Leszek A. Utracki
Charles A. Wilkie
Editors

Polymer Blends Handbook

Second Edition

Springer Reference

Polymer Blends Handbook

Leszek A. Utracki • Charles A. Wilkie
Editors

Polymer Blends Handbook

Second Edition

With 491 Figures and 388 Tables

Springer Reference

Editors
Leszek A. Utracki (1931–2012)
Industrial Materials Institute
National Research Council of Canada
Boucherville, QC, Canada

Charles A. Wilkie
Department of Chemistry and Fire Retardant Research Facility
Marquette University
Milwaukee, WI, USA

Printed on acid-free paper

Preface to the Second Edition

The field of polymer blends is one that continues to grow year by year. More and more blends are now available and can consist of several polymers, all combining to give enhanced properties for a specific application. The preface that was included in the first edition clearly states the state of the field both then and now. Certainly there have been changes, and this new edition reflects those changes.

The biggest changes to this edition occur in the second section on applications where the content has been rearranged in better keeping with current thinking. New to this edition are chapters on degradation, stabilization and flammability of polymer blends, polymer blends with nanoparticles, and polyethylenes and their blends. Also there are three new appendices, on trade names, commercialization dates, and notations and symbols.

The first edition of the *Polymer Blends Handbook* was edited by Leszek A. Utracki who also wrote several of the chapters in that book. It was his idea that the time was ripe for a new edition of the book, and he arranged for all of the chapter authors and had the book well underway. Unfortunately, Leszek left this world on July 11, 2012. Just before, while he was hospitalized, he completed the work on the new chapter on polyethylene and its blends. His last update to the chapter took place on July 7, 2012.

This book is really a tribute to Leszek A. Utracki, the man and the scientist. He was proud of the first edition, and we think that he would be proud of this edition as well.

I would like to express my gratitude to Leszek for inviting me to serve as a coeditor of this book and to all of those, especially the authors of the chapters and the section reviewers, who have made this book possible. Finally, I thank my family, and I am also quite confident that the Utracki family was instrumental in enabling him to do the work.

June 2014
<div align="right">Charles A. Wilkie
Milwaukee, WI, USA</div>

Preface to the First Edition

Science as a methodical investigation of nature's capacities evolved from the humble craft tradition. Its goal is to provide the most general and the simplest possible description of the observable character of nature. In the past, the singular concept of "science" comprised all aspects of intellectual endeavor: the arts, the sciences, and the crafts. It was Diderot's *Encyclopédie ou Dictionnaire Raisonné des Sciences*, *des Arts et des Métiers* of 1751–1766 that first divided the old "science" into these three parts. The next split – that between the basic and applied sciences – is barely a century old. Basic science has been described as motivated by the desire to discover connections between natural phenomena, while applied science is the application of the discovered laws of nature for the material benefits of mankind. The boundary between the two is not rigid since experimental observation frequently provides a spur to fundamental discoveries.

In the golden times of the scientific institutions in Europe and North America, the most prominent scientists, often the Nobel Prize winners, directed the work. In the USA, during the years 1945–1975, basic scientific research was considered "essential for the national security, economic growth and survival of the basic democratic values" (J. Krige & D. Pestre, *Science in the 20th Century*, 1997). In the 1960s, several major corporations supported research institutes with total freedom of the research topics.

During the last two decades of the twentieth century, there has been an apparent reversal in the appreciation of science. Except for a few domains (e.g., astrophysics or atomic physics, project *genome*), intellectual efforts are being directed toward short-term developmental work of a commercially pertinent nature. This tendency is global, evident in the industrial, academic, as well as state-supported laboratories. The CEOs hired for a contract to manage an institution are focused on the present. Managing has become a profession divorced from technical knowledge – a research institute, finance company, or pig farm may "benefit" from guidance by the same person. These tendencies are reflected in the evolution of polymer science and technology.

The history of synthetic polymers is incredibly short. The term *polymer* was introduced in 1832. The first synthetic polymer (phenol-formaldehyde) was commercialized as *Bakelite*™ in 1909, while the first thermoplastic (polystyrene, *Trolitul*™), 6 years later. The early polymer industry was developed by entrepreneurs that had little if any technical background. The commercial successes (and

less known but more numerous failures) predated even the fundamental idea of what constitutes the polymeric species. As late as 1926, Hermann Staudinger unsuccessfully advocated the concept of a linear, covalently bonded macromolecule. This idea was finally accepted during the Faraday Society meeting in 1935, only after Carothers reported on his polymerization studies and demonstrated the validity of the polycondensation theory, developed by his younger colleague from du Pont de Nemours, Paul Flory. The theory provided the relationships between the molecular weights and the reaction kinetics, thus making it possible to ascertain the validity of the newly formulated polycondensation principles that postulated the sequential addition of bifunctional units to form linear macromolecules.

In 1900, the world production of plastics was 25 kton, doubling during the following 30 years, then redoubling in 5. The most spectacular growth was recorded in the early 1940s when the demand created by the convulsions of World War II engendered a spectacular growth of 25 % per annum. During the first 30 post-war years, the global plastics industry sustained an average growth rate of 15 %/year. By 1992, the world production of plastics had reached 102 million m^3/year, while that of steel was 50 million m^3/year. Furthermore, from 1980 to 1990 plastics production increased by 62 %, while that of steel decreased by 21 %. Only during the past 20 years or so has plastics consumption shown smaller and more erratic advances. It is expected that by the year 2000, the world production of plastics will be 151 million tons/year. Considering the uneven polymer consumption around the world, polymer production has the potential to increase tenfold by the mid-twenty-first century. Polymers are the fastest growing structural materials.

Rubber blending predates that of thermoplastics by nearly a century. In 1846, Parkes introduced the first blends of *trans*- and *cis*-1,4-polyisoprene, i.e., natural rubber (NR) with gutta-percha (GP). By varying the composition and/or adding fillers, the blends were formed into a variety of flexible or rigid articles.

Polymer blends were developed alongside the emerging polymers. Once nitrocellulose (NC) was invented, it was mixed with NR. Blends of NC with NR were patented in 1865 – 3 years before the commercialization of NC. The first compatibilization of polyvinylchloride (PVC) by blending with polyvinylacetate (PVAc) and their copolymers dates from 1928. PVC was commercialized in 1931, while its blends with nitrile rubber (NBR) were patented in 1936 – 2 years after the NBR patent was issued. The modern era of polymer blending began in 1960, after Alan Hay discovered the oxidative polymerization of 2,4-xylenols that led to polyphenylene ether (PPE). Its blends with styrenics, *Noryl*[TM], were commercialized in 1965.

At present, polymer alloys, blends, and composites consume over 80 wt% of all plastics. In addition, the polymer blends segment of the plastics industry increases about three times faster than the whole plastics industry. Blending has been recognized as the most versatile, economic method to produce materials able to satisfy complex demands for performance. By the year 2000, the world market for polymer blends is expected to reach 51 million tons per annum, worth well over US$ 200 billion. The tendency is to offer blends that can be treated as any other

resin on the market; hence, their processibility must closely match that of single-phase polymers but offer a much greater range of performance possibilities.

In the economically advanced countries, plastics have displaced conventional materials for most applications. Today, the market pressure forces the resin manufacturers to provide better, more economic materials with superior combinations of properties, not as a replacement for wood or steel but rather to replace the more traditional polymers. This has resulted in:

- Increased scale of production
- Use of multicomponent and multiphase materials
- New processing methods

For example, twin-screw extruders with 80 t/h throughput and injection (100,000 kN) molding presses with shot size of 100 l of polymer are available. Composites where the matrix is a polymer blend that comprises six different polymers have been introduced. Gas and multiple injection processes, melt-core technology, solid-state forming, and microcellular foams all lead to new products with advanced performance. The polymer industry is becoming increasingly sophisticated.

To support these new tendencies, the research community has been asked to provide better predictive methods for the multicomponent blends as well as improved sensors for the closed-loop process control. In particular, the evolution of morphology during the compounding and processing steps is of paramount importance. Microrheology and coalescence are the keys to describing the structure evolution of polymer blends.

In the early 1990s, the first mathematical models capable of predicting the evolution of morphology during compounding of polymer blends were developed. The fully predictive model provided good agreement with the experimentally determined variation of morphology inside a twin-screw extruder. However, it must be recognized that the morphology developed inside the compounding or the processing unit is dynamic. Upon removal of stress and in the absence of effective compatibilization, the morphology changes with time.

Today, very few unmodified resins are being used. Some polymers require less modification than others. For example, the semicrystalline polymers that already have a two-phase structure may need modification less urgently. By contrast, the amorphous resins, such as PVC, PS, PPE, or polycarbonate of bisphenol A (PC), are brittle and require blending more frequently. The advantages of blending fall into two categories.

(a) Blending may improve resin or product performance by:

1. Producing materials having a full set of the desired properties at lowest cost
2. Extending the engineering resins performance by incorporation of less expensive polymers
3. Improving specific properties:
   - Toughening brittle polymers eliminates the need of using low-molecular-weight additives (e.g., plasticizer in the flexible PVC formulations).
   - Blending with a more rigid and more heat-resistant resin may lead to improved modulus and dimensional stability.

- Incorporation of a semicrystalline polymer into an amorphous resin improves solvent and chemical resistance (e.g., in blends of PC with PEST).
- Incorporation of a nonflammable resin into a flammable one improves flame resistance (e.g., styrenics or acrylics with PVC).
- Blends with polymers having either −OH or −SH functionality result in permanently antistatic blends (e.g., ethylene oxide-co-epichlorohydrin with ABS/PC blend).
- Biodegradable materials can be produced by incorporation of a biodegradable resin.
- Blending makes it possible to produce integrated multilayer structures.
4. Providing means for recycling of industrial and/or municipal plastics waste
5. Rebuilding high molecular weights of partially degraded polymers, thus making it possible to produce high-performance articles from the plastics waste

(b) Blending may lead to improved processibility in the following ways:

1. Incorporation of a miscible resin with a lower glass transition temperature (T_g) makes it possible to process the high-T_g resin at temperatures well below the thermal degradation limit (e.g., PS/PPE blends).
2. Incorporation of an immiscible, low-viscosity resin makes it possible to reduce pressure drop across dies or runners, thereby increasing productivity (e.g., LCP/PEEK blends).
3. Blending with a resin that either by itself shows high strain hardening (SH) (e.g., LDPE in blends with another PO) or when reactively blended forms long-chain branches (e.g., PS in blends with PO) results in blends having a controllable degree of SH. These materials show better processibility in technologies where the extensional flow field is important, namely, film blowing, blow molding, wire coating, and foaming.
4. Incorporation of elastomeric particles improves nucleation of gas bubbles; thus, it stabilizes the foaming process and reduces bubble size and the final foam density.
5. Incorporation of a degradable resin into an engineering or specialty one provides the means for generation of a controllable amount of foaming gas during the ensuing stages of processing, namely, injection molding.
6. Blending different grades of the same resin broadens the molecular weight distribution, which in turn results in easier, more stable processing (as well as better mechanical performance).
7. Blending improves product uniformity (scrap reduction) and plant economy.
8. Blending ascertains quick formulation changes and, thus, plant flexibility and productivity.
9. Blending reduces the number of grades that need to be manufactured and stored.
10. Blending technology offers methods for producing higher-aesthetic-value materials, e.g., films or coatings without gel particles (or "fish eyes") and moldings with streak-free surface finish.

The aim of the *Polymer Blends Handbook* (PBH) is to provide the most comprehensive information on all aspects of polymer blend science and technology. The book will be useful for students entering the field as well as for seasoned professionals. The contributors to PBH are renowned experts from eight countries and four continents, who work in academe, government laboratories, and industry.

In consequence, the book may be considered as comprising two parts: 1. fundamental principles (nine chapters) and 2. technology (eight chapters and four appendices). Each chapter provides an introduction to the pertinent topic, discusses the principal aspects and the typical approaches used by the experts in the area, provides numerical values of pertinent parameters, and gives extensive references that facilitate further topical studies.

PBH comprises 17 chapters with the following topics: 1. Introduction to polymer blends, 2. Thermodynamics, 3. Crystallization, 4. Interphase and compatibilization by addition of a compatibilizer, 5. Reactive compatibilization, 6. Interpenetrating polymer networks, 7. Rheology, 8. Morphology, 9. Compounding, 10. Processing, 11. Use of radiation, 12. Properties and performance, 13. Applications, 14. Degradation and aging, 15. Commercial blends, 16. Role of polymer blends' technology in polymer recycling, and 17. Perspectives. Furthermore, the appendices provide information on 1. International abbreviations for polymers and polymer processing, 2. Miscible polymer blends, 3. Examples of commercial polymer blends, and 4. Dictionary of terms used in polymer science and technology.

Finally, the editor wishes to express thanks and personal appreciation to the contributors. They invested much time outside their regular duties, collecting the material and setting it into uniform text. They showed a high spirit of cooperation and great patience. The *Polymer Blends Handbook* is a testimonial of their efforts.

25 December, 1999   Leszek A. Utracki
                                                                                         Montreal, Canada

Section Editors

Miriam Rafailovich Program in Chemical and Molecular Engineering, Department of Materials Science and Engineering, Stony Brook University, Stony Brook, NY, USA

Evangelos Manias Department of Materials Science and Engineering, Pennsylvania State University, PA, USA

About the Editors

Leszek A. Utracki, 1931–2012, was Senior Research Officer at the National Research Council of Canada, Industrial Materials Institute, and adjunct professor at McGill University, Department of Chemical Engineering, in Montreal, Quebec. Professor Utracki was the author/editor of 21 books and had written 48 book chapters, hundreds of journal articles, as well as meeting proceedings, which placed him on the ISI list of Highly Cited Researchers. He was the cofounder and President of the Canadian Rheology Group and the Polymer Processing Society (International). He also organized and served as the series editor of the book series "Progress in Polymer Processing" and as a member in the editorial boards of several research journals. He was the recipient of many international awards, but one is specifically worth mentioning: just a few months after he passed away, he was awarded the Queen Elizabeth II Diamond Jubilee Medal of Distinction, which is to honor significant contributions and achievements by Canadians.

Leszek A. Utracki was born and educated in Poland. After completing his postdoctorate at USC in Los Angeles with Robert Simha, he settled in Canada. He was a passionate researcher in the fields of thermodynamics, rheology, and processing of multicomponent/multiphase polymeric systems. Sadly, he passed away a few months after embarking on the work for the second edition of the *Polymer Blends Handbook*, during which he had made important contributions to the work. This edition of the handbook is dedicated to his memory.

Charles A. Wilkie is currently Professor Emeritus of Chemistry at Marquette University. He received his B.S. degree from the University of Detroit and his Ph.D. in Inorganic Chemistry from Wayne State University, following which he joined Marquette University. He has been assistant, associate, and full professor and retired as the Habermann-Pfletschinger Professor in 2009. His main areas of interest for the past several years have been polymer nanocomposites and fire retardancy.

Contents

Contributors

Abdellah Ajji CREPEC, Department of Chemical Engineering, Ecole Polytechnique de Montreal, Montreal, QC, Canada

M. K. Akkapeddi York, PA, USA

V. Arrighi Institute of Chemical Sciences, School of Engineering and Physical Sciences, Heriot-Watt University, Edinburgh, Scotland, UK

Z. Bartczak Department of Polymer Physics, Centre of Molecular and Macromolecular Studies Polish Academy of Sciences, Lodz, Poland

S. Bruce Brown Hill Country Patent Services, Inc, Austin, TX, USA

J. M. G. Cowie Institute of Chemical Sciences, School of Engineering and Physical Sciences, Heriot-Watt University, Edinburgh, Scotland, UK

Mark T. DeMeuse MTD Polymer Consulting, Charlotte, NC, USA

V. Everaert Department of Chemistry, Division of Molecular and Nanomaterials, Laboratory of Macromolecular Structure Chemistry, Catholic University of Leuven, Heverlee, Belgium

A. Galeski Department of Polymer Physics, Centre of Molecular and Macromolecular Studies Polish Academy of Sciences, Lodz, Poland

Lloyd A. Goettler Department of Polymer Engineering, The University of Akron, Akron, OH, USA

Suat Hong Goh Department of Chemistry, National University of Singapore, Singapore, Singapore

R. Gonzalez-Núñez Department of Chemical Engineering, Universidad de Guadalajara, Guadalajara, Jalisco, Mexico

G. Groeninckx Department of Chemistry, Division of Molecular and Nanomaterials, Laboratory of Macromolecular Structure Chemistry, Catholic University of Leuven, Heverlee, Belgium

R. K. Gupta Department of Chemical Engineering, West Virginia University Benjamin M. Statler College of Engineering and Mineral Resources, Morgantown, WV, USA

C. Harrats Laboratoire de Chimie Appliquée (LAC) DGRSDT, Institut des Sciences et Technologies, Ctr Univ Ain Temouchent, Ain Temouchent, Algeria

R. Hu Arkema Coating Resins, Cary, NC, USA

Takashi Inoue Department of Polymer Science and Engineering, Yamagata University, Yonezawa, Japan

Musa R. Kamal Department of Chemical Engineering, McGill University, Montreal, QC, Canada

Francesco Paolo La Mantia Department of Civil, Environment, Aerospace and Materials Engineering, University of Palermo, Palermo, Italy

Evangelos Manias Department of Materials Science and Engineering, Pennsylvania State University, University Park, PA, USA

Zvonimir Matusinovic Faculty of Chemical Engineering and Technology, University of Zagreb, Zagreb, Croatia

A. Mirzadeh Department of Chemical Engineering, McGill University, Montreal, QC, Canada

P. Mukhopadhyay IPEX Technologies Inc., Montreal, Canada

Toshiaki Ougizawa Department of Chemistry and Materials Science, Tokyo Institute of Technology, Meguro-ku, Tokyo, Japan

D. R. Paul Department of Chemical Engineering and Texas Materials Institute, The University of Texas at Austin, Austin, TX, USA

D. Rodrigue Department of Chemical Engineering, Université Laval, Quebec, QC, Canada

Roberto Scaffaro Department of Civil, Environment, Aerospace and Materials Engineering, University of Palermo, Palermo, Italy

James J. Scobbo SABIC-Innovative Plastics, Mount Vernon, IN, USA

Andreas Schönhals BAM Federal Institute for Materials Research and Testing, Berlin, Germany

G. Z.-H. Shi Industrial Materials Institute, National Research Council of Canada, Boucherville, QC, Canada

Rehau Inc, Leesburg, VA, USA

L. H. Sperling Chemical Engineering and Materials Science and Engineering, Whitaker Laboratory, Lehigh University, Bethlehem, PA, USA

R. R. Tiwari Department of Chemical Engineering and Texas Materials Institute, The University of Texas at Austin, Austin, TX, USA

Leszek A. Utracki National Research Council Canada, Industrial Materials Institute, Boucherville, QC, Canada

M. Vanneste Textile Functionalisation & Surface Modification, R&D/ CENTEXBEL, Zwijnaarde, Algeria

Charles A. Wilkie Department of Chemistry and Fire Retardant Research Facility, Marquette University, Milwaukee, WI, USA

S. F. Xavier Parul Innovation Center, Parul Institute of Technology, Vadodara, Gujarat, India

Formerly at Research Center, Indian Petrochemicals Corporation Ltd., Vadodara, Gujarat, India

Huajie Yin BAM Federal Institute for Materials Research and Testing, Berlin, Germany

Part I

Fundamentals

Polymer Blends: Introduction

<div align="right">**1**</div>

Leszek A. Utracki, P. Mukhopadhyay, and R. K. Gupta

Contents

Leszek A. Utracki: Deceased.

L.A. Utracki
National Research Council Canada, Industrial Materials Institute, Boucherville, QC, Canada

P. Mukhopadhyay
IPEX Technologies Inc., Montreal, Canada
e-mail: Prithu.Mukhopadhyay@ipexna.com

R.K. Gupta
Department of Chemical Engineering, West Virginia University Benjamin M. Statler College of Engineering and Mineral Resources, Morgantown, WV, USA
e-mail: rakesh.gupta@mail.wvu.edu

Abstract

While this chapter serves as an introduction to all the subsequent chapters, it is quite comprehensive. A brief history as well as information on polymer synthesis, nomenclature, and properties is provided. The need to formulate polymer alloys and blends and the resulting benefits are explained. Since the vast majority of polymer pairs are thermodynamically immiscible, compatibilization and reactive extrusion are necessary to improve interfacial adhesion and to optimize blend performance. How polymer morphology is influenced both by blend

composition and the imposed process conditions is discussed first. This provides the theoretical basis for understanding the concept of polymer blending.

The raison d'etre of polymer blending is developing materials having enhanced performance. Performance itself depends on the polymer pair types employed, their relative amounts, extent of miscibility, nature and amount of compatibilizer used, and the method of blending. A key issue is the process of mixing polymers during which blends undergo a complex combination of shear and elongation and the evolution of blend microstructure becomes crucial and requires close attention. Each category of polymer pairs, from commodity resins and their blends, to engineering resins and their blends, and to specialty polymers and their blends is discussed in detail. Pertinent theoretical as well as experimental results are presented and reviewed.

The concern over environmental issues and sustainability has opened up another vibrant research field, namely, biobased and biodegradable polymer blends. An overview of major developments and recent trends in biodegradable blends with an emphasis on PLA blends are also discussed. This chapter closes with an outlook for the future of this important subject.

1.1   Introduction

The world production of plastics in 1900 was about 30,000 t – in the year 2010 it had reached 265 Mt, with thermoplastics contributing about 90 % of this amount, while the rest was thermosets. For the last 20 years, plastic production has increased at the rate of about 5 % per year, with no saturation in sight. In 2010, China accounted for 23.5 % of plastic production, whereas Europe and the North American (NAFTA) region contributed 21.5 % and 20.5 %, respectively (Plastics-the facts 2011, PlasticsEurope, 20th ed). According to a report by Global Industry Analysts Inc., global plastic consumption is set to reach 297.5 Mt by 2015.

Polymers are classified as either *natural*, those that resulted from natural biosynthesis, or *synthetic*. The *natural* (polysaccharides, proteins, nucleic acids, natural rubbers, cellulose, lignin, etc.) has been used for tens of thousands of years. In Egypt the musical string instruments, papyrus for writing, and styrene (in a tree balsam) for embalming were used 3,000 BC. For millennia shellac has been used in Indian turnery (Chattopadhyaya 1986). The natural rubber was used by *Olmecs* at least 3,000 years ago (Stuart 1993).

The term *synthetic* polymer refers equally well to linear, saturated macromolecules (i.e., *thermoplastics*), to unsaturated polymers (i.e., *rubbers*), or to any substance based on cross-linkable monomers, macromers, or prepolymers (i.e., *thermosets*). The focus of this handbook is on blends of thermoplastics made of predominantly saturated, linear macromolecules.

In the last quarter century, there have been two major developments, one technical and one economic, which have given a new direction to the polymer industry. There has been a revolution in polyolefin technology that started during the last decade of the

twentieth century, and this is related to the development of metallocene and single-site catalysts. The use of these catalysts allows for the synthesis of improved polymers with well-defined structures and closely controlled molecular architectures. Separately, there has been a shift toward green chemistry, promoted by concerns about sustainability and raw material availability. The need to provide alternatives to petroleum-based products has led to the development and commercialization of biobased plastics. Simultaneously, there has been increasing emphasis on the recycling of postconsumer plastics (Yeh et al. 2009). Additionally, there has been consolidation in the industry and an overall shift in production of commodity resins to countries in Asia.

There are many sources of information about polymer history (Martuscelli et al. 1987; Seymour and Cheng 1987; Vogl and Immergut 1987; Alper and Nelson 1989; Morris 1989; Seymour 1989; Sperling 1992; Mark 1993; Sparke 1993; Utracki 1994, 1998a; Freinkel 2011; Strom and Rasmussen 2011).

The abbreviations used in this text are listed at the end of this chapter.

1.2   Early Polymer Industry

1.2.1   The Beginnings

The polymer industry traces its beginning to the early modifications of shellac, natural rubber (NR, an amorphous *cis*-1,4-polyisoprene), gutta-percha (GP, a semicrystalline *trans*-1,4-polyisoprene), and cellulose. In 1846, Parkes patented the first polymer blend: NR with GP partially co-dissolved in carbon disulfide. Blending these two polyisoprene isomers resulted in partially cross-linked (co-vulcanized) materials whose rigidity was controllable by composition. The blends had many applications ranging from picture frames, tableware, ear trumpets, to sheathing the first submarine cables.

1.2.2   Modified Natural Polymers

The first man-made polymer was nitrocellulose (NC). The main use of the NC resins was a replacement of the natural and expensive materials, viz., ivory, tortoise shell products, amber, ebony, onyx, or alabaster. The use of cellulose acetate (CA), as a thermoplastic, began in 1926. Cellulose ethers and esters became commercially available in 1927. Casein cross-linked by formaldehyde gave hornlike materials – *Galalith*™ has been used to manufacture shirt buttons or as imitation of ivory and porcelain (Pontio 1919).

1.2.3   Synthetic Rubbers

The first polymerization of isoprene in sealed bottles was reported in 1884 by Tilden. *Methyl rubber* was thermally polymerized at 70 °C – the reaction

required 3–6 months, giving poor quality products. In 1926 BASF developed sodium-initiated polymerization of butadiene known as *Buna*™ for butadiene + natrium. The first successful, general-purpose rubbers were copolymers of butadiene with either styrene, *Buna-S*, or acrylonitrile, *Buna-N* (Tschunkur and Bock 1933; Konrad and Tschunkur 1934). Poly(2-chlorobutadiene), *chloroprene* (Carothers et al. 1931), was introduced in 1931 by du Pont. Elastomeric polysulfides (Patrick 1932), were commercialized in 1930 as *Thiokol*™. In 1937 butyl rubber (copolymer of isobutylene with isoprene) was invented. The synthetic rubber production took a big leap during the Second World War (WW2) (Morton 1982).

1.2.4   Synthetic Thermosetting Polymers

The first commercially successful *synthetic* polymer was phenol-formaldehyde (PF) resin (Smith 1899). The resin was introduced in 1909 by Baekeland as *Bakelite*™. The urea-formaldehyde (UF) resins were discovered in 1884, but production of *Beetle*™ moldable resin commenced in 1928. Three years later, *Formica*™, phenolic paper covered with decorative layer protected by UF, was introduced. The thiourea-formaldehyde molding powders were commercialized in 1920, while in 1935, Ciba introduced *Cibanite*™, aniline-formaldehyde (AF) resins, molding materials, and then, 2 years later, the melamine formaldehyde (MF).

Epoxy compounds were discovered by Prileschaiev in 1909, but its importance was realized only during WW2. In 1956, glass fiber reinforcements were introduced. The thermoset polyesters (TS) were developed by Ellis in 1933–1934. The first use of glass-reinforced TS dates from 1938.

1.2.5   Synthetic Thermoplastic Polymers

The synthetic polymers are divided into three categories:
1. Commodity
2. Engineering
3. Specialty

The five large-volume polymeric families that belong to the commodity resins are polyethylenes (PE), polypropylenes (PP), styrenics (PS), acrylics (PMMA), and vinyls (PVC). According to the web site, www.icis.com, the market share of these plastics in 2011 was 178 Mt – in other words, they represent about 70 % of all plastics.

The five engineering polymer families are polyamides (PA), thermoplastic polyesters (PEST), polycarbonates (PC), polyoxymethylenes (POM), and polyphenylene ethers (PPE). According to a March 2013 Industry Experts report entitled "Engineering Plastics – A Global Market," 19.6 Mt of engineering plastics were produced in 2012. In other words, these polymers constitute only about 10 % by volume of all polymers produced. However, due to superior properties, they command a much larger percentage by value of the plastic consumption.

Table 1.1 High-performance materials: a comparison

No.	Material	Strength (GPa)		Modulus (GPa)	
		Theoretical	Observed	Theoretical	Observed
1.	Polyethylene (standard)	21	≤ 0.03	316	0.2
2.	Polyethylene gel-spun	21	6.0	316	220
3.	Polyester (standard)	24	0.07	124	2.2
4.	Polyester oriented	24	1.2	124	21
5.	Aromatic polyamide	21	3.6	190	125
6.	Aromatic polyester (EFK)	–	4.1	–	139
7.	Poly(phenylene benzothiazole)	–	4.2	371	365
8.	Polyazomethin	–	4.7	–	125
9.	Carbon fiber	–	3.1	–	235
10.	Steel	29	2.1–3.5	–	210

The engineering and specialty polymers show high mechanical performance, and the continuous use temperature $150 \leq \text{CUT}(°\text{C}) \leq 500$.

The polymer industry increasingly favors high technology and high value-added materials. These are obtained either by means of new polymerization methods, by new processing technologies, or by alloying and reinforcing. For example, new syndiotactic PP or PS (sPP or sPS, respectively) surpasses the performance of their predecessors. The gel-spun PE fibers have 200 times higher tensile strength than standard PE. Aromatic polyester (EKF from Sumitomo) has tensile strength of 4.1 GPa, to be compared with 70 MPa of a standard polyester resin (see Table 1.1).

New types of polymers are also being introduced, e.g., dendritic-structure polymers (Fréchet et al. 1992; Schluter and Rabe 2000), carbosilane dendritic macromolecules (Roovers et al. 1993), the "hairy rod" molecular structures where rigid-rod chain macromolecules are provided with short and flexible side branches (Wegner 1992), etc. However, the polymer technology invariably moves away from the single-phase materials to diverse combinations of polymers, additives, and reinforcements. While synergistic effects are often cited, the main reason is a need for widening the range of properties, for development of materials that would have the desired combination of properties – tailor-made polymeric systems. With single-phase polymers, one can only change the molecular weight or form copolymers. This can require significant effort. By contrast, blending is easy and inexpensive, and it is especially useful when only small volumes are required. Also, scale-up is straightforward. At present, about a third of the synthetic resins are used in blends and another third in composites.

1.2.6   Compounding and Processing

The first mixer was an annular container with a spiked rotor for rubber compounding (Hancock 1823). The calendar/two-roll mill was patented by Chaffe in 1836 and manufactured by Farrel Co. A counterrotating twin-shaft internal mixer

with elliptical rotating disks or sigma blades was developed by the end of the 1800s (Freyburger 1876; Pfleiderer 1880). The first hand-operated extruder was a ram press, used for forming NR or GP and then later NC.

The first belt-driven extruders with Archimedean screw were patented much later (Gray 1879). In 1939, Paul Leistritz Maschinenfabrik built electrically heated, air-cooled extruder, with nitrided barrel, having $L/D = 10$, an automatic temperature control, variable screw speed. The machine is considered a precursor of the modern single-screw extruders, SSE. During the WW2 breaker plates, screen packs, crosshead dies, coextrusion, monofilament extrusion, film blowing, and biaxial sheet orientation were introduced. In the 1950s, a coextrusion process, venting, and two-stage screws were developed. In the 1980s the microprocessor control evolved into computer-integrated manufacturing, and the helical grooved feed barrels, high-pressure gear pumps, air lubricated die flow, and biaxial film orientation were introduced (Utracki 1991a, c).

Pfleiderer patented the first modular counterrotating twin-screw extruder (TSE) in 1882. An intermeshing, corotating TSE, the predecessor of the modern machines, was designed for extrusion of CA. The TSE was used by I. G. Farbenindustrie for the production of PA-6 (Colombo 1939). In 1959, Werner and Pfleiderer introduced ZSK machines (vented, intermeshing, corotating, with segmented screw and barrel, twin-screw extruders). These provided good balance between the dispersive and distributive mixing at relatively high output rates. In 1979 Japan Steel Works (JSW) developed TEX-series TSEs for reactive compounding, permitting an easy change of the screw direction from co- to counterrotation. In collaboration with Sumitomo Chem., barrel elements with sampling ports were designed, providing ready access to the processed material for determining the reaction progress and morphology (Nishio et al. 1990). American Leistritz has been active in designing TSE kneading elements that improved mixing capability by maximizing the extensional flow field. More information on the evolution of the extrusion technology can be found in ▶ Chap. 9, "Compounding Polymer Blends".

Injection molding of NC dates from 1872. The early machines were hand operated. They used an axially movable screw or plunger and were equipped for devolatilization. The commercial-scale injection molding of PS has begun in 1931. In 1932 Gastrow developed the first automatic unit, *Isoma-Automat* (30 g capacity per shot), with torpedo-type heating chamber. In 1951, Willert invented an in-line reciprocating screw plasticization that revolutionized the injection molding industry. The first automated injection molding plant was developed by Eastman Kodak in 1950.

Hayatt used blow molding in 1880 to produce baby rattles out of CA tubes or sheets. In 1942, Plax Corp. started manufacturing *squeezable* LDPE bottles. By the end of the 1950s, blow molding was the most rapidly developing processing method. In 1965 Wyeth, using the stretch blow molding, produced polyethylene terephthalate (PET) bottles. In 1972, Toyo Seikan started to produce multilayered blow molded bottles from PP and EVAl. In 1976 Ishikawajima-Harima introduced intermittent coextrusion blow-molding system for large parts.

1.2.7 Development of Polymer Science

1.2.7.1 Polymerization

Cellulose modification dates from 1833 (Braconnot). In 1838 Regnault photopolymerized vinylidene chloride. A year later, Simon observed that heating styrene in the presence of air generated a tough gelatinous material – a low molecular weight PS. Polyoxymethylene (acetal) was discovered in 1859. In 1872 several new polymers were announced, viz., PVC, polyvinyl bromide (PVB), and phenol-formaldehyde (PF). Polymethacrylates were discovered by Kahlbaum in 1880, polymethylene in 1897, 1 year later polycarbonate by Einhorn, polyamide-6 (PA-6) in 1907, etc. In the 1920s, the list of polymers rapidly started to increase, viz., polysulfide (PSF), polyvinyl alcohol (PVAl), poly(styrene-co-maleic anhydride) (SMA), polyvinyl formal (PVFO), etc. During the next decade, polyacetylene (PACE), styrene-acrylonitrile copolymer (SAN), low-density polyethylene (LDPE), polyvinylidene chloride (PVDC), epoxy resins (EP), polyamides (e.g., PA-66, PA-610, PA-106), polysiloxanes (PDMS), polychlorotrifluoroethylene (PCTF), polytetrafluoroethylene (PTFE), and many others were discovered (Utracki 1989a).

Most early thermoplastics, e.g., PVC or PS, were obtained in the free radical polymerization, initiated either by heat or by sunlight. The first systematic studies of the free radical chemistry commenced 80 years later (Ostromislensky 1911, 1915, 1916). Fikentscher empirically determined which one of the 30-or-so monomers *liked* or *disliked* to copolymerize with each other. The advantage of latex blending was also established. The theory of the free radical copolymerization was only developed in the 1940s (Alfrey et al. 1952).

The polycondensation reactions have been known since the mid-1800 (Lourenço 1859; Wurtz 1859, 1860). In 1927, Carothers and his colleagues provided the basis for understanding the nature of these reactions (Carothers, 1931). Good agreement between Flory's theoretical predictions and the experimental observations of the average molecular weight (MW) provided convincing arguments for the acceptance of the linear macromolecule model.

The alkyl-lithium-initiated, *living* anionic polymerization of elastomers was described in 1928 by Ziegler. To polymerize styrene-isoprene block copolymers, Szwarc et al. (1956) used sodium naphthalene as an anion-radical di-initiator, while Shell used an organolithium initiator. The polymerization mechanism was described by Bywater (1965).

In the early 1950s, Ziegler found that in the presence of $ZrCl_4 + AlR_3$ ethylene can be polymerized at low temperature and pressure into linear, high-density polyethylene (HDPE). The catalysts developed by Ziegler, and later by Natta, become known as *Ziegler-Natta*, *Z-N* catalysts. These can be defined as polymerization initiators created from a catalyst (1) and cocatalyst (2), where (1) is halide or oxyhalide of transition metals from groups IV to VII and (2) is an organometallic compound of metal from groups I to III. The *Z-N* catalyst is prepared by mixing ingredients (1) and (2) in a dry, oxygen-free solvent (Natta and Danusso 1967). A more recent Z-N catalyst development is

$MgCl_2$-supported catalysts that have a 100-fold more active sites per mole of Ti and about ten times higher propagation rate (Rieger et al. 1990).

The newest, single-site metallocene catalyst makes it possible to control MW, molecular weight distribution (MWD), comonomer placement, stereoregularity, and lifetime of the reactive chain end (Kaminsky et al. 1985, 1992; Kaminsky 1998; Swogger 1998; Choi and Soares 2012). The use of either $(Cp)_pR'_s(Cp)MeQ_{3-p}$ or $R''_s(Cp)_2MeQ'$ (where Cp is cyclopentadienyl (substituted or not) radical; Me is metal from group 4b, 5b, or 6b; and R', R'', Q, and Q' are radicals (viz., aryl, alkyl, alkenyl, alkylaryl, or arylalkyl), s = 0–1, p = 0–2), for the polymerization of ethylene copolymers, provides independent control of MW and density. The catalyst is used in combination with a large amount of alumoxanes.

In 1975 Mitsui Petrochemicals introduced metallocene-made LLDPE *Tafmer*™, with controlled comonomer placement, but rather low MW. In 1991, Dow Plastics produced developmental quantities of ethylene copolymers with up to 25 mol% of butene, hexene, or octene, *Affinity*™ resins. The use of a metallocene catalyst with a single cyclopentadiene ring resulted in a certain degree of randomization of the polymerization process. The catalyst produced PP with narrow molecular weight distribution, *and a long-chain branching*, similar to LDPE. In the early 1990s, Exxon Chemical Company (now ExxonMobil) worked to develop metallocene catalysts for use in Union Carbide's (now Dow Chemical) gas-phase UNIPOL™ PE process. Later, in 1997, the two companies formed a joint venture called Univation Technologies which introduced XCAT™ metallocene catalysts. The resulting linear low-density polyethylene finds application in flexible packaging, pallet stretch wrap, and food packaging and agricultural films. The most recent development is PRODIGY™ bimodal catalyst that allows for the synthesis of bimodal film resins in a single reactor, resulting in a PE with improved performance and processability.

The metallocene catalysts are also used to produce high melting point polymers out of *commodity* monomers, e.g., sPS, with $T_g = 100\ °C$, and $T_m = 266\ °C$, or syndiotactic poly(*p*-phenyl styrene), (sPhPS), with $T_g = 196\ °C$, $T_m = 352\ °C$, and the decomposition temperature, $T_{decomp} = 380\ °C$. Since sPhPS is miscible with sPS in the whole range of concentration, blends of these two syndiotactic polymers can be processed at any temperature above $266\ °C$ (Watanabe et al. 1992). Polycyclohexylethylene (PCHE) is a metallocene resin, developed by Dow as a replacement for PC in the production of optical disks. PCHE has low shrinkage (0.02 % after 24 h), higher light transmission than PC (91.9 % vs. 89.8 %, respectively) and high flex modulus of 71 GPa.

1.2.7.2 Polymer Physics
Molecular Weight (MW)
Osmotic pressure measurements for the determination of MW were used in 1900 to characterize starch. Twenty years later, the solution viscosity measurements were introduced by Staudinger for this purpose. However, it was Mark and his collaborators who developed the concept of the intrinsic viscosity ([η]) and demonstrated that it provides information on the volume of individual colloidal particles, thus on MW.

For the freely rotating chains, the dependence (today known as *Mark-Houwink-Sakurada* equation) was obtained (Guth and Mark 1934):

$$[\eta] \equiv \lim_{c \to 0}[(\eta/\eta_o) - 1]/c = KM_v^a \tag{1.1}$$

where η and η_o are viscosities of the solution and solvent, M_v is the viscosity-average molecular weight, and K and a 0.5–0.7, are equation parameters. In 1933 the ultracentrifugation was developed (Kraemer and Lansing 1933). Utility of light scattering for the determination of MW was demonstrated 11 years later (Debye 1944, 1946).

Free-Volume Concept

The free-volume theory of liquids dates from the beginning of the twentieth century. Two expressions for *the free-volume fraction*, f, have been proposed, either $f = (V - V_{occ})/V$ or less frequently used $f = (V - V_{occ})/V_{occ}$ (V_{occ} is the occupied volume). The theory was used to interpret the temperature (T) and pressure (P) dependencies of liquid viscosity (Batschinski 1913). The V_{occ} was defined as the specific volume at which the liquid viscosity is immeasurably high, $\eta \to \infty$. Good correlation was found between V_{occ} and either the critical volume or the van der Waals constant b, viz.

$V_{occ}/(V_{crit}/3) = V_{occ}/b = 0.921 \pm 0.018$. Batschinski wrote:

$$\eta = a_o + a_1/f = a_o + a_1 V/(V - V_{occ}) \tag{1.2}$$

where a_i are equation parameters. Forty years later, more accurate data of viscosity (spanning several orders of magnitude) and specific volume for a series of paraffin's with molecular weight MW = 72–1,000 g/mol led to the logarithmic dependence (Doolittle 1951):

$$\ln \eta = a_o + a_1 V/(V - V_{occ}) \tag{1.3}$$

where v_o is the value of v at a characteristic solidification temperature, T_o, at which the fluid viscosity increases to infinity. Equation 1.3 provided a basis for the derivation of well-known WLF time-temperature shift factor a_T (Williams et al. 1955).

The free-volume model has been also incorporated into thermodynamic theories of liquids and solutions (Prigogine et al. 1957), and it is an integral part of theories used for the interpretation of thermodynamic properties of polymer blends (Utracki 1989a). In particular, it is a part of the most successful equation of state (EoS) derived for liquids and glasses (Simha and Somcynsky 1969), critically examined using data for 56 principal polymers (Rodgers 1993). Since the mid-1960s, the lifetime of ortho-positronium has been used to measure the free-volume fraction f. Accordingly, f increases linearly with the temperature:

$$f = -0.13556 + 6.2878(T/T^*) \quad \text{for} \quad 0.0165 \leq T/T^* \leq 0.0703$$

where T* is the temperature reducing parameter in Simha-Somcynsky theory (Utracki 1998b). More detailed analysis indicated that the free volume should be discussed in terms of distribution of the holes. For example, the measurements showed that above T_g the number of holes does not increase, but their volume does (Kobayashi et al. 1989). In PS/PPE blends, the size of the free-volume spaces in PS was found smaller than that in PPE (Li et al. 1999b).

Viscoelasticity

In 1874, Boltzmann formulated the theory of viscoelasticity, giving the foundation to the modern rheology. The concept of the relaxation spectrum was introduced by Thompson in 1888. The spring-and-dashpot analogy of the viscoelastic behavior (Maxwell and Voigt models) appeared in 1906. The statistical approach to polymer problems was introduced by Kuhn (1930).

Busse (1932) observed that "green" rubber under stress shows a dual behavior, suggesting the presence of two types of interactions: few widely separated strong ones, acting as physical cross-links, and many weak ones of the van der Waals type, which make it possible for one macromolecule to slip by the others. This postulate was the first connotation of the chain entanglement. Bueche (1952, 1956, 1962) adopted the entanglements' concept for the interpretation of polymer flow. He calculated the molecular friction constant per statistical segment as the unit force needed to pull the undeformed macromolecule through the surrounding medium at unit speed, $f_o = F/N$ (with N being the number of statistical segments per macromolecule), deriving the relations (see Eq. 1.4) between the diffusion constant, D, or zero-shear viscosity, η_o, and such molecular parameters as density, ρ, molecular weight, M, and radius of gyration, R_g:

$$
\begin{aligned}
&D\eta_o = (\rho N_A/36)\left(R_g^2/M\right)k_B T; \quad \text{and} \quad \eta_o = (\rho N_A/36)\left(R_g^2/M\right)N^* f_o \\
&\text{for:} \quad M \le 2M_e \quad N^* = M/M_o \\
&\text{for:} \quad M > 2M_e \quad N^* = \beta(M/M_o)(\rho N_A/48)(M/M_e)^2\sqrt{M}\left(R_g^2/M\right)^{3/2}
\end{aligned}
\tag{1.4}
$$

where numerical constant $\beta \cong 0.6$. The dependence predicts that for low molecular weight liquids (M below the value of the critical molecular weight for entanglement, $M_c = 2M_e$, where M_e is the molecular weight between entanglements), η_o should be proportional to M, while for high molecular weight macromolecules (above M_c), to $M^{3.5}$. Thus, predictions of the entanglement-based theory are in good agreement with the observations: $\eta_o \propto M^{3.4}$ (Gupta 2000). The correlation between the plateau modulus and entanglement concentration soon followed (Ferry et al. 1955). The long disputes on the nature of entanglement led to defining it as "a special type of interactions, affecting mainly the large-scale motions of the chains, and through them, the long time end of the viscoelastic relaxation time spectrum" (Graessley 1974).

Entanglement-based theories have now been largely superseded by reptation theories that owe their origins to the work of de Gennes (1979) and of Doi and Edwards (1986) and Doi (1995). The essential idea here is that entangled polymer molecules can be considered to be contained within a tube; the orientation of the tubes and the motion of the chains within the tubes relax over different timescales. This concept has been developed by a large number of authors over the years, and a simple and readable model that accounts for the main mechanisms has been published by Marrucci and Ianniruberto (2003). A major success of the reptation theory has been in establishing the molecular weight dependence of polymer diffusion.

Work to further expand the reptation-tube model has been explored. Pokrovskii (2008), for example, has shown that the underlying stochastic motion of a macromolecule leads to two modes of motion, namely, reptative and isotropically diffusive. There is a length of a macromolecule $M^* = 10M_e$ where M_e is "the macromolecule length between adjacent entanglements" above which macromolecules of a melt can be regarded as obstacles to motions of each other and the macromolecules reptate. The transition to the reptation mode of motion is determined by both topological restriction and the local anisotropy of the motion.

1.3 Polymer Structure and Nomenclature

1.3.1 Basic Considerations

A *polymer* is a substance composed of *macromolecules*, built by covalently joining at least 50 molecular mers, or the *constitutional repeating units or CRU*. The longest sequence of CRU defines the *main chain* of a macromolecule. The main chain may be composed of a series of *subchains*, identified by some chemical of physical characteristic (e.g., tactic placement). The main chain may also contain long or short *side chains* or *branches*, attached to it at the *branch points*. A small region in a macromolecule from which at least four chains emanate constitutes a *cross-linking point*. A macromolecule that has only one cross-link is the *star macromolecule*.

A macromolecule consisting of several cross-linked chains, but having a finite molecular weight, is a *micronetwork*. A highly ramified macromolecule in which each CRU is connected to every other CRU is a *polymer network*. When the main chain of a macromolecule has numerous branch points from which linear side chains emanate, it is *comb macromolecule*. The CRU is defined as a bivalent organic group, not necessarily identical to the source from which the macromolecule was prepared – it is the largest identifiable group in the polymer dictated by the macromolecular structure. To discuss the structure of polymer molecules, one may consider the chemical nature of CRU, type of the linkages, the global macromolecular arrangement, and the topochemical character of the macromolecule, tacticity, etc. These are summarized in Table 1.2.

Table 1.2 Macromolecular structures

No.	Characteristic	Examples
1	*Recurring constitutional repeating units, CRU*	
1.1	*Structure*	Aliphatic, aromatic, heterocyclic, metallo-organic
1.2	*Joining similar CRU*	Homopolymers (linear, branched, dendritic, cross-linked, etc.)
1.3	*Joining different CRUs*	Copolymers, multipolymers, polyadducts, polycondensates…
1.4	*Joining polymer segments*	Block copolymers, graft copolymers, ladder polymers
2	*The nature of bond between CRU*	For example, ether, ester, amide, urethane, sulfite
3	*Macromolecular structure*	Linear, branched, cross-linked, dendritic
4	*Topochemical characteristics of macromolecule*	
4.1	*Geometrical isomers*	For example, rubber and gutta-percha are poly(1,4-isoprene), *cis-* and *trans-*, respectively
4.2	*Optical isomers*	Having optically active C*; e.g., polypeptides, polysaccharides
4.3	*Tacticity*	Isotactic, syndiotactic, and atactic
4.4	*Helical structures*	Polypeptides, tactic polymers
4.5	*Head-to-tail, head-to-head*	For example: PIB or PS

1.3.2 Polymer Nomenclature

Macromolecular compounds can be classified according to (Kumar and Gupta 2003):

1. The chemical structure of the repeating unit (viz., polyamides, polyesters, polyolefins)
2. The structure (viz., linear, branched, ladder, or cross-linked)
3. The phenomenological behavior or technological use
4. The source of the compounds (viz., synthetic, natural, and derived products)

The Commission on Macromolecular Nomenclature defined 52 terms related to polymer structure, including *polymer*, *constitutional units*, *monomer*, *polymerization*, *regular polymer*, *tactic polymer*, *block polymer*, *graft polymer*, *monomeric unit*, *degree of polymerization*, *addition polymerization*, *condensation polymerization*, *homopolymer*, *copolymer*, *bipolymer*, *terpolymer*, *and copolymerization* (IUPAC 1974). The Commission remains the leading nomenclature body in the polymer field. Table 1.3 lists the pertinent sources for information on the nomenclature of polymeric materials.

Since there are difficulties in assigning systematic and unique abbreviations to polymers, only a short list has the IUPAC's official sanction. The IUPAC Macromolecular Nomenclature Commission has published three sets of rules for naming polymers:

1. Traditional, *trivial names* are sanctioned by the historical use and approved by IUPAC as an alternative (examples are listed in Table 1.4)
2. *Structure-based* nomenclature
3. *Source-based* nomenclature proposed by the Commission

Table 1.3 Polymer nomenclature proposed by the IUPAC

No.	Title	References
1.	*Report on Nomenclature Dealing with Steric Regularity in High Polymers*	Huggins et al. 1962, 1966
2.	*Basic Definitions of Terms Relating to Polymers*	IUPAC 1974, 1996
3.	*Nomenclature of Regular Single-Strand Organic Polymers*	IUPAC 1976
4.	*Stereochemical Definitions and Notations Relating to Polymers*	IUPAC 1981
5.	*Note on the Terminology for Molar Masses in Polymer Science*	IUPAC 1984
6.	*Nomenclature for Regular Single-Strand and Quasi-Single-Strand Inorganic and Coordination Polymers*	IUPAC 1985a
7.	*Source-Based Nomenclature for Copolymers*	IUPAC 1985b
8.	*Use of Abbreviations for Names of Polymeric Substances*	IUPAC 1987
9.	*Definitions of Terms Relating to Individual Macromolecules, Their Assemblies, and Dilute Polymer Solutions*	IUPAC 1989a
10.	*Definitions of, Terms Relating to Crystalline Polymers*	IUPAC 1989b
11.	*A Classification of Linear Single-Strand Polymers*	IUPAC 1989c
12.	*Compendium of Macromolecular Nomenclature*	Metanomski 1991
13.	*Source-Based Nomenclature for Non-Linear Macromolecules and Macromolecular Assemblies*	Jenkins et al. 1993

Table 1.4 Traditional and systematic names of polymers

No.	Traditional name	Systematic name
1.	Polyethylene	Poly(methylene)
2.	Polypropylene	Poly(propylene)
3.	Polyisobutylene	Poly(1,1-dimethyl ethylene)
4.	Polybutadiene	Poly(1-butenylene)
5.	Polyisoprene	Poly(1-methyl- 1-butenylene)
6.	Polystyrene	Poly(1-phenyl ethylene)
7.	Polyacrylonitrile	Poly(1-cyano ethylene)
8.	Polyvinyl alcohol	Poly(1-hydroxy ethylene)
9.	Polyvinylacetate	Poly(1-acetoxy ethylene)
10.	Polyvinylchloride	Poly(1-chloro ethylene)
11.	Polyvinylidenefluoride	Poly(1,1-difluoro ethylene)
12.	Polytetrafluoroethylene	Poly(difluoro methylene)
13.	Polyvinylbutyral	Poly[(2-propyl-1,3-dioxane-4,6-diyl) methylene]
14.	Polymethylacrylate	Poly[1-(methoxycarbonyl) ethylene]
15.	Polymethylmethacrylate	Poly[1-(methoxycarbonyl)-1-methyl ethylene]
16.	Polyformaldehyde	Poly(oxy methylene)
17.	Polyethylene oxide	Poly(oxy ethylene)
18.	Polyphenylene ether	Poly(oxy-1,4-phenylene)
19.	Polyethylene terephthalate	Poly(oxyethylene-oxyterephthaloyl]
20.	Poly-ε-caprolactam	Poly[imino(1-oxohexamethylene)]
21.	Polyamide-6,6 or polyhexamethyleneadipamide	Poly[imino(1,6-dioxohexa methylene) iminohexa methylene]; or poly(iminoadipoyliminohexa methylene)

1.3.2.1 Structure-Based Nomenclature

For organic, regular, single-strand polymers, the structure-based system of naming polymers should be used. This nomenclature describes chemical structures rather than substances. Three steps are to be followed in a sequence:

1. Identify the constitutional repeating unit, CRU.
2. Orient the CRU.
3. Name the CRU.

The name of the polymer is *poly(CRU)*. The preferred CRU is one beginning with the subunit of highest seniority. The order of seniority is heterocyclic rings, chains containing heteroatoms (in the descending order O, S, Se, Te, N, P), carbocyclic rings, and chains containing only carbon. The seniority is expressed by brackets and internal parentheses (see examples in Table 1.4).

After the CRU and its orientation, reading left to right, have been established, the CRU or its constituent subunits are named. The name (the largest identifiable unit) includes description of the main chain and the substituents. The subunits are named according to the rules for nomenclature of organic chemistry. The name of the CRU is formed by citing, in order, the names of the largest subunits within the CRU. More complicated, regular single-strand polymers can be represented as multiples of repeating units, such as [ABC]$_n$. The name of the polymer is *poly(ABC)*, where (ABC) stands for the names of A, B, and C, taken in the order of seniority. An extension of the structure-based method to linear inorganic and/or coordination polymers is limited by the general lack of a system for naming bivalent radicals. Few polymers with inorganic, covalently bonded backbones have trivial names (viz., poly(dimethylsiloxane) or poly(dichlorophosphazene)), some can be named by (as organic polymers) using bivalent radicals, e.g., poly[oxy(dimethyl silylene)] or poly[nitrilo (dichlorophosphoranylidyne)].

Structure-based nomenclature is also applicable to copolymers having a regular structure, regardless of the starting materials used (viz., poly(oxyethylene-oxyterephthaloyl)). In principle, it should be possible to extend the existing structure-based nomenclature beyond regular, single-strand polymers to polymers that have reacted, cross-linked polymers, ladder polymers, and other more complicated systems.

1.3.2.2 *Source-Based* Nomenclature

Traditionally, polymers have been named by attaching the prefix *poly* to the name of the CRU, real or assumed monomer, the source from which it is derived. Thus, PS is the polymer made from styrene. When the name of the monomer consists of two or more words, parentheses should be used, but for common polymers such as polyvinylchloride, polyvinylacetate, etc., it is customary to omit them. Different types of polymerization can take place with many monomers, and there are different ways for obtaining a polymer. For example, name such as polyvinyl alcohol refers to a hypothetical source, since this polymer is obtained by hydrolysis of polyvinylacetate. In spite of deficiencies, the source-based nomenclature is still entrenched in the literature. It is also the basis for naming and classifying copolymers (see Table 1.5).

Table 1.5 Nomenclature of copolymers

No.	Type	Connective	Example
1.	Short sequences		
1.1.	Unknown or unspecified	-co-	Poly(A-co-B)
1.2.	Statistical	-stat-	Poly(A-stat-B)
1.3.	Random	-ran-	Poly(A-ran-B)
1.4.	Alternating	-alt-	Poly(A-alt-B); (AB)n
1.5.	Periodic with at least three monomeric units	-per-	Poly(A-per-B-per-C); (ABC)$_n$; (ABAC)$_n$; (AABB)$_n$
2.	Long sequences		
2.1.	Block	-block-, or -b-	Poly A-block-poly B; poly(A-b-B)
2.2.	Graft (polymeric side chain different)	-graft-or -g-	Poly A-graft-poly B; poly(A-g-B); AAAAA (g-BBB)AAAAAAA
2.3.	Star	-star-	Star-poly A
2.4.	Star block	-star-...-block-	Star-poly A-block-poly B
3.	Networks		
3.1.	Cross-linked	-cross-	Cross-poly A
3.2.	Interpenetrating	-inter-	Cross-poly A-inter-cross-poly B
3.3.	Conterminous	-cross-	Poly A-cross-poly B

1.3.3 Copolymers

When mers are not identical, the polymerization leads to a *copolymer*. For divalent mers, a *linear copolymer* is obtained, but when at least some mers are able to join more than two units, the polymerization leads to *branched* or *cross-linked copolymer*. When the polymerization starts on a polymer chain of different chemical character than the one that is subsequently forming, the resulting structure is known as *grafted copolymer*. Thus, the arrangement of the different types of monomeric units must be specified. Several types of arrangements are shown in Table 1.5, where A, B, and C represent different CRUs. The systematic source-based nomenclature for copolymers involves identification of the constituent monomers and description of their arrangement. This is achieved by citing the names of the constituent monomers after the prefix "poly" and by placing between the names of each pair of monomers an italicized connective to denote the kind of arrangement by which those two types of monomeric units are related in the structure.

The structures listed in Table 1.5 are divided into three categories: *short sequences, long sequences, and networks.* Within the first category, a sequence of placement of individual CRU is considered, within the second the placement of long sequences of CRU defines the copolymer type, while to the third belong cross-linked networks, cross-linked polymers, and chemical-type interpenetrating polymer networks. The network is a cross-linked system in which macromolecules of polymer A are cross-linked by macromolecules of polymer B (Sperling 1992). The composition can be expressed as, e.g., *block*-co-poly(butadiene/styrene) (75:25 wt%) or *graft*-co-poly[isoprene/(isoprene; acrylonitrile)] (85:15 mol%).

Table 1.6 Descriptors for nonlinear macromolecules and macromolecular assemblies

Polymer structure	Descriptor
Cyclic	*cyclo*
Branched (unspecified)	*branch*
Short-chain	*sh-branch*
Long-chain	*l-branch*
With f (give numerical value) branch points	*f-branch*
Comb	*comb*
Star (unspecified)	*star*
With f (give numerical value) arms	*f-star*
Network	*net*
Micronetwork	*m-net*
Polymer blend	*blend*
Interpenetrating polymer network	*ipn*
Semi-interpenetrating polymer network	*sipn*
Macromolecule-macromolecule complex	*compl*

1.3.4   Macromolecular Assemblies

To describe polymers or polymer blends with greater precision, the qualifiers listed in Table 1.6 have been suggested (Jenkins et al. 1993). In a series of four papers, Wilks (1997a–d) has compared the polymer nomenclature styles and structure representation systems used by Chemical Abstracts Service (CAS), the IUPAC, and MDL Information Systems, Inc. (MDL).

1.3.5   Polymer Blend Terminology

The terminology used in polymer blends' science and technology is summarized in Table 1.7 (Utracki 1989a, b). Universal adoption of a consensus nomenclature is vital to the description of chemical structures in online searching and in publishing works. For instance, different kinds of surfaces, interfaces, and interphases provide challenges to develop consistent nomenclature. This is a continuous process as polymers, its variations, and their blends are studied. The definition and nomenclature relating to polymer liquid crystals are recommended in IUPAC (2001), regular single-stranded polymers in IUPAC (2002), terms related to polymers containing ionizable or ionic groups and of polymers containing ions in Jones (2009), and so is the graphical representation of single-strand (copolymers) and irregular polymers in IUPAC (2012).

1.4   Introduction to Polymer Blends

Polymer blends constitute almost one third of the total polymer consumption, and their pertinence continues to increase. According to bcc Research, the global

Table 1.7 Terminology of polymer blends

Term	Definition
Polymer	A substance composed of large molecules, the *macromolecules*, built by covalently joining at least 50 molecular mers, segments, or recurring *constitutional repeating units*, *CRU*. Commercial polymers may contain up to 2 wt% of another polymeric modifier
Copolymer	Polymeric material synthesized from more than a single monomer
Engineering polymer (EP)	Processable polymeric material, capable of being formed to precise and stable dimensions, exhibiting high performance at the continuous use temperature CTU > 100 °C and having tensile strength in excess of 40 MPa
Polymer blend (PB)	Mixture of at least two macromolecular substances, polymers or copolymers, in which the ingredient contents is above 2 wt%.
Homologous polymer blend	Mixture of two homologous polymers (usually a mixture of narrow molecular weight distribution fractions of the same polymer)
Miscible polymer blend	Polymer blend, homogenous down to the molecular level, associated with the negative value of the free energy of mixing: $\Delta G_m \approx \Delta H_m \leq 0$ and a positive value of the second derivative $\partial^2 \Delta G_m \partial \phi^2 > 0$. Operationally, it is a blend whose domain size is comparable to the dimension of the macromolecular statistical segment
Immiscible polymer blend	Polymer blend whose free energy of mixing $\Delta G_m \approx \Delta H_m > 0$
Compatible polymer blend	Term to be avoided! At best a utilitarian, nonspecific term indicating a marketable, visibly homogeneous polymer mixture, with enhanced performance over the constituent polymers
Polymer alloy	Immiscible, compatibilized polymer blend with modified interface and morphology
Compatibilization	Process of modification of the interfacial properties in immiscible polymer blend, resulting in reduction of the interfacial tension coefficient and stabilization of the desired morphology, thus leading to the creation of a polymer alloy
Interphase	Third phase in binary polymer alloys, enhanced by interdiffusion or compatibilization. Thickness of this layer varies with the blend components and compatibilization method from 2 to 60 nm
Compatibilizer	Polymer or copolymer that either added to a polymer blend or generated there during reactive processing modifies its interfacial character and stabilizes the morphology
Chemical compatibilization	Compatibilization by incorporation of a compatibilizer, usually either a copolymer or multipolymer
Physical compatibilization	Compatibilization by physical means: high stress field, thermal treatment, irradiation, etc.
Reactive compatibilization	Compatibilization during reactive processing, extrusion, or injection molding
Engineering polymer blend	Polymer blend or polymer alloy that either contains or has properties of an engineering polymer
Interpenetrating polymer network (IPN)	Polymer alloy, containing two or more polymers in the network form, each chemically cross-linked. Sequential, simultaneous (SIN), and latex type IPNs are known
Thermoplastic IPN	Polymer alloy, containing two or more polymers in a co-continuous network form, each physically cross-linked. The cross-linking originates in crystallinity, ion cluster formation, presence of hard blocks in copolymers, etc.

market in volume for engineering resins and their blends was more than 22 billion pounds in 2012; polycarbonates and polyamides are the most prominent, and these account for about 60 % of the total market.

1.4.1 Benefits and Problems of Blending

The following material-related benefits can be cited:
  (i) Providing materials with a full set of desired properties at the lowest price
 (ii) Extending the engineering resins' performance
(iii) Improving specific properties, viz., impact strength or solvent resistance
(iv) Offering the means for industrial and/or municipal plastic waste recycling
    Blending also benefits the manufacturer by offering:
  (i) Improved processability, product uniformity, and scrap reduction
 (ii) Quick formulation changes
(iii) Plant flexibility and high productivity
(iv) Reduction of the number of grades that need to be manufactured and stored
 (v) Inherent recyclability, etc.

1.4.2 Compatibilization

The topic is extensively treated in ▶ Chap. 4, "Interphase and Compatibilization by Addition of a Compatibilizer" and ▶ Chap. 5, "Reactive Compatibilization", and thus only the key features are mentioned below. Several books and reviews also provide extensive information on the topic (Newman and Paul 1978; Kotliar 1981; Porter et al. 1989; Porter and Wang 1992; Brown 1992; Ajji and Utracki 1996; Datta and Lohse 1996; Utracki 1998a; Bucknall and Paul 2000; Robeson 2007).

It is noteworthy that in the absence of the configurational entropy effects (see ▶ Chap. 2, "Thermodynamics of Polymer Blends"), the miscibility of polymer blends depends on the balance of small enthalpic and/or non-configurational entropic effects. Sensitivity of this balance to small variation of the macromolecular structure is illustrated in the series of papers on miscibility of model polyolefins – e.g., see (Rabeony et al. 1998). Another example is provided by the photoisomerization initiated, reversible phase separation of PVME blends with stilbene-substituted PS (Ohta et al. 1998).

While miscibility is limited to a specific set of conditions, the immiscibility dominates – most polymers form immiscible blends that require compatibilization. Alloys' performance depends on the ingredients, their concentration, and morphology. The alloying process must result in *stable* and *reproducible* properties of polymer blends. Thus, the morphology must either be stable, unchanged during the forming steps, or the changes must be well predicted. The alloying makes use of an appropriate dispersing method (viz., mechanical mixing, solution, or latex blending) and compatibilization.

The latter process must accomplish three tasks:

1. Reduce the interfacial tension, thus giving a finer dispersion.
2. Stabilize the morphology against thermal or shear effects during the processing steps.
3. Provide interfacial adhesion in the solid state.

The compatibilization strategies comprise (i) addition of a small quantity of cosolvent – a third component, miscible with both phases, (ii) addition of a copolymer whose one part is miscible with one phase and another with another phase, (iii) addition of a large amount of a core-shell copolymer – a compatibilizer-cum-impact modifier, (iv) reactive compounding that leads to modification of at least one macromolecular species that result in the development of local miscibility regions, and (v) addition of a small quantity of nanoparticles which influence blend structure similarly to particle-stabilized water/oil emulsions.

Commercial alloys may comprise six or more polymeric ingredients. The increased number of components, n, increases the number of interfaces between them: $N = n(n-1)/2$. For such complex systems, it may be necessary to use an ingredient with highly reactive groups, capable of interacting with several polymeric components, e.g., such multicomponent copolymer as ethylene-glycidyl methacrylate, triglycidylisocyanurate, etc. Alternatively, one may carry a sequential blending, incorporating one polymer within another and then combining the preblends into the final alloy, hence reducing the number of interfaces that must be simultaneously controlled.

While the reduction of the interfacial tension, ν, is relatively easy by introduction of a macromolecular "surfactant," the stabilization of morphology and improvement of the interfacial adhesion in the solid state may not be so. One may use either a single compatibilizer that can perform all three compatibilization tasks, or a combination of agents, each playing one or two different roles. For example, stabilization of the desired dispersion (accomplished by addition of "surfactant" to mechanically mixed compound) may be accomplished by partial cross-linking of one of the three phases: matrix, dispersed, and the interphase. In the latter case, the interfacial adhesion in the solid state is also improved.

The density profile across the interface follows an exponential decay (see Fig. 1.1). The intercepts of the steepest tangential line with the horizontal lines defining the volume fraction of either one of the two polymeric ingredients, $\phi = 0$ and 1, define the thickness of the interphase, Δl (Helfand and Tagami 1971, 1972). Experimentally Δl varies from 2 to 60 nm (Kressler et al. 1993; Yukioka and Inoue 1993, 1994). Measurements of Δl have been used to map the miscibility region of PC/SAN blends when varying the AN content and temperature (Li et al. 1999a).

For high molecular weight polymer blends (M $\rightarrow \infty$), the Helfand and Tagami theory predicts that in binary blends (i) the interfacial thickness, Δl_∞, is inversely proportional to the interfacial tension coefficient, v_∞, the product, $\Delta l_\infty v_\infty$, being independent of the thermodynamic interaction parameter, χ; (ii) the surface free energy is proportional to $\chi^{1/2}$; (iii) the chain ends of both polymers concentrate at the interface; (iv) any low molecular weight third component is repulsed to the interface; and (v) the interfacial tension coefficient increases with molecular weight

Fig. 1.1 Density profile
across the interface, defining
thickness of the interphase
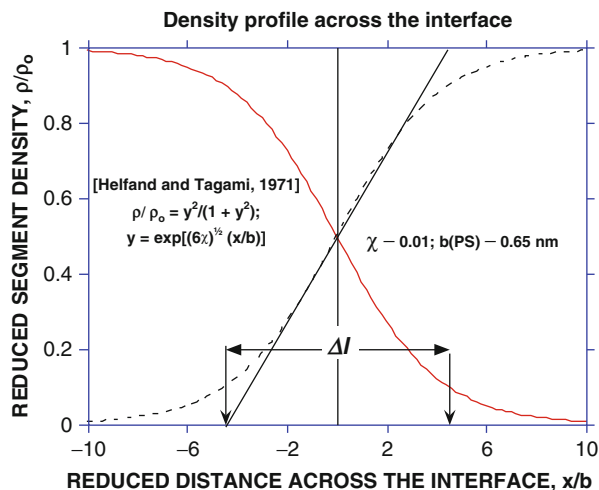
to an asymptotic value: $v = v_{\infty} - a_o M^{-2/3}$. The value of v can be measured or calculated from the molecular structure of two polymers, e.g., by means of the Hoy's group contribution method. The computed and experimental values of v for 46 polymer pair showed good correlation with an average error of $\pm$ 36 % (Luciani et al. 1996, 1997).

The concentration dependence of v_{∞} may be expressed as (Tang and Huang 1994; Ajji and Utracki 1996)

$$v = v_{CMC} + (v_o - v_{CMC})\exp\{-a\chi Z_c\phi\};$$
$$d = d_{CMC} + (d_o - d_{CMC})\exp\{-a\chi Z_c\phi\} \tag{1.5}$$

where a and a_1 are adjustable parameters, Z_C is the copolymer's degree of polymerization, and subscript CMC indicates the "critical micelles concentration." It is important to note that v and the diameter of the dispersed phase follows the same mathematical dependence.

The amount of compatibilizer required to saturate the interface, w_{cr}, can be expressed by the two limiting equations:

$$w_{cr} = 3\phi M/aRN_A; \qquad w_{cr} = 27\phi M/[\langle r^2\rangle RN_A] \tag{1.6}$$

where ϕ is the volume fraction of the dispersed phase, R is the radius of the dispersed drop, N_{Av} is the Avogadro number, M is the copolymer molecular weight, $a \geq 5$ nm^2 is the specific cross-sectional area of the copolymer macromolecule, $\langle r^2\rangle = KM$ is square end-to-end distance of the copolymer, and K is the characteristic parameter of the polymeric chain. The first equation in Eq. 1.6 was derived assuming that *all* compatibilizer's molecules cross the interface once, while the second assuming that di-block copolymer macromolecular coils are randomly

deposited on the interface (Mathos 1993; Ajji and Utracki 1996). The reality is somewhere in between these two ideal cases. Both relations predict that the amount of copolymer required to saturate the interface is proportional to the total interfacial area expressed as ϕ/R.

Measurements of ν for the commercial resins' blends depended on the contact time of the two polymers. Helfand et al. theory predicts that owing to diffusion of low molecular weight ingredients to the interphase, ν should decrease with time. This indeed was observed for most blends, but an opposite effect was also seen for some PA/PO blends. The effect depended on the nature and amount of antioxidants and stabilizers in each resin. POs frequently contain acidic stabilizers, viz., sterically hindered phenols, (hydro)-peroxide decomposers (e.g., tris(2,4-di-tert-butyl phenyl)-phosphite), radical scavengers such as thio-derivatives (Herbst et al. 1995, 1998). When blending thus stabilized PO with PA, chemical reactions between the acidic stabilizers and $-NH_2$ of the PA chain ends result in formation of a rigid membrane. Measuring the interfacial tension coefficient as a function of the contact time shows increasing values of the interfacial tension coefficient. These time effects should be incorporated when predicting the blends' morphology (Luciani et al. 1996, 1997).

Initially, the most common method of compatibilization was an addition of a third polymeric component, either a block or a graft copolymer. It was assumed that the compatibilizer would migrate to the interface, broadening of the segmental concentration profile, Δl. There are several reports indicating that addition of a block or graft copolymer reduces ν and alters the molecular structure at the interface, but it rarely increases the interphase thickness. Another disadvantage of the addition method is the tendency for a copolymer to migrate to at least five different locations, forming saturated solutions and micelles in both phases, as well as the interphasial layer (block copolymers may also form mesophases). Hence, the copolymeric compatibilizer that is to be added to a blend should have:

(i) Maximum miscibility with the respective polymeric components.
(ii) Molecular weight of each block only slightly higher than the entanglement M_e.
(iii) Concentration just above CMC. In industry the time effects are important – the higher is the viscosity of the blend's components, the longer is the diffusion time, thus the slower the processing.

The morphology of commercial blends usually is far from equilibrium. Preparation of the alloys must take thermodynamic and kinetic parameters into account if the desired effects are to be achieved. The effects of copolymer addition on the dispersion size and blend performance have been studied (Hobbs et al. 1983; Fayt et al. 1986a; Armat and Moet 1993; Alsewailem and Gupta 2002). The interface/morphology relationship in polymer blends with thermoplastic starch has also been studied (Taguet et al 2009).

From the economic as well as the performance points of view, the reactive compatibilization is most interesting (see ▶ Chap. 5, "Reactive Compatibilization"). The process involves (i) sufficient dispersive and distributive mixing to ascertain required renewal of the interface; (ii) presence of a reactive functionality, suitable to react across the interphase; (iii) sufficient reaction rate making it

possible to produce sufficient quantity of the compatibilizing copolymer within the residence time of the processing unit. The method leads to particularly thick interphase, thus good stability of morphology.

The reactive blending has been used since the beginning of the plastic industry. For example, two polyisoprene isomers, NR and GP, were softened by addition of $SCl_2 + CS_2$ and milled in a hot rubber mill. During milling, the solvent partially decomposed co-vulcanizing NR with GP (Parkes 1846). A patent from 1939 describes reactive blending of PVAl with multicomponent acrylic copolymers containing maleic anhydride (I. G. Farbenindustrie 1939). In the early 1940s, BASF used a corotating TSE for reactive extrusion of PA-6. Since the mid-1960, the reactive extrusion has been used for toughening and general modification of the engineering resins, viz., PA, PET, PC, or PBT. In 1971, Exxon patented styrene grafting of PE in reactive extrusion followed by blending with PPE for improved processability and excellent performance. Oxazoline-grafted polymers were used as compatibilizers in reactive blending of PC with PA. In 1975 du Pont started to manufacture the *super tough PA*, *Zytel-ST™*, by reactive blending of PA-66 with maleated ethylene-propylene-diene elastomer (EPDM-MA). The reactive compatibilization of the PPE/PA was developed in 1977 (Ueno and Maruyama 1979). More details on reactive compatibilization can be found in ▶ Chap. 5, "Reactive Compatibilization" as well as in a monograph published by Utracki (1998a).

It has been known for a long time that emulsions of low viscosity liquids can be stabilized not just by the use of surfactants but also by means of added nanoparticles (Pickering 1908). This behavior is found to carry over to polymer blends as well (Vermant et al. 2008; Fenouillot et al. 2009; Yoo et al. 2010). It is found that the morphology that results with the use of nanoparticles is finer than that in the case of pure blends since the interfacial tension is lowered. The morphology is also more stable against annealing. This effect is the result of the nanoparticles locating themselves at the blend interface and forming a solid barrier that inhibits drop coalescence. For this result to be observed, though, the size, shape, surface chemistry, and loadings of the nanoparticles must be tailored such that the Gibb's free energy of the interface is minimized when nanoparticles are located there. Else, there can even be transfer of nanoparticles from one phase to another (Goldel et al. 2012). A benefit of using nanofillers like carbon nanotubes in immiscible polymer blends is that the electrical percolation threshold can be significantly lowered (Goldel and Potschke 2011). This topic is explored in ▶ Chap. 17, "Polymer Blends Containing "Nanoparticles"".

It is imperative to mention that component polymer surfaces and interfaces play a major role in the properties and applications of blends such as in biocompatibility, switching, or adaptive properties. Whether it is an everyday plastic part or parts in automotives or in an airplane, not only the development of interfacial morphology but also the analyses of blends interfaces are equally important. The compatibilizing effect is primarily due to the interfacial activity of the constituent partners. This in turn raises the question of what are the effects of the molecular weight, concentration, temperature, and molecular architecture of the

compatibilizer. Anastasiadis (2011) has reviewed interfacial tension in binary polymeric blends and the effects of copolymers as emulsifying agents. The diffused interface widths in binary blends such as PVC/EVA and PS/PMMA have been studied (Ramya 2013). When there is a large difference in compressibility between constituent polymers, Cho (2013) interpreted pressure coefficient of interfacial tension and argued that there exist a region that $\delta_\gamma/\delta P < 0$. Polymer surface and interface characterization techniques differ based on the environments (such as air, vacuum, liquid, etc.). Stamm (2008) has lucidly described several aspects of surface and interface characterization and provided a list of different techniques in which those could be applied. The other technique known as grazing incidence small-angle neutron scattering is also gaining attention due to its surface sensitivity in the investigation of nanostructures in thin films and at surfaces (Buschbaum 2013).

1.4.3 Morphology

The morphology depends on the blend concentration. At low concentration of either component, the dispersed phase forms nearly spherical drops, and then, at higher loading, cylinders, fibers, and sheets are formed. Thus, one may classify the morphology into dispersed at both ends of the concentration scale and co-continuous in the middle range. The maximum co-continuity occurs at the phase inversion concentration, ϕ_I, where the distinction between the dispersed and matrix phase vanishes. The phase inversion concentration and stability of the co-continuous phase structure depend on the strain and thermal history (Song et al. 2009, 2011). For a three-dimensional (3D) totally immiscible case, the percolation theory predicts that $\phi_{perc} = 0.156$. In accord with the theory, the transition from dispersed to co-continuous structure occurs at an average volume fraction, $\phi_{onset} = 0.19 \pm 0.09$ (Lyngaae-Jørgensen and Utracki 1991; Lyngaae-Jørgensen et al. 1999). The co-continuity contributes to synergism of properties, e.g., advantageous combination of high modulus and high impact strength in commercial blends. Detailed discussion of the phase co-continuity and its effect on morphology and rheology is given in ▶ Chap. 7, "Rheology of Polymer Alloys and Blends".

When discussing the morphology, it is useful to use the *microrheology* as a guide. At low stresses in a steady uniform shear flow, the deformation can be expressed by means of three dimensionless parameters – the viscosity ratio, the capillarity number, and the reduced time, respectively:

$$\lambda \equiv \eta_d/\eta_m; \quad \kappa = \sigma d/v; \quad t^* = t\dot{\gamma}/\kappa = \gamma/\kappa \quad (1.7)$$

where σ is the local stress, η_d and η_m is the dispersed phase and matrix viscosity, respectively, $\dot{\gamma}$ is the deformation rate, and d is the droplet diameter. The capillarity number may be used in its reduced form $\kappa^* \equiv \kappa/\kappa_{cr}$, where the critical capillarity number κ_{cr} is defined as the minimum capillarity number sufficient to cause breakup of the deformed drop. The drop can break when $1 < \kappa^* < 2$.

For $\kappa^* > 2$ the drops deform into stable filaments, which only upon reduction of κ^* disintegrate by the capillarity forces into mini-droplets. The deformation and breakup processes require time – in shear flows the reduced time to break is $t_b^* \geq 100$. When values of the capillarity number and the reduced time are within the region of drop breakup, the mechanism of breakup depends on the viscosity ratio, λ – in shear flow, when $\lambda > 3.8$, the drops may deform, but they cannot break. Dispersing in extensional flow field is not subjected to this limitation. Furthermore, for this deformation mode κ_{cr} (being proportional to drop diameter) is significantly smaller than that in shear (Grace 1982).

The use of microrheology for the description of drop deformation and break was found to provide a surprisingly good agreement with experimental observations for the morphology evolution during compounding in a TSE (Utracki and Shi 1992; Shi and Utracki 1992; 1993). The predictive model (without adjustable parameters) was further improved by incorporation of the coalescence (Huneault et al. 1995a). A similar model has also been proposed (Moon and Park 1998).

The flow affects the blend morphology, but the structure variations also engender changes to the rheological response. The flow affects morphology in two ways – it changes the degree and type of dispersion on a local level and imposes global changes of morphology in formed parts. The latter effects originate from the flow-imposed migration of the dispersed phase that, for example, may cause formation of skin-core structures, weld lines, etc. The flow-imposed morphologies can be classified as (i) dispersion (mechanical compatibilization), (ii) fibrillation, (iii) flow coalescence, (iv) interlayer slip, (v) encapsulation, and others (Utracki 1995).

Flow may also cause mechanochemical degradation that generates reactive components, viz., radicals, peroxides, acids, etc. Transesterification, *trans*-amidation, and ester-amide exchange reactions during processing are well documented (their rate depends on the total interfacial area that in turn depends on flow) (Walia et al. 1999). These reactions may be responsible for the formation of compatibilizers that increase the interfacial area, affect the phase equilibria and the regularity of the main chain, and thus modify the degree of dispersion, blend's crystallinity, and, hence, performance. Use of cross-linked PE (XLPE) and different elastomers (EPDM, EVAc, butyls) as insulation materials is well known in the power distribution cable industries. Flow behavior and morphology of melt mixed blends of XLPE and silicone elastomers with and without compatibilizer (vinyl silane) have been studied (Mukhopadhyay et al. 1990). Surface morphology of the blends revealed the presence of a cross-linked microgelled silicone elastomer that seemed to disperse as a filler in the continuous XLPE matrix.

Miscibility of the blend components has an obvious effect on morphology (for detailed discussions, see ▶ Chap. 8, "Morphology of Polymer Blends"). During processing, the hydrostatic and shear stresses can change the lower critical solubility temperature (LCST) by at least 60 °C. This may result in formation (inside the processing unit) of a miscible blend. The blend emerging from the extruder may phase separate by the spinodal decomposition mechanism into a co-continuous structure, whose degree of dispersion can be controlled, for example, PBT/PC blends.

Stress-induced fibrillation occurs in a steady-state shearing or extension, when the capillarity ratio $\kappa > 2$. Under these conditions, flow is co-deformational. Since, $\kappa \propto d$, it is easier to fibrillate coarser dispersions where $\phi > a\lambda^b$ (the numerical value of the a and b parameters depends on the composition of the blend) (Krasnikova et al. 1984). Flow through a capillary of POM dispersed in a copolyamide (CPA) at $T = T_m(POM) + 6\ °C$ resulted in fibrils with diameters of about 20 μm and length 3.2 mm. Fibrillation of POM in EVAc strongly varied with λ. For $\lambda \approx 1$, the finest morphology was found (Tsebrenko et al. 1976, 1982). At temperatures slightly above the melting point, $T > T_m$, coalescence combined with stress-induced crystallization resulted in the formation of long fibers. The effect has been explored for performance improvement of blends comprising liquid-crystal polymers (LCP) (La Mantia 1993; Champagne et al. 1996).

The shear-induced interlayer slip was theoretically predicted – it creates a tree-ring structure in the extrudates (Utracki et al. 1986; Utracki 1991b; Bousmina et al. 1999). The relation may be used to describe the steady-state viscosity of antagonistically immiscible polymer blends, such as PP/LCP (Ye et al. 1991; Utracki 1986, 1991b).

The shear-induced segregation takes place in any system comprising flow elements with different friction coefficient, either miscible or immiscible (Doi and Onuki 1992). Migration of the low viscosity component toward the high stress regions may result in a flow-induced encapsulation. The effect has been well documented and successfully explored in polymer processing (Utracki 1987, 1988, 1989a, 1991a, 1995). For example, the high viscosity engineering resins with poor resistance to solvents, e.g., PC, PEST, or PEEK, can be blended with a low melt viscosity LCP. Extrusion through a die with sufficiently long land causes LCP to migrate toward the high stress zone near the die land, thus lubricating the die flow, improving the throughput, and enveloping the resin in a protective layer of LCP (Cogswell et al. 1981, 1983, 1984).

From an industrial viewpoint, polymer morphology can change due to physical aging even after a part has been extruded or injection molded, and this has implications on the performance of a polymer during service. Amorphous polymer melts when rapidly cooled to below their T_g form nonequilibrium structures which can relax over time by losing free volume (Struik 1978). As a consequence, mechanical properties can change, often for the worse. The use of polymer blends can retard this process since specific interactions such as hydrogen bonding and dipole-dipole interactions can restrict molecular mobility and increase long-term stability (Cowie and Arrighi 2010). Cowie and Ferguson (1989) have studied the physical aging of blends of PS and PVME using enthalpy relaxation and determined that the blend aged at a slower rate as compared to PVME alone.

In closing this section, we note that research interest in polymer blend miscibility is quite active as it affects final blend morphology. Recently, using a lattice-based equation of state, White and Lipson (2012) provided new correlations between the microscopic character of blend components and their bulk miscibility. These authors studied twenty-five polymer blend systems divided into two categories UCST and LCST and have found that the averaged difference between pure component energy parameters is significantly greater for LCST blends than for UCST blends.

1.4.4 Rheology

The rheology of polymer blends is discussed in detail in ▶ Chap. 7, "Rheology of Polymer Alloys and Blends". Here only an outline will be given. Since the flow of blends is complex, it is useful to refer to a simpler system, e.g., for miscible blends to solutions or a mixture of polymer fractions, for immiscible blends to suspensions or emulsions, and to compatibilized blends to block copolymers (Utracki 1995; Utracki 2011). It is important to remember that *the flow behavior of a multiphase system should be determined at a constant stress*, *not at a constant deformation rate*.

For miscible blends, the free-volume theory predicts a positive deviation from the log-additivity rule, PDB. However, depending on the system and method of preparation, these blends can show either a positive deviation, negative deviation, or additivity (Utracki 1989a). Upon mixing, the presence of specific interactions may change the free volume and degree of entanglement, which in turn affect the flow behavior (Steller and Żuchowska 1990; Couchman 1996). For immiscible blends, the flow is similarly affected, but in addition there are at least *three* contributing phases: those of polymeric components and the interphase in between. Flow of suspensions provides good model for blends with high viscosity ratio, $\lambda > 4$, while for blends with $\lambda \approx 1$, the emulsion model is preferred. The block copolymer is a good model for well-compatibilized polymer alloys.

The fundamental assumption of the classical rheological theories is that the liquid structure is either stable (Newtonian behavior) or its changes are well defined (non-Newtonian behavior). This is rarely the case for flow of multiphase systems. For example, orientation of sheared layers may be responsible for either dilatant or pseudoplastic behavior, while strong interparticle interactions may lead to yield stress or transient behaviors. Liquids with yield stress show a *plug flow*. As a result, these liquids have drastically reduced extrudate swell, $B \equiv \equiv d/d_o$ (d is diameter of the extrudate, d_o that of the die) (Utracki et al. 1984). Since there is no deformation within the plug volume, the molecular theories of elasticity and the relations they provide to correlate, for example, either the entrance pressure drop or the extrudate swell, are not applicable.

The concentration dependence of the constant-stress viscosity provides information on the inherent flow mechanism. The experimental data should be evaluated considering the log-additivity rule, $\ln \eta_b = \sum \phi_i \ln \eta_i$. There are five possible types of behavior, described as (1) positively deviating blend (PDB), (2) negatively deviating blends (NDB), (3) log-additive blends, (4) PNDB, and (5) NPDB. These can be described combining the emulsion model of polymer blends with the interlayer slip (Utracki 1991b; Bousmina et al. 1999). Owing to the variability of the blend structure with flow, the rheological responses are sensitive to the way they are measured. Since the structure depends on strain, the responses measured at high and low values of strain are different. For this reason, the selected test procedure should reflect the final use of the data. When simulation of flow through a die is attempted, the large strain capillary flow is useful. However, when the material characterization is important, the dynamic tests are recommended. The dynamic

measurements of polymer blends at small strains are simple and reliable. The storage and loss shear moduli (G' and G'', respectively) should be first corrected for the yield stress and then analyzed for the relaxation spectrum (Utracki and Schlund 1987; Riemann et al. 1995; Friedrich et al. 1995).

Two types of rheological phenomena can be used for the detection of blend's miscibility: (1) influence of polydispersity on the rheological functions and (2) the inherent nature of the two-phase flow. The first type draws conclusions about miscibility from, e.g., coordinates of the relaxation spectrum maximum; cross-point coordinates (G_x, ω_x) (Zeichner and Patel 1981); free-volume gradient of viscosity, $\alpha = d(\ln\eta)/df$; the initial slope of the stress growth function, $S = d(\ln\eta_E^+)/d\ln t$; the power-law exponent $n = d(\ln\sigma_{12})/d\ln\dot{\gamma} \cong S$, etc. The second type involves evaluation of the extrudate swell parameter, $B \equiv \equiv D/D_o$, strain (or form) recovery, apparent yield stress, etc.

Compatibilization enhances dispersion, increases the total apparent volume of the dispersed phase, rigidifies the interface, and increases interactions not only between the two phases but also between the dispersed drops. These changes usually increase the blend's viscosity, elasticity, and the yield stress. The compatibilizer effects are especially evident at low frequencies. There are two mechanisms that may further affect these behaviors: (i) the copolymer may form micelles inside one or both polymeric phases instead of migrating to the interphase and (ii) an addition of compatibilizer may increase the free volume resulting in decreased viscosity.

The time-temperature, t-T, superposition principle is not valid even in miscible blends well above the glass transition temperature, T_g (Cavaille et al. 1987; Ngai and Plazek 1990; Chung et al. 1994). In miscible blends, as either the concentration or temperature changes, the chain mobility changes and relaxation spectra of polymeric components in the blends show different temperature dependence, thus the t-T principle cannot be obeyed. Furthermore, at the test temperatures, the polymeric components are at different distance from their respective glass transition temperatures, $T - T_{g1} \neq T - T_{g2}$, which affects not only the t-T superposition but also the physical aging time (Maurer et al. 1985). In immiscible PO blends, such as PE/PP, at best, the superposition is limited to the melt within narrow temperature ranges (Dumoulin 1988).

For most blends, the morphology changes with the imposed strain. Thus, it is expected that the dynamic low strain data will not follow the pattern observed for the steady-state flow. One may formulate it more strongly: *in polymer blends the material morphology and the flow behavior depend on the deformation field*, *thus under different flow conditions*, *different materials are being tested*. Even if low strain dynamic data could be generalized using the t-T principle, those determined in the steady state will not follow the pattern. Chuang and Han (1984) reported that for blends at constant composition, the plots of N_1 versus σ_{12} and G' versus G'' are independent of T. However, for immiscible blends, the steady-state relation may be quite different from the dynamic one. The agreement can be improved by means of the Sprigg's theory (Utracki 1989a).

Four measures of melt elasticity have been used: the first normal stress difference, N_1; the storage modulus, G'; and the two indirect ones, the entrance-exit

pressure drop, P_e (*Bagley correction*), and the extrudate swell, B. In homogeneous melts, the four measures are in a qualitative agreement. In the blends where the dispersed phase is rigid, B and P_e is small. By contrast, for the readily deformable dispersed phase, the deformation-and-recovery provides a potent mechanism for energy storage, leading to a large elastic response. In short, neither Bagley's entrance-exit pressure drop correction, P_e, nor the extrudate swell, B, should be used as a measure of blends' elasticity. In both cases, not the molecular deformation but the *form recovery* dominates the observed dependence.

Two contributions to the tensile stress growth function, η_E^+, should be distinguished: one due to the linear viscoelastic response, η_{EL}^+, and the other originating in the structural change of the specimen during deformation, η_{ES}^+. The first can be calculated from any linear viscoelastic function, while the second depends on the intermolecular interactions or entanglements, and its value depends on the total strain, $\varepsilon = t\dot{\varepsilon}$, and either strain rate $\dot{\varepsilon}$ or straining time, t (Utracki 1988, 1989, 1995; Takahashi 1996). Owing to the industrial importance of strain hardening, $SH \equiv \log(\eta_{ES}^+/\eta_{EL}^+)$, a large body of literature focuses on the optimization of blend composition to maximize SH. Since SH depends on the entanglement, either interchain reactions that lead to branched macromolecules, blending linear polymers with branched ones, synthesizing bimodal resins, or widening the molecular weight distribution may result in improved SH. Extensive work on SH has been done for PE blends, especially the ones comprising LDPE (Utracki and Schlund 1987). Several other resins with long-chain branching (viz., bPC, bPP, or a biodegradable polybutylenesuccinate, etc.) have been introduced as special grades for, e.g., film blowing, blow molding, wire coating, or foaming (Imaizumi et al. 1998).

The convergent flow at the die entrance provides strong elongational flow. In 1989 Laun and Schuch derived for Newtonian liquids that $P_e \approx 1.64\sigma_{12}$. The relation is satisfactory for homopolymers, but for the blend, the prediction is about one decade too low. On the other hand, this type of flow provides excellent means for mixing highly viscous dispersed phase. An extensional flow mixer (EFM) was developed. The device provides good mixing for multicomponent polymer systems, e.g., for blends with components having widely different viscosities, viz., PE with UHMWPE, PP with high elasticity EPR, and PC with PTFE (Nguyen and Utracki 1995; Utracki and Luciani 1996a; Luciani and Utracki 1996; Tokohisa et al. 2006).

1.4.5 Developing Commercial Blends

There are several methods of blending, viz., mechanical (dominant), solution, latex, fine powder, as well as several techniques adopted from the IPN technology. Not always the finest dispersion is desirable – the size and shape of the dispersed phase must be optimized considering the final performance of the blend.

The polymer blends' performance depends on the properties of the ingredients, their content, and morphology. Since the cost is virtually fixed by the material and

the compounding method, the economy depends on blend's morphology, tailored for a specific application. Blends have been developed for economic reasons, viz., improvement of either a specific property (e.g., impact strength) or engendering a full set of required properties, extending engineering resin performance, improving processability, recycling, etc.

There are several approaches to evaluation of the blend economy. For example, the cost of a blend equals the weight average of material cost, plus the compounding cost per unit mass, e.g., $C_b = \Sigma w_i C_i + K$. Another approach is to calculate the cost-to-performance ratios for diverse materials and/or compositions. For example, one may ask *how much a unit of the tensile modulus or the strength at yield will cost* and optimize the composition accordingly. However, with growing frequency, the blend economy is based on the replacement calculations, comprising the total cost, that of material, compounding, forming, assembling, customer satisfaction, esthetics, service life-spans, and then the ease of disposal or recycling.

For a major resin manufacturer, blending provides means to improve and broaden the resin performance, and therefore, it enhances the demands and sale. By contrast, the resin user starts with a set of performance parameters that the material must possess. In both cases, the basic preposition is the same: *to have a blend with desired characteristics*, one must use a component that already shows this characteristic, or simply, *one cannot create something out of nothing*.

While extension of the engineering resin performance constitutes the largest part of the high-performance blends' production, the most difficult and interesting task is the development of blends with a full set of desired properties. To achieve this goal, a systematic approach has been developed (Utracki 1994). The procedure starts with the selection of blend components, each possessing at least one of the desired properties. For example, to improve impact strength, an elastomer should be used; to induce flame retardancy, a nonflammable polymer; to improve modulus, a stiffer resin should be incorporated; etc. Since for each property there are several candidates to select from, the selection is guided by the principle of the compensation of properties – advantages of one component should compensate for deficiencies of the other, e.g., the disadvantages of PPE (processability and impact strength) can be compensated for by those of HIPS. Next, the method of compatibilization, compounding, and processing must be selected. Since polymer blends' performance depends on morphology, the goal is to ascertain the desired structure by selecting an appropriate resin grade (rheology) as well as the methods of compatibilization, compounding, and processing.

Interesting studies on the morphology development during dispersive mixing were published by Kozlowski (1994, 1995). In this fundamental work, a rotating disk mixer was used. The disk had a milled grove in which stationary spreader was inserted. The gap clearance, speed of rotation, temperature, shape of the spreader, and pressure were controlled. The device simulated the dispersive processes that take place in internal mixers or extruders. A model of stepwise generation of morphology was proposed, where the original pellet (of the dispersed phase) undergoes deformation into elongated plates, which under stress break into fibers and finally into drops. The final morphology is a result of dispersion and

coalescence processes that depend on the viscoelastic character of the component, the interfacial tension properties, and the stress history (see ▶ Chap. 9, "Compounding Polymer Blends").

The ideal compounding unit should have (i) uniform elongational and shear stress field; (ii) flexible control of temperature, pressure, and residence time; (iii) capability for homogenization of liquids having widely different rheological properties; (iv) efficient homogenization before onset of degradation; and (v) flexibility for the controllable change of mixing parameters.

Most blends described in the patent literature have been prepared using either an internal mixer or a single-screw extruder (SSE). In standard configuration, SSE is inadequate for the preparation of blends with controlled morphology. Furthermore, due to the presence of "dead spaces," the run-to-run reproducibility of the SSE-extruded blends may be poor. SSE should not be used for reactive blending. However, there are several designs of mixing screws, profiled barrel elements, and add-on mixing devices that ameliorate SSE mixing capability. From between the latter devices, RAPRA's cavity transfer mixer (CTM) or the patented extensional flow mixer (EFM) should be mentioned. The first of these is a sort of "dynamic motionless mixer," where material is transferred from the cavities in the barrel to those on the screw, enhancing the distributive mixing (Gale 1980). The EFM is a motionless device in which the extensional forces provide dispersive mixing for blends with components having widely different viscosities, viz., PE with UHMWPE, PP with high elasticity EPR, PC with PTFE, gel particles in reactor powders, etc. (Utracki and Luciani 1996a).

More expensive but easier to control is a twin-screw extruder, TSE. Owing to the modular design with many types of elements fulfilling different functions, TSE can be optimized for specific tasks. The ratio of the dispersive-to-distributive mixing can be adjusted, and the width of the residence time can be controlled. TSE is excellent chemical reactor for polymerization, modification of polymers, and reactive compatibilization (Rauwendaal 2001). As a result, the blend quality and run-to-run reproducibility are improved. Computer models have been developed to predict variation of blend's morphology along the screw length in these machines (Shi and Utracki 1992, 1993; Huneault et al. 1993, 1995b).

1.4.6 Blends' Performance

The quality of compounded blend affects the processing and performance. Layering, poor weld lines in injection molded parts, and skin-core extrudate structure with low notched Izod impact strength all indicate poor blend quality – either not adequate dispersion or poor stabilization of morphology. Compounding demands precise control of process variables. At the present, most alloys are prepared by reactive processing. It has been reported that pellet blending of two blend lots may lead to apparent immiscibility and bad weld-line strength. Evidently, even a small variation in the extent of reaction may make them immiscible. The mixed lots may pass standard tests, but still yield unacceptable products.

Historically, blending was used to improve the impact strength of the early resins, i.e., toughening of PS, PVC, PMMA, PET, PA, etc. With time, blends evolved into multipolymer systems that not only have to be impact modified but also compatibilized. Many blends have been formulated with a multicomponent modifier that simultaneously compatibilizes and impact-modifies the mixtures.

The following observations can be made: (1) The maximum toughening of brittle polymers has been obtained dispersing ca. 10 vol.% of a ductile resin with domain diameter of d ≈ 0.1–1.0 μm –the lower limit is for resins that fracture by the shear banding, whereas the higher for those that fracture by the crazing and cracking (Bucknall 1977; Bucknall et al. 1984). (2) The phase co-continuity provides the best balance of properties, e.g., high rigidity in the presence of large deformability (or elongation). The properties depend on the thickness of the interpenetrating strands, thus also on compatibilization. (3) For the best barrier properties, the lamellar structure is desirable. To create it, the blend should comprise large but stable drops with diameter d ≈ 5–50 μm. During biaxial stretching (e.g., in blow molding or film-blowing processes), the large drops easily deform into lamellae.

Two types of mechanical tests are recognized: low speed (tensile, compressive, or bending) and high speed (impact). Poor compatibilization affects both. For example, in tensile tests the maximum strain at break and the yield stress can be dramatically reduced by poor inter-domain adhesion. Similarly, the lack of adhesion is responsible for low-impact strength – the specimens are brittle. Several toughening mechanisms have been proposed, viz., crazing, shear-banding, cavitation, particle debonding, elastic deformation of the toughening particles, etc. (Arends 1996).

Polymeric systems are roughly classified as either brittle or pseudo-ductile. The first type has low crack initiation as well as propagation energy and it fails by the crazing-and-cracking mechanism. Typical examples are PS, PMMA, and SAN. The second type has high crack initiation energy, but low crack propagation energy, and it tends to fail by yielding and shear banding. Typical examples are PA, PEST, and PC. As usual, there are some polymers, e.g., POM and PVC, which show intermediate behaviors – in many systems the fracture takes place by a mixed mode. The transition from brittle to ductile mode of fracture depends on the intrinsic properties of the material as well as on the external variables such as geometry, temperature, loading mode, test rate, etc. To detect the mechanism of fracture, the stress-strain, and the volume-strain dependencies should be known. "Toughness" is defined as the total area under the stress-strain curve, thus abruptly ending curves without the yield point are characteristic of brittle materials. The volume-strain dependence provides means for quantitative identification of the fracture mode – pure shear banding shows no volume expansion, whereas pure crazing and cracking show the maximum volume expansion.

Wu (1985, 1987, 1988, 1990) postulated that the brittle/ductile behavior of a neat amorphous polymer is controlled by two intrinsic molecular parameters: the entanglement density, ν_e, and the chain stiffness (given by the characteristic chain constant, C_∞). Assuming that crazing involves chain scission, the stress, σ_z,

Fig. 1.2 Izod impact
strength at room temperature
as a function of diameter of
elastomeric particles in
methylmethacrylate-
butadiene-styrene copolymer
used for toughening
polyvinylchloride resin
(After Bartelo and Mori 1994)
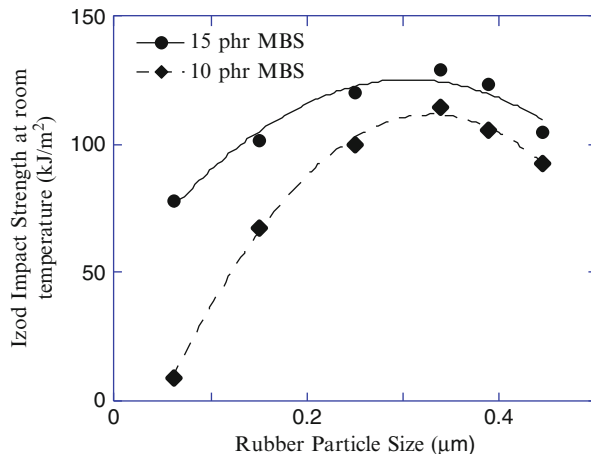
should be proportional to $\nu_e^{1/2}$ and the yield stress, σ_y, proportional to C_∞. In consequence, $\sigma_z/\sigma_y \propto \nu_e\sqrt{3M_v/\rho_a}$, where M_v is the average molecular weight of a statistical segment and ρ_a is the polymer density. For brittle polymers, $\nu_e < 7.5$.

Effectiveness of the toughening process depends on the diameter of the elastomeric particles and their concentration. At constant concentration, the toughness versus particle diameter dependence goes through a maximum – abscissa of its location, d_{opt}, does not depend on concentration, whereas the ordinate does (see Figure 1.2). The optimum particle size, d_{opt}, depends on the entanglement density of the matrix resin, as well as on the fracturing and toughening mechanisms. In general, small particles, having weight-average diameters in the range of 0.2–0.4 μm, work well in the presence of shear yielding, while larger particles in the range of 2 and 3 μm are more effective in the presence of crazing (Bucknall and Paul 2009). Another important characteristic is interparticle spacing (Bucknall and Paul 2009, 2013).

However, the determination of the d_{opt} may be ambiguous, owing to the polydispersity of sizes as well as to inclusion of the matrix polymer inside the elastomeric particle. For example, it has been accepted that to toughen PS into HIPS, the optimum diameter is defined as a diameter of the elastomeric particles expanded by inclusion of the PS mini-drops. In PVC, the diameter of the elastomer was defined as the diameter of the original butadiene latex particle before grafting it with styrene and methylmethacrylate. In PC, the "optimum" diameter was defined by availability of the core-shell toughening agent – it is difficult to find toughness with elastomeric particles having diameter $d < 100$ nm. The strategy for the preparation of polymer blends with stable morphology demands that blends have thick interphase, $\Delta l \leq 60$ nm. Frequently it is impossible to decide how far the toughening by rubber core extends into the interphase. Many impact-resistant engineering resin blends have been formulated using a core-shell multicomponent copolymer with a *rigid* core and elastomeric shell whose thickness and affinity with the matrix resin was adjusted.

In many cases, toughening of a brittle polymer can be achieved by introduction of stiffness heterogeneity, viz., incorporation of an elastomer, immiscible polymer, solid particles, gas bubbles (i.e., foaming or microfoaming), etc. However, the size and concentration of these heterogeneities should be optimized. For most thermoplastics, the optimum diameter of the dispersed elastomeric particle is d < 3 μm and its volume fraction $0.05 < \phi < 0.10$. The accepted mechanism of toughening considers the heterogeneity to be a stress concentrator, generating excessive crazing and/or shear banding of the matrix, thus requiring higher amount of energy to cause fracture. The stress concentration factor was defined as $\gamma \propto 1/(1 - a\phi^{2/3})$ where the parameter a depends on the matrix (Bucknall 1977; Partridge 1992). For blends with pseudo-ductile matrix, d_{opt} depends on concentration, as it is important to keep the distance between the elastomeric particles approximately constant.

During the early works on compatibilization of PE/PS blends in Prof. Heikens laboratories, it was noted that addition of a small amount of one polymer to another improved impact properties. Since these two polymers are antagonistically immiscible and upon solidification void formed around the dispersed particles, it was concluded that it is the presence of the voids that accounts for the toughening effect (D. Heikens, 1982, private communication). About 15 odd years later, the microcellular blends have been introduced. For example, microfoamed blends of HDPE with PP (using CO_2 in an autoclave) showed significantly improved impact strength (Dorudiani et al. 1998). Similar enhancement of mechanical performance was reported earlier for N_2-microfoamed PS, SAN, or PC (Collias and Baird 1995). Now, microfoaming is being used to reduce the material consumption, part weight (by 30–50 %) (Kumar and Suh 1990), but it can also help to improve the mechanical performance, especially of the injection molded parts.

Under the triaxial stresses in the region ahead of the sharp crack, a particle may cavitate at a certain strain, changing the stress field of the matrix from the dilatation to the distortion dominated. Thus, the matrix may deform plastically, what consumes energy. The mechanism depends on the size of the dispersed toughening particles and the inherent plastic deformation capability of the matrix (Borggreve and Gaymans 1989; Lazzeri and Bucknall 1993; Yee and Shi 1995; Groeninckx et al. 1995). In PC cavitation occurred well before shear yielding (Parker et al. 1992). Blends comprising relatively high concentration of two engineering resins may require toughening of both phases by sequential reactive blending.

Formation of co-continuous structures in blends of either a brittle or pseudo-ductile resin with an elastomer may result in a quantum jump of toughness, without greatly affecting the key engineering properties of the high-performance resin. Commercial blends of this type, e.g., POM, PA, PC, or PET with an elastomer, are available (viz., *Triax*™ series).

1.4.7 Evolution of Polymer Alloys and Blends

The historical evolution of the polymer blend technology is presented in the following order:

1. Commodity resins (styrenics, PVC, acrylics, PE's, PP)
2. Engineering resins (PA, PEST, PC, POM, PPE)
3. Specialty resins (PSF, PAE, PARA, PAr, PPS, LCP, PEI, PEA, etc.)

Blends of polymer A with polymer B will be discussed following the adopted rules: (i) symbol A/B is used to identify any mixture of polymer A with B, independently of the concentration range or morphology, and (ii) the A/B blends are discussed under the name of the lower category polymer, i.e., blends of engineering or specialty polymers with a commodity resin are discussed in the category of commodity resin blends, blends of specialty polymers with engineering resins are discussed in the category of engineering resins, hence "specialty resin blends" consider only mixtures of two (or more) specialty resins.

1.5 Commodity Resins and Their Blends

Five large-volume polymeric groups belong to this category: polyethylenes, polypropylene, styrenics, acrylics, and vinyls. Their world market share remains relatively stable – the commodity resins represent 71 % of all consumed plastics.

1.5.1 Polystyrene (PS)

Simon in 1839 named the distillate of *Styrax officinalis* a *styrol*. By 1845, the thermal polymerization of styrene as well as the thermal depolymerization of PS was known. In 1915, I. G. Farbenindustrie started commercial production of PS, *Trolitul™*. Until the 1950s, PS was produced in small quantities – the resin was brittle, thermally unstable, with poor solvent and scratch resistance. The main use of styrene was in the manufacture of styrenics, viz., *Buna-S*, SBR, or ABS.

Common PS is atactic and amorphous. It has good optical clarity, low dielectric loss factor, modulus E = 3.2 GPa, strength σ = 45–65 MPa, density ρ = 1,050 kg/m^3, and CUT = 50–70 °C. Because of brittleness and low chemical resistance, the demand for neat PS has decreased, and except for foaming, PS is rarely used. PS can also be polymerized into crystalline forms: isotactic (iPS) or syndiotactic (sPS) with T_m = 230 °C or 272 °C, respectively. The former was polymerized using Ziegler-Natta catalyst (Ishihara et al. 1986), while the latter using a single-site metallocene titanium-based catalyst (Imabayashi et al. 1994).

The high-impact PS, HIPS, has been known since 1911 (Matthews 1911, 1913). In the USA, Ostromislensky (1924, 1926–1928) patented copolymerization of styrene with *rubber*, *balata*, *or other elastic and plastic gum*. Production of HIPS, *Victron™*, by the Naugatuck Chemical started in 1925, but soon it was discontinued.

PS is miscible with several polymers, viz., polyphenylene ether (PPE), polyvinylmethylether (PVME), poly-2-chlorostyrene (PCS), polymethylstyrene (PMS), polycarbonate of tetramethyl bisphenol-A (TMPC), co-polycarbonate of bisphenol-A and tetramethyl bisphenol-A, polycyclohexyl acrylate (PCHA),

polyethylmethacrylate (PEMA), poly-*n*-propyl methacrylate (PPMA), polycyclohexyl methacrylate (PCHMA), copolymers of cyclohexyl methacrylate and methylmethacrylate, bromobenzylated or sulfonated PPE, etc. Information on other miscible blends may be found in ▶ Chap. 21, "Miscible Polymer Blends".

Similarly, poly-α-methylstyrene is miscible with PMMA, PEMA, PBMA, and PCHMA. Poly-*p*-methylstyrene and poly-*p*-t-butylstyrene show miscibility with polyalkyl(meth)acrylates. However, PS is immiscible with PMMA, PMA, polyethylacrylate (PEA), polybutylacrylate (PBA), or PBMA (Somani and Shaw 1981).

In miscible blends, it is important that both components are in the entangled state. In particular, during processing in the extensional flow field (e.g., blow molding, film blowing, wire coating, calendering, or foaming), an enhancement of strain hardening (SH) can only be obtained when the concentration of the high molecular weight component is at least comparable to the critical concentration of entanglement, $c \geq c^*$. Under these circumstances, large increases of SH were observed, e.g., for PS blended with ultra-high molecular weight PS (UHMW-PS) or SAN blended with ultra-high molecular weight PMMA (UHMW-PMMA). By contrast, addition of immiscible UHMW-PS to SAN did not show any improvement of SH (Takashi 1996; Takahashi et al. 1996; Koyama et al. 1997; Minegishi et al. 1997, 1998). Examples of blends that were evaluated for SH are listed in Table 1.8.

1.5.1.1 PS/Commodity Resin Blends

The most common immiscible PS blends are those prepared to improve the impact strength of PS or its copolymers, viz., HIPS or SBR (Table 1.9).

It was reported that incorporation of 0.1–18 vol.% of either acrylic or olefinic elastomer particles (e.g., in HIPS) into a thermoplastic (viz., PE, PP, PS, SAN, PEST, PPE/HIPS, PC, PEI, PA, fluoropolymers, etc.) resulted in excellent control of the foaming process (Campbell and Rasmussen 1994). The bubble diameter could be calculated from the concentration of rubber particles. When these were lightly cross-linked, the stretched membrane provided an excellent barrier against coalescence of gas bubbles. Thus, reliable nucleation and absence of coalescence lead to foaming stability. For example, in autoclave foaming of PS with N_2, the cell size was less than 40 μm, independently of the saturation pressure and only slightly increasing with the foaming temperature.

Postulating that the rubber particles are stretched to membranes all having the same thickness, the foam cell size can be expressed as

$$D_{cell} = D_o + \left(d_{rubber}^3 / nt\right)^{1/2}; \quad n = 3 \text{ to } 6 \tag{1.8}$$

where D_{cell} is the cell size, d_{rubber} is the initial diameter of rubber particle, D_o is the diameter of foam cell in the absence of rubber particles, and t is thickness of the rubber shell after foaming. Depending on the initial assumption of

Table 1.8 Strain hardening in molten polymer blends

Polymers	Type	SH behavior (references)
PMMA/ UHMW-PMMA	Miscible	General rule: large enhancement of SH only for c(UHMW) > c* = 1.2 wt%; SH ≤ 10 (Minegishi et al. 1997)
PS/UHMW-PS	Miscible	Large enhancement of SH increasing with T; SH ≤ 10 (Minegishi et al.1998)
SAN/UHMW-PS	Immiscible	At 145 °C no effect on SH; SH ≤ 2 (Koyama et al. 1997)
SAN/UHMW-PMMA	Miscible	Large enhancement of SH; SH ≤ 10 (Koyama et al. 1997)
PE/UHMWPE	Miscible	Large enhancement of SH; SH ≤ 10 (Okamoto et al. 1998a, b; Kotaka 1998)
Bimodal POs	Miscible	Large enhancement of SH; SH ≤ 10 (Münstedt and Kurzbeck 1998)
LLDPE/LLDPE	Miscible	Average SH for the narrow and broad MWD LLDPEs (Schlund and Utracki 1987)
LLDPE/LDPE	Immiscible	Presence of LDPE increased linearly SH of LLDPE (Schlund and Utracki 1987)
		Enhancement of SH for c ≥ 10 wt% LDPE
LDPE/PS	With 0–5 wt% of SEBS	SEBS (micelles in LDPE phase) reduced the strain at break; additive SH; yield stress (Utracki and Sammut 1987, 1990)
LDPE/PS	Compatibilized	Better SH; the blends are suitable for foaming (Y. Horiuchi, 1998, personal communication)
PMMA/PVDF	Miscible	30 wt% of PVDF reduced SH of PMMA at 160 °C (Kotaka 1998)

Table 1.9 Toughening of PS

Composition	Reason	References
PS with SBR	Impact performance	Seymour 1951
PS with PIB and PSIB	Toughness	Sparks and Turner 1952
PS with PB and SBR	Toughness	Hayes 1956, 1967
PS with SBR and a cross-linked SBR	Toughness	Conrad and Reid 1963
PS with SBR and PEG	Toughness, adhesion, electrostatic dissipation	Briggs and Price 1963
HIPS (PS toughened by styrene-grafted EPR)	To improve weatherability	*Hostyren*™
HIPS with SBS	Enhanced properties	Durst 1970
PB reacted with styrene, ethyl- or methylstyrene, t-butyl styrene, and/or vinyl silanes	Low-density PO foams for marine or submarine applications	Dawans and Binet 1981
PS with SBR, (SB)$_n$, and PP	Toughness	Grancio et al. 1981, 1983
HIPS with a star-block copolymer, (SB)$_n$	Enhanced properties	Gausepohl et al. 1982
HIPS with a SB-block copolymer having small size of the rubber particles	Transparent HIPS	Asahi Chemical Industry 1982
HIPS with HDPE and SEBS	Enhanced properties	Murray 1982
HIPS with BS(B′S′)$_n$ terminated with 2,4-di-*tert*-butyl-*p*-cresol and *tris* (nonyl-phenyl)phosphite	For adhesiveness	Shiraki et al. 1986

Fig. 1.3 Cell size versus the initial rubber particle diameter. Data points: (Campbell and Rasmussen 1994) *solid line* – Eq. 1.8 with n = 6, and the cell wall thickness t = 85 nm
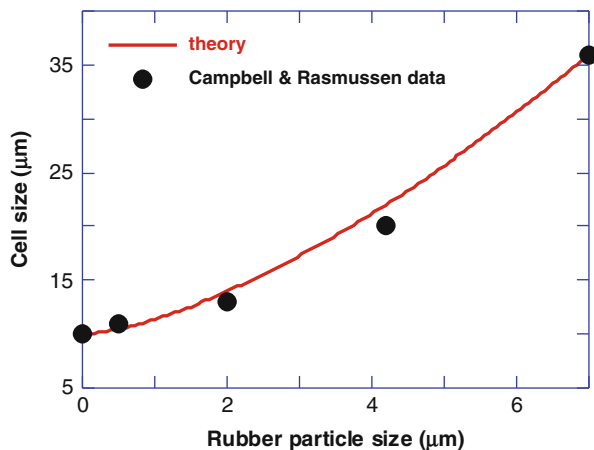
Table 1.10 PS or HIPS with polyolefins

Additive	References
PE and CSR	Herbing and Salyer 1963
PE and styrene-ethylene bulk copolymer	Gorham and Farnham 1964
PO and EVAc	Yamamoto et al. 1971
Either PP or PE	Ogawa et al. 1973
5–95 wt% PS with 95–5 wt% PO and 0.5–10 wt% SEBS (foaming)	Zeitler and Mueller-Tamm 1977
PP and SEBS	Holden and Gouw 1979
1–99 wt% of either LDPE, LLDPE, HDPE, EVAc, PP, or EPR (chemical foaming to open-cell structures)	Tashiro et al. 1983
LLDPE	Canterino and Freudemann 1985; Canterino et al. 1986
Reprocessed PE/PS, compatibilized with 0.5–40 wt% of EVAc	McCullough and Stevens 1985
$\geq$ 60 wt% of partially neutralized ionic PS (e.g., a copolymer of styrene and acrylic acid) with $\geq$ 1 wt% PE ionomers, foamed with 3–20 wt% of $NaHCO_3$	Park 1986a, 1986b, 1988
PE or PP compatibilized with a nonsymmetrical 3-block copolymer, S1-D-S2	Hoenl et al. 1993
HDPE and either SBS or SIS	Swartzmiller et al. 1993, 1994

the cell geometry, the geometrical factor can be calculated as n = 3 to 6. Adequacy of Eq. 1.8 is shown in Fig. 1.3.

The second large group of styrenic blends comprises these with polyolefins – they are summarized in Tables 1.10 and 1.11. These blends are mainly used in packaging. Formulated for extrusion, injection, and blow molding, they show excellent processability, improved impact strength, low moisture absorption, and shrinkage. The performance characteristics (e.g., modulus, toughness, ductility, transparency, or gloss) can be controlled by composition and morphology.

Table 1.11 Addition of styrenics to PO

Additive to PE	Reason	References
1. Addition of styrenics to PE		
SAN	Improved crack resistance	Jankens 1963
5–20 wt% SBR	Impact strength	Dow Chem. 1963
SB, SBS, or a *p*-methylstyrene-b-isoprene copolymer	Improved crack resistance	Minekawa et al. 1971
Styrene-grafted HDPE	Higher modulus	Yui et al. 1978
ABS with CPE or low molecular weight PS	Impact strength	Kamosaki et al. 1978
SEBS	Mechanical properties	Davison and Gergen 1977, 1980
SBS or SEBS as compatibilizers for PS/PE	Recyclability	Lindsey et al. 1981
HIPS with HDPE and SEBS	Impact strength	Castelein 1982
PS/LDPE; MI ratio $R = MI_{PS}/MI_{PE} = 790$, weight ratio $Y = 10$ to $Y = [394.7 + 1.18R - 295.1 \log D]$; density: $D = \rho = 15$–$30 kg/m^3$. R and Y control the co-continuous blends morphology	Flexibility, dumping small vibrations, stiffness, heat insulation, low water permeability	Hoki and Miura 1987
5–50 wt% PS with LDPE a chemical blowing agent and a peroxide (0.05–0.1 pph DCP)	Dimensionally stable, $\rho = 20$–$30 kg/m^3$, cells 1.5 mm	Park 1986c, 1987, 1995
LDPE/PS = 80/20 blends compatibilized in a twin-screw extruder with supercritical CO_2	Studies of the rheology during closed-cell foaming	Lee et al. 1998
2. Addition of styrenics to PP		
PS or HIPS	For nacreous soda-straw tubes	Ogawa et al. 1973
ABS with either CPE or low molecular weight PS	Impact strength	Kamosaki et al. 1978
PS with HIPS and SEBS	Mechanical performance	Holden and Gouw 1979
PS was compatibilized by adding either SBS or (SB)$_n$	Higher modulus	Grancio et al. 1981, 1983
PS or HIPS and a nonsymmetrical, linear 3-block copolymer of styrene and butadiene, S1-D-S2, where the polystyrene blocks $S1 \geq S$	Processability, impact and stress-cracking resistance, impermeability to H_2O	Hoenl et al. 1993
PS with recycled PP – co-continuous morphology	Performance, recyclability	Morrow et al. 1994
sPP-co-sPS from single-site metallocene catalyst	Compatibilization of sPP/sPS	Razavi 1994
PP, EPR, EVAc, and PS blended with 1–50 wt% of the silane-modified-based resin, cross-linking catalyst and 1–20 wt% of a foaming agent	Resilient foams with superior, compression strength, and heat-insulating properties	Kobayashi et al. 1997

Other patents described similar blends prepared either by different methods or comprising different compatibilizer. For example, PO was mixed with styrene in the presence of an initiator that caused polymerization at temperatures below melting point of PO (Vestberg and Lehtiniemi 1994).

Interesting blends, having a broad range of properties, were prepared in two steps: (1) BR was grafted and cross-linked with either styrene or methylmethacrylate to produce a core-shell copolymer. (2) Next, it was blended with PO for improved processability, impact resistance, rigidity, etc. (Aoyama et al. 1993, 1994). Structural blends of styrene-grafted PP with either SBR, SBS, or an acrylic elastomer were developed (DeNicola and Conboy 1994).

Since the early 1990s, the constrained geometry metallocene catalysts have been used by Dow to produce either alternating or pseudo-random ethylene-co-styrene interpolymers (ESI) (Stevens et al. 1991). ESI with up to 50 wt% styrene is semicrystalline; it is known to compatibilized PE/PS blends since it forms domain structures into which the homopolymers can dissolve. ESI also has good melt strength, mechanical, impact, and damping characteristics (Ellebrach and Chum 1998). Flow and processing information on ESI were published (Karjala et al. 1998).

Himont (now Lyondell Basell) introduced a family of PP-based blends under the trade name of *Hivalloy*™. Some grades seem to be mechanical alloys of PP/PS, compatibilized and impact modified by incorporation of SEBS and EPR. Others are reactor made – here porous grains of PP serve as reaction beds for the polymerization and grafting of PS, SMA, acrylics, etc.

PS is one of the most frequently foamable thermoplastic resin. Blends that belong to this category are presented in Table 1.12. Blends containing ≥ 50 wt% PS (MW = 200 kg/mol) and acrylic copolymers were described as particularly useful for the manufacture of low-density foams. The acrylic copolymer contained methylmethacrylate and, e.g., 5 wt% of ethylacrylate. The presence of the copolymer facilitated foaming, but it reduced the foam compressive strength. The best balance was obtained using about 22 wt% of the copolymer. The foam had closed cells with cell diameter varying from 0.1 to 1 mm (Smith and Cross 1996).

1.5.1.2 PS/Engineering Resin Blends

The majority of PS blends that belong to this category are mixtures with PPE. Discovery of PPE miscibility with PS led to a family of *Noryl*™ blends, commercialized in 1965. Since that time, the PPE/PS blends were modified by the incorporation of a variety of additives. The PPE/PS blends show the glass transition temperature, $T_g = 100$–210 °C, continuously increasing with PPE content. The most often used compositions contain less than 30 wt% of PPE (PPE is about three times more expensive than PS).

PPE is the most "natural" additive that upgrades performance of PS to the required level. PS/PPE blends have been used as a replacement for PS in applications where higher HDT and/or impact strength is required. These alloys are easy to foam for the manufacture of, e.g., hot water piping insulation, in automotive applications, etc. Examples of PPE/PS blends are listed in Table 1.13.

Table 1.12 Foamable PS blends

Blend	Comment	References
PS with low concentration of siloxane-oxyalkylene copolymers	Reduced interface tension, easier bubble nucleation and growth, smaller cells	Granda et al. 1977
PS with radial teleblock SBS, PMS, naphthenic extender oil, formed at P = 1.4 MPa and then foamed using microwaves at 10–100 MHz	Molded articles had thin skin and uniformly foamed interior	Siedenstrang and Thorsrud 1984
PS with SAN, ABS, and 15–50 wt% of SMA	Chemical foaming ($NaHCO_3$) during injection molding	Sprenkle 1980
75–98 wt% of PS, 2–25 wt% of a BR (MW = 200–300 kg/mol)	Easy to foam due to fine dispersion of BR spheres	Henn et al. 1996
Mixtures of emulsion copolymers comprising acrylonitrile, butadiene, styrene, and acrylic or methacrylic acid	Low-density foams for non-wovens, carpets, fleece, or cardboard	Matner et al. 1977
SBR blends with 10–50 wt% of plastisol PVC	For foamed, flame-resistant carpet backing	Morgan and Ribaudo 1980
SBR, ABS, MABS, and/or SBS, with either PS, PO, PVC, PPE, PA, POM, PC, PSF, or PEST	For high impact strength moldings	Aoki et al. 1981
Polymer alloys of SMA and cellulose esters at a ratio varying from 1:100 to 100:1	Reaction between anhydride and cellulosic – OH facilitated foaming and gave good product performance	Heslinga and Greidanus 1982
5–35 wt% of SEBS, 65–90 wt% of PB-1, 5–30 wt% of EPR or EPDM, 2–15 wt% of LDPE	Foams had excellent bending capability, tear strength, stiffness, and HDT	Hwo 1996
Two SBR copolymers, (1) with of 53–75 wt% of styrene and (2) with 42–75 wt% of styrene	Cured foams for shoe soles with high shock absorption	Hashimoto and Ohashi 1985
ABS compositions	Foamed with supercritical CO_2 at P ≤ 5 MPa	Kumar et al. 1995
45–90 wt% of PS or styrene-acrylic acid copolymer with 10–55 wt% of PVDC or vinylidenechloride-methyl acrylate copolymer	Physically foamed products had improved O_2 and H_2O permeability, toughness, and flame resistance	Romesberg 1991
PS, SMA, SAN, PMS, or HIPS blended with SBS and an extending oil and then incorporated into PA, PEST, PPS, SAN, ABS, ASA, PC, PPE, PO, their copolymers, or blends	A general method for the production of a variety of foamable injection moldings	Burnell 1993
75–97 wt% of either PS or HIPS and 3–25 wt% of an elastomeric (co)polymer having a T_g < −20 °C	Foamable materials with good performance characteristics	Blumenstein et al. 1994
Latex copolymers were blended, cross-linked, and foamed: (1) 20 wt% styrene, 20 wt% divinylbenzene, 60 wt% 2-ethylhexyl acrylate with (2) 80 wt% styrene, 20 wt% divinylbenzene	Pen-cell foams with great absorbency were prepared for baby dippers, for paint rollers, filters, etc.	Brownscombe et al. 1997

(*continued*)

Table 1.12 (continued)

Blend	Comment	References
ABS with ASA and two SAN copolymers were foamed with a physical foaming agent	Easy formability, excellent physical properties, and Freon resistance	Kim and Choi 1998
Blends of NR, SBR, BR, and SB copolymer that had 0–30 wt% of styrene and MW $\geq$ 30 kg/mol	Foamable rubber blend, suitable for tires or belts	Kawauzra et al. 1997

Table 1.13 Examples of PS/PPE blends

Modifier of PPE/PS blend	References
Elastomers such as PB, SBR, or NBR	Lauchlan and Shaw 1970
PB	Huels 1971
Poly(methylmethacrylate-co-styrene) and PO	Izawa et al. 1973a, b
Either SBR or ABS	Nishioka et al. 1973
Vinyl-terminated ethylene-propylene-styrene terpolymer (SEP)	Haaf 1979
PA-66	Mitsubishi Petrochemical 1982
Foaming with dry gases generated by the thermal decomposition of a dihydro-oxadiazinone + azodicarboxylic acid amide or ester	Kochanowski 1982
PPE-polyolefin graft copolymer and NBR	Mitsubishi Petrochemical 1983
Epoxy-terminated liquid PB, with either PP-MA or SEBS	Mitsubishi Petrochemical 1983
SBR and SBS copolymer	Mitsubishi Gas 1985
ABS and SAN	Japan Synthetic Rubber 1985
Hydroxynaphthoic acid	Tamura 1985
Ethylene glycol-propylene glycol copolymer (PEG-PPG)	Vaughan 1985
SBR and radial-SB copolymer	Sugio et al. 1987
PPE/PS closed-cell insulating foams, with high compressive strength	Allen et al. 1989; Weber et al. 1990
PPE/SAN with cross-linking and C3–C6 hydrocarbon blowing agents	Hahn et al. 1992
PPE with, e.g., PS, PMS, PES, PEI, PC, PA, PEST, PP, or PE and the blowing and nucleating agents	Bland and Conte 1993

Five *Caril*™ grades of expandable PPE/PS beads (diameter 0.3–0.5 mm) offer HDT up to 120 °C, thus are suitable for the production of microwavable and steam-cleanable packaging with the wall thickness $\geq$ 1 mm. The recommended density of molded product is $\rho = 60$ kg/m^3. Other foamable, flame-retardant PPE/PS blends, with good acoustic and thermal insulation properties, have been produced in suspension polymerization of a PPE solution in styrene and pentane. Resulting beads had diameter d = 0.5–1.0 mm and could be steam pre-foamed and compression molded in a standard equipment. The cited advantages are high HDT, non-flammability, dimensional stability, strength, stiffness, low molding cost, low density, easy lamination with decorative and weather-resistant ASA, and recyclability (Koetzing and Diebold 1995).

Table 1.14 Compatibilization of PS/PC blends by SAN

Additive to PC	Reason	References
Either SAN or styrene-allyl methacrylate-butyl acrylate-methyl methacrylate copolymer or with a *multilayered copolymer* from styrene, allyl methacrylate, benzyl acrylate, divinylbenzene	Toughening, high mechanical performance, solvent resistance	Kishida et al. 1978a, b
SAN and a styrene-grafted acrylic rubber	Improved mechanical properties	Kamata et al. 1979
PS and MBS	Higher modulus	Lee 1980

PS is antagonistically immiscible with all other engineering resins, viz., PA, PC, POM, and PEST. PS has been added to these polymers to improve processability and reduce cost without unduly affecting the performance (the so-called extension of the engineering performance).

Non-compatibilized blends of PS with either PEST or PEST and PMMA have been used for decorative applications or as the so-called plastic paper (Kamata et al. 1980). Similarly, PAr blends with either SAN (Brandstetter et al. 1983a, b, c) or high-performance blends of LCP with thermoplastic polymers (e.g., PP, PS, PC, PI) (Haghighat et al. 1992) showed adequate performance for the envisaged applications. However, most PS blends with engineering resins require compatibilization. Thus, for example, PS with PA-6 was compatibilized by addition of either methylmethacrylate-styrene copolymer (SMM) (Fayt et al. 1986b) or SMA (e.g., used in PARA/PS blends) (Lee and Char 1994). POM was blended with a small amount of either PS poly(α-methyl styrene) (MPS) or SAN and with particulate fillers (Tajima et al. 1991). PAr/PS blends were compatibilized with PAr-PS segmented copolymer (Unitika Ltd. 1983).

Several blends comprising PC and diverse styrenics, viz., ABS, SAN, SB, SBS, MBS, etc., are known (see Table 1.14). Similarly as for PVC blends (see Table 1.15), the strong interactions between AN and carbonyl groups of PC (in PVC it is the tertiary carbon) are responsible for the good performance. An interesting variation of the compatibilization procedure involved dispersing PC in water with vinyl monomer(s) that subsequently were polymerized. The in situ formed graft copolymers acted as a compatibilizer (Kanai et al. 1978; Kakizaki et al. 1979a). In 1974, polyphenylenesulfide, PPS, was blended with either PS or a styrene copolymer (Miyanishi 1976). Acid-base forces are responsible for strong molecular interactions. An understanding of specific forces is required if polymer blend systems are to be formulated, so as to satisfy steadily increasing demands on their performance and durability (Mukhopadhyay and Schreiber 1995).

Later, to provide a complete set of the required performance characteristics, multicomponent blends were promoted, for example, PC, PPE, ASA, SAN, PS, phosphate esters, PTFE, and SEBS (Niessner et al. 1993) or PC, PEST, ABS modified by incorporation of alkyl (meth)acrylates and glycidyl methacrylate, and PPE with either PS, HIPS, or SEBS and a polyalkyl(meth)acrylate (Laughner 1993).

Table 1.15 PVC/ABS-type blends

Additive to PVC	Reason	References
ABS	For either phonographic records or artificial leathers	Parker 1951; Schule 1952
5–30 wt% of either methylmethacrylate-acrylonitrile-butadiene-styrene(MABS)	High impact strength, mechanical properties	Himei et al. 1967
1–50 wt% ABS and post-chlorinated PVC	Improved processability, impact strength, and thermal stability	Kojima et al. 1970
ABS grafted with acrylonitrile-ethyl acrylate-styrene	Improved toughness	Tanaka et al. 1971a, b, c
ABS and SBS	Improved impact strength	Minekawa et al. 1971
MBS or MABS	Impact strength	Kumabe et al. 1973
Multilayer butadiene-styrene-divinylbenzene-butylacrylate-methyl methacrylate	Processability and high impact resistance	Usami and Ochiai 1976
Poly(2-cyano-5-norbornene) and ABS	Impact strength	Matsuura et al. 1978
PB grafted with styrene, methylmethacrylate, and maleic anhydride (ABSM-MA) or a mixture of ABS and SMM-MA	Processability, high impact strength, mechanical properties	Dufour 1982
Methylstyrene-styrene-acrylonitrile-grafted polybutadiene or with maleated styrene-methylmethacrylate-butadiene (ABS-MA)	Processability, high impact strength, mechanical properties	Dufour 1988
ABS and vinylchloride-ethylhexyl acrylate	Abrasion resistance	Greenlee et al. 1992
Core-shell copolymer: EPDM grafted with styrene-butadiene methacrylate or allyl cyanurate	Processability, high notched impact strength	Siol et al. 1993a, 1995
CPVC and PMMA, methylstyrene-acrylonitrile-methyl methacrylate, methylstyrene-acrylonitrile-styrene, imidized-PMMA, imidized-SMA, and SAN	Economy, high HDT and impact strength	Soby et al. 1994

1.5.2 Acrylonitrile-Butadiene-Styrene (ABS)

The first mechanical blends of NBR with SAN, known as "type-A ABS," date from 1936. In the mid-1940s, Dow started emulsion polymerization of "ABS-type G." By the late 1950s, the *high heat ABS* were invented, viz., interpolymers of α-methylstyrene and acrylonitrile (Irving 1961), a mixture of methylmethacrylate-α-methylstyrene either with styrene-grafted polybutadiene (SBR) or with an ABS (Kanegafuchi 1967, 1984), a mixture of SMA and ABS (Stafford and Adams 1972), a mixture of SMA with ABS and MBS (Tatuhiko and Akira 1982), a mixture of SMA-MMA with ABS, etc.

Acrylonitrile-styrene-acrylate terpolymers, known as either ASA or AAS, constitute another class of ABS resins, viz., *Centrex™*, *Luran™* S, *Richform™*, *etc*. These materials may also contain reactive groups, viz., maleic anhydride or glycidyl methacrylate.

Weather-resistant ABS can be obtained either by the incorporation of EVAc (Fukushima and Mitarai 1971) or by replacing PB with EPDM to obtain AES (Wefer 1984, 1985, 1988). Alternatively, blends of SAN with maleated EPDM and CPE may be used (Kim et al. 1992). However, the non-weatherable styrenics are frequently prepared by dissolving an elastomer in methylmethacrylate and either styrene or α-methylstyrene, and then polymerizing them into methyl methacrylate-butadiene-styrene graft copolymers (MBS) (Ruffing et al. 1964; Schmitt et al. 1967). There is a great diversity of the MBS copolymers, viz., graft, core-shell, or multilayer type – lately also with acidic or epoxy groups (Lee and Trementozzi 1979, 1980, 1981, 1982; McKee et al. 1982; Keskkula et al. 1984).

1.5.2.1 ABS/SMA Blends

The ABS/SMA blends show excellent processability, high heat deflection temperature (HDT) low warpage, stiffness at high temperature, good impact strength, as well as solvent and chemical resistance. They successfully compete with PPE or PC alloys for the automotive applications (trim, instrument panels, roof linings, hubcaps, headlight housings), electronics, and electrical industry, houseware, appliances, power tools, industrial machinery, plumbing products, parts for washing machines and vacuum cleaners, etc. An example of commercial blends is *Cadon™*.

1.5.2.2 ABS/PVC Blends

There are several reasons for blending PVC with ABS-type copolymers, viz., to improve processability, mechanical properties, and low-temperature toughness. Good properties of these blends originate from the miscibility between PVC and SAN part of ABS. In some commercial blends, viz., *Geloy™*, ABS may be replaced by ASA to obtain improved miscibility and weatherability. For enhancement of HDT, SMA may also be added. The blends with more than 30 wt% PVC are self-extinguishing but are more difficult to process.

1.5.2.3 ABS/PC Blends

Blends of PC with 5–70 wt% ABS were developed in the early 1960s. The basic technology has been used to produce such alloys as *Bayblend™*, *Cycoloy™*, *Idemitsu™ PC/ABS*, *Iupilon™*, or *Triax™ 2000*. The consumption of ABS/PC blends is increasing as the cost-to-performance ratio is low and properties are predictable (Khan et al. 2005). The alloys combine good processability of ABS with excellent mechanical properties, impact, and heat resistance of PC. The opaque blends show dimensional stability, low shrinkage and moisture absorption, high stiffness and hardness, good impact resistance at temperatures (T ≥ −50 °C), excellent UV stability, processability, mechanical properties, heat resistance, flame retardancy, good chemical resistance, but poor to gasoline, aromatic hydrocarbons, esters, ketones, and some chlorinated hydrocarbon. The ABS/PC blends are being manufactured with either a dispersed or co-continuous morphology.

There are many similarities between ABS/PVC and ABS/PC blends. Both are immiscible, having three distinct phases of PVC or PC, SAN, and an elastomer

Table 1.16 PC/ABS-type blends

Reason	Additive to PC/ABS	References
Toughness	10–70 wt% ABS	Grabowski 1964a
HDT and stiffness	Styrene-α-methylstyrene-acrylonitrile, PSF	Grabowski 1970, 1971, 1972
HDT an impact resistance	MBS and PAES	Yamauchi et al. 1974
Processability, HDT, impact resistance	Polyethersulfone, PES	Weaver 1972
Flow, weatherability, thermal, and mechanical performance	EVAc	Hasegawa et al. 1974
Pearl-like iridescence, dyeability	PMMA	Ikura et al. 1974
Heat resistance, dimensional stability	PVC	Hardt et al. 1975
Mechanical performance	CPE grafted with SAN	Kabuki et al. 1973
Processability, impact strength	Skin-core graft copolymers of styrene and acrylonitrile on elastomeric latex particles	Sakano et al. 1978
Solvent and impact resistance	MBS and acrylic elastomer	Kitamura 1986

(Suarez and Barlow 1984). The blends are compatibilized by the dipole-dipole interactions between PC and SAN, particularly evident in SAN with ≥ 25 wt% AN (Kim and Burns 1988, 1990). ABS/PC blends can also be compatibilized by incorporation of either acrylic, acidic, or epoxy groups (see Table 1.16).

In the late 1970s, the reactive blending of PC/ABS began to dominate the technology. Initially, the PC blends with ABS modified by incorporation of the maleic anhydride moieties (ABS-MA), later ABS with acrylic acid groups (ABS-AA) were developed. The third generation blends comprise ABS modified by copolymerization with glycidyl methacrylate (ABS-GMA). Examples are listed in Table 1.17.

In 1983, Monsanto developed blends with co-continuous morphology, *Triax™ 2000*. These alloys comprised PC, ABS, and styrene-methylmethacrylate-maleic anhydride (SMMA-MA) (Jones and Mendelson 1985). One year later, PC was reactively blended with either ABS, SAN-GMA, or NBR or with graft copolymers of acrylonitrile-butadiene-α-methyl styrene-methyl-methacrylate (MeABS) and acrylonitrile-α-methyl styrene-methyl methacrylate copolymer (MeSAN) (Kress et al. 1986). The blends were commercialized by Bayer as *Bayblend™*.

In 1992, low gloss and moldable blends, with electrostatic discharge properties, were developed. They comprised PC, ABS, and either a graft copolymer of styrene, hydroxyethyl methacrylate, and acrylonitrile bonded onto a 1,3-butadiene rubber (ABS-HEMA), styrene-acrylonitrile-methacrylic acid copolymer (SAN-MAc), styrene-acrylonitrile-hydroxyethyl methacrylate (SAN-HEMA) or an acrylonitrile polymer containing gels (Vilasagar and Rawlings 1994). *Cycoloy™* is the PC/ABS blend from General Electric Co (now SABIC).

Table 1.17 PC/ABS reactive blends

Composition	Reason	References
PC with ABS and rubber-modified SMA	Processability, impact strength, heat resistance	Henton 1980, 1982
PC with SAA and EMMA	Impact strength, mechanical properties	Thomas 1982
PC with ACM and SAA	Impact strength and HDT	Henton 1984
PC/ABS with EAA acidic compatibilizer	Processability and impact strength	Grigo et al. 1984
PC/ABS with SMA-AA	High HDT and impact strength	Brandstetter et al. 1982a, b, c; 1983a, b, c
PC/ABS with SMM-GMA	Processability, impact strength, and heat resistance	Daicel 1982, 1983, 1984
PC/MBS with SAN and PEST	Impact strength and thermal stability	Teijin Chem. 1980
PBT, PC, ABS, and PB grafted with acrylate esters and AN, ACM	Rigidity, flowability, solvent resistance, impact strength, dimensional stability	Bier and Indner 1982; Neuray et al. 1982
PC, PEST, polyester carbonate, etc., with 30–90 wt% of SMA + ABS and 2.5–20 wt% of a chemical blowing agent	Foamable engineering blends having excellent physical performance	White and Krishnan 1989
PC, PEST, or PEI with 1–50 wt% of ABS and a chemical foaming agent	Moldable blends for chemical foaming	Allen and Avakian 1987

1.5.2.4 ABS/PA Blends

ABS/PA mixtures are immiscible; hence, the standard three strategies are applicable: (i) addition of a small amount of ABS to improve PA toughness without a compatibilizer, (ii) generation of non-compatibilized blends with co-continuous morphology, and (iii) compatibilized blends in the full range of composition. ABS is an amorphous resin, while PAs are semicrystalline; hence, it is advantageous to incorporate ABS as either a dispersed or a co-continuous phase – the latter being preferred. However, addition of semicrystalline PA to ABS increases mold shrinkage, and thus, addition of filler is advised. Owing to high processing temperatures of PA, it is essential to use high heat ABS. For the adequate impact performance, at least 10 wt% of ABS should be added, but at this level, the compatibilization is required. The reactive compatibilization involves the use of ABS that has been modified by incorporation of either acrylic acid, maleic anhydride, or polyvinylphenol (PVPh).

The reason for blending ABS with PA is to reduce moisture sensitivity, improve toughness, and reduce shrinkage and warpage of the latter resin. The alloys show good processability; surface finish; high heat stability; a chemical, oil, wear, and abrasion resistance; dimensional stability; low-temperature impact strength; reduced moisture sensitivity; and economy. Synergistic properties have been reported. Examples of commercial alloys are *Stapron™ N*, *Novalloy™-A*, *Techniace™ TA*, *Triax™ 1000*, *Ultramid™*, and *Macslloy™* (Utracki 1994). Also, in a series of papers, Kitayama et al. (2000a, b, 2001) have described the blending of PA6 with SAN.

The first ABS/PA blends were announced in 1961 (Grabowski 1964b, 1966) and much later introduced as *Elemid™*. *Triax™-1000* is an alloy of PA-66 with ABS-MA, having the phase co-continuity (Lavengood et al. 1986, 1988). PA-6 was also blended with BR grafted with styrene and MA (SBMA) (Asahi-Dow Ltd. 1981). Later, transparent blends of copolyamide(s), PA, and ABS were developed (Fox et al. 1989). Blending either ABS-MA or EPR-MA, with amine-terminated PA or PEST, resulted in alloys with excellent performance (Akkapeddi et al. 1990, 1992a, 1993; Okada et al. 2004). Similarly, either ABS-MA or ABS-GMA copolymer was used to compatibilize and to toughen PA blends with other resins, viz., PC, PEST, or PAr (Yuichi and Suehiro 1989). Later the role of elastomer, its type, and location in the PA-66/SAN/Elastomer system was studied (Nair et al. 1997, 1998).

1.5.2.5 ABS/PEST Blends

The thermoplastic polyesters (PEST) are dominated by two resins: polyethylene terephthalate (PET) and polybutylene terephthalate (PBT). There are similarities between ABS/PA and ABS/PEST blends.

In blends with ABS, a part of PEST may be replaced by PC, and 10–20 wt% of an impact modifier may also be added, e.g., MBS, poly(methylmethacrylate-g-butadiene-co-styrene), poly(MMA-g-n-BuA), high rubber ABS ($\geq$ 50 wt% PB), or ASA with $\geq$ 50 wt% acrylate rubber, etc. Examples of commercial blends are *Alphaloy™ MPB*, *Cycolin™*, *Diaaloy™ B*, *Malecca™ B*, *Maxloy™*, *Lumax™*, *Triax™ 4000*, and *Ultrablend™ S*. The alloys show excellent moldability, low post-molding shrinkage and warpage, stress-crack resistance, high gloss, high temperature stiffness, toughness and mechanical strength, high heat resistance at temperatures T $\leq$ 140 °C, low shrinkage, good dimensional stability, impact strength, good wear and abrasion resistance, good thermal and weathering resistance, as well as solvent (e.g., to gasoline and motor oils) and chemical resistance. An abbreviated evolution of the PEST/ABS technology is summarized in Table 1.18.

Table 1.18 PEST/ABS blends

Composition	Reason	References
PET with MBS	Notched impact strength and embrittlement resistance	Sauers and Barth 1970
PAr with ABS	Processability and impact strength	Koshimo 1973
PBT/ABS/SEBS	Stable morphology	Gergen and Davison 1978
PBT with carboxyl-modified ABS	Chemical, solvent, and impact resistance	Tanaka et al. 1979
PBT + PET or PC, with ABS or ACM (rubber particle diameters $d \cong 0.4$ μm)	Impact strength and balance of other properties	Bier and Indner 1982; Binsack et al. 1982
PBT with either ABS-MA or ABS-GMA	Heat, chemical, and impact resistance	Orikasa et al. 1989
PET or PBT with an AES-GMA (*Techniace™*)	Flowability and good balance of properties	Hirai et al. 1988, 1989, 1992

1.5.2.6 ABS/TPU Blends

Developed in the early 1960s, ABS/TPU blends combine TPU's toughness and paintability with ABS's low-temperature impact strength and adequate HDT. The main advantage is the excellent impact behavior at $T \geq -40\,^{\circ}C$. Furthermore, TPU improves antifriction properties, abrasion, and chemical resistance. Stiffness is also increased and the flowability of injection molding compounds is good. ABS is usually dispersed in the TPU matrix. TPU was also successfully blended with SBR grafted with acrylonitrile, acrylate, or methacrylate esters (MABS) (Abe et al. 1977), with SMM-MA copolymer (Gomez 1992), and with bulk-polymerized ABS (Henton et al. 1992). Depending on the type of TPU, compatibilization may be necessary. Examples of commercial alloys are *Prevail*™ and *Techniace*™ *TU*.

1.5.2.7 ABS/PSF Blends

In these blends, ABS's role is to improve flowability and reduce cost, while that of PSF is to improve the shape retention at high temperatures. ABS/PSF blends are compatibilized either by *phenoxy*, EVAc-GMA, or SMA copolymers. They have good processability, high notched Izod impact strength, plateability, hydrolytic stability, and economy. However, they may show poor surface and weld-line strength. *Arylon*™ and *Mindel*™ *A* are examples of the commercial ABS/PSF alloys, while *Ucardel*™ is an example of PSF blends with SAN. Evolution of ABS/PSF blends' technology is summarized in Table 1.19.

Table 1.19 PSF/ABS blends

Composition	Reason	References
PSF with 40–52 wt% ABS and poly (α-methyl styrene-co-AN)	Excellent flow, good impact resistance, non-flammability	Ingulli and Alter 1969, 1970
Polyarylethersulfone (PAES) with AES	Toughness and impact strength	Barth 1970
ABS with equal amount of PSF and PC	Processability, rigidity, and impact strength	Grabowski 1971, 1972
PAES with EVAc and/or MBS	Tensile, flexural, and impact strength	Lauchlan 1971
PAES with PC and either MBS or ABS	High HDT and impact resistance	Yamauchi et al. 1974
PSF with 10 wt% anhydride-terminated PSF and MABS	Excellent HDT and impact resistance	Aya et al. 1979
PSF with AES	Thermal stability and impact strength	Sumitomo 1982
PSF with cross-linked acrylate copolymer, cross-linked SAN, and uncross-linked SAN	Good tensile modulus, yield strength, impact resistance, and respectable HDT $= 106\,^{\circ}C$	Robeson 1985
PSF/ABS with EVAc-GMA	Processability, HDT, and impact strength	Orikasa and Sakazume 1990, 1992
PSF with 25–45 wt% semicrystalline PPS and 0–10 wt% MBS	resistance to impact, high temperatures, and adverse environmental conditions	Golovoy and Cheung 1994

1.5.3   SBS Block Copolymers

In 1961, using lithium catalyst, a series of styrene-isoprene (SI) and styrene-butadiene (SB) block copolymers were synthesized (Bull and Holden 1977). The resins had $T_g \approx -90$ to $+90$ °C. Full-scale production started in 1965. Since then, numerous two- and three-block copolymers have been developed, with hydrogenated and maleated block copolymers also being offered. With the world consumption of 330 kt/year, the block copolymers constitute the largest part of the commercial TPE market. Large quantity of SBS resin is used in blends. Commercial resins include *Elexar™*, *Collimate™*, *Finaclear™*, *Kraton™*, *Thermolastic™*, and *Tufprene™*.

1.5.3.1 SBS/SEBS Blends with Commodity Resins

SBS copolymers are used in blends as compatibilizers, impact modifiers, or stabilizers of morphology and performance. As shown in Table 1.20, they have been

Table 1.20 SBS blends with other styrenics

Composition	Reason	References
PVC with ABS and SBS	Toughness and performance	Minekawa et al. 1971
SBS with PS, EVAc, and other ingredients	For elastic films	Hinselmann et al. 1973
HIPS with 12.5 wt% PB and SBS	Excellent impact strength	Durst 1970, 1975
SIS with PS and/or IR	Optical and mechanical properties	Kawai et al. 1978
PS and/or HIPS with PP and SEBS	Impact and tensile strength, solvent resistance	Holden and Gouw 1979
Poly-*p*-methylstyrene (P*p*MS) with SBS	Impact strength and clarity	Sherman 1981, 1983
AN-grafted SEBS with SAN	Weatherability, impact strength	Paddock 1981
PS with (SB)$_n$ and SBR	Impact strength, transparency	Asahi Chemical 1982
SEBS dissolved in styrene, methacrylic acid, and isoprene and then polymerized	Thermoplastic IPN, with superior mechanical properties	Siegfried et al. 1984
SEBS-type IPN with carbon black, CB	Electrically conductive blends	Sorensen 1984
PS with AXBXA or (AXB)$_n$ (A = styrene, B = butadiene, X = AB tapered block)	Impact strength, and transparency, superior to that observed for SBS/PS blends	Toyama et al. 1985
SBS (acidic, amino, imido-terminated) and PA, PEST, TPU, POM, PVAl, PC, PSF, PPE, PPS, or PVC	Water-swelling materials for civil engineering, construction, etc.	Shiraki and Hattori 1986, 1994
SMMA, a tapered SB and ductile SBS, *Zylar™*	Transparent (extremely low haze), impact resistant	Blasius 1992, 1994
HIPS, PE, and either SBS or SIS; a co-continuous morphology	Chemical, solvent, and stress-cracking resistance	Hoenl et al. 1993; Seelert et al. 1993
SMMA and either a mixture of SBS and a tapered BSB triblock copolymer or SBR	Transparent, low haze, high impact, craze, and γ-radiation resistance	Hauser et al. 1993

Table 1.21 SBS Blends with polyolefins

Composition	Reason	References
PP with 20 wt% of either SBS or SIS	High impact strength, without adverse effect on other properties	Japan Synthetic Chemical Ind. 1971
PP blends with 6–8 wt% SEBS	Transparency and impact strength	Porter 1972
SBS with 20–30 wt% PO	Processability, mechanical properties	Tabana and Maki 1976
PS with HIPS, PP, and SEBS	Performance, co-continuous morphology	Holden and Gouw 1979
SEBS with diverse polymers, including PE	Dispersed drops of d = 200 nm	Davison and Gergen 1980
PP/PS with either SBS or (SB)$_n$	Moldability and mechanical properties	Grancio et al. 1981, 1983
HDPE with PS and SEBS	Superior performance over HDPE/PS	Lindsey et al. 1981
HIPS with HDPE SEBS	Impact strength	Castelein 1982
LLDPE with SEBS	Transparent, impact resistant	Holden and Hansen 1989
PS, LLDPE, and SEBS	Impact strength, lack of yellowing	Seelert et al. 1993
PP and PET reactively blended with maleated SEBS	Rigid blends with good impact strength and adhesion to solids	Tekkanat et al. 1993, 1994
PA/PO/SEBS compatibilized by SMA	Moldable, good impact strength	Chundury 1993, 1994
PO with PA, PET and styrenics	Recycled commingled scrap	Weber et al. 1994
SBS, EVAc, PS, and LLDPE or ULDPE	Elastomeric films	Djiauw 1994
PO with SEBS, SEPS, SEB grafted with maleic anhydride acrylic or sulfonic acid	Moldable resin with good impact strength, scratch, and abrasion resistance	O'Leary and Musgrave 1993
PP with either SBR, SBS, or an acrylic elastomer, and PP grafted with styrene	Stand-alone structural materials	DeNicola and Conboy 1994

frequently incorporated along other styrenics. There are many patents for mixtures of PO with SBS-type copolymers. Their history is outlined in Table 1.21.

1.5.3.2 SBS Blends with Engineering Resins

Since the anionically polymerized block copolymers are relatively expensive, they have been more frequently used in blends with engineering than commodity resins. Owing to miscibility of styrene blocks with PPE, the SBS and SEBS are "natural" tougheners for this polymer. However, for blending with PEST, PC, POM, or PA, the copolymer should be modified by incorporation of acidic, acid anhydride, or epoxy moieties.

SBS with Polyphenylene Ether (PPE)

Evolution of PPE blends with SBS-type block copolymers is summarized in Table 1.22. SBS or its derivatives have been frequently used to stabilize the morphology in more complex blends. In Table 1.23 examples of this type of system are presented.

Table 1.22 SBS Blends with polyphenylene ether

PPE modifiers	Reason	References
PPE with 10–90 wt% SBS	Processability and toughness	Kambour 1970
PPE with SEBS	Processability	Haaf 1979
SBS- or EPDM-modified PS and SEBS	Flow, impact, and thermal properties	Lee 1979, 1980, 1982, 1983, 1985
HIPS and SB di-block copolymer	Impact strength and solvent resistance	Brandstetter et al. 1982a, b, c
Styrene-phenyl-maleimide copolymer and either SB, SBS, or SEBS	HDT, chemical, solvent, and impact resistance	Fukuda and Kasahara 1982
HIPS, styrene-grafted EPDM and/or SB grafted with EGMA	Impact strength and processability	Ueno et al. 1982a, b
SBR, SBS, and EPR	Processability and impact strength	Mitsubishi Gas 1982
HIPS, SEBS, and PE	Processability and impact strength	Haaf 1983
Styrene-grafted PPE, PPE-S with SBR and SB	Processability, gloss, toughness, and tensile strength	Izawa et al. 1983
HIPS, SBS, SBR, EPR, and hydrogenated poly(bisphenol-A-phosphite)	Impact strength, processability, and flame retardancy	Sugio et al. 1984
ABS and SEBS	Moldability, toughness, strength	Ueda and Sasame 1986
PS, SBR, and SBS	Plateability and mechanical properties	Mitsubishi Gas Co. 1985
HIPS, SEBS, and LLDPE	High impact strength	Hambrecht et al. 1986
HIPS and either SB, SBS, or $(SB)_n$	Cracking and impact resistance	DeMunck and Lohmeijer 1986

SBS with Polyamides (PA)

SBS or SEBS has been used as an impact modifier in PPE/PA blends, with PA usually being the matrix and PPE an organic, low-density filler. The blends were developed in the early 1970s by the Asahi Chemical. By the end of the decade, the first reactive blends were announced by the Sumitomo Chemical (Ueno and Maruyama 1981) and General Electric (Van der Meer et al. 1989).

The simple, SBS/PA blends were in parallel development with the PPE/SBS/PA ones. Addition of SBS to PA improved the tensile and impact strength of the latter resin. The blends comprise either 1–25 wt% SBS as a dispersed or at higher concentration as co-continuous phase (see Table 1.24).

SBS with Thermoplastic Polyesters (PEST)

The development of PEST/SBS blends parallels that of the PA/SBS ones. First, blends of PBT, ABS, and SEBS were disclosed (Gergen and Davison 1978). Four years later, the reactive compatibilization was discovered – PBT was blended with SEBS and SMA (Durbin et al. 1983). By the end of 1970s, multicomponent blends comprising PBT, PET, PC, and either SEBS, $(SB)_n$, butadiene-caprolactone-styrene,

Table 1.23 SBS in PPE multicomponent blends

Additives	References
PPE with PA-66, PS, maleated PP, and SEBS	Fujii et al. 1987
PPE reactively blended with SBS and MA and then mixed with PA or PEST	Van der Meer and Yates 1987
Reactive blends of carboxylated PPE with PA-66 and SEBS	Grant and Jalbert 1987, 1989
PPE, PA, SBS, and a reactive mixture of styrene-glycidyl methacrylate with styrene and a peroxide	Mawatari et al. 1987
PPE, PBT, SEBS, and PC [PBT – matrix; PPE + SEBS – dispersed phase; PC at the interface]	Brown et al. 1987
PPE, HIPS, PEST, PS with reactive (2-oxazoline) groups, PC, and SBS	Avakian et al. 1988
PPE with PBT (or PET), SEBS, PC, and mica	Yates 1987, 1989
PPE grafted with fumaric acid, reactively blended with PC and SEBS	Ishihara 1989
Grafted PPE, blended with dimethylsiloxanes, PC, PBT, and SEBS	Brown 1992
PPE, with PBT, PC, SEBS, and/or acrylate copolymer	Yates and Lee 1990
PPE, HIPS, an ethylene-methacrylic acid copolymer, EMAA, SEBS, and SGMA	Fuji and Ting 1987
PPE with PVDF, SEBS, and poly(styrene-co-methyl-methacrylate)	Van der Meer et al. 1989
PPE with HIPS, PE, and SEBS	Ting 1990
PPE with PP and SEBS	Lee 1990
PPE/PET or PPE/PA reactively compatibilized with SEBS-GMA	Mayumi and Omori 1988
PPE/PET or PPE/PA reactively compatibilized with SEBS-MA	Modic and Gelles 1988
PPE/PBT, toughened by addition of urea-butylated resin and SEBS	Mizuno and Maruyama 1990
PPE with PC, PBT, and either SBS, SEBS, or a core-shell copolymer	Brown and Fewkes 1992, 1994
Epoxy- or phosphate-functionalized PPE, with PBT or PET, palmitamide, SEBS, and PC	Yates 1993
PPE with PA-66, SEBS, SB; a styrene-butadiene radial copolymer; citric acid; and either citric acid or chloro-epoxy triazine	Gianchandai et al. 1993
PPE with PA-6 or PA-66, MA and toughened with SB	Lee 1994
PPE-MA or PPE-GMA, with sPS, SEBS, and fillers	Okada and Masuyama 1994

or butadiene-caprolactone block copolymer were developed (Wambach and Dieck 1980). Reactive compatibilization of PEST/SEBS by addition of MA was disclosed in 1984. The method was general, applicable to polyamides as well as to polyesters (Shiraishi and Goto 1986).

SBS with Polycarbonates (PC)

Similarly to blends of SBS with PA or PEST, these with PC were first described in 1976. However, owing to the weak interactions between SBS and PC, these systems require compatibilization. Thus, either SBS must be acidified (e.g., with SEBS-MA) or acidified acrylate added, viz., MABS, MBS, SMA, etc. Selected examples are listed in Table 1.25.

Table 1.24 Evolution of the SBS/PA blends

Composition	Reason	References
PA-66, SEBS, *phenoxy*, and bisphenol-A-epichlorohydrin	Tensile and impact strength of PA	Freed 1975
PA-6 with SEBS	Toughness, balance of properties	Bull and Holden 1977
PA-6 or PA-66 with SBS	Improved toughness and reduced modulus	Cerny and Troncy 1981
PA-6 with SEBS-MA and/or LLDPE	Tensile and impact strength	Mitsubishi Chem. 1982
PA-6 and SEBS-MA	Processability, mechanical properties, impact strength	Asahi Chem. 1983, 1984, 1987
PA, or PEST with SEBS-MA	High notched Izod impact strength	Gelles et al. 1987
PA-66 with SEBS, SEBS-MA, PO	Moldable alloys with high impact strength	Gelles et al. 1988
COPO, with PA-6 and SEBS-MA	Good balance of strength and toughness	Machado 1992
PA + acidified SEBS, EPR, or EPDM; the adduct incorporated into PA	Processability, mechanical properties, and low-temperature toughness	Ohmae et al. 1991, 1992
PA-66 + 1:1 blend SEBS and SEBS-MA	Processability and toughness	Gelles et al. 1994

Table 1.25 SBS/PC blends

Composition	References
PC with 30 wt% SEBS for co-continuous morphology	Gergen and Davison 1977
PC with PE and hydrogenated and chlorosulfonated SBS	Bussink et al. 1978
PEST with PC, SEBS, and mineral filers	Dieck and Wambach 1980
PC/ABS/PP compatibilized and toughened by SEBS-MA	Gallucci and Bookbinder 1989
PC with SB-teleblock and SEBS	Lee 1983
PC with either SBS and MBA or SEBS, EEA, and LLDPE	Liu 1982, 1984
PC with PE and SEBS	Idemitsu Kosan 1983
PC with either SBS, EGMA, or MBS	Sumitomo Chemical 1982, 1983
PC with SMA and SBS	Daicel Chem. 1984
PC, COPO, PEST, SEBS + butylacrylate-methylmethacrylate grafted rubber	Laughner et al. 1992
PC, PPE, ASA, SAN, PS, phosphate esters, PTFE, and SEBS	Niessner et al. 1993
PC, modified SEBS, and hydroxyethyl acrylate-terminated ε-caprolactone	Wilkey 1994

1.5.3.3 SBS Blends with Specialty Resins

SEBS must be processed below 280 °C; thus, its use with specialty resins has been limited to polyphenylenesulfide (PPS) (Garcia and Martinovich 1984). Sometimes SBS and a specialty resin are parts of a multicomponent blend, viz., PPS, PPE, either PA- 6 or PA-12, SEBS (*Kraton™ G*), an acidified polyolefin (e.g., EPR-MA, PE-GMA, or EVAc-GMA), and reactive compatibilizer

(citric, maleic, or agaric acid). Here, PPS was a matrix, and PA was the dispersed phase that contained PPE/SEBS and a filler (Ishida and Kabaya 1994).

1.5.4 Polyvinylchloride (PVC)

PVC was first synthesized by Regnault in 1835. The first patent on vinyl chloride monomer (VCM) polymerization was granted in 1912 to Ostromislensky. However, to make commercially viable articles, PVC must be stabilized and either plasticized or blended. In 1927, B. F. Goodrich started production of plasticized PVC, *Vinylite™* (Semon 1933).

The first patented PVC alloys were prepared by latex blending with PVAc and poly(vinylchloride-co-vinylacetate) (PVCAc) (Voss, and Dickhäuser 1930, 1933, 1935, 1936). I. G. Farbenindustrie commercialized PVC extruder blended with polyacrylic ester – the so-called rigid formulation (Fikentscher and Heuce 1930; Fikentscher and Wolff 1931). *Troluloid™* and *Astralon™* were the first commercial thermoplastic polymer blends.

PVC blended with *Buna-N* produced excellent thermoplastic materials (Badum 1942). These blends were prepared either in a rubber mill, by latex blending, or powder blending and then extruding. The rigid PVC not only had higher heat HDT than the flexible one, but it was *permanently* plasticized. In 1940 also B. F. Goodrich patented the NBR/PVC blends. Many forms of PVC and its copolymers have been developed over the years to fit specific uses, viz., latex, plastisol, organosol, flexible, and mostly the rigid formulation. In 1991 world production of PVC was 22.0 Mt or 21.6 wt% of the thermoplastic resin market.

1.5.4.1 PVC/NBR Blends

The PVC/NBR blends were commercialized in 1936 by Bergisch-Gladbach. Nearly identical alloys, *Geon™ Polyblends*, were introduced by B.F. Goodrich 1947. To ascertain adequate interaction between PVC and NBR, the AN content in NBR should be at least 25 wt%. Most commercial blends contain 50–90 wt% NBR that acts as a solid plasticizer and processing aid. PVC blends with cross-linked NBR have been foamed since the 1940s, initially for the production of buoyancy vests, shock absorption and insulation (McCracken 1984), and later for shoe soles. Still later, acidification of NBR made it possible to incorporate the NBR/PVC blends into PA, PC, or PEST (Iwanaga et al. 1990). It was also found that NBR provides good compatibilization and toughening in blends of PVC with carbon monoxide-ethylene-vinylacetate copolymer (COPO-VAc) (Lund and Agren 1993). There are several commercial PVC/NBR blends, viz., *Geon™*, *JSR NV*, *Krynac™ NV*, *Nipol™*, *Paracril™ OZO*, or *Vynite™*.

1.5.4.2 PVC/Acrylics Blends

The most common acrylic, PMMA, shows limited miscibility with chlorinated hydrocarbons (e.g., PVDC, PVC, CPVC, or CPE). The miscibility depends on the type of chlorinated polymer, tacticity of PMMA, and molecular weights

Table 1.26 Toughened PVC/acrylic blends

Modifier	References
Butadiene-MMA-styrene copolymer (MBS, *Acryloid*™)	Fujii and Ohtsuka 1954
PMMA and poly(butadiene-g-MMA)	Jarrett and Williams 1960
Ethylene-ethylacrylate copolymer	Van Cleve and Mullins 1962
MBS with controlled size of the elastomeric particles, transparent	Saito 1975
Copolymer of vinylchloride, alkyl acrylate, and vinylidene chloride	Hoshi and Kaneko 1962, 1963, 1965
Butadiene-styrene-methylacrylate-ethylacrylate	Ichinoe 1967
Core-shell: cross-linked ABS with grafted onto it PMMA shell	Michel 1969
PB grafted with MMA, styrene, and vinyl acetate	Kakefuda and Ito 1971
Poly(butadiene-co-butyl acrylate-co-styrene)	Ide and Deguchi 1971
Core-shell: poly(AN-co-MMA) or poly(AN-co-ethylhexyl acrylate-co-MMA)	Tanaka et al. 1971a, b, c; 1972
Poly(styrene-co-AN-co-MMA-g-butyl acrylate-g-MMA)	Ide et al. 1972
5–20 phr of MMA-AN-butadiene-styrene (MABS) with 10–40 wt% AN and/or styrene, 50–80 wt% 1,3-butadiene, and 25–75 wt% MMA for foamed profiles, bottles, pipes, boards, moldings, etc.	Parks 1976
Core-shell: poly(butadiene-co-styrene-divinylbenzene-co-butylacrylate-co-MMA)	Usami and Ochiai 1976
$\leq$ 20 wt% of either poly(vinylchloride-co-vinyl acetate) or EVAc – the blends were though and easy to foam	Barth et al. 1976; Goswami 1977
CPE and poly(MMA-co-butyl acrylate)	Maruyama et al. 1977
MMA and styrene grafted onto an acrylic elastomer	Kishida et al. 1977
AN-b-MMA block copolymer	Iwata et al. 1979
PMMA with dehydrochlorinated PVC were found miscible and easy to foam for the cryogenic insulation in space vehicles	Jayabalan 1982; Jayabalan and Balakrishnan 1985
Copolymer of ethylene, 1–60 % acrylic ester and 1–30 % CO_2 or SO_2	Rys-Sikora 1983, 1984
Core, cross-linked silicone rubber; inner shell, cross-linked acrylate elastomer; outer shell, styrene-AN copolymers	Lindner et al. 1990

of the two polymers. The origin of miscibility is the interaction between the -CHCl- group of PVC and the carboxyl group of the acrylic (Jager et al. 1983). Acrylics have been incorporated into PVC blends quite early (Small and Small 1951). In spite of PVC miscibility with PMMA, blends of these two polymers are not commercially important. To be useful, the blends must be toughened, preferably by acrylic elastomers. Some of the toughening agents are listed in Table 1.26.

Examples of commercial PVC/acrylics blends are *Acrylivin*™, *Decoloy*™, *Enplex*™, *Hostalit*™, *Kane-ace*™, *Kydene* ™, *Metabulen*™, or *Vinidur*™. The blends have been used for industrial, commercial, and consumer goods; in medical, electrical, and chemical engineering equipment; for food or beverage; as aircraft or mass transit interior components; for power tool housings; etc.

Table 1.27 PVC toughening by non-acrylic elastomers

Modifier	References
PIB, NR, IR, or CR	Goodrich 1941
Thio-rubbers (TM)	Rittershausen 1949
CR and NBR	Signer and Beal 1953
Chlorinated polybutadiene (CPB)	Esso 1960
Polyisobutylene (PIB)	Lonza Ltd. 1964
Di-butyl fumarate and butadiene copolymer	Koenig et al. 1964
TM and CSR	Allied Chemicals 1965, 1966
BR and/or poly(ethylene-co- vinyl or acrylic monomer), e.g., EVAc	Kasuya et al. 1969
EPDM and polynorbornene having carboxylic and carboxylic ester groups	Mitsubishi Chem. 1983
PVC blends with cross-linked NBR for foamed floating devices	McCracken 1984
DOP plasticized PVC blended with TPU and EVAc	Shin et al. 1998

1.5.4.3 PVC/Elastomer Blends

These blends, usually with 30–60 wt% PVC, are represented by *Carloy*™, *OxyBlend*™, or *Vynaprene*™. They have been formulated for extrusion, calendering, injection, or blow molding, e.g., into bottles, sheets for exterior signs, window accessories, cables and hoses, printing plates and rollers, shoe soles, profiles, military coax jacketing, etc. PVC blends with ABS and modified ABS were already discussed. In Table 1.27 an abbreviated list of PVC blends comprising non-acrylic elastomer(s) is provided.

1.5.4.4 PVC/Polyolefin Blends

PVC is antagonistically immiscible with PO. Thus, the standard strategies are applicable: (i) addition of a small amount of PO to improve processing and impact strength, (ii) co-continuous morphology, (iii) incorporation of PO as part of a copolymer comprising miscible with PVC segments, and (iv) compatibilized blends. Owing to difficulties in compatibilization, the PVC/PO blends are not commercial (Liang et al. 1999). Evolution of these systems is outlined in Table 1.28.

1.5.4.5 PVC/CPE and PVC/CSR Blends

PVC blends with CPE were patented and commercialized in 1956 as *Hostalit*™. Blends with CSR soon followed. By the mid-1970s, the emphasis shifted toward blends with acrylic elastomers. Ternary alloys were developed, viz., of PVC with CPE and poly(methyl methacrylate-co-butyl acrylate) (MMBA) (Maruyama et al. 1977) or PVC, CPVC, and either MABS or a mixture of PMMA with imidized-PMMA or imidized-SMA (Soby et al. 1994). These blends have been used for outdoor applications, flame-retardant wall coverings, and automobile interiors. Injection molded components include gullies in sewage systems, caps for road reflector posts and bench slats, etc. Evolution of these blends is traced in Table 1.29.

Table 1.28 PVC blends with PO

Composition	Reason for blending	References
PO with PVC	For extrusion or milling	Rosenfelder and Rosen 1962
PVC with either PP, PE, PS, or SBR and ethylene-vinylchloride	HDT, flame resistance, impact, and tensile strength	Montgomery 1966
PVC with either PE or PP and MBS	Impact strength formulations for pipes or electrical insulation	Baer and Hankey 1967
PVC with either PE or PP and ABSM	Impact performance	Himei et al. 1967
PP with PVC and either PMMA or PC	Layered, wood-like materials	Yahata et al. 1971
PP and either EVAc-VC, EVAc, or HDPE	Low-temperature impact resistance	Kojima and Tanahashi 1972
PVC was copolymerized with PP	Flame retardancy	Unitika Ltd. 1984
PVC, HDPE, and CPE	Compatibilized blends	Nippon Zeon 1984
PVC/PO + poly(ethylene-co- alkyl, aryl, alkaryl or methylmethacrylate ester)	Mechanical and impact performance	Williams and Ilenda 1993

Table 1.29 PVC blends with either CPE or CSR

Composition	References
PVC with CPE	Frey 1958
PVC with CSR	Matsuda 1960
PVC with CPB	Esso 1960
Latex blending: PVC with CR	Nyori et al. 1962
PVC with PO, compatibilized by either CPE or MBS	Baer and Hankey 1963
Solution-blended PVC with CPE or CSR	Beer 1963
PVC with CPE and a diamine (an interfacial agent)	Hankey and Kianpour 1964
PVC with equal amount of CSR and SAN	Salyer and Holladay 1964
PVC with equal amount of CPE or CSR	Hedberg and Magner 1965
PVC with EVAc and CPE	Dow Chemical Co. 1965
PVC with chlorinated-SBR (C-SBR)	Takkosha Co. 1967
PVC with chlorinated EPDM (C-EPDM)	Watanabe et al. 1967
Powder blending: PVC and PE and then chlorinating and milling	Kato et al. 1967
PVC with two heterogeneously chlorinated LDPEs	Willott 1968
PVC with CPVC and ABS	Kojima et al. 1970
PVC with PS and C-SBR	Falk 1981
PVC/CPE with SMA	Bourland 1983
PVC with HDPE and C-SBR	Nippon Zeon 1984
PVC/CPE with glycidyl *p*-tert-butyl-benzoate	Sugiara and Takayama 1988
PVC/CPE with either SMMA or PS-VAc	Liou and Sun 1993

1.5.4.6 PVC/TPU (Mainly Polyester-Type) Blends

Initially, two-component, PVC/TPU blends were proposed (B. F. Goodrich Co. 1960), but soon, PVC/TPU blends with a modifier, e.g., ABS (Waugaman et al. 1963); NBR or PA (Képes 1959) were disclosed. Blending was also carried out by mixing PVC with polyols and isocyanates and then polymerizing these two (Dainichiseika Color & Chemicals 1982, 1983). Commercial PVC/TPU blends (with NBR) are represented by *Duralex™*. The materials are usually formulated for extrusion, e.g., for wire and cable insulation, hoses, and packaging.

Later, foamable, recyclable PVC blends were disclosed. They comprise PVC plasticized with DOP and/or epoxidized soybean oil, blended with either TPU and/or EVAc. The formulation could be foamed either during extrusion or injection molding. The material is used to produce anti-slip shoe soles with good abrasion resistance (Shin et al. 1998).

1.5.4.7 PVC/EVAc and PVC/EVAc-VC Blends

The miscibility of PVC with EVAc depends on the VAc content. Blends of PVC with PVAc were patented in 1938. PVC, or poly(vinylchloride-co-acetate) (PVCAc), was also blended with polyvinylacetal (PVA) (Lonza Elektrizitätswerke & Chem. 1948). In later patents, PVC instead of being mechanically blended with PVAc was copolymerized with vinyl acetate. The copolymer still required toughening; thus, it was emulsion polymerized in the presence of styrene-butadiene-vinylacetate latex (Farbwerke Hoechst 1970). Latex blending (followed by spray drying) was a simple and efficient mixing method (Hammer 1971). Similarly, PVC and/or PVCAc was blended with a variety of butadiene-butyl acrylate-styrene copolymers (Ide and Deguchi 1971). PVC blends with ethylene-vinyl acetate-carbon monoxide copolymer (EVAc-CO) and a methylmethacrylate graft copolymer, *Kane-Ace™*, are also commercially interesting (Mitsui Petrochemicals 1983).

Commercial PVC blends with either EVAc or PVC-VAc have been offered for outdoor applications since the 1970s as high impact strength, rigid formulations (e.g., *Denkovinyl™*, *Hostalit™*, *Vinidur™*, *Solvic™*, or *Trosiplast™*). The resins show good hardness, rigidity, adequate heat, chemical, and flame resistance.

1.5.4.8 PVC Blends with COPO

The first PVC/COPO blends were developed in 1960 (Mullins 1964). It was reported that PVC melt viscosity decreased by addition of COPO (Hammer 1973). Later, the compositions were modified – PVC was blended with ethylene-carbon monoxide-vinylacetate copolymer (COPO-VAc) and BMMM (Reardon 1982).

1.5.4.9 PVC Blends with Engineering Resins

Owing to poor thermal stability of PVC, the high temperature blending must be avoided. Thus, only few PVC/engineering resin blends are known. These are summarized in Table 1.30.

The first commercial blend of this type is *Cylon™*. Here PVC is the matrix, and PA (that melts below 215 °C!) the dispersed phase. The two resins were compatibilized using the well-known PVC plasticizer – *Elvaloy™* (a terpolymer

Table 1.30 PVC blends with engineering resins

Composition	References
PVC with 5–25 wt% polypropylene terephthalate (PPT)	Hurwitz and DeWitt 1970
PVC + copolymer of PET with polybutyleneglycol, PBG, and 1,4-butanediol	Crawford and Witsiepe 1972
PVC with PC and ABS	Hardt et al. 1975
Low friction coefficient blends of PVC with POM	Doerffurt and Waeteraere 1977
Styrene-grafted PC with neat PC, PS and other styrenics, acrylics or PVC	Kakizaki et al. 1979b
PVC with polyethylene carbonate	Dixon and Ford 1979
High HDT blends: PVC, MBS, and polyimide (PI)	Kopchik 1981
PVC with poly(butanediol-terephthalate-adipate) and 30 wt% GF	Yang 1987
Vinylchloride polymerized in the presence of PI, blended with PVC and MBA	Clikeman et al. 1987
PVC with poly(methylmethacrylate-co-maleimide-co-vinyl cyanide) and styrene-cyclohexyl-maleimide-grafted butadiene	Ito et al. 1990
PVC with imidated polymethacrylate (polyglutarimide, PGI)	Fromuth et al. 1992
Plasticized PVC with an aliphatic polyester-b-aromatic polyester	Jean and Devauchelle 1993
Miscible blend: PVC/PC and a bishydroxyphenyl-hexafluoropropane (6F-PC)	Drzewinski 1993, 1994

of ethylene, carbon monoxide, and acrylics). These soft to semirigid alloys were commercialized for wire coating, automotive applications, and blow molding (Grande 1997; Hofmann 1998). They are flame, abrasion, and chemicals resistant, easy to process, and tough.

1.5.5 Polyvinylidenechloride (PVDC)

Polyvinylidenechloride, PVDC, was discovered in 1838 by Regnault but commercialized 100 years later as *Saran™*. The commercial PVDC is modified by the incorporation of either 15–20 wt% vinyl chloride or 13 wt% vinyl chloride and 2 wt% acrylonitrile. PVDC blends are summarized in Table 1.31.

1.5.6 Polyvinylidenefluoride (PVDF)

PVDF was patented in 1948 and commercialized by Pennsalt in 1962. It is a semicrystalline polymer with $T_g = -56$ to $-35\ °C$, 50 % crystallinity, and $T_m = 160–180\ °C$. PVDF has been blended mainly with PMMA (Lin and Burks 1993). The blends are suitable for the use as stable electrets or weather-resistant architectural coatings. Nearly 25 wt% of PVDF consumption is in weather-resistant architectural spray finishing or coating to metals, roofing, curtain walls, wall panels,

Table 1.31 Examples of PVDC blends

Composition: PVDC with	References
NBR and CR	Signer and Beal 1951
Polyurethanes	McCready 1976
Ethylene-carbon monoxide-vinyl chloride copolymer, *Alcryn*™ blends	Loomis and Statz 1984, 1986
PO and ethylene-methylacrylate compatibilizing ionomer	Burgert 1987
PA-6, PA-1212, or PARA and poly(ethylene-co-alkyl (meth)acrylate-co-vinyl acetate-co-CO-co-maleic anhydride)	Hofmann 1994
PVDC-VC with vinylidene chloride-methyl acrylate copolymer (PVDC-MeA)	Paleari and Fornasiero 1994

Table 1.32 Examples of PVDF blends

Composition: PVDF with	References
PCTFE for wire coating	Kaufman 1963
30 wt% PMMA for outdoor films with good clarity, chemical, and UV stability	Koblitz et al. 1966
PMMA and polyethylacrylate	Schmitt and Miller 1970
Solution blended with PA-610 to lower PA's water absorption	Saito 1975
PC and acrylic copolymer for clear, yellowish films with single $T_g \approx 120\ °C$	Leibler and Ringenberg 1986
PPE/SEBS and SMMA for weatherability, chemical, and solvent resistance	Van der Meer et al. 1989
Compatibilized PA for impact resistance and gas barrier properties	Hizasumi et al. 1989
COPO, PVP, PSF, polyester rubbers, or poly-2-oxazoline	Gergen and Lutz 1989
POM for resistance to frictional wear, heat, and UV stability	Shibata et al. 1992

window frames, doors, hand rails, fascias, awnings, louvers, and canopies. PMMA/ PVDF blends are commercially available, e.g., *Polycast*™ from Royalite. PVDF blends are summarized in Table 1.32.

1.5.7 Acrylic Blends

Polymethylacrylate (PMA) and polymethylmethacrylate (PMMA) were discovered, respectively, in 1880 and 1930. The resins have been used for the production of transparent plastic sheets, viz., *Plexiglas*™ or *Perspex*™, and used for the military aircraft cockpit canopies, gunner's turrets, and the like (Riddle 1954). Acrylic elastomers (ACM or ANM) were developed by Röhm in 1901 and commercialized in 1948 as *Hycar*™ vulcanizable copolymers of ethyl acrylate, allyl maleated lactones, chloroethyl vinyl ether, butadiene, isoprene, acrylonitrile, etc. (Mast et al. 1944). Since the 1950s, a wide variety of acrylic compatibilizers and impact modifiers have been developed.

Table 1.33 Acrylic compatibilizers-*cum*-impact modifiers, MBA and MBS

Composition	References
Methylmethacrylate-butadiene-styrene terpolymer (MBS)	Fujii and Ohtsuka 1954
methylmethacrylate-butadiene-styrene-α-methylstyrene, for weather resistance	Ruffing et al. 1964
Butadiene-styrene-methylacrylate-ethylacrylate (ASA)	Ichinoe 1967
Partially cross-linked ABS core and PMMA shell (a MABS)	Michel 1969
Copolymers of styrenics (e.g., PS, SAN, SMMA, etc.) with, e.g., 0.1 wt% of hydroxyethyl acrylate	Rubens 1986

1.5.7.1 Co-poly(meth)acrylates (MBA and MBS)

In the 1950s, the core-shell, emulsion-type methylmethacrylate-butadiene-styrene terpolymer (MBS) was developed to toughen PVC or PC. These blends could also contain other polymers, viz., SAA (Murdock et al. 1960), SMM and PS (Murdock et al. 1962), SMM-AN (Schmitt et al. 1967), *high heat* ABS (Kanegafuchi Chemical Industry 1967), HIPS (Ward 1970), MMVAc-AA (Holland et al. 1970), SMMA (Blasius 1992), etc. Table 1.33 traces the evolution of these systems. Later, these multipolymers were modified by incorporation of MA, AA, or GMA units to serve as reactive compatibilizers and toughening agents for PA, PEST, or PC blends.

1.5.7.2 Impact modification of PMMA

PMMA, like PS, is brittle and requires toughening. These efforts are summarized in Table 1.34.

1.5.7.3 PO Blends with Acrylic Polymers

PMMA is antagonistically immiscible with polyolefins – blends of this type have been used in non-critical applications, viz., PP/PMMA blends with EVAc were used as plastic paper (Yamamoto et al. 1971), while those with PVC (or CA) as wood-like materials (Yahata et al. 1971). For more demanding applications, either PO should be blended with an acrylic copolymer comprising a PO block, or PO should be grafted with acrylic moieties. Examples of the PO/Acrylics blends are listed in Table 1.35.

Blends of a PO (PE, PP, PB, P4MP, their blends, and copolymers, e.g., with 1-alkenes, vinyl esters, vinyl chloride, methacrylic esters, and methacrylic acid) with 0.2–50 wt% of a graft copolymer showed high tensile modulus and high sag resistance without increased melt viscosity. The blends could be shaped into foamed profiles at T = 200–230 °C.

To prepare the graft copolymer, a PO (MW = 50–1,000 kg/mol) was either dissolved or swollen in an inert hydrocarbon, monomers (≥80 wt% of a methacrylic ester, $CH_2 = C(CH_3)COOR$), and an initiator was added to the heated mixture while stirring. As a result, acrylic branches of a relatively high molecular weight (MW = 20–200 kg/mol) were grafted onto the PO macromolecules. The graft copolymer could be used as a compatibilizer-cum-impact modifier in a variety

Table 1.34 Impact modification of PMMA

PMMA impact modifier	References
PVAc	E. I. du Pont de Nemours 1942
Copolymers of methacrylonitrile, ethylacrylate, and/or α-methylstyrene	Coover and Wooten 1962
Ethylene-vinyl acetate-vinyl chloride copolymer (EVAc-VC)	Kishikawa et al. 1971
SMA and methylmethacrylate-methylacrylate copolymer (MMMA)	Bronstert et al. 1971
MBA: copolymer of butadiene, butylacrylate, and methylmethacrylate	Kotama 1972
Styrene-acrylonitrile copolymer (SAN)	Sugimura et al. 1972
SAN, PS, and poly(methyl norbornene-2-carboxylate)	Ikeda et al. 1976
IPN: cross-linked PBA, cross-linked and uncross-linked SAN	Silberberg 1982
Poly(p-hydroxy styrene), PVPh, and EVAl	La Fleur et al. 1992, 1994
Acrylic core-shell copolymer and either PBT or PET	Bright et al. 1993
Poly(allyl methacrylate-co-butyl acrylate-co-butanediol dimethacrylate-co-styrene-co-methyl methacrylate) or poly(acrylonitrile-co-butyl acrylate-co-tricyclodecenyl acrylate-co-styrene)	Farwerck et al. 1993
Poly(acrylate-N-cyclohexyl maleimide), PMI, and a copolymer: PMMA – core, cross-linked butyl acrylate-styrene copolymer – middle layer and PMMA shell, $d = 200–300\ nm$	Shen 1994
PEG/atactic PMMA blends were characterized by PVT at T = 20–200 °C and P = 0–200 MPa. Free-volume fraction was calculated from an equation of state	Schmidt and Maurer 1998

Table 1.35 Polyolefin/acrylic blends

PMMA impact modifier	References
40–90 wt% of ethylene-co-acrylic or methacrylic acid with ethylene-co-vinylacetate or ethyl acrylate for foam production	Park 1978, 1980
Ionomer with (1) a terpolymer of ethylene, vinylacetate and CO or SO_2, and (2) an elastomer (e.g., NR, IR, PU)	Enderle 1984
PE with EVAc, CPE, BR, etc., have been chemically foamed at T = 150–210 °C	Kuhnel and Spielau 1981
5 to 95 wt% of LDPE or LLDPE with EAA	Park 1985, 1986d
PE with either poly(ethylene-co-vinylcarboxylate) or an acrylate	Broadhed 1987
PP with an ionomer and EBA-GMA	Saltman 1988, 1989, 1992
PP with an ionomer, EBA-GMA, and EPDM	Dawson 1993
PO with a core-shell graft copolymer MBS type	Aoyama et al. 1993, 1994
PP with acidified PP, or a carboxylic acid-modified EPR, SMM-MA, and either EMMA-GMA or EVAc-GMA	Abe et al. 1994
LLDPE, PMMA and SEBS, EPR, or ethylene-styrene block copolymer (ES)	Dobreski and Donaldson 1994
At least two elastomers and an ethylene-methacrylate-acrylic acid ionomer	Arjunan 1994, 1995
PE with alkyl acrylate or alkyl methacrylate	Godfrey 1995

of polymers selected from between PO, acrylic polymers, SAN, EVAc, PA, PEST, PC, POM, PAr, PVC, ABS, PVDC, cellulosics, polyester-polyether block copolymers, PEA, PEEK, PEI, PES, CPVC, PVDF, PPE, PPS, PSF, TPU, PAI, PCL, polyglutarimide, and blends of PEST with PC or PVC (Ilendra et al. 1992, 1993).

1.5.7.4 PC Blends with Acrylic Polymers

PMMA has been blended with PC since 1971. Two types of PMMA/PC systems are of interest: (i) impact-modified alloys and (ii) miscible blends. To the first category belong *Meta-marble*™ blends of PMMA/PC with ABS (Ikura et al. 1974) or with ASA (Giles and Sasserath 1986). Blends of PC with two acrylic copolymers showed good processability, notched impact strength, and HDT (Eckel et al. 1993).

Acrylic polymers are recognized for their miscibility with a variety of polymers, viz., miscibility of PMA with PVAc (Kern 1957). PMMA is miscible with standard PC at T < LCST ≈ 140 °C. The miscibility range can be greatly increased by modifying the PC chain ends (LCST ≤ 300 °C) (Kambour 1988). Demixing PMMA/PC blends by the spinodal decomposition mechanism generated alloys with excellent mechanical properties (Kyu 1990).

PMMA is also miscible with fluorinated PC (Drzewinski 1993, 1994).

1.5.7.5 PEST Blends with Acrylic Polymers

Blends of PEST with acrylic polymers are limited to systems with acrylic elastomers. Examples are listed in Table 1.36. PBT and PET were reported to form miscible blends with either a poly-*p*-methoxyphenyl methacrylate or poly(phenyl methacrylate) (Siol et al. 1993b, 1994).

1.5.7.6 PPE Blends with Acrylic Polymers

Poly(2,6-dimethyl-*p*-phenylene ether) (PPE) was rarely blended with acrylics, viz., with styrene-methylmethacrylate-co-*cis*-polyisoprene (Abolins and Reinhardt 1976) and PMMA (Izawa and Nakanishi 1973; Matsunaga et al. 1974).

Table 1.36 Polyester/acrylic blends

1. Acrylic impact modifiers for PEST	References
Ethylene-methylmethacrylate copolymer (EMMA)	Dijkstra and Jones 1969
Graft copolymer: acrylonitrile-butadiene-styrene-methylmethacrylate, ABSM, and PDMS	Sauers and Barth 1970
Ethylene-hydroxyethyl methacrylate (EHEMA)	Jones et al. 1971
Ethylene-vinylacetate (EVAc)	Jones et al. 1971
methylmethacrylate-methyl acrylate copolymer (MMMA)	Kamata et al. 1974
Ethylene-vinylacetate-methacrylic acid copolymer	Gander et al. 1977
2. Blends of PMMA with	
1,4-butanediol terephthalate-co-polybutylene glycol (PBT-PBG)	Charles and Gasman 1979
PET and PS	Kamata et al. 1980
PBT and CH_3NH_2 (to convert PMMA into polyglutarimide)	Toray Ind. 1984

1.5.7.7 PA Blends with Acrylic Polymers

Polyamides, PA, can be impact modified by addition of acrylic multipolymers, e.g., methylmethacrylate-co-methacrylic acid-co-ethylacrylate (Halliwell 1965, 1966), ethylene-2-hydroxy ethyl methacrylate-methylmethacrylate (Hepworth et al. 1970), or ethylene-ethylacrylate-acrylic acid ionomer (Meyer and Tacke 1978).

1.5.7.8 POM Blends with Acrylic Polymers

These systems are not of industrial importance. However, addition of an acrylic was reported to improve processability, abrasion resistance, and weatherability of POM. For example, to improve weatherability, POM was blended with polythioisocyanate, TPU, PMMA, and benzotriazole (Endo et al. 1990). POM/TPU with EMMA and benzotriazole show enhanced performance (Okuda 1990). POM was also blended with EGMA (Takahashi and Kobayashi 1992), EGMA/AS, EGMA/PMMA, or their mixture (Kobayashi and Shinohara 1993).

1.5.8 Polyethylenes (PE)

1.5.8.1 Homopolymers

Properties of PE depend on molecular weight (MW), molecular weight distribution (MWD), as well as on the degree and type of branching (Peacock 2000). The density and modulus of PEs increase with crystallinity. As shown in Table 1.37, seven principal categories of PE are recognized. Commercial polyethylenes are generally copolymers of ethylene with varying amounts of α-olefins, and the comonomer has the effect of reducing crystallinity and density.

The first polymethylene was obtained in 1897 by the thermal decomposition of diazomethane. In 1931, about half a gram of PE was obtained in a free radical polymerization at high T and P. In 1937, *Telcothene*™, a blend of PE and polyisobutylene (PIB) was produced for submarine cables, and in 1939, the first LDPE, *Alketh*™, plant with 100 t/year capacity went into operation (Kennedy 1986). In 1951, HDPE was polymerized using the Z-N catalyst (Zletz 1954).

Table 1.37 Polyethylenes

No.	Type	Code	Density (kg/m^3)	Characteristics
1.	Ultra-high MW	UHMWPE	$\rho \approx 969$	MW > 3,000 kg/mol
2.	High density	HDPE	941–969	High MW and crystallinity
3.	Medium density	MDPE	926–940	
4.	Low density	LDPE	910–925	Long-chain branching, $T_m = 115\ °C$
5.	Linear low density	LLDPE	910–925	Ziegler Natta type with short branching, $T_m = 120–135\ °C$
6.	Very low density	VLDPE	900–910	
7.	Ultra low density	ULDPE	855–900	$T_m = 40–85\ °C$

In 1957, Du Pont Canada developed LLDPE, *Sclairtech*™ (Lank and Williams 1982). In the 1980s, new catalysts made it possible to polymerize VLDPE and ULDPE, commercialized in 1986. The newest PEs (*Tafmer*™ was introduced by Mitsui Petrochemicals in 1975) are prepared using the single-site metallocene catalysts (Choi and Soares 2012). These new resins have controlled MW, MWD, comonomer placement, and density. Their melting point, T_m = 70–120 °C, increases linearly with density, ρ = 880–930 kg/m^3. Details of the different catalysts used for olefin polymerization and the resulting molecular structures and attendant properties may be found in the recent review by Posch (2011). We note that Exxon Mobil has developed a grade for tough, high clarity films called Enable™ mPE 35-05HH resin that can extend downgauging opportunities on LLDPE and LDPE film equipment. This resin and its blends are useful for making compression packaging film, lamination film, stand-up pouch film, and medium- and heavy-duty bag film.

1.5.8.2 PE Blends

As much as 30% of all polyolefin products involve blends (Robeson 2007). It has been found, for example, that blending metallocene-catalyzed linear low-density polyethylenes (mLDPEs) with HDPE improves the Izod impact strength and some tensile properties of HDPE. Adding mLLDPE to LDPE increases the ductility of LDPE (Cran and Bigger 2009). In general, PE blends can be divided into three categories: (1) PE lots blended to meet standard specifications for density and melt flow, (2) PE modified with ≤ 15 wt% of other polymer(s), and (3) PE bends with other thermoplastics or thermoplastic elastomers.

PEs are immiscible with nearly all polymers; thus the standard strategies are applicable: (i) non-compatibilized blends with low concentration of the dispersed phase, e.g., blends of either PP or PE with 2 wt% PVAl; (ii) non-compatibilized blends for the use in noncritical applications; (iii) non-compatibilized blends having co-continuous morphology, e.g., PE, blended with neoprene rubber at a ratio 1:1 and then irradiated by electron beam; and (iv) compatibilized blends.

PE/Elastomer Blends

Polyolefins have been modified by the incorporation of elastomers to improve low-temperature impact strength and elongation. Table 1.38 provides examples of these systems.

PE/EPR or EPDM Blends

The first patent on PE/EPR blends was deposited before commercialization of EPR (Corbellini 1962). Several similar inventions were disclosed, viz., HDPE blends with EPR (Crawford and Oakes 1963, 1966), PE with EPDM (Prillieux et al. 1962), PE/EPDM blends with either PP or PB (Schreiber 1966), PE with EPR and ethylene-acetoxybicycloheptene copolymer (Shirayama and Iketa 1971), or VLDPE with EPR, EPDM, or their mixtures (Nishio et al. 1992). To improve PE/EPDM adhesion to polar materials, PE was first grafted with MA and then blended with EPDM (Honkanen et al. 1983).

Table 1.38 PE/elastomer blends

Modifier	Reason	References
Rubber	Impact modification	Standard Oil 1937
Cyclo-rubber	Adhesion to metal	Child et al. 1942
PIB	Transparent, impermeable, shrink-wrap films	Briggs et al. 1958;
CSR	For films or coatings	Boger and Thomas 1958
BR	Improve elongation	Cole 1959
Poly-1-butene	Processability and ESCR	Rudin and Schreiber 1964
BR and EVAc	Improved extensional behavior	Ceresa et al. 1968
An ionomer, with or without EVAc	Films with good tear and yield strength	Willott 1968
0.1–5 wt% aPP	Blown or stretched packaging films	Nakamura et al. 1973
EVAc and EVAl	Transparency and impact strength	Pritchett 1980, 1981
Polytransoctanamer (PTO)	Impact modification	Kita and Hashimoto 1987
Poly(ethylene-co-vinylcarboxylate)	High impact strength	Broadhed 1987
ULDPE/CSR or CPE, dynamically vulcanized and then dispersed into fresh CSR or CPE	Processability, hot-weld strength, adhesion and crack resistance for single-ply roofing membranes	Ainsworth 1990, 1994
Starch and at least one ionic compound	High-frequency sealable packagings	Dehennau et al. 1994

The first reactor-type thermoplastic polyolefin (R-TPO) was LLDPE/PP (Yamazaki and Fujimaki 1970, 1972). The three-component R-TPOs (PE with PP and EPR) soon followed (Strametz et al. 1975). PE was also polymerized in the presence of active catalyst and an olefinic copolymer (Morita and Kashiwa 1981). Blending amorphous co-polyolefins with crystalline POs (HDPE, LLDPE, PP) and a filler resulted in moldable blends, characterized by excellent sets of properties (Davis and Valaitis 1993, 1994). Blends of polycycloolefin (PCO) with a block copolymer (both polymerized in metallocene-catalyzed process) and PE were reported to show outstanding properties, viz., strength, modulus, heat resistance, and toughness (Epple and Brekner 1994).

Later, blends of a partially cross-linked thermoplastic elastomer with 5–40 parts of a PO (viz., LLDPE, PP, EPR, or PB-1) were developed for low-density, foamable alloys (Okada et al. 1998a). The density was reduced at least by a factor of two. In the following patent, 1–17 wt% of a long-chain branched PP was also added (Okada et al. 1998b). The extruded foam was free of surface roughness caused by defoaming, was soft to the touch, and showed excellent heat and weathering resistance.

For the power distribution cable industries, insulation compounds are selected primarily to obtain required electrical properties for their intended service and anticipated conditions of use. PE insulation is very sensitive to partial discharges,

while XLPE insulation is better where temperature stability is concerned. PE can be cross-linked either by chemical reaction (such as peroxides) or by γ-ray or by high-energy electron beam irradiation. However, in cable fabrication, chemical cross-linking of PE is used almost exclusively. Cross-linking of PE decreases modulus and elongation but increases ultimate tensile strength. However, enhanced thermal characteristics and excellent electrical properties coupled with mechanical toughness and good resistance to chemicals make XLPE an ideal insulant for applications in many types of electrical cables. Blends of various synthetic elastomers (EPM, EPDM, EVAc, Butyls, Silicones) with XLPE have been studied (Blodgett 1979; Mukhopadhyay and Das 1989, 1991). The effects of ethylene to propylene ratio (E/P) on the flow behavior, structure, mechanical properties, and failure mechanisms of XLPE and EPDM blends have also been studied (Mukhopadhyay et al. 1989; Mukhopadhyay and Das 1990).

PE/PE Blends

Molten polyethylenes of different type chain structures usually are immiscible (see ► Chap. 2, "Thermodynamics of Polymer Blends"). Upon crystallization the spherulites of one PE (having higher T_m) are encapsulated by those of the other PEs. Co-crystallization of two PEs into a single-type isomorphic cell is rare (Utracki 1989a). However, due to low interfacial tension coefficient, the phase coarsening is slow.

Alloys of different PEs constitute a large and important part of the PO technology. For example, in some countries, 70 wt% of PE is sold after blending (e.g., LLDPE with LDPE). As the technology evolves, these blends are prepared from resins of widely different rheological character, giving the viscosity ratios $\lambda \geq 10,000$. Usually, they do not require compatibilization, but owing to such a large value of the viscosity ratio, blending in shear flow is inefficient. Mixing in the extensional flow field is the potential solution (Luciani and Utracki 1996; Utracki and Luciani 1996a). Once cooled below the crystallization point of one component, the blend's morphology is fixed by crystalline cross-links. Blending of different grades and types of PE improves processability and mechanical performance. Blending, as it will be evident from the examples in Table 1.39, also may lead to transparency, improved abrasion resistance, stress-crack resistance, etc.

PE/PP Blends

PE has been used to improve the low-temperature impact strength of PP (see Table 1.40). The blends are mostly immiscible, compatibilized either by addition of EPR, EPDM, by reactive blending, or by post-blending co-cross-linking, e.g., by electron beam or γ-radiation (Utracki and Dumoulin 1995). Recently, Sonnier et al. (2008) showed that the use of 5wt% metallocene random copolymers of ethylene-olefin (mPE) as a compatibilizer increased the elongation at break of an 80/20 blend of high impact PP/HDPE from 60 % to 340 %. This was due to better interfacial adhesion. The comonomer content in mPE ranged from 8.3 % to 19.2% and the comonomer was either butene or octene.

Table 1.39 PE/PE blends

Blend	Advantage	References
LDPE with LLDPE	Processability, stiffness, abrasion resistance, H_2O vapor permeability	Wissbrun et al. 1962; 1965; Golike 1962
LDPE, HDPE, and EPDM or aPP	Soft, thin films	Sakane et al. 1979
Two types of LLDPE	Processability, impact strength, mechanical performance	Larsen 1982
LLDPE with LDPE, PP, TPOs, rubbers, EVAc, PP-MA, EPR	Improved processability	Haas and Raviola 1982; Cowan 1983; Fukui et al. 1983
HDPE with LLDPE	Improved strength, toughness, and transparency	Showa Denko 1983; Ogah 2012
LDPE with HDPE, PP, and EP-block	Modulus, strength, no sagging	Shin-Kobe Electric Machinery 1984
LLDPE, LDPE, and PP or EPR	High stiffness and film clarity	Bahl et al. 1985
HDPE with either LLDPE or LDPE	High stress-crack resistance	Boehm et al. 1992
VLDPE and LLDPE	Processability	Godbey and Martin 1993, 1994
Metallocene LLDPE and ionomer	Heat shrinkable films	Babrowicz et al. 1994
High and low molecular weight PE	Processability and physical properties	Coutant 1994
Reactor blends of LLDPE	Improved MD/TD tear balance	Ali et al. 1994
100 parts of LDPE (ρ = 890–925 kg/m^3), 1–110 parts of a HDPE	Expandable compositions for a small diameter electric wire insulation	Sakamoto et al. 1994
LLDPE with EVAc (10–20 % VAc)	Processability, tear strength, transparency	Benham and McDaniel 1994
LDPE with LLDPE	Improved tear strength and haze	Benham et al. 1995
70–98 wt% of LDPE (with $\leq$ 60 wt% LLDPE) and 2–30 wt% HDPE	For physical foaming of recycled HDPE	Lee 1995, 1996
Bimodal PEs (LCB = 0.01–3; $M_{n1}/M_{n2} > 7$) was lightly cross-linked. The PE-1 was prepared in the first reactor, and PE-2 was prepared in the presence of 15–65 wt% of PE-1 in the second reactor. The reaction could be carried out in the slurry, solution, or gas phase	Blends ($\rho \leq$ 885 kg/m^3) were used for wire/cable coating; weather stripping; seals; foamed articles with closed, open, or mixed cells; containers; medical appliances; drapes and coverings; fibers; tapes; tubes; pipes and hoses: bellows: boots; gaiters; footwear; etc.	Cree et al. 1998

PE/Other Commodity Polymer Blends

The PEs are frequently used as impact modifiers for a variety of other thermoplastics. For example, addition of either PE, CPE, or CSR to PVC improved its moldability, stability, impact strength, and chemical resistance (Matsuda et al. 1960). Blends of PO/PVAl were developed to improve the antistatic properties (Minekawa et al. 1969). LDPE was blended with poly(2-ethyl-2-oxazoline) (PEOX) for improved adhesion, e.g., to PET (Hoenig et al. 1984). Blends of PE, PP, PS, or their copolymers with ethylene-fluorinated vinyl ether copolymer were

Table 1.40 PE/PP blends

Composition	Reason	References
PP/LLDPE	Mechanical properties at low temperature	Holzer and Mehnert 1963, 1966
PP/LLDPE	Impact resistance and low-T brittleness	Martinovitch and March 1963
PP/LDPE	Impact strength and low brittle temperature	Sun Oil 1964
PE/PP compatibilized with EPR	Low-T brittleness and Izod impact strength	Rayner et al. 1964
PE/PP compatibilized with PIB	Low-temperature impact strength	Lehane 1964
Isotactic PP with sPP	Low-temperature impact strength	Emrick 1966
PE/PP compatibilized with EPDM	Improved impact properties of PEs	Schreiber 1966
PE grafted with methacrylic acid and PP with dimethylaminoethylmethacrylate	Blended at a ratio 1:1 showed excellent mechanical properties	Langworth 1967
PE/PP compatibilized with EPR	High impact strength	Sumitomo Chem. 1968
Isotactic PP with aPP	Impact strength at low temperature	Tanahashi and Kojima 1970
PE/PP compatibilized with EP-block copolymers	Mechanical, low-temperature impact, and optical properties	Leugering and Schaum 1970
Reactor blends: PE with PP and EPR	Reactor-*thermoplastic polyolefin*, R-TPO	Yamazaki and Fujimaki 1970
PP/EPR and 5–30 wt% of hexene- or octene-type LLDPE	Improvement of mechanical properties	Shirayama et al. 1972
PP/HDPE = 1:1	Processability, weld-line strength, low-T impact strength	Moorwessel et al. 1974
PP with 5–20 wt% LDPE and EPR	Transparency and mechanical performance	Oita et al. 1978
PP with EPR and then with PE	Co-continuous morphology – impact and mechanical properties	Huff 1978
Blending PP with EPR and then with PE	Co-continuous morphology, high performance	Huff 1980
PP, LDPE, HDPE, and an EP-block copolymer	Films with good modulus, tear strength, and sagging properties	Shin-Kobe Electric Machinery 1984
PP, LLDPE, LDPE, and/or EPR	High modulus and clarity	Bahl et al. 1985
PP, LLDPE, and a *Plastomer*™ (a metallocene ethylene-co-butene)	For melt-spun or melt-blown fibers or fabrics	Bartz et al. 1993a
EPR with *Plastomer*™	Packaging films, tubes, and trays	Mehta and Chen 1994
HDPE with PP autoclave-foamed with CO_2	Foam with $\geq 10^9$ cells/mL and cell diameter, d $\leq$ 10 μm. High impact strength	Dorudiani et al. 1998

Table 1.41 PE/PA blends

Composition	Reason	References
LDPE or PP with either PA-6 or PA-66	For sheets, films, fibers, or bottles	Mesrobian and Ammondson 1962
PE with a PE-PA-6 copolymer	Transparency and low permeability	Craubner et al. 1962
PE mixed with a lactam and then polymerized	Low water absorption, strength	Hill et al. 1970
PA-6/LDPE or PIB/N-stearyl stearamide	Low-temperature impact, tenacity	Gilch and Michael 1970
PA-66, PE, PBT, and PC with SEBS	Co-continuous morphology	Gergen and Davison 1978
Aromatic polyamide (PARA) compounded with PE	Processability, elongation at break, tensile, and impact strength	Paschke et al. 1983
PA with carboxylated EPDM and PE	For improved impact resistance	Unitika Ltd. 1983
PA blended with a mixture of PP, HDPE, and EPR	Processability, mechanical properties even after water immersion	Hasuo et al. 1985
PA with HDPE, EPR, and maleated PP	Rigidity and low-T impact strength	Kondo and Tominari 1987
PARA with PE or PP-MA and hydrazine	Resistance to thermal degradation	Yoshihara 1990
PO-g-GMA, acrylamide, vinylpyrrolidone, acrylic, and/or methacrylic acid ester and then blended with either PA or PEST	Adhesion to fillers, excellent performance of filled compositions	Teraya et al. 1994

used for the electrical insulation of high-voltage, submarine cables (Barraud et al. 1993). Blends of LLDPE with EVAc or EEA have comparable physical properties and cost to plasticized PVC (Rifi 1994).

PE/PA Blends

The reasons for blending PE with PA are (1) a desire to improve the impact strength and moisture absorption of PA and (2) to improve rigidity and barrier properties (to oxygen and solvents) of PE. Films and containers manufactured from the latter blends show overlapping lamellar structures that cause high tortuosity for molecular diffusion and significant reduction of oxygen or solvent (e.g., gasoline) permeability. The technology became particularly attractive after the reactive grafting of PO with either maleic anhydride, acrylic acid, or glycidyl methacrylate was invented (Steinkamp and Grail 1976). These modified POs could be directly used in blends with either PA or PEST (Davis 1975). In Table 1.41 examples of PE/PA blends are given.

PE/PC Blends

To increase rigidity of PE, the resin has been blended with about 5 wt% of a high-modulus polymer, e.g., PC (Peters and Schuelde 1963). PC also stabilized PO against the thermal degradation (Schutze et al. 1972). Addition of 3–5 wt% PO

Table 1.42 Compatibilized PE/PC blends

Compatibilizer/impact modifier	References
0.01–2 wt% ABS	O'Connell 1974
Hydrogenated chlorosulfonated butadiene-styrene block copolymer	Bussink et al. 1978
Maleated LLDPE	Mitsubishi Chemical Ind. 1980
Ethylene-glycidyl methacrylate copolymer (EGMA)	Sumitomo Chem. 1982, 1983
Methyl-phenyl siloxane	Rosenquist 1982
Acrylic *and* hydrocarbon elastomers (viz., BR, EPR, EPDM, IR, IIR)	Teijin Chem. 1982, 1983, 1984
EPR or EPDM	D'Orazio et al. 1982
1–5 wt% SEBS	Idemitsu Kosan 1983
Acrylic rubber or maleated PO	Idemitsu Petrochem. 1983, 1984
4 wt% poly(butylacrylate-co-methylmethacrylate) copolymer	O'Connell 1983
ABS with polysiloxanes containing Si-H bonds	Liu 1983, 1984
Ethylene-ethyl acrylate copolymer (EEA) and SEBS	Overton and Liu 1984, 1985
0.2–15 wt% acrylic impact modifier (MBA, *Acryloid™ KM*)	Endo and Ishii 1984
TPE (acrylic rubber, butyl rubber, EPDM, or SBS)	Kozakura et al. 1992, 1994

Table 1.43 PPE/styrenics blends with PE

Composition	References
PPE with LDPE	General Electric 1966
PPE with either SBR or HIPS and LDPE	Summers et al. 1972
PPE was blended with SEBS and PE	Yonemitsu et al. 1976
PPE with HIPS, SEBS, and PE	Haff and Lee 1978
PPE with PS, SEBS, and PE	Haaf 1979
PE with 0–35 wt% PP, PDMS, and 5–35 wt% PPE, PC, PET, or PA	Plochocki et al. 1979
PPE with hydrogenated SB block copolymer and LDPE	General Electric 1984
PPE with HIPS, SEBS, and LLDPE	Hambrecht et al. 1986
PPE with styrenics and high molecular weight HDPE	Bopp and Balfour 1993

toughened PC (Yamada 1963). For good dispersion, the blending should be carried out at T > 290 °C, using PE grades with the viscosity ratio $\eta(PE)/\eta(PC) \leq 0.3$–0.9. Several impact-modified grades of PC (viz., *Lexan™ EM*) comprise PE (Freitag et al. 1991). However, as Table 1.42 illustrates, most PE/PC blends also contain a polymeric compatibilizer-*cum*-impact modifier.

PE/PPE Blends

The PPE/PE blends are not commercial, but a small amount of PE is frequently added to PPE/HIPS or PPE/SBR blends to improve processability and solvent resistance (see Table 1.43).

To enhanced rigidity of PO, 5–35 wt% of modified PPE was added. In this application, PPE can be considered a low-density filler. Similar effects can be obtained adding a small quantity of other polymers, viz., PC, POM, PPS, etc.

Table 1.44 PEST/PE blends

Composition	References
PET with 0.5–50 wt% PE, for impact strength	Glanzstoff 1967
PET with poly(ethylene-co-acrylic acid) ionomer	Cope 1969
PET with oxidized and carboxylated PE and glass fibers	Segal 1973
Poly(ethylene-2,6-naphthalene dicarboxylate) (PEN) with MDPE and/or PP	Tokai and Sakai 1973
PBT (or PET) with PC and LLDPE	Boutni and Liu 1983
PBT (or PET) with PC and PB	Dieck and Kostelnik 1983
PET with LLDPE	Smith and Wilson 1984
PET with either PE, PP, PO-GMA, vinyl- or acrylic-grafted PO, and GF	Mukohyama 1993
PBT with PC, and PE, PP, and/or EPR grafted with GMA or MA	Fujie 1993
HDPE and copolymer of n-butylterephthalate with ethylene- and propylene glycol	Abu-Isa and Graham 1993
PET with 30–70 wt% LDPE, HDPE, or LDPE and EEA-GMA	Natarajan et al. 1993, 1994

Table 1.45 POM/PE blends

Composition	References
POM was blended with 1–5 wt% of either PE, EVAc, or PEG	Burg et al. 1972
POM was blended with 90–99 wt% of LDPE	Rudin and Schreiber 1964b
PE or PP with EVAc and either POM, PMMA, PS, or SMM	Yamamoto et al. 1971
POM was blended with EVAc and HDPE	Ishida and Masamoto 1974
POM was first blended with TPU and then with either PA, LLDPE, PP, PBT, or PET	Flexman 1992

PE/PEST Blends

Addition of PE to PEST is known to improve impact strength, processability, solvent resistance, and weatherability. When more than 5 wt% of PE is required, compatibilization is advisable. Examples of these systems are listed in Table 1.44.

PE/POM Blends

POM is difficult to compatibilize, and without compatibilization only ≤ 10 wt% of POM in PE, or vice versa PE in POM, can be used. For example, addition of a small amount of PE to POM improves its processability, impact and abrasion resistance, hardness, surface finish, and rigidity, while addition of POM to PE improved its modulus and abrasion resistance – see Table 1.45.

PE/Specialty Resin Blends

Most specialty resins are processed at temperatures that limit the possibility of blending them with PE. The PE/specialty resin blends usually contain low concentration, ≤ 5 wt%, of either component. Addition of PE improves the processability, surface finish, chemical, solvent, and impact resistance. Addition of specialty polymer to PE may improve rigidity and processability (viz. PE/LCP). Examples are given in Table 1.46.

Table 1.46 Specialty polymer blends with PE or PP

Composition	References
Polyarylene polyether sulfone (PAES) with $\leq$ 5 wt% of PE or PP	Gowan 1969
Polysulfone (PSF) with either PE, PP, BR, EPR, or EPDM	Hart 1971
Polyarylamideimide (PAI) with a small amount of PE	Toray Ind. 1981
Polysulfide (PPS) blends with PDMS and either PE or PP	Liang 1987
PPS/PE compatibilized by addition of an aromatic nitro compound	Köhler et al. 1992
Polyoxycyanoarylene (POCA) with PO, compatibilized by EGMA	Hashimoto et al. 1990
PE blends with liquid crystal polyester (LCP)	Alder et al. 1993

1.5.9 Polypropylene (PP)

1.5.9.1 Homopolymers

There are three types of polypropylene: amorphous (aPP), isotactic (PP), and syndiotactic (sPP) (Karian 2003). Performance of these resins depends on the tacticity content. PP was commercialized in 1957 by Hoechst. The slurry process in hexane used the Ziegler-Natta (AlEt$_2$Cl + TiAlCl$_6$) catalyst (Sailors and Hogan 1982). The new metallocene catalysis leads to isomer purity in excess of 96 % (see, for example, Posch 2011). It is also possible to produce branched, *high melt strength PP*, with extensional stress hardening, similar to that of LDPE (Phillips et al. 1992). The new PPs show the melting point, T$_m$ = 120–164 °C. To enhance the performance, PP is usually blended (in the reactor or outside the reactor) with much more viscous PP-copolymers. As a consequence, one of the most serious industrial problem is homogenization of these materials (Luciani and Utracki 1996; Utracki and Luciani 1996b).

Most industrial polypropylenes are isotactic, but a few syndiotactic polypropylenes are available (De Rosa and Auriemma 2006). The advantage of sPP over PP is that impact strength and tensile modulus of sPP are significantly higher. While PP has a planar zigzag helical structure, the sPP has a three-dimensional one that leads to lower crystallinity and melting point: T_m(PP) ≈ 165 vs. T_m(sPP) ≈ 133 °C.

1.5.9.2 PP Blends

PP is brittle, especially at T $\leq$ T$_g$ ≈ 0 °C. The resin fractures by the crazing-cracking mechanism (Friedrich 1983). The discovery of PP immediately followed by search for methods of improvement the low-T impact behavior. PP was blended with EPR or EPDM (Hogan and Banks 1953, 1955), PE (Holzer and Mehnert 1963), sPP (Emrick 1966), aPP (Tanahashi and Kojima 1970), etc.

PP/Other Polyolefin Blends

PP is often made using two reactors in series: the first reactor makes isotactic PP, while the second reactor makes a random copolymer of PP and PE. The copolymer is amorphous, and it is blended with the PP homopolymer to enhance impact resistance (Tan et al. 2005). PP blends with elastomers will be discussed in the following parts. In Table 1.47 few examples of PP blends with other POs are given.

Table 1.47 PP/PO blends

Elastomer added to PP	Comment	References
PP/PIB miscible (?) blends	Low-temperature impact properties	Ranalli 1958
PP miscible with aPP or polybutene-1	Reduction of T_g by up to 20 °C	Romankevich and Frenkel 1980
10–60 wt% PP or LLDPE with EPDM and ≤ 95 wt% PIB or butyl rubber	Soft, easy foamable blends (due to strain hardening)	Matsuda et al. 1981, 1988
PP with polytransoctanamer (PTO)	Fivefold increased impact strength	Kita and Hashimoto 1987
PP with polyoctadecene (POD)	Temperature sensitive transparency	Tanaka et al. 1988
PP/PB and *Plastomer*™	Impact and mechanical properties	Bartz et al. 1993b
PP/PB and a poly(*1*-butene-co-ethylene)	Processability, impact strength, and optical properties	Hwo 1994
High MW aPP blended with high MW of either PP or sPP	aPP was immiscible with PP and partially miscible with sPP	Silvestri and Sgarzi 1998
Addition of EPR to PP	To strengthen spherulites boundary	Lustiger et al. 1998

PP/Elastomer Blends

These blends constitute a large, commercially important group. Usually 5–20 wt% of elastomer have been used. Alloying improves processability (e.g., in blow molding) and impact strength at low temperature. Diverse elastomers have been used, e.g., EPR, BP, PIB, BR, uncured PB, and SBR; *dynamically co-vulcanized* CBR; and BR, CSM, and EPDM (Reid and Conrad 1960, 1962; Dow Chem. 1963; Gessler and Haslett 1962; Esso R&E 1962; Coran and Patel 1978). Blends with amorphous CSR showed good mechanical properties (Shikata et al. 1973). Partially vulcanized blends of CSR with PP and/or ULDPE had good processability, hot-weld strength, interplay adhesion, and crack resistance (Ainsworth 1990, 1994). Addition of CPE improved PP's processability and properties (Newe et al. 1984).

Many EPR and EPDM elastomers show a block copolymer behavior. When blended with PP, they form emulsion-like dispersions. For the ease of compounding, a small amount of PE may also be added. Furthermore, if the elastomeric phase is lightly cross-linked, the morphology is more stable. The PP/EPR blends can be processed by all methods used for PP. They are characterized by good processability, dimensional stability, low shrinkage, high stiffness, tear strength and softening temperature, good mechanical properties (at T = −40 °C to 150 °C), ozone resistance, fatigue, and abrasion resistance (see Table 1.48). These materials have been used in more than 200 applications, in automotive industry, appliances, hardware and plumbing, medical, shoe industry, sports equipment, toys, etc. Examples of commercial PP/EPR blends are *Buna*™, *Dutral*™, *Epcar*™, *Epichlomer*™, *Epsin*™ and *Santoprene*™, *Esprene*™, *Ferrocline*™, *Gafply*™, *Intolan*™, *Kelburon*™, *Larflex*™, *Milastomer*™, *Nordel*™, *Royaltherm*™, *Trilene*™, and *Vistalon*™.

Table 1.48 PP/EPR blends

Elastomer(S) added to PP	Reason	References
0.1–60 wt% EPR, containing 2–25 % ethylene – the earliest patents	Increased impact and tensile strength, superior mechanical properties	Schilling 1964, 1966; Short 1967; Shirayama et al. 1971
EPDM (EPR with dicyclopentadiene or ethylidene-norbornene), partially cross-linked with peroxides	Alloys could be shaped into articles with good properties without further vulcanization	Fischer 1972
EPDM	Unexpectedly high tensile strength	Stricharczuk 1977
Dynamic vulcanization of PP with either EPR or EPDM; *Santoprene*™	A range of Shore hardness, toughness, elongation, impact strength	Coran and Patel 1978
Dynamically blended PP/EPR and a peroxide-containing co-polyolefin	A masterbatch that subsequently was blended with EPDM into TPO	Yamamoto and Shimizu 1979
Sequential compounding of PP, first with EPR and then with PE	Co-continuous morphology, good impact and mechanical properties	Huff 1980
Amorphous EPR + crystalline EPR	Balance of properties, impact strength	Galli and Spataro 1983
Bimodal EPR	Impact strength and mechanical properties	Makino et al. 1986
PP/PE, EPR, EPDM, SBS, ionomers, EVAc, EEA, or ESI. Styrene-grafted PP added and "visbreaking"	Blends foamed with isopentane; good dimensional stability	Fudge 1987
Reactive preblend of PP with either EPR or EPDM (in a ratio from 1:0.01 to 1:0.5) added to PP	Improved homogeneity, heat resistance, impact resistance, and greater flowability	Yeo et al. 1989
Dynamically vulcanized BR or CBR and EPDM	High tensile strength	Puydak et al. 1990, 1992
PP, PE, PS, PMMA, or PVC was blended with either EPR or EPDM	Sequentially cured and foamed blends	Cakmak and Dutta 1992; Dutta and Cakmak 1992
EPR blends with sPP	Transparent, low-T impact resistance	Asanuma et al. 1992
EPR, EPDM, or their mixtures, with a metallocene-type VLDPE, PP, and talc	Moldability, surface appearance, hardness, and impact resistance	Nishio et al. 1992
Ethylene-α-olefin copolymers, stereo-block polypropylene, or EPR	Enhanced inter-spherulitic and interlamellar strength	Lustiger 1993
Isotactic EPR, $T_g < -20\ °C$	Modulus, low-T impact strength	Winter et al. 1993
Random crystalline terpolymers – EPR	For fibers with high resiliency and shrinkage, for pile fabrics	Clementini et al. 1993
EPDM with ethylene-methacrylate-zinc, glycidyl methacrylate-acrylate or epoxy	To improve the scuff resistance	Dawson 1993

(*continued*)

Table 1.48 (continued)

Elastomer(S) added to PP	Reason	References
Dynamically vulcanized blends of PP with EPDM, mineral oil, and PDMS	For slush molding large plastic parts	Hikasa et al. 1994
Poly(4-methyl-1-pentene) with PIB	For food overwrap films	Nagase et al. 1994
Olefinic, partially cross-linked elastomer: EPDM, EPR, BR, NR, IR, CBR, etc.	For manufacturing automotive components	Ellul 1994
Metallocene PP was alloyed with EPR	For low-temperature heat sealability	Shichijo 1994
PP blended with EPR and EPDM and then irradiated in the presence of O_2	Easily foamed blends with high strain hardening	DeNicola et al. 1995, 1997
Long branch containing PP with partially cross-linked EPR and a foaming agent	Reduction of density by ≥ 2, smooth surface, heat and weathering resistance	Okada et al. 1998

PP/EVAc blends are immiscible; thus, in two-component systems, only a small amount of EVAc can be used, e.g., to improve dyeability, flexibility, electrostatic dissipation, or barrier properties. The hydrolyzed EVAc (EVAl) was also used (Minekawa et al. 1969). In most cases, the PP/EVAc blends are part of more a complex, multicomponent system comprising a reactive compatibilizer (see Table 1.49).

1.5.10 Thermoplastic Olefin Elastomers (TPO)

Ziegler-Natta catalyst makes it possible to polymerize α-olefins into elastomers with controlled degree of crystallinity and cross-likability. The first EPR's were manufactured in 1960, 3 years later, the first EPDM. It is advantageous to produce block copolymers with PP being the rigid and PE the soft block. A direct sequential polymerization of propylene and ethylene-propylene mixture leads to the reactor blends (R-TPO) (Cecchin and Guglielmi 1990).

EPR may be cross-linked by peroxides, while EPDM by the standard methods of the rubber industry. By varying the composition and process variables, a wide range of properties can be obtained. The resin with vulcanized, dispersed phase has CUT ≈ 125 °C, higher than standard TPO, and they are known as the *thermoplastic vulcanizates*, *TPV* (Fritz and Anderlik 1993). Diverse TPOs with properties that range from flexible to rigid (but tough) are manufactured by the large resin producers, as well as by the compounding houses (Utracki and Dumoulin 1995).

Polytransoctanamer (PTO) has been used as a high-performance elastomer and in blends with commodity and engineering resins. Polyoctadecene (POD) blends with PP are thermochromic. The most interesting are the metallocene-type polycyclic polyolefins, e.g., polycyclopentene or polynorbornene, either syndiotactic or isotactic with $T_m = 400–600$ °C.

Table 1.49 PP/EVAc blends

Elastomer added To PP	Comment	References
PP with 18–32 wt% EVAc and/or ethylene-ethylacrylate copolymer (EEA)	Impact strength, elongation, and low-T brittleness	Miller and Reddeman 1962
PP with EVAc	Dyeability, flexibility, barrier properties, and toughness	Sakata et al. 1968
PP/EVAc and POM, PMMA, PS, or SMM	For paperlike films	Yamamoto et al. 1971
70 wt% PP and EVAc, PVCAc, HDPE	Low-temperature impact resistance	Kojima and Tanahashi 1972
PP/EVAc with maleated LDPE	Melt strength and rigidity	Idemitsu Petrochem. 1983
35 wt% PP, 50% PIB, and 15% EVAc	For films, moldings, and extrusions	Shulman 1984
PP/PC with 2–35 wt% EVAc	Excellent solvent resistance	Giles and Hirt 1986
10–90 wt% PP, 5–60 wt% EVAc, and 5–50 wt% PEOX	Miscible (?) alloy for intermediate layer in recyclable barrier films	Sanchez et al. 1991
PP/EVAc with PP-MA	Low permeability by gases or liquids	Kamal et al. 1992
PP/EVAc with EAA and polybutene	Tough, radiation resistant, heat sealable	Wilfong and Rolando 1993

1.5.11 PP/Engineering Resin Blends

1.5.11.1 PP/PA Blends

There are three types of PP/PA blends: (1) with a small percentage of PO, either acidified or not, (2) alloys with high component ratio where PA is a matrix, (3) and blends with a small amount of dispersed PA to increase rigidity. Table 1.50 gives some examples of these systems.

To toughen PA, 2–5 wt% of either PO, elastomer, *ionomer*, acidified, or epoxidized copolymer may be added. PA/PO blends of type (2) were developed to improve dimensional stability and to reduce water absorbency of PA. Alloying PA with PO reduces the *rate* of water migration to and from the blend, but not the inherent water absorption of PA (Utracki and Sammut 1991, 1992). The alloying is either a two- or three-step reactive process: (1°) acidification of PO, (2°) preparation of a compatibilizer, and (3°) compounding PP, PA, and the compatibilizer. Usually, the reactive blending is carried out in a twin-screw extruder (Nishio et al. 1990; Hu and Cartier 1998). Since it may cause reduction of the blend crystallinity (thus performance), the extent must be optimized. The rigid PA/PP blends usually comprise PA:PP = 3:2 with 12 wt% of a compatibilizing copolymer. Finally, in type (3), incorporation of PA improves processability, solvent resistance, CUT, HDT, and surface finish. For enhanced performance, the blends should be compatibilized.

Table 1.50 PP/PA blends

Composition	Comment	References
1. Toughened PA		
PA, PP, and 0.5 wt% of PP-MA	Compatibilized blends	Davis 1975
PA/PO and ionomer	*Surlyn*™ as a compatibilizer	Toyobo 1981
PA/PO and PO grafted with MA or a compound containing two epoxy groups	High impact strength	Subramanian 1980, 1983, 1984
PO grafted with glycidyl methacrylate, acrylamide, vinylpyrrolidone, acrylic acid esters, and/or methacrylic acid esters and then blended with PA or PEST	Two-stage, reactive impact modification: preparation of reactive compatibilizer and then blending	Teraya et al. 1994
2. Rigid PA/PP blends		
Non-compatibilized PP/PA blends	For films, sheets, or bottles with good printability and low liquid permeability	Mesrobian and Ammondson 1962
PP with PA-6 or PA-66 and GF	Rigid, non-compatibilized blends	Asahi Fiber Glass 1981
PP/PA-6 compatibilized by EPR-MA	Impact-resistant blends	Katsura 1986
PP was maleated and then reactively blended with PA to obtain 12 wt% of PP-co-PA	Two-step blending: maleation of PP, incorporation of PA	Glotin et al. 1989
PA was blended with acidified PP and GF	Moldability, water resistance, HDT, low-T impact strength	Iwanami et al. 1989
Reactive blending of PP/PA-6 with either EPR-MA or SEBS-MA	SEBS-MA gave better impact strength, yield stress, toughness, and modulus	Rösch and Mülhaupt 1994
3. PA/Elastomer blends		
PP, PA-6-co-PA-66, PP-MA with NBR and EPDM	Impact strength, high stress at break, high elongation, good ductility, and high gloss	Tokas 1981
PP, EPR, PA, and SMA, SEBS-MA, EPR-MA, MBA, ASA, etc.	For automotive, electrical, electronics, building, furniture, small appliances, etc.	Chundury and Scheibelhoffer 1994
PP, EPR, PA, and 2 compatibilizers from between SEBS, SEBS-MA, and poly(ethylene-co-acrylic ester-co-MA)	Recyclable high impact strength blends	Chundury 1994
PP-MA was blended with PB	Adhesive to metals and polar polymers: PA, PET, or PC	Lee et al. 1994

1.5.11.2 PP/PC Blends

PP and PC are immiscible; thus, excepting the exploratory use as a "plastic paper," only the two ends of the concentration range have been explored, viz., addition of 5 wt% PP to PC (to improve processability of PC) (Dobkowski 1980) or addition of ≤ 10 wt% of PC (to improve PP processability, enhance crystallinity and crystallization temperature, the appearance, modulus, and impact strength) (Liang and Williams 1991). For concentrations ≥ 10 wt%, compatibilization is necessary.

Table 1.51 PP/PEST blends

Composition	Comment	References
PAr with low concentration of PO, elastomer, or EVAc	Uncompatibilized blends	Koshimo et al. 1973
PBT with PP	Improved moldability of PBT	Seydl and Strickle 1976
PET, PO, and either glycidyl methacrylate-modified PO or vinyl-grafted PO	High heat and moisture absorption resistance	Mukohyama 1993
PBT/PC with PE, PP, or EPR modified with 0.05–15 wt% glycidyl methacrylate and/or 0.1–2 wt% MA	Processability, toughness, rigidity, strength, dimensional stability, and flexural modulus	Fujie 1993
PPE, PA, or PEST with EPDM, SBS, SEBS, or EPR, and PP grafted with styrene and a glycidyl moiety	Flexural and tensile strength	Okamoto et al. 1993, 1994
Recycled PET/PP = 2:3–3:2 and SEBS-MA	For molding battery containers	Tekkanat et al. 1993, 1994
PP with PET or PBT and a polyolefin-polyester graft copolymer	Compatibilized	Fujita et al. 1994
PEST, PA, PP-MA, and either PET or PBT with sodium dimethyl 5-sulfoisophthalate	High tensile and impact strength	Tajima et al. 1994

This is accomplished using ethylene-acrylic copolymer, cellulosics, PA, PVAc, or TPU (Goldblum 1963, 1964); an acrylic elastomer, acrylic elastomer with PP-MA, and either butyl rubber or isobutene-isoprene rubber (Teijin Chem. 1982, 1983); SBR and EEA (Liu 1984); MBS (Overton and Liu 1984); or EVAc (Giles and Hirt 1986).

1.5.11.3 PP/PEST Blends

PP is antagonistically immiscible with PEST, and when the concentration of the dispersed phase exceeds 5–10 wt%, compatibilization is necessary. Initially, the uncompatibilized blends were formulated within the low concentration region of the dispersed phase. By the end of 1980s, reactive compatibilization started to dominate the technology. Examples of PP/PEST blends are listed in Table 1.51.

1.5.11.4 PP/PPE Blends

Two-component blends of PP with PPE are unknown. To get a reasonable performance out of a PP/PPE mixture, first PPE must be toughened using a styrenic resin, and then the blend compatibilized. Thus (see Table 1.52), PP is only one ingredient in multicomponent PPE blends.

1.5.11.5 PP/POM Blends

PP/POM blends are antagonistically immiscible, not available on the market. The early blends contained a small amount of one resin in another, viz., either PP or LDPE, with 1–10 wt% POM showed improved processability, good appearance,

Table 1.52 PP/PPE Blends

Composition	Comment	References
PPE-MA with PP-MA, SBR, glycidyl methacrylate copolymer, and/or phenylenediamine binder	Solvent resistance, moldability, impact, and mechanical properties	Togo et al. 1988
PPE dispersed in PP, PE, PA, PEST, POM, PPS, or PEEK, compatibilized by EPR-MA, EVAc-GMA, and either maleic anhydride or bis(4-phenyl isocyanate)	Processability, heat resistance, and mechanical properties	Nishio et al. 1988, 1994
PPE, PP, and SEBS	Modulus, rigidity, tensile strength, and HDT	Lee 1990
PPE with PP grafted with styrene and MA and EVAc-GMA, styrene-grafted EPDM	Rigidity as well as high heat, chemical, and impact resistance	Furuta and Maruyama 1990
PPE, PP, and PPS with hydrogenated styrene-isoprene block copolymers	Heat, impact, and solvent resistance	Maruyama and Mizuno 1990
PPE modified by glycidol or epichlorohydrin with PP-MA or PP-GMA and PA or PEST	Moldability and mechanical strength	Nakano et al. 1992
PPE with PP, compatibilized with styrene-grafted propylene-methyloctadiene (or hexadiene)	Stiffness and impact strength	Tanaka et al. 1992
PPE/PS, styrene-grafted polypropylene (PP-PS), SEBS and PP	Processability, HDT, impact and tensile strength, stiffness solvent resistance, gloss	DeNicola and Giroux 1994
PPE/PP compatibilized with PO grafted with ethylenically unsaturated *t*-alkylcarbamate	Copolymers used as decomposable compatibilizing agents	Campbell and Presley 1995

and improved performance (Rudin and Schreiber 1964a). However, blends containing higher concentration of ingredients must be compatibilized, viz., by addition of muconic acid-grafted PP (Chen et al. 1991) or by TPU and EBA-GMA (Subramanian 1992).

1.5.12 PP/Specialty Polymer Blends

Most specialty resins require high processing temperatures, while PP usually has $T_{proc} < 250\,°C$. Thus, only few blends of this type are known. For example, addition of PP enhanced throughput of PAES (Gowan 1968, 1969), PEI, PC/PEST blends, etc.

Linear, aromatic polyamides (PARA) are either liquid crystalline, semicrystalline, or amorphous. Mainly the latter resins are used in blends with PP, viz., PARA with PP-MA (Iwanami et al. 1990), PARA with PE-MA, or PP and hydrazine (Yoshihara 1990). Blends of copolyphthalamide (PPA) with PP were compatibilized using either PP-MA (Paschke et al. 1993, 1994) or PP grafted with acrylic acid (Brooks et al. 1993, 1994).

Table 1.53 PP/LCP blends

Composition	Comment	References
Low concentration of LCP in a resin	To improve processability	Cogswell et al. 1981
10 wt% of LCP was blended with, e.g., PP, PS, PC, or PI	Molecular orientation imposed by extrusion through a rotating die	Haghighat et al. 1992
LCP and PP, PET, PA, PC, PE, PVC, PVDC, PPS, PVDF, PVF, or PMMA	To produce oriented films with protrusions that resulted in low friction	Wong 1990, 1994
PP was blended with LCP	2 extruders with a static mixer, to stretch LCP into microfibrils	Sukhadia et al. 1991, 1992
PP/LCP compatibilized with PP-MA	(Processing as described above)	Baird and Datta 1992
LCP with either PP, PPE, PPE/PS, PC, or PEI	(1) Prepregs from an extruder, mixer, and rolls; (2) prepregs consolidated at $T < T_m$	Isayev 1991, 1993

PP blends with a small amount of LCP are of industrial interest for two reasons: (i) to improve processability or (ii) to improve the mechanical performance. The second effect depends on the blend's morphology, i.e., on the orientation of LCP domains. The latter depends on the concentration, viscosity and elasticity ratios, interfacial tension coefficient, flow type and intensity, total strain, drawdown ratio, etc. Three stages of orientation are (1) drop deformation, (2) fibrillation of the domains, and (3) stretching of the LCP chains (Champagne et al. 1996). Only the latter provides a reasonable cost-to-performance ratio. Examples of PP/LCP systems are listed in Table 1.53.

1.6 Engineering Resins and Their Blends

The term *engineering polymer* is applied to a processable resin, capable of being formed to precise and stable dimensions, having high performance at CUT $\geq 100\,^{\circ}$C, and the tensile strength of $\sigma \geq 40$ MPa (Utracki 1989a). Five polymer families belong to this category: PA, PEST, PC, POM, and PPE. While the relative size of the engineering resin market varies from country to country, these polymers constitute about 13 % by volume and 34 % by value of the total plastic's consumption. Since the blends of engineering/commodity resins have already been discussed, here only engineering/engineering and engineering/specialty resins will be considered.

Engineering resins and their blends have been foamed using mainly chemical foaming agents, e.g., hydrazodicarboxylates, benzazimides, or 5-phenyltetrazole. However, products of decomposition of these agents (e.g., alcohol, ammonia, water, etc.) were found to hydrolyze PC, PA PC/ABS, or PEST, reducing the performance of foamed products. For this reason, dihydro-oxadiazinones were proposed as the preferred chemical foaming agents for the engineering resins, their compositions, and blends (including PPE/HIPS) (Nizik 1978, 1979). Another method for foaming high temperature polymers profits from thermal

Table 1.54 Comparative properties of PAs

Property	PA-6	PA-66	PA-11	PA-12	PA-46	PA-610	PA-63T
Tensile modulus (MPa)	1,400	2,000	1,000	1,600	1,700	1,500	$\geq 2,000$
Tensile stress (MPa)	40	65	50	45	59	40	≥ 75
Maximum elongation (%)	200	150	500	300	60	500	50–150
Density (kg/m^3)	1,130	1,140	1,040	1,020	1,100	1,080	1,060–1,120
T_g(°C),	57	57	46	37	295	50	145
T_m (°C)	220	255	185	180		215	240
HDT (°C)	80	105	55	140	90	95	150

instability of polypropylene carbonate (PPCO, MW = 1–1,000 kg/mol) (Kuphal et al. 1990). The process involves blending PPCO with a resin or its blend that is to be foamed. The blend is then heated to T > 300 °C, sufficient to melt the principal resin and to decompose PPCO. Talc, wollastonite, clay, $CaCO_3$, or citric acid can be used as a nucleating agent. The densities of the molded articles were reduced by at least 50 %. Today foaming of the engineering resins with supercritical CO_2 is practiced.

1.6.1 Polyamides (PA)

Polyamides are abbreviated as PA, followed by the number of carbons in a diamine and dicarboxylic acid, viz., PA-66 has six carbons in each component, etc. Poly-ε-caprolactam or polyamide-6 (PA-6) was first studied by Von Brown in 1905–1910, and 30 years later commercialized as *Perlon*™. In the year 1936, PA-66 and several other aliphatic and semi-aromatic polyamides were disclosed (Carothers 1937). Two years later, du Pont introduced *Nylon*™. PA-11 was commercialized in 1955, PA-12 in 1966, PA-612 in 1970, and PA-46 in 1987. In 1976 du Pont started production of the *super tough* PA blends (Damm and Matthies 1990). In 1991 consumption of the thermoplastic PAs was estimated at 1.2 Mt. Comparative properties of the better-known PAs are listed in Table 1.54.

Liquid crystal aromatic polyamides (PARA), poly(*meta*-phenylene isophthalamide), *Nomex*™, and poly(*para*-phenylene terephthalamide), *Kevlar*™-49, were commercialized in 1961 and 1965, respectively. Amorphous aromatic polyamide, *Trogamid*™, was introduced in 1969, and polyphthalamide *Amodel*™ in 1991.

PA started to be blended with other engineering resins at the end of the 1960s, viz., PA with POM (Moncure 1969; Asahi Chem. 1969), PA with POM and PET (Fujiwara 1971), PA-6 reactively compatibilized with PET (Reimschussel and Dege 1969), PA-6-co-diisocyanate copolymer with PET (Illing 1970), etc. By the year 1970, the number of PA blends rapidly started to increase. The main efforts were directed toward improvement of toughness and processability of PA. Reactive compatibilization and impact modification became an integral part of the PA-blends technology.

Table 1.55 PA(1)/PA(2) blends

PA(1)	PA(2)	Comment	References
PA-66	PA-6 or PA-610	Reduced residual stresses in moldings	Stott and Hervey 1958
X-linked PA-66	PA-6 or PA-11	Excellent impact resistance	Uniroyal 1968
PARA	PA-6, PA-66, PA-610, PA-11, or PA-12	To improve the impact strength	Dynamit Nobel 1969
PA(1)	PA(2)	Miscibility/immiscibility studies	Zimmerman et al. 1973
PA-6I6T	Another PA at 1:1	Tough and strong fibers or films	Unitika 1982
PA-6	PA-11	Toughened by sulfonated EPDM	Weaver 1983, 1985
PA-66	Either PA-6, PA-612, PA-11, or PA-12	Printability, clarity, barrier, and dimensional stability	Mollison 1984
PA-6	Poly(trimethyl hexamethylene terephthalamide)	Resistant to cracking when exposed to metal halides	Ube Ind., 1984, 1985
PA-66	PA-6	SMM-MA and mineral filler	Asahi Chemical Industry 1985
PA-66	PA-6	With aminosilane-treated GF	Toray Ind., 1985
PA-mXD6	PA-66 and PBT, or PA-6	Tough, high-T, films; good barrier against O_2 permeation	Mitsubishi Gas Chem. 1985
PA-12	PARA	Transparent blends	Maj and Blondel 1993
PA-6I6T	PA-612 or PA-666, with PA-6, PA-11, or PA-12	At least 5 % shrinkage at 90 °C in at least one direction	Vicik 1994
PA-6 or PA-66	Semi-aromatic copolyamide	Compatibilized with either SMA, maleated EPDM, or MBA	Schmid and Thullen 1994
PA-66	PARA	Maleated elastomer and filler; low-T impact strength and HDT	Heger and Oeller 1994

1.6.1.1 PA(1)/PA(2) Blends

These blends are commercially available, e.g., *Zytel 3100*™ and *Grilon*™ *BT*. They show improved processability, solvent resistance, elongation, low-temperature impact and tensile strength, as well as enhanced barrier properties (see Table 1.55). They have been also incorporated into more complex, multicomponent systems, e.g., PA/PARA = 1:1, PPE, PCL, *ionomer*, EPR, a monomeric mixture of oxide and/or carbonate (e.g., ethylene carbonate, ethylene oxide, etc.), and a polyhydric alcohol (e.g., ethylene glycol or trimethylene glycol). The alloys were used to mold parts for the automotive, electrical, or electronic industries (Hamada et al. 1994).

1.6.1.2 PA/PPE Blends

PAs are excellent candidates for blending with PPE – each ingredient compensates for deficiency of the other. Since the resins are immiscible and brittle, they must be compatibilized and toughened. In consequence, PA/PPE blends comprise minimum four polymeric components: PA, PPE, a styrenic modifier, and an acidic compatibilizer. Usually PA is the matrix in which PPE/styrenic resin domains are dispersed. As time progresses, these blends are getting more complex – examples

are shown in Table 1.56. Commercial blends are *Artley*, *Dimension™*, *Luranyl™*, *Lynex™ A* and *Xyron™*, *Noryl™ GT*, *Remarry™*, *Ultranyl™*, *Vestoblend™*, etc.

1.6.1.3 PA Blends with POM, PEST, or PC

The immiscible blends with ≤ 5 wt% of either component were introduced first (e.g., POM with PA or PARA) before adequate methods of compatibilization were developed. Owing to the crystalline nature of these resins, the blends should also be impact modified. It is noteworthy that in blends of semicrystalline resins, the total crystallinity tends to increase (Nadkarni and Jog 1991). The compatibilization and impact modification are often accomplished using a multipolymer. For example, POM/PA-66 blends have been modified by adding either an ethylene-methylacrylate copolymer (EMAC), PEG (Kohan 1982), or a melamine-derivative "dispersant" (Tsukahara and Niino 1992, 1994).

In PA/PEST blends, PA improves the processability, mechanical properties, and solvent resistance of PEST. Examples of the developed PA/PEST blends are listed in Tables 1.57–1.58. PA blends with PC are similar to those with PEST. Since addition of PA to PC may lead to crystallization of the latter resin, also these blends should be compatibilized *and* impact modified (see Table 1.59).

1.6.1.4 PA/Specialty Polymer Blends

Addition of a small amount of PA improves processability of the specialty resin and is beneficial to performance of the GF-reinforced systems. Addition of specialty resin to PA enhances the thermal behavior and rigidity of the latter resin. For higher concentration of these ingredients, compatibilization and impact modification are required. Since PA is sensitive to heat, oxygen, and moisture, the compounding requires a special care. Examples are listed in Table 1.60.

1.6.2 Thermoplastic Polyesters (PEST)

Aromatic polyesters show good performance and have high T_m and HDT (see Table 1.61). Polyethylene terephthalate (PET) was invented in 1941 and commercialized as *Terylene™* fibers. The catalytic transesterification also lead to PPT, PBT, PHMT, PEN, etc. Polybutylene terephthalate (PBT) has better processability than PET and lower T_m. Poly(ethylene-2,6-naphthalene dicarboxylate) (PEN) has high modulus, strength, HDT, and excellent barrier properties. Polypropylene terephthalate (PPT) is a resin from shell. It combines the high crystallization rate of PBT with performance of PET. Polyarylates [-O-ϕ-C(CH$_3$)$_2$-ϕ-CO$_2$-ϕ-CO-]$_n$ (PAr) are linear amorphous polyesters, usually of bisphenol-A with isophthalic and terephthalic acids – they show intermediate performance between that of PC and PEST – high strength, stiffness, excellent impact strength, and HDT. Polyethyleneterephthalateglycol (PETG) is an amorphous copolymer of ethylene glycol and 1,4-cyclohexanedimethanol, with terephthalic and isophthalic acids. The block copolymers, having hard PBT segments and soft polyetherglycol ones, are versatile elastomers (e.g., *Hytrel™* from du Pont).

Table 1.56 PA/PPE blends

Composition	Comment	References
PPE/PA-12	Processability and performance	Komoto 1972
PPE/PA-66 = 1:1 with SBR-MA	First reactive compatibilization	Ueno and Maruyama 1981, 1982
PPE/PA and a compatibilizer	Compatibilized by SMA	Kasahara et al. 1982
PPE/PA and a compatibilizer	Polycarboxylic acid derivatives	Abolins et al. 1985
PPE/PA and a compatibilizer	With citric acid	Gallucci et al. 1985
PPE/PA and a compatibilizer	With oxalic dihydrazide	Lohmeijer et al. 1986
PPE/PA and a compatibilizer	Acid chloride of trimellitic, terephthalic, or 1-acetoxyacetyl-3,4-dibenzoic acid	Aycock and Ting 1986, 1987, 1994
PPE blended with PTO and MA and then compounded with PA-12	Processability, impact strength, solvent resistance, and HDT = 156 °C	Droescher et al. 1986
PPE/PA and a compatibilizer	Core butylacrylate-MMA; shell SMA	Van der Meer and Yates 1987
Amino-terminated PPE with PA-MA	Mechanical properties, low-T ductility	Fujii et al. 1987
PPE/PA and a compatibilizer	Addition of SEBS-MA	Modic and Gelles 1988
PPE-MA with bis-2-hydroxy ethyl fumaramide, PA, and functionalized ethylene-α-olefin elastomer	*Dimension*™ commercial blends with high elongation, impact strength, HDT, and dimensional stability	Akkapeddi et al. 1988, 1992b
PPE/PA and a compatibilizer	Either EPR-MA, EVAc-GMA, MA, or bis(4-phenyl isocyanate)	Nishio et al. 1988, 1994
PPE functionalized with trimellitic anhydride acid chloride and dimethyl-*n*-butyl amine, PA and PDMDPhS	PDMDPhS with carboxylic acid, amine, epoxy, anhydride, or ester groups	Smith et al. 1990, 1994
PPE/PA and a compatibilizer	Compatibilized by organic diisocyanates	Pernice et al. 1992
PPE/PA and a compatibilizer	By aromatic nitro-derivative	Bencini and Ghidoni 1993
The above blends were modified with styrene-butadiene radial copolymer	Threefold increase of the Izod impact strength	Gianchandai et al. 1993
The above blends were modified with tapered block copolymer	Further improvement of the impact strength	Yates 1993
PPE capped with trimellitic anhydride acid chloride and blended with PA-66	Toughened by addition of SEBS	Aycock and Ting 1994
PPE/PA and a compatibilizer	Either EPR-MA, E/GMA, or E/VAc/GMA, citric, malic, or agaric acid	Ishida and Kabaya 1994
Modified PPE with PA and SEBS	Moldability and mechanical properties	Kodaira et al. 1994
PPE modified with glycidol or epichlorohydrin, with PA or PEST	Either PP-MA, PP-GMA, *ionomers*, or EVAl was added	Arashiro et al. 1994

(*continued*)

Table 1.56 (continued)

Composition	Comment	References
PPE-MA with PA and SEB	Selectively hydrogenated S-B di-block	Lee 1994
PPE capped with salicylic ester and SBS dispersed in PS, PA, PEST, or PEI	Resistance to loss of impact strength after recycling	Richards and White 1994
PPE, PA, POM, and a Lewis acid (e.g., trialkylboran or borate, boric acid or halogenated boron)	For automotive applications	Takayanagi et al. 1994
PPE dissolved in lactam(s) and then compatibilized and polymerized	The compatibilizer was either PPE-MA, SAA, or SMA	Samuels 1994

PESTs and PCs are known to have low melt strength and are difficult to process in operations involving elongational flows, viz., blow molding, stretching, or foaming. During foaming the cell size distribution is broad, the wall thickness variable and the mechanical properties are poor. To improve the melt strength, a diacid anhydride and a metal compound may be added during extrusion (Hirai and Amano 1993). These additives induce branching, increase MW, and strain hardening. Alternatively, linear and branched resins may be blended.

The branched macromolecules can be produced in reactions with polyols having 3–6 hydroxyl groups. This approach has been successful even for recycling post-consumer PET. For example, ≥ 25 wt% of a bPET with recycled PET were extruder blended with ≤ 20 wt% of a chain extender (e.g., partially neutralized ethylene-methacrylic acid ionomers, copolymers of maleic anhydride or glycidyl methacrylate, etc.). Downstream up to 5 wt% of a chemical or physical blowing agent was incorporated. The blends were used to produce rigid insulation, trays, food packaging, microwave cookware, oxygen and moisture barrier films, etc. (Muschiatti and Smillie 1995).

1.6.2.1 Polyester Blends

The largest group comprises the impact-modified PESTs – these were summarized while discussing commodity resin blends. The commercial blends with, e.g., SMA or acrylic rubber show good processability, rigidity, impact and tensile strength, as well as excellent weatherability, viz., *Arloy™* 2000, *Bexloy™*, *Celanex™*, *Pibiter™ HI*, *Rynite™*, and *Ultradur™ KR*.

The second largest group comprises different combinations of PEST, for example, PET/PBT, PBT/PAr, or PET/PEN. These have been mainly developed for improved processability, good surface properties, HDT, impact strength, and dimensional stability, viz., *Celanex™*, *EMC™*, *Valox™*, etc. Examples of their formulations and performances are given in Table 1.62.

1.6.2.2 PEST Blends with PC

The PEST/PC blends are immiscible (T_g of PC is depressed by ca. 20 °C) and brittle, requiring toughening. Usually, PC blends with PEST contain 10–20 wt% of ABS, ASA, or MBS. In most commercial blends, PC is the matrix, but blends

Table 1.57 PA/PET blends

Composition	Comment	References
PA/PET blends		
PET/PA-6	With α,α-dimethylol-propionic acid	Reimschussel and Dege 1969
PET with PA-6-co-diisocyanate	Compatibilized and toughened blends	Illing 1970, 1973
PET with PA-66	Crystallization rates and mechanical properties	Nakamura and Neki 1981
Reactive PA/PEST blends	Direct coupling	Mitsubishi Petrochem. 1984
Reactive PA/PEST blends	Catalyst, *p*-toluenosulfonic acid	Pillon and Utracki 1984, 1986
Reactive PA/PEST blends	With *phenoxy*	Robeson 1988
PA/PET blends	Polyamide-polyester block copolymer	Maresca and Shafer 1988
Reactive PA/PET blends	Butylacrylate-methyl-acrylate block copolymer	Tsumiyama et al. 1988
Reactive PA/PET blends	Phosphoryl azide reactive coupler	Bhattacharje et al. 1990
Reactive PA/PET blends	PET containing toluenosulfonic acid groups	Van Sluijs et al. 1992
PA blends with PBT or PAr		
Non-compatibilized PA/PBT	To enhance PBT crystallinity	Toray Ind. 1983
Reactive PA/PBT blends	Acidified ethylene copolymer	Sheer 1982
Reactive PA/PBT blends	Maleated PS	Mitsubishi Petrochem. 1985
Reactive PA/PBT blends	Epoxy compounds	Urabe and Ikuhara 1989
Reactive PA/PBT blends	Either SGMA or SMA	Watanabe and Inozuka 1991
Compatibilized PA/PBT	Low molecular weight PBT	Goetz et al. 1993
1:1 PAr with PA, PET, or PBT	Transparent, impact resistant	Asahara et al. 1977a, b
PAr with PA-6 and Si-compounds or PET	Processability, high gloss, chemical, mechanical, electrical properties, and HDT	Unitika 1982, 1983, 1984
PAr with PA or PARA	PA-co-PAr added; single T_g	Dean 1990, 1992

formulated for low-T impact strength (down to $-40\ °C$) have co-continuous morphology and are reinforced by addition of ≤ 30 wt% of GF. It is vital to avoid reduction of PET crystallinity during blending or processing. The main advantage of the PC/PEST alloys is the increased stiffness, reduced susceptibility to stress cracking on contact with fuels, and an improved resistance to chemicals and fuels. The blends show good processability, heat resistance, ductility, HDT, high modulus at high temperature, good electrical properties, thermal stability, impact, tensile and flexural strength over a wide temperature range, low shrinkage,

Table 1.58 Multicomponent PA/PEST blends

Composition	Compatibilizer	References
Amorphous PA or PARA, with either PEST, PC, PEC, or PAr	A polyamide-polyester block copolymer, PA-b-PEST	Maresca and Shafer 1988
PA blends with either PAr or PC	EGMA	Yuichi and Suehiro 1989
PAr/PA	Either ABS-MA or ABS-GMA	Yasue et al. 1989
PET, PA-6, and PO	EEA-GMA	Natarajan et al. 1994
PEST, EVAl, PA, and PEST (with Na- dimethyl 5-sulfoisophthalate groups)	An *ionomer* and PP-MA	Tajima et al. 1994
PEST/PA	Reactively blended in solid state	Al Ghatta 1994

Table 1.59 PA/PC blends

Composition	Comment	References
PA-12/PC	For electrical insulation	Okuzono and Kifune 1975
PA-12/PC with PSF, PPE, or PET	Moldability and mechanical performance	Okuzono and Kifune 1976
PA/PC	Toughened with SEBS	Gergen and Davison 1978
PARA/PC	Pearly looking, resistance to oils and water, good mechanical properties	Mitsubishi Chem. 1980
Polyestercarbonate (PEC) with PA	Compatibilized and toughened by MABS	Sakano et al. 1981, 1982
PC/PA-6	Compatibilized by addition of SMA	Dainippon Ink. 1983
PA/PC commercial alloys *Dexcarb™*	Polyesteramide, an elastomer, and either PP-MA or EPR-MA	Perron 1984, 1988
PC end-capped with trimellitic anhydride acid chloride and then reactively blended with PA-6 and MBS	Moldability, excellent Izod impact strength, and elongation	Hathaway and Pyles 1988, 1989
PA-6I with PC	High impact and tensile strength	Gambale et al. 1988, 1994
PC/PA-6; compatibilized	Polyethyloxazoline, PEOX, added	Thill 1989
PA blends with, either PAr or PC	Compatibilized and modified by EGMA	Yuichi and Suehiro 1989
PA blends with, either PAr or PC	With ABS-MA or ABS-GMA	Yasue et al. 1989
PA with, PAr or PC and PA-co-PC	With glycidyl isocyanurate	Derudder 1990
Branched, bPC, and ≥ 1 polymer from: PEST, styrenics, PA, PO, and TPE	Processability, solvent and impact resistance, mechanical properties	Kozakura et al. 1992, 1994
PC and/or PEC with PA-6	With acrylic elastomer	Heger et al. 1992
PC/PA-6/ABS	With imidized polyacrylates	Leitz et al. 1992
PC/PA-6 with PEI and/or TPU	With butyl glycidyl ether, EPR-MA, or EPDM-MA	Perron et al. 1993
PA-6/PC/SEBS/SEBS-MA	20-fold increase of impact strength, 50-fold increase of elongation	Industrial Technology Institute, Japan 1996

Table 1.60 PA specialty polymer blends

Composition	Comment	References
1. PA/PSF blends		
PSF with PA-11	For improved impact properties	Nield 1971
PA/PSF with poly(sulfone-g-lactam)	Processability and mechanical properties	McGrath and Matzner 1972
PA-6/PSF	Processability, thermal and mechanical properties	Kyo and Asai 1978
PARA/PES	HDT = 172 °C and mechanical properties	Hub et al. 1986
PA-46/PES	Mechanical and thermal properties	Koning and Vroomans 1992
PARA/PES	Mechanical and thermal performance	Bapat et al. 1992
PAES or PES blended with PA-6T6	High heat resistance and stiffness	Weber and Muehlbach 1993
2. PA/PPS blends		
PARA with a small amount of PPS	Moldability, HDT, and impact strength	Shue and Scoggins 1981
PA-46 with PPS	Impact and mechanical properties, HDT, heat, and chemical resistance	Chiba et al. 1978
PPS with polyphthalamide (PPA)_	Heat and chemical resistance, HDT, mechanical properties	Chen and Sinclair 1990
PPS with PPA and GF	Mechanical properties	Davies 1990
PPS/PA with EPDM and MA	Compatibilized-*cum*-impact modified	Yu and Beever 1992
PPSS with either PA or PEST	Mechanical properties, HDT, dimensional and chemical stability	Ishio and Kobayashi 1992
PPS, either PA-66 or PA-MXD6 and Mg(OH)$_2$	Tensile strength, arc tracking, and heat resistance	Dubois et al. 1993
3. PA/*phenoxy* blends		
PA-6 with *phenoxy*	Excellent ESCR	Schober 1973
PA-66 with *phenoxy* and SEBS	Tensile and impact strength	Freed 1975
PA with PEST, *phenoxy*, and MBS	Tensile and impact properties	Robeson 1988
4. PA/PEA blends		
PA-12 with PEA	Tough, flexible, heat and hot oil resistant	Sumitomo Chem. 1984
PEBA/PA (ABS, MBS, NBR, SBR, or EPDM)	Impact strength at low-T, *Rilsan*™	Arraou 1986
5. PA/PAI blends		
PAI with PA-66 or PARA and inorganic filler	Moldings with high mechanical performance	Toray Ind. 1979
PI, PA, PAI, or PI + PA and aromatic PI	Miscible blends for selective permeation	Ekiner and Simmons 1993
6. PA/PEI blends		
PEI with PA or PEST	Processability	Giles and White 1983

Table 1.60 (continued)

Composition	Comment	References
PEI with PA-6 and PEI-b-PA	Impact strength	Robeson and Matzner 1984
PEI with PA-6 or PA-66	Compatibilized by nonyl-phenolic	Gallucci 1988
PEI with PA-12	Reduced shrinkage and water absorption	Giles 1987
Copolyesteretherimide, PEEI *Lomod*™, blended with either PA or PARA	Thermal aging behavior	Angeli 1992

Table 1.61 Comparative properties of PEST's

Property	PC	PET	PPT	PBT	PEN	PETG	PAr
Tensile modulus (MPa)	2,300	2,800	2,500	2,600	2,400	6,700	2,200
Tensile strength (MPa)	62	81	68	52	82	34	60–70
Maximum elongation (%)	120	70	–	200	100	110	7–100
Density (kg/m^3)	1,200	1,375	1,350	1,300		1,250	1,190–1,210
T_g (°C)	149	98	80	60	117	88	> 180
T_m (°C)	220	255	225	223	337	–	–
HDT (°C)	280	167	149	136	109	70	120–175

and good dimensional stability, but they may have poor weatherability, and their solvent resistance (while superior to that of PC) is moderate. The commercial blends include *Alphaloy*™ *MPB*, *Baitaloy*™ *VL*, *Cycolin*™, *Dialoy*™, *Ektar*™, *Hyperlite*™, *Eastalloy*™, *Idemitsu*™ *S*, *Impact*™, *Lumax*™, *Malecca*™ *B*, *Makroblend*™, *Maxloy*™, *Novadol*™, *Novaloy*™ *B*, *Petsar*™, *Pocan*™, *Sabre*™, *Stapron*™, *Techniace*™ *TB*, *Triax*™ *400*, *Ultrablend*™, *Valox*™, and *Xenoy*™. The blends are mainly used for automotive body panels, in outdoor power or recreational equipment, appliance housings, telecommunications, etc.

The PC/PEST blends were first described in 1966. The first, three-component blends were disclosed in 1972 (see Table 1.63). Many multicomponent alloys comprise PC and PEST. From between them, these with PPE are particularly important – see the following part.

1.6.2.3 PEST Blends with PPE

Blending PPE with either PEST or PC poses similar problems – the polymers are immiscible and brittle, hence require compatibilization and toughening. The PEST/PPE blends are multicomponent systems, with ≥ 5 components: PEST, PPE, styrenic copolymer, compatibilizer, and impact modifier. Examples of commercial blends are *Dialoy*™ *X*, *Gemax*™, or *Iupi-ace*™. For improved modulus and dimensional stability, they are usually reinforced with GF. These alloys are known for excellent processability, high solvent resistance, and dimensional stability. Evolution of these systems is outlined in Table 1.64.

Table 1.62 Examples of PEST blends

Composition	Comment	References
First PET/PBT blends	Enhanced crystallizability, miscibility	Heywang 1966
PBT with 40 wt% PAr	For electrical insulation, films, moldings	Wiener 1969
First modified PET/PBT blends	Toughening with butyl rubber	Hiri and Kotama 1971
PET with PA	For good frictional resistance	Fujiwara 1971
PAr with either PC or PEST	Moldability and impact strength	Koshimo et al. 1973
PBT with PET or PHT	High elongation and impact strength	Tsunawaki et al. 1973
PBT with PC	Impact resistance and elongation	Matsukane and Azo 1973
PBT with PPE	Processability and mechanical properties	Nakamura and Toyomoto 1974
PET with PC	High stress corrosion resistance	Horiuchi and Kamiya 1974
PAr with PEST and PA-6 or PPS	Further enhancement properties	Asahara et al. 1977a, b
PET/PBT blends	Modified by of acrylic elastomers	Kamata et al. 1978a
PAr with acetate-capped POM	Processability of POM	Gale 1978
PAr with either PET or PBT	Transparency, HDT, and impact strength	Fukushima et al. 1979
PET/PBT/SEBS	Impact, heat, and tensile strength	Wambach and Dieck 1980
PBT/PET/PC	Impact strength, rigidity, strain at break	Goedde et al. 1980
PBT/PET/*phenoxy* and a toughener	Butylacrylate-glycidyl methacrylate-MMA	Charles and Coleman 1981
PAr with PCT	Processability, weatherability, impact	Robeson 1981
PAr/PEST with TPU	High modulus while retaining strength	Robeson et al. 1981
PAr, PET, and EEA, TPU, etc.	To improve impact resistance and HDT	Robeson 1981, 1982
PET/PBT or PEST/PC, toughened	Toughener: MBS, ACM, or ABS, etc.	Bier and Indner 1982
PBT with either POM or PA	Impact modified by an ionomer	Sheer 1982
PET/PBT and, e.g., EGMA	Processability and performance	Memon and Myers 1983
PBT reactively blended with PAr	High impact strength	Toga and Okamoto 1983
PET with PAr and PA-6	Processability, gloss, HDT, transparency	Unitika Ltd. 1983
PAr with PEST and PC, ABS, PA	Processability blends, set of properties	Robeson 1985
PAr/PEST with EGMA or EPR grafted with glycidyl oxybenzyl acrylamide	Excellent processability and performance	Toyoda et al. 1986
PET/PC/PCT, EPR, and/or MBA	High impact resistance	Romance 1990

(*continued*)

Table 1.62 (continued)

Composition	Comment	References
POM, POM-copolymer, aliphatic polyester and polyether	Processability, crystallization, low shrinkage, HDT, and mechanical prop.	Makabe et al. 1991
POM/TPU/EBA-GMA/PA or PEST	Processability and mechanical properties	Subramanian 1992
PEST/POM and isocyanate or isothiocyanate coupling agent	Processability, mechanical properties, and low gloss	Katsumata and Matsunaga 1992, 1993, 1995
Solution-prepared PAr/PET	Immiscible: two Tgs and $\chi > 0$	Chung and Akkapeddi 1993
Blend of linear and branched PET	For high-quality mineral water bottles	Greaves et al. 1993
PET with PCT	High impact strength at low-T	Stewart and Bell 1995
PET with PEN	Transesterification reducing crystallinity	Wu and Cuculo 1998

1.6.2.4 PEST Blends with Specialty Resins

PESTs are immiscible with polyphenyl sulfides (PPS) or polyphenylenesulphidesulfone (PPSS). The customary three types of uncompatibilized blends are known, with 5–10 wt% of the dispersed (either PPS or PEST) phase and the phase co-continuity. The compatibilized blends (with a copolymer containing either epoxy or acid anhydride groups) show high tensile and impact strength (Nishiyama et al. 1990, 1991a, b) that can further be improved by addition of a TPE (Nishiyama and Nakakita 1991). PPS/PEST blends were also compatibilized by addition of a PPS-PEST copolymer (Suenaga and Ishikuwa 1991). The alloys could be reinforced with GF, talc, mica, wollastonite, or clay (Gary 1993).

Polyarylethersulfone (PAES) (-[O-ϕ-O-ϕ-SO$_2$-ϕ-]$_{0.25n}$-[O-ϕ-SO$_2$-ϕ-]$_{0.75n}$-) blended with either PAr, PEST, PC, or their mixtures showed well-balanced mechanical properties and good environmental stress-cracking resistance (Robeson and Harris 1985, 1986). For improvement HDT, mechanical properties, and flame retardancy, PET was blended with a PAES: (-[-ϕ-SO$_2$-ϕ-O-ϕ-C (CH$_3$)-ϕ-O]$_n$-) (El-Hibiri et al. 1992). Blends of this type PAES with PC, PET, ZnBO$_3$, and PTFE had high flame retardancy (Jack et al. 1993).

Polyetherimide (PEI) was blended with PAr for improved moldability and mechanical properties (Holub and Mellinger 1981). Similarly, polyestercarbonate (PEC) was blended with either PEI, PA, PI, PAI, or their mixtures, to give alloys characterized by high HDT and tensile strength (Quinn 1984). Blends of PEI, PAr, and PC showed good moldability, flexural strength, and modulus (Holub 1990). Also PEI, PET, and PEC blends had good processability and impact strength similar to PEI (Quinn and Holub 1986). Adding ABS to PEI/PEST blends enhanced the impact resistance (Gaafar 1990). PEI was also blended with PBT and a cross-linking triallyl cyanurate and triallyl isocyanurate (Hosoi 1991). To produce soft, flexible, dimensional stable, and water-resistant materials, polyesteramide (PEA) was blended with PET (and/or PA-6) (Toray Industries, Inc. 1982).

Table 1.63 PEST/PC blends

Composition	Comment	References
PBT with PC and MBS	Processability, chemical resistance, impact	Nakamura and Toyomoto 1974
PET/PC with a compatibilizer-impact modifier	Butylacrylate-styrene-triallyl isocyanurate, grafted with MMA and styrene	Kamata et al. 1978b
PCT with PC and branched PC	Good clarity, tensile strength, and notched Izod impact strength	Mohn et al. 1979
PBT/PC with *Acryloid*™	Moldability and high impact strength	Motz 1980
PBT/PC and PEC	High impact strength and strain at break	Dieck and Cohen 1980
PEST/PC, SEBS, PVAc, or (SB)$_n$ and butadiene-caprolactone-styrene	*Xenoy*™ alloys, with mineral filers or not	Dieck and Wambach 1980
PEST/PC, BR, and an impact modifier; *Makroblend*™	With (meth)acrylic esters (and acrylonitrile, acrylate rubber, ACM, EVAc, and/or ABS)	Cohen 1980, 1982; Bier and Indner 1982
PET/PC, butyl rubber (BR)	Good overall performance	Teijin Chem. 1983
PEST, PC, PO, and MBA	High impact strength alloys	Boutni and Liu 1983
PEST, PC, BR, an acrylic elastomer, *HIA-15*, and PMP	Good sets of mechanical properties	Teijin Chem. 1983
Reactively blended PEST, PC, and an acidified elastomer	Tensile strength, impact resistance, and electrical conductivity; *Tafmer*™	Mitsubishi Chem. 1983
PEST/PC/ styrene-α-methylstyrene-acrylonitrile-butadiene	Good moldability, mechanical properties, and heat resistance	Biglione and Fasulo 1983
PEST/PC/2-methyl-1,3-propanediol	Improved HDT, elongation, and impact strength	Yoga et al. 1983
PBT/PC with AES	Greatly improved impact strength	Sumitomo Naug 1983
PC/PEST with EVAc	For uniaxially drawn shrink films	Weyer et al. 1984
PET/PC and 10–15 wt% *Acryloid*™	High impact resistance	Hepp 1984
PEST, PC, and an ethylene-acrylic acid-butylacrylate	High impact strength moldable compositions	Portugall et al. 1984
PC/PEST/elastomer/*phenoxy*	Impact-modified blends	Liu and Giles 1986
PC/PET, or PETG, EEA, and an impact modifier	Extrusion-blended, foamed, and then injection molded; $\rho = 900$ kg/m^3, good performance	Avakian and Jodice 1986
PEST, PC, and MBS-AA or GMA	High impact strength; *Ultrablend*™	Lausberg et al. 1987
PC/PEST and siloxane copolymer	Chemical, weather, impact resistance; *Dialoy*™	Hongo et al. 1987
PC/PET with ≥ 90 wt% PES	PES foamed by degradation of PET/PC	Haggard 1987
PC/PEST with acrylic elastomer	Improved impact strength	Sakai et al. 1989
PC/PEST and PE-MA wax	Improved impact strength	Liang 1989

(*continued*)

Table 1.63 (continued)

Composition	Comment	References
PET/PC/EPDM/PCL/EEA-MA	Chemically resistant, impact properties	Natarajan and Mininni 1991
PBT/PC, PO-GMA, or PO-MA	Moldability, toughness, strength, and stability	Fujie 1993
PBT/PC/ABS/PE-GMA or -MA, vinyl, styrene or (meth)acrylate	Impact strength conditions	Steendam et al. 1993

Table 1.64 PEST blends with PPE

Composition	Comment	References
Blends with unmodified PPE		
PPE/PBT/SBS	Processability, impact, and tensile strength	Lee 1978
PPE, PC, SEBS, and either PBT or PET	Stable morphology, processability, high impact strength, and solvent resistance	Brown et al. 1987
PPE/PET/PC/EGMA	For automotive applications	Yonetani et al. 1987
PPE/PET with SEBS-GMA	Excellent solvent resistance, moldability, impact and mechanical properties	Mayumi and Omori 1988
PPE/PET, EPR-MA, EVAc-GMA, MA or bis(4-phenyl isocyanate)	Processability, heat resistance, and mechanical properties	Nishio et al. 1988, 1994
PPE, PEST, PS, PC, SEBS, and/or acrylic modifier	High impact strength PPE alloys; *Gemax*™	Yates and Lee 1990
PPE/PBT with PC-b-PS-b-PC, PC, and either SEBS or MBS	Processability, tensile elongation and strength, as well as chemical and impact resistance	Brown and Fewkes 1992, 1994
PPE, PEST or TMPC, PS-VPh, HIPS	PEST is miscible with PVPh, thus PS-VPh is an efficient compatibilizer	Colby et al. 1993, 1994
PPE, PEST, PC-PBT, and SEBS	Excellent rigidity and impact strength	Chambers et al. 1995
Blends with modified PPE		
PPE modified with unsaturated dicarboxylate, e.g., fumaric acid	Reactively blended with PBT, PC, and SEBS for improved mechanical performance	Ishihara 1989
PPE modified with dimethylsiloxanes,	Blends with PPE, PEST, and SEBS for enhanced solvent and impact resistance	Brown 1989
PPE modified with an epoxy-compound	Blended with PPE, PEST, and hydrogenated poly-α-olefin for processability and impact resistance	Hasson and Yates 1993
PPE modified with end-capped with salicylic acid ester	Blended with SEBS and then dispersed in either PA, PEST, PEI, or PS; for processability, resistance to loss of impact strength after recycling	Richards and White 1994
PPE modified with either glycidol or epichlorohydrin	Blended with PP-MA, PP-GMA, *ionomers*, EVAl, PA, and PEST; for moldability, solvent and heat resistance, mechanical strength	Arashiro et al. 1994

The low-temperature phosphate glasses (LTG: -[-Zn-O-P(O_2Na)-O-P(O_2Li)-O-Zn-O-P(O_2Na)-O]-) have been blended with PET, PBT, PEK, PEEK, PPS, PEI, LCP, PC, etc. (Bahn et al. 1991). The blends containing up to 65 vol.% of LTG were reported to have good mechanical properties (Frayer 1993, 1994). The technology makes it possible to generate controlled morphology of the dispersed LTG phase as well as to ascertain its good bonding to the organic matrix.

1.6.3 Polyurethanes (TPU)

The polyester-type thermoset polyurethanes were commercialized in 1942, and the linear thermoplastic ones (TPU) 10 years later. Polyester-type TPUs, *Texin*™ resins for extrusion and injection molding, were introduced in 1961, whereas polyether-type, *Roylar*™, in 1971. Owing to great diversity of the ingredients, the TPU performance can be readily modified. For this reason, as well as because of the cost, TPUs are seldom blended. Their use can be divided into three groups: (i) blends with POM, (ii) blends in which TPU is used as a compatibilizer and impact modifier, and (iii) others.

1.6.3.1 POM/TPU Blends

The oldest and most common method of POM toughening is by incorporation of TPU. *Delrin*™ POM/TPU blends were commercialized in 1960. The others followed, e.g., *Celcon*™, *Duraloy*™, *Formaldafil*™, *Fulton*™ *KL*, *Hostaform*™, *RTP 800*, *TC*, or *Ultraform*™. These alloys have high impact strength and elastic recovery that depend on composition, morphology, as well as on the compounding and processing methods. Examples of these blends are listed in Table 1.65.

1.6.3.2 PC/TPU Blends

TPU has been used to toughen PC, to enhance its mechanical behavior and ESCR. The blends have been used in industrial and medical applications (De Boer and Heuschen 1988; Pinchuck 1991). Blends of PC/PET/TPU with EVAc-GMA and optionally MBS or ABS have good flexural modulus, strength, weld-line strength, solvent resistance, and impact behavior (Laughner 1994). PC blends with a polycaprolactone-polyurethane resin, TPU *Pellethane*™, and either MBS or MBA showed similar behavior (Henton et al. 1993).

Texin™ *3000* and *Texin*™ *4000* are the commercial blends. In the first TPU is the matrix, while in the second PC plays this role. The resins are used for the production of gears, tubings, housings, top-lifts, extruded profiles, and for the automotive industry and consumer goods.

1.6.4 Polycarbonate (PC)

Polycarbonates are polyesters of polyhydric phenols and carboxylic acid. Except for the lack of crystallinity, their properties resemble those of PEST. The most

Table 1.65 POM/TPU blends

Composition	Comment	References
POM with OH- NCO- or NCS-terminated TPU	To improve POM elasticity	McAndrew 1971
POM/TPU with mineral fillers	For enhanced stiffness	Reske and Wolters 1984
POM/TPU and polycarbodiimide and ethylene-*bis*-stearamide	Moldability and impact strength (POM was acetate end-capped)	Richardson 1984
POM/TPU	High impact strength at low-T	Drzal et al. 1986
POM, PC and TPU	High impact strength	Silvis et al. 1990
POM with polythioisocyanate-TPU	Impact and flexural strength	Sugiyama and Mochizuki 1990
POM/TPU and acrylics	Abrasion resistance and weatherability	Endo et al. 1990
POM/TPU and ABS	Processability, thermal and dimensional stability, chemical and creep resistance	Guest et al. 1991
POM/TPU, with SAN, ABS, AES, PC, PA, PAr, PPE, HIPS, acrylics, imidized acrylics, or SMA	For lower mold shrinkage, good stiffness, elongation, toughness, etc.	Flexman 1992
POM/TPU and EBA-GMA, with PA-612, PA-6, PP, or PET	Good modulus, impact strength, and processability	Subramanian 1992
POM/TPU and di-glycerin, pentaerythritol, *phenoxy*, or PVAl	Tensile strength and elongation at break, impact resistance, etc.	Nagai et al. 1993, 1994

common polycarbonate is that of bisphenol-A (PC), which was commercialized in 1956. PC is tough, transparent, self-extinguished, dimensionally stable, resistant to salts and oxidation, but susceptible to abrasion, stress cracking, and attacks by solvent, acids, and alkali. It is $T_g = 149\ °C$, but the ductile-brittle transition is at 0–10 °C. The resin ought to be toughened, for example, by addition of ABS, MBA, or MBS. The annual consumption and its growth rate of PC are, respectively, 700 kt and 5 %. About 40 % of PC is used in blends.

Originally, the commercial PC resins were linear polymers with high shear viscosity and low melt strength, thus difficult to process in operation involving extensional flows, viz., blow-molding stretching and foaming. Several years ago, branched PC (bPC) became available. The resin is usually blended with linear PC at the ratio that on the one hand is economically viable and on another that provides sufficient melt strength for the required process. For example, 60–95 wt% bPC (MW = 32–45 kg/mol) was blended with 5–40 wt% PC (MW = 15–27 kg/mol). The blends with MFR = 2–8 g/10 min were suitable for extrusion, injection molding, blow molding, and/or foaming at $T_{process}$ = 250–310 °C (Van Nuffel et al. 1998).

1.6.4.1 PC Blends with PPE

Blends of PPE with PC are immiscible and brittle; thus, they must to be compatibilized and toughened (see Table 1.66).

Table 1.66 Examples of PPE/PC blends

PPE/PC and	Comment	References
PS or SMMA and PEST	Compatibilizer: acrylic elastomer, *phenoxy*; or Cl-SBR	Izawa and Nakanishi 1973
PBT and SEBS	Processability, impact strength, solvent resistance	Brown et al. 1987
HIPS/PEST/SBS and PS grafted with 2-oxazoline (PSOX)	Advantageous set of performance characteristics	Avakian et al. 1988
Fumaric acid-grafted PPE and SEBS	Mechanical properties and low gloss	Ishihara 1989
PS, PEST, SEBS, and/or MBA	High impact strength	Yates and Lee 1990
PBT, PC-PS-PC block copolymer, and impact modifier	Excellent rigidity and impact strength	Brown and Fewkes 1992, 1994
SAN/PS – compatibilized	Poly(butylacrylate-co-styrene-co-acrylonitrile)	Niessner et al. 1993
PEST/ABS with PS, HIPS, SEBS, PA, PC, and/or PEST	Multicomponent blends prepared by reactive processing	Laughner 1993, 1994
PEST, PC-PBT copolymer, and SEBS	Good rigidity and impact strength	Chambers et al. 1995

1.6.4.2 PC/POM Blends

These blends are immiscible, thus should be compatibilized and toughened. Addition of POM to PC improves the solvent and chemical resistance (Miller 1972). PC blends with POM and TPU were easy to mold into articles having high impact strength (Silvis et al. 1990). POM-b-PC was used either as a compatibilizer or as a modifier of performance for such polymers as PES, PEEK, PA, and PAN (Dhein et al. 1993).

1.6.4.3 PC Blends with Specialty Resins

There is a great diversity of polyimides (PI) having $T_g = 180$–$420\,^\circ$C. Several were blended with PC to improve its stiffness, HDT, and strength. PEI/PC blends were commercialized in 1992 as *Ultem™ LTX*, for injection molding or extrusion. They show higher impact resistance than PEI and higher heat resistance than PC, as well as they retain the strength, chemical resistance, and the hydrolytic stability of PEI.

Fluoropolymers are notoriously immiscible with any other polymer. Usually, they are dispersed in blends of engineering and specialty polymers either to improve processability or to induce lubricity and abrasion resistance. Examples of the PC/specialty resin blends are listed in Table 1.67.

1.6.5 Polyoxymethylene (POM)

Polycondensation of formaldehyde was reported by Butlerov in 1859, but only in 1950 du Pont developed end-capping that prevented unzipping. POM is crystalline, thus rigid, brittle, and chemically nonreactive. Production of *Delrin™* and *Celcon™* started in 1959 and 1962, respectively. The world consumption of POM and its annual growth rate are 500 kt and 5 %.

Table 1.67 PC blends with specialty polymers

Composition	Comment	References
1. PC/Siloxane resin blends		
PC with PDMS	Solution cast films with good properties	Caird 1961
PC and/or PEST with siloxane-based vinyl copolymer	For chemical, weather, and low-temperature impact resistance	Hongo et al. 1987
PC with poly(dimethyl siloxy biphenylene oxide)	Transparent, flame, and impact-resistant alloys	Jordan and Webb 1992
PC with siloxane/vinyl-based copolymer	Thermal stability, ductility at low-T, and impact resistance	Derudder and Wang 1993
PC, or polyestercarbonate with PC-b-PDMS	Low-flammability, impact strength over a wide T	Hoover 1993
PC/PArSi and SBS	Excellent mechanical properties	Jordan and Webb 1994
2. PC/PSF blends		
PAES: [-φ-C(CH$_3$)$_2$-φ-O-φ-SO$_2$-φ-O-]$_n$, with PC	Impact, tensile strength, elongation at break	Union Carbide Corp. 1966
PC with PAES and MBS or AES	Impact and tensile strength, HDT	Grabowski 1971
PC with PAES and CHR	Good impact and fire resistance	Lauchlan and Snodgrass 1973
PSF with linear *and* branched PC	Improved solvent resistance	Binsack et al. 1979
PSF with PEC	Impact strength and flame retardancy	Quinn and Rosenquist 1982
PC and polycarbonate-sulfone grafted with ethylhexyl acrylate	High impact strength	Tyrell et al. 1984
PAES with PC, PAr or PEST	Well-balanced mechanical properties	Robeson and Harris 1985, 1986
PSF/PC with PET or PBT and GF	Performance, solvent, and chemical resistance	Militskova et al. 1993
PC/PAES with MBA	BR grafted with MMA, styrene, and/or AN; then (shell) MMA, styrene, AN	Weber and Muehlbach 1993
3. PC/Fluoropolymer blends		
PC with ETFE	Processability, lubricity, and abrasion	Kawai and Miyauchi 1974
PC with PP and with PTFE	Improved performance	Kishimoto 1976
PC/PVDF with co-polyacrylics	Miscible, yellowish films, T$_g$ = 120 °C	Leibler and Ringenberg 1986
PC with PTFE	Processability, lubricity, and abrasion	Akega 1991
PC with PTFE, ABS, and cresol novolak phosphate oligomers	Improved performance, flame resistance	Fuhr et al. 1992
4. PC/Polyimide blends		
PC with SMI	Improved stiffness, HDT, and strength	Fava 1979, 1981
PC with PEI	Processability, flexural and impact strength	Giles 1983, 1984

(*continued*)

Table 1.67 (continued)

Composition	Comment	References
PEI/PAr, PC, and phenyl phosphate	Improved melt stability	Peters and Rock 1989
PEI with PAr, PC and HIPS	Flexibility and impact resistance	Holub and Rock 1989
PEI with PAr and PC	HDT, flame, and impact resistance	Holub 1990
PC with PAI	Mechanical and antistatic properties	Shimamura and Suzuki 1991
PC with a carbodiimide: $(X)_m$-$(-N = C = N-Y-)_p$-$(-N = C = N-X)_m$	For sheath optical fibers	Kamps et al. 1994

The most common POM blends are homologous mixtures of POMs having different molecular structures (linear, branched, cross-linked) (Matsuzaki 1991), different molecular weights (Ishida and Sato 1970), or with different end groups (Nagasaki et al. 1991; Hanezawa and Ono 1991). On the second place are blends of POM with TPU, preferably polyester type. POMs are also blended with core-shell acrylic elastomers, MBS or MBA. Commercial blends of POM with PEST are available. To improve weatherability of POM, the resin was blended with PMMA and a fluoropolymer (viz. PTFE, PVF, PVDF) (Katsumata 1991).

For the manufacture of sliding parts, POM blends were developed with PTFE (Ishioka 1991); with PVDF (Shibata et al. 1992); with either wax, PTFE, silicone oil, or PEG; and with EBA-GMA (Takahashi and Kobayashi 1993). Later blending technology of POM involved introduction of the reactive end groups – it makes compatibilization with other polymers relatively simple.

Addition of PPE/PS to POM was used to improve processability, HDT, and mechanical properties (Ishida and Masamoto 1974). Then, POM with a Lewis acid was incorporated into PPE/PA blends to improve compatibilization and induce high heat and impact resistance (Takayanagi et al. 1994). POM blends with specialty polymers are formulated either to take advantage of POM (the resistance to abrasion) or of the specialty resin (e.g., to improve stiffness and wear resistance by incorporation of PEEK or PEI) (Suzuki and Nagahama 1987). POM is miscible with polyvinylphenol, PVPh; thus addition of PVPh to blends of POM with COPO compatibilizes the system (Machado 1993).

1.6.6   Polyphenylene Ether (PPE)

In 1956, by oxidative coupling of *2,6*-dimethyl phenol, poly(2,6-dimethylphenyl ether) was obtained (PPE) (Hay 1959, 1964, 1967, 1968). The resin was commercialized in 1964. PPE is amorphous (T_g = 210 °C), but it can crystallize (T_m = 257 °C). It is thermally stable only to T $\leq$ 150 °C (CUT = 125 °C). It has good rigidity, creep resistance, dimensional stability, and high electrical, chemical, moisture, and flame resistance. The main disadvantages are processability, oxidative degradation, low-impact strength, and weatherability. The resin is usually

"plasticized" by blending with styrenics. The annual production and growth rate of PPE are, respectively, 300 kt and 9 %.

1.6.6.1 PPE Blends

The first PPE blends with PS and polydiphenylsiloxane (PDPS) were reported to be transparent, colorless solids that turn into liquid at 85 °C (Boldebuck 1962). Since then PPE has been modified by blending (e.g., with HIPS, ASA, MBA, SBS or SEBS, etc.), by grafting (Brown 1989), or by reacting its end groups (Richards and White 1994).

Modified PPE is mainly blended with other engineering resins – most of these were already discussed. The principal types of PPE blends are with styrenics, with PA, and with PEST. Owing to miscibility of PPE with PS, the compatibilization is relatively simple. However, blending PPE with either PA or PEST is more challenging, since these systems require reactive compatibilization. Development of PPE grafted with acidic functionality was motivated by this need.

PPE has been blended with most specialty resins – the latter usually as a minor component. Exceptions are the PPE/PPS alloys. Their performance depends on the level of PPS crystallinity. The commercial blends, *DIC PPS* (introduced in 1982), were developed for the electrical, electronic, and mechanical industry. These show good processability, reduced flash in injection molding, toughness, high heat, and chemical resistance.

Several blends of PPE with specialty resins are parts of multicomponent systems. For example, PI was blended with PPE and then cured. The alloys were used as rigid and stable matrices for manufacturing fiber-reinforced composites (Camargo et al. 1986). Similarly, end-capped PPE was blended with SEBS and then dispersed in either PEI, PA, PEST, or PS, to give improved resistance to loss of impact strength after thermal recycling (Richards and White 1994). Blends of PAI with PPS and at least one of either PA, PEST, PC, PPE, PSF, PES, PEI, PEK, PEEK, PPS, PEST, PA, PEA, or siloxanes were compatibilized with aromatic polyisocyanates. The systems showed excellent flowability, high heat resistance, and mechanical strength (Kawaki et al. 1995). Examples of PPE/specialty polymer blends are listed in Table 1.68.

1.6.6.2 Miscible PPE Blends

Miscibility of PPE with PS has been known since 1960. Later, two other PPE blends were announced miscible. PPE blends with polytransoctanylene (PTO) can be processed at 260 °C and have HDT ≥ 194 °C. The patents suggested that PTO is miscible with PPE (Jadamus et al. 1986, 1987). The PPE blends with polyphenyl methacrylate, poly(*p*-methoxy phenyl methacrylate), poly(benzyl methacrylate), or poly(3-phenyl propyl methacrylate) were reported to have the lower critical solution temperature, LCST = 105–150 °C (Fischer and Siol 1993, 1995).

Immiscible, but transparent, are blends of PPE with a copolymer of cyclohexanedimethanol, ethylene glycol, and terephthalic acid (PCTG) – the clarity was achieved by closely matching the refractive indices at the use temperature. The alloys also show good processability, thermal dimensional stability, and economy (Stewart and Massa 1993).

Table 1.68 PPE specialty polymer blends

Composition	Comments	References
1. PPS/PPE blends		
PPS with PPE/PSF and/or PC, GF	The first, reactively compatibilized blends	Bailey 1977
PPS with a styrene-grafted PPE and polyetherester rubber	Good toughness, impact, and tensile strength	Dainippon Ink and Chem., Inc. 1982
PPS/PPE with EPR-MA, EBA-MA, SGMA, EVAc-GMA, etc.	Reactive blending, yielded reinforcing spherical PPE particles $d = 0.01–10\ \mu m$	Nishio et al. 1988, 1994
PPS/PPE/core-shell graft copolymer	Toughened by silicone elastomer particles	Sasaki et al. 1989
PPS/PPE with SEBS and PP	Tough blends	Maruyama and Mizuno 1990
PPS + ABS, PPE, PC, PA, PEST	Presence of macromers with epoxy group	Tsuda and Azuma 1991
PPSS with PPE, PC, PA, or POM	Impact strength, mechanical properties	Ono et al. 1991
PPE/PPS and polymethylene-phenylene-isocyanate with GF	Mechanical and welding properties, solvent resistance	Gotoh and Nagaoka 1993
PPE/PPS/core-shell MBS or SEBS	PPE reacted with trimellitic anhydride acid chloride and dimethyl-n-butylamine	Dekkers 1994
PPS/PPE/EBA-GMA blends with particle size $d = 0.001–10\ \mu m$	Impact resistance, stiffness, heat resistance, moldability, appearance	Orikasa and Sakazume 1994
PPE with co-poly(arylene sulfide), $[(-\phi\text{-S-})_{1-x}(-\phi\text{-S-S-})_x]_n$	Processability, good mechanical properties	Bagrodia et al. 1994a
2. PSF/PPE blends		
PSF, POM with PPE	High HDT	Ikeguchi and Nagata 1974
PC/PA-12 and PPE/PSF	Moldability and mechanical performance	Okuzono and Kifune 1975, 1976
3. PI/PPE blends		
PPE/SBR grafted (SBMI)	Improved performance	Fava and Doak 1980
PPE/SBS, styrene-phenyl-maleimide	HDT, impact, and solvent resistance	Fukuda and Kasahara 1982
PI with PPE, PPS, PEI, or PSF	Moldability, stability, mechanical strength	Ohta et al. 1988
PEI with PPE-MA	Mechanical performance	White and van der Meer 1989
Two PPEs with polyetherimide-silane copolymer	Processability, flame-retardant properties, and impact strength	Haaf 1992
4. PEBA/PPE blends		
PEBA with PPE and triglycidylisocyanurate	Non-delaminating behavior, good rigidity, and strength	Brown et al. 1992

Table 1.68 (continued)

Composition	Comments	References
5. PPE/fluoropolymer blends		
PPE with poly (hexafluoropropylene-co-vinylidene fluoride)	Thermoformable, high HDT, and flame resistance	Snodgrass and Lauchlan 1972
PPE with PVDF, SMMA, and SEBS	Improved impact strength and elongation	Van der Meer et al. 1989

1.7   Specialty Polymers and Their Blends

The *specialty* resins are expensive, produced in relatively small volumes either for a specific application or looking for a market niche. Their $T_g > 200$ °C and modulus > 3 GPa. In 1991 the total world consumption of polysulfones (PSF) and polyethersulfones (PES) was 8.5 kt. Blends of the following polymers are known: polyfluorocarbons, polysiloxanes, sulfur-containing polymers (PPS, PPSS, PES, and PSF), polyetherketones (PEK, PEEK, PEKK), polyimides (PI, PEI, and PAI), PAr, COPO, polyphosphazene (PHZ), and LCP.

1.7.1   Fluorocarbon Polymers

Known in Germany since 1933, polytetrafluoroethylene (PTFE) is a semicrystalline resin (92–98 % crystallinity), with $T_m = 342$ °C and melt viscosity of $\eta \approx 10$ GPas. Other more common fluoropolymers are polychlorotrifluoroethylene (PCTFE), *Hostaflon™* commercialized in 1934, fluorinated ethylene-propylene (FEP), *Teflon™-FEP* introduced in 1972, and numerous copolymers with $T_m = 260$–304 °C, processable at $T_{process} = 315$–425 °C and having the degradation temperature $T_{deg} = 425$–440 °C. The fluoropolymers are characterized by stability at high temperatures; toughness and flexibility at low temperatures; low friction, insolubility, and inertness to chemicals; low dielectric losses; and high dielectric strength. The world consumption of fluoropolymers in 1991 was 72 kt.

In blends, fluoropolymers are used in small quantities to enhance throughput, reduce the frictional properties, and increase the wear resistance. Blends comprising 0.3–50 wt% of a low molecular weight PTFE ($T_m \leq 350$ °C) with engineering resin showed improved antifriction properties (Asai et al. 1991). LLDPE generally exhibits sharkskin melt fracture, but the use of fluoropolymer additives, such as the copolymer of vinylidene fluoride and hexafluoropropylene, can help to eliminate the extrusion instability (Hatzikiriakos and Migler 2005).

PPS and PEEK which blended with fluoro(co)polymers and reinforced with either CF or GF were wear resistant with a short break-in period for forming a self-lubricating film (Davies and Hatton 1994). Many commercial blends contain fluoropolymers (primarily PTFE) for the improved weatherability and wear and solvent resistance: *SUPEC™* – "self-lubricating" blend of crystalline PPS with

PTFE and 30 wt% GF, *Lubricomp*™ blends from LNP and similar *RTP*™ blends from RTP Co. (e.g., 15 wt% PTFE, 30 wt% GF, and any of the following resins: ABS, PA, PEST, PC, PE, PEI, POM, PP, PPE, PPS, PS, PSF, PVDF, SAN, TPU, PEEK, PES, etc.), *Sumiploy*™ from Sumitomo Chem. Co., etc. (Utracki 1994).

1.7.2 Siloxane Polymers

Polysiloxanes, [-O-Si(RR′)-], are linear resins that can be branched or cross-linked into elastomers. They have high compressibility, permeability to gases, low T_g and viscosity, exceptional weatherability, low surface tension coefficient, and are relatively expensive. Siloxane polymers or copolymers have been incorporated into engineering or specialty resins to improve processability, toughness, HDT, and solvent and weather resistance.

The main polymers of this type are polydimethylsiloxane (PDMS) and polymethylphenylsiloxane (PMPhS). Their $T_g = -127$ and -86 °C, respectively. They start oxidizing at 290 °C and 375 °C and undergo structural rearrangement at 435 °C and 410 °C. Polysiloxanes have been used as high temperature impact modifiers that improve the flame resistance, processability, and optical properties. Several commercial blends are on the market, viz., *Rimplast*™ (high tensile, flexural, and Izod impact strength PAs), *Dialoy*™ (PC/PET blends with good chemical, weather, and low-T impact resistance), etc. Evolution of polysiloxane blends with engineering and specialty resins is summarized in Table 1.69.

1.7.3 Polyarylene Sulfide (PPS)

Polyarylene sulfides (PPS), (-φ-S-)$_n$, was commercialized in 1971 as *Rayton*™ *R*. The resin is semicrystalline with $T_g = 194$ °C and $T_m = 288$ °C; thus $T_{process} \geq 290$ °C. PPS is difficult to mold – it tends to adhere to the mold surface and to flow into mold crevices. It has also relatively poor impact resistance. Blends have been developed to alleviate these problems, e.g., with 25 wt% of either PSF, PPE, or PC (Bailey 1977). Commercial PPS blends are available with PPE (e.g., *DIC PPS* commercialized in 1982, *Noryl*™ *APS*), PARA (*RTP 1300*), or PTFE (*Lubricomp*™ *PPS*). They show good processability with reduced flash, are tough, excellent wear, as well as high heat, solvent, chemical, and oxidation resistance.

PPS has been frequently blended with PSFs. The latter resins are mainly amorphous, frequently transparent, with $T_g = 196–288$ °C, able to maintain high-performance characteristics over a wide temperature range, but poor weatherability, notched impact strength, and ESCR. The PPS/PSF blends have been developed to improve PPS processability and/or the mechanical performance over a wide range of temperatures, to improve PSF weatherability, impact, and ESCR characteristics. Evolution of these blends is outlined in Table 1.70.

PArs are aromatic amorphous polyesters, viz., *U-polymer*™, *Ardel*™ *D-100*, *Durel*™, *Arylon*™, etc. Their $T_g \approx 188$ °C and HDT = 120–175 °C. Blends with

Table 1.69 Polysiloxane blends

Composition	Comments	References
1. PA blends		
PA, vinyl-terminated PDMS, siloxane with Si-H groups and Pt	Tensile, flexural, and notched Izod impact strength	Arkles 1983, 1985
Acidified PPE, PA, PDMDPhS	Flame resistance	Smith et al. 1990, 1994
2. PEST blends		
PET with PDMS and MABS	Impact and embrittlement resistance	Sauers and Barth 1970
PEST and/or PC with siloxane-based vinyl-grafted copolymer	Chemical, weather, and low-temperature impact resistance	Hongo et al. 1987
PEST/PC/PPE/star-block copolymer	Impact-modified engineering resins	Hoxmeier 1994
PEST and siloxane-acrylic elastomer	Impact strength at low temperature	Yamamoto et al. 1992, 1994
3. PC blends		
PC with PDMS	Solution cast films	Caird 1961
PC with siloxane and elastomer	Impact resistance	De Boer and Heuschen 1988
PC with PArSi	Transparent, flame and impact resistant	Jordan and Webb 1992, 1994
PC or PEC with PC-b-PDMS	Low flammability and good impact strength,	Hoover 1993
PC with elastomeric polysiloxane/polyvinyl-based graft copolymer	thermally stable, low-T ductility, impact, and heat resistance	Derudder and Wang 1993
4. POM blends		
POM/PDMS adsorbed on silicone	For sliding parts with high wear resistance	Takayama et al. 1991
5. PPE blends		
PPE, PS, and PDPS	Clear, transparent, colorless solids at 65 °C	Boldebuck 1962
PPE-g-siloxane and SEBS	Enhanced solvent and impact resistance	Brown 1989
Poly(bisphenol-A dimethylsiloxane) with PPE, PAr, PI, PEST, or PC	HDT, reduced melt viscosity	Herrmann-Schoenherr and Land 1993, 1994
PArSi with PPE and SBS	Flame retardancy	Jordan and Webb 1994
6. PEI blends		
PEI with poly(carbonate-b-siloxane) and EPDM, ABS, MBS, or MMBA	Processability, impact strength	Giles and White 1983
PEI with PArSi	Processability, flame retardancy	Jordan and Webb 1994
PArSi with PPE and SBS	Flame retardancy	Jordan and Webb 1994
7. PPS blends		
PPS/PDMS, trialcoxysilane, and PO	Processability and impact strength	Liang 1987
PPS/PBT, silane, and GF	Chemical resistance and toughness	Serizawa et al. 1992

(*continued*)

Table 1.69 (continued)

Composition	Comments	References
PPS with silicone and acrylate elastomer lattices	Improved heat and impact resistance	Koshirai et al. 1992, 1994
PPS-g-amine with PDMS-g-epoxy	Improved tensile elongation and strength	Han 1994
8. PHZ blends		
PHZ or its copolymer with a siloxane polymer and/or elastomer	Bisazoformamide (foaming agent) gave semirigid, highly flame-retardant foams	Dieck and Quinn 1977

PPS have been developed to improve the performance of PAr – processability, rigidity, and hydrolytic stability.

To the category of amorphous, aromatic polyamides (PARA) belong polyphthalamides (PPhA), e.g., *Amodel*™ (T_g = 127 °C, T_m = 310 °C, HDT = 285 °C, CUT = 180 °C). PPS/PARA blends were formulated to increase the reinforcing effects of GF on PPS. They show good processability, mechanical performance, and resistance to thermal degradation.

Polyimides (PI) were introduced in 1962 as thermally non-processable *Kapton*™. To improve processability, the main-chain flexibility was enhanced by incorporating segments with higher mobility, viz., polyamide-imide (PAI), polyetherimide (PEI), polyimide-sulfone (PISO), etc. These polymers are characterized by high T_g = 150–420 °C and thermal resistance. They are blended with PPS to enhance its moldability, thermal stability, and mechanical performance.

Polyaryletherketone (PEEK), [-ϕ-CO-ϕ-O-ϕ-O]$_n$, was commercialized in 1980 as *Victrex*™. It is a tough resin with T_g = 143 °C and T_m = 334 °C. Blends of PEEK with PPS show synergistic effects toward tensile and flexural strength as well as the impact resistance.

The inorganic low-temperature glasses (LTG) with $T_g \leq 300$ °C are durable and water resistant. LTG was blended with either PPS, PET, PBT, PEK, PEEK, PEI, LCP, PC, or fluorinated polymers (Frayer 1993, 1994).

Oxidation of PPS by addition of N_2O_4 in a sulfuric acid solution results in the incorporation of surfoxide groups, leading to either polyphenylenesulfidesulfoxide or polyphenylenesulfoxide. Their blends with high temperature resins (viz., PSF, PES, PPS, PEI, PAr, PEEK, PC, PI, PAI, LCP, fluoropolymers, cycloolefins, and their alloys or composites) produced high temperature-resistant foams by heating for 5–60 min at T = 300–470 °C (Scheckenbach et al. 1998). The process reduced the moldings' density by at least 50 %.

1.7.4   Polysulfone (PSF)

Polyarylsulfones (PSF or PSU), or polyarylethersulfones (PAES), have the chain structure (-ϕ-SO$_2$-)$_n$. The commercial resins include *Udel*™ PSF,

Table 1.70 PPS blends

Composition	Comments	References
1. PPS/PSF		
PSF/PPS with 45 parts of a styrene-butadiene rubber (SBR)	The first PPS/PSF blends – to improve the impact strength	Asahi Chem. Ind. Co., Ltd. 1981
PPS with PSF and 5–40 wt% PTFE	Processability and resistance to corrosives	Bailleux et al. 1984
PSF/PPS/PSF-b-PPS copolymer	Impact strength, uniformity, and cohesion	Hashimoto 1986
PPS/PPSS {PPE, PC, PA, POM}	Impact strength and mechanical properties	Ono et al. 1991
PPS with either PSF or PPSS	Improved interfacial adhesion and moldability	Bagrodia et al. 1993, 1994a, b
45–60 wt% PSF, 25–45 wt% PPS, and 0–10 wt% MBS	Resistance to impact, high-T performance, weatherability – for car body panels	Golovoy and Cheung 1994
2. PPS/PAr		
PAr with 40 wt% PET and PPS	Enhancement of properties	Kyo et al. 1978
PAr with 1–99 wt% PPS	Processability, impact, fire, and abrasion resistance	Matsunaga et al. 1978
PAr/PPS and chloro-hydro-dimethano-di-benzocyclo octene	good hydrolytic stability, moldability, and flame retardancy	Salee 1980, 1981
PAr/PPS, ABS, or acrylic elastomer	Excellent hydrolytic stability	Salee, 1982
3. PPS/PARA		
PARA with a small amount of PPS	Moldability, HDT, and impact strength	Shue and Scoggins 1981
PPS with a small amount of PPhA and GF	Mechanical properties, adhesion (NH_2 with GF), and aromatic parts of PPhA with PPS	Davies 1990
Reinforced blends of PPS with PPhA and POCA	High degradation temperature, chemical resistance, HDT, mechanical properties	Chen and Sinclair 1990
95–5 wt% PARA with PPS	High resistance to heat and thermal aging; improved melt flow	Yamamoto and Toyota 1992
PPS with 25–95 parts of either PA-66 or PA-MXD6 and $Mg(OH)_2$	Excellent tensile strength as well as arc, tracking, and heat resistance	Dubois et al. 1993
4. PPS/PI		
PPS with 60 wt% PI	To improve moldability at 310 °C	Alvarez 1977
PI with PPS, PPE, PEI, or PSF	To improve the moldability of PI	Ohta et al. 1988
PPS, 20–65 wt% PAI, and 4,4′-diphenyl methane diisocyanate	Processability, heat, chemical, and solvent resistance, mechanical strength	Kawaki et al. 1992, 1994, 1995
5. PPS with PEEK and LTG		
PPS with 10–90 wt% PEEK	Processability, strength, and impact resistance	Robeson 1982
PPS/PEEK/PMP, GF, organosilane	Mold release and reduced molding flash	Hindi et al. 1994
Low-temperature glasses (LTG) with 35 wt% PPS	Rigidity, dimensional stability, strength	Frayer 1993, 1994

$[-\phi-C(CH_3)_2-\phi-O-\phi-SO_2-\phi-O-]_n$ (T_g = 196 °C and CUT = 160 °C), *Astrel*™ $[-\phi-\phi-SO_2-\phi-O-\phi-SO_2-]_n$ (T_g = 288 °C), *Victrex*™ PES $[-\phi-SO_2-\phi-O-]_n$ (T_g = 228–232 °C), *Radel*™ *R* PPSF $[-\phi-\phi-O-\phi-O-\phi-SO_2-\phi-O-]_n$ (T_g = 220 °C), *Ultrason*™ *E*, *Talpa*™ *1000*, *Sumilite*™, polyimidesulfone, PISO, *Amoron*™ polythioethersulfone, PTES, etc. Then there is the sinterable polyphenylenesulfone, *Ceramer*™ $[-\phi-SO_2-\phi-]_n$ (T_g = 360 °C, $T_{decomp.}$ > 450 °C), used as an "additive" to high-performance polymers used in harsh environment (Ceramer 1996).

PSFs are transparent; flame resistant; have high strength, modulus, and hardness; and HDT > 200 °C. They show excellent resistance to thermal and irradiation degradation, but are difficult to process (high melt viscosity) and have low ESCR and poor weatherability. The latter properties can be improved by blending and/or reinforcing. PSF blends comprise high-performance resins, viz., PPE, PPS, PTFE, etc., with such compatibilizers/impact modifiers as *phenoxy*, EVAc-GMA (Gaafar 1990), SMA copolymers (Golovoy and Cheung 1994), siloxane-polyarylene polyether copolymers, or high temperature MBS. *Mindel*™ *A* and *Arylon*™ are examples of the commercial ASA/PSF blends. They show good processability, toughness, plateability, and heat and water resistance.

Addition of a small amount of PSF to a variety of resins improves hardness, the notched Izod impact strength, plateability, hydrolytic stability, and shape retention at high temperatures. Many PSF blends of or with engineering resins have been developed, viz., with PA, PEST, PC, PPE, or POM. They have high HDT, heat resistance, strength, stiffness, mechanical properties, and ESCR. Polysulfone blends have been foamed using water and either N_2 or CO_2 (Bland and Conte 1991). The blend comprised at least two sulfone polymers, e.g., PES and PSF, and at least one non-sulfone polymer (e.g., PS, PPE, PEI, PC, PA, PEST, PP, or PE). The nucleating agent was either talc, mica, silica, Zn-stearate, Al-stearate, TiO_2, or ZnO. The foams were used as insulation for high temperature structural applications. Since in the preceding part PPS blends with PSF were described, in Table 1.71 examples of PSF blends with other specialty resins are listed.

1.7.5 Polyetheretherketone (PEEK)

Polyaryletherketones (PAEK) are aromatic polymers with ether and ketone linkages in the chain, viz., PEK, PEEK, PEEKK, etc. Polyetheretherketone (*Victrex*™ PEEK), $[-\phi-CO-\phi-O-\phi-O-]_n$, was commercialized in 1980 (T_g = 143 °C, T_m = 334 °C). Commercial blends of PEEK include *Sumiploy*™ PEEK/PES/ PTFE, PEEK/LCP, *Cortem*™ PEEK/LTG, etc. Evolution of PEEK blends' technology is outlined in Table 1.72.

1.7.6 Polyimides (PI, PEI, or PAI)

Polyimides (PI) have imide group, $-R-N = (CO)_2 = R'-$, in the main chain. Owing to a variety of possible R and R' groups, their T_g = 180–420 °C. To improve

Table 1.71 PSF/PI blends

Composition	Comments	References
1. PSF/PI		
PAI with 0.1–50 wt% of either PSF, PA, or PARA	Improved melt flow and good mechanical properties	Toray Industries, Inc. 1979, 1980, 1981
PES/PPBA (T_g = 200–300 °C)	For lacquers and homogenous, clear films	Patton and LaMarre 1983
PEI with PSF, PP, PEC, or PAr; with PC and PEST, PAr or PA, etc.	For good processability, improved flexural and impact strength	Giles, 1983, 1984
PI with 0.01–10 phr PSF solution cast	For films with good blocking resistance	Mitsubishi Chem., 1984
PI with PEI, PES, PAr, PC, PEEK, or PPE, e.g., PI: PEEK: PEI = 1:1:1	T_g = 175 °C, used as crack-resistant coatings with good adhesion to metal	Camargo et al. 1986
PI with PSF, PPS, PPE, or PEI	Moldability, heat and chemical resistance	Ohta et al. 1988
PES with PEI	Improved HDT	Melquist 1993
PES/sulfonyl *bis*(phthalic anhydride)-co-*bis*(*p*-amino cumyl) benzene	Processability, solubility, mechanical, and thermal properties	El-Hibri and Melquist, 1993
LCP-type PI with PES, PI, PEI, PAI, PEK, or PEEK	Remarkably good processability and excellent thermal stability	Okawa et al. 1994
PES/PI (e.g., *XU*-218 or *PI*-2080) miscible blends (single T_g, UCST)	High moduli, tensile strengths, and impact strengths	Karasz and MacKnight 1994
2. PSF blends with fluoropolymers		
PSF/PPS/5–40 wt% PTFE fibrils	Processability, lubricity, anticorrosive	Bailleux et al. 1984
PES/0.3–50 wt% low MW PTFE	Self-lubricity	Asai et al. 1991
PSF/PC or PET, ZnBO$_3$, and PTFE	Flame-retardant, synergistic properties	Jack et al. 1993
Fluorine-containing polycyanurates with PSF, PP, or PEEK	Flame-retardant, low thermal expansion, T_g = 180–320 °C, stable to 430–500 °C	Ardakani et al. 1994
3. PSF blends with other specialty resins		
PES, with poly(*p*-phenylene ether-co-*p*-phenylenesulfonyl)	Miscible, transparent solvent-cast films, with good water and chemical resistance	Newton 1981
PSF with 70 wt% polyether-amide (PEA)	Moldability, high HDT and mechanical properties	Hitachi Chemical Co., Ltd., 1983
PSF/acrylic elastomer/ polyphosphates	Thermal stability, flame retardancy, toughness	Schmidt, 1983
PEEK/PAES with HDT = 157 °C	Low warpage and shrinkage, rigidity, stress-cracking, solvent, and impact resistance	Harris and Robeson 1986, 1987
PES, PEEK, and 20 wt% PEI	Mechanical properties and heat resistance	Rostami 1987
PES/95-75 wt% PEEK	Chemical and hot-water resistance	Tsumato et al. 1987

<div align="right">(<i>continued</i>)</div>

Table 1.71 (continued)

Composition	Comments	References
PAEK, PAE, or PPE, blended with LCP, PI, PAES, or PEST	Processability (warp-free moldings), mechanical properties, and high HDT	Harris and Michno 1988
PES with phenoxy	Chemical resistance and tensile strength	Kraus et al. 1991
PSF with PVP or PEG, radiation cross-linked	For selectively permeable membranes or hollow fibers	Kobayashi and Tanaka 1992
Biodegradable PLA with either PSF, PC, PI, PPE, etc.	To improve the thermal properties	Nemphos and Kharas 1993
PES dissolved in oligooxybenzoyl acid and then polymerized to POBA	Molecular composites, polymerizing while shearing	Tochioka 1993

Table 1.72 PEEK blends with specialty resins

Composition	Comments	References
PEEK/PAI and optionally with PPS	Solvent resistance, hydrolytic stability	Harris and Gavula 1986
95–75 wt% PEEK with PES	Chemical and hot-water resistance	Tsumato et al. 1987
POM/10 phr of PEEK and/or PEI	Wear resistance without loss of slipperiness	Suzuki and Nagahama 1987
PEK/PAI and zinc sulfate hydrate	Good moldability and high impact strength	Smyser and Brooks 1990
LTG with either PEK, PEEK, PPS, PEI, LCP, PC, PET, PBT, or fluorinated polymers	Processability, mechanical properties, stiffness – *Cortem™ Alloys* with either LCP or with PEEK	Bahn et al. 1991
Crystalline and amorphous PEK with PAr	Good flowability and processability	Falk and Herrmann-Schoenherr 1992
POM-b-PC with PES, PEEK, PA, or PAN	Film-forming thermoplastic polymeric alloys	Dhein et al. 1993
ASA, PC, PEST, PEC, PPE, PPS, PEEK, PES, PSF, and/or PPE	Toughened by 30–80 wt% elastomer, e.g., SEBS and core-shell graft copolymers	Niessner et al. 1994
PPS blends with PEEK	Improved mold release and reduced flash	Hindi et al. 1994
PI, PAI, PSF, PEI, PES, PEEK, PPS, or PPE and a polyether-b-polyamide or polyether-b-polyester	Easy to mold blends, flexible and elastic, with excellent chemical and thermal resistance	Movak et al. 1994
PEKK/PEI = 70/30 w/w co-reacted through the terminal amine group of PEI and ketone one of PEKK	Resulted compound with strain hardening was water foamable at T = 335–350 °C, whereas neither PEKK nor PEI can be foamed	Brandom et al. 1997

Table 1.73 PI blends

Composition	Comments	References
PEI with PAr	Moldability and mechanical properties	Holub and Mellinger 1981
PEI/PAI = 1:1	Mechanical properties and ESCR	Maresca et al. 1981
Polyarylethers with PEI	Good ESCR	Robeson et al. 1981
PEI, poly(carbonate-b-siloxane), and EPDM, ABS, MBS or MMBA	Processability and impact strength	Giles and White 1983
PEI, PA-6, and PEI-b-PA	Moldability and impact strength	Robeson and Matzner 1984
PEI with polyestercarbonate (PEC)	High HDT and tensile strength	Quinn 1984
PEI/0.5–20 wt% of a fluoropolymer	Mold release, heat resistance, and shrinkage	Sumitomo Chem. 1985
PI with PAI in the full range of composition	Foamed during the final stage of the condensation reaction at T = 120–320 °C	Long and Gagliani 1986
PI, with PPS, PPE, PEI, and PSF	Moldability, heat stability, chemical resistance, and mechanical strength	Ohta et al. 1988
PEI with PPE-MA	Mechanical performance	White and van der Meer 1989
PEK with either PES, PEI, PEEK, PEST, PAr or PPS, and filler	Processability, mechanical strength, as well as heat and flame resistance	Murakami et al. 1991
PEI, PBT, and triallyl cyanurate and triallyl isocyanurate	High thermal deformation resistance and HDT	Hosoi 1991
Low-temperature glasses with PEI	High modulus, mechanical performance	Bahn et al. 1991
Polyether-b-polyimide-b-siloxane copolymer with low MW PEI	Impact-resistant materials with excellent processability and HDT	Durfee and Rock 1993
PPS/PEI with 30 wt% GF	High flow and no flash	*Supec™ CTX530*
Fluoro-elastomers dispersed in a resin, e.g., PI, PAI, PSF, PEI, PES, PEEK, PPS, PPE, etc.	Moldings: flexible, elastic, self-lubricating, having excellent chemical and thermal resistance	Movak et al. 1994
LCP-PI with either PI, PEI, PAI, PES, PEK or PEEK	Remarkably good processability and excellent thermal stability	Okawa et al. 1994
PBI with 0–95 wt% of PEI	Thermo-oxidative stability	Haider and Chenevey 1994
PI blended with PMS and then foamed by the thermal decomposition of PMS	Nano-foams showed increased craze zone size and higher crack stability than the not-foamed PI films	Plummer et al. 1995; Charlier et al. 1995

processability, flexible groups were incorporated into the main chain. Examples of blends of these resins are listed in Table 1.73.

Polyamideimides (PAI) were obtained by polycondensation of imides with aromatic diamines, $[-N=(CO)_2=\phi-CO-NH-R-NH-CO-\phi=(CO)_2=N-]_n$ ($T_g = 275$ °C, HDT = 265–280 °C). The resin has high tensile and impact strength from T = −190 to T = 260 °C, dimensional stability, good dielectric properties, solvent and chemical

resistance, flame retardancy, good UV stability, and low outgassing in high vacuum. To improve processability, PAI was blended with PA, PSF, or PEST (Toray Industries, Inc. 1979).

Polyetherimide (PEI), [-N(CO)$_2$-ϕ-O-ϕ-C(CH$_3$)$_2$-ϕ-O-ϕ(CO)$_2$CN-ϕ-]$_n$ (T$_g$ = 215–220 °C, HDT = 217 °C, CUT = 170 °C, no weight loss at T $\leq$ 400 °C), was commercialized as *Ultem™*. The resin has high tensile modulus (even at elevated temperatures), approaching that of many glass-reinforced resins. Commercial PEI blends include these with PC (*Ultem™ LTX* introduced in 1990), with PPS (*Supec™ CTX530*) (Utracki 1994), or with polyphenylsulfone (Sanner and Gallucci 2011).

Polyimidesulfone (PISO) was introduced in 1986 *Celazole™* (T$_g$ = 249–349 °C). This transparent resin with flexural modulus of 4.8 GPa and tensile strength of 63 MPa has shown excellent solvent and creep resistance.

1.7.7 Aromatic Amorphous Polyamides (PARA)

There is a great diversity of amorphous aromatic or semi-aromatic polyamides (PARA). The commercial resins include *Trogamid™*, *Quiana™*, *Amodel™*, etc. They have been blended to improve the mechanical properties and impact strength, as well as to enhance the barrier properties of the matrix resin to permeation by gases or liquids. Examples of blends with PARA are listed in Table 1.74. Blends of PARA were also discussed along other blends of polyamides.

Table 1.74 Blends with aromatic amorphous polyamides (PARA)

Composition	Composition	References
PARA with POM	Toughness and impact strength	Asahi Chem. Ind. 1969
PARA with semicrystalline PA	Improved oxygen barrier properties	Dynamit Nobel 1969
PAI with PA-66 or PARA	Processability and mechanical properties	Toray Ind. 1979, 1981
PARA with PC	Nacreous, resistant to oils and boiling water	Mitsubishi Chem. 1980
PARA with 5–95 wt% PPS	Improved moldability, HDT, and impact strength	Shue and Scoggins 1981
PARA with PA-6I6T	For strong fibers or films	Unitika Co., Ltd. 1982
PARA with PES	Increased HDT and mechanical performance	Hub et al. 1986
PPS with PPhA and GF	Stiff, high-performance reinforced alloys	Davies 1990
PARA with maleated PP or PE	Sliding electrical parts, resistance to thermal degradation in contact with Cu	Iwanami et al. 1990
PARA with rubber-modified PS	Transparent, having near-zero birefringence	Angeli and Maresca 1990
PARA with PAr are miscible	Processability, mechanical properties, solvent, weather, HDT, impact and stress-crack resistance	Bapat et al. 1992

Table 1.75 Blends with linear, aromatic polyesters (PAr)

Composition	Comments	References
PAr with PC and PET	Improved impact resistance	Koshimo 1973
PAr blends with PET	Transparent and impact resistant commercial blends	*U 8000* from Unitika or *Ardel™ D-240* from Amoco
PAr/PET = 1:1 with PA-6 or PPS	Enhanced mechanical properties	Asahara et al. 1977a, b
PAr with 1–99 wt% PPS	Processability, impact strength, fire and abrasion resistance	Matsunaga et al. 1978
PAr/PPS and dodecachloro-dodeca-hydro-dimethano-di-benzocyclooctene	Good hydrolytic stability, moldability, and flame retardancy	Salee 1980, 1981
PAr/PET/PPS with ABS or MBS	Improved hydrolytic stability	Salee 1982
PAr with PA-6, *U-polymer™* X-9	Processability, mechanical properties	Unitika, Ltd. 1982, 1983
PAr with polybenzimidazole (PBI)	Miscible blends	Chen et al. 1990

1.7.8 Polyarylates (PAr)

These polyesters, $[\text{-O-}\phi\text{-C(CH}_3)_2\text{-}\phi\text{-CO}_2\text{-}\phi\text{-CO-}]_n$ ($T_g \approx 188$ °C and HDT = 120–175 °C), were introduced in 1974. The commercial resins include *U-polymer™*, *Ardel™*, *Durel™*, and *Arylon™*. Their advantages include transparency, good weatherability, and high HDT. PAr has been blended with nearly all resins, including ABS, EPDM, *ionomers*, LCP, PA, PB, PBI, PBT, PC, PEI, PEK, PET, *phenoxy*, PMB, PS, PPE, PPS, etc. Three types of PAr blends are of particular importance – those with polyesters, PEST, polyamides, PA, and polyphenylenesulfide, PPS. A summary of PAr blends is provided in Table 1.75.

1.7.9 Aliphatic Polyketone (COPO)

This copolymer of carbon monoxide with ethylene and propylene is semicrystalline, with $T_g = 15\text{–}20$ °C, $T_m = 110\text{–}242$ °C (Ballauf et al. 1941). *Carilon™* resin (introduced in 1995) is a strictly alternating copolymer, $[\text{-CO-C}_2\text{H}_4\text{-}]_n$, obtained using metallocene catalyst. It has $T_m \approx 220$ °C, tensile strength $\sigma = 80$ MPa, and elongation at break $\varepsilon = 25\%$. The moldings have outstanding wear and friction resistance, high resilience over a wide temperature range, low sensitivity to water and organic solvents, and good barrier properties, but they are sensitive to UV. Several blends of COPO have been patented, e.g., with SAN (miscible blends), PA-6, and SEBS-MA (Machado 1992), with TPU (George 1992), and with POM and PVPh (Machado 1993).

1.7.10 Blends with Rigid-Rod Polymers

Three types of blends belong to this group: (1) molecular composites, i.e., the molecular LCP solutions, (2) immiscible blends of LCP, and (3) blends of electroconductive polymers.

1.7.10.1 Molecular Composites

In fiber-reinforced composites, the absolute size of the reinforcing fibers is not important, but good adhesion to matrix and the length-to-diameter ratio of the fiber, L/D ≥ 500, are (Piggott 1986). Accordingly, reduction of the reinforcing particle size from, e.g., GF or CF, to rigid-rod molecules seems desirable. If the reinforcement is to be provided by individual macromolecules, the rigid-rod polymer must form molecular solution in selected thermoplastic resin. Such systems are known as *molecular composites*, MC, first generated in the late 1970s (see Table 1.76).

MC can be prepared by dissolution of either the rigid-rod polymer in a monomer that subsequently can be polymerized or by dissolving monomer of the rigid-rod polymer in a thermoplastic resin and then polymerizing it. The selections of the soluble monomer/polymer pair as well as control of the polymerization and phase

Table 1.76 Molecular composites

Composition	Comments	References
Poly(*p*-phenylenebenzobisthiazole) with poly(2,5,(6′)-benzimidazole)	MC of oriented macromolecules; films and fibers had high modulus and strength	Hwang et al. 1983
Poly(*p*-phenylene terephthalamide) (PPTA) with PA-6 or PA-66 in methanesulfonic acid	Coagulation resulted in MC that upon thermal treatment phase separated	Chuah et al. 1989a, b
Poly(2,5,(6′)-benzimidazole) with PAr	MC miscible system	Chen et al. 1990
Rigid-rod [-CO-ϕ(CF₃)-ϕ(CF₃)-CONH-ϕ(CF₃)-ϕ(CF₃)-NH-] in vinylpyridine or pyrrolidone	Polymerization of the monomeric solvent resulted in MC	Stein et al. 1992
Polybenzimidazoles, 5–95 wt% with PARA blended in DMF	Miscible by film transparency, single T_g, FTIR, and X-ray diffraction	Calundann et al. 1992; 1994
PES dissolved in polyoxybenzoyl or *p*-aceto-aminobenzoic acid, polymerizing the latter at the shear rate of 2.0–13 1/s	Solvent-free MC, high modulus and strength, for the manufacture of fibers or rod-shaped extrudates	Tochioka 1993
70–99 wt% PGI, and either PBI or LCP, with PET or PC	Good balance of toughness, tensile modulus, and HDT	Hallden-Abberton et al. 1994
Dissolution of PA or PO in lactams and then polymerizing it into a rigid-rod, e.g., poly(*p*-aminoethyl benzoate) (PAEB)	MC: N-(*p*-amino benzoyl) caprolactam in molten maleated PP, PA-6, PA-66, or PARA and then polymerized; PA modulus x2	Mülhaupt et al. 1994
Poly[2,2′-(*m*-phenylene)-5,5′-bis benzimidazole] (PBI) with 0–65 wt% PEEK	Mechanical, thermal, and chemical properties; for gaskets, seals, valve seats, and O-rings	Andres et al. 1995

separation rates are critical. The IPN approach may "lock" the dispersed structure into a metastable system with sufficient stability for processing (Utracki 1994).

1.7.10.2 Liquid-Crystal Polymers (LCP)

There are several commercial LCPs, viz., *Ekkcel*™ (degrades at $T_{process}$ 400 °C), *Xydar*™, *Vectra*™, *E-konol*™, *X-7G*, *Ultrax*™, *KU 1-90*, *Granlar*™, *Novoaccurate*™, *Rodron*™, *Victrex*™, etc. LCPs are mainly used for injection molding of parts that require exact dimensions and high performance.

Large quantity of LCP is used in blends. These are immiscible, highly oriented systems, where LCP domains provide reinforcement. Since LCPs are expensive, either the desired performance must be achieved using a small amount of melt processable LCP, or the other component of the blend is similarly priced. In blends LCP can (i) improve processability of engineering and specialty polymer (Froix et al. 1981; Cogswell et al. 1981, 1983, 1984), (ii) enhance crystallization of semicrystalline polymers (Hong et al. 1992), (iii) improve stiffness and other mechanical properties in applications where fatigue strength is important (Yamauchi et al. 1991), (iv) provide external protective layer for solvent and/or abrasion sensitive resins, etc. Excepting those with PP, the LCP blends with commodity resins are scarce (see Table 1.77).

1.7.10.3 Electro-Dissipative and Electroconductive Blends

Most organic polymers are insulators. However, there are applications requiring dissipation of the electrostatic charge (ESD) or even electrical conductivity (ECP) that would be comparable to that of metals. The ESD materials should have the surface resistivity $10^{12} \geq R \geq 10^5$ Ω cm. The resistivity of ECP should be $10^5 \geq R \geq 10^{-2}$ Ω cm.

The ESD behavior can be provided by blending in a flexible-chain polymer with an active -OH or -SH group, viz., polyvinyl alcohol (PVAl), ethylene-vinylacetate (EVAc), polyvinylphenol (PVPh), a copolymer of ethylene oxide and epichlorohydrin (EO-CHR), maleated copolymer, aliphatic polysulfides, etc. These low performance resins have been incorporated into a variety of alloys and blends (see Table 1.78).

By contrast, the ECP must have conjugated rigid-rod macromolecules. Several such polymers show high electrical conductivity (usually after doping), viz., polyacetylene (PAc), polyaniline (PANI), polypyrrole (PPy), polyparaphenylenes (PPP), or poly-3-octyl thiophene (POT). The resins are expensive, difficult to process, brittle, and affected by ambient moisture, thus blending is desirable. For uniaxially stretched fibers, the percolation threshold is 1.8 vol.%; hence, low concentration of ECP (usually 5–6 vol.%) provides sufficient phase co-continuity to ascertain conductivity similar to that of copper wires (see Table 1.78).

As a synthetic strategy, simple and versatile reactive blending will continue to play a pivotal role in the development of newer materials. For example, the blending technique is being used to produce bulk heterojunction polymer solar cells (polymer/fullerene) and to develop electrically conductive polymer blends using electrically conductive fillers and additives (Huang and Kipouras 2012).

Table 1.77 Liquid-crystal polymer blends

Composition	Comments	References
1. LCP blends with commodity resins		
PP/LCP with PP-MW as a compatibilizer	LCP macromolecules stretched by simultaneous flow and crystallization in a static mixer	Baird and Datta 1992
PP/LCP	LCP macromolecules stretched in a counterrotating pipe die	Haghighat et al. 1992
PP/LCP	LCP macromolecules stretched under high injection molding stresses	Heino et al. 1993
LCP/PE	Viscosity reduction	Alder et al. 1993
LCP/cycloolefins (COP)	Processability	Epple et al. 1992
LCP and radiation cross-linkable resins	For articles that strain recover upon heating	Toy et al. 1994
2. LCP blends with engineering resins		
Poly(1,4-benzamide) or terephthalamide dispersed in PA	Rigid microfibrils enhanced modulus and improved the thermal behavior	Takayanagi et al. 1980
PET with 2 phr of poly[bis (4-methoxy phenyl)terephthalate]	Processability and excellent mechanical properties	Toray Industries, Inc. 1980
30 wt% PET with LCP	Processability, mechanical properties, HDT = 167 °C	Celanese Corp. 1981, 1984
PC with a wholly aromatic polyester, LCP	Mechanical, tensile and flexural, properties	Froix et al. 1981
PPE or PAEK with LCP, PI, PAES, or PEST	Processability, mechanical properties, and HDT	Harris and Michno 1988
PS/PPE/2–98 wt% of a LCP, stretched into submicroscopic fibers	Tensile strength, high modulus, satisfactory elongation, good impact strength, and high HDT	Isayev 1991, 1993, 1994
PBT with p-hydroxybenzoic acid-ethyleneterephthalate ($T_m \leq 300$ °C)	Co-reaction to increase η, thus orientability and mechanical performance	Dekkers et al. 1992
PC with PAr and LCP	Low anisotropy, high HDT, heat, and impact resistance	Izumi et al. 1992
LCP with PP, PS, PC, PI, etc.	Multiaxial molecular orientation of LCP	Haghighat et al. 1992
LCP with PC and PET or PBT	Ductility, toughness, strength, HDT modulus	Cottis et al. 1993
PBT with segmented block copolymer, LCP-b-PBT	For fibers having high modulus and strength	Farris and Jo 1993
PEI-LCP with PC, PBT, or PA	Processability and mechanical behavior	Bonfanti et al. 1993
LCP block copolymer of the type [rod]$_x$-[coil]$_y$ with PET, PBT, PA	For spinning fibers with high mechanical properties and low shrinkage	Dashevsky et al. 1993, 1994
LCP dispersed in either PEST, PC, PA, or modified PPE	Replacements for fiber-reinforced plastics – recyclable blends	Tomita et al. 1993, 1994

(*continued*)

Table 1.77 (continued)

Composition	Comments	References
LCP with PA, ABS, PC, PBT, PPE, PP, PC, or their blends	Compatibilized blends, used as replacement for glass fiber composites	Tomita et al. 1993, 1994
LCP with 3–15 wt% PAr	Matrices for conventional composites	Roemer and Schleicher 1993, 1994
LCP with PEST, PC, PAs, PI, etc.	Polymerization of LCP in polymeric matrix	Gupta et al. 1994
Poly(*p*-phenylene terephthalamide)/PA or PARA, and PEKK or PAN	Biphasic solution in sulfuric acid, spun, coagulated, stretched into PPD-T fibrils	Coburn and Yang 1994
Hydroxyalkylated PPE, hydroxyl-containing PO, PA, and LCP	Moldability, solvent and heat resistance, mechanical strength	Arashiro et al. 1994
Compatibilized blends of PET with 10–15 wt% LCP	Processing, nontransparent material with good mechanical properties	Bonis and Adur 1995
3. LCP blends with specialty resins		
PES with a small amount of LCP	Improved flowability and processability	Cogswell et al. 1981
PPS, LC-polyesters and LC-poly (esteramides)	Processability and physical properties	Froix et al. 1981
PEI with 35–95 wt% LCP, self-reinforced polymer compositions	LCP fibers, tensile strength, modulus, elongation, impact strength, HDT	Isayev and Swaminathan 1989
LCP with PI, PAES, or PEST and either PAEK, PAE, or PPE	Processability, good mechanical properties, and high HDT	Harris et al. 1988
$\geq$ 0.01 wt% LCP with PET, PA, PC, PE, PP, PVC, PVDC, PPS, PVDF, PVF, or PMMA	Oriented films with small protrusions that resulted in low friction	Wong, C. P. 1990, 1994
LCP with either a *phenoxy* or an esteramide-based LC	Processability, thermal stability, and mechanical properties	Koning et al. 1990
LTG/LCP	*Cortem™ Alloys*: matrix LCP and $\leq$ 80 wt% of dispersed LTG; E = 14 GPa	Bahn et al. 1991
Amino-terminated PEI with polyester-type LCP	High tensile strength	Bookbinder and Sybert 1992
LCP with 2–98 wt% PEK	Toughness, excellent elasticity, and impact strength	Falk and Hermann-Schoenherr 1992
PPS with polyesteramide-type LCP	Accelerated crystallization rate of PPS	Minkova et al. 1992
LCP from *p*-hydroxybenzoic and 2,6-hydroxynaphthoic acids, with a non-thermotropic polymer, silane	Good phase morphology, interfacial adhesion, good thermal and mechanical behavior	Haider et al. 1993
PEI with 5–95 wt% LCP and *p*-amino benzoic acid or pyromellitic anhydride	Compatibilized moldable blends, useful as matrix for composites	Roemer and Schleicher 1993

(continued)

Table 1.77 (continued)

Composition	Comments	References
PI with polyimide-type LCP, $T_m \geq 300\ ^\circ C$	Processability, chemical resistance, flame retardancy and mechanical strength	Asanuma et al. 1993
PI with PEK and/or LCP and other additives; *Aurum*™ PI/LCP	Processability, HDT $\geq 230\ ^\circ C$, strength, thermal, and chemical resistance	Tsutsumi et al. 1994
LC-type polyimide with either PI, PEI, PAI, PES, or PEK	Remarkably good processability and excellent thermal stability	Okawa et al. 1994
Polyglutarimide with PBI, or LCP, and PET or PC	Good balance of toughness, tensile modulus, and HDT	Hallden-Abberton et al. 1994
PAI, with 3–30 wt% LCP	Lower viscosity, unaffected mechanical properties	Lai et al. 1994
PPS with a polymer of 6-hydroxy-2-naphthoic acid and 4-hydroxybenzoic acid, or terephthalic acid and 4-amino phenol	Processability and properties, used to mold parts for the electronic industry, particularly connectors	Yung and Linstid 1995
LCP blended with another LCP	Processability, HDT $\geq 200\ ^\circ C$, impact strength	Charbonneau et al. 1995

Table 1.78 Electro-dissipative and electroconductive blends

Composition	Comments	References
1. Electro-dissipative blends: ESD systems		
Aliphatic polysulfides (TM) with polybutadienes (PB)	To mold static charge-free rolls and guides for textile industry	Patric 1942
PO with 2 wt% PVAl	Mechanical, hygroscopic, antistatic properties	Minekawa et al. 1969
PC, with PET and ≥ 1 wt% of an elastomer containing acidic groups	High tensile strength, good impact resistance, and electrical conductivity	Mitsubishi Chemical Industries Co. Ltd. 1983
ABS and ≤ 20 wt% EO-CHR	Antistatic thermoplastic compositions	Federl and Kipouras 1986
EO-CHR with ABS, HIPS, MBS, SMA or PS/PPE, and an acrylic (co)polymer	Rapid dissipation of static charge, reduced delamination, and improved ductility	Gaggar et al. 1988; 1989
PVC, CPVC, PC, PEST, EP, PF, or styrenics with EO-CHR	Antistatic properties	Barnhouse and Yu 1988; Yu 1988
PC/PAI and a $C_{2\text{-}10}$ diamine	Processability, impact strength, appearance, mechanical, and antistatic properties	Shimamura and Suzuki 1991
PS with EO-CHR and PCL	static dissipative and tensile elongation	Giles and Vilasagar 1994

Table 1.78 (continued)

Composition	Comments	References
2. Electroconductive blends: ECP systems		
PAc was polymerized into PE	PE with catalyst exposed to acetylene	Galvin and Wnek 1982
Polypyrrole electrochemically polymerized within a matrix resin	Electrically conducting material with improved mechanical properties over those of PPy	Lindsey and Street 1985
PVC with "doped" PANI and an additive	Intrinsically electrically conductive films or fibers	Kulkarni and Wessling 1992, 1993, 1994
Amine-terminated PANI melt-blended with SMA	Materials were suitable for the use as electric conductors	Jongeling 1993
Polyaniline tosylate (PANI) and PETG	For films, inks, fibers, and coatings, in shielding, antistatic, and adhesives	Shacklette et al. 1993
Poly-3-octyl thiophene with PP, PVC, PS, PE, EVAc, PVC/ABS, etc., and dopant, e.g., I_2	Blends were formed into desired shapes and used either as EMI or ESD materials	Kokkonen et al. 1994
PANI with dodecylbenzene sulfonic acid heat treated and then mixed with either PS, PE, PS, ABS, or PP	Soluble thermoplastic ECPBs could be modified by mixing with protonic acid and metallic salts	Karna et al. 1994
Fluorine-containing polycyanurates and a thermoplastic polymer, e.g., PSF, PPE, PEEK	Heat or electrically conducting materials, for electronic packaging, adhesives, in the fabrication of electronic parts	Ardakani et al. 1994
PANI or PPy with polymeric dopant – sulfonated: -PE, -SEBS, -PS, etc.	Electrically conductive polymeric systems with good mechanical properties	Cross and Lines 1995
Matrix polymer and an electrically conducting thermotropic liquid-crystal polymer, LCP	Matrix: PO, EPR, CPE, CSR, PS; dispersed: PANI, PAc, PPy, poly (3-undecylthiophene), poly (3-dodecylthiophene), or polyparaphenylene	Ho and Levon 1995
SBR matrix and PANI filler	Conductivity, swelling, thermal and mechanical properties found to depend on PANI concentration and ratio between PANI-DBSA and PSS	Martins et al. 2006

The material developed by these authors consists of two polyolefin copolymers with different melt flow rates and filled with electrically conductive fillers and other additives. Two of the resins used are propylene/ethylene copolymers with different flow rates and flow ratios ranging from 2:3 to 1:90. The conductive filler particles include copper, silver, iron, or carbon black. These conductive resins can be molded or extruded, and applications range from circuit boards to shielding to implants.

Clearly, blending is an important technique to obtain conducting materials based on intrinsically conductive polymers and conventional as well as rubbery plastics. In a recent study, Martins et al. (2006) prepared an electrically conductive thermoplastic elastomer by blending butadiene-styrene copolymer (SBR) and

polyaniline (PANI) doped with dodecylbenzene sulfonic acid (DBSA) and poly (styrene sulfonic acid) (PSS). PSS also acted as a compatibilizer between PANI and SBR. PANI was doped by reactive processing with DBSA and PSS to produce the conductive complex PANI-DBSA-PSS. This complex was mixed with 90, 70, and 50% (w/w) SBR in an internal mixer with counterrotating blades. A similar strategy can be utilized to formulate thermally conducting plastics (Agarwal et al. 2008).

1.8   Biobased and Biodegradable Blends

In the recent past, there have been intense efforts aimed at developing alternatives to oil-based chemicals and polymers to reduce reliance on petroleum and natural gas (Stewart 2007). Biomass is the feedstock of the biobased economy, and, in practice, this means the use of corn and soybeans (for polyurethanes), although the hope is to eventually utilize agricultural and forest residues. Enzymes or microbial action are employed to convert biomass into useful chemicals and plastics. All the major plastic companies have initiated research programs in this area (Reisch 2002).

Only a few biobased polymers are commercially available (Mohanty et al. 2005). Polymers known as polyhydroxyalcanoates (PHA) are polyesters that are synthesized using bacteria, starting from either sucrose or starch. Varying the nutrient composition changes the chemical makeup of the polymer obtained (Hodzic 2005). This polymer has been commercialized by the Metabolix company under the trade name Mirel, and there are other similar products as well. Alternatively, one may obtain monomers from biomass and then carry out the polymerization using standard techniques. The most important polymer produced in this manner is polylactic acid (PLA) which is a linear polyester; here lactic acid is obtained from the fermentation of corn stover. In the past, the major application of PLA was in resorbable surgical sutures and in implantable drug-delivery devices. Although implantable medical devices are still being made from PLA and its blends (Wang et al. 2012), the material is increasingly being used in packaging where mechanical and thermal properties are not especially important. PLA production has increased significantly in the last 20 years since Cargill Inc. was able to produce high molecular weight PLA using ring-opening polymerization of lactide (Auras et al. 2010). The biodegradability property of PLA is due to the fact that the ester linkages are susceptible to hydrolysis, especially at high temperatures and in the presence of water; once the molecular weight is reduced, bacteria can degrade the material easily.

Biodegradable polymers are attractive since they are less likely to end up in landfills or contribute to the buildup of plastic trash that persists in the environment for a very long time. Biodegradability has also been explored in agriculture to prevent excessive moisture loss and weeds growth and to alleviate the recyclability problems – an agricultural film should last as long as it is needed and then disintegrate under the influence of either microorganisms and/or UV irradiation.

A biodegradable polymer is one that can decompose to small molecules, such as carbon dioxide, under the action of microorganisms is a specified amount of time (Mohanty et al. 2005). Most biopolymers are biodegradable, e.g., a large family of polysaccharides. They have been used in biodegradable blends with synthetic polymers. Some synthetic polymers, viz., PET, are susceptible to biodegradation when copolymerized with polylactones. Polymers with controlled, reversed misci-bility, viz., polyglycoles, are also biodegradable. Polymers with carbon backbones, viz., PE or PP, may be susceptible to biodegradation after incorporation of ketone side groups, -C(R)(COR′)- (Guillet 1973). Biodegradable polybutylene succinate or adipate, *Bionolle™*, has been commercially introduced in 1996 by Showa Denko. Similarly, Novamont introduced fully biodegradable *Mater-Bi™*. The latter mate-rials are blends of starch and other polymers, viz., poly-ε-caprolactone, ethylene-vinyl alcohol, etc.

1.8.1   PLA Blends

Lactic acid produced from the fermentation route is 99.5 % L-lactic acid and condensation polymerization leads to low molecular weight PLLA or poly (L-lactide) (Nampoothiri et al. 2010; Rasal et al. 2010). High molecular weight polymer can be produced by ring-opening polymerization, and one can also adjust the ratio of L- to D-lactic acid units (Auras et al. 2010). Even so, it is not considered to be an engineering polymer since it has poor thermal and hydrolytic stability. Although it has stiffness and strength comparable to commercial polymers like polystyrene and PET (Imre and Pukanszky 2013), it suffers from low values of ductility, HDT, and toughness. Some of these properties can be improved by blending PLA with plasticizers or with other plastics.

The elongation to break of PLA is less than 10 %, but it can be significantly enhanced by the incorporation of low molecular weight plasticizers which are also biocompatible; these include oligomeric lactic acid and low molecular weight polyethylene glycol (PEG) (Martin and Averous 2001). As is normal with the use of plasticizers, however, there is a concomitant reduction in both the elastic modulus and the glass transition temperature. A variation of this procedure has been reported by Rasal and Hirt (2010) who blended PLA with polyacrylic acid followed by physical blending with PEG in solution. Films made from the mixture showed a tenfold increase in toughness compared to neat PLA with little or no decrease in tensile strength and modulus. Note that with time, low molecular weight additives can migrate to the surface of a part due to reasons such as physical aging and this phenomenon may be accompanied by an increase in polymer crystallinity (Auras et al. 2010; Rasal et al. 2010); an increase in crystallinity is usually accompanied by a reduction in ductility.

A lowering in PLA modulus and T_g can be avoided if PLA is blended with other polymers. However, it is not miscible with many plastics, and the use of block copolymers or the use of reactive blending is generally necessary. Candidate poly-mers may be biodegradable or nonbiodegradable. In the former category are starch,

PGA, and PHA (Yu et al. 2006), while in the latter category are polyolefins, vinyl and vinylidene polymers, and elastomers and rubber (Detyothin et al. 2010). PLA has been blended extensively with starch due to its plentiful supply, low cost, and biodegradable nature (Yu et al. 2010). However, it is hydrophilic, and it tends to swell in the presence of water. To promote compatibility of starch with the hydrophobic PLA, one may use coupling agents such as methylene diphenyl diisocyanate (MDI) or functionalize the polyester by grafting highly reactive groups such as maleic anhydride with the expectation that covalent bonds will be formed by reaction with the hydroxyl groups on starch (Rzayev 2011). It is found that mechanical properties of PLA such as modulus, yield strength, and impact strength can all be improved by blending with starch in the presence of MDI. The use of other additives, such as resorcinol di(phenyl phosphate), can endow the blends with flame retardancy (Pack et al. 2012). Several PLA blends have now been commercialized, and these find application mainly in packaging and agriculture. The recent review by Imre and Pukanszky (2013) may be consulted for details.

Approaches that can be employed to toughen PLA with the use of different blend constituents and how the toughening protocols modify mechanical properties have been described by Anderson et al. (2008). The most significant improvement in toughness of PLA has been reported by McCarthy et al. (1999) who made blends of PLA with polybutylene-succinate adipate (PBSA). PBSA is a biodegradable polymer, but it is not biobased. A 70/30 (weight%) PLA/PBSA blend exhibited about a 5-fold increase in tensile elongation to break and about a 25-fold increase in tensile toughness. More recently, Krishnaswamy (2013) and Krishnaswamy et al. (2013) have described blends of PLA and PHA which have about 31–58 % increase in tensile elongation and 21–35 % greater tensile toughness than PLA alone.

As mentioned earlier, a major application of PLA is in food packaging. Cheung et al. (2012) have described blends of PLA with styrenic polymers compatilbilized with styrene-based copolymers like SEBS, SMA, and SMMA that can be extruded and thermoformed to produce very low-density food service foam articles with good mechanical properties. Li et al. (2012) have described the development of a biodegradable gloss film that contains 60–99 % PLA and the rest PP. In general, biodegradable polymer blends are prepared by blending a thermoplastic resin with a biodegradable one. Specific examples are given in Table 1.79. Blending must produce dispersion that after disintegration of the biodegradable part, the thermoplastic powder will not contaminate the environment.

1.9   Blending and Recycling

Recycling is becoming increasingly important. Its methods depend on the polymer type and source. Within the resin manufacturers' plant recycling is the easiest. This is known as postindustrial recycling. In processing plants, where commingled polymeric scrap is generated, it is more difficult, but it is still possible by separating the different components (Jody et al. 1997). The most difficult is recycling of

Table 1.79 Biodegradable polymer blends

Composition	Comments	References
PVAl/vinylacetate grafted starch	Biodegradable, better properties than PVAl	Yoshitake et al. 1978
PHBA, with 10–40 wt% CPE	Biodegradability, impact properties and HDT	Holmes et al. 1982
PLA/PEO, EVAc, EVAl, EPDM, SBR, etc.	Biodegradable, flexible alloys	Kharas and Nemphos 1992
EVAl/poly(hydroxybutyrate-valerate)	Biodegradability and good impact properties	Webb et al. 1992
PS, PO, NR, SBR, PI, PB, or CA, a polysaccharide and bioagent	Cellulose with 1 wt% of bacteria, fungi, and/or enzymes	Guttag 1992, 1994
LDPE, starch, and a copolyacrylate	Biodegradable blends	Willett 1992
Maleated starch, PE or PP, and 1–35 wt% acrylic copolymer	Biodegradable films with good mechanical properties	Tomka 1992; Tomka et al. 1993
Amylose/PA/PEST/POM/gelatins	For manufacturing transparent packaging films	Meier 1993
Starch, latex of either polymer or elastomer, and 0–20 phr fillers	The mixture could be molded or extruded to form parts useful for food packaging	Munk 1993
Starch/poly [unsaturated fatty acids + diamines + diol-based glycols]	The blends were used to manufacture packaging films or moldings	Ritter et al. 1993
PO/PHB/A-B block copolymers of poly(meth)acrylic esters	For disposable napkins, ostomy bags, and ordinary wrapping	Ballard and Buckmann 1993
Plasticized polylactic or a lactic acid-hydroxycarboxylic acid copolymer	Flexible and hydrolyzable materials, useful for absorbing oils and body fluids	Morita et al. 1993
PLA/PC or PSF, PI, PPE, siloxanes, silicones, PMMA, etc.	Improved HDT of biodegradable polymers	Nemphos and Kharas 1993, 1994
Hydroxypropyl-starch or urea-starch, and either PA or PEST	For the manufacture of printable moldings or films	Buehler et al. 1993, 1994
PS, PE, PP, TPU, PEST, PA, etc., with 5–99 wt% of either carbohydrates, proteins, or lipids	Reactively blended biodegradable interpolymers, with good mechanical properties, and limited water absorption	Vaidya and Bhattacharya 1994
A polar polymer, polysaccharide, and fatty acid (hydroxy) peroxide	Good performance until exposed to suitable environment for degradation	Chapman and Downie 1994
Synthetic polymer, peracid, and starch	Superior mechanical properties, biodegradability	Hsu et al. 1994
LLDPE with starch and ≥ 1 ionic compound	For high-frequency sealable multilayer packaging films, biodegradation	Dehennau et al. 1994
Nonconsumable agricultural products with an adhesive	Biodegradable tableware from impact-molded, coated particles	Liebermann 1994
PEG with PA, PE-co-acrylic or methacrylic acid, EVAc, EVAl	Degradable and/or recyclable plastic articles with inverse solubility characteristic	Petcavich 1994

(continued)

Table 1.79 (continued)

Composition	Comments	References
TPU and/or *phenoxy*, EVAl, COPO, cellulose, and/or polyalkylene oxide	Attractive physical, optical, and barrier properties and were melt processable without PVAl degradation	La Fleur et al. 1994
Starch with biologically degradable aliphatic polyesters, hydrophobic protein, PVAl, or cellulose esters and a hygroscopic material	Absorbed water was released during either extrusion or injection molding at T = 200 °C, causing the mixture to foam to density ρ = 160 kg/m³	Tomka 1998

postconsumer polymers which show up in municipal solid waste (MSW) and ultimately end up in landfills. Indeed, the magnitude of the problem has been increasing at a rapid rate. The plastic component of MSW in the USA has risen from 390,000 t in 1960 to 30.7 million tons in 2007 (Merrington 2011). Three basic methods of recycling have been used: (i) direct, where cleaned resins are incorporated into virgin material, (ii) reprocessing the commingled plastics either by blending or transforming into plastic wood or plastic concrete, and (iii) feedstock type that may involve depolymerization or pyrolysis. To the following text, only the method (ii) is important. It can be subdivided into (1) compatibilization and upgrading of resins in direct recycling, (2) compatibilization and upgrading of commingled plastics for reprocessing, and (3) recycling of polymer blends (Akovali et al. 1998).

The essential difficulty in recycling commingled plastic is the fact that mixed plastics have poor mechanical, thermal, and flow properties even when the individual components have very desirable ones. In particular, plastic mixtures have low ductility and poor impact strength (Liang and Gupta 2001). This limits their use to less demanding applications such as flower pots, park benches, and plastic lumber. To reuse postconsumer plastics in high-value applications, it is necessary to first separate plastic waste by chemical type. A variety of techniques, such as float-sink tanks and hydrocyclones, can be used to separate mixed plastics based on differences in density. For plastics with overlapping density, other methods, such as froth flotation, can be employed (Merrington 2011). A relevant question then is the purity level that must be attained in such a separation process. The higher the purity, the better is the performance, but the higher also is the cost of the separation process.

One way to address the issue of residual contaminants present in polymer recovered from postconsumer waste is to use regrind in an inner layer in a multilayer article. Shelby et al. (2012) have described several such transparent polymer compositions made from a variety of polymer pairs that exhibit excellent barrier properties while retaining processability and good mechanical property. Another approach is to blend the separated plastic with virgin plastic. This procedure also allows one to standardize the flow properties if the virgin polymer is available in different molecular weights (Liang and Gupta 2002). Even so, it is necessary to compatibilize the recycled material since it remains a multicomponent blend.

To do this, one may (i) add at least one ingredient with highly reactive groups that can interact with several polymeric components, e.g., ethylene-acrylate-maleic anhydride, glycidyl methacrylate-ethylene-vinylacetate, and ethylene-glycidyl methacrylate-methylmethacrylate (the copolymer may compatibilize and toughen); (ii) add a low molecular weight additive that at different stages of the reactive blending binds to different components, viz., ethylene-glycidyl methacrylate, triglycidyliso-cyanurate, etc.; and (iii) add a cosolvent, for example, *phenoxy*. A significant penetration of properly designed copolymer into the homopolymer phases has been reported (Brown 1989).

The morphology can be stabilized by (i) thick interphase, (ii) partial cross-linking, or (iii) addition of an immiscible polymer with a suitable spreading coefficient (Yeung et al. 1994). The adhesion between the phases in the solid state is improved by (i) addition of a copolymer that covalently bonds the phases, (ii) reduction of size of the crystalline domains, (iii) adequate adhesion, e.g., by the use of polyetherimine, PEIm (Bjoerkengren and Joensson 1980), and (iv) dispersing at high stresses, either in the melt (Patfoort 1976) or in solid state (Shaw 1993; Khait 1994, 1995).

Chemical re-stabilization of recycled material against the thermal- and light-induced degradation is essential. Addition of 0.1–0.5 wt% of a sterically hindered phenol and a phosphite at a ratio varying from 10:1 to 1:10 is recommended (Pauquet et al. 1994). For outdoor applications, hindered amine light stabilizers with UV absorbers of the benzotriazole type are to be used (Herbst et al. 1995, 1998). Examples of blends used for polymer recycling are listed in Table 1.80. For more details, see ▶ Chap. 20, "Recycling Polymer Blends" in this book.

1.10   Conclusions and Outlook

Blends like composites are integral parts of the plastic industry. Their sales are estimated at more than US$ 100 billion per annum. The blends provide widening selection of performance characteristics, tunable for specific applications at a reasonable cost. In effect, this technology is a shortcut to development of complex polymeric species.

Considering the range of possibilities and constraints, polymer blends provide a fertile field of polymer research. Polymer blending not only requires understanding of intrinsic properties of polymers but also a broad knowledge of numerous disciplines such as thermodynamic principles of miscibility and compatibilization, surface and interfacial properties, morphology, rheology, processing, and performance during the service life of the material. Decades of research have enriched our understanding about the science and technology of polymer blends. As a result, polymer blends and blending techniques are finding applications in multidisciplinary fields.

Performance during its service life is crucial to the widespread application of any material. It has been estimated, for example, that at least 15–25 % of all failures of plastic materials in commercial use are related to the problem of environmental

Table 1.80 Polymer blends for recycling

Composition	Comments	References
PS with 1–10 wt% PE and CSR	Improved impact, elongation, and strength (CPE or CSR is a compatibilizer for scrap)	Herbing and Salyer 1963
LLDPE/PS shear-compatibilized	Blends with good mechanical properties	Patfoort 1976
PS or HIPS, with PP and SEBS	SEBS is expensive but useful in recycling	Holden and Gouw 1979
PS with PO, S-b-B stabilizers	Recycling requires higher concentration of stabilizers than virgin resins	Sadrmohaghegh et al. 1985
sPS and sPS copolymer with MA or GMA and an elastomer reactive with it	Recyclable, impact resistant, good elongation, and retention of physical properties	Okada 1994
PO with 30–40 wt% PS recycled without compatibilization	High properties due to stable co-continuous morphology	Morrow et al. 1994
PA with PA/LDPE, EGMA	Recyclable blends, good performance	Timmermann et al. 1994
$\geq$ 2 PO, PS, polydienes – either virgin, recycled, or both	Blending at T in between the melting points of the components	Lai and Edmondson 1995
Rubber scrap with rosin and fatty acids, esters and unsaponifiables, and PE, PET, TPU, PU, PVC, etc.	Cryogenically comminuting rubber, drying it, blending with plasticizer/binding agent, heating, and blending with polymers	Segrest 1995
Automotive scrap plastic parts comprising PC, PEST, ABS, PA, etc., with 5–15 wt% MBS	Compounding in a TSE, devolatilization, filtering of paint flakes; closed-loop control system for properties	Lieberman 1995
Branched PET with recycled PET and a chain extender or a cross-linking agent	Foaming and extruding the mixture	Muschiatti and Smillie 1995
Recycling of manufactured polymer blends	Recent concepts in polymer blends recycling	Jose et al. 2011

stress cracking (ESCR) (Arnold 1996). The development of polymer blends technology has provided a strategic route to avoid ESCR of amorphous engineering polymers and allowed these engineering blends (Xenoy®, Noryl®, Gemax®, Triax, Elemid, Macroblend) to be used in various aggressive environments. For automotive applications, blends have been formulated with high T_g polymers (PC, PPO) with crystalline polymers (PBT, PA 66) (Robeson 2007). As applications of amorphous polymers expand in adverse environments, newer commercial blends will be developed, and the reader is referred to the recent review by Robeson (2013). This effort is likely to be aided by computational methods that have been developed in the science and technology of polymer blends. Molecular dynamics provide means of computation of the specific interactions and miscibility (Coleman et al. 1991) or the interfacial energy in a polymer blend (Yao and Kamei 1995).

Indeed, commercial computer programs are available for designing blends with specific sets of properties.

The phase behavior and morphology of phase-separated polymer blends play a vital role in the design of membrane transport properties (Robeson 2010). Numerous applications of polymeric membranes involving gas and liquids are known. Although different transport models have been utilized successfully to relate morphology with transport properties, there is enough room for improvements as membrane applications continue to grow in such areas as gas separation.

Formulation of biodegradable polymer blends is already on the rise, and these blends are being used successfully in applications ranging from agriculture to consumer goods, to packaging, and to automotives. Blends of biodegradable polymers, however, behave differently than those of commodity polymers. Miscibility-structure-property relationship of these blends will continue to emerge. Progress has been made in developing self-extinguishing biodegradable polymer blends (PLA/ECOFLEX). As the use of biodegradable polymer blends increases, demand for flame-retardant formulations will rise as well.

Another rapidly evolving field is biomedical engineering and particularly tissue engineering that seeks to regenerate or repair damaged or diseased tissues and organs. Scaffolds are being fabricated by combining the solid-state foaming and immiscible polymer blending methods. Biodegradable dipeptide-based polyphosphazene-PLAGA blends have been reported to be a promising material for mechanically competent scaffolds for bone tissue engineering (Deng et al. 2010). Undoubtedly, biodegradable and biocompatible polymer blends will play an increasing role in the fabrication of tissue engineering scaffolds in the future.

One usually wishes to know what would be the final properties of a polymer blend once it has been conceptually designed but before it is actually made. That is what molecular modeling does. However, there is always a compromise between simulation complexity, accuracy, and speed of prediction. Studies are being carried out which could open up the possibility of computer-aided design of polymer blends with desired physical and mechanical properties.

Although great strides have been made in the past, opportunities still exist to improve and solve numerous polymer blend problems. Research and technical innovation will continue to impact polymer blend development and production. We are confident that polymer blends will continue to contribute to the development of our modern society.

1.11   Cross-References

Abbreviations

aPP Amorphous polypropylene
AA Acrylic acid
AAS Copolymer from acrylonitrile, styrene and acrylates; ASA
ABS Acrylonitrile-butadiene-styrene
ABSM Acrylonitrile-butadiene-styrene-methylmethacrylate
ACM Copolymer of acrylic acid ester and 2-chloroethyl vinyl ether
AES Quarterpolymer from acrylonitrile, ethylene, propylene, and styrene
AF Aniline-formaldehyde
AN Acrylonitrile
ANM Acrylate rubber, based on ethyl acrylate with acrylonitrile
ASA Copolymer from acrylonitrile, styrene and acrylates
BMMM Butyl methacrylate-methylmethacrylate copolymer
bPC Branched polycarbonate
BR Butadiene rubber; polybutadiene
CA Cellulose acetate
CAS Chemical Abstracts Service
CB Carbon black
CBR Cis-polybutadiene rubber
CF Carbon fiber
CHR Epichlorohydrin
CMC Critical micelle concentration
COP Cycloolefin
COPO Copolymer of carbon monoxide with polyolefins (ethylene or propylene)
COPO-VAc Carbon monoxide-ethylene-vinylacetate copolymer
CPA Copolyamide
CPB Chlorinated polybutadiene
CPE Chlorinated polyethylene
CPVC Chlorinated polyvinylchloride
CR Elastomeric polychloroprene
CRU Constitutional repeating unit
CSM Chlorosulfonated polyethylene rubber
CSR Core-shell rubber

CTM Cavity transfer mixer
CUT Continuous use temperature
DBSA Dodecylbenzene sulfonic acid
DOP Dioctyl phthalate
EAA Ethylene-acrylic acid copolymer
EBA Ethylene butyl acrylate
ECP Electroconductive polymer
EEA Ethylene-ethylacrylate copolymer
EFK Aromatic polyester
EFM Extensional flow mixer
EGMA Poly(ethylene-glycidyl methacrylate)
EHEMA Ethylene-hydroxyethyl methacrylate
EMAA Ethylene-methacrylic acid copolymer
EMAC Ethylene-methacrylate copolymer
EMMA Ethylene-methylmethacrylate copolymer
EO Ethylene oxide
EoS Equation of state
EP Epoxy resin. Also engineering polymer
EPDM Ethylene-propylene-diene elastomer
EPDM-MA Maleated ethylene-propylene-diene elastomer
EPR Ethylene propylene rubber
ESCR Environmental stress-cracking resistance
ESD Electrostatic charge dissipation
ESI Ethylene-co-styrene interpolymer
ETFE Ethylene-tetrafluoroethylene
EVAc Ethylene-vinylacetate
EVAc-CO Ethylene-vinyl acetate-carbon monoxide copolymer
EVAl Ethylene vinyl alcohol
FEP Fluorinated ethylene-propylene
GF Glass fiber
GMA Glycidyl methacrylate
GP Gutta-percha
HDPE High-density polyethylene
HDT Heat deflection temperature, heat distortion temperature
HEMA Hydroxyethyl methacrylate
HIPS High impact polystyrene
IIR Isobutene-isoprene rubber (butyl rubber)
IPN Interpenetrating polymer network
iPS Isotactic polystyrene
IR Synthetic *cis*-1,4-polyisoprene
IUPAC International Union of Pure and Applied Chemistry
JSW Japan steel works
LCP Liquid-crystal polymer
LCST Lower critical solubility temperature

LDPE Low-density polyethylene
LLDPE Linear low-density polyethylene
LTG Low-temperature glass
MA Maleic anhydride
MABS Methylmethacrylate-acrylonitrile-butadiene-styrene
MBA Copolymer from methylmethacrylate, butadiene and acrylonitrile
MBS Copolymer from methylmethacrylate, butadiene and styrene
MC Molecular composite
MDI Methylene diphenyl diisocyanate
MDL MDL Information Systems, Inc.
MDPE Medium density polyethylene
MD/TD Machine direction/transverse direction
MeABS Graft copolymer of ABS and methylmethacrylate
MeSAN Graft copolymer of SAN and methylmethacrylate
MF Melamine formaldehyde
MI Melt index
MFR Melt flow rate
mLDPE Metallocene-catalyzed low-density polyethylene
mLLDPE Metallocene-catalyzed linear low-density polyethylene
MMA Methylmethacrylate
MMBA Poly(methylmethacrylate-co-butyl acrylate)
MMMA Methylmethacrylate-methylacrylate copolymer
MMVAc-AA Copolymer of methylmethacrylate, vinylacetate and acrylic acid
MPS Poly(α-methyl styrene)
MSW Municipal solid waste
MW Molecular weight
MWD Molecular weight distribution
NBR Elastomeric copolymer from butadiene and acrylonitrile; nitrile rubber
NC Nitrocellulose
NDB Negatively deviating blend
NPDB Negative and positive deviating blend
NR Natural rubber
P4MP Poly(4-methyl-1-pentene)
PA Polyamides, nylon
PAc Polyacetylene
PACE Polyacetylene
PAE Polyarylether
PAEB Poly(*p*-aminoethyl benzoate)
PAEK Polyaryletherketone
PAES Polyarylethersulfone
PAI Polyamide-imide
PAN Polyacrylonitrile
PANI Polyaniline
PAr Polyarylate

PARA Polyarylamide; aromatic amorphous polyamide
ParSi Poly(aryloxysiloxane)
PB Polymer blend; polybutadiene
PB-1 Poly-1-butene
PBA Polybutylacrylate
PBG Polybutyleneglycol
PBI Polybenzimidazole
PBMA Poly(butyl methacrylate)
PBSA Polybutylene-succinate adipate
PBT Polybutylene terephthalate
PC Polycarbonate
PCHA Polycyclohexyl acrylate
PCHE Polycyclohexylethylene
PCHMA Polycyclohexyl methacrylate
PCL Polycaprolactone
PCO Polycycloolefin
PCS Poly-2-chlorostyrene
PCTF Polychlorotrifluoroethylene
PCTFE Polychlorotrifluoroethylene
PCTG Copolymer of cyclohexanedimethanol, terephthalic acid and ethylene glycol
PDB Positively deviating blend
PDMDPhS Poly(dimethyl-diphenyl siloxane)
PDMS Polydimethylsiloxane, polysiloxane
PDPS Polydiphenylsiloxane
PE Polyethylene
PEA Polyethylacrylate; polyesteramide; polyether-amide
PEBA Polyether-block-amide
PEC Polyestercarbonate
PEEI Copolyesteretherimide
PEEK Polyether ether ketone; polyaryletherketone
PEG Polyethylene glycol
PEI Polyetherimide
PEIm Polyetherimine
PEK Polyetherketone
PEKK Polyetherketone
PEMA Polyethylmethylacrylate
PEN Poly(ethylene-2,6-naphthalene dicarboxylate)
PEO Polyethylene oxide
PEOX Poly(2-ethyl-2-oxazoline)
PES Polyethersulfone
PEST Thermoplastic polyester
PET Polyethylene terephthalate
PETG Polyethyleneterephthalateglycol

PF   Phenol-formaldehyde
PGA   Polyglycolic acid
PGI   Polyglutarimide
PHA   Polyhydroxyalcanoate
PHB   Poly-3-hydroxybutyrate
PHBA   Poly(β-hydroxybutyric acid)
PHT   Polyhexamethyleneterephthalate
PHZ   Polyphosphazene
PI   Polyimide
PIB   Polyisobutylene
PISO   Polyimide-sulfone
PLA   Polylactic acid
PMA   Polymethacrylate
PMB   Poly*p*-methylenebenzoate
PMI   Polymethacrylimide
PMMA   Poly(methylmethacrylate), acrylic
PMP   Poly-4-methyl-1-pentene
PMPhS   Polymethylphenylsiloxane
PMS   Polymethylstyrene
PNDB   Positive and negative deviating blend
PO   Polyolefin
POBA   Polyoxybenzoyl acid, rigid-rod polymer
POCA   Polyoxycyanoarylene
POD   Polyoctadecene
POM   Polyoxymethylene
POT   Poly-3-octyl thiophene
PP   Polypropylene
PPA   Polyphthalamide
PPBA   Polyparabanic acid
PPCO   Polypropylene carbonate
PPE   Polyphenylene ether
PPG   Propylene glycol
PPhA   Polyphthalamide
PPMA   Poly-*n*-propyl methacrylate
PpMS   Poly-*p*-methylstyrene
PPP   Polyparaphenylene
PPS   Polyphenylenesulfide
PPSS   Polyphenylenesulfidesulfone
PPT   Polypropylene terephthalate
PPTA   Poly(*p*-phenylene terephthalamide)
PPy   Polypyrrole
PS   Polystyrene, styrenic
PSF   Polysulfide; polysulfone
PSIB   Polyisobutylene-block-polystyrene

PSOX Polystyrene grafted with 2-oxazoline
PSS Poly(styrene sulfonic acid)
PSU Polyarylsulfone
PTES Polythioethersulfone
PTFE Polytetrafluoroethylene
PTO Polytransoctanamer
PVA Polyvinylacetate
PVAl Polyvinyl alcohol
PVB Polyvinyl bromide
PVC Polyvinyl chloride, vinyl
PVCAc Poly(vinylchloride-co-vinylacetate)
PVDC Polyvinylidenechloride
PVDC-MeA Vinylidenechloride-methylacrylate copolymer
PVDF Polyvinylidene fluoride
PVF Polyvinyl fluoride
PVFO Polyvinyl formal
PVME Poly vinyl methyl ether
PVP Polyvinylpyrrolidone
PVPh Polyvinylphenol
SAA Poly(styrene-acrylic acid)
SAN Styrene-acrylonitrile copolymer
SAN-MAc Copolymer of SAN and methacrylic acid
SB Styrene-butadiene block copolymer
SBR Styrene-butadiene rubber
SBS Styrene-butadiene-styrene block copolymer
SEB Styrene-ethylene/butylene
SEBS Styrene-ethylene-butylene-styrene block copolymer
SEP Styrene-ethylene-propylene block copolymer
SH Strain hardening
SI Styrene-isoprene block copolymer
SIS Styrene-isoprene-styrene block copolymer
SMA Poly(styrene-co-maleic anhydride)
SMI Copolymer from styrene and maleimide
SMM Styrene-methylmethacrylate copolymer
SMMA Styrene methylmethacrylate
sPhPS Syndiotactic poly(*p*-phenyl styrene)
sPP Syndiotactic polypropylene
sPS Syndiotactic polystyrene
SSE Single-screw extruder
TM Thio-rubber
TMPC Polycarbonate of tetramethyl bisphenol-A
TPE Thermoplastic elastomer
TPU Thermoplastic polyurethane
TPV Thermoplastic vulcanizate

TS Thermoset polyester
TSE Twin-screw extruder
UF Urea-formaldehyde
UHMWPE Ultra-high molecular weight polyethylene
UHMW-PMMA Ultra-high molecular weight poly(methylmethacrylate)
UHMW-PS Ultra-high molecular weight polystyrene
ULDPE Ultra low-density polyethylene
VCM Vinyl chloride monomer
VPh Vinylphenol
VLDPE Very low-density polyethylene
XLPE Cross-linked polyethylene

References

H. Abe, T. Fujii, M. Yamamoto, S. Date, U.S. Patent 5,278,233, 11 Jan 1994, to Sumitomo Chem

K. Abe, H. Sakano, A. Inoue, S. Tajima, Jap. Pat. 093,465, 05 Aug 1977, to Sumitomo Naugatuck

V. Abolins, D.L. Reinhardt, U.S. Patent 3,983,090, 28 Sept 1976; Can. Pat. 994,040, 27 July 1976, to General Electric Co.

V. Abolins, J.E. Betts, F.F. Holub, Europ. Pat. Appl. 129,825, 02 Jan 1985, to General Electric Co.

I.A. Abu-Isa, P.M. Graham, U.S. Patent 5,194,468, 16 Mar 1993, to General Motors Corp.

S. Agarwal, M.M.K. Khan, R.K. Gupta, Polym. Eng. Sci. **48**, 2474 (2008)

O.C. Ainsworth, U.S. Patent 4,978,703, 18 Dec 1990, to The Dow Chemical

O.C. Ainsworth, U.S. Patent 5,286,795, 15 Feb 1994, to The Dow Chemical

A. Ajji, L.A. Utracki, Polym. Eng. Sci. **36**, 1574 (1996)

M. Akega, Jap. Pat. 03 92,324, 17 Apr 1991, to Teijin Chem.

M.K. Akkapeddi, B. Van Buskirk, A.C. Brown, PCT Int. Appl. W088/08433, 03 Nov 1988, to AlliedSignal

M.K. Akkapeddi, B. Van Buskirk, T.J. Kraft, U.S. Patent 4,902,749, 20 Feb 1990, to AlliedSignal

M.K. Akkapeddi, B. Van Buskirk, A.C. Brown, U.S. Patent 5,162,440, 10 Nov 1992a, to AlliedSignal

M.K. Akkapeddi, B. Van Buskirk, T.J. Kraft, U.S. Patent 5,115,018, 19 May 1992b, to AlliedSignal

M.K. Akkapeddi, B. Van Buskirk, T.J. Kraft, U.S. Patent 5,210,134, 11 May 1993, to AlliedSignal

G. Akovali, C.A. Bernardo, J. Leidner, L.A. Utracki, M. Xanthos (eds.), *Frontiers in the Science and Technology of Polymer Recycling*. NATO ASI Series E, vol. 351 (Kluver, Dordrecht, 1998)

H.A.K. Al Ghatta, PCT Int. Appl. WO 94 09,069, 28 Apr 1994, to M. & G. Ricerche

P.T. Alder, J.G. Dolden, D.G. Othen, PCT Int. Appl. 008,231, 29 Apr 1993, to British Petroleum

T. Alfrey, J.J. Bohrer, H.F. Mark, *Copolymerization* (Interscience, New York, 1952)

A.H. Ali, J.T.T. Hsieh, K.J. Kauffman, Y.V. Kissin, S.C. Ong, G.N. Prasad, A.L. Pruden, S.D. Schregenberger, U.S. Patent 5,284,613, 08 Feb 1994, to Mobil Oil Corp.

R.B. Allen, R.W. Avakian, U.S. Patent 4,683,247, 28 July 1987, to General Electric Co.

R.B. Allen, B.M. Bacskai, D.L. Roberts, R.C. Bopp, U.S. Patent 4,857,390, 15 Aug 1989, to General Electric Co.

Allied Chemical Corp., Neth. Pat. Appl. 6,410,654, 12 Mar 1965

Allied Chemical Corp., Neth. Pat. Appl. 6,410,561; 6,515,314, 31 May 1966

J. Alper, G.L. Nelson, *Polymeric Materials: Chemistry for the Future* (ACS, Washington, DC, 1989)

F.D. Alsewailem, R.K. Gupta, J. Disp. Sci. Technol. **23**, 135 (2002)

R.T. Alvarez, U.S. Patent 4,017,555, 12 Apr 1977

S.H. Anastasiadis, Adv. Polym. Sci. **238**, 179 (2011)

K.S. Anderson, K.M. Schreck, M.A. Hillmyer, Polym. Rev. **48**, 85 (2008)

T. Andres, H. Alvarez, O. R. Hughes, W. Cooper, C. Wang, U.S. Patent 5,391,605, 21 Feb 1995, to Hoechst Celanese Corp.

S.R. Angeli, L.M. Maresca, Europ. Pat. Appl. 370,243, 30 May 1990, to General Electric Co.

S.R. Angeli, Can. Pat. 2,059,914, 28 Aug 1992, to General Electric Co.

A. Aoki, T. Shiraki, T. Ibaragi, U.S. Patent 4,304,881, 08.12.1981, to Asahi Kasei Kogyo

T. Aoyama, K. Hara, Y. Okimura, A. K. Shu, H. Kobayashi, M. Izumi, Europ. Pat. Appl. 575,809, 29 Dec 1993; Jap. Pat. 53 39,433; Jap. Pat. 53 39,434, 21 Dec 1993, to Kanegafuchi Kagaku Kogyo

T. Aoyama, K. Hara, Y. Okimura, A. K. Shu, H. Kobayashi, M. Izumi, Jap. Pat. 60 73,192, 15 Mar 1994, to Kanegafuchi Kagaku Kogyo

Y. Arashiro, M. Kihara, H. Ohmura, F. Yamada, U.S. Patent 5,360,866, 01 Nov 1994, to Mitsubishi Petrochemical

A.A. Ardakani, J.T. Gotro, J.C. Hedrick, K. Papathomas, N.M. Patel, J.M. Shaw, A. Viehbeck, Europ. Pat. Appl. 581,314, 02 Feb 1994; Jap. Pat. 61 07,958, 19 Apr 1994, to IBM Corp.

C.B. Arends (ed.), *Polymer Toughening* (Marcel Dekker, New York, 1996)

P. Arjunan, U.S. Patent 5,281,651, 25 Jan 1994

P. Arjunan, U.S. Patent 5,391,625, 21 Feb 1995; U.S. Patent 5,397,833, 14 Mar 1995, to Exxon

B.C. Arkles, Ger. Offen. 3,314,355, 27 Oct 1983, to Petrarch Systems

B.C. Arkles, U.S. Patent 4,500,688, Feb 19, 1985, to Petrarch Systems

R. Armat, A. Moet, Polymer **34**, 977 (1993)

J.C. Arnold, Trends Polym. Sci. **4**, 403 (1996)

J.-L. Arraou, Caoutch. Plast., Juin-Juil., 1986, p. 79

H. Asahara, Y. Asai, K. Yasue, Jap. Pat. 100,552, 23 Aug 1977a, to Unitika, Ltd.

H. Asahara, Y. Asai, K. Yasue, Y. Okabayashi, Jap. Pat. 100,553, 23 Aug 1977b, to Unitika, Ltd.

Asahi Chemical Industry Co., Brit. Pat. 1,154,447, 11 June 1969; Fr. Pat. 1,570,281, 06 June 1969

Asahi Chemical Industry Co., Jap. Pat. 118,456, 17 Sept 1981

Asahi Chemical Industry Co., Jap. Pat. 021,442; 021,443; 021,449, 04 Feb 1982; Jap. Pat. 030,747; 030,748, 19 Feb 1982; Jap. Pat. 085,847, 28 May 1982

Asahi Chemical Industry Co., Jap. Pat. 007,443, 17 Jan 1983

Asahi Chemical Industry Co., Jap. Pat. 020,354, 02 Feb 1984; U.S. Patent, 4,438,236, 31 Jan 1984

Asahi Chemical Industry Co., Jap. Pat. 044,540, 09 Mar 1985; Jap. Pat. 047,063, 14 Mar 1985; Jap. Pat. 060,158, 06 Apr 1985; Jap. Pat. 071,661, 23 Apr 1985

Asahi Chemical Industry Co., Europ. Pat. Appl. 219,973, 29 Apr 1987

Asahi Fiber Glass Co., Jap Pat. 030,451, 27 Mar 1981

Asahi-Dow Limited, Jap. Pat. 112,957, 05 Sept 1981

K. Asai, T. Kobayashi, M. Maeda, Europ. Pat. Appl. 444,589, 04 Sept 1991, to Sumitomo Chemical Co.

T. Asanuma, T. Sasaki, S. Nakanishi, T. Inoue, Europ. Pat. Appl. 499,216, 19 Aug 1992, to Mitsui Toatsu

T. Asanuma, N. Koga, H. Oikawa, Y. Okawa, A. Yamaguchi, Europ. Pat. Appl. 564,299, 06 Oct 1993, to Mitsui Toatsu

R. Auras, L.-T. Lim, S.E.M. Selke, H. Tsuji (eds.), *Poly (Lactic Acid)* (Wiley, Hoboken, 2010)

R.W. Avakian, R.E. Jodice, U.S. Patent 4,587,272, 06 May 1986, to General Electric Co.

R.W. Avakian, C.M.E. Bailly, W.J.L. Hamersma, W.J.L.A. Hamersma, Europ. Pat. Appl. 274,140, 13 July 1988, to General Electric Co.

T. Aya, Y. Kubo, T. Sasagawa, Jap. Pat. 097,655, 01 Aug 1979, to Toray Industries

D.F. Aycock, S.P. Ting, U.S. Patent 4,600,741, 15 July 1986, to General Electric Co.

D.F. Aycock, S.P. Ting, U.S. Patent 4,642,358, 1987 to General Electric Co.

D.F. Aycock, S.P. Ting, U.S. Patent 5,331,060, 19 July 1994, to General Electric Co.

R. Babrowicz, B.C. Childress, K.R. Ahlgren, G.P. Shah, Europ. Pat. Appl. 597,502, 18 May 1994, to W. R. Grace & Co.

E. Badum, U.S. Patent 2,297,194, 29 Sept 1942, to Bergisch-Gladbach

M. Baer, E.H. Hankey, U.S. Patent 3,085,082, 09 Apr 1963, to Monsanto Chem.

M. Baer, E.H. Hankey, U.S. Patent 3,312,756, 04 Apr 1967; U.S. Patent 3,316,327, 25 Apr 1967, to Monsanto Chem.

S. Bagrodia, D.R. Fagerburg, J.J. Watkins, P.B. Lawrence, PCT Int. Appl. WO 01,240, 21 Jan 1993; PCT Int. Appl. WO 05,115 A1, 18 Mar 1993, to Eastman Kodak

S. Bagrodia, D.R. Fagerburg, P.B. Lawrence, J.J. Watkins, U.S. Patent 5,276,111, 04 Jan 1994a, to Eastman Kodak

S. Bagrodia, D.R. Fagerburg, J.J. Watkins, P.B. Lawrence, PCT Int. Appl. WO 94 09,071, 28 Apr 1994b, to Eastman Kodak

S.K. Bahl, P.J. Canterino, R. Shaw, Brit Pat. 2,152,515, 07 Aug 1985, to Mobil Oil

W.A. Bahn, G.H. Beall, J. Ference, C.J. Monahan, C.J. Quinn, P.S. Roussel, U.S. Patent 5,043,369, 27 Aug 1991, to Corning Inc.

F.W. Bailey, U.S. Patent 4,021,596, 03 May 1977, to Phillips Petroleum

C. Bailleux, M. Bernard, B. Dupont, G. Lozach, J.P. Mata, Fr. Pat. 2,535,332, 04 May 1984, to Electricité de France

D.G. Baird, A. Datta, PCT Int. Appl. 218,568, 29 Oct 1992, to Virginia Polytechnic Inst.

D.G.H. Ballard, A.J.P. Buckmann, PCT Int. Appl. 93 17,064, 02 Sept 1993, to Zeneca Ltd.

F. Ballauf, O. Bayer, L. Leichmann, Ger. Pat. 863,711, 27 Aug 1941, to Bayer

P.M. Bapat, J.E. Harris, Y.T. Chen, Europ. Pat. Appl. 477,757, 01 Apr 1992, to Amoco Corp.

J.P. Barnhouse, S.H. Yu, U.S. Patent 4,719,263, 12 Jan 1988, to B. F. Goodrich

J. Barraud, B. Boutevin, S. Gervat, Y. Parasie, J. Parisi, Europ. Pat. Appl. 565,424, 13 Oct 1993, to Alcatel Alsthom

C.A. Bartelo, M.Mori, *Adv. Additives & Modifiers for Polymer & Blends*, 3rd International Conference, Clearwater Beach, 23–25 Feb 1994

B.P. Barth, U.S. Patent 3,510,415, 05 May 1970, to Union Carbide Corp.

H.-J. Barth, H. Reinecke, G. Hottenbach, E. Kurtz, U.S. Patent 3,944,508, 16 Mar 1976, to Wacker Chem.

K.W. Bartz, L.P. Land, A.K. Mehta, A.A. Montagna, PCT Int. Appl. WO 06,169 A1, 01 Apr 1993a, to Exxon

K.W. Bartz, J.C. Floyd, P. Meka, F.C. Stehling, PCT Int. Appl. WO 006,168, 01 Apr 1993b, to Exxon

A.J. Batschinski, Z. Physik. Chem. **84**, 643 (1913)

L.A. Beer, Belg. Pat. 633,818, 19 Dec 1963, to Monsanto

E. Bencini, D. Ghidoni, Europ. Pat. 560,447, 15 Sept 1993, to Enichem Polimeri SARL

E.A. Benham, M.P. McDaniel, U.S. Patent 5,344,884, 06 Sept 1994, to Phillips

E.A. Benham, F.W. Bailey, J.D. Wehmeyer, M.P. McDaniel, U.S. Patent 5,378,764, 03 Jan 1995, to Phillips

H.R. Bhattacharjee, Y.P. Khanna, R. Kumar, J.J. Belles, PCT Int. Appl. 012,836, 1 Nov 1990, to AlliedSignal

P. Bier, C. Indner, Europ. Pat. Appl. 063,263, 27 Oct 1982, to Bayer

G. Biglione, G.C. Fasulo, Ger. Offen. 3,310,757, 29 Sept 1983, to Montedison

R. Binsack, E. Reese, J. Wank, Ger. Pat. 2,735,092, 15 Feb 1979; Ger. Pat. 2,755,025; 2,755,026, 13 June 1979, to Bayer

R. Binsack, D. Rempel, P. Bier, C. Lindner, Europ. Pat. Appl. 056,243, 21 July 1982, to Bayer

C.A.B.. Bjoerkengren, E.S. Joensson, Swed. Pat. 413,031, 31 Mar 1980, to Aktiebolag Akerlund och Rausing

D.G. Bland, J.J. Conte, U.S. Patent 5,017,622, 21 May 1991, to Dow Chemical

D.G. Bland, J.J. Conte, U.S. Patent 5,179,130, 12 June 1993; U.S. Patent 5,218,007, 08 June 1993, to Dow Chemical

W.G. Blasius Jr., Intl. Pat. Appl. PCT WO 92 013,917, 20 Aug 1992, to Novacor Chem.

W.G. Blasius Jr., U.S. Patent 5,290,862, 01 Mar 1994, to Novacor Chem.

R.B. Blodgett, Rubber Chem. Technol. **52**, 410 (1979)

U. Blumenstein, P. Klaerner, H. Schuch, H.-M. Walter, U.S. Patent 5,334,658, 02 Aug 1994, to BASF

L. Boehm, H.F. Enderle, H. Jastrow, Europ. Pat. Appl. 517,222, 09 Dec 1992, to Hoechst

V.C. Boger, A.G. Thomas, U.S. Patent 2,854,425, 30 Sept 1958, to B. F. Goodrich

E. M. Boldebuck, U.S. Patent 3,063,872, 13 Nov 1962, to General Electric Co.

C. Bonfanti, A. Lezzi, U. Pedretti, A. Roggero, F.P. La Mantia, Europ. Pat. Appl. 565,195, 13 Oct 1993, to Eniricerche

L.J. Bonis, A.M. Adur, SPE Techn. Pap. **41**, 3156 (1995)

D.C. Bookbinder, P.D. Sybert, U.S. Patent 5,135,990, 04 Aug 1992, to General Electric Co.

R.C. Bopp, K.G. Balfour, Europ. Pat. Appl. 550,204, 07 July 1993, to General Electric Co.

R.J.M. Borggreve, R.J. Gaymans, Polym. Commun. **30**, 71 (1989)

L.G. Bourland, U.S. Patent 4,388,443, 14 June 1983, to Atlantic Richfield

M. Bousmina, J.F. Palierne, L.A. Utracki, Polym. Eng. Sci. **39**, 1049 (1999)

O.M. Boutni, P.Y. Liu, Europ. Pat. Appl. 110,222, 13 June 1983, to General Electric Co.

D.K. Brandom, J.P. Desouza, D.G. Baird, G.L. Wilkes, J. Appl. Polym. Sci. **66**, 1543 (1997)

F. Brandstetter, A. Echte, H. Gausepohl, H. Naarmann, Europ. Pat. Appl. 048,400, 31 Mar 1982a, to BASF

F. Brandstetter, A. Echte, J. Hambrecht, H. Naarmann, Ger. Offen. 3,115,368, 18 Nov 1982b; Europ. Pat. Appl. 048,399, 31 Mar 1982, to BASF

F. Brandstetter, J. Hambrecht, B. Scharf, Europ. Pat. Appl. 062,838, 20 Oct 1982c, to BASF

F. Brandstetter, J. Hambrecht, H. Muenstedt, Ger. Offen. 3,149,812, 21 July 1983a, to BASF

F. Brandstetter, J. Hambrecht, B. Scharf, Ger. Offen. 3,203,488, 11 Aug 1983b, to BASF

F. Brandstetter, J. Hambrecht, G. Blinne, K.H. Illers, Ger. Offen. 3,202,370, 04 Aug 1983c, to BASF

R.L. Briggs, R.L. Price, U.S. Patent 3,096,300, 02 July 1963, to Dow Chemical

J.R. Briggs, R.G. Newburg, R.E. Clayton, U.S. Patent 2,854,435, 30 Sept 1958, to Esso

T.A. Bright, A. Deckers, M. Knoll, Ger. Offen., 4,138,574, 27 May 1993, to BASF

T.O. Broadhed, Europ. Pat. Appl. 209,294, 21 Jan 1987, to Du Pont Canada

K. Bronstert, R. Jung, J. Schwaab, D. Stein, Ger. Offen. 2,024,940, 02 Dec 1971, to BASF

G.T. Brooks, B.L. Joss, C.L. Myers, Europ. Pat. Appl. 572,267, 01 Dec 1993, to Amoco Corp.

G.T. Brooks, B.L. Joss, C.L. Myers, U.S. Patent 5,283,284, 01 Feb 1994, to Amoco Corp.

S.B. Brown, U.S. Patent 4,831,087, 16 May 1989, to General Electric Co.

S.B. Brown, in *Reactive Extrusion: Principles and Practice*, ed. by M. Xanthos (Hanser, Munich, 1992)

S.B. Brown, E.J. Fewkes Jr., Europ. Pat. Appl. 493,675, 08 July 1992, to General Electric Co.

S.B. Brown, E.J. Fewkes Jr., U.S. Patent 5,189,114, U.S. Patent 5,290,863, 01 Mar 1994, to General Electric Co.

S.B. Brown, D.J. McFay, J.B. Yates III, G.F. Lee PCT Int. Pat. Appl. WO 87 00,850, 12 Feb 1987, to General Electric Co.

T.F. Brownscombe, R.M. Bass, P.K. Wong, G.C. Blytas, W.P. Gergen, M. Mores, U.S. Patent 5,646,193, 08 July 1997, to Shell Oil

C.B. Bucknall, *Toughened Plastics* (Applied Science, London, 1977)

C.B. Bucknall, I.K. Partridge, M.V. Ward, J. Mater. Sci. **19**, 2064 (1984)

C.B. Bucknall, D.R. Paul, *Polymer Blends: Formulations and Performance*, vol. 1 and 2 (Wiley, New York, 2000)

C.B. Bucknall, D.R. Paul, Polymer **50**, 5539 (2009)

C.B. Bucknall, D.R. Paul, Polymer **54**, 320 (2013)

F. Bueche, J. Chem. Phys. **20**, 1959 (1952)

F. Bueche, J. Chem. Phys. **25**, 599 (1956)

F. Bueche, *Physical Properties of Polymers* (Interscience, New York, 1962)

F. Buehler, E. Schmid, H.J. Schultze, Europ. Pat. Appl. 536,679, 14 Apr 1993, to Ems-Inventa

F. Buehler, E. Schmid, H.J. Schultze, U.S. Patent 5,346,936, 13 Sept 1994, to Ems-Inventa

A.L. Bull, G. Holden, J. Elastom. Plast. **9**, 281 (1977)

K. Burg, E. Wolters, H. Cherdron, Ger. Offen. 2,037,823, 03 Feb 1972, to Hoechst

W.E. Burgert, Europ. Pat. Appl. 215,150, 25 Mar 1987, to Dow Chemical

A.M. Burnell, U.S. Patent 5,272,182, 21 Dec 1993, to General Electric Co.

P.M. Buschbaum, Polym. J. **45**, 34 (2013)

W.F. Busse, J. Phys. Chem. **36**, 2862 (1932)

J.D. Bussink, J.W.J. De Munck, P.C.A.M. van Abeelen, U.S. Patent 4,122,131, 24 Oct 1978, to General Electric Co.

S. Bywater, Adv. Polym. Sci. **4**, 66 (1965)

D.W. Caird, U.S. Patent 3,087,908, 30 Apr 1961, to Osaka Kinzoku Kogyo

M. Cakmak, A. Dutta, U.S. Patent 5,114,987, 19 May 1992, to Edison Polymer Innovation Corp.

G.W. Calundann, F. Herold, E.C. Chenevey, T.S. Chung, Europ. Pat. Appl. 510,818, 28 Oct 1992, to Hoechst Celanese Corp.

G.W. Calundann, F. Herold, E.C. Chenevey, T.S. Chung, U.S. Patent 5,290,884, 01 Mar 1994, to Hoechst Celanese Corp.

R. Camargo, F. Mercer, T.-C. Cheng, PCT. Intl. Appl. WO 86 04,079, 17 July 1986, to Raychem Corp.

G.A. Campbell, D.H. Rasmussen, U.S. Patent 5,358,675, 25 Oct 1994; U.S. Patent 5,369,135, 29 Nov 1994, to Mobil Oil Corp.

J.R. Campbell, J.R. Presley, U.S. Patent 5,380,796, 10 Jan 1995, to General Electric Co.

P.J. Canterino, J.P. Freudemann, Europ. Pat. Appl. 148,567, 17 July 1985, to Mobil Oil

P.J. Canterino, D.V. Dobreski, R.G. Shaw, U.S. Patent 4,579,912, 01 Apr 1986, to Mobil Oil

W.H. Carothers, Chem. Rev. **8**, 353 (1931)

W.H. Carothers, U.S. Patent 2,071,250; 2,071,251; 2,071,252; 2,071,253, 16 Feb 1937, to E. I. du Pont

W.H. Carothers, I. Williams, A.M. Collins, J.E. Kirby, J. Am. Chem. Soc. **53**, 4203 (1931)

J. Castelein, Europ. Pat. Appl. 060,525, 22 Sept 1982, to Montefina

J.Y. Cavaille, J. Perez, C. Jourdan, G.P. Johari, J. Polym. Sci. B Polym. Phys. **25**, 1847 (1987)

G. Cecchin, F. Guglielmi, Europ. Pat. Appl. 373,660, 20 June 1990, to Himont

Celanese Corporation, Fr. Demand, 2,484,430, 18 Dec 1981

Celanese Corporation, U.S. Patent 4,489,190, 30 June 1984

Ceramer™ Hoechst-Ticona, Techn. Inf. (1996)

R.J. Ceresa, N.E. Davenport, T.L. Trudgian, Brit. Pat. 1,112,024, 01 May 1968, to W. R. Grace & Co.

J. Cerny, R. Troncy, Fr. Pat. 2,473,534, 17 July 1981, to Rhône-Poulenc

G.R. Chambers, G.F. Smith, J.B. Yates III, U.S. Patent 5,384,359, 24 Jan 1995, to General Electric Co.

M.F. Champagne, M.M. Dumoulin, L.A. Utracki, J.P. Szabo, Polym. Eng. Sci. **36**, 1636 (1996)

G.M. Chapman, R.H. Downie, U.S. Patent 5,352,716, 04 Oct 1994, to Ecostar International

L.F. Charbonneau, B. Gupta, H.C. Linstid, L.C. Sawyer, J.P. Shepherd, U.S. Patent 5,393,848, 28 Feb 1995, to Hoechst Celanese Corp.

J.J. Charles, E.A. Coleman, Europ. Pat. Appl. 033,393, 12 Aug 1981, to GAF Corp.

J.J. Charles, R.C. Gasman, Ger. Offen. 2,825, 236, 25 Jan 1979, to GAF Corp.

Y. Charlier, J.L. Hedrick, T.P. Russell, Polymer **36**, 4529 (1995)

D. Chattopadhyaya, *History of Science and Technology in Ancient India* (Firma KLM PVT, Calcutta, 1986)

Y.T. Chen, D.P. Sinclair, Europ. Pat. Appl. 361,636, 04 Apr 1990, to Amoco Co.

P.N. Chen, T.S. Chung, P.J. Harget, U.S. Patent 4,963,628, 16 Oct 1990, to Hoechst Celanese Corp.

P.N. Chen, A. Forschirm, M. Glick, M. Jaffe, U.S. Patent 5,070,144, 03 Dec 1991, to Hoechst Celanese Corp.

Y.W. Cheung, D.V. Dobreski, R. Turner, M. Wheeler, Y.P. Handa, U.S. Patent 8,304,499, 6 Nov 2012, to Pactiv Corp.

K. Chiba, K. Yamada, T. Muraki, Jap. Pat. 079,942, 14 July 1978, to Toray Ind.

C.L. Child, R.B.F.F. Clarke, B.J. Habgood, Brit. Pat. 544,359, 09 Apr 1942, to ICI

J. Cho, Macromol. Res. **21**, 1360 (2013)

Y. Choi, J.B.P. Soares, Can. J. Chem. Eng. **90**, 646 (2012)

H.H. Chuah, T. Kyu, T.E. Helminiak, Polymer **30**, 1591 (1989a)

H.H. Chuah, L.-S. Tan, F.E. Arnold, Polym. Eng. Sci. **29**, 107 (1989b)

H.-K. Chuang, C.D. Han, Adv. Chem. Ser. **204**, 171 (1984)

D. Chundury, PCT Int. Appl. WO 013,170, 08 July 1993, to Ferro Corp.

D. Chundury, U.S. Patent 5,278,231, 11 Jan 1994, to Ferro Corp.

D. Chundury, A.S. Scheibelhoffer, U.S. Patent 5,321,081, 14 June 1994, to Ferro Corp.

J.C. Chung, M.K. Akkapeddi, Polymer Prepr. **34**(1), 614 (1993)

G.C. Chung, J.A., Kornfield, S.D. Smith, Macromolecules **27**, 964, 5729 (1994)

L. Clementini, A.F. Galambos, G. Lesca, K. Ogale, L. Spagnoli, M.E. Starsinic, L. Giuseppe, Europ. Pat. Appl. 552,810, 28 July 1993, to Himont Inc.

R.R. Clikeman, D.S. Cinoman, E.D. Weiler, E.D., U.S. Patent 4,650,824, 17 Mar 1987, to Rohm & Haas Co.

J.C. Coburn, H.H. Yang, U.S. Patent 5,366,781, 22 Nov 1994, to E. I. du Pont

F.N. Cogswell, B.P. Griffin, J.B. Rose, Europ. Pat. Appl. 030,417, 17 June 1981, to ICI

F.N. Cogswell, B.P. Griffin, J.B. Rose, U.S. Patent 4,386,174, 1983, to ICI

F.N. Cogswell, B.P. Griffin, J.B. Rose, U.S. Patent 4,433,083, 1984, to ICI

S.C. Cohen, WO Pat. 00,972, 1980, to General Electric Co.

S.C. Cohen, Can. Pat. 1,123,534, 11 May 1982, to General Electric Co.

R.H. Colby, C.J.T. Landry, M.R. Landry, T.E. Long, D.J. Massa, D.M. Teegarden, Europ. Pat. Appl. 530,648, 10 Mar 1993, to Eastman Kodak

R.H. Colby, C.J.T. Landry, M.R. Landry, T.E. Long, D.J. Massa, D.M. Teegarden, U.S. Patent 5,276,089, 04 Jan 1994, to Eastman Kodak

Q.P. Cole, U.S. Patent 2,912,410, 10 Nov 1959, to General Electric Co.

M.M. Coleman, J.F. Graf, P.C. Painter, *Specific Interactions and the Miscibility of Polymer Blends* (Technomics Publishing, Lancaster, 1991)

D.I. Collias, D.G. Baird, Polym. Eng. Sci. **35**, 1178 (1995)

R. Colombo, Ital. Pat. Appl. 370,578, 1939, to Lavorazione Materie Plastiche

W.R. Conrad, R.J. Reid, U.S. Patent 3,098,839, 23 July 1963, to Firestone Tire & Rub

H.W. Coover Jr., W.C. Wooten Jr., U.S. Patent 3,0058,949, 16 Oct 1962, to Eastman Kodak

O.J. Cope, U.S. Patent 3,435,093, 25 Mar 1969, to E. I. du Pont

A.Y. Coran, R. Patel, Ger. Offen. 2,757,430, 06 July 1978; U.S. Patent 4,130,534, 19 Dec 1978, to Monsanto

L. Corbellini, Ger. Offen. 1,137,859, 11 Oct 1962, to Montecatini

S. Cottis, H. Chin, W.H. Shiau, D. Shopland, U.S. Patent 5,262,473, 16 Nov 1993, to Enichem America

P.R. Couchman, J. Appl. Polym. Sci. **60**, 1057 (1996)

W.R. Coutant, Europ. Pat. Appl. 588,147, 23 Mar 1994, to Phillips

M.A. Cowan, Europ. Pat., Appl. 095,299, 30 Nov 1983, to Intercont. Plast.

J.M.G. Cowie, R. Ferguson, Macromolecules **22**, 2307 (1989)

J.M.G. Cowie, V. Arrighi, in *Polymer Physics: From Suspensions to Nanocomposites and Beyond*, ed. by L.A. Utracki, A.M. Jamieson (Wiley, Hoboken, 2010)

M.J. Cran, S.W. Bigger, Polym. Plast. Technol. Eng. **48**, 272 (2009)

H. Craubner, G. Illing, A. Hrugesch, Ger. Offen. 1,138,922, 31 Oct 1962, to BASF

J.W. Crawford, W.G. Oakes, Brit. Pat. 941,083, 06 Nov 1963, to ICI

J.W. Crawford, W.G. Oakes, Ger. Offen. 1,217,608, 16 May 1966, to ICI

R.W. Crawford, W.K. Witsiepe, Ger. Offen. 2,224,678, 30 Nov 1972, to E. I. du Pont

S.H. Cree, C.A. Wilson, S. A. de Vries, U.S. Patent 5,795,941, 18 Aug 1998, to Dow Chemical

M.G. Cross, R. Lines, U.S. Patent 5,378,402, 0 3 Jan 1995, to Raychem Limited

Daicel Chemical Industries, Jap. Pat. 049,656, 23 Mar 1982; Jap. Pat. 117,563, 22 July 1982

Daicel Chemical Industries, U.S. Patent 4,393,169, 12 July 1983

Daicel Chemical Industries, Jap. Pat. 06,253, 13 Jan 1984

Dainichiseika Color & Chem. Co., Jap. Pat. 053,552, 30 Mar 1982

Dainichiseika Color & Chem. Co., Jap. Pat. 83,039, 18 May 1983

Dainippon Ink & Chem., Jap. Pat. 025,355, 10 Feb 1982

Dainippon Ink & Chem., Jap. Pat. 008,760, 18 Jan 1983

P.O. Damm, P. Matthies, in *Handbook of Plastics Materials and Technology*, ed. by I.I. Rubin (Wiley, New York, 1990)

S. Dashevsky, K.S. Kim, S.W. Palmaka, PCT Int. Appl. 013,172, 08 July 1993, to Akzo

S. Dashevsky, K.-S. Kim, S.W. Palmaka, R.L. Johnston, L.A.G. Busscher, J.A. Juijn, U.S. Patent 5,346,970, 13 Sept 1994, to Akzo Nobel

S. Datta, D.J. Lohse, *Polymeric Compatibilizers: Uses and Benefits in Polymer Blends* (Hanser, Munich, 1996)

G.J. Davies, U. K. Patent Appl. 2,220,416, 10 Jan 1990, to T&N Technology

M. Davies, P.M. Hatton, Europ. Pat. Appl. 611,384, 24 Aug 1994, to ICI

J.H. Davis, Brit. Pat. 1,403,797, 20 Aug 1975, to ICI

J.A. Davis, J.K. Valaitis, Europ. Pat. Appl. 564,961, 13 Oct 1993, to Bridgestone/Firestone

J.A. Davis, J.K. Valaitis, U.S. Patent 5,286,798, 15 Feb 1994, to Bridgestone/Firestone

S. Davison, W.P. Gergen, U.S. Patent 4,041,103, 09 Aug 1977, to Shell Oil

S. Davison, W.P. Gergen, U.S. Patent 4,242,470, 30 Dec 1980, to Shell Oil

F. Dawans, D. Binet, U.S. Patent 4,255,524, 10 Mar 1981, to Institut Francais du Petrole

R.L. Dawson, U.S. Patent 5,206,294, 27 Apr 1993, to E. I. du Pont

J. De Boer, J.M.H. Heuschen, U.S. Patent 4,788,252, 29 Nov 1988, to General Electric Co.

C. De Rosa, F. Auriemma, Prog. Polym. Sci. **31**, 145 (2006)

B.D. Dean, U.S. Patent 4,937,297, 26 June 1990, to Amoco

B.D. Dean, U.S. Patent 5,115,046, 19 May 1992, to Amoco

P. Debye, J. Appl. Phys. **15**, 338 (1944)

P. Debye, J. Appl. Phys. **17**, 319 (1946)

P.G. de Gennes, *Scaling concepts in polymer physics* (Cornell University Press, Ithaca, 1979)

C. Dehennau, T. Depireux, I. Claeys, Europ. Pat. Appl. 587,216, 16 Mar 1994, to Solvay

M.E.J. Dekkers, U.S. Patent 5,290,881, 01 Mar 1994, to General Electric Co.

M.E.J. Dekkers, D.K. Yoshimura, M.P. Laughner, U.S. Patent 5,171,778, 15 Dec 1992, to General Electric Co.

J.W. DeMunck, J.H.G. Lohmeijer, Europ. Pat. Appl. 177,989, 16 Apr 1986, to General Electric Co.

M. Deng, L.S. Nair, S.P. Nukavarapu, T. Jiang, W.A. Kanner, X. Li, S.G. Kumbar, A.L. Weikel, N.R. Krogman, H.R. Allcock, C.T. Laurencin, Biomaterials **31**, 4898 (2010)

A.J. DeNicola Jr., M.R. Conboy, U.S. Patent 5,286,791, 15 Feb 1994, to Himont

A.J. DeNicola, T.A. Giroux, U.S. Patent 5,370,813, 06 Dec 1994, 26 Mar 1990, to Himont

A.J. DeNicola Jr., J.A. Smith, M. Felloni, U.S. Patent 5,414,027, 09 May 1995, to Montell North America

A.J. DeNicola Jr., J.A. Smith, M. Felloni, U.S. Patent 5,605,936, 25 Feb 1997, to Montell North America

J.L. Derudder, U.S. Patent 4,960,836, 02 Oct 1990, to General Electric Co.

J.L. Derudder, I.-C.W. Wang, Europ. Pat. Appl. 537,014, 14 Apr 1993, to General Electric Co.

S. Detyothin, A. Kathuria, W. Jaruwattanayon, S.E.M. Selke, R. Auras, in *Poly (Lactic Acid)*, ed. by R. Auras, L.-T. Lim, S.E.M. Selke, H. Tsuji (Wiley, Hoboken, 2010)

R. Dhein, W. Ebert, H. Hugl, H. Ohst, Ger. Pat. 4,142,765, 24 June 1993, to Bayer

R.L. Dieck, S.C. Cohen, PCT Int. Appl. 000,972, 15 May 1980, to General Electric Co.

R.L. Dieck, R.J. Kostelnik, Europ. Pat. Appl. 071,773, 16 Feb 1983, to General Electric Co.

R.L. Dieck, E. J. Quinn, U.S. Patent 4,026,839, 31 May 1977; U.S. Patent 4,055,520, 25 Oct 1977; U.S. Patent 4,061,606, 06 Dec 1977, to Armstrong Cork

R.L. Dieck, A.D. Wambach, PCT Int. Appl. 001,167, 12 June 1980, to General Electric Co.

L.K. Djiauw, U.S. Patent 5,320,899, 14 June 1994, to Shell Oil

A.J. Dijkstra, M.E.G. Jones, Ger. Offen. 1,814,073, 24 July 1969, to ICI

D.D. Dixon, M.E. Ford U.S. Patent 4,137,280, 30 Jan 1979, to Air Products & Chemicals

F.Z. Dobkowski, Polymer **25**(3), 110 (1980)

D.V. Dobreski, J.J. Donaldson, U.S. Patent 5,290,866, 01 Mar 1994, to Mobil Oil Corp.

H. Doerffurt, F. Waeteraere, Ger. Offen. 2,555,691, 16 June 1977, to Dynamit Nobel

M. Doi, *Introduction to polymer physics* (Clarendon, Oxford, 1995)

M. Doi, S.F. Edwards, *The Theory of Polymer Dynamics* (Oxford University Press, New York, 1986)

M. Doi, A. Onuki, J. Phys. (Paris) **2**, 1631 (1992)

A.K. Doolittle, J. Appl. Phys. **22**, 1031 (1951)

L. D'orazio, R. Greco, C. Mancarella, E. Martucelli, G. Ragosta, C. Silvester, Polym. Eng. Sci. **22**, 536 (1982)

S. Dorudiani, C.B. Park, M.T. Kortschot, Polym. Eng. Sci. **38**, 1205 (1998)

Dow Chemical Co., Brit. Pat. 942,363, 20 Nov 1963

Dow Chemical Co., Neth. Pat. Appl. 6,507,478, 20 Dec 1965

M. Droescher, M. Bartmann, K. Burzin, R. Feinauer, C. Gerth, W. Neugebauer, H. Jadamus, W. Ribbing, J. Lohmar, Europ. Pat. Appl. 205,816, 30 Dec 1986 to Hüls

R.S. Drzal, B.S. Ehrlich, L.H. La Nieve III, Europ. Pat. Appl. 116,450, 02 Jan 1986, to Upjohn Co.

M.A. Drzewinski, U.S. Patent 5,248,732, 28 Sept 1993, to Enichem

M.A. Drzewinski, U.S. Patent 5,286,794, 15 Feb 1994; U.S. Patent 5,292,809, 08 Mar 1994, to Enichem

M. Dubois, B. Guyot, R. Thommeret, Europ. Pat. Appl. 554,932, 11 Aug 1993, to Solvay

D.L. Dufour, U.S. Patent 4,329,272, 11 May 1982, to Monsanto

D.L. Dufour, Europ. Pat. Appl. 272,239, 22 June 1988, to Monsanto

M.M. Dumoulin, Ph.D. thesis, Ecole Polytechnique, Montreal, 1988

D.P. Durbin, R.L. Danforth, R.G. Lutz, U.S. Patent 4,377,647, 22 Mar 1983, to Shell Oil

N.E. Durfee Jr., J.A. Rock, Can. Pat. Appl. 2,050,182, 01 Mar 1993, to General Electric Co.

R.R. Durst, Ger. Offen. 2,009,407, 12 Nov 1970, to General Tire & Rubber

R.R. Durst, U.S. Patent 3,907,929, 23 Sept 1975, to General Tire & Rubber

A. Dutta, M. Cakmak, Rubber. Chem. Techn. **65**, 932 (1992)

Dynamit Nobel, Fr. Pat. 2,004,607, 28 Nov 1969

E. I. du Pont de Nemours & Company, Brit. Pat. 550,931, 01 Feb 1942

T. Eckel, G. Fennhoff, W. Jakob, K. Oott, J. Schoeps, D. Wittmann, Europ. Pat. Appl. 570,797, 24 Nov 1993, to Bayer

O.M. Ekiner, J.W. Simmons, U.S. Patent 5,248,319, 28 Sept 1993, to E. I. du Pont

M.J. El-Hibiri, G.S. Jack, W.E. Kelly, S.R. Patel, U.S. Patent 5,151,462, 29 Sept 1992, to Amoco Corp.

M.J. El-Hibri, J.L. Melquist, U.S. Patent 5,206,311, 27 Apr 1993, to Amoco Corp.

S. Ellebrach, S. Chum, SPE Techn. Pap. **44**, 1795 (1998)

M.D. Ellul, U.S. Patent 5,290,886, 01 Mar 1994, to Advanced Elastomer System

D.D. Emrick, U.S. Patent 3,268,627, 23 Aug 1966, to Standard Oil Co.

S.J. Enderle, U.S. Patent 4,480,054, 30 Oct 1984, to E. I. Du Pont

H. Endo, T. Ishii, Europ. Pat. Appl. 122,601, 24 Oct 1984, to Idemitsu Petrochem.

T. Endo, O. Kanoto, N. Matsunaga, Europ. Pat. Appl. 354,802, 14 Feb 1990, to Polyplastics

U. Epple, M.-J. Brekner, U.S. Patent 5,359,001, 25 Oct 1994, to Hoechst

U. Epple, M.-J. Brekner, H. Cherdron, PCT Int. Appl. 016,585, 01 Oct 1992, to Hoechst

Esso, Brit. Pat. 851,028, 12 Oct 1960

Esso, Brit. Pat. 893,540, 11 Apr 1962

J.C. Falk, U.S. Patent 4,302,555, 24 Nov 1981, to Borg-Warner Chem.

U. Falk, O. Hermann-Schoenherr, Europ. Pat. Appl. 513,655, 19 Nov 1992, to Hoechst

Farbwerke Hoechst, Fr. Pat. 1,588,354, 10 Apr 1970

R.J. Farris, B.W. Jo. PCT Int. Appl. WO 93 01,238, 21 Jan 1993, to University of Massachusetts

K.-P. Farwerck, H. Lauke, G.E. McKee, F. Seitz, N. Guentherberg, H. Ohlig, S. Besecke, H. Kroeger, W. Loth, N. Niessner, L. Schlemmer, D. Wagner, Europ. Pat. Appl. 534,235, 31 Mar 1993, to BASF

R.A. Fava, U.S. Patent 4,160,792, 10 July 1979, to ARCO

R.A. Fava, U.S. Patent 4,284,735, 18 Aug 1981, to ARCO

R.A. Fava, K.W. Doak, U.S. Patent 4,221,880, 09 Sept 1980, to ARCO

R. Fayt, R. Jerôme, Ph. Teyssié, J. Polym. Sci., Polym. Lett. Ed. **24**, 25 (1986a); Makromol. Chem. **187**, 837 (1986)

R. Fayt, Ph. Teyssié, D. Hanton, Fr. Pat. 2,582,659, 05 Dec 1986b, to Isover Saint Gobain

A.R. Federl, G. Kipouras, U.S. Patent 4,588,773, 13 May 1986, to Borg-Warner Chem.

F. Fenouillot, P. Cassagnau, J.-C. Majeste, Polymer **50**, 1333 (2009)

J.D. Ferry, R.F. Landel, M.L. Williams, J. Appl. Phys. **26**, 359 (1955)

M. Fikentscher, C. Heuce, Ger. Offen. 654,989, 1930, to I. G. Farbenindustrie

M. Fikentscher, W. Wolff, Ger. Offen. 660,793, 1931, to I. G. Farbenindustrie

W.K. Fischer, So. Afric. Pat. 72 00,388, 23 Aug 1972, to Uniroyal

J.-D. Fischer, W. Siol, U.S. Patent 5,218,050, June 1993, to Röhm

J.-D. Fischer, W. Siol, U.S. Patent 5,380,801, 10 Jan 1995, to Röhm

E.D. Flexman Jr., U.S. Patent 5,318,813, 07 June 1992, to E. I. du Pont

D.W. Fox, S.J. Shafer, L.M. Maresca, D.C. Clagett, Europ. Pat. Appl. 322,558, 05 July 1989, to General Electric Co.

P.D. Frayer, *NRCC/IMI symposium Polyblends-'93*, Boucherville, 26–27 Oct 1993

P.D. Frayer, *PPS Regional Meeting*, Akron, 4–7 Apr 1994

J. M. J. Fréchet, I. Gitsov, C. J. Hawker, L. Lochman, K. Wooley, *4th SPSJ International Polymer Conference*, Yokohama, 29 Nov–3Dec 1992

W.T. Freed, U.S. Patent 3,920,602, 18 Nov 1975, to Celanese Corp.

S. Freinkel, *Plastic: A Toxic Love Story* (Houghton Mifflin Harcourt, Boston, 2011)

D. Freitag, G. Fengler, L. Morbitzer, Angew. Chem. Int. Ed. **30**, 1598 (1991)

H.H. Frey, Ger. Offen. 1,045,089, 20 Nov 1958; Ger. Offen. 1,111,383, 13 Oct 1958, to Hoechst

P. Freyburger, U.S. Patent 180,568, 1876

K. Friedrich, in *Crazing in Polymers*, ed. by H. H. Kausch. Adv. Polym. Sci. **52/53** (Springer, Berlin, 1983)

Chr. Friedrich, W. Gleinser, E. Korat, D. Maier, J. Wesse, J. Rheol. **39**, 1411 (1995)

H.G. Fritz, R. Anderlik, Kautschuk Gummi Kunstst. **46**, 374 (1993)

M.F. Froix, N.S. Trouw, R.R. Schwarz, Fr. Demand 2,483,442, 04 Dec 1981, to Celanese Corp.

H.C. Fromuth, L.A. Cohen, W.T. Freed, D.S. Cinoman, Europ. Pat. Appl. 494,542, 15 July 1992, to Röhm & Haas

K.D. Fudge, U.S. Patent 4,666,946, 19 May 1987, to Atlantic Richfield

K. Fuhr, F. Mueller, K.H. Ott, J. Schoeps, H. Peters, W. Ballas, Europ. Pat. Appl. 463,495, 02 Jan 1992, to Bayer

S. Fuji, S.P. Ting, Europ. Pat. Appl. 226,851, 01 July 1987, to General Electric Co.

H. Fujie, Europ. Pat. 558,256, 01 Sept 1993, to Teijin

M. Fujii, Y. Ohtsuka, Chem. High Polym. **13**, 54 (1954)

S. Fujii, H. Ishida, M. Morioka, A. Saito, R. van der Meer, PCT Intl. Appl. 005,304, 11 Sept 1987, to General Electric Co.

Y. Fujita, T. Kawamura, K. Yokoyama, K. Yokomizo, S. Toki, U.S. Patent 5,298,557, 29 Mar 1994, to Tonen Corp.

G. Fujiwara, Jap. Pat. 041,456, 07 Dec 1971, to Toray Industries

K. Fukuda, H. Kasahara, Europ. Pat. Appl. 044,703, 27 Jan 1982; Jap. Pat. 105,452, 30 June 1982, to Asahi-Dow

O. Fukui, Y. Inuizawa, S. Hinenoya, Y. Takasaki, Fr. Pat. 2,522,331, 02 Sept 1983, to Ube Industries

M. Fukushima, H. Mitarai, Jap. Pat. 022,852, 30 June 1971, to Japan Synthetic Chem.

N. Fukushima, I. Namazue, T. Saito, K. Hieda, Jap. Pat. 116,053, 10 Sept 1979, to Sumitomo Chem.

M. Furuta, T. Maruyama, Europ. Pat. Appl. 356,194, 28 Feb 1990, to Sumitomo Chem.

G.M. Gaafar, Europ. Pat. Appl. 383,977, 29 Aug 1990, to General Electric Co.

S.K. Gaggar, J.M. Dumler, T.B. Cleveland, Europ. Pat. Appl. 294,722, 14 Dec 1988, to Borg-Warner Chem.

S.K. Gaggar, J.M. Dumler, T.B. Cleveland, U.S. Patent 4,857,590, 15 Aug 1989, to Borg-Warner Chem.

D.M. Gale, U.S. Patent 4,117,033, 26 Sept 1978, to E. I. du Pont

G.M. Gale, U. K. Pat. Appl. 80 30,586, 1980, to RAPRA

P. Galli, M. Spataro, Europ. Pat. Appl. 077,532, 27 Apr 1983, to Montedison

R.R. Gallucci, PCT Intl. Appl. 006,168; 006,169, 25 Aug 1988, to General Electric Co.

R.R. Gallucci, D.C. Bookbinder, U.S. Patent 4,806,597, 21 Feb 1989, to General Electric Co.

R.R. Gallucci, R. van der Meer, R.W. Avakian, PCT Intl. Appl. 005,372, 05 Dec 1985, to General Electric Co.

M.E. Galvin, G.E. Wnek, Polym. Commun. **23**, 795 (1982)

R.J. Gambale, D.C. Clagett, L.M. Maresca, S.J. Shafer, U.S. Patent 5,280,088, 18 Jan 1994, to General Electric Co.

R.J. Gambale, L.M. Maresca, D.C. Clagett, S.J. Shafer, Europ. Pat. Appl. 285,692; 285,693, 12 Oct 1988, to General Electric Co.

F.W. Gander, E.F. Hoegger, W.P. Kane, U.S. Patent 4,020,126, 26 Apr 1977, to E. I. du Pont

R.A. Garcia, R.J. Martinovich, U.S. Patent 4,451,607, 29 May 1984, to Phillips

K.N. Gary, Can. Pat. Appl. 2,063,492, 20 Sept 1993

H. Gausepohl, G. Heinz, B. Schmitt, Europ. Pat. Appl. 048,388, 31 Mar 1982, to BASF

R. Gelles, W.P. Gergen, R.G. Lutz, Europ. Pat. Appl. 211,467, 25 Feb 1987, to Shell

R. Gelles, R.G. Lutz, W.P. Gergen, Europ. Pat. Appl. 261,748, 30 Mar 1988, to Shell

R. Gelles, W.P. Gergen, R.G. Lutz, M.J. Modic, U.S. Patent 5,371,141, 06 Dec 1994, to Shell

General Electric Company, Neth. Pat. Appl. 6,517,152, 06 July 1966

General Electric Company, Jap. Pat. 100,159, 09 June 1984

E.R. George, U.S. Patent 5,166,252, 24 Nov 1992, to Shell Oil

W.P. Gergen, S. Davison, U.S. Patent 4,090,996, 05 May 1977, to Shell Oil

W.P. Gergen, S. Davison, U.S. Patent 4,088,711, 09 May 1978, to Shell Oil

W.P. Gergen, R. G. Lutz, U.S. Patent 4,818,786, 04 Apr 1989, to Shell Oil

A.M. Gessler, W.H. Haslett Jr., U.S. Patent 3,037,954, 05 June 1962, to Esso

J.K. Gianchandai, A. Hasson, R.J. Wroczynski, J B. Yates III, Europ. Pat. Appl. 550,206, 07 July 1993, to General Electric Co.

H. Gilch, D. Michael, Ger. Offen. 1,901,552, 13 Aug 1970, to Bayer

H.F. Giles Jr., U.S. Patent 4,390,665, 28 June 1983, to General Electric Co.

H.F. Giles Jr., U.S. Patent 4,455,410, 19 June 1984, to General Electric Co.

H.F. Giles Jr., U.S. Patent 4,657,987, 14 Apr 1987, to General Electric Co.

H.F. Giles Jr., R.P. Hirt Jr., U.S. Patent 4,579,910, 01 Apr 1986, to General Electric Co.

H.F. Giles Jr., J.N. Sasserath, U.S. Patent 4,579,909, 01 Apr 1986, to General Electric Co.

B.S. Giles, S. Vilasagar, Europ. Pat. Appl. 596,704, 11 May 1994, to General Electric Co.

H.F. Giles Jr., D.M. White, U.S. Patent 4,387,193, 28 June 1983, to General Electric Co.

Glanzstoff, Brit. Pat. 1,091,256, 15 Nov 1967

M. Glotin, R. Parsy, P. Abadie, Ger. Offen. 3,909,273, 05 Oct 1989, to Atochem.

K.J. Godbey, P.G. Martin, U.S. Patent 5,264,219, 23 Nov 1993, to Minnesota Mining & Manufacturing

K.J. Godbey, P.G. Martin, PCT Int. Appl. WO 94 03,539, 17 Feb 1994, to Minnesota Mining & Manufacturing

D.A. Godfrey, U.S. Patent 5,382,615, 17 Jan 1995, to Eastman Chemical

E.J. Goedde, F.F. Holub, P.S. Wilson, Ger. Offen. 2,917,941, 13 Nov 1980, to General Electric Co.

W. Goetz, M. Laun, W. Betz, W. Heckmann, Ger. Offen. 4,127,720, 25 Feb 1993, to BASF

K.B. Goldblum, Ger. Offen. 1,266,974, 10 July 1963, to General Electric Co.

K.B. Goldblum, Belg. Pat. 634,842, 13 Jan 1964, to General Electric Co.

A. Goldel, P. Potschke, in *Polymer Carbon Nanotube Composites*, ed. by T. McNally, P. Potschke (Woodhead Publishing, Cambridge, 2011)

A. Goldel, G. Kasaliwal, P. Potschke, G. Heinrich, Polymer **53**, 411 (2012)

R.C. Golike, Belg. Pat. 619,351, 27 Dec 1962, to E. I. du Pont

A. Golovoy, M. Cheung, U.S. Patent 5,281,664, 25 Jan 1994, to Ford Motor Co.

P.M. Gomez, Europ. Pat. Appl. 515,344, 25 Nov 1992, to Monsanto

Goodrich (B. F.) Co., Brit. Pat. 539,834, 25 Sept 1941

Goodrich (B. F.) Co., Brit. Pat. 830,226, 09 Mar 1960

W.F. Gorham, A.G. Farnham, U.S. Patent 3,117,945, 14 Jan 1964, to Union Carbide Corp.

J.C. Goswami, U.S. Patent 4,031,045, 21.06.1977, to Stauffer Chem.

S. Gotoh, K. Nagaoka, Europ. Pat. 570,972, 24 Nov 1993, to Sumitomo Chem.

A.C. Gowan, U.S. Patent 3,361,851, 02 Jan 1968, to General Electric Co.

A.C. Gowan, U.S. Patent 3,472,810, 14 Oct 1969, to General Electric Co.

T.S. Grabowski, U.S. Patent 3,130,177, 21 Apr. 1964a, to Borg-Warner Corp.

T.S. Grabowski, U.S. Patent 3,134,746, 26 May 1964b, to Borg-Warner Corp.

T.S. Grabowski, U.S. Patent 3,267,175, 16 Aug 1966, to Borg-Warner Corp.

T.S. Grabowski, So. Afric. Pat. 07,675, 25 Apr 1970, to Borg-Warner Corp.

T.S. Grabowski, Brit. Pat. 1,253,226, 10 Nov 1971; Ger. Offen. 2,051,890, 06 May 1971, to Borg-Warner Corp.

T.S. Grabowski, Fr. Pat. 1,604,656, 11 Feb 1972; U.S. Patent 3,649,712, 14 Mar 1972, to Borg-Warner Corp.

H.P. Grace, Chem. Eng. Commun. **14**, 225 (1982)

W.W. Graessley, Adv. Polym. Sci. **16**, 1 (1974)

M.R. Grancio, D.F. Steward, J.F. Cass, Europ. Pat. Appl. 042,153, 23 Dec 1981, to Sweetheart Plastics

M.R. Grancio, D.F. Steward, J.F. Cass, U.S. Patent 4,386,187, 31 May 1983, to Sweetheart Plastics

J.E. Granda, J.J. Quinlan, J.J. Garland, U.S. Patent 4,013,597, 22.03.1977, to ARCO

J.A. Grande (ed.), Modern Plast. **74**, 37 (Sept 1997)

T.S. Grant, R.L. Jalbert, Europ. Pat. Appl. 226,910, 01 July 1987; U.S. Patent 4,654,405, 31 Mar 1987, to Borg-Warner Chemicals, Inc.

T.S. Grant, R.L. Jalbert, Europ. Pat. Appl. 305,878, 08 Mar 1989, to Borg-Warner Chemicals, Inc.

M. Gray, Brit. Pat. 5,056, 1879

S.J. Greaves, D.A. Harrison, K.M. Jones, PCT Int. Appl. WO 93 23,449, 25 Nov 1993, to ICI

W.S. Greenlee, J.C. Vyvoda, R.W. Wypart, U.S. Patent 5,157,076, 20 Oct 1992, to B. F. Goodrich Co.

U.R. Grigo, N.R. Lazear, M.W. Witmann, Ger. Offen. 3,325,702, 26 Jan 1984, to Mobay Chem.

G. Groeninckx, D. Dompas, T. Hasegawa, M. Isogawa, M. Kadokura, *NRCC/IMI symposium Polyblends-'95*, Boucherville, 9–20 Oct 1995

M.J. Guest, P.F.M. Van der Berghen, L.M. Aerts, A. Gkogkidis, A. De Bert, Europ. Pat. Appl. 440,441, 07 Aug 1991, to Dow Chemical

J.E. Guillet, in *Polymer Science and Technology*, vol. 3, ed. by J. E. Guillet (1973), Plennm, New York, p. 1

R.K. Gupta, *Polymer and Composite Rheology*, 2nd edn. (Marcel Dekker, New York, 2000)

B. Gupta, J.P. Shepherd, L.F. Charbonneau, PCT Int. Appl. WO 94 04,612, 03 Mar 1994, to Hoechst Celanese Corp.

E. Guth, H.F. Mark, Monatsh **65**, 93 (1934)

A. Guttag, U.S. Patent 5,120,089, 1992

A. Guttag, U.S. Patent 5,346,929, 13 Sept 1994

W.R. Haaf, U.S. Patent 4,167,507, 11 Sept 1979, to General Electric Co.

W.R. Haaf, PCT Int. Appl. 001,254, 14 Apr 1983, to General Electric Co.

W.R. Haaf, Europ. Pat. Appl. 491,191, 24 June 1992, to General Electric Co.

W.R. Haaf, G.F. Lee Jr., Ger. Offen. 2,750,515, 29 June 1978, to General Electric Co.

A. Haas, F. Raviola, Europ. Pat. Appl. 042,743, 13 Jan 1982, Soc. Chim. Charbonnages

M.T. Haggard, 4,710,522, 01 Dec 1987, to Mobil Oil Corp.

R.R. Haghighat, R.W. Lusignea, L. Elandjian, PCT Int. Appl. WO 92 17,545, 15 Oct 1992, to Foster-Miller

K. Hahn, U. Guhr, H. Hintz, R. Gellert, U.S. Patent 5,093,375, 03 Mar 1992, to BASF

M.I. Haider, E.C. Chenevey, U.S. Patent 5,277,981, 11 Jan 1994, to Hoechst Celanese Corp.

I.M. Haider, S. Kenig, V.J. Sullivan, Europ. Pat. 568,945, 10 Nov 1993, to Hoechst Celanese Corp.

M.P. Hallden-Abberton, N.M. Bortnick, W.J. Work, Eur. Pat. Appl. 594,433, 27 Apr 1994, to Rohm & Haas

R.H. Halliwell, Fr. Pat. 1,411,274, 17 Sept 1965, to E. I. du Pont

R.H. Halliwell, Brit. Pat. 1,047,069, 02 Nov 1966, to E. I. du Pont

T. Hamada, S. Yakabe, A. Ito, U.S. Patent 5,283,282, 01 Feb 1994, to Asahi Kasei Kogyo

J. Hambrecht, K. Gerberding, W.F. Mueller, B. Schmitt, Ger. Offen. 3,434,977, 03 Apr 1986, to BASF

C.F. Hammer, Macromolecules **4**, 69 (1971)

C.F. Hammer, U.S. Patent 3,780,140, 18 Dec 1973, to E. I. du Pont

C.Y. Han, U.S. Patent 5,324,796, 28 June 1994, to General Electric Co.

T. Hancock, Brit. Pat. 004,768, 1823

H. Hanezawa, Y. Ono, Jap. Pat. 03 292,314, 24 Dec 1991, to Asahi Chem.

E.H. Hankey, A. Kianpour, U.S. Patent 3,145,187, 18 Aug 1964, to Monsanto

D. Hardt, V. Serini, H. Vernaleken, H.E. Braese, Ger. Offen. 2,402,176, 1975, to Bayer

J.E. Harris, J.P. Gavula, Europ. Pat. Appl. 116,450, 02 Jan 1986, to Upjohn

J.E. Harris, M.J. Michno Jr., U.S. Patent 4,755,556, 05 July 1988, to Amoco Corp.

J.E. Harris, L.M. Robeson, Europ. Pat. Appl. 176,989, 09 Apr 1986, to Union Carbide Corp.

J.E. Harris, L.M. Robeson, Europ. Pat. Appl. 215,580, 25 Mar 1987, to Union Carbide Corp.

J.E. Harris, L.M. Robeson, B.H. Eckstein, M.D. Clifton, Europ. Pat. Appl. 257,150, 02 Mar 1988, to Amoco Corp.

C.R. Hart, Ger. Pat. 2,122,734, 02 Dec 1971, to ICI

R. Hasegawa, T. Kawamura, Y. Nakamura, H. Kubota, Jap. Pat. 041,444, 18 Apr 1974, to Teijin Chem.

M. Hashimoto, Jap. Pat. 246,755, 04 Nov 1986, to Dainippon Ink & Chemicals

T. Hashimoto, T. Ohashi, U.S. Patent 4,546,127, 08.10.1985, to Bridgestone Tire

M. Hashimoto, Y. Akana, H. Hori, Europ. Pat. Appl. 368,281, 16 May 1990, to Mitsui Petrochem

A. Hasson, J.B. Yates, Europ. Pat. 557,654, 01 Sept 1993, to General Electric Co.

M. Hasuo, T. Okano, M. Ito, Jap. Pat. 262,853, 26 Dec 1985, to Mitsubishi Chem.

S.J. Hathaway, R. A. Pyles, U.S. Patent 4,732,934, 1988, to General Electric Co.

S.J. Hathaway, R. A. Pyles, U.S. Patent 4,800,218, 1989, to General Electric Co.

S.G. Hatzikiriakos, K.B. Migler (eds.), *Polymer Processing Instabilities* (Marcel Dekker, New York, 2005)

D.I. Hauser, M.B. Colella, W.G. Blasius Jr., J.M. Haines, Europ. Pat. Appl. 532,171, 17 Mar 1993, to Novacor Chem.

A.S. Hay, J. Am. Chem. Soc. **81**, 6335 (1959)

A.S. Hay, Belg. Pat. 635,349, 24 Jan 1964, to General Electric Co.

A.S. Hay, U.S. Patent 3,306,874; 3,306,875, 28 Feb 1967, to General Electric Co.

A.S. Hay, U.S. Patent 3,402,144, 17 Sept 1968, to General Electric Co.

R.A. Hayes, U.S. Patent 2,755,270, 17 July 1956, to Firestone Tire & Rubber

R.A. Hayes, Ger. Offen. 1,232,741, 19 Jan 1967, to Firestone Tire & Rubber

J.G. Hedberg, L.M. Magner, U.S. Patent 3,209,055, 28 Sept 1965, to E. I. du Pont

G. Heger, M. Oeller, Eur. Pat. Appl. 583,706, 23 Feb 1994, to Bayer

G. Heger, E. Piejko, J. Buekers, L. Morbitzer, A. Karbach, Ger. Offen. 4,110,484, 01 Oct 1992, to Bayer

M. Heino, J. Seppaelae, M. Westman, PCT Int. Appl. WO 93 24,574, 09 Dec 1993, to Neste Oy

E. Helfand, Y. Tagami, J. Polym. Sci. Polym. Lett. **9**, 741 (1971)

E. Helfand, Y. Tagami, J. Chem. Phys. **56**, 3593 (1972)

R. Henn, K. Hahn, W. Loth, W. Heckmann, U. Blumenstein, H.-D. Schwaben, K.-H., Wassmer, H. Tatzel, U.S. Patent 5,525,636, 11 Jun 1996, to BASF

D.E. Henton, U.S. Patent 4,218,544, 19 Aug 1980, to Dow Chemical

D.E. Henton, Europ. Pat. Appl. 056,246; 056,247, 21 July 1982, to Dow Chemical

D.E. Henton, U.S. Patent 4,439,582, 27 Mar 1984, to Dow Chemical

D.E. Henton, A. Chen, P.J. Moses, B.S. Ehrlich, D.E. Beyer, PCT Int. Appl. WO 92 20,744, 26 Nov 1992, to Dow Chemical

D.E. Henton, D.M. Naeger, F.M. Plaver, U.S. Patent 5,219,933, 15 June 1993, to Dow Chemical

L.R. Hepp, Europ. Pat. Appl. 113,096, 11 July 1984, to General Electric Co.

S.J. Hepworth, J.D. Seddon, J.E. Priddle, Ger. Offen. 2,011,608, 01 Oct 1970, to ICI

J.A. Herbing, I.O. Salyer, U.S. Patent 3,092,607, 4 June 1963, to Monsanto Chemical Co.

H. Herbst, K. Hoffmann, R. Pfaendner, F. Sitek, *Proceed. of National Seminar on Emerging Trends in Plastic Recycling Technologies and Waste Management*, Goa, 27–28 May 1995

H. Herbst, K. Hoffmann, R. Pfaendner, H. Zweifel, in *Frontiers in the Science and Technology of Polymer Recycling*, ed. by G. Akovali, C.A. Bernardo, J. Leidner, L.A. Utracki, M. Xanthos. NATO ASI Series, vol. 351 (Kluver, Dordrecht, 1998)

O. Herrmann-Schoenherr, H.T. Land, Eur. Pat. Appl. 568,917, 10 Nov 1993, to Hoechst

O. Herrmann-Schoenherr, H.T. Land, Jap. Pat. 60 57,160, 01 Mar 1994, to Hoechst

A. Heslinga, P.J. Greidanus, U.S. Patent 4,332,917, 01 June 1982; U.S. Patent 4,338,417, 06 June 1982, to Nederlandse Centrale Organisatie voor Toegepast-Natuurwetenschappelijk Onderzoek

H. Heywang, Ger. Offen. 1,221,323, 21 July 1966, to Siemens and Halske

T. Hikasa, H. Mendori, T. Hamanaka, T. Igarashi, Y. Shida, U.S. Patent 5,308,700, 03 May 1994, to Sumitomo Chem.

R.W. Hill, R.P. Anderson, S.V. Scroggins, U.S. Patent 3,539,662, 10 Nov 1970, to Gulf R&D Co.

S. Himei, M. Takine, K. Akita, Jap. Pat. 000,949, 18 Jan 1967, to Kanegafuchi Chem.

M.H. Hindi, M.W. Woods, N. Harry, T. Wakida, U.S. Patent 5,300,552, 05 Apr 1994, to Phillips

K. Hinselmann, V. Ladenberger, K. Bronstert, G. Fahrbach, Ger. Offen. 2,137,274, 08 Feb 1973, to BASF

M. Hirai, T. Tatsuda, T. Yoshida, Europ. Pat. Appl. 284,086, 28 Sept 1988, to Sumitomo Naugatuck

M. Hirai, T. Tatsuda, T. Yoshida, U.S. Patent 4,855,355, 08 Aug 1989, to Sumitomo Naugatuck

M. Hirai, T. Tatsuda, T. Yoshida, Can. Pat. 1,307,863, 22 Sept 1992, to Sumitomo Naugatuck

T. Hirai, N. Amano, SPE Techn. Pap. **39**, 1256 (1993)

T. Hiri, H. Kotama, Jap. Pat. 005,224, 09 Feb 1971, to Toray Industries

Hitachi Chemical Company, Ltd., Jap. Pat. 052,348, 28 Mar 1983

N. Hizasumi, T. Uehara, H. Ohba, K. Hirose, Europ. Pat. Appl. 336,680, 11 Oct 1989, to Kureha Chem.

K.-S. Ho, K. Levon, U.S. Patent 5,391,622, 21 Feb 1995, to Neste Oy

S.Y. Hobbs, R.C. Bopp, V.H. Watkins, Polym. Eng. Sci. **23**, 380 (1983)

A. Hodzic, in *Natural Fibers, Biopolymers and Biocomposites*, ed. by A.K. Mohanty, M. Misra, L.T. Drzal (Taylor and Francis, Boca Raton, 2005)

S.M. Hoenig, D.P. Flores, S.P. Ginter, U.S. Patent 4,474,928, 02 Oct 1984, to Dow Chemical

H. Hoenl, A. Jung, P. Klaerner, B. Ostermayer, S. Seelert, Europ. Pat. Appl. 545,181, 09 June 1993, to BASF

G.H. Hofmann, U.S. Patent 5,352,735, 04 Oct 1994, to E. I. du Pont

G.H. Hofmann, Plast. Technol. **55** (1998)

J.P. Hogan, R.L. Banks, U. S. Pat. Appl. 333,576, 27 Jan 1953, to Phillips

J.P. Hogan, R.L. Banks, Belg. Pat. 530,617, 24 Jan 1955, to Phillips

T. Hoki, N. Miura, U.S. Patent 4,652,590, 24 Mar 1987, to Dow Chemical Co.

G. Holden, L.H. Gouw, Europ. Pat. Appl. 004,685, 17 Oct 1979, to Shell.

G. Holden, D.R. Hansen, Europ. Pat. Appl. 308,001, 22 Mar 1989, to Shell

W.D. Holland, J.M. Schmitt, R.M. Griffith, Ger. Offen. 2,018,606, 29 Oct 1970, to American Cyanamid

P.A. Holmes, A.B.. Newton, F.M. Willmouth, Europ. Pat. Appl. 052,460, 26 May 1982, to ICI

F.F. Holub, U.S. Patent 4,908,418; 13 Mar 1990, to General Electric Co.

F.F. Holub, G.A. Mellinger, U.S. Patent 4,258,155, 24 Mar 1981, to General Electric Co.

F.F. Holub, J.A. Rock, Europ. Pat. Appl. 325,718; 325,719, 02 Aug 1989, to General Electric Co.

R. Holzer, K. Mehnert, Ger. Offen. 1,145,792, 21 Mar 1963, to Hoechst

R. Holzer, K. Mehnert, U.S. Patent 3,262,292, 1966, to Hoechst

S.M. Hong, B.C. Kim, K.U. Kim, I.J. Chung, Polym. J. **24**, 727 (1992)

M. Hongo, H. Shigemitsu, N. Yamamoto, A. Yanagase, Europ. Pat. Appl. 249,964, 23 Dec 1987, to Mitsubishi Rayon

A. Honkanen, M. Arina, R. Holstii, Finn. Pat. 064,805, 30 Sept 1983, to Neste Oy

J.F. Hoover, Europ. Pat. Appl. 524,731, 27 Jan 1993, to General Electric Co.

K. Horiuchi, T. Kamiya, Jap. Pat. 001,639, 16 Jan 1974, to Teijin Chem.

Y. Hoshi, A. Kaneko, Jap. Pat. 014,220, 17 Sept 1962, to Kureha Chemical Works

Y. Hoshi, A. Kaneko, Brit. Pat. 928,799, 12 June 1963, to Kureha Chemical Works

Y. Hoshi, A. Kaneko, Belg. Pat. 635,851, 01 Feb 1965, to Kureha Chemical Works

N. Hosoi, Jap. Pat. 03 167,258, 19 July 1991, to Sumitomo Electric Industries

R.J. Hoxmeier, U.S. Patent 5,276,095, 04 Jan 1994, to Shell Oil

H.-W. Hsu, S.-C. Liuo, S.-F. Jiang, J.-H. Chen, H.-M. Lin, H.-D. Hwu, M.-L. Chen, M.-S. Lee, T. Hu, U.S. Patent 5,308,897, 14 Jan 1994, to Industrial Technology Research Institute, Taiwan

G.-H. Hu, H. Cartier, Intl. Polym. Process. **13**, 111 (1998)

J. Huang, GP. Kipouras, U.S. Patent 8,273,268, 25 Sept 2012, to PolyOne Corp.

H.H. Hub, G. Blinne, H. Reimann, P. Neumann, G. Schaefer, Ger. Offen. 3,444,339, 05 June 1986, to BASF

Huels., Brit Pat., 1,247,068, 22 Sept 1971

T. Huff, U.S. Patent 4,087,485, 02 May 1978, to Exxon

T. Huff, Europ. Pat. Appl. 015,066, 03 Sept 1980, to Exxon

M.L. Huggins, G. Natta, V. Desreux, H. Mark, J. Polym. Sci. **56**, 153 (1962)

M.L. Huggins, G. Natta, V. Desreux, H. Mark, Pure Appl. Chem. **12**, 645 (1966)

M.A. Huneault, Z.H. Shi, L.A. Utracki, "Polyblends-'93," *NRCC/IMI Symposium*, Boucherville, 26–27 Oct 1993

M.A. Huneault, M.F. Champagne, A. Luciani, J.-F. Hetu, L.A. Utracki, *Polymer Processing Society European Meeting*, Stuttgart, 25–28 Oct 1995a

M.A. Huneault, Z.H. Shi, L.A. Utracki, Polym. Eng. Sci. **35**, 115 (1995b)

M.J. Hurwitz, W.G. DeWitt III, Ger. Offen. 2,017,398, 22 Oct 1970, to Rohm & Haas

W.-F. Hwang, D.R. Wiff, C. Verschoore, G.E. Price, Polym. Eng. Sci. **23**, 784 (1983)

C.C. Hwo, U.S. Patent 5,369,181, 29 Nov 1994, to Shell Oil

C.C. Hwo, U.S. Patent 5,585,411, 17 Dec 1996, to Shell Oil

I.G. Farbenindustrie, Brit. Pat. 505,651, 08 May 1939

S. Ichinoe, Jap. Pat. 002,149, 31 Jan 1967, to Kureha Chem.

F. Ide, K. Deguchi, Jap. Pat. 035,175, 11 Nov 1971, to Mitsubishi Rayon

F. Ide, K. Okano, K. Deguchi, Jap. Pat. 023,645, 01 July 1972, to Mitsubishi Rayon

Idemitsu Kosan Co., Jap. Pat. 057,456, 05 Apr 1983

Idemitsu Petrochemical Company, Limited, Jap. Pat. 096,640, 08 June 1983

Idemitsu Petrochemical Company, Limited, Jap. Pat. 027,947, 14 Feb 1984

H. Ikeda, S. Aotani, K. Takahashi, K. Arai, Jap Pat. 001,561, 08 Jan 1976, to Japan Synthetic Rubber

M. Ikeguchi, Y. Nagata, Jap. Pat. 083,741, 12 Aug 1974, to Nippon Steel Chem.

K. Ikura, H. Shigemori, N. Nawa, Y. Sugimura, Jap. Pat. 041,444, 18 Apr 1974, to Teijin Chem.

C.S. Ilendra, N. Bortnick, R.K. Graham, W.J. Work, U.S. Patent 5,128,410, 07 July 1992, to Rohm & Haas

C.S. Ilendra, N. Bortnick, W.J. Work, U.S. Patent 5,229,456, 20 July 1993, to Rohm and Haas

G. Illing, U.S. Patent 3,536,680, 1970; Ger. Offen. 1,900,179, 30 July 1970, to Werner & Pfleiderer

G. Illing, Ger. Offen. 2,140,041, 22 Feb 1973, to Werner & Pfleiderer

H. Imabayashi, K. Ishikawa, Y. Ishida, U.S. Patent 5,306,790, 26 Apr 1994, to Idemitsu Petrochem.

M. Imaizumi, R. Fujihira, J. Suzuki, K. Yoshikawa, R. Ishioka, *14th International Polymer Processing Society Meeting, PPS-14*, Yokohama, 08–12 June 1998

B. Imre, B. Pukanszky, Europ. Polym. J. (2013, in press), **49**, 1215

Industrial Technology Institute, Japan, *Japan New Materials Report*, 9/10, 2 (1996)

A.F. Ingulli, H.L. Alter, So. Afric. Pat. 6,806,262, 06 Mar 1969, 10 Dec 1970, to Uniroyal

A.F. Ingulli, H.L. Alter, Ger. Offen. 2,025,467, 10 Dec 1970, to Uniroyal

H.H. Irving, U.S. Patent 3,010,936, 1961, to Borg Warner Chemicals

A.I. Isayev, U.S. Patent 5,021,475, 1991, to University of Akron

A.I. Isayev, U.S. Patent 5,260,380, 1993, to University of Akron

A.I. Isayev, U.S. Patent 5,283,114, 01 Feb 1994, to University of Akron

A.I. Isayev, S. Swaminathan, U.S. Patent 4,835,047, 30 May 1989, to University of Akron

H. Ishida, H. Kabaya, U.S. Patent 5,292,789, 08 Mar 1994, to GE Plastics Japan

S. Ishida, J. Masamoto, Jap. Pat. 018,144, 18 Feb 1974; Jap. Pat. 040,346, 15 Apr 1974, to Asahi Chem.

S. Ishida, K. Sato, Jap. Pat. 035,188, 11 Nov 1970, to Asahi Chem.

T. Ishihara, U.S. Patent 4,814,393, 21 Mar 1989, to General Electric Co.

N. Ishihara, T. Seimiya, M. Kuramoto, M. Uoi, Macromolecules **19**, 2464 (1986)

A. Ishio, K. Kobayashi, Europ. Pat. Appl. 463,738, 02 Jan 1992, to Toray

K. Ishioka, Jap. Pat. 03 217,448, 25 Sept 1991, to NOK Corp.

H. Ito, Y. Kawachi, M. Morimoto, Europ. Pat. Appl. 379 154, 25 July 1990, to Mitsubishi Rayon

IUPAC (International Union of Pure and Applied Chemistry), Pure Appl. Chem. **40**, 479 (1974)

IUPAC, Pure Appl. Chem. **48**, 373 (1976)

IUPAC, Pure Appl. Chem. **53**, 733 (1981)

IUPAC, J. Polym. Sci. Polym. Lett. Ed. **22**, 57 (1984)

IUPAC, Pure Appl. Chem. **57**, 149 (1985a)

IUPAC, Pure Appl. Chem. **57**, 1427 (1985b)

IUPAC, Pure Appl. Chem. **59**, 691 (1987)

IUPAC, Pure Appl. Chem. **61**, 1769 (1989a)

IUPAC, Pure Appl. Chem. **61**, 769 (1989b)

IUPAC, Pure Appl. Chem. **61**, 234 (1989c)

IUPAC, Pure Appl. Chem. **68**, 2287 (1996)

IUPAC, Pure Appl. Chem. **73**, 845 (2001)

IUPAC, Pure Appl. Chem. **74**, 1921 (2002)

IUPAC, Pure Appl. Chem. **84**, 2167 (2012)

K. Iwanaga, Y. Tanaka, K. Takemoto, Jap. Pat. 2,077,429, 16 March 1990, to Tosoh Corp.

K. Iwanami, K. Kitano, K. Narukawa, K. Aoki, Y. Yagi, M. Sakuma, T. Mikami, M. Esaki, F. Kato, Europ. Pat. Appl. 333 518, 20 Sept 1989, to Nippondenso

K. Iwanami, K. Kitano, Y. Yagi, T. Mikami, Europ. Pat. Appl. 382,559, 16 Aug 1990, to Tonen Sekiyu Kagaku

H. Iwata, T. Otani, S. Arakawa, S. Deguchi, Jap. Pat. 157,153, 11 Dec 1979, to Mitsubishi Rayon

S.I. Izawa, A. Nakanishi, Jap. Pat. 22,590, 22 Mar 1973, to Asahi-Dow

S.I. Izawa, K. Sotoyama, Y. Sugawara, Jap. Pat. 39,015; 39,017; 39,018, 21 Nov 1973a, to Asahi-Dow

S.I. Izawa, J. Sugiyama, N. Kosaka, Can. Pat. 1,144,680, 12 Apr 1983, to Asahi-Dow

S.I. Izawa, K. Toyama, K. Harada, Y. Sugawara, U.S. Patent 3,781,382, 25 Dec 1973b, to Asahi-Dow

M. Izumi, M. Kajioka, T. Yamagishi, K. Yoshino, T. Wakui, Europ. Pat. Appl. 470,557, 12 Feb 1992, to Kawasaki Steel Corp.

G.S. Jack, M.J. El-Hibri, W.E. Kelly, S.R. Patel, Europ. Pat. Appl. 535,785, 07 Apr 1993, to Amoco Corp.

H. Jadamus, W. Ribbing, R. Feinauer, W. Schaefer, Ger. Offen. 3,442,273, 22 May 1986 to Hüls

H. Jadamus, W. Ribbing, R. Feinauer, W. Schaefer, U.S. Patent 4,656,220, 07 Apr 1987 to Hüls

H. Jager, E.J. Vorenkamp, G. Challa, Polym. Commun. **24**, 290 (1983)

A.L. Jankens, Belg. Pat. 625,004, 20 May 1963, to Dow Chemical

Japan Synthetic Chem. Ind., Fr. Pat. 2,000,728, 04 Mar 1971

Japan Synthetic Rubber Co., Jap. Pat. 053,553, 27 Mar 1985; Jap. Pat. 079,060, 04 May 1985; Jap. Pat. 086,151, 15 May 1985; Jap. Pat. 108,454, 13 June 1985

K.B. Jarrett, A.A. Williams, Brit. Pat. 850,947, 12 Oct 1960, to ICI

M. Jayabalan, J. Appl. Polym. Sci. **27**, 43 (1982)

M. Jayabalan, T. Balakrishnan, J. Cellular. Plast. **21**(6), 399 (1985)

D. Jean, G. Devauchelle, Fr. Pat. 2,682,960, 30 Apr 1993, to Labinal

A.D. Jenkins, J. Kahovec, P. Kratochvil, I. Mita, I.M. Papisov, L.H. Sperling, R.F.T. Stepto, *Source-Based Nomenclature for Non-Linear Macromolecules and Macromolecular Assemblies*, draft report for the IUPAC Commission on Macromolecular Nomenclature, May 1993

B.J. Jody, B. Arman, D.E. Karvelas, J.A. Pomykala, E.J. Daniels, U.S. Patent 5,653,867, 1997

R.G. Jones (ed.) *The Purple Book*, 2nd edn. (RSC Publishers, 2009), Cambridge, UK

W.J. Jones, R.A. Mendelson, Europ. Pat. Appl. 135,492, 27 Mar 1985, to Monsanto

M.E.B. Jones, E. Nield, C.R. Hart, U.S. Patent 3,562,200, 09 Feb 1971, to ICI

T.J.M. Jongeling, Eur. Pat. Appl. 538,939, 28 Apr 1993, to DSM

T.C. Jordan, J.L. Webb, Europ. Pat. Appl. 497,004, 05 Aug 1992, to General Electric Co.

T.C. Jordan, J.L. Webb, U.S. Patent 5,334,672, 02 Aug 1994, to General Electric Co.

J. Jose, P. Jyotishkumar, S.M. George, S. Thomas, in *Recent Developments in Polymer Recycling*, ed. by A. Fainleib, O. Grigoryeva (Transworld Research Network, Trivandrum, 2011)

K. Kabuki, K. Matsuno, O. Tanaka, Jap. Pat. 73 055,948, 06 Aug 1973, to Tokyo Shibaura Electric.

G. Kakefuda, T. Ito, Jap. Pat. 034,904, 13 Oct 1971, to Hitachi Chemical

T. Kakizaki, S. Horie, T. Mizutani, Jap Pat. 117,555, 12 Sept 1979a

T. Kakizaki, S. Horie, H. Sano, Jap Pat. 146,887, 16 Nov 1979b, to Mitsubishi Petrochem.

M.R. Kamal, G. Lohfink, L. Arghyris, S. Hozhabr-Ghelichi, PCT Int. Appl. 006,837, 30 Apr 1992, to McGill University

K. Kamata, R. Handa, M. Hongo, Jap. Pat. 121,855, 21 Nov 1974, to Mitsubishi Rayon

K. Kamata, Y. Kinoshita, M. Hongo, H. Nakanishi, Jap. Pat. 129,246, 11 Nov 1978a, to Mitsubishi Rayon

K. Kamata, I. Sasaki, M. Hongo, Jap. Pat. 137,251, 30 Nov 1978b, to Mitsubishi Rayon

K. Kamata, Y. Kinoshita, H. Nakanishi, Jap. Pat. 000,055, 05 Jan 1979, to Mitsubishi Rayon

K. Kamata, I. Sasaki, H. Mori, Jap. Pat. 003,471, 11 Jan 1980, to Mitsubishi Rayon

R.P. Kambour, U.S. Patent 3,639,508, 1970, to General Electric Co.

R.P. Kambour, Europ. Pat. Appl. 263,378, 13 Apr 1988, to General Electric Co.

W. Kaminsky, Pure Appl. Chem. **70**, 1229 (1998)

W. Kaminsky, K. Kulper, H.H. Brintzinger, F.R.W.P. Wild, Angew. Chem. Int. Ed. Engl. **24**, 507 (1985)

W. Kaminsky, R. Engehausen, K. Zoumis, W. Spaleck, J. Rohrmann, Makromol. Chem. **193**, 1643 (1992)

M. Kamosaki, S. Tokuhara, M. Kita, N. Nakashima, Jap. Pat. 146,748; 146,753, 20 Dec 1978, to Daicel

R. Kamps, G. Lange, G. Leimann, F. Paul, W. Pfandl, P. Friedemann, Europ. Pat. Appl. 598,213, 25 May 1994, to Siemens

A. Kanai, S. Hata, M. Miura, Jap. Pat. 031,796, 25 Mar 1978, to Mitsubishi Petrochem.

Kanegafuchi Chem. Co., Fr. Pat. 1,499,542, 27 Oct 1967

Kanegafuchi Chem. Co., Jap Pat. 004,642, 11 Jan 1984

F.E. Karasz, W.J. MacKnight, U.S. Patent 5,286,812, 15 Feb 1994, to University of Massachusetts

H.G. Karian (ed.), *Handbook of Polypropylene and Polypropylene Composites* (Marcel Dekker, New York, 2003)

T.P. Karjala, Y.W. Cheung, M.J. Guest, in *Metallocene-Catalyzed Polymers*, ed. by G.M. Benedict, B.L. Goodall (SPE Plastics Design Library, Norwich, 1998)

T. Karna, J. Laakso, T. Niemi, H. Ruohonen, E. Savolainen, H. Lindstrom, E. Virtanen, O. Ikkala, A. Andreatta, U.S. Patent 5,340,499, 23 Aug 1994, to Neste Oy

H. Kasahara, K. Fukuda, H. Suzuki, Europ. Pat. Appl. 046,040, 17 Feb 1982, to Asahi-Dow

T. Kasuya, T. O. Omichi, H. Maehara, Jap. Pat. 011,546, 27 May 1969, to Asahi Chem.

R. Kato, I. Soematsu, T. Mori, Jap. Pat. 003,108, 09 Feb 1967, to Toa Gosei Chem.

T. Katsumata, Jap. Pat. 03 119,048, 21 May 1991, to Polyplastics

T. Katsumata, N. Matsunaga, Europ. Pat. Appl. 519,749, 23 Dec 1992, to Polyplastics

T. Katsumata, N. Matsunaga, Europ. Pat. Appl. 549,338, 30 June 1993, to Polyplastics

T. Katsumata, N. Matsunaga, U.S. Patent 5,378,748, 03 Jan 1995, to Polyplastics

S. Katsura, Jap. Pat. 028,539, 08 Feb 1986, to Mitsubishi Petrochem.

H.S. Kaufman, U.S. Patent 3,105,827, 01 Oct 1963, to Minnesota Mining and Manufacturing

M. Kawai, M. Miyauchi, Jap. Pat. 124,150, 27 Nov 1974, to Teijin Chem.

H. Kawai, T. Munemaru, T. Inoue, R. Kimura, Jap. Pat. 043,539, 21 Nov 1978, to Institute for Production and Development Science

T. Kawaki, A. Amagai, M. Ishikawa, T. Yamada, Y. Hirai, H. Ban, Eur. Pat. Appl. 492,947, 01 July 1992, to Mitsubishi Gas Chem.

T. Kawaki, A. Amagai, M. Ishikawa, T. Yamada, Y. Hirai, H. Ban, U.S. Patent 5,321,097, 14 June 1994, to Mitsubishi Gas Chem.

T. Kawaki, A. Amagai, T. Yamada, H. Harada, H. Ban, U.S. Patent 5,387,652, 07 Feb 1995, to Mitsubishi Gas Chem.

T. Kawauzra, S. Aibe, M. Kawazoe, U.S. Patent 5,679,744, 21 Oct 1997, to The Yokohama Rubber Co., Ltd.

C. Kennedy, *ICI, The Company That Changed Our Lives* (Hutchinson Limited, London, 1986)

A. Képes, Fr. Pat. 1,175,241, 23 Mar 1959, to Soc. anon. des manufacturers des glaces et produits chimiques de Saint-Gobain, Chauny & Cirey

R.J. Kern, U.S. Patent 2,806,015, 10 Sept 1957, to Monsanto Chem.

H. Keskkula, D.A. Maass, K.M. McCreedy, U.S. Patent 4,460,744, 17 July 1984, to Dow Chemical

K. Khait, SPE Techn. Pap. **40**, 3006 (1994)

K. Khait, SPE Techn. Pap. **41**, 2066 (1995)

M.M.K. Khan, R.F. Liang, R.K. Gupta, S. Agarwal, Korea Australia Rheol. J. **17**, 1 (2005)

G.B. Kharas, S.P. Nemphos, Europ. Pat. Appl. 515,203, 25 Nov 1992, to Novacor Chem.

W.N. Kim, C.M. Burns, Polym. Eng. Sci. **28**, 1115 (1988)

W.N. Kim, C.M. Burns, J. Polym. Sci. Polym. Phys. **28**, 1409 (1990)

S.-K. Kim, J.-W. Choi, U.S. Patent 5,747,587, 05 May 1998, to Cheil Industries

B.K. Kim, M.S. Kim, H.M. Jeong, K.J. Kim, J.K. Jang, Angew. Makromol. Chem. **194**, 91 (1992)

H.S. Kim, B.S. Jin, Y.C. Kwon, K. Seong, in *Encyclopaedic Dictionary of Commercial Polymer Blends*, ed. by L.A. Utracki (ChemTec, Toronto, 1994)

K. Kishida, J. Kobayashi, N. Ohsaka, Jap. Pat. 077,858, 26 Nov 1977, to Mitsubishi Rayon

K. Kishida, H. Mori, M. Kaneta, Jap. Pat. 001,246, 09 Jan 1978a, to Mitsubishi Rayon

K. Kishida, H. Mori, H. Fukunaga, H. Nakanishi, Jap. Pat. 018,661, 21 Feb 1978b, to Mitsubishi Rayon

H. Kishikawa, K. Yasuno, S. Kitamura, Ger. Offen. 2,119,376, 11 Nov 1971, to Sumitomo Chem.

T. Kishimoto, Jap. Pat. 059,952, 25 May 1976, to Mitsui Petrochem.

M. Kita, K. Hashimoto, Jap. Pat. 131,043, 13 June 1987, to Daicel Huels

K. Kitamura, Jap. Pat. 002,748, 08 Jan 1986, to Teijin Chem.

N. Kitayama, H. Keskkula, D.R. Paul, Polymer **41**, 8041 (2000a)

N. Kitayama, H. Keskkula, D.R. Paul, Polymer **41**, 8053 (2000b)

N. Kitayama, H. Keskkula, D.R. Paul, Polymer **42**, 3751 (2001)

T. Kobayashi, K. Shinohara, PCT Int. Appl. WO 93 05,107, 18 Mar 1993, to E. I. du Pont

T. Kobayashi, K. Tanaka, Can. Pat. 2,064,301, 29 Sept 1992, to Toray

T. Kobayashi, K. Miyazaki, M. Nakamura, U.S. Patent 5,594,038, 14 Jan 1997; U.S. Patent 5,646,194, 08 July 1997, to Sekisui Chemical

Y. Kobayashi, W. Zheng, E.F. Meyer, J.D. McGervey, A.M. Jamieson, R. Simha, Macromolecules **22**, 2302 (1989)

F.F. Koblitz, R.G. Petrella, A.A. Dukert, A. Christofas, U.S. Patent 3,253,060, 28 Nov 1966, to Pennwalt Chemical

J.E. Kochanowski, U.S. Patent 4,334,030, 08 Jun 1982, to General Electric Co.

T. Kodaira, H. Ishida, H. Kabaya, U.S. Patent 5,310,821, 10 May 1994, to GE Plastics Japan

H. Koenig, G. Wick, F. Thomczik, A. Thielemann, Ger. Offen. 1,165,255, 12 May 1964, to Hüls

P. Koetzing, K. Diebold, Kunststoffe **85**, 2046 (1995)

M.I. Kohan, U.S. Patent 4,351,916, 28 Sept 1982; Europ. Pat. Appl. 047,529, 17 Mar 1982, to E. I. du Pont

B. Köhler, W. Rüsseler, B. Sarabi, K. Reinking, F. Jonas, Europ. Pat. Appl. 510,475, 28 Oct 1992, to Bayer

H. Kojima, A. Taoka, K. Takiguchi, Jap. Pat. 027,905, 11 Sept 1970, to Mitsubishi Monsanto Chem.

M. Kojima, M. Tanahashi, Jap. Pat. 014,710, 02 May 1972, to Chisso

T. Kokkonen, T. Karna, J. Laakso, P. Nuholm, J.-E. Sterholm, H. Stubb, U.S. Patent 5,279,769, 18 Jan 1994, to Neste Oy

H. Komoto, Jap. Pat. 020,243, 28 Sept 1972, to Asahi Chem.

M. Kondo, K. Tominari, Jap. Pat. 079,260, 11 Apr 1987, to Mitsui Petrochem.

C.E. Koning, J.A.J. Kingma, L. Prinsen, Europ. Pat. Appl. 365,101, 25 Apr 1990, to Stamicarbon

C.E. Koning, H.J. Vroomans, Europ. Pat. Appl. 463,238, 02 Jan 1992, to Stamicarbon

E. Konrad, E. Tschunkur, U.S. Patent 1,973,000, 1934, to I. G. Farbenindustrie

R.M. Kopchik, U.S. Patent 4,255,322, 10 Mar 1981, to Rohm & Haas

A. Koshimo, Jap. Pat. 025,053, 02 Apr 1973, to Unitika

A. Koshimo, H. Sakata, T. Okamoto, H. Hasegawa, Jap. Pat. 051,945, 051,946, 051,947, 051,948, 21 July 1973, to Unitika

A. Koshirai, A. Nakata, N. Yamamoto, Europ. Pat. Appl. 468,772, 11 Mar 1992, to Mitsubishi Rayon

A. Koshirai, A. Nakata, N. Yamamoto, U.S. Patent 5,288,798, 22 Feb 1994, to Mitsubishi Rayon

T. Kotaka, *International Symposium on Elongational Flow of Polymeric Systems*, Yamagata U., Yonezawa, 13–15 June 1998

K. Kotama, Jap. Pat. 009,740, 23 Mar 1972, to Mitsubishi Rayon

A.M. Kotliar, J. Polym. Sci. Macromol. Rev. **16**, 367 (1981)

K. Koyama, T. Takahashi, Y. Naka, J. Takimoto, *13th International Annual Meeting* (Polymer Processing Society, New York, 1997)

S. Kozakura, S. Kuze, K. Tanaka, Europ. Pat. Appl. 496,257; 496,258, 29 July 1992, to Idemitsu Petrochem.

S. Kozakura, S. Kuze, K. Tanaka, U.S. Patent 5,314,949, 24 May 1994, to Idemitsu Petrochem.

M. Kozlowski, Polym. Networks Blends **4**, 39 (1994)

M. Kozlowski, Polym. Networks Blends **5**, 163 (1995)

E.O. Kraemer, W.D. Lansing, J. Am. Chem. Soc. **55**, 4319 (1933)

N.P. Krasnikova, E.V. Kotova, E.P. Plotnikova, M.P. Zabugina, G.V. Vinogradov, V.E. Dreval, Z. Pelzbauer, Kompoz. Polim. Mater. **21**, 37 (1984)

M. Kraus, I. Katsnelson, M. Heisler, PCT Int. Appl. 018,664, 12 Dec 1991, to Gelman Sci.

H.J. Kress, C. Lindner, L. Morbitzer, H. Peters, K.H. Ott, J. Schoeps, Ger. Offen. 3,514,185, 23 Oct 1986, to Bayer

J. Kressler, N. Higashida, T. Inoue, W. Heckmann, F. Seitz, Macromolecules **26**, 2090 (1993)

R.K. Krishnaswamy, U.S. Patent Appl. 2013006546, Mar 2013

R.K. Krishnaswamy, J. van Walsem, O.P. Peoples, Y. Shabtai, A.R. Padwa, U.S. Patent Appl., June 2013

W. Kuhn, Kolloid Z. **68**, 2 (1930)

W. Kuhnel, P. Spielau, U.S. Patent 4,255,372, 10 Mar 1981, to Dynamit Nobel

V.G. Kulkarni, B. Wessling, Europ. Pat. Appl. 497,514, 05 Aug 1992, to Americhem.

V.G. Kulkarni, B. Wessling, Europ. Pat. Appl. 536,915, 14 Apr 1993, to Americhem.

V.G. Kulkarni, B. Wessling, U.S. Patent 5,290,483, 01 Mar 1994, to Americhem.

H. Kumabe, A. Morimoto, Y. Kitagawa, N. Shiraishi, Fr. Pat. 2,151,639, 25 May 1973, to Japan Synthetic Rubber

A. Kumar, R.K. Gupta, *Fundamentals of Polymer Engineering*, 2nd edn. (Marcel Dekker, New York, 2003)

V. Kumar, N.P. Suh, Polym. Eng. Sci. **30**, 1323 (1990)

V. Kumar, J.E. Weller, R. Murray, SPE Techn. Pap. **41**, 2202 (1995)

J.A. Kuphal, L.M. Robeson, J.G. Santangelo, U.S. Patent 4,940,733, 10 July 1990, to Air Products & Chem.

K. Kyo, Y. Asai, Jap Pat. 129,248, 11 Nov 1978, to Unitika

T. Kyu, Europ. Pat. Appl. 392,763, 17 Oct 1990, to Edison Polym. Innov. Corp.

E.E. La Fleur, R.M. Amici, W.T. Freed, W.J. Work, W.G. Carson, U.S. Patent 5,147,930, 1992, to Rohm & Haas

E.E. La Fleur, R.M. Amici, W.J. Work, U.S. Patent 5,189,097, U.S. Patent 5,322,892, 21 June 1994a, to Rohm & Haas

E.E. La Fleur, R.M. Amici, W.T. Freed, W.J. Work, W.G. Carson, U.S. Patent 5,296,537, 22 Mar 1994b, to Rohm & Haas

E.E. La Fleur, W.J. Work, R.M. Amici, N.M. Bortnick, N.L. Holy, Eur. Pat. Appl. 583,109, 16 Feb 1994c, to Rohm & Haas

F.P. La Mantia (ed.), *Thermotropic Liquid Crystal Polymer Blends* (Technomics, Lancaster, 1993)

S.-Y. Lai, M.S. Edmondson, U.S. Patent 5,408,004, 18 Apr 1995, to Dow Chemical

X.-Y. Lai, D.-F. Zhao, F. Lai, U.S. Patent 5,344,895, 06 Sept 1994, to University of Massachusetts Lowell

R. Langworth, U.S. Patent 3,299,176, 17 Jan 1967, to E. I. du Pont

H.H. Lank, E.L. Williams, *The Du Pont Canada History* (Du Pont Canada, Montréal, 1982)

O.E. Larsen, Can. Pat. 1,120,630, 23 Mar 1982, to Phillips

R.L. Lauchlan, Ger. Offen. 2,035,147, 28 Jan 1971, to Uniroyal

R.L. Lauchlan, G.A. Shaw, Fr. Pat. 2,011,783, 06 Mar 1970, to Uniroyal

R.L. Lauchlan, H.E. Snodgrass, Ger. Pat. 2,312,971, 27 Sept 1973, to Uniroyal

M.K. Laughner, PCT Int. Appl. WO 93 19,128, 30 Sept 1993; U.S. Patent 5,262,476, 16 Nov 1993, to Dow Chemical

M.K. Laughner, U.S. Patent 5,286,790, 15 Feb 1994, to Dow Chemical

M.K. Laughner, C.P. Bosnyak, B.N. Herron, PCT Int. Appl. 003,504, 05 Mar 1992, to Dow Chemical

D. Lausberg, C. Taubitz, M. Knoll, Ger. Offen. 3,617,070, 26 Nov 1987, to BASF

R.E. Lavengood, A.F. Harris, A.R. Padwa, Europ. Pat. Appl. 202,214, 20 Nov 1986, to Monsanto

R.E. Lavengood, R. Patel, A.R. Padwa, U.S. Patent 4,777,211, 11 Oct 1988, to Monsanto

A. Lazzeri, C.B. Bucknall, J. Mater. Sci. **28**, 6788 (1993)

G.F. Lee Jr., U.S. Patent 4,123,410, 31 Oct 1978; U.S. Patent 4,128,602; 4,128,603; 4,128,604; 05 Dec 1978, to General Electric Co.

G.F. Lee Jr., U.S. Patent 4,143,095, 06 Mar 1979, to General Electric Co.

G.F. Lee Jr., U.S. Patent 4,242,263, 39 Dec 1980, to General Electric Co.

G.F. Lee Jr., U.S. Patent 4,311,633, 19 Jan 1982, to General Electric Co.

G.F. Lee Jr., U.S. Patent 4,383,082, 10 May 1983, to General Electric Co.

G.F. Lee Jr., Europ. Pat. Appl. 133,487, 27 Feb 1985, to General Electric Co.

G.F. Lee Jr., U.S. Patent 4,972,021, Nov 20, 1990, to General Electric Co.

G.F. Lee Jr., U.S. Patent 5,324,782, 28 June 1994, to General Electric Co.

S.-T. Lee, SPE Techn. Pap. **42**, 1948 (1996)

S.-T. Lee, U.S. Patent 5,428,093, 27 June 1995, to Sealed Air Corp.

Y.S. Lee, K.H. Char, Macromolecules **27**, 2603 (1994)

Y.C. Lee, Q.A. Trementozzi, Europ. Pat. Appl. 002,961, 11 July 1979, to Monsanto

Y.C. Lee, Q.A. Trementozzi, Europ. Pat. Appl. 007,931, 20 Feb 1980; U.S. Patent 4,223,096, 16 Sept 1980, to Monsanto

Y.C. Lee, Q.A. Trementozzi, U.S. Patent 4,305,869, 1981, to Monsanto

Y.C. Lee, Q.A. Trementozzi, U.S. Patent 4,341,695, 27 July 1982, to Monsanto

R.W. Lee, M.S. Ott, C.O. Castro, U.S. Patent 5,281,670, 25 Jan 1994, to Shell Oil

M.-H. Lee, C. Tzoganakis, C.B. Park, Polym. Eng. Sci. **38**, 1112 (1998)

J.P. Lehane Jr., U.S. Patent 3,137,672, 16 June 1964, to Hercules Powder

R. Leibler, W. Ringenberg, Ger. Offen. 3,518,538, 27 Nov 1986, to Roehm

E. Leitz, D. Wittmann, K.-H. Ott, A. Karbach, Ger. Offen. 4,114,589, 05 Nov 1992, to Bayer

H.J. Leugering, H. Schaum, So. Afric. Pat. 004,328, 08 Jan 1970, to Hoechst

H. Li, Y. Yang, R. Fujitsuka, T. Ougizawa, T. Inoue, Polymer **40**, 927 (1999a)

H.-L. Li, Y. Ujihira, A. Nanasawa, Y.C. Jean, Polymer **40**, 349 (1999b)

F. Li, T.J. Coffy, Daumerie, U.S. Patent 8,268,913, 18 Sept 2012 to Fina Technology

Y.F. Liang, U.S. Patent 4,708,983, 24 Nov 1987, to Phillips

Y.F. Liang, U.S. Patent 4,889,898, 26 Dec 1989, to Plastics Engineering

R. Liang, R.K. Gupta, SPE ANTEC **3**, 2753 (2001)

R. Liang, R.K. Gupta, SPE ANTEC **3**, 2948 (2002)

Z. Liang, H.L. Williams, J. Appl. Polym. Sci. **43**, 379–392 (1991)

H. Liang, B.D. Favis, Y.S. Yu, A. Eisenberg, Macromolecules **32**, 1637 (1999)

M. Lieberman, U.S. Patent 5,424,013, 13 June 1995

B.E. Liebermann, U.S. Patent 5,354,621, 11 Oct 1994, to Beltec International

S.-C. Lin, S. Burks, *Optimization of PVDF Performance via Polymer Blends*, SPI Fluoropolymer Conference, Oct 1993

C. Lindner, V. Damrath, K.E. Piejko, K.H. Ott, Ger. Pat. Appl. 3,822,667, 11 Jan 1990; Europ. Pat. Appl. 349,845, 10 Jan 1990, to Bayer

S.E. Lindsey, G.B. Street, Synth. Met. **10**, 67 (1985)

C.R. Lindsey, D.R. Paul, J.W. Barlow, J. Appl. Polym. Sci. **26**, 1 (1981)

D.W. Liou, Y.C. Sun, Ger. Offen. 4,311,436, 21 Oct 1993, to Dow Chem.

P.Y. Liu, PCT Int. Appl. 003,222, 30 Sept 1982, to General Electric Co.

P.Y. Liu, Ger. Offen. 3,300,855; 3,300,857, 11 Aug 1983, to General Electric Co.

P.Y. Liu, U.S. Patent 4,424,303, 03 Jan 1984; PCT Intl. Appl. 001,164, 29 Mar 1984; Europ. Pat. Appl. 119,533, 26 Sept 1984, to General Electric Co.

P.Y. Liu, H.F. Giles Jr., U.S. Patent 4,629,760, 16 Dec 1986, to General Electric Co.

J.H.G.M. Lohmeijer, J. Bussink, J.W.M. Noordermeer, U.S. Patent 4,618,637, 21 Oct 1986, to General Electric Co.

J.V. Long, J. Gagliani, U.S. Patent 4,621,015, 04 Nov 1986

Lonza Elektrizitätswerke & Chem. Fabriken, Swiss Pat. 253,413; 253,414, 01 Nov 1948

Lonza Limited, Brit. Pat. 964,578, 02 July 1964

G.L. Loomis, R.J. Statz, Europ. Pat. Appl. 101,833, 07 Mar 1984, to E. I. du Pont

G.L. Loomis, R.J. Statz, U.S. Patent 4,613,533, 1986, to E. I. du Pont

A.-V. Lourenço, Compt. Rend. **49**, 813 (1859)

A. Luciani, L.A. Utracki, Intl. Polym. Process. **6**, 299–309 (1996)

A. Luciani, M.F. Champagne, L.A. Utracki, Polym. Network Blends **6**(41), 51 (1996)

A. Luciani, M.F. Champagne, L.A. Utracki, J. Polym. Sci. B Polym. Phys. Ed. **35**, 1393 (1997)

A. Lund, L. Agren, PCT Int. Appl. 000,548, 07 Jan 1993, to Uponor Innovation

A. Lustiger, Can. Pat. Appl. 2,083,664, 21 June 1993, to Exxon

A. Lustiger, C.N. Marzinsky, R.R. Mueller, SPE Techn. Pap. **44**, 1506 (1998)

J. Lyngaae-Jørgensen, L.A. Utracki, Makromol. Chem. Macromol. Symp. **48/49**, 189 (1991)

J. Lyngaae-Jørgensen, K. Lunde Rasmussen, E.A. Chtcherbakova, L.A. Utracki, Polym. Eng. Sci. **39**, 1060 (1999)

J.M. Machado, U.S. Patent 5,175,210, 29 Dec 1992; U.S. Patent 5,369,180, 29 Nov 1992, to Shell Oil

J.M. Machado, U.S. Patent 5,210,137, 11 May 1993, to Shell Oil

P. Maj, P. Blondel, Europ. Pat. Appl. 550,308, 07 July 1993, to Elf Atochem.

Y. Makabe, T. Hatsu, Y. Yamamoto, Jap. Pat. 03 126,752, 29 May 1991, to Toray

K. Makino, I. Umeda, K. Sugiura, Jap. Pat. 016,943, 24 Jan 1986, to Japan Synthetic Rubber

L.M. Maresca, S.J. Shafer, U.S. Patent 4,788,249, 29 Nov 1988, to General Electric Co.

L.M. Maresca, M. Matzner, L.M. Robeson, U.S. Patent 4,250,279, 10 Feb 1981, to Union Carbide Corp.

H. Mark, in *ACS Book Series: Profiles, Pathways, and Dreams*, ed. by J.I. Seeman (ACS, Washington, DC, 1993)

G. Marrucci, G. Ianniruberto, Phil. Trans. R. Soc. Lond. A **361**, 677 (2003)

O. Martin, L. Averous, Polymer **42**, 6209 (2001)

R.J. Martinovitch, R.P. March, U.S. Patent 3,074,616, 22 Jan 1963, to Phillips

C.S. Martins, R. Faez, M.C. Rezende, M.A. De Paoli, J. Appl. Polym. Sci. **101**, 681 (2006)

E. Martuscelli, C. Marchetta, L. Nicolais, *Future Trends in Polymer Science and Technology — Polymers: Commodities or Specialties?* (Technomics, Lancaster, 1987)

T. Maruyama, Y. Mizuno, Europ. Pat. Appl. 388,308, 16 May 1990, to Sumitomo Chem.

H. Maruyama, Y. Shinagawa, K. Nishida, O. Kakishita, Jap. Pat. 093,459, 05 Aug 1977, to Mitsubishi Plastics

W.C. Mast, C.E. Rehberg, T.J. Dietz, C.H. Fisher, Ind. Eng. Chem. **36**, 1022 (1944)

M. Mathos, Master thesis, Ecole Polytechnique de Montréal, 1993

M. Matner, E. Schwinum, L. Mott, U.S. Patent 4,001,163, 04 June 1977, to Monsanto

Y. Matsuda, Jap. Pat. 007,579, 1960, to Dainippon Celluloid

Y. Matsuda, T. Kinoshita, H. Marusawa, M. Saito, Jap. Pat. 05,384, 1960a, to Dainippon Celluloid

Y. Matsuda, T. Kinoshita, H. Marusawa, S. Yabumoto, T. Fujii, Jap. Pat. 06,135, 1960b, to Dainippon Celluloid

A. Matsuda, S. Shimizu, S. Abe, U.S. Patent 4,247,652, 27 Jan 1981, to Mitsui Petrochemical Ind.

A. Matsuda, S. Shimizu, S. Abe, U.S. Patent 4,212,787, 15 July 1988, to Mitsui Petrochemical Ind.

M. Matsukane, C. Azo, Jap. Pat. 054,160, 30 July 1973, to Teijin Chemicals

H. Matsunaga, S. Nakashio, K. Yonetani, T. Takemura, Jap. Pat. 74 38,954, 11 Apr 1974, to Sumitomo Chem.

H. Matsunaga, Y. Uemura, T. Saito, H. Ishida, Jap. Pat. 057,255, 24 May 1978, to Sumitomo Chem.

T. Matsuura, Y. Katayama, J. Shimada, Jap. Pat. 060,947, 31 May 1978, to Nippon Telegraph & Telephone Public Corp.

K. Matsuzaki, Jap. Pat. 03 0,756, 07 Jan 1991, to Asahi Chem. Co.

F.E. Matthews, Brit. Pat. 016,278, 14 July 1911

F.E. Matthews, Fr. Pat. 459,134, 27 Aug 1913

F.H.J. Maurer, J.H.M. Palmen, H.C. Booij, Rheol. Acta **24**, 243 (1985)

M. Mawatari, T. Tetsuo, S. Tsuchikawa, S. Kimura, Europ. Pat. Appl. 244,090, 04 Nov 1987, to Japan Synthetic Rubber

J. Mayumi, H., Omori, Europ. Pat. Appl. 268,981, 01 June 1988, to Mitsubishi Petrochem.

F.B. McAndrew, Ger. Pat. 2,051,028, 29 Apr 1971, to Celanese Corp.

S.P. McCarthy, R.A. Gross, W. Ma, U.S. Patent 5,883,199, 1999

W.J. McCracken, J. Cellular. Plast. **20**(2), 150 (1984)

J.E. McCready, U.S. Patent 3,947,403, 30 Mar 1976, to Goodyear Tire and Rubber

T.W. McCullough, B.D. Stevens, U.S. Patent 4,515,907, 07 May 1985, to Dow Chemical

J.E. McGrath, M. Matzner, U.S. Patent 3,655,822, 11 Apr 1972, to Union Carbide Corp.

G.H. McKee, F. Haaf, J. Hambrecht, K. Benker, R. Stephan, H. Breurer, Ger. Offen. 3,113,627, 21 Oct 1982, to BASF

A.K. Mehta, M.C. Chen, U.S. Patent 5,358,792, 25 Oct 1994, to Exxon

P. Meier, Ger. Pat. 4,139,468, 03 June 1993, to Ems-Inventa

J.L. Melmquist, U.S. Patent 5,189,115, 23 Feb 1993, to Amoco Corp.

N.A. Memon, C.S. Myers, U.S. Patent 4,391,938, 05 July 1983, to Rohm & Haas

A. Merrington, in *Applied Plastics Engineering Handbook*, ed. by M. Kutz (Elsevier, Amsterdam, 2011)

R.B. Mesrobian, C.J. Ammondson, Brit. Pat. 889,354, 14 Feb 1962, to Continental Can Company

V. Metanomski (ed.), *Compendium of Macromolecular Nomenclature*, IUPAC Macromol. Div. (Blackwell, Oxford, 1991)

R.V. Meyer, P. Tacke, Ger. Offen. 2,654,168, 01 June 1978, to Bayer

J.M. Michel, Fr. Pat. 1,566,235, 09 May 1969, to Pechiney-Saint Gobain

E.A. Militskova, E.A. Pavlova, I.O. Stalnova, V.B. Cherkashin, USSR. Pat. 1,788,958, 15 Jan 1993, to USSR

A. Miller, N.G. Reddeman, Belg. Pat. 620,703, 14 Nov 1962, to Miliprint

G.W. Miller, U.S. Patent 3,646,159, 29 Feb 1972, to Baychem Corp.

A. Minegishi, Y. Naka, T. Takahashi, Y. Masubuchi, J. Takimoto, K. Koyama, Nihon Reor. Gakk. **25**, 215 (1997)

A. Minegishi, A. Nishioka, T. Takahashi, Y. Masubuchi, J. Takimoto, K. Koyama, *International Symposium on Elongational Flow of Polymeric Systems*, Yamagata U., Yonezawa, 13–15 June 1998

S. Minekawa, K. Yamaguchi, K. Toyomoto, E. Fujimoto, Y. Takeuchi, Jap. Pat. 008,585, 12 Sept 1969, to Asahi Chem.

S. Minekawa, K. Yamaguchi, K. Toyomoto, E. Fujimoto, Y. Takeuchi, Jap. Pat. 016,429, 06 May 1971, to Asahi Chem.

L.I. Minkova, M. Paci, M. Pracella, P. Magagnini, Polym. Eng. Sci. **32**, 57 (1992)

Mitsubishi Chem. Ind. Co., Jap. Pat. 157,648, 08 Dec 1980

Mitsubishi Chem. Ind. Co., Jap. Pat. 137,347, 24 Aug 1982

Mitsubishi Chem. Ind. Co., Jap. Pat. 076,448, 09 May 1983

Mitsubishi Chem. Ind. Co., Jap. Pat. 020,351, 02 Feb 1984

Mitsubishi Gas Chem. Co., Jap. Pat. 174,344, 27 Oct 1982

Mitsubishi Gas Chem. Co., Jap. Pat. 020,953, 02 Feb 1985

Mitsubishi Petrochem. Co., Jap. Pat. 195,147, 30 Nov 1982

Mitsubishi Petrochem. Co., Jap. Jap. Pat. 007,448, 17 Jan 1983; Jap. Pat. 162,653, 27 Sept 1983

Mitsubishi Petrochem. Co., Jap. Pat. 022,956, 06 Feb 1984

Mitsubishi Petrochem. Co., Jap. Pat. 086,161; 086,164, 15 May 1985

Mitsui Petrochem. Ind., Jap. Pat. 168,646, 05 Oct 1983; Jap. Pat. 213,039, 10 Dec 1983

K. Miyanishi, Y. Manabe, Jap Pat., 047,043, 22 Apr 1976, to Teijin Chemicals

Y. Mizuno, T. Maruyama, Europ. Pat. Appl. 349,339, 03 Jan 1990, to Sumitomo Chem.

M. J. Modic, R. Gelles, Europ. Pat. Appl. 255,184, 03 Feb 1988, to Shell

A.K. Mohanty, M. Misra, L.T. Drzal (eds.), *Natural Fibers, Biopolymers and Biocomposites* (Taylor and Francis, Boca Raton, 2005)

R.N. Mohn, D.R. Paul, J.W. Barlow, C.A. Cruz, J. Appl. Polym. Sci. **23**, 575 (1979)

A.N. Mollison, U.S. Patent 4,461,808, 24 July 1984, to DuPont Canada

H. Moncure Jr., U.S. Patent 3,480,694, 25 Nov 1969, to E. I. du Pont

C.W. Montgomery, Fr. Pat. 1,445,876, 15 July 1966, to Ethyl Corp.

D.Y. Moon, O.O. Park, Adv. Polym. Technol. **17**, 203 (1998)

D. Moorwessel, R. Glasser, G. Pfirrmann, Ger. Offen. 2,306,893, 22 Aug 1974, to BASF

A.W. Morgan, R.G., Ribaudo, U.S. Patent 4,228,245, 14 Oct 1980, to Bayer

Y. Morita, N. Kashiwa, Europ. Pat. Appl. 022,376, 14 Jan 1981, to Mitsui Petrochem.

K. Morita, K. Uchiki, H. Shinoda, U.S. Patent 5,223,546, 29 June 1993a; U.S. Patent 5,238,968, 24 Aug 1993b, to Mitsui Toatsu Chemicals

P.J.T. Morris, *The American Synthetic Rubber Research Program* (University of Pennsylvania Press, Philadelphia, 1989)

D.R. Morrow, T.J. Nosker, K.E. VanNess, R.W. Renfree, U.S. Patent 5,298,214, 29 Mar 1994, to Rutgers State University

M. Morton, in *History of Polymer Science and Technology*, ed. by R.B. Seymour (Marcel Dekker, New York, 1982)

G.S. Motz, U.S. Patent 4,226,961, 07 Oct 1980, to General Electric Co.

C.T. Movak, P.N. Nelson, S. Nam, W. DeMoully, K.D. Goebel, U.S. Patent 5,371,143, 06 Dec 1994, to Minnesota Mining & Manufacturing

P. Mukhopadhyay, C.K. Das, Polym. Plast. Technol. Eng. **28**, 537 (1989)

P. Mukhopadhyay, C.K. Das, J. Appl. Polym. Sci. **39**, 49 (1990)

P. Mukhopadhyay, C.K. Das, Int. J. Polym. Mater. **15**, 57 (1991)

P. Mukhopadhyay, H.P. Schreiber, Colloids Surf. A Physicochem. Eng. Asp. **100**, 47 (1995)

P. Mukhopadhyay, G. Chowdhury, C.K. Das, Kautschuk Gummi Kunststoffe **42**, 308 (1989)

P. Mukhopadhyay, G. Chowdhury, C.K. Das, J. Appl. Polym. Sci. **40**, 1833 (1990)

A. Mukohyama, Int. Pat. Appl. 08,233, 29 Apr 1993, to E. I. du Pont

R. Mülhaupt, J. Rosch, S. Hopperdietzel, E. Weinberg, H. Klein, U.S. Patent 5,312,875, 17 May 1994, to Rehau

D.H. Mullins, Brit. Pat. 958,399, 21 May 1964, to Union Carbide Corp.

W.G. Munk, Ger. Offen. 4,204,083 A1, 04 Mar 1993, to Nordmann Rassmann GmbH & Co.

H. Münstedt, S. Kurzbeck, *International Symposium on Elongational Flow of Polymeric Systems*, Yamagata U., Yonezawa, 13–15 June 1998

S. Murakami, H. Higuchi, S. Matsuo, Jap. Pat. 03 190,961, 20 Aug 1991, to Idemitsu Kosan

J.D. Murdock, N. Nelan, G.H. Segall, Ger. Offen. 1,217,606, 26 May 1960, to Canadian Industries

J.D. Murdock, N. Nelan, G.H. Segall, Brit. Pat. 901,386, 18 July 1962, to Canadian Industries

J.G. Murray, U.S. Patent 4,352,908, 05 Oct 1982, to Mobil Oil Corp.

L.C. Muschiatti, B.A. Smillie, U.S. Patent 5,391,582, 21 Feb 1995, to E. I. Du Pont

V.M. Nadkarni, J.P. Jog, in *Two – Phase Polymer Systems*, ed. by L.A. Utracki (Hanser, Munich, 1991)

S. Nagai, M. Hasegawa, H. Mimura, M. Kobayashi, Eur. Pat. Appl. 565,304, 13 Oct 1993, to Mitsubishi Gas Chem.

S. Nagai, M. Hasegawa, H. Mimura, M. Kobayashi, U.S. Patent 5,326,846, 05 July 1994, to Mitsubishi Gas Chem.

K. Nagasaki, T. Hata, K. Matsuzaki, Jap. Pat. 03 263,454, 22 Nov 1991, to Asahi Chem.

Y. Nagase, M. Kobayashi, T. Kato, S. Imuta, U.S. Patent 5,338,792, 16 Aug 1994, to Mitsui Petrochem.

S.V. Nair, A. Subramaniam, L.A. Goettler, J. Material Sci. **32**, 5347 (1997)

S.V. Nair, A. Subramaniam, L.A. Goettler, J. Material Sci. **33**, 3455 (1998)

K. Nakamura, K. Neki, Europ. Pat. Appl. 039,155, 04 Nov 1981, to Asahi Chem.

K. Nakamura, K. Toyomoto, Jap. Pat. 075,662, 22 July 1974, to Asahi Chem.

K. Nakamura, T. Kimura, H. Tsunoda, Jap. Pat. 083,174, 06 Nov 1973, to Sanyo Pulp.

H. Nakano, T. Inoue, S. Gotoh, M. Kihira, Europ. Pat. Appl. 484,941, 13 May 1992, to Mitsubishi Petrochem.

K.M. Nampoothiri, N.R. Nair, R.P. John, Bioresource Technol. **101**, 8493 (2010)

K.M. Natarajan, R. Mininni, Europ. Pat. Appl. 428,178, 22 May 1991, to Enichem.

K.M. Natarajan, P. Arjunan, D. Elwood, Europ. Pat. Appl. 540,120, 05 May 1993, to Enichem.

K.M. Natarajan, P. Arjunan, D. Elwood, U.S. Patent 5,296,550, 22 Mar 1994, to Enichem.

G. Natta, F. Danusso (eds.), *Stereoregular Polymers and Stereospecific Polymerization* (Pergamon Press, New York, 1967)

S.P. Nemphos, G.B. Kharas, Eur. Pat. Appl. 540,182, 05 May 1993, to Novacor Chem.

S.P. Nemphos, G.B. Kharas, U.S. Patent 5,300,576, 05 Apr 1994, to Novacor Chem.

D. Neuray, W. Nouverte, R. Binsack, D. Rempel, P.R. Mueller, Europ. Pat. Appl. 064,648, 17 Nov 1982, to Bayer

R. Newe, E. Lange, H. Hoffmann, K. Wetzel, East Ger. Offen. 207,381, 29 Feb 1984, to VEB Chemiekombinat Bitterfeld

S. Newman, D.R. Paul, *Polymer Blends*, vol. I and II (Academic, New York, 1978)

A.B.. Newton, Europ. Pat. Appl. 037,181, 07 Oct 1981, to ICI

K.L. Ngai, D.J. Plazek, Macromolecules **23**, 4282 (1990)

X.Q. Nguyen, L.A. Utracki, U.S. Patent 5,451,106, 19 Sept 1995, to National Research Council Canada

E. Nield, Ger. Offen. 2,122,735, 25 Nov 1971, to ICI

N. Niessner, G.E. Mac Kee, K. Ruppmich, Ger. Pat. 4,200,247, 15 July 1993, to BASF

N. Niessner, F. Seitz, W. Fischer, N. Guentherberg, K. Ruppmich, R. Moors, R. Weiss, Europ. Pat. Appl. 576,960, 05 Jan 1994, to BASF

Nippon Zeon Co., Jap. Pat. 129,245, 25 July 1984

T. Nishio, T. Sanada, T. Okada, Europ. Pat. Appl. 270,247, 08 June 1988, to Sumitomo Chem.

T. Nishio, Y. Suzuki, K. Kojima, M. Kakugo, Kobunshi Robunshu **47**, 331 (1990)

T. Nishio, T. Nomura, N. Kawamura, H. Sato, A. Uchikawa, I. Tsutsumi, Y. Goto, Europ. Pat. Appl. 519,725, 23 Dec 1992, to Mitsubishi Petrochem.

T. Nishio, T. Sanada, S. Hosoda, K. Nagaoka, T. Okada, U.S. Patent 5,288,786, 22 Feb 1994, to Sumitomo Chem.

A. Nishioka, S. Kato, Y. Kiyomatsu, M. Ichikawa, Y. Kitagawa, Jap. Pat. 074,552, 08 Oct 1973, to Japan Synthetic Rubber

A. Nishiyama, T. Nakakita, Jap. Pat. 03 252,455, 11 Nov 1991, to Ube Industries

M. Nishiyama, K. Ohtsuki, Y. Nakakita, H. Ozawa, Europ. Pat. Appl. 360,544, 28 Mar 1990, to Ube

M. Nishiyama, T. Nakakita, K. Ohtsuka, Jap. Pat. 03 100,055, 25 Apr 1991a, to Ube

M. Nishiyama, K. Ohtsuka, T. Nakakita, Jap. Pat. 03 91,562, 17 Apr 1991b, to Ube

G.E. Nizik, U.S. Patent 4,097,425, 27 Jan 1978, to General Electric Co.

G.E. Nizik, U.S. Patent 4,174,432, 13 Nov 1979, to General Electric Co.

K. Nyori, A. Kinoshita, I. Hatano, Jap. Pat. 010,928; 012,919, 04 Sept 1962, to Kanegafuchi Chem.

W.J.J. O'Connell, Fr. Dem. 2,213,959, 09 Aug 1974, to General Electric Co.

W.J.J. O'Connell, Jap. Pat. 076,450, 09 May 1983, to General Electric Co.

A.O. Ogah, J.L. Afikuwa, Int. J. Eng. Management Sci. **3**, 85 (2012)

T. Ogawa, N. Ito, K. Ohishi, R. Samejima, Jap. Pat. 031,241, 24 Apr 1973, to Sumitomo Chem.

T. Ohmae, Y. Toyoshima, K. Mashita, N. Yamaguchi, J. Nambu, U.S. Patent 5,010,136, 23 Apr 1991, to Sumitomo Chem.

T. Ohmae, Y. Toyoshima, K. Mashita, N. Yamaguchi, J. Nambu, Europ. Pat. Appl. 480,770, 15 Apr 1992, to Sumitomo Chem.

M. Ohta, K. Iiyama, S. Kawashima, S. Tamai, H. Oikawa, A. Yamaguchi, Europ. Patent Appl. 294,144, 07 Dec 1988, to Mitsui Toatsu Chem.

T. Ohta, O. Urakawa, Q. Tran-Cong, Macromolecules **31**, 6845 (1998)

T. Oita, T. Hara, R. Samejima, K. Tanabe, Jap Pat. 108,146, 20 Sept 1978, to Sumitomo Chem.

A. Okada, U.S. Patent 5,352,727, 04 Oct 1994, to Idemitsu Kosan

A. Okada, A. Masuyama, U.S. Patent 5,326,813, 05 July 1994, to Idemitsu Kosan

K. Okada, M. Karaiwa, A. Uchiyama, U.S. Patent 5,728,744, 17 Apr 1998a, to Mitsui Petrochem.

K. Okada, M. Karaiwa, A. Uchiyama, U.S. Patent 5,786,403, 28 July 1998b, to Mitsui Petrochem

O. Okada, H. Keskkula, D.R. Paul, J. Polym. Sci. Part B Polym. Phys. **42**, 1739 (2004)

K.T. Okamoto, K.D. Eastenson, S.C. Guyaniyogi, Europ. Pat. Appl. 566,106, 20 Oct 1993, to Himont

K.T. Okamoto, K.D. Eastenson, S.C. Guyaniyogi, U.S. Patent 5,290,856, 01 Mar 1994, to Himont

M. Okamoto, A. Kojima, T. Kotaka, Polymer **39**, 2149 (1998a)

M. Okamoto, H. Kubo, T. Kotaka, *14th International Polymer Processing Society Meeting*, *PPS-14*, Yokohama, 08–12 June 1998b

Y. Okawa, N. Koga, H. Oikawa, T. Asanuma, A. Yamaguchi, U.S. Patent 5,321,096, 14 June 1994, to Mitsui Toatsu Chem.

S. Okuda, Europ. Pat. Appl. 356,167, 28 Feb 1990, to Polyplastics

T. Okuzono, M. Kifune, Jap. Pat. 001,147, 08 Jan 1975, to Mitsubishi Gas Chem.

T. Okuzono, M. Kifune, Jap. Pat. 030,255; 030,256, 11 Sept 1976, to Mitsubishi Gas Chem

J. O'Leary, S. Musgrave, PCT Int. Appl. WO 93 21,269, 28 Oct 1993, to ICI, Australia

Y. Ono, K. Iida, K. Murata, Y. Noto, Jap Pat. 03 97,756, 23 Apr 1991, to Dainippon Ink & Chem.

Y. Orikasa, S. Sakazume, Europ. Pat. Appl. 361,400, 04 Apr 1990, to Nippon Petrochem.

Y. Orikasa, S. Sakazume, Europ. Pat. Appl. 506,006, 30 Sept 1992, to Nippon Petrochem.

Y. Orikasa, S. Sakazume, U.S. Patent 5,296,538, 22 Mar 1994, to Nippon Petrochem.

Y. Orikasa, S. Sakazume, S. Nishimura, Y. Maki, Europ. Pat. Appl. 314,188, 03 May 1989, to Nippon Petrochem.

I.I. Ostromislensky, J. Russ. Phys. Chem. Soc. **44**, 204 (1911)

I.I. Ostromislensky, J. Russ. Phys. Chem. Soc. **47**, 1772, 1915, 1928 (1915)

I.I. Ostromislensky, J. Russ. Phys. Chem. Soc. **48**, 1132 (1916)

Ostromislensky, Iwan I., of New York, N. Y., Brit. Pat. 233,649, 07 May 1924; Can. Pat. 261,327, 01 June 1926; U.S. Patent 1,613,620, 11 Jan 1927; U.S. Patent 1,676,281, 10 July 1928, to Naugatuck Chem.

D.E. Overton, P.Y. Liu, Europ. Pat. Appl. 119,531, 26 Sept 1984, to General Electric Co.

D.E. Overton, P.Y. Liu, U.S. Patent 4,532,282, July 1985, to General Electric Co.

S. Pack, M. Lewin, M.H. Rafailovich, *Fire and Polymers VI: New Advances in Flame Retardant Chemistry and Science*, ACS Symposium Series, Plennm, New York, vol. 1118 (2012), American Chemical Society, Washington, DC

C.F. Paddock, U.S. Patent 4,264,747, 28 Apr 1981, to Uniroyal

M. Paleari, T. Fornasiero, Europ. Pat. Appl. 593,837, 27 Apr 1994, to W. R. Grace & Co.

C.P. Park, U.S. Patent 4,129,530, 12 Dec 1978, to Dow Chemical

C.P. Park, U.S. Patent 4,215,202, 29 July 1980, to Dow Chemical

C.P. Park, U.S. Patent 4,554,293, 19 Nov 1985, to Dow Chemical

C.P. Park, U.S. Patent 4,623,671, 18 Nov 1986a, to Dow Chemical

C.P. Park, U.S. Patent 4,567,209, 28 Jan 1986b, to Dow Chemical

C.P. Park, U.S. Patent 4,605,682, 12 Aug 1986c, to Dow Chemical

C.P. Park, U.S. Patent 4,581,383, 08 Apr 1986d, to Dow Chemical

C.P. Park, U.S. Patent 4,652,588, 24 Mar 1987, to Dow Chemical

C.P. Park, U.S. Patent 4,722,972, 02 Feb 1988, to Dow Chemical

C.P. Park, U.S. Patent 5,469,818, 24 Oct 1995, to Dow Chemical

C.L. Parker, U.S. Patent 2,539,385, 30 Jan 1951, to Radio Corporation of America

D.S. Parker, H.-J. Sue, J. Huang, A.F. Yee, Polymer **31**, 2267 (1992)

A. Parkes, Brit. Pat. 1,147, 25 Mar 1846; Brit. Pat. 1,313, 07 Nov 1865

C.E. Parks, U.S. Patent 3,975,315, 17 Aug 1976, to BFGoodrich

I.K. Partridge, in *Multicomponent Polymer Systems*, ed. by I.S. Miles, S. Rostami (Longman Scientific & Technical, Harlow, 1992)

E.F. Paschke, M.A. Stasi, E.F. Rader, U.S. Patent 4,383,084, 10 May 1983, to Standard Oil

E.E. Paschke, C.L. Myers, G.P. Desio, Europ. Pat. Appl. 572,266, 01 Dec 1993, to Amoco Corp.

E.E. Paschke, C.L. Myers, G.P. Desio, U.S. Patent 5,292,805, 08 Mar 1994, to Amoco Corp.

G.A.R. Patfoort, Belg. Pat. 833,543, 18 Mar 1976

J.C. Patrick, U.S. Patent 1,890,191, 1932, to Thiokol Chem.

J.C. Patrick, U.S. Patent 2,278,128, 31 Mar 1942, to Thiokol Chem.

T. Patton, LaMarre, Europ. Pat. Appl. 068,695, 05 Jan 1983, to Exxon

J.-R. Pauquet, F. Sitek, R. Todesco, U.S. Patent 5,298,540, 29 Mar 1994, to Ciba-Geigy Corp.

A.J. Peacock, *Handbook of Polyethylene* (Marcel Dekker, New York, 2000)

R. Pernice, C. Berto, A. Moro, R. Pipa, Europ. Pat. Appl. 528,477, 31 July 1992, to ECP Enichem Polimeri

P.J. Perron, Adv. Polymer Technol. **6**, 79 (1984)

P.J. Perron, U.S. Patent 4,782,114, 01 Nov 1988, to Dexter Corp.

P.J. Perron, K. Nangrani, E. Bourbonais, U.S. Patent 5,187,228, 16 Feb 1993, to Dexer Corp.

R.J. Petcavich, U.S. Patent 5,367,003, 22 Nov 1994.

E.N. Peters, J.A. Rock, Europ. Pat. Appl. 325,719, 02 Aug 1989, to General Electric Co.

H. Peters, F. Schuelde, Ger. Offen. 1,146,251, 28 Mar 1963, to Hoechst

P. Pfleiderer, Ger. Offen. 10,164, 1880, to Maschinenfabrik Werner und Pfleiderer

E.M. Phillips, K.E. McHugh, K. Ogale, M.B. Bradley, Kunststoffe **82**, 671 (1992)

S.U. Pickering, J. Chem. Soc. Abstr. **91–92**, 2001 (1908)

M.R. Piggott, in *Failure of Plastics*, ed. by W. Brostow, R.D. Corneliussen (Hanser, Munich, 1986)

L.Z. Pillon, L.A. Utracki, Polym. Eng. Sci. **4**, 1300 (1984)

L.Z. Pillon, L.A. Utracki, Polym. Process Eng. **24**, 375 (1986)

L. Pinchuck, Europ. Pat. Appl. 461,375, 18 Dec 1991, to Corvita Corp.

A. Plochocki, T. Bek, J. Bojarski, L. Czarnecki, L. Grabiec, J. Kepka, P. Machowski, Polish Pat. 100,160, 17 Apr 1979, to Institute Chem. Ind., Polish Academy of Sci.

C.J.G. Plummer, J.L. Hedrick, H.-H. Kausch, J.G. Hilborn, J. Polym. Sci. Part B Polym. Phys. **33**, 1813 (1995)

V.N. Pokrovskii, J. Exp. Theoretical Phys. **106**, 604 (2008)

M. Pontio, U.S. Patent 1,293,191, 1919

L.M. Porter, Ger. Offen. 2,156,681, 18 May 1972, to Shell

R.S. Porter, L.H. Wang, Polymer **33**, 2019 (1992)

R.S. Porter, J.M. Jonza, M. Kimura, C.R. Desper, E.R. George, Polym. Eng. Sci. **29**, 55 (1989)

M. Portugall, G. Blinne, W. Ziegler, M. Walter, H. Reimann, K. Schlichting, Ger. Offen. 3,234,174, 15 Mar 1984, to BASF

W. Posch, in *Applied Plastics Engineering Handbook*, ed. by M. Kutz (Elsevier, Amsterdam, 2011)

I. Prigogine, A. Bellemans, V. Mathot, *The Molecular Theory of Solutions* (North-Holland, Amsterdam, 1957)

M. Prillieux, P. Delbende, M. Moulin, Fr. Pat. 1,289,580, 06 Apr 1962, to Esso

E.G. Pritchett, U.S. Patent 4,228,250, 14 Oct 1980, to National Distillers & Chemical Corp.

E.G. Pritchett, U.S. Patent 4,264,746, 1981, to National Distillers & Chemical Corp.

R.C. Puydak, D.R. Hazelton, T. Ouhadi, PCT Int. Appl. WO 90 014,389, 29 Nov 1990, Oct 1992, to Exxon

R.C. Puydak, D.R. Hazelton, T. Ouhadi, U.S. Patent 5,157,081, Oct 1992, to Exxon

C.B. Quinn, U.S. Patent 4,430,484, 07 Feb 1984, to General Electric Co.

C.B. Quinn, F.F. Holub, Europ. Pat. Appl. 187,416, 16 July 1986, to General Electric Co.

C.B. Quinn, N.R. Rosenquist U.S. Patent 4,358,569, 09 Nov 1982, to General Electric Co.

M. Rabeony, D.J. Lohse, R.T. Garner, S.J. Han, W.W. Graessley, K.B. Migler, Macromolecules **31**, 6511 (1998)

P. Ramya, J. Phys. Conf. Ser. **443**, 012048 (2013)

F. Ranalli, Ital. Pat. 583,501, 14 Oct 1958, to Montecatini S. G.

R.M. Rasal, D.E. Hirt, Macromol. Mater. Eng. **295**, 204 (2010)

R.M. Rasal, A.V. Janorkar, D.E. Hirt, Progr. Polym. Sci. **35**, 338 (2010)

C. Rauwendaal, *Polymer Extrusion*, 4th edn. (Hanser, Munich, 2001)

L.S. Rayner, J.A. Bond, M. Clark, R.E. Nott, Brit. Pat. 958,079, 13 May 1964, to ICI

A. Razavi, U.S. Patent 5,278,265, 11 Jan 1994, to Fina Technology

J.E. Reardon, U.S. Patent 4,329,278, 11 May 1982, to E. I. du Pont

R.J. Reid, W.R. Conrad, U.S. Patent 2,929,795, 22 Mar 1960, to Firestone Tire & Rubber

R.J. Reid, W.R. Conrad, Belg. Pat. 617,870, 21 Nov 1962, to Firestone Tire & Rubber

H.K. Reimschussel, G.J. Dege, Ger. Offen. 1,918,499, 13 Nov 1969, to Allied Chem. Corp.

M.S. Reisch, *Chem. Eng. News*, 22–27, 15 Apr 2002

E. Reske, E. Wolters, Ger. Pat. 3,303,760; 3,303,761, 09 Aug 1984, to Hoechst

W.D. Richards, D.M. White, Europ. Pat. Appl. 592,144, 13 Apr 1994, to General Electric Co.

P.N. Richardson, Europ. Pat. Appl. 117,748, 05 Sept 1984, to E. I. du Pont

E.H. Riddle, *Monomeric Acrylic Esters* (Reinhold, New York, 1954)

B. Rieger, X. Mu, D.T. Mallin, M.D. Rausch, J.C.W. Chien, Macromolecules **23**, 3559 (1990)

R.-E. Riemann, W. Gleinser, Friedrich, *Polymer Processing Society European Meeting*, Stuttgart, 26–28 Sept 1995

M.R. Rifi, U.S. Patent 5,326,602, 05 July 1994, to Union Carbide Chem.

W. Ritter, R. Bergner, M. Schäfer, Ger. Offen. 4,121,111 A1, 07 Jan 1993, to Henkel

E.P. Rittershausen, U.S. Patent 2,489,674, 29 Nov. 1949, to Socony Vacuum Oil Co.

L.M. Robeson, Europ. Pat. Appl. 24,245, 25 Feb 1981, to Union Carbide Corp.

L.M. Robeson, U.S. Patent 4,324,869, 13 Apr 1982, to Union Carbide Corp.

L.M. Robeson, U.S. Patent 4,532,288, 30 July 1985, to Union Carbide Corp.

L.M. Robeson, PCT Int. Appl. 000,220, 14 Jan 1988, to Amoco Corp.

L.M. Robeson, *Polymer Blends* (Hanser, Munich, 2007)

L.M. Robeson, Ind. Eng. Chem. Res. **49**, 11859 (2010)

L.M. Robeson, Polym. Eng. Sci. **53**, 453 (2013)

L.M. Robeson, J.E. Harris, Europ. Pat. Appl. 133,907, 13 Mar 1985, to Union Carbide Corp.

L.M. Robeson, J.E. Harris, Europ. Pat. Appl. 176,988, 09 Apr 1986, to Union Carbide Corp.

L.M. Robeson, M. Matzner, Europ. Pat. Appl. 104,659, 04 Apr 1984, to Union Carbide Corp.

L.M. Robeson, M. Matzner, L.M. Maresca, Europ. Pat. Appl. 33,394, 12 Aug 1981, to Union Carbide Corp.

P.A. Rodgers, J. Appl. Polym. Sci. **48**, 1061 (1993)

M. Roemer, A. Schleicher, PCT Int. Pat. Appl. 002,144, 04 Feb 1993, to Hoechst

M. Roemer, A. Schleicher, Jap. Pat. 60 49,338, 22 Feb 1994, to Hoechst

K.A. Romance, U.S. Patent 4,897,448, 30 Jan 1990, to Eastman Kodak

O.V. Romankevich, S. Ya. Frenkel, Acta Polymerica, **31**, 287(1980)

F.E. Romesberg, U.S. Patent 5,051,452, 24 Sept 1991, to Dow Chemical Co.

J. Roovers, L.-L. Zhu, P.M. Toporowski, M. van der Zwan, H. Iatrou, N. Hadjichristidis, Macromolecules **26**, 4324 (1993)

J. Rösch, R. Mülhaupt, Polym. Bull. **32**, 697 (1994)

W.J. Rosenfelder, J.J. Rosen, U.S. Patent 3,046,237, 24 July 1962, to Dublon

N.R. Rosenquist, U.S. Patent 4,335,032, 15 June 1982, to General Electric Co.

S. Rostami, Europ. Pat. Appl. 211,604, 25 Feb 1987, to ICI

L.C. Rubens, U.S. Patent 4,604,426, 05.08.1986, to Dow Chemical

A. Rudin, H.P. Schreiber, Fr. Pat. 1,349,823, 17 Jan 1964a, to Canadian Industries Ltd. (CIL)

A. Rudin, H.P. Schreiber, Can. Pat. 688,416, 09 June 1964b, to Canadian Industries Ltd. (CIL)

N.R. Ruffing, B.A. Kozakiewicz, B.B. Cave, J.L. Amos, Belg. Pat. 632,377, 1964, to Dow Chemical

J. Rys-Sikora, U.S. Patent 4,391,923, 05 July 1983, to E. I. Du Pont

J. Rys-Sikora, U.S. Patent 4,434,253, 28 Feb 1984, to E. I. Du Pont

Z.M.O. Rzayev, Int. Rev. Chem. Eng. **3**, 153 (2011)

C. Sadrmohaghegh, G. Scott, E. Setudeh, Polym. Plast. Technol. Eng. **24**, 149 (1985)

H.R. Sailors, J.P. Hogan, in *History of Polymer Science and Technology*, ed. by R.B. Seymour (Marcel Dekker, New York, 1982)

T. Saito, Jap. Pat. 007,850, 27 Jan 1975, to Showa Denko

I. Sakai, J. Oshima, M. Yamada, Europ. Pat. Appl. 299,468; 299,469, 18 Jan 1989, to Takeda Chem.

T. Sakamoto, Kumai, K. Kenichiro, S. Gotoh, U.S. Patent 5,346,926, 13 Sept 1994, to Nippon Unicar.

S. Sakane, K. Minato, M. Takashige, Jap. Pat. 000,052, 05 Jan 1979, to Idemitsu Petrochem.

H. Sakano, A. Ito, M. Terada, Ger. Pat. 3,027,957, 12 Feb 1981, to Sumitomo-Naugatuck

H. Sakano, A. Ito, M. Terada, U.S. Patent 4,317,891, 1982, to Sumitomo-Naugatuck

H. Sakano, K. Motomatsu, I. Tsukino, I. Yoshida, T. Shima, H. Kojima, T. Yoshida, Jap. Pat. 07,757, 24 Jan 1978, to Sumitomo Naugatuck

R. Sakata, T. Kuroda, K. Masuda, Y. Nakayama, M. Tanaka, Jap. Pat. 003,964, 13 Feb 1968, to Mitsubishi Petrochem.

G. Salee, U.S. Patent 4,211,687, 08 July 1980, to Hooker Chemicals and Plastics Corp.

G. Salee, U.S. Patent 4,304,709, 08 Dec 1981, to Hooker Chemicals and Plastics Corp.

G. Salee, U.S. Patent 4,327,012, 27 Apr 1982, to Hooker Chemicals and Plastics Corp.

R.P. Saltman, PCT Int. Appl. WO 88 003,453, 19 Mar 1988, to E. I. du Pont

R.P. Saltman, U.S. Patent 4,871,810, 03 Oct 1989, to E. I. du Pont

R.P. Saltman, U.S. Patent 5,091,478, 25 Feb 1992, to E. I. du Pont

I.O. Salyer, H.P. Holladay, U.S. Patent 3,149,183, 15 Sept 1964, to Monsanto

G.J. Samuels, U.S. Patent 5,336,732, 09 Aug 1994, to AlliedSignal

I.C. Sanchez, W.M. Balaba, L.T. Stevenson, U.S. Patent 5,032,434, 16 July 1991, to Aluminum
   Company of America

M.A. Sanner, R.R. Gallucci, *Proc. SPE ANTEC*, 2684 (2011)

I. Sasaki, N. Yamamoto, A. Yanagase, U.S. Patent 5,011,887; Europ. Patent Appl. 332,188,
   13 Sept 1989, to Mitsubishi Rayon

M.E. Sauers, B.P. Barth, Ger. Offen. 1,954,671, 06 May 1970, to Union Carbide Corp.

H. Scheckenbach, A. Schonfeld, S. Weis, U.S. Patent 5,708,041, 13 Jan 1998, to Höchst

W.M. Schilling, Brit. Pat. 975,877, 18 Nov 1964, to Hercules Powder

W.M. Schilling, U.S. Patent 3,200,173, 10 Aug 1966, to Hercules Powder

B. Schlund, L.A. Utracki, Polym. Eng. Sci. **27**, 380 (1987); ibid. **27**, 1523 (1987)

A.D. Schluter, J.P. Rabe, Angew. Chem. Int. Ed. **39**, 865 (2000)

M. Schmidt, Europ. Pat. Appl. 077,493, 27 Apr 1983, to Mobay Chemical Corp.

M. Schmidt, F.H.J. Maurer, J. Polym. Sci. Part B Polym. Phys. **36**, 1061 (1998)

E. Schmid, H. Thullen, U.S. Patent 5,288,799, 22 Feb 1994, to EMS-Inventa

J.M. Schmitt, C.H. Miller Jr., U.S. Patent 3,524,906, 18 Aug 1970, to American Cyanamid

J.M. Schmitt, L.A. Landers, J.F. Terenzi, U.S. Patent 3,354,238, 21 Nov 1967, to American
   Cyanamid

D.L. Schober, U.S. Patent 3,714,289, 30 Jan 1973, to Union Carbide Corp.

H.P. Schreiber, Brit. Pat. 1,037,820, 03 Aug 1966, to Canadian Industries Ltd. (CIL)

E.C. Schule, U.S. Patent 2,605,247, 29 July 1952, to Firestone Tire & Rubber

H.G. Schutze, H.C. Williams, N.P. Neureiter, D.E. Bown, U.S. Patent 3,655,718, 11 Apr 1972, to
   Esso

S. Seelert, P. Klaerner, A. Jung, H. Hoenl, B. Ostermayer, Ger. Pat. 4,139,627, 03 June 1993a, to
   BASF

S. Seelert, R. Weiss, D. Zeltner, Ger. Pat. 4,209,032, 23 Sept 1993b, to BASF

L. Segal, U.S. Patent 3,769,260, 30 Oct 1973, to Allied Chem. Corp.

N. Segrest, U.S. Patent 5,397,825, 14 Mar 1995

W.L. Semon, U.S. Patent 1,929,453, 10 Oct 1933, to B. F. Goodrich

H. Serizawa, M. Kubota, H. Sano, Europ. Pat. Appl. 468,772, 29 Jan 1992, to Polyplastics

W. Seydl, E. Strickle, U.S. Patent 3,937,757, 10 Feb 1976, to BASF

R.B. Seymour, U.S. Patent 2,574,439, 06 Nov 1951, to Monsanto Chem.

R.B. Seymour (ed.), *Pioneers in Polymer Science* (Kluwer, Boston, 1989)

R.B. Seymour, T. Cheng (eds.) *Advances in Polyolefins*, ACS Symp., Miami Beach, Spring 1985
   (Plenum Press, New York, 1987)

L.W. Shacklette, G.G. Miller, C.C. Han, R.L. Elsenbaumer, PCT Int. Appl. WO 93 024,555,
   09 Dec 1993, to AlliedSignal

W.J.D. Shaw, Can. Pat. Appl. 2,071,707, 20 Dec 1993, to University of Calgary

M.L. Sheer, U.S. Patent 4,317,764, 02 Mar 1982, to E. I. du Pont

M.D. Shelby, W.R. Hale, T.J. Pecorini, M.E. Rogers, S.A. Gilliam, M.D. Cliffton, M.E. Stewart,
   U.S. Patent 8,304,499, 6 Nov 2012 to Eastman Chemical Co.

J.S.J. Shen, U.S. Patent 5,328,962, 12 July 1994, to ICI, Ltd., Acrylics

A.M. Sherman, Europ. Pat. Appl. 027,312, 22 Apr 1981, to Mobil Oil Corp.

A.M. Sherman, U.S. Patent 4,397,988, 09 Aug 1983, to Mobil Oil Corp.

Z.H. Shi, L.A. Utracki, in *Proceedings of the Canadian Society of Chemical Engineers Annual
   Meeting*, Toronto, Oct 1992; Polym. Eng. Sci. **32**, 1834 (1992)

Z.H. Shi, L.A. Utracki, in *Proceedings of the Polymer Processing Society Annual Meeting*,
   Manchester, Apr 1993

A. Shibata, S. Nagai, M. Kobayashi, M. Kimura, H. Mimura, Europ. Pat. Appl. 500,269, 26 Aug
   1992, to Mitsubishi Gas Chem.

K. Shichijo, Europ. Pat. Appl. 593,221, 20 Apr 1994, to Mitsubishi Petrochem.

K. Shikata, K. Okamura, S. Nakamura Jap. Pat. 097,946, 13 Dec 1973, to Tokuyama Soda

K. Shimamura, Y. Suzuki, Jap Pat. 03 24,153, 01 Feb 1991, to Asahi Chem.

B.S. Shin, J.Y. Lee, D.K. Kim, S.J. Kim, S.O. Cho, U.S. Patent 5,776,993, 07 July 1998, to Korea Inst. Footwear & Leather Technology

Shin-Kobe Electric Machinery Company, Limited, Jap. Pat. 096,156, 02 June 1984

M. Shiraishi, M. Goto, Jap. Pat. 106,653, 24 May 1986, to Mitsubishi Petrochem.

T. Shiraki, Y. Hattori, U.S. Patent 5,115,035, Appl. 25 Nov 1986, to Asahi Kasei Kogyo

T. Shiraki, Y. Hattori, U.S. Patent 5,332,784, 26 July 1994, to Asahi Kasei Kogyo

T. Shiraki, S. Nakajima, M. Karaushi, Jap. Pat. 61 116,541, 04 June 1986, to Asahi Chem.

K. Shirayama, K. Iketa, Jap. Pat. 021,303; 021,305, 16 June 1971, to Sumitomo Chem.

K. Shirayama, S. Shiga, H. Watanabe, Jap Pat. 008,370, 10 Mar 1972, to Sumitomo Chem.

G.A. Short, U.S. Patent 3,354,239, 21 Nov 1967, to Shell Oil

K.K. Showa Denko, Jap. Pat. 059,242, 08 Apr 1983; Jap. Pat. 157,837, 20 Sept 1983; Jap. Pat. 176,234, 15 Oct 1983

R.S. Shue, L.E. Scoggins, U.S. Patent 4,292,416, 29 Sept 1981, to Phillips

C.B. Shulman, Europ. Pat. Appl. 116,783, 29 Aug 1984, to Exxon

R.W. Siedenstrang, A.K. Thorsrud, U.S. Patent 4,456,706, 26 June 1984, to Phillips

D.L. Siegfried, D.A. Thomas, L.H. Sperling, U.S. Patent 4,468,499, 28 Aug 1984, to Lehigh University

R.J. Signer, K.F. Beal, U.S. Patent 2,547,605, 03 Apr 1951, to Visking Corp.

R.J. Signer, K.F. Beal, U.S. Patent 2,658,050, 03 Nov 1953, to Visking Corp.

J. Silberberg, Europ. Pat. Appl. 045,875, 17 Feb 1982; U.S. Patent 4,342,846, 03 Aug 1982; U.S. Patent 4,360,636, 23 Nov 1982, to Stauffer Chemical

R. Silvestri, P. Sgarzi, Polymer **39**, 5871 (1998)

H.C. Silvis, B.A. King, V.K. Berry, J.R. Schroeder, U.S. Patent 4,968,755, 06 Nov 1990, to Dow Chemical

R. Simha, T. Somcynsky, Macromolecules **2**, 341 (1969)

W. Siol, J.-D. Fischer, T. Sufke, E. Felger, K. Frank, U.S. Patent 5,250,623, 1993a, to Rohm GmbH Chemische Fabrik

W. Siol, J.-D. Fischer, U. Terbrack, K. Koralewski, Europ. Pat. Appl. 547,481, 23 June 1993b, to Röhm GmbH Chemische Fabrik

W. Siol, J.-D. Fischer, T. Sufke, E. Felger, K. Frank, U.S. Patent 5,374,487, 20 Feb 1994, to Rohm GmbH Chemische Fabrik

W. Siol, J.-D. Fischer, U. Terbrack, K. Koralewski, U.S. Patent 5,380,797, 10 Jan 1995, to Röhm GmbH Chemische Fabrik

K.W. Small, P.A. Small, U.S. Patent 2,555,062, 29 May 1951, to ICI

A. Smith, Brit. Pat. 16,274, 1899

P.J. Smith, B.J. Cross, PCT. WO 96/00257, 04 Jan 1996, to ICI

R.R. Smith, J.R. Wilson, Europ. Pat. Appl. 105,826, 18 Apr 1984, to Goodyear Tire & Rubber

H.J.E. Smith, R. van der Meer, A.H.L. Groothuis, Europ. Pat. Appl. 369,169, 23 May 1990, to General Electric Co.

H.J.E. Smith, R. van der Meer, A.H.L. Groothuis, U.S. Patent 5,357,003, 18 Oct 1994, to General Electric Co.

G.L. Smyser, G.T. Brooks, Europ. Patent Appl. 376,347, 04 July 1990, to Amoco Corp.

H.E. Snodgrass, R.L. Lauchlan, Fr. Pat. 2,086,141, 04 Feb 1972, to Uniroyal

L.M. Soby, M.H. Lehr, E.D. Dickens Jr., M. Rajagopalan, W.S. Greenlee, U.S. Patent 5,354,812, 11 Oct 1994, to B. F. Goodrich

R.H. Somani, M.T. Shaw, Macromolecules **14**, 1549 (1981)

D. Song, W. Zhang, R.K. Gupta, E.G. Melby, Can. J. Chem. Eng. **87**, 862 (2009)

D. Song, W. Zhang, R.K. Gupta, E.G. Melby, AIChE J. **57**, 96 (2011)

R. Sonnier, V. Massardier, P. Cassagnau, Int. J. Mater. Form. (Suppl. 1), 657 (2008), Volume 1.

I.W. Sorensen, U.S. Patent 4,465,804, 14 Aug 1984, to Allied Corp.

P. Sparke (ed.), *The Plastics Age* (The Overlook Press, Woodstock, 1993)

W.J. Sparks, L.B. Turner, U.S. Patent 2,618,624, 18 Nov 1952, to Standard Oil Development Co.

L.H. Sperling, *Introduction to Physical Polymer Science*, 2nd edn. (Wiley, New York, 1992)

W.E. Sprenkle, U.S. Patent 4,207,402, 10 Jun 1980, to Monsanto

O.L. Stafford, J.J. Adams, U.S. Patent 3,642,949, 15 Feb 1972, to Dow Chemical

M. Stamm, *Polymer Surfaces and Interfaces – Characterization, Modification and Applications* (Springer, Berlin/Heidelberg, 2008)

Standard Oil Development Co., Fr. Pat. 812,490, 11 May 1937

W.J.D. Steendam, F.R. Mooijman, T.P. Kempers, Europ. Pat. Appl. 573,680, 15 Dec 1993, to General Electric Co.

R.S. Stein, M. Sethumadhavan, R.A. Gaudiana, T. Adams, D. Guarrera, S.K. Roy, J. Macromol. Sci. Pure Appl. Chem. **A29**, 517 (1992)

R.A. Steinkamp, T.J. Grail, U.S. Patent 3,953,655, 27 Apr 1976, to Exxon

R. Steller, D. Zuchowska, J. Appl. Polym. Sci. **41**, 1595 (1990)

J.C. Stevens, F.J. Timmers, D.R. Wilson, G.F. Schmidt, P.N. Nickias, R.K. Rosen, G.W. Knight, S. Lai, Europ. Pat. Appl. 416,815, 1991

R. Stewart, Plast. Eng. **63**, 24 (2007)

J.L. Stewart, E.T. Bell, U.S. Patent 5,382,628, 17 Jan 1995, to Eastman Chemical

M.E. Stewart, D.J. Massa, U.S. Patent 5,235,001, 10 Aug 1993, to Eastman Kodak

L.L. Stott, L.R.B. Hervey, Brit. Pat. 792,955, 09 Apr 1958, to Polymer Corp.

H. Strametz, H.J. Leuering, K. Rust, M. Engelmann, Ger. Offen. 2,417,093, 06 Nov 1975, to Hoechst

P.T. Stricharczuk, Ger. Offen. 2,644,644, 07 Apr 1977, to B. F. Goodrich

E.T. Strom, S.E. Rasmussen (eds.), *100+ Years of Plastics: Leo Baekeland and Beyond*. ACS Symposium Series (ACS, Washington, DC, 2011)

L.C.E. Struik, *Physical Ageing in Amorphous Polymers and Other Materials* (Elsevier, Amsterdam, 1978)

G.E. Stuart, Nat. Geosci. **184**(5), 88 (1993)

H. Suarez, J.W. Barlow, J. Appl. Polym. Sci. **29**, 3253 (1984)

P.M. Subramanian, Europ. Pat. Appl. 015,556, 17 Sept 1980, to E. I. du Pont

P.M. Subramanian, U.S. Patent 4,410,482, 1983, to E. I. du Pont

P.M. Subramanian, U.S. Patent 4,444,817, 24 Apr 1984, to E. I. du Pont

P.M. Subramanian, U.S. Patent 5,096,964, 17 Mar 1992, to E. I. du Pont

Y. Suenaga, T. Ishikuwa, Jap. Pat. 03 137,123, 11 June 1991, to Tosoh Corp.

M. Sugiara, S. Takayama, Jap. Pat. 88 92,663, 23 April 1988, to Fuso Kagaku Kogyo

Y. Sugimura, H. Moriyama, K. Iikura, Y. Shigemori, Jap. Pat. 020,241, 28 Sept 1972, to Teijin, Ltd.

A. Sugio, M. Masu, M. Okabe, E. Ukita, Europ. Pat. Appl. 099,231, 25 Jan 1984, to Mitsubishi Gas Chem.

A. Sugio, K. Okabe, T. Kobayashi, Jap. Pat. 010,162, 19 Jan 1987, to Mitsubishi Gas Chem.

N. Sugiyama, M. Mochizuki, Europ. Pat. Appl. 350 223, 10 Jan 1990, to Polyplastics

A.M. Sukhadia, A. Datta, D.G. Baird, Conf. Proceed. SAMPE **36**, 913 (1991); SPE Techn. Pap. **37**, 1008 (1991)

A.M. Sukhadia, A. Datta, D.G. Baird, Int. Polym. Process. **7**, 218 (1992)

Sumitomo Chem. Co., Brit. Pat. 1,114,589, 22 May 1968

Sumitomo Chem. Co., Jap. Pat. 125,253; 125,252, 04 Aug 1982

Sumitomo Chem. Co., Jap. Pat. 059,259, 08 Apr 1983

Sumitomo Chem. Co., Jap. Pat. 193,957, 02 Nov 1984

Sumitomo Chem. Co., Jap. Pat. 038,464, 28 Feb 1985

R.M. Summers, M. Kramer, D.B.G. Jaquiss, Ger. Offen. 2,229,550, 21 Dec 1972, to General Electric Co.

Sun Oil Company, Brit. Pat. 952,089, 11 Mar 1964

K. Suzuki, M. Nagahama, Jap. Pat. 004,748, 10 Jan 1987, to Toray Industries

S.B. Swartzmiller, R.J. Donald, J.E. Bonekamp, PCT Int. Appl. 013,168, 08 July 1993, to Dow Chemical

S.B. Swartzmiller, R.J. Donald, J.E. Bonekamp, U.S. Patent 5,334,657, 02 Aug 1994, to Dow Chemical

K.W. Swogger, SPE Techn. Pap. **44**, 1790 (1998)

M. Szwarc, M. Levy, R. Milkovich, J. Am. Chem. Soc. **78**, 2656 (1956)

M. Tabana, H. Maki, Jap Pat. 031,745, 031,746, 18 Mar 1976, to Sumitomo Chem.

A. Taguet, M.A. Huneault, B.D. Favis, Polymer **50**, 5733 (2009)

Y. Tajima, K. Kawaguchi, T. Nakane, 5,300,572, 05 Apr 1994, to Polyplastics

Y. Tajima, K. Miyawaki, H. Sano, Europ. Pat. Appl. 494,533, 23 Dec 1991, to Polyplastics

T. Takahashi, Ph.D. thesis, Yamagata University, Yonezawa (1996)

T. Takahashi, T. Kobayashi, PCT Int. Appl. WO 92 20,745, 26 Nov 1992, to E. I. du Pont

T. Takahashi, T. Kobayashi, PCT Int. Appl. 011,206, 10 June 1993, to E. I. du Pont

T. Takahashi, Y. Naka, J. Takimoto, K. Koyama, *Sen-i Gakkai Prep*. 67–68 (1996)

K. Takayama, T. Endo, O. Kanoto, N. Matsunaga, Jap. Pat. 03 134,050, 07 June 1991, to Polyplastics

M. Takayanagi, T. Ogata, M. Morikawa, T. Kai, J. Macromol. Sci. Phys. **B17**, 591 (1980)

K. Takayanagi, K. Nishida, K. Suzuki, U.S. Patent 5,352,721, 04 Oct 1994, to Mitsubishi Petrochem.

Takkosha Company Ltd., Jap. Pat. 010,736, 13 June, 1967

Y. Tamura, Jap. Pat. 258,253, 20 Dec 1985, to Mitsubishi Petrochem.

H. Tan, L. Li, Z. Chen, Y. Song, Q. Zheng, Polymer **10**, 3522 (2005)

M. Tanahashi, M. Kojima, Jap. Pat. 012,225, 04 May 1970, to Chisso Corp.

A. Tanaka, H. Anno, T. Kawahara, T. Hattori, Ger. Offen. 2,013,570, 07 Oct 1971a, to Japanese Geon.

H. Tanaka, M. Matsuo, N. Izawa, Jap. Pat. 005,065, 08 Feb 1971b, to Japanese Geon.

H. Tanaka, S. Futamura, K. Kato, Jap. Pat. 001,866; 001,868, 18 Jan 1971c, to Japanese Geon.

A. Tanaka, T. Hattori, H. Anno, T. Kawahara, Brit. Pat. 1,275,332, 24 May 1972, to Japanese Geon.

C. Tanaka, S. Nakajima, M. Morikawa, Jap. Pat. 040,851, 31 Mar 1979, to Toray

S. Tanaka, J. Sakai, T. Fukao, K. Wakatsuki, K. Wakamatsu, Europ. Pat. Appl. 285,414, 05 Oct 1988, to Sumitomo Chem.

T. Tanaka, H. Nakano, H. Satoh, S. Gotoh, Europ. Pat. Appl. 506,076, 30 Sept 1992, to Mitsubishi Petrochem.

T. Tang, B. Huang, Polymer **35**, 281 (1994)

H. Tashiro, H. Naito, M. Takayama, I. Yoshimura, U.S. Patent 4,384,032, 17 May 1983, to Asahi-Dow

I. Tatuhiko, O. Akira, Ger. Pat. 3,150,341, 01 July 1982, to Daicel Chem.

Teijin Chem., Jap. Pat. 082,151, 20 June 1980

Teijin Chem., Jap. Pat. 153,042, 21 Sept 1982

Teijin Chem., Jap. Pat. 017,153, 01 Feb 1983; Jap. Pat. 129,045, 01 Aug 1983

Teijin Chem., Jap. Pat. 043,053, 09 Mar 1984

B. Tekkanat, H. Faust, B.L. McKinney, Europ. Pat. Appl. 533,304, 24 Mar 1993, to Johnson Service Company, Globe-Union

B. Tekkanat, H. Faust, B.L. McKinney, U.S. Patent 5,280,066, 18 Jan 1994, to Johnson Service Company, Globe-Union

T. Teraya, S. Kikuchi, K. Yokoyama, Y. Fujita, Jap. Pat. 61 45,261, 24 May 1994, to Tonen Corp.

B.P. Thill, U.S. Patent 4,883,836, 28 Nov 1989, to The Dow Chemical

L.S. Thomas, U.S. Patent 4,335,038, 15 June 1982, to Dow Chemical

R. Timmermann, R. Dujardin, P. Orth, E. Ostlinning, H. Schulte, R. Dhein, E. Grigat, Europ. Pat. Appl. 583,595, 23 Feb 1994, to Bayer

S.P. Ting, U.S. Patent 4,892,904, 27 June 1990, to General Electric Co.

T. Tochioka, Europ. Pat. Appl. 553,846, 04 Aug 1993, to Mazda Motor Corp.

Y. Toga, I. Okamoto, Ger. Offen. 3,314,257, 20 Oct 1983, to Daicel Chem.

S. Togo, A. Amagai, Y. Kondo, T. Yamada, Europ. Pat. Appl. 268,486, 25 May 1988, to Mitsubishi Gas Chem.

Y. Tokai, K. Sakai, Jap. Pat. 047,942, 07 July 1973, to Teijin

E.F. Tokas, U.S. Patent 4,308,355, 29 Dec 1981, to Monsanto

M. Tokihisa, K. Yakemoto, T. Sakai, Polym. Eng. Sci. **46**, 1040 (2006)

T. Tomita, M. Ohsugi, D. Adachi, Europ. Pat. Appl. 566,149, 20 Oct 1993, to Mazda Motor Corp.

T. Tomita, M. Ohsugi, D. Adachi, Jap Pat. 60 41,444, 15 Feb 1994, to Mazda Motor Corp.

I. Tomka, Ger. Offen. 4,116,404, 19 Nov 1992, to Bio-Tec Biologische Naturverpackungen

I. Tomka, J. Meissner, R. Menard, Ger. Offen. 4,134,190, 22 Apr 1993

I. Tomka, U.S. Patent 5,705,536, 06 Jan 1998; U.S. Patent 5,844,023, 01 Dec 1998, to Bio-Tec Biologische Naturverpackungen

Toray Ind., Jap. Pat. 080,458, 17 June 1979

Toray Ind., Jap. Pat. 102,651, 06 Aug 1980

Toray Ind., Jap. Pat. 004,653, 19 Jan 1981

Toray Ind., Jap. Pat. 034,152, 24 Feb 1982

Toray Ind., Jap. Pat. 017,151, 01 Feb 1983

Toray Ind., Jap. Pat. 027,946, 14 Feb 1984

Toray Ind., Jap. Pat. 038,460, 28 Feb 1985

L.T. Toy, A.N.K. Lau, C.-W. Leong, PCT Int. Appl. WO 94 014,890, 07 July 1994, to Raychem Corp.

Y. Toyama, T. Miyaji, E. Okuya, Jap. Pat. 179,449, 13 Sept 1985, to Japan Synthetic Rubber

Toyobo Company Limited, Jap. Pat. 167,740, 23 Dec 1981

Y. Toyoda, K. Yasue, T. Okamoto, F. Ohama, Jap. Pat. 61 190,552, 25 Aug 1986, to Unitika

E. Tschunkur, W. Bock, Ger. Offen. 570,980, 1933, to I. G. Farbenindustrie

M.V. Tsebrenko, N.M. Rezanova, G.V. Vinogradov, *Nov. Reol. Polim. 11th Mater. Vses Simp. Reol.* **2**, 136 (1982)

M.V. Tsebrenko, A.V. Yudin, T.I. Ablazowa, G.V. Vinogradov, Polymer **17**, 831 (1976)

T. Tsuda, K. Azuma, Jap Pat. 03 62,853, 18 Mar 1991, to Toa Gosei Chem.

H. Tsukahara, M. Niino, Fr. Demande 2,665,904, 21 Feb 1992, to Asahi Kasei Kogyo

H. Tsukahara, M. Niino, U.S. Patent 5,354,798, 11 Oct 1994, to Asahi Kasei Kogyo

T. Tsumato, K. Asai, Y. Suzuki, Jap. Pat. 010,161, 19 Jan 1987, to Sumitomo Chem.

T. Tsumiyama, T. Shimada, Y. Akagawa, S. Nakamoto, T. Takada, Europ. Pat. Appl. 294,062, 07 Dec 1988, to Ube Ind.

K. Tsunawaki, S. Sasama, K. Watanabe, K. Nawata, Jap. Pat. 031,247, 24 Apr 1973, to Teijin

T. Tsutsumi, T. Nakakura, S. Morikawa, K. Shimamura, T. Takahashi, A. Morita, N. Koga, A. Yamaguchi, M. Ohta, Y. Gotoh, M. Amano, H. Oochi, K. Ito, U.S. Patent 5,312,866, 17 May 1994, to Mitsui Toatsu Chem.

J.A. Tyrell, O.M. Boutni, G.L. Freimiller, U.S. Patent 4,469,852, 04 Sept 1984, to General Electric Co.

Ube Ind. Ltd., Jap. Pat. 043,057, 09 Mar 1984

Ube Ind. Ltd., Jap. Pat. 69,159, 19 Apr 1985

S. Ueda, S. Sasame, Jap. Pat. 062,551, 31 Mar 1986, to Asahi Chem. Ind.

K. Ueno, T. Maruyama, Jap. Pat. 030,247, 06 Mar 1979, to Sumitomo Chem.

K. Ueno, T. Maruyama, Europ. Pat. Appl. 024,120, 25 Feb 1981, to Sumitomo Chem.

K. Ueno, T. Maruyama, U.S. Patent 4,315,086, 09 Feb 1982, to Sumitomo Chem.

K. Ueno, H. Inoue, A. Furuta, S. Ebisu, Europ. Pat. Appl. 052,854, 02 June 1982a; Jap. Pat. 108,153, 06 July 1982b, to Sumitomo Chem.

Union Carbide Corp., Neth. Pat. Appl. 6,604,731, 10 Oct 1966

Uniroyal Incorporated, Brit. Pat., 1,128,121, 25 Sept 1968

Unitika Ltd., Jap. Pat. 115,452, 17 July 1982

Unitika Ltd., Jap. Pat. 067,749, 22 Apr 1983

Unitika Ltd., Jap Pat. 112,929, 23 Jan 1984

H. Urabe, I. Ikuhara, Europ. Pat. Appl. 341,623, 15 Nov 1989, to Mitsubishi Kasei Corp.

S. Usami, Y. Ochiai, Jap. Pat. 034,941, 25 Mar 1976, to Kureha Chem.

L.A. Utracki, J. Rheol. **30**, 829 (1986)

L.A. Utracki, in *Current Topics in Polymer Science*, ed. by R.M. Ottenbrite, L.A. Utracki, S. Inoue (Hanser, Munich, 1987)

L.A. Utracki, in *Rheological Measurements*, ed. by A.A. Collyer, D.W. Clegg (Elsevier, London, 1988)

L.A. Utracki, *Polymer Alloys and Blends* (Hanser V, Munich, 1989a) [Japanese translation Tokyo Kagaku Dozin Co. Ltd., Tokyo (1991)]

L.A. Utracki, in *Multiphase Polymers: Blends and Ionomers*, ed. by L.A. Utracki, R.A. Weiss. ACS Symposium Series, vol. 395 (American Chemical Society, Washington, DC, 1989b)

L.A. Utracki (ed.), *Two-Phase Polymer Systems* (Hanser V, Munich, 1991a)

L.A. Utracki, J. Rheol. **35**, 1615 (1991b)

L.A. Utracki, in *Frontiers of Materials Research, Electronic and Materials Research*, ed. by M. Kong, L. Huang (Elsevier, Amsterdam, 1991c)

L.A. Utracki (ed.), *Encyclopaedic Dictionary of Commercial Polymer Blends* (ChemTec, Toronto, 1994)

L.A. Utracki, in *Rheological Fundamentals of Polymer Processing*, ed. by J.A. Covas (Kluver Academic, Dordrecht, 1995)

L.A. Utracki, *Commercial Polymer Blends* (Chapman & Hall, London, 1998a)

L.A. Utracki, *Foaming Polymer Blends, NRCC/IMI Internal report*, Boucherville, 1998b

L.A. Utracki, in *Encyclopedia of Polymer Blends*, ed. by A.I. Isayev (Wiley, Weinheim, 2011)

L.A. Utracki, M.M. Dumoulin, in *Polypropylene: Structure, Blends and Composites*, ed. by J. Karger-Kocsis (Chapman & Hall, London, 1995)

L.A. Utracki, A. Luciani, Can. Pat Appl., Sept 1996a

L.A. Utracki, A. Luciani, Intl. Plast. Eng. Technol. **2**, 37 (1996b)

L. A. Utracki, P. Sammut, *VAMAS TWP-PB Meeting*, Berlin, 13 Apr 1987

L.A. Utracki, P. Sammut, Polym. Eng. Sci. **30**, 1019 (1990)

L.A. Utracki, P. Sammut, Plast. Rubber Compos. Process. Appl. **16**, 221 (1991)

L.A. Utracki, P. Sammut, Polym. Networks Blends **2**, 23 (1992); ibid. **2**, 85 (1992)

L.A. Utracki, B. Schlund, Polym. Eng. Sci. **27**, 367 (1987); ibid **27**, 380 (1987); ibid. **27**, 1512 (1987); SPE Techn. Papers **33**, 1002 (1987)

L.A. Utracki, Z.H. Shi, Polym. Eng. Sci. **32**, 1824 (1992)

L.A. Utracki, M.M. Dumoulin, P. Toma, Polym. Eng. Sci **26**, 37 (1986)

L.A. Utracki, M.R. Kamal, N.M. Al-Bastaki, SPE-Techn. Pap. **30**, 417 (1984)

U.R. Vaidya, M. Bhattacharya, U.S. Patent 5,321,064, 14 June 1994, to University of Minnesota

R. Van Cleve, D. H. Mullins, U.S. Patent 3,062,778, 06 Nov 1962, to Union Carbide Corp.

R. Van der Meer, J.B. Yates III, PCT Int. Appl. 000,540, 29 Jan 1987, to General Electric Co.

R. Van der Meer, R. de Jong, R. Avakian, J. M. Heuschen, Europ. Pat. Appl. 300 178, 25 Jan 1989, to General Electric Co.

C.T.E. Van Nuffel, H. T. Pham, S. Namhata, J. Eiffler, U.S. Patent 5,804,673, 08 Sept 1998, to Dow Chemical

C. P. Van Sluijs, J. F. Repin, P. J. Van Asperen, W. G. M. Bruls, Europ. Pat. Appl. 481,558, 22 Apr 1992, to DSM

J.M. Vaughan, U.S. Patent 4,524,179, 18 June 1985, to Borg-Warner Chem.

J. Vermant, S. Vandebril, C. Dewitte, P. Moldenaers, Rheol. Acta **47**, 835 (2008)

T. Vestberg, I. Lehtiniemi, U.S. Patent 5,300,578, 05 Apr 1994, to Neste Oy

S.J. Vicik, U.S. Patent 5,344,679, 06 Sept 1994, to Viskase Corp.

S. Vilasagar, H.S. Rawlings, U.S. Patent 5,302,646, 12 Apr 1994, to General Electric Co.

O. Vogl, E.H. Immergut, *Polymer Science in the Next Decade: Trends, Opportunities, Promises* (Wiley, New York, 1987)

A. Voss, Dickhäuser, Ger. Offen. 540,101, 26 June 1930, to I. G. Farbenindustrie

A. Voss, Dickhäuser, Ger. Offen. 579,048, 20 June 1933; Ger. Offen. 579,254, 22 June 1933, to I. G. Farbenindustrie

A. Voss, Dickhäuser, U.S. Patent 2,012,177, 20 Aug 1935, to I. G. Farbenindustrie

A. Voss, Dickhäuser, U.S. Patent 2,041,502, 19 May 1936; U.S. Patent 2,047,398, 14 July 1936, to I. G. Farbenindustrie

P.S. Walia, R.K. Gupta, C.T. Kiang, Polym. Eng. Sci. **39**, 2431 (1999)

A.D. Wambach, R.L. Dieck, PCT Intl. Appl. 001,276, 26 June 1980, to General Electric Co.

Y. Wang, D.C. Gale, B. Huang, U.S. Patent 8,262,723, 11 Sept 2012, to Abbott, Inc.

G.F. Ward, U.S. Patent 3,548,032, 15 Dec 1970, to Shell Oil

K. Watanabe, A. Inozuka, Europ. Pat. Appl. 409,152, 23 Jan 1991, to Daicel Chem.

K. Watanabe, M. Ozaki, J. Hara, Jap. Pat. 007,700, 29 Mar 1967, to Toyo Koatsu

M. Watanabe, T. Tazaki, S. Machida, N. Ishihara, *4th SPSJ International Polymer Conference*, Yokohama, 1992, pp. 11.29–12.03

C.A. Waugaman, J.C. Taylor, J.C. Anthony, Belg. Pat. 626,029, 13 June 1963, to B. F. Goodrich Co.

E.P. Weaver, Ger. Offen. 2,154,445, 04 May 1972, to Uniroyal

E.P. Weaver, Europ. Pat. Appl. 086,069, 17 Aug 1983; Europ. Pat. Appl. 086,069, 17 Aug 1983, to Uniroyal

E.P. Weaver, U.S. Patent 4,529,776, 16 July 1985, to Uniroyal

A. Webb, A.W. Carlson, T.J. Galvin, PCT Int. Appl. 001,733, 06 Feb 1992, to ICI

H. Weber, E. Nintz, M. Walter, D. Ballweber, B. Ostermayer, U.S. Patent 4,927,859, 22 May 1990, to BASF

M. Weber, K. Muehlbach, Ger. Offen. 4,121,705, 07 Jan 1993; Europ. Pat. Appl. 561,197, 22 Sept 1993; Ger. Pat. 4,208,339, 23 Sept 1993, to BASF

M. Weber, F. Seitz, A. Jung, N. Guentherberg, Ger. Pat. 4,227,742, 24 Feb 1994; Europ. Pat. Appl. 586,898, 16 Mar 1994; Jap. Pat. 61 72,595, 21 June 1994, to BASF

J.M. Wefer, Europ. Pat. Appl. 107,303, 02 May 1984; U.S. Patent 4,485,212, 27 Nov 1984, to Uniroyal Chem.

J.M. Wefer, U.S. Patent 4,493,921, 15 Jan 1985, to Uniroyal Chem.

J.M. Wefer, Europ. Pat. Appl. 287,207, 19 Oct 1988, to Uniroyal Chem.

G. Wegner, *4th SPSJ International Polymer Conference*, Yokohama, 1992, pp. 11.29–12.03.

K. Weyer, L. Bottenbruch, D. Neuray, W. Stix, Ger. Offen. 3,227,028, 26 Jan 1984; Ger. Offen. 3,227,029, 26 Jan 1984, to Bayer

D.M. White, R. van der Meer, PCT Int. Appl. 000,179, 12 Jan 1989, to General Electric Co.

R.J. White, S. Krishnan, U.S. Patent 4,837,243, 06 June 1989, to Mobay Corp.

R.P. White, J.E.G. Lipson, Macromolecules **45**, 1076 (2012)

M.V. Wiener, U.S. Patent 3,466,348, 09 Sept 1969, to Goodyear Tire and Rubber

D.L. Wilfong, R.J. Rolando, Europ. Pat. Appl. 547,834, 23 June 1993, to 3M Co.

J.D. Wilkey, U.S. Patent 5,288,800, 22 Feb 1994, to Shell Oil

E.S. Wilks, J. Chem. Inf. Comput. Sci. **37**, 171 (1997a); ibid. **193** (1997b); ibid. **209** (1997c); ibid. **224** (1997d)

J.L. Willett, U.S. Patent 5,087,650, 11 Feb 1992, to Fully Comp. Plastics

D.R. Williams, C.S. Ilenda, Europ. Pat. Appl. 560,496, 15 Sept 1993, to Rohm & Haas

M.L. Williams, R.F. Landel, J.D. Ferry, J. Am. Chem. Soc. **77**, 3701 (1955)

M.C.K. Willott, Brit. Pat. 1,118,545, 03 July 1968, to ICI

A. Winter, B. Bachmann, V. Dolle, Europ. Pat. Appl. 552,681, 28 July 1993, to Hoechst

K.F. Wissbrun, R.H. Ball, P.J. Rossello, Belg. Pat. 614,282, 22 Aug 1962, to Celanese Corp.

K.F. Wissbrun, R.H. Ball, P.J. Rossello, Brit. Pat. 994,376, 10 June 1965, to Celanese Corp.

C.P. Wong, U.S. Patent 5,124,184, 11 Oct 1990, to 3M Co.

C.P. Wong, U.S. Patent 5,330,697, 19 July 1994, to 3M Co.

S. Wu, Polymer **26**, 1855 (1985)

S. Wu, Polym. Eng. Sci. **27**, 225 (1987)

S. Wu, J. Appl. Polym. Sci. **35**, 549 (1988)

S. Wu, Polym. Eng. Sci. **30**, 753 (1990)

G. Wu, J.A. Cuculo, Polymer **40**, 1011 (1998)

A. Wurtz, Compt. Rend. **49**, 813 (1859)

A. Wurtz, Compt. Rend. **50**, 1195 (1860)

A. Yahata, H. Kitada, S. Tanaka, Jap. Pat. 040,756, 02 Dec 1971; Jap. Pat. 041,103, 04 Dec 1971, to Sanyo Kako

S. Yamada, Ger. Offen. 1,569,448, 04 July 1963, to Teijin Chem. Co.

N. Yamamoto, A. Nakata, A. Koshiari, A. Yanagase, Europ. Pat. Appl. 488,263, 03 June 1992, to Mitsubishi Rayon

N. Yamamoto, A. Yanagase, A. Nakata, A. Koshirai, T. Yanai, U.S. Patent 5,334,656, 02 Aug 1994, to Mitsubishi Rayon Co.

S. Yamamoto, H. Shimizu, Jap. Pat. 038,347, 22 Mar 1979, to Teijin

S. Yamamoto, A. Toyota, Europ. Pat. Appl. 489,437, 10 June 1992, to Mitsui Petrochem.

S. Yamamoto, S. Honda, H. Shimizu, Jap. Pat. 043,470, 23 Dec 1971, to Sekisui Chem.

M. Yamauchi, T. Magome, A. Takahara, T. Kajiyama, Reports Prog. Polym. Phys. Japan **34**, 229 (1991)

S. Yamauchi, K. Yasuno, S. Kitamura, Jap. Pat. 013,855, 03 Apr 1974, to Sumitomo Chem

I. Yamazaki, T. Fujimaki, Jap. Pat. 007,627, 03 Mar 1970, to Showa Denko

I. Yamazaki, T. Fujimaki, Jap. Pat. 007,141, 29 Feb 1972, to Showa Denko

W.Y. Yang, Europ. Pat. Appl. 212,449, 04 Mar 1987, to B. F. Goodrich

S. Yao, E. Kamei, Nihon Reor. Gakk. **23**, 103 (1995)

K. Yasue, T. Marutani, Y. Fukushima, T. Ida, Europ. Pat. Appl. 301,663, 01 Feb 1989, to Stamicarbon

J.B. Yates III, G.F. Lee Jr., Europ. Pat. Appl. 349,747, 10 Jan 1990, to General Electric Co.

J.B. Yates III, PCT Int. Appl. 005,311, 11 Sept 1987, to General Electric Co.

J.B. Yates III, Europ. Pat. Appl. 303,077, 15 Feb 1989, to General Electric Co.

J.B. Yates III, Europ. Pat. Appl. 550,208, 07 July 1993, to General Electric Co.

Y.-C. Ye, F.P. La Mantia, A. Valenza, V. Citta, U. Pedretti, A. Roggero, Europ. Polym. J. **27**, 723 (1991)

A.F. Yee, Y. Shi, SPE Techn. Pap. **41**, 2642 (1995)

S.-K. Yeh, S. Agarwal, R.K. Gupta, Comp. Sci. Technol. **69**, 2225 (2009)

J.K. Yeo, J.M. Oh, S.K. Chang, E.S.H. Lee, U.S. Patent 4,829.125, 09 May 1989, to Lucky

C. Yeung, R.C. Desai, J. Noolandi, Macromolecules **27**, 55 (1994)

Y. Yoga, I. Okamoto, K. Watanabe, Ger. Offen. 3,313,442, 27 Oct 1983, to Daicel Chem.

E. Yonemitsu, A. Sugio, M. Masu, T. Kawaki, Y. Sasaki, Jap. Pat. 057,754, 20 May 1976, to Mitsubishi Gas-Chem.

K. Yonetani, S. Nakamura, S. Inoue, Jap. Pat. 121,757; 121,760, 03 June 1987, to Toray

Y. Yoo, R.R. Tiwari, Y.-T. Yoo, D.R. Paul, Polymer **51**, 4907 (2010)

Y. Yoshihara, Europ. Pat. Appl. 397,531, 14 Nov 1990, to Mitsui Petrochem

T. Yoshitake, T. Tasaka, R. Sato, Jap. Pat. 050,254; 050,264, 08 May 1978, to Kuraray

S.H.P. Yu, Europ. Pat. Appl. 282,985, 21 Sept 1988; Jap. Pat. 63 314,261, 22 Dec 1988, to B. F. Goodrich

M.C.C. Yu, W.H. Beever, Europ. Pat. Appl. 473,038, 04 Mar 1992, to Phillips

L. Yu, K. Dean, L. Li, Prog. Polym. Sci. **31**, 576 (2006)

L. Yu, E. Petinakis, K. Dean, H. Liu, in *Poly (Lactic Acid)*, ed. by R. Auras, L.-T. Lim, S.E.M. Selke, H. Tsuji (Wiley, Hoboken, 2010)

H. Yui, T. Kakizaki, H. Sano, Jap. Pat. 014,752, 09 Feb 1978, to Mitsubishi Petrochem.

O. Yuichi, S. Suehiro, Europ. Pat. Appl. 304,041, 22 Feb 1989, to Nippon Petrochem.

S. Yukioka, T. Inoue, Polymer **34**, 1256 (1993)

S. Yukioka, T. Inoue, Polymer **35**, 1182 (1994)

P.C. Yung, H.C. Linstid III, U.S. Patent 5,418,281, 23 May 1995, to Hoechst Celanese Corp.

G.R. Zeichner, P.D. Patel, *Second World Congress of Chemical Engineering*, Montreal, 1981, vol. 6, p. 333

G. Zeitler, H. Mueller-Tamm, U.S. Patent 4,020.025, 26 Apr 1977, to BASF

J. Zimmerman, E.M. Pearce, I.K. Miller, J.A. Muzzio, I.G. Epstein, E.A. Hosegood, J. Appl. Polym. Sci. **17**, 849 (1973)

A. Zletz, U.S. Patent 2,692,257, 19 Oct 1954, to Standard Oil of Indiana

Thermodynamics of Polymer Blends

<div style="text-align:right">**2**</div>

Evangelos Manias and Leszek A. Utracki

Contents

Leszek A. Utracki: deceased.

E. Manias (✉)
Department of Materials Science and Engineering, Pennsylvania State University, University Park, PA, USA
e-mail: manias@psu.edu

L.A. Utracki
National Research Council Canada, Industrial Materials Institute, Boucherville, QC, Canada

Abstract

This chapter summarizes the thermodynamics of multicomponent polymer systems, with special emphasis on polymer blends and mixtures. After a brief introduction of the relevant thermodynamic principles – laws of thermodynamics, definitions, and interrelations of thermodynamic variables and potentials – selected theories of liquid and polymer mixtures are provided: Specifically, both *lattice theories* (such as the Flory-Huggins model, Equation of State theories, and the gas-lattice models) and *off-lattice theories* (such as the strong interaction model, heat of mixing approaches, and solubility parameter models) are discussed and compared. Model parameters are also tabulated for the each theory for common or representative polymer blends. In the second half of this chapter, the thermodynamics of phase separation are discussed, and experimental methods – for determining phase diagrams or for quantifying the theoretical model parameters – are mentioned.

2.1   Introduction

Performance of polymer blends depends on the properties of polymeric components, as well as how they are arranged in space. The spatial arrangement is controlled by the thermodynamics and flow-imposed morphology. The word "thermodynamics" invariably brings to mind "miscibility." However, thermodynamics has a broader use for the practitioners of polymer science and technology than predicting miscibility. The aim of this chapter is to describe how to measure, interpret, and predict the thermodynamic properties of polymer blends, as well as where to find the relevant information and/or numerical values.

Determination of such thermodynamic properties as the phase diagram or the Flory-Huggins binary interaction parameter, χ_{12}, is in principle difficult. The difficulties originate in high viscosity of macromolecular species, thus slow diffusion toward the equilibrium, heat generation when mixing, and thermal degradation at processing relevant temperatures.

For these reasons, there is a tendency to use values obtained from low molecular homologues or solutions. Furthermore, it is an accepted practice to purify the polymers before measuring their thermodynamic properties. However, most industrial polymers are modified by incorporating low molecular weight additives. Furthermore, they are processed under high flow rates and stresses that preclude the possibility of thermodynamic equilibrium. For these and other reasons, a direct application of the laboratory data to industrial systems may not always be appropriate or advisable.

Another difficulty originates in the lack of theories able to predict variation of thermodynamic properties for commercially relevant systems with modifiers. Different additive compositions are used by different manufacturers of the same polymer. Some of these are even being "used up" during processing or during the products' lifetime, their content, and chemical structure change. They may significantly affect the thermodynamic properties of a polymeric mixture, by the physical, viz., that of a cosolvent, and the chemical effects. For example, additives of one polymeric component of a blend may chemically react with additives of another polymeric component, mutually neutralizing each other. In particular, these effects may be large as far as the surface and interface energies are concerned.

2.2 Thermodynamic Principles

2.2.1 Definitions

For convenience, thermodynamic systems are usually assumed closed, isolated from the surroundings. The laws that govern such systems are written in terms of two types of variables: *intensive* (or intrinsic) that do not depend on the mass and *extensive* that do. By definition, extensive variables are additive, that is, their value for the whole system is the sum of their values for the individual parts. For example, volume, entropy, and total energy of a system are extensive variables, but the specific volume (or its reciprocity – the density), molar volume, or molar free energy of mixing are intensive. It is advisable to use, whenever possible, intensive variables.

The main independent variables are the temperature (T), pressure (P), and composition (expressed as number of molecules, N_i, for each component molecule species, i, or through the respective molar fractions, x_i, or volume fractions, ϕ_i). The principal thermodynamic terms are listed in Table 2.1, whereas Table 2.2 provides values of constants often used in thermodynamic calculations.

2.2.1.1 Thermodynamic Potentials and the Concept of Free Energy

In thermodynamics, any energy definition for a system is expressed in terms of pairs of thermodynamic variables, termed as *conjugate variables*. Conjugate pairs are T and S (with TS relating to heat), P and V (with PV related to mechanical work), μ and N, and so on. In each pair, one of the variables is an *intensive variable* (e.g., T, P, μ, etc., that can be considered as a "generalized force"), and the other variable is *extensive* (e.g., S, V, N, respectively, that is considered as the respective "generalized displacement"). The construction of all energy expressions, i.e., thermodynamic potentials, is based on conjugate variables pairs, and all energy changes are associated with products of the absolute value of one conjugate variable multiplied by the change of the other from each pair, i.e., $T \Delta S$, $S \Delta T$, $P \Delta V$, $V \Delta P$, $\mu \Delta N$, and so on.

For every thermodynamic system, there is a finite number of D conjugate pairs describing it (Alberty 2001), or, equivalently, D independent variables are needed to describe the extensive state of the system (*natural variables*). D is also called the "thermodynamic dimensionality" of the system, or, equivalently, the thermodynamic

Table 2.1 Definition of principal thermodynamic terms

Term	Symbol	Definition
Internal energy	U	$U = U(N, V, S)$ comprises of heat, Q, work, W
Entropy	S	$S = S(N, V, U)$ with $S = k \ln \Omega$; where Ω is a measure of the multiplicity of states
Enthalpy	H	$H = H(N, P, S)$ with $H = U + PV$
Helmholtz potential	F	$F = F(N, V, T)$ with $F = U - TS = H - PV - TS$
Gibbs potential	G	$G = G(N, P, T)$ with $G = U + PV - TS = H - TS$
Landau potential	Ω	$\Omega = \Omega(T, V, \mu)$ with $\Omega = U - TS - \mu N$
Extensive properties of a mixture	Z_m	Z_m can be E_m or S_m or F_m or H_m, etc.
Change of an extensive property due to mixing	ΔZ_m	$\Delta Z_m = Z_m - \Sigma x_i Z_i = \Sigma x_i (Z_i - Z_i^0) = \Sigma x_i \Delta Z_i$
Ideal solutions	ΔG^I	$\Delta G^I = -T\Delta S^I = kTN\Sigma x_i \ln x_i$, thus no interactions, $\Delta H^I = 0$, and total randomness of molecular placement, $\Delta V^I = 0$
Regular solutions	ΔG^R	$\Delta G^R = \Delta H^P - T\Delta S^I$; $\Delta H^R \propto \frac{1}{2}(\varepsilon_{11} + \varepsilon_{22}) - \varepsilon_{12}$. The molecular interactions are nonspecific, without associations, hydrogen or dipole-dipole bonding, distribution, orientation, etc.
Excess properties	ΔZ^E	$\Delta Z^E = \Delta Z - \Delta Z^I$
Athermal solutions	ΔG^A	$\Delta G^A = -T\Delta S$; $\Delta H^A = 0$
Combinatorial entropy	ΔS^{comb}	That part that originates from the number of possible placements of molecules in the lattice of an athermal solution (the latter assumption usually is abandoned in the following derivations)
Equation of state (EoS)	PVT	The relation between P, V, and T for a material
Reducing variables	P^*, V^*, T^*	Reducing variables are characteristic materials' parameters used to reduce the corresponding independent variables, making them to follow respective corresponding state equation(s)
Corresponding states	$\tilde{P}\tilde{V}\tilde{T}$	Describing behavior of material by relations of its reduced variables, e.g., $\tilde{P} \equiv P/P^*, \tilde{V} \equiv V/V^*, \tilde{T} \equiv T/T^*$
Free volume	V_f	$V_f = V - V_o$, where $V_o \simeq \lim_{T \to 0} V$
Solubility parameter	δ	Can be calculated from the heat of vaporization ΔH^V $(\Delta H^V = RT^2(\partial \ln P/\partial T)_{sat})$ by $\delta = \sqrt{(\Delta H^V - RT)/V}$ or can also be calculated from the molecular structure

space of the system has D dimensions. For example, in the simplest case of a single-phase ideal gas, there are three pairs of conjugate variables and, thus, $D=3$. By definition of the thermodynamic energy functions (thermodynamic potentials, cf. Table 2.1), this means that there will be 2^D unique thermodynamic potentials. The various thermodynamic potentials are defined considering as its independent variables one thermodynamic parameter from each conjugate pair; these are the D *natural variables* of this thermodynamic potential (e.g., $U = U(N, V, S)$, $F = F(N, V, T)$, $G = G(N, P, T)$, etc., see also Table 2.1). For the same example as above, the single-phase ideal gas, there will be $2^3 = 8$ thermodynamic potentials that can be

Table 2.2 Useful constants

Constant	Symbol	Value
Avogadro's number	N_A	6.02205×10^{23} [mol^{-1}]
Boltzmann constant	k_B	1.38065×10^{-23} [JK^{-1}]
Molar gas constant	$R = N_A k_B$	8.31441 [JK^{-1}mol^{-1}]
Molar volume at standard conditions	$V_o = RT_o/P_o$	22.41383×10^{-3} [m^{3}mol^{-1}]
Origin of Celsius scale	T_o	273.15 [K]
Planck's constant	h	6.62618×10^{-34} [Js]
Standard atmospheric pressure	P_o	1.01325×10^5 [Nm^{-2}]

defined to quantify its energy at a given state, or its energy change upon undergoing any arbitrary thermodynamic process. All 2^D thermodynamic potentials can be calculated for any system, and its corresponding differential can be calculated for any arbitrary process to quantify the corresponding energy change for this process (Alberty 2001). However, only one of these 2^D energy definitions adopts appropriate values and has appropriate behaviors/changes for each thermodynamic process, and this energy (thermodynamic potential) is the *free energy* of the system for this thermodynamic process. For a system undergoing a thermodynamic process, by definition:

1. The free energy adopts a minimum value at equilibrium.
2. The free energy change is negative for spontaneous processes.

Both the above are satisfied by a thermodynamic potential, when the thermodynamic process happens under conditions where its *natural variables* remain constant. For example, for a closed system ($N = $ constant) undergoing a process under controlled temperature and volume (T, V are also constant), the Helmholtz potential $F = F(N, V, T)$ is the corresponding free energy; similarly, for the same system undergoing a process where NPT are constant, the Gibbs potential $G = G(N, P, T)$ is now the free energy in this case; and so on.

New energy terms need to be added in the form of conjugate pairs when the system has additional energy contributions: e.g., if there exist more than one species of molecules, a separate $\mu_i N_i$ term is needed for each species i; if there are magnetic dipoles or spins, a BM term is needed (B is the magnetic field, M the system magnetization, and $B \, dM$ would be the associated energy change contribution in dU); and so on. Also, there may be additional mechanical work terms (beyond $P \, dV$), such as work associated with interfaces, $\gamma \, dA_{inter}$; work associated with mechanical deformation, $V \sum_{ij}\tau_{ij}d\varepsilon_{ij}$; or work associated for uniaxial deformation, $F \, dl$.

2.2.2 The Three Laws of Thermodynamics

Thermodynamics focuses on the state of material, usually in *a closed system*. Historically, the laws were empirically formulated using the well-accepted process of hypothesis, observation, and analysis. However, since the energetic state of a closed system is a sum of all the molecular and atomic motions, the statistical physics re-derived these laws from the first principles (Waldram 1985; Gupta 1990).

2.2.2.1 The First Law (Conservation of Energy)

In a closed system, the total energy remains constant (also known as *sine perpetuum mobile*). Thus, for a closed system, the change of internal energy (dU):

$$dU = dW + dQ = 0 \tag{2.1}$$

where dW represents the work done on or by the system and dQ represents the change of the thermal energy content. Note that there are several forms of energy that can be classified as "work," for example, compression, friction, electromagnetic interaction, etc.

For a perfect gas at constant pressure, $P = $ const., Eq. 2.1 gives the relationship between the heat capacities at constant pressure and at constant volume, viz., $C_P - C_V = R$ (R is the gas constant). Similarly, at $T = $ const., Eq. 2.1 predicts that the external work can only be performed at a cost of the internal energy: $PdV = -dU$.

2.2.2.2 The Second Law (The Principle of Entropy Increase)

The energy always flows from a higher to a lower level; hence, the system tends to move toward a more uniform distribution of the local energetic states. Since the entropy provides a measure of randomness, in a closed system, the entropy never decreases:

$$dS = \frac{dQ}{T} \geq 0 \tag{2.2}$$

The second law of thermodynamics is also known as the Carnot cycle principle that specifies that "heat can never pass from a colder to a warmer body without some other changes, connected therewith, occurring at the same time" (Clausius).

Equation 2.2 can also be written as:

$$
\begin{aligned}
\left(\frac{\partial S}{\partial V}\right)_T &= \frac{1}{T}\left(\frac{\partial Q}{\partial V}\right)_T = \left(\frac{\partial P}{\partial T}\right)_V \\
\left(\frac{\partial S}{\partial P}\right)_V &= \frac{1}{T}\left(\frac{\partial Q}{\partial P}\right)_V = \left(\frac{\partial V}{\partial T}\right)_S
\end{aligned}
\tag{2.2a}
$$

2.2.2.3 The Third Law (Entropy Vanishes at Absolute Zero)

In 1906, Nernst showed (experimentally) that the equilibrium entropy tends toward zero as the absolute temperature approaches zero:

$$
\begin{aligned}
&\lim_{T \to 0} S = \lim_{T \to 0} dS = 0, \quad \text{or equivalently} \\
&S = \int_0^T \frac{dQ_{rev}}{T}\left(\text{assuming } S_{T=0} \overset{emp}{=} 0\right)
\end{aligned}
\tag{2.3}
$$

As a corollary, near zero K the change of entropy in any process is negligibly small. Thus, the third law is empirical, but so far no contradictory observation was reported. As a consequence of Eq. 2.3, near the absolute zero the coefficient of thermal expansion and the pressure coefficient are expected to vanish:

$$\lim_{T \to 0} \left(\frac{\partial S}{\partial P} \right)_T = \lim_{T \to 0} \left(\frac{\partial S}{\partial V} \right)_T = 0$$

$$\lim_{T \to 0} \left(\frac{\partial V}{\partial T} \right)_P = -\lim_{T \to 0} \left(\frac{\partial P}{\partial T} \right)_V = 0$$

(2.3a)

In summary, the first law is simply a statement of the law of conservation of energy, the second law is concerned only with differences in the entropy between (two) states, and the third law allows for the calculation of the absolute entropy of a state (assuming knowledge of the system's entropy at the absolute zero of temperature, that is at $T = 0$ K).

2.2.3   Interrelations Between Thermodynamic Variables

The full differentials (or the total changes) of the principal thermodynamic potentials for a closed system ($N = $ const.) cast in terms of their natural variables are

$$
\begin{aligned}
dF &= -SdT - PdV \\
dH &= TdS + VdP \\
dG &= -SdT + VdP
\end{aligned}
$$

(2.4)

Note that Eq. 2.4 implies that $F = F(T, V)$, $H = H(S, P)$, and $G = G(T, P)$ and that the thermodynamic definitions of pressure, P, and temperature, T, are

$$
\begin{aligned}
P &= \frac{(\partial S/\partial V)_U}{(\partial S/\partial U)_V} = \left(\frac{\partial F}{\partial V} \right)_T \\
T &= \left(\frac{\partial H}{\partial S} \right)_P = \left(\frac{\partial U}{\partial S} \right)_V
\end{aligned}
$$

(2.5)

These relations are important when deriving an equation of state by statistical methods. In addition, they can naturally lead to another set of useful identities through the derivation of the mixed second derivatives of the thermodynamic potentials (known as Maxwell relations):

$$
\begin{aligned}
\frac{\partial^2 U}{\partial S \partial V} &= + \left(\frac{\partial T}{\partial V} \right)_S = - \left(\frac{\partial P}{\partial S} \right)_V \\
\frac{\partial^2 H}{\partial S \partial P} &= + \left(\frac{\partial T}{\partial P} \right)_S = + \left(\frac{\partial V}{\partial S} \right)_P \\
\frac{\partial^2 F}{\partial T \partial V} &= - \left(\frac{\partial S}{\partial V} \right)_T = - \left(\frac{\partial P}{\partial T} \right)_V \\
\frac{\partial^2 G}{\partial T \partial P} &= - \left(\frac{\partial S}{\partial P} \right)_T = + \left(\frac{\partial V}{\partial T} \right)_P
\end{aligned}
$$

(2.6)

Whereas, since the heat capacity C is $\delta Q \equiv C\delta T$, using the second law of thermodynamics ($\delta S = \delta Q/T$, or $\delta Q = T\delta S$) and Eq. 2.4 the heat capacities at

constant pressure (or at constant volume) can directly connect the enthalpy and entropy gradients between two temperatures, for example,

$$C_P \equiv T\left(\frac{\partial S}{\partial T}\right)_P = -\left(\frac{\partial H}{\partial T}\right)_P \quad \text{and} \quad C_V \equiv T\left(\frac{\partial S}{\partial T}\right)_V = -\left(\frac{\partial H}{\partial T}\right)_V \qquad (2.7)$$

Based on the Maxwell relations, the definitions of the isothermal compressibility (K_T or β_T), the isoentropic compressibility (K_S or β_T), and the thermal expansion coefficient (α) can be written with the ln V removed as, respectively,

$$
\begin{aligned}
K_T \text{ or } \beta_T &\equiv \left(\frac{\partial P}{\partial \ln V}\right)_T = -\frac{1}{V}\left(\frac{\partial V}{\partial P}\right)_T \\
K_S \text{ or } \beta_S &\equiv \left(\frac{\partial P}{\partial \ln V}\right)_S = -\frac{1}{V}\left(\frac{\partial V}{\partial P}\right)_S \\
\alpha &\equiv \left(\frac{\partial \ln V}{\partial T}\right)_P = +\frac{1}{V}\left(\frac{\partial V}{\partial T}\right)_P
\end{aligned}
\qquad (2.8)
$$

The parameter K_T is also known as the isothermal bulk modulus and α as the volume expansion coefficient; these are interrelated by means of the Grüneisen constant, γ:

$$\gamma = -\frac{V}{C_V}\frac{(\partial V/\partial T)_P}{(\partial V/\partial P)_T} = \frac{\alpha V}{C_V \beta_T} \qquad (2.9)$$

Similarly, through the definition of isothermal and isoentropic compressibility, the ratio and difference of C_P and C_V can also be simplified to

$$
\begin{aligned}
\frac{C_P}{C_V} &= \frac{(\partial P/\partial V)_S}{(\partial P/\partial V)_T} = \frac{\beta_T}{\beta_S} \\
C_P - C_V &= T\left(\frac{\partial S}{\partial T}\right)_P - T\left(\frac{\partial S}{\partial T}\right)_V = VT\frac{\alpha^2}{\beta_T}
\end{aligned}
\qquad (2.7a)
$$

2.2.4 Multicomponent Systems

In a multicomponent, closed system comprising N_i moles of component i, the changes dX in an extensive function of state X (e.g., U, F, G, S, H, C_P, C_V, etc.) caused by the variation of composition are given by

$$
\begin{aligned}
dX &= \sum_i X_i dN_i \\
\text{defining } X_i &\equiv \left(\frac{\partial X}{\partial N_i}\right)_{N_{j \neq i}} \quad \text{and, thus: } X = \sum_i X_i N_i
\end{aligned}
\qquad (2.10)
$$

where the functions X_i are known as partial molar quantities. Thus, the full differentials of the state functions (viz., Eq. 2.4) can be expressed as

$$
\begin{aligned}
dU &= TdS - PdV + \sum_i \mu_i dN_i \\
dF &= -SdT - PdV + \sum_i \mu_i dN_i \\
dH &= TdS + VdP + \sum_i \mu_i dN_i \\
dG &= -SdT + VdP + \sum_i \mu_i dN_i
\end{aligned}
\tag{2.11}
$$

where $\mu_i = \partial G / \partial N_i$ is the chemical potential of component i and N_i being a natural variable for all four above state functions, that is, $U = U(S, V, N)$, $F = F(T, V, N)$, $H = H(S, P, N)$, and $G = G(T, P, N)$. The relationships in Eq. 2.11 indicate that in a closed multicomponent system (N_i = const.) any change of the independent variables must be reflected in a change of the chemical potentials (μ_i):

$$
-SdT + VdP - \sum_i N_i d\mu_i = 0
\tag{2.12}
$$

Equation 2.12 is known as the Gibbs-Duhem relationship and is a depiction that the free energy of this grand canonical ensemble remains unchanged.

2.3 Thermodynamics of a Single-Component System

2.3.1 Equation of State (EoS) or PVT Relationships

2.3.1.1 Equation of State (EoS)

All theoretical equations of state suggest a corresponding state behavior of PVT properties that requires three scaling parameters (P^*, V^*, and T^*). These define the corresponding state and are used to scale/reduce the PVT toward $\tilde{P} \equiv P/P^*, \tilde{V} \equiv V/V^*, \tilde{T} \equiv T/T^*$. In his Ph.D. thesis of 1873, van der Waals proposed the first EoS formulated in terms of corresponding state (reduced) variables. The relation can be written in terms of PVT or in terms of reduced variables $\tilde{P}\tilde{V}\tilde{T}$, indicating expected observance of the corresponding state principle:

$$
\begin{aligned}
P &= \frac{RT}{V - b} - \frac{a}{V^2} \\
\frac{\tilde{P}}{\tilde{T}} &= \frac{8}{3\tilde{V} - 1} - \frac{3}{\tilde{T}\tilde{V}^2}
\end{aligned}
\tag{2.13}
$$

$$
\left(\text{where}\, \tilde{P} \equiv P/P^*, \tilde{V} \equiv V/V^*, \tilde{T} \equiv T/T^*, \right.
$$
$$
\left. \text{with}\, V^* = 3b; P^* = a/27b^2; T^* = 8a/27Rb \right)
$$

This approach demonstrated that the V^* and P^* are related to the van der Waals excluded volume (b) and the cohesive energy density ($\propto a$) of a system, a fact that has been largely used thereafter in subsequent EoS theories. Equation 2.13 also introduced the free volume concept; note that as $T \to 0$, $V \to b$. van der Waals

considered that molecules move in "cells" defined by the surrounding molecules with a uniform potential. Furthermore, Eq. 2.13 allows, through the definition of the critical point (P_c, T_c) in the P-T phase diagram (*vide infra*), to connect a and b to the critical values of pressure and temperature, P_c and T_c, which can be found tabulated from experimental data for various systems (viz., $a = 27R^2T_c^2/64P_c$, and $b = RT_c/8P_c$). This enables improved predictive capability over the ideal gas EoS. Finally, van der Walls also proposed a method to extend the single-component EoS of Eq. 2.13 to multicomponent mixtures by using the same relation with weight-averaged values of a_m, b_m of the mixture calculated based on the mole compositions (y_i) and the single-component a_i, b_i of each component i: $a_m = \sum_i \sum_j y_i y_j \sqrt{a_i a_j}$ and $b_m = \sum_i y_i b_i$. Thus, although the van der Walls EoS is not used today for any practical purpose, it is purely pedagogical, it does clearly demonstrate the corresponding state principle, it predicts continuity of matter between gas and liquid phases, it provides a mixture rule for EoS application in multicomponent mixtures, and it laid the foundations for modern EoS theories.

The volume, within which the center of a molecule can freely move, is what defines its free volume (or, more accurately, free volume relates to the excess empty volume beyond the per-molecule unoccupied volume). Thus, one may distinguish and define:

1. Total volume, V.
2. Occupied volume, V_o (usually defined as the V at $T = 0$ K).
3. Free volume, $V_f = V - V_o$.
4. Doolittle's free volume fraction, $f_D = V_f/V_o$.
5. Free volume fraction, $f = V_f/V = 1/(1 + 1/f_D)$ (to be used here).

Detailed methods of computation of the van der Waals excluded volume (for any chemical structure) have been developed (van Krevelen 1976). Thermodynamically, the free volume is expressed in terms of the entropy of vaporization:

$$P = \frac{RT}{V_f}\exp\left(-\frac{\Delta H^V}{RT}\right) = \frac{RT}{V_f}\exp\left(-\frac{\Delta S^V}{R}\right) = \frac{RT}{V}$$
$$\text{or} : \Delta S^V = R\ln\left(V/V_f\right) \text{ and } \Delta H^V = T^V \Delta S^V$$

(2.14)

Over the years, many versions of the EoS theories have been proposed (see, e.g., Table 2.3). Several comprehensive reviews of the EoS used in polymer thermodynamics have been published. For example, one review (Curro 1974) discussed applications of EoS within a full range of materials and variables, viz., to crystals, glasses, molten polymers, and monatomic liquids. This review discusses fundamentals of the theories and it provides a list of available experimental data. The comparison between different EoS was made on two levels, first by comparing the derived expressions for physical quantities (e.g., the characteristic reducing parameters, cohesive energy density, or internal pressure) and then comparing how well the EoS describes the observed PVT dependencies for polymers. A second type of reviews focused on summarizing PVT parameters for the molten state of polymers (Zoller 1989; Rodgers 1993a, b; Cho 1999). The authors here examined and compared several EoS theories, e.g., Spencer and Gilmore (1949) (S-G),

Table 2.3 A summary of a few EoS, mentioned in this section

Cell models

Flory-Orwoll-Vrij (FOV)

$$\frac{\tilde{P}\tilde{V}}{\tilde{T}} = \frac{\tilde{V}^{1/3}}{\left(\tilde{V}^{1/3}-1\right)} - \frac{1}{\tilde{T}\tilde{V}}$$

$\tilde{P} \equiv \frac{P}{P^*}, \tilde{V} \equiv \frac{V}{V^*}, \tilde{T} \equiv \frac{T}{T^*}$ Eq. 2.15

Prigogine (P)

$$\frac{\tilde{P}\tilde{V}}{\tilde{T}} = \frac{\tilde{V}^{1/3}}{\left(\tilde{V}^{1/3}-2^{-1/6}\right)} - \frac{2}{\tilde{T}}\left(\frac{1.2045}{\tilde{V}^2} - \frac{1.011}{\tilde{V}^4}\right)$$

$\tilde{P} \equiv \frac{P}{P^*}, \tilde{V} \equiv \frac{V}{V^*}, \tilde{T} \equiv \frac{T}{T^*}$ Eq. 2.17

Dee and Walsh (D-W)

$$\frac{\tilde{P}\tilde{V}}{\tilde{T}} = \frac{\tilde{V}^{1/3}}{\left(\tilde{V}^{1/3}-2^{-1/6}q\right)} - \frac{2}{\tilde{T}}\left(\frac{1.2045}{\tilde{V}^2} - \frac{1.011}{\tilde{V}^4}\right)$$

$\tilde{P} \equiv \frac{P}{P^*}, \tilde{V} \equiv \frac{V}{V^*}, \tilde{T} \equiv \frac{T}{T^*}$ $q = 1.07$

Simha and Somcynsky (S-S) hole model

$$\frac{\tilde{P}\tilde{V}}{\tilde{T}} = \frac{y\tilde{V}^{1/3}}{\left[(y\tilde{V})^{1/3}-\vartheta y\right]} - \frac{2y}{\tilde{T}}\left(\frac{1.2045}{(y\tilde{V})^2} - \frac{1.011}{(y\tilde{V})^4}\right)$$

$$\frac{s}{3c}\left[1+\frac{\ln(1-y)}{y}\right] = \frac{\frac{1}{3}(y\tilde{V})^{1/3}-\vartheta y}{(y\tilde{V})^{1/3}-\vartheta y} - \frac{y}{6\tilde{T}}\left(\frac{2.409}{(y\tilde{V})^2} - \frac{3.033}{(y\tilde{V})^4}\right)$$

System of two equations; $\vartheta = 2^{-1/6}$ cf. hexagonal cells; y = fraction of occupied sites; $s/3c \simeq 1$ for polymers
$\tilde{P} \equiv \frac{P}{P^*}, \tilde{V} \equiv \frac{V}{V^*}, \tilde{T} \equiv \frac{T}{T^*}$ Eq. 2.19

Lattice fluid models

Sanchez and Lacombe (S-L)

$$\frac{\tilde{P}\tilde{V}}{\tilde{T}} = -\tilde{V}\left[\ln\left(1-\frac{1}{\tilde{V}}\right) - \frac{1}{\tilde{V}}\right] - \frac{1}{\tilde{T}\tilde{V}}$$

$\tilde{P} \equiv \frac{P}{P^*}, \tilde{V} \equiv \frac{V}{V^*}, \tilde{T} \equiv \frac{T}{T^*}$ Eq. 2.16

Jung

$$\frac{\tilde{P}\tilde{V}}{\tilde{T}} = -\tilde{V}\left[\ln\left(1-\frac{1}{\tilde{V}}\right) + \frac{1}{\tilde{V}}\right] - \frac{4}{\tilde{T}}\left(\frac{1.2045}{\tilde{V}^2} - \frac{1.011}{\tilde{V}^4}\right)$$

$\tilde{P} \equiv \frac{P}{P^*}, \tilde{V} \equiv \frac{V}{V^*}, \tilde{T} \equiv \frac{T}{T^*}$ Eq. 2.18

Empirical PVT relations

Tait equation (4-parameter)

$$V(P,T) = V(0,T)\left[1 - C\ln\left(1 + \frac{P}{B(T)}\right)\right]$$

with $C = 0.0894$; $V(0,T) = V_o e^{\alpha T}$; $B(T) = B_o e^{-B_1 T}$ Eq. 2.22

Hartmann and Haque (H-H)

$$\tilde{P}\tilde{V}^5 = \tilde{T}^{3/2} - \ln\tilde{V}$$

$P^* = B_o, V^* = V_o, T^* = T_o$ Eq. 2.23

Sanchez and Cho (S-C)

$$\tilde{V} = \frac{1}{1-\tilde{T}}\exp\left[\frac{\omega}{(1-\omega)B_1}\left\{1 - \left(1 + \frac{B_1\tilde{P}\exp(9\tilde{T})}{\omega}\right)^{1-\omega}\right\}\right]$$

$B_1 = 10.2$; $\omega = 0.9$ Eq. 2.24

Flory et al. (1964) (FOV), Sanchez-Lacombe (1976, 1977, 1978) (S-L), Simha and Somcynsky (1969) (S-S), Prigogine et al. (1953, 1957) (P), Dee and Walsh (1988) (D-W), Hartmann and Haque (1985) (H-H), and Sanchez and Cho (1995) (S-C), and tabulated the respective corresponding state values (P^*, V^*, and T^*) for most common polymers. These comparisons span across the different types of EoS models, from cell models (FOV, P, D-W), to lattice-fluid (S-L) and hole (S-S) models, to semiempirical approaches (H-H, S-C), comparing the validity of distinctly different EoS approaches across large numbers of different homopolymers and copolymers. All reviews seem to build a consensus on the comparative accuracy of the various EoS: Zoller (1989) reported large deviations (≤ 0.01 mL/g)

for S-G, the FOV and S-L were useful only at low P and over small P ranges, whereas S-S and S-C consistently provided the best representation of data over extended ranges of T and P, with average deviations in volume of ≤ 0.003 mL/g (S-S) and ≤ 0.0004 mL/g (S-C), compared to the experimental values. Rodgers (1993a, b) and Cho (1999) reach similar comparative conclusions, based on additional experimental PVT data, reporting that the D-H modified cell, the S-S hole, the P cell models, and the semiempirical H-H and S-C models, were all found to provide good fits of polymer liquid PVT data over the full range of experimental pressures, whereas the FOV and the S-L EoS were both significantly less accurate when applied over wide pressure ranges.

The FOV model can be summarized as

$$\frac{\tilde{P}}{\tilde{T}} = \frac{1}{\tilde{V}^{2/3}\left(\tilde{V}^{1/3} - 1\right)} - \frac{1}{\tilde{T}} \cdot \frac{1}{\tilde{V}^2} \tag{2.15}$$

with: $\quad V^* = \rho_*^3; \quad P^* = ck_BT^*/V^*; \quad T^* = s_*\eta_*/(2cV^*k_B)$

where ρ_* is the "hard-sphere" radius, s_* the number of contacts per segment, η_* the segment-segment interaction energy, and c the coordination number (k_B is the Boltzmann constant).

The S-L model, better known as the "lattice-fluid model," introduces vacancies into the classical incompressible Flory-Huggins model (*vide infra*). The lattice vacancy is treated as a pseudoparticle in the system. This model can be summarized as

$$\frac{\tilde{P}}{\tilde{T}} = -\left[\ln\left(1 - \frac{1}{\tilde{V}}\right) + \frac{1}{\tilde{V}}\right] - \frac{1}{\tilde{T}} \cdot \frac{1}{\tilde{V}^2} \tag{2.16}$$

with $V^* = M_W/r\rho^*$ (where M_W is the weight-averaged molecular weight, while ρ^* is the characteristic density parameter, $\rho^* = 1/V^*$), $P^* = rN_1\varepsilon^*/V^*$, and $T^* = \varepsilon^*/k_B$ (where ε^* is the van der Walls interaction energy). The parameter r represents the number of lattice sites occupied by the r-mer – its presence in the EoS negates the principle of corresponding states. The latter can be recovered only for $r \rightarrow \infty$.

The Prigogine simple cell model (P) considers each monomer in the system to be trapped in the cell created by its surroundings. The general cell potential, generated by the surroundings, is simplified to be athermal (cf. free volume theory), whereas the mean potential between the centers of different cells are described by the Lennard-Jones 6–12 potential. The P model EoS can be summarized as

$$\frac{\tilde{P}}{\tilde{T}} = \frac{1}{\tilde{V}^{2/3}\left(\tilde{V}^{1/3} - 2^{-1/6}\right)} - \frac{2}{\tilde{T}} \cdot \left(\frac{1.2045}{\tilde{V}^3} - \frac{1.011}{\tilde{V}^5}\right) \tag{2.17}$$

where the factor $2^{-1/6}$ originates from the hexagonal close packing lattice used as a cell geometry and the factors 1.2045 and 1.011 correct the effects of higher coordination shells on the internal energy. Another, largely unnoticed,

EoS was proposed (Jung 1996), by employing a continuous lattice and using a Lennard-Jones 6–12 potential to modify the S-L simple lattice fluid. This method combines elements from both S-L and P models, and the obtained EoS can be summarized as

$$\frac{\tilde{P}}{\tilde{T}} = -\left[\ln\left(1 - \frac{1}{\tilde{V}}\right) + \frac{1}{\tilde{V}}\right] + \frac{4}{\tilde{T}} \cdot \left(\frac{1.2045}{\tilde{V}^3} - \frac{1.011}{\tilde{V}^5}\right) \qquad (2.18)$$

with the same definitions as the S-L simple lattice-fluid EoS. To examine the ability of this EoS to describe *PVT* dependencies, the author used experimental data of eight polymers and compared with the FOV, S-L, S-S, and D-W relations. The evaluation was performed computing errors in describing the volume (ΔV), as well as thermal expansivity and isothermal compressibility. As in the previous evaluations, S-S dependence performed the best. For the description of *PVT*, the new EoS performed as well as that of D-W, but for the expansivity and compressibility, it outperformed the latter EoS.

The S-S EoS derived by Simha and Somcynsky (1969) is based on the Prigogine cell model by introducing lattice imperfections (holes, unoccupied sites). In S-S, a liquid is represented as a mixture of *y* occupied and *h* ($=1 - y$) unoccupied sites; thus, following the "Significant Liquid Structures" nomenclature (Eyring and Jhon 1969), the model considers a liquid as being an intermediate between solid and gas. To derive the EoS, the authors first calculated the partition function, *Z*, for all possible number of arrangements of occupied sites and empty holes in a lattice with *z* coordination number. The Helmholtz free energy is directly given, $F = -k_B T \ln Z$, and its differentiation gives the pressure and, thus, the equation of state. Minimization of the Helmholtz free energy *F* provides a second relation that must be solved simultaneously with the EoS:

$$\frac{\tilde{P}}{\tilde{T}} = \frac{y}{\tilde{V}^{2/3}\left[(y\tilde{V})^{1/3} - 2^{-1/6}y\right]} - \frac{2y^2}{\tilde{T}} \cdot \left(\frac{1.2045}{(y\tilde{V})^3} - \frac{1.011}{(y\tilde{V})^5}\right)$$

$$\frac{s}{3c}\left[1 + \frac{\ln(1-y)}{y}\right] = \frac{\frac{1}{3}(y\tilde{V})^{1/3} - 2^{-1/6}y}{(y\tilde{V})^{1/3} - 2^{-1/6}y} - \frac{y}{6\tilde{T}}\left(\frac{2.409}{(y\tilde{V})^2} - \frac{3.033}{(y\tilde{V})^4}\right) \qquad (2.19)$$

with : y = fraction of occupied sites;

$s/3c \simeq 1$ in normal practice for polymers

Of all the EoS used for polymeric species, the one derived by S-S was the first to explicitly consider the hole fraction, $h = 1-y$. Equation 2.19 provides a corresponding state description of *PVT* behavior of any liquid. Once the four characteristic parameters: *P**, *V**, *T**, and *3c/s* are known, the specific volume and all its derivatives are known in the full range of *P* and *T*. For linear polymers, where $3c/s \simeq 1$, only the three usual parameters (*P**, *V**, and *T**) are required. Values of

P^*, V^*, and T^* for selected polymers are listed in Table 2.4. At atmospheric pressure, $\tilde{P} = 0$, and within the range of reduced volumes, $0.95 < \tilde{V} 1.40$, Eq. 2.19 predicts that the volume expansion with T should follow the dependence (Simha and Weil 1970):

$$\ln \tilde{V}_i = S_1(s_i, c_i) + S_2(s_i, c_i)\tilde{T}_i^{3/2} \tag{2.20}$$

2.3.1.2 Frozen Free Volume Fraction

The S-S EoS theory defined through Eq. 2.19 is valid for any liquid. However, upon cooling when the temperature reaches the glass transition region, part of the free volume fraction is no longer accessible for the molecular motion. The S-S theory can also be used in this glassy region, if it can be estimated what part of the free volume is frozen as T approaches the glass transition temperature, T_g. Experimentally, the frozen fraction of the free volume, FF, depends on the absolute value of T_g. This finding was first reported for several polymers at ambient pressure (Simha and Wilson 1973). Subsequently, the generality of this observation was confirmed by analyzing isobaric thermal expansion of PS for a wide range of pressures (Utracki and Simha 1997).

As shown in Fig. 2.1, the frozen fraction of the free volume, FF, follows the same dependence whether T_g changes are caused by the polymeric chemical structure or by imposed pressure. The observed, general dependence follows the empirical relation:

$$FF = 0.997 - 4.75 \times 10^{-4} \; T_g - 1.52 \times 10^{-6} \; T_g^2 \quad (R_{\text{fit}} = 0.975) \tag{2.21}$$

It is gratifying to see that as the glass transition temperature approaches the absolute zero, $T_g \rightarrow 0\text{K}$, Eq. 2.21 predicts that all free volume should freeze, $FF(T_g = 0\text{K}) = 1$. On the other hand, at the high-temperature range, as T_g exceeds 669 K (396 °C), all free volume should be accessible to thermal motion in the glassy state, i.e., $FF(T_g \geq 400\,°\text{C}) = 0$. Thus, it is to be expected that polymers at high temperature will have the same thermal expansion coefficient across the glass transition temperature, viz., $\alpha_L = \alpha_G$, where subscripts L and G indicate liquid and glassy state, respectively.

2.3.1.3 Empirical PVT Relations

Starting from a different viewpoint, one can reach empirically justified EoS by phenomenological arguments used to build universal behaviors (functions) and fit them to experimental PVT data. The most common such approach for polymers is an isothermal compressibility V-P model (Tait 1888) known as the Tait equation:

$$\begin{aligned} &V(P,T) = V(0,T)\left[1 - C \ln\left(1 + P/B(T)\right)\right] \\ &\text{with } V(0,T) = V_o\exp(\alpha T); \quad B(T) = B_o\exp(-B_1 T) \end{aligned} \tag{2.22}$$

where $C = 0.0894$ is treated as a universal constant, α is the thermal expansion coefficient, and $B(T)$ is known as the Tait parameter. This renders the Tait

Table 2.4 A list of polymers (homopolymers and random copolymers), the S-S characteristic parameters (P^*, V^*, and T^*), as well as the difference between the measured and computed volumes (ΔV) averaged over the data's temperature range (ΔT) and pressure range (ΔP) (Rodgers 1993a, b)

Polymer		P^* (bar)	T^* (K)	V^* (mL/g)	ΔV (ΔT, ΔP) (μL/g) (°C, bar)
Homopolymers					
PDMS	Poly(dimethyl siloxane)	5014	7864	0.9592	0.48 (25–70, 0–1000)
PS	Polystyrene	7159	12840	0.9634	0.35 (115–196, 0–2000)
PoMS	Poly(o-methylstyrene)	7461	13080	0.9814	0.46 (139–198, 0–1800)
PMMA	Poly(methyl methacrylate)	9264	11940	0.8369	0.10 (114–159, 0–2000)
PcHMA	Poly(cyclohexyl methacrylate)	7722	12030	0.9047	0.66 (123–198, 0–2000)
PnBMA	Poly(n-butyl methacrylate)	8560	10310	0.9358	1.31 (34–200, 0–2000)
PMA	Poly(methyl acrylate)	9691	10460	0.8431	0.93 (37–220, 0–1960)
PVAc	Poly(vinyl acetate)	9474	9348	0.8126	0.14 (35–100, 0–800)
PTFE	Poly(tetrafluoroethylene)	6581	8126	0.4339	1.36 (330–372, 0–390)
PSF	Polysulfone	11160	12770	0.7903	0.36 (202–371, 0–1960)
PEG	Poly(ethylene oxide)	9145	10150	0.8812	0.41 (88–224, 0–685)
PTHF	Poly(tetrahydrofuran)	7255	10280	1.0087	0.40 (62–166, 0–785)
BPE	Branched polyethylene	6923	10390	1.1674	0.99 (125–198, 0–2000)
LPE	Linear polyethylene	7864	9793	1.1406	0.90 (142–200, 0–2000)
HMLPE	High MW linear polyethylene	9213	9207	1.1278	1.10 (137–200, 0–2000)
PIB	Polyisobutylene	6866	11360	1.0940	0.20 (53–110, 0–1000)
PMP	Poly(4-methyl-1-pentene)	5453	11030	1.2050	1.79 (241–319, 0–1960)
PBD	cis-1,4-polybutadiene	8150	9225	1.0766	0.36 (4–55, 0–2835)
HDPE	High-density polyethylene	5063	12290	1.2190	1.43 (140–203, 0–1960)
LDPE	Low-density polyethylene	7936	9595	1.1380	2.26 (121–175, 0–1960)
LDPE-A	Low-density polyethylene "A"	7162	10580	1.1664	0.65 (112–225, 0–1960)
LDPE-B	Low-density polyethylene "B"	7036	10860	1.1734	0.59 (112–225, 0–1960)
LDPE-C	Low-density polyethylene "C"	7188	10660	1.1679	0.61 (112–225, 0–1960)
a-PP	a-Polypropylene	6277	9494	1.1274	0.74 (80–120, 0–1000)
i-PP	i-Polypropylene	5730	11060	1.1884	1.26 (170–297, 0–1960)
i-PB	i-Poly(1-butene)	6037	10920	1.1666	0.75 (133–246, 0–1960)
PET	Poly(ethylene terephthalate)	11940	11800	0.7426	0.57 (274–342, 0–1960)
PPE	Poly(2,6-dimethyl phenylene oxide)	9294	10580	0.8602	0.91 (203–320, 0–1765)
PC	Bisphenol-A polycarbonate	10200	11830	0.8156	0.37 (151–340, 0–1765)
PAr	Polyarylate (Ardel)	10030	12390	0.8091	0.26 (177–310, 0–1765)
Phenoxy	Phenoxy	11390	11730	0.8529	0.35 (68–300, 0–1765)
PEEK	Poly(ether ether ketone)	10860	12580	0.7705	0.85 (346–398, 0–2000)
PVME	Poly(vinyl methyl ether)	8481	10360	0.9632	0.68 (30–198, 0–2000)
PA-6	Polyamide 6	5499	16870	0.8327	0.44 (236–296, 0–1960)

(*continued*)

Table 2.4 (continued)

Polymer		P^* (bar)	T^* (K)	V^* (mL/g)	$\Delta V (\Delta T, \Delta P)$ (µL/g) ($^\circ$C, bar)
PA-66	Polyamide 6,6	7069	12640	0.8195	0.52 (246–298, 0–1960)
PEA	Poly(ethyl acrylate)	8308	10040	0.8773	0.88 (37–217, 0–1960)
PEMA	Poly(ethyl methacrylate)	9870	10190	0.8710	0.81 (113–161, 0–1960)
TMPC	Tetramethyl bisphenol-A PC	8192	11540	0.8794	0.96 (218–290, 0–1600)
HFPC	Hexafluoro bisphenol-A PC	8510	10550	0.6317	0.66 (159–280, 0–2000)
BCPC	Bisphenol chloral PC	9878	12190	0.6975	0.47 (155–284, 0–2000)
PECH	Poly(epichlorohydrin)	9131	11370	0.7343	0.31 (60–140, 0–2000)
PCL	Poly(ε-caprolactone)	7845	10870	0.9173	0.30 (100–148, 0–2000)
PVC	Poly(vinyl chloride)	8495	12350	0.7230	0.42 (100–150, 0–2000)
Random copolymers					
EP50	Ethylene/propylene 50 %	5720	12220	1.2227	1.58 (140–250, 0–625)
EVAc18	Ethylene/vinyl acetate 18 %	7056	10630	1.1341	0.47 (112–219, 0–1765)
EVAc25	Ethylene/vinyl acetate 25 %	6978	10440	1.1040	0.56 (94–233, 0–1765)
EVAc28	Ethylene/vinyl acetate 28 %	7472	10310	1.0949	0.67 (94–233, 0–1765)
EVAc40	Ethylene/vinyl acetate 40 %	7539	10360	1.0446	0.54 (75–235, 0–1765)
SAN3	Styrene/acrylonitrile 2.7 %	7642	12070	0.9416	0.81 (105–266, 0–2000)
SAN6	Styrene/acrylonitrile 5.7 %	8238	11490	0.9352	0.70 (96–267, 0–2000)
SAN15	Styrene/acrylonitrile 15.3 %	7792	12360	0.9299	0.50 (132–262, 0–2000)
SAN18	Styrene/acrylonitrile 18 %	7853	12380	0.9255	0.42 (104–255, 0–2000)
SAN40	Styrene/acrylonitrile 40 %	8118	12900	0.9124	0.56 (100–255, 0–2000)
SAN70	Styrene/acrylonitrile 70 %	8747	13790	0.8906	0.36 (100–270, 0–2000)
SMMA20	Styrene/methyl methacrylate 20 %	7640	11800	0.9186	0.42 (110–270, 0–2000)
SMMA60	Styrene/methyl methacrylate 60 %	7911	11780	0.8739	0.55 (110–270, 0–2000)

Fig. 2.1 Frozen fraction of free volume (*FF*) versus glass transition temperature (T_g). *Triangles*: values for different polymers at ambient pressures (Simha and Wilson 1973). *Squares*: PS data at pressures *P*: 0–400 MPa (Data: Rehage 1980; calculations Utracki and Simha 1997)
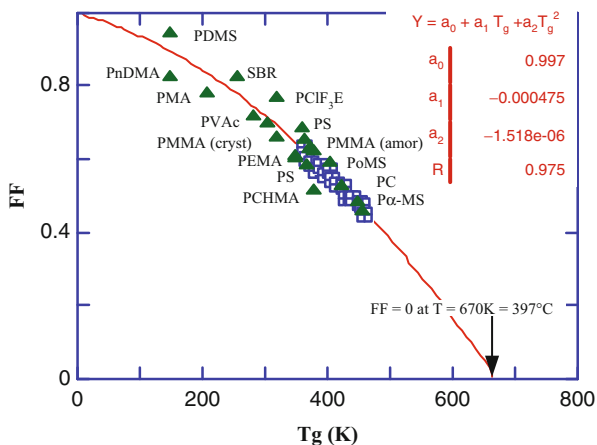
equation as a 4-parameter (V_o, α, B_o, B_1) representation of the *PVT* behavior. About a century later, the H-H empirical PVT relation was proposed (Hartmann and Haque 1985), which is a three-parameter empirical EoS approach, that is, it has the form of a dimensionless EoS connecting $\tilde{P}\tilde{V}\tilde{T}$, with the usual definition of $\tilde{P} \equiv P/P^*$, $\tilde{V} \equiv V/V^*$, $\tilde{T} \equiv T/T^*$ and by using characteristic state values (P^*, V^*, and T^*) for a given polymer. The H-H relation is noteworthy due to the simplicity of its form and respectable agreement with the experimental data:

$$\tilde{P}\tilde{V}^5 = \tilde{T}^{3/2} - \ln\tilde{V}$$
$$\text{with:} \quad V^* = V_o; \quad P^* = B_o; \quad T^* = T_o \tag{2.23}$$

In Eq. 2.23, the characteristic pressure-reducing parameter, B_o, has been identified as the isothermal bulk modulus extrapolated to $T = 0$ and $P = 0$. Subsequently, Sanchez et al. (Sanchez 1993; Sanchez and Cho 1995) used a temperature-pressure (T-P) superposition which allows for the compressional strain, $\ln(V/V_o)$, to be written as a function of the reduced pressure, $\Delta P = (P - P_o)/B_o$, following the same general curve independent of T (here, B is again the bulk modulus, and B_o is its isothermal value evaluated at a reference pressure, P_o). The Sanchez-Cho (S-C) relation seems to provide the most faithful reproduction of experimental data among empirical three-parameter models. The S-C relation can be summarized as

$$\tilde{V} = \frac{1}{1-\tilde{T}}\exp\left[\frac{\omega}{(1-\omega)B_1}\left\{1 - \left(1 + \frac{B_1\tilde{P}}{\omega}\exp(9\tilde{T})\right)^{1-\omega}\right\}\right] \tag{2.24}$$
$$\text{with:} \quad B_1 = 10.2; \quad \omega = 0.9$$

the corresponding P^*, V^*, and T^* are tabulated for various polymers in Table 2.5. An excellent agreement with experimental data was achieved, indicating validity of the relation.

2.3.2 Solid–Liquid and Vapor–Liquid Equilibria

For a single component, the phase diagram provides a map of the solid, liquid, and vapor states, as well as their coexistence regions. It is customary to construct such single-component phase diagrams as log-log plots of P versus V relation at constant T. Fig. 2.2 shows a phase diagram of argon. Dividing the three variables by the corresponding reducing parameters, the dependence can be cast in a general plot of reduced pressure versus reduced volume, $\tilde{P}$ versus $\tilde{V}$, at constant reduced temperature, $\tilde{T}$. For simple low molecular weight liquids, the van der Waals equation, Eq. 2.13, provides a reasonable description.

Guggenheim further demonstrated that near the critical point the coexistence curve of liquid and vapor follows a simple proportionality:

$$\tilde{T} - 1 \propto |(1 - \tilde{\rho})^3|/3 \tag{2.25}$$

This dependence is shown in Fig. 2.3 as a solid line – the dashed line represents the van der Waals parabolic prediction.

Table 2.5 Characteristic parameters (P^*, V^*, and T^*) for the Sanchez-Cho empirical EoS model for various polymers (Cho 1999)

Polymer	(Monomer or description)	P^* (bar)	T^* (K)	V^* (mL/g)
PDMS	Dimethyl siloxane	62129	1375.1	0.8071
PS	Styrene	78676	2277.2	0.8165
PoMS	o-Methylstyrene	77721	2380.6	0.8368
PMMA	Methyl methacrylate	98730	2184.2	0.7139
PBMA	rc-Butyl methacrylate	90253	1855.9	0.7963
PCHMA	Cyclohexyl methacrylate	85151	2195.1	0.7710
PEA	Ethyl acrylate	91318	1747.4	0.7398
PEMA	Ethyl methacrylate	112570	1771.2	0.7332
PMA	Methyl acrylate	106239	1829.0	0.7121
PVAC	Vinyl acetate	103999	1696.9	0.6918
LPE	Linear polyethylene (PE)	99435	1655.0	0.9491
BPE	Branched-PE	86307	1751.9	0.9723
LDPE-A	Low-density PE-A	82145	1865.4	0.9852
LDPE-B	Low-density PE-B	79838	1923.8	0.9937
LDPE-C	Low-density PE-C	82253	1880.5	0.9869
PBD	Butadiene	94432	1633.8	0.9115
PBD8	Butadiene with 8 % 1,2 content	91363	1798.6	0.9308
PBD24	Butadiene with 24 % 1,2 content	87080	1819.0	0.9359
PBD40	Butadiene with 40 % 1,2 content	83520	1842.9	0.9357
PBD50	Butadiene with 50 % 1,2 content	77573	1892.0	0.9408
PBD87	Butadiene with 87 % 1,2 content	72418	1905.6	0.9498
PB	1-Butene	68911	1924.1	0.9854
PAr	Arylate	115573	2243.9	0.6839
PCL	Caprolactone	95301	1849.0	0.7671
PC	Carbonate (PC)	121061	2070.3	0.6871
BCPC	Bisphenol chloral PC	99313	2249.1	0.5971
HFPC	Hexafluoro bisphenol-A PC	101731	1788.2	0.5264
TMPC	Tetramethyl bisphenol-A PC	105730	1908.0	0.7261
PET	Ethylene terephthalate	152788	2022.2	0.6199
PIB	Isobutylene	70453	2130.2	0.9382
PI8	Isoprene with 8 % 3,4 content	76696	1921.0	0.9453
PI14	Isoprene with 14 % 3,4 content	82199	1911.3	0.9366
PI41	Isoprene with 41 % 3,4 content	81123	1912.7	0.9370
PI56	Isoprene with 56 % 3,4 content	86001	1854.5	0.9330
i-PP	Isotactic polypropylene	61181	1991.5	1.0116
a-PP	Atactic polypropylene	62028	1776.2	0.9690
Phenoxy	Phenoxy	127281	2103.4	0.7242
PSO	Sulfone	132864	2232.2	0.6655
PEO	Ethylene oxide	108054	1789.1	0.7441
PVME	Vinyl methyl ether	92705	1861.3	0.8187

(*continued*)

Table 2.5 (continued)

Polymer	(Monomer or description)	P^* (bar)	T^* (K)	V^* (mL/g)
PEEK	Ether ether ketone	143355	2126.5	0.6395
PTFE	Tetrafluoroethylene	97575	1400.7	0.3638
PTHF	Tetrahydrofuran	81602	1843.0	0.8561
PMP	4-Methyl-i-pentene	64525	1885.0	1.0089
PA6	Amide 6	57184	3140.3	0.7130
PA66	Amide 66	83919	2195.2	0.6887
PECH6	Epichlorohydrine	88993	2068.9	0.6269
PVC	Vinyl chloride	75512	2395.4	0.6252
PPO	Phenylene oxide	117769	1810.4	0.7181
EP50	Ethylene/propylene 50 %	64210	2384.7	1.0582
EVAc18	Ethylene/vinyl acetate 18 %	81075	1878.9	0.9585
EVAc25	Ethylene/vinyl acetate 25 %	79575	1848.3	0.9338
EVAc28	Ethylene/vinyl acetate 28 %	86221	1812.5	0.9241
EVAc40	Ethylene/vinyl acetate 40 %	84419	1856.1	0.8864
SAN3	Styrene/acrylonitrile 2.7 %	78785	2185.7	0.8030
SAN6	Styrene/acrylonitrile 5.7 %	88968	2010.7	0.7896
SAN15	Styrene/acrylonitrile 15.3 %	86020	2170.4	0.7860
SAN18	Styrene/acrylonitrile 18 %	84956	2208.4	0.7854
SAN40	Styrene/acrylonitrile 40 %	77726	2435.2	0.7853
SAN70	Styrene/acrylonitrile 70 %	91770	2546.6	0.7616
SMMA20	Styrene/methyl methacrylate 20 %	85313	2105.6	0.7789
SMMA60	Styrene/methyl methacrylate 60 %	88589	2099.5	0.7408

2.3.3 Gibbs Phase Rule

The state variables are those intensive or extensive quantities that describe a system, for example, by means of the "equation of state." The total number of variables required to describe a system with i number of components is $i+2$ (cf. Eq. 2.11, i accounts for the i composition variables, N_i, and 2 accounts for, e.g., P and T). For the discussions of phase diagrams, it is important to know how many of the state variables can be varied without going through a phase transition. For a closed system with i number of components and Π number of phases, the number of intensive variables (cf. thermodynamic degrees of freedom, #f) is given by the "Gibbs phase rule":

$$\#f = i + 2 - \Pi \tag{2.26}$$

For example, for a phase equilibrium of a two-component blend ($i = 2$), in order to follow the two-phase ($\Pi = 2$) coexistence, Eq. 2.26 predicts #$f = 2$, i.e., two
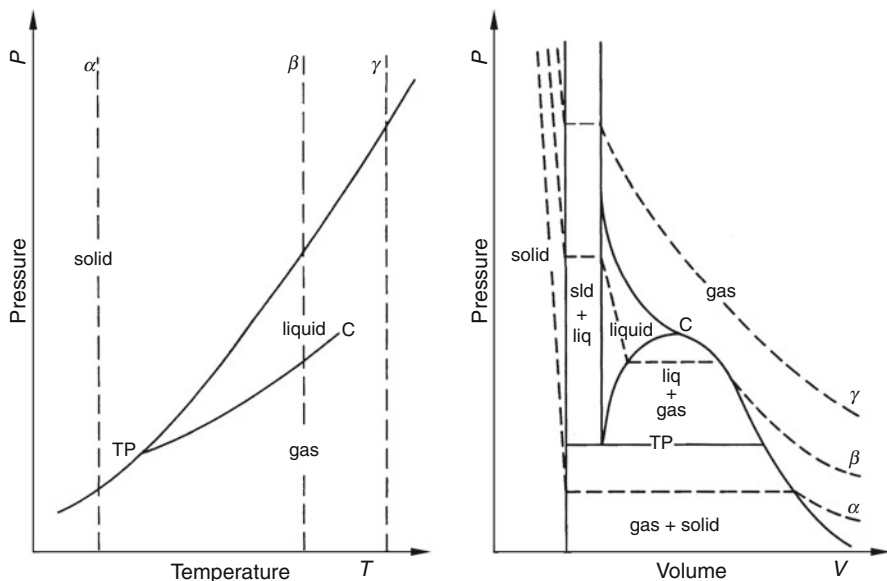
Fig. 2.2 The van der Waals-type phase diagram in T-P (*left*) and P-V (*right*) axes. *C* is the critical point; *TP* is the triple point of the coexistence between solid, liquid, and vapor (TP is a line in the P-V phase diagram). *Solid lines* are the phase boundaries, whereas the *dashed lines* are isotherms at different temperatures (α below T_C, β slightly below T_C, and γ above T_C). The liquid–gas, solid–liquid, and solid-vapor coexistence regions are also shown (After Flowers and Mendoza 1970)
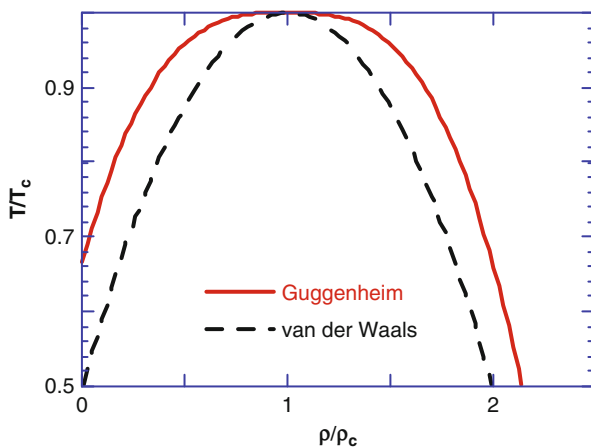
Fig. 2.3 The liquid–vapor coexistence curves, $\tilde{T}$ versus $\tilde{\rho}$, as predicted by Guggenheim (*solid line*) and by van der Waals

variables must be simultaneously changed (e.g., T and composition), whereas, for the same system within the single-phase ($\Pi = 1$) miscible region, three variables are available (e.g., composition, T and P). For a discussion based on general phase equilibria conditions, see Sect. 1.2.3 (Klenin 1999).

2.4 Polymeric Mixtures

Polymeric mixtures are conveniently divided into *polymer solutions* (containing one or more low molecular weight liquids, termed as solvent) and *polymer blends* (containing only macromolecular species). They will be briefly described in the following Sects. 2.5.1 and 2.5.2, respectively. More detailed discussion of the theoretical foundations is given in Sect. 2.6.

2.4.1 Polymer Solutions

In contrast to the mixtures of low molecular weight species, where composition is customarily expressed as a concentration or mole fraction, x_i, in the case of polymer solutions, composition must be given as volume fraction, ϕ_i, to correctly account for the much larger space (volume) occupied by a given concentration of a polymer, cf. for a polymer with degree of polymerization n, $\phi_i \sim x_i n$. For dilute solutions, the wt/vol concentration, c, can be also used accounting for weight of polymer per volume of solvent (e.g., in g/100 mL). As in mixtures of small molecules, also in polymer solutions, the solubility originates mainly from entropic reasons (Yamakawa 1971).

Traditionally, solutions have been used in polymer characterization, e.g., to measure its molecular weight averages (number, weight, and z-averaged molecular weight, M_n, M_w, and M_z), or the size of its macromolecular coil. The latter may be expressed as the unperturbed end-to-end distance (R_o), or through the related radius of gyration ($R_{g,\,o}$), viz.,

$$\langle R_o^2 \rangle = 6 \left\langle R_{g,o}^2 \right\rangle = \sigma^2 n l^2 \frac{1 + \langle \cos\theta \rangle}{1 - \langle \cos\theta \rangle} \tag{2.27}$$

In Eq. 2.31, σ is the steric hindrance factor of the macromolecular chain, n is the number of statistical segments (each statistical segment having a length l and the bond angle between two consecutive segments is equal to θ).

Solutions can also be used to measure of the thermodynamic interactions between polymer segments and solvent molecules. These intermolecular interactions are best discussed in terms of the virial coefficients, A_i. The change of the solvent chemical potential upon dissolution of a polymer is given by

$$\Delta\mu = \left(\frac{\partial G_m}{\partial N_2}\right)_{T,P,N_1} = RT \ \ln a_o = -V_1 \Pi \tag{2.28}$$

where a_o is the activity and Π the osmotic pressure, usually expressed as

$$\frac{\Pi}{c} = RT\left(\frac{1}{M_n} + A_2 c + A_3 c^2 + \dots\right) \quad \text{with} \quad A_2 = \frac{4\pi^{3/2} N_A}{M_n^2} \left\langle R_g^2 \right\rangle^{3/2} \Psi(z) \tag{2.29}$$

The second virial coefficient in Eq. 2.29 contains two functionals that depend on the binary interactions, the perturbed radius of gyration R_g, and the function $\Psi(z)$, which is

$$\Psi = \frac{1 - \exp(-5.73z)}{5.73} \quad \text{with} \quad z = \frac{4}{3^{3/2}} C_M \left(\frac{1}{2} - \chi \right) M_n^{1/2} \qquad (2.30)$$

As z increases from 0 (*theta conditions*) to 2 (*good solvent*), the Ψ function also increases from 0 to about 0.2. For simplicity, dilute solutions are used to avoid the need for determination of higher-order virial coefficients. In this case, A_2 provides a direct measure of the intermolecular interactions in polymer solutions and can be directly related to the respective Flory-Huggins parameter (χ, *vide infra*, Sect. 2.6.1.1). However, since $A_3 \propto A_2 M_n$, Eq. 2.29 can be written as

$$\left(\frac{\Pi M_n}{RT} \right)^{1/2} = 1 + \frac{M_n A_2}{2} \qquad (2.31)$$

In another approach, light scattering also makes it possible to determine A_2, viz.,

$$\frac{Kc}{R_\theta} = \frac{1}{M_w \ \langle P_1(\theta) \rangle} + 2A_2'c + 3A_3'c^2 + \dots \qquad (2.32)$$

where K is an experimental quantity ($K = 4\pi^2(dn/dc)^2\eta_o^2(1+\cos^2\theta)/N_A\lambda^4$), c is the concentration of the solution, $R_\Theta(c)$ is the Rayleigh ratio, and $\langle P_1(\theta) \rangle$ is the intramolecular interference factor, i.e., the angular dependence of the scattered light. Equation 2.32 provides the polymer's molecular weight, M_w, from the dilute solution limit where all higher-order terms of the virial expansion become negligible: $\lim_{c \to 0, \ \theta \to 0}(Kc/R_\theta) = 1/M_w$. Similar to the osmotic pressure (Eq. 2.29), light scattering (Eq. 2.32) also allows to calculate virial coefficients, with the second virial coefficient again being related to the solvent-solute interactions.

The thermodynamic interactions and the size of polymer coil also enter dependencies that describe the transport behavior of polymer solutions, viz., viscosity, diffusion, sedimentation, etc. To complete this short summary, the viscosity relations should be mentioned. Defining η as the solution viscosity and η_o as the solvent viscosity, the following, relative (η_r), specific (η_{sp}), and intrinsic ($[\eta]$) viscosities, are typically expressed as

$$
\begin{aligned}
\eta_r \quad &\equiv \quad \eta/\eta_o \\
\eta_{sp} \quad &\equiv \quad (\eta - \eta_o)/\eta_o = \eta_r - 1 \\
[\eta] \quad &\equiv \quad \lim_{c \to 0} \left(\eta_{sp}/c \right) = \lim_{c \to 0} \frac{\ln \eta_r}{c} \\
\eta_{sp}/c \quad &\cong \quad [\eta] + k_H[\eta]^2 c \qquad \text{(Huggins equation)}
\end{aligned}
\qquad (2.33)
$$

which can also be fitted to a virial-type expansion (e.g., $\eta_r = 1 + [\eta]c + k'([\eta]\,c)^2 + \cdots$). Many relations have been proposed connecting the intrinsic viscosity, $[\eta]$, to the polymer/solvent interaction parameters. One of the better known is that credited to Inagaki et al. (1966):

$$[\eta]^{4/5}/M_v^{2/5} = 0.786K^{4/5} + 0.454K^{2/15}\Phi_o^{2/3}B^{2/3}M_v^{1/3} \qquad (2.34)$$

where $K = 2.5 \times 10^{23}[\langle R_o^2 \rangle/M_v]^{3/2}$ and $B = (2\rho_s^2/V_o)(0.5 - \chi)$, with ρ_s and V_o being the segmental density and the molar volume of the solvent.

It is worth noting that the three methods of evaluation of the solution behavior, osmometry, light scattering, and intrinsic viscosity, provide different molecular weight averages, respectively, number average, M_n, weight average M_w, and "viscosity" average, M_v. Knowing at least two of them, one can also estimate the width of the molecular weight distribution through polydispersity factors, e.g., through M_w/M_n.

2.4.2 Polymer Blends: Definitions and Miscibility

In contrast to solutions, polymer blends are mostly immiscible. As shown in Appendix 2 by Krause and Goh, over 1,000 cases of miscibility have been found; however, these are so infrequent and poorly defined that one may consider them as exceptions to the general rule of polymer/polymer immiscibility.

While the thermodynamic definition of miscibility is unambiguous (see Table 2.6), there is a significant amount of discussion as to the methods of miscibility detection and the size of heterogeneity in miscible blends.

The methods of miscibility detection (sometimes wrongly labeled as "compatibility" experiments) will be discussed later in this chapter. Opacity (turbidity) can provide limited only information on miscibility – since light scattering manifests when the size of heterogeneity becomes larger than 100 nm and the difference in refractive index is greater than about 0.01; further complications arise when one or both polymer phases are semicrystalline. The most widely used tool for the "detection of miscibility" relates to measurement of the glass transition temperature, T_g. There is a widely accepted belief that blends which display a single T_g are miscible. The glass transition temperature is relatively simple to measure, but there are inherent uncertainties of the measurements that need to be carefully examined (Utracki 1989). For example, T_g is insensitive when the amount of one component is less than about 10 wt% or when the component T_g's occur at similar temperatures. On the latter, the T_g method should not be used for blends containing polymers whose T_g's differ by less than 10 °C from each other.

Along these lines, it has been shown, first by Schultz and Young (1980) and then by many others, that T_g is not sensitive to the thermodynamic miscibility of the components, but rather to the degree of dispersion. For example, in solvent-mixed PS/PMMA blends that were not allowed to phase separate, a single T_g has been detected, but when the specimens were annealed, double peaks were observed. In another example, solvent cast blends of PVC with caprolactone-grafted lignin showed a single T_g, while the measured domain size ranged between 10 and 30 nm, indicating immiscibility (De Oliveira and Glasser 1994).

Table 2.6 Terms related to polymer blend miscibility (see also ▶ Chap. 1, "Polymer Blends: Introduction")

Miscible polymer blend: polymer blend, homogenous down to the molecular level, in which the domain size is comparable to the macromolecular dimension; associated with negative value of the free energy of mixing, $\Delta G_m \simeq \Delta H_m \leq 0$, and within the phase stability condition $\partial^2 \Delta G_{ml}/\partial^2 \phi > 0$

Immiscible blends: polymer blends whose free energy increases upon mixing, i.e., $\Delta G_m \simeq \Delta H_m > 0$

Polymer alloy: immiscible but compatibilized polymer blend; implies a modified interphase and, thus, morphology

Interphase: a nominal third phase in binary polymer alloys, engendered by interdiffusion or compatibilization at the interfaces between the two polymer domains. The interphase thickness Δl varies between 1 and 60 nm depending on polymers' miscibility and compatibilization

Compatibilization: process of modification of the interphase in immiscible polymer blends, resulting in reduction of the interfacial energy, development, and stabilization of a desired morphology, leading to the creation of a polymer alloy with enhanced performance

Fig. 2.4 The glass transition temperature versus composition for PEK/N-TPI blends. The two *black squares*, connected by a *straight line*, are the T_g's of the two polymers; open circles are data for blends prepared at 455 °C; *solid circles* are for the same blends prepared at 400 °C. The lines are only guides to the eye (Data from Sauer et al. 1996)
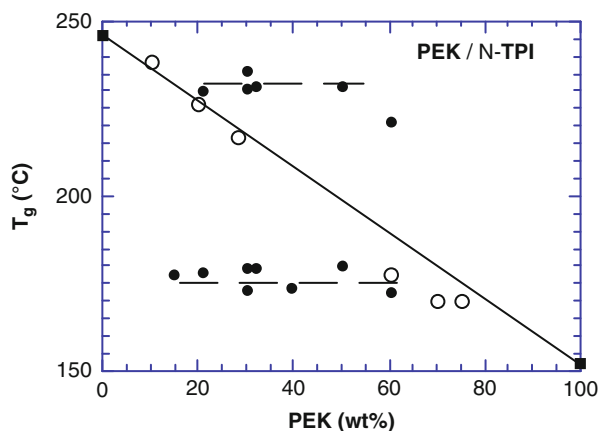
For PEK/PI blends, the T_g's of the neat components are separated by about 90 °C; however, depending on the chemical nature of the components, as well as on the blend composition and blending conditions, three types of the glass transition behavior were observed: Specifically, three T_g behaviors for PEK blended with N-TPI were obtained, as shown in Fig. 2.4 after (Sauer et al. 1996) (N-TPI stands for: "new thermoplastic polyimide," obtained from condensation of 4,4-bis (3-aminophenoxy)biphenyl with pyromellitic dianhydride). At "low" blending temperature, of 400 °C, the mixture showed two T_g's, but when the same polymers were blended at $T = 440$ °C, the blend showed a single T_g; interestingly, when the two polymers were blended at intermediate temperatures, 400 °C$< T <$440 °C, a single, broad, overlapping T_g was obtained. Clearly, the glass transition behavior reflected different degrees of dispersion for the PEK/PI system, rather than phase miscibility (the degradation temperature is 410 °C). Finally, it is frequent that blends of rubber-containing copolymers (such as SBS or ABS type), e.g., PPE/SBS,

PC/ABS, or PPE/MBS, are identified as miscible, on the basis of T_g measurements. Obviously, this T_g measurement probes the mixing of the viscoelastic components of the blend, effectively neglecting the elastomeric (rubber) domains. The elastomeric domains remain immiscible in the blends, much like they were in the copolymers, and may show (or not, depending on their content) another T_g at much lower temperatures.

In any liquid, either single or multicomponent one, there is a significant amount of heterogeneity, usually expressed by density/composition fluctuation functions. Thus, along the above discussion, it is justified to ask two questions:

1. What is the maximum size, d_d, of heterogeneity in a polymer blend that fulfills the conditions of the thermodynamic miscibility (viz., $\Delta G_m \leq 0$ and $\partial^2 \Delta G_m / \partial^2 \phi \geq 0$)?
2. At what level of heterogeneity T_g is a monotonic function of composition?

Various answers have been given to the first question. On the basis of the size of the cooperative segmental motion required at T_g, it was estimated that d_d is 2–3 nm (Boyer 1966; Warfield and Hartmann 1980). The local segmental dynamics of a flexible polymer chain was found to be affected by the neighboring chains lying within 2–7 nm (Callaghan and Paul 1994a, b). Other authors consider that miscibility is achieved when the heterogeneity diameter becomes comparable to the unperturbed radius of gyration of the macromolecule, thus $d_d = \langle R_{g,\,o}^2 \rangle^{1/2}$ typically 3–10 nm (Silberberg and Kuhn 1952; Wolf 1980, 1984). Many others' estimates fall within these limits (e.g., Kaplan 1976; Bair and Warren 1980; Cowie 1989). Thus, it seems that the thermodynamic miscibility is associated with a size of compositional heterogeneity d_d smaller than about 10 nm, cf. smaller than the polymer size, an intuitively expected answer for intimate mixing of chain-type objects.

The answer to the second question has been given as well. Depending on the chemical nature of the system and its morphology, double peak of T_g has been reported to appear for domain sizes d_d as small as 15–20 nm (Frisch et al. 1982; Utracki 1989; De Oliveira and Glasser 1994).

From a fundamental point of view, the glass transition reflects a change in the molecular mobility upon cooling and can be viewed as associated with "freezing" of a portion of the free volume. However, the frozen fraction depends on the absolute value of T_g – as the T_g absolute value increases, more free volume becomes accessible to the thermal motion in the glassy state. Judging by data presented in Fig. 2.1, for organic macromolecules, the fundamental mechanism of the glass transition is not expected to be valid for T_g larger than about 400 °C. In short, even under the most favorable conditions, T_g should be unable to discriminate between the presence and absence of thermodynamic miscibility, i.e., when a system is miscible, a single T_g will indeed be found, but also a single T_g will also be manifested for immiscible systems having finely dispersed phases. In many cases, T_g may be able to detect the "technological miscibility," i.e., to identify systems that are so well homogenized that the phase domains will not be affected by the processing conditions. The method may be used as a pragmatic scan for industrially useful blends, or evaluation of a compatibilization scheme.

It is noteworthy that "homogeneity at fairly fine level is necessary for optimum performance, but some degree of microheterogeneity is usually desirable to preserve the individual properties of respective polymer components" (Hess et al. 1993). Note that nearly all commercial polymer blends (with the notable exception of the PVDF/PMMA blend) are immiscible. One tends to study miscibility not so much as to develop single-phase commercial blends, but mainly to design better compatibilizers and compatibilization strategies.

Since the standard test methods for detecting miscibility, viz., T_g measurements, microscopy, small-angle X-ray scattering, etc., are limited to $d_d \geq 15$ nm, other methods should be used for studies of true thermodynamic miscibility. Such approaches mostly capitalize on advanced scattering methods, such as high-resolution or multidimensional nuclear magnetic resonance (NMR) techniques, spin-diffusion NMR measurements, non-radiative energy transfer, excimer fluorescence, thermally stimulated depolarization current, small-angle neutron scattering (SANS), Fourier transfer infrared spectroscopy (FTIR), etc. Even simple NMR measurement of spin–lattice relaxation times, T_1, is capable to distinguish down to domain sizes of 2–3 nm. The method can be used for either molten or solidified mixture specimens. For example, these methods produced the following results:

a-PVC/PMMA: Homogenous at 20 nm, but heterogeneous at 2 nm. After deuteration of PMMA, the miscibility extended down to 1–2 nm.

PS/PVME, PnBMA/PS (2 mol% –OH): Homogenous at 20 nm.

SAN/PMMA: Homogenous at 20 nm, but heterogeneous at 2–15 nm (McBrierty et al. 1978).

a-PET/PC, a-PVDF/PMMA, a-PCL/PVC: Homogenous at 2 nm (Douglass and McBrierty 1978; Douglass 1979).

PS/PPE: Only about 30 wt% blend components participate in intimate interactions on the scale of less than 2 nm. The rest show the same nuclear resonance pattern as the one recorded for the two homopolymers (Stejskal et al. 1981; Takahashi et al. 1990).

2.5 Theories of Liquid Mixtures

2.5.1 Lattice, Cell, and Hole Theories

The statistical mechanics methods that use a pseudocrystalline model of regularly placed elements on a "lattice" are known as lattice theories. Many theories, known under the names of free volume, cell-hole, tunnel, Monte Carlo, or molecular dynamics belong here. Of these, only two will be mentioned. The first, and the best known, was originally developed by Huggins (1941) and, independently, by Flory (1941), then extended by many authors (Utracki 1962; Koningsveld 1967). The second is the cell-hole Simha and Somcynsky (1969) theory that has been incessantly evolving during the intervening years. The theory makes it possible to interpret and predict different material's behavior in a wide range of

states and independent variables, viz., gases, low molecular weight organic liquids, metals, and polymers in a glassy or molten state, to determine miscibility of gases or liquids in polymers, to compute the phase diagrams of polymer blends, etc.

2.5.1.1 Flory-Huggins Theory

For binary systems that contain two components denoted as i (i.e., $i=1$ or 2 and, traditionally, for polymer solutions the subscript 1 indicates solvent, and 2 polymer) the Flory-Huggins, FH, relation has been expressed in several equivalent forms:

$$\frac{\Delta G_m}{RT} = \frac{\phi_1}{V_1}\ln \phi_1 + \frac{\phi_2}{V_2}\ln \phi_2 + \chi'_{12}\phi_1\phi_2 \quad \left[\text{with} \quad \chi'_{12} \equiv \chi_{12}/V_{ref}\right]$$

$$\Delta G_m = RTV \left[\frac{\phi_1}{V_1}\ln \phi_1 + \frac{\phi_2}{V_2}\ln \phi_2\right] + B\phi_1\phi_2 \quad \left[\text{with} \quad B \equiv \chi_{12}RT\left(V/V_{ref}\right)\right]$$

$$(2.35)$$

In Eq. 2.35, ϕ_i is the volume fraction and V_i is the molar volume of component "i." The first two logarithmic terms give the combinatorial entropy of mixing, which are by definition of ϕ negative and always promote mixing, while the third term is the enthalpy of mixing. For polymer blends V_i are both large; thus the combinatorial entropy becomes vanishingly small, and, therefore, the miscibility or immiscibility of the system is determined by the value of the last term, $\chi'_{12}\phi_1\phi_2$. Using $\phi_2 + \phi_1 = 1$ and the monomeric volume as a reference volume, the free energy of mixing ΔG_m, expressed now in a per monomer basis, can be rewritten as

$$\frac{\Delta G_m}{kT} = \frac{\phi}{N_1}\ln \phi + \frac{1-\phi}{N_2}\ln(1-\phi) + \chi'_{12}\phi(1-\phi) \qquad (2.35a)$$

where N_i is the degree of polymerization of the i component ($N_i = 1$ for i being a solvent). For the purposes of determining phase behavior or miscibility, it does not matter if one uses the change in free energy of mixing expressed per unit volume, per mole of lattice sites, or per monomeric volume. Due to the assumption of the FH model, in its unaltered original form, the model predicts UCST only behavior (Fig. 2.5).

Applying to Eq. 2.35 the critical point conditions (the critical point is located on the spinodal, thus, $\partial^2\Delta G_m/\partial^2\phi = 0$, and is the extremum of the spinodal curve, thus, $\partial^3\Delta G_m/\partial^3\phi = 0$) and treating the so-called binary interaction parameter, χ_{12} or B, as composition independent, the critical conditions for phase separation can be expressed as

$$\chi'_{12,cr} = \frac{1}{2}\left(\frac{1}{\sqrt{V_1}} + \frac{1}{\sqrt{V_2}}\right)^2 = \frac{1}{2}\left(\frac{1}{\sqrt{N_1}} + \frac{1}{\sqrt{N_2}}\right)^2$$

$$B_{cr} = \frac{RTV}{2}\left(\frac{1}{\sqrt{V_1}} + \frac{1}{\sqrt{V_2}}\right)^2 = \frac{RT}{2}\left(\frac{1}{\sqrt{N_1}} + \frac{1}{\sqrt{N_2}}\right)^2$$

$$(2.36)$$
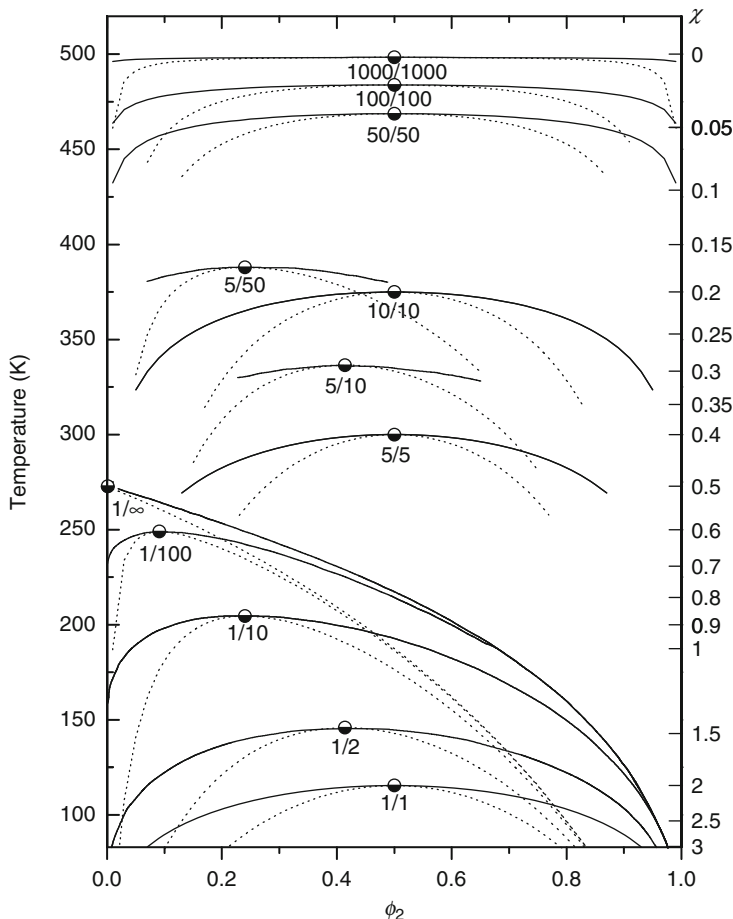
Fig. 2.5 Phase diagrams predicted by the Flory-Huggins (*FH*) model for various ratios of molar sizes (N_1/N_2, as indicated): *solid lines* are *binodals* and *dashed lines* are *spinodals*; for all phase diagrams, a generic $\chi_{12} = -0.6 + 300/T$ was assumed; see right-side y-axis. Three groups of phase diagrams are distinguished: the group in the *bottom* corresponds to solutions, with component 1 being the solvent ($N_1 = 1$); the *middle* group corresponds to mixtures of oligomeric molecules; and only for the *top* three phase diagrams correspond to mixtures that resemble polymer blends ($N_1 N_2 \gg 1$). All spinodals, UCST critical points, and the binodals of the symmetric, $N_1 = N_2$, mixtures were analytically calculated from the derivatives of Eq. 2.35 (critical points from Eq. 2.36), and the rest of the binodals are from numerical solutions

Equation 2.36 gives the miscibility conditions for systems with species of different molecular weight. The relations are rather accurate, as they are markedly insensitive to the FH assumptions and approximations (Fig. 2.6). Three special cases can be distinguished:

1. Small molecule mixtures ($V_1 \simeq V_2$ or $N_1 = N_2 \approx 1$) are miscible when $\chi_{12} < 2$, viz., $\chi_{12} < \chi_{12, \, cr}$ and from Eq. 2.36 $\chi_{12,cr} = 2$ (for $N_1 = N_2 = 1$).

Fig. 2.6 Critical temperatures, both UCST and LCST, as a function of polymer M_w, for polystyrene solutions in methyl-cyclohexane. In the inset, the critical temperatures are fitted to Eqs. 2.36 and 2.39 (*vide infra*) showing an excellent agreement over the whole ensemble of data (Data from Wohlfarth (2008); collected from 71 systems, from 18 independent studies published from 1963 to 2002)

In the inset:

$$\chi_c = 1 + \frac{1}{\sqrt{N}} + \frac{1}{2N}$$

assuming $T_c = B/(\chi_c - A)$

yields : $\chi = -0.015 + \frac{177.29}{T}$

fitted as :
$\chi = A + B/T$ $A = -0.015 \pm 0.0002$
$(R^2 = 0.98341)$ $B = 177.29 \pm 0.05$

PS/methyl-cyclohexane
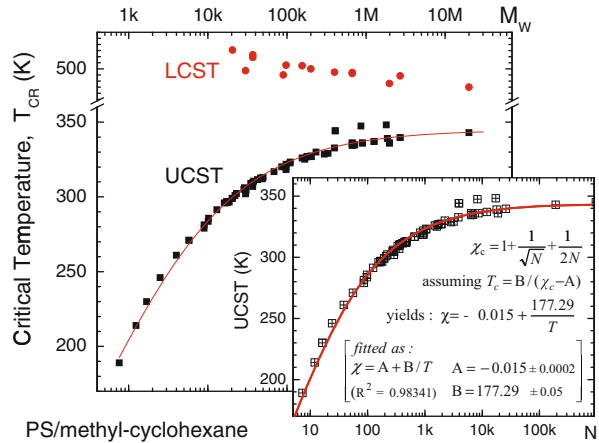
2. Polymer solutions ($V_1 \gg V_2$ or $N_2 \gg N_2 \approx 1$) are miscible when $\chi_{12} < 1/2$, viz., $\chi_{12} < \chi_{12,cr}$ and from Eq. 2.36 $\chi_{12,cr} = 1/2 + 1/\sqrt{N} + 1/2N \approx 1/2$ (for $N = N_2$).
3. Polymer blends (V_1 and $V_2 \gg 1$, or $N_1 \approx N_2 \gg 1$) are miscible when $\chi_{12} < 0$, viz., $\chi_{12} < \chi_{12,cr}$ and from Eq. 2.36 $\chi_{12,cr} = 2/N \approx 0$ (for $N = N_1 = N_2$).

Originally, after Hildebrand, the parameter χ_{12} was assumed to have a single, characteristic value for a given mixture. However, it was soon found that even for polymer solutions χ_{12} is a complex function of many independent variables, viz., concentration, temperature, pressure, molecular weight, molecular weight distribution, etc. For calculating isobaric phase diagram, the influence of the first two variables should be expressed as (Koningsveld 1967) $\chi_{12} = \sum_{j=0}^{j \leq 2} a_j \phi_2^j$ with $a_j = \sum_{k=1}^{m \leq 2} a_{jk} T^k$. Thus, at constant pressure, it takes nine parameters to describe variation of χ_{12} with concentration and temperature.

In a first approximation, the temperature dependence of χ_{12} can be simplified by keeping only one temperature term, i.e., $\chi_{12} = A + B/T$, which for polymer solutions most often gives a rather good estimation. For example, in Fig. 2.6, we fitted tabulated UCST's PS/methyl-cyclohexane solutions from 71 different PS M_w's from 22 different studies, obtaining $\chi_{12} = -0.015 + 117.29/T$ with a pretty good accuracy across multiple works and experiments. For polymer blends and for less demanding thermodynamic calculations, the concentration dependence must also be included, and most often χ_{12} is simplified by keeping one composition term and one temperature term. Thus, to express conditions of miscibility in PS blends with poly(styrene-*co*-4-bromostyrene), the binary interaction parameter per mer of styrene (when T within the 440–500 K region) was expressed as $\chi_{12}/N = -0.02208 + 20/T - 0.01482\phi_2$ (Strobl et al. 1986). Similarly, for PS blends, the following relation was proposed (Ahn et al. 1997a, b): $B_{12}(\phi_2, T) = B_0 + B_1\phi_2 + B_2 T/1{,}000$ where experimental/fitted or calculated values can be used for the B_i parameters. However, in polymer blends, there is typically a nonnegligible concentration dependence of the binary interaction parameter, i.e., $\chi = \chi(T, \phi)$, and in order to model blends by FH a relation of the form $\chi(T, \phi) = D(T) \cdot B(\phi)$ is used (the

separation of variables is for simplifying the fittings to experimental data series). For example, for PS/PVME, setting

$$\chi(T, \phi) = (1 - 0.4\phi) \; (0.02215 - 8.0/T) \qquad (2.37)$$

provided reasonable prediction of the phase behavior across various M_w's (Qian et al. 1991); more accurate prediction of the spinodals, for the same PS/PVME blends, necessitated the concentration term to be expanded to $(1 - 1.5\phi + 0.815\phi^2)$ and the T term to be adjusted for each polystyrene M_w (Qian et al. 1991):

$$
\begin{aligned}
\chi(T, \phi) &= \left(1 - 1.5\phi + 0.815\phi^2\right) \; \left(0.02754 - 9.0/T\right) \; \text{low } M_W \\
\chi(T, \phi) &= \left(1 - 1.5\phi + 0.815\phi^2\right) \; \left(0.0436 - 18.0/T\right) \; \text{medium } M_W \quad (2.37a) \\
\chi(T, \phi) &= \left(1 - 1.5\phi + 0.815\phi^2\right) \; \left(0.00644 - 2.5/T\right) \; \text{high } M_W
\end{aligned}
$$

The above compare well with results from a prior experimental approach, which employed SANS to map out the spinodal for d-PS/PVME, albeit parameterized using different functionals, with a linear ϕ dependence for both the $\chi_H \propto 1/T$ and the χ_S terms (Schwahn et al. 1987), which are based on a EoS model.

By redefining the T dependence of $\chi(T)$, e.g., to include $1/T^2$ or $\ln T$ terms, one can use the FH equation to predict other type of phase diagrams, such as LCST, closed-loop, chimney, etc. (Qian et al. 1991; Eitouni and Balsara 2007). In fact, a number of reasonably accurate, within the applicable T range, FH model $\chi(T)$ relations exist in literature for a number of polymer blends (often including a second T term (i.e., C/T^2), see Table 2.8).

More generally, the interaction parameter dependencies on T and ϕ can be written as

$$
\begin{aligned}
\chi_{12}(\phi_2, T, M_1, M_2, \ldots) &= \chi_H(\phi_2, M_1, M_2, \ldots) &+& \chi_S(\phi_2, M_1, M_2, \ldots)/T \\
B_{12}(\phi_2, T, M_1, M_2, \ldots) &= B_H(\phi_2, M_1, M_2, \ldots)T &+& B_S(\phi_2, M_1, M_2, \ldots)
\end{aligned}
\qquad (2.38)
$$

In this notation, the T dependence is explicitly provided using the standard second virial coefficient functionality, i.e., $\chi \propto 1/T$, and χ_{12} is now expressed in terms of enthalpic and entropic parts, i.e., χ_H and χ_S, respectively, each being a function of concentration, molecular weight of both polymers, and other independent variables. In other words, Eq. 2.38 attempts to account for nonrandom mixing, i.e., contribution of the non-combinatorial entropy to the interactions. This idea is particularly important for polymer blends. Here, the miscibility mainly originates from strong interactions that are expected to cause changes of intersegmental orientation, hence nonrandom mixing that entails strong entropic effects. Table 2.7 gives a few example values of Eq. 2.38 parameters for selected, simple polymer blends.

As one would expect from the definition of χ_{12} (cf. viewed as the excess enthalpy/interaction between monomers in a mixed pair vs. in their single phase)

Table 2.7 Enthalpic, χ_H, and entropic, χ_S, contributions to the Flory-Huggins binary interaction parameter, χ_{12}, see Eq. 2.38

Polymer-1	Polymer-2	ϕ_2	$\chi_H \times 10^4$	χ_S(K)	Reference
PE, $N = 2{,}538$	d-PE, $N = 2{,}464$	0.221	−0.012	0.132	1
PE, $N = 3{,}308$	d-PE, $N = 3{,}275$	0.087	2.761	0.069	1
PE, $N = 3{,}308$	d-PE, $N = 3{,}275$	0.457	0.242	0.089	1
PE, $N = 4{,}598$	d-PE, $N = 4{,}148$	0.044	1.628	0.325	1
PE, $N = 4{,}598$	d-PE, $N = 4{,}148$	0.087	0.759	0.138	1
PE, $N = 4{,}598$	d-PE, $N = 4{,}148$	0.131	0.808	0.100	1
PE, $N = 4{,}598$	d-PE, $N = 4{,}148$	0.221	−0.907	0.139	1
PE, $N = 4{,}598$	d-PE, $N = 4{,}148$	0.457	−0.843	0.127	1
PE, $N = 4{,}598$	d-PE, $N = 4{,}148$	0.708	−0.859	0.133	1
PS, $N = 15{,}400$	d-PS, $N = 8{,}700$	0.500	−2.900	0.200	1
PpMS, $N = 498$	d-PS, $N = 291$	0.250	−0.011	70	2
PpMS, $N = 498$	d-PS, $N = 291$	0.500	−0.0081	57	2
PpMS, $N = 498$	d-PS, $N = 291$	0.749	−0.0081	61	2
PpMS, $N = 1{,}108$	d-PS, $N = 291$	0.249	−0.0119	72	2
PpMS, $N = 835$	d-PS, $N = 3{,}123$	0.5	−2	2.16	3

Notes: N is the degree of polymerization, d-PE deuterated PE, d-PS deuterated PS, *PpMS* poly(*p*-methylstyrene)
References: **1**. Londono et al. 1994; **2**. Londono and Wignall 1997; **3**. Jung and Fischer 1988

there is marked independence of χ_{12} on the molecular weight of the polymers, N. However, large variability of χ_{12} has been observed with the concentration of the polymer blends, showing often linear and, in some cases, quadratic dependencies of χ_{12} on ϕ (e.g., Han et al. 1988; Krishnamoorti et al. 1994a) and on T (e.g., Eitouni and Balsara 2007, and references therein).

A compilation of $\chi_{12}(T)$ parameters, spanning numerous polymer blends, showed that it is often necessary that a second T term is added to Eq. 2.38 to obtain satisfactory accuracy; thus, the following the empirical dependence of χ_{12} on T

$$\chi_{12}(T) = A + B/T + C/T^2 \tag{2.39}$$

is obtained, and a compilation of $\chi_{12}(T)$ such functions for about 120 polymer blends can be found in the second edition of "Physical Properties of Polymers Handbook" (Eitouni and Balsara 2007) (see also Table 2.8). Most of these data were obtained by applying RPA (random phase approximation) to small-angle neutron scattering (SANS) profiles measured from homogenous homopolymer blends. This approach was pioneered by Hadziioannou and Stein (1983, 1984), Murray et al. (1985), and Herkt-Maetzky and Schelten (1983). In these cases, one needs to consider also the dependence of χ_{12} on the deuteration effects of polymers, whereby there can be appreciable changes in χ depending on deuteration (see Tables 2.7, 2.8); indicatively, appreciable interaction parameters can manifest even between the hydrogenated and deuterated homologues of the same polymer,

Table 2.8 Temperature dependence of $\chi_{12}(T)$ parameterized as $\chi_{12}(T) = A + B/T + C/T^2$ (Eq. 2.39), including the temperature range of parameter validity. Selected polystyrene (PS) and polypropylene (PP) blends are tabulated here. A much more extensive compilation can be found in (Eitouni and Balsara 2007)

Polymer-1	Polymer-2	A	B (K)	C(K^2)	T range (°C)
d-PS	PMMA	0.0174	2.39	–	120–180
PS	d-PMMA	0.0180	1.96	–	170–210
PS	PMMA	0.0129	1.96	–	100–200
d-PS	d-PMMA	0.0154	1.96	–	130–210
d-PS	PVME	0.0973	−41.6	–	60–150
PS	PVME	0.103	−43.0	–	60–150
PS	d-PXE	0.058	−37.7	–	100–280
d-PS	PXE	0.059	−32.5	–	180–330
PS	PI$_{(7)}$	0.00785	17.6	–	100–180
d-PS	PCHA	0.067	−35	–	120–155
PS	P2VP	0.018	35	–	155–230
d-PS	PPMA	0.0515	−27.2	5127	80–130
d-PS	PBMA	0.107	−60.4	9807	20–130
PS	P4MS	0.0046	3.2	–	160–230
PP	d_3-SPB$_{(97)}$	0.00454	−4.71	1364	30–130
d_4-PP	SPB$_{(97)}$	0.00244	−3.27	1051	30–130
PP	SPB$_{(97)}$	0.00349	−3.99	1208	30–130
PP	d_3-SPB$_{(78)}$	0.00747	−6.38	1426	50–170
d_4-PP	SPB$_{(78)}$	0.00381	−3.50	895	50–170
PP	SPB$_{(78)}$	0.00564	−4.94	1161	50–170
PP	d_5-SPI$_{(7)}$	0.00302	4.59	944	30–170
d_4-PP	SPI$_{(7)}$	0.00392	5.39	969	30–170
PP	SPI$_{(7)}$	0.00347	4.99	957	30–170
HHPP	d_2-SPB$_{(78)}$	0.00153	1.24	–	110–170
d_4-HHPP	SPB$_{(78)}$	0.00220	1.40	–	30–170
HHPP	SPB$_{(78)}$	0.00187	1.32	–	110–170
HHPP	d_3-SPB$_{(66)}$	0.00716	−6.17	1338	30–170
d_4-HHPP	SPB$_{(66)}$	0.00675	−5.84	1280	30–170
HHPP	SPB$_{(66)}$	0.00696	−6.01	1309	30–170
HHPP	d_3-PEB	0.00127	−0.96	282	30–170
d_4-HHPP	PEB	0.00243	−1.86	457	30–170
HHPP	PEB	0.00185	−1.41	370	30–170
HHPP	d_5-SPI$_{(7)}$	0.00806	−5.71	1046	30–170
d_4-HHPP	SPI$_{(50)}$	0.00220	1.24	–	30–170
HHPP	d_5-SPI$_{(50)}$	0.00174	1.29	–	50–170
HHPP	SPI$_{(50)}$	0.00197	1.27	–	50–170
HHPP	d_4-PP	0.00427	2.13	–	30–130

(*continued*)

Table 2.8 (continued)

Polymer-1	Polymer-2	A	B (K)	$C(K^2)$	T range (°C)
d_4-HHPP	PP	0.00301	1.54	–	30–130
HHPP	PP	0.00364	1.84	–	30–130
d_4-HHPP	PIB	0.0180	−7.74	–	30–170

Notes: The values of A, B, and C and thus χ are based on a reference volume $V_{ref} = 0.1$ nm^3

Polymer notation: A d- label preceding the polymer acronym indicates a per-deuterated polymer; partially deuterated polymers are labeled as d_3-, d_4-, etc., for selective deuteration of 3, 4, etc., hydrogens. Numbers in subscripted parentheses after the polymer name indicate the primary comonomer fraction, e.g., SPB$_{(66)}$ is a saturated polybutadiene with 66 mol% butadiene

Polymer acronyms: *P2VP* poly(2-vinyl pyridine), *P4MS* poly(4-methylstyrene), *PBMA* poly(*n*-butyl methacrylate), *PCHA* poly(cyclohexyl acrylate), *PEB* poly(ethyl butylene), *PIB* polyisobutylene, *PI* polyisoprene, *PMMA* poly(methyl methacrylate), *PPMA* poly(*n*-pentyl methacrylate), *PP* polypropylene, *HHPP* head-to-head polypropylene, *PS* polystyrene, *PVME* poly(vinyl methyl ether), *PXE* poly(2,6-dimethyl-1,4-phenylene oxide), *SPB* saturated polybutadiene, *SPI* saturated polyisoprene
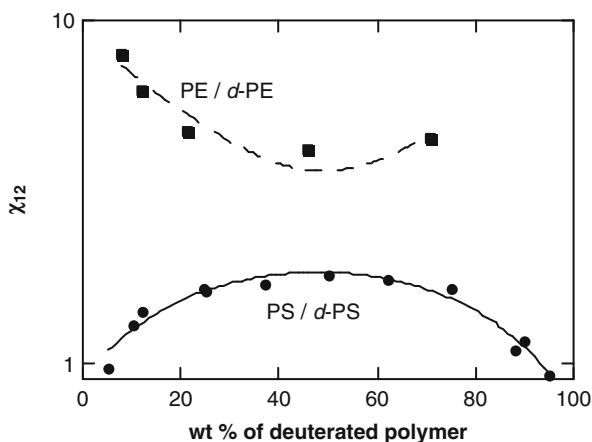
Fig. 2.7 The binary interaction parameter for blends of PS with d-PS at $T = 433$ K and for PE with d-PE at $T = 443$ K (Londono et al. 1994)

oftentimes leading to phase separation of such, especially at large molecular weights. For example, in Fig. 2.7, the experimental values of this parameter are shown for blends of a hydrogenated polymer with its deuterated homologue, i.e., PE with d-PE at $T = 443$ K and PS with d-PS at $T = 433$ K (Londono et al. 1994). The data can be described in terms of Eq. 2.38. A formal analysis of these data was published by Bidkar and Sanchez (1995).

Even at a superficial view, it is rather obvious that the FH theory has limitations, even when all its restrictive assumptions (weak interactions, entropy-independent enthalpy, etc.) are satisfied. For example, the χ for polymers, as defined by FH ($\chi = z\Delta\varepsilon/kT$; z is coordination number and $\Delta\varepsilon$ the excess enthalpy of interaction for one mixed pair) allows for z solvent neighbors around each monomer, neglecting that

Table 2.9 Structural parameters for model polyolefins (Dudowicz and Freed 1996a, b)

Polyolefin		r	p	q
PE	Polyethylene	1	0	0
PEP	Poly(ethylene propylene)	1.2	0.2	0.25
PPE	Poly-1-pentene [poly(propyl ethylene)]	1.2	0.2	0.25
PEE	Poly-1-butene [poly(ethyl ethylene)]	1.25	0.25	0.33
PP	Polypropylene	1.33	0.33	0.5
P2B	Poly-2-butene	1.5	0.5	1
PDMB	Poly(4,4-dimethyl 1-butene)	1.67	0.5	1
PIB	Polyisobutylene	1.75	0.5	1

there are always (at least) two other monomers of either side of an internal monomer; this leads to a gross overestimation of the nearest neighbor heterocontacts, which, however, can be addressed by a simple correction, replacing z by $z - 2$ (Guggenheim 1944, 1952). A number of other extensions of the FH theory also address the type and geometry of monomer, the stiffness of the backbone, the existence of unsaturated carbons, etc.; the reader is referred to a recent review (Freed and Dudowicz 2005, and references cited therein). More arguments along these same lines led to correction terms or extensions in the FH theory that can address, beyond chain connectivity, also monomer size, monomer geometry including pending groups, restricted bond rotations, etc., details that can become very important when comparing to sensitive experimental data, such as SANS measurements of χ. The details of such corrections go beyond the scope of this chapter; the interested reader is again referred to Freed and Dudowicz (2005); in most cases, such extensions retain the FH equation for the free energy of mixing, Eq. 2.35, and redefine the χ' parameter as an appropriate function, rather than a system-specific constant. Thus, such corrections lead to a binary interaction parameters with functionals such as

$$\chi'(\phi, T) = a + \frac{b + c\phi}{T} \quad \text{or} \quad \chi'(\phi, T) = a' + \frac{b'}{T} + c'\phi \qquad (2.40)$$

where a, b, and c are corrections due to monomer geometry, packing (see also Table 2.9 *ff.*), and other (b', c') considerations, often rather involved in their definition (e.g., Eq. 11a vs. Eq. 2.10 in Freed and Dudowicz 2005). Finally, another drawback of the FH theory is the assumption of a fully occupied lattice, i.e., the assumption that all space is occupied by units, either solvent molecules or polymeric segments, of equal and constant size. As a consequence, the free volume contributions are largely neglected. It was pointed out that dissolution of polymer is associated with volume changes (Maron 1959), leading to a modification of the FH theory extended to account for ternary systems comprising of polydispersed polymers (Utracki 1962).

2.5.1.2 Equation of State Theories

Starting in the early 1960s considerable effort was made to develop what become known as the equation of state theories (Flory et al. 1964; Eichinger and Flory 1968;

Simha and Somcynsky 1969; Patterson 1969, 1982; Patterson and Robard 1978; Sanchez and Lacombe 1976, 1977; Sanchez 1983, 1984). The equation of state (EoS) theories of mixtures are based on the principles discussed in Sect. 2.4.1. Formally, the computation of the partition function for a single component or for a mixture of components is similar, yielding the Helmholtz free energy of mixing.

Different EoS use different measures of the binary interactions between components. For example, in Flory's extension of the FH approach, the binary interaction parameter, χ_{12}, is still present (Flory 1970). In S-L EoS (see Eq. 2.16), the characteristic pressures for the mixture of species are assumed to be pairwise additive:

$$P^* = \sum_i \phi_i P_i^* - \sum_{i<j} \sum_j \phi_i \phi_j \Delta P^* \qquad (2.41)$$

For such systems, the difference of the interaction energy density, ΔP^*, has been considered a measure of the binary interactions between polymeric segments, proportional to either χ_{12} or B (Sanchez 1989).

The most successful statistical thermodynamic theory of liquids is that proposed by Simha and Somcynsky, S-S (Simha and Somcynsky 1969; Jain and Simha 1980, 1981, 1982, 1984). From the corresponding partition function, the Helmholtz free energy and then the pressure were computed using the general derivatives, Eq. 2.5. For a single-component system, the S-S yielded PVT relationships (Eq. 2.19). Initially, the theory has been used to compute PVT behavior of homopolymers. Later, it was extended to full thermodynamic description of multicomponent systems, viz., thermodynamics of mixtures, gas-liquid and liquid-liquid phase equilibria, etc. Thus, using the derived expression for the free energy of neat components, the molar Helmholtz free energy was derived for a binary mixture (Jain and Simha 1980; 1984; Stroeks and Nies 1988):

$$
\begin{aligned}
\frac{F_m}{RT} = \quad & x_1 \ln x_1 + x_2 \ln x_2 + \frac{\langle s \rangle}{y}(1-y)\ln(1-y) - (\langle s \rangle - 1)\ln\frac{z-1}{e} \\
& -\langle c \rangle \left[\ln \frac{\langle V^* \rangle (1-\eta)^3}{Q} - \left(\frac{yQ^2}{2T^*} \right)\left(AQ^2 - 2B \right) \right] \\
& -\frac{3}{2}\left[x_1 c_1 \ln\left(2\pi \frac{\langle M_{o1} \rangle}{(N_A h)^2} \right) + x_2 c_2 \ln\left(2\pi \frac{\langle M_{o2} \rangle}{(N_A h)^2} \right) \right]
\end{aligned}
\qquad (2.42)
$$

where N_A and h are Avogadro's and Planck's constants, respectively and the nomenclature follows the typical variables of the S-S EoS, such as y the fraction of occupied lattice cells; Q the dimensionless quantity $1/(yV^*)$; η the dimensionless quantity $2^{-1/6}yQ^{1/3}$; s_i the number of segments per chain of molar mass M_i; M_{oi} the segmental molar mass, $M_{oi} = M_i/s_i$; as well as the three principal reducing variables $P_i^* (= zq_i\epsilon_{ii}^*/s_i v_{ii}^*)$, $T_i^* (= zq_i\epsilon_{ii}^*/Rc_i)$, and $V_i^* (= v_{ii}^*/M_{oi})$, which relate to the component's maximum molar intermolecular attraction energy per segment (ϵ_{ii}^*) and the number of intermolecular contacts ($q_i z = s_i(z-2) + 2$), with the subscripts i, in all

Fig. 2.8 The binary
interaction parameters S_ε and
S_v of the Simha-Somcynsky
(S-S) EoS for PS/PPE blends
(T range, T_g to 330 °C;
P range, 0–180 MPa) (Jain
et al. 1982)
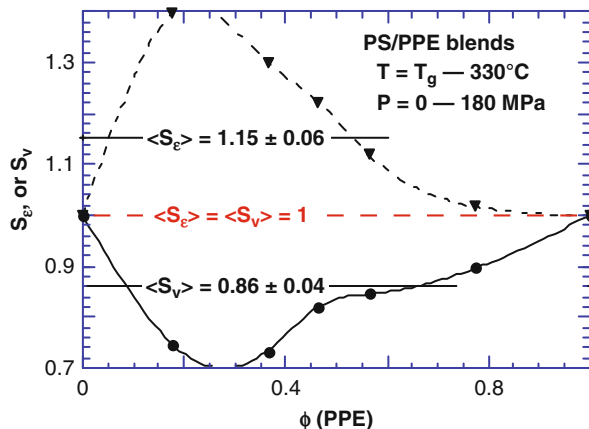
cases, indicating the value for component i. And the mixture variables, the values in
angle brackets, $\langle\rangle$, which are compositional averages based on the components'
properties and their molar fractions, x_i, in the mixture:

$$\langle s \rangle = x_1 s_1 + x_2 s_2 \quad \text{and} \quad \langle c \rangle = x_1 c_1 + x_2 c_2$$
$$\langle M_o \rangle = (x_1 s_1 M_{o1} + x_2 s_2 M_{o2})/(x_1 s_1 + x_2 s_2)$$
$$\langle \epsilon^* \rangle \langle v^* \rangle^k = X_1^2 \epsilon_{11}^* v_{11}^{*\,k} + X_2^2 \epsilon_{22}^* v_{22}^{*\,k} + 2X_1 X_2 \epsilon_{12}^* v_{12}^{*\,k} \quad (k = 2, 4)$$
$$\text{where} \quad X_1 = 1 - X_2 = x_1 [s_1(z-2) + 2]/\langle qz \rangle$$

$$(2.43)$$

In Eq. 2.43, there are two cross-interaction parameters, quantified through
weight-averaged mixing rules, that characterize the binary system:

1. The interaction energy, $\epsilon_{12}^* = S_\epsilon \sqrt{\epsilon_{11}^* \epsilon_{22}^*}$
2. The repulsion volume, $v_{12}^* = S_v [(v_{11}^{*\,1/3} + v_{22}^{*\,1/3})/2]^3$

For nearly athermal systems, the proportionality factors, S_ε and S_v, are taken as
equal to 1. Thus, for the systems without strong interactions, the binary parameters
are well approximated by the geometric and algebraic averages. For example, for
PS/PVME blends, the assumption $S_\varepsilon = S_v = 1$ resulted in 0.1 % deviation for the
experimental values of the cross-parameters (Xie et al. 1992; Xie and Simha, 1997,
"private communication"). In contrast, it is to be expected that for systems with
strong intermolecular interactions such mixture rules may fail and experimental
values for the cross-factors may have to be found. However, least squares fit of
Eqs. 2.42 and 2.43 to experimental values of CO_2 miscibilities in PS (in a wide
range of P and T) yielded values for S_ε and S_v close to 1 (Xie et al. 1997).

The S-S equations were used for the description of *PVT* dependencies for PS,
PPE, and their blends (Jain et al. 1982). The data are presented in Fig. 2.8, where the
best-fit values for each composition: $S_\varepsilon(P, T, \phi)$ and S_v (P, T, ϕ) are plotted
versus PPE volume fraction, ϕ(PPE). The plot shows concentration, a nontypical
dependence for these two parameters, i.e., a behavior not previously observed for
mixtures of solvents or for polymer solutions; the variation is not large – the

averages of S_ε and S_v are, respectively, 1.15 ± 0.06 and 0.86 ± 0.04. From a theoretical point of view, it is highly satisfying that these values are not far from unity. Furthermore, the larger (than 1) value of S_ε and the smaller (than 1) value of S_v indicate the presence of specific interactions between PS and PPE, larger than the geometric average energetic interactions, and a contraction of the binary volume contribution, smaller than the algebraic mean. It should be stressed that, as shown by the original authors, the S_ε and S_v values provided excellent description of the *PVT* dependencies over the full range of variables. The observed compositional variability may, thus, be caused by inadequacies of the theory, or the computational method, or the experimental data. Analysis of these and other blends by means of the S-S EoS is continuously being pursued.

2.5.1.3 Gas-Lattice Model

The gas-lattice model considers liquids to be a mixture of randomly distributed occupied and vacant sites. P and T can change the concentration of holes, but not their size. A molecule may occupy m sites. Binary liquid mixtures are treated as ternary systems of two liquids (subscripts "1" and "2") with holes (subscript "0"). The derived equations were used to describe the vapor-liquid equilibrium of *n*-alkanes; they also predicted well the phase behavior of *n*-alkanes/PE systems. The gas-lattice model gives the non-combinatorial Helmotz free energy of mixing expressed in terms of composition and binary interaction parameters, quantified through interaction energies per unit contact area (Kleintjens 1983; Nies et al. 1983):

$$
\begin{aligned}
\Delta F_m/N_\phi kT = \quad & \phi_0 \ln \phi_0 + (\phi_1/m_1) \ln \phi_1 + (\phi_2/m_2) \ln \phi_2 + \\
& \left[\alpha_{11} + g_{11}^L(1-\gamma_1)/(1-\gamma_1\phi_1-\gamma_2\phi_2)\right]\phi_0\phi_1 + \\
& \left[\alpha_{22} + g_{22}^L(1-\gamma_2)/(1-\gamma_1\phi_1-\gamma_2\phi_2)\right]\phi_0\phi_2 + \\
& \left[\alpha_{12} + g_{12}^L(1-\gamma_1)/(1-\gamma_1\phi_1-\gamma_2\phi_2)\right]\phi_1\phi_2
\end{aligned}
\tag{2.44}
$$

with $N_\phi = n_0 + n_1 m_1 + n_2 m_2$ and $\gamma_i = 1 - \sigma_i/\sigma_0$; the superscript L is used to indicate that the relation was derived from the gas-lattice model; the parameter s_i is the interacting surface area of species "i"; the binary interaction parameters include two terms, as usual, the α_{ij} empirical entropy corrections and the g_{ij} temperature dependencies ($g_{ij} = -w_{ij}/2\sigma_0 kT$, with w_{ij} is the interaction energy per unit contact surface area involved in $i - j$ contact, $i = j$ corresponds to same-species interactions). This approach is rather versatile, and, among other, it has been extended and adapted to describe the empirical parameters through a molecular basis (Koningsveld et al. 1987), as well as orientation-dependent interactions (Besseling and Scheutjens 1994). According to the gas-lattice theory, four factors determine the polymer/polymer miscibility (Koningsveld et al. 1982: Koningsveld 1986):

1. Interacting surface areas of segments
2. Coil dimensions (dependent on T, ϕ, and M_W)
3. Molecular weight polydispersity
4. Free volume fraction

   In an effort to address some of the FH and gas-lattice models simplifications, the lattice cluster theory (LCT) was developed (Dudowicz et al. 1991; Dudowicz

and Freed 1991, 1993, 1995, 1996a, b; Freed and Dudowicz 1995; 1996a, b; 2005).
LCT is a mean-field lattice-based model, but in comparison to FH theory, it
incorporates two modifications: (1) It includes local packing and interactions,
and (2) it distinguishes different structures of the monomeric units, allowing the
monomeric units to occupy different adjacent sites, as dictated by their structure
(e.g., pending side groups). The theory represents polymer chains as strings of beads,
called *united atoms*, freely jointed by flexible bonds. For example, it considers CH_x
(x = 0, 1, 2, or 3) as a single bead (or group) that occupies one lattice site. LCT also
incorporates vacant sites (free volume) and uses the nonrandom mixing principle.
Thus, the free energy of mixing is given by

$$\frac{\Delta F_m}{NkT} = \sum_i \frac{\phi_i}{M_i} \ln \phi_i + \phi_v \ln \phi_v + \sum_i g_i(\phi_i)\phi_i\phi_v + \sum_{i \neq j} g_{ij}\left(\phi_i, \phi_j\right)\phi_i\phi_j \quad (2.45)$$

The first two terms of Eq. 2.45 are the combinatorial entropy contributions, one
for each species i and one, the second term, for the free volume contribution to
the entropy of mixing (where the subscript v indicates the free volume fraction).
The third term represents the non-combinatorial contribution ($g_i(\phi_i)$ is the
non-combinatorial energy of a molten state of polymer i having the free volume
fraction ϕ_v). The fourth term represents the energetic contribution originating from
interaction between unlike species, $i \neq j$. Here, $g_{ij}(\phi_i, \phi_j)$ is the interaction term
expressed as a polynomial with coefficients that depend on the structure of the
polymer chains; these coefficients are computed as double expansions in $1/z$ (z is
the lattice coordination number) and ε_{ij}/kT (ε_{ij} is the van der Waals interaction
energies between groups i and j). Through curve fitting to experimental data, it has
been shown that the binary interaction parameter, Flory-Huggins' χ_{12} or g_{12} above,
is a thermodynamic function of such independent variables as T, P, ϕ_i, molecular
weight, and others. LCT shows that the binary interaction parameter has strong
sensitivity also to composition, monomeric structure, and local correlation. The
theory was quite successful describing observed dependencies for PS/PVME blends
using four parameters: $\varepsilon_{S/S}$, $\varepsilon_{VME/VME}$, $\varepsilon_{S/VME}$, and the cell volume. Except for the
heterocontact parameter $\varepsilon_{S/VME}$ (which must be determined by a fitting procedure),
the values of the other three parameters are determined from the *PVT* dependencies
of neat resins and are not adjustable in the blend phase calculations.

LCT, originally developed for di-block copolymers, was found to be particularly
useful to explain miscibility of polyolefin blends, where the two resins differ in the
type and size of short-chain branching. These polymers comprise of structural units
with two carbons in the main chain (backbone), i.e., polyethylene, PE = $[CH_2–CH_2]_n$;
polypropylene, PP = $[CH_2–CH (CH_3)]_n$; poly-2-butene, P2B = $[CH (CH_3)–CH$
$(CH_3)]_n$; polyisobutylene, PIB = $[CH_2–C (CH_3)_2]_n$; poly(4,4-dimethyl 1-butene),
PDMB = $[CH_2–CH (C_4H_9)]_n$; etc. Structural parameters (e.g., ratio of end to interior
groups, number of bonds, volume of submonomer units, etc.) are used to distinguish
between different monomer structures and geometries and account for differences in
the blend phase behavior by redefining $\chi(\phi, T)$ (see Eq. 2.40). For example, three such

Table 2.10 Binary interaction parameters, $\chi = \chi_s + \chi_H/T$, for model polyolefin 1:1 blends at 500 K (Freed and Dudowicz 1996a, b). See also Tables 2.9 and 2.8

Blends	T_c (K)	r	$1,000\chi_s$	χ_H (K)	100χ
PE/PIB	488	0.75	−0.3248	5.8188	1.13
PEP/PIB	477	0.55	0.4560	2.8443	0.615
PE/P2B	432	0.5	1.877	1.6352	0.510
PP/PIB	395	0.417	1.840	0.9062	0.354
PP/PE	383	0.333	1.356	0.5150	0.229
PEP/P2B	365	0.3	1.327	0.3259	0.187
P2B/PIB	351	0.25	1.049	0.2119	0.135
PE/PEP	340	0.2	0.6486	0.1249	0.083
PP/P2B	328	0.167	0.5463	0.0569	0.061
PEP/PP	311	0.133	0.3249	0.0424	0.037

parameters, r, p, and q, were used for the polyolefins above (values for model polyolefin macromolecules are summarized in Table 2.9). A number of derivative models (simplified-LCT, basic-LCT, etc.) were also developed by the same scientists (Freed and Dudowicz 2005).

Miscibility is expected for blends of polyolefins having similar values of these structural parameters. In Table 2.10, examples of the computed binary interaction parameters for 1:1 composition polyolefin blends at 500 K are shown (Freed and Dudowicz 1996a, b). The experimental values of these parameters have also been measured (Balsara et al. 1992, 1994; Graessley et al. 1993, 1994a, b, 1995; Krishnamoorti et al. 1994a, b, 1995, 1996; Lin et al. 1996; Schipp et al. 1996; Reichart et al. 1997). Experimental data were determined using either small-angle neutron scattering (SANS), cloud-point curve determination (CPC), or *PVT* measurements. The experimental results will be discussed later, *vide infra* SANS measurements.

2.5.2 Off-Lattice Theories

2.5.2.1 Strong Interactions Model

For incompressible systems having strong interactions, e.g., acid–base type, the directional-specific model of segmental interactions may be used (Walker and Vause 1982; ten Brinke and Karasz 1984). By appropriate definition of $\chi(T)$, the familiar FH expression was derived for a symmetric ($N_1 = N_2 = N$) blend:

$$\frac{\Delta G_m}{RT} = \frac{\phi_1}{N} \ln \phi_1 + \frac{\phi_2}{N} \ln \phi_2 + \chi(T)\phi_1\phi_2$$
$$\text{with } \chi = \frac{U_2}{RT} + \ln(1 - \lambda) + \ln\left(1 + \frac{1}{q}\right) \text{ and } \lambda = \left[1 + qe^{(U_1 - U_2)/RT}\right]^{-1} \quad (2.46)$$

where U_1 and U_2 are the attractive and repulsive energies, respectively, and q is the degeneracy number; the familiar FH expression was obtained by splitting the binary interaction parameter χ in an enthalpic and an entropic term:

$$
\begin{aligned}
\chi_H/z &= [\lambda U_1 + (1 - \lambda U_2)]/RT \text{ and} \\
\chi_S/z &= \ln(1 - \lambda) + \ln(1 + 1/q) - \lambda(U_1 - U_2)/RT
\end{aligned}
\tag{2.46a}
$$

respectively, with q and λ as above. Depending on the relative magnitudes of U_1 and U_2, Eq. 2.46 predicts either UCST or LCST.

2.5.2.2 Heat of Mixing Approach

For most polymers, $N \gg 1$ and the configurational entropy of a polymer blend become vanishingly small; thus, to a very good approximation $\Delta G_m \approx \Delta H_m$ (the enthalpic effects dominate) and, hence, adiabatic calorimetry should be able to predict polymer/polymer miscibility (Cruz et al. 1979).

$$
\Delta G_m \approx \Delta H_m = B\phi_1\phi_2 = \chi_{12}RT(V/V_1)\phi_1\phi_2
\tag{2.47}
$$

After experimentally confirming the validity of this idea, the principal authors attempted to use this approach for explanation of the so-called miscibility windows (Paul and Barlow 1984). The latter term refers either to polymer/copolymer blends that show miscibility only within a limited range of copolymer compositions (e.g., Balazs et al. 1985; Fernandes et al. 1986; Goh and Lee 1987) or to blends of two copolymers having a common monomer (Shiomi et al. 1986). As earlier, in Koningsveld's treatment of χ_{12}, here also the parameter B has an enthalpic contribution and a non-combinatorial entropic contribution. For multicomponent systems, Eq. 2.47 can be generalized (Barlow and Paul 1987):

$$
\frac{\Delta G_m}{V} \approx \frac{\Delta H_m}{V} = \sum_i \sum_{j \neq i} B_{ij}\phi_i\phi_j - \sum_k \Psi_k \sum_i \sum_{j \neq i} B_{ij}\phi_i^k\phi_j^k
\tag{2.48}
$$

where Ψ_k is the volume fraction of polymer k and the usual constraints for the component volume fractions are extended to $\sum \phi_i \equiv 1$ and $\sum \phi_i^k \equiv 1$. For simple systems, containing a copolymer A (mers #1 and #2) and either a homopolymer B (mers #3) or a copolymer B (mers #1 and #3), Eq. 2.48 can be simplified to read:

$$
\frac{\Delta G_m}{V} \approx \frac{\Delta H_m}{V} = B\Psi_1\Psi_2
\tag{2.49}
$$

where B is now, respectively,

$$
\begin{aligned}
B &= B_{13}\phi_1' + B_{23}\phi_2' - B_{12}\phi_1'\phi_2' \text{ or} \\
B &= B_{12}\phi_2(\phi_2' - \phi_3'') + B_{13}\phi_3(\phi_3' - \phi_2'') + B_{23}\phi_2'\phi_3''
\end{aligned}
\tag{2.49a}
$$

where ϕ_i' and ϕ_i' ′ denote the volume fraction of i-type monomer in copolymers A and B, respectively. Over the years, values of the parameter B for many polymer mixtures have been published. As shown in Table 2.11, similar to χ_{12}, also the binary B varies with composition, temperature, and other blend variables.

Table 2.11 Binary interaction parameters: B, ΔP^*, or χ_{12} (see earlier data in Utracki 1989). To convert cal/mL to J/m^3, multiply the listed values by 4.187×10^6

Polymer-1	Polymer-2	T (°C)	B(cal/mL)	ΔP^* (cal/mL)	χ_{12}	References
PS	TMPC	30	−0.13	−0.17 ± 0.01		1
PS	TMPC	300	0.11	−0.17 ± 0.01		1
PS	Pα-MS	50	0.012–0.025	0.011 − 0.025		2
PS$_{(50)}$	Pα-MS		−0.0833 + 0.001034 T			2
PS	PMMA	160	0.542	0.620		2
PS	PMMA	245	0.464	0.532		2
PS	PMMA	153	0.457	0.520		2
PS	PMMA	250	0.392	0.455		2
PS	PMMA	195	0.21 ± 0.02	0.24 ± 0.05		2
PS$_{(50)}$	PMMA		0.542 + 10^{-4}			2
Pα-MS	PMMA	150	0.354			2
Pα-MS	PMMA	250	0.458			2
PS	PC	50	0.43	0.44		3
PS	DMPC	50	0.20–0.49	–		3
PS	TMPC	240	0.036	−0.17		3
PS	TCPC	50	>0.72	–		3
PS	PCZ	50	0.28	–		3
PS	HFPC	300	>14	>1.6		3
PS	BCPC	50	1.5	>0.33		3
PS	TMPC-P	180	0.16	0.023		3
Pα-MS	PC	50	0.39–0.44	0.42–0.49		3
Pα-MS	DMPC	50	>0.18	–		3
Pα-MS	TMPC	180	0.26	0.068		3
Pα-MS	TCPC	300	>0.31	–		3
Pα-MS	PCZ	200	>0.24	-		3
Pα-MS	HFPC	50	0.22–0.72	0.12–1.4		3
Pα-MS	BCPC	300	>0.33	>0.44		3
Pα-MS	TMPC-P	180	0.21–0.29	0.001–0.006		3
PMMA	PC	50	0.057–0.066	0.043		3
PMMA	DMPC	196	0.16	–		3
PMMA	TMPC	214	0.29	0.40		3
PMMA	TCPC	300	0.45–0.77	–		3
PMMA	PCZ	50	0.17	–		3
PMMA	HFPC	160	−0.072	−0.30		3
PMMA	BCPC	150	0.01	−0.077		3
PMMA	TMPC-P	235	0.22	0.31		3
PS	PSF	248	0.85	1.18		4
PS	DMPSF	300	>0.67	–		4
PS	TMPSF	228	0.31	0.33		4
PS	HMBIPSF	300	>1.25	–		4
PS	PES	300	−1.27	–		4

(*continued*)

Table 2.11 (continued)

Polymer-1	Polymer-2	T (°C)	B(cal/mL)	ΔP^* (cal/mL)	χ_{12}	References
PS	HFPSF	300	>136	–		4
PS	TMHFPSF	50	0.63	–		4
PS	TMHFPSF	240	1.12	–		4
PS	TMPSF-P	174	0.34			4
Pα-MS	PSF	50	0.32	0.37		4
Pα-MS	PSF	300	>0.43	>0.53		4
Pα-MS	DMPSF	300	>0.30	–		4
Pα-MS	TMPSF	50	>0.35	>0.36		4
Pα-MS	HMBIPSF	300	>0.29	–		4
Pα-MS	PES	300	>0.31	–		4
Pα-MS	HFPSF	50	>0.20	–		4
Pα-MS	TMHFPSF	300	>0.30	–		4
Pα-MS	TMPSF-P	300	>0.29	–		4
PMMA	PSF	50	0.25–0.34	0.19–0.27		4
PMMA	DMPSF	300	>0.77	–		4
PMMA	TMPSF	231	0.39	0.44		4
PMMA	HMBIPSF	300	>0.76	–		4
PMMA	PES	300	>0.78	–		4
PMMA	HFPSF	50	0.10–0.15	–		4
PMMA	TMHFPSF	50	0.25	–		4
PMMA	TMHFPSF	293	0.77	–		4
PMMA	TMPSF-P	300	>0.76	–		4
PAN	PSF	50	3.6	4.1		4
PET	PETG	280			−0.12	5
PBT	20 % PAr	249			−0.65	6
PBT	40 % PAr	246			−0.40	6
PBT	60 %PAr	236			−0.31	6
PBT	80 %PAr	232			−0.22	6
PBT	65 wt% PEE				0.13	7
PBT	70 wt% PEE				0.10	7
PBT	75 wt% PEE				0.07	7
PBT	80 wt% PEE				0.048	7
PBT	85 wt% PEE				0.032	7
PBT	90 wt% PEE				0.012	7
PS	75 % P_p-MS	140			−0.008	8

(*continued*)

Table 2.11 (continued)

Polymer-1	Polymer-2	T (°C)	B(cal/mL)	ΔP^* (cal/mL)	χ_{12}	References
PS	50 % P$_p$-MS	140			−0.006	8
PS	25 % P$_p$-MS	140			−0.006	8
PB	50 % d-PB	130			0.00053	9
PB	50 % d-PB	121			0.00055	9
PB	43 % d-PB	130			0.00032	9
PMMA	50 % PnBMA	25			0.081	10
PMMA	50 % PiBMA	25			0.068	10
PiBMA	50 % PnBMA	25			0.0019	10
PS	PCSt	30			0.07 ± 0.02	11
PVDF	PMMA	170	−2.93			12
PVDF	MMA-GMA$_{(8)}$	170	−4.1			12
PVDF	MMA-GMA$_{(14)}$	170	−4.5			12
PVDF	MMA-GMA$_{(28)}$	170	−3.7			12
PC	PNP	200			0.175	13
PC	PMS	200			0.031	13
PCEMA	PCL				−0.99	14
PCEMA	PHS				−0.48	14
PS	PAN		4.59			15
Pα-MS	PAN		6.02			15
Pα-MS	PS		0.022 ± 0.001			16
BR	PAN		8.60			17
BR	PVC		0.72 ± 0.07			17
PVC	PAN		3.84 ± 0.43			17
PVAl	PAA		−19.9		−1.24	18
PA-6	Zn-SPS	220			−1.3	19
PA-6	Li-SPS	240	−215			20
PA-6	PS	240	28.7			20
PVDF	PMMA	160	−4.43			21
PVDF	PEMA	160	−2.66			21
PEMA	PMMA	160	3.25			21
PA-6	Mn-SPS$_{(10)}$	190	−1.9			22
PA-6	Mn-SPS$_{(20)}$	180	−2.0			22
PA-6	Mn-SPS$_{(30)}$	175	−1.8			22
PA-6	Mn-SPS$_{(50)}$	166	−1.5			22

<div align="right">(continued)</div>

Table 2.11 (continued)

Polymer-1	Polymer-2	T (°C)	B(cal/mL)	ΔP^* (cal/mL)	χ_{12}	References
PS	PPE	150			−0.2	23
PVC	PCL$_{(50)}$	250			−0.5	23
PI	d-PB$_{(50)}$	150			0.0023	24
PHS	PCEMA		−4.67		−0.76	25
PHS	PCMMA		−8.39		−1.2	25
PHS	PVC		−3.8		−0.76	26
PCL	SAN$_{(25)}$		−0.61			27
PCL	PC		−0.39			27
PC	SAN$_{(25)}$		0.2 ± 0.3			27
PVDC	PDPS		−0.2		Fig. 2.7	28
PVDC	PDPA		−1.1		Fig. 2.7	28
PVDC	PCL		−2.0		Fig. 2.7	28
PVDC	PCDS		−3.1		Fig. 2.7	28
PVDF	PBA	175	−1.0		−0.19	29
PVME	d-PS$_{(50)}$	100–150			0.0702–30.9/T	30
PVME	d-PS$_{(70.6)}$	100–150			0.0817–36.8/T	30
PB	d-PB	−50–80			0.5–1.29	30
PSiαMS	PS$_{(50)}$	100–200			0.0032–5.46/T	31
Pα-MS	PS$_{(50)}$	180–300			0.0044–0.0046	31
PMMA	PS				0.006–0.022	32
P4VP	PS	165			7.5 ± 2.5	33
P4VP	PS	180			3.5 ± 1.5	33
P4VP	PS	183			0.4	33
PIB$_{[82k]}$	EB$_{[85k]}$			Fig. 2.8	0.0194–6.36/T	34
PIB$_{[82k]}$	EB$_{[114k]}$			Fig. 2.8	0.0232–8.306/T	34
PIB$_{[160k]}$	EB$_{[114k]}$			Fig. 2.8	0.0228–8.14/T	34
PIB$_{[82k]}$	EB$_{[73k]}$			Fig. 2.8	0.0151–5.149/T	34
PIB$_{[82k]}$	HHPP$_{[27.5k]}$			Fig. 2.8	0.0194–6.36/T	34
d-PP	HHPP			Fig. 2.9	−0.00639 + 3.305/T	35
d-PP	EB$_{(97)}$			Fig. 2.9	−0.00883 + 4.200/T	35
d-PP	EB$_{(78)}$			Fig. 2.9	−0.00320 + 1.685/T	35
d-HHPP	PEB			Fig. 2.9	−0.00137 + 1.011/T	35
d-HHPP	PEP			Fig. 2.9	−0.00036 + 0.517/T	35
PVDF	PMA	160			−0.221 ± 0.002	36

Table 2.11 (continued)

Polymer-1	Polymer-2	T (°C)	B(cal/mL)	ΔP^* (cal/mL)	χ_{12}	References
P(VF$_2$-co-VF$_4$)	PMA	160			$-0.005 \pm$ 0.0005	36
HDPE	LDPE	150			$0.000402 \pm$ 4×10^{-5}	37
HDPE	LDPE	180			$0.000390 \pm$ 4×10^{-5}	37
HDPE	LDPE	190			$0.000387 \pm$ 4×10^{-5}	37
PEP$_{(25)}$	PEB	27–167			$-0.00167 +$ 0.954/T	38
PEP$_{(57.5)}$	PEB	27–167			$-0.00143 +$ 0.883/T	38
PEP$_{(89.1)}$	PEB	27–167			$-0.00219 +$ 1.138/T	38
PEMA$_{(70)}$	CR	42			-0.122	39
PEMA$_{(50)}$	CR	40			-0.053	39
PEMA$_{(30)}$	CR	39			-0.030	39
PCL	P4HS	50			-1.1	40
PVP	CDA 90 wt %	24.5			-4.20	41
PVP	CDA 65 wt %	24.5			-1.64	41
PVP	CDA 40 wt %	24.5			-0.60	41
PVP	CDA 15 wt %	24.5			-0.36	41
PMMA	Phenoxy	170			-0.61	42
PMMA	PEG				-0.35	43
PEG	Phenoxy				-1.90	44
PA-6	MXD	275			$-0.185/$ -0.194	45
PEEK	PEI	180			-0.3	46
PP	SEBS + oil	160			-0.043	47
PCl$_{(high\ \phi)}$	PVDC				-0.02	48
PCl$_{(low\ \phi)}$	PVDC				-0.21	48
PCl$_{(high\ \phi)}$	P(VCl$_2$-VAc)				-0.01	48
PCl$_{(low\ \phi)}$	P(VCl$_2$-VAc)				-0.28	48
PS	PPE	210	-0.89 ± 0.04			49
PS	PPE	210	-0.31 ± 0.15			50
PS	PPE	232	-1.62 ± 0.07			51
PS	PPE	210	$-1.46 +$ 0.00238 T		0.121–77.9/T	52

Table 2.11 (continued)

Polymer-1	Polymer-2	T (°C)	B(cal/mL)	ΔP^* (cal/mL)	χ_{12}	References
PS	P1,4PE	30	-0.005 ± 0.43			53
PS	PC	30	0.41 ± 0.13			54
PS	TMPC	30	0.19 ± 0.34			54
PS	PAN	30	7.63 ± 0.12			54
PES-C	PEG	65	4.65			55

Abbreviations: *BCPC* bisphenol chloral polycarbonate, *CDA* cellulose diacetate, *CR* polychloroprene, *DMPC* dimethyl bisphenol-A polycarbonate, *DMPSF* dimethyl bisphenol-A polysulfone, *EB* ethylene-butene copolymer (with indicated, in subscripts, butene content, or MW in g/mol), *HFPC* hexafluoro bisphenol-A polycarbonate, *HFPSF* hexafluoro polysulfone, *HMBIPSF* hexamethyl biphenol polysulfone, *MXD* poly(*m*-xylene adipamide), *P1,4PE* poly (1,4-phenylene ether), *P4VP* poly(4-vinylpyridine), *PAN* polyacrylonitrile, *PBA* poly (1,4-butylene adipate), *PB* polybutadiene, *d-PB* deuterated polybutadiene; *PC* bisphenol-A polycarbonate, *PCDS* poly(1,4-cyclohexanedimethylene succinate), *PCEMA* poly-1-chloroethyl methacrylate, *PCMMA* poly-1-chloromethyl methacrylate, *PCZ* bisphenol-Z polycarbonate, *PDPA* poly(2,2-dimethyl-1,3-propylene adipate), *PDPS* poly(2,2-dimethyl-1,3-propylene succinate), *PEB* polyethylene-butene, *PEE* polyester-ether aromatic block copolymer, *PEP* polyethylene-propylene, *PES-C* phenolphthalein polyetherether sulfone, *PES* polyethersulfone, *PHS* polyhexamethylene sebacate, *PI* polyisoprene, *PMS* poly(methylmethacrylate-*co*-*p*-methylstyrene), *PNP* poly(methylmethacrylate-*co*-*N*-phenylmaleimide), *d-PP* deuterated amorphous polypropylene, HH*PP* head-to-head amorphous polypropylene, *d-HHPP* deuterated head-to-head amorphous polypropylene, *PPE* poly(2,6-dimethyl-1,4-phenylene ether), *PSF* bisphenol-A polysulfone, *P4HS* poly(4-hydroxy styrene), *PS* polystyrene, *PCSt* poly-*p*-chlorostyrene, *Pα-MS* poly(α-methylstyrene), *PSiαMS* poly(sila-α-methylstyrene), *Pp-MS* poly-*para*-methylstyrene, *SAN(x)* copolymer of styrene with *x* % acrylonitrile, *Li-SPS* Li-sulfonated PS, *Mn-SPS* Mn-sulfonated PS, *Zn-SPS* Zn-sulfonated PS, *TCPC* tetrachloro bisphenol-A polycarbonate, *TMPC-P* tetramethyl bisphenol-P polycarbonate, *TMPC* tetramethyl bisphenol-A polycarbonate, *TMHFPSF* tetramethyl hexafluoro polysulfone, *TMPSF-P* tetramethyl bisphenol-P polysulfone, *TMPSF* tetramethyl bisphenol-A polysulfone

References: 1. Kim and Paul 1992; **2.** Callaghan and Paul 1993; **3.** Callaghan and Paul 1994a; **4.** Callaghan and Paul 1994b; **5.** Papadopoulou and Kalfoglu 1997; **6.** Huo and Cebe 1993; **7.** Gallagher et al. 1993; **8.** Londono and Wignall 1997; **9.** Alamo et al. 1997; **10.** Sato et al. 1996a, b; **11.** Ogawa et al. 1986; **12.** Gan and Paul 1995; **13.** Ikawa and Hosoda 1991; **14.** Peng et al. 1994; **15.** Cowie et al. 1992a; **16.** Cowie et al. 1992b; **17.** Cowie and Harris 1992; **18.** Diniliuc et al. 1992; **19.** Lu and Weiss 1992; **20.** Molnar and Eisenberg 1992; **21.** Goh and Siow 1988; **22.** Lu and Weiss 1991; **23.** Lu and Weiss 1992; **24.** Hasegawa et al. 1991; **25.** Neo and Goh 1992; **26.** Woo et al. 1985; **27.** Shah et al. 1986; **28.** Woo et al. 1983; **29.** Pennings and Manley 1996; **30.** Takeno et al. 1996; **31.** Maier et al. 1996; **32.** Pinder 1997; **33.** Clarke et al. 1997; **34.** Krishnamoorti et al.; **35.** Graessley et al. 1995; **36.** Maiti and Nandi 1995; **37.** Schipp et al. 1996; **38.** Lin et al. 1995; **39.** Kundu et al. 1996; **40.** Lezcano et al. 1996; **41.** Jinghua et al. 1997; **42.** Hong et al. 1997; **43.** Martuscelli et al. 1984; **44.** Iriarte et al. 1989; **45.** Shibayama et al. 1995; **46.** Goodwin and Simon 1996; **47.** Ohlsson and Tørnell 1996; **48.** Aubin et al. 1983; **49.** ten Brinke et al. 1983; **50.** Kambour et al. 1980; **51.** Plans et al. 1984; **52.** Maconnachie et al. 1984; **53.** Ziaee and Paul 1996; **54.** Ziaee and Paul 1997; **55.** Zheng et al. 1997

Determination of *B* for a series of blends made it possible to establish empirical rules for the observed miscibilities. Thus, for example, Prud'homme (1982) reported a systematic variation of miscibility in a series of halogenated polymer blends with aliphatic polyesters. The highest miscibility was observed for

Fig. 2.9 The binary interaction parameter B for PVDC/aliphatic polyester blends plotted as a function of the number of methylene groups ($-CH_2-$) per ester group ($-COO-$) in the second polymer (Data from Woo et al. 1986)
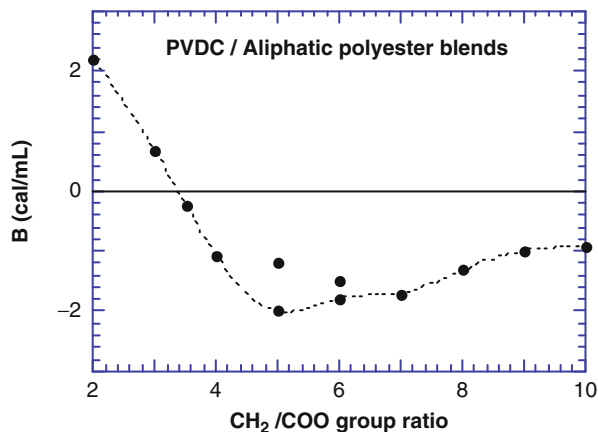

Fig. 2.10 The binary interaction parameters for two PIB resins ($M_w = 81.6$ and 114 kg/mol) with either ethylene-butene copolymers (of different M_w and composition) or with an atactic head-to-head polypropylene (HHPP), based on SANS data (Krishnamoorti et al. 1995)
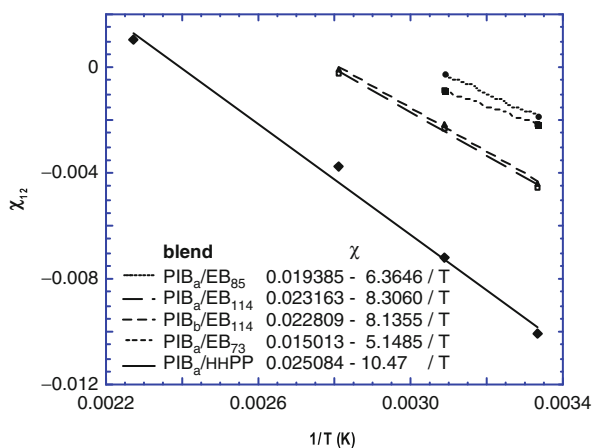
chlorinated polymers, e.g., PVC, and the lowest for fluorinated, e.g., PVF, with the brominated PVB, having an intermediate behavior. Furthermore, when the chlorinated polymer was mixed with a series of polyesters, the highest miscibility was observed when the ratio of the $-CH_2-$ to $-COO-$ groups reached an optimum value. This optimum value depended on the chemical nature of the halogenated polymer – as shown in Fig. 2.9, for PVDC blends with aliphatic polyesters this optimum value is between 5 and 6.

In Table 2.11 along the parameters χ_{12} and B, the available values of ΔP^* are also listed. The latter parameter originates from S-L EoS, and it has been considered a measure if the interaction energy is proportional to χ_{12} or B (Sanchez 1989). All these parameters, being proportional to each other, are expected to show similar variability with the independent variables; for example, see the variation with composition and temperature of χ_{12} in Figs. 2.10 and 2.11 and of ΔP^* in Fig. 2.12.

Fig. 2.11 Temperature
dependence of the binary
interaction parameter, χ, for
blends of deuterated
amorphous polypropylene
(either head-to-tail or head-to-
head) with polyethylene
copolymers. The values were
determined from SANS data
(Graessley et al. 1995)
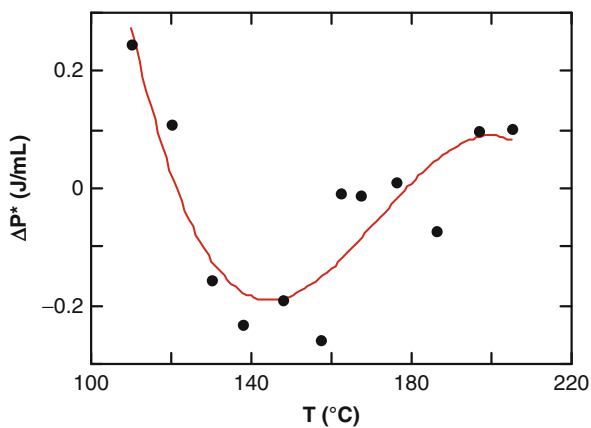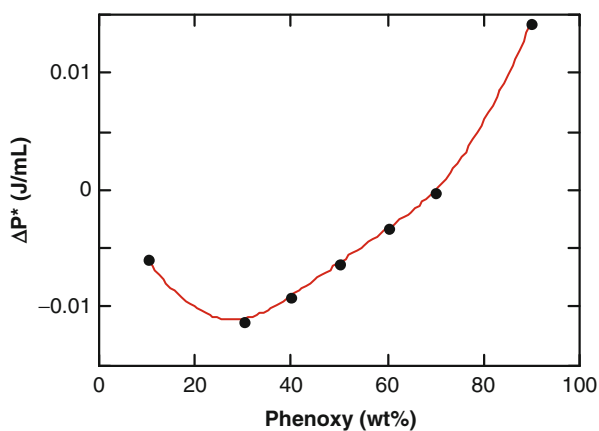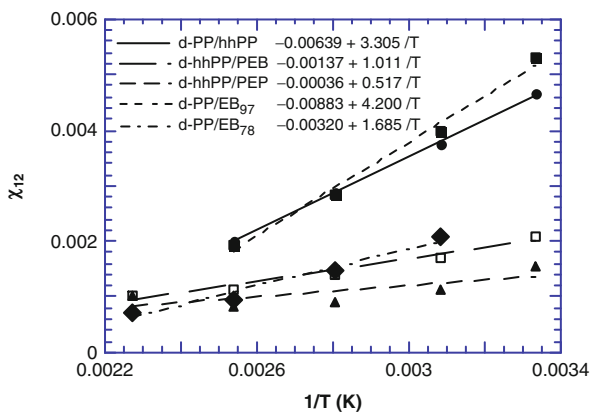
Fig. 2.12 (*Top*)
Compositional variation of
the interaction parameter ΔP^*
in phenoxy/polyvinyl methyl
ether blends at the spinodal
temperature, T_s. (*bottom*)
Temperature dependence of
ΔP^* (Data after Etxeberria
et al. 1997)

Fig. 2.13 Compositional variation of the interaction parameter, B, in a copolymer (mers #1 and #2)/ homopolymer (mers #3) blend. Even when all three binary interaction parameters are positive ($B_{23} = 1$, $B_{13} = 2$, and $B_{12} = 0-10$), for a copolymer with strong repulsive interactions, $B_{12} = 10$, a "window of miscibility" is predicted

Copolymer-A (mers #1 & #2) with polymer-B (mers #3) blends:

$$B = B_{13}\phi + B_{23}(1 - \phi) - B_{12}\phi (1 - \phi)$$
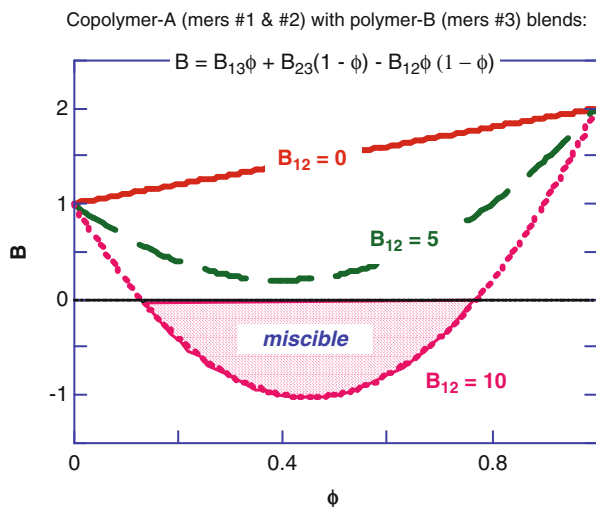
The observed regularity in the miscibility behavior of polymers can be understood considering the polymers as composed of individual interacting groups. For example, taking the case illustrated in Fig. 2.9, one may consider that PVDC is an alternating copolymer of units, $-CH_2-$ and $-CCl_2-$, whereas the aliphatic polyester is composed of $-CH_2-$ and $-COO-$ units. Equations 2.48 and 2.49 predict that even systems with all positive values of the binary interaction parameter, $B_{ij} > 0$, (repulsive interactions) may have a window of miscibility, where the overall parameter B becomes negative. The magnitude of this effect depends primarily on the value of the repulsive interactions within the copolymer molecule, $B_{12} > 0$; a schematic representation of Eq. 2.49 is shown in Fig. 2.13.

Since B_{ij} characterizes the enthalpic and non-configurational entropy of interaction between segments i and j, they should be pairwise and additive, to a good approximation; thus, one could tabulate these parameters per group and, in turn, use them for predicting miscibility in any arbitrary system composed of polymers and/or copolymers built from these groups/segments (Paul and Barlow 1984). This idea is similar in concept with the group-contribution approach of calculating solubility parameters. Table 2.12 provides examples of B_{ij} values published over the years, as well as χ_{ij}. The χ_{ij} dimensionless parameter is directly proportional to B_{ij} (Eq. 2.47), whereas ΔP^* is the binary interaction energy density calculated from S-L EoS. Since ΔP^* is also proportional to B_{ij} (Sanchez 1989), one may apply S-L theory to experimental data and compute the segmental contributions, ΔP_{ij}^*, in analogy to B_{ij}:

$$\Delta P^* = \Delta P_{12}^* \phi_2' \left(\phi_2' - \phi_3''\right) + \Delta P_{13}^* \phi_3'' \left(\phi_3'' - \phi_2'\right) + \Delta P_{23}^* \phi_2' \phi_3'' \qquad (2.50)$$

The segmental interaction parameters have been also used to explain the "miscibility window" or "miscibility chimney" in polymer/copolymer or

Table 2.12 Binary segmental interaction parameters, B_{ij} or χ_{ij}

Unit 1	Unit 2	B_{ij} (cal/mL)	χ_{ij}	Reference
–CH$_2$–	Phenoxy	8.34		1
–CH$_2$–	–COO–	250.3		1
–COO–	Phenoxy	154.9		1
–CH$_2$–	S	5.72		2
–CH$_2$–	AN	97.5		2
–CH$_2$–	–COO–	136.5		2
S	AN	122		2
S	–COO–	103		2
AN	–COO–	104		2
–CH$_2$–	–CH(C$_6$H$_5$)–	8.07		2
–CH$_2$–	–CH(CN)–	234		2
–CH(C$_6$H$_5$)–	–CH(CN)–	277		2
–CH(C$_6$H$_5$)–	–COO–	96.8		2
–CH(CN)–	–COO–	170		2
–CH$_x$–	(C$_6$H$_5$)–	10.4		2
–CH$_x$–	–CN	508		2
–CH$_x$–	–COO–	136		2
(C$_6$H$_5$)–	–CN	579		2
(C$_6$H$_5$)–	–COO–	93.0		2
–CN	–COO–	351		2
VAc	C(VC)		0.17	3
VAc	VC		0.27	3
VAc	–CH$_2$–		1.01	3
VC	C(VC)		0.042	3
VC	–CH$_2$–		0.15	3
S	MMA	0.22		4
S	MA	7.32		4
MA	MMA	9.30		5
MA	EMA	10.4		5
MA	nPNM	11.9		5
MA	S	14.9		5
MA	AN	−0.381		5
AN	MMA	5.00		5
AN	EMA	5.33		5
AN	nPMA	5.85		5
AN	S	8.14		5
S	MMA	0.181		5
S	EMA	−0.0361		5
S	nPMA	−0.0309		5
S	MMA	0.26		6
α-MS	MMA	0.26		6
α-MS	S	0.018		6
TMPC	S	−0.15		7

(*continued*)

Table 2.12 (continued)

Unit 1	Unit 2	B_{ij} (cal/mL) χ_{ij}	Reference
TMPC	MMA	0.26	7
HFPC	S	1.5	7
HFPC	MMA	−0.07, −0.73	7
HFPC	TMPC	0.25 ± 0.04	7
S	MMA	0.18, 0.26	7
S	MMA	0.22	8
MA	MMA	7.18	8
S	MA	10.7	8
S	AN	6.8	8
MA	AN	−0.31	8
S	TMPC	−0.14	8
MA	TMPC	11.5	8
S	PPE	≤−0.37	8
MA	PPE	14.6 ± 0.5	8
MMA	VC	0.54	9
S	VC	2.85	9
MMA	S	2.93	9
AN	S	95.52	9
TMPAr	PAr	5.36	10
TMPAr	S	2.18	10
TMPAr	AN	99.04	10
PAr	S	10.52	10
PAr	AN	89.09	10
S	AN	117.89	10
$-p\mathrm{C_6H_4-O-}$	$-p\mathrm{C_6H_4-CO-}$	1.44	11
t-BMA	S (130 °C)	0.34	12
t-BMA	S (150 °C)	0.50	12
t-BMA	S (180 °C)	3.03	12
t-BMA	MAN (130 °C)	1.47	12
t-BMA	MAN (150 °C)	2.29	12
t-BMA	MAN (180 °C)	7.40	12
t-BMA	MMN (130 °C)	0.76	12
t-BMA	MMN (150 °C)	1.00	12
t-BMA	MMN (180 °C)	4.37	12
S	MAN (130 °C)	1.20	12
S	MAN (150 °C)	2.02	12
S	MAN (180 °C)	2.15	12
S	MMA (130 °C)	0.221	12
S	MMA (150 °C)	0.229	12
S	MMA (180 °C)	0.242	12
S	CHMA (130 °C)	−0.15	12
S	CHMA (150 °C)	−0.43	12

(*continued*)

Table 2.12 (continued)

Unit 1	Unit 2	B_{ij} (cal/mL)	χ_{ij}	Reference
S	CHMA (180 °C)	−0.10		12
MMA	MAN (130 °C)	0.28		12
MMA	MAN (150 °C)	0.84		12
MMA	MAN (180 °C)	0.91		12
CHMA	MAN (130 °C)	1.40		12
CHMA	MAN (150 °C)	2.65		12
CHMA	MAN (180 °C)	2.11		12
CHMA	MMA (130 °C)	0.75		12
CHMA	MMA (150 °C)	0.64		12
CHMA	MMA (180 °C)	0.50		12
S (140–170 °C)	MMA		−0.635 + 287/T	13
S (140–170 °C)	AN		−11.0 + 4,940/T	13
S (140–170 °C)	CL		−0.913 + 412/T	13
AN (140–170 °C)	MMA		−4.44 + 2,000/T	13
AN (140–170 °C)	CL		−4.76 + 2,140/T	13
MMA (130–200 °C)	nBMA		−0.216 + 95.7/T	14
MMA (130–200 °C)	iBMA		−0.157 + 73.1/T	14
iBMA (130–200 °C)	nBMA		0.0179 − 10 − 7(846 T − T2)	14
S (80–130 °C)	AN		0.12	15
S (80–130 °C)	CL		0.0077	15
CL (80–130 °C)	AN		0.049	15
CL	DTC		0.001	16
S	DTC		0.02	16
AN	DTC		0.042	16
VCVAc-90	iBMA	−5.49		17
VCVAc-90	iBMA-nBMA50	−2.22		17
VCVAc-90	iBMA-nBMA13	−0.11		17
VCVAc-90	nBMA	−1.73		17
iBMA	nBMA	0.00002		17
SAN$_{(75\ \%\ S)}$	SMMA$_{(90\ \%\ MMA)}$		−0.0134	18
MAN$_{(90\ \%\ MMA)}$	SMMA$_{(90\ \%\ MMA)}$		0.0083	18
MAN$_{(90\ \%\ MMA)}$	SAN$_{(75\ \%\ S)}$		−0.0108	18
SAN$_{(80\ \%\ S)}$	SMMA$_{(95\ \%\ MMA)}$		−0.0154	18
MAN$_{(95\ \%\ MMA)}$	SMMA$_{(95\ \%\ MMA)}$		0.0021	18
MAN$_{(95\ \%\ MMA)}$	SAN$_{(80\ \%\ S)}$		−0.011	18
–CH$_2$–	–NHCO–		8.534	19
–CH$_2$–	–COO–		2.233	19

(*continued*)

Table 2.12 (continued)

Unit 1	Unit 2	B_{ij} (cal/mL)	χ_{ij}	Reference
–CH₂–	–CHCl–		0.500	19
–COO–	–NHCO–		3.880	19
–CHCl–	–NHCO–		6.750	19
–COO–	–CHCl–		0.038	19
S	VME	0.0167		20
S	DNS	1.79		20
DNS	VME	1.50		20
DNS	PPE	2.936		20

Abbreviations for the polymeric units: (C_6H_5)– phenyl ring, *α-MS* alpha-methylstyrene, *AN* acrylonitrile, *BMA* butylmethacrylate, *CHMA* cyclohexyl methacrylate, *CL* caprolactone, *C(VC)* unit of chlorinated PVC, *DNS* 2,4-dinitrostyrene-*co*-styrene, *DTC* 2,2-dimethyltrimethylenecarbonate, *HFPC* hexafluoro bisphenol-A carbonate, *MA* maleic anhydride, *MMA* methylmethacrylate, *PAr* unit of polyarylate, *Phenoxy* unit of poly(hydroxy ether) of bisphenol-A, *PPE* unit of poly(2,6-dimethyl-1,4-phenylene ether), *S* styrene, *TMPAr* unit of tetramethyl bisphenol-A polyarylate, *TMPC* unit of tetramethyl bisphenol-A polycarbonate, *VAc* vinyl acetate, *VC* vinyl chloride, *VCVAc90* VC-*co*-VAc copolymer with 90 % VC, *VME* vinyl methyl ether

References: 1. Paul and Barlow 1984; **2.** Fernandes et al. 1986; **3.** Shiomi et al. 1986; **4.** Kim et al. 1989; **5.** Brannock et al. 1991; **6.** Callaghan and Paul 1993; **7.** Takakuwa et al. 1994; **8.** Gan and Paul 1994a; **9.** Dompas et al. 1997; **10.** Ahn et al. 1997a, b; **11.** Harris and Robeson 1987; **12.** Nishimoto et al. 1995; **13.** Higashida et al. 1995; **14.** Sato et al. 1996a, b; **15.** Schulze et al. 1993; **16.** Kammer and Kumerlowe 1996; **17.** Sato et al. 1997; **18.** Cowie et al. 1992c; **19.** van Ekenstein et al. 1997; **20.** Fernandez et al. 1997

copolymer/copolymer blends (Lath and Cowie 1988). These parameters have been found useful to predict miscibility of blends containing one component whose structure is systematically varied, e.g., polyesters with either halogenated polymers or phenoxy (Prud'homme 1982; Harris et al. 1983; Woo et al. 1985, 1986), polyamide blends (Ellis 1989), ternary blends (Shah et al. 1986), and other systems, viz., SAN/PMMA, SAN/PC, polyethyloxazoline/polyester, PPE with a mixture of P*o*ClS and P*p*ClS, PC/PCL/phenoxy, and many more.

Ellis (1988, 1989, 1990a, b) used the same approach to evaluate miscibility of polyamide blends. He treated the polyamide molecules as copolymers, viz., comprised of units A, B, and C in the form $A_xB_yC_{1-x-y}$, where A, –CH₂–; B, –NHCO–; and C, $–C_6H_4–$ (phenyl). The analysis made it possible to systematize the experimental observations and predict conditions of miscibility for aliphatic and semi-aromatic polyamides. The method was applied to a 1:1 composition of blends, and χ_{12} values were assumed to be temperature independent. Examples of the segmental interaction parameters, χ_{ij}, used are given in Table 2.13. For binary mixtures of aliphatic polyamides A_xB_{1-x} with A_yB_{1-y} (where A and B groups were as defined above), the binary interaction parameter of the blend was expressed as $\chi_{12} = 7.984(x-y)^2$, a positive number; thus, these polymers are expected to be immiscible. The miscibility, if observed, may be explained by either the presence of hydrogen bonding or *trans*-reactions (transamidation) resulting in rapid homogenization of the system (e.g., PA-6/PA-46 at 310 °C becomes homogenous in 4 min) (Ellis 1992).

Table 2.13 Segmental interaction parameters, χ_{ij}, for polyamide blends (Ellis 1990b, 1993, 1995, 1997)

Segment-1	Segment-2	χ_{12}
$-CH_2-$	$-NHCO-$	7.984; 8.534
$-CH_2-$	$-CH_2-NHCO-CH_2-$	1.479
$-CH_2-$	$-COO-$	2.233
$-CH_2-$	$-C_6H_4-$	-0.288; -0.308
$-CH_2-$	$-mC_6H_4-$	0.1
$-CH_2-$	$-NHCO-C_6H_4-NHCO-$	1.571
$-CH_2-$	$-NHCO-pC_6H_4-NHCO-$	1.680
$-CH_2-$	$-NHCO-mC_6H_4-NHCO-$	1.693
$-NHCO-$	$-C_6H_4-$	7.460; 7.974
$-NHCO-$	$-COO-$	3.880
$-NHCO-$	$-mC_6H_4-$	8.000
$-NHCO-$	$-NHCO-C_6H_4-NHCO-$	2.275
$-NHCO-$	$-NHCO-pC_6H_4-NHCO-$	2.432
$-NHCO-$	$-NHCO-mC_6H_4-NHCO-$	2.445
$-CH_2-NHCO-CH_2-$	$-NHCO-C_6H_4-NHCO-$	-0.083
$-CH_2-$	$-COO-$	2.233
$-NHCO-$	$-COO-$	3.880
$-C_6H_4-$	$-COO-$	1.692
$-mC_6H_4-$	$-COO-$	1.500
$-mC_6H_4-$	$-NHCO-mC_6H_4-NHCO-$	1.680

It has been known since the early days that behavior of the aromatic polyamides (aramids) depends critically on the type of isomeric substitutions – *para*-substitutions result in crystalline, while *meta*-substitutions in amorphous polymers (Kwolek et al. 1962). Similarly, the two aramids: poly(*m*-xylene adipamide) and poly (hexamethylene isophthalamide), MXD6 and PA-6I, respectively, show different miscibility, e.g., with aliphatic polyamides. Clearly, blind application of the segmental interaction strategy to aromatic or semi-aromatic polyamides leads to conflicts. However, the problem can be resolved considering *p*- and *m*-substituted phenyl as two different statistical segments (Ellis 1995). This idea is indeed evident in the segmental contributions listed in Table 2.14.

The segmental interaction values of χ_{ij} from Table 2.13 were used to compute the binary interaction parameters, χ_{12}, for blends of a semi-aromatic polyamide, PA-3Me6T (Trogamid^{TM} T) with aliphatic polyamides, PA-4 to PA-12. These values are listed in Table 2.14, along with the observations of miscibility, in good agreement (Ellis 1989). The data of Table 2.14 were used to construct Fig. 2.14. Similar to the case for the miscibility of halogenated polymers with polyesters, here also the miscibility depends on the CH_2/NHCO ratio – with the best miscibility found when the group ratio was 7, e.g., for PA-410.

Later, this analysis was extended to PA blends with polyesters (Ellis 1993, 1995; 1997). Thus, in the simplest case of PA blends with aliphatic polyesters, i.e., blends of A_xB_{1-x} with A_yD_{1-y}, where the units are A, $-CH_2-$; B, $-NHCO-$; and

Table 2.14 Calculated binary interaction parameters, χ_{12}, based on segmental contributions values (from Table 2.13) for blends of aliphatic polyamides with PA-3Me6T and experimental observation of miscibility (Ellis 1989)

Aliphatic PA	Aromatic PA	χ_{12}	Observation
PA-4	PA-3Me6T	0.0400	Immiscible
PA-46	PA-3Me6T	0.0065	Immiscible
PA-6	PA-3Me6T	−0.0050	Miscible
PA-66	PA-3Me6T	−0.0050	Miscible
PA-69	PA-3Me6T	−0.0069	Miscible
PA-610	PA-3Me6T	−0.0058	Miscible
PA-612	PA-3Me6T	−0.0023	Miscible
PA-11	PA-3Me6T	0.0061	Immiscible
PA-12	PA-3Me6T	0.0104	Immiscible
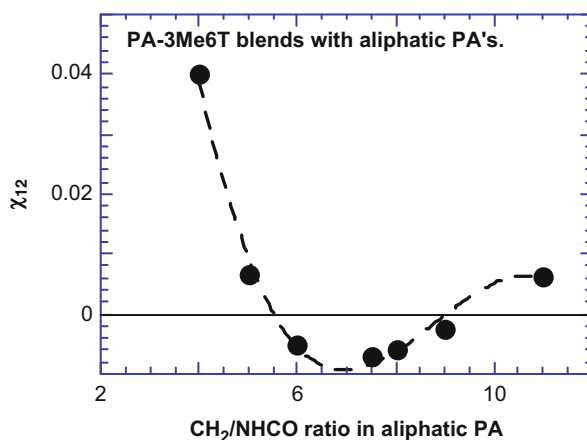
Fig. 2.14 The calculated binary interaction parameter for blends of PA-3Me6T with aliphatic polyamides as a function of the –CH$_2$–/–NHCO– group ratio of the aliphatic polyamide (Data from Ellis 1989)

D, –COO– (ester) and the subscripts x, y refer to the polymers' mer volume fractions, the binary χ based on segmental contributions is (Ellis 1993) $\chi_{12} = (y-x)(1-x) \chi_{AB} + (x-y)(1-y) \chi_{AD} + (1-x)(1-y) \chi_{BD}$. The values of χ_{ij} are also listed in Table 2.13. A similar principle was used to apply the LCT to polyolefin copolymer blends (Freed and Dudowicz 2005).

After 30 years since its conception, the heat of mixing (or analog calorimetry) method for the determination of polymer/polymer miscibility is becoming increasingly sophisticated. The low molecular weight analogs are selected on the basis of detailed calculations of the electrostatic charges on the atoms and molecules, using molecular orbital theories. The following principles have been formulated (Sandler and Wu 1991; Ziaee and Paul 1996; 1997):

The geometry of a functional group (in the polymer and selected analog molecule) should be the same.

The electrostatic charge of each atom in a functional group should be approximately the same.

Table 2.15 Segmental binary interaction parameters, B_{ij}, at 0.5 volume fraction, for polar groups related to bisphenol-A carbonates and acrylonitriles (Ziaee and Paul 1996, 1997)

Group-1	Group-2	T (°C)	B_{ij} (cal/mL)
$-C_6H_5$	$-CH_2-$	30	8.74 ± 0.16
$-C_6H_5$	$-CH_2-$	80	7.74 ± 0.16
$-C_6H_5$	$-CH_2-$	130	5.93 ± 0.20
$-C_6H_5$	C_6H_5-O-	80	-2.11 ± 0.30
$-CH_2-$	C_6H_5-O-	80	5.44 ± 0.15
$-C_6H_4-O-$	C_6H_5-	80	-0.60 ± 0.45
$-C_6H_4-O-$	$-CH_2-$	80	7.24 ± 0.26
$-C_6H_5$	$-mXO-$	80	-0.91 ± 0.14
$-CH_2-$	$-mXO-$	80	3.13 ± 0.18
$-C_6H_5$	$-CO-$	80	-36.9 ± 18
$-C_6H_5$	$-CO-$	90	15.1
$-CH_2-$	$-CO-$	80	-19.1 ± 15
$-CH_2-$	$-CO-$	90	41.4
C_6H_5-O-	$-CO-$	90	-8.97
$-C_6H_5$	$-Ph_2OCOO-$	90	0.55 ± 0.21
$-CH_2-$	$-Ph_2OCOO-$	90	10.1 ± 0.2
$-C_6H_5$	$-mX_2OCOO-$	130	0.40 ± 0.06
$-CH_2-$	$-mX_2OCOO-$	130	4.56 ± 0.06
$-C_6H_5$	$-CH_2-CN$	30	19.1 ± 0.2
$-CH_2-$	$-CH_2-CN$	30	60.8 ± 0.5

Notes: Most groups are the obvious common compounds (methylene, $-CH_2-$ (cf. alkyl); phenyl, $-C_6H_5$; carbonyl, $-CO-$; phenol, C_6H_5-O-; etc.). The rest of the groups relate to the segments of bisphenol-A polycarbonate and tetramethyl bisphenol-A polycarbonate: mX is m-xylyl: $-C_6H_2(CH_3)_2-$ (cf. di(2,6-dimethyl)phenyl); mXO, m-xylyl ether: $-C_6H_2(CH_3)_2-O-$; Ph_2OCOO, diphenyl carbonate: $-C_6H_4-O-CO-O-C_6H_4-$; mX_2OCOO, di(m-xylyl)carbonate, viz., di (2,6-dimethyl)phenyl carbonate, $-[C_6H_2(CH_3)_2]-O-CO-O-[C_6H_2(CH_3)_2]-$, i.e., a diphenyl carbonate with each of the two phenyls being a 2,6-dimethyl substituted phenyl (m-xylyl)

The functional group should be approximately electroneutral.

The functional group should be the smallest entity, identified by dividing the analog molecule into a collection of electroneutral groups.

Going beyond effectively apolar polymers – those whose miscibility is determined by van der Walls interactions (dispersion forces) – for polar polymer, the partial charges can also be accounted for and incorporated in segmental binary interaction parameters. A careful analysis of such data makes it possible to determine binary interaction parameters, B_{ij}, as those listed in Table 2.15. For these data, the authors calculated the (enthalpic) binary interaction parameters for several polymer/oligomer pairs, from Eq. 2.49 using the B_{ij} values, where the heat of mixing was determined at $T = 80$ °C for 1:1 blend/mixture compositions (Ziaee and Paul 1996; 1997). The calculated values were in good agreement with the measured ones, based mostly on polystyrene blends with bisphenol-A polycarbonate and tetramethyl bisphenol-A polycarbonate, as well as with acrylonitrile-containing polymers.

In summary, the heat of mixing approach and the corresponding segmental binary interaction parameters entail several simplifying assumptions. The numerical values of the parameters do vary depending on method of evaluation, selected system/pair, concentration, temperature, etc. However, the method has been found useful for the identification of potentially miscible systems and conditions. Furthermore, the approach provided a valid tool for interpretation of the blends' behavior at higher concentration, viz., 1:1 compositions, where the interaction parameters are relatively insensitive to the variability of concentration. Under these conditions, the segmental binary interaction parameters have been successfully employed to describe:

Miscibility in systems without strong specific interactions

Behavior of blends of a homopolymer with copolymer

Miscibility of polymer series (chemically similar polymers, e.g., polyamides, polycarbonates)

Window of miscibility in two- or three-component systems

Chimney of miscibility in two- or three-component systems

2.5.2.3 Solubility Parameter Approach

The concept of the solubility parameter originates from Hildebrand's work on enthalpy of regular solutions (Hildebrand and Scott 1950, 1962; Shinoda 1978) and was defined as the square root of the cohesive energy density $\left(\delta \equiv \sqrt{E/V}\right)$. Accordingly, in a strict sense, the molecular interactions should be nonspecific, without forming associations or orientation, hence not polar or hydrogen-bonding interactions. Another fundamental assumption was that the intermolecular interactions 1-2 are geometric mean of the intramolecular interactions, 1-1 and 2-2:

$$\Delta H_m \approx \Delta G_m^{non\ comb} = \phi_1 \phi_2 V_m (\delta_1 - \delta_2)^2 \geq 0$$

$$\Delta H_m \approx \phi_1 \phi_2 V_m \left[\sqrt{\frac{E_1^V}{V_1}} - \sqrt{\frac{E_2^V}{V_2}} \right]^2 = \left[\frac{E_1^V}{V_1} - \frac{2E_{12}^V}{\sqrt{V_1 V_2}} + \frac{E_2^V}{V_2} \right] \quad (2.51)$$

where E_i^V is the molar energy of vaporization of substance i and δ_i is its solubility parameter. Comparing Eq. 2.51 to Eq. 2.35 makes it evident that the binary interaction parameter *chi* can be written in solubility parameter terms:

$$\chi'_{12} \approx \left(V_{ref}/RT \right) (\delta_1 - \delta_2)^2 \quad (2.52)$$

where the reference volume is usually taken as $V_{ref} = 100$ mL/mol (viz., the liquid density is 1). It is important to note that, as stated by Eq. 2.51, the above interaction parameter is limited to the enthalpic part of binary interaction parameter, i.e.,

$$\chi'_{12} = \chi_S + \chi_H = \chi_S + \left(V_{ref}/RT \right) (\delta_1 - \delta_2)^2 \quad (2.53)$$

The entropic term in Eq. 2.53, χ_S, originates from local configurational effects, as well as combinatorial entropy contributions. When Eq. 2.52 is used, then χ_S must be accounted for through other means.

For molecules without polar groups, the solubility parameter δ_i may be determined or approximated:

1. From the δ_i definition (see Eq. 2.51):

$$\delta_i^2 = E_i^V/V = \left(\Delta H_i^V - PV\right)/V \approx \left(\Delta H_i^V - RT\right)/V \qquad (2.54)$$

2. From empirical correlation, as, for example, with the surface tension coefficient (γ_i) or the dipole moment (μ_i):

$$\delta_i^2 = 14\gamma_i/V^{1/3} \quad \text{or} \quad \delta_i = 37.4\mu_i/V^{1/2} \qquad (2.55)$$

3. By solving Eq. 2.51 for δ_1, knowing the experimental values of ΔH_m for material 1 in a series of solvents with known values of δ_2

For small molecules without strong interactions, the values of the solubility parameter vary from 5.9 (for C_6F_{14}) to 14.1 (for I_2), whereas it is about 30 for H_2O (Hansen 2000); the standard error of these estimates is ± 0.2, much larger for water. Given that polymer (melt) evaporation experiments are impossible, the solubility parameter of a polymer is usually determined by measurements of its oligomeric liquids or by indirect measurements of its behavior in a solvent of known solubility parameter. The solvent approach allows for the polymer to be cross-linked (the degree of swelling (D_s) is measured) or simply dissolved in the solvent (the intrinsic viscosity ($[\eta]$) is usually measured). From the plot of either D_s or $[\eta]$ versus $\delta_{solvent}$, the value of $\delta_{polymer}$ is determined as the value that corresponds to the peak location (Utracki 1972), or by appropriately fitting the whole curve (Hansen 2000). For copolymers, the volume additivity of the monomeric solubility parameters is assumed, i.e., $\delta = \sum \phi_i \delta_i$. This assumption also follows from the group-contribution method used to compute δ from the chemical and structural characteristics of polymeric chain, *vide infra* (Grulke 1989; van Krevelen 1992; Coleman et al. 1992, 2006). Correlation between the solubility parameter theory and the EoS based on the Flory model was also explored (Biros et al. 1971). The authors demonstrated that $\delta = P^{*1/2}V^*/V$, where P^* and V^* are the pressure-reducing and volume-reducing parameters, respectively.

Given the definition of δ, the temperature and pressure gradients of the solubility parameter can be approximated by

$$\left.\frac{\partial \ln\delta}{\partial T}\right|_P \cong -\alpha_P \quad \text{and} \quad \left.\frac{\partial \ln\delta}{\partial P}\right|_T \cong +\beta_T \qquad (2.56)$$

where α_P is the isobaric thermal expansion coefficient and β_T is the isothermal compressibility. These relations can be used to correct/extrapolate the value of δ to any temperature and pressure of interest (δ values are usually given at 298 K and ambient pressure).

For completeness of the above discussion, a few examples of solubility parameters for selected polymers are given in Table 2.16. More extensive listings can be found in the source literature (Shinoda 1978; Van Krevelen 1976; Grulke 1989;

Table 2.16 Solubility parameters, experimental and calculated, for various common polymers at 298 K. All δ values are in $(J/mL)^{1/2}$ the calculated values have a nominal error of ± 0.8 $(J/mL)^{1/2}$

Polymer	Experimental δ			Calculated δ
	Shinoda [1978]	van Krevelen [1976]	Grulke [1989]	Coleman 1990
PTFE	12.69	12.7	–	–
PDMS	14.94	–	14.90–15.59	–
PE	16.17	15.8	15.76–17.09	16.4
PP	–	16.8–18.8	18.80–19.20	15.2
PPG	–	15.4–20.3	19.20	17.4
PIB	16.58	16.0–16.6	14.50–16.47	14.8
PS	18.63	17.4–19.0	17.40–19.80	19.5
PVAc	19.24	19.1–22.6	18.00–22.61	19.7
PMMA	19.44	18.6–26.2	18.58–26.27	18.5
PVC	19.65	19.2–22.1	19.20–22.10	20.3
PET	21.90	19.9–21.9	21.54	23.6
PMAN	21.90	21.9	–	24.4
CA	22.31	–	22.30–23.22	–
PA-66	27.84	27.8	22.87–23.37	–
PAN	31.52	25.6	25.60–31.50	28.3

Note: The calculated values of δ in the last column can be reproduced by the CD-ROM tool provided in (Coleman and Painter [2006a], [b]). Although the tool allows for the input of almost any arbitrary polymer, and even provides a calculated δ value for these, care must be given to the uncertainty associated with certain groups' contributions, e.g., $-CF_2-$, $>Si<$, etc., whose attraction values are denoted as "rough estimates"; rather inaccurate numbers for δ are obtained for polymers that are comprised primarily by such groups, e.g., using $-CF_2-$ group contributions for PTFE above would result in $\delta = 10.2$, but this value is with ± 5 uncertainty. Calculated δ's with large uncertainties are omitted above. These limitation are outlined in the accompanying booklet (Coleman and Painter [2006a], [b])

Coleman et al. [1990]). As evident, by comparing data from different studies, cf. Table [2.16], one complication of the solubility parameter method is poor reproducibility of the measured values. Selection of different commercial polymers and solvents, or using different sets of solvents, may significantly change the value of the measured δ. Also, more recent and arguably more accurate calculated δ values exist (Hansen [2000]; Coleman and Painter [2006a], [b]), *vide infra*.

The biggest drawback of the solubility parameter approach, as described above, is the omission of the entropic and specific interactions' effects. Furthermore, the fundamental dependencies do not take into account either the structural (isomeric), orientation, or the neighboring group effects (e.g., steric effects, intermolecular screening, functional group accessibility) (Coleman and Painter [2006a], [b]). However, solubility parameters can provide a guide toward miscibility: Since the contributions that are included in the solubility parameter calculation are indeed detrimental to miscibility, minimizing their value must but help the miscibility.

In the simplest approach, the solubility parameter of a polymer can be calculated by a summation of group contributions (Coleman and Painter 1988, 1989, 1990, [2006a], [b]). The essence of this approach is to assume pairwise additivity for the interaction of sub-monomeric building blocks, "groups," which can be added to

Table 2.17 Selected group contributions for the calculation of solubility parameters based on Eq. 2.57; molar volume V_i^g [cm^3/mole] and molar attraction F_i^g [(cal · cm^3)$^{1/2}$/mole] (Coleman and Painter 2006a, b). The source contains additional groups and important instructions of how, and when, meaningful solubility parameters for polymers can be obtained

Group	V_i^g	F_i^g
–CH$_3$	31.8	218
–CH$_2$–	16.5	132
>CH–	1.9	23
>C<	−14.8	−97
>C$_6$H$_3$–	41.4	562
–C$_6$H$_4$–	58.5	652
–C$_6$H$_5$	75.5	735
=CH$_2$	29.7	203
–CH=	13.7	113
>C=	−2.4	18
–OCO–	19.6	298
–CO–	10.7	262
–O–	5.1	95
–Cl	23.9	264
–CN	23.6	426
–NH$_2$	18.6	275
>NH	8.5	143
>N–	−5.0	−3

form the monomer units. For example, a simple hydrocarbon, such as *n*-octane, is assumed to consist of six –CH$_2$– and two –CH$_3$ groups; using the energy of vaporization for a series of such paraffins with varied length, Coleman and Painter estimated molar attraction constants for –CH$_2$– and –CH$_3$.

Further, by including branched hydrocarbons, and molecules containing other functional groups (ether oxygens, esters, nitriles, etc.), a table of constants was obtained (Table 2.17) and, subsequently, used to calculate the solubility parameter for various polymers, using the relationship:

$$\delta = \frac{\sum_i F_i^g}{\sum_i V_i^g} \tag{2.57}$$

In the late 1980s, a new approach to the solubility parameter concept was developed (Painter et al. 1988, 1989a, b, 1990, Coleman et al. 1988, 1989, 1990, 1991, 1995), which was later further refined to address some of the drawbacks mentioned above (Coleman and Painter 2006a, b). The authors start by recasting Flory-Huggins Eq. 2.35 into the form (Painter et al. 1988):

$$\frac{\Delta G_m}{RT} = \frac{V}{V_{ref}} \left[\frac{\phi_1}{N_1} \ln\phi + \frac{\phi_2}{N_2} \ln\phi_2 + \chi'_{12}\phi_1\phi_2 \right] + \frac{\Delta G_H}{RT} \tag{2.35b}$$

where V is the total molar volume of the two components and $V_{ref} = 100$ mL/mol is the reference volume. Originally, the new term, ΔG_H, was introduced to express the effects of hydrogen bonding in blends (where one polymer self-associates, the other does not – but it is capable to hydrogen bond to the first one). Since then, this term has been extended to describe all specific interactions (hydrogen bonding, ion-ion, ion-dipole, charge transfer, $\pi-\pi$ electron interactions, etc.) that provide negative contributions to the free energy of mixing. Equation 2.35b distinguishes three contributions to the free energy of mixing: the configurational entropy (given by the two logarithmic terms), the dispersive or van der Waals interactions (given by the positive $\chi'_{12}\phi_1\phi_2$ term), and the strong interaction term, ΔG_H. For systems with no specific interactions ($\Delta G_H \approx 0$), Eq. 2.35b becomes the FH equation. The interactions of the van der Waals type are accounted for by the $\chi'_{12}\phi_1\phi_2 \geq 0$ term, with χ'_{12} quantified through Hildebrand's solubility parameters via Eq. 2.52. The degree of polymerization dependence of miscibility was assumed to follow Eq. 2.36.

The novelty of the Coleman-Painter theory is the calculation of the hydrogen-bonding contributions in the free energy of mixing (Painter et al. 1988, 1995, 2000). Previous attempts to describe blends with specific interactions, including hydrogen bonds, usually employed the FH theory and allowed the χ parameter to become negative. However, such an approach is rather unsatisfactory because:

1. The hydrogen-bonded contacts are not random (i.e., the interaction term cannot take the usual $\chi\phi_1\,\phi_2$ form, because only for strictly random mixing the term $\phi_1\phi_2$ provide the probability of a 1–2 contact).
2. The formation of hydrogen bonds results in a high loss of degrees of rotational freedom in the molecules or segments involved and, hence, introduces significant entropic as well as enthalpic changes in ΔG_m.
3. It is rather unreasonable to lump both specific and nonspecific interactions into one overall interaction parameter, not only because they are very different in character (composition dependence, temperature dependence, etc.), but also because it is often the balance between the two, i.e., specific and nonspecific interactions, that determines the blend phase behavior.

In contrast, the Coleman-Painter theory quantified the hydrogen-bonding contributions implicitly by re-enumerating an "equilibrium distribution" of the various species in the mixture after accounting for hydrogen-bonding formation (in pairs, hydrogen-bonded dimers, or longer sequences h-mers). Specifically, starting from Eq. 2.35b, the final result for the specific interaction term ΔG_H can be written as

$$\frac{\Delta G_H}{RT} = \begin{aligned} &\frac{\phi_1}{r}\ln\phi_{01} + \phi_2\ln\frac{\phi_{21}}{\phi_{21}^0} \\ &+ K\phi_2\left(\phi_{21} - \phi_{21}^0\right) + \phi_2(1 - K\phi_{21})\frac{X}{1+X} \\ &- \left[\frac{\phi_2}{n_H^0}\ln\phi_2 + \frac{\phi_1}{r}\ln\phi_1\right] \end{aligned} \qquad (2.58)$$

with

$$r = V_1/V_2 \quad \left(\text{equiv. } V_{ref} = V_2\right) \quad \text{and} \quad X = K_1\phi_{01}/r$$

where the volume fractions ϕ_1 and ϕ_2 are the usual volume fraction of polymer 1 and 2, respectively, in the blend; ϕ_{01} is the volume fraction of polymer 1 that remains unassociated; ϕ_{21} and ϕ_{21}^0 represent the nonbonded monomers of polymer 2 in the blend and in the neat state, respectively; and n_H^0 is the equilibrium length of the hydrogen-bonded sequence of monomers. Note that a term describing the energy of hydrogen bond formation does not appear explicitly in the result (Eq. 2.58). To compute the thermodynamic contribution of the strong interactions to the overall thermodynamic behavior of a blend, one must first determine the three principal constants: K_A, K_B, and K_2; these are defined as association equilibrium constants for the formation of hydrogen bond between B and A units (of polymer 2 and 1), respectively, the formation of self-association between sequences of multiple B units, and the formation of doublets of the hydrogen-bonded B units (Coleman and Painter 1995; Painter and Coleman 2000). The K_A, K_B, and K_2 can be quantified experimentally, e.g., by IR spectroscopy, they are interrelated (only two of the three Ks need to be determined independently) and are constrained by stoichiometry (the total number of i-type mers is the sum of the associated and non-associated mers); the fraction of hydrogen-bonded A groups, f_A^{HB} which can be determined experimentally, can yield

$$f_A^{HB} = 1 - \frac{\phi_{0A}}{\phi_A} = 1 - \left[\frac{1}{1 + K_A\phi_B\Gamma_1}\right] \quad \text{with} \quad \Gamma_1 = 1 - \frac{K_2}{K_B} + \frac{K_2/K_B}{1 - K_B\phi_{0B}}$$
and
$$\phi_B = \phi_{0B}\Gamma_2\left[1 + \frac{K_A\phi_{0A}}{r}\right] \quad \text{with} \quad \Gamma_2 = 1 - \frac{K_2}{K_B} + \frac{K_2/K_B}{(1 - K_B\phi_{0B})^2}$$

$$\text{(2.58b)}$$

For the computation of an isobaric phase diagram, the temperature dependence of the association constants has to be known: $K_A(T)$, $K_B(T)$, and $K_2(T)$; the polymer-specific T dependence follows an Arrhenius-type dependence:

$$K_i = K_i^o \exp\left(\frac{-h_i}{R}\left[\frac{1}{T} - \frac{1}{T^o}\right]\right) \quad\quad\quad \text{(2.58c)}$$

where h_i is the enthalpy of formation of a hydrogen bond, which can be determined from experimental data (Painter and Coleman 2000). When the pressure influence on blend miscibility is of interest, the K_i functions must be evaluated within the appropriate range of pressures as well: $K_A(T, P)$, $K_B(T, P)$, and $K_2(T, P)$.

As mentioned, one of the strong points of this theory is that, since the three equilibrium association constants are defined in terms of chemical repeating units, these constants can, thus, be measured by spectroscopic means (Painter et al. 1989a, b, 2000). Infrared spectroscopy is sensitive to hydrogen bonding, but selection of the

Table 2.18 Association equilibrium constants for polyvinylphenol (PVPh), blends at 25 °C (Coleman et al. 1989; Xu et al. 1991)

Polymer		N	K_A	K_B	K_2
PVPh		60	37.1	66.8	21.0
StVPh	[75 % VPh]	371	27.5	49.6	15.6
StVPh	[43 % VPh]	223	16.5	29.8	9.4
StVPh	[25 % VPh]	131	9.7	17.5	5.5
StVPh	[8 % VPh]	37	2.8	5.0	1.6
StVPh	[2 % VPh]	11	0.8	1.4	0.5
PMA		350	53.2	–	–
PEA		700	46.8	–	–
PVAc		3,000	64.0	–	–
EVAc	[70 % VAc]	3,000	61.6	–	–
PCL		3,000	66.2	–	–
h_i (kcal/mol)		–	3.8	5.2	5.6

Note: StVPh [x% VPh] stands for poly(styrene-*co*-vinylphenol) with x% of vinylphenol comonomer

most appropriate vibration band is essential. For example, instead of N-H or O-H stretching, the carbonyl group (C=O) may be a better choice. Examples of the association constants for blends of poly(4-vinyl phenol), PVPh, with acrylic polymers are given in Table 2.18. These values were used to compute the phase diagrams for blends of styrene-*co*-vinyl phenol (comprising of 2–100 % VPh), with either acrylic polymers, poly(alkyl$_{i\,=\,1..6}$-methacrylates), or polyethers (Serman et al. 1989, 1991; Xu et al. 1991). The experimental data confirmed the theoretical prediction, thus corroborating the validity of the model. Since then, more blends, as well as polymer solutions, have been investigated experimentally and compared favorably against the theoretical predictions (Painter et al. 2000).

As stated before, the Hildebrand solubility parameter concept was developed for nonpolar, low molecular weight liquids at room temperature. For polar molecules, the method did not provide consistent information. To avoid trouble, initially all liquids were divided into three categories for poorly, moderately, and strongly interacting systems. Another route was taken by Hansen (1967) who postulated that all intermolecular forces:

• London dispersion forces between nonpolar molecules
• Repulsive forces between nonpolar molecules
• Coulombic ion/ion interactions
• Dipole/dipole interactions between the permanent dipoles
• Permanent dipole/ion interactions
• Induced dipole/ion interactions
• Permanent dipole/induced dipole interactions
• Charge-transfer forces
• Hydrogen bonding
• Coordination bonding
• Metallic bonding, etc.

Fig. 2.15 Schematic representation of Hansen's miscibility sphere, Eq. 2.60
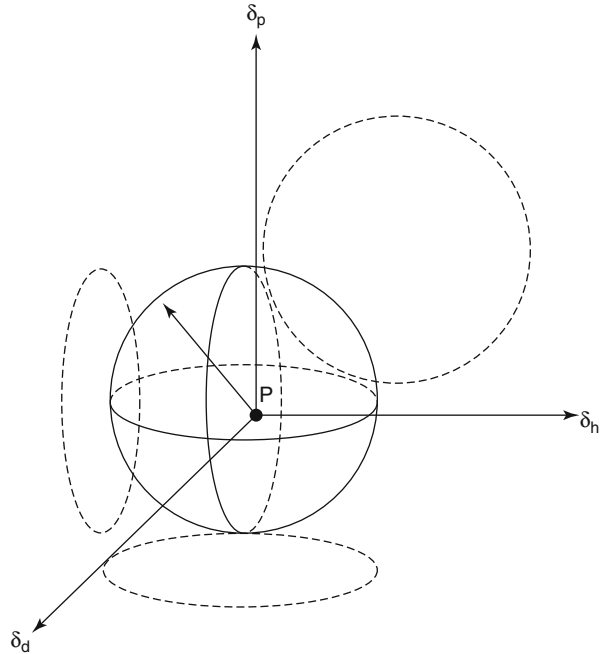
can be combined and grouped into three types of interactions, dispersive, polar, and hydrogen bonding, and a substance's total solubility parameter can thus be written as

$$\delta_i^2 = \delta_{id}^2 + \delta_{ip}^2 + \delta_{ih}^2 \tag{2.59}$$

where the subscripts d, p, and h represent the dispersive, polar, and hydrogen-bonding interactions, respectively. Accordingly, two substances would be miscible only when their solubility parameters place them within the critical radius of a spheroid, defined as (Hansen 1967, 1995)

$$R_{12}^2\text{crit} = \Theta(\delta_{1d} - \delta_{2d})^2 + \left(\delta_{1p} - \delta_{2p}\right)^2 + \left(\delta_{1h} - \delta_{2h}\right)^2 = \chi_{12} \geq 0 \tag{2.60}$$

where the semiempirical fudge parameter: Θ assumes values of 4–5 and accounts for the dominant role that the dispersion forces play in binary solubility. The concept is illustrated in Fig. 2.15. Examples of the numerical value of the Hansen's parameters are given in Table 2.16 (Hansen 1967, 1994, 1995; Hansen and Beerbower 1971; Grulke 1989; Luciani et al. 1996b), whereas a comprehensive collection of values has been compiled in a handbook (Hansen 2000). As reported by Hansen (1995, 2000), values of these parameters may greatly vary from one commercial polymer resin to another, reflecting diversity of molecular weights,

molecular weight distribution, the presence or absence of catalyst, and a great diversity of additives (caution is advised for their use). The values of the solubility parameters for solvents are considered more dependable.

Much like the Coleman-Painter approach, the solubility method also allows for the values of the Hansen's partial solubility parameters, δ_{id}, δ_{ip}, and δ_{ih}, to be calculated from the molecular structure of a polymer by using additive group contributions. van Krevelen (1976) demonstrated usefulness of the method using contributions from individual atoms, structural groups, and configurations. However, care must be given when such solubilities are employed in mixture that contain dissimilar in interactions polymers. For example, comparing to the calculations of interfacial surface tensions based on dispersive and polar components, it becomes necessary for the polar component to be further broken down in an electron-donor and an electron-acceptor component, e.g., $\delta_{ip} \propto \delta_{ip}^{+}\delta_{ip}^{-}$, and enter Eq. 2.60 as $(\delta_{1p}^{+}-\delta_{2p}^{+})(\delta_{1p}^{-}-\delta_{2p}^{-})$, rather than as $(\delta_{1p}-\delta_{2p})^2$, otherwise one is led to rather unreasonable predictions (van Oss et al. 1988); thus, it becomes obvious that Eq. 2.60 is a simplification, which works well for polar substances 1 and 2 that are similar in polarity, but it becomes problematic when, for example, an electronegative and an electropositive substance are considered (Table 2.19).

While the tabulated data for the group contributions are given for amorphous materials at room temperature, $T = 25\ {}^{\circ}\text{C}$ (298 K), miscibility at processing temperatures (200–300 $^{\circ}$C) is most often of interest; thus, it is necessary to correct the solubility parameter values for any temperature effects. The solubility parameters are, in principle, insensitive to temperature. However, although interaction energies are not expected to be a function of T, the corresponding interaction volumes, either for the polymers or for the corresponding groups, are indeed T dependent. To account for the T dependence, either Eq. 2.20 or 2.56 can be used. The calculated values of δ_{id}, δ_{ip}, and δ_{ih} at 150 $^{\circ}$C (423 K) for selected polymers are listed in Table 2.20.

Equation 2.60 was also used to calculate the interfacial (interphasial) tension coefficients, γ_{12}, for two polymers forming an immiscible blend, based on their chemical structures.

$$\begin{aligned}
\gamma_{12} &= k_1(\rho RT)^{n-1}\left[\Theta(\delta_{1d} - \delta_{2d})^2 + (\delta_{1p} - \delta_{2p})^2 + (\delta_{1h} - \delta_{2h})^2\right]^n \\
&= k\left[\Theta(\delta_{1d} - \delta_{2d})^2 + (\delta_{1p} - \delta_{2p})^2 + (\delta_{1h} - \delta_{2h})^2\right]
\end{aligned} \quad (2.61)$$

where k, k_1 are constants and ρ is the density. Good agreement was found between the computed and experimental values of the coefficient for 46 polymer blends (Fig. 2.16). The best correlation was found for the values $0.3 \le \Theta \le 0.5$. Thus, contrary to the dissolution processes dominated by the dispersive forces ($\Theta = 4\sim5$), for interphasial phenomena, the dispersive forces seem less important than the polar ones (Luciani et al. 1996a, 1997). A more detailed experimental approach, providing also M_w and T dependencies of the interfacial

Table 2.19 Hansen solubility parameters for selected polymers at 25 °C. All values are in $(J/mL)^2$. For some polymers, more than one set of δ values are provided (a, b, etc.), indicating variability in experiments/fittings or polymer structure effects (comonomer, M_w, additives, etc.). A much more comprehensive collection of such values can be found in the relevant handbook (Hansen 2000)

Polymer		δ_d	δ_p	δ_h
ABS	(a)	18.60	8.80	4.20
ABS	(b)	16.30	2.70	7.10
ABS	(c)	17.60	8.60	6.40
CA		18.60	12.73	11.01
CR		19.00	8.00	0
HDPE		18.01	0	0
LLDPE		17.35	0	0
PA-6	(a)	17.39	12.71	11.14
PA-6	(b)	17.00	3.40	10.60
PA-66	(a)	18.62	5.11	12.28
PA-66	(b)	17.40	9.80	14.60
PAN		21.70	14.10	9.10
PB		16.98	0	1.02
PC	(a)	19.10	10.90	5.10
PC	(b)	18.10	5.90	6.90
PIB		14.53	2.52	4.66
PDMS		16.60	1.90	8.00
PES		19.60	10.80	9.20
PET	(a)	19.44	3.48	8.59
PET	(b)	19.10	6.30	9.10
PET	(Mylar)	18.00	6.20	6.20
PMA		15.22	11.54	7.63
PnBA		16.38	8.97	5.77
PMMA		18.64	10.52	7.51
PP		17.19	0	0
PPS		18.70	5.30	3.70
PS		21.28	5.75	4.30
PSF		19.03	0	6.96
PTFE		16.20	1.80	3.40
PVAc		20.93	11.27	9.66
PVC		18.82	10.03	3.07
PVDF		9.65	5.87	6.66
PVP		21.40	11.60	21.60
SBR		17.55	3.36	2.70

tension in immiscible blends, scattering or pendant drop approaches can be applied (Anastasiadis et al. 1988); this work showed good agreement with interfacial tension theoretical approaches, based on lattice models in the spirit of the Flory-Huggins approach (Helfand 1975a, b, c, Roe 1975). For more details

Table 2.20 Calculated partial solubilities at 298 K and at 423 K (Luciani et al. 1996b)

Polymer	T^* (K)	V_{298}/V_{423}	δ_d^{298K}	δ_p^{298K}	δ_h^{298K}	δ_d^{423K}	δ_p^{423K}	δ_h^{423K}
HDPE	11,560	0.934	18.01	0	0	15.54	0	0
LLDPE	9,710	0.915	17.35	0	0	14.32	0	0
PVAc	9,389	0.911	15.22	11.54	7.63	12.44	9.43	6.23
PMA	10,360	0.923	15.22	11.54	7.63	12.78	9.69	6.41
PS	12,680	0.942	16.72	8.25	5.15	14.71	7.26	4.53
PEA	9,929	0.918	15.75	10.45	6.83	13.08	8.68	5.67
PnBA	8,590	0.899	16.38	8.97	5.78	13.00	7.12	4.59
PiBA	8,590	0.899	16.12	8.99	4.61	12.80	7.14	3.66
PtBA	8,590	0.899	14.37	8.16	8.34	11.41	6.48	6.62
PMMA	11,880	0.937	13.59	9.25	10.30	11.79	8.03	8.94
PEHA	8,160	0.891	16.81	7.27	3.69	13.10	5.67	2.87
PCP	10,752	0.927	15.95	10.52	6.98	13.53	8.92	5.92
PET	11,740	0.936	15.03	13.13	10.54	13.01	11.36	9.12
PA-6	15,290	0.956	17.39	12.71	11.14	15.78	11.53	10.11
PA-66	11,980	0.937	17.39	12.71	11.14	15.12	11.05	9.69
PEG	10,170	0.921	16.74	10.14	8.74	14.00	8.48	7.31
PTMG	10,300	0.922	17.33	7.51	6.24	14.53	6.30	5.23
PP	11,260	0.932	16.70	0	0	14.32	0	0
PnBMA	10,080	0.920	15.00	7.75	8.52	12.51	6.46	7.10
PtBMA	13,340	0.946	13.45	7.17	9.58	11.94	6.36	8.50
PVDF	10,440	0.924	9.65	5.87	6.66	8.13	4.94	5.61
PDMS*	7,825	0.885	16.60	1.90	8.00	12.73	1.46	6.14
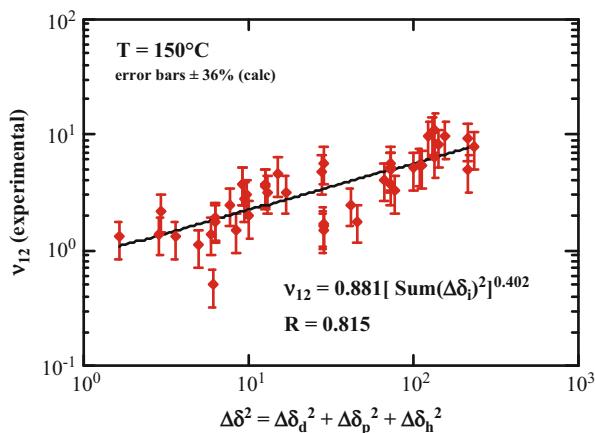
Fig. 2.16 Interfacial tension coefficient at 150 °C for 46 polymer blends plotted versus the solubility parameter contributions. R is the correlation coefficient

In figure:
T = 150°C
error bars ± 36% (calc)

$v_{12} = 0.881[\ Sum(\Delta\delta_i)^2]^{0.402}$

R = 0.815

$\Delta\delta^2 = \Delta\delta_d^2 + \Delta\delta_p^2 + \Delta\delta_h^2$

on the thermodynamics of interfacial tension in polymer blends, see Anastasiadis (2011).

A pragmatic modification of the solubility parameter approach was proposed by Bush et al. (1996). Recognizing that ΔH_m can be negative, the authors wrote

$$\Delta G_m \approx \Delta H_m = \phi_1 \phi_2 \left[(\delta_1 - \delta_2)^2 - e_h \right] \qquad (2.62)$$

where the correction e_h is a positive number, associated with the energy density that originates from specific interactions. In other words, Eq. 2.62 implies that, in the presence of favorable specific interactions, in order to maximize miscibility the solubility parameters of the two blend components should be the same.

2.5.3 Polymer Reference Interaction Site Model (PRISM)

Thermodynamic properties of a system can also be obtained from atomistic considerations. Molecular dynamics or Monte Carlo methods have been successfully used to study polymers. The success stems from the fact that many properties can be projected from dynamics of relatively simple, oligomeric models. Unfortunately, miscibility strongly depends on the molecular weight, and so far it cannot be examined by these methods.

Another similar route that considers interactions between individual elements of a system is the reference interaction site model (RISM). The theory involves computations of the system structure by means of the probability density function, which describes location of all N particles of the system. The binary interactions define the pair-density function:

$$\rho_N^{(2)} = \frac{N!}{(N-2)!} \int P_N \, dr^{(N-2)} = \rho^2 \, g(r) \qquad (2.63)$$

P_N is the probability density of N particles, r is the particle coordinate, and $g(r)$ is the radial distribution function. The potential energy of the system is given as a product of the potential energy of a single particle with all others, multiplied by a factor $N/2$:

$$U = \frac{N\rho}{2} \int_0^\infty 4\pi r^2 \, u(r)g(r) \, dr \qquad (2.64)$$

Thus, the total description of the thermodynamic state hinges on accurate quantification of $g(r)$. Ornstein and Zernike suggested separating the influence of this parameter into direct and indirect parts. The first describes direct interaction of the reference particle 1 with particle 2, while the indirect one that of particle 1 with particle 3, which in turn interacts with particle 2:

$$g_{12}(r) = c_{12}(r) + \rho \int c_{13}(r)[g_{13}(r) - 1] \, dr_3 \qquad (2.65)$$

where $c(r)$ is the direct correlation function. The advantage of the Ornstein-Zernike equation is that it can be readily generalized to more complex systems with inter- and

intramolecular interactions. RISM has been applied to progressively more complex liquids, from monatomic to diatomic, CCl_4, C_6H_6, etc. (Chandler and Andersen 1972). In the late 1980s, RISM has been applied to polymers, termed PRISM (Curro and Schweizer 1987; Schweizer and Curro 1989). The PRISM requires less computing time than atomistic simulations, but still makes it possible to incorporate structural details of polymeric molecules that the lattice models have been unable to account for. For example, bond lengths, their angles, chain conformation statistics, and different interaction potentials can be included in the mathematical simulations (Honeycutt 1992a, b, Curro 1994).

For polymer blends, PRISM provides good correlation with the experimental data obtained by SANS and light scattering (Eitouni and Balsara 2007). The agreement very much depends on selection of the "closure" approximation. Initial selection of the most appropriate closure for a given system can be quite difficult. Nevertheless, the method gave encouraging results, predicting details of phase separation in PO blends (Schweizer 1993). The deuteration effects as well as these related to structural differences between homopolymer and copolymers were well described (Schweizer 1993; Eitouni and Balsara 2007). The PRISM approach for polymer blends is still undergoing development and expansion; thus, more details here would simply be a snapshot at the moment of writing; the interested reader is therefore referred to seek a recent review or book chapter on PRISM.

2.5.4 Summary of Theoretical Approaches

Three theoretical approaches to the thermodynamics of polymer blends were briefly discussed: (1) the lattice theories, including the newer equation of state theories, (2) the off-lattice theories, and (3) the computational methods.

The lattice theories are the oldest and most frequently used to interpret and to predict the thermodynamic properties of multicomponent systems containing polymers. The Flory-Huggins theory is the best known. To use the theory, one must know the temperature, pressure, and concentration dependence of the enthalpic and entropic contributions to the binary interaction parameter, $\chi_{12} = \chi_H (T, P, \phi, \ldots) + \chi_s (P, \phi, \ldots)/T$. Two types of extension of the FH theory were discussed, the first that evolved from Paul and Barlow is a heat of mixing approach, and the second was a solubility approach developed by Coleman and Painter. The first of these two makes it possible to treat a homopolymer as a copolymer composed of subunits of the chain, thus to generalize and predict behavior of a great number of polymer blends. The second divides all thermodynamic influences into three groups: the configurational entropy, the van der Waals interactions, and the specific interactions. The novelty of this modification is the method of treatment of the latter interactions that combines the FTIR-measured kinetics of associations with the FH theory. All these approaches suffer from the fundamental drawbacks of the FH theory: inability to take into account the fine structure of polymeric chains, nonrandomness, orientation, and free volume. The interaction parameters depend on many variables, and the reported numerical values vary widely.

Fig. 2.17 Pressure dependence of the binodal and spinodal temperatures for the three *d*-PB/PS blends, with varied butadiene monomer structure. All phase boundaries increase with *P*, as expected from reduced free volume effects, but those for *d*-PB(1,2)/PS blends increase with a parabolic shape, while the increase is linear for the other two blends (Schwahn 2005)
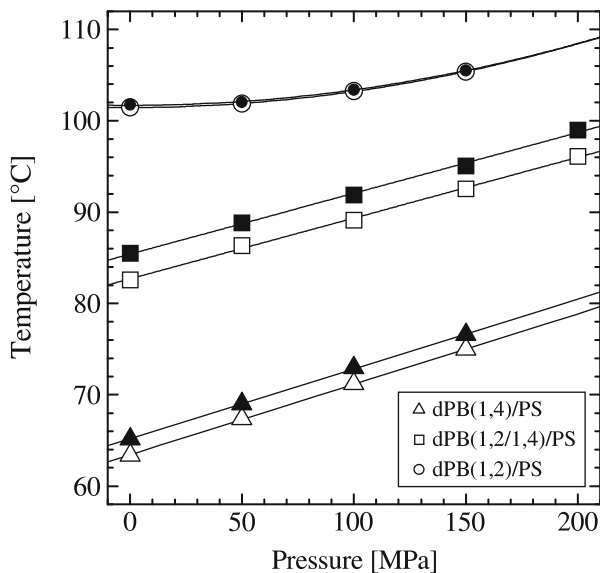
The theories based on the equation of state are more versatile. The model developed by Simha and many of his collaborators is most useful. By contrast with the FH theory, it leads to two binary interaction parameters, one energetic, the other volumetric, that are constant in the full range of independent variables. Furthermore, it has been found that the numerical values of these two parameters can be approximated by the geometric and algebraic averages, respectively. The nonrandom mixing can easily be incorporated into the theory. The non-lattice approaches, viz., strong interactions, heat of mixing, and solubility parameter approaches have more limited use. Their application should be confined to cases where the assumptions used in the derivations are well fulfilled.

The influence of pressure, *P*, on the miscibility needs a comment. Since pressure reduces the effects of the free volume contributions, for most blends the miscibility increase with *P* (Walsh and Zoller 1987; Schwahn 2005). The effects are very sensitive to the monomer structure, as one would expect from free volume considerations, as, for example, in PB/PS blends (Fig. 2.17): In the case of *d*-PB/PS blends, the general trend of an increase of the phase boundaries with pressure is observed for all systems (viz., increased binodal and spinodal temperatures with *P*, due to the reduction of free volume), but the shapes of $T_{binodal}(P)$ and $T_s(P)$ are linear for *d*-PB(1,4)/PS and *d*-PB(1,4-*co*-1,2)/PS blends and are more parabolic for the blend with *d*-PB(1,2)/PS; also the compatibility of PS is best for *d*-PB(1,4) and worst for *d*-PB(1,2), with the *d*-PB(1,4-*co*-1,2) copolymer being in between the two, as expected (Fig. 2.17). The *P* effect generally depends on the magnitude of the heat of mixing: For systems with $\Delta H_m < 0$, the miscibility is enhanced by compression, whereas for those with $\Delta H_m > 0$ it is reduced (Rostami and Walsh, 1984, 1985; Walsh and Rostami 1985). For PS solutions, the pressure gradient of

the critical solution temperature was found to be a function of the molecular weight – the higher the M_w, the more negative the gradient value (Stroeks and Nies 1990). For polymer blends, the gradient is usually positive: for PPE blends with a random copolymer of o- and p-fluorostyrene, the gradient $d(UCST)/dP = 64$ to 108 °C/GPa (Maeda et al. 1986), and for PS/PVME, $d(LCST)/dP = 300$ °C/GPa (Hiramatsu et al. 1983), whereas for blends of PEA/PVF the LCST showed a complex dependence (Suzuki et al. 1982). The prediction of the pressure effects on solubility poses great challenges for the precision of the theoretical description. It should be noted that, according to the conditions for phase separation (*vide infra*, e.g., Eq. 2.66, Fig. 2.20), the critical point is given by third partial derivative of the free energy of mixing, and its pressure gradient – the stability condition – by the forth partial derivative.

2.6 Phase Separation

2.6.1 Thermodynamics of Phase Separation

The thermodynamic conditions for phase separation and, also, the definitions of the respective phase diagram are given by

$$
\begin{aligned}
&\text{binodal}: (\partial \Delta G_m / \partial \phi_i)_{P,T,n_j}^{\text{phase 1}} = (\partial \Delta G_m / \partial \phi_i)_{P,T,n_j}^{\text{phase2}} \left(cf. \mu_i^{\text{phase 1}} = \mu_i^{\text{phase 2}} \right) \\
&\text{spinodal}: \left(\partial^2 \Delta G_m / \partial \phi_2^2 \right)_{P,T} = 0 \\
&\text{critical point}: \left(\partial^3 \Delta G_m / \partial \phi_2^3 \right)_{P,T} = 0 \\
&\text{stability condition}: \left(\partial^4 \Delta G_m / \partial \phi_2^4 \right)_{P,T} > 0
\end{aligned}
$$

$$(2.66)$$

Schematic of a phase diagram of a binary system is shown in Fig. 2.18. There are three regions of different degree of miscibility: (1) the single-phase miscible region between the two binodals, (2) the four fragmented metastable regions between binodals and spinodals, and (3) the two-phase separated "spinodal" regions of immiscibility bordered by the spinodals. The diagram also shows two critical solution temperatures, the lower, LCST (at higher temperature), and the upper, UCST (at lower temperature). The phase diagram with two critical points is a rule for measurements of mixtures with low molecular weight component(s). Whereas for polymer blends usually only one critical point is accessible for normal conditions, e.g., P, and typically shows either the LCST (most often) or the UCST. A few blends having UCST are PS blends with SBS, PoClS, PBrS, or poly(methyl-phenyl siloxane), and BR blends with SBR, SAN with NBR (Utracki 1989).

The origin of the critical point can be traced to the temperature effects on miscibility: In a first approach, one can distinguish three principal contributions to the binary interaction parameter, χ_{12} (Patterson 1982), with rather distinct T dependences: in general, the dispersive forces contributions in χ_{12}, with a $1/T$

Fig. 2.18 A schematic of the phase diagram for liquid mixtures with the upper and lower critical solution temperature, UCST and LCST, respectively. The placement of the critical compositions at about $\phi_{cr} = 0.5$ denotes that this is a symmetric blend ($N_1 = N_2$). In the general case, the phase diagram is qualitatively the same, but much less symmetric with respect to ϕ, with a ϕ_{cr} appearing in very small polymer concentrations, e.g., $\phi_{cr} \approx 1/\sqrt{N}$, cf. FH theory
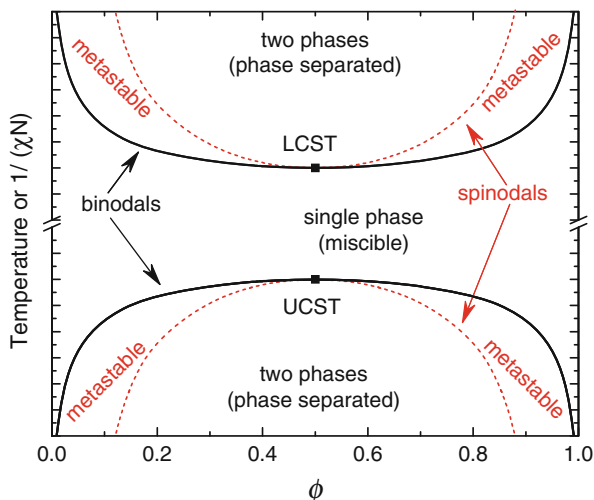
dependence; the free volume contributions, increasing with T; and the specific interaction contributions in χ_{12}, typically increasing with T (e.g., Arrhenius). As schematically illustrated in Fig. 2.19, the different temperature dependencies of these contributions affect χ_{12} in very different manner. For low molecular weight systems, where the dispersion interactions and free volume effects dominate the χ_{12}, the sum of these two has a U-shape, intersecting the critical value of the binary interaction parameter in two places – hence, two critical points, UCST and LCST (Fig. 2.19a). In contrast, most polymer blends owe their miscibility to the presence of specific interactions that contribute a negative value in the interaction parameter, but increase with T until they are balanced out by the free volume contributions (as well as by the ubiquitous dispersion forces, which in this case can be ignored). The sum of the two most important contributions in χ_{12} reaches the critical value at one temperature (e.g., an LCST, Fig. 2.19b).

To predict the phase behavior for a given system, the following steps are typically taken:

1. Select the most appropriate theoretical model for the free energy of mixing, ΔG_m.
2. Determine values of the characteristic material parameters required by the selected theory.
3. Solve Eq. 2.66 for the selected theory.
4. Readjust the fitting parameters of the theory to optimize the fit.
5. Make predictions of the thermodynamic behavior and then verify experimentally.

The most important step is the selection of the theoretical model, i.e., the form of ΔG_m. The balance between the complexity of its form and the adequacy of the description of experimental behavior must be preserved, also its applicability to the relevant P and T ranges must be checked, e.g., the existence of parameters with

Fig. 2.19 Interactions in polymer solutions and blends usually comprise of dispersive forces, the free volume effects, and specific interactions. (**a**) The χ_{12} of polymer solutions are typically dominated by the contributions from dispersive forces and free volume, whose T dependence can result in a UCST and LCST. (**b**) In polymer blends, the contributions from the free volume and the contributions from specific interactions usually control the T dependence of χ_{12}, giving rise to an LCST
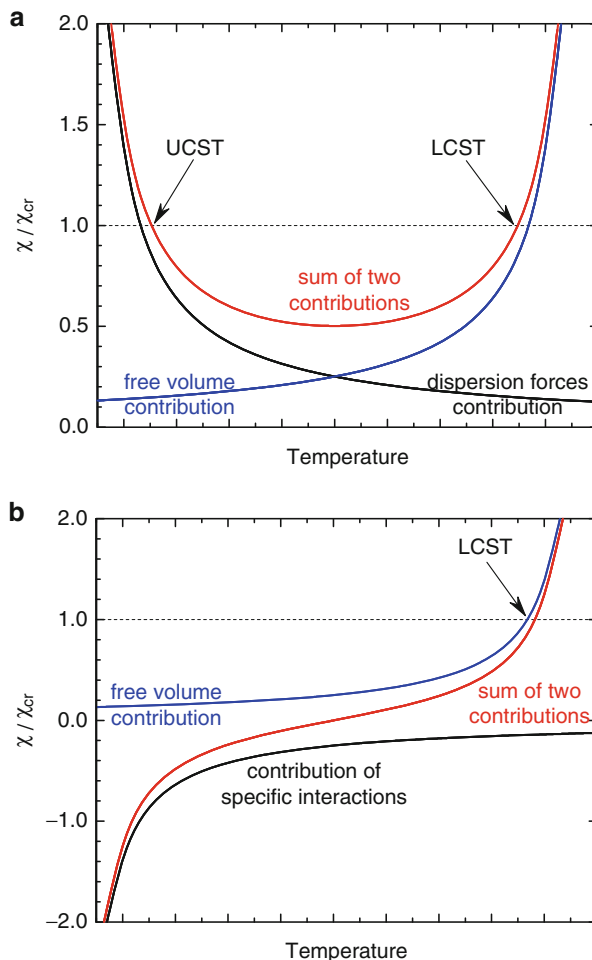
values of confidence in these ranges. One fundamental question is whether the pressure dependence of the phase diagram is important or not. Most data in literature deal with ambient pressures, whereas most industrial applications, viz., processing, compounding, and forming, are done at high pressures (e.g., extrusion $P \sim 70$ MPa, injection molding $P \sim 500$ MPa, etc.). The accuracy demanded from the theory to account for large variations of pressure is severe. It suffices to note that according to Eq. 2.66 the critical point is given by the third derivative of the free energy of mixing – its pressure dependence (stability criterion) is given by the fourth derivative!

The sometimes complicated forms of the free energy equations require, in most cases, that Eq. 2.66 are solved numerically, especially for the binodal determination (Jain and Simha 1984; Nies et al. 1990; Kisselev and Manias 2007). Often authors described the computational procedures, e.g., Nies et al. (1990), for the modified

Fig. 2.20 Calculated phase diagrams for *n*-hexane/PE systems at varied pressures ($P = 1$, 50, and 100 bar); x_2 is the mole fraction of PE with $M_w = 8$ kg/mol (Nies et al. 1990)
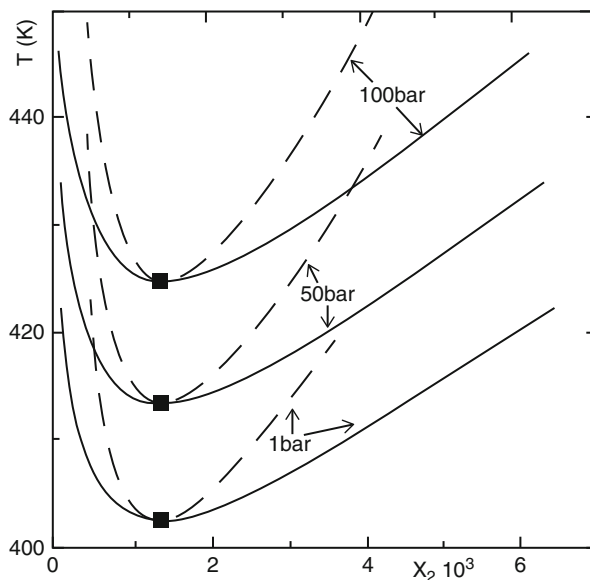
S-S theory giving Eqs. 2.42 and 2.43, and Kisselev and Manias (2007), for the LF theory with specific interactions. In the case of the S-S theory, the Helmholtz free energy is explicitly provided, which, in turn, can easily be converted into Gibbs free energy, viz., $G = F + PV$, or $\Delta G_m = \Delta F_m + P\Delta V_m$, where the terms with Δ represent the excess values due to mixing (differences from the single-phase values for each component, i.e., the function values of the mixture less the contributions of the pure components). Results of these computations are exemplified by the three isobaric phase diagrams of PE solutions in *n*-hexane, shown in Fig. 2.14, whereas a number of examples of polymer phase diagrams are available in literature (e.g., Koningsveld et al. 2001) (Fig. 2.20).

2.6.2 Mechanisms of Phase Separation

Phase separation takes place when a single-phase system undergoes either a change of composition or, more usually, a change in T or P that forces it to move from the single-phase region and enter either the metastable or the two-phase/spinodal region (Fig. 2.18). There is a substantial difference between the phase separation mechanisms that take place for moving from single phase to metastable and for moving from single phase to two phase. When the system enters from the single-phase region into the metastable region, phase separation typically occurs by mechanisms resembling crystallization, i.e., slow nucleation followed by growth of the phase separated domains. Thus, this process is known as the "nucleation and growth," or NG for short. In contrast, when the system is forced to jump from a single phase into the spinodal/two-phase immiscible region, the phases separate
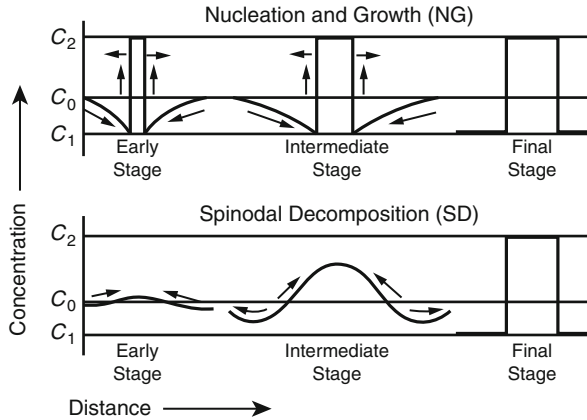
Fig. 2.21 Schematic representation of the density fluctuations during the spinodal decomposition mechanism (*SD*, *bottom*) and the nucleation and growth (*NG*, *top*). Three stages are shown: early, where in SD the wavelength is constant but the amplitude increases; intermediate, where both the wavelength and the amplitude change; and final, where the concentration amplitude is at maximum and the wavelength increases only due to coarsening processes

spontaneously: This process starts with instantaneous segmental density fluctuation that progressively increases in amplitude and later in wavelength. The process is known as the "spinodal decomposition," or SD for short.

These two processes are schematically illustrated in Fig. 2.21, as composition versus distance. Three stages of the phase separation process are distinguished: early, intermediate, and late/final. The upper and lower limits of the concentration are given by the tie-line limits intersecting the binodal at $T = $ constant, for the temperature of the experiment (Fig. 2.18). Following the late stage of phase separation, the process continues into a series of coalescence steps, which increase the lateral dimension d of the phases: Coalescence starts with Ostwald ripening ($d \propto t^{1/3}$; see Eq. 2.67), followed by surface tension-controlled coarsening ($d \propto t$; see Eq. 2.68), ending with gravitational or divergent coalescence that leads to formation of large size (macroscopic) separate phases.

$$d \; V_d \propto \frac{\gamma_{12}\phi_c V D_t}{RT}dt \Rightarrow (d/d_o)^{n_c} = 1 + K_c t \qquad (2.67)$$

where V_d is the drop volume, γ_{12} is the interfacial tension, ϕ_c is the equilibrium concentration of the phase separated system (binodal concentration at T), V is the molar volume of the drop fluid, n_c is the coarsening exponent, and K_c is the coarsening rate constant. For a steady-state coarsening, $n_c = 3$, whereas for sheared systems $n_c = 3/2$ (Ratke and Thieringer 1985). Subsequently,

$$\frac{RT}{\gamma_{12}} \le d^2 \le \frac{\gamma_{12}}{g\Delta\rho} \Rightarrow d \propto t \qquad (2.68)$$

where g is the gravitational constant (acceleration) and $\Delta\rho$ is the density difference between the two phases.

For fundamental studies of phase separation, to ensure that phase separation will proceed by the SD mechanism, a composition near the critical point is usually selected. The blend is then quenched (temperature jump) from the miscible to the spinodal region passing through or near the critical point. For this reason, SD studies are often called "critical quenching." Conversely, to study the NG mechanism (a significantly less popular subject), compositions for temperature jumps are selected away from the critical concentration; these studies are then known as "off critical." Reviews on phase separation are continuously published (the reader is strongly encouraged to do a fresh literature search); some such reviews were used next to highlight phase separation behaviors (Kwei and Wang 1978; Olabisi et al. 1979; Herkt-Maetzky 1984; Aifantis 1986, 1987; Hashimoto 1987; Nose 1987; Binder 1987; Hashimoto 1988; Han et al. 1988; Utracki 1989, 1994; etc.).

2.6.2.1 Spinodal Decomposition (SD)

Early theories of the phase separation dynamics are based on a mean-field approach developed for metallurgical applications (Cahn and Hilliard 1958; Cahn 1978). In the spinodal region, the concentration fluctuations are delocalized, leading to long-range spontaneous phase separation by SD. This type of mean-field theory is not adequate to describe the phase dynamics of small molecule liquids (especially near the critical point), but it has been successful in describing phase separation in polymeric systems, due to the slow diffusion rates owing to the large-chain dimension. The time-dependent probability distribution function for concentration can be determined directly by digital image analysis method (Tanaka and Nishi 1987).

For SD, three stages and three mechanisms of domain growth are traditionally identified (Siggia, 1979): diffusion, liquid flow, and coalescence. The earliest diffusion stage follows the Ostwald equation, Eq. 2.67, and is limited to the period when $d_o \leq d \leq 5d_o$, where d_o is the initial diameter of the segregated region ($d_o \approx$ 2–9 nm Voigt-Martin et al. 1986). The subsequent flow region dominates when $5d_o \leq d \approx 1$ μm. Within these two regions, the SD structure is regular and the growth can be observed by scattering methods. At the last, coalescence, stage of SD, diffusion becomes bimodal and then irregular. Thus, at this stage, the kinetics of phase separation has been studied using time-resolved scattering techniques, with light, neutrons, or other irradiation sources. There is a direct relation between the virtual structure function, $S(q, t)$, and the scattering intensity function, $I(q, t)$:

$$
\begin{aligned}
I(q,t) &= I_b + K\ S^2(q,t) \\
&= (I_b + K\ S_\infty) + K(S_o - S_\infty)\exp\big[2R(q)t\big] \\
&= I_\infty + (I_o + I_\infty)\exp\big[2R(q)t\big]
\end{aligned}
\tag{2.69}
$$

where I_b is the background scattering intensity, K is a constant, and S_o and S are the values of the structure function at time 0 and at time t. To extract the concentration

fluctuation function $R(q)$, a semilogarithmic plot of $\ln(I - I_\infty)$ versus t is used. However, in many cases, since the scattering intensity at equilibrium is low, the concentration fluctuation function is determined as

$$R(q) \cong \frac{1}{2} \frac{d \; \ln I(q,t)/I_o(q,t)}{dt} \tag{2.70}$$

As Eq. 2.69 indicates, the scattering intensity $I(q, t)$ is proportional to $S^2(q, t)$. For this reason, the plot of $I(q, t)$ versus q (at constant decomposition time and temperature) already provides evidence of the dynamics of phase separation in polymer blends.

The mechanism of phase separation is analyzed from the R versus q dependence. The dynamics of phase separation within the SD domain starts with a balance between the thermodynamics and material flux. The mean-field theory of phase separation leads to the following simple form of the structure function, $S(q)$ (Cahn and Hilliard 1958):

$$\begin{aligned}
S(q) &= S_o \exp\left[R(q)t\right] \\
R(q) &= -Mq^2 \left[\frac{\partial^2 G}{\partial \phi^2} + 2q^2 k\right] \\
q &= \frac{4\pi}{\lambda} \sin\left(\Theta/2\right) = \frac{2\pi}{\Lambda}
\end{aligned} \tag{2.71}$$

where M is the Onsager mobility factor, G is the free energy for the homogenous system, ϕ is the segmental volume fraction, and κ is the gradient energy coefficient arising from local composition fluctuations; the wavevector, q, is a function of the wavelength, λ, and the scattering angle, Θ. It has been shown that near the spinodal $\partial^2 G/\partial \phi^2 \propto 1 - (T/T_s)$, where T_s is the spinodal temperature, whereas the maximum wavelength for SD phase separation is $\lambda_{\max} \propto [1 - (T/T_s)]^{-1/2}$ (van Aarsten 1970). According to Eq. 2.71, the concentration fluctuation function, $R(q)$, can be linearized by plotting $R(q)/q^2$ versus q^2. The linearity provides evidence of the SD mechanism independently of the scale of the phase separation.

From the intersection at $q = 0$, the mutual diffusion coefficient D_M is obtained:

$$\begin{aligned}
\lim_{q\to 0} \left(\frac{R(q)}{q^2}\right) &= D_M = -M\frac{\partial^2 G}{\partial \phi^2} \\
D_M &= 2\phi_1\phi_2(\chi_{12s} - \chi_{12})(N_1 D_1 \phi_2 + N_2 D_2 \phi_1) \\
\chi_{12\ s} &= (N_1\phi_1)^{-1} + (N_2\phi_2)^{-1}
\end{aligned} \tag{2.72}$$

Evidently, D_M depends on the second derivative of the free energy, which in turn can be expressed in terms of the self-diffusion coefficients of polymers, D_1 and D_2, and the $\chi(T)$-distance from spinodal. The method of determining D_M is presented in Fig. 2.22, whereas its dependence on T across the spinodal is shown in Fig. 2.23. From D_M, one may calculate the binary interaction parameter and,
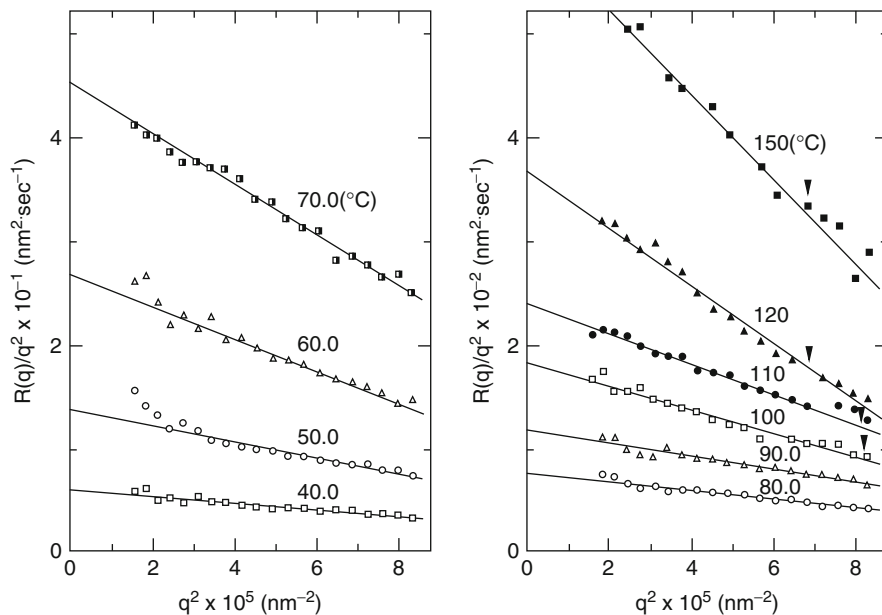
Fig. 2.22 Determination of the mutual diffusion coefficient, D_M, from the early stage data of the spinodal decomposition, SD, in SBS/PBD blends (Izumitani and Hashimoto 1985)

Fig. 2.23 Mutual diffusion coefficient D_M versus T for a PS/PVME blend undergoing spinodal decomposition. T-jumps, across the spinodal temperature $T_s = 151.2\ °C$, were performed in both directions, quenching into SD region, and reverse, quenching from the SD region (Sato and Han 1988)
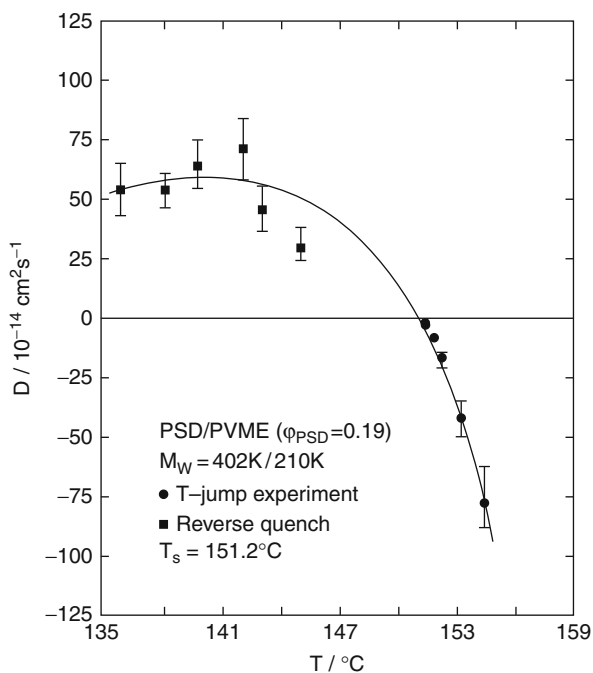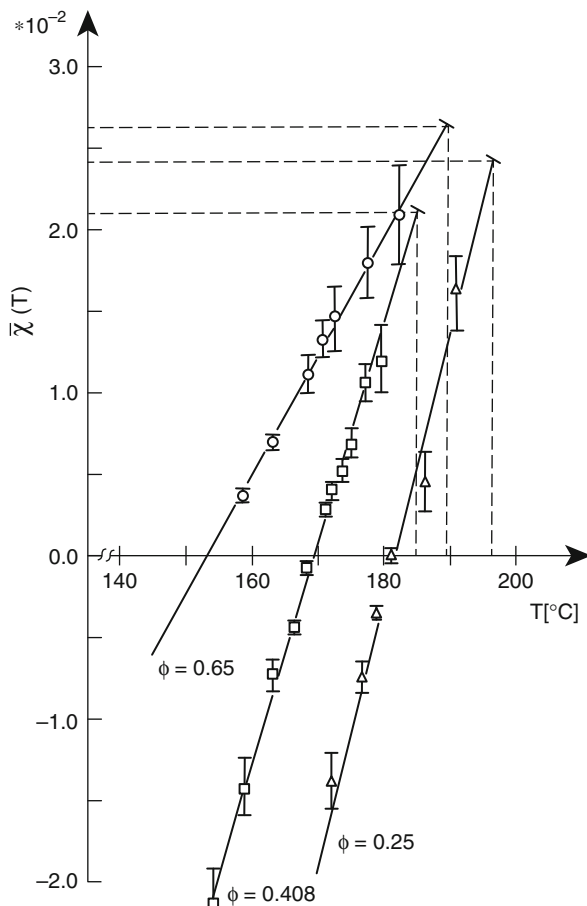
hence, determine conditions for the thermodynamic miscibility. Fig. 2.24 shows the χ_{12} dependence on T and ϕ.

Coarsening of the structure continues through a series of steps that lead to a gross (macroscopic) phase separation. However, under certain conditions, the coarsening progresses only up to a certain stage, where the structure becomes fixed or "pinned." The pinning originates in a transition from the percolation to cluster formation then freezing-in of the molecular diffusion. In simple term, the generated structure is relatively regular; thus, there is little energetic incentive for the molecules to diffuse from one drop, through "unfriendly" territory of the other phase, to another drop. An example of this has been given for blends of PI containing 20, 30, and 50 wt% of SBR (Takenaka et al. 1989). Evidently, stirring the mixture disrupts the fine balance of forces that make the pinning process possible; thus, pinning is not expected to take place during processing.

Most work on SD focuses on the effects of temperature and composition on phase equilibria in binary polymer mixtures. However, in industrial processes, other

variables may be of equal importance, e.g., the shear stress, shear stress rate, and pressure. It is known that these variables are important for miscibility and, hence, for the morphology and performance. For example, during extrusion of PC/PBT blends the LCST was increased by at least 60 °C, causing miscibility; the blend, upon exit from the extruder, phase separated by the SD mechanism, which resulted in co-continuity of phases and excellent performance. Solvent casting of polymer blends and controlled evaporation can also lead to SD. This technology has been used for industrial production of semipermeable, selective membranes. The product characterized by co-continuity of phases also showed excellent mechanical performance. The type of solvent, concentration, temperature, and method of casting are used to control the blend morphology and its final performance (Inoue et al. 1985, 1987; Nauman et al. 1986).

Phase separation was computer simulated using finite-difference in time and space Runge–Kutta and Monte Carlo with a Hamiltonian methods (Petschek and Metiu 1983; Meakin and Reich 1982; Meakin et al. 1983). Both methods were found equivalent, reproducing the observed pattern of phase separation in both NG and SD regions. The unity of the phase separation dynamics on both sides of the spinodal has been emphasized (Leibler 1980; Yerukhimovich 1982).

2.6.2.2 Nucleation and Growth (NG)

As shown in Fig. 2.25, there is a significant difference in the scattering pattern evolution for NG and SD mechanisms, especially during the early stages of phase separation: SD follows a semilogarithmic time dependence (see Eq. 2.71), whereas NG follows a linear time dependence.

When the concentration of the minor phase is above 10–15 %, SD occurs by rapid growth of regularly spaced concentration waves, while NG is a slower and more random process. On the other hand, at low concentrations of the minor phase, neglecting the fine structure of the dispersed phase, phase separation by NG and SD mechanism looks similar. Also the reverse quenching of SD and NG morphologies is similar, both being controlled by (Kumaki and Hashimoto 1986):

$$\left(\frac{\partial^2 G}{\partial \phi^2}\right)_{\text{spinodal}} = -\lim_{q \to 0} \frac{R(q)}{Mq^2} = \text{constant} \tag{2.73}$$

The relation shows that the rate depends on the conditions for SD, the same for systems on both sides of the spinodal.

The NG is an activated process with a linear growth rate (Matsuda 1991):

$$\begin{aligned}
\text{Nucleation}: \quad & \frac{dN}{dt} = k_N \exp[-\Delta E_{aN}/k_B T] \\
& \Delta E_{aN} = \frac{4}{3}\pi r_{N,cr}^3 \Delta G_m + 4\pi r_{N,cr}^3 \gamma_{12} = \frac{16\pi}{3}\gamma_{12}^3 \Delta G_m^2 \\
\text{Growth}: \quad & \frac{\partial \phi}{\partial t} = D\nabla^2 \phi
\end{aligned} \tag{2.74}$$

Fig. 2.25 A plot of the scattering intensity versus time for 70 % PVME/30 % PS blends (SE-70), at wavevector $q = 5.6 \times 10^4$ cm^{-1} (the spinodal temperature was estimated at $T_s = 99.2$ °C); the data at higher T (99.7 °C, 100 °C, and 101 °C) are for the SD regime, and the data for 99 °C are for the ND regime (Hashimoto et al. 1983)
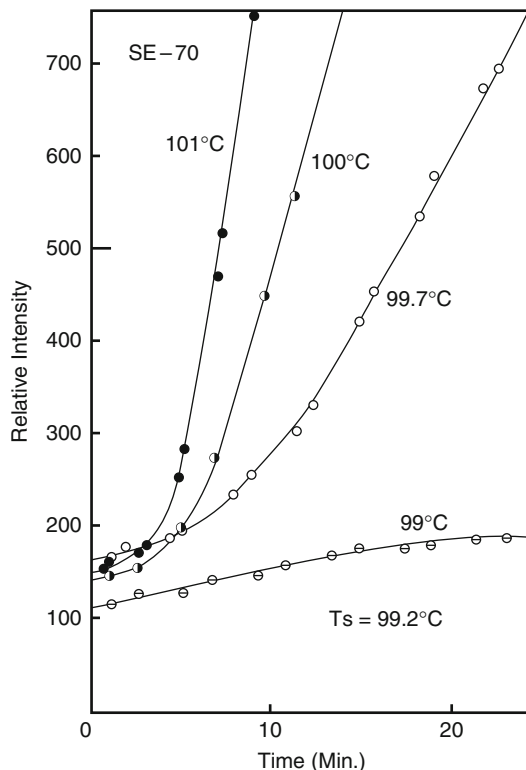
where $r_{N,cr}$ is the critical radius of the nucleating particle and D is the diffusion constant. Accordingly, the nucleation process requires activation energy for nucleation (ΔE_{aN}). However, once nucleated, the phases separate and grow spontaneously. The nucleation is initiated by the local fluctuations of density. The activation energy ΔE_{aN} depends on the local gradient of the free energy of mixing (ΔG_m) and the interfacial tension (γ_{12}). Once formed, the drops grow by diffusion of macromolecules into the nucleated domains, with the rate given by the Ostwald ripening. The diffusion stage is followed by coalescence (Hashimoto et al. 1986; Hashimoto 1988).

In principle, during the initial stage of phase separation the NG mechanism leads to a drop/matrix morphology over the full range of concentrations. However, the morphology at the later stages depends on the volume fraction of the dispersed phase, as well as the method and extent of stabilization. Furthermore, since nucleation depends on the local density fluctuations, whose amplitude depends on the distance from the critical conditions, near the spinodal, phase separation can occur either by the NG or SD mechanism (Langer 1977, 1980). This ambiguity is further exacerbated in applications by compounding and by processing stresses.

Table 2.21 Phase equilibrium studies for polymer/solvent systems, including mixed solvents

Polymer	Solvent
PE	Diphenyl-ether, *n*-hexane, ethylene, nitrobenzene, amyl acetate, xylene, 1,2,4,5-tetrachlorobenzene (TCB), xylene/glycol, toluene, petroleum ether, bromonaphthalene
PP	Benzene, *o*-dichlorobenzene, isopropyl ether, *n*-heptane, tetralin/butyl carbitol, TCB
PDMS	Oligo-isobutylene, carbon tetrachloride/cyclohexane/methanol
PS	Cyclohexane, methyl-cyclohexane, acetone, *tert*-butyl acetate, ethyl acetate, ethyl oxalate, vinyl acetate, ethyl malonate, methyl acetate, methyl succinate, octene, polyvinyl acetal/chloroform, rubber/benzene, toluene/ethanol
PVC	Tetrahydrofuran/water, cyclohexanone/methanol, chlorobenzene, cyclohexane/acetone
PVP	Water/acetone
PVAc	Acetone, water, methyl-isobutyl ketone, dioxane/isopropanol
PVA1	Water, water/acetone, water/propanol
PMMA	Benzene, toluene, 3-heptanone, *n*-propanol, *p*-cymene, MEK/isopropanol, acetone/hexane, butanone/cyclohexane
PBMA	Benzene
PCHMA	Dioxane/methanol
PEG	Water, chloroform/hexane
PPG	Water, isopropanol/water, isooctane
PIB	Di-isobutyl ketone, benzene/acetone, tri-methyl pentene, 2-methylheptane, toluene/methanol
CR	Benzene, benzene/acetone, benzene/methanol
PIP	Acetone/ethanol
PAN	Dimethyl formamide, dimethyl sulfoxide/toluene
PC	Methylene chloride/methanol
PET	Phenol/cyclohexane, dimethyl formamide, trifluoroacetic acid/chloroform
PA-6	*m*-Cresol/cyclohexane, phenol, formic acid
NC	Acetone, butyl acetate, acetone/water, ethyl acetate/heptane
SBR	Benzene

2.6.3 Phase Diagrams

There is a large body of literature on phase diagrams for binary and ternary polymer solutions (Flory 1953; Tompa 1956; Cantow 1967; Utracki 1989) and extensive compilations of data (phase diagrams, cloud points, critical temperatures) for numerous systems (e.g., Wohlfarth 2004, 2008; Koningsveld et al. 2001). A few examples of such systems are listed in Table 2.21.

Phase diagrams of polymer blends, including binary polymer/polymer systems and ternary polymer/polymer/solvent systems, are scarcer (Koningsveld 2001). Furthermore, owing to the recognized difficulties in determination of the equilibrium properties, the diagrams are oftentimes either partial or approximate or built using low molecular weight polymers. Examples are listed in Table 2.22.

Table 2.22 Phase equilibrium studies for polymer/polymer blend systems. CST stands for critical solution temperature: L indicates lower CST, while U indicates upper CST (see Fig. 2.18)

Polymer-1		Polymer-2		CST (°C)	References
PS	$(M_w = 237)$	PVME	$(M_w = 13.3)$	$L = 120$	1
PS		TMPC		$L < 220$	2
PS	$(M_w = 29)$	PoClS		$L = 350$	3
PS	$(M_w = 22)$	P(S-co-BrS)	$(M_w = 22)$	$U = 218$	4
PS	$(M_w = 10)$	PMPS	$(M_w = 2.8)$	$U = 103$	5
PS	$(M_w = 2.7)$	PIP	$(M_w = 2.7)$	$U = 173$	6
SAN	$(M_w = 223)$	PMMA	$(M_w = 92)$	$L = 150$	7
SAN	$(M_w = 223)$	PCL	$(M_w = 35)$	$L = 90$	8
SAN	$(M_w = 194)$	NBR	$(M_w = 297)$	$L = 52$	9
PVC	$(M_w = 55)$	PMMA	$(M_w = 60)$	$L = 190$	10
PVC	$(M_w = 160)$	NBR	$(M_w = 340)$	$L > 180$	11
PVDF	$(M_w = 100)$	PEMA	$(M_w = 332)$	$L = 200$	12
αMSAN	$(M_w = 160)$	PMMA	$(M_w = 126)$	$L = 185$	13
CPE	$(M_w = 190)$	PMMA	$(M_w = 42)$	$L = 100$	14
PES		PEG	$(M_w = 20–200)$	$L = 80$	15
BR	$(M_w = 390)$	SBR	$(M_w = 480)$	$U = 103$	16
PHMA	$(M_n = 55)$	StVPh	$(M_n = 11)$	$L = 159$	17
PHMA	$(M_n = 55)$	StVPh	$(M_n = 14)$	$L = 84$	17
PPE		PFSt copolymer		$U = 270$	18
PVME		StVPh (0–0.4 % –OH)		$L = 153–193$	19
PEK		N-TPI		$U = 445$	20
PC-co-TMPC	$(M_w = 72)$	PS	$(M_w = 330)$	$L = 175$	21
PC-co-TMPC	$(M_w = 72)$	SAN	$(M_w = 160)$	$U = 290$	21
PC-co-TMPC	$(M_w = 72)$	SMMA	$(M_w = 160)$	$U = 230$	21
P-n-BMA	$(M_w = 270)$	PMMA	$(M_w = 100)$	$U = 160$	22
SMAN	$(M_w = 101)$	PMMA		$L = 135$	23
PVME	$(M_w = 99)$	PS	$(M_w = 114)$	$L = 119$	24
PVME	$(M_w = 389)$	PS	$(M_w = 230)$	$L = 152$	25
PEG	$(M_w = 300)$	PMMA	$(M_w = 130)$	$L = 227$	26
PI	$(M_w = 101)$	d-PB	$(M_w = 53)$	$L = 85$	27
PVDC	$(M_w = 101)$	PHEDO		$L = 174$	28
PVDF	$(M_w = 428)$	PMA	$(M_w = 257)$	$L = 332$	29
PVDF	$(M_w = 736)$	PMA	$(M_w = 257)$	$L = 300$	29
PVDF	$(M_w = 140)$	PBA	$(M_w = 14)$	$L = 233$	30
PIB	$(M_w = 1,000)$	LLDPE	$(M_w = 125)$	$L = 85$	31
PC	$(M_w = 58)$	PMMA	$(M_w = 87)$	$L = 240$	32
PVC	$(M_w = 170)$	PPrA	$(M_w = 87)$	$L = 129$	33
PVC	$(M_w = 170)$	PPeA	$(M_w = 415)$	$L = 107$	33
PVC	$(M_w = 170)$	PBA	$(M_w = 383)$	$L = 126$	33
TMPC	$(M_w = 33)$	SMMA	$(M_w = 281)$	$L = 250$	34

(*continued*)

Table 2.22 (continued)

Polymer-1		Polymer-2		CST (°C)	References
TMPC	($M_w = 33$)	SMMA	($M_w = 106$)	$L = 264$	34
PMMA	($M_w = 94$)	SMMA	($M_w = 81$)	$L = 150$	35
GMA/MMA	($M_w = 471$)	SAN	($M_w = 152$)	$U = 350$	36
PPE	($M_w = 39$)	PαMS	($M_w = 55$)	$L = 253$	37
PVC	($M_w = 213$)	αMSAN	($M_w = 55$)	$U = 261$	37
PVC	($M_w = 213$)	SAN (20%AN)	($M_w = 178$)	$U = 150$	37

Polymer abbreviations: *PHMA* poly-*n*-hexyl methacrylate, *StVPh* polystyrene-*co*-vinylphenol, *PFSt* poly(*o*-fluorostyrene-*co*-*p*-fluorostyrene), *P(S-co-BrS)* poly(styrene-*co*-4-bromostyrene), *N-TPI* "new thermoplastic polyimide" (see reference), *PPrA* poly-*n*-propyl acrylate, *PPeA* poly-*n*-pentyl acrylate; the rest of the polymer acronyms as usual

References: 1. Voigt-Martin et al. 1986; **2.** Shaw 1974; **3.** Takahashi et al. 1985; **4.** Strobl et al. 1986; **5.** Nojima et al. 1982; **6.** Koningsveld et al. 1974; **7.** McBrierty et al. 1978; **8.** McMaster and Olabisi 1975; **9.** Ougizawa and Inoue 1986; **10.** Jagger et al. 1983; **11.** Inoue et al. 1985; **12.** Saito et al. 1987; **13.** Goh et al. 1982; **14.** Walsh et al. 1982; **15.** Walsh and Rostami 1985; **16.** Ougizawa et al. 1985; **17.** Bhagwagar et al. 1994; **18.** Kambour et al. 1980; **19.** Hoy 1970; **20.** Sauer et al. 1996; **21.** Kim and Paul 1992; **22.** Sato et al. 1996a, b; **23.** Nishimoto et al. 1995; **24.** Ougizawa et al. 1991; **25.** Han et al. 1988; **26.** Fernandes et al. 1986; **27.** Hasegawa et al. 1992; **28.** Woo et al. 1986; **29.** Maiti and Nandi 1995; **30.** Pennings and Manley 1996; **31.** Krishnamoorti et al. 1995; **32.** Kyu et al. 1991; **33.** Sham and Walsh 1987; **34.** Kim and Paul 1992; **35.** Andradi and Hellmann 1993; **36.** Gan and Paul 1994b; **37.** Gan et al. 1994

2.7 Experimental Methods

The thermodynamic properties of a polymer blend determine its performance. Many authors have focused on miscibility – this aspect has been extensively discussed in the literature (Olabisi et al. 1979; Solc 1982; Utracki 1989; Coleman et al. 1991; Paul and Bucknall 2000; Koningsveld et al. 2001), and few selected results, with the emphasis of what is not covered in details in the following chapters, are briefly mentioned here. The characterization methods of the thermodynamic behavior of polymer blends can be divided into groups:

Thermodynamic studies not directly related to miscibility (e.g., PVT measurements)

Determination of the interaction parameter (χ_{12} quantified through SAXS, SANS, melting point depression, from the Hess cycle, etc.)

Direct methods of miscibility determination (turbidity measurements, microscopy, combinatorial approaches, etc.)

Studies of the phase equilibria (determined by scattering methods, viz., turbidity, PICS, SAXS, and SANS; fluorescence techniques; ultrasonic measurements; etc.).

Indirect methods of miscibility determination (e.g., from the glass transition temperature, viz., T_g from thermal, dielectric, or mechanical tests, NMR, spectroscopic methods, ODT through rheology, etc.)

2.7.1 PVT and Related Measurements

Equilibrium thermodynamics controls the PVT behavior of any system and its thermal expansion coefficient, compressibility, bulk modulus, hardness, etc. The thermodynamic pressure, which can be defined as a partial derivative of the Helmholtz free energy (see Eq. 2.5), for multicomponent systems, comprises of two interaction parameters, e.g., $\langle \varepsilon^* \rangle \langle v^* \rangle^k$; $k = 2,4$. These values can as easily be determined from dilatometric measurements as from the phase diagram (Jain et al. 1982). With the advance of other methods, dilatometry has been largely neglected: It is still being used to characterize the compressibility of neat resins, but rarely nowadays to study the behavior of polymeric blends (Plochocki 1982, 1983, 1986; Zoller 1989; Steller and Zuchowska 1990; Zoller and Walsh 1995).

The interaction parameters can be calculated from the PVT data of polymer blends (Jain et al. 1982; Privalko et al. 1985); however, due to the need for subtraction of two large numbers, the resulting values were often erratic, with errors up to ± 6 %. Such errors may be acceptable for some applications, but not for the construction of phase diagrams. A more straightforward experimental route is the computation of the reducing parameters, P^*, V^*, and T^*, by, e.g., two possible approaches:

1. Experimental values are compared with theoretical predictions, assuming an EoS and an averaging scheme, e.g., Eq. 2.43. This approach was used, for example, to interpret the thermodynamic behavior of PS/PVME blends, for T, 25–200 °C, and P, 0–200 MPa (Ougizawa et al. 1991), and for a series of polyolefins (EPR, a-PP, PP, PEP, PEB, i-PB, PIB, etc.) whose miscibility was studied using PVT and SANS measurements (Krishnamoorti et al. 1996). The results were interpreted using Hildebrand's solubility parameter formalism. For regular blends, a close agreement was found.
2. From P^*, V^*, and T^*, the molar attractive energy, ε_{12}, and repulsion volume, v_{12}, can be calculated and, subsequently, compared with theoretically derived averages, viz., the geometric mean for the former and the algebraic mean for radius for the latter (see Sect. 2.4.1). For miscible systems, the dependence of these values on composition can be easily derived. Usually, these compare reasonably well with the experimental data, since immiscibility causes large variations from the monotonic dependence.

Several interesting observations relate to such thermodynamic measurements. For example, the exothermic effects, associated with phase separation in LCST-type polymer blends, showed a correlation between the exothermic enthalpy and the interactions between the components (Natansohn 1985); however, the specific interaction parameter χ_{12} was not calculated. In another example, there are definitive correlations between the thermodynamic and the transport properties (see ▶ Chap. 7, "Rheology of Polymer Alloys and Blends"). Thermodynamic properties of multiphase polymeric systems affect the flow, and vice versa. As discussed in ▶ Chap. 7, "Rheology of Polymer Alloys and Blends", the effects of stress can engender significant shift of the spinodal temperature, $\Delta T_s = 16$ °C. While at low stresses the effects can vary, i.e., the miscibility can either increase or decrease,

at higher stress values an enhancement of miscibility is expected. Flow has also been used to establish whether the molten blends are miscible or not (Schlund and Utracki 1987a, b, Utracki and Schlund 1987a, b).

Finally, thermodynamics also plays a dominant role in interfacial phenomena, viz., value of interfacial tension, thickness of the interphase, Δl, rheological properties, adhesion, compatibilization, etc. It is worth recalling that most lattice theories directly relate the magnitudes of γ_{12} and Δl to the value of the binary interaction parameter, χ_{12} (Helfand and Tagami 1971a, b, 1972; Helfand 1975a, b, c; Helfand and Sapse 1975; Roe 1975; Joanny and Leibler 1978; Broseta et al. 1990; Anastasiadis 2011). For example, the interfacial tension, as measured from pedant drop or scattering experiments, can be used to obtain binary interaction parameters, χ_{ij} (Anastasiadis 2011). In another example, the equilibrium interfacial thickness, Δl, in PMMA blends with PS and SAN was determined by ellipsometry (Higashida et al. 1995); from the Δl values, the authors computed the temperature dependence of the binary interaction parameter, $\chi_{ij}(T)$, and then the phase diagrams. However, since these topics are of prime importance for Chap. 4, they will not be discussed here.

2.7.2   Determination of Interaction Parameters

2.7.2.1 Binary Systems

All types of radiation scattering techniques, viz., light, X-ray, and neutron, have been used to measure the interaction parameters and study the phase equilibria in polymer blends and solutions. Using the relations derived for polymer solutions (see Eqs. 2.27, 2.28, 2.29, 2.30, 2.31, and 2.32), scattering methods can be used to measure molecular weight, M_w; end-to-end distance or radius of gyration, $\langle s_o^2 \rangle^{1/2}$; and the second virial coefficient, A_2, thus χ_{12}.

The relation between the characteristic dimension of the scattering phase, d_{av}; the wavelength of irradiation, λ; and the scattering angle, Θ, is given by (see Eq. 2.71)

$$d_{av} = \Lambda = \frac{\lambda}{2} \sin\left(\Theta/2\right) \tag{2.71a}$$

Depending on the experimental values of λ and Θ, the experimentally accessible values of d_{av} vary accordingly. Approximate ranges of the dimensions of scattering phases for the light, neutron, and X-ray techniques are given in Table 2.23.

The great majority of polymer blends have domain sizes in the range of 50 nm to 5 µm. Thus, LS and SAXS methods albeit more proliferated have limited use for studies of phase morphology, while SANS is much better suited. SANS has been used to study macromolecular size and conformation, morphology, in a single or multicomponent system, in molten or solid state. Since the contrast, phase discrimination, is based on the mass number, it is very useful to replace the hydrogen atoms in one polymer, or parts of a polymer, by deuterium. The deuterated polymer is mixed with its hydrogenated homologue at a selected low concentration, usually ∼0.1 %, providing a means to control contrast. The mixture can be then used as one of the

Table 2.23 Spatial ranges for the scattering phase dimensions accessible to various scattering methods

Method	Origin of contrast	Scattering domain size (μm)
Light scattering (LS)	Refractive index	1–100
Small-angle neutron scattering (SANS)	Mass number	0.01–3
Small-angle X-ray scattering (SAXS)	Electron density	1–100
Wide-angle X-ray scattering (WAXS)	Electron density	0.1–1

blend's components, or for the study of homopolymer properties. Several reviews of the SANS application for the characterization of polymer conformation and morphology have been published (Sperling 1984; Rennie 1992; Balsara et al. 1992; Lohse 1994; Krishnamoorti et al. 1995; Takeno et al. 1996; Hammouda 2010).

It should be noted that deuteration will change the conformation of macromolecules and also their miscibility/solubility, especially for high M_w (Utracki 1989). Theory predicts phase separation (with UCST) for a blend of hydrogenated with deuterated polymer (Buckingham and Hentschel 1980; Edwards 1983; Honeycutt 1992a, b); see also Fig. 2.7, a behavior that has been experimentally observed in multiple systems (Eitouni 2007): Phase separation of poly-1,4-butadiene with its deuterated analog confirmed the prediction (Bates et al. 1985, 1986; Bates and Wignall 1986; Bates and Wilzinius 1989; Schelten et al. 1977; Yang et al. 1983; Atkin et al. 1984). Similarly, blends of hydrogenated with deuterated PDMS show immiscibility (Lapp et al. 1985). Apparently, there are three principle origins for these isotopic effects: (i) position of the isotope, (ii) conditions for SANS measurements, and (iii) difference in segmental volume upon deuteration. In conclusion, SANS is an excellent method for determination of molecular size and intermolecular interaction in polymer blends, provided that the isotopic effects are either absent or appropriately corrected for. The method is precise in quantifying the dependencies on molecular weight, molecular structure, macromolecular architecture, chemical substituents and additives, as well as on independent variables, P, T, deformation, etc. In Table 2.24, a few examples of blend studies are summarized. The interested reader is referred to consult specialized publications (Utracki 1989; Balsara et al. 1992; Lohse 1994; Krishnamoorti et al. 1995; Eitouni 2007; Hammouda 2010) or books.

SANS has been used extensively to determine χ_{12} of polymer blends, by fitting SANS profiles measured from blends to RPA. This approach was pioneered by Hadziioannou and Stein (1983, 1984), Murray and Stein (1985), and Herkt-Maetzky and Schelten (1983). In particular, the phase diagram in PVME/d-PS was among the first blends studied and has been extensively studied since then (Hadziioannou et al. 1983, 1984; Schwahn et al. 1987; Hammouda et al. 1995; Takeno et al. 1996; Choi et al. 1998, 2000; etc.), partly due to its well-documented LCST and the small difference in LCST ($\Delta T_{cr}^{LCST} \approx 40\,^\circ$C) upon deuteration. In the vicinity of the critical point, a non-mean-field behavior was observed. The SANS results can be summarized as follows (Utracki 1989):

- The M_w determined by the solution methods agreed with values obtained by SANS; the average ratio $M_w^{(sol)}$ to $M_w^{(SANS)}$ was found to be 1.02;

Table 2.24 Example SANS studies of polymer blends (*d* before an acronym indicates a deuterated polymer). See also Table 2.8 for selected $\chi_{12}(T)$ based on SANS data

Blend	Comment	References
d-PS/P*p*MS	For 1:1 polystyrene/poly(*p*-methylstyrene) blend: $1000\chi_{12} = -(0.2 \pm 0.1) + (2160 \pm 60)/T$	1
d-PS/P*p*MS	M_w, ϕ, and T dependence of χ_{12}	2
PS/P*o*CS	PS/poly(*o*-chloro styrene) blends showed both LCST and UCST; χ_{12} was independent of ϕ and T	3
d-PB/PI	χ_{12} and phase diagrams for various blend compositions (3/7; 5/5; 7/3); LCST from SANS and SALS	4
PVE/PI	QENS showed PI dynamics same as in homopolymer, but PVE α-relaxation plasticized by PI	5
LDPE/HDPE	Studies of PE/PE miscibility	6
PE/PE	Blends of linear-PE/branched-PE showed difficulties in interpretation of SANS data	7
d-PE/EEA	PE/EEA (18 % EA copolymer) showed immiscibility (EA domains of 3–4 nm)	8
PIB/PP and EB	Composition and T dependence of $\chi_{12}(\phi, T)$	9
PIB/PP and EB, *d*-PS/PS	Compressibility effects, cf. Sanchez-Lacombe theory	10
PP/polyolefins	Isotopic, ϕ, and T effects on χ_{12}	11
Polyolefin blends	PP/EPR, etc., comparison between SANS and *PVT* data	12
Polyolefin blends	LDPE/HDPE immiscible at 143 °C with $\chi_{12} = +0.00056$; *d*-HDPE/*d*-PB had $\chi_{12} = +0.0004$; PB/*d*-PB had $\chi_{12} = +0.00053$ at 130 °C	13
Polyolefin blends	PP/poly(ethylene-*co*-1-hexene): χ_{12} showed a min at 50 % 1-hexene comonomer	14
PMB/PEB	Poly(methyl butylene)/poly(ethyl butylene) binary and ternary systems; $\chi_{12} = 0.0028 - 2.30/T + 584.45/T^2$	15
PMB/PEB	P dependence of $\chi_{12}(T)$ (χ_{12} becomes $\propto 1/T$ at higher P)	16
d-PS/PVME, *d*-PB/PB, *d*-PB/PI	Blends studied over various T regions (regions $\gg T_g$, $\sim T_g$, and $< T_g$)	17
PP/PI	$\chi_{12}(\phi, T)$ of binary and ternary blends of head-to-head PP with head-to-tail PP and PI	18

References: **1.** Jung and Fischer 1988; **2.** Londono and Wignall 1997; **3.** Murray et al. 1985; **4.** Hasegawa et al. 1991; **5.** Arbe et al. 1999; **6.** Londono et al. 1994; **7.** Schipp et al. 1996; **8.** Marr 1995; **9.** Krishnamoorti et al. 1995; **10.** Taylor et al. 1996; **11.** Graessley et al. 1995; **12.** Krishnamoorti et al. 1996; **13.** Alamo et al. 1997; **14.** Seki et al. 2000; **15.** Lin et al. 1996; **16.** Lefebvre et al. 2000, 2002; **17.** Takeno et al. 1996; **18.** Reichart et al. 1997

- Increasing the blends' temperature causes the second virial coefficient, A_2, to decrease, thus, leading to an LCST as a rule for the studied systems.
- The radius of gyration, $\langle s_o^2 \rangle^{1/2}$, of the deuterated polymer decreased with M_w, in the matrix of the same chemical character. In most cases, the coil size of the probe molecules was found to be slightly increasing with A_2.
- Given the small positive values of A_2, blends of PMMA/SAN, PVC/PMMA, PPE/PS, and PVME/PS are miscible. However, in each system, the value of A_2

decreased with M_w, indicating worsening miscibility. In these systems $\langle s_o^2 \rangle^{1/2} \propto M_W^n$, with the exponent n depended on the system and temperature. Specifically, for PS/PVME, $n = 0.57$ (25 °C) or 0.52 (120 °C); for PPE/PS, $n = 0.55$; whereas, for PS in PS and for PMMA in PMMA, $n = 0.5$; and for PMMA in PSAN-19, $n = 0.60$, and for PSAN-19 in PMMA, $n = 0.64$.

SAXS and SANS were used to study PMMA with PVDF blends (Wendorff 1980, 1982; Hadziioannou and Stein 1984). The binary interaction parameter χ_{12} was plotted versus PVDF content, and the isothermal data (at $T = 200$ °C) could be expressed by a linear dependence (Wendorff 1980, 1982): $-1/(\chi_{12} + 0.0035) = -0.72 + 0.76\phi_{PVDF}$. Several authors reported data of $\langle s_o^2 \rangle^{1/2}$ and A_2 for polymer blends (Hadziioannou et al. 1983; Ree 1987; Maconnachie et al. 1984). The binary interaction parameter χ_{12} can be extracted from the second virial parameter A_2. As discussed in Sect. 2.5.1, $\langle s_o^2 \rangle^{1/2}$ and A_2 are measured using scattering methods, including light scattering (LS). One innovative way of using LS involves polymer/polymer/solvent ternary systems: This approach requires either that one of the polymers is iso-refractive with the solvent or that the polymers have equal contrast (Pinder 1997). The method was successfully used to measure χ_{12} for PS/PMMA blends of different M_w. Similarly, A_2 can be determined from osmotic pressure measurements of polymer/polymer/solvent ternary systems, yielding $\chi_{12}(\phi)$ for PVCVAc with acrylic copolymers in cyclohexanone (Sato et al. 1997).

SAXS has been mainly used to study morphology of the semicrystalline blends, cf. how it is affected by composition, crystallization rate, compatibilization, additives, etc. However, it can also be used to study local structures in molten polymer blends, for example, within the interphasial region. The method has been used for liquid, glassy, and crystalline systems to determine the spinodal and binodal temperatures as well as to measure χ_{12}. A reasonable agreement between the values measured by different methods was obtained (Harris et al. 1983; Riedl and Prud'homme 1984; Barlow and Paul 1987).

The depression of the melting point, T_m, has also been used to determine χ_{12}. Development of the method is credited to Nishi and Wang (1975, 1977). T_m depends on two factors: (1) the unit cell geometry, as well as the type and dimensions of the crystals/crystallites, and (2) the interactions between the crystalline polymer and other ingredients. To determine χ_{12} from T_m, it is important that there are no chemical reactions and all specimens (e.g., representing different compositions) are identically treated (identical thermal history), as well as that the mutual solubility of low molecular weight fractions is either small or independent of the blend composition.

However, it is important to ascertain that incorporation of other ingredients changes crystallinity only through thermodynamic interactions, while other effects on crystallinity are negligibly small. Blending can affect crystallinity in diverse ways, due to the effects of added components on nucleation and growth rates. Thus, blending method and parameters, especially rates, can have serious effects on crystallizability and crystal size. Experimentally, the presence of a miscible amorphous polymer in the blend usually slows down, or even prevents, crystallization of the semicrystalline polymer. For fewer systems, enhancement of crystallinity and increase in T_m upon blending have also been reported (Harris and Robeson 1987;

Table 2.25 Examples of determination of χ_{12} from melting point depression studies

Blend	Comment	References
PCL/PVDC-x	PCL blends with PVDC, PVDC-VC, PVDC-VAc, or PVDC-AN: $\chi_{12}(\phi_{PCL})$ showed a maximum at ca. 30 wt% and small T dependence	1
PVDF/acrylates	PVDF blends with PMMA, PEMA, PMHA copolymers: B_{12} was negative for all PVDC/acrylate blends	2
PVDF/PMMA	PVDF blends with PMMA and review of procedures used to determine χ_{12}	3
PVDF/PMA PVF-VDF/PMA	T dependence of $\chi_{12}(\phi)$ was determined; miscibility turns into immiscibility with increased PVF content	4
PVDF/PBA	PVDF blends with poly(1,4-butylene adipate) were miscible over full range of compositions: $\chi_{12} = -0.19$	5
PA/M-sPS	PA blends with Mn- or Zn-sulfonated PS were miscible (with $\chi_{12} < 0$); results confirmed by FTIR and SAXS	6
PBT/PAr	PAr depressed PBT's T_m by 17 °C; calculated χ_{12} varied from -0.65 (20 wt% PAr) to -0.22 (80 wt% of PAr)	7
PBT/ester-ethers	PBT blends with segmented/block poly(ester-co-ether): miscibility depended on the copolymer composition	8
PA/MXD	PA-g blends with poly(m-xylene adipamide): $\chi_{12} < 0$ indicated miscibility in amorphous phase; miscibility increased with transamidation during aging.	9
PP/SEBS/oil PP/EPR/oil	Miscibility was concluded for PP/SEBS/oil, $\chi_{12} = -0.043$, and immiscibility for PP/EPR/oil	10
PCL/P4HS	PCL blends with poly(4-hydroxy styrene): $\chi_{12}/V = -0.013$ and single T_g indicated miscibility	11
CR/PEMA	Miscibility concluded from the negative χ_{12}: -0.030 to -0.122, and from FTIR	12
PET/PETG	Miscibility concluded from the negative $\chi_{12} = -0.122$ (280 °C)	13

References: **1.** Zhang and Prud'homme 1987; **2.** Goh and Siow 1988; **3.** Runt and Gallagher 1991; **4.** Maiti and Nandi 1996; **5.** Pennings and Manley 1996; **6.** Lu and Weiss 1991, 1992; **7.** Huo and Cebe 1993; **8.** Gallagher et al. 1993; **9.** Shibayama et al. 1995; **10.** Ohlsson and Tørnell 1996; **11.** Lezcano et al. 1996; **12.** Kundu et al. 1996; **13.** Papadopoulou and Kalfoglu 1997

Dumoulin et al. 1987). As a result, despite its simplicity, obtained values of χ_{12} from the T_m method should be confirmed by other techniques (Utracki 1989; Groeninckx et al. 1998). Enthalpic interaction parameters determined for low molecular analogs via direct calorimetric measurements of the enthalpy of melting, ΔH_m, provide data which correlate well with χ_{12} determined by other methods (Barlow and Paul 1987; Rana et al. 1996; Ziaee and Paul 1996, 1997). The most crucial aspect here is the selection of suitable analogs. In this task, consideration of the partial charges of the atoms in each molecule can be used as guide (Ziaee and Paul 1996, 1997); as discussed in the heat of mixing Sect. 2.6.2.2, there are several disadvantages in such an approach, for example, inability to account for structural and/or polydispersity effects. Another method that can address some of these concerns is the microcalorimetric determination of ΔH_m using low viscosity oligomeric mixtures (Singh and Walsh 1986; Sham and Walsh 1987) (Table 2.25).

2.7.2.2 Ternary Systems Containing Solvent

The difficulties in the calorimetric determination of the interaction parameters are caused by the high viscosity of most commercially relevant or academically interesting polymers and the accompanying slow diffusion rates, heat generation during mixing or processing, etc. These problems do not exist for solutions.

One way to overcome such problems is to consider solvent(1)/polymer(2)/ polymer(3) ternary systems; any method that determines either ΔG_m or its derivatives should make it possible to calculate χ_{23}. Thus, for example, osmotic pressure measurements were used to characterize PS/PVME blends dissolved in either toluene or ethylbenzene (Shiomi et al. 1985). The χ_{23} was found to depend on the blends' composition. Elimination of the solvent effects gave $\chi_{23}/V_1 = -10^4$ $(7.41-11.01\phi_3)$. Thus, the system was expected to remain miscible up to a PVME volume fraction of $\phi_3 = 0.67$. Osmotic pressure has also been used to determine $\chi_{23} = 0.070$ for PS with poly(p-chloro styrene) in toluene, 2-butanone, and cumene (Ogawa et al. 1986). For the same system, $\chi_{23} = 0.087$ was calculated from intrinsic viscosity measurements. Thus, the system is thermodynamically immiscible. More recently, osmotic pressure measurements in cyclohexanone of a ternary system resulted in $\chi_{23}(\phi)$ for poly(vinylchloride-co-vinylacetate) blends with a series of acrylic copolymers (Sato et al. 1997).

Vapor sorption of PS/poly(α-methylstyrene) gave $\chi_{23} = 0.504$, varying with T and polymer concentration, indicating that this system is immiscible with UCST > 100 °C (Saeki et al. 1981). Light-scattering measurements of ternary systems, polymer(1)/polymer(2)/solvent(3), were also successfully used to determine polymer/polymer interaction parameters, $\chi_{12}(\phi)$. The method is particularly easy to use either if one of the two polymers is iso-refractive with the solvent or if the polymers have equal contrast (Pinder 1997). The method was successfully used to measure χ_{12} for PS/PMMA blends of different M_w.

Over the years, several authors tried to correlate polymer/polymer miscibility with solution viscosity in a common solvent (e.g., Bohdanecky and Kovar 1982). An interesting report in this field was (Chee 1990) considered that the parameter $b = k_H[\eta]^2$ (k_H is the Huggins constant of Eq. 2.33, and $[\eta]$ is the intrinsic viscosity) can be set as a measure of the interactions between the solvent and the polymeric species. For polymer blends, the author wrote

$$\left. \begin{array}{l} [\eta]_{blend} = w_2[\eta]_2 + w_3[\eta]_3 \\ b_{blend} = w_2^2 b_{22} + w_3^2 b_{33} + 2w_2 w_3 b_{23} \end{array} \right\} \Rightarrow \mu \equiv \frac{[b_{23} - (b_{22} + b_{33})/2]}{\left([\eta]_3 - [\eta]_2\right)^2} \quad (2.75)$$

where the parameter μ as defined in Eq. 2.75 is a measure of the polymer/polymer miscibility (viz., negative μ values indicate immiscibility, and positive μ miscibility). Three series of blends were examined: (1) PVC/PMMA, (2) PiBMA/PMMA, and (3) PiBMA/PVC. In agreement with the calculated values of the parameter μ, the first of these three blends was found miscible, whereas the two other immiscible in the full range of composition. However, the method is, at best, qualitative. For example, the effect of the common solvent on the parameter μ was not investigated,

but fundamentals of intermolecular interactions make it dubious that nonpolar solvents will lead to the same value of the parameter μ as strongly polar ones. The author observed that the method breaks down for polymer pairs that can form associations. Intrinsic viscosity measurements were also used to evaluate intermolecular interactions in blends of cellulose diacetate with poly(vinyl pyrrolidone) (Jinghua et al. 1997).

Another method is based on the principle that the change in any thermodynamic state function depends only on the initial and final states (Hess cycle). For example, in path I, two polymers are dissolved separately in the same solvent and then mixed together; in path II, polymers are first blended together and then dissolved in the same solvent. From the balance of the dissolution enthalpies, the heat of mixing of two polymers, ΔH_m, can be calculated at the corresponding temperature. However, since ΔH_m, in the above example, is a small number determined by subtracting two large values from each other, the error of these estimation can be large. Furthermore, χ_{23} determined from ΔH_m above is from dilute systems, and its extrapolation to melt may be impractical (Koningsveld et al. 1974). ΔH_m measurements have been used to characterize PPE blends with either PS, halogenated PS, or copolymers (Zacharius et al. 1983). At 34.8 °C, the heat of mixing of PS/PPE blend was small and negative, indicating weak specific interactions. By contrast, in blends of PS with poly(2-chloro styrene), ΔH_m was small and positive, dependent on molecular weight and temperature. In agreement with the observations, for PS/poly (2-chloro styrene-*co*-4-chloro styrene), $\Delta H_m = 0.31$ J/g was found in the full range of copolymer compositions, confirming immiscibility.

Size exclusion chromatography, SEC, has also been used for the determination of polymer/polymer interaction coefficients in solvent/polymer/polymer three-component systems (Narasimhan et al. 1979, 1983, 1984). The method was found precise and thermodynamically significant. Strong solvent concentration dependence of $\chi_{23} > 0$ was reported from tests of toluene/PMMA/PS system (Lau et al. 1984, 1985).

In conclusion, it is important to note that the determination of χ_{23} is of dubious value for predicting polymer/polymer miscibility, especially for processing conditions. The chi parameter is a complex function of many variables, including T and P that can become extreme during processing. The solution methods require high polymer dilution and low temperatures, significantly lower than those used for compounding or forming of polymer blends. Methods capable to accurately extrapolate solution data to the processing conditions do not exist. The above comments are pertinent to any of the ternary solvent methods of χ_{23} determination.

2.7.3 Phase Diagrams

2.7.3.1 Turbidity Measurements

The method consists of preparation of a series of mixtures of varied concentrations (near the phase separation condition) then causing the separation to occur, e.g., by ramping the temperature. The onset of turbidity is observed visually, using

a photoelectric cell, or by a UV-visible spectrophotometer. The ensemble of the cloud points defines the cloud-point curves (CPC) that closely follow the system's binodal. The method can be extended to rigorous studies of phase separation by measuring the light-scattering intensity.

For polymer blends, the CPC is usually determined by preparing films under conditions of miscibility, in a wide range of compositions. The films are then heated through the cloud point at a rate not exceeding 0.1 °C/min. Depending on the rate, type of system, and polydispersity, the hysteresis (difference between CPC on heating and cooling) can be significant. Examples of blends whose phase diagrams were determined are listed in Table 2.26.

The scattered intensity of light due to concentration fluctuations, extrapolated to zero-scattering angle, is inversely proportional to the second derivative of ΔG_m. Thus, it can be used to determine the location of a spinodal, i.e., the spinodal temperature, T_s, for the given mixture. As Eq. 2.32 indicates, LS makes it possible to determine also the second virial coefficient (A_2) and from it the binary interaction parameter (χ or B). However, this technique is applicable only to homogenous systems, i.e., at temperatures $T \leq T_s$ for LCST systems or at $T \geq T_s$ for those having UCST. As mentioned in Sect. 2.8.2.2, the LS methods has been used primarily to study the phase equilibria of polymer solutions.

Pulse-induced critical scattering, PICS, is an elegant method of LS measurements that makes it possible to extend the measurements closer to the spinodal. It uses a small mass of a homogenous liquid mixture very rapidly heated or cooled into the metastable region. The laser light-scattering intensity is measured after thermal equilibrium is reached, but before the system can phase separate, the mixture is brought out into the homogenous region and the cycle repeated (Gordon et al. 1973). The temperature change can be accomplished in milliseconds, afforded by the small specimen size, and the time of one full cycle is less than a minute.

One of the most serious obstacles in the phase equilibrium studies of polymer blends is the viscosity of the system. At the accessible temperatures, between softening point and thermal degradation, the self-diffusion coefficient of macromolecules is of the order of 10^{-4} to $10^{-6} \text{m}^2/\text{s}$ (Kausch and Tirrell 1989). As a result, phase separation is very slow. To accelerate the process, a low-speed centrifuge, the "centrifugal homogenizer" (CH), with PICS has been used (Koningsveld et al. 1982). In short, centrifugation within the immiscibility zone permits determination of binodal and critical points, while use of the PICS mode allows location of the spinodal.

2.7.3.2 Scattering Methods

Turbidity, light scattering, and PICS methods, discussed in the preceding paragraphs, are based on the scattering of light by liquid systems with optical heterogeneities. These principles have been extended to other types of radiation, e.g., X-rays and neutrons, cf. SAXS and SANS, which have been used to study polymer blend structures. In contrast to light scattering, SAXS uses the regularity of crystalline, or pseudocrystalline arrays of atoms, whereas SANS that of different mass of atoms. The data are treated via a relation derived for the conventional light-scattering equation (Eq. 2.32):

Table 2.26 Examples of polymer blends with known phase diagram(s)

Blend	Comment	References
PS/PVME	LCST. A rare case of miscible homopolymers. M_w only slightly affects the critical concentration (about 10 wt% of PS), but strongly changes the critical temperature 102–145 °C	Nishi and Kwei 1975
		Nishi et al. 1975
		Reich 1986
		Qian et al. 1991
		Radusch et al. 1996
SAN/PMMA	LCST. PMMA miscibility with SAN (5.7–38.7 wt% AN; at $T = 140$–170 °C). Interfacial thickness data. PMMA is immiscible with both PS and PAN	McMaster 1975
		McBrierty et al. 1978
		Higashida et al. 1995
SAN/PCL	LCST. Miscibility chimney dependent on the blend composition and AN content in SAN	McMaster 1973;
		Schulze et al. 1993;
		Kammer et al. 1996
		Higashida et al. 1995
PS/4MPC	LCST = 220 °C	Shaw 1974
PVDF/i-PEMA	LCST = 220 °C	Saito et al. 1987
		Hahn et al. 1987
PMMA/α-MSAN	LCST = 185 °C	Goh et al. 1982
PMMA/CPE	LCST = 100 °C	Walsh et al. 1982
PMMA/PVC	LCST = 190 °C	Jagger et al. 1983
PMMA/Phenoxy	LCST = 158 °C (30 wt% phenoxy). Phase diagram from turbidity	Chiou and Paul 1991;
		Etxeberria et al. 1997
PES/Phenoxy	LCST = 194 °C (57 wt% of phenoxy)	Walsh and Singh 1986
PES/PEO	LCST = 80 °C	Walsh and Rostami 1985
PVC/NBR/plasticizer	Miscibility only for the PVC/AN part	Inoue et al. 1985
PVC/Acrylates	LCST = 106 °C for PVC/PPrA	Sham and Walsh 1987
	LCST = 127 °C for PVC/PBA	
	LCST = 131 °C for PVC/PPeA	
PS/PMPS	UCST = 103 °C	Takahashi et al. 1986
SBR-45/BR	UCST = 140 °C	Ougizawa et al. 1985
NBR-40/SAN	UCST = 140 °C	Ougizawa and Inoue 1986

$$\frac{K\ c_2}{R(q)} = \frac{A_1}{M_{w,2}\ P(q)} + 2A_2\ c^2 + \dots \tag{2.76}$$

where $q \equiv (4\pi/\lambda)\sin\theta$ is the scattering vector (cf. Eq. 2.71); c_2 is the polymer concentration, $M_{W,2}$ the polymer molecular weight, and A_2 the polymer second virial coefficient (the subscript 2 indicates that the polymer is present in lower concentration); $R(q) \equiv I(q)\omega^2/I_o V_{sc}$ is the ratio of scattered to incident intensities (Rayleigh ratio); $P(q)$ is Debye's one-particle scattering form function, same with the one used in light scattering; λ is the neutron wavelength; and θ is the scattering

half-angle. The constant K contains the scattering lengths of hydrogen (^{1}H) and deuterium (^{2}H) as the most important quantities, whereas the average scattering radius of the polymer, cf. R_g^{sc} or $(R_g^{2\ sc}/M_W)^{1/2}$, is calculated from $P(q)$.

The phase equilibria in systems containing di-block poly(styrene-*b*-butadiene), SB, mixed with either a homopolymer or a random copolymer were established by plotting the reciprocal of the intensity of the main SAXS peak as a function of 1/T; thus, the spinodal, T_s, and binodal, T_B, temperatures were measured (Zin and Roe 1984). SAXS has been typically used to study the morphology of polymer blends in the solid state (Khambatta 1976; Russel, 1979; Russel and Stein, 1982, 1983). For example, in the interlamellar regions of PCL/PVC blend, the system is miscible on a molecular scale. Addition of PVC impeded crystallization of PCL. At high PVC concentration, PCL remained in solution. The radius of gyration was larger than that under unperturbed conditions, in spite of the fact that the second virial coefficient, A_2, was virtually zero. SAXS was also used to study the morphology of LDPE/HDPE blends (Reckinger et al. 1984, 1985). It was found that during the crystallization, macromolecules segregate. This segregation was also observed during rapid quenching at about 100 °C/min; at the high rates associated with the process, the segregation distance was comparable to coil dimension in the melt.

2.7.3.3 Fluorescence Techniques

"Excitation fluorescence" is the principle of the fluorescence techniques used for studying polymer blends. The method comprises of three steps: incorporation of an excimer, its excitation, and recording the excitation delay. The excimer can be an aromatic polymer component of the blend (viz., PS, poly(vinyl-dibenzyl), polyvinylnaphthalene, an aromatic group grafted onto the macromolecular chain, etc.), or it can be added as "probe" molecule (e.g., anthracene). There are three possibilities for the aromatic rings to form excimers: intramolecular adjacent, intramolecular nonadjacent, and intermolecular types. Each of these types is sensitive to different aspects of the chain conformation and environment, thus, sensitive to blend miscibility effects. The most important of these for studies of polymer blends is the intermolecular, usually identified from concentration measurements (Winnik et al. 1988).

In a second method, the "non-radiative energy transfer" method (NRET), the energy is transferred from a donor to a receptor chromophore, when the distance between them is of the order of 2–5 nm. Phase separation is concluded from a decrease of the chromophore energy transfer. The method has been used to study PVC miscibility with PMMA or with SAN; PS or poly-α-methylstyrene (PαMS) with PS-αMS copolymer; PS or PαMS or PBS [poly(tert-butyl styrene)] or PS + PBS with PS-BS copolymer; etc. (Morawetz 1980, 1981, 1983; Albert et al. 1986).

2.7.3.4 Ultrasonic Velocity

For homogenous systems, the ultrasonic velocity is related to the ratio of modulus to density. Thus, one may expect that any method that determines density changes with adequate precision can provide a measurement or an indication of

miscibility (Singh and Singh 1983). The ultrasonics can also be used as a fast screening method for the optimization of processing and its parameters, e.g., employed as online characterization of polymers blends (Piau and Verdier 1993; Verdier and Piau 1995; Gendron et al. 1995).

The compressive ultrasonic velocity (6 MHz, at room temperature) was used to study cast blend films of PMMA/PVAc, PMMA/PS, PVC/CR, and PS/EPDM (Singh and Singh 1983; Shaw and Singh 1987). A linear correlation between the sound velocity and the composition was observed for miscible blends, whereas immiscibility, viz., in PMMA/PS blends, the same dependence was irregular. Phase separation in PVC/CR was detected at $w = 70$ wt% of CR, indicated by a sudden departure from linear correlation. The ultrasonic absorption versus composition gave even stronger evidence of immiscibility. Ultrasonics have been also successfully used to study the phase behavior in polyurethanes (Volkova 1981).

Acoustic emission has been frequently used in studies of the fracture behavior of fiber-reinforced composites. This method was also adopted to studies of blends. Since the sound is most frequently generated by debonding of two phases, there should be a drastic difference in the acoustic activity for blends located on the two sides of spinodal. To quantify miscibility between PVC and EVAc, acoustic emission measurements during a peel test of a-PVC/EVAc/PVC sandwich were carried out (Muniz et al. 1992). The authors considered that the acoustic emissions at slow rates of peeling are related not to the viscoelastic dissipation processes, but rather to the work necessary to pull apart polymeric chains or break bonds. The highest acoustic emission was obtained for VAc content in EVAc of 18 and 29 wt%.

2.7.4 Indirect Methods for Polymer/Polymer Miscibility

These methods do not provide data for the binodal, spinodal, or the numerical value of the interaction parameter, but general information about the polymer/polymer miscibility. However, the information can frequently be used, e.g., to construct a map of miscibility – a simplified phase diagram.

2.7.4.1 Glass Transition Temperature (T_g) Measurements

When polymer is cooled, from either the liquid or rubbery state, its molecular motion slows down, and eventually it undergoes a glass transition, or vitrification, preceeded by crystallization for semicrystalline polymers. The glass formation is a nonequilibrium phenomenon and is kinetic in nature, i.e., not a genuine first-order thermodynamic transition; thus, its characteristic temperature, T_g, is detected at different temperature values depending on the cooling rate, the probing method, the thermal history, etc. Nevertheless, most theoretical treatments consider the glass to be at a pseudo-equilibrium state, endowing T_g with characteristics of a critical temperature of a second-order thermodynamic transition. The thermodynamics of such a state demands knowledge of "order parameters," z_i:

$$dG = \left(\frac{\partial G}{\partial T}\right)_{P,z_i} dT + \left(\frac{\partial G}{\partial P}\right)_{T,z_i} dP + \sum_{i=1}^{n} \left(\frac{\partial G}{\partial z_i}\right)_{P,T,z_j} dz_i \qquad (2.77)$$

At equilibrium, the affinity coefficients, $A_i \equiv (\partial G/\partial z_i)_{P,T,z_j} \rightarrow 0$, and the equilibrium equation, Eq. 2.11, regain validity.

When liquids are viewed as collections of inherently non-crystallizable macromolecules, they are expected to show equilibrium amorphous properties in all T ranges. Furthermore, in the thermodynamic description of the glassy state, it was postulated that cooling a liquid causes its configurational entropy to decrease, becoming zero at T_g (DiMarzio and Gibbs 1958; Dong and Fried 1997). This concept gives legitimacy to the pseudo- or semi-equilibrium theories of the glassy state, viz., Couchman's theories (Couchman 1978, 1979a, b). It is widely accepted that when the test methods are slow enough (usually less than 1 °C/min and/or 1 Hz) the glass behaves in a semi-equilibrium manner and its behavior can be generalized.

In a first approximation, the polymer's glass transition is related to the cooperative segmental motion involving 50–100 backbone chain carbon atoms, or 15–30 statistical segments, i.e., a domain of a size $d_d = 2$–3 nm (Boyer 1966; Warfield and Hartmann 1980). However, the glass transition is not a phenomenon occurring at constant free volume. Along these lines, the most common use of T_g in determination of polymer/polymer miscibility is based on the premise that a single T_g indicates that a uniform blend domain size comparable to the macromolecular cooperative length or to the macromolecular radius of gyration, i.e., $2 \leq d_d \leq 15$ nm. This approach has already been discussed in Sect. 2.5.2. It is important to recognize that a single T_g is not a measure of miscibility, but rather an indication of the state of dispersion. There are several equations relating T_g to composition (Utracki 1989). One approach (Couchman 1978) proposed the following relation for the T_g of miscible systems:

$$\ln T_g = \frac{\sum_i w_i \Delta C_{Pi} \ln T_{gi}}{\sum_i w_i \Delta C_{Pi}} \qquad \left(\text{with } \Delta C_{Pi} \equiv C_P^{\text{liquid}} - C_P^{\text{glass}} \text{ for polymer } i\right) \quad (2.78)$$

where w_i and T_{gi} are, respectively, the weight fraction and glass transition temperature of polymer i in the blend and ΔC_{Pi} is a difference of the isobaric heat capacity, C_P, in the liquid and glass states of polymer i, assumed to be independent of T. From this relationship, several empirical and semiempirical formulas were derived, including the Gordon-Taylor equation, as well as the Fox equation. Note that these relations are valid only for miscible systems. The latter one

$$\frac{1}{T_g} = \sum_i \frac{w_i}{T_{gi}} \qquad \left(\text{or}: \quad \sum_i w_i \left(1 - \frac{T_g}{T_{gi}}\right) = 0\right) \qquad (2.79)$$

is particularly simple and ubiquitously used, even applied to calculate blends' composition from measured values of T_g (this use should be limited to situations where

the T_g versus composition was "calibrated" and confirmed to follow Eq. 2.79). Comparing Eqs. 2.78 and 2.79, it is obvious that the Fox equation ignores the contributions of ΔC_{Pi}. To account for this omission, a different relation can be derived, also for miscible blends, for example, in a two-component system (Lu and Weiss 1991, 1992):

$$T_g = \frac{w_1 T_{g1} + k\ w_2 T_{g2}}{w_1 + k\ w_2} - \frac{\chi_{12}\ R\big(T_{g2} - T_{g1}\big)b\ w_1 w_2}{\Delta C_{P1}(w_1 + k\ w_2)(w_1 + b\ w_2)^2} \qquad (2.80)$$

where k and b are ratios of, respectively, ΔC_P's and densities of polymers 1 and 2 and χ_{12} is the binary interaction parameter. Thus, the relation makes it possible to compute the interaction parameter of miscible blends from T_g versus composition dependencies.

In a different approach, starting from Eq. 2.78, the following dependence was derived for binary blends (Utracki and Jukes 1984):

$$w_1 \ln\big(T_g/T_{g1}\big) + k\ w_2 \ln\big(T_g/T_{g2}\big) = 0 \qquad (2.81)$$

For a miscible blend, the parameter k is equal to $k = \Delta C_{P1}/\Delta C_{P2}$ (relaxing this condition, transforms Eq. 2.81 into a semiempirical one, valid for either miscible or immiscible systems). The dependence should be symmetrical, i.e., it must be valid when the indices are exchanged. Thus, miscibility requires that $k = 1/k = 1$. The larger the difference between k and $1/k$, the larger is the immiscibility of the system. The dependence should not be used for strongly associating polymer blends where blend T_g may reach values higher than those observed for either pure component. Such miscible, hydrogen-bonded, or donor-acceptor pairs are well described by a single parameter relation (Utracki 1989):

$$T_g = (1 + K^*\ w_1 w_2)\Big[w_1 T_{g1}^{3/2} + w_2 T_{g2}^{3/2}\Big]^{2/3} \qquad (2.82)$$

where K^* is a material parameter, with a value that increases with stronger polymer/polymer association.

Several methods of T_g determination make it possible to measure the width of the glass transition temperature (TW). The value of TW can be more reliable in assessing the degree of miscibility than T_g. For example, TW of 6 °C was determined for neat polymers, TW = 10 °C for miscible blends, and TW = 32 °C for blends approaching immiscibility (Fried et al. 1978). By measuring T_g and TW for samples annealed at different temperatures and then quenched, one may be able to determine the level of miscibility and hence construct a simplified phase diagram. This has been done for numerous blends, like those listed in Table 2.26, and others, e.g., for PS/PTMPC, PVC/poly(α-methylstyrene-co-methylmethacrylate-co-acrylonitrile), and NBR/EVAc (Casper and Morbitzer 1977) (vide infra, Table 2.27).

To construct the phase diagram, thin blend specimens should be prepared. The preferred method is to cast film from a common solvent. However, it has been

Table 2.27 A few examples of T_g measurements of polymer blends

Blend	Comment	References
PVDC/aliphatic polyesters	THF cast films; T_g measured by DSC on samples annealed at 460 K	1
Oligo(styrene-*co*-allyl alcohol)/ aliphatic polyesters	Specimens mechanically mixed at $T = T_g +$ 70 °C; DSC at 20 °C/min; UCST directly observed	2
PS/poly(styrene-*co*-4-bromostyrene)	Films cast from $CHCl_3$ of CH_2Cl_2; DSC (10 mg) at 20 °C/min. UCST reported	3
Poly(aryl ether ketone) blends	T_g linear dependence on mole fraction of ketone groups	4
PMMA/SAN/SMA PEM/SAN/SMA MAN/SAN/SMA	Samples were either cast from MEK or melt blended; DSC at 20 °C/min; T_g from the onset during the second heating cycle	5
1,2-PB/1,4-PI	Polymers co-dissolved in benzene, then freeze-dried; DSC at 10 °C/min' T_g and TW measured in duplicate or triplicate	6
SAN/SMMA/MAN	Ternary blends prepared in THF, precipitated by MeOH, then dried; DSC at 20 °C/min over $T = 310–430$ K	7
PC/TMPC/SAN/SMMA	Samples cast from THF; DSC at 20 °C/min; T_g taken at onset. Phase diagrams constructed	8
SMMA/poly(butyl-*co*-hexafluoro-carbonate)	Samples dissolved in CH_2Cl_2, precipitated by MeOH, and dried. T_g taken at onset during the second heating	9
Poly(α-MSAN)/SAN, TMPC, PVC, PPE or PMMA; PMMA-GMA/SAN or TMPC	Samples either cast from THF, or hot cast from DMF or acetonitrile, dried at 150 °C for 2 days; DSC at 20 °C/min. Diverse phase diagrams	10
PC/poly(ET-*co*-caprolactone)	Samples cast from $CHCl_3$; DSC at 20 °C/min $T \leq 530$ K. T_g taken at half-height	11
PMMA-GMA/PVDF	Samples cast from DMF; DSC at 20 °C/min to 190 °C; miscibility only for PMMA-GMA with GMA <35.7 wt%	12
PS/PC or oligo(cyclic-carbonate)	Samples hot cast from *o*-dichlorobenzene; DSC at 20 °C; samples annealed at 200 °C for 5 min	13
PS/PCHMA	Dissolved in THF, precipitated by MeOH; DSC at 10 °C/min; T_g taken at midpoint of inflection	14
PBT/Poly(ester carbonate)	DSC at 20 °C/min; T_g from second scan. Solution cast samples gave two T_g's; precipitated from solution or melt mixed (at 250 °C) systems had only one T_g	15
PEI/PAr	Melt mixed at 300 °C; DSC at 20 °C/min. T_g taken at onset	16
CR/PEMA	Melt mixed at 100 °C; DSC at 20 °C/min	17

(*continued*)

Table 2.27 (continued)

Blend	Comment	References
PMMA/PBMA	Samples prepared by MeOH precipitation of acetone solutions; DSC (20 mg) at 10 °C/min	18
PEEK/PEI	Melt mixed at 400 °C, quenched in ice water into 0.2–0.4 mm sheets. DSC (10 mg) at 20 °C/min. Miscible blends	19
Poly(aryl ether ketone)/aromatic thermoplastic polyimides	Melt mixed at 400–455 °C (ca. 50 mg, between two sheets of Kapton^{TM}); DSC at 20 °C/min	20
Poly(styrene-*co*-2,4-dinitrostyrene)/ PVME or PPE	Samples cast from DMF; DSC at 20 °C/min. Phase diagram with LCST found	21
PVC or c-PVC/poly(caprolactam-*co*-caprolactone)	Samples co-precipitated from *p*-xylene, THF, or DMSO; DSC at 10 °C; T_g from onset and inflection point	22
Cellulose diacetate/PVP	Samples by solution casting; DSC at 10 °C	23
PMMA/PEG/Phenoxy	Samples melt mixed; DSC at 20 °C/min. Immiscibility window found	24
SAN/PAr-*co*-TMPAr	Samples MeOH precipitated from CH_2Cl_2; DSC at 20 °C/min. Miscibility map given	25
PVC/SMMA	Samples melt mixed; DSC at 20 °C/min (contrast enhanced by physical aging, 46 h at 60 °C)	26

References: 1. Aubin et al. 1983; **2.** Woo et al. 1984; **3.** Strobl et al. 1986; **4.** Harris and Robeson 1987; **5.** Brannock and Paul 1990; **6.** Roovers and Toporowski 1992; **7.** Cowie et al. 1992c; **8.** Kim and Paul 1992; **9.** Takakuwa et al. 1994; **10.** Gan et al. 1994; Gan and Paul 1994b; **11.** Dezhu et al. 1995; **12.** Gan and Paul 1995; **13.** Nachlis et al. 1995; **14.** Friedrich et al. 1996; **15.** Rodriguez et al. 1996; **16.** Bastida et al. 1996; **17.** Kundu et al. 1996; **18.** Sato et al., 1996a, b; **19.** Goodwin and Simon 1996; **20.** Sauer et al. 1996; **21.** Fernandez et al. 1997; **22.** van Ekenstein et al. 1997; **23.** Jinghua et al. 1997; **24.** Hong et al. 1997; **25.** Ahn et al. 1997; **26.** Dompas et al. 1997

observed that the blend thermograms depend on the type of solvent used for casting the film. For example, PVC/PHMT blends cast from toluene had a single T_g, whereas when cast from 1,4-dioxane it exhibited two T_g's, a fact that it is not completely unexpected, since small differences in the polymer/solvent χ results in quite substantial enthalpic contributions in the free energy of mixing, in the order of χN, N being the size (degree of polymerization) of the polymer, which would cause in a better dissolution of one of the two polymers in any given solvent and, in turn, would result in differences in the miscibility of the cast blend. Clearly, caution is advised: Preferably the procedure should be carried out using specimens prepared by different methods; specimens should be annealed at temperatures located on both sides of the expected spinodal and then quenched. The most popular method for detecting T_g is the differential scanning calorimetry (DSC), owing to the simplicity of the experiments and the small specimen sizes required (a few mg). Using substantially more complex experiments and analysis, more information can be obtained from a dynamic test: either dielectric relaxation spectroscopy, or dynamic mechanical analysis (shear, bending or tensile, preferably at low and

constant test frequency). T_g can also be determined by dilatometry. The method extends testing of the blend miscibility to higher pressures, as those expected during processing (Jain et al. 1982; Walsh and Zoller 1987; Zoller and Walsh 1995). The pressure effects are not negligible, for example, for PPE/PS system, the pressure gradient of T_g (dT_g/dP) was reported to range from 4.3 to 8.2 °C/GPa, depending on the composition (Zoller and Hoehn 1982).

One shortcoming of the method can be demonstrated by the fact that, even for immiscible blends, rarely two T_g's can be detected for compositions containing less than 20 wt% of the dispersed phase. Beyond any instrumental detection limits, the experimental range of resolution depends also on the difference between the T_g's of the two polymers ($\Delta T_g = T_{g1} - T_{g2}$). Since the width of the glass transition can be as large as TW = 40 °C, this method of assessment of miscibility should not be used for systems with $\Delta T_g \leq TW/2 \approx 20$ °C. Table 2.27 provides some examples studies of blend miscibility by means of T_g measurements; older data can be found in Utracki (1989).

2.7.4.2 Spectroscopic Methods: NMR

For the studies of interactions in polymer blends, nuclear magnetic resonance (NMR) and Fourier transform infrared spectroscopy (FTIR) are of principal significance. The NMR methods for the studies of polymer blends are well described in textbooks as well as in several reviews (Olabisi et al. 1979; Robeson 1980; Martuscelli et al. 1983; Kaplan 1984; McBrierty and Packer 1993; Cheng et al. 2011). The NMR parameters used in the determination of polymer/polymer miscibility are mainly the times related to the half-life of the spin relaxation, such as the spin–lattice relaxation time (T_1), the spin-spin (T_2), and the spin–lattice in the rotating frame ($T_{1\rho}$). The shorter the relaxation time, the broader is the NMR line width (for solid samples the lines are broad, a manifestation of slow reorientation of bonds, whereas for liquids and solution they are narrow, as expected from faster bond reorientation). The position of the lines, i.e., the precessional frequency of the nucleus, depends on its chemical environment, spatial configuration, and interactions. The position of the peak or the so-called chemical shift (usually quoted as d in parts-per-million, ppm) is a reflection of the energetic state of the nucleus, while the line intensity is that of its population. For example, $T_{1\rho}$ was used to analyze interactions between PVC and polymethacrylates: poly(cyclohexyl methacrylate) (PCHMA), poly(phenyl methacrylate) (PPMA), and poly(benzyl methacrylate) (PBzMA) (Sankarapandian and Kishore 1996). The NMR-detected domain size was between 3 and 15 nm. The miscibility of the same systems was also analyzed by measuring T_g. Both methods indicated miscibility for the PVC/PCHMA blends and immiscibility for the PVC/PBzMA system; however, for the PVC/PPMA 1:1 blends, while T_g indicated miscibility, the $T_{1\rho}$ NMR data showed that the same system is immiscible.

Modern solid-state NMR involves the use of very short radio-frequency pulses (of variable duration from 1 to 200 ms) and can be complemented with real-time Fourier transform analysis and multiple scan capability. Standard NMR enhancements nowadays, such as scalar (low power, ca. 4 kHz) and dipolar (about 45 kHz) decoupling, magic angle spinning, spectra of multiple elemental isotopes beyond

Fig. 2.26 An example of NMR used to probe local environment of a polymer in a blend. [15]N CPMAS (cross-polarization, magic angle spinning) NMR spectra of polyamide-6 in a blend with polyketone. PA-6 in a PK/PA 6:4 blend (**a**) shows primarily (70 %) its α-crystal phase, whereas in its pure form (**b**) PA-6 shows a 60 % γ and 40 % α crystal (Data from Asano, Chap. 5 in Cheng et al. 2011)
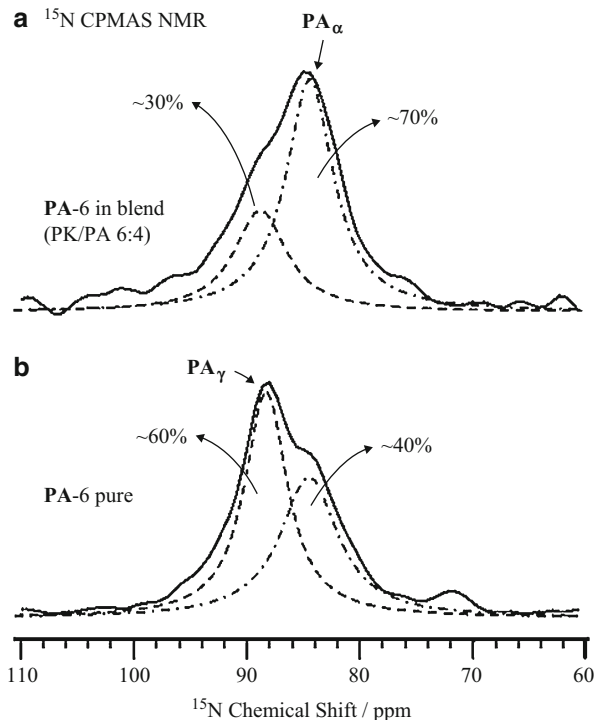
[1]H and ^{13}C, multi-pulse (multidimensional NMR), and cross-polarization methods, enable spectra for solid samples with resolutions similar to those known for liquids (Webb 2006; White and Wachowicz 2008). Such spectra provide precise information on the local environment of selected nuclei, configuration, interactions, and sample morphology (Fig. 2.26).

The interactions between PVDF with PMMA, PVAc, or PVME were studied by dipolar-dipolar decoupling, cross-polarization, magic angle spinning, and high-resolution ^{13}C NMR (Lin 1983; Ward and Lin 1984). Clear peak assignment for each carbon was made, and peak intensities were measured. It was found that blending has little effect on the peak frequency but a significant effect on its intensity. For example, the attenuation (A_t as a % of the observed to the expected intensities) varied with the method of blend preparation. For PVDF/PMMA 1:1 blends, when cast from DMF A_t was 100 % (immiscible), while when cast from MEK A_t was 60–75 %, and for extruded blends A_t was 26–49 % (miscible). Much clearer differences were obtained in PMAA/PVAc blends studied by ^{13}C CPMAS (cross-polarization, magic angle spinning) NMR (Fig. 2.27).

Information on short-distance spatial proximity between different segments of molecules can be obtained using the proton spin-diffusion NMR method. This is a particularly valuable method for the characterization of polymer blends. For example, in case of PS/PVME cast films, the method provided information on blend composition, fraction of interacting groups (phenyl from PS with ether from
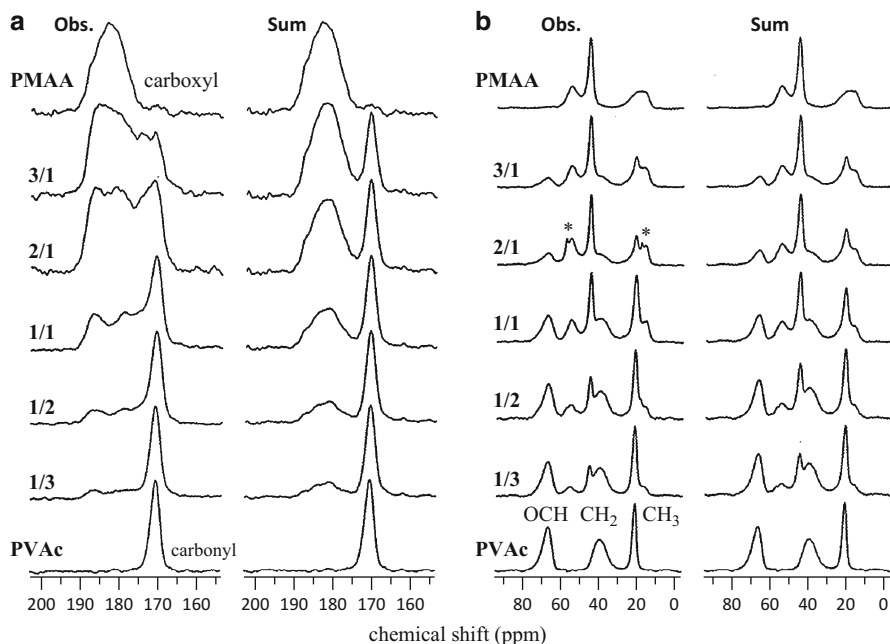
Fig. 2.27 ^{13}C CPMAS NMR spectra of PMAA (*top line*), PVAc (*bottom line*), and several PMAA/PVAc blends. (**a**) carboxyl regions of PMAA and carbonyl regions of PVAc; (**b**) aliphatic regions. The weighted sums (of the pure PMAA and pure PVAc ^{13}C NMR spectra) are also depicted on the right of the corresponding observed spectra (*left columns*). The blend formation results in strong qualitative changes in the OC=O carbon, but not so much in the carbons of the aliphatic region (Data from Asano et al. 2002)

PVME), and group mobility within each of the three domains (PS, PVME, and PS-PVME). Again, it was found that different degree of dispersion is obtained when casting films from different solvents (Caravatti et al. 1985; 1986).

Miscibility of PEEKK/PEI 1:1 blend was analyzed using solid-state NMR (Schmidt-Rohr et al. 1990). This work involved tagging of ^{1}H magnetization, based on chemical shift difference, ^{1}H spin diffusion for controlled mixing times (tuned to probe 0.5–50 nm length scales), and high-resolution ^{13}C detection. The sample was prepared by compounding at 653 K. Intimate mixing on a molecular scale was concluded. An extension of this method employed 2D ^{13}C-^{13}C CPMAS NMR combined with multiple alternating depolarization (MAD) ^{13}C(HH) ^{13}C pulses, to probe PS/PXE blends (Hou et al. 2004); albeit tedious and lengthy, this method yielded substantially improved sensitivity in unlabeled samples and much better contrast between blend components compared to ^{1}H spin-diffusion NMR.

Two-dimensional ^{2}H NMR was used to analyze miscibility in blends of poly-1,4-polyisoprene with polyvinylethylene (PI/PVE) (Arendt et al. 1994; Chung et al. 1994). The blends were prepared by casting 3 wt% toluene solution. The rate of reorientation as a function of temperature near T_g was determined for both components. It was found that the system is miscible, but the glass transition is

broad owing to the wide distribution of segmental motions arising from the differences in the rates of the two polymers. As a result, the PIP/PVE blends were found to be rheologically complex: In spite of miscibility, the time-temperature superposition was found to be invalid.

High-resolution ^{13}C NMR spectroscopy was used to analyze miscibility of POM with terphenol ($M_w = 600$ g/mol). The size of the heterogeneity in the amorphous phase was estimated as 1 nm. The ^{1}H spin-diffusion analysis indicated a homogenous mixing on the molecular level (Egawa et al. 1996).

2.7.4.3 Spectroscopic Methods: Infrared

The use of infrared spectroscopy for the characterization of polymer blends is extensive (Olabisi et al. 1979; Coleman and Painter 1984; Utracki 1989; He et al. 2004 and references therein; Coleman et al. 1991, 2006). The applicability, fundamental aspects, as well as principles of experimentation using infrared dispersive double-beam spectrophotometer (IR) or computerized Fourier transform interferometers (FTIR) were well described (e.g., Klopffer 1984).

FTIR has been extensively used to study hydrogen bonding in polymer blends (Ting 1980; Cangelosi 1982; Moskala 1984; Pennacchia 1986; He et al. 2004; Coleman et al. 1991, 2006). These interactions affect not only the –OH absorption region (3,500–3,600 cm^{-1}), but also the =CO stretching (1,737 cm^{-1}), the –CH$_2$ symmetric stretching (2,886 cm^{-1}), as well as the fingerprint frequency region (1,300–650 cm^{-1}). As discussed in Sect. 2.6.2.3, FTIR has been used to calculate the strong interaction term of the free energy of mixing, ΔG_H (see Eqs. 2.35b and 2.58) (Painter et al. 1988, 2006). The combination of FTIR spectra, which can yield a miscibility map for specific systems, with the fitted model parameters, which can give "theoretical" phase boundaries, can be combined to construct phase diagrams for specific polymer blend systems (Fig. 2.28).

FTIR was also used to analyze the mechanism of interactions in blends of aliphatic polyesters with chlorinated polymers, viz., PVC, PVDC, or PVC-DC. In miscible blends, the polyesters' carbonyl stretching absorption frequency (1,700–1,775 cm^{-1}) was shifted – the shift was absent in immiscible systems – revealing hydrogen bonding between C–O and α- or β-hydrogen. However, there are indications that the interaction mechanism does vary from system to system, e.g., the dipolar C=O with C–Cl interactions have been also identified (Coleman et al. 1983; Prud'homme 1982; Garton et al. 1983; Morra and Stein 1984; Albert et al. 1986). A typical approach to construct a miscibility map from FTIR data is shown in Fig. 2.28, and a short summary of FTIR studies of polymer blends in Table 2.28.

There are publications on the use of other spectroscopic techniques, such as Brillouin scattering, photoacoustic, and Raman spectroscopy. The primary application of these has been to study the heterogeneities in polymer blends, viz., crystallization or phase separation.

2.7.4.4 Microscopy

Microscopy methods, in the broader sense of methods that provide direct morphology imaging, can be divided into several categories: optical microscopy (OM),
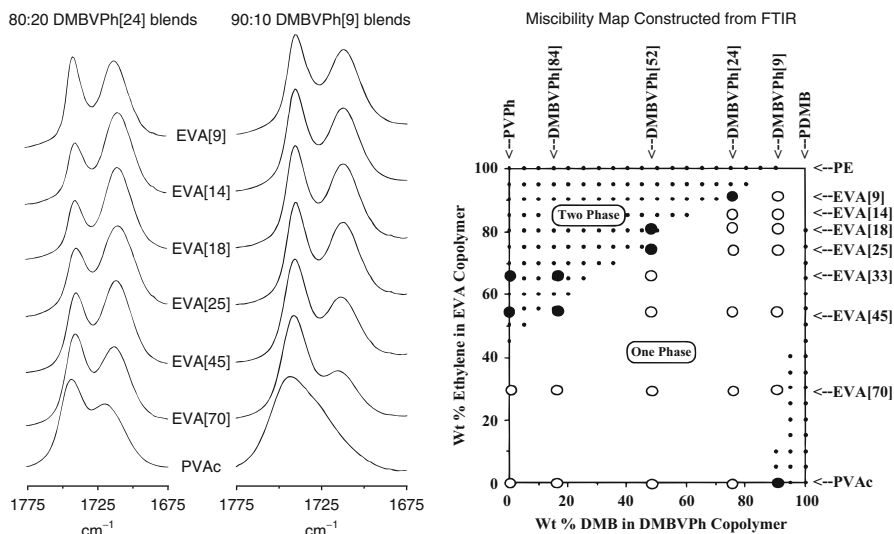
Fig. 2.28 IR spectra in the carbonyl stretching region for blends of 2,3-dimethylbutadiene-*co*-4-vinylphenol (DMBVPh) with PVAc, EVA[70], EVA[45], EVA[25], EVA[18], EVA[14], and EVA[9] recorded at 100 °C; numbers in brackets indicate the % of the comonomer, Ph or VA, in each polymer. (*Left*) IR spectra of 80:20 wt% DMBVPh-[24] blends; (*Middle*) IR spectra of 90:10 wt% DMBVPh-[9] blends; (*Right*) Miscibility map calculated at 100 °C for DMBVPh/EVA blends: areas encompassed by small black dots denote the predicted two-phase regions; experimentally determined single- and two-phase blends are denoted by the open and filled large circles, respectively (Data from Pehlert et al. (1997)

scanning electron microscopy (SEM), transmission electron microscopy (TEM), atomic force microscopy (AFM), and several modifications of these techniques. For example, the scanning transmission electron microscopy (STEM) and low-voltage scanning electron microscopy (LVSEM, at 0.1–2 kV accelerating voltage) are particularly useful for polymer blends (Vesely and Finch 1988). STEM uses ultrathin stained films, providing images with a few nanometers resolution. LVSEM provides about tenfold increased image contrast (in comparison to the conventional SEM) with almost no charging problem (Berry 1988). Owing to shallow sampling depth and low energy of the secondary electrons, conductive coating is not needed. The method uses flat, microtomed specimens providing image quality comparable to that of TEM (Vesely 1996; a nice review of microscopy methods for blends). In all cases, microscopy is considered a necessary second method of characterization for polymer blends, since it provides the required morphological information needed to explain results from spectroscopy, T_g, or other measurements.

In most cases, some mode of sample "preparation" has to be used after the blend formation, viz., staining, swelling, fracturing, or etching. These are very appropriate for and have been extensively used to characterize morphology of immiscible blends, but they have obvious severe shortcomings in miscible or partially miscible

Table 2.28 A few examples of FTIR measurements of polymer blends

Blend	Comment	References
PVDF/PMMA	Blending slightly affected the carbonyl stretching near 1,735 cm^{-1}	1
PPE/PS	FTIR peak ratio 1,030/700 cm^{-1} used for the determination of composition	2
PPE/PS	Strongest interactions for 30 wt% PPE	3
PPE/PS	FTIR was used for characterizing macromolecular orientation in solid state	4
PC/PCL	Miscibility in the amorphous phase	5
PC/PBT	Miscibility in the amorphous phase	6
PCL/Phenoxy	H-bonding between the -OH group of phenoxy and C=O of PCL	7
PS/PVME	Changes in molecular environment were easiest detected using the vibrations: in PS the out-of-plane CH, and in PVME the COCH$_3$ at 700 and 1,100 cm^{-1}	8
PF (Novolac)/PS, SAN, PEA, PVAc, PEMA, PMMA, PMPS, PC, or PVME	Novolac (PF) blends: frequency shifts in CO vibration from 1,774 to 1,752 cm^{-1} due to hydrogen bonding in miscible blends	9
PET/PC	FTIR used to study transesterification	10
PET/PA-6	Studies of ester-amide exchange reactions	11
PU/poly(EG-co-PG)	The N-H stretching (3,500–3,100 cm^{-1}) was found sensitive to interactions	12
PVPh/PVAc, EVAc, PCL, PPL, PMA, PEA, PBA, or P2EHA	Poly(4-vinyl phenol) blends: the amount of free and bonded C=O vibrations were determined fort the PVPh/hydrogen-bonding polymer blends, using a curve fitting procedure	13
poly(DMB-co-VPh)/ EVA	2,3-dimethylbutadiene-co-4-vinylphenol (DMBVPh) blends with EVA (VA comonomer: 0 % to 100 %). Miscibility map constructed (see also Fig. 2.28)	14
poly(S-co-VPh)/ PBMA, PHMA, or PTHF	Poly(styrene-co-4-vinyl phenol) blends: the hydroxyl stretching (3,100–3,700 cm^{-1}) and "fingerprint" (600–1,650 cm^{-1}) regions were analyzed. The bands 3,525 and 3,100–3,500 cm^{-1} were assigned, respectively, to free and hydrogen-bonded structures	15
PVC/SAN	Nitrile stretch vibration region (2,260–2,220 cm^{-1}) and C-Cl absorption (660–580 cm^{-1}) were used to characterize the interactions	16
PPE/PS	New method of IR-data treatment was proposed. Weight fraction of polymer-1 in the blend: $x_1 = a_o + a_1R/(1 + a_2R)$, where a_i are parameters, and $R = A_1/(A_1 + A_2)$ is the absorbency fraction	17
PVPh/PMMA	Measurements of solvent cast films showed the H-bonding extent depended on solvent	18

References: 1. Saito et al. 1987; **2.** Mukherji et al. 1980; **3.** Koenig and Tovar-Rodriguez 1981; **4.** Wang and Porter 1983; **5.** Coleman et al. 1984; **6.** Birley and Chen 1984; **7.** Garton 1983, 1984; **8.** Garcia 1987; **9.** Coleman and Varnell 1982; Fahrenholtz 1982; **10.** Huang and Wang 1986; **11.** Pillon and Utracki 1986; **12.** Coleman et al. 1988; **13.** Coleman et al. 1989; **14.** Pehlert et al. 1997; **15.** Xu et al. 1991; Serman et al. 1991; **16.** Kim et al. 1996; **17.** Cole et al. 1996; **18.** Dong and Ozaki 1997

blends. There are numerous factors that reduce resolution in blends, well above instrumental capabilities, and several sources for introduction of artifacts in electron microscopy, e.g., metallization in SEM and OsO_4 staining in TEM, introduce an artificial grain structure, especially under greater magnifications. However, even at the highest resolution, it is difficult to obtain sufficient confidence to declare whether the blend is thermodynamically miscible. One of the better sources of this information comes from studies of the diffusion rate of one polymer into another using any of the previously mentioned techniques. Preparation of samples for the observation under TEM is more tedious and exacting than that used for SEM. The specimens have to be hardened and microtomed into ca. 200 nm thin slices, and most often stained with Br_2, OsO_4, or RuO_4. Frequently, the SEM and TEM methods are being used in parallel (Karger-Kocsis and Kiss 1987; Kyotani and Kanetsuna 1987; Hsu and Geil 1987; Vesely 1996).

For example, the effects of AN content on miscibility of SAN with PMMA were studied by measuring the thickness of the interphase (Higashida et al. 1995). The effects of concentration, compatibilization, and annealing for PA with either PS or PE (compatibilized by 5 wt% of PP-MAh or SMA) were studied by SEM (Chen et al. 1988). Compatibilization reduced the diameter of dispersed phases by a factor of ten and stabilized the system against coalescence at the annealing temperature ($T = 200$–$230\ ^\circ C$, for at least 1.5 h).

Interesting studies of phase coarsening in PMMA/SMMA blends were followed using interference contrast light microscopy and/or TEM (Andradi and Hellmann 1993). Films, cast from toluene, were homogenized at low temperature and then brought to the spinodal region for phase separation and coarsening; owing to the difference in the refractive indices, good contrast was obtained without etching. The kinetics of phase coarsening in blends of PS with poly(sila-α-methylstyrene) was followed under an optical microscope (Maier et al. 1996). The blends have UCST that depends on M_w. Annealing within the single-phase region, and then jumping to the spinodal region, causes SD and phase coarsening. Similarly, optical and SEM methods were used to study phase separation in blends of PP with isotactic poly(1-butene) (Cham et al. 1994); this system was found to have an UCST.

Reactive compatibilization of PA/SAN blends was followed with careful TEM (Mujumdar et al. 1994a, b). Better contrast was obtained using phosphotungstic acid than RuO_4. The binary interaction parameter, χ_{12}, was calculated from the micelle spacing in microphase-separated PS-b-PVP system (Clarke et al. 1997). The spacing was determined using an AFM. Details of the polymer blends' morphology and the methods of its characterization were discussed in ▶ Chap. 8, "Morphology of Polymer Blends" in the first edition of this handbook.

Finally, a creative approach employing optical microscopy involved high-throughput (combinatorial) methods: Here, a single sample was made with a gradient of blend composition in one direction and a linear change in temperature in the normal direction. After sufficient annealing of the samples, the LCST phase diagram can be directly observed with optical microscopy (Meredith et al. 2000, 2002; Karim et al. 2002; Yurekli et al. 2004); see also Fig. 2.29.

Fig. 2.29 Optical microscopy photograph of a PS and poly(vinyl methyl ether) (PS/PVME) T-ϕ combinatorial sample (library) after 16 h of annealing, showing the lower critical solution temperature (*LCST*) cloud-point curve. *White points* are conventional *light*-scattering cloud points measured independently on separate uniform samples (Meredith et al. 2000)
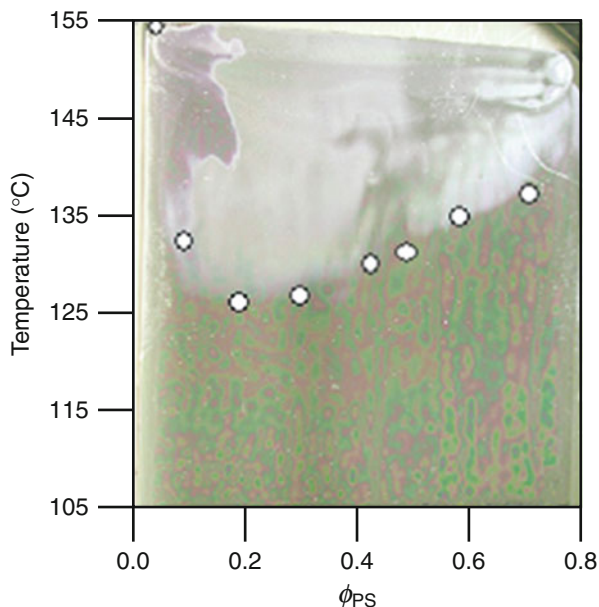
2.8 Summary and Conclusions

The information provided in this chapter can be divided into four parts: 1. introduction, 2. thermodynamic theories of polymer blends, 3. characteristic thermodynamic parameters for polymer blends, and 4. experimental methods. The introduction presents the basic principles of the classical equilibrium thermodynamics, describes behavior of the single-component materials, and then focuses on the two-component systems: solutions and polymer blends. The main focus of the second part is on the theories (and experimental parameters related to them) for the thermodynamic behavior of polymer blends. Several theoretical approaches are presented, starting with the classical Flory-Huggins lattice theory and, those evolving from it, solubility parameter and analog calorimetry approaches. Also, equation of state (EoS) types of theories were summarized. Finally, descriptions based on the atomistic considerations, in particular the polymer reference interaction site model (PRISM), were briefly outlined.

As the volume of tabulated values of thermodynamic parameters indicates, the largest pool of data is based on Flory-Huggins type of relations. This is only to be expected since the theory, and the related concept of the binary interaction parameters, either B or χ_{12}, was introduced to polymer science very early, more than a half century ago, in 1941 to be precise. Even with its rather limited applicability, due to its strict assumptions, and the well-recognized complexity of functional dependence [viz., $\chi = chi(T, P, \phi, M_w, \text{MWD, molecular}$

structure, stresses, ...), needed for most practical applications] the FH model remains to broadest used and continually developed theoretical framework for blend thermodynamics.

In hindsight, due to its ability to address high T and P, the EoS approach has been used with growing frequency to describe the thermodynamic behavior of multicomponent polymer-based systems. Such problems as the temperature- and pressure-dependent miscibility of low molecular weight liquids or polymeric liquids in selected polymers have been successfully solved. For binary blends, the EoS uses two parameters, the first related to the change of specific volume and the other to the energetic interactions. It has been shown that for many cases the values of these experimental constants can be well predicted using the algebraic and geometric means, respectively. Since during polymer processing pressure plays a major role, the EoS is potentially a very valuable tool for polymer researchers and engineers.

Biography The second edition of this chapter was written after Les Utracki had passed away. In an effort to maintain the look and feel of the chapter's first edition, we retained the structure of the original chapter and only updated the content to reflect developments within the last decade. All shortcomings and concerns regarding this chapter should be addressed to manias@psu.edu.

EM would like to dedicate this chapter to the memory of Les Utracki, as well as to my Ph.D. advisors Gerrit ten Brinke and Georges Hadziioannou; all three of these exceptional scientists have seminal and pioneering accomplishments in the field of polymer blends, as reflected in the contents of this chapter, and made invaluable contributions to the first author's education in thermodynamics and blends.

2.9   Cross-References

▶ Crystallization, Micro- and Nano-structure, and Melting Behavior of Polymer Blends
▶ Interphase and Compatibilization by Addition of a Compatibilizer
▶ Mechanical Properties of Polymer Blends
▶ Morphology of Polymer Blends
▶ Polymer Blends Containing "Nanoparticles"
▶ Properties and Performance of Polymer Blends
▶ Recycling Polymer Blends

Notations and Abbreviations

Most of the abbreviations used in this chapter are listed in Appendix 1. Pertinent ones are listed under Tables 2.11 and 2.12.

References

J.-H. Ahn, C.-K. Kang, W.-C. Zin, Eur. Polym. J **33**, 1113 (1997a)

T.O. Ahn, U. Nam, M. Lee, H.M. Feong, Polymer **38**, 577 (1997b)

R.G. Alamo, W.W. Graessley, R. Krishnamoorti, D.J. Lohse, J.D. Lonono, L. Mandelkern, F.C. Stehling, G.D. Wignall, Macromolecules **30**, 561 (1997)

B. Albert, R. Jerome, P. Teyssie, B. Baeyens-Volant, J. Polym. Sci. Polym. Chem. Ed. **24**, 551, 2577 (1986)

R.A. Alberty, Pure Appl. Chem. **73**, 1349 (2001)

S.H. Anastasiadis, I. Gancarz, J.T. Koberstein, Macromolecules **21**, 2980 (1988)

S.H. Anastasiadis, Interfacial tension in binary polymer blends and the effects of copolymers as emulsifying agents, in *Polymer Thermodynamics*. Advances in Polymer Science, vol 238 (2011), p. 179

L.N. Andradi, G.P. Hellmann, Polymer **34**, 925 (1993)

A. Arbe, A. Alegria, J. Colmenero, S. Hoffmann, L. Willner, D. Richter, Macromolecules **32**, 7572 (1999)

B.H. Arendt, R.M. Kannan, M. Zewail, J.A. Kornfield, S.D. Smith, Rheol. Acta. **33**, 322 (1994)

A. Asano, M. Eguchi, M. Shimizu, T. Kurotsu, Macromolecules **35**, 8819 (2002)

M. Aubin, Y. Bdard, M.-F. Morrissette, R.E. Prud'homme, J. Polym. Sci. Polym. Phys. Ed. **21**, 233 (1983)

H.E. Bair, P.C. Warren, J. Macromol. Sci. Phys. **B20**, 381 (1980)

N.P. Balsara, L.J. Fetters, N. Hadjichristidis, D.J. Lohse, C.C. Han, W.W. Graessley, R. Krishnamoorti, Macromolecules **25**, 6137 (1992)

N.P. Balsara, D.J. Lohse, W.W. Graessley, R. Krishnamoorti, J. Chem. Phys. **100**, 3894 (1994)

S. Bastida, J.I. Eugizabal, J. Nazabal, Polymer **37**, 2317 (1997)

F.S. Bates, G.D. Wignall, Macromolecules **19**, 932 (1986)

F.S. Bates, P. Wilzinius, J. Chem. Phys. **91**, 3258 (1989)

F.S. Bates, G.D. Wignall, W.C. Koechler, Phys. Rev. Lett. **55**, 2425 (1985)

F.S. Bates, S.B. Dierker, G.D. Wignall, Macromolecules **19**, 1938 (1986)

V.K. Berry, Scanning **10**, 19 (1988)

N.A.M. Besseling, J.M.H.M. Scheutjens, J. Phys. Chem. **98**, 11597 (1994)

D.E. Bhagwagar, P.C. Painter, M.M. Coleman, Macromolecules **27**, 7139 (1994)

U.R. Bidkar, I.C. Sanchez, Macromolecules **28**, 3963 (1995)

A.W. Birley, X.Y. Chen, Brit. Polym. J. **16**, 77 (1984)

J. Biros, L. Zeman, D.D. Patterson, Macromolecules **4**, 30 (1971)

M. Bohdanecky, J. Kovar, *Viscosity of Polymer Solutions* (Elsevier, Amsterdam, 1982)

R.F. Boyer, J. Polym. Sci. Part C **14**, 267 (1966)

J. Brandrup, E.H. Immergut (eds.), *Polymer Handbook*, 3rd edn. (Wiley, New York, 1989)

G.R. Brannock, D.R. Paul, Macromolecules **23**, 5240 (1990)

G.R. Brannock, J.W. Barlow, D.R. Paul, J. Polym. Sci. Part B Polym. Phys. Ed. **29**, 413 (1991)

D. Broseta, G.H. Frederickson, E. Helfand, L. Leibler, Macromolecules **23**, 132 (1990)

S.F. Bush, J.M. Methven, D.R. Blackburn, High Perform. Polym. **8**, 67 (1996)

T.A. Callaghan, D.R. Paul, Macromolecules **26**, 2439 (1993)

T.A. Callaghan, D.R. Paul, J. Polym. Sci. Part B Polym. Phys. **32**, 1813 (1994a)

T.A. Callaghan, D.R. Paul, J. Polym. Sci. Part B Polym. Phys. **32**, 1847 (1994b)

F. Cangelosi, Ph.D. thesis, University of Connecticut, Storrs, 1982

M.J.R. Cantow, *Polymer Fractionation* (Academic, New York, 1967)

P. Caravatti, P. Neuenschwander, R.R. Ernst, Macromolecules **18**, 119 (1985)

P. Caravatti, P. Neuenschwander, R.R. Ernst, Macromolecules **19**, 1889 (1986)

P.M. Cham, T.H. Lee, H. Marand, Macromolecules **27**, 4263 (1994)

D. Chandler, H.C. Andersen, J. Chem. Phys. **57**, 1930 (1972)

K.K. Chee, Europ. Polym. J. **26**, 423 (1990)

C.C. Chen, E. Fontan, K. Min, J.L. White, Polym. Eng. Sci. **28**, 69 (1988)

H.N. Cheng, T. Asakura, A.D. English (eds.), *NMR Spectroscopy of Polymers: Innovative Strategies for Complex Macromolecules*. ACS Symposium Series, vol. 1077 (Oxford University Press, New York, 2011)

J.S. Chiou, D.R. Paul, J. Appl. Polym. Sci. **42**, 279 (1991)

J. Cho, I.C. Sanchez, in *Polymer Handbook*, ed. by J. Brandrup, E.H. Immergut, E.A. Grulke, 4th edn. (Wiley, New York, 1999)

S. Choi, X. Liu, R.M. Briber, J. Polym. Sci. B Polym. Phys. **36**, 1 (1998)

S. Choi, X. Liu, R.M. Briber, Macromolecules **33**, 6495 (2000)

G.-C. Chung, J.A. Kornfield, S.D. Smith, Macromolecules **27**, 964, 5729 (1994)

C.J. Clarke, A. Eisenberg, J. La Scala, M.H. Rafailovich, J. Sokolov, Z. Li, S. Qu, D. Nguyen, S.A. Schwarz, Y. Strzhemechny, B.B. Sauer, Macromolecules **30**, 4184 (1997)

K.C. Cole, Y. Thomas, E. Pellerin, M.M. Dumoulin, R.M. Paroli, Appl. Spectrosc. **50**, 774 (1996)

M.M. Coleman, P.C. Painter, Appl. Spectrosc. Rev. **20**, 255 (1984)

M.M. Coleman, P.C. Painter, Prog. Polym. Sci. **20**, 1 (1995)

M.M. Coleman, P.C. Painter, *Miscible Polymer Blends: Background and Guide for Calculations and Design* (DEStech Publications, Lancaster, 2006a)

M.M. Coleman, P.C. Painter, Aust. J. Chem. **59**, 499 (2006b)

M.M. Coleman, D.F. Varnell, Macromolecules **15**, 59 (1983)

M.M. Coleman, D.F. Varnell, J.P. Runt, Polym. Sci. Technol. **20**, 937 (1982)

M.M. Coleman, D.F. Varnell, J.P. Runt, Contemp. Topics Polym. Sci. **4**, 807 (1984)

M.M. Coleman, D.J. Skrovanek, J. Hu, P.C. Painter, Macromolecules **21**, 59 (1988)

M.M. Coleman, A.M. Lichkus, P.C. Painter, Macromolecules **22**, 586 (1989)

M.M. Coleman, C.J. Serman, D.E. Bhagwar, P.C. Painter, Polymer **31**, 1187 (1990)

M.M. Coleman, J.T. Graf, P.C. Painter, *Specific Interactions and the Miscibility of Polymer Blends* (Technomic Publishing, Lancaster, 1991)

P.R. Couchman, Macromolecules **11**, 1156 (1978)

P.R. Couchman, Phys. Lett. A **70**, 155 (1979a)

P.R. Couchman, J. Appl. Phys. **50**, 6043 (1979b)

J.M.G. Cowie, J.H. Harris, Polymer **33**, 4592 (1992)

J.M.G. Cowie, in *Encyclopedia of Polymer Science and Engineering*, Supplement to 2nd edn, ed. by H.F. Mark, N.M. Bikales, C.G. Overberger, Menges G. (Wiley, New York, 1989)

J.M.G. Cowie, E.M. Elexpuru, I.J. McEwen, Polymer **33**, 1993 (1992a)

J.M.G. Cowie, M.D. Fernandez, M.J. Fernandez, I.J. McEwen, Polymer **33**, 2744 (1992b)

J.M.G. Cowie, G. Li, R. Ferguson, I.J. McEwen, J. Polym. Sci. Polym. Phys. Ed. **30**, 1351 (1992c)

J.G. Curro, Polymeric equations of state. J. Macromol. Sci. Rev. Macromol. Chem. **C11**, 321–366 (1974)

J.G. Curro, Macromolecules **27**, 4665 (1994)

J.G. Curro, K.S. Schweizer, Macromolecules **20**, 1928 (1987)

J.G. Curro, R.R. Lagasse, R. Simha, J. Appl. Phys. **52**, 5892 (1981)

J.G. Curro, R.R. Lagasse, R. Simha, Macromolecules **15**, 1621 (1982)

W. De Oliveira, W.G. Glasser, J. Appl. Polym. Sci. **51**, 563 (1994)

G.T. Dee, D.J. Walsh, Macromolecules **21**, 811, 815 (1988)

M. Dezhu, Z. Ruiyun, L. Xiaolie, Polym. Commun. **36**, 3963 (1995)

E.A. DiMarzio, J.H. Gibbs, J. Chem. Phys. **28**, 373 (1958)

L. Dinililuc, C. DeKesel, C. David, Eur. Polym. J. **28**, 1365 (1992)

D. Dompas, G. Groeninckx, M. Isogawa, T. Hasegawa, M. Kadukura, Polymer **38**, 421 (1997)

Z. Dong, J.R. Fried, Comp. Theor. Polym. Sci. **7**, 53 (1997)

J. Dong, Y. Ozaki, Macromolecules **30**, 286 (1997)

D.C. Douglass, ACS Polym. Prepr. **20**(2), 251 (1979)

D.C. Douglass, V.J. McBrierty, Macromolecules **11**, 766 (1978)

J. Dudowicz, K.F. Freed, Macromolecules **24**, 5076, 5112 (1991)

J. Dudowicz, K.F. Freed, Macromolecules **26**, 213 (1993)

J. Dudowicz, K.F. Freed, Macromolecules **28**, 6625 (1995)

J. Dudowicz, K.F. Freed, Macromolecules **29**, 7826 (1996a)

J. Dudowicz, K.F. Freed, Macromolecules **29**, 8960 (1996b)

J. Dudowicz, M.S. Freed, K.F. Freed, Macromolecules **24**, 5096 (1991)

Y. Egawa, S. Imanishi, A. Matsumoto, F. Horii, Polymer **25**, 5569 (1996)

H.B. Eitouni, N.P. Balsara, Thermodynamics of polymer blends, Chapter 19, in *Physical Properties of Polymers Handbook*, ed. by J.E. Mark, 2nd edn. (Springer, New York, 2007)

T.S. Ellis, Polymer **29**, 2015 (1988)

T.S. Ellis, Macromolecules **19**, 72 (1989)

T.S. Ellis, Polymer **31**, 1057 (1990a)

T.S. Ellis, Polym. Eng. Sci. **30**, 998 (1990b)

T.S. Ellis, Polymer **33**, 1469 (1992)

T.S. Ellis, Polymer **36**, 3919 (1995)

T.S. Ellis, Polymer **38**, 3837 (1997)

A. Etxeberria, A. Unanue, C. Uriarte, J.J. Iruin, Polymer **38**, 4085 (1997)

H. Eyring, M.S. Jhon, *Significant Liquid Structures* (Wiley, New York, 1969)

S.R. Fahrenholtz, Macromolecules **15**, 937 (1982)

A.C. Fernandes, J.W. Barlow, D.R. Paul, J. Appl. Polym. Sci. **32**, 5357 (1986)

M.D. Fernandez, M.J. Fernandez, I.J. McEwen, Polymer **38**, 2767 (1997)

P.J. Flory, J. Chem. Phys. **9**, 660 (1941)

P.J. Flory, *Principles of Polymer Chemistry* (Cornell University Press, Ithaca, 1953)

P.J. Flory, Dicus. Faraday Soc. **49**, 7 (1970)

P.J. Flory, R.A. Orwoll, A. Vrij, J. Am. Chem. Soc. **86**, 3507 (1964)

B.H. Flowers, E. Mendoza, *Properties of Matter* (Wiley, London, 1970)

K.F. Freed, J. Dudowicz, Trends. Polym. Sci. **3**, 248 (1995)

K.F. Freed, J. Dudowicz, Macromolecules **29**, 625 (1996a)

K.F. Freed, J. Dudowicz, Macromol. Symp. **112**, 17 (1996b)

K.F. Freed, J. Dudowicz, Adv. Polym. Sci. **183**, 63 (2005)

C. Friedrich, C. Schwarzwlder, R.-E. Riemann, Polymer **37**, 2499 (1996)

K.C. Frisch, D. Klempner, H.L. Frish, Polym. Eng. Sci. **22**, 1143 (1982)

K.P. Gallagher, X. Zhang, J.P. Runt, G. Hyunh-ba, J.S. Lin, Macromolecules **26**, 588 (1993)

P.P. Gan, D.R. Paul, J. Appl. Polym. Sci. **54**, 317 (1994a)

P.P. Gan, D.R. Paul, Polymer **35**, 3513 (1994b)

P.P. Gan, D.R. Paul, J. Polym. Sci. Part B Polym. Phys. **33**, 1693 (1995)

P.P. Gan, D.R. Paul, A.R. Padwa, Polymer **35**, 1487, 3351 (1994)

D. Garcia, in *Current Topics in Polymer Science*, ed. by R.M. Ottenbrite, L.A. Utracki, S. Inoue (Hanser, Munich, 1987)

A. Garton, Polym. Eng. Sci. **23**, 663 (1983)

A. Garton, Polym. Eng. Sci. **24**, 112 (1984)

R. Gendron, J. Tatiboueet, J. Guevremont, M.M. Dumoulin, L. Piche, Polym. Eng. Sci. **35**, 79 (1995)

S.H. Goh, K.S. Siow, Polym. Bull. **20**, 393 (1988)

S.H. Goh, D.R. Paul, J.W. Barlow, Polym. Eng. Sci. **22**, 34 (1982)

A.A. Goodwin, G.P. Simon, Polymer **37**, 991 (1996)

W.W. Graessley, R. Krishnamoorti, N.P. Balsara, L.J. Fetters, D.N. Schulz, J.A. Sissano, Macromolecules **26**, 1137 (1993)

W.W. Graessley, R. Krishnamoorti, N.P. Balsara, L.J. Fetters, D.J. Lohse, D.N. Schulz, J.A. Sissano, Macromolecules **27**, 2574 (1994a)

W.W. Graessley, R. Krishnamoorti, N.P. Balsara, A. Butera, L.J. Fetters, D.J. Lohse, D.N. Schulz, J.A. Sissano, Macromolecules **27**, 3896 (1994b)

W.W. Graessley, R. Krishnamoorti, G.C. Reichart, N.P. Balsara, L.J. Fetters, D.J. Lohse, Macromolecules **28**, 1260 (1995)

E.A. Grulke, in *Polymer Handbook*, ed. by J. Brandrup, E.H. Immergut, 3rd edn. (Wiley, New York, 1989)

E.A. Guggenheim, Proc. R. Soc. Lond. A **183**, 203 (1944)

E.A. Guggenheim, *Mixtures* (Oxford University Press, Oxford, 1952)

M.C. Gupta, *Statistical Thermodynamics* (Wiley, New York, 1990)

G. Hadziioannou, R.S. Stein, J. Polym. Sci. B Polym. Phys. **21**, 159 (1983)

G. Hadziioannou, R.S. Stein, Macromolecules **17**, 567 (1984)

B.R. Hahn, O. Herrmann-Schnherr, J.H. Wendorff, Polymer **28**, 201 (1987)

B. Hammouda, J. Macromol. Sci. Part C Polym. Rev. **50**, 14 (2010)

B. Hammouda, B.J. Bauer, Macromolecules **28**, 4505 (1995)

C.C. Han, J.W. Baurer, J.C. Clark, Y. Muroga, Y. Matsushita, M. Okada, Q. Tran-Cong, T. Chang, I. Sanchez, Polymer **29**, 2002 (1988)

C.M. Hansen, J. Paint Technol. **39**, 104 (1967)

C.M. Hansen, Europ. Coat. J. **5/94**, 305 (1994)

C.M. Hansen, *Paint Testing Manual* (ASTM, Philadelphia, 1995)

C.M. Hansen, *Hansen Solubility Parameters: A Users Handbook* (CRC Press, Boca Ratton, 2000)

C. M. Hansen, A. Beerbower, *Encyclopaedia of Chemical Technology*, A. Standen (eds.), Suppl vol 2 (Interscience, New York, 1971)

J.E. Harris, L.M. Robeson, J. Polym. Sci. Part B Polym. Phys. **25**, 311 (1987)

B. Hartmann, M.A. Haque, J. Appl. Polym. Sci. **30**, 1553 (1985)

M. Hasegawa, S. Sakurai, M. Takenaka, T. Hashimoto, C.C. Han, Macromolecules **24**, 1813 (1991)

T. Hashimoto, in *Current Topics in Polymer Science*, ed. by R. Ottenbrite, L.A. Utracki, S. Inoue (Carl Hanser, Munich, 1987)

T. Hashimoto, Phase Trans. **12**, 47 (1988)

T. Hashimoto, J. Kumaki, H. Kawai, Macromolecules **16**, 641 (1983)

T. Hashimoto, T. Takebe, S. Suehiro, Polym. J. **18**, 123 (1986)

Y. He, B. Zhu, Y. Inoue, Prog. Polym. Sci. **29**, 10211051 (2004)

E. Helfand, Macromolecules **8**, 552 (1975a)

E. Helfand, J. Chem. Phys. **62**, 999 (1975b)

E. Helfand, J. Chem. Phys. **63**, 2192 (1975c)

E. Helfand, A. Sapse, J. Chem. Phys. **62**, 1327 (1975)

E. Helfand, Y. Tagami, Polym. Lett. **9**, 741 (1971a)

E. Helfand, Y. Tagami, J. Chem. Phys. **57**, 1812 (1971b)

E. Helfand, Y. Tagami, J. Chem. Phys. **56**, 3592 (1972)

C. Herkt-Maetzky, J. Schelten, Phys. Rev. Lett. **51**, 896 (1983)

W.M. Hess, C.R. Herd, P.C. Vegvari, Rubber Chem. Technol. **66**, 329 (1993)

N. Higashida, J. Kressler, T. Inoue, Polymer **36**, 2761 (1995)

H. Higuchi, Z. Yu, A.M. Jamieson, R. Simha, J.D. McGgervey, J. Polym. Sci.: Polym. Phys. **33**, 2295 (1995)

J. Hildebrand, R.L. Scott, *The Solubility of Nonelectrolytes*, 3rd edn. (Reinhold, New York, 1950)

J. Hildebrand, R.L. Scott, *Regular Solutions* (Prentice-Hall, Englewood Cliffs, 1962)

J.D. Honeycutt, SPE Tech. Pap. **38**, 1602 (1992a)

J.D. Honeycutt, ACS Polym. Prepr. **33**, 529 (1992b)

B.K. Hong, J.Y. Kim, W.H. Jo, S.C. Lee, Polymer **38**, 4373 (1997)

K.G. Honnell, J.G. Curro, K.S. Schweizer, Macromolecules **23**, 3496 (1990)

K.G. Honnell, J.D. McCoy, J.G. Curro, K.S. Schweizer, A.H. Narten, A. Habenschuss, J. Chem. Phys. **94**, 4659 (1991)

S.-S. Hou, Q. Chen, K. Schmidt-Rohr, Macromolecules **37**, 1999 (2004)

K.L. Hoy, J. Paint Technol. **42**, 76 (1970)

C.C. Hsu, P.H. Geil, Polym. Eng. Sci. **27**, 1542 (1987)

Z.H. Huang, L.H. Wang, Makromol. Chem. Rapid Commun. **7**(255) (1986)

M.L. Huggins, J. Chem. Phys. **9**, 440 (1941)

P.P. Huo, P. Cebe, Macromolecules **26**, 3127 (1993)

K. Ikawa, S. Hosoda, Polym. Netw. Blends **1**, 102 (1991)

H. Inagaki, H. Suzuki, M. Kurata, J. Polym. Sci. **C15**, 409 (1966)

T. Inoue, T. Ougizawa, O. Yasuda, K. Miyasaka, Polym. Commun. **18**, 57 (1985)

M. Iriarte, J.I. Iribarren, A. Etxeberria, J.J. Iruin, Polymer **30**, 1160 (1989)

T. Izumitani, T. Hashimoto, J. Chem. Phys. **83**, 3694 (1985)

H. Jagger, E.J. Vorenkamp, G. Challa, Polym. Commun. **24**, 290 (1983)

R.K. Jain, R. Simha, Macromolecules **13**, 1501 (1980)

R.K. Jain, R. Simha, Macromolecules **17**, 2663 (1984)

R.K. Jain, R. Simha, P. Zoller, J. Polym. Sci. Polym. Phys. Ed. **20**, 1399 (1982)

Y. Jinghua, C. Xue, G.C. Alfonso, A. Turturro, E. Pedemonte, Polymer **38**, 2127 (1997)

F. Joanny, L. Leibler, J. Phys. (Paris) **39**, 951 (1978)

H.Y. Jung, Polym. J. **28**, 1048 (1996)

W.G. Jung, E.W. Fischer, Makromol. Chem. Macromol. Symp. **16**, 281 (1988)

R.P. Kambour, R.C. Bopp, A. Maconnachie, W.J. MacKnight, Polym. Commun. **21**, 133 (1980)

H.W. Kammer, C. Kumerlowe, Polym. Eng. Sci. **36**, 1608 (1996)

D.S. Kaplan, J. Appl. Polym. Sci. **20**, 2615 (1976)

S. Kaplan, ACS Polym. Prepr. **25**(1), 356 (1984)

J. Karger-Kocsis, L. Kiss, Polym. Eng. Sci. **27**, 254 (1987)

A. Karim, K. Yurekli, J.C. Meredith, E.J. Amis, R. Krishnamoorti, Polym. Eng. Sci. **42**, 1836 (2002)

C.K. Kim, D.R. Paul, Polymer **33**, 1630, 2089 (1992)

J.H. Kim, J.W. Barlow, D.R. Paul, J. Polym. Sci. Part B Polym. Phys. Ed. **27**, 223 (1989)

C.H. Kim, J.-K. Park, T.-S. Hwang, Polym. Eng. Sci. **36**, 535 (1996)

A.M. Kisselev, E. Manias, Fluid Phase Equilibria **261**, 69 (2007)

L.A. Kleintjens, Fluid Phase Equilibria **10**, 183 (1983)

V.J. Klenin, *Stability and Phase Separation* (Elsevier, Amsterdam, 1999)

W. Klopffer, *Introduction to Polymer Spectroscopy* (Springer, Berlin, 1984)

J.L. Koenig, M.J.M. Tovar-Rodriguez, Appl. Spectrosc. **35**, 543 (1981)

R. Koningsveld, Ph.D. thesis, University Leiden (1967)

R. Koningsveld, L.A. Kleintjens, H.M. Schoffaleers, Pure Appl. Chem. **39**, 1 (1974)

R. Koningsveld, L.A. Kleintjens, A.M. Leblans-Vinck, J. Phys. Chem. **91**, 6423 (1987)

R. Koningsveld, W.H. Stockmayer, E. Nies, *Polymer Phase Diagrams: A Textbook* (Oxford University Press, New York, 2001)

R. Krishnamoorti, W.W. Graessley, N.P. Balsara, D.J. Lohse, J. Chem. Phys. **100**, 3894 (1994a)

R. Krishnamoorti, W.W. Graessley, N.P. Balsara, D.J. Lohse, Macromolecules **27**, 3073 (1994b)

R. Krishnamoorti, W.W. Graessley, L.J. Fetters, R.T. Garner, D.J. Lohse, Macro-molecules **28**, 1252 (1995)

R. Krishnamoorti, W.W. Graessley, G.T. Dee, D.J. Walsh, L.J. Fetters, D.J. Lohse, Macromole-cules **29**, 367 (1996)

P.P. Kundu, D.K. Tripathy, S. Banners, Polymer **37**, 2423 (1996)

S.L. Kwolek, P.W.,Morgan, W.R. Sorenson, U.S. Patent 3,063,966, 13 Nov 1962, Appl. 5 Feb 1958, to E. I. du Pont de Nemours & Company

M. Kyotani, H. Kanetsuna, J. Macromol. Sci. Phys. **B26**, 325 (1987)

T. Kyu, J.M. Saldanha, M.K. Kiesel, in *Two-Phase Polymer Systems*, ed. by L.A. Utracki (Hanser Publications, Munich, 1991)

D. Lath, J.M.G. Cowie, Makromol. Chem. Macromol. Symp. **16**, 103 (1988)

A.A. Lefebvre, J.H. Lee, N.V. Balsara, B. Hommouda, Macromolecules **33**, 7977 (2000)

A.A. Lefebvre, J.H. Lee, N.V. Balsara, B. Hommouda, Macromolecules **35**, 7758 (2002)

E.G. Lezcano, C.S. Coll, M.G. Prolongo, Polymer **37**, 3603 (1996)

T.S. Lin, Ph.D. thesis, Virginia Polytechnic Institute (1983)

C.C. Lin, S.V. Jonnalagadda, N.P. Balsara, C.C. Han, R. Krishnamoorti, Macromolecules **29**, 661 (1996)

D. Lohse, Rubber Chem. Technol. **67**, 367 (1994)

J.D. Londono, G.D. Wignall, Macromolecules **30**, 3821 (1997)

J.D. Londono, A.H. Narten, G.D. Wignall, K.G. Honnell, E.T. Hsieh, T.W. Johnson, F.S. Bates, Macromolecules **27**, 2864 (1994)

X. Lu, R.A. Weiss, Macromolecules **24**, 4381 (1991)

X. Lu, R.A. Weiss, Macromolecules **25**, 6185 (1992)

A. Luciani, M.F. Champagne, L.A. Utracki, Polym. Netw. Blends **6**, 41 (1996a)

A. Luciani, M.F. Champagne, L.A. Utracki, Polym. Netw. Blends **6**, 51 (1996b)

A. Luciani, M.F. Champagne, L.A. Utracki, J. Polym. Sci. B Polym. Phys. **35**, 1393 (1997)

A. Maconnachi, J. Kressler, B. Rudolf, P. Reichert, F. Koopmann, H. Frey, R. Mülhaupt, Macromolecules **29**, 1490 (1996)

R.-D. Maier, R.P. Kambour, D.M. White, S. Rostami, D.J. Walsh, Macromolecules **17**, 2645 (1984)

R.-D. Maier, J. Kressler, B. Rudolf, P. Reichert, F. Koopmann, H. Frey, R. Mülhaupt, Macromolecules **29**, 1490 (1996)

P. Maiti, A.K. Nandi, Macromolecules **28**, 8511 (1995)

W.M. Marr, Macromolecules **28**, 8470 (1995)

E. Martuscelli, G. Demma, E. Rossi, A.L. Segre, Polym. Commun. **6**, 125 (1983)

E. Martuscelli, M. Pracella, W.P. Yue, Polymer **25**, 1097 (1984)

S. Matsuda, Polym. J. **23**, 435 (1991)

V.J. McBrierty, K.J. Packer, *Nuclear Magnetic Resonance in Solid Polymers* (Cambridge University Press, Cambridge, 1993)

V.J. McBrierty, D.C. Douglass, T.K. Kwei, Macromolecules **11**, 1265 (1978)

J.E. McKinney, R. Simha, Macromolecules **7**, 894 (1974)

L.P. McMaster, Macromolecule **6**, 760 (1973)

L.P. McMaster, ACS Adv. Chem. Ser. **142**, 43 (1975)

L.P. McMaster, O. Olabisi, ACS Org. Coat. Plast. Chem. Prepr. **35**, 322 (1975)

J.C. Meredith, A. Karim, E.J. Amis, Macromolecules **33**, 5760 (2000)

J.C. Meredith, A. Karim, E.J. Amis, MRS Bull. **27**, 330 (2002)

A. Molnar, A. Eisenberg, Macromolecules **25**, 5774 (1992)

B.S. Morra, R.S. Stein, Polym. Eng. Sci. **24**, 311 (1984)

E.J. Moskala, Ph.D. thesis, Pennsylvania State University (1984)

B. Mujumdar, H. Keskkula, D.R. Paul, N.G. Harvey, Polymer **35**, 4263 (1994a)

B. Mujumdar, H. Keskkula, D.R. Paul, Polymer **35**, 5453, 5468 (1994b)

A.K. Mukherji, M.A. Butler, D.L. Evans, J. Appl. Polym. Sci. **25**, 1145 (1980)

E.C. Muniz, P.A.M. Vasquez, R.E. Bruns, S.P. Nunes, B.A. Wolf, Makromol. Chem. Rapid Commun. **13**, 45 (1992)

C.T. Murray, J.W. Gilmer, R.S. Stein, Macromolecules **18**, 996 (1985)

W.L. Nachlis, J.T. Bendler, R.P. Kambour, W.J. MacKnight, Macromolecules **28**, 7869 (1995)

M.K. Neo, S.H. Goh, Polymer **33**, 3203 (1992)

E. Nies, A. Stroeks, R. Simha, R.K. Jain, Colloid Polym. Sci. **268**, 731 (1990)

T. Nishi, T.K. Kwei, Polymer **16**, 285 (1975)

T. Nishi, T.T. Wang, Macromolecules **8**, 909 (1975)

T. Nishi, T.T. Wang, Macromolecules **10**, 421 (1977)

T. Nishi, T.T. Wang, T.K. Kwei, Macromolecules **8**, 227 (1975)

M. Nishimoto, Y. Takami, A. Tohara, H. Kasahara, Polymer **36**, 1441 (1995)

S. Nojima, K. Tsutsumi, T. Nose, Polym. J. **14**, 225, 289, 907 (1982)

E. Ogawa, N. Yamaguchi, M. Shima, Polym. J. **18**, 903 (1986)

B. Ohlsson, B. Törnell, Polym. Eng. Sci. **36**, 1547 (1996)

T. Ohnaga, T. Sato, S. Nagata, Polymer **38**, 1073 (1997)

O. Olabisi, R. Simha, J. Appl. Polym. Sci. **21**, 149 (1977)

O. Olabisi, L.M. Robeson, M.T. Shaw, *Polymer-Polymer Miscibility* (Academic, New York, 1979)

T. Ougizawa, T. Inoue, Polym. J. **18**, 521 (1986)

T. Ougizawa, T. Inoue, H.W. Kammer, Macromolecules **18**, 2089 (1985)

T. Ougizawa, G.T. Dee, D.J. Walsh, Macromolecules **24**, 3834 (1991)

P.C. Painter, M.M. Coleman, Hydrogen bonding systems, Chapter 4, in *Polymer Blends*, ed. by D.R. Paul, C.B. Bucknall, vol. 1 (Wiley, New York, 2000)

P.C. Painter, Y. Park, M.M. Coleman, Macromolecules **21**, 66 (1988)

P.C. Painter, Y. Park, M.M. Coleman, Macromolecules **22**, 570 (1989a)

P.C. Painter, Y. Park, M.M. Coleman, Macromolecules **22**, 580 (1989b)

P.C. Painter, J. Graf, M.M. Coleman, J. Chem. Phys. **92**, 6166 (1990)

C.P. Papadopoulou, N.K. Kalfoglu, Polymer **38**, 631 (1997)

D.D. Patterson, Polym. Eng. Sci. **22**, 64 (1982)

D.R. Paul, J.W. Barlow, Polymer **25**, 487 (1984)

D.R. Paul, C.B. Bucknall (eds.), *Polymer Blends: Vol. 1: Formulation and Vol. 2: Performance* (Wiley, New York, 2000)

G.J. Pehlert, P.C. Painter, B. Veytsman, M.M. Coleman, Macromolecules **30**, 3671 (1997)

J. Peng, S.H. Goh, S.Y. Lee, K.S. Siow, Polym. Netw. Blends **4**, 139 (1994)

J. Pennacchia, Ph.D. thesis, Polytechnic Institute, New York (1986)

J.P. Pennings, St. R. Manley, Macromolecules **29**, 77 (1996)

M. Piau, C. Verdier, Ultrason. Int. **93**, 423 (1993)

L.Z. Pillon, L.A. Utracki, Polym. Proc. Eng. **4**, 375 (1986)

D.N. Pinder, Macromolecules **30**, 226 (1997)

J. Plans, W.J. MacKnight, F.E. Karasz, Macromolecules **17**, 810 (1984)

I. Prigogine, N. Trappeniers, V. Mathot, Disc. Faraday Sci. **15**, 93 (1953)

I. Prigogine, A. Bellemans, V. Mathot, *The Molecular Theory of Solutions* (North-Holland, Amsterdam, 1957)

R.E. Prud'homme, Polym. Eng. Sci. **22**, 1138 (1982)

M. Puma, Polym. Adv. Technol. **8**, 39 (1997)

C. Qian, S.J. Mumby, B.E. Eichinger, Macromolecules **24**, 1655 (1991)

H.-J. Radusch, N.T. Tung, C. Wohlfarth, Angew. Makromol. Chem. **235**, 175 (1996)

D. Rana, B.M. Mandal, S.N. Bhattacharyya, Polymer **37**, 2439 (1996)

L. Ratke, W.K. Thieringer, Acta Metal. **33**, 1793 (1985)

S. Reich, Phys. Lett. **114A**, 90 (1986)

G.C. Reichart, W.W. Graessley, R.A. Register, R. Krishnamoorti, D.J. Lohse, Macromolecules **30**, 3363 (1997)

A.R. Rennie, *Characterization of Solid Polymers*, S.J. Spells (eds.), (Chapman & Hall, London, 1992)

L.M. Robeson, in *Polymer Compatibility and Incompatibility*, ed. by K. Solc (Harwood Academy, New York, 1980)

P.A. Rodgers, J. Appl. Polym. Sci. **48**, 1061 (1993a)

P.A. Rodgers, J. Appl. Polym. Sci. **50**, 2075 (1993b)

J.L. Rodriguez, J.I. Eguizabal, J. Nazabal, Polym. J. **28**, 501 (1996)

J.M. Rodriguez-Parada, V. Percec, J. Polym. Sci. Chem. Ed. **24**, 579 (1986)

R.J. Roe, J. Chem. Phys. **62**, 490 (1975)

J. Roovers, P.M. Toporowski, Macromolecules **25**, 3454 (1992)

B. Rudolf, J. Kressler, K. Shimomami, T. Ougizawa, T. Inoue, Acta Polym. **46**, 312 (1995)

J. Runt, K.P. Gallagher, Polym. Comm. **32**, 180 (1991)

H. Saito, Y. Fujita, T. Inoue, Polym. J. **19**, 405 (1987)

I.C. Sanchez, Polymer **30**, 471 (1989)

I.C. Sanchez, J. Cho, Polymer **36**, 2929 (1995)

I.C. Sanchez, R.H. Lacombe, J. Phys. Chem. **80**, 2352 (1976)

I.C. Sanchez, R.H. Lacombe, J. Polym. Soc. Polym. Lett. Ed. **15**, 71 (1977)

I.C. Sanchez, R.H. Lacombe, Macromolecules **11**, 1145 (1978)

I.C. Sanchez, J. Cho, W.-J. Chen, Macromolecules **26**, 4234 (1993)

S.I. Sandler, H.S. Wu, Ind. Eng. Chem. Res. **30**, 881, 889 (1991)

M. Sankarapandian, K. Kishore, Polymer **37**, 2957 (1996)

T. Sato, C.C. Han, J. Chem. Phys. **88**, 2057 (1988)

T. Sato, M. Endo, T. Shiomi, K. Imai, Polymer **37**, 2131 (1996a)

T. Sato, M. Tohyama, M. Suzuki, T. Shiomi, K. Imai, Macromolecules **29**, 8231 (1996b)

T. Sato, M. Suzuki, M. Tohyama, M. Endo, T. Shiomi, K. Imai, Polym. J. **29**, 417 (1997)

B.B. Sauer, B.S. Hsiao, K.L. Faron, Polymer **37**, 445 (1996)

C. Schipp, M.J. Hill, P.J. Barham, V.M. Clocke, J.S. Higgins, L. Oiarzabal, Polymer **37**, 2291 (1996)

B. Schlund, L.A. Utracki, Polym. Eng. Sci. **27**, 1523 (1987a)

B. Schlund, L.A. Utracki, Polym. Eng. Sci. **27**, 359, 380 (1987b)

K. Schmidt-Rohr, J. Clauss, B. Blmich, H.W. Spiess, Magn. Reson. Chem. **28**, S3–S9 (1990)

K. Schulze, J. Kressler, H.W. Kammer, Polymer **34**, 3704 (1993)

D. Schwahn, Adv. Polym. Sci. **183**, 1 (2005)

D. Schwahn, K. Mortensen, T. Springer, H. Yee-Madeira, R. Thomas, J. Chem. Phys. **87**, 6078 (1987)

K.S. Schweizer, Macromolecules **26**, 6050 (1993)

K.S. Schweizer, J.G. Curro, J. Chem. Phys. **91**, 5059 (1989)

M. Seki, H. Uchida, Y. Maeda, S. Yamauchi, K. Takagi, Y. Ukai, Y. Matsushita, Macromolecules **33**, 9712 (2000)

C.J. Serman, Y. Xu, J. Graf, P.C. Painter, M.M. Coleman, Macromolecules **22**, 2019 (1989)

C.J. Serman, Y. Xu, J. Graf, P.C. Painter, M.M. Coleman, Polymer **32**, 516 (1991)

V.S. Shah, J.D. Keitz, D.R. Paul, J.W. Barlow, J. Appl. Polym. Sci. **32**, 3863 (1986)

C.K. Sham, D.J. Walsh, Polymer **28**, 804 (1987)

M.T. Shaw, J. Appl. Polym. Sci. **18**, 449 (1974)

M. Shibayama, K. Uenoyama, J.-I. Oura, S. Nomura, T. Iwamoto, Polymer **36**, 4811 (1995)

K. Shinoda, *Principles of Solutions and Solubility* (Marcel Dekker, New York, 1978)

T. Shiomi, F.E. Karasz, W.J. MacKnight, Macromolecules **19**, 2274 (1986)

G.O. Shonaike, G.P. Simon (eds.), *Polymer Blends and Alloys* (Marcel-Dekker, New York, 1999)

A.R. Shultz, A.L. Young, Macromolecules **13**, 663 (1980)

A. Silberberg, W. Kuhn, Nature **170**, 450 (1952)

A. Silberberg, W. Kuhn, J. Polym. Sci. **13**, 21 (1954)

R. Simha, T. Somcynsky, Macromolecules **2**, 342 (1969)

R. Simha, C.E. Weil, J. Macromol. Sci. Phys. **B4**, 215 (1970)

R. Simha, P.S. Wilson, Macromolecules **6**, 908 (1973)

R. Simha, U. Yahsi, Statistical thermodynamics of hydrocarbon fluids. J. Chem. Soc. Faraday Trans. **91**, 2443 (1995)

K. Solc (ed.), *Polymer Compatibility and Incompatibility* (Harwood Academic Publishers, New York, 1982)

R.S. Spencer, G.D. Gilmore, J. Appl. Phys. **20**, 504 (1949)

E.O. Stejskal, J. Schaefer, M.D. Sefcik, R.A. McKay, Macromolecules **14**, 2683 (1981)

R. Steller, D. Zuchowska, J. Appl. Polym. Sci. **41**, 1595 (1990)

G.R. Strobl, J.T. Bendler, R.P. Kambour, A.R. Schulz, Macromolecules **19**, 2683 (1986)

A. Stroeks, E. Nies, Macromolecules **23**, 4092 (1990)

P.G. Tait, Phys. Chem. **3**, 1 (1888)

M. Takahashi, S. Kinoshita, T. Nose, Polym. Prepr. Jap. **34**, 2421 (1985)

M. Takahashi, H. Hirouchi, S. Kinoshita, T. Nose, J. Phys. Soc. Jap. **55**, 2687 (1986)

H. Takahashi, Y. Inoue, O. Kamigaito, K. Osaki, Kobunshi Ronbunshu **47**, 7, 611 (1990)

K. Takakuwa, S. Gupta, D.R. Paul, J. Polym. Sci. Part B Polym. Phys. **32**, 1719 (1994)

M. Takenaka, K. Tanaka, T. Hashimoto, in *Contemporary Topics in Polymer Science*, ed. by W.M. Culberston, vol. 6 (Plenum Press, New York, 1989)

H. Takeno, S. Koizumi, H. Hasegawa, T. Hashimoto, Macromolecules **29**, 2440 (1996)

G. ten Brinke, F.E. Karasz, Macromolecules **17**, 815 (1984)

G. ten Brinke, F.E. Karasz, W.J. MacKnight, Macromolecules **16**, 1827 (1983)

S.-P. Ting, Ph.D. thesis, Polytechnic Institute, New York (1980)

H. Tompa, *Polymer Solutions* (Butterwords Scientific Publications, London, 1956)

L.A. Utracki, J. Appl. Polym. Sci. **6**, 399 (1962)

L.A. Utracki, Polym. J. **3**, 551 (1972)

L.A. Utracki, Polym. Eng. Sci. **25**, 655 (1985)

L.A. Utracki, J. Rheol. **30**, 829 (1986)

L.A. Utracki, *Polymer Alloys and Blends* (Hanser, Munich, 1989)

L.A. Utracki, J. Rheol. **35**, 1615–1637 (1991)

L.A. Utracki, in *Rheological Fundamentals of Polymer Processing*, ed. by J.A. Covas, J.F. Agassant, A.C. Diogo, J. Vlachopoulos, K. Walters (Kluver Academic, Dordrecht, 1995)

L.A. Utracki, B. Schlund, Polym. Eng. Sci. **27**, 367 (1987a)

L.A. Utracki, B. Schlund, Polym. Eng. Sci. **27**, 1512 (1987b)

L.A. Utracki, R. Simha, U. Yahsi, Interrelationships between P-V-T and flow behavior of hydrocarbons. in *Proceedings of the XII International Congress on Rheology*, Quebec, 18–23 Aug 1996

L.A. Utracki, R. Simha, in *Free-Volume Application to Foaming*, NRCC/IMI Symposium on Polymer Foaming, Boucherville 28, Jan 1997

J.J. van Aarsten, Eur. Polym. J. **6**, 919 (1970)

G.O.R.A. van Ekenstein, H. Deuring, G. ten Brinke, T.S. Ellis, Polymer **38**, 3025 (1997)

D.W. van Krevelen, *Properties of Polymers*, 2nd edn. (Elsevier, Amsterdam, 1976)

D.W. van Krevelen, in *Computational Modeling of Polymers*, ed. by J. Bicerano (Marcel Dekker, New York, 1992)

C.J. van Oss, M.K. Chaudhury, R.J. Good, Chem. Rev. **88**, 927 (1988)

C. Verdier, M. Piau, Recent Prog. Genie Procedes, **9**(38), (Genie des Procedes dans la Chaine des Polymeres et dans la Chaine Catalytique), 25–30 (1995)

D. Vesely, Polym. Eng. Sci. **36**, 1586 (1996)

D. Vesely, D.S. Finch, Makromol. Chem. Macromol. Symp. **16**, 329 (1988)

I.G. Voigt-Martin, K.-H. Leister, R. Rosenau, R. Koningsveld, J. Polym. Sci. Part B Polym. Phys. **24**, 723 (1986)

J.R. Waldram, *The Theory of Thermodynamics* (Cambridge University Press, Cambridge, 1985)

D.J. Walsh, S. Rostami, Macromolecules **18**, 216 (1985)

D.J. Walsh, P. Zoller, Makromol. Chem. **188**, 2193 (1987)

D.J. Walsh, J.S. Higgins, C. Zhikuan, Polymer **22**, 1005 (1982)

L.H. Wang, R.S. Porter, J. Polym. Sci. Polym. Phys. Ed. **21**, 1815 (1983)

T.C. Ward, T.S. Lin, ACS Adv. Chem. Ser. **206**, 59 (1984)

R.W. Warfield, B. Hartmann, Polymer **21**, 31 (1980)

G. Webb (ed.), *Modern Magnetic Resonance* (Springer, Dordrecht, 2006)

J.L. White, M. Wachowicz, Polymer blend miscibility – NMR, Chapter 7. in *Annual Reports on NMR Spectroscopy*, vol. 64 (Academic Press, Elsevier, London, 2008)

C. Wohlfarth, *CRC Handbook of Thermodynamic Data of Aqueous Polymer Solutions* (CRC Press, Boca Raton, 2004)

C. Wohlfarth, *CRC Handbook of Liquid-Liquid Equilibrium Data of Polymer Solutions* (Taylor & Francis, Boca Raton, 2008)

B.A. Wolf, Makromol. Chem. Rapid Commun. **189**, 1613 (1980)

B.A. Wolf, Macromolecules **17**, 615 (1984)

E.M. Woo, J.W. Barlow, D.R. Paul, J. Appl. Polym. Sci. **28**, 1347 (1983)

E.M. Woo, J.W. Barlow, D.R. Paul, J. Appl. Polym. Sci. **29**, 3837 (1984)

E.M. Woo, J.W. Barlow, D.R. Paul, Polymer **26**, 763 (1985)

E.M. Woo, J.W. Barlow, D.R. Paul, J. Appl. Polym. Sci. **32**, 3889 (1986)

H.-K. Xie, E. Nies, A. Stroeks, R. Simha, Polym. Eng. Sci. **32**, 1654 (1992)

H.-K. Xie, R. Simha, P. Moulin, in *FoamTech Meeting*, NRCC/IMI, Boucherville, 12 Sept 1997

Y. Xu, J. Graf, P.C. Painter, M.M. Coleman, Polymer **32**, 3103 (1991)

U. Yahsi, Ph.D. thesis, Case Western Reserve University, Department of Physics, Cleveland (1994)

H. Yamakawa, *Modern Theory of Polymer Solutions* (Harper & Row, New York, 1971)

H. Yang, G. Hadziioannou, R.S. Stein, J. Polym. Sci. B: Polym. Phys. **21**, 159 (1983)

K. Yurekli, A. Karim, E.J. Amis, R. Krishnamoorti, Macromolecules **37**, 507 (2004)

S. Zhang, R. Prud'homme, J. Polym. Sci. Part B Polym. Phys. **24**, 723 (1987)

S. Zheng, J. Huang, Y. Li, Q. Guo, J. Polym. Sci. Part B Polym. Phys. **35**, 1383 (1997)

S. Ziaee, D.R. Paul, J. Polym. Sci. Part B Polym. Phys. **34**(1996), 2641 (1996)

S. Ziaee, D.R. Paul, J. Polym. Sci. Part B Polym. Phys. **35**, 489, 831 (1997)

P. Zoller, in *Polymer Handbook*, ed. by J. Brandrup, E.H. Immergut, 3rd edn. (Wiley, New York, 1989)

P. Zoller, H.H. Hoehn, J. Polym. Sci. Polym. Phys. Ed. **20**, 1385 (1982)

P. Zoller, D. Walsh, *Standard Pressure-Volume-Temperature Data for Polymers* (Technomic Publishing Company, Lancaster-Basel, 1995)

Crystallization, Micro- and Nano-structure, and Melting Behavior of Polymer Blends

3

G. Groeninckx, C. Harrats, M. Vanneste, and V. Everaert

Contents

G. Groeninckx (✉) • V. Everaert
Department of Chemistry, Division of Molecular and Nanomaterials, Laboratory of
Macromolecular Structure Chemistry, Catholic University of Leuven, Heverlee, Belgium
e-mail: gabriel.groeninckx@chem.kuleuven.ac.be; valja.everaert@gmail.com

C. Harrats
Laboratoire de Chimie Appliquée (LAC) DGRSDT, Institut des Sciences et Technologies,
Ctr Univ Ain Temouchent, Ain Temouchent, Algeria
e-mail: charrats@gmail.com

M. Vanneste
Textile Functionalisation & Surface Modification, R&D/CENTEXBEL, Zwijnaarde, Algeria
e-mail: myriam.vanneste@centexbel.be

Abstract

When the melt of a crystalline polymer is cooled to a temperature between the glass transition and the equilibrium melting point, the thermodynamic requirement for crystallization is fulfilled.

In a crystallizable miscible blend, however, the presence of an amorphous component, either thermoplastic or thermosetting, can either increase or decrease the tendency to crystallize depending on the effect of the composition of the blend on its glass transition and on the equilibrium melting point of the crystallizable component and also on the curing extent and conditions in case of thermosetting amorphous component. The type of segregation of the amorphous component, influenced by parameters such as crystallization conditions, chain microstructure, molecular weight, blend composition, and curing extent, determines to a large extent the crystalline morphology of a crystallizable binary blend. Separate crystallization, concurrent crystallization, or cocrystallization can occur in a blend of two crystallizable components. The spherulite growth of the crystallizable component in miscible blends is influenced by the type and molecular weight of the amorphous component, the former affecting the intermolecular interactions between both components and the latter the diffusion of the amorphous component. The blend composition, the crystallization conditions, the degree of miscibility and the mobility of both blend components, and the nucleation activity of the amorphous component are important factors with respect to the crystallization kinetics. The melting behavior of crystallizable miscible blends often reveals multiple DSC endotherms, which can be ascribed to recrystallization, secondary crystallization, or liquid-liquid phase separation. Complex crystallization behavior develops in miscible blends containing a crystallizable thermoplastic and a curable thermosetting component. That depends on the temperature and time of curing the thermosetting and also on whether crystallization is initiated before, during, or after the curing process.

For the discussion of the crystallization and melting behavior in immiscible polymer blends, a division into three main classes is proposed.

In blends with a crystallizable matrix and an amorphous dispersed phase, both the nucleation behavior and the spherulite growth rate of the matrix can be affected. Nucleation of the matrix always remains heterogeneous; however, the amount of nuclei can be altered due to migration of heterogeneous nuclei during melt-mixing. Blending can also influence the spherulite growth rate of the matrix. During their growth, the spherulites can have to reject, occlude, or deform the dispersed droplets. In general, the major influence of blending is a change in the spherulite size and semicrystalline morphology of the matrix.

A completely different behavior is reported for blends in which the *crystallizable phase is dispersed*. Fractionated crystallization of the dispersed droplets, associated with different degrees of undercooling and types of nuclei, is the rule. The most important reason is a lack of primary heterogeneous nuclei within each crystallizable droplet. An important consequence of fractionated crystallization may be a drastic reduction in the degree of crystallinity.

When two crystallizable components are blended, a more complex behavior due to the influence of both phases on each other is expected. In general, the discussion for matrix crystallization and droplet crystallization can be combined. However, crystallization of one of the phases can sometimes directly induce crystallization in the second phase. As a consequence, the discussion of blends of this type has been subdivided with respect to the physical state of the second phase during crystallization. The special case of "coincident crystallization," in which the two phases crystallize at the same time, is discussed. Finally, the effect of compatibilization of crystalline/crystalline polymer blends is briefly reviewed.

A new section has been added, introduced to deal with crystallization phenomena in immiscible polymer blends containing nanoparticles. Recent reports, although few, discuss the effect of nanoparticles on crystallization and melting in immiscible polymer blends.

3.1   General Introduction

The study of the processing-morphology-property relations of polymer blends has become a topic of major scientific importance during the past three decades mainly because of intensified technological interest in this area.

The science and technology of polymer blends has now acquired an important position in the area of development of new polymeric materials. Moreover, the application of polymer blends has increased significantly and is expected to continue to grow. Of the total consumption of engineering polymers, more than 20 % is currently thought to be composed of blends with important and various applications in the automotive, electrical, and electronic industry, in computer and business equipment housings, in medical components, etc. Annually about 4,900 patents related to polymer blends are published worldwide.

These are various reasons for today's focus on polymer blends. Design of new polymers with special properties by chemical synthesis is always more expensive than the costs of the constituent existing polymers and the blending operation. A proper selection and combination of polymeric components in a certain ratio might result in a blend material with optimal properties for a specific application. The resulting blend will be the more successful; the more of the desired properties of the components are expressed in its property profile. A remarkable broad spectrum of properties can often be achieved by blending. These properties include mostly mechanical strength and stiffness, toughness, processability, heat distortion

temperature, chemical and weathering resistance, flame retardancy, thermal and dimensional stability, aging resistance, elongation, permeability, transparency, and gloss.

A fundamental question, which has to be addressed first about any blend system of interest, is of course whether the components are miscible or not. Polymer mixtures of chemically dissimilar polymers can be divided on the basis of the miscibility of their components being miscible, partially miscible, or fully immiscible.

While miscibility of polymers was considered as rather rare three decades ago, it is now recognized as an achievable phenomenon with probably well over 500 noted miscible combinations. The conceptual key toward forming miscible polymer blends is to choose polymer pairs with chemical structures capable of specific interactions leading to exothermic heats of mixing. Miscibility studies on homopolymer/copolymer blends indicate that strong repulsive interactions between the segments of the copolymer larger than those between its segments and the homopolymer might also lead to miscibility.

Miscible polymer blends behave similar to what is expected of a single-phase system. Their properties are a combination of the properties of the pure components, and in many cases, they are intermediate between those of the components. The characteristics of the components affecting the properties of miscible blends are their chemical structure and molecular weight, their concentration, and their intermolecular interactions, including crystallizability.

While miscible blend systems are of considerable scientific and practical interest, it should not be concluded that miscibility is always the preferred situation with respect to the properties. In fact, immiscibility leading to two or multiple phases during blending is desired in various cases since the property combinations that one seeks require essentially a system in which each phase can contribute its own characteristics to the blend material.

For thermodynamic reasons, i.e., small entropy gain on mixing, most arbitrary selected polymer pairs are immiscible and, as a consequence, display a two-phase behavior. Melt-mixing of immiscible polymers can result in a variety of phase morphologies depending on the blend composition, the rheological characteristics of the components such as viscosity and elasticity, the interfacial tension between the phases, and the intensity and type of flow that is applied. In the case of immiscible polymer blends, important characteristics with respect to their properties are the chemical nature of the components, the blend composition, the phase morphology (size and shape), the degree of crystallinity and semicrystalline structure of the phases in the case of crystallizable components, and the interfacial interactions between the phases.

A number of miscible polymer blends are only completely miscible and form one-phase systems over a limited concentration, temperature, and pressure range. Under certain conditions of temperature, pressure, and composition, miscible binary blends may phase separate into two liquid phases with different compositions, called partially miscible blends. Important characteristics of this type of blends are the overall blend composition, the morphology, and the composition of the different phases as well as the nature of the interface between the phases.

A large number of polymer blends contain one or two crystallizable components. The crystallization behavior of a polymer component in a blend is expected to be altered by the presence of the second blend component, whether both are completely miscible, partially miscible, or totally immiscible. Therefore, a profound scientific understanding of the crystallization behavior and the resulting semicrystalline structure in polymer blends is necessary for effective manipulation and control of their properties.

There are a number of important factors governing the change of the crystallization rate and semicrystalline structure of a polymer in blend systems. Those include the degree of miscibility of the constituent polymers, their concentration, their glass-transition and melting temperature, the phase morphology and the interface structure in the case of immiscible blends, etc.

This chapter, related to the crystallization, morphological structure, and melting of polymer blends, has been divided into two main parts. The first part (Sect. 3.2) deals with the crystallization kinetics, semicrystalline morphology, and melting behavior of miscible polymer blends. The crystallization, morphological structure, and melting properties of immiscible polymer blends are described in the second part of this chapter (Sect. 3.3).

3.2 Crystallization, Morphological Structure, and Melting Behavior of Miscible Polymer Blends

The crystallization of miscible and immiscible polymer blends can differ remarkably from that of the neat crystallizable component(s). In the case of crystallizable miscible blends (discussed in this section), important polymer characteristics with respect to crystallization are the chemical nature and molecular mass of the components, their concentration in the blend, and the intermolecular interactions between the components.

The thermodynamic requirement for crystallization in a miscible blend is that the blend exhibits a free energy on crystallization that is more negative than the free energy of the liquid-liquid mixture. A liquid-solid phase separation can occur when the miscible melt is cooled to a temperature between the glass transition of the blend and the equilibrium melting point of the crystallizable component(s) (Sect. 3.2.1). The presence of an amorphous component in a crystallizable binary blend can either increase or decrease the tendency to crystallize, depending on the effect of composition on the glass transition of the blend and on the equilibrium melting point of the crystallizable component.

The morphology of a semicrystalline polymer blend is largely determined by the type of segregation of the amorphous component (Sect. 3.2.2.1). In the case of interspherulitic segregation of the amorphous component, where the spherulites of the crystalline component are imbedded in an amorphous matrix, the semicrystalline morphology will be influenced to a lesser extent than when the amorphous component is located within the spherulites (interlamellar and interfibrillar segregation). The parameters determining the type of segregation are not fully understood.

Recent studies (Defieuw 1989) indicate that the crystallization conditions, blend composition, chain rigidity and microstructure, and molecular weight of the components are important. Blends consisting of two crystallizable components (Sect. 3.2.2.2) can exhibit separate crystallization or concurrent crystallization (cocrystallization).

Spherulite growth of the crystallizable component in miscible blend (Sect. 3.2.3) will be influenced by the type and molecular weight of the amorphous component (the former affecting the intermolecular interactions between both components and the latter the diffusion of the amorphous component).

The blend composition, the crystallization condition, the degree of miscibility and the mobility of both blend components, and the nucleation activity of the amorphous component are important factors with respect to the crystallization kinetics (Sect. 3.2.4).

The melting behavior of miscible crystallizable blends (Sect. 3.2.5) is often complex, revealing multiple DSC endotherms, which can be ascribed to several causes such as recrystallization, secondary crystallization, liquid-liquid phase separation (Sect. 3.2.6), etc.

3.2.1 Crystallization Temperature Range of Crystallizable Miscible Blends

The crystallization of a polymer can only proceed in a temperature range limited on the low temperature side by the glass-transition temperature (T_g) and on the high temperature side by the equilibrium melting point ($T_m°$). Below T_g the mobility of the polymer chains is hindered, while in the proximity of $T_m°$, crystal nucleation is inhibited.

When dealing with crystallizable miscible blends, the glass transition is located in between those of the neat components (Fig. 3.1). The presence of an amorphous component in a crystallizable miscible polymer blend can increase or decrease the tendency to crystallize depending on the T_g of the amorphous component with respect to that of the crystallizable one. If the T_g of the amorphous component is lower than that of the crystallizable one, the crystallization envelope ($T_m° - T_g$) is widened, and the crystallization is facilitated. In the opposite case, where the T_g of the amorphous component is higher than that of the crystallizable one, the blend T_g is increased and the temperature range over which crystallization can occur becomes smaller. A limiting case of this is the inhibition of crystallization due to the fact that the blend T_g is higher than the $T_m°$ of the crystallizing component, a phenomenon that is often seen in blends with a high concentration of amorphous component. An even more complex situation is observed when two miscible components are crystallizable.

Some examples are given in Table 3.1. In PCL/CPE blends, the PCL crystallization is enhanced when CPE is added (Defieuw et al. 1989a). The crystallization range becomes narrower in blends such as PCL/PECH (Runt and Martynowicz 1986), PEG/PEMA (Cimmino et al. 1989), PCL/SAN (Defieuw et al. 1989d), and
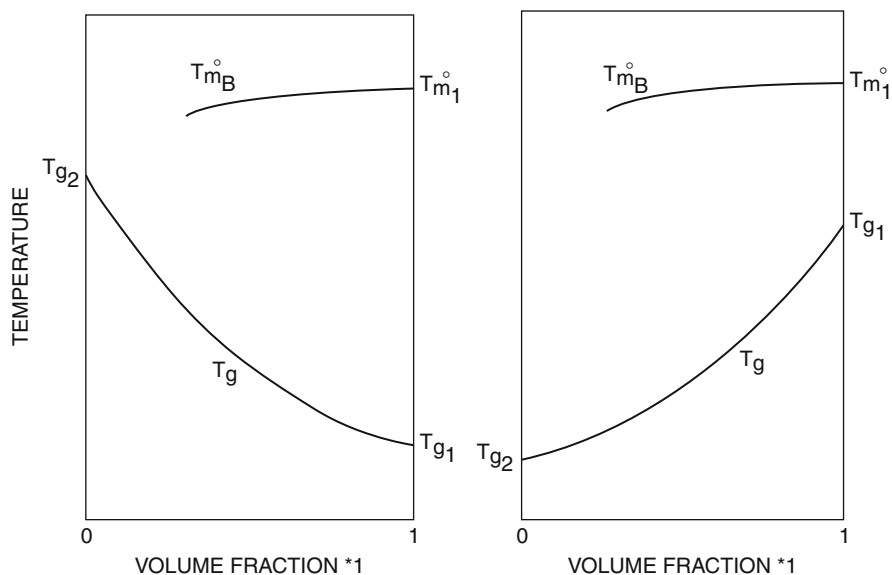
Fig. 3.1 Possible crystallization temperature ranges for a crystallizable miscible polymer blend (*1* crystallizable component, *2* amorphous component) (Runt and Martynowicz 1986)

PBT/PAr (Iruin et al. 1989), PEO/Aramide 34I (Dreezen et al. 1999a), and PEO/PES (Dreezen et al. 1999b). It should be noted that the PBT/PAr 10/90 blend does not show any tendency to crystallize although the blend's T_g is located beneath the melting point of PBT. A possible explanation for this observation is that crystallization is too slow to be noticed within the observation time limit.

3.2.2 Crystallization Phenomena in Miscible Polymer Blends

When crystallized from the melt, most polymers show a spherulitic texture (Fig. 3.2). The spherulites then consist of lamellar stacks of alternating crystalline and amorphous layers, radiating from the center (the primary nucleus).

3.2.2.1 Modes of Segregation of the Amorphous Component During Crystallization in Crystalline/Amorphous blends

In blends of a crystallizable polymer with an amorphous one, the morphology is largely determined by the type of segregation of the amorphous component. Crystallization in a miscible blend involves two types of polymer transport: diffusion of the crystallizable component toward the crystallization front and simultaneous rejection of the amorphous component. This latter phenomenon is called segregation; it can take place at three different levels: interspherulitic, interfibrillar, and interlamellar (Fig. 3.3).

Table 3.1 Influence of T_g of the amorphous component on the crystallization ability of the crystallizable component in miscible binary polymer blends

Polymer blend[a]	Blend composition (wt/wt)	T_g and $T_m°$ (°C) of crystallizable component		T_g (°C) of amorphous component	Blend T_g (°C)	Crystallization[b]	References
PCL/CPE42	50/50[c]	−63	60	1.5	34	y	Defieuw et al. (1989a)
PCL/CPE49	50/50[c]	−63	60	18.5	44	y	
PCL/PECH	10/90	−60	60	−15	Ns[d]	y	Runt and Martynowicz (1986)
PCL/PSMA14	90/10 step − 10 %/+10 %	−63, 4	56.7	127.1	Na	y	Balsamo et al. (2006)
PCL/SAN24	50/50[c]	−63	60	110	30	y	Defieuw et al. (1989c)
PBT/PAr	70/30	31	219	179	43	y	Iruin et al. (1989)
	50/50				51	y	
	30/70				87	y	
	10/90				147	n	
PEG/PEMA	90/10	−55	75	71	−47[e]	y	Cimmino et al. (1989)
	80/20				−39[e]	y	
	70/30				−30[e]	y	
PEO/PA (Aramide 34I)	95/05 to 50/50 step −5 %/+5 %	−60	73	224			Dreezen et al. (1999a)
PEO/PES	85/15	−60	73	225	−50	y	Dreezen et al. (1999b)
	80/20				−40	y	
	75/25				−30	y	

[a]The crystallizable component is listed first
[b]Ability to crystallize: yes (y) or no (n)
[c]More compositions are reported in the article
[d]ns not stated
[e]Calculated from the Fox equation
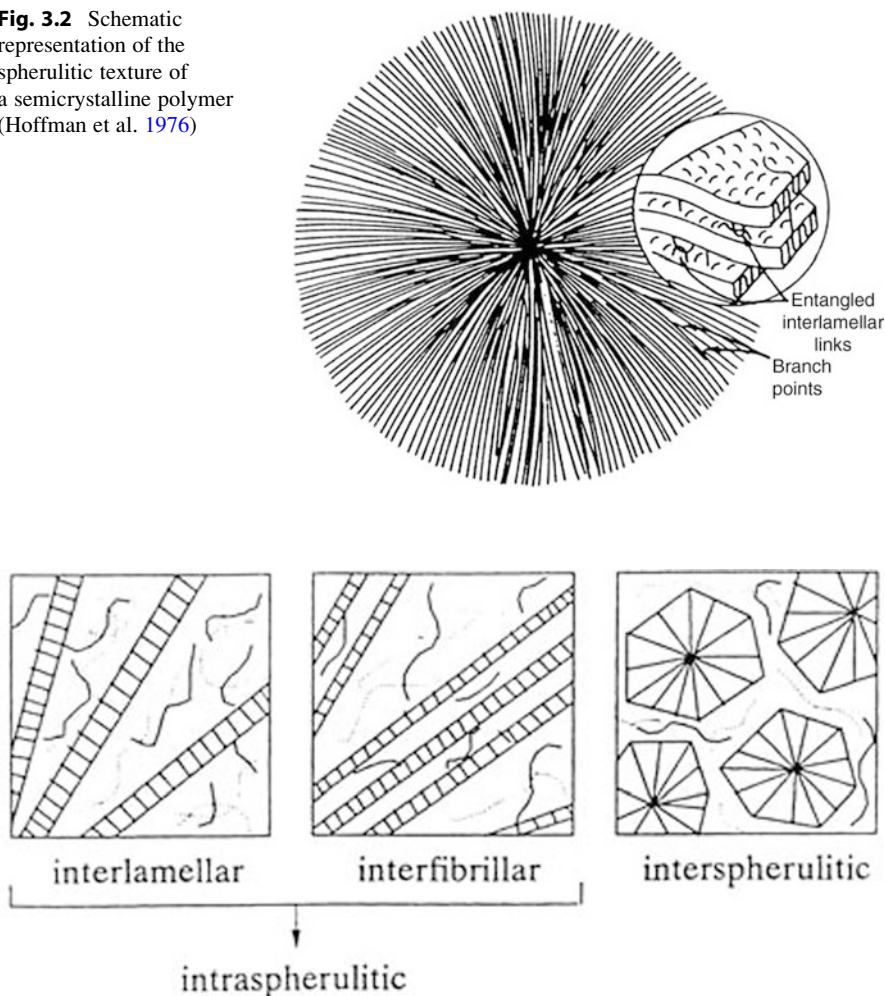
Fig. 3.3 Schematic representation of the different types of segregation of the amorphous component in crystallizable miscible polymer blends (*full lines*: crystallizable component, *dotted lines*: amorphous component)

Interspherulitic segregation, in which the spherulites are imbedded in an amorphous matrix, can be distinguished from the other two types using optical microscopy. In the case of intraspherulitic segregation, a volume-filling texture is observed; the amorphous components can be located either between the lamellae (interlamellar) or between stacks of lamellae (interfibrillar). To find out whether or not interlamellar segregation occurs, small-angle X-ray scattering (SAXS) can be used. The increase of the long spacing, which is the sum of the average thickness of the crystalline and amorphous layers, as well as the increase of the thickness of the

amorphous layers between the crystalline lamellae, with increasing concentration of the amorphous component, are parameters that are often used as indications for interlamellar segregation. In Table 3.2 some examples are presented together with the parameter and/or technique used to make conclusions about the type of segregation.

Most studies concerning the segregation behavior of amorphous components in a miscible crystallizable blend deal with PCL as the crystallizable component. In their blends with PCL, PVC has shown to segregate interlamellar (Stein et al. 1978, 1981; Khambatta et al. 1976a, b; Ong and Price 1978a; Russell and Stein 1980, 1983), PC interfibrillar or interspherulitic (Vandermarliere 1986; Cruz et al. 1979; Fernandez et al. 1986), CPE either interfibrillar or interspherulitic (depending on the amount of amorphous component) (Defieuw et al. 1989a), SMA interlamellar (Defieuw et al. 1989a; Defieuw et al. 1989b, c; Vanneste et al. 1995), SAN interlamellar (Defieuw et al. 1989c; Vanneste et al. 1995), and Phenoxy interlamellar/interfibrillar (Defieuw et al. 1989d; Vanneste 1993).

An intensively studied blend is the PEEK/PEI blend for which interlamellar (Chen and Porter 1994), interfibrillar (Crevecoeur and Groeninckx 1991: Hsiao and Sauer 1993), and interspherulitic segregations (Crevecoeur and Groeninckx 1991) were reported. In PEKK/PEI blends, PEI is segregated interspherulitically (Hsiao and Sauer 1993).

Warner et al. (1977) have shown that in iPS/PS blends the noncrystallizable atactic PS was mainly segregated between the fibrils inside the spherulites. Similar observations have been reported recently by Chi Wang et al. (2006) by using TEM and SEM tools on 50 wt% atactic PS/50 wt% syndiotactic PS miscible blends. On the other hand, Wenig et al. (1975) determined the segregation of PPE to be interlamellar region in the iPS/PPE blends. The influence of the tacticity of PMMA on segregation in PEG/PMMA blends was investigated by Silvestre et al. (1987a). Atactic and syndiotactic PMMA were found located in between the lamellae of PEG, whereas isotactic PMMA was reported to segregate interfibrillar or interspherulitic. It should, however, be noted that a low molecular weight iPMMA was used in this study. In other PEG blends, the amorphous component resided in the interlamellar (EVAc; Cimmino et al. 1994), interspherulitic (PEMA; Cimmino et al. 1989), and interlamellar and interfibrillar regions (PVAc; Silvestre et al. 1987b; Kalfoglou et al. 1988). Atactic PMMA (Canetti et al. 1994) and atactic polyhydroxybutyrate (PBH; Abe et al. 1994) were located between the lamellae in blends with iPHB. Interlamellar segregation was also reported in blends of 1-octene LLDPE fractions with different short-chain branching contents (Defoor et al. 1993).

Blends of PVDF with PMMA have been studied by several authors. All three types of segregation were detected, which was attributed to variation of the crystallization temperature by Stein et al. (1981) and Morra and Stein (1982). Hahn et al. (1987) reported the existence of a compositional interphase (a region of varying polymer composition) between the lamellae and the amorphous interlayer. The order-disorder interphase seemed to contain pure PMMA, while in the remaining interlamellar region, a homogeneous mixture of PMMA and amorphous PVDF was located.

Table 3.2 Type of segregation of the amorphous component in some crystallizable miscible polymer blends

Polymer blend	Amorphous comp. (wt%)[a]	Type of segregation	Parameter	Technique[b]	References
PCL/PVC	0–50% PVC	Interlamellar	Long spacing	SAXS, OM	Stein et al. (1978, 1981), Khambatta et al. (1976a, b), Ong and Price (1978a), Russell and Stein (1980, 1983)
PCL/PC		Interfibrillar or interspherulitic	Long spacing	SAXS	Vandermarliere (1986), Cruz et al. (1979), Fernandez et al. (1986)
PCL/CPE	0–30% CPE[c]	Interfibrillar	Long spacing	SAXS, OM	Defieuw et al. (1989a), Defieuw (1989)
	>30% CPE[c]	Interspherulitic	Long spacing	SAXS, OM	Defieuw et al. (1989a)
PCL/SMAx[d]	0–40% SMA	Interlamellar	Long spacing	SAXS, OM	Defieuw (1989), Defieuw et al. (1989b, c)
PCL/PSMA14	0–10% SMA14	Interlamellar	Amorphous layer thickness	SAXS	Vanneste (1993)
	0–100% PCL	Interlamellar	Amorphous layer thickness	TEM	Balsam et al. (2006)
PCL/SANy[e]	0–50% SAN24	Interlamellar	Long spacing	SAXS, OM	Defieuw et al. (1989c)
	0–20% SAN15	Interlamellar	Amorphous layer thickness	SAXS	Vanneste and Groeninckx (1995)
PCL/Phenoxy	0–50% Phenoxy	Interlamellar/interfibrillar	Long spacing	SAXS, OM	Defieuw (1989), Defieuw et al. (1989d)
	0–10% Phenoxy	Interlamellar	Amorphous layer thickness	SAXS	Vanneste (1993)
PEG/aPMMA	0–40% PMMA	Interlamellar	Long spacing	SAXS	Silvestre et al. (1987a)
PEG/sPMMA	0–40% PMMA	Interlamellar	Long spacing	SAXS	Silvestre et al. (1987a)
PEG/iPMMA	0–40% PMMA	Interfibrillar or interspherulitic	Long spacing	SAXS	Silvestre et al. (1987a)
PEG/PVAc	0–40% PVAc	Interlamellar and interfibrillar	Amorphous thickness	SAXS, OM	Silvestre et al. (1987b)
		Interfibrillar			Kalfoglou et al. (1988)

(continued)

Table 3.2 (continued)

Polymer blend	Amorphous comp. (wt%)[a]	Type of segregation	Parameter	Technique[b]	References
PEG/PEMA		Intraspherulitic			Cimmino et al. (1989)
PEG/EVA[f]	0–20% EVA	Interlamellar		OM	Cimmino et al. (1993b)
PEO/Aramid 34I	0–50% Armd	Intraspherulitic		OM,SAXS	Dreezen et al. (1999)
PEO/PES		Intraspherulitic		OM, SAXS	Dreezen et al. (1999)
aPHB/iPHB		Interlamellar and interfibrillar[g]			Abe et al. (1994)
aPMMA/iPHB		Interlamellar			Canetti et al. (1994)
PVDF/PMMA	ns	Interlamellar, interfibrillar, or interspherulitic[h]	Amorphous layer thickness	SAXS, OM	Morra et al. (1982, 1984), Stein et al. (1981)
PVDF/PMMA	0% and 40% PMMA	Partially interlamellar/partially interfibrillar		SAXS, OM	Saito and Stuhn (1994)
PVDF/PMMA	0–75% PMMA	Interlamellar	Amorphous layer thickness	SAXS	Ullmann and Wendorff (1985)
PVDF/iPEMA[i]	0–50% iPEMA	Interlamellar	Long spacing	SAXS	Eshuis et al. (1982)
iPS/PPE	0–30% PPE	Interlamellar	Lamellar thickness	SAXS	Wenig et al. (1975)
iPS/PS	0–30% PS	Interfibrillar	Amorphous layer thickness	SAXS	Warner et al. (1977), Stein et al. (1981), Russell and Stein (1980)
aPS/sPs	0–80% aPS	Interfibrillar	Long spacing	SAXS, TEM	Wang et al. (2004)
LLDPE/LLDPE[j]		Interlamellar	Long spacing	SAXS	Defoor et al. (1993)
PEEK/PEI	0–50% PEI	Interfibrillar or interspherulitic	Long spacing	SAXS	Crevecoeur and Groeninckx (1991)

PEEK/PEI	0–50% PEI	Interlamellar	Melting behavior	DSC	Chen and Porter (1994)
PEEK/PEI[k]	<50% PEI	Interfibrillar	Long spacing	SAXS	Hsiao and Sauer (1993)
PEKK/PEI[l]	0–50% PEI	Interspherulitic	Long spacing	SAXS	Hsiao and Sauer (1993)

[a] ns not specified

[b] $SAXS$ small-angle X-ray scattering, OM optical microscopy

[c] CPE containing 42.1 and 49.1 wt% chlorine

[d] x = wt% MA in SMA, i.e., 14 and 25 wt% MA

[e] y = wt% AN in SAN, i.e., 15 and 24 wt% AN

[f] PEG/EVA is only miscible for a vinyl acetate content of 56% and higher (Cimmino et al. 1993)

[g] Two different molecular weights were used

[h] Depending on the crystallization temperature (Stein et al. 1981)

[i] PVDF/iPEMA shows an LCST phase behavior (LCST = 183 °C), the experiments were performed on blends prepared and studied below this temperature

[j] A blend of 1-octene LLDPE fractions with different short-chain branching contents was investigated, i.e., 3 and 33 methyl groups per 1000 carbon atoms

[k] Rapid crystallization conditions, interfibrillar segregation occurred in blends with a PEI concentration below 50 %; at higher contents of the amorphous component, interspherulitic segregation was observed

[l] Slow crystallization conditions

Miscibility, isothermal crystallization kinetics, crystal structure, and microstructure of biodegradable PBSA/PVPh blends were investigated with DSC, Polarized OM, WAXD, and SAXS (Yang et al. 2009).

The investigation revealed the following features with respect to the crystallization of PBSA in the presence of PVPh:

1. PBSA and PVPh are miscible crystalline/amorphous polymer blends. Miscibility of PBSA/PVPh blends was evidenced by the single composition-dependent glass-transition temperature over the entire blend compositions. The negative polymer-polymer interaction parameter, obtained from the melting depression of PBSA, indicates that PBSA/PVPh blends are thermodynamically miscible.
2. Isothermal crystallization kinetics study of neat and blended PBSA indicates that the crystallization mechanism of PBSA does not change, but the crystallization rate decreases with increasing the PVPh content in the blends.
3. The crystal structure of PBSA is not modified in the PBSA/PVPh blends. However, the values of LP, Lc, and La become larger with increasing the PVPh content, indicating that PVPh mainly resides in the interlamellar region of PBSA spherulites.

## Typical Examples of Supramolecular and Semicrystalline Morphology

PEO (semicrystalline)/Aramide 34I (amorphous) blend was observed by polarized microscope to identify the supramolecular structure and characterized by SAXS to identify the type of semicrystalline morphology (Dreezen et al. 1999). The supramolecular structure of pure PEO consists of different types depending on the molecular weight and the crystallization temperature. Allen and Mandelkern (1982) compiled a morphological map for PEO in which three different supramolecular structures are present: a spherulitic, a hedritic, and an intermediate spherulitic-hedritic structure. Figure 3.4 reveals that pure PEO displays a non-structured-birefringence structure. Blending PEO with Aramide 34I results in the formation of well-defined Maltese-cross spherulites above 15 % Aramide 34I. Figure 3.4a represents an intermediate pattern of spherulitic-hedritic structure. All the blends containing up to 25 % amorphous Aramide 34I exhibit volume-filling spherulites indicating intraspherulitic segregation of the amorphous component. This change was attributed to lower diffusion rate and increased secondary nucleation when crystallizing PEO in blends with Aramide 34I, the T_g of which is very high. Calculation from SAXS reveals that both the long period and the amorphous thickness increase with the amount of the amorphous component, whereas the crystalline lamellae thickness slightly decreases; this effect is synonymous of interlamellar segregation. A model in which thin lamellae are located between the primary formed thick lamellae in the same stack was proposed to describe the secondary crystallization of PEO in PEO/Aramide 34I blends (Fig. 3.4). Similar crystallization, melting, and supramolecular structure and mode of segregation behavior were also reported when PEO is blended with polyethersulfone (Dreezen et al. 1999b; Fig. 3.5).

The concept of a crystal-amorphous (also order-disorder) interface was first proposed by Flory (1962) for binary semicrystalline/amorphous blends.
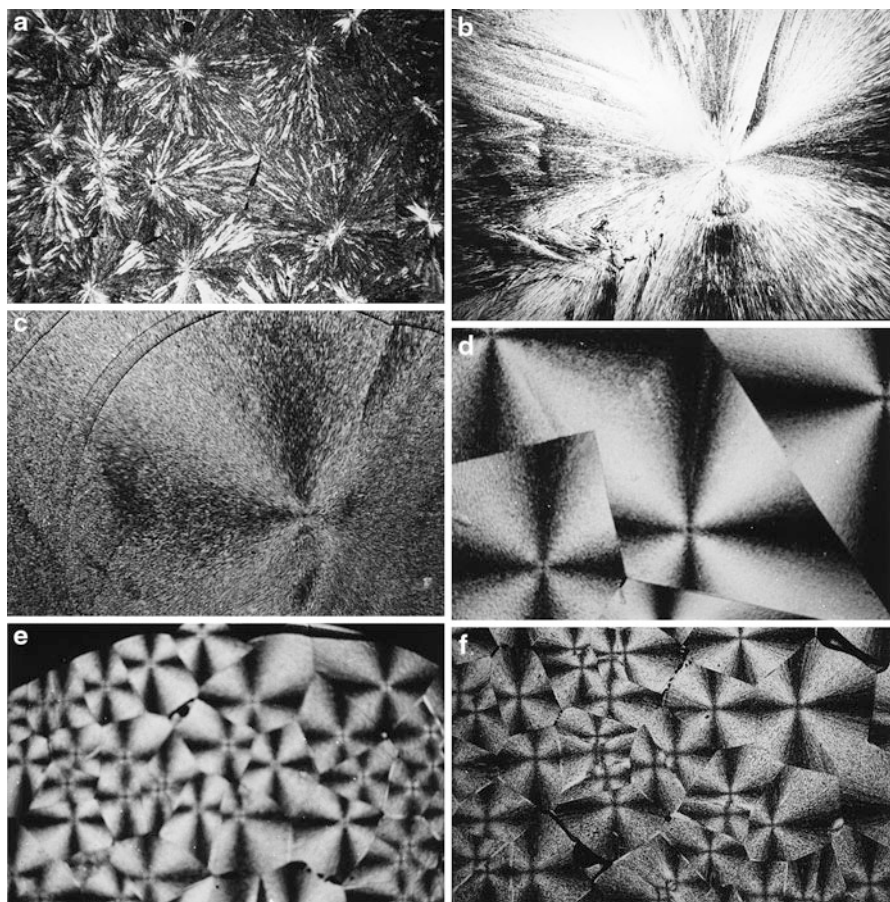
Fig. 3.4 Optical micrographs of PEO/Aramide 34I blends: (**a**) 100/0 $T_c = 47$ °C, magn. 5×; (**b**) 95/5 $T_c = 42$ °C, magn. 5×; (**c**) 90/10 $T_c = 44$ °C, magn. 10×; (**d**) 85/15 $T_c = 32$ °C, magn. 10×; (**e**) 80/20 $T_c = 28$ °C, magn. 10×; (**f**) 75/25 $T_c = 28$ °C, magn. 10× (Dreezen et al. 1999)

The *order-disorder interphase* was defined as the region of loss of crystalline order. Kumar and Yoon (1991) examined this interface and found that in blends the thickness of this transition zone was essentially independent of the interaction parameter between the two polymers (when χ_{12} varied from -1 to -0.005). Following the theoretical predictions, the thickness of this region increases only slightly when stiffer chains are considered. Due to the higher degree of order of segments of the crystallizable component in this zone, the penetration of the amorphous component is limited. The *compositional interphase*, however, is influenced by the stiffness of both chains and by the interaction parameter (the interfacial thickness varies with the reciprocal of $|\chi_{12}|^{1/2}$). This prediction seems to be confirmed by experiments. Blends of iPS and PS as well as HDPE/LDPE blends (at a temperature above the melting point for the latter blend) have a χ_{12} that is
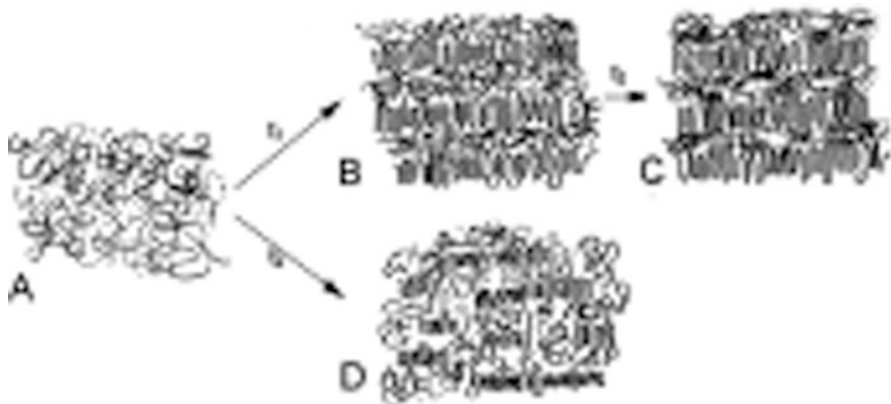
Fig. 3.5 Model describing the crystallization behavior of (**a**) 80/20 PEO/Aramide 34I blend; (**b**) after fast primary crystallization; (**c**) secondary crystallization; and (**d**) a 65/35 PEO/Aramide blend after crystallization (Dreezen et al. 1999)

nearly zero; as a consequence, they will not form a mixed phase in the interlamellar region – the amorphous polymer will be excluded from the interlamellar zone. This seems to be in agreement with the experimental observations for iPS/PS (Warner et al. 1977) and HDPE/LDPE (Song et al. 1988). The presence of a pure order-disorder interphase has been observed in PVDF/PMMA blends (Wenig et al. 1975) using small-angle X-ray scattering and dielectric relaxation experiments. Jonas et al. (1995) estimated the spatial extension of the order-disorder interphase of PEEK in its blends with PEI.

A check of the theoretical predictions of Kumar and Yoon can be made comparing several miscible crystallizable blends with components having a similar stiffness but exhibiting variable interactions (i.e., different values of χ_{12}). Such experimental work was done by Runt et al. (1991) who examined blends of crystallizable PEG with three different amorphous components (PMMA, PVAc and polyhydroxystyrene, PHS). The first two amorphous polymers (PMMA and PVAc) exhibited a small interaction with PEG, while PHS (being able to form hydrogen bonds with PEG) displayed large interactions. A pure PEG interphase was found for the PEG blends with PMMA and PVAc, whereas a relaxation suggestive for the presence of a mixed interphase for the PEG/PHS blend was observed. Barron et al. (1992) studied strongly interacting PCL blends with PC, PVC, Phenoxy, etc., by means of dielectric relaxation measurements. The blends exhibit a dielectric relaxation in between the relaxation of the pure components, indicating the presence of a mixed amorphous interphase. The possibility to observe this transitional behavior depended on the frequency used; a frequency of 10 Hz was used in this case. Therefore, it was impossible to study these transitions by means of dynamic mechanical experiments (DMA, usually 1 Hz is used) or differential scanning calorimetry (DSC). For the PCL/PVC blends (PVC segregates interlamellar (Russell and Stein 1983), three transitions were noticed: (1) a pure amorphous PCL region (γ-relaxation); (2) a mixed amorphous phase,

located at a higher temperature than the former and which shifts to higher temperatures with increasing PVC content; and (3) an interphase transition that shifts to higher temperatures the stronger the interaction between both polymers. A frequency lower than 10Hz results in an overlap of the transitions associated with the mixed and phase and with the interphase, while at higher frequencies, the γ-relaxation merges with the interphase transition.

Excellent work was reported by Balsamo et al. (2006) on the semicrystalline morphology of PCL/PSMA14 miscible blends as well as on their crystallization kinetics. The authors used a combination of dielectric, calorimetric, and microscopy characterization tools to investigate crystallization features of PCL in miscible PCL/PSMA14 blends over the whole composition range. The results achieved allowed to draw the following conclusions with respect to the miscibility effect on the blend relaxation dynamics and crystallization kinetics of PCL:

(a) Crystallization of PCL in the blend occurs when the PCL content reaches 30 wt% or more. A depression of the PCL melting point and a significant cold crystallization process are detected for the 40/60 blend, showing the intimate mixing of the components with the existence of interactions on a molecular level. This is supported by the interlamellar insertion of the PSMA14, the formation of ring-banded spherulites, and the significant increase in the half-crystallization times.

(b) The existence of a miscible interlamellar region leads to a spherulitic extinction ring spacing that becomes larger upon increasing crystallization temperature. Interestingly, it also increases with PSMA14 content. The latter differentiates the PSMA14/PCL system from other PCL blends.

(c) With respect to the chain dynamics, the thermally stimulated depolarization current (TSDC) results indicate that even the short-range reorientations of the PCL dipoles are affected by blending. The addition of the rigid PSMA14 to PCL causes the hindering of the pre-cooperative motions usually assigned to the β relaxation in the presence of PCL crystalline regions.

For example, Fig. 3.6 shows the spherulites formed after isothermal crystallization at the indicated temperatures. Indeed, in addition to the typical Maltese-cross, extinction rings appear, leading to ring-banded spherulites. This kind of superstructures has been observed, for example, in blends of PCL with SAN (Wang and Jiang 1997; Li et al. 1992; Wang et al. 1998) and PVC (Eastmond 2000) as well as in block copolymers (Balsamo et al. 1996; Albuerne et al. 2003; Nojima et al. 1991). Note that the spherulites fill all the space, indicating the absence of interspherulitic segregation. In all cases, a linear increase of the radii of the spherulites with time was found until their impingement, evidencing that the growth rate is not controlled by diffusion. These results are in agreement with the interlamellar location of the PSMA14 evidenced here with TEM and are the consequence of the low flexibility of the PSMA chains and its affinity toward the PCL.

It is well known that banding is the result of the cooperative twisting of the lamellae during growth. Although such twisting has been associated with internal stresses produced on the lamellae surfaces, the reason for its occurrence is still controversial (Lotz and Cheng 2005). It has also been reported in case of polymer
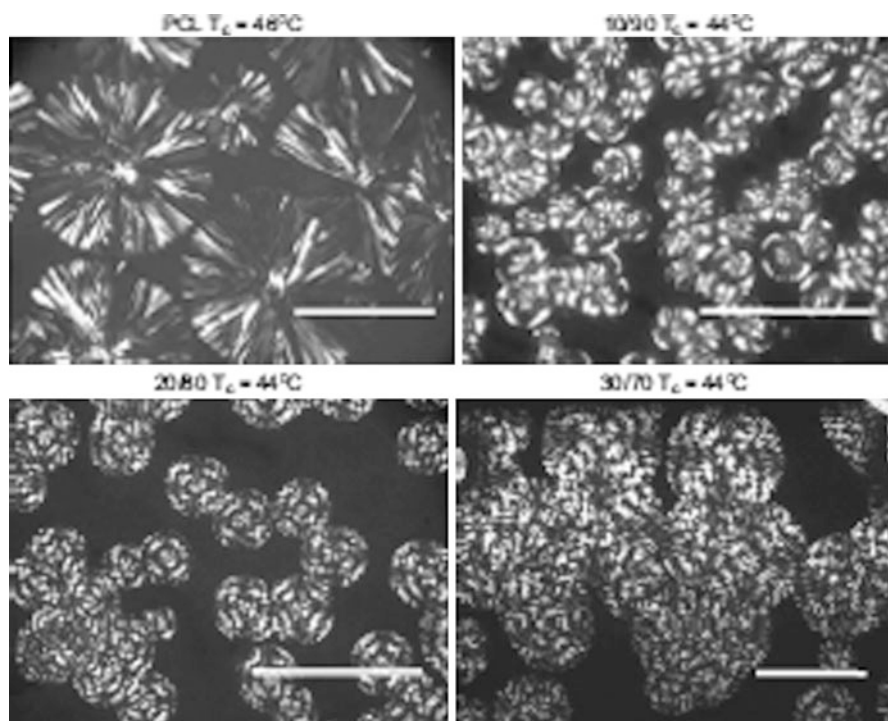
Fig. 3.6 POM images obtained during isothermal crystallization of PSMA14/PCL blends at the indicated crystallization temperatures. The *bars* represent 100 μm. Top left: PCL Tc = 46 °C, Top right: 10/90 Tc = 44 °C, Bottom left: 20/80 Tc = 44 °C, Bottom right: 30/70 Tc = 44 °C. (Balsamo et al. 2006 with Permission)

blends that the periodicity of the rings depends on composition (Morin et al. 2001). To characterize the superstructure, the periodicity of the rings was measured in PSMA14/PCL 20/80 and 30/70. The results presented in Fig. 3.7 reveal that the periodicity increases with the content of the amorphous component, a fact that is contrary to the results obtained by other authors in blends containing PCL (Nojima et al. 1991; Wang et al. 1996; Schulze et al. 1993). Nevertheless, Briber and Khoury (1987, 1993) reported a similar trend in poly(vinylene fluoride)/poly(ethyl acrylate) blends. This could be related to the dependence of the interaction parameter on composition. Additionally, the periodicity markedly increases with the crystallization temperature, due to the higher segmental mobility within the blend.

3.2.2.2 Modes of Crystallization in Crystalline/Crystalline Blends

When dealing with miscible blends containing two crystalline components, several modes of crystallization are possible: separate crystallization, concurrent crystallization, cocrystallization, etc. Only those blends in which both components are miscible in the melt are considered here (Table 3.3). PET/PBT blends were reported to be an example of separate crystallization (Escala and Stein 1979;

Fig. 3.7 Dependence of the ring periodicity measured from POM micrographs as a function of crystallization temperature for PSMA14/PCL 30/70 and 20/80 (Balsamo et al. 2006)
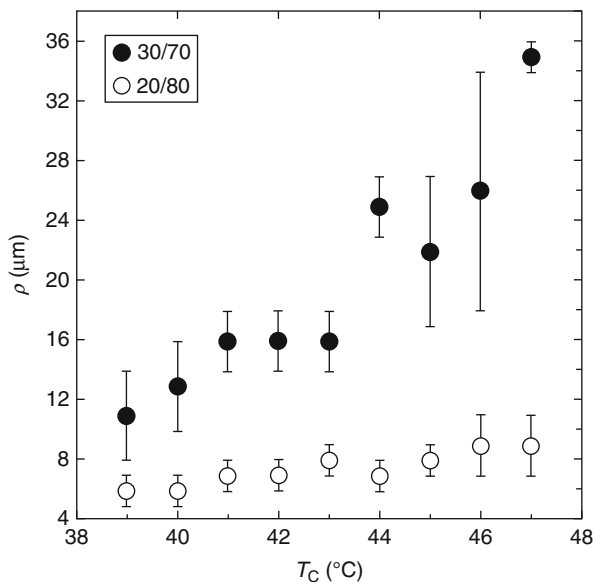
Stein et al. 1981). A spherulitic crystallization was observed for the neat components as well as for blends with small amounts of one component, and the crystals of the minor component were included within the spherulites of the major component, which results in a coarsening of the spherulitic texture. Transesterification is, however, the reason for the homogenous amorphous phase.

Run et al. (2009) have recently shown that in the miscible blends of PET and PTT, PET component will crystallize first, and the formed crystallites serve as the nucleating agent for PTT crystallization at higher temperatures. The content of each component in the blend affects the crystallization growth rate of the other blend partner. PTT constitutes a diluting agent for the PET crystallization process. The spherulite's size, however, is much smaller than that of those formed in pure PTT. A completely different situation was reported by Chen et al. (2009) when the crystallization of miscible PET/PLA blend was considered. Due to the phenomenon of rigid amorphous fraction (RAF) formed by one component, the crystallization of the other partner is perturbed or even altered. PET can crystallize in all blends, regardless of whether PLA is amorphous or crystalline, and the degree of crystallinity of PET decreased as the fraction of PLA was increased in the blend. Whereas, the PLA crystallization is strongly affected by the mobility of the PET fraction. In the presence of an amorphous PET, PLA can crystallize, albeit weakly, even in a 70PLA/30PET blend. But when the PET is crystalline, PLA cannot crystallize below a 0.9 fraction in the blend. This phenomenon has been attributed of the ability of PET and PLA to form rigid amorphous fractions (RAF) which, like crystals, may inhibit the growth of crystals of the other blend partner.

A simultaneous (or concurrent) crystallization can only occur when the crystallization temperature ranges overlap and if the crystallizability of both blend's

Table 3.3 Crystallization types of miscible polymer blends consisting of two crystallizable components

Polymer blend	Crystallization type[a]	References
LDPE/LLDPE	Concurrent crystallization	Hu et al. (1977)
	Separate crystallization	Kyu et al. (1987)
LDPE/VLDPE	Cocrystallization	Chen et al. (2001)
UHMWPE/HDPE	Concurrent crystallization	Kyu and Vadhar (1986)
UHMWPE/LLDPE	Concurrent crystallization	Kyu and Vadhar (1986)
	Cocrystallization/ separate[b]	Vadhar and Kyu (1987)
UHMWPE/LDPE	Separate crystallization	Kyu and Vadhar (1986, 1987)
LLDPE/LLDPE[c]	Cocrystallization	Rego Lopez and Gedde (1988)
LDPE/EPDM[d]	Cocrystallization	Starkweather, Jr. (1980)
HDPE/LLDPE[e]	Cocrystallization[f]	Hu et al. (1987), Edward (1986), Gupta et al. (1994)
LLDPE/VLDPE	Cocrystallization	Huang et al. (1990)
LDPE/VLDPE	Partial cocrystallization	Huang et al. (1990)
HDPE/VLDPE	Cocrystallization	Huang et al. (1990)
DHDPE[g]/LLDPE[h]	Cocrystallization[i]	Tashiro et al. (1992a, b; 1994a, b, c, d)
DHDPE/LLDPE[j]	Partial cocrystallization	Tashiro et al. (1994a, b, c, d)
DHDPE/HDPE	Partial cocrystallization[k]	Tashiro et al. (1994a, b, c, d)
PEEK/PEK	Cocryst./separate cryst.[l]	Sham et al. (1988)
PEEK/PEK	Cocrystallization	Harris and Robeson (1987)
PEEK/PEEEK	Cocrystallization	Harris and Robeson (1987)
PEEK/PEEKK	Cocrystallization	Harris and Robeson (1987)
PEEK/P(E)$_{0.43}$(K)$_{0.57}$[m]	Cocrystallization	Harris and Robeson (1987)
PEEK/PEK/PEI	Cocryst. of PEEK and PEK	Harris and Robeson (1988)
PVF/PVDF	Cocrystallization	Natta et al. (1965)
VDF-TFE/VDF-HFA	Cocrystallization[n]	Cho et al. (1993)
iPS/iP(p-Me-S)[o]	Cocrystallization	Natta et al. (1961)
P(iPr-vinylether)/P(sec-But-vinyl ether)	Cocrystallization	Wunderlich (1973)
P(4-Me-pentene)/P (4-Me-hexene)	Cocrystallization	Wunderlich (1973)
PBT/PEE[p]	Cocrystallization	Gallagher et al. (1993)
PET/PBT	Separate crystallization	Stein et al. (1978)

<div align="right">(continued)</div>

Table 3.3 (continued)

Polymer blend	Crystallization type[a]	References
PET/PTT	Separate crystallization	Run et al. (2009)
iPMMA/sPMMA	Cocrystallization	Liquori et al. (1965)
PCL/PC	Separate crystallization	Vandermarliere (1986)
PCL/PBT	Separate crystallization	Righetti et al. (2007)
PPE/iPS	Separate crystallization	Hammel et al. (1975)
PED/EVAc[q]	Cocrystallization	Clough et al. (1994)
PET/PLA	Separate crystallization	Chen et al. (2009)

[a]It should be noted that not all authors use the same terminology concerning the type of crystallization. Especially the terms "cocrystallization" and "concurrent crystallization" are often confused. Since some authors did not examine whether the lattice parameters change or not, it is not possible to decide if they mean cocrystallization or concurrent crystallization

[b]Depending on the blend preparation: cocrystallization when sequentially mixed and separate crystallization when simultaneously mixed

[c]Different molecular weight fractions

[d]Ethylene/propylene/1,4-hexadiene with an ethylene/propylene ratio of 4.5 mol%

[e]LLDPE: ethylene butene-1 copolymer, 18 branches/1,000 C

[f]Valid as well for slowly as rapidly (quenched) cooled blends

[g]DHDPE: deuterated HDPE

[h]LLDPE with a branching content of ca. 17 ethyl groups/1,000 carbons

[i]The lattice parameters vary continuously with composition of the blend, and the cocrystallization process is ascribed to the closeness of the crystallization rate of both species

[j]LLDPE with a branching content of ca. 41 ethyl groups/1,000 carbons

[k]The tendency to cocrystallize increases with increasing HDPE concentration

[l]Cocrystallization occurs when the blends are quenched rapidly from the melt (± 100 °C/min); separate crystallites are formed when isothermally crystallized, annealed at high temperatures, precipitated from solution, or slowly cooled from the melt (1 °C/min)

[m]$P(E)_{0.43}(K)_{0.57}$ is a random copolymer composed of phenyl ether and phenyl ketone units

[n]The type of crystallization depends on the thermal treatment of the samples: cocrystallization takes place in samples that are quenched or annealed at 110 °C for 6 h; separate crystallization is observed when annealed at 100 °C for 6 h. This is due to the existence of an UCST phase behavior between 100°C and 110 °C

[o]Copolymer of styrene and *p*-methyl styrene containing 30 mol% of the latter comonomer

[p]Miscibility of PBT/PEE depends on the copolymer composition of PEE, and cocrystallization occurs under all crystallization conditions and is possible because the unit cell parameters of PBT and PEE are the same. To avoid interchain chemical reactions, the blends were prepared by solvent casting

[q]EVAc has a molar ratio of ethylene to vinyl acetate of 7:1 and is amorphous, an increase of the lattice parameters was noticed when adding EVAc

components is similar. Cocrystallization is only possible when the components are isomorphic or miscible in the amorphous as well as in the crystalline phase. In both cases, mixed crystals can result, but in the case of concurrent crystallization, no changes in crystal structure may be induced. Cocrystallization requires chemical

compatibility, close matching of the chain conformations, lattice symmetry, and comparable lattice dimensions (Olabisi et al. 1979). Some examples of miscible polymer blends with two crystalline components are given in Table 3.3 together with the type of crystallization.

3.2.3   Spherulite Growth of the Crystallizable Component

3.2.3.1 Spherulite Growth Rate in Homopolymers

In the case of homopolymers, the growth rate of a lamellar crystal is controlled by two processes: on the one hand by the ability of forming a surface nucleus (determined by the degree of undercooling, $\Delta T = T_m{}^\circ - T_g$) and on the other hand by the ability of diffusion of the chain molecules toward the crystal growth front (determined by the difference between the crystallization temperature, T_c, and the glass-transition temperature, T_g). Both processes are inversely dependent on temperature; a maximum rate of crystal growth is usually observed at temperatures close to $T_{\max} \approx (T_g + T_m)/2$.

The growth rate kinetics of bulk semicrystalline homopolymers have been described in the past by Mandelkern et al. (1954) and Hoffman and Lauritzen (1976, 1973), using a modified version of the theory of nucleation of Turnbull and Fisher (1949):

$$G = G^\circ \exp[-\Delta E/R(T_c - T_o)]\exp[-\Delta F^*/k_B T] \tag{3.1}$$

G° is a constant dependent on the regime of crystallization, independent of temperature, and inversely proportional to the polymer molecular weight (Van Antwerpen and Van Krevelen 1972); T_o is the temperature at which motions necessary for the transport of molecules through the liquid-solid boundary cease; T_c is the temperature of crystallization; and k_B is the Boltzmann constant.

The rate of growth of a crystal, G, is governed by two processes: the activation energy required to transport crystalline molecules across the solid-liquid interface (ΔE) and the work necessary to form a critical nucleus (ΔF^*). At low supercooling, the growth rate is nucleation controlled, while at high supercooling, it is diffusion controlled; as a consequence, Eq. 3.1 produces a bell-shaped curve. Such a behavior for iPS (curve a) is shown in Fig. 3.8.

3.2.3.2 Spherulite Growth Rate in Miscible Polymer Blends

When dealing with crystallizable miscible polymer blends containing a noncrystallizable component, some refinements had to be made. Some modifications were proposed by Alfonso and Russell (1986) and by Cimmino et al. (1989) for blends in which the amorphous component is segregated into the interlamellar region (see also Sect. 3.2.2.1). First, the chemical potential of the liquid phase might be altered by the specific interactions that are often responsible for the miscibility of polymers (Olabisi et al. 1979). Such interactions may change the free energy required to form a critical nucleus as well as the mobility of both the crystalline and amorphous components. Second, the noncrystallizable component has to

Fig. 3.8 Spherulitic growth rate in iPS and iPS/PS blends (the values represent the percentage of atactic PS present in the blend) (Keith and Padden 1964)
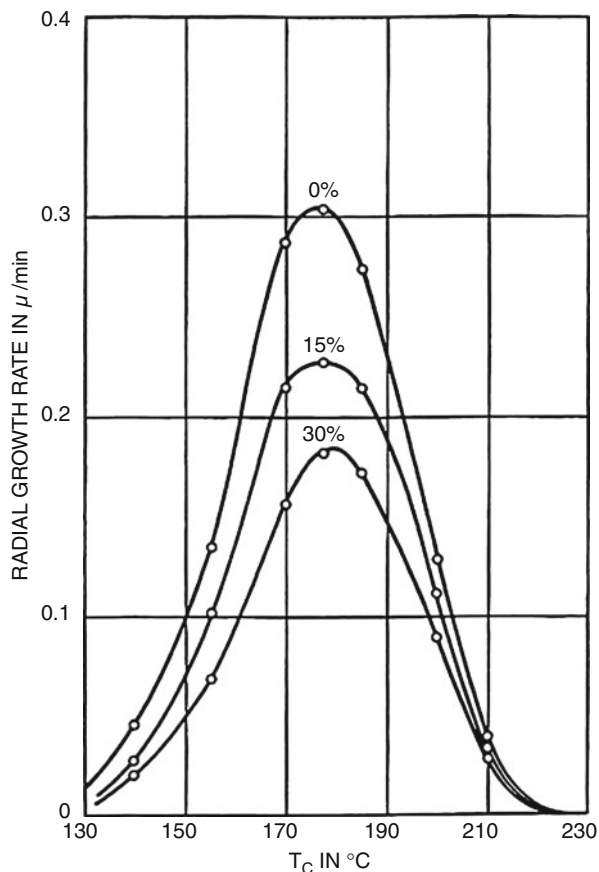
diffuse away from the crystal growth front into the interlamellar region. Thus, the rate at which the growth front progresses depends on the competition between the inherent capability of the crystal to grow and on the rate of rejection (segregation) of the amorphous component. The kinetics of crystal growth will ultimately be determined by the slower of these two phenomena. A direct consequence of this consideration is the dependence of the crystal growth rate on the molecular weight of both components. Third, the concentration of the crystallizable component at the growth front will decrease during crystallization. And finally, the glass-transition temperature and the melting temperature can be influenced by addition of an amorphous polymer. As already mentioned in Sect. 3.2.1, the T_g of miscible blend lies in between the glass-transition temperatures of the neat components, its value being a function of the blend's composition. Depending on the T_g value of the noncrystallizable component (higher or lower than the T_g of the crystallizable component), the crystallization temperature range will be, respectively, narrowed or widened.

Incorporating the concepts discussed above, the equation describing the crystal growth rate in a miscible polymer blend can be expressed as

$$G_m = (\phi_2 k_1 k_2)/(k_1 + k_2)\exp(-\Delta F_m{}^*/k_B T_c) \tag{3.2}$$

ϕ_2 is the volume fraction of the crystallizable component; T_c is the crystallization temperature; k_1 is the rate of transport of the crystallizable molecules across the liquid-solid boundary:

$$k_1 = G° \exp[-\Delta E/R(T_c - T_o{}')] \tag{3.3}$$

$T_o{}'$ is the value of T_o in the blend and can be written in terms of the glass transition and a constant C (associated with the WLF constant C_2) (Rostami 1990); and k_2 is the rate at which the amorphous component segregates

$$k_2 = D/d = 2\overline{D}/L \tag{3.4}$$

d is the maximum distance over which the amorphous component has to diffuse away during crystallization ($d = L/2$, with L the crystal lamellae thickness), and D is the diffusion coefficient. Since a simultaneous diffusion of the amorphous and the crystalline component takes place, the diffusion coefficient of interest is the mutual diffusion coefficient, $\overline{D}$; $\Delta F_m{}^*$ is the free energy of nucleus formation (secondary nucleation) in the presence of a noncrystallizable component.

The rate of crystal growth in a semicrystalline blend, G_m, will depend on the magnitude of k_1, k_2, and $\Delta F_m{}^*$. At low undercooling, $\Delta T = T_m° - T_c$, $\Delta F_m{}^*$ is high and hence G_m is small. However, if the blend T_g approaches or exceeds the melting point ($T_m°$), k_2 can prohibit crystallization regardless of the value of $\Delta F_m{}^*$.

Table 3.4 refers to a number of crystallizable miscible polymer blends for which the spherulite growth rate as a function of the crystallization temperature has been investigated. For most blends, only a part of the bell-shaped curve could be measured. In Fig. 3.8, the complete bell-shaped spherulitic growth rate curve of iPS in iPS/PS blends containing 0, 15, and 30 wt% PS is shown. Due to the addition of impurity (e.g., the amorphous PS), a suppression of the growth rate is observed, which is greater than the concentration of the impurity added. Important parameters of the impurity added to the crystallizable component are the type, concentration, and molecular weight (Keith and Padden 1964).

By means of several optical techniques, viz., small-angle laser light scattering (SALLS), optical microscopy, etc., the spherulite structure can be studied. From the photographic scattering pattern, the spherulitic radius, R, can be calculated as a function of the crystallization time and/or blend composition (Stein 1964):

$$R = 4.1\lambda/4\pi\{1/\sin(0.5\ \theta_m)\} \tag{3.5}$$

θ_m represents the azimuthal angle of the intensity maximum; R the spherulite radius; and λ the light wavelength in the medium.

A general observation is a decrease of the spherulitic radius with increasing content of the amorphous polymer when a same crystallization time is used (see Fig. 3.9 and Table 3.5: PCL/PVC).

Table 3.4 Spherulitic growth rate measurements in miscible polymer blends (G vs. T_c)

Polymer blend	Amorphous comp. (wt%)	Temperature range studied (T_c, °C)	Bell-shaped curve	References
iPS/PS	0–30% PS	130–230	Complete	Keith and Padden (1964)
PEG/PMMA	0–30% PMMA	40–55	Part	Cimmino et al. (1989)
PEG/PMMA[a]	0–30% PMMA	10–60	Part	Alfonso and Russell (1986)
PEG/PMMA[b]	0–40% PMMA	35–55	Part	Martuscelli (1984)
PEG/PMMA	0–40% PMMA	44–58	Part	Calahorra et al. (1982)
PEG/PVAc	0–40% PVAc	45–55	Part	Martuscelli (1984)
PEO/PES	0–50 % PES	17–55	Part	Dreezen et al. (1999)
PEO/Aramid	0–50 % Aramid	25–45	Part	Dreezen et al. (1999)
PVDF/PMMA	0–50% PMMA	110–160	Part	Wang and Nishi (1977)
	30% PMMA	148–162	Complete[c]	Okabe et al. (2010)
PCL/PVC	25–50% PVC	20–35	Part	Ong and Price (1978)
	0–10% PVC	30–41	Part	Nojima et al. (1986)

[a]Several PMMA polymers with different molecular weights were used
[b]Several PEG polymers with different molecular weights were used
[c]A temperature of 162 °C has been used and allowed a spherulite growth rate of bell-shaped curve

3.2.3.3 Determination of the Lateral and Fold Surface Free Energies from the Growth Rate

Alfonso and Russell (1986) related the different terms in Eq. 3.2 to the measurable or characteristic properties of the blend, which resulted in the following relation for blends in which the amorphous component segregated into the interlamellar regions:

$$G_m = \left\{\phi_2 G\degree \exp[-\Delta E / R(T_c - T_o{}')] 2\overline{D}/L\right\} / \left\{G\degree \exp[-\Delta E / R(T_c - T_o{}')] + 2\overline{D}/L\right\}$$
$$\exp\left\{(-2b\sigma\sigma_e)/\left(k_B T \Delta h_u f\left[1 - T_c/T_m\degree - RTV_{2u}\chi(1 - \phi_2)^2 / \Delta h_u f\, V_{1u}\right]\right)\right\} \quad (3.6)$$

where b is the thickness of a monomolecular layer; $\sigma\sigma_e$ is the product of the lateral and fold surface free energies; V_{iu} is the molar volume of component i; χ is the Huggins-Flory interaction parameter; and Δh_u is the heat of fusion per mole of monomer of the crystallizable component, the temperature dependence of which is taken into account by the parameter f:

$$f = \left[2T_c/\left(T_c + T_m\degree\right)\right] \quad (3.7)$$

Both $\sigma\sigma_e$ and χ are assumed to be independent of temperature and composition.
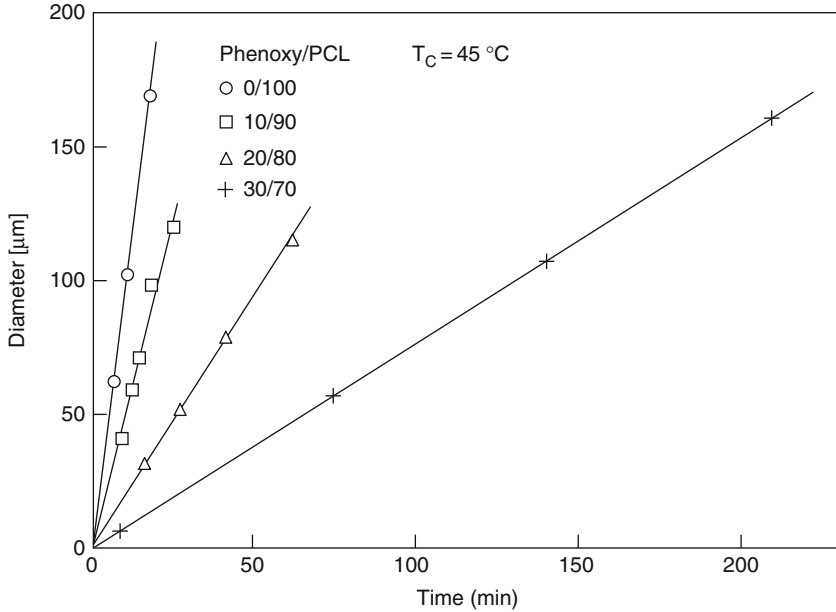
Fig. 3.9 Spherulite growth of PCL/Phenoxy blends at $T_c = 45\ ^\circ$C (Defieuw et al. 1989d)

In Eq. 3.6 the ratio $\overline{D}/G$, a modified version of the δ-parameter (Keith and Padden, 1963, 1964), appears. This length, relative to the thickness of the crystalline lamellae (L), is critical for the consideration of the crystal growth in crystallizable miscible polymer blends.

Equation 3.6 can be written as

$$\alpha = -\sigma\sigma_{ei}\beta \tag{3.8}$$

where

$$\begin{aligned}\alpha = \ln G_m - \ln\phi_2 - \ln G^\circ + \Delta E/R(T_c - T_o') \\ + \ln\{1 + [G^\circ L \exp[-\Delta E/R(T_c - T_o')]/2\overline{D}]\}\end{aligned} \tag{3.9}$$

and

$$\alpha = \ln G^\circ - (K_g/T_c\Delta Tf) \tag{3.10}$$

with

$$K_g = (n\, b\, \sigma\sigma_e T_m^\circ)/(\Delta h_u k_B) \tag{3.11}$$

Table 3.5 Maximum spherulite radius, R, as a function of crystallization time (t_c) and blend composition

Polymer blend	Composition (wt%)	T_c (°C)	R_{max} measured (μm)[a]	t_c (min) required to obtain R_{max}[a]	References
PCL/PVC	100/0	30	21[b]	[c]	Khambatta et al. (1976a, b)
	90/10	30	36[b]	[c]	
	80/20	30	31[b]	[c]	
	70/30	30	26[b]	[c]	
	60/40	30	19[b]	[c]	
	50/50	30	10[b]	[c]	
	75/25	20	33	7	Ong and Price (1978b)
		25	32	9	
		30	60	20	
		35	63	33	
	90/10	33.2	136	8	Nojima et al. (1986)
		35.1	157	12	
		37.8	150	19	
		39.2	122	31	
PCL/CPE 42.1[d]	100/0	45	70	3	Defieuw et al. (1989a)
	90/10	45	150	25	
	80/20	45	119	43	
PCL/Phenoxy	100/0	45	168	19	Defieuw et al. (1989b)
	90/10	45	119	25	
	80/20	45	114	61	
	70/30	45	160	209	
PCL/SMA 14[e]	100/0	45	165	16	Defieuw et al. (1989b)
	90/10	45	169	77	
	80/20	45	111	187	
PEG/iPS	100/0	Ns	Ns		Wenig et al. (1975)
	90/10				
	70/30				

[a]Extrapolated values from figures
[b]A mean value is given, obtained by various optical techniques
[c]The crystallization was allowed to proceed for more than five halftimes of crystallization for each composition
[d]CPE with 42.1 wt% chlorine; PCL/CPE 42.1 shows an LCST behavior (LCST = 147 °C); the experiments were performed on specimens prepared below the LCST
[e]SMA with 14 wt% MA

where n is 2 or 4 depending on the regime of crystallization (Hoffman 1982; Ong and Price 1978b; Runt and Martynowicz 1986). The value of $n = 2$ refers to intermediate growth behavior (regime II), while the value of $n = 4$ corresponds with regime I and III in which low and high undercooling, respectively, is taking place. Furthermore, based on the WLF relation (Williams et al. 1955), the growth rate can be written as (Ong and Price 1978b)

Fig. 3.10 Plot of α versus $T_m/(T_c\Delta T)$ for various compositions of a PEG/PMMA blend (*triangles*, 100/0; *circles*, 90/10; *squares*, 80/20; *crosses*, 70/30; *filled circles*, 60/40) (Calahorra et al. 1982)
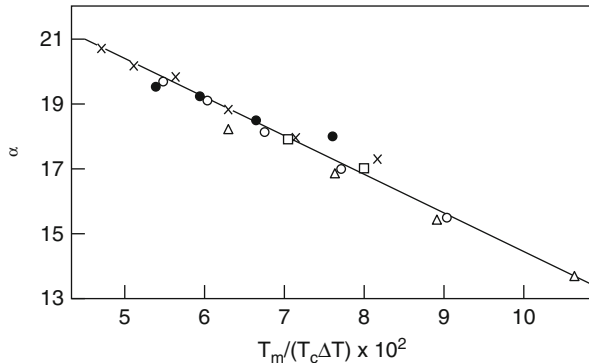
$$\alpha = \ln G^\circ - C_3\left\{T_m^\circ/T_c\left(T_m^\circ - T_c\right)\right\} \tag{3.12}$$

where

$$C_3 = (4\,b\,\sigma\sigma_e)/(k_B\,\Delta h_u) \tag{3.13}$$

Note that $K = C_3\,T_m$ when $n = 4$ (regime I or III)
and

$$\beta = (2b/k_B T_c)\left\{\left(\Delta h_u f\Delta T/Tm^\circ\right) - \left[RTV_{2u}\chi(1 - \phi_2)^2\right]/V_{1u}\right\}^{-1} \tag{3.14}$$

α contains parameters associated with the kinetic processes, while thermodynamic variables are met in β. If the product $\sigma\sigma_e$ is independent of the blend composition and temperature, then, according to Eq. 3.8, a curve of α versus β should produce a straight line, regardless of the concentration and molecular weight of the amorphous component. The slope of such a plot is a measure of the product $\sigma\sigma_e$.

Another way to rewrite Eq. 3.6 is (Cimmino et al. 1989)

$$\alpha = \ln G_m - \ln\phi_2 + C_1/[R(C_2 + T_c - T_o] - \left[\left(0.2T_m^\circ\ln\phi_2\right)/\left(T_m^\circ - T_c\right)\right] \tag{3.15}$$

Although equilibrium melting points, $T_m^\circ = T_c$, should be used in Eq. 3.13, generally the experimental T_m values are used.

Considering the Eqs. 3.11 and 3.13, a plot of α versus $1/(T_c\Delta Tf)$ and $T_m^\circ/(T_c\Delta T)$, respectively, should result in a straight line from which $\sigma\sigma_e$ can be obtained – see Fig. 3.10 where a plot of α as a function of $T_m^\circ/(T_c\Delta T)$ is shown.

The straight line in Fig. 3.10 represents a fit of Eq. 3.13 to the experimental values using the WLF constants, $C_1 = 17,250$ cal/mol and $C_2 = 72$ K (see Eq. 3.15), the latter value being higher than the true WLF value of 51.6. Other authors,

however, also had to use higher C_2 values to fit their growth rate data (Hoffman and Weeks [1962a](); Magill [1964](); Boon et al. [1968]()). The good fit in Fig. [3.10]() indicates that the temperature dependence of the spherulite growth rate of a crystallizable component in miscible blends is quite similar to that of homopolymers. It is also obvious from this figure that σ_e is independent of the concentration of the amorphous component (PMMA). Caution should be taken to generalize these data since (1) the high concentration diluent was not investigated and (2) the temperature range was near the melting point. The same observations were, however, made by Ong and Price ([1978b]()) and by Wang and Nishi ([1977]()).

3.2.3.4 Influence of the Molecular Weight of the Amorphous Component

Alfonso and Russell ([1986]()) found a significant curvature in the α versus β plots of PEG/PMMA blends (see Eq. [3.8]()) while they were linear for neat PEG. The curvature could be due to an increase of $\sigma\sigma_e$ with a decreasing temperature. These authors also studied the influence of the molecular weight of the amorphous component (PMMA) on the spherulite growth rate of PEG. Noteworthy is the discrepancy seen at low undercooling for one of the blends containing PMMA with a molecular weight corresponding to the critical molecular weight for entanglement. Superposing all data for different molecular weights (above the critical value) results in a true master curve (see Fig. [3.11]()), which shows that Eq. [3.8]() accounts quite well for the effect of molecular weight.

3.2.3.5 Influence of the Molecular Weight of the Crystallizable Component

Martuscelli ([1984]()) studied the influence of the molecular weight of the crystallizable component (PEG) on the spherulite growth rate of PEG/PMMA blend. In contrary to Calahorra et al. ([1982]()), they found that the fold surface free energy, σ_e, decreases with increasing PMMA content in the blend. It should be mentioned, however, that the molecular weight of PEG used by Calahorra is much higher ($M_w = 400$ kg/mol) compared to the PEG used by Martuscelli (2 and 10 kg/mol). The value of σ_e was seen to depend on the molecular weight of PEG (Martuscelli [1984]()), being smaller in the case of blends containing PEG with lower molecular weight (see Fig. [3.12]()).

Several authors (Ong and Price [1978b](); Alfonso and Russell [1986](); Runt and Martynowicz [1986](); Cimmino et al. [1989]()) used one of the equations mentioned above to calculate $G°$, σ, σ_o, and/or $\sigma\sigma_o$ (see Table [3.6]()). The following empirical relationship (Thomas and Staveley [1952](); Geil [1963](); Vidotto et al. [1969]()) was developed:

$$\sigma = 0.1\, b\, \Delta h_u \tag{3.16}$$

3.2.3.6 Influence of Copolymer Composition

The influence of the SAN copolymer composition on the spherulitic growth rate of PCL has been studied at a fixed crystallization temperature by

Fig. 3.11 Master curve of α
versus β for blends of PEG
(145) with PMMA (125) and
PMMA (525) (values between
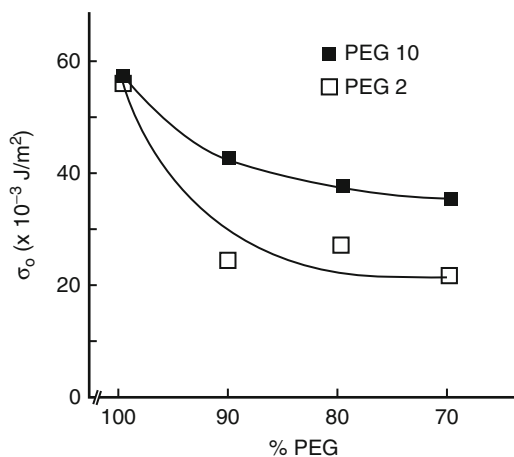brackets refer to the
molecular weight of the
components in kg/mol)
(Alfonso and Russell 1986)
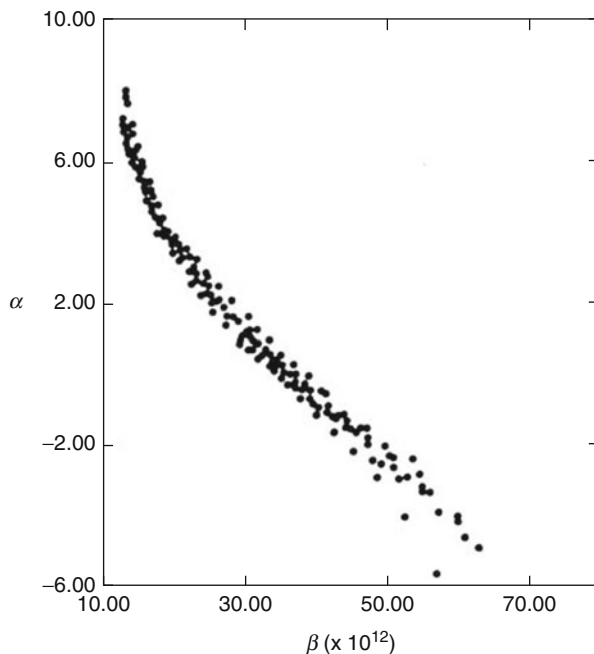
Fig. 3.12 Surface free
energy of folding, σ_o, as
a function of the PMMA
content for PEG/PMMA
blends using two PEG
polymers differing in
molecular weight (2 and
10 kg/mol) (Martuscelli 1984)

Kressler et al. (1992, 1993). A minimum has been observed at about 20 wt% AN in
SAN for several compositions (see Fig. 3.13), due to a minimum in the value of the
interaction parameter, χ, at the same copolymer composition that is responsible for
a reduced chain mobility.

Table 3.6 Pre-exponential factor ($G°$), lateral (σ), and fold surface (σ_e) free energy and/or their product ($\sigma\sigma_e$) as calculated from Eqs. 3.8, 3.11, or 3.13

Polymer blend	Composition	$G°$ ($\times10^{-3}$ m/s)	$\sigma\sigma_e$ ($\times10^6$ J²/m⁴)	σ_e ($\times10^3$ J/m²)	σ ($\times10^3$ J/m²)	References
PEG/PMMA	100/0[a]					Alfonso and Russell (1986)
	13,000	3.6	363			
	145,000	2.2	496			
	594,000	8.0	627			
	990,000	48.3	724			
PEG/PMMA	0–40% PMMA	4.1	186	18.8	9.9[b]	Calahorra et al. (1982)
PEG/PMMA	100/0			58/60/57[c]		Martuscelli et al. (1984)
	90/10			43/48/26[c]		
	80/20			38/39/27[c]		
	70/30			36/39/22[c]		
	60/40			36/37/—[c]		
PEG/PEMA	100/0			58	[d]	Cimmino et al. (1989)
	90/10			28	[d]	
	80/20			24	[d]	
	70/30			14	[d]	
PCL/PVC	25–50 wt% PVC[e]	0.72	175	27	6.5[f]	Ong and Price (1978b)
PCL/SAN19.5[g]	90/10		567			Kressler et al. (1993)
	80/20		507			
	70/30		518			
	60/40		491			

(continued)

Table 3.6 (continued)

Polymer blend	Composition	$G°$ ($\times 10^{-3}$ m/s)	$\sigma\sigma_e$ ($\times 10^6$ J²/m⁴)	σ_e ($\times 10^3$ J/m²)	σ ($\times 10^3$ J/m²)	References
PVDF/PMMA[h]	100/0	0.182	464	47	9.76[h]	Wang and Nishi (1977)
	75/25	0.131	495	51	9.76[h]	
	50/50	0.012	396	40	9.76[h]	

[a]Several molecular weight PEG polymers were used

[b]Other compositions have been studied too

[c]This parameter has been calculated using a modified version of Eq 3.16: $\sigma = 0.1\,(\Delta h_u)\,(a_o b_o)^{0.5}$, where $a_o = 5.43$ A, $b_o = 4.45$ A, and $\Delta h_u = 1.986 \times 10^6$ J/m³

[d]σ was calculated by Eq. 3.16, using $b = 4.65$ A (Vidotto et al. 1969)

[f]σ was calculated by Eq. 3.16, using $b = 4.38$ A and $\Delta h_u = 1.48 \times 10^{+8}$ J/m³

[g]Since all compositions could be superposed on one straight line in the α versus $T_m/T\Delta T$ plot, all blend compositions have the same value for $G°$, σ, σ_e, and $\sigma\sigma_e$

[h]SAN with 19.5% AN; other copolymers have been used by the author leading to the same tendencies

[i]The first value is calculated from the spherulitic growth rate data of PEG(10)/PMMA, the second one from the overall crystallization data of PEG(10)/PMMA, and the third one from the spherulitic growth rate data of PEG(2)/PMMA (Martuscelli and Demma 1980) (the value between brackets refers to the molecular weight of PEG in kg/mol)

[j]This parameter has been calculated using Eq. 3.16 where $b_o = 4.65$A and $\Delta h_u = 2.13 \times 10^6$ J/m³ (Van Krevelen 1976)

Fig. 3.13 Dependence of the spherulite growth rate G on the copolymer composition of SAN in PCL/SAN blends at 45 °C (Kressler et al. 1992, 1993)
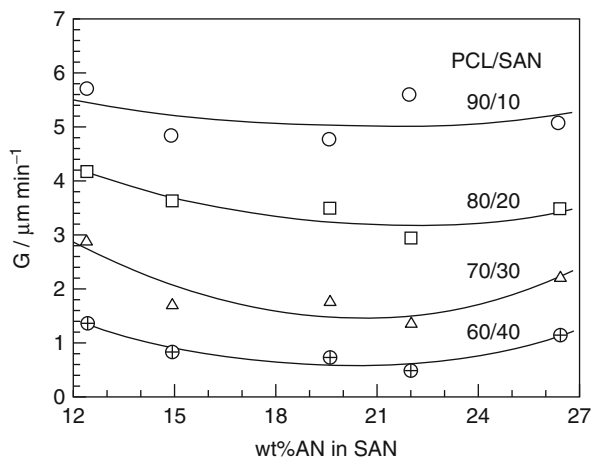
Fig. 3.14 Values of $(\sigma\sigma_e)^{1/2}$ versus the copolymer composition of SAN in PCL/SAN blends (Kressler et al. 1992, 1993)
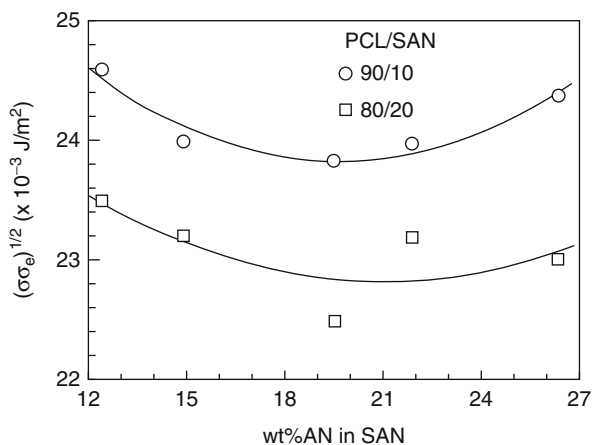
The same authors also investigated the influence of the copolymer composition of SAN in PCL/SAN blends on $G°$ and $(\sigma\sigma_e)^{1/2}$. The plot of $(\sigma\sigma_e)^{1/2}$ versus the acrylonitrile content in SAN shows a minimum (Fig. 3.14), suggesting that the addition of SAN results in a stabilization of the growing PCL crystallites. This effect was more pronounced when the interactions between SAN and PCL, indicated by χ, are more favorable. Since $G°$ is proportional to $\left|\chi - \chi_s\right|$ (Saito et al. 1991), with χ_s the interaction parameter at the spinodal, a minimum was also noticed in the $G°$ versus the copolymer composition of SAN (see Figs. 3.14 and 3.15).

Fig. 3.15 The pre-exponential factor G° SAN in PCL/SAN blends (Kressler et al. 1992, 1993)
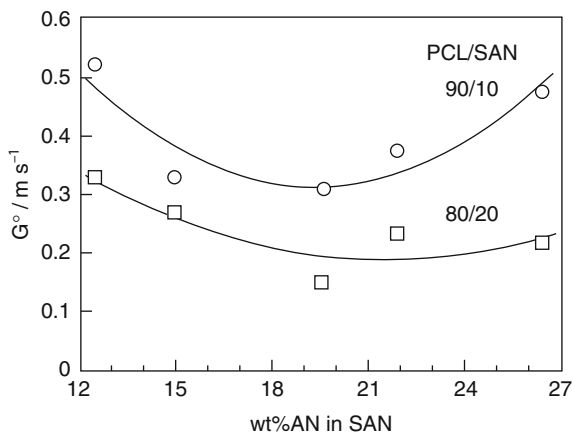
3.2.3.7 Other Aspects Related to Crystallization in Miscible Blends

(a) Chen et al. (2001) are among the few authors who considered the study of the effect of chain branching on the crystallization behavior of polyethylenes blends. Simple DSC techniques were used to differentiate, in terms of crystallization and melting, between blends of LDPE and VLDPE containing short branches. A stepwise isothermal crystallization was applied to thermally fractionate species based on their branching densities. The fractionated curves were used to determine the short-chain branching distribution, crystallization, and miscibility of the blends. When the two blend partners have similar unbranched segments, they may cocrystallize provided miscibility exists in the melt. Cocrystallization was found in all series of blends investigated but to varying extent depending on the branches densities of each blend couple.

(b) Svoboda et al. (2008) by choosing PCL/SAN containing 27.5 wt% AN could elucidate an interesting phenomenon of the competition between the phase dissolution and the crystallization of PCL in the blend. The authors qualified the crystallization as the liquid-solid phase transition and the phase dissolution as the liquid-liquid phase transition. A blend of 80/20 PCL/SAN phase separates via spinodal decomposition (SD) above the LCST, yielding a regularly phase-separated SD structure. By quenching a sample at temperatures below the Tm of the crystallizable PCL component, it was possible to have both crystallization and phase separation. TEM observations revealed that during isothermal annealing (after quenching to temperature as 51 °C close to T_m of PCL), the SD structure disappeared, and then the crystallization started from a single-phase mixture to yield normal crystalline structure similar to a neat PCL phase. At lower temperatures (e.g., 40 °C), crystallization set in quickly, and the SD was preserved implying the crystallization prevailed over the dissolution process, resulting in a bi-continuous structure consisting of amorphous (SAN-rich) and crystalline (PCL-rich) regions. At intermediate temperatures (e.g., 45 °C), the phase dissolution competed with the crystallization,

Fig. 5.16 Crystallization isotherms for the PEG/PEMA 80/20 blend crystallized at different T_c (Cimmino et al. 1989)
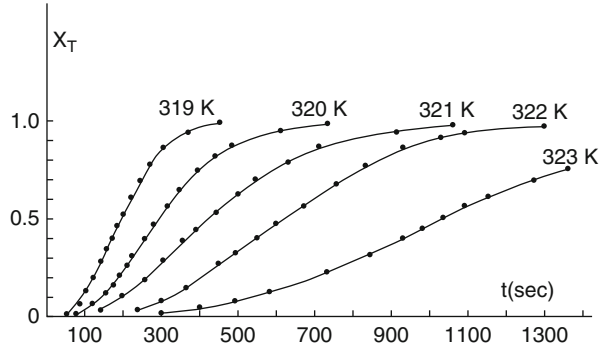
resulting in a bi-continuous structure with longer periodic distance and a broad boundary having a gradient in composition of amorphous region between PCL lamellae crystals.

3.2.4   Overall Crystallization Kinetics

3.2.4.1 General Aspects of the Avrami Theory Under Isothermal Conditions

The overall crystallization kinetics of blends can often be described by the Avrami equation (Avrami 1939):

$$\alpha = 1 - \exp\{-kt^n\} \tag{3.17}$$

α is the weight fraction of crystallinity at time t, n is the Avrami index depending on the type of nucleation and the crystal growth geometry, and k is the Avrami constant related to the crystallization rate:

$$k = \ln\left(2/t^n_{1/2}\right) \tag{3.18}$$

where $t^n_{1/2}$ is the halftime of crystallization (the time for half the crystallinity to develop), which is often used as a measure for the overall rate of crystallization. The theory was applied to polymer systems, e.g., by Morgan (1954) and Mandelkern et al. (1954).

In Fig. 3.16 typical crystallization isotherms were obtained by plotting α versus the crystallization time for the PEG/PEMA 80/20 blend at different crystallization temperatures. From such curves, the halftime of crystallization, $t^n_{1/2}$, can be deduced.

Equation 3.17 can be rewritten as

$$\log\{-\ln(1-\alpha)\} = \log k + n\log t \tag{3.19}$$

Plotting the left part of this equation against log t should result in a straight line, from which both Avrami parameters, n (slope) and k (intercept), can be obtained.

In Table 3.7 some literature data on the Avrami constants and the halftime of crystallization are presented. The Avrami n index (smaller than three for all the crystallization temperatures studied) of PCL/PBT system as investigated recently by Righetti et al. (2007) suggests a not fully three-dimensional crystalline growth. For the calculation of the crystallization growth rate, the authors plotted the reciprocal of the crystallization time needed to reach 20 % (and not half) of the crystallinity as a function of undercooling. As illustrated in Fig. 3.17, the dependence of the crystallization rate on the PCL molecular weight for both miscible and phase-separated PBT/PCL 80/20 blends, at the undercoolings accessible to DSC, parallels perfectly the trends exhibited by the linear growth rate curves that refer to lower undercoolings. Indeed and in contrast to many miscible systems, the low molecular weight PCL induces an increase in the crystallization rate of the PBT because of the higher molecular mobility the PCL oligomer causes as a plasticizer.

Cimmino et al. (1989) calculated the halftime of crystallization ($t_{1/2}$) for some PEG blends, PEG/PEMA, PEG/PVAc, and PEG/PMMA, using the same blend composition and the crystallization temperature. Blends of PEG with PVAc had the smallest $t_{1/2}$, while the PEG/PEMA blends showed the highest values for the halftime of crystallization. The type of amorphous component added to PEG seems to be important. The differences observed in $t_{1/2}$ (and also in the values of G) depend on:

– The degree of miscibility and mobility of the crystallizable and amorphous components
– The influence of the amorphous component on the nucleation of PEG
– Influence of the noncrystallizable component on the secondary nucleation or the crystallization regime (neat PEG and PEG/PEMA crystallize in regime I, whereas PEG/PVAc and PEG/PMMA crystallize in regime II)

Adding PMMA to PEG results in a decrease of $k = \ln 2/t^{n}_{1/2}$ (see Eq. 3.18), an effect that is clearly seen in Fig. 3.18 where $1/t_{1/2}$ is plotted against crystallization temperature (Martuscelli et al. 1984).

3.2.4.2 Modified Avrami Expression

It was often found that, contrary to the theoretical prediction, the value of n is noninteger (Avrami 1939). The Avrami model is based on several assumptions, such as constancy in shape of the growing crystal, constant rate of radial growth, lack of induction time, uniqueness of the nucleation mode, complete crystallinity of the sample, random distribution of nuclei, constant value of radial density, primary nucleation process (no secondary nucleation), and absence of overlap between the growing crystallization fronts. These assumptions are often not met in polymer (blend) crystallization. Also, erroneous determination of the "zero" time and an overestimation of the enthalpy of fusion of the polymer at a given time can lead to noninteger values for n (Grenier and Prud'homme 1980).

Pérez-Cardenas et al. (1991) developed a modified Avrami expression, taking into account the secondary crystallization effects. The weight fraction of crystallinity, α, can be written as the sum of two terms:

Table 3.7 Overall kinetic rate constant, k; Avrami index, n; and halftime of crystallization, $t^n_{1/2}$; as function of the crystallization temperature and blend composition for some crystallizable miscible blends

Polymer blend	Composition	T_c (°C)	k (s^{-n})	n	$t^n_{1/2}$ (min)	Reference
PCL/PVC	70/30	5	4.36×10^{-2}	2.86	3.6	Ong and Price (1978b)
		15	1.41×10^{-2}	2.60	6.2	
		25	1.95×10^{-3}	2.55	20	
	65/35	5	1.99×10^{-3}	2.82	10	
		15	7.60×10^{-4}	2.70	15	
		25	9.57×10^{-5}	2.93	37	
	60/40	5	4.57×10^{-6}	3.23	46	
		15	8.50×10^{-6}	3.14	35	
		25	2.62×10^{-6}	3.26	58	
	50/50	5	2.45×10^{-9}	3.16	630	
		15	3.98×10^{-9}	3.22	480	
		25	3.16×10^{-9}	3.08	595	
PCL/PVC[a]	100/0	29.6	19.95×10^{-3}	3.5	45[b]	Nojima et al. (1986)
		38.0	3.88×10^{-3}	2.2	217[b]	
		42.1	1.01×10^{-3}	2.4	848[b]	
	90/10	28.4	13.80×10^{-3}	2.1	61[b]	
		38.4	2.16×10^{-3}	1.7	374[b]	
		40.4	0.87×10^{-3}	1.9	949[b]	

(*continued*)

Table 3.7 (continued)

Polymer blend	Composition	T_c (°C)	k (s^{-n})	n	$t''_{1/2}$ (min)	Reference
PEG/PMMA[a]	100/0	47	1.09[c]	2.53	0.8	Martuscelli et al. (1984)
		51	5.18×10^{-3c}	2.78	5.8	
		54	3.52×10^{-5c}	2.63	42.9	
	90/10	46	2.84×10^{-1c}	2.52	1.4	
		50	7.53×10^{-3c}	2.67	5.4	
		53	8.46×10^{-5c}	2.57	33.3	
	80/20	42	3.57×10^{-2c}	2.45	3.4	
		47	4.94×10^{-4c}	2.46	19.0	
		50	5.40×10^{-5c}	2.50	39.1	
	70/30	39	9.26×10^{-3c}	2.56	5.7	
		44	2.90×10^{-4c}	2.82	16.8	
		49	6.05×10^{-6c}	2.72	72.4	
PEG/PEMA[a]	100/0	47	4.171×10^{-4}	2.1	0.5	Cimmino et al. (1989)
		50	6.144×10^{-5}	2.0	1.2	
		53	2.840×10^{-6}	2.4	4.7	
	90/10	47	2.068×10^{-6}	2.5	4.2	
		49	4.614×10^{-7}	2.1	8.1	
		51	3.306×10^{-8}	2.3	30.5	
	80/20	47	5.082×10^{-7}	2.4	4.7	
		49	7.686×10^{-8}	2.8	10.1	
		51	4.823×10^{-9}	2.3	30.5	
	70/30	43	2.497×10^{-7}	2.8	—	
		45	5.829×10^{-8}	2.1	—	
		47	1.315×10^{-8}	2.4	—	

PBT/PCL MW = 1250; Miscible blend	80/20	$T_m^\circ - T_c = 47.4$	n.a	2.4	n.a.	Righetti et al. (2007)
		45.4	–	2.5	–	
		43.4	–	2.4	–	
		41.4	–	2.2	–	
		39.4	–	2.3	–	
		37.4	–	2.5	–	
		35.4	–	2.8	–	
		33.4	–	2.8	–	
		31.4	–	2.7	–	

[a]The authors investigated a wide range of crystallization temperatures, from which only a few are presented here
[b]The halftime of crystallization is expressed in seconds (!)
[c]The overall kinetic rate constant is expressed in $\min^{-n}$ (!)

Fig. 3.17 Reciprocal of the time needed to reach 20 % of the final crystallinity ($1/\tau 0.2$) for PBT and PBT/PCL blends, plotted as a function of the undercooling. The *lines* are a guide for eyes (Righetti et al. 2007)
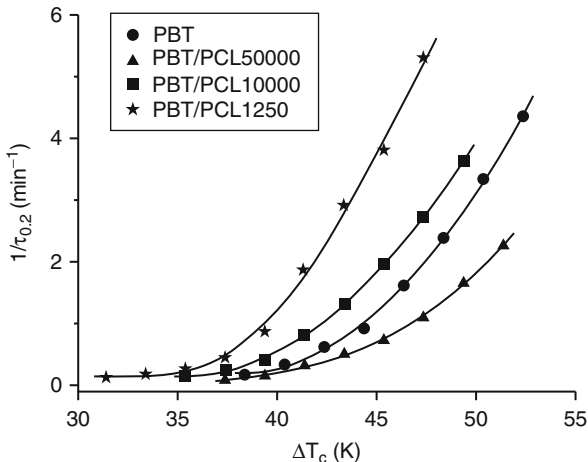
Fig. 3.18 Reciprocal of the halftime of crystallization, $t_{1/2}$, versus T_c for neat PEG (10) and PEG (10) blends with PMMA (the value between brackets refers to the molecular weight of PEG in kg/mol) (Martuscelli 1984)
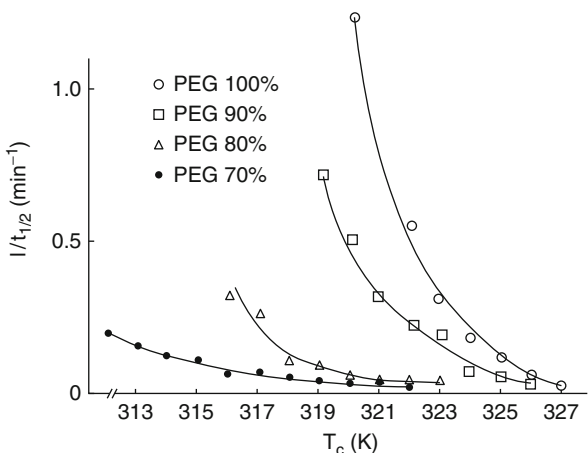
$$\alpha = \alpha_p + \alpha_s \qquad (3.20)$$

where the subscripts "*p*" and "*s*" refer to primary and secondary crystallization, respectively.

The crystallization process is divided in three regions (Fig. 3.19): (I) the initial primary crystallization region, (II) a region in which both primary and secondary crystallization takes place, and finally (III) a region in which only secondary crystallization occurs.

A parameter, ζ, was introduced, which is the weight fraction of the polymer crystallized by primary and secondary crystallization at the moment that the primary crystallization has ended (end of region II). The whole crystallization process is then described by two equations:

Fig. 3.19 Comparison between a typical experimental crystallization isotherm (*solid line*) and the Avrami equation (Eq. 3.17, *broken line*). The three regions I, II, and III correspond to primary, primary and secondary, and secondary crystallization, respectively (Pérez-Cardenas et al. 1991)
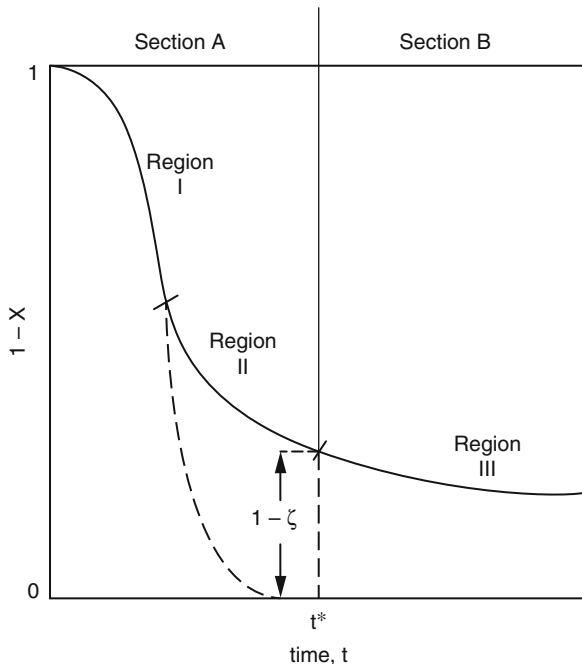
$$1 - \alpha = \exp\left(-kt^{n} - k't^{n'}\right)\left[kn(1 - \zeta)\int_{o}^{t}\exp\left(k\tau^{n} + k'\tau^{n'}\right)\tau^{n-1}d\tau + 1\right] \quad (3.21)$$

$$1 - \alpha = (1 - \zeta)\exp(k't^{*n'})\exp\left(-k't^{n'}\right) \quad (3.22)$$

Equation 3.21 is valid for $\alpha \leq \zeta$ and Eq. 3.22 for $\alpha > \zeta$. Instead of two Avrami parameters, five parameters are required to describe the process. They have the following physical meaning: k and n (the primary crystallization parameters) depend on crystallization temperature, nature of primary nucleation, and the fast growth; the secondary crystallization parameters, k' and n', depend on the conditions under which the slow crystallization of the remaining amorphous regions takes place; and a fifth parameter, ζ, indicates the weight fraction of material crystallized up to the moment the primary crystallization ends. t^* is the moment at which the third region starts (e.g., pure secondary crystallization).

Some literature data concerning isothermal crystallization experiments of linear PE at 128 °C (Doremus et al. 1958) have been fitted using different values for the parameters in Eqs. 3.21 and 3.22 (Fig. 3.20). The most accurate fit was obtained using the following parameters: $n = 4$, $k = 3.7 \times 10^{-10}$, $n' = 2$, $k' = 4 \times 10^{-6}$, and $\zeta = 0.68$.

Fig. 3.20 Theoretical isotherms (*solid lines*) using Eqs. 3.21 and 3.22 for three different sets of values of the five parameters (Pérez-Gardenas et al. 1991) fitted to the experimental values (*points*) of Doremus et al. (1958)
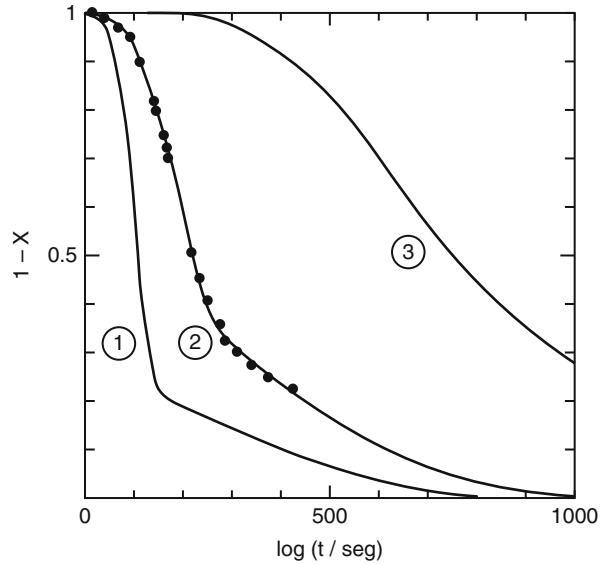
In the case of miscible polymer blends, the temperature dependence of the overall kinetic rate constant, k, can be calculated from (Boon and Azcue 1968; Wunderlich 1973; Hoffman 1982)

$$1/n \ln k - \ln \phi_2 + \Delta E / \{R(T_c - T_o)\} - \{(0.2 T_m^\circ \ln \phi_2)/\Delta T\} = \alpha_2$$
$$= \ln A_n - \{K_g / T_c \Delta T f\} \tag{3.23}$$

with K_g the same as in Eq. 3.12

3.2.4.3 Determination of the Surface Free Energy of Folding from Overall Kinetic Data

A plot of α_2 versus $1/(T_c \Delta T f)$ results in a straight line and from the slope, values of σ_e can be obtained. In Table 3.8 and Fig. 3.21, the free energy of folding, σ_e, for some PEG/PEMA and PEG/PMMA blends, respectively, derived from the overall kinetics of crystallization (Eq. 3.23), is compared with the values obtained from the radial growth rate data (Eq. 3.11). The compositional dependence of σ_e derived from both methods is similar, although higher values were obtained using Eq. 3.23 (overall kinetics of crystallization).

The σ_e values obtained from both analyses almost coincide. The dependence of σ_e on the composition of the PEG/PMMA blends may be partly accounted for by the effect of concentration, since the concentration-dependent part of σ_e is only a few joule per square meter (Martuscelli 1984). It is possible that PMMA molecules located in the interlamellar regions easily form entanglements with PEG molecules, favoring the formation of large loops on the surface of the PEG crystals.

Table 3.8 Free energy of folding (σ_e) for some PEG/PEMA blends calculated using Eqs. 3.11 and 3.23

Polymer blend	Composition (wt%)	σ_e ($\times 10^3$J/m^2) (Eq. 3.11)	σ_e ($\times 10^3$J/m^2) (Eq. 3.23)	References
PEG/PEMA	100/0	58	75	Cimmino et al. (1989)
	90/10	28	42	
	80/20	24	34	
	70/30	14	29	
PEG/PMMA	100/0	58	60	Martuscelli et al. (1984)
	90/10	43	48	
	80/20	38	39	
	70/30	36	39	
	60/40	36	37	
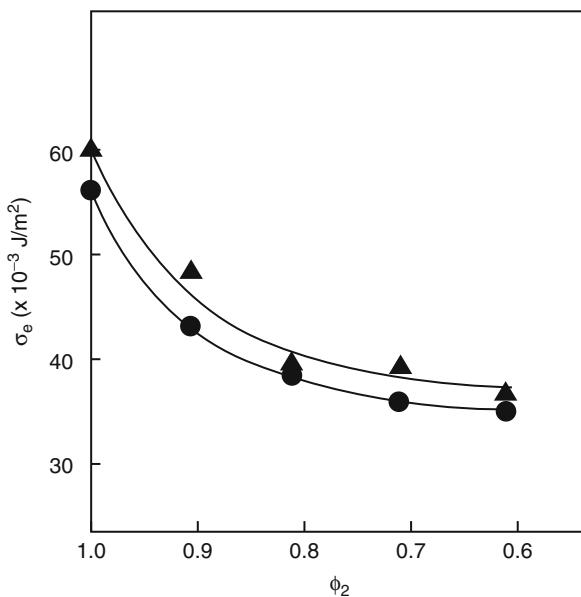
Fig. 3.21 Surface free energy of folding, σ_e, versus the volume fraction of the crystallizable component, ϕ_2, for blends of PEG (10) with PMMA from spherulite growth rate data (*circles*) and from overall rates of crystallization data (*triangles*) (the value between brackets refers to the molecular weight of PEG in kg/mol) (Martuscelli et al. 1984)

This can lead to an increase of both the surface enthalpy and the entropy of folding which contribute to σ_e ($\sigma_e = H_e - TS_e$). The decrease of σ_e when adding PMMA suggests that the entropic term overwhelms the enthalpic one.

3.2.4.4 Nonisothermal Kinetics

The theory of Avrami is limited to isothermal processes. Since polymer processing is mostly performed under nonisothermal conditions, the theory has been extended (Ziabicki 1967; Ozawa 1971; Ziabicki 1976).

According to Ozawa ([1971](#)), the crystallinity at any temperature is given by

$$-\ln(1 - \alpha) = C(t)/q^{n''} \tag{3.24}$$

where q is the heating or cooling rate; $C(t)$ is a cooling function of the process; and n'' is the Ozawa exponent.

Ziabicki ([1967](#), [1976](#)) based his analysis on the assumption that any nonisothermal process can be treated as a combination of several isothermal crystallization steps:

$$E(t) = kt^n = \ln2\left\{\int_0^t ds/t_{1/2}[\alpha(s)]\right\}^n \tag{3.25}$$

This equation is an analogue of Eq. [3.18](#).

Under nonisothermal conditions, the ultimate Avrami parameters will be averages of the parameters of the subsequent steps.

Gupta et al. ([1994](#)) used the following equation, based on the theory described by Ziabicki ([1967](#), [1976](#)) and by Kamal and Chu ([1983](#)), to describe the nonisothermal behavior of cocrystallizing HDPE/LLDPE blends.

$$\left[\alpha_p' \left(T_p - T_{ons}\right)\right]/\left[\beta\left(1 - \alpha_p\right)\right] = (n - 1) - \left[E\left(T_p - T_{ons}\right)\right]/\left[RT_p^2\right] \tag{3.26}$$

where $\alpha' = d\alpha/dt = nkt^{(n-1)}\left(1 - \alpha\right)$ and β is the heating rate. In the case of a cooling experiment, β will be negative and β should be replaced by $-\beta$ in the equation.

T_{ons} is the onset temperature and T_p is the temperature after time t $(T_p - T_{ons} = \beta t)$, where the subscript "p" denotes the peak temperature and E is the activation energy of the crystallization process.

A plot of the left part of Eq. [3.26](#) against $(T_p - T_{ons})/T_p^2$ should be linear with slope and intercept equal to E/R and $(n - 1)$, respectively (see Fig. [3.22](#)). The quantity α was evaluated from the ratio of the area under the crystallization peak per unit mass of the sample. α_p is the extent of crystallization at the peak maximum and is determined by the fractional area under the exotherm from the onset temperature T_{ons} to the peak temperature T_p relative to the total area under the exotherm.

The Avrami exponent and the activation energy decrease with increasing LLDPE content (see Table [3.9](#)).

The authors suggested that the Avrami constant could be seen as the sum of two processes: a contribution due to nucleation and a contribution due to growth:

$$n = n_{\text{ucleation}} + n_{\text{growth}} \tag{3.27}$$

Since both components cocrystallize (Edward [1986](#); Hu et al. [1987](#); Gupta et al. [1994](#)), the crystalline growth can be considered to be identical. As a consequence, the differences seen in the Avrami exponent, n, in the blends

Fig. 3.22 Plot of $[\alpha_p' (T_p - T_o)]/[\beta (1 - \alpha_p)]$ versus $(T_p - T_o)/T_p^2$ for HDPE, LLDPE, and the 50/50 blend (Gupta et al. 1994)
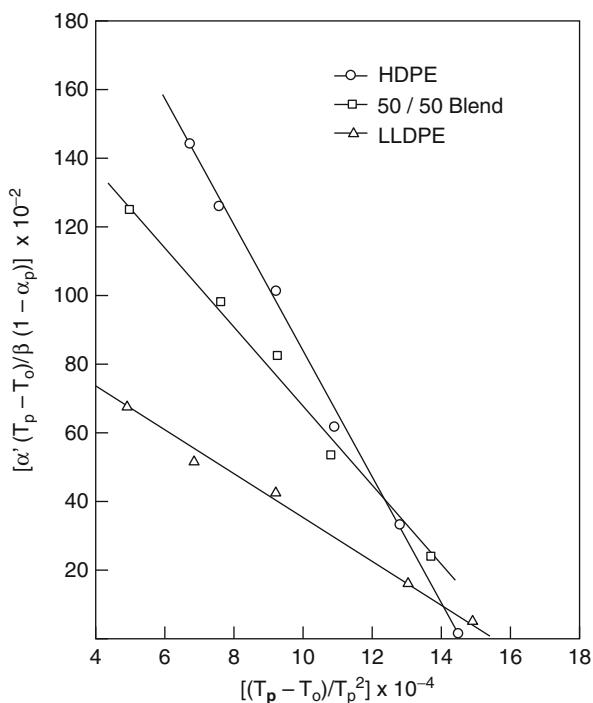
Table 3.9 Avrami exponent, n, for HDPE, LLDPE, and their blends

Blend composition (wt%)[a] HDPE/LLDPE	Avrami exponent, n	Activation energy, E (kJ/mol)
100/0	2.94	121.67
75/25	2.65	99.44
50/50	2.30	85.83
20/80	1.93	59.04
0/100	1.72	49.16

[a]More compositions were mentioned in the article (Gupta et al. 1994)

must be due to a difference in the nucleation behavior that depends on the blend composition. A value varying from 0 (instantaneous nucleation) to 1 (sporadic nucleation) was attributed to the contribution of the nucleation of LLDPE and HDPE, respectively, to the Avrami constant, n. The remaining part of n (e.g., 1.94 for HDPE and 1.74 for LLDPE) represents the value for the growth process.

The lower activation energy for LLDPE compared to HDPE seems to be due to a storage of thermal energy by the crystallites caused by the presence of bulky pendant groups at the crystalline boundary that exert repulsive forces. Cocrystallization enhances these forces due to the greater abundance of the bulky groups that results in a decrease of the activation energy.

3.2.5   Melting Behavior of Crystallizable Miscible Blends

3.2.5.1 The Equilibrium Melting Temperature in Miscible Blends: Hoffman-Weeks Plot

In a semicrystalline homopolymer, the change in free energy of melting per mole of monomer unit is given by

$$\Delta G_u(T) = \Delta H_u - T\Delta S_u \tag{3.28}$$

where ΔH_u and ΔS_u are the enthalpy and the entropy changes on melting, respectively. For blends, the difference in free energy of the crystalline unit can be written as (Sanchez and Di Marzio 1971)

$$\Delta G_{ub}(T) = \Delta G_u(T) + \Delta g_M = \Delta H_u - T\Delta S_u + \Delta h_M - T\Delta s_M \tag{3.29}$$

where $\Delta G_u(T)$ has the same meaning as in Eq. 3.28, i.e., the heat of fusion of the crystalline component in the blend is assumed to be equal to that of the homopolymer. For athermal blends ($\Delta h_M = 0$) Eq. 3.29 becomes

$$\Delta G_{ub}(T) = \Delta H_u - T\Delta S_u - T\Delta s_M = \Delta H_u - T\Delta S_{ub} \tag{3.30}$$

For an infinitely thick crystal with an equilibrium melting temperature in the blend of $T_{mb}°$, $\Delta G_{ub}(T_{mb}°)$ is equal to 0 and

$$T_{mb}° = \Delta H_u/\Delta S_{ub} \tag{3.31}$$

substituting Eq. 3.31 into Eq. 3.30 results in

$$\Delta G_{ub}(T_{mb}) = \Delta H_u(1 - T_{mb}/T_{mb}°) - T_{mb}\Delta s_M \tag{3.32}$$

At T_m:

$$\Delta G_{ub}(T_{mb}) = 2(\sigma_{eb}/n_b) \tag{3.33}$$

Combining and rearranging Eqs. 3.32 and 3.33 gives a relation between the experimental and equilibrium melting point in athermal polymer blends:

$$1/T_{mb} = \{1/T_{mb}° + \Delta s_M/\Delta H_u\}\{1/[1 - (2\sigma_{eb}/\Delta H_u n_b)]\} \tag{3.34}$$

with $\sigma_{eb} = \phi_1^{\alpha} \sigma_e$ and $n_b = (1 - \phi_1)^{\beta} n$ with α and β constants which need to be evaluated for each system (Cimmino et al. 1988). For $\Delta s_M \to 0$, the dependence can be simplified to

$$T_{mb} = T_{mb}°[1 - (2\sigma_{eb}/\Delta H_u n_b)] \tag{3.35}$$

If the heat of mixing is not ignored ($\Delta h_M \neq 0$), then the same treatment of Eq. 3.29 as used to obtain Eq. 3.35 results in

Fig. 3.23 Hoffman-Weeks plot for PCL-rich PCL/PC blends (the data are displaced by 5 °C to discern the different blend compositions) (Jonza and Porter 1986)
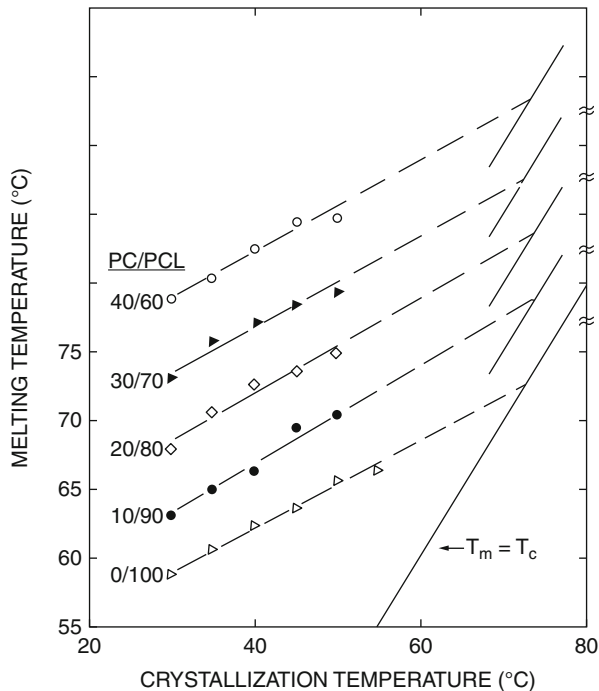
$$T_{mb} = T_{mb}°\{1 - [(2\sigma_{eb}/\Delta H_u n_b) + (\Delta g_M/\Delta H_u)]\} \tag{3.36}$$

This equation is a general form of the relation between the experimental and equilibrium melting temperature of the blend.

The equilibrium temperature of a polymer (blend) can experimentally be determined by a Hoffman-Weeks plot, which is a plot of the experimental melting point versus the crystallization temperature (T_m vs. T_c) as presented in Fig. 3.23. Extrapolation from experimental data to the $T_m = T_c$ line results in the value of $T_{mb}°$.

The influence of T_c on T_m is due to morphological contributions such as degree of perfection and the finite size of crystals (Hoffman and Weeks 1962b; Mandelkern 1964). If the crystals are perfect, of finite size and no recrystallization takes place during the melting, the T_m versus T_c data can be described by Nishi and Wang (1975)

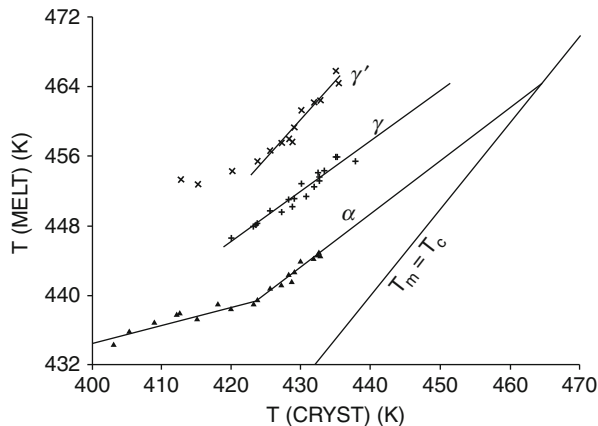$$T_m° - T_m = \phi(T_m° - T_c) \tag{3.37}$$

or

$$T_m = T_m°(1 - \phi) + \phi T_c \tag{3.38}$$

$T_m°$ and T_m are the equilibrium and observed melting point, respectively; ϕ is the stability parameter that depends on the crystal thickness and assumes

Fig. 3.24 Hoffman-Weeks plot for PVDF/PMMA blends with 50.1 vol% of PVDF (Stein et al. 1981)

values between 0 and 1 (sometimes ϕ is replaced by $1/\gamma$, where γ is the thickening factor of the crystal).

The value of $\phi = 0$ implies $T_m = T_m^\circ$ for all T_c, whereas $\phi = 1$ implies $T_m = T_c$. Therefore, the crystals are most stable at $\phi = 0$ and inherently unstable at $\phi = 1$. Nishi and Wang (1975) examined the polymer system PVDF/PMMA and found a value for $\phi = 0.2$ for all compositions studied, which suggests that the crystals are fairly stable. A comparable value has been found for other polymer crystals (Hoffman and Weeks 1962b).

The same polymer blend was studied by Stein et al. (1981), Morra and Stein (1984). Since PVDF crystallizes into several types of morphologies, different lines are shown in the Hoffman-Weeks plot (Fig. 3.24). The curve representing the melting point of PVDF as a function of the crystallization temperature for the α modification shows a break that was associated with defect exclusion from the crystal (Stein et al. 1981) and by entrapment of head-to-head defects of the PVDF chains into the crystals during rapid crystallization at large undercooling (Morra and Stein 1984).

Hoffman-Weeks plots have also been drawn for several other amorphous/crystalline miscible blends, such as PVDF/PEMA (Eshuis et al. 1982), PEG/PMMA (Martuscelli 1984), PCL/SARAN (Zhang and Prud'homme 1987), as well as for some miscible blends containing two semicrystalline components, PCL/PC (Jonza and Porter 1986) and PCL/Penton (Guo 1990). Table 3.10 represents equilibrium melting points derived from T_m versus T_c plots for some of these systems.

In Fig. 3.25 Hoffman-Weeks plot for PCL/PBT blends is compared to pure PBT sample. A nonlinear extrapolation procedure was applied for the determination of the equilibrium melting temperature of the crystallizing phase. The linear extrapolation as proposed initially by Hoffman-Weeks neglects the contribution of the increment of the lamellar thickness. Note that the PCL is miscible with PBT only when the PCL molecular weight is equal or lower than MW = 1,250. The blend samples having a PCL molecular weight of 10,000 or 50,000 form immiscible mixture for which the crystallization behavior of pure PBT is recovered. The T_m° of

Table 3.10 Equilibrium melting points derived from Hoffman-Weeks plots for several crystallizable miscible blends

Polymer blend	Composition[a]	$T_m°$ (°C)	References
PVDF/PMMA	100/0	173.8	Nishi and Wang (1975)
	50/50	165.2	
PCL/PC[b]	100/0	71	Jonza and Porter (1986)
	10–40 % PC	71 ± 2	
PCL/P(VCl$_2$-VC)[c]	100/0	58.1	Zhang and Prud'homme (1987)
	50/50	55.4	
PCL/P(VCl$_2$-VA)[c]	50/50	55.3	
PCL/P(VCl$_2$-AN)	50/50	53.6	
PCL/Penton	0/100	185	Guo (1990)
	50/50	172.5	
PEEK/PEI	0–60 % PEI	384	Chen and Porter (1993)
		389	Lee and Porter (1987)
iPS/PPE	0–35 % PPE	240	Plans et al. (1984)

[a]Most authors studied more compositions than the ones presented here
[b]Both polymers crystallize in this blend, but no $T_m - T_c$ plots could be made for PC since the blends are reactive at the higher crystallization temperatures required for this component
[c]Both polymers crystallize in this blend

Fig. 3.25 Melting temperature of non-thickened crystals ($\beta = 1$) as a function of T_c for PBT and PBT/PCL blends. The *curved* lines are the nonlinear fit to the experimental data. The *straight* line $T_m = T_c$ is also depicted. The *inset* shows an enlargement of the plot (Righetti et al. 2007)
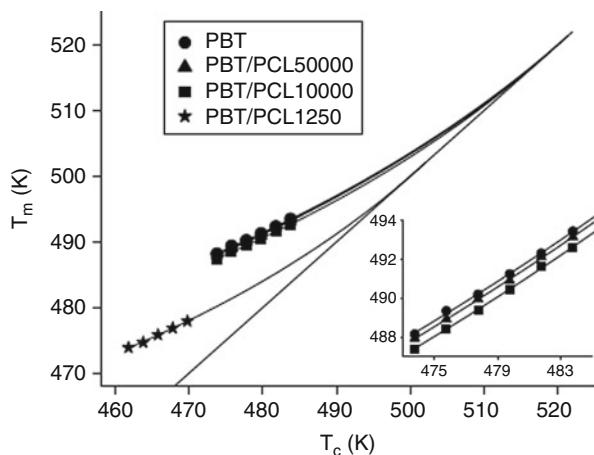
the PBT/PCL1250 is equal to 501 °K, much lower than that of pure PBT (522 °K) or its blends with higher MW PCL samples (PCL10000: $T_m° = 519$°K; PCL50000: $T_m° = 521$ °K).

It should, however, be noted that several blends do not show a linear T_m versus T_c relation (Rim and Runt 1984; Jonza and Porter 1986). The absence of linearity originates from several effects, such as recrystallization, crystal defects, etc.

Fig. 3.26 Schematic diagram of the free energy of a crystalline phase (G_c) and the free energy of a melt phase of a homopolymer (G_m°) and a miscible blend (G_{mb}°) as function of the temperature
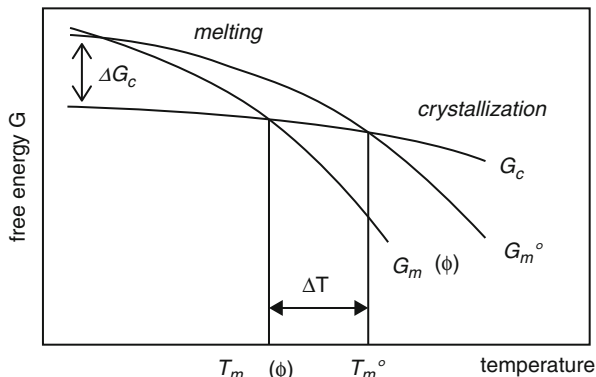
3.2.5.2 Melting-Point Depression

The melting behavior of a semicrystalline component in a miscible blend strongly depends on the blend composition. In several blends, a depression of the melting point has been observed after addition of an amorphous polymer. This behavior results from the kinetic, morphological, and thermodynamic factors (Cimmino et al. 1989). *Kinetic* effects originate from the crystal formation at temperatures below the equilibrium melting point. They can be avoided by using equilibrium values derived from Hoffman-Weeks plots. Melting-point depression, caused by *morphological* effects (see Eq. 3.38), is associated with changes in crystal thickness, perfection and geometry, as well as different thermal histories of the samples. When a miscible diluent is added to a semicrystalline polymer, the equilibrium melting point of the crystallizable component can be depressed due to interaction between both components. The free energy of the crystallizable component will decrease from G_m° to G_{mb}°, when the crystallites are surrounded by a mixed melt phase. The free energy of the crystalline phase, G_c, is not affected by mixing. The melting temperature, defined as the cross section of G_c and G_m (e.g., when $\Delta G = 0$), may be depressed (Fig. 3.26).

The melting-point depression resulting from *thermodynamic* effects can be described by the following equation (Flory 1953; Nishi and Wang 1975):

$$\left(1/T_{mb}^\circ\right) - \left(1/T_m^\circ\right) = -[(RV_{2u})/(\Delta h_u V_{1u})]$$
$$\left[(\ln\phi_2/m_2) + (1/m_2 - 1/m_1)(1 - \phi_2) + \chi_{12}(1 - \phi_2)^2\right] \tag{3.39}$$

T_{mb}° and T_m° are the equilibrium melting point of the blend and the neat crystallizable component, respectively; V_u is the molar volume of the repeating unit of the components (1 = amorphous component and 2 = crystallizable component); Δh_u is the heat of fusion per mole of repeating unit; m is the number of units in the molecule, i.e., the degree of polymerization; ϕ is the volume fraction; and χ_{12} is the polymer-polymer interaction parameter.

Since, for polymers $m \to \infty$, Eq. 3.39 can be reduced to

$$\left(1/T_{mb}^{\circ}\right) - \left(1/T_{m}^{\circ}\right) = -[(RV_{2u})/(\Delta h_u V_{1u})]\chi_{12}(1 - \phi_2)^2 \qquad (3.40)$$

Instead of χ_{12}, the interaction energy density, B_{12}, can be used; both parameters are related by

$$\chi_{12} = B_{12}V_{1u}/RT \qquad (3.41)$$

Melting-point depression data are often used to determine the Huggins-Flory interaction parameter, χ_{12} (see Table 3.11), that is a measure for the miscibility of the blend, i.e., χ_{12} is negative for a miscible blend. A lack of melting-point depression means that χ_{12} is zero. Equation 3.39 is only valid for systems in which the crystalline morphology is not affected by the composition.

Many authors (Hay 1976; Kwei and Frisch 1978; Rim and Runt 1984; Plans et al. 1984; Alfonso and Russell 1986), however, encountered difficulties when fitting Eq. 3.40 to their experimental data, due to (Rostami 1990):

– The use of observable melting temperatures instead of the thermodynamic equilibrium temperatures.
– The plot of the left-hand side of Eq. 3.40 versus the right-hand side has no zero-intercept. The intercept contains information about the crystalline morphology (Kwei and Frisch 1978; Walsh et al. 1985) that has been ignored. Following Eq. 3.39 the intercept should equal $1/m_1$. When high molecular weight polymers are used, $1/m_1$ equals zero. This was observed for PVDF/PMMA and PVDF/PEMA blends (Kwei and Frisch 1978).
– The concentration dependence of the interaction parameter adds a restriction on plotting the left-hand side of Eq. 3.40 versus ϕ_1 to obtain a single value for χ_{12} (Kwei and Frisch 1978; Plans et al. 1984; Walsh et al. 1985).

A modified version of this equation has been used by some other authors (Kwei and Frisch 1978; Walsh et al. 1985), who added a constant that is related to the morphology of the crystalline region:

$$\Delta h_u\left(T_m^{\circ} - T_{mb}^{\circ}\right)/\phi_1 RT_m^{\circ} - T_{mb}^{\circ}/m_1 - \phi_1 T_{mb}^{\circ}/2m_2 = C/R - b\phi_1 \qquad (3.42)$$

where C is a constant taking into account the morphological contributions (which were assumed to be proportional to ϕ_1) and b is a constant derived from the equation relating the interaction parameter with temperature: $\chi_{12} = a + b/T$ with $a \ll b/T$ near the melting point. This approach was, however, not satisfactory (Walsh et al. 1985).

It should be noted that in Eq. 3.42 the assumption of infinite molecular weights has not been included as was done in Eq. 3.40.

Balsamo et al. (2006) presented a nice comparison in Fig. 3.27 of the effect of equilibrium melting-point depression in miscible blends of PCL with various partners including PVC, PSMA14 (14 wt% MA), Phenoxy, and SAN19,5 (19,5 wt% AN). It is clear that PSMA14 caused the greatest depression of the T_m° of PCL compared to the other partners. The authors ascribed this effect to the

highest interaction PCL develops with PSMA14 and that hinders the formation of perfect and complete lamellae. The peak temperature was used for the calculations instead of the onset due to the presence of a low melting endotherm that introduces some error in the determination of the onset of the melting point corresponding to the primary crystallization. Using at least eight experimental points, a linear dependence was observed in the T_c range used in this work. Thus, the extrapolation to $T_c = T_m$ by a linear least squares fit could be performed to calculate T_m°. For neat PCL, a T_m° of 69.9 °C, was observed in agreement with values reported in the

Table 3.11 Interaction parameters, χ_{12} and B_{12}, derived from the melting-point depression data

Polymer blend	Interaction parameter, χ_{12}	Interaction parameter, B_{12} ($\times 10^6 \text{J/m}^3$)	References
PVDF/PMMA	−0.295 (160 °C)	−12.48	Nishi and Wang (1975)
PVDF/PEMA	−0.34 (160 °C)	−11.94	Kwei et al. (1976)
		−13.11	Imken et al. (1976)
PEG(20,000)/PMMA[a]	−1.93 (76 °C)	−65.32	Martuscelli and Demma (1980)
PEG(100,000)/PMMA	−0.35 (74 °C)	−11.93	Martuscelli et al. (1984)
PEG/PVC[b]	−0.094 (65 °C)	−6.56 (65 °C)	Marco et al. (1993)
PCL/SAN 19.2[c]	−0.18		Kressler and Kammer (1988)
PBA/Phenoxy		−16.20 (61 °C)	Harris et al. (1982)
PEA/Phenoxy		−9.67 (49 °C)	Harris et al. (1982)
PCL/Phenoxy		−10.09 (56 °C)	Harris et al. (1982)
PCL/Penton[d]		−15	Guo (1990)
PCL/P(VCl$_2$-VC) 80/20[e,d]	−0.46		Zhang and Prud'homme (1987)
PCL rich	−0.02		Aubin et al. (1983)
P(VCl$_2$-VC) rich	−0.21		Aubin et al. (1983)
PCL/P(VCl$_2$-VA) 80/20[e,d]	−0.53		Zhang and Prud'homme (1987)
PCL rich	−0.01		Aubin et al. (1983)
P(VCl$_2$-VA) rich	−0.28		Aubin et al. (1983)
PCL/P(VCl$_2$-AN) 80/20[e,d]	−0.37		Zhang and Prud'homme (1987)
P(VCl$_2$/VCl)/PDPS[d]		−0.84	Woo et al. (1983)
P(VCl$_2$/VCl)/PDPA[d]		−4.60	Woo et al. (1983)
P(VCl$_2$/VCl)/PCL[d]		−8.37	Woo et al. (1983)
P(VCl$_2$/VCl)/PCDS[d]		−12.98	Woo et al. (1983)
PCL/PVDF[d,f]	−1.5		Jo et al. (1992)
FVA/EVAc[g]	−0.06	−15.07	Clough et al. (1994)
PI/EVAc[g]	−0.02	−7.12	Clough et al. (1994)

(*continued*)

Table 3.11   (continued)

Polymer blend	Interaction parameter, χ_{12}	Interaction parameter, B_{12} ($\times 10^6 J/m^3$)	References
PED/EVAc[g]	−0.38	−115.56	Clough et al. (1994)
PEEK/PEI	−0.40 (400 °C)	−5.02	Chen and Porter (1993)
iPS/PS (2,200)	−0.002		Runt (1981)
iPS/PS (50,000)	−0.003		Runt (1981)
iPS/PPE	0.17		Plans et al. (1984)
	−0.022		Runt (1981)

[a]The absolute value of χ_{12} is too large in comparison with the other literature data on miscible blends. The authors (Martuscelli et al. 1984) suggested that for this blend non-negligible entropic effects occur during mixing of the two polymers, noncompliance with the assumption inherent in the extrapolation of T_m (observed melting point) by using the Hoffman-Weeks plot and the inadequacies of the Huggins-Flory theory to describe the melting behavior of such polymer-polymer system
[b]EVAc (molar ratio ethylene to vinyl acetate: 7:1) is amorphous
[c]SAN containing 19.2 wt% AN
[d]Both polymers are semicrystalline
[e]More compositions have been investigated by the authors
[f]Units: J/mL
[g]This system shows an LCST behavior for PCL-rich blends, while blends with a high concentration on PVDF are phase separated; the blends considered here are only the miscible ones below their LCST (blends with a content of PVDF less than 30 wt%)
[h]The polymer blend PEG/PVC is only miscible when the concentration on PVC is $\geq$40 %
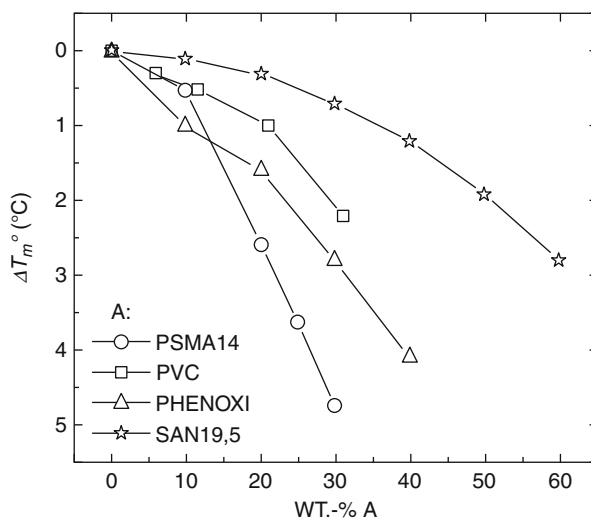
Fig. 3.27 Equilibrium melting-point depression of the PCL fraction in blends A/PCL as a function of the amorphous polymer A content. (○) Author's work, (Δ) (10), (□) (5), (☆) (15) (Balsamo et al. 2006)

literature (Balsamo et al. 2001; Wang and Jian 1997; Jonza and Porter 1986; Neo and Goh 1991). The melting-point depression exhibited by the PCL fraction with increasing PSMA14 (68.3 ± 2.2 °C and 64.2±1.4 °C for PSMA14/PCL 10/90 and 30/70, respectively) indicates miscibility between PCL and PSMA14 as was previously discussed from the standard DSC scans.
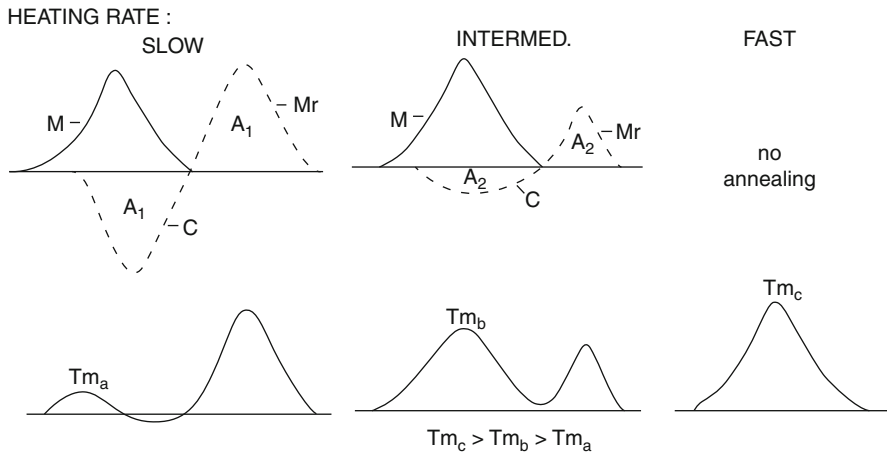
Fig. 3.28 Schematic representation of the melting mechanism proposed to account for the heating rate dependence of recrystallizing material. The *top* of the figure shows the melting of the original crystals (M), recrystallization (C), and remelting (M_r). The *bottom* portion of the figure shows the resultant thermograms that are experimentally observed (Rim and Runt 1983)

For some miscible blends, a melting-point elevation has been reported with respect to that of the neat crystallizable component, both crystallized at the same temperature (Eshuis et al. 1982; Rim and Runt 1983, 1984). These observations may originate from recrystallization, enhanced crystal perfection, and increased crystal size.

3.2.5.3 Multiple Melting Endotherms

The melting behavior of binary crystallizable blends often reveals multiple melting endotherms that can be ascribed to recrystallization, secondary crystallization effects, phase separation, etc.

Recrystallization is a process in which the initial, rather imperfect, lamellae melt and recrystallize to produce thicker and more perfect lamellae that as a consequence melt at a higher temperature. As a result of this process, a double melting behavior may be observed. Recrystallization has been observed for neat polymers and blends.

A method that is often used to determine if the dual melting behavior is caused by recrystallization is the variation of the heating rate in DSC experiments. It is suggested that during the DSC run, an annealing of the crystalline lamellae occurs (see Fig. 3.28; Rim and Runt 1983). At slow heating rates, the original crystals are given sufficient time to reorganize, and the melting behavior is then mainly caused by lamellae originating from recrystallization (C) and melting of the recrystallized material (M_r). The resulting behavior is a composite of the peaks due to the melting of the original crystals (M), the recrystallization exotherm, and the melting of the recrystallized material. As the heating rate is increased, the crystals have less time to reorganize, thus C and M decrease in magnitude.

A plot of the observed melting point of both melting endotherms as function of the crystallization temperature (Hoffman-Weeks plot) is another method to detect whether recrystallization occurs. The melting point of recrystallized material is independent of T_c; thus a horizontal line is observed in the T_m versus T_c plot.

During crystallization of a miscible polymer blend, the composition of the amorphous phase changes, i.e., becomes poorer on the crystallizable component. In some cases, a liquid-liquid phase separation can take place as a result of the crystallization. This phenomenon will be discussed more in detail in the next section.

A complex melting behavior is also observed when a semicrystalline polymer exhibits two different types of crystal structure. A second crystal structure can be introduced by a variation in temperature, pressure, elongation, etc. This phenomenon is known for neat PE. Adding an amorphous polymer to a crystallizable component can result in a change of the unit cell dimensions of the crystal structure. This has been observed for LDPE blended with EPDM (Starkweather 1980), where the unit cell expanded in the a-direction (a raises from 7.515–8.350 A) when increasing the amount of EPDM, while the b- and c-directions remained almost unchanged. The composition of EPDM plays also an important role. EPDM with an ethylene/propylene mole ratio of 4:5 (EPDM-1) exhibits the behavior as mentioned above. Decreasing the ethylene content in the EPDM copolymer results in an amorphous polymer (designated EPDM-2 and EPDM-3; Starkweather 1980) that do not alter the unit cell dimensions as much as EPDM-1 does. The latter copolymer is thought to cocrystallize (at least partially) with LDPE.

Several blends prepared by coprecipitation followed by crystallization from the melt exhibit a double melting behavior, due to the occurrence of the secondary crystallization process. The amorphous component causes a retarded crystallization of some of the crystallizable chains, which form lamellae smaller than and located between the primary ones constituting the spherulites (see Fig. 3.29).

This is a phenomenon often observed in PCL blends. In DSC scans as a function of crystallization time (t_c), a single melting behavior is observed after short t_c, while a second melting endotherm is noticed at long t_c (see Fig. 3.30). This second melting endotherm becomes more important as the more amorphous component is added (Vanneste and Groeninckx 1995; Fig. 3.31).

In Table 3.12 some blends are presented exhibiting a complex melting behavior due to one or more of the abovementioned reasons.

It should be mentioned that several homopolymers (of which polyethylene is probably the best known sample) also exhibit a complex melting behavior. Branched polyethylenes (LDPE, LLDPE, and VLDPE) show multiple melting endotherms, due to the presence of fractions with different branching contents (Schouterden et al. 1985; Defoor et al. 1993). This was clearly illustrated by Defoor et al. who fractionated LLDPE with respect to the short-chain branching content and blended the fractions with the highest and the lowest branching content. It was shown that they both crystallized and melted separately. Both fractions determined the spherulitic morphology in a cooperative way.

< melting process

tc=0   short tc   long tc

crystallization process >
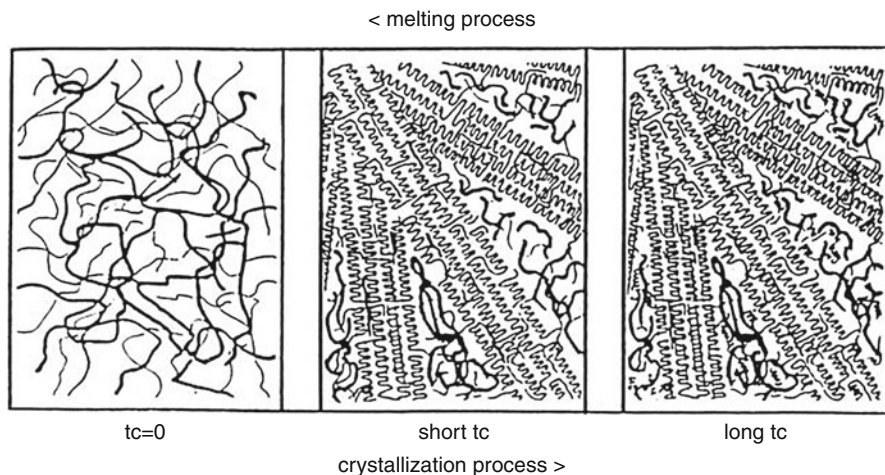
Fig. 3.29 Schematic presentation illustrating the secondary crystallization process (*thin lines*: crystallizable component, *thick lines*: amorphous component)
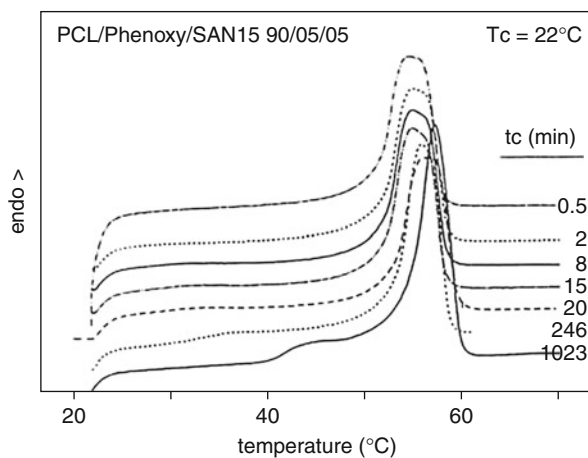
Fig. 3.30 Influence of the crystallization time on the melting behavior of the ternary PCL/Phenoxy/SAN 15 = 90/05/05 blend (Vanneste and Groeninckx 1994)

Other examples are PPS (which shows a double melting behavior due to the obstructive effect of branching or cross-linking of the molecules on crystallization at high temperature; Mai et al. 1994) and PEEK. Much controversy exists about the cause of the double melting behavior of PEEK – recrystallization or secondary crystallization. According to one group of authors (Prasad et al. 1991; Hudson et al. 1991; Bassett et al. 1992; Lattimer et al. 1992), PEEK that was crystallized

Fig. 3.31 Influence of the concentration of the amorphous component on the amount of secondary crystallization in PCL/SAN 15/SMA 14 polymer blends (Vanneste and Groeninckx 1995)
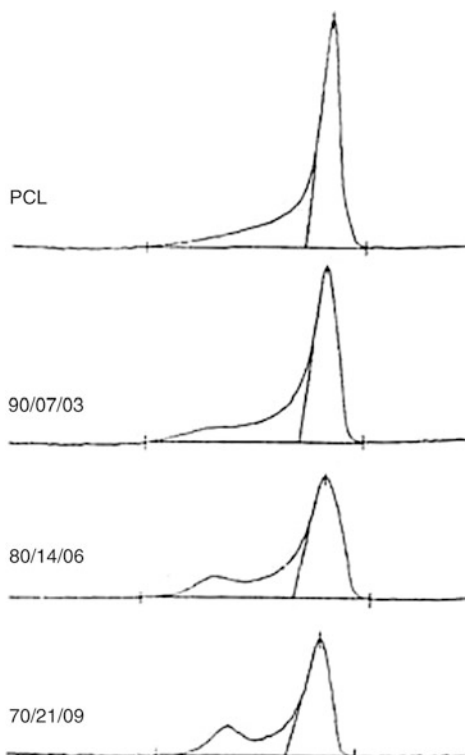
from the melt contains crystals with two types of lamellar thickness. The thicker ones grow first, while the smaller ones grow later within the thicker lamellae. Thermal analysis, however, indicates that a process of melting, recrystallization, and remelting occurs (Cheng et al. 1986; Lee and Porter 1987; Lee et al. 1989; Crevecoeur and Groeninckx 1991).

PEO/amorphous polyamide (Aramide 34I) blends investigated by Dreezen et al. (1999) displayed a double melting behavior. By varying the crystallization time of a 85 wt% PEO/15 wt% Aramide 34I from 33 to 451 h, the authors could demonstrate that the primary melting endotherm visible at 65 °C does not change, whereas the second melting endotherm increased in intensity and shifted to higher temperatures (from 41 °C to 50 °C) with increasing crystallization time (Fig. 3.32). They attributed the presence of a second melting endotherm, situated at lower temperatures than the main peak, to secondary crystallization of PEO after the primary crystallization process. The crystallization of some PEO-chains was retarded and crystallized slowly after the formation of the spherulitic structure. With time the thin lamellae thicken and melt at higher temperatures. During heating at low heating rates,

Table 3.12 Examples of crystallizable miscible polymer blends exhibiting a complex melting behavior

Polymer system	Type of melting behavior	Required conditions	References
PCL/SAN	Recrystallization	Melt crystallized	Rim and Runt (1983, 1984)
PCL/SAN	Dual melting behavior[a]	Melt crystallized	Kressler and Kammer (1988)
PCL/SAN	Recrystallization	Melt crystallized	Vandermarliere (1986)
PCL/Phenoxy/ SAN 15[b]	Recrystallization	Short crystallization times	Vanneste (1993), Vanneste and Groeninckx (1994)
PEEK/PEI[c]	Recrystallization	Melt crystallized	Crevecoeur and Groeninckx (1991)
LDPE/EPDM	Different crystal types	Ethylene/propylene ratio: 4:5	Starkweather(1980)
PCL/P(VCl$_2$-VC)	Secondary crystallization	High P(VCl$_2$-VC) content[d]	Zhang and Prud'homme (1987)
PCL/CPE[e]	Secondary crystallization	Coprecipitation technique + melt crystallization	Defieuw et al. (1989b)
PCL/SMA x[f]	Secondary crystallization	Coprecipitation technique + melt crystallization	Defieuw et al. (1989b)
PCL/Phenoxy	Secondary crystallization	Coprecipitation technique + melt crystallization	Defieuw et al. (1989d)
PCL/SAN x/SAN y[g]	Secondary crystallization	Coprecipitation technique + melt crystallization	Defieuw et al. (1989c), Vanneste (1993)
PCL/Phenoxy/ SAN 15[b]	Secondary crystallization	Coprecipitation technique + melt crystallization[h]	Vanneste and Groeninckx (1994)
PEEK/PEI	Secondary crystallization	Melt blended and crystallized	Bassett et al. (1992), Hsiao and Sauer (1994)
LLDPE/LLDPE[c]	Secondary crystallization	Coprecipitation technique + melt crystallization	Defoor et al. (1993)
PCL/PSMA14	Dual crystallization	Melt crystallized	Balsamo et al. (2006)

[a]Reason for this dual melting behavior "is not completely clear," but recrystallization is possibly occurring
[b]SAN containing 15 wt% AN
[c]A blend of 1-octene LLDPE fractions with different short-chain branching content was investigated, i.e., 3 and 33 methyl groups per 1,000 carbon atoms
[d]Solution cast blends followed by melt crystallization
[e]PCL/CPE is only totally miscible for CPE containing 49.1 wt% chlorine
[f]$x = 14$ and 25 wt%
[g]x and y are 25 and 24 wt% and 15 and 14 w%, respectively, in both references
[h]Only the blends with 90 wt% are dealt with since only those combinations were found to be miscible

the lamellae melt and recrystallize, resulting in lower melting endotherm that shifted to lower temperatures the recrystallized lamellae melt at slightly higher temperatures than the thick primary lamellae with a shift to higher temperature and an increase in intensity of the higher melting endotherm (Fig. 3.33).

Fig. 3.32 DSC-heating curves of 85/15 PEO/Aramide blends crystallized at 28 °C for different times (Dreezen et al. 1999)
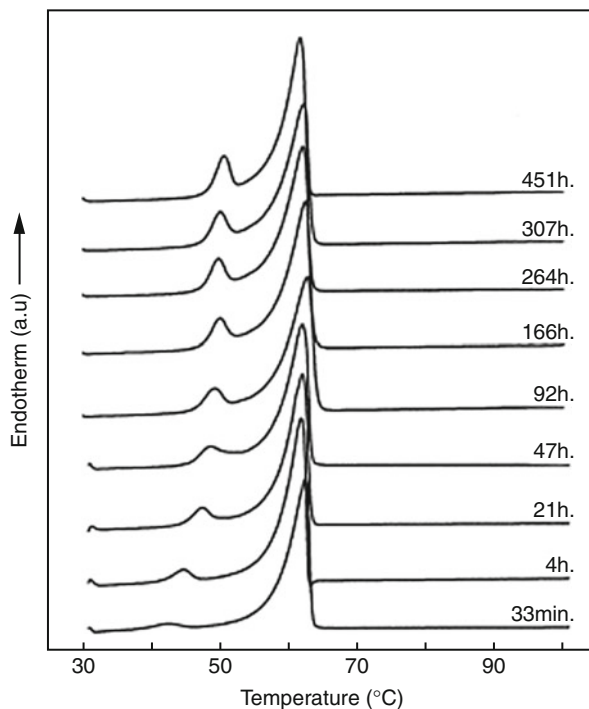
3.2.6 Crystallization Phenomenon in Miscible Thermoplastic/ Thermosetting Blends

Because of the additional parameter of curing a phase, crystallization of blends of a curable amorphous thermosetting with a crystallizable thermoplastic has been poorly reported in literature. Nevertheless, the few blend systems covered are very interesting and show attractive phenomena in terms of crystallization, melting, and phase separation when the thermosetting is cured. Crystallization in thermosetting polymer blends containing a crystallizable thermoplastic component will be affected by the miscibility of the components, the phase behavior of the cross-linked blends, and the topological effect of the formed network. Except for the particular three-dimensional network formed upon chemical curing, the effect of thermosetting curing is almost similar to that of a solidifying phase (cooling below T_g for an amorphous phase or crystallization of a crystallizable phase) in thermo-plastic/thermoplastic blend system. Therefore, we can consider that the utmost effect of the cured phase on the crystallizable phase is the chain mobility restriction. How does the segregation of the cured thermosetting component take place during the crystallization of the semicrystalline component? Prior to any deep investigation of the crystallization phenomenon, a deep understanding of the miscibility of the thermosetting/thermoplastic blends is crucial. The determination of the glass

Fig. 3.33 Schematic representation of the melting mechanism proposed to account for the heating rate dependence of recrystallizing blends. The *left* side of the figure shows the melting of the original crystals (*full line*) and the recrystallization, remelting phenomenon (*dashed line*), while the *right* side shows the resulting experimentally observed thermogram: (**a**) for an 80/20 PEO/Aramide blend; (**b**) for a 65/35 PEO/Aramide blend at fast, intermediate, and slow heating rates (Dreezen et al. 1999)
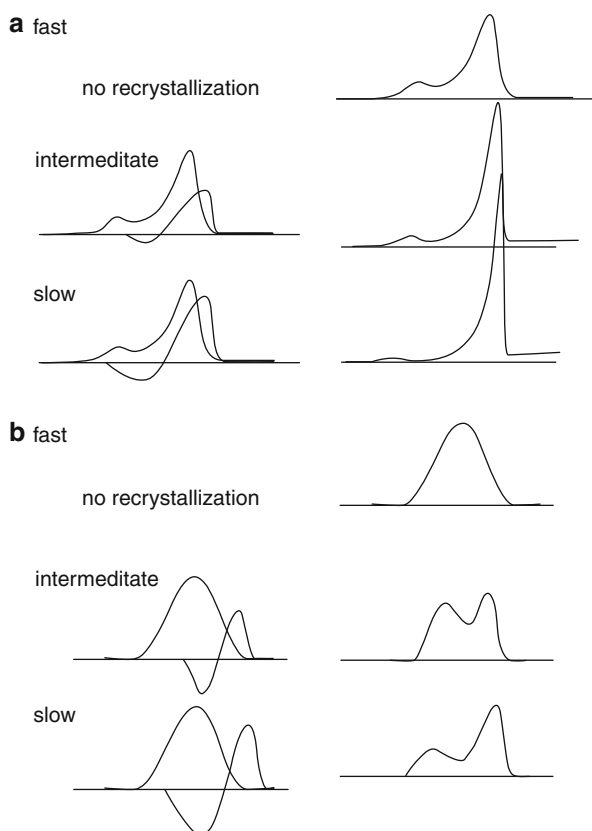
transition as a function of the extent of curing of the thermosetting resin helps for the interpretation of the crystallization results. Other questions remain poorly elucidated including, e.g., to which extent the chains of the thermoplastic component remain intimately in contact to the thermosetting network when curing is achieved. One can expect that a part of the crystallizable phase is entrapped in the formed network of the thermosetting and does not participate to the overall crystallization.

Blends of bisphenol A type epoxy resin (ER) with PEO (Guo et al. 2001a), PCL (Guo et al. 2001b), and POM (Goossens et al. 2006a, b, 2007) are typical examples of thermosetting/thermoplastic blend system studied. The curing of the epoxy resin is usually ensured by using MCDEA curing agent. In Fig. 3.34 the T_g of the blend and the T_c and T_m of the PEO component as a function of the ER/PEO blend composition are plotted. It is clear that the presence of PEO phase reduces the cross-linking density of the ER resin, and hence it is T_g via a dilution and eventually a plasticizing mechanism. Blends with 60 wt% or more ER do not exhibit any crystallization and behave as an amorphous phase. Blends with 50–60 wt% PEO crystallize at higher T_c, indicating chain mobility constraints imposed by the formation of a cross-linked ER network.

Fig. 3.34 Thermal properties of the second scan of the MCDEA-cured ER/PEO blends. (●) Experimental plot of T_g versus overall blend composition, (□) plot of T_g versus calculated amorphous composition, and (————) theoretical curve of T_g versus composition as predicted by the Gordon-Taylor equation using a k value of 0.25. The T_c (cooling) (□) as a function of composition is also given (Guo et al. 2001)
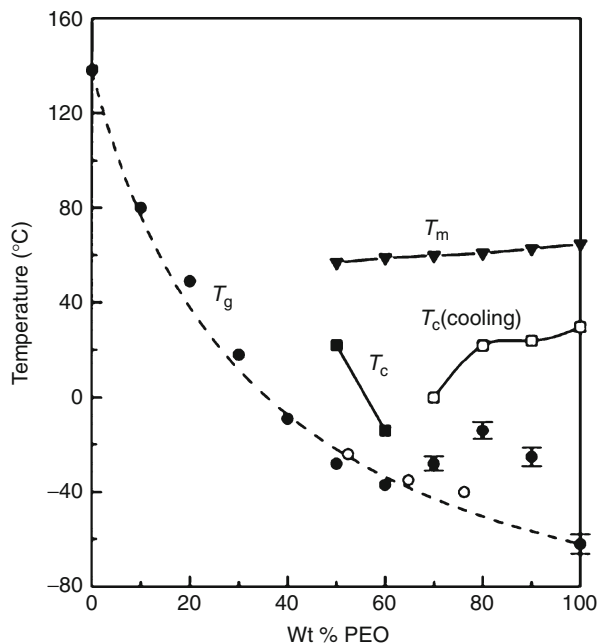
Blends of uncured thermosetting component DGEBA with PCL were compared to blends of cured resin ER with PCL (Guo et al. 2001). In Fig. 3.35 are plotted the measured experimental T_g of the uncured DGEBA/PCL blends as a function of composition. The curve exhibits a mixing rule trend indicating a strong miscibility of the two components. Note that in blends containing 70 wt% or more PCL, the T_g exhibits a positive deviation with respect to the fox mixing rule (broken line), indicating a high crystallinity of the PCL phase. Figure 3.36 shows the T_g of the cured ER/PCL blends, the T_c and T_m as a function of the blend composition. Comparison of the two figures reveals that the uncured DGEBA resin is less constraining the crystallinity of the PCL phase than the cured ER resin. Indeed, the crystallization temperature, T_c, increases with increasing ER content synonymous of the difficult crystallization of PCL in the presence of the cured resin.

The melting depression is less pronounced in the uncured blend than in the cured one. A smaller difference of the Tm's of the two endothermic peaks is depicted between the cured and the uncured DGEBA/PCL blend system. Big differences with respect to the melting behavior compared to classical thermoplastic/thermoplastic miscible blends are revealed. The crystallization of the crystallizable phase was found to be very sensitive to the thermal history as manifested by crystallization peaks observed during the first heating scan, the second heating scan, or the phenomenon of the double melting behavior. Figure 3.37 illustrates these effects for the degree of crystallinity as a function of the PCL content in the cured ER/blend. Substantial differences exist between samples as-prepared, cooled from the melt or quenched. No significant effect is depicted for the cooled or the quenched samples when the content

Fig. 3.35 Thermal transitions of the quenched samples of uncured DGEBA/PCL blends. ($\bullet$) Experimental T_g versus overall blend composition, ($\square$) T_g versus calculated amorphous composition, (——) theoretical curve of T_g according to the fox equation, and ($\square$) T_c cooling (Guo et al. 2001)
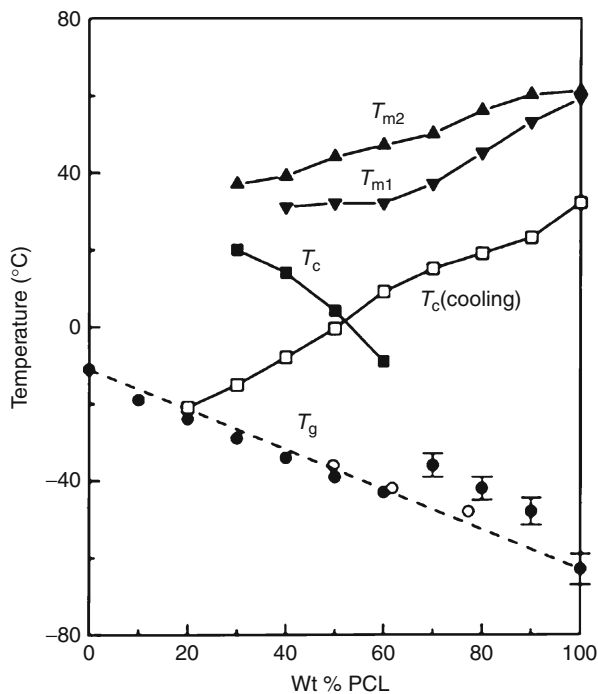
Fig. 3.36 Thermal transitions of the quenched samples of uncured MCDEA-cured ER/PCL blends. ($\bullet$) Experimental T_g versus overall blend composition, ($\square$) T_g versus calculated amorphous composition, (——) theoretical curve of T_g versus blend composition as predicted by the Gordon-Taylor equation using a value of $k = 0.37$, and ($\square$) T_c cooling (Guo et al. 2001)
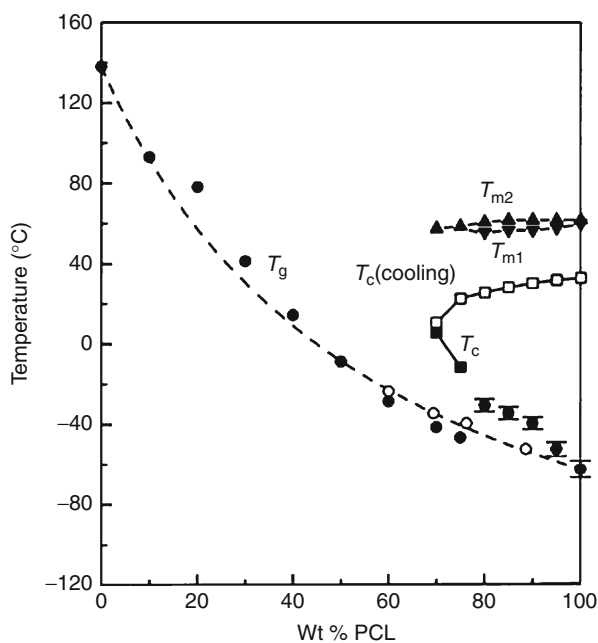
X_c PCL versus
PCL weight fraction of the
MCDEA-cured ER/PCL
blends. (□) as-prepared
samples, (●) quenched
samples, and (□) X_c PCL
developed during the cooling
scan (Guo et al. 2001)
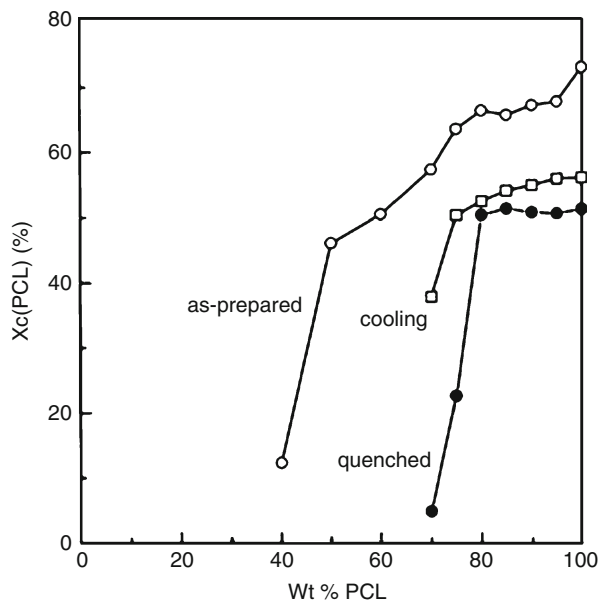
of PCL is equal or above 80 wt%. A drastic decrease of crystallinity is however
registered below this critical concentration. The as-prepared samples exhibit
a decreasing degree of crystallinity when the concentration of PCL is between
100 and 40 wt%.

3.2.6.1 Crystallization Kinetics

The overall crystallization rate of the crystallizable phase in thermosetting/thermo-
plastic miscible blends is greatly affected by the presence of the thermosetting resin
either cured or not (ER cured with MCDEA or uncured DGEBA resin). The
crystallinity of PCL in the cured ER/PCL blend decreases much more rapidly
with increasing amorphous cured ER content than that of the uncured amorphous
DGEBA/PCL blends. The authors ascribed this behavior to the higher T_g of the
cured ER restraining the chain mobility for the PCL and thus limiting the extent and
rate of crystallization ($T_g = 138\ °C$ for the cured ER and $T_g = -11\ °C$ for the
uncured DGEBA system).

Halftime of crystallization $t_{1/2}$ as a function of crystallization T_c for cured
ER/EO blend reveals that addition of cured ER resin to PEO crystallizable ther-
moplastic depresses the overall crystallization rate of PEO, and at a fixed T_c, the
overall crystallization rate decreases significantly with increasing the concentration
of the cured resin ER (Fig. 3.38). Application of the Avrami extrapolation resulted
in *n* values comprised between 3.5 and 5, not changing as the content of ER in the
blend is increased. That means the incorporation of cured ER does not affect
significantly the nucleation, and growth process is under the conditions the authors
selected for the crystallization of PEO.

Fig. 3.38 Halftime of crystallization $t_{1/2}$ as a function of crystallization temperature T_c (Guo et al. 2001)
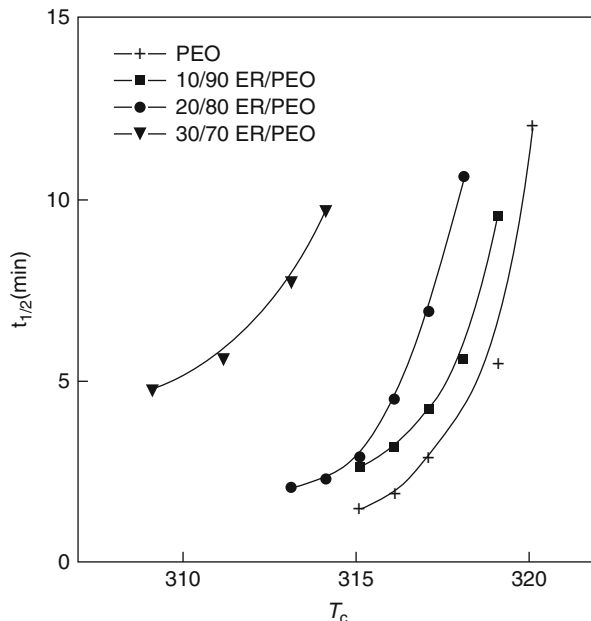
Goossens et al. (2006b, 2007) studied the most challenging aspect which consists of curing the DGEBA and monitoring the crystallization of the POM phase in the DGEBA thermosetting/POM thermoplastic blends system.

The influence of the curing reaction and the resulting reaction-induced phase separation on the crystallization and melting of POM in POM/DGEBA has been studied at two different cure temperatures (180 °C situated above the melting point of POM and 145 °C below it). Various phase morphologies have been generated which allows to investigate the POM crystallization in either a particle-in-matrix or in a phase-inverted phase morphology of POM/DGEBA blends. By using DSC and OM characterization techniques, the authors could demonstrate that at the curing temperature of 180 °C, large differences exist between particle-in-matrix (for 10 wt% POM blends) and phase-inverted structures (20 wt% POM blends) with respect to crystallization behavior. The melting temperatures were almost similar, indicating reorganization in the small POM-rich droplets in the 10 wt% POM blend upon heating. When lowering the curing temperature to 145 °C, isothermal crystallization was induced followed by interspherulitic reaction-induced phase separation (RIPS). Substantial differences were noticed between dynamically and isothermally crystallized POM.

3.2.6.2 Semicrystalline Morphology Development

As in classical amorphous thermoplastic/crystallizable thermoplastic miscible blends, the chains of the thermosetting are rejected from the crystallizing front when the crystallizable thermoplastic is crystallizing in thermosetting/thermoplastic blends. The curing process allows the formation of a network that is not involved
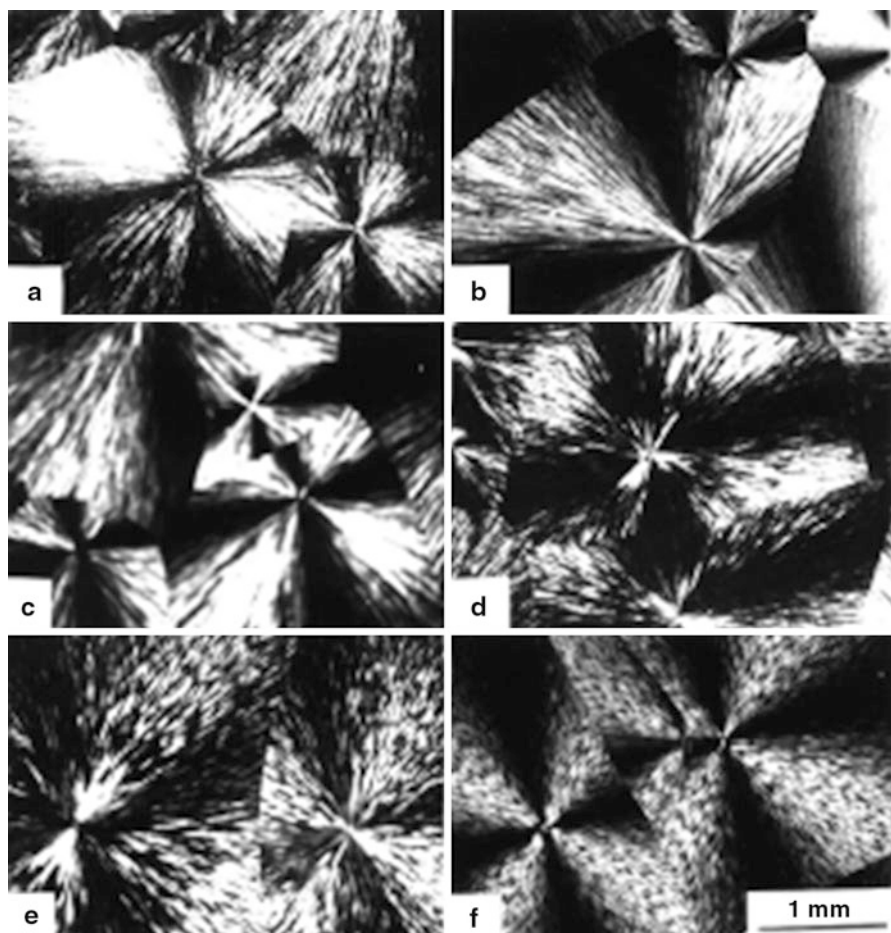
Fig. 3.39 Optical micrographs of ER/PEO blends crystallized at 23 °C. ER/PEO: (**a**) 0/100; (**b**) 10/90; (**c**) 20/80; (**d**) 30/70; (**e**) 40/60; and (**f**) 50/50 (Guo et al. 2001)

in crystallization and is segregated in own domain upon crystallization. The liquid-solid phase separation occurring during the crystallization process of PEO in miscible MCDEA-cured ER/PEO blends requires the segregation and diffusion of amorphous ER away from the crystalline nucleus. The cured ER molecules have a rather limited mobility compared to the linear polymer diluents. Well-defined spherulites were observed in cured ER/PEO blends with ER content up to 50 wt% isothermally crystallized at 23 °C (Fig. 3.39). The spherulitic morphology does not become irregular or coarser with increasing ER content as revealed by OM characterization tools. That indicates that the MCDEA-cured ER is not segregated in the interspherulitic space but must be interlamellarly or interfibrillarly segregated during the process of PEO crystallization. This semicrystalline morphology has been confirmed by using SAXS characterization. The long period increased

Fig. 3.40 Long period, L, as a function of composition for MCDEA-cured ER/PCL blends (Guo et al. 2001)
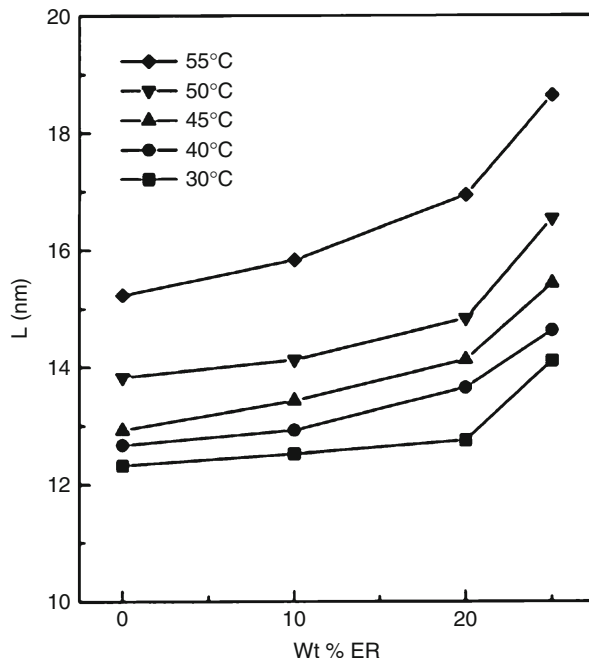
drastically with increasing ER content at all crystallization temperatures. The interlamellar segregation resulting in an increase of the long period has been reported in a number of cases of miscible polymer blends as, e.g., PVC/PCL (Khambatta et al. 1976a, b) or PSMA/PCL (Defieuw et al. 1989a). In contrast to linear (not cross-linked) polymers, cured resins exhibit high viscosity and slow chain mobility which makes its diffusion at the crystallizing front difficult. Similar trends of the long period increase have been reported for PCL/MCDEA-cured ER blends using SAXS techniques (Guo et al. 2001). When the content of the cured ER was increased from 0 to 25 wt%, the long period was increased by almost 1.5 nm at all crystallization temperatures (Fig. 3.40). That is synonymous of interlamellar segregation of the ER resin upon crystallization of PCL.

3.2.7 Coupling of Demixing and Crystallization Phenomena

3.2.7.1 Thermoplastic/Thermoplastic Blends

Tanaka and Nishi (1985) were the first to report about the existence of coupling between crystallization and demixing in crystallizable blends. A competition between demixing and crystallization is seen in binary blends of a semicrystalline and an amorphous polymer when the crystallization curve and the miscibility gap intersect. The morphology of blends exhibiting such behavior is determined by the ratio of the rate of crystallization and of demixing. Four important situations can be distinguished (Fig. 3.41):

Fig. 3.41 Phase diagram of a binary polymer blend with miscibility gap (UCST) and intersecting crystal/melt coexistence curve. The $T_m{}^\circ$ curve is extrapolated into the miscibility gap. Quenching routes *A* to *D* are explained in the text. For routes *B* and *C*, the quenching-induced phase separation and crystallization are indicated. —— binodal, ——— spinodal, and —. crystal/melt coexistence curve (Li et al. 1991)
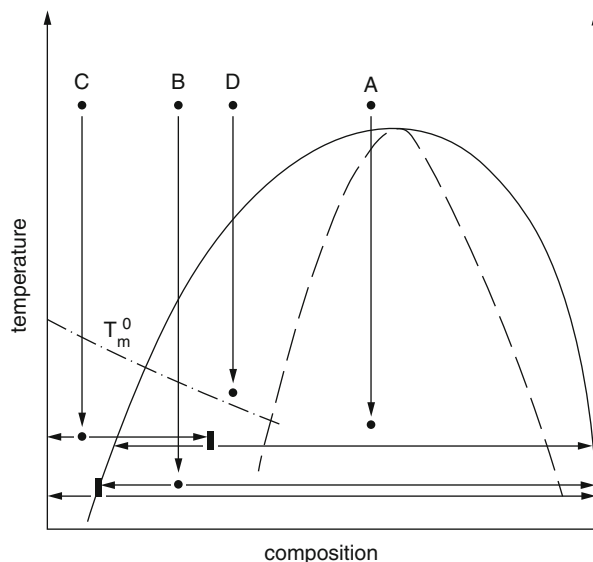
A. **Simultaneous spinodal decomposition and crystallization**
   The blend is quenched into the unstable region of the miscibility gap and to a temperature below the crystallization/melt coexistence curve.
B. **Simultaneous binodal decomposition and crystallization**
   This type is similar to spinodal decomposition, but a composition is quenched into the metastable region of the miscibility gap.
C. **Crystallization induced decomposition**
   The blend is quenched outside the miscibility gap to a temperature below the crystallization/melt coexistence curve. The concentration of the noncrystallizable component increases with crystallization until the miscibility gap is reached inducing demixing.
D. **Decomposition-induced crystallization**
   The blend is quenched into the miscibility gap to a temperature that lies above the crystallization/melt coexistence curve for the actual composition but lies below the crystallization curve for the binodal composition. When the blend is quenched, demixing occurs resulting in two coexisting phases of which one is able to crystallize. The demixing can result in spinodally as well as in binodally decomposed material.

Only few experimental studies have been performed on polymer blends exhibiting one or more of the phenomena described above (see Table 3.13).

Routes A and C of Fig. 3.41 were discussed by Tanaka and Nishi (1985, 1989) for a system consisting of PCL and PS. In case A coarse spherulite results including PS droplets, while in case C the spherulites are separated and show large droplets on their surface (see Fig. 3.42).

Li et al. (1991, 1993) investigated case B and C for the same system, i.e., PCL/low molecular weight PS, for which the phase diagram is presented in Fig. 3.43.

Table 3.13 Polymer blends showing coupling of demixing and crystallization. The routes describing the type of coupling are explained in the text

Polymer blend	Composition	Type of coupling	References
PCL/PS	40/60	Route B	Li et al. (1991)
	60/40	Route C	
PPE/PEG	12.1/87.9	Route B	Shibanov and Godovsky (1989)
	46/54	Route A	
	93.7/6.3	Route B	
PEG/PPG	88/12	Route B	Shibanov and Godovsky (1991)
	54/46	Route A	
	10.3/89.7	Route B	
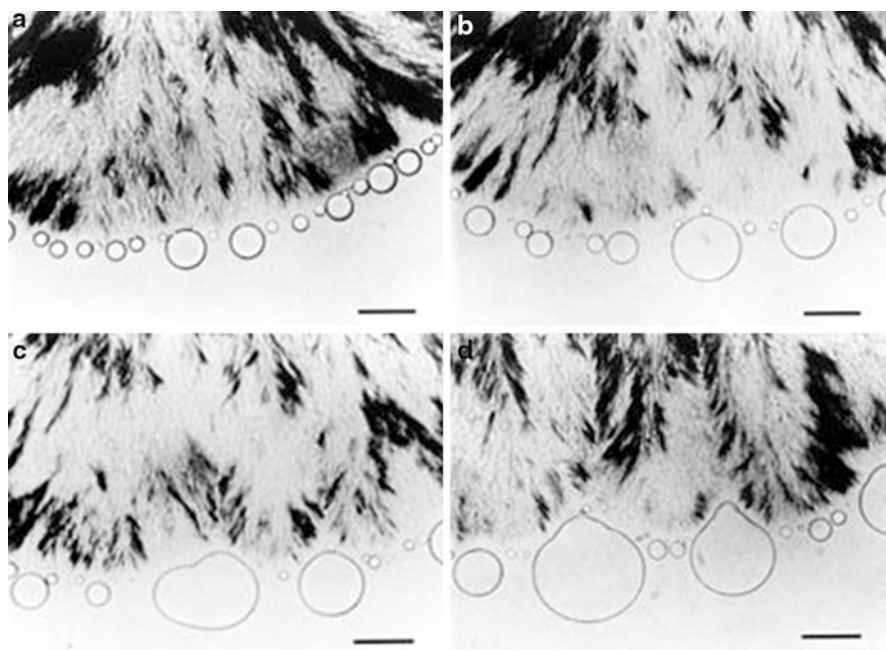
Fig. 3.42 Phase separation behavior at the growth front of the spherulites of PCL during the crystallization process in the PCL/PS 70/30 blend at $T_c = 50$ °C. These morphologies were observed at (**a**) 1,860 min, (**b**) 2,790 min, (**c**) 3,250 min, and (**d**) 4,230 min after quenching (bars: 20 μm) (Tanaka and Nishi 1989)

For route C three different regimes (Fig. 3.44) can still be distinguished depending upon the rate of crystallization, $G = dR/dt$, and the rate of diffusion of the noncrystallizable component, $v_d = (D/t_c)^{1/2}$ (D = diffusion constant and t_c is the correlation time of the macromolecules). Parameters, v_d and G, show a different dependence on temperature (see Fig. 3.45). The growth rate, G, has a maximum

Fig. 3.43 Phase diagram of the PCL/PS blend (*triangles*: homogeneous melt/PCL crystal coexistence curve, *filled circles*: glass-transition curve, *open circles*: spinodal, and *squares*: binodal) (Li et al. 1991)
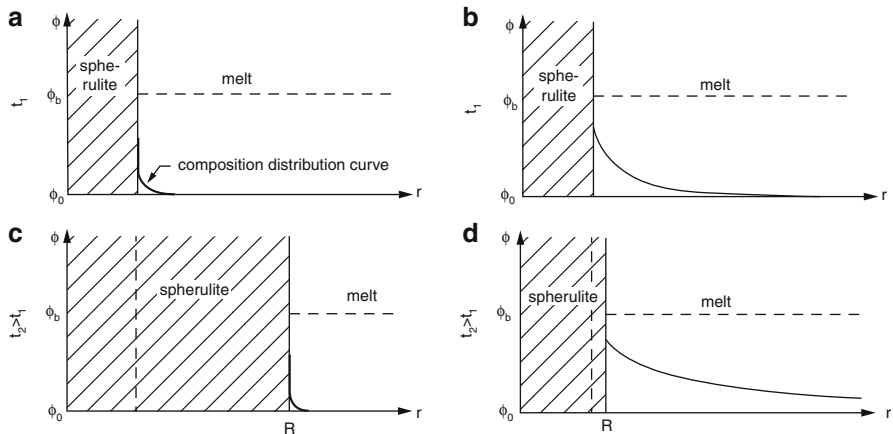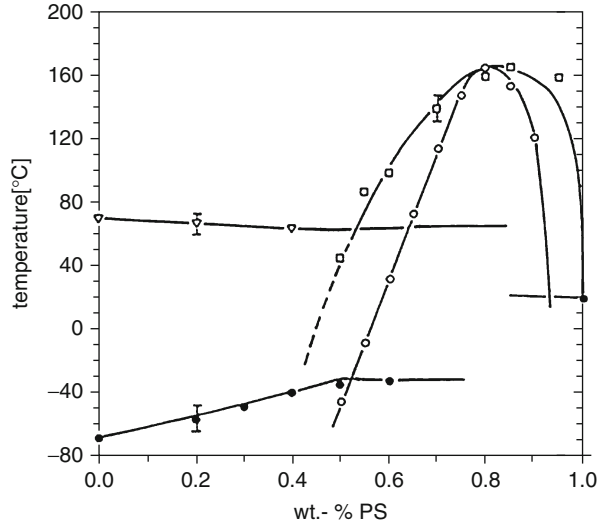
Fig. 3.44 Concentration distribution of PS around a spherulite at different times t and for different ratios G/v_d. ϕ_o, start composition; ϕ_b, binodal composition; and r, local coordinate. (**a**) Regime 1, (**b**) regime 2: the binodal composition is not exceeded, (**c**) as in (**b**) but the binodal composition is exceeded, (**d**) superposition of the concentration distribution curves (*dashed lines*) according to the transition between regime 2 and 3 of two adjacent spherulites (Li et al. 1991)

between the melting temperature and the glass-transition temperature of the blend, whereas the diffusion rate of the amorphous component, v_d, increases with temperature.

1. $v_d \ll G$: the noncrystallizable component is trapped within the growing crystals. Depending on the composition of the amorphous phase, liquid-liquid

Fig. 3.45 Temperature dependence of the diffusion-driven displacement of the noncrystallizing component, v_d, and the spherulitic growth rate G (Li et al. 1991)
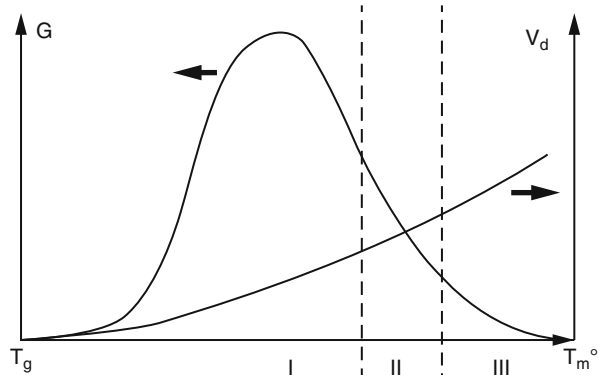
demixing may occur resulting in droplets of noncrystallizing polymer inside the spherulites.

2. $v_d \approx G$: a part of the amorphous component is trapped and another part is segregated from the growing crystals. The concentration of this component increases with crystallization, and finally demixing occurs resulting in the formation of droplets at the spherulite surface.

3. $v_d >> G$: the noncrystalline component is fully segregated into the bulk melt. When the miscibility gap is reached, the melt phase separates homogeneously and binodally.

The crystallization rate is retarded for all regimes, but the extent of hindrance increases from regime 1 to 3. It should be noted that the diffusion of the crystalline polymer occurs on a lamellar scale (about 10 nm), whereas the diffusion of the amorphous component, induced by demixing, takes place on a spherulitic scale (10–20 μm). Under normal processing conditions, crystallization presumably takes place at a higher rate than the demixing.

The morphology resulting from the three regimes are presented in the Fig. 3.46 (regime 1), Fig. 3.47 (regime 2), and Fig. 3.48 (transition from regime 2 to 3) for the PCL/PS system.

A demixing-induced crystallization is shown in Fig. 3.49 (route B in Fig. 3.41) for the binary PCL/PS 40/60 blend.

3.2.7.2 Thermoplastic/Thermosetting Blends

Curing of the thermosetting component and crystallization of the semicrystalline thermoplastic blend partner are two processes that induce phase separation in thermosetting/thermoplastic miscible blend. The new phase morphology that could be generated from the intimately miscible molecules of both components depends on the temperature and kinetics of the curing reaction of the thermosetting resin and of the crystallization of the thermoplastic phase. Semicrystalline thermoplastics like PCL (Guo et al. 2001a, b), PBT (Kulshreshtha et al. 2003a, b), and syndiotactic polystyrene (Schut et al. 2003; Salmon et al. 2005) have been used with curable thermosetting partners with which they form miscible blends before
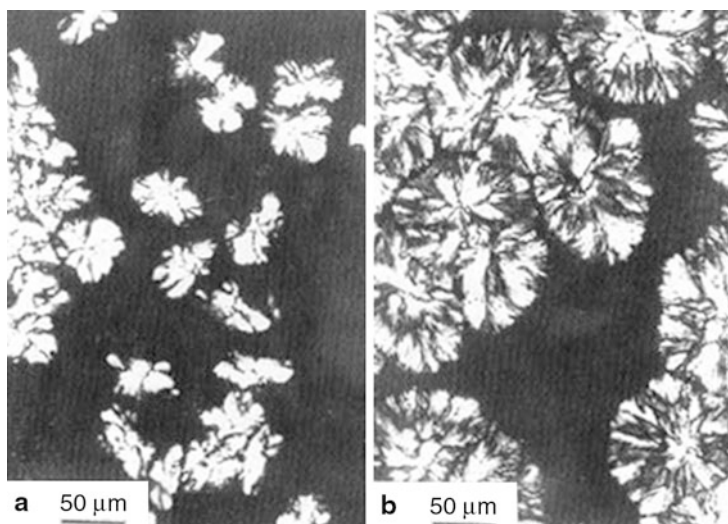
Fig. 3.46 Morphology development in a PS blend with 60 wt% PCL at 44 °C after (**a**) 55 min and (**b**) 126 min (bar: 50 μm) (Li et al. 1991)
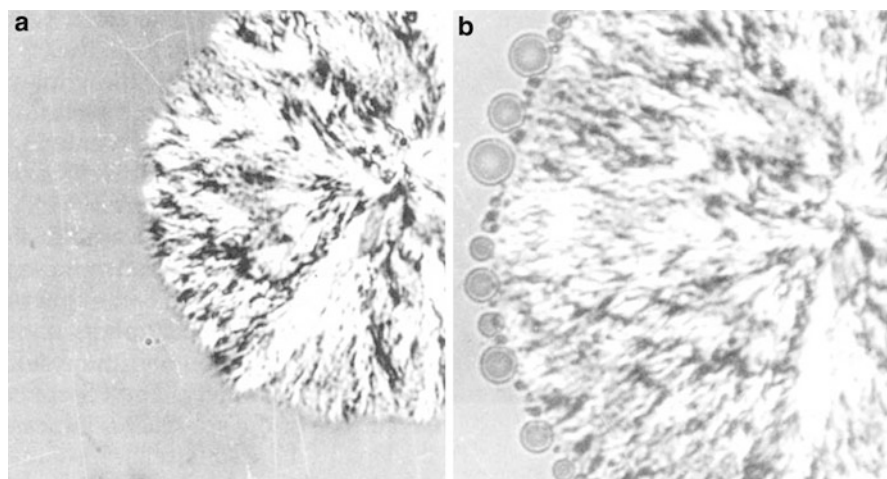
Fig. 3.47 Morphology development in a PS blend with 60 wt% PCL at 49 °C after (**a**) 92 h and (**b**) 142 h (bar: 25 μm) (Li et al. 1991)

any curing or crystallization. Crystallization in thermosetting blends containing a crystallizable thermoplastic component will be affected by the miscibility, the phase behavior and the morphology of the cross-linked blends, and the topological effect of the network (Guo et al. 1991, 2004; Lu et al. 2003; Zheng et al. 2003).
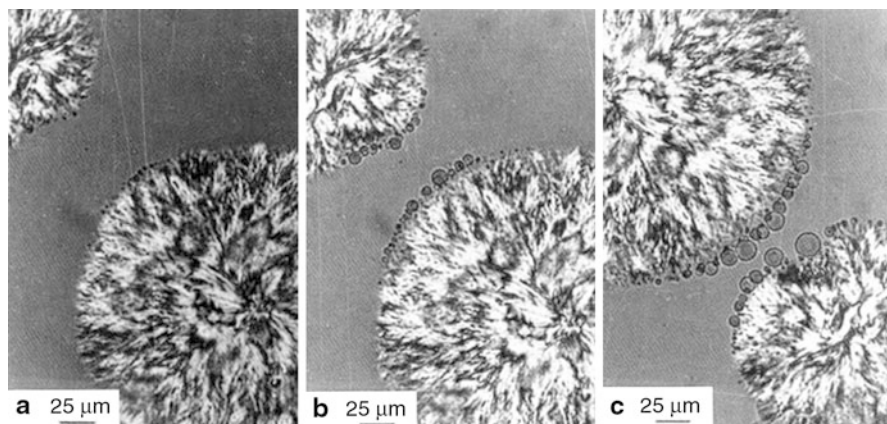
Fig. 3.48 Morphology development in a PS blend with 60 wt% PCL at 51 °C after (**a**) 91.5 h, (**b**) 100 h, and (**c**) 109 h (Li et al. 1991)
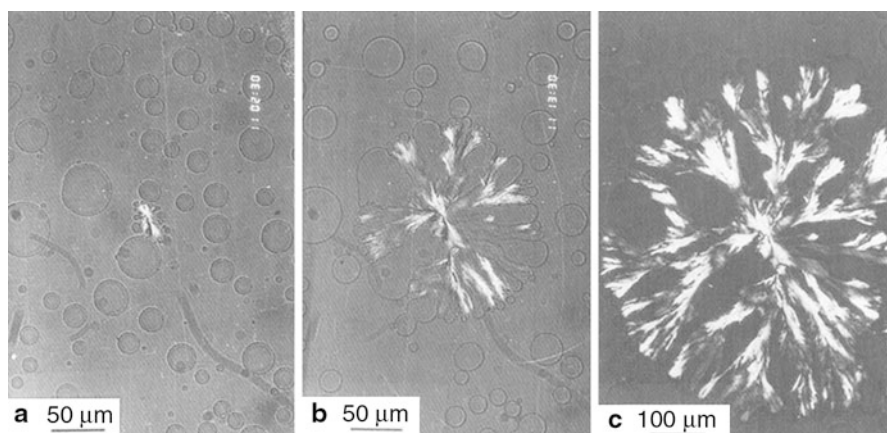
Fig. 3.49 Phase separation followed by crystallization in a PS blend of 40 wt% PCL at 46 °C after (**a**) 2.5 h, (**b**) 13.5 h, and (**c**) 27 h (Li et al. 1991)

By selecting POM/DGEBA/DDS thermosetting/thermoplastic miscible blends, Goossens et al. (2006a, b) could elucidate how the phases are reorganized upon curing of the thermosetting and crystallization of the thermoplastic. Depending on the experimental conditions chosen, crystallization of POM can be investigated before or after the reaction (curing)-induced phase separation (RIPS), i.e., crystallization in homogeneous blend or in a phase-separated one. Three cure temperatures (150, 145, and 140) situated below the melting point of POM were examined. Curing at these temperatures will alter the starting order of the RIPS and crystallization of POM. Both processes will mutually affect each other, leading to complex blend morphologies. Curing at 150 °C is a situation where:
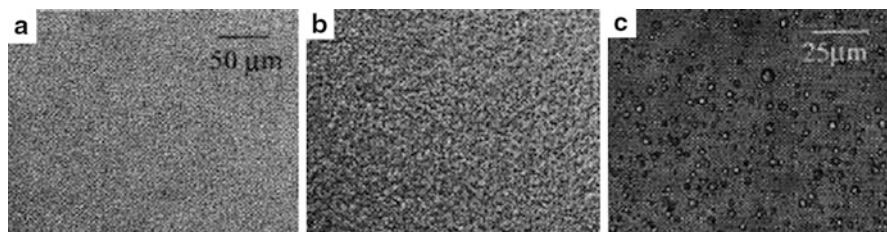
Fig. 3.50 OM pictures of a blend with 10 wt% POM cured at 150 °C for different times: (**a**) 29 min, (**b**) 44 min, and (**c**) 120 min (Goossens et al. 2006a)
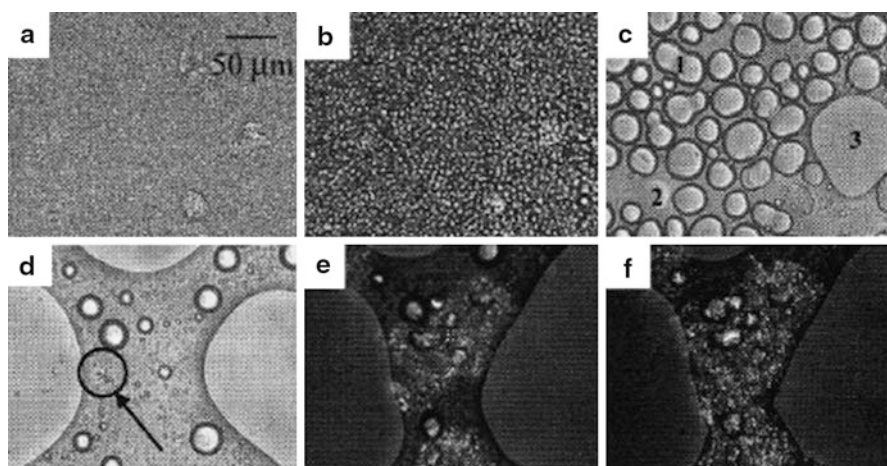
Fig. 3.51 OM pictures of a blend with 20 wt% POM cured at 150 °C for different times: (**a**) 31 min, (**b**) 35 min, (**c**) 41 min, (**d**) 45 min, (**e**) 66 min, and (**f**) 71 min (Goossens et al. 2006a)

(i) *Phase separation precedes the isothermal crystallization* (*curing at* 150 °C).
As a consequence of RIPS due to curing, the three initially miscible blends, containing 10, 20, and 30 wt% POM, evolved to a co-continuous and then to a droplet (POM rich)-in-matrix (epoxy rich) phase morphologies (Figs. 3.50, 3.51 and 3.52). For the blends with 10 wt% POM, no isothermal crystallization was depicted because the difference between the cure temperature (150 °C) and the homogeneous crystallization temperature (85 °C) was too large to induce homogeneous crystallization in the dispersed POM-rich droplets. In contrast, at a content of 20 wt%, POM isothermal crystallization was observed after phase separation has set in via successive spinodal demixing, break up into epoxy-rich droplets dispersed in a POM-rich matrix and coalescence which increased particle size. Fifteen minutes after, the liquid-liquid demixing has set in, and growing spherulites were observed in the POM-rich matrix phase in between the epoxy droplets. The growth of spherulites in the POM-rich matrix was also observed during the phase separation process of a 30 wt% POM blend, cured at 150 °C.
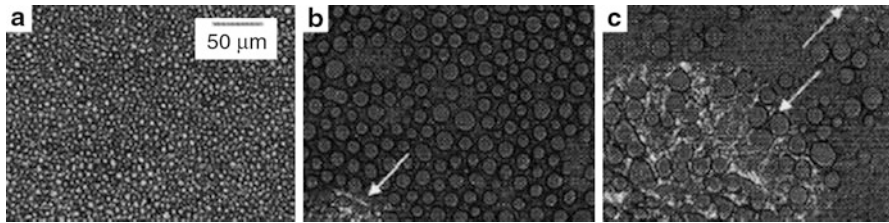
Fig. 3.52 OM pictures of a blend with 30 wt% POM cured at 150 °C for different times: (**a**) 50 min, (**b**) 66 min, and (**c**) 92 min (Goossens et al. 2006a)

(ii) *Isothermal crystallization followed by phase separation* (*curing at* 145 °C).
At this curing temperature, isothermal crystallization starts before the liquid-liquid phase separation as caused by the curing of the epoxy resin. Homogeneous blends containing 5 wt% POM developed spherulites after 22 min. Thirty three minutes later, interspherulitic zone starts to phase separate leading to a co-continuous phase structure. While the liquid-liquid phase separation proceeds, the spherulites continue to grow through the POM-rich continuous part of the co-continuous structure. Crystallization stops as the phase structure evolved to a droplet-matrix as POM molecules need to diffuse through the highly viscous cured epoxy. The authors could differentiate between three zones within the POM spherulite: zone 1 is the spherulite growth in the homogeneous sample where no RIPS occurs yet, zone 2 is the spherulite growth in the co-continuous structure, zone 3 is limited because of the slow diffusion of very diluted POM molecules in the epoxy-rich matrix, and, finally, zone 4 which represents the volume hat has been phase separated but did not undergo crystallization at 145 °C. Blends containing 10 wt% POM exhibits the same trend. In contrast, increasing the POM content beyond 10 wt% gave a different phase-separated process. For example, the co-continuous structure was found to break up in a phase-inverted structure instead of a particle/matrix structure. Increasing the amount of POM resulted in higher nucleation density and an increased crystallization growth rate.

(iii) *Isothermal crystallization without phase separation* (*curing at* 140 °C).
Decreasing the cure temperature to 140 °C will increase the supercooling and consequently the nucleation density. Indeed, when a blend with 20 wt% POM was cured at 140 °C, spherulites appeared as early as 1 min which is a direct result of the higher supercooling. After 20 min the spherulites are almost volume filling due to higher nucleation density and the higher local crystallization rate. This suggests that nearly all the epoxy resin is rejected interlamellar or interfibrillar.

3.2.8 Conclusions

Most of the fundamental and experimental aspects related to the crystallization phenomena occurring in miscible polymer blends are relatively well known. Much research has been done in the 1970s and 1980s, especially the development of the

general theory concerning the crystallization process itself and the concomitant kinetics. These theories could be adapted to simple systems under quiescent conditions. Later, modifications have been made to the original concepts to take into account the effects occurring under processing conditions (for instance, the nonisothermal Avrami theory), unusual phenomena not responding to the simple theory (for instance, the nonlinearity of Hoffman-Weeks plots), coupling of the crystallization with demixing processes, etc.

The addition of a second component to a crystallizable polymer has several profound consequences:

1. Depending on the glass-transition temperature of the added component, the crystallization window is widened or narrowed.
2. The type of added component is also important. Crystallization in the presence of an amorphous component is paralleled to segregation. The segregation can occur into three regions: interspherulitic, interfibrillar, and interlamellar, depending on the ratio of the diffusion rate of the amorphous component and of the crystallization rate of the crystallizable component. In blends of two crystallizable polymers, the phenomena such as separate crystallization, concurrent crystallization, and cocrystallization may take place.
3. The spherulite growth rate changes by blending due to interactions between the components, the necessity of diffusion of both components, the concentration change in the amorphous phase during crystallization, and the possible changes of the glass-transition and melting temperature.
4. The overall kinetics are strongly affected by the type of amorphous component, its influence on the nucleation of the crystallizable component, the degree of miscibility, the presence of secondary nucleation effects, and the molecular weight of both components.
5. The melting behavior is often complex due to phenomena such as reorganization, secondary crystallization, demixing, etc. A depression of the equilibrium melting temperature is often observed.
6. In case of thermosetting/thermoplastic initially miscible blends, the duration and the curing temperature of the thermosetting are crucial conditions which determine the crystallization kinetics, the type of semicrystalline phase morphology generated, as well as the melting behavior of the semicrystalline partner of the blend. Depending on the temperature at which crystallization is carried out, competition between demixing and crystallization can take place.

3.3 Crystallization, Morphological Structure, and Melting Behavior of Immiscible Polymer Blends

3.3.1 Introduction

From a commercial point of view, semicrystalline polymers are of prime importance. Among the four mostly used commodity plastics (PE, PS, PVC, and PP), only PS is completely amorphous. The three semicrystalline polymers account for the

largest volume of the commercial polymer blends. A majority of the polymer blends contains at least one crystalline component. Most polymer blends are immiscible.

The immiscible semicrystalline polymer blends may be classified in terms of crystalline/crystalline systems in which both components are crystallizable and crystalline/amorphous systems in which only one component can crystallize, being either the matrix or the dispersed phase (Utracki 1989). Numerous authors have been investigating the crystallization behavior of immiscible blends. In Tables 3.14 and 3.15, an overview is given of a number of important immiscible crystallizable blend systems.

The properties of the finished articles made from immiscible blends are governed by the morphology created as a result of the interplay of processing conditions and inherent polymer characteristics, including crystallizability. Therefore, a scientific understanding of the crystallization behavior in immiscible polymer blends is necessary for the effective manipulation and control of properties by compounding and processing of these blends.

In the following part, a discussion on the crystallization behavior in immiscible polymer blends is given, including the nucleation behavior, spherulite growth, overall crystallization kinetics, and final semicrystalline morphology. Each topic is illustrated with several examples from the literature to allow the reader to find enough references on the discussed subject for further information.

3.3.2 Factors Affecting the Crystallization Behavior of Immiscible Polymer Blends

The discussion on the crystallization behavior of neat polymers would be expected to be applicable to immiscible polymer blends, where the crystallization takes place within domains of nearly neat component, largely unaffected by the presence of other polymers. However, although both phases are physically separated, they can exert a profound influence on each other. The presence of the second component can disturb the normal crystallization process, thus influencing crystallization kinetics, spherulite growth rate, semicrystalline morphology, etc.

Important factors are:
– Molecular structure and molecular mass of the components
– Blend composition
– Type and degree of dispersion of the phases in the melt state
– Phase interactions (e.g., nature of the interface, migration of nuclei, etc.)
– Melt history (T_{melt}, t_{melt}, etc.)
– Crystallization conditions (e.g., T_c, cooling rate, etc.)
– Physical crystallization conditions (surrounded by melt or solidified material)

These factors influence the crystalline morphology development, resulting in changes of crystallization parameters such as:
– Nucleation density, N
– Spherulite growth rate, G

Table 3.14 Thermal data on immiscible crystalline/amorphous blends (After Nadkarni and Jog 1991)

Comp. A (cryst.)	Comp. B (amorph.)	$T_{g,A}$ (°C)	$T_{g,B}$ (°C)	$T_{c,pure\ A}$ (10°C/min)	$T_{m,\ pure\ A}$	Physical state of the amorph. comp. at T_c	References
LDPE	PS	−123	103	101	115–123	±solidified	Baïtoul et al. (1981)
LDPE	PMMA	−123	100–123	101	115–123	Solidified	
LDPE	PC	−123	147	101	115–123	Solidified	
LLDPE	PS	−123	103	102–110	125	Viscous melt/ ±solid	Müller et al. (1995), Morales et al. (1995)
HDPE	PS	−123	103	118	132–140	Melt	Aref-Azar et al. (1980)
HDPE	PC	−123	147	118	132–140	Solidified	Kunori and Geil (1980)
PP	EPDM[a,b]	−10	100	121	165	Melt	Martuscelli (1984, 1985), Bartczak et al. (1984), Martuscelli et al. (1983), Karger-Kocsis et al. (1979), Greco et al. (1987)
PP	EPR[a,b]	−10	±−45	121	165	Melt	Martuscelli et al. (1982), Coppola et al. (1987), Bartczak et al. (1984), Kalfoglou (1985), Karger-Kocsis et al. (1979), Martuscelli (1985)
PP	PIB[b]	-10	–	121	165	Melt	Martuscelli (1984, 1985), Bartczak et al. (1984), Martuscelli et al. (1982, 1983), Bianchi et al. (1985)
PP	PS	−10	103	121	165	Melt	Bartczak et al. (1987), Wenig et al. (1990), Wei-Berk (1993), Santana and Müller (1994), Han et al. (1977), Hlavatá and Horák (1994)

(continued)

Table 3.14 (continued)

Comp. A (cryst.)	Comp. B (amorph.)	$T_{g,A}$ (°C)	$T_{g,B}$ (°C)	$T_{c,pure\ A}$ (10°C/min)	$T_{m,pure\ A}$	Physical state of the amorph. comp. at T_c	References
PP	PC	−10	147	121	165	Solidified	Ghijsels et al. (1982), Karger-Kocsis et al. (1979)
PP	TR (SBS)	−10	–	121	165	Melt	Nadkarni and Jog (1987)
PET	PMMA	70	100–123	150	257	Melt	Quirk et al. (1989)
PET	PS	70	103	150	257	Melt	Quirk et al. (1989), Liang and Pan (1994)
PET	PPE	70	215	150	257	Solidified	
PVDF	PVME	−45		140	172		
PEG	PS	−60	103	40	65	Solidified	Lotz and Kovacs (1969)[c], O'Malley et al. (1969)[c]
PEG	PI	−60	10	40	65	Viscous melt	Robitaille and Prud'homme (1983)[d]
POM	PS	−80	103	143	170	Melt	Chang et al. (1991)
POM	PC	−80	147	143	170	±solidified	
PA-6	PC	52	147	199	210	Viscous melt	Ide and Hasegawa (1974), Chen et al. (1988)
PA-6	PS	52	103	199	210	Melt	Martuscelli (1984)
PA-6	Elastomer	52	–	199	210		
sPS	PVME[e]	95	−28	±245	270	Melt	Cimmino et al. (1991, 1993)
PEMA	PMMA	67	105				Kwei et al. (1977)

[a] EPR and EPDM are amorphous only if they are random copolymers

[b] Small and defective PP molecules or amorphous PP chains are partially soluble in the elastomer phase; this can lead to a slightly deviating behavior Martuscelli et al. (1983), Kalfoglou (1985)

[c] Studies have been done on block copolymers of either PEG-PS-PEG or PEG-PS

[d] Studies were done on liquid/liquid phase-separated triblock copolymer PEG-PI-PEG

[e] sPS/PVME is immiscible as long as the PVME content is higher than 10 %

Table 3.15 Thermal data on immiscible crystalline/crystalline blends (After Nadkarni and Jog (1991))

Comp. A (matrix)	Comp. B (minor)	$T_{g,A}$	$T_{g,B}$	$T_{c,A}$	$T_{c,B}$	$T_{m,A}$	$T_{m,B}$	Physical condition for cryst. of A/B		References
LLDPE	PP	−123	−10	102–110	121	125	165	Solid	Melt	Zhou and Hay (1993), Long et al. (1991), Müller et al. (1995), Morales et al. (1995)
LDPE	PP	−123	−10	101	121	115–123	165	Solid	Melt	Teh (1983)
HDPE	EPR[a]	−123	±−40	118		132–140		Viscous melt	Solid	Greco et al. (1987a)
HDPE	PA-6	−123	52	118	199	132–140	225	Solid	Melt	Chen et al. (1988)
HDPE	PP	−123	−10	118	121	132–140	165	Solid	Melt	Bartczak and Galeski (1986), Martuscelli et al. (1980), Rybnikâr (1988)
HDPE	POM	−123	−80	101	143	115–123	170	Solid	Melt	Frensch et al. (1989), Klemmer and Jungnickel (1984)
HDPE	PPS	−123	80	118	256	132–140	280	Solid	Melt	Nadkarni et al. (1987), Nadkarni and Jog (1986), Chen and Su (1993)
PE	PA-11	−123	47	100–120		115–140	180	Solid	Melt	Chen et al. (1988)
PP	LLDPE	−10	−123	121	102–110	165	125	Melt	Solid	Long et al. (1991), Flaris et al. (1993), Zhou and Hay (1993), Plawky and Wenig (1994), Müller et al. (1995)
PP	HDPE	−10	−123	121	118	165	132–140	Supercooled melt	Solid	Bartczak et al. (1986), Noel and Carley (1984), Teh et al. (1994a), Lovinger and Williams (1980),

(continued)

Table 3.15 (continued)

Comp. A (matrix)	Comp. B (minor)	$T_{g,A}$	$T_{g,B}$	$T_{c,A}$	$T_{c,B}$	$T_{m,A}$	$T_{m,B}$	Physical condition for cryst. of A/B		References
PP	LDPE	−10	−123	121	101	165	115–123	Melt	Solid	Wenig and Meyer (1980), Teh et al. (1994b), Gupta et al. (1982), Martuscelli et al. (1980), Rybnikár (1988), Bartczak et al. (1984), Martuscelli (1985), Galeski et al. (1984), Teh (1983), Teh et al. (1994a)
PP	EPR[a]	−123	±−30	121		165	±125	Melt	Solid	Greco et al. (1987b), Martuscelli (1984)
PP	PA-6	−10	52	121	199	165	210	Solid	Melt	Liang et al. (1983)[b], Ikkala et al. (1993), Moon et al. (1994), Park et al. (1990), Grof et al. (1989)[b], Ide and Hasegawa (1974)
PP	PA-12	−10		121	154	165	171–179	Solid	Melt	Tang et al. (1994)
PP	PEG	−10	−60	121	38	165	65	Melt	Solid	Bartczak and Galeski (1986), Tang and Huang (1994b)
PP	PVDF	−10	−45	121	140	165	172	Solid	Supercooled melt	
Shingankuli et al. (1988)										
PET	HDPE	70	−123	150	118	257	132–140	Melt	Solid	Wilfong et al. (1986)
PET	LLDPE	70	−123	150	102–110	257	125	Melt	Solid	Wilfong et al. (1986)
PET	PP	70	−10	150	121	257	165	Melt	Solid	Wilfong et al. (1986)
PET	PPS	70	80	150	256	257	280	Solid[c]	Melt[c]	Shingankuli et al. (1988)
PPS	HDPE	80	−123	256	118	280	132–140	Superheated melt	Solid	Nadkarni et al. (1987), Nadkarni and Jog (1986), Jog et al. (1993)

PPS	PET	80	70	256	150	280	257	Supercooled melt	Solid	Shingankuli et al. (1988), Jog et al. (1993)
PA-6	PP	52	−10	199	121	225	165	Melt	Solid	Ikkala et al. (1993), Holsti-Mietinen et al. (1992), Park et al. (1990), Ide and Hasegawa (1974), Tang and Huang (1994a)
PA-6	HDPE	52	−123	199	118	225	132–140	Melt	Solid	Chen et al. (1988)
PA-6	LLDPE	52	−123	199	102–110	225	125	Melt	Solid	
PA-6	PVDF	52	−45	199	140	225	172	Melt	Solid	Frensch and Jungnickel (1989, 1991), Frensch et al. (1989)
PA-66	PVDF	60	−45	229	140	264	172	Melt	Solid	Frensch and Jungnickel (1991)
PA-6	POM	52	−80	199	143	225	170	Melt	Solid	
PVDF	PA-6	−45	52	140	199	172	210	Solid[c]	Melt[c]	Frensch and Jungnickel (1989), Frensch et al. (1989)
PVDF	PA-66	−45	60	140	229	172	264	Solid	Melt[c]	Frensch and Jungnickel (1991)
PVDF	PBT	−45	35	140	180	172	225	Solid[c]	Melt[c]	Frensch and Jungnickel (1989), Frensch et al. (1989)
PVDF	PCL	−45	−60	140	172	172	60	Melt	Solid	

[a]EPDM and EPR copolymers are crystalline if block copolymer and depending on the ethylene/propylene ratio; in blends with PE or PP, they can extract to some extent (depending on the ethylene/propylene ratio) amorphous low molecular weight molecules from the PP or PE phase that slightly influence the crystallization and melting behavior

[b]Study done on fibers

[c]Sometimes coincident crystallization occurs in finely dispersed morphology

– Overall crystallization rate, K
– Total degree of crystallinity, X_c
– Semicrystalline morphology, i.e., shape, size, and texture of the spherulites, interspherulitic boundaries, etc.

To discuss these topics in a systematic way, a distinction will be made between three main blend categories, namely:
1. Blends with a crystallizable matrix and an amorphous dispersed phase
2. Blends with an amorphous matrix and a crystallizable dispersed phase
3. Blends containing two crystallizable components

3.3.3 Blends with a Crystallizable Matrix and an Amorphous Dispersed Phase

In immiscible blends, the phases are separated in the molten state, thus before crystallization of the matrix starts. The dispersed amorphous phase is assumed to be homogeneously distributed in the melt in droplet-like domains.

3.3.3.1 Nucleation Behavior of the Crystallizable Matrix
General Considerations Related to Heterogeneous Nucleation
When a crystallizable component forms the matrix phase in a polymer blend, nucleation can occur via *heterogeneous nucleation* by heterogeneities in a similar way as in the pure component. The heterogeneities, available in the melt, can be residual catalysts, fillers, impurities, crystalline residues (due to incomplete melting), etc. Each type of "heterogeneity" has its own typical activation energy for the formation of an "active nucleus of critical size," corresponding to a certain degree of undercooling $(T_m - T_c)$. When $T_{c,1}$ is reached during cooling from the melt, all heterogeneities of type 1 (which have the lowest activation energy) become active and the nucleation of the crystallizable phase is induced. Once the crystallization is initiated by the primary nucleation, it can further spread over the whole available material via secondary nucleation, before any other type of heterogeneity can become active.

Since in immiscible blends the phases are physically separated, the same heterogeneities that nucleate the homopolymer at $T_{c,pure}$ may nucleate the crystallizable matrix. As a result, the crystallization temperature, T_c, of the blend during cooling from the melt will in general not differ that much from the T_c of the pure component.

Some general principles governing the crystallization behavior of homopolymers also remain valid for immiscible polymer blends in which the crystallizable component forms the continuous phase.

The *premelting temperature*, T_{melt}, may have a profound influence on the crystallization temperature of the matrix, T_c, during cooling from the melt (Table 3.16).

The higher the temperature at which the blend is kept in the melt prior to crystallization, the less residual crystalline parts (otherwise leading to self-seeded

Table 3.16 Influence of T_{melt} and $T_{c,iso}$ upon the nucleation behavior in crystalline/amorphous polymer blends

Blend system	Influence of T_{melt}	Influence of $T_{c,iso}$	References
PP/EPDM		x	Martuscelli et al. (1983)
		x	Martuscelli (1985)
PP/EPR		x	Martuscelli et al. (1982)
	x	x	Martuscelli (1985)
PP/PIB		x	Bianchi et al. (1985)
		x	Martuscelli (1985)
PP/PS	x	x	Bartczak et al. (1987)
		x	Wenig et al. (1990)
sPS/PVME[a]		x	Cimmino et al. (1993a)

[a]sPS/PVME is only immiscible in those blends where the amount PVME exceeds 10 %

nucleation) remain in the melt. As a result, fewer nuclei are available to nucleate the melt phase, thus leading to the formation of fewer but larger spherulites.

Another less important factor is the *isothermal crystallization temperature*, $T_{c,iso}$, when the crystallization is carried out at a constant temperature (Table 3.16). When a crystallization experiment is performed at lower temperatures, the activation energy for nucleation of several types of heterogeneities can be overcome. At that $T_{c,iso}$, more nuclei become active, leading to the formation of a larger number of smaller spherulites.

Although most principles for the crystallization of homopolymers remain valid for immiscible blends with a crystallizable matrix, the crystallization behavior can be altered by two phenomena, inherently correlated with immiscible two-phase systems, namely, migration of impurities during melt-mixing and the nucleating activity of the interface between two phases.

Migration of Impurities During the Melt-Mixing Process
During the melt-mixing process, heterogeneous impurities can migrate across the interface between both blend phases (Bartczak et al. 1986). The driving force for this migration is the interfacial free energy of the impurity with respect to its melt phase, $\sigma_{i,1}$. If this interfacial free energy is higher than the interfacial free energy of that impurity within the second melt phase, $\sigma_{i,2}$, it is energetically more favorable for the impurity to move to the second phase. As soon as it has the "possibility," it will migrate across the interface (Galeski et al. 1984).

Several factors determine the "possibility" for the impurities to migrate from one phase to the other phase during the melt-mixing process.

Because the migration of heterogeneities can only occur when they find themselves close enough to the interface, the melt-mixing conditions play an important role (Bartczak et al. 1987; Fig. 3.53). It must be clear that the longer the mixing or the more intense the mixing, the higher the probability that nuclei find themselves somewhere at an interface, where they can easily migrate. Thus, the effect of migration on the crystallization behavior will be more pronounced – migration of
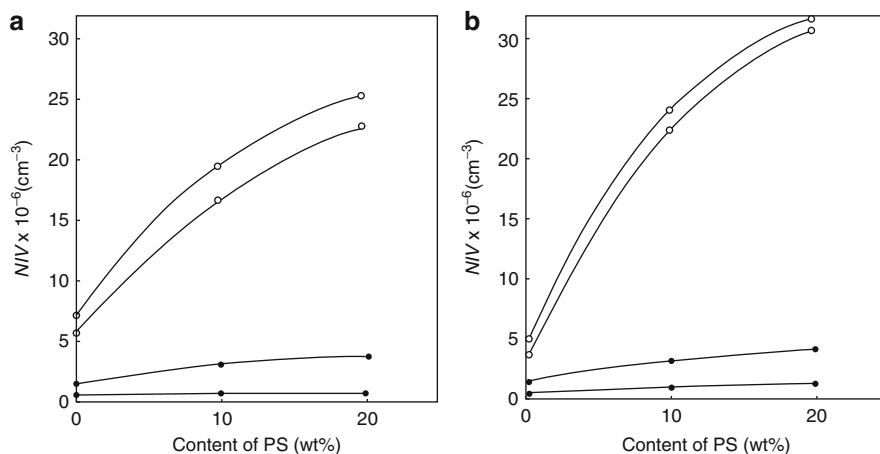
Fig. 3.53 Influence of the amount of dispersed phase, mixing time, and crystallization temperature, T_c, on the amount primary nuclei active for crystallization at T_c in a PP/PS blend. All samples have been molten up at 220 °C; (**a**) 2× mixing, (**b**) 3× mixing; $T_{c,iso}$ was set to 119 °C (∇), 123 °C (Δ), 125 °C ($\bigcirc$), and 130 °C ($\square$) (Bartczak et al. 1987)

heterogeneities across the interface will not proceed in the absence of mechanical mixing (Bartczak et al. 1987). Furthermore, the possibility for impurities to be located close enough to an interface stands in direct relation to the phase morphology generated during the melt-mixing (Bartczak et al. 1987).

As the relative amount of the phases changes, the amount of nuclei that can migrate varies, and the effect of these migrating nuclei on the crystallization behavior changes. This can be understood if one assumes an amorphous/crystalline blend system in which heterogeneities migrate from the crystallizable matrix toward the second phase. With increasing amount of the second phase, the total amount of available nuclei is lower, and they will migrate toward a larger volume of the second phase, which may lead to a more than proportional decrease of the nucleation density in the crystallizable phase.

However, the melt morphology also changes with varying content of the phases. By increasing the amount of the second phase, the dispersion becomes coarser due to coalescence of droplets. This implies that larger droplets are formed, and as a consequence, a lower total interfacial contact area is available. Hence, less impurities will find themselves located close enough to the interface to be able to migrate. It should be remarked that a critical volume fraction of the second component could exist, which is able to absorb all active nuclei of the crystallizable matrix. Adding higher amounts of the second component will no longer decrease the number of active nuclei per volume unit of the crystallizable matrix. An example is given for the PP/LLDPE blend, where LLDPE is in the molten state during PP crystallization (and thus can be considered as an amorphous melt) (Fig. 3.54).

Fig. 3.54 Influence of LLDPE on the nucleation of PP at various temperatures: (**a**) measured as blend volume and (**b**) calculated as PP volume fraction (Long et al. 1991)
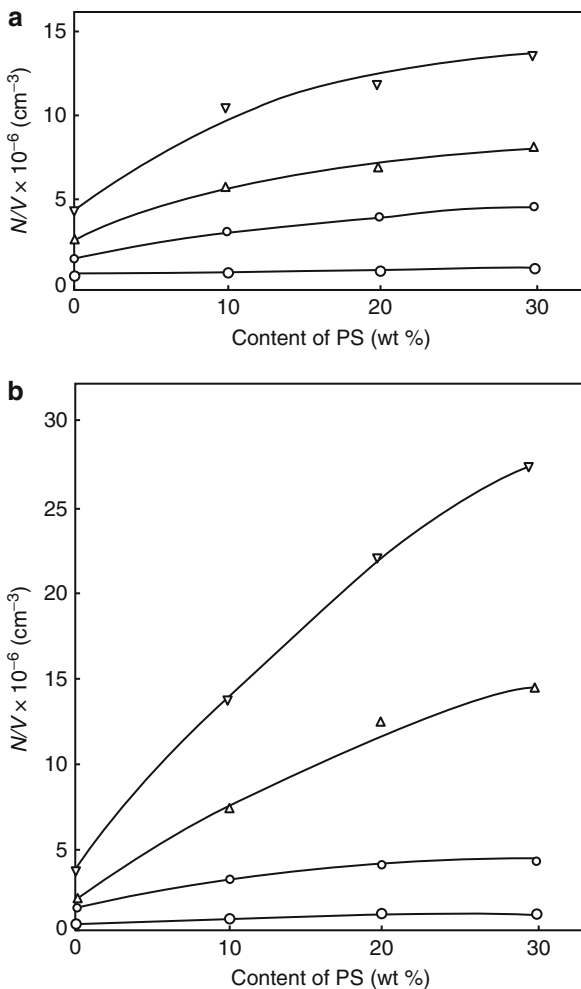
Finally, a factor that also may influence the degree of migration is found to be the *interfacial free energy between both phases of the blend in the melt*, $\sigma_{1,2}$. If $\sigma_{1,2}$ is high, due to a high degree of immiscibility between the phases, a sharper interface will be formed. Nuclei close to such a sharp interface are found to migrate fast and efficient (Bartczak et al. 1987), in contrary to partially miscible blends where no evidence could be found for such a fast migration (Galeski et al. 1984; Bartczak et al. 1986).

In general, the migration of heterogeneities from one phase to the other in blends with a crystallizable matrix only slightly affects the crystallization temperature of the matrix during cooling from the melt (Bartczak et al. 1987). More important should be the influence of migration on the final semicrystalline morphology. This aspect will be discussed in Sect. 3.3.3.4.

Nucleating Activity of the Interface

The second phenomenon found to influence the crystallization behavior in immiscible polymer blends is the nucleating activity of the interface (Bartczak et al. 1987; Wenig et al. 1990; Wei-Berk 1993).

In immiscible polymer blends with a high degree of immiscibility such as PP/PS, it has been shown that nucleation at the interface affects the crystallization behavior. Wenig et al. (1990) showed that with increasing the amount of PS in a blend with PP, the nucleation shifted from preferentially thermal (related to the degree of undercooling) to more athermal. This was explained by the effect of heterogeneous surface nucleation at PS interfaces (Fig. 3.53).

However, not all interfaces can produce additional nucleating centers. For immiscible and highly incompatible polymer blends, since their interfacial tension is higher, the interface is very sharp (Helfand and Tagami 1972). Such interfaces can rarely induce new nuclei. Furthermore, on a molecularly smooth surface, a new layer can only be grown after secondary nucleation, and a somewhat lower energy barrier is present, since the surface area which must be created is smaller (Hoffmann et al. 1992). Only an interface which wets well with the crystallizable matrix, so that a crystalline chain can deposit on it, can cause heterogeneous nucleation (Turnbull 1950; Geil 1973). The wetting ability between two melt phases can be calculated from the spreading coefficient F_{12}. An example can be given by the immiscible polymer blend pair PP/PS (Bartczak et al. 1987; Fig. 3.53).

Furthermore, the *physical state* of the second component at the time of matrix nucleation is of importance. It may be presumed that the mode of nucleation of a polymer in the presence of solidified domains of the second polymeric phase is heterogeneous, and therefore the nucleation rate should be higher than in the pure homopolymer. The effect of blending on the nucleation behavior is more subtle and complex in the presence of a molten second component. Factors such as miscibility, relative melt viscosity, and inherent crystallizability all influence the formation of critical size nuclei (Nadkarni and Jog 1991).

Nucleation by the interfaces contributes to the crystallization behavior proportionally to the *total amount of interface* in the blend system. The finer the amorphous droplets are dispersed, the larger the total interfacial contact surface, and thus the higher is the possibility of nucleation at these interfaces.

The main factors determining the melt morphology are the blend composition, the difference in melt viscosity between both phases, and the interfacial tension. Hence, the nucleation effect on the crystallization behavior should be more pronounced in blends containing a higher amount of the dispersed phase, or in blends composed of components with nearly equal melt viscosities. It has to be noticed that due to coalescence, upon increasing the amount of the amorphous component, larger domains are formed. As a result, the total interfacial contact area may not increase proportionally, leading to a less-than-linear increase of T_c with increasing amount of the amorphous component (see Figs. 3.55 and 3.53).

Fig. 3.55 Influence of the amount of dispersed phase, mixing time, T_{melt} and $T_{c,iso}$ on the amount of nuclei per volume unit in the immiscible PP/PS blend (**a**) after $2\times$ mixing, (**b**) after $3\times$ mixing; T_{melt} was set to 190 °C (*open symbols*) or 220 °C (*filled symbols*); $T_{c,iso}$ for experiments was 125 °C (*circles*) or 130 °C (*blocks*) (Bartczak et al. 1987)
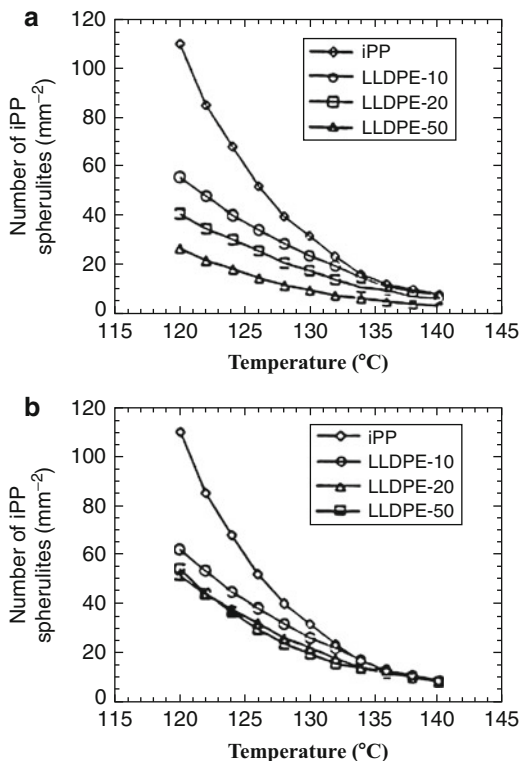
An interesting application of the direct relationship between nucleating interfaces and the total amount of the interfacial contact surface can be found in *compatibilized* immiscible blends. In these systems, the dispersed phase size becomes much smaller, strongly increasing the total amount of interface at which nucleation can occur. Some authors reported that this could cause an upward shift in the T_c by up to 10 °C (Wei-Berk 1993). However, other studies in which the crystallization behavior of a compatibilized blend was investigated did not always mention such a clear nucleating activity (Table 3.17).

Finally, the degree of nucleation at the amorphous/semicrystalline interfaces was found to be *temperature dependent*. When the crystallization temperature was raised, the nucleating efficiency of the interface was found to decrease (Bartczak et al. 1987).

In conclusion, the polymer interface can induce some limited number of nucleation events, but does not cause transcrystallinity, as some other crystal surfaces do. Consequently, the amorphous droplet surfaces, either in the solid or molten state, only act as a weak nucleating agent (Bartczak et al. 1987).

Nucleation Behavior of Some Selected Polymer blends
See Table 3.18

Table 3.17 Influence of compatibilizers on the nucleation behavior of the semicrystalline matrix in crystalline/amorphous polymer blends

Blend system	Observations	Explanation	Reference
PA-6/EPR + g-SA	Compatibilization ↓ spherulite size (which was not found in PA-6/EPR blends) + serious ↑ of the interfacial adhesion	Strong nucleation effect of EPR-g-SA on the PP phase	Martuscelli (1984)
PP/PS +PP/PS block	T_c increased (116 → 126 °C) (DSC) along with copolymer content up to 20–25 % of PS phase	Copolymer lowers the interfacial tension → finer dispersion → more surface available for nucleation at interface + more formation of α-phase PP crystals as T_c rises above 125 °C	Wei-Berk (1993)

3.3.3.2 Spherulite Growth of the Crystallizable Matrix

For homopolymers, the temperature dependence of the isothermal spherulite growth rate, G, is described by Eq. 3.43 (Turnbull and Fischer 1949):

$$G_I = G^{\circ} \exp[-\Delta E / kT_c [\exp] - \Delta F^* / kT_c] \tag{3.43}$$

In the case of immiscible blends with a crystallizable matrix, the spherulite growth can be disturbed to a certain degree by the presence of an amorphous phase component, dispersed in the crystallizable melt.

Phenomena Affecting the Spherulite Growth Rate: Energetic Considerations
Prior to crystallization, the amorphous component exists in the form of droplet-like domains, which at T_c can either be in the molten or glassy state. During the spherulite growth of the crystallizable matrix, small domains may be rejected by the spherulitic growth front either completely to the amorphous interspherulitic zone or only partly over some distance. Furthermore, somewhat larger domains can be occluded by the growing stacks of lamellae after which they eventually can be deformed (Martuscelli 1984; Bartczak et al. 1984). In most cases, a combination of the above-described processes is observed; small droplets are rejected over some distance, coagulate at the growth front, and are engulfed and/or deformed subsequently by the growing lamellar stacks.

The presence of droplet-like domains along the path of the crystallizing growth front can markedly disturb the spherulite growth. The outlined processes require the growth front to perform work against the interfaces, thus dissipating energy. Such energies constitute new energy barriers, controlling the spherulite growth in immiscible blends.

The spherulite growth rate depression is proportional to the type of energy barrier that has to be overcome and can be quantitatively expressed by a modified equation of the spherulite growth rate (Martuscelli 1984):

Table 3.18 Examples of the nucleation behavior of the crystallizable matrix in crystalline/amorphous polymer blends

Blend system (preparation)	Comp.[a]	Observed nucleation behavior (technique used)	Explanation	Reference
LDPE/PS (melt-mix)	90/10 80/20 70/30 60/40	No change		Baïtoul et al. (1981)
HDPE/PS (melt-mix)	90/10 80/20	No change		Aref-Azar et al. (1980)
PP/EPR (melt-mix)	95/5 90/10	Spherulite size ↓ to less than 1/2 size of PP pure with (EPR)↑ (SALS, O. M.)	EPR is nucleating agent for the production of α-type spherulites (most stable and dense packed)	Karger-Kocsis et al. (1979)
	80/20	Formation of more α-type spherulites with (EPR) ↑ (WAXS, O. M.)		
	60/40	T_c ↑ with (EPR) ↑ (DSC)		
PP/EPR (solvent-mix + melt-mix)	90/10 80/20 (70/30)	N/S in PP phase ↑ with (EPR) ↑, mainly at higher (EPR) ⇒ spherulite size ↓ (O. M.)		Martuscelli et al. (1982), Coppola et al. (1987), Kalfoglou (1985)
PP/EPR (melt-mix)	95/5 90/10 80/20 70/30	N/S with (EPR) ↑ (5–7x) This effect is more pronounced when the % ethylene ↑ or the MW ↓ of the used EPR (O. M.)	EPR acts as a nucleating agent, probably due to migration of nuclei from EPR to PP phase	Martuscelli (1985)
PP/EPDM (solvent cast film)	90/10 80/20 70/30	N/S in PP phase ↑ with (EPDM) ↑, mainly at higher (EPDM) ⇒ spherulite size ↓ (O. M.)		Martuscelli et al. (1983)

(continued)

Table 3.18 (continued)

Blend system (preparation)	Comp.[a]	Observed nucleation behavior (technique used)	Explanation	Reference
PP/PIB (melt-mix)	90/10 80/20 70/30	N/S is not affected by addition of PIB (O. M., thick sheet cross section)	No additional nucleation effects	Bianchi et al. (1985), Martuscelli (1985)
PP/PIB (solvent-mix)	90/10	N/S seriously ⇈ with addition of PIB up to 30 times N/S in PP pure (O. M., thin film)	PIB seems to be an effective nucleating agent	Martuscelli et al. (1983), Martuscelli (1985)
PP/SBS (melt-mix)	75/25 50/50	T_c ↑ slightly ($\pm2\,^\circ$C) with addition of SBS (DSC)	SBS is a weak nucleating agent for PP	Ghijsels et al. (1982)
PP/SBS (melt-mix)	95/5 90/10	Spherulite radius ↓ with addition of SBS (O. M., SALS)	SBS is a weak nucleating agent for PP	Karger-Kocsis (1979)
PP/PS (melt-mix)	90/10 80/20	N/V ↑ with (PS)↑ (up to 7x N/V found in pure PP)	Mainly migration of nuclei from PS phase to PP phase	Bartczak et al. (1987)
	70/30	This effect is more pronounced with longer mixing times (O. M.)	Some limited nucleating activity of PS droplets at interface because of their high interfacial tension	
PP/PS (solvent-mix)	90/10	N/S ↑ due to addition of PS up to 20 % PS (4×)	Nucleating activity of PS at the interface	Wenig et al. (1990)
	80/20 70/30	This increase becomes less pronounced with further (PS)↑ (O. M.)	When (PS) > 20%, coalescence of droplets occurs ⇒ less ↑ interfacial area	
	60/40 50/50	Avrami exponent n ↓ from 3 to 2 (DSC)	Nucleation changes from thermal to athermal due to nucleation at interfaces	

PP/PS (melt-mix)	96/4 77/23 65/35 60/40	$T_c \uparrow$ from 121°C (4%PS) to 127°C (40% PS) (DSC)	Nucleating activity of the PS interface on PP	Wei-Berk (1993)
PP/PS (melt-mix)	90/10 80/20 70/30 50/50	No significant change in T_c visible		Santana and Müller (1994)
sPS/PVME[b] (solvent-mix and molten up)	80/20	Formation of larger spherulites with (PVME) $\uparrow$ (O. M.)	Migration of impurities during mixing from sPS to PVME phase	Cimmino et al. (1993a)
	70/30 50/50	$t_{0.5} \uparrow$ during isothermal crystallization (DSC)		

[a]Other compositions than the ones mentioned have been investigated sometimes
[b]PVME and sPS are immiscible as long as the concentration PVME remains larger than 10 % of the blend

Table 3.19 Expressions for the dissipation energy terms and corresponding spherulite growth rates in a crystalline/amorphous polymer blend system (Martuscelli 1984; Bartczak et al. 1984)

Rejection of droplets by growing spherulites	Occlusion of droplets in growing lamellae	Deformation of occluded droplets[a]
$E_1 = 1.5 \, (EGR_s\mu_Mc/\rho_Mr^2)$	$E_3 = 3C\mu_M\Delta F/\rho_Mr$	$E_4 = U(K) \, (3C\mu_M\gamma_{PS}/\rho_Mr)$
$G = G_1/(1 + (3\mu_McEG_1R_s/2\rho_M{}^2RT))$	$G = G_1 \exp(-3C\mu_M\Delta F/\rho_MrRT)$	$G = G_1 \exp(-U(K). (3C\mu_M\gamma_{PS}/\rho_MrRT))$
$E_2 = C\mu_M\rho_PG^2/2\rho_M$		
$G = G_1 \exp(-C\mu_M\rho_PG^2/2\rho_MRT)$		

G_1 is the undisturbed spherulite growth rate

μ_M is the molecular mass of the repetitive unit of the macromolecular chain of the crystallizable matrix

γ_{PS} is the interfacial free energy between the crystallizing solid and the inclusions

ρ_M and ρ_P is the density of the matrix and of the dispersed component

R_s and r is the radius of spherulite and of the dispersed particles, respectively

c is the volume concentration of the noncrystallizable component

R is the gas constant

E is the kinetic energy supply required to move the dispersed droplet along with the motion of the crystallizing front $= 2/3 \, G^2 \, \Pi r^2 \, \rho_P$

[a]The energy of deformation is the sum of two terms: the first is related to change of the surface of particles and the second to deformation of viscoelastic material. U(K) is a complicated function of the coefficient of deformation K of the particles. In the expression of E_4, only the change in surface is taken into consideration with reference to the case where $\Delta F > 0$

$$G = G_1\exp[-(E_1 + E_2 + E_3 + E_4)/kT_c] \qquad (3.44)$$

where G_1 is the spherulite growth rate of the plain crystallizable polymer (theoretically described by the Turnbull-Fisher equation); E_1 is the energy dissipated for rejection (proportional to the melt viscosity); E_2 is the energy needed to overcome the inertia of the drops; E_3 is the energy needed to form a new interface if drops are engulfed; and E_4 is the energy dissipated for deformation of occluded particles.

Theories for the description of these energies for a non-polymeric solidification front were developed by Cissé and Bolling (1971) and by Omenyi et al. (1981). Bartczak et al. (1984) have modified these theories in order to apply them to the case of a crystalline polymeric front that grows according to a spherulite-like morphology, while in the melt, noncrystallizable polymeric domains of spherical shape are present (Table 3.19).

The driving force for rejection, occlusion, or deformation processes is equal to the difference of interfacial free energies (Martuscelli 1984):

$$\Delta F = \gamma_{PS} - \gamma_{PL} \qquad (3.45)$$

where γ_{PS} is the interfacial free energy between crystallizing solid and the inclusions, and γ_{PL} is the interfacial free energy between the melt and the inclusions. When ΔF is positive, the particle droplet will be rejected (Wei-Berk 1993).

Table 3.20 Energy dissipated in PP/TR blends for rejection, occlusion, and deformation of the TR droplets by the growing PP lamellae (Martuscelli 1984; Bartczak et al. 1984)

Process	Energy (J/mol PP repeating units)
Rejection	10^1–10^4
Kinetic energy of rejection	10^{-15}–10^{-14}
Occlusion	10^{-2}–10^{-1}
Deformation: surface change term	10^{-1}–10^0
Deformation: viscous term	10^{-7}–10^{-6}

Martuscelli (1984) and Bartczak et al. (1984) have calculated the energies dissipated by growing PP spherulites in a blend with dispersed rubber particles for all the abovementioned phenomena that may disturb the spherulite growth (Table 3.20).

It can be concluded that mainly rejection of small particles and to a lesser extent deformation of large engulfed droplets (requiring the formation of new surface boundaries) cause a depression in the spherulite growth rate.

Factors Influencing the Spherulite Growth Rate, *G*

Several factors determine the amount of energy required by the growth front to be overcome in order to allow the crystallizable matrix to form spherulites.

The first and most important of these is the *crystallization temperature*, T_c. The higher the isothermal crystallization temperature above $T_{c,\text{max}}$, the slower the spherulites will grow. However, higher T_c also implies a lower melt viscosity. In such case, small droplets will be rejected easier, consuming less energy. This is reflected in a spherulite growth rate, nearly independent on the total amount of small amorphous droplets to be rejected, while at lower T_c, it could be clearly seen that the growth rate is much affected by the amount of fine droplets (Fig. 3.56)

The temperature dependence of the spherulitic growth rate has been theoretically treated (Wenig et al. 1990), for several blends composed of a PP matrix in which PS droplets were dispersed. This temperature dependence could be calculated based on the work done by Hoffmann (1983) and by Suzuki and Kovacs (1970) and is defined as follows (Fig. 3.57a):

$$\text{for } T < T_g - C_2 : G(T) = 0$$
$$\text{for } T_g - C_2 < T < T_m{}^\circ : G(T) = G{}^\circ \exp\left[-C_1 C_2 / (C_2 + T - T_g)\right] \exp\left[(-C_3)/T(T_m{}^\circ - T)\right]$$
$$\text{for } T > T_m{}^\circ : G(T) = 0$$

$$(3.46)$$

where T_g is the glass-transition temperature of the crystallizable component; $T_m{}^\circ$ is the theoretical melting temperature of the crystalline component; G°, C_1, C_2, and C_3 are parameters describing the growth rate behavior in the blends.

For the crystalline component, the parameters from the WLF equation, C_1 and C_2, can be found from literature (Icenogle 1985). T_g and $T_m{}^\circ$ can be measured for pure crystallizable component. The parameters G° and C_3 can be calculated from the experiments that give the spherulite growth rate G as

Fig. 3.56 Theoretical estimation for spherulite growth rate depression in immiscible PP-based blends in the case of *rejection* of particles: influence of particle size, $T_{c,iso}$, and volume concentration of the second component (Martuscelli 1984)
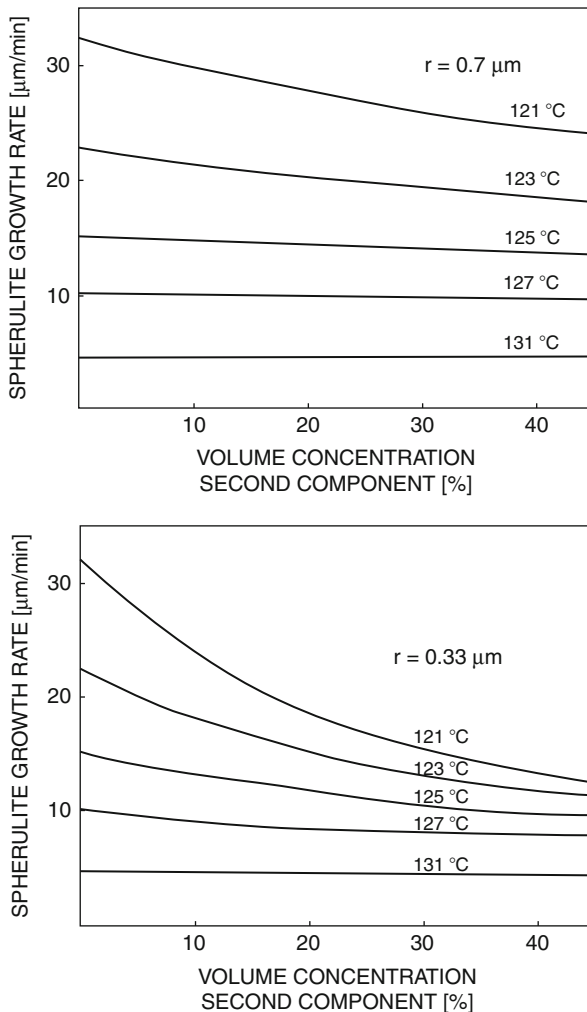
a function of temperature T. By plotting the value $\ln G + C_1C_2/(C_2 + T - T_g)$ versus $1/(T(T_m - T))$ for the entire crystallization temperature range, a linear plot is obtained from which the values of $G°$ (intercept) and C_3 (slope) for all the blend compositions can be determined (Fig. 3.57b). Once all these parameters are known, the growth rate can be estimated as a function of temperature for all blend compositions, according to Eq. 3.46.

Secondly, the *blend composition* is of importance as well. The finer the dispersion (i.e., at low content of the amorphous phase, nearby equal melt viscosities of matrix and dispersed phase, etc.), the more droplets need to be rejected. This high energy-consuming process reduces the spherulite growth rate (see Fig. 3.57).

Fig. 3.57 (**a**) Temperature dependence of the spherulite growth rate, G, for PP (experimental values were fitted using the function defined in Eq. 3.46); (**b**) plot to determine the parameters $G°$ and C_3 ($C_1 = 25$, $C_2 = 30$ K, $T_g = 260$ K, $T_m° = 460.5$ K) (Wenig et al. 1990)
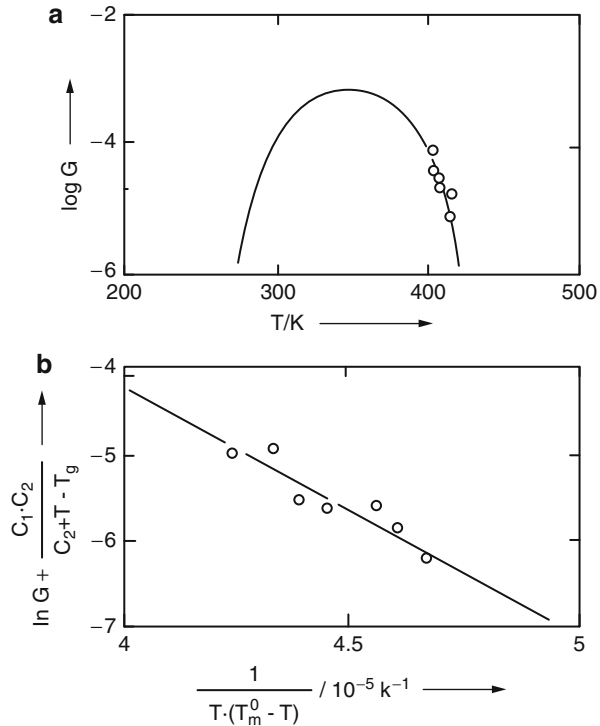
Spherulite Growth Rate Investigations in Some Typical Polymer Blends
See Table 3.21

3.3.3.3 Overall Crystallization Kinetics

The effect of blending on the overall crystallization rate is the net combined effect of the nucleation and spherulite growth. Martuscelli (1984) observed that in blends of PP with LDPE, crystallized at a T_c high enough to prevent any LDPE crystallization, the overall rate of crystallization of the PP matrix phase (thus in the presence of the LDPE molten droplets) was progressively depressed with increasing content of LDPE (Fig. 3.58).

This can be seen in the plot of $t_{1/2}$ (halftime of crystallization at a fixed $T_{c,iso}$) versus blend composition. The observations agree very well with the findings that the growth rate of the PP spherulites is almost unaffected, while the nuclei density decreases with increasing LDPE content due to impurity migration from PP to LDPE phase.

A different case has also been explored by Martuscelli (1984) for PA-6 blended with an EPR-rubber. As shown in Fig. 3.59, $t_{1/2}$ of the PA-6/EPR blend decreased (faster overall crystallization rate) as the content of the rubbery phase increased, especially at lower concentrations of the EPR phase.

Table 3.21 Examples of the spherulite growth rate, G, of the crystallizable matrix in crystalline/amorphous polymer blends

Blend system	Comp.	G (µm/min)[a] (from O. M.)	$\neq T_c$[b]	Final semicrystalline morphology	Comments	Reference
PP/EPR (thin film)	100/0	32	x	Some droplets are ejected interspherulitically	Small ↓ of G which is composition dependent	Martuscelli et al. (1982)
	90/10	±30				
	80/20	±27		At low (EPR): droplets are ejected for a short distance and then occluded intraspherulitically		Martuscelli (1985)
	70/30	±27				
		at 121 °C				
PP/EPDM (thin film)	100/0	15	x	Droplets are occluded intraspherulitic	Only small ↓ of G independent of the blend composition	Martuscelli et al. (1983)
	90/10	11				
	80/20	12		Droplets are aligned along radial direction due to coalescence of droplets upon rejection for short distance, followed by deformation		Martuscelli (1985)
	60/40	13				
		at 125 °C				
PP/PIB (thin film)	100/0	32	x	Most droplets (3–5 µm) are occluded intraspherulitically	Clear depression of G on addition of PIB which is strongly dependent on MW PIB and composition[c]	Martuscelli et al. (1982)
						Martuscelli et al. (1983)
	90/10	23		Sometimes droplets are rejected (for short distance or even interspherul.) if MW PIB low (PIB) low (<10 %)		Martuscelli (1985)
	80/20	20				
		at 121 °C				

PP/PS	100/0	2.5	x	PS droplets are occluded intraspherulitically (no rejection or deformation)	G is not changed and is independent on blend composition	Bartczak et al. (1987)
	90/10	2.3			
	80/20	2.5			
	70/30	2.5			
		at 133 °C			
PP/PS	100/0	3.2	x		G is only slightly ↓ except for 90/10 composition (no explanation)	Wenig et al. (1990)
	90/10	1.6			
	80/20	3.1			
	70/30	2.8			Globally G is independent on composition
	60/40	2.2			
		at 133 °C			
sPS/PVME	100/0	2.5	x	Droplets are occluded intraspherulitically	G is ± independent on composition	Cimmino et al. (1991)
	80/20	6.0			
	70/30	7.0			G↑ with (PVME) ↑ due to facilitated transport of chains (PVME and PS chains are partially miscible ⇒ Tg↓)	Cimmino et al. (1993)
	50/50	–			
		at 244 °C			

[a]Some of the listed data were extracted from plots presented in the article

[b]x indicates that the influence of different crystallization temperatures T_c has been investigated

[c]PIB is shown to be partially miscible with the amorphous phase of PP at low concentrations. Hence, the behavior can deviate and exhibit some typical characteristics as in miscible systems
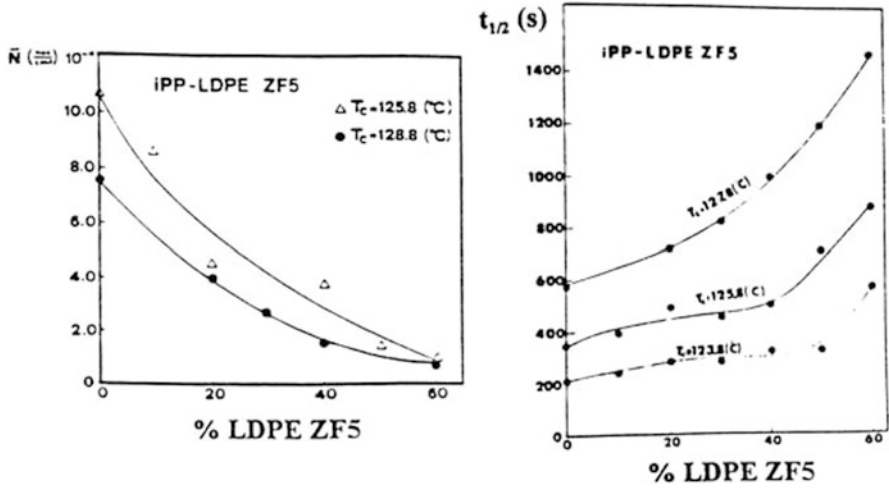
Fig. 3.58 Global crystallization kinetics in immiscible PP/LDPE blends; influence of the amount dispersed phase and the crystallization temperature, T_c, on the halftime for crystallization, $t_{1/2}$ (Martuscelli 1984)
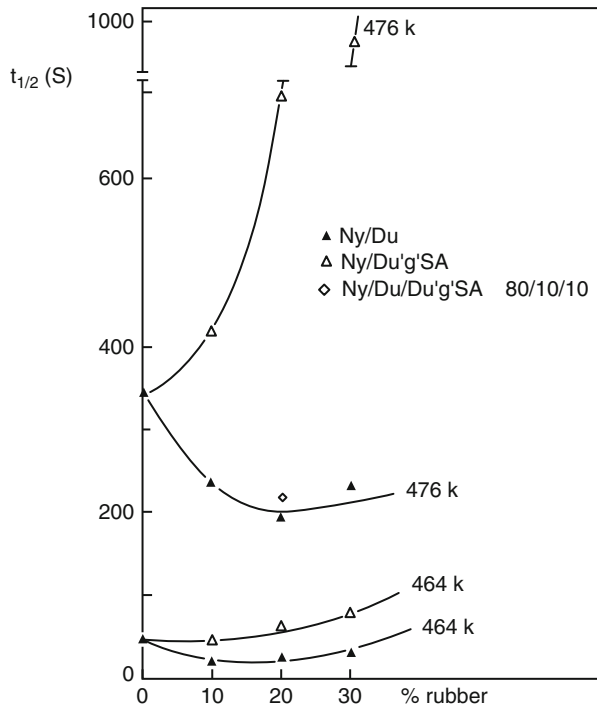
Fig. 3.59 Variation of the halftime of crystallization, $t_{1/2}$, with the percent of added rubber component (EPR) and T_c for PA-6/Dutral and the compatibilized blend PA-6/Dutral-g-SA (Martuscelli 1984)

Fig. 3.60 Evolution of DSC crystallinity from cooling (▼) and melting curves (■) versus PA6 droplet size for various (PS/SMA2)/PA6 blend compositions (Tol et al. 2005c)
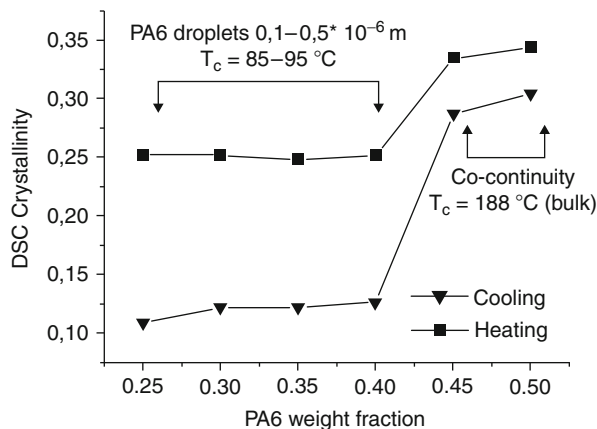
The reverse could be observed in a compatibilized blend. Because in these blends a serious decrease of the spherulite size was observed, the authors concluded that the compatibilizer acted as a nucleating agent for the PP phase. However, due to the increase of the melt viscosity upon compatibilization, the overall crystallization kinetics was retarded. Additionally, they observed experimentally that ΔF^* (free energy for the formation of a nucleus of critical size) and σ_e (surface free energy of folding) in compatibilized blends were larger than in PA-6 homopolymer. An opposite trend was observed for the physical PA-6/EPR blends. No further investigations have been done to elucidate this phenomenon.

The crystallization kinetics of PA6 in immiscible blends of PS/PA6 and (PS/SMA2)/PA6 have been investigated over very broad temperature range using high cooling rates (Tol et al. 2005c). For immiscible blends with PA6 droplets of micrometer size, exhibiting moderate decrease of crystallization temperature compared to the PA6 bulk crystallization, an athermal nucleation mechanism was suggested based on nucleation process in a very small temperature interval. Blends of PA6/PS compatibilized using SMA2 having submicrometer-sized PA6 droplets, crystallizing at 90 °C (i.e., a supercooling of 100 °C compared to Tc bulk), a random nucleation event was found using isothermal DSC experiments, which is characteristic of a homogeneous nucleation process. This effect was persistent up to 40 wt% PA6 (Fig. 3.60). This concentration is the highest concentrated heterogeneous system reported, exhibiting homogeneous nucleation kinetics. Crystallinities were strongly affected by the confining conditions of the droplets. For 1–30 μm-sized PA6 droplets crystallizing at intermediate temperatures, the crystallinity decreased with decreasing PA6 droplets size from 36 % for bulk PA6 to 22 %. For the submicrometer-sized PA6 droplets, a very strong decrease in crystallinity was found down to 10 %.

3.3.3.4 Final Semicrystalline Morphology

The addition of a second noncrystallizable component to a crystallizable matrix can cause drastic variations of important morphological and structural parameters of the
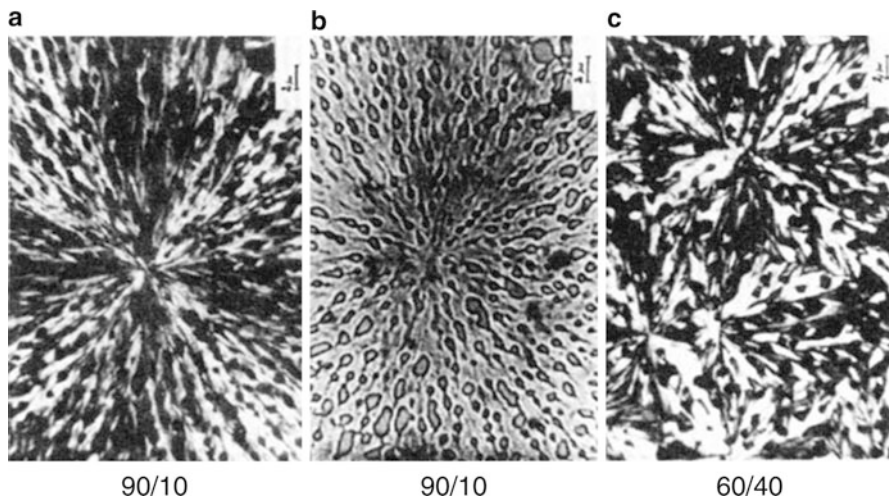
Fig. 3.61 Optical micrographs of melt-crystallized films of PP/EPDM blends at $T_c = 135\,^{\circ}\mathrm{C}$; (**a**) 90/10, crossed polarizers; (**b**) 90/10, parallel polarizers; (**c**) 60/40, crossed polarizers (Martuscelli et al. 1983)

semicrystalline phase, such as the shape, size, regularity of spherulites and interspherulitic boundary regions, lateral dimensions of the lamellae, etc. These factors may greatly influence the mechanical behavior and, in particular, the fracture mechanisms and thus are of great importance, especially when the toughening of semicrystalline polymer blends is considered.

The first important parameter determining the final crystalline morphology is the *nucleation density*, N (see Sect. 3.3.3.1). An increase in the nucleation density (per volume unit of the crystallizable material) due to migration of nuclei from one phase toward the other, or due to a nucleating activity at the polymer/polymer interface, results in the formation of more numerous but smaller spherulites.

The spherulite *growth rate*, G, also plays a role.

- At low G values, there is a higher probability that all dispersed particles can diffuse fast enough away from the growth front and be pushed along until complete crystallization. The second phase component will then be found mainly in the interspherulitic regions.
- At high G values, even small particles will not be rejected anymore. Hence, the homogeneously distributed droplets will be as such engulfed, rejected into newly formed boundaries behind occluded particles, and eventually deformed. This results in a radial-like distribution of the droplets within the spherulite (Fig. 3.61).
- At intermediate growth rates, the dispersed drops will first be pushed along, but due to an increase of the amount of droplets at the solidification front, they will coagulate and subsequently be engulfed. This results in a spherulite center consisting of pure crystalline material and an outer layer in which dispersed particles are occluded.
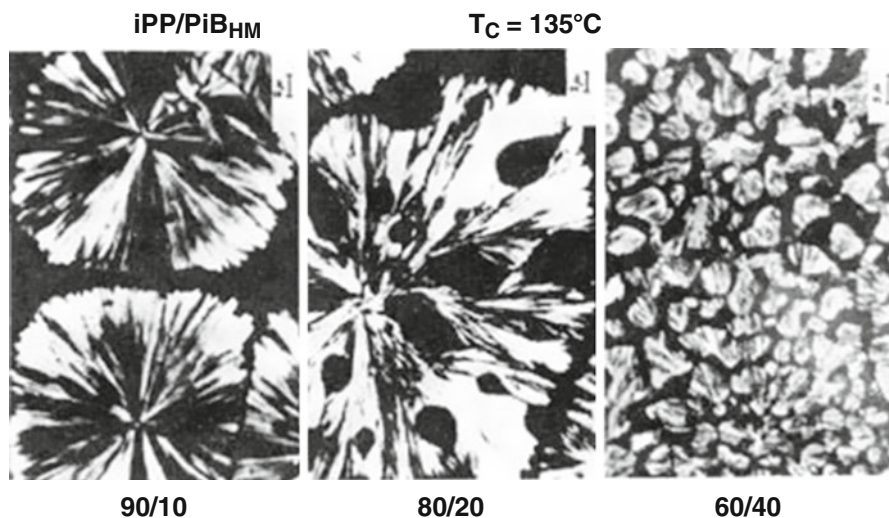
Fig. 3.62 Optical micrographs of isothermally ($T_c = 135$ °C) crystallized thin films of PP/PIB (HM) blends with different compositions (Martuscelli et al. 1983)

Another parameter strongly influencing the final crystalline morphology is the *blend composition* (Fig. 3.62).

The higher the amount of the amorphous phase, the higher the chance to have a coarse melt morphology containing lots of large, easily coalescing amorphous droplets. In such a case, the crystallizing growth front will mainly engulf and deform these droplets. The resulting crystalline morphology will be heavily disturbed by the second phase component.

Some examples of the final semicrystalline morphology in several immiscible crystalline/amorphous blend systems have already been given in Tables 3.21 and 3.22 for the discussion of the spherulite growth rate (Sect. 3.3.3.2). Some more information about this topic can be found in the articles listed in Table 3.23.

3.3.3.5 Melting Behavior of the Crystalline Matrix in Crystalline/ Amorphous Blends

The behavior of binary blends with only one crystallizable component has been studied by several authors, who have investigated different systems. The crystals of the crystallizable matrix have grown in equilibrium with their own melt phase. The presence of separate domains of noncrystallizable component, dispersed in the molten matrix during the crystallization process (owing to the kinetic and morphological effects), may cause a depression of the observed melting temperature, T_m' (Martuscelli 1984). However, the changes in T_m' will be only in the range of a few degrees C.

Some binary systems do not show any depression at all, indicating that T_m' and T_m do not depend on blend composition. This is found when the second dispersed

Table 3.22 Global crystallization kinetics of the crystallizable matrix in some crystalline/amorphous blend systems

Blend system	Comp.	Parameter	$\neq T_c{}^a$	Comments	References
HDPE/PS	100/0	Avrami exponent (DSC) $t_{0.5}$ (DSC)	x	Unaffected cryst. kinetics (insensitive to blend morphology)	Aref-Azar et al. (1980)
	90/10				
	80/20				
PP/EPR	100/0	$X_{c,iso}$ (DSC)		At (EPR) < 20 %: slight ↓ of X_c due to limited miscibility of aPP and EPR → hindered crystal growth	Kalfoglou (1985)
	90/10				
	80/20			At (EPR) > 20 % : X_c ↑ with (EPR) ↑ due to nucleating activity of EPR	
	60/40				
PP/PIB	100/0	$X_{c,iso}$ (WAXS, DSC)		X_c ↓ with (PIB) ↑	Bianchi et al. (1985)
	90/10				Martuscelli (1985)
	80/20				
	70/30				
PP/PS	100/0	Avrami exp., n (DSC)		n ↓ from 3 to 2 with (PS) ↑ (due to surface nucleation at PS droplets), and G = cte ⇒ crystallization rate is enhanced and strongly dependent on blend composition	Wenig et al. (1990)
	90/10				
	80/20				
	70/30				
	60/40				
PA-6/EPR	100/0	$t_{0.5}$ (DSC)	x	Serious ↓ in $t_{0.5}$, which is most pronounced at low conc. EPR ⇒ enhanced crystallization kinetics	Martuscelli (1984)
	90/10				
	80/20				
	70/30				
sPS/PVME	100/0	$t_{0.5}$ (DSC)	x	Seriously retarded kinetics of sPS phase ($t_{0.5}$ ↑) which is composition dependent Effect of N/S ↓ is larger than that of G ↑	Cimmino et al. (1993)
	80/20				

[a]x indicates that the influence of different T_c on the overall crystallization kinetics has been investigated in the article mentioned

phase does not influence the normal crystallization behavior of the matrix polymer: no nucleating activity, no influence on spherulite growth rate, etc.

Some examples of the melting behavior in previously discussed blend systems are given in Table 3.24.

3.3.4 Blends with a Crystallizable Dispersed Phase in an Amorphous Matrix

In immiscible polymer blends, the minor component often forms the dispersed phase, whose shape and size are complex functions of the blend composition, the

Table 3.23 Overview of literature in which the final semicrystalline morphology in immiscible crystalline/amorphous polymer blends has been studied

Blend system	Reference	Composition[a]	Growth rate[b] (rejection ↔ occlusion)	Nucleation density[c] (spherulite size)
PP/EPR	Martuscelli et al. (1982)	x		x
	Coppola et al. (1987)	x		x
	Kalfoglou (1985)	x		x
	Karger-Kocsis et al. (1979)	x		x
	Martuscelli (1985)	x		
PP/EPDM	Martuscelli et al. (1983)	x	x	x
	Martuscelli (1985)	x		
PP/PIB	Martuscelli et al. (1982)	x	x	x
	Martuscelli et al. (1983)	x	x	x
	Bianchi et al. (1985)	x	x	x
	Martuscelli (1985)	x	x	x
PP/PS	Bartczak et al. (1987)	x		x
PEG/PS	Lotz and Kovacs (1969)	x		
sPS/PVME	Cimmino et al. (1991)	x		x
	Cimmino et al. (1993)	x		x

[a]Influence of compositional variations on the semicrystalline morphology has been investigated
[b]Influence of different spherulite growth rates on semicrystalline morphology is discussed
[c]Final spherulite size has been evaluated

melt viscosity of the dispersed phase and the matrix, the viscosity ratio, the interfacial tension, and the processing conditions (Utracki 1989; Folkes and Hope 1993).

The crystallization behavior of a dispersed melt phase, for example, discrete melt droplets, in an amorphous matrix can be dramatically affected compared to that of the bulk polymer. It has been reported by several authors that crystallizable dispersed droplets can exhibit the phenomenon of *fractionated crystallization* originating from the primary nucleation of isolated melt particles by species with different nucleating activities (heterogeneities, local chain ordering)

Table 3.24 Examples of the melting behavior of the crystallizable matrix in some crystalline/amorphous blend systems

Blend system	$T_{m\downarrow}$	$T_m \uparrow$	References
PP/EPR		$T_m \uparrow$ with (EPR) ↑	Martuscelli et al. (1982)
		Effect is largest at high ethylene content and low MW of EPR	Martuscelli (1984)
		EPR is able to extract selectively defective PP chains ⇒ $T_m \uparrow$ and $X_c \uparrow$	Martuscelli (1985)
PP/EPR	$T_m \downarrow$ with (EPR) ↑ (2 to 3 °C) due to $T_c \downarrow$ ⇒ formation of smaller lamellae which melt at slightly lower T_m		Kalfoglou (1985)
PP/EPR	$T_m \downarrow$ with (EPR) ↑ (3 to 4 °C) due to the formation of smaller spherulites with lower C_p (although T_c ↑)		Karger-Kocsis et al. (1979)
PP/EPDM	$T_m \downarrow$, min. is observed at 20 % EPDM EPDM is able to dissolve aPP at low conc. EPDM (≈ diluent-effect)		Martuscelli et al. (1983)
PP/PIB	$T_m \downarrow$ with (PIB) ↑ This effect is largest at high conc. PIBLM or low conc. PIBHM PIB dissolves aPP in low amounts (≈ dilution effect)		Martuscelli et al. (1983)
PP/PS	$T_m \downarrow$ with (PS) ↑ (2 to 3 °C) due to some specific interactions at the interface		Mucha (1986) Wei-Berk (1993)
POM/PC	$T_m \downarrow$ with (PC) ↑ (2 to 3 °C) ΔH_m = cte (per g POM)		Chang et al. (1991)
PEG/PS	$T_m \downarrow$ with (PS) ↑ (max. 8 °C) due to formation of smaller lamellae if the (PS) in the block copolymer ↑		O'Malley et al. (1969)
PET/PPE		$T_m \uparrow$ upon addition of PPE to a PET matrix (≈ 2 °C)	Liang and Pan (1994)
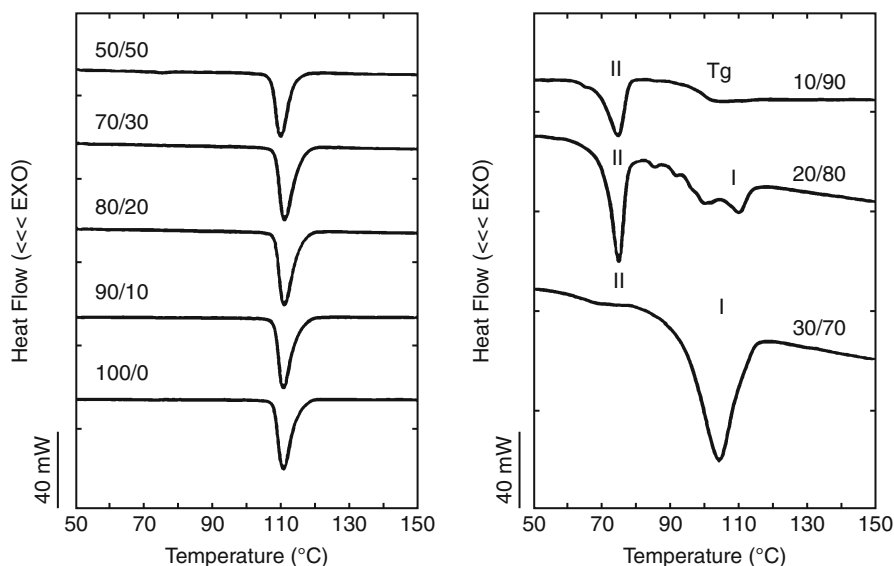
Fig. 3.63 DSC cooling curves (10 °C/min) for PP/PS blends; difference in the crystallization behavior in blends with PP as a matrix phase and as a dispersed phase (Santana and Müller 1994)

(Aref-Azar et al. 1980; Baïltoul et al. 1981; Ghijsels et al. 1982; Robitaille and Prud'homme 1983; Frensch et al. 1989; Santana and Müller 1994; Müller et al. 1995; Morales et al. 1995; Fig. 3.63).

3.3.4.1 The Phenomenon of Fractionated Crystallization of a Dispersed Phase

Crystallization is a phase transition that is controlled by nucleation and growth (Wunderlich 1976). As it has been outlined in Sect. 3.2.2, crystallization during cooling from the melt in homopolymers is initiated by impurities (primary heterogeneous nucleation), after which the crystallizing front spreads over the whole material via the secondary nucleation, before other heterogeneities, requiring a larger degree of undercooling, $\Delta T_{c,i} = T_{mo} - T_{c,i}$, can become active. A single crystallization exotherm is generally observed in DSC thermograms. So, the primary nucleation is the rate-determining step of crystallization. The dynamics of the process depend for a given component only on the temperature.

However, for polymer blends in which the crystallizable phase is dispersed into fine droplets in the matrix, crystallization upon cooling from the melt can sometimes occur in several steps (fractionated crystallization) that are initiated at different undercooling, often ending up with a crystallization at the homogeneous crystallization temperature $T_{c,hom}$ (Aref-Azar et al. 1980; Baïltoul et al. 1981; Ghijsels et al. 1982; Santana and Müller 1994).

The first investigations concerning the crystallization in discrete droplets date from 1880; Van Riemsdyk reported that small gold melt droplets solidify at much

Table 3.25 Crystallization behavior in finely dispersed crystalline droplets

Polymer	Dispersion method	Average droplet size (μm)	ΔT_c, bulk (°C)	ΔT_c, droplets (°C)	Reference
PE	Thermodyn. inert liquid	Some μm	±20	±55[a]	Cormia et al. (1962)
PP	Thermodyn. inert liquid	Some μm	±50	±102[a]	Burns and Turnbull (1966)
PEG	Thermodyn. inert liquid	5	±20	±65[b]	Cormia et al. (1962)
PE	Suspended in silicon oil and sprayed on slides*	1–2	±20	55[a]	Koutsky et al. (1967)
PP	*	1–2	±50	100[a]	Koutsky et al. (1967)
PEG	*	1–2	±20	65[b]	Koutsky et al. (1967)
POM	*	1–2	±30	84[a or b]	Koutsky et al. (1967)
iPS	*	1–2	±	102[b]	Koutsky et al. (1967)
PA-6	*	1–2	±15	100[b]	Koutsky et al. 1967

[a]Crystallization by homogeneous nucleation at $T_{c,hom}$
[b]Nucleating activity of the suspending medium prevents to detect the real undercooling needed to obtain a homogeneous crystallization

larger undercoolings than the bulk material (Van Riemsdyk 1880). Similar observations were made later for other metals (Perepezko and Paik 1982), indicating this to be a basic crystallization phenomenon.

The creation of sufficiently small polymer droplets as a stable suspension was much more difficult. It was therefore only first in 1959 that similar experiments have been reported for polymers (Frensch et al. 1989; Table 3.25).

It was clearly observed that the phenomenon of delayed crystallization was directly related to the size of the dispersed droplets (Koutsky et al. 1967). Only the smallest droplets showed crystallization at much larger undercooling, droplets having a sufficiently large diameter crystallized at temperatures approaching the bulk crystallization temperature, T_c. The explanation for this behavior is obvious: the spectrum of undercoolings at which several crystallization steps occur reflects the difference in nucleating activity of the various heterogeneities available in the melt (Frensch et al. 1989). It can be assumed that if the dispersion of the polymer is so fine that not every droplet contains at least one heterogeneity of type 1, only those droplets containing the latter will crystallize at an undercooling $\Delta T_{c,1}$. Since the droplets are physically not in contact with each other, further growth via secondary nucleation in other crystallizable droplets is impossible. During further cooling, heterogeneities of type 2 requiring the second lowest degree of undercooling, $\Delta T_{c,2}$, can become active in some of the remaining droplets, resulting

Fig. 3.64 Isothermal homogeneous crystallization of finely dispersed polymer droplets as a function of time (**a**) linear PE, (**b**) PP (Koutsky et al. 1967)
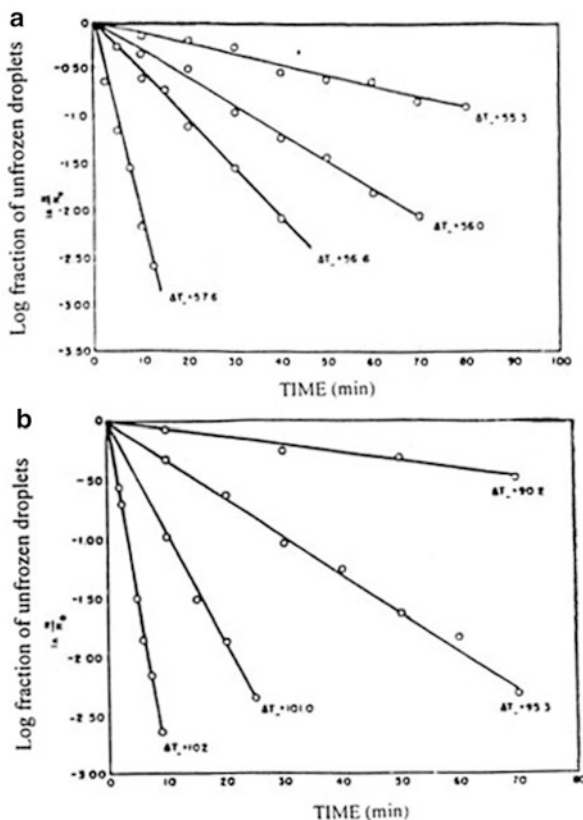
in a second crystallization exotherm. This process goes on until finally some very fine droplets that have not yet been nucleated by the heterogeneous species will crystallize in a homogeneous mode.

In isothermal experiments, the fractionated crystallization of finely dispersed crystallizable droplets is reflected by longer crystallization times before the same degree of crystallinity X_c is obtained. This has been illustrated clearly by Koutsky et al. (1967) in experiments (see Table 3.25) in which finely dispersed droplets of PE and PP in a suspension of silicon oil were crystallized at different undercoolings ΔT_c (Fig. 3.64).

It should be mentioned that the occurrence of a fractionated crystallization is related only to the number densities of dispersed polymer particles and primary heterogeneous nuclei. No direct physical relationship has been found with the number or size of spherulites. These parameters are additionally influenced by the cooling rate and the crystallization temperature (Frensch et al. 1989).

Several factors can influence the fractionated crystallization behavior. An important parameter that has already been discussed is the thermal history of the sample. Crystallizable dispersed droplets that were submitted to premelting at higher temperatures or longer times generally display a shift in the heterogeneous

Table 3.26 Influence of compatibilization on the crystallization behavior of the dispersed phase in amorphous/crystalline polymer blends

Blend system	Compositions	Matrix at T_c	Comments	References
PP/PS +SBS	18/80/2	Melt	SBS did not ↓ particle size (bad compatibilizer because immisc. with PP)	Santana and Müller (1994)
	9/90/1		Nucleation density ↑ because homogeneous nucleation process becomes more heterogeneous (higher T_c)	
			SBS transfers heterogeneities to PP	
LDPE/PS + Kraton G	15/77.8/7.2	Solid	Kraton enhances the formation of a finer dispersed PE phase	Bailtoul et al. (1981)
			Shift of multiple crystallization to lower temp.	
PET/PS +PET-b-PS	23.75/71.25/5	Melt	Addition of block copolymers caused a serious ↓ of droplet size (± 5 μm → 0.2 to 4 μm)	Quirk et al. (1989)
			Compatibilization caused large ↓ of X_c (≈ -10 %)	
PET/PPE +PET-b-PS	23.75/71.25/5	Solid	Addition of block copolymers caused a ↓ of droplet size (± 5 μm → 2 to 4 μm)	Quirk et al. (1989)
			Compatibilization caused X_c ↑ (≈ -10 to 20 %)	

nucleation spectrum to greater undercooling. The homogeneous crystallization temperature however is not displaced and thus independent of the thermal history (Koutsky et al. 1967). This may become less evident for blends with unstable phase morphology (rapid phase coarsening upon annealing); long residence times in the melt will cause fine droplets to coarsen. Consequently, the newly formed larger droplets have a higher probability to crystallize close to the bulk crystallization temperature of the homopolymer.

The degree of dispersion of the minor phase plays a crucial role. Important factors here are the blend composition, the interfacial tension between both components, the melt viscosity of both components, the processing device and mixing conditions, the blend preparation method, etc.

In this context, it is interesting to evaluate also the influence of compatibilization on the crystallization behavior of the dispersed phase. Since compatibilization reduces the droplet size of the minor phase even more drastically, it can be expected that this can lead to a serious shift of the crystallization temperature toward lower temperatures, resulting in more pronounced fractionated crystallization or even in a homogeneous crystallization. However, this issue is more complex due to numerous other factors involved in the nucleation process. Some examples from the literature are listed in Table 3.26. They illustrate how differently the compatibilization can influence the crystallization behavior of the dispersed phase.

3.3.4.2 Theoretical Considerations of the Fractionated Crystallization

In crystallizable dispersed droplets, several different nucleating heterogeneities (type i) can be present, each having a typical free energy for the formation of a nucleus of critical size, ΔF^*, at an undercooling $\Delta T_{c,i}$:

$$\Delta F^* \approx \Delta y_{pn}/\left(\Delta T_{c,i}\right)^2 \tag{3.47}$$

This free energy is proportional to the specific interfacial free energy difference Δy_{pn} defined as (Wunderlich 1976)

$$\Delta y_{pn} = y_p(m, c) - y_{pn}(m) + y_{pn}(c) \tag{3.48}$$

where the indices refer to polymer (p), melt (m), crystal (c), and nucleus (n); $y_{pn}(m)$ is the interfacial energy between the nucleating species and the polymer melt; $y_{pn}(c)$ is the interfacial energy between the nucleating species and the polymer crystal; and $y_p(m, c)$ is the lateral surface free energy between the crystal and its own melt.

In the case of a homogeneous nucleation, the expression for Δy_{pn} can be simplified to read: $\Delta y_{pn} = 2\, y_p(m, c)$

If one assumes that for the onset of crystallization $\Delta F^*/kT$ must be smaller than a certain critical value (i.e., a nucleus of critical size can be formed at the given temperature), independent of the material, and if one neglects that the crystallization also depends on the temperature-dependent mobility of the crystallizable segments, the following expression for the relation between Δy and the degree of undercooling for two heterogeneities of type 1 and type 2 can be given (Frensch et al. 1989):

$$\Delta y1/\Delta y2 \approx \left(T_{c,1}/T_{c,2}\right)\cdot\left(\Delta T_{c,1}/\Delta T_{c,2}\right)^2 \tag{3.49}$$

where $T_{c,1}$ and $T_{c,2}$ represent the temperatures at which nucleation is induced by the heterogeneity of type 1 and 2, respectively (Fig. 3.65).

In the special case of a homogeneous nucleation, Eq. 3.49 can be simplified to read

$$\Delta T_{c,\,hom} = T_c^\circ - T_{c,\,hom} = T_c^\circ/5;\ \ i.e., T_{c,\,hom} = 0.8 T_c^\circ \tag{3.50}$$

where T_c° is the crystallization temperature in the bulk polymer (in K).

From the latter (Eq. 3.50), the homogeneous crystallization temperature for each polymer can be estimated in a simple way.

Furthermore, from Eq. 3.49 for heterogeneity of type 1, one may write

$$\Delta y1/y_p(m, c) \approx 62.5\, \left(T_{c,1}/T_c^\circ\right)\left(\Delta T_{c,1}/T_c^\circ\right)^2 \tag{3.51}$$

From this dependence, the relative values of Δy for different heterogeneities can be calculated at the corresponding degrees of undercooling.

Fig. 3.65 Plots of the relative specific interfacial energy difference $\Delta y/y$ versus the relative undercooling $\Delta T/T°_m$ at which a heterogeneity nucleates the polymer; (1) and (2), two different heterogeneous nucleations; (3) homogeneous nucleation (Frensch and Jungnickel 1989)
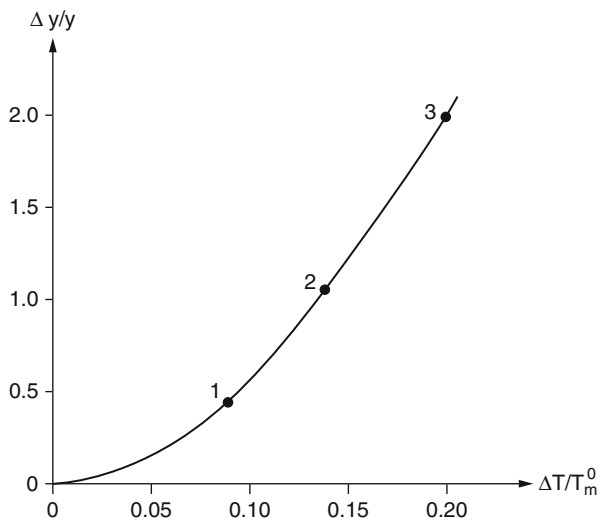
From the fractionated crystallization behavior and the blend morphology, one can determine the number density of the nucleating active species. Among a large number of small polymer droplets, each having a volume V_D, the fraction of droplets that contain exactly z heterogeneities of type 1 (inducing normally crystallization in the bulk polymer at $T_c°$) follows a Poisson distribution function (Pound and LaMer 1952):

$$f_z^{(1)} = \left[\left(M^{(1)} \cdot V_D \right)^Z / z! \right] \exp\left(-M^{(1)} \cdot V_D \right) \tag{3.52}$$

where $M^{(1)}$ is the concentration of heterogeneities of type 1 and $M^{(1)}.V_D$ is the mean number of heterogeneities of type 1 per droplet with volume V_D.

Hence, the fraction of droplets that contain at least one heterogeneity of type 1 can be given by

$$f_{z>0}^{(1)} = 1 - f_0^{(1)} = 1 - \exp\left(-M^{(1)} \cdot V_D \right) \tag{3.53}$$

Now considering that not all droplets have the same size, $f_{z>0}^{(1)}$ describes that fraction of the droplets (with average volume V_D) that crystallize induced by heterogeneity of type 1. The other droplets will crystallize at a different crystallization step. From the relative intensities of the fractionated crystallization steps, one can estimate the concentration of the different heterogeneities, if the mean size of these droplets is known.

In the special case where the usual crystallization from heterogeneity of type 1 is completely suppressed, Eq. 3.52 can be written as

$$M^{(1)} \cdot V_D << 1 \tag{3.54}$$

Table 3.27 Evaluation of the blend morphology and thermal behavior in immiscible PS/HDPE blends in which HDPE was the minor phase (Aref-Azar et al. 1980)

wt% HDPE	Size-dispersed phase (μm)	Number droplets (cm^{-3})	ΔH_m^a (J/g)	X_c^b (%)
1	0.1–0.3	10^{11}–10^{12}	–	–
5	0.3–0.5	10^{10}–10^{11}	163	55
10	2.0–3.0	10^7–10^8	159	54
20	5–10	10^6–10^7	184	63

[a]ΔH_m for pure HDPE is 293 J/g
[b]Degree of crystallinity, X_c, for HDPE homopolymer is 80 %

3.3.4.3 Droplet Crystallization in the Presence of a Matrix Melt

In most immiscible crystalline/amorphous polymer blends, the crystallization of the dispersed phase occurs in the presence of a molten matrix phase. In the following description, examples will be categorized according to the major classes, as listed in Table 3.14.

Polyethylene Blends

Blends of PS/HDPE have been investigated by Aref-Azar et al. (1980). Table 3.27 gives an overview of the crystallization behavior in the crystallizable dispersed phase.

It should be noted that the crystallization kinetics is related to the size of the dispersed HDPE droplets and the nucleation density. An increase in the amount amorphous PS caused the HDPE phase to be dispersed into finer droplets that, as a result, exhibited a lower degree of crystallinity, X_c, when isothermally crystallized. Furthermore, a higher degree of undercooling was needed to reach the same X_c in blends where the HDPE phase was dispersed into finer droplets, indicating that crystallization depends on the temperature. The melting behavior of the HDPE phase did not seem to be affected by blending.

Recently, Müller et al. (1995) and Morales et al. (1995) have reported on the crystallization of LLDPE that was finely dispersed in a PS matrix. A good correlation was found between the size of the LLDPE phase and the tendency to crystallize in a fractionated way. The authors showed that the relationship is only sensitive to the volume of the dispersed crystallizable droplets and not to the shape of the droplets.

Polypropylene Blends

Numerous studies have been performed on the crystallization behavior of PP in blends with an amorphous component. However, only few authors paid attention to the crystallization behavior of the PP phase when it formed the minor phase of the blend.

Ghijsels et al. (1982) investigated the multiple crystallization behavior of blends in which the crystallizable PP phase was finely dispersed into a SBS-rubber (TR). In the case where the latter was finely dispersed, the authors found the PP phase to crystallize at much higher undercooling. A serious drop in the degree of crystallinity, X_c, was also reported. The melting behavior of the fractionated crystallized blend did not seem to be markedly affected, e.g., ΔH_m and T_m remained constant, independent of the amount TR added.

Wei-Berk (1993) reported on the crystallization behavior of PP droplets dispersed in a PS matrix. A slight drop in $T_{c,PP}$ (as the PP phase became the minor phase) was observed. However, the author only investigated the behavior in blends containing more than 35 % PP, and did not correlate the crystallization behavior with the blend morphology.

Recently, Santana and Müller (1994) investigated the same polymer blend. These authors reported that droplets having a diameter of less than 6 μm crystallized at higher undercooling ($T_c \approx 78$ °C), while the larger droplets crystallized at $T_c \approx 105$ °C – the latter temperature corresponding to the bulk T_c for the PP used in the studies. The authors referred to the fractionated crystallization behavior caused by a lack of heterogeneities in some of the finely dispersed PP droplets, ending up with the appearance of the homogeneous crystallization peak. Hence, the nucleation mechanism was found to be strongly influenced by the blend morphology.

Polyester Blends

Quirk et al. (1989) investigated the crystallization behavior of PET in a PET/PS 25/75 blend. The PET particle diameter as determined by SEM was found to be in the range of 5 μm, being quite large due to the large difference in interfacial tension between both phases (hindering easy droplet breakup during mixing). Suppression of the cold crystallization in the PET droplets quenched from the melt was observed, along with serious depression of the total degree of crystallinity with increasing content of the amorphous phase.

PBS/PBA crystalline/crystalline miscible blends were recently studied for their crystallization behavior by Yang et al. (2011). Upon blending with PBS, PBA was found to exhibit fractionated crystallization during the nonisothermal crystallization process. The higher isothermal crystallization temperature (TIC) of PBS (e.g., 100 °C) was favorable for the fractionated crystallization of PBA, which was probably attributed to the distribution of PBA in the preexisting PBS matrix. At high TIC of PBS, the phase segregation of PBA was more obvious, that is, PBA can be distributed in the interspherulitic region as well as interfibrillar/interlamellar region of the PBS matrix. However, at low TIC of PBS, the phase segregation was not obvious. The parameters of the crystallization kinetics suggest that PBS suppresses the crystallization of PBA, which was mainly ascribed to the physical confinement effect of PBS on PBA. From the WAXD and FTIR analyses, it was concluded that PBS facilitates the formation of the PBA α-crystal, namely, the PBA polymorphic crystallization can be regulated. From polarized OM observation, the spherulite growth direction and morphology of PBA were found to be controlled by those of PBS. This was mainly ascribed to the induction effect of growth direction of PBS lamellae on PBA ones.

Polyamide Blends

Tol et al. (2005a) intensively described the crystallization phenomenon of polyamide (PA6) semicrystalline component in an immiscible blend with pure PS or (PPE/PS) amorphous miscible mixture. The idea was to have a controlled and a varying glass-transition temperature of the amorphous phase. Two situations

were studied: uncompatibilized blends and reactively compatibilized blends using SMA reactive copolymer. The composition and viscosity ratios of the blend have been selected to generate versatile phase morphologies including the most important ones for the study, i.e., PA6 droplets in (PPE/PS) matrix.

Uncompatibilized PA6/(PPE/PS) Blends

Multiple crystallization peaks were observed in blend systems where PA6 constitutes the dispersed droplets (s 65 and 66). The blends having continuous PA6 phase do not show significant differences in crystallization behavior compared to pure PA6 homopolymer. In contrast, as PA6 content decreases, it forms discrete droplet in the matrix. The multiple crystallization peaks correspond to different degrees of supercooling. As the size of the droplet exceeds a critical size, the PA6 crystallizes around its bulk crystallization temperature (188 °C). When the morphology becomes finer and the concentration of PA6 droplets per unit volume increases, a significant part of the droplets crystallize at higher degree of supercooling as translated by the intensity of the new crystallization peaks. This was ascribed to a heterogeneous nucleation of nuclei having different activities. Three crystallization peaks have been identified in blends with (PPE/PS) matrix. One of these peaks has been formed below ($T_c = 90$ °C), the average vitrification temperature of the matrix ($T_g = 150$ °C). It has been ascribed to a homogeneous nucleation after all the heterogeneities in the droplets have been exhausted. The authors concluded that:

- When the droplet size is small enough and the number of PA6 droplets exceeds the number of nuclei active at T_c bulk, crystallization takes place in different steps, at larger degrees of supercooling, via nucleation by different types of nuclei that need a larger supercooling to become active.
- The crystallization can be affected by the thermal history.
- Self-nucleation experiments generating a larger number of nuclei crystallizing at T_c bulk can lead to a complete suppression of the fractionated crystallization phenomena.
- When the amorphous phase is vitrified prior to crystallization, the nucleation densities increase, leading to less fractionated crystallization in the dispersed droplets.
- The overall crystallization rate, determined after self-nucleation, decreases with decreasing PA6 droplet size (20–1 μm), indicating the disturbing effect of the small dimensions of the micrometer-sized PA6 particles.
- The degree of fractionated crystallization, characterized by the fraction of the droplets that crystallized at temperature below T_c bulk, can be fairly related to the volume average droplet diameter.
- The number of crystallization peaks T_c bulk is very dependent on the droplet size distribution, leading to more peaks for broader distributions (Figs. 3.66 and 3.67).

Reactively Compatibilized PA6/(PPE/PS) Blends

The authors used SMA reactive copolymer that reacts via the anhydride group with the amine groups of the PA6 semicrystalline component of the blend and the

Fig. 3.66 DSC cooling curves for a number of (PPE/PS)/PA6 blend compositions with PA6 droplets (Tol et al. 2005a)
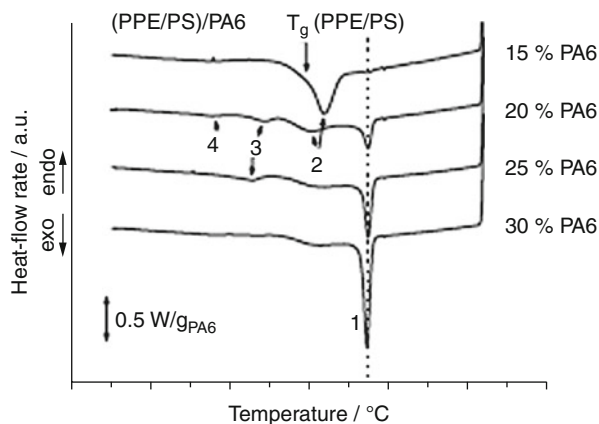
styrene segment ensures miscibility with the PS/PPE mixture. The effects of two copolymers, SMA2 (2 % MA content) and SMA17 (17 % MA), on the crystallization of PA6 in the immiscible (PA6/(PPE/PS)) blends were compared. Figure 3.68 is very illustrative of the effect of the SMA copolymer on the crystallization behavior of the blend. A very strong transition in crystallization behavior is observed when the blend phase morphology evolves from a co-continuous to a PA6-dispersed droplets. Reactive compatibilization with SMA2 strongly decreases the PA6 droplet size in the blend by a factor of 10 (from 1–2 to 0.1–0.2 μm on average). In addition, due to compatibilization, the droplet distribution is less polydisperse compared to uncompatibilized blends. An enormous retardation of the crystallization is induced by the reactive compatibilization. The bulk crystallization around 188 °C (peak1) is completely suppressed, and a crystallization peak emerges around 85 °C (peak 3 in Fig. 3.68a, peak4 in Fig. 3.68b), about 100 °C lower than the bulk crystallization temperature. The authors performed additional experiments combining the phase morphology (droplet size and distribution measurement) and crystallization phenomena and draw the following conclusions on the effect of the reactive compatibilization on crystallization of PA6 in compatibilized immiscible PA6/(PPE/PS) blends:

– Fractionated crystallization is strongly enhanced in the submicron-sized PA6 droplets per unit volume leading to a marked delay of crystallization to very high supercooling and ultimately to crystallization at temperatures as low as 85 °C.
– A clear relation between the number of dispersed PA6 droplets per unit volume and the intensity of the homogeneous nucleation peak at this very low crystallization temperature has been found.
– Abundant reaction of the reactive copolymer with the PA6 seems to reduce the mobility of PA6 chain segments, leading to an increased fractionated crystallization in the PA6 droplets.

Ethylene-1-octene copolymer was also used as an amorphous blend partner of PA6 in PA6/ethylene-1-octene blend reactively compatibilized using PE-g-MA reactive copolymer (Sanchez et al. 2006). Because of the dispersed phase
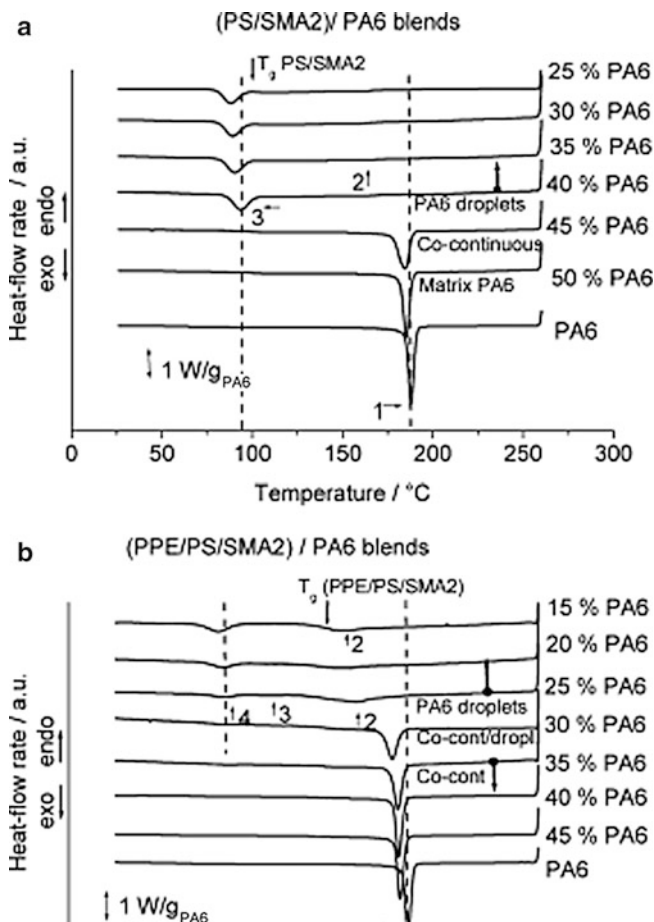
Fig. 3.67 DSC cooling curves at 10 K/min for (**a**) PS/PA6 and (**b**) (PPE/PS)/PA6 blend compositions (Tol et al. 2005a)

morphology, fractionated crystallization was observed, leading to an extra supercooling of PA6 (50 °C compared to bulk crystallization temperature). Self-nucleation experiments the authors used were able to demonstrate, as expected, that a lack of heterogeneities is at the origin of the fractionated crystallization.

Yordanov et al. (2005) have considered fractionated crystallization in blends of LDPE/PA6 reactively compatibilized using each of the three different types of reactive copolymers: EAA, EGMA, and SEBS-g-MA. As expected the SEBS-MA, owing to the efficient reaction of the maleic anhydride groups with the amine groups of PA6, resulted in the most significant particle size reduction of the dispersed phase. As a direct consequence, the most visible fractionated crystallization was obtained with this copolymer. Compatibilization with EGMA could not lead to PA6/LDPE blends that exhibit fractionated crystallization because of a lack of interfacial

Fig. 3.68 DSC crystallization curves for different compositions of (**a**) (PS/SMA2)/PA6 blends and (**b**) (PPE/PS/SMA2)/PA6 blends. (PS/SMA2 ratio 92/8 w/w, (PPE/PS/SMA2)/PA6 80/20, and 85/15: 95/5 w/w (PPE/PS)/SMA2 (Tol et al. 2005b)
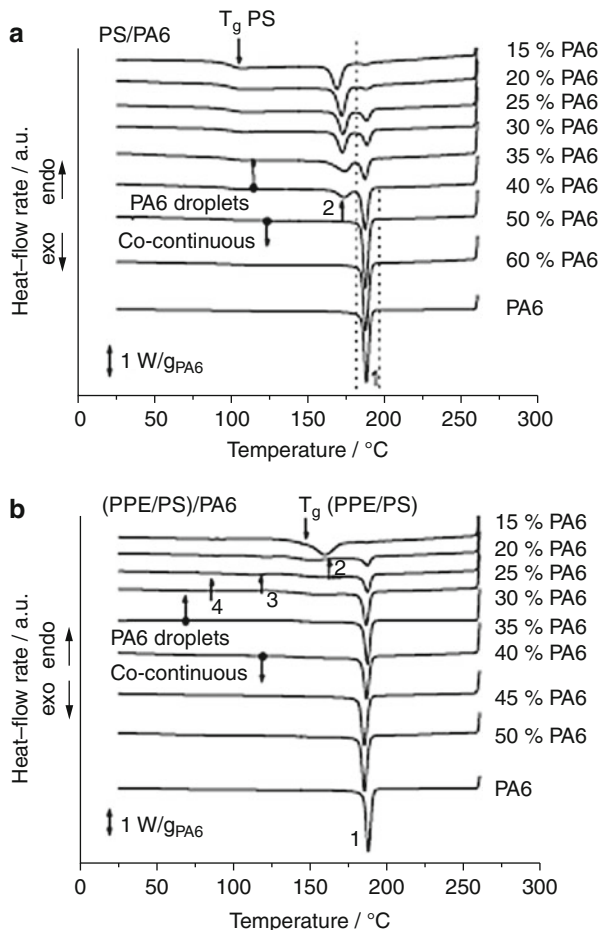
reaction and thus inefficiency in reducing particle size. The authors performed self-nucleation experiments and concluded that the lack of nuclei is responsible for the fractionated crystallization at high supercooling and not the absolute particle size reduction.

Other Blends

Robitaille and Prud'homme (1983) studied the crystallization in the liquid/liquid phase-separated melt of the triblock copolymer PEG-PI-PEG having a minor amount of PEG. The authors reported a lower degree of crystallinity of the PEG domains along with a slight melting-point depression. Due to the fine dispersion of PEG, the droplets only crystallized at much higher undercoolings (up to 60 °C lower than the bulk T_c), and less perfect crystalline lamellae were formed. These lamellae consequently melted at lower temperatures than the usual T_m. The bulk T_c has disappeared completely. The authors related this behavior to the
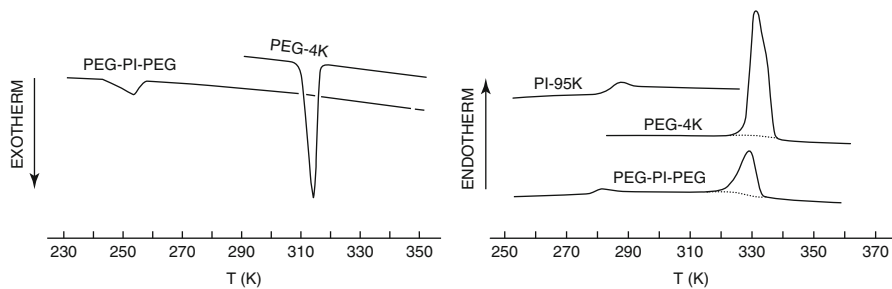
Fig. 3.69 DSC cooling and heating curves for the PEG-PI-PEG block copolymer, a pure PEG sample, and PI; the homogeneous crystallization of the PEG segment at much higher degrees of undercooling does not really influence its melting behavior (Robitaille and Prud'homme 1983)

lack of heterogeneities available in the PEG microdomains, which are hence nucleated at much lower temperatures by a homogeneous nucleation mechanism (Fig. 3.69).

Tang and Huang (1994a) investigated that the crystallization behavior of PA-6 is an EPDM matrix. The fractionated crystallization of the PA-6 occurs when the PA-6 content decreased below 15 wt%. Two crystallization peaks were observed, one around the bulk $T_{c,PA-6}$ and another at about 25 °C lower, caused by the smaller PA-6 droplets having a lack in heterogeneous nuclei. The ratio of the α/γ crystalline form was not altered by the fractionated crystallization, indicating that the lower crystallizing droplets do not crystallize in another crystalline form as in the bulk.

Fractionated crystallization of the POM crystalline phase in (PS/PPE) miscible amorphous phase has been investigated by DSC, and the results were correlated to the blend phase morphology (Everaert et al. 2000). This model blend was selected to investigate both the influence of the blend phase morphology and of the physical state of the amorphous PS/PPE matrix on the crystallization behavior of the minor POM phase. To have a varying Tg of the amorphous matrix, the PS/PPE composition has been varied as 85/15, 60/40, 50/50, and 40/60 wt:wt% to have tg's of 114 °C, 134 °C, 144 °C, and 156 °C, respectively. Interesting relationships were established between the crystallization features and the parameters of the phase morphologies developed in the blend. Figure 3.70 shows the absolute degree of crystallinity of the POM crystalline phase as a function of the average particle diameter of the POM dispersed as minor phase in PS/PPE amorphous matrix (the composition of Ha4 and Ha7 are 85/15 and 50/50 PS/PPE, respectively). The authors could not correlate the degree of crystallinity to the POM particle diameter. In contrast, as the fraction of POM droplets should reflect all homogeneously crystallized material, a correlation between both parameters could be found (Fig. 3.71). To elucidate a possible effect of the phase morphology of the blend on the crystallization of the crystalline polymer, the authors have asked and discussed the following key questions: (i) What determines the onset of fractionated crystallization and/or the offset of heterogeneous nucleation at T_c, bulk?

Fig. 3.70 Relationship between the absolute degree of crystallinity, X_c, of the POM phase and the average particle diameter of the POM droplets (Everaert et al. 2000)
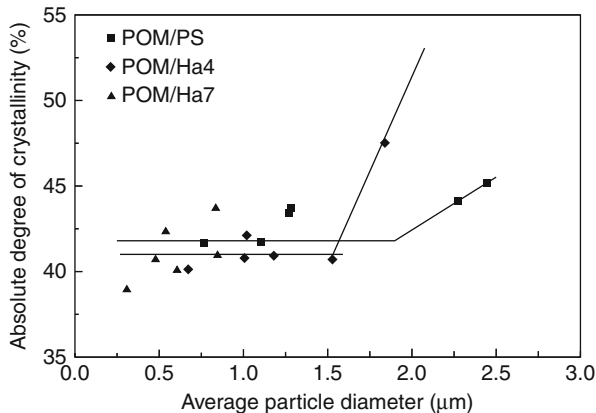
Fig. 3.71 Correlation between the fraction of POM droplets in POM/Ha7 blends with a composite-like phase morphology and the intensity of the homogeneous crystallization peak (Everaert et al. 2000)
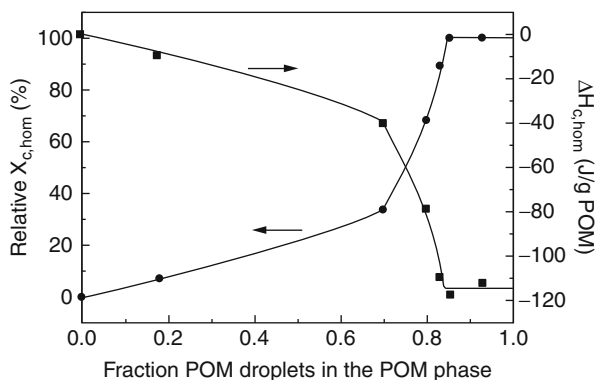
(ii) Is fractionated crystallization solely related to the blend phase morphology? (iii) Under what conditions are multiple crystallization peaks possible, and what determines their number and extent? (iv) What causes the decrease of the crystallinity in fractionated crystallizing samples? The onset of fractionated crystallization was found to coincide with the center of the phase inversion region. In contrast, the morphological parameters and blend composition that could influence the offset of fractionated crystallization were less evidenced. The data presented in Table 3.28 reveal the effect of the POM content in POM/(PS/PPE) blend systems on the final degree of crystallinity, X_c, as calculated directly from fractionated crystallization.

The semicrystalline phase morphology and crystallinity of POM in POM/(PS/PPE) blends were studied with respect to fractionated crystallization (Everaert et al. 2003). The degree of crystallinity decreases with decreasing POM content with a visible shift from bulk to homogeneous crystallization. Analysis of WAXD reflections indicate that the decrease in X_c is not solely due to the formation of thinner lamellae at higher degrees of undercooling.

Table 3.28 Influence of the POM content in POM/(PS/PPE) blend systems on the final degree of crystallinity, X_c, as calculated directly from fractionated crystallization curves. X_c for POM is 54 %

Wt % POM	POM/PS	POM/Ha4	POM/Ha6	POM/Ha7	POM/Ha8
5	42[a]	41[a]	40[a]	39[a]	47[a]
10	42	41[a]	41[a]	41[a]	36[a]
15	43[a]	43[a]	39[a]	43	46
20	43	41	39	41	46
30	44	41	42	41	47
40	45	48	45	44	51
60	53[b]	46	51	53	52[b]

[a]Only one crystallization exotherm around 95 °C (homogeneous nucleation)
[b]Only one crystallization exotherm around 145 °C (bulk nucleation)

3.3.4.4 Droplet Crystallization in the Presence of a Glassy Amorphous Matrix

The crystallization of dispersed domains in the presence of a solidified matrix has not yet been a field of active research. Some examples are given below.

Polyethylene Blends

The thermal behavior of PS/LDPE blends has been investigated by Baitoul et al. (1981). A clear indication of the fractionated crystallization was deduced from the appearance of two additional crystallization peaks around 71 °C and 64 °C in all blends in which LDPE was the dispersed phase. Furthermore, the crystallization kinetics was found to slow down severely when the content of PS was raised.

Kunori and Geil (1980) investigated the melting behavior of the binary PC/HDPE blends, in which the weight percentage PE varied between 2 % and 10 %. The melting temperature of the HDPE droplets did not seem to be affected.

Polypropylene Blends

The majority of published papers on the crystallization of PP in blends concerns those blends in which the T_g of the amorphous component falls below the crystallization temperature of PP. The crystallization of PP in the presence of a glassy amorphous matrix has seldom been reported.

The well-known blend PC/PP has been intensively investigated by Favis and his co-workers (1987, 1988, 1990, 1992). Morphology development, rheology, compatibilization, etc., were studied, but no results on the thermal behavior of these blends were reported.

Polyester Blends

Quirk et al. (1989) have reported the crystallization behavior in blends of PPE with PET. Since the blend components showed only a small difference in the interfacial tension, quite small dispersions could be obtained ($d \approx 4$ μm). The authors reported that the glassy PPE matrix enhanced the cold crystallization of PET after being quenched. Decreasing the PPE content from 75 to 50 wt% resulted in the nearly

disappearance of the cold crystallization exotherm. This behavior was found to be opposite to that in a PS/PET blend (where PET crystallizes surrounded by a PS melt). No clear explanation has been given here.

A similar result for PPE/PET blends has been reported by Liang and Pan (1994). The authors found the cold crystallization temperature, $T_{c, cold}$, in the dispersed PET phase to be markedly lower than that of the virgin PET, indicating that PPE may partly act as nucleating agent to promote the nucleation of the PET component.

Other Blends

O'Malley et al. (1969) described the thermal behavior of PEG/PS blends in which PEG was dispersed into fine droplets. A clear indication of fractionated crystallization combined with a simultaneous decrease in the total degree of crystallinity with increasing weight fraction of PS has been observed. Again, a slight decrease of the melting temperature, T_m, with about 2 °C was detected, although ΔH_m remained unaffected. This was attributed by the authors to the formation of less perfect crystalline lamellae during the crystallization at higher undercooling.

Chang et al. (1991) reported on the melting behavior in PC/POM blends. The blends were found to behave in a similar way as the above-described PEG/PS blend.

3.3.5 Conclusions

It can be stated that the crystallization behavior of a semicrystalline polymer phase, dispersed into an amorphous matrix, is characterized by:

 (i) Fractionated crystallization or homogeneous nucleation if the minor phase is finely dispersed. Annealing or large droplets resulted in the appearance of a crystallization peak close to the bulk T_c° of the homopolymer.
 (ii) A decrease in the overall degree of crystallinity, X_c, after cooling from the melt, most pronounced in finely dispersed blend morphologies.
(iii) A slight decrease of the melting temperature due to the formation of less perfect crystalline lamellae at higher undercoolings. A decrease of the overall melting enthalpy, ΔH_m, could be observed clearly, only in blends where the crystallizable dispersed phase did not undergo recrystallization upon heating.

3.3.6 Binary Polymer Blends Containing Two Crystallizable Phases

A large number of polymer blends consists of two crystallizable phases (Table 3.15); hence, more studies have been carried out on the thermal behavior of crystalline/crystalline polymer blends.

The morphology of a polyblend consisting of two crystallizable polymers can vary depending on the processing conditions and the relative rates and temperature of crystallization of the constituent polymers. These can either crystallize at the same time (coincident crystallization, see further) or separately in a sequential

manner, leading to different morphologies and hence different properties. As such, in blends of two semicrystalline polymers, the physical properties may be altered not only by the blend composition and the phase morphology but also by changing their relative crystallization behavior. Therefore, it is important to study the effect of blending on the crystallization behavior of each component in the blend, to understand the structure development as influenced by melt-processing.

Because the phases are physically separated in the melt, the theory concerning the crystallization behavior as discussed above can be combined to understand the crystallization and melting behavior of most crystalline/crystalline polymer blends. In general, both crystallizable phases crystallize separately around their characteristic bulk T_c-value (as long as the minor phase is not dispersed into very fine droplets). The T_c-values can be somewhat shifted due to the migration of heterogeneities from one phase toward the other phase or due to the nucleating activity of one – crystalline or crystallizing – phase at the interface with the second phase. However, changes in the nucleation density of both phases will be more clearly reflected in the spherulite size of each blend component with respect to the homopolymer. This can have important consequences for the final mechanical properties of the blend (Friedrich 1978, 1979).

In the following overview, a survey of the most important topics concerning crystallization behavior in immiscible crystalline/crystalline polymer blends is given. Because the physical state of the second phase affects the crystallization mode of the phase under consideration, a distinction has been made for blends crystallizing in a melt environment and those crystallizing when the second phase has solidified.

3.3.6.1 Crystallization of the Matrix in the Presence of a Molten Dispersed Phase

For most commonly studied polymer blends, crystallization of the matrix occurs in the presence of a molten dispersed phase. The crystallization behavior of the continuous phase can be compared to that found for crystalline/amorphous blend systems in which the dispersed amorphous phase was in the molten state.

Polyethylene Blends

Because of the low crystallization temperature of the polyethylenes (HDPE, LDPE, LLDPE, etc.) (see Table 3.15), in most commonly used blends, the dispersed phase has already solidified before the PE matrix starts crystallizing. However, Greco et al. (1987a) studied the crystallization of HDPE ($T_c \approx 118\ ^\circ\text{C}$) in an 80/20 binary blend with EPR elastomers containing a different ethylene/propylene ratio. The HDPE phase was reported to exhibit higher T_c-values during cooling from the melt, indicating enhanced nucleation, due to the nucleating effect of the EPR copolymers on the HDPE matrix. Furthermore, the melting point, T_m, shifted to slightly higher temperatures relative to the homopolymer due to better crystal perfection as a result of the dissolution of some low molecular weight ("defective") HDPE molecules into the EPR copolymer phase during the melt-mixing process. The latter phenomenon was directly related to the ethylene content in the copolymer.

Polypropylene Blends

Blends of isotactic polypropylene, PP, with a polyethylene are immiscible and, owing to their commercial importance, have been the subject of intensive studies. In these blends, PP crystallization mostly takes place in the presence of molten PE droplets.

Long et al. (1991) investigated the crystallization behavior in blends of PP with LLDPE. They found the crystallization temperature of the PP matrix, T_c, to decrease slightly upon the addition of LLDPE. However, the degree of crystallinity, X_c, and the spherulite growth rate, G, were not affected. The authors concluded that the overall crystallization rate of PP in the matrix decreased due to a decreasing primary nuclei density. The latter was confirmed in O. M. experiments by the increased size of the PP spherulites upon the addition of LLDPE. However, Zhou and Hay (1993) reported that with the addition of LLDPE to PP, the crystallization rate remained similar as for the PP homopolymer.

Flaris et al. (1993) investigated also the same blend system and reported that blending had a pronounced effect on the lamellar morphology. Furthermore, the isothermal crystallization experiments indicated that the spherulite growth rate, G, and the nucleation density of the PP phase were enhanced. The authors suggested that these observations could be related to the formation of additional nucleation sites, which arise from the polymer-polymer interfaces created by the blending.

Because three different observations were reported on the crystallization of the PP matrix in which LLDPE droplets are dispersed, no unambiguous conclusions on this matter can be given. A serious investigation of all factors playing a role here is necessary in the future.

Blends composed of a PP matrix with LDPE as the minor dispersed phase have been intensively investigated by Teh (1983), Bartczak et al. (1984), Galeski et al. (1984), and recently Teh et al. (1994a). All authors found LDPE to act primarily as an efficient nucleating agent for the PP matrix, reducing the average PP spherulite size, and to induce the formation of some large β-form PP crystals at the interface with the LDPE phase that melt at a lower temperature, $T_m = 155\,°C$ as compared to normal α-form PP crystals with $T_m = 165\,°C$. Galeski et al. (1984) and Bartczak et al. (1984) revealed that the nucleating activity of the LDPE phase was mainly attributed to the migration of heterogeneous impurities from LDPE to PP during the melt-mixing process. Furthermore, Galeski et al. (1984) showed the spherulite growth rate of the PP matrix to be unaffected by the dispersed molten LDPE droplets and showed that these droplets were not rejected by the growing PP spherulites.

In the case of PP/HDPE blends, the influence of the HDPE component was more complex and dependent on the physical state of the dispersed HDPE droplets. At a T_c high enough to prevent any HDPE crystallization, the overall rate of crystallization of the PP matrix in isothermal crystallization was found to be strongly reduced by the addition of HDPE (Bartczak et al. 1986). Since the spherulite growth rate of PP was found to be constant and independent of the blend composition (Teh et al. 1994a), this decrease has been attributed to a decrease in the nucleation density of the PP phase. Bartczak et al. (1986) related this to the migration of heterogeneous nuclei from the PP phase toward the HDPE melt during

melt-blending. As a result, the PP spherulite size was found to increase (Bartczak et al. 1986; Teh et al. 1994b). The same observations were reported for PP/HDPE blends cooled slowly from the melt (Plesek and Malac 1986).

However, in the case of either an isothermal crystallization at temperatures below the crystallization temperature of HDPE or crystallization at a higher cooling rate, there may have been migration of nuclei from the PP toward the HDPE phase, but the overall number of heterogeneous nuclei was increased due to the presence of HDPE crystallites that may have acted as additional nucleating centers for PP (Lovinger and Williams 1980; Gupta et al. 1982; Bartczak et al. 1986; Plesek and Malac 1986; Teh et al. 1994a, b). This results in a drastic reduction of the PP spherulite size (Noel and Carley 1984; Lovinger and Williams 1980; Plesek and Malac 1986). Moreover, Bartczak and Galeski (1986) reported that spherulitic crystallization of a polymer near the interface can cause its deformation, increasing the interfacial area, and can lead to an improvement of toughness and impact properties.

Greco et al. (1987b) studied the crystallization in immiscible PP/EPR blends. The average spherulite size in the PP phase was smaller than in the homopolymer. The higher the PP contents (C-3) in EPR, the stronger the nucleating effect for the matrix. The authors experimentally showed that migration of impurities could not cause this effect and that the copolymer composition was the most important factor. An increase in the PP content of the EPR caused a higher miscibility (defective PP molecules could be partially dissolved in the EPR phase), leading to more perfect PP crystallites melting at a higher T_m, and also caused a stronger nucleating effect.

Pukansky et al. (1989) investigated both the crystallization and melting behavior and the global blend morphology in PP/EPDM blends over the whole composition range. Blends quickly cooled from the melt did not show significant changes in the crystallization behavior of the PP matrix. However, blends crystallized at a fixed rate of 10 °C/min behaved differently. Thermograms of the blends containing between 5 and 50 vol% EPDM showed a second melting peak at lower temperature, corresponding to the melting of the β-form of PP. Furthermore, the authors reported that small amounts of EPDM slightly increased the $T_{c,PP}$, but did not affect the degree of crystallinity. Dispersed EPDM droplets thus seem to promote the formation of the hexagonal β-form of PP.

An overview of the effects affecting the primary nucleation in immiscible PP-based blends is provided in Table 3.29.

Polyethylene Terephthalate Blends

Wilfong et al. (1986) reported on the effects of blending low concentrations (1–10 wt%) **polyolefin** with PET on the crystallization and toughening behavior of the latter. The authors studied blends of PET with LLDPE, HDPE, PP, and poly (4-methylpentene-1), all of them having a lower melting point than PET (Table 3.15). Polyolefin melts did not enhance the nucleation of PET, although the spherulite size of the PET matrix was found to be 2.5–3 times larger than for the homopolymer, with a broader spherulite size distribution. Both the crystallization

Table 3.29 Overview of the phenomena influencing heterogeneous primary nucleation in polypropylene-based immiscible blends (After Bartczak et al. 1995)

Blend system[a]	Migration of impurities[b]	Crystallization of the second component[b]	Influence of the interface[b]	References
PP/LLDPE	—[c]	—	-	Zhou and Hay (1993)
	↓↓	—		Long et al. (1991)
	—		↑↑	Flaris et al. (1993)
PP/LDPE	↑↑	↑[c]	↑	Bartczak et al. (1984), Teh (1983), Galeski et al. (1984), Teh et al. (1994a)
PP/HDPE	↓↓↓			Bartczak et al. (1986), Teh et al. 1994a, b
	↓↓↓[d]	↑↑↑[d]		Lovinger and Williams (1980), Gupta et al. (1982), (Bartczak et al. (1986), Teh et al. (1994)
PP/EPR	——	—		Greco et al. (1987b)

[a]Data concerning the crystallization of the matrix polymer (mentioned first in the blend code)
[b]↑ indicates an increase of the nucleation density in the blend, ↓ indicates a decrease of the nucleation density (the number of arrows is related to the intensity of the effect)
[c]— indicates that the authors did not find evidence explicitly for the mentioned topic to influence the nucleation of PP in the blend system described
[d]Found for samples crystallized nonisothermally

rate and the degree of crystallinity were found to be reduced by blending. This was attributed to the expense of energy that was required by the crystallizing growth front to reject and deform the polyolefin dispersed molten droplets. Martuscelli (1984) and Bartczak et al. (1984) have calculated that the rejection and/or deformation of dispersed droplets by the crystallizing growth front can cause a marked depression of the spherulite growth rate, G.

Poly(phenylene sulfide) Blends
Poly(phenylene sulfide), PPS, is an expensive, high-performance but brittle specialty resin. Blending can offer a good alternative both in toughness improvement and cost reduction (Nadkarni and Jog 1991).

Shingankuli et al. (1988) and Jog et al. (1993) investigated the influence of blending PPS with PET on its thermal and crystallization behavior. Blending was found to enhance the PPS nucleation. Isothermal crystallization experiments revealed that the crystallization time of PPS decreases along with the crystallization induction time. Both parameters were found to depend on composition. Optical microscopy confirmed this and revealed that the size of PPS spherulites in PPS/PET blends was drastically reduced as compared to the homopolymer. Furthermore, the degree of crystallinity of the PPS phase decreased with increasing PET concentration. However, dynamic crystallization experiments showed a constant value of $T_{c,PPS}$. The authors have related the accelerated crystallization of PPS in a blend with PET to the nucleation at the interface of the PET droplets. Owing to its supercooled state, the PPS matrix consists of highly ordered chains.

Nadkarni and Jog (1986), Nadkarni et al. (1987), and Jog et al. (1993) investigated the crystallization in blends of PPS with three types of HDPE, having a different melt flow index. In contrast to the PPS/PET blends, PPS crystallizes now in a superheated HDPE melt environment. From the dynamic cooling experiments, it was found that the presence of the HDPE melt suppresses the crystallization of PPS. The crystal growth rate, G, of PPS was found to remain unchanged, but its nucleation density was reduced as the concentration of HDPE in the blend increased or when the melt viscosity of the HDPE phase decreased. As a consequence, the overall crystallization rate of PPS was found to be retarded.

Other Blends
Chen et al. (1988) reported about blends of polyamides with a polyolefin. PA-11/LDPE blends and PA/HDPE blends both showed an increase of the melting temperature of the PA-11 matrix due to the addition of the polyolefin. No further attention was paid to this phenomenon.

Holsti-Miettinen et al. (1992) and Ikkala et al. (1993) recently studied the crystallization behavior of PA-6 blended with PP. No shift of the crystallization temperature of the PA-6 matrix was observed in the blends; the dispersed PP droplets did not influence the crystallization behavior of the matrix.

Frensch and Jungnickel (1989) investigated the influence of blend composition on the crystallization and melting behavior of PA-6/PVDF blends and PBT/PVDF blends. The crystallization of the PA-6 matrix and PBT matrix was promoted by the dispersed molten PVDF phase, as indicated by the rise in their T_c in the blends, while their relative crystallinity remained unaffected. The authors assigned this increase in T_c to migration of nucleating heterogeneities from the dispersed PVDF phase toward the matrix phase during melt-mixing of the blends.

3.3.6.2 Crystallization of the Matrix in the Presence of a Solidified Dispersed Phase

The crystallization of a polymer in the presence of solidified domains of the second phase takes place through a heterogeneous nucleation process. Since the rate of heterogeneous nucleation is higher than that of homogeneous nucleation, and since primary nucleation is the rate-controlling step for polymer crystallization, the crystallization rate is expected to be higher in such blends when compared to homopolymers (Nadkarni and Jog 1991).

Polyethylene Blends
On account of their commercial interest, the crystallization of HDPE, LDPE, and LLDPE in blends with PP has been extensively investigated. In these systems, the PP phase solidified already before the PE matrix starts crystallizing.

In the case of LDPE/PP blends, not much attention has been focused on the case where the LDPE phase forms the matrix. Teh (1983) reported no shift in the melting temperature of the LDPE matrix in the presence of solidified PP domains. Bartczak and Galeski (1986) observed that the LDPE crystallinity remained unaffected by blending.

Zhou and Hay (1993) investigated the crystallization behavior in LLDPE/PP blends. The crystallization rate of the LLDPE matrix, measured from isothermal DSC experiments, was not really affected by the dispersed PP domains. However, its degree of crystallinity slightly decreased with increasing PP content in the blend. According to the authors, this could be ascribed to the lower degree of perfection of the LLDPE crystals.

More extensive investigations have been performed on HDPE/PP blends by Martuscelli et al. (1980) and Bartczak and Galeski (1986). From the isothermal crystallization experiments, it was found that the rate of crystallization of the HDPE matrix was markedly reduced upon addition of small amounts of PP (10 wt%). The authors attributed this phenomenon to the increased melt viscosity of the sample caused by the presence of solidified PP domains. Moreover, Plesek and Malac (1986) have calculated from the surface tensions of the homopolymers at T_c that PP crystallization will not cause the nucleation of the HDPE phase, while in the reverse case HDPE crystals will induce the nucleation of PP.

Similar results were reported by Nadkarni and Jog (1986) and Nadkarni et al. (1987) for HDPE/PPS blends. The degree of crystallinity of HDPE in blends with a HDPE matrix was not affected by blending. The degree of supercooling required for initiating nonisothermal crystallization of HDPE was surprisingly not affected by the presence of solid PPS domains. However, isothermal crystallization halftimes for HDPE in the blends containing more than 10 wt% PPS were longer than for the HDPE homopolymer. Again, this has been attributed by the authors to the increased melt viscosity due to the presence of solidified PPS domains.

Frensch et al. (1989) reported on the crystallization of HDPE in a blend with POM. The HDPE matrix crystallized in all samples at almost the same temperature and to the same extent, independent of the extrusion time.

Polypropylene Blends
The majority of papers related to the crystallization of isotactic polypropylene(PP)-based blends concern those where the PP matrix crystallizes in the presence of a molten dispersed phase of polyethylenes and olefinic elastomers. As a result, crystallization of a PP matrix in the presence of a solidified dispersed polymer has seldom been reported (Nadkarni and Jog 1991).

Shingankuli (1990) studied the crystallization behavior of PP in the presence of solidified PVDF domains. A higher crystallization temperature of the PP matrix phase was observed, indicating an enhanced nucleation in the blends. The degree of crystallinity of PP was found to increase by about 30 % to 40 % with increasing PVDF content. Isothermal crystallization studies also confirmed the acceleration of the overall crystallization rate in terms of shorter crystallization halftimes for PP.

More efforts have recently been dedicated in understanding the crystallization behavior in PP/PA-6 blends. Holsti-Miettinen et al. (1992), Moon et al. (1994), and Ikkala et al. (1993) found that the crystallization temperature of the PP matrix by cooling from the melt rises by about 10 °C by adding PA-6. Ikkala et al. (1993) observed that the largest temperature increase was caused at a PA-6 concentration of about 20 wt%; in this case, the PA-6 dispersion size was quite small (2.5 μm).

Moon et al. (1994) have related this temperature shift to the migration of heterogeneous nuclei toward the PP matrix during the melt-mixing process, together with the nucleating agent-like behavior of the solidified PA-6 domains. No change of the melting peak has been noticed (Park et al., 1990). Grof et al. (1989) performed some isothermal crystallization experiments on fibers of the PP/PA-6 blend. In accordance with the cited findings, the latter authors reported a decrease both in the crystallization halftime and the induction time for crystallization of PP in PP/PA-6 blends, while no change in the degree of crystallinity was observed.

Tang and co-workers (1994) investigated briefly the crystallization behavior of PP in blends with PA-12. The melting point remained unaffected by blending. However, a slight shift of the crystallization peak (about 2.5 °C), upon cooling from the melt, was reported for blends comprising 33 wt% PA, along with an increase of the height of the T_c peak. The PP matrix has been nucleated by the dispersed PA-12 domains. The authors related this to the fine morphology; at the interface of the phases, epitaxial crystallization had also been observed. This was also the reason why the PA-12 phase in the blends only existed in the γ-form. However, it should be mentioned that these PP/PA-12 blends were prepared from solution.

Polyethylene Terephthalate Blends

Only few papers related to the crystallization of a PET matrix in immiscible crystalline/crystalline blends have been published.

Shingankuli et al. (1988) investigated the thermal behavior of PET blends with the glass fiber-reinforced polymer PPS. Dynamic crystallization experiments revealed that the PET crystallization behavior was significantly altered by blending. Upon the addition of PPS, both the onset temperature for crystallization and the peak value, T_c, showed a dramatic shift to higher temperatures (up to 20 °C). Also, the degree of crystallinity significantly increased in the blends. The author attributed the phenomenon to the heterogeneous nucleation induced by the glass fibers in the PPS phase and the nucleating activity of the already solidified PPS domains. As a result, the PET matrix in the blends became richer in heterogeneous nucleating sites as compared to virgin PET. Isothermal experiments confirmed these conclusions and showed that the crystallization halftime of PET decreased drastically in the blends (attributed to the enhanced nucleation). Furthermore, an increase of the onset of melting of the PET matrix (15 °C) with increasing content of PPS in the blends has been observed. The melting behavior PET in the blends has been explained by the formation of larger and more perfect crystallites (due to the nucleation at higher temperatures) with a narrower size distribution and by an increased degree of crystallinity.

Other Blends

Frensch and Jungnickel (1989, 1991) and Frensch et al. (1989) have investigated the thermal behavior of polyvinylidene fluoride, PVDF, in blends with polyamides, in relation to the blend morphology. PA-6 droplets could be finely dispersed into the PVDF matrix. The crystallization temperature of the PVDF matrix did not seem to be affected in the blends. A similar behavior was observed in PVDF/PA-66 blends.

Investigations on the crystallization behavior of PVDF in a blend with polybutyleneterephthalate, PBT, have been reported by Frensch and Jungnickel (1989) and Frensch et al. (1989). PBT dispersed droplet size was found to be an order of magnitude larger than the dispersed PA droplets in PVDF blends. However, in this case, the $T_{c,PVDF}$ displayed a shift to higher temperatures (2–8 °C) upon blending with PBT, which was attributed to the nucleating efficiency of amorphous or crystallizing PBT domains (which subsequently crystallized coincidentally with the PVDF matrix).

3.3.6.3 Crystallization of the Dispersed Phase in the Presence of a Matrix Melt

Immiscible blends most often show a two-phase morphology consisting of a continuous matrix and a droplet-like dispersed phase beyond the phase inversion region. From Sect. 3.2.3, it is clear that the crystallization behavior of droplets can be dramatically affected as compared to the homopolymer.

In summary, (i) dispersed drops can have an altered nucleation density, caused by the migration of heterogeneous nuclei during the melt-mixing process, they can be nucleated by a crystallizing or solidified matrix, the interface can induce some additional nucleating centers, etc. (ii) The smallest dispersed droplets can suffer from the lack of heterogeneous impurities in each droplet, what may result in a fractionated crystallization. In some cases, this can give rise to the coincident crystallization of the dispersed phase with the (lower crystallizing) matrix (see Sect. 3.2.4.6).

Polyethylene as Dispersed Phase

Because of the low crystallization temperature of all polyethylenes as compared to most other commonly used thermoplastics, crystallization will proceed most often in an already solidified matrix. No literature could be found on the crystallization behavior of PE in a molten matrix environment.

Polypropylene as Dispersed Phase

Typical polymer blends with isotactic polypropylene, PP, are the PP/PE blends, in which PP is the first crystallizing component.

Zhou and Hay (1993) investigated the crystallization in LLDPE/PP blends. They reported that the extent of crystallization in PP droplets is seriously hindered by the low nucleation density of PP, resulting in a serious drop of the degree of crystallinity during the isothermal measurements. From these experiments, it could be predicted that cooling from the melt would result in a fractionated crystallization (30 wt% PP) or even homogeneous crystallization (10 wt% PP). Similar results had already been reported by Long et al. (1991), Pukanszky et al. (1989), and recently Müller et al. (1995) and Morales et al. (1995). The latter authors even mentioned that the retarded crystallization of PP droplets in some cases finally resulted in the coincident crystallization of PP with the LLDPE matrix. Furthermore, a partial change in the crystallographic form from α to the lower melting β-form was observed. Lovinger et al. (1977) reported that the β-form is nucleated at a lower rate than the α-form and hence promoted on homogeneous nucleation.

Teh (1983) reported only the melting behavior of LDPE/PP blends – no shift in $T_{m,PP}$ was seen. An enhancement in the formation of the β-form PP spherulites in the LDPE melt was observed.

Blends of HDPE with PP have been studied by several authors. However, not much attention has been focused on the crystallization behavior of the dispersed phase yet.

Polyamide as Dispersed Phase

Several blends with polyamides, crystallizing at high temperatures, have been studied. Chen et al. (1988) investigated the phase morphology and melting behavior of HDPE/PA-11 and LDPE/PA-11 75/25 blends. The melting point of the dispersed PA-11 phase was found to be unaffected by blending.

Several studies have been performed on the thermal behavior of PP/PA-6 blends. Park et al. (1990) reported a melting-point depression for the dispersed PA-6 phase (about 4 °C), having an average particle size of 2–5 μm at 25 wt% PA-6 in the blend. However, the relations between the crystallization phenomena and the blend morphology were not explored. Ikkala et al. (1993) have investigated the correlation between the blend morphology, crystallization, and melting behavior of the minor component in PP/PA-6 blends. The PA-6 phase was reported to crystallize at its bulk temperature. However, compatibilization (resulting in the formation of a finer dispersion) did not show any crystallization exotherm around the bulk $T_{c,PA\text{-}6}$. This could be explained by the retarded crystallization caused by a lack of heterogeneous nuclei in the PA-6 droplets. Finally, the nucleating activity of both blend components on each other caused the coincidental crystallization of the PA-6 with the PP matrix.

Moon et al. (1994) also investigated the thermal behavior of PP/PA-6 70/30 blends. The authors reported the T_c of the PA-6 droplets to rise remarkably (by about 14 °C) as compared to the T_c of the virgin PA-6. This rise in $T_{c,PA\text{-}6}$ was explained by analogy to findings of Khanna et al. (1988a, b) on pure virgin PA-6 homopolymer, suggesting that melt extrusion of PA-6 would lead to a more ordered molecular arrangement that persisted in the molten state due to hydrogen bonding, and as such caused a faster crystallization. This has been confirmed by crystallization experiments on melt-extruded PA-6 homopolymer. The results of the blends as compared to melt-mixed pure PA-6 agree with those reported by Ikkala et al. (1993) – no shift in the $T_{c,PA\text{-}6}$ was caused by blending. Furthermore, they also reported that compatibilization of the blends caused a decrease of the dispersed phase size, leading to fractionated and subsequently coincident crystallization.

Frensch and Jungnickel (1989) and Frensch et al. (1989) tried to elucidate the crystallization behavior of the minor phase in the binary PVDF/PA-6 blends, in relation to the final blend morphology. They reported that the crystallization of the PA-6 droplets was fractionated and/or retarded, depending on the number of mixing cycles and dispersion size. The smaller the PA-6 droplets, the more pronounced the retardation of the crystallization peak ($\Delta T \approx 40$ °C). Nevertheless, the melting endotherm remained unaffected. They concluded that part or all of the PA-6 phase finally coincidentally crystallized with the PVDF matrix due to the specific mutual nucleating efficiency of both components.

A similar behavior has been reported by Frensch and Jungnickel (1991) for PVDF/PA-66 blends. In this case, the undercooling associated with the retarded crystallization was about 90 °C higher than the one for the bulk crystallization! The size of the dispersed PA-66 droplets has been found to be only about 0.3 μm. The authors concluded that the appearance of fractionated and coincident crystallization is correlated with the low interfacial energies between the amorphous melt phases, providing a high level of dispersion, and between the crystalline phases, providing a nucleating efficiency.

Other Blends

Shingankuli et al. (1988) reported on the crystallization of dispersed PPS domains in a PET matrix. The onset of crystallization of the dispersed PPS domains decreased (by about 7 °C) with decreasing PPS content, together with the crystallization peak and the degree of crystallinity. The authors concluded that the PPS crystallization was retarded mainly when the PPS content in the blends was below 20 wt%. Furthermore, the onset of melting of the PPS fraction remained nearly unaffected, except for those blends containing less than 20 wt% PPS. In the latter case, the onset of melting seriously decreased (by about 30 °C), whereas the melting peak temperature and heat of fusion remained constant. This can be attributed to the lower crystallization temperature of the PPS droplets leading to the formation of less perfect, lower melting crystallites.

Klemmer and Jungnickel (1984) have reported on the fractionated crystallization of POM in an HDPE matrix. They found an additional crystallization peak of POM to occur 14 °C lower than the bulk crystallization peak. This was attributed to the fractionated crystallization of POM, caused by an interface-induced additional inhomogeneous nucleation and crystallization. It was shown that this phenomenon only occurs in those blends where the number of the dispersed particles was higher than the number of available heterogeneous particles. Moreover, the preparation method clearly influenced the fractionation due to the change of the particle sizes – fractionated crystallization has been observed only in melt-mixed blends.

Frensch and Jungnickel (1989) and French et al. (1989) have investigated PVDF/PBT blends and related their thermal behavior with the blend morphology. Similar to PVDF/PA-6 blends, the PBT droplet crystallization was completely suppressed in an 85/15 blend and finally crystallized coincidentally with the PVDF matrix. Again this phenomenon could be related to the fine dispersion of PBT droplets, in number exceeding the available nuclei. Shorter melt-mixing cycles caused a coarser dispersion leading only to a fractionated crystallization of PBT at $T_{c,bulk}$ and at $T_{c,PVDF}$.

3.3.6.4 Crystallization of the Dispersed Phase in the Presence of an Already Solidified Matrix

Polyethylene as Dispersed Phase

PP/PE blends have been studied extensively by several authors. Zhou and Hay (1993) reported that the dispersed LLDPE droplets in PP/LLDPE blends showed problems in nucleating at the normally expected bulk crystallization temperature, T_c. Also, a serious decrease of the degree of crystallinity from isothermal measurements, as the LLDPE content decreased, could be observed. Contrary to these

observations, Müller et al. (1995) recently stated that the LLDPE droplets do not exhibit fractionated crystallization when they are dispersed in a PP matrix (although they do in a PS matrix), because of the nucleating effect of the solidified PP matrix on the LLDPE droplets.

Galeski et al. (1984) and Teh et al. (1983) have investigated PP/LDPE blends. No shift of the melting peak for LDPE has been observed. Both authors showed migration of the impurities during the melt-mixing process from the PP toward the LDPE phase. No further details on the crystallization behavior of the LDPE droplets themselves were reported.

Nadkarni and Jog (1986) have reported on PPS/HDPE blends. The degree of crystallinity of HDPE was reduced when HDPE was the minor phase. Furthermore, the $T_{c,HDPE}$ shifted to somewhat lower temperatures (by about 5 °C) but only in those blends with a low HDPE content. Isothermal crystallization halftimes for HDPE in its blends with PPS decreased as the HDPE content decreased, indicating an enhanced nucleation from the solidified PPS interfaces.

Chen et al. (1988) have investigated the melting behavior of 75/25 PA-6/HDPE and PA/LDPE **blends**. No shift has been observed in the melting point. No attention has been focused to the crystallization of the PE droplets.

Polypropylene Blends

Blends of PA-6 with PP dispersed as fine droplets have been examined recently by several authors.

Ikkala et al. (1993) investigated the thermal behavior and morphology of blends of PA-6 in which PP had been dispersed. In binary blends, PP droplets crystallized even at somewhat higher temperature (by about 5 °C) than the PP homopolymer, attributed to the nucleating activity of the solidified PA-6 matrix toward the dispersed PP phase. Morphological investigations revealed that the PP dispersion in the blends was quite coarse; so nearly every droplet contained the heterogeneities that usually nucleate PP. However, upon compatibilization, this behavior changed. Compatibilizers that formed an immiscible interlayer between PA-6 and PP and caused a reduction of the dispersed particle size gave rise to a retarded crystallization of the PP phase in a PA-6/PP 80/20 blend, decreasing the $T_{c,PP}$ by 50° C! This behavior was directly caused by the small size of the dispersed phase and the prevented nucleation from the solidified matrix. Blends containing 40 wt% PP did not crystallize in a retarded way due to their coarser droplet size, but clearly were not nucleated by the PA-6 phase as seen from $T_{c,PA-6} = T°_{c,PA-6}$. Similar results have been presented by Holsti-Miettinen et al. (1992).

Other Blends

Tang and Huang (1994b) investigated the relation between blend morphology and crystallization behavior in PP/PEG blends, prepared by solution blending. They reported that the PEG phase crystallized fractionated at different degrees of undercooling, but was always nucleated heterogeneously. The authors related the different crystallized fractions to PEG droplets of different sizes; the largest droplets crystallized at the bulk crystallization temperature.

Shingankuli et al. (1988) studied the crystallization behavior of dispersed PET droplets in a PPS matrix. A serious increase of the crystallization temperature of the dispersed PET phase (by about 20° C) during cooling experiments from the melt was explained as a result of the nucleating activity of the glass fibers in the PPS matrix, but also from the solidified PPS itself. As a result, the crystallization became more heterogeneous and the crystallization peak width decreased drastically. A corresponding increase in the onset of melting for PET (about 15 °C) was attributed to the formation of thicker and more perfect PET crystallites in the blends.

Frensch and Jungnickel (1989) and Frensch et al. (1989) have studied PA-6/PVDF blends. The authors reported that the finely dispersed PVDF droplets crystallized fractionated at different undercoolings. Again this could be directly related to the lack of heterogeneous nuclei in some of the smallest droplets. Increasing the blend composition or decreasing the mixing cycles caused the crystallization of the PVDF droplets to shift to higher temperatures, due to the formation of a coarser morphology. A similar behavior has been reported for PA-66/PVDF blends (Frensch and Jungnickel 1991).

A reverse case however has been reported by the same authors for the crystallization of dispersed PVDF droplets in a solidified PBT matrix. In the latter case, $T_{c,PVDF}$ even shifted to higher temperatures (by about 5 °C) than for homopolymer crystallization. The shift seemed to become less pronounced as the number of mixing cycles increased. No explanation for this behavior was reported. The melting endotherm of the PBT droplets was not affected by the blending.

3.3.6.5 Coincident Crystallization in Crystalline/Crystalline Polymer Blends

A few authors have observed coincident crystallization of both phases in crystalline/crystalline immiscible blends. This phenomenon was reported for blends in which the minor phase exhibits a higher degree of undercooling for crystallization due to its fine dispersion (see Sect. 3.2.3) and the matrix phase crystallizes at its bulk T_c that is lower than that of the minor phase. An additional factor that should be taken into account is that a heterogeneous nucleation is promoted on surfaces with a high interfacial tension (Helfand and Sapse 1975) (i.e., a crystallizing phase boundary). This can lead to the "coincident crystallization" of both phases, as it has been reported by Frensch and Jungnickel (1989, 1991) and by Frensch et al. (1989).

Principle of Coincident Crystallization

It has been observed that this phenomenon is connected with the phase dispersion of the minor component and is enhanced when the dispersion becomes finer. Upon cooling from the melt, a finely dispersed phase can exhibit fractionated crystallization, what implies that none, or only part of the dispersed droplets crystallize at their bulk T_c. This type of crystallization is related to the lack of heterogeneities in the droplets, required for nucleation at the bulk T_c.

When the blend is now further cooled, two possible ways of primary nucleation are possible. In the first case, the matrix phase is nucleated by heterogeneous species present in this phase, and, instantly, newly created crystals appear. Hence,

the crystallization temperature of the matrix will be situated at its bulk T_c. The second possibility for coincident crystallization occurs in the case one finds again a single crystallization peak for the matrix phase, which however takes place above its bulk T_c. Some novel mutual nucleating mechanism was suggested in such blends; a molten component (minor phase) acts as nucleating substrate for the matrix, which instantaneously crystallizes (Frensch and Jungnickel 1989).

For both cases, when the Δy-value (see Sect. 3.2.3.2) between these newly formed crystals and the melt of the minor phase is smaller than that of all other heterogeneities present in the minor phase (except probably the nuclei of "type 1" normally nucleating around the bulk $T_{c,minor}$), its associated specific undercooling must be so small that the crystals can induce the crystallization of that minor phase from the instant of their own creation (Frensch et al. 1989). Consequently, a single *coincident* crystallization peak will be registered in DSC thermograms.

It is clear that this phenomenon is phase morphology-dependent. Only in those blends where the minor phase is dispersed into sufficiently fine droplets, this phase has the opportunity to exhibit fractionated crystallization. Hence, only at low blend compositions and/or good matching viscosities of both phases (where the capillary number C_a predicts droplet breakup being dominant above coalescence) the occurrence of coincident crystallization is possible.

Examples of Coincident Crystallization
Frensch and Jungnickel (1989, 1991) and Frensch et al. (1989) have investigated the crystallization behavior of PVDF/PA-6, PVDF/PA-66, and PVDF/PBT blends. The PVDF/PA-6 blends showed a composite droplet-type morphology (finely dispersed matrix droplets encapsulated in the minor phase droplets) that disappeared after sufficiently long mixing cycles. Along with these observations, coincident crystallization was found in PVDF/PA-6 blends for an 85/15 and 75/25 composition only. The influence of morphological changes could be significant; after four mixing cycles, the dispersed PA-6 droplets became finer and did not contain small PVDF inclusions anymore. Along with this observation, only one single coincident crystallization peak could be found from DSC. The small exotherm at 184 °C caused by some larger PA-6 domains containing the PVDF inclusions with a small exotherm at 113 °C had disappeared completely by the mixing (Fig. 3.72). PVDF crystallization was found to be initiated by nucleation from heterogeneities of "type 1" at the bulk $T_{c,PVDF}$. A similar behavior has been reported for PVDF/PA-66 blends by Frensch and Jungnickel (1991).

A second system investigated by the authors was the PVDF/PBT blend. Similar effects could be observed. However, coincident crystallization in the PVDF/PBT 85/15 blend occurred at a somewhat higher temperature than the bulk $T_{c,PVDF}$. It could be concluded that in this case, the PBT melt induced the crystallization of the PVDF matrix phase.

Besides the cases of coincident crystallization reported previously, recent investigations on PP/PA-6 blends in which a compatibilizing agent had been used to obtain finer and more homogeneous dispersed phase morphology also mentioned coincident crystallization of the PA-6 droplets with the PP matrix (Ikkala et al. 1993; Moon et al. 1994). However, this has not been observed in the binary blend.
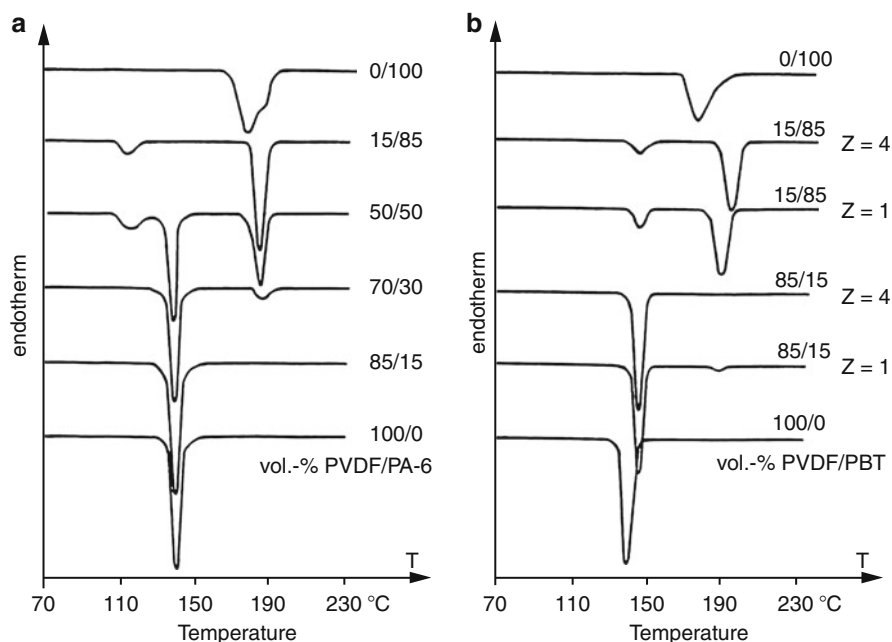
Fig. 3.72 Retarded and/or fractionated crystallization causing coincident crystallization in PVDF/PA-6 and PVDF/PBT blends. Influence of the blend composition (**a**) and the number of extrusion cycles *Z* (**b**) (Frensch and Jungnickel 1989)

3.3.6.6 Effect of Compatibilization on the Crystallization Behavior in Crystalline/Crystalline Polymer Blends

Blending offers an interesting means of tailoring product properties to specific applications. However, in the case of immiscible polymer pairs, the desired properties are not achieved readily without a compatibilizer, which enhances the phase dispersion and stability, as well as a good adhesion between the phases. This can be effectuated by physical or reactive methods (Folkes and Hope 1993). Compatibilization strongly affects the blend phase morphology, and as such, it also may influence the crystallization behavior of the blend (Flaris et al. 1993). Because both factors are related to the final properties of the blend, it is worth paying attention to these phenomena.

Several authors have investigated the influence of compatibilization on the global blend morphology. However, only a few authors really tried to understand the effect of compatibilization in crystalline/crystalline polymer blends on the crystallization kinetics, melting behavior, and semicrystalline morphology of the components. In Table 3.30, some recent results on this topic are summarized.

From the data presented in this table, it appears that in contrast to binary blends without a compatibilizer, the crystallization of the minor component in compatibilized blends cannot be solely explained by the size of the dispersion (Ikkala et al. 1993; Flaris et al. 1993; Tang and Huang 1994a; Holsti-Miettinen et al. 1995). Other factors

Table 3.30 Influence of a compatibilizing agent on the crystallization behavior of binary crystalline/crystalline polymer blends

Blend system[a] +compatibilizer	Studies on the influence of	Crystallization	Explanation	Reference
PP/PA-6 + MAH-g-PP 70/30	Concentration compatibilizer (in phr)	PP matrix: $T_{c,PP}$ matrix $\approx$ cte PA-6 droplets: $T_{c,PA-6}$ ↓ from 195 °C (0phr) to 188 °C (1.5 phr) $X_{c,PA-6}$ also ↓ From > 2 phr MA => coincident crystallization of PA-6 with PP matrix ($\Delta T = 60$ °C)	Increase of phr MA-g-PP => Interfacial tension ↓ => Dispersion size PA-6 ↓↓ => Lack of heterogeneities in each droplet => Retarded crystallization Constraint effect of grafted PA-6 chains is negligible	Moon et al. (1994)
PP-g-MA/PA-6 77/23 50/50	Composition	*PP matrix: $T_c \approx T_{c,bulk}$ *PA-6 dispersed: fractionated crystallization => Coincident cryst. with PP	Compatibilization => Interfacial tension ↓ => Droplet size ↓ => Lack of heterogeneity of type 1 —> crystallization by nuclei of type 2 which in his turn induces PP-MA crystallization	Tang and Huang (1994a)
PA-6/PP +MAH-g-PP +MAH-g-SEBS +FA-g-EBA +GMA-g-E EA 80/20 60/40	Composition Type of compatibilizer	*PA-6 matrix: $T_c \approx T_{c,bulk}$ *PP dispersed 20 % – > Depending on type of compatibilizer: • Cryst. around $T_{c,bulk}$ • Retarded cryst. ($\Delta T \approx 50$ °C) *PP dispersed 40 %: no large shift down of T_c	* If PA-6/PP phases in direct contact (no comp or analog. comp. as MA-g-PP) => PA-6 nucleates PP droplets => No lack of nuclei in droplets => $T_c \approx T_{c,bulk}$ *If SEBS, EBA, or E EA => immiscible interlayer between phases => Small droplets with lack of nuclei => T_c ↓↓ *PP droplets are large (coalescence) and contain enough heterogeneities to cryst. at $T_{c,PP}$	Holsti-Miettinen et al. (1992) Ikkala et al. (1993)
PP/PA-6 +MAH-g-PP +MAH-g-SEBS +FA-g-EBA +GMA-g-E EA 80/20 60/40	Composition Type of compatibilizer	*PP matrix: $T_c \approx T_{c,bulk}$ but slight ↑ in T_c (10 °C) in case of binary blend and MAH-g-PP *PA-6 dispersed: coincident crystallization with PP	*PA-6 has nucleating effect on PP cryst. at interface if in direct contact SEBS, EBA, and E EA form immiscible interlayer between PA-6 and PP => no nucleation => $T_{c,PP} \approx T_{c,bulk}$ *Compatibilization => serious reduction of PA-6 droplet size => lack of nucleating species => retarded cryst.	Holsti-Miettinen et al. (1992) Ikkala et al. (1993)

(continued)

Table 3.30 (continued)

Blend system[a] +compatibilizer	Studies on the influence of	Crystallization	Explanation	Reference
PP/PEG + (PP-MA)-g-PEG 75/25 50/50	Composition	*Isothermal cryst. rate of both PP and PEG ↑ with compatibilizer. Growth rate remains cte. Avrami exp. PP = cte. Avrami exp. PEG: 1 - > 2. *Fractionated cryst. of PEG is reduced by adding the compatibilizer	Mutual nucleation between PP and PEG	Tang and Huang (1994b)
PP/LLDPE + EP blockpol. + SEBS triblock + SEBS-g-MA 72/18/10	Type of compatibilizer	• Nucleation density at T_c = 135 °C: – ↑↑ with EP – ↓ with SEBS • Spherulite growth rate ↑ upon compatibilization • Interfacial free energy of PP crystal surfaces ↓ with compatibilization	• Compatibilization changes the interface morphology = > Additional nucleation sites from interfaces • Finer dispersion of LLDPE can cause more unidimensional growth of crystals	Flaris et al. (1993)
PP/LLDPE + EP blockpol. + Butyl rubber + EPR + SEBS triblock 72/18/10	Type of compatibilizer	• $T_{c,PP}$ ↑ (3–4 °C) when compat. is added: – Peak temp. independent on type of compat. – Onset temp. is dependent on type compat. • Half-width of exotherm ↓ strongly by addition of compat., independent of type used	• Rate of nucleation ↑ • Crystal size distribution becomes more uniform due to higher nucleation rate	Plawky and Wenig (1994)
PA-6/ionomer 90/10 80/20 70/30 60/40	Concentration of ionomer	• Dramatic ↑ in crystallization halftimes • $T_{c,PA-6}$ ↓ with [ionomer] ↑ (by ±4 °C) • Relative X_c ↓ with [ionomer] ↑ • Much wider distribution of PA-6 crystallite sizes	Strong interactions between PA-6 and ionomer impeded the crystallization of PA-6	Willis et al. (1993)

[a] All blend systems listed have been prepared by melt-mixing, except when indicated with

affecting the crystallization are the type of compatibilizer and its degree of miscibility with one or both of the blend components, the amount of compatibilizer added, the amount of interface created, and other effects.

The general influence of a compatibilizer on the crystallization behavior of an immiscible polymer blend system is still far from being well understood. However, abstract can be made between two main classes. A first class consists of compatibilizers that form a kind of "immiscible" interlayer between the two phases. Examples are given by Holsti-Miettinen et al. (1992) and Ikkala et al. (1993) for PP/PA-6 blends to which MAH-g-SEBS, FA-g-EBA, and GMA-g-E EA have been added. The compatibilizer prevents direct nucleating effects from one phase on the other. As such, only the size of the dispersion relative to the nucleation density of the dispersed phase and the nucleating effect of the compatibilizing agent itself play a role in the crystallization behavior (Fig. 3.73). Remark however that the size of the dispersion is often directly related to the concentration of the compatibilizer added (Moon et al. 1994).

A second class consists of compatibilizers that have an analogous chemical structure compared to one or two of the blend components. Here, the influence of a compatibilizer on the crystallization behavior of both phases is complex. Several factors have to be taken into account: nucleating effect of the matrix on the dispersed phase or from the dispersed phase on the matrix, the size of the dispersed phase relative to the nucleation density of that phase (and thus to the composition, content of the compatibilizer, etc.), nucleating effect of the compatibilizer itself, interactions of the compatibilizing agent and one or both phases which can impede the crystallization, cocrystallization of the compatibilizer with one of the phases, etc. An illustration is given in Figs. 3.72 and 3.73. Again, the concentration of compatibilizer plays a crucial role (Fig. 3.74).

Compatibilization seems to be of industrial interest in several ways: besides the improvement of the phase dispersion and adhesion, leading to superior mechanical properties, it also often can prevent the minor crystallizable dispersed phase from fractionated or retarded crystallization, which make faster production times and higher thermal stability of the products possible.

3.3.6.7 Conclusions on the Crystallization Behavior of Immiscible Crystalline/Crystalline Polymer Blends

The scientific literature on crystallization in polymer blends clearly indicates that the crystallization behavior and the semicrystalline morphology of a polymer are significantly modified by the presence of the second component even when both phases are physically separated due to their immiscibility. The presence of the second component, either in the molten or solid state, can affect both nucleation and crystal growth of the crystallizing polymer. The effect of blending on the overall crystallization rate is the net combined effect on nucleation and growth.

From the above literature survey, it is clear that the physical state of the second phase at the moment of crystallization is of utmost importance.

The crystallization of a *continuous matrix in which the dispersed phase is in the molten state* can be influenced by several phenomena. One of the most important
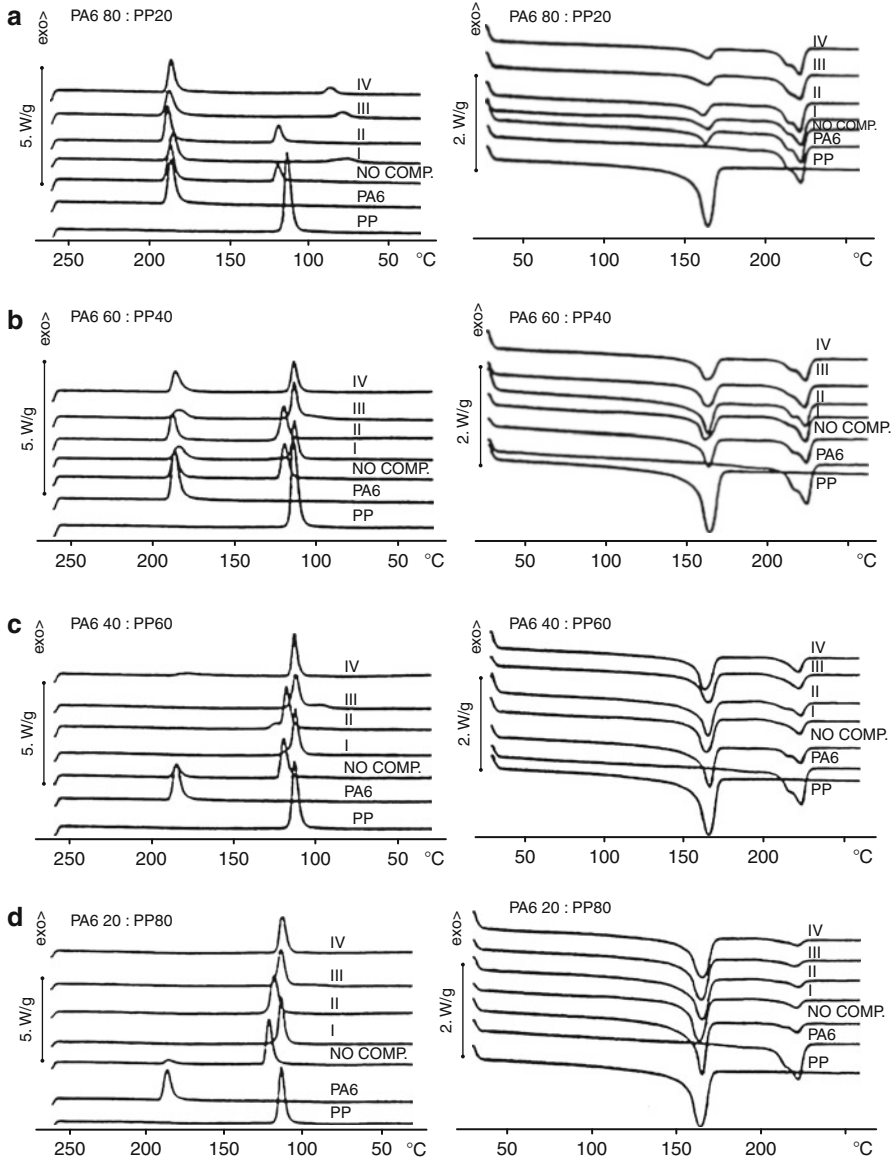
Fig. 3.73 Influence of compatibilization (10 wt%) on the crystallization and melting behavior of PA-6/PP blends with various blend compositions. Compatibilizer types used were EBA-g-FA (I), PP-g-MAH (II), SEBS-g-MAH (III), and E EA-GMA (IV) (Ikkala et al. 1993)

factors that play a role here is the possibility that impurities and nuclei migrate during the melt-mixing process, hence altering the nucleation density of the components. Furthermore, the interface may enhance the nucleation, mostly due to highly ordered structures in supercooled melt droplets.
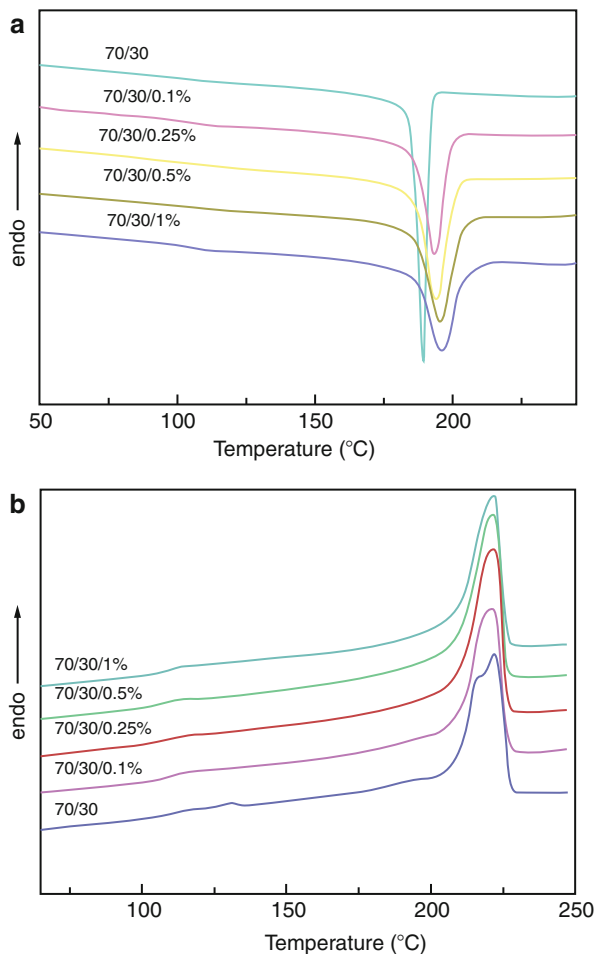
It should however be mentioned that the crystal growth rate, G, is generally not affected. Only in some exceptional cases where the growing crystallizing front rejects and/or deforms finely dispersed melt droplets, a decrease of G has been reported. It can thus be concluded that the matrix always crystallizes around its bulk temperature. Migration of nuclei, nucleation effects, etc., result in a shift of the $T_{c,matrix}$ by 5–10 °C, on average. The melting behavior of the matrix remains in general unaffected.

In the case of the *crystallization of the matrix in the presence of already solidified or crystallizing particles*, migration of nuclei still can play an important role. However, several other phenomena have to be taken into account. First of all, the solidified domains can act as efficient nucleators. Furthermore, retarded crystallization of finely dispersed droplets can nucleate the matrix and leads to coincident crystallization of both phases. Finally, it has been reported that epitaxial crystallization at the interfaces sporadically occurs. All these phenomena lead to an increased heterogeneous nucleation of the matrix phase.

Although most often also here the crystal growth rate is not affected, some authors have reported that finely dispersed solidified domains can increase the melt viscosity of the matrix in such a way that the crystallization rate becomes depressed. Again, the matrix component will crystallize around its bulk temperature. The abovementioned phenomena can eventually alter the spherulite size and shift the T_c of the matrix on average by 5–10 °C. The melting behavior remains normally unaffected.

The crystallization and melting behavior of a dispersed phase is highly different from the behavior of the continuous phase and much more sensitive for changes.

Droplets crystallizing in a melt matrix can just crystallize at their bulk temperature or show shifts of their T_c as a result of migration of nuclei, as has been outlined for matrix crystallization in the melt.

However, an important additional factor that plays a role here is the size of the dispersed phase. When the number of finely dispersed droplets exceeds the available heterogeneities of "type 1," fractionated or even homogeneous crystallization will occur, leading to shifts in the crystallization temperature by sometimes up to 100 °C (as compared to the homopolymer). This can result in a change of the crystal polymorphic form, coincident crystallization with a lower crystallizing matrix component, etc. However, the melting peak in the latter case will only be slightly depressed (by 2–4 °C) due to the formation of less perfect crystallites at lower temperatures. Additionally, it has been demonstrated that compatibilization can induce drastic changes in the blend phase morphology and thus in the crystallization and melting behavior.

In the case where *dispersed droplets crystallize in an already solidified matrix*, the same phenomena as in the previously described case can influence the thermal behavior of the dispersed phase. Additionally, nucleation from the already solidified matrix will play a distinguished role. An induction of heterogeneous nuclei often can reduce the fractionated crystallization or even bring the T_c back at its bulk temperature.

3.3.7 Crystallization in Immiscible Polymer Blends Containing Nanoparticles

Solid particles can be used as fillers dispersed in a matrix composed of one polymer or copolymer but can also be added in a miscible and immiscible binary, ternary, or multicomponent blend. The objective of the addition of fillers is diverse. They can be used as fillers to reduce the price of the composite and to improve the properties of the material (mechanical, aspect, chemical, etc.). Nanoparticles are among the category of fillers, the particle size of which is in the nanometer scale. They are considered as a new generation of particles which is progressively occupying a strategic position in the area of material development. Carbon nanotubes (CNTs) are nanoparticles that have been widely used in various fields owing to their remarkable mechanical, thermal, and electrical properties. One of the most intriguing applications of CNTs is the polymer/CNTs composites. Because of the combination of low density,

nanometer scale diameter, high aspect ratio, and, more importantly, unique physical properties such as extremely high mechanical strength and modulus, CNTs have emerged as potential reinforcing filler in polymer composites with excellent performance and multifunction. Nanoparticles can also be added to polymer matrices for specific effect of modifying a single but discrete property such as crystallization of homopolymers. In this application, they are nucleating agents as they enhance the crystallization of the polymer matrix where they are dispersed via a heterogeneous nucleation process. The use of nanoparticles as nucleating agents and more generally as crystallization modifiers in polymer blends is poorly reported in literature. Only few reports deal with this particular application of nanoparticles. Bose et al. (2007) performed an interesting investigation on fractionated crystallization in reactively compatibilized PA6/(amorphous)ABS blends. They added multiwall carbon nanotubes (MWNT) as heterogeneous nucleating agents. SMA- or SMA-modified MWNT were able to reduce significantly the particle size of PA6 up to a concentration of 1 wt% SMA. Fractionated crystallization was observed in both reactively compatibilized and non-compatibilized 20 PA6/80ABS blends. Delayed crystallization was reported for both types of blends due to lack of heterogeneities because of indirect but crucial effect of particle size reduction.

Pillin and Feller (2006) investigated the crystallization of the PBT minor phase in an EEA continuous matrix by DSC and SEM. When PBT is the minor phase, PBT crystallizes at a lower temperature of 105°C. Introducing different CB nanoparticles into the EEA continuous phase at contents increasing from 0.02 to 5 wt% resulted in important modifications of the PBT crystallization. A new PBT exotherm appeared at $T_c = 144$ °C on the addition of CB, becoming really visible at $T_c = 158$ °C and finally moving to $T_c = 185$ °C at high content. The areas corresponding to the new peaks were found to increase to the detriment of that of the fractionated crystallization at $T_c = 105$ °C. Morphological studies and interfacial tension measurements were made to understand the surprising activity of the CB. Moreover, the substitution of the EEA phase with a less polar component as, e.g., LLDPE, confirmed the importance of the strong interactions developed by EEA with CB aggregates.

Liu et al. (2012) have recently investigated the morphology, melting, crystallization, and mechanical properties for similar blend combination of PA6/ABS with MWNT nanotubes. PA6/ABS blends (70/30 and 50/50 wt) with 0, 0.1, 0.25, 0.5, and 1 wt% MWNTs were studied. Figures 3.75 and 3.76 show the crystallization and melting behaviors of PA6/ABS (70/30 wt) and (50/50 wt) blends with different contents of MWNTs. By incorporating MWNTs, the crystallization peak of PA6 shifted to higher temperature regions, the same effect has been reported in various polymer/CNTs composites (Li et al. 2006; Assouline et al. 2003; Valentini et al. 2003). The crystallization onset temperature (Tco) and the crystallization peak temperature (Tcp) increase with increasing the content of MWNTs. In PA6/ABS (70/30 wt) blends, PA6 crystallized at 191.4 °C, and with the incorporation of 1 wt% MWNTs, PA6 started to crystallize at 203.6, i.e., 12.2 °C higher than that of PA6 in simple (nonmodified blends). In PA6/ABS (50/50 wt) blend, the increment in Tco is also 12.2 °C. The long fibrillar MWNTs provided ideal

Fig. 3.75 DSC (**a**) cooling and (**b**) heating curves of PA6/ABS (50/50 wt) blends with various contents of MWNTs (Liu et al. 2012)
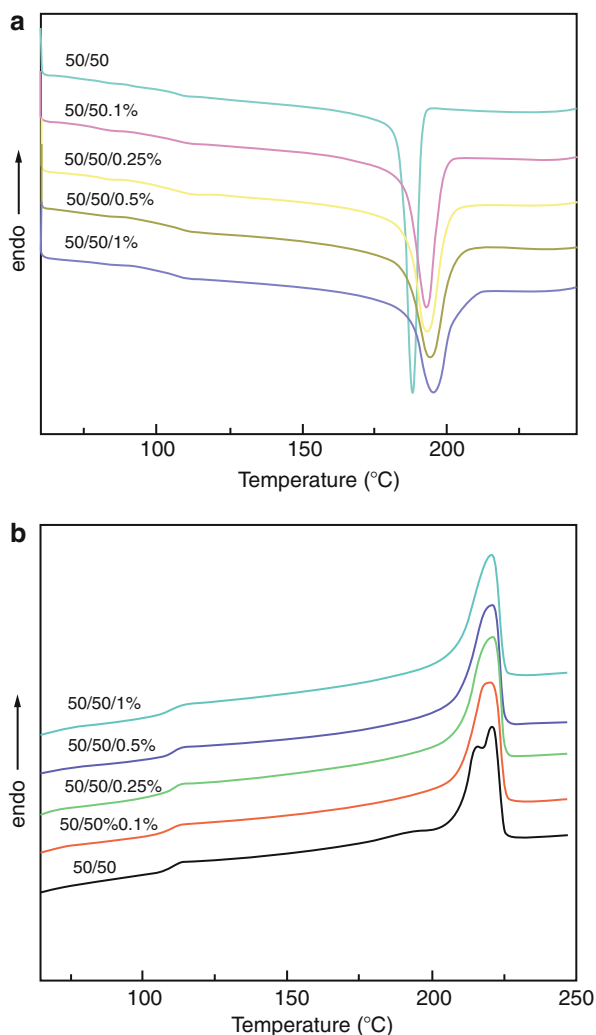
nucleation sites for PA6 chains (Gong et al. 2000). Indeed, the nucleation ability of MWNTs was quite high and effective. When the content of MWNTs in PA6 increases, more heterogeneous nucleation sites are available, leading to higher Tco and Tcp. Additionally, a weak exotherm at about 110 °C is found in Fig. 3.75a, c, which is often referred to as fractionated crystallization. This phenomenon often appears when the crystallizable polymer exists as the minor phase in a dispersed droplets form. In the composition the authors selected, PA6 acts mainly as the matrix. Indeed, fractionated crystallization is less visible, because numerous new interfaces are introduced during melt-mixing which can cause heterogeneous nucleation (Turbull et al. 1950; Helfand et al. 1977). In the melting endotherms,

Fig. 3.76 The effect of compatibilizers (SEBS) and (EP) on the nucleation of isotactic PP at various temperatures: (**a**) measured as blend volume and (**b**) calculated as PP volume fraction (Long et al. 1995)
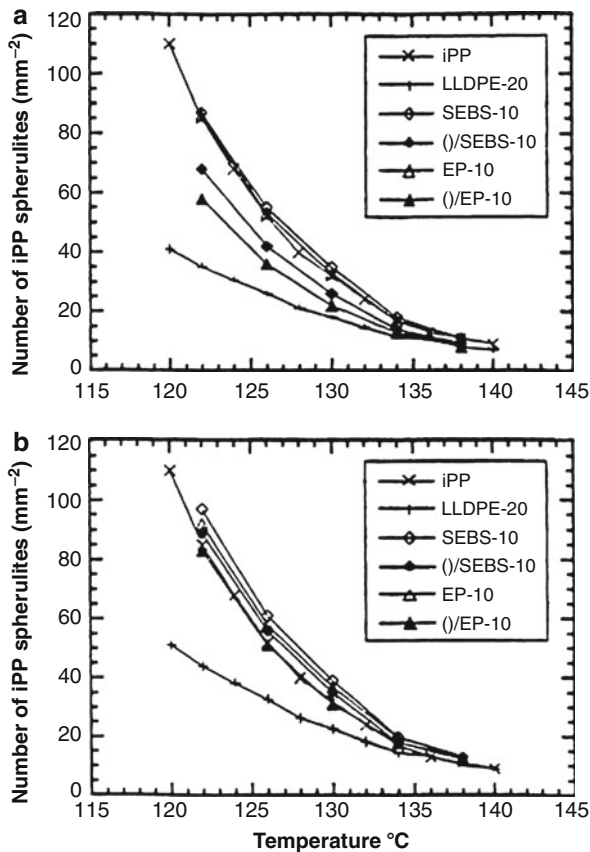
PA6 forms two melting peaks in both PA6/ABS (70/30 wt) and PA6/ABS (50/50 wt) simple blends. The double melting peaks were not due to the existence of two crystal forms but originated from the different distribution of the lamellar thickness (Helfand et al. 1977). According to the authors, the introduction of MWNTs in the blends provides a large amount of nucleation sites for end tethering of PA6 chains to form the α-phase crystals with similar lamellar thickness and restrain reorganization or recrystallization during the heating process in DSC scanning (Phang et al. 2006), which results in only one melting peak of PA6. The favorable formation of α-phase crystals in the presence of MWNTs also facilitates the enhancement of mechanical properties of the blends (Zhang et al. 2004).

The fractionated crystallization behavior of polypropylene (PP) droplets in its 20PP/80PS blends in the presence of hydrophilic or hydrophobic fumed silica nanoparticles was studied by using differential scanning calorimetry, scanning electron microscopy, and transmission electron microscopy by Huang et al. (2013). The fractionated crystallization of PP droplets in the PS matrix was promoted by adding a low content of hydrophobic or hydrophilic nanoparticles due

to their morphological refinement effect. However, discrepancies in the fractionated crystallization behavior of PP droplets occurred as the nanoparticle content increased. The crystallization became dominated by the heterogeneous nucleation effect of high content of hydrophilic nanoparticles. The authors ascribed this decrease to possible migration of the nanoparticles preferentially into PP droplets during mixing, significantly suppressing their fractionated crystallization (cause heterogeneous nucleation).

3.4   General Conclusion

Crystallization and melting phenomena in multicomponent polymer-based materials has been and is still a subject of scientific activity for a large number of academic and industrial research centers. That is because a wide spectrum of properties of many polymer materials depends on the crystallization process and on their extent of crystallinity as a result of the processing operations. The huge volume of literature of various types dealing with the crystallization and melting features is a strong witness of the above statements. The present chapter can be considered as a smart guide rather than an exclusive review work for people involved with the study of crystallization both for academic and applied research programs. The chapter has been split, although not really simple to achieve, into miscible, immiscible, and nanoparticles containing polymer blends. The miscible blends section has been divided into subsections of thermoplastic/thermoplastic and thermoplastic/thermosets. In the former system, the segregation of the molecules of the amorphous component from the crystallizing front is affected by the T_g, the kinetics of diffusion of the amorphous component, the crystallization kinetics, and the supercooling. In the latter blend system, the temperature and time of curing of the thermosetting affect strongly the crystallization features of the crystallizable thermoplastic component.

In miscible blends, segregation of the amorphous component competes with crystallization of the crystallizable one. Interspherulitic, interfibrillar, and interlamellar are the regions where segregation can take place during the crystallization of the crystallizable componenet. The balance between the diffusion rate of the amorphous component and the crystallization rate of the crystallizable component determines one or the other of the segregation type. In miscible blends of two crystallizable components, separate crystallization, concurrent crystallization, or cocrystallization may take place upon cooling from above the two individual melting temperatures of both blend components. Examples of blend systems leading to similar behavior were selected from literature and summarized herein. These phenomena were already reported in the first edition of the handbook and are maintained unmodified in the present chapter as no important new concepts were reported since then.

In immiscible blend systems, the accent was put on the fractionated crystallization features. A new and interesting work has been done since the first edition. This is extensively highlighted in the present chapter. The phenomenon is significant when the crystallizable phase is dispersed in the amorphous phase of the second blend component. Reactively compatibilized blends were compared to uncompatibilized

ones. The effect of compatibilization was shown to indirectly affect the crystallization behavior of the blends as it effects only and mainly causes particle size reduction. That results in more fractionated crystallization as the number of heterogeneities becomes insufficient to locate in all the crystallizable dispersed particles.

Dedication and Acknowledgments Professor Emeritus Dr. Gabriël Groeninckx would like to dedicate this chapter to all his former master and Ph.D. students, postdocs, and colleagues of the Laboratory for Macromolecular Structure Chemistry of the Catholic University of Leuven (KU Leuven, Heverlee, Belgium) for their valuable contribution in the field of polymer blends and related domains. He also would like to fully express his acknowledgments to the KU Leuven where he spent his scientific career from 1965 to 2010. And last but not least, he also has the great pleasure of dedicating this chapter 5 to his wife Anne-Marie and his children Christine, Filip, and Mark but also to his grandchildren Maartje, Nikolaas, Lineke, Noortje, and Luca. Each of them made him very happy in their own way.

3.5   Cross-References

▶ Interphase and Compatibilization by Addition of a Compatibilizer
▶ Miscible Polymer Blends
▶ Morphology of Polymer Blends
▶ Polymer Blends Containing "Nanoparticles"
▶ Reactive Compatibilization

Notations and Abbreviations

AN Acrylonitrile
aPMMA Atactic poly(methyl methacrylate)
aPS Atactic polystyrene
BR Butyl rubber
CPE Chlorinated polyethylene
DDS 4,4′-diaminodiphenylsulfone
DGEBA Diglycidyl ether of bisphenol A
DHDPE Deuterated high-density polyethylene
EBA Ethylene butylacrylate
EEA Elastomeric copolymer from ethylene and ethyl acrylate
EGMA Ethylene glycidyl methacrylate
EPDM Elastomeric terpolymer from ethylene, propylene, and a non-conjugated diene
EPR Elastomeric ethylene-propylene copolymer
EPR-g-SA Elastomeric ethylene-propylene copolymer grafted with styrene acrylonitrile
ER Epoxy resin
EVAc Poly(ethylene-*co*-vinyl acetate) (random)
FVA Poly(vinyl acetate-*co*-di-*n*-tetradecyl fumarate) (alternating)

GMA Glycidyl methacrylate copolymer
HDPE High-density polyethylene
iP(*p*-Me-S) Isotactic copolymer of styrene and *p*-methyl styrene
iPEMA Isotactic poly(ethyl methacrylate)
iPMMA Isotactic poly(methyl methacrylate)
iPS Isotactic polystyrene
LDPE Low-density polyethylene
LLDPE Linear low-density polyethylene
MA or MAH Maleic anhydride
MCDEA 4,4′-methylenebis(3-chloro-2,6-diethylaniline
P(4-Me-pentene) Poly(4-methyl pentene)
P(E)$_{0.43}$(K)$_{0.57}$ Random copolymer of phenyl ether and phenyl ketone
P(iPr-vinyl ether) Poly(isopropyl-vinyl ether)
P(sec-But-vinyl ether) Poly(sec-butyl vinyl ether)
PA-11 Polyamide 11
PA-12 Polyamide 12
PA-6 Polyamide 6
PA-66 Polyamide 66
PAr Polyarylate
PBA Poly(1,4.butylene adipate)
PBT Polybutyleneterephthalate
PC Bisphenol-A polycarbonate
PCDS Poly(1,4-cyclohexane-dimethylene succinate)
PCL Poly-e-caprolactone
PDPA Poly(2,2-dimethyl-1,3-propylene adipate)
PDPS Poly(2,2-dimethyl-1,3-propylene succinate)
PE Polyethylene
PEA Poly(ethylene adipate)
PECH Poly(epichlorohydrin)
PED *n*-Dodecyl ester terminated poly(ethylene glycol)
PEE Poly(ester-ether) segmented block copolymers
PEEEK Poly(ether ether ether ketone)
PEEK Poly(ether ether ketone)
PEEKK Poly(ether ether ketone ketone)
PEG Polyethylene glycol (also PEO)
PEI Poly(ether imide)
PEK Poly(ether ketone)
PEKK Poly(ether ketone ketone)
PEMA Polyethylmethacrylate
Penton Poly[3,3-bis(chloromethyl)oxetane]
PET Polyethyleneterephthalate
PET-b-PS Block copolymer of PET and PS segments
Phenoxy Poly(hydroxy ether of bisphenol A)
PI Di-*n*-octadecyl ester of itaconic acid

PI Polyisoprene
PIB Polyisobutene
PMMA Polymethylmethacrylate
POM Polyoxymethylene
PP Isotactic polypropylene
PPE, PPO Poly(2,6-dimethyl 1,4-phenylene ether), GE Co. trade name
PPG Poly(propylene glycol)
PPS Poly(phenylene sulfide)
PS Atactic polystyrene
PSMA Poly(styrene-*co*-maleic anhydride)
PVAc Poly(vinyl acetate)
PVC Polyvinyl chloride
PVDF Poly(vinylidene fluoride) (sometimes expressed as PVF_2)
PVF Poly(vinyl fluoride)
PVME Polyvinylmethylether
RIPS Reaction-induced phase separation
SAN Poly(styrene-*co*-acrylonitrile)
SARAN $P(VCl_2$-VC), $P(VCl_2$-VA), or $P(VCl_2$-AN) random copolymers of vinyl-idene chloride (VCl_2) with vinyl chloride (VC), vinyl acetate (VA), and acrylo-nitrile (AN), respectively
SBS Elastomeric styrene-butadiene-styrene triblock polymer (also TR)
SD Spinodal decomposition
SEBS Styrene-ethylene/butylene-styrene triblock polymer
SMA Poly(styrene-*co*-maleic anhydride)
sPMMA Syndiotactic poly(methyl methacrylate)
sPS Syndiotactic polystyrene
TR Thermoplastic rubber (also SBS)
UHMWPE Ultra-high-molecular-weight polyethylene
VDF-HFA Copolymer of vinylidene fluoride and hexafluoro acetone
VDF-TFE Copolymer of vinylidene fluoride and tetrafluoro ethylene
VLDPE Very low-density polyethylene
compat. Compatibilization, compatibilized, etc.
conc. Concentration
cryst. Crystallization, crystalline, crystallize
cte Constant
DSC Differential scanning calorimetry
etc. Et cetera
exp. Exponent
HM High molecular weight
LCST Lower critical solution temperature
O. M. Optical microscopy (also OM)
phr. Parts per hundred
[(*polymer*)] Amount/concentration of the cited polymer
SALS Small-angle light scattering (also SALLS)

SAXS Small-angle X-ray scattering

SEM Scanning electron microscopy

temp. Temperature

UCST Upper critical solution temperature

WAXS Wide-angle X-ray scattering

WLF Williams, Landel, and Ferry

C_1, C_2, C_3 WLF constants

C-2 Carbon chain with 2 C-atoms; i.e., ethylene

C-3 Carbon chain with 3 C-atoms; i.e., propylene

C_p Heat capacity under constant pressure

E_1 Energy dissipated for rejection of droplets during spherulite growth

E_2 Energy to overcome the inertia of droplets during spherulite growth

E_3 Energy required to form new interfaces when droplets are engulfed

E_4 Energy dissipated for deformation of occluded particles during spherulite growth

F_{12} Spreading coefficient

$f_z^{(1)}$ Fraction of dispersed droplets of volume V_D that contain z heterogeneities of type 1

G Isothermal spherulite growth rate

G^o Theoretical spherulite growth rate

G_1 Undisturbed spherulite growth rate of the homopolymer described by the Turnbull-Fisher equation

$M^{(1)}$ Concentration of heterogeneities of type 1

MW Molecular weight

n Avrami exponent

N Nucleation density

N/S Nucleation density normalized per unit area

K Overall crystallization rate

$t_{0.5}$ Halftime of crystallization at a fixed $T_{c,iso}$

T_c Bulk crystallization temperature upon cooling from the melt

T_c^o Crystallization temperature of the bulk homopolymer

$T_{c,cold}$ Cold crystallization temperature

$T_{c,hom}$ Homogeneous crystallization temperature

$T_{c,i}$ Crystallization temperature at which heterogeneities of type i become active

$T_{c,iso}$ Isothermal crystallization temperature

$T_{c,max}$ Optimal isothermal crystallization temperature which yields the highest overall crystallization

T_g Glass-transition temperature

T_m Measured melting temperature of the crystalline phase

T_m^o Theoretical melting temperature for crystalline lamellae of infinite thickness

T_m' Observed melting temperature of the crystalline phase in blends

T_{melt} Premelting temperature

t_{melt} Time the polymer is kept in the melt

V_D Average volume of dispersed polymer droplets

Vol% Volume percentage

wt% Weight percentage

X_c Total degree of crystallinity

y_p **(m, c)** Lateral surface free energy between the crystal and its own melt

y_{pn} **(m)** Interfacial energy between the nucleating species and the polymer melt

y_{pn} **(c)** Interfacial energy between the nucleating species and the polymer crystal

z Number of heterogeneities of type 1, inducing crystallization in the bulk polymer at $T_c{}^o$

Symbols: Greek Letters

$\boldsymbol{\Delta E}$ Activation free energy for the transport of chains through the liquid–solid interface

$\boldsymbol{\Delta F}$ Difference of interfacial energies; driving force for rejection, engulfing, and/or deformation of dispersed droplets during spherulite growth

$\boldsymbol{\Delta F^*}$ Free energy for the formation of a nucleus of critical size

$\boldsymbol{\Delta H_m}$ Total melting enthalpy of the crystalline polymer fraction

$\boldsymbol{\Delta T_{c,hom}}$ Degree of undercooling required for homogeneous crystallization

$\boldsymbol{\Delta T_{c,i}}$ Degree of undercooling required before a heterogeneity of type i can become active

$\boldsymbol{\Delta y_i}$ Specific interfacial energy difference between a nucleating species of type i and the polymer

$\boldsymbol{\Delta y_{pn}}$ Specific interfacial energy difference between a nucleating species and the polymer

$\boldsymbol{\gamma_{PS}}$ Interfacial free energy between the crystallizing solid and the inclusions

$\boldsymbol{\gamma_{PL}}$ Interfacial free energy between the liquid polymer melt and the inclusions

$\boldsymbol{\sigma_o}$ Surface free energy of folding

$\boldsymbol{\sigma_{1,2}}$ Interfacial free energy between two phases of a blend in the melt

$\boldsymbol{\sigma_{i,1}}$ Interfacial free energy of an impurity with respect to melt phase 1

$\boldsymbol{\sigma_{i,2}}$ Interfacial free energy of an impurity with respect to melt phase 2

References

H. Abe, Y. Doi, M. Satkowski, I. Noda, Macromolecules **27**, 50 (1994)

J. Albuerne, L. Marquez, A.J. Muller, J.M. Raquez, P. Degee, P. Dubois, Macromolecules **36**, 1633 (2003)

G.C. Alfonso, T.P. Russell, Macromolecules **19**, 1143 (1986)

A. Aref-Azar, J. Hay, B. Marsden, N. Walker, J. Polym. Sci., Polym. Phys. Ed. **B18**, 637 (1980)

E. Assouline, A. Lustiger, A.H. Barber, C.A. Cooper, E. Klein, E. Wachtel, J. Polym. Sci. Part B: Polym. Phys. **41**(520) (2003)

M. Aubin, Y. Bédard, M.-F. Morrissette, R.E. Prudhomme, J. Polym. Sci., Polym. Phys. Ed. **B21**, 233 (1983)

M.J. Avrami, Chem. Phys. **7**, 1103 (1939)

M. Baïtoul, H. Saint-Guirons, P. Xans, P. Monge, Eur. Polym. J. **17**, 1281 (1981)

V. Balsamo, F. von Gyldenfeldt, R. Stadler, Macromol. Chem. Phys. **33**, 197 (1996)

V. Balsamo, D. Newman, L. Gouveia, L. Herrera, M. Grimau, E. Laredo, Polymer **47**, 5810 (2006)

C.A. Barron, S.K. Kumar, J.P. Runt, ACS Polym. Prepr. **2**, 610 (1992)

Z. Bartczak, A. Galeski, Polymer **27**, 544 (1986)

Z. Bartczak, A. Galeski, E. Martuscelli, Polym. Eng. Sci. **24**, 1155 (1984)

Z. Bartczak, A. Galeski, M. Pracella, Polymer **27**, 537 (1986)

Z. Bartczak, A. Galeski, N.P. Krasnikova, Polymer **28**, 1627 (1987)

Z. Bartczak, E. Martuscelli, A. Galeski, in *Polypropylene: Structure*, *Blends and Composites*, vol. 2, ed. by J. Karger-Kocsis (Chapman & Hall, London, 1995)

D.C. Bassett, R.H. Olley, I.A.M. Al Raheil, Polymer **29**, 1745 (1992)

L. Bianchi, S. Cimmino, A. Forte, R. Greco, F. Riva, C. Silvestre, J. Mater. Sci. **20**, 895 (1985)

J. Boon, J.M. Azcue, J. Polym. Sci., Part A-2 **6**, 885 (1968)

J. Boon, G. Challa, D.W. Van Krevelen, J. Polym. Sci., Part A-2 **6**, 1791 (1968)

J.R. Burns, D. Turnbull, J. Appl. Phys. **37**, 4021 (1966)

E. Calahorra, M. Cortazar, G.M. Guzman, Polymer **23**, 1322 (1982)

M. Canetti, P. Sadocco, A. Siciliano, A. Seves, Polymer **35**, 2884 (1994)

F.-C. Chang, M.-Y. Yang, J.-S. Wu, Polymer **32**, 1394 (1991)

H.-L. Chen, R.S. Porter, J. Polym. Sci., Polym. Phys. Ed. **B31**, 1845 (1993)

T.H. Chen, A.C. Su, Polymer **34**, 4826 (1993)

C.C. Chen, E. Fontan, K. Min, J.L. White, Polym. Eng. Sci. **28**, 69 (1988)

F. Chen, R.A. Shanks, G. Amarasinghe, Polymer **42**, 4579 (2001)

H. Chen, M. Pyda, P. Cebe, Thermochim. Acta. **492**, 61 (2009)

S.Z.D. Cheng, M.-Y. Cao, B. Wunderlich, Macromolecules **19**, 1868 (1986)

J.W. Cho, S. Tasaka, S. Miyata, Polym. J. **25**, 1267 (1993)

S. Cimmino, E. Martuscelli, C. Silvestre, Macromol. Chem. **16**, 147 (1988)

S. Cimmino, E. Martuscelli, C. Silvestre, M. Canetti, C. De Lalla, A. Seves, J. Polym. Sci., Polym. Phys. Ed. **B27**, 1781 (1989)

S. Cimmino, E. Di Pace, E. Martuscelli, C. Silvestre, Polym. Comm. **32**, 251 (1991)

S. Cimmino, E. Di Pace, E. Martuscelli, C. Silvestre, Polymer **34**, 2799 (1993a)

S. Cimmino, E. Martuscelli, C. Silvestre, A. Cecere, M. Fontelos, Polymer **34**, 1207 (1993b)

J. Cissé, G. Bolling, J. Cryst. Growth **10**, 56 (1971)

N.E. Clough, R.W. Richards, T. Ibrahim, Polymer **35**, 1044 (1994)

F. Coppola, R. Greco, E. Martuscelli, H.W. Kammer, C. Kummerlowe, Polymer **28**, 47 (1987)

R. Cormia, F. Price, D. Turnbull, J. Chem. Phys. **37**, 1333 (1962)

G. Crevecoeur, G. Groeninckx, Macromolecules **24**, 1190 (1991)

G. Crevecoeur, Ph.D. dissertation, KU Leuven, 1991

C.A. Cruz, J.W. Barlow, D.R. Paul, Macromolecules **12**, 726 (1979)

G. Defieuw, Ph.D. dissertation, KU Leuven, 1989

G. Defieuw, G. Groeninckx, H. Reynaers, Polymer **30**, 2158 (1989a)

G. Defieuw, G. Groeninckx, H. Reynaers, Polymer **30**, 595 (1989b)

G. Defieuw, G. Groeninckx, H. Reynaers, *Contemporary Topics in Polymer Science: Multiphase Macromolecular Systems*, vol. 6 (Plenum, New York, 1989c), p. 423

G. Defieuw, G. Groeninckx, H. Reynaers, Polymer **30**, 2164 (1989d)

F. Defoor, G. Groeninckx, H. Reynaers, P. Schouterden, B. Van Der Heyden, J. Appl. Polym. Sci. **47**, 1839 (1993)

G. Dreezen, M.H.J. Koch, H. Reynaers, G. Groeninckx, Polymer **40**, 6451 (1999a)

G. Dreezen, Z. Fang, G. Groeninckx, Polymer **40**, 5907 (1999b)

G.C. Eastmond, Adv. Polym Sci. **59**, 40 (2000)

G.H. Edward, Br. Polym. J. **18**, 88 (1986)

A. Escala, R. S. Stein, in *Multiphase Polymers*, ed. by S. L. Cooper, G. M. Ester. Advance in Chemistry Series, vol. 176 (American Chemical Society, Washington, DC, 1979), p. 455

A. Eshuis, E. Roerdink, G. Challa, Polymer **23**, 735 (1982)

V. Everaert, G. Groeninckx, L. Aerts, Polymer **41**, 1409 (2000)

V. Everaert, G. Groeninckx, M.H.J. Koch, H. Reynaers, Polymer **44**, 3491 (2003)

B.D. Favis, J. Appl. Polym. Sci. **39**, 285 (1990)

B.D. Favis, Makromol. Chem., Macromol. Symp. **56**, 143 (1992)

B.D. Favis, J.P. Chalifoux, Polym. Eng. Sci. **27**, 1591 (1987)

B.D. Favis, J.P. Chalifoux, Polymer **29**, 1761 (1988)

B.D. Favis, C. Lavallee, A. Derdouri, J. Mater. Sci. **27**, 4211 (1992)

A.C. Fernandez, J.W. Barlow, D.R. Paul, Polymer **27**, 1799 (1986)

V. Flaris, A. Wasiak, W. Wenig, J. Mater. Sci. **28**, 1685 (1993)

M.J. Folkes, P.S. Hope (eds.), *Polymer Blends and Alloys* (Blackie Academic and Professional, London, 1993)

H. Frensch, B.-J. Jungnickel, Colloid Polym. Sci. **267**, 16 (1989)

H. Frensch, B.-J. Jungnickel, Plast. Rubber Compos. Process. Appl. **16**, 5 (1991)

H. Frensch, P. Harnischfeger, B.-J. Jungnickel, in *Multiphase Polymers: Blends and Ionomers*, eds. by L. Utracki, R. A. Weiss. ACS Symposium Series, vol. 395 (American Chemical Society, Washington, DC, 1989), p. 101

C. Friedrich, Progr. Colloid Polym. Sci. **66**, 299 (1979)

A. Galeski, Z. Bartczak, M. Pracella, Polymer **25**, 1323 (1984)

K.P. Gallagher, X. Zhang, J.P. Runt, G. Huynh-ba, J.S. Lin, Macromolecules **26**, 588 (1993)

P.H. Geil, *Polymer Single Crystals* (Wiley, New York, 1963), p. 229

P.H. Geil, *Polymer Single Crystals* (R. E. Krieger, New York, 1973)

A. Ghijsels, N. Groesbeek, C.W. Yip, Polymer **23**, 1913 (1982)

X.Y. Gong, J. Liu, S. Baskaran, R.D. Voise, J.S. Young, Chem. Mater. **12:1**, 1049 (2000)

S. Goossens, G. Groeninckx, Macromolecules **39**, 8049 (2006)

S. Goossens, G. Groeninckx, J. Polym. Sci.: Part B: Polym. Phys. **45**, 2456 (2007)

S. Goossens, B. Goderis, G. Groeninckx, Macromolecules **39**, 2953 (2006)

R. Greco, M. Mancarella, E. Martuscelli, G. Ragosta, Y. Jinghua, Polymer **28**, 1922 (1987a)

R. Greco, M. Mancarella, E. Martuscelli, G. Ragosta, Y. Jinghua, Polymer **28**, 1929 (1987b)

D. Grenier, R.E. Prud'homme, J. Polym. Sci., Polym. Phys. Ed. **B18**, 1655 (1980)

I. Grof, O. Durcova, A. Marcincin, Acta Polym. **40**, 344 (1989)

Q. Guo, Makromol. Chem. **191**, 2639 (1990)

Q. Guo, G. Groeninckx, Polymer **42**, 8647 (2001)

Q. Guo, X. Peng, Z. Wang, Polymer **32**, 53 (1991)

Q. Guo, C. Harrats, G. Groeninckx, M.H.J. Koch, Polymer **42**, 4127 (2001a)

Q. Guo, C. Harrats, G. Groeninckx, H. Reynaers, M.H.J. Koch, Polymer **42**, 6031 (2001b)

Q. Guo, S. Slavov, P.J. Halley, J. Polym. Sci.: Part B: Polym. Phys. **42**, 2833 (2004)

A.K. Gupta, V.B. Gupta, R.H. Peters, W.G. Harland, J.P. Berry, J. Appl. Polym. Sci. **27**, 4669 (1982)

A.K. Gupta, S.K. Rana, B.L. Deopura, J. Appl. Polym. Sci. **44**, 719 (1992)

A.K. Gupta, S.K. Rana, B.L. Deopura, J. Appl. Polym. Sci. **51**, 231 (1994)

B.R. Hahn, O. Herrmann-Schönherr, J.H. Wendorff, Polymer **28**, 201 (1987)

C.D. Han, C.A. Villamizar, Y.W. Kim, S.J. Chen, J. Appl. Polym. Sci. **21**, 353 (1977)

J.E. Harris, L.M. Robeson, J. Polym. Sci., Polym. Phys. Ed **B25**, 311 (1987)

J.E. Harris, L.M. Robeson, J. Appl. Polym. Sci. **35**, 1877 (1988)

J.E. Harris, S.H. Goh, D.R. Paul, J.W. Barlow, J. Appl. Polym. Sci. **27**, 839 (1982)

J.N. Hay, J. Polym. Sci., Polym. Chem. Ed. **A14**, 2845 (1976)

E. Helfand, A. Sapse, J. Chem. Phys. **62**, 1327 (1975)

E. Helfand, Y. Tagami, J. Chem. Phys. **56**, 3592 (1972)

E. Helfand, Z.R. Wasserman, J. Appl. Phys. **56**, 251 (1977)

D. Hlavatá, Z. Horák, Eur. Polym. J. **30**, 597 (1994)

J.D. Hoffman, Polymer **24**, 3 (1983)

J.D. Hoffman, J.J. Weeks, J. Chem. Phys. **37**, 1723–1741 (1962a)

J.D. Hoffman, J.J. Weeks, J. Res. Natl. Bur. Stand., Sect. A **66**, 13–28 (1962b)

J. D. Hoffman, G. T. Davis, J. I. Lauritzen, in *Treatise on Solid State Chemistry*, vol. 3, chapter 7, ed. by N. B. Hannay (Plenum, New York, 1976)

J.D. Hoffmann, R.L. Miller, H. Marand, D.B. Roitman, J. Nat. Bur. Stand. **79A**, 671 (1992)

R. Holsti-Miettinen, J. Seppälä, O.T. Ikkala, Polym. Eng. Sci. **32**, 868 (1992)

R. Holsti-Miettinen, M. Heino, J. Seppälä, J. Appl. Polym. Sci. **57**, 573 (1995)

B.S. Hsiao, B.B. Sauer, J. Polym. Sci., Polym. Phys. Ed. **B31**, 901 (1993)

S.-R. Hu, T. Kyu, R.S. Stein, J. Polym. Sci., Polym. Phys. Ed. **B25**, 71 (1987)

B. Huang, J. Wang, D. Pang, in *Third European Symposium on Polymer Blends* (PRI), Cambridge, UK, 1990, p. B3

S.D. Hudson, D.D. Davis, A.J. Lovinger, Macromolecules **25**, 3446 (1991)

R.D. Icenogle, J. Polym. Sci., Polym. Phys. Ed. **B23**, 1369 (1985)

F. Ide, A. Hasegawa, J. Appl. Polym. Sci. **18**, 963 (1974)

O.T. Ikkala, R.M. Holsti-Miettinen, J. Seppälä, J. Appl. Polym. Sci. **49**, 1165 (1993)

R.L. Imken, D.R. Paul, J.W. Barlow, Polym. Eng. Sci. **16**, 593 (1976)

J.J. Iruin, J.I. Eguiazabal, G.M. Guzman, Eur. Polym. J. **25**, 1169 (1989)

W.H. Jo, S.J. Park, I.H. Kwon, Polym. Int. **29**, 173 (1992)

J.P. Jog, V.L. Shingankuli, V.M. Nadkarni, Polymer **34**, 1966 (1993)

A.M. Jonas, T.P. Russell, Y.D. Yoon, Macromolecules **28**, 8491 (1995)

J.M. Jonza, R.S. Porter, Macromolecules **19**, 1946 (1986)

N.K. Kalfoglou, Angew. Makromol. Chem. **129**, 103 (1985)

N.F. Kalfoglou, D.D. Sotiropoulou, A.G. Margaritis, Eur. Polym. J. **24**, 389 (1988)

M.R. Kamal, E. Chu, Polym. Eng. Sci. **3**, 27 (1983)

J. Karger-Kocsis, A. Kallo, A. Szafner, G. Bodor, U.S. Senyei, Polymer **20**, 37 (1979)

H.D. Keith, F.J. Padden Jr., J. Appl. Phys. **34**, 2409 (1963)

H.D. Keith, F.J. Padden Jr., J. Appl. Phys. **35**, 1286 (1964)

F.H. Khambatta, F.P. Warner, T.P. Russell, R.S. Stein, J. Polym. Sci-A2 **14**, 1391 (1976a)

F.B. Khambatta, F. Warner, T. Russell, R.S. Stein, J. Polym. Sci., Polym. Phys. Ed. **B14**, 1391 (1976b)

Y.P. Khanna, R. Kumar, A.C. Reimschuessel, Polym. Eng. Sci. **28**, 1607 (1988a)

Y.P. Khanna, A.C. Reimschuessel, A. Banerjie, C. Altman, Polym. Eng. Sci. **28**, 1600 (1988b)

N. Klemmer, B.-J. Jungnickel, Colloid Polym. Sci. **262**, 381 (1984)

J.A. Koutsky, A.G. Walton, E. Baer, J. Appl. Phys. **38**, 1832 (1967)

J. Kressler, H.W. Kammer, Polym. Bull. **19**, 283 (1988)

J. Kressler, P. Svoboda, T. Inoue, in *ACS Polymer Preprints*, vol. 33, p. 612. Papers presented at the Washington, DC. Meeting, August 1992

J. Kressler, P. Svoboda, T. Inoue, Polymer **34**, 3225 (1993)

B. Kulshreshtha, A. Ghost, A.K. Misra, Polymer **44**, 4723 (2003a)

B. Kulshreshtha, A.K. Ghost, A. Misra, J. Macromol. Sci. Phys. **B42**, 307 (2003b)

S.K. Kumar, D.Y. Yoon, Macromolecules **24**, 5414 (1991)

T. Kunori, P.H. Geil, J. Makromol. Sci., Phys. Ed. **B18**, 135 (1980)

T.K. Kwei, H.L. Frisch, Macromolecules **11**, 1267 (1978)

T.K. Kwei, G.D. Patterson, T.T. Wang, Macromolecules **9**, 780 (1976)

T.K. Kwei, H.L. Frisch, W. Radigan, S. Vogel, Macromolecules **10**, 157 (1977)

T. Kyu, P. Vadhar, J. Appl. Polym. Sci. **32**, 5575 (1986)

T. Kyu, S.-R. Hu, R.S. Stein, J. Polym. Sci., Polym. Phys. Ed. **B25**, 89 (1987)

M.P. Lattimer, J.K. Hobbs, M.J. Hill, P.J. Barham, Polymer **33**, 3971 (1992)

J.I. Lauritzen, J.D. Hoffman, J. Appl. Phys. **44**, 4340 (1973)

Y. Lee, R.S. Porter, Macromolecules **20**, 1336 (1987)

Y. Lee, R.S. Porter, J.S. Lin, Macromolecules **22**, 1756 (1989)

Y. Li, B.-J. Jungnickel, Polymer **34**, 9 (1993)

Y. Li, M. Stein, B.-J. Jungnickel, Colloid Polym. Sci. **269**, 772 (1991); and '*Mitteilungen aus dem Deutschen Kunststoff-Institut*', Nr° 53, April, Darmstadt, 1991

W. Li, R. Yan, B. Jian, Polymer **33**, 889 (1992)

P. Li, Y. Huang, M. Kong, Y. Lv, Y. Luo, Q. Yang, G. Li, Colloid Polym. Sci. **291**, 1693 (2013)

B. Liang, L. Pan, J. Appl. Polym. Sci. **54**, 1945 (1994)

B.R. Liang, J.L. White, J.E. Spruiel, B.C. Goswami, J. Appl. Polym. Sci. **28**, 2011 (1983)

A.M. Liquori, G. Anzuino, V.M. Coiro, M. D'Alagni, P. de Santis, M. Savino, Nature **206**, 358 (1965)

X.Q. Liu, W. Yang, B.H. Xie, M.B. Yang, Mater. Design. **34**, 355 (2012)

Y. Long, Z. Stachurski, R.A. Shanks, Polym. Int. **26**, 143 (1991)

B. Lotz, A.J. Kovacs, ACS Div. Polym. Chem., Polym. Prepr. **10**, 820 (1969)

A.J. Lovinger, M.L. Williams, J. Appl. Polym. Sci. **25**, 1703 (1980)

A.J. Lovinger, J.O. Chua, C.C. Gryte, J. Polym. Sci., Polym. Phys. Ed. **B15**, 641 (1977)

H. Lu, S.X. Zheng, Polym. **44**, 4689 (2003)

J.H. Magill, J. Appl. Phys. **35**, 3249 (1964)

K. Mai, M. Zhang, H. Zeng, S. Qi, J. Appl. Polym. Sci. **51**, 57 (1994)

L. Mandelkern, *Crystallization of Polymers* (McGraw-Hill, New York, 1964)

L. Mandelkern, F.A. Quinn, P.J. Flory, J. Appl. Phys. **25**, 830 (1954)

C. Marco, M.A. Gomez, J.G. Fatou, A. Etxeberria, M.M. Elorza, J.J. Iruin, Eur. Polym. J. **29**, 1477 (1993)

E. Martuscelli, Polym. Eng. Sci. **24**, 563 (1984)

E. Martuscelli, in *Polymer Blends and Mixtures*, ed. by D. J. Walsch (Dordrecht, Springer, 1985), pp. 217–243

E. Martuscelli, G.B. Demma, in *Polymer Blends: Processing, Morphology and Properties*, ed. by E. Martuscelli, M. Kryszewski, R. Palumbo (Plenum, New York, 1980a)

E. Martuscelli, M. Pracella, M. Avella, R. Greco, G. Ragosta, Makromol. Chem. **181**, 957 (1980b)

E. Martuscelli, C. Silvestre, G. Abate, Polymer **23**, 229 (1982)

E. Martuscelli, C. Silvestre, L. Bianchi, Polymer **24**, 1458 (1983)

E. Martuscelli, M. Pracella, P.Y. Wang, Polymer **25**, 1097 (1984)

H.-S. Moon, B.-K. Ryoo, J.-K. Park, J. Polym. Sci., Polym. Phys. Ed. **B32**, 1427 (1994)

R.A. Morales, M.L. Arnal, A.J. Müller, Polym. Bull. **35**, 379 (1995)

L.B. Morgan, Phila. Trans. Roy. Soc. Lond. **247**, 13 (1954)

D. Morin, Y. Zhao, R.E. Prud'homme, J. Appl. Polym. Sci. **81**, 1683 (2001)

B.S. Morra, R.S. Stein, J. Polym. Sci., Polym. Phys. Ed. **B20**, 2261 (1982)

B.S. Morra, R.S. Stein, Polym. Eng. Sci. **24**, 311–318 (1984)

B.S. Morra, Ph.D. dissertation, University of Amherst, MA, 1980

M. Mucha, Colloid Polym. Sci. **264**, 859 (1986)

A. J. Müller, M. L. Arnal, R. A. Morales, in *Europhysics Conference Abstracts*, 19D, P2, Prague, 17–20 July 1995

V.M. Nadkarni, J.P. Jog, J. Appl. Polym. Sci. **32**, 5817 (1986)

V.M. Nadkarni, J.P. Jog, Polym. Eng. Sci. **27**, 451 (1987)

V.M. Nadkarni, V.L. Shingankuli, J.P. Jog, Int. Polym. Proc. **2**, 53 (1987)

V.M. Nadkarni, J. P. Jog, in *Two-phase Polymer Systems*, ed. by L. A. Utracki (Hanser Publishing, Munich/New York, 1991)

G. Natta, P. Corradini, D. Sianesi, D. Morero, J. Polym. Sci. **51**, 527 (1961)

G. Natta, I.W. Bassi, D. Sianesi, G. Caporiccio, E. Torti, J. Polym. Sci., Polym. Chem. Ed. **A3**, 4263 (1965)

M.K. Neo, S.H. Goh, Eur. Polym. J. **27**, 927 (1991)

T. Nishi, T.T. Wang, Macromolecules **8**, 909 (1975)

O.F. Noel, J.P. Carley, Polym. Eng. Sci. **24**, 488 (1984)

S. Nojima, H. Tsutsui, M. Urushihara, W. Kosaka, N. Kato, T. Ashida, Polym. J. **18**, 451 (1986)

S. Nojima, D.J. Wang, T. Ashida, Polym. J. **23**, 1473 (1991)

O. Olabishi, L.M. Robeson, M.Y. Shaw, *Polymer-Polymer Miscibility* (Academic, New York, 1979)

J.J. O'Malley, R.G. Crystal, P.F. Erhardt, ACS Div. Polym. Chem., Polym. Prepr. **10**, 796 (1969)

S. Omenyi, A. Neumann, W. Martin, G. Lespinard, R. Smith, J. Appl. Phys. **52**, 789 (1981)

C.J. Ong, F.P. Price, J. Polym. Sci. Polym. Symp. **63**, 45 (1978a)

C.J. Ong, F.P. Price, J. Polym. Sci. Polym. Symp. **63**, 59 (1978b)

T. Ozawa, Polymer **12**, 150 (1971)

S.J. Park, B.K. Kim, H.M. Jeong, Eur. Polym. J. **26**, 131 (1990)

J.H. Perepezko, J.S. Paik, Undercooling Behaviour of Liquid Metals, in *Rapidly solidified Amorphous and Crystalline Alloys*, ed. by B.H. Kear, B.C. Giessen, M. Cohen (North Holland, New York, 1982)

F.C. Pérez-Cardenas, D.E.L. Felipe, L. Castillo, R. Vera-graziano, J. Appl. Polym. Sci. **43**, 779 (1991)

I.Y. Phang, J.H. Ma, L. Shen, T.X. Liu, W.D. Zhang, Polym. Int. **55**, 71 (2006)

I. Pillin, J.-F. Feller, Macomol. Mater. Eng. **291**, 1375 (2006)

J. Plans, W.J. MacKnight, F.E. Karasz, Macromolecules **17**, 810 (1984)

U. Plawky, W. Wenig, J. Mater. Sci. Lett. **13**, 863 (1994)

M. Plesek, Z. Malac, in *Morphology of Polymers*, ed. by B. Sedlacek, Proceedings of the 17th Europhysics Conference on Macromolecular Physics, Prague, 15–18 July 1985 (1986)

G.M. Pound, V.K. LaMer, J. Am. Chem. Soc. **74**, 2323 (1952)

A. Prasad, H. Marand, Bull. Am. Phys. Soc. **36**, 632 (1991)

B. Pukanszky, F. Tudos, A. Kallo, G. Bodor, Polymer **30**, 1399 (1989)

R.P. Quirk, J.-J. Ma, C.C. Chen, K. Min, J.L. White, in *Contemporary Topics in Polymer Science*, *Vol. 6*, *Multiphase macromolecular Systems*, ed. by B. M. Culbertson (Plenum, New York/ London, 1989)

J.M. Rego Lopez, U.W. Gedde, Polymer **29**, 1037 (1988)

M.C. Righetti, M.L. Di Lorenzo, M. Angiuli, E. Tombari, P. La Pietra, Eur. Polym. J. **43**, 4726 (2007)

P.B. Rim, J.P. Runt, Macromolecules **16**, 762–768 (1983)

P.B. Rim, J.P. Runt, Macromolecules **17**, 1520–1526 (1984)

C. Robitaille, J. Prud'homme, Macromolecules **16**, 665 (1983)

S. Rostami, Polymer **31**, 899–904 (1990)

M. Run, Y. Hao, C. Yao, Thermochim. Acta. **51**, 495 (2009)

J.P. Runt, Macromolecules **14**, 420 (1981)

J. Runt, P.B. Rim, S.E. Howe, Polym. Bull. **11**, 517 (1984)

J.P. Runt, L.M. Martynowicz, in *Multicomponent Polymer Materials*, ed. by D. R. Paul, L.H. Sperling, Advance in Chemistry Series, vol. 211 (American Chemical Society, Washington, DC, 1986)

J.P. Runt, C.A. Barron, X.-F. Zhang, S.K. Kumar, Macromolecules **24**, 3466 (1991)

T.P. Russell, R.S. Stein, J. Macromol. Sci., Phys. Ed. **B17**, 617 (1980)

T.P. Russell, R.S. Stein, J. Polym. Sci. Polym. Phys. Ed. **B21**, 999 (1983)

F. Rybnikâr, J. Macromol. Sci. Phys. Ed. **B27**, 125 (1988)

H. Saito, B. Stühn, Macromolecules **27**, 216 (1994)

H. Saito, T. Okada, T. Hamane, T. Inoue, Macromolecules **24**, 4446 (1991)

N. Salmon, V. Carlier, J. Schut, P.M. Remiro, I. Mondragon, Polym. Int. **54**, 667 (2005)

I. Sanchez, E.A. Di Marzio, Macromolecules **4**, 677 (1971)

O.O. Santana, A.J. Müller, Polym. Bull. **32**, 471 (1994)

P. Schouterden, G. Groeninckx, H. Reynaers, C. Riekel, M.H.J. Koch, Polym. Bull. **13**, 533 (1985)

K. Schulze, J. Kressler, H.W. Kammer, Polymer **34**, 3704 (1993)

J. Schut, M. Stamm, M. Dumon, J. Galy, J.F. Gerard, Macroml. Symp. **202**, 25 (2003)

C.K. Sham, G. Guerra, F.E. Karasz, W.J. MacKnight, Polymer **29**, 1016 (1988)

Y.D. Shibanov, Y.K. Godovsky, Progr. Colloid Polym. Sci. **80**, 110 (1989)

Y.D. Shibanov, Y.K. Godovsky, Makromol. Chem., Macromol. Symp. **44**, 61 (1991)

V.L. Shingankuli, J.P. Jog, V.M. Nadkarni, J. Appl. Polym. Sci. **36**, 335 (1988)

V. L. Shingankuli, Ph.D. thesis, Bombay University, India, 1990

C. Silvestre, S. Cimmino, E. Martuscelli, F.E. Karasz, W.J. MacKnight, Polymer **28**, 1190 (1987a)

C. Silvestre, F.E. Karasz, W.J. MacKnight, E. Martuscelli, Eur. Polym. J. **23**, 745 (1987b)

H.H. Song, D.-Q. Wu, M. Ree, R.S. Stein, J.C. Phillips, L. LeGrand, B. Chu, Macromolecules **21**, 1180 (1988)

H.W. Starkweather Jr., J. Appl. Polym. Sci. **25**, 139 (1980)

R.S. Stein, in *Newer Methods of Polymer Characterization*, chapter 4 (Wiley, New York, 1964)

R.S. Stein, F.B. Khambatta, F.P. Warner, T. Russell, A. Escala, E. Balizer, J. Polym. Sci., Polym. Symp. **63**, 313 (1978)

R.S. Stein, T.P. Russell, B.S. Morra, M. Wai, J. Gilmer, in *Structural Order in Polymers*, ed. by F. Ciardelli, P. Giusti (Pergamon, New York, 1981), p. 195

T. Suzuki, A. Kovacs, Polym. J. **1**, 82 (1970)

P. Svoboda, D. Svobodova, T. Chiba, T. Inoue, Eur. Polym. J. **44**, 329 (2008)

H. Tanaka, T. Nishi, Phys. Rev. Lett. **55**, 1102 (1985)

H. Tanaka, T. Nishi, Phys. Rev. A **39**, 783 (1989)

T. Tang, B. Huang, J. Appl. Polym. Sci. **53**, 355 (1994a)

T. Tang, B. Huang, J. Polym. Sci., Polym. Phys. Ed. **B32**, 1991 (1994b)

T. Tang, H. Li, B. Huang, Macromol. Chem. Phys. **195**, 2931 (1994)

K. Tashiro, M.M. Satkowski, R.S. Stein, Y. Li, B. Chu, S.L. Hsu, Macromolecules **25**, 1809 (1992a)

K. Tashiro, R.S. Stein, S.L. Hsu, Macromolecules **25**, 1801 (1992b)

K. Tashiro, M. Izuchi, F. Kaneuchi, C. Jin, M. Kobayashi, R.S. Stein, Macromolecules **27**, 1140 (1994a)

K. Tashiro, M. Izuchi, M. Kobayashi, R.S. Stein, Macromolecules **27**, 1121 (1994b)

K. Tashiro, M. Izuchi, M. Kobayashi, R.S. Stein, Macromolecules **27**, 1128 (1994c)

K. Tashiro, M. Izuchi, M. Kobayashi, R.S. Stein, Macromolecules **27**, 1134 (1994d)

J.W. Teh, J. Appl. Polym. Sci. **28**, 605 (1983)

J.W. Teh, H.P. Blom, A. Rudin, Polymer **35**, 1680 (1994a)

J.W. Teh, A. Rudin, J.C. Keung, Adv. Polym. Technol. **13**, 1 (1994b)

D.G. Thomas, L.A.K. Staveley, J. Chem. Soc. 4569 (1952)

R.T. Tol, V.B.F. Mathot, G. Groeninckx, Polymer **46**, 369 (2005a)

R.T. Tol, V.B.F. Mathot, G. Groeninckx, Polymer **46**, 383 (2005b)

R.T. Tol, V.B.F. Mathot, G. Groeninckx, Polymer **46**, 2955 (2005c)

D. Turbull, J. Chem. Phys. **18**, 198 (1950)

D. Turnbull, J. Chem. Phys. **18**, 198 (1950)

D. Turnbull, R.E. Cech, J. Appl. Phys. **21**, 804 (1950)

D. Turnbull, J.C. Fisher, J. Chem. Phys. **17**, 71 (1949)

W. Ullmann, J.H. Wendorff, Compos. Sci. Technol. **23**, 97 (1985)

L.A. Utracki, *Polymer Alloys and Blends* (Hanser Publishers, Munich, 1989)

P. Vadhar, T. Kyu, Polym. Eng. Sci. **27**, 202 (1987)

L. Valentini, J. Biagiotti, J.M. Kenny, S. Santucci, Compos. Sci. Technol. **63**, 1149 (2003)

F. Van Antwerpen, D.W. Van Krevelen, J. Polym. Sci., Polym. Phys. Ed. **B10**, 2423 (1972)

D.W. Van Krevelen, *Properties of Polymer* (Elsevier, New York, 1976)

A.D. Van Riemsdyk, Ann. Chim. Phys. **20**, 66 (1880)

M. Vandermarliere, Ph.D. dissertation, KU Leuven, 1986

M. Vanneste, G. Groeninckx, Polymer **35**, 1051 (1994)

M. Vanneste, G. Groeninckx, Polymer **36**, 4253 (1995)

M. Vanneste, Ph.D. dissertation, KU Leuven, 1993

G. Vidotto, D.L. Levy, A.J. Kovacs, Kolloid Z. Z. Polym. **230**, 289 (1969)

D.J. Walsh, S. Rostami, V.B. Singh, Macromol. Chem. **186**, 145 (1985)

Z. Wang, B. Jiang, Macromolecules **30**, 6223 (1997)

T.T. Wang, T. Nishi, Macromolecules **10**, 421 (1977)

Z. Wang, X. Wang, D. Yu, B. Jiang, Polymer **38**, 5897 (1997)

Z. Wang, A.N. Lijia, B. Jiang, X. Wang, H. Zhao, Polym. J. **30**, 206 (1998)

F.P. Warner, W.J. MacKnight, R.S. Stein, J. Polym. Sci., Polym. Phys. Ed. **B15**, 2113 (1977)

C. Wei-Berk, ACS **68**, 299 (1993)

W. Wenig, K. Meyer, Colloid Polym. Sci. **258**, 1009 (1980)

W. Wenig, F.E. Karasz, W.J. MacKnight, J. Appl. Phys. **46**, 4194 (1975)

W. Wenig, H.-W. Fiedel, A. Scholl, Colloid Polym. Sci. **268**, 528 (1990)

D.L. Wilfong, A. Hiltner, E. Baer, J. Mater. Sci. **21**, 2014 (1986)

M.L. Williams, R.F. Landel, J.D. Ferry, J. Am. Chem. Soc. **77**, 3701 (1955)

J.M. Willis, B.D. Favis, C. Lavallé, J. Mater. Sci. **28**, 1749 (1993)

E.M. Woo, J.W. Barlow, D.R. Paul, J. Appl. Polym. Sci. **28**, 1347 (1983)

B. Wunderlich, *Macromolecular Physics* (Academic, New York, 1973)

B. Wunderlich, in *Macromolecular Physics*, *Vol.2*, *Crystal Nucleation-Growth-Annealing* (Academic, New York/San Francisco/London, 1976)

J. Yang, P. Pan, L. Hua, Y. Xie, T. Dong, B. Zhu, Y. Inoue, X. Feng, Polymer **52**, 3460 (2011)

C. Yordanov, L. Minkova, Eur. Polym. J. **41**, 527 (2005)

H. Zhang, R.E. Prud'homme, J. Polym. Sci., Polym. Phys. Ed. **B24**, 723 (1987)

W.D. Zhang, L. Shen, I.Y. Phang, T.X. Liu, Macromolecules **37**, 256 (2004)

S.X. Zheng, Q. Guo, Y.L. Mi, Polymer **44**, 867 (2003)

X.-Q. Zhou, J.N. Hay, Polymer **34**, 4710 (1993)

A. Ziabicki, Appl. Polym. Symp. **6**, 1 (1967)

A. Ziabicki, *Fundamentals of Fibre Formation: The Science of Fibre Spinning and Drawing* (Wiley, New York, 1976), p. 111

Interphase and Compatibilization by Addition of a Compatibilizer

4

Abdellah Ajji

Contents

A. Ajji
CREPEC, Department of Chemical Engineering, Ecole Polytechnique de Montreal, Montreal, QC, Canada
e-mail: abdellah.ajji@polymtl.ca

Abstract

Polymer blends are mixtures of at least two macromolecular species, polymers
and/or copolymers. For practical reasons, the name *blend* is given to a system
only when the minor component content exceeds 2 wt%. Depending on the sign
of the free energy of mixing, blends are either miscible or immiscible. In
a general sense, the polymer/polymer miscibility does not exist – it is always
limited to a "miscibility window," a range of independent variables, such as
composition, molecular weight, temperature, pressure, etc. More than 1,600 of
these "miscibility windows" have been identified for two-, three-, or four-
component blends. The immiscibility dominates the field (Utracki 1989). For
more details on the thermodynamics of mixing and phase diagrams, the reader is
referred to ▶ Chap. 2, "Thermodynamics of Polymer Blends" in this volume.
This chapter is an updated version of the 1998 version and addresses the aspects
related to the interphase in immiscible polymer blends and their compatibi-
lization by the addition of a compatibilizer. In the first part, theoretical aspects
treating on the prediction of the distribution profiles, interface thickness, and
interfacial tension are presented for immiscible homopolymer blends, copoly-
mers, copolymer/homopolymer blends, and finally copolymer-added homopol-
ymer blends. The second part deals with experimental aspects such as
measurement techniques and comparisons of experimentally measured results
with theory for the interfacial tension and thickness for the systems mentioned
above. Finally, some information on patented polymer blends is presented in
table form. The first two parts are updated at their end with related information
from recent literature.

4.1 Introduction

4.1.1 Definition of the Surface and Interface Tension Coefficients

The surface tension is the reversible work required to create a unit surface area at
constant temperature (T), pressure (P), and composition (n) (Wu 1982):

$$v_i = (\partial G / \delta A)_{T,P,n} \tag{4.1}$$

where v_i is the surface tension coefficient of the substance i, G is Gibbs free energy
of the system, and A is the surface area. In immiscible liquids, interactions between

components are located at the physical boundary creating the interface. The energy required to reversibly separate the two liquids is expressed as the work of adhesion:

$$W = v_1 + v_2 - v_{12} \tag{4.2}$$

where v_1 and v_2 are surface tension coefficients of neat components and v_{12} is the interfacial tension coefficient between the liquids 1 and 2.

4.1.2 Importance of the Interfacial Properties in Polymer Blends

The structure and morphology of immiscible blends depends on many factors among which the flow history and the interfacial properties are the most important. At high dilution and at low flow rates, the morphology of polymer blends is controlled by three dimensionless microrheological parameters: (i) the viscosity ratio, $\lambda = \eta_1/\eta_2$, where η_1 is the viscosity of the dispersed liquid and η_2 that of the matrix; (ii) the capillarity number, $\kappa = \sigma_{12}\, d/v_{12}$, where σ_{12} and d are, respectively, the shear stress and the initial drop diameter; and (iii) the reduced time, $t^* = t\dot{\gamma}/\kappa$, where t is deformation time and $\dot{\gamma}$ is the rate of shear (Utracki 1989, 1994). Thus, the interfacial and rheological properties are keys for the morphological development in polymer blends, which in turn is the controlling factor for their performance.

To improve performance of immiscible blends, usually they need to be compatibilized. There are three aspects of compatibilization: (1) reduction of the interfacial tension that facilitates fine dispersion, (2) stabilization of morphology against its destructive modification during the subsequent high stress and strain processing (e.g., during the injection molding), and (3) enhancement of adhesion between phases in the solid state, facilitating the stress transfer, hence improving the mechanical properties of the product. Compatibilization can be either carried out by adding a compatibilizer to a polymer blend or prepared during the reactive processing or blending. During the latter process, the compatibilizing species are chemically formed in situ, directly across the interface.

In this chapter, compatibilization of polymer blends by means of the addition of a compatibilizer will be discussed. First, the theories will be summarized as follows: (i) interface, (ii) interphase, and (iii) compatibilization process. Reference to some recent work in the area will also be performed in this updated version. This brief summary is to provide a general framework for understanding the phenomena associated with compatibilization and guidance for optimization of the process to gain maximum performance. The theoretical part is followed by the experimental part, where the methods for the determination of interfacial properties are presented. Most of the chapter is dedicated to provide comprehensive information on the characteristic properties of blends compatibilized by the addition of a compatibilizing agent, also with updates from recent literature.

4.2   Theoretical Aspects of the Interface

4.2.1   Binary Immiscible Polymer Blends

Mixing two polymers usually results in an immiscible system, characterized by a coarse, easy to alter morphology, and poor adhesion between the phases. These blends have large size domains of dispersed phase and poor adhesion between them. As a result, their performance is poor and irreproducible. In particular the impact strength, maximum strain at break, and the yield strength are affected. The irreproducibility originates from instability of morphology – blend structure developed during the compounding step is unstable and irreproducible. To be able to solve these three problems (degree of dispersion, stability of morphology, and adhesion between the phases in solid state), one must learn about the region between the two phases in binary polymer blends, the interface or rather the interphase.

Let us consider a molten, immiscible, binary blend of polymers A and B, without compatibilizer. Helfand and Tagami (1971a, b), Helfand (1975a, b, c), Roe (1975), and Helfand and Sapse (1975) have developed a quantitative lattice theory of the interphase that 20 years later still provides good basis for understanding.

Helfand and Tagami model is based on self-consistent field that determines the configurational statistics of macromolecules in the interfacial region. At the interface, the interactions between statistic segments of polymers A and B are determined by the thermodynamic binary interaction parameter, χ_{12}. Since the polymers are immiscible, there are "repulsive" enthalpic effects that must be balanced by the entropic ones that cause chains A and B to intermingle.

In the first simplified mean-field approach, (i) the two homopolymers were assumed to have the same degree of polymerization; (ii) the complex set of equations derived for the segmental density profile, ρ_i (where $i = A$ or B), was solved for infinitely long macromolecules, $M_w \to \infty$; (iii) the isothermal compressibility was assumed to be negligibly low; and (iv) there was no volume change upon blending (i.e., the attractive or repulsive forces between two polymers were assumed weak).

The analytical solution of the interfacial composition profile was found to follow an exponential decay function (Helfand and Tagami 1972):

$$
\begin{aligned}
\rho_i &= \rho_{i,o} y^2/(1+y^2) \\
y &\equiv \exp\left\{(6\chi_{AB})^{1/2}(x/b)\right\}
\end{aligned}
\tag{4.3}
$$

where b is the lattice parameter and i can be either A or B. A typical dependence is shown in Fig. 4.1 (Utracki 1994).

Similarly, for the symmetrical polymers A and B whose $M_w \to \infty$, the interfacial thickness, Δl_∞, and the interfacial tension coefficient, v_∞, were derived as:

$$
\Delta l_\infty = 2b(6\chi_{AB})^{-1/2}
\tag{4.4}
$$

Fig. 4.1 Representation of
the interface, with the
definition of the interphase
thickness, Δl; χ and b are,
respectively, the binary
interaction and the lattice
parameters
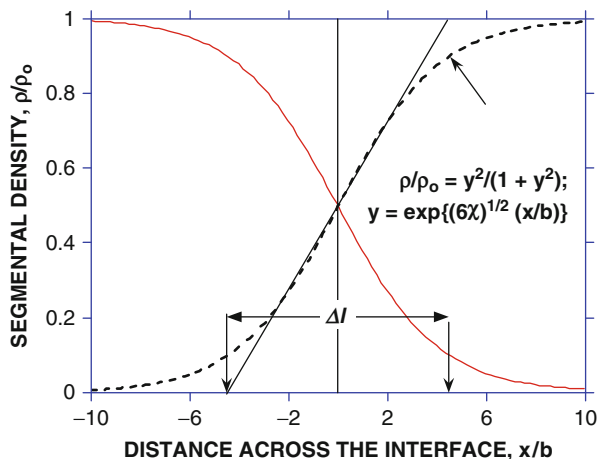
$$v_\infty = b\rho T k_b (\chi_{AB}/6)^{1/2} \tag{4.5}$$

where k_b is the Boltzmann constant and T is the absolute temperature.

Predictions of Eq. 4.5 were compared with the experimental data for three polymeric blends: polystyrene/polymethylmethacrylate, PS/PMMA; polybutyl methacrylate/polyvinylacetate, PBMA/PVAc; and PMMA/PBMA. It was found that v_∞ agreed with the experimental value of v_{12} determined for PBMA/PVAc. However, the agreement for PMMA/PBMA was not as good, while for PS/PMMA the difference was 50 %. In consequence, the authors postulated that for large values of χ_{12}, the thickness of the interphase is too small for the mean-field theory to be valid. Equation 4.5 also predicts that the interfacial tension coefficient is a linear function of the temperature. Furthermore, since to the first approximation $\chi_{AB} = a + b/T$, the slope dv_{12}/dT should be negative. Figure 4.2 indeed confirms these predictions.

The Helfand-Tagami lattice theory predicts that there is reciprocity between the interfacial tension coefficient and the interfacial thickness, and the product, $v_\infty \Delta l_\infty$, is independent of the thermodynamic binary interaction parameter, χ_{12}. Furthermore, the theory led to the conclusions that (i) the surface free energy is proportional to $\chi_{12}^{1/2}$; (ii) the chain ends of both polymers concentrate at the interface; (iii) any low molecular weight third component is repulsed to the interface; (iv) the interfacial tension coefficient is a linear function of temperature (see Eq. 4.5 and Fig. 4.2); and (v) the interfacial tension coefficient increases with molecular weight to an asymptotic value, v_∞, as illustrated in Fig. 4.3:

$$v = v_\infty - a_o M_n^{-2/3} \tag{4.6}$$

Four years later, Helfand and Sapse removed the restriction of the original theory for the symmetric character of both polymers, obtaining for v_∞ the following expression:
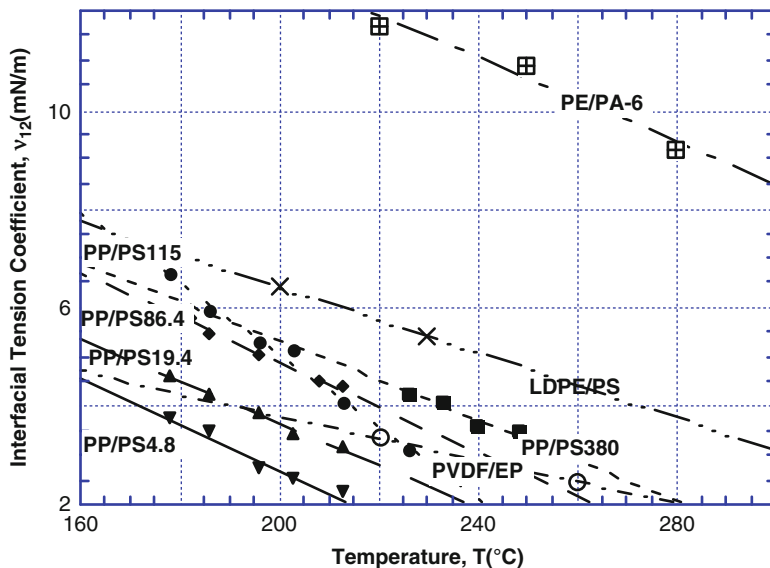
Fig. 4.2 Temperature dependence of the interfacial tension coefficient for PP/PS (data from Demarquette and Kamal 1994) and for PE/PA, LDPE/PS, and PVDF/EP
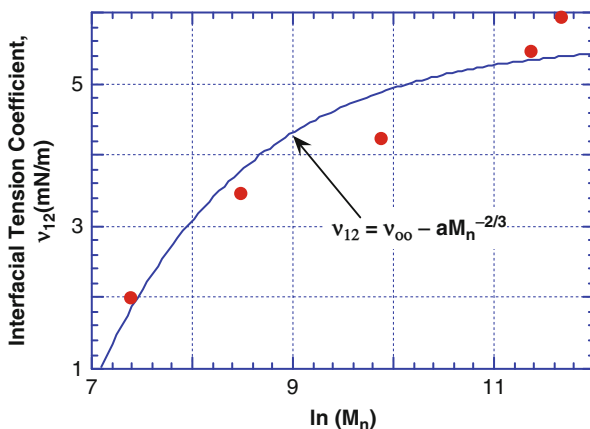
Fig. 4.3 Verification of the molecular weight dependence of the interfacial tension coefficient, as predicted by the Helfand-Tagami theory (see Eq. 4.6)

$$v_\infty = (2/3)k_b T\alpha^{1/2}(\beta_A^3 - \beta_B^3)/(\beta_A^2 - \beta_B^2)$$
$$\alpha \equiv \chi_{AB}(\rho_{oA}\rho_{oB})^{1/2} \tag{4.7}$$
$$\beta_i^2 = \rho_{oi}b_i^2/6$$

where $b_i^2 = \langle R_i^2\rangle/Z_i$ and b_i is the Kuhn statistical segment length.

Substituting in Eq. 4.7, $\rho_{oA} = \rho_{oB}$ and $\beta_A = \beta_B$ result in the recovery of Eq. 4.5.

A generalized gradient theory of the interface was developed by Anastasiadis et al. (1988). The approach is based on the assumption that the composition gradient is small compared to the reciprocity of the intermolecular distances. Under these circumstances the free energy density, g, can be written as a power series, truncated after the square term. In essence, the theory determines the difference in the density fluctuation per unit interfacial area between a polymer mixture and a system in which the properties are homogenous. The theory predicts that:

$$
\begin{aligned}
v_{12} &= \int_{\phi_\alpha}^{\phi_\beta} \left[\overline{\kappa} \Delta g(\phi) \right]^{1/2} d\phi \\
\overline{\kappa} &\equiv -\left[\partial^2 g / \partial\phi\partial\nabla^2\phi \right] + \left[\partial^2 g / \partial |\nabla\phi|^2 \right]
\end{aligned}
\tag{4.8}
$$

Thus, to calculate v_{12}, one has to select an appropriate expression for the energy density gradient and then integrate Eq. 4.8 within the limit of composition in both phases, ϕ_A and ϕ_B. Huggins-Flory and Cahn-Hilliard theories were used with good success to predict the temperature gradient, but poor as far as the effects of molecular weight were concerned.

Roe (1975) developed a quasicrystalline lattice model for conditions where $\chi_{12} >> \chi_{cr}$ (where χ_{cr} is the critical value of the interaction parameter at the phase separation) and for $\chi_{12} - \chi_{cr} << \chi_{cr}^2$. Under the first conditions (high immiscibility), the theory predicted a proportionality between v_{12} and χ_{12}, whereas under the second (near the phase separation), a proportionality between v_{12} and $\chi_{12}^{3/4}$ was predicted. By contrast with the previously summarized Helfand and Tagami predictions, Roe's theory indicates that the product $v_{12}\Delta l$ should be proportional to $\chi_{12}^{1/2}$.

Kammer (1977) considered the interface between two polymers from the basic thermodynamic point of view. He derived a simple relation: $v_{12} = \Delta\mu_{B/S}$, where $\Delta\mu_B$ is the excess chemical potential of polymer B in the mixture and S is the molar area of the interface. Near the spinodal decomposition, using the Cahn-Hilliard gradient theory, he calculated:

$$
\begin{aligned}
v_{12} &= v_o + RT\phi_B^{1/2}\varepsilon^{1/2} \\
\varepsilon &\equiv (\chi - \chi_{cr})/\chi_{cr}
\end{aligned}
\tag{4.9}
$$

The following year, from similar assumptions, Joanny and Leibler (1978) derived:

$$
\begin{aligned}
v_{12} &= (2/3)k_B T b^2 Z_B^{-1/2}\varepsilon^{3/2} \\
\Delta l &= (1/3)b Z_B^{1/2}\varepsilon^{-1/2} \\
\therefore v\Delta l &= (2k_B T/9b)\varepsilon
\end{aligned}
\tag{4.10}
$$

where $Z_B = Z_A$ is the degree of polymerization. The proportionality $v_{12} \sim \varepsilon^{3/2}$ and $\Delta l \sim \varepsilon^{-1/2}$ are in agreement with the classical approach to the interface (de Gennes 1977). Thus, it seems that the prediction of the Helfand-Tagami lattice

theory that the product, $v_{12}\Delta l$, is independent of the thermodynamic binary interaction parameter, χ_{12}, may not be correct in the whole range of variables. The authors observed that the relation breaks down in antagonistically immiscible blends where $\chi_{12} >> \chi_{cr}$. Nowadays, there is growing theoretical evidence that the prediction is not valid for $\chi_{12} \rightarrow \chi_{cr}$.

More recently, Eq. 4.4 was modified to account for finite M_w (Broseta et al. 1990). For blends of polystyrene with polyvinylpyridine, PS/PVP, the authors obtained:

$$\Delta l = 2b\,(6\chi_{12})^{-1/2}[1 + (\ln\ 2)(1/Z_{PS} + 1/Z_{PVP})/\chi_{12}] \tag{4.11}$$

where Z is the degree of polymerization. Equation 4.11 was corrected for entropic effects. For $M_w \rightarrow \infty$, Eq. 4.4 is recovered. Polydispersed systems were also considered by assuming the same bimodal distribution of chain lengths for both A and B components. As expected, chains of higher M_w tended to localize in the bulk phases rather than near the interfacial region. The loss of translational entropy associated with the confinement of the chain into half the space is more easily accepted by large chains than by small ones.

Muller and Binder investigated recently (Muller and Binder 2000) the structure and thermodynamics of interfaces in dense polymer blends using Monte Carlo (MC) simulations and self-consistent held (SCF) calculations. A quantitative agreement between the MC simulations and the SCF calculations was found for structurally symmetric blends for interfacial properties such as interfacial tension or enrichment of copolymers at the interface. Some capillary wave contributions had, however, to be taken into account for quantitative comparison of the profiles across the interface in the MC simulations and the SCF calculations. SCF calculations led to profiles of a perfectly fiat interface and the local, interfacial position fluctuated for the MC simulations. Asymmetric blends' interfacial properties were investigated by considering the polymers having different stiffnesses. At high incompatibilities, the interfacial width is not much larger than the persistence length of the stiffer component. Deviations from the predictions of the Gaussian chain model were found indicating that while the Gaussian chain model yields an increase of the interfacial width upon increasing the persistence length, no such increase was found in the MC simulations. The details of the chain architecture on all length scales could be taken into account using a partial enumeration technique in the SCF calculations, and a good agreement with the MC simulations was achieved.

There have been also some recent theoretical approaches addressing mainly the thermodynamic properties of binary and ternary polymer blends. Campos et al. (1996) extended the Flory-Huggins theory to predict the thermodynamic properties of binary polymer blends and blends in solution. Their approach was applied for PVDF/PS dry blend and in solution in dimethylformamide (DMF) with inclusion of an interaction function. It could be inferred that this blend behave as slightly incompatible under environmental conditions, in agreement with previously reported data. That incompatibility was suppressed when a low molar mass component, such as DMF, was added, reaching the semidilute regime (total

polymer volume fraction of about 0.35). Values of the Gibbs free energy of mixing as a function of the blend composition were also evaluated for both ternary solution and dry blend and discussed in terms of their stability.

Rudolf et al. (1998) used the modified cell model of Dee and Walsh and the Simha-Somcynsky theory to investigate the phase behavior, excess volumes, the influence of pressure on miscibility, and the causes of miscibility. It was found that the theory of Dee and Walsh yields results similar to the previously investigated theories, whereas the Simha-Somcynsky theory does not. A modification of the latter theory for mixtures again resulted in predictions similar to that of Dee and Walsh and the earlier investigated theories.

Buta et al. (2001) tested the Monte Carlo approach for the lattice cluster theory to derive the thermodynamic properties of binary polymer blends. They considered the two polymers to have the same polymerization indices, i.e., M = 40, 50, or 100. The results confirm that this lattice cluster theory had a higher accuracy compared to the Flory-Huggins theory and the Guggenheim's random mixing approximation. However, some predictions for the specific heat were found to be inaccurate because of the low order cutoff of the high temperature perturbative expansion.

Finally, a review was done by Higgins et al. (2005) in which they combined the experiments and a theory based on the lattice Born-Green-Yvon (BGY) approach to predict coexistence curves, neutron scattering intensities, and pressure-volume-temperature surfaces. This work allowed to better understand some of the correlations between the microscopic structure and macroscopic behavior of several common polymer mixtures.

4.2.2   Copolymers

Block copolymers are polymers constituted of at least two different monomers arranged in a specific manner – they could be diblock, triblock, multi-block, linear, star shaped, etc. Those based on styrene and butadiene, SB or SBS, are the earliest to be applied and studied, as well as the largest as far as the volume of production is concerned (Holden et al. 1967).

4.2.2.1 Block Copolymers: Fundamentals

To ascertain control of the molecular weight, structure, and composition, block copolymers are usually synthesized in anionic polymerization. The block copolymers of commercial interest are specifically prepared from monomers that upon polymerization yield immiscible macromolecular blocks, a smaller one rigid and the other flexible. The rigid blocks form physical cross-links that upon heating above the transition point make the copolymer flow. Thus, these materials belong to the growing family of thermoplastic elastomers.

There are two distinct differences between the phase diagram of a block copolymer and the one obtained for a mixture of two homopolymers. In block copolymers, owing to the chemical links between blocks, microdomains instead of macroscopic phases are observed. The size of microdomains can be

controlled by varying the molecular weight and composition. Furthermore, since the type of morphology depends on the concentration as well as on the transition temperatures of the individual phases, the phase diagram of block copolymers shows comparable complexity to those of metallic alloys.

The domain size and shape, as well as the interfacial thickness, depend on the following factors: (i) magnitude of the repulsive interactions between the A and B blocks, χ_{AB}; (ii) the conformation entropy loss necessary to maintain constant segment density; (iii) the localization entropy loss that causes the chemical links to be present at the interface; and (iv) the composition. These mutually compensating factors (i vs. ii + iii) depend on molecular weight of each block and the binary interaction parameter (Helfand 1975; Helfand and Wasserman 1976, 1978, 1980; Hashimoto et al. 1974, 1980a, b; Inoue et al. 1969; Krause 1980; Meir 1969, 1987; Hashimoto et al. 1983).

4.2.2.2 Interphase in Block Copolymers

Theories of block copolymers are usually complex, involving computation of the domain size, the interphase thickness between the blocks, the structure, and the order–disorder transitions. Helfand and Wasserman (1976, 1978, 1980), using the narrow interphase approximation, showed that Eq. 4.4 is valid in the limit of infinitely immiscible blocks having $M_w \to \infty$ (i.e., the strong segregation limit, SSL). The authors' approach was based on the confined chain statistics. Expressions for the free energy of different structure formation, interfacial tension, and interfacial thickness (in the case of an infinite M_w) were derived. For large $\chi_{12}Z_c$ values (Z_c is the copolymer degree of polymerization), the narrow interface approximation was assumed valid; thus, the boundary thickness should be similar to that in an A/B mixture. This interfacial thickness Δl was expressed as:

$$\Delta l = 2\left[\left(\beta_A^2 + \beta_B^2\right)/2\chi_{12}\right]^{1/2} \tag{4.12}$$

with $\beta_i^2 = (\rho_{oi}b_i^2)/6$ and $b_i^2 = <R_i^2>/Z_i$, where b_i is the Kuhn statistical segment length, Z_i is the degree of polymerization, ρ_{oi} is the density, and $<R_i^2>$ is the radius of gyration of the block i. For identical chains and the lattice size, $b^2 = b_i^2\rho_i$ and Eq. 4.12 converts to Eq. 4.4.

The thermodynamic properties of block copolymers in disordered state have been studied by Leibler (1980). Using the random phase approximation (de Gennes 1979), the author developed a relation between the segmental density correlation function and the scattering vector. An order parameter, related to the reduced segmental density, was introduced. In the disordered state, this order parameter is zero, whereas for the ordered phase, it is a periodic nonzero function. Leibler demonstrated that the critical condition for microphase separation in diblock copolymers is $\chi_{AB}Z_c = 10.5$.

The work was extended by Olvera de la Cruz and Sanchez (1986) to block copolymers with more complex architectures. For diblock copolymers, the authors confirmed Leibler's results, $\chi_{AB}Z_c = 10.5$. The same value was also found for the star copolymers having the same number of A and B arms, each of the same length:

Fig. 4.4 Interphase thickness in styrene-isoprene block copolymers versus total molecular weight. *Points* are experimental (Hashimoto et al. 1980; Richars and Thomason 1983); the *line* was computed from Eq. 4.13 using $\Delta l_o = 1.9$ nm and $\chi = 1,000$ $\chi_{AB}/M_o = 0.6$
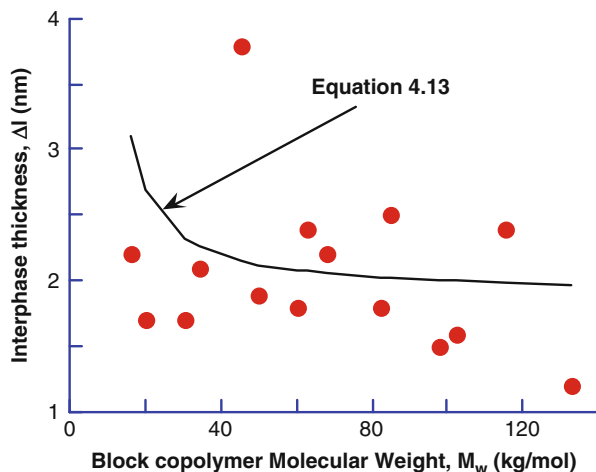
$Z_A = Z_B$. Computations for triblock copolymers gave $\chi_{AB}Z_c = 8.86$, indicating poorer miscibility than that computed for diblocks.

More recently, a theory based on confined chain statistics (CCS) predicted that Δl should be a decreasing function of Z_c. Thus, the modification of Eq. 4.4 resulted in an expression valid for $\chi_{AB}Z_c \geq 20$ (Spontak and Zielinski 1993):

$$\Delta l = \Delta l_\infty [1 - (8\ln 2)/(\chi_{AB}Z_c)]^{-1/2} \tag{4.13}$$

Equations 4.12 and 4.13 are similar, but differences in the range of 40 % have been found in the low $\chi_{AB}Z_c$ region. The prediction of Eq. 4.13 is compared in Fig. 4.4 with the small-angle neutron scattering and small-angle X-ray scattering data (Hashimoto et al. 1980; Richars and Thomason 1983).

4.2.3   Copolymer/Homopolymer Blends

4.2.3.1 Blends of Block Copolymer with Homopolymer

Information on the phase diagrams of copolymer/homopolymer blends can be found in reviews by Ajji and Utracki (1996, 1997) and in ▶ Chap. 2, "Thermodynamics of Polymer Blends" in this handbook. The interface thickness of A/A-B mixtures was not theoretically calculated, but experimental measurements indicate that the presence of the homopolymer leaves the domain boundary unchanged (Bates et al. 1983; Hashimoto et al. 1990a; Tanaka et al. 1991; Zin and Roe 1984; Green et al. 1989). On the other hand, the part of the phase diagram where the concentration of the block copolymer in the mixture is low was studied in detail (Whitmore and Noolandi 1985; Leibler et al. 1983; Leibler 1988). The proposed models were similar. In both, the conditions for the formation of spherical micelles

were investigated and expressions of the critical micelle concentration, $\phi_{CMC}^{\text{spherical}}$, were derived. For example (Leibler 1988):

$$\phi_{CMC}^{\text{spherical}} = \exp\left\{ 1.72(\chi_{AB}Z_C)^{1/3}f^{4/9}\left(1.74f^{-1/3}-1\right)^{1/3} - f\chi_{AB}Z_C \right\} \qquad (4.14)$$

where f is the fraction of A-polymer in A-B copolymer.

The predictions of ϕ_{CMC} were extended to cylindrical and lamellar micelle morphologies (Shull et al. 1991). In all cases, geometric parameters, e.g., core radius and corona thickness, can be computed, assuming that the interfacial thickness between the core and the corona is equal to Δl_∞.

Experimental studies of micellar systems were carried out using scattering methods (Selb et al. 1983; Rigby and Roe 1984, 1986; Kinning et al. 1990, 1991). Theoretical simulations of the scattering curves have been based on the assumptions that either an infinitely sharp boundary thickness or a diffuse interfacial thickness is equal to Δl_∞. In spite of these seemingly diverse principles, the simulations were reasonably correct.

The enthalpy associated with the addition of a homopolymer having high M_w to a block copolymer in the disordered state is not compensated by sufficient entropic gains; hence, a mesophase is formed. This effect was observed by Cohen and Torradas (1984). This contrasts with other reports (Ptaszynski et al. 1975; Hashimoto et al. 1990; Winey et al. 1991) where upon the addition of a homopolymer with molecular weight smaller than that of the corresponding block, the average area per junction point was found to increase. SAXS scattering patterns obtained from samples having lamellar morphology followed an idealized model, in which layers of styrene and butadiene (with randomly varying thickness and a diffuse interface) were parallel.

Green and Russel (1991) theoretically and experimentally studied effects of the addition of a low molecular weight symmetric block copolymer of P(S-b-MMA) on the interfacial tension in blends comprising a high molecular weight homopolymer, either PS or PMMA. The theory was based on a mean-field argument (similar to that of Leibler), valid within the low compatibilizer concentration range. The theory predicted that:

$$v = v_o - k_B T[\rho\phi_C a\exp\{\chi_{AB}Z_C\}]/Z_C \qquad (4.15)$$

where ϕ_c is the volume fraction of the copolymer. The calculations were consistent with experimental data on similar systems. The estimated value of χ_{AB} compared well with that determined in neutron scattering experiments.

Floudas et al. (1997) studied theoretically and experimentally microphase segregation in block copolymer/homopolymer blends for an asymmetric diblock copolymer and homopolymer concentrations of less than 25 %. It was observed that the minority phase could solubilize only a small amount of added homopolymer. The addition of higher amounts resulted in the formation of nonequilibrium structures. Theoretical predictions in the strong segregation limit showed that $(\chi N)_c$,

where N is the degree of polymerization, always increases with the addition of the minority phase. Experiments agreed with experiments in the two extreme cases of N much larger than N_h (homopolymer degree of polymerization) and N much smaller than N_h. Their results showed that the degree of compatibility between the two blocks of the diblock AB can be effectively controlled by adding a small amount of homopolymer A or B.

Choksi and Ren (2005) derived a density functional theory for diblock copolymer/homopolymer blends. Their numerical results were shown to capture the multiscale separation in the system: (i) macrophase separation into homopolymer- and copolymer-rich macrodomains followed by (ii) microphase separation into A- and B-rich microdomains within the copolymer-rich macrodomains. They also demonstrated a result on local minimizers in one space dimension, confirming a lamellar multiscale phase separation.

More recently, Martinez-Veracoechea and Escobedo (2009) used a self-consistent theory and particle-based simulations for the case of bicontinuous phases in diblock copolymer/homopolymer blends. They were able to predict the spontaneous formation of double-diamond phase (DD) and plumber's nightmare phase (P) in the range of homopolymer volume fraction simulated via coarse-grained molecular dynamics for the first time. The self-consistent field theory was used to explore the DBC/homopolymer phase diagram in more detail. They showed that although the two-phase coexistence of a DBC-rich phase and a homopolymer-rich phase does precede the stability of complex bicontinuous phases in many cases, the DD phase can be stable in a relatively wide region of the phase diagram. The P phase was always metastable with respect to macrophase separation under the thermodynamic conditions explored with SCFT. It was sometimes nearly stable, suggesting that full stability could be achieved in other unexplored regions. Moreover, the predicted DD and P phases could be observed in experiments as "long-lived" metastable phases.

Finally, a comparison of self-consistent field theory (SCFT) results with experiments for micelle formation in block copolymer/homopolymer blends was performed by Greenall et al. (2009) for a blend of poly(styrene-butadiene) diblocks and homopolystyrene. They found that the micelle core radii R_c shape and variation with molecular parameters could be reproduced much more accurately than scaling theories. For the corona thickness, the accuracy of the predictions was at least as good as that of scaling theories. For copolymers with lighter core blocks, SCFT predictions for the critical micelle concentration improved over those of scaling theories by an order of magnitude. In the case of heavier core blocks, however, SCFT predicted the critical micelle concentration less well due to inaccuracies in the modeling of the bulk chemical potential.

4.2.3.2 Blends of Graft or Random Copolymer with Homopolymer

There are only few papers dealing with systems comprising a graft copolymer and a homopolymer. For example, blends of graft A-B copolymer with homopolymer A (identical with the backbone of the copolymer) were found to have unusual morphologies (Eastmond and Phillips 1977, 1979). The most common of these

were spherical structures (named *onions*) consisting of alternating concentric layers of *A* and *B* components. The conclusion was that the *onions* had their origin in the immiscibility of copolymer with homopolymer, even when the molecular weight of chemically identical blocks was comparable (Eastmond et al. 1987). Other studies reported similar findings, even when the molecular weight of homopolymer was lower than that of the corresponding block (Jiang et al. 1985). It was suggested that the immiscibility and the *onion*-type morphology originated in molecular structure of copolymer.

For the case of homopolymer blends with a random copolymer, Shimomai et al. (1996) studied their miscibility using the equation of state theory and compared the results for poly(methyl methacrylate) (PMMA) and styrene-acrylonitrile random copolymers (SAN) blends. They used the Flory-Orwoll-Vrij equation of state theory. To obtain the equation of state parameters (P*, V*(sp), T*: characteristic parameters), the pressure-volume-temperature (PVT) behavior was measured for PMMA and a series of SANs with various acrylonitrile contents. The Flory-Huggins interaction parameter X was separated into two contributions based on the equation of state theory for mixtures: an exchange energy term and a free volume term. Both their temperature and copolymer composition dependences were estimated by calculations using the equation of state parameters. There exists a region in which the part due to the exchange energy term is negative, leading to a miscibility window in PMMA/SAN blends. However, the immiscibility at high temperatures in the blends could not be explained only by term; it was caused by the free volume contribution.

4.2.4 Blends of Two Homopolymers with a Compatibilizer

4.2.4.1 Blends of Two Polymers with a Copolymer

Ternary blends that comprise two immiscible polymers and a copolymer are of a particular interest. They not only represent an ideal model for studying compatibilization of polymer blends, but also they have found direct commercial applications. Phase diagram information can be found in reviews by Ajji and Utracki (1996, 1997) and in ▶ Chap. 2, "Thermodynamics of Polymer Blends," ▶ Chap. 21, "Miscible Polymer Blends," and ▶ Chap. 8, "Morphology of Polymer Blends" in this handbook.

The theories discussed in Sect. 4.2.1 dealt with binary polymer blends without compatibilizer. Hong and Noolandi (1980, 1981a, b) developed a theory, similar to that of Helfand, for the interfacial region in three-component polymeric systems comprising polymers *A* and *B* and either a cosolvent or a block copolymer. The theory is based on the lattice model – it uses the mean-field approximation. It is formulated using the reduced equation of state variables. Finite molecular weights and conformational entropy effects were considered, but the excluded volume effects were not (this aspect was later treated by Broseta et al. (1987)). The resulting system of equations can be solved numerically for the interfacial composition profile, interfacial tension coefficient, thickness of the interphase, etc. At low values of M_w, the theory well predicts v_{12}, but for higher M_w, the prediction was up to 20 % too high.

Calculations of the Interfacial Tension Coefficient and CMC

The emulsifying effects of a small quantity of a block copolymer, *A-B*, added to immiscible blend of homopolymers *A* and *B*, were examined by Leibler (1988). The theory predicted the reduction of the interfacial tension coefficient, v_{12}, caused by equilibrium adsorption of a copolymer at the interface. For well-chosen compositions and molecular weights of the copolymer, low values of v_{12} are to be expected. This suggests a possible existence of thermodynamically controlled stable droplet phase, in which the minor phase homopolymer drops are protected by an interfacial film of the copolymer, interfacing the matrix polymer. The size distribution of the droplets is expected to depend on the rigidity and spontaneous radius of curvature of the interfacial film that can be controlled by molecular structure of the copolymer.

For long copolymer chains (in strongly immiscible, or the "wet brush case"), the reduction of the interfacial tension coefficient should follow the relation:

$$\Delta v \equiv v - v_o = -\left(k_B T/a^2\right)(3/4)^{1/3}\left(\Sigma/a^2\right)^{-5/3}\left[Z_{CA}Z_A^{-2/3} + Z_{CB}Z_B^{-2/3}\right] \quad (4.16)$$

where Z_{CA} and Z_{CB} are, respectively, the number of *A* and *B* monomeric segments in copolymer; $Z_c = Z_{CA} + Z_{CB}$ is the total number of segments in copolymer; Z_A and Z_B are the degrees of polymerization in homopolymer *A* and *B*, respectively; a is the monomer length; and Σ is the interfacial area per copolymer joint ($\Sigma = A/Q$, where Q is the number of copolymer chains at the interface between *A* and *B* and *A* is the total interface surface area). For short copolymer chains ($Z_c < Z_i^{-2/3}$ and $\Sigma < Z_c^{1/2}a^2$), Eq. 4.16 can be simplified to read:

$$\Delta v = -3Z_C\left(k_B T/a^2\right)\left(\Sigma/a^2\right)^{-3} \quad (4.17)$$

Both Eqs. 4.16 and 4.17 predict that when adsorption density (Σ/a^2) is high, the interfacial tension coefficient is low. For the same surface area per chain, longer copolymer chains are predicted to be more efficient. The expressions of Σ/a^2 can be obtained, for both "wet" and "dry" brushes, as a function of the copolymer chemical potential, μ. The ratio was found to depend on the logarithm of the copolymer concentration (Leibler 1988).

From Eq. 4.14, the critical micelle concentration, *CMC*, was derived:

$$\phi_{CMC}^+ = \exp\{\mu_{CMC} - f\chi_{AB}Z_C\} \quad (4.18)$$

where ϕ_{CMC}^+ is the volume fraction of copolymer in B-rich phase and μ_{CMC} is its chemical potential at *CMC*:

$$\mu_{CMC} = (3/2)^{4/3}f^{4/9}\left(1.74f^{-1/3} - 1\right)^{1/3}(\chi_{AB}Z_C)^{1/3} \quad (4.19)$$

As copolymers are added, v_{12} decreases until ϕ^+ reaches the ϕ_{CMC}^+ value, at which the limiting value of the interfacial tension coefficient, v_{CMC}, is obtained.

A question arises whether the copolymer can saturate the interface so that $\Delta v = v_o = (k_B T/a^2)(\chi/6)^{1/2}$, and effectively the interfacial tension vanishes. This saturation may occur when $\mu = \mu_{sat} = (3/4^{2/3})(\chi N)^{1/3}$. For a flat interface, v_{12} should vanish when $f > 0.31$. The theory also predicts that for $f < 0.31$, spherical micelles may appear. In the latter case, the limiting reduction of v_{12} is given by:

$$\Delta v/v_o = -3^{1/2} f^{2/3} \left(1.74 f^{-1/3} - 1\right)^{1/2} \tag{4.20}$$

Typically, for $f = 0.33, 0.2$, and 0.15, $\Delta v/v_o$ is expected to be $1.00, 0.83$, and 0.42 respectively; hence, $\Delta v = v_o$ for $f = 1/3$. Thus, the more asymmetric is the chain, the less it is efficient as an interfacial agent. Since the theory does not differentiate between polymers A and B, evidently the most efficient copolymer composition must be as follows: $1/3 < f_{opt} < 2/3$, or $f_{opt} = 1/2$.

For more symmetric chains $f > 0.31$, $v = 0$ can be reached when:

$$\phi_{sat}^+ = \exp\left\{ \left(3/4^{2/3}\right)(\chi_{AB} Z_C)^{1/3} - f\chi_{AB} Z_C \right\} \tag{4.21}$$

For a flat interface saturated by the copolymer, the copolymer film thickness was calculated as:

$$\Delta l = a Z_C^{2/3} \left(v_o a^2/3 k_B T\right)^{1/3} \tag{4.22}$$

The above expressions are valid for flat interface. For interface with a curvature R, e.g., for droplets having a radius $R \gg \Delta l$, the following expressions were derived (dry film) (Leibler 1988):

$$v(\mu, R) = v(\mu) - [K(\mu)/R\psi(\mu)] + K(\mu)/2R^2 \tag{4.23}$$

$$\Delta l = Z_C a^2/\Sigma \tag{4.24}$$

The droplet size is given by:

$$R = \{K(\mu)/[v(\mu)\psi(\mu)]\}\left[1 - \left(1 - v(\mu)\psi^2(\mu)/K(\mu)\right)^{1/2}\right] \tag{4.25}$$

For copolymer content close to the saturation of a flat interface, the R-value becomes:

$$R = K(\mu)/[v(\mu)\psi(\mu)] = (3/2)\psi(\mu) \tag{4.26}$$

The limiting value is obtained for the saturation value of μ.

In Eqs. 4.23, 4.24, 4.25, and 4.26:

$$
\begin{aligned}
K(\mu) &= 2\Sigma^{-5}[7\beta(f) - 32\varepsilon^2]Z_C^3 \\
\Sigma &= a^2(3/2^{1/2})(Z_C/\mu)^{1/2} \\
\psi(\mu) &= (L/3\varepsilon)[7\beta(f) - 32\varepsilon^2] \\
L &= Z_C a^3/\Sigma \\
\beta(f) &= f^3 + (1-f)^3 \\
\varepsilon &= (1/2) - f
\end{aligned}
\tag{4.27}
$$

Equations 4.23, 4.24, 4.25, and 4.26 are valid at equilibrium, without taking into account the kinetic effects. The latter effects may be important when comparing theoretical predictions with experimental data.

There are other theories of the interface, some of which lead to different dependencies. For example, Noolandi (1984; 1985) considered a binary polymer system compatibilized by addition of a diblock copolymer. For $\chi_{AB}Z_c\phi_p \leq 2$, he derived:

$$
\begin{aligned}
v_{12} &= v_o + \Delta l\phi_C\{\chi_{AB}\phi_P/2 + (1/Z_C)[1 - \exp(\chi_{AB}Z_C\phi_P/2)]\} \\
\therefore \Delta v_{12} &\cong -\exp(\chi_{AB}Z_C\phi_P/2)
\end{aligned}
\tag{4.28}
$$

where a_o is a numerical parameter, while ϕ_c, ϕ_p, and Z_c are, respectively, the volume fraction of the copolymer, the volume fraction of the polymer, and the degree of polymerization of the copolymer.

It is noteworthy that Leibler's (see Eqs. 4.20 and 4.22) and Noolandi's theories (see Eq. 4.28) predict that the product $v_{12}\Delta l$ depends on the binary interaction parameter χ_{12}. Thus, the reciprocity between v_{12} and Δl predicted by Helfand and Tagami for binary systems is not expected to exist in compatibilized binary blends.

Two semiempirical relations between the interfacial tension coefficient and compatibilizer concentration were derived. The first was obtained assuming an analogy between the addition of a block copolymer to a polymer blend and titration of an emulsion with surfactant (Utracki and Shi 1992):

$$
\begin{aligned}
v_{12} &= (\phi v_{CMC} + \phi_{\text{mean}}v_o)/(\phi + \phi_{\text{mean}}) \\
v_{CMC} &\equiv v_{12}(\phi_C = \phi_{CMC}) \\
\phi_{\text{mean}} &\equiv (\phi_{CMC} + \phi_o)/2
\end{aligned}
\tag{4.29}
$$

The other was proposed by Tang and Huang (1994):

$$
v = v_{CMC} + (v_o - v_{CMC})\exp\{-K\phi\}
\tag{4.30}
$$

The latter authors proposed a similar relation for the particle's radius:

$$
R = R_{CMC} + (R_o - R_{CMC})\exp\{-K\phi\}
\tag{4.31}
$$

In Eqs. 4.30 and 4.31, K is treated as an adjustable parameter. Its functional dependence can be deduced from the comparison with Noolandi's Eq. 4.28, since $K \propto \chi_{AB} Z_c$. These dependencies were found useful in describing the experimental data.

Cho et al. (2000) studied the segregation dynamics of block copolymers to the interface of an immiscible polymer blend and compared experimental results to the predictions of various theories for a poly(styrene-b-dimethylsiloxane) [P(S-b-DMS); $M_n = 13,000$] symmetric diblock copolymer system added to a molten blend of the corresponding immiscible homopolymers. They used the pendant drop technique at intermediate times and compared their results to the predictions of diffusion-limited segregation models proposed by Budkowski, Losch, and Klein (BLK) and by Semenov that have been modified to treat interfacial tension data. The apparent block copolymer diffusion coefficients obtained from the two analyses fall in the range of 10^{-5}–10^{-6} cm^2/s, in agreement with the estimated self-diffusion coefficient of the PDMS homopolymer matrix.

More recently, Reynolds et al. (2004) used mean-field theories and scattering to study the thermodynamic organization of a polymer blend by the addition of balanced block copolymers. They used parameters determined from binary experiments to predict the behavior of multicomponent A/B/A-C polymer blends, where A was saturated polybutadiene with 90 % 1,2-addition (sPB90), B was polyisobutylene (PIB), and C was also saturated polybutadiene but with 63 % 1,2-addition (sPB63). The polymers were chosen such that the binary interactions (A/B, A/C, and B/C) were similar to those in oil (A)/water (B)/nonionic surfactant (A-C) systems. The Flory-Huggins interaction parameters and the statistical segment lengths were all determined experimentally by fitting the random phase approximation (RPA) to small-angle neutron scattering (SANS) data from the three binary homopolymer blends. These parameters were successfully used to predict the scattering from concentration fluctuations in a homogeneous A/B/A-C blend using multicomponent RPA. These same binary parameters were also used as the only inputs to self-consistent field theory (SCFT) calculations of ordered multicomponent polymer blends. The SCFT calculations enabled quantitative interpretation of the SANS profiles from microphase-separated A/B/A-C blends. The phase separation temperatures predicted by the theory for the blends were within the experimental error, and the theoretical domain spacings were within 10 % of the experimental values.

Finally, a review of the experimental and theoretical investigations of the interfacial tension in phase-separated homopolymer blends with the effect of copolymers and emulsifying agents was published by Anastasiadis (2011) recently. The effects of temperature and molecular weight on the behavior were emphasized: interfacial tension γ decreases with increasing temperature (for polymer systems exhibiting upper critical solution temperature behavior) with a temperature coefficient of the order of 10^{-2} dyn/(cm.degrees C), whereas it increases with increasing molecular weight. The increase followed a dependence of the type:

$$\gamma = \gamma_{oo} \left(1 - k_{\text{int}}.Mn^{-z} \right)$$

(with z approximatively 1 for high molecular weights), where γ_{oo} is the limiting interfacial tension at infinite molecular weight and M_n the number average molecular weight.

The effects of concentration, molecular weight, composition, and macromolecular architecture of the copolymeric additives were discussed. An issue that could influence the efficient utilization of a copolymeric additive as an emulsifier is the possibility of micelle formation within the homopolymer matrices when the additive is mixed with one of the components. These micelles will compete with the interfacial region for copolymer chains. A second issue related to the possible trapping of copolymer chains at the interface, which could lead to stationary states of partial equilibrium. The in situ formation of copolymers by the interfacial reaction of functionalized homopolymers was also discussed.

Blends with an Arbitrary X-Y Block Copolymer

Vilgis and Noolandi (1988) investigated, by means of statistical thermodynamics, the use of an arbitrary block copolymer *X-Y* in *A/B* blends. The aim was to predict v_{12}, Δl, and the concentration profile across the interphase of the blocks. This was achieved by generalizing the theory of the interfacial properties of immiscible polymer blends in the presence of a block copolymer. The diffusion equations for the density profiles were solved numerically. Despite the use of chemically different blocks, their addition resulted in the reduction of v_{12}, increasing as M_w of the blocks increased. The computations were performed assuming different values of the binary interaction parameters and degree of polymerization. Strong localization effects of the *XY* emulsifier were observed when the interactions between the blocks and the homopolymers were increased. Thus, the competitive interactions of the blocks with different homopolymers were shown to promote strong interfacial activity. As a result, a selective orientation of the *XY* blocks in the *A/B* polymer mixture is expected to be similar to that computed for the *A/A-B/B* system.

A simplified analytical calculation for the case where the interaction parameters obey the assumed relationships led to the following relation for the reduction of the interfacial tension coefficient in the *A/B* blend upon the addition of copolymer *XY*:

$$\Delta v = -(1/Z_C)\exp\{Z_C[(\chi_1/2) + \chi_2]\}$$
$$\chi_1 \equiv \chi_{BY} = \chi_{AX} = \chi_{XY} = \chi_{AB} \qquad (4.32)$$
$$\chi_2 \equiv \chi_{AY} = \chi_{BX} > \chi_1$$

This suggests that it is possible to design a universal compatibilizer operating on the principle of competitive repulsive interactions between the homopolymers and the different blocks of the copolymer.

Critical Compatibilizer Concentration

Matos (1993) showed that the critical concentration of interfacial agents is directly related to the interfacial area of the dispersed phase, thus related to interface saturation. The chemical structure played an important role in the emulsification

ability of copolymers. Many block or graft copolymers were selected such that their segments were identical to those of the homopolymers. Alternatively, the blocks could be chemically different but miscible, each with different homopolymers. However, complete miscibility of all blocks in a single phase should be avoided.

The morphological analysis showed that diblock copolymers of the type polystyrene-b-hydrogenated polybutadiene, P(HB-b-S), have a higher interfacial activity than triblock or graft copolymers. It is possible that owing to the steric restriction at the interface, graft and triblock copolymers form micelles in the homopolymer phases. This adds to the complexity of the system morphology without fulfilling the basic functions of a copolymer. The diblock copolymer more readily interacts with the two homopolymeric phases, forming appropriate entanglements that result in the reduction of the interfacial tension coefficient, and enhanced interphasial adhesion in the solid state. These observations have been confirmed by measuring the mechanical properties. In blends prepared in solution, M_w of the homopolymers should be lower than those of the corresponding blocks. This rule seemed to be less critical for blends prepared in the molten state (Fayt et al. 1986a, b, 1989) – only one copolymer was reported to follow this rule.

The amount of the interfacial agent required to saturate the interface, w_{cr}, is related to its M_w, the total surface area of the interface, and the specific cross-sectional area of the copolymer macromolecule, a. Paul and Newman (1978) proposed the following relation for the critical amount of copolymer necessary to saturate the interface:

$$w_{cr} = 3\phi M_w/(RaN_{Av}) \tag{4.33}$$

where ϕ is the volume fraction of the dispersed phase, R is the radius of the dispersed drop, and N_{Av} is Avogadro's number. The authors also suggested (not derived from molecular parameters) that for a diblock copolymer, $a \geq 5$ nm^2.

Similarly, Matos (1993) developed an expression for the minimum copolymer amount required to cover the surface of spherical particles. The model was based on the division of an outer shell surrounding the particle into pseudo-cubic elements, each containing randomly oriented (random coil configuration) blocks of diblock copolymer:

$$w_{cr} = 9(3\phi/R)(M_A + M_B)/\left[N_{Av}\langle r^2 \rangle\right] = 3\phi M_w/\left[RN_{Av}\langle r^2 \rangle/9\right] \tag{4.34}$$

where M_A and M_B are molecular weights of the A and B blocks, respectively, $M_A + M_B = M_w$, and $< r^2 >$ is the square of the end-to-end distance of the copolymer chain. Since $< r^2 >$ is proportional to M_w, the above relation depends on the A/B ratio rather than on M_w's. Equations 4.33 and 4.34 are identical if $a = < r^2 >/9$. The density of A-blocks around the particle was expressed as:

$$\rho_A = 3^{5/2} M_A/\left[N_{Av}\langle r^2 \rangle^{3/2}\right] \tag{4.35}$$

In the most general case, the periphery of a drop contains A chains of the matrix and the copolymer. Since $< r^2 >$ is proportional to M_w, then the density should be proportional to $M_A^{-1/2}$. Clearly, for long copolymer chains, the segmental density will tend to zero, thus implying higher contribution from the A chains.

For blends containing diblock copolymers, interface enrichment by the copolymers as well as the potential reduction of the interfacial tension was investigated by Muller and Binder recently (Muller and Binder 2000). For weak segregation, the addition of copolymers led to compatibilization. At high incompatibilities, the homopolymer-rich phase could accommodate only a small fraction of the copolymer before the formation of a copolymer lamellar phase. The analysis of interfacial fluctuations yielded an estimate for the bending rigidity of the interface. The latter quantity is important for the formation of a polymeric microemulsion at intermediate segregation.

4.2.4.2 Blends of Two Polymers with "Cosolvent"

Another way of compatibilizing immiscible polymer blends is by the addition of a mutually miscible ingredient, a "cosolvent," usually polymeric in nature. The objective here is not to generate a wholly miscible three-component system but to add just enough mutually miscible polymers. The cosolvent is to induce interactions between the immiscible polymers, thus compatibilizing the blend but preserving its two-phase structure. To help in the judicious selection of appropriate cosolvent for a given immiscible blend, a partial list of miscible systems is given in Table 4.1.

In polymer blends, the thermodynamic miscibility depends primarily on specific interactions. For the entropic reasons, high molecular weight homopolymers are expected to be immiscible when the specific interactions are absent. Many types of interactions may exist between two polymers. These include London dispersion forces between nonpolar molecules, Coulombic ion/ion and ion/dipole interactions, dipole/dipole interactions between permanent or induced dipoles, charge-transfer forces, hydrogen bonding, etc. Polymer/polymer miscibility has been generally identified as mainly caused by hydrogen bonding (e.g., PPE/PS, PVME/PS, PVC/PCL, Phenoxy/PCL, PEG/PAA) and, for specific cases, by ionic and dipolar interactions.

Some polymers have been found miscible with many other resins, or in other words, there are many immiscible blends whose components are miscible with the same polymer. The addition of this polymer can be used to partially homogenize the system, i.e., to compatibilize the blend. The added polymer is a cosolvent. Of particular interest are systems in which the presence of a cosolvent makes it possible for the two immiscible components to form three-body interactions. In this case, the blend is indeed compatibilized, with the cosolvent being located in the interphase. For thermodynamic reasons, mostly copolymers belong to this type of cosolvents. In the left-hand side column of Table 4.1, there are polymers that may be used as cosolvents for pairs of resins listed in the other column. Some of the latter resins may show local miscibility (e.g., PS with styrenic copolymers), but the vast majority is immiscible.

Table 4.1 Some examples of miscible polymers

Potential cosolvent	Polymers miscible with the potential cosolvent
PEEK	PEK, PEI, PES, etc.
PEG	Phenoxy, PVC, TPU, EP, PAA, PES, EVAc, PVP, poly(meth)acrylates, etc.
Phenoxy	PES, PMMA, PVME, PVP, TPU, PBT, PET, etc.
PMMA	PC, MSAN, EPA, poly(meth)acrylates, PF, NC, PPG, PVAc, PVC, PVC-VAc, CPVC, PVDF, etc.
PPE	PS, CPS, SMA, P(α-MeS), SBS, SAN, ABS, etc.
PS	PC(TM-BPA), PPE, CHMA, PVME, etc.
PVAc	PVDF, halogenated-PMMA, etc.
PVC	PCL, EVAc, PVAc, PBT, poly(meth)acrylates, etc.
SAN	PCL, PVC, PPE, co-polymethacrylates, etc.
SMA	PCL, PVME, methacrylates, vinyl butyral, etc.
Co-polyacrylic acid	PVP, PAs, PEG, etc.
Epichlorohydrin	SAN, (meth-)acrylates, PVAc
NBR	Chloroprene, NC, PVC, PVCAc, etc.
PAr	Phenoxy, PET, PBT, PARA, PVC, etc.
PARA	PAs, PET, PBT, PAr
PB	EPDM, PI, etc.
PBT, PET	PEST, Phenoxy, PVC, PVDC-VAc, LCP, etc.
PC	Carbonates, adipates, (co-)polyesters, PCL, PMMA, SMA, etc.
PCL	Phenoxy, PC, PVC, PVB, CPE, NC, c-PP, PVDC-VAc, EPI, etc.

Note that according to the discussed strategy, the added polymer is to be *miscible* with the principal polymeric ingredients of the blend. On the other hand, it has been reported in the open and patent literature that the addition of a small amount of a third *immiscible* polymer to a blend of two immiscible ones also improves the degree of dispersion. A "classical" example is a blend of PE with $\leq$ 15 wt% PS – here the addition of $<$ 2 wt% of PMMA reduced the domain size of PS by a factor of ten. In this case, the drop size reduction originates from hindered coalescence. The immiscible polymer preferentially migrates to the interface between the two principal resins, providing protection to the dispersed phase against coalescence. This phenomenon has been commercially explored, e.g., in blends comprising PPE/SEBS drops dispersed in PBT matrix – an addition of immiscible PC improved the degree of dispersion and stabilized the morphology by reducing the risk of coalescence.

In principle, any polymer that is miscible with two others can be used as cosolvent. As the data in Table 4.1 indicate, Phenoxy, PMMA, PPE, PC, and PCL are miscible with several polymers; hence, they are the best candidates for cosolvents of many systems. It is noteworthy that acrylic multipolymers are often used as additives to many blends. Their role is to enhance compatibilization as well as to toughen the blends.

Table 4.2 Examples of *Phenoxy* compatibilized blends

Blend	Comments	References
PA with SEBS	0.5–3.0 wt% Phenoxy significantly improved the tensile and impact strength above the values for PA	Freed 1975
PC/PET/Akryloid™ KM660	10 wt% Phenoxy compatibilized the three-ingredient mixture. The materials showed excellent impact strength, ductility, and solvent resistance	Liu and Giles 1986
PA-6, PA-66, or PA-610, with either PET or PBT	0.5–15 wt% Phenoxy increased elongation, tensile strength, Izod impact strength, and uniformity	Robeson 1988
PSF/ABS	Either Phenoxy, EVAc-GMA, SMA copolymers, or MBS were used as compatibilizers. The blends showed good processability, toughness, plateability, and heat and water resistance	Gaafar 1990a; Orikasa and Sakazume 1990; Golovoy and Cheung 1994
LCP/PEST	Addition of Phenoxy™ was also found to provide good compatibilization	Dashevsky et al. 1993, 1994

Finally, in a very recent study, Pakravan Lonbani et al. (2012) used the rheological technique to investigate the phase separation and miscibility of chitosan/PEO solutions at different compositions in aqueous acetic acid solutions. Lower critical solution temperature (LCST) phase behavior was observed for chitosan/PEO solution blends. Phase separation temperature, miscibility range, and correlation length of the solutions were determined from isochronal dynamic temperature sweep experiments. The effect of the chitosan/PEO ratio on the binodal and spinodal decomposition temperatures was studied. Finding phase separation information on polymer solutions through rheological measurement was very promising. Isothermal steady shear rheological measurements were also carried out on chitosan/PEO solutions over a temperature range in which phase separation occurs. Viscosity increase was observed at low shear rates above the phase separation temperature (but in its vicinity), which confirms the validity of the theoretical approach employed to determine the critical temperatures through dynamic rheological measurements. Finally, the Flory-Huggins interaction parameters were estimated from critical solution temperature and concentration results.

One of the most frequently used cosolvents is the poly(hydroxy ether) of bisphenol-A, *Phenoxy*. Owing to the presence of the phenolic group, the resin forms strong hydrogen bonding with numerous polymers. In 1970, Mitsubishi Chemical discovered that toughness of engineering resin blends could be improved by incorporation of a Phenoxy. This commenced a widespread use of the resin. Phenoxy has been used as a compatibilizer in many blends (see Table 4.2). It is, however, to be noted that adding too much Phenoxy can make the blend miscible, which may reduce the mechanical performance, especially the impact strength. For

example, *Phenoxy* was reported to lead to single-phase blends, viz., PBT/PEST or PC; PCL/PVME, PC, or PEST; etc.

4.2.5 Conclusions and Outlook

In the case of binary A/B blends, Helfand and his coauthors provided the basic relations and the theoretical guidance to the properties of the interface, as well as to their modification by incorporation of a compatibilizer. The theory is based on strong, limiting assumptions (e.g., infinitely long macromolecules); thus, one should not expect a quantitative agreement with experimental data. However, the theoretical predictions offer a powerful guidance for the best compatibilization strategies.

The interfacial thickness, Δl_∞, and the interfacial tension coefficient, v_∞, are both related to the square root of the thermodynamic binary interaction parameter, $\chi_{AB} - \Delta l_\infty$ directly, whereas v_∞ inversely – thus, their product, $\Delta l_\infty \cdot v_\infty$, is to be independent of thermodynamic interactions. The latter conclusion may have limited validity, but the general tendency – the reciprocity between the interfacial tension coefficient and the interphase thickness – is correct. The theory correctly predicted the magnitude of the interphasial thickness, $\Delta l_\infty = 1–4$ nm. Note that the theory is for *A/B* binary systems, thus extending these predictions to compatibilized systems, where $\Delta l_\infty \leq 65$ nm may lead to erroneous expectations. For the latter system, the reciprocity between v_∞ and Δl_∞ is not to be expected.

For the strategies of compatibilization, Helfand's theory provides three important conclusions: (1) the chain ends of both polymers concentrate at the interface, (2) any low molecular weight third component is forced by the thermodynamic forces to the interface, and (3) the interfacial tension coefficient increases with molecular weight up to an asymptotic value.

Noolandi et al. developed a theory for the interfacial region in three-component polymeric systems comprising diblock copolymers. There are two aspects to consider: the phase separation in block copolymers upon the addition of one or two homopolymers and the modification of the *A/B* blend properties upon addition of a block copolymer (either *A-B* or *X-Y* type). The second aspect is more pertinent for the polymer blend technology. In particular, the ternary blends comprising two homopolymers and a copolymer, either *A/B/A-B* or *A/B/X-Y*, are of industrial interest.

The addition of a block copolymer, *A-B*, to an immiscible blend of homopolymers *A* and *B* reduces the interfacial tension coefficient similarly as the addition of a surfactant affects emulsions. Thus, the idea of the critical micelle concentration, *CMC*, and the limiting value of the interfacial tension coefficient, v_{CMC}, can be applied to polymer blends. This suggests possible existence of a thermodynamically controlled stable droplet phase, in which the minor phase homopolymer drops, protected by an interfacial film of copolymer, are dispersed within the major phase polymer. The theory

predicts that *CMC* depends exponentially on the product $\chi_{AB}Z_c$ – the larger are the repulsive interactions and/or the higher is the molecular weight of a copolymer, the lower is the concentration for saturation of the interface. Once the concentration of the added copolymer exceeds *CMC*, the micelles are formed. The interfacial tension coefficient exponentially decreases with $-\phi_c\chi_{AB}Z_c$, toward the limiting value at *CMC*, v_{CMC}.

Vilgis and Noolandi investigated the effects of the addition of a block copolymer *X-Y* to blends of *A* and *B* polymers. Similar dependencies as those derived for *A-B* copolymer were found. The work suggested that it is possible to design universal compatibilizers based on the principle of competitive repulsive interactions between the homopolymer and copolymer blocks.

4.3   Determination of the Interfacial Parameters

4.3.1   Interfacial Tension Coefficient

As seen in Sect. 4.2, several theoretical approaches have been proposed for the description of the interfacial phenomena. The lattice theories by Helfand, Roe, Noolandi, and their collaborators are based on the study of conformation and molecular environment. The derived relations are written in terms of the binary thermodynamic interaction parameter χ_{12} and the lattice constants. The theories do agree that the interfacial tension coefficient is a function of χ_{12}, but the predicted functional dependencies are different: $v_{12} \propto \chi_{12}^n$, with exponent $n = 1/2$ to $3/2$, depending on the assumptions.

These and more recent theories can be considered as guides for the expected dependencies, but they cannot be used directly to calculate either the interfacial tension coefficient or the interphase thickness. Since there is a significant disagreement between the theoretical relationships derived for the interfacial tension coefficient, several attempts were made to calculate its approximate values from other physical quantities. Two methods have been considered, the first using the surface tension coefficients, v_i, as an intermediate physical quantity, and the second the solubility parameters.

4.3.1.1 Calculations of the Interfacial Tension Coefficient
From Surface Tension Coefficients
Among the different approaches used to calculate the surface tension coefficient, v_i, the most useful seems to be the parachor method (Sugden 1924; Van Krevelen 1976; Wu 1982). This parameter was defined as (Sugden 1924):

$$P_i \equiv M_i v_i^{1/4}/\Delta\rho_i \tag{4.36}$$

where M_i is the molecular weight of a liquid i and $\Delta\rho_i$ is its liquid-minus-vapor density difference. The value of P_i can be calculated for any chemical compound
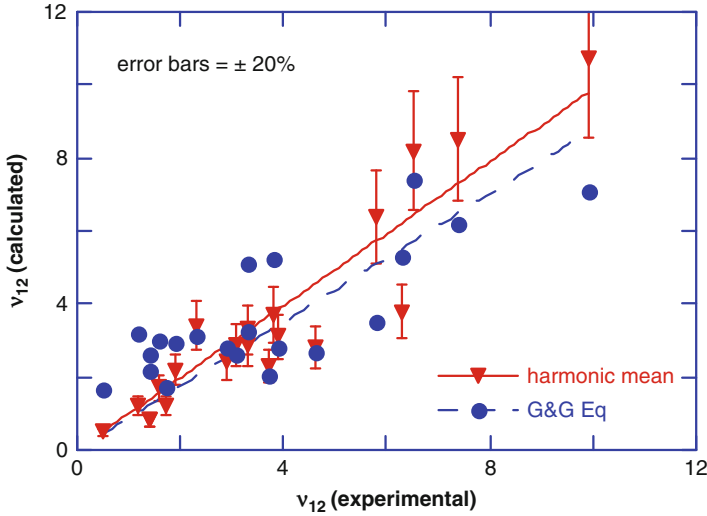
Fig. 4.5 Comparison between calculated and measured values of the interfacial tension coefficient from Girifalco and Good Eq. 4.37 and from the harmonic mean Eq. 4.38, incorporating the dispersive and polar contributions

from the contributions of structural elements. Once the surface tensions are known, the second step for calculating the interfacial tension coefficient, v_{12}, requires a relationship between v_i and v_{12}. Two dependencies have been proposed, first one by Girifalco and Good (1957):

$$v_{12} = v_1 + v_2 - 2\varphi(v_1 v_2)^{1/2} \tag{4.37}$$

(here φ is a semiempirical interaction parameter) and the second by Wu (1982). The latter one is based on the concept of fractional polarity that assumes the molecular forces originate from the polar and dispersive interactions:

$$
\begin{aligned}
v_{12} &= v_1 + v_2 - 4v_{1d}v_{2d}/(v_{1d} + v_{2d}) - 4v_{1p}v_{2p}/(v_{1p} + v_{2p}) \\
&= (v_{1d} - v_{2d})^2/(v_{1d} + v_{2d}) + (v_{1p} - v_{2p})^2/(v_{1p} + v_{2p})
\end{aligned}
\tag{4.38}
$$

The subscripts d and p refer to dispersive and polar components of the surface tension coefficients. Equation 4.38 is called the harmonic-mean equation. The idea can also be written in the form of a geometric mean equation:

$$v_{12} = v_1 + v_2 - 2\left(v_1^d v_2^d\right)^{1/2} - 2\left(v_1^p v_2^p\right)^{1/2} \tag{4.39}$$

In Fig. 4.5, the interfacial tension coefficients calculated from Eqs. 4.37 and 4.38 are compared with the experimental values. For the selected pairs of polymers, the latter seems to provide a better correlation with the measured values of v_{12}.

From the Solubility Parameters

The cohesive properties of a material are related to the solubility parameter, δ_i, that originates from different types of interactions: dispersive or atomic, molecular of the type polar and hydrogen bonding, induced dipoles, metallic, etc. The first three types are the most important; thus, respectively:

$$\delta_i^2 = \delta_{id}^2 + \delta_{ip}^2 + \delta_{ih}^2 \tag{4.40}$$

The values of the δ_i-components can be calculated for any chemical substance from the tabulated group and bond contributions. Once δ_i is known for both polymers in the blend, the Huggins-Flory binary thermodynamic interaction parameter, χ_{12}, can be calculated from:

$$\chi_{12} = (V/RT)[\delta_1 - \delta_2]^2 \tag{4.41}$$

From Eq. 4.41 and predictions of the lattice theories, the interfacial tension coefficient can be written as (Luciani et al. 1996):

$$v_{12} = kRT\chi_{12}^n = k_1(\rho RT)^{n-1}\left\{\left(\delta_{1,d} - \delta_{2,d}\right)^2 + \left(\delta_{1,p} - \delta_{2,p}\right)^2 + \left(\delta_{1,h} - \delta_{2,h}\right)^2\right\}^n$$

$$\therefore v_{12} = k_1(T)\left\{\left(\delta_{1,d} - \delta_{2,d}\right)^2 + \left(\delta_{1,p} - \delta_{2,p}\right)^2 + \left(\delta_{1,h} - \delta_{2,h}\right)^2\right\}^n \tag{4.42}$$

To evaluate the validity of Eq. 4.42, the experimental data of v_{12} for 46 polymer blends are plotted in Fig. 4.6 as a function of the computed values of the bracketed sum (Brandrup and Immergut 1989). The straight line represents the least squares fit. It is noteworthy that the exponent $n = 0.402$ is close to 1/2, predicted by Helfand et al.; lower than 3/4, predicted by Roe et al.; and significantly lower than the value of 3/2 derived by Joanny and Leibler.

4.3.1.2 Determination of the Interfacial Tension Coefficient

For low-viscosity Newtonian fluids, several methods for the measurements of v_{12} have been developed (Wu 1974). However, the high viscosity of industrial polymer melts makes most of them irrelevant. The few remaining ones that can be used for the determination of v_{12} in polymer blends can be divided into equilibrium and dynamic methods (Luciani et al. 1997).

Equilibrium Methods

Pendant Drop Method

The pendant drop method, schematically shown in Fig. 4.7, was used in many studies of polymeric blends, usually with low molecular weight fractions of given polymer pairs (Wu 1974). The technique is based on the analysis of the drop shape of component-1 emerging from the extremity of a capillary, immersed in component-2 (Anastasiadis et al. 1987, 1988, 1989b; Owens et al. 1989a, b).
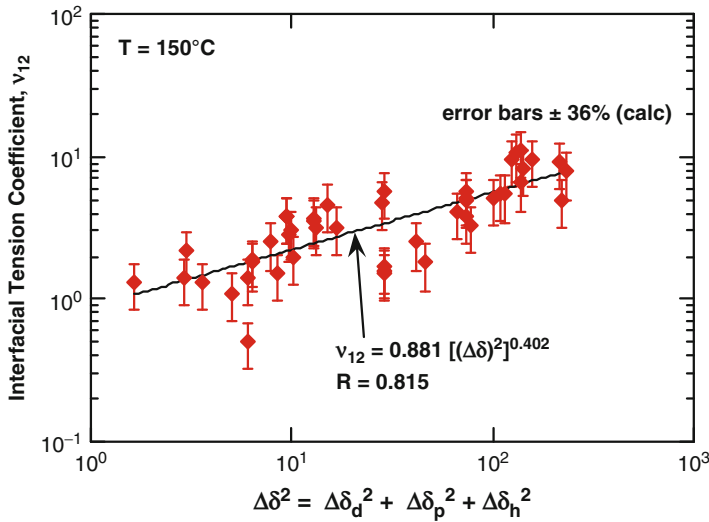
Fig. 4.6 Interfacial tension coefficient at 150 °C for 46 polymer blends plotted versus the solubility parameter contributions (see Eq. 4.42)

The interfacial tension coefficient can be calculated from the drop shape using the relation:

$$v_{12} = g\Delta\rho d_e/H(S) \tag{4.43}$$

where g is the gravitational constant, $\Delta\rho$ is the density difference between the two molten polymers, and $H(S)$ is a function of the form factor S, defined as:

$$S \equiv d_s/d_e \tag{4.44}$$

where d_s and d_e are defined in Fig. 4.7. The values of $H(S)$ are tabulated (Adamson 1982). The application of this method requires the knowledge of the polymer melts' density at the processing temperature.

Sessile Drop Method
The sessile drop method is similar to the pendant drop one (Sakai 1965). The same scheme is used, but in this case, the droplet is resting on a plane surface immersed in the second component (see Fig. 4.8) – v_{12} is calculated from the analysis of the drop shape at equilibrium (characterized by the relative magnitude of the shape parameters, X and Z, defined in Fig. 4.8), knowing the densities of the polymeric fluids at the temperature of measurement.

Spinning Drop Method
In the spinning drop method, a droplet of polymer-1 immersed in polymer-2 is submitted to extensional deformation through the use of centrifugal forces

Fig. 4.7 Schematic representation of the interfacial tension measurements by the pendant drop method; d_e is the maximum drop diameter, and d_s is the diameter located at the distance d_e from the drop apex
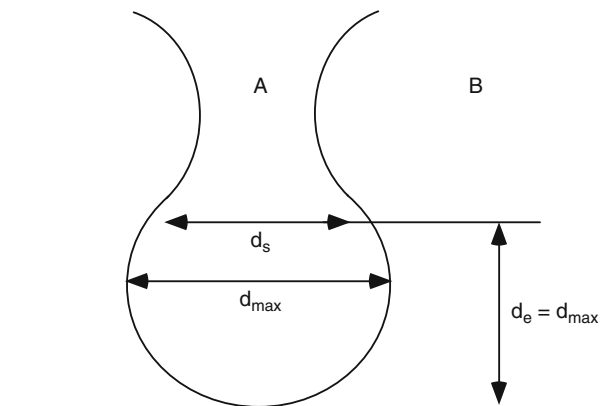
Fig. 4.8 Schematic representation of the interfacial tension measurements by the sessile drop method; X is the equatorial radius, and Z is the distance from the equator to the drop apex
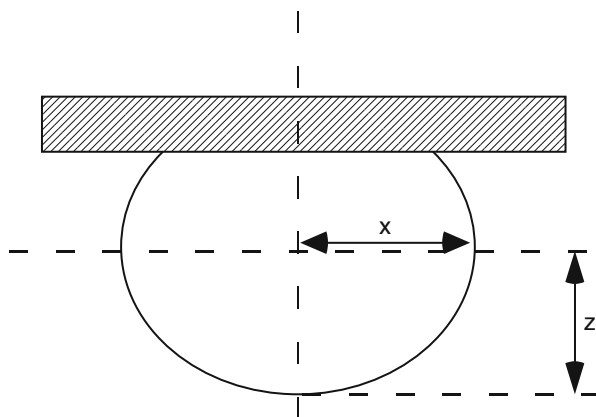
(Elmendorp and De Vos 1986). The extent of deformation is controlled by the rotational speed imposed on the system contained in a cylindrical tube (see Fig. 4.9). The rotational energy is balanced by the increased interfacial area. The interfacial tension coefficient is calculated from the equilibrium drop deformation. For drops with length to diameter ratio larger than 4, the following dependence was suggested (Vonnegut 1942):

$$v_{12} = \omega^2 d^3 \Delta\rho/32 \tag{4.45}$$

where d is diameter of the spinning drop and ω is the angular velocity of the cylinder. The technical difficulties of constructing an apparatus suitable for handling highly viscous polymer melts make this method too elaborate to be commonly used.

All these equilibrium techniques are rarely applicable for the measurements of the interfacial tension coefficient of common, industrial polymers. A long time is

Fig. 4.9 Schematic representation of the interfacial tension measurements by the spinning drop method; ω is the angular velocity, and d the deformed drop diameter
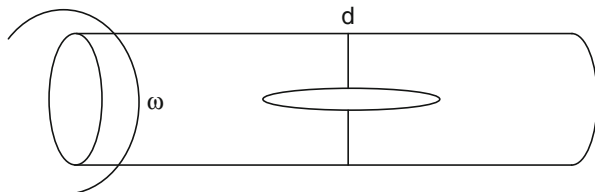
usually required to reach the equilibrium. Since the rate is determined by the ratio of the interfacial tension coefficient to viscosity, v_{12}/η, the time to reach an equilibrium can take either minutes or days – this may lead to the thermal degradation and uncertain validity of the measured v_{12}. As the degradation products are preferentially adsorbed at the interface, the determined interfacial tension coefficient may not reflect the blend behavior during compounding or forming. The influence of the equilibration time (thus degradation and contamination) on the v_{12} value is expected to be significant (Grace 1982).

The pendant and spinning drop methods were to determine v_{12} for different polymer pairs as well as the effect of temperature and compatibilizer (Garmabi and Kamal 1998). The authors found a linear relationship between the temperature (T) and v_{12} for PE/PA and PP/EVAl (see Fig. 4.2), as well as strong effect of compatibilizers. The pendant drop method and T-effects on v_{12} for different PS/PP blends were also described (Demarquette and Kamal 1994).

Dynamic Methods

In dynamic methods, determination of v_{12} is based on the time evolution of a fluid element shape, from a nonequilibrium to an equilibrium state. The evolution is driven by the interfacial tension, and depending on the initial shape of the element, it can follow different dependencies.

Capillary Breakup Method

The capillary breakup method is based on Tomotika's theory (Tomotika 1935, 1936). The author was the first to investigate the development of Rayleigh's instabilities in cylinders of one fluid imbedded in another (see Figs. 4.10 and 4.11) (Rayleigh 1879). The amplitude variations of the sinusoidal distortions, α, can be described by:

$$\alpha \equiv (b - a)/2d_0 = \alpha_0 \exp\{qt\} \qquad (4.46)$$

with

$$q = v_{12}\Omega(x, \lambda)/\eta_m d_0 \qquad (4.47)$$

where λ is the relative viscosity of the system ($\lambda = \eta_d/\eta_m$) and $\Omega(x, \lambda)$ is a complex function of λ and the observed wavelength, Λ, of the distortion, expressed as $x = \pi d_0/\Lambda$.
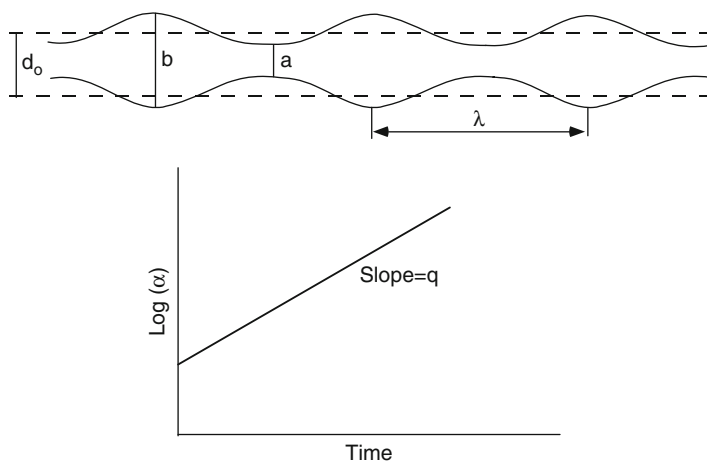
Fig. 4.10 Schematic representation of the interfacial tension measurements by the capillary breakup method; d_0 is the initial diameter of the fiber, b and a are the maximum and minimum diameters observed during the breakup process, respectively
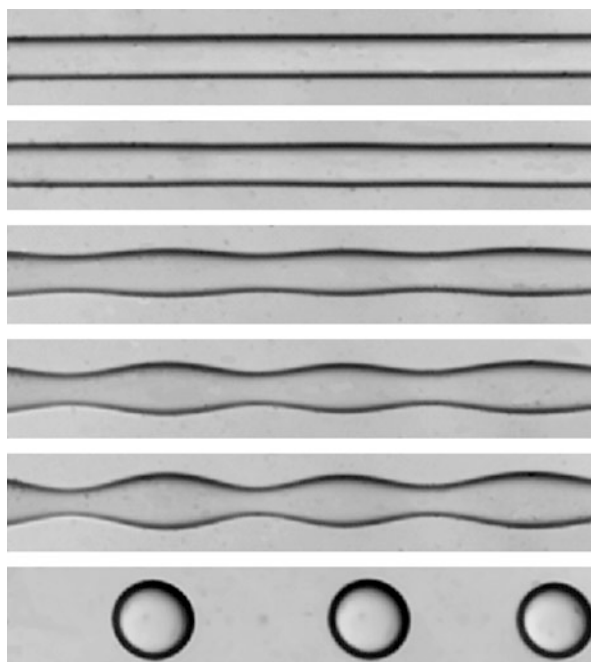
Fig. 4.11 Optical micrographs of a PA-6 fiber imbedded in PS matrix at 230 °C. The initial diameter of the fiber was 46 μm. The photographs were taken (from the *top*) after: $t = 0$, 10, 19, 23, 25, and 29 min

The values of $\Omega(x, \lambda)$ can be calculated from Tomotika's equations. The linear dependence of $\ln(\alpha)$ on the fiber disintegration time enables estimation of q and, consequently, v_{12}.

Table 4.3 Interfacial tension coefficient as determined using the capillary breakup method (Luciani et al. 1997)

Matrix	Fiber	T(°C)	v_{12}(mN/m)
PS 103-300	PA-6 Z211	230	6.3
LDPE 1001	PA-6 Z211	230	8.9
PE 300	PA-6 C316	220	11.7
		250	10.9
		280	9.2
PS 220	LDPE 1001	200	6.4
		230	**5.4**
PS 220	PMMA V920	200	**1.8**
PMMA V920	LDPE 1001	200	5.9
PMMA V920	PA-6 Z211	230	6.9
EP	PVDF	220	3.4
		260	2.5
EP	PA-6 C316	220	10.3
		240	9.4
EP	PA-6 C316 + Lotader	220	2.8
LDPE 1001 + 0.5 % Irganox MD 1024	PS 220	200	6.4
LDPE 1001 + 0.5 % Irganox MD 1024	PA-6 Z211	230	14.4

It seems that Chappelear (1964) was the first who applied this technique to measure the interfacial tension coefficient of polymer blends. Further refinements have been published (Elemans 1989; Elemans et al. 1990; Elmendorp 1986). The method is simple, not requiring special equipment, but the zero-shear viscosity of the investigated polymers at the processing temperature must be known. Typical results obtained through this method are shown in Table 4.3.

Deformed Drop Retraction Method (DDRM)

The deformed drop retraction method (DDRM) has been recently proposed. It makes it possible to determine v_{12} from the time evolution of deformed ellipsoidal drops toward its spherical equilibrium form (Luciani et al. 1997). Assuming an ellipsoidal shape for a drop of initial radius R_0 deformed under simple shear, the following relation was found:

$$D = D_o \exp\left\{ -t\left[\frac{40(\lambda + 1)}{(2\lambda + 3)(19\lambda + 16)} \frac{v_{12}(t_c)}{\eta_m R_o} \right] \right\} = D_o \exp\{-t/\tau\} \qquad (4.48)$$

with $D = (L - B)/(L + B)$ (where L and B represent the long and short diameters of the prolate ellipsoid, respectively), λ is the viscosity ratio, η_m is the matrix viscosity, $v_{12}(t_c)$ is the interfacial tension at the polymer-polymer contact time t_c, and D_0 is the initial value of D at $t = 0$. In principle, this relation is valid only for Newtonian systems. However, the method can be used to characterize viscoelastic materials

Fig. 4.12 Interfacial tension
coefficient in LDPE/PS
system as a function of the
contact time at 200 °C.
Vertical bars correspond
to ± 6 % error
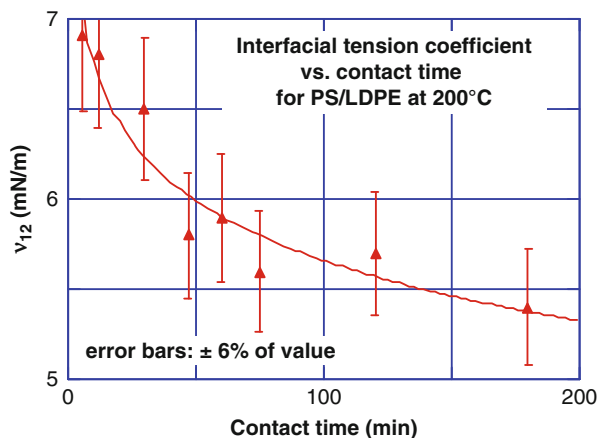
provided that (1) the retraction rate is sufficiently slow to ensure that the material
behave as Newtonian and (2) the elastic relaxation of the materials after deforma-
tion is faster than the ellipsoidal droplet retraction, that is, a clear separation of the
two mechanisms is achieved.

DDRM is particularly useful for the binary polymer blends. The dynamic interfa-
cial tension coefficient, v_{12}, is determined from the time evolution of a distorted fluid
drop toward its equilibrium form. Measurements of either low-viscosity model
systems or high-viscosity industrial polymer mixtures led to a good agreement with
values obtained from the widely used breaking-thread method. DDRM enables to
measure v_{12} in polymeric blends of commercial interest – the high-viscosity systems
that frequently are impossible to characterize by other techniques. Furthermore, for
the first time, it is possible to follow the time dependence of v_{12} thus unambiguously
determining its dynamic and equilibrium values. For example, in LDPE/PS blends
v_{12}, presented in Fig. 4.12, decreased with the polymer-polymer contact time, t_c, from
$v_{12} = 6.9$ mN/m at $t_c = 12$ min to $v_{12} = 5.2$ mN/m at $t_c \geq 75$ min – the latter may
represent the true thermodynamic equilibrium value, $v_{12\varepsilon\theta}$. Such a large reduction of
v_{12} may be due to the thermodynamically driven migration of chain ends, low
molecular weight fractions and additives, as well as thermal degradation. The contact
time dependence of v_{12} explained some of the differences reported for the data
obtained using different measurement techniques, viz., pendant drop, capillary
breakup, or ellipsoid retraction techniques (Luciani et al. 1997).

4.3.2 Interphasial Thickness

Much less information is available on the methods for the determination of the
interphasial thickness in polymer blends, Δl, than that of v_{12}. For binary systems,
assuming that these two parameters are interrelated, one may estimate Δl from v_{12},
the latter determined using one of the above-described methods. To determine the
experimental value of Δl in any system, diverse methods have been used, viz.,

electronic microscopy, X-ray scattering, ellipsometry (Yukioka and Inoue 1991; Fayt et al. 1986a, b), light scattering, etc. Results of these measurements are presented in the next section (see Table 4.6).

4.3.2.1 Microscopy

Since the dimensions to be probed are of the order of few nanometers, the most useful microscopic method would be that of the transmission electron microscopy (TEM). Using this technique, Fayt et al. (1986a, b) observed the location of the P(S-b-HB) compatibilizer in PE/PS blends. The authors inserted a short sequence of isoprene between the styrenic and hydrogenated butadiene blocks. After staining the isoprene double bonds with OsO_4, the authors were able to observe the presence of the copolymer at the interface between the matrix and dispersed phase. The thickness of the interphase could then be measured. The experiments also demonstrated the presence of the added compatibilizer as dispersed micelles inside the PE phase. This technique is applicable, however, only when selective staining affects only the compatibilizer.

4.3.2.2 Ellipsometry

The ellipsometric method has been developed by Yukioka and Inoue (1991, 1994). The principles of the technique and the model used for calculating the thickness of the interphase are schematically illustrated in Figs. 4.13 and 4.14, respectively. The retardation (Δ) and reflection ratio ($\tan(\psi)$) can be determined from the ellipsometric readings. The adopted model assumes the existence of four layers: air, thin polymer-1, interphase, and thick polymer-2 (see Fig. 4.14). In the interphase the refractive index is assumed to be an average: $n_3 = (n_1 + n_2)/2$. Thus, one can compute the best value of the interfacial thickness, d_3, to fit the observed values of Δ and $\tan(\psi)$. The following relations were derived for the computation of d_3:

$$\rho = \frac{R_i^p}{R_i^s} = \frac{|R_i^p|\exp(i\Delta_p)}{|R_i^s|\exp(i\Delta_s)} = \frac{|R_i^p|}{|R_i^s|}\exp\left[i(\Delta_p - \Delta_s)\right] = \tan(\psi)\exp(i\Delta)$$

$$\text{where}: \quad R_i^j = \frac{r_i^j + R_{i+1}^j\exp(-iD_{i+1})}{1 + r_i^j R_{i+1}^j\exp(-iD_{i+1})}; \quad D_i = 4\pi n_i d_i \cos(\theta_i)/\lambda;$$

$$\text{and} \quad r_i^p = \frac{n_{i+1}\cos(\theta_i) - n_i\cos(\theta_{i+1})}{n_{i+1}\cos(\theta_i) + n_i\cos(\theta_{i+1})}; \quad r_i^s = \frac{n_i\cos(\theta_i) - n_{i+1}\cos(\theta_{i+1})}{n_i\cos(\theta_i) + n_{i+1}\cos(\theta_{i+1})}$$

$$n_1\sin(\theta_1) = n_2\sin(\theta_2) = n_3\sin(\theta_3) = n_4\sin(\theta_4)$$

$$(4.49)$$

In Eq. 4.49, superscripts p and s designate parallel and perpendicular polarization of light, and λ is the true interfacial thickness. The other quantities in these equations are defined in Fig. 4.14. The interface thickness needs to be corrected using the composition profile. The true interfacial thickness is then determined as $\Delta l = \lambda = d_3/1.7$.

For example, the ellipsometric technique was used to determine the interfacial thickness in SAN/PA blends, compatibilized by the addition of SMA
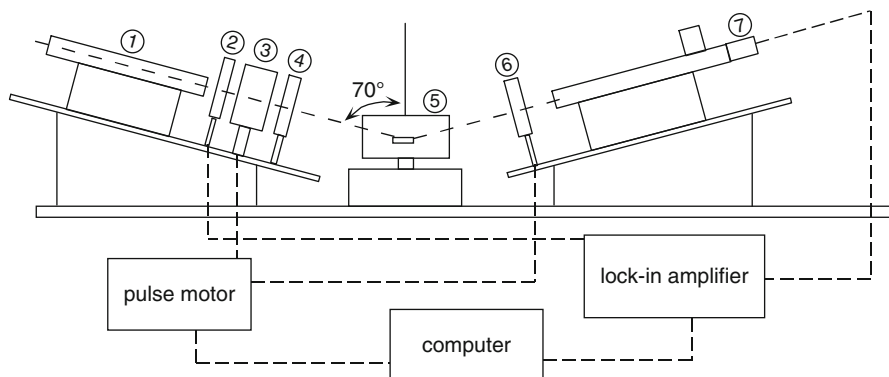
Fig. 4.13 Experimental setup for the ellipsometric measurements: *1.* is a He-Ne laser, *2.* is a chopper, *3.* is a polarizer, *4.* is a compensator, *5.* is a sample chamber, *6.* is an analyzer, and *7.* is a detector (e.g., a photodiode) (After Yukioka and Inoue)

Fig. 4.14 The four-layer model used for the calculations of the interfacial thickness. n_i designates the refractive index, θ_i the incidence angle, r_i the Fresnel reflection coefficient, R_i the reflection coefficient in the incident plane, and d_i the thickness of the layer
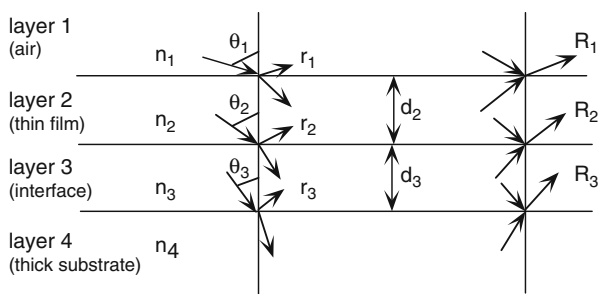
(Yukioka and Inoue 1991, 1994). A thin bilayer film of SMA/SAN was prepared and then mounted on a thick PA substrate. The interfacial thickness varied with the compatibilization time from $\Delta l = 2$ to 30 nm. The method was also used to study the interphasial thickness variation in PCL blends with CTBN or CTBR. Without a reactive modifier (aminopropyltriethoxysilane, APS), the measured thickness was $\Delta l = 3$ nm, upon addition increasing to 6 nm (Okamoto and Inoue 1993).

4.3.2.3 X-Ray Scattering

Small-angle X-ray scattering (SAXS) has been used by many authors to determine the interfacial thickness. An excellent review of this subject can be found in Perrin and Prud'homme (1994). Many methods of calculations can be used. One of these involves an analysis of the deviation from Porod's law, in which the desmearing procedure is avoided. This procedure was applied to blends of PS with PMMA added with a P(S-b-MMA) block copolymer. Upon the addition of a copolymer, the interface thickness changed from $\Delta l = 2$ to 6 nm (Perrin and Prud'homme 1994).

4.3.2.4 Atomic Force Microscopy

Another technique of interest is the atomic force microscopy (AFM). The method can be used to any system where properties of the separated phases significantly differ. For example, the method was used to determine the thickness of the interphase in blends of PA with soft elastomers. In this case the rigidity scanning procedure was the most appropriate. Since the difference in moduli between the dispersed phase and the matrix was large, scanning in this mode gave a rigidity profile across the thickness. The interfacial thickness was found to be about 20 nm (M. Champagne, private communication, 1996).

4.3.2.5 Other Methods

Several other methods, more or less tedious, have been described in the literature. They include welding cleavage experiments (Foster and Wool 1991), neutron reflectivity (Fernandez et al. 1988), etc.

4.3.3 Update on Recent Results on Interfacial Tension and Characteristics

In this section, some of the recent results reported in literature on the measurements of interfacial tension and characteristics are reported.

Sigillo et al. (1997) used several experimental methods for the measurement of interfacial tension of a model polymer blend. Common to all methods presented here are two main points. The first is that a is obtained from experiments where the shape of the interface between the liquids is directly observed by means of optical microscopy techniques. The second point is that the interface geometry is controlled by a balance between the interfacial force and the viscous stresses generated by some flow applied to the system. Measurements have been carried out on a model polymer blend, whose constituents are a polyisobutylene and a polydimethylsiloxane, both transparent and liquid at room temperature. When compared with each other, the values of interfacial tension obtained from the different methods show a good quantitative agreement. Excellent agreement is also found with results for the same system previously published in the literature.

Temperature dependence of interfacial tension of demixed polystyrene/poly (dimethylsiloxane) melts was studied by Nose (1997) using the sessile drop technique. The results were described as a scaled relation of reduced interfacial tension versus reduced segregation strength. The scaled relation was discussed on the basis of the mean-field theory, and a semiempirical expression has been presented for the scaled relation covering a wide temperature range.

The effect of molecular weight on the interfacial excess ($z(B)^*$), tension (γ_{ABC}), and width (w_{ABC}) in polystyrene/poly(d(8)-styrene-co-4-bromostyrene)/poly (styrene-co-4-bromostyrene) ($AB{:}C$) system was studied by Genzer and Composto (1998). Low-energy forward recoil spectrometry (LE-FRES) was used to measure $z(B)^*$ as a function of the B volume fraction in the $B{:}C$ blend. The experimental $z(B)^*$'s were found to be in excellent agreement with those calculated using the

self-consistent field (SCF) model of the $A/B{:}C$ interface. In addition, the SCF model was used to evaluate γ_{ABC} and the widths for the $A/B{:}C$, A/B, and A/C interfaces (i.e., $w(ABC)$, $w(AB)$, and $w(AC)$, respectively). Their results demonstrated that increasing the number of B segments, N_B, greatly increases the magnitude of $z(B)^*$, particularly at low B contents. On the other hand, varying N_A had only a minor effect on $z(B)^*$. Concurrent with the segregation of B, γ_{ABC} and $w(AB)$ rapidly decreased and increased, respectively, as B content initially increases. Upon calculation of the entanglement length, $w(e)$, for each component, $w(AB)$ was found to approach $w(e)$ when B content approximated 0.30. As a result, the mechanical strength of the interface should greatly improve. The optimum amount of B to achieve good compatibilization correlated with the B content at which $z(B)^*$ is a maximum.

Luciani et al. (1998) critically examined the experimental methods used for the measurements of the interfacial coefficient in polymer blends as well as the theoretical models for its evaluation. A new working relation was derived that makes it possible to compute the interfacial tension from the chemical structure of two polymers. The calculations involve the determination of the dispersive, polar, and hydrogen-bonding parts of the solubility parameter from the tabulated group and bond contributions. The computed values for 46 blends were found to follow the experimental ones with a reasonable scatter of $+/-$ 36 %. The authors mentioned also that since many experimental techniques have been developed for low-viscosity Newtonian fluids, most were irrelevant to industrial polymeric systems. For their studies, two were selected: capillary breakup method and a newly developed method based on the retraction rate of deformed drop.

The effect of a compatibilizer on interfacial tension reduction and coalescence suppression was also studied by Lepers and Favis (1999) on an 80 % polystyrene and 20 % ethylene-propylene copolymer compatibilized by diblock copolymers of poly (styrene-hydrogenated butadiene). The diblocks differed in that one contained 53 % styrene (symmetric diblock) and the other 30 % styrene (asymmetric diblock). The interfacial tension was measured using the breaking-thread technique, and the results were compared to both the theoretical predictions of Noolandi and Hong and Leibler. The morphology was tracked using an emulsification curve, comparison of which with the interfacial tension results made it possible to estimate the relative role of interfacial tension and coalescence reduction in particle-size reduction phenomena.

Willemse et al. (1999) studied the influence of interfacial tension on the composition range within which fully co-continuous polymer blend structures can exist for different blends with selected matrix viscosities and viscosity ratios. The critical composition for full co-continuity was found to increase with increasing interfacial tension, narrowing the composition range. The effect of the interfacial tension on the critical composition was found to be composed of two counteracting effects: the stability of the co-continuous morphology and the phase dimensions. The latter effect was smaller than the former.

Guerrica-Echevarria et al. (2000) used the interfacial tension as a parameter to characterize the miscibility level of polymer blends. Fourteen polymer pair interfacial tensions were determined by means of contact angle measurements

of the surface of each polymer component, with at least two liquids, and the relation with the different miscibility levels of the corresponding blends evaluated. Although exceptions were found, the values obtained appeared to be related to the miscibility level of the blend, immiscible blends giving high interfacial tension values that decreased as miscibility increased. The relation was possibly affected by additional parameters and was clearer when the components of the blends compared were similar.

Xing et al. (2000) compared five different techniques for the measurement of interfacial tension in a model polystyrene (PS)/polyamide-6 (PA-6) system at a constant temperature. The techniques include three dynamic methods (the breaking thread, the imbedded fiber retraction, and the retraction of deformed drop), one equilibrium method (the pendant drop), and a rheological method based on linear viscoelastic measurements. The advantages, the limitations, and the difficulties of each technique were discussed and compared.

The effect of copolymer molecular weight, architecture, and composition on the interfacial tension of a binary polymer blend was studied by Retsos et al. (2001, 2004). The system investigated was polystyrene/polyisoprene blends in the presence of polystyrene-block-polyisoprene copolymers using the pendant drop method. The interfacial tension decreased with the addition of small amounts of copolymer and reached a plateau at higher copolymer concentration, in agreement with previous studies. However, the reduction of the interfacial tension was a nonmonotonic function of the copolymer molecular weight at constant copolymer concentration in the plateau region. As the additive molecular weight increases, the interfacial tension reduction went through a maximum. This should be related with the increased tendency of micelle formation for high copolymer molecular weights, which was confirmed by small-angle X-ray scattering. The results were also discussed in relation to theoretical predictions for polymer/polymer/copolymer mixtures.

For the effect of architecture, graft copolymers with constant molecular weight and varying composition are utilized as additives (Retsos et al. (2004)). The interfacial tension decreased with the addition of small amounts of copolymer and reached also a plateau at higher copolymer concentration. The interfacial tension at interfacial saturation depended on copolymer composition exhibiting a minimum and was lower than that using a symmetric diblock with the same molecular weight. Moreover, the interfacial tension at saturation depended on the side of the interface the copolymer was introduced; its addition to the polyisoprene phase was much more efficient than to polystyrene. This was interpreted as due to the asymmetric architecture of the copolymer and pointed to the fact that a local equilibrium could only be attained in such systems: the copolymer reaching the interface from one homopolymer phase probably does not diffuse to the other phase. The fact that this behavior was not a kinetic effect was also verified.

For the interface thickness, there are also a number or recent studies that addressed this issue that was less studied before. Yeung and Shi (1999) performed a dynamic mean-field study on the formation of interfaces in immiscible polymer blends. They studied the interdiffusion dynamics of a polymer interface toward its

equilibrium profile using a dynamic mean-field method, in which the nonequilibrium chemical potentials were evaluated numerically using the full polymer mean-field free energy. Their results demonstrated that the interfacial width grows as $t^{1/4}$ at early times and saturates to the equilibrium thickness at long times, in agreement with previous, more approximate analyses based on Cahn-Hilliard-type theories. Furthermore, it was shown that the dynamic exponent can only be obtained unequivocally via a scaling analysis. The interdiffusion of a polymer interface in the single-phase regime was also studied.

Rharbi and Winnik (2001) and Yang et al. (2003) from the same research group studied the interface thickness of two systems: styrene-methyl methacrylate and isoprene-methyl methacrylate block copolymers using an energy transfer technique. First, films were prepared from mixtures of two PS-PMMA copolymers of identical length and compositions, labeled at their junctions with either a 9-phenanthryl or 2-anthryl group. The fluorescence decays were analyzed in terms of a model that takes account of the Helfand-Tagami distribution profile of polymer segments at the interface. An interface thickness of 4.8 nm was determined after careful corrections. A theoretical value of 4.2 nm was obtained when using Semenov's finite-chain correction to Helfand-Tagami prediction and the Flory-Huggins interaction parameter recovered by Russell for partially deuterated d-PS-PMMA copolymer. When the Callaghan and Paul interaction parameter value was employed for undeuterated PS + PMMA blends, an interfacial thickness of 4.9 nm was obtained.

In a second study, they evaluated the interfacial thickness of two poly(isoprene-b-methyl methacrylate) block copolymers (PI-PMMA) using the same approach. Small-angle X-ray scattering experiments showed that films of the mixed diblock copolymers have a lamellar morphology with a spacing that varies with composition from 24 to 26 nm. Fluorescence decay profiles from these films were analyzed in terms of an energy transfer model that takes into account the distribution of junctions across the interface and calculated an interface thickness of 1.6 +/− 0.1 nm. This value was independent of the acceptor/donor ratio (i.e., the acceptor concentration) in the films.

Farinha et al. (2000) used an energy transfer study to evaluate the interface thickness in blends of poly(butyl methacrylate) (PBMA) and poly(2-ethylhexyl methacrylate) (PEHMA). A model that describes the energy transfer between donors and accepters chemically attached to the two different components of a polymer blend is proposed. The model describes the case of one polymer dispersed as spheres of identical diameter in a continuous matrix of the second polymer. The model takes explicit account of the segment distribution of the two polymers at the interface region. This model was used to characterize the interface between PBMA and PEHMA domains in a binary blend. By using a 14:1 particle ratio of PEHMA to PBMA, films in which the 120 nm PBMA particles were surrounded by the PEHMA matrix were obtained. For the ion-exchanged latex blend, the interface thickness (Δ) in the film freshly prepared at room temperature was $\Delta = 21$ +/− 2 nm and upon annealing broadened to 25 +/− 2 nm. Because of the low degrees of polymerization for the samples, it was difficult to have

confidence in the value of the Flory-Huggins interaction parameter calculated from the experimental value of Δ because the correction for the finite length of the component was larger than the term that depends on the interface width. Keeping in mind the limitations of this calculation, the interaction parameter was estimated to 0.02–0.03.

Finally in two recent studies from the same research group (Meghala and Ranganathaiah 2012; Ramya and Ranganathaiah 2013), the interfaces of ternary and binary polymer blends were characterized. In the first study (Ramya and Ranganathaiah 2013), the interface widths in two immiscible polymer blends (polyvinyl chloride (PVC)/polystyrene (PS) and PVC/ethylene vinyl acetate (EVA)) were determined experimentally using hydrodynamic interaction approach through free volume measurement by positron annihilation lifetime spectroscopy. For comparison, the same study was performed on a miscible blend (styrene-acrylonitrile (SAN)/polymethyl methacrylate (PMMA)). The interfacial width (Δ) was evaluated from the hydrodynamic interaction (a) based on the Kirkwood-Riseman theory and friction coefficient from Stokes equation. Friction at the interface of a binary blend evidences how close the surfaces of the polymer chains come or stay apart, which in turn depends on the type of force/interaction at the interface. In this study, the interface width was defined from a different perspective of Flory-Huggins interaction approach. Measured composition-dependent interface widths in the three blends studied demonstrated the sensitivity of the method. In miscible blend, high friction at the interface resulted in stronger hydrodynamic interaction and hence smaller interface widths, whereas weak or no interaction in immiscible blends produce wider widths.

The second study (Meghala and Ranganathaiah 2012) was dedicated to the evaluation of interfaces in poly(styrene-co-acrylonitrile) (SAN)-based ternary polymer blends using also positron lifetime spectroscopy. The method successfully applied for binary blends (single interface), mentioned above, was theoretically modified for ternary blends and experimentally verified by measuring free volume content in blends and their constituents. They tested the efficacy of this method in two ternary blends: SAN/PVC/PMMA and SAN/EVA/PVC at different compositions. The effective hydrodynamic parameter evaluated using individual values turned out to be handy in predicting the overall miscibility level of a ternary blend.

4.4   Compatibilization by Addition of a Compatibilizer

There are several strategies of compatibilization, e.g., (i) the addition of a small quantity of a third component that either is miscible with both phases (a cosolvent) or is a precisely tailored copolymer whose one part is miscible with one phase and another with another phase (0.5–2 wt%, usually block-type, less frequently graft one); (ii) the addition of a large quantity, ≤ 35 wt%, of a core-shell copolymer(s) that behaves like a multipurpose compatibilizer-*cum*-impact modifier; and (iii) reactive compatibilization, designed to enhance

the domain interactions and generate finer morphology by creating chemical bonds between the two homopolymers during the compounding or forming processes. The latter type of compatibilization is treated in ▶ Chap. 5, "Reactive Compatibilization" in this handbook.

In the following part, aspects related to the morphology of the blends with and without an added compatibilizer (from the nm to the μm scale) will be presented. These include information on the interfacial characteristics (interfacial tension coefficient and thickness of the interphase), morphology, crystallization, and performance of the blends. This information will be presented mainly in a tabulated form, summarizing the main features from the referenced publications.

4.4.1 Interfacial Characteristics

Experimentally, it has been shown that diblock copolymers, especially of the type polystyrene-b-hydrogenated polybutadiene, P(S-b-HB), have a higher interfacial activity than triblock or graft copolymers. Diblocks more readily interact with the homopolymer phases, forming appropriate entanglements that result in the reduction of v_{12} in the melt and enhanced interphasial adhesion in the solid state. When properly selected and added in optimum quantity, they were also found to stabilize the morphology against the shear degradation during abusive processing. Experimental data are listed in Tables 4.4, 4.5, and 4.6.

The addition of graft copolymers is much less frequent. Some blends of this type were reported to have unusual onion-like morphology. This observation is not universally valid – the compatibilizing effect must depend on the structure and composition of the copolymer. Owing to the complexity of these structures, the theoretical analysis has not been attempted.

Effective compatibilization of binary polymer blends by the addition of a copolymer reduces the dispersed particles' size and v_{12} (Anastasiadis et al. 1987; Wu 1987; Patterson et al. 1971). An illustration is shown on Fig. 4.15. The effect of compatibilizer addition is similar to the emulsification of the classical emulsions. In the former systems, the compatibilizer effect on the drop size and v_{12} follows the same behavior as the emulsion drop size reduction upon the addition of a surfactant. The latter behavior is usually described as the "titration curve" that characterizes the surfactant efficiency. The shape of the titration curve depends on the type of emulsifier and the emulsification process, e.g., mixing time and equipment. However, the amount of emulsifier to saturate the interface also depends on the affinity of the emulsifier to the dispersed phase, the size of the dispersion, the orientation of the emulsifier at the interface, and its ability to prevent flocculation and coalescence (Djakovic et al. 1987). A similar behavior is to be expected for polymer blends upon the addition of a compatibilizer.

Recently, the effect of a reactively formed compatibilizer on v_{12} was studied using the pendant drop method (Garmabi and Kamal 1998). Their results are shown in Fig. 4.16. A small quantity of MAH drastically reduced the interfacial tension coefficient, but the amount of formed graft was not determined.

Table 4.4 General interfacial characteristics of blends

Blend system	Techniques and results	References
PE/PS with P(HB-b-S) or P(HB-b-I-S)	Used TEM and other methods. Copolymer located at the interface	Fayt et al. 1986a, b, 1989; Hobbs et al. 1983
PS/PMMA	Embedded fiber retraction technique at 190 °C. $v_{12} = v_{\infty} - C_1 M_n^z$, $z = 0.73 \pm 0.24$. For M_n exceeding 48 kg/mol, v_{12} was independent of M_n with a mean value of 1.2 mN/m	Ellingson et al. 1994

The efficiency of a block copolymer is limited by the formation of micelles in bulk phases and by the kinetic factors. Consequently, the block copolymer used as a compatibilizer should be designed by taking thermodynamic and kinetic parameters into account to achieve the desired effects. Thus, the structure and transitions in copolymers and homopolymer/copolymer systems are of great interest.

The formation of gradient interfaces between PS- and PB-rich microphases in SBS block copolymers was investigated by means of solid-state NMR and solution NMR as well as TEM, AFM, and SAXS by Thomann et al. (2009). Its molecular architecture, linear and star-shaped asymmetric block structures, and gradient as well as random incorporation of styrene comonomer into the PB-rich blocks were compared. Although all studied SBS possess a very similar total styrene content, different morphologies and mechanical properties were found in the extruded SBS/PS blends, whose origin could be related to the formation of a compositional interface gradient. Employing the sensitivity of solid-state NMR for hard (glassy) and soft (rubbery) phases as well as their respective chemical compositions, it was found that upon raising the temperature up to the PS glass transition, different amounts of polystyrene from the hard PS phase "soften" and integrate into the soft PB-rich phase ("PS softening"). The degree of "PS softening" characterizes the interfacial gradients of SBS block copolymers at elevated temperatures up to the melt. The softened PS was found to partially mix into the soft phase and partially remain at the interface, thus forming different gradient interfaces, depending primarily on the amount of styrene randomly incorporated in the PB mobile blocks and much less on a compositional gradient at the block linkages in SBS chains.

In SBS/PS blends, SBS with a substantial "PS softening" effect was found to preferentially form elongated PB lamellar morphologies, which led to improved mechanical ductility. The purpose of the study was to apply different characterization methods and correlate their results in order to gain important compositional and morphological information as well as their effects on the SBS/PS blend mechanical properties. Rapid and robust low-cost pulsed solid-state NMR methods were established as versatile analytical tools for the application in high-output polymer screening (HOPS) and quality control systems, enabling online monitoring of structure–property correlations as well as product quality of SBS-based materials.

Table 4.5 Copolymers and homopolymer with copolymer systems

System	Techniques and results	References
Homopolymer/copolymer	Solubilization of homopolymer by copolymer. The homopolymer A dissolves in microdomains of A-blocks of the A-B copolymer, until a limit of miscibility is reached. Above this limit, excess of homopolymer forms macroscopic domains	Hashimoto et al. 1990; Tanaka et al. 1991
PS with P(S-b-VP) copolymer	PS-block with $M_w = 9.5$ and PVP-block with $M_w = 10.6$ kg/mol. SAXS was used. Blends containing PS with $M_w < 9.5$ were transparent; those with $M_w > 13.7$ kg/mol were opaque. The solubility limit increased when M_w of PS decreased	Skoulios et al. 1971
PS with P(S-b-I) copolymer	SAXS. Polymer dissolved in domains of block of the same nature as long as its M_w is lower than that of the block	Ptaszynski et al. 1975
Copolymer	Used X-ray scattering. Microdomain measured repeat distance: $D \propto M_w^{0.643}$, theoretical $D \propto M_w^{2/3}$	Hashimoto et al. 1980; Matsushita et al. 1990; Ohta and Kawasaki 1986
PS/PMMA and symmetric P(S-b-MMA) copolymer	Used SAXS and TEM. Stabilization of the interface, the formation of micelles, and the micro- and macrophase separation. The same morphology was observed in solution and after solvent evaporation	Lowenhaupt and Hellmann 1990, 1991, 1994
Copolymer	The effect of temperature, M_w, preparation history, etc., on D. The interphasial thickness, ΔI, was found to remain constant	Spontak and Zielinski 1993; Ohta and Kawasaki 1986; Roe et al. 1981; Anastasiadis et al. 1989a, 1990; Bates et al. 1983; Hashimoto et al. 1977; Todo et al. 1977; Todo, Hashimoto and Kawai 1978
PS/SB/S-B	SALS, TEM, and SAXS were used to study PS-solubilization in S-b-B copolymer (50 wt% styrene). The solubility of PS in the S-block was governed by the ratio of the homopolymer M_w to the block's M_w. The lamellar repeat period increased linearly as more PS was added. The butadiene layer thickness remained constant	Jeon and Roe 1994
PPE, with SAN, SMMA, SAA, or SMA	Miscibility of copolymers with PPE when the amount of comonomer is small. The interfacial energy between the blend components was significantly reduced by adding either a PS-b-PMMA or PS-b-PEB-b-PMMA. The copolymers had a profound influence on the morphology, phase adhesion, and mechanical properties of the blend	Gottschalk et al. 1994

Table 4.6 Interfacial thickness in polymer blends

Polymer or blend	Copolymer	Techniques and results	References
Polymer A	P(A-b-B)	The interfacial thickness did not change upon the addition of homopolymer, $\Delta l \cong 2$ nm	Ptaszynski et al. 1975; Bates et al. 1983; Zin and Roe 1984; Hashimoto et al. 1990; Tanaka et al. 1991
PS/PMMA	P(S-b-MMA)	Neutron reflectivity using blends with high copolymer content and an equal amount of homopolymers. The microdomain boundary thickness was found to increase by 25 % from the pure copolymer to a mixture containing 17 % homopolymer; $\Delta l \cong 2$ nm	Russel et al. 1991b
PS	P(S-b-VP)	Studied M_w effects of diblock copolymer segregation at the interface using the segregation isotherms. A normalized interfacial thickness was found as a universal function of that portion of the block copolymer chemical potential due to chain stretching	Dai and Kramer 1994
PS/PVP	Poly(styrene-b-2-vinyl pyridine)	Forward recoil spectrometry, FRES, was used to study the diffusion of copolymer randomly dispersed in the PS layer of a PS/PVP bilayer sample. Free copolymer chains were detected at the interface below ϕ_{CMC}, whereas, above it, copolymer chains were also found at the PS/air surface as well as micellar segregation at the interface was visually confirmed	Shull et al. 1991
PS/PMMA		Determined $\Delta l = 6$ nm by the welding cleavage experiments	Foster and Wool 1991
		For spin-coated samples, $\Delta l = 5$ nm was determined by neutron reflectivity	Fernandez et al. 1988
		Similar experiments as above also gave $\Delta l = 5$ nm	Anastasiadis et al. 1989a
PS/PMMA	P(S-b-MMA)	Increasing thickness of the P(S-b-MMA) layer between PS and PMMA to 23.9 nm caused a gradual increase of Δl from 5 to 8.4 nm	Russel et al. 1991

Table 4.6 (continued)

Polymer or blend	Copolymer	Techniques and results	References
		Micellar segregation at the interface of samples was not observed by the elastic recoil detection method	Jeon and Roe 1994
		SAXS method was used. Upon addition of the copolymer, the interface thickness changed from $\Delta l = 2$ to 6 nm	Perrin and Prud'homme 1994
PCL with CTBN or CTBR	APS	Ellipsometric methods. $\Delta l = 3$ nm without APS and 6 nm with APS (a reactively generated copolymer)	Okamoto and Inoue 1993
PE/PP	EPR	The interfacial thickness was $\Delta l = 1.5$–2.8 nm without copolymer. The blend was compatibilized by adding EPR	Teh et al. 1994
PE/PS	P(HB-b-S) or P(HB-b-I-S)	Copolymer migrated to the interface. Observed a continuous layer around each dispersed particle, either of PE in PS or PS in PE. $\Delta l = 10$–12 nm was determined. 2 wt% of P(HB-b-S) was sufficient to reduce the v_{12}, the particles size, as well as prevent coalescence. At 5 wt%, the copolymer effect was stable	Fayt et al. 1986a, b, 1989; Hobbs et al. 1983

Fig. 4.15 Interfacial tension coefficient as a function of diblock copolymer in the minor phase. System: matrix, polybutadiene; dispersed phase (pendant drop technique), polystyrene with styrene-b-butadiene diblock copolymer (Data: Anastasiadis et al. 1988). *Dotted* and *solid lines* were computed from Eqs. 4.29 and 4.30, respectively
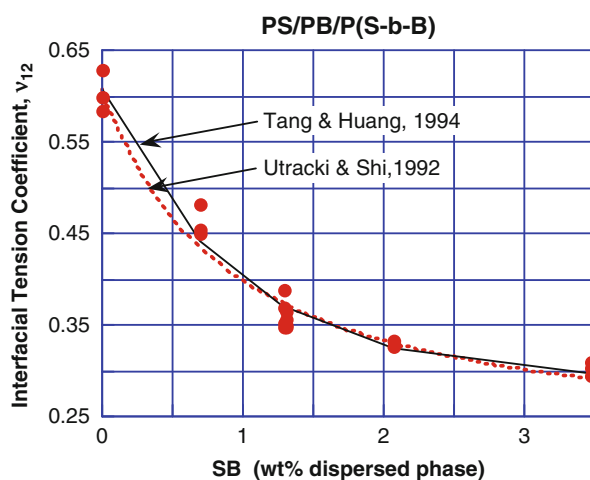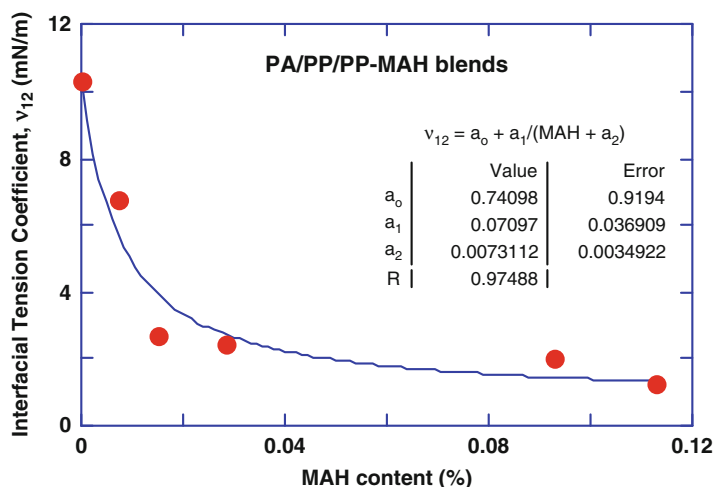
Fig. 4.16 Interfacial tension as a function of added maleic anhydride for PE/PA-6 blend

4.4.2 Thickness of the Interphase

In contrast to measurements of the interfacial tension coefficient, only few measurements of the interphase thickness have been reported (Wlochowicz and Janicki 1989; Janicki et al. 1986). For example, domain boundary thickness were measured in PS/PMMA blends (Foster and Wool 1991; Fernandez et al. 1988; Russel et al. 1991a; Perrin and Prud'homme 1994). Generally, values in the range of 2–6 nm were reported for the interface thickness.

4.4.3 Morphology

As shown in Tables 4.7 and 4.8, several methods have been used to characterize the morphology of polymer blends containing a block copolymer. In the pioneering works, transparency of films cast from solutions was used as a measure of the emulsifying agent efficiency (Riess et al. 1967; Banderet et al. 1967). Other studies have focused on the observation of phase size reduction in the scanning or transmission electron microscopy, SEM and TEM, respectively (Ouhadi et al. 1986; Fayt and Jerome 1990; Heuschen et al. 1990; Jo et al. 1991; Sakellariou et al. 1991). For block copolymers, the spherical, cylindrical, lamellar, and many other morphologies (including newly discovered ordered bicontinuous and grain boundary structures) have been reported for the copolymers' microphase-separated state and for their blends with homopolymers. New structures were characterized by hyperbolic interfaces (Hasegawa et al. 1993).

Table 4.7 Morphology in copolymer and homopolymer/copolymer blends

System	Techniques and results	References
P(S-b-I) blends with PS	Lamellar-catenoid or double-diamond morphologies as well as microstructural disorder have been reported	Spontak et al. 1993
PS with P(S-b-B), (K-resin)	Mesh-and-strut morphology consisting mostly of hyperbolic interfaces, found between the lamellar and spherical phases, was observed	Hashimoto et al. 1992
P(S-b-B-b-MMA) triblock copolymers and their hydrogenated analogs	At 17 % B-block, a "cylinder at the wall" morphology was observed – here PB and PHB cylinders were located at the lamellar PS/PMMA interface. At 6 % B-block, PB formed spheres at this interface. Hydrogenation of PB induced significant changes	Stadler et al. 1995
P(S-b-BMA) and blends with PPE	From dilute 2-propanol solutions, 42 wt% copolymer formed micelles with PS in the core. From THF solutions, ordered cylindrical structures were obtained. The addition of 10 wt% PPE turned the cylinders into spheres with PPE cores insulated by swollen PS blocks from a PBMA matrix. In PPE/P(S-b-BMA) 50/50 blends, multilayer vesicles and lamellar structures coexisted. In blends having less than 5 % of P(S-b-BMA), micelles with PBMA cores were observed in PPE matrix	Siqueira and Nunes 1994
PMMA or PS with P(S-b-MMA)	The microphase separation was observed only when low M_w homopolymers were used. Blends of a polymer C having strong specific interactions with A did not show any M_w limit for the microphase segregation	Lowenhaupt et al. 1994
PE with SB, SBS, SI, or SIS copolymers	In low-viscosity PE matrix, SB, SBS, and statistical SB copolymers formed spheres or ellipsoids. Broken filaments have been observed for SBS at 240 °C and for SIS at 270 °C. When PE was blended with high molecular weight of either SB or SIS, at 240 and 220 °C, respectively, co-continuous, elongated structures were observed	Getlichermann and David 1994

4.4.4   Crystallization

Another important aspect of compatibilization is the effect on blends' micromorphology, i.e., on the total crystallinity and the crystalline morphology (Utracki 1989; Xavier 1991; Nadkarni and Jog 1991).

Crystallization may take place only within the temperature region limited on the upper side by the melting point, T_m, and on the lower side by the glass transition temperature, T_g. The crystallization behavior very much depends on the state of

Table 4.8 Blends of two homopolymers with or without a copolymer

Blend	Additive	Techniques and results	References
PE/PP	EPR	Processing conditions, melt viscosity and elasticity ratios, M_w, and MWD affect the melt and solid morphology and hence the performance	Teh et al. 1994
PAr/PVDF	PAr-b-PMMA	PVDF/PMMA is a miscible blend. The addition of PAr to the PAr/PVDF/PAr-b-PMMA resulted in the reduction of PVDF T_m and an increase of PAr T_g. These effects were enhanced by the addition of PAr-b-PMMA. Finer dispersion was obtained for higher block copolymer content. Contact angle measurements showed that v_{12} was greatly influenced by the presence of block copolymer	Ahn et al. 1994
PP/PC	SEBS –*Kraton G*	Distinct changes of morphology were observed for 10–20 wt% PC, when the PP/SEBS ratio varied from 95/5 to 90/10. SEM studies showed composite PC droplets with SEBS envelopes, embedded in PP matrix. This suggests stronger interfacial interactions between SEBS and PP than between PC and PP	Srinivasan and Gupta 1994
PPE/PE ionomer	P(S-b-VP)	Melt mixing at 290 °C. The addition of a small amount of PS-b-PVP was found to reduce the domain size	Jo et al. 1994a
PBT/ PMMA	Phenoxy	When a small amount of polyhydroxy ether of bisphenol-A (*Phenoxy*) was added to the PBT/PMMA blends, the morphology changed into more regular and finer. For > 50 wt% *Phenoxy,* the blend converted to single phase	Jo et al. 1994b
PS/PP	PSiS	Excellent dispersions in PS with up to 5 % of polydimethylsilylene-co-phenylmethylsilylene (PSiS) were obtained. In PP at > 1 wt% PSiS, segregation was observed. The blending of PSiS with PS decreased surface resistance, increased hardness, and provided protection from degradation by sunlight	Asuke et al. 1994
PS/PVC	Graft copolymer	A block-graft copolymer was prepared by grafting a diblock copolymer of styrene and butadiene, with cyclohexyl methacrylate monomers. PS/PVC blends comprising a small amount of the block-graft copolymer showed excellent behavior. The copolymer had strong effect on the blends' morphology	Braun et al. 1994

miscibility, as well as on the nature of other blend's components. In miscible blends T_g is a monotonic function of the components' T_g's. When the second component is amorphous, its presence can either decrease or increase the tendency of the first resin to crystallize. The process depends on the blending effects on T_g and on the chain mobility (the free volume effect). When T_g of the amorphous component is

lower than that of the semicrystalline, the crystallization envelope is increased and the crystallization is facilitated. The effect is similar to the crystallization from a solvent – both the T_g and chain mobility tend to maximize the total crystallinity. Such blending may induce the crystallization of polymers that are known to be amorphous, e.g., PC. In the opposite case, the addition of an amorphous component increases T_g of the blend, reduces the crystallization envelope, and thus hinders crystallization.

When the blends are immiscible in the molten state, the crystallinity is an even more complex function of the ingredients' properties, compatibilization method, processing parameters, and post-processing treatments. The following factors have been identified to play a major role: (i) the molecular constitution and M_w of the components; (ii) composition; (iii) the type of phase morphology and the degree of dispersion; (iv) the interphase, thus interactions between the phases, nature of the interface, migration of nuclei from one phase to the other, etc.; (v) melt history, in particular the time the polymers were exposed to $T > T_m$; (vi) crystallization conditions, T_c, cooling rates, annealing, etc.; and (vii) physical conditions of crystallization, viz., presence of nucleating impurities; discontinuities, e.g., gas bubbles or filler particles; confinement by molten, crystalline, or glassy phase; etc.

As predicted by Helfand and Tagami, the interface is the locus of low molecular weight impurities that have been shown to nucleate crystallization, as, for example, in PS/PP blends (Wening et al. 1990). Compatibilization by the addition of a third component may either reduce or enhance the tendency for crystallization. On the one hand, the addition of a compatibilizer increases the interfacial area, thus increasing the nucleation rate – an increase of T_c by 10 °C was reported (Wei-Berk 1993). However, the compatibilization also may increase thickness of the interphase, Δl, thus hindering the diffusion of the nucleating agent to the crystallizable phase. It has been reported that when the size of domains containing the crystallizable polymer falls below certain limit, the crystallization rate is drastically reduced. In blends having widely different drop diameters, this may lead to fractionated crystallization with large undercooling required for the smallest drops. The presence of undercooling reflects the difference in nucleating activity of the heterogeneity existing in the dispersed phase. When the drop size is reduced beyond a certain limit, it may no longer have a nucleus for the heterogeneous crystallization – it may crystallize by the homogenous mechanism at much lower T_c (Frensch et al. 1989). Table 4.9 presents data on selected semicrystalline blends. More details on crystallization can be found in ▶ Chap. 3, "Crystallization, Micro- and Nano-structure, and Melting Behavior of Polymer Blends."

4.4.5 Mechanical Performance

Since blends are mainly used as structural materials, the most important properties are mechanical, especially the impact strength, stiffness, and elongation. Historically, blending was developed to improve these properties in the early

Table 4.9 Crystallization with and without compatibilizer

Blend	Additive	Technique and results	References
PA-6/EPR	EPR-g-SA	Compatibilizer had strong nucleating capability, reducing the spherulite size and increasing adhesion between the phases	Martuscelli 1984
PP/PA-6	Maleated PP (PP-MA)	Thermal analysis and optical microscopy. One or two crystallization peaks were affected by PP-MA. T_c of PA-6 initially decreased then leveled off with PP-MA content, whereas that of PP was not affected. Blends with PP-MA showed concurrent crystallization at the T_c of PP	Moon et al. 1994
PP/PS	P(P-b-S)	T_c increased from 116 °C to 126 °C upon the addition of PP-b-PS. Its presence lowered v_{12}, reduced PS drop diameter, and thus produced higher surface for nucleation of the α-PP crystals	Wei-Berk 1993
PP/PS	SBS	The drop size of PP did not change, but T_c increased, owing to the immiscibility of PP with polybutadiene block. SBS is a poor compatibilizer but capable to transfer nucleating heterogeneity to PP	Santana and Müller 1994
PP/HIPS	SB	WAXS and SAXS methods. The addition of an SB slightly reduced crystallinity of α-PP	Hlavata and Horak 1994
PET/PPE	P(ET-b-S)	The addition of a compatibilizer reduced the PS drop size (from $d = 5$ to 0.2 μm) as well as increased the total crystallinity	Quirk et al. 1995

resins, viz., PS, PVC, PMMA, PET, PA, etc. When blending started to involve mixtures of polymers, the impact modification has progressively changed into compatibilization. However, even today, many blends profit from the simultaneous compatibilization and impact modification by the addition of multicomponent modifiers. Many patents and papers in the open literature address this question, some of which will be presented in this section and the following one on patented blends. More information on various aspects of the mechanical performance can be found in ▶ Chap. 11, "Mechanical Properties of Polymer Blends" and ▶ Chap. 10, "Properties and Performance of Polymer Blends" in this handbook.

Two types of mechanical tests have been used: the low rate of deformation (tensile, compressive, or bending tests) and the high-speed impact tests. The immiscibility of polymers is reflected in both. For example, in tensile tests, the maximum strain at break (or the maximum elongation) and the yield stress (or the maximum strength) can be dramatically decreased by poor adhesion between the phases in the solid state. Similarly, this lack of adhesion is responsible for low values of impact strength – the specimens are brittle.

Polymeric systems can be classified as either brittle or pseudo-ductile. The first type tends to fail by the crazing mechanism and has low crack

Fig. 4.17 Izod impact strength at room temperature as a function of diameter of elastomeric particles in methyl methacrylate-butadiene-styrene copolymer used for toughening polyvinyl chloride resin
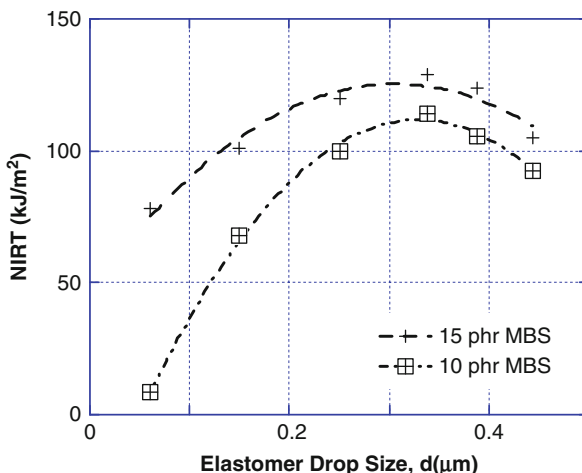
initiation as well as propagation energy – typical examples: PS, PMMA, and SAN. The second type tends to fail by yielding and has high crack initiation energy and low crack propagation energy – typical examples: PA, PEST, and PC. As usual, there are some polymers, e.g., POM and PVC, which show an intermediate behavior. The transition from brittle to ductile behavior depends on the intrinsic performance characteristics of the material as well as on external variables, such as the test temperature, rate of testing, geometry, loading mode, etc.

It is a common practice to toughen brittle resins by the addition of elastomeric particles. The effectiveness of the process depends on their diameter and concentration. It has been found that at constant concentration of the toughening agent, its effectiveness, i.e., the plot of toughness versus particle diameter, follows a bell-shaped curve, defining the optimum particle diameter. As shown in Fig. 4.17, the optimum does not change with concentration.

The optimum particle size, d_{opt}, was found to depend on the entanglement density of the matrix resin (see Fig. 4.18). However, the dependence can be used only as a general guide. Both the fracturing and toughening mechanisms change from one resin to the next. The determination of the d_{opt} also is ambiguous owing to the polydispersity of sizes as well as to the presence of other macromolecular chains. For example, it has been accepted that to toughen PS into HIPS, the optimum diameter is defined as a diameter of the elastomeric particles expanded by the occlusion of the PS matrix. In PVC the diameter of the elastomer was defined as the diameter of the original butadiene latex, before grafting it with styrene and methyl methacrylate. In PC the "optimum" diameter was defined rather from the point of view of availability of the core-shell toughening agent than the true optimum performance – it is becoming increasingly difficult to find tougheners with elastomeric particles having diameter $d < 100$ nm. Furthermore, the strategy of the preparation of polymer
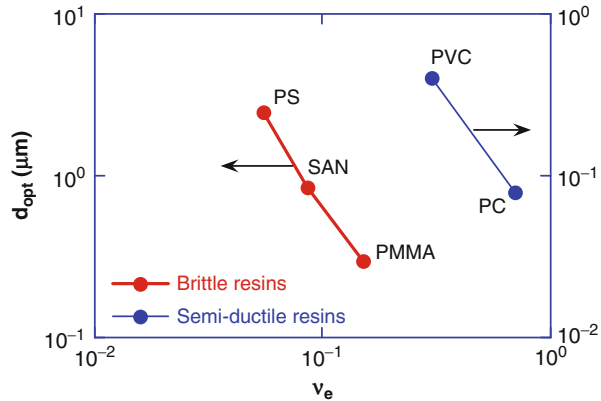
blends with stable morphology demands that blends have a thick interphase, $\Delta l \leq 60$ nm. Frequently it is impossible to decide how far the toughening by rubber core extends to the interphase. Many impact-resistant engineering resin blends have been formulated using the core-shell multicomponent with rigid core and elastomeric shell whose thickness and affinity to the matrix resin can be adjusted.

By contrast with brittle resins where d_{opt} is independent of concentration, in pseudo-ductile, one of these two variables is related – when the concentration of the toughening agent decreases, the elastomeric particle size must be reduced. In other words, in the latter systems, it is the distance between the elastomeric particles that seems to control the fracture mechanism. Again, there are resins showing intermediate behavior between these two limits.

The above discussion focused on the addition of discrete elastomeric particles. However, there have been reports that the formation of co-continuous structures of brittle or pseudo-ductile resin and an elastomeric one can produce a quantum jump in toughness, without greatly affecting the key engineering properties of the high-performance resin. Commercial blends of this type, e.g., comprising POM, PA, PC, or PEST, are available. When the blends are formulated with relatively large content of two resins, it may be necessary to toughen both phases. This is often done using sequential reactive blending. Examples of mechanical properties of blends toughened by the addition of block copolymers are given in Table 4.10. More information on this topic is presented in the section on patented blends.

4.4.6   Solvent and Chemical Resistance

In many applications the chemical and solvent resistance is of paramount importance. To improve these properties, blending with a resin having the required performance characteristics is used. By nature, the modifying resins must have

Table 4.10 Examples of compatibilized and impact modified polymer blends

Blend	Additive	Comments	References
PE/PA-6	SEBS-MA, ≤ 10 wt%	Reactive blending, reduced v_{12}, increased adhesion	Armat and Moet 1993
PS/PP = 1:1	5 wt% of low MW SEBS	Threefold increase of the impact strength	Appleby et al. 1994
PPE/PE ionomer	PS-b-PVP	In PPE matrix blends, tensile strength and elongation increased	Jo et al. 1994
PS/PVC/CPE	#1. SEB-GMA #2. (SEB-GMA)3 #3. random S-r-EB-GMA	Compatibilization depends on GMA content and degree of chlorination of the CP; best #1, worst #3	Koklas and Kalfoglou 1994
PP + 0–30 wt% PC	SEBS (5, 10, and 20 wt%)	Improved impact, reduced tensile, and flexural moduli	Srinivasan and Gupta 1994
HIPS/PBT	PS-GMA	Reactive processing to form PBT-b-PS	Chang et al. 1994

very much different chemical compositions, which leads to antagonistic immiscibility and a need for compatibilization. The examples listed in Table 4.11 illustrate some commercial solutions.

4.4.7 Electrostatic Dissipating Blends

Polymer blends have been often used as electrical insulating materials. Polymers do not readily conduct electrical current, are inexpensive in comparison to other known insulating materials, and are sufficiently durable and heat resistant. However, in some applications, owing to the accumulation of surface charge that may discharge rapidly and cause damage to electronic components and cause fires or explosions, they may pose problems. A need has existed for electrostatic dissipating polymeric compositions, ESD.

The ESD compositions must have sufficient resistivity to cause slow dissipation of a static charge, but not too low as to allow the charge to move too quickly through the material, thereby causing an arc or spark. The surface resistivity $105 \leq R \leq 1,012 \ \Omega$ cm is considered desirable. Attempts have been made to coat an electrostatic dissipative material onto plastic, add graphite, or metal particles, but coating can easily be wiped out and the additives are expensive, make processing difficult, and often lower the mechanical performance of the plastic part. Incorporation of organic semiconducting materials, or other low molecular weight antistatic agents, also is disadvantageous. These additives must migrate to the surface and pose similar problems as coatings.

For ESD the surface resistivity should be $105 \leq R \leq 1,012 \ \Omega$ cm. The best strategy for development of such materials is by the incorporation of organic semiconducting polymers. Selected examples are listed in Table 4.12.

Table 4.11 Blends with enhanced chemical and solvent resistance

Blend	Additive	Comments	References
HIPS/HDPE	SBS or SIS	High impact strength and resistance to solvents	Swartzmiller et al. 1993
PA/ABS	SAN-MA	Excellent solvent resistance and toughness	Lavengood et al. 1988
PPE/PA	SBR-MA, SGMA, SMA, or EMAA	Solvent and impact resistance	Ueno and Maruyama 1981; Fuji and Ting 1987
PPE/PA	PPE-MA	Reactive extrusion	Akkapeddi et al. 1988
PPE/PC/ PEST	SEBS	Improved impact and solvent resistance	Hobbs et al. 1992
PPE/PBT	PC/EGMA	High solvent, temperature resistance, and dimensional stability	Yates 1987
PP/PA	Maleic, fumaric, acrylic, or methacrylic acid grafted PP or SEBS	Low water absorption and permeability	Nishio et al. 1990
PEST/ABS	AES-GMA, ABS-MA, or ABS-GMA	Outstanding heat, chemical, and impact resistance	Yasue et al. 1989; Hirai et al. 1988
PET/PO	PO-GMA or EEA-GMA	High heat and moisture absorption resistance	Mukohyama 1993; Natarajan et al. 1993

4.5   Patented Blends with Added Compatibilizer

Patented or commercial polymer blends are in most cases multiphase, compatibilized systems. In the old but still popular blends of polyvinyl chloride or polycarbonate with acrylonitrile-butadiene-styrene copolymer, PVC/ABS or PC/ABS, the styrene-acrylonitrile copolymer, SAN, ascertains adequate compatibilization in the systems. Note that ABS went through a series of process and composition modifications to enhance performance in blends.

In this brief description of selected patented and/or commercial blends, first the commodity then the engineering and specialty materials will be presented in a tabulated form (Utracki 1997). Further information on the topic can be found in ▶ Chap. 9, "Compounding Polymer Blends" in this handbook.

More than 550 patents were identified from 1976 to 2013 with the research term polymer blends in the abstract. The approximate number of patents found between 1995 and May 2013 were as follows:

2006–2013: 100 patents
2003–2013: 150 patents
2000–2013: 200 patents
1995–2013: 300 patents

Interested reader can consult the web site of the US patent office for the details on these patents.

Table 6.12 Examples of ESD blends

Blend	Additive	Comments	References
ABS/PMMA	5–25 wt% EO-CHR epihalohydrin copolymer	ESD, reduced delamination, and improved ductility	Gaggar et al. 1988
PS/PCL	2–50 wt% EO-ECH	Excellent ESD and elongation	Giles and Vilasagar 1994

4.5.1 Commodity Resin Blends

4.5.1.1 Polyolefin Blends
The information about polyolefin, styrenic, vinyl, and acrylic blends is presented in tabulated form in Tables 4.13, 4.14, and 4.15 below.

4.5.1.2 Styrenic Blends
See Table 4.14.

4.5.1.3 Vinyl and Acrylic Blends
See Table 4.15.

4.5.2 Engineering and Specialty Resin Blends

The information about engineering and specialty blends are presented in tabulated form in Table 4.16 below.

4.6 Conclusions and Outlook

To select proper compatibilizer, it is imperative to know whether the copolymer is capable to (i) engender a fine dispersion during blending, (ii) preferentially migrate to the homopolymers' interface, (iii) stabilize the morphology against segregation, and (iv) enhance the adhesion between the phases. It is only when all these conditions are satisfied that the idea of interfacial activity of classical emulsifiers can be applied to copolymers added to immiscible blends.

The effective compatibilization of binary polymer blends by the addition of a copolymer should reduce the interfacial tension coefficient. Often, it also alters the molecular structure of the interface (as measured by the scattering methods). The process is similar to the emulsification in the classical emulsions. The emulsifier effect on the droplet size follows generally the same behavior as the interfacial tension. This behavior is described by the emulsification curves (evolution of the particle's size with the emulsifier content) and characterizes the additives' efficiency. The shape of the emulsifying curve depends greatly on the type of emulsifier and the emulsification process. If the selected compatibilizer is miscible only with one component of the blend, its efficiency

Table 4.13 Typical polyolefin polymer blends and their characteristics

Blend	Additive	Comments	References
PP and/or LLDPE	EPR	Enhanced mechanical performance	Yamazaki and Fujimaki 1970, 1972
PCO/PE	Block copolymers with ethylene or propylene and norbornene blocks	Low melt viscosity, thus good processability, high elongation at break, impact strength, toughness, hardness, and modulus	Epple and Brekner 1994
PE/PPE	Styrenic copolymers (SB, SBS, SEBS)	Had excellent impact strength, good solvent resistance and aging characteristics	Haaf and Lee 1978
PE/PET	Block copolymer: n-butyl terephthalate/ ethyleneglycol and propylene glycol, Hytrel™4074, and a mixture of two aromatic phosphites	Improved impact strength and flame resistance, as well as low permeation to gasoline	Abu-Isa and Graham 1993
PE/POM	EVAc	Abrasion resistant, glossy moldings, high elongation, excellent impact strength, dimensional stability, and high environmental stress cracking	Ishida and Masamoto 1974
PE and PP	EPR	Good flow properties and a very good low-temperature impact strength	Schreck et al. 1994
PP/SBR	PP grafted with styrene	Useful as stand-alone structural materials	DeNicola and Conboy 1994
PE or PP with PS or HIPS	3-block copolymer of styrene and butadiene or isoprene	Good processability, stress cracking resistance, impermeability to water vapor, and improved impact resistance	Hoenl et al. 1993
PP/PC	EVAc	Good mechanical properties and excellent solvent resistance	Giles and Hirt 1986
PP with PET or PBT	Polyolefin-polyester graft copolymer	Excellent impact strength, flexural modulus, HDT, and peel resistance	Fujita et al. 1994
PP/LCP	Maleated PP	Compatibilization improved the performance well above that observed for two-component LCP/PP blends	Baird and Datta 1992

is negligible. The efficiency of a block copolymer is limited by the formation of micelles in bulk phases as well as by the kinetic factors.

The morphology of blends may be complex. The addition of compatibilizer not only affects the size and shape of the separated phases (the macro-morphology), but it may also affect the crystalline form, the size of crystalline entities, as well as the total crystallinity (the micromorphology). In a blend of two semicrystalline polymers, e.g., PE/PP, four phases may coexist:

Table 4.14 Typical blends with styrenic polymers and their characteristics

Blend	Additive	Comments	References
PS or HIPS with polyolefins	SEBS	2–30 wt% PP and 5–20 wt% SEBS. Good impact, flexural strength, and tensile yield retention were reported	Holden and Gouw 1979
PS/PP	$(SB)^n$ block copolymer	Thermoformable blends	Grancio et al. 1981
PS/LLDPE	SEBS	10–90 wt% PS, 10–90 wt% LLDPE, and 5–40 wt% SEBS – the system showed good resistance to impact and yellowing	Seelert et al. 1993
PS/EVAc	SB	Improved elasticity, tensile strength, and reduced die buildup. Further improvement by replacing a part of the EVAc with a low crystallinity PO	Djiauw and Mitchell 1990; Djiauw 1994
45–70 wt% HIPS with 15–40 wt% HDPE	5–25 wt% SBS or SIS	Thermoformable blends with good interfacial properties for refrigerator or freezer liners. They are easy to process into parts with high impact strength and solvent resistance	Swartzmiller et al. 1993

PE-crystalline, PP-crystalline, PE-amorphous, and PP-amorphous. The situation can be more complex if the polymorphism of PP (with four potential crystalline structures) is taken into account. The spherulites' size, lamellar thickness, interlamellar amorphous zones, perfection of the crystallites, total crystallinity, and a possibility of epitaxial crystallization are additional factors that affect the final morphology and performance. Processing conditions, such as the extent of shearing, the cooling rate, and annealing history, all affect the melt and solid morphology. The addition of a compatibilizer multiplies the factors that must be taken into account. More details on the effect of processing and compounding can be found in ▶ Chap. 9, "Compounding Polymer Blends" in this handbook.

Polymer blends must provide a variety of performance parameters. Usually it is a set of performance criteria that determines if the material can be used or not. For specific application more weight can be given to one or another material property. The most important properties of polymer blends are mechanical. Two types of tests have been used: the low rate of deformation (tensile, compressive, or bending) and the high-speed impact. Immiscibility affects primarily the maximum elongation at break and the yield stress.

Polymers are either brittle or pseudo-ductile. The first type tends to fail by the crazing mechanism and has low crack initiation as well as propagation energy, while the second tends to fail by yielding and has high crack initiation energy and low crack propagation energy. The transition from brittle to ductile behavior depends on the intrinsic performance characteristics of the material as well as on external variables, such as test temperature, rate of testing, geometry, loading

Table 4.15 Typical blends of vinyl and acrylic polymers

Blend	Additive	Comments	References
PVDC or PVC with 70–20 wt% CR	10–25 wt% NBR	Transparent blends, thermoplastic, heat sealable, printable, odorless, and tasteless, suitable for a wide range of applications	Signer and Beal 1953
PVC with 5–13 phr of SBR	NBR	The alloys showed improved impact strength at low temperature	Bataafse Petroleum 1960
PVC	MBS	Butadiene methyl methacrylate styrene copolymer, MBS as an impact modifier	Feuer 1958
PVC or PVCAc	Poly(B-co-BA-co-S), or poly(S-co-AN-co-MMA-g-BA-g-MMA)	3–40 wt% P(S-co-BA-co-S). The alloys were transparent, with good weatherability and high impact strength	Ide and Deguchi 1971
			Ide and Miura 1971
			Ide et al. 1972
PVC/SAN	ABS-type G	10 phr of SAN and 10 phr of ABS-type G. Give resins with *low sensitivity to mechanical working*. For vacuum forming the blend performance could be improved by addition of ≤ 20 % PVCAc	Parks and Jennings 1956
5–50 wt% PVC with 1–50 % ABS	Post-chlorinated PVC	The alloys showed improved processability, impact strength, and thermal stability	Kojima et al. 1970
PVC	5–30 wt% MABS	PVC with MABS showed high impact strength	Himei et al. 1967
PVC/ABS	ABS core and grafted with AN-co-Et- acrylate-co-styrene	Excellent mechanical properties, high impact strength, transparency, surface smoothness, and whitening resistance	Tanaka et al. 1971
PVC/ABS	ABS (core) grafted with PMMA	PMMA improved PVC/ABS miscibility. The alloys displayed excellent mechanical properties and impact strength	Michel 1969

mode, etc. To toughen a brittle polymer, elastomeric particles with optimum diameter, d_{opt}, should be used. It has been found that d_{opt} depends on the entanglement density of the matrix resin, $d_{opt} \propto v_e^n$, where the exponent $n = -2$ to -3. For pseudo-ductile polymers, a similar dependence is valid, but since for them the entanglement density is significantly higher, the required size of the elastomeric zones is small, in order of nm. Furthermore, it has been found that not only the size but also the separating distance between the elastomeric zones is important. Thus, for these polymers, the toughening strategy is based on the creation of proper size elastomeric interphase, with rigid core that provides

Table 4.16 Engineering and specialty polymer blends

Blend	Additive	Comments	References
PPE/PEST	SBS	Low viscosity, good impact, fire resistance, and tensile strength	Lee 1978
PC/ACM	Styrene-acrylic acid copolymer, SAA	High impact strength and HDT	Henton 1980, 1982, 1983, 1984, 1986
PC/ABS	SMMA-MA	Co-continuous morphology	Jones and Mendelson 1985
PC/MeABS	AN-co-α-methyl styrene-co-MMA, MeSAN	Good compatibility, toughness, and thermal stability	Kress et al. 1986
PC/PBT/LLDPE	MBA	Impact and solvent resistance	Boutni and Liu 1984, 1986
PPE/PA	Styrene-butadiene radial copolymer (*K-Resin*™) with citric acid or chloro-epoxytriazine or tapered block copolymer	Izod impact strength was improved (in comparison to blends with HIPS) by a factor of three	Gianchandai et al. 1993; Yates 1993
PA/PAr or PA/PEST	PA-co-PAr	Good processability, mechanical properties, UV stability, heat, solvent, and stress-crack resistance	Dean 1990
PA/PC or PA/PAr	EGMA	Impact modification	Yuichi and Suehiro 1989
PA/PVDF	A compatibilizer	Suitable for parts that are impact resistant and impermeable to gases	Hizasumi et al. 1989
PA/PEI	Phenolic compounds, e.g., a nonylphenolic	Have reduced water absorption, had less swelling, and have good dimensional stability	Gallucci 1988; Gallucci and Rock 1992

proper separation. The ultimate in the toughening method for pseudo-ductile polymers is the generation of co-continuous structure having proper size of the phases.

For brittle polymers the impact strength can be improved by engendering proper size heterogeneity in the matrix – rubber particles that may or may not be joined to the matrix or even gas bubbles. Toughening is accomplished by increasing the number of crazes, thus increasing the total energy of fracture. However, this strategy rarely leads to maximum improvement of impact strength, and as a rule, it decreases several other performance parameters. Thus, for good balance of properties, e.g., improved processability, dispersion, impact strength, and other mechanical properties, it is imperative that the impact modifier is well bonded to the polymeric phases, i.e., that it plays the broader role of compatibilizer.

In PO blends, the preferred compatibilizer has been EPR, while in styrenic blends, SBS or SEBS maintains high visibility in spite of the price. Both compatibilizers can also improve the impact strength. However, the excessive

amount of elastomer can lower the modulus and strength of the alloy; thus, the elastomeric particles' size should be optimized.

The PVC blends are usually compatibilized by the addition of an acrylic copolymer, viz., ABS, MABS, MBS, or a core-shell-type copolymer (consisting of ABS core and grafted with acrylonitrile-ethyl acrylate-styrene) was introduced by Japanese Geon in 1966.

Owing to miscibility, PPE has been compatibilized by adding a styrenic copolymer, capable of interacting with the other polymer, e.g., either PS or HIPS, SEBS, or SBS. Since the most interesting second polymer was either PA or PEST, in the early 1980s, the technology moved to reactive blending. The use of PC that preferentially migrated to the interface between the dispersed drops of PPE and SEBS, dispersed in PBT matrix, is an excellent example of the use of the third polymer to prevent coalescence, thus to stabilize the optimized morphology. In several engineering blends, e.g., ABS/PSF, the nearly universal cosolvent, *Phenoxy*, has been used. However, majority of modern commercial blends is prepared by reactive compatibilization.

Strong research and development activity is still ongoing on polymer blends, with a variety of new functional applications such as biomedical, energy, environment, etc.

4.7   Cross-References

Abbreviations

ABS   Acrylonitrile-butadiene-styrene
APS   Aminopropyltriethoxysilane
CPE   Chlorinated polyethylene
CTBN   Butadiene acrylonitrile copolymer with $\alpha, \omega -$ carboxyl groups
CTBR   Butadiene oligomer with $\alpha, \omega -$ carboxyl groups
DMF   Dimethylformamide
DSC   Differential scanning calorimetry
EGMA   Ethylene-graft-maleic anhydride

EPDM Ethylene-propylene-diene terpolymer
EPR Ethylene-propylene rubber
EVOH, EVAl Ethylene vinyl alcohol copolymer
FRES Forward recoil spectroscopy
HIPS High-impact polystyrene
LLDPE Linear low-density polyethylene
MA Maleic anhydride
PA Polyamide
PAr Polyarylate
PB Polybutadiene
PBMA Polybutyl methacrylate
PBT Polybutylene terephthalate
PC Polycarbonate
PCL Poly(ε-caprolactone)
PE Polyethylene
PEI Polyether imide
PES Polyether sulfone
PEST Polyester
PET Polyethylene terephthalate
PETG Polyethylene terephthalate glycol
PHB Polyhydrogenated butadiene
Phenoxy Polyhydroxy ether of bisphenol-A
PMMA Polymethylmethacrylate
PO Polyolefin
POM Polyoxymethylene
PP Polypropylene
PPE Polyphenylene ether
PS Polystyrene
PSF Polysulfone
PVAc Polyvinyl acetate
PVAl Polyvinyl alcohol
PVC Polyvinyl chloride
PVDF Polyvinylidene fluoride
PVP Polyvinyl pyridine
SAN Styrene-acrylonitrile
SANS Small-angle neutron scattering
SAXS Small-angle X-ray scattering
SB Styrene-butadiene copolymer
SBS Styrene-butadiene-styrene three-block copolymer
SEBS Styrene-ethylene/buthylene-styrene three-block copolymer
SEM Scanning electron microscopy
SI Styrene-isoprene copolymer
SIS Styrene-isoprene-styrene three-block copolymer
SMA Styrene-maleic anhydride

SMMA Styrene-methyl methacrylate block copolymer
TEM Transmission electron microscopy
THF Tetrahydrofuran

Nomenclature

Notation

A	Total interface surface area
a, b, c, k, K, n, u	Equation constants
a, b_i	Segment or monomer length or lattice parameter
a_1, a_2	Long and short axis of a deforming particle
CMC	Critical micelles concentration
D	Domain period in copolymer
$\boldsymbol{D}$	Drop deformability parameter
d	Droplet diameter
d_{eq}	Equilibrium droplet diameter
ΔE_S	Elastic energy
f	Fraction of a component in copolymer
f^*	Transition concentration from microphase to macrophase separation
g	Energy density
ΔG_m	Gibbs free energy of mixing
ΔH_m	Heat of mixing
k_B	Boltzmann constant
l	Mean length of statistical skeletal segment
$\Delta l, \Delta l_o$	Interfacial thickness and initial interfacial thickness
Δl_∞	Interfacial thickness for infinite molecular weight
LCST	Lower critical solubility temperature
M_A, M_B, Mv	Molecular weight of monomer-A, monomer-B, and a statistical segment
M_e	Entanglement molecular weight
M_n, M_w, M_z	Number, weight, and z-average molecular weight
N_{Av}	Avogadro's number
N_v	Number of statistical skeletal segments
Q	Number of copolymer chains at the interface
R	Ideal gas constant, droplet radius
$\langle r^2 \rangle$	End-to-end distance of the polymer chains
$\langle R_i^2 \rangle$	Radius of gyration of chain i
S	Interfacial area per unit volume of the blend
t, t^*	Time and dimensionless breakup time
T, T_g, T_m	Temperature, glass transition temperature, and melting point
T_{cr}, T_s	Critical and spinodal temperature
UCST	Upper critical solubility temperature

V	Specific volume
w_{cr}	Minimum amount of copolymer to cover surface of spherical particle
w_i	Weight fraction of i
Z_i	Degree of polymerization of polymer i (or copolymer)
χ, χ_{AB}	Binary thermodynamic interaction parameter
ϕ_1, ϕ_2	Volume fraction of the dispersed and matrix phase, respectively
ϕ_d, ϕ_m	Volume concentration of dispersed phase and the matrix
ϕ_p	Polymer volume fraction
γ	Shear strain
$\dot{\gamma}$	Shear rate
η, η', η^*	Shear viscosity, dynamic viscosity, and complex viscosity
$[\eta]$	Intrinsic viscosity
η_1, η_2	Viscosity of the dispersed and matrix phase, respectively
η_d, η_m	Viscosity of the dispersed and matrix phase, respectively
$\eta_i, \eta_{Si}, \eta_{Ei}$	Interfacial, shear interfacial, and extensional interfacial viscosity
η_o, η_r	Zero-shear viscosity and relative viscosity
$\kappa = \sigma d/v_{12}$	Capillarity number
κ_{cr}	Critical capillarity number
$\lambda = \eta_1/\eta_2$	Viscosity ratio
μ	Chemical potential
$\Delta\mu$	Excess chemical potential
v	Surface tension coefficient
v_{12}	Interfacial tension coefficient between phases 1 and 2
v_e	Entanglement density
v_o	Initial interfacial tension
v_∞	Interfacial tension for infinite molecular weight
ρ	Density
Σ	Interfacial area per copolymer joint
σ	Stress
σ_{12}	Shear stress
s_m	Stress for the matrix phase
σ_y	Yield stress
τ, t_y	Relaxation or residence time, and characteristic relaxation time
ω	Angular frequency
ζ_o	Rouse friction coefficient

References

I.A Abu-Isa, P.M. Graham, U.S. Patent 5,194,468, 16 Mar 1993, Appl. 19 June 1992, to General Motors Corporation

A.W. Adamson, *Physical Chemistry of Surfaces*, 4th edn. (Wiley, New York, 1982)

T.O. Ahn, J.H. Lee, H.M. Jeong, K.W. Cho, Eur. Polym. J. **30**, 353 (1994)

A. Ajji, L.A. Utracki, Polym. Eng. Sci. **36**, 1574 (1996)

A. Ajji, L.A. Utracki, Prog. Rubber. Plast. Technol. **13**, 153 (1997)

M.K. Akkapeddi, B. VanBuskirk, A.C. Brown, PCT Int. Appl. W088/08433, 03 Nov 1988, Appl. 24 Aug 1987; U.S. Patent 5,162,440, 10 Nov 1992, Appl. 24 Apr 1987, to AlliedSignal, Inc

S.H. Anastasiadis, Adv. Polym. Sci. **238**, 179 (2011)

S.H. Anastasiadis, J.K. Chen, J.T. Koberstein, A.F. Siegel, J.E. Sohn, J.A. Emerson, J. Colloid Interface Sci. **119**, 55 (1987)

S.H. Anastasiadis, I.S. Gancarz, J.T. Koberstein, Macromolecules **21**, 2980 (1988)

S.H. Anastasiadis, T.P. Russel, S.K. Satija, C.F. Majkrzak, Phys. Rev. Lett. **62**, 1852 (1989a)

S.H. Anastasiadis, I.S. Gancarz, J.T. Koberstein, Macromolecules **22**, 1449 (1989b)

S.H. Anastasiadis, T.P. Russel, S.K. Satija, C.F. Majkrzak, J. Chem. Phys. **92**, 5677 (1990)

T. Appleby, F. Cser, G. Moad, E. Rizzardo, C. Stavropoulos, Polym. Bull. **32**, 479 (1994)

R. Armat, A. Moet, Polymer **34**, 977 (1993)

T. Asuke, Y. Chienhua, R. West, Macromolecules **27**, 3023 (1994)

D.G. Baird, A. Datta, PCT Int. Appl. 218,568, 29 Oct 1992, U.S. Appl. 17 Apr 1991, to Virginia Polytechnic Institute and State University

A. Banderet, C. Tournut, G. Riess, J. Polym. Sci. **C16**, 2601 (1967)

Bataafse Petroleum Maatschappij N.V., British Patent 853,804, 9 Nov 1960

F.S. Bates, C.V. Berney, R.E. Cohen, Macromolecules **16**, 1101 (1983)

O.M. Boutni, P.Y. Liu, US Patent 4,444,949, 24 Apr 1984, Appl. 1981; US Patent 4,626,572, 02 Dec 1986, Appl 1985, to General Electric Company

Brandrup and Immergut, Polymer handbook, Wiley intersceince publ. (1989)

D. Braun, M. Fischer, G.P. Hellmann, Macromol. Symp. **83**, 77 (1994)

D. Broseta, L. Leibler, L.O. Kaddour, C. Strazielle, J. Chem. Phys. **87**, 7248 (1987)

D. Broseta, G.H. Frederickson, E. Helfand, L. Leibler, Macromolecules **23**, 132 (1990)

D. Buta, K.F. Freed, I. Szleifer, J. Chem. Phys. **114**, 1424 (2001)

A. Campos, C.M. Gomez, R. Garcia, J.E. Figueruelo, V. Soria, Polymer **37**, 3361 (1996)

D.-Y. Chang, W.-F. Kuo, F.-C. Chang, Polym. Netw. Blends **4**, 157 (1994)

D.C. Chappelear, Polym. Prepr. **5**, 363 (1964)

D.M. Cho, W.C. Hu, J.T. Koberstein, J.P. Lingelser, Y. Gallot, Macromolecules **33**, 5245 (2000)

R. Choksi, X.F. Ren, Phys. D-Nonlinear Phenom. **203**, 100 (2005)

R.E. Cohen, J.M. Torradas, Macromolecules **17**, 1101 (1984)

K.H. Dai, E.J. Kramer, J. Polym. Sci. Polym. Phys. Eds. **32**, 1943 (1994)

S. Dashevsky, K.S. Kim, S.W. Palmaka, PCT Int. Appl. 013,172, 08 Jul 1993; PCT Int. 013,173, 08 Jul 1993, Appl. 23 Dec 1991, to Akzo N. V

S. Dashevsky, K.-S. Kim, S.W. Palmaka, R.L. Johnston, L.A.G. Busscher, J.A. Juijn, U.S. Patent 5,346,970, 13 Sep 1994, Appl. 22 July 1993, 23 Dec 1991, to Akzo Nobel

P.G. De Gennes, J. Phys. Lett. **38**, L-441 (1977)

P.G. De Gennes, *Scaling Concepts in Polymer Physics* (Cornell University Press, Ithaca, 1979)

B.D. Dean, U.S. Patent 4,937,297, 26 June 1990, Appl. 1988; U.S. Patent 5,115,046, 19 May 1992, Appl. 06 May 1991, to Amoco Corporation

N.R. Demarquette, M. Kamal, Polym. Eng. Sci. **34**, 1823 (1994)

A.J. DeNicola Jr., M.R. Conboy, U.S. Patent 5,286,791, 15 Feb 1994, Appl. 29 May 1992, to Himont, Incorporated

L. Djakovic, P. Dokic, P. Radivojevic, I. Seffer, V. Sovilj, Colloid Polym. Sci. **265**, 993 (1987)

L.K. Djiauw, U.S. Patent 5,320,899, 14 June 1994, Appl. 15 Oct 1992, to Shell Oil Company

L.K. Djiauw, N.F. Mitchell, U.S. Patent 4,977,014, 11 Dec 1990, Appl. 22 Aug 1989 to Shell Oil Company

G.C. Eastmond, in *Polymer Surfaces and Interfaces*, ed. by W.J. Feast, H.S. Munro (Wiley, New York, 1987)

G.C. Eastmond, D.G. Phillips, in *Polymer Alloys*, ed. by D. Klempner, K.C. Frisch. Polymer Science and Technology, vol. 10 (Plenum, New York, 1977)

G.C. Eastmond, D.G. Phillips, Polymer **20**, 1501 (1979)

P.H.M. Elemans, Ph.D. thesis, Technische Universiteit Eindhoven, 1989

P.H.M. Elemans, J.M.H. Janssen, H.E.H. Meijer, J. Rheol. **34**, 131 (1990)

P.C. Ellingson, D.A. Strand, A. Cohen, R.L. Sammler, C.J. Carriere, Macromolecules **27**, 1643 (1994)

J.J. Elmendorp, G. De Vos, Polym. Eng. Sci. **26**, 415 (1986)

J.J. Elmendorp, Ph.D. thesis, Delft University, 1986

U. Epple, M.-J. Brekner, U.S. Patent 5,359,001, 25 Oct 1994, Appl. 20 Apr 1993, Ger. Appl. 22 Apr 1992, to Hoechst A.-G

J.P.S. Farinha, O. Vorobyova, M.A. Winnik, Macromolecules **33**, 5863 (2000)

R. Fayt, R. Jerôme, Polym. Eng. Sci. **30**, 937 (1990)

R. Fayt, R. Jerôme, P. Teyssié, J. Polym. Sci. Polym. Lett. Ed. **24**, 25 (1986a)

R. Fayt, R. Jerôme, P. Teyssié, Makromol. Chem. **187**, 837 (1986b)

R. Fayt, R. Jerôme, P. Teyssié, J. Polym. Sci. Polym. Phys. Ed. **27**, 775 (1989)

M.L. Fernandez, J.S. Higgins, J. Penfold, R.C. Ward, C. Shackleton, D.J. Walsh, Polymer **29**, 1923 (1988)

S.S. Feuer, U.S. Patent 2,857,360, 21 Oct 1958, to Röhm and Haas

G. Floudas, N. Hadjichristidis, M. Stamm et al., J. Chem. Phys. **106**, 3318 (1997)

K.L. Foster, R.P. Wool, Macromolecules **24**, 1397 (1991)

W.T. Freed, U.S. Patent 3,920,602, 18 Nov 1975, Appl. 12 Aug 1974, to Celanese Corporation

H. Frensch, P. Harnischfeger, B.-J. Jungnickel, in *Multiphase Polymers: Blends and Ionomers*, ed. by L.A. Utracki, R.A. Weiss. ACS Symposium Series, vol. 395 (American Chemical Society, Washington, DC, 1989)

S. Fuji, S.P. Ting, European Patent Appl. 226,851, 01 July 1987, U.S. Appl. 1985, to General Electric Company

Y. Fujita, T. Kawamura, K. Yokoyama, K. Yokomizo, S. Toki, U.S. Patent 5,298,557, 29 Mar 1994, Appl. 01 Feb 1991, Jap. Appl. 02 Feb 1990, to Tonen Corporation

G.M. Gaafar, European Patent Appl. 352,485, 31 Jan 1990a; European Patent Appl. 383,977, 29 Aug 1990b, Appl. 1989, to General Electric Company

S.K. Gaggar, J.M. Dumler, T.B. Cleveland, European Patent Appl. 294,722, 14 Dec 1988; Australian Patent 88 16,570, 08 Dec 1988; Japan Patent 64 001,748, 06 Jan 1989; U.S. Patent 4,857,590, 15 Aug 1989; Ca. Patent 1,320,774, 27 July 1993; Ger. Offen. 3,883,614, 07 Oct 1993, U.S. Appl. 08 June 1987, to Borg-Warner Chem.; GE Chemicals, Inc

R.R. Gallucci, PCT Intl. Appl. 006,168; 006,169, 25 Aug 1988, Appl. 12 Feb 1987; European Patent Appl. 303,075; 15 Feb 1989, Appl. 29 Oct 1987, to General Electric Company

R.R. Gallucci, J.A. Rock, U.S. Patent 5,166,246, 24 Nov 1992, Appl. 05 Apr 1989, to General Electric Company

H. Garmabi, N. Demarquette, M. Kamal, Inter. Polym. Process. **13**, 183 (1998)

J. Genzer, R.J. Composto, Macromolecules **31**, 870 (1998)

M. Getlichermann, C. David, Polymer **35**, 2542 (1994)

J.K. Gianchandai, A. Hasson, R.J. Wroczynski, J.B. Yates III, European Patent Appl. 550,206, 07 July 1993, Appl. 31 Dec 1991, to General Electric Company

H.F. Giles Jr., R.P. Hirt Jr., U.S. Patent 4,579,910, 01 Apr 1986, Appl. 02 Jan 1985, to General Electric Company

B.S. Giles, S. Vilasagar, European Patent Appl. 596,704, 11 May 1994, Appl. 02 Nov 1993, US Appl. 04 Nov 1992, to General Electric Company

L.A. Girifalco, R.J. Good, J. Phys. Chem. **61**, 904 (1957)

A. Golovoy, M. Cheung, U.S. Patent 5,281,664, 25 Jan 1994, Appl. 20 July 1992, to Ford Motor Company

A. Gottschalk, K. Muhlbach, F. Seitz, R. Stadler, C. Auschra, Macromol. Symp. **83**, 127 (1994)

H.P. Grace, Chem. Eng. Commun. **14**, 225 (1982)

M.R. Grancio, D.F. Steward, J.F. Cass, European Patent Appl. 042,153, 23 Dec 1981, Appl. 11 June 1980; U.S. Patent 4,386,187, 31 May 1983, Appl. 11 June 1981, to Sweetheart Plastics, Inc

P.F. Green, T.P. Russel, Macromolecules **24**, 2931 (1991)

P.F. Green, T.P. Russel, R. Jérôme, M. Granville, Macromolecules **22**, 908 (1989)

M.J. Greenall, D.M.A. Buzza, T.C.B. McLeish, Macromolecules **42**, 5873 (2009)

G. Guerrica-Echevarria, J.I. Eguiazabal, J. Nazabal, Polym. Test. **19**, 849 (2000)

W.R. Haaf, G.F. Lee Jr., Ger. Offen. 2,750,515, 29 June 1978, Appl. 1976, to General Electric Company

H. Hasegawa, Y. Nishikawa, S. Koizumi, T. Hashimoto, S.T. Hyde, in *Proceedings of the 3rd IMURS*, Tokyo, Sept 1993

T. Hashimoto, A. Todo, H. Ito, H. Kawai, Macromolecules **10**, 377 (1977)

T. Hashimoto, K. Nagatoshi, A. Todo, H. Hasegawa, H. Kawai, Macromolecules **7**, 374 (1974)

T. Hashimoto, M. Fujimura, H. Kawai, Macromolecules **13**, 1237 (1980a)

T. Hashimoto, M. Shibayama, H. Kawai, Macromolecules **13**, 1660 (1980b)

T. Hashimoto, M. Shibayama, H. Kawai, Macromolecules **16**, 1093 (1983)

T. Hashimoto, H. Tanaka, H. Hasegawa, Macromolecules **23**, 4378 (1990a)

T. Hashimoto, T. Takebe, K. Fujioka, in *Dynamics and Patterns in Complex Fluids*, ed. by A. Onuki, K. Kawasaki (Springer, New York, 1990b)

T. Hashimoto, K. Koizumi, H. Hasegawa, T. Izumitani, S.T. Hyde, Macromolecules **25**, 1433 (1992)

E. Helfand, Macromolecules **8**, 552 (1975a)

E. Helfand, J. Chem. Phys. **62**, 999 (1975b)

E. Helfand, J. Chem. Phys. **63**, 2192 (1975c)

E. Helfand, A. Sapse, J. Chem. Phys. **62**, 1327 (1975)

E. Helfand, Y. Tagami, Polym. Lett. **9**, 741 (1971a)

E. Helfand, Y. Tagami, J. Chem. Phys. **57**, 1812 (1971b)

E. Helfand, Y. Tagami, J. Chem. Phys. **56**, 3592 (1972)

E. Helfand, Z.R. Wasserman, Macromolecules **9**, 879 (1976)

E. Helfand, Z.R. Wasserman, Macromolecules **11**, 960 (1978)

E. Helfand, Z.R. Wasserman, Macromolecules **13**, 994 (1980)

D.E. Henton, U.S. Patent 4,218,544, 19 Aug 1980; U.S. Patent 4,367,310, 04 Jan 1983, Appl. 03 May 1979; European Patent Appl. 056,246; 056,247, 21 July 1982, Appl. 09 Jan 1980; European Patent Appl. 056,247, 21 July 1982, Appl. 09 Jan 1980; U.S. Patent 4,439,582, 27 Mar 1984, Appl. 03 May 1979; U.S. Patent 4,619,968, 28 Oct 1986, Appl. 12 Aug 1985, to Dow Chemical Company

J. Heuschen, J.M. Vion, R. Jerôme, P. Teyssié, Polymer **31**, 1473 (1990)

J.S. Higgins, M. Tambasco, J.E.G. Lipson, Prog. Polym. Sci. **30**, 832 (2005)

S. Himei, M. Takine, K. Akita, Japan Patent 000,949, 18 Jan 1967, Appl. 1963, to Kanegafuchi Chem. Ind. Co., Ltd

M. Hirai, T. Tatsuda, T. Yoshida, European Patent Appl. 284,086, 28 Sep 1988; Japan Patent 63 241,062, 06 Oct 1988, 94 015,659, 02 Mar 1994; Australian Patent 88 13,737, 29 Sep 1988; U.S. Patent 4,855,355, 08 Aug 1989, Appl. 28 Mar 1987; Ca. Patent 1,307,863, 22 Sep 1992, Jap. Appl. 27 Mar 1987, to Sumitomo Naugatuck KK; Sumitomo Dow, Ltd

N. Hizasumi, T. Uehara, H. Ohba, K. Hirose, European Patent Appl. 336,680, 11 Oct 1989, Appl. 1988, to Kureha Chem. Industry Company, Limited

D. Hlavata, Z. Horak, Eur. Polym. J. **30**, 597 (1994)

S.Y. Hobbs, R.C. Bopp, V.H. Watkins, Polym. Eng. Sci. **23**, 380 (1983)

S.Y. Hobbs, T. Stanley, O. Phansteil, ACS Polym. Prepr. **33**(2), 614 (1992)

H. Hoenl, A. Jung, P. Klaerner, B. Ostermayer, S. Seelert, European Patent Appl. 545,181, 09 June 1993, Appl. 03 Dec 1991, to BASF A.-G

G. Holden, E.T. Bishop, N.R. Legge, in *Proceedings of the International Rubber Conference*, (1967). MacLaren & Sons Pub., London (1968)

G. Holden, L.H. Gouw, European Patent Appl. 004,685, 17 Oct 1979, Appl. 30 Mar 1978, to Shell International Research Maatschappij B. V

K.M. Hong, J. Noolandi, Macromolecules **13**, 964 (1980)

K.M. Hong, J. Noolandi, Macromolecules **14**, 727 (1981a)

K.M. Hong, J. Noolandi, Macromolecules **14**, 736 (1981b)

F. Ide, K. Deguchi, Japan Patent 035,175, 11 Nov 1971, Appl. 1966, to Mitsubishi Rayon Co., Ltd

F. Ide, M. Miura, Ger. Offen. 2,054,719, 24 June 1971, Appl. 7 Nov 1969, to Mitsubishi Rayon Co., Ltd

F. Ide, K. Okano, K. Deguchi, Japan Patent 023,645, 01 July 1972, Appl. 05 June 1968; 030,098, 05 Aug 1972, Appl. 1969, to Mitsubishi Rayon Co. Ltd

T. Inoue, T. Soen, T. Hashimoto, H. Kawai, J. Polym. Sci. Part A-2 **7**, 1283 (1969)

S. Ishida, J. Masamoto, Japan Patent 018,144, 18 Feb 1974, Appl. 13 June 1972; Japan Patent 040,346, 15 Apr 1974, Appl. 28 Aug 1972, to Asahi Chemical Industry Company, Limited

J. Janicki, A. Wlochowicz, S. Rabek, Acta Polym. **37**, 229 (1986)

K.J. Jeon, R.J. Roe, Macromolecules **27**, 2439 (1994)

M. Jiang, X. Huang, T. Yu, Polymer **26**, 1689 (1985)

W.H. Jo, H.C. Kim, D.H. Baik, Macromolecules **24**, 2231 (1991)

W.H. Jo, B.C. Jo, J.C. Cho, J. Polym. Sci. Polym. Phys. Ed. **32**, 1661 (1994a)

W.H. Jo, J.Y. Kim, M.S. Lee, Polym. J. **26**, 465 (1994b)

J.F. Joanny, L. Leibler, J. Phys. (Paris) **39**, 951 (1978)

W.J. Jones, R.A. Mendelson, European Patent Appl. 135,492, 27 Mar 1985, U S. Appl. 1983, to Monsanto Company

H.-W. Kammer, Z. Phys. Chem. Leipz. **258**, 1149 (1977)

D.J. Kinning, E.L. Thomas, L.J. Fetters, J. Chem. Phys. **90**, 5806 (1990)

D.J. Kinning, E.L. Thomas, L.J. Fetters, Macromolecules **24**, 3893 (1991)

H. Kojima, A. Taoka, K. Takiguchi, Japan Patent 027,905, 11 Sep 1970, Appl. 10 Apr 1963, to Mitsubishi Monsanto Chem. Ind. Co., Ltd

S.N. Koklas, N.K. Kalfoglou, Polymer **35**, 1433 (1994)

S. Krause, Macromolecules **13**, 1602 (1980)

H.J. Kress, C. Lindner, L. Morbitzer, H. Peters, K.H. Ott, J. Schoeps, Ger. Offen. 3,514,185, 23 Oct 1986; U.S. Patent 4,683,265, Appl. 19 Apr 1985, to Bayer A.-G

R.E. Lavengood, R. Patel, A.R. Padwa, U.S. Patent 4,777,211, 11 Oct 1988, App. 09 July 1985, to Monsanto Company

G.F. Lee Jr., U.S. Patent 4,123,410, 31 Oct 1978, Appl. 30 Sep 1977; U.S. Patent 4,128,602; 4,128,603; 4,128,604; 05 Dec 1978, Appl. 24 Apr 1970, to General Electric Company

L. Leibler, Macromolecules **13**, 1602 (1980)

L. Leibler, Makromol. Chem. Macromol. Symp. **16**, 1 (1988)

L. Leibler, H. Orland, J.C. Wheeler, J. Chem. Phys. **79**, 3550 (1983)

J.C. Lepers, B.D. Favis, AIChE J. **45**, 887 (1999)

P.Y. Liu, H.F. Giles Jr., U.S. Patent 4,629,760, 16 Dec 1986, Appl. 1985, to General Electric Company

B. Lowenhaupt, G.P. Hellmann, Colloid Polym. Sci. **268**, 885 (1990)

B. Lowenhaupt, G.P. Hellmann, Polymer **32**, 1065 (1991)

B. Lowenhaupt, G.P. Hellmann, Colloid Polym. Sci. **272**, 121 (1994)

B. Lowenhaupt, A. Steurer, G.P. Hellmann, Y. Gallot, Macromolecules **27**, 908 (1994)

A. Luciani, M.F. Champagne, L.A. Utracki, Polym. Netw. Blends **6**, 41 (1996)

A. Luciani, M.F. Champagne, L.A. Utracki, J. Polym. Sci. Polym. Phys. Ed. **35**, 1393 (1997)

A. Luciani, M.F. Champagne, L.A. Utracki, Macromol. Symp. **126**, 30–37 (1998)

F.J. Martinez-Veracoechea, F.A. Escobedo, Macromolecules **42**, 1775 (2009)

E. Martuscelli, Polym. Eng. Sci. **24**, 563 (1984)

M. Matos, Master thesis, Ecole Polytechnique de Montréal, 1993

Y. Matsushita, K. Mori, R. Saguchi, Y. Naka, I. Noda, M. Nagasawa, Macromolecules **23**, 4313 (1990)

D. Meghala, C. Ranganathaiah, Polymer **53**, 850 (2012)

D.J. Meir, J. Polym. Sci. Part C **26**, 81 (1969)

D.J. Meir, in *Thermoplastic Elastomers*, ed. by N.R. Legge, G. Holden, H.E. Schroeder (Hanser Pub, Munich, 1987)

J.M. Michel, French Patent 1,566,235, 09 May 1969; Ger. Offen. 1,900,978, 04 Sep 1969; 1,906,747, 18 Sep 1969, Appl. 1968, to Pechiney-Saint Gobain

H.S. Moon, B.K. Ryoo, J.K. Park, J. Polym. Sci. Polym. Phys. Ed. **32**, 1427 (1994)

A. Mukohyama, International Patent Appl. 08,233, 29 Apr 1993, Appl. 15 Oct 1991, to E. I. du Pont de Nemours & Company

M. Muller, K. Binder, Macromol. Symp. **159**, 97 (2000)

V.M. Nadkarni, J.P. Jog, in *Two-Phase Polymer Systems*, ed. by L.A. Utracki (Hanser Verlag, Munich, 1991)

K.M. Natarajan, P. Arjunan, D. Elwood, European Patent Appl. 540,120, 05 May 1993; U.S. Patent 5,296,550, 22 Mar 1994, Appl. 01 Nov 1991, to Enichem S.p.A

T. Nishio, Y. Suzuki, K. Kojima, M. Kakugo, Kobunshi Robunshu **47**, 331 (1990)

J. Noolandi, Polym. Eng. Sci. **24**, 70 (1984)

J. Noolandi, Ber. Bunsenges. Phys. Chem. **89**, 1147 (1985)

T. Nose, Polym. J. **29**, 218 (1997)

T. Ohta, K. Kawasaki, Macromolecules **19**, 2621 (1986)

M. Okamoto, T. Inoue, Polym. Eng. Sci. **33**, 175 (1993)

M. Olvera de la Cruz, I. Sanchez, Macromolecules **19**, 2501 (1986)

Y. Orikasa, S. Sakazume, European Patent Appl. 361,400, 04 Apr 1990, Appl. 1988; European Patent Appl. 506,006, 30 Sep 1992; U.S. Patent 5,296,538, 22 Mar 1994, Appl. 25 Mar 1991, to Nippon Petrochemicals Company, Limited, and Nippon Oil Fats Company, Limited

T. Ouhadi, R. Fayt, R. Jerôme, P. Teyssié, J. Appl. Polym. Sci. **32**, 5647 (1986)

J.N. Owens, I.S. Gancarz, J.T. Koberstein, T.P. Russel, Macromolecules **22**, 3380 (1989a)

J.N. Owens, I.S. Gancarz, J.T. Koberstein, T.P. Russel, Macromolecules **22**, 3388 (1989b)

M. Pakravan Lonbani, M.-C. Heuzey, A. Ajji, Macromolecules **45**, 7621 (2012)

C.E. Parks, G.B. Jennings, U.S. Patent 2,753,322, 03 July, 1956, to Monsanto Chemical Company

H.T. Patterson, K.H. Hu, T.H. Grindstaff, J. Polym. Sci. Part C **34**, 31 (1971)

D.R. Paul, S. Newman, in *Polymer Blends*, ed. by D.R. Paul, S. Newman (Academic Press, New York, 1978)

P. Perrin, R.E. Prud'homme, Macromolecules **27**, 1852 (1994)

B. Ptaszynski, P.J. Teyssié, A. Skoulios, Makromol. Chem. **176**, 3483 (1975)

R.P. Quirk, J.-J. Ma, C.C. Chen, K. Min, J. L. White, Contemporary topics in Polymer science, vol. 6, Multiphase Macromolacular systems, 107 (1989)

P. Ramya, C. Ranganathaiah, J. Appl. Polym. Sci. **127**, 190 (2013)

L. Rayleigh, Proc. R. Soc. **29**, 71 (1879)

H. Retsos, I. Margiolaki, A. Messaritaki, S.H. Anastasiadis, Macromolecules **34**, 5295 (2001)

H. Retsos, S.H. Anastasiadis, S. Pispas, J.W. Mays, N. Hadjichristidis, Macromolecules **37**, 524 (2004)

B.J. Reynolds, M.L. Ruegg, N.P. Balsara, C.J. Radke, T.D. Shaffer, M.Y. Lin, K.R. Shull, D.J. Lohse, Macromolecules **37**, 7401 (2004)

Y. Rharbi, M.A. Winnik, Macromolecules **34**, 5238 (2001)

R.W. Richars, J.L. Thomason, Polymer **24**, 1089 (1983)

G. Riess, J. Kohler, C. Tournut, A. Banderet, Makromol. Chem. **101**, 58 (1967)

D. Rigby, R.J. Roe, Macromolecules **17**, 1778 (1984)

D. Rigby, R.J. Roe, Macromolecules **19**, 721 (1986)

L.M. Robeson, PCT Int. Appl. 000,220, 14 Jan 1988, Appl. 1986, to Amoco Corporation

R.J. Roe, J. Chem. Phys. **62**, 490 (1975)

R.J. Roe, M. Fishkis, J.C. Chang, Macromolecules **14**, 1091 (1981)

B. Rudolf, T. Ougizawa, T. Inoue, Macromol. Theory Simul. **7**, 1 (1998)

T.P. Russel, A. Menele, W.A. Hamilton, G.S. Smith, S.K. Satija, C.F. Majkrzak, Macromolecules **24**, 5721 (1991a)

T.P. Russel, S.H. Anastasiadis, A. Menelle, G.P. Felcher, S.K. Satija, Macromolecules **24**, 1575 (1991b)

T. Sakai, Polymer **6**, 59 (1965)

P. Sakellariou, G.C. Eastmond, I.S. Miles, Polymer **32**, 2351 (1991)

O.O. Santana, A.J. Müller, Polym. Bull. **32**, 471 (1994)

M. Schreck, A. Winter, V. Dolle, H. Kondoch, M. Antberg, J. Rohrmann, U.S. Patent 5,322,902, 21 June 1994, Appl. 19 Dec 1990, German Appl. 21 Dec 1989, to Hoechst A.-G

S. Seelert, P. Klaerner, A. Jung, H. Hoenl, B. Ostermayer, Ger. Pat. 4139627, 03 Jun 1993, Appl. 30 Nov 1991, to BASF A.-G

J. Selb, P. Marie, A. Rameau, R. Duplessix, Y. Gallot, Polym. Bull. **10**, 444 (1983)

K. Shimomai, N. Higashida, T. Oujizawa et al., Polymer **37**, 5877 (1996)

K.R. Shull, E.J. Kramer, G. Hadziioannou, W. Tang, Macromolecules **24**, 2748 (1991)

I. Sigillo, L. di Santo, S. Guido, N. Grizzuti, Polym. Eng. Sci. **37**, 1540 (1997)

R.J. Signer, K.F. Beal, U.S. Patent 2,658,050, 03 Nov 1953, to Visking Corp

D.F. Siqueira, S.P. Nunes, Polymer **35**, 490 (1994)

A. Skoulios, P. Helfter, Y. Gallot, J. Selb, Makromol. Chem. **148**, 105 (1971)

R.J. Spontak, J.M. Zielinski, Macromolecules **26**, 396 (1993)

R.J. Spontak, S.D. Smith, A. Ashraf, Polymer **34**, 2233 (1993)

K.R. Srinivasan, A.K. Gupta, J. Appl. Polym. Sci. **53**, 1 (1994)

R. Stadler, C. Auschra, J. Beckmann, U. Knappe, I. Voigt-Martin, L. Leibler, Macromolecules **28**, 3080 (1995)

S. Sugden, J. Chem. Sci. **125**, 1117 (1924)

S.B. Swartzmiller, R.J. Donald, J.E. Bonekamp, PCT Int. Appl. 013,168, 08 Jul 1993; U. S. Patent 5,334,657, 02 Aug 1994, Appl. 18 Dec 1992, Appl. 20 Dec 1991, to Dow Chemical Company

H. Tanaka, S. Futamura, K. Kato, Japan Patent 001,866; 001,868, 18 Jan 1971, Appl. 28 Dec 1966, to Japanese Geon Co., Ltd

H. Tanaka, H. Hasegawa, T. Hashimoto, Macromolecules **24**, 240 (1991)

T. Tang, B. Huang, Polymer **35**, 281 (1994)

J.W. Teh, A. Rudin, J.C. Keung, Adv. Polym. Technol. **13**, 1 (1994)

Y. Thomann, R. Thomann, A. Hasenhindl, R. Mulhaupt, B. Heck, K. Knoll, H. Steininger, K. Saalwachter, Macromolecules **42**, 5684 (2009)

A. Todo, K. Miyoshi, T. Hashimoto, H. Kawai, Polym. Eng. Sci. **17**, 587 (1977)

A. Todo, T. Hashimoto, H. Kawai, J. Appl. Crystallogr. **11**, 558 (1978)

S. Tomotika, Proc. R. Soc. **A150**, 322 (1935)

S. Tomotika, Proc. R. Soc. **A153**, 302 (1936)

K. Ueno, T. Maruyama, European Patent Appl. 024,120, 25 Feb 1981, Appl. 08 Aug 1979; U.S. Patent 4,315,086, 09 Feb 1982, App. 16 Jul 1980, to Sumitomo Chemical Co., Ltd

L.A. Utracki, *Polymer Alloys and Blends* (Hanser Pub, Munich, 1989)

L.A. Utracki (ed.), *Encyclopaedic Dictionary of Commercial Polymer Blends* (ChemTec Pub, Toronto, 1994)

L.A. Utracki, *Commercial Polymer Blends* (Chapman and Hall, London, 1997)

L.A. Utracki, Z.H. Shi, Polym. Eng. Sci. **32**, 1824 (1992)

B.W. Van Krevelen, *Properties of Polymers*, 2nd edn. (Elsevier, Amsterdam, 1976)

T.A. Vilgis, J. Noolandi, Makromol. Chem. Makromol. Symp. **16**, 225–234 (1988)

B. Vonnegut, Rev. Sci. Instrum. **13**, 6 (1942)

C. Wei-Berk, Am. Chem. Soc. Polym. Mater. Sci. Eng. **68**, 299 (1993)

W. Wening, H.-W. Fiedel, A. Scholl, Colloid Polym. Sci. **268**, 528 (1990)

M.D. Whitmore, J. Noolandi, Macromolecules **18**, 657 (1985). 2486

R.C. Willemse, A.P. de Boer, J. van Dam, A.D. Gotsis, Polymer **40**, 827 (1999)

K.I. Winey, E.L. Thomas, L.J. Fetters, Macromolecules **24**, 6182 (1991)

Wlochowicz and Janicki, J. Appl. Ppolym. Sci. **38**, 1469 (1989)

S. Wu, J. Makromol. Sci. Macromol. Chem. **10**, 1 (1974)

S. Wu, *Polymer Interface and Adhesion* (Marcel Dekker, New York, 1982)

S. Wu, Polym. Eng. Sci. **27**, 225 (1987)

S.F. Xavier, in *Two-Phase Polymer Systems*, ed. by L.A. Utracki (Hanser Verlag, Munich, 1991)

P.X. Xing, M. Bousmina, D. Rodrigue, M.R. Kamal, Macromolecules **33**, 8020 (2000)

I. Yamazaki, T. Fujimaki, Japan Patent 007,627, 03 Mar 1970, Appl. 24 Dec 1969; 007,141, 29 Feb 1972, Appl. 26 Nov 1969, to Showa Denko K.K

J. Yang, J.P. Lu, Y. Rharbi, L. Cao, M.A. Winnik, Y.M. Zhang, U.B. Wiesner, Macromolecules **36**, 4485 (2003)

K. Yasue, T. Marutani, Y. Fukushima, T. Ida, European Patent Appl. 301,663, 01 Feb 1989, Appl. 26 July 1988, Jap. Appl. 1987, to Stamicarbon B. V

J.B. Yates III, PCT Int. Appl. 005,311, 11 Sep 1987; European Patent Appl. 303,077, 15 Feb 1989; European Patent Appl. 550,208, 07 Jul 1993; European Patent Appl. 550,210, 07 July 1993, Appl. 31 Dec 1991, to General Electric Company

C. Yeung, A.C. Shi, Macromolecules **32**, 3637 (1999)

O. Yuichi, S. Suehiro, European Patent Appl. 304,041, 22 Feb 1989, Appl. 17 Aug 1988, Jap. Appl. 1987, to Nippon Petrochemicals Company, Limited

S. Yukioka, T. Inoue, Polym. Commun. **32**, 17 (1991)

S. Yukioka, T. Inoue, Polymer **35**, 1183 (1994)

W.C. Zin, R.J. Roe, Macromolecules **17**, 183 (1984)

Reactive Compatibilization

<div style="text-align:right">5</div>

S. Bruce Brown

Contents

Formerly with Polymer Materials Laboratory, General Electric Co. Global Research Center,
Schenectady, New York 12309

S.B. Brown
Hill Country Patent Services, Inc, Austin, TX, USA
e-mail: hcpatents@earthlink.net

5.1   Introduction

Reactive compatibilization of immiscible polymer blends by in situ copolymer formation is reviewed using approximately 1,100 examples taken from both journal articles and patents. Selected references in English through approximately 2013 to early 2014 are included. Important chemical reactions are illustrated which are useful for copolymer formation across a melt-phase boundary during melt processing of the immiscible blends. Focus is on irreversible chemical reactions taking place within typical extrusion residence times for polymer processing. Examples of block, graft, cross-linked, and degradative copolymer formation are shown. The illustrated chemical reactions and processes are also generally useful for compatibilization of immiscible polymer blends either not illustrated or not yet conceived.

Commercial polymer products are frequently derived from blending two or more polymers to achieve a favorable balance of physical properties. As described in ▶ Chap. 2, "Thermodynamics of Polymer Blends" in this handbook, from the thermodynamic point of view, there are two basic types of polymer blends: miscible and immiscible. The vast majority of polymer pairs are immiscible. There are only a few commercially important polymer blends based on miscible or partially miscible (i.e., miscible within a low range of concentration) polymer pairs. It is seldom possible to mix two or more polymers and create a blend with useful properties. Instead, when preparing a new polymer blend from immiscible resins, it is necessary to devise a specific strategy for compatibilizing the mixture to provide for optimum physical performance and long-term stability. Although there do exist a very small number of commercial blends of immiscible polymers that are not compatibilized, most commercially available blends of immiscible polymers have been compatibilized by some specific mechanism.

The majority of polymer blends containing elastomeric, thermoplastic, and/or liquid crystalline polymers are processed by melt extrusion at some point in their history. After melt extrusion with intensive mixing, the morphology of an immiscible polymer blend on a microscopic scale will often consist of a dispersed phase of the more viscous polymer in a continuous matrix of the less viscous polymer (depending upon the relative amounts and viscosities of the two polymers in the blend). A good analogy from everyday experience is a dispersed mixture of viscous oil droplets in an immiscible water matrix.

The formation of optimum dispersed phase particle size and the long-term stabilization of the resulting blend morphology are critical if the blend is to have optimum properties and in particular good mechanical properties. If this

morphology is not stabilized, then the dispersed phase may coalesce during any subsequent heat and/or high stress treatment, such as injection molding. Coalescence may result in gross-phase segregation of the two polymers and delamination on a macroscopic scale and/or brittleness or poor surface appearance in the final molded part. Good analogies from everyday experience would be the separation on standing of a not stabilized oil-in-water dispersion into two separate liquid phases. Therefore, an important aspect of all compatibilization strategies is the promotion of morphology stabilization. Morphology stabilization may be provided by sufficient interfacial adhesion and/or lowered interfacial tension between the two polymer phases.

Of the various compatibilization strategies that have been devised, an increasingly common method is either to add a block, graft, or cross-linked copolymer of the two (or more) separate polymers in the blend or to form such copolymers through covalent or ionic bond formation in situ during a reactive compatibilization step. The first of these methods was described in ▶ Chap. 4, "Interphase and Compatibilization by Addition of a Compatibilizer," in this handbook, while the second method is the topic of this chapter.

The said copolymer can reside at the interface between the dispersed and matrix phases, acting as an emulsifying agent that effectively stabilizes the dispersed phase particles against coalescence and providing interfacial adhesion between dispersed and continuous phases in the solid state. In this manner such a copolymer can both promote optimum dispersed phase particle size formation during compounding and prevent phase coalescence of the dispersed phase during any subsequent heat treatment and/or high stress processes. Again, the analogy from everyday experience is the addition of a soap or other emulsifying agent to stabilize an oil-in-water emulsion. Often, as little as 0.5–2.0 wt% copolymer is sufficient to achieve morphology stabilization of an immiscible polymer blend. However, frequently higher amounts, for example, as much as 10–20 wt% copolymer, may be necessary to obtain optimum physical properties of the blend, e.g., impact strength.

The majority of commercially important, immiscible polymer blends rely for compatibilization on the presence of a copolymer of the blended polymers. However, such a copolymer is almost never synthesized in a separate step and then added as a distinct entity to the blend of immiscible polymers. Instead, a compatibilizing copolymer is most economically formed simultaneously with generation of morphology during extrusion processing, a process referred to as reactive compatibilization. The reactive compatibilization process is logically a subcategory of the broader class of interchain copolymer formation reactions performed by reactive extrusion (Brown 1992a), because there are other commercial reasons for preparing copolymers of immiscible polymers aside from using them as in situ generated compatibilizing agents for immiscible blends.

Copolymer formation by reactive compatibilization is a *heterogeneous reaction taking place across a melt-phase boundary*. Often this process occurs by direct reaction between chemical functionalities on some fraction of each of the two

polymers. In some cases a third reactive species may be added to the blend to promote copolymer formation by one of several mechanisms.

Reactive compatibilization has at least two advantages:

1. First, the compatibilizing copolymer is automatically formed at the interface between the two immiscible polymers where it is needed to stabilize morphology. In contrast, when a compatibilizing copolymer is added as a separate entity to a polymer blend, it must diffuse to the polymer-polymer interface to be effective for promoting morphology stabilization and interfacial adhesion between dispersed and continuous phases. However, that added copolymer may prefer to self-associate in micelles and form a separate phase that is useless for compatibilization.

2. A second advantage of in situ copolymer formation is that the molecular weight of each of the two distinct polymeric segments in the copolymer is usually the same as that of the individual bulk polymer phase in which the segment must dissolve. Even approximate molecular weight matching between copolymer segment and bulk phase can result in optimum copolymer/bulk phase interaction for maximum interfacial adhesion. See, for example, Jiao et al. (1999).

5.2   Purpose

Only a relatively small number of chemical reactions have been devised to form a compatibilizing copolymer during extrusion processing. Therefore, a purpose of this chapter is to identify these different chemical reactions and give selected examples illustrating their scope to form block, graft, or cross-linked copolymers as compatibilizers for immiscible polymer blends. The emphasis is on copolymer formation during melt reaction occurring during development of morphology. With few exceptions, the examples are limited to processes that require mixing in the molten state. This includes processes run in single-screw or twin-screw extruders, or similar continuous or semicontinuous processing equipment, as well as in batch mixers.

The references in this review include both journal articles and selected published or issued patents. A large number of reactive compatibilization examples are found in industrial research and are documented mostly in patents. Patent references are included in this chapter if they reveal a novel compatibilization strategy apparently not otherwise documented until later in the journal literature. Numerous examples of industrial compatibilization methods have also been provided in a book based on the patent literature (Utracki 1998).

It is not the purpose of this chapter to describe "compatibilization" of layers of immiscible polymers in laminates. Strategies similar to those used to compatibilize intimately mixed polymer blends have also been used to prepare stable laminates, and in those cases, where a chemical reaction takes place between laminate layers, similar types of chemical reaction have been used.

Nevertheless, laminate macroscopic morphology is essentially fixed, and formation of stable laminates is better treated as an adhesion problem. Similarly, composite compositions which may comprise a blend of one or more functionalized polymers with a second, less tractable component such as starch, lignin, clay, silica, POSS, carbon nanotubes, etc. are outside the scope of this chapter.

It is also not the purpose of this chapter to summarize examples of "compatible" polymer blends formed in a solution step involving dissolution of the polymer components, whether or not a chemical reaction takes place between them. In some cases, particularly when no reaction takes place, such blends are only "pseudo-stable," since they may not have been processed above the Tg of one or both of the polymer components. Also, mixing in solution followed by devolatilization is rarely economical for practice in industry, particularly since many commercially important compatibilized polymer blends comprise at least one semicrystalline component (e.g., PA) which is poorly soluble in common solvents. There are included in the Tables a small number of examples of solution blended polymer blends when these complement similar examples prepared by melt processing.

It is also not the purpose of this chapter to describe examples of compatibilized polymer blends formed by polymerization of a monomer in the presence of a second polymer. In these cases, the growing polymer chain may react with functionality on the second polymer to form a certain fraction of compatibilizing copolymer.

The coverage of this chapter is arranged by binary polymer *Blend Type*, in alphabetical order of the first polymeric component. Thus, "polyamide blend" is the first category discussed herein. Subcategories within each Blend Type category are arranged by the specific chemical reactions that have been described in the literature for reactive compatibilization processes.

The emphasis is on illustrating the scope of these particular reactions and not on presenting every known example of a particular compatibilization strategy. For example, polyamide-polyolefin (PA-PO) blends compatibilized by reaction of PA amine end-groups with anhydride-functionalized PO have been studied in hundreds of different published examples, as have immiscible pairs of polyesters (or polycarbonate) compatibilized by transesterification reactions and polyester-polyolefin blends compatibilized using anhydride-grafted PO. Although these studies contribute to understanding the physics and property optimization of such blends, the underlying chemistry is basically the same in each case, and limitations of space preclude comprehensively listing all such examples. It should also be noted that many published studies listed herein actually represent a series of papers or patents. In some cases, only one paper or patent in the series is referenced. Also included in this chapter are some examples of blends which illustrate simple copolymer formation between two functionalized polymers although a corresponding blend with either of the unfunctionalized polymers is not exemplified, because it is

perfectly possible that the said copolymer could be a compatibilizer in corresponding blends with one or both unfunctionalized polymers.

5.3   Definitions of Compatibilization and Polymer Alloys

As defined in the appendix "Dictionary of Terms Used in Polymer Science and Technology" in this handbook, compatibilization means "A process of modification of interfacial properties of an immiscible polymer blend, leading to creation of polymer alloy." A polymer alloy in turn is defined as "An immiscible polymer blend having a modified interface and/or morphology," whereas a polymer blend is simply "A mixture of at least two polymers or copolymers." In other words, all polymer alloys are blends, but not all polymer blends are alloys. A somewhat more elaborate definition of a polymer alloy would describe a blend of at least two immiscible polymers stabilized either by covalent bond or ionic bond formation between phases or by attractive intermolecular interaction, e.g., dipole-dipole, ion-dipole, charge-transfer, hydrogen-bonding, van der Waals forces, etc. Only stabilization by covalent bond formation or ionic association (including acid-base and ion-neutral donor group interaction) is covered in this chapter.

 Thermodynamic compatibility describes a miscible polymer blend that displays a single glass transition temperature, Tg, within the full range of composition of the two polymers. For the purposes of this chapter, we will be more concerned with *Technological Compatibility*. This term describes a polymer blend that does not separate into its individual components and does not lose useful technological properties over the expected lifetime of a molded part (which has been estimated by the Society of Plastics Engineers to be about 10 years) (Gaylord 1989; Rudin 1982). Taking a somewhat different view, Coran and Patel have defined compatibilization as a process for improving ultimate properties by making polymers in a blend less incompatible (Coran and Patel 1983b).

5.4   Types of Polymer Blends

The market for commercial polymer blends has grown steadily over the past four decades. A recent estimate of the polymer alloy/blend market by volume for 2012 was about 2.2 billion pounds. The market was projected to grow to about 2.6 billion pounds by 2018 (BCC Research 2013). The principal markets for all blends include the automotive industry; phone, computer, and other business machine housings; electrical components such as connectors; appliances; consumer products; recreational equipment; and construction and industrial applications.

 Commercial activity is mirrored by technological activity. It was estimated that roughly 87,000 patents appeared worldwide on all aspects of polymer blends between 1970 and 1987 averaging almost 5,000 patents per year (Juliano 1988). The pace appears to have slowed little since then although the emphasis has
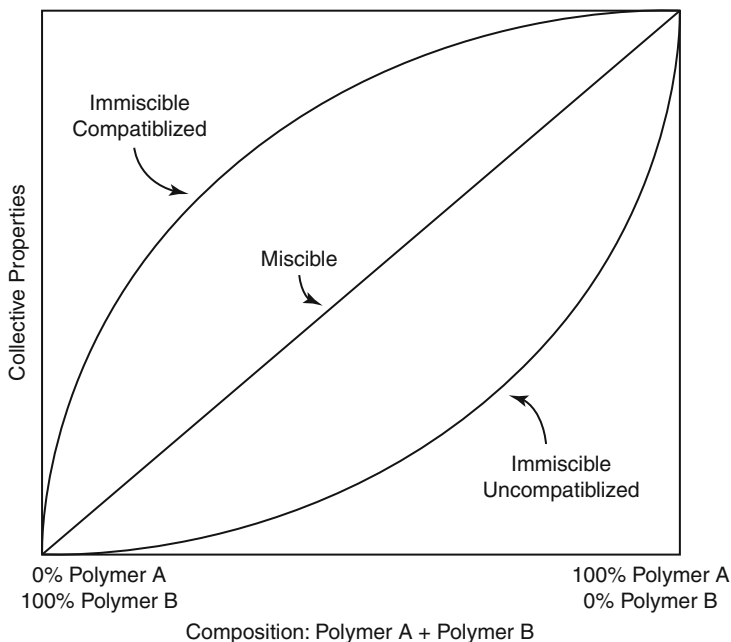
Fig. 5.1 Potential effect on polymer blend properties as component concentration changes

changed from simple blends (e.g., binary blends with additives) to more complex compositions for specialty applications.

Common polymer blend building blocks arranged in a hierarchy of price and performance are shown in Fig. 19.2 of ▶ Chap. 19, "Commercial Polymer Blends" in this handbook. As the price gets higher, one is typically paying for higher heat stability and higher modulus. High performance thermoplastics such as PPS, PEI, and LCP and engineering thermoplastics such as PPE, PBT, and PC have high heat stability and are often designed to take the place of metals in typical applications. Lower modulus, commodity plastics such as PE, EPDM, and modified styrenics have lower heat stability and are often used in applications requiring high flexibility.

The goal of combining two or more polymers such as polymer pairs from those categories described above (e.g., an engineering thermoplastic plus a commodity polyolefin) is to achieve in the blend a combination of favorable properties from each polymer. Figure 5.1 shows idealized expected properties from blending two polymers that are either miscible (straight center line), immiscible and uncompatibilized (curved bottom line), or immiscible and compatibilized (curved top line). In the case of polymers that are miscible in all proportions, one can only hope to obtain in their blend an average of their physical properties depending upon the proportion of each polymer present. In a common example, the Tg of a miscible blend will vary linearly from that of the lower Tg polymer to that of the higher Tg polymer as the higher Tg polymer increases in proportion in the blend.

When two immiscible polymers are blended without compatibilization, one generally obtains a mixture with physical properties worse than those of either individual polymer. Usually such a blend has poor structural integrity and poor heat stability since there is no mechanism for stabilizing a dispersion of one polymer in a matrix of the other. On a macroscopic scale, the blend may appear heterogeneous and in the extreme case grossly delaminated, e.g., in a molded part.

When two immiscible polymers are blended with compatibilization, one may expect a synergistic combination of properties derived from each polymer. A common example is a blend of a thermoplastic (to provide high heat stability) with an immiscible, rubbery impact modifier (to provide impact resistance), e.g., a rubber-toughened PA. A second common example is a blend of a semicrystalline thermoplastic with an amorphous thermoplastic. Because of their semicrystalline nature, polymers such as PA, PBT, PPS, or PP often have high chemical solvent resistance but low ductility, low dimensional stability, and low Tg. In contrast, amorphous polymers such as PPE, PEI, PC, and PE typically have poor solvent resistance and stress crack sensitivity but higher ductility, dimensional stability, and Tg. Often a binary blend includes a third, lower modulus polymer to provide optimum impact strength. A good example is a rubber-toughened blend of PPE with PA. In commercial examples, PPE and PA are combined in amounts such that PPE is the dispersed phase and PA is the continuous, matrix phase so that the blend possesses adequate solvent resistance (e.g., to common solvents used in automotive applications) but also higher heat stability compared to unmodified PA. Again, because of its inherent solvent resistance, this type of blend is prepared by melt processing and cannot economically be prepared by combining the components in solution.

Quite generally, the goal in preparing any polymer blend is to obtain one or all of the following benefits: higher heat distortion temperature (HDT), improved variable temperature impact resistance, solvent resistance, dimensional tolerance, higher flow, utilization of recycle/regrind, and lower cost.

5.5   Characteristics of Immiscible Polymer Blends

The general characteristics of immiscible polymer blends have been described in a large number of references (e.g., many of those listed in Sect. 5.6 on "General Stractegies for Compatibilization of Immiscible Polymer Blends"). Commercial polymer blends are most often prepared by some form of processing in a molten state, usually extrusion. Among the factors that determine which polymer will be the dispersed phase and the continuous matrix are the relative volume proportions and relative viscosities of the two polymers. During intensive mixing in a twin-screw or single-screw extruder, the less viscous molten polymer in a simple 1:1 mixture of two polymers will form an easily deformable matrix, while the more viscous polymer will form a difficultly deformable dispersed phase. Generally, the more viscous polymer will form the dispersed phase even in some cases when it represents more than 50 vol% of the blend.
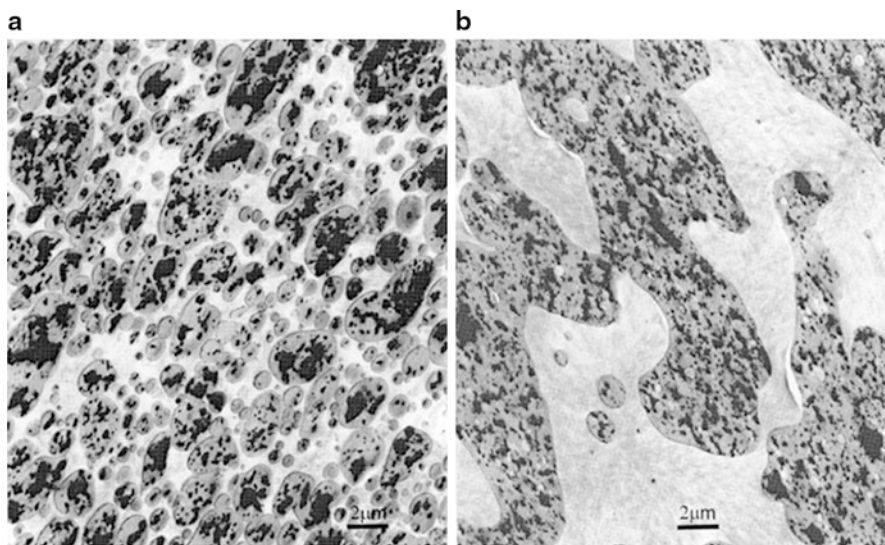
Fig. 5.2 Morphology of PPE dispersed phase in a PBT matrix (**a**) as extruded and (**b**) after molding

Blend properties depend strongly on which polymer is the continuous phase. The majority of commercially important compatibilized blends of semicrystalline polymers with amorphous polymers are prepared in compositions such that the semicrystalline component is the matrix and the amorphous component is the dispersed phase. Such blends show adequate solvent resistance since in this morphology the surface consists largely of the dominant, matrix phase of semicrystalline polymer.

The formation of optimum dispersed phase particle size and the stabilization of the resulting blend morphology are critical if the blend is to have optimum properties and in particular good mechanical properties. Figure 5.2 shows a morphology generated by processing an uncompatibilized blend of PPE dispersed phase in a PBT matrix (Brown, unpublished results, 1988). Figure 5.2a shows that a reasonably uniform dispersion of PPE may be formed simply by suitable degree of mixing during extrusion. Figure 5.2b, however, demonstrates phase coalescence of PPE particles to form large, irregularly shaped islands when the extrudate of the uncompatibilized blend is molded at normal processing temperature. In this blend there is no interfacial adhesion between the two phases and, hence, no mechanism for morphology stabilization. Even in the presence of an impact modifier, the resulting molded parts are quite brittle since there are no uniform dispersed phase particles of proper size to dissipate impact energy.

Table 5.1 shows further examples of dispersed phase coalescence in blends of PA as the dispersed phase in a less viscous PE or PS matrix. The data show that the mean PA particle size increases dramatically with simple heating under static conditions in the absence of any mechanism for morphology stabilization. The same coalescence can occur in molded parts of uncompatibilized polymer blends

Table 5.1 Change of dispersed phase dimensions in uncompatibilized polymer blends upon annealing (Adapted from White and Min 1989)

Blend	Mean dimension after annealing (µm)		
	30 min	60 min	90 min
PS/PA-6 (60/40)	90	140	310
LDPE/PA-6 (50/50)	251	314	319
LDPE/PA-11 (50/50)	162	275	303

subjected to further thermal treatment after molding (e.g., in a paint drying oven). The mechanical properties of these blends are quite poor.

In summary, a frequent goal in making a technologically compatible blend of immiscible polymers is to stabilize an appropriate morphology of the dispersed phase polymer in the matrix polymer by promotion of interfacial adhesion and/or by lowering the interfacial tension. These conditions are critical for providing good mechanical properties, toughness, molded part dimensional integrity, and maximum solvent resistance in the blend.

5.6 General Strategies for Compatibilization of Immiscible Polymer Blends

Numerous reviews have been published which discuss general (or specific) aspects of strategies for compatibilization of immiscible polymer blends, including but not limited to those by Fink (2013), Imre and Pukanszky (2013) (bio-based and biodegradable polymer blends including reactive compatibilization), Karaağaç and Deniz (2013) (rubber based blends), Covas et al. (2011), Jiang et al. (2010) (reactive compatibilization), Nwabunma and Kyu (2008) (polyolefin blends), Robeson (2007), Yu et al. (2006) (polymer blends from renewable resources), Feldman (2005), Macosko et al. (2005) (reactive compatibilization), Mangaraj (2005) (recycling ground rubber waste), Harrats and Groeninckx (2004) (reactive compatibilization) Paul (2004) (reactive compatibilization), Platé et al. (2004) (theoretical considerations), Horák et al. (2002), Litmanovich et al. (2002) (theoretical considerations), Baker et al. (2001), Prut and Zelenetskii (2001), Bussink and van de Grampel (2000), Paul and Bucknall (2000), Fakirov (1999) (transreactions in condensation polymers), Shonaike and Simon (1999), Xanthos (1999) (polypropylene), Koning et al. (1998), Robeson et al. (1998) (PVAl-PO blends), Tran-Cong (1998), Al-Malaika (1997), Baranov (1997), Gao et al. (1997) (ionomer blends), Lohse et al. (1997), Datta and Lohse (1996), Utracki and Dumoulin (1995) (polypropylene), Folkes and Hope (1993), Brown (1992a) (reactive compatibilization). Liu and Baker (1992a) (reactive compatibilization), Elmendorf and Van der Vegt (1991), Xanthos and Dagli (1991) (reactive compatibilization), Menges (1989), Utracki (1989, 1998), Brown and Orlando (1988) (reactive compatibilization), Paul et al. (1988), Teyssie et al. (1988), Sperling (1987), Fox and Allen (1985), Solc (1981), Rudin (1980), Paul and Newman (1978), and Bucknall (1977). The basic strategies for compatibilization of two-phase polymer blends can be divided into at least four major categories.

5.6.1   Co-crystallization of Two Phases

This particular strategy is limited to those cases in which an immiscible polymer blend contains two semicrystalline polymers that can co-crystallize. Nadkarni and Jog (1989, 1991) have reviewed examples of this type of compatibilized blend. Co-crystallization may also occur as a secondary process in an intimately mixed blend containing a copolymer resulting in concomitant effects on blend properties as shown in a few of the examples of this review.

5.6.2   In Situ Immobilization of One Phase: Dynamic Vulcanization

In these examples a dispersed phase of a cross-linkable rubber is vulcanized in the presence of a matrix of a second, immiscible, non-vulcanizable polymer during the residence time of melt processing. Examples have also been reported in which a mixture of two vulcanizable polymers has been employed. Coran (1995) has summarized five key requirements for preparing optimum compositions by dynamic vulcanization:

1. Good match between surface energies of the dispersed phase and the matrix
2. Low entanglement molecular length (high entanglement density) of the rubber
3. Crystalline plastic matrix
4. Stable rubber and plastic at blend processing temperatures
5. Availability of appropriate curing system for rubber under desired processing conditions

Coran and others have reviewed work in this area (Coran and Patel 1995, 1996, 2004; Karger-Kocsis 1999; Abdou-Sabet et al. 1996; Coran 1987, 1990, 1995).

Most examples of dynamically vulcanized blends do not involve covalent bond formation between the immiscible phases. However, other work has shown that covalent bond formation between phases in conjunction with dynamic vulcanization of one phase can lead to blends with improved properties in certain cases. This is particularly true in blends where certain of Coran's five key requirements above are not met. Some examples of dynamically vulcanized blends that also feature copolymer formation between the two immiscible phases are summarized in this review under the appropriate categories.

5.6.3   Inclusion of a Third Material as a Compatibilizing Agent

5.6.3.1 Addition of a Separate Compatibilizing Agent

A separate compatibilizing agent included in a blend may be a third material not derived from either of the two immiscible polymers. Representative examples include certain plasticizers, random copolymers, and block copolymers, which may lower the interfacial tension between the two immiscible polymer components.

Table 5.2 Change of dispersed phase dimensions in compatibilized polymer blends upon annealing (Adapted from White and Min 1989)

Blend	Mean dimension after annealing (μm)		
	30 min	60 min	90 min
PS/PA-6/SMA (57/38/5)	4	5	5
PE/PA-6/PP-MA (47/47/5)	5	7	13
PE/PA-11/PP-MA (47/47/5)	5	6	4

Examples also exist where the separate compatibilizing agent is a chemically unreactive *analog* of one (or both) of the two immiscible polymers that has an attractive interaction with each polymer. In any case this is often a semiempirical compatibilization strategy since precedent may be the only basis for choosing an effective compatibilizer. Reviews on addition of this type of compatibilizing agent as a separate component to an immiscible polymer blend have appeared in addition to ▶ Chap. 4, "Interphase and Compatibilization by Addition of a Compatibilizer," in this handbook. They include but are not limited to those listed above in Sect. 5.6 and those by Gaylord (1989), Xanthos (1988), and Paul (1978).

5.6.3.2 Inclusion of a Copolymer of the Two Immiscible Polymers

As stated earlier, a copolymer of the two immiscible polymers themselves would seem to be ideally suited to act as a compatibilizing agent for an immiscible blend. If the copolymer is at the interface of the two phases, then the segments of the copolymer dissolve in the respective bulk phases of the same identity. The copolymer acts as emulsifying agent for the blend resulting in reduced interfacial energy and improved interfacial adhesion.

Table 5.2 shows dramatic examples of the stabilization of dispersed phase morphology in the presence of a compatibilizing copolymer, in these cases formed through reaction of PA amine end-groups with anhydride-functionalized matrix polymer. In all examples, essentially no change in dispersed phase particle size occurs after annealing under static conditions for up to 90 min. The data shown in Table 5.2 should be compared with those presented in Table 5.1, where the dispersed phase mean dimensions were presented for similar, uncompatibilized blends.

There are two basic options for inclusion of a copolymer compatibilizer in a blend of immiscible polymers. First, the copolymer can be synthesized in a separate step followed by addition to the blend. One disadvantage is that this requires a new product synthesis with expensive and time-consuming process development, and, hence, a significant number of years before profitability, since scale of copolymer manufacture will be initially low.

A second and more important disadvantage is that adding the copolymer as a separate species to the blend requires that the copolymer diffuse to the phase interface of the immiscible polymers to be effective as a compatibilizer.

Diffusion to the interface may not be efficient within the residence time of a typical extrusion blending process (usually 2–5 min). In addition, high concentrations of added copolymer may form micelles as a third, distinct phase that does not contribute to compatibilization (see, e.g., Jeon et al. 2005).

A third, potential disadvantage is that for optimum interfacial interaction, a copolymer synthesized in a separate reaction step must have carefully controlled segment lengths to best match the molecular weight of the bulk phase in which the segment must dissolve (see, e.g., Cercle and Favis 2012; see also Gani et al. 2010, for an approach to solving this dilemma). It is often desired to offer for different applications a series of commercial blends containing the same two polymers but with different molecular weights for the polymers in each blend. Any copolymer synthesis process would then have to be capable of producing a series of copolymers with a variety of controlled segment molecular weights for optimum compatibilization efficiency, an economically difficult task.

Commonly, the most economical and efficient process for including a copolymer in a blend of immiscible polymers is to form the copolymer in situ by a chemical reaction during the extrusion process during establishment of the immiscible phase morphology – the process known as reactive compatibilization. In summary the advantages of such a process include:

- The copolymer is made only as needed and a separate copolymer commercialization process need not be developed.
- The copolymer is formed directly at the phase interface where it can serve as a compatibilizer, and no diffusion process dependent on extruder residence time is involved.
- The copolymer, except when formed in a degradative process, typically has segment molecular weights similar to the molecular weights of the bulk phases in which the segments must dissolve, which should promote optimum interaction between copolymer and bulk phases. This also facilitates commercialization of a series of blends containing polymers with quite different molecular weight since the copolymer formed in situ will usually have ideal segment molecular weights.
- A disadvantage of forming copolymer in situ is that such a process often requires that each of the immiscible polymers bear an appropriate chemical functionality for reaction across a melt-phase boundary.

As practiced commercially, reactive compatibilization is a continuous extruder process with material residence time usually 1–5 min. Such a process permits large-scale preparation of a polymer blend as needed ("Just-In-Time" inventory control). Because reactive compatibilization involves a heterogeneous reaction across a phase boundary, the reaction is limited by the interfacial volume available at this phase boundary. Most often, twin-screw extruders (having screw diameter from about 20 to >120 mm) are employed. The screws are designed using an appropriate sequence of screw elements and auxiliary conditions (e.g., subsequent vacuum venting of volatiles) to promote generation of a large interfacial area for the desired chemical reaction to form copolymer.

5.7   Generic Processes and Specific Types of Reactions to Form Copolymer in a Reactive Compatibilization Process

When it is desired to form in situ a compatibilizing graft, block, or cross-linked copolymer, there are at least two distinct *generic* processes available for copolymer formation:

1. *Direct Reaction*, wherein reactive functionalities on each of the two immiscible polymers react with each other across the melt-phase boundary.

2. *Addition of a Third, Reactive Species* to effect or promote copolymer formation. This situation is a typical "three-body" reactive extrusion problem requiring that three chemical species (at least two of which are immiscible) react within the short residence time of extrusion processing. In some cases, the third, reactive species is simply a catalyst that activates functionality on one polymer for reaction with functionality on the second polymer. Such cases produce results similar to the direct reaction process. Frequently, however, the added reactive species is a *coupling agent* capable of reacting with each of the polymers individually (as opposed to reacting with and activating only one of the two polymers). If the coupling agent is preferentially soluble in one of the two phases (e.g., a polar coupling agent in the more polar polymer phase), it may give predominantly homogeneous reaction instead of promoting heterogeneous reaction (copolymer formation) across the melt-phase boundary. Hu et al. (1997) have studied one type of polymer melt reaction (carboxylic acid + epoxide) in which the kinetic efficiency depends upon the partition coefficient of reactant between two immiscible polymer phases. Such considerations must be applied to all reactive compatibilization processes involving three or more reactive species. Coupling agents are further discussed herein below.

As subcategories of the two generic processes, there are at least five *specific* processes for achieving interchain copolymer formation between two polymers during reactive compatibilization in an extruder. The following sections and their accompanying tables show these five processes starting with two idealized homopolymers, one derived from monomer "A" with structure AAAAAAAA and the other derived from monomer "B" with structure BBBBBBBB. Each process produces a specific type of copolymer compatibilizing agent by particular types of chemical reactions.

5.7.1   Compatibilization by a Redistribution Reaction to Produce Block and Random Copolymer: Reaction Type #1

As summarized in Table 5.3, redistribution reactions (often referred to as "transreactions") occur by chemical interchange of block segments of one polymer chain for corresponding segments of a second polymer chain. Such reactions may be homogeneous (self-reaction) or heterogeneous. In the homogeneous case, the molecular weight distribution of a polymer may reach equilibrium. In the heterogeneous case, redistribution reactions can form a copolymer between two

Table 5.3 Redistribution reaction ("transreaction") to form block and random copolymer (Adapted from Brown 1992a)

Reaction type	Characteristics	Type of copolymer obtained
1a	By reactive end-groups of one polymer attacking main chain of second polymer	**AAAAABBBBB + AABBBBBAAA + AABBAAABBB + BBB + BB, etc.**
1b	By chain cleavage/recombination involving each polymer	**(Same as from 1a)**
Summary of characteristics		
In theory all the chains of each polymer participate in the redistribution reaction. The reacting polymers can be diluted with different, nonreactive polymers. In process (a), the extent of reaction depends on concentration of reactive end-groups		
In processes (a) and (b), the initial reaction product is a block copolymer, which is often an effective compatibilizer. Further reaction leads to random copolymer with loss of phase integrity and loss of properties associated with uniform sequence distribution of each polymer (e.g., crystallinity)		
The reaction may be catalyzed. Preferably, the catalyst is one that may be easily quenched or thermally degraded before a significant amount of the random copolymer is formed		

different polymers. This type of reaction is typically dependent upon reaction time and temperature and is not often used to form polymer alloys in a reactive compatibilization process because the time for forming a stable compatibilizing copolymer may be longer than a typical extrusion process time.

Redistribution reactions can occur by several different mechanisms. In one common example, nucleophilic end-groups of one polymer react with electrophilic linkages in the main chain of a second polymer resulting in chain cleavage (e.g., acidolysis or alcoholysis). The initial product is a block copolymer of the two polymers along with a lower molecular weight fragment of the second polymer. Since the initial block copolymer can participate in further redistribution reactions, the net product after sufficient time may be a random copolymer. The propensity to form random copolymer is further increased if both polymers have nucleophilic end-groups and also electrophilic linkages in the main chain that can participate in redistribution. Redistribution during thermal processing is also a common self-reaction in condensation polymers such as PA, PEST, and PC that often contain nucleophilic amine, hydroxy, or phenolic end-groups, along with electrophilic groups such as amide, ester, or carbonate linking the individual monomer units.

In common examples, essentially all of the polymer chains in each of the immiscible polymers are capable of participating in the copolymer-forming reaction by redistribution. This is in contrast to many other processes for in situ copolymer formation where only those few chains bearing reactive functionality participate. Unless the redistribution process is carefully controlled, it is difficult to stop the process to make stable, compatibilized polymer blends. If the reaction is thermally initiated, the blend processing temperatures and residence times must be strictly and reproducibly controlled within narrow limits to achieve reproducible properties. For prolonged reaction times at a temperature above that necessary to initiate the reaction, one may obtain a broad distribution of block lengths and

eventually random copolymer. The random copolymer may not be as efficient a compatibilizer for the immiscible polymer blend as the block copolymer initially formed. More importantly, a high degree of random copolymer formation may destroy desirable properties in the polymer blend such as crystallinity in one of the polymers and, hence, solvent resistance in the final blend. In the extreme case, phase separation is lost and the mixture may become homogeneous and transparent. The problem of controlling the redistribution process does not necessarily stop at the manufacturing stage. After a compatibilized polymer blend leaves the manufacturer, it typically undergoes further thermal histories such as molding or paint-oven drying at the processing facilities of the final user. Continued redistribution reaction in the hands of a final user may cause deterioration and non-reproducibility in blend properties.

When applicable, a common method for controlling a redistribution process is to initiate the reaction with a catalyst. Control may then be achieved by quenching the catalyst at the desired extent of reaction. Certain types of redistribution catalyst may thermally decompose under controlled processing conditions that make quenching unnecessary. In these cases, a predominance of block copolymer may be formed that serves as an effective compatibilizer for an immiscible polymer blend. Just as importantly, only a relatively small fraction of the polymer chains may actually participate in the redistribution process so that phase separation and the properties attributable to the original sequence distribution may be maintained.

The redistribution reaction is a degradative process for making a compatibilizing copolymer. A common feature of all redistribution reactions to form copolymer between two different polymers is that the molecular weight of at least one segment of the initially formed block copolymer is less than that of the bulk polymer phase from which it is derived. Therefore, even when the redistribution process is carefully controlled to give predominantly block copolymer, the copolymer may not be as efficient a compatibilizer as a similar type of block copolymer formed by an end-group/end-group reaction (see herein below). With a low molecular weight block segment, one may have poor penetration into the corresponding bulk polymer phase and less than optimum interfacial adhesion between the immiscible phases with copolymer at the interface. As discussed before, an optimum interfacial adhesion is usually obtained when the segmental molecular weights of the block copolymer are similar to the molecular weights of the individual bulk polymer phases. A general review of "Interchange Reactions Involving Condensation Polymers" describes early work on redistribution reactions in the melt blends of polyesters, polyamides, and polyester + polyamide (Kotliar 1981).

5.7.2 Compatibilization by Graft Copolymer Formation: Reaction Type #2

Graft copolymer formation has been the most common method of forming a compatibilizing copolymer between two immiscible polymers during reactive compatibilization. As shown in Table 5.4, there are at least four processes for

Table 5.4 Graft copolymer formation processes (Adapted from Brown 1992a)

Reaction type	Characteristics	Type of copolymer obtained		
2a	By *direct reaction* of end-group of the 1st polymer with pendent groups of the 2nd polymer	A A - BBBBB A + A A	A A - BBBBB A A - BBBBB A	etc.
2b	By reaction of end-group of the 1st polymer with pendent group of the 2nd polymer in the presence of a *condensing agent*	**(Same as from process a)**		
2c	By reaction of end-group of the 1st polymer with pendent group of the 2nd polymer in the presence of a *coupling agent* ("c")	A A -c- BBBBB A + A A	A A -c- BBBBB A A -c- BBBBB A	
2d	By reaction of pendent groups of the 1st polymer with main chain of the 2nd polymer in a *degradative process*	A A - BBB A + A A	A A - BBB A A - BB A + BBB + BB	etc.

Summary of characteristics

Only chains bearing reactive functionality participate in the copolymer-forming reactions. A small amount of cross-linked copolymer may be formed when the end-group-functionalized polymer has functional groups at both ends

Graft copolymer formation between two polymers *each with different functionality* may occur either by *direct reaction* (e.g., A-acid end-group + B-pendent epoxy group) or by addition of a *condensing agent* that activates functionality of one polymer for reaction with functionality of the second polymer (e.g., A-acid end-group + B-pendent alcohol + triaryl phosphite)

Graft copolymer formation between two polymers *each with the same type of functionality* may be obtained using a *coupling agent* that links the two groups (e.g., A-acid + B-acid + diepoxide). The reaction may be inefficient if the coupling agent segregates into one phase, instead of concentrating at the interface. The coupling agent is incorporated into the final copolymer as a linking group

Graft copolymer formation may occur by a *degradative process* through reaction between a pendent functionality on one polymer and main-chain linkages on the second polymer. Small amounts of cross-linked copolymer may be formed if degradable segments of the graft copolymer react further

forming graft copolymer in a melt reaction. In the direct reaction process, the reaction occurs between one polymer containing reactive sites along its main chain and a second polymer with reactive sites only at end-groups. Depending upon stoichiometry and concentration of functional groups, copolymer structures of the general type 2a and 2b are obtained. In this particular type of graft copolymer formation, the average molecular weight of the copolymer is the simple sum of the average molecular weights of the two reacting species.

Graft copolymers may also be formed through reaction of a bi- or multifunctional coupling agent with one polymer containing reactive sites along its main chain and a second polymer with reactive sites only at end-groups (Type 2c). Typical coupling agents include multifunctional epoxy resins, oxazolines, carbodiimides, and isocyanates that react with nucleophilic end-groups of condensation polymers. The coupling agent is incorporated into the copolymer. When the coupling agent is an epoxide, a new secondary alcohol is formed when the epoxide ring is opened by a nucleophile. This alcohol may also be reactive to one or more polymeric components (particularly polyesters) similar to the reactivity of alcohol groups on phenoxy resin (see, e.g., Su et al. 1997).

A third, less common process for forming graft copolymer as shown in Table 5.4 is Type 2d. In this process, multiple reactive sites pendent on one polymer chain can bite into the linkages of a second type of polymer chain. The reaction creates a copolymer having segments with average molecular weight less than the sum of the two initial reacting species. This is a degradative method for forming a compatibilizing copolymer. A common example is the transesterification reaction between the poly(hydroxy ether) of bisphenol A (a phenoxy resin) and a polyester. Pendent hydroxy groups on phenoxy resin can undergo transesterification with ester linkages in the polyester chains resulting in graft copolymer formation accompanied by lower molecular weight polyester fragments. Because the molecular weight of the grafted polyester species is less than that of the homopolymer from which it was derived, the grafted chain segments may be below optimum molecular weight necessary for most efficient chain entanglement with the remaining homopolymer phase. This may result in less than optimum physical properties. Furthermore, if there is a large number of pendent reactive sites, then degradation of the second polymer may reach the point where it has lost the physical properties that made it useful for blending. Consequently, formation of a graft copolymer compatibilizing agent by a degradative process is not a common method for immiscible blend compatibilization.

Many commercial thermoplastics for high-impact strength applications are two-phase blends in which a higher modulus thermoplastic matrix is toughened by the presence of a lower modulus, dispersed phase polyolefin. In the majority of cases, such blends are compatibilized by graft copolymer formation between at least some fraction of the chains of the two immiscible polymers. Rubber-toughened PAs are the most common examples. In most of these cases, PA amine end-groups react with pendent anhydride or epoxy groups along the main chain of an immiscible rubbery polyolefin to form sufficient copolymer to compatibilize a dispersed polyolefin phase in a matrix phase of PA. Rubber-toughened PEST are also often compatibilized through graft copolymer formation formed through reaction between polyester acid end-groups and epoxy-functionalized polyolefins.

In rubber-toughened thermoplastic blends, the efficiency of compatibilization depends among other things upon sufficient concentrations of both thermoplastic reactive end-groups and polyolefin reactive pendent groups to give adequate levels of copolymer under the mixing, temperature, and residence time protocol of the extrusion process. Concentrations of thermoplastic reactive end-groups are

usually controlled during the manufacturing process, e.g., through control of stoichiometry in condensation polymerization and/or through addition of reactive or unfunctionalized chain-capping agents either during synthesis or in a subsequent processing step.

Functionality in rubbery polyolefins is usually introduced in one of two ways:

1. Copolymerization of olefin monomer(s) with another functionalized monomer (e.g., poly(ethylene-*co*-acrylic acid), poly(ethylene-*co*-glycidyl methacrylate), etc.)
2. Graft functionalization of polyolefin in a separate processing step (e.g., polyethylene-g-maleic anhydride, polypropylene-g-maleic anhydride, etc.)

Graft functionalization may be performed either by reactive extrusion in the molten state (see, e.g., Brown 1992a), in solution, or by solid-state processes. In these cases, concentration of functionality is controlled by temperature, physical phase of the polymer substrate, stoichiometry of functionalization agent, and (optional) catalyst among other factors.

When graft functionalization is performed by extrusion, the removal of unbound functionalization agent from functionalized PO is critical for success of subsequent copolymer formation with reactive thermoplastic end-groups. Unbound functionality (e.g., free maleic anhydride) in the PO phase may tie up reactive end-groups of the thermoplastic resin during subsequent reactive compatibilization processing, making these end-groups unavailable for copolymer formation. For functionalization during a separate extruder grafting reaction, unbound functionalization agent is removed by efficient devolatilization, and for solution functionalization, by solubilization of excess functionalization agent during isolation of solid, functionalized polymer.

5.7.3 Compatibilization by Block Copolymer Formation: Reaction Type #3

Compatibilized polymer blends have been prepared through block copolymer formation between immiscible polymers. In the direct reaction process, during melt processing, the functionalized end-groups on some fraction of chains in each of the polymers react across a melt-phase boundary to form block copolymers. Depending upon stoichiometry, either A-B or A-B-A or both copolymer structures may be obtained as shown in Table 5.5 (Type 3a or 3b). The average molecular weight of the copolymer corresponds to the sum of the average molecular weights of the reacting polymers.

Block copolymers may also be formed through reaction of the end-group on one polymer with a condensing agent which activates that end-group for reaction with a nucleophilic end-group on a second immiscible polymer. Typical condensing agents include phosphite esters that react with acid and hydroxy end-groups on condensation polymers. A by-product from the condensing agent is always formed in the copolymer reaction and is often removed by devolatilization of the blend melt. Since the condensing agent is not incorporated into the copolymer, the process is similar to that shown in Table 5.5, Type 3a.

Table 5.5 Block copolymer formation processes (Adapted from Brown 1992a)

Reaction type	Characteristics	Type of copolymer obtained
3a	By *direct reaction* of end-group of the 1st polymer with end-group of the 2nd polymer	**AAAAA-BBBBB**
3b	By reaction of end-group of the 1st polymer with end-group of the 2nd polymer in the presence of a *condensing agent*	**(Same as from process a)**
3c	By reaction of end-group of the 1st polymer with end-group of the 2nd polymer in the presence of a *coupling agent* ("c")	**AAAAA-c-BBBBB**
3d	By reaction of end-group of the 1st polymer with main chain of the 2nd polymer in a *degradative process*	**AAAAA-BBB + BB**
Summary of characteristics		

Only chains that bear reactive functionality participate in the copolymer-forming reaction. A-B-A block copolymer may result from the reaction if least one polymer is functional at both ends

Block copolymer formation between two polymers *each with different functionality* may occur either by *direct reaction* (e.g., A-acid end-group + B-epoxy end-group) or by addition of a *condensing agent* that activates functionality on one polymer for efficient reaction with functionality on the second polymer (e.g., A-acid end-group + B-alcohol end-group + triaryl phosphite)

Block copolymer formation between two polymers *each with the same type of functionality* may occur by adding a *coupling agent* capable of linking the two end-groups (e.g., A-acid + B-acid + diepoxide). The method may be inefficient if the coupling agent segregates to one phase instead of concentrating at the interface. The coupling agent is incorporated into the final copolymer as a linking group

Block copolymer formation may occur by a *degradative process* through reaction between end-group functionality on one polymer and main-chain linkages in the second polymer

    Block copolymers may also be formed through reaction of end-groups on each of the immiscible polymers with a coupling agent. Typical coupling agents are the same as for graft copolymer formation and include multifunctional epoxy resins, oxazolines, carbodiimides, and isocyanates that react with nucleophilic end-groups of condensation polymers. The coupling agent is incorporated into the copolymer. The process is shown in Table 5.5 (Type 3c). When the coupling agent is an epoxide, a new secondary alcohol is formed when the epoxide ring is opened by a nucleophile. This alcohol may also be reactive to one or more polymeric components (particularly polyesters) similar to the reactivity of alcohol groups on phenoxy resin.

    Block copolymers may also be formed by a degradative process in which end-groups on one polymer undergo transreaction with linkages in the main chain of a second, immiscible polymer. A low molecular weight fragment of the second polymer is formed as by-product. The block copolymer has lower average molecular weight than the sum of the average molecular weights of the reactants. The process shown in Table 5.5 (Type 3d) is essentially the same as Reaction Type 1a in Table 5.3 terminating at the block copolymer. A typical copolymer architecture in this process is an A-B block. An A-B-A block can form if the degradable segment is further degraded through transreaction with another end-group-functionalized polymer.

5.7.4 Compatibilization by Covalently Cross-Linked Copolymer Formation: Reaction Type #4

As shown in Table 5.6, compatibilizing copolymers may be formed in situ by a covalent cross-linking process.

The cross-linking reactions have been performed by at least five processes. In Reaction Type 4a, direct cross-linking occurs by covalent bond formation between functionalities on each of the two immiscible polymers without degradation of either polymer. The cross-linking is most often performed by reaction of pendent, nucleophilic sites of one multifunctional polymer with pendent, electrophilic sites of the second multifunctional polymer. Common examples include reactions of pendent acid or amine nucleophiles on one functionalized polymer with pendent electrophilic groups such as epoxide, oxazoline, or ortho ester on a second functionalized polymer.

Covalent cross-linking reactions mediated by a third, added reagent may give the same type of copolymer structure as that which results from direct cross-linking reactions (Table 5.6, Type 4b and 4c). In this case, the added reagent may be a radical initiator or other type of activating agent such as a condensing agent. Such activating agents are not incorporated into the final copolymer. Radical initiators may promote radical formation on each of two immiscible polymers. A cross-linked copolymer results through radical-radical coupling between the two polymers at a melt-phase interface. Self-coupling of each polymer may compete with cross-coupling as is the case with most three-body reactions in which an added reagent is capable of reacting with each of the two immiscible polymers.

Covalent cross-linking by covalent bond formation arising from mechanochemical radical generation and recombination in the absence of an added radical initiator may also be performed (Table 5.6, Type 4d). The method is less frequently used than other cross-linking reaction types. When two immiscible polymers can both form radicals on their main chains in the absence of added radical initiator, then a copolymer results when radical sites on the two different polymers recombine at the phase interface. If radical formation occurs without chain degradation, then the copolymer becomes cross-linked as multiple sites on each chain participate in the reaction. Alternatively, one radical-forming polymer can form a cross-linked copolymer with a second polymer containing a radical trap such as an unsaturated site (e.g., EPDM). This cross-linking process may be difficult to control since it only stops when thermal and/or shear conditions are below some threshold level. Casale and Porter (1975, 1978) and La Mantia and Valenza (1994) have briefly reviewed mechanochemical radical generation and its use to form copolymers in immiscible blends. Ahn et al. (1995) have described radical generation and copolymer formation in immiscible polymer blends subjected to elastic strain pulverization in specially modified extruders building on earlier Russian work. Pulverization occurs in an extruder section kept below the polymer melting points. The compatibilizing copolymer formed in these cases may be a block, graft, or cross-linked copolymer depending upon the polymers involved. See also the more recent review

Table 5.6 Covalently cross-linked copolymer formation processes (Adapted from Brown 1992a)

Reaction type	Characteristics	Type of copolymer obtained		
4a	Covalent cross-linking by *direct reaction* of pendent functionality of 1st polymer with pendent functionality of 2nd polymer	**A B** **A - - B** **A B** or **A - - B** **A B**	**A B A** **A B ----- A** **A ----- B A** **A B A** **A B A**	
4b	Covalent cross-linking by reaction of a pendent functionality of the 1st polymer with pendent functionality of the 2nd polymer in the presence of a *condensing agent*	**(same as from process a)**		
4c	Main chain of the 1st polymer reacts with main chain of the 2nd polymer in the presence of a *radical initiator*	**(same as from process a)**		
4d	Main chain of the 1st polymer reacts with main chain of the 2nd polymer through mechanochemical radical generation	**(same as from process a)**		
4e	Covalent cross-linking by reaction of pendent functionality of the 1st polymer with pendent functionality of the 2nd polymer in the presence of a *coupling agent* ("c")	**A B** **A -c- B** **A B** or **A -c- B** **A B**	**A B A** **A -c- B A** **A B A** **A B -c- A** **A B A**	

Summary of characteristics

Only chains bearing reactive functionality participate in copolymer-forming reactions

Cross-linked copolymer formation between two polymers *each with different functionality* may occur either by *direct reaction* (e.g., A-pendent acid + B-pendent epoxide) or by addition of a *condensing agent* that activates functionality on one polymer for efficient reaction with functionality on the second polymer (e.g., A-pendent acid + B-pendent alcohol + triaryl phosphite) (process 4a and 4b)

Cross-linked copolymer formation may also occur via *direct reaction* of mechanochemically generated free radicals of each polymer in the absence of added radical initiator, or through radical trapping by a reactive site, such as olefin or acetylene groups in the second polymer (process 4a) Alternatively, a radical initiator may be added to generate radical sites on one or both polymers (process 4c). A cross-linked copolymer results if the polymers involved are not degraded. When the polymers are degraded, then the copolymer structure may be as shown in Table 5.3

Cross-linked copolymer formation between two polymers *each with the same type of functionality* may occur by adding a *coupling agent* capable of linking the two pendent groups (e.g., A-pendent acid + B-pendent acid + diepoxide). The method may be inefficient if the coupling agent segregates to one phase instead of concentrating at the interface. The coupling agent is incorporated into the final copolymer as a linking group

In all the above cases, the initial copolymer formed is a *graft copolymer*, but this product may react further to form cross-linked copolymer as additional functionalities of one or both of the two segments of the copolymer react

by Beyer and Clausen-Schaumann (2005) concerning mechanochemical radical generation in polymers.

Covalent cross-linking reactions to form a compatibilizing copolymer may also be performed by addition of a coupling agent. Coupling agents react with the same

type of functionality in each of the immiscible polymers and remain bound in the cross-linked product as linking agents. Examples include diepoxide reaction with pendent carboxylic acid groups on each of two immiscible polymers. In this case, the structure of the cross-linked copolymer is shown in Table 5.6 (Type 4e). Most commonly, coupling agents are multifunctional reagents with molecular weights less than about 1,000. When immiscible polymer pairs are employed, each bearing multiple pendent nucleophilic groups (such as carboxylic acids), then low molecular weight coupling agents such as bis-, tris, tetra-, and higher epoxides; bis-oxazolines; and other multifunctional electrophilic species are used. A low molecular weight coupling agent bearing multiple olefinic sites may be used to promote cross-linking in blends containing POs. Common examples include commercially available tris-acrylates and triallyl isocyanurate. Often these cross-linking reactions are performed in the presence of radical initiator. Self-coupling of each polymer may compete with cross-coupling as is the case with most three-body reactions in which an added reagent is capable of reacting with each of the two immiscible polymers.

5.7.5 Compatibilization by Ionic Interaction to Form Copolymer: Reaction Type #5

Immiscible polymer blends have been compatibilized through formation of a compatibilizing copolymer linked by ionic association instead of by covalent bonding. Although many examples have been published, most of these involve solution mixing of the two immiscible polymers (see Natansohn et al. 1990). Most examples given in this chapter describe only such polymer blends prepared by melt mixing.

In theory, the possible architectures of a compatibilizing copolymer arising from ionic association may be the same as all those architectures arising from covalent bond formation that were previously discussed. However, in practice only a small number of copolymer architectures have been reported for compatibilizing agents arising from ionic association. In the most common examples (Table 5.7; Type #5a), ionizable groups such as carboxylic, sulfonic, or phosphonic acid are present in low concentrations (e.g., about 5 % or less) on both polymers. The ionizable groups may be at least partially neutralized by a mono-, di-, or trivalent metal cation, such as Na^{+1}, Zn^{+2}, or Al^{+3}. Multivalent cations may form a bridging linkage between the ionizable groups of the two immiscible polymers resulting in interchain copolymer formation by ion-ion association. Monovalent cations such as Na^{+1} or K^{+1} may also be used to promote association through ion-dipole association. With either type of cation, a morphology is formed in which there are concentrated domains of associated ionic species (ion clusters) in a matrix of the immiscible homopolymers.

In the first type of ionic association (Type #5a), the ionizable functionalities of the two polymers are located in the pendent side groups. These polymers are prepared either through copolymerization with ion-containing monomers (or latent ion-containing monomers) or through subsequent grafting with such

Table 5.7 Ionic copolymer formation processes (Adapted from Brown 1992a)

Reaction type	Characteristics	Type of copolymer obtained
5a	Ion-ion association mediated by metal cations as linking agents ("c")	A B A B A A -c- B A -c- B A A B **or** A B A A -c- B A B -c- A A B A B A
5b	Ion-neutral donor group association mediated by metal cations	**(Similar to structure from process a)**
5c	Ion-ion association mediated by interchain protonation of a basic polymer by an acidic polymer ("acid-base" reaction)	A B A B A A - - B A B ----- A A B **or** A ----- B A A - - B A B A A B A B A

Summary of characteristics

Only chains bearing reactive functionality participate in copolymer-forming reactions

In theory, it is possible to form block, graft, or cross-linked copolymers by ionic associations. However, in practice, telechelic polymers with ionic functionality at the chain ends are uncommon. Therefore, the majority of reported examples involve *cross-linked copolymer formation* between two immiscible polymers bearing pendent ionic groups

Ionic groups include carboxylic, sulfonic, and (less frequently) phosphonic acid groups. The acidic groups may be at least partially neutralized with monovalent, divalent, or trivalent metal cations, e.g., Na^+, Zn^{+2}, Al^{+3}. Ionic cross-linking of immiscible polymers bearing acidic groups may be mediated by such metal cations or by low molecular weight dibasic molecules such as diamines. Both these agents may link ions of different polymers

Masked ionomeric groups may also be used. They generate ions during melt processing. Examples include phosphonate esters that form phosphonic acid salt in the melt by transesterification with a salt, e.g., zinc stearate

monomers. Consequently, the resulting compatibilizing agents are most often cross-linked copolymers with the structure shown in Table 5.7 as Type 5a.

In a second type of ionic association (Type #5b) metal cations may mediate association between ionic groups on one polymer and neutral donor groups on a second immiscible polymer. Typical ionic groups are again carboxylic, sulfonic, and phosphonic acids. Neutral donor groups contain atoms, usually nitrogen or phosphorus, having unshared pairs of electrons capable of coordinating to metal cations. Such groups include pyridine, quinoline, and phenanthroline. These are usually introduced into a polymer via copolymerization with the vinyl analog, e.g., vinylpyridine. Again, the structure of the compatibilizing copolymer is usually cross-linked.

In a third type of ionic association (Type #5c), acidic groups such as carboxylic acids bound to one polymer may mediate interchain copolymer formation by protonation of basic groups on a second, immiscible polymer. In this case, the compatibilizing agent is again most often a cross-linked copolymer.

General discussions of the properties of polymers containing ionizable groups (ionomers) have been published (see, e.g., Kim et al. 2002; Hara and Sauer 1994;

Lundberg 1987; Rees 1986). Ionic cross-links are usually thermally reversible, which may limit the usefulness of blends containing them in certain commercial applications. Since ionomers are initially self-associated through ionic bonds, thermal reversibility of ionic cross-links in the melt is necessary to overcome homogeneous, self-cross-linking within each homopolymer before heterogeneous, interchain cross-linking can occur. Often a high degree of plasticization of the ion-containing polymer melt is required so that high processing temperatures that might lead to polymer decomposition need not be used. In some cases, polymers containing masked ionomeric functionality, i.e., chemical groups that form ionic species during extrusion, have been used to form copolymers during reactive processing. Use of masked ionomers may require lower energy during extrusion since ionic self-association does not have to be overcome before interchain copolymer formation can occur.

5.8   Polyamide Blends

Examples of polyamide blends are listed in alphabetical order of the second polymer in the blend unless otherwise noted. When copolymer characterization was not performed, the structure of the compatibilizing copolymer is inferred from the functionality location on each of the two polymers. In some cases, more than one type of compatibilizing copolymer may have formed.

Many of the copolymer-forming reactions employed to compatibilize PA blends with a second immiscible polymer have been studied by Orr et al. (2001) who determined that the order of increasing reactivity in functionalized polymer pairs is acid/amine, hydroxyl/(anhydride or acid), aromatic amine/epoxy, aliphatic amine/epoxy, acid/oxazoline, acid/epoxy, aromatic amine/anhydride, and aliphatic amine/anhydride (most reactive).

5.8.1   Polyamide + Polyamide Blends

5.8.1.1 Copolymer Formation by Redistribution Reaction
Examples of copolymer formation by redistribution reactions (sometimes referred to as transreactions) in PA/PA blends are given in Table 5.8. In related work, Liu and Donovan (1995) failed to find evidence for transamidation in PA-6 blends with an aromatic polyamide during molding and annealing. Aspects of transreactions in PA/PA blends have been described in Eersels et al. (1999) and in portions of other chapters included in Fakirov (1999) (transreactions in condensation polymers).

5.8.1.2 Copolymer Formation by Amine + Carboxylic Acid Reaction: Blends Containing a Condensing Agent
Aharoni et al. (1984) and Aharoni (1983) have shown that blends of immiscible polyamides may be compatibilized through copolymer formation mediated by addition of a phosphite condensing agent. A block copolymer results when the phosphite-activated end-group of one PA reacts at the phase interface with a

Table 5.8 PA/PA blends: copolymer formation by redistribution reaction

Polyamide/polyamide	Characterization and comments	References
PA-66 (70-60)/PA-6I (30-40); also PA-66/PA-6	Biaxial extruder at 280 °C/mixture of various phosphite catalysts with calcium hypophosphite/Tm, Tg, GPC, NMR, mechanical properties	Aramaki et al. 2004
PA-6/PA-610 or PA-46	Melt mixing at 290–310 °C/MALDI/^{13}C NMR/DSC/sequence analyses of copolyamides	Samperi et al. 2004
PA-46 (70-0)/PA-6I (30-100)	Mini-extruder at 295–325 °C or TSE at 315 °C/DSC/influence of processing conditions on extent of transamidation	Eersels et al. 1998; Eersels and Groeninckx 1996, 1997, (see also Powell and Kalika 2000)
PA-6 (100-0)/poly(m-xylene adipamide) (0-100)	Film extrusion using SSE at 275 °C/DSC/ study of heat-aged films/transamidation vs. time	Shibayama et al. 1995
PA-6 (100-0)/poly(m-xylene adipamide) (0-100)	SSE at 290 °C/mechanical properties/ DMTA/DSC/NMR/effects of annealing and of different transamidation levels on properties	Takeda et al. 1992a; Takeda and Paul 1991
PA-6 (85)/PA-66 (15)	Wayne extruder at 280 °C/diphenyl phosphoryl azide additive/DSC	Bhattacharjee and Khanna 1990
PA-6 (85)/PA-66 (15)	Wayne extruder at 280 °C/various bisulfate or biphosphate catalysts/DSC	Khanna 1989
PA-6 (20-80)/PA-66 (80-20)	Wayne extruder at 280 °C/various phosphite catalysts/Tm, heat of fusion, mechanical properties	Khanna et al. 1983
PA-6 (95-5)/PA-66 (5-95)	Thermal redistribution in extruder at 215–280 °C/DSC	Schott and Sanderford 1977

nucleophilic end-group on the second PA. The reaction also produces a secondary phosphite by-product. The relative proportions of copolymer vs. simple chain-extended PA may depend upon the relative solubility of the condensing agent in each of the immiscible polymer phases. For example, blends of 95-50 parts PA-6 were extruded using an SSE at 265–315 °C with 5-50 parts PA-11 (or PA-12 or PA-66 or PA-6T) in the presence of 0-1 part triphenyl phosphite or other trialkyl phosphite. Copolymer-containing blends were characterized by selective solvent extraction, FTIR, ^{13}C NMR, and ^{31}P NMR. Model compound studies were done to understand the mechanism of copolymer formation.

5.8.1.3 Copolymer Formation by Amine + Anhydride Reaction: Blends Containing a Coupling Agent

Xie and Yang (2004) have prepared blends of PA-6 (70 parts) and PA-12,12 (30 parts) through addition of SEBS-g-MA (15 wt%) which may serve as a coupling agent between the two PA. Blend characterization included SEM.

5.8.2   Polyamide + Polyester (or Polycarbonate) Blends

5.8.2.1 Copolymer Formation by Amine + Anhydride Reaction

Qu et al. (2008) reported blends of PA-6 with PET compatibilized through addition of ethylene-acrylate-maleic anhydride terpolymer.

John and Bhattacharya (2000) reported that PBT may be modified by extrusion with MA. The modified PBT forms compatibilized blends with PA-66 characterized by FTIR, ^{13}C NMR, SEM, and mechanical properties.

PA/PC ternary blends have also been compatibilized through copolymer formation between PA amine end-groups and anhydride-functionalized styrene copolymer. Kim et al. (1999a) employed SAN-co-MA in PA-6,12/PC blends. Lee et al. (1999b) and Horiuchi et al. (1996, 1997a, b, c) employed SEBS-g-MA with PA-6/PC blends.

PA/PC blends have also been compatibilized by block copolymer formation through reaction of PA amine end-groups with PC anhydride end-groups (Hathaway and Pyles 1988, 1989). PC phenolic end-groups were anhydride-functionalized by reaction with trimellitic anhydride acid chloride. Extruded blends of PA-6 and PC were characterized by selective solvent extraction and mechanical properties of test parts. An amorphous polyamide could also be compatibilized with PC using this strategy.

5.8.2.2 Copolymer Formation by Amine + Carboxylic Acid Reaction: Blends Containing a Condensing Agent

PA/PEST blends have been compatibilized through block copolymer formation mediated by addition of a phosphite condensing agent (Aharoni et al. 1984; Aharoni 1983; Aharoni and Largman 1983). Block copolymer results when the phosphite-activated end-group of a PEST (or PA) reacts with a nucleophilic end-group on a PA (or PEST) at the phase interface with generation of secondary phosphite by-product. The relative proportions of copolymer vs. simple chain-extended PA or PEST may depend upon the relative solubility of condensing agent in each of the immiscible polymer phases. For example, blends of 95-5 parts PA-6 (or PA-66 or PA-12) were extruded using an SSE at 265–315 °C with 5-95 parts PET (or PBT or PCT) in the presence of 0-1 part triphenyl phosphite or trialkyl phosphite. Copolymer-containing blends were characterized by morphology, viscosity, selective solvent extraction, FTIR, ^{13}C NMR, and ^{31}P NMR. Model compound studies were done to understand the mechanism of copolymer formation. Various other PEST and PA resins were also used.

5.8.2.3 Copolymer Formation by Carboxylic Acid + Epoxide Reaction: Blends Containing a Coupling Agent

As shown in Table 5.9, PA/PEST blends can be compatibilized through block copolymer formation mediated by addition of a multifunctional epoxide coupling agent. The coupling agent may react with nucleophilic end-groups on each of the two immiscible polymers at the phase interface to give a block copolymer containing the coupling agent as linking group. The relative proportions of copolymer vs. simple chain-extended PA or PEST may depend upon the relative solubility of coupling agent in each of the immiscible polymer phases. See, e.g., Jeziórska (2005) wherein a bis-oxazoline coupling agent was used, but the predominant reaction was PEST chain extension.

Table 5.9 PA/PEST blends – blends containing a coupling agent: copolymer formation by carboxylic acid + epoxide reaction

Polyamide/polyester	Characterization and comments	References
PA-6/PC/epoxy resin	Mechanical properties/DSC/SEM/ dynamic rheometry/effects of 3 different mixing sequences	Wang et al. 2012c
PA-6/PET/multifunctional epoxide resin (0–10 wt%)	SEM/WAXD/polarizing microscopy/ DMTA/mechanical properties/DSC/FTIR	Huang et al. 1998
PA-66 (70-50)/PBT (30-50)/multifunctional epoxide resin (0–5 phr)	TSE at 275 °C/SEM/TEM/extrudate swell/DSC/torque rheometry/capillary rheometry/effects of PA:PBT ratio and epoxy content on mechanical properties/ blends optionally + core-shell elastomer	Huang and Chang 1997a, b (see also Chiou and Chang 2000)
PA-6 (17)/PBT (83)/ multifunctional epoxide resin (0-12)	TSE at 230–250 °C/mechanical properties/SEM/DSC/DMA/WAXD	An et al. 1996

5.8.2.4 Copolymer Formation by Degradative Process

Examples of compatibilizing copolymer formation in PA/PEST blends by reaction of PA end-groups with PEST main-chain units by a degradative process (including PA/PC blends) are given in Table 5.10. The degradative process in this instance may also be considered a transreaction. Reviews of transreactions in PA/PEST blends include those described in chapters of Fakirov (1999) (transreactions in condensation polymers).

5.8.3 Polyamide + Polyesteramide LCP + Polyolefin Blends

5.8.3.1 Copolymer Formation by Amine + Anhydride Reaction

Seo (1997) prepared compatibilized PA blends with LCP polyesteramide (Hoechst Vectra® B950) in the presence of anhydride-functionalized polyolefin. Specifically, 60 parts PA-6 was mixed with 25 parts LCP and 15 parts EPDM-g-MA in a TSE at 290 °C. The blend was characterized by SEM, optical microscopy, Raman spectroscopy, mechanical properties, selective solvent extraction, and FTIR.

5.8.4 Polyamide + Polyester LCP + Polypropylene Blends

5.8.4.1 Copolymer Formation by Amine + Anhydride Reaction

Tjong and Meng (1997) have described PA/LCP polyester blends with improved properties through addition of anhydride-terminated PP-MA. A block copolymer may form between PA amine end-groups and anhydride-terminated PP. For example, 86 parts PA-6 was mixed in an internal mixer with 14 parts PP-MA at 220 °C followed by injection molding with 5-40 parts LCP (Hoechst Vectra® A950). The blends were characterized by torque rheometry, mechanical properties, DMA, and SEM.

Table 5.10 PA/PEST blends: copolymer formation by degradative process

Polyamide/polyester	Characterization and comments	References
Poly(hexamethylene isophthalamide-*co*-terephthalamide/poly (butylene succinate)	TSE/selective solvent extraction/ FTIR/^{13}C NMR/SEM/p-toluene sulfonic acid catalyst	Yao et al. 2012
Poly(*m*-xylene adipamide) (50) PET (50)/terephthalic acid (1 wt%)	Melt reaction at 285 °C/^{1}H and^{13}C NMR/DSC/progress of reaction study	Samperi et al. 2010
PA-12/PBT/hyperbranched poly(ethyleneimine)-g-PA-12	DSC/^{13}C NMR/optical microscopy/ morphology	Wang et al. 2009b
PA-66 (70-60)/PET (30-40) also PTT or PBT	Biaxial extruder at 280 °C/mixture of various phosphite catalysts with calcium hypophosphite/Tm/Tg/GPC/NMR/ mechanical properties	Aramaki et al. 2004
PA-6/PBT or PET	Reaction at 260 °C and 280 °C/NMR/ MALDI/mechanism of reaction/role of added p-toluene sulfonic acid	Samperi et al. 2003a, b
PA-6/PC	Haake mixer at 280 °C/evidence for copolymer formation/reaction kinetics/ also blends including poly(propylene oxide)	Costa and Oliveira 1998, 2002
PA-66 (95-50)/LCP (Hoechst Vectra A950) (5-50)	SSE or Brabender/mechanical properties/ morphology/selective solvent extraction/ spectroscopic and thermal analysis/ variation of PA end-group concentrations and acid/amine ratios	Costa et al. 2001
PA-11 or PA-66 or PA-6,10 or PA-6,12/block copolyetherester	Morphology/mechanical properties/DSC/ rheology/selective solvent extraction/ FTIR/micro-Raman spectroscopy	Koulouri et al. 1999b
PA-6 (50)/PET (50)	Extrusion in capillary rheometer at 280 °C then annealing/SEM/selective solvent extraction/FTIR/DMTA/WAXS	Evstatiev et al. 1996; Serhatkulu et al. 1995
PA-6 (70-0)/PC (30-100)	Thermal redistribution in internal mixer at 260 °C/NMR/TLC/DSC	Konyukhova et al. 1994
PA-6 (90-0)/PC (10-100)	Internal mixer at 240 °C/torque rheometry/SEM/GPC/mechanical properties/effects of mixing time/effects of PA amine and acid end-group concentrations	La Mantia and Valenza 1994; Valenza et al. 1994
PA-6 (80-20)/PC (20-80)	Internal mixer at 240 °C/selective solvent extraction/NMR/TGA/MS/IV/model studies/kinetics/also data from solution reactions	Montaudo et al. 1994
PA-6 (100-0)/PC (0-100)	Thermal redistribution in internal mixer at 240 °C or SSE at 250 °C/DSC/selective solvent extraction/SEC/FTIR/SEM vs. time/ rheology/mechanical properties/DMTA	Gattiglia et al. 1989a, b, 1990, 1992

(*continued*)

Table 5.10 (continued)

Polyamide/polyester	Characterization and comments	References
PA-6 (85)/PET (15)	SSE at 280 °C/diphenyl phosphoryl azide additive/DSC	Belles et al. 1991
PA-6 (75-25)/PC (25-75)	Low degree of thermal redistribution in internal mixer at 240–250 °C/torque vs. time and temperature/DSC/selective solvent extraction	Eguiazábal and Nazábal 1988
PA-66 (54-10)/PET (46-90)	Internal mixer/FTIR/NMR/DSC/ mechanical properties vs. degree of redistribution/H bonding between phases/ toluenesulfonic acid catalyst (0.2)	Pillon et al. 1987a, b
PA-66 (0-54)/PET (100-46)	Internal mixer at 265–295 °C or TSE at 290–370 °C/NMR/23 % max. copolymer level/toluenesulfonic acid catalyst (0.2)	Pillon and Utracki 1984

5.8.5 Polyamide + Polyethersulfone Blends

Kanomata et al. (2011) prepared compatibilized blends of PA-6 and polyethersulfone using PES having hydroxyphenyl end-groups. Blends prepared in a Brabender mixer were characterized using TEM and torque rheometry in comparison with control blends.

Weber and Güntherberg (1999) have prepared compatibilized blends of PA and polyethersulfone in the presence of S-MA-(N-phenylmaleimide) terpolymer. In the examples, the PA was derived either from hexamethylenediamine-isophthalic acid or from hexamethylenediamine-caprolactam-terephthalic acid. Blends comprising PA, an amine-terminated polyethersulfone, and S-MA-(N-phenylmaleimide) ter-polymer prepared in a Haake mixer were characterized using mechanical properties testing, selective solvent extraction, DSC, and Vicat B test. Blends optionally contained phenoxy resin.

5.8.6 Polyamide + Polyolefin Blends (Excepting Polypropylene)

Blends in these sections include those with either a single PA or a mixture of semicrystalline PAs or a mixture of amorphous and semicrystalline PAs.

5.8.6.1 Copolymer Formation by Amide-Ester Exchange
Graft copolymer compatibilizing agents have been prepared by direct reaction (Table 5.11) through amide-ester exchange reaction between polyamide amine end-groups and pendent ester groups on polyolefin copolymers such as EEA. In these cases, a low molecular weight alcohol is generated as a by-product.

5.8.6.2 Copolymer Formation by Amine + Anhydride Reaction
The most common method for compatibilizing PA/amorphous polyolefin blends involves graft copolymer formation by reaction of polyamide amine end-groups

Table 5.11 PA/PO blends: copolymer formation by amide-ester exchange

Polyamide/polyolefin	Characterization and comments	References
PA-1010/EVAc/tetrabutyl titanate catalyst	Melt mixing at 240 °C/mechanical properties/SEM/DMA/MFI/FTIR/NMR/also used acrylate rubber in place of EVAc (2013b)	Lu et al. 2013a, b
PA-11/poly(lactic acid)/titanium isopropoxide catalyst (0–0.1 wt%)	Melt blended/failure of catalyst to promote copolymer formation over simple degradation irrespective of catalyst level and mixing time/DSC/SEM/mechanical properties/^{13}C NMR	Patel et al. 2013
PA-6 (60)/EVAc rubber (40)/dibutyltin oxide (1)	Melt mixing at 230 °C/NMR/characterization confirmed exchange reaction extent and copolymer yield/rate constant determination	Wu et al. 2013
PA-6 (85-25)/EEA (18 % EA) (15-75)	Melt mixing at 230 °C/optical microscopy/selective solvent extraction/SEM/DSC/DMA/mechanical properties/FTIR	Koulouri et al. 1996, 1997
PA-6 (100-75)/LDPE (0-25)/LDPE-g-BA (18 % BA) (0-2.4)	Internal mixer coupled to SSE at 260 °C/SEM/torque rheometry/mechanical properties/water absorption/hardness/effect of premixing LDPE + LDPE-g-BA	Raval et al. 1991

with pendent anhydride groups on an appropriate polyolefin to form a compatibilizing copolymer linked through an imide bond. Anhydride groups may be incorporated into suitable POs through grafting or through copolymerization with maleic anhydride, citraconic anhydride, itaconic anhydride, and congeners or through grafting or copolymerization with potentially latent anhydrides such as vicinal diacids or acid-esters including fumaric acid, maleic acid monoalkyl ester, and congeners. Selected examples are listed in Table 5.12.

5.8.6.3 Copolymer Formation by Amine + Carboxylic Acid Reaction

As shown by examples listed in Table 5.13, PA/PO blends have been compatibilized through block copolymer formation between PA amine end-groups and terminal carboxylic acid groups of polyolefins. PA blends with oxidized PE should fall into this category since carboxylic acid groups are believed to be located at PE chain ends (see El'darov et al. 1996).

Compatibilized PA/PO blends have also been prepared by graft copolymer formation between the amine end-groups of PA and PO pendent carboxylic acid groups to give a new amide linkage (Table 5.14). Water is the by-product of this reaction. The work by Aharoni is noteworthy in that it employs a condensing agent to effect copolymer formation between polyamide end-groups and pendent carboxylic acid groups on EAA.

Mascia and Hashim (1997, 1998) have prepared compatibilized blends of PA with PVDF by using carboxylic acid-functionalized PVDF. In an example, 20 parts PA-6 was combined with 80 parts PVDF-g-methacrylic acid (10 % MAA) in an internal mixer at 240 °C. The graft copolymer-containing blend was characterized by SEM, FTIR, mechanical properties, selective solvent extraction, and rheology. The effects of adding zinc acetate were studied.

Table 5.12 PA/PO blends: copolymer formation by amine + anhydride reaction

Polyamide/polyolefin	Characterization and comments	References
PA-6/HDPE/HDPE-g-MA	Broad range of compositions/selective solvent extraction/SEM/rheology/finding of two dispersed phase sizes and its implications	Argoud et al. 2014
PA-6/HDPE/EPDM-g-MA	Internal mixer/mechanical properties/ morphology/DSC/rheology	Dou et al. 2013
PA-6/PMP/PMP-g-MA	Melt kneaded in biaxial extruder/mechanical properties/melt tension	Enna et al. 2013
PA-6/EPDM/EPDM-g-MA	Mechanical properties/SEM morphology/DSC/ Molau test/best properties at 80-10-10 ratio	Xu et al. 2013b
PA-6/HDPE/EPDM/ EPDM-g-MA	Mechanical properties/morphology/DSC/effect of EPDM molecular weight	Zhou et al. 2013
PA-6/HDPE/EPDM-g-MA	Mechanical properties/rheology/morphology/ effect of one-step or two-step processing protocol	Li et al. 2012a
PA-6/HDPE-g-MA	Dispersed phase particle size characterized by ultrasonic velocity and attenuation as function of HDPE-g-MA amount	Wang et al. 2012a
PA-6 (25 wt%)/LLDPE/ PB-g-MA	Grafting of PB-g-MA onto LLDPE using DCP RI, followed by extrusion with PA/co-continuous morphology	Shi et al. 2010
PA-6/polyolefin elastomer/ PO elastomer-g-MA	Mechanical properties/morphology/Molau test/ MA grafted through ultrasound-assisted extrusion/comparison of blend properties to those containing PO with MA grafted using peroxide	Xie et al. 2010
PA-6/EBA-g-MA	Morphology/rheology/effect of using unfunctionalized EBA	Balamurugan and Maiti 2008a, b
PA-6/metallocene PE/metallocene PE-g-MA	TSE/mechanical properties/SEM/capillary rheometry/FTIR/also used metallocene EPDM, metallocene EPDM-g-MA, and metallocene EP-g-MA	Lopez-Quintana et al. 2008
PA-6/ETFE/ETFE-g-MA/ LDPE-g-MA/PO-f-GMA	TSE/mechanical properties/abrasion test	Atwood et al. 2007
PA-6/UHMWPE/ HDPE-g-MA	Brabender mixer/mechanical and tribological properties/FTIR	Wang et al. 2007b
PA-6/EPDM-g-MA	One-step melt grafting and copolymer formation/ SEM/DSC/selective solvent extraction/FTIR/ NMR/mechanical properties/comparison to two-step process	Coltelli et al. 2006 (see also Komalan et al. 2008)
PA-6/ethylene-octene copolymer-g-MA	TEM/mechanical properties/also used amorphous PA	Huang and Paul 2006 (see also Huang et al. 2006a, b; Yu et al. 1998)
PA-6/PMMA-f-anhydride	PA-amine reaction with glutaric anhydride in PMMA chain/morphology/physical properties	Iliopoulos et al. 2006; Freluche et al. 2005
PA-6/ethylene-octene copolymer/PE-g-MA	Mechanical properties/morphology/dimensional stability	Sanchez et al. 2006

Table 5.12 (continued)

Polyamide/polyolefin	Characterization and comments	References
PA-6/EPDM-g-MA	Dynamic packing injection molding/mechanical properties/SEM/impact strength vs. interparticle distance/blend properties vs. those prepared by conventional molding	Wang et al. 2006
PA-6/EVAc/EVAc-g-MA	Attenuated total reflectance IR/mechanical properties/morphology/properties vs. MA content (1–6 %)	Bhattacharyya et al. 2001, 2005
PA-6/EPDM/EPDM-g-MA	TSE/morphology/effects of temperature and extruder residence time/monitoring of chemical conversion and morphology	Covas and Machado 2005
PA-11/PE/EPDM-g-MA	Mechanical properties/SEM	Hu et al. 2004
PA-6/EP/EP-g-MA	Rheology/morphology/effect of EP-g-MA content level	Oommen et al. 2004
PA-6/LDPE/PE-g-MA	Brabender mixer/SEM/DSC/selective solvent extraction/comparison of blend properties to those of blends with EAA in place of PE-g-MA	Jiang et al. 2003
PA-6/EP/EP-g-MA	Morphology development along extruder screw axis	Machado et al. 1999, 2002
PA-6/EPDM/EPDM-g-MA	Melt mixing/TEM/effect of viscosity ratio/effect of partially cross-linking rubber phase	Oderkerk and Groeninckx 2002
PA-6 (20)/EEA-g-MA (80; 17 wt% EA; 1 wt% MA)	TSE at 220 °C/TEM/selective solvent extraction/ NMR/FTIR/SEC/DSC/mechanical properties/ also used EEA with 0.5 wt% MA/PA amine-terminated at one end	Pernot et al. 2002
PA-11/ethylene-octene copolymer-g-MA	Morphology, ductile-brittle transition temps. and mechanical properties as a function of MA grafting level	Li et al. 2001
PA-6/NR-f-MA	Melt processing/rheology/DMA/morphology	Carone et al. 2000
PA-6/VLDPE-g-MA	TSE/SEM/optical microscopy/mechanical properties/DSC/DMTA/comparison to commercial (PA-6/ULDPE) blend/also used VLDPE-g-DEM	Lazzeri et al. 1999 (see also Gadekar et al. 1998)
PA-6/EP-g-MA	Melt blending/rheology/mechanical properties/ DMTA/morphology/effect of component ratio/ also addition of MgO	Okada et al. 1999
PA-6/EVAc/EVAc-g-MA	Morphology/mechanical properties/interfacial adhesion	Piglowski et al. 1999
PA-6/EP/EP-g-MA	Melt mixing/SEM/effect of processing conditions, content of EP-g-MA, PA-6 MW, and mode of mixing	Thomas and Groeninckx 1999
PA-6/EPDM-g-MA	DSC/morphology/amount of PA graft vs. blend composition/length of PA graft/also used PA-66	Van Duin et al. 1998
PA-6 (75)/EPDM-g-MA (25) or EP-g-MA or ULDPE-g-MA	TSE at 270 °C/mechanical properties/SEM/ rheology/comparison to SEBS-g-MA impact modifier	Burgisi et al. 1997
PA-66 (75)/EPDM-g-MA (0.4–1 % MA) (25)	TSE at 255 °C/mechanical properties	Roberts et al. 1997

Table 5.12 (continued)

Polyamide/polyolefin	Characterization and comments	References
PA-6 (9-6)/PE (90)/ HDPE-g-MA (1-4)	PA + HDPE-g-MA extruded on TSE at 240 °C followed by blow molding with 90 % PE/DSC/SEM/rheology/permeation test/ mechanical properties/selective solvent extraction + FTIR for PA-HDPE copolymer characterization	Yeh et al. 1997
PA-6 (70-0)/LDPE (30-100)/ E-BA-MA (0-6) or EVAc-g-MA	SSE at 235 °C/DSC/SEM/WAXD/tensile properties/selective solvent extraction/interfacial tension estimates/also ternary blends containing EP (30 %)	Beltrame et al. 1996
PA-6 (80)/EP (0-20)/ EP-g-MA (1.1 % MA) (0-20)	SSE at 240 °C or TSE at 280 °C/torque rheometry/TEM/titration of residual amine groups/effects of extruder type and PA mol. wt. and amine end-group concentration on morphology, mechanical properties, and ductile-brittle transition temperature/effects of di- vs. monofunctional PA	Oshinski et al. 1996a, b, c, d
PA-6 (100-0)/aromatic PA-(0-100)/EP-g-MA (0-20)	TSE at 280–300 °C/DSC/DMA/rheology/ mechanical properties/MFI/TEM/selective solvent extraction/effects of different extrusion sequences	Xanthos et al. 1996
PA-6 (70)/EP (0-30)/ EP-g-MA (0-30)	Internal mixer at 240 °C/SEM/effects of adding phthalic anhydride to consume amine end-groups/model reactions to assess roles of amine- vs. amide-anhydride reactions	Marechal et al. 1995
PA-66 (100-80)/ EPDM-g-MA (0-20)	TSE/mechanical properties/SAXS/SEM/ TEM/effects of rubber level and functionality/factors affecting ductile-brittle transition temperature/analysis of fracture surfaces	Muratoglu et al. 1995a, b
PA-6 (95-80)/EP-g-MA (0.7 % MA) (5-20)	TSE at 290 °C/blends made from PA + masterbatch of 20 wt% EP-g-MA/ SEM/deformation and fracture behavior vs. strain retention and rubber content	Dijkstra et al. 1994
PA-6 (100-80) or PA-66/ EP-g-MA (1.5 % MA) (0-20)	Processing study with SSE and TSE/TEM/ mechanical properties vs. extrusion conditions and morphology/effects of using PA + rubber masterbatch	Majumdar et al. 1994g
Amorphous PA (80)/ EP-g-MA (0.7 % MA) (20)	Internal mixer at 200 °C/torque rheometry/ selective solvent extraction/SEM study of morphology development in reactive and in nonreactive blends	Scott and Macosko 1994a, 1995b
Aromatic PA (50)/ hydrogenated NBR (50)/ NBR-co-MA (30 % MA) (0-10)	Miniature mixer at 250 °C/morphology/ ellipsometry/L101 (0.9 phr) added for vulcanization of rubber phase/effects of mixing protocol/other carboxylated rubbers also used	Bhowmick et al. 1993
PA-46 (90)/EP-g-MA (1 % MA) (10)	TSE at 310 °C/SEM/mechanical properties/also blends containing polysulfone and PA-polysulfone copolymer	Koning et al. 1993a

(*continued*)

Table 5.12 (continued)

Polyamide/polyolefin	Characterization and comments	References
PA-11 (20) or PA-6/ HDPE-g-MA (80)	Internal mixer or TSE at 210 °C/torque rheometry/mechanical properties/SEM/selective solvent extraction/DSC/simultaneous addition of PA + PE + MA + radical initiator	Lambla and Seadan 1992, 1993
PA-6 (80)/EP-g-MA (1.3–4.4 % MA) (20)	Internal mixer at 260 °C/FTIR/mechanical properties/SEM	Abbate et al. 1992
PA-6 (90)/EEA-MA (1.5 % MA) (10)	TSE/mechanical properties/DSC/SEM/MFI/also blends containing glass fiber	Crespy et al. 1992
PA-6/PMMA-f-glutaric anhydride	TSE/mechanical properties/selective solvent extraction/FTIR/optional NaOH catalyst/PMMA partially functionalized by extrusion with dimethylamine	Harvey et al. 1992
PA-6 (100-0) or PA-66/ EP-g-MA (1.2 % MA) (0-100)	Double extruded in SSE at 240 °C or 280 °C/ mechanical properties/torque rheometry/lap shear adhesion/DMA/effects of mixing protocol	Oshinski et al. 1992a, b
PA-6 (50)/(88 HDPE +12 LLDPE) (0-50)/(88 HDPE + 12 LLDPE)-g-MA (0.27 % MA) (0-50)	TSE at 275 °C/mechanical properties/melt viscosity/rheology/SEM/effects of functionalized PE mol. wt./MA grafted to mixture of HDPE + LLDPE	Padwa 1992
PA-6 (100-0)/HDPE (0-100)/ HDPE-g-MA (0.8 % MA) (0-5)	SSE at 245 °C/SEM/DSC/capillary rheometry	Kim et al. 1991
PA-6 (30-10)/HDPE (70-90)/ EPDM-g-MA (1.8 % MA) (1, 3, or 5 parts)	Internal mixer at 250 °C/DSC/DMA/optical microscopy/SEM/also binary blends containing 95 PA + 5 EPDM-g-MA	Kim and Kim 1991
PA-6 (90-10) or PA-11/ HDPE (10-90) or MDPE/ PE-g-MA (0-10)	Internal mixer at 200–300 °C/torque rheometry/ capillary rheometry/SEM/selective solvent extraction/FTIR	Serpe et al. 1990
PA-66 (80)/EP-g-MA (20)	TSE at 280 °C/morphology vs. unfunctionalized EP use/DSC/DMA/EELS	Ban et al. 1988, 1989
PA-6 (90)/EPDM-g-MA (10)	SSE/selective solvent extraction/%N/FTIR/ mechanical properties vs. MA level	Borggreve and Gaymans 1989
PA-6 (90)/EPDM-g-MA (10) or EP-g-MA or PE-g-MA	SSE/selective solvent extraction/mechanical properties/morphology/dilatometry tests/also used unfunctionalized poly(etherester) TPE	Borggreve et al. 1989a, b
Aromatic PA (84 parts)/ EPDM-g-FA (8.4 parts; 1.5–2.0 % FA)/ionomer resin (7.6 parts; 72 % Zn neutralized)	TSE at 321 °C/mechanical properties vs. blends with less EPDM-g-FA or without ionomer	Dunphy 1989
PA-6 (35 %)/polyarylate (35 %)/EP-g-nadic anhydride (15 %)/EVAc-co-GMA (15 %)	TSE at 270 °C/mechanical properties vs. blends with only one functionalized rubber/other PA used	Okamoto et al. 1989
PA-6 (100-80)/EPDM-g-MA (0-20)	SSE/0.4 wt% MA/morphology/mechanical properties correlation with interparticle distance	Borggreve et al. 1988a, b
PA-6 (90-80)/EP-g-MA (0-10)/unfunctionalized EP (10-20)	Internal mixer at 260 °C/mechanical properties vs. morphology	D'Orazio et al. 1988

Table 5.12 (continued)

Polyamide/polyolefin	Characterization and comments	References
Copolyamide of 60 % polyhexamethylene adipamide and 40 % polyhexamethylene adipamide-terephthamide/ EP-g-MA	Melt extrusion/mechanical properties	Neilinger et al. 1988
PA-66,6 copolymer (84)/ ethylene-butene copolymer-g-FA (16; 1 wt% FA)	Extruded at 232 °C/mechanical properties vs. blend with unfunctionalized EB copolymer	Sawden 1988
PA-6 (80)/LDPE-g-S-MA (20)	TSE at 240 °C/mechanical properties/also used PA-66 and PA-46	Vroomans 1988
PA-6 (100-80)/EP (0-20)/ EP-g-MA (0-20)	Internal mixer at 260 °C/0.6–4.5 wt% MA/morphology/mechanical properties	Greco et al. 1987
PA-6 (100-70)/EP (0-20)/ EP-g-MA (0-30)	Internal mixer at 260 °C/mechanical properties vs. morphology	Cimmino et al. 1986
PA-66 (100-96)/ EPDM-g-MA (0-4)	TSE at 204–347 °C/FTIR/DSC/SEM/mechanical properties vs. MA level (0–10 %)	Crespy et al. 1986
PA-6 (50)/EP-g-MA (50; 1.7–1.9 % MA)	SSE at 215–232 °C/mechanical properties vs. higher MW EPDM-g-MA	Olivier 1986a (cf. Phadke 1988a)
PA-6 (100-70)/EP (0-30)/ EP-g-MA (10-30)	internal mixer at 260 °C/crystallinity by DSC/SAXS/WAXS/SEM/optical microscopy	Martuscelli et al. 1985
PA-6 (80 parts)/ hydrogenated poly-butadiene-g-MA (20 parts; 0.4 wt% MA)	TSE at 288 °C/mechanical properties/also used other MA-grafted polyolefins	Hergenrother et al. 1984, 1985
PA-6 (100-80)/EP (0-20)/ EP-g-MA (0-20)	Internal mixer at 260 °C/2.9 % MA/morphology/ mechanical properties vs. EP-g-MA fraction	Cimmino et al. 1984
PA-66 (41 parts)/PA-6 (40 parts)/EPDM (9 parts)/ EPDM-g-FA (10 parts; 1.5–2.0 % FA)	TSE at 310–320 °C/mechanical properties vs. blends with single PA	Roura 1982, 1984
PA-66 (100-60)/PE-g-MA (0-40)	TSE at 270 °C/0.4 % MA/mechanical properties/ adverse effect of blocking anhydride groups/ morphology	Hobbs et al. 1983
PA-6 (80)/ethylene-butene copolymer-g-MA (20; 0.35 % MA)	Extruded at 250 °C/mechanical properties	Ohmura et al. 1982
PA-6/EP-hexadiene-norbornadiene copolymer-g-FA	TSE at 270 °C/mechanical properties	Richardson 1981
PA-66 or amorphous PA/functionalized ethylene copolymer	TSE/anhydride- or carboxylic acid- or epoxide-functionalized ethylene copolymer/mechanical properties	Epstein 1979
PA-66 (24 parts)/ LDPE-g-MA (10 parts)	TSE at 271 °C/mechanical properties vs. control/ effect of different radical initiators for grafting LDPE/PA-6 also used	Swiger and Juliano 1979; Swiger and Mango 1977

Table 5.13 PA/PO blends: block copolymer formation by amine + carboxylic acid reaction

Polyamide/polyolefin	Characterization and comments	References
PA-66/oxidized LLDPE	Mechanical properties/morphology	Zhu et al. 2010
Aromatic PA (50)/ hydrogenated NBR (50)/ carboxy-terminated NBR (0-5)	Miniature mixer at 250 °C/ morphology/ellipsometry/L101 (0.9 phr) added for vulcanization of rubber phase/effects of mixing protocol/other carboxylated rubbers also used	Bhowmick et al. 1993
PA-6 (75)/oxidized LDPE (25)	Internal mixer at 240 °C/ morphology/mechanical and rheological properties vs. functionalization level	Curto et al. 1990
PA-6 (47.5)/PE (47.5)/ oxidized LDPE (5)	1 in. extruder at 222 °C/heat-aged morphology/mechanical properties	Armstrong 1968

Table 5.14 PA/PO blends: graft copolymer formation by amine + carboxylic acid reaction

Polyamide/polyolefin	Characterization and comments	References
PA-6/carboxylated nitrile rubber	TSE/DMTA/TEM/effects of carboxylation level on blend properties/rubber cured during mixing	Chowdhury et al. 2007
PA-6/LDPE/EAA (6 wt% AA)	Morphology/interfacial tension measured by breaking thread method/also used EAA partially Zn neutralized	Minkova et al. 2002, 2003
PA-6/EAA/optionally with LDPE	SEM/effect on blend properties of different AA content in EAA/also used EAA partially Zn neutralized	Filippi et al. 2002
PA-6/EVAc/EAA	Mechanical properties/morphology/ rheology/comparison to blend without either of EVAc or EAA	Wang et al. 2001
PA-6/PE-g-AA	DSC/WAXS	Psarski et al. 2000
PA-6 (60)/PE-f-(10-undecenoic acid) (40)	TSE/morphology/mechanical properties/ Molau test/FTIR/f-PE synthesized using metallocene catalyst/also used 10-undecen-1-ol or N-methyl-10-undecenylamine	Anttila et al. 1999
PA-6/EVAl-f-carboxylic acid	FTIR/SEM/DSC/DMTA/rheology/ selective solvent extraction/ionic linkage postulated	De Petris et al. 1998
PA-6/LLDPE-g-AA	Internal mixer/SEM/DSC	Qui et al. 1999
PA-6 (9-6)/PE (90)/EAA (11 % AA; 40 % Zn neutralized) (1-4)	PA + EAA extruded on TSE at 240 °C followed by blow molding with 90 % PE/DSC/SEM/rheology/permeation test/ mechanical properties/selective solvent extraction + FTIR for PA-EAA copolymer characterization	Yeh and Fan-Chiang 1997; Yeh et al. 1997
PA-1010 (75)/EP (5-25)/ EP-g-AA (1 % AA) (0-20)	SSE at 210 °C/mechanical properties/ SEM/DSC/WAXD	Xiaomin et al. 1996

(*continued*)

Table 5.14 (continued)

Polyamide/polyolefin	Characterization and comments	References
PA-6 (90-10)/HDPE (10-90)/ EMAA ionomer (0-30)	Internal mixer at 250 °C/torque rheometry/ SEM/dispersed phase particle size vs. interfacial modifier concentration/ emulsification curves/effects of mixing protocol/also blends containing PP in place of HDPE	Favis 1994; Willis and Favis 1988
PA-6 (75-25)/HDPE (25-75)/ EMAA ionomer (0-5)	SSE/interfacial tension measurements/ morphology before and after annealing/ mechanical properties	Chen and White 1993
PA-6 (40-20)/HDPE (60-80)/ EMAA ionomer (2)	TSE at 250 °C/use of PE + 10 % EMAA ionomer masterbatch/rheology/SEM/also ribbon extruded blends	Gonzalez-Nunez et al. 1993
PA-6 (100-0)/EMAA ionomer (0-100)	Internal mixer at 250 °C/torque rheometry/ SEM/selective solvent extraction/FTIR/ DSC	Willis et al. 1993
PA-6 (90)/EAA (10 % AA) (10)	TSE/mechanical properties/DSC/SEM/ MFI/also blends containing glass fiber	Crespy et al. 1992
PA-6 (80-90)/EAA (20-10)	TSE at ≥270 °C/FTIR/NMR/DTA/GPC/ selective solvent extraction/morphology/ amine, acid quantification/% chains grafted	Braun and Illing 1987
PA-66 (85)/acid-functionalized EP (15)	TSE at 230–280 °C/rheology/SEM/ dispersed phase particle size vs. interfacial tension/effect of component viscosity ratio	Wu 1987
PA-6 (90)/EMAA (10)	Internal mixer at 250 °C/mechanical properties and morphology as function of MAA content/FTIR/selective solvent extraction/DSC/role of H-bonding	MacKnight et al. 1985
PA-6 (90-80)/EAA (10-20) or EMAA ionomer/TPPite (1) or trialkyl phosphite condensing agent	SSE at 265–315 °C/selective solvent extraction/model compound reactions/ FTIR/^{13}C NMR/^{31}P NMR	Aharoni et al. 1984; Aharoni 1983
PA-66/EMAA (11–12 wt% acid; 66 % Zn neutralized)	TSE at 280 °C/mechanical properties vs. using unneutralized EMAA	Murch 1974
PA-66/EMAA (9.8–16.4 wt% acid)	SSE at 280 °C/mechanical properties/effect of amine end-group concentration	Kohan et al. 1972
PA-6 (50)/PE (40)/EMAA (10; 4 mol% acid; 38 % Na neutralized)	Double-pass extrusion/mechanical properties	Mesrobian et al. 1968
PA-66/EMAA (5.7 mol% acid)	SSE at 280 °C/morphology/barrier properties	Anonymous 1965

5.8.6.4 Copolymer Formation by Amine or Carboxylic Acid + Epoxide Reaction

Table 5.15 shows examples of PA/PO blends compatibilized through graft copolymer formation between PA amine or carboxylic acid end-groups and pendent epoxy groups on polyolefins.

Table 5.15 PA/PO blends: copolymer formation by amine or carboxylic acid + epoxide reaction

Polyamide/polyolefin	Characterization and comments	References
PA-6/MDPE-g-GMA	Mechanical properties/morphology/GMA grafting optionally performed in presence of styrene monomer and differing concentration of DCP RI	Daneshvar and Masoomi 2012
PA-12/ENR	Mechanical properties/morphology/temperature scanning stress relaxation measurement/ optionally with dynamic vulcanization/ comparison to blends with unfunctionalized NR	Narathichat et al. 2011
PA-6/PE-g-GMA	TSE/SEM/DSC	Huang et al. 2008
PA-6 (25-75)/LDPE (75-25)/E-GMA	Brabender mixer/SEM/rheology/DSC/ morphology as function of blend composition, compatibilizer concentration, and GMA content/ also used LDPE-g-GMA, SEBS-g-GMA	Wei et al. 2005; Minkova et al. 2002
PA-6/LDPE/E-g-GMA	Melt blending/morphology/thermal properties/ selective solvent extraction/comparison of properties to those of blends with EAA and PE-g-MA in place of E-g-GMA	Chiono et al. 2003
PA-6/LDPE-g-GMA (3.5 wt% GMA)	Internal mixer/torque rheometry/SEM/DSC/ FTIR/Molau test/GMA grafting with addition of styrene monomer in presence of peroxide/ comparison to blends with unfunctionalized LDPE	Wei et al. 2003
PA-6/ENR	Morphology/DSC/mechanical properties/FTIR/ compatibilization of PO blends	Xie et al. 2003
PA-6/PE-f-GMA	Melt mixing at 240 °C/morphology/pull-out of in situ formed graft copolymer/also used PE-g-MA in place of PE-f-GMA	Pan et al. 2001, 2002
PA-6/EPDM-f-epoxide	Melt mixing/morphology/comparison to blend with unfunctionalized EPDM	Wang et al. 1998b
PA-6 (75)/SB core-MMA-GMA shell impact modifier (25)	Mini-extruder at 240 °C/TEM/dispersed phase agglomeration as function of epoxide concentration on shell surface	Aerdts et al. 1997
PA-6 (100-0 parts)/ PE-g-GMA (0-100 parts)	Custom mixer at 230 °C/SEM/DSC/DMA/ mechanical properties/selective solvent extraction/FTIR/also used PA-11, PA-12, PA-612, or PA-610/optionally + HDPE	Koulouri et al. 1997
PA-6 (80)/EPDM-g-GMA (20; 2.8 % GMA)	Mechanical properties	Olivier 1986b

5.8.6.5 Copolymer Formation by Miscellaneous Reactions

Miscellaneous compatibilization methods belonging to this category are listed in Table 5.16. Chen and Wang (2001) reported that pan-milling a blend of PA-6 and PP resulted in chain scission and subsequent copolymer formation resulting in a blend with improved properties compared to the same blend prepared by extrusion. Li et al. (1993) have shown that PA-PO copolymer may be formed through displacement reaction between PA amine end-groups and benzylic bromide groups

Table 5.16 PA/PO blends: copolymer formation by miscellaneous reactions

Polyamide/polyolefin	Characterization and comments	References
PA-6/NBR/NBR-f-oxazoline (5–7 phr)	Mechanical properties/morphology/DSC/ rheology/swelling/creep behavior	Gomes et al. 2013
PA-6/EPDM-g-MA/epoxy resin	TSE/mechanical properties/morphology/ DSC/rheology/effects of blending protocol on blend properties	Wang et al. 2012f
PA-6/EP-g-isocyanate	Mechanical properties/morphology/FTIR/ DSC/rheology/EP grafted with allyl (3-isocyanato-4-tolyl) carbamate	Ding et al. 2003
PA-6 (80)/LDPE (20)/EAA (2 phr)/bis-oxazoline coupling agent (0.2–0.35 phr)	TSE/SEM/rheology/DSC/mechanical properties/Molau test/used 2,2′-(1,3-phenylene)-bis(2-oxazoline)	Scaffaro et al. 2003 (see also Canfora et al. 2004; and La Mantia et al. 2005)
PA-6/ULDPE-g-DEM	TSE/rheology/morphology/dielectric spectroscopy/selective solvent extraction/ FTIR/DSC/impact strength	Sanchez et al. 2001
PA-6/oxazoline-f-nitrile rubber	DSC/impact strength/portion of nitrile groups on rubber converted to oxazoline groups in separate reaction	Piglowski et al. 2000
PA-6/polyepichlorohydrin	Banbury mixer/rheology/TEM/diffuse reflectance IR/Molau test/X-ray diffractometry/also used poly (epichlorohydrin-co-ethylene oxide)	Da Costa et al. 1999; Da Costa and Felisberti 1999
PA-6/EP-g-isocyanate	morphology/mechanical properties/DSC/ comparison to blends made with unfunctionalized EP/EP grafted with reaction product of 2-hydroxyethyl methacrylate and isophorone diisocyanate	Jun et al. 1999
PA-6/PE/oxazoline-f-PE	TSE/mechanical properties/morphology/ comparison to blends with unfunctionalized PE/also used PP, oxazoline-f-PP, oxazoline-f-EP, and oxazoline-f-SEBS	Vocke et al. 1998, 1999
PA-6 (90-10)/LDPE-g-isocyanate (10-90)	Internal mixer at 245 °C/SEM/rheology/ mechanical properties/comparison to blends made with unfunctionalized LDPE/ FTIR/PE grafted with 2 wt% reaction product of 2-hydroxyethyl methacrylate and isophorone diisocyanate	Park et al. 1997
PA-6 (100-70)/brominated poly (isobutylene-co-p-methylstyrene) (2.3 mol% p-methylstyrene; 0.7 wt% Br) (0-30)	TSE/TEM/SEM/optical microscopy/DSC/ mechanical properties/fracture mechanism	Li et al. 1993
PA-6 (80 parts)/EP-g-N-methacrylyl caprolactam (20 parts)	TSE at 270 °C/PA-6 was mixture of two grades with different amine end-group content/mechanical properties vs. blends with unfunctionalized EP/also used PA-66 and PA-46/also used N-acrylyl caprolactam and N-methacrylyl laurolactam	Akkapeddi et al. 1989

Table 5.16 (continued)

Polyamide/polyolefin	Characterization and comments	References
PA-6 (100-0) or PA-6,66,610 terpolymer or PA-69/ chlorinated PE (0-100)/L101 RI	Internal mixer at 225 °C/selective solvent extraction/FTIR/mechanical properties/ also blends containing m-phenylene bismaleimide or trimethylolpropane triacrylate + RI	Coran and Patel 1983a
PA-66 (2.7 parts)/EA-BA-vinyl benzyl chloride copolymer (0.9 parts; 0.23–0.33 % reactive chloride)	SSE at 280 °C/multiple pass extrusion/ mechanical properties/also used vinyl chloroacetate as reactive chloride source	Moncur 1982

pendent on brominated poly(isobutylene-*co-p*-methylstyrene) (see also Bhadane et al. 2008, 2011; and Tsou et al. 2009, 2011). Coran and Patel (1983a) suggest that PA-PO copolymer may be formed by a displacement reaction between PA amine end-groups and PO chloride groups, simultaneous with dynamic vulcanization of the PO phase. Moncur (1982) reported that PA-PO copolymer may form through PA amine end-group displacement of chloride from a PO copolymer bearing reactive chloride.

5.8.7   Polyamide + Polyolefin + Polypropylene Blends

5.8.7.1 Copolymer Formation by Amine + Carboxylic Acid Reaction
Favis (1994) and Willis and Favis (1988) prepared compatibilized PA blends with PP and carboxylic acid-functionalized EMAA ionomer. Blends containing 90-10 parts PA-6, 0-30 parts EMAA ionomer, and 10-90 parts PP were combined in an internal mixer at 250 °C and characterized by torque rheometry and SEM. Dispersed phase particle size vs. interfacial modifier concentration was determined. Emulsification curves were constructed. Effects of mixing protocol on blend properties were studied. Blends were also prepared containing HDPE in place of PP.

5.8.7.2 Copolymer Formation by Amine + Anhydride Reaction
PA/PP blends have been compatibilized through graft copolymer formation between polyamide amine end-groups and pendent anhydride groups on a functionalized polyolefin as exemplified in Table 5.17.

Chen and White (1993) and Chen et al. (1988) have reported properties for blends containing 75-25 parts PA-6 (or PA-11), 25-75 parts LDPE (or HDPE), and 0-5 parts PP-MA. The blends were prepared in an SSE at 200–230 °C and characterized by mechanical properties and DSC. Morphology and capillary rheometry were done before and after annealing. Interfacial tension measurements for the blends were also reported.

5.8.7.3 Copolymer Formation by Amine or Carboxylic Acid + Epoxide Reaction
As shown in Table 5.18, PA/PP blends can be compatibilized through graft copolymer formation between polyamide amine end-groups and pendent epoxide groups

Table 5.17 PA/PO/PP blends: copolymer formation by amine + anhydride reaction

Polyamide/polyolefin/PP	Characterization and comments	References
PA-11 (60)/EB-g-MA (10)/PP (30)	Twin-screw melt kneader/ mechanical properties/SEM/ EDXA/PA-EB premixed/ comparison to other orders of mixing	Kawada et al. 2013
PA-6 (0-40)/ethylene-octene copolymer-g-MA (0-20)/PP	PP continuous phase/morphology by SEM and TEM/mechanical properties	Bai et al. 2004 (see also Liu et al. 2004, 2006)
PA-6 (30)/EP-g-MA (0-20) PP (50-70)	Internal mixer at 240 °C/TEM/ mechanical properties vs. volume fraction of compatibilizer	Rösch et al. 1996; Rösch 1995; Rösch and Mülhaupt 1994
PA-6 (100-0)/EP-g-MA (1.1 % MA) (0-20)/PP (0-100)	SSE at 240 °C/mechanical properties/ductile-brittle transition temperatures/DMA/tensile dilatometry/SEM/TEM/effects of PP and PA molecular weight/ effects of adding PP-MA	Gonzalez-Montiel et al. 1995a, b, c
PA-6 (100-0)/E-BA-g-FA (0.4 % FA) (10)/PP (0-100)	TSE at 245 °C/DSC/SEM/ mechanical properties	Ikkala et al. 1993; Holsti-Miettinen et al. 1992
PA-66 (1.8 parts)/mixture of EP and PP grafted with MA (1 part; 1 wt% MA)	TSE at 271 °C/moisture absorption vs. blends without functionalized polymers	Perron and Bourbonais 1988
PA-6 (30 parts)/PP (50 parts)/70:30 mixture of EP and PP grafted with nadic anhydride (20 parts; 0.2 wt% NA)	TSE at 250 °C/mechanical properties vs. blends with mixture of EP and PP functionalized separately instead of as a mixture	Fujita et al. 1987

Table 5.18 PA/PO/PP blends: copolymer formation by amine or carboxylic acid + epoxide reaction

Polyamide/polyolefin/PP	Characterization and comments	References
PA-6 (30) or PA-66/PP (70)/ E-BA-GMA (2.5 % GMA) (3.5)	TSE at 250–280 °C/SEM/interfacial tension measurements by imbedded fiber retraction/comparison to blend without compatibilizer/masterbatch prepared from PP + 5 % E-BA-GMA	Kirjava et al. 1995
PA-6 (100-0)/PP (0-100)/ E-EA-GMA (8 % GMA) (0-10)	TSE at 245 °C/mechanical properties/ DSC/SEM	Ikkala et al. 1993; Holsti-Miettinen et al. 1992

on a functionalized PO. Since there are multiple epoxide sites on the polyolefin, some cross-linked copolymer may result as well if the PA is functionalized at both ends. The proportion of cross-linked copolymer formed also depends upon blend composition and processing conditions.

5.8.8 Polyamide + Polyolefin + Styrene Copolymer Blends

5.8.8.1 Copolymer Formation by Amide-Ester Exchange

Horak et al. (1997) prepared compatibilized PA blends with ABS in the presence of polyacrylate copolymer bearing pendent ester groups. A graft copolymer is obtained when PA amine end-groups undergo transreaction with the pendent ester groups. In an example, 50-45 parts PA-6 was mixed with 45-50 parts ABS and 0-10 parts MMA-co-AN (80 % MMA) in an internal mixer at 240 °C. The blend was characterized by SEM, WAXS, and mechanical properties. The effects of premixing PA + MMA-co-AN or of adding dibutyltin dilaurate or Ti(OBu)$_4$ catalyst were examined.

5.8.8.2 Copolymer Formation by Amine + Anhydride Reaction

As shown in Table 5.19, PA/PO blends have been compatibilized through graft copolymer formation between polyamide amine end-groups and pendent anhydride groups on a functionalized styrene copolymer or alternatively through copolymer formation between PA and anhydride-functionalized PO in the presence of PS or a styrene copolymer.

5.8.8.3 Copolymer Formation by Amine or Carboxylic Acid + Epoxide Reaction

Huang et al. (2011) prepared blends of PA-6 with ABS in the presence of ethylene-acrylate-GMA copolymer. Characterization techniques included SEM, DSC, HDT, and mechanical properties.

Filippi et al. (2004) prepared blends of PA-6 with LDPE in the presence of SEBS-g-GMA. Inefficient compatibilization of PA/PE was observed in comparison to the use of SEBS-g-MA apparently due to cross-linking reactions involving both amine and carboxylic acid end-groups on PA.

An interesting study by Kudva et al. (1998) showed that PA-6/ABS blends were poorly compatibilized through graft copolymer formation between PA amine or carboxylic acid end-groups and MMA-co-GMA. Extensive characterization indicated that, although the epoxy-functionalized MMA is miscible with the SAN domain, the difunctionality of PA end-groups led to PA cross-linking rather than formation of a compatibilizing copolymer.

5.8.9 Polyamide + Polyphenylene Ether Blends

PA/PPE blends in these sections include those containing PPE-miscible PS or a functionalized PS. These blends often contain a rubbery impact modifier, such as SEBS.

5.8.9.1 Blends Containing PPE Melt Functionalized with Anhydride Groups: PA-PPE Copolymer Formation by Amine + Anhydride Reaction

Anhydride groups are readily introduced into polyphenylene ethers such as poly (2,6-dimethylphenylene ether) (PPE) by extrusion with maleic anhydride (MA) or

Table 5.19 PA/PO/styrene copolymer blends: copolymer formation by amine + anhydride reaction

Polyamide/polyolefin/styrene copolymer	Characterization and comments	References
PA-66/polybutadiene-g-MA/ABS	FTIR/Molau test/MFI/DMA/SEM	Yang et al. 2012
PA-1010/PP-g-(styrene-co-MA)/ABS	Mechanical properties/SEM/ crystallization behavior	Zhang et al. 2012
PA-6/PP-g-(styrene-co-MA)/PS	SEM morphology	Wang et al. 2011
Recycle PA-PP (75-25)/SEBS-g-MA	SEM/rheology/mechanical properties/ also used PP-g-MA in place of SEBS-g-MA	Hong et al. 2006
PA-6/PP/PP-g-(styrene-co-MA)	SEM/rheology/DMA/mechanical properties/enhancement in properties compared to use of PP-g-MA or PP-g-styrene	Wang and Xie 2006
PA-6/LDPE/styrene-b-(ethylene-co-propylene)-g-MA	Morphology/thermal and mechanical properties/comparison to binary PA and LDPE blends with SEP-g-MA and to ternary blends with HDPE-g-MA or SEBS-g-MA in place of SEP-g-MA	Filippi et al. 2004, 2005
PA-6 (15)/PP (70)/SEBS + SEBS-g-MA (15)	TSE/TEM/thermal and mechanical properties/progressive replacement of SEBS with SEBS-g-MA	Wilkinson et al. 2004
PA-6/ABS/PMMA-co-MA	Mechanical properties/morphology/ also used PMMA-co-GMA in place of PMMA-co-MA	Araujo et al. 2003a, b
PA-6/LDPE/SEBS-g-MA (2 wt% MA)	Morphology/interfacial tension measured by breaking thread method	Minkova et al. 2003
PA-66 (60)/PP (20)/SEBS-g-MA (20)	Blend characterization using microscopic techniques/effect of different levels of MA	Wong and Mai 1999, 2000
PA-6/EP-g-MA/SMA	Melt extrusion/mechanical properties/ morphology	Kelnar et al. 1999
PA-6 (75)/PMMA (25)/SMA (20 % MA) (5-35)	Melt extrusion/morphology vs. extrusion time and parts of SMA in blend	Dedecker and Groeninckx 1998
PA-6 (50)/PP (50)/SEBS-g-MA (5–25 wt%)	Morphology/mechanical properties/ effects of different mixing protocols	Ohlsson et al. 1998a, b
PA-6 (85-75)/SAN (25% AN) (12-25)/ imidized acrylate copolymer (56% methyl glutarimide, 40% MMA, 2% MAA, 3% glutaric anhydride) (0-8)	TSE at 240°C/torque rheometry/SEM/ morphology development in extruder vs. screw design and processing conditions/also PA-6 and PA-66 blends with SEBS-g-MA/titration of residual amine end-groups	Majumdar et al. 1997
PA-6 (10)/HDPE (80-90)/SEBS-g-MA (0-10)	TSE at 230 °C/rheology/mechanical properties/DSC/SEM	Chandramouli and Jabarin 1995

(*continued*)

Table 5.19 (continued)

Polyamide/polyolefin/styrene copolymer	Characterization and comments	References
PA-6 (78-55)/EP-g-MA (1.1 % MA) (0-22)/EPDM-g-SAN (0-45) or ABS	SSE at 240 °C/TEM/mechanical properties	Lu et al. 1995
PA-6 (25)/LDPE (75)/SEBS-g-MA (0-5)	TSE at 250 °C/SEM/observation of morphology development along extruder screw axis	Lim and White 1994
PA-6 (50-45) or PA-66 or PA-11 or PA-612 or PA-610 or PA-1212 or PA-6-66 copolymer/ABS (45-50)/imidized acrylate copolymer (56% methyl glutarimide, 40% MMA, 2% MAA, 1% glutaric anhydride) (0-10)	SSE at 240°C or two different types of TSE/torque rheometry/TEM/DSC/ mechanical properties vs. extrusion conditions and morphology/ductile-brittle transition temperatures/effects of PA amine end-group concentration	Majumdar et al. 1994a
PA-6 (100-0)/ABS (0-100)/imidized acrylate copolymer with various acid + anhydride concentrations (0-20)	SSE at 240°C/TEM/torque rheometry/ mechanical properties vs. compatibilizer content, functionalization level, rubber conc. and mixing protocol/ductile-brittle transition temperatures	Majumdar et al. 1994b
PA-6 (75) or PA-66 or PA-6,66 copolymer/SAN (6-40% AN) (0-25)/ imidized acrylate copolymer with various acid + anhydride concentrations (0-25)	SSE at 240°C/torque rheometry/DSC/ TEM/mechanical properties/effects of AN content/effects of acid + anhydride concentration/effects of PA amine end-group concentration	Majumdar et al. 1994g
PA-6 (75)/LDPE (25)/SEBS-g-MA (2 % MA) (0-15)	SSE at 240 °C/mechanical properties/ SEM/optical microscopy/DSC	Armat and Moet 1993
PA-6 (75-25)/HDPE (25-75)/ SEBS-g-MA (0-5)	SSE/interfacial tension measurements/ morphology before and after annealing/ mechanical properties	Chen and White 1993

congeners such as fumaric acid (FA), itaconic acid, citraconic acid, and related compounds. Evidence has been presented that such anhydride groups are predominantly located along the PPE main chain and with a fraction also at chain ends (Glans and Akkapeddi 1991b). This functionality distribution depends on the type and level of functionalization agent and on the mixing protocol during extrusion processing. PPE that has been melt functionalized, for example, with FA or MA reacts with PA to give predominantly graft copolymer by reaction of anhydride pendent groups on PPE with amine end-groups of PA. There is certainly a proportion of block copolymer formation as well since some anhydride functionality may be present at the chain ends on PPE. In the examples given in Table 5.20, PPE was functionalized in either a separate extrusion step before mixing with PA or in the front section of an extruder with downstream feeding of PA.

Son et al. (2000a, b) have studied the effect of processing conditions on the morphology of PA blends with PPE compatibilized through addition of MA.

PPE has also been melt functionalized with various esters of trimellitic anhydride substituted in the 4-position (Sivavec and M?cCormick 1991). A phosphite catalyst

Table 5.20 PA/PPE blends – blends containing PPE melt functionalized with anhydride groups: copolymer formation by amine + anhydride reaction

Polyamide/PPE	Characterization and comments	References
PA-66 (48)/PPE-g-FA (37)/ EPDM-g-cyclic ortho ester (15)	TSE/impact strength vs. control blends/also used oxidized PPE and PPE-f-citric acid/EPDM reacted in separate extrusion step with graftable cyclic ortho ester	Khouri and Campbell 1997
PA-6 (40 parts)/PPE (50 parts)/ SEBS (10 parts)/vinyl trimellitic anhydride (1.5 wt%)	TSE at 290 °C/mechanical properties/PPE preextruded with anhydride/also used 2-isopropenyl oxazoline, 2-styryl oxazoline, cinnamic acid, and other functionalized species	Akkapeddi et al. 1992
PA-6 (41)/PPE-g-MA (0–3 % MA) (49)/SEBS (10)	TSE at 280 °C/selective solvent extraction/mechanical properties/ ductile-brittle transition temperatures/SEM/TEM	Campbell et al. 1990
PA-6 (40)/PPE-g-FA (60)	SSE at 275 °C/X-ray diffraction for compositional analysis and crystallinity level/comparison to blend made with unfunctionalized PPE	Murthy et al. 1990
PA-6 (50 parts)/PPE (50 parts)/ MA (0.5 parts)	TSE at 290 °C/impact strength vs. ratio of PA amine end-groups to PA carboxylic acid end-groups/ also used PA-66/also used citric acid, malic acid, or n-phenyl citric amide	Fujii et al. 1989
PA-66 (41 parts)/PPE (40 parts)/SEBS copolymer (10 parts)/citric acid (0.25 parts)	TSE at 300 °C/PPE precompounded with functionalization agent/mechanical properties/malic acid also used/ other PA also used	Gallucci et al. 1989
PA-66 (50 parts)/PPE (50 parts)/SEBS (5 parts)/ 1,2,3,4-cyclopentane tetracarboxylic acid (0.5 parts)	TSE at 315–321 °C/mechanical properties/PPE preextruded with acid/also used 1,4,5,8-naphthalene tetracarboxylic acid, pyromellitic dianhydride, tetrabromophthalic anhydride	Grant and Jalbert 1989
PA-66 (60)/PPE (36)/ polyoctenylene (4)/anthracene-MA adduct (1)	Double screw kneader/adduct precompounded with PPE/morphology and mechanical properties compared to blends with MA in place of adduct/also used PA-6, PA-12	Dröscher and Jadamus 1988
PA-66 (40 parts)/PPE (50 parts)/SB copolymer (10 parts)/MA (0.5 parts)	TSE at 300 °C/all components throat fed/radial teleblock SB copolymer/effect of S block length on mechanical properties/PA-6 also used	Ueda et al. 1988 (see also Abe et al. 1988; Shibuya et al. 1988a, b; Shibuya and Kosegaki 1987)

Table 5.20 (continued)

Polyamide/PPE	Characterization and comments	References
PA-66 (41 parts)/PPE (49 parts)/SBS (10 parts)/ triethylammonium fumarate (0.7-1.5 parts)	TSE/mechanical properties/PPE, SBS, fumarate preextruded before mixing with PA/effect of fumarate loading/other ammonium fumarates also used in place of triethyl	Yates 1988
PA-66 (41 parts)/PPE (49 parts)/EPDM (10 parts)/ MA (0.6-3.1 parts)	TSE/mechanical properties/PPE, EPDM, MA preextruded before mixing with PA/SBS, SEBS, and EP also used in place of EPDM	Yates and Ullman 1988
PA-66 (1 part)/PPE-g-MA (1 part; 0.1–3.0 wt% MA)	SSE/insolubles analysis/ mechanical properties/detrimental effect of using RI for grafting MA to PPE/also used itaconic acid in place of MA/control blends changing grafting protocol/also used other PA types	Jalbert and Grant 1987; Grant et al. 1988
PA-66 (41 parts)/PPE (49 parts)/SEBS (10 parts)/FA (0.7-1.5 parts)	TSE at 285 °C/mechanical properties/PPE, SEBS, FA preextruded before mixing with PA/SEBS + EPDM also used/PA-6 also used	Van der Meer and Yates 1987 (see also Taubitz et al. 1991)
PA-66 (3 parts)/PPE (7 parts)/ MA (1 part)	Brabender mixer at 250–300 °C/ mechanical properties vs. blend without MA	Ueno and Maruyama 1982a

was used to promote transesterification and functionalization at PPE phenolic chain ends. As an example, 412 g PPE was extruded with 8 % 4-(*o*-carbophenoxyphenyl)-trimellitic anhydride and 0.5 % triphenyl phosphite on a TSE at 170–300 °C. Analysis of the extrudate showed 40 % carboxylation and 55 % capping of PPE phenolic end-groups. Extrusion of 49 parts capped PPE with 41 parts PA-66 and 10 parts SEBS provided molded test parts with Izod impact strength of 247 J/m. The PPE-PA copolymer in this case is primary block type. For melt functionalization of PPE with various trimellitamides and subsequent compatibilized blends with PA, see also Sivavec and Fukuyama (1992).

5.8.9.2 Blends Containing PPE Solution Functionalized with Anhydride Groups: PA-PPE Block Copolymer Formation by Amine + Anhydride Reaction

Campbell et al. (1990) have reported properties for compatibilized PA-PPE blends made using anhydride-terminated PPE. Anhydride-terminated PPE was made by capping PPE phenolic end-groups with trimellitic anhydride acid chloride in solution. A block copolymer may form between PA amine end-groups and PPE-anhydride during subsequent melt mixing. For example, a blend containing 49 parts

PPE-anhydride, 41 parts PA-6, and 10 parts SEBS impact modifier was extruded using a TSE at 280 °C. The copolymer-containing blend was characterized by selective solvent extraction, mechanical properties, SEM, and TEM. Ductile-brittle transition temperatures were determined. The same anhydride-terminated PPE was also used to prepare compatibilized blends with PA-66 (Aycock and Ting 1986, 1987).

5.8.9.3 Blends Containing PPE Solution or Melt Functionalized with Aryloxy Triazine Groups: PA-PPE Copolymer Formation by Amine + Ester Exchange Reaction

PPE has been functionalized in solution with a variety of chloro aryloxy triazine derivatives in the presence of a base to provide a reactive diaryloxy triazine-capped PPE (Brown 1991b, 1993). Diaryloxy triazine-capped PPE can also be prepared by melt functionalization through transesterification of the cyanuric acid phenyl ester (i.e., aryloxy triazine) with PPE phenolic end-groups (Brown 1992b). Extrusion of the functionalized PPE with an amine-functionalized polymer such as amine-terminated PA results in formation of a compatibilizing block copolymer through displacement of at least one aryloxy group from the diaryloxy triazine end-cap. Typically, a 2,6-unfunctionalized aryloxy group is displaced from the triazine end-cap during extrusion in preference to displacement of more hindered 2,6-dimethylphenoxy PPE terminal unit. The reaction may also be viewed as an esteramide exchange reaction between a cyanuric acid ester (i.e., the diaryloxy triazine terminal group on PPE) and PA-amine end-group. In one example, 41 % PA-66 extruded with 49 % diaryloxy triazine-capped PPE, and 10 % impact modifier showed Izod impact strength of 753 J/m and tensile elongation of 122 % compared to 37 J/m and 11 % for the same blend containing unfunctionalized PPE. The effect of PA amine end-group concentration on blend properties was examined.

5.8.9.4 Blends Containing PPE Functionalized with Carboxylic Acid: Copolymer Formation by Amine + Carboxylic Acid Reaction

Yates and White (1989) introduced carboxylic acid functionality into PPE by metalation in solution with alkyl lithium and treatment with carbon dioxide. Extrusion of this functionalized PPE (45 parts) with PA-66 (45 parts) and SEBS (10 parts) provided a composition which showed eightfold improvement in impact strength compared to a similar blend made with unfunctionalized PPE.

5.8.9.5 Blends Containing Functionalized PPE: PA-PPE Copolymer Formation by Amine or Carboxylic Acid + Electrophile Reaction

PA/PPE blends have been compatibilized through copolymer formation between PA amine or carboxylic acid end-groups and an electrophile-functionalized PPE (Table 5.21). Typically, the PPE is functionalized in a separate reaction either in the melt or in solution to introduce an electrophilic moiety (such as epoxide, carbodiimide, cyclic ortho ester, imide, or the like) at a phenolic end-group or along the PPE main chain or both.

Table 5.21 PA/PPE blends – blends containing functionalized PPE: PA-PPE copolymer formation by amine or carboxylic acid + electrophile reaction

Polyamide/PPE	Characterization and comments	References
PA-6/PPE/PPE-f-phthalimide/SEBS	Brabender mixer/torque rheometry/FTIR/NMR/mechanical properties/PPE end-capped using N-methyl-4-nitrophthalimide/maximum impact strength at 1.65 % functionalized PPE in blend	Ghidoni et al. 1996
PA-66 (41 parts)/PPE-f-cyclic ortho ester (49 parts)/SBS (10 parts)/Lewis acid catalyst	TSE at 120–288 °C/mechanical properties vs. blend with no catalyst/ortho ester functionalization either in solution or in the melt	Khouri et al. 1992, 1993
PA-66 (41 parts)/PPE-f-dialkylphosphatoethoxy triazine (49 parts)/impact modifier (10 parts)	TSE at 120–288 °C/mechanical properties vs. blends with unfunctionalized PPE/chloroethoxy and bromoethoxy triazine could be used in place of dialkylphosphatoethoxy triazine	Phanstiel and Brown 1991, 1992
PA-66 (41 parts)/PPE-g-GMA (49 parts)/impact modifier (10 parts)	TSE at 185–345 °C/mechanical properties/various other graftable epoxides also used	Brown 1991a
PA-66 (41 parts)/PPE-f-epoxytriazine (49 parts)/impact modifier (10 parts)	TSE at 120–320 °C/mechanical properties vs. blend with unfunctionalized PPE/PPE capped with various chloro-epoxy triazines/also used other PA	Brown et al. 1991b
PA-12 (60 parts)/PPE-f-oxazoline (40 parts)	TSE at 290 °C/mechanical properties vs. blend with unfunctionalized PPE/also used imide-functionalized PPE and EPDM impact modifier	Neugebauer et al. 1991

5.8.9.6 Blends Containing Unfunctionalized PPE: Copolymer Formation by Coupling Agent Addition

Unfunctionalized PPE has been compatibilized with immiscible PA by addition of a coupling agent capable of reacting with both PPE and PA end-groups. In one example, 4,4′-methylenediphenyl diisocyanate (1 part) was used to compatibilize PPE (49 parts) with PA-6 (41 parts) in the presence of an impact modifier. Properties of compatibilized blends were compared to those without coupling agent and without impact modifier (Pernice et al. 1993). Similar work was performed by Chiang et al. (1998). Chiang and Chang (1998) employed a multifunctional epoxy resin for the same purpose.

5.8.9.7 Blends Containing Unfunctionalized PPE + Functionalized PS: PA-PS Copolymer Formation by Miscellaneous Reactions

Unfunctionalized PPE may be compatibilized with immiscible PA by addition of functionalized polystyrene capable of forming copolymer with PA (Table 5.22). This is a common compatibilization strategy for PPE blends since both PS itself and

Table 5.22 PA/PPE/PS blends – blends containing unfunctionalized PPE + functionalized PS: PA-PS copolymer formation by miscellaneous reactions

Polyamide/PPE/polystyrene	Characterization and comments	References
PA-6 (70)/PPE (30)/SMA (21.8 % MA)	FTIR/DSC/SEM/mechanical properties/ also blends containing SEBS-g-MA/also blends containing PPE-g-MA	Wang et al. 2010b, c, d
PA-6/PPE/PS/SMA	Morphology/DSC/effect of different mixing protocols/also studied blends without PPE	Tol et al. 2004, 2005
PA-6/PPE/SEBS-g-MA	Melt extrusion/rheology/TEM/DSC/ mechanical properties	Wu et al. 2006a (see also Wu et al. 2004)
PA-6 (70-30)/PPE (30-70)/ SMA (8 % MA) (0-10)	TSE at 290 °C/FTIR/SEM/capillary rheometry/DMA/mechanical properties	Chiou et al. 1999; Chiang and Chang 1997
PA-6/PPE/SMA	Morphology/FTIR/effect of blending protocol/effects of wt% MA in SMA and PA-6 MW	Dedecker and Groeninckx 1999
PA-6 (70-50)/PPE (30-50)/ S-GMA (0-10)	TSE at 280 °C/torque rheometry/capillary rheometry/SEM/DMA/mechanical properties	Chiang and Chang 1996
PA-6 (70-50)/PPE (30-50)/ SAA (11–46 % AA) (0-3)	Internal mixer or TSE at 280 °C/rheology/ SEM/mechanical properties/MFI/effect of different AA contents in SAA	Jo and Kim 1992
PA-6 (40 parts)/PPE (40 parts)/ SBS (10 parts)/styrene-chloromethylstyrene copolymer (10 parts; 3 % chloromethylstyrene)	TSE at 280 °C/mechanical properties vs. blends without chloro-functionalized copolymer/also used S-GMA or styrene-vinyl oxazoline copolymer	Taubitz et al. 1990
PA-66 (63 parts)/PPE (27 parts)/EP-g-MA (8 parts; 0.08 % MA)/PS-g-GMA (2 parts)	TSE at 320 °C/mechanical properties vs. blends with unfunctionalized EP or EP-g-MA made without RI/also used PA-46	Mawatari et al. 1989
PA-66 (50 parts)/PPE-g-MA (25 parts)/SEBS-g-MA (25 parts; 0.6 wt% MA)	TSE at 300 °C/insolubles analysis/ mechanical properties vs. blends with unfunctionalized PPE or SEBS/also used PA-6	Nakazima and Izawa 1989
PA-6 (20 parts)/PPE (60 parts)/ SMA (20 parts)	TSE at 280 °C/PA preextruded with SMA/mechanical properties vs. blends with either PS or SMMA copolymer/also used SMMA-MA or styrene-N-phenyl maleimide copolymer	Kasahara et al. 1982

functionalized polystyrenes with a relatively low level of functionality are miscible with PPE. The examples in the table include use of anhydride-, acid-, and epoxide-functionalized polystyrenes, all of which are capable of reacting with nucleophilic end-groups on PA to form a graft copolymer.

5.8.10 Polyamide + Polyphenylene Sulfide Blends

Gui et al. (2013) prepared blends of an elastomeric PA with PPS in the presence of an epoxy resin. Blend characterization techniques included rheology, FTIR, and mechanical properties.

Yamao and Kosaka (2000) have prepared compatibilized blends of PA-66 or PA-46 with an amine-functionalized PPS in the presence of either pyromellitic acid anhydride or a multifunctional epoxy resin as coupling agent. See also Ishio et al. (2011).

Blends containing PA and an anhydride-modified polyphenylene sulfide have been prepared by Kadoi et al. (1996). For example, PPS was extruded with either maleic anhydride, itaconic anhydride, or succinic anhydride to form a PPS shown to have carbonyl incorporation by FTIR after selective solvent extraction to remove unreacted anhydride. Blends of modified PPS and PA-66 were extruded at 290–310 °C and molded to provide test parts with improved properties compared to blends with unmodified PPS.

5.8.11 Polyamide + Polypropylene Blends

5.8.11.1 Copolymer Formation by Amine + Anhydride Reaction
Immiscible blends of PA and PP have been compatibilized through copolymer formation between PA amine end-groups and maleic anhydride-functionalized PP to form a new imide linkage (Table 5.23). The structure of maleic anhydride-functionalized PP has been discussed, e.g., by De Roover et al. (1995) and Sclavons et al. (1996). The authors demonstrated that the free radical initiated maleation of PP in the molten state leads to anhydride groups locating mainly at PP chain ends. Consequently, unless PP has been functionalized by a process that suppresses PP chain degradation, the reaction product of amine-terminated PA with MA-functionalized PP may be predominantly a block copolymer.

5.8.11.2 Copolymer Formation by Amine + Carboxylic Acid Reaction
As shown in Table 5.24, PA/PP blends can be compatibilized through graft copolymer formation between PA amine end-groups and pendent acid groups grafted at more than one site along the PP chain or with acid groups along a poly(acrylic acid) segment grafted at a single PP site.

5.8.11.3 Copolymer Formation by Amine or Carboxylic Acid + Epoxide or Oxazoline Reaction
Deng et al. (2007) compatibilized PA-66 blends with PP through addition of alpha-methylstyrene-GMA copolymer. Evidence was presented that the copolymer acts to functionalize PP in situ with GMA groups. PA-6 blends with PP or PE were also prepared using this method.

Table 5.23 PA/PP blends: copolymer formation by amine + anhydride reaction

Polyamide/PP	Characterization and comments	References
Amorphous PA/PP/PP-MA (20 %)	Morphology/Young's modulus/mechanical properties	Aranburu and Eguiazábal 2013
Recycle PA-6/PP/PP-g-MA	TSE/thermal and mechanical properties/morphology	Jaziri et al. 2008
PA-6/PP/PP-g-MA	Torque rheometry/mechanical properties/SEM/no effect seen using PP with different MFI/comparison to blends with unfunctionalized PP or using PP-g-AA	Agrawal et al. 2007
PA-12/PP/PP-g-MA	Mechanical properties/SEM/critical concentration of compatibilizer for optimum properties/comparison to compatibilization theories	Jose et al. 2006b, c (see also Wu et al. 2006b)
PA-1010/PP/PP-g-MA	Melt mixing/mechanical properties/SEM	Yan and Sheng 2006
PA-6/PP/PP-g-MA	Melt mixing/fracture toughness measured using asymmetric double cantilever beam test/X-ray diffraction/XPS	Seo and Ninh 2004
PA-6/PP/PP-g-MA (2.5–10 wt%)	Internal batch mixer/morphology/rheology/DSC/laser scanning confocal microscopy	Afshari et al. 2002
PA-6/PP/PP-g-MA	Melt mixing/morphology/effect of processing conditions including screw speed and configuration	Tabtiang and Venables 2002
PA-6/PP-g-MA	Melt mixing/SEM/TEM/interfacial tension studied using Neumann Triangle method	Zhaohui et al. 2001
PA-66/PP-g-MA	Morphology/comparison to blends compatibilized by addition of PA-66-PP copolymer	Champagne et al. 2000
Poly(m-xylene adipamide)/PP-g-MA	Brabender at 265 °C/FTIR/model reactions/copolymer structure	De Roover et al. 2000
PA-6/PP-g-MA	TSE/morphology development over extruder screw length/mechanical properties/development of 1-pass extruder process for grafting and compatibilization	Cartier and Hu 1999 (see also Franzheim et al. 2000; Barangi et al. 2008)
Amorphous PA/PP/PP-MA	Melt blending/SEM/XPS/interfacial fracture toughness/effects of PP-MA level	Cho and Li 1998
Amorphous PA (30)/PP (70-0)/PP-MA (0-70)	Mini-Max molder at 240 °C/laser light scattering/TEM/SEM/ellipsometry	Li et al. 1997
PA-6 (30)/PP (60-70)/PP-MA (0.4 % MA) (0-10)	TSE at 230 °C/rheology/DSC/WAXS/FTIR/FT-Raman/optical microscopy	Marco et al. 1997
PA-66 (100-0)/PP (0-100)/PP-MA (0-5)	TSE at 255 °C/mechanical properties	Roberts et al. 1997
PA-6/PP-MA	Interfacial fracture energies between molded plaques as function of temperature/video imaging, ESCA and SEM of fracture surfaces/DSC	Bidaux et al. 1996

<div align="right">(continued)</div>

Table 5.23 (continued)

Polyamide/PP	Characterization and comments	References
PA-6 (30-25) or PA-12/PP (60-70)/PP-MA (0-20)	Internal mixer at 240 °C/TEM/mechanical properties and dispersed phase domain size vs. vol. fraction of compatibilizer/also blends containing EP rubber	Rösch et al. 1996; Rösch 1995; Rösch and Mülhaupt 1993, 1995a, b
PA-6 (100-25)/PP (25-100)/ PP-MA (5.3 % MA) (0-9)	Internal mixer at 235 °C/mechanical properties/DSC/water absorption/SEM/ DMA	Sathe et al. 1996
PA-12 (25)/PP (0-75)/PP-MA (0-75)	Solution precipitation followed by heat treatment at 180 °C/SEM/DMA/DSC/ effects of annealing/selective solvent extraction	Tang et al. 1995, 1996
PA-6 (60)/PP-MA (40)	SSE or TSE/mechanical and thermal properties/use of recycle PP containing 5–10 % EVAl + 2–5 % LDPE vs. virgin PP	Akkapeddi et al. 1995
PA-6 (100-0)/PP (0-100)/PP-MA (0.4–3.1 % MA) (0-100)	SSE or internal mixer at 240 °C/torque rheometry/mechanical properties/TEM	Gonzalez-Montiel et al. 1995b, d
PA-66 (30-0)/PP (40-100)/ PP-MA (0-30)	Internal mixer at 240–270 °C/SAXS/ effects of extrusion temperature on dispersion	Lin et al. 1995
PA-6 (75-68)/PP (25-23)/ PP-MA (10)	TSE at 240 °C/SEM/mechanical and thermal properties/rheometry/effects of PA mol. wt./also glass filled blends	Wu et al. 1995
PA-66 (75-25)/PP (25-75)/ PP-MA (0.2–2.7 % MA) (0-25)	TSE at 285 °C/morphology and mechanical properties vs. 0.2 or 2.7 wt% MA content PP/DSC crystallization behavior	Duvall et al. 1994a, b, c
PA-66 (50-20)/PP-MA (0.9–2.1 % MA) (50-80)	Mechanical properties/rheology/SEM/ copolymer analysis	Fritz et al. 1994
PA-66 (76-19)/PP (19-76)/ PP-MA (0.4 % MA) (0-5)	TSE at 280 °C/morphology and mechanical properties vs. PA-PP viscosity ratio	Hietaoja et al. 1994
PA-6 (80-30)/PP (18-56)/ PP-MA (0-14)	Internal mixer or TSE at 240 °C/SEM/ mechanical and rheological properties/ DMA/water absorption	Speroni 1994
PA-12 (80)/PP (20)/PP-MA (6 % MA) (4) or PP-g-AA	Internal mixer at 210 °C/torque rheometry/ SEM/DSC/rheology/mechanical properties	Valenza and Acierno 1994
PA-6 (100-0)/PP (0-100)/ PP-MA (0.2 % MA) (0-10)	TSE at 245 °C/DSC/SEM/mechanical properties	Ikkala et al. 1993; Holsti-Miettinen et al. 1992
PA-6 (100-0)/PP (0-100)/ PP-MA (5 % MA) (0-6)	Internal mixer at 240 °C/rheology/ mechanical properties/SEM/DSC/effects of processing conditions	La Mantia 1993
PA-6 (30)/PP (50-70)/PP-MA (0-20)	Internal mixer/TEM/SEM/creep measurements	Schlag et al. 1993

(*continued*)

Table 5.23 (continued)

Polyamide/PP	Characterization and comments	References
PA-6 (60)/PP (40)/PP-MA (12)	Round-robin DMTA study of commercial blend supplied as extrudate	Wippler 1993
PA-6 (100-0)/PP (0-100)/ PP-MA (0-5)	Fiber extrusion at 260 °C/mechanical properties/SEM/SALS	Grof et al. 1992
PA-6 (100-10)/PP (0-75)/ PP-MA (3 % MA) (0-90)	Extruder at 245 °C/SEM/DSC/rheology	Park et al. 1990
PA-66 (85 parts)/PP-g-MA (10 parts; 0.11 % MA)/ EVAc-co-GMA (5 parts; 10 % GMA)	Extruded at 280 °C/mechanical properties vs. blends without both functionalized polymers/also used PA-6, PE-g-GMA, or EP-g-MA	Mashita et al. 1988
(PA-6,66 copolymer (35)-NBR (65) vulcanizate) (50)/(PP (50)-EPDM (50) vulcanizate) (50)/PP-MA (10)	Internal mixer at 220 °C/PA + rubber vulcanization and PP + rubber performed in separate steps before blending/ mechanical properties vs. use of unfunctionalized PP/comparison to use of functionalized PP in initial vulcanizate/ PP-f-carboxymethyl maleamic acid	Coran et al. 1985
PA-6/PP-MA	Extrusion molding at 230 °C/selective solvent extraction/DSC/morphology/ mechanical properties vs. MA content/ residual amine conc.	Ide and Hasegawa 1974

Pompe et al. (2002) have prepared compatibilized PA/PP blends using oxazoline-modified PP.

Zhang and Yin (1998), Xiaomin et al. (1997, 1998), and Zhang et al. (1996, 1997) have prepared compatibilized PA/PP blends by adding epoxide-grafted PP. Graft copolymers result from reaction between PA amine end-groups and pendent epoxide groups on PP (or with epoxide groups along a poly(GMA) segment grafted at a single PP site). For example, 100-15 parts PA-1010 was mixed with 0-85 parts PP and 0-25 parts PP-g-GMA in either an SSE or TSE at 200–210 °C. The resulting blends were characterized by selective solvent extraction, SEM, rheology, DSC, ESCA nitrogen analysis, FTIR, mechanical properties, and peel test. Since there may be multiple epoxide sites on the polypropylene, some cross-linked copolymer may result if the polyamide is functionalized at both ends. The proportion of cross-linked copolymer formed also depends upon blend composition and processing conditions.

5.8.11.4 Copolymer Formation by Miscellaneous Reactions

Lin and Isayev (2006) prepared blends of PA-6 and PP by treatment with high-intensity ultrasound during extrusion. Mechanical properties, crystallinity, and morphology were investigated. The competition between polymer degradation and partial in situ compatibilization was assessed.

Table 5.24 PA/PP blends: copolymer formation by amine + carboxylic acid reaction

Polyamide/PP	Characterization and comments	References
PA-6/PP/PP-g-AA	TSE/blends containing tracer monitored by optical detector during extrusion	Pinheiro et al. 2008; Melo and Canevarolo 2005
PA-6 (25-75)/PP (0-75)/ oxidized PP (10-60)	TSE at 240 °C/mechanical properties and MFR vs. blends without oxidized PP/also used oxidized PP-Na or -Zn ionomer	Dang et al. 2005
PA-66/PP-g-COOH	Mechanical properties/PP functionalized by grafting with a peroxide-COOH/ comparison to blends containing PP-g-MA in place of PP-g-COOH	Bohn et al. 2001
PA-6/PP-f-AA	DSC/WAXS	Psarski et al. 2000
PA-1010 (75)/PP (5-25)/ PP-g-AA (5 % AA) (0-20)	Internal mixer at 205 °C/SEM/rheology/ mechanical properties/selective solvent extraction/ESCA nitrogen analysis	Zhang and Yin 1997
PA-6 (85)/PP (7.5-15)/ PP-g-AA (6 % AA) (0-7.5)	Internal mixer or TSE at 235–255 °C/ selective solvent extraction/morphology/ mechanical and viscosity properties/ reaction kinetics from torque measurements	Dagli et al. 1994
PA-6 (100-0)/PP (0-100)/ PP-g-AA (2 % or 6 % AA) (0-6)	Internal mixer at 240 °C/rheology/ mechanical properties/SEM/DSC/effects of processing conditions	La Mantia 1993
PA-11 (100-0)/PP (0-100)/ PP-g-AA (6 % AA) (0-100)	TSE at 240 °C/torque rheometry/DMA/ SEM	Liang and Williams 1992

5.8.12 Polyamide + Polypropylene + Styrene Copolymer Blends

5.8.12.1 Copolymer Formation by Amine + Anhydride Reaction

As shown by examples listed in Table 5.25, PA/PP blends have been compatibilized through graft copolymer formation between polyamide amine end-groups and pendent anhydride groups on a functionalized styrene copolymer.

5.8.13 Polyamide + Polysiloxane + Styrene Copolymer Blends

Maric et al. (2001) have studied PA blends with poly(dimethylsiloxane) (PDMS) either in binary blends of the functionalized polymers or in ternary blends with a functionalized styrene copolymer. The efficiency of copolymer formation concurrent with morphology development and stabilization was studied for reactions between PA-amine and PDMS-anhydride, between PA-amine and PDMS-epoxy, and between PA-carboxylic acid and PDMS-epoxy. The effects of relative melt viscosities on interfacial reactivity and resulting morphology were noted.

Table 5.25 PA/PP/styrene copolymer blends: copolymer formation by amine + anhydride reaction

Polyamide/PP/styrene copolymer	Characterization and comments	References
PA-6/PP-g-(S)MA/PS	SEM/selective solvent extraction/ effect of order of component addition/PP grafted with MA in presence of styrene monomer	Li et al. 2011c
PA-6/PP/PS/PP-g-MA/SMA	TSE/SEM/DSC/selective solvent extraction/comparison to compatibilized and uncompatibilized binary blends of PA/PS and PA/PP	Omonov et al. 2005
PA-6 (100-0)/PP (0-100)/ SEBS-g-MA (2 % MA) (0-10)	TSE at 245 °C/TEM/SEM/ mechanical and viscosity properties/DSC/DMTA/fracture mechanical study	Heino et al. 1997a; Holsti-Miettinen et al. 1992, 1994
PA-6 (30)/PP (50-70)/ SEBS-g-MA (0-20)	Internal mixer at 240 °C/TEM/ mechanical properties and dispersed phase domain size vs. volume fraction of compatibilizer	Rösch et al. 1996; Rösch 1995; Rösch and Mülhaupt 1993, 1994
PA-6 (100-0)/PP (0-100)/ SEBS-g-MA (0–1.8 % MA) (0-20)	SSE at 240 °C/mechanical properties/ductile-brittle transition temperatures/DMA/TEM/SEM/ effects of rubber functionality level/ effects of adding PP-MA/tensile dilatometry	Gonzalez-Montiel et al. 1995a, b, c
PA-6 (100-0)/PP (0-100)/ SEBS-g-MA (2 % MA) (10)	TSE/DSC/SEM	Ikkala et al. 1993

5.8.14 Polyamide + Polysulfone Blends

5.8.14.1 Copolymer Formation by Amine + Carboxylic Acid Reaction

PA blends with polysulfone have been compatibilized through graft copolymer formation between polyamide amine end-groups and pendent carboxylic acid groups on a polysulfone functionalized using 4,4′-bis(4-hydroxyphenyl)pentanoic acid (Marechal et al. 1998). Characterization was by mechanical properties and morphology. A similar strategy was used by Ibuki et al. (1999) who in addition studied anhydride-terminated or anhydride-grafted polysulfone. See also Charoensirisomboon et al. (1999a, b, 2000) and Koriyama et al. (1999) and further papers by these authors.

5.8.15 Polyamide + Polystyrene or Styrene Copolymer Blends

5.8.15.1 Copolymer Formation by Acid-Base Interaction

Villarreal et al. (2004) have prepared blends of PA-6 with PS compatibilized by addition of poly(styrene-*co*-sodium acrylate). Characterization techniques included mechanical properties and SEM. See also Rodríguez-Ríos et al. (2004) for related work.

Compatibilized blends of PA-6 with syndiotactic PS (sPS) were prepared by melt blending in the presence of sulfonated sPS (Li et al. 2002). Blends were characterized by morphology, mechanical properties, and DSC. Sulfonated sPS at a level of 20 wt% or less was reported to be miscible with sPS. For related work involving PA-6 and sulfonated PS, see Molnar and Eisenberg (1991, 1992).

5.8.15.2 Copolymer Formation by Amine + Anhydride Reaction

Immiscible blends of PA and PS or styrene copolymer have been compatibilized through graft copolymer formation between PA amine end-groups and anhydride-functionalized styrene copolymer to form a new imide linkage (Table 5.26).

PA/PS blends have also been compatibilized through block copolymer formation between amine-terminated PA and anhydride-terminated PS. Anhydride end-groups were introduced into PS through reaction of either anion-terminated PS or hydroxy-terminated PS with trimellitic anhydride acid chloride. For example, Park et al. (1992) blended 80 parts PA-6 with 10-16 parts PS and 4-10 parts anhydride-terminated PS in an internal mixer at 240 °C. The blends were characterized by torque rheometry, SEM, selective solvent extraction, DSC, morphological stability to annealing, and lap shear adhesion. The effect of mixing protocol on properties was studied. Properties were also compared to those for blends compatibilized by added PA-PS graft copolymer that had been synthesized in a separate step.

5.8.15.3 Copolymer Formation by Amine + Carboxylic Acid Reaction

Melt reactions between amine-terminated PA and carboxylic acid groups on styrene-acrylic acid copolymer have been demonstrated (Table 5.27). The initial reaction product is a graft copolymer, but longer reaction times may result in cross-linking, since the polyamides (PA-66 and PA-69) can have two amine end-groups per chain (Kuphal et al. 1991). Monoamine-terminated polyamides were reported in the same study to exhibit miscibility with SAA through hydrogen-bonding depending upon AA content. For PA-1010 blends with carboxylated PS, see Li and Li (1999).

Kausar et al. (2013) prepared blends of PS and amine-f-PS with an aramid prepared from 1,5-diaminonaphthalene and 1,4-phenylenediamine with isophthaloyl chloride. Morphological and thermophysical properties were investigated. Formation of an aramid-g-PS copolymer was proposed, perhaps through an amine-carboxylic acid reaction. For related blends of amine-f-PS and aramid, see Shabbir et al. (2008, 2010).

5.8.15.4 Copolymer Formation by Amine or Carboxylic Acid + Epoxide Reaction

Sun et al. (2005) prepared compatibilized blends of PA-6 with ABS-co-GMA. See also Singh and Gupta (2011).

Chen et al. (2003) have studied PA-6 blends with sPS compatibilized using S-co-GMA in a torque rheometer. Blends were characterized using SEM, mechanical properties, and DSC.

Chang and Hwu (1991) prepared compatibilized PA/PS blends through addition of epoxide-functionalized S-GMA copolymer. A graft copolymer

Table 5.26 PA/PS or styrene copolymer blends: copolymer formation by amine + anhydride reaction

Polyamide/PS or styrene copolymer	Characterization and comments	References
PA-6 (70)/PS (30)/PS-f-MA (1.5 phr)	SEM/TEM/DSC	Cai and Wu 2014
PA-6/ABS/SAN-MA copolymer	Viscosity monitoring/SEM/mechanical properties	Handge et al. 2012
PA-6/ASA-f-MA	SEM/Molau test/mechanical properties	Liu et al. 2012b
PA-6/ABS-g-MA/epoxy resin	DSC/mechanical properties/DMA/SEM/TEM	Shulin et al. 2011
PA-6/ABS/SAN/SAN-co-MA	TSE/rheology/Vicat B/mechanical properties	Weber et al. 2010
PA-6/SB-g-MA	TSE/SEM/DMTA/DSC/mechanical properties	Ding and Dai 2008
PA-6/ABS/SAN-co-MA	Mechanical properties/morphology/crystallinity	Ren et al. 2008
PA-6/SAN/SAN-f-MA	Melt mixing/morphology/rheology/AFM	Sailer and Handge 2007a, b, 2008
PA-6/ABS-g-MA	TEM/FTIR/Molau test/mechanical properties/also used ABS-g-AA and ABS-g-GMA	Sun et al. 2008 (see also Xu et al. 2008; Fu et al. 2013)
PA-6/PS/SMA	Morphology/rheology/DMA/effects of processing conditions on blend properties	Choi et al. 2006
PA-12/SEBS-g-MA	TSE/TGA/SEM/DMTA/DSC/comparison to blend with unfunctionalized SEBS	Jose et al. 2006a
Amorphous PA or PA-6 or PA-66/SEBS/SEBS-g-MA	Effect of different processing conditions TSE vs. SSE/morphology/mechanical properties	Huang et al. 2004
PA-66 (70)/PS (30/SMA or phthalic anhydride-terminated PS (<10 wt%)	Morphology/fluorescent label to visualize copolymer/also used syndiotactic PS	Jeon et al. 2004a
PA-12/PS/anhydride-end-capped PS-b-polyisoprene copolymer	Melt blending/morphology/morphology is PA-12 core with polyisoprene shell in PS matrix	Koulic et al. 2004
PA-6/syndiotactic PS-g-MA	FTIR/mechanical properties/morphology/DSC	Zhang and Son 2003
PA-6 (50 wt%)/ABS/SAN-f-MA	TSE/morphology/rheometry/mechanical properties	Jafari et al. 2002a, b
PA-1010 (75)/HIPS (15)/HIPS-g-MA (10; 1–5 % MA)	Melt mixed/mechanical properties/SEM	Chen et al. 1999; Chen and Liu 1999
PA-6/PS/MA-terminated PS	Melt mixing/mechanical properties/SEM/effect of PS MW/MA-terminated PS synthesized using ATRP	Koulouri et al. 1999a

Table 5.26 (continued)

Polyamide/PS or styrene copolymer	Characterization and comments	References
Amorphous PA (80)/SAN (20)/SMA	Morphology/mechanical properties/ interfacial adhesion strength measured using an asymmetric double cantilever beam fracture test	Cho et al. 1997, 1998
PA-6/SMA (28 % MA)	DSC/morphology/amount of PA graft vs. blend composition/length of PA graft/also used PA-66	Van Duin et al. 1998
PA-6 (75)/SMA (20 % MA) (0-5)/ SB core + MMA shell impact modifier (20-25)	Mini-extruder at 240 °C/TEM/ comparison to blends containing core-shell impact modifier with GMA grafted onto shell	Aerdts et al. 1997
PA-6 (75)/SEBS-g-MA (25)	TSE at 270 °C/mechanical properties/SEM/rheology/ comparison to PO-g-MA impact modifiers	Burgisi et al. 1997
PA-6 (80)/SEBS (0-15)/ SEBS-g-MA (0.5–1.8 % MA) (0-20)	SSE at 240 °C/mechanical properties/TEM/effects of different MA levels	Kayano et al. 1997
PA-6 (95-60)/SMA (5-40)	Internal mixer at 250 °C/mechanical properties/SEM/WAXS/SAXS/also blends with SMA pre-reacted with 0–100 % octadecylamine based on MA content	Kelnar et al. 1997
PA-6 (20)/ABS (80)/poly (N-phenylmaleimide-S-MA) (3 % MA) (0-20)	TSE at 250 °C/rheology/ SEM/selective solvent extraction/ FTIR/effects of processing conditions	Lee et al. 1997
PA-6 (80)/PS-g-MA (0.08–0.18 % MA) (20)	Internal mixer at 230 °C/ SEM/tensile properties/rheology/ FTIR/NMR/selective solvent extraction	Jo et al. 1996
PA-6 (80-70) or PA-66/SMA (0-10)/ SB core + MMA shell impact modifier (20) or BA core + MMA	SSE at 240–280 °C/torque rheometry/mechanical properties/ ductile-brittle transition temperatures/TEM/effects of mixing protocol	Lu et al. 1993, 1996
PA-6 (80)/SEBS (0-20)/SEBS-g-MA (0.5–2 % MA) (0-20)	SSE at 240 °C or TSE at 280 °C/ torque rheometry/TEM/titration of residual amine groups/effects of extruder type and PA mol. wt. and amine end-group concentration on morphology, mechanical properties, and ductile-brittle transition temperature/effects of di- vs. monofunctional PA	Oshinski et al. 1996a, b, c, d

<div align="right">(continued)</div>

Table 5.26 (continued)

Polyamide/PS or styrene copolymer	Characterization and comments	References
PA-6 (80-20)/PS (20-80)/PS-g-MA (0.08–0.68 % MA) (5)	Internal mixer at 230 °C/SEM/ tensile properties/rheology/ laminate butt joint test/effect of PS mol. wt. in PS-g-MA/effect of mixing sequence	Park et al. 1996
PA-6 (78-55)/EPDM-g-SAN (0-45) or ABS/SEBS-g-MA (1.8 % MA) (0-22)	SSE at 240 °C/TEM/mechanical properties	Lu et al. 1995
amorphous PA (20)/SMA (17 % MA) (80)	Internal mixer at 200 °C or TSE/selective solvent extraction/ SEM study of morphology development in reactive and in nonreactive blends/comparison of mixer efficiencies	Scott and Macosko 1995a; Sundararaj et al. 1995
Amorphous PA/SMA (8–23 % MA)/ SAN (25 % AN)	Melt-pressed, spin-coated film layers/ellipsometer measurement for interfacial area vs. MA content and annealing time	Yukioka and Inoue 1994
PA-6 (95-60)/SEBS-g-MA (28 % S/2 % MA) (5-40)	TSE at 245 °C/TEM/mechanical and viscosity properties/DMTA	Holsti-Miettinen et al. 1992, 1994
PA-6 (60)/ABS (36-40)/SMA (25 % MA) (0-4)	Double extrusion on SSE/mechanical properties vs. SMA content/TEM	Majumdar et al. 1994c
PA-6 (100-80) or PA-66 or PA-11 or PA-12 or PA-1212 or PA-612 or PA-610 or PA-69 or PA-46/SEBS (0-20)/SEBS-g-MA (1.8 % MA) (0-20)	SSE at 240 °C/torque rheometry/ mechanical properties/TEM/ ductile-brittle transition temperatures/ interfacial tension estimates/effects of PA amine end-group concentration on copolymer formation (titration before and after extrusion)/torque rheometry	Majumdar et al. 1994d, e
PA-6 (100-80) or PA-66 or PA-12 or PA-1212 or PA-6,66 copolymer/ SEBS (0-20)/SEBS-g-MA (29 % S + 1.8 % MA) (0-20)	Processing study with SSE and two different types of TSE/TEM/ mechanical properties vs. extrusion conditions and morphology/effects of using PA + rubber masterbatch	Majumdar et al. 1994f
PA-6 (100-85)/SEBS (0-15)/ SEBS-g-MA (8–13 % MA) (0-4)	TSE at 260 °C/SEM/WAXS/DMA/ mechanical properties	Wu et al. 1994
PA-6 (80-20)/PS (20-80)/ SEBS-g-MA (0-5) or SMA	SSE at 230 °C/DSC/capillary rheometry and morphology before and after annealing/mechanical properties/interfacial tension measurements/comparison to blends containing SAN in place of SMA	Chen and White 1993; Chen et al. 1988
PA-6 (100-0)/ABS (0-100)/SMA (8 % MA) (0-10)	Internal mixer at 220–240 °C/ DMA/rheology/SEM/effect of preblending of PA + SMA or ABS + SMA	Kim et al. 1993

(*continued*)

Table 5.26 (continued)

Polyamide/PS or styrene copolymer	Characterization and comments	References
PA-6 (70-0)/ABS (30-100)/ S-MMA-MA (25 % MA) (0-8)	SSE at 260 °C/mechanical properties/SALS/optical microscopy/SEM	Misra et al. 1993
PA-6 (80) or PA-66/SEBS (0-16)/ SEBS-g-MA (0.5–2 % MA) (0-20)	TSE at 250 °C/mechanical properties/TEM	Modic and Pottick 1993
PA-6 (100-70)/SBS (0-10)/ SBS-g-MA (0.5–1.5 % MA) (0-30)	TSE at 240 °C/rheology/solvent swelling/SEM/TEM/mechanical properties	Seo et al. 1993
PA-6 (85)/SEBS (11-15)/ SEBS-g-MA (0-4)	TSE at 260 °C/SEM/WAXS/ mechanical properties	Wu et al. 1993
PA-6 (100-0) or PA-66/SEBS (0-100)/SEBS-g-MA (1.8 % MA) (0-100)	Double extruded on SSE at 240 °C or 280 °C/TEM/ mechanical properties/torque rheometry/lap shear adhesion/ DMA/DSC/effects of mixing protocol	Oshinski et al. 1992a, b
PA-6 (80)/PS (10-16)/SMA (2 % MA) (4-10)	Internal mixer at 240 °C/torque rheometry/SEM/selective solvent extraction/DSC/morphological stability to annealing/lap shear adhesion/comparison to PA-PS block copolymer-compatibilized blends	Park et al. 1992
PA-6 (100-0) + poly(m-xylene adipamide) (0-100)/SEBS (0-20)/ SEBS-g-MA (1.8 % MA) (0-20)	SSE at 260 °C/torque rheometry/ mechanical properties/ductile-brittle transition temp./TEM/DMTA/DSC/ effects of mixing protocol/effects of PA-PA transamidation on properties	Takeda et al. 1992a
PA-6 (100-80) or PA-66 or PA-11 or PA-12 or PA-1212 or poly(m-xylene adipamide)/SEBS-g-MA (1.8 % MA) (0-20)	SSE at 260–280 °C/torque rheometry/ mechanical properties/TEM/effects of di- vs. monofunctional PA/effects of preextrusion of PA-6 with 10 wt% of different PA	Takeda et al. 1992b
PA-66 (90-10)/PS (10-90)/SMA (11 % or 25 % MA) (0-0.5)	TSE/rheology/DSC/SEM/TEM/ selective solvent extraction/FTIR/ mechanical properties/also binary blends of PA + SMA	Chang and Hwu 1991
PA-6 (100-0)/SMA (8 % MA) (0-100)	TSE at 240 °C/rheology/SEM/DSC/ mechanical properties/HDT/FTIR	Kim and Park 1991
PA-6 (100-0)/SAN (0-100) or ABS/SMA (14 % or 25 % MA) (0-10) or imidized acrylate copolymer with 1 % MA content or SAN-co-IPO (1 % oxazoline)	Double extrusion on SSE/torque rheometry/mechanical properties/ selective solvent extraction/SEM/ lap shear adhesion/SAN + SMA double extruded in separate step followed by extrusion with PA	Triacca et al. 1991
PA-6 (100-70)/SAN (0-30)/SMA (15 % or 30 % MA) (0-7.5)	Mini-max molder at 230 °C/SEM/ mechanical properties/selective solvent extraction/FTIR	Angola et al. 1988

<div align="right">(continued)</div>

Table 5.26 (continued)

Polyamide/PS or styrene copolymer	Characterization and comments	References
PA-6 (50 parts)/ABS-g-MA (50 parts; 1 wt% MA)	TSE at 260 °C/mechanical properties vs. blend with unfunctionalized ABS/also used PA-66 and amorphous PA	Grant and Howe 1988
PA-6 (80 parts)/hydrogenated styrene-butadiene copolymer-g-MA (20 parts; 0.5–2.3 wt% MA)	TSE/mechanical properties vs. blend with unfunctionalized copolymer/ also used PA-66 or hydrogenated styrene-butadiene copolymer-g-AA	Shiraki et al. 1986, 1987a, b
PA-6 (50 parts)/S-MMA-MA copolymer (50 parts; 9 wt% MA)	TSE at 260 °C/morphology/ copolymer analysis/mechanical properties vs. blend with S-MMA copolymer/also used PA-66, SMA, or SAN-MA	Kasahara et al. 1983
PA-6 (358 parts)/PS (90 parts)/SMA (2.3 parts; 50 % MA)	Extruded at 227–232 °C to form rods/ properties vs. blends without SMA	Sims 1976
PA-6 (80-20)/S-MAA (20-80)	Extrusion molding at 230 °C/ selective solvent extraction/DSC/ mechanical properties	Ide and Hasegawa 1974

Table 5.27 PA/styrene copolymer blends: copolymer formation by amine + carboxylic acid reaction

Polyamide/styrene copolymer	Characterization and comments	References
PA/ABS-f-carboxylic acid	Order in its place of reactivity in the melt was ABS-g- undecylenic acid > ABS-g-oleic acid > ABS-g-crotonic acid > ABS-g-acrylic acid	Zhou et al. 2004
PA-6 (100-87.5)/SAA (8 % AA) (0-12.5)	SSE at 240 °C/torque rheometry/mechanical properties/TEM/effects of adding 20 % BA core + MMA shell impact modifier	Lu et al. 1994
PA-66 (50) or PA-69/SAA (20 % AA) (50)	Internal mixer at 220 °C or 265 °C/melt flow/ DSC	Kuphal et al. 1991
PA-6 (70-50)/PS (0-90)/ PS-MMA-MAA (3-11 % MAA) (0-30)	Two-roll mill at 230 °C/SEM/optical microscopy/selective solvent extraction	Fayt and Teyssie 1989

results from reaction of pendent epoxide groups with either amine or acid end-groups on PA. A blend of 50 parts PA-66, 50 parts PS, and 0-0.5 parts S-GMA (3 % GMA) was prepared on a TSE and characterized by rheology, SEM, and mechanical properties. Since there are multiple epoxide sites on S-GMA, some cross-linked copolymer may result if the polyamide is functionalized at both ends. The proportion of cross-linked copolymer formed also depends upon blend composition and processing conditions. See also Martens et al. (2004).

Table 5.28 PA/styrene copolymer blends: copolymer formation by amine or carboxylic acid + oxazoline reaction

Polyamide/styrene copolymer	Characterization and comments	References
Amorphous PA (99-80)/S-IPO (1 % IPO) (1-20)	Internal mixer at 210 °C/SEM/interfacial fracture toughness/flexural properties/selective solvent extraction/FTIR	Tan et al. 1996
Amorphous PA (20)/S-IPO (1 % IPO) (80)	Internal mixer at 200 °C/torque rheometry/ selective solvent extraction/SEM study of morphology development in reactive and in nonreactive blends	Scott and Macosko 1995a

5.8.15.5 Copolymer Formation by Amine or Carboxylic Acid + Isocyanate Reaction

Zhang et al. (2013a) prepared compatibilized PA/PS blends through addition of an isocyanate-functionalized PS. For example, blends comprising PA-6 and PS-*co*-(3-isopropenyl-α,α-dimethylbenzene isocyanate) were characterized using FTIR, DSC, and morphology determination. The effects of different functionalized PS loading and the isocyanate level in the PS copolymer were investigated.

Yin et al. (2009b) prepared blends of PA-6 with SEBS which had been functionalized with ε-caprolactam-blocked allyl (3-isocyanate-4-tolyl) carbamate.

5.8.15.6 Copolymer Formation by Amine or Carboxylic Acid + Oxazoline Reaction

As shown in Table 5.28, blends of PA and PS have been compatibilized through graft copolymer formation between PA amine or acid end-groups and oxazoline-functionalized styrene copolymer.

5.8.16 Polyamide + Polyurethane Blends

5.8.16.1 Copolymer Formation by Carboxylic Acid or Amine + Isocyanate Reaction: Blends Containing a Coupling Agent

PA/TPU blends have been compatibilized by addition of a bis-isocyanate coupling agent that is capable of reacting with nucleophilic end-groups on both polymers to form a block copolymer. Franke et al. (1993) have extruded PA-6 (20-0 parts) with polyester-urethane (78-100 parts) using a TSE at 230 °C in the presence of 0.5-2 parts diphenylmethane diisocyanate. The coupling agent was added downstream of the extruder feed throat. The blends were characterized by TEM, SEC, DSC, DMA, and FTIR.

5.9 Polyester Blends

Examples of polyester blends not shown in earlier sections are listed in alphabetical order of the second polymer in the blend unless otherwise noted. Polycarbonate blends are also included as polyesters. When copolymer characterization was not performed, the structure of the compatibilizing copolymer is inferred from the

Table 5.29 PEST/PEST blends – blends containing a condensing agent: copolymer formation by alcohol + carboxylic acid reaction

Polyester/polyester	Characterization and comments	References
PET (75)/PBT (25)/various phosphite condensing agents (0–5 %)	Internal mixer at 275–280 °C/GPC/DSC/ torque rheometry/viscometry/selective solvent extraction/phosphorus analysis/ effect of PET end-group concentrations/ FTIR for end-groups concentration/effect of phosphite structure/model study with OH + COOH-terminated acrylic polymer/ detailed mechanistic study	Jacques et al. 1993, 1996a, b, 1997
PET (80-70)/TPE polyester (20-30)/various phosphite condensing agents (0–3 %)	Internal mixer at 271 °C/torque rheometry/mechanical properties/^{31}P NMR/GPC/DSC/environmental stress cracking/use of recycle PET	Abu-Isa et al. 1996

functionality location on each of the two polymers. In some cases, more than one type of compatibilizing copolymer may have formed.

Copolymer-forming reactions for compatibilizing immiscible blends, some of which are applicable to PEST blends, have been studied by Orr et al. (2001) who determined that the order of increasing reactivity in functionalized polymer pairs is acid/amine, hydroxyl/ (anhydride or acid), aromatic amine/epoxy, aliphatic amine/epoxy, acid/oxazoline, acid/ epoxy, aromatic amine/anhydride, and aliphatic amine/anhydride (most reactive).

For reviews of reactive compatibilization of poly(lactic acid) (sometimes referred to as polylactide) with other immiscible polymers, see Imre and Pukanszky (2013) and Liu and Zhang (2011).

5.9.1 Polyester + Polyester (or Polycarbonate) Blends

5.9.1.1 Copolymer Formation by Alcohol + Carboxylic Acid Reaction: Blends Containing a Condensing Agent

As shown in Table 5.29, blends of immiscible polyesters may be compatibilized through copolymer formation mediated by addition of a phosphite condensing agent. Block copolymer results when the phosphite-activated end-group of one PEST reacts with a nucleophilic end-group of another PEST. The reaction takes place at the phase interface. A secondary phosphite is a by-product. The relative proportions of copolymer vs. simple chain-extended PEST may depend upon the relative solubility of condensing agent in each of the immiscible polymer phases.

5.9.1.2 Copolymer Formation by Carboxylic Acid + Epoxide or Oxazoline or Isocyanate Reaction: Blends Containing a Coupling Agent

Blends of poly(lactic acid) and poly((butylene-adipate)-*co*-terephthalate) have been prepared with the addition of either 2,2′-(1,3-phenylene)-bis(2-oxazoline) or phthalic anhydride (Dong et al. 2013). Blends were characterized using DSC, SEM, and mechanical properties.

Polycarbonate blends with poly(lactic acid) have been compatibilized through addition of bis(isocyanate), bis(carbodiimide), oxazoline-f-PS, or epoxy resin (Wang et al. 2012e; Mukawa et al. 2011).

Blends of aliphatic-aromatic polyester (75-25 parts) and poly(lactic acid) (25-75 parts) have been compatibilized through extrusion with a copolymer of styrene, GMA, and isomethacrylates (0-5 parts) (Hale 2008). Polyesters included those derived from adipic acid-terephthalic acid-butanediol. Mechanical properties were greatly improved compared to those for blends with no compatibilizer.

Poly(ε-caprolactone) blends with poly(lactic acid) have been compatibilized in the presence of polyepoxide or either di- or trisisocyanate (Harada et al. 2008).

Harada et al. (2007) have prepared compatibilized blends of PLA with poly (butylene succinate) through addition of lysine trisisocyanate. Characterization techniques included MFR, mechanical properties, SEC, and laser scanning confocal microscopy.

The crystallization behavior of PTT-PC blends in the presence of either epoxy resin or EPDM-g-GMA has been studied by Xue et al. (2005).

PET-PEN blends have been compatibilized in the presence of a bis-oxazoline coupling agent (Yang et al. 2002b).

Ju et al. (2000) prepared compatibilized blends of polyarylate with an LCP in the presence of tetraglycidyl-4,4′-diaminodiphenyl methane coupling agent.

Chin and Chang (1997) and Chin et al. (1996) have compatibilized blends of immiscible PEST through addition of a multifunctional epoxide coupling agent capable of reacting with nucleophilic end-groups on each of the two immiscible PEST at the phase interface to give a block copolymer containing the coupling agent as linking group. In one example 100-85 parts PET was extruded using a TSE at 270–285 °C with 0-15 parts LCP (Hoechst Vectra® A900) and 0-2 parts tetrafunctional epoxy resin. The blends were characterized by torque rheometry, capillary rheometry, DSC, SEM, and FTIR. Mechanical properties were determined vs. composition and morphology. Ethyltriphenylphosphonium bromide was added as a catalyst to promote the reaction of polyester acid or alcohol end-groups with epoxy resin. The relative proportions of copolymer vs. simple chain-extended PEST depend at least partly upon the relative solubilities of coupling agent and catalyst in each of the immiscible polymer phases. See also Tjong and Meng (1999) and Dekkers et al. (1992).

5.9.1.3 Copolymer Formation by Radical Coupling

Krishnaswamy et al. (2013) prepared blends of poly(lactic acid) with poly (3-hydroxybutyrate-*co*-4-hydroxybutyrate) containing 17–40 wt% 4-hydroxybutyrate in the presence of radical initiator. Blends were characterized by melt strength, viscosity, and mechanical properties. Blend properties were compared to control blends without RI.

Wang et al. (2009a) have compatibilized the biodegradable polymers poly(L-lactic acid) and poly(butylene succinate) in the presence of DCP radical initiator (0.05–0.2 phr). For related work, see Lan et al. (2013).

For blends of poly(butylene succinate) with poly(hydroxybutyrate-*co*-hydroxyvalerate or poly(hydroxybutyrate) compatibilized in the presence of radical initiator, see Ma et al. (2012a).

Blends of poly(lactic acid) and poly(butylene-adipate-*co*-terephthalate) were prepared in the presence of varying concentrations of L101 RI by Coltelli et al. (2010). The blends were characterized by morphology, rheology, and mechanical properties.

Other radical-radical coupling reactions used to compatibilize blends of immiscible polyesters include those by Avella et al. (1996); Immirzi et al. (1994); and Cavallaro et al. (1993). Specifically, 70-30 parts poly(hydroxybutyrate-*co*-hydroxyvalerate) (4 mol% valerate) or poly(hydroxybutyrate) was mixed with 30-70 parts PCL in an internal mixer at 100 °C or 160 °C in the presence of 0-0.5 parts DCP or DBP radical initiator. Blends were characterized by SEM, mechanical properties, selective solvent extraction, and FTIR.

5.9.1.4 Copolymer Formation by Redistribution Reaction

Brief reviews covering redistribution reactions (often referred to as transesterification reactions or simply transreactions) in polyester and in polycarbonate binary blends have been prepared by Porter et al. (1989) and Porter and Wang (1992). Carrot et al. (2007) have surveyed more recent knowledge relating to PET/PC blends. Pesneau et al. (2001) have studied the relative effectiveness of different transesterification catalysts, finding that dibutyltin oxide had the highest activity of those studied. Other reviews of transreactions in polyester blends include Montaudo et al. (1999), Pilati et al. (1999), Economy et al. (1999), and also portions of other chapters in Fakirov (1999) (transreactions in condensation polymers).

Selected references for redistribution processes in PEST/PEST blends are listed in Table 5.30. Early studies of these processes focused on measuring the extent of redistribution under specific processing conditions rather than on producing compatibilized polymer blends with an attractive balance of properties. A number of other studies have reported the limits of miscibility for certain melt-mixed polyester pairs in the absence of transesterification – see, for example, the NMR study of PC/PET blends (Abis et al. 1994). Table 5.30 omits references in which transesterification in PEST/PEST blends is brought about under static conditions either by annealing or heating in a DSC chamber.

5.9.2 Polyester + Polyether Blends (Including Polycarbonate)

5.9.2.1 Copolymer Formation by Transesterification

A graft copolymer may be formed through transesterification between pendent hydroxy groups on phenoxy polyether resin and ester linkages in the chains of an immiscible polyester or polycarbonate phase (Table 5.31). Since the product is a graft copolymer accompanied by a low molecular weight fragment from the polyester, this is a degradative copolymer-forming process. The initial product of the transreaction is a graft copolymer as the alcohol reacts into the polyester chain. Longer reaction time may result in a cross-linked copolymer since the pendent polyester segment is capable of further reaction with OH on a different phenoxy chain. These types of blends have also been prepared by solution casting followed by annealing. Blends of LCP with phenoxy resin provide an example (Kodama 1992).

Table 5.30 PEST/PEST blends: copolymer formation by redistribution reaction

Polyester/polyester	Characterization and comments	References
Poly(lactic acid)/PC	NMR/GPC/DMA/effects of catalysts: Zn borate, Ti pigment, or tetrabutyl titanate	Liu et al. 2013a
Poly(lactic acid)/poly (butylene succinate)	Melt blended/torque rheometry/SEM/ mechanical properties/TPPite catalyst	Ojijo et al. 2013
PEN/PET	Influence of capping PET OH end-groups on extent of transesterification	Blanco et al. 2012 (see also Becker et al. 2002)
PC/poly(lactic acid)/ tetrabutylammonium tetraphenyl borate	TSE/mechanical properties/DMTA/ comparison to blend with no catalyst	Penco et al. 2012
PTT/poly(butylene succinate)	Melt blended at 270 °C for various times or for 2 h. at various temperatures/mechanical properties/DSC/morphology/polarized optical microscopy	Zhou et al. 2012
PET/PTT	DSC/WAXD/effect of mixing time	Castellano et al. 2011
PET (20)/PC (80)/cobalt catalyst	DSC/DMA/MFR/mechanical properties/ detrimental effect of transesterification on properties	Mendes et al. 2011
PTT/PC	DMTA/TGA/morphology/DSC/WAXD/ FTIR	Aravind et al. 2010a
PET/PTT ($\leq$30 wt%)	Melt extrusion/DSC/mechanical properties/ comparison to product obtained either from solution or by melt spinning	Safapour et al. 2010
Poly(lactic-co-glycolic) acid/poly(trimethylene carbonate)	Morphology/mechanical properties	Zhang et al. 2010
PEN/LCP (Hoechst Vectra A950)	DSC/mechanical properties/morphology/ selective solvent extraction	Caligiuri et al. 2009
PC/LCP/ABS	DSC/^{13}C NMR/SEM/rheology/mechanical properties/determination of optimum transreaction vs. properties/phosphorus-containing LCP	Chen et al. 2009
PEN/PTT	DMA/DSC/NMR/effect of melt processing time and temperature	Jafari et al. 2009
Polyestercarbonate/PC/ tetrabutylphosphonium hydroxide catalyst	TSE or SSE/mechanical properties/rheology/ HDT/haze/effects of different catalysts and catalyst loading/polyestercarbonate derived from resorcinol-isophthalate-terephthalate	Berkstresser et al. 2008
PET (90-50)/poly [ethylene 5,5′-isopropylidene-bis(2-furoate)] (10-50)	DSC/NMR/MALDI/TGA	Kamoun et al. 2006
PC (50)/PET (50)/alkyl titanate catalyst	Torque rheometer at 270 °C/DSC/SALS/ FTIR/SEM/TEM/DMTA	Wilkinson et al. 2005
PEN/poly(pentylene terephthalate)	SEM/optical microscopy/X-ray analysis/^{1}H NMR/effect of reaction time	Woo et al. 2005
PC (30-50)/PBT (70-50); also PC/PTT; PET/PTT	Biaxial extruder at 280 °C/mixture of various phosphite catalysts with calcium hypophosphite/ Tm/Tg/GPC/NMR/mechanical properties	Aramaki et al. 2004

Table 5.30 (continued)

Polyester/polyester	Characterization and comments	References
PEN/PET	TSE/kinetics of reaction vs. model compounds	Medina et al. 2004; Alexandrova et al. 2002
PET (80)/poly(ethylene isophthalate) (20)	Melt mixed at 270 °C/mechanical properties/NMR/DSC/monitoring of block copolymer to random copolymer transition/also used poly(ethylene terephthalate-*co*-isophthalate)	Kint et al. 2003
PET/LCP	Internal mixer/LCP derived from p-hydroxybenzoic acid + ethylene terephthalate (80:20 or 60:40)/DSC/NMR/SEM/also used PEN in place of PET	Park and Kim 2003
PET/PC	TSE/with and without lanthanum acetyl acetonate catalyst/DSC/SEM/mechanical properties	Kong and Hay 2002
PBT/polyester-urethane	Melt mixed/mechanical properties/DMA/DSC/SEM/NMR	Archondouli and Kalfoglou 2001
PEN/PET	Deuterated PET/small-angle neutron scattering/effects of temperature and heating time/reaction kinetics/NMR	Collins et al. 2001
PET (70)/PC (30)	Extruder mixing/mechanical properties/effects of processing conditions	García et al. 2001
PBT/PET	Structural analysis of copolyester formed by interchange reaction/^{13}C NMR/effect of reaction time/solubility/dibutyltin dilaurate vs. Ti(OBu)$_4$ catalyst	Kim et al. 2001b
PEN/LCP	Melt blended/mechanical properties/DSC/DMA/SEM/evidence for transreaction between PEN and PET segments of LCP	Xie et al. 2001b
PBT/PET	Deuterated PET/small-angle neutron scattering/effects of temperature and heating time/reaction kinetics	Backson et al. 1999
PC/LCP	LCP derived from ethylene glycol-*p*-hydroxybenzoic acid-terephthalic acid/^{13}C NMR/reaction kinetics showing which LCP segment was most active in transreaction	Ho and Wei 1999 (see also Bum et al. 2001)
PEN/LCP	LCP derived from ethylene glycol-*p*-hydroxybenzoic acid-terephthalic acid/dibutyltin dilaurate catalyst/mechanical properties/thermal and rheological properties	Kim et al. 1999b (see also Hong et al. 2001)
PBT/PC	Melt mixed/monitoring reaction to determine structure of copolymer and mechanism of reaction/also used PET	Montaudo et al. 1998a
PET (50)/PC (50)	Internal mixer at 270 °C/selective solvent extraction/NMR/GPC/lanthanide catalyst comparison	Fiorini et al. 1997
PET (100-90)/LCP (0-10) (Unitika LC3000)	TSE at 290 °C/DSC/SEM/capillary rheometry/WAXD/NMR/fiber tensile properties/dibutyltin dilaurate catalyst (0–0.1 wt%)	Hong et al. 1997

(continued)

Table 5.30 (continued)

Polyester/polyester	Characterization and comments	References
PBT (70-30)/PC (30-70)	TSE at 270 °C/DSC/NMR/FTIR/optical microscopy	Hopfe et al. 1997; Pompe et al. 1996
PC (100-0)/PET (0-100)	Internal mixer or TSE at 270–280 °C/DSC/ SEM/selective solvent extraction/NMR/SEC/ rheology/torque rheometry/catalyst comparison	Ignatov et al. 1996, 1997a, b; Fiorini et al. 1995
PC (100-0) or PET/LCP (0-100) (Hoechst Vectra B950)	TSE at 280 °C/DSC/annealing studies	Lin and Yee 1997
Polyarylate (90-10)/ PETG (10-90)	Internal mixer at 235 °C/torque variation/ DSC/NMR/FTIR/selective solvent extraction	Oh et al. 1997
PEN (40)/PET (60)	TSE at 280 °C/NMR/time-resolved light-scattering measurements during annealing	Okamoto and Kotaka 1997
PC (70-30)/PBT (30-70)	TSE at 270 °C/DSC/NMR/copolyester content vs. annealing time/miscibility vs. copolymer content	Pompe and Häubler 1997
PC (50)/LCP (50) (Unitika LC3000 or Eastman X-7G)	Internal mixer at 300 °C/SEM/DMTA/ selective solvent extraction/NMR/rheology/ Ti(OBu)$_4$ catalyst (0–0.3 wt%)	Stachowski and DiBenedetto 1997
Amide-modified PBT (30)/PC (70)/TPPite (0–2.2 %)	Mini-TSE at 270°/DMA/DSC/NMR/amine end-group titration	Van Bennekom et al. 1997
PC (70-30)/LCP (30-70)	Internal mixer at 310 °C/DSC/NMR/FTIR/ LCP was poly(p-oxybenzoate-co-p-phenylene-isophthalate)	Wei et al. 1997
PC (90-60)/LCP (10-40) (poly(oxybenzoate-co-ethyleneterephthalate))	Internal mixer at 240–290 °C/DSC/NMR/ SEM/use of copolymer as compatibilizer for PC + different LCP/transesterification inhibition with TPP/also catalysis by Ti(OBu)$_4$	Wei and Ho 1997; Wei et al. 1996; Wei and Su 1996; Su and Wei 1995
PBT (50)/PC (50)/ Ti(OR)$_4$ catalyst	Internal mixer at 230 °C/SEM/DSC/SAXS/ WAXS	Wilkinson et al. 1997 (see also Tatum et al. 2000)
PET (50)/PEN (50)	Extent of reaction vs. time at 280 °C/IV/MW/ hydrodynamic radius	Yoon et al. 1997
Polyarylate (50-10)/ PBT (50-90)/Ti(OBu)$_4$ catalyst (0.005–0.2 %)	Mini-max molder at 260–280 °C/mechanical properties/DSC/NMR including model compounds	Eguiazábal et al. 1996; Fernandez-Berridi et al. 1995; Espinosa et al. 1993; Valero et al. 1990
PBT (25)/PET (75)/ Ti(OBu)$_4$ catalyst (0–1,050 ppm)	Internal mixer at 275–280 °C/^{13}C NMR determination of transesterification level/ stabilizing effect of TPPite (0–5 %)	Jacques et al. 1996c
PET (100-20)/LCP (0-80) (poly (oxybenzoate-co-ethyleneterephthalate))	Internal mixer at 275–293 °C/NMR/SEM/ DSC/degree of reaction vs. mixing time and ratio of LCP monomer units	Ou and Lin 1996a, b (see also Ou et al. 1999; Ou 1998)
PBT (100-0)/PCE (42 % or 70 % ester) (0-100)	Internal mixer at 250 °C/DSC/selective solvent extraction	Rodriguez et al. 1996

(*continued*)

Table 5.30 (continued)

Polyester/polyester	Characterization and comments	References
Polyarylate (100-0)/ PET (0-100)	Injection molded mixture/torque rheometry/ DSC/NMR/SEM/DMTA/mechanical properties	Martinez et al. 1992, 1994
PBT (50)/PC (50)	TSE at 290 °C/TEM/time-resolved light scattering/effect of transesterification on phase separation	Okamoto and Inoue (1994)
PC (90-70)/PCL (10-30)	Internal mixer or SSE at 240–250 °C/DSC/ selective solvent extraction/FTIR/rheology/ toluene sulfonic acid (0.1-2) or Ti(OBu)$_4$ or dibutyltin dilaurate catalyst/other catalysts ineffective	Shuster et al. 1994
PC (91-39) or PBT or polyarylate/ polypivalolactone (9-61)	Mini-TSE at 280 °C/selective solvent extraction/FTIR/DSC/Ti(OBu)$_4$ catalyst (0–0.5 wt%)	Tijsma et al. 1993, 1994
PC (50)/LCP (50) (poly (oxybenzoate-co- ethyleneterephthalate))	Internal mixer at 260 °C/Ti(OBu)$_4$ catalyst (0–0.5 wt%)/FTIR/GPC/SEM/use of copolymer as compatibilizer for PC + LCP	Amendola et al. 1993
PBT (25-75)/PC (75-25)	Melt mixing or solution precipitation/TGA/ mass spectroscopy/viscometry	Montaudo et al. 1993
PEN (100-0)/PET (0-100)	SSE at 275–315 °C/effect of multiple extrusion passes/NMR/DSC/effect of residual titanium catalyst levels	Stewart et al. 1993a
PC (80-20)/LCP (20-80) (poly(4,4-dioxy- diphenyl-co-iso-or terephthalate))	Internal mixer at 290 °C/rheology/selective solvent extraction/FTIR/NMR/TEM/DSC	Belousov et al. 1992
PET (43)/PC (57)	Internal mixer at 270 °C/FTIR/NMR/DSC/ TGA/DMA/IV/model reactions	Berti et al. 1992a, b
Polyarylate (50)/ PBT (50)	TSE at 260–320 °C/DSC/NMR/Ti(OBu)$_4$ catalyst (60–270 ppm)	Miley and Runt 1992
Poly(hexamethylene terephthalate) (67-20)/ LCP (80-33) (poly (oxybenzoate-co- ethyleneterephthalate))	Mini-max molder at 260 °C/selective solvent extraction/DSC/NMR/SEM/WAXS/DMTA/ effects of added phosphite stabilizer	Croteau and Laivins 1990; Laivins 1989
Polyarylate (50)/PC (20)/PET (30)	Thermal redistribution in SSE at 280–325 °C/ DSC/FTIR/also stabilizers added to prevent thermal	Cheung et al. 1989
PC (50) or polyarylate/ PET (50) or PBT	Stabilizers to prevent thermal redistribution/^{31}P NMR study of stabilizer fate	Golovoy et al. 1989
PC (90-10)/PET (10-90)	Thermal redistribution/DSC/FTIR/optical microscopy	Suzuki et al. 1989
Polyarylate (15-85)/ PC (85-15)	Thermal redistribution in SSE vs. TSE 260–300 °C/DSC/mechanical properties	Golovoy et al. 1987
Polyarylate (50)/ PBT (50)	Capillary rheometry at 280–300 °C/selective solvent extraction/FTIR	Arruabarrena et al. 1986

(continued)

Table 5.30 (continued)

Polyester/polyester	Characterization and comments	References
PET (60)/PC (40)	Thermal redistribution in internal mixer 260 °C/FTIR/DSC/DMA	Huang and Wang 1986
Polyarylate/PC	Thermal redistribution in internal mixer 250–300 °C/torque vs. time, temperature/DSC/DMA	Mondragon and Nazábal 1985, 1986
PET (50)/PC (50)	Stirred batch reactor at 275 °C/selective solvent extraction/selective degradation/IV measurements/optional addition of Ti(OBu)$_4$ catalyst	Pilati et al. 1985
Polyarylate (100-0)/PET (0-100) or PETG or PC	SSE at 265–270 °C/thermal redistribution on molding 260–350 °C/time, temp. effects/DMA/DSC/selective solvent extraction	Robeson 1985
Polyarylate (80-10)/PC (20-90)	TSE at 220–320 °C gradient/redistribution during devolatilization of mixtures in solution/DSC/impact strength/comparison to control compositions	Freitag et al. 1985
PC (100-0)/copolyester of cyclohexanedimethanol and iso-and terephthalic acids (0-100)	SSE at 275–300 °C/IV/DSC/use of arsenic trioxide to quench residual titanate catalyst	Smith et al. 1981

5.9.3 Polyester + Polyetherimide Blends

5.9.3.1 Copolymer Formation through Coupling Agent Addition
PEST blends with PEI (derived from 2,2-bis[4-(3,4-dicarboxyphenoxy)phenyl] propane dianhydride and meta-phenylene diamine) have been compatibilized in the presence of various multifunctional epoxy resins and a catalyst (Brown et al. 2000b). PEST types included mixtures of PCT and PETG; catalysts included sodium stearate. Mechanical properties and HDT were compared to properties for blends without either epoxy resin or catalyst.

Silvi et al. (1997) have compatibilized an immiscible blend of LCP and similar PEI through copolymer formation in the presence of a coupling agent. Representative coupling agents included PE-co-GMA and the *o*-cresol novolak reaction product with epichlorohydrin. Mechanical properties and HDT were compared to properties for blends without polyepoxide. PEI could be diluted with polyarylate, polyestercarbonate, PET, or PEN.

5.9.3.2 Copolymer Formation by Transreaction
A copolymer may be formed through transreaction between a bisphenol A polyestercarbonate resin and imide linkages in the chains of an immiscible PEI phase in the presence of a catalyst (Brown et al. 1998b). This is a degradative

Table 5.31 PEST/polyether blends: copolymer formation by transesterification

Polyester/polyether	Characterization and comments	References
PTT/phenoxy	NMR/SEM/rheometry	Farmahini-Farahani et al. 2008
LCP (Hoechst Vectra A950) (90-0)/phenoxy (10-100)	Mini-max molder at 290 °C/ rheology/DSC/SEM/mechanical properties/selective solvent extraction/FTIR	Choi et al. 1995
PBT (30-0)/PC (0-100)/ phenoxy (0-100)	Internal mixer at 240 °C/torque rheometry/DSC/DMTA/selective solvent extraction/also PC + phenoxy binary blends	Remiro and Nazábal 1991a, b
PBT (50)/phenoxy (50)	Internal mixer at 230 °C or 250 °C/ torque rheometry/selective solvent extraction/FTIR/DSC/DMTA/ mechanical properties	Eguiazábal and Nazábal 1990
PC (0-100)/phenoxy (100-0)	Internal mixer at 200–250 °C; torque vs. time, temperature/DSC/ DMA/improved modulus and tensile strength as copolymer forms	Mondragon et al. 1986, 1988; Mondragon and Nazábal 1987
Polyarylate (100-0)/ phenoxy (0-100)	Internal mixer at 230 °C, 250 °C, or 270 °C/torque rheometry/DSC/ mechanical and thermal properties	Mondragon et al. 1987
Polyarylate (70-20)/ phenoxy (30-80)	SSE at 265–270 °C/thermal redistribution during molding at 270–320 °C/DMA	Robeson 1985

process initially forming block copolymer and eventually random copolymer as chains continue to react. The final product may be transparent. Various phosphite catalysts were used. PC and polyarylate could be used in place of polyestercarbonate. Bookbinder and Sybert (1992) prepared compatibilized blends of Hoechst Vectra® A950 with amine-terminated PEI. A copolymer may form through reaction of PEI amine groups with main-chain ester units of LCP in a degradative process.

5.9.4 Polyester + Polyethersulfone Blends

Kanomata et al. (2011) prepared compatibilized blends of either PBT or PET and polyethersulfone using PES having hydroxyphenyl end-groups. Blends prepared in a Brabender mixer were characterized using TEM and torque rheometry in comparison with control blends.

5.9.5 Polyester + Polyolefin Blends (Excepting Polypropylene)

5.9.5.1 Copolymer Formation by Alcohol + Anhydride Reaction
As shown in Table 5.32, PEST/PO blends have been compatibilized through copolymer formation between polyester alcohol end-groups and pendent anhydride

Table 5.32 PEST/PO blends: copolymer formation by alcohol + anhydride reaction

Polyester/polyolefin	Characterization and comments	References
PETG/EVAc-g-MA	Internal mixer/mechanical properties/Young's modulus/gel content/effect of MA and DCP RI level on EVAc properties	Hwang et al. 2012
Poly(lactic acid)-g-MA (50)/PVAl (50)	Brabender mixer/mechanical properties/NMR/ also blends containing unfunctionalized PLA	Quintana et al. 2012
Poly(lactic acid)-g-MA/ PEG	Melt blended/DSC/rheometry/comparison to blend with unfunctionalized PLA	Hassouna et al. 2011
PTT/EPDM-g-MA	Morphology/rheology/comparison to blends with unfunctionalized EPDM	Aravind et al. 2010b
Recycle PET/ LLDPE-g-MA	Low-temperature solid-state extrusion/ mechanical properties/DSC/morphology/FTIR	Zhang et al. 2008
PTT/(ethylene-octene copolymer)-g-MA	Melt mixing/mechanical properties/morphology	Guerrica-Echevarría et al. 2007
PET/HDPE/HDPE-g-MA	Mechanical and thermal properties/MA-grafted PO prepared using UV preirradiation process resulting in different grafting and cross-linking degrees/comparison of blend properties to those containing PO-g-MA prepared using RI process/ also used LDPE and LLDPE and their corresponding MA-grafted species	Martinez et al. 2007
PBT/HDPE-g-MA	Mechanical properties/morphology/rheology/ comparison to blends with unfunctionalized HDPE	Qi et al. 2006
PTT/EPDM/EP-g-MA	DSC/positron annihilation lifetime measurements	Ravikumar et al. 2006
PBT (80)/EVAc-g-MA (20)	Haake mixer/torque rheometry/FTIR/SEM/ mechanical properties vs. blend with unfunctionalized EVAc	Kim et al. 2003, 2001a
PET/HDPE/MA	Mechanical properties/SEM	Lusinchi et al. 2000
LCP (Hoechst Vectra A950)/PP-g-MA	Extruder/rheology/SEM/mechanical properties vs. LCP concentration	Tjong et al. 1998
PBT (100-20)/EVAc-g-MA (0.8 % MA) (0-80) or EMM-g-MA	TSE at 260 °C/GPC/SEM/DSC/mechanical properties vs. use of unfunctionalized EVAc or EMM	Kang et al. 1997
PBT (60)/LCP (Hoechst Vectra A950) (25)/ EPDM-g-MA (15)	TSE at 290 °C/SEM/optical microscopy/Raman spectroscopy/mechanical properties/selective solvent extraction/FTIR	Seo 1997
PET/HDPE/HDPE-g-MA (5 parts per 100 parts PET) or EVAc-g-MA	TSE at 270 °C/rheology/interfacial tension measurements	Ihm and White 1996
PET (100-0)/HDPE (0-20)/ EMAc-MA (1.4 % MA) (0-100)	TSE at 280 °C/DMA/DSC/mechanical properties/ SEM/FTIR/optical microscopy/use of recycle PET	Kalfoglou et al. 1995

<div align="right">(continued)</div>

Table 5.32 (continued)

Polyester/polyolefin	Characterization and comments	References
PET (85-20)/HDPE (10-75)/PO-g-MA (0-5)	TSE at 270 °C/SEM/DSC/optical microscopy/ mechanical properties	Sambaru and Jabarin 1993
PBT (80)/EP-g-MA (2.3 % MA) (20)	Internal mixer at 240 °C/mechanical properties/ SEM/rheology/DSC/selective solvent extraction	Cecere et al. 1990

functionality on a polyolefin such as maleic anhydride-grafted polyolefin. Because this alcohol-anhydride reaction is reversible with the equilibrium lying on the side of unreacted anhydride, only a relatively small amount of copolymer may be formed. Consequently, the dispersed polymer phase may not be well stabilized against coalescence upon further thermal treatment (for a discussion, see, e.g., Sun et al. (1996) and Boyer et al. (2005)). Alternatively, at least some copolymer may be formed by a degradative mechanism through transesterification between polyester main-chain linkages and a low concentration of pendent acid groups in anhydride functionalized polyolefin. In addition copolymer may possibly form through anhydride exchange between PEST-CO_2H end-groups and PO-anhydride. Alternatively, it may also happen that compatibilization results from hydrogen-bonding interaction.

5.9.5.2 Copolymer Formation by Carboxylic Acid + Cyclic Ortho Ester or Epoxide Reaction

Table 5.33 shows examples of PEST/PO blends that have been compatibilized through graft copolymer formation either by reaction of polyester carboxylic acid end-groups with either pendent cyclic ortho ester or pendent epoxide groups on a polyolefin or by reaction of polycarbonate epoxide end-groups with carboxylic acid groups on a polyolefin. In any case, the copolymer is joined through a new ester linkage. Since there may be multiple electrophilic sites or multiple carboxylic acid sites on the polyolefin, some cross-linked copolymer may result if the polyester is functionalized at both ends. The proportion of cross-linked copolymer formed also depends upon blend composition and processing conditions.

When the new ester linkage is formed, a secondary alcohol group forms as well through ring opening of the epoxide group. The new secondary alcohol may also react with polyester main-chain linkages to form copolymer through a degradative transesterification process. Consequently, two very different types of copolymer may be formed in certain blends of this section.

Perret et al. (1996) have encapsulated a third polymer within a PO phase dispersed in a PEST matrix; the third polymer was PA-66, having higher Tm than the matrix. In this ternary blend, the epoxy-functionalized PO was capable of reacting with terminal functional groups on both of the other two polymers. The blend was formed either by preextrusion of PO with PA, followed by extrusion with PEST, or by feeding PO and PA to the feed throat of an extruder, then adding PEST downstream. The morphology showed a PEST matrix in which shells of PO

Table 5.33 PEST/PO blends: copolymer formation by carboxylic acid + cyclic ortho ester or epoxide reaction

Polyester/polyolefin	Characterization and comments	References
Poly(lactic acid)/ethylene-octene copolymer-g-GMA (>10 wt%)	Mechanical properties/FTIR/Molau test/morphology/critical interparticle distance of dispersed domains	Feng et al. 2013a
Poly(lactic acid)/ethylene-co-methyl acrylate-co-GMA	Mechanical properties/FTIR/morphology/addition of N,N-dimethylstearylamine catalyst (0.2 wt%)	Feng et al. 2013b; Zhang et al. 2013b
Poly(lactic acid)/E-GMA	Mechanical properties/SEM/TEM/thermal expansion properties/comparison to blends with SEBS-g-MA or unfunctionalized ethylene-octene copolymer in place of E-GMA	Jiang et al. 2013
Poly(lactic acid)/NR/NR-g-GMA	Internal mixer/thermal and mechanical properties/morphology/effect of GMA level on properties	Juntuek et al. 2012
Poly(lactic acid)/EBA-GMA/EMAA-Zn ionomer	TSE/mechanical properties/DMA/morphology/also effect of different ionomer cations	Liu et al. 2011b, 2012a, 2013b; Song et al. 2012b
PET/EMA + EMA-co-GMA (25:75 wt%:wt%)	SSE/DSC/ductile-brittle transition temperature/IV measurement/effect of catalyst system used in preparing PET/also used PET containing isophthalic acid residues and recycle PET	Colhoun et al. 2011
Recycle PET/E-GMA	Mechanical properties/morphology/density/effect of processing conditions on blend properties	Kunimune et al. 2011
Poly(lactic acid)/ethylene-octene copolymer/E-GMA (10 phr)	Mechanical properties/morphology/rheology/FTIR	Pai et al. 2011; Li et al. 2011a
PET/ethylene-octene copolymer/ethylene-octene copolymer-g-GMA	Use of recycle PET/morphology/mechanical properties/thermal properties/evidence for copolymer formation	Liu et al. 2009a, 2010a
Poly(lactic acid)/EBA-GMA/EMAA partially Zn neutralized	Extrusion blending/TEM/mechanical properties/effects of blending temperature and elastomer/ionomer ratio	Liu et al. 2010b
Poly(lactic acid)/EB/PP-PO copolymer/E-GMA	Twin-screw kneader/DSC/TEM/mechanical properties/two-step vs. one-step mixing process/also used ethylene-octene copolymer in place of EB	Shimano and Moritomi 2010

(*continued*)

Table 5.33 (continued)

Polyester/polyolefin	Characterization and comments	References
Poly(lactic acid)/E-GMA	Mechanical properties	Oyama 2009
Poly(lactic acid)/LLDPE/ethylene-octene copolymer-g-GMA	SEM/DSC/WAXD/FTIR/spreading coefficient calculation	Su et al. 2009
PET/HDPE/EBA-g-GMA	Haake torque rheometer/capillary rheometry/SEM morphology/effect of EBA-g-GMA level on blend properties	Li and Lu 2008; Li et al. 2009d
Recycle PET/PC/EBA-co-GMA	Low-temperature solid-state extrusion/mechanical properties/SEM/DSC/FTIR/effect of blending sequence on properties	Peng et al. 2008
PBT/NBR/EPDM-g-GMA	Two-step mixer process/DSC/SEM/TEM/DMTA/mechanical properties/indirect dynamic vulcanization/also used EPDM-g-ally(3-isocyanato-4-tolyl) carbamate	Shi et al. 2008
PBT/EP-g-GMA	Mechanical properties/morphology/effect of GMA grafting level on properties	Sun et al. 2006
PET/EP-g-GMA	Internal mixer/rheology/SEM/DMA/FTIR/Molau test/EP functionalized with GMA in the presence of trimethylol propane triacrylate/comparison to blends containing unfunctionalized EP or EP functionalized with GMA in absence of triacrylate	Al-Malaika and Kong 2005
PBT/EMA/EMA-g-GMA	TEM/DMTA/reaction kinetics/compatibilization accompanied by dynamic vulcanization of rubber phase	Martin et al. 2003, 2004a, b, c
PBT/(ethylene-octene copolymer)-g-GMA	Extrusion processing/mechanical properties/morphology/also blends containing unfunctionalized ethylene-octene copolymer	Aróstegui and Nazábal 2003a, b
PET/EP/E-g-GMA (8 wt% GMA)	Deformation mechanisms/fractography of impact fractured samples/tensile dilatometry/DMA	Loyens and Groeninckx 2003a, b
PET/EP/EP-g-GMA	Morphology/critical interparticle distance/mechanical properties	Loyens and Groeninckx 2002
Recycle PET/HDPE/E-GMA	Morphology/rheology/DSC/FTIR/NMR/capillary rheometry/mechanical properties/comparison to blends containing various MA- or AA-f-PO in place of E-GMA	Pracella et al. 2002

Table 5.33 (continued)

Polyester/polyolefin	Characterization and comments	References
LCP/PE-f-epoxide	TSE/morphology/mechanical and thermal properties/effect of blend component ratios and of different PE epoxy levels	Tynys et al. 2002
PBT (80)/EMA-GMA (20)	SEM/selective solvent extraction/EMA-GMA modified with benzoic acid to vary the amount of epoxide present/quantification of PBT-PO copolymer formation vs. PO cross-linking	Martin et al. 2001
PET/UHMWPE-f-epoxide	TSE or batch mixer/morphology/mechanical properties/UHMWPE powder irradiated, then reacted first with AA, then with a difunctional cycloaliphatic epoxy resin to introduce epoxide functionality/comparison of properties to those of blends containing UHMWPE-f-AA	Mascia and Ophir 2001
PET/HDPE/HDPE-g-GMA	Internal mixer/SEM/also grafting of GMA in presence of styrene monomer	Pazzagli and Pracella 2000
PET/E-GMA	Mechanical properties/morphology/also used ethylene-ethyl acrylate-GMA copolymer/effect of GMA level on blend properties	Pietrasanta et al. 1999
PBT (100-85)/EPDM-g-GMA (0-15)	Internal mixer at 245 °C/SEM/mechanical properties vs. use of unfunctionalized EPDM	Wang et al. 1997
PBT (80-60)/EMAc-GMA (12-24)/PA-66 (8-16)	Buss Ko-kneader/pre-compounding of PA + EMAc-GMA at 270 °C followed by compounding with PBT at 250 °C/SEM/mechanical properties	Perret et al. 1996
PET (60) or PC + PE/EEA-GMA (25) or E-GMA/EEA (15) or EP	SSE or TSE/mechanical properties/TEM	Akkapeddi et al. 1995
PBT (100-0) or LCP (Hoechst Vectra A950)/EEA-GMA (0-100)	TSE at 240 °C/DSC/SEM/FTIR/rheology/mechanical properties/comparison vs. properties of EEA-GMA blends with PBT or LCP + PP	Holsti-Miettinen et al. 1995
PET (100-0)/HDPE (0-20)/E-GMA (0-100) or EEA-GMA	TSE at 280 °C/DMA/DSC/mechanical properties/SEM/FTIR/optical microscopy/use of recycle PET	Kalfoglou et al. 1995
PET (80-70)/EEA-GMA (20-30)	TSE at 280 °C/mechanical properties/SEM/rheology/properties comparison to properties comparison to blends with unfunctionalized rubbers/effects of amine catalyst addition	Penco et al. 1995

(*continued*)

Table 5.33 (continued)

Polyester/polyolefin	Characterization and comments	References
PET (20-18)/HDPE (73-78)/ E-GMA (2-9)	Internal mixer or TSE at 270–290 °C/DSC/selective solvent extraction/FTIR/rheology/ mechanical properties/morphology vs. order of mixing	Dagli and Kamdar 1994
PBT (80-50)/E-GMA (3 % GMA) (20-50)	TSE at 260 °C/adipic acid (0.1) optionally added as rubber vulcanization agent/mechanical properties/TEM	Okamoto et al. 1994
PET (50) or PETG/E-GMA (6 % GMA) (50)	Internal mixer at 270 °C/torque rheometry/GPC/effects of residual levels of different catalysts used to synthesize polyesters	Stewart et al. 1993b
PBT (50)/EPDM-g-GMA (1.5 %, 3 %, or 6 % GMA) (50)	TSE at 250 °C/extrusion of PBT + EPDM -g-GMA followed by re-extrusion with vulcanization agent (either L130 or 6-aminohexyl carbamic acid)/ mechanical properties/SEM/TEM	Moffett and Dekkers 1992 (see also Hepp 1985; Olivier 1986b; Phadke 1988b; Pratt 1988; Pratt et al. 1988)
PBT (50-95)/EPDM-g-cyclic ortho ester (50-5)	TSE at 250 °C/different cyclic ortho esters used/tensile properties vs. blends with unfunctionalized EPDM or EPDM-g-GMA/other PEST also used	Shea et al. 1992
Epoxy triazine-capped PC (50)/ acid- or anhydride-functionalized PO (50)	Solution reaction/copolymer analysis by selective solvent extraction/numerous functionalized PO used/also used SMA in melt reaction in place of functionalized PO	Brown et al. 1991a

surround cores of PA. The blend was an impact-modified PEST with higher impact strength than the corresponding blend containing epoxy-functionalized PO alone. One reason for the improvement may be that the volume fraction of PO impact modifier was effectively increased by inclusion of PA core. Copolymer formation between PEST and PO may also be combined with subsequent dynamic vulcanization of the PO phase in either the same or a separate processing step (Okamoto et al. 1994; Moffett and Dekkers 1992).

5.9.5.3 Copolymer Formation by Carboxylic Acid + Oxazoline Reaction

PEST/PO blends have been compatibilized through graft copolymer formation by reaction of polyester carboxylic acid end-groups with pendent oxazoline groups on an appropriate PO. The copolymer contains a new esteramide linkage. Wörner et al. (1997) have blended 0-20 parts oxazoline-functionalized rubbers containing more than one oxazoline group per chain with 100-80 parts acid-terminated PBT in

an internal mixer at 240 °C. Oxazoline-functionalized B-AN or E-B-AN was used. The copolymer structure was initially a graft copolymer. However, if additional oxazoline groups on the rubber react with additional PBT acid groups, then a cross-linked copolymer structure can arise. The blends of Wörner et al. were characterized by torque rheometry, mechanical properties, DMA, SEM, DSC, and level of oxazoline groups on the rubber (fraction of nitrile groups on AN-containing rubber that had been converted to oxazoline groups). Improved blend properties were obtained through addition of a bis-oxazoline chain extender for PBT.

5.9.5.4 Copolymer Formation through Coupling Agent Addition

Zhang et al. (2013c) prepared compatibilized blends of poly(lactic acid) and EVAl in the presence of a multifunctional epoxy resin and zinc stearate. Characterization techniques included morphology, dynamic light scattering, and barrier properties.

Compatibilized blends of PBT with EVAc have been prepared through addition of 2,2′-(1,3-phenylene)-bis(2-oxazoline) coupling agent (Scaffaro and La Mantia 2006; Scaffaro et al. 2004). The effect of EAA addition was studied. Evidence was presented that chain extension of the reactive polymers by the coupling agent was negligible. Blends characterization included mechanical properties and morphology in comparison to uncompatibilized blends.

Zhang and Hourston (1999) prepared blends of PBT and either LDPE or EPDM in the presence of a bismaleimide in a Haake mixer. A copolymer formation mechanism involving radical coupling was proposed.

Okamoto and Inoue (1993) have compatibilized an immiscible blend of terminally functionalized PEST and PO through block copolymer formation in the presence of a coupling agent. For example, 80 parts hydroxy-terminated PCL was mixed in a custom melt reactor at 120 °C with 20 parts carboxyl-terminated butadiene oligomer (or carboxyl-terminated NBR) in the presence of 0-1 part aminopropyltriethoxysilane coupling agent. Morphology development could be followed through analysis of successive samples taken periodically from the reactor. Samples were characterized by light-scattering photometry, ellipsometric analysis, and GPC.

5.9.5.5 Copolymer Formation by Diels-Alder Reaction

The benzocyclobutene functionality can thermally form an intermediate that can function as the diene partner in a classical Diels-Alder ring-forming reaction with an olefin. When benzocyclobutene and olefin are located on two immiscible polymers, the reaction can in theory lead to copolymer formation. Dean (1993) has postulated that copolymer is formed when 50-15 parts benzocyclobutene-terminated polyarylate is mixed with olefin-containing EPDM in an internal mixer at 265 °C. Blends were characterized by mechanical properties and DMTA.

5.9.5.6 Copolymer Formation by Transesterification

Polyester-polyolefin copolymer compatibilizers have been made through catalyzed or thermal transesterification of polyester or polycarbonate or polyestercarbonate main-chain ester linkages with pendent ester or acid groups (acidolysis) in a polyolefin copolymer such as EVAc or EMAA (Table 5.34). In a separate example,

Table 5.34 PEST/PO blends: copolymer formation by transesterification

Polyester/polyolefin	Characterization and comments	References
PC/PMMA/tin 2-ethylhexanoate catalyst (0.5 wt%)	DSC/TGA/FTIR/selective solvent extraction/^{1}H NMR/optical transparency/ also SnCl$_2$ · 2H$_2$O catalyst	Singh et al. 2011, 2012
PET/PE-f-dibutyl succinate/Zn acetate catalyst	Mechanical properties/morphology/ selective solvent extraction/FTIR/also used ZnO, Ti(OBu)$_4$, and TiO(OCCH$_3$)$_2$ as catalysts	Coltelli et al. 2008
PET (70)/PO-f-dibutyl maleate (30)/Zn acetate catalyst	Mechanical properties/SEM/DSC/ selective solvent extraction	Coltelli et al. 2007
PC/HDPE/EAA/dibutyltin oxide catalyst	Haake mixer/SEM/DSC/rheology/ formation of PC-EAA copolymer	Yin et al. 2007
PC/phenolic-f-PMMA	Melt mixed at 280 °C/ tetraphenylphosphonium benzoate catalyst/MMA copolymerized with alpha-methyl-*p*-hydroxystyrene	Bolton et al. 2005
LCP (50)/poly(ethylene acrylic acid) ionomer (50)	SSE or batch mixer/assessment of acidolysis to form graft copolymer compatibilizer	Son and Weiss 2001, 2002; Zhang et al. 2000
PC/poly(ethylene-co-butylene) diol	Melt mixing/NMR/UV spectroscopy/ amine catalysis/DSC/GPC	Lee et al. 2001
PC/poly(MMA-co-AA) (6 mol% AA; partially neutralized with Zn cations)	Melt reaction at 235 °C/unneutralized poly(MMA-co-AA) does not form copolymer with PC/ternary blends with PVDF/morphology/mechanical properties	Moussaif et al. 2000
PC/PMMA/SnOBu$_2$ catalyst	NMR/SEC/thermogravimetry/MS	Montaudo et al. 1998b
PC (50-30)/imidized acrylate copolymer (77 % glutarimide, 19 % MMA, 3 % MAA, 2 % glutaric anhydride) (70-50)	Internal mixer at 260–270 °C or solution casting/FTIR/optical microscopy/SEM/ TEM/SEC/model reactions/selective solvent extraction/comparison to blends with PMMA or with imidized acrylate copolymer containing different imide levels, or no acid or anhydride/details of reaction mechanism	Debier et al. 1995, 1997a, b
PBT (70)/EVAc (10-20)/PE (10-20)	Internal mixer at 230 °C/SEM/dibutyltin oxide catalyst (0–4 %)/encapsulation of PE dispersed phase by PBT-EVAc copolymer	Legros et al. 1997
PBT (50-10)/EVAc (9 % or 28 % VAc) (50-90)	Internal mixer at 230 °C/selective solvent extraction/NMR/FTIR/SEM/model reactions/dibutyltin oxide catalyst (0–1 %)/blends optionally + PE	Pesneau et al. 1997
PETG (90-80)/EVAc (10-20)	Internal mixer at 210 °C/SEM/NMR model study/rheology/DMA/interfacial tension measurements by breaking thread method/dibutyltin oxide catalyst (0–1 %)	Lacroix et al. 1996a, b

Table 5.34 (continued)

Polyester/polyolefin	Characterization and comments	References
PET (100-0)/EEA (0-100)	Glass mixer at 260–290 °C/DMA/SEM/ mechanical properties/selective solvent extraction/FTIR/DSC	Gravalos et al. 1995
PET (68-23)/LLDPE (23-68)/EMAA ionomer (5-15)	Extruded at 280 °C/DMA/DSC/ mechanical properties/SEM/optical microscopy	Kalfoglou et al. 1994
PETG (70-30)/EVAc (28 % VAc) (30-70)	Internal mixer at 180 °C or 210 °C/SEM/ rheology/DSC/mechanical properties/ dibutyltin oxide catalyst (0–4 %)	Legros et al. 1994
PC (95-50)/HDPE (0-20)/ EMAA ionomer (5-50)	Internal mixer at 220 °C/torque rheometry/FTIR/DSC/selective solvent extraction/mechanical properties/SEM	Mekhilef et al. 1992
Poly(hydroxybutyrate) (80)/ EP-g-MA (4 % MA) (20) or EP-g-dibutyl maleate or partially hydrolyzed EVAc	Internal mixer at 180 °C/mechanical properties/SEM	Abbate et al. 1991

polyester-polyolefin copolymer has been formed through transesterification between a carbonate ester linkage and an anhydride in a second polymer chain. All these examples represent degradative copolymer formation since the PEST chains are cleaved and the average molecular weight of the new copolymer is less than the sum of the average molecular weights of the two immiscible polymers.

In Table 5.34, Debier et al. (1995, 1997) present evidence that copolymer formation occurs in PC + PMMA blends through transesterification between PC carbonate ester linkages and acid groups produced by hydrolysis on PMMA. The table omits references in which transesterification in appropriate polyester-polyolefin blends is brought about under static conditions either by annealing or heating in a DSC chamber.

A block copolymer may be formed through transesterification between nucleophilic end-groups of one polymer and ester linkages in the chains of an immiscible polyester phase. Sek and Kaczmarczyk (1997) and Minkova et al. (1996) used oxidized PE as the acid-terminated polymer and an LCP with ester linkages susceptible to transesterification with PE acid end-groups. Since the product is a block copolymer accompanied by low molecular weight fragments from the polyester, this type of copolymer-forming reaction is degradative. The process is not redistributive since the PE chain cannot participate in redistribution. In an example, 50 parts LCP polyester (a copolymer of sebacic acid, dihydroxybiphenyl, and p-hydroxybenzoic acid) and 50 parts oxidized PE were mixed in an internal mixer at 240 °C. The blend was characterized by selective solvent extraction, FTIR, DSC, and SEM. Optionally, $Ti(OBu)_4$ catalyst was added to promote reaction.

5.9.5.7 Copolymer Formation by Miscellaneous Reactions

Chen et al. (2013a) prepared blends of PCL with NR in the presence of peroxide which, in addition to cross-linking NR, served to enhance the compatibility of PCL and NR as shown by FTIR and SEM. The blend was studied as a shape-memory composition.

Hachemi et al. (2013) prepared blends of poly(lactic acid) with PVC in the presence of DCP RI and MA. Characterization techniques included DSC, TGA, SEM, and mechanical properties.

Gramlich et al. (2010) prepared blends of maleimide-terminated poly(lactic acid) with conjugated soybean oil. A compatibilizing copolymer was formed through Diels-Alder reaction between maleimide double bond and diene units in conjugated soybean chains. Blends were characterized by morphology and mechanical properties.

Pan et al. (2007) prepared compatibilized blends of PC with EMAc-g-GMA. Characterization concluded that copolymer was formed through reaction of PC phenolic end-groups and epoxy groups.

Jung et al. (2003) have prepared compatibilized blends of PET with LDPE comparing a variety of functionalized LDPEs as compatibilizing agents, including LDPE-co-AA, LDPE-f-MA, LDPE-f-GMA, and LDPE functionalized with either masked or naked NCO monomers.

Park et al. (1998b) have prepared compatibilized blends of PET with PE using PE grafted with 2-hydroxyethyl methacrylate-isophorone diisocyanate. See also Park et al. (2002), Bae et al. (2001), and Kim et al. (2000a, b). For PBT/ethylene-octene copolymer blends compatibilized using masked isocyanate, see Yin et al. (2009a).

Hourston et al. (1991) have prepared compositions of 60-0 parts PBT and 16-40 parts EPDM in the presence of 0-60 parts copolymer of PBT with maleate ester (3.5 % maleate) using a TSE at 255 °C. A compatibilizing copolymer was postulated from the cross-linking reaction between maleate olefinic groups and EPDM olefinic groups. Blends were characterized by mechanical properties and TEM. Model studies were performed to understand the cross-linking process. Blends were also prepared using an internal mixer at 250 °C.

5.9.6   Polyester + Polyolefin + Polypropylene Blends

5.9.6.1 Copolymer Formation by Carboxylic Acid + Epoxide Reaction

PEST/PP blends have been compatibilized through graft copolymer formation by reaction of polyester carboxylic acid end-groups with pendent epoxide groups on an appropriate PO with potentially some miscibility with PP (Table 5.35). The copolymer is joined through a new ester linkage. Some cross-linked copolymer may also form. When the new ester linkage is formed, a secondary alcohol group forms as well. The new secondary alcohol may also react with polyester main-chain linkages to form copolymer through a degradative transesterification process.

5.9.7   Polyester + Polyolefin + Styrene Copolymer Blends

5.9.7.1 Copolymer Formation by Alcohol + Anhydride Reaction

Examples of PEST/PO/styrene copolymer blend compatibilization in which a copolymer may be formed between polyester alcohol end-groups and pendent

Table 5.35 PEST/PO/PP blends: copolymer formation by carboxylic acid + epoxide reaction

Polyester/polyolefin/polypropylene	Characterization and comments	References
PET/EBA-GMA/PP	Rheology/SEM	Khonakdar et al. 2013
Poly(lactic acid)/PB-f-epoxide/PP	Haake mixer/torque rheology/DSC/ comparison to blend without PB-f-epoxide or with unfunctionalized PB	Li et al. 2012b
Poly(hydroxybutyrate)/EMA-GMA/ PP	Morphology/mechanical properties	Sadi et al. 2012
PBT/EPDM-f-epoxide/PP	Haake mixer/SEM/FTIR/torque rheometry/mechanical properties/EPDM functionalized using performic acid	Ao et al. 2007b
PBT (70-30)/E-GMA (6 % GMA) (0-20)/PP (30-70)	TSE at 255 °C/torque/capillary rheometry/ FTIR/SEM/TEM/mechanical properties/ catalysis of acid + epoxide reaction using phosphonium salt	Tsai and Chang 1996
PBT (100-0) or LCP (Hoechst Vectra A950)/EEA-GMA (5)/PP (0-100)	TSE at 240 °C/DSC/SEM/FTIR/rheology/ mechanical properties/comparison vs. properties of binary EEA-GMA blends with PBT or LCP	Holsti-Miettinen et al. 1995
PBT (29 parts)/EVAc-co-GMA (5 parts; 10 parts GMA)/PP-g-MA (66 parts; 0.11 wt% MA)	Extruded at 240 °C/mechanical properties vs. blends without functionalized polymers/PET and E-GMA also used	Mashita et al. 1991

anhydride functionality on a styrene copolymer are shown in Table 5.36. Because the alcohol-anhydride reaction is reversible (with the equilibrium lying on the side of unreacted anhydride), only a relatively small amount of copolymer may be formed. In consequence, the dispersed phase polymer may not be well stabilized against coalescence upon further thermal treatment (for a discussion, see, e.g., Sun et al. (1996) and Boyer et al. (2005)). Alternatively, at least some copolymer may be formed by a degradative mechanism through transesterification between PEST main-chain linkages and a low concentration of pendent acid groups in anhydride-functionalized styrene copolymer or in anhydride-functionalized PO. In addition copolymer may possibly form through anhydride exchange between PEST-CO_2H end-groups and either anhydride-functionalized styrene copolymer or anhydride-functionalized PO. Alternatively, it may also happen that compatibilization results from H-bonding interaction. For related work in PET/PP blends compatibilized using SEBS-g-MA (or PP-g-MA), see Papadopoulou and Kalfoglou (2000).

5.9.7.2 Copolymer Formation by Carboxylic Acid + Epoxide Reaction

Larocca et al. (2010) prepared blends of PBT and SAN in the presence of MMA-co-EA-co-GMA. Blend characterization techniques included morphology. PBT samples with different molecular weight were used to change the PBT/SAN viscosity ratio. In related work, AES was used in place of SAN (Larocca et al. 2005).

Table 5.36 PEST/PO/styrene copolymer blends: copolymer formation by alcohol + anhydride reaction

Polyester/polyolefin/styrene copolymer	Characterization and comments	References
Recycle PET/recycle HDPE/ PE-g-MA/SEBS	Morphology/mechanical properties/crystallinity level/optionally with addition of methylene di(phenyl isocyanate) coupling agent	Lei et al. 2009
PET/HDPE/SEBS-g-MA (1-5 parts per 100 parts PET)	TSE at 270 °C/rheology/interfacial tension measurements	Ihm and White 1996
PET (80)/HDPE (20)/ SEBS-g-MA (0-20)	SSE at 270 °C/rheology/SEM/mechanical properties/use of recycle PET	La Mantia et al. 1994
PET (100-0)/HDPE (0-100)/ SEBS-g-MA (5–20 phr)	TSE at 270 °C/mechanical properties/SEM/DSC/ WAXD	Carte and Moet 1993

5.9.8 Polyester + Polyphenylene Ether Blends

PEST/PPE blends in these sections include those containing PPE-miscible PS or a functionalized PS. These blends often contain a rubbery impact modifier, such as SEBS, as well.

5.9.8.1 Blends Containing Functionalized PPE: PEST-PPE Copolymer Formation by Degradative Process

Furuta et al. (1994) have prepared compatibilized blends of LCP with an amine-functionalized PPE. For example, an LCP derived from p-acetoxybenzoic acid, terephthalic acid, isophthalic acid, and 4,4′-diacetoxydiphenyl was blended with an amine-functionalized PPE to provide a blend with improved properties compared to those with unfunctionalized PPE. PPE was melt functionalized with either p-aminostyrene, diallylamine, allylamine, or vinylimidazole. Other LCP were also used.

5.9.8.2 Blends Containing Functionalized PPE: PEST-PPE Copolymer Formation by Carboxylic Acid + Electrophile Reaction

PEST/PPE blends have been compatibilized through copolymer formation between polyester and a functionalized PPE (Table 5.37). Typically, the PPE is functionalized in a separate reaction either in the melt or in solution to introduce an electrophilic moiety (such as epoxide, carbodiimide, cyclic ortho ester, or the like) at a phenolic end-group or along the PPE main chain or both. The electrophilic moiety can react with PEST carboxylic acid end-groups in the melt resulting in a compatibilizing copolymer.

PEST-PPE blends have been compatibilized through block copolymer formation between carboxylic acid end-groups on polyesters, such as PBT, and epoxy-terminated PPE (Brown and Lowry 1992a). PPE was functionalized in solution with a variety of chloro-epoxy triazine derivatives in the presence of a base to provide a reactive epoxy triazine-capped PPE (Brown and Lowry 1992b; Yates et al. 1992). Melt functionalization of PPE was also possible (Brown et al. 2009). Representative chloro-epoxy triazine capping agents included

Table 5.37 PEST/PPE blends – blends containing functionalized PPE: PEST-PPE copolymer formation by carboxylic acid + electrophile reaction

Polyester/PPE	Characterization and comments	References
PBT (70)/PPE (30)/ ricinol-2-oxazoline maleate/radical initiator	Brabender at 260 °C/SEM/melt index/HDT/mechanical properties vs. control blend containing 2-ricinol-2-oxazoline/1,3-bis(t-butylperoxyisopropyl)benzene RI	Oshima et al. 1998
PET/epoxy or cyclic ortho ester-functionalized PPE/PE-co-GMA/SEBS	TSE at 280–300 °C/mechanical properties/morphology vs. blends with unfunctionalized PPE or without functionalized PE	Hwang et al. 1996
PBT (2 parts)/PPE-g-glycidyl acrylate (1 part; 4 % GA)/SEBS (0.33 parts)	TSE at 120–288 °C/PPE grafted in presence of a lubricant/mechanical properties vs. PPE grafting conditions	Khouri et al. 1994
PBT (55)/PPE-g-GMA (36)/SEBS (9)	TSE/mechanical properties/numerous other functionalized PPE and functionalized PEST were prepared, primarily in solution	Sybert et al. 1991
PBT (45 %)/ carbodiimide-functionalized PPE (45 %)/SEBS (10 %)	TSE/PPE functionalized in solution with 4,4′-bis (4-cyclohexylcarbodiimido) diphenylmethane/ mechanical properties/copolymer analysis by selective solvent extraction/PET also used	Han and Gately 1987

2-chloro-4-(2,4,6-trimethylphenoxy)-6-glycidoxy-1,3,5-triazine. For example, blends containing PBT, PPE-epoxide, and SEBS impact modifier were prepared using a TSE and characterized by selective solvent extraction, morphology, and mechanical properties. Numerous other polyesters, polyestercarbonates, and polyesteramides were used in these blends (see, e.g., Brown and Lowry 1992b).

PEST-PPE blends have also been compatibilized through block copolymer formation between carboxylic acid end-groups on polyesters, such as PBT, and PPE bearing reactive dialkylphosphatoethoxy triazine terminal groups (Phanstiel and Brown 1991, 1992). In this case PPE was functionalized in solution with a variety of chloro dialkylphosphatoethoxy triazine derivatives in the presence of a base to provide a reactive triazine-capped PPE. Representative chloro dialkylphosphatoethoxy triazine capping agents included 2-chloro-4-(2-di-n-butylphosphatoethoxy)-6-(2,6-xylenoxy)-1,3,5-triazine. For example, a blend containing 60 parts PBT, 30 parts functionalized PPE, and 10 parts impact modifier was prepared using a TSE. Molded test parts showed Izod impact strength of 860 J/m compared to 48 J/m for a similar blend containing unfunctionalized PPE. 2-Chloro-4-(2-chloroethoxy)-6-(2,4,6-trimethylphenoxy)-1,3,5-triazine or 2-chloro-4-(2-bromoethoxy)-6-(2,4,6-trimethylphenoxy)-1,3,5-triazine could be used in place of phosphatoethoxy triazine (Phanstiel and Brown 1993). See also Schmidhauser and Longley (1991).

PEST-PPE blends have also been compatibilized through block or graft copolymer formation between carboxylic acid end-groups on polyesters, such as PBT, and PPE bearing cyclic ortho ester groups. PPE could be either end-capped in solution using a chloro ortho ester triazine derivative such as 2-chloro-4-(2-methoxy-2-methyl-1,3-dioxolanyl)methoxy-6-phenoxy-1,3,5-triazine) (Khouri et al. 1992; Khouri and Phanstiel 1992) or functionalized in the melt using a graftable cyclic ortho ester such as 4-methacryloyloxymethyl-2-methoxy-2-methyl-1,3-dioxolane

(Khouri et al. 1993). In either case, blends of various polyesters with cyclic ortho ester-functionalized PPE showed markedly better mechanical properties compared with control blends containing unfunctionalized PPE. Polyolefin grafted with cyclic ortho ester could also be used in PEST blends comprising PPE grafted with cyclic ortho ester (Khouri 1996).

5.9.8.3 Blends Containing Functionalized or Unfunctionalized PPE: PEST-PPE Copolymer Formation through Coupling Agent or Condensing Agent Addition

As illustrated in Table 5.38, coupling agents have been employed to compatibilize PEST-PPE blends through copolymer formation between PEST carboxylic acid

Table 5.38 PEST/PPE blends: PEST-PPE copolymer formation through coupling agent addition

Polyester/PPE	Characterization and comments	References
PBT (55 parts)/PPE-g-FA (32 parts; 2 % FA)/PE-co-GMA (12 % GMA)	TSE at 250–290 °C/mechanical properties vs. control blends/bis- and tris-cyclic ortho ester and EPDM-g-cyclic ortho ester used in place of PE-co-GMA/SEBS or ZnSt optionally added/PET, PEN, PBN also used	Brown et al. 1997b
PET (100-0)/PPE (0-100)/ tetrafunctional epoxy resin (0-0.5)	TSE at 265–290 °C/torque rheometry/ mechanical properties/FTIR/SEM/ DSC/ethyltriphenylphosphonium bromide catalyst added/property comparison vs. blend with difunctional epoxy resin	Lo et al. 1997 (see also Jana et al. 2001, for PBT blends)
PET (48.5)/PPE (48.5)/ phosphorus tris(lactam) (3)	SSE at 270–280 °C/copolymer level by selective solvent extraction/mechanical properties vs. without tris(lactam)/ different tris(lactams) used/PET-PC-PPE also studied	Glans and Akkapeddi 1991a
PET (3 parts)/PPE-g-MA (2 parts; 1 % MA)/N,N′-bis (2-methyl-2-nitropropyl)-1,4-diaminobenzene (0.1 parts)	TSE at 270–300 °C/mechanical properties vs. blends without dinitrodiamine/also used PBT, other functionalized PPEs, and other dinitrodiamines	Mizuno et al. 1991
PBT (42)/PPE-g-FA (42)/SEBS (10-12)/bis- or trisisocyanate (2-9)	TSE at 265 °C/tris(6-isocyanatohexyl) isocyanurate or 2,4-bis (4-isocyanatophenylmethyl)phenyl isocyanate/mechanical properties vs. control blends/PET and elastomeric PEST also used	Han 1988
PET/PPE/epoxidized polybutadiene (0.5-5.0 parts; 7.5 % oxirane oxygen content)	TSE/mechanical properties vs. blends with unfunctionalized PB/SB copolymer optionally added	Kobayashi et al. 1988
PBT (50)/PPE-g-MA (50)/ diglycidyl ester of fatty acid dimer (2)	Injection molded/mechanical properties/HDT/melt viscosity vs. blends with less epoxide	Nakamura et al. 1988

end-groups and either PPE phenolic end-groups (unfunctionalized PPE) or PPE-g-carboxylic acid or PPE-g-anhydride (functionalized PPE). Numerous similar examples using epoxide coupling agents in PEST-PPE blends have been patented. Tang et al. (1992) have employed a phosphite condensing agent in similar manner to form compatibilizing copolymer. See also van Aert et al. (2001). Chen et al. (1993) employed a catalyst of boric acid with either polyphosphoric acid or sulfuric acid as a condensing agent to link PPE phenolic end-groups with LCP carboxylic acid end-groups.

5.9.8.4 Blends Containing Unfunctionalized PPE + Functionalized PS: PEST-PS Copolymer Formation by Carboxylic Acid + Epoxide Reaction

PEST/PPE blends have been compatibilized through graft copolymer formation between polyester and a PPE-miscible functionalized styrene copolymer (Table 5.39). In this instance, the reaction is between polyester carboxylic acid

Table 5.39 PEST/PPE/styrene copolymer blends – blends containing unfunctionalized PPE + functionalized PS: PEST-PS copolymer formation by carboxylic acid + cyclic ortho ester or epoxide reaction

Polyester/PPE/styrene copolymer	Characterization and comments	References
PBT (60)/PPE (40)/SB core + MMA shell impact modifier with GMA grafted onto shell (5)	Mini-extruder at 240 °C/TEM/ comparison of morphology with and without addition of epoxy-functionalized impact modifier	Aerdts et al. 1997
PBT (70-50)/PPE (30-50)/S-co-GMA (2–15 % GMA) (0-20 parts)	TSE at 260 °C/mechanical properties/ SEM/DSC/torque rheometry/DMA/ ethyltriphenyl phosphonium bromide catalyst (0-0.05 parts)	Liu et al. 1996 (see also Han et al. 2011)
LCP (Hoechst Vectra A950) (20-5)/PPE (40-47)/PS (40-47)/ S-co-GMA (2 %, 5 %, or 10 % GMA) (0-5)	TSE at 290 °C/torque rheometry/ HDT/capillary rheometry/SEM/FTIR/ mechanical properties/ ethyltriphenylphosphonium bromide catalyst (0-0.02 parts)	Chang and Chang 1995
PET (50-20)/PPE (50-80)/PS (0-20)/S-co-GMA (15 % GMA) (0-10 parts)	TSE at 290 °C/DSC/DMA/SEM/also addition of phenoxy resin	Liang and Pan 1994 (see also Sano and Ohno 1988)
PBT (20-80)/PPE (15-50)/SEBS (5-25)/styrene-cyclic ortho ester copolymer (2-15)	TSE at 270 °C/impact strength vs. blends with unfunctionalized PS/PS copolymer prepared using styrene and 4-methacryloyloxymethyl-2-methoxy-2-methyl-1,3-dioxolane, for example	Khouri 1993
PBT (60)/PPE (30)/styrene-isopropenyl oxazoline copolymer (10 parts)/PC (8 parts)/SEBS (12 parts)	TSE at 320 °C/mechanical properties vs. blend without functionalized PS or using SMA	Hamersma et al. 1991
PET (30)/PPE (70)/SEBS-g-S-GMA (20)	TSE/mechanical properties vs. blend without functionalized SEBS	Mayumi and Omori 1988

end-groups and pendent electrophilic groups on the styrene copolymer such as epoxide, oxazoline, cyclic ortho ester, and the like typically leading to a new ester linkage in the resulting copolymer. In the examples where the new ester linkage is formed from an epoxide group, a secondary alcohol group forms as well. The new secondary alcohol may also react with polyester main-chain linkages to form copolymer through a degradative transesterification process. Since there are typically multiple epoxide sites on the styrene copolymer, some cross-linked copolymer may result as well if the polyester is functionalized at both ends. The proportion of cross-linked copolymer formed also depends upon functionality concentration on both PEST and PS, blend composition, and processing conditions.

5.9.9 Polyester + Polyphenylene Sulfide Blends

Luo et al. (2013) employed a disulfide-modified PPS in compatibilized blends with LCP blend characterization techniques including rheological, mechanical, and thermal properties. Gopakumar et al. (1999) reported transesterification of thermotropic LCP with carboxylic acid-terminated PPS. Blends were characterized by morphology, mechanical properties, and DSC. Hanley et al. (1999) used a similar compatibilization strategy for blends of PET and carboxylic acid-terminated PPS. Chen et al. (1993) employed a catalyst of boric acid with either polyphosphoric acid or sulfuric acid as a condensing agent to link PPS thiol end-groups with LCP carboxylic acid end-groups.

5.9.10 Polyester + Polyphosphonate Blends

Kauth et al. (1988) have disclosed transesterification of aromatic polyesters and a polyphosphonate in a devolatilizing extruder. For example, a polyester derived from bisphenol A and 1:1 iso/terephthalic acid dissolved in dichloromethane/chlorobenzene was devolatilized along with a similar solution of a polyphosphonate derived from methanephosphonic acid and 4,4′-dihydroxybiphenyl in a TSE at 340 °C. The isolated transparent product had a single Tg by DSC and improved impact strength compared to test parts of the individual homopolymers. Polycarbonate and polyestercarbonates were also successfully transesterified with polyphosphonate using this procedure.

5.9.11 Polyester + Polypropylene Blends

5.9.11.1 Copolymer Formation by Alcohol + Anhydride Reaction
Bettini et al. (2013) prepared PET/PP blends in a TSE with addition of PP-g-MA, the latter grafted polymer prepared using MA alone or MA in the presence of styrene monomer. The extent of PP degradation and MA incorporation was measured as a function of styrene monomer level. The effect of styrene level in PP-g-(S)MA

on subsequent blend properties was assessed using rheology, mechanical properties, and SEM. A similar study was performed by Khonakdar et al. (2013). See also Zhidan et al. (2011) for PET/PP/PP-g-MA blends incorporating recycle PET.

Akbari et al. (2007) prepared PET/PP blends using 5, 10, or 15 wt% PP-g-MA, the latter grafted polymer being prepared by solid-state grafting. Characterization methods included DSC, optical microscopy, SEM, and EDXA.

Xue et al. (2007a, b) investigated the effects of PP-g-MA addition for compatibilizing blends of PTT and PP. Rheological, morphological, thermal and mechanical properties were measured. For blends of poly(esteramide) LCP with PP-g-MA, see Seo et al. (2006).

5.9.11.2 Copolymer Formation by Carboxylic Acid + Epoxide Reaction

PEST/PP blends have been compatibilized through graft copolymer formation by reaction of polyester carboxylic acid end-groups with pendent epoxide groups on an appropriate PP or on a PO or styrene-polyolefin copolymer showing some miscibility with PP (Table 5.40). The copolymer is joined through a new ester linkage. When the new ester linkage is formed, a secondary alcohol group forms as well through ring opening of the epoxide. It is theoretically possible that the new secondary alcohol may also react with polyester main-chain linkages to form copolymer through a degradative transesterification process. Since there are multiple reactive sites on the epoxide-containing polymers, some cross-linked copolymer may result if the acid-containing polymer is functionalized at both ends. The proportion of cross-linked copolymer formed also depends upon blend composition and processing conditions. An example is also included in this section where a compatibilizing copolymer is postulated to form by reaction between acidic phenolic end-groups on polycarbonate and epoxide groups grafted to PP (Zhihui et al. 1998, 1997).

Using a TSE at 180 °C, Vainio et al. (1996b) have prepared blends of 42 parts poly(butyl acrylate-*co*-GMA) (2–5 mol% GMA) with 53-58 parts PP and 0-5 parts PP-g-AA (6 % AA) as a compatibilizer. A cross-linked copolymer may result through reaction of epoxide groups along the copolyester main chain with acid groups grafted at more than one site along the PP chain (or with acid groups along a poly(acrylic acid) segment grafted at a single PP site). The blends were characterized by DMTA, gel content, FTIR, and TEM. Other functionalized poly(butylacrylate) copolymers for use in these blends were also prepared by copolymerization with olefinic oxazoline-, amine-, carboxylic acid-, and hydroxyl-containing monomers.

5.9.11.3 Copolymer Formation by Carboxylic Acid + Oxazoline Reaction

Vainio et al. (1997, 1996a) have compatibilized PEST/PP blends by graft copolymer formation between acid-terminated polyester and oxazoline-grafted PP. Specifically, 30 parts PBT was mixed with 0-70 parts PP and 0-70 parts PP-g-oxazoline in an internal mixer at 250 °C or TSE at 240 °C. Blends were characterized by SEM, torque rheometry, DMA, and DSC. Oxazoline-functionalized PP was prepared by grafting PP with ricinol oxazoline maleinate in the presence of styrene monomer + RI. The inclusion of styrene monomer suppresses radical-induced decomposition of PP. Some cross-linked copolymer

Table 5.40 PEST/PP blends: copolymer formation by carboxylic acid + epoxide reaction

Polyester/polypropylene	Characterization and comments	References
Poly(lactic acid)/PP-g-GMA	Extrusion/MFR/AFM/effects of varying GMA content (0–3 %)/PP grafted with GMA in presence of multifunctional acrylate monomer	Li et al. 2012d
PET (80-50)/PP-g-GMA (20-50; 5.2 wt% GMA)	Brabender mixer/SEM/DSC/melt viscosity/PP grafted with GMA in presence of styrene monomer	Pracella and Chionna 2003
PBT/PP/PP-g-MA/ multifunctional epoxy resin	Mechanical properties/morphology/ rheometry	Shieh et al. 2001
LCP (Rodrun LC3000)/PP/ PP-g-GMA	Morphology/DSC	Yu et al. 2000
PC (30-10)/PP (70-90)/ PP-g-GMA (0.46 mol% GMA) (2.5-20)	TSE at 250 °C/mechanical properties/ selective solvent extraction/SEM/ DSC/WAXS	Zhihui et al. 1997, 1998
PET (80-17.5)/PP (17.5-80)/ SEBS-g-GMA (0-5) or SEBS-g-MA	TSE at 275 °C/mechanical properties/ SEM/rheology/DMTA	Heino et al. 1997b
LCP/PP/E-GMA	Morphology, DSC, mechanical properties	Chiou et al. 1996b
PBT (30)/PP-g-GMA (70)	TSE at 240 °C/one-step grafting of GMA to PP followed by downstream feeding and copolymer formation with PBT/comparison to two-step process/ effects of processing conditions/ mechanical properties/SEM/rheology/ failure of PP-MA or PP-g-AA to act as compatibilizer	Hu et al. 1996; Sun et al. 1996; Champagne et al. 1999
Poly(butyl acrylate)-co-GMA (2–5 mol% functional monomer) (42)/PP (53-58)/ PP-MA (0.4 % MA)	TSE at 180 °C/mechanical properties/ DMTA/gel content/FTIR/TEM/poly (butyl acrylate) also copolymerized with olefinic oxazoline, amine, carboxylic acid, or hydroxyl	Vainio et al. 1996b

may also form in this blend if the polyester is acid-functionalized at both chain ends. See also Vocke et al. (1998) and Jeziórska (2001).

5.9.11.4 Copolymer Formation through Ionomeric Cross-Linking
Compatibilized blends of 90 parts PBT and 10 parts oxidized PP or its corresponding Na ionomer were prepared in TSE at 240 °C (Dang et al. 2005). Blends were characterized by mechanical properties, morphology, and MFR compared to blends with unfunctionalized PP.

5.9.11.5 Copolymer Formation by Radical Coupling
Li et al. (2012c) prepared blends of poly(lactic acid) with PP in the presence of radical initiator. Blend characterization techniques included DSC. The effects of different radical initiators and different concentrations of RI were studied.

5.9.12 Polyester + Polysulfone Blends

Zhang and He (2002) have compatibilized LCP polyester (Hoechst Vectra® B950) with polysulfone-g-MA, the functionalized polysulfone having been prepared in solution. Blend characterization techniques included XPS, DMA, morphology and melt viscosity.

5.9.13 Polyester + Styrene Copolymer Blends

5.9.13.1 Copolymer Formation by Alcohol + Anhydride or Carboxylic Acid Reaction

Studies have been made of PEST/styrene copolymer compatibilization in which a copolymer is formed between polyester alcohol end-groups and pendent anhydride functionality on a styrene copolymer (Table 5.41). Because the alcohol-anhydride reaction is reversible with the equilibrium lying on the side of unreacted anhydride, only a relatively small amount of copolymer may be formed. Thus, the dispersed phase polymer may not be well stabilized against coalescence upon further thermal treatment (for a discussion, see, e.g., Sun et al. 1996 and Boyer et al. 2005). Alternatively, at least some copolymer may be formed by a degradative mechanism through transesterification between polyester main-chain linkages and a low concentration of pendent acid groups in anhydride-functionalized styrene copolymer. See also the work of Wu et al. (2010) for blends comprising PBT and ultrafine, vulcanized ABS wherein a copolymer was postulated to form between PBT-OH groups and surface carboxyl groups on ABS.

5.9.13.2 Copolymer Formation by Carboxylic Acid + Epoxide Reaction

As the examples of Table 5.42 demonstrate, PEST/styrene copolymer blends may be compatibilized through graft copolymer formation by reaction of polyester carboxylic acid end-groups with pendent epoxide groups on an appropriate styrene copolymer. Also included in the table is an example of graft copolymer formation in PC-styrene copolymer blends through reaction of styrene copolymer carboxylic acid pendent groups with epoxide end-groups on an appropriately functionalized PC. In either case, the copolymer formed is joined through a new ester linkage. When the new ester linkage is formed, a secondary alcohol group is also formed through ring opening of the epoxide. The new secondary alcohol may also react with polyester main-chain linkages to generate copolymer through a degradative transesterification process. When there are multiple reactive sites on at least one of the two polymers, some cross-linked copolymer may result depending upon functionalized polymer type, blend composition, and processing conditions.

5.9.13.3 Copolymer Formation by Transreaction

Bolton et al. (2005) prepared a copolymer of S-AN and alpha-methyl-*p*-hydroxystyrene. The copolymer was shown to be an effective compatibilizer for PC/SAN blends extruded in the presence of tetraphenylphosphonium benzoate catalyst.

Table 5.41 PEST/styrene copolymer blends: copolymer formation by alcohol + anhydride reaction

Polyester/styrene copolymer	Characterization and comments	References
PC/SEBS-g-MA/ triazabicyclodecene catalyst	260 °C optimum T/SEC/rheology + Van Gurp-Palmen plot/DSC/also studied stannous octoate catalyst	Chevallier et al. 2013
PET/ABS-g-MA	Torque rheometer/SEM/DMA/use of recycle PET	Wang et al. 2012d
PET/SB-g-MA	Correlation of rheology, mechanical properties, and morphology	Sanchez-Solis et al. 2001
PET/PS/SMA	Melt mixing at 280 °C/morphology/ mechanical properties/thermal properties/ selective solvent extraction/viscosity change	Yoon et al. 2000
PBT (70)/ABS (30)/SMA (2.5-7.5)	SSE at 255 °C/mechanical properties	Basu and Banerjee 1997
PET (99-95)/SEBS-g-MA (0–4.5 % MA) (1-5)	TSE at 260–280 °C/IV/SEM/DSC/selective solvent extraction/mechanical properties/ rheology	Tanrattanakul et al. 1997a, b
PET (100-0)/ABS (0-100)/ ABS-g-MA (3.5 % MA) (0-100)	Extruded at 280 °C/DMA/DSC/mechanical properties/SEM/FTIR/optical microscopy	Kalfoglou et al. 1996
PET (100-0)/SEBS-MA (1.8 % MA) (0-100)	TSE at 280 °C/DMA/DSC/mechanical properties/SEM/FTIR/optical microscopy/use of recycle PET/ternary blends with HDPE also prepared	Kalfoglou et al. 1995 (see also Yu et al. 2004)

Su et al. (2001a, b) have prepared blends of PBT with hydroxy-functionalized polystyrenes which differed in the number of hydroxy groups per chain. The effects of triphenyl phosphite and titanium butoxide on PBT chain degradation and copolymer formation were studied. Blends were characterized by FTIR, DSC, GPC, morphology, rheology, and mechanical properties.

Wildes et al. (1999) have reported compatibilized blends of PC with amine-functionalized SAN.

In a study by Landry et al. (1994), 50 parts PBT (or PET) was extruded with 50 parts poly(vinylphenol) using a mini-SSE at 254 °C or 293 °C, followed by annealing at 265 °C or 290 °C. The blends were characterized by DSC. Copolymer formation evidently occurs through a degradative reaction between pendent phenolic groups on poly(vinylphenol) and ester linkages in the polyester main chain. A low molecular weight polyester fragment results from this process.

5.9.13.4 Copolymer Formation by Miscellaneous Reactions

Liu et al. (2011a) prepared compatibilized PBT-ASA blends by addition of epoxy resin coupling agent. Blends were characterized by mechanical properties and morphology (TEM and FESEM).

Lee and Park (2001) prepared compatibilized PC-PBT-PS blends through reacting PBT with oxazoline-functionalized PS. See Becker and Schmidt-Naake (2003) for compatibilized blends of PC with oxazoline-functionalized SAN and

Table 5.42 PEST/styrene copolymer blends: copolymer formation by carboxylic acid + epoxide reaction

Polyester/styrene copolymer	Characterization and comments	References
PET (90)/S-BA copolymer (10)/PS-co-GMA (5)	TEM/optical microscopy/mechanical properties/also used S-MMA or SEBS in place of S-BA/also PC-ABS and PC-HIPS blends with PS-g-GMA	Gonzalez-Montiel et al. 2013
Poly(lactic acid) (5-10)/ S-co-GMA (0–10 wt% GMA; 95-90)	Batch mixer at 210 °C/PLA phase domain size by solution light scattering/also used isocyanate functionalized PS	Wang et al. 2013a
Poly(lactic acid)/GMA-f-ABS/ethyltriphenyl phosphonium bromide catalyst	FTIR/DMA/SEM/TEM/mechanical properties	Sun et al. 2011
Poly(lactic acid)/ABS/ SAN-co-GMA/ethyltriphenyl phosphonium bromide catalyst	DMA/SEM/TEM/mechanical properties	Li and Shimizu 2009
PBT/SBS/PS-co-GMA	Morphology/mechanical properties/effect of SBS styrene content and block length/effect of GMA level	Canto et al. 2006
PBT/SAN-GMA	Mechanical properties/also blends with unfunctionalized SAN or with poly-isocyanate	Lumlong et al. 2006
PBT/ABS-co-GMA (optionally with PC)	DMA/DSC/SEM/morphology/rheology/ mechanical properties/effect of GMA content	Sun et al. 2005 (see also Sun et al. 2013)
PET/SEBS-g-GMA	DSC/rheometry/morphology/mechanical properties	Pracella and Chionna 2004
PEN/PS/S-co-GMA	Mechanical properties/morphology/rheology also blends with PTT	Huang 2003; Huang et al. 2003
PBT/HIPS-g-GMA	Mechanical properties/SEM/DMA	Yang et al. 2002a
LCP/SAN-co-GMA	Morphology/mechanical properties/addition of ethyl triphenylphosphonium bromide catalyst	Huang et al. 2001
PBT/ABS/MMA-EA-GMA copolymer	TSE/morphology stability/ mechanical properties/SAN used in place of ABS	Hale et al. 1999a, b
PBT/PS/S-GMA	Melt blending/selective solvent extraction/ GPC/FTIR/SEM/comparison to solution blend	Jeon and Kim 1998a, b
PBT (90-10)/PS (10-90)/ S-GMA (0-9)	Internal mixer at 200 °C/SEM/TEM/rheology	Kim et al. 1997a
LCP (75-10) (Hoechst Vectra A900)/PS (25-90)/S-GMA (5 % GMA) (5)	TSE at 290 °C/torque vs. time measurements/ rheology/mechanical properties/FTIR/SEM/ catalysis using phosphonium salt	Chiou et al. 1996a
PBT (75-25)/PS (25-75)/ S-GMA (0-10 parts)	Internal mixer at 230–240 °C/DSC/DMTA/ rheology/SEM	Kim and Lee 1996

(*continued*)

Table 5.42 (continued)

Polyester/styrene copolymer	Characterization and comments	References
PBT (75-25)/ABS (25-75)/ SAN-GMA (0-5) (2, 4, and 10 % GMA in copolymer)	TSE/FTIR/morphology/mechanical properties vs. use of unfunctionalized SAN/melt flow/titration of residual acid groups/use of ethyltriphenylphosphonium bromide catalyst	Lee et al. 1994
PET (75-25)/PS (25-75)/ S-GMA (5 % GMA) (0-5) (2, 5, and 10 % GMA in copolymer)	TSE at 270 °C/torque rheometry/mechanical properties/SEM/melt viscosity/use of ethyltriphenylphosphonium bromide catalyst	Maa and Chang 1993
PET (50) or PETG/S-GMA (5 % GMA) (50)	Internal mixer at 270 °C/torque rheometry/ GPC/effects of residual levels of different catalysts used to synthesize polyesters	Stewart et al. 1993b
Epoxy triazine-capped PC (1 part)/SMA (1 part; 14 % MA)	TSE at 125–265 °C/copolymer analysis by selective solvent extraction	Brown et al. 1991a

Becker and Schmidt-Naake (2004) for compatibilized blends of PC with oxazoline- or benzoxazole-functionalized ABS.

Lee and Park (2000) found evidence for copolymer formation in blends of anhydride-terminated PC and oxazoline-functionalized PS prepared in a Haake mixer. Blends were characterized by torque rheometry, SEM, FTIR, NMR, and mechanical properties. Anhydride-terminated PC was prepared by reaction of PC phenolic end-groups with trimellitic anhydride acid chloride (cf. Hathaway and Pyles 1988, 1989).

Lee et al. (2000) prepared compatibilized PET-PS blends through reacting PET with carbamate-functionalized PS, the carbamate serving as a masked isocyanate.

Ju and Chang (1999) prepared compatibilized PET-PS blends through blending PET and PS with SMA in the presence of a tetra-epoxide coupling agent.

Krabbenhoft (1986) prepared copolymers of PC with SEBS by extrusion with a disulfonyl azide. In one example, a blend of PC (1 part), SEBS (2 parts), and 4,4′-biphenyl disulfonyl azide was extruded on an SSE at 182 °C. This extrudate was melt blended with EEA and additional PC to give a blend comprising 82.5 % PC, 7.5 % SEBS, and 10 % EEA. Copolymer formation was shown by selective solvent extraction. Improved impact strength was seen in comparison to blends prepared without disulfonyl azide.

5.9.14 Polyester + Polyurethane Blends

Dogan et al. (2013) prepared blends of poly(lactic acid) with TPU through addition of 1,4-phenylene diisocyanate coupling agent. Characterization techniques included mechanical, thermal, morphological, and rheological properties.

Imre et al. (2013) also prepared compatibilized blends of poly(lactic acid) with polyurethane elastomer by coupling reaction under extrusion conditions. Copolymer formation was shown by SEM, AFM, DMA, and mechanical property measurement.

Archondouli et al. (2003) studied blends of PC with polyester-type polyurethane using SEM, mechanical properties, DMA, DSC, TGA, FTIR, and NMR. Formation of copolymer was shown by selective solvent extraction and spectroscopic analysis.

Samios et al. (2000) prepared PET blends with polyester polyurethane. Blends were characterized by mechanical properties, DMA, NMR, and morphology. An esteramide interchange reaction was proposed as the mechanism for compatibilizing copolymer formation.

5.10   Polyether or Polyphenylene Ether Blends

Examples of polyether blends not shown in earlier sections are listed in alphabetical order of the second polymer in the blend unless otherwise noted. Included in this section are polyphenylene ether blends not described in sections on PA, PEST, or PO. When copolymer characterization was not performed, the structure of the compatibilizing copolymer is inferred from the functionality location on each of the two polymers. In some cases, more than one type of compatibilizing copolymer may have formed.

5.10.1   Polyether + Polyolefin Blends

5.10.1.1 Copolymer Formation by Alcohol + Anhydride Reaction

Compatibilizing copolymers have been formed by direct reaction between pendent alcohol groups of phenoxy resin and pendent anhydride groups on MA-grafted polyolefins. Again, the initial product of the reaction was a graft copolymer, but longer reaction time resulted in a cross-linked copolymer since the pendent phenoxy chain is capable of further reaction with MA on a different polyolefin chain. Mascia and Bellahdeb (1994a, b) have blended 75-25 parts phenoxy resin with 25-75 parts EP-g-MA (0.7 % MA) in either an internal mixer or a TSE at 180–200 °C. The blends were characterized by selective solvent extraction, SEM, DSC, and rheology. Increased cross-linking was observed with increasing MA-to-phenoxy ratio and with the addition of either NaOEt or sodium benzoate (2 %). The resulting copolymers were used to compatibilize PET + HDPE blends.

5.10.1.2 Copolymer Formation by Alcohol + Ester Transreaction

Kim and Choi (1996b) have compatibilized blends of phenoxy resin with PMMA. Compatibilizing cross-linked copolymer resulted from transreaction between phenoxy pendent alcohol groups and pendent PMMA ester groups.

Compositions of 100-0 parts phenoxy resin and 0-100 parts PMMA were prepared in an internal mixer at 240 °C. The blends were characterized by DSC, FTIR, mechanical properties, rheology, and DMA. Mascia and Bellahdeb (1994a, b) have compatibilized phenoxy polyether resin with an acid-functionalized polyacrylate resin through cross-linking. A base capable of forming alkoxide from the polyether hydroxy groups was used. Thus, 75-25 parts phenoxy resin and 25-75 parts E-tBA-AA terpolymer (or EMAA Na ionomer) were blended in an internal mixer or TSE at 180–200 °C in the presence of 2 parts NaOEt. Blends were characterized by selective solvent extraction, SEM, DSC, and rheology. The resulting cross-linked copolymers were used to compatibilize PET + HDPE.

5.10.1.3 Copolymer Formation by Miscellaneous Reactions
Frick et al. (2013) prepared compatibilized blends of PEEK and PTFE (component ratios 0-100 to 100-0) using melt-processable PTFE treated by electron beam radiation to introduce –COF and –COOH functional groups by chain scission. Blend characterization techniques included mechanical properties and morphology.

5.10.2   Polyether + Styrene Copolymer Blends

5.10.2.1 Copolymer Formation by Alcohol + Anhydride Reaction
Bayam and Yilmazer (2002) have reported compatibilization of poly (tetramethylene ether glycol) with SMA prepared in a batch mixer or in a TSE in the presence of zinc acetate hydrate. Blends were characterized using thermal, mechanical, morphological, and spectroscopic techniques. FTIR analysis indicated the presence of copolymer from ester formation.

5.10.2.2 Copolymer Formation by Alcohol + Epoxide Reaction
Compatibilizing copolymers have been formed by direct reaction between pendent alcohol groups of phenoxy resin and pendent epoxide groups on GMA-grafted styrene copolymer. Again, the initial product of the reaction was a graft copolymer, but longer reaction time resulted in a cross-linked copolymer since the pendent phenoxy chain was capable of further reaction with GMA. Furthermore, the new hydroxy group arising from ring-opened epoxy groups may also participate in cross-linking reactions. It is also possible that some cross-linked copolymer resulted from transesterification between pendent hydroxy groups on phenoxy resin and the GMA ester groups. Chen and Chang (1994) have prepared blends of 75-45 parts phenoxy resin and 25-50 parts ABS with addition of 0-10 parts SAN-GMA (5 % GMA) copolymer in an internal mixer or a TSE at 230 °C. The blends were characterized by torque rheometry, SEM, viscosity behavior, and mechanical properties. Sodium lauryl sulfonate (0.02-0.10 parts) was added as a catalyst to promote the copolymer-forming reaction.

5.10.2.3 Copolymer Formation by Amine + Anhydride Reaction
Schaefer et al. (1995) prepared blends of poly(tetrahydrofuran) with SMA in the presence of bis(amine)-terminated poly(tetrahydrofuran). Characterization

techniques included FTIR and microscopy. Reaction rate constants were determined. The effects of temperature and poly(tetrahydrofuran) MW were studied.

5.10.3   Polyetherimide + Polyphenylene Ether Blends

PEI-PPE blends have also been compatibilized through copolymer formation between functionalized PPE and PEI in the presence of a multifunctional epoxy resin such as PE-co-GMA (Brown et al. 2000a). Functionalized PPE included PPE-g-FA. Catalysts such as sodium stearate were optionally added.

PEI-PPE blends have also been compatibilized through copolymer formation between anhydride-functionalized PPE such as PPE-g-FA and amine-terminated PEI (White et al. 1989). Amine-terminated PEI was prepared from bisphenol A-diphthalic acid anhydride and m-phenylene diamine, the latter used in excess. Copolymer analysis was by selective solvent extraction. Mechanical properties and morphologies were compared to blends with unfunctionalized PPE and PEI.

5.10.4   Polyetherimide + Polyphenylene Sulfide Blends

PEI-PPS blends have also been compatibilized through copolymer formation between amine-containing PEI and PPS in the presence of a multifunctional epoxy resin such as epoxy cresol novolak (Nazareth 1996).

5.10.5   Polyphenylene Ether + Polyphenylene Sulfide Blends

Some early work on copolymer-compatibilized PPE-PPS blends is summarized in Arashiro et al. (1992). PPE-PPS blends have also been compatibilized through copolymer formation between citric acid-functionalized PPE (e.g., 162 parts) and PPS (e.g., 225-275 parts) in the presence of a multifunctional epoxy resin (0-17.5 parts) and a minor amount of PBT (25-50 parts) (Brown et al. 1997a) or in the presence of a epoxy-functionalized PO and a catalyst (Brown et al. 2001) or in the presence of a bifunctional cyclic ortho ester compound (Brown et al. 1998a). See also Dekkers (1989) and Inoue et al. (1990). Okabe et al. (1989) have prepared compatibilized blends comprising PPE-g-MA and amine-functionalized PPS in the presence of 4,4′-diphenylmethane diisocyanate coupling agent.

PPE-PPS blends have also been compatibilized through copolymer formation between a PPS bearing nucleophilic functional groups and either epoxy-functionalized PPE (Han et al. 1992) or cyclic ortho ester-functionalized PPE (Brown et al. 1996). In the former case, PPE was functionalized by reaction with a chloro-epoxy triazine and, in the latter, by reaction with either a chloro (cyclic ortho ester) triazine or a graftable cyclic ortho ester.

Kubo and Masamoto (2002) have prepared compatibilized blends of PPE and PPS through addition of styrene-co-GMA.

5.10.6 Polyphenylene Ether + Polysiloxane Blends

PPE-polysiloxane blends have also been compatibilized through copolymer formation between amine-terminated polydimethylsiloxane and either epoxy-functionalized PPE (Blohm et al. 1995) or anhydride-functionalized PPE (Shea et al. 1989). Compatibilized blends have also been formed by extrusion of PPE with epoxy-functionalized polydimethylsiloxane (Cella et al. 2002) and by kneading of anhydride-functionalized PPE with carboxylic acid-functionalized polydimethylsiloxane in the presence of a diamine coupling agent (Moritomi and Iji 2002).

5.10.7 Polyphenylene Ether + Styrene Copolymer Blends

PPE is not miscible with SMA containing as much as 28 % MA (Witteler et al. 1993). To compatibilize these two resins, Koning et al. (1993b, 1996) have added a monoamine-terminated PS that can form a graft copolymer with SMA. Since the amine-terminated PS is miscible with PPE, compatibilized PPE-SMA blends are obtained. Specifically, 30 parts of unfunctionalized PPE was blended (internal mixer at 220 °C, or mini-SSE at 280 °C, or TSE at 326 °C) with 56 parts SMA (28 % MA) and 14 parts amine-functionalized PS. The blend was characterized by TEM, SEM, mechanical and thermal properties, DMA, and GPC copolymer detection. The effect of pre-reacting amine-terminated PS with SMA was studied. The blend properties were compared to those for uncompatibilized blends. Blends were also made containing ABS + SEBS. Further examples of compatibilizing copolymer formation in PPE-styrene copolymer blends are shown in Table 5.43.

5.11 Polyolefin Blends

Examples of polyolefin blends not shown in earlier sections are listed in alphabetical order of the second polymer in the blend unless otherwise noted. PVC is included as a polyolefin. When copolymer characterization was not performed, the structure of the compatibilizing copolymer is inferred from the functionality location on each of the two polymers. In some cases, more than one type of compatibilizing copolymer may have formed.

5.11.1 Polyolefin + Polyolefin Blends (Excepting Polypropylene)

5.11.1.1 Copolymer Formation by Alcohol + Anhydride Reaction
Yang et al. (2013) prepared compatibilized blends of EVAl with maleic anhydride-grafted ethylene-octene copolymer (0–25 wt%). Blends were characterized using mechanical, thermal, FTIR, and morphological techniques.

Table 5.43 PPE/styrene copolymer blends: copolymer formation by miscellaneous reactions

PPE/styrene copolymer	Characterization and comments	References
PPE (30)/sPS (70)/S-IPO (0-25)/ SEBS (0-20)/SEBS-g-MA (0-20)	TSE/SEM/rheology/DMA/DSC/mechanical properties/effect of mixing protocol	Choi et al. 1999
PPE-g-MA/ABS/SAN-g-GMA	Mechanical properties/morphology/different mixing regimes/use of different ABS types	Lee et al. 1999a
PPE-g-FA (5 parts; 1 % FA)/PS (0.25 parts)/ABS-FA (4 parts; 1 % FA)/SEBS (0.95 parts)/hexanediol (0.03 parts)	TSE/mechanical properties vs. blends with unfunctionalized polymers or without diol/also used PPE-g-MA and SAN-g-MA/also used PPE-g-maleic acid monoethyl ester and ABS-g-GMA/also used hexamethylenediamine or glycerindiglycidyl ether	Taubitz et al. 1988a, b, c, d
PPE-g-FA (4.5 parts)/SAN (2.3 parts)/SBS (1.2 parts)/core-shell impact modifier derived from a cross-linked butyl acrylate core and a SAN-GMA shell (2 parts; 3 % GMA)	TSE/mechanical properties vs. blends with unfunctionalized PPE	Taubitz et al. 1988f
PPE (400)/SAN (600)/p-quinone dioxime (2)	Brabender or TSE/mechanical properties vs. blends without dioxime or with RI/copolymer determined by selective solvent extraction/PS used in place of SAN/also used p-dinitrosobenzene	Ueno and Maruyama, 1982b

Wang et al. (2007c) prepared blends of HDPE and EVAl compatibilized through addition of HDPE-g-MA. Characterization methods included mechanical, thermal, and rheological properties.

Boyer et al. (2005) have reported that hydroxy-functionalized oligomers have little tendency to form a stable graft to PP-g-MA under the conditions studied.

Lee and Kim (1998) prepared compatibilized blends of EVAl with LDPE by addition of LDPE-g-MA (1–12 phr).

Schmukler et al. (1986a, b) prepared compatibilized blends of PVAl with an anhydride-functionalized polyethylene. For example, 50 wt% PVAl was reacted at 325 °C in a Brabender mixer with 50 wt% HDPE grafted with 1.5 wt% methylbicyclo(2.2.1)-hept-5-ene-2,3-dicarboxylic anhydride. Characterization showed evidence for copolymer formation and no gross phase separation.

5.11.1.2 Copolymer Formation by Carboxylic Acid + Epoxide Reaction
As shown in Table 5.44, immiscible blends containing at least two polyolefins have been compatibilized through cross-linked copolymer formation between carboxylic acid groups at multiple sites on one polyolefin and epoxide groups at multiple sites on another polyolefin.

5.11.1.3 Copolymer Formation through Coupling Agent Addition
Examples in Table 5.45 show use of coupling agents that can, in theory, react at sites along the main chain of each of the two immiscible polyolefins. The work of Inoue (1994a, b) and of Naskar et al. (1994) involve concomitant dynamic vulcanization of an elastomeric phase with an added cross-linking agent.

Table 5.44 PO/PO blends: copolymer formation by carboxylic acid + epoxide reaction

Polyolefin/ polyolefin	Characterization and comments	References
HDPE-g-MA/ENR	Morphology/mechanical properties/also used phenolic-modified HDPE in place of HDPE-g-MA	Nakason et al. 2008
Poly(acrylic acid) (50)/ENR (50)	Internal mixer at 180 °C/rheology/solvent swelling/SEM/mechanical properties/DMA/ carbon black filler (0–25 phr)/effects of mixing sequence	Mallick et al. 1993, 1997
PE-g-AA (6 % AA) (100-0)/ENR (0-100)	Internal mixer at 150 °C/mechanical properties/DMA/solvent swelling/effects of adding ZnO or ZnSt to form ionomeric network/DSC/FTIR/UV/SEM	Mohanty et al. 1995, 1996, 1997; Mohanty and Nando 1997
NBR-g-AA (71-0)/ ENR (7-75)/PVC (14-75)	Internal mixer at 180 °C/mechanical and thermal properties/FTIR	Ramesh and De 1993
PE (23)/PE-g-MA (3)/NR (58)/ENR (17)	Internal mixer at 150 °C/mechanical properties vs. omission of functionalized polymers/morphology	Choudhury and Bhowmick 1989

Table 5.45 PO/PO blends: copolymer formation through coupling agent addition

Polyolefin/polyolefin	Characterization and comments	References
EPDM/PVC/benzoyl peroxide/ trimethylolpropane trimethacrylate	Melt mixing/physical characterization/also vulcanization using phenolic resin and tin chloride	Stelescu 2008
HDPE (50)/PVC (50)/NBR (0-15)/ TAIC (0-2)/DCP RI (0-1.5)	Two-roll mill at 160 °C/SEM/mechanical properties vs. NBR presence/selective solvent extraction	Fang et al. 1997
LDPE (80)/PVC (20)/TAIC (4)/ DBP (0.5-1) or DCP RI	Internal mixer at 180 °C/mechanical properties/SEM/10 % EA-MMA added as processing aid/also use of recycled PVC and PE	Ajji 1995
EPDM (20)/EP (80)/m-phenylene bismaleimide (0.075-0.6)	TSE at 210 °C/mechanical and thermal properties/morphology/selective solvent extraction/evidence for EP-EPDM copolymer	Inoue 1994a, b
NR (100-0)/NBR-AA (0-100)/bis (diisopropyl) thiophosphoryl disulfide (3)	Lab mill/SEM/swelling index/rheology/ mechanical properties	Naskar et al. 1994

5.11.1.4 Copolymer Formation through Ionomeric Cross-Linking Mediated by Metal Cations

Examples of some immiscible polyolefin blends that have been compatibilized through ionomeric cross-linking between ionic groups on each polyolefin are listed in Table 5.46.

Table 5.46 PO/PO blends: copolymer formation through ionomeric cross-linking mediated by metal cations

Polyolefin/polyolefin	Characterization and comments	References
Carboxylated nitrile rubber Zn ionomer (90-50)/EAA Zn ionomer (10-50)	Physical properties vs. blends of non-ionomeric polymers/FTIR/DMA/also use of recycle	Antony et al. 2000
EPDM-g-MA/ HDPE-g-MA/Zn stearate	Melt blended/physical properties vs. blends with unfunctionalized polymers	Antony and De 1999
PVDF-g-MAA/ PO-ionomer/Zn(acac)$_2$	Morphology/viscosity/solid-state grafting of methacrylic acid to PVDF powder by irradiation	Valenza et al. 1998
EMAA-Zn salt (100-0)/ EPDM-g-MA (1 % MA) (0-100)/zinc oxide (10)	Internal mixer at 170 °C/mechanical properties/DMA/ FTIR/effects of multiple thermal histories	Datta et al. 1996
EMAA-Zn salt (70-30)/ EPDM-SO$_3$ Zn salt (30-70)	Internal mixer at 170 °C/mechanical properties/DMA/ dielectric thermal analyses/FTIR/effects of multiple thermal histories	Kurian et al. 1996

Table 5.47 PO/PO blends: copolymer formation involving mechanochemical radical formation

Polyolefin/polyolefin	Characterization and comments	References
NBR (75-25) or hydrogenated NBR/PVC (25-75)	Internal mixer at 180 °C/rheometry/DMTA/ DSC/FTIR/solvent swelling	Manoj et al. 1993a, b
LDPE (100-80)/PVC (0-20)	Torque rheometer at 180 °C/selective solvent extraction/FTIR/effects of PVC stabilizers	Ghaffar et al. 1980–1981

5.11.1.5 Copolymer Formation Involving Mechanochemical Radical Formation

Radicals may be formed on polyolefins under high-shear mixing conditions in a process termed mechanochemical radical generation. Two immiscible polyolefins may both be subject to mechanochemical radical generation during extrusion processing. In blends of PO that are not prone to degradation upon radical formation, a cross-linked copolymer may result from the recombination of radicals from each polymer. As a result, a compatibilized blend with improved physical properties may be obtained. In blends of PO subject to chain scission under high-shear mixing conditions, radical recombination reactions may lead to block and eventually random copolymer formation similar to other degradative copolymer formation processes. The examples listed in Table 5.47 show cross-linked copolymer formation in PVC blends with PO. For a general review of polymer reactions under the action of mechanical forces, see Prut (2009). Other aspects of mechanochemical processes in polymers may be found in Beyer and Clausen-Schaumann (2005). For a study of similarities between mechanochemical and high-energy radiation processes in polymer processing, see, e.g., Smith et al. (2001).

Casale and Porter ([1975]) reported that copolymer formation between NBR and PVC may occur via mechanochemical radical generation on each polymer followed by recombination. The proposed mechanism was based on earlier studies by Akutin ([1968]). Later, Manoj et al. ([1993b]) postulated another mechanism for the same system involving hydrolysis of nitrile groups to amide or carboxylic acid followed by displacement of allylic chloride on PVC by amide-NH_2 or acid-OH.

5.11.1.6 Copolymer Formation by Miscellaneous Reactions

Song et al. ([2012a]) prepared blends of PMMA with various functionalized poly (propylene-ethylene) copolymers. Blends were characterized by mechanical, morphological, and adhesion tests. Compatibility was found to increase in the order of unfunctionalized poly(propylene-ethylene), MA-grafted poly(propylene-ethylene), hydroxy-grafted poly(propylene-ethylene), and secondary amine-grafted poly (propylene-ethylene) which latter species exhibited the best compatibilization efficiency.

Lopattananon et al. ([2007]) have prepared blends of maleated natural rubber and carboxylated nitrile rubber in the presence of zinc acetate to form a compatibilizing copolymer through ionic cross-links. The effect of different maleation levels was studied. Blend properties were compared to those for blends with unfunctionalized rubbers.

Oliveira et al. ([2004]) prepared compatibilized blends of EPDM and NBR using mercapto-modified EPDM with oxazoline-functionalized NBR. Mercapto-modified EVAc was also used. Blends were characterized by techniques including mechanical properties and morphology.

Soares et al. ([2004]) prepared blends of partially hydrolyzed EVAc and NBR using oxazoline-functionalized NBR. Blends were characterized by techniques including mechanical properties, morphology, selective solvent extraction, and FTIR.

Dalai and Wenxiu ([2002b, c]) have reported blends of either HDPE or LDPE with EVAc effected by radiation cross-linking. Blend characterization techniques included morphology and thermal properties.

Nugay and Nugay ([2000]) prepared blends of poly(methyl methacrylate)-b-poly(4-vinylpyridine) with poly(acrylic acid), possibly compatibilized through copolymer formation by ion-neutral donor group association.

Some unusual ester cross-linking reactions have been proposed as copolymer-forming processes for immiscible PO blends (Table [5.48]). Alternative mechanisms include consideration of the possible contributions of simpler processes such as IPN formation, radical-radical coupling, or ionomeric cross-linking.

5.11.1.7 Copolymer Formation through Radical Initiator Addition

As shown in the examples listed in Table [5.49], immiscible blends of polyolefins have been compatibilized by copolymer formation brought about by radical coupling in the presence of a radical initiator. The work of Kim et al. ([1997a]) and Xu et al. ([1997]) involved copolymer formation between immiscible rubber and plastic phases simultaneous with the dynamic vulcanization of the elastomeric phase.

Table 5.48 PO/PO blends: copolymer formation by miscellaneous reactions

Polyolefin/polyolefin	Characterization and comments	References
Recycled LDPE/PE-g-AA/ BR/isocyanate-terminated butadiene rubber	Mechanical properties/X-ray analysis/DMA/ morphology/effect of varying functional group ratio	Fainleib et al. 2003
HDPE-g-diisocyanate/ EVAl	Mechanical properties vs. uncompatibilized blend/HDPE grafted with 2-hydroxyethyl methacrylate-isophorone diisocyanate	Park et al. 1998
Chlorosulfonated PE (50)/ carboxylated NBR (50)	Two-roll mill/selective solvent extraction/ DMA/FTIR/proposed carboxylate ester cross-link through displacement of chloride on PE by carboxylate	Roychoudhury and De 1997
EPDM-SO$_3$ Zn ionomer (100-0)/ENR (0-100)	Two-roll mill/capillary rheometry/FTIR/ 10–25 meq. per 100 g. sulfonate level/ proposed sulfonate ester cross-link rather than ionomer cross-link	Manoj et al. 1994

Table 5.49 PO/PO blends: copolymer formation through radical initiator addition

Polyolefin/polyolefin	Characterization and comments	References
Metallocene cycloolefin copolymer (70-25)/ethylene-octene copolymer (30-75)/RI	Mechanical properties/SEM/rheology/DMA	Doshev et al. 2011
NR/LLDPE/MA + DCP RI	Internal mixer at 150 °C/FTIR/TEM/AFM/ selective solvent extraction/comparison to blends without DCP	Magaraphan et al. 2007
LDPE (100-0)/LLDPE (0-100)/ DCP RI (0-1)	Internal mixer at 160 °C/torque vs. component ratio and DCP level/mechanical properties/ selective solvent extraction	Abraham et al. 1992, 1998
LDPE (100-0)/PVC (0-100)/ butadiene rubber (0-5)/ DCP RI (0-2)	Two-roll mill at 155 °C/SEM/optical microscopy/mechanical properties vs. BR presence	Xu et al. 1997
EPDM (100-0)/LLDPE (0-100)/DCP RI (0.7)	Roll mill at 80 °C/mechanical properties/ rheology/DSC/SEM/X-ray diffraction	Kim et al. 1996
Recycle mix of LDPE (45), HDPE (15), PVC (15), <10 PS, HIPS, PP, PET/L101 RI (0-2)	TSE at 210 °C melt T/morphology/selective solvent extraction/mechanical properties vs. RI level/rheology of mix and of individual resins vs. RI level (0–1 %)	Vivier and Xanthos 1994
LDPE (85)/EVAc (15)/ DCP RI (1)	Internal mixer at 150–210 °C/torque rheometry/effects of processing conditions on cross-linking/DSC/FTIR/DMA	Vogel and Heinze 1993
LDPE (40-38)/PVC (57-60)/ NBR (0-4)/DCP RI (0-0.02)	Two-roll mill at 155 °C/morphology/ mechanical properties vs. DCP level and NBR presence	Xu et al. 1993
HDPE (100-0)/LLDPE (0-100)/ DCP RI (0-1)	Internal mixer at 220 °C/torque rheometry/ mechanical properties	Kurian et al. 1992
LDPE (50)/PVC (50)/CHP RI (0-0.1)	Torque rheometer at 120–170 °C/selective solvent extraction/FTIR/mechanical properties/ DMTA/addition of copolymer to PE + PS	Hajian et al. 1984

Table 5.50 PO/PO blends: copolymer formation by transesterification

Polyolefin/polyolefin	Characterization and comments	References
EVAc (48)/EMAc (48)	TSE at 165–200 °C optionally with on-line microwave treatment to effect transreaction/morphology development along screw axis vs. processing conditions in three different extruders/rheology/TGA-GC/selective solvent extraction/SEM/mechanical properties/use to fix morphology of EVAc + EMAc dispersed phase in PP matrix/dibutyltin oxide catalyst (0-4)	De Loor et al. 1994, 1997; Cassagnau and Michel 1994; Cassagnau et al. 1993
EVAc (90-5)/EMAc (10-95)	TSE at 165 °C under which conditions no cross-linking occurred/cross-linked through heating between parallel plates in presence of dibutyltin oxide/swelling monitored by analysis for methyl acetate/rheology	Espinasse et al. 1994

5.11.1.8 Copolymer Formation by Transesterification of Pendent Ester Groups

Immiscible polyacrylates have been compatibilized through transesterification between pendent ester groups on one polyacrylate with pendent ester groups on another polyacrylate. Selected examples are listed in Table 5.50.

5.11.2 Polyolefin + Polyoxymethylene Blends

Compatibilized blends of hydroxylated polyoxymethylene (polyacetal) with carboxylic acid-functionalized PP have been prepared (Chen et al. 1991). The formation of ester linkages between the polymers was proposed. For example, blends comprising hydroxylated polyoxymethylene and muconic acid-grafted PP were made into film by calendering at 200 °C to provide compositions with markedly improved mechanical properties compared to similar blends containing unfunctionalized PP or unfunctionalized polyoxymethylene.

5.11.3 Polyolefin + Polyphenylene Ether Blends

5.11.3.1 Blends Containing Functionalized PPE: PO-PPE Copolymer Formation by Carboxylic Acid + Cyclic Ortho Ester or Epoxide Reaction

As shown in Table 5.51, immiscible blends containing a functionalized polyolefin and a functionalized polyphenylene ether have been compatibilized through cross-linked or graft copolymer formation between carboxylic acid groups at multiple sites on one polymer and either cyclic ortho ester groups or epoxide groups at sites on another polymer.

Table 5.51 PO/PPE blends: copolymer formation by carboxylic acid + cyclic ortho ester or epoxide reaction

Polyolefin/PPE	Characterization and comments	References
PE-co-GMA (10-40 parts; 12 % GMA)/PPE (30-90 parts)/PPE-g-FA (30-90; 2 % FA)	TSE at 250–290 °C/mechanical properties vs. blend with unfunctionalized PPE/other functionalized PPE also used/unfunctionalized PP optionally included	Brown et al. 1999
EPDM-g-cyclic ortho ester (1)/PPE-g-FA (9)	TSE at 302 °C/mechanical properties/also used oxidized PPE and PPE-f-citric acid/EPDM reacted in separate extrusion step with graftable cyclic ortho ester	Khouri and Campbell 1997
PE-g-MA (45.5 parts)/epoxy triazine-capped PPE (45.5 parts)/EPDM (9 parts)	SSE at 245–275 °C/mechanical properties vs. blend with unfunctionalized PPE/PP-g-MA and various PE grades used	Campbell et al. 1991
LLDPE-g-(t-butylmethacrylate)/epoxy triazine-capped PPE	Melt or solution blended/selective solvent extraction/also used t-butylallylcarbamate in place of t-butylmethacrylate, both grafted to LLDPE in the melt in presence of RI	Campbell 1990
EPDM-g-GMA (10 parts; 5.4 wt% GMA)/PPE-g-FA (90 parts; 0.7 wt% FA)	TSE at 300 °C/mechanical properties vs. blends with unfunctionalized polymers	Weiss 1989
PP-g-GMA (1 part)/PPE-g-MA (1 part)	Laboratory mixer at 270 °C/mechanical properties vs. blends with unfunctionalized polymers/PP grafted in separate extrusion with 10 wt% styrene and 3 wt% GMA/also used p-phenylenediamine as coupling agent	Togo et al. 1988

5.11.3.2 Blends Containing Functionalized PPE: PO-PPE Copolymer Formation through Coupling Agent Addition

Togo et al. (1988) compatibilized PP with PPE by combining carboxylic acid-functionalized PP with carboxylic acid-functionalized PPE in the presence of a diamine. For example, a 1:1 mixture of PP-g-MA and PPE-g-MA was melt kneaded with 1 wt% p-phenylenediamine at 270 °C. The product was formed into sheet with high tensile strength. PP was grafted with MA in the presence of styrene. BPA or a polyepoxide resin was also used in place of diamine.

5.11.4   Polyolefin + Polyphenylene Ether + Styrene Copolymer Blends

5.11.4.1 Blends Containing Unfunctionalized PPE + Functionalized PS: PO-PS Copolymer Formation by Carboxylic Acid + Epoxide Reaction

Immiscible blends containing a polyolefin, an unfunctionalized polyphenylene ether and a functionalized styrene copolymer, have been compatibilized through cross-linked

copolymer formation between carboxylic acid groups at multiple sites on polyolefin and epoxide groups at multiple sites on styrene copolymer. Fujii and Ting (1988) reported compatibilized blends of EMAA (15 parts), PPE (47 parts), HIPS (30 parts), SEBS (8 parts), and S-co-GMA (1 part) prepared on a TSE at 288 °C. Characterization included mechanical properties vs. blends without functionalized polymers. Abe et al. (1984) prepared blends of EVAc-co-GMA (1 part; 8 wt% VAc; 4 wt% GMA) with SMA (1 part; 8 wt% MA) in a kneader at 200 °C and characterized the copolymer by selective solvent extraction. Blends of the copolymer with PPE/PS had greatly improved mechanical properties compared to blends without copolymer.

5.11.4.2 Blends Containing Unfunctionalized PPE + Functionalized PS: PO-PS Copolymer Formation by Carboxylic Acid + Oxazoline Reaction

Hohlfeld (1986) prepared compatibilized blends of EAA and unfunctionalized PPE by extrusion with styrene-isopropenyl oxazoline copolymer (S-IPO). In one example, a blend of EAA (30 parts), PPE (35 parts), and S-IPO (35 parts) was mixed in a Brabender mixer at 280 °C. Torque level was higher and mechanical properties were significantly improved compared to blends with PS used in place of S-IPO. See also Xu et al. (1999b) for a study of similar blends.

5.11.4.3 Copolymer Formation through Ionomeric Cross-Linking Mediated by Metal Cations

Immiscible polyolefin impact modifiers have been compatibilized with PPE/PS blends by employing a polyolefin sulfonate ionomer and also including PS-sulfonate ionomer in the blend (Table 5.52). Alternatively, PPE-sulfonate ionomer could be used in place of PS-sulfonate ionomer. In these compositions, the polyolefin ionomer can cross-link with PS ionomer through metal cations. The PS-sulfonate ionomer is at least partially miscible with PS, which in turn is miscible with PPE. Simple ionomers have been used (Golba and Seeger 1987; Campbell et al. 1986, 1989). In similar blends, a masked ionomer, such as a polyolefin phosphonate ester, could also be used (Brown and McFay 1986, 1987). The masked ionomer is melt processable but generates a polyolefin phosphonate ionomer through ester hydrolysis in situ during extrusion in the presence of zinc stearate. The polyolefin phosphonate ionomer can cross-link with PS sulfonate ionomer that is miscible with PS which in turn is miscible with PPE.

5.11.5 Polyolefin + Polyphenylene Sulfide

5.11.5.1 Copolymer Formation by Nucleophile + Epoxide Reaction

Immiscible blends containing an epoxy-functionalized polyolefin and a polyphenylene sulfide have been compatibilized by Oyama et al. (2011) through graft copolymer formation between epoxide groups at multiple sites on either EMA-GMA or E-GMA-g-PMMA and nucleophilic end-groups such as amine,

Table 5.52 PO/PPE/styrene copolymer blends: ionomeric cross-linking mediated by metal cations

Polyolefin/PPE/styrene copolymer	Characterization and comments	References
EPDM-SO$_3$ Zn salt (12)/PPE (52)/ PPE-SO$_3$ Zn salt (13) or PS-SO$_3$ Zn salt/PS (23)/TPP (18)/ZnSt (12)	TSE at 270 °C/mechanical properties vs. omission of PPE-SO$_3$ Zn salt/ replacement of EPDM-SO$_3$ Zn salt with PDMS-SO$_3$ or B-AN-AA Na salt	Golba and Seeger 1987; Campbell et al. 1986, 1989
EP-PO$_3$Et (9-0)/PPE (50)/PS (9-20)/ PS-SO$_3$ Zn salt (0-9)/ZnSt (0-9)/ TPP (14)	TSE at 240 °C/mechanical properties vs. use of unfunctionalized rubber or unfunctionalized PS/model compound studies/EP-PO$_3$Et forms EP-PO$_3$ Zn salt in presence of ZnSt	Brown and McFay 1986, 1987

carboxylic acid, or thiophenol on PPS. Blend characterization techniques included morphology and mechanical properties.

Horiuchi and Ishii (2000) prepared PPS blends with LDPE-g-MA and PE-f-GMA in a TSE. Blend characterization techniques included morphology, TEM, EELS, DSC, tribological tests, and mechanical properties.

Hwang et al. (1998) effected graft copolymer formation between epoxide groups at multiple sites on PE-co-GMA and nucleophilic end-groups on PPS (see also Bailly et al. (1997) and Sugie et al. (1985)). SEBS impact modifier was also used in these blends. Han (1991a, b) employed amine- and carboxylic acid-terminated PPS in similar blends. Numerous similar examples of this compatibilization strategy have appeared, as documented, for example, in patents assigned to Toray Industries.

5.11.5.2 Copolymer Formation by Miscellaneous Reactions

Lehmann (2011) prepared compatibilized blends of PPS and PTFE (component ratios 0-100 to 100-0) using melt-processable PTFE treated by radiation to introduce –COF and –COOH functional groups by chain scission. It was proposed that functional groups on PTFE may react with thiol end-groups on PPS. Blend characterization techniques included mechanical and tribological properties.

5.11.6   Polyolefin + Polypropylene Blends

5.11.6.1 Copolymer Formation by Alcohol + Anhydride Reaction

Cascone et al. (2001) prepared compatibilized blends of PP-g-MA with poly(vinyl butyral) having different content of vinyl alcohol units. Demarquette and Kamal (1998) have prepared compatibilized blends of EVAl and PP through inclusion of

Table 5.53 PO/PP blends: copolymer formation by amine + anhydride or amine + carboxylic acid reaction

Polyolefin/polypropylene	Characterization and comments	References
Poly[2-(t-butylamino)ethyl methacrylate]-f-amine/PP-g-MA	Melt processed as fibers/antibacterial activity against *E. coli*/copolymer formation prevented release of the polymethacrylate biocide from surface of fibers	Thomassin et al. 2007
NBR (50-25)/amine-terminated NBR (0-10)/PP (45-50)/PP-MA (0-5)	Internal mixer at 190 °C/mechanical properties vs. omission of functional polymers/dimethylol phenol (3.75 %) + SnCl$_2$ (0.5 %) added as vulcanization agent for NBR	Coran and Patel 1983b
Carboxyl-terminated NBR (50)/amine-terminated PP (50)	Internal mixer at 190 °C/mechanical properties vs. use of unfunctionalized PP/dimethylol phenol (3.75 %) + SnCl$_2$ (0.5 %) added as vulcanization agent for NBR	Coran and Patel 1983b

PP-g-MA (0.1 mol% MA). Characterization methods included SEM, ESCA, and interfacial tension measurement. Tselios et al. (1998) have prepared compatibilized blends of LDPE and PP through inclusion of PP-g-MA (0.8 mol% MA) and EVAl (7.5 mol% vinyl alcohol). Blends were characterized using SEM, torque rheometry, mechanical properties, FTIR, and micro-Raman spectroscopy.

5.11.6.2 Copolymer Formation by Amine + Anhydride or Amine + Carboxylic Acid Reaction

Coran and Patel (1983b) have shown that the mechanical properties of dynamically vulcanized NBR-PP blends can be improved through copolymer formation between the two immiscible polymers concurrent with vulcanization. In the first example in Table 5.53, block copolymer resulted from reaction of amine-terminated NBR with anhydride-terminated PP. The latter was prepared through functionalization of PP with MA in the presence of radical initiator. In the second example, a block copolymer may have resulted from reaction of acid-terminated NBR with a primary amine-terminated PP. The latter was prepared in a prior reaction between maleic anhydride-terminated PP and triethylenetetramine. It is also possible that the block copolymer may be linked through ionomeric association resulting from protonation of PP-amine with NBR acid.

5.11.6.3 Copolymer Formation by Carboxylic Acid + Epoxide Reaction

A compatibilizing copolymer may be formed through reaction between carboxylic acid groups grafted onto a PO chain and acrylate epoxide groups grafted onto a PP chain. In an internal mixer, Liu et al. (1993) have prepared compositions comprising 20 parts NBR-g-AA, 0-75 parts PP, and 0-25 parts PP-g-GMA (0.8 % GMA). The blends were characterized by torque rheometry, SEM, FTIR, and mechanical properties. Control blends were made using either unfunctionalized NBR or PP

with different GMA levels. Although the exact structure of the copolymer is not known, it is convenient to consider that the reaction leads to a cross-linked copolymer based on the assumption that the acrylate epoxide groups are truly grafted onto the PP chains and are not all at terminal sites. Ao et al. (2006) compatibilized EPDM/PP blends using epoxidized EPDM and PP-g-AA.

Interestingly, Wang et al. (2012b) have reported that solid-state chlorination of PP in the presence of GMA results in high levels of GMA grafting. The PP-g-GMA was shown to form compatibilized blends with hydroxy-terminated butadiene-acrylonitrile rubber.

5.11.6.4 Copolymer Formation by Carboxylic Acid + Oxazoline Reaction

A compatibilizing copolymer may be formed through reaction of carboxylic acid groups grafted onto a PO chain and olefinic oxazoline groups grafted onto a PP chain. Again, it is reasonable to consider that this copolymer may be cross-linked based on the assumption that the oxazoline groups are truly grafted along the PP chains and are not all at terminal sites. Liu and Baker (1994) and Liu et al. (1993) have prepared PO-PP blends containing 20 parts NBR-g-AA, 0-80 parts PP, and 80-0 parts PP-g-IPO (0.2 % grafted isopropenyl oxazoline) in an internal mixer. The blends were characterized by torque rheometry, SEM, FTIR, and mechanical properties. Control blends were made using either unfunctionalized NBR or different IPO levels on PP.

5.11.6.5 Copolymer Formation through Coupling Agent Addition

As shown in Table 5.54, PO/PP blends have been compatibilized by copolymer formation formed through addition of a coupling agent such as a tris-acrylate and a radical initiator that can react with both PO and PP in an immiscible blend. Although PP may have at most one unsaturated site per chain (see Coran and Patel 1983b), the immiscible rubber phase may have multiple reactive sites. Depending upon stoichiometry of coupling agent and reactant polymers, the reaction may lead to a cross-linked copolymer. In the examples from Coran and coworkers, an additional coupling agent could be used to dynamically vulcanize the elastomeric phase following copolymer formation with the PP matrix.

5.11.6.6 Copolymer Formation by Displacement Reaction

Solid-state chlorination of PP may lead to low levels of chlorine incorporation along the PP chain with minimal PP molecular weight degradation. Coran and Patel (1983b) have blended (internal mixer at 190 °C) 50 parts chlorinated PP with 45 parts NBR containing 5 parts amine-terminated NBR. The blend was characterized by mechanical properties and compared to those for blends using unfunctionalized PP. Compatibilization resulted from copolymer formation through displacement reaction of chloride by amine groups. The blend was prepared in the presence of a vulcanization agent (3.75 % of dimethylol phenol plus 0.5 % of $SnCl_2$) to cause concomitant vulcanization of the rubber phase.

Table 5.54 PO/PP blends: copolymer formation through coupling agent addition

Polyolefin/polypropylene	Characterization and comments	References
EPDM/PP/Zn dimethacrylate/ peroxide RI	Melt mixing/mechanical properties/ TEM/SEM/DMA	Chen et al. 2013b
NBR/PP/Zn dimethacrylate/ peroxide RI	Melt mixing/torque rheometry/mechanical properties/TEM/SEM/TGA	Xu et al. 2013a
PP/ENR/triallyl cyanurate	Brabender mixer coupled with an electron accelerator to introduce functional groups into PP/FTIR/SEM/DMA/DSC/ mechanical properties/effect of order of component mixing	Rooj et al. 2011
HDPE-g-MA/PP-g-MA/ dodecane diamine	TSE/mechanical properties/also used Zn or Na salt in place of diamine to promote ionomeric interaction	Colbeaux et al. 2004, 2005
EPDM/PP/DCP RI	Internal mixer/torque measurement/ estimate of interfacial tension/also added trimethylolpropane triacrylate coupling agent	Shariatpanahi et al. 2002
EPDM-g-MA/PP-g-MA/ polyoxypropylenediamine	TSE/SEM/mechanical properties vs. diamine level	Phan et al. 1998
PE (25-10)/PP (75-90)/Luperox 101 RI (0-0.4)	TSE at 210 °C/rheology/DSC/DMA/ addition of trimethylolpropane triacrylate coupling agent	Graebling et al. 1997
HDPE (10-0)/EPR (10-20)/PP (80)/RI (0-0.01)	TSE at 230 °C/rheology/SEM/optical microscopy/DSC/mechanical properties/ unidentified RI/unidentified methacrylate additive (0-0.3)	Do et al. 1996
EPDM (30-0) or PB/PP (70-100)/ m-phenylene bismaleimide (0.075-0.6)	TSE at 210 °C/mechanical and thermal properties/DMA/ductile-brittle transition temperatures/SEM/selective solvent extraction/DSC/MFR/evidence for PP-EPDM copolymer	Inoue and Suzuki 1995, 1996; Ishikawa et al. 1996; Inoue 1994a, b
HDPE (8)/PP (80)/EPDM (12)/ 1,3-bis(t-butylperoxy-isopropyl) benzene RI (0-0.3)	TSE at 230 °C/MFI/SEM/rheology/ mechanical properties/use of PE-EPDM masterbatch/addition of trimethylolpropane triacrylate coupling agent	Kim and Choi 1996a
EP (20)/PP (80)/1,3- bis(t-butylperoxy-isopropyl) benzene RI (0–0.05 %)	TSE at 230 °C/rheology/SEM/DSC/ mechanical properties/optical microscopy/ increased coupling efficiency + retardation of PP degradation by addition of trimethylolpropane triacrylate coupling agent	Kim and Do 1996
NR (10)/PP (90)/1,3- bis(t-butylperoxy)benzene RI (0–0.05 %)	TSE at 230 °C/DSC/capillary rheometry/ SEM/mechanical properties/increased coupling efficiency + retardation of PP degradation by addition of trimethylolpropane triacrylate coupling agent	Yoon et al. 1995

(*continued*)

Table 5.54 (continued)

Polyolefin/polypropylene	Characterization and comments	References
EPDM (55 parts)/ethylene 4-methyl-1-pentene copolymer (20 parts)/PP (25 parts)/L130 RI (0.2 parts) + divinylbenzene (0.3 parts)	TSE at 230 °C/tensile and film properties vs. blend made without ethylene-methylpentene copolymer	Yonekura et al. 1988 (see also Otawa et al. 1988)
NBR (67.5-22.5)/dimethylol phenol-modified PP (25-75)/ dimethylol phenol (0-10)/SnCl$_2$ curing agent (0-1.1)	Internal mixer at 190 °C/mechanical properties vs. use of unfunctionalized PP/PP and dimethylol phenol (2–4 %) premixed before addition of rubber/ optional addition of additional coupling agent/addition of 0–7.5 % amine-terminated NBR	Coran and Patel 1983b

5.11.6.7 Copolymer Formation through Radical Coupling

PO/PP blends have been compatibilized by addition of a radical initiator. Early examples were summarized in a review by Teh et al. (1994); additional examples are listed in Table 5.55. PP can undergo chain scission in the presence of radical initiator to give a terminal radical site. Coupling of this PP radical with a PE radical located on the PE chain may initially yield a graft copolymer. Since the new copolymer may participate in further coupling reactions, a cross-linked copolymer may eventually be formed depending upon reaction time and radical concentration among other factors.

EPDM/PP blends have been compatibilized by exposure to high-intensity ultrasonic waves during extrusion (Feng and Isayev 2004; Chen and Li 2005), as have blends of PP with natural rubber (Oh et al. 2003). HDPE/PP (or HDPE/ground tire rubber) blends have been compatibilized through copolymer formation promoted by gamma irradiation (Sonnier et al. 2010). Dalai and Wenxiu (2002a) have reported blends of PP and EVAc with copolymer formation effected by radiation cross-linking. Blend characterization techniques included morphology and thermal properties.

5.11.7   Polyolefin + Polypropylene + Styrene Copolymer Blends

Dharmarajan et al. (1995) have prepared compatibilized blends of PP/styrene copolymer with or without functionalized PO. Blends of 100-0 parts PP, 0-100 parts SMA, 0-15 parts EP-g-(primary amine) (0.3 mol% amine), and 0-5 parts PP-(secondary amine) (0.4 wt% amine) were combined in an internal mixer at 220 °C. Blends were characterized by FTIR, DMTA, TEM, rheology, mechanical properties, lap shear adhesion, and paint adhesion. Properties were compared for blends containing either of the two amine-functionalized polymers alone. Reaction of EP-g-(primary amine) with SMA should result in a cross-linked copolymer because EP-g-(primary amine) contains randomly distributed amine functionality in the backbone. The secondary amine-terminated PP was prepared by first extruding PP with MA to form predominantly anhydride-terminated PP, followed by extrusion with N-methyl-1,3-propanediamine to give the secondary amine-terminated PP through reaction of

Table 5.55 PO/PP blends: copolymer formation through radical initiator addition

Polyolefin/polypropylene	Characterization and comments	References
HDPE/PP/RI	TSE either corotating or counterrotating/ butyl methacrylate added to feed components/mechanical properties/ morphology	Hettema et al. 1999
EPDM (15 vol%)/PP (85 vol%)/RI	TSE/MFI/impact strength/matrix crystallinity/morphology	van der Wal et al. 1998
LLDPE/PP/RI	Extrusion/SEC/FTIR/comparison to different mathematical models for changes in MWD/effect of different RI	Cheung and Balke 1997
LDPE (100-0)/PP (0-100)/ L130 RI (0-3) or t-butyl perbenzoate	Internal mixer at 150 °C or 180 °C/ mechanical properties vs. RI and PP content/DSC/selective solvent extraction/ optional addition of hydroquinone (0.75 %)/also silica-filled blends	Chodak et al. 1996; Chodak and Chorvath 1993; Chodak et al. 1991
LDPE (100-0)/PP (0-100)/ L101 RI (0-1)	Internal mixer or TSE at 180 °C/torque rheometry/rheology/SEM/mechanical properties/SEC/DSC/DMA/effects of PP-PE viscosity ratios/comparison to radiation induced cross-linking	Yu et al. 1990, 1992, 1994
LLDPE (50)/PP (50)/ L101 RI (0-0.25)	SSE at 185 °C followed by static mixer at 200–220 °C/mechanical properties/SEM/ DSC/SEC/TREF	Cheung et al. 1990

the primary amine of the diamine with the PP-anhydride. Dharmarajan et al. suggested that PP-MA is mostly end-group functionalized with a smaller portion of main-chain-functionalized species as the result of trapping PP radicals before chain scission. Chains with combinations of end-group and main-chain functionalization should also be present since the authors report that their PP-MA contains a significant amount of highly functionalized PP-MA oligomer. Therefore, in these examples, the copolymers prepared from PP-MA and SMA may consist of a mixture of cross-linked and grafted species.

5.11.8   Polyolefin + Polysiloxane Blends

5.11.8.1 Copolymer Formation by Amine + Anhydride Reaction

DeLeo et al. (2011) and DeLeo and Velankar (2008) prepared compatibilized blends of polyisoprene-PDMS (70-30 and 30-70) with addition of 0.1–3.0 wt% copolymer of MA-f-polyisoprene and amine-f-PDMS. Characterization methods included optical microscopy and rheology.

Kole et al. (1995) postulated the formation of a cross-linked copolymer through reaction between amine groups distributed along the main chain of a polysiloxane and anhydride groups distributed along the main chain of a PO. A unique feature of this example is the use of acrylamide-grafted siloxane rubber as the source of amine groups. Amine groups alpha to carbonyl groups (as in acrylamide) are much

Table 5.56 PO/polysiloxane blends: copolymer formation involving mechanochemical radical formation

Polyolefin/polysiloxane	Characterization and comments	References
EMAc (100-0)/vinyl-functionalized PDMS (3.8 % vinyl) (0-100)	Internal mixer at 85–180 °C/capillary rheometry/DMA/FTIR	Bhattacharya et al. 1995; Santra et al. 1993a
LDPE (50)/EMAc (0-10)/vinyl-functionalized PDMS (3.8 % vinyl) (50)	Internal mixer at 180 °C/mechanical properties/DMA/FTIR/SEM/WAXS/X-ray diffraction/lap shear adhesion	Santra et al. 1993b

less nucleophilic than typical amine functionality. In an example, 50/50 blends of EPDM-g-MA (1 % MA) with acrylamide-grafted silicone rubber were mixed in an internal mixer at 35 °C, 70 °C, or 150 °C. The blends were characterized by DMA, FTIR, mechanical properties, solvent swelling, and TGA.

5.11.8.2 Copolymer Formation Involving Mechanochemical Radical Formation

As shown in Table 5.56, copolymer formation was postulated between mechanochemically generated radicals at sites on EMAc and vinyl-functionalized PDMS during melt processing (Santra et al. 1993a, b). The substitution pattern of vinyl groups on PDMS was not reported. Assuming that the vinyl groups are distributed along the PDMS chains (and not present only as end-groups), then the compatibilizing copolymer formed is a cross-linked copolymer. EMAc-PDMS copolymer formed in situ has also been used to compatibilize PDMS with thermoplastic polyurethane (Santra et al. 1995).

5.11.8.3 Copolymer Formation by Acid-Base Interaction

Blends of carboxylic acid-terminated polybutadiene and amine-terminated PDMS have been prepared by Fleischer et al. (1994). A copolymer with block-like structure was postulated to form. Blends were characterized using pendant drop tensiometry and FTIR.

5.11.8.4 Copolymer Formation by Miscellaneous Reactions

PMMA/polydimethylsiloxane blends have been compatibilized in the presence of methacryloxypropyl trimethylsiloxane (dos Anjos et al. 2010). Formation of covalent bonds between PMMA and silane coupling agent was examined using FTIR. Modulus and tensile strength were improved in the compatibilized blends.

5.11.9 Polyolefin + Polystyrene or Styrene Copolymer Blends (Including Polypropylene)

An interesting publication by Martini et al. (2006) describes a method for separating a reactively compatibilized PP/PS blend into its individual polymeric components for analysis. The method involved use of high-temperature, high-pressure, near-critical

solvent extraction with n-alkane. The effects of different n-alkanes and different temperatures and the influence of blend morphology and composition on separation efficiency were studied. The compatibilizing copolymer could be isolated and quantified using this procedure.

5.11.9.1 Copolymer Formation by Acid-Base Interaction

Compatibilized blends of ethylene-methacrylic acid copolymer and PS were prepared by Kim et al. (1998) through addition of S-co-4-vinylpyridine. Similarly, blends of poly(isobutyl methacrylate) were compatibilized with poly(styrene-co-methacrylic acid) using poly(isobutyl methacrylate-co-2-(N,N-dimethylamino) ethyl methacrylate) or poly(isobutyl methacrylate-co-4-vinylpyridine) (Habi and Djadoun 1999). Turcsáyii (1995) has reported compatibilized blends of PE-g-(N-vinylimidazole) with acrylic acid-modified PP.

5.11.9.2 Copolymer Formation by Alcohol + Anhydride Reaction

Tang et al. (2002) prepared blends of PS and ethylene-vinyl acetate-vinyl alcohol in the presence of SMA using a TSE. Characterization techniques included morphology, mechanical properties, and FTIR.

Tselios et al. (1997) have compatibilized PO/styrene copolymer blends through cross-linked copolymer formation between PO alcohol groups and anhydride groups on styrene copolymer. Specifically, 50 parts EVAl (1.6–7.5 % VAl) was mixed with 50 parts SMA (8.4–14.7 mol% MA) in an internal mixer at 200 °C. The blends were characterized by torque rheometry, FTIR, DSC, TGA, selective solvent extraction, and mechanical properties as a function of mole ratio alcohol to anhydride. Blend properties were compared to those with EVAc in place of EVAl.

5.11.9.3 Copolymer Formation by Amine + Anhydride Reaction

As shown in Table 5.57, PO/styrene copolymer blends have been compatibilized through cross-linked copolymer formation between amine-functionalized PO and anhydride-functionalized styrene copolymer.

Dharmarajan et al. (1995) have compatibilized PP/styrene copolymer blends by formation of a graft copolymer through reaction of secondary amine-terminated PP (0.4 wt% amine) with SMA. The secondary amine-terminated PP was prepared by first extruding PP with MA to form anhydride-terminated PP followed by extrusion with N-methyl-1,3-propanediamine to give the secondary amine-terminated PP through reaction of the primary amine of the diamine with the PP-anhydride. Blends within the range PP to SMA from 0-100 to 100-0, containing 0-5 parts amine-terminated PP, were prepared in an internal mixer at less than 220 °C. They were characterized by FTIR, DMTA, TEM, mechanical properties, rheology, lap shear adhesion, and paint adhesion. Some cross-linked copolymer may be present if the PP-MA contains more than one anhydride group. A similar compatibilization strategy was used (Datta et al. 1993a) wherein EP-g-MA or PP-g-MA was extruded with an excess of diaminopropane to yield an amine-functionalized PO which was used in blends with SMA and also in combination with an engineering thermoplastic such as PPE, PBT, and SAN (Dekoninck 1993).

Table 5.57 PO/PS or styrene copolymer blends: copolymer formation by amine + anhydride reaction

Polyolefin/PS or styrene copolymer	Characterization and comments	References
PE-g-MA (20)/amine-terminated PS (80)	Melt blended at 180 °C/SEM morphology/stability upon annealing compared to nonreactive blend	Oxby and Maric 2013
Polyisoprene/PS/telechelic polyisoprene diamine/telechelic PS dianhydride	Internal mixer/SEM/evolution of domain size/effects of telechelic polymer MW and loading	Ashcraft et al. 2009
PP-g-MA/amine-terminated PS	Extrusion/morphology/varying viscoelastic properties of blend components/comparison to uncompatibilized blend	Omonov et al. 2007
PP-g-MA (1 or 8 wt% MA)/ polycyclohexylmethacrylate/ amine-terminated PS	Melt blend/selective solvent extraction/SEM	Harrats et al. 2004
PMMA-f-phthalic anhydride/ amine-terminated PS	Melt blend/comparison of reaction rate between end-functionalized PMMA and mid-chain-functionalized PMMA/also used amine-terminated PMMA	Jeon et al. 2004b; Moon et al. 2001
PMMA-f-anhydride/PS-f-amine	Melt blended at 180 °C/monitoring of reaction progress/morphology/ PMMA end-capped with phthalic anhydride/used PS with either terminal or pendant primary amine groups	Yin et al. 2001, 2003a, b
EP-g-MA/EPDM/amine-f-SAN	Melt blended/morphology/kinetics/ also used carbamate-functionalized SAN forming amine-functionalized SAN on thermolysis	Pagnoulle and Jérôme 2001a, b; Pagnoulle et al. 2000a, b
Anhydride-terminated PMMA/ amine-terminated PS	TEM/AFM/structure of interface induced by block copolymer	Lyu et al. 1999
Amine-functionalized EP (0.3–0.5 mol% amine) (30-0)/ HDPE (0-25)/SMA (8–14 % MA) (65-100)	Internal mixer at 180–220 °C/ mechanical properties/SEM/TEM/ rheology/pre-reaction of functionalized EP and SMA/selective solvent extraction	Datta et al. 1993b
Amine-functionalized EP (0.3–0.5 mol% amine) (35-0)/ SMA (8–14 % MA) (65-100)	Internal mixer at <220 °C/ mechanical properties/DSC/FTIR/ SEM/rheology/selective solvent extraction	Dharmarajan and Datta 1992
Amine-functionalized LLDPE (100-0)/SMA (6 % MA) (0-100)	Internal mixer at 220 °C/torque rheometry/SEM/mechanical properties/DSC/FTIR/MFI/PE grafted with dimethylamino-ethyl methacrylate or t-butyl-aminoethyl methacrylate	Song and Baker 1992

Table 5.58 PO/PS or styrene copolymer blends: copolymer formation by carboxylic acid + cyclic ortho ester or epoxide reaction

Polyolefin/PS or styrene copolymer	Characterization and comments	References
Polyisoprene/PS/telechelic polyisoprene dicarboxylic acid/telechelic PS diepoxide	Internal mixer/SEM/evolution of domain size/ effects of telechelic polymer MW and loading	Ashcraft et al. 2009
PP/PP-g-GMA/SEBS-g-MA	Haake mixer/FTIR/mechanical properties/ SEM/torque rheometry/effect of GMA and of MA loading	Ao et al. 2007a
EMA-co-GMA/SMA	Brabender mixer or TSE/mechanical properties/rheology/morphology/comparison to blend with unfunctionalized EMA	Bayam et al. 2001
PMMA-GMA (25)/ PS-monocarboxylic acid (75)	NMR/GPC/study of copolymer structure vs. that of homogeneous blend of PS-acid + PS-GMA/effect of reaction rate on morphology	Jeon et al. 2001; Jeon and Kim 2000
PP-g-AA/PS/PS-f-GMA	Morphology/rheology/effect of poly(acrylic acid) homopolymer present in PP-g-AA	Kim et al. 1999c
PE-g-AA (70-10 parts)/PS (30-90 parts)/S-co-GMA (0-3 parts)	Internal mixer at 200 °C/SEM/TEM/rheology/ DMA/effects of AA content on properties	Kim et al. 1997a, b, c
EPDM-g-cyclic ortho ester (50)/SAN-co-AA (50; 1 mol% AA)	TSE at 230 °C/% insolubles and mechanical properties vs. blend with unfunctionalized SAN/copolymer could be used as impact modifier for PC	Khouri and Stoddard 1995a, b

5.11.9.4 Copolymer Formation by Carboxylic Acid + Cyclic Ortho Ester or Epoxide Reaction

PO/styrene copolymer blends have been compatibilized through cross-linked or graft copolymer formation between acid-functionalized PO and epoxide-functionalized PS or vice versa (Table 5.58). Also, acid-functionalized styrene copolymer has been compatibilized with PO grafted with cyclic ortho ester. Anhydride-functionalized polymer is also effective in these blends since some acid groups are present from ring-opened anhydride. Epoxide groups are most frequently introduced into PO or PS by copolymerization with GMA, while cyclic ortho ester groups are introduced by grafting or copolymerization with olefinic cyclic ortho ester.

5.11.9.5 Copolymer Formation by Carboxylic Acid + Oxazoline Reaction

PO/styrene copolymer blends have been compatibilized through cross-linked copolymer formation between acid-functionalized PO and oxazoline-functionalized PS (Table 5.59). Anhydride-functionalized PO is also effective in these blends since some acid groups may be present from ring-opened anhydride. Oxazoline groups are most frequently introduced into PS by copolymerization of styrene with isopropenyl oxazoline (IPO).

Table 5.59 PO/PS or styrene copolymer blends: copolymer formation by carboxylic acid + oxazoline reaction

Polyolefin/PS or styrene copolymer	Characterization and comments	References
EP-g-MA/S-IPO/syndiotactic PS	Mechanical properties/SEM/rheology	Choi et al. 2002
PP-f-oxazoline/PS-f-COOH	Melt blended at 200 °C/morphology/ functionalization with 3 different oxazoline monomers	Kaya et al. 2002 (see also Pionteck et al. 2004)
Ethylene-octene copolymer-g-oxazoline/SAN/SMA	Mechanical properties/TEM/DSC	Mader et al. 1999
PMMA-f-oxazoline/carboxylic acid-terminated PS	TEM/solid-state NMR/static light scattering	Hölderle et al. 1998
EP-g-MA (0.7 % MA) (20)/S-IPO (1 % IPO) (80)	Internal mixer at 200 °C/torque rheometry/selective solvent extraction/ SEM study of morphology development in reactive and in nonreactive blends	Scott and Macosko 1994a
NBR-g-AA (7 % AA) (20)/S-IPO (1.7 % IPO) (80)	Internal mixer at 260 °C/torque vs. time and temperature/SEM/FTIR/ mechanical properties vs. use of unfunctionalized PS and oxazoline content in blend	Liu and Baker 1992b
EAA (9 % AA) (50-20)/PS (0-50)/ S-IPO (1.2 % IPO) (30-60)	Internal mixer at 240 °C/FTIR/torque rheometry/capillary rheometry/also TSE with on-line rheometry and FTIR controls/optical microscopy	Curry and Andersen, 1991/1992
PE-g-MA (30)/S-IPO (1.7 % IPO) (70)	Internal mixer at 190 °C/torque rheometry/FTIR/SEM	Liu et al. 1990
EAA (9 % AA) (90-10)/S-IPO (1 % IPO) (10-90)	Internal mixer at 225 °C/FTIR/SEM/ selective solvent extraction/DSC/ mechanical properties vs. processing conditions/effects of diluting with unfunctionalized LDPE and PS/effect of zinc chloride catalyst	Saleem and Baker 1990; Baker and Saleem 1987a, b (see also Schuetz et al. 1989)
B-AN-AA (20)/S-IPO (80) or combined with unfunctionalized PS	Internal mixer at 185 °C/torque vs. functionalization concentration/ morphology/mechanical properties/ detrimental effect of >5 % IPO (too small dispersed phase particle size)	Fowler and Baker 1988
LLDPE (25 parts)/LLDPE-g-MA (25 parts)/PS (30 parts)/S-IPO (20 parts; 1 % IPO)	Brabender at 280 °C/mechanical properties vs. blend with unfunctionalized polymers	Hohlfeld 1986

Sundararaj et al. (1995) have prepared blends containing PP-MA and oxazoline-functionalized PS. A graft copolymer may form through reaction between pendent oxazoline groups on PS and terminal acid groups (from some hydrolysis of anhydride groups) on PP. Specifically, 80 parts S-IPO (1 % IPO) was blended with 20 parts PP-MA (0.1 % MA) in either an internal mixer at 200 °C or in a TSE. The blends were characterized by selective solvent extraction and SEM. Morphology

Table 5.60 PO/PS or Styrene copolymer blends: copolymer formation through coupling agent addition

Polyolefin/PS or styrene copolymer	Characterization and comments	References
PP-g-MA/SMA/diphenyl diamino methane tetraglycidyl ether	Mechanical properties/morphology	Hung et al. 2008
PP-g-AA/SEBS-g-MA/ p-phenylenediamine	Extrusion/mechanical properties/ morphology	Bassani and Pessan 2002, 2003
PP-g-MA/SBS-g-MA/ 4,4′-diaminodiphenylmethane	Mechanical properties/also blends containing unfunctionalized isotactic PP	Wilhelm and Felisberti 2002a, b
EPDM (30)/PS (70)/divinylbenzene or trimethylolpropane triacrylate (5 %)	Torque rheometer/selective solvent extraction/DSC/mechanical properties/ addition of peroxide RI	Al-Malaika and Artus 1998
LLDPE (90-10)/PS (10-90)/TAIC (0-0.35) + styrene monomer (0-7)/ DCP RI (0-0.35)	TSE at 200 °C/mechanical properties/ selective solvent extraction/DSC/SEC/ FTIR/SEM/rheology	Teh and Rudin 1991, 1992
LLDPE (50)/styrene-co-vinylbenzaldehyde (50)/TAIC/ DCP RI	TSE at 200 °C/mechanical properties/ selective solvent extraction (1–8 % copolymer)/FTIR/morphology	Van Ballegooie and Rudin 1988

development in the different mixing equipment was studied in both reactive and nonreactive blends (i.e., unfunctionalized PS and PP).

5.11.9.6 Copolymer Formation through Coupling Agent Addition

PO/styrene copolymer blends have been compatibilized by cross-linked copolymer formation in the presence of coupling agent as shown in Table 5.60.

In addition, PP/styrene copolymer blends have also been compatibilized by addition of a bismaleimide coupling agent capable of reacting with both polymers. For example, Inoue (1994a, b) has prepared blends containing 80 parts PP and 20 parts SIS (or SBS) in the presence of 0-0.3 parts m-phenylene bismaleimide coupling agent using a TSE at 210 °C. The blends were characterized by mechanical properties, melt flow rate, DSC, morphology, and selective solvent extraction. Evidence was presented for PP-SIS copolymer formation.

Bromobutyl rubber and SMA blends have been compatibilized through addition of a bifunctional coupling agent (Willis et al. 1990). The authors assumed that a low molecular weight amino alcohol reacted with rubber bromo groups to form a quaternary ammonium salt. The resulting alcohol-functionalized rubber could form cross-linked copolymers through reaction of hydroxy groups with anhydride of SMA. Blends of 30-5 parts bromobutyl rubber with 70-95 parts SMA and 0-8 parts 2-dimethylaminoethanol coupling agent were prepared in an internal mixer at 150–200 °C, followed by TSE processing at 200 °C. The blends were characterized by FTIR, SEM, and mechanical properties. The effects of premixing rubber with amine and the effects of processing conditions were studied. Model reactions for the proposed copolymer-forming reaction were carried out in solution.

5.11.9.7 Copolymer Formation by Friedel-Crafts Coupling

The Friedel-Crafts alkylation reaction is one of the oldest known methods for attaching an alkyl group to an aromatic ring. The process typically proceeds by reaction between an alkyl cation precursor and an aromatic compound in the presence of a Lewis acid catalyst. In one example, Sun and Baker (1997) obtained copolymer in blends of 80-20 parts LLDPE with 20-80 parts PS and 0.3 parts aluminum chloride. The proposed mechanism involved cation formation on PE through Lewis acid-catalyzed degradation, followed by attachment of PE cation to aromatic rings of PS. Blends were prepared in an internal mixer at 180 °C and characterized by selective solvent extraction, GPC, SEM, FTIR, and mechanical properties. The effects of added styrene monomer were also studied. This process is an example of degradative copolymer formation since the PE graft segment attached to the PS chain has lower molecular weight than the PE phase from which it was derived. Although the initial copolymer formed in this process is a graft copolymer, the grafted PE segments may still be capable of reacting with catalyst with subsequent cation formation and attachment to a different PS chain leading potentially to a cross-linked copolymer. For related work, see also Sun et al. (1998), Diaz et al. (2002, 2005, 2007), Guo et al. (2007), Liu et al. (2009b), Jian-Ping et al. (2011), and Shahbazi et al. (2012). Li et al. (2009a, b, 2011b) employed aluminum chloride in compatibilized blends of PP and PS. A potential issue with any Friedel-Crafts process employed to form a compatibilizing copolymer is removal of residual catalyst from the blend to prevent adverse effects on blend properties during the lifetime of any formed plastic part.

5.11.9.8 Copolymer Formation by Ion-Neutral Donor Group Association

Compatibilized blends of 77 parts EPDM-SO$_3$Zn salt and 9 parts S-co-4-vinylpyridine with 4 parts zinc stearate (ZnSt) plasticizer were prepared in an internal mixer at 200 °C (Lundberg et al. 1988; Agarwal et al. 1987; Peiffer et al. 1986). The blends were characterized by FTIR, DMA, melt viscosity, DSC, and SEM. Mechanical properties were compared to blends containing unfunctionalized PS or containing EPDM-SO$_3$Na or Mg salts. A copolymer linked by ion-neutral donor group cross-links may form between sulfonate anion and pyridine nitrogen mediated by Zn cation. Related blends comprising sulfonated EPDM and styrene/maleimide/2-vinyl pyridine copolymer have been described by Dean (1986).

5.11.9.9 Copolymer Formation by Radical Coupling

As shown in Table 5.61, PO blends with either PS or styrene copolymer have been compatibilized through radical coupling reaction. In these examples, radicals were generated either through addition of radical initiators, through addition of a peroxide-containing polymer, through addition of an azide species, through use of ultrasonic oscillation during extrusion, through mechanochemical processing, or through preirradiation.

Table 5.61 PO/PS or styrene copolymer blends: copolymer formation through radical coupling

Polyolefin/PS or styrene copolymer	Characterization and comments	References
EPDM/SAN/MA + L101 RI	SEM morphology/FTIR/DMTA/effect of different mixing protocols/also used DCP RI	Taheri et al. 2011
PTFE/SBS or SB or ABS	Laboratory kneader/PTFE irradiated to form long-lived radical centers/selective solvent extraction/FTIR/tribological properties/also used NBR in place of styrene copolymer	Lehmann and Kluepfel 2010
PP/PS/di-t-butyl peroxide	SEM/rheology/DSC/addition of tetraethyl thiuram disulfide to control the degradation process	Li et al. 2009c
EPDM/SAN/RI	TSE/mechanical properties/rheology/FTIR/ comparison of various RIs	Hrnjak-Murgic et al. 2004 (see also Kratofil et al. 2007)
HDPE/PS	Extrusion with ultrasonic oscillation to form radicals/mechanical properties/morphology/ rheology/selective solvent extraction	Chen et al. 2002
PMMA/PS	Radical generation through solid-state shear pulverization/effects of MW, composition ratio, and screw design on blend properties/ both PMMA and PS were pyrene labeled for fluorescence-detection GPC to confirm copolymer formation	Lebovitz et al. 2002 (see also Furgiuele et al. 2000)
LDPE/PS/liquid PB/dialkyl peroxide RI	Morphology/mechanical properties/effect of different lubricants/use of LDPE-PS comingled waste	Hlavata et al. 2001
PP/SAN/DCP	FTIR/MFR/SEM/effect of RI concentration and blend component ratio on properties	Xie et al. 2001a
PP/PS/DCP	TSE/morphology/MFR/suppression of PP degradation by addition of multifunctional monomers	Xie and Zheng 2000
PE/PS/SEBS/DCP	Mixer at 165 °C/PE partially cross-linked with RI and then mixed with SEBS for further reaction/SEM/TEM/mechanical properties	Wang et al. 1998a
EPDM (19)/S-EP (3)/PS (78)/ various RI	TSE at 235 °C/SEM/solvent swelling/ mechanical properties vs. RI concentration	Crevecoeur et al. 1995
PB (20)/PS (80)/aromatic sulfonyl azide (0.25-2)	Internal mixer at 180 °C/mechanical properties/FTIR/TEM/radical formation through hydrogen abstraction by thermally generated nitrene in triplet state	Radusch et al. 1993
EEA (30-50)/PS-co-butyl acrylate-co-(t-butylperoxy methacryloyloxyethyl carbonate) (70-50)	Brabender mixer at 180 °C/selective solvent extraction/effect of temperature on grafting efficiency/also blends of peroxide-containing polymer with PP	Moriya et al. 1988; (see also Moriya et al. 1989)
LDPE (50)/PS (50)/CHP RI (0-1)	Torque rheometer at 120–170 °C/selective solvent extraction/FTIR/mechanical properties/DMTA/addition of copolymer to PE + PS	Hajian et al. 1984

5.11.9.10 Copolymer Formation by Thiol-Alkene Coupling

In a series of papers by Soares and coworkers (see, e.g., Soares et al. 2001), compatibilized blends have been prepared through copolymer formation between a thiol-functionalized polymer (also termed a mercapto-functionalized polymer) and a second polymer comprising a double bond (alkene). In a specific example, styrene-butadiene copolymer/EVAc blends with different ratios of components were compatibilized through addition of mercapto-modified EVAc. Evidence for copolymer formation came from FTIR and DMA. Morphology, mechanical properties, and DSC results were also reported.

5.11.9.11 Copolymer Formation by Transesterification

Hu and Lambla (1995) have blended EMAc (90-65 parts) with monohydroxy-terminated PS (10-35 parts) in an internal mixer at 180–220 °C in the presence of dibutyltin dilaurate or dibutyltin oxide catalyst. A compatibilizing copolymer arises from transesterification between pendent ester groups of EMAc and terminal hydroxy groups of PS. The effects on blend properties of PS molecular weight were reported. The effects of processing conditions and addition of solvent on conversion kinetics were studied.

5.11.10 Polyolefin + Polyurethane Blends

Ma et al. (2012b) reported compatibilized PVDF-TPU blends comprising PVDF-g-acrylic acid. Farah and Lerma (2010) prepared hydroxy-functionalized PP by reaction of PP-g-MA with 2-aminoethanol and used this functionalized PP in blends with TPU and unfunctionalized PP. Ethylene-octene copolymer was also used in place of PP.

Wang et al. (2007a) prepared compatibilized ethylene-octene copolymer blends with polyurethane using maleated ethylene-octene copolymer and amine-functionalized polyurethane. However, a study by Stutz et al. (1996) found no evidence for copolymer formation between thermoplastic polyurethane and either EAA or SMA under the specific conditions studied.

Qureshi (2009) prepared PP/TPU blends compatibilized using an amine-functionalized PP, which functionalized PP had been prepared in a separate step by extrusion of PP-g-MA with either hexamethylenediamine or dodecamethyl-enediamine. Blends characterization techniques included SEM, rheology, and mechanical properties.

Lu and Macosko (2004) and Lu et al. (2003) have prepared compatibilized blends of polyurethane with functionalized PP characterizing the blends by rheology, DMA, tensile properties, and morphology. Primary and secondary amine-functionalized PP were more efficient compatibilizers than was PP-g-MA. A degradative mechanism for copolymer formation involving polyurethane chain cleavage was postulated. See also Kobayashi et al. (2011) for related PE/TPU blends.

With regard to reactively compatibilized TPU blends, Lu et al. (2002) determined the relative reactivity of various functionalities toward TPU using model compounds. The ranking of relative reactivity was found to be primary amine (most reactive) > secondary amine >> hydroxyl $\sim$ carboxylic acid $\sim$ anhydride >> epoxide (least reactive).

5.12   Polyphenylene Sulfide Blends

Examples of polyphenylene sulfide blends not shown in other sections are listed in alphabetical order of the second polymer in the blend unless otherwise noted. Included in this section are polyphenylene sulfide blends not containing PA, PEST, or PO. When copolymer characterization was not performed, the structure of the compatibilizing copolymer is inferred from the functionality location on each of the two polymers. In some cases, more than one type of compatibilizing copolymer may have formed.

5.12.1   Polyphenylene Sulfide + Polysiloxane Blends

5.12.1.1 Copolymer Formation by Amine + Epoxide Reaction
Compatibilized blends of polyarylene sulfide with epoxy-functionalized polydimethylsiloxane have been prepared by Han (1994). An amine-terminated polysiloxane was functioned in solution with a chloro-epoxy triazine. Blends of 95:5 PPS:polysiloxane were extruded at 130–290 °C to provide compositions with markedly improved mechanical properties compared to a similar blend containing unfunctionalized polysiloxane.

5.12.2   Polyphenylene Sulfide + Styrene Copolymer Blends

Compatibilized blends of polyarylene sulfide with SEBS-g-MA have been prepared by Hisamatsu et al. (2000). Possibly an amine-terminated PPS reacts with anhydride to form a compatibilizing copolymer. Blend properties were measured as a function of MA content on SEBS. Nam et al. (2003) prepared compatibilized blends of PPS with ABS-g-MA in a TSE. Blends were characterized using optical microscopy, SEM, FTIR, DMA, and heat distortion temperature.

5.13   Polystyrene or Styrene Copolymer Blends

Examples of polystyrene blends not shown in earlier sections are listed in alphabetical order of the second polymer in the blend unless otherwise noted.

5.13.1   Polystyrene + Styrene Copolymer Blends

Xu et al. (1999a) prepared compatibilized blends of PS and the Zn salt of sulfonated PS by addition of poly(styrene-b-4-vinylpyridine) diblock copolymer. Characterization methods included SEM, DSC, SAXS, and FTIR. The effect of block copolymer level was studied. Evidence was found for Zn-mediated cross-linking between sulfonate groups and pyridine nitrogen.

Taubitz et al. (1988e) prepared ABS-g-GMA by reactive extrusion and used the product to make compatibilized blends with carboxylic acid-terminated PS. In one example, ABS-g-GMA (40 parts; 1.5 % GMA) was extruded with carboxylic acid-terminated PS (40 parts) on a TSE at 210 °C. The product showed only 15 % unbound PS by selective solvent extraction and GPC. For comparison blends prepared with unfunctionalized ABS showed 96–100 % unbound PS.

5.13.2   Polystyrene + Polyurethane Blends

Cassu and Felisberti (2001) prepared compatibilized PS/polyurethane blends by reactive extrusion in the presence of SMA. Blends were characterized by rheology, solubility tests, GPC, and SEM to confirm the presence of copolymer.

5.13.3   Styrene Copolymer + Polysiloxane Blends

Livengood et al. (2002) prepared compatibilized blends of amine-terminated polydimethylsiloxane and SMA by extrusion at 135–210 °C. The products were formulated into toner compositions with improved properties.

5.14   Summary

This chapter has not presented every known example of a reactive compatibilization strategy, nor has it included every known polymer that has been compatibilized in an immiscible blend with one or more other polymers. However, the compatibilization strategies presented herein illustrate broadly general methods which may be applied to new polymer blends or applied to known polymer blends for a higher return on cost vs. performance ratio.

The papers cited in this chapter reach similar conclusions concerning the effects on immiscible blend properties of a copolymer formed by reactive compatibilization. In virtually all cases, the generated blend morphology shows a smaller dispersed phase particle size than that observed in the absence of copolymer formation. In the majority of cases, this morphology is stabilized against agglomeration and coalescence of the dispersed phase during subsequent thermal processing. The specific morphology size distribution and its stability result in improved mechanical properties, not observed in uncompatibilized blends. A few

efforts have been made to characterize the phase interface and to correlate the interfacial thickness with the level of copolymer formed. However, in most older papers, the existence of copolymer is simply inferred from secondary evidence and its level is not quantified.

Except for a few notable cases, there was seldom consideration in these papers about the architectures of copolymers generated and their possible effects on compatibilization efficiency and morphological stability. Furthermore, since morphological stability alone may not result in optimum physical properties, it is sometimes not possible to know if optimum physical properties have been obtained. In numerous papers, clearly more than one type of copolymer architecture can form. For example, in acid-epoxide reactions, a new secondary alcohol may form that may possibly equilibrate into polyester constituting one blend component (see, e.g., Su et al. 1997). Only a few papers discuss the consequences of using di- vs. mono-end-group-functionalized polymers and their possible effects on generating graft vs. cross-linked copolymers. In many papers, the level and type of functionality on the reacting polymers are not specified.

There are numerous cited examples of blends where at least one polymeric component is vulcanizable. Such systems may be quite difficult to analyze after processing. In some cases, formation of an interpenetrating network (IPN) may be mistaken for covalently bonded copolymer. This is particularly so when no deliberate effort has been made to promote vulcanization and its occurrence was adventitious. Selective solvent extraction experiments to detect copolymer can be misinterpreted if some polymer is physically occluded in a matrix of the second polymer.

Some polymers contain reactive functionality but are also themselves subject to mechanochemical radical generation. When such polymers are blended under high-shear mixing with a second functionalized polymer, the architectures of formed copolymer may derive both from the primary, expected reaction and also from an unexpected, radical-radical coupling process.

In some cited examples, a third, multifunctional reagent is added that reacts with both polymers, for example, as a coupling agent. The relative solubility of many such reagents in particular polymers is often unknown. In immiscible blends, the reagent may segregate into one phase and selectively couple or cross-link that phase, in competition with the desired interpolymer reaction at the phase interface. Again, IPN formation may result, leading to confusion when interpreting selective solvent extraction data. For some types of reagents the problem of phase segregation can be solved by preparing a masterbatch in which a slight stoichiometric excess of the reagent is added to one of the polymers. The reagent caps the reactive functionality, but it does not couple or chain extend the polymer in which it is selectively soluble. Thus, reaction of the newly functionalized polymer at a phase interface with a second polymer is facilitated when the two polymers are blended. This strategy often works when using a coupling agent and in certain cases when using a condensing agent but not always when using a nonselective activating agent. However, relative stoichiometries of reacting species are often not considered in older cited examples.

There have been only a few studies of kinetics of copolymer-forming reactions under melt processing conditions because it is quite difficult to generate these data. In the papers cited in this chapter, there are many examples where not only the level of copolymer formed but also the architecture of the copolymer strongly depends on the melt processing time. Many of the blends are "living" in the sense that more copolymer would be generated with additional time. In contrast, some types of copolymer linkage (e.g., the reaction product of an alcohol and a cyclic anhydride) may degrade, and copolymer may be lost with additional processing time or at higher processing temperature. Different copolymer architecture may form with additional processing time, particularly when a redistribution reaction is possible as either the primary or as the secondary reaction (e.g., when a reactive alcohol is generated from epoxide ring opening with acid). It is usually difficult to isolate and characterize a copolymer from a melt-processed polymer blend. Model studies of copolymer formation between immiscible polymers have been performed either in solution (where there is unlimited interfacial volume for reaction) or using hot-pressed films of the polymers (where the interfacial volume for reaction is strictly controlled at a fixed phase interface). Model studies using low molecular weight analogs of the reactive polymers are useful, but their applicability to high molecular weight reacting systems may be limited. Nevertheless, excellent insight into reactive compatibilization processes has been obtained in recent years (such as through bilayer film studies) in publications including, but limited to, those by Scott and Macosko (1994b) (model experiments for interfacial reaction between SMA and either PA-11 or amine-terminated butadiene-acrylonitrile copolymer during reactive polymer blending); Merfeld et al. (1998) (interfacial thickness in bilayers of PPE and styrenics copolymers), Karim et al. (1999) (transesterification at a polymer blend layer examined by multiple physical techniques), Hayashi et al. (2000) (study of interfacial reaction between PA and anhydride-terminated polysulfone by neutron reflectivity and small-angle neutron scattering), Schulze et al. (2000) (reaction kinetics of end-functionalized chains at an amino-terminated PS/anhydride-terminated PMMA interface), Koulic et al. (2001) (premade vs. in situ formed compatibilizer at the PS/PMMA interface), Schulze et al. (2001) (measuring copolymer formation from end-functionalized chains at anhydride-terminated PMMA and amino-terminated PS interface using forward recoil spectrometry and SEC/fluorescence detection), Cheng et al. (2003) (computational modeling of reactive extrusion process), Yeung and Herrmann (2003) (computational modeling of reactive extrusion process), Coote et al. (2003) (neutron reflectometry investigation of polymer-polymer reactions at the interface between immiscible polymers), Jones et al. (2003) (effect of thermodynamic interactions on reactions of anhydride-terminated PMMA and amino-terminated PS in bilayer film), Harton et al. (2005) (diffusion-controlled reactive coupling at polymer-polymer interfaces), Kho et al. (2005) (morphological development at a bilayer film interface of PMMA-GMA/PS-COOH under electric field), Yu et al. (2005) (interfacial reaction kinetics at a PA-6/SMA reactive interface), Zhang et al. (2005) (interfacial morphology development during reactive coupling of anhydride-terminated PMMA and amino-terminated PS in bilayer film),

Kim et al. (2006) (bilayer film study of COOH-terminated PS and PMMA-GMA reaction), Chi et al. (2007) (kinetics of interfacial reaction between carboxylic acid-terminated PB and amino-terminated PDMS studied by interfacial tension measurements), Wang et al. (2010a) (investigation of reactive polymer-polymer interface using nanomechanical mapping), and Wang et al. (2013b) (interfacial interchange reaction between PC and amorphous PA).

It is to be hoped that future work on reactive compatibilization will continue to combine the excellent materials science that has been done to date with additional investigations of the more exact nature of chemical processes occurring and their quantitative effect on blend properties. Such knowledge of the chemistry, coupled to fluid mechanics and morphology development models, would provide powerful tools for optimization of known and invention of new reactive compatibilization processes to prepare commercially valuable polymer blends.

5.15 Cross-References

▶ Commercial Polymer Blends
▶ Compounding Polymer Blends
▶ Crystallization, Micro- and Nano-structure, and Melting Behavior of Polymer Blends
▶ High Performance Polymer Alloys and Blends for Special Applications
▶ Interphase and Compatibilization by Addition of a Compatibilizer
▶ Mechanical Properties of Polymer Blends
▶ Morphology of Polymer Blends
▶ Polyethylenes and Their Blends
▶ Properties and Performance of Polymer Blends
▶ Recycling Polymer Blends
▶ Rheology of Polymer Alloys and Blends

Abbreviations

AA Acrylic acid
ABS Acrylonitrile-butadiene-styrene terpolymer
AES Terpolymer from acrylonitrile, ethylene-propylene elastomer and styrene
AFM Atomic force microscopy
AN Acrylonitrile
ASA Acrylonitrile-styrene-acrylate terpolymer
ATRP Atom transfer radical polymerization
B Butadiene
BA n-Butyl acrylate
tBA t-Butyl acrylate
BPA Bisphenol A
CHP Cumene hydroperoxide

CL Caprolactone
DBP Dibenzoyl peroxide
DCP Dicumyl peroxide
DEM Diethylmaleate
DMA Dynamic mechanical analysis
DMTA Dynamic mechanical thermal analysis
DSC Differential scanning calorimetry
E Ethylene
EA Ethylacrylate
EAA Ethylene acrylic acid copolymer
EB Ethylene-butene copolymer
EBA Ethylene butyl acrylate copolymer
EDXA Energy dispersive X-ray analysis
EEA Ethylene ethylacrylate copolymer
EELS Electron energy loss spectroscopy
E-GMA Ethylene glycidyl methacrylate copolymer
EMA Ethylene methyl acrylate copolymer
EMAA Ethylene-methacrylic acid copolymer
EMAc Ethylene methyl acrylate copolymer
EMM Ethylene methyl methacrylate copolymer
ENR Epoxidized natural rubber
EP Ethylene-propylene copolymer
EPDM Ethylene-propylene-diene modified rubber
ESCA Electron spectroscopy for chemical analysis
ETFE Ethylene-tetrafluoroethylene copolymer
EVAc Ethylene-vinyl acetate copolymer
EVAl Ethylene-vinyl alcohol copolymer
-f- Functionalized (or functionalized with)
FA Fumaric acid
FESEM Field emission scanning electron microscopy
FTIR Fourier transform infrared spectroscopy
GMA Glycidyl methacrylate
GPC Gel permeation chromatography
HDPE High density polyethylene
HDT Heat distortion temperature
HIPS High-impact polystyrene
I Isoprene
IA Isobutyl acrylate
IM Impact modifier
IPO Isopropenyl oxazoline
IV Intrinsic viscosity
L101 Luperox® 101 (2,5-di-(t-butylperoxy)-2,5-dimethylhexane)
L130 Luperox® 130 (2,5-dimethyl-2,5-di-(t-butylperoxy) hexyne-3)
LCP Liquid crystalline polymer(s) (polyester-type unless noted)

LDPE Low-density polyethylene
LLDPE Linear low-density polyethylene
MA Maleic anhydride
MAA Methacrylic acid
MAc Methyl acrylate
MALDI Matrix-assisted laser desorption/ionization mass spectrometry
MDPE Medium density polyethylene
MFI Melt flow index
MFR Melt flow rate
MMA Methyl methacrylate
MS Mass spectrometry
MW Molecular weight
MWD Molecular weight distribution
NA Nadic anhydride
NBR Nitrile-butadiene rubber
NMR Nuclear magnetic resonance spectroscopy
NR Natural rubber
PA Polyamide(s)
PB Polybutadiene
PBN Polybutylene naphthalate
PBT Polybutylene terephthalate(s)
PC Bisphenol A polycarbonate
PCE Polycarbonate ester copolymer
PCL Polycaprolactone
PCT Poly(cyclohexanedimethanol terephthalate)
PDMS Polydimethylsiloxane
PE Polyethylene
PE-g-MA Maleic anhydride-grafted polyethylene
PEEK Polyetheretherketone
PEG Polyethylene glycol
PEI Polyetherimide
PEN Polyethylene naphthalate
P-E-P Propylene-ethylene-propylene block copolymer
PES Polyethersulfone
PEST Polyester(s)
PET Polyethylene terephthalate(s)
PETG Polyethylene terephthalate glycol modified (glycol is typically cyclohexanedimethanol)
Phenoxy Copolymer of BPA and epichlorohydrin
Phr Parts per 100 parts resin
PLA Poly(lactic acid)
PMMA Poly(methyl methacrylate)
PMP Poly-4-methylpentene-1
PO Polyolefin(s)

PP Polypropylene
PPE Polyphenylene ether(s)
PPS Polyphenylene sulfide
PPVL Polypivalolactone
PS Polystyrene
PTFE Polytetrafluoroethylene
PTT Poly(trimethylene terephthalate)
PVAc Polyvinyl acetate
PVAl Polyvinyl alcohol
PVC Polyvinylchloride
PVDF Polyvinylidene difluoride
RI Radical initiator
S Styrene
SAA Styrene-acrylic acid copolymer
SALS Small-angle light scattering
SAN Styrene-acrylonitrile copolymer
SAXS Small-angle X-ray scattering
SB Styrene-butadiene copolymer
SBS Styrene-butadiene-styrene copolymer
SEBS Styrene-(ethylene/butylene)-styrene copolymer
SEC Size-exclusion chromatography
SEM Scanning electron microscopy
SEP Styrene (ethylene-propylene) block copolymer
SI Styrene-isoprene copolymer
S-IPO Styrene-isopropenyl oxazoline copolymer
SIS Styrene-isoprene-styrene copolymer
SMA Styrene-*co*-maleic anhydride copolymer
sPS Syndiotactic polystyrene
SSE Single-screw extruder
Tg Glass transition temperature
Tm Melting temperature
TAIC Triallyl isocyanurate
TBAB Tetrabutylammonium bromide
TEM Transmission electron microscopy
TGA Thermogravimetric analysis
TPE Thermoplastic elastomer
TPP Triphenyl phosphate
TPPite Triphenyl phosphite
TPU Thermoplastic polyurethane
TSE Twin-screw extruder
UHMWPE Ultra high molecular weight polyethylene
ULDPE Ultra low-density polyethylene
UV Ultraviolet
VLDPE Very-low-density polyethylene

VTMS Vinyl trimethoxysilane
WAXD Wide-angle X-ray diffraction
WAXS Wide-angle X-ray scattering
XPS X-ray photoelectron spectroscopy
ZnSt Zinc stearate

References

M. Abbate, E. Martuscelli, G. Ragosta, G. Scarinzi, J. Mater. Sci. **26**, 1119 (1991)

M. Abbate, V. Di Liello, E. Martuscelli, P. Musto, G. Ragosta, Polymer **33**, 2940 (1992)

S. Abdou-Sabet, R.C. Puydak, P. Rader, Rubber Chem. Technol. **69**, 476 (1996)

K. Abe, S. Yamauchi, A. Ohkubo, US Patent 4,460,743, 17 July 1984 to Mitsubishi Petrochemical

H. Abe, T. Nishio, Y. Suzuki, T. Sanada, S. Hosoda, T. Okada, Eur. Pat. Appl., 295,103, 12 Dec 1988 to Sumitomo Chemical

L. Abis, R. Braglia, I. Camurati, E. Merlo, K.M. Natarajan, D. Elwood, S.G. Mylonakis, J. Appl. Polym. Sci. **52**, 1431 (1994)

D. Abraham, K.E. George, D.J. Francis, Angew. Makromol. Chem. **200**, 15 (1992)

D. Abraham, K.E. George, D.J. Francis, J. Appl. Polym. Sci. **67**, 789 (1998)

I.A. Abu-Isa, C.B. Jaynes, J.F. O'Gara, J. Appl. Polym. Sci. **59**, 1957 (1996)

A.M. Aerdts, G. Groeninckx, H.F. Zirkzee, H.A.M. van Aert, J.M. Geurts, Polymer **38**, 4247 (1997)

M. Afshari, R. Kotek, M.H. Kish, H.N. Dast, B.S. Gupta, Polymer **43**, 1331 (2002)

P.K. Agarwal, I. Duvdevani, D.G. Peiffer, R.D. Lundberg, J. Polym. Sci. B Polym. Phys. **25**, 839 (1987)

P. Agrawal, S.I. Oliveira, E.M. Araujo, J.A. Tomas, J. Mater. Sci. **42**, 5007 (2007)

S.M. Aharoni, Polym. Bull. **10**, 210 (1983)

S.M. Aharoni, T. Largman, US Patent 4,417,031, 22 Nov 1983, to Allied

S.M. Aharoni, W.B. Hammond, J.S. Szobota, D. Masilamani, J. Polym. Sci. A Polym. Chem. **22**, 2567 (1984)

D. Ahn, K. Khait, M.A. Petrich, J. Appl. Polym. Sci. **55**, 1431 (1995)

A. Ajji, Polym. Eng. Sci. **35**, 64 (1995)

M. Akbari, A. Zadhoush, M. Haghighat, J. Appl. Polym. Sci. **104**, 3986 (2007)

M.K. Akkapeddi, J.C. Haylock, J.A. Gervasi, US Patent 4,847,322, 11 July 1989, to Allied-Signal

M.K. Akkapeddi, B. Van Buskirk, A.C. Brown, US Patent 5,162,440, 10 Nov 1992, to Allied-Signal

M.K. Akkapeddi, B. Van Buskirk, C.D. Mason, S.S. Chung, X. Swamikannu, Polym. Eng. Sci. **35**, 72 (1995)

M.S. Akutin, A.V. Melik-Kasumov, R.V. Torneu, V.N. Kotrelev, Plast. Massy **12**, 45 (1968)

A. Alexandrova, A. Cabrera, M.A. Hernandez, M.J. Cruz, M.J.M. Abadie, O. Manero, D. Likhatchev, Polymer **43**, 5397 (2002)

S. Al-Malaika (ed.), *Reactive Modifiers for Polymers* (Springer, New York, 1997)

S. Al-Malaika, K. Artus, J. Appl. Polym. Sci. **69**, 1933 (1998)

S. Al-Malaika, W. Kong, Polymer **46**, 209 (2005)

E. Amendola, C. Carfagna, P. Netti, L. Nicolais, S. Saiello, J. Appl. Polym. Sci. **50**, 83 (1993)

J. An, J. Ge, Y. Liu, J. Appl. Polym. Sci. **60**, 1803 (1996)

J.C. Angola, Y. Fujita, T. Sakai, T. Inoue, J. Polym. Sci. B Polym. Phys. **26**, 807 (1988)

Anonymous, GB Patent 998,439, 14 July 1965, to DuPont

P. Antony, S.K. De, Polymer **40**, 1487 (1999)

P. Antony, S. Bandyopadhyay, S.K. De, Polymer **41**, 787 (2000)

U. Anttila, K. Hakala, T. Helaja, B. Löfgren, J. Seppälä, J. Polym. Sci. A Polym. Chem. **37**, 3099 (1999)

Y.H. Ao, S.L. Sun, Z.Y. Tan, C. Zhou, H.X. Zhang, J. Appl. Polym. Sci. **102**, 3949 (2006)

Y.H. Ao, K. Tang, N. Xu, H.-D. Yang, H.-X. Zhang, Polym. Bull. **59**, 279 (2007a)

Y.H. Ao, S.L. Sun, Z.Y. Tan, C. Zhou, N. Xu, K. Tang, H.D. Yang, H.X. Zhang, Polym. Bull. **58**, 447 (2007b)

M. Aramaki, T. Saitou, T. Maekawa, US Patent 6,794,463, 21 Sept 2004, to Asahi

N. Aranburu, J.I. Eguiazábal, J. Appl. Polym. Sci. **127**, 5007 (2013)

Y. Arashiro, S. Yamauchi, H. Ohmura, F. Yamada, M. Kihira, Eur. Pat. Appl. 472,960, 4 Mar 1992 to Mitsubishi Petrochemical

E.M. Araujo, E. Hage Jr., A.J.F. Carvalho, J. Appl. Polym. Sci. **87**, 842 (2003a)

E.M. Araujo, E. Hage Jr., A.J.F. Carvalho, J. Mater. Sci. **38**, 3515 (2003b)

I. Aravind, A. Boumod, Y. Grohens, S. Thomas, Ind. Eng. Chem. Res. **49**, 3873 (2010a)

I. Aravind, S. Jose, K.H. Ahn, S. Thomas, Polym. Eng. Sci. **50**, 1945 (2010b)

P.S. Archondouli, N.K. Kalfoglou, Polymer **42**, 3489 (2001)

P.S. Archondouli, J.K. Kallitsis, N.K. Kalfoglou, J. Appl. Polym. Sci. **88**, 612 (2003)

A. Argoud, L. Trouillet-Fonti, S. Ceccia, P. Sotta, Eur. Polym. J. **50**, 177 (2014)

R. Armat, A. Moet, Polymer **34**, 977 (1993)

R.G. Armstrong, US Patent 3,373,222, 12 Mar 1968, to Continental Can

A. Aróstegui, J. Nazábal, Polym. Adv. Technol. **14**, 400 (2003a)

A. Aróstegui, J. Nazábal, Polym. J. **35**, 56 (2003b)

L. Arruabarrena, M.E. Munoz, J.J. Pena, A. Santamaria, Polym. Commun. **27**, 92 (1986)

E. Ashcraft, H. Ji, J. Mays, M. Dadmun, ACS Appl. Mater. Interfaces **1**, 2163 (2009)

K.B. Atwood, M.J. Brown, D.C. Urian, US Patent Appl. 20070232170, 4 Oct 2007, to DuPont

M. Avella, B. Immirzi, M. Malinconico, E. Martuscelli, M.G. Volpe, Polym. Int. **39**, 191 (1996)

D.F. Aycock, S.-P. Ting, US Patent 4,600,741, 15 July 1986, to General Electric

D.F. Aycock, S.-P. Ting, US Patent 4,642,358, 10 Feb 1987, to General Electric

S.C.E. Backson, R.W. Richards, S.M. King, Polymer **40**, 4205 (1999)

T.-Y. Bae, K.-Y. Park, D.-H. Kim, K.-D. Suh, J. Appl. Polym. Sci. **81**, 1056 (2001)

S.-L. Bai, G.-T. Wang, J.-M. Hiver, C. G'Sell, Polymer **45**, 3063 (2004)

C.M.E. Bailly, J.P. Shaw, C.-F.R. Hwang, US Patent 5,681,893, 28 Oct 1997, to General Electric

W.E. Baker, M. Saleem, Polymer **28**, 2057 (1987a)

W.E. Baker, M. Saleem, Polym. Eng. Sci. **27**, 1634 (1987b)

W.E. Baker, C.E. Scott, G.-H. Hu (eds.), *Reactive Polymer Blending* (Hanser/Gardner Publications, Cincinnati, 2001)

G.P. Balamurugan, S.N. Maiti, Polym. Eng. Sci. **48**, 2482 (2008a)

G.P. Balamurugan, S.N. Maiti, Polym. Test. **27**, 752 (2008b)

L.L. Ban, M.J. Doyle, M.M. Disko, G.R. Smith, Polym. Commun. **29**, 163 (1988)

L.L. Ban, M.J. Doyle, M.M. Disko, G. Braun, G.R. Smith, Subinclusion morphology in compatibilised polymer blends, in *Integration of Fundamental Polymer Science and Technology*, ed. by P.J. Lemstra, L.A. Kleintjens (Elsevier Applied Science, New York, 1989), p. 117

L. Barangi, F.A. Taromi, H. Nazockdast, Macromol. Symp. **274**, 166 (2008)

A.O. Baranov, A.V. Kotova, A.N. Zelenetskii, E.V. Prut, Russ. Chem. Rev. **66**, 877 (1997)

A. Bassani, L.A. Pessan, J. Appl. Polym. Sci. **86**, 3466 (2002)

A. Bassani, L.A. Pessan, J. Appl. Polym. Sci. **88**, 1081 (2003)

D. Basu, A. Banerjee, J. Appl. Polym. Sci. **64**, 1485 (1997)

G. Bayam, U. Yilmazer, J. Appl. Polym. Sci. **83**, 2148 (2002)

G. Bayam, U. Yilmazer, M. Xanthos, J. Appl. Polym. Sci. **80**, 790 (2001)

BCC Research (2013), cited at http://www.bccresearch.com/market-research/plastics/engineering-resins-polymer-alloys-blends-pls020c.html

H.G. Becker, G. Schmidt-Naake, J. Appl. Polym. Sci. **90**, 2322 (2003)

H.G. Becker, G. Schmidt-Naake, Chem. Eng. Technol. **27**, 909 (2004)

O. Becker, G.P. Simon, T. Rieckmann, J.S. Forsythe, R.F. Rosu, S. Völker, J. Appl. Polym. Sci. **83**, 1556 (2002)

J.J. Belles Jr., H.R. Bhattacharjee, Y.P. Khanna, R. Kumar, US Patent 5,055,509, 8 Oct 1991, to Allied-Signal

S.I. Belousov, Y.K. Godovskii, V.V. Matveev, I.V. Sapozhnikova, A.E. Chalykh, Polym. Sci. USSR **34**, 254 (1992)

P.L. Beltrame, A. Castelli, M.D. Pasquantonio, M. Canetti, A. Seves, J. Appl. Polym. Sci. **60**(579) (1996)

G.A. Berkstresser IV, B.D. Mullen, P.D. Sybert, US Patent 7,323,535, 29 Jan 2008, to General Electric

C. Berti, V. Bonora, F. Pilati, Makromol. Chem. **193**, 1679 (1992a)

C. Berti, V. Bonora, F. Pilati, Makromol. Chem. **193**, 1665 (1992b)

S.H.P. Bettini, L.C. de Mello, P.A.R. Munoz, A. Ruvolo-Filho, J. Appl. Polym. Sci. **127**, 1001 (2013)

M.K. Beyer, H. Clausen-Schaumann, Chem. Rev. **105**, 2921 (2005)

P.A. Bhadane, A.H. Tsou, J. Cheng, B.D. Favis, Macromolecules **41**, 7549 (2008)

P.A. Bhadane, A.H. Tsou, J. Cheng, M. Ellul, B.D. Favis, Polymer **52**, 5107 (2011)

H.R. Bhattacharjee, Y.P. Khanna, US Patent 4,946,909, 7 Aug 1990, to Allied-Signal

A.K. Bhattacharya, R.N. Santra, V.K. Tikku, G.B. Nando, J. Appl. Polym. Sci. **55**, 1747 (1995)

A.R. Bhattacharyya, A.K. Ghosh, A. Misra, Polymer **42**, 9143 (2001)

A.R. Bhattacharyya, A.K. Ghosh, A. Misra, K.-J. Eichhorn, Polymer **46**, 1661 (2005)

A.K. Bhowmick, T. Chiba, T. Inoue, J. Appl. Polym. Sci. **50**, 2055 (1993)

J.-E. Bidaux, G.D. Smith, N. Bernet, J.-A.E. Manson, J. Hilborn, Polymer **37**, 1129 (1996)

I. Blanco, G. Cicala, C.L. Restuccia, A. Latteri, S. Battiato, A. Scamporrino, F. Samperi, Polym. Eng. Sci. **52**, 2498 (2012)

M.L. Blohm, S.B. Brown, G.T. Seeger, P.P. Anderson, US Patent 5,385,984, 31 Jan 1995, to General Electric

C.C. Bohn, S.C. Manning, R.B. Moore, J. Appl. Polym. Sci. **79**, 2398 (2001)

D.H. Bolton, D.M. Derikart, N. Kohncke, P. Moulinie, Eur. Pat. Appl. 1,153,981, 15 June 2005, to Bayer

D.C. Bookbinder, P.D. Sybert, US Patent 5,135,990, 4 Aug 1992, to General Electric

R.J.M. Borggreve, R.J. Gaymans, Polymer **30**, 63 (1989)

R.J.M. Borggreve, R.J. Gaymans, A.R. Luttmer, Makromol. Chem. Makromol. Symp. **16**, 195 (1988a)

R.J.M. Borggreve, R.J. Gaymans, J. Schuijer, J.F. Ingen Housz, Polymer **28**, 1489 (1988b)

R.J.M. Borggreve, R.J. Gaymans, H.M. Eichenwald, Polymer **30**, 78 (1989a)

R.J.M. Borggreve, R.J. Gaymans, J. Schuijer, Polymer **30**, 71 (1989b)

C. Boyer, B. Boutevin, J.J. Robin, Polym. Degrad. Stab. **90**, 326 (2005)

D. Braun, W. Illing, Angew. Makromol. Chem. **154**, 179 (1987)

S.B. Brown, US Patent 4,994,525, 19 Feb 1991a, to General Electric

S.B. Brown, US Patent 4,997,885, 5 Mar 1991b, to General Electric

S.B. Brown, Reactive extrusion: a survey of chemical reactions of monomers and polymers during extrusion processing, chapter 4, in *Reactive Extrusion Principles and Practice*, ed. by M. Xanthos (Hanser Publishers, New York, 1992a), p. 75

S.B. Brown, in *Symposium on Blends of Amorphous and Crystalline Polymers sponsored by the Division of Polymer Chemistry, 204th ACS Meeting*, Washington, DC, 24 Aug 1992b

S.B. Brown, US Patent RE. 34,364, 31 Aug 1993, to General Electric

S.B. Brown, R.C. Lowry, US Patent 5,089,566, 18 Feb 1992a, to General Electric

S.B. Brown, R.C. Lowry, US Patent 5,096,979, 17 Mar 1992b, to General Electric

S.B. Brown, D.J. McFay, Polym. Prepr. Am. Chem. Soc. Div. Polym. Chem. **27**(1), 333 (1986)

S.B. Brown, D.J. McFay, US Patent 4,680,329, 14 July 1987, to General Electric

S.B. Brown, C.M. Orlando, Reactive extrusion, in *Encyclopedia of Polymer Science and Engineering*, ed. by J.I. Kroschwitz, vol. 14, 2nd edn. (Wiley, New York, 1988), pp. 169–189

S.B. Brown, R.J. Gambale, L.L. McCracken, US Patent 5,030,693, 9 July 1991a, to General Electric

S.B. Brown, J.S. Trent, J.C. Golba Jr., R.C. Lowry, US Patent 5,041,504, 20 Aug 1991b, to General Electric

S.B. Brown, C.-F.R. Hwang, F.F. Khouri, S.T. Rice, J.J. Scobbo Jr., J.B. Yates, US Patent 5,504,165, 2 Apr 1996, to General Electric

S.B. Brown, K.H. Dai, C.-F.R. Hwang, S.T. Rice, J.J. Scobbo Jr., J.B. Yates, US Patent 5,612,401, 18 Mar 1997a, to General Electric

S.B. Brown, C.-F.R. Hwang, F.F. Khouri, S.T. Rice, J.J. Scobbo Jr., J.B. Yates, US Patent 5,698,632, 16 Dec 1997b, to General Electric

S.B. Brown, C.-F.R. Hwang, S.T. Rice, J.J. Scobbo Jr., J.B. Yates, F.F. Khouri, US Patent 5,837,758, 17 Nov 1998a, to General Electric

S.B. Brown, S.M. Cooper, B.A. Giles, US Patent 5,852,085, 22 Dec 1998b, to General Electric

S.B. Brown, J.R. Campbell, C.-F.R. Hwang, S.T. Rice, P.A. Rodgers, J.J. Scobbo Jr., J.B. Yates, US Patent 5,939,490, 17 Aug 1999, to General Electric

S.B. Brown, B.A. Giles, Y. Jin, D. Nazareth, S.T. Rice, R. Puyenbroek, B.J. McKinley, US 6,166,137, 26 Dec 2000a, to General Electric

S.B. Brown, Y. Jin, J.F. Kelley, J. Liao, M.T. Takemori, R.L. Utley, US Patent 6,150,473, 21 Nov 2000b, to General Electric

S.B. Brown, C.-F.R. Hwang, H. Ishida, J.J. Scobbo Jr., J.B. Yates III, US Patent 6,303,708, 16 Oct 2001, to General Electric

S.B. Brown, H.-P. Brack, J.A. Cella, D. Karlik, US Patent 7,547,749, 16 June 2009, to SABIC Innovative Plastics

C.B. Bucknall, *Toughened Plastics* (Applied Science, London, 1977)

S. Bum, Kil, O. Ok, Park, K.H. Yoon, J. Appl. Polym. Sci. **82**, 2799 (2001)

G. Burgisi, M. Paternoster, N. Peduto, A. Saraceno, J. Appl. Polym. Sci. **66**, 777 (1997)

J. Bussink, H.T. van de Grampel, Polymer blends, in *Ullman's Encyclopedia of Industrial Chemistry*. In: B. Elvers (ed.) (Wiley-VCH Verlag, Weinheim, 2000) doi:10.1002/14356007.a21_273; published on-line

X. Cai, G. Wu, J. Macromol. Sci. B Phys. **53**, 347 (2014)

L. Caligiuri, P. Stagnaro, B. Valenti, G. Canalini, Eur. Polym. J. **45**, 217 (2009)

J.R. Campbell, US Patent 4,980,415, 25 Dec 1990, to General Electric

J.R. Campbell, P.M. Conroy, R.A. Florence, Polym. Prepr. Am. Chem. Soc. Div. Polym. Chem. **27**(1), 331 (1986)

J.R. Campbell, R.E. Williams, S.B. Brown, P.M. Conroy, R.A. Florence, US Patent 4,840,982, 20 June 1989, to General Electric

J.R. Campbell, S.Y. Hobbs, T.J. Shea, V.H. Watkins, Polym. Eng. Sci. **30**, 1056 (1990)

J.R. Campbell, T.J. Shea, S.Y. Hobbs, S.B. Brown, US Patent 5,068,286, 26 Nov 1991, to General Electric

L. Canfora, S. Filippi, F.P. La Mantia, Polym. Eng. Sci. **44**, 1732 (2004)

L.B. Canto, E. Hage Jr., L.A. Pessan, J. Appl. Polym. Sci. **102**, 5795 (2006)

E. Carone Jr., U. Kopcak, M.C. Goncalves, S.P. Nunes, Polymer **41**, 5929 (2000)

C. Carrot, S. Mbarek, M. Jaziri, Y. Chalamet, C. Raveyre, F. Prochazka, Macromol. Mat. Eng. **292**, 693 (2007)

T.L. Carte, A. Moet, J. Appl. Polym. Sci. **48**, 611 (1993)

H. Cartier, G.-H. Hu, Polym. Eng. Sci. **39**, 996 (1999)

A. Casale, R.S. Porter, Adv. Polym. Sci. **17**, 1 (1975)

A. Casale, R.S. Porter, *Polymer Stress Reactions*, vol. 1 (Academic, New York, 1978), p. 226 ff

E. Cascone, D.J. David, M.L. DiLorenzo, F.E. Karasz, W.J. MacKnight, E. Martuscelli, M. Raimo, J. Appl. Polym. Sci. **82**, 2934 (2001)

P. Cassagnau, A. Michel, Polym. Eng. Sci. **34**, 1011 (1994)

P. Cassagnau, M. Bert, V. Verney, A. Michel, Polymer **34**, 124 (1993)

S.N. Cassu, M.I. Felisberti, J. Appl. Polym. Sci. **82**, 2514 (2001)

M. Castellano, E. Marsano, A. Turturro, M. Canetti, J. Appl. Polym. Sci. **122**, 698 (2011)

P. Cavallaro, B. Immirzi, M. Malinconico, E. Martuscelli, M.G. Volpe, Angew. Makromol. Chem. **210**, 129 (1993)

A. Cecere, R. Greco, G. Ragosta, G. Scarinzi, A. Taglialatela, Polymer **31**, 1239 (1990)

J.A. Cella, J. Liska, V.L. Ulery, G.W. Yeager, S.A. Nye, H. Guo, N. Sing, US Patent 6,339,131, 15 Jan 2002, to General Electric

C. Cercle, B.D. Favis, Polymer **53**, 4338 (2012)

M.F. Champagne, M.A. Huneault, C. Roux, W. Peyrel, Polym. Eng. Sci. **39**, 976 (1999)

M.F. Champagne, A. Helmert, M.M. Dumoulin, Polym. Mater. Sci. Eng. **83**, 465 (2000)

K. Chandramouli, S.A. Jabarin, Adv. Polym. Technol. **14**, 35 (1995)

D.-Y. Chang, F.-C. Chang, J. Appl. Polym. Sci. **56**, 1015 (1995)

F.-C. Chang, Y.-C. Hwu, Polym. Eng. Sci. **31**, 1509 (1991)

P. Charoensirisomboon, T. Chiba, S.I. Solomko, T. Inoue, M. Weber, Polymer **40**, 6803 (1999a)

P. Charoensirisomboon, T. Chiba, K. Torikai, H. Saito, T. Ougizawa, T. Inoue, M. Weber, Polymer **40**, 6965 (1999b)

P. Charoensirisomboon, T. Chiba, T. Inoue, M. Weber, Polymer **41**, 5977 (2000)

S.-H. Chen, F.-C. Chang, J. Appl. Polym. Sci. **51**, 955 (1994)

Y. Chen, H. Li, Polymer **46**, 7707 (2005)

G. Chen, J. Liu, J. Appl. Polym. Sci. **74**, 857 (1999)

Y. Chen, Q. Wang, Polym. Int. **50**, 966 (2001)

C.C. Chen, J.L. White, Polym. Eng. Sci. **33**, 923 (1993)

C.C. Chen, E. Fontan, K. Min, J.L. White, Polym. Eng. Sci. **28**, 69 (1988)

P.N. Chen Sr., A. Forschrim, M. Glick, M. Jaffe, US Patent 5,070,144, 3 Dec 1991, to Hoechst Celanese

P. Chen Sr., V. Sullivan, T. Dolce, M. Jaffe, US Patent 5,182,334, 26 Jan 1993, to Hoechst Celanese

G. Chen, J. Yang, J.J. Liu, J. Appl. Polym. Sci. **71**, 2017 (1999)

G. Chen, S. Guo, H. Li, J. Appl. Polym. Sci. **86**, 23 (2002)

B. Chen, T. Tang, S. Xu, X. Zhang, B. Huang, Polymer Journal **35**, 141 (2003)

L. Chen, H.-Z. Huang, Y.-Z. Wang, J. Jow, K. Su, Polymer **50**, 3037 (2009)

W.-C. Chen, S.-M. Lai, M.Y. Chang, Z.-C. Liao, J. Macromol. Sci. B Phys. (2013a). doi:10.1080/00222348.2013.860304; published online

Y. Chen, C. Xu, X. Liang, L. Cao, J. Phys. Chem. B **117**, 10619 (2013b)

M.H. Cheng, A.C. Balazs, C. Yeung, V.V. Ginzburg, J. Chem. Phys. **118**, 9044 (2003)

P.C. Cheung, S.T. Balke, Ind. Eng. Chem. Res. **36**, 1191 (1997)

M.-F. Cheung, A. Golovoy, R.O. Carter, H. van Oene, Ind. Eng. Chem. Res. **28**, 476 (1989)

P. Cheung, D. Suwanda, S.T. Balke, Polym. Eng. Sci. **30**, 1063 (1990)

C. Chevallier, F. Becquart, C. Benoit, J.-C. Majeste, M. Taha, Polym. Eng. Sci. (2013). doi:10.1002/pen.23816; published online

C. Chi, Y.T. Hu, A. Lips, Macromolecules **40**, 6665 (2007)

C.-R. Chiang, F.-C. Chang, J. Appl. Polym. Sci. **61**, 2411 (1996)

C.-R. Chiang, F.-C. Chang, Polymer **38**, 4807 (1997)

C.-R. Chiang, F.C. Chang, J. Polym. Sci. B Polym. Physics 36, 1805 (1998)

C.-R. Chiang, M.-Y. Ju, F.-C. Chang, Polym. Eng. Sci. **38**, 622 (1998)

H.-C. Chin, F.-C. Chang, Polymer **38**, 2947 (1997)

H.-C. Chin, K.-C. Chiou, F.-C. Chang, J. Appl. Polym. Sci. **60**, 2503 (1996)

V. Chiono, S. Filippi, H. Yordanov, L. Minkova, P. Magagnini, Polymer **44**, 2423 (2003)

K.-C. Chiou, F.-C. Chang, J. Polym. Sci. B Polym. Phys. **38**, 23 (2000)

Y.-P. Chiou, D.-Y. Chang, F.-C. Chang, Polymer **37**, 5653 (1996a)

Y.-P. Chiou, K.-C. Chiou, F.-C. Chang, Polymer **37**, 4099 (1996b)

K.-C. Chiou, S.-C. Wu, H.-D. Wu, F.-C. Chang, J. Appl. Polym. Sci. **74**, 23 (1999)

K. Cho, F. Li, Macromolecules **31**, 7495 (1998)

K. Cho, K.H. Seo, T.O. Ahn, Polymer Journal **29**, 987 (1997)

K. Cho, K.H. Seo, T.O. Ahn, J. Appl. Polym. Sci. **68**, 1925 (1998)

I. Chodak, I. Chorvath, Makromol. Chem. Macromol. Symp. **75**, 167 (1993)

I. Chodak, I. Janigova, A. Romanov, Makromol. Chem. **192**, 2791 (1991)

I. Chodak, H. Repin, W. Bruis, I. Janigova, Macromol. Symp. **112**, 159 (1996)

G.D. Choi, S.H. Kim, W.H. Jo, M.S. Rhim, J. Appl. Polym. Sci. **55**, 561 (1995)

S.H. Choi, I. Cho, K.U. Kim, Polymer Journal **31**, 828 (1999)

W.-M. Choi, C.-I. Park, O.O. Park, J.-G. Lim, J. Appl. Polym. Sci. **85**, 2084 (2002)

J.-H. Choi, H.-G. Kim, D.-H. Han, J.-C. Lim, D.-H. Oh, K.-E. Min, J. Appl. Polym. Sci. **101**, 1 (2006)

N.R. Choudhury, A.K. Bhowmick, J. Appl. Polym. Sci. **38**, 1091 (1989)

R. Chowdhury, M.S. Banerji, K. Shivakumar, J. Appl. Polym. Sci. **104**, 372 (2007)

S. Cimmino, L. D'Orazio, R. Greco, G. Maglio, M. Malinconico, C. Mancarella, E. Matuscelli, R. Palumbo, G. Ragosta, Polym. Eng. Sci. **24**, 48 (1984)

S. Cimmino, F. Coppola, L. D'Orazio, R. Greco, G. Maglio, M. Malinconico, C. Mancarella, E. Matuscelli, G. Ragosta, Polymer **27**, 1874 (1986)

A. Colbeaux, F. Fenouillot, J.-F. Gérard, M. Taha, H. Wautier, J. Appl. Polym. Sci. **93**, 2237 (2004)

A. Colbeaux, F. Fenouillot, J.-F. Gérard, M. Taha, H. Wautier, J. Appl. Polym. Sci. **95**, 312 (2005)

F.L. Colhoun, M.E. Stewart, S. Weinhold, R.D. Peters, R.L. Martin, US Patent Appl. 20110318519, 29 Dec 2011, to Grupo Petrotemex

S. Collins, S.K. Peace, R.W. Richards, W.A. MacDonald, P. Mills, S.M. King, Polymer **42**, 7695 (2001)

M.-B. Coltelli, E. Passaglia, F. Ciardelli, Polymer **47**, 85 (2006)

M.-B. Coltelli, S. Bianchi, M. Aglietto, Polymer **48**, 1276 (2007)

M.-B. Coltelli, M. Aglietto, F. Ciardelli, Eur. Polym. J. **44**, 1512 (2008)

M.-B. Coltelli, S. Bronco, C. Chinea, Polym. Degrad. Stab. **95**, 332 (2010)

M.L. Coote, D.H. Gordon, L.R. Hutchings, R.W. Richards, R.M. Dalgliesh, Polymer **44**, 7689 (2003)

A.Y. Coran, in *Thermoplastic Elastomers*, ed. by N.R. Legge, G. Holden, H.E. Schroeder (Hanser Publishers, New York, 1987), pp. 133–161, chapter 7

A.Y. Coran, Rubber Chem. Technol. **63**, 599 (1990)

A.Y. Coran, Rubber Chem. Technol. **68**, 351 (1995)

A.Y. Coran, R. Patel, Rubber Chem. Technol. **56**, 210 (1983a)

A.Y. Coran, R. Patel, Rubber Chem. Technol. **56**, 1045 (1983b)

A.Y. Coran, R. Patel, in *Polypropylene: Structure, Blends, and Composites*, ed. by J. Karger-Kocsis (Chapman and Hall Publishers, London, 1995), pp. 162–201, chapter 6

A.Y. Coran, R. Patel, in *Thermoplastic Elastomers*, ed. by G. Holden, N.R. Legge, R.P. Quirk, H.E. Schroeder, 2nd edn. (Hanser/Gardner Publishers, Cincinnati, 1996), pp. 153–190, chapter 7

A.Y. Coran, R. Patel, in *Thermoplastic Elastomers*, ed. by G. Holden, H.R. Kricheldorf, R.P. Quirk, 3rd edn. (Carl Hanser Verlag, Munich, 2004), pp. 143–182, chapter 7

A.Y. Coran, R. Patel, D. Williams-Headd, Rubber Chem. Technol. **58**, 1014 (1985)

D.A. Costa, C.M.F. Oliveira, J. Appl. Polym. Sci. **69**, 857 (1998)

D.A. Costa, C.M.F. Oliveira, J. International, Polym. Mater. **51**, 393 (2002)

G. Costa, D. Meli, Y. Song, A. Turturro, B. Valenti, M. Castellano, L. Falqui, Polymer **42**, 8035 (2001)

J.A. Covas, A.V. Machado, Int. Polym. Process. **20**, 121 (2005)

J.A. Covas, L.A. Pessan, A.V. Machado, N.M. Larocca, Polymer blend compatibilization by copolymers and functional polymers, chapter 7, in *Encyclopedia of Polymer Blends*, ed. by A.I. Isayev, S. Palsule, vol. 2 (Wiley, New York, 2011), p. 315

A. Crespy, B. Joncour, J.P. Prevost, J.P. Cavrot, C. Caze, Eur. Polym. J. **22**, 505 (1986)

A. Crespy, C. Caze, D. Coupe, P. Dupont, J.P. Cavrot, Polym. Eng. Sci. **32**, 273 (1992)

J.J. Crevecoeur, L. Nelissen, M.C.M. van der Sanden, P.J. Lemstra, H.J. Mencer, A.H. Hogt, Polymer **36**, 753 (1995)

J.-F. Croteau, G.V. Laivins, J. Appl. Polym. Sci. **39**, 2377 (1990)

J. Curry, P. Andersen, Adv. Polym. Technol. **11**, 3 (1991/1992)

D. Curto, A. Valenza, F.P. La Mantia, J. Appl. Polym. Sci. **39**, 865 (1990)

L. D'Orazio, C. Mancarella, E. Martuscelli, J. Mater. Sci. **23**, 161 (1988)

S.C.G. Da Costa, M.I. Felisberti, J. Appl. Polym. Sci. **72**, 1835 (1999)

S.C.G. Da Costa, M.D.C. Goncalves, M.I. Felisberti, J. Appl. Polym. Sci. **72**, 1827 (1999)

S.S. Dagli, K.M. Kamdar, Polym. Eng. Sci. **34**, 1709 (1994)

S.S. Dagli, M. Xanthos, J.A. Biesenberger, Polym. Eng. Sci. **34**, 1720 (1994)

S. Dalai, C. Wenxiu, J. Appl. Polym. Sci. **86**, 3420 (2002a)

S. Dalai, C. Wenxiu, J. Appl. Polym. Sci. **86**, 1296 (2002b)

S. Dalai, C. Wenxiu, J. Appl. Polym. Sci. **86**, 553 (2002c)

M. Daneshvar, M. Masoomi, J. Appl. Polym. Sci. **124**, 2048 (2012)

V.A. Dang, D. Dong, T.T.M. Phan, C.Q. Song, US Patent 6,887,940, 3 May 2005, to Basell Poliolefine Italia

S. Datta, D.J. Lohse, *Polymeric Compatibilizers* (Hanser/Gardner Publications, Cincinnati, 1996)

S. Datta, N. Dharmarajan, J.-M. Dekoninck, D.A. White, US Patent 5,225,483, 6 July 1993a, to Exxon

S. Datta, N. Dharmarajan, G. Ver Strate, L. Ban, Polym. Eng. Sci. **33**, 721 (1993b)

S. Datta, P.P. De, S.K. De, J. Appl. Polym. Sci. **61**, 1839 (1996)

A. De Loor, P. Cassagnau, A. Michel, B. Vergnes, J. Appl. Polym. Sci. **53**, 1675 (1994)

A. De Loor, P. Cassagnau, A. Michel, B. Vergnes, J. Appl. Polym. Sci. **63**, 1385 (1997)

S. De Petris, P. Laurienzo, M. Malinconico, M. Pracella, M. Zendron, J. Appl. Polym. Sci. **68**, 637 (1998)

B. De Roover, M. Sclavons, V. Carlier, J. Devaux, R. Legras, A. Momtaz, J. Polym. Sci. A Polym. Chem. **33**, 829 (1995)

B. De Roover, J. Devaux, R. Legras, J. Polym. Sci. A Polym. Chem. **35**, 901 (2000)

B.D. Dean, US Patent 4,568,724, 4 Feb 1986, to Atlantic Richfield

B.D. Dean, J. Appl. Polym. Sci. **47**, 2013 (1993)

D. Debier, J. Devaux, R. Legras, J. Polym. Sci. A Polym. Chem. **33**, 407 (1995)

D. Debier, J. Devaux, R. Legras, J. Polym. Sci. B Polym. Phys. **35**, 749 (1997a)

D. Debier, S. Vanclooster, J. Devaux, R. Legras, J. Polym. Sci. B Polym. Phys. **35**, 735 (1997b)

K. Dedecker, G. Groeninckx, Polymer **39**, 4985 (1998)

K. Dedecker, G. Groeninckx, J. Appl. Polym. Sci. **73**, 889 (1999)

M.E.J. Dekkers, Eur. Pat. Appl. 341,421, 15 Nov 1989, to General Electric

M.E.J. Dekkers, D.K. Yoshimura, M.P. Laughner, US Patent 5,171,778, 15 Dec 1992, to General Electric

J.-M. Dekoninck, US Patent 5,244,971, 14 Sept 1993, to Exxon

C. DeLeo, S. Velankar, J. Rheol. **52**, 1385 (2008)

C. DeLeo, K. Walsh, S. Velankar, J. Rheol. **55**, 713 (2011)

N.R. Demarquette, M.R. Kamal, J. Appl. Polym. Sci. **70**, 75 (1998)

J. Deng, S. Liang, C. Zhang, W. Yang, Macromol. Rapid Commun. **28**, 2163 (2007)

N. Dharmarajan, S. Datta, Polymer **33**, 3848 (1992)

N. Dharmarajan, S. Datta, G. Ver Strate, L. Ban, Polymer **36**, 3849 (1995)

M.F. Diaz, S.E. Barbosa, N.J. Capiati, Polymer **43**, 4851 (2002)

M.F. Diaz, S.E. Barbosa, N.J. Capiati, Polymer **46**, 6096 (2005)

M.F. Diaz, S.E. Barbosa, N.J. Capiati, Polymer **48**, 1058 (2007)

K. Dijkstra, J. ter Laak, R.J. Gaymans, Polymer **35**, 315 (1994)

Q. Ding, W. Dai, J. Appl. Polym. Sci. **107**, 3804 (2008)

Y. Ding, Z. Xin, Y. Gao, X. Xu, J. Yin, G. Costa, L. Falqui, B. Valenti, Macromol. Mat. Eng. **288**, 446 (2003)

I.H. Do, L.K. Yoon, B.K. Kim, H.M. Jeong, Eur. Polym. J. **32**, 1387 (1996)

S.K. Dogan, E.A. Reyes, S. Rastogi, G. Ozkoc, J. Appl. Polym. Sci. (2013). doi:10.1002/app.40251; published online

W. Dong, B. Zou, P. Ma, W. Liu, X. Zhou, D. Shi, Z. Ni, M. Chen, Polym. Int. **62**, 1783 (2013)

D.S.C. Dos Anjos, E.C.V. Revoredo, A. Galembeck, Polym. Eng. Sci. **50**, 606 (2010)

P. Doshev, D. Tomova, A. Wutzler, H.-J. Radusch, J. Polym. Eng. **25**, 375 (2011)

R. Dou, W. Wang, Y. Zhou, L.-P. Li, L. Gong, B. Yin, M.-B. Yang, J. Appl. Polym. Sci. **129**, 253 (2013)

M. Dröscher, H. Jadamus, US Patent 4,760,115, 26 July 1988, to Huls

J.F. Dunphy, US Patent 4,851,473, 25 July 1989, to DuPont

J. Duvall, C. Sellitti, C. Myers, A. Hiltner, E. Baer, J. Appl. Polym. Sci. **52**, 207 (1994a)

J. Duvall, C. Sellitti, C. Myers, A. Hiltner, E. Baer, J. Appl. Polym. Sci. **52**, 195 (1994b)

J. Duvall, C. Sellitti, V. Topolkaraev, A. Hiltner, E. Baer, C. Myers, Polymer **35**, 3948 (1994c)

J. Economy, L.A. Schneggenburger, D. Frich, in *Transreactions in Condensation Polymers*, ed. by S. Fakirov (Wiley-VCH, Weinheim, 1999), p. 195

K.L.L. Eersels, G. Groeninckx, Polymer **37**, 983 (1996)

K.L.L. Eersels, G. Groeninckx, J. Appl. Polym. Sci. **63**, 573 (1997)

K.L.L. Eersels, G. Groeninckx, M.H.J. Koch, H. Reynaers, Polymer **39**, 3893 (1998)

K.L.L. Eersels, A.M. Aerdts, G. Groeninckx, in *Transreactions in Condensation Polymers*, ed. by S. Fakirov (Wiley-VCH, Weinheim, 1999), p. 267

J.I. Eguiazábal, J. Nazábal, Makromol. Chem. Macromol. Symp. **20/21**, 255 (1988)

J.I. Eguiazábal, J. Nazábal, J. Mater. Sci. **25**, 1522 (1990)

J.I. Eguiazábal, M.J. Fernandez-Berridi, J.J. Iruin, I. Maiza, J. Appl. Polym. Sci. **59**, 329 (1996)

E.G. El'darov, F.V. Mamedov, V.M. Gol'dberg, G.E. Zaikov, Polym. Degrad. Stab. **51**, 271 (1996)

J.J. Elmendorf, A.K. Van der Vegt, Fundamentals of morphology formation in polymer blending, chapter 6, in *Two-Phase Polymer Systems*, ed. by L.A. Utracki (Hanser Publishers, New York, 1991), pp. 165–184

M. Enna, K. Fujihara, Y. Tsugane, Y. Aso, R. Seki, Eur. Pat. Appl. 2,631,270, 28 Aug 2013 to Mitsui Chemicals

B.N. Epstein, US Patent 4,174,358, 13 Nov 1979, to DuPont

I. Espinasse, P. Cassagnau, M. Bert, A. Michel, J. Appl. Polym. Sci. **54**, 2083 (1994)

E. Espinosa, M.J. Fernandez-Berridi, I. Maiza, M. Valero, Polymer **34**, 382 (1993)

M. Evstatiev, N. Nicolov, S. Fakirov, Polymer **37**, 4455 (1996)

A. Fainleib, O. Grigoryeva, O. Starostenko, I. Danilenko, L. Bardash, Macromol. Symp. **202**, 117 (2003)

S. Fakirov (ed.), *Transreactions in Condensation Polymers* (Wiley-VCH, Weinheim, 1999)

Z. Fang, C. Xu, S. Bao, Y. Zhao, Polymer **38**, 131 (1997)

H. Farah, F. Lerma Jr., Eur. Pat. Appl. 1,235,879, 25 Aug 2010, to Dow Global Technologies

M. Farmahini-Farahani, S.H. Jafari, H.A. Khonakdar, F. Böhme, H. Komber, A. Yavari, M. Tarameshlou, Polym. Int. **57**, 612 (2008)

B.D. Favis, Polymer **35**, 1552 (1994)

R. Fayt, P. Teyssie, J. Polym. Sci. C Polym. Lett. **27**, 481 (1989)

D. Feldman, J. Macromol. Sci. A Pure Appl. Chem. **42**, 587 (2005)

W. Feng, A.I. Isayev, Polym. Eng. Sci. **44**, 2019 (2004)

Y. Feng, Y. Hu, J. Yin, G. Zhao, W. Jiang, Polym. Eng. Sci. **53**, 389 (2013a)

Y. Feng, G. Zhao, J. Yin, W. Jiang, Polym. Int. (2013b). doi:10.1002/pi.4632; published online

M.J. Fernandez-Berridi, J.J. Iruin, I. Maiza, Polymer **36**, 1357 (1995)

S. Filippi, V. Chiono, G. Polacco, M. Paci, L.I. Minkova, P. Maganini, Macromol. Chem. Phys. **203**, 1512 (2002)

S. Filippi, H. Yordanov, L. Minkova, G. Polacco, M. Talarico, Macromol. Mat. Eng. **289**, 512 (2004)

S. Filippi, L. Minkova, N. Dintcheva, P. Narducci, P. Maganini, Polymer **46**, 8054 (2005)

J.K. Fink, *Reactive Polymers Fundamentals and Applications : A Concise Guide to Industrial Polymers*, 2nd edn. (Elsevier, Waltham, 2013)

M. Fiorini, C. Berti, V. Ignatov, M. Toselli, F. Pilati, J. Appl. Polym. Sci. **55**, 1157 (1995)

M. Fiorini, F. Pilati, C. Berti, M. Toselli, V. Ignatov, Polymer **38**, 413 (1997)

C.A. Fleischer, A.R. Morales, J.T. Koberstein, Macromolecules **27**, 379 (1994)

M.J. Folkes, P.S. Hope, *Polymer Blends and Alloys* (Blackie Academic, London, 1993)

M.W. Fowler, W.E. Baker, Polym. Eng. Sci. **28**, 1427 (1988)

D.W. Fox, R.B. Allen, Compatibility, in *Encyclopedia of Polymer Science and Engineering*, ed. by J.I. Kroschwitz, vol. 3, 2nd edn. (Wiley, New York, 1985), p. 772

C. Franke, P. Pötschke, G. Ratzsch, G. Pompe, K. Sahre, D. Voigt, A. Janke, Angew. Makromol. Chem. **206**, 21 (1993)

O. Franzheim, T. Rische, M. Stephan, W.J. MacKnight, Polym. Eng. Sci. **40**, 1143 (2000)

D.L. Freitag, L. Bottenbruch, M. Schmidt, US Patent 4,533,702, 6 Aug 1985, to Bayer

M. Freluche, I. Iliopoulos, J.J. Flat, A.V. Ruzette, L. Leibler, Polymer **46**, 6554 (2005)

A. Frick, D. Sich, G. Heinrich, D. Lehmann, U. Gohs, C. Stern, J. Appl. Polym. Sci. **128**, 1815 (2013)

H.G. Fritz, Q. Cai, U. Bölz, R. Anderlik, Macromol. Symp. **83**, 93 (1994)

Y. Fu, H. Song, C. Zhou, H. Zhang, S. Sun, Polym. Bull. **70**, 1853 (2013)

S. Fujii, S.-P. Ting, US Patent 4,728,461, 1 Mar 1988 to General Electric

S. Fujii, H. Ishida, M. Morioka, A. Saito, R. van der Meer, US Patent 4,873,276, 10 Oct 1989, to General Electric

Y. Fujita, M. Sakuma, K. Kitano, M. Sakaizawa, Y. Yagi, N. Yamamoto, T. Yokokura, Eur. Pat. Appl. 235,876, 9 Sept 1987, to Tonen Sekiyu

N. Furgiuele, A.H. Lebovitz, K. Khait, J.M. Torkelson, Macromolecules **33**, 225 (2000)

M. Furuta, I. Murase, T. Yamaguchi, US Patent 5,278,254, 11 Jan 1994, to Sumitomo

R. Gadekar, A. Kulkarni, J.P. Jog, J. Appl. Polym. Sci. **69**, 161 (1998)

R.R. Gallucci, R. van der Meer, R.W. Avakian, US Patent 4,873,286, 10 Oct 1989, to General Electric

L. Gani, S. Tence-Girault, M. Millequant, S. Bizet, L. Leibler, Macromol. Chem. Phys. **211**, 736 (2010)

Z. Gao, A. Molnar, A. Eisenberg, Blend compatibilization, in *Ionomers: Synthesis, Structure, Properties and Applications*, ed. by M.R. Tant, K.A. Mauritz, G.L. Wilkes (Blackie Academic and Professional, London, 1997), p. 390

M. García, J.I. Eguiazábal, J. Nazábal, J. Appl. Polym. Sci. **81**, 121 (2001)

E. Gattiglia, F.P. La Mantia, A. Turturro, A. Valenza, Polym. Bull. **21**, 47 (1989a)

E. Gattiglia, A. Turturro, E. Pedemonte, J. Appl. Polym. Sci. **38**, 1807 (1989b)

E. Gattiglia, A. Turturro, E. Pedemonte, G. Dondero, J. Appl. Polym. Sci. **41**, 1411 (1990)

E. Gattiglia, A. Turturro, F.P. La Mantia, A. Valenza, J. Appl. Polym. Sci. **46**, 1887 (1992)

N.G. Gaylord, J. Macromol. Sci. Chem. **A26**, 1211 (1989)

A. Ghaffar, C. Sadrmohaghegh, G. Scott, Polym. Degrad. Stab. **3**, 341 (1980–1981)

D. Ghidoni, E. Bencini, R. Nocci, J. Macromol. Sci. **31**, 95 (1996)

J.H. Glans, M.K. Akkapeddi, US Patent 5,037,897, 6 Aug 1991a, to Allied-Signal

J.H. Glans, M.K. Akkapeddi, Macromolecules, **24**, 383 (1991b)

J.C. Golba Jr., G.T. Seeger, Plast. Eng. **43**, 57 (1987)

A. Golovoy, M.F. Cheung, H. van Oene, Polym. Eng. Sci. **27**, 1642 (1987)

A. Golovoy, M.-F. Cheung, K.R. Carduner, M.J. Rokosz, Polym. Eng. Sci. **29**, 1226 (1989)

A.C.O. Gomes, B.G. Soares, M.G. Oliveira, L.A. Pessan, C.M. Paranhos, J. Appl. Polym. Sci. **127**, 2192 (2013)

A. Gonzalez-Montiel, H. Keskkula, D.R. Paul, Polymer **36**, 4621 (1995a)

A. Gonzalez-Montiel, H. Keskkula, D.R. Paul, Polymer **36**, 4605 (1995b)

A. Gonzalez-Montiel, H. Keskkula, D.R. Paul, Polymer **36**, 4587 (1995c)

A. Gonzalez-Montiel, H. Keskkula, D.R. Paul, J. Polym. Sci. B Polym. Phys. **33**, 1751 (1995d)

A. Gonzalez-Montiel, L.F. Santos, E.S. Guerra, US Patent Appl. 20130144009, 6 June 2013, to CID Centro de Investigacion y Desarrollo Tecnologico SA de CV

R. Gonzalez-Nunez, B.D. Favis, P.J. Carreau, Polym. Eng. Sci. **33**, 851 (1993)

T.G. Gopakumar, S. Ponrathnam, A. Lele, C.R. Rajan, A. Fradet, Polymer **40**, 357 (1999)

D. Graebling, M. Lambla, H. Wautier, J. Appl. Polym. Sci. **66**, 809 (1997)

W.M. Gramlich, M.L. Robertson, M.A. Hillmyer, Macromolecules **43**, 2313 (2010)

T.S. Grant, D.V. Howe, US Patent 4,740,552, 26 Apr 1988, to Borg-Warner

T.S. Grant, R.L. Jalbert, US Patent 4,826,933, 2 May 1989, to Borg-Warner Chemicals

T.S. Grant, R.L. Jalbert, D. Whalen, US Patent 4,732,938, 22 Mar 1988, to Borg-Warner

K.G. Gravalos, J.K. Kallitsis, N.K. Kalfoglou, Polymer **36**, 1393 (1995)

R. Greco, M. Malinconico, E. Matuscelli, G. Ragosta, G. Scarinzi, Polymer **28**, 1185 (1987)

I. Grof, M.M. Sain, O. Durcova, J. Appl. Polym. Sci. **44**, 1061 (1992)

G. Guerrica-Echevarría, J.I. Eguiazábal, J. Nazábal, Eur. Polym. J. **43**, 1027 (2007)

H. Gui, T. Zhou, L. Li, T. Zhou, F. Liu, Y. Zhan, A. Zhang, J. Appl. Polym. Sci. **130**, 3411 (2013)

Z. Guo, L. Tong, Z. Xu, Z. Fang, Polym. Eng. Sci. **47**, 951 (2007)

A. Habi, S. Djadoun, Eur. Polym. J. **35**, 483 (1999)

R. Hachemi, N. Belhaneche-Bensemra, V. Massardier, J. Appl. Polym. Sci. (2013). doi:10.1002/app.40045; published online

M. Hajian, C. Sadrmohaghegh, G. Scott, Eur. Polym. J. **20**, 135 (1984)

W.R. Hale, US Patent 7,368,503, 6 May 2008, to Eastman Chemical

W. Hale, J.-H. Lee, H. Keskkula, D.R. Paul, Polymer **40**, 3621 (1999a)

W. Hale, H. Keskkula, D.R. Paul, Polymer **40**, 365 (1999b)

W.J.L.A. Hamersma, R.W. Avakian, C.M.E. Bailly, US Patent 5,011,889, 30 Apr 1991, to General Electric

C.Y. Han, US Patent 4,792,586, 20 Dec 1988, to General Electric

C.Y. Han, PCT Intl. Appl. WO 91/018054, 28 Nov 1991a, to General Electric

C.Y. Han, PCT Intl. Appl. WO 91/018055, 28 Nov 1991b, to General Electric

C.Y. Han, US Patent 5,324,796, 28 June 1994, to General Electric

C.Y. Han, W.L. Gately, US Patent 4,689,372, 25 Aug 1987, to General Electric

C.Y. Han, S.B. Brown, E.W. Walles, T. Takekoshi, A.J. Caruso, US Patent 5,122,578, 16 June 1992, to General Electric

S.Y. Han, T.O. Ahn, H.M. Jeong, J. Polym. Eng. **21**, 421 (2011)

U.A. Handge, A. Galeski, S.C. Kim, D.J. Dijkstra, C. Gotz, F. Fischer, G.T. Lim, V. Alstadt, C. Gabriel, M. Weber, H. Steininger, J. Appl. Polym. Sci. **124**, 740 (2012)

S.J. Hanley, J.J. Rafalko, K.A. Steele, H.C. Linstid, T.J. Dolce, L.H. Sperling, J. Polym. Sci. A Polym. Chem. **37**, 3473 (1999)

M. Hara, J.A. Sauer, J. Macromol. Chem. Rev. Macromol. Chem. Phys. **C34**, 325 (1994)

M. Harada, T. Ohya, K. Iida, H. Hayashi, K. Hirano, H. Fukuda, J. Appl. Polym. Sci. **106**, 1813 (2007)

M. Harada, K. Iida, K. Okamoto, H. Hayashi, K. Hirano, Polym. Eng. Sci. **48**, 1359 (2008)

C. Harrats, G. Groeninckx, in *Modification and Blending of Synthetic and Natural Macromolecules, NATO Science Series*, ed. by F. Ciardelli, S. Penczek, vol. 175 (Kluwer, Dordrecht, 2004), p. 155

C. Harrats, T. Omonov, G. Groeninckx, P. Moldenaers, Polymer **45**, 8115 (2004)

S.E. Harton, F.A. Stevie, H. Ade, Macromolecules **38**, 3543 (2005)

N.G. Harvey, N.M. Bortnick, M.P. Hallden-Abberton, R.B. Queenan, T.D. Goldman, Eur. Pat. Appl. 0500361, 26 Aug 1992, to Rohm and Haas

F. Hassouna, J.-M. Raquez, F. Addiego, P. Dubois, V. Toniazzo, D. Ruch, Eur. Polym. J. **47**, 2134 (2011)

S.J. Hathaway, R.A. Pyles, US Patent 4,732,934, 22 Mar 1988, to General Electric

S.J. Hathaway, R.A. Pyles, US Patent 4,800,218, 24 Jan 1989, to General Electric

M. Hayashi, T. Hashimoto, H. Hasegawa, M. Takenaka, H. Grüll, A.R. Esker, M. Weber, S.K. Satija, C.C. Han, M. Nagao, Macromolecules **33**, 8375 (2000)

M. Heino, P. Hietaoja, J. Seppälä, T. Harmia, K. Friedrich, J. Appl. Polym. Sci. **66**, 2209 (1997a)

M. Heino, J. Kirjava, P. Hietaoja, J. Seppälä, J. Appl. Polym. Sci. **65**, 241 (1997b)

L.R. Hepp, Eur. Pat. Appl. 149,192, 24 July 1985, to General Electric

W.L. Hergenrother, M.G. Matlock, R.J. Ambrose, US Patent 4,427,828, 24 Jan 1984, to Firestone Tire & Rubber

W.L. Hergenrother, M.G. Matlock, R.J. Ambrose, US Patent 4,508,874, 2 Apr 1985, to Firestone Tire & Rubber

R. Hettema, J. Van Tol, L.P.B.M. Janssen, Polym. Eng. Sci. **39**, 1628 (1999)

P.T. Hietaoja, R.M. Holsti-Miettinen, J.V. Seppälä, O.T. Ikkala, J. Appl. Polym. Sci. **54**, 1613 (1994)

T. Hisamatsu, S. Nakano, T. Adachi, M. Ishikawa, K. Iwakura, Polymer **41**, 4803 (2000)

D. Hlavata, Z. Krulis, Z. Horak, F. Lednicky, J. Hromadkova, Macromol. Symp. **176**, 93 (2001)

J.-C. Ho, K.-H. Wei, Polymer **40**, 717 (1999)

S.Y. Hobbs, R.C. Bopp, V.H. Watkins, Polym. Eng. Sci. **23**, 380 (1983)

R.W. Hohlfeld, US Patent 4,590,241, 20 May 1986, to Dow

M. Hölderle, M. Bruch, H. Lüchow, W. Gronski, R. Mülhaupt, J. Polym. Sci. A Polym. Chem. **36**, 1821 (1998)

R.M. Holsti-Miettinen, J.V. Seppälä, O.T. Ikkala, Polym Eng. Sci. **32**, 868 (1992)

R.M. Holsti-Miettinen, J.V. Seppälä, O.T. Ikkala, I.T. Reima, Polym Eng. Sci. **34**, 395 (1994)

R.M. Holsti-Miettinen, M. Heino, J.V. Seppälä, J. Appl. Polym. Sci. **57**, 573 (1995)

S.M. Hong, S.S. Hwang, Y. Seo, I.J. Chung, K.U. Kim, Polym. Eng. Sci. **37**, 646 (1997)

S.M. Hong, H.O. Yoo, S.S. Hwang, K.J. Ihn, C.H. Lee, Polym. J. **33**, 457 (2001)

S.M. Hong, S.S. Hwang, J.S. Choi, H.J. Choi, J. Appl. Polym. Sci. **101**, 1188 (2006)

I. Hopfe, G. Pompe, K.-J. Eichhorn, Polymer **38**, 2321 (1997)

Z. Horak, Z. Krulis, J. Baldrian, I. Fortelný, D. Konecny, Polym. Netw. Blends **7**, 43 (1997)

Z. Horák, I. Fortelný, J. Kolařík, D. Hlavatá, A. Sikora, Polymer blends, in *Encyclopedia of Polymer Science and Engineering*, ed. by J.I. Kroschwitz, 4th edn. (Wiley, New York, 2002)

S. Horiuchi, Y. Ishii, Polym. J. **32**, 339 (2000)

S. Horiuchi, N. Matchariyakul, K. Yase, T. Kitano, H.K. Choi, Y.M. Lee, Polymer **37**, 3065 (1996)

S. Horiuchi, N. Matchariyakul, K. Yase, T. Kitano, Macromolecules **30**, 3664 (1997a)

S. Horiuchi, N. Matchariyakul, K. Yase, T. Kitano, H.K. Choi, Y.M. Lee, Polymer **38**, 6317 (1997b)

S. Horiuchi, N. Matchariyakul, K. Yase, T. Kitano, H.K. Choi, Y.M. Lee, Polymer **38**, 59 (1997c)

D.J. Hourston, S. Lane, H.X. Zhang, J.P.C. Bootsma, D.W. Koetsier, Polymer **32**, 1140 (1991)

Z. Hrnjak-Murgic, L. Kratofil, Z. Jelcic, J. Jelencic, Z. Janovic, Intl. Polym. Process. **2004/02**, 139 (2004)

G.-H. Hu, M. Lambla, J. Polym. Sci. A Polym. Chem. **33**, 97 (1995)

G.-H. Hu, Y.-J. Sun, M. Lambla, J. Appl. Polym. Sci. **61**, 1039 (1996)

G.-H. Hu, S. Triouleyre, M. Lambla, Polymer **38**, 545 (1997)

G. Hu, B. Wang, X. Zhou, Mater. Lett. **58**, 3457 (2004)

J.-M. Huang, J. Appl. Polym. Sci. **88**, 2247 (2003)

C.-C. Huang, F.-C. Chang, Polymer **38**, 4287 (1997a)

C.-C. Huang, F.-C. Chang, Polymer **38**, 2135 (1997b)

J.J. Huang, D.R. Paul, Polymer **47**, 3505 (2006)

Z.H. Huang, L.H. Wang, Makromol. Chem. Rapid Commun. **7**, 255 (1986)

Y. Huang, Y. Liu, C. Zhao, J. Appl. Polym. Sci. **69**, 1505 (1998)

J.-M. Huang, M.-F. You, F.-C. Chang, J. Appl. Polym. Sci. **82**, 3321 (2001)

J.-M. Huang, M.-Y. Ju, C.-J. Hung, W.-C. Luoh, F.-C. Chang, J. Appl. Polym. Sci. **87**, 967 (2003)

J.J. Huang, H. Keskkula, D.R. Paul, Polymer **45**, 4203 (2004)

J.J. Huang, H. Keskkula, D.R. Paul, Polymer **47**, 639 (2006a)

J.J. Huang, H. Keskkula, D.R. Paul, Polymer **47**, 624 (2006b)

J.-W. Huang, C.-C. Chang, C.-C. Kang, M.-Y. Yeh, Thermochim. Acta **468**, 66 (2008)

B. Huang, D. Li, Z. Li, X. Li, W. Zhou, J. Appl. Polym. Sci. **122**, 586 (2011)

C.-J. Hung, H.-J. Chuang, F.-C. Chang, J. Appl. Polym. Sci. **107**, 831 (2008)

C.-F.R. Hwang, J.J. Scobbo Jr., J.B. Yates, US Patent 5,583,179, 10 Dec 1996, to General Electric

C.-F.R. Hwang, J.J. Scobbo Jr., S.B. Brown, US Patent 5,723,542, 3 Mar 1998, to General Electric

S.W. Hwang, H.C. Ryu, S.W. Kim, H.Y. Park, K.H. Seo, J. Appl. Polym. Sci. **125**, 2732 (2012)

J. Ibuki, P. Charoensirisomboon, T. Chiba, T. Ougizawa, T. Inoue, M. Weber, E. Koch, Polymer **40**, 647 (1999)

F. Ide, A. Hasegawa, J. Appl. Polym. Sci. **18**, 963 (1974)

V. Ignatov, C. Carraro, V. Tartari, R. Pippa, F. Pilati, C. Berti, M. Toselli, M. Fiorini, Polymer **37**, 5883 (1996)

V. Ignatov, C. Carraro, V. Tartari, R. Pippa, M. Scapin, F. Pilati, C. Berti, M. Toselli, M. Fiorini, Polymer **38**, 201 (1997a)

V. Ignatov, C. Carraro, V. Tartari, R. Pippa, M. Scapin, F. Pilati, C. Berti, M. Toselli, M. Fiorini, Polymer **38**, 195 (1997b)

D.J. Ihm, J.L. White, J. Appl. Polym. Sci. **60**, 1 (1996)

O.T. Ikkala, R.M. Holsti-Miettinen, J. Seppälä, J. Appl. Polym. Sci. **49**, 1165 (1993)

I. Iliopoulos, L. Leibler, M. Freluche, J.-J. Flat, P. Gerard, Macromol. Symp. **245–246**, 371 (2006)

B. Immirzi, M. Malinconico, E. Martuscelli, M.G. Volpe, Macromol. Symp. **78**, 243 (1994)

B. Imre, B. Pukanszky, Eur. Polym. J. **49**, 1215 (2013)

B. Imre, D. Bedo, A. Domjan, P. Schon, J. Vancso, B. Pukanszky, Eur. Polym. J. **49**, 3104 (2013)

T. Inoue, J. Appl. Polym. Sci. **54**, 723 (1994a)

T. Inoue, J. Appl. Polym. Sci. **54**, 709 (1994b)

T. Inoue, T. Suzuki, J. Appl. Polym. Sci. **56**, 1113 (1995)

T. Inoue, T. Suzuki, J. Appl. Polym. Sci. **59**, 1443 (1996)

K. Inoue, A. Saito, M. Morioka, Eur. Pat. Appl. 368,413, 16 May 1990, to GE Plastics Japan

M. Ishikawa, M. Sugimoto, T. Inoue, J. Appl. Polym. Sci. **62**, 1495 (1996)

A. Ishio, K. Saitoh, S. Kobayashi, US Patent 8,076,423, 13 Dec 2011, to Toray Industries

B. Jacques, R. Legras, J. Devaux, E. Nield, Makromol. Chem. Macromol. Symp. **75**, 231 (1993)

B. Jacques, J. Devaux, R. Legras, E. Nield, Polymer **37**, 4085 (1996a)

B. Jacques, J. Devaux, R. Legras, E. Nield, Polymer **37**, 1189 (1996b)

B. Jacques, J. Devaux, R. Legras, E. Nield, J. Polym. Sci. A Polym. Chem. **34**, 1189 (1996c)

B. Jacques, J. Devaux, R. Legras, E. Nield, Polymer **38**, 5367 (1997)

S.H. Jafari, P. Pötschke, M. Stephan, H. Warth, H. Alberts, Polymer **43**, 6985 (2002a)

S.H. Jafari, P. Pötschke, M. Stephan, G. Pompe, H. Warth, H. Alberts, J. Appl. Polym. Sci. **84**, 2753 (2002b)

S.-H. Jafari, H.A. Khonakdar, A. Asadinezhad, L. Haussler, F. Bohme, H. Komber, Macromol. Chem. Phys. **210**, 1291 (2009)

R.L. Jalbert, T.S. Grant, US Patent 4,654,405, 31 Mar 1987, to Borg-Warner Chemicals

S.C. Jana, N. Patel, D. Dharaiya, Polymer **42**, 8681 (2001)

M. Jaziri, N. Barhoumi, V. Massardier, F. Melis, J. Appl. Polym. Sci. **107**, 3451 (2008)

H.K. Jeon, J.K. Kim, Macromolecules **31**, 9273 (1998a)

H.K. Jeon, J.K. Kim, Polymer **39**, 6227 (1998b)

H.K. Jeon, J.K. Kim, Macromolecules **33**, 8200 (2000)

H.K. Jeon, O.H. Taek, J.K. Kim, Polymer **42**, 3259 (2001)

H.K. Jeon, B.J. Feist, S.B. Koh, K. Chang, C.K. Macosko, R.P. Dion, Polymer **45**, 197 (2004a)

H.K. Jeon, C.W. Macosko, B. Moon, T.R. Hoye, Z. Yin, Macromolecules **37**, 2563 (2004b)

H.K. Jeon, J. Zhang, C.K. Macosko, Polymer **46**, 12422 (2005)

R. Jeziórska, Macromol. Symp. **170**, 21 (2001)

R. Jeziórska, Polym. Degrad. Stab. **90**, 224 (2005)

C. Jiang, S. Filippi, P. Magagnini, Polymer **44**, 2411 (2003)

G. Jiang, H. Wu, S. Guo, Polym. Eng. Sci. **50**, 2273 (2010)

J. Jiang, L. Su, K. Zhang, G. Wu, J. Appl. Polym. Sci. **128**, 3993 (2013)

X. Jian-Ping, C. Jian-Ding, C. Ming-Lian, J. Appl. Polym. Sci. **119**, 2961 (2011)

J. Jiao, E.J. Kramer, S. de Vos, M. Moller, C. Koning, Polymer **40**, 3585 (1999)

W.H. Jo, H.C. Kim, Polym. Bull. **27**, 465 (1992)

W.H. Jo, C.D. Park, M.S. Lee, Polymer **37**, 1709 (1996)

J. John, M. Bhattacharya, Polym. Int. **49**, 860 (2000)

T.D. Jones, J.S. Schulze, C.W. Macosko, T.P. Lodge, Macromolecules **36**, 7212 (2003)

S. Jose, P.S. Thomas, S. Thomas, J. Karger-Kocsis, Polymer **47**, 6328 (2006a)

S. Jose, B. Francis, S. Thomas, J. Karger-Kocsis, Polymer **47**, 3874 (2006b)

S. Jose, S.V. Nair, S. Thomas, J. Karger-Kocsis, J. Appl. Polym. Sci. **99**, 2640 (2006c)

M.-Y. Ju, F.-C. Chang, J. Appl. Polym. Sci. **73**, 2029 (1999)

M.-Y. Ju, M.-Y. Chen, F.-C. Chang, Macromol. Chem. Phys. **201**, 2298 (2000)

P.C. Juliano, General Electric Co., personal communication based on literature survey, 1988

J.-B. Jun, J.-G. Park, K.-D. Suh, J. Appl. Polym. Sci. **74**, 465 (1999)

W.-C. Jung, K.-Y. Park, J.-Y. Kim, K.-D. Suh, J. Appl. Polym. Sci. **88**, 2622 (2003)

P. Juntuek, C. Ruksakulpiwat, P. Chumsamrong, Y. Ruksakulpiwat, J. Appl. Polym. Sci. **125**, 745 (2012)

S. Kadoi, H. Yabe, K. Kobayashi, US Patent 5,488,084, 30 Jan 1996, to Toray Industries

N.K. Kalfoglou, D.S. Skafidas, D.D. Sotiropoulou, Polymer **35**, 3624 (1994)

N.K. Kalfoglou, D.S. Skafidas, J.K. Kallitsis, J.-C. Lambert, L. Van der Stappen, Polymer **36**, 4453 (1995)

N.K. Kalfoglou, D.S. Skafidas, J.K. Kallitsis, Polymer **37**, 3387 (1996)

W. Kamoun, S. Salhi, B. Rousseau, R. El Gharbi, A. Fradet, Macromol. Chem. Phys. **207**, 2042 (2006)

T.-K. Kang, Y. Kim, G. Kim, W.-J. Cho, C.-S. Ha, Polym Eng. Sci. **37**, 603 (1997)

A. Kanomata, K. Yamauchi, S. Horiuchi, H. Sakata, S. Honda, I. Asano, US Patent Appl. 20110311816, 22 Dec 2011, to Toray Industries

B. Karaağaç, V. Deniz, in *Advances in Elastomers I*, ed. by P.M. Visakh, S. Thomas, A.K. Chandra, A.P. Mathew (Springer, Berlin/Heidelberg, 2013), p. 263

J. Karger-Kocsis, Thermoplastic rubbers via dynamic vulcanization, chapter 5, in *Polymer Blends and Alloys*, ed. by G.O. Shonaike, G.P. Simon (Marcel Dekker, New York, 1999), pp. 125–154

A. Karim, J.F. Douglas, S.K. Satja, C.C. Han, R.J. Goyette, Macromolecules **32**, 1119 (1999)

H. Kasahara, K. Fukuda, H. Suzuki, US Patent 4,339,376, 13 July 1982, to Asahi-Dow

H. Kasahara, K. Tazaki, K. Fukuda, H. Suzuki, US Patent 4,421,892, 20 Dec 1983, to Asahi-Dow

A. Kausar, S. Zulfiqar, M.I. Sarwar, J. Appl. Polym Sci. (2013). doi:10.1002/app.39954; published online

H. Kauth, K. Reinking, D. Freitag, US Patent 4,782,123, 1 Nov 1988, to Bayer

J. Kawada, M. Mouri, O. Watanabe, A. Usuki, M. Kito, A. Amari, O. Kito, PCT Intl. Appl. WO 2013/191307, 27 Dec 2013, to Toyota

A. Kaya, G. Pompe, U. Schulze, B. Voit, J. Pionteck, J. Appl. Polym Sci. **86**, 2174 (2002)

Y. Kayano, H. Keskkula, D.R. Paul, Polymer **38**, 1885 (1997)

I. Kelnar, M. Stephan, L. Jakisch, I. Fortelný, J. Appl. Polym. Sci. **66**, 555 (1997)

I. Kelnar, M. Stephan, L. Jakisch, I. Fortelný, J. Appl. Polym. Sci. **74**, 1404 (1999)

Y.P. Khanna, US Patent 4,861,838, 29 Aug 1989, to Allied-Signal

Y.P. Khanna, E.A. Turi, S.M. Aharoni, T. Largman, US Patent 4,417,032, 22 Nov 1983, to Allied Corporation

D.H. Kho, S.H. Chae, U. Jeong, H.Y. Kim, J.K. Kim, Macromolecules **38**, 3820 (2005)

H.A. Khonakdar, S.H. Jafari, S. Mirzadeh, M.R. Kalaee, D. Zare, M.R. Saehb, J. Vinyl & Additive Tech. **19**, 25 (2013)

F.F. Khouri, US Patent 5,231,132, 27 July 1993, to General Electric

F.F. Khouri, US Patent 5,567,780, 22 Oct 1996, to General Electric

F.F. Khouri, J.R. Campbell, US Patent 5,691,411, 25 Nov 1997, to General Electric

F.F. Khouri, R.J. Halley, J.B. Yates III, US Patent 5,247,006, 21 Sept 1993, to General Electric

F.F. Khouri, O. Phanstiel, US Patent 5,162,448, 10 Nov 1992, to General Electric

F.F. Khouri, G.J. Stoddard, US Patent 5,391,616, 21 Feb 1995a, to General Electric

F.F. Khouri, G.J. Stoddard, US Patent 5,393,833, 28 Feb 1995b, to General Electric

F.F. Khouri, S.B. Brown, J.T. Jackman, US Patent 5,115,042, 19 May 1992, to General Electric

F.F. Khouri, R.J. Halley, J.B. Yates III, US Patent 5,281,667, 25 Jan 1994, to General Electric

B.K. Kim, C.H. Choi, J. Appl. Polym. Sci. **60**, 2199 (1996a)

B.K. Kim, C.H. Choi, Polymer **37**, 807 (1996b)

B.K. Kim, I.H. Do, J. Appl. Polym. Sci. **61**, 439 (1996)

J.W. Kim, S.C. Kim, Polym. Adv. Technol. **2**, 177 (1991)

J.K. Kim, H. Lee, Polymer **37**, 305 (1996)

B.K. Kim, S.J. Park, J. Appl. Polym. Sci. **43**, 357 (1991)

B.K. Kim, S.Y. Park, S.J. Park, Eur. Polym. J. **27**, 349 (1991)

B.K. Kim, Y.M. Lee, H.M. Jeong, Polymer **34**, 2075 (1993)

K.-H. Kim, W.-J. Cho, C.-S. Ha, J. Appl. Polym. Sci. **59**, 407 (1996)

J.K. Kim, S. Kim, C.E. Park, Polymer **38**, 2155 (1997a)

S. Kim, J.K. Kim, C.E. Park, Polymer **38**, 2113 (1997b)

S. Kim, J.K. Kim, C.E. Park, Polymer **38**, 1809 (1997c)

D.H. Kim, W.H. Jo, S.C. Lee, H.C. Kim, J. Appl. Polym Sci. **69**, 807 (1998)

Y.H. Kim, M. Kikuchi, S. Akiyama, K. Sho, S. Izawa, Polymer **40**, 5273 (1999a)

S.H. Kim, S.M. Hong, S.S. Hwang, H.O. Yoo, J. Appl. Polym. Sci. **74**, 2448 (1999b)

J.K. Kim, D.K. Yi, H.K. Jeon, C.E. Park, Polymer **40**, 2737 (1999c)

D.H. Kim, K.Y. Park, K.-D. Suh, J.-Y. Kim, J. Macromol. Sci. A Pure Appl. Chem. **37**, 1141 (2000a)

D.H. Kim, K.Y. Park, J.-Y. Kim, K.-D. Suh, J. Appl. Polym. Sci. **78**, 1017 (2000b)

S.J. Kim, B.-S. Shin, J.-L. Hong, W.-J. Cho, C.-S. Ha, Polymer **42**, 4073 (2001a)

J.H. Kim, W.S. Lyoo, W.S. Ha, J. Appl. Polym. Sci. **82**, 159 (2001b)

J.-S. Kim, M. Luqman, J.-M. Song, Ionomers, in *Encyclopedia of Polymer Science and Engineering*, ed. by J.I. Kroschwitz, 4th edn. (Wiley, New York, 2002)

S.J. Kim, C.-J. Kang, S.R. Chowdhury, W.-J. Cho, C.-S. Ha, J. Appl. Polym. Sci. **89**, 1305 (2003)

H.Y. Kim, H.J. Kim, J.K. Kim, Polymer Journal **38**, 1165 (2006)

D.P.R. Kint, A.M. de Ilarduya, A. Sansalvado, J. Ferrer, S. Munoz-Guerra, J. Appl. Polym. Sci. **90**, 3076 (2003)

J. Kirjava, T. Rundqvist, R. Holsti-Miettinen, M. Heino, T. Vainio, J. Appl. Polym. Sci. **55**, 1069 (1995)

Y. Kobayashi, T. Itoh, T. Inoue, Eur. Pat. Appl. 282,052, 14 Sept 1988, to Mitsubishi Petrochemical

S. Kobayashi, J. Song, H.C. Silvis, C.W. Macosko, M.A. Hillmyer, Ind. Eng. Chem. Res. **50**, 3274 (2011)

M. Kodama, Polym. Eng. Sci. **32**, 267 (1992)

M.I. Kohan, W.H. Martin, C.K. Rosenbaum, US Patent 3,676,400, 11 July 1972, to DuPont

S. Kole, S. Roy, A.K. Bhowmick, Polymer **36**, 3273 (1995)

C. Komalan, K.E. George, S. Jacob, S. Thomas, Polym. Adv. Technol. **19**, 351 (2008)

Y. Kong, J.N. Hay, Polymer **43**, 1805 (2002)

C. Koning, R. Fayt, W. Bruls, L. Vondervoort, T. Rauch, P. Teyssie, Makromol. Chem. Macromol. Symp. **75**, 159 (1993a)

C. Koning, A. Ikker, R. Borggreve, L. Leemans, M. Möller, Polymer **34**, 4410 (1993b)

C. Koning, W. Bruis, F. Op Den Buijsch, L. Vondervoort, Macromol. Symp. **112**, 167 (1996)

C. Koning, M. van Duin, C. Pagnoulle, R. Jérôme, Prog. Polym. Sci. **23**, 707 (1998)

E.V. Konyukhova, S.I. Belousov, Y.V. Kuz'mina, N.P. Bessonova, Y.K. Godovsky, Polym. Sci., Ser. A **36**(9), 1209 (1994).

H. Koriyama, H.T. Oyama, T. Ougizawa, T. Inoue, M. Weber, E. Koch, Polymer **40**, 6381 (1999)

A.M. Kotliar, J. Polym. Sci. Macromol. Rev. **16**, 367 (1981)

C. Koulic, Z. Yin, C. Pagnoulle, B. Gilbert, R. Jérôme, Polymer **42**, 2947 (2001)

C. Koulic, G. Francois, R. Jérôme, Macromolecules **37**, 5317 (2004)

E.G. Koulouri, K.G. Gravalos, J.K. Kallitsis, Polymer **37**, 2555 (1996)

E.G. Koulouri, K.G. Gravalos, J.K. Kallitsis, Polymer **38**, 4185 (1997)

E.G. Koulouri, J.K. Kallitsis, G. Hadziioannou, Macromolecules **32**, 6242 (1999a)

E.G. Koulouri, E.C. Scourlis, J.K. Kallitsis, Polymer **40**, 4887 (1999b)

H.O. Krabbenhoft, US Patent 4,579,905, 1 Apr 1986, to General Electric

L.J. Kratofil, A. Pticek, Z. Hrnjak-Murgic, J. Jelencic, M. Mlinac-Misak, J. Elastomers & Plastics **39**, 371 (2007)

R.K. Krishnaswamy, J. Van Walsem, O.P. Peoples, Y. Shabtai, A.R. Padwa, PCT Intl. Appl. WO 2013/184822, 12 Dec 2013, to Metabolix

K. Kubo, J. Masamoto, J. Appl. Polym. Sci. **86**, 3030 (2002)

R.A. Kudva, H. Keskkula, D.R. Paul, Polymer **39**, 2447 (1998)

N. Kunimune, K. Yamada, Y.W. Leong, S. Thumsorn, H. Hamada, J. Appl. Polym. Sci. **120**, 50 (2011)

J.A. Kuphal, L.H. Sperling, L.M. Robeson, J. Appl. Polym. Sci. **42**, 1525 (1991)

P. Kurian, K.E. George, D.J. Francis, Eur. Polym. J. **28**, 113 (1992)

T. Kurian, S. Datta, D. Khastgir, P.P. De, D.K. Tripathy, S.K. De, D.G. Peiffer, Polymer **37**, 4787 (1996)

F.P. La Mantia, Adv. Polym. Technol. **12**, 47 (1993)

F.P. La Mantia, A. Valenza, Angew. Makromol. Chem. **216**, 45 (1994)

F.P. La Mantia, M. Vinci, F. Pilati, Polymer Recycling **1**, 33 (1994)

F.P. La Mantia, L. Canfora, N.T. Dintcheva, Polym. Eng. Sci. **45**, 1297 (2005)

C. Lacroix, M. Bousmina, P.J. Carreau, B.D. Favis, A. Michel, Polymer **37**, 2939 (1996a)

C. Lacroix, M. Bousmina, P.J. Carreau, M.F. Llauro, R. Petiaud, A. Michel, Polymer **37**, 2949 (1996b)

G.V. Laivins, Macromolecules **22**, 3974 (1989)

M. Lambla, M. Seadan, Polym. Eng. Sci. **32**, 1687 (1992)

M. Lambla, M. Seadan, Macromol. Symp. **69**, 99 (1993)

X. Lan, X. Li, Z. Liu, Z. He, W. Yang, M. Yang, J. Macromol. Sci. A Pure Appl. Chem. **50**, 2013 (2013)

M.R. Landry, D.J. Massa, C.J.T. Landry, D.M. Teegarden, R.H. Colby, T.E. Long, P.M. Henrichs, J. Appl. Polym. Sci. **54**, 991 (1994)

N.M. Larocca, E. Hage Jr., L.A. Pessan, J. Polym. Sci. B Polym. Phys. **43**, 1244 (2005)

N.M. Larocca, E.N. Ito, C.T. Rios, L.A. Pessan, R.E.S. Bretas, E. Hage Jr., J. Polym. Sci. B Polym. Phys. **48**, 2274 (2010)

A. Lazzeri, M. Malanima, M. Pracella, J. Appl. Poly. Sci. **74**, 3455 (1999)

A.H. Lebovitz, K. Khait, J.M. Torkelson, Macromolecules **35**, 9716 (2002)

S.Y. Lee, C. Kim, J. Appl. Poly. Sci. **68**, 1245 (1998)

S. Lee, O.O. Park, J. Appl. Poly. Sci. **77**, 1338 (2000)

S. Lee, O.O. Park, Polymer **42**, 6661 (2001)

P.-C. Lee, W.-F. Kuo, F.-C. Chang, Polymer **35**, 5641 (1994)

C.W. Lee, S.H. Ryu, H.S. Kim, J. Appl. Polym. Sci. **64**, 1595 (1997)

C.-H. Lee, S.K. Lee, S.-W. Kang, S.-H. Yun, J. Ho Kim, S. Choe, J. Appl. Polym. Sci. **73**, 841 (1999a)

C.H. Lee, Y.M. Lee, H.K. Choi, S. Horiuchi, T. Kitano, Polymer **40**, 6321 (1999b)

J.-S. Lee, K.-Y. Park, D.-J. Yoo, K.-D. Suh, J. Polym. Sci. B Polym. Phys. **38**, 1396 (2000)

S. Lee, J.S. Park, H. Lee, J. Appl. Poly. Sci. **82**, 1725 (2001)

A. Legros, P.J. Carreau, B.D. Favis, A. Michel, Polymer **35**, 758 (1994)

A. Legros, P.J. Carreau, B.D. Favis, A. Michel, Polymer **38**, 5085 (1997)

D. Lehmann, US Patent Appl. 20110040017, 17 Feb 2011, to Leibniz-Institut fuer Polymerforschung

D. Lehmann, B. Kluepfel, US Patent Appl. 20100249333, 30 Sept 2010, to Leibniz-Institut fuer Polymerforschung

Y. Lei, Q. Wu, C.M. Clemons, W. Guo, J. Appl. Polym. Sci. **113**, 1710 (2009)

H. Li, Z. Li, Poly. Int. **48**, 124 (1999)

S.-C. Li, L.-N. Lu, J. Appl. Polym. Sci. **108**, 3559 (2008)

Y. Li, H. Shimizu, Eur. Polym. J. **45**, 738 (2009)

D. Li, A.F. Yee, K.W. Powers, H.-C. Wang, T.C. Yu, Polymer **34**, 4471 (1993)

H. Li, T. Chiba, N. Higashida, Y. Yang, T. Inoue, Polymer **38**, 3921 (1997)

Q.F. Li, D.G. Kim, D. Wu, K. Lu, R.G. Jin, Polym. Eng. Sci. **41**, 2155 (2001)

H.-M. Li, Z.-G. Shen, F.-M. Zhu, S.-A. Lin, Eur. Polym. J. **38**, 1255 (2002)

J. Li, G. Ma, J. Sheng, J. Macromol. Sci. B Phys. **48**, 979 (2009a)

J. Li, G. Ma, J. Sheng, J. Macromol. Sci. B Phys. **48**, 471 (2009b)

R. Li, X. Zhang, L. Zhou, J. Dong, D. Wang, J. Appl. Polym. Sci. **111**, 826 (2009c)

S.-C. Li, L.-N. Lu, W. Zeng, J. Appl. Polym. Sci. **112**, 3341 (2009d)

D. Li, B. Shentu, Z. Weng, J. Macromol. Sci. B Phys. **50**, 2050 (2011a)

J. Li, G. Ma, J. Sheng, J. Macromol. Sci. B Phys. **50**, 741 (2011b)

Y. Li, D. Wang, J.-M. Zhang, X.-M. Xie, Polym. Bull. **66**, 841 (2011c)

L.-P. Li, B. Yin, Y. Zhou, L. Gong, M.-B. Yang, B.-H. Xie, C. Chen, Polymer **53**, 3043 (2012a)

F. Li, J. Ashbaugh, D. Rauscher, R. Dotter, PCT Intl. Appl. WO 2012112266, 23 Aug 2012b, to Fina Technology

F. Li, J. Ashbaugh, D. Rauscher, R. Dotter, PCT Intl. Appl. WO 2012112263, 23 Aug 2012c, to Fina Technology

F. Li, T.J. Coffy, M. Daumerie, US Patent Appl. 20120080822, 5 Apr 2012d, to Fina Technology

B. Liang, L. Pan, J. Appl. Polym. Sci. **54**, 1945 (1994)

Z. Liang, H.L. Williams, J. Appl. Polym. Sci. **44**, 699 (1992)

S. Lim, J.L. White, Polym Eng. Sci. **34**, 221 (1994)

H. Lin, A.I. Isayev, J. Appl. Polym. Sci. **102**, 2643 (2006)

O. Lin, A.F. Yee, J. Mater. Sci. **32**, 3961 (1997)

J.S. Lin, E.Y. Sheu, Y.H.R. Jois, J. Appl. Polym. Sci. **55**, 655 (1995)

A.D. Litmanovich, N.A. Platé, Y.V. Kudryavtsev, Prog. Polym. Sci. **27**, 915 (2002)

N.C. Liu, W.E. Baker, Adv. Polym. Technol. **11**, 249 (1992a)

N.C. Liu, W.E. Baker, Polym. Eng. Sci. **32**, 1695 (1992b)

N.C. Liu, W.E. Baker, Polymer **35**, 988 (1994)

Y. Liu, J.A. Donovan, Polymer **36**, 4797 (1995)

H. Liu, J. Zhang, J. Polym. Sci. B Polym. Phys. **49**, 1051 (2011)

N.C. Liu, W.E. Baker, K.E. Russell, J. Appl. Polym. Sci. **41**, 2285 (1990)

N.C. Liu, H.Q. Xie, W.E. Baker, Polymer **34**, 4680 (1993)

W.-B. Liu, W.-F. Kuo, C.-J. Chiang, F.-C. Chang, Eur. Polym. J. **32**, 91 (1996)

H. Liu, T. Xie, Y. Zhang, Y. Ou, X. Fang, G. Yang, Polym. J. **36**, 754 (2004)

H. Liu, T. Xie, Y. Zhang, Y. Ou, G. Yang, Polym. J. **38**, 21 (2006)

Y. Liu, W. Guo, Z. Su, B. Li, C. Wu, J. Macromol. Sci. B Phys. **48**, 414 (2009a)

Y. Liu, Q. Shi, Z. Ke, L. Yin, J. Yin, Polym. Bull. **63**, 411 (2009b)

Y. Liu, Z. Su, W. Guo, B. Li, C. Wu, J. Macromol. Sci. B Phys. **49**, 615 (2010a)

H. Liu, F. Chen, B. Liu, G. Estep, J. Zhang, Macromolecules **43**, 6058 (2010b)

S. Liu, S. Qin, Z. Luo, J. Yu, J. Guo, M. He, J. Macromol. Sci. B Phys. **50**, 1780 (2011a)

H. Liu, W. Song, F. Chen, L. Guo, J. Zhang, Macromolecules **44**, 1513 (2011b)

H. Liu, L. Guo, X. Guo, J. Zhang, Polymer **53**, 272 (2012a)

Z. Liu, Y. Deng, Y. Han, M. Chen, S. Sun, C. Cao, C. Zhou, H. Zhang, Ind. Eng. Chem. Res. **51**, 9235 (2012b)

N.C. Liu, S. Lin, C. Zhou, W. Yu, Polymer **54**, 310 (2013a)

H. Liu, X. Guo, W. Song, J. Zhang, Ind. Eng. Chem. Res. **52**, 4787 (2013b)

B.P. Livengood, B.W. Baird, G.P. Marshall, US Patent 6,350,552, 26 Feb 2002, to Lexmark

D.-W. Lo, C.-R. Chiang, F.-C. Chang, J. Appl. Polym. Sci. **65**, 739 (1997)

D.J. Lohse, T.P. Russell, L.H. Sperling (eds.), *Interfacial Aspects of Multicomponent Polymer Materials* (Plenum Press, New York, 1997)

N. Lopattananon, A. Kraibut, R. Sangjan, M. Seadan, J. Appl. Polym. Sci. **105**, 1444 (2007)

S. Lopez-Quintana, C. Rosales, I. Gobernado-Mitre, J.C. Merino, J.M. Pastor, J. Appl. Polym. Sci. **107**, 3099 (2008)

W. Loyens, G. Groeninckx, Polymer **43**, 5679 (2002)

W. Loyens, G. Groeninckx, Polymer **44**, 4929 (2003a)

W. Loyens, G. Groeninckx, Polymer **44**, 123 (2003b)

Q.-W. Lu, C.W. Macosko, Polymer **45**, 1981 (2004)

M. Lu, H. Keskkula, D.R. Paul, Polymer **34**, 1874 (1993)

M. Lu, H. Keskkula, D.R. Paul, Polym. Eng. Sci. **34**, 33 (1994)

M. Lu, H. Keskkula, D.R. Paul, J. Appl. Polym. Sci. **58**, 1175 (1995)

M. Lu, H. Keskkula, D.R. Paul, J. Appl. Polym. Sci. **59**, 1467 (1996)

Q.-W. Lu, T.R. Hoye, C.W. Macosko, J. Polym. Sci. A Polym. Chem. **40**, 2310 (2002)

Q.-W. Lu, C.W. Macosko, J. Horrion, Macromol. Symp. **198**, 221 (2003)

X. Lu, H. Zhang, Y. Zhang, J. Appl. Polym. Sci. (2013a). doi:10.1002/app.40064; published online

X. Lu, H. Zhang, Y. Zhang, J. Appl. Polym. Sci. **130**, 4587 (2013b)

S. Lumlong, K. Kuboyama, T. Chiba, T. Ougizawa, Macromol. Symp. **233**, 17 (2006)

R.D. Lundberg, Ionic polymers, in *Encyclopedia of Polymer Science and Engineering*, ed. by J.I. Kroschwitz, vol. 8, 2nd edn. (Wiley, New York, 1987), p. 393

R.D. Lundberg, I. Duvdevani, D.G. Peiffer, P.K. Agarwal, in *Advances in Polymer Blends and Alloys Technology*, ed. by M.A. Kohudic, vol. 1 (Technomic Publishing, Lancaster, 1988), p. 131

R. Luo, X. Zhao, P.C. Yung, US Patent Appl. 20130069001, 21 Mar 2013, to Ticona

J.M. Lusinchi, B. Boutevin, N. Torres, J.J. Robin, J. Appl. Polym. Sci. **79**, 874 (2000)

S.-P. Lyu, J.J. Cernohous, F.S. Bates, C.W. Macosko, Macromolecules **32**, 106 (1999)

P. Ma, D.G. Hristova-Bogaerds, P.J. Lemstra, Y. Zhang, S. Wang, Macromol. Mat. and Eng. **297**, 402 (2012a)

H. Ma, Z. Xiong, F. Lu, C. Li, Y. Yang, Macromol. Mat. and Eng. **297**, 136 (2012b)

C.-T. Maa, F.-C. Chang, J. Appl. Polym. Sci. **49**, 913 (1993)

A.V. Machado, J.A. Covas, M. van Duin, J. Polym. Sci. A Polym. Chem. **37**, 1311 (1999)

A.V. Machado, J.A. Covas, M. van Duin, Polym. Eng. Sci. **42**, 2032 (2002)

W.J. MacKnight, R.W. Lenz, P.V. Musto, R.J. Somani, Polym. Eng. Sci. **25**, 1124 (1985)

C.W. Macosko, H.K. Jeon, T.R. Hoye, Progress in Polymer Science **30**, 939 (2005)

D. Mader, J. Kressler, R. Mülhaupt, J. Appl. Polym. Sci. **73**, 1685 (1999)

R. Magaraphan, R. Skularriya, S. Kohjiya, J. Appl. Polym. Sci. **105**, 1914 (2007)

B. Majumdar, H. Keskkula, D.R. Paul, Polymer **35**, 5468 (1994a)

B. Majumdar, H. Keskkula, D.R. Paul, Polymer **35**, 5453 (1994b)

B. Majumdar, H. Keskkula, D.R. Paul, Polymer **35**, 3164 (1994c)

B. Majumdar, H. Keskkula, D.R. Paul, Polymer **35**, 1399 (1994d)

B. Majumdar, H. Keskkula, D.R. Paul, Polymer **35**, 1386 (1994e)

B. Majumdar, H. Keskkula, D.R. Paul, J. Appl. Polym. Sci. **54**, 339 (1994f)

B. Majumdar, H. Keskkula, D.R. Paul, N.G. Harvey, Polymer **35**, 4263 (1994g)

B. Majumdar, D.R. Paul, A.J. Oshinski, Polymer **38**, 1787 (1997)

A. Mallick, D.K. Tripathy, S.K. De, J. Appl. Polym. Sci. **50**, 1627 (1993)

A. Mallick, A.K. Bhattacharya, B.R. Gupta, D.K. Tripathy, S.K. De, J. Appl. Polym. Sci. **65**, 135 (1997)

D. Mangaraj, Rubber Chem. Technol. **78**, 536 (2005)

N.R. Manoj, P.P. De, S.K. De, J. Appl. Polym. Sci. **49**, 133 (1993a)

N.R. Manoj, P.P. De, S.K. De, Rubber Chem. Technol. **66**, 550 (1993b)

N.R. Manoj, P.P. De, S.K. De, D.G. Peiffer, J. Appl. Polym. Sci. **53**, 361 (1994)

C. Marco, G. Ellis, M.A. Gomez, J.G. Fatou, J.M. Arribas, I. Campoy, A. Fontecha, J. Appl. Polym. Sci. **65**, 2665 (1997)

P. Marechal, G. Coppens, R. Legras, J.-M. Dekoninck, J. Polym. Sci. A Polym. Chem. **33**, 757 (1995)

P. Marechal, T. Chiba, T. Inoue, M. Weber, E. Koch, Polymer **39**, 5655 (1998)

M. Maric, N. Ashurov, C.W. Macosko, Polym. Eng. Sci. **41**, 631 (2001)

M.M. Martens, R. Koshida, J.L. Bohan, W.R. Fielding, US Patent 6,774,174, 10 Aug 2004, to DuPont

P. Martin, J. Devaux, R. Legras, M. van Grup, M. van Duin, Polymer **42**, 2463 (2001)

P. Martin, C. Gallez, J. Devaux, R. Legras, L. Leemans, M. van Grup, M. van Duin, Polymer **44**, 5251 (2003)

P. Martin, C. Maquet, R. Legras, C. Bailly, L. Leemans, M. van Grup, M. van Duin, Polymer **45**, 5111 (2004a)

P. Martin, C. Maquet, R. Legras, C. Bailly, L. Leemans, M. van Grup, M. van Duin, Polymer **45**, 3277 (2004b)

P. Martin, J. Devaux, R. Legras, L. Leemans, M. van Grup, M. van Duin, J. Appl. Polym. Sci. **91**, 703 (2004c)

J.M. Martinez, J.I. Eguiazábal, J. Nazábal, J. Appl. Polym. Sci. **45**, 1135 (1992)

J.M. Martinez, J. Nazábal, J.I. Eguiazábal, J. Appl. Polym. Sci. **51**, 223 (1994)

J.G. Martinez, R. Benavides, C. Guerrero, J. Appl. Polym. Sci. **104**, 560 (2007)

R.E. Martini, S. Barbosa, E. Brignole, Ind. Eng. Chem. Res. **45**, 3393 (2006)

E. Martuscelli, F. Riva, C. Sellitti, C. Silvestre, Polymer **26**, 270 (1985)

L. Mascia, F. Bellahdeb, Adv. Polym. Technol. **13**, 99 (1994a)

L. Mascia, F. Bellahdeb, Adv. Polym. Technol. **13**, 37 (1994b)

L. Mascia, K. Hashim, J. Appl. Polym. Sci. **66**, 1911 (1997)

L. Mascia, K. Hashim, Polymer **39**, 369 (1998)

L. Mascia, A. Ophir, J. Appl. Polym. Sci. **81**, 2972 (2001)

K. Mashita, T. Fujii, T. Omae, US Patent 4,780,505, 25 Oct 1988 to Sumitomo

K. Mashita, T. Fujii, T. Oomae, US Patent 5,004,782, 2 Apr 1991 to Sumitomo

M. Mawatari, T. Itoh, S. Tsuchikawa, S. Kimura, US Patent 4,839,425, 13 June 1989, to Japan Synthetic Rubber

J. Mayumi, H. Omori, Eur. Pat. Appl. 268,981, 1 June 1988 to Mitsubishi Petrochemical

R.M. Medina, D. Likhatchev, A. Alexandrova, A. Sanchez-Solis, O. Manero, Polymer **45**, 8517 (2004)

N. Mekhilef, A.A. Kadi, A. Ajji, Polym. Eng. Sci. **32**, 894 (1992)

T.J.A. Melo, S.V. Canevarolo, Polym. Eng. Sci. **45**, 11 (2005)

L.C. Mendes, P.S.C. Pereira, V.D. Ramos, Macromol. Symp. **299–300**, 183 (2011)

G. Menges, Macromol. Chem. Macromol. Symp. **23**, 13 (1989)

G.D. Merfeld, A. Karim, B. Majumdar, S.K. Satija, D.R. Paul, J. Polym. Sci. B Polym. Phys. **36**, 3115 (1998)

R.B. Mesrobian, P.E. Sellers, D. Adomaitis, US Patent 3,373,224, 12 Mar 1968, to Continental Can

D.M. Miley, J. Runt, Polymer **33**, 4643 (1992)

L.I. Minkova, T. Miteva, D. Sek, B. Kaczmarczyk, P.L. Magagnini, M. Paci, F.P. La Mantia, R. Scaffaro, J. Appl. Polym. Sci. **62**, 1613 (1996)

L. Minkova, H. Yordanov, S. Filippi, Polymer **43**, 6195 (2002)

L. Minkova, H. Yordanov, S. Filippi, N. Grizzuti, Polymer **44**, 7925 (2003)

A. Misra, G. Sawhney, R.A. Kumar, J. Appl. Polym. Sci. **50**, 1179 (1993)

Y. Mizuno, T. Maruyama, S. Yachigo, US Patent 5,019,615, 28 May 1991, to Sumitomo

M.J. Modic, L.A. Pottick, Polym. Eng. Sci. **33**, 819 (1993)

A.J. Moffett, M.E.J. Dekkers, Polym. Eng. Sci. **32**, 1 (1992)

S. Mohanty, G.B. Nando, Polymer **38**, 1395 (1997)

S. Mohanty, S. Roy, R.N. Santra, G.B. Nando, J. Appl. Polym. Sci. **58**, 1947 (1995)

S. Mohanty, G.B. Nando, K. Vijayan, N.R. Neelakanthan, Polymer **37**, 5387 (1996)

S. Mohanty, K. Vijayan, N.R. Neelkantan, G.B. Nando, Polym. Eng. Sci. **37**, 1395 (1997)

A. Molnar, A. Eisenberg, Polym. Commun **32**, 370 (1991)

A. Molnar, A. Eisenberg, Polym. Eng. Sci. **32**, 1665 (1992)

M.V. Moncur, US Patent 4,350,794, 21 Sept 1982, to Monsanto

I. Mondragon, J. Nazábal, Polym. Eng. Sci. **25**, 178 (1985)

I. Mondragon, J. Nazábal, J. Appl. Polym. Sci. **32**, 6191 (1986)

I. Mondragon, J. Nazábal, J. Mater. Sci. Lett. **6**, 698 (1987)

I. Mondragon, M. Gaztelumendi, J. Nazábal, Polym. Eng. Sci. **26**, 1478 (1986)

I. Mondragon, P.M. Remiro, J. Nazabal, Eur. Polym. J. **23**, 125 (1987)

I. Mondragon, M. Gaztelumendi, J. Nazábal, Polym. Eng. Sci. **28**, 1126 (1988)

G. Montaudo, C. Puglisi, F. Samperi, J. Polym. Sci. A Polym. Chem. **31**, 13 (1993)

G. Montaudo, C. Puglisi, F. Samperi, J. Polym. Sci. A Polym. Chem. **32**, 15 (1994)

G. Montaudo, C. Puglisi, F. Samperi, Macromolecules **31**, 650 (1998a)

G. Montaudo, C. Puglisi, F. Samperi, J. Polym. Sci. A Polym. Chem. **36**, 1873 (1998b)

G. Montaudo, C. Puglisi, F. Samperi, in *Transreactions in Condensation Polymers*, ed. by S. Fakirov (Wiley-VCH, Weinheim, 1999), p. 159

B. Moon, T.R. Hoye, C.W. Macosko, Macromolecules **34**, 7941 (2001)

S. Moritomi, M. Iji, US Patent 6,339,131, 2 July 2002, to Sumitomo

Y. Moriya, N. Suzuki, Y. Okada, US Patent 4,753,990, 28 June 1988 to Nippon Oil and Fats

Y. Moriya, N. Suzuki, H. Goto, US Patent 4,839,423, 13 June 1989 to Nippon Oil and Fats

N. Moussaif, C. Pagnoulle, R. Jérôme, Polymer **41**, 5551 (2000)

M. Mukawa, Y. Hayata, A. Nodera, H. Yasuda, K. Watanabe, US Patent 7,994,239, 9 Aug 2011, to Idemitsu Kosan

O.K. Muratoglu, A.S. Argon, R.E. Cohen, M. Weinberg, Polymer **36**, 4771 (1995a)

O.K. Muratoglu, A.S. Argon, R.E. Cohen, M. Weinberg, Polymer **36**, 921 (1995b)

L.E. Murch, US Patent 3,845,163, 29 Oct 1974, to DuPont

N.S. Murthy, H. Minor, M.K. Akkapeddi, B. Van Buskirk, J. Appl. Polym. Sci. **41**, 2265 (1990)

V.M. Nadkarni, J.P. Jog, Crystallization of polymers in thermoplastic blends and alloys, in *Handbook of Polymer Science and Technology*, ed. by N.P. Cheremisinoff, vol. 4 (Marcel Dekker, New York, 1989), pp. 81–120

V.M. Nadkarni, J.P. Jog, Crystallization behavior in polymer blends, chapter 8, in *Two-Phase Polymer Systems*, ed. by L.A. Utracki (Hanser Publishers, New York, 1991), pp. 213–239

K. Nakamura, K. Kometani, A. Koshino, K. Horiuchi, PCT Intl. Appl. WO 88/00953, 11 Feb 1988, to Toray Industries

C. Nakason, M. Jarnthong, A. Kaesaman, S. Kiatkamjornwong, J. Appl. Polym. Sci. **109**, 2694 (2008)

O. Nakazima, S. Izawa, US Patent 4,863,996, 5 Sept 1989, to Asahi

J.-D. Nam, J. Kim, S. Lee, Y. Lee, C. Park, J. Appl. Polym. Sci. **87**, 661 (2003)

M. Narathichat, C. Kummerlöwe, N. Vennemann, C. Nakason, J. Appl. Polym. Sci. **121**, 805 (2011)

N. Naskar, T. Biswas, D.K. Basu, J. Appl. Polym. Sci. **52**, 1007 (1994)

A. Natansohn, R. Murali, A. Eisenberg, CHEMTECH **20**, 418 (1990)

D. Nazareth, Eur. Pat. Appl. 697,442, 21 Feb 1996, to General Electric

W. Neilinger, D. Wittman, U. Westeppe, L. Bottenbruch, J. Kirsch, H.-J. Fullmann, Eur. Pat. Appl. 291,796, 11 Nov 1988, to Bayer

W. Neugebauer, M. Bartmann, U. Kowalczik, J. Mugge, US Patent 5,039,746, 13 Aug 1991, to Huels

N. Nugay, T. Nugay, Eur. Polym. J. **36**, 1027 (2000)

D. Nwabunma, T. Kyu (eds.), *Polyolefin Blends* (Wiley-Interscience, Hoboken, 2008)

J. Oderkerk, G. Groeninckx, Polymer **43**, 2219 (2002)

T.S. Oh, J.H. Ryou, Y.S. Chun, W.N. Kim, Polym. Eng. Sci. **37**, 838 (1997)

J.S. Oh, A.I. Isayev, M.A. Rogunova, Polymer **44**, 2337 (2003)

B. Ohlsson, H. Hassander, B. Tornell, Polymer **39**, 6705 (1998a)

B. Ohlsson, H. Hassander, B. Tornell, Polymer **39**, 4715 (1998b)

Y. Ohmura, S. Maruyama, H. Kawasaki, US Patent 4,339,555, 13 July 1982, to Mitsubishi Chemical Industries

V. Ojijo, S.S. Ray, R. Sadiku, ACS Appl. Mater. Interfaces **5**, 4266 (2013)

M. Okabe, A. Amagai, H. Eto, Y. Tanaka, UK Patent GB 2,218,996, 29 Nov 1989, to Mitsubishi Gas Chemical

O. Okada, H. Keskkula, D.R. Paul, Polymer **40**, 2699 (1999)

M. Okamoto, T. Inoue, Polym. Eng. Sci. **33**, 175 (1993)

M. Okamoto, T. Inoue, Polymer **35**, 257 (1994)

M. Okamoto, T. Kotaka, Polymer **38**, 1357 (1997)

T. Okamoto, K. Yasue, T. Marutani, Y. Fukushima, US Patent 4,804,707, 14 Feb 1989, to Unitika

M. Okamoto, K. Shiomi, T. Inoue, Polymer **35**, 4618 (1994)

M.G. Oliveira, A.C. Gomes, C.O. Ana, M.S.M. Almeida, B.G. Soares, Macromol. Chem. Phys. **205**, 465 (2004)

E.J. Olivier, US Patent 4,594,386, 10 June 1986a, to Copolymer Rubber & Chemical

E.J. Olivier, PCT Intl. Appl. WO 86/04076, 17 July 1986b, to Copolymer Rubber & Chemical

T.S. Omonov, C. Harrats, G. Groeninckx, Polymer **46**, 12322 (2005)

T.S. Omonov, C. Harrats, G. Groeninckx, P. Moldenaers, Polymer **48**, 5289 (2007)

Z. Oommen, S.R. Zachariah, S. Thomas, G. Groeninckx, P. Moldenaers, J. Mewis, J. Appl. Polym. Sci. **92**, 252 (2004)

C.A. Orr, J.J. Cernohous, P. Guegan, A. Hirao, H.K. Jeon, C.W. Macosko, Polymer **42**, 8171 (2001)

A. Oshima, H. Ishida, T. Shinohara, US Patent 5,780,548, 14 July 1998, to General Electric

A.J. Oshinski, H. Keskkula, D.R. Paul, Polymer **33**, 284 (1992a)

A.J. Oshinski, H. Keskkula, D.R. Paul, Polymer **33**, 268 (1992b)

A.J. Oshinski, H. Keskkula, D.R. Paul, Polymer **37**, 4919 (1996a)

A.J. Oshinski, H. Keskkula, D.R. Paul, Polymer **37**, 4909 (1996b)

A.J. Oshinski, H. Keskkula, D.R. Paul, Polymer **37**, 4891 (1996c)

A.J. Oshinski, H. Keskkula, D.R. Paul, J. Appl. Polym. Sci. **61**, 623 (1996d)

Y. Otawa, A. Uchiyama, K. Hiraoka, K. Okamoto, S. Shimizu, Eur. Pat. Appl. 269,274, 1 June 1988, to Mitsui Petrochemical Industries

C.-F. Ou, J. Appl. Polym. **68**, 1591 (1998)

C.-F. Ou, C.-C. Lin, J. Appl. Polym. **61**, 1455 (1996a)

C.-F. Ou, C.-C. Lin, J. Appl. Polym. **61**, 1379 (1996b)

C.-F. Ou, M.S. Chao, S.L. Huang, J. Appl. Polym. **74**, 2727 (1999)

K.J. Oxby, M. Maric, Macromol. Reaction Eng. (2013). doi: 10.1002/mren.201200081; published online

H.T. Oyama, Polymer **50**, 747 (2009)

H.T. Oyama, M. Matsushita, M. Furuta, Polym. J. **43**, 991 (2011)

A.R. Padwa, Polym. Eng. Sci. **32**, 1703 (1992)

C. Pagnoulle, R. Jérôme, Macromolecules **34**, 965 (2001a)

C. Pagnoulle, R. Jérôme, Polymer **42**, 1893 (2001b)

C. Pagnoulle, C. Koning, L. Leemans, R. Jérôme, Macromolecules **33**, 6275 (2000a)

C. Pagnoulle, P. Martin, R. Jérôme, Macromol. Chem. Phys. **201**, 2181 (2000b)

F.-C. Pai, H.-H. Chu, S.-M. Lai, J. Polym. Eng. **31**, 463 (2011)

L. Pan, T. Chiba, T. Inoue, Polymer **42**, 8825 (2001)

L. Pan, T. Inoue, H. Hayami, S. Nishikawa, Polymer **43**, 337 (2002)

M.-M. Pan, B. Yin, W. Yang, Y. Zhao, M.-B. Yang, J. Macromol. Sci. B Phys. **46**, 1267 (2007)

C.P. Papadopoulou, N.K. Kalfoglou, Polymer **41**, 2543 (2000)

D.S. Park, S.H. Kim, J. Appl. Polym. Sci. **87**, 1842 (2003)

S.J. Park, B.K. Kim, H.M. Jeong, Eur. Polym. J. **26**, 131 (1990)

I. Park, J.W. Barlow, D.R. Paul, J. Polym. Sci. B Polym. Phys. **30**, 1021 (1992)

C.D. Park, W.H. Jo, M.S. Lee, Polymer **37**, 3055 (1996)

K.Y. Park, S.H. Park, K.-D. Suh, J. Appl. Polym. Sci. **66**, 2183 (1997)

S.H. Park, G.J. Lee, S.S. Im, K.D. Suh, Polym. Eng. Sci. **38**, 1420 (1998)

K.Y. Park, S.-S. Lee, J.-Y. Kim, K.-D. Suh, J. Macromol. Sci. A Pure Appl. Chem. **39**, 787 (2002)

R. Patel, D.A. Ruehle, J.R. Dorgan, P. Halley, D. Martin, Polym. Eng. Sci. (2013). doi:10.1002/pen.23692; published online

D.R. Paul, Interfacial agents for polymer blends, in *Polymer Blends*, ed. by D.R. Paul, S. Newman, vol. 2 (Academic, New York, 1978), pp. 35–62

D.R. Paul, in *Modification and Blending of Synthetic and Natural Macromolecules, NATO Science Series*, ed. by F. Ciardelli, S. Penczek, vol. 175 (Kluwer, Dordrecht, 2004), p. 293

D.R. Paul, C.B. Bucknall (eds.), *Polymer Blends: Formulation and Performance*, vols. 1 & 2 (Wiley, New York, 2000)

D.R. Paul, S. Newman (eds.), *Polymer Blends*, vols. 1 & 2 (Academic, New York, 1978)

D.R. Paul, J.W. Barlow, H. Keskkula, Polymer blends, in *Encyclopedia of Polymer Science and Engineering*, ed. by J.I. Kroschwitz, vol. 12 (Wiley, New York, 1988), p. 417

F. Pazzagli, M. Pracella, Macromol. Symp. **149**, 225 (2000)

D.G. Peiffer, I. Duvdevani, P.K. Agarwal, R.D. Lundberg, J. Polym. Sci. C Polym. Lett. **24**, 581 (1986)

M. Penco, M.A. Pastorini, E. Occhiello, F. Garbassi, R. Braglia, G. Giannotta, J. Appl. Polym. Sci. **57**, 329 (1995)

M. Penco, A. Lazzeri, T.V. Phuong, P. Cinelli, PCT Intl. Appl. WO 2012025907, 1 Mar 2012, to Universita' di Pisa

Y. Peng, W. Guo, P. Zhu, C. Wu, J. Appl. Polym. Sci. **109**, 483 (2008)

R. Pernice, C. Berto, A. Moro, R. Pippa, US Patent 5,210,125, 11 May 1993, to ECP Enichem Polimeri

H. Pernot, M. Baumert, F. Court, L. Leibler, Nat. Mater. **1**, 54 (2002)

P. Perret, A. Bouilloux, M. Hert, I. Leclere, Macromol. Symp. **112**, 183 (1996)

P.J. Perron, E.A. Bourbonais, PCT Intl. Appl. WO 88/06174, 14 Sept 1988 to Dexter

I. Pesneau, M.F. Llauro, M. Gregoire, A. Michel, J. Appl. Polym. Sci. **65**, 2457 (1997)

I. Pesneau, M. Gregoire, A. Michel, J. Appl. Polym. Sci. **79**, 1556 (2001)

S.V. Phadke, US Patent 4,757,112, 12 July 1988a, to Copolymer Rubber & Chemical

S.V. Phadke, Eur. Pat. Appl. 279,502, 24 Aug 1988b, to Copolymer Rubber & Chemical

T.T.M. Phan, A.J. DeNicola Jr., L.S. Schadler, J. Appl. Polym. Sci. **68**, 1451 (1998)

O. Phanstiel, S.B. Brown, US Patent 5,010,144, 23 Apr 1991, to General Electric

O. Phanstiel, S.B. Brown, US Patent 5,089,567, 18 Feb 1992, to General Electric

O. Phanstiel, S.B. Brown, US Patent 5,210,191, 11 May 1993, to General Electric

Y. Pietrasanta, J.-J. Robin, N. Torres, B. Boutevin, Macromol. Chem. Phys. **200**, 142 (1999)

J. Piglowski, M. Trelinska-Wlaźlak, B. Paszak, J. Macromol. Sci. B Phys. **38**, 515 (1999)

J. Piglowski, I. Gancarz, M. Wlaźlak, Polymer **41**, 3671 (2000)

F. Pilati, E. Marianucci, C. Berti, J. Appl. Polym. Sci. **30**, 1267 (1985)

F. Pilati, M. Fiorini, C. Berti, in *Transreactions in Condensation Polymers*, ed. by S. Fakirov (Wiley-VCH, Weinheim, 1999), p. 79

L.Z. Pillon, L.A. Utracki, Polym. Eng. Sci. **24**, 1300 (1984)

L.Z. Pillon, J. Lara, D.W. Pillon, Polym. Eng. Sci. **27**, 984 (1987a)

L.Z. Pillon, L.A. Utracki, D.W. Pillon, Polym. Eng. Sci. **27**, 562 (1987b)

L.A. Pinheiro, G.-H. Hu, L.A. Pessan, S.V. Canevarolo, Polym. Eng. Sci. **48**, 806 (2008)

J. Pionteck, P. Poetschke, U. Schulze, N. Proske, A. Kaya, H. Zhao, H. Malz, Macromol. Symp. **214**, 279 (2004)

N.A. Platé, A.D. Litmanovich, Y.V. Kudryavtsev, in *Modification and Blending of Synthetic and Natural Macromolecules, NATO Science Series*, ed. by F. Ciardelli, S. Penczek, vol. 175 (Kluwer, Dordrecht, 2004), p. 241

G. Pompe, L. Häubler, J. Polym. Sci. B Polym. Phys. **35**, 2161 (1997)

G. Pompe, L. Häubler, W. Winter, J. Polym. Sci. B Polym. Phys. **34**, 211 (1996)

G. Pompe, P. Pötschke, J. Pionteck, J. Appl. Polym. Sci. **86**, 3445 (2002)

R.S. Porter, L.-H. Wang, Polymer **33**, 2019 (1992)

R.S. Porter, J.M. Jonza, M. Kimura, C.R. Desper, E.R. George, Polym. Eng. Sci. **29**, 55 (1989)

C.S. Powell, D.S. Kalika, Polymer **41**, 4651 (2000)

M. Pracella, D. Chionna, Macromol. Symp. **198**, 161 (2003)

M. Pracella, D. Chionna, Macromol. Symp. **218**, 173 (2004)

M. Pracella, L. Rolla, D. Chionna, A. Galeski, Macromol. Chem. Phys. **203**, 1473 (2002)

C.F. Pratt, PCT Intl. Appl. WO 88/07065, 22 Sept 1988, to General Electric

C.F. Pratt, S.V. Phadke, E.J. Olivier, PCT Intl. Appl. WO 88/05452, 28 July 1988, to General Electric

E.V. Prut, Polym. Sci. Ser. D **2**, 1 (2009)

E.V. Prut, A.N. Zelenetskii, Russ. Chem. Rev. **70**, 65 (2001)

M. Psarski, M. Pracella, A. Galeski, Polymer **41**, 4923 (2000)

R. Qi, J. Nie, C. Zhou, D. Mao, B. Zhang, J. Appl. Polym. Sci. **102**, 6081 (2006)

C. Qu, R. Su, Q. Zhang, R. Du, Q. Fu, Polym. Int. **57**, 139 (2008)

W. Qui, K. Mai, K. Fang, Z. Li, H. Zeng, J. Appl. Polym. Sci. **71**, 847 (1999)

R. Quintana, O. Persenaire, L. Bonnaud, P. Dubois, Y. Lemmouchi, PCT Intl. Appl. WO 2012131370, 4 Oct 2012, to British American Tobacco

N.M. Qureshi, US Patent Appl. 20090163663, 25 June 2009, to Escalator Handrail Co.

H.-J. Radusch, J. Ding, M. Schulz, Angew. Makromol. Chem. **204**, 177 (1993)

P. Ramesh, S.K. De, J. Appl. Polym. Sci. **50**, 1369 (1993)

H. Raval, S. Devi, Y.P. Singh, M.H. Mehta, Polymer **32**, 493 (1991)

H.B. Ravikumar, C. Ranganathaiah, G.N. Kumaraswamy, M.V. Deepa Urs, J.H. Jagannath, A.S. Bawa, S. Thomas, J. Appl. Polym. Sci. **100**, 740 (2006)

R.W. Rees, Reversible crosslinking, in *Encyclopedia of Polymer Science and Engineering*, ed. by J.I. Kroschwitz, vol. 4, 2nd edn. (Wiley, New York, 1986), p. 395

P.M. Remiro, J. Nazábal, J. Appl. Polym. Sci. **42**, 1639 (1991a)

P.M. Remiro, J. Nazábal, J. Appl. Polym. Sci. **42**, 1475 (1991b)

J. Ren, H. Wang, L. Jian, J. Zhang, S. Yang, J. Macromol. Sci. B Phys. **47**, 712 (2008)

P.N. Richardson, US Patent 4,283,502, 11 Aug 1981, to DuPont

D.H. Roberts, R.C. Constable, S. Thiruvengada, Polym. Eng. Sci. **37**, 1421 (1997)

L.M. Robeson, J. Appl. Polym. Sci. **30**, 4081 (1985)

L.M. Robeson, *Polymer Blends : A Comprehensive Review* (Hanser/Gardner Publications, Cincinnati, 2007)

L.M. Robeson, A. Famili, J.F. Nangeroni, in *Science and Technology of Polymers and Advanced Materials*, ed. by P.N. Prasad, J.E. Mark, S.H. Kandil, Z.H. Kafafi (Springer, New York, 1998), p. 9

J.L. Rodriguez, J.I. Eguiazábal, J. Nazábal, Polym. J. **28**, 501 (1996)

H. Rodríguez-Ríos, S.M. Nuño-Donlucas, J.E. Puig, R. González-Núñez, P.C. Schulz, J. Appl. Polym. Sci. **91**, 1736 (2004)

S. Rooj, V. Thakur, U. Gohs, U. Wagenknecht, A.K. Bhowmick, G. Heinrich, Polym. Adv. Technol. **22**, 2257 (2011)

J. Rösch, Polym. Eng. Sci. **35**, 1917 (1995)

J. Rösch, R. Mülhaupt, Makromol. Chem. Rapid Commun. **14**, 503 (1993)

J. Rösch, R. Mülhaupt, Polym. Bull. **32**, 697 (1994)

J. Rösch, R. Mülhaupt, J. Appl. Polym. Sci. **56**, 1599 (1995a)

J. Rösch, R. Mülhaupt, J. Appl. Polym. Sci. **56**, 1607 (1995b)

J. Rösch, R. Mülhaupt, G.H. Michler, Macromol. Symp. **112**, 141 (1996)

M.J. Roura, US Patent 4,346,194, 24 Aug 1982, to DuPont

M.J. Roura, US Patent 4,478,978, 23 Oct 1984, to DuPont

A. Roychoudhury, P.P. De, J. Appl. Polym. Sci. **63**, 1761 (1997)

A. Rudin, J. Macromol. Chem. Rev. Macromol. Chem. **C19**, 267 (1980)

A. Rudin, *The Elements of Polymer Science and Engineering* (Academic, New York, 1982)

R.K. Sadi, R.S. Kurusu, G.J.M. Fechine, N.R. Demarquette, J. Appl. Polym. Sci. **123**, 3511 (2012)

S. Safapour, M. Seyed-Esfahani, F. Auriemma, O.R. de Ballesteros, P. Vollaro, R. Di Girolamo, C. De Rosa, A. Khosroshahi, Polymer **51**, 4340 (2010)

C. Sailer, U.A. Handge, Macromol. Symp. **254**, 217 (2007a)

C. Sailer, U.A. Handge, Macromolecules **40**, 2019 (2007b)

C. Sailer, U.A. Handge, Macromolecules **41**, 4258 (2008)

M. Saleem, W.E. Baker, J. Appl. Polym. Sci. **39**, 655 (1990)

P. Sambaru, S.A. Jabarin, Polym. Eng. Sci. **33**, 827 (1993)

C.K. Samios, K.G. Gravalos, N.K. Kalfoglou, Eur. Polym. J. **36**, 937 (2000)

F. Samperi, M. Montaudo, C. Puglisi, R. Alicata, G. Montaudo, Macromolecules **36**, 7143 (2003a)

F. Samperi, C. Puglisi, R. Alicata, G. Montaudo, J. Polym. Sci. A Polym. Chem. **41**, 2778 (2003b)

F. Samperi, M.S. Montaudo, C. Puglisi, S. Di Giorgi, G. Montaudo, Macromolecules **37**, 6449 (2004)

F. Samperi, M.S. Montaudo, S. Battiato, D. Carbone, C. Puglisi, J. Polym. Sci. A Polym. Chem. **48**, 5135 (2010)

A. Sanchez, C. Rosales, E. Laredo, A.J. Muller, M. Pracella, Macromol. Chem. Phys. **202**, 2461 (2001)

M.S. Sanchez, V. Mathot, G. Groeninckx, W. Bruls, Polymer **47**, 5314 (2006)

A. Sanchez-Solis, F. Calderas, O. Manero, Polymer **42**, 7335 (2001)

H. Sano, H. Ohno, Eur. Pat. Appl. 268,280, 25 May 1988, to Mitsubishi Petrochemical

R.N. Santra, S. Roy, A.K. Bhowmick, G.B. Nando, Polym. Eng. Sci. **33**, 1352 (1993a)

R.N. Santra, B.K. Samantaray, A.K. Bhowmick, G.B. Nando, J. Appl. Polym. Sci. **49**, 1145 (1993b)

R.N. Santra, S. Roy, V.K. Tikku, G.B. Nando, Adv. Polym. Technol. **14**, 59 (1995)

S.N. Sathe, S. Devi, G.S.S. Rao, K.V. Rao, J. Appl. Polym. Sci. **61**, 97 (1996)

F.H. Sawden, Eur. Pat. Appl. 274,424, 13 July 1988, to DuPont Canada

R. Scaffaro, F.P. La Mantia, Macromol. Chem. Phys. **207**, 265 (2006)

R. Scaffaro, F.P. La Mantia, L. Canfora, G. Polacco, S. Filippi, P. Maganini, Polymer **44**, 6951 (2003)

R. Scaffaro, F.P. La Mantia, C. Castronovo, Macromol. Chem. Phys. **205**, 1402 (2004)

R. Schaefer, J. Kressler, R. Neuber, R. Muelhaupt, Macromolecules **28**, 5037 (1995)

S. Schlag, J. Rösch, Chr. Friedrich, Polym. Bull. **30**, 603 (1993)

J.C. Schmidhauser, K.L. Longley, Tetrahedron Lett. **32**, 7155 (1991)

S. Schmukler, M. Shida, J. Machonis Jr., US Patent 4,600,746, 15 July 1986a to Norchem

S. Schmukler, M. Shida, J. Machonis Jr., US Patent 4,575,532, 11 Mar 1986b to Norchem

N.R. Schott, B. Sanderford, Coat. Plast. Prepr. Am. Chem. Soc. Div. Org. Coat. Plast. Chem. **37**(2), 73 (1977)

J.E. Schuetz, R.W. Hohlfeld, B.C. Meridith, US Patent 4,864,002, 5 Sept 1989, to Dow

J.S. Schulze, J.J. Cernohous, A. Hirao, T.P. Lodge, C.W. Macosko, Macromolecules **33**, 1191 (2000)

J.S. Schulze, B. Moon, T.P. Lodge, C.W. Macosko, Macromolecules **34**, 200 (2001)

M. Sclavons, V. Carlier, B. De Roover, P. Franquinet, J. Devaux, R. Legras, J. Appl. Polym. Sci. **62**, 1205 (1996)

C.E. Scott, C.W. Macosko, Polymer **35**, 5422 (1994a)

C.E. Scott, C.W. Macosko, J. Polym. Sci. B Polym. Phys. **32**, 205 (1994b)

C.E. Scott, C.W. Macosko, Polymer **36**, 461 (1995a)

C.E. Scott, C.W. Macosko, Int. Polym. Process. **10**, 36 (1995b)

D. Sek, B. Kaczmarczyk, Polymer **38**, 2925 (1997)

Y. Seo, J. Appl. Polym. Sci. **64**, 359 (1997)

Y. Seo, T.H. Ninh, Polymer **45**, 8573 (2004)

Y. Seo, S.S. Hwang, K.U. Kim, J. Lee, S.I. Hong, Polymer **34**, 1667 (1993)

Y. Seo, T.H. Ninh, S.M. Hong, S. Kim, T.J. Kang, H. Kim, J. Kim, Langmuir **22**, 3062 (2006)

T. Serhatkulu, B. Erman, I. Bahar, S. Fakirov, M. Evstatiev, D. Sapundjieva, Polymer **36**, 2371 (1995)

G. Serpe, J. Jarrin, F. Dawans, Polym. Eng. Sci. **30**, 553 (1990)

S. Shabbir, S. Zulfiqar, Z. Ahmad, M.I. Sarwar, Polym. Eng. Sci. **48**, 1793 (2008)

S. Shabbir, S. Zulfiqar, S.I. Shah, Z. Ahmad, M.I. Sarwar, J. Phys. Chem. B **114**, 13241 (2010)

K. Shahbazi, M.K.R. Aghjeh, F. Abbasi, M.P. Meran, M.M. Mazidi, Polym. Bull. **69**, 241 (2012)

H. Shariatpanahi, H. Nazokdast, B. Dabir, K. Sadaghiani, M. Hemmati, J. Appl. Polym. Sci. **86**, 3148 (2002)

T.J. Shea, J.R. Campbell, D.M. White, L.A. Socha, US Patent 4,814,392, 21 Mar 1989, to General Electric

T.J. Shea, A.J. Moffett, J.R. Campbell, M.E.J. Dekkers, F.F. Khouri, US Patent 5,132,361, 21 July 1992, to General Electric

Q. Shi, P. Stagnaro, C.-L. Cai, J.-H. Yin, G. Costa, A. Turturro, J. Appl. Polym. Sci. **110**, 3963 (2008)

H. Shi, D. Shi, X. Wang, L. Yin, J. Yin, Y.-W. Mai, Polymer **51**, 4958 (2010)

M. Shibayama, K. Uenoyama, J. Oura, S. Nomura, T. Iwamoto, Polymer **36**, 4811 (1995)

N. Shibuya, K. Kosegaki, Eur. Pat. Appl. 248,526, 9 Dec 1987 to Mitsubishi Petrochemical

N. Shibuya, K. Takagi, S. Hattori, T. Kobayashi, H. Sano, Eur. Pat. Appl. 270,796, 15 June 1988a, to Mitsubishi Petrochemical

N. Shibuya, Y. Sobajima, H. Sano, US Patent 4,743,651, 10 May 1988b, to Mitsubishi Petrochemical

Y.-T. Shieh, T.-N. Liao, F.-C. Chang, J. Appl. Polym. Sci. **79**, 2272 (2001)

M. Shimano, S. Moritomi, US Patent Appl. 20100261846, 14 Oct 2010, to Sumitomo Chemical

T. Shiraki, F. Hayano, H. Morita, US Patent 4,628,072, 9 Dec 1986, to Asahi

T. Shiraki, F. Hayano, H. Morita, US Patent 4,657,970, 14 Apr 1987a, to Asahi

T. Shiraki, F. Hayano, H. Morita, US Patent 4,657,971, 14 Apr 1987b, to Asahi

G.O. Shonaike, G.P. Simon (eds.), *Polymer Blends and Alloys* (Marcel Dekker, New York, 1999)

S. Shulin, C. Zhuo, S. Lili, Z. Huixuan, J. Appl. Polym. Sci. **121**, 909 (2011)

M. Shuster, M. Narkis, A. Siegmann, J. Appl. Polym. Sci. **52**, 1383 (1994)

N. Silvi, S.B. Brown, M.H. Giammattei, K.L. Howe, US Patent 5,939,490, 27 May 1997, to General Electric and DuPont

W.M. Sims, US Patent 3,966,839, 29 June 1976, to Foster Grant

H. Singh, N.K. Gupta, J. Polym. Res. **18**, 1365 (2011)

A.K. Singh, R. Prakash, D. Pandey, J. Phys. Chem. B **115**, 1601 (2011)

A.K. Singh, R. Prakash, D. Pandey, RSC Adv. **2**, 10316 (2012)

T.M. Sivavec, S.J. McCormick, US Patent 5,066,719, 19 Nov 1991, to General Electric

T.M. Sivavec, S.M. Fukuyama, US Patent 5,140,077, 18 Aug 1992, to General Electric

W.A. Smith, J.W. Barlow, D.R. Paul, J. Appl. Polym. Sci. **26**, 4233 (1981)

A.P. Smith, R.J. Spontak, H. Ade, Polym. Degrad. Stab. **72**, 519 (2001)

B.G. Soares, F.F. Alves, M.G. Oliveira, A.C.F. Moreira, F.G. Garcia, M.F.S. Lopes, Eur. Polym. J. **37**, 1577 (2001)

B.G. Soares, M.S.M. Almeida, P.I.C. Guimaraes, Eur. Polym. J. **40**, 2185 (2004)

K. Solc (ed.), *Polymer Compatibility and Incompatibility. Principles and Practice* (Harwood Academic Publishers, New York, 1981)

Y. Son, R.A. Weiss, Polym. Eng. Sci. **41**, 329 (2001)

Y. Son, R.A. Weiss, Polym. Eng. Sci. **42**, 1322 (2002)

Y. Son, K.H. Ahn, K. Char, Polym. Eng. Sci. **40**, 1376 (2000a)

Y. Son, K.H. Ahn, K. Char, Polym. Eng. Sci. **40**, 1385 (2000b)

Z. Song, W.E. Baker, J. Appl. Polym. Sci. **44**, 2167 (1992)

J. Song, C.M. Thurber, S. Kobayashi, A.M. Baker, C.W. Macosko, H.C. Silvis, Polymer **53**, 3636 (2012a)

W. Song, H. Liu, F. Chen, J. Zhang, Polymer **53**, 2476 (2012b)

R. Sonnier, V. Massardier, L. Clerc, J.M. Lopez-Cuesta, A. Bergeret, J. Appl. Polym. Sci. **115**, 1710 (2010)

L.H. Sperling, Microphase structure, in *Encyclopedia of Polymer Science and Engineering*, ed. by J.I. Kroschwitz, vol. 9, 2nd edn. (Wiley, New York, 1987), p. 770

F. Speroni, Macromol. Symp. **78**, 299 (1994)

M.J. Stachowski, A.T. DiBenedetto, Polym. Eng. Sci. **37**, 252 (1997)

M.-D. Stelescu, Macromol. Symp. **263**, 70 (2008)

M.E. Stewart, A.J. Cox, D.M. Naylor, Polymer **34**, 4060 (1993a)

M.E. Stewart, S.E. George, R.L. Miller, D.R. Paul, Polym. Eng. Sci. **33**, 675 (1993b)

H. Stutz, P. Pötschke, U. Mierau, Macromol. Symp. **112**, 151 (1996)

K.-F. Su, K.-H. Wei, J. Appl. Polym. Sci. **56**, 79 (1995)

C.C. Su, E.M. Woo, C.-Y. Chen, R.-R. Wu, Polymer **38**, 2047 (1997)

W.-Y. Su, K. Min, R.P. Quirk, Polymer **42**, 5121 (2001a)

W.-Y. Su, Y. Wang, K. Min, R.P. Quirk, Polymer **42**, 5107 (2001b)

S. Su, Q. Li, Y. Liu, H. Xu, W. Guo, C. Wu, J. Macromol. Sci. B Phys. **48**, 823 (2009)

T. Sugie, R. Ishikawa, F. Kobata, US Patent 4,528,346, 9 July 1985, to Dainippon Ink and Chemicals

Y.-J. Sun, W.E. Baker, J. Appl. Polym. Sci. **65**, 1385 (1997)

Y.-J. Sun, G.-H. Hu, M. Lambla, H.K. Kotlar, Polymer **37**, 4119 (1996)

Y.-J. Sun, R.J.G. Willemse, T.M. Liu, W.E. Baker, Polymer **39**, 2201 (1998)

S.L. Sun, X.Y. Xu, H.D. Yang, H.X. Zhang, Polymer **46**, 7632 (2005)

S.L. Sun, Z.Y. Tan, M.Y. Zhang, H.D. Yang, H.X. Zhang, Polymer International **55**, 834 (2006)

S. Sun, Z. Chen, H. Zhang, Polym. Bull. **61**, 443 (2008)

S. Sun, M. Zhang, H. Zhang, X. Zhang, J. Appl. Polym. Sci. **122**, 2992 (2011)

S. Sun, F. Zhang, Y. Fu, C. Zhou, H. Zhang, J. Macromol. Sci. B Phys. **52**, 861 (2013)

U. Sundararaj, C.W. Macosko, A. Nakayama, T. Inoue, Polym. Eng. Sci. **35**, 100 (1995)

T. Suzuki, H. Tanaka, T. Nishi, Polymer **30**, 1287 (1989)

R.T. Swiger, L.A. Mango, DE Patent 2,722,270, 1 Dec 1977, to General Electric

R.T. Swiger, P.C. Juliano, US Patent 4,147,740, 3 Apr 1979, to General Electric

P.D. Sybert, C.Y. Han, S.B. Brown, D.J. McFay, W.L. Gately, J.A. Tyrell, R.A. Florence, US Patent 5,015,698, 14 May 1991, to General Electric

A. Tabtiang, R.A. Venables, Polymer **43**, 4791 (2002)

M. Taheri, J. Morshedian, H. Ali Khonakdar, J. Appl. Polym. Sci. **119**, 1417 (2011)

Y. Takeda, D.R. Paul, Polymer **32**, 2771 (1991)

Y. Takeda, H. Keskkula, D.R. Paul, Polymer **33**, 3394 (1992a)

Y. Takeda, H. Keskkula, D.R. Paul, Polymer **33**, 3173 (1992b)

N.C.B. Tan, S.-K. Tai, R.M. Briber, Polymer **37**, 3509 (1996)

R.T.H. Tang, M.C. Bochnik, F. Mares, S. Arnold, US Patent 5,124,411, 23 June 1992, to Allied-Signal

T. Tang, Z. Lei, X. Zhang, H. Chen, B. Huang, Polymer **36**, 5061 (1995)

T. Tang, Z. Lei, B. Huang, Polymer **37**, 3219 (1996)

L.W. Tang, K.C. Tam, C.Y. Yue, X. Hu, Y.C. Lam, L. Li, J. Appl. Polym. Sci. **85**, 209 (2002)

V. Tanrattanakul, A. Hiltner, E. Baer, W.G. Perkins, F.L. Massey, A. Moet, Polymer **38**, 4117 (1997a)

V. Tanrattanakul, A. Hiltner, E. Baer, W.G. Perkins, F.L. Massey, A. Moet, Polymer **38**, 2191 (1997b)

S.B. Tatum, D. Cole, A.N. Wilkinson, J. Macromol. Sci. B Phys. **39**, 459 (2000)

C. Taubitz, E. Seiler, K. Boehlke, H. Gausepohl, B. Ostermayer, Eur. Pat. Appl. 285,966, 12 Oct 1988a, to BASF

C. Taubitz, E. Seiler, K. Boehlke, B. Ostermayer, H. Gausepohl, Eur. Pat. Appl. 285,969, 12 Oct 1988b, to BASF

C. Taubitz, E. Seiler, K. Boehlke, B. Ostermayer, H. Gausepohl, Eur. Pat. Appl. 285,975, 12 Oct 1988c, to BASF

C. Taubitz, E. Seiler, K. Boehlke, B. Ostermayer, H. Gausepohl, V. Muench, Eur. Pat. Appl. 285,976, 12 Oct 1988d, to BASF

C. Taubitz, E. Seiler, R. Bruessau, D. Wagner, Eur. Pat. Appl. 285,968, 12 Oct 1988e, to BASF

C. Taubitz, E. Seiler, H. Gausepohl, K. Boehlke, R. Bueschl, Eur. Pat. Appl. 289,780, 9 Nov 1988f, to BASF

C. Taubitz, E. Seiler, J. Hambrecht, K. Mitulla, K. Boehlke, US Patent 4,959,415, 25 Sept 1990, to BASF

C. Taubitz, E. Seiler, K. Boehlke, D. Wagner, US Patent 5,053,458, 1 Oct 1991, to BASF

J.W. Teh, A. Rudin, Polym. Eng. Sci. **31**, 1033 (1991)

J.W. Teh, A. Rudin, Polym. Eng. Sci. **32**, 1678 (1992)

J.W. Teh, A. Rudin, J.C. Keung, Adv. Polym. Technol. **13**, 1 (1994)

P. Teyssie, R. Fayt, R. Jérôme, Macromol. Chem. Macromol. Symp. **16**, 41 (1988)

S. Thomas, G. Groeninckx, Polymer **40**, 5799 (1999)

J.-M. Thomassin, S. Lenoir, J. Riga, R. Jérôme, C. Detrembleur, Biomacromolecules **8**, 1171 (2007)

E.J. Tijsma, L. van der Does, A. Bantjes, I. Vulic, G.H.W. Buning, Makromol. Chem. Macromol. Symp. **75**, 193 (1993)

E.J. Tijsma, L. van der Does, A. Bantjes, I. Vulic, G.H.W. Buning, Macromol. Chem. Phys. **195**, 1577 (1994)

S.C. Tjong, Y.Z. Meng, Polymer **38**, 4609 (1997)

S.C. Tjong, Y.Z. Meng, J. Appl. Polym. Sci. **74**, 1827 (1999)

S.C. Tjong, R.K.Y. Li, Y.Z. Meng, J. Appl. Polym. Sci. **67**, 521 (1998)

S. Togo, A. Amagai, Y. Kondo, T. Yamada, Eur. Pat. Appl. 268,486, 25 May 1988, to Mitsubishi Gas Chemical

R.T. Tol, G. Groeninckx, I. Vinckier, P. Moldenaers, J. Mewis, Polymer **45**, 2587 (2004)

R.T. Tol, V.B.F. Mathot, G. Groeninckx, Polymer **46**, 383 (2005)

Q. Tran-Cong, Phase separation and morphology of chemically reacting polymer blends, in *Structures and Properties of Multiphase Polymeric Materials*, ed. by T. Araki, Q. Tran-Cong, M. Shibayama (Marcel Dekker, New York, 1998), p. 155

V.J. Triacca, S. Ziaee, J.W. Barlow, H. Keskkula, D.R. Paul, Polymer **32**, 1401 (1991)

C.-H. Tsai, F.-C. Chang, J. Appl. Polym. Sci. **61**, 321 (1996)

C. Tselios, D. Bikiaris, J. Prinos, C. Panayioutou, J. Appl. Polym. Sci. **64**, 983 (1997)

C. Tselios, D. Bikiaris, V. Maslis, C. Panayioutou, Polymer **39**, 6807 (1998)

A.H. Tsou, B.D. Favis, Y. Hara, P.A. Bhadane, Y. Kirino, Macromol. Chem. Phys. **210**, 340 (2009)

A.H. Tsou, Y. Soeda, Y. Hara, M.B. Measmer, US Patent 8,021,730, 20 Sept 2011, to Exxonmobil and Yokohama Rubber

B. Turcsáyii, J. Macromol. Sci. A Pure Appl. Chem. **32**, 255 (1995)

A. Tynys, U. Hippi, J. Seppälä, J. Appl. Polym. Sci. **86**, 1886 (2002)

S. Ueda, H. Harada, K. Yoshida, K. Kasei, US Patent 4,772,664, 20 Sept 1988, to Asahi

K. Ueno, T. Maruyama, US Patent 4,315,086, 9 Feb 1982a, to Sumitomo Chemical

K. Ueno, T. Maruyama, US Patent 4,338,410, 6 July 1982b, to Sumitomo Chemical

L.A. Utracki, *Polymer Blends and Alloys* (Hanser Publishers, New York, 1989)

L.A. Utracki, *Commercial Polymer Blends* (Chapman and Hall, London, 1998)

L.A. Utracki, M.M. Dumoulin, Polypropylene alloys and blends with thermoplastics, in *Polypropylene Structure, Blends and Composites*, ed. by J. Karger-Kocsis (Chapman and Hall, London, 1995), pp. 50–94

T. Vainio, G.-H. Hu, M. Lambla, J.V. Seppälä, J. Appl. Polym. Sci. **61**, 843 (1996a)

T. Vainio, H. Jukarainen, J.V. Seppälä, J. Appl. Polym. Sci. **59**, 2095 (1996b)

T. Vainio, G.-H. Hu, M. Lambla, J.V. Seppälä, J. Appl. Polym. Sci. **63**, 883 (1997)

A. Valenza, D. Acierno, Eur. Polym. J. **30**, 1121 (1994)

A. Valenza, F.P. La Mantia, E. Gattiglia, A. Turturro, Int. Polym. Process. **9**, 240 (1994)

A. Valenza, G. Carianni, L. Mascia, Polym. Eng. Sci. **38**, 452 (1998)

M. Valero, J.J. Iruin, E. Espinosa, M.J. Fernandez-Berridi, Polym. Commun. **31**, 127 (1990)

H.A.M. Van Aert, G.J.M. van Steenpaal, L. Nelissen, P.J. Lemstra, J. Liska, C. Bailly, Polymer **42**, 2803 (2001)

P. Van Ballegooie, A. Rudin, Polym. Eng. Sci. **28**, 1434 (1988)

A.C.M. Van Bennekom, D.T. Pluimers, J. Bussink, R.J. Gaymans, Polymer **38**, 3017 (1997)

R. Van der Meer, J.B. Yates, PCT Intl. Appl. WO 87/00540, 29 Jan 1987, to General Electric

A. Van der Wal, J.J. Mulder, J. Oderkerk, R.J. Gaymans, Polymer **39**, 6781 (1998)

M. Van Duin, M. Aussems, R.J.M. Borggreve, J. Polym. Sci. A Polym. Chem. **36**, 179 (1998)

M.E. Villarreal, M. Tapia, S.M. Nuño-Donlucas, J.E. Puig, J. Gonzalez-Nunez, J. Appl. Polym. Sci. **92**, 2545 (2004)

T. Vivier, M. Xanthos, J. Appl. Polym. Sci. **54**, 569 (1994)

C. Vocke, U. Anttila, M. Heino, P. Hietaoja, J. Seppälä, J. Appl. Polym. Sci. **70**, 1923 (1998)

C. Vocke, U. Anttila, J. Seppälä, J. Appl. Polym. Sci. **72**, 1443 (1999)

J. Vogel, C. Heinze, Angew. Makromol. Chem. **207**, 157 (1993)

H.J. Vroomans, Eur. Pat. Appl. 286,734, 19 Oct 1988, to Stamicarbon

D. Wang, X.-M. Xie, Polymer **47**, 7859 (2006)

X.-H. Wang, H.-X. Zhang, Z.-G. Wang, B.-Z. Jiang, Polymer **38**, 1569 (1997)

Z. Wang, C.-M. Chan, S.H. Zhu, J. Shen, Polymer **39**, 6801 (1998a)

X.-H. Wang, H.-X. Zhang, W. Jiang, Z.-G. Wang, C.-H. Liu, H.-J. Liang, B.-Z. Jiang, Polymer **39**, 2697 (1998b)

X. Wang, H. Li, E. Ruckenstein, Polymer **42**, 9211 (2001)

C. Wang, J.X. Su, J. Li, H. Yang, Q. Zhang, R.N. Du, Q. Fu, Polymer **47**, 3197 (2006)

J.S. Wang, X.D. Chen, B.Y. Mai, M.Q. Zhang, M.Z. Rong, J. Appl. Polym. Sci. **105**, 1309 (2007a)

H.-G. Wang, L.-Q. Jian, B.-L. Pan, J.-Y. Zhang, S.-R. Yang, H.-G. Wang, Polym. Eng. Sci. **47**, 738 (2007b)

Q. Wang, R. Qi, Y. Shen, Q. Liu, C. Zhou, J. Appl. Polym. Sci. **106**, 3220 (2007c)

R. Wang, S. Wang, Y. Zhang, C. Wan, P. Ma, Polym. Eng. Sci. **49**, 329 (2009a)

P. Wang, K. Meng, H. Cheng, S. Hong, J. Hao, C.C. Han, H. Haeger, Polymer **50**, 2154 (2009b)

D. Wang, S. Fujinami, H. Liu, K. Nakajima, T. Nishi, Macromolecules **43**, 5521 (2010a)

S. Wang, B. Li, Y. Zhang, J. Appl. Polym. Sci. **118**, 3545 (2010b)

S. Wang, B. Li, Y. Zhang, Plast. Rubber Compos. **39**, 379 (2010c)

S. Wang, B. Li, Y. Zhang, Polym. Polym. Compos. **18**, 219 (2010d)

D. Wang, Y. Li, X.-M. Xie, B.-H. Guo, Polymer **52**, 191 (2011)

S. Wang, C. Lin, H. Sun, F. Chen, J. Li, S. Guo, Polym. Eng. Sci. **52**, 338 (2012a)

S. Wang, L. Shao, Z. Song, J. Zhao, Y. Feng, J. Appl. Polym. Sci. **124**, 4827 (2012b)

Q. Wang, Y. Jiang, L. Li, P. Wang, Q. Yang, G. Li, J. Macromol. Sci. B Phys. **51**, 96 (2012c)

H. Wang, Q. Qian, X. Jiang, X. Liu, L. Xiao, B. Huang, Q. Chen, J. Appl. Polym. Sci. (2012d). doi:10.1002/app.36984; published online

Y. Wang, S.M. Chiao, T.-F. Hung, S.-Y. Yang, J. Appl. Polym. Sci. (2012e). doi:10.1002/app.36920; published online

Q. Wang, J. Zhu, P. Wang, L. Li, Q. Yang, Y. Huang, J. Appl. Polym. Sci. **124**, 5064 (2012f)

W. Wang, D.K. Knoeppel, F. Li, J.M. Sosa, US Patent Appl. 20130005852, 3 Jan 2013a, to Fina Technology

M. Wang, G. Yuan, C.C. Han, Polymer **54**, 3612 (2013b)

M. Weber, N. Güntherberg, US Patent 5,907,101, 25 May 1999, to BASF

M. Weber, H. Honl, P. Ittemann, W. Haensel, US Patent Appl. 20100036043, 11 Feb 2010, to BASF

K.-W. Wei, J.-C. Ho, J. Appl. Polym. Sci. **63**, 1527 (1997)

K.-W. Wei, K.-F. Su, J. Appl. Polym. Sci. **59**, 787 (1996)

K.-W. Wei, W.-J. Hwang, H.-L. Tyan, Polymer **37**, 2087 (1996)

K.-W. Wei, H.-C. Jang, J.-C. Ho, Polymer **38**, 3521 (1997)

Q. Wei, D. Chionna, E. Galoppini, M. Pracella, Macromol. Chem. Phys. **204**, 1123 (2003)

Q. Wei, D. Chionna, M. Pracella, Macromol. Chem. Phys. **206**, 777 (2005)

K.A. Weiss, US Patent 4,816,515, 28 Mar 1989, to General Electric

J.L. White, K. Min, in *Comprehensive Polymer Science*, ed. by S.L. Aggarwal, vol. 7 (Pergamon Press, New York, 1989), p. 285

D.M. White, L.A. Socha, R. van der Meer, PCT Intl. Appl. WO 89/000179, 12 Jan 1989, to General Electric

G. Wildes, H. Keskkula, D.R. Paul, J. Polym. Sci. B Polym. Phys. **37**, 71 (1999)

H.M. Wilhelm, M.I. Felisberti, J. Appl. Polym. Sci. **85**, 847 (2002a)

H.M. Wilhelm, M.I. Felisberti, J. Appl. Polym. Sci. **86**, 366 (2002b)

A.N. Wilkinson, S.B. Tattum, A.J. Ryan, Polymer **38**, 1923 (1997)

A.N. Wilkinson, M.L. Clemens, V.M. Harding, Polymer **45**, 5239 (2004)

A.N. Wilkinson, E.M.I. Nita, M.L. Clemens, E. Jobstl, J.P.A. Fairclough, J. Macromol. Sci. B Phys. **44**, 1087 (2005)

J.M. Willis, B.D. Favis, Polym. Eng. Sci. **28**, 1416 (1988)

J.M. Willis, B.D. Favis, J. Lunt, Polym. Eng. Sci. **30**, 1073 (1990)

J.M. Willis, B.D. Favis, C. Lavallee, J. Mater. Sci. **28**, 1749 (1993)

C. Wippler, Polym. Eng. Sci. **33**, 347 (1993)

H. Witteler, G. Lieser, M. Dröscher, Makromol. Chem. Rapid Commun. **14**, 401 (1993)

S.-C. Wong, Y.-W. Mai, Polymer **40**, 1553 (1999)

S.-C. Wong, Y.-W. Mai, Polymer **41**, 5471 (2000)

E.M. Woo, S.-S. Hou, D.-H. Huang, L.-T. Lee, Polymer **46**, 7425 (2005)

C. Wörner, P. Müller, R. Mülhaupt, J. Appl. Polym. Sci. **66**, 633 (1997)

S. Wu, Polym. Eng. Sci. **27**, 335 (1987)

C.-J. Wu, J.-F. Kuo, C.-Y. Chen, Polym. Eng. Sci. **33**, 1329 (1993)

C.-J. Wu, J.-F. Kuo, C.-Y. Chen, E. Woo, J. Appl. Polym. Sci. **52**, 1695 (1994)

J.-Y. Wu, W.-C. Lee, W.-F. Kuo, H.-C. Kao, M.-S. Lee, J.-L. Lin, Adv. Polym. Technol. **14**, 47 (1995)

D. Wu, X. Wang, R. Jin, Eur. Polym. J. **40**, 1223 (2004)

D. Wu, X. Wang, R. Jin, J. Appl. Polym. Sci. **99**, 3336 (2006a)

Y. Wu, Y. Yang, B. Li, Y. Han, J. Appl. Polym. Sci. **100**, 3187 (2006b)

F. Wu, T. Xie, G. Yang, Polym. Bull. **65**, 731 (2010)

W. Wu, C. Wan, H. Zhang, Y. Zhang, J. Appl. Polym Sci. (2013). doi:10.1002/pen.40272; published online

M. Xanthos, Polym. Eng. Sci. **28**, 1392 (1988)

M. Xanthos, in *Polypropylene*, ed. by J. Karger-Kocsis (Kluwer, Dordrecht, 1999), p. 694

M. Xanthos, S.S. Dagli, Polym. Eng. Sci. **31**, 929 (1991)

M. Xanthos, J.F. Parmer, M.L. LaForest, G.R. Smith, J. Appl. Polym. Sci. **62**, 1167 (1996)

Z. Xiaomin, W. Dongmei, Y. Zhihui, Y. Jinghua, J. Appl. Polym. Sci. **62**, 67 (1996)

Z. Xiaomin, Y. Zhihui, N. Tainhai, Y. Jinghua, Polymer **38**, 5905 (1997)

Z. Xiaomin, L. Gang, W. Dongmei, Y. Zhihui, Y. Jinghua, L. Jingshu, Polymer **39**, 15 (1998)

T. Xie, G. Yang, J. Appl. Polym. Sci. **93**, 1446 (2004)

X.-M. Xie, X. Zheng, Mater. Design **22**, 11 (2000)

X.-M. Xie, Y.-Y. Liu, B.-H. Guo, J. Feng, T. Ishikawa, T. Morinaga, J. Appl. Polym. Sci. **82**, 1284 (2001a)

W.B. Xie, K.C. Tam, C.Y. Yue, X. Hu, Y.C. Lam, L. Li, J. Appl. Polym. Sci. **82**, 477 (2001b)

B.-H. Xie, M.-B. Yang, S.-D. Li, Z.-M. Li, J.-M. Feng, J. Appl. Polym. Sci. **88**, 398 (2003)

T. Xie, H. Wu, W. Bao, S. Guo, Y. Chen, H. Huang, H. Chen, S.-Y. Lai, J. Jow, J. Appl. Polym. Sci. **118**, 1846 (2010)

C. Xu, Z. Fang, J. Zhong, Angew. Makromol. Chem. **212**, 45 (1993)

C. Xu, Z. Fang, J. Zhong, Polymer **38**, 155 (1997)

S. Xu, T. Tang, B. Chen, B. Huang, Polymer **40**, 2239 (1999a)

S. Xu, H. Zhao, T. Tang, L. Dong, B. Huang, Polymer **40**, 1537 (1999b)

X.Y. Xu, S.L. Sun, Z.C. Chen, H.X. Zhang, J. Appl. Polym. Sci. **109**, 2482 (2008)

C. Xu, Z. Fang, Y. Chen, Polym. Eng. Sci. (2013a). doi:10.1002/pen.23789; published online

M. Xu, W. Qiu, G. Qiu, J. Macromol. Sci. B Phys. **52**, 155 (2013b)

M.L. Xue, Y.-L. Yu, J. Sheng, H.H. Chuah, J. Macromol. Sci. B Phys. **44**, 531 (2005)

M.L. Xue, Y.-L. Yu, H.H. Chuah, J. Macromol. Sci. B Phys. **46**, 603 (2007a)

M.L. Xue, Y.-L. Yu, H.H. Chuah, G.X. Qiu, J. Macromol. Sci. B Phys. **46**, 387 (2007b)

S. Yamao, W. Kosaka, US Patent 6,037,422, 14 Mar 2000, to Idemitsu Petrochemical

L.-T. Yan, J. Sheng, Polymer **47**, 2894 (2006)

H. Yang, M. Lai, W. Liu, C. Sun, J. Liu, J. Appl. Polym. Sci. **85**, 2600 (2002a)

H. Yang, J. Ma, W. Li, B. Liang, Y. Yu, Polym. Eng. Sci. **42**, 1629 (2002b)

H. Yang, X. Cao, Y. Ma, J. An, Y. Ke, X. Liu, F. Wang, Polym. Eng. Sci. **52**, 481 (2012)

L. Yang, A. Zhang, L. Wang, R. Chen, Y. Zeng, W. Wu, Polym. Eng. Sci. **53**, 2093 (2013)

Z. Yao, J.-M. Sun, Q. Wang, K. Cao, Ind. Eng. Chem. Res. **51**, 751 (2012)

J.B. Yates, US Patent 4,755,566, 5 July 1988, to General Electric

J.B. Yates, T.J. Ullman, US Patent 4,745,157, 17 May 1988, to General Electric

J.B. Yates, D.M. White, US Patent 4,859,739, 22 Aug 1989, to General Electric

J.B. Yates, S.B. Brown, R.C. Lowry, J.C. Blubaugh, D.F. Aycock, US Patent 5,115,043, 19 May 1992, to General Electric

J.T. Yeh, C.C. Fan-Chiang, J. Appl. Polym. Sci. **66**, 2517 (1997)

J.T. Yeh, C.C. Fan-Chiang, S.-S. Yang, J. Appl. Polym. Sci. **64**, 1531 (1997)

C. Yeung, K.A. Herrmann, Macromolecules **36**, 229 (2003)

Z. Yin, C. Koulic, C. Pagnoulle, R. Jérôme, Macromolecules **34**, 5132 (2001)

Z. Yin, C. Koulic, C. Pagnoulle, R. Jérôme, Langmuir **19**, 453 (2003a)

Z. Yin, C. Koulic, C. Pagnoulle, R. Jérôme, Macromol. Symp. **198**, 197 (2003b)

B. Yin, Y. Zhao, M.-M. Pan, M.-B. Yang, Polym. Adv. Technol. **18**, 439 (2007)

L. Yin, D. Shi, Y. Liu, J. Yin, Polym. Int. **58**, 919 (2009a)

L. Yin, J. Yin, D. Shi, S. Luan, Eur. Polym. J. **45**, 1554 (2009b)

K. Yonekura, A. Uchiyama, A. Matsuda, US Patent 4,785,045, 15 Nov 1988, to Mitsui Petrochemical Industries

L.K. Yoon, C.H. Choi, B.K. Kim, J. Appl. Polym. Sci. **56**, 239 (1995)

K.H. Yoon, S.C. Lee, I.H. Park, H.M. Lee, O.O. Park, T.W. Son, Polymer **38**, 6079 (1997)

K.H. Yoon, H.W. Lee, O.O. Park, Polymer **41**, 4445 (2000)

D.W. Yu, M. Xanthos, C.G. Gogos, Adv. Polym. Technol. **10**, 163 (1990)

D.W. Yu, M. Xanthos, C.G. Gogos, Adv. Polym. Technol. **11**, 295 (1992)

D.W. Yu, M. Xanthos, C.G. Gogos, J. Appl. Polym. Sci. **52**, 99 (1994)

Z.-Z. Yu, Y.-C. Ou, G.-H. Hu, J. Appl. Polym. Sci. **69**, 1711 (1998)

L. Yu, G. Simon, R.A. Shanks, M.R. Nobile, J. Appl. Polym. Sci. **77**, 2229 (2000)

Z.-Z. Yu, M.-S. Yang, S.-C. Dai, Y.-W. Mai, J. Appl. Polym. Sci. **93**, 1462 (2004)

X. Yu, Y. Wu, B. Li, Y. Han, Polymer **46**, 3337 (2005)

L. Yu, K. Dean, L. Li, Prog. Polym. Sci. **31**, 576 (2006)

S. Yukioka, T. Inoue, Polymer **35**, 1182 (1994)

J. Zhang, J. He, Polymer **43**, 1437 (2002)

H.X. Zhang, D.J. Hourston, J. Appl. Polym. Sci. **71**, 2049 (1999)

X.Q. Zhang, Y. Son, J. Appl. Polym. Sci. **89**, 2502 (2003)

X. Zhang, J. Yin, Polym. Eng. Sci. **37**, 197 (1997)

X. Zhang, J. Yin, Macromol. Chem. Phys. **199**, 2631 (1998)

X. Zhang, Z. Yin, J. Yin, J. Appl. Polym. Sci. **62**, 893 (1996)

X. Zhang, X.L. Li, D. Wang, Z. Yin, J. Yin, J. Appl. Polym. Sci. **64**, 1489 (1997)

H. Zhang, R.A. Weiss, J.E. Kuder, D. Cangiano, Polymer **41**, 3069 (2000)

J. Zhang, T.P. Lodge, C.W. Macosko, Macromolecules **38**, 6586 (2005)

H. Zhang, Y. Zhang, W. Guo, D. Xu, C. Wu, J. Appl. Polym. Sci. **109**, 3546 (2008)

J. Zhang, L. Luo, S. Lyu, J. Schley, B. Pudil, M. Benz, A. Buckalew, K. Chaffin, C. Hobot, R. Sparer, J. Appl. Polym. Sci. **117**, 2153 (2010)

J. Zhang, Y. Li, Y. Zhu, M. Cui, X. Jiang, J. Polym. Eng. **32**, 487 (2012)

C.-L. Zhang, T. Zhang, L.-F. Feng, J. Appl. Polym. Sci. (2013a). doi:10.1002/app.39972; published online

X. Zhang, Y. Li, L. Han, C. Han, K. Xu, C. Zhou, M. Zhang, L. Dong, Polym. Eng. Sci. **53**, 2498 (2013b)

W. Zhang, Z. Gui, C. Lu, S. Cheng, D. Cai, Y. Gao, Mater. Lett. **92**, 68 (2013c)

L. Zhaohui, X. Zhang, S. Tasaka, N. Inagaki, Mater. Lett. **48**, 81 (2001)

L. Zhidan, S. Juncai, C. Chao, Z. Xiuju, J. Appl. Polym. Sci. **121**, 1972 (2011)

Y. Zhihui, Z. Xiaomin, Z. Yajie, Y. Jinghua, J. Appl. Polym. Sci. **63**, 1857 (1997)

Y. Zhihui, Z. Yajie, Z. Xiaomin, Y. Jinghua, Polymer **39**, 547 (1998)

Z.F. Zhou, N.C. Liu, H. Huang, Polymer **45**, 7109 (2004)

W.-H. Zhou, S.-W. Ye, Y.-W. Chen, Y.-L. Huang, S.-S. Yuan, J. Macromol. Sci. B Phys. **51**, 2361 (2012)

Y. Zhou, W. Wang, R. Dou, L.-P. Li, B. Yin, M.-B. Yang, Polym. Eng. Sci. **53**, 1845 (2013)

X. Zhu, Z. Yang, S. Wu, J. Thermoplast. Compos. Mater. **23**, 351 (2010)

Interpenetrating Polymer Networks

6

L. H. Sperling and R. Hu

Contents

L.H. Sperling (✉)
Chemical Engineering and Materials Science and Engineering, Whitaker Laboratory, Lehigh University, Bethlehem, PA, USA
e-mail: lhs0@lehigh.edu

R. Hu
Arkema Coating Resins, Cary, NC, USA
e-mail: maria.hu@arkema.com

Abstract

An interpenetrating polymer network, IPN, can be defined as a combination of two
polymers in network form, at least one of which is synthesized and/or cross-linked
in the immediate presence of the other. This chapter presents the synthesis, mor-
phology, and properties of IPNs made in different ways emphasizing bulk syntheses
and latex syntheses. Some of the most interesting materials have a glassy polymer
and a rubbery polymer combined. Usually, polymer I is synthesized, followed by
polymer 2. If the reactions are noninterfering, both monomers can be mixed with
their respective cross-linkers and initiators and polymerized simultaneously. Appli-
cations of IPN technology are broad, including sound and vibration damping,
biomedical applications, coatings, adhesives, and golf ball components.

The morphology of IPNs has been widely investigated via electron microscopy
and dynamical mechanical spectroscopy. Many IPNs have dual-phase continuity,
with phase domain sizes of the order of several hundred angstroms. For sound and
vibration damping over broad temperature ranges, the two polymers are mixed in
different extents in different parts of the material, usually in the submicron range.

As examples of the biomedical materials, films to cover serious skin burns are
used because of their capability of transporting moisture away from the burn site
by diffusion while simultaneously transporting in oxygen to help keep the still
living tissue cells alive and multiplying. The films are transparent, so that the
doctors can see how the healing is progressing. Quite different materials make
up false teeth, which are hard and tough and very crack resistant.

Structured latex particles were also introduced to provide multifunctional
properties. Three component latexes with IPN cores as impact and damping
improvers were prepared by three-stage emulsion polymerization. The IPN cores
were composed of one impact part and one damping part.

6.1   Introduction

An interpenetrating polymer network, IPN, is defined as a blend of two or more
polymers in a network form, at least one of which is synthesized and/or cross-linked
in the immediate presence of the other(s). An IPN can be distinguished from
polymer blends, blocks, or grafts in two ways: (1) An IPN swells, but does not
dissolve in solvents, and (2) creep and flow are suppressed.

6.1.1   Definitions

There are several kinds of IPNs:

Sequential IPN. First, polymer network I is synthesized. Then, monomer II plus cross-linker and activator are swollen into network I and polymerized in situ; see Fig. 6.1a.

Simultaneous Interpenetrating Network, SIN. The monomers and/or prepolymers plus cross-linkers and activators of both components are mixed, followed by simultaneous polymerization via noninterfering reactions; see Fig. 6.1b. Typical syntheses involve chain and step polymerization kinetics. While both polymerizations proceed simultaneously, the rates of the reaction are rarely identical.

Latex IPN. The polymers are made in the form of latexes, each particle constituting a micro-IPN. Depending on the rates of monomer addition relative to the rates of
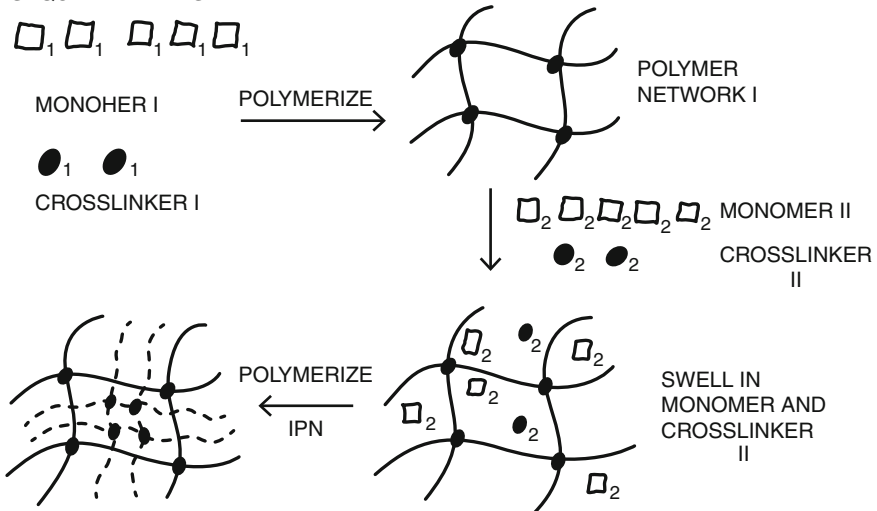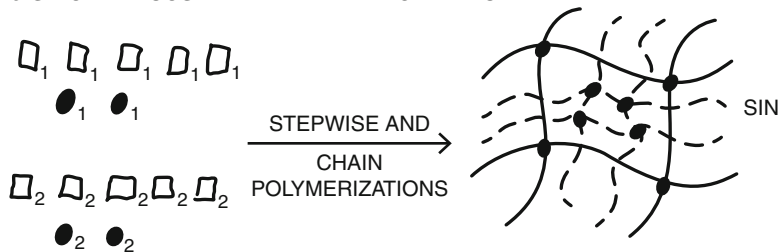
Fig. 6.1 Two synthetic methods for preparing interpenetrating polymer networks. (**a**), sequential IPNs and, (**b**), simultaneous interpenetrating networks, SINs

polymerization, various degrees of interpenetration and/or core/shell morphologies may develop. There are several kinds of latex IPNs; see Sect. 6.4.

Gradient IPN. In this case, the overall composition or cross-link density of the material varies from location to location on the macroscopic level. One way of preparing these materials involves partial swelling of polymer network I by the monomer II mix, followed by rapid polymerization before diffusional equilibrium takes place. Films can be made with polymer network I predominantly on the surface and polymer network II predominantly on the other surface with a gradient composition existing throughout the interior.

Thermoplastic IPN. When physical cross-links rather than chemical cross-links are utilized, the materials may flow at elevated temperatures. As such, they are hybrids between polymer blends and IPNs. Such cross-links commonly involve block copolymers, ionomers, and/or semicrystallinity.

Semi-IPN. These are compositions in which one or more polymers are cross-linked and one or more polymers are linear or branched.

6.1.2 History of IPNs

While the field of IPNs is considered younger than the corresponding field of polymer blends, blocks, and grafts, some of the early materials predated those commonly ascribed to the corresponding blend, block, and graft fields. To complicate the issue, the patent literature reveals that the topology of IPNs was invented over and over again. A brief summary is given in Table 6.1.

The first such invention was by Aylsworth (1914) (Table 6.1, No. 1), who was at the time the chief chemist of Thomas A. Edison in the latter's West Orange, NJ laboratory. He was also an independent inventor, working part time in his own laboratory (Sperling 1987).

Table 6.1 Early IPN patents

No.	Polymer 1	Polymer 2	Application	Inventor	Pat. No.
1	Phenol formaldehyde	Natural rubber	Toughen phonograph records	J. W. Aylsworth	*U.S. Pat.*, 1,111,284; 1914
2	Natural rubber	PVC	Plastic materials	H. Hopff	*Ger. Pat.*, 623,351; 1935
3	Poly(methyl methacrylate)	Poly(methyl methacrylate)	Smooth-surfaced plastics	J. J. P. Staudinger and H. M. Hutchinson	*U.S. Pat.*, 2,539,377; 1951
4	Positively charged network	Negatively charged network	Ion-exchange resin	G. S. Solt	*Br. Pat.*, 728,508; 1955

In those years, Edison had switched from the cylinder-type phonograph records to the platter type. The latter ones were made of the new phenol formaldehyde material, just invented by Leo Baekeland. The problem with the new material was that it was extremely brittle, hence the new platters needed to be very thick. Aylsworth's solution to the problem was to mix in natural rubber and sulfur, which on heating forms a network. Since the phenol formaldehyde compositions are all densely cross-linked, the overall composition was a simultaneous interpenetrating network.

In 1935, Dr. Heinrich Hopff of I. G. Farbenindustrie patented two major advances in emulsion polymerization and latex formation (see Table 6.1, No. 2):

1. Various vinyl monomers such as vinyl chloride were added to a natural rubber latex dispersion and polymerized to make a core-shell structure.
2. Various vinyl latexes, previously polymerized, were mixed with natural rubber latex, both still in aqueous dispersion, and then coagulated. Thus, core-shell latex and latex blend materials were known very early.
3. The coagulated masses of both (1) and (2) above could be masticated with sulfur and vulcanized, as mentioned in the patent, producing semi-IPNs.

Staudinger and Hutchinson (No. 3 in Table 6.1) were concerned with the surface unevenness of the new cast-polymerized plastics, as prepared between glass plates (Staudinger and Hutchinson, 1951). While the plastics were clear, objects behind them appeared distorted. They started with either cross-linked PMMA or cross-linked PS and added the same monomer mix as before and polymerized in situ. This creates a homo-IPN. The intent was that by stretching polymer network I taut via the swelling action of monomer mix II, the surface waviness would be reduced, thus improving the visual characteristics for windows, etc. It must be remarked that J. J. P. Staudinger was Herman Staudinger's son. The latter was the person who enunciated the now famous Macromolecular Hypothesis in 1920, stating that there was a certain class of colloids actually composed of long chains.

In 1955, Solt discovered that IPNs with one network charged negatively and the other charged positively made superior ion-exchange resins (Solt 1955). An important feature of these materials relates to having the two phases in juxtaposition on a very small scale. If the system is mutually miscible, however, efficiency declines due to the interactions between the opposite polymer ions, kicking out the mobile salt ions.

The term *interpenetrating polymer networks* was coined by John Millar in 1960, who prepared homo-IPNs (an IPN with both polymers identical) of polystyrene (Millar 1960). Millar knew about Solt's work, and his objective was to increase the size of suspension particles of polystyrene intended for ion-exchange applications.

Starting in the late 1960s, the field of IPNs was examined by three teams of investigators. Papers by Frisch et al. on IENs (1969a, b), Sperling and Friedman on sequential IPNs (1969), and Lipatov and Sergeeva (1967) on filled materials started systematic research to establish the field of IPNs. By the year 1979, there were

approximately 75 patents and 125 papers in the field (Lipatov and Sergeeva 1967; Sperling and Friedman 1969; Frisch et al. 1969a). Later on, that many IPN patents and papers are produced each year (Kim and Sperling 1997).

6.1.3 A Brief Literature Survey

Some of the IPN literature includes a book by Sperling (1981) and edited works by Klempner and Frisch (1993), Klempner et al. (1994), Sperling and Kim (1996), and Kim and Sperling (1996). A book by Sperling appeared in 1997 with a chapter on IPNs (Sperling 1997). Today, IPNs are widely accepted as a branch of multicomponent polymer materials and as such are discussed in many general polymer textbooks (Elias 1997) as well as more specialized monographs (Utracki 1989) and edited works (Gergen 1996).

A valuable review of IPN research was published by Yu. S. Lipatov and T. T. Alekeeva in 2007 (Lipatov and Alekeeva 2007). This review covers IPN research and development throughout the world from the beginning in the early twentieth century with 356 references. A good deal of theory is introduced relative to the problems of phase mixing and separation during the synthesis stage.

Sperling recently published a history of IPNs, going back to the early 1900s (Sperling 2011) as well. The first man known to invent an IPN was Jonas W. Aylsworth, who was associated at times with Thomas Edison. Aylsworth added natural rubber and sulfur to Leo Baekeland's Bakelite (Alysworth 1914), based on phenol and formaldehyde. As it was, Thomas Edison was using the original Bakelite for his phonograph records when he switched from spools to the platters. The platters needed to be very thick, lest they break on dropping, etc. Since both the Bakelite and the rubber and sulfur composition were cross-linked, they made an IPN, the first known such composition. Then, Edison's phonograph records suddenly got much thinner. The reader should note that this advance was carried out long before the idea of a polymer being a chain structure was considered. Sperling goes on to describe how IPNs were reinvented by several people, as revealed in the patent literature. Most of the works were largely forgotten, until the late 1960s.

6.2 Synthetic Methods

All interpenetrating polymer networks utilize two different polymers. The exception involves the homo-IPNs, where both polymers are identical (Millar 1960; Siegfried et al. 1979). While these polymers may be synthesized by any of the known methods of polymer synthesis, some methods clearly work better in given objectives than others. The principal kinetic methods used are chain and step polymerization.

Many sequential IPNs have used two chain polymerizations, where monomer mix I is polymerized and monomer mix II is swelled in, followed by polymerization

of monomer mix II. Typical examples involve poly(ethyl acrylate) and PS (Huelck et al. 1972) and SBR and PS (Curtius et al. 1972).

A host of cross-linkers have been employed; see Table 6.2. The mixed functionality cross-linkers often serve as grafting sites between networks of quite different nature, perhaps one network chain polymerized and the other step polymerized. Then, each type of functionality reacts with each type of monomer during polymerization.

Where a step polymerization is used, almost always it is for the first polymer synthesized in a sequential IPN. The reasons involve the slow diffusion into a preexisting network of most monomers used in step polymerization and the relatively high glass transition temperature of step-polymerized polymers. The latter reason is important because in order for diffusion and concomitant polymerization to occur rapidly, polymer network I should be above its glass transition at the temperature of polymerization of monomer mix II. Table 6.2 presents glycerol as a simple trifunctional cross-linker for step-polymerized materials, suitable for polyesters and polyurethanes.

For simultaneous interpenetrating networks (SINs), two independent, noninterfering reactions are required. Thus, a chain and a step polymerization have been the method of choice for many such polymerizations. Typical examples have involved PS, polyurethanes (Hourston and Schafer 1996; Mishra et al. 1995), and PMMA. A key factor in the kinetics of such polymerizations is the keeping of the system above the glass transition temperature of both components. If the glass transition of either the polymer network I or polymer network II rich phase vitrifies, the polymerization in that phase may slow dramatically.

There are several interesting polymerization schemes intermediate between a sequential IPN and an SIN. For example, in in situ prepared sequential IPNs, both monomers are polymerized via free radical reaction (He et al. 1993; Rouf et al. 1994). The two monomers must have quite different reactivities toward the free radicals. This situation arises with vinyl or acrylic double bonds and allylic double bonds. The allylic double bonds react about 100 times slower than acrylic or methacrylic bonds. Often, two initiators are used, one reacting at a lower temperature and the other at a higher temperature. In one of the systems studied, based on methyl methacrylate and diallyl carbonate of bisphenol-A (DACBA), first, cross-linked PMMA was formed at moderate temperatures. Then, by just increasing the temperature after completion of the first polymerization, the synthesis of the allylic network followed. In this case, the initiator azobisisobutyronitrile, AIBN, was used to polymerize the MMA at 60 °C, and then the sample was heated to 95 °C for the polymerization of the DACBA with t-butyl peroxy isononanoate (TBPIN).

Latex IPNs offer unique synthetic opportunities. Since an IPN double network, ideally, is contained in each submicroscopic latex particle, special effects are possible. The simplest case involves a cross-linked seed latex particle that is polymerized first. Then, monomer mix II is added. There are two subclasses. First, all of the monomer mix II can be added at once or at least far more rapidly than the polymerization takes place. In that case, the monomer will first swell the latex particle, and then the excess monomer forms a shell around the swollen core.

Table 6.2 Selected cross-linkers for network formation

Dysfunctional cross-linkers

$H_2C=CH$

$H_2C=CH$

$H_2C=CH$

$CH=CH_2$

Divinylbenzene

Tetraethylene glycol dimethacrylate

Higher-functionality cross-linkers

Trimethylolpropane trimethacrylate

Triallyl cyanurate

Mixed functionality cross-linkers

Step functionality cross-linkers

CH_3
$H_2C=C-$
CH_2
$O-CH-CH_2$
O

$H_2C-CH-CH_2$
$OH OH OH$

H_3C $O-Si-O$ CH_3
O O
H_3C CH_3

Glycidyl methacrylate

Glycerol

Tetraethyl orthosilicate

If the monomer mix II is added slowly, or more slowly than the initiator can polymerize the material, little monomer can swell into the particle, and a better defined core/shell structure develops.

There are other cases to consider, such as the polarity of the two polymers. Usually, the more polar polymer will prefer to be in contact with the aqueous phase (thermodynamics considerations). Without cross-linking, there can be a phase inversion from what was stated in the previous paragraphs. The presence of cross-linking, however, limits such inversion (where polymer network II forms the core) because of the swelling restrictions on polymer network I imposed by the cross-links. Then, in the general case, one must ask what relative rates of polymerization are taking place, what level of cross-linkers are employed, etc., leading to many current research topics (Lovell and El-Aasser 1997).

6.3   Morphology and Glass Transitions

The previous section showed how IPNs and related materials can be synthesized. The several synthetic methods, such as sequential, simultaneous, latex, and thermoplastic IPN formation, will result in different morphologies. One of the main advantages of IPN synthesis relates to the ease of promoting dual-phase continuity, i.e., for a two-component system, the two components will be phase separated, and each will exhibit phase continuity throughout the material.

Because most IPNs are phase separated, they usually exhibit multiple glass transition, one for each phase. However, since the phases are small with large volumes of interphase material, the glass transitions may be broadened or moved toward each other.

Another advantage of using IPNs involves its thermosetting characteristics. By definition, IPNs will not flow when heated. A partial exception is the thermoplastic IPNs, which behave cross-linked at ambient temperatures, but flow at elevated temperatures. While some IPNs are tough, impact-resistant plastics, the cross-linking permits many other types of applications, such as sound and vibration damping; biomedical, adhesive, and coating uses; etc. (see Sect. 6.5).

6.3.1   Morphology via Electron Microscopy

A powerful method of examining the morphology of many multicomponent polymer materials utilizes transmission electron microscopy (Woodward 1989). If the two phases are nearly equal in electron density, staining with osmium tetroxide or other agents can be used. For more detailed discussion on the methods of morphology characterization, see ▶ Chap. 8, "Morphology of Polymer Blends."

Donatelli et al. (1976) examined the morphology of *net*-polybutadiene-*internet*-polystyrene and compared these with those of the corresponding semi-IPNs and polymer blends; see Fig. 6.2. In the absence of cross-links, then a solution
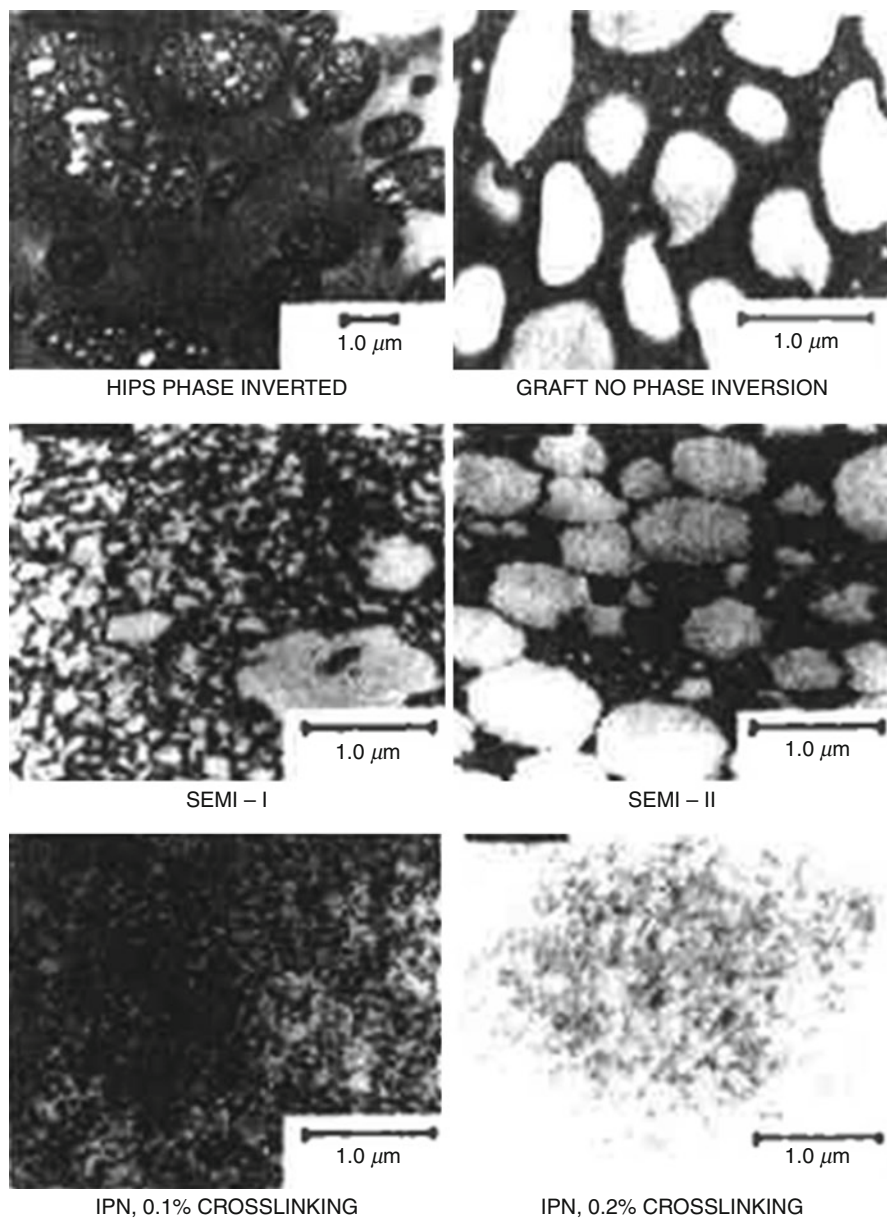
Fig. 6.2 Selected morphologies of IPNs based on SBR and polystyrene, SBR stained with osmium tetroxide. *Upper left*, commercial high-impact polystyrene. *Upper right*, Ostromislensky's material, with no phase inversion; *middle left*, semi-IPN, SBR cross-linked; *middle right*, semi-II IPN, PS cross-linked; *lower left*, full IPN; *lower right*, full IPN, higher cross-linking in the SBR

graft copolymer develops. If the solution is stirred during the polymerization, and then a phase inversion takes place, see Fig. 6.2, upper left. This material is the well-known high-impact polystyrene, HIPS. On quiescent polymerization, the material fails to undergo phase inversion, and polybutadiene remains the continuous phase; see Fig. 6.2, upper right. This last material was invented by Ostromislensky (1927). The middle left and right compositions are, respectively, the semi-I and semi-II compositions of the polybutadiene and the polystyrene. The bottom left and right are the full sequential IPNs, with lower and high cross-link levels in the polybutadiene, as indicated.

The full IPNs shown here (as in numerous other cases) have dual-phase continuity. The domains, as cut in thin section for transmission electron microscopy, appear to be ellipsoidal. Actually, they are more probably thin sections of cylinders, cut at various angles. Other studies show that both phases may be continuous. Spinodal decomposition kinetics, thought to apply in many such cases, results in interconnected cylinders (Utracki 1994).

The upper left has an Izod impact resistance of approximately 80 J/m, the middle left about 150 J/m, and the bottom left about 250 J/m. These early results encouraged the development of these materials.

The domain size of sequential IPNs (such as shown in Fig. 6.2) is controlled by several features: the interfacial tension coefficient between the two polymers, γ; the volume fraction of polymers 1 and 2, v_1 and v_2, respectively; effective network concentration of the two polymers v_1 and v_2, respectively; and the gas constant times the absolute temperature, RT.

Basic equations were derived by Donatelli et al. 1977 and Yeo et al. 1983. Both assumed spheres of polymer 2 dispersed in polymer 1, although the spinodal decomposition model and much electron microscopy suggest that interconnected cylinders may be more prevalent, as discussed above. The Yeo et al. equation is the more general:

$$D_2 = \frac{4\gamma}{RT(Av_1 + Bv_2)} \tag{6.1}$$

where

$$A = \frac{1}{2v}\left(3v_1^{1/3} - 3v_1^{4/3} - v_1 \ln v_1\right)$$

and

$$B = \frac{1}{2}\left(\ln v_2 - 3v_2^{2/3} + 3\right)$$

For lightly cross-linked systems of 50/50 composition, the value of D_2 is of the order of several hundred angstroms. Even though spheres rather than cylinders were specified in the derivation, the numerical result is surprisingly accurate.

6.3.2   Phase Diagram Control of SIN Morphology

While the morphology of sequential IPNs is mainly controlled by the volume fractions of the two polymers and the thermodynamics of mixing, that of SINs depends primarily on the time order of three key events:

1. The gelation of polymer 1
2. The gelation of polymer 2
3. Phase separation of the two polymers

If gelation of one or both polymers precedes phase separation, the polymer gelling first will tend to be more continuous. If phase separation precedes gelation, then a rather coarse morphology may develop. Of course, both gelation and phase separation are controlled by the kinetics of polymerization and the concentration of the cross-linkers, as well as the thermodynamics of mixing.

To determine the time order of the three quantities indicated above, a metastable phase diagram was developed by Mishra et al. (1995). These authors studied polyurethane-based SINs, with poly(methyl methacrylate) constituting the other polymer. The system has proved very popular for research, over 50 papers now being in the literature on PU/PMMA and PU/PS SINs (Mishra and Sperling 1996). The morphologies of these systems vary widely, from two well-defined glass transitions to one broad glass transition or two glass transitions shifted inward toward each other. It appears that the differences in the morphology may have arisen through a different time sequence of the three critical events. (Mathematically, three factorial yields six different possibilities for the finished product.)

As shown in Fig. 6.3, Mishra et al. (1995) presented a tetrahedron as the spatial form of their metastable phase diagram, the corners of which represented MMA, PMMA, urethane prepolymer "U", and PU. The PMMA contained 0.5 % tetraethylene glycol dimethacrylate, causing it to gel after about 8 % conversion; see the G_1-"U"-PU plane. The phase separation curve for the ternary system MMA-PMMA-"U" (front triangle) on polymerization of only the MMA is indicated by the points C-D-A-E. Similarly, the phase separation curve for the MMA-PMMA-PU system (see rear triangle, Fig. 6.3) is represented by the points J-B-K-L. Thus, the entire tetrahedron volume is divided into two regions: one phase separated and the other single phased, separated by the curvilinear construction C-D-A-E-L-B-J. This surface exhibits a characteristic sail-like shape.

The inset in Fig. 6.3 illustrates the actual experimentally determined curve, C-D-A-E, of the tetrahedron. To the left of the diagram, the results were one phased and to the right, two phased. The curve down the middle of the triangle indicates where phase separation was first noted.

The intersection of the PMMA gelation plane with that of the phase separation sail-like surface, the curvilinear line A-B, represents the critical line along which simultaneous gelation of PMMA and phase separation of the PU from the PMMA exists. Reactions passing to the left of this curve will have the PMMA gel before phase separation, while reactions to the right of A-B will phase separate before gelation takes place.
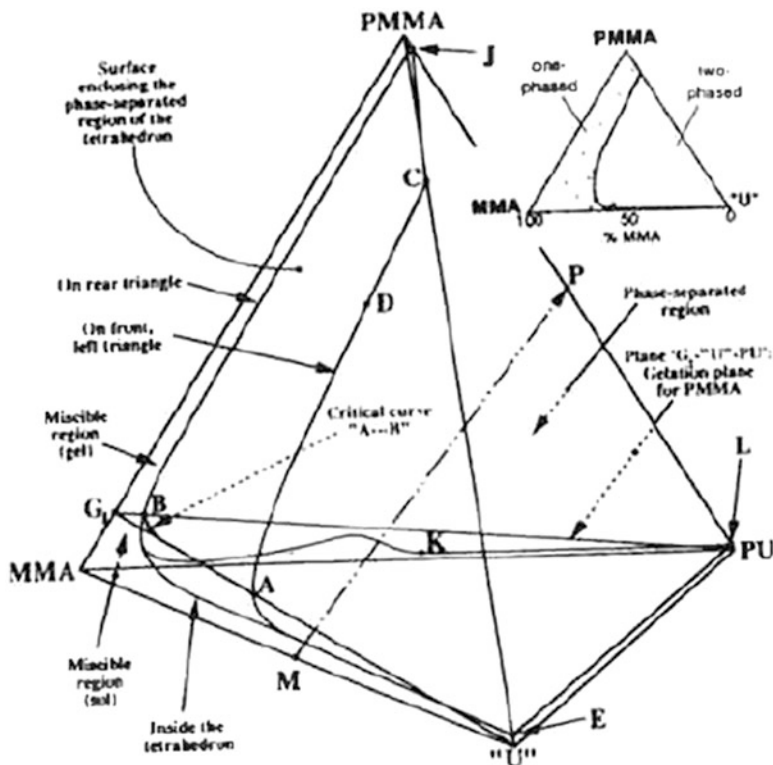
Fig. 6.3 The metastable phase diagram for the polyurethane-poly(methyl methacrylate) SIN at 60 °C. The PMMA gels at and above the plane G_1-"U"-PU. The intersection of the PMMA gelation plane and the surface along the curve A represents the condition of simultaneous phase separation and PMMA gelation

The gelation plane of the polyurethane is illustrated in Fig. 6.4; see G_2-MMA-PMMA. For completeness, the gelation plane G_1 of the PMMA from Fig. 6.3 is also shown. The gelation plane G_2 occurred after about 67 % conversion of the PU. The intersection of the two planes, G_1-G_2, illustrates the line of simultaneous gelation of the two polymers. Reactions passing to one side or the other of this line will have one polymer or the other gelling first. It must be noted that the line G_1-G_2 also intersects the line A-B of Fig. 6.3, not shown. The intersection of these two curves expresses the presence of a triple critical point, where both polymers simultaneously gel and phase separate. While this triple critical point represents the ideal SIN synthesis condition, it would not, in general, produce the best physical or mechanical properties.

The tetrahedron construction represents the synthesis of sequential IPNs as well as the SINs. It must be noted that in real SIN syntheses, it is almost impossible to have the kinetics of polymerization of both polymers proceeding at identical rates. Sequential IPN polymerization represents the other extreme, where first one polymer is completely synthesized and then the other follows sequentially.

Fig. 6.4 The metastable phase diagram, same compositions as Fig. 6.3, illustrating the PU gelation plane, G_2-MMA-PMMA
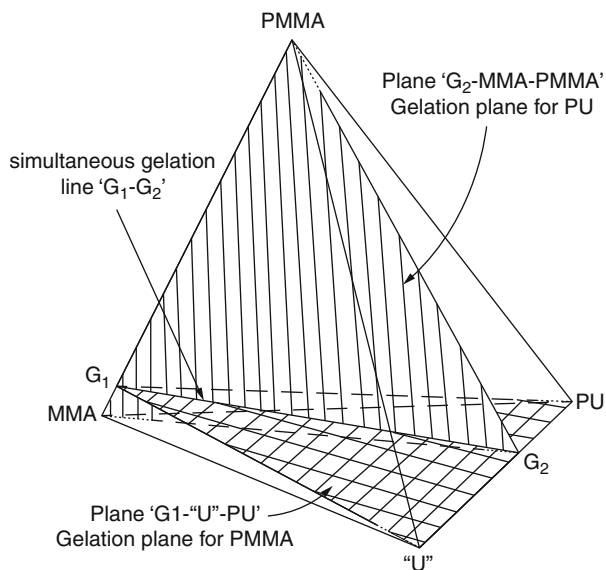
Both sequential IPN and SIN polymerizations begin somewhere along the edge of the line connecting the two monomers, MMA-"U" in the present case. However, the polymerization lines need not be straight or even continue as single lines. When the polymerization line intersects the sail-like phase separation surface illustrated in Fig. 6.3, the line divides into two portions. Both these lines must conclude somewhere along the line connecting the two polymers, in this case the line PMMA-PU. Since it is impossible to have complete phase separation, the lines cannot be exactly at either apex. However, the more complete the phase separation will be, the closer to the apices the ends of the polymerization will be.

Sophiea et al. published the first classical composition-temperature phase diagram, working with the semi-IPN *net*-polyurethane-*inter*-poly(vinyl chloride) (Sophiea et al. 1994). They found a lower critical solution temperature, LCST $\cong 120\,^{\circ}\mathrm{C}$; below this temperature the system was one phased and above two phased. Such behavior is now known to be characteristic of most polymer blends (see ▶ Chap. 2, "Thermodynamics of Polymer Blends").

On the other hand, DuPrez et al., investigating the behavior of a poly(ethylene oxide)-*inter-net*-poly(methyl methacrylate) semi-II IPN, found what appears to be the lower-temperature portion of an upper critical solution temperature, UCST (DuPrez et al. 1996). However, since the temperatures were all below any possible critical temperature, conclusions are difficult to draw.

A TTT cure diagram was developed by Kim et al. for the system poly (ether sulfone)-*inter-net*-epoxy semi-II IPN (Kim et al. 1993). They showed that the transformation of the monomers to the polymers involved five steps: onset of phase separation, gelation of the epoxy component, a fixation of the domain size and shape morphology, end of phase separation, and (in this case)

vitrification of the epoxy component. In their system, the onset of phase separation preceded gelation.

Thermoplastic IPNs are defined above as being hybrid materials between the IPNs and the mechanical blends. Many of these materials consist of polypropylene, a semicrystalline polymer (the crystallinity contributing to the physical cross-linking of the system), and EPDM. The EPDM is lightly cross-linked during the mechanical blending, such that a dual-phase continuity is developed with the EPDM forming cylindrical structures inside of the polypropylene matrix. The basic physical requirements for dual-phase continuity in such blends were expressed by Paul and Barlow and by Jordhamo et al. (Paul and Barlow 1980; Jordhamo et al. 1986):

$$\frac{V_I}{V_{II}} x \frac{\eta_{II}}{\eta_I} = X \tag{6.2}$$

where if:

X > 1, phase I is continuous

X ≅ 1, dual-phase continuity or phase inversion is likely

X < 1, phase II is continuous

In Eq. 6.2, the quantity V is the volume fraction, and η represents the melt viscosity of phase I or phase II, depending on the subscript. Equation 6.2 represents the limiting case for zero shear. Utracki has proposed more complete relationships for finite shear stresses (Utracki 1989). However, although the forces involved in melt blending are large, the shear rates in blending are considerably smaller than on mixing lower viscosity fluids, such as oil and water. More information on this topic can be found in ▶ Chap. 7, "Rheology of Polymer Alloys and Blends" in this handbook.

Davison and Gergen developed thermoplastic IPNs based on SEBS triblock copolymers (where the S hard blocks provide physical cross-linking) and semicrystalline polymers (Davison and Gergen 1977; Gergen and Davison 1978; Gergen et al. 1996). Figure 6.5 illustrates the dual-phase characteristics of a thermoplastic IPN of SEBS and PA-12, the latter having been extracted (Gergen et al. 1996).

The important points developed in this section are that sequential IPN synthesis tends to make dual-phase continuous materials. For both sequential and simultaneous syntheses, a metastable phase diagram can be developed to study the kinetics of phase separation and gelation, so that better control of the morphology can be attained. The thermoplastic IPNs depend on equal volume and viscosity ratios to attain the dual-phase continuity.

6.3.3   Glass Transition Behavior

Due to the small size of the domains, the glass transitions tend to be either broadened or moved toward one another on the temperature or frequency axis; see Table 6.3. This is a direct consequence of the greater extent of mixing and/or greater interphase volume fraction encountered in these materials. The glass transition temperatures

Fig. 6.5 An SEM fracture surface of an extracted thermoplastic IPN, 25/75 PA-11/SEBS. The SEBS phase was extracted

Table 6.3 Dynamic mechanical behavior of IPNs

No.	Observation	Comments
1	Two sharp T_gs near homopolymer values	Little or no mixing
2	T_gs moved toward each other	Molecular mixing in interphase and/or inside domains
3	One broad T_g spans both original T_g ranges	Extensive but incomplete mixing
4	One sharp T_g	Possibly miscible; T_g following the Fox equation
5	One or both T_gs increased	Cross-linking causes the T_g to increase. Can be part of no. 2

depend on the cross-linker level, as that influences the extent of mixing and/or interpenetration of the chains (Nemirovski et al. 1996). Of course, the glass transition temperature of any polymer increases slightly with increasing cross-link level. In this case, the polymer with the higher glass transition temperature may actually decrease as it is mixed with the other polymer. In such cases, within each phase, the Fox equation, often used for statistical copolymers, may be applied.

The volume fraction of the two polymers also plays critical roles; see Fig. 6.6 (Hsieh et al. 1996). This behavior is similar to many polymer blends, where the intensity of the transition depends on the volume fraction. In Fig. 6.6, an inward shift may also be observed. The glass transition temperature of three-polymer latex IPNs will be treated in Sect. 6.4.7.4.

6.4   Latex-Based Materials

Latex-based polymer materials can be either nature made, as natural rubber (Stern 1967; White 1995), or synthetically made. The synthetically made latexes are

Fig. 6.6 Loss modulus temperature behavior of PU (PTMO2000)/UPMI (PEG600) IPNs at various PU/UBMI ratios: _____ 100/0, __ __ __ 90/10, __.. __.. __.. 70/30, ... 0/100
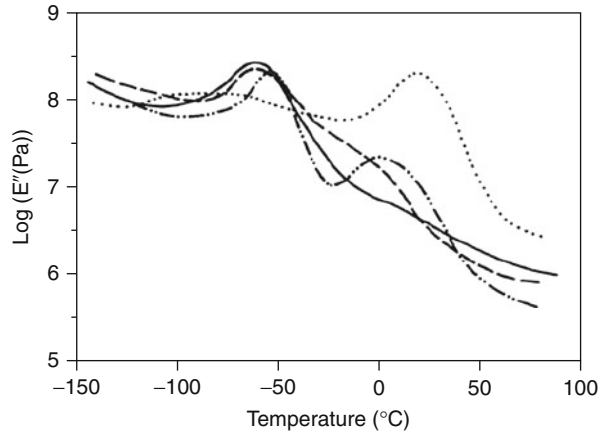
commonly based on recipes of monomer, water, surfactant, and free radical initiator to induce chain polymerization (Lovell and El-Aasser 1997; Wickson 1993). However, recipes based on step polymerization are also well known, often resulting in cross-linked films (Walker and Shaffer 1996). The resulting latex material consists of small particles, usually spherical, of 50–500 nm in diameter, dispersed in water. Alternately, polymers are sometimes emulsified after polymerization (direct emulsification, the product sometimes called artificial latexes) via agitation of a melt in the presence of water and surfactant (emulsifier) and sometimes organic solvent or plasticizer (Piirma 1989).

6.4.1 Definitions

Latexes have long been used in IPNs and related materials. Some of the material types described in the literature are the following:

Latex Blends. These are combinations of two or more kinds of latexes, differing in chemical makeup. Blends of the same kind of latex, but differing in such characteristics as particle size, are of great interest, but will not be considered here (Gilicinski and Hegedus 1996). A latex blend used in coatings involves hard and soft latexes, serving to increase the modulus of the coating as well as improve block resistance (the ability to resist adhesion between two such films) (ASTM 1989; Friel 1992; Rajasingham et al. 2003), film formation properties (Robeson et al. 2003), dirt pickup resistance (Notta 2011), etc.

Core-Shell Latexes. First, a seed latex of polymer 1 is synthesized. Then, a second monomer is added to the system, usually with no added surfactant. Often, a starved polymerization route is employed, i.e., the rate of polymerization equals or exceeds the rate of monomer addition. This reduces the swelling of the seed latex by monomer 2, producing a two-layer latex having a spherical core and an overlaying shell. Obviously, multiple shells can be added.

Latex IPNs. A cross-linked seed latex of polymer 1 is synthesized first. Then, monomer 2 and cross-linker and initiator are added, usually without new surfactant. If the monomer 2 mix is added either all at once or rapidly, then swelling of polymer 1 by monomer 2 is encouraged, with subsequent greater interpenetration.

Latex IENs. Latex interpenetrating elastomer networks, latex IENs, are latex blends that have been cross-linked after film formation. They are named after the early works of Frisch and co-workers, who called these materials interpenetrating elastomer networks (Frisch et al. 1969b). Many latex blends, as used in coatings especially, are cross-linked as finally used in service.

Pre-cross-linked Latex Blends. In these materials the individual latexes are cross-linked during synthesis and then blended, and a film is formed. Because of limited deformation and/or interdiffusion capabilities, such films tend to be weak and only used for special purposes (Zosel and Lay 1993; Lesko and Sperry 1997). However, light cross-linking, as occurs in SBR latexes, may be tolerated. Pre-cross-linked latex blend materials are actually not IPNs, because the definition requires that at least one of the polymers be polymerized and/or cross-linked in the immediate presence of the other. An application of pre-cross-linked suspension-polymerized blends, in anionic and cationic form, is as ion-exchange resins. In suspensions, the particles are larger, usually of the order of 10–200 μm.

6.4.2   History of Latex Blends and Latex IPNs

The early research on core-shell and latex blend materials has already been mentioned; see Table 6.1. Hopff's materials (1935) were intended to be used vulcanized, in semi-IPN form.

A still earlier patent by I. G. Farbenindustrie prepared core/shell latexes from nitrocellulose and poly(ethyl acrylate) (Farbenindustrie 1931). Example 6 of the patent shows the level of sophistication already obtained 10 years after Staudinger's Macromolecular Hypothesis:

> 20 parts of nitrocellulose are dissolved in 80 parts of acrylic ethyl ester and emulsified in 200 parts of water, which contain 0.3 % of Marseilles soap (saponified from olive oil) and 0.5 % of sodium isopropylnaphthalene sulphonate and which has been adjusted with the aid of N/100 aqueous sulphuric acid to a hydrogen ion concentration corresponding to a pH value of 6.2. 2.5 parts of 30 %. aqueous hydrogen peroxide are added to the emulsion. After heating for 2 h at from 80 °C to 90 °C, the emulsion is freed from any non-polymerized ester with the aid of steam, and coagulated with the aid of aqueous 5 %. hydrochloric acid. The product is readily soluble in organic solvents and yields very elastic films.

While no cross-linker is mentioned in the patent, poly(ethyl acrylate) usually gels. That it was "readily soluble" suggests a low molecular weight. These early patents set the stage for today's latex blends and IPNs.

6.4.3 Types of Cross-Links

Klein and Daniels point out three basic categories of cross-linking in latexes (Klein and Daniels 1997): homogeneous or intraparticle cross-linking, interfacial cross-linking, and interstitial cross-linking. If two different polymer latexes are involved, the interfacial cross-linking actually constitutes a type of grafting. In interstitially cross-linked systems, cross-linking occurs in the aqueous phase, where water-soluble or water-swellable polymers undergo cross-linking (or grafting) reactions. These, for example, may involve melamine formaldehyde resins.

The principal types of cross-linking (or grafting) systems include carboxyl groups, hydroxyl groups, chloride (or other halogen) moieties, dimethyl meta-isopropyl benzyl isocyanate, TMI® or related materials, derivatives of acrylamide (such as N-methyl ethers), epoxy groups, and sulfonate groups. Ureido-functional monomers can also be used (Merger et al. 1988). Hydrogen and ionic bonding constitute effective physical cross-linking or grafting methods. Acetoacetoxyethyl methacrylate (AAEM) (Del Rector 1988) and diacetone acrylamide (DAAM)/adipic dihydrazide (ADH) (Kessel 2008; Zhang et al. 2012) are used extensively in coatings industry as well. Blocked cross-linking agents are also introduced by Yang et al. (2011) to be used in water-based coating.

A widely used self-condensable monomer is N-methylolacrylamide. This monomer undergoes a self-condensation reaction as well as reactions with hydroxyl and carboxyl moieties. The methylol functional groups can also react with epoxides or other methylol or methylol ether groups. Typically, N-methylol acrylamide is employed at concentrations of 3–7 wt% in latex coatings formulations (Daniels and Klein 1991).

6.4.4 Strategies for Low-VOC Latex Coatings

Low-VOC (volatile organic compounds, <50 g/l) and 0-VOC coatings (<5 g/l) are increasing in importance in the waterborne coating market due to increasing customer desire to minimize exposure to perceived chemical toxins in paint products and government regulations. To meet the needs, coating resins are moving toward lower T_g to achieve a good film formation property in the absence of a conventional coalescent (typically a VOC). However, this results in a softer film which impacts other coating properties, such as block resistance, hardness, and dirt pickup.

Feng et al. discussed some of the possibilities for producing low-VOC latex coatings (Feng et al. 1995). They pointed out that low-T_g latex materials produce low-T_g films, tacky to touch. The ability to resist adhesion (between two such films) is called *block resistance* in the coatings industry (ASTM 1989). Historically, people added organic solvents, transient plasticizers, etc., promoting particle deformation and interdiffusion, which on evaporation increased block resistance.

Reactive plasticizers that polymerize after film formation can also be used. They form an independent network (sometimes topologically resembling bailing wire) or

cross-link the polymer. Thus, the reaction results in a nonvolatile IPN. The chemistry of the latex surface region can be arranged such that it can be plasticized with water. This may be satisfactory for situations where the surface chemistry will be altered later or that water will not reach the final film in deleterious quantities. On the other hand, if still using higher-T_g IPN resin, high boiling-point ($>285\ ^{\circ}C$) coalescent can also be used in the formulation to improve the film formation property of the low- or near-zero VOC (0-VOC) coatings.

A newer alternative relates to the blending of hard and soft latex particles. The soft particles flow to form a film, while the hard ones tend to raise the modulus and, if on the surface, increase scratch resistance, etc.

Another alternate involves the post-drying of the film via cross-linking. Any number of reactions can be used, including double bonds pendent to the chain or condensable groups. Kessel et al. studied DAAM cross-linking reaction and its influence film formation of an acrylic latex (Kessel et al. 2008). They reported that the cross-linking reaction takes place during film formation process through "keto-hydrazide" reaction. They found that the cross-linking reaction is acid catalyzed and the reaction rate increases as pH decreases. Therefore, for ammonia-neutralized latex, the cross-linking reaction is favored by the loss of water during drying and the decrease in pH arising from the evaporation of ammonia. The cross-linking influences the later stages of film formation when particles are close packed. With the help of DAAM/ADH post cross-linking reaction, the film formation property can be improved. In some cases, heat, radiation, or high-temperature peroxides might be used. If two different latexes or core-shell structures are present, then the product will be an IPN.

6.4.5 Selected Patents in Latex Blends and Cross-Linked Systems

The field of latex blends and their cross-linked counterparts has been especially active; see Tables 6.4 and 6.5. Even in Table 6.4, where no cross-linkers are specified in the claims, it is likely that in many instances, the final product will contain some cross-linking. No. 4 in Table 6.4, for example, mentions a *gelling agent*. All the materials in Table 6.5 have a cross-linker in either one or both of the latexes. Both the N-methylol acrylamides and the ureido-functional groups described above appear in Table 6.5. The reader should note the use of both large and small latex pairs, as well as hard and soft latex pairs, in terms of making useful materials.

As defined in Sect. 6.1 and above, the compositions described in Table 6.5 are all latex IENs, where two latexes are blended and then cross-linked.

Patents rarely include the description of the system morphology. Patel et al. (1996) examined blends of hard and soft particles via atomic force microscopy, finding that when the soft component is present in amounts larger than 40 %, smoothed bumps were observed that appeared larger than either the hard or soft particles alone. The smoothness of each bump, supported by other evidences, suggests that the soft particles have coalesced into a virtual

Table 6.4 Selected patents in latex blend applications

No.	Polymer 1	Polymer 2	Application	References
1	Styrene/acrylic	SBR	Toner aggregation processes	Croucher et al., *U.S. Pat.* 5,496,676, 1995, Xerox
2	Nitrile based	Olefinically unsaturated polymers	Corrosion-resistant coatings	Duke et al., *U.S. Pat.* 4,510,204, 1985, Standard Oil
3	SBR	PMMA	Partitioning agent for crumb rubber	Grimm and Gunnerson, *U.S. Pat.* 4,271213, 1981, Goodyear
4	SBR	NBR	Foam rubber backings	Peltier et al., *U.S. Pat.* 4,55,591, 1985, Polysar
5	PVC (small diameter)	Core-shell acrylic (large diameter)	Bimodal vinyl dispersion resins	Yang *U.S. Pat.* 4,461,869, 1984, Goodrich
6	ABS	SAN	High surface gloss	Leach and Murray, *U.S. Pat.* 3,624,183, 1971, U.S. Rubber Co.
7	Acrylic binder (soft)	Acrylic binder (hard)	Dimensionally stable backings	Grose and Carlson, *U.S. Pat.* 4,609,431, 1986, Congoleum
8	Aromatic vinyl monomer based	Conjugated diene based	Adhesives for palm fibers, bedding	Mori et al., *Jap. Pat.*, 082 69,274, 1995, Nippon Zeon
9	Acrylic acid based	Urethane based	Adhesive resistant to fuels	Heiner and Coates, *Eur. Pat.*, 741,005, 1995, 3M
10	Vinylidene chloride-co-butadiene	PVC	Protection of wood	Kalinina et al., *Rus. Pat.*, 2,055,843, 1992, Im. Acad. Lebedeva
11	Rubber grafted with vinyl cyanides	ABS	Impact-resistant thermoplastics	Nakajima et al., *Jap. Pat.*, 08 169,999, 1994, Toray Ind.

continuum at the surface. The overall surface unevenness was thought to be indicative of underlying hard particles. The hard particles were thought to be submersed because of the lower surface energy of the soft polymer. Gilicinski and Hegedus (1996) also used atomic force microscopy to identify hard and soft domains by supplementing topographic data with mechanical property maps. A third such study by Geurts et al. examined the effect of blending two sizes of monodisperse poly(butyl methacrylate) latexes via minimum film formation techniques (Geurts et al. 1996). Usually, the addition of increasing amounts of small particles beyond a certain concentration level leads to a disruption of the particle matrix until the point at which the matrix changes from a continuous matrix of large particles into a continuous matrix of small particles. While these model materials were not cross-linked, it is easy to imagine the effects of cross-linking such materials, as indicated in Table 6.5.

Table 6.5 Selected patents in latex IEN applications

No.	Polymer 1	Polymer 2	Comments/ cross-linker	Application	Reference
1	Poly(vinyl chloride)	Poly(vinyl acetate)	Hydroxymethyl diacetone acrylamide	Wet primed paint adhesion	Nickerson et al., *US Pat.*, 3,935,151, 1976, Bordon
2	PI	PB	Vulcanizing rubber compound	Golf ball thread rubber	Hamada., *US Pat.*, 5,340,112, 1994, Sumitomo
3	Vinyl esters	Resorcinol formaldehyde	N-methylol acrylamide	Woodworking adhesives	Mudge et al., *US Pat.*, 5,434,216, 1995, National Starch
4	Acrylic ester	PVC	Polymer 3: melamine formaldehyde; N-methylol acrylamide	Water-based coating	Leeson and Ludwig., *US Pat.*, 4,007,147, 1977, B. F. Goodrich
5	SBR	PVC	N-methylol acrylamide in SBR-based latex	Heat-sealable PVC films	Wietsma and Stam., *US Pat.*, 5,166,269, 1992, BASF
6	Poly(vinyl halide)	Acrylic	N-methylol acrylamide in acrylic	Dielectric sealing	Yannich and Katz., *US Pat.*, 4, 684,689, 1989, National Starch
7	Acrylic	Heterocycles	Ureido-functional monomers	Paint dispersions and leather assists	Merger et al., *US Pat.*, 4,777,265 1988, BASF
8	Acrylic (soft)	Acrylic (hard)	Ureido-functional monomers	Polymeric binder for aqueous coatings	Friel, *Eur. Pat. Appl.*, 0,466,409 A1 1992, Rohm and Haas

6.4.6 Core/Shell Latexes

Core/shell latexes refer to systems with a submicroscopic particle morphology of one polymer forming the center part (the core) and the other polymer covering the core (the shell layer). Core/shell latexes are made via two consecutive emulsion polymerization stages, usually forming a particle structure with the initially polymerized material at the center and the later-formed polymer as the outer layer. If more than two stages are employed in the emulsion polymerization process, latex particles with multilayered morphology can be obtained.

The morphology of latex particles is controlled by the thermodynamic and kinetic factors. The thermodynamic factors determine the ultimate stability of the multiphase system, inherent in the production of a composite latex particle, while the kinetic factors determine the ease with which such a thermodynamically favored state can be achieved. The parameters affecting the thermodynamics of the system include the particle surface polarity, the relative phase volumes, and the

core particle size. The parameters affecting the kinetics of the morphological development include the mode of monomer addition (monomer starved or batch) and the use of cross-linking agents. Of course, cross-linked core/shell latexes constitute IPNs; see Sect. 6.4.1.

The core/shell morphology is usually more favorable if the latex contains a hydrophobic/hydrophilic polymer pair polymerized in that order, the volume fraction of the second-stage polymer is higher, the core particle size is larger (in the range from 100 to 900 nm), semicontinuous polymerization process (monomer-starved-feeding mode) for polymer 2 is employed, and cross-linking agents in both core and shell phases are used (Lee and Ishikawa 1983; Cho and Lee 1985; Berg et al. 1986; Lee and Rudin 1989, 1992; Jonsson et al. 1991; Xu et al. 1991; Lee 1981; Min et al. 1983; Hourston et al. 1986a; Sundberg et al. 1990; Winzor and Sungberg 1992; Durant and Sundberg 1995; Kong et al. 1996).

To a large degree, the physical and mechanical properties of the final product depend on the particle morphology. By properly selecting polymer pairs for the core and the shell stage, latex particles can be designed to have unique properties for a wide range of potential applications, from paints, coatings, adhesives, organic opacifiers, to impact modifiers for plastics or carriers for biomolecules (Kowalski et al. 1984; Dong et al. 1995; Qian et al. 1995; Segall et al. 1995; Hu et al. 1995, 1997c; Lindemann and Deacon 1993; Lee et al. 1986).

6.4.7   Latex IPNs (LIPNs)

LIPNs are also prepared through a two-stage emulsion polymerization (Kim and Sperling 1997; Nagarajan et al. 1996a; Sperling et al. 1972, 1973; Hourston and Satgurunathan 1984). First, a cross-linked seed latex is synthesized. For the second stage, one variation consists of swelling cross-linked latex particles (as the seed) with the second monomer, cross-linker, and initiator/catalyst, followed by polymerization. Another method is to feed the second monomer (together with a cross-linking agent and initiator/catalyst) slowly in a monomer-starved condition during the polymerization (Sperling 1997). The morphology of LIPNs is controlled by many factors, as will be discussed in Sect. 6.4.7.2.

The LIPNs are a special type of IPNs that combine both networks in a single latex particle, which differs from bulk IPNs, because the thermosetting character is limited to the size of the latex particles (of the order of several tens to a few hundred nanometers). Such IPNs have unique features in morphology, as well as in physical and mechanical properties (Zhong and Zhu 1991; Shu et al. 1990b; Zhang et al. 1991).

6.4.7.1 Cross-Linking and Grafting

For an ideal IPN, the two or more polymer networks are at least partially interlaced on a molecular scale but not covalently bonded to each other and cannot be separated unless chemical bonds are broken (Mita and Akiyama 1997).

The cross-linking of each polymer network is simply controlled by the type and concentration of the cross-linker employed in the system. The higher the cross-linker level (especially in polymer network I), the finer the morphology.

For a real IPN, however, especially for LIPNs, cross-linking or grafting of the polymer 1 with polymer 2 is likely to occur, based on the following three reasons:

1. The LIPNs are typically prepared through a two-stage emulsion polymerization process by a free radical polymerization mechanism. The cross-linking agents usually have two or more double bonds. Depending on the polymerization conditions, part of the double bonds from cross-linker I could be left during the first-stage polymerization, subject during the second-stage polymerization to act as graft sites.

2. If polymer 1 has residual double bonds, such as polybutadiene, part of the residual double bonds may be reacted in the second-stage free radical polymerization process, forming grafting sites for polymer 2.

3. If polymer 1 has an active α-hydrogen in the molecular structure, such as poly (butyl acrylate), hydrogen abstraction easily occurs in the second-stage polymerization. Actually, in many cases, to improve the compatibility between two networks, a graft site is intentionally added in polymer network I to enhance the grafting of polymer 2 on polymer 1.

The grafting reaction between two polymers can usually be minimized if the two polymer networks are formed through different polymerization mechanisms, such as polycondensation and free radical polymerization. In this case, a grafting agent may be needed in polymer 1 to improve the compatibility between the two networks. Again, the higher the graft site level, the higher the grafting efficiency of polymer 2 on polymer 1, the better the compatibility of the two phases. With very high graft levels, an AB-cross-linked copolymer may be created (Sperling 1997). However, for most purposes, the graft site concentration should be low enough to prevent miscibility of the two polymers.

6.4.7.2 Morphology

The morphology of latex IPNs refers to the degree of phase separation, the number of the phases, the shape and size and the domains, the degree of phase continuity, and the structure of the interface. On film formation, the ensemble of latex particles presents further unique morphologies. For LIPNs, the morphology is complicated because the swelling, polymerization, cross-linking, and phase separation are all taking place within the submicron polymer particles in an aqueous phase. Different LIPNs have different morphologies. Even for LIPNs with the same chemical composition, the morphology can be different when different synthesis processes are used (Peng and Li 1995). Since an LIPN is typically prepared by sequential emulsion polymerization, a core/shell morphology often forms, similar to that of the latex particles synthesized by a two-(or more)stage emulsion polymerization process (Sperling and Sarge 1972). However, if the cross-linking density of the first prepared polymer and the monomer 2 concentration are controlled properly, a cellular-type morphology can also be obtained (Silverstein et al. 1989; Hu et al. 1995; Sionakidis et al. 1979).

Similarly as in the core/shell latex particles, the LIPN morphology is controlled by the miscibility of the polymers, the volume fraction of each polymer, the cross-linking density of the polymers, and the sequence or the order of the synthesis (which polymer is synthesized first) (Sionakidis et al. 1979; Hourston and Satgurunathan 1987). The effects of those factors on the LIPN morphology are summarized as follows:

1. The more miscible the two polymer compositions, the less the phase separation between them and/or the smaller the domain size for each of them. The misci-bility is partially indicated by the solubility parameters (δ) of the two polymers. The closer the two δs, the more miscible the system (Yin et al. 1991).

2. Effect of the volume fraction of each phase in LIPN morphology depends on the nature of the two compositions. Phase separation can be reduced with increasing the content of the first component (Krause 1972) or with increasing the volume fraction of the second component (Geng 1992), i.e., by staying away from 50/50 compositions. If polymer 1 is hydrophobic (synthesized first) and polymer 2 is hydrophilic (synthesized later), a normal core/shell morphology is more easily formed; vice versa, an inverted core/shell morphology may result (Narkis et al. 1985, 1986). In addition, the longer the swelling time for the monomer 2 in polymer 1, the more nearly thermodynamic equilibrium is achieved for the system (Hourston et al. 1987).

3. Increasing the cross-linking density of polymer I (the seed) reduces the phase size (Sheu et al. 1990a). However, greater phase separation can occur when the cross-linking density of polymer I is high enough to reduce the diffusion of the monomer 2 into polymer 1. The higher the cross-linking density of polymer 2, the more efficient for the molecular interlocking, the less phase separation results (Sheu et al. 1990b; Yin et al. 1988).

The morphology of LIPNs can be investigated optically by either TEM or SEM and mechanically via the glass transition behavior. Nemirovski et al. studied elasto-meric LIPNs by a two-stage emulsion polymerization of styrene [with a comonomer to lightly cross-link the PS] upon a lightly cross-linked polyacrylate (PAcr) seed latex (75:25 PAcr:PS) (Nemirovski et al. 1996). The influence of the sequence and composition upon the morphology is schematically illustrated in Fig. 6.7 (Silverstein and Narkis 1989). They proposed a schematic diagram of the molded LIPN showing both the interparticle and the intraparticle microdomains and the bicontinuous IPN structure inside the particles; see Fig. 6.8 (Silverstein et al. 1989).

Wu and Zhao studied LIPN systems by a two-stage emulsion polymerization technique (Wu and Zhao 1995). A latex seed (polymer 1) was synthesized first in a semicontinuous emulsion polymerization, swollen by the second-stage monomer or monomer mixture (forming polymer 2), and followed by polymerization to form IPN materials. Six kinds of monomers were used: acrylonitrile (AN), vinyl acetate (VAc), n-butyl acrylate (nBA), methyl methacrylate (MMA), ethyl methacrylate (EMA), and ethyl acrylate (EA). The effect of composition, cross-linking level, feeding sequence of polymer 1 and polymer 2 on the IPN miscibility, and

Fig. 6.7 Schematic cross section of LIPNs at 100 %, 75 %, 50 %, and 25 % seed polymer: (**a**) hydrophobic seed; (**b**) hydrophilic cross-linked seed, both polymers cross-linked; and (**c**) hydrophilic seed, second-stage cross-linked
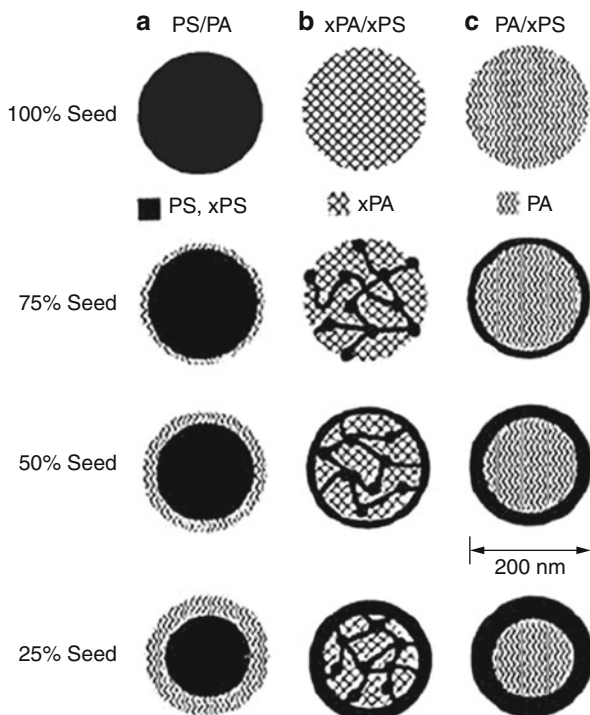
Fig. 6.8 Schematic cross section of molded LIPN showing intraparticle and interparticle PS nanodomains and an interwoven network structure
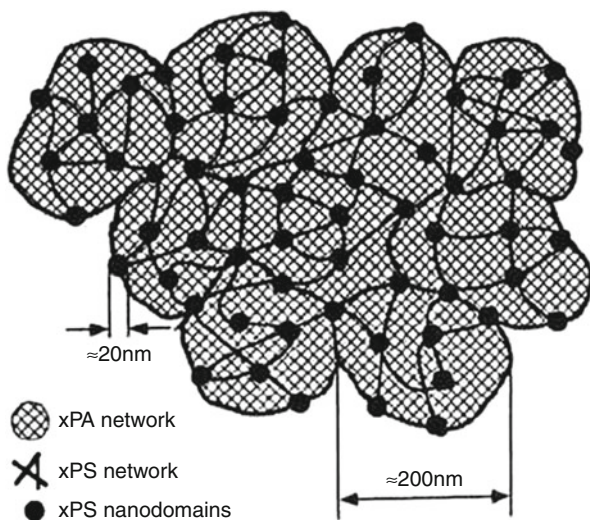
Fig. 6.9 Dynamic
mechanical spectroscopy
curve of the LIPN with
different synthetic orders:
C–1 = P(AN-*co*-EMA)/P*n*BA
and C–5 = P*n*BA/P(AN-*co*-
EMA)
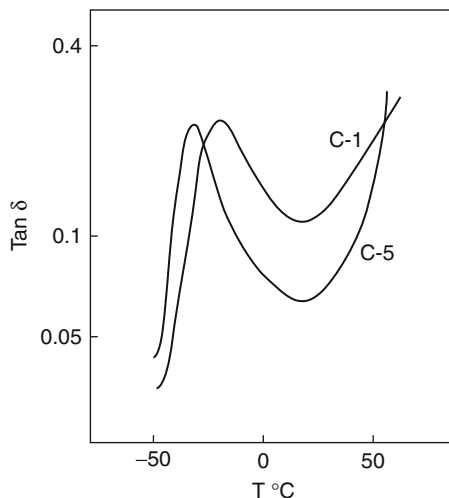
mechanical behavior were investigated via TEM, equilibrium swelling ratio, density, and DMS measurements. They found that the latex IPN particles had a core/shell-type morphology. Introduction of a third component as a comonomer (which had good miscibility with the original two polymers) improved the IPN miscibility. Their IPNs with higher cross-linking density had a higher phase miscibility. They also found that the IPNs with a hard core and a soft shell morphology, called an inverted IPN, had a higher miscibility than the IPNs with the opposite morphology, called normal IPNs (soft core and hard shell), as shown in Fig. 6.9.

Another kind of LIPN material, P(MMA-*stat*-S)/P(BA-*stat*-AA), with a core/shell structure, was synthesized by Chen and Wang (1995a, b). P(MMA-*stat*-S) seed was synthesized first by batch emulsion polymerization, and then PBA-PAA was semicontinuously polymerized. The effects of emulsifier concentration, cross-linking agent, and initiator on the final latex films were investigated. They found that the core was a hard MMA-S statistical copolymer with PBA located in the inner layer of the shell and the PAA located in the outer layer of the shell (due to a poor miscibility of PAA with P(MMA-*stat*-S) and the hydrogen bonding between PAA and water). An interpenetrated structure was formed at the interface of the core and the shell. These 0.1–0.2 μm latex particles were initially dispersed in the aqueous phase. After the evaporation of water, these latex particles formed a film, the particles coalescing with the soft shell becoming the continuous phase sticking these particles together. This kind of IPN can be used in coatings and adhesives. It was also shown that on increasing the core/shell ratio (hard to soft monomer weight ratio) from 2/8 to 8/2, the state of the film changed from an adhesive to one cracked into a powder. At the 1/1 core/shell ratio, increasing the AA concentration to 2.5 %, the film was still uniform and clear; but at higher AA levels, the latex stability decreases in the presence of electrolyte (due to a thinner electronic double layer) and higher water absorbance (due to the hydrophilicity of the –COOH). From DSC, the core/shell LIPN showed two broad T_gs at −36 and 103 °C and one small T_g at 10 °C.

Besides two-component LIPNs, three-component LIPNs have also been studied through three-stage emulsion polymerization processes (Zhang et al. 1991, 1994; Isao et al. 1992). These authors synthesized poly(n-butyl acrylate) cross-linked with ethylene glycol dimethacrylate as the seed latex. Styrene and divinylbenzene were added at the second stage. The third stage was linear poly(methyl methacrylate). Starved polymerization conditions resulted in more regular-shaped latex particles than batch addition of monomer.

Another interesting three-component LIPN consists of cross-linked polyorgano-siloxane (tetraethoxysilane as cross-linker) as the first stage, swollen by butyl acrylate monomer (allyl methacrylate as cross-linker) and then polymerized to form the second component, and finally, poly(methyl methacrylate) was grafted onto the IPN core as the shell layer (Isao et al. 1992). Such kind of LIPNs is found to be good impact modifiers in thermoplastics; i.e., they are toughened by the addition of finely divided low-T_g phase.

6.4.7.3 Damping

Polymers with sound and vibration damping properties are finding numerous applications, especially in the aircraft, automotive, tall buildings, and appliance industries (Aklonis and MacKnight 1983; Thurman and Miller 1986; Corsaro and Sperling 1990; Sophiea et al. 1994). The damping properties of polymers are dominated by their glass transitions. Usually, homopolymers or statistical copolymers possess efficient damping in a temperature range of only 20–30 °C around the T_g (Aklonis and MacKnight 1983). For most outdoor or machinery applications, however, good damping materials should exhibit a high loss factor (tan $\delta > 0.3$) over a temperature range of at least 60–80 °C (Yak 1994; Yao et al. 1991).

Why use IPNs as damping materials? It is because the introduction of cross-links in IPNs restricts the domain size to the order of 10–20 nm, which enhances the formation of a microheterogeneous morphology. This results in broad glass transitions, making them effective as broad temperature or frequency damping materials (Wang et al. 1996; Fay et al. 1991; Sperling and Fay 1991).

The damping behavior of LIPNs can be improved by proper design of the chemical composition in the system and effective control of the IPN morphology. The same factors should be considered as controlling core/shell LIPN morphology, such as the miscibility of the system, chemical structure of the polymer molecule, glass transition temperatures, cross-linking density of the two networks, and the feeding sequence in the polymerization. But here, to develop an LIPN with broad temperature damping behavior, a more miscible or microheterogeneous morphology is needed instead of a core/shell-type morphology. By contrast, if only a narrow temperature range is needed, such as an indoor, room temperature application, a homopolymer or simple statistical copolymer with a sharp T_g will serve better. An example would be slightly plasticized poly(vinyl acetate), $T_g = 25$ °C.

Based on damping theory (Kim and Sperling 1997; Sophiea et al. 1994a), the damping behavior of a polymer can be evaluated from its dynamic mechanical behavior by expressing it as the area under the tan δ versus temperature curve (Keskkula et al. 1971) or the area under the linear loss modulus versus temperature

curve (Fradkin et al. 1986a, b; Chang et al. 1987). The broad temperature damping performance improves if the polymer system is more miscible, the glass transition peak is broader, and the tan δ or loss modulus peak intensity is higher. The damping performance can also be predicted and improved via group contribution analysis (Fradkin et al. 1986b; Chang et al. 1987, 1988; Fay et al. 1990; Foster et al. 1987). However, the group contribution analysis may be unable to predict the partially miscible two-peaked (microheterogeneous) IPNs (Lipatov 1989), because the analysis is based only on molecular structure, not considering the interaction between the polymer phases.

Sperling et al. first developed a prototype "Silent Paint," which is a two-layer coating system, PEMA/PnBA LIPN, capable of attenuating noise and vibration over −30 °C to +100 °C (Sperling et al. 1974). Later, they further investigated P(EMA-EA)/P(BA-EA) and PVC/P(B-AN) LIPNs for more effective damping applications (Grates et al. 1975; Lorenz et al. 1976; Sperling et al. 1975). The damping capability was controlled by varying the chemical composition of the LIPN systems.

Liu et al. also studied LIPN systems for damping control in coating applications (Liu et al. 1995). A polystyrene (PS)/polyacrylate (PAcr) latex IPN was synthesized in a two-stage emulsion polymerization. Cross-linked PS was synthesized first as the seed polymer by a semicontinuous process, followed by an nBA-MA-BMA monomer mix with cross-linking agent, again feeding semicontinuously into the PS seed to polymerize, forming an IPN latex. The effect of PS and PAcr ratio and the addition of inorganic fillers, such as mica, graphite, $CaCO_3$, and TiO_2 on the damping of the final coating film, were studied. They found that the damping behavior of PS/PAcr IPN at room temperature was improved with increasing PS amount in the system, as shown in Table 6.6. This is because the presence of the benzene ring (from PS) enhances the friction of molecular chain movement. The introduction of a monomer with polar group to the PAcr backbone improved the miscibility of the IPN system and increased the adhesion of the coating film. This is because the polarity can increase the interchain attraction, favoring the permeation of the molecular chains, enhancing the mutual entanglement between the networks, and increasing the friction between the polymer molecular chains. Consequently, the damping property was improved. The addition of inorganic fillers increased the damping effective value, as well as expanded the temperature range for effective damping, with flake structure fillers, e.g., mica, showing the best result. This was confirmed by the DMS measurement, with the broadest tan δ peak and the highest valley value obtained.

Peng and Li synthesized a series of PS/P(EA-*stat*-nBA) LIPNs by two-stage emulsion polymerization method to investigate the effect on the damping properties of composition, cross-linker content, chain transfer agent, polar group, and feeding sequence (Peng and Li 1995). The results show that the PS/P(EA-*stat*-nBA) LIPNs are a partially miscible system. The effect of cross-linker content of network I on the damping properties is not the same as that of network II. The damping properties of the PS/P(EA-*stat*-nBA) LIPN (hard component synthesized first) are superior to that of P(EA-*stat*-nBA)/PS LIPN (soft component synthesized first). The introduction of

Table 6.6 Effect of PS/PAcr ratio on damping

PS/PA	25/75	35/65	45/55	50/50
Noise reduce, dB/mm	3.0	3.5	3.9	5.3

polar groups into the system can increase the damping properties by increasing the tan δ and broadening the damping range, while the addition of a chain transfer agent can broaden the damping temperature range.

6.4.7.4 Development of LIPNs with Multifunctional Properties

A type of three-component latex with IPN cores as impact and damping improvers was prepared by three-stage emulsion polymerization (Hu et al. 1995, 1997a). The IPN cores were composed of one impact part (polybutadiene based, with T_g around $-75\ ^\circ$C) and one damping part (acrylic based, with T_g around $+10\ ^\circ$C). The synthesis procedure was as follows: First, component A, a seed latex of poly (butadiene-*stat*-styrene), P(Bd/S) 90/10, was prepared at both 95 % and 40 % gel fraction. After stripping the residual monomer in the seed latex, a mixture of acrylate monomer (butyl acrylate or ethylhexyl methacrylate) and styrene or methyl methacrylate monomer together with tetraethylene glycol dimethacrylate and initiator was added and swollen for 24 h at room temperature and then polymerized to form an IPN hybrid core, A + B. Finally, the third component, C, poly(styrene-*stat*-acrylonitrile) (72/28) copolymer, was synthesized under monomer-starved conditions to form a uniform glassy shell layer covering on the IPN cores. This last made the latex particles compatible with a polycarbonate matrix (Tanrattanakul et al. 1996). A core/shell-type phase separation was observed for IPN particles when using P(Bd/S) with 95 % gel fraction, while a cellular IPN morphology with a distribution of polyacrylate-based copolymer in P(Bd/S) phase was formed with 40 % gel fraction P(Bd/S). Also, the domain size of the second polymer was larger when increasing the volume fraction of the second polymer. In order to study the effect of interfacial interaction between the two polymer components in an IPN particle (polymer A and polymer B), separate core/shell particles and multilayered structured particles were prepared, as molded in Fig. 6.10 (Hu et al. 1997b).

Dynamic mechanical spectroscopy (DMS) was used to characterize the glass transitions of the above LIPN particles. It was found that poly(butyl acrylate)-based copolymer provides higher miscibility with P(Bd/S) than poly(ethylhexyl methacrylate)-based copolymer, which has a longer side chain in the molecular structure. As a comparison to the IPN core/shell system, a blend of separate core/shell latex particles, A (poly(butadiene-*stat*-styrene) (90/10))/C (poly(styrene-*stat*-acrylonitrile) (72/28)) and B (poly(butyl acrylate)-based copolymer or poly (ethylhexyl methacrylate)-based copolymer)/C latexes were also synthesized and evaluated. Figure 6.11 (Hu et al. 1997a) shows three glass transitions for the IPN core/shell latex particles. Figure 6.12 (Hu et al. 1997a) shows a better-developed middle glass transition for component B and a lower-temperature P(Bd/S) glass transition. The polymer B appears more miscible with polymer A in the IPN form.

Fig. 6.10 Models of different types of core-shell modifiers: (**a**) traditional core/shell, (**b**) IPN core/shell, (**c**) blend of separate core/shell, and (**d**) multilayered core/shell. Possible polymer compositions are polybutadiene copolymer as polymer A, acrylic copolymer as polymer B, and SAN as polymer C
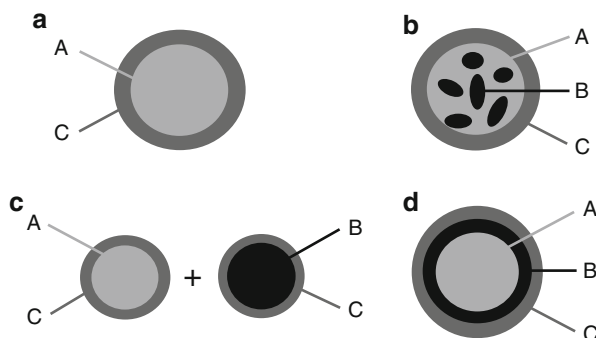
Fig. 6.11 DMS results for IPN core/shell latex film: (0.5 + 0.5)/1 (A + B)/C, A = P(Bd/S), B = P(EHMA/S), and C = SAN
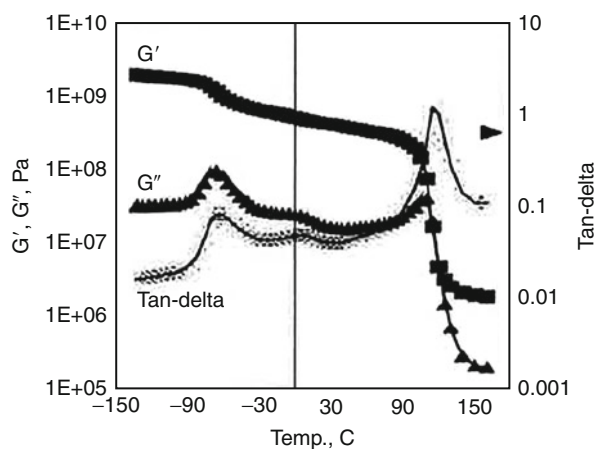
In the same work, the damping behavior of those three-component LIPNs was evaluated from the integrals of the linear loss shear modulus versus temperature (loss area, LA) and linear tan δ versus temperature (tan δ area, TA) curves measured by DMS (Hu et al. 1997b). Baselines were used for subtraction, as is common in spectroscopy calculations (Fay et al. 1991). The IPN core/shell particles showed the highest damping, comparing with separate and multilayered core/shell particles. Also, normal synthesized (rubbery polymer was synthesized first) and inverted synthesized (glassy polymer was synthesized first) semi-I IPN and semi-II IPN latexes were compared for their damping performance. The inverted synthesized ones provided much higher LA and TA values, due to their finer morphology.

Tables 6.7 and 6.8 summarize selected LIPN systems developed for two- and three-stage systems, respectively. For the latter, polymer 3 is usually a linear overcoat. Of great interest throughout are morphology and concomitant behavior. Applications for coatings, damping, and impact improvement are discussed in many of the works.

Fig. 6.12 Dynamic
mechanical spectroscopy
results for lend of separate
core/shell latex film – 1/1 A/C
and 1/1 B/C at a 1/1 blend
ratio: A = P(Bd/S), B = P
(EHMA/S), and C = SAN.
More distinctive glass
transitions are shown here,
particularly for polymer B
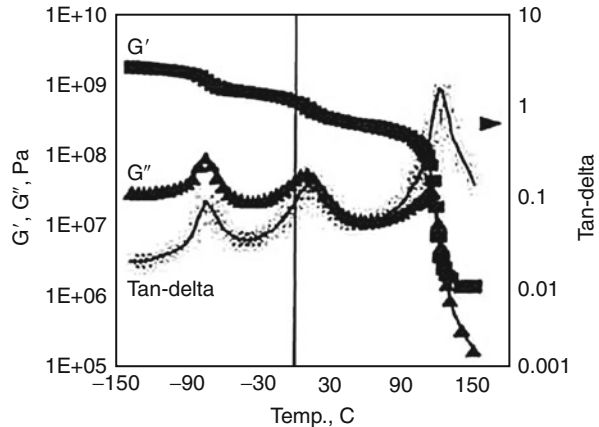
6.5   Actual and Proposed Applications of IPNs

While the field of IPNs is relatively young compared with those of polymers, the
number of applications are growing rapidly. In 1979, the total number of scientific
papers was about 125; there were about 75 patents. Today, about that many are
published each year. Major advances include thermoplastic IPNs, renewable
resource materials, biomedical materials, and nonlinear optical materials.

6.5.1   Thermoplastic IPNs

The thermoplastic IPNs utilize physical cross-links, rather than chemical cross-
links. Usually, these materials will flow when heated to sufficiently high tempera-
ture (hence the terminology *thermoplastic*), but behave as thermosets at ambient
temperature, with IPN properties, often possessing dual-phase continuity. Most
often, physical cross-links are based on triblock copolymers (thermoplastic elasto-
mers being the leading material), ionomers, or semicrystalline materials.

Sometimes one of the components is chemically cross-linked. Usually, such mate-
rials undergo dynamic vulcanization, i.e., chemical cross-linking during melt shearing.
The resulting action yields a dual-phase continuity product, where the chemically
cross-linked component forms cylinders within the matrix of the other component.

Coran and Patel (1996) list several examples of the improvements possible:
Reduced permanent set
Improved ultimate mechanical behavior
Improved fatigue resistance
Improved fluid resistance, i.e., to hot oils
Improved high-temperature stability
Greater stability of phase morphology in the melt (i.e., the phase domain size does
    not increase)

Table 6.7 Selected two-stage LIPN systems

Polymer 1	Polymer 2	Property investigated	References
Polyacrylate (PAcr)	Poly(n-butyl acrylate) (PnBA)	Damping behavior	Wu and Zhao (1996)
Polystyrene (PS)	Polyacrylate (PAcr)	Damping coating	Wang et al. (1996)
PAcr	MAA, PMMA, P (MMA/S)	Mechanical behavior	Nagarajan et al. (1996a, b, c, d)
PS	P(EA-nBA)	Damping	Li et al. (1995)
Acrylic	Acrylic	Coating behavior	Rearick et al. (1996)
Natural rubber	PBA	Impact modifier in PC	Schneider et al. (1996a)
PAcr	PS or PMMA	Film formation	Nagarajan et al. (1996e)
PAcr	PS	Structure and properties	Nemirovski et al. (1996)
PAcr	PAcr	Powder paint	Mizoguchi et al. 1996
PS	PAcr	Damping	Liu et al. (1997)
PAcr	P(S/MMA) copolymer	Film formation	Nagarajan et al. (1997)

Table 6.8 Selected three-stage LIPN systems

Polymer 1	Polymer 2	Polymer 3	Property investigated	References
PBd-based copolymer	PBA-based copolymer	SAN	Morphology and damping	Hu et al. (1995, 1997a, b), Tanrattanakul et al. (1996)
Natural rubber	PS	PMMA	Morphology	Schneider et al. (1996b)
PBA	PS	PMMA	Impact modifier	Zhang et al. (1996)
PU	PBMA	PS	Miscibility, damping	Hourston et al. (1996)

Greater melt strength (i.e., green strength)

More reliable thermoplastic fabricability

Some materials that have achieved importance include EPDM/PP, NBR/PA, PU/PA, SEBS/PA, EPDM/PBT, and epichlorohydrin rubber/PA. Usually, these materials are made more processable through plasticizing oils. Holden (1996) provided trade names of selected compositions, emphasizing those based on hard polymer-elastomer combinations; see Table 6.9.

6.5.2 Renewable Resource IPNs

Renewable resources are those agricultural products that can be grown repeatedly. A closely related term is natural products. However, the latter may not be renewable, i.e., coal or petroleum oil. Renewable resource materials have long been based on

Table 6.9 Selected plastic-elastomer thermoplastic IPNs by trade name[b]

Trade name (manufacturer)	Synthetic method	Polymer	Elastomer	Notes
Ren-Flex[TM] (Dexter), Hifax[R] (Himont), Polytrope[R] (Schulman), Telcar[R] (Teknor Apex), Ferroflex[R] (Ferro), Flexothene[R] (Quantum)	Blend	PP	EPDM or EPR	Relatively hard, low density, not highly filled
Santoprene[R] (AES), Sarlink[R] (Novacor, DSM), Uniprene[R] (Teknor Apex), Hifax[R] (Himont)	Dynamic vulcanizate[a]	PP	EPDM	Better oil resistance, low compression set, softer
Trefsin[R] (AES), Sarlink 2000 (Novacor, DSM)	Dynamic vulcanizate	PP	Butyl rubber	Low permeability, high damping
Vyram[R] (AES)	Dynamic vulcanizate	PP	Natural rubber	Low cost
Geolast[R] (AES)	Dynamic vulcanizate	PP	Nitrile rubber	Oil resistant
Alcryn[R] (DuPont)	Blend	Chlorinated polyolefin	Ethylene reactive blend	Single phase, soft, oil resistant
Sarlink[R] 1000 (Novacor, DSM)	Dynamic vulcanizate	PVC	Nitrile rubber	Oil resistant
Chemigum[R] (Goodyear), Apex[R] N (Teknor Apex), Elastar[R] (Nippon Zeon)	Blend	PVC	Nitrile rubber	Oil resistant
Rimplast[R] (Petrarch Systems)	Blend	PA	Silicone rubber	Medical applications
Kraton IPN[R] (Shell)	Blend	Polyester	SEBS	Automotive

[a]Dynamic vulcanizate: usually, the EPDM is cross-linked via free radical methods during a shearing action of the blend, often accompanied by a partial phase inversion to dual-phase continuity

[b]Based on Holden (1996), Chap. 16, Table 16.10; AES advanced elastomer systems

cellulose, triglyceride oils, and natural rubber, among other materials. Some IPNs based on renewable resources are summarized in Table 6.10. These materials suffer from two drawbacks in the current era: Research on them is passé and rather poorly funded. Secondly, the price of many renewable resources, such as castor oil and cellulose, is actually above the corresponding prices for petroleum-based products.

6.5.3 Biomedical IPNs

It has been said that people working on new applications are more willing to consider new materials than people working on established applications. This is certainly a truism when considering the biomedical applications of polymeric materials; see Table 6.11. The emphasis on soft contact lenses is remarkable.

Table 6.10 Renewable resource IPNs

Polymer 1	Polymer 2	Application	References
Castor oil urethanes	Acrylics	Coatings for hydroelectric dams and iron, tough plastics	Tan (1994), Xie et al. (1993), Sperling et al. (1981)
PEG	Dextran	Multistimuli-responsive drug	Kurisawa et al. (1995)
Natural rubber	PMMA	Rubber-toughened plastics	Natural Producers (1997), Schneider et al. (1996), Hourston and Romain (1990)
Allyl cellulose cinnamonate	Styrenics and acrylics	Improved thermal stability	Kamath et al. (1996)
Hyaluronic acid	Synthetic polymer	Biomedical and sanitary fields	Giusti and Callegaro (1997)

Table 6.11 Biomedical applications of IPNs

Polymer 1	Polymer 2	Application	References
Poly(vinylpyrrolidone)	HEMA	Gradient, refractive index soft contact lenses	Calderara et al. (1996)
Polytetrafluoroethylene	Poly(dimethyl siloxane)	Burn dressing	Dillon (1989, 2006)
Poly(dimethyl siloxane)	Poly(acrylic acid)	High-permeability soft contact lenses	Robert et al. (1995)
Acrylic	PEO/PPE	Controlled transdermal drug delivery	Cho et al. (1995)
Poly(ε-caprolactone)	PEG	Bioerodible drug release	Kim et al. (1995)
PU	Maleimide-PU	Blood compatibility	Hsieh et al. (1997)
Polyurea	Poly (2-hydroxyethyl methacrylate)	Contact lenses via reaction injection molding	Hill et al. (1996)
PEG	Dextran	Drug delivery	Kurisawa et al. (1995)
Poly(methyl methacrylate)	Poly(methyl methacrylate)	Artificial teeth	Roemer and Tateosian (1984)
Silicone rubber	Polyurethanes	Steam sterilizable tubing	Anon. (1983)
Poly(N-isopropyl acrylamide)	Polyurethane or poly(acrylic acid)	Drug release	Lim et al. (1997)
Poly(ethylene glycol)	Poly(acrylic acid)	Body parts improvement or replacement	Waters et al. (2011)
Poly(ethylene glycol methyl ether methacrylate)	Poly(acrylic acid)	Body parts improvement or replacement	Naficy et al. (2012)

The first item, showing a gradient IPN being used to form a gradient refractive index material, is the most interesting. Of course, there are two ways to bend light, either to have a curved surface, the basis of most lenses, or to have a variable refractive index. This invention combines the two. The second item in Table 6.11 addresses burn dressings. In this case, a polytetrafluoroethylene film is filled with silicone rubber to prepare a dual-phase continuity structure. The silicone rubber provides high permeability allowing moisture to escape, while the polytetrafluoroethylene provides mechanical strength. Together, they are transparent, allowing better observation of the healing burn wound. A similar type of material is also used for applications, such as wound care, scar management, and others (Dillon 1997, 2006).

Over the years, the interest in IPNs for biomedical applications has increased. One "trick" being developed is to have one network with low cross-link density and the other with high cross-link density. The result has been shown to yield stronger, more fracture-resistant materials. As will be shown below, this idea works even if the two polymers are otherwise identical, i.e., homo-IPNs. Also, many of the new, proposed materials are versions of hydrogels. Since these materials are intended for improvement or replacement of body parts, many are studied at body pH: 7.4.

Waters et al. (2011) investigated IPN hydrogels based on a tightly cross-linked poly(ethylene glycol) network and a loosely cross-linked poly(acrylic acid) network, with emphasis on pH = 7.4. This idea of having one network tight and one loose was originated by Gong et al. (2003). This yields a self-reinforced material, with one network able to stretch under applied strain and the other able to stop crack growth. This idea dominates much of what follows for the hydrogels that will be mentioned below.

Another paper using the idea above as modified is a hydrogel based on poly (ethylene glycol methyl ether methacrylate) with poly(acrylic acid) (Naficy et al. 2012). Network I has a structure termed "bottle brush," signifying long chains attached to a master backbone chain. Poly(acrylic acid) constitutes the second network. Here, the second network contributes the larger part of the structure. These materials became transparent at a pH greater than 5. These materials are able to retain a large fraction of water. Due to their soft nature, etc., they are very similar to real biological systems.

An important possible application of these materials is as drug delivery systems with antibacterial properties (Silan et al. 2012). Compositions such as poly (acrylonitrile-co-(3-acrylamidoproplyl trimethyl ammonium chloride led to core-shell nanoparticles. Further, IPN microgels were prepared by mixing double quaternized poly(acrylonitrile-co-vinylpyridine). Suitable inherently antibacterial materials include silvery nanoparticles, copper nanoparticles, copper oxide nanoparticles, and chitosan, among many others. Also, the electrostatic interactions between positively charged polymers and the negative charges on the cell walls of bacteria cause disruption of the cell wall, leading to death of the bacteria.

Table 6.12 IPNs for nonlinear optical applications

Polymer 1	Polymer 2	Application	References
Polyurethane	Polyacrylate	Good temporal stability	Xie et al. (1997)
Epoxy	Phenoxysilicon polymer	Frequency doubling	Tripathy et al. (1995)
Epoxy	Phenoxy	Optical wave guide	Martununkul et al. (1995)
Polycarbonate	Acrylic	Second-order nonlinear optics	Tripathy et al. (1996)

6.5.4 Nonlinear Optical Materials

Nonlinear optics is concerned with the manipulation of electromagnetic energy, particularly into different wavelengths than the original. For second-order nonlinear optics, an asymmetric molecule is required. While such molecules clearly do not need to be polymeric, the use of asymmetric polymer chains and side chains produces materials with spatial and temporal stability. Such asymmetric groups have the capability of holding one photon until another arrives, and then the energies may be added, with a single photon of twice the frequency produced, or other algebraic manipulations may be undertaken. As may be expected, a wider range of mechanical behavior patterns arise through the application of IPN technology; see Table 6.12. A leader in the field is Tripathy, with a patent (Tripathy et al. 1996) in nonlinear optic applications for IPNs.

6.5.5 Sound and Vibration Damping

One of the major effects of having extensive but incomplete mixing in two polymers, whether cross-linked or not, is that a very broad glass transition region may result, one that spans the temperature range between the two original glass transitions. Compared to their non-cross-linked counterparts, it is easier to prepare such materials with IPN technology; see Table 6.13. While the evidence is debatable whether such IPNs have more total damping (it seems to depend on the composition), having substantially the same damping level over a broad temperature range is good for outdoor and machinery applications. For example, a car door will be equally damped in winter and summer, and over broad frequency ranges, as well as at the standard 25 °C, 600 Hz standard conditions. However, the vinyl-phenolic composition (Yamamoto and Takahashi 1990) (in Table 6.13) damps specifically at the elevated temperatures at which machinery operates, but only weakly at room temperature.

6.5.6 Compatibilizing Phase-Separated IPNs

Most IPNs consist of two polymers that phase separate during synthesis. While the domains are usually very small, the dual network structure and positive heat of mixing result in two phases.

Table 6.13 Sound and vibration damping materials via IPN formation

Polymer 1	Polymer 2	Comments	References
Polystyrene	Polyacrylate	Latex IPNs	Wang et al. (1996)
Polyacrylate	Polystyrene	Latex IPNs	Liu et al. (1997)
PU	Poly(butyl methacrylate)	Good damping	Brovko et al. (1995)
SBR	Acrylic	Latex IPN, polymer 3: SAN	Hu et al. (1997)
Vinyl	Phenolic	Damps machinery at high temperatures	Yamamoto and Takahashi (1990)
Polyurethane	Acrylic	Full and semi-IPNs	Hourston et al. (1986b)

There are, however, several pairs of IPN polymers that have been made miscible (Lipatov and Alekeeva 2007). The most useful way consists of introducing compatibilizers that react or interact at the interfaces of both polymers of the synthesis. These compatibilizers form an intermediate region between the two phases in question. Major results include a decrease in the interfacial tension between the two networks, allowing greater contact at the interfaces between the two networks, which permits greater contact at the interface between the two polymers. Depending on the IPN pair, frequently used compatibilizers include 2-hyroxyethylmethacrylate, oliourethane dimethacrylate, and triblock urethane with both ends containing $CH_3–CH_2–O–CH_2–CH_2–$.

These compatibilizers form an intermediate region between the two original phases in question. Major results include a decrease in the interfacial tension between the two networks, allowing greater contact at the interface between the two polymers. The compatibilizers should be distributed throughout the mix of the two polymers, improving the thermodynamics interactions. Note that the compatibilizer should have a negative value of the thermodynamic quantity X. However, Lipatov and Alekseeva (2007) point out that there are actually two types of compatibilization: non-equilibrium compatibilization and true thermodynamic stability of the two polymer components after network polymerization is complete. A simple test of the compatibilizer's success is via dynamic mechanical characterization. If the blend shows two tan (delta) maxima, and the compatibilized system only one maximum, that is a measure of success. In other words, if the polymer mix has only one glass transition, it is usually considered miscible (of course, the two polymers separated should have different glass transition temperatures). Sometimes, a range of glass transitions are noted, resulting in an apparent but incomplete miscibility.

There are other ways of increasing compatibilization. These may be through grafting reactions between the two networks, etc. On very rare occasions, true miscibility may exist without compatibilizers.

Some important ways of establishing compatibility include changing the polymerization sequences, introduction or prior presence of oppositely charged groups, and the formation of hydrogen bonds. Of course, one very broad glass transition range may be found, substantially running from T_{g1} to T_{g2} of the two polymers, representing partial mixing with all possible compositions coexisting in the mix. Some examples of compatibilized IPNs are collected in Table 6.14.

Table 6.14 Compatibilized IPNs

Polymer I	Polymer II	References
Poly(butyl acrylate) or poly(butyl methacrylate)	Diallyl network	Derrough et al. (1993)
Polyurethane	Polyacrylate	Yu et al. (1999)
Poly(dimethyl)siloxane urethane	Poly(methyl methacrylate)	Zhou et al. (1994)
Polyurethane	Unsaturated polyesters	Kim and Kim (1987)
Polyurethane	Poly(butyl methacrylate)	Lipatov et al. (2007)
Polyurethane	Polystyrene	Hourston and Schafer (1997)

6.5.7   Current Status of IPNs

Today, the rate of publications in the area of IPNs is approaching 100 papers per year. As may be expected, a relatively large fraction is devoted to applications (Sperling 2011). Some interesting examples relate to electronic devices. Plesse et al. (2004), for example, synthesized conducting IPNs, useful for actuators. The IPN synthesis was based on poly(ethylene oxide) and polybutadiene networks, containing a conducting polymer poly(3,4-ethylenedioxytheiophene (Plesse et al. 2004). High modulus and dimensionally stable polyimide IPN substrates were claimed to be used in flexible printed circuits, tape-automated bonding tapes, metal interconnectors for integrated circuits, and other similar types of electronic applications (Uhara 2004). Tran-Van et al. described IPNs for electrochromic devices (Tran-Van et al. 2008). Some other applications include fuel cell membranes (Morin. et al. 2010). The readers of this article may expect to see the list go on and on.

6.5.8   A Few More Exciting Materials

One interesting invention is a poly(2,6-dimethylphenylene oxide)-poly(styrene-HEMA)-based IPN that is useful for solar heating (Eck et al. 1995). The IPN has an adjustable lower critical solution temperature, so that when coated onto the glass panels, it clouds up if the temperatures inside get too hot. Polymer blends will not work so effectively for this application, because when they phase separate, the phases may continue to grow; thus the time to come back to a one-phased material may be long. The IPN structure restrains phase domain growth, so that the material, acting as a *smart material*, clouds and clears relatively rapidly, reacting to the temperature of the structure it is protecting.

Other areas of IPN application cover circuit boards (Tate and Varnell 1989; Takahashi et al. 1996) and, via gradient IPN technology, improved optical fibers (Bukhbinder and Kosjakov 1996). This last works by having a gradient refractive index from the axis to the surface, curving the light back away from the surface and

reducing the fraction of light leaving the fiber for the exterior. Another area of interest involves coatings and adhesives. An overcoat layer comprising a polyolefin/epoxy semi- or full IPN for a metal substrate was claimed in several patents (Ylitalo et al. 1997; Perez et al. 2007, 2010). The metal article can be a pipe, vessel, conduit, rod, profile-shaped article, or tube. Such kind of coating can provide a good resistance to various chemicals, such as petroleum, water, natural gas, methane, ammonia, gasoline, oxygen, hydrogen, as well as various industrial chemicals. Golf balls containing IPNs have also been claimed in several patents since 2007 (Kuntimaddi and Bulpett 2007; Kuntimaddi et al. 2008, 2010, 2011, 2013). Since a golf ball has multiple layers (up to 4 layers), the IPN technology is used to form one or more of the layers. At least two polymeric compounds are included. The first polymeric system may include a polyurethane-based or polyurea-based system and the second polymeric system may include an epoxy-based or acrylic-based system. For a golf ball, a high shear resistance, which indicates the ability of a material to maintain its mechanical stability and integrity upon the application of a shear stress to that material, is required. With IPN technology in the particular layer (e.g., core, intermediate, or cover layer), the shear resistance of that layer is increased. In addition, the resistance to moisture penetration of that layer is also increased. Consequently, the mechanical properties, such as tensile or flexural modulus and impact resistance, and durability of such golf ball will be less affected, resulting in longer lifetime. Some recent patents also claimed highly microporous thermoplastic/bismaleimide semi-IPNs to be used as a gas separation membrane (Kumar and Kurdi 2010) and porous IPNs to be used for chromatography and filtration of various compounds including biomolecules (Bonner et al. 2012).

   In summary, many of the IPN applications do not depend on high modulus or impact resistance (but some do!); these materials often show their best properties in the leathery, rubbery, or swollen states. Thus, it is seen that the applications for IPNs cover a broad range today.

6.6   Conclusions

The field of IPNs is simultaneously one of the oldest in multicomponent polymer literature and one of its newest and fastest growing fields. With IPNs, it is relatively easy to prepare very small domain sizes and/or materials with dual-phase continuity. IPNs can be made via a multitude of ways: sequential, simultaneous, latex, gradient, and thermoplastic, to name some of the more prominent materials.

   While IPNs can be and have been made extremely tough and impact resistant, many of the proposed applications involve such diverse fields and sound and vibration damping, biomedical materials, and nonlinear optics. This is because the presence of cross-links in both polymers reduces creep and flow, allowing relatively stable materials with a wide range of moduli to be prepared. Thus, those materials with leathery mechanical behavior, combinations of elastomers and plastics, are especially interesting to scientists, inventors, and engineers.

6.7   Cross-References

Abbreviations and Acronyms

AA   Acrylic acid
Bd   Butadiene
DACBA   Diallyl carbonate of bisphenol-A
DMS   Dynamic mechanical spectroscopy
EA   Ethyl acrylate
EMA   Ethyl methacrylate
EPDM   Ethylene-propylene-diene copolymer
HEMA   Hydroxyethyl methacrylate
IENs   Interpenetrating elastomer networks
IPN   Interpenetrating polymer network
LA   Loss area
LIPN   Latex interpenetrating polymer network
nBA   *n*-butyl acrylate
NBR   Nitrile butadiene rubber
PA   Polyamide
PAA   Poly(acrylic acid)
PAcr   Polyacrylate
PB   Polybutadiene
PI   Polyisoprene
PMMA   Poly(methyl methacrylate)
PP   Polypropylene
PPE   Poly(2,6-dimethyl phenylene oxide)
PS   Polystyrene
PU   Polyurethane
PVC   Poly(vinyl chloride)
S   Styrene
SBR   Styrene butadiene rubber
SEBS   Styrene ethylene butylene styrene
SIN   Simultaneous interpenetrating network
TA   Tan(delta) area
TBPIN   *t*-butyl peroxyisononanoate
U   Urethane
VAc   Vinyl acetate
VOC   Volatile organic compounds

References

J.J. Aklonis, W.J. MacKnight, *Introduction to Polymer Viscoelasticity*, 2nd edn. (Wiley, New York, 1983)

Anonymous, Mod. Plast. Feb 12 (1983)

ASTM, D 4946 89, ASTM, Philadelphia (1989)

J.W. Aylsworth, U. S. Patent 1,111,284, 1914

J. Berg, D. Sundberg, B. Kronberg, Polym. Mat. Sci. Eng. **54**, 367 (1986)

A.G. Bonner, L. Udell, D.W. Andrews, F.D. Tsai, G.D.L. Reyes, U.S. Patent 8,298,657, 2012

A.A. Brovko, L.M. Sergeeva, L.M. Karabanova, L.A. Gorbach, Ukr. Khim. Zh. **61**, 58 (1995)

T.L. Bukhbinder, V.I. Kosjakov, Vysokomol. Soed., Ser. B **28**, 625 (1996)

I. Calderara, D. Baude, D. Jayeux, D.J. Lougnot, Polym. Mat. Sci. Eng. (Prepr.) **75**, 244 (1996)

M.C.O. Chang, D.A. Thomas, L.H. Sperling, J. Appl. Polym. Sci. **34**, 409 (1987)

M.C.O. Chang, D.A. Thomas, L.H. Sperling, J. Polym. Sci. Polym. Phys. Ed. **26**, 1627 (1988)

J.H. Chen, L. Wang, Gaofenzi Cailiao Kexue Yu Gong Cheng **11**(2), 46 (1995a)

J.H. Chen, L. Wang, Gongneng Gaofenzi Xuebao **8**(2), 220 (1995b)

I. Cho, K.W. Lee, J. Appl. Polym. Sci. **30**, 1903 (1985)

S.C. Cho, S.O. Choi, Y.H. Bae, Y.H. Kim, Drug Deliv. Syst. **10**, 437 (1995)

A.Y. Coran, R.P. Patel, in *Thermoplastic Elastomers*, ed. by G. Holden, N.R. Legge, R. Quirk, H.E. Schroeder, 2nd edn. (Hanser, Munich, 1996)

R.D. Corsaro, L.H. Sperling (eds.), *Sound and Vibration Damping with Polymers*. ACS Symposium Series, vol. 421 (American Chemical Society, Washington, DC, 1990)

A.J. Curtius, M.J. Covitch, D.A. Thomas, L.H. Sperling, Polym. Eng. Sci. **12**, 101 (1972)

E.S. Daniels, A. Klein, Prog. Org. Coat. **19**, 359 (1991)

S. Davison, W.P. Gergen, U.S. Patent 4,041,103, 1977

S.N. Derrough, C. Rout, J.M. Widmaier, J. Appl. Polym. Sci. **48**, 1183 (1993)

M.E. Dillon, U.S. Patent 4,832,009, 1989

M.E. Dillon, U.S. Patent 5,656,279, 1997

M.E. Dillon, U.S. Patent 7,087,135, 2006

A.A. Donatelli, L.H. Sperling, D.A. Thomas, Macromolecules **9**, 671 (1976)

A.A. Donatelli, L.H. Sperling, D.A. Thomas, J. Appl. Polym. Sci. **21**, 1189 (1977)

L.S. Dong, Y. Tong, Y.X. An, H. Tang, Y.G. Zhang, Z.L. Feng, Gaofenzi Cailiao Kexue Yu Gongcheng **11**(6), 9 (1995)

F.E. DuPrez, P. Tan, E.J. Goethals, Polym. Adv. Technol. **7**, 257 (1996)

Y.G. Durant, D.C. Sundberg, J. Appl. Polym. Sci. **58**, 1607 (1995)

W. Eck, H.R. Wilson, H.J. Cantow, Adv. Mater. **7**, 800 (1995)

H.G. Elias, *An Introduction to Polymer Science* (VCH, Weinheim, 1997)

I.G. Farbenindustrie, British. Patent 358,534, 1931

J.J. Fay, C.J. Murphy, D.A. Thomas, L.H. Sperling, in *Sound and Vibration Damping with Polymers*, ed. by R.D. Corsaro, L.H. Sperling (American Chemical Society, Washington, DC, 1990)

J.J. Fay, C.J. Murphy, D.A. Thomas, L.H. Sperling, Polym. Eng. Sci. **31**, 1731 (1991)

J. Feng, M.A. Winnik, R. Shivers, B. Clubb, Macromolecules **28**, 7671 (1995)

J.N. Foster, L.H. Sperling, D.A. Thomas, J. Appl. Polym. Sci. **33**, 2637 (1987)

D.G. Fradkin, J.N. Foster, L.H. Sperling, D.A. Thomas, Rubber Chem. Technol. **59**, 255 (1986a)

D.G. Fradkin, J.N. Foster, L.H. Sperling, D.A. Thomas, Polym. Eng. Sci. **26**, 730 (1986b)

J.M. Friel, European Patent Application 0 466 409 A1, 1992

H.L. Frisch, D. Klempner, K.C. Frisch, J. Polym. Sci. Polym. Phys. Ed. **7**, 775 (1969a)

H.L. Frisch, D. Klempner, K.C. Frisch, Polym. Lett. **7**, 775 (1969b)

Y.Z. Geng, Tuliao Gongye **4**, 11 (1992)

W.P. Gergen, S. Davison, U.S. Patent 4,101,605, 1978

W.P. Gergen, R.G. Lutz, S. Davison, in *Thermoplastic Elastomers*, ed. by G. Holden, N.R. Legge, R. Quirk, H.E. Schroeder, 2nd edn. (Hanser, Munich, 1996)

J.M. Geurts, M. Lammers, A.L. German, Colloids. Surf., A **108**(295) (1996)

A.C. Gilicinski, C.R. Hegedus, in *Film Formation in Waterborne Coatings*, ed. by T. Provder, M.A. Winnik, M.W. Urban (ACS Books, Washington, DC, 1996)

P. Giusti, L. Callegaro, U.S. Patent 5,644,049, 1997

J.P. Gong, Y. Katsuyama, T. Kurokawa, Y. Osada, Adv. Mater. **15**(14), 1155 (2003)

J.A. Grates, D.A. Thomas, E.C. Hickey, L.H. Sperling, J. Appl. Polym. Sci. **19**, 1731 (1975)

X. He, J.M. Widmaier, G.C. Meyer, Polym. Int. **32**, 295 (1993)

G.A. Hill, K.C. Frisch, V. Sendijarevic, S. Wong, Japan Patent 08294936 A2, 1996, to Johnson and Johnson

G. Holden, in *Thermoplastic Elastomers*, ed. by G. Holden, N.R. Legge, R. Quirk, H.E. Schroeder, 2nd edn. (Hanser, Munich, 1996)

H. Hopff, German Patent 623,351, 1935

D.J. Hourston, J. Romain, J. Appl. Polym. Sci. **39**, 1587 (1990)

D.J. Hourston, R. Satgurunathan, J. Appl. Polym. Sci. **29**, 2969 (1984)

D.J. Hourston, R. Satgurunathan, J. Appl. Polym. Sci. **33**, 215 (1987)

D.J. Hourston, F.U. Schafer, Polym. Adv. Technol. **7**, 273 (1996)

D.J. Hourston, F.U. Schafer, in *IPNs Around the World: Science and Engineering*, ed. by S.C. Kim, L.H. Sperling (Wiley, New York, 1997), p. 155

D.J. Hourston, M.G. Huson, J.A. McCluskey, J. Appl. Polym. Sci. **32**, 3881 (1986a)

D.J. Hourston, R. Satgurunthan, H.C. Varma, J. Appl. Polym. Sci. **31**, 1955 (1986b)

D.J. Hourston, R. Satgurunathan, H.C. Varma, J. Appl. Polym. Sci. **34**, 901 (1987)

K.H. Hsieh, D.C. Liao, C.Y. Chen, W.Y. Chiu, Polym. Adv. Technol. **7**, 265 (1996)

K.H. Hsieh, C.Y. Chen, D.C. Liao, W.Y. Chiu, in *IPNs Around the World: Science and Engineering*, ed. by S.C. Kim, L.H. Sperling (Wiley, Chichester, 1997)

R. Hu, V.L. Dimonie, M.S. El-Aasser, R.A. Pearson, L.H. Sperling, A. Hiltner, S.G. Mylonakis, J. Appl. Polym. Sci. **58**, 375 (1995)

R. Hu, V.L. Dimonie, M.S. El-Aasser, J. Appl. Polym. Sci. **64**, 1123 (1997a)

R. Hu, V.L. Dimonie, M.S. El-Aasser, R.A. Pearson, A. Hiltner, S.G. Mylonakis, L.H. Sperling, J. Polym. Sci. A: Polym. Chem. **35**, 2193 (1997b)

R. Hu, V.L. Dimonie, M.S. El-Aasser, R.A. Pearson, A. Hiltner, S.G. Mylonakis, L.H. Sperling, J. Polym. Sci. B: Polym. Phys. **35**, 1501 (1997c)

V. Huelck, D.A. Thomas, L.H. Sperling, Macromolecules **5**, 340,348 (1972)

S. Isao, Y. Naoki, Y. Akira, U.S. Patent 5,132,359, 1992

J.L. Jonsson, H. Hassander, L.H. Jansson, B. Tornell, Macromolecules **24**, 126 (1991)

G.M. Jordhamo, J.A. Manson, L.H. Sperling, Polym. Eng. Sci. **26**, 518 (1986)

M. Kamath, J. Kincaid, B. Mandal, J. Appl. Polym. Sci. **59**, 45 (1996)

H. Keskkula, S.G. Turley, R.F. Boyer, J. Appl. Polym. Sci. **15**, 351 (1971)

N. Kessel, D.R. Illsley, J.I. Keddie, J. Coat. Technol. Res. **5**(3), 285–297 (2008)

J.H. Kim, S.C. Kim, Polym. Eng. Sci. **27**, 1243, 1252 (1987)

S.C. Kim, L.H. Sperling (eds.), *IPNs Around the World: Science and Engineering* (Wiley, Chichester, 1997)

B.S. Kim, T. Chiba, T. Inoue, Polymer **34**, 2809 (1993)

S.O. Kim, J.H. Ha, Y.J. Jung, C.S. Cho, Arch. Pharmacal Res. **18**, 18 (1995)

S.C. Kim, L.H. Sperling, (eds.), Polym. Adv. Technol. (Special IPN issue) (Apr 1996)

A. Klein, E.S. Daniels, in *Emulsion Polymerization and Emulsion Polymers*, ed. by P.A. Lovell, M.S. El Aasser (Wiley, Chichester, 1997)

D. Klempner, K.C. Frisch, in *Advances in Interpenetrating Polymer Networks*, vol. I (1989), vol. II (1990), vol. III (1993), vol. IV (1993) (Technomic, Lancaster)

D. Klempner, L.H. Sperling, L.A. Utracki, *Interpenetrating Polymer Networks*. Advances in Chemistry Series, vol. 239 (American Chemical Society, Washington, DC, 1994)

X.Z. Kong, C.Y. Kan, Q. Yuan, Polym. Adv. Technol. **7**, 888 (1996)

A. Kowalski, M. Vogel, R.M. Blankenship, U.S. Patent 4,468,498, 1984

S.J. Krause, J. Macromol. Sci., Rev. Macromol. Chem **C7**(2), 251 (1972)

A. Kumar, J. Kurdi, U.S. Patent 7,785,397, 2010

M. Kuntimaddi, D.A. Bulpett, U.S. Patent 7,175,545, 2007

M. Kuntimaddi, S. Wu, K.M. Harris, M. Rajagopalan, D.A. Bulpett, M.E. Lutz, U.S. Patent 7,429,220, 2008

M. Kuntimaddi, S. Wu, M. Rajagopalan, U.S. Patent 7,851,561, 2010

M. Kuntimaddi, S. Wu, M. Rajagopalan, U.S. Patent 7,888,448, 2011

M. Kuntimaddi, S. Wu, K.M. Harris, M. Rajagopalan, D.A. Bulpett, M.E. Lutz, U.S. Patent 8,353,788, 2013

M. Kurisawa, M. Terano, N. Yui, Macromol. Rapid Commun. **16**, 663 (1995)

P.I. Lee, in *Emulsion Polymers and Emulsion Polymerization*, ed. by D.R. Bassett, A.E. Hamielec. ACS Symposium Series, vol. 165, 1981, p. 405

D.I. Lee, T. Ishikawa, J. Polym. Sci., Polym. Chem. **21**, 147 (1983)

S. Lee, A. Rudin, Macromol. Chem. Rapid Commun. **10**, 655 (1989)

S. Lee, A. Rudin, in *Polymer Latex: Preparation, Characterization and Application*, ed. by E.S. Daniels, D. Sudol, M.S. El-Aasser. ACS Symposium Series, vol. 492 (American Chemical Society, Washington, DC, 1992)

D.I. Lee, T. Kawamura, E.F. Stevens, U.S. Patent 4,569,964, 1986

P.M. Lesko, P.R. Sperry, in *Emulsion Polymerization and Emulsion Polymers*, ed. by P.A. Lovell, M.S. El-Aasser (Wiley, Chichester, 1997)

S.C. Li, W.J. Peng, X.P. Lu, Int. J. Polym. Mater. **29**(12), 37 (1995)

Y.H. Lim, D. Kim, D.S. Lee, J. Appl. Polym. Sci. **64**, 2647 (1997)

M.K. Lindemann, K. Deacon, U.S. Patent 4,616,057, 1986; 4,686,260, 1987; 5,169,884, 1992;, 5,177,128, 1993 and 5,190,997, 1993

Y.S. Lipatov, in *Advances in Interpenetrating Polymer Networks*, ed. by D. Klempner, K. Frisch (Technomic, Lancaster, 1989)

Y.S. Lipatov, T.T. Alekeeva, *Phase Separated Interpenetrating Polymer Networks* (Springer, Berlin, 2007). This book is an exact reproduction of a review article published in Adv. Polym. Sci., 1–227, 208 (2007)

Y.S. Lipatov, L.M. Sergeeva, Russ. Chem. Rev. **45**(1), 63 (1967)

R.Y. Liu, J.Y. Wang, S.R. Tang, Y.W. Li, X.Y. Tang, Tuliao Gongye **3**, 4 (1995)

R. Liu, J. Wang, Q. Han, Y. Li, X. Tang, Gaofenzi Xuebao **2**, 213 (1997)

J.E. Lorenz, D.A. Thomas, L.H. Sperling, in *Emulsion Polymerization*, ed. by I. Piirma, J.L. Gardon. ACS Symposium Series, vol. 24 (American Chemical Society, Washington, DC, 1976). Chapter 20

P.A. Lovell, M.S. El-Aasser (eds.), *Emulsion Polymerization and Emulsion Polymers* (Wiley, Chichester, 1997)

S. Martununkul, J.I. Chen, L. Li, X.L. Jiang, R.J. Jeng, S.K.I. Sengupta, J. Kumar, S.K. Tripathy, *Polymers for Second Order Nonlinear Optics* (American Chemical Society, Washington, DC, 1995)

F. Merger, H.M. Hutmacher, W. Schwarz, G. Nestler, M.G. Szucksanyi, R. Mueleer Mall, U.S. Patent 4,777,265, 1988

J.R. Millar, J. Chem. Soc. **263**, 1311 (1960)

T.T. Min, A. Klein, M.S. El-Aasser, J.W. Vanderhoff, J. Polym. Sci. Polym. Chem. Ed. **21**, 2845 (1983)

V. Mishra, L.H. Sperling, *The Polymeric Materials Encyclopedia: Synthesis, Properties and Applications* (CRC Press, Boca Raton, 1996)

V. Mishra, F.E. DuPrez, E. Gosen, E.J. Goethals, L.H. Sperling, J. Appl. Polym. Sci. **58**, 331 (1995)

I. Mita, S. Akiyama, Plast. Eng. **40**, 393 (1997)

M. Mizoguchi, Y. Fuseya, Y. Fujita, Y. Ishino, M. Seki, T. Miyawaki, European Patent 750023Al, 1996

A. Morin, B. Ameduri, L. Chikh, O. Fichet, G. Gebel, M. Mercier, WO/2010/066964

S. Naficy, J.M. Razal, P.G. Whitten, G.G. Wallace, G.M. Spinks, Polym. Phys. **50**, 423 (2012)

P. Nagarajan, C.K. Mital, M.K. Trivedi, J. Appl. Polym. Sci. **59**, 191 (1996a)
P. Nagarajan, C.K. Mital, M.K. Trivedi, J. Appl. Polym. Sci. **59**, 197 (1996b)
P. Nagarajan, C.K. Mital, M.K. Trivedi, Paint India **46**(2), 19 (1996c)
P. Nagarajan, M.K. Trivedi, C.K. Mital, J. Appl. Polym. Sci. **59**, 203 (1996d)
P. Nagarajan, M.K. Trivedi, C.K. Mital, J. Appl. Polym. Sci. **59**, 209 (1996e)
P. Nagarajan, M.K. Trivedi, C.K. Mital, Polym. Mater. Sci. Eng. **76**, 348 (1997)
M. Narkis, Y. Talmon, M. Silverstein, Polymer **26**, 1359 (1985)
M. Narkis, Y. Talmon, M. Silverstein, J. Elastom. Plast. **18**(3), 136 (1986)
Natural Rubber Producers Research Association, Technical Information Sheet No. 9, Revised (1997)
N. Nemirovski, M.S. Silverstein, M. Narkis, Polym. Adv. Technol. **7**, 247 (1996)
H.D. Notta, in *Proceeding of the Waterborne Symposium*, New Orleans, 28 Feb–4 Mar 2011,
    p. 110
I. Ostromislensky, U.S. Patent 1,613,673, 1927
A.A. Patel, J. Feng, M.A. Winnik, G. Vancso, Polymer **37**, 5577 (1996)
D.R. Paul, J.W. Barlow, J. Macromol. Sci. Rev. Macromol. Chem. **C18**, 109 (1980)
W.J. Peng, S.C. Li, J. Appl. Polym. Sci. **58**, 967 (1995)
M.A. Perez, T.L. Wood, S.M. Attaguile, U.S. Patent 2007/0036982, 2007
M.A. Perez, T.L. Wood, S.M. Attaguile, U.S. Patent 7,790,288, 2010
I. Piirma, in *Encyclopedia of Polymer Science and Engineering*, ed. by J.I. Kroschwitz, 2nd edn.
    (Wiley, New York, 1989) (Supplement Volume)
C. Plesse, F. Vidal, H. Randrianahazaka, D. Teyssie, C. Chevrot, Polymer **46**, 7771 (2004)
J.Y. Qian, R.A. Pearson, V.L. Dimonie, M.S. El-Aasser, J. Appl. Polym. Sci. **58**, 439 (1995)
S. Rajasingham, B. Jan, A. Jack, WO 03/031526 A1, 2003
B. Rearick, S. Swarup, P. Kamarchik, J. Coat. Technol. **68**(862), 25 (1996)
C. Robert, C. Bunel, J.P. Vairon, European Patent Application 643,083, 1995
L.M. Robeson, L.A. Vratsanos, S.A. Miller, US6656998, 2003
F.D. Roemer, L.H. Tateosian, European Patent, 0 014 515, 1984
C. Rouf, S. Derrough, J.J. Andre, J.M. Widmaier, G.C. Meyer, in *Interpenetrating Polymer
    Networks*, ed. by D. Klempner, L.H. Sperling, L.A. Utracki. Advances in Chemistry Series,
    vol. 239 (ACS Books, Washington, DC, 1994)
M. Schneider, T. Pith, M. Lambla, Poly. Adv. Technol. **7**, 577 (1996a)
M. Schneider, T. Pith, M. Lambla, Polym. Adv. Technol. **7**, 425 (1996b)
I. Segall, V.L. Dimonie, M.S. El-Aasser, P.R. Soskey, S.G. Mylonakis, J. Appl. Polym. Sci.
    58, 385, 401, and 419 (1995)
H.R. Sheu, M.S. El-Aasser, J.W. Vanderhoff, J. Polym. Sci: Part A: Polym. Chem. **28**, 653 (1990a)
H.R. Sheu, M.S. El-Aasser, J.W. Vanderhoff, J. Polym. Sci. Part A: Polym. Chem. **28**, 629 (1990b)
D.L. Siegfried, D.A. Thomas, L.H. Sperling, Macromolecules **12**, 586 (1979)
C. Silan, A. Akcali, M.T. Otkun, N. Ozbey, S. Butun, O. Ozay, N. Sahiner, Colloids Surf.
    B Biointerfaces **89**, 248 (2012)
M.S. Silverstein, M. Narkis, Polym. Eng. Sci. **29**, 824 (1989)
M.S. Silverstein, Y. Talmon, M. Narkis, Polymer **30**, 416 (1989)
J. Sionakidis, L.H. Sperling, D.A. Thomas, J. Appl. Polym. Sci. **24**, 1179 (1979)
G.S. Solt, British Patent 728,508, 1955
D. Sophiea, D. Klempner, V. Senjijarevic, B. Suthar, K.C. Frisch, in *Interpenetrating Polymer
    Networks*, ed. by D. Klempner, L.H. Sperling, L.A. Utracki. ACS Symposium Series, vol.
    239 (American Chemical Society, Washington, DC, 1994), p. 39
L.H. Sperling, *Interpenetrating Polymer Networks and Related Materials* (Plenum, New York,
    1981)
L.H. Sperling, Polym. News **12**, 332 (1987)
L.H. Sperling, *Polymeric Multicomponent Materials: An Introduction* (Wiley, New York, 1997)
L.H. Sperling, Chap. 5: History of interpenetrating polymer networks starting with bakelite-based
    compositions, in *100+ Years of Plastics. Leo Baekeland and Beyond*, ed. by E. Thomas Strom,
    S.C. Rasmussen. ACS symposium series, vol. 1080 (Oxford University Press, NewYork, 2011)

L.H. Sperling, J.J. Fay, Polym. Adv. Technol. **2**, 49 (1991)

L.H. Sperling, D.W. Friedman, J. Polym. Sci. **A2**(7), 425 (1969)

L.H. Sperling, H.D. Sarge III, J. Appl. Polym. Sci. **16**, 3041 (1972)

L.H. Sperling, T.W. Chiu, C.P. Hartman, D.A. Thomas, Int.. J. Polym. Mater. **1**, 331 (1972)

L.H. Sperling, T.W. Chiu, D.A. Thomas, J. Appl. Polym. Sci. **17**, 2443 (1973)

L.H. Sperling, T.W. Chiu, R.G. Gramlich, D.A. Thomas, J. Paint Technol. **46**, 47 (1974)

L.H. Sperling, D.A. Thomas, J.E. Lorenz, E.J. Nagel, J. Appl. Polym. Sci. **19**, 2225 (1975)

L.H. Sperling, J.A. Manson, N. Devia Manjarres, U. S. Patent 4,254,002, 1981

J.J. Staudinger, H.M. Hutchinson, U.S. Patent 2,539,377, 1951

H.J. Stern, *Rubber: Natural and Synthetic*, 2nd edn. (Maclaren and Sons Ltd, London, 1967)

D.C. Sundberg, A.P. Casassa, J. Pantazopoulos, M.R. Muscato, J. Appl. Polym. Sci. **41**, 1425 (1990)

A. Takahashi, T. Horiuchi, M. Nomoto, K. Nanaumi, K. Yamamoto, Polym. Adv. Technol. **7**, 329 (1996)

P. Tan, in *Interpenetrating Polymer Networks*, ed. by D. Klempner, L.H. Sperling, L.A. Utracki. Advances in Chemistry Series, vol. 239 (ACS Books, Washington, DC, 1994)

V. Tanrattanakul, E. Baer, A. Hiltner, R. Hu, V.L. Dimonie, M.S. El Aasser, L. Sperling, S.G. Mylonakis, J. Appl. Polym. Sci. **62**, 2005 (1996)

M. Tate, D.F. Varnell, U.S. Patent 4,855,212, 1989

A. Thurman, R.K. Miller, *Fundamentals of Noise Control Engineering* (Fairmont Press, Atlanta, 1986)

F. Tran-Van, L. Beouch, F. Vidal, P. Yammine, D. Teyssie, C. Chevrot, Electrochim. Acta **53**, 4336 (2008)

S. Tripathy, J. Kumar, S. Marturunkakul, J.I. Chen, L. Li, SPE Technol. Pap. **41**, 1611 (1995)

S.K. Tripathy, R.J. Jeng, J. Kumar, S. Marturunkakul, J.I. Chen, U.S. Patent 5,532,320, 1996

K. Uhara, U.S. Patent 6,828,390, 2004

L.A. Utracki, *Polymer Alloys and Blends* (Hanser Publisher, Munich, 1989)

L.A. Utracki, in *Interpenetrating Polymer Networks*, ed. by D. Klempner, L.H. Sperling, L.A. Utracki. Advances Chemistry Series, vol. 239 (ACS Books, Washington, DC, 1994)

F.H. Walker, O. Shaffer, in *Film Formation in Waterborne Coatings*, ed. by T. Provder, M.A. Winnik, M.W. Urban. ACS Symposium Series, vol. 648 (American Chemical Society, Washington, DC, 1996)

J.Y. Wang, R.Y. Liu, W.H. Li, Y.W. Li, X.Y. Tang, Polym. Intern. **39**(2), 101 (1996)

D.J. Waters, K. Engberg, R. Parke-Houben, C.N. Ta, A.J. Jackson, M.F. Toney, C.W. Frank, Macromolecules **44**, 5776 (2011)

J.L. White, *Rubber Processing: Technology, Materials, and Principles* (Hanser Publisher, Munich, 1995)

E.J. Wickson (ed.), *Handbook of PVC Formulating* (Wiley, New York, 1993)

C.L. Winzor, D.C. Sungberg, Polymer **33**, 3797 (1992)

A.E. Woodward, *Atlas of Polymer Morphology* (Hanser Publisher, Munich, 1989)

Z. Wu, D.R. Zhao, Gongneng Gaofenzi Xuebao **8**(4), 480 (1995)

Z. Wu, D.R. Zhao, Gongneng Gaofenzi Xuebao **9**(2), 257 (1996)

H.Q. Xie, J.S. Guo, G.G. Wang, Eur. Poly. J. **29**, 1547 (1993)

H.Q. Xie, X.D. Huang, J.S. Guo, in *IPNs Around the World: Science and Engineering*, ed. by S.C. Kim, L.H. Sperling (Wiley, Chichester, 1997)

Y.S. Xu, T.Y. Cao, F. Long, W.P. Han, Huagong Xuebao **42**(6), 683 (1991)

S. Yak, in *Advances in Interpenetrating Polymer Networks*, ed. by D. Klempner, K.C. Frisch, vol. IV (Technomic Publishing Company, Lancaster, 1994)

K. Yamamoto, A. Takahashi, in *Sound and Vibration Damping with Polymers*, ed. by R.D. Corsaro, L.H. Sperling. ACS Symposium Series, vol. 424 (American Chemical Society, Washington, DC, 1990)

Y. Yang, Y. Chen, R.J. Sheerin, J.F. Mauck, N. Tilara, J. Gracia De Visicaro, WO 2011/153534

S. Yao, M. Jia, X. Yan, Y. Wang, in *Polymers and Biomaterials*, ed. by H. Feng, Y. Han, L. Huang (Elsevier, Amsterdam, 1991)

J.K. Yeo, L.H. Sperling, D.A. Thomas, Polymer **24**, 307 (1983)

Y.L. Yin, X.Z. Zheng, S.R. Yao, Gaofenzi Xuebao **1**, 55 (1988)

Y.L. Yin, S.Z. Zheng, S.R. Yao, B.Z. Zhang, Gaofenzi Cailiao Kexue Yu Gong Cheng (Polym. Mat. Sci. Eng.) **2**, 76 (1991)

D.A. Ylitalo, M.A. Perez, T.M. Clausen, R.J. Devoe, K.E. Kinzer, M.D. Swan, WO Patent 97 11,122 A1, 1997, to 3M

X. Yu, G. Gao, J. Wang, F. Li, X. Tang, Polym. Int. **48**, 805 (1999)

L.C. Zhang, X.C. Li, T.C. Liu, J. Appl. Polym. Sci. **42**, 891 (1991)

L.C. Zhang, X.C. Li, T.C. Liu, in *Interpenetrating Polymer Networks*, ed. by D. Klempner, L.H. Sperling, L.A. Utracki. Advances in Chemistry Series, vol. 239 (ACS Books, Washington, DC, 1994)

L.C. Zhang, H.W. Tai, Y.D. Liu, Polym. Adv. Technol. **7**(4), 281 (1996)

X. Zhang, Y. Liu, H. Huang, Y. Li, H. Chen, J. Appl. Polym. Sci. **123**(3), 1822 (2012)

Y. Zhong, P. Zhu, Xiangtang Daxue Ziran Kexue Xuebao **13**(3), 57 (1991)

P. Zhou, Q. Xu, H.L. Frisch, Macromolecules **27**, 938 (1994)

A. Zosel, G. Lay, Macromolecules **26**, 2222 (1993)

Rheology of Polymer Alloys and Blends

7

Musa R. Kamal, Leszek A. Utracki, and A. Mirzadeh

Contents

Leszek A. Utracki: deceased.

M.R. Kamal (✉) • A. Mirzadeh
Department of Chemical Engineering, McGill University, Montreal, QC, Canada
e-mail: musa.kamal@mcgill.ca; amin.mirzadeh@mcgill.ca

L.A. Utracki
National Research Council Canada, Industrial Materials Institute, Boucherville, QC, Canada

Abstract

This chapter presents an overview of some of the important principles and characteristics associated with the rheological behavior of polymer blends. Initially, the chapter reports the observations and the scientific laws that illustrate and govern the rheological behavior of classical suspensions and emulsions of simple non-polymeric liquids. It is indicated that one of the main characteristics that differentiates the rheological behavior of polymer blends from that of simpler liquids is the viscoelastic nature of polymers and their blends. The discussion also points out the relationship between blend morphology and rheology and the importance of surface energy effects, such as interparticle and interfacial interactions. The general rheological characteristics of miscible polymer systems are considered. However, since the majority of polymers are immiscible, the rheological behavior of immiscible polymer blends is considered in more detail, with allowance for both thermodynamic and morphological factors. The influence of flow on morphology, as in phase separation, drop deformation, breakup, and fiber formation are discussed. Both viscous and viscoelastic characteristics of blend behavior are described, under the influence of shear and elongational flow fields. Various examples are presented, based on the study of rheological behavior of blends in both rheological testing devices (parallel plate, rotational, steady state, oscillatory, capillary, elongational, etc.) and processing equipment (extruders, mixers, molds, dies, etc.). In many cases, the observed rheological behavior is compared to the predictions of theoretical, computational, or empirical models.

7.1 Introduction

7.1.1 Rheology of Multiphase Systems

The rheology of multiphase systems is an extension of the general rheological dependencies observed for single component fluids. Obviously, the basic definitions of rheological functions, e.g., viscosity, η, dynamic shear moduli, G' and G'', dynamic shear compliance, J' and J'', etc., are identical. However, owing to the numerous influences, viz., concentration, morphology, flow geometry, time scale, type of flow field, thermodynamic interactions between the phases, and many others, more complex relationships prevail between the measured rheological functions of multiphase system and the intrinsic physical properties of the constituent fluids.

Table 7.1 Characteristics of flow fields

| No. | Type | γ | Vorticity | Uniformity of | | Comment |
				σ	γ	
1.	**Steady-state shear**					
1.1.	Sliding plate, and rotational cone-and-plate	Large	Yes	Homogeneous	Homogeneous	For small gap, or for cone angle $< 4°$
1.2.	Poiseuille (capillary or slit), Couette, and rotational parallel plates	Large	Yes	Functions of spatial coordinates	Functions of spatial coordinates	For laminar flows small measuring thickness is required
2.	**Dynamic shear**					
2.1.	Cone-and-plate	Small	Yes	Homogeneous	Homogeneous	For cone angle $< 4°$
2.2.	Parallel plates	Small	Yes	Linear	Linear	Gap 0.8–2.0 mm
2.3.	Couette	Small	Yes	Variable	Variable	Gap 0.2–0.5 mm
3.	**Extensional flows**					
3.1.	Uniaxial	Mid	No	Homogeneous	Homogeneous	
3.2.	Biaxial	Mid	No	Homogeneous	Homogeneous	

Rheological measurements in multiphase systems should be designed so that the length scale of flow is significantly larger than the size of the flow element. This makes it possible to treat the multiphase system as being homogeneous, having an average, "specific" rheological behavior. For example, Brenner (1970) showed that magnitude of relative viscosity, η_r, of diluted spherical suspensions, measured in capillary flows, depends on the $(d/D)^2$ factor, where d is the sphere diameter and D is the diameter of the capillary – for $D \cong 10d$, the error in η_r, was 1 %. Thus, if 1 % error is the acceptable limit, the size of the dispersion should be at least 10 times smaller than the characteristic dimension of the measuring device, viz., radius of a capillary in capillary viscometers, distance between stationary and rotating cylinders or plates in, respectively, the Couette or Weissenberg rheometer, etc. However, for many systems of industrial interest, the data are usually generated with a smaller factor, mainly for comparative purposes.

Another aspect of multiphase rheometry is related to the interrelations between the flow field and system morphology. In the present context, the term "morphology" will refer to the overall physical structure and/or arrangement of the components, usually described as a dispersed phase (particles or domains), co-continuous lamellae, fibrils, spherulites, etc. Furthermore, multiphase morphology deals with the distribution and orientation of the phases, the interfacial area, the volume of the interphase, etc. Flow may induce modifications of morphology, such as concentration gradients and orientation of domains.

Three types of flow are mainly used in rheological measurements: steady-state shearing, dynamic shearing, and elongation (Table 7.1). The three can be classified according to the strain, γ, vorticity, as well as uniformity of stress, σ, and strain within the measuring space.

Steady-state flows have a strong influence on the morphology, whereas dynamic flows have small influence. Extensional flows are characterized by uniform deformation with no vorticity; thus they are the most effective in changing the morphology and orientation of the system.

The rheological functions must be volume averaged (Hashin 1964). The averaged quantities are sometimes known as *bulk quantities*. For example, the bulk rate of strain tensor, $\langle \dot{\gamma}_{ij} \rangle$, is expressed as

$$\langle \gamma_{ij} \rangle = \frac{1}{2} \left(\left\langle \frac{\partial v_i}{\partial x_j} \right\rangle + \left\langle \frac{\partial v_j}{\partial x_i} \right\rangle \right) = \frac{1}{\Delta V} \int\limits_{\Delta v} \dot{\gamma}_{ij} dV \tag{7.1}$$

where $\left\langle \frac{\partial v_i}{\partial x_j} \right\rangle = \frac{1}{\Delta V} \int\limits_{\Delta V} \frac{\partial v_i}{\partial x_j} dV$

The stress tensor, $\langle \sigma_{ij} \rangle$, in multiphase systems, is given by

$$\langle \sigma_{ij} \rangle = -p \delta_{ij} + 2\eta_0 \langle \dot{\gamma}_{ij} \rangle + \frac{1}{\Delta V} \sum \left(S_{ij} - x_i F_j \right) \tag{7.2}$$

In Eqs. 7.1 and 7.2, v_i is local velocity, x_i is local coordinate, ΔV is an elementary volume, p is pressure, δ_{ij} is unit tensor, η_o is viscosity of the continuous phase, while S_{ij} and F_i represent hydrodynamic and non-hydrodynamic forces acting on a particle. These two functionals are usually coupled, as the thermodynamic interactions affect the hydrodynamic forces and vice versa.

The first two terms on the right-hand side (rhs) of Eq. 7.2 are identical to those for a homogeneous fluid. For a multiphase system, they represent the stress tensor of the matrix liquid, while the third term describes the perturbing influences of the dispersed phase (Batchelor 1974, 1977). Owing to difficulties in deriving exact forms of the S_{ij} and F_i functions in the full range of concentrations, Eq. 7.2 is usually written as a power series in volume fraction, ϕ, of the suspended particles.

The rheological behavior of multiphase systems within the linear, dilute region ($\phi < 0.05$) is relatively well described. For example, for dilute suspensions of spherical particles in Newtonian liquids, Eq. 7.2 reduces to Einstein's formula for the relative viscosity, η_r:

$$\begin{aligned} \langle \sigma_{ij} \rangle &= -p\delta_{ij} + 2\eta_0[1 + (5/2)\phi]\dot{\gamma}_{ij} \\ \text{or } \eta_r &= 1 + (5/2)\phi \end{aligned} \tag{7.3}$$

Equation 7.2 has been also solved for dilute suspension of anisometric particles (Hinch and Leal 1972), elastic spheres (Goddard and Miller 1967; Roscoe 1967), and emulsions (Oldroyd 1953, 1955; Barthès-Biesel and Chhim 1981). These works were reviewed by Barthès-Biesel (1988).

In the higher concentration range, where particle–particle interactions must be taken into account, Eq. 7.2 is often approximated by a second-order polynomial. However, even for hard-sphere suspensions, the theoretical extension of Eq. 7.3 has been found difficult:

$$\eta_r = 1 + (5/2)\phi + K\phi^2 + O(\phi^3)$$ (7.4)

where the second-order coefficient was calculated as K = 5.2–7.6. Such theoretical predictions should be compared with experimental results. Thomas (1965) compiled relative viscosity data, η_r versus ϕ, measured in 16 laboratories for different types of hard-sphere suspensions, e.g., pollen in water, steel balls in oil, etc. After correcting the data (e.g., for the immobilized adsorbed layer of the suspending liquid), the results superimposed and were fitted to the following relation (valid within the experimentally explored range of concentration, $\phi \leq 0.6$):

$$\eta_r = 1 + (5/2)\phi + 10.05\phi^2 + 0.00273\ \exp\{16.6\phi\}$$ (7.5)

Allowance for the last term in Eq. 7.5 yields K = 10.43 as the second-order coefficient of Eq. 7.4.

Owing to difficulties in deriving general constitutive equations for multiphase systems, rheologists had to resort to simplified theoretical or semiempirical dependencies derived for specific types of rheological tests and/or for specific multiphase systems. These, experimentally well-established relations, constitute the basic tools for the interpretation of rheological data for multiphase systems. They will be discussed in the following parts of the text.

7.1.2 Basic Concepts of Polymer Blends

The following standard definitions will be used (Utracki 1989a, 1991a; see also *Nomenclature* in ▶ Chap. 1, "Polymer Blends: Introduction" of this handbook).

7.1.2.1 Definitions
(a) **Polymer blend** is a mixture of two or more polymers and/or copolymers, terpolymers, etc., containing at least 2 wt% of the dispersed phase.
(b) **Miscible blend** is a blend with domain size comparable to the dimension of a macromolecular statistical segment, or in other words, whose free energy of mixing is negative, $\Delta G_m < 0$, and its second derivative of concentration with volume, is positive: $\partial^2 \Delta G_m / \partial \phi^2 > 0$. Usually, miscibility is restricted to a relatively narrow range of independent variables, viz., molecular weight, composition, temperature, pressure, etc. Thus, immiscibility dominates.
(c) **Polymer alloy** is an otherwise immiscible blend, which is compatibilized, with modified interphase and morphology.

Table 7.2 Rheological models for miscible and immiscible blends	**1. Miscible blends**	**2. Immiscible blends**
	1.1. Solutions	2.1. Suspensions
	1.2. Homologous polymer blends	2.2. Emulsions
		2.3. Block copolymers

Alloying involves several operations that must result in blends showing *stable* and *reproducible* properties. These processes comprise compatibilization, mixing, and stabilization. Compatibilization may be accomplished either by addition of a compatibilizer or by reactive processing. Its role is to facilitate dispersion, stabilization of the morphology, and enhancement of the interaction between phases in the solid state. Commercial alloys may comprise up to six polymeric ingredients. Development of such an alloy is complex, requiring knowledge of thermodynamics, rheology, and processing and their influences on morphology, thus performance.

If the rheology of suspensions and emulsions is difficult to describe theoretically and to determine experimentally, the difficulties increase substantially in the case of polymer blends. For example, both phases in polymer blends are likely to be viscoelastic, the viscosity ratio varies over a wide range, and morphology can be very complex. As a guide to characterization of the rheology of blends, it is useful to refer to the behavior of simpler systems, i.e., models that can offer important insight. The following systems (Table 7.2) are considered commonly. They will be treated in the following discussion.

7.1.2.2 Phase Co-continuity

When a small quantity of one polymer is intimately mixed with another polymer, the resulting system is a blend composed of a matrix (the major component) and the dispersed phase (the minor component). When the concentration of the dispersed phase is increased, the morphology may change from a discontinuous dispersion of nearly spherical drops to progressively interconnected drops, then rods, fibers, and sheets. At a certain concentration, labeled as *the phase inversion volume fraction*, ϕ_I, the distinction between the dispersed and matrix phases vanishes – the system morphology becomes co-continuous. Phase co-continuity is one of the most important aspects of blend morphology (Lyngaae-Jørgensen et al. 1999).

Since the morphology is strongly affected by large strain flow, it is expected that the method of specimen preparation influences the co-continuity. Both the phase inversion concentration and stability of the co-continuous phase structure depend on the strain and thermal history.

It has been reported that the onset of co-continuity occurs at an average volume fraction, $\phi_{onset} = 0.19 \pm 0.09$. In many branches of physics, the concept of percolation has been found useful. For example, when the concentration of conductive spheres in nonconductive medium exceeds the percolation threshold volume fraction, ϕ_{perc}, there is a sudden increase of electrical conductivity. For the three-dimensional case, 3D, theory predicts that $\phi_{perc} = 0.156$, while for 1D it is $\phi_{perc} = 0.019$. It has been postulated that the observed changes of morphology in polymer blends, when co-continuity occurs, belong to the group of percolation

Fig. 7.1 For immiscible blends the onset of phase co-continuity should coincide with the percolation threshold. Theoretically, $\phi_{perc} = 0.156$ for 3D flow of immiscible system. Experimentally, $\phi_{2perc} = 0.19 \pm 0.09$ was found (Lyngaae-Jørgensen and Utracki 1991)
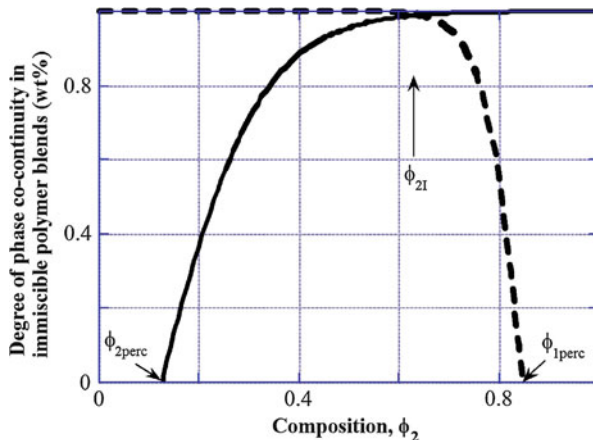
phenomena (Lyngaae-Jørgensen and Utracki 1991). Figure 7.1 depicts the variation of phase co-continuity in blends of high-density polyethylene with polystyrene, HDPE/PS. The data (obtained by selective extraction of the matrix phase) indicate that the onset of phase co-continuity occurred at $\phi_{1perc} = 0.16$ and $\phi_{2perc} = 0.15$, whereas $\phi_I = 0.64$.

Co-continuity contributes to synergism of properties, e.g., advantageous combination of high modulus and high impact strength in commercial blends. Therefore, it is of interest to determine the composition at which co-continuity can be formed. Practically, the breadth of the co-continuity composition range depends on the experimental concentration step size used during the selective extraction tests. The following simple equation was proposed to relate the phase inversion composition to volume fractions and viscosity ratio:

$$\phi_{I1}/\phi_{I2} = \eta_1/\eta_2 \equiv \lambda \;\; \text{or} \;\; \phi_{I2} = (1 + \lambda)^{-1}$$
$$\phi_{I2} = (1 + F(\lambda)\lambda)^{-1} \tag{7.6}$$

where

$$F(\lambda) = 1 + 2.25\log\lambda + 1.81(\log\lambda)^2 \tag{7.7}$$

Note that $\phi_{I1} = 1 - \phi_{I2}$ and ϕ_{I1} and ϕ_{I2} are the volume fractions of liquids 1 and 2, respectively, at the phase inversion. Equation 7.6 is empirical, proposed by Paul and Barlow (1980) as a generalization of the experimental observations reported by Avgeropoulos et al. (1976). Equation 7.7 was derived from the filament instability equation by Metelkin and Blekht (1984). These relations are applicable to systems prepared at low stresses; thus in these equations, the viscosity ratio, λ, should correspond not to the ratio of the zero-shear viscosities, but to its value at the shear stress used to prepare the blends. The relations were found to describe the phase inversion for systems with nearly equal polymer viscosities, where $\lambda \to 1$. As the viscosity ratio increases, these equations predict more rapid change of ϕ_{I2}.

Fig. 7.2 Concentration dependence of emulsion viscosity. *Solid line* represents $\eta = \eta_1(\phi_2)$ while the other lines the same dependence for $\eta = \eta_2 \cdot \eta_r(\phi_1)$. To calculate these dependencies $[\eta] = 2$ and $\phi_m = 0.8$ were assumed. The intercepts correspond to the iso-viscous conditions defining the phase inversion concentration, $\phi_{2I} = 1 - \phi_{1I}$ (Utracki 1991)
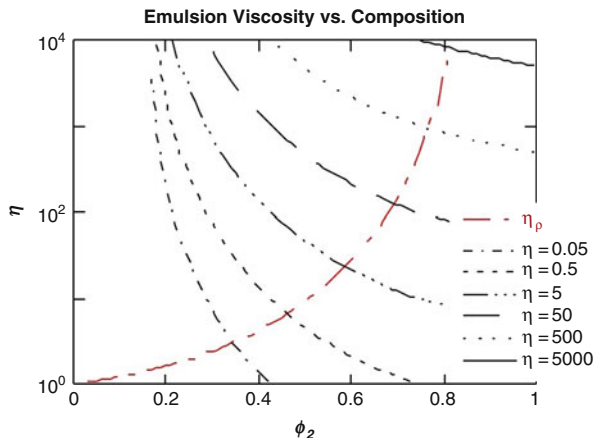
To derive a more general relation for the phase inversion concentration, one may start by computing $\eta(A) = \eta_B^o \eta_r(\phi_A)$ and $\eta(B) = \eta_A^o \eta_r(\phi_B)$, where η_r is the relative viscosity. The latter dependence can be expressed as (Krieger and Dougherty 1959)

$$\eta_r = [1 - (\phi/\phi_m)]^{-[\eta]\phi_m} \qquad (7.8)$$

In Eq. 7.8, ϕ_m is the maximum packing volume fraction, and $[\eta]$ is the intrinsic viscosity. The computed curves are shown in Fig. 7.2. To calculate these dependencies, $\phi_m = 0.8$ and $[\eta] = 2$ were assumed. The six points of intersection represent the iso-viscous conditions for dispersion of liquid 1 in 2 and liquid 2 in 1, or in other words, the conditions for phase inversion.

Based on Eq. 7.8, the iso-viscous point can be expressed as

$$\lambda = [(\phi_m - \phi_{2I})/(\phi_m - \phi_{1I})]^{[\eta]\phi_m}; \quad \text{where} \quad \phi_m = 1 - \phi_{perc} \qquad (7.9)$$

Equation 7.9 can be expanded into MacLaurin's series, then truncated after the second term to give a simplified version, valid within the range $-1 < \phi_{Ii}/\phi_m < 1$:

$$\phi_{I2} = [1 - (\log\lambda)/[\eta]]/2 \qquad (7.10)$$

Figure 7.3 shows the experimental dependence of λ on ϕ_{2I} for thermoplastic polymer blends. The horizontal and vertical lines represent the conditions between which the phase inversion took place. The straight line represents Eq. 7.10. For most polymer blends the values of parameters in Eq. 7.9: $[\eta] \cong 1.9$; $\phi_m \cong 1 - \phi_{perc} = 0.84$ provide good approximation.

It should be noted that the steady-state viscosity ratio should be taken at a constant stress (not deformation rate). The "sharpness" of the phase inversion peak depends on the distribution of stresses within the mixing device, as well as on

Fig. 7.3 Experimental ϕ_{2I} versus λ dependence for mechanically prepared thermoplastics blends. The *dotted*, *solid*, and *broken lines* represent Eq. 7.6, 7.9, and Eq. 7.10, respectively; the values: $[\eta] = 1.9$ and $\phi_m = 0.84$ were used (Utracki 1991)
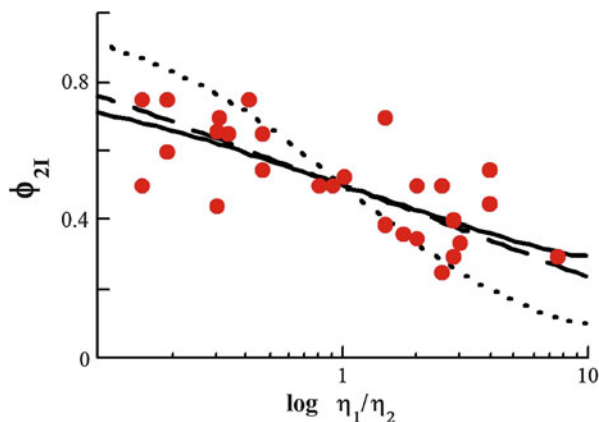
the absolute magnitude of polymer viscosity – the wider the distribution of stresses and/or the higher the viscosity, the wider the range of concentrations at which the phase inversion takes place. Since many experiments are conducted using an internal mixer known to possess a wide range of flow conditions, instead of a single point, usually a range of concentrations for the phase co-continuity has been reported (see Fig. 7.3).

Another relation was proposed for predicting the phase inversion concentration. It assumes that, at the phase inversion, the morphology of both phases is fibrillar and that the rate of fiber disintegration is the same for both components (Metelkin and Blekht 1984). The validity of the model is limited to viscosity ratios ranging from 0.25 to 4 (Luciani 1993, 1996):

$$\lambda \equiv \eta_1/\eta_2 = [\Omega_2(\Lambda,\lambda)/\Omega_1(\Lambda,\lambda)](R_{0,1}/R_{0,2})$$
$$= [\Omega(\eta_1/\eta_2)/\Omega(\eta_2/\eta_1)](\phi_1/\phi_2)^{1/2} \tag{7.11}$$

The significance of the function $\Omega(\Lambda, \lambda)$ will be discussed in the Sect. 7.3.1.2, dedicated to emulsion microrheology. Steinmann et al. suggested that, at the phase inversion point, the shape relaxation times of domains of the components meet at a maximum (Steinmann et al. 2002).

Since these models do not always completely agree with phase inversion compositions found experimentally, melt elasticity effects were examined to verify if the observed deviations could be attributed to elasticity effects. A model was proposed, using the storage moduli and loss tangent ratios instead of viscosity ratios in Eq. 7.6 (Table 7.3) (Bourry and Favis 1998). Based on their results, the more elastic component tends to encapsulate the less elastic one. Therefore, the elastic contribution of the blends was found to be an important factor in determination of co-continuity.

The validity of Cox–Merz rule should be verified by measuring G′ and tan δ at frequency ω corresponding to the shear rate γ_p. The use of the ratio of storage moduli for the experimental data evaluated at a constant matrix shear stress

Table 7.3 Summary of some available semiempirical phase inversion models

Equation	Reference
Viscosity ratio-based models	
$\frac{\phi_{I1}}{\phi_{I2}} \times \frac{\eta_2}{\eta_1} = 1$	Avgeropoulos et al. (1976)
$\phi_{I1}/\phi_{I2} = A(\eta_1/\eta_2)^B$	Paul and Barlow (1980)
$\phi_{I2} = (1 + F(\lambda) \times \lambda)^{-1}$ $F(\lambda) = 1 + 2.2g \log(\lambda) + 1.8[\log(\lambda)]^2$	Metelkin and Blekht (1984)
$\lambda = \left[\frac{(\phi_m - \phi_{2I})}{(\phi_m - \phi_{1I})}\right]^{[\eta]\phi_m}$	Utracki (1991)
$\phi_{2I} = \frac{1 - (\lambda^2 \Omega^2(\lambda))}{[\lambda^2 \Omega^2(\lambda) + \Omega^2(1/\lambda)]}$	Lucuani and Jarrin (1996)
$\Phi_I = k(\phi - \phi_{cr})^x$	Lyngaae-Jorgensen et al. (1999)
$\phi_{2I} = \frac{1}{(\lambda^{1/Z} + 1)}$	Steinmann et al. (2002)
Elasticity ratio-based models	
$\frac{\phi_{1I}}{\phi_{2I}} = \frac{G'_2(\omega)}{G'_1(\omega)}, \frac{\phi_{1I}}{\phi_{2I}} = \frac{\tan \delta_1(\omega)}{\tan \delta_2(\omega)}$	Bourry and Favis (1998)

(Sarazin and Favis 2003; Shahbikian et al. 2011) and the loss tangent ratio for the data obtained at a constant shear rate (Shahbikian et al. 2011; Steinmann et al. 2001) yields better agreement with the predictions of the Bourry and Favis model.

It should be noted that phase inversion prediction models focus on only a single composition, whereas in reality, co-continuous structures are observed over a composition range. Considering the definition of co-continuous structure and equations based on the percolation theory, a model was proposed to correlate a continuity index (Φ_I) with the volume fraction at onset of co-continuity (ϕ_{cr}) (see Table 7.3) (Lyngaae-Jorgensen et al. 1999). Numerical simulation predicted ϕ_{cr} to be about 0.2 for classical percolation in three-dimensional systems (Dietrich and Amnon 1994; Potschke and Paul 2003).

The co-continuous structure and the final rheological properties of an immiscible polymer blend are generally controlled by not only the viscoelastic and interfacial properties of the constituent polymers but also by the processing parameters. For example, the effect of plasticizer on co-continuity development in blends based on polypropylene and ethylene-propylene-diene-terpolymer (PP/EPDM), at various compositions, was studied using solvent extraction. The results showed more rapid percolation of the elastomeric component in the presence of plasticizer. However, the same fully co-continuous composition range was maintained, as for the non-plasticized counterparts (Shahbikian et al. 2011). It was also shown that the presence of nanoclay narrows the co-continuity composition range for non-plasticized thermoplastic elastomeric materials (TPEs) based on polypropylene and ethylene-propylene-diene-terpolymer and influences their symmetry. This effect was more pronounced in intercalated nanocomposites than in partially exfoliated nanocomposites with improved clay dispersion. It seems that the smaller, well-dispersed particles interfere less with thermoplastic phase continuity (Mirzadeh et al. 2010). A blend of polyamide 6 (PA6) and a co-polyester of

Fig. 7.4 Co-continuity index versus BioFlex concentration (Kucharczyk et al. 2012)
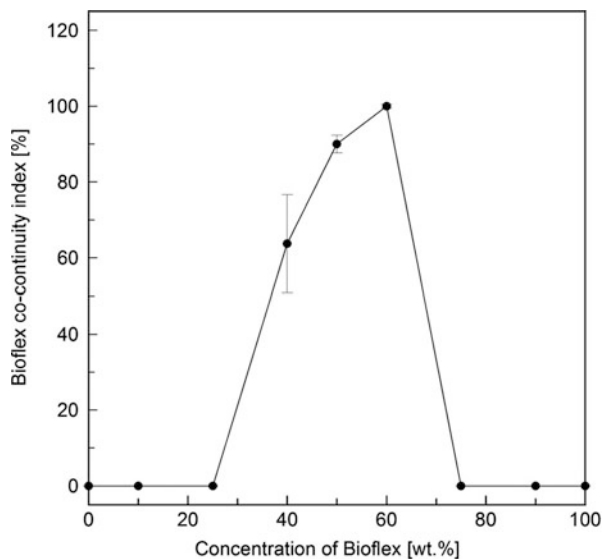
polylactide (BioFlex) was studied using scanning electron microscopy (SEM) and dynamic rheological measurements (Kucharczyk et al. 2012). SEM showed the formation of co-continuity for the blends containing 50–60 wt% of BioFlex. Rheological measurements and solvent extraction showed a broader co-continuity interval, even for blends with over 25 wt% BioFlex. All methods indicated maximum co-continuity at 60 wt% BioFlex. The best fit of experimental data was for the model including the contribution of elasticity to interfacial tension (Bourry and Favis 1998; Fig. 7.4).

7.1.2.3 The Interphase

Lattice theory predicts that the density profile across the interface follows the exponential decay function (Helfand and Tagami 1971, 1972):

$$\begin{aligned} \rho/\rho_o &= y^2/(1 + y^2) \\ \text{where} \quad y &\equiv \exp\left\{ (6\chi_{AB})^{1/2}(x/b) \right\} \end{aligned} \tag{7.12}$$

In Eq. 7.12, χ_{AB} is the thermodynamic binary interaction between polymers A and B, and b is a lattice parameter. The dependence is shown in Fig. 7.5. The intercept of the tangential line at the place of the steepest decline (or incline for the other component) defines thickness of the interphase, Δl.

The lattice theory of the interface predicts that there is a reciprocity between the interfacial tension coefficient and the interfacial thickness (Helfand and Sapse 1975):

$$\begin{aligned} v_{12} &= k_B T a^{-1} (m\chi_{AB})^{1/2} \quad \text{and} \quad \Delta l = 2(m/\chi_{AB})^{1/2} \\ \therefore \Delta\lambda \cdot v_{12} &= 2mk_B T/a \end{aligned} \tag{7.13}$$

Density profile across the interface

$\rho/\rho_o = y^2/(1 + y^2)$;
$y = \exp[(6\chi)^{1/2}\,(x/b)]$ $\chi \approx 0.01$; $b(PS) \approx 0.65$ nm

Δl

REDUCED SEGMENT DENSITY, ρ/ρ_o

REDUCED DISTANCE ACROSS THE INTERFACE, x/b
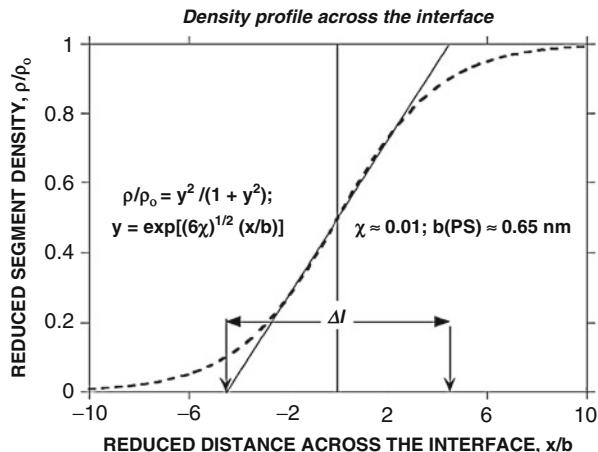
where a, b, and m are lattice parameters. Notice that according to this theory, the product, $v_{12}\Delta l$, is independent of the thermodynamic binary interaction parameter, χ_{AB}. The theory leads to the conclusions that (i) surface free energy is proportional to the square root of χ_{AB}, (ii) the chain ends of both polymers concentrate at the interface, (iii) any small molecular weight third component will be repulsed to the interface, and (iv) interfacial tension coefficient increases with molecular weight to an asymptotic value: $v_{12} = v_\infty - a_o M_n^{-2/3}$. These conclusions were found to offer good guidance for development of compatibilization strategies.

There are several other theories of the interface, some of which lead to quantitatively different results (Ajji and Utracki 1996, 1997). For example, Noolandi (1984) considered a binary system compatibilized by addition of a block copolymer. For $\chi_{AB}N_c\phi_p \leq 2$ he derived:

$$v_{12} = v_{o|} + \Delta L\phi_c\{\chi_{AB}\phi_p/2 + (1/N_c)[1 - \exp\{\chi_{AB}N_c\phi_p/2\}]\}$$
$$\therefore \quad v_{12} \cong v_o - a_o\Delta L\phi_c + O(\phi_c^2) \tag{7.14}$$

where a_o is a numerical parameter, while ϕ_c, ϕ_p, and N_c are, respectively, volume fraction of copolymer, of polymer, and degree of polymerization of the copolymer. A semiempirical dependence of the interfacial tension coefficient on compatibilizer concentration can be derived from an analogy to titration of an emulsion with surfactants (Utracki 1992):

$$v_{12} = (\phi v_{CMC} + \phi_{mean}v_o)/(\phi + \phi_{mean})$$
$$\text{where;}$$
$$v_{CMC} = v_{12}(\phi_c = CMC) \tag{7.15}$$
$$\phi_{mean} = (v_{CMC} + v_o)/2$$

where v_o is the initial interfacial tension coefficient at zero concentration of copolymer, v_{CMC} is the interfacial tension at saturation of the interface, and

Fig. 7.6 Interfacial tension coefficient versus concentration of compatibilizer for polystyrene blends with polybutadiene, compatibilized with styrene-butadiene block copolymer. Data points (Anastasiadis and Koberstein 1988), line computed from Eq. 7.15
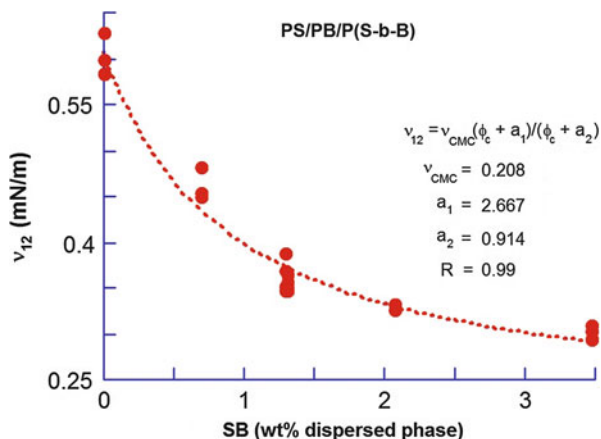
ϕ is the copolymer concentration. Eq. 7.15 adequately described the interfacial tension coefficient in the system polystyrene/polybutadiene compatibilized by addition of styrene-butadiene block copolymer; see Fig. 7.6 (Anastasiadis et al. 1988, 1989).

Recently an exponential decay relation was proposed (Tang and Huang 1994):

$$v_{12} = v_{CMC} + (v_o - v_{CMC})\exp\{-K\phi\} \tag{7.16}$$

where K is a parameter – from Eq. 7.14, its value should be proportional to $K \propto \chi_{AB}N_c$.

There have been several efforts to provide means for computation of the interfacial tension coefficient from characteristic parameters of the two fluids (Luciani et al. 1996). The most interesting relation was that found between the interfacial tension coefficient and the solubility parameter contributions that are calculable from the group contributions. The relation makes it possible to estimate the interfacial tension coefficient from the unit structure of macromolecules at any temperature. The correlation between the experimental and calculated data for 46 polymer blends were found to be good – the correlation coefficient R = 0.815 – especially when the computational and experimental errors are taken into account.

There are several methods for measuring the interfacial tension coefficient for low-viscosity liquids, e.g., spherical shape recovery after slight deformation, liquid thread breakup, rotating bubble or drop, pendant drop, sessile bubble or drop, du Nuouy ring, or light scattering. For high-viscosity polymeric melts, they can be used with decreasing reliability. The most recent and highly successful method involves spherical shape recovery of a drop deformed by about 15 % either in shear or (preferably) in elongation. Since the drop can be repetitively deformed and its shape recovery follows, this method is the only one that makes

Table 7.4 Interphase
thickness

Type of blend	Thickness (nm)
Immiscible blend	2
Block copolymer interphase	4–6
Immiscible blends filled with nanoclay	4–20
Polymer/copolymer	30
Reactive compatibilization	30–60
Radius of gyration, $\langle R_g^2 \rangle^{1/2}$	5–35

it possible to follow the time evolution of the interfacial tension coefficient. Furthermore, the method also makes it possible to examine whether, for a given polymer pair, the interfacial energy is symmetrical, i.e., if $\nu_{\alpha\beta} = \nu_{\beta\alpha}$ (Luciani et al. 1996).

There are fewer methods available to measure the interphase thickness, e.g., ellipsometry, microscopy, and scattering. For example, Ville et al. investigated the interphase in polyethylene (PE)/polyamide (PA) blends with nodular morphology, filled with modified montmorillonite, using morphological and rheological experimental techniques (Ville et al. 2012). The average interphase thickness was determined at several points (from more than 200 local interphase thickness measurements) by using an image analysis software. It was shown that the average interphase thickness increased with clay fraction, from about 7 nm at 1 % clay to about 20 nm at 4 % clay, which was expected since clay particles were localized exclusively at the interphase (Huitric et al. 2009; Khatua et al. 2004). However, based on rheological characterization, which showed not very long dominant relaxation times (nodule form relaxation time and interphase relaxation time), Ville et al. mentioned that using microscopy method to characterize the interphase is certainly insufficient due to the presence of a continuous rigid nanocomposite shell that misrepresents the physical reality of the interphase in these systems (Ville et al. 2012).

A summary of the measured Δl is given in Table 7.4. The temperature dependence of Δl in PMMA/SAN and PMMA/PS blends is presented in Fig. 7.7.

7.2   Rheological Models for Miscible Blends

By definition, miscible polymer blends are single-phase mixtures. Miscibility depends on the molecular weight, concentration, temperature, pressure, deformation rate, etc. Flow of these systems can be compared to that of solutions of low molecular weight, miscible components, or to flow of mixtures of polymeric fractions. Both models are far from perfect, but they serve to illustrate the basic behavior of miscible systems. In the first case one can learn about the effects of the thermodynamic interactions between chemically different components on the flow behavior. In the second case, it is the effect of molecular weight and molecular weight distribution that can be observed.

Fig. 7.7 Interphase thickness versus temperature for polymethylmethacrylate blends with (from *top*) styrene-acrylonitrile copolymer and polystyrene (Kressler et al. 1993)
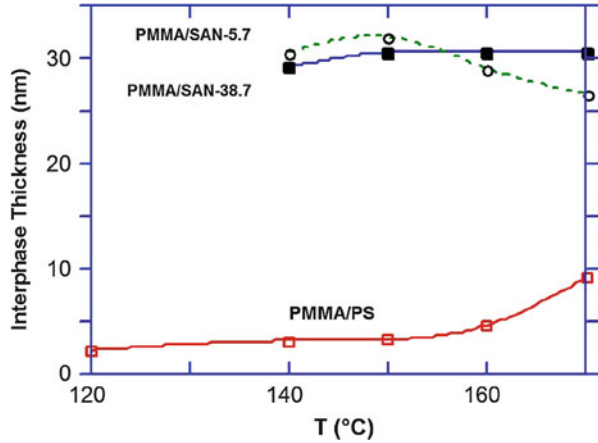
7.2.1 Solutions

For solutions (Glasstone et al. 1941):

$$\ln[V\eta_0] = \sum_i x_i \ln[V_i \eta_{0i}] - \prod_i x_i \Delta H_m / 2.45RT \tag{7.17}$$

where V is the specific volume and x_i is the mole fraction. For miscible blends, $\Delta H_m < 0$ and the above relations predict a positive deviation from the log-additivity rule, PDB. The latter rule, the log-additivity, was formulated by Arrhenius (1887):

$$\ln\eta_0 = \sum_i x_i \ln \eta_{0i} + \ln\eta^E \tag{7.18}$$

with the excess viscosity term, $\ln \eta^E \to 0$.

There are several other blending rules for solution viscosity, e.g., (McAllister 1960):

$$
\begin{aligned}
\ln\eta_{k,b} = {} & x_1^3 \ln\eta_{k,1} + x_2^3 \ln\eta_{k,2} + 3x_1^2 x_2 \ln\eta_{k,12} \\
& + 3x_1 x_2^2 \ln\eta_{k,21} + 3x_1^2 x_2 \ln[(2M_1 + M_2)/3] \\
& + 3x_1 x_2^2 \ln[(M_1 + 2M_2)/3] + x_1^3 \ln M_1 \\
& + x_2^3 \ln M_2 - \ln(x_1 M_1 + x_2 M_2)
\end{aligned}
\tag{7.19}
$$

where $\eta_{k,i}$ indicates the kinematic viscosity, M_i is the molecular weight, and the two kinematic viscosities with double subscripts are the empirical interaction viscosities. Equation 7.19 was derived from a three-body model of a miscible mixture comprising two low molecular weight liquids with two interaction viscosities.

7.2.2   Homologous Polymer Blends

The homologous macromolecular blends are simply mixtures of fractions of the same polymer having the same molecular constitutions. On the one hand, any commercial polymer may be treated as a homologous macromolecular blend, and on the other, blending narrow molecular weight distribution fractions provides important information on the rheological behavior of commercial materials. Since the zero-shear viscosity for narrow molecular weight distribution samples can be expressed as

$$\eta_0 = KM_w^\alpha \quad \text{thus} \quad M_w = (\eta_0/K)^{1/\alpha} \tag{7.20}$$

(where K and $\alpha = 1$ or 3.4 are parameters), but since

$$M_w = \sum_i w_i M_i \tag{7.21}$$

then it follows that (Friedman and Porter 1975)

$$\eta_o = \left[\sum_i w_i \eta_{o,i}^{1/\alpha} \right]^\alpha \tag{7.22}$$

For binary mixtures, Eq. 7.22 predicts that viscosity should show a positive deviation from the log-additivity rule, PDB.

There is a mounting evidence that PDB is not a rule for miscible polymer blends. Depending on the system and method of preparation, polymer blends can show a positive deviation, negative deviation, or additivity. Note that miscibility in polymeric systems requires strong specific interactions, which in turn affect the free volume, thus the rheological behavior. It has been demonstrated that Newtonian viscosity can be described by the relation (Utracki 1983, 1985, 1986)

$$\ln\eta_0 = a_0 + a_1/(f + a_2) \tag{7.23}$$

where a_i are equation parameters $a_o \equiv \ln \eta_o^*$ with η_o^* being the iso-free volume viscosity, a_1 is a function of the molecular architecture and polydispersity ($a_1 = 0.79$ was found for all paraffin's and their mixtures), and $a_2 = 0.07$ is the linearization parameter. The key to Eq. 7.23 is the free volume fraction, f, computed from Simha's statistical theory (Simha and Somcynsky 1969; Simha and Jain 1984). This approach was successful in describing pressure, temperature, and concentration dependence of the viscosities of solvents and polymer melts (Utracki 1983, 1985, 1986).

7.3   Model Systems for Immiscible Blends

Most polymer blends are immiscible. Their flow is complex not only due to the presence of several phases having different rheological properties (as it will be

demonstrated later, even in blends of two polymers the third phase, the interphase, must be taken into account) but also due to strain sensitivity of blends' morphology. Such a complexity of flow behavior can be best put in perspective by comparing it to flow of better understood systems, suspensions, emulsions, and block copolymers.

Flow of suspensions of solid particles in Newtonian liquids is relatively well understood, and these systems provide good model for flow of polymer blends, where the viscosity of dispersed polymer is much higher than that of the matrix polymer.

Flow of emulsions provides the best model for polymer blends, where the viscosity of both polymers is comparable. The microrheology of emulsions provides the best, predictive approach to morphological changes that take place during flow of polymer blends. The effect of emulsifiers on the drop size and its stability in emulsions has direct equivalence in the compatibilization effects in polymer blends.

Finally, the rheological behavior of block copolymers serves as a model for well-compatibilized blends, with perfect adhesion between the phases. The copolymers provide important insight into the effects of the chemical nature of the two components and the origin of the yield phenomena.

7.3.1 Suspensions

The dispersions of solid particles in viscous fluids can be found in a wide range of natural and industrial applications. There are some interactions determining the microstructure of the suspension, such as interactions arising from Brownian, interparticle, and flow-induced forces. In the equilibrium state, there is a balance between Brownian and interparticle forces. Under the influence of flow, hydrodynamic interactions become considerable, in comparison with thermal and interparticle forces.

The rheological properties of the suspension are strongly influenced by the spatial distribution of the particles. The relationship between microstructure and rheology of suspensions has been studied extensively (Brader 2010; Morris 2009; Vermant and Solomon 2005). Most of earlier studies dealt with the simplest form of suspensions, in which dilute hard-sphere suspensions are subjected only to hydrodynamic and thermal forces near the equilibrium state (i.e., Péclet number $<< 1$) (Bergenholtz et al. 2002; Brady 1993; Brady and Vicic 1995). In shear flows of such suspensions, the structure is governed only by the particle volume fraction and the ratio of hydrodynamic to thermal forces, as given by the Péclet number.

The main problem in extending the microstructural theories to high Péclet number and volume fraction is related to the formulation of the many-body interactions. Recently, based on the Smoluchowski equation, Nazockdast and Morris (2012) developed a theory for concentrated hard-sphere suspensions under shear. The theory resulted in an integro-differential equation for the pair distribution function. It was used to capture the main features of the hard sphere structure and to predict the rheology of the suspension, over a wide range of volume fraction (≤ 0.55) for $0 < \mathrm{Pe} \leq 100$ (Nazockdast and Morris 2012).

There are two reasons for discussing the solid-in-liquid dispersions in the chapter dedicated to flow of polymer blends (Utracki 1995). Historically, the first

systematically studied multiphase systems were suspensions in Newtonian liquids, initially at infinite dilution (Einstein 1906, 1911), than at increasingly concentrated limits (Simha 1952). Knowledge of these derivations is fundamental to understanding the energy dissipation during flow in any multiphase system. Furthermore, the suspensions in viscoelastic matrix are good models for polymer blends having viscous polymer dispersed in a significantly less viscous matrix polymer.

7.3.1.1 Suspensions in Newtonian Liquids

The following assumptions are often used: (i) The size of a rigid particle is large in comparison to the suspending medium molecules, but small compared to the smallest characteristic diameter of the flow channel so the continuum theories are applicable. (ii) The flow is steady state, without inertia or sedimentation. (iii) The suspending medium perfectly adheres to the particles. Depending on the system (as well as the author), additional assumptions may be made, e.g., regarding interparticle interactions, orientation, etc.

Denisov et al. (1985) as well as Brady and Bossis (1985) reported on numerical simulation of suspension rheology. The first authors used the 6–12 *Lennard-Jones potential* with the usual meaning of ε^* and σ^* characteristic constants (with dimensions of energy and length, respectively) of the interacting species. Taking R_o as a measure of distance from the center of the particle at which action of the potential begins, the necessary conditions for dilatant behavior were: (i) $R_o \geq \sigma^*$ and (ii) particle concentration exceeding a critical value dependent on the system. The Stokesian dynamic's method was used by the other authors. The simulation provided valuable information on the influence of various microstructural elements on the macroscopic viscosity. The relative velocity of two particles in suspension provided the most important contribution to energy loss. As ϕ increased, the correlation of interparticle motion also increased. Hydrodynamic lubrication resulted in an increased number of particles acting as single agglomerate. The maximum packing volume fraction, ϕ_m, takes on a meaning as a percolation-like threshold for the viscosity to increase to infinity owing to the formation of infinite clusters.

Microstructural theories of suspensions appear to be particularly well suited to solve problems associated with time-dependent flows, thixotropy and rheopexy (anti-thixotropy) (Russel 1983; Utracki 1989, 1995).

Relative Viscosity of Suspensions

One of the most interesting derivations of the η versus ϕ dependence (covering the full range of concentration) was published by Simha (1952). He considered the effects of concentration on the hydrodynamic interactions between suspended particles of finite size. (Note that previously the particles were simply considered point centers of force that decayed with cube of the distance.) Simha adopted a cage model, placing each solid, spherical particle of radius a inside a spherical enclosure of radius b. At distances $x < b$, the presence of other particles does not influence

flow around the central sphere and the Stokes relation is satisfied. This assumption leads to a modified Einstein (1906, 1911) relation

$$\eta_r = 1 + (5/2)\lambda(y)\phi \tag{7.24}$$

where $\lambda(y)$ is the modifying (or shielding) function of the relative cage size, $y \equiv a/b$:

$$\lambda(y) = \frac{4(1 - y^7)}{4(1 + y^{10}) - 25y^3(1 + y^4) + 42y^5}$$
$$\text{with} \quad y = \left[2\left(1/\widetilde{\phi}\right)^{1/3} - 1\right]^{-1} \tag{7.25}$$

In Eq. 7.25, ϕ_m is the maximum packing volume fraction. Thus, the magnitude of the shielding function $\lambda(y)$ depends on the reduced volume fraction, $\widetilde{\phi} \equiv \phi/\phi_m$. At low concentration, $\widetilde{\phi} \to 0$, the shielding factor vanishes and Einstein's relation is recovered. However, at high concentration, $\widetilde{\phi} \to 1$, the shielding function and relative viscosity both go to infinity, $\lambda(y)$, $\eta_r \to \infty$. Substituting Eq. 7.25 into Eq. 7.24 and expanding it into power series make it possible to write simplified versions, valid respectively within the low (viz., Eq. 7.26) and high (viz., Eq. 7.27) concentration range:

$$\eta_{sp} \equiv \eta_r - 1 = (5\phi/2)\left[1 + \frac{25}{32}\widetilde{\phi} - \frac{21}{64}\widetilde{\phi}^{5/3} + \frac{625}{128}\widetilde{\phi}^2 + \ldots\right] \tag{7.26}$$

and

$$\lim_{\phi \to \phi_m} \eta_r = 27\phi/20\left[\widetilde{\phi}\left(1 - \widetilde{\phi}\right)^{-3}\right] \tag{7.27}$$

Two other semiempirical relations have been often used to describe the concentration dependence of suspension viscosity. The first was derived for the first time by Mooney (1951):

$$\ln\eta_r = [\eta]/\left(1 - \widetilde{\phi}\right) \tag{7.28}$$

where $[\eta]_s$ is the intrinsic viscosity. The subscript s indicates that the parameter refers to solid particles. The intrinsic viscosity is defined as

$$[\eta] = \lim_{\phi, \dot{\gamma} \to 0} (\eta - \eta_o)/\eta_o\phi = \lim_{\phi, \dot{\gamma} \to 0} d(\eta_r - 1)/d\phi = \lim_{\phi, \dot{\gamma} \to 0} d \ln \eta_r/d\phi \tag{7.29}$$
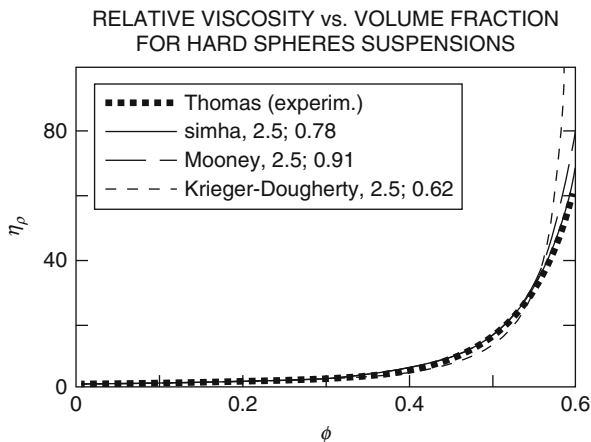
Fig. 7.8 Relative viscosity of hard-sphere suspension in Newtonian fluid as a function of the volume fraction. Thomas curve represents the generalized behavior of suspensions as measured in 19 laboratories. The remaining curves were computed from Simha's, Mooney's, and Krieger–Dougherty's relations assuming Einstein value for intrinsic viscosity of hard spheres, $[\eta] = 2.5$, but different values for the maximum packing volume fraction, $\phi_m = 0.78, 0.91$, and 0.62, respectively

The second dependence is the already cited Eq. 7.8, derived by Krieger and Dougherty (1959). The relation belongs to a large group of dependencies of the type, discussed in detail a few years back (Utracki 1989):

$$\eta_r = (1 + \alpha\phi)^{\beta} \tag{7.30}$$

In Eq. 7.30, the values of the semiempirical parameters, α and β, are usually constant, e.g., respectively 2.5 and 1, or -2.5 and -1, or -1.73 and -2.0, etc. However, in the Krieger–Dougherty relation, these two parameters depend on the system $\alpha = 1/\phi_m$ and $\beta = [\eta]\phi_m$.

In Fig. 7.8, the plots of η_r versus ϕ calculated from Simha's Eq. 7.24, Mooney's Eq. 7.28, and Krieger–Dougherty's Eq. 7.8 are compared with the empirical curve-fitted relation, Eq. 7.5. For all the relations, the intrinsic viscosity $[\eta]_s = 2.5$ was used. However, to optimize the fit, different values for the maximum packing volume fraction, $\phi_m = 0.78, 0.91$, and 0.62, respectively, had to be used. Detailed analysis of Thomas' data made it possible to conclude that Simha's relations provide the best fit with more realistic values of the physical parameters (Utracki and Fisa 1982).

To summarize, the dependence of relative viscosity on the volume fraction of suspended particles can be expressed by any of several theoretical or semiempirical relations. These can be written in terms of the two parameters, $[\eta]$ and ϕ_m; thus $\eta_r = \eta_r([\eta], \phi/\phi_m)$. As it will be shown, the generality of this dependence extends beyond the monodispersed hard-sphere suspensions.

The relationships between η_r and ϕ have been derived for suspensions of monodispersed hard spheres in Newtonian liquids. However, most real systems are polydispersed in size and do not necessarily consist of spherical particles. It has been found that here also Simha's Eq. 7.24, Mooney's Eq. 7.28, or Krieger–Dougherty's Eq. 7.8 are useful, provided that the intrinsic viscosity and the maximum packing volume fraction are defined as functions of particle shape and size polydispersity. For example, by allowing ϕ_m to vary with composition, it was possible to describe the η_r versus ϕ variation for bimodal suspensions (Chang and Powell 1994). Similarly, after values of $[\eta]$ and ϕ_m were experimentally determined, Eq. 7.24 provided good description for the η_r versus ϕ dependence of several multiphase systems, e.g., PVC emulsions and plastisols, mica-reinforced polyolefins, and sealant formulations (Utracki 1988, 1989).

The problem of packing a maximum volume of solids into a given space is common to numerous branches of physics and technology. It suffices to note that the relative viscosity of suspensions is a function of the reduced volume fraction, $\widetilde{\phi} \equiv \phi/\phi_m$, to realize the importance of ϕ_m. Experimentally, it was demonstrated that ϕ_m calculated from *dry packing* of solid particles agrees well with the value determined for a suspension.

Theoretically and experimentally polydispersity increases the ϕ_m value, for example, from 0.62 observed for random packing of uniform spheres to values exceeding 0.9. An interesting recipe for ϕ_m maximization requires four generations of nearly spherical particles with the diameter ratios 1:3:9:17. Blending them at the volume ratios 4:1:1:4 result in $\phi_m = 0.78$. However, what was important, the suspensions were found to be nonsedimenting, and when dried they gave solid bed with uniform porosity (Ritter 1971; Lord 1971).

In industrial practice it may be important to use mixtures of filler particles not only of spheroidal shape (as discussed above) but also of different shapes, e.g., filling and reinforcing polymer with $CaCO_3$ particles and glass fibers. The theoretical basis for optimization of such systems was developed by Wieckowski and Streg (1966) and later by Milewski (Milewski 1973, 1977, 1978; Milewski and Katz 1987). These studies are also important for polymer blends where at concentrations exceeding the percolation threshold the morphology is complex, comprising spheres, fibers, and lamellas.

For anisometric particles it is useful to use the particle aspect ratio, p, defined as a ratio of two orthogonal axes. For prolate ellipsoids (fibers) $p > 1$ is the length-to-diameter ratio, whereas for oblate ellipsoids (plates) $p < 1$ is the thickness divided by the largest dimension of the plate. It was observed that both, the intrinsic viscosity, $[\eta]$, and the inverse of the maximum packing volume fraction, $1/\phi_m$, increase linearly with p. Thus, the relative viscosity of suspensions of anisometric particles is higher than that observed for spheres. For example, Doi and Edwards predicted (1978) that for rods $\eta_r \propto \phi^3$.

In the extensional, irrotational field, under the steady-state conditions, the particles remain oriented in the direction of stress. In uniaxial flow they align with the main axis in the flow direction, while in biaxial they lie on the stretch

plane (Batchelor 1970, 1971). For dilute spherical suspensions in Newtonian liquid, the extensional viscosity follows the Trouton rule, i.e., $\eta_E \cong 3\eta$. However, for anisometric particles the Trouton ratio η_E/η is a strong function of p. For example, at $\phi = 0.01$ extensional viscosity of rods with aspect ratio p $= 1,000$ is 1,000 times higher than that for suspension of spheres.

Particle Orientation in Flow

The orientation of particles in flow is of particular interest to microrheology. To predict the macroscopic rheological properties of a multiphase system, a detailed description of each phase behavior is required. In this field, contributions from the Pulp and Paper Research Institute of Canada by Mason et al. and later by van de Ven and his coauthors are particularly valuable. The earlier results were summarized by Goldsmith and Mason (1967), the latter by Van de Ven (1989). The microrheology has been particularly well developed for infinitely dilute systems in Newtonian matrix – either solid particles or liquid drops. In the present part, only the former system will be summarized. More extensive discussion of microrheology of the liquid–liquid systems will be presented later, while considering the rheological behavior of polymer blends.

For suspension of solid particles in a liquid, the theoretical and experimental works indicate that the angle of orientation of a spheroid can be expressed as

$$\phi_1 = \arctan\left[p \tan\left(2\pi t/t_p\right)\right] \tag{7.31}$$

where the period of rotation of a particle with an aspect ratio, p, is given by

$$t_p = 2\pi\left(p + p^{-1}\right)/\dot{\gamma} \tag{7.32}$$

Accordingly, for rods, the maximum velocity of rotation occurs at $t/t_p = 0$, 1/2, 3/4, 5/4, ... For spheres with p $= 1$, $\phi_1 = 2\pi\,t/t_p$, i.e., constant rotational velocity. In nonuniform shear fields, such as that observed during flow through a capillary (Poiseuille flow), the particles rotate with velocity predicted by Eqs. 7.31 and 7.32, according to the value of the shear rate existing at the radial location of the sphere in the capillary. Near the wall, for finite diameter spheres, the immobile layer of the suspending medium causes a reduction of rotational and translational velocity. The effect scales with the square of the sphere diameter.

The wall also causes a geometric exclusion effect, i.e., a lower-than-average concentration of particles near the wall and a retardation of their motion. The phenomena are complicated by the axial migration of particles, dependent on the Reynolds number, $\mathrm{Re} = \rho\dot{\gamma}d^2/\eta_o$, where ρ and d are the particle density and diameter, respectively.

To control the orientation of the fibers during composites manufacturing, it is helpful to have an insight about the relation between the suspension structure and rheological properties. Determination of the position, orientation history, and shape of fibers due to bending and twisting in a fluid are the main stream of the studies in this area (Joung et al. 2001; Schmid et al. 2000; Switzer Iii and Klingenberg 2003).

There are a few studies about the role of the fiber flexibility. Recently, Keshtkar et al. (2009) investigated the effect of fiber flexibility on the rheological behavior and orientation of fibers suspended in a Newtonian fluid under simple shear flow using conventional rheometry and rheo-microscopy. The ability of the mesoscopic model of Rajabian et al. (2005) to predict the rheological behavior and orientation of the fibers was also examined (Keshtkar et al. 2010). The advantage of using the abovementioned mesoscopic model is related to the compatibility of thermodynamics with its equations. The results showed that by increasing the fiber flexibility, both the viscosity and first normal stress difference increased. The main conclusion based on rheo-microscopy of the various suspensions is that at low shear rates, the most rigid fibers are more easily oriented than flexible fibers. High shear rate data indicated negligible difference in the orientation state of the flexible and rigid fibers. However, the model predictions for the fiber orientation were qualitatively consistent with the experimental data; it was suggested that GENERIC model (Grmela and Öttinger 1997) should be extended to predict the formation of agglomerates in the fiber-filled suspensions (Keshtkar 2009).

Shear-Induced Particle Migration

There are at least two possible mechanisms for particle migration during shear flow, inhomogeneity of the stress field and strong interparticle interactions (Graham et al. 1991). In the first case, the particles tend to migrate to low shear stress regions, while in the second case the situation is more complex involving a coupled relationship between the thermodynamic and hydrodynamic forces.

The Newtonian behavior of suspensions in Newtonian liquids is limited to low concentrations. An exception seems to be the extensional flow of anisometric particles (irrotational flow field) where the rate of strain independent region extends to concentrations where strong non-Newtonian behavior would be expected in shear. This rate of deformation-dependent phenomena will be summarized below.

During the capillary flow of concentrated suspensions, the difference in velocities of particles located at different radial positions results in the formation of transient multiplets or stacks, behaving similarly to rods. Under these circumstances the rate of axial migration is accelerated, and the flow profile flattens. For example, experimentally, for $\phi = 1/3$ suspensions of spheres flowing through a tube at the Reynolds number Re $\equiv 2\rho Q/\pi R_1 \eta = 0.056$, a partial plug flow was observed. However, when Re reached the value of 0.112, a complete plug flow was observed – the flow was no longer Newtonian (Karnis et al. 1966; Vadas et al. 1973).

Matsumoto et al. (1986) reported that in the cone-and-plate geometry, the storage G' and loss G'' shear moduli of uniform, nonrigid spheres decrease monotonically with test time (or number of shearing cycles). G' and G'' were observed to decrease by four decades, but steady-state shearing for 15 s returned them to the initial values. Since the phenomenon depended on the rigidity as well as on the uniformity of shape and size, development of a structure during the dynamic test must be postulated.

In Couette flow the spheres migrate toward the outer cylinder. In shearing, a *shear fractionation* of spherical particles has been observed. For example, Giesekus (1981) observed that, during torsional shearing of binary sphere suspensions, the larger and the smaller spheres separated into two different annular volumes, i.e., for each sphere size a critical equilibrium radial distance had to be postulated. On the other hand, Prieve et al. (1984, 1985) reported that for each sphere diameter and speed of rotation there is a critical radius, r_c; in the parallel plate rheometer, a particle located at $r < r_c$ was observed to migrate inward, whereas that placed at $r > r_c$ migrated outward. There is no theoretical explanation for either observation.

In a wide-gap Couette rheometer, migration of spheres was followed by a nuclear magnetic resonance imaging (Abbott et al. 1991). Migration to the low shear rate region was found to be determined by the total strain, proportional to the shear rate and square of the particle diameter, but independent of the (Newtonian) viscosity of the matrix liquid. More recently, similar studies were undertaken for suspensions of rods with $p = 2$–18 and $\phi = 0.3$ or 0.4 (Mondy et al. 1994). At the same ϕ, the composition gradient of rods of different aspect ratios was indistinguishable, the same as the one earlier reported for spheres. The rate of migration was found to increase with concentration.

Owing to the periodically accelerated rotation of fibers in a shear field, alignment of fibers in Couette flow is to be expected. Theory indicates that the shear field is about half as efficient at causing fiber alignment as extension. However, the shear field is rarely homogeneous, and during the flow fibers undergo breaking, bending, or coiling, which causes further reduction of alignment efficiency. Further details on various modes of orientation behavior of flowing suspensions can be found in reviews by Cox and Mason (1971), Batchelor (1974), and Leal (1980).

The evidence accumulated so far indicates that there is a full spectrum of structures, from a liquid-like where the yield stress, $\sigma_y = 0$, to a solid-like with large σ_y. For anisometric particles at $\phi > 1/p$, yield may originate in mechanical interlocking of particles, but for spheres it stems from the interparticle interactions. When these interactions are weak, $\sigma_y \to 0$ is observed, with the arrow indicating the time effect. If the experiment is conducted at low rates of shear, no yield behavior would be noted.

In uniaxial extensional (convergent) flow, there is evidence of spherical particles moving toward the center of the stream. Convergent flow of a dilute suspension of glass fibers, $p = 200$–800, in Newtonian liquids was studied by Murty and Modlen (1977). The fiber orientation angle (defined as an average angle between the fiber axis and flow direction) changed from $45°$ (random) to about $15°$. The orientation started upstream from the convergence. For low viscosity liquids, jamming at the entrance region was responsible for as much as 60 % of fibers being "filtered out."

At higher fiber loading, $\phi_p > 1$, the rheological responses of aligned fiber suspensions resemble those of liquid crystals. Becraft and Metzner (1992) analyzed the rheological behavior and orientation of glass fibers (GF), in polyethylene (PE), and polypropylene (PP). The experimental data were interpreted using a modified

Doi theory for liquid crystalline fluids, LCF (Doraiswamy and Metzner 1986). The kinetics of the distribution function, f, is given by

$$\frac{Df}{Dt} = \nabla \cdot \overline{D}_r \nabla f + \nabla \cdot \overline{D}_r \frac{f \nabla V}{k_B T} - \nabla \cdot (uf) \qquad (7.33)$$

where $\overline{D}_r$ is the rotational diffusivity of the rods and u denotes a unit vector corresponding to rod orientation. The first term on the rhs of Eq. 7.33 accounts for the contribution of Brownian motion to the orientation distribution function, the second for the effects of the liquid crystalline interaction potential between the rods, while the third term for the effects of flow.

Doraiswamy and Metzner noted that use of the LCF approach is permissible at concentrations above that which would correspond to the transition from isotropic to aligned morphology, $\phi > 8/p$. The theory provided fair description of the stress–strain dependence for systems containing 10 wt% GF and excellent agreement for those with 40 wt% GF. Also, the approach gave good predictions of the diagonal terms of the second-order orientation tensor.

Aggregation and Yield Stress

One of the fundamental assumptions of the continuum theories is stability of structure (Newtonian behavior) or, alternatively, a well-defined process of structural changes (non-Newtonian behavior). However, as it was already mentioned, orientation effects in sheared layers of suspensions are responsible for either dilatant or pseudoplastic behavior, while strong interparticle interactions may lead to yield stress or a transient behavior. In short, there is an intimate relation between the liquid structure and its rheological response; change in one causes a corresponding change in the other. Some of these changes have been theoretically treated, viz., Eq. 7.32. The aggregation is the result of the attractive forces or the flow conditions. It could be categorized in two groups: flocculation which is the reversible aggregation and coagulation which is a fast irreversible aggregation (Larson 1999). A physical change in the system may cause flocculation. Flocculates can be re-dispersed in the suspension using mechanical processes such as shaking or stirring (deflocculation). Aggregation, agglomeration, and flocculation are structural phenomena ranging from transient rotating doublets observed within dilute region to a pseudo-solid-like behavior of flocculated suspensions with yield stress. Aggregation can occur due to thermodynamic interparticle interactions, chemical bonding, or geometric crowding. The latter type prevails in shear flows of suspensions of anisometric particles.

It was shown that even in the absence of attractive interparticle interactions, shear forces can make aggregates of the particles interacting by large friction forces (Switzer Iii and Klingenberg 2003). For example, flow-induced aggregation has been observed for stiff fibers (Schmid et al. 2000) and carbon nanotube suspensions (Khalkhal et al. 2011).

There are numerous theories based on structural models of suspensions (Mikami 1980). Wildemuth and Williams (1984) considered that the maximum packing

volume fraction, ϕ_m, is a function of *normalized* shear stress, $\widetilde{\sigma}_{12} \equiv \sigma_{12}/M$, where M is a numerical parameter. The authors derived the relation

$$\phi_m = \left(\phi_{m,o} + \phi_{m,\infty}\widetilde{\sigma}_{12}^m\right)/\left(1 + \widetilde{\sigma}_{12}^m\right) \tag{7.34}$$

where m = 1.00–1.17 is an experimental constant, while $\phi_{m,o}$ and $\phi_{m\infty}$ are values of the maximum packing volume fraction at $\widetilde{\sigma}_{12}$ and $\widetilde{\sigma}_{12} = \infty$, respectively. Defining the yield stress as $\widetilde{\sigma}_{12}$ when $\phi = \phi_m$, one can rearrange Eq. 7.34 to read

$$\widetilde{\sigma}_y = \left(\phi - \phi_{m,o}\right)/\left(\phi_{m,\infty} - \phi\right) \tag{7.35}$$

Hoffman (1972, 1974) also reported that at low rates of shear and high solid content, $\phi > 0.54$, the power law index $n = d\ln\sigma_{12}/d\ln\dot{\gamma}$ approaches zero.

For the system styrene-acrylonitrile (SAN) latex in ethylene glycol, addition of salt decreased *n* to zero. The experiment was performed to demonstrate that increased interparticle interaction causes the onset of dilatation to move to higher rate of shear. However, the work also demonstrated that at these high concentrations there is a yield stress, σ_y. Onogi and Matsumoto (1981) reported that in PS suspension with particles having strong attractive forces, the yield phenomenon was observed, while suspensions of PS particles having repulsive forces behaved like Newtonian liquids. Thus, the yield stress is associated with formation of a three-dimensional structure by interacting particles, resulting in a behavior similar to an elastic solid. Similarly, impact modification of PMMA by incorporation of 0–50 wt% of core-shell latex particles of poly(butylacrylate-co-styrene) demonstrated that the particles form a co-continuous network at $\phi \leq 0.2$ that result in a low frequency rubbery plateau. The high-frequency data were found independent of composition (Bousmina and Muller 1992). There are several methods for determining σ_y. Among these is the modified Casson equation (Utracki 1982):

$$F^{1/2} = F_y^{1/2} + aF_m^{1/2} \tag{7.36}$$

where F may be any rheological function (viz., shear stress σ_{12}, elongational stress σ_{11}, shear loss modulus G'', etc.), F_y indicates the yield value of F, F_m is the F-value of the matrix liquid at the same deformation rate as F, and a is a measure of the relative value of F. Another method requires a simultaneous fit of experimental data to a constitutive equation in which a parameter or parameters are related to σ_y (Utracki 1987).

Measurements of creep and elastic recovery also provide a sensitive, direct mean of detecting yield stress, either by simultaneous fit of time-dependent strain, $\gamma(\tau)$, at a constant stress, σ_{12}, to the compliance equation:

$$J(t) \equiv \gamma_{12}(t)/\sigma_{12} = J_0 + J_e^0\Psi(t) + t/\eta \tag{7.37}$$

(where $\Psi(t)$ is the retardation function), or by plotting the recoverable strain versus stress. In the latter case, the maximum value of stress below which the Hookean behavior is obtained gives the value of σ_y.

Polymer lattices and suspensions of carbon black in linseed oil and clay or calcium carbonate in aqueous media provide examples (Amari and Watanabe 1983). The values of σ_y determined from creep and those from shear viscosity were found to be in good agreement.

There are several direct methods of measurement of a yield stress. The constant stress rheometer is most frequently used to determine σ_y value in shear. Dzuy and Boger (1983, 1985) used a rotational vane viscometer. Yield stresses in compression can be calculated from the unrelaxed stress values in parallel plate geometry. Its value in elongation has been directly measured as the critical stress value below which no sample deformation was observed during 30 min of straining in an extensional rheometer.

Khalkhal and Carreau (2011) examined the linear viscoelastic properties as well as the evolution of the structure in multiwall carbon nanotube–epoxy suspensions at different concentration under the influence of flow history and temperature. Initially, based on the frequency sweep measurements, the critical concentration in which the storage and loss moduli shows a transition from liquid-like to solid-like behavior at low angular frequencies was found to be about 2 wt%. This transition indicates the formation of a percolated carbon nanotube network. Consequently, 2 wt% was considered as the rheological percolation threshold. The appearance of an apparent yield stress, at about 2 wt% and higher concentration in the steady shear measurements performed from the low shear of $0.01 \ s^{-1}$ to high shear of $100 \ s^{-1}$, confirmed the formation of a percolated network (Fig. 7.9). The authors used the Herschel–Bulkley model to estimate the apparent yield stress. As a result they showed that the apparent yield stress scales with concentration as $\tau_y \sim \varphi_v^{2.64\pm0.16}$ (Khalkhal and Carreau 2011).

For unoriented particle systems, the von Mises criterion for plastic flow of solids should be obeyed; the yield stress in elongation and compression should be equal to each other and larger by the factor of $\sqrt{3}$ than the yield stress in shear, σ_y. However, for highly concentrated suspensions of anisometric particles, von Mises criterion should not be used.

For suspensions, the concentration dependence of σ_y was found to follow either of the following two dependencies:

$$\sigma_y = a_1(\phi - \phi_0)^{a_2} \quad \text{and} \quad \sigma_y = a_3\exp\{a_4\phi\} \tag{7.38}$$

where a_i are adjustable parameters. The exponent a_2 depends on the particle geometry as well as the interparticle interactions. For human blood $\sigma_y = 26.87\phi^3$ (mPa) was reported (Picart et al. 1998).

It has been observed that for many systems the value of yield stress depends on the time scale of the measurements. Setting all controversies aside, pragmatically it is advantageous to consider that in these systems there are aggregates of different size, characterized by the dynamic interparticle interactions. For a given system these interactions have specific strength, σ_y^∞, and the aggregates have a characteristic relaxation time, τ_y. This model leads to the following relation:

$$\sigma_y(\xi) = \sigma_y^\infty \left[1 - \exp\{-\tau_y\xi\}\right]^u; \quad \text{for} \quad \xi = \omega, \ \dot{\gamma} \ \text{or} \ \dot{\varepsilon} \tag{7.39}$$

where u = 0.2–1.0 characterizes polydispersity of the aggregates. Equation 7.39 was found to be easy to use, and the parameters computed from curve fitting of the experimental data, $\sigma_{apparent} = \sigma_y + \sigma_{true}$, agreed quite well with the independently determined values.

Leonov (1994) introduced kinetics of interactions into his rheological equation of state. The new relation can describe systems with a dynamic yield stress, without resorting to a priori introducing the yield stress as a model parameter (as it has been done in earlier models).

Time-Dependent Flows

Two types of flow are recognized: thixotropy, defined as *a decrease of apparent viscosity under shear stress*, *followed by a gradual recovery when the stress is removed*, and its opposite, anti-thixotropy, or rheopexy. Both are related to molecular or macroscopic changes in interactions. In thixotropic liquids, the aggregate bonding must be weak enough to be broken by flow-induced hydrodynamic forces. If dispersion is fine, even slight interactions may produce thixotropic effects. When

Table 7.5 Definitions of viscoelastic and thixotropic systems

No.	Viscoelastic systems	Thixotropic systems
1.	Yield stress defined by the conditions: $\dot{\gamma} = 0$ when $\sigma_{12} < \sigma_y$	Critical stress defined by the conditions: $\dot{\gamma}(t) = 0$ when $\sigma_{12} < \sigma_{crit}(t)$
2.	Initial slope of the flow curve: $\lim_{\dot{\gamma} \to 0} \partial \ln \eta_{app} / \partial \ln \dot{\gamma} = 1$	Initial slope of the flow curve: $\lim_{\dot{\gamma} \to 0} \partial \ln \eta_{app} / \partial \ln \dot{\gamma} \leq 1$
3.	Elastic effects are present	Lack of elastic effects
4.	After step increase of $\dot{\gamma}$ the shear stress, σ_{12}^{+} increases	After step increase of $\dot{\gamma}$ the shear stress, σ_{12}^{+} decreases
5.	Smaller equilibrium strains than those for thixotropic systems	Larger equilibrium strains than those for viscoelastic systems

the dispersion coarsens, larger forces are required to engender the same effects. In the case of suspensions of anisometric particles, the interactions are particularly strong, while for spheres, the effect can be controlled by changing the type and concentration of ionic groups on the surface. Similarly, in polymer blends the interdomain interactions can be controlled by addition of a compatibilizer – its presence enhances the interphase interactions.

Breakup and recreation of the associated structure follow exponential decay kinetics. The simplest, single exponential relation representing thixotropic behavior is

$$\eta(t) - \eta_{\infty}^{t} = \left(\eta_0^{t} - \eta_{\infty}^{t} \right) \exp\{-t/\tau^{*}\} \qquad (7.40)$$

where t is the shearing time, η_0^t and η_∞^t are values of shear viscosity at $t = 0$ and ∞, respectively, and τ^* is the relaxation time of the system.

Time dependency also enters into the consideration of the rheological response of any viscoelastic system. In steady-state testing of materials such as molten polymers, the selected time scale should be sufficiently long for the system to reach equilibrium. Frequently, the required period, $t > 10^4$ s, is comparable to that in thixotropic experiments. More direct distinctions between these two types of flow are the usual lack of elastic effects and the larger strain values at equilibrium observed for thixotropic materials (see Table 7.4). There is a correlation between these two phenomena, and theories of viscoelasticity based on thixotropic models have been formulated by Leonov (1972, 1994). Inherent to the concept of thixotropy is the yield stress. Both the microstructural and continuum theories postulate that the material behaves as a Bingham body at stresses below a critical value (Table 7.5).

Steady-State Flows

There are three types of melt behavior in a simple shear flow: dilatant (D) (shear thickening); Newtonian (N), and pseudoplastic (P) (shear thinning). Similarly, in an extensional flow, the liquids may be stress hardening (SH), Troutonian (T), or stress softening (SS). By definition, the response considered here is taken at sufficiently

long times to ensure steady state, and the yield effect, Y, is subtracted. In consequence, within the experimental range of stress or deformation rate, several types of behavior may be observed. There exist a great variety of flow curves observed for different materials.

Pseudoplastic Flows

For suspensions, the most common type is a pseudoplastic flow curve with the so-called upper, η_o, and lower, η_∞, Newtonian plateaux (Cross 1965, 1970, 1973):

$$\eta - \eta_\infty = (\eta_0 - \eta_\infty)/(1 + a_0\dot{\gamma}^{a_1}) \tag{7.41}$$

In this relation a_o is the parameter describing how fast the viscosity changes between the two plateaux. In viscoelastic systems, the lower plateau is several orders of magnitude smaller than the upper one, $\eta_\infty << \eta_o$, and it is frequently neglected.

Equation 7.41 resembles the one derived by Carreau (1972) for monodispersed polymer melts, which later was generalized for polydispersed systems (Utracki 1984, 1989):

$$\eta = \eta_0[1 + (\tau\dot{\gamma})^{m_1}]^{-m_2} \tag{7.42}$$

In Eq. 7.42, τ is the relaxation time and m_1 and m_2 are polydispersity parameters, with a bound: $n = 1 - m_1 m_2$, where n is the power-law exponent in the relation:

$$\sigma_{12} = K\dot{\gamma}^n \tag{7.43}$$

Equation 7.42 well describes the flow behavior of polymeric systems, and it was found useful for polymer blends. It should be stressed that Eqs. 7.41, 7.42, and 7.43 describe the flow behavior of fluids without yield stress or thixotropicity.

Dilatant Flows

Krieger and Choi (1984) studied the viscosity behavior of sterically stabilized PMMA spheres in silicone oil. In high viscosity oils, thixotropy and yield stress were observed. The former is well described by Eq. 7.41. The magnitude of σ_y was found to depend on ϕ, the oil viscosity, and temperature. In most systems, lower Newtonian plateau was observed for the reduced shear stress value: $\sigma_r \equiv \sigma_{12}d^3/RT > 3$ (d is the sphere diameter, R is the gas constant, and T is the absolute temperature). However, when shear stress was further increased, dilatant behavior was observed. Dilatancy was found to depend on d, T, and silicone oil viscosity. The authors reported small and erratic normal stresses.

To describe the above behavior, the following relation was derived (Utracki 1989):

$$\eta - \eta_\infty = (\eta_0 - \eta_\infty)\left[1 + a_0\exp\{\tau\dot{\gamma} - a_1\}^{2a_2}\right]\left[1 + (\tau\dot{\gamma})^{m_1}\right]^{-m_2} \tag{7.44}$$

where a_i are equation parameters. Excepting the assumptions that $\eta_\infty \neq 0$ and insertion of the middle square bracket on the rhs of Eq. 7.44, the dependence is the same as Eq. 7.42.

Hoffman (1972, 1974), Strivens (1976), van de Ven (1984, 1985), Tomita et al. (1982, 1984), and Otsubo (1994) reported pseudoplastic/dilatant flow of concentrated suspensions of uniform and polydispersed spheres. A dramatic change in light diffraction pattern was systematically observed at the shear rate corresponding to the onset of dilatancy. Van de Ven and his collaborators demonstrated that, depending on concentration and shear rate, the distance between the sliding layers of uniform spheres in a parallel plate rheometer can vary by as much as 10 %.

The dilatant behavior of binary sphere suspensions in capillary flow was reported by Goto and Kuno (1982, 1984). At constant loading, dilatancy was observed only within a relatively narrow range of composition, $0.714 < x < 0.976$, where x represents the fraction of larger spheres.

Suspensions, even in Newtonian liquids, may exhibit elasticity. Hinch and Leal (1972) derived relations expressing the particle stresses in dilute suspensions with small Peclet number, $Pe = \dot{\gamma}/D_r \sim 1$ (D_r is the rotary diffusion coefficient), and small aspect ratio. The origin of the elastic effect lies in the anisometry of particles or their aggregates. Rotation of asymmetric entities provides a mechanism for energy storage, Brownian motion for its recovery. For suspensions of spheres, this mechanism does not exist and the first normal stress, N_1, is expected to vanish. However, when at higher ϕ the spherical particles aggregate into anisometric clusters, the system may and does show a viscoelastic behavior. Indeed, large N_1 (Kitano and Kataoka 1981), Weissenberg rod climbing (Nawab and Mason 1958), and large capillary entrance–exit pressure drops were reported (Goto et al. 1986). On the other hand, owing to the yield stress, no extrudate swell was observed in suspensions of anisometric particles in Newtonian liquids (Roberts 1973).

Theoretically, interparticle interactions contribute directly to the elastic stress component of spherical suspensions as well as by modification of the microstructure (Batchelor 1977):

$$\langle S^P \rangle N = \sum_{i=2}^{N} \sum_{j<i}^{N} r_{ij} F_{ij} \tag{7.45}$$

where N is the number of particles and r_{ij} center-to-center separation of i and j particles with pairwise interparticle interaction force F_{ij}. Gadala-Maria (1979) reported that, for suspensions of PS spheres in silicone oil, N_1 linearly increased with σ_{12}. Other theories have been discussed by Van Arsdale (1982), Bibbo et al. (1985), Brady (1993), Becraft and Metzner (1994), and many others.

The dynamic mechanical testing of suspensions is particularly suitable for studying systems with anisometric particles with well-defined structures (Ganani and Powell 1985). The authors studied the dynamic behavior of spheres in Newtonian liquids. They reported that dynamic viscosity, η', behaves similarly as the steady-state viscosity, η, while the storage modulus $G' \cong N_1 \cong 0$.

Transient Effects

In system where the structure changes with time upon imposition of stress, transient effects are important. For example, semi-concentrated fiber suspensions in shear and extension show large transient peaks in the first and the second normal stress differences (Dinh and Armstrong 1984; Bibbo et al. 1985). It is interesting that the peaks appear at different times, first for N_2, then for N_1, and finally for σ_{12}.

7.3.1.2 Suspensions in Non-Newtonian Liquids

Filled and reinforced polymer melts belong in this category. There are numerous reviews on the topic (Chaffey 1983; Goettler 1984; Metzner 1985; Utracki 1987, 1988; Utracki and Vu-Khanh 1992). There is particularly strong interest in flow of polymeric composites filled with anisometric, reinforcing particles, with properties that strongly depend on the flow-induced morphology and distribution of residual stresses.

In the absence of interlayer slip, addition of a second phase leads to an increase of viscosity. The simplest way to treat the system is to consider the relative viscosity as a function volume fraction of the solids, ϕ, particle aspect ratio and orientation.

There is no difference between the flow of suspensions in Newtonian liquids and that of polymeric composites, when the focus is on the Newtonian behavior phase. The non-Newtonian behavior of suspensions originates either from the non-Newtonian behavior of the medium or from the presence of filler particles. The problems associated with this behavior can originate in interparticle interactions (viz., yield stress) and orientation in flow (Leonov 1990; Mutel and Kamal 1991; Vincent and Agassant 1991; Shikata and Pearson 1994).

7.3.1.3 Flow-Induced Orientation

The most efficient orientation fields are extensional. Using convergent and divergent flow one may control orientation of anisometric particles. Most of the work in this area has been done with fiber-filled materials, but the effects are equally important for flow of neat semicrystalline polymer melts or liquid crystal polymers (Goettler and Shen 1983; Goettler 1984). In extensional flow, platelets are less susceptible to orientation. Two-stage orientation mechanism was observed in converging flow (Utracki 1988).

The nonlinear rheological behavior of platelet dispersions is a response to flow-induced rearrangements. Some methods have been developed to provide information on flow-induced orientation of platelets. These methods, generally, consist of performing in situ small-angle X-ray scattering (SAXS) (Bihannic et al. 2010) or small-angle neutron scattering (SANS) (Hanley et al. 1994; Kalman and Wagner 2009; Ramsay and Lindner 1993) experiments under shear flow applied in a Couette shear cell apparatus. For example, SAXS patterns obtained from radial and tangential incident beams relative to flow velocity field in a Couette apparatus showed biaxial orientation of natural clay particles (Bihannic et al. 2010). To correlate shear-induced particle orientation and the corresponding suspension viscosity, the effective volume fraction was first calculated based on parameters

Fig. 7.10 Comparison
between experimental and
calculated viscosities
(Bihannic et al. 2010)
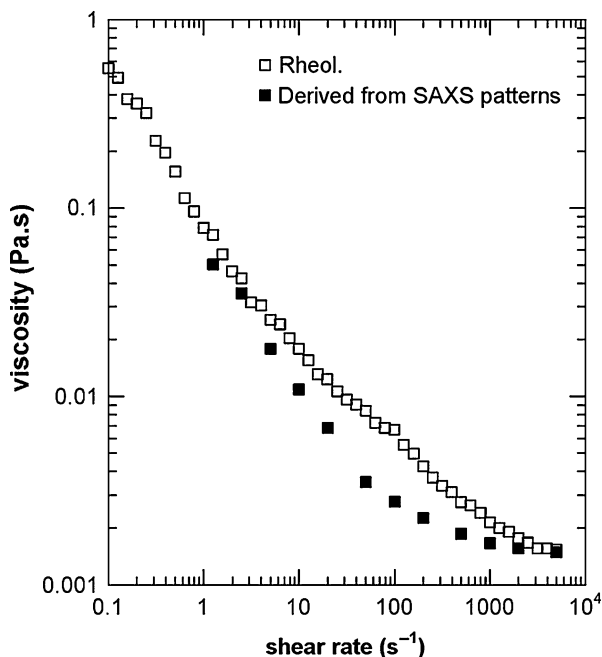
derived from SAXS patterns (using an orientation distribution function) for differ-
ent shear rates. Then the viscosity was calculated using the model proposed by
Quemada (Quemada 1977; Quemada and Berli 2002) that relates suspension
viscosity to effective volume fraction. Figure 7.10 depicts the experimental and
calculated viscosities for the clay suspension. It reveals that the proposed approach
is successful in relating anisotropy of SAXS patterns to rheological behavior of the
suspension.

However, in shear-thinning dispersion, flow-induced orientation develops as
shear rate increases. Moreover, the shape factor of the particles affects the orien-
tational order. Evaluation of the shape factor effect on the orientation of particles
and, consequently, the rheological properties of suspensions showed that the shape
factor distribution provides more precise information than the median value of the
shape factor, specially at high shear rates (>105 s^{-1}) (Lohmander and Rigdahl
2000). Comparing two suspensions prepared using particles with a broad shape
factor distribution and a narrow one, with the same average value, showed higher
viscosity for the latter due to the different orientational order.

The orientation affects flow profoundly, hence processability, as well as the
product performance. It plays an important role in extrusion or injection molding
where the anisometric particles may become oriented in a complex manner.
Layered structures, weld lines, splice lines, swirls, and surface blemishes are well
known. Mold geometry (e.g., inserts) and transient effects make predictions diffi-
cult. It has been theoretically and experimentally shown that, when designing

a mold for composites with anisometric particles, the principles developed for single-phase melts do not apply (Crowson and Folkes 1980; Crowson et al. 1980, 1981; Folkes 1982; Vincent and Agassant 1986, 1991).

Yield Stress

Yield occurs as a result of structure formation due to physical crowding of particles, interparticle interactions, or steric–elastic effects of the medium. Depending on the stability of the structure, true or apparent (i.e., time-dependent) yield stress can be obtained. As a consequence, the magnitude of yield stress increases with aspect ratio of the particles, their rigidity, and concentration. The phenomenon is visible in steady-state shear, dynamic, or extensional flow, especially at low rates of deformation, where the slope of the flow curve, $\log\eta$ versus $\log\dot{\gamma}$, is often $\partial\log\eta/\partial\log\dot{\gamma} = -1$ (time-independent yield). Neglecting the yield stress may have serious consequences on interpretation of elasticity.

Yield stress and plug flow are interrelated. The viscous loss energy is dissipated in a relatively small volume of material, where the concentration of solids differs from average. This may lead to excessive shear heating (effects as large as $\Delta T \geq 80\,°C$ have been observed), degradation of polymeric matrix, strong change of skin morphology during polymer blends extrusion, as well as to attrition of anisometric particles, fibers, or flakes. Thus, the skin layer may not only have different concentration, but different chemical and physical composition as well. At high flow rates, this situation may lead to slip at the wall.

In capillary flow, slip velocity at the wall, s, can be calculated from (Reiner 1930, 1931)

$$
\begin{aligned}
&\dot{\gamma} = \dot{\gamma}_N(3 + 1/n) - (s/R)(n^* + 3) \\
&n \equiv \partial\ln\sigma_{12}/\partial\ln\dot{\gamma} \\
&n^* \equiv \partial\ln s/\partial\ln\sigma_{12} \\
&s = s_o(\sigma_{12} - \sigma_y)^{s_1}
\end{aligned}
\tag{7.46}
$$

where the first expression on the rhs of Eq. 7.46 is the well-known Rabinowitsch correction and the second expression represents the contribution of the slip. Here s is the slip velocity, R is the radius of the capillary, and s_i are parameters. Experimentally, it was observed that the slip velocity depends on the difference between shear stresses, $\sigma_{12} - \sigma_y$. Exponent values as large as $s_1 = 6.3$ were determined for rigid PVC. Slip may occur in any large strain flow, in capillary, cone-and-plate, or parallel plate flow (Kalyon et al. 1993, 1998).

Further consequences of the yield stress (i.e., plug flow) are (i) a drastic reduction of the extrudate swell, $B \equiv d/d_o$ (d is diameter of the extrudate, d_o that of the die) (see, e.g., Crowson and Folkes 1980; Utracki et al. 1984), and (ii) significant increase of the entrance–exit pressure drop, P_e (also known as Bagley correction). For single-phase fluids, these parameters have been related to elasticity by molecular mechanisms (Tanner 1970; Cogswell 1972; Laun and Schuch 1989). However, in multiphase systems, both B and P_e depend primarily on the

inter-domain interactions and morphology, not on deformation of the macromolec-
ular coils. Thus, in multiphase systems (i.e., blends, filled systems, or composites),
only direct measures of elasticity, such as that of N_1, N_2, or G' should be used. It is
customary to plot the measure of the elastic component versus that of the shear
components, viz., N_1 versus σ_{12}, or G' versus G'', etc. For rheologically simple
systems, the relationships are independent of temperature, but for the multiphase
systems the viscoelastic time–temperature principle does not hold.

A viscoelastic–plastic model for suspensions of small particles in polymer melts
was proposed (Sobhanie et al. 1997). The basic assumption is that the total stress is
divided into that in the matrix and the network of immersed interacting particles.
The model leads to nonlinear viscoelastic relations with the yield function, which is
defined in terms of structure rupture and restoration.

Many parameters like the size, size distribution, and shape of the particles along
with the particle–particle and particle–fluid interactions, viscoelastic properties of
the suspending fluid, and the flow geometry complicate the modeling of suspension
behavior. Chateau et al. proposed a homogenization approach to estimate the
behavior of suspensions of noncolloidal particles in an incompressible yield stress
fluids (Chateau et al. 2008). The study involve treats the non-Newtonian suspension
as a continuous medium based on the properties of its constituents. The problem is
simplified by using the secant method of Castañeda (1991) and Suquet (1993).
According to Chateau et al., where Herschel–Bulkey law is valid, the yield stress
($\tau_c{}^{hom}$) of the suspension may be estimated as the product of the suspending fluid
yield stress (τ_c) and a function of solid volume fraction, φ: ($\tau_c{}^{hom}/\tau_c = ((1 - \varphi)$
$g(\varphi))^{1/2}$). Using the Krieger–Dougherty law (Krieger and Dougherty 1959) to
determine the ratio of the macroscopic to the microscopic properties ($g(\varphi)$), it
was found that the experimental results are in a good agreement with the simple
law $\tau_c{}^{hom}/\tau_c = (1 - \varphi)^{1/2}(1 - \varphi/\varphi_m)^{-1.25\varphi m}$ (Chateau et al. 2008). This means that
as long as the noncolloidal particles are spherical, only the close packing density,
yield stress, and power law index of the suspending medium are necessary to
identify the macroscopic properties of these suspensions (Chateau et al. 2008).

Extensional Flows

The yield stress is also observed in extensional flows (Kamal et al. 1984a, b; Utracki
1988). Yield stress is manifested in two related ways: (i) as a vertical displacement
in the stress growth function at decreasing strain rates, contrasting with the normal
linear viscoelastic behavior of single-phase polymeric melts, and (ii) as a deviation
from the relation $\lim_{\dot{\varepsilon}\to0} \eta_E(\dot{\varepsilon}) = 3\eta_0$.

In qualitative agreement with the von Mises criterion, $\sigma_{11,y}/\sigma_{12,y} = 1.3 - 2.0$
was reported (Utracki 1984). The Trouton ratio

$$R_T \equiv \lim_{\dot{\varepsilon}\to0} \eta_E(\dot{\varepsilon})/3\eta_0 \qquad (7.47)$$

was found to decrease by half, as the concentration of glass beads in SAN increased
($\phi \leq 0.37$) (Martischius 1982). It was argued that in extensional flow only the liquid

undergoes deformation; thus both the extensional strains and viscosities should be corrected for the "diluting" effect of the filler volume (Nicodemo et al. 1975).

The relative extensional viscosity of suspensions in a power-law liquid can be expressed as (Goddard 1978)

$$\eta_{E,r} \equiv \eta_E(\phi,\dot{\varepsilon})/\eta_E(0\dot{\varepsilon}) = 1 + 2\phi R_T p^{n+1} \left\{ (1/n - 1)\left[1 - (\pi/\phi)^{(1-1/n)/2}\right] \right\}^{n/(2+n)}$$

(7.48)

Equation 7.48 described the extensional viscosity behavior of a PE/mica system well, after subtracting the yield stress using Casson's equation (Utracki and Lara 1984).

7.3.2 Emulsion Rheology

Liquid-in-liquid systems can be divided into three categories: those in which both liquids are Newtonian, those in which both phases are viscoelastic, and those systems comprising one Newtonian and one viscoelastic liquid. The first of these categories refers to emulsions (E), the second to polymer blends (B), and the third class is used as models (M) to gain some insight into the effects of elasticity on the flow and morphology. Some polymer blends may also be classified as M. Several reviews are available on emulsion rheology (Sherman 1963, 1968; Barry 1977; Nielsen 1977; Utracki 1988, 1989; Pal 1996) and on emulsions containing high volume fraction of the dispersed phase, $\phi > 0.74$ (Cameron and Sherrington 1996).

7.3.2.1 Newtonian Flow

Einstein's treatment of suspensions was extended to emulsions by Taylor (1932, 1934) who derived the following expression for the relative viscosity of emulsions:

$$\eta_r = 1 + (5/2)\sigma[\lambda + 2/5]/[\lambda + 1]$$
$$\therefore [\eta]_e = (5/2)\sigma[\lambda + 2/5]/[\lambda + 1]$$
$$\text{where} \quad \lambda \equiv \eta_d/\eta_\mu$$

(7.49)

Oldroyd (1953, 1955) modified this theory by incorporating effects of the interface:

$$[\eta]_e = (5/2)[\Lambda + 2/5]/[\Lambda + 1]$$
$$\text{where} \quad \Lambda \equiv (\eta_d + \eta_i/5d)/\eta_m$$
$$\text{and} \quad \eta_i = 2\eta_{Si} + 3\eta_{Ei}$$

(7.50)

In Eq. 7.50 the interfacial viscosity, η_i, is expressed in terms of the interfacial shear (subscript Si) and extensional (subscript Ei) components. The plot of emulsion viscosity as a function of the dimensionless viscosity ratio, Λ, is shown in Fig. 7.11.

Fig. 7.11 Intrinsic viscosity of emulsion versus the viscosity ratio (defined in the Figure) (Oldroyd 1953, 1955)
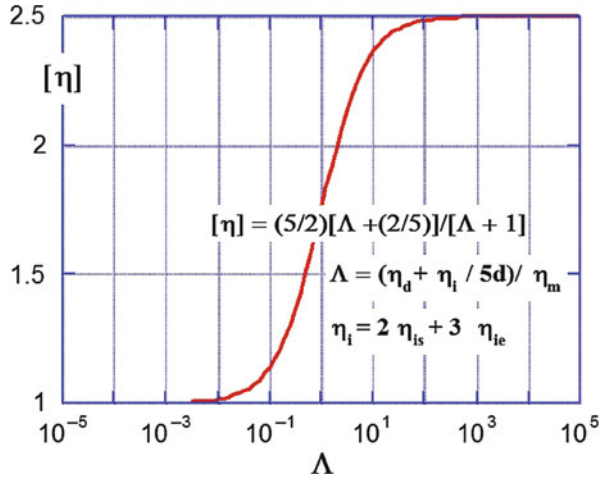
Note that the upper bound of the emulsion intrinsic viscosity is Einstein's value for hard-sphere suspension $[\eta] = 2.5$. This limit is observed for $\Lambda > 100$. For $\Lambda = 1$ (solutions), $[\eta] = 1.75$. The lower values are expected for emulsions of low viscosity liquids in highly viscous one – for $\Lambda < 0.01$, $[\eta] \approx 1$. Equation 7.50 was found valid in a wide range of $1.3 < \Lambda < \infty$.

Oldroyd (1953, 1955), Choi and Schowalter (1975), Oosterbroek et al. (1980, 1981), and many others considered the interphase between the dispersed phase and the matrix liquid to be a physical, three-dimensional entity endowed with its own specific rheological properties. These considerations led to calculations of two relaxation's times for Newtonian emulsions (Choi and Schowalter 1975)

$$\eta_r = 1 + \phi[(5\lambda + 2)/(2\lambda + 2)] + (5/8)[\phi(5\lambda + 2)/(\lambda + 1)]^2$$
$$\tau_1 = \tau_0[1 + 5\phi\{(19\lambda + 16)/[4(\lambda + 1)(2\lambda + 3)]\}]$$
$$\tau_2 = \tau_0[1 + 3\phi\{(19\lambda + 16)/[4(\lambda + 1)(2\lambda + 3)]\}]$$
$$\tau_0 = (\eta_2 R/\nu_{12})\{(19\lambda + 16)(2\lambda + 3)/[40(\lambda + 1)]\}$$

$$(7.51)$$

For the relative viscosity of emulsions, in the absence of deformation and coalescence, Eqs. 7.24, 7.25, 7.26, 7.27, 7.28, 7.29, and 7.30 may also be used, provided that the intrinsic viscosity is calculated from Eq. 7.50 and that the maximum packing volume fraction is treated as an adjustable parameter, dependent on the interphase. This pragmatic approach has been successfully used to describe $[\eta]$ versus ϕ variation for such complex systems as industrial lattices (at various stages of conversion), plastisols, and organosols.

Industrial emulsions are usually prepared as concentrated systems, containing $\phi_m \leq 0.94$. Owing to interface interactions and deformability of droplets, these systems behave rather like elastic, soft solids without any sign of Newtonian behavior. Between the highly concentrated and dilute regions, there is a wide zone of structural change reflected in a spectrum of non-Newtonian behavior.
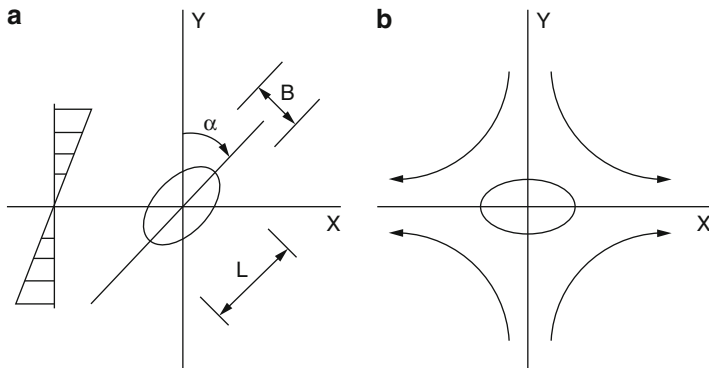
Fig. 7.12 Deformation of drops in shear (**a**) and extensional (**b**) flow field (Taylor 1932, 1934)

7.3.2.2 Emulsion Microrheology
Drop Deformability

When a neutrally buoyant, initially spherical droplet is suspended in another liquid and subjected to shear or extensional stress, it deforms and then breaks up into smaller droplets. Taylor (1932, 1934) extended the work of Einstein (1906, 1911) on dilute suspensions of solid spheres in a Newtonian liquid to dispersions of single Newtonian liquid droplet in another Newtonian liquid, subjected to a well-defined deformational field. Taylor noted that, at low deformation rates in both uniform shear and planar hyperbolic fields, the sphere deforms into a spheroid (Fig. 7.12).

At low stress in steady uniform shearing flow, the deformation can be described by three dimensionless parameters: the viscosity ratio, the capillary number, and the reduced time:

$$\lambda \equiv \eta_1/\eta_2; \quad \kappa \equiv \sigma_{ij} d/v_{12} \quad \text{and} \quad t^* = \gamma/\kappa \tag{7.52}$$

where η_1 and η_2 are the viscosities of the dispersed and the matrix phases, respectively, σ_{ij} is the stress (either in shear $ij = 12$ or in extension $ij = 11$), d is the initial drop diameter, v_{12} is the interfacial tension coefficient between two phases, and γ is the generated strain.

During shear or uniaxial extensional flow, the initially spherical drop deforms into a prolate ellipsoid with the long axis, a_1, and two orthogonal short axes, a_2. It is convenient to define the drop deformability parameter, D, as

$$
\begin{aligned}
D &\equiv (a_1 - a_2)/(a_1 + a_2) \\
&= \left\{ \left[1 + \gamma^2/2 + (\gamma/2)(4 + \gamma^2)^{1/2} \right]^{3/4} - 1 \right\} \Big/ \left\{ \left[1 + \gamma^2/2 + (\gamma/2)(4 + \gamma^2)^{1/2} \right]^{3/4} + 1 \right\} \\
&= [\exp\{3\varepsilon/2\} - 1]/[\exp\{3\varepsilon/2\} + 1]
\end{aligned}
\tag{7.53}
$$

where γ and ε are shear and uniaxial extensional strains, respectively.

According to Taylor, the equilibrium deformability of drops is a complex function, which has simple solutions at two limits. On the one hand, at low stresses, when the interfacial tension effects dominate the viscous ones (low value *of* λ), the deformability D and the orientation angle α (see Fig. 7.12) of the droplet can be expressed as

$$D = (\kappa/2)[(19\lambda + 16)/(16\lambda + 16)] \quad \text{and} \quad \alpha = \pi/4 \qquad (7.54a)$$

Since, for $\lambda = 0$ to ∞, the quantity in the square bracket ranges from 1.00 to 1.18, the drop deformability $D \cong 0.55\kappa$. Thus, a small deformation of Newtonian drops in Newtonian matrix varies linearly with the capillary number. This proportionality was indeed demonstrated in Couette-type rheometer for a series of corn syrup/silicon oil emulsions (Elemans 1989).

On the other hand, when the interfacial tension is negligibly small in comparison to viscosity (high value of λ):

$$D = (\kappa/2)[(19\lambda + 16)/(16\lambda + 16)] \quad \text{and} \quad \alpha = \pi/4 \qquad (7.54b)$$

Taylor predicted that droplet breakup will occur at $D \geq D_{crit} = 0.5$.

Cox (1969) extended Taylor's theory to systems with the full range of viscosity ratios:

$$\begin{aligned} &D = (\kappa/2)[(19\lambda + 16)/(16\lambda + 16)]/\left[(19\lambda\kappa/40)^2 + 1\right]^{1/2} \\ &\alpha = (\pi/4) + (1/2)\arctan\{19\lambda\kappa/20\} \end{aligned} \qquad (7.55)$$

The above relations are valid for Newtonian systems undergoing small, linear deformation, smaller than that, which would lead to breakup. Furthermore, experimental data indicate that it takes time to reach the equilibrium deformation. It is convenient to use the reduced time scale (see Eq. 7.52), $t_d^* \cong 25$ is required to reach the equilibrium deformation (Elemans 1989).

Taylor's theory makes it also possible to predict the retraction of slightly deformed drops toward an equilibrium spherical form:

$$\begin{aligned} D(t) &= D_o\exp\{-[80(\lambda + 1)/(2\lambda + 3)(19\lambda + 16)](tv_{12}/\eta_2 d)\} \\ &= D_o\exp\{-t/\tau_{ret}\} \\ \text{where}: \quad &\tau_{ret} = \eta_{eq}d/v_{12}; \quad \eta_{eq} = \eta_2[(2\lambda + 3)(19\lambda + 16)/80(\lambda + 1)] \end{aligned} \qquad (7.56)$$

where t is the retraction time and the relaxation time, τ_{ret}, is expressed as a ratio of the equivalent viscosity, η_{eq}, divided by the interfacial tension coefficient scaled by drop diameter. Thus, knowing the time evolution of D and the viscosity of the

Drop Deformation in Shear Field
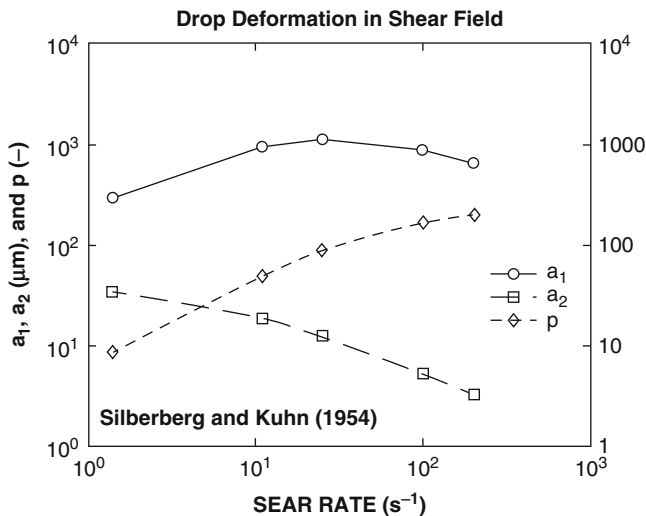
Fig. 7.13 Drop deformability versus shear rate (Silberberg and Kuhn 1954)

materials, one can calculate the interfacial tension coefficient. In principle, Eq. 7.56 is valid for Newtonian systems, but the method can also be used to characterize viscoelastic materials, provided that the following two conditions are valid: (1) the retraction rate is sufficiently slow to ensure that materials behave as Newtonian, and (2) the elastic relaxation of the materials after deformation is faster than the ellipsoidal droplet retraction, i.e., a clear separation of the two mechanisms is possible (Luciani et al. 1996).

The deformability of drops in a three-component Newtonian system (comprising 1.1 % PS and 1.7 % ethyl cellulose dissolved in benzene) was studied by Silberberg and Kuhn (1952, 1954). The authors reported that as the rate of shear increased, the spherical drops changed shape into prolate ellipsoids, with the long axis, a_1, and two orthogonal short semiaxes, a_2. The data are presented in Fig. 7.13. The observed maximum on the a_1 curve may be associated with the rheological effect on solubility.

Owing to elasticity of the interphase, the first normal stress difference and the relaxation time can be calculated as (Schowalter et al. 1968)

$$N_1 = \phi(\sigma_{12}d\kappa)^2/40v_{12}$$
$$\text{and} \quad \tau^* = \eta dD\kappa(2\lambda + 3)/40v_{12} \tag{7.57}$$

It is convenient to express the capillary number in its reduced form $\kappa^* \equiv \kappa/\kappa_{cr}$, where the critical capillary number, κ_{cr}, is defined as the minimum capillary number sufficient to cause breakup of the deformed drop. Many experimental studies have been carried out to establish dependency of κ_{cr} on λ. For simple

Table 7.6 Parameters of the critical capillary number for drop burst in shear and extension in Newtonian systems (R. A. de Bruijn 1989)

Flow	$1000c_1$	$1000c_2$	$1000c_3$	$1000c_4$	$1000c_5$
Shear	−506.0	−99.4	124.0	−115.0	−611.0
Elongational	−648.5	−24.42	22.21	−0.56	−6.45

shear and uniaxial extensional flow, De Bruijn (1989) found that droplets break most easily when $0.1 < \lambda < 1$, but do not break for $\lambda > 4$:

$$\log(\kappa_{cr}/2) = c_1 + c_2\log\lambda + c_3(\log\lambda)^2 + c_4(\log\lambda + c_5) \qquad (7.58)$$

Parameters of Eq. 7.58 are listed in Table 7.6 (see also Fig. 7.45).

Note that in shear for $\lambda = 1$, the critical capillary number $\kappa_{cr} = 1$, whereas for $\lambda > 1$, κ_{cr} increases with λ and becomes infinite for $\lambda > 3.8$. This means that breakup of the dispersed phase in pure shear flow becomes impossible for $\lambda > 3.8$. This limitation does not exist in extensional flows.

The deformation of dispersed drops in immiscible polymer blends with viscosity ratio $\lambda = 0.005$–13 during extensional flow was studied by Delaby et al. (1994, 1995). The time-dependent drop deformation during start-up flow at constant deformation rate was derived. The model is restricted to small drop deformations.

Milliken and Leal (1991) used a computer-controlled four-roll mill to investigate the deformation of polymeric drops in an imiscible Newtonian fluid in planar extensional flow. They showed that deformation curves differ, based on the viscosity ratio. Steady drop shapes were observed only for emulsions with viscosity ratio higher than one. However, for the low-viscosity polymeric dispersed phase, the deformation of drops does not follow that of Newtonian fluids anymore, and the critical capillary number was significantly smaller. For both cases, the transient deformation and breakup of polymeric drops were found to be different from Newtonian drops (Milliken and Leal 1991). Other geometries, such as Couette, torsional parallel plate, torsional cone and plate, and rectilinear parallel plate, have been used extensively (Fischer and Erni 2007). Comparison between these experimental results and numerical data regarding the deformation behavior arising from shear or elongational flow of emulsions verifies the consistency of the Volume of Fluid (VoF) method (Renardy et al. 2002) and the Boundary Integral Method (BIM) (Feigl et al. 2003) for the simulation of concentrated emulsion flow.

Drop Breakup

With regard to drop deformation and breakup, there are four regions of reduced capillary numbers, κ^*, both in shear and elongation:

For $-0.1 > \kappa^*$-droplets do not deform.

For $-0.1 < (\kappa^*) < 1$-droplets deform, but they do not break.

For $-1 < \kappa^* < 2$-droplets deform then split into two primary droplets.

For $-\kappa^* > 2$-droplets deform into stable filaments.
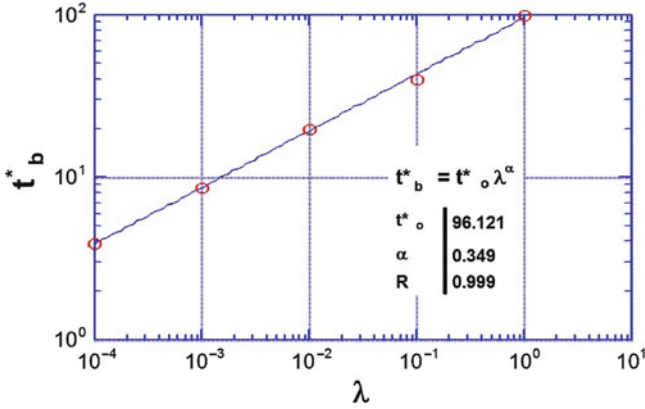
Fig. 7.14 Effect of the viscosity ratio on the critical time to break (Huneault et al. 1994)

As for κ_{cr}, Fig. 7.14 shows that the critical time for drop breakup t_b^* varies with λ.

When values of the capillary number and the reduced time are within the region of drop breakup, the mechanism of breakup depends on the viscosity ratio, λ.

In shear, four regions have been identified (Goldsmith and Mason 1967):

For $-0.1 >> \lambda$-small droplets are shed from sigmoidal drops – *tip spinning*.

For $-0.1 < \lambda < 1$-drop breaks into two principal and odd number of satellite droplets.

For $-1 < \lambda < 3.8$-drop deforms into fiber, which then disintegrates into small droplets.

For $-\lambda > 3.8$-drops may deform, but they do not break.

Critical capillary numbers for elongational flows are lower than for shear flows. In other words, the elongational flow field is much more effective for droplet breakup in a dispersive mixing regime (Grace 1982).

Drop Fibrillation and Breakup

In addition to the previously discussed drop breakup into two principal drops (and an odd number of small satellite droplets), there is another mechanism for dispersing one liquid in another. This is based on the "capillarity instability principle" of long cylindrical bodies. For $\kappa^* > 2$, drops deform affinely with the matrix into long fibers. When subsequently the deforming stress decreases, causing the reduced capillary number to fall below two, $\kappa^* < 2$, the fibers disintegrate under the influence of the interfacial tension. The problem was theoretically treated by Rayleigh (1879), Taylor (1932, 1934), and Tomotika (1935, 1936). The latter author showed that the degree of instability can be described by the growth rate parameter of a sinusoidal distortion:

$$q = v_{12}\Omega(\Lambda,\lambda)/2\eta_m R_0 \tag{7.59}$$

where Λ is the distortion wavelength, $\Omega(\Lambda, \lambda)$ is a function tabulated by Tomotika, and R_o is the initial fiber radius. The hydrodynamic instability is characterized by a maximum for the dominant wavelength Λ_m that leads to thread breakup. For $0.01 \leq \lambda \leq 10$:

$$\Omega(\Lambda_m, \lambda) = \exp\left\{ \sum_{i=0}^{4} b_i (\log \lambda)^i \right\} \tag{7.60}$$

where $b_0 = -2.588$, $b_1 = -1.154$, $b_2 = 0.03987$, $b_3 = 0.0889$, and $b_4 = 0.01154$. The distortion amplitude α grows exponentially with time, t:

$$\alpha = \alpha_0 \exp\{qt\} \tag{7.61}$$

where α_0 is the distortion at t = 0. Assuming that the initial distortion is due only to thermal fluctuations, Kuhn (1953) estimated that

$$\alpha_0 = (21k_B T)\left(8\pi^{3/2} v_{12}\right)^{-1/2} \tag{7.62}$$

where k_B is Boltzmann constant and T is the absolute temperature. The thread breakup occurs when $\alpha = R \cong 0.81 R_o$. The time required to reach this stage can be expressed as

$$t_b^* \equiv t_b \dot{\gamma}/\kappa = 2[\ln(0.81 R_0/\alpha_0)]/\Omega(\Lambda_m, \lambda) \tag{7.63}$$

Thus, t_b^* is an important parameter describing the breakup process for fibers subjected to lower stresses than those required for fibrillation, i.e., $\kappa^* < 2$. The above indicates that breakup is less likely at low interfacial tension. Since the matrix viscosity appears in the left side of the equation (in the capillary number), one may expect shorter breakup times with lower matrix viscosity, but it is noteworthy that this term also changes the Tomotika function on the right side of the equation. Figure 7.15 shows the distortion growth rate at the dominant wavelength as a function of viscosity ratio. To obtain a low value of $\Omega(l, \lambda)$, thread viscosity should be high and the matrix viscosity has to be low (Potschke and Paul 2003).

In practice, one of the most serious obstacles for quantitative use of Timotika's theory is estimation of the initial distortion, α_0.

The time corresponding to the complete breakup, t_b, was measured (Grace 1982; Elemans 1989). The data are presented in Fig. 7.14. Numerically they can be expressed as

$$t_b^* \cong 84 \lambda^{0.355} \kappa^{*-0.559} \tag{7.64}$$
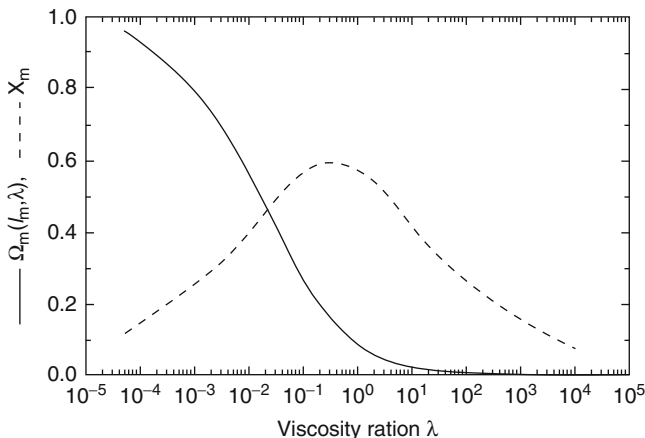
Fig. 7.15 Distortion growth rate at dominant wavelength and dominant wave length versus λ (Potschke and Paul 2003)

Coalescence

During mixing, the dispersed phase progressively breaks down until a minimum drop diameter is reached. As the drop diameter decreases, further breakup becomes increasingly difficult. For emulsions, the size of the smallest drop that can be broken can be calculated from Taylor's theory, but experiments have shown that, in most cases, the equilibrium droplet size is larger than predicted. Furthermore, the deviation increases with concentration of the dispersed phase, $\phi_d - \phi_o$, where experimentally the smallest value for which the deviation occurs, $\phi_o \approx 0.005$ (Utracki and Shi 1992).

The fusion of the two or more droplets due to the local thinning and disruption of the matrix is called coalescence. Complete phase separation is expected as the limiting case of coalescence. Two types of coalescence must be recognized: the first is determined by equilibrium thermodynamics (e.g., liquid–liquid miscibility, interfacial tension coefficient, rheological conditions of the interphase, etc.); the second is determined by dynamics, and it is dominated by rheology and flow conditions. In the following text, only the second type will be discussed.

Utracki (1973) studied steady-state shear coagulation of PVC lattices for a wide range of variables. Assuming that the locus of coagulation is at the particle–matrix interface and that the rate of coagulation depends on the frequency of particle collisions, the critical time for coalescence was calculated as

$$
\begin{aligned}
t_c &= a_0 E^+ d^3 / \left[\rho_d \left(1 + N^+ + N^0 \right) \phi_d^{8/3} \dot{\gamma}^2 \right] \\
\text{or} \quad t_c &= 2.940 E^+ (\phi_m - \phi_d) / \left[\eta_m (V_x/V) \phi_d^{8/3} \dot{\gamma}^2 \right]
\end{aligned}
\tag{7.65}
$$

where a_o is a numerical parameter; E^+ is the threshold energy of coagulation; N^o and N^+ are the number of coagulating drops, respectively, initially and at $t = t_o$; V_x/V is the volume fraction of emulsion undergoing uniform shearing; and ρ_d is the drop density. Validity of these relations was confirmed on many lattices. In particular, $t_c \propto \dot{\gamma}^{-2}$ and $dt_c/d\phi_d < 0$ (thus, coagulation rate increases with ϕ_d) were experimentally confirmed. Since the coagulation was assumed to be related to the projected area of the drop, $d \propto \phi_d^{2/3}$ was implicitly assumed.

Fortelny et al. (1988, 1990) assumed that Brownian motion is the principal driving force for coalescence in polymer blends. Applying Smoluchowski's theory, the authors obtained:

$$S = S_0 \left\{ 1 + (2/3\pi)[k_B T/(\eta_m \phi_d)]^{1/2} S_0^{3/2} t^{1/2} \right\}^{-2/3} \tag{7.66}$$

where S_o and S are the interface areas in the unit volume of the blend having monodisperse spherical particles, respectively, before and after coalescence. The experimental data confirmed the linearity of $(S/S_o)^{-3/2}$ as a function of $t^{1/2}$. However, it is to be noted that Brownian motion affects particles that usually are below the size of dispersions in polymer blends. Furthermore, coalescence should be independent of the stress field intensity and magnitude of the interfacial energy. The efficiency of particle collisions due to Brownian motion leading to coalescence should also be taken into account.

Coagulation is a result of collision between two spherical drops of diameter, d, that approach each other with certain velocity gradient to a distance smaller than their radius. Coalescence can occur only if the liquid remaining between two flattened drops will be removed sooner than the global velocity field will force the drops to separate. The instabilities in the layer of the entrapped film will break it when the separation between drops is smaller than the critical separation distance, $h_c \cong 5$ nm, the critical coalescence time for systems with mobile interface is expected to follow the relation: $t_c = 3\kappa[\ln(d/4h_c)]/4\dot{\gamma}^2$ (Elmendorp 1986; Chesters 1991a). The relation was derived for isolated pairs of drops, and as such it does not take into account the concentration effect. It predicts that, in shear, the coalescence of two isolated drops is proportional to the exerted stress and it is easier for larger spheres with high surface energy. It was observed that $t_c \propto \dot{\gamma}^{-2}$, in agreement with Eq. 7.65. Experimentally, coalescence probability was found to rapidly decrease with increasing κ and d.

7.3.2.3 Non-Newtonian Flows

Only dilute emulsions or systems undergoing slow deformation show Newtonian, deformation rate-independent flow. As the concentration and deformation rate increases, the flow progressively changes into pseudoplastic. Since the rheological response is a reflection of the inner structure of the material, modifications of the emulsion morphology accompany such a change.

Morphology

Even in the dilute region, individual emulsion droplets rarely exist. In most cases, droplets are polydisperse in size, forming doublets, chain structures, or aggregates. Two types of emulsion morphology can be distinguished: (A) formed by the shear field (e.g., skin-core structures developed during flows through long tubes) and (B) formed by particle–particle interaction. Knowledge of type A structures is important for proper interpretation of the flow phenomena. Their formation is influenced by the differences in the flow behavior of the components, as well as by shear coagulation. Knowledge of type B structures is important for the utilization of suspension rheology in processing. Since the effective volume fraction of dispersed particles increases with increase of association, the relative viscosity of emulsion is strongly influenced by these variables.

By contrast with polymer blends, emulsions are prepared by carefully designing the interface system and by sequential addition of ingredients. Both elements are essential when 96 vol% of one liquid must be dispersed in 4 vol% of another. If, due to interactions of emulsifiers, the continuous phase becomes viscoelastic, the emulsion has high consistency or a *body*. There is gradual passage of structures, from rotating doublets in dilute systems to entrapment of the dispersed phase in a continuous network of interacting interfaces. Consequently, emulsions can show a Newtonian as well as a complex thixotropic and viscoelastic character (Nielsen 1977).

Theoretical Treatment

The theoretical treatment of two-phase flow was reviewed by Cox and Mason (1971), Leal (1980), and Barthès-Biesel (1988). As indicated before, dispersions of one Newtonian liquid in another result in systems that are characterized by elasticity and relaxation times, e.g., Eq. 7.57.

For dilute emulsions, with neither hydrodynamic interactions nor interfacial effects, Fröhlich and Sack (1946) developed the following time-dependent constitutive equation:

$$
\begin{aligned}
&[1 + \tau_1(d/dt)]\tau = 2\eta[1 + \tau_2(d/dt)]d \\
&\text{where} \quad \eta = \eta_m\big[1 + (5\phi/2) + 0\big(\phi^2\big)\big], \\
&\qquad \tau_1 = [3\eta_m/2G](1 + 5\phi/3), \\
&\qquad \tau_2 = [3\eta_m/2G](1 - 5\phi/2)
\end{aligned}
\tag{7.67}
$$

where G is the Hookean modulus of the elastic, dispersed spheres, while λ_i is the relaxation time of the emulsion. Thus, the theory considered viscoelasticity of dilute emulsions to originate in elastic deformability of the dispersed phase.

Nearly a decade later, Oldroyd (1953, 1955) proposed a constitutive model similar to that of Fröhlich and Sack, valid at small deformations. The model considered low concentration of monodisperse drops of one Newtonian liquid in another. The interfacial tension and the viscoelastic properties of the interfacial film

were incorporated by means of convected derivatives. The model provided the following relation for the complex modulus:

$$G^* = G_m^*[1 + 3\phi H]/[1 - 2\phi H]$$

$$H = \frac{(4/R')\left(2G_m^* + 5G_d^*\right) + \left(G_d^* - G_m^*\right)\left(16G_m^* + 19G_d^*\right)}{(40/R')\left(G_m^* + G_d^*\right) + \left(2G_d^* + 3G_m^*\right)\left(16G_m^* + 19G_d^*\right)} \quad (7.68)$$

$$G_i^* = G_i^*(\omega); \quad R' = R/v_{12}; \quad \text{thus:} \quad H = H(\omega; R')$$

where v_{12} the interfacial tension coefficient, R is the drop radius, $G_i^*(\omega)$ is the complex modulus, and subscripts i = m, d indicate matrix or disperse phase, respectively.

Oldroy's model was extended by Palierne (1990) to emulsions with polydisperse spherical drops. The model considered viscoelastic liquids, the concentration range was extended up to that at which drop–drop interactions start complicating the flow field. However, the drops must be spherical, undergoing small deformation, and the interfacial tension coefficient was considered constant, independent of stress and the interfacial area. The following relation was derived for the complex modulus:

$$G^* = G_m^*\left[1 + 3\sum_{i=1}^{n}\phi_i H_i\right]/\left[1 - 2\sum_{i=1}^{n}\phi_i H_i\right]$$

$$H_i = \frac{(4/R_i')\left(2G_m^* + 5G_d^*\right) + \left(G_d^* - G_m^*\right)\left(16G_m^* + 19G_d^*\right)}{(40/R_i')\left(G_m^* + G_d^*\right) + \left(2G_d^* + 3G_m^*\right)\left(16G_m^* + 19G_d^*\right)} \quad (7.69)$$

$$G_i^* = G_i^*(\omega); \quad R_i' = R_i/v_{12}; \quad \text{thus:} \quad H_i = H_i(\omega; R')$$

Here ϕ_i and R_i are, respectively, the volume fraction and the drop radius. The main feature of this model is the inclusion of a contribution from the interfacial tension to the viscoelastic properties and the inclusion of the effect of particle size polydispersity. For example, knowing $G_i^*(\omega)$ of the two main components of the blend, one can predict the dynamic moduli of the emulsion (as well as dilute polymer blends) from the knowledge of the interfacial tension coefficient and distribution of drop sizes. This model has been used extensively to determine the interfacial tension or droplet size of emulsions (Guschl and Otaigbe 2003; Mekhilef et al. 2000; Xing et al. 2000; Yoo et al. 2010). It has been shown that the volume average droplet radius could be employed instead of R_i, as long as the ratio of volume to number average radius of an emulsion is less than two (Graebling et al. 1993a). The theory is applicable to low strains and to the concentration range where yield stress is absent (Graebling and Muller 1990, 1991; Graebling et al. 1993b).

Low-viscosity mixtures of PDMS and PI, with $\lambda = 0.155$, 0.825, and 4.02 were studied at room temperature (Kitade et al. 1997). The dynamic data were analyzed using Eq. 7.69. Good agreement was found. However, for the $\lambda = 4.02$ system, the drops were insensitive to the flow field. They neither broke nor coalesced. Similar observations were reported for PDMS/PIB system (Vinckier et al. 1996). The latter

authors also observed that agreement with Palierne's model becomes weaker for blends pre-sheared at higher shear rate, i.e., blends with finer drop dispersion.

Palierne emulsion model failed to describe the dynamic modulus of the PP/EPDM blends after radiation, because the viscosity ratio increased significantly and the rubber phase changed from deformed droplets to hard domains after radiation (Cao et al. 2007). Interconnections among inclusions of the dispersed phase (Shi et al. 2006) and the existence of multiple emulsion (emulsion-in-emulsion) structure exhibiting different relaxation domains in compatibilized systems are other factors contributing to the failure of Palierne's model (Friedrich and Antonov 2007; Pal 2007).

Honerkamp and Weese (1990) reported on the use of Tikhonov's regularization for the determination of material functions. This method of data treatment was found particularly useful for the computation of the relaxation and retardation spectra (Elster et al. 1991; Honerkamp and Weese 1993). It has also been used to compute the sphere-size distribution of the dispersed phase in binary blends (Gleisner et al. 1994a), as well as the ratio of the dispersed drop diameter divided by the interfacial tension coefficient, d/ν_{12} (Gleisner et al. 1994b).

Friedrich et al. (1995) modified Palierne's Eq. 7.69 by a continuous function:

$$G^*(\omega) = G_M^*(\omega) \left[1 + 3 \int_{-\infty}^{\infty} H(\omega, R') u(R') R' d\ln R' \right] \Big/ \left[1 - 2 \int_{-\infty}^{\infty} H(\omega, R') u(R') R' d\ln R' \right]$$
(7.70)

where $R' = R/\nu_{12}$ and $u(R') = \nu_{12}v(R)$ is the scaled, volume-weighted distribution of sphere sizes. Using Tikhonov's regularization method, the distribution function, $u(R')$, could be computed. The experimental data (storage and loss shear moduli, G' and G'', respectively, within six decades of frequency and transmission electron microscopy, TEM) were determined for 2, 5, 10, and 20 wt% PS in the PMMA matrix. From the dynamic viscoelastic data of the neat components and the blends, the monomodal distribution of the distribution function $u(R')$ versus log $R' = \log (R/\nu_{12})$ was computed and compared with data obtained from TEM. Excellent agreement was found for blends containing 2 and 5 wt%, fair for 10 wt%, and poor for 20 wt% PS. In the latter case, TEM showed a bimodal distribution (possibly resulting from coalescence), whereas a monomodal distribution was obtained from the rheological data. The interfacial tension coefficient computed from these results varied from $\nu_{12} = 2.08$ to 3.10 mN/m. The average value, $\nu_{12} = 2.5$ mN/m at 190 °C, is comparable to the literature data $\nu_{12} = 0.8$ to 1.8 mN/m at 200 °C (Luciani et al. 1996).

For infinitely dilute viscoelastic emulsions, the shear dependence of inherent viscosity was derived as (Barthès-Biesel and Acrivos 1973)

$$\eta_{inh} \equiv (\eta_{rel} - 1)/\phi = [(5/2)\lambda + 1]/[\lambda + 1] - f(\lambda)(\sigma_{12}/E_{int})^2 + 0(\sigma_{12}^3) \quad (7.71)$$

where $f(\lambda) > 0$ is a rational function of λ. The relation predicts that in dilute emulsions subjected to small deformations, the η_{inh} should decrease with the square

of the shear stress. The effect of stress is moderated by interphase elasticity expressed as E_{int}. The theory was experimentally verified. Note the similarity of the first term on the rhs of Eq. 7.71 to the expression derived by Oldroyd for the intrinsic viscosity of emulsions, Eq. 7.50. Accordingly, Eq. 7.71 may be modified by replacing λ by Λ, as derived by Oldroyd.

Semi-concentrated emulsions were examined theoretically and experimentally only within the linear viscoelastic region (Oosterbroek and Mellema 1981; Oosterbroek et al. 1980, 1981; Eshuis and Mellema 1984). Recognizing that the interphase has a finite thickness (sometimes the total volume of the interphase is comparable to, or even exceeds, the volume of the dispersed phase), the authors postulated that the interphase should have two interfacial coefficients, v' and v'' facing the two principal polymer domains. Then, two models of the interphase were evaluated: (i) a two-dimensional viscoelastic film and (ii) the interphase of finite thickness. Both led to at least two relaxation times:

$$\begin{aligned} \tau_1 &= \left\{ (1 + R/\Delta L)^2 \eta (R + \Delta L)(1/v' + 1/v'') \right\} \\ \tau_2 &= \left\{ \eta(R + \Delta L)/(v' + v'') \right\}; \text{where } v_{12} = v' + v'' \end{aligned} \tag{7.72}$$

The experimental data employing dynamic testing in the kHz region for ionic emulsions was equally well described using either model. The emulsion elasticity was found to originate in droplet deformation. For nonionic emulsions, only one relaxation time was observed. The data were interpreted in terms of the second Oldroyd's model in which the interfacial tension is more important than the viscoelasticity of the interphase. The steady-state viscosities of both ionic and nonionic systems at the volume fraction $\phi \leq 0.2$ were found to follow Simha's Eq. 7.24.

For concentrated emulsions and foams, Princen (1983, 1985) proposed a stress–strain theory based on a two-dimensional cell model. Consider steady-state shearing of such a system. Initially, at small strains, the stress increases linearly as in an elastic body. As the strain increases, the stress reaches the yield value, then at still higher deformation, it catastrophically drops to negative values. The reason for the latter behavior is the creation of unstable cell structure that generates a recoil mechanism. The predicted dependencies for modulus and the yield stress were expressed as

$$\begin{aligned} G &\equiv \sigma/\gamma \quad \propto \quad v_{12}\phi^{1/3}/d \\ \text{and} \quad \sigma_y &\propto G\tilde{F}_{max}(\phi) \end{aligned} \tag{7.73}$$

where the function $\tilde{F}_{max}(\phi)$ is the concentration-dependent, dimensionless contribution to stress per single drop. The theory was evaluated using a concentrated oil-in-water system.

Princen's work was followed by (Reinelt 1993), who considered theoretical aspects of shearing three-dimensional, highly concentrated foams and emulsions. Initially, the structure is an assembly of interlocked tetrakaidecahedra (which have

six square surfaces and eight hexagonal ones). An explicit relation for the stress tensor up to the elastic limit was derived. When the elastic limit is exceeded, the stress–strain dependence is discontinuous, made of a series of increasing parts of the dependence, displaced with a period of $\gamma = 2^{3/2}$.

The validity of Princen's theory for concentrated water-in-oil emulsions was also investigated by Ponton et al. (2001), using the droplet size distribution determined by laser diffractometry based on the Mie theory model. Comparing the surface–volume diameter and the mass fractions of emulsions depicted an increase in the particle size with the volume fraction reduction. They showed that their experimental data (as obtained by oscillatory measurements and droplet-size distribution) corroborated the expression of the elastic shear modulus for the two-dimensional model proposed by Princen and Kiss (1986). In this model, G′ is proportional to $(\sigma/R_{SV})\Phi_v^{1/3}(\Phi_v\text{-}\Phi_c)$ where σ is the interfacial tension, R_{SV} is the volume–surface radius (as obtained by laser diffractometry), and Φ_v and Φ_C are the volume fraction and the critical volume fraction, respectively (Ponton et al. 2001). The latter was found to be 0.714 experimentally, which is close to the value obtained by Princen ($\sim$0.712) (Ponton et al. 2001).

Paruta-Tuarez et al. (2011) analyzed the Princen and Kiss equation (Princen and Kiss 1986) associated with the linear form of the function $E(\Phi_v)$, ($E(\Phi_v) = A(\Phi_v - \Phi_c)$). This function was proposed to take into account the experimental dependence of storage modulus (G′) on the dispersed-phase volume fraction (Φ_v). However, it was found that the Princen and Kiss equation underestimates the storage modulus values in some cases, due to the particular set of experimental data used for derivation of $E(\Phi_v)$. Thus, despite the applicability of the linear form of the function $E(\Phi_v)$ as proposed by Princen and Kiss, it is not universal and another choice of experimental data could lead to other mathematical functions (Paruta-Tuarez et al. 2011).

Experimental Data

Experimentally, there are three concentration regions of emulsion flow: (i) dilute for $\phi < 0.3$, characterized by nearly Newtonian behavior; semi-concentrated at $0.3 < \phi < \phi_m$ with mainly pseudoplastic character; and concentrated at $\phi_m < \phi < 1.0$, showing solid-like properties with modulus and yield.

The necessary condition for non-Newtonian flow to occur is droplet deformation, expressed either by the deformability parameter, $D = (a_1 - a_2)/(a_1 + a_2)$, or by the aspect ratio, $p = a_1/a_2$.

Figure 7.16 illustrates the effect of shear rate, initial drop diameter, and the viscosity ratio on the droplet aspect ratio, p. For low and high values of λ, a pseudoplastic dependence has been observed (Talstoguzov et al. 1974).

The shear viscosity of polymer-thickened oil-in-water emulsions was studied by Pal (1992). Addition of polyethyleneglycol, PEG, made it possible to vary the matrix liquid viscosity. The flow was pseudoplastic, following Ellis dependence:

$$\eta_r = 1/\left[1 + A\eta_o\sigma_{12}^{\alpha-1}\right] \tag{7.74}$$

Fig. 7.16 Effect of the shear
rate (*top*), the initial drop
diameter (*middle*), and the
viscosity ratio (*bottom*)
on the drop aspect
ratio for the systems:
water–gelatin–dextran
(W–G–D, *circles*) and
water–gelatin–polyvinyl
alcohol (W-G-P, *squares*)
(Talstoguzov et al. 1974)

Drop deformability in water-gelatine
systems with either PVAl or dextran
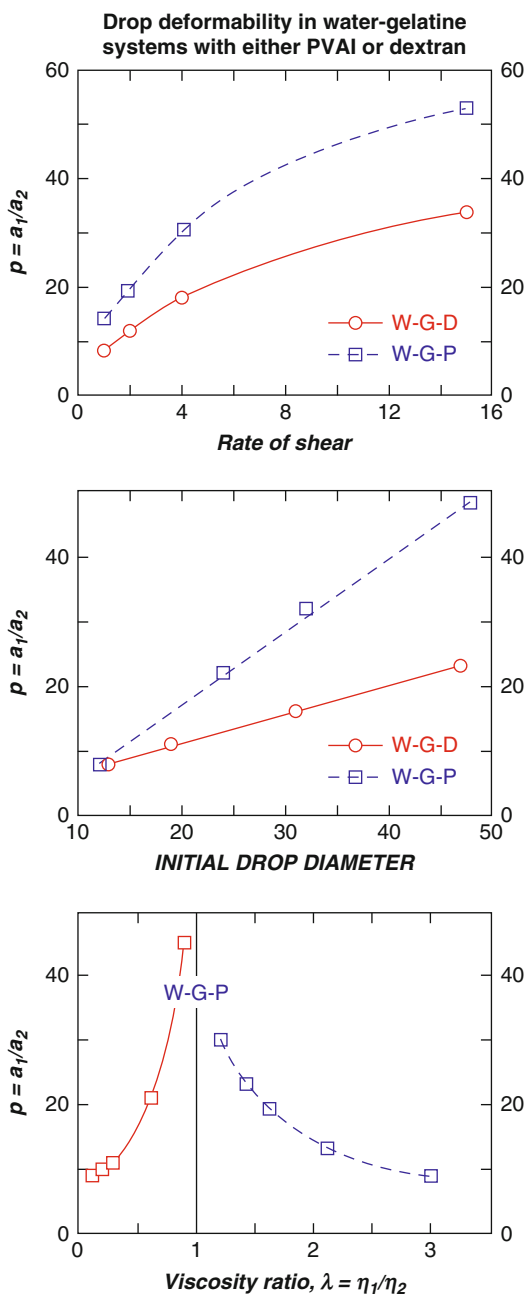
where A and α are equation parameters. The zero-shear viscosity, η_o, was found to follow a modified Mooney dependence (see Eq. 7.28):

$$\ln\eta_r = 2.5K_1\phi/[1 - K_2\phi] \tag{7.75}$$

where K_i are equation parameters. It was observed that η_r of the thickened emulsions is lower than that for the emulsions without PEG.

In liquid–liquid systems, upon increase of concentration of the dispersed phase, at certain concentration suddenly the dispersed and continuous liquids exchange roles. This is known as a *phase inversion*. Salager et al. (1983) and Minana-Perez et al. (1986) reported two types of phase transition in ionic emulsions – in the first, viscosity goes through a minimum, whereas in the second it goes through a maximum. The first type of transition (normal) is associated with a decrease of the interfacial tension coefficient and formation of a microemulsion. The second (catastrophic) transition is associated with an inversion of unstable structure to a stable one.

The extensional viscosity of non-Newtonian emulsions, η_E, at the dispersed phase volume fraction $\phi = 0.3$–0.8, was measured using the opposed nozzles configuration. For more diluted emulsions, $\phi < 0.6$, the elongational viscosity, η_E, was found to decrease with the rate of elongation, $\dot{\varepsilon}$, mimicking the flow curves in a shear field, η versus $\dot{\gamma}$. Furthermore, the Trouton rule, $\eta_E \cong 3\eta$, was found to be reasonably obeyed. However, for more concentrated emulsions, $\phi \geq 0.7$, owing to the presence of yield stress, η_E was found to depend on the test geometry, viz., nozzle diameters and their separation (Anklam et al. 1994). Since in more concentrated emulsions, the structure is engendered by close packing of interacting spheres, its destruction must depend on the type of imposed deformation as well as on strain. In consequence, the lack of correlation between the shear flow and extensional flow data was expected.

Compliance, J, of concentrated oil-in-water emulsions at $0.4 \leq \phi \leq 0.7$ was found to follow a two-retardation time process:

$$J(t) - J_0 + J_1\exp\{-t/\tau_1^*\} + J_2\exp\{-t/\tau_2^*\} \tag{7.76}$$

where J_o and J_i are, respectively, instantaneous compliance and retarded values, all three decreasing with concentration of the dispersed phase (Gladwell et al. 1986).

For a similar system, the shear viscosity was found to follow the power law model with yield (Pal et al. 1986). Owing to the presence of yield stress, the flow of concentrated emulsion was found to be facilitated by superposition of 10 Hz oscillation on the steady-state shear flow – up to 40 % energy saving was reported (Jezequel et al. 1985). More recently, the relative viscosity of emulsions was described in terms of scaling parameters (Pal 1997). Ten principal variables were incorporated into six dimensionless groups: λ, κ, reduced time, $t_r = t/(\eta_m d^3/8\,k_B\,T)$, relative density, $\rho_r = \rho_d/\rho_m$, Peclet number, $Pe = \eta_m\dot{\gamma}d^3/8k_BT$, and Reynolds number, $Re = \rho_m\dot{\gamma}d^2/4\eta_m$. For the steady-state flow of well-stabilized emulsions, it was argued that the relative viscosity of emulsions should depend only on two

parameters: volume fraction of the dispersed phase and Re, i.e., $\eta_r = f(\phi, Re)$. At constant composition, the experimental data for coarse and fine oil-in-water emulsions plotted versus the deformation rate, $\dot{\gamma}$, showed different dependencies (higher η_r for finer dispersion), but when plotted versus Re, a single dependence was found.

The understanding rheology of dilute and concentrated multiple emulsions is necessary to provide information related to mixing, processing, and storage of such systems. To predict the relative viscosity of multiple emulsions of type B, containing several small internal droplets, and type C, containing a large number of small internal droplets, four variables were introduced in the proposed viscosity models (Pal 2008) : K_{21} (viscosity ratio of primary-emulsion matrix to multiple-emulsion matrix), K_{32} (viscosity ratio of internal droplet to primary-emulsion matrix), φ^{PE} (volume fraction of internal droplets within a multiple emulsion droplet), and φ^{ME} (volume fraction of total dispersed phase in the whole multiple emulsion). Based on experimental data and model predictions, it was shown that the viscosity generally increases with increase in any of these variables. Comparison between experimental data and predictions of various models showed that the model based on the Yaron and Gal-Or equation (Yaron and Gal-Or 1972) was reasonably in agreement with experimental data. However, the model based on the Oldroyd equation under predicted and the model obtained using the Choi–Schowalter equation (Choi and Schowalter 1975) overestimated the viscosity of multiple emulsion systems (Pal 2008).

7.3.2.4 Melt Flow of Block Copolymers

Block copolymers, BC, are macromolecular species in which long chains of one polymer are joined to long chains of another polymer. Thus, BCs are made of at least two chemically different chains arranged linearly, in form of multi-branch stars, combs, etc. Linear block copolymers are the most common – diblock, AB, triblock, ABA, or multiblock, $A(BA)_n$.

Commercial BCs are prepared from monomers that, upon polymerization, yield immiscible macromolecular blocks, one rigid and the other flexible, that separate into a two-phase system with "rigid" and "soft" domains. The concentration and molecular weights provide control of the size of the separated domains, thus the morphology and the interconnection between the domains. The existence of a dispersed rigid phase in an elastomeric matrix is responsible for its *thermoplastic elastomer* behavior. For symmetric block copolymers, Leibler (1980) showed that a sufficient condition for microphase separation is $(\chi_{AB}N) = 10.5$, where χ_{AB} is the binary thermodynamic interaction parameter and N is the degree of BC polymerization (Folkes 1985).

As in polymer blends, also in BC the phase transition is affected by flow. Theoretically it was predicted that homogeneous melt can be obtained at $T < UCST$, provided that the stress field exceeds the critical value for the phase demixing, $\sigma_{12} > \sigma_{12, \text{ crit}}$ (Lyngaae-Jørgensen 1989).

For most BCs the phase diagram is characterized by the presence of an upper critical solution temperature, UCST, also known as an order–disorder transition temperature or a microphase separation temperature. Below UCST the block

copolymers phase separate, while above it, an isotropic melt is obtained. Owing to the chemical link between the blocks, during phase separation in BCs, micro-domains instead of macroscopic phases are usually obtained. Furthermore, since the micro-morphology depends on the concentration as well as on the temperature, the phase diagram is complex, similar to those of metallic alloys. Under thermodynamic equilibrium conditions, depending on the composition, magnitude of the interaction parameter, and temperature, spherical, cylindrical, lamellar, or some other structures are formed. There are three elements to BC morphology: domain size, domain shape, and the interfacial thickness – they lead to a wide variety of rheological responses (Inoue et al. 1969; Meir 1969; Hashimoto et al. 1980a,b; Krause 1980).

For A-B block copolymers, the thickness of the interphase, Δl, is theoretically derived by Helfand and Wasserman (1976, 1978, 1980):

$$\Delta l = 2\sqrt{(\beta_A^2 + \beta_B^2)/2\chi_{AB}}$$
$$\text{where}: \quad \beta_i^2 = (\rho_{oi} b_i^2)/6; \quad \text{and} \quad b_i = <R_i^2>/Z_i \tag{7.77}$$

where b_i is length of Kuhn's statistical segment, Z_i is degree of polymerization, ρ_{oi} is density, and $<R_i^2>$ is the radius of gyration of the block. For immiscible systems $\chi_{AB} \geq 0$; thus as the "antipathy" of the two types of blocks toward each other decreases and $\chi_{AB} \to 0$, the interphase thickness increases.

Recently, another theoretical expression for Δl was derived for symmetric diblock copolymer with $N_A = N_B = N/2$ with lamellar morphology (Spontak and Zielinski 1993):

$$\Delta l = \Delta l_\infty [1 - (8\ln2)/(\chi_{AB}N)]^{-1/2} \tag{7.78}$$

where N is the degree of BC polymerization and Δl_∞ is the interface thickness when $N \to \infty$. The dependence should only be used for $\chi_{AB}N \geq 20$. The theory predicts that as $\chi_{AB}N$ decreases, the thickness of the interphase increases – nearly three times more rapidly for block copolymers than for homopolymer blends.

Considering melt flow of BCs, it is usually assumed that the test temperature is $UCST > T > T_{gc}$, where T_{gc} stands for glass transition temperature of the continuous phase. However, at $T_{gc} < T < T_{gd}$ (T_{gd} is T_g of the dispersed phase), the system behaves as a cross-linked rubber with strong viscoelastic character. At $UCST > T > T_{gd,}$ the viscosity of BC is much greater than would be expected from its composition. The reason for this behavior is the need to deform the domain structure and pull filaments of one polymer through domains of the other. Viscosity increases with increase of the interaction parameter between the BC components, in a similar way as the increase of the interfacial tension coefficient in concentrated emulsions causes viscosity to rise (Henderson and Williams 1979).

In shear, the block copolymers exhibit time-dependent flow with yield stress (Liu et al. 1983):

$$\sigma_{12}(t) = \sigma_y + \eta_0\dot{\gamma}\{\beta + [(1 - \beta)/(1 + b\dot{\gamma}^m)][1 + b\dot{\gamma}^m\exp\{-kt(1/b = \dot{\gamma}^m)\}]\}$$
(7.79)

where β represents the relative residual viscous dissipation parameter, b and m are parameters originating from the structural breakdown and reformation of structure, while k is the loss rate constant. The relation can describe multiple phenomena: yield, upper and lower Newtonian plateaus, pseudoplasticity, stress growth and overshoot, thixotropy, hysteresis, etc.

The multiplicity of rheological phenomena observed in BC is related to sensitivity of the melt structure to independent molecular and rheological variables. For example, for styrene-butadiene-styrene (SBS), the activation energy of flow $\Delta E_\eta = 80$ or 160 kJ/mol for compositions containing less or more that 31 vol% of styrene. The difference originates in the structure; it is dispersed below 31 % and interconnected above (Arnold and Meier 1970).

Block polymers, owing to the tendency for formation of regular structures tailored by molecular design, are ideal models for compatibilized, two-phase polymer blends or alloys. Blends do show similar rheological behaviors, e.g., yield, pseudoplasticity, thixotropy, structural rearrangements, but since the morphology is more difficult to control, the interpretation of data could present serious difficulties.

7.4 Rheology of Miscible Blends

7.4.1 General Observations

Miscible polymer blends are less common that immiscible ones. The miscibility is usually confined to a specific range of independent variables, such as chain configuration, molecular weight, composition (viz., for alternate copolymers), temperature, pressure, etc. Nevertheless, Krause reported that 1680 two-, three, or four-component polymeric mixtures were identified as miscible in 780 publications (Krause 1980).

It is noteworthy that even in miscible polymers of similar molecular structure, viz., 1,4-polyisoprene with 1,2-polybutadiene, time–temperature superposition fails. With the glass transition temperatures separated by 60 °C, the polymers preserve their different dynamics in the blends (Kannan and Kornfield 1994). Thus, even miscible systems can be rheologically complex. The rheological behavior of blends in the vicinity of phase separation is of great fundamental importance. It will be discussed in Sect. 7.4.3.

PPE/PS mixtures are considered classical examples of miscible polymer blends. Within the accessible range of temperatures, single-phase melts have been observed with the size of homogeneity below 20 nm. Dynamic flow behavior of PPE/PS blends, with molecular weight ratio MW(PS)/MW(PPE) $\cong$ 1, was studied in a wide range of temperatures and compositions (Prest and Porter 1972). The authors assumed additivity of the free volumes of the components and characterized the blend flow behavior under iso-free volume conditions. Increasing PPE content

resulted in higher values of the storage and loss shear moduli, G′ and G″. The same blends, but with MW(PS)/MW(PPE) = 100 were studied by Araujo and Stadler (1988).

Blends of atactic polymethylmethacrylate with polyethyleneglycol, PMMA/PEG, were reported miscible (Colby 1989). Their rheology, PMMA/PEG = 50/50 and 80/20 at T = 160–210 °C, was studied in a dynamic shear field (Booij and Palmen 1992). By contrast with homopolymers, the blends did not follow the time–temperature superposition. The deviation was particularly poor at low temperatures. The reason for the deviation is most likely based on the different temperature dependence of the relaxation functions. The authors concluded that in miscible blends, the temperature dependence of the relaxation times of individual macromolecules depends on composition. This leads to different degree of mutual entanglement and hence the rubber plateau moduli.

In contrast with PPE/PS blends, those of PS with PVME are known to have lower critical solution temperature, LCST, in the middle of the experimentally accessible temperature range, LCST = 100–180 °C (depending on composition and MW of the components). Rheology of these systems was studied within the miscible and immiscible as well as across the phase separation region. Within the miscible region, addition of PVME was reported to plasticize PS, thus shifting the terminal zone of G′ and G″ to higher frequencies (Schneider and Brekner 1985; Brekner et al. 1985; Yang et al. 1986). It was also reported that the time–temperature superposition principle for the blends breaks down as the temperature approaches the glass transition temperature, T_g (Cavaille et al. 1987). For the PS/PVME blends, with molecular weight ratio MW(PS)/MW(PVME) $\cong$ 40, separate relaxation times were found in the entanglement region (Stadler et al. 1988) (in homologous polymer blends having significantly different molecular weights, the relaxation spectra also show separate relaxation times for the components). Time–temperature superposition was obtained up to T = LCST + 40 °C (Stadler et al. 1988). For the PS/PVME blends, with molecular weight ratio MW(PS)/MW (PVME) $\cong$ 2, phase separation was found to increase G′ but not G″; thus the time–temperature superposition breaks down (Ajji et al. 1989; Ajji and Choplin 1991). For similar blends, with MW(PS)/MW(PVME) $\cong$ 0.8, total breakdown of the time–temperature superposition principle was reported for the phase-separated region. Large increases in both G′ and G″ were observed (Mani et al. 1992).

Sharma and Clarke (2004) reported experiments on a lower critical solution temperature blend of PSD and PVME, in order to determine the miscibility of the blend based purely on rheology. The investigation was done in the temperature range of T_g (glass-transition temperature) + 45 K to T_g + 155 K in which the blend morphology was expected to change from homogeneous to two-phase structure. Dynamic temperature sweep was found to be sensitive to the phase-separation temperature and the miscibility region. They suggested that the first change in the slope of the smoothly varying storage modulus is associated with the binodal temperature. Three different zones identified in the tan δ-temperature curve (peak zone and off-peak zones) were shown to correspond to the miscible, metastable, and phase-separated regions of the phase diagram (Sharma and Clarke 2004).
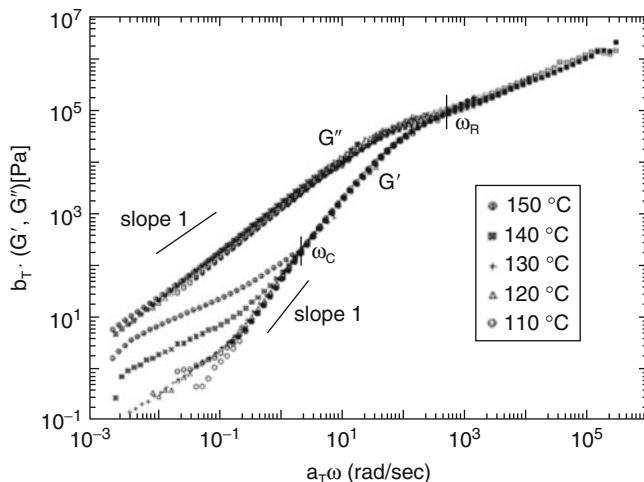
Fig. 7.17 Master curves of storage modulus (G′) and loss modulus (G″) for a 50:50 PSD/PVME blend, as a function of frequency ω (Sharma and Clarke 2004)

Time–temperature superposition works well in the homogeneous region of LCST (e.g., polystyrene and poly(vinyl methyl ether)) or UCST (e.g., polystyrene and poly(α-methylstyrene))systems. This suggests scaling behavior of $G' \sim \omega^2$ and $G'' \sim \omega^1$ at low frequencies. However, time–temperature superposition fails in the metastable region of these blends, which exhibit an increase in the magnitude of G′ in the terminal zone (Kim et al. 1998; Sharma and Clarke 2004). Figure 7.17 depicts clear deviation from scaling behavior of homogeneous blends of PSD/PVME, just after the rheologically determined binodal temperature (only the temperatures at which the time–temperature superposition failure occurs are listed in the fig., i.e., above 104 °C). It was suggested that the observed thermo-rheological complexity is related to the different morphologies formed by different coarsening kinetics. It seems that concentration fluctuation induced stress, which is mostly of elastic origin, causes storage modulus to be more sensitive to phase transitions than loss modulus (Kapnistos et al. 1996; Sharma and Clarke 2004).

The investigation of the Han plots, which is the log–log plot of storage modulus versus loss modulus, is another effective method to determine the onset of phase separation. This method is more sensitive to concentration fluctuations than data obtained from time–temperature superposition. The Han plot of homogeneous phases shows two main features: temperature independence and terminal slope of two (Han et al. 1990, 1995). Deviations from these two criteria were reported only for Han plots above the LCST and below the UCST (Kim et al. 1998; Sharma and Clarke 2004). Therefore, it has been suggested to use this method to infer the phase-separation (binodal) temperature rheologically.

There are other fingerprints that may be used to track the critical point of the phase transition in polymer blends, using the linear regime of rheological

Fig. 7.18 Cole–Cole plot
of the 80:20 blend at
different temperatures
(Ajji et al. 1988a)
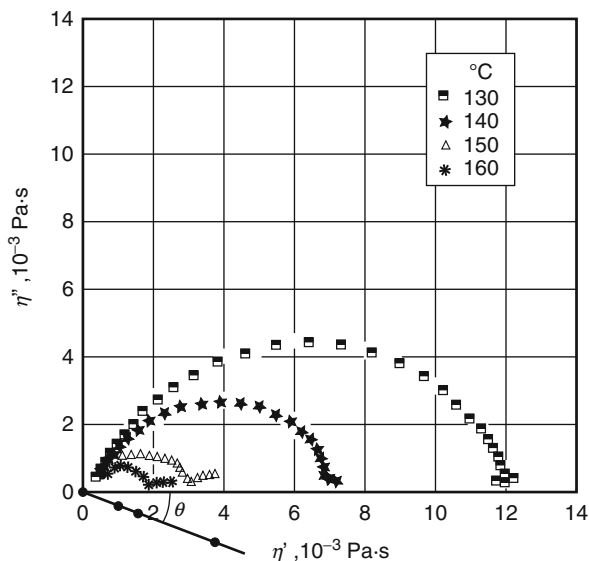
experiments. One method is the so-called Cole–Cole diagram showing the
relationship between the dynamic viscosity (η') and the loss viscosity (η'').
For example, Ajji et al. (1988a) used the Cole–Cole representations to estimate
the phase-transition temperature of the 80:20 PS/PVME blend, as shown in
Fig. 7.18 at different temperatures. The characteristic of the Cole–Cole plot for
homogeneous blends is the presence of only one circular arc. Therefore, the
temperature at which a second circular arc begins to appear is the phase-transition
temperature of the system. Close to this temperature on the right-hand side of the
first arc, a tail develops and forms a second arc. Phase-transition temperature was
found to be about 140 °C by this technique, which was close to the value of 138 °C
found by cloud point measurements (Ajji et al. 1988a,b). Phase separation of
polymer blends can be also identified in the relaxation spectrum $H(\tau)$ of polymer
blends in the form of an additional relaxation (Bousmina et al. 2002; Zuo and
Zheng 2006).

According to Onuki (1987), the shear viscosity increases in phase-separating
fluids near the critical point. However, Sharma and Clarke (2004) claimed that
Onuki's prediction of features specific to the transition from a homogeneous to
a two-phase regime was not observed for PSD/PVME blends.

Blends of tetramethyl polycarbonate, TMPC, with PS were reported miscible
(Wisniewsky et al. 1984). Couchman (1996) demonstrated that the concentration
dependence of η_o at 230 °C can be predicted from the characteristic parameters of
the two components, assuming absence of specific interactions.

Fig. 7.19 The experimental (points) and computed from Eq. 7.80 relation between viscosity and composition for polypropylene blends with styrene-ethylene-butene-styrene block copolymer (Steller and Zuchowska 1990)
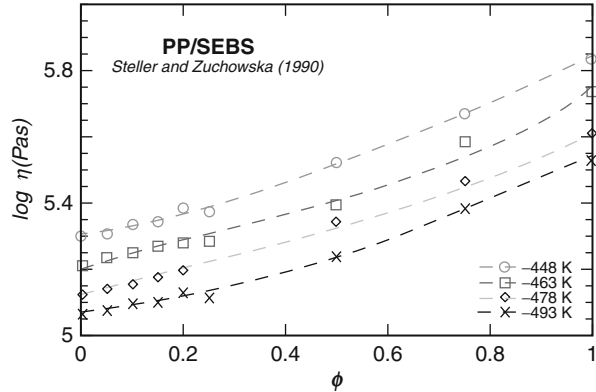
In miscible blends, flow behavior depends on free volume, entanglements, and specific interactions. From Doolittle's equation, assuming additivity of the occupied volume and non-additivity of the free volume, Steller and Zuchowska (1990) derived:

$$\ln\eta_b = \sum_{i=1}^{n}\phi_i\ln\eta_i = \frac{\sum_{i=1}^{n}w_i[(\delta_i-1)/(\delta_{i+1})]V_i}{2\sum_{i=1}^{n}w_iV_i/(\delta_i+1)} - (1/2)\sum_{i=1}^{n}\phi_i(\delta_i-1)$$

$$\delta \equiv [1-4(\partial\ln\eta/\partial T)/(\partial\ln V/\partial T)/B]^{1/2} = (2V_0+V_f)/V_f \tag{7.80}$$

where w_i and V_i are, respectively, weight fraction and specific volume of i-th component, while V_o and V_f are the occupied and free volume, respectively. Since the parameter δ can be determined experimentally (from the temperature gradient of the viscosity and specific volume – see Eq. 7.80), the dependence is fully predictive, as shown in Fig. 7.19.

The reptation model provides simple mixing rules for miscible systems (Doi and Edwards 1986):

$$G_N^o = \sum G_{Ni}^o\phi_i; \quad \eta_o = \sum \eta_{oi}\phi_i; \quad J_e^o\eta_o^2 = \sum J_{ei}^o\eta_{oi}^2\phi_i \tag{7.81}$$

where G_N^o is the plateau modulus, η_o is the zero-shear viscosity, and J_e^o is the recoverable shear compliance. This "single reptation model" neglects the thermodynamic interactions and constraints release. Viscoelasticity of miscible polymer blends was also analyzed by Tsenoglou (1988). The "double reptation model" resulted in the following mixing rules for the miscible blends:

$$G_N^o = \left[\sum_{i=1}^{2} \left(G_{Ni}^o \right)^{1/2} \phi_i \right]^2$$

$$\eta_o = \eta_{o1} \phi_1^2 + \eta_{o2} \phi_2^2 + 4 \left(G_{N1}^o G_{N2}^o \right)^{1/2} \phi_1 \phi_2 \left[\left(G_{N1}^o / \eta_{o1} \right) + \left(G_{N2}^o / \eta_{o2} \right) \right]^{-1} \quad (7.82)$$

$$J_e^o \eta_o^2 = J_{e1}^o \eta_{o1}^2 \phi_1^2 + J_{e2}^o \eta_{o2}^2 \phi_2^2 + 8 \phi_1 \phi_2 \left[\frac{\left(G_{N1}^o / G_{N2}^o \right)^{1/4}}{\left(J_{e1}^o \eta_{o1}^2 \right)^{1/2}} + \frac{\left(G_{N2}^o / G_{N1}^o \right)^{1/4}}{\left(J_{e2}^o \eta_{o2}^2 \right)^{1/2}} \right]^{-1}$$

Validity of Eqs. 7.81 and 7.82 was examined for mixtures of entangled, nearly monodisperse blends of poly(ethylene-*alt*-propylene) with head-to-head PP (Gell et al. 1997). The viscoelastic properties, compared at constant distances from the respective glass transition temperatures of each component, were found to obey the time–temperature superposition principle. The data agreed better with the predictions of Eq. 7.82 than Eq. 7.81. However, for blends of linear and branched PE, the relations were found valid only when MW and rheological properties of the two components were similar (Groves et al. 1996).

The double reptation model was used to evaluate viscoelastic behavior of metallocene-catalyzed polyethylene and low-density polyethylene blends by Peon et al. (2003). They compared their results with those obtained for HDPE/BPE blends prepared under similar conditions. Since this model assumes miscibility between the mixed species, the experimental viscosity of HDPE/BPE blends showed only small deviation compared to that expected according to the reputation miscible model. However, the model underestimated the compositional dependence of the zero-shear viscosity for mPE/LDPE blends, especially at intermediate levels. The enhanced zero-shear viscosity in immiscible blends such as PETG/EVA, PP/EVA, or EVA/PE blends was found to be more abrupt than it is for mPE/LDPE blends (Lacroix et al. 1996, 1997; Peon et al. 2003).

The enhanced viscoelastic functions are attributable to additional relaxation processes that occur at low frequencies associated with deformation of the dispersed phase. Therefore, for cases such as mPE/LDPE, where partial miscibility at high LDPE content and the extremely different relaxation times of the phases in the blends rich in mPE are observed, a hybrid model including the double reptation approach for the matrix and the linear Palierne approach for the whole system could successfully explain the viscoelastic response of these blends (Peon et al. 2003).

Yu et al. (2011) studied rheology and phase separation of polymer blends with weak dynamic asymmetry ((poly(Me methacrylate)/poly(styrene-*co*-maleic anhydride)). They showed that the failure of methods, such as the time–temperature superposition principle in isothermal experiments or the deviation of the storage modulus from the apparent extrapolation of modulus in the miscible regime in non-isothermal tests, to predict the binodal temperature is not always applicable in systems with weak dynamic asymmetry. Therefore, they proposed a rheological model, which is an integration of the double reptation model and the self-concentration model to describe the linear viscoelasticity of miscible blends. Then, the deviation of experimental data from the model predictions for miscible

blends determines the binodal temperature. This method was successfully applied in PMMA/SMA blend with weak dynamic asymmetry (Yu et al. 2011).

7.4.2 Relaxation Spectrum and Linear Viscoelasticity

Substituting Eq. 7.42 into Gross frequency relaxation spectrum, H_G, results in the following expression:

$$\tilde{H}_G \equiv H_G/\eta_0 = (2/\pi)r^{-m_2}\sin(m_2\Theta)$$
$$r = \left[1 + 2(\omega\tau)^{m_1}\cos(m_1\pi/2) + (\omega\tau)^{2m_1}\right]^{\frac{1}{2}} \tag{7.83}$$
$$\Theta \equiv \text{arc}\sin\left\{(\omega\tau)^{m_1}r^{-1}\sin(m_1\pi/2)\right\}$$

Thus, once the four parameters of Eq. 7.42 are known, the relaxation spectrum and then any linear viscoelastic function can be calculated. For example, the experimental data of the dynamic storage and loss shear moduli, respectively G' and G'', or the linear viscoelastic stress growth function in shear or uniaxial elongation can be computed from the following relations (Utracki and Schlund 1987):

$$G'(\omega) = \int_{-\infty}^{+\infty}\left\{sH_G(s)/\left[1 + (s/\omega)^2\right]\right\}d\ln s$$
$$G''(\omega) = \int_{-\infty}^{+\infty}\left\{\omega H_G(s)/\left[1 + (\omega/s)^2\right]\right\}d\ln s \tag{7.84}$$
$$\eta_E^+(t) = \int_{-\infty}^{+\infty}\{H_G(\omega)[1 - \exp(-\omega t)]\}d\ln\omega$$

Since Gross frequency relaxation spectrum can be computed from η', i.e., from the loss modulus, $G'' = \eta'\omega$, the agreement between the computed and measured G' values provides good means of verifying both the computational and experimental procedures. It has been found that Eqs. 7.83 and 7.84 are useful to evaluate the rheological performance of systems that obey linear viscoelastic principles.

According to the definition of the reduced relaxation spectrum, the integral:

$$\int_{-\infty}^{+\infty}\tilde{H}_G(s)d\ln s \equiv 1 \tag{7.85}$$

Thus, the coordinates of the maximum, $\tilde{H}_{G,\max}; \omega_{\max}$, are related respectively to the system polydispersity and molecular weight. However, if the system is miscible,

these functions are fully predictable from the composition, polydispersity, and molecular weight of the components. Note that in miscible blends, the general relation between the relaxation spectrum of a mixture and its composition follows the third-order blending rule:

$$H(\tau) = \sum w_{ijk} H_{ijk}\left(t/\tau_{ijk}\right) \qquad (7.86)$$

The dependence can be significantly simplified, when all fractions are either entangled or not (the situation that exists in most polymer blends):

$$H_G(\omega) = \sum w_i H_{Gi}(\omega) \qquad (7.87)$$

Thus, for miscible polymer blends, the relaxation spectrum is a linear function of the relaxation spectra of the components and their weight fractions, w_i. Hence, one may use rheological functions to detect miscibility/immiscibility of polymer blends. An example is presented in Fig. 7.20 (Utracki and Schlund 1987).

Two principles can be used for the rheological methods of miscibility detection:
1. Effect of polydispersity on the rheological functions
2. Effect of the inherent nature of the two-phase flow

The first principle makes it possible to draw conclusions about miscibility from, e.g.:
- Coordinates of the relaxation spectrum maximum (Utracki and Schlund 1987)
- Cross-point coordinates (G_x, ω_x) (Zeichner and Patel 1981)
- Free volume gradient of viscosity: $\alpha = d(\ln\eta)/df$
- Initial slope of the stress growth function: $S \equiv d\ln\eta_E^+/d \ln t$ (Schlund and Utracki 1987)
- The power-law exponent $n \equiv d\ln\sigma_{12}/d\ln\dot{\gamma} \cong S$

The second principle involves evaluation of, e.g.:
- Extrudate swell parameter, $B = D/D_o$
- Strain (form) recovery
- Yield stress

These effects, associated with immiscibility, will be discussed in later in this chapter.

7.4.3 Phase Separation and Flow

The phase behavior of polymer blends under flow was reviewed by Kammer et al. (1993).

For most polymer blends, the phase diagram is characterized by the presence of the lower critical solution temperature, LCST. Thus, as the temperature increases, miscible polymer blends may phase-separate. Theoretically, the miscibility region stretches up to the binodal. However, as the system approaches the binodal,

Fig. 7.20 Coordinates of the maximum of the Gross frequency relaxation function, $\tilde{H}_{G,max}$ (*top*), and, ω_{max} (*bottom*), versus, respectively, the polydispersity index, M_w/M_n, and the zero shear viscosity, η_o, a measure of the molecular weight (Utracki and Schlund 1987)
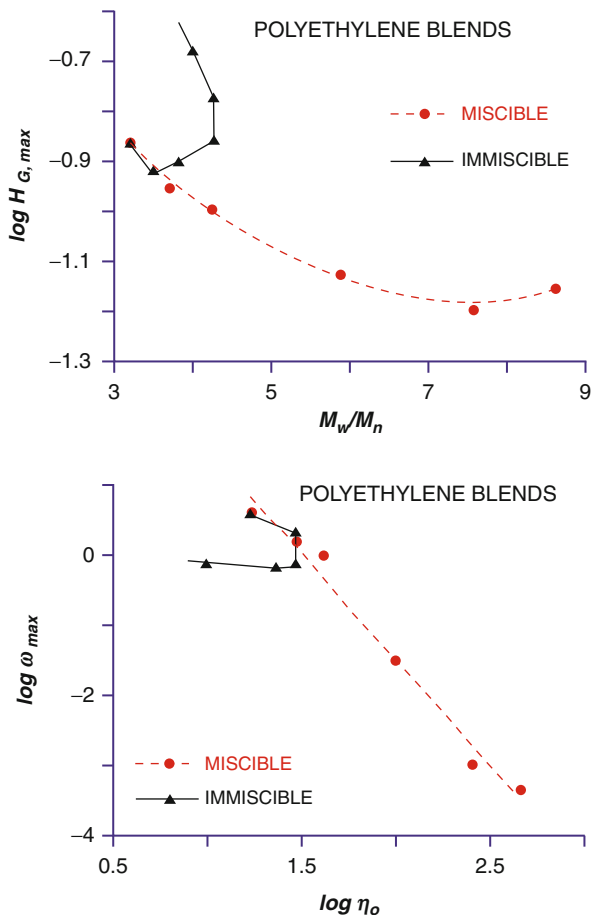
there is strong mutual interaction between the rheology and thermodynamics (Rangel-Nafaile et al. 1984; Larson 1992).

For systems of small molecules, the phase diagram does not change by the kinetic energy. However, due to the viscoelastic nature of polymer blends, a part of the flow energy could be stored as the free elastic energy. This influences the Gibbs free energy of the blend. Therefore, the phase diagram and miscibility would change. Various studies attempted to correlate this energy to the properties and the conditions of flow. One approach involves modification of the free energy of the system by the addition of the elastic free energy, which is expressed in terms of the viscosity and the shear modulus. Berrayah and Maschke (2011) considered the effects of shear on the phase diagram of binary polymer blends of poly(styrene acrylonitrile) copolymer and poly(methyl methacrylate) characterized by a lower critical solution temperature (LCST). Using the above theoretical formulism, they showed that predictions are in good agreement with cloud point data of the PSAN/PMMA

Fig. 7.21 The equilibrium phase diagram of PSAN/ PMMA under shear flow at several shear rates. Symbols represent the cloud point data of the system PSAN/PMMA in the quiescent (Berrayah and Maschke 2011)
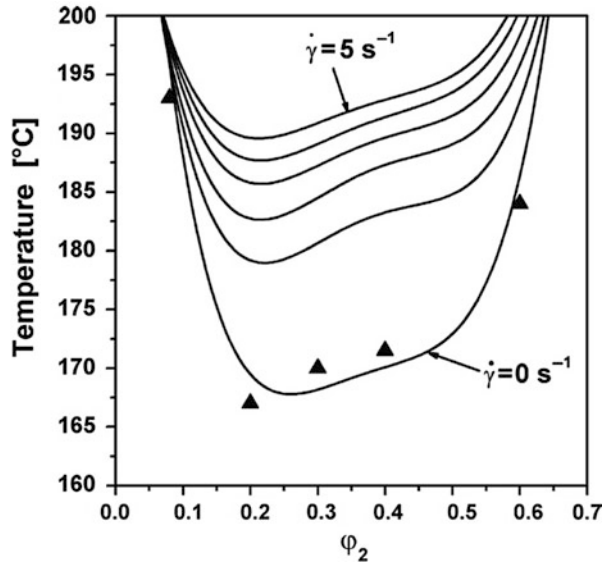
blend in the quiescent state and the miscibility was enhanced with increasing shear rate (Fig. 7.21) (Berrayah and Maschke 2011).

The interaction between stress and composition in single-phase polymer solutions and blends is of theoretical and experimental concern. Flow-induced encapsulation has been known for a long time. Recently, the focus has shifted to miscible systems of nonuniform compositions placed in a nonuniform stress field. Two mechanisms have been proposed: the first postulating that long chains migrate to lower stress regions to decrease the elastic energy stored by deformation of the macromolecular coil (Metzner et al. 1979), the second assumes that long chains can support stress more than the short ones, creating imbalance of stresses and relative motion of the components (Doi and Onuki 1992). The latter theory makes it possible to calculate the concentration gradients in sheared blends. For example, in cone-and-plate geometry, the theory predicts migration of the high molecular weight fractions toward the center. Phenomenologically, the effect may be considered to originate from the hoop stress created in shearing of the larger polymeric chains that force them to migrate toward the center, engendering what is known as *Weissenberg effect*. The effect is related to the normal stress, $\sigma_N = N_1 + 2\,N_2$, and the osmotic pressure gradient, $d\pi/d\phi$, while the diffusion time is determined by the ratio (l/D_m), where l is the diffusion length scale and D_m is the mutual diffusion coefficient – the process is rather slow.

7.4.3.1 Influence of Thermodynamics on Rheology

For linear viscoelastic functions near phase separation at low strains, Larson and Fredrickson (1987) derived:

$$G'(\omega) = \omega^2 \Delta^{-5/2}; \quad \psi_1 = \psi_2 = \Delta^{-5/2} \atop G''(\omega) = \omega \Delta^{-3/2}; \quad \eta(\dot{\gamma}) = \Delta^{-3/2} \left.\right\} \tag{7.88}$$

where $\Delta = 2((\chi N)_s - (\chi N))$ is a measure of thermodynamic distance from the spinodal. The theory indicates that, at spinodal, the linear viscoelastic functions go to infinity or, in other words, the system becomes rheologically nonlinear. Numerically, near the spinodal, the theory predicts that the ratio $\Psi_2/\Psi_1 \cong -1.35$, instead of the usual $\Psi_2/\Psi_1 = -0.05$ to -0.20. All the data for diverse liquid systems indicate that when approaching phase separation, the viscosity should increase with the correlation length, but the rate of the increase and the absolute magnitude may vary from one system to another. The effect depends on the deformation rate and is more pronounced in high molecular weight systems.

This prediction was found qualitatively valid for blends of low density polyethylene, LDPE, with linear low density polyethylene, LLDPE. At about 20 wt% of LDPE, a sharp peak in the plot of $a_1 \equiv dln\eta/dlnY$ (where $Y = 1/(f + 0.07)$ with f being the free volume fraction) versus composition. This behavior was associated with the phase separation in the blends (Utracki and Schlund 1987).

In contrast to the predictions of Eq. 7.88, the effective viscosity at the spinodal was described by the fluidity additivity relation (Onuki 1994, 1997):

$$1/\eta_{eff} = \phi_1/\eta_1 + \phi_2/\eta_2; \quad N_1 \propto \dot{\gamma}(\phi_1\eta_2/\phi_2) \atop \text{at SD}: \quad \phi_1/\eta_1 \approx \phi_2/\eta_2; \quad \text{where} \quad \phi_1 = 1 - \phi_2 \tag{7.89}$$

Similarly, the first normal stress difference, N_1, is also predicted to be proportional to the shear stress. The phase co-continuity condition was derived from the equal shear stress principle between two phase-separating phases. The dependence is the same as empirically derived by Paul and Barlow – see Eq. 7.6.

The effect of phase separation on the dynamic shear flow of PS/PVME blends was frequently studied (Schneider and Brekner 1985; Brekner et al. 1985; Yang et al. 1986; Cavaille et al. 1987; Stadler et al. 1988; Ajji et al. 1989; Ajji and Choplin 1991; Mani et al. 1992). The results seem to differ, depending on the relative magnitude on the molecular weight, MW(PS)/MW(PVME). When the ratio was large, PVME acts as a plasticizer. When the ratio was about 2, a passage through the phase-separation region affected the dynamic storage shear modulus, G', but not the loss modulus, G''. Finally, for ratios less than one, it was reported that neither the storage nor loss dynamic shear modulus, G' and G'', respectively, indicated any significant change near the phase separation region, but upon entering the phase separation region both functions increased. By measuring the fluorescence intensity, the authors were able to map the phase separation region well. The time–temperature superposition principle was found to be valid only within the miscible blends region (Mani et al. 1992).

Dynamic shear flow within the linear viscoelastic region was used to determine binodal and spinodal temperatures (T_b and T_s, respectively) in LCST-type

blends (Vlassopoulos 1996). The system of interest was PMMA (containing 12 wt% ethyl acrylate) with 10–60 wt% SMA. The demixing temperature was determined in temperature sweeps, by plotting log G′ versus T – departure from a straight line was taken as T_b. Determination of T_s involved plotting $[G''(\omega)]^2/[TG'(\omega)]^{2/3}$ versus 1/T. Again, linear extrapolation was used to determine T_s. The rheologically determined data were found to correspond reasonably well to those determined by turbidity and light scattering.

The viscoelastic properties of model blends with UCST were studied in dynamic and steady-state shearing (Vlassopoulos et al. 1997). Low molecular weight PS and poly(methyl phenyl siloxane), PMPS, were used – the neat resins showed Newtonian behavior. The equilibrium phase diagram was determined by optical means. Within the miscible region, blend viscosity followed the log-additivity rule, provided that the concentration was corrected for the difference in the surfaces (Mertsch and Wolf 1994):

$$\ln\eta = w_1\ln\eta_1 + w_2\ln\eta_2 + \left\{\ln(\eta_1/\eta_2)\frac{\varsigma w_1 w_2}{1 + \varsigma w_1}\right\}$$
$$\text{where}: \quad \varsigma(\text{Bondi}) = \left.\frac{S_1/S_2}{V_1/V_2}\right|_{\text{Bondi}} - 1 \tag{7.90}$$

where w_i is the weight fraction of polymer i. The correcting factor, ς, can either be treated as a fitting parameter ($\varsigma = -0.54$ was determined for PS/PMPS system) or it can be calculated using Bondi's values of the surface, S_i, and volume, V_i, for each component ($\varsigma = -0.5$ was calculated). The phase separation resulted in rheologically complex behavior. However, the rapid increases of the rheological functions near SD, predicted by Eq. 7.88, were not observed.

7.4.3.2 Influence of Rheology on Thermodynamics

The response of heterogeneous systems to a stress field allows them to be placed in two categories: (i) those in which stress induces irreversible changes (e.g., precipitation, denaturation of protein, crystallization, etc.) and (ii) those in which the changes are reversible. The classification is not perfect, as the type and magnitude of stress field can be crucial, but it provides a guide: in most cases, miscibility in systems (i) is reduced by stress, while in systems (ii) it is increased. In other words, if a system can be irreversibly modified by rheological means, its solubility will be reduced. An excellent review on the phase transition in shear flow has been published (Onuki 1997).

Microrheology indicates that drops burst when the capillarity parameter $\kappa \approx 1$ (see Eq. 7.52). Thus, in shear, the equilibrium drop diameter $d \propto \nu_{12}/\sigma_{12}$ – the higher is the shear stress in the matrix or the lower is the interfacial tension coefficient, the smaller is the drop size. In other words, it is natural to expect that shearing improves dispersion. When the drop diameter becomes comparable to the radius of gyration of the macromolecules, miscibility is achieved (Silberberg and Kuhn 1952; Wolf 1980, 1984).

The above argument is correct for infinitely diluted systems. In the practical case at finite concentrations, drop coalescence may limit the dispersion process. However, when shearing takes place near the critical point, phase separation can only occur when the rate of shear is smaller than $1/\tau_c$, where τ_c is the thermodynamic relaxation time for the concentration fluctuations.

Strain compatibilization at low, steady-state stress was considered by Lyngaae-Jørgensen (1985):

$$\sigma_{cr}^2 \cong a_o T(T_s - T); \quad T \leq T_s \tag{7.91}$$

where a_o is a material parameter. Subjecting block copolymers to above-critical stresses at low deformation rates made it possible to change T_s by $\Delta T = 29\ ^\circ C$. For systems with lower critical solution temperature, LCST, the spinodal was shifted to higher temperatures. The values $a_o = 0.26$ and 0.53 $(kPa/K)^2$ were calculated, for block copolymers and poly(styrene-*co*-acrylonitrile)/poly(methyl methacrylate) blends, respectively. Equation 7.91 is in qualitative agreement with experimental observations that, in polystyrene/polybutadiene/dioctylphthalate systems, the critical point shifted as according to $\Delta T_o(\dot\gamma) \approx a_o T_o \dot\gamma^{1/2}$, where a_o is a numerical (Hashimoto et al. 1990).

A thermodynamic theory of strain demixing was proposed (Horst and Wolf 1991, 1992, 1994). The authors postulated that the Gibbs free energy of mixing for flowing blends can be expressed as a sum of the equilibrium thermodynamic free energy of mixing, ΔG_m, and the flow-induced stored energy term ΔE_S:

$$\Delta G\dot\gamma = \Delta G_m - \Delta E_s = \left(\sum_{i=1}^{n} x_i V_i\right)\langle J_e^o\rangle[\langle\eta_o\rangle\dot\gamma]^{2n} \tag{7.92}$$

where the averaged values of the zero-shear viscosity and the steady-state shear compliance can be calculated from, respectively

$$\langle\eta_o\rangle = \left(\sum_{i=1}^{n} w_i\eta_i^{1/3.4}\right)^{3.4}$$
$$\langle J_e^o\rangle\langle\eta_o\rangle^{4.4/3.4} = \sum_{i=1}^{n} w_i J_{ei}^o\eta_i^{4.4/3.4} \tag{7.93}$$

The theory was found to predict complex behavior near the phase-separation conditions. As the rate of shear increases, first, the system undergoes homogenization, then demixing, followed by another homogenization and demixing. At high rates of shear, the system should behave similarly as in the quiescent state. These predictions were found to be in qualitative agreement with experimental data, e.g., for blends of ethylene-vinyl acetate copolymer with chlorinated polyethylene, EVAc/CPE, or polystyrene with poly(vinylmethylether), PS/PVME (Hindawi et al. 1992; Fernandez et al. 1993a, 1995).

The first observation of shear-induced increase of the LCST was reported for PS/PVME by Mazich and Carr (1983). The authors concluded that shear stress can enhance miscibility by 2–7 °C. Larger effects, $\Delta T \leq 12$ °C, were reported for the same system in hyperbolic flow (Katsaros et al. 1986). In a planar extensional flow at $\dot{\varepsilon} = 0.012 - 26$ s^{-1}, the phase-separated PS/PVME was homogenized at temperatures 3 to 6 °C above T_s. The critical parameter of homogenization was found to be the extensional strain, $\varepsilon = \dot{\varepsilon} t_c = 44 \pm 14$, where t_c is the critical time to achieve miscibility at various levels of ϕ, T, and $\dot{\varepsilon}$. The constancy of ε_c indicates that the main mechanism of flow-induced miscibility is related to deformation; after cessation of flow, the deformation dissipates and the homogenized blend phase separates within 20–70 s. By contrast, large stresses can cause demixing in colloidal (e.g., denaturation of proteins) and polymeric systems. In the latter case, precipitation from poor solvent solution, shear crystallization, and stress-related phase separation, are known. For example, PS/PVME under planar stresses at $\sigma_{11} < 10$ MPa shows the previously discussed strain compatibilization, whereas at $\sigma_{11} \geq 30$ MPa it exhibits stress demixing (Katsaros et al. 1986). The demixing may be related to differences in the rheological behavior of the two blend components.

The correlation between rheology and thermodynamics in polymer blends is not straightforward. The concept of stored energy is useful in describing the interaction of rheology with thermodynamics in partially miscible polymer blends (Soontaranum et al. 1996). Flow-induced stored energy determines the deviation of the stored energy of the blend from the linear additivity rule ($\Delta E_S = E_s (\phi_1 E_1 + \phi_2 E_2)$. It is reasonable to consider that the miscibility region of the system is extended when flow-induced stored energy is negative ($\Delta G \gamma = \Delta G_m + \Delta E_s$). This is called flow-induced mixing (shear-induced mixing) and has been observed in a number of systems, such as PS/PIB blends exhibiting UCST (Wu et al. 1992), PSAN-PMMA blends exhibiting LCST (Kammer et al. 1991), and PSAN-PMMA blends in which the spinodal curve is shifted upward upon imposition of shear (Soontaranum et al. 1996). In contrast, positive deviation of the flow-induced stored energy from additivity leads to flow-induced phase separation (de-mixing) (Fernandez et al. 1993b).

For true shifting of the critical point to occur, the suppression of long-range concentration fluctuation must be anisotropic. This has not been observed in PS/PVME blends. Using neutron scattering, it was demonstrated that shearing suppresses the fluctuations only parallel to the flow, leaving the concentration gradients in other directions unchanged (Nakatani et al. 1990). Viscoelastic effects (caused by the presence of a high-MW polymer) during the early stage of spinodal decomposition (SD) were discussed (Clarke et al. 1997). The data were verified using PVME blended with PS having MW = 1,610 kg/mol. Good agreement was observed.

The relation between rheology and morphology during late stages of SD in PS/PVME blends was investigated by means of several techniques (Polios et al. 1997). The results were interpreted using Doi-Ohta (1991) theory.

Shear-induced mixing was reported for polystyrene/polyisobutylene, PS/PIB, blends (Wu et al. 1992). Optical measurements indicated that shearing within the

miscible blend region did not cause demixing, while shearing within the two-phase region reduced turbidity. The latter observation was interpreted as most probably resulting from the shear-induced mixing of the blends.

Blends of PI with PB were dynamically sheared at large amplitude ($\gamma_o = 0.8$) and frequency $\omega = 0.63$ and 6.3 rad/s (Matsuzaka et al. 1997). After a temperature jump, the spinodal decomposition (SD) was in situ observed at the lower frequency, but not at the higher frequency. In the latter case, after stopping the oscillation, a modified SD pattern emerged. The authors postulated that the dynamic flow induced a structure in the miscible system, quite different from that which exists in the non-sheared specimens.

7.5   Rheology of Immiscible Blends

7.5.1   Rheological Equation of State

Based on the principles of the flow behavior of simpler systems, viz., suspensions, emulsions, and block copolymers, as well as an understanding of the mutual interactions between rheology and thermodynamics near phase separation, it may be possible to consider the flow of more complex systems where all these elements may play a role. Evidently, any constitutive equation to describe flow of immiscible polymer blends should combine three elements: (i) the stress-induced effects on the concentration gradient, (ii) an orientation function, and (iii) the stress–strain description of the systems, including the flow-generated morphology. The first steps toward a theory of blend flow behavior were proposed by Helfand and Fredrickson (1989), then by Doi and Onuki (1992). A greatly simplified constitutive equation for immiscible 1:1 mixture of two Newtonian fluids having the same viscosity and density was also derived (Doi and Ohta 1991). The derivation considered time evolution of the area and orientation of the interface in flow, as well as the interfacial tension effects. The relation predicted scaling behavior for the stress and the velocity gradient tensors:

$$\sigma(t,[\widetilde{\kappa}(t)]) = c\sigma(ct, [\kappa(t)]) \quad \text{and} \quad \widetilde{\kappa}(t) = c\kappa(ct)$$
$$\sigma(c\dot{\gamma}) = c\sigma(\dot{\gamma}); \quad \sigma_{12} \propto \dot{\gamma} \quad \text{and} \quad (\sigma_{11} - \sigma_{22}) \propto \dot{\gamma} \tag{7.94}$$

Experimental verification of Eqs. 7.94 indicated that the scaling relationships are valid, but the shape of the experimental transient stress curves, after a step-change of shear rate, did not agree with Doi-Ohta's theory (Takahashi et al. 1994). Similar conclusions were reported for PA-66 blends with 25 wt% PET (Guenther and Baird 1996). For steady shear flow, the agreement was poor, even when the strain-rate dependence of the viscosities of the components was incorporated. Similarly, the recovery of the overshoot (or that of undershoot for step-down experiments) and the shear thinning were not predicted by that theory. However, the theory could predict the extra stress arising from the interfacial tension. Also, the transients (η and N_1) at the start-up of steady-state flow agreed qualitatively with the theory. Doi-Ohta's theory was also compared to the experimental data of semi-concentrated mixtures

of PIB in PDMS (Vinckier et al. 1997). The theory described reasonably well the transient effects at the start-up of steady-state shearing. The scaling laws were also obeyed by these slightly viscoelastic blends.

Following the work of Doi and Ohta, a more general theory was derived for immiscible polymer blends by Lee and Park (1994). A constitutive equation for immiscible blends was proposed. The model and the implied blending laws were verified by comparison with dynamic shear data of PS/LLDPE blends in oscillatory shear flow. This new approach considered the influence of morphology in determining the rheological behavior in a given flow field. Thus, instead of formulating a single droplet problem, as microrheology does for the dilute dispersions, the authors considered the complex interfaces formed between two phases of immiscible fluids created by deformations, breakup, and coalescence of drops (caused by flow and interfacial tension). A semi-phenomenological kinetic equation was derived that described the time evolution of the interfacial area per unit volume, Q, and its anisotropy in a given flow field, q_{ij}:

$$Q = (1/V)\int ds; \quad q_{ij} = (1/V)\int \left[n_i n_j - (1/3)\delta_{ij}\right]ds \tag{7.95}$$

where n_i denotes the unit normal vector to the interfaces, V the total system volume, and dS an interface element. The time evolutions of Q and q_{ij} are affected by the flow that deforms the interface to an anisotropic state:

$$dQ/dt = -d_{ij}q_{ij}$$
$$dq_{ij}/dt = -q_{ik}d_{kj} - q_{jk}d_{ik} + (2/3)d_{ij}d_{lm}q_{lm} - (Q/3)(d_{ij} + d_{ji}) + (q_{lm}d_{lm})/Qq_{ij} \tag{7.96}$$

where $d_{ij} = \partial u_i/\partial x_j$ is the macroscopic velocity gradient tensor. For a mixture of fluids with equal viscosity, the stress tensor may be expressed as

$$\sigma_{ij} = \eta_m\left(d_{ij} + d_{ji}\right) - v_{12}q_{ij} - Pd_{ij}; \quad d_{ij} \equiv du_i/dx_j \tag{7.97}$$

where η_m is the matrix viscosity and v_{12} is the interfacial tension coefficient. In Eq. 7.97, the excess shear stress is proportional to the spatial anisotropy of the interfaces, q_{ij}, and the structure of the interface distorted by the competition between flow and interfacial tension.

The resulting constitutive equation can be used not only for arbitrary volume fractions but also for arbitrary flow fields. It is advantageous to consider that the time evolution of Q and q_{ij} originates in the external flow as well as in the interfacial tension:

$$dQ/dt = (dQ/dt)_{\text{flow}} + (dQ/dt)_{\text{interf.tens.}}$$
$$dq_{ij}/dt = (dq_{ij}/dt)_{\text{flow}} + (dq_{ij}/dt)_{\text{intenf.tens.}} \tag{7.98}$$

For concentrated systems, dimensional analysis of the retraction caused by interfacial tension makes it possible to express the second terms in Eq. 7.98 as

$$dQ/dt = -c_1 c_2 (v_{12}/\eta_m)Q^2 - c_1 c_3 (v_{12}/\eta_m)q_{ij}q_{ij} \tag{7.99}$$

$$dq_{ij}/dt = -c_1(v_{12}/\eta_m)Qq_{ij} - c_1 c_3(v_{12}/\eta_m)(q_{lm}q_{lm}/Q)q_{ij} \tag{7.100}$$

where the dimensionless parameters, c_i, are, respectively, the total relaxation, the size relaxation, and the breakup and shape relaxation. They all depend on the volume fraction ϕ.

The macroscopic stress tensor for the two-phase fluid can be expressed as σ_{ij} = (pressure term) + $\eta_m(d_{ij} + d_{ji})$ + (viscosity ratio term) + (morphology-dependent term) or respectively

$$\sigma_{ij} = -P\delta_{ij} + [1 + 3\phi(\lambda - 1)/5(\lambda + 1)]\eta_m\left(d_{ij} + d_{ji}\right) - v_{12}q_{ij} \tag{7.101}$$

To complete the constitutive equation, contributions originating from flow must be incorporated. These are expressed as

$$dQ/dt = -d_{ij}q_{ij} \tag{7.102}$$

$$dq_{ij}/dt = -q_{ik}d_{kj} - q_{jk}d_{ki} + (2/3)\delta_{ij}d_{lm}q_{lm} - (Q/3)(d_{ij} + d_{ji}) + (q_{lm}d_{lm}/Q)q_{ij} \tag{7.103}$$

Substitution of Eqs. 7.99, 7.100, 7.102, and 7.103 into the two dependencies in Eq. 7.98 provides two relations that, when combined with Eq. 7.101, form the rheological equation of state. Note that at t = 0: $Q = Q_o$ and $q_{ij} = q_{ijo}$. For dynamic oscillatory flow, the relationships between the complex shear moduli $G^* = i\omega\eta^*$ can be written as

$$G_b^* = \left\{1 + \left[6\phi\left(G_i^* - G_m^*\right)/10\left(G_i^* + G_m^*\right)\right]G_m^* + G_{int}^*\right\} \tag{7.104}$$

where G_b^*, G_m^*, and G_i^* are the complex moduli of the blend, the matrix, and the dispersed phase, respectively. The term G_{int}^* is the complex modulus attributed to the interfaces. Imposition of sinusoidally varying strain, $\gamma(\omega) = \gamma_o \sin(\omega t)$ results in frequency-dependent stress at the interface $v_{12}q_{ij}$. The latter also sinusoidally changes with the stress amplitude, δ_{int}, and is out of phase with the strain. The interfacial stress amplitude σ_{int} and its phase lag by δ_{int} can be calculated by solving Eqs. 7.102, and 7.103 assuming the initial values of Q_o, q_{ijo} as well as of the parameters, c_i. The interfacial moduli G_{int}^*, G'_{int}, and G''_{int} can be expressed as

$$G_{int}^*(i\omega) = G'_{int}(\omega) + iG''_{int}(\omega) \tag{7.105}$$
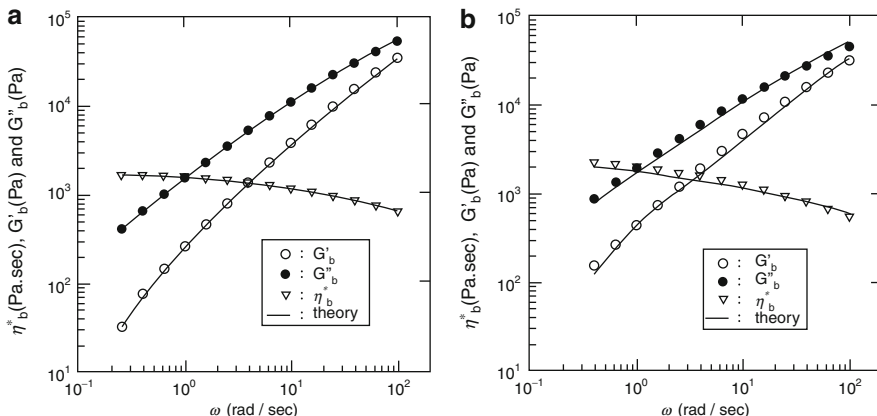
Fig. 7.22 Comparison of model predictions with experimental results for (**a**) 10 wt% and (**b**) 30 wt% of PS in LLDPE (After Lee and Park 1994)

$$G' = (\sigma_{int}/\gamma_0) \cos(\delta_{int}) \tag{7.106}$$

$$G'' = (\sigma_{int}/\gamma_0) \sin(\delta_{int}) \tag{7.107}$$

where γ_o is the strain amplitude.

The effects of shear flow on the PS/LLDPE morphology were investigated by observing the structure of quenched samples under the scanning electron microscope, SEM. Predictions based on the constitutive equations were compared with observations from the dynamic shear experiments at 200 °C (see Fig. 7.22). The frequency variations of G_b', G_b'', and η_b^* were found to be in good agreement with computations based on Eqs. 7.101, 7.102, and 7.103. However, to get such agreement, seven parameters (viz., ν_{12}, ϕ, initial value of the anisotropy parameter, q_{ijo}, initial size of the dispersion, and three dimensionless equation parameters) were required (Lee and Park 1994).

It should be noted that the Doi and Ohta theory predicts only an enhancement of viscosity, the so-called emulsion-like behavior that results in the positive deviation from the log-additivity rule, PDB. However, the theory does not have a mechanism that may generate an opposite behavior that may result in a negative deviation from the log-additivity rule, NDB. The latter deviation has been reported for the viscosity versus concentration dependencies of PET/PA-66 blends (Utracki et al. 1982). The NDB deviation was introduced into the viscosity–concentration dependence of immiscible polymer blends in form of an interlayer slip caused by steady-state shearing at large strains that modify the morphology (Utracki 1991).

A complete set of governing relationships was derived from the requirements of the compatibility of dynamics and thermodynamics (Grmela and Ait-Kadi 1994, 1998; Grmela et al. 1998). The authors developed a set of equations governing the

time evolution of the functions Q and q_{ij} (see Eqs. 7.95), as well as the extra stress tensor expressed in their terms. The rheological and morphological behavior was expressed as controlled by two potentials: thermodynamic and dissipative. Under specific conditions for these potentials, the Lee and Park formalism can be recovered.

Lacroix et al. (1997, 1998) attempted to evaluate three approaches (those of Palierne, Lee and Park, and Grmela and Aït-Kadi). They are capable in describing the experimental data of different types of polymer blends, viz., PS/PE, PETG/EVAc, PP/EVAc, and PP with EVAc and poly(ethyl methacrylate) (PEMA). Since EVAc is miscible with PEMA, the latter blend is also a two-phase blend with PP being the matrix. All blends were prepared within the concentration range that assured dispersed morphology. The Palierne model was found to describe well the linear viscoelastic behavior, whereas the model of Lee and Park was found useful for describing the rheological behavior under large strains. In the later paper, it was shown that the overshoot at the start-up of shearing was described well using either the Lee and Park or Grmela and Aït-Kadi model.

Based on the morphological features, the proposed models can be divided into two categories (Yu and Zhou 2007). The first group is based on local coarse-grained morphology such as the models of Doi and Ohta, Lee and Park, and Grmela. The second group includes the models based on droplet morphology, such as the models proposed by Maffettone and Minale (1998), Jackson and Tucker Iii (2003), and Yu and Bousmina (2003).

The first group used a statistical area tensor or interfacial anisotropic tensor to explain the complex interface by applying some modification on the Doi and Ohta model. The general advantage of these models is their ability to describe the blends with co-continuous structure or irregular phase morphology. On the other hand, the main drawback is attributed to the model parameters that can be used for a specific system and are non-generalizable. More quantitative morphological studies should be done to extend their applications.

The second group involves an ellipsoidal shape tensor representing the shape of the droplets. They lead to good description of droplet deformation, droplet relaxation, and rheological properties, along with the ability to incorporate the viscoelastic effects of components (Maffettone and Greco 2004; Yu et al. 2004; Yu et al. 2005). However, they fail to describe the systems that undergo droplet breakup and coalescence phenomena. To overcome this problem, Dressler and Edwards (2004) assumed that the variable droplet distribution can be considered in terms of two thermodynamic variables: the droplet shape tensor and the number density of representative droplets. They used a single time scale for breakup and coalescence to track droplet numbers. However, while this approach worked well for the PIB/PDMS blend, it was suggested that more quantitative rheological and morphological studies are needed to compare model predictions and experiments, especially for systems in which the breakup process dominates (e.g., transient process under large step shear) (Yu and Zhou 2007).

As another approach to predict the rheological behavior of immiscible blends, Almusallam et al. (2003) and Zkiek et al. (2004) constructed "hybrid" models based

on local coarse-grained morphology by casting Tomotika's theory to consider thread breakup under quiescent conditions. Yu and Zhou (2007) proposed a simple constitutive equation for immiscible blends. The theory predicts the overshoot in the first normal stress difference in the transient start-up of shear and morphology of droplets under varying shear histories. This model is based on the ellipsoidal description of droplets and includes the breakup and coalescence processes. The main assumption is that the discrete droplet breakup/coalescence process can affect droplet size only and it can be approximated by a continuous dynamic equation. A simple mapping approach was suggested to unify the variation of droplet volume due to the breakup/coalescence process and the conservation of droplet volume during the deformation (Yu and Zhou 2007).

7.5.2 Morphology of Immiscible Blends

In immiscible blends, the properties are related to the interface as well as to the size and shape of the dispersed phase. The morphology is controlled by both equilibrium and nonequilibrium thermodynamics, as well as by the flow field. As discussed in Sect. 7.1.2.2, at equilibrium and within the region of low volume fraction of the dispersed phase, $\phi < \phi_{perc} = 0.16$, droplets are expected, while at $\phi > \phi_{perc} = 0.16$ a co-continuous morphology, e.g., fibers or lamellae, are usually observed.

When the polymers are miscible under one set of conditions (e.g., within a specified range of concentration (ϕ), pressure (P), and temperature (T)), but immiscible under other conditions, the nonequilibrium morphology depends on the quench depth and time scale. Shallow quenching into the metastable region (between the binodal and spinodal curves) results in nucleation of the dispersed drops, followed by their growth. The mechanism of this phase separation is appropriately called *nucleation and growth*, NG. By contrast, deep quenching into the spinodal region results in *spinodal decomposition*, SD. Here there is an instantaneous generation of regularly spaced co-continuous structures, with progressive increase of the concentration difference between the two adjacent regions and increased spacing. The co-continuity of structures has been reported for scales varying from a few nanometers to hundreds of micrometers.

Both the NG and SD morphologies are transient, progressively coarsening. At a late stage, both NG and SD mechanisms follow similar ripening patterns, leading to an appropriate equilibrium morphology. Without compatibilization, the two phases may totally separate into two layers. In the case of well-compatibilized blends, the action of a compatibilizing agent is similar to that of surfactants in emulsions – one may assign specific surface area coverage per single molecule of the compatibilizer. However, dimensions of the dispersed, compatibilized phase do change with time after cessation of flow. By contrast, addition of a stabilizing agent (e.g., a third polymer immiscible in the two others) may prevent coalescence, preserving the degree of dispersion (but not the orientation) generated during the flow.

7.5.3 Microrheology of Polymer Blends

In this part, the breakup of polymer drops will be discussed, initially dealing with diluted systems (isolated drops) and subsequently with concentrated dispersions where coalescence is of equal importance. Dispersion in Newtonian systems was discussed in Sect. 7.3.2.2.

The mechanisms governing deformation and breakup of drops in Newtonian liquid systems are well understood. The viscosity ratio, λ, critical capillary number, κ_{crit}, and the reduced time, t^*, are the controlling parameters. Within the entire range of λ, it was found that elongational flow is more effective than shear flow for breaking the drops. However, it is always important to realize that both rheological and thermodynamic considerations play an important role in the development of morphology in polymer blends. The role of thermodynamics is illustrated in the following example. Ravati and Favis (2013) reported three completely different interfacial tension-driven structures for the ternary blends: partial wetting for PBS/PLA/PCL, complete wetting tri-continuous morphology for PBS/PLA/PBAT, and combined partial-complete wetting cases for the PBS/PBAT/PCL blend. The variety of structures was achieved since the interfacial tensions between the phases were very low and the spreading coefficients were close to zero. Simply replacing one component with another changed the sign of the spreading coefficient and led to a different wetting behavior, as shown in Fig. 7.23. The observed partial and complete wetting cases were supported by Harkins theory of the spreading of liquids (Harkins 1941).

7.5.3.1 Deformation and Breakup of Viscoelastic Drops

The shear deformation of viscoelastic drops in a Newtonian medium has been the subject of several studies. Gauthier et al. (1971) found higher values of the critical capillary number than those determined for Newtonian drops. Prabodh and Stroeve (1991) observed that, during shearing, some drops are greatly extended and only break when the flow is stopped. The authors concluded that, at $\lambda < 0.5$, the drop elasticity has a stabilizing effect, but for $\lambda > 0.5$ the opposite is true. Interestingly, the experimental observations of De Bruijn (1989) seem to contradict the latter conclusion. He found that the critical capillary number for the viscoelastic droplets is always higher (sometimes much higher) than for the Newtonian drops, whatever the λ-value. De Bruijn concluded that drop elasticity always hinders drop breakup.

For Newtonian drops suspended in a viscoelastic fluid, Flumerfelt (1972) reported the existence of a minimum drop size below which breakup cannot be achieved. The author pointed out that the elasticity of the medium tends to increase this minimum value for breakup, that is, to stabilize the droplets.

In the case when both the droplets and the suspending medium are viscoelastic liquids, Wu (1987) reported that drops can break up during extrusion even when $\lambda > 4$. However, owing to the complex nature of the deformation during flow through an extruder, it was difficult to even speculate on the origin of this phenomenon. Van Oene (1978) studied the mechanisms of two-phase formation in a mixture of two viscoelastic fluids. He pointed out that, besides the viscosity ratio and the equilibrium interfacial tension of the two liquids, the elasticity of the liquids plays an important
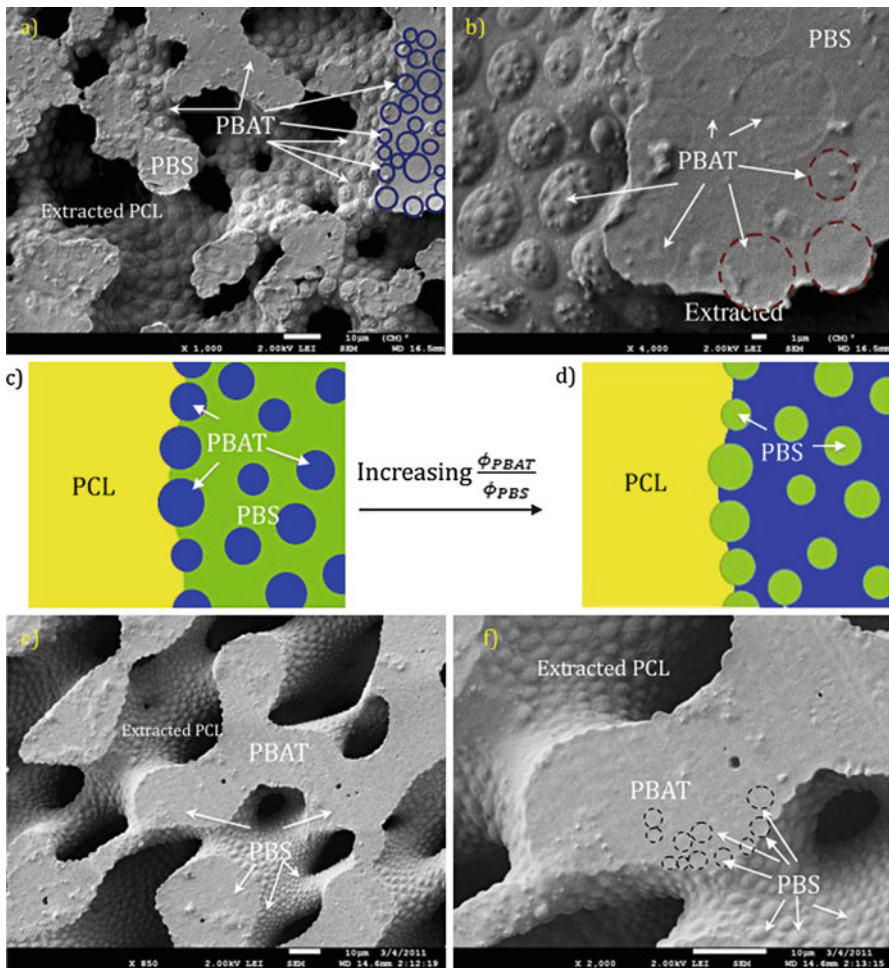
Fig. 7.23 Micrographs and schematics of combined partial-complete wetting morphology for ternary PBS/PBAT/PCL blends showing the effect of composition. (**a**, **b**) 25%PBS/25%PBAT/50%PCL after extraction of the PCL phase by acetic acid and annealing; (**c**) schematic of 25% PBS/25%PBAT/50%PCL; (**d**) schematic of 10%PBS/40%PBAT/50%PCL; (**e**, **f**) 10%PBS/40% PBAT/50%PCL after extraction of PCL phase by acetic acid and annealing. The *white bar* indicates 10 μm except for (**b**) which is 1 μm (Ravati and Favis 2013)

role in deformability of drops. Thermodynamic considerations led to the following relation for the dynamic interfacial tension coefficient:

$$v_{12} = v_{12}^0 + (d_0/12)\left[(\sigma_{11} - \sigma_{22})_d - (\sigma_{11} - \sigma_{22})_m\right] \tag{7.108}$$

where v_{12}^0 is the interfacial tension in a quiescent polymer blend, d_o is the initial diameter of the dispersed drop, and $(\sigma_{11} - \sigma_{22})_i$ is the first normal stress difference of

the dispersed (i = d) and of the matrix (i = m) phase, respectively. For $(\sigma_{11} - \sigma_{22})_d > (\sigma_{11} - \sigma_{22})_m$ the dependence predicts that higher elasticity of the dispersed than the continuous phase results in more stable drops. On the other hand, for $(\sigma_{11} - \sigma_{22})_d < (\sigma_{11} - \sigma_{22})_m$ Eq. 7.108 predicts that $\nu_{12} < \nu_{12}^o$; thus the flow tends to enhance the dispersing process (flow compatibilization). Note that ν_{12} cannot be negative; for large differences of the normal stress difference and for large drop diameters (thus, for higher concentration of the dispersed phase), this translates into co-continuous morphology, for which the above relation is no longer valid.

Since flow affects miscibility of blends near the spinodal, the interfacial tension coefficient must also change with the flow conditions. This theory leads to $\nu_{12}(\dot{\gamma}) = \nu_{12}^o \left[1 - a\kappa^{1/3b}\right]^{2b}$, where a and b are parameters (Onuki 1986).

Han and Funatsu (1978) studied droplet deformation and breakup for viscoelastic liquid systems in extensional and nonuniform shear flow. The authors found that viscoelastic droplets are more stable than the Newtonian ones; in both Newtonian and viscoelastic media, they require higher shear stress for breaking. The critical shear rate for droplet breakup was found to depend on the viscosity ratio; it was lower for $\lambda < 1$ than for $\lambda > 1$. In a steady extensional flow field, the viscoelastic droplets were also found less deformable than the Newtonian ones. In the viscoelastic matrix, elongation led to large deformation of droplets (Chin and Han 1979).

Bousfield et al. (1986) studied the surface-tension-driven breakup of Newtonian and viscoelastic filaments. The authors found that disturbances grow more rapidly in viscoelastic filaments than in the Newtonian ones but that there is a retardation of the growth and stabilization at long times, resulting from large extensional stresses (see Fig. 7.24). The formation of satellite drops was found to be retarded by the elasticity. The authors analyzed the problem using the Galerkin finite element method, as well as a one-dimensional theory for viscoelastic filaments. Their findings were successfully used to interpret existing experimental data on Newtonian and viscoelastic jet disintegration, where the initial disturbance was imposed by nozzle vibration. For viscoelastic jets, an asymptotic solution was offered for the later stages of the process:

$$\ln(R/R_0) = a_0 - t/3\tau; \quad \text{for} \quad t >> \tau \qquad (7.109)$$

where a_o and τ are, respectively, the numerical constant and the relaxation time. This work should have direct bearing on disintegration of viscoelastic filaments in a Newtonian matrix, but application of these findings to polymer blends is more difficult.

Lyngaae-Jørgensen et al. (1993) developed a predictive model of morphology variation during simple shear flow of diluted polymer blends. The model considers the balance between the rate of breakup and the rate of drop coalescence. It was assumed that (i) the viscosity and elasticity of the dispersed phase are significantly lower than those of the matrix, (ii) only the cylindrical, large drops (defined by the long and short semiaxes a_1 and a_2) are able to break and form small drops, and

Fig. 7.24 Computed radius at the neck for disintegrating jet stream of Newtonian (*solid line*) and Maxwell fluid (*dashed line*) (Bousfield et al. 1986)
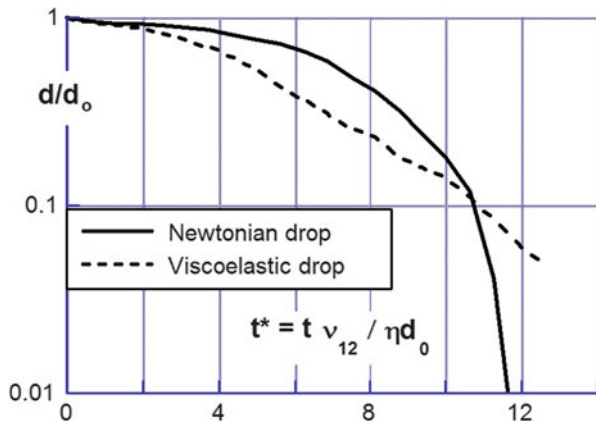
(iii) the coalescence can occur between all types of the dispersed entities. The dynamics of drop formation and breakup can be described by

$$dN_S/dt = N_b R_{Lb} - 2R_{SSC} - R_{LSC}$$
$$dN_L/dt = R_{SSC} - R_{Lb} - R_{LSC}$$
$$da_2/dt = (a_2/dt)_{V,\,\text{flow}} + (a_2/dt)_{\text{coalescense}}$$

(7.110)

where dN_S/dt, dN_L/dt, and da_2/dt are the rates of change of the numbers of small drops and large drops and the rate of change of drop dimension correspondingly; R_{Lb} is the rate at which the number of small drops, N_b, are produced by breakage of the large drops; R_{LSC} and R_{SSC} are the number rates at which small drops are destroyed by coalescence with large and small drops, respectively; R_{LSC} is the number rate of coalescence between large drops. The first term on the right side of the last relation in Eq. 7.110 describes the contribution due to the flow process, and the second reflects that the average thickness of the large domains increases during coalescence.

The theory makes it possible to compute the drop aspect ratio, $p = a_1/a_2$, a parameter that can be directly measured in either a transient or steady-state flow. Following the derivation by Hinch and Acrivos (1980), the flow-induced changes to the drop aspect ratio were assumed to be proportional to the first normal stress coefficient of the matrix fluid. The coalescence was assumed to follow the Silberberg and Kuhn (1954) mechanism. These assumptions substituted into Eq. 7.110 gave a simple dependence for the aspect ratio:

$$p = 4\phi_d p_r \eta_m \dot{\gamma}/\pi a_1 (\sigma_{11} - \sigma_{12})_m - a_2$$

(7.111)

where a_i are adjustable parameters.

Fig. 7.25 Deformability of PS drops in PMMA during steady-state shear flow at 180 °C. The points are experimental; the line is to guide an eye (Lyngaae-Jørgensen et al. 1993)
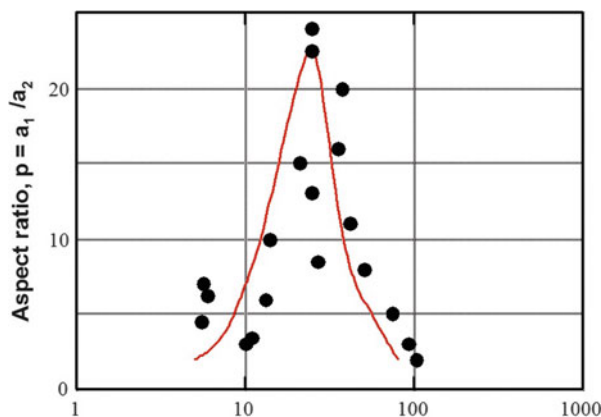
A special unit, equipped for light-scattering measurements, was attached to a Rheometrics Mechanical Spectrometer with cone and plate to follow the transitional events during shearing of polymer blend melts. The predictions of p obtained by the proposed model were found to be in a reasonable agreement with the experimental observations for poly(methyl methacrylate) blends with either 8 or 10 wt% polystyrene, PMMA/PS. The most interesting finding that came out of this work was that, both theoretically and experimentally, under steady-state flow conditions, the aspect ratio plotted versus shear stress showed a sharp peak at the stresses corresponding to transition of PMMA viscosity from the Newtonian plateau to the power-law flow, i.e., to the onset of the elastic behavior. The dependence is presented in Fig. 7.25.

Mighri and Huneault (2002) investigated the drop deformation and breakup mechanisms in Boger fluid in PDMS as a viscoelastic model fluid system and PPS/PE and EPR/PP polymer blends under high shear rate conditions. Flow visualization was carried out in a transparent Couette shearing setup. Two non-Newtonian deformation and breakup mechanisms were presented. The first one was attributed to normal force buildup in the droplet. It was manifested in contraction of the dispersed droplet in the flow direction and its elongation in the vorticity direction at high deformation rates. The second deformation/breakup mechanism was the erosion mechanism. Erosion at the drop surface would occur only in highly viscous molten polymer systems, in which shear stresses could reach the required level. It was suggested that the ends of highly elongated particles would be located in different planes due to flow disturbance. Consequently, clouds of very small ribbons and sheets were formed around the drop, which then elongated and broke into very small droplets (Mighri and Huneault 2002). They also mentioned that the breakup process for the high interfacial tension PS/PE blends was very similar to that of low interfacial tension the EPR/PP system, probably due to the fact that viscosity ratio of both blends was very high.

Aggarwal and Sarkar (2008) used a three-dimensional front-tracking finite-difference method to study the effects of matrix viscoelasticity on viscous and viscoelastic drop deformation in shear flow. They used the Oldroyd-B constitutive equation to model the viscoelasticity of the system and to predict numerically the drop deformation and orientation. It was observed that increasing matrix viscoelasticity changed the drop inclination angle with the flow direction significantly. Also the steady-state drop deformation first decreased and then increased with increasing Deborah number. The change in drop orientation angle along with localized stretching of the polymer molecules at the drop tips was shown to play a critical role in the observed non-monotonic behavior. It was mentioned that the breakup of a viscous drop in a viscoelastic matrix is more pronounced for high De and restricted at smaller De. They showed that polymer to total viscosity ratio (β) affects the drop inclination angle through the combined parameter βDe, pointing out the effect of the first normal stress difference in a steady shear ($N_1 = 2\beta De$) (Aggarwal and Sarkar 2008).

In another attempt, Sirivat et al. (2011) investigated the effects of three different parameters on droplet oscillatory deformation and breakup in polystyrene/high-density polyethylene by using a flow cell mounted on an optical microscope: (i) the effect of time scale ratio (4.0, 16.6, 33.2, and 63.8), (ii) the effect of viscosity ratio (0.58, 0.12, and 0.06), and (iii) the effect of droplet elasticity. The authors defined a modified deformation parameter as Def* $= (a^* - c)/(a^* + c)$ where a^* and c denote the apparent drop principal axes and the minor axes of the droplets as obtained from the droplet image projected onto the flow-vorticity plane from the time series of images. The difference between the maximum and minimum values of Def* divided by two (as a measure of amplitudes of deformation parameters) showed the linear correlation with small capillary numbers, whereas the dependences became nonlinear at large capillary numbers. The increase in critical capillary number was considerable with increasing viscosity ratio, but capillary number changed slightly with the time scale ratio. On the other hand, at a fixed capillary number, amplitudes of deformation parameters increased with decreasing the droplet elasticity (Sirivat et al. 2011) which is in agreement with the main conclusion of the previous studies showing the elasticity of the droplet suppresses droplet deformation and breakup (Lerdwijitjarud et al. 2003, 2004). Furthermore, Sirivat et al. suggested two different drop breakup patterns for PS/HDPE blends; (i) the nonsymmetric one-end tearing pattern that forms many smaller drops for the high-viscosity ratio system and (ii) the two-end stretching and twisting pattern that makes only few satellite drops at each end for the lower-viscosity ratio blend (Sirivat et al. 2011). Lee et al. (2009, 2010) studied the effect of steady shear on the phase separation in LCP/PC blends, using a shear stage, in conjunction with polarized light microscopy (Linkam stage). The phase diagram was divided into three regions with two phase-separation temperatures, Tsp1 and Tsp2, as the internal boundaries. Below Tsp1, phase separation can hardly occur. Between Tsp1 and Tsp2, phase separation can occur to a small extent. Above Tsp2, phase separation in the blends can proceed to a large extent. At low shear rates, both Tsp1 and Tsp2 are shifted to a lower position

(relative to the quiescent conditions) on the phase diagram, indicating that the LCP/PC blends exhibited shear-induced phase-separation behavior. The phase-separated morphology of the blends showed significant changes under shear. For low LCP contents (10 wt%), the blends did not form the droplet-type morphology under shear, as was observed under quiescent conditions. Instead, the blends formed interconnected-type structure, and the network-like LCP-rich domains were transformed to short and thick fragments, due to the breakup of the network. For moderate LCP contents (20–30 wt%), the blends exhibited interconnected structure. However, the LCP-rich domains were thicker and shorter than those formed under quiescent conditions. For high LCP content (40–60 wt%), the blend exhibited droplet-type morphology, with the PC-rich phase appearing as dispersed domains. However, these dispersed domains were not distributed uniformly spatially. The effect of shear, at a shear rate of 0.40 s^{-1}, on the temporal morphological development in 50 wt% LCP/PC blends at 290 °C was examined and compared to the situation under quiescent conditions. Both cases showed that phase separation started quickly and then slowed down at the later stages of the process. The speed and magnitude of phase separation in the blend was enhanced significantly under shear, because of the shift of the phase diagram.

The dynamic mechanical shear behavior of several blends, viz., PS with PMMA, PDMS with PEG, and PS with PEMA, were studied by Graebling et al. (1989, 1993b). The linear viscoelastic behavior of these blends with the volume fraction of the dispersed phase $\phi \leq 0.15$ was found to follow predictions of Palierne's emulsion model, which makes use of the viscoelastic behavior of component polymers and a single parameter that characterizes the interface, i.e., the ratio of the interfacial tension coefficient and drop radius, ν_{12}/R. The values of the interfacial tension coefficient determined from the viscoelastic measurements were found to be in good agreement with results obtained from the pendant drop method. However, the theory seems to break down for polymer blends with $\phi \geq 0.2$. The observed agreement between the experimental data and the theory means that the emulsion model can indeed be used for interpretation of the viscoelastic behavior of polymer blends. The noted deviations at higher concentration range are not in conflict with the basic premises of the approach. They originate from the imposed limitations of the model (see Sect. 7.3.2.3.2).

7.5.3.2 Coalescence of Viscoelastic Drops

For diluted Newtonian systems, the size of the smallest drop that can be broken is calculable from Taylor's theory. However, for polymer systems, many studies have shown that equilibrium drop size is usually larger than predicted and the deviation increases with concentration of the dispersed phase, $\phi_1 - \phi_o$, where ϕ_1 is the volume fraction of the dispersed phase and $\phi_o \approx 0.005$ is the smallest concentration for which the deviation occurs. Roland and Bohm (1984) studied the shear-induced coalescence in two-phase polymeric fluids by small-angle neutron scattering. The coalescence rate was high, dependant on the rheological properties of the two phases and the flow field.

Coalescence occurs in shear as well as quiescent systems. In the latter case, the effect can be caused by molecular diffusion to regions of lower free energy, by Brownian motion, dynamics of concentration fluctuation, etc. Diffusion is the mechanism responsible for coalescence known as *Ostwald ripening*. The process involves diffusion from smaller drops (high interfacial energy) to the larger ones. Shear flow enhances the process (Ratke and Thieringer 1985):

$$(d/d_0)^n = 1 + a_0 t, \quad n = n(y) = 3/2 \text{ to } 3 \tag{7.112}$$

where d_o is the drop diameter at the moment of imposition of stress and a_o is a constant. The exponent n decreases from the classical value of 3, for quiescent systems, to 3/2 at high shear rates.

Flow-induced coalescence is accelerated by the same factors that favor drop breakup, e.g., higher shear rates, reduced dispersed-phase viscosity, etc. Most theories start with calculation of probabilities for the drops to collide, for the liquid separating them to be squeezed out, and for the new enlarged drop to survive the parallel process of drop breakup. As a result, at dynamic equilibrium, the relations between drop diameter and the independent variables can be derived.

Tokita (1977) calculated the total number of collisions per unit volume and time. The author assumed that coalescence is proportional to this number and to the number of particles. The latter was assumed to increase with mixing time, being proportional to the shearing energy, $\dot{\gamma}\sigma_{12}$, and inversely proportional to the interfacial tension coefficient, v_{12}. At equilibrium, the rates of coalescence and breakup are equal. Thus, the equilibrium drop size can be expressed as

$$d = (24/\pi)p_r v_{12}\phi_1 / [\sigma_{12}\dot{\gamma} - (4/\pi)p_r E\phi_1] \tag{7.113}$$

where p_r is the probability of collision and E is the macroscopic bulk breaking energy. In agreement with experimental findings, the relation predicts that the equilibrium drop diameter increases with concentration and the interfacial tension coefficient, but it decreases with shear stress. At the low concentration limit, $\phi_1 \leq \phi_o$, Eq. 7.113 also agrees with the conclusions of Taylor's theory, but for $\phi_{d\to0}$, it predicts an unrealistic limit, $d \to 0$.

Under steady-state flow conditions, the morphology is fully defined by the dynamic breakup and coalescence processes. However, behind is an implicit assumption that the flow conditions are strong enough to erase the initial morphology. The presence of the critical value of shear rate, $\dot{\gamma}_{cr}$, has been documented (Minale et al. 1997). The authors reported that the unique morphology was observed only above $\dot{\gamma}_{cr}$. Below this limit, multiple pseudo-steady-state structures were observed for the model PDMS/PIB system. No attempt was made to generalize this observation. In principle, the phenomenon should be related to the critical value of the capillary number, κ_{cr}, and a ratio of the polymer(s) relaxation time to

the rate of shearing. The presence of $\dot{\gamma}_{cr}$ can also be used to explain observations on morphology evolution of PDMS/PIB blends (Grizzuti and Bifulco 1997).

Following a procedure similar to that of Tokita (1977), for equilibrium drop diameter in steady simple shear flow, the following dependence was proposed (Fortelny et al. 1988, 1990):

$$d = d_T + [(v_{12}p_r\phi_1)/\eta_2 f(\kappa)] \tag{7.114}$$

where d_T is Taylor's equilibrium diameter (e.g., calculable from Eq. 7.52) and $f(\kappa)$ is a function of the capillary number and the rheological properties of the system. Equation 7.114 predicts that as $\phi_{1\to0}$, the drop diameter is determined by the Taylor breakup conditions. As the concentration increases, d becomes proportional to the expression in square bracket. The authors reported that, in the system PP/EPDM, coalescence was more intense than predicted by the dependence.

A theory for the dynamic equilibrium drop diameter also started from separate calculations of the drop breakup and coalescence during steady-state shearing. The rate of particle generation was taken to be determined by microrheology, viz., Eq. 7.52, (Huneault et al. 1995a):

$$(dN_d/dt)_{\text{break-up}} = \dot{\gamma} N_d/\kappa_{cr}t_b^* \tag{7.115}$$

Since the dispersed phase volume is constant, the number of drops, N_d, can be related to the volume fraction of the dispersed phase, ϕ, and to the drop diameter, $N_d = 6\phi V/\pi d^3$. The coalescence rate is a function of the collision probability and the dynamics of the collision process. From Eq. 7.65 coalescence rate can be written as

$$(dN_d/dt)_{\text{coalescence}} = -C\dot{\gamma} N_d\phi^{8/3}/d^2 \tag{7.116}$$

where C is a coalescence constant. At equilibrium, the diameter rate of change is zero.

From Eqs. 7.115, and 7.116, the dynamic drop diameter is

$$d_{eq} = d_{eq}^0 + \left(6C\kappa_{cr}t_b^*\phi^{8/3}\right)^{1/2} \tag{7.117}$$

where d_{eq} is the equilibrium drop diameter (at steady-state shearing), in a blend with the volume fraction of the dispersed phase, ϕ, mixed under a given set of processing conditions, while $d_{eq}^o = d_T$ is its value extrapolated to zero concentration. The only unknown in Eq. 7.117 is the coalescence constant, C. Its value can be determined from a plot of d_{eq} versus ϕ (Fig. 7.26).

Domingues et al. (2010) developed a model to predict the morphology of immiscible systems in a single screw extruder. This model considers the stretching, breakup, and coalescence phenomena. The authors followed the approach proposed

Fig. 7.26 Equilibrium drop
diameter as a function of
polyethylene volume fraction
in polystyrene matrix. The
blend was compounded for
5 min in an internal mixer at
200 °C – line is theoretical,
Eq. 7.117, the points are
experimental (Huneault
et al. 1995)
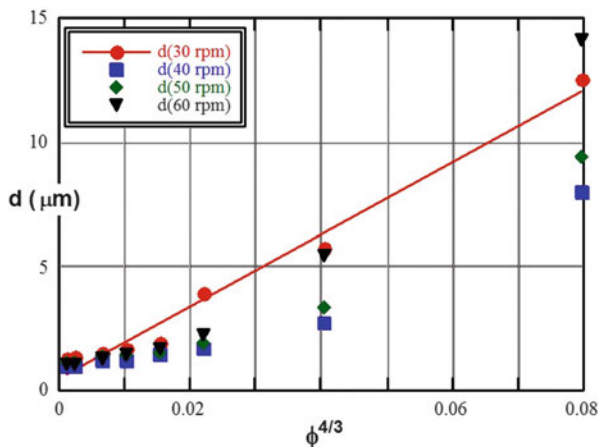
Table 7.7 Expressions for the probabilities of collision and expulsion h* and the new particle size after coalescence R* (Delamare and Vergnes 1996)

$P_{col} = \exp\left(-\frac{\pi}{8\gamma\varphi t_{loc}}\right)$	For all the cases
$P_{\exp} = \exp\left[-\frac{9}{8}\left(\frac{R}{h^*}\right)^2\kappa^2\right]$	For immobile interfaces ($\lambda \gg 1$)
$P_{\exp} = \exp\left[-\frac{\sqrt{3}}{4}\left(\frac{R}{h^*}\right)\lambda\kappa^{3/2}\right]$	For partially mobile interfaces
$P_{\exp} = \exp\left[-\frac{3}{2}Ln\left(\frac{R}{h^*}\right)\kappa\right]$	For mobile interfaces ($\lambda \ll 1$)
$h^* = \left(\frac{10^{-20}R}{8\pi v_{12}}\right)^{1/3}$	For all the cases
$R^* = R\left(\frac{2}{2-P_{Coal}}\right)^{1/3}$	For all the cases

by Chesters (1991b) and Delamare and Vergnes (1996). They assumed that coalescence occurs by collision of two identical spherical drops in a shear flow, while the polymer film between them will be excluded and flow into the main stream. Therefore, the probability of the coalescence was defined as the product of the probability for expulsing the film separating the drops (P_{exp}) and the probability of the two drops colliding (P_{col}). P_{col} increases exponentially with the local residence time (t_{loc}), the volume fraction of the dispersed phase (ϕ), and shear rate. On the other hand, the probability for expulsing the liquid film depends on the viscosity ratio determining the type of interface. As seen in Table 7.7, P_{exp} is expressed differently using h*, the critical value for the breaking of the liquid film, the viscosity ratio (λ), capillary number (κ), the droplet radius (R), and the interfacial tension (v_{12}). Finally the new particle size after coalescence, R*, was computed from volume conservation to develop a model of morphology evolution (Delamare and Vergnes 1996).

The coarsening of the phase structure due to the matrix crystallization process is an important issue to be considered. Dimzoski et al. (2013) attempted to clarify the coalescence of dispersed phase particles induced by crystallizing matrix domains

during the cooling of an immiscible polymer blend in the quiescent state. The study was carried out using PP/EPR blends for which the coalescence during annealing in the quiescent state was studied in detail (Dimzoski et al. 2011). It is known that changes in the size of the rubber particles, during the cooling of the melt mixed blend, determine the effectiveness of EPR in the toughening of the PP matrix. Therefore, the authors investigated the possible changes in blend morphology during the crystallization of PP via the rejection of the EPR domains from the spherulites growth front, which consequently could lead to collision and coalescence. They suggested that molecular forces and/or coalescence induced by the Brownian motion caused a primary coarsening of the phase structure before reaching the temperature of PP crystallization. The contribution of crystallization to coalescence of the dispersed phase particles was found to be largest at a finite rate of cooling. This was explained by the rejection energy required to exclude particle from the growing spherulite (Dimzoski et al. 2013).

7.5.3.3 Predicting Drop Size Changes During Processing

Mohr et al. (1957) analyzed the degree of mixing in a single screw extruder (SSE), using the concept of striation thickness suggested by Spencer and Wiley (1957). The amount of shear strain experienced by an element of fluid in the extruder screw channel was calculated for a number of flow paths. Decreased helix angle, increased ratio of pressure flow to drag flow, and an increased flight height were predicted to improve mixing. The ratio of the viscosities of the minor and matrix phases significantly influenced the degree of mixing.

Schrenk et al. (1963) analyzed the degree of mixing in a simple annular mixer, which might be helpful for understanding mixing in a SSE. To evaluate the mixedness of the two-component polymers, the striation thickness was measured, when the inner shaft was rotated and the outer cylinder was stationary. Near the shaft, the thickness was substantially reduced, but only slightly near the external cylinder.

Bigg and Middleman (1974) studied the transverse flow in a rectangular cavity, similar to that in an SSE. They used the Marker and Cell technique to calculate the degree of mixing, which was described by the interfacial perimeter per cavity width. As the viscosity ratio decreased, the degree of mixing was enhanced.

Chella and Ottino (1985) studied the degree of mixing in an SSE by theoretical analysis of the kinematics of mixing. They evaluated the degree of mixing as a function of the ratio of screw length to height of flight, helix angle, the ratio of pressure flow and drag flow, and the direction of the shearing plane. The stretch of the minor phase increased with axial distance. Mixing was relatively insensitive to the initial feed conditions. The results of the studies on the dependence of mixing on extruder dimensions and operating conditions were in qualitative agreement with Mohr's analysis (Mohr et al. 1957).

The initial morphology generated during the melting and mixing stages in an extruder is important in the development of the final morphology of the extrudate. Lindt and Ghosh (1992) suggested that an abrupt morphological change occurs during the simultaneous melting and striation formation in the melting zone in an SSE. Within a fraction of a second, the scale of mixing drops by several orders of

magnitude. High stress in the thin molten film in the melting zone causes a reduction of striation thickness of the minor phase. The lamellar layers may be developed when the minor component pellets melt at the interface between the melt film and the solid bed. The layers could become threads as they undergo breakup. Finally, the threads change into droplets, as they are broken.

Scott and Macosko (1991) proposed a mechanism of morphology development based on experiments carried out in a batch mixer. When the minor component pellet melts, sheets or ribbons of the dispersed phase are formed, due to dragging of the pellets on the hot surface of the mixing equipment. Next, holes are formed in the sheets or ribbons of the dispersed phase, as the interfacial instability starts, and sheet or ribbon morphology changes into a lace structure. Then, the lace breaks into irregularly shaped pieces with diameters equal to the ultimate sphere morphology.

The above two proposed mechanisms incorporate concepts involving distributive and dispersive mixing. Layer or sheet morphology development is mainly due to distributive mixing. Distributive mixing refers to the physical process of blending two fluids such that the physical separation distances are reduced to a scale where diffusion or a chemical reaction can occur (Bigio and Conner 1995). Breakup of layers into threads, laces, or spheres could be attributed to dispersive mixing which is related to instability of the minor phases.

Other studies attempted to develop a model describe morphology evolution during polymer blending in a twin screw extruder. The first model (Shi and Utracki 1992) was based on a simplified flow analysis, and the microrheological considerations of the dispersed-phase drop disintegration. The effects of coalescence were neglected. A later model comprised more refined flow analysis, two mechanisms of dispersion (the fibrillation mechanism and a drop splitting mechanism for low supercritical capillary numbers, with the choice of breakup mechanism based on locally computed microrheological criteria), as well as coalescence effects (Huneault et al. 1995a). The latter effects were taken into account by determining the coalescence constant in Eq. 7.117 from the plot shown in Fig. 7.26. Thus, this model was self-consistent, fully predictive, without any adjustable parameters. The validity of the theoretical assumptions was evaluated by comparing the two model predictions with the experimentally measured drop diameters at different axial positions in the twin screw extruder. Experimentally, after the extrusion reached steady state, the screw rotation was stopped and the molten blend was quenched within a specially designed extruder barrel. It was estimated that the PS/PE blends were quenched within 7–10 s. The second model yielded reasonable predictions of morphology evolution of non-compatibilized blends of PS in PE and of PE in PS.

Based on microrheology, it is possible to expect that (i) the drop size is influenced by the following variables: viscosity and elasticity ratios, dynamic interfacial tension coefficient, critical capillary number, composition, flow field type, and flow field intensity; (ii) in Newtonian liquid systems subjected to a simple shear field, the drop breaks most easily when the viscosity ratio falls within the

range $0.3 < \lambda < 1.5$, while drops having $\lambda \geq 3.8$ do not break under shear; (iii) droplet breakup is easier in an elongational flow field than in a shear flow field; the relative efficiency of the elongational field dramatically increases for large values of $\lambda \geq 1$; (iv) drop deformation and breakup in viscoelastic systems seems to be more difficult than that observed for Newtonian systems; (v) when the concentration of the minor phase exceeds a critical value, $\phi_d > \phi_c \approx 0.005$, the effect of coalescence must be taken into account; (vi) even when the theoretical predictions of droplet deformation and breakup are limited to infinitely dilute, monodispersed Newtonian systems, they can be successfully used for predicting the development of blend morphology during compounding in twin-screw extruders.

Other experiments were conducted in a corotating, intermeshing twin-screw extruder using the same PE/PS system as described above (Huneault et al. 1995b). The screw geometry consisted of five zones: melting, melt conveying (no pressure), mixing (kneading), pumping, and flow through a die. The specimens were scooped from three ports and quenched within a second. After dissolution of the matrix, the dispersed phase was divided into fibers and droplets, characterized separately. Immediately after melting, the dispersed phase formed into fibers and droplets, both with diameters below 10 μm. Contrary to the previous model assumptions, fibers did not break in the unfilled conveying region that followed the melting section. Instead, they were mainly destroyed in the kneading section. Fibers were present after melting even at concentrations of the dispersed phase as low as 2 wt%. The effect of increasing the concentration was not only to increase the final diameter of droplets but also to increase the fiber content. The observations indicated that coalescence was not limited to drops. However, near the die, the average drop diameter did decrease to about $d \cong 1$ μm range (as observed earlier).

Cho and Kamal (2002) derived equations for the affine deformation of the dispersed phase, using a stratified, steady, simple shear flow model. It includes the effects of viscosity ratio and volume fraction. According to the equation, for viscosity ratio > 1, the deformation of the dispersed phase increases with the increase of the dispersed phase fraction. For compatibilized PE/PA-6 blends at high RPM (i.e., 100, 150, and 200 RPM) in the Haake mixer, the particle size decreases with concentration of the dispersed phase up to 20 wt%. This occurs because the total deformation of the dispersed phase before breakup increases as the volume fraction increases, and coalescence is suppressed. The increase of the particle sizes between 20 and 30 wt% results from the increase of coalescence due to the high dispersed phase fractions. The data for 1 wt% blends suggest that mixing in the Haake mixer follows the transient deformation and breakup mechanism, and that shear flow is dominant in the mixer.

Clearly, the microrheology of polymeric systems is more complex than the classical microrheology of Newtonian, low viscosity liquids. Near the liquefaction point (either T_m or T_g) the viscosity is of the order of 10^{12} Pas, and the relaxation time is of the order of 100 s (Angell 1997). As temperature

increases along the barrel, these values decrease according to the Vogel–Tamman–Fulcher relation:

$$\eta = \eta_o \exp\{B/(T - T_o)\}$$
$$\tau = \tau_o \exp\{B/(T - T_o)\}$$
$$\text{where}: \quad T_o \approx T_g + 50 \tag{7.118}$$

The long relaxation times are responsible for nonequilibrium structures, generated by the mechanical action of the compounding equipment that is not taken into account by microrheology. The microrheological model provided good agreement with the experimental data obtained after 7–10 s quenching. However, these data were on purpose collected from the second half of the TSE barrel, where the temperature was reasonably stable (isothermal model). Evidently, evolution of blend morphology is more complex than a simple, "steady-state" model can predict. The rapid variations of morphology will be particularly important for computations of reactive compatibilization.

The evolution of morphology along the extrusion direction, in a twin screw extruder, for thermoplastic vulcanizates (TPVs) and TPV nanocomposites at high EPDM content during dynamic vulcanization was studied by Mirzadeh et al. (2013). Figure 7.27 shows that the coarse co-continuous morphology in the first mixing zone changed to droplet matrix structure, as a result of cross-linking of the rubber phase. The breakup of highly elongated threads observed in the second mixing zone led to a line of small rubber droplets in the third mixing zone. It seems that the TPV nanocomposites reach this morphological state sooner due to the faster cross-linking reaction. Morphology evolution continued by the transition of the droplets into a network made by irregular rubber particles in the second and third mixing zones. The SEM micrographs of the samples taken from the die exit showed the coexistence of a small number of rubber droplets in the vicinity of the smaller irregular rubber particles connected to each other by some rubber fibrils. The existence of irregular shape rubber particles was also observed by Shahbikian et al. using the AFM technique (Shahbikian 2010). The evolution of morphology in this case is in agreement with the conceptual mechanism of morphology evolution in thermoplastic vulcanizates proposed by Bhadane et al. (2006). They suggested that a network (namely, β-network) forms due to the viscosity mismatch between the non-cross-linked rubber (in the center of rubber domains) and cross-linked rubber (at the outer envelope of the rubber phase), during the dynamic cross-linking. Again, it is obvious that the drop size changes during processing in the case of reactive blends are also complex.

Different morphological changes during blending were reported by Sundararaj et al. (1992, 1995). Similar morphological features were observed for reactive or nonreactive blends in an extruder, internal mixer, or a miniature cup-and-rotor mixer. Initially, during melting, the polymers were stretched into sheets and ribbons, which broke into fibers, then in turn into drops. However, the two studies reported different morphologies, most likely due to differences in the concentration of the dispersed phase (5 % and 20 %, respectively).
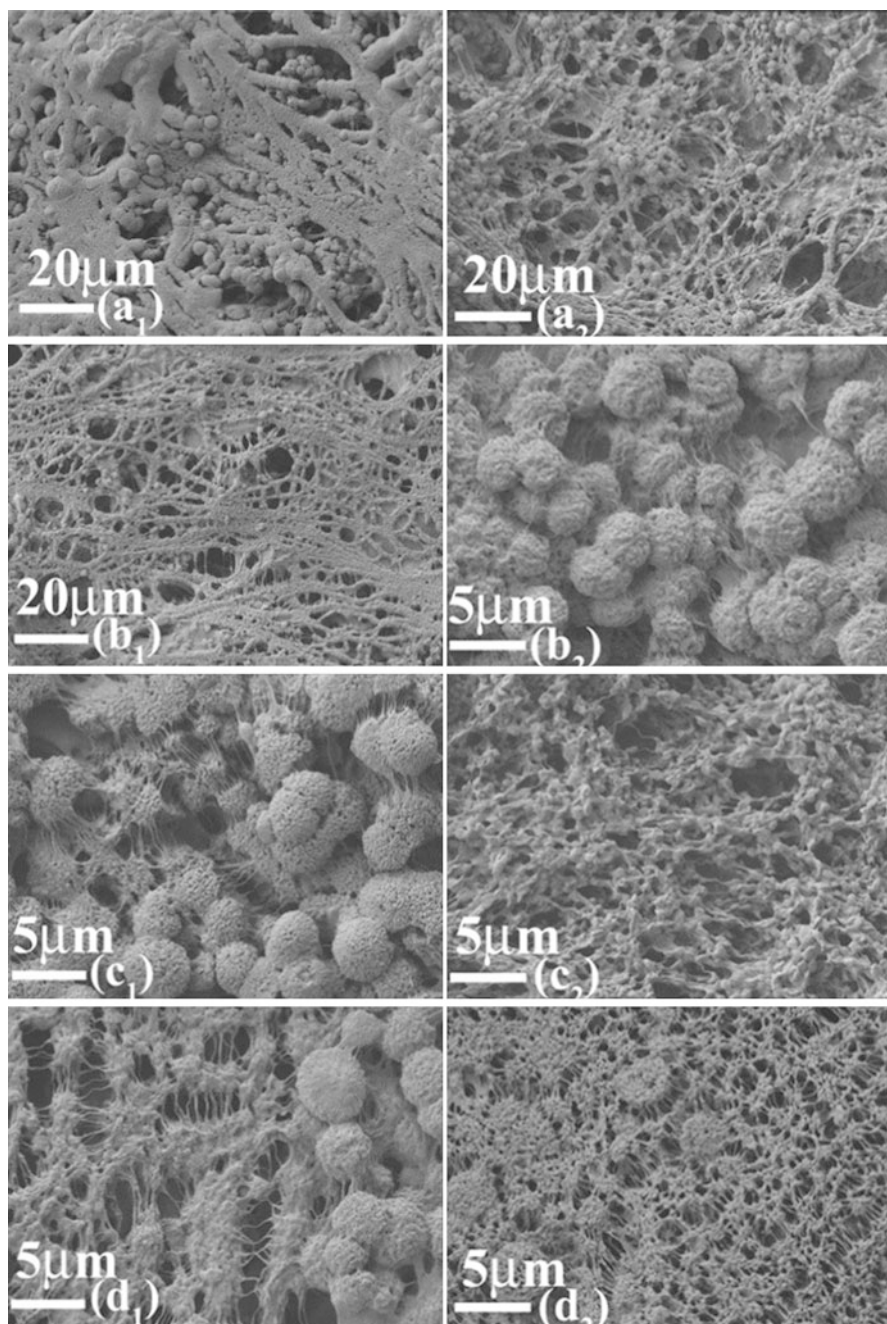
Fig. 7.27 SEM micrographs of TPV (X1; the first row) and TPV nanocomposite (*X2*:the second row) for the samples taken at the first mixing zone (**a**), the second mixing zone (**b**), the third mixing zone (**c**), and the die exit (**d**) (Mirzadeh et al. 2013)

7.5.3.4 Mixing and Blending in Extensional Flow Field

Most works on liquid mixing in the extensional flow field considered convergent flow of a Newtonian liquid from a reservoir to a capillary (Tsebrenko et al. 1974, 1976; Ablazova et al. 1975; Krasnikova et al. 1978; Han and Funatsu 1978; Chin and Han 1979, 1980; Han 1981; Han and Yu 1981; Suzaka 1982; Vinogradov et al. 1982; Utracki et al. 1986). A device capable of mixing polymeric liquids (having widely ranging viscosity ratios) in an extensional field was constructed (Nguyen and Utracki 1995). The extensional flow mixer, EFM, was designed incorporating the following principles, based on the microrheological analysis:

1. The blend must be exposed to the extensional flow fields and to semi-quiescent zones.
2. The convergences and divergences should be of progressively increasing intensity.
3. The convergent–divergent flow should be generated in the radial not axial direction.
4. To reduce the pressure drop, and to prevent blockage, slit restrictions should be used.
5. The extensional flow mixer must be adjustable.
6. The rate of flow, upstream from the plates, should be approximately constant.

In EFM, the material flows from the rim between two facing each other circular convergent–divergent plates with ridges, toward the opening in the center of the lower plate. To assess the relative merit of the extensional mixing, EFM was attached to an SSE. For comparison, the blends were also prepared in a corotating, intermeshing TSE. The same temperature profiles were used for SSE + EFM as for TSE. In all cases the dispersed phase was significantly more viscous than the matrix, $\lambda \geq 4$. The efficiency was judged considering:

1. The degree of dispersion in PS/PE blends of PS with either 5 or 10 wt% HDPE. At the exit from SSE + EFM, either fibrillar or nodular morphology was observed. The number average fiber diameter decreased with pressure across the c–d plates from $d_n = 1.2$–0.7 μm to d = 0.2–3 μm, at respectively P = 10.3 to 18.6 MPa. The blends prepared in a TSE showed much coarser morphology, containing mainly infinitely long HDPE fibers with diameter varying from d = 1 to 10 μm.
2. The results of PP impact strength improvement by incorporation of EPR are summarized in Fig. 7.28. As evident, impact strength at room temperature increased with EPR content. Clearly, SSE + EFM compounding resulted in higher impact strength (points) than that obtained from TSE (broken line).
3. The ability to homogenize resins with widely different molecular weight can be exemplified by UHMWPE/HDPE blends. Addition of high MW polymer is expected to increase G′, G″, η, and the first normal stress coefficient, Ψ_1. For the linear polymers, these parameters at low deformation rates, η_o and Ψ_{1o}, are proportional to $M_w^{3.5}$ and M_w^7, respectively. Thus, the elasticity is more sensitive to the high MW fractions. For this reason, the frequency dependence of the storage modulus ratio G′(blend)/G′(PE), at 200 °C, for HDPE and its blends with 3 wt% UHMWPE was measured. The blends prepared in TSE had the worst
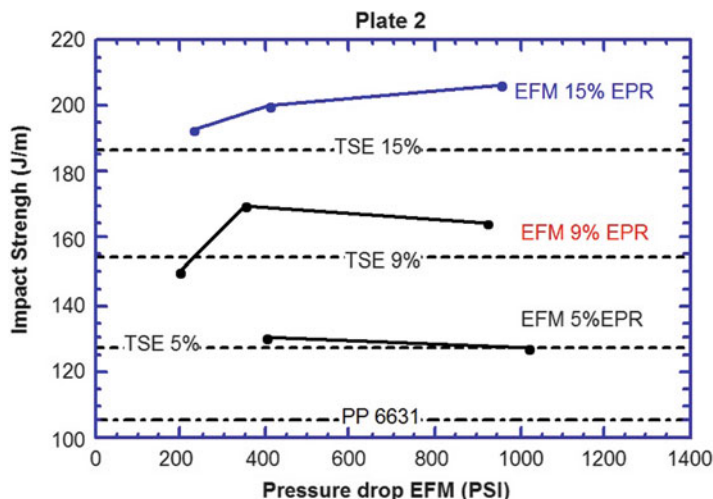
Fig. 7.28 Effect of EPR addition on PP's notched impact strength at room temperature. The specimens were prepared either in a TSE (*horizontal lines*) or in an SSE/EFM with c–d plates #2. In the latter case the results depended on the pressure drop across EFM (Utracki and Luciani 1996)

performance: G′ at ω = 0.01 rad/s increased by 90 %, while in EFM + SSE the increase was up to 210 % at P = 18.6 MPa.

4. Elimination of gel particles in the reactor powder. The gel particles can form during polymerization of EVAc or TPO. Since they may be considered very high molecular weight fractions of the same resins, SSE + EFM was used to eliminate or reduce the blemishes and improve the mechanical performance. On both counts, the performance was found at least equivalent to that obtained using a TSE.

One may calculate the pressure drop, ΔP, in EFM starting with well-known expressions (Cogswell 1972; Binding 1988; Tremblay 1989). An expression derived from Binding's theory was found to provide excellent prediction (no adjustable parameters) of the pressure across EFM.

Historically, the counterrotating TSEs were known as "calendaring" extruders, with high stresses existing between the two screws and low stresses outside this region. Owing to the high calendering pressures, the screws could rub against the barrel causing premature wear. Thus, slower speeds (up to 150 rpm) and large intermeshing gaps were recommended. One of the advantages of these counterrotating machines has been the presence of the elongational flow field within the calendering zone. The machines have been successfully used in numerous applications requiring high dispersive stresses.

The analysis of TSE performance resulted in modification of the screw profiles (higher free volume of the process), as well as in development of new mixing (or kneading) elements. The increased free volume (thus slender screw profile) resulted in lowering the average shear rate; thus the screw speeds needed to be

increased. New kneading and mixing elements have been designed to improve either the distributive or dispersive mixing. The kneading blocks (mono- and bi-lobal, to be used either in co- or counterrotating TSE, the tri- and hexa-lobal only in counterrotating TSE) were designed to maximize the extensional flow field within the lobal pools and reduce the shear field in the intermeshing and overflight regions. These designs improved mixing capabilities greatly, even for polymeric systems having large differences in the rheological flow parameters (Thiele 1995).

The influence of these complex flow fields on morphology development in blends of HDPE/PA6 (Wang 2005) and also immiscible polymer blends of PS/PMMA (Mours et al. 2003) was investigated. Droplet formation, breakup, and coalescence in these flows were studied by different microscopic techniques. The results showed that drop deformation and breakup were sensitive to both shear and extensional flow fields. However, extensional flow was more effective than shear flow in generating well-developed laminar phase. The main conclusion of these attempts points out the significant effect of the elongational flow fields on the final morphology. Therefore, it should be emphasized that the description of shear flow alone is insufficient for modeling purposes in processing machines (Mours et al. 2003).

7.5.4   Flow-Imposed Morphology

In this part, focus will be on the changes of morphology imposed by different flow fields and on the influence of variations in morphology on flow behavior. It must be evident that the degree of dispersion and the type of structure strongly relate to the type and intensity of imposed stresses during flow. Note that both concentrated suspensions and emulsions show yield stress and time-dependent flow. These macroscopic observations are related to the structural changes occurring on the microscale. Similar behavior of polymer blends is to be expected. One has to keep in mind that, during polymer processing, neither the thermodynamic miscibility, the macromolecular configuration (e.g., entanglement), nor the morphology is in an equilibrium state.

Most models of the morphological changes in polymer blends assume that an average response (e.g., an average size drop is being broken, or average size drops coalesce) provides good representation of the whole system. This assumption should be reasonably correct for blends with narrow distribution of drop sizes. However, there are reports in which (e.g., during the initial stages of blending in a twin-screw extruder) the domain sizes may differ by three orders of magnitude. Here the "average size" response may not be valid. A kinetic theory of structure development in moderately concentrated polymer blends was proposed (Patlazhan and Lindt 1996). The breakup and coalescence under steady-state shearing were considered, assuming a temporal population balance. This development provides a framework for incorporation of the elementary phenomena of drop breakup and coalescence to an overall model.

The effect of flow on miscibility of polymer blends is another area of industrial importance. There is evidence that during processing, the imposed stresses can change the critical temperature by at least 60 °C, causing miscibility inside the processing equipment. The blends, upon release of pressure, may undergo spinodal decomposition that results in superior performance (Inoue 1993).

Flow may also result in mechanochemical degradation processes that generate reactive sites, viz., radicals, peroxides, acids, etc. Furthermore, transesterification and ester–amide exchange reactions are well documented. These reactions affect the phase equilibrium as well as the regularity of the chain structure, thus dispersion in the blend and its crystallinity.

Blend morphology refers to the spatial arrangement of the blend components forming either a dispersed, a stratified (e.g., lamellar or a sandwich-type), or a co-continuous structure. Generation of morphology depends on the viscosity and elasticity ratios of the polymeric blend components (at constant stress). Both ratios vary with the type and the intensity of the flow field. While the viscosity ratio seems to control the ease of dispersing the component, thus the degree of dispersion, the elasticity ratio contributes to shaping the phases – the type of morphology. Two other pertinent parameters are the concentration and the level of interfacial interactions. To modify the interfacial energy, blends are usually compatibilized either by the addition of compatibilizer or by reactive blending. Once formed, the morphology needs to be stabilized against a possible destruction during the forming steps.

The rheological properties of a two-phase system depend not only on the rheological behavior of the components but also on the size, size distribution, and the shape of the discrete phase droplets dispersed in the continuous matrix phase. Flow affects morphology in two different ways:

- It changes the degree and type of dispersion at the local level, viz., drop breakup and coalescence.
- It causes migration of the dispersed phase, thus imposing global changes of morphology in the formed parts, viz., skin-core structures, weld lines, blush lines, etc.

In consequence, the flow-imposed morphologies can be classified as (i) dispersion (mechanical compatibilization), (ii) fibrillation, (iii) lamellae formation, (iv) coalescence, (v) interlayer slip, (vi) encapsulation, etc. These types will be discussed below under appropriate headings.

There is a reciprocal relation between morphology and flow behavior. Plochocki (1978, 1983) defined the particular rheological composition (PRC) most frequently observed in polyolefin blends. At PRC the $\eta = \eta(\phi)$ function reaches a local maximum or minimum. The existence of the maximum is related to a change of the dispersed phase, e.g., from spherical to fibrillar or from dispersed to co-continuous, while that of the minimum is related to a reciprocal change and/or to variation of the specific volume.

Table 7.8 provides a partial reference to studies on the effects of flow on the morphology of polymer blends (Lohfink 1990; Walling 1995). The dispersed phase morphology development has been mainly studied in a capillary flow. To explain the fibrillation processes, not only the viscosity ratio but also the elasticity effects and the interfacial properties have to be considered. In agreement with the microrheology of

Table 7.8 Studies of flow field effects on polymer blends morphology

Flow type	Blend	Observations	Reference
1. Theory	Viscoelastic fluids	Elastic free energy approach	Van Oene 1972
2. Shear field	PS/PE	Particle size distribution for $\lambda > 1$, coarse; $\lambda \leq 1$, fine	Starita 1972
	PMMA/PS	$0.5 < \lambda < 2.0$, composition dependent: PS – droplet breakup; PMMA – elongated droplets	Chuang and Han 1984
	LLDPE/PS	$\lambda < 1$, long PE fibers	Dreval et al. 1983a,b
		$\lambda > 1$, long PE fibers	
	PMMA/PS	Maximum aspect ratio at the transition from the Newtonian to power-law flow region	Lyngaae-Jørgensen et al. 1993
	Immiscible Blend	A transition from a droplet-dispersed structure to a network structure	Orihara et al. 2006
	PIB/PDMS	The morphology evolution and the rheological material functions in shear flow both under transient and steady-state conditions	Deyrail et al. 2007
	PIB/PDMS	Effect of silica nanoparticles	Peng et al. 2011
3. Capillary flow	HDPE/PS	$\lambda < 1$, long PE fibers	Han and Yu 1971, 1972
	PS/PP	$\lambda > 1$, long PS fibers	Han et al. 1975
	PP/EP	$\lambda < 1$, PP fibers, high shear stress dependent length	Danesi and Porter 1978
	POM/CPA	$\lambda \leq 1$, POM fibers, shear stress dependent shape	Ablazova et al. 1975
			Tsebrenko et al. 1976
			Tsebrenko 1978
	PP/PS	$\lambda < 1$, PP fibers, relaxation dependent length	Krasnikova et al. 1978
	POM/EVAc	$\lambda \leq 1$, POM films and fibers; $\lambda = 1.32$, POM microfibers; $\lambda = 4.3$, POM fibers and particles	Tsebrenko et al. 1980
	PE/PP	$\lambda > 1$, continuous fibers	Alle and Lyngaae-Jørgensen 1980; Alle et al. 1981
		$\lambda < 1$, breakup, small droplets	
	HDPE/PS	$\lambda < 0.7$, fibers; $0.7 < \lambda < 1.7$, undulant fibers & rods; $\lambda > 2.2$, undeformed droplets	Min et al. 1984
	EVAl/PP	$\lambda > 1$, EVAl fibers	Lepoutre 1989

(*continued*)

Table 7.8 (continued)

Flow type	Blend	Observations	Reference
4. Annular and slit flow	HDPE/PA-6	PA-6 platelets and lamellas permeability barrier	Subramanian 1985, 1987
5. Convergent flow	model fluids	Single drop deformation in axi-symmetric convergence/divergence	Mighri et al. 1997
	model fluids	Single drop deformation in a slit convergence/divergence	Bourry et al. 1998
	PP/PA6	The dispersed phase featured a droplet structure and a fibrous structure near the center line and wall of the channel	Wang et al. 2012
6. Flow in mixing devices	PP/PC	PC drop size depends on viscosity and λ	Favis and Chalifoux 1987, 1984
	PA-66/EPR	EP particle size depends on ν_{12}, κ, and λ	Wu 1987
	PET/EP		
	EVAl/PP	EVAl particle size dependence on concentration	Lepoutre 1989
	HDPE/PA-6	Developing laminar morphology by controlling flow fields in a single-screw extruder	Huang et al. 2005
	Cellulose Acetate Butyrate (CAB)/Polyolefin	The microfibrillar and lamellar hybrid morphologies	Wang and Sun 2006
	binary and ternary PS, PA and PE blends	Nonuniformity of the phase structure by nonuniform flow field in a mixing device	Fortelny et al. 2009
7. Flow in mixing devices With compatibilization (Interfacial tension Modification)	PA-6/PP	Maleic anhydride grafted PP (PP-MA)	Ide and Hasegawa 1974
	LDPE/PS	Surface active compounds	Heikens and Barentsen 1977
	PA-6/PE	Chemically modified dispersed phase	Chuang and Han 1984
	PA-6/PE/EVAc	Chemically modified dispersed phases	Chuang and Han 1985; Han and Chuang 1985
	LDPE/PS	Hydrogenated butadiene-b-styrene diblock copolymer (HPB-b-PS)	Fayt et al. 1981, 1982, 1986
	LLDPE/PS		
	HDPE/PS		
	PVF/PE	Poly(hydrogenated butadiene-b-methylmethacrylate)	Ouhadi et al. 1986
	LDPE/ABS		Fayt and Teyssie 1989

(*continued*)

Table 7.8 (continued)

Flow type	Blend	Observations	Reference
	PP/EVAl	PP-MA	Lepoutre 1989
	PLA/glycerol-plasticized thermoplastic starch	MA-grafted- PLA	Huneault and Li 2007
	PP/PA6	PP-MA	Barangi et al. 2008
8. Slit flow and compatibilization	HDPE/PA	Modified PA: platelet formation, permeability barrier	Subramanian 1985, 1987
	PP/EVAl	Maleic anhydride grafted PP: lamellar formation, permeability barrier	Lohfink 1990
	PP-MA/EVAl		Lohfink and Kamal 1993
	HDPE/PA-6	Methacrylic acid/isobutyl acrylate: lamellas, post extrusion calendering/elongation	Gonzalez-Nunez et al. 1993
	PP-MA/EVAl; PE-MA/PA-6	Maleic anhydride grafted PP & HDPE: lamellas for permeability barrier	Kamal et al. 1995; Garmabi and Kamal 1995
	PET/iPP	The transcrystallites fabricated through a slit extrusion hot stretching-quenching process	Li et al. 2004
9. Flows in injection molding	ABS/rubber reinforced	Delamination layer of rubber particles arranged in rows	Kato 1968
	PP/EPDM	Skin: 350 to 400 μm; thin, elongated minor phase; core: isotropic spherical inclusions	Ho and Salovey 1981
	PP/PE/EPDM		
	PA-6/EVAc	Skin: no other distinct layer; EVAc concentrated near core	D'Orazio et al. 1986, 1987
	PP/TPO	Skin: major deformation; core: dispersed spherical drops	Karger-Kocsis 1987
	POM – rubberized tough	Skin: semicrystalline and rubber sheets; core: rod shaped rubber particles aligned in flow direction	Percorine et al. 1990
	PA-6/PE	Maximum anisotropy at intermediate position near the mold wall	Ghiam and White 1991
	PP/EPDM	Maximum particle deformation 100 μm under surface	Michaeli et al. 1993

Table 7.8 (continued)

Flow type	Blend	Observations	Reference
	PP/EVAl	Skin: small rectangular platelets; shear zone: lamellar morphology	Walling 1995
		core: undeformed EVAl particles	
	PC/ABS	Effects of polycarbonate oligomer on morphological and mechanical properties of the weldline in injection molded blend	Uemura et al. 2008
	PC/ABS	The importance of the shear stress and solidification time of the resin in determining the final morphology	O-Charoen et al. 2008

Newtonian systems, an upper bound for the viscosity ratio, λ, has also been reported for polymer blends – above certain value of λ (which could be significantly larger than the Newtonian value of 3.8) the dispersed phase could not be deformed. By contrast, lower bounds of λ were not established for polymer blends.

Incorporation of compatibilizers (a third phase) into immiscible blends improves the adhesion between blend phases and helps to achieve mechanical properties comparable to those of homopolymers. The formation of lamellar structures with specifically designed arrangement of the dispersed phase in the matrix phase could provide barrier properties comparable to those achieved in multilayer parts.

7.5.4.1 Dispersion

Microrheology can provide information regarding the temporal evolution of the drop diameter, d, under steady-state shearing, in the absence of coalescence. Assume that drops breakup occurs only if the shearing time at each appropriate shear stress exceeds the required time to break, $t > t_b$ (for shearing times $t < t_b$ the average drop remains unchanged). Then, Eq. 7.115 yields the following expression for the relative change of drop diameter as

$$
\begin{aligned}
&\ln(d_o/d) = \dot{\gamma}\,(t - t_b)/3\kappa_{cr}t_b^* = [(\gamma/\gamma_b) - 1]/3 \\
&\text{since}: \quad \gamma_b \cong 2 \quad \rightarrow \quad \therefore d = d_o\exp\{(1 - \gamma/2)/3\}
\end{aligned}
\tag{7.119}
$$

Since derivation of this relation considered only the drop-splitting mechanism and neglected coalescence, its validity may be limited to small capillary numbers, $\kappa^* = 1\text{–}2$, and low concentrations.

The drop diameter usually decreases with an increase of shear rate (see Fig. 7.29). However, microrheology indicates that there are different mechanisms operating in different flow types (e.g., shear and elongation) or at different field intensity. Furthermore, there is usually a difference in the quench time between the outer layer and the core of specimen. The data in Fig. 7.29 were obtained using capillary flow. The morphology was affected by the extensional flow field upstream

Fig. 7.29 Reduced drop diameter versus rate of shear at 250 °C. The blend comprising 10 wt% PA-6 in HDPE was extruded through a capillary with the L/D = 40 (Utracki et al. 1986)
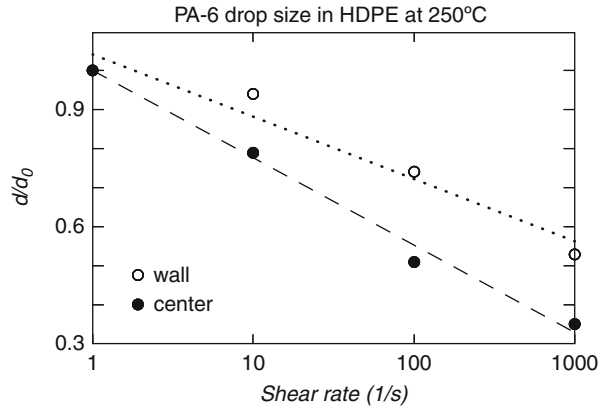
from the die, shear flow (and flow-induced encapsulation) inside the die, and slower cooling in the center than at the core of the extrudate. After such complex morphological changes, empirically the drop diameter decreases with logarithm of the deformation rate, $d/d_o = 1 - a_o \ln \dot{\gamma}$, where $a_o \cong 0.3$–0.6 is a material parameter.

Huang et al. (2008) simulated the effect of three different screw geometries on morphology development of an immiscible polymer blend based on polypropylene/polyamide-6 (PP/PA 6). Samples collected from four different points along the extruder using a specially designed sampling device during blending by conventional screw elements, a fluted mixing element, and also by pineapple mixing element. Morphology evolution was evaluated using scanning electron microscopy, and it was interpreted considering the flow fields occurring along screw elements. The coarsest and most nonuniform morphology at the exit of the extruder was produced with the screw with conventional screw elements, whereas the finest and most uniform morphology was produced using the screw with a fluted mixing element. The chaotic mixing characteristic of the pineapple mixing element produced thin laminar layers of dispersed phase (Huang et al. 2008).

7.5.4.2 Fibrillation

The mechanism responsible for formation of fibers or fibrils is extensional, e.g., at the entrance to a capillary. Once inside the capillary, the blend undergoes shear flow, with intensity dependent on the radial position. The evolution of morphology of PMMA blends with core-shell elastomeric latex particles, poly(butylacrylate-*co*-styrene) was studied (Bousmina and Muller 1996). It was found that, within the plug flow region, the particles were randomly distributed, but in the outer part of the extrudate the particles were aligned into straight pearl strings. Had coalescence been possible, these would form fibers. The authors proposed a mechanism for string formation within the steady-state shear zone of the flow field. It is possible to postulate that there are at least two possible fibrillation mechanisms: the extensional flow at the entrance to capillary and the "stringing" process described by Bousmina and Muller.

Fig. 7.30 Stress-dependent values of the orthogonal axis of deformed polypropylene drops in shear at 250 °C. The blend comprised PP/PA-6 = 1:5, with and without an acrylic compatibilizer, AA (Søndergaard et al. 1992)
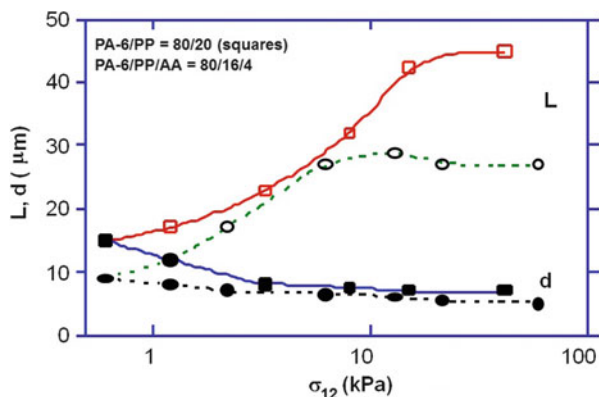
Stress-induced fibrillation occurs under steady-state shearing or elongation when $\kappa > 2$. Under these conditions, the dispersed phase is co-deformational with the matrix. Since the capillary parameter is proportional to diameter (viz., Eq. 7.52), it is easier to fibrillate coarser dispersions at concentrations exceeding a limited value: $\phi_{\text{limit}} \approx a\lambda^b$, where the numerical values of a, b depend on the blend (Krasnikova et al. 1984).

Fibrillation is also affected by the presence of a compatibilizer. From the perspective of the capillary parameter, κ, addition of a surface tension modifier has two effects: it lowers the interfacial tension coefficient (thus increasing κ) and decreasing the initial drop diameter (thus increasing κ) – the net result is difficult to predict. An illustration is provided in Fig. 7.30. Here PP drops in PA-6 matrix were observed during shearing in a cone-and-plate geometry, without and with an acrylic compatibilizer, AA. For both systems, the dimensions (long and short axes of a prolate ellipsoid) were approached a plateau at shear stress $\sigma_{12} \geq 10$ kPa. Evidently, the plateau value of the long axis, $a_1 = L$, was higher for the system without AA than that with it. However, the rate of elongation indicates that AA facilitated the fibrillation process (Søndergaard et al. 1992).

Tsebrenko et al. (1976) reported on fibrillation of POM in a copolyamide (CPA) matrix as a result of flow through a capillary. Fine fibrils with diameters of about 20 μm and length 3.2 mm were obtained during extrusion at $T = T_m(\text{POM}) + 6$ °C. The low extrusion temperature facilitated stress-induced crystallization of the POM fibers, preserving the morphology engendered at the entrance to the spinneret.

As evident from data in Table 7.9, fibrillation of POM in poly(ethylene-*co*-vinyl acetate), PEVAc, strongly depended on the viscosity ratio, λ (Tsebrenko et al. 1982). These data also indicate that for low-viscosity dispersed phase, the coalescence that results in formation of plate-like objects complicates the blend morphology. Furthermore, since the diameter of the fibrils remains virtually constant, low-viscosity ratios result in short fibers. On the other hand, for $\lambda \geq 1.7$, the diameter drops again and platelets were detected. In short, for the best results $\lambda \cong 1$ is preferred.

Table 7.9 Effect of viscosity ratio on fibrillation of POM in POM/PEVAc = 20/80 (Tsebrenko et al. 1982)

| λ = ηd/η_m | d ± σ (μm) | Number of fibrils | POM dispersion form (wt%) | | |
			drops	Fibers	plates
0.35	5.3 ± 2.5	61,500	0	83	17
0.91	4.2 ± 1.8	13,200	0	100	0
1.05	5.5 ± 3.6	6,800	0	100	0
1.70	6.2 ± 3.6	4,300	0	80	20
4.10	7.3 ± 5.8	4,400	48	50	2

Polymer blends were prepared comprising a poly(etheresteramide) block copolymer, PEBA, with liquid crystalline copolymers, LCP (Champagne et al. 1996). The minor component was deformed into fibrillar-type morphology that enhanced the mechanical properties in the draw direction, in a manner comparable to unidirectional continuous-fiber reinforced composites. Films prepared using a single screw extruder were melt drawn on calendering rolls. The storage modulus of blends containing 30 wt% LCP increased with draw ratio, DR ≤ 12, nearly 50-fold in comparison to neat PEBA (from 18 MPa to almost 1 GPa). The blend morphology was characterized by dissolving the PEBA matrix, followed by gravimetric and microscopic analysis of the LCP phase. As expected, the average fiber diameter decreased as a function of $DR^{-0.5}$. It was noted that only relatively large drops were deformed into fibers, leaving nearly 50 % of LCP in the form of small dispersed nodules. The fiber content as a function of DR followed a trend parallel to that of the mechanical properties. Longitudinal and transverse moduli followed the Halpin-Tsai predictions for unidirectional fiber composites. Properties of compression-molded specimens prepared from these blends compared favorably with glass fiber composites.

Drop deformation in shear that leads to fibrillation was examined using microscopy, light scattering, and fluorescence (Kim et al. 1997). They selected systems near the critical conditions of miscibility, thus where the flow affects miscibility and reduces the value of ν_{12}. The drop aspect ratio, p, plotted as a function of the capillary number, κ, showed two distinct regimes. For $\kappa < \kappa_{cr}$, p was directly proportional to κ, whereas for $\kappa > \kappa_{cr}$, p followed more complex behavior, with an asymptote that corresponds to flow-induced homogenization.

7.5.4.3 Lamellar Morphology

Lamellar morphology occurs in flow regimes where the dispersed phase undergoes two dimensional stretching with the formation of multilayers. In immiscible blends, such a structure may enhance barrier properties when the dispersed phase is a barrier material (e.g., PA, EVAl) and the matrix phase is a commodity polymer (e.g., PE, PP, etc.). Well-developed lamellas increase the length of the pathway for permeants diffusing through the blend. The longer path causes a lowering of the concentration gradient across the blend material, thus reducing the mass flux or permeability.

Subramanian (1985, 1987) was the first to develop a method for generating lamellar morphologies in polymer blends during melt processing. The method has been used to impart permeability barriers to low-cost polyolefins, PO, using small amounts of a barrier polymer. For example, blending under controlled conditions HDPE and a modified polyamide, either PA-6 or PA-66, led to compositions that during the subsequent blow molding or film blowing, generated lamellar PA dispersions. In particular, the lamellar morphology blends of PE and PA-6 were produced in a blow-molding machine. The product exhibited good barrier properties. The optimum performance was obtained using 18 wt% PA. The work resulted in commercialization of the *Selar*™ technology.

PP/EVAl blends with lamellar morphology were produced either in a single screw extruder with a specially designed die (Lohfink and Kamal 1993), using the injection molding machine (Walling 1995; Walling and Kamal 1996), or in an extruder with an annular blown film die (Lee and Kim 1997). To produce PP/EVAl sheets with lamellar morphology, Lohfink and Kamal (1993) designed and constructed a biaxially stretching slit die, which had converging and diverging sections to achieve the desirable extensional flow. In the PP matrix, EVAl lamellae were formed in the sheet core. The optimum barrier performance for oxygen transmission was obtained using 25 wt% EVAl. The barrier properties of the blends were superior to those obtained later in the blow molding process (Walling and Kamal 1996). During the injection molding of PP/EVAl blends, a complex morphology was obtained. In the core region, small relatively undeformed EVAl particles were found. By contrast, in the high shear zone near the skin, lamellas were present. Formation of the lamellar structure was enhanced by increasing EVAl concentration, compatibilization, and reduced mold thickness (Walling 1995; Walling and Kamal 1996).

The study by Kamal et al. (1995) showed that it is possible to control the flow-induced morphology to generate discontinuous overlapping platelets of PA-6 or EVOH dispersed phase in a polyolefin matrix phase. They considered the effects of feeding order, melt temperature, composition, compatibilizer level, die design, screw type, and cooling conditions. The results confirmed that screw type and processing conditions are key factors in developing a laminar morphology. For example, the combination of metering screw, 1.0 mm die exit gap, and 270 °C die temperature results in a laminar morphology. However, a mixing screw, 0.5 mm die exit gap, and 250 °C die temperature lead only to an alignment of the PA-6 domains in the flow direction without well-developed laminar morphology. For the optimized case, the toluene permeability of extruded ribbons of HDPE/PA-6 blends was found to be in the range of values obtained only with multilayer systems (Kamal et al. 1995).

In another attempt, the effects of processing conditions, such as different screw speeds, screw geometries, metering and mixing screws, on the morphology of the extruded ribbons of HDPE/PA-6 blends prepared by single screw extruder equipped with a convergent die were studied by Huang et al. (2005). The results showed that, in contrast to previous studies, even with a viscosity ratio larger than one, a laminar morphology with an aspect ratio of about 100 could be generated by appropriate combination of the screw type and shear intensity. Also, the formation of

well-developed laminar PA-6 phase is more effective using an extensional flow field rather than shear flow (Huang et al. 2005).

Morphology of blends is strongly influenced by the mixing mechanism. Well-developed lamellar morphology is produced when deformation of the minor phase is high, and its breakup is minimized. Coalescence of the deformed minor phase could also contribute to lamellar morphology (Lohfink and Kamal 1993). Thus, from the microrheological point of view, the best results are to be expected from systems where (1) the domain size of the dispersed phase is relatively homogeneous, with d $\cong$ 50 μm; (2) the viscosity of the dispersed phase is lower than that of the matrix, i.e., $\lambda < 1$ (which is not in agreement with the work done by Huang et al. (2005)); (3) the dispersed phase shows a strain hardening behavior. Breakup of the minor phase has been discussed in detail in the former sections.

Kinematics of Mixing

Spencer and Wiley (1957) found that the deformation of an interface, subject to large unidirectional shear, is proportional to the imposed shear and that the proportionality factor depends on the orientation of the surface prior to deformation. Erwin (1978) developed an expression, which described the stretch of area under deformation. The stretch ratio (i.e., deformed area to initial area) is a function of the principal values of the strain tensor and the orientation of the fluid. Deformation of a plane in a fluid is a transient phenomenon. So, the Eulerian frame of deformation that is traditionally used in fluid mechanical analysis is not suitable for the general analysis of deformation of a plane, and a local Lagrangian frame is more convenient (Chella 1994).

A general equation for the kinematics of distributive mixing was developed in a Lagrangian frame. The degree of mixing was described in terms of inter-material area density, or striation thickness, which could be obtained experimentally. Using an ideal laminar mixing model, the thickness of an individual particle of the minor phase was expressed as $\delta_d = 2\phi_1/a_v$, where ϕ_1 is the volume fraction of the minor phase and a_v is the interfacial area density (Ottino et al. 1981). As a result of deformation, the lamellar thickness and the interfacial area density change with the local strain, γ_l, viz., $\delta_d = \delta_d^o/\gamma_l$; $a_v = a_v^o \gamma_l$, where the symbols with upperscript "o" indicate the initial conditions. For simple shear flow deformation, when the deforming interface has the same direction as the flow, the local area strain is related to the linear strain of the flow field, $\gamma = t\dot{\gamma}$:

$$\delta_d = \delta_d^o \left[1 + (t\dot{\gamma})^2 \right]^{-1/2} \tag{7.120}$$

The above equation could be used for the interpretation of lamellar morphology development, when breakup of the minor phase is excluded, and the interfacial tension coefficient is vanishingly small.

Parameters Determining Lamellar Morphology Development

Distributive lamellar mixing depends on the deformation rate, deformation time, and the initial direction of the interface. The degree of mixing increases as the

deformation rate and time increase. The initial direction of the interface, favorable for maximum mixing, is also needed for achieving a high degree of mixing (Ottino et al. 1981).

Lohfink and Kamal (1993) observed that, in single screw extrusion through a flat die, an increase of die gap size yielded fewer, but thicker layers. On the other hand, a smaller die gap size resulted in an increased number of stacked thin layers. Higher screw rpm produced a more pronounced lamellar structure. In real mixing equipment, such as an SSE, deformation time (residence time) could be limited by the deformation rate (screw speed). Lee and Kim (1997) reported that an increase in screw speed reduced the degree of mixing, because the residence time decreased and the minor phase melting was insufficient.

The viscosity ratio, λ, is one of the major parameters in determining the deformation of the minor phase layer. When the viscosity ratio varies from zero to infinity, Taylor's Eq. 7.49 predicts that deformability of a small drop would change from 1.0λ to 1.18λ. For viscoelastic systems, Gonzalez-Nunez et al. (1993) and Lee and Kim (1997) obtained higher deformation for lower viscosity ratio, when they changed the viscosity ratio by changing the viscosity of matrix material.

Lamellar morphology development also depends on the volume fraction of the minor phase. The individual thickness of EVAl phase in PP matrix phase decreased when the concentration of EVAl phase decreased from 30 to 20 vol% (Kamal et al. 1995). In the experiment, for the processing conditions the viscosity ratio was $\lambda > 1$.

The minor phase layers become thinner as interfacial tension coefficient, v_{12}, decreases (Kamal et al. 1995; Lee and Kim 1997). This confirms that the decrease of v_{12} results in a more efficient transfer of stress from the matrix to the minor phase layer (Gopalakrishnan et al. 1995). As the v_{12} is reduced further, the layers of minor phase transform into fibers (Kamal et al. 1995). These results are in agreement with the morphology development mechanisms (Ottino et al. 1981; Lindt and Ghosh 1992; Scott and Macosko 1991).

7.5.4.4 Coalescence

Droplet–droplet coalescence was already discussed in Part 9.4.2.2. Here, the effects of coalescence on morphology will be summarized. Under normal circumstances, there is a dynamic equilibrium between coalescence and dispersion processes; thus it is difficult to assign a particular effect as due to coalescence. However, during flow at temperatures near the melting point, the effects of coalescence dominate the final morphology. For example, blends of HDPE with up to 30 wt% of PA-6 were extruded using a capillary viscometer at T = 150, 200 and 250 °C. All the extrudates contained PA-6 fibrils, independently at T below or above the melting point of PA-6, $T_m = 219$ °C (Utracki et al. 1986). Judging by the diameter of the resulting PA-6 domains and their internal structure, the fibrillation originated mainly from the flow-induced coalescence.

For capillary flow at 150 °C, the extensional stress, $\sigma_{11} = 50$–800 kPa, at the entrance to capillary was calculated from (Cogswell 1972)

$$\eta/\eta_E = 2\tan^{-2}\alpha; \quad \alpha = \arctan(2\dot{\varepsilon}/\dot{\gamma});$$
$$\sigma_{12}\dot{\gamma} = 2\sigma_{12}\dot{\varepsilon} \tag{7.121}$$

Since the tensile yield stress for "solid" PA-6 at 150 °C was determined as $\sigma_y = 15$ kPa, independent of the rate of straining, the extensional stress in the capillary entrance was more than sufficient to deform the amorphous part of PA-6. Owing to crystallization, the elongated structures, once created, could neither disintegrate nor elastically retract to spherical shapes.

Similarly, at $T > T_m$, coalescence of semicrystalline dispersed domains combined with stress-induced crystallization leads to formation of long fibers. This effect was explored for the improvement of performance of blends comprising liquid crystal polymers, LCP (La Mantia 1993).

Velankar et al. (2001) conducted shear-induced coalescence experiments on immiscible polymer blends with a droplet–matrix morphology. The study was carried out on model blends of polyisobutylene (PIB) and polydimethylsiloxane (PDMS), with various amounts of a PIB–PDMS diblock copolymer as a compatibilizer. This kind of compatibilizer promotes intimate mixing of thermodynamically immiscible homopolymers through their effect on the interfacial tension between them. The authors determined the mean capillary number of the droplets using dynamic mechanical measurements. The results showed that increasing the amount of a surface-active compatibilizer increased the steady shear capillary number of droplets to values well above the Ca_{cr} required for breakup of uncompatibilized droplets. This suggests that a simple decrease in interfacial tension is not the only effect of adding the compatibilizer to these immiscible blends. The hydrodynamic stress required for breakup of uncompatibilized blends, based on interfacial tension arguments, is lower than that required for breaking compatibilized droplets. Previous simulations by Stone and Leal (1990) and Li and Pozrikidis (1997) indicated the flow-induced gradients in the concentration of the compatibilizer on the droplet surface. Therefore, Valenkar et al. explained their results by assuming the existence of gradients in interfacial tension induced by the gradients of compatibilizer concentration due to flow. Microscopy experiments were in agreement with this interpretation (Velankar et al. 2001).

7.5.4.5 Interlayer Slip

The interlayer slip originates in the low entanglement density region at the interface (Helfand and Tagami 1971, 1972). There is a preponderance of chain ends and the low molecular weight species in the interphase. This leads to the low viscosity – in binary PS/PMMA blends, the interphase viscosity was determined as $\eta_{Interph} \approx 90$ Pas, hence three orders of magnitude smaller than viscosities of the two comprised polymers (Valenza et al. 1991). The net result of the interlayer slip is a drastic reduction of viscosity for mixtures of two immiscible liquids. The phenomenon, first observed for mixtures of low molecular weight liquids, was empirically described, using the fluidity additivity equation. The latter dependence was first derived by Bingham (1922):

Fig. 7.31 Concentration dependence of shear viscosity of PP/LCP blends; dotted line represents the fluidity equation, Eq. 7.122 (Data from Ye et al. 1991)
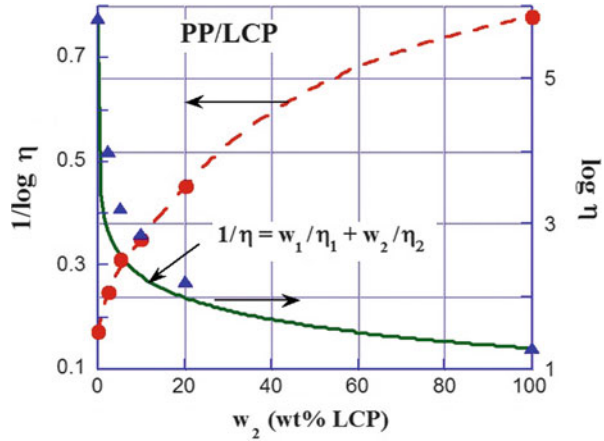
$$1/\eta = (w_1/\eta_1) + (w_2/\eta_2)$$
$$\text{or general,} \quad 1/\eta = \sum_{1=1}^{n} w_i/\eta_i \tag{7.122}$$

where w_i and η_i are the volume or weight fraction and the viscosity of the component i, respectively (see Fig.. 7.31).

The dependence was re-derived later for a telescopic flow of two polymers through a pipe (Heitmiller et al. 1964). The two liquids formed a large number of concentric layers, each of the same cross-sectional areas. The fundamental condition that leads to the fluidity additivity relation was the continuity of the shear stress across the multi-stratified structure. Lin (1979) followed this derivation with an additional assumption that the shear stress of each layer can be modified by the presence of an additional frictional stress, $Z = (\beta - 1)(R\Delta P/2L)$, where R is the capillary radius, ΔP is the pressure drop, and β is a characteristic material parameter (interlayer slip factor) in

$$1/\eta = \beta[(w_1/\eta_1) + (w_2/\eta_2)] \tag{7.123}$$

For a mixture of two liquids having the same viscosity, $\eta_1 = \eta_2$, Eq. 7.122 predicts additivity, while Eq. 7.123 with $\beta > 0$ predicts a negative deviation form additivity (NDB). For $\beta = 1$ Bingham's relation is recovered. However, there are serious reservations about the fundamental consequences of the frictional extra stress Z (Bousmina et al. 1999). In a rigorous derivation for a telescopic flow with the interfacial slip, the following dependence was obtained:

Table 7.10 Calculated viscosity of the interphase

Blend (1/2)	η_1 (Pas)	η_2 (Pas)	$\eta_{Interphase}$ (Pas)	Reference
POM/CPA	349	583	0.69	Bousmina et al. 1999
PP/PS	214	693	1.64	Bousmina et al. 1999
PE/PS	4000	582	25.22	Bousmina et al. 1999
PS/PMMA	1172	4610	13.31	Bousmina et al. 1999
PS/PMMA	3400	15500	90.00	Valenza et al. 1991

$$1/\eta = (w_1/\eta_1) + (w_2/\eta_2) + \theta\sqrt{\phi_1\phi_2}$$
$$\text{where}: \quad \theta \propto 1/\Delta l\eta_{Interphase} \tag{7.124}$$

Equations 7.123 and 7.124 predict a negative deviation from the log-additivity rule.

The material parameter θ in Eq. 7.124 governs the NDB behavior. It was shown that its value is inversely proportional to the thickness of the interphase, Δl, and its viscosity, $\eta_{Interphase}$ (Bousmina et al. 1999). Theoretically, the same molecular mechanism should be responsible for both factors, viz., better miscibility, better interdiffusion, thus higher Δl and $\eta_{Interphase}$. However, the low molecular weight components of the blend, that are forced by the thermodynamics to diffuse to the interphase, may not change much the former parameter, but drastically reduce the latter. For immiscible blends, Δl is small, typically 2–6 nm. Thus θ is large, and interlayer slip takes place. For compatibilized blends, the macromolecules of the two phases interact and interlace, which increases both factors; thus, the slip effects are negligible. Measured or calculated values of the interphase viscosity are listed in Table 7.10.

Interlayer slip creates a tree-ring structure in extrusion, e.g., observed in samples containing 30 wt% PA-6 in HDPE matrix, extruded at T = 250 °C. The HDPE/PA-6 capillary viscosities at 250 °C followed Lin's Eq. 7.123 (Utracki et al. 1986). The simplest fluidity equation, Eq. 7.122, may be useful in describing steady-state viscosity of antagonistically immiscible polymer blends, such as PP/LCP shown in Fig. 7.31. When the volume of the interphase is known, the general form of the Bingham formula in Eq. 7.122 can be used to calculate the interphase viscosity. This indeed has been done, in the case of shear flow of a multilayer PS/PMMA sandwich (Lyngaae-Jørgensen et al. 1988).

Yang et al. (2003) investigated the rheological behavior of PBT/LLDPE and PBT/LLDPE-*g*-acrylic acid, using a capillary rheometer. They used an equation proposed by Utracki (1991) successfully to depict the viscosity–composition dependence of the blends at low shear stresses. Morphological studies showed a droplet–matrix morphology at low shear rates. On the other hand, at high shear rates, the droplet–matrix morphology at the center of the extruded bar was observed in vicinity of a stratified PBT phase (co-continuous morphology) which contributed to lowering the viscosity of the blending system. This also caused the above equation to fail to predict the rheological behavior of these two systems. It was

concluded that the parameter β (interlayer slip factor) in the equation (see Eqs. 7.123 and 7.125) was related not only to the shear stress but also to the elasticity difference of the two components of the blend, the composition, and the interactions of the blend components at high shear stresses (Yang et al. 2003).

7.5.4.6 Encapsulation

Shear-induced segregation of polymer domains is related to differences in the magnitudes of the rheological properties of blend components. During large strain flow, segregation takes place not only in immiscible blends, in which the viscosities and elasticity of the two phases differ, but also in miscible blends comprising components of different MW. In the latter case, it is the difference in chain lengths that causes an imbalance of stresses and relative motion of the components (Doi and Onuki 1992).

Migration of the low viscosity component toward the high stress regions results in flow encapsulation of one phase by another. The effect has been well documented and successfully explored in polymer processing. For example, this mechanism is responsible for the lubricated, high-throughput flow of POs upon addition of either fluoro- or siloxane polymers. Similarly, enhancement of flow of engineering and specialty resins by incorporation of low viscosity (when molten) LCP is attributed to flow segregation (Utracki 1987, 1988, 1989).

7.5.5   Shear Flows

The easiest way to discuss flow of polymer blends is to compare them to simpler, low molecular weight homologues, viz., Sect. 7.3. For immiscible blends, the best model is that of emulsions. Like blends, emulsions comprise one liquid dispersed in another. The emulsion morphology is stabilized by addition of a surfactant or an emulsifier, similarly as immiscible blend is stabilized by addition of a compatibilizer. Both systems, emulsions and blends, show phase inversion, viz., Sect. 7.3.2. In emulsions, the phase inversion concentration, ϕ_{I1}, depends mainly on the type and concentration of emulsifier, while in blends it is dominated by relative rheological properties of the two polymers. In emulsion technology, by carefully selecting surfactants and the sequence of liquid addition, it is possible to generate (at the same concentration) two emulsions having different morphologies, viscosities, and other properties (Utracki 1989).

7.5.5.1 Concentration Dependence of Viscosity

In miscible blends, where the free energy of mixing is negative, $\Delta G_m < 0$, experimental data indicate that, in most system, either the log-additivity rule (see Eq. 7.18) or small positive deviations from it are generally observed. Near the phase separation region, where $\Delta G_m \approx 0$, the rheological response is complex as the free energy of mixing is precariously balanced by the term describing the energy input by the flow. Finally, in immiscible systems, where $\Delta G_m > 0$, five different types of behavior have been identified. In Fig. 7.32, curves
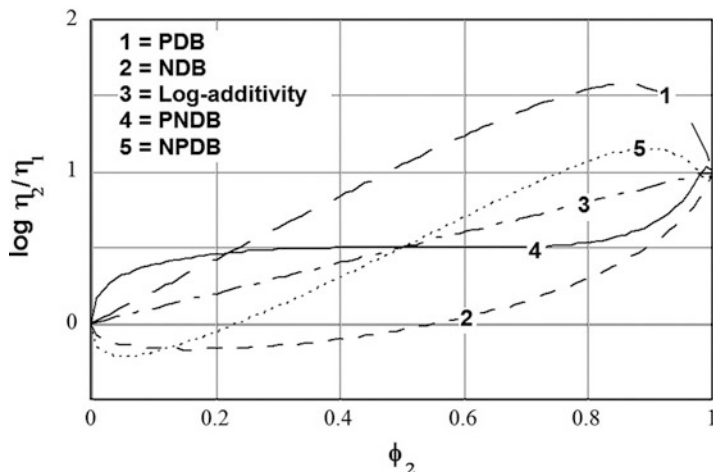
Fig. 7.32 Five types of the relation between shear viscosity and concentration for immiscible polymer blends: *1*. PDB, *2*. NDB, *3*. additivity, *4*. PNDB, and *5*. NPDB (Utracki 1991)

1–5 represent, respectively, (i)) positively deviating blend (PDB), (ii) negatively deviating blends (NDB), (iii) log-additivity, (iv) PNDB, and (v) NPDB (Utracki 1991). To understand the origins of these types of behavior, it is necessary first to evaluate morphology and flow-imposed morphology in polymer blends.

From the discussion of phase inversion in Sect. 7.1.2, the emulsion model predicts that immiscible blends should show positive deviation, PDB, from the log-additivity rule: $\ln \eta = \sum w_i \ln \eta_i$. However, while PDB has been found in about 60 % of such blends, the remaining four types (see Fig. 7.32) must also be accounted for. This means that at least one other mechanism must be considered when modeling the viscosity–concentration dependence of polymer blends. This second mechanism should lead to the opposite effect, which is to the negative deviation from the log-additivity rule, NDB.

The simplest mechanism that explains the NDB behavior is interlayer slip, which leads to derivation of Eq. 7.123 and Eq. 7.124. One may postulate that at constant stress, the net η versus ϕ dependence can be written as a sum of two contributions: the interlayer slip, expressed by η_Λ (calculated from either Eq. 7.123 or Eq. 7.124), and the emulsion-like viscosity enhancement given by an excess term, $\Delta \log \eta^E$ (Utracki 1991):

$$\ln \eta = \ln \eta_L + \Delta \ln \eta^E$$
$$\Delta \ln \eta^E = \eta_{\max} \left\{ 1 - \left[(\phi_1 - \phi_{1I})^2 / \left(\phi_1 \phi_{2I}^2 + \phi_2 \phi_{1I}^2 \right) \right] \right\} \tag{7.125}$$

As mentioned in Sect. 7.1 for polymer blends, the relation between the steady-state shear viscosity and concentration can be quite complex. In the following discussion, the *constant stress* (not the constant rate) *viscosity*, corrected for the

Fig. 7.33 Concentration
dependence of blend viscosity
at five levels of shear stress
(from top: $\sigma_{12} = 10^1$ to 10^5),
indicating a gradual change of
dominant flow mechanism
from emulsion-type to
interlayer slip
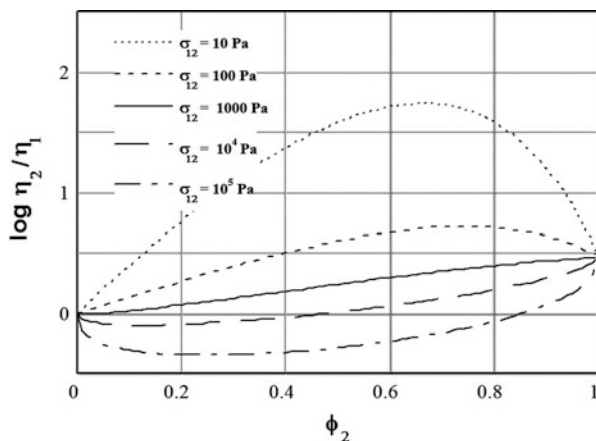
Fig. 7.34 Concentration
dependence of blend viscosity
for polymer-1/polymer-2
blends; three different
molecular weight grades of
polymer-2 were used. For the
lowest molecular weight
PDB, whereas for the highest
NDB behavior is to be
expected
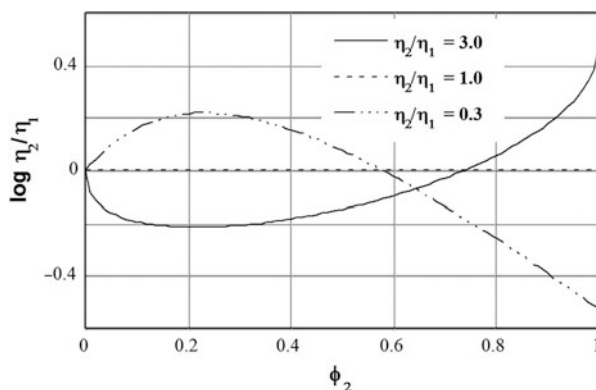
yield and time effects, will be considered. To illustrate flexibility of Eq. 7.125 to
describe (and thus to facilitate interpretation of the rheological results) η versus ϕ,
dependence examples of computations are shown in Figures 7.33, 7.34, 7.35, 7.36,
7.37, 7.38, 7.39, and 7.40.

The numerical values of the phase inversion concentration, ϕ_{2I}, as well as the
two material parameters that enter Eq. 7.125 are listed in Table 7.11.

7.5.5.2 Dynamic Flow

Blend structure changes with flow conditions. Therefore, the observed rheological
responses must be sensitive to method of measurement. Since modification of
structure is related to strain, responses measured at high and low strain values
will be different. For this reason, the selected type of test procedure should reflect
the final use of the data. When simulation of flow through a die is considered, large
strain capillary flow is useful. On the other hand, if material characterization is
important, low strain dynamic testing should be used. Because of morphology

Fig. 7.35 Concentration dependence of shear viscosity of PS/PMMA blends. Points are experimental (Lyngaae-Jørgensen 1983), while the lines were computed from Eq. 7.125
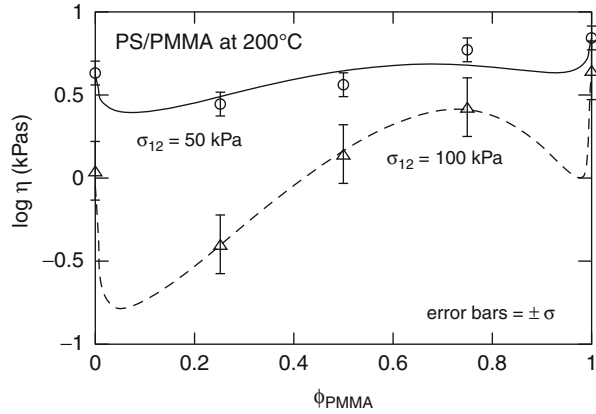
Fig. 7.36 Concentration dependence of zero shear viscosity of polypropylene blends with two linear low density polyethylenes at 190 °C. Points are experimental with error bars indicating the standard deviation (Dumoulin 1988). Lines are computed from Eq. 7.125
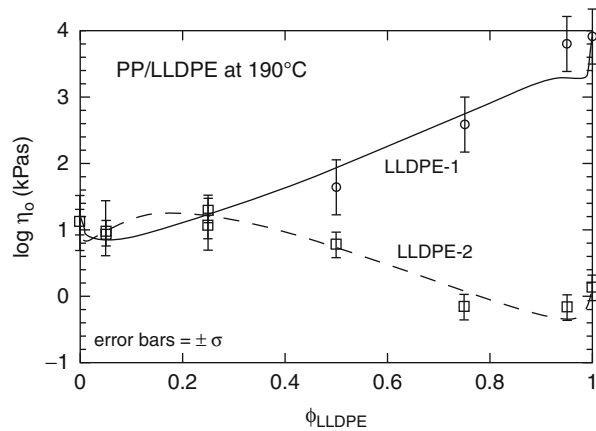
Fig. 7.37 Concentration dependence of η' and η, shear viscosities of LLDPE/PC blends at 245 °C and at constant stresses: $G'' = 1$, 10 and 100 kPa and $\sigma_{12} = 100$ kPa, respectively. Points – experimental; error bars of measurements $\pm 2\%$ (Utracki and Sammut 1990)
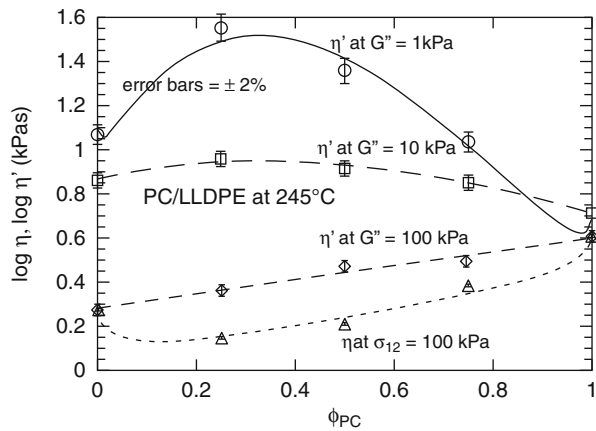
Fig. 7.38 Concentration
dependence of zero shear
viscosity at 260, 280, and
300 °C of polyethylene
terephthalate blended with
polyamide-6,6. Points are
experimental with the error
bars indicating the error of
measurements ± 2 % (Utracki
et al. 1982)
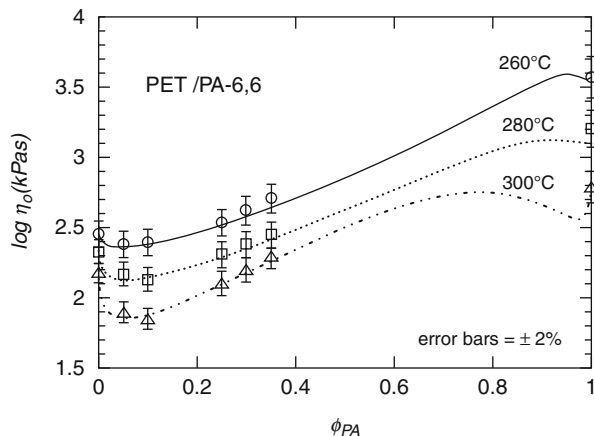
Fig. 7.39 Concentration
dependence of zero shear
viscosity of PS/PMMA blends
at 180 and 210 °C. Points are
experimental (Valenza
et al. 1991); solid lines are
computed from Eq. 7.125
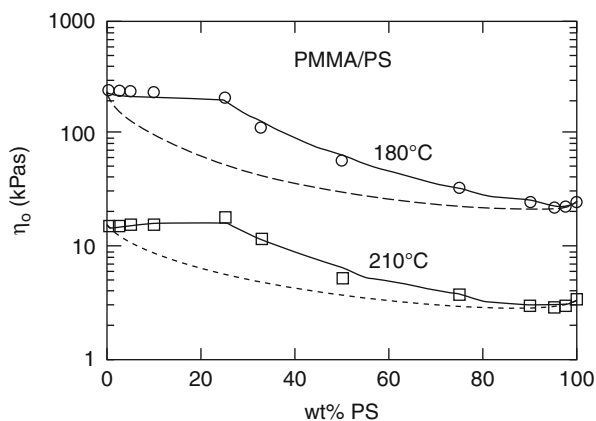
Fig. 7.40 Concentration
dependence of zero shear
viscosity at 200 °C of
PS/LDPE blends without
(*solid line*) and with (*broken
line*) 5 wt% SEB.
Points – experimental; error
bars of measurement ±3 %
(Ausin et al. 1987)
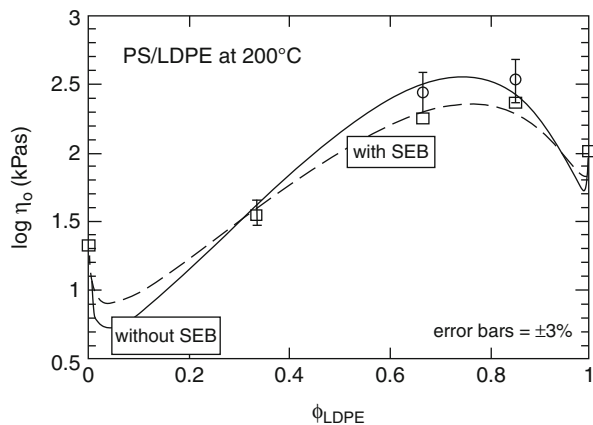
Table 7.11 Parameters used for curve fitting of viscosity versus concentration data to Eqs. 7.9 and 7.123 (Utracki 1991)

System	Conditions	ϕ_{I2} from Eq. 7.9	Eq. 7.125 parameters		
			η_{max}	β	r^2
PS/PMMA	180 °C	0.886	0.5597	1.6797	0.9956
PS/PMMA	210 °C	0.820	0.4882	2.1336	0.9882
PP/LLDPE-1	190 °C	0.998	1.7138	10.0212	0.9789
PP/LLDPE-2	190 °C	0.093	1.4890	15.4634	0.9804
LLDPE/PC	$G'' = 1$ kPa, 245 °C	0.306	0.9523	2.4706	0.9855
LLDPE/PC	$G'' = 10$ kPa, 245 °C	0.417	0.1521	0.0111	0.9929
LLDPE/PC	$G'' = 100$ kPa, 245 °C	0.681	0.0365	0.0100	0.9897
LLDPE/PC	Capillary flow, 245 °C	0.681	0.1164	1.8245	0.9903
PA-66/PET	260 °C	0.928	0.5897	2.0757	0.9996
PA-66/PET	280 °C	0.882	0.6371	4.0414	0.9991
PA-66/PET	300 °C	0.796	0.9166	8.6473	0.9968
LDPE/LLDPE-I	190 °C	0.956	0.4321	0.0161	0.9999
LDPE/LLDPE-II	190 °C	0.288	0.2972	0.0100	0.9825
PS/PMMA	Without compatibilizer	0.711	1.6172	39.9755	–
PS/PMMA	With compatibilizer	0.888	0.9822	6.1057	–
PE/PMMA	η' at $G'' = 1$ kPa, 160 °C	0.913	0.4173	0.0010	0.9922
PE/PMMA	η at $\sigma_{12} = 1$ kPa, 160 °C	0.888	0.3723	0.0010	0.9965
PS/PMMA	200 °C at $\sigma_{12} = 50$ kPa	0.619	0.4495	4.6611	0.9476
PS/PMMA	200 °C at $\sigma_{12} = 100$ kPa	0.804	1.3651	41.6292	0.9991
PS/LDPE	With SEB	0.827	1.933	22.2605	0.9754
PS/LDPE	Without SEB	0.827	1.483	11.8930	0.9806

Table 7.12 Comparison of continuum-based predictions for simple fluid with experimental observations for polymer blends

Rheological function	Simple fluid	Polymer blend
Viscosity at vanishing deformation rates	$\eta(\dot{\gamma}) = \eta'(\omega) = \eta_E(\dot{\varepsilon})/3$	$\eta(\dot{\gamma}) \neq \eta'(\omega) = \eta_E(\dot{\varepsilon})/3$
Extensional viscosity (from entrance effects)	$\eta_E = \eta_E(Cogswell)$	$\eta_E \neq \eta_E(Cogswell)$
First normal stress difference (from extrudate swell)	$N_1 = N_1$(B-swell); Tanner 1970	$N_1 \neq N_1$(B-swell)

sensitivity to test conditions, there is a serious disagreement between predictions of the continuum-based theories and experiments. This is summarized in Table 7.12.

A study using confocal Raman spectrometry was carried out to determine the concentration profile within the extrudate of rubbery particles in a polyethylene matrix during capillary flow (Chartier et al. 2010). Chartier et al. reported that the effect of the concentration of particles on the apparent viscosity of polymer melts measured using capillary flow was the opposite of that based on observations made using linear dynamic viscosity measurements (Fig. 7.41). Shear-induced migration can be detected from the concentration profile of the components of the

Fig. 7.41 (*top*) the dynamic viscosity versus frequency and (*bottom*) apparent capillary viscosity of various concentrations of rubber in uncompatibilized PE/Sunigum blends at 180 °C (Chartier et al. 2010)
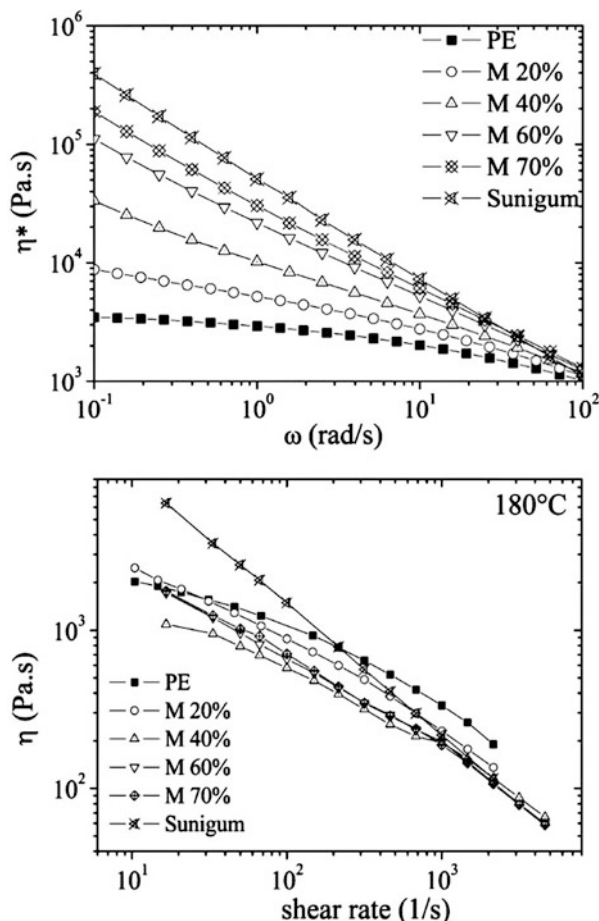
blends inside the material. They discovered that the lowest viscosity component migrates toward the capillary wall. The addition of a compatibilizers inhibited this migration.

Dynamic testing of polymer blends at small amplitude is a relatively simple and reliable procedure. The resulting storage and loss shear moduli, G' and G'', respectively, should be first corrected for yield stress then the loss data can be fitted to Eq. 7.42 to determine the value of the four parameters, η_o, τ, m_1, and m_2. Once these parameters are known, the Gross frequency relaxation spectrum, and as a result all linear viscoelastic functions, can be calculated (see Eqs. 7.85, 7.86, and 7.87).

The dependence of rheological functions of liquid mixtures on the content and the rheological functions of neat ingredients has been discussed, to some extent, in Sect. 7.3.2.3. A summary of these results is given in Table 7.13.

Table 7.13 Blend viscoelasticity from emulsion models (Graebling and Muller 1991)

Author	Concentration	Liquids	Drops	Results
Taylor 1932	Dilute	Newtonian	Undeformable	$\eta = \eta(\lambda, \phi)$
Oldroyd 1953	Dilute	Newtonian	Deformable	$G', G'', \eta = f(\lambda, \phi, \nu)$
Palierne 1990	Moderately concentrate	Viscoelastic	Deformable, polydispersed	$G^*, H = f(G^*_m, G^*_d, \nu_{12}/d, \phi)$

The last entry in Table 7.13 refers to the theory by Palierne (1990). The theory is based on the following assumptions: (i) the system consists of two viscoelastic liquids; (ii) the concentration of the dispersed phase is moderate; (iii) the drops are spherical, polydisperse, and deformable; (iv) the drop deformation is small, so the blend behavior is linear viscoelastic; and (v) the interfacial tension coefficient, ν_{12}, is constant, independent of stress and interfacial area. The theoretical analysis leads to Eq. 7.70. Note that the ratio ν_{12}/d is the only parameter of the equation. The model was found to provide good description of the dynamic behavior for several blends, supporting the idea that the long relaxation times in blends originate from geometrical relaxation of droplets (Graebling et al. 1989, 1993b).

7.5.5.3 Compatibilization Effects

Most immiscible polymer blends require compatibilization to reduce the interfacial tension. This helps to increase the degree of dispersion to stabilize the morphology developed during compounding against extensive damage during high stress and strain processing (e.g., during injection molding) and to enhance adhesion between the phases in the solid state, facilitating the stress transfer and improving the mechanical properties of the product. Compatibilization is achieved either by addition of a small quantity, 0.5–2 wt%, of a precisely tailored (usually) block copolymer; an addition of a multipurpose core-shell copolymer, ≤ 35 wt%, that also improves toughness of the blend; or by reactive processing.

Compatibilization strategy for either addition or reactive blending requires that the copolymer migrates to the interface, thus, on the one hand, lowering the thermodynamic immiscibility barrier between the two phases, and, on the other, engendering formation of the third phase, the interphase.

From the point of view of blend morphology in the molten state, compatibilization enhances the dispersion, increases the total apparent volume of the dispersed phase, rigidifies the interface, and increases interaction not only between the two phases, but also between the dispersed drops. Furthermore, reactive compatibilization may involve chemical bonding between the two polymer macromolecules, resulting in significant increase of the molecular weight at the interface.

The rheological consequences of these changes can be predicted from a model system. The emulsion model indicates that making the interface more rigid causes the intrinsic viscosity of the emulsion to increase (see Eq. 7.50). Similarly, an increase of the apparent volume of the dispersed phase causes the relative viscosity to increase (see Eqs. 7.24 and 7.25). Furthermore, enhanced interactions between

the phases will reduce the possibility of the interlayer slip and increase formation of associative network formation, which may result in the yield stress. In short, compatibilization is expected to increase melt viscosity, elasticity, and the yield stress.

There are two mechanisms that may invalidate this prediction: (i) In spite of the best efforts of researchers and technologist the added copolymer may prefer to form micelles inside one of the polymeric phases than to migrate to the interphase. This has been frequently observed in blends with block copolymers, e.g., for blends of PS with PE, "compatibilized" by addition of a hydrogenated styrene-butadiene block copolymer, SEBS (Utracki and Sammut 1988, 1990). (ii) Depending on the blend composition, an addition of compatibilizer may affect the total free volume of the system. These changes are difficult to predict. An increase of the free volume (evidenced by reduction of melt density) is expected to result in increased fluidity of the system.

Effects of addition of hydrogenated styrene-butadiene di-block copolymers (one strictly di-block and the other tapered) on properties of HDPE/HIPS blends were investigated (Brahimi et al. 1991). The rheological behavior of the blends, especially in the low-frequency region, was sensitive to the copolymer content. However, at high frequencies, the copolymer only slightly affected the flow. Furthermore, addition of a small amount of compatibilizer reduced the zero-shear viscosity, η_o, while higher loading had an opposite effect. This behavior was interpreted as due to the change in the copolymer state in the blend, i.e., saturation of the interface followed by micelle formation.

The results were compared with prediction of Palierne model, viz., Eq. 7.39. For diluted, uncompatibilized blends, PS/PE = 10/90 or 90/10, relatively good agreement was found. The agreement was poor for blends containing 3 wt% of the tapered di-block copolymer. In the latter case, the reduction of storage and loss shear moduli, especially at low frequencies, could not be explained by the emulsion model. The effect of the interfacial tension and particle size over a relatively wide range did not significantly affect the model predictions. These observations confirmed an earlier report for the same system (Aït-Kadi et al. 1992). Since, at low frequencies, slip is less likely to occur than at high frequencies, low values of G' and G'' could not be explained by this mechanism. The most likely explanation is an increase of the free volume by incorporation of the copolymer. The nonlinear variation of specific volume as a function of composition has been frequently observed for systems with limited miscibility.

Blends of PS with LDPE were compatibilized by addition of di- and tri-block copolymers, *Kraton*™ G 1701 and G 1605 (Pascault et al. 1994). A continuous decrease of PS-drop size and an increase of shear viscosity with addition of copolymer were reported.

Blends of PP with a polyamide (PA-6, PA-66, or PA-12) were the object of intensive studies. Linear viscoelastic shear moduli were measured for PP/PA-6 blends comprising different amount of PP-g-PA-6 copolymer. It was reported that, in spite of the expected reduction of the particle size with increase of the compatibilizer content, no qualitative effect of the flow was observed (Scholz et al. 1989).

In a thorough study, PP, PA-6, and their compatibilized blends were studied at 225–250 °C, in steady-state and dynamic shear, as well as extensional flow conditions (Utracki and Sammut 1992). The dynamic flow curves for the blend were significantly higher than what could be predicted from the component flow behavior. The blends showed a regular, pseudoplastic flow behavior, without yield stress. By contrast, capillary flow was found to be insensitive to temperature, suggesting a major modification of morphology during these large strain tests. Similarly, the extensional viscosity of the blends was one order of magnitude higher than what could be expected from the component polymer behavior. During extensional flow, the blends showed strain hardening, absent for either PP or PA-6. This could be explained by postulating that reactive compatibilization significantly increased the molecular weight of the system – strain hardening is to be expected for highly entangled, high MW systems. It was also reported that the measured elongational viscosity, η_E, for two homopolymers agreed quite well with the value calculated from the entrance pressure drop in capillary flow, P_e. However, for the blend, the calculated value of η_E was one order of magnitude higher than measured.

Reactive compatibilization in a specially designed twin-screw extruder was carried out during compounding maleated polypropylene, PP-MA (0–0.14 wt% MA), with PA-6. During the reaction a di-block copolymer was formed at the interface. As the copolymer content increases from zero to 20 wt%, the number average diameter of PA-6 drops decreased from the initial value $d_o = 20$ to $d = 0.14$ μm at 20 wt% copolymer. The concentration dependence of shear viscosity also changed with compatibilization from negative deviation from the log additivity rule, NDB, to positive deviation, PDB (Nishio et al. 1992).

The effect of compatibilization on the shear flow of PP/PA-6 and PP/PA-12 blends was also studied (Germain et al. 1994). Here the copolymer flow curve was one order of magnitude lower than that of PA. The authors reported that, at low deformation rates, emulsion-type morphology dominated the flow, whereas, at higher rates, concentric layered-type morphology, with appropriate flow behavior, was observed. At low shear rates, the blend viscosity was higher than the viscosity of the matrix, while at high shear rates the contrary was observed. The low shear rate behavior was analyzed by means of Palierne theory, assuming that the copolymer is located at the interface. Good agreement was obtained for the low-concentration blends. For high stress (and strain) deformation, a model of lamellar telescopic flow for power-law fluid was derived. The skin-core model represented the flow of blends well. Thus, it can be postulated that, in blends with low MW copolymeric compatibilizers, the stress may cause its disentanglement from at least one phase, forming a layered morphology, and resulting in flow lubricated by the presence of the low molecular weight compatibilizer.

Effects of addition of a compatibilizing block copolymer, poly(styrene-b-methyl methacrylate), P(S-b-MMA) on the rheological behavior of an immiscible blend of PS with SAN were studied by dynamic mechanical spectroscopy (Gleisner et al. 1994a). Upon addition of the compatibilizer, the average diameter of PS particles decreased from $d \cong 400$ to 120 nm. The data were analyzed using

weighted relaxation-time spectra. A modified emulsion model, originally proposed by Choi and Schowalter (1975), made it possible to correlate the particle size and the interfacial tension coefficient with the compatibilizer concentration. It was reported that the particle size reduction and the reduction of ν_{12} occur at different block copolymer concentrations.

In another attempt, TPVs based on ENR/PP blends were prepared by melt mixing via dynamic vulcanization, using two different types of compatibilizers: phenolic-modified polypropylene (Ph-PP) and graft copolymer of maleic anhydride on polypropylene molecules (PP-g-MA) (Nakason et al. 2006). A high compatibilizing effect was found because of the chemical interaction between the polar groups in ENR and Ph-PP or PP-g-MA. The TPVs prepared from ENR/PP with Ph-PP as a compatibilizer showed the highest rheological and mechanical properties, while those based on ENR/PP exhibited the lowest values. Moreover, the TPV, compatibilized with Ph-PP, showed smaller rubber particles dispersed in the PP matrix, compared to the corresponding TPV based on ENR/PP-g-MA (Nakason et al. 2006).

Huitric et al. (2007) studied the effect of different concentrations of polyethylene-graft-maleic anhydride on the morphology evolution of blends of low density polyethylene and nylon 12, using a method based on quenching following deformation of the samples, which were kept between the parallel plates of a rheometer. They determined droplet size and transient viscosity of the blends as functions of the total strain. The results revealed that the droplet size was governed by coalescence at low strain values. Due to the important interfacial coverage of the interface by the grafted copolymer chains, a significant coalescence inhibition was observed for the blends with high concentration of compatibilizer. In that case, the intensity of the coalescence did not change by the applied shear rate. On the contrary, increasing shear rate favored the coalescence for the blends without compatibilizer or with low compatibilizer concentration. The authors introduced an additional parameter for non-affine deformation (slip parameter) in a modified version of the Lee and Park model. The results showed great improvement in the predictions of droplet size evolution by this adjustment.

Kordjazi and Ebrahimi (2010) investigated the rheological properties and morphology of compatibilized and noncompatibilized PP/PET blends, using SEBS-g-MA as a compatibilizer. They suggested that the behavioral changes of rheological properties by increasing the compatibilizer are related to the aggregation of the dispersed particles encapsulated with elastomeric shell, which is responsible for the failure of Palierne's model predictions. Based on frequency sweep and step strain experiments in the linear region, after pre-shearing using various shear rates, the authors also suggested that the aggregated structure was destroyed and replaced by an alignment in the flow direction (Kordjazi and Ebrahimi 2010).

DeLeo et al. (2011) considered the formation of a compatibilizer between two multifunctional reactive polymers that leads to a cross-linked copolymer at the interface. The study was conducted on model blends PDMS/PI. In this case a chemical reaction between amine-functional PDMS and maleic anhydride-functional PI formed the compatibilizer. The effects of interfacial cross-linking

on rheological behavior and morphological characteristics were found to be highly asymmetric for the samples with PI:PDMS ratio of 30:70 or 70:30. The PI-continuous blends showed unusual features including drop clusters, nonspherical drops, and "gel-like" behavior, which increased by increasing reactive compatibilizer loading. Contrarily, PDMS-continuous blends displayed typical droplet–matrix morphology with round drops and showed liquid-like behavior that was qualitatively similar to that of compatibilizer-free blends. The authors speculated that the asymmetry of the compatibilizer architecture on the two sides of the interface is the factor causing the structural and rheological asymmetry (DeLeo et al. 2011).

Entezam et al. (2012) studied the effect of interfacial activity and micelle formation on rheological behavior and microstructure of reactively compatibilized PP/PET blends. They used different interfacial modifiers, i.e., PTW or PP-g-MAH. They also used dynamic and start-up shear flow experiments as well as their subsequent recovery. Reactive compatibilization, in concentrations close to the critical micelle concentration, at which the interface is saturated with the compatibilizer, changed the rheological behavior from emulsion to solid-like behavior due to the interconnectivity between dispersed phase domains. They suggested that PTW micelles in the bulk phase of the blend favored physical network-like structure formation and enhanced the time and intensity of the relaxation process. However, the PP-g-MAH micelles restricted interconnectivity between the dispersed domains. The analysis of fractional Zener models (FZMs) showed nonzero value of G_e (the elastic modulus of spring element of FZM) for the compatibilized blends with network-like structure. It was suggested that the increase of G_e with formation of PTW micelles and its zero value for the blends consisting of PP-g-MAH micelles indicate a dual role for micelles influencing rheological and morphological properties of PP/PET blends (Entezam et al. 2012).

7.5.5.4 Time–Temperature Superposition

The time–temperature superposition principle, t-T, has been a cornerstone of viscoelastometry. It has been invariably used to determine the viscoelastic properties of materials over the required 10 to 15 decades of reduced frequency, ωa_T (Ferry 1980). Measuring the rheological properties at several levels of temperature, T, over the experimentally accessible frequency range (usually two to four decades wide), then using the t-T shifting, has made it possible to construct the complete isothermal function.

As demonstrated before, the shifting involves three shift factors, one horizontal, usually expressed as $a_T = b_T \eta_o(T)/\eta_o(T_o)$, where $b_T = \rho_o T_o/\rho T$ is the first vertical shift factor that originates in the thermal expansion of the system (ρ is density). The subscript o indicates the reference conditions, defined by the selected reference temperature T_o, usually taken in the middle of the explored T-range. For homopolymer melts as well as for amorphous resins, the two shift factors, a_T and b_T, are sufficient. However, for semicrystalline polymers the second vertical factor v_T has been found necessary – it accounts for variation of

the crystallinity content during frequency scans at different temperatures (Ninomiya and Ferry 1967; Dumoulin 1988).

Only when all the relaxation times in a given system are multiplied by the same factor, when the temperature is changed, the t-T principle can be observed. In single-phase homologous polymer blends, the relaxations are mainly controlled by the segmental mobility; thus the t-T superposition has been observed in a wide range of conditions. Similarly, for polymers filled with high modulus particles, the filler is responsible for enhancement of modulus without affecting the relaxation spectrum, and as a consequence t-T superposition is obeyed. However, in rheologically complex heterogeneous systems, individual polymeric components contribute to the relaxation and since their activation energies are usually different, a change of temperature affects them differently – lack of t-T is a result.

Fesko and Tschoegl (1971) demonstrated that the simplest form of the time–temperature superposition relation for a function $G(t, T) = G[t, a(T)]$ is

$$
\begin{aligned}
[\partial G(t,T)/\partial T]_t &= \left\{[\partial G(t,T)]/[\partial \ln t]_T\right\}\{d[\ln a(t,T)]/dT\} \\
d[\ln a(t,T)]/dt &= \sum_i N_i(t)d[\ln a_i(T)]/dT; i = 1, \ldots, n \\
N_i(t) &= \phi_i L_i(t,T_0)/\sum_i \phi_i L_i(t,T_0) \\
L_i(t,T_0) &= \partial G_i[(\ln t),T_0]/\partial \ln t
\end{aligned}
\tag{7.126}
$$

where the summation extends over every species in the system. Equation 7.126 assumes that the effects of time and temperature can be separated, $G(t, T) = G[t \cdot a(t, T)]$. Similar derivation was published by Goldman et al. (1977).

There is growing evidence that t-T superposition is not valid even in miscible blends well above the glass transition temperature. For example, Cavaille et al. (1987) reported lack of superposition for the classical miscible blends – PS/PVME. The deviation was particularly evident in the loss tangent versus frequency plot. Lack of t-T superposition was also observed in PI/PB systems (Roovers and Toporowski 1992). By contrast, mixtures of entangled, nearly monodispersed blends of poly(ethylene-*alt*-propylene) with head-to-head PP were evaluated at constant distance from the glass transition temperature of each system, homopolymer or blend (Gell et al. 1997). The viscoelastic properties were best described by the "double reptation model," viz., Eq. 7.82. The data were found to obey the time–temperature superposition principle.

The explanation proposed by Ngai and Plazek (1990) was based on the postulate that the number of couplings between the macromolecules varies with concentration and temperature of the blend. The number of couplings, n, can be calculated from the shift factor, $a_T = [\varsigma_o(T)/\varsigma_o(T_o)]^{1/(1 - n)}$, where $\varsigma_o(T)$ is the Rouse friction coefficient. Thus, in miscible, single-phase systems, as either the concentration or temperature changes, the chain mobility changes and relaxation spectra of polymeric components in the blends show different temperature dependence, i.e., the t-T principle cannot be obeyed. Similar conclusions were reached from a postulate

that the deviation originates from different temperature dependence of the relaxation functions of the blend components (Booij and Palmen 1992).

In immiscible blends, the t-T principle does not hold. For immiscible amorphous blends, it was postulated that two processes must be taken into account: the t-T superposition and the aging time (Maurer et al. 1985). On the other hand, in immiscible blends, at the test temperature, the polymeric components are at different distances from their respective glass transition temperatures, $T - T_{g1} \neq T - T_{g2}$. In blends of semicrystalline polymers, such as PE/PP, the superposition is limited to the molten state, within a narrow, high temperature range (Dumoulin 1988).

As an alternative to t-T superposition, plot of the elastic stress tensor component as a function of the viscous one has been used, e.g., $(\sigma_{11} - \sigma_{22})$ versus σ_{12} or G' versus G''. For systems in which the t-T is obeyed, such plots provide a temperature-independent master curve, without the need for data shifting and calculating the three shift factors. Indeed, from Doi and Edwards tube model, the following relation was derived:

$$\ln G' = 2\ln G'' + \ln(6M_e/5\rho RT) \qquad (7.127)$$

where M_e is the entanglement molecular weight (Han and Kim 1993). The dependence suggests that a plot of G' versus G'' should be insensitive to temperature. Indeed, good superposition was obtained for several blends where the structure remained unchanged within the range of independent variables, e.g., in such miscible systems as PS/PVME and PEO/PMMA, or even in some immiscible blends whose components have similar glass transition temperature, viz., PS/PMMA. However, lack of superposition was noted in other systems, where the structure did change, viz., PS/PVME heated across the binodal, block copolymer across the microphase separation temperature, LCP across the nematic transition temperature, etc.

7.5.5.5 Steady-State Versus Dynamic Viscosities

For most blends, the morphology changes with the imposed strain. Thus, it is expected that the dynamic low strain data will not follow the pattern observed for steady-state flow. One may formulate it more strongly: in polymer blends, the morphology and the flow behavior depend on the deformation field; thus under different flow conditions, different structures are being tested. Even if low strain dynamic data can be generalized using the t-T principle, those determined in steady state will not follow the pattern.

Chuang and Han (1984) reported that, for miscible and immiscible blends at constant composition, the plots of N_1 versus σ_{12} and G' versus G'' are independent of T. However, while for single phase systems, the two dependencies are approximately parallel, the steady-state relation may be quite different from the dynamic one for immiscible blends, such as PS/PMMA.

The agreement can be improved by means of the Sprigg's theory (1965). The general theory leads to the conclusion that

$$\eta(\dot{\gamma}) = \eta'(\omega), \quad \text{or} \quad \sigma_{12}(\dot{\gamma}) = G''(\omega)/C$$
$$\psi_1(\dot{\gamma}) = 2G'(\omega)/\omega^2, \quad \text{or} \quad N_1(\dot{\gamma}) = 2G'(\omega)/C^2 \tag{7.128}$$

where $C \equiv \omega/\dot{\gamma} = [(2 - 2e - e^2)/3]^{1/2}$ and e is a model parameter. For a series of PMMA/ABS blends, the plot of C versus composition was nonlinear, with C = 1 found only for PMMA homopolymer. Variation of this structural parameter seems to be related to differences of morphology existing in dynamic and steady-state flow fields (Utracki 1989).

Capillary flow of EPDM with poly(vinylidene-*co*-hexafluoropropylene), *Viton*™, showed a sixfold reduction of shear viscosity upon addition of about 2 % of the other component (Shih 1976, 1979), whereas in dynamic tests, the complex viscosity behavior of EPDM and EPDM with 5 % Viton™ was similar over a wide range of frequency and strain (Kanu and Shaw 1982). The latter authors postulated accumulation of the second component at the capillary entrance, which periodically feeds into the capillary, lubricating the main stream by a sort of roll bearing effect. In this particular case, the difference is related not only to material properties but also to a flow segregation enhanced by the geometry of the measuring device. Since the effect is strongly affected by flow geometry, the data obtained in capillary flow have little value for process design requirements.

The phenomenon of flow segregation has been exploited commercially. For example, high viscosity engineering resin that has poor resistance to solvents, e.g., polycarbonate or polyetheretherketone (PC or PEEK, respectively), can be blended with low melt viscosity liquid crystal polymer, LCP. Extruding such a blend through die with long enough land forces LCP to migrate toward the high stress surface, thus lubricating die flow and in addition engendering a protective layer on the surface of PC or PEEK. The reduction of viscosity of a polymer melt upon addition of LCP was originally described in 1979, in a patent deposition from ICI (Cogswell et al. 1981, 1983, 1984). The rheological behavior of LCP blends with polyether imide *Ultem*™ was studied by Nobile et al. (1990) in steady-state capillary and dynamic mechanical modes of deformation. The flow of LCP was reported to be sensitive to pressure; thus the flow of blends was carried out using a short capillary.

Another, more common commercial use of the phenomenon is addition of fluoropolymers to polyolefins. In this case, a small amount of fluoropolymer progressively migrates to the die surface, reducing the die pressure drop and making it possible to extrude the resin at high throughput without melt fracture. It has been shown that this approach also works for other polymers, viz., PEEK. Thus blends of PEEK with polytetrafluoroethylene, 1–5 wt% PTFE, were extruded. The pressure drop across the die was reported to decrease with time to an equilibrium value, P_{lim}. The value of P_{lim} depended on PTFE content, whereas the time to reach it depended on the rate of extrusion – the higher was the rate, the shorter was the saturation time (Chan et al. 1992).

Over the years, dynamic testing has become the preferred method of testing the rheological behavior of the multiphase systems. For example, Nishi et al. (1981) carried out careful studies on the dynamic behavior of PS/PVME. The specimens were cast at temperatures either below or above the lower critical solution temperature, LCST $\cong$ 95 °C. While those prepared at T < LCST (single-phase system) showed superimposition of dynamic data onto a master curve, those that were cast at T > LCST did not.

7.5.5.6 Blend Elasticity

Four measures of melt elasticity are commonly used: in steady-state shearing, the first normal stress difference (N_1); in dynamic tests, the storage modulus (G'); and the two indirect and controversial ones, namely, entrance–exit pressure drop (Bagley correction) (P_e) and the extrudate swell (B). In homogeneous melts, the four measurements are in qualitative agreement. More complex behavior is expected for blends. If the blend can be regarded as an emulsion, without interlayer slip the PDB behavior for the elastic measurements is to be expected. On the other hand, in systems where the dispersed phase is difficult to deform (as in suspensions), extrudate swell should be small. Deformation and recovery of the dispersed phase shape provides a potent mechanism for the elastic energy that result in large elastic response – this does not have anything to do with the molecular energy storage.

The direct measurements of N_1 and σ_{12} indicate a parallel dependence of both these functions plotted versus ϕ, even when they have a sigmoidal form. Considering the steady shear flow of a two-phase system, it is generally accepted that the rate of deformation may be discontinuous at the interface, and it is more appropriate to consider variation of the rheological functions at constant stress than at constant rate, i.e., $N_1 = N_1 (\sigma_{12})$. Using a similar argument for the dynamic functions, it should be concluded that $G' = G'(G'')$ should be used. Note that, as discussed above, the steady-state and dynamic data for polymer blends rarely superimpose.

Another method for estimating the elasticity contribution is through the Bagley entrance–exit pressure drop correction, P_e. For single-phase systems, the plot of P_e versus σ_{12} is independent of capillary diameter, temperature, and molecular weight, but rather sensitive to changes in flow profile (Utracki 1985). The plot was found to be useful for interpretation of the stress, temperature, and composition-dependent morphological changes in immiscible polymer blends (Dumoulin et al. 1985). However, it could not be used to estimate the elasticity of blends.

Extrudate swell, B, has been used to calculate the recoverable shear strain, γ_R, for single-phase materials (Utracki et al. 1975). Introduction of the interface negates the basic theoretical assumptions on which the calculation of γ_R was based. In addition, presence of the yield stress, frequently observed in multiphase systems, prevents B from reaching its equilibrium value required to calculate γ_R and then N_1. Nevertheless, B is used as a qualitative measure of blend elasticity.

Note that the presence of the dispersed, deformable phase leads to *form recovery*, i.e., shrinkage of the prolate ellipsoids motivated by the interfacial energy, which results in unduly large enhancement of B. The phenomenon has little to do with deformability of macromolecular coil – the postulated mechanism of swelling

in single-phase polymeric system. The main origin of blend swelling is the elastic recovery of domains extended during the convergent flow in the capillary entrance. The observed *form swelling* of blends could be large, giving strain recovery, $\gamma_R \leq 6.5$.

It is worth pointing out that strain recovery can be nonsymmetrical as far as the blend composition is concerned. In the case when the viscosity ratio at low deformation rate exceeds the limiting value $\lambda_{cr} = 3.8$, there is a significant difference in the mechanism of dispersion. During compounding in a twin-screw or twin-shaft instrument, the material undergoes stretching in shear and extensional flow fields. Depending on the composition, the stretched forms undergo different recovery. For blends with $\lambda > \lambda_{cr}$ the prolate ellipsoids cannot be broken; thus they slowly retract into large spheres. For blends with $\lambda < 1/\lambda_{cr}$ the prolate ellipsoids will disintegrate by the capillarity instability mechanism (El Khadi et al. 1995).

Similar observations were reported for PMMA/PS blends (Gramespacher and Meissner 1995). The elastic creep compliance for PMMA/PS = 16/84 behaved regularly, similar to what has been observed for single-phase polymers. However, when the composition was reversed, i.e., PMMA/PS = 84/16, the recovery creep compliance showed a maximum at which the recovery direction was reversed. The authors attributed the dissymmetry of behavior to different retardation times of the blend components.

7.5.6 Elongational Flows

Owing to experimental difficulties, there are but few publications on uniaxial deformation of blends. To prepare specimens for testing, samples usually are transfer molded and relaxed, both operations requiring relatively long heating time, during which only well-stabilized blends will not coarsen.

It is convenient to distinguish two contributions to the tensile stress growth function, η_E^+, one due to the linear viscoelastic response, η_{EL}^+, and the other originating in the structural change of the specimen during deformation, η_{ES}^+. The first can be calculated from any linear viscoelastic response, while the second (which originates in either intermolecular interactions or entanglements) depends on both the total strain, $\varepsilon = \dot{\varepsilon}t$, and either strain rate $\dot{\varepsilon}$ or straining time t. Owing to the industrial importance of strain hardening (SH), a large body of literature focuses on the optimization of blend composition to maximize SH. Since SH depends on the entanglements, blending branched polymers usually affects SH even in the low concentration range.

Most of the work on uniaxial extensional flow of immiscible polymer blends has focused on the behavior of systems containing PE. The main reason is the need for better, easier-to-process film resins, moreover for a relative stability of polyolefin blend morphology. Film blowing conceptually involves two different engineering operations, extrusion and blowing. For most production lines the latter limits productivity. For low density LDPE resins, strain hardening provides a self-regulating, self-healing mechanism. For HDPE and LLDPE, only small SH

can be obtained for the high MW and MWD resins. As a result, most LLDPE resins on the market are blends with LDPE, rubbers, copolymers, or another type of LLDPE. SH was also found to be an important resin characteristic for wire coating. Here the surface finish and uniformity of the deposited layer were superior for blends with high strain hardening and low shear viscosity (Utracki 1988).

Among biodegradable polymers, poly(lactic acid) (PLA) is a popular candidate for a wide variety of packaging applications because of its excellent gloss and clarity, high tensile strength, good heat sealability, and low coefficient of friction. However, drawbacks, including a low melt strength and brittleness, limit its end-use applications. Eslami and Kamal (2012) examined three different potential approaches to overcome these limitation by proper rheological and mechanical experiments: (i) the blending of PLA with poly((butylene succinate)-*co*-adipate) (PBSA) as another biodegradable polymer, (ii) the modification of the clay by formation of a blend/clay nanocomposite (Eslami and Kamal 2013b), and (iii) the introduction of by branching using chain extender (Eslami and Kamal 2013a). In the first approach, a series of blends based on poly(lactic acid) (PLA) and biode-gradable poly((butylene succinate)-*co*-adipate) (PBSA) and their nanocomposites with nanoclay (PLA/PBSA/Clay ternary nanocomposites) were prepared using a twin-screw extruder. The morphology and structure of the blends and the nanocomposites were examined using field emission scanning electron micros-copy, transmission electron microscopy, and X-ray diffraction. Rheological prop-erties of the blends, nanocomposites, and pure components were also studied in dynamic oscillatory shear measurements and elongational mode at different Hencky rate.

The authors calculated the strain hardening intensity values as a measure of melt strength using the ratio of $\eta_{E,nonlinear}/\eta_{E,linear}$ (λ_n). The slope of log λ_n versus Hencky strain defines the strain hardening intensity. As seen in Fig. 7.42 (a), effective improvements in melt strength required over 50 wt% PBSA which decreases the tensile modulus.

It was mentioned that the incorporation of nanoclay had only a minor effect on melt strength; however it increased the tensile modulus. On the other hand, Cole–Cole plot of the melts showed that the chain extender can promote the development of chain branching by time. The use of an epoxy based multifunctional chain extender resulted in significant enhancement of the melt strength and processability of the blends even at 30 wt% PBSA (Fig. 7.39b). These blends also exhibited interesting mechanical properties (Eslami and Kamal 2013a).

Blends of LLDPE/PP = 50:50, with or without compatibilizing ethylene-propylene copolymer, EPR, was studied by Dumoulin et al. (1984a, b, c). In spite of the expected immiscibility, the blends showed additivity of properties with good superposition of the stress growth functions in shear and elongation, as well as with the zero deformation rate Trouton ratio, $R_T \cong 1$. In earlier work, blends of medium density PE (MDPE) with small quantities of ultra-high molecular weight polyethylene (UHMWPE) were studied in shear and extension. Again, SH and $R_T \cong 1$ was observed.
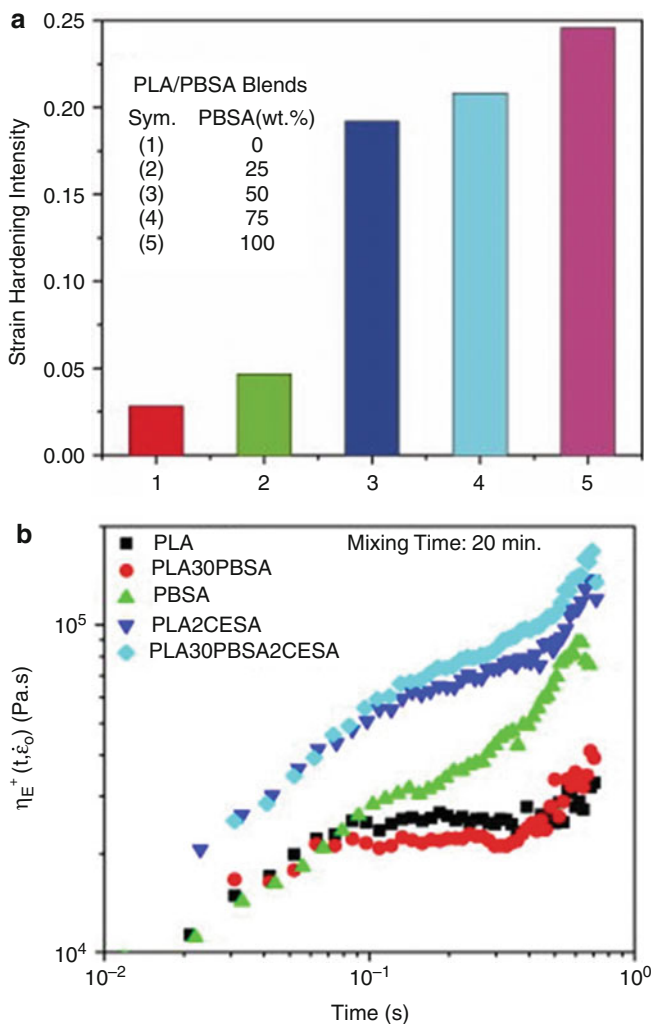
Fig. 7.42 (**a**) Rheological properties of PLA/PBSA blends without chain extender (**b**) with chain extender (Eslami and Kamal 2013a, b)

It has been shown that the stress growth function, in uniaxial extension, provides three important pieces of information on the polymer. The initial slope of the stress growth function

$$S_i = \lim_{t \to 0} d\ln\eta_E^+ / d\ln t \qquad (7.129)$$

was found to correlate with polydispersity of the molecular weights, M_z/M_n, where M_z and M_n are respectively z- and number average molecular

weights (Schlund and Utracki 1987). The observation agrees with Gleissle's principle (1980):

$$
\eta(\dot{\gamma}) = \eta^{+}(t) \quad \text{for} \quad \dot{\gamma} = 1/t
$$
$$
\therefore \quad \lim_{t \to 0} \partial \ln \eta^{+}(t)/\partial \ln t = \lim_{t \to 0} \partial \ln \eta(\dot{\gamma})/\partial \ln \dot{\gamma} = n - 1 \tag{7.130}
$$

The plateau or equilibrium value provides information on the weight average molecular weight, M_w, and the stress hardening part, $\eta_{ES}^{+}(t)$ on the entanglements, i.e., branching, association, etc. The parameter S_i could provide information regarding blend miscibility. Solubility usually broadens the width of the MW distribution, causing S_i to increase. By contrast, immiscibility causes separation of high molecular weight fractions and narrowing MWD. The miscibility can also be reflected in a maximum strain at break, ε_b. In "antagonistically" immiscible blends of PA-6 in LLDPE, a sharp decrease of ε_b was observed. However, in blends with co-continuous morphology ε_b may increase to an average value, with negative deviations on both sides (Min 1984).

Li et al. (1990) studied the elongational viscosity of specially prepared blends of styrene-acrylonitrile copolymer, SAN, with different loadings of cross-linked polybutadiene, BR, particles having diameter, $d = 170$ nm. At higher rates of extension, the SAN showed strong strain hardening behavior. As the volume of rubber particles in the system increased, the strain hardening became less evident. By contrast, the low deformation rate elongational viscosity was shown to increase with BR loading, and as its content increased, the system progressively showed increased sensitivity to strain.

Delaby et al. (1994) attempted to experimentally examine the relation between droplet deformability and the extensional viscosity ratio, $D_E = D_E(\lambda_E)$. The authors demonstrated that the theories proposed by Taylor (1932, 1934) and Palierne (1990) predict the same dependence:

$$
(\gamma_d - 1)/(\gamma_m - 1) = 5/(2\lambda_E + 3) \tag{7.131}
$$

where γ_d and γ_m are respectively strain of the dispersed phase (defined as a ratio of the long axis to the original drop diameter) and the matrix. Only for $\lambda_E = 1$ co-deformation of drop is to be expected. The dependence is shown in Fig. 7.43. The experiments show good agreement with the behavior predicted by Eq. 7.131 in the full range of the viscosity ratios used in the studies, $\lambda_E = 0.005$ to 13. Drop deformability computed in 2D, using the boundary element method, resulted in higher value than 5/3, given for 3D by Eq. 7.131; independently, two research teams found the limit for $\lambda_E \to 0$ to be 2 (Khayat et al. 1996; Stradins and Osswald 1996).

Convergent flow at the die entrance provides strong elongational flow. Laun and Schuch [1989 derived the following relation between the entrance pressure drop in capillary flow and the shear stress at the capillary wall:

Fig. 7.43 Relative deformation of the dispersed phase versus the viscosity ratio (Delaby et al. 1994)

Drop-to-Matrix Deformation in Elongational Flow

$(\gamma_d - 1)/(\gamma_m - 1) = 5/(2\lambda_E + 3)$
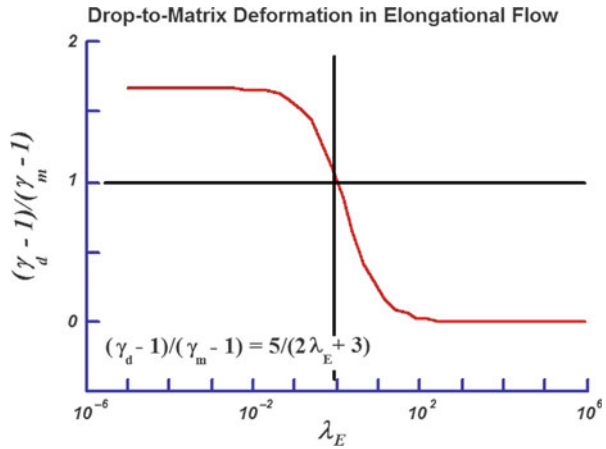
Fig. 7.44 Entrance–exit pressure drop in capillary flow of polypropylene, polyamide-6, and commercial PP/PA-6 blend, Orgalloy at 230 °C – line computed from Eq. 7.132
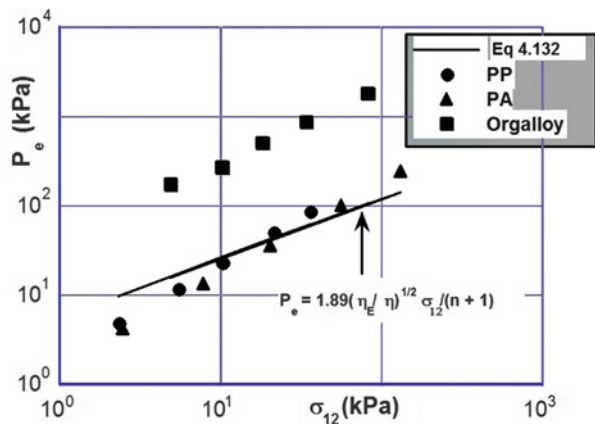
$P_e = 1.89(\eta_E/\eta)^{1/2}\sigma_{12}/(n+1)$

$$P_e = 1.89(\eta_E/\eta)^{1/2}\sigma_{12}/(n+1) \tag{7.132}$$

For Newtonian liquids Eq. 7.132 predicts $P_e \approx 1.64\sigma_{12}$, This proportionality is shown in Fig. 7.44 along with the experimental values determined for ORGALLOY™, PP, and PA-6. Evidently, Eq. 7.132 provides satisfactory approximation for the homopolymers, but for the blend, the prediction is again about one decade too low. Similarly, as for the shear flows, here also the elongational properties of blends show a different behavior under different extensional flow field conditions.

Extensional flow is important for the dispersion process. As the microrheology indicates, the minimum of the κ versus λ curve is very narrow for the shear flow, but very broad (and lower) for the extensional flow (see Fig. 7.45). This suggests that it should be much easier to disperse fluids in extensional than in shear flow fields.
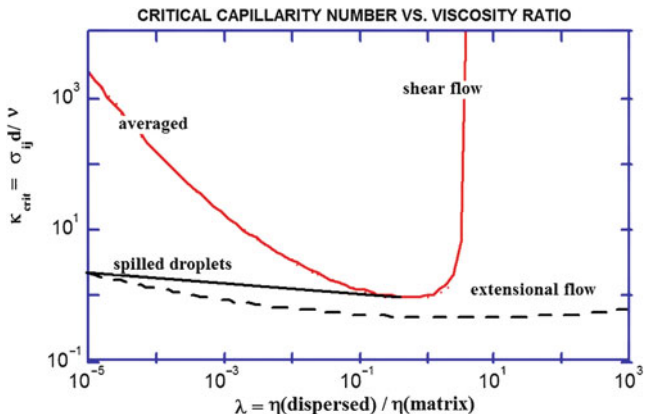
Fig. 7.45 Critical capillary number versus viscosity ratio is shear flow (*solid lines*) and extension (*dash line*)

In particular, the benefits are obvious for high and low values of the viscosity ratio. It has been demonstrated theoretically and experimentally that drops can be deformed but not broken by shear flow if $\lambda > 3.8$. This is not the case for the inverse ratio, but the drop spinning mechanism in this region is slow, which makes the dispersion process inefficient. These theoretical findings have been confirmed by constructing an extensional flow mixer, EFM, and performing experiments with polymer blends having large difference of viscosity (Luciani and Utracki 1996; Utracki and Luciani 1996).

7.6   Concluding Remarks

The rheological behavior of polymer blends is a complex phenomenon that is not only an extension of the rheological behavior of simple multicomponent systems, such as solutions, emulsions, and suspensions. Also, it is not the combination of the rheological behavior of the individual polymeric components or additive. However, the rheological behavior of polymer blends is governed by the same general rules of thermodynamics, mechanics, surface science, and other physical and chemical principles that govern the behavior of all materials, when they respond to stress or strain or forces that produce a rheological response.

In this chapter, we have attempted to provide some of the fundamental background regarding the behavior of simpler systems and to indicate how polymer blends behave similarly to these systems in some respects, while in many other respects they behave in a much more complex manner. Much of our discussion related to simple two-component blend systems. However, there are many

multicomponent systems that are of commercial interest in many applications. Even more complex blends, such as those involving biosystems and systems involving natural polymers, are gaining interest. The understanding of the flow and rheological behavior of these systems is certainly very difficult. However, in the final analysis, these materials must obey the same laws of physics and chemistry. Complex as they might be, it is certain that the modern tools of science and technology will deal with the relevant issues.

It should be apparent from the aspects covered in this chapter that the rheological behavior of polymer blends, as many aspects of the behavior of polymer systems, cannot be understood or explained in terms of fundamentals and observations associated with rheology alone. Many aspects of polymer and blend behavior are involved. Therefore, we suggest to the reader to refer to other chapters in this handbook for a more complete understanding of the issues involved.

7.7 Cross-References

▶ Compounding Polymer Blends
▶ Interpenetrating Polymer Networks
▶ Interphase and Compatibilization by Addition of a Compatibilizer
▶ Miscible Polymer Blends
▶ Morphology of Polymer Blends
▶ Polymer Blends Containing "Nanoparticles"
▶ Thermodynamics of Polymer Blends

Notation and Abbreviations

Notations (Roman Letters)

a, b, k, K, n, u, β Equation constants
a_v Interfacial area density
B_{AB} Reduced binary thermodynamic interaction parameter, $B_{AB} = \chi_{AB}RT/V$
B Droplet width
b_i Segment length
c_i Lee and Park relaxation parameters
D Deformation
d Droplet diameter
d^* Equilibrium droplet diameter
D, D_M, D_s Diffusion, inter diffusion and self diffusion coefficient, respectively
D_p Particle diffusion coefficient
E^+ Threshold energy of coagulation
E_{DK} Macroscopic bulk breaking energy

F Intrinsic thermodynamic function

f Frequency

G*, G′, G″ Complex, storage and loss shear modulus, respectively

H(τ) Relaxation time spectrum

H̃(ω) Reduced frequency relaxation spectrum

H̃$_G$(ω) Gross' frequency relaxation spectrum

H$_{max}$ Maximum of the relaxation spectrum

h$_c$ Critical separation distance

k$_B$ Boltzmann constant

L Droplet length

M Onsager-type mobility factor

M$_n$, M$_w$, M$_z$ Number, weight and z-average molecular weight, respectively

N$_1$ = σ$_{11}$ − σ$_{22}$ First normal stress difference

N$_{o,N}$ Initial and final number of particles respectively

N^o, N$^+$ Number of coagulating drops, initially and at t = t$_c$

N$_T$ Total number of collisions per unit time

n Number of particles

n$_i$ Number of moles unit volume

P Pressure

Pe Peclet number

p$_r$ Probability that two particles that have collided result in coalescence

q Wave vector, or sinusoidal distortion

R Ideal gas constant

Re Reynolds number or real part of a complex function

R(q) Fluctuation function

r̄ Reduced drop radius

⟨r$_\Theta^2$⟩$^{1/2}$ Unperturbed, average radius of gyration

rad Radian

r$_N$ Radius of the critical nucleus

S(q), S$_0$ Virtual structure function

S$_o$, S Interfacial area per unit volume of the blend for monodispersed spherical particles before and after coalescence, respectively

s Spinodal

T Absolute temperature

T$_g$ Glass transition temperature

t Time

t$_b$ Necessary time for breakup of droplets

t$_b$* Dimensionless breakup time

t$_c$ Coalescence time

UCST Upper critical solubility temperature

V Volume

V$_x$/V Volume fraction of emulsion undergoing uniform shear

z Reduced frequency, $f \cdot \tau$

Notation (Greek Letters)

$\boldsymbol{\alpha}$ Orientation angle

$\boldsymbol{\alpha_o}$ The distortion at $t = 0$

$\boldsymbol{\beta_{12}}$ Interlayer slip factor

$\boldsymbol{\chi_{AB}}$ Binary thermodynamic interaction parameter between polymers A and B

$\boldsymbol{\Delta}$ Thermodynamic distance from the spinodal; $\Delta \equiv 2((\chi_{AB}N)_{s-} (\chi_{AB}N))$

$\boldsymbol{\Delta E}$ Activation energy, e.g., of flow: ΔE_η

$\boldsymbol{\Delta G_m}$ Gibbs free energy of mixing

$\boldsymbol{\Delta H_m, \Delta S_m}$ Enthalpy and entropy of mixing, respectively

$\boldsymbol{\varepsilon, \dot{\varepsilon}}$ Hencky strain and Hencky strain rate in extension, respectively

$\boldsymbol{\phi_1, \phi_2}$ Volume fraction of dispersed and matrix phase, respectively

$\boldsymbol{\phi_c}$ Volume fraction of the cross-linked monomer units

$\boldsymbol{\phi_i}$ Volume fraction of phase i at phase inversion

$\boldsymbol{\phi_m}$ Maximum packing volume fraction

$\boldsymbol{\phi_{perc}}$ Percolation threshold

$\boldsymbol{\gamma, \dot{\gamma}}$ Shear strain and rate of shearing, respectively

$\boldsymbol{\eta}$ Viscosity

$\boldsymbol{\eta_o}$ Zero-shear viscosity

$\boldsymbol{\eta_r}$ Relative viscosity

$\boldsymbol{[\eta]}$ Intrinsic viscosity

$\boldsymbol{\eta'}$ Dynamic viscosity

$\boldsymbol{\eta^*}$ Complex viscosity

$\boldsymbol{\eta_1, \eta_2}$ Viscosity of dispersed and matrix phase, respectively

$\boldsymbol{\kappa = \sigma_{\iota\varphi}d/\nu_{12}}$ Capillary number

$\boldsymbol{\kappa_{crit}}$ Critical capillary number

$\boldsymbol{\Lambda}$ Distortion wavelength

$\boldsymbol{\lambda = \eta_1/\eta_2}$ Viscosity ratio

$\boldsymbol{\lambda_s}$ Wavelength

$\boldsymbol{\nu_{12}^o}$ Interfacial tension in a quiescent blends

$\boldsymbol{\nu_{12}}$ Interfacial tension coefficient between phase 1 and 2

$\boldsymbol{\rho}$ Density

$\boldsymbol{\rho_d}$ Droplet density

$\boldsymbol{\sigma}$ Stress

$\boldsymbol{\sigma_{11}}$ Extensional stress

$\boldsymbol{\sigma_{11} - \sigma_{22} = N_1}$ First normal stress difference

$\boldsymbol{\sigma_{12}}$ Shear stress

$\boldsymbol{s_m}$ Stress in the matrix phase

$\boldsymbol{\sigma_y}$ Yield stress

$\boldsymbol{\sigma_y^o}$ Permanent yield stress

$\boldsymbol{\tau}$ Relaxation time

$\boldsymbol{t^*}$ Mean relaxation time

$\boldsymbol{\Omega(\Lambda, \lambda)}$ Tabulated function for capillary instability

ω Angular frequency
ω_max Frequency at which $\tilde{H}(\omega)$ is maximum
ω_x Crossover frequency
ψ_1, ψ_2 First and second normal stress difference coefficient, respectively

Abbreviations

ABS Acrylonitrile-butadiene-styrene
EFM Extensional flow mixer
EPDM Ethylene-propylene-diene terpolymer
EPR Ethylene-propylene rubber
EVAc Ethylene-vinyl acetate copolymer
HDPE High density polyethylene
HIPS High impact polystyrene
IPN Interpenetrating networks
LDPE Low density polyethylene
LLDPE Linear low density polyethylene
NG Nucleation and growth
NR Natural rubber
PA Polyamide
PAA Polyacrylic acid
PB Polybutadiene
PC Polycarbonate
PCL Polcaprolactone
PE Polyethylene
PEO Polyethylene oxide (or polyethyleneglycol, PEG)
PEMA Poly(ethyl methacrylate)
Phenoxy Polyhydroxyether of bis-phenol A
PMMA Polymethylmethacrylate
PnBA Poly(*n*-butyl)acrylate
PP Polypropylene
PPE Polyphenyleneether
PS, PSD Polystyrene, deuterated PS
PSF Polysulfone
PVC Polyvinyl chloride
PVME Polyvinylmethylether
RMS Rheometrics Mechanical Spectrometer
RSR Rheometrics Stress Rheometer
SBR Styrene-butadiene rubber
SBS Styrene-butadiene-styrene three block copolymer
SD Spinodal decomposition
SEBS Styrene-ethylene/butene-styrene three block copolymer
SEC Size exclusion chromatography
SIN Simultaneous interpenetrating polymer networks

SSE Single-screw extruder
TP Thermoplastic resin
TS Thermoset resin
TSE Twin-screw extruder

References

J.R. Abbott, N. Tetlow, A.L. Graham, S.A. Altobelli, E. Fukushima, L.A. Mondy, T.S. Stephens, J. Rheol. **35**, 773 (1991)

T.I. Ablazova, M.B. Tsebrenko, A.V. Yudin, G.V. Vinogradov, B.V. Yarlykov, J. Appl. Polym. Sci. **19**, 1781 (1975)

D.D. Acierno, D. Curto, F.P. La Mantia, A. Valenza, in *NRCC/IMRI symposium "Polyblends- '85"*, Boucherville, QC, Canada, 16–17April 1985

D.D. Acierno, D. Curto, F.P. La Mantia, A. Valenza, Polym. Eng. Sci. **26**, 28 (1986)

N. Aggarwal, K. Sarkar, J. Fluid Mech. **601**, 63–84 (2008)

T.O. Ahn, J.H. Kim, H.M. Jeong, S.W. Lee, L.S. Park, J. Polym. Sci. Part B Polym. Phys. **32**, 21 (1994)

A. Aït-Kadi, A. Ajji, B. Brahimi, in *Theoretical and Applied Rheology*, ed. by P. Moldenaers, R. Keunings. 11th International Congress on Rheology (Elsevier, Brussels, 1992)

A. Ajji, P.A. Gignac, Polym. Eng. Sci. **32**, 903 (1992)

A. Ajji, L. Choplin, Macromolecules **24**, 5221 (1991)

A. Ajji, L.A. Utracki, Polym. Eng. Sci. **36**, 1574 (1996)

A. Ajji, L.A. Utracki, Prog. Rubber Plast. Technol. **13**, 153 (1997)

A. Ajji, L. Choplin, R.E. Prud'homme, J Polym Sci B **26**, 2279–2289 (1988a)

A. Ajji, L. Choplin, R.E. Prud'homme, J. Polym. Sci. Part B Polym. Phys. **26**, 2279 (1988b)

A. Ajji, L. Choplin, R.E. Prud'homme, J. Polym. Sci. Part B Polym. Phys. **29**, 1573 (1994)

G. Akovali, J. Polym. Sci. A-2 **5**, 875 (1967)

P.S. Allan, M.J. Bevis, Plast. Rubber Proc. Appl. **3**, 85, 331 (1983)

P.S. Allan, M.J. Bevis, Plast. Rubber Proc. Appl. **5**, 71 (1985)

P.S. Allan, M.J. Bevis, Plast. Rubber Proc. Appl. **7**, 3 (1987)

P.S. Allan, M.J. Bevis, in *Proceedings of 5-th Annual PPS Meeting*, Kyoto, 11–14 April 1989

N. Alle, J. Lyngaae-Jørgensen, Rheol. Acta **19**, 94, 104 (1980)

N. Alle, F.E. Andersen, J. Lyngaae-Jørgensen, Rheol. Acta **20**, 222 (1981)

A.S. Almusallam, R.G. Larson, M.J. Solomon, J. Non-Newtonian Fluid Mech. **113**, 29–48 (2003)

S.H. Anastasiadis, I. Gancarz, J.T. Koberstein, Macromolecules **21**, 2980 (1988)

S.H. Anastasiadis, I. Gancarz, J.T. Koberstein, Macromolecules **22**, 1449 (1989)

C.A. Angell, Polymer **38**, 6261 (1997)

M.R. Anklam, G.G. Warr, R.K. Prud'homme, J. Rheol. **38**, 797 (1994)

Y. Aoki, M. Watanabe, Polym. Eng. Sci. **32**, 878 (1992)

M.A. Araujo, R. Stadler, Makromol. Chem. **189**, 2169 (1988)

K.R. Arnold, D.J. Meier, J. Appl. Polym. Sci. **14**, 427 (1970)

S. Arrhenius, Z. Physik. Chem. (Leipzig) **1**, 285 (1887)

A. Ausin, I. Eguiazabal, M.E. Munoz, J.J. Pena, A. Santamaria, Polym. Eng. Sci. **27**, 529 (1987)

G.N. Avgeropoulos, F.C. Weissert, P.N. Biddison, G.G.A. Böhm, Rubber Chem. Technol. **49**, 93 (1976)

M. Bains, S.T. Balke, D. Reck, J. Horn, Polym. Eng. Sci. **34**, 1260 (1994)

L. Barangi, H. Nazockdast, F.A. Taromi, J. Appl. Polym. Sci. **108**, 2558–2563 (2008)

A.O. Baranov, V.V. Nizhegorodov, I.I. Perepechko, M.I. Knunyants, E. Pruts, Vysokomol. Soedin. **A34**, 66 (1992)

W.M. Barentsen, D. Heikens, P. Piet, Polymer **15**, 119 (1974)

I. Barrar, G.N. Mathur, Polymer **35**, 2631 (1994)

B.W. Barry, Adv. Colloid Interface Sci. **5**, 37 (1977)

D. Barthès-Biesel, A.A. Acrivos, J. Fluid Mech. **61**, 1 (1973)

D. Barthès-Biesel, V. Chhim, Int. J. Multiphase Flow **7**, 493 (1981)

D. Barthès-Biesel, in *Rheological Measurements*, ed. by A.A. Collyer, D.W. Clegg (Elsevier, London, 1988)

D.W. Bartlett, J.W. Barlow, D.R. Paul, J. Appl. Polym. Sci. **27**, 2351 (1982)

G.K. Batchelor, J. Fluid Mech. **44**, 419 (1970)

G.K. Batchelor, J. Fluid Mech. **46**, 813 (1971)

G.K. Batchelor, Annu. Rev. Fluid Mech. **6**, 227 (1974)

G.K. Batchelor, J. Fluid Mech. **83**, 97 (1977)

C.G. Bazuin, A. Eisenberg, J. Polym. Sci. Part B Polym. Phys. **24**, 1021, 1121, 1137, 1155 (1986)

M.L. Becraft, A.B.. Metzner, J. Rheol. **36**, 143 (1992)

D. Beery, S. Kenig, A. Siegmann, Polym. Eng. Sci. **31**, 451 (1991)

D. Beery, S. Kenig, A. Siegmann, M. Narkis, Polym. Eng. Sci. **32**, 6 (1992)

J. Bergenholtz, J.F. Brady, M. Vicic, J. Fluid Mech. **456**, 239–275 (2002)

A. Berrayah, U. Maschke, J Polym Sci B **49**, 310–317 (2011)

P.A. Bhadane, N. Virgilio, B.D. Favis, M.F. Champagne, M.A. Huneault, F. Tofan, AIChE J. **52**, 3411–3420 (2006)

M.A. Bibbo, S.M. Dinh, R.C. Armstrong, J. Rheol. **29**, 905 (1985)

D.I. Bigg, S. Middleman, Ind. Eng. Chem. Fundam. **13**, 113 (1974)

D.I. Bigio, J.H. Conner, Polym. Eng. Sci. **35**, 1527 (1995)

I. Bihannic, C. Baravian, J.F.L. Duval, E. Paineau, F. Meneau, P. Levitz, J.P. de Silva, P. Davidson, L.J. Michot, J. Phys. Chem. B **114**, 16347–16355 (2010)

D.M. Binding, J. Non-Newtonian Fluid Mech. **27**, 173 (1988)

E.C. Bingham, *Fluidity and Plasticity* (McGraw-Hill, New York, 1922), p. 86

K.G. Blizard, R.R. Haghighat, Polym. Eng. Sci. **33**, 799 (1993)

L.S. Bolotnikova, A.K. Evseer, Y.N. Panov, S.Y. Frenkel, Vysokomol. Soed. **B24**, 154 (1982)

H.C. Booij, J.H.M. Palmen, in *11 Congress Rheology*, Brussels, 17–21 Aug 1992 (1992)

D. Bourry, B.D. Favis, J Polym Sci B **36**, 1889–1899 (1998)

D.W. Bousfield, R. Keunings, G. Marucci, M.M. Denn, J. Non-Newtonian Fluid Mech. **21**, 79 (1986)

M. Bousmina, R. Muller, in *11th Congress on Rheology*, Brussels, 17–21 Aug 1992 (1992)

M. Bousmina, R. Muller, Rheol. Acta **35**, 369 (1996)

M. Bousmina, A. Lavoie, B. Riedl, Macromolecules **35**, 6274–6283 (2002)

M. Bousmina, J.F. Palierne, L.A. Utracki, Polym. Eng. Sci. **39**, 1049 (1999)

J.M. Brader, J. Phys. Condens. Matter **22**, 363101 (2010)

J.F. Brady, G. Bossis, J. Fluid Mech. **155**, 105 (1985)

J.F. Brady, J. Chem. Phys. **99**, 567 (1993)

J.F. Brady, M. Vicic, J. Rheol. **39**, 545–566 (1995)

B. Brahimi, A. Aït-Kadi, A. Ajji, R. Fayt, J. Rheol. **35**, 1069 (1991)

M.J. Brekner, H.J. Cantow, H.A. Schneider, Polym. Bull. **14**, 17 (1985)

H. Brenner, J. Fluid Mech. **4**, 641 (1970)

R.E.S. Bretas, C. Granado, Eur. Polym. **290**, 769 (1994)

R.E.S. Bretas, D. Collias, D.G. Baird, Polym. Eng. Sci. **34**, 1492 (1994)

D.J. Bye, I.S. Miles, Eur. Polym. J. **22**, 185 (1986)

N.R. Cameron, D.C. Sherrington, Adv. Polym. Sci. **126**, 163 (1996)

Y. Cao, W. Fan, J. Wang, R. Chen, Q. Zheng, Suliao Gongye **35**, 41–43 (2007)

P.J. Carreau, Trans. Soc. Rheol. **16**, 99 (1972)

P. Cassagnau, M. Bert, V. Verney, A. Michel, Polym. Eng. Sci. **32**, 998 (1992)

P.P. Castañeda, J. Mech. Phys. Solids **39**, 45–71 (1991)

J.Y. Cavaille, J. Perez, C. Jourdan, G.P. Johari, J. Polym. Sci. B Polym. Phys. **25**, 1847 (1987)

C.E. Chaffey, Ann. Rev. Mater. Sci. **13**, 43 (1983)

C. Chartier, L. Benyahia, J.F. Tassin, H.D. Ngoc, J.F. Bardeau, Polym. Eng. Sci. **50**, 773–779 (2010)

M.F. Champagne, M.M. Dumoulin, L.A. Utracki, J.P. Szabo, Polym. Eng. Sci. **36**, 1636 (1996)

C.-M. Chan, A. Nixon, S. Venkatraman, J. Rheol. **36**, 807 (1992)

C. Chang, R.L. Powell, J. Rheol. **38**, 85 (1994)

N. Chapleau, P.J. Carreau, C. Peleteiro, P.-A. Lavoic, T.M. Malik, Polym. Eng. Sci. **32**, 1876 (1992)

X. Chateau, G. Ovarlez, K.L. Trung, J. Rheol. **52**, 489–506 (2008)

R. Chella, in *Mixing and Compounding of Polymers*, ed. by I. Manas-Zloczower, Z. Tadmor (Hanser, Munich/Vienna/New York, 1994)

R. Chella, J.M. Ottino, Ind. Eng. Chem. Fundam. **24**, 170 (1985)

C. Chen, F.S. Lai, Polym. Eng. Sci. **34**, 472 (1994)

A.K. Chesters, Chem. Eng. Res. Des. **69**, 259–270 (1991a)

A.K. Chesters, Trans. Ind. Chem. Eng. **A69**, 259 (1991b)

H.B. Chin, C.D. Han, J. Rheol. **23**, 557 (1979)

H.B. Chin, C.D. Han, J. Rheol. **24**, 1 (1980)

Y.G. Cho, M.R. Kamal, Polym. Eng. Sci. **42**, 2005–2015 (2002)

S.J. Choi, W.R. Schowalter, Phys. Fluids **18**, 420–427 (1975)

H.-K. Chuang, C.D. Han, in *Polymer Blends and Composites in Multiphase Systems*, ed. by C.D. Han. Advances in Chemistry, Vol. 206 (American Chemical Society, 1984)

H.-K. Chuang, C.D. Han, J. Appl. Polym. Sci. **29**, 2205 (1984); Adv. Chem. **204**, 171 (1984); J. Polym. Sci. **29**, 2205 (1984)

H.-K. Chuang, C.D. Han, J. Appl. Polym. Sci. **30**, 165, 2457 (1985)

N. Clarke, T.C.B. McLeish, S. Pavawongsak, J.S. Higgins, Macromolecules **30**, 4459 (1997)

F. Cogswell, N. Polym. Eng. Sci. **12**, 69 (1972); Trans. Soc. Rheol. **16**, 383 (1972)

F.N. Cogswell, B.P. Griffin, J.B. Rose, Eur. Pat. Appl. **030,417**, 17 June 1981, Appl. 07 Nov 1980

F.N. Cogswell, B.P. Griffin, J.B. Rose, U.S. Patent **4,386,174**, 1983

F.N. Cogswell, B.P. Griffin, J.B. Rose, U.S. Patent **4,433,083**, 1984; U.S. Patent **4,438,236**, 1984, U.K. Appl. 1979, to Imperial Chemical Industries, PLC

R.H. Colby, Polymer **30**, 1275 (1989)

A.A. Collyer, D.W. Clegg (eds.), *Rheological Measurements* (Elsevier, London, 1988)

A.A. Collyer, L.A. Utracki (eds.), *Polymer Rheology and Processing* (Elsevier, London, 1990)

P.R. Couchman, J. Appl. Polym. Sci. **60**, 1057 (1996)

R.G. Cox, S.G. Mason, Annu. Rev. Fluid Mech. **3**, 291 (1971)

R.G. Cox, J. Fluid Mech. **37**, 601 (1969)

M.M. Cross, J. Colloid Sci. **20**, 417 (1965)

M.M. Cross, J. Colloid Sci. **33**, 30 (1970)

M.M. Cross, J. Colloid Sci. **44**, 175 (1973)

R.J. Crowson, M.J. Folkes, Polym. Eng. Sci. **20**, 934 (1980)

R.J. Crowson, M.J. Folkes, P.F. Bright, Polym. Eng. Sci. **20**, 925 (1980)

R.J. Crowson, A.J. Scott, D.W. Saunders, Polym. Eng. Sci. **21**, 1014 (1981)

D. Curto, F.P. La Mantia, D. Acierno, Rheol. Acta **22**, 197 (1983)

S. Danesi, R.S. Porter, Polymer **19**, 448 (1978)

C. David, M. Getlichermann, M. Trojan, R. Jacobs, Polym. Eng. Sci. **32**, 6 (1992)

R.A. De Bruijn, Ph.D. Thesis, Eindhoven University of Technology, 1989

R.D. Deanin, G.E. d'Isidoro, ACS Div. Org. Coat. Plast. Prepr. **43**, 19 (1980)

I. Delaby, B. Ernst, R. Muller, Rheol. Acta **34**, 525 (1995)

I. Delaby, B. Ernst, Y. Germain, R. Muller, J. Rheol. **38**, 1705 (1994)

L. Delamare, B. Vergnes, Polym. Eng. Sci. **36**, 1685–1693 (1996)

C. DeLeo, K. Walsh, S. Velankar, J. Rheol. **55**, 713–731 (2011)

I.E. Denisov, A.I. Krasheninnikov, V.G. Chervin, Kolloid. Z. **47**, 790 (1985)

B.L. Deopura, S. Kadam, J. Appl. Polym. Sci. **31**, 2145 (1986)

F. Deri, O. Behar, Polym. Intl. **28**, 63 (1992)

Y. Deyrail, Z. El Mesri, M. Huneault, A. Zeghloul, M. Bousmina, J. Rheol. **51**, 781–797 (2007)

S. Dietrich, A. Amnon, *Introduction to Percolation Theory* (Taylor & Francis, 1994)

K. Dimov, M. Savov, Vysokomol. Soed. **A22**, 65 (1980)

B. Dimzoski, I. Fortelny, M. Slouf, M. Nevoralova, D. Michalkova, J. Mikesova, *e-Polymer* (2011)

B. Dimzoski, I. Fortelný, M. Šlouf, A. Sikora, D. Michálková, Polym. Bull. **70**, 263–275 (2013)

S.M. Dinh, R.C. Armstrong, J. Rheol. **28**, 207 (1984)

V. Dobrescu, V. Cobzaru, J. Polym. Sci. Polym. Symp. **64**, 27 (1978)

V. Dobrescu, in *Rheology*, ed. by G. Astarita, G. Marrucci, L. Nicolais, vol. 2 (Plenum, New York, 1980), p. 555

M. Doi, S.F. Edwards, J. Chem. Soc. Faraday Trans. **11**, 74, 560, 918 (1978)

M. Doi, T. Ohta, J. Chem. Phys. **95**, 1242 (1991)

M. Doi, A. Onuki, J. Phys. Paris **2**, 1631 (1992)

N. Domingues, A. Gaspar-Cunha, J.A. Covas, Polym. Eng. Sci. **50**, 2194–2204 (2010)

M. Doraiswamy, A.B.. Metzner, Rheol. Acta **25**, 580 (1986)

L. D'Orazio, C. Mancarella, E. Martuscelli, A. Casale, A. Filippe, F. Speroni, J. Mater. Sci. **21**, 989 (1986)

L. D'Orazio, C. Mancarella, E. Martuscelli, A. Casale, A. Filippe, F. Speroni, J. Mater. Sci. **22**, 429 (1987)

M. Dressler, B.J. Edwards, J. Non-Newtonian Fluid Mech. **120**, 189–205 (2004)

V.Y. Dreval, A. Kassa, Y.K. Borisenkova, M.L. Kerber, G.V. Vinogradov, M.S. Akutin, Vysokomol. Soed. **A25**, 156 (1983a)

V.Y. Dreval, G.V. Vinogradov, M.P. Zabugina, N.P. Krasnikova, E.V. Kotova, Z. Pelzbauer, Rheol. Acta **22**, 102 (1983b)

M.M. Dumoulin, C. Farha, L.A. Utracki, Polym. Eng. Sci. **24**, 1319 (1984a)

M.M. Dumoulin, Ph.D. Thesis, Ecole Polytechnique, Montreal, 1988

M.M. Dumoulin, P. Toma, L.A. Utracki, I. Jinnah, M.R. Kamal, SPE Techn. Pap. **31**, 534 (1985)

M.M. Dumoulin, L.A. Utracki, P.J. Carreau, in *36ᵗʰ Conference of the Canadian Society of Chemical Engineering*, Sarnia, 5–8 Oct 1986

M.M. Dumoulin, L.A. Utracki, C. Farha, SPE Techn. Pap. **30**, 443 (1984b)

M.M. Dumoulin, L.A. Utracki, J. Lara, Polym. Eng. Sci. **24**, 117 (1984c)

N.Q. Dzuy, D.V. Boger, J. Rheol. **27**, 321 (1983)

N.Q. Dzuy, D.V. Boger, J. Rheol. **29**, 335 (1985)

P. Edel, Ph.D. Thesis (3e cycle), Univ. Pau, 1984

A. Einstein, Ann. Phys. **19**, 289 (1906)

A. Einstein, Ann. Phys. **34**, 591 (1911)

H. El Khadi, J. Denault, D. Tapin, M.F. Champagne, L.A. Utracki, M.M. Dumoulin, SPE Techn. Pap. **41**, 3143 (1995)

P.H.M. Elemans, Modeling of the processing of incompatible polymer blends, Ph.D. Thesis, Eindhoven University of Technology, 1989

J.J. Elmendorp, Ph.D. Thesis, Delft University of Technology, The Netherlands, 1986; Polym. Eng. Sci. **26**, 418 (1986)

C. Elster, J. Honerkamp, J. Weese, Rheol. Acta **30**, 161 (1993)

M. Entezam, H.A. Khonakdar, A.A. Yousefi, S.H. Jafari, U. Wagenknecht, G. Heinrich, B. Kretzschmar, Macromol. Mater. Eng. **297**, 312–328 (2012)

L. Erwin, Polym. Eng. Sci. **18**, 1044 (1978)

A. Eshuis, J. Mellema, Colloid Polym. Sci. **262**, 159 (1984)

H. Eslami, M.R. Kamal, Annu. Tech. Conf. Soc. Plast. Eng. **70**, 155–158 (2012)

H. Eslami, M.R. Kamal, J. Appl. Polym. Sci. **127**, 2290–2306 (2013a)

H. Eslami, M.R. Kamal, J. Appl. Polym. Sci. **129**, 2418–2428 (2013b)

B.D. Favis, J.P. Chalifoux, Polymer **29**, 1761 (1988)

R. Fayt, P. Teyssie, Polym. Eng. Sci. **29**, 538 (1989)

R. Fayt, R. Jerome, P. Teyssie, J. Polym. Sci. Makromol. Chem. **187**, 837 (1986a)

R. Fayt, R. Jerome, P. Teyssie, J. Polym. Sci. Polym. Lett. Ed. **19**, 79, 1269 (1981)

R. Fayt, R. Jerome, P. Teyssie, J. Polym. Sci. Polym. Lett. Ed. **24**, 25 (1986b)

R. Fayt, R. Jerome, P. Teyssie, J. Polym. Sci. Polym. Lett. Ed. **20**, 2209 (1982)

K. Feigl, S.F.M. Kaufmann, P. Fischer, E.J. Windhab, Chem. Eng. Sci. **58**, 2351–2363 (2003)

M.L. Fernandez, J.S. Higgins, S.M. Richardson, Chem. Eng. Res. Des. **71**, 239–244 (1993a)

M.L. Fernandez, J.S. Higgins, S.M. Richardson, Trans. IChemE **71A**, 239 (1993b)

M.L. Fernandez, J.S. Higgins, R. Horst, B.A. Wolf, Polymer **36**, 149 (1995)

J.D. Ferry, *Viscoelastic Properties of Polymers*, 3rd edn. (Wiley, New York, 1980)

D.G. Fesko, N.W. Tschoegl, J. Polym. Sci. **C35**, 51 (1971)

P. Fischer, P. Erni, Curr. Opin. Colloid Interf. Sci. **12**, 196–205 (2007)

R.W. Flumerfelt, Ind. Eng. Chem. Fundam. **11**, 312 (1972)

M.J. Folkes, *Short Fiber Reinforced Thermoplastics* (Wiley, New York, 1982)

M.J. Folkes (ed.), *Processing, Structure and Properties of Block Copolymers* (Elsevier, London, 1985)

I. Fortelny, D. Kamenicka, J. Kovar, Angew. Makromol. Chem. **164**, 125 (1988)

I. Fortelny, D. Michalkova, J. Koplikova, E. Navratilova, J. Kovar, Angew. Makromol. Chem. **179**, 185 (1990)

I. Fortelny, M. Lapcikova, F. Lednicky, Z. Stary, Z. Krulis, Polimery (Warsaw, Pol.) **54**, 139–144 (2009)

A. Frank, J. Meissner, Rheol. Acta **23**, 117 (1984)

H.R. Frederix, R. Fayt, A. Gilliquet, Comportement Industriel des Alliages Polymeriques – Analyse et Perspectives Nouvelles, internal report No. PL 15 CRIF, Bruxelles, July 1981

E.M. Friedman, R.S. Porter, Trans. Soc. Rheol. **19**, 493 (1975)

C. Friedrich, W. Gleinser, E. Korat, D. Maier, J. Weese, J. Rheol. **39**, 1411 (1995)

C. Friedrich, Y.Y. Antonov, Macromolecules **40**, 1283–1289 (2007)

F.A. Gadala-Maria, Ph.D. Thesis, Stanford University, 1979

E. Ganani, R.L. Powell, J. Comp. Mater. **19**, 194 (1985)

H. Garmabi, M.R. Kamal, SPE Techn. Pap. **41**, 3182 (1995)

F. Gauthier, H.L. Goldsmith, S.G. Mason, Rheol. Acta **10**, 344 (1971)

C.B. Gell, R. Krishnamoorti, E. Kim, W.W. Graessley, L.J. Fetters, Rheol. Acta **36**, 217 (1997)

A.A. Gerasimchuk, O.V. Romankevich, E.M. Aizenshtein, Khim. Volok. **2**, 21 (1986)

Y. Germain, B. Ernst, O. Genelot, L. Dhamani, J. Rheol. **38**, 681 (1994)

F. Ghiam, J.L. White, Polym. Eng. Sci. **31**, 76 (1991)

A. Ghijsels, J.J.S.M. Ente, J. Raadsen, in *Integration of Fundamental Polymer Science and Technology-2*, ed. by P.J. Lemstra, L.A. Kleintjens (Elsevier, Amsterdam, 1988)

H. Giesekus, private communication, 1981

N. Gladwell, R.R. Rahalkar, P. Richmond, Rheol. Acta **25**, 55 (1986)

S. Glasstone, K.L. Laidler, H. Eyring, *Theory of Rate Processes* (McGraw-Hill, New York, 1941)

W. Gleisner, H. Braun, C. Friedrich, H.J. Cantow, Polymer **35**, 128 (1994a)

W. Gleisner, D. Maier, M. Schneider, J. Weese, C. Friedrich, J. Honerkamp, J. Appl. Polym. Sci. **53**, 39 (1994b)

W. Gleissle, in *Rheology*, ed. by G. Astarita, G. Marruci, L. Nicolais, vol. 2 (Plenum, New York, 1980), p. 457

J.D. Goddard, C. Miller, J. Fluid Mech. **28**, 657 (1967)

L.A. Goettler, K.S. Shen, Rubber Chem. Technol. **56**, 619 (1983)

L.A. Goettler, Polym. Compos. **5**, 60 (1984)

A.Y. Goldman, G.K. Murzakhanov, O.A. Soshina, Mekh. Polim. **4**, 614 (1977)

H.L. Goldsmith, S.G. Mason, in *Rheology*, ed. by F.R. Eirich, vol. 4 (Academic, New York, 1967)

A. Golovoy, M. Kozlowski, M. Narkis, Polym. Eng. Sci. **32**, 854 (1992)

R. Gonzalez-Nunez, B.D. Favis, P.J. Carreau, Polym. Eng. Sci. **33**, 851 (1993)

R. Gopalakrishnan, M. Shultz, R.M. Gohil, J. Appl. Polym. Sci. **56**, 1749 (1995)

H. Goto, H. Kuno, J. Rheol. **26**, 387 (1982)

H. Goto, H. Kuno, J. Rheol. **28**, 197 (1984)

S. Goto, H. Nagazono, H. Kato, Rheol. Acta **25**, 119, 246 (1986)

H.P. Grace, Chem. Eng. Commun. **14**, 225–277 (1982)

D. Graebling, R. Muller, Colloids Surf. **55**, 89 (1991)

D. Graebling, A. Benkira, Y. Gallot, R. Muller, Eur. Polym. **30**, 301 (1994)

D. Graebling, R. Muller, J.F. Palierne, J. Phys. IV **3**, 1525–1534 (1993a)

D. Graebling, R. Muller, J.F. Palierne, Macromolecules **26**, 320 (1993b)

A.L. Graham, S.A. Altobelli, E. Fukushima, L.A. Mondy, T.S. Stephens, J. Rheol. **35**, 191 (1991)

H. Gramespacher, J. Meissner, J. Rheol. **39**, 151 (1995)

N. Grizzuti, O. Bifulco, Rheol. Acta **36**, 406 (1997)

M. Grmela, A. Ait-Kadi, L.A. Utracki, J. Non-Newtonian Fluid Mech. **77**, 253 (1998)

M. Grmela, A. Ait-Kadi, J. Non-Newtonian Fluid Mech. **55**, 191 (1994)

M. Grmela, A. Ait-Kadi, J. Non-Newtonian Fluid Mech. **55**, 191 (1998)

M. Grmela, M. Bousmina, J.-F. Palierne, Rheol. Acta **40**, 560 (2001)

M. Grmela, H.C. Öttinger, Phys. Rev. E **56**, 6620–6632 (1997)

D.J. Groves, T.C.B. McLeish, R.K. Chohan, P.D. Coates, Rheol. Acta **35**, 481 (1996)

G.K. Guenther, D.G. Baird, J. Rheol. **40**, 1 (1996)

A.K. Gupta, K.R. Srinivasan, J. Appl. Polym. Sci. **47**, 167 (1993)

A.K. Gupta, B.K. Ratnam, K.R. Srinivasan, J. Appl. Polym. Sci. **46**, 281 (1992)

P.C. Guschl, J.U. Otaigbe, J. Colloid Interface Sci. **266**, 82–92 (2003)

C.D. Han, H.-K. Chuang, J. Appl. Polym. Sci. **30**, 2431 (1985)

C.D. Han, K. Funatsu, J. Rheol. **22**, 113 (1978)

C.D. Han, J.K. Kim, Polymer **34**, 2533 (1993)

C.D. Han, H.-H. Yang, J. Appl. Polym. Sci. **33**, 1199, 1221 (1987)

C.D. Han, T.C. Yu, J. Appl. Polym. Sci. **15**, 1163 (1971)

C.D. Han, T.C. Yu, Polym. Eng. Sci. **12**, 81 (1972)

C.D. Han, T.C. Yu, J. Appl. Polym. Sci. **15**, 1163 (1981)

C.D. Han, Y.W. Kim, S.J. Chen, J. Appl. Polym. Sci. **19**, 2831 (1975)

C.D. Han, *Multiphase Flow in Polymer Processing* (Academic, New York, 1981)

C.D. Han, D.M. Baek, J.K. Kim, Macromolecules **23**, 561–570 (1990)

C.D. Han, D.M. Baek, J.K. Kim, T. Ogawa, N. Sakamoto, T. Hashimoto, Macromolecules **28**, 5043–5062 (1995)

H.J.M. Hanley, G.C. Straty, F. Tsvetkov, Langmuir **10**, 3362–3364 (1994)

W.D. Harkins, J. Chem. Phys. **9**, 552–568 (1941)

T. Hashimoto, M. Fujimura, H. Kawai, Macromolecules **13**, 1237 (1980a)

T. Hashimoto, K. Nagatoshi, A. Todo, H. Kawai, Macromolecules **13**, 1237 (1980b)

T. Hashimoto, T. Takebe, K. Fujioka, in *Dynamics and Patterns in Complex Fluids*, ed. by A. Onuki, K. Kawasaki (Springer, New York, 1990)

Z. Hashin, Appl. Mech. Rev. **17**, 1 (1964)

K. Hayashida, T. Yoshida, Bull. Fac. Text. Sci. Kyoto Univ. **9**, 65 (1979)

D. Heikens, W. Barentsen, Polymer **18**, 69 (1977)

R.F. Heitmiller, R.Z. Naar, H.H. Zabusky, J. Appl. Polym. Sci. **8**, 873 (1964)

E. Helfand, G.H. Fredrickson, Phys. Rev. Lett. **62**, 2468 (1989)

E. Helfand, A.M. Sapse, J. Chem. Phys. **62**, 1327 (1975)

E. Helfand, Y. Tagami, J. Polym. Sci. Polym. Lett. **9**, 741 (1971)

E. Helfand, Y. Tagami, J. Chem. Phys. **56**, 3593 (1972)

E. Helfand, Z.R. Wasserman, Macromolecules **9**, 879 (1976)

E. Helfand, Z.R. Wasserman, Macromolecules **11**, 960 (1978)

E. Helfand, Z.R. Wasserman, Macromolecules **13**, 994 (1980)

C.P. Henderson, M.C. Williams, J. Polym. Sci. Polym. Lett. Ed. **17**, 257 (1979)

E.J. Hinch, A.A. Acrivos, J. Fluid Mech. **98**, 305 (1980)

E.J. Hinch, L.G. Leal, J. Fluid Mech. **52**, 683 (1972)

I.A. Hindawi, J.S. Higgins, R.A. Weiss, Polymer **33**, 2522 (1992)

G. Hinrichsen, W. Green, Kunststoffe **71**, 99 (1981)

W.-J. Ho, R. Salovey, Polym. Eng. Sci. **21**, 839 (1981)

R.L. Hoffman, Trans. Soc. Rheol. **16**, 155 (1972)

R.L. Hoffman, J. Colloid Interface Sci. **46**, 491 (1974)

J. Honerkamp, J. Weese, Continuum Mech. Thermod. **2**, 17 (1990)

J. Honerkamp, J. Weese, Rheol. Acta **32**, 57, 65 (1993)

S.M. Hong, B.C. Kim, Polym. Eng. Sci. **34**, 1605 (1994)

S.M. Hong, B.C. Kim, S.S. Hwang, K.U. Kim, Polym. Eng. Sci. **33**, 630 (1993)

R. Horst, B.A. Wolf, Macromolecules **24**, 2236 (1991)

R. Horst, B.A. Wolf, Macromolecules **25**, 5291 (1992)

H.X. Huang, G. Jiang, X.J. Li, Int. Polym. Process. **23**, 47–54 (2008)

H.-X. Huang, Y.-F. Huang, S.-L. Yang, Polym. Int. **54**, 65–69 (2005)

J.-C. Huang, H.-F. Shen, Y.-T. Chu, Adv. Polym. Technol. **13**, 49 (1994)

J. Huitric, M. Moan, P.J. Carreau, N. Dufaure, J. Non-Newtonian Fluid Mech. **145**, 139–149 (2007)

J. Huitric, J. Ville, P. Mederic, M. Moan, T. Aubry, J. Rheol. **53**, 1101–1119 (2009)

M.A. Huneault, M.F. Champagne, A. Luciani, J.-F. Hetu, L.A. Utracki, *Generation of Polymer Blends' Morphology* (Polymer Processing Society, Stuttgart, 1995a)

M.A. Huneault, Z.H. Shi, L.A. Utracki, Polym. Eng. Sci. **35**, 115 (1995b)

M.A. Huneault, H. Li, Polymer **48**, 270–280 (2007)

J.P. Ibar, Polym. Plast. Technol. Eng. **17**, 11 (1981)

J.P., Ibar, U.S. Patent **4,469,649**, 04 Sept 1984, priority 14 March 1979

J.P. Ibar, Plast. News 18 Oct 1993

F. Ide, A. Hasegawa, J. Appl. Polym. Sci. **18**, 963 (1974)

O.T. Ikkala, I.T. Reima, Polym. Eng. Sci. **34**, 395 (1994)

T. Inoue, Private communication, 1993

T. Inoue, T. Soen, T. Hashimoto, H.J. Kawai, Polym. Sci. Part A-2 **7**, 1283 (1969)

N.E. Jackson, C.L. Tucker Iii, J. Rheol. **47**, 659–682 (2003)

S.E. Jang, B.S. Kim, Polym. Eng. Sci. **34**, 847 (1994)

P.H. Jezequel, P. Flaud, D. Quemada, Chem. Eng. Commun. **32**, 85 (1985)

H.-F. Jin, J. Tao, Plast. Rubber Compos. Process. Appl. **16**, 45 (1991)

C.G. Joung, N. Phan-Thien, X.J. Fan, J. Non-Newtonian Fluid Mech. **99**, 1–36 (2001)

D.P. Kalman, N.J. Wagner, Rheol. Acta **48**, 897–908 (2009)

D.M. Kalyon, A. Lawal, R. Yazici, P. Yaras, S. Railkar, Polym. Eng. Sci. **36**, 00 (1998)

D.M. Kalyon, P. Yaras, B. Aral, U. Yilmazer, J. Rheol. **37**, 35 (1993)

M.R. Kamal, H. Garmabi, S. Hozhabr, L. Arghyris, Polym. Eng. Sci. **35**, 41–52 (1995)

M.R. Kamal, I.A. Jinnah, L.A. Utracki, Polym. Eng. Sci. **24**, 1337 (1984a)

M.R. Kamal, A.T. Mutel, L.A. Utracki, Polym. Compos. **5**, 289 (1984b)

H.W. Kammer, M. Socher, Acta Polym. **33**, 658 (1982)

H.W. Kammer, J. Kressler, R. Kummerloewe, Adv. Polym. Sci. **106**, 31 (1993)

H.W. Kammer, C. Kummerloewe, J. Kressler, J.P. Melior, Polymer **32**, 1488–1492 (1991)

R.M. Kannan, J. Kornfield, J. Rheol. **38**, 1127 (1994)

R.C. Kanu, M.T. Shaw, Polym. Eng. Sci. **22**, 507 (1982)

M. Kapnistos, A. Hinrichs, D. Vlassopoulos, S.H. Anastasiadis, A. Stammer, B.A. Wolf, Macromolecules **29**, 7155–7163 (1996)

J. Karger-Kocsis (ed.), *Polypropylene: Structure, Blends and Composites* (Elsevier, Barking, UK, 1994)

J. Karger-Kocsis, Polym. Eng. Sci. **27**, 241 (1987)

T.E. Karis, D.C. Prieve, S.L. Rosen, J. Rheol. **28**, 381 (1984)

A. Karnis, H.L. Goldsmith, S.G. Mason, J. Colloid Interface Sci. **22**, 531 (1966)

M. Kasajima, K. Ito, A. Suganuma, D. Kunti, Kobun. Robunshu **38**, 239, 245 (1981)

K. Kato, Polymer **9**, 225 (1968)

J.D. Katsaros, M.F. Malone, H.H. Winter, Polym. Bull. **16**, 83 (1986)

J.D. Katsaros, M.F. Malone, H.H. Winter, Polym. Eng. Sci. **29**, 1434 (1989)

M. Keshtkar, M.C. Heuzey, P.J. Carreau, J. Rheol. **53**, 631–650 (2009)

M. Keshtkar, M.C. Heuzey, P.J. Carreau, M. Rajabian, C. Dubois, J. Rheol. **54**, 197–222 (2010)

M. Keshtkar, *Rheological Study and Rheo-microscopy of Semi-flexible Fiber Suspensions* (Ecole Polytechnique, Montreal, 2009), p. 249

F. Khalkhal, P.J. Carreau, Rheol. Acta **50**, 717–728 (2011)

F. Khalkhal, P.J. Carreau, G. Ausias, J. Rheol. **55**, 153–175 (2011)

B.B. Khatua, D.J. Lee, H.Y. Kim, J.K. Kim, Macromolecules **37**, 2454–2459 (2004)

R.E. Khayat, A. Luciani, L.A. Utracki, Boundary Elem. **8**, 515 (1996)

B.K. Kim, C.D. Han, Y.J. Lee, Polym. J. **24**, 205 (1992)

B.K. Kim, in *37ᵗʰ Symposium on Macromolecules* (Society for Polymer Science Japan (SPSJ), Fukuoka, 1989)

J.K. Kim, H.H. Lee, H.W. Son, C.D. Han, Macromolecules **31**, 8566–8578 (1998)

S. Kim, E.K. Hobbie, J.-W. Yu, C.C. Han, Macromolecules **30**, 8245 (1997)

S. Kitade, A. Ichikawa, N. Imura, Y. Takahashi, I. Noda, J. Rheol. **41**, 1039 (1997)

T. Kitano, T. Kataoka, Rheol. Acta **20**, 390 (1981)

T. Kitano, T. Kataoka, Y. Nagatsuka, Rheol. Acta **23**, 20 (1984)

D. Klempner, K.C. Frisch (eds.), *Polymer Alloys III* (Plenum, New York, 1983)

D. Klempner, L.H. Sperling, L.A. Utracki (eds.), *Interpenetrating Polymer Networks*. Advances in Chemistry, vol. 239 (American Chemical Society, Washington, DC, 1994)

A. Kohli, N. Chung, R.A. Weiss, Polym. Eng. Sci. **29**, 573 (1989)

Z. Kordjazi, N.G. Ebrahimi, J. Appl. Polym. Sci. **116**, 441–448 (2010)

N.P. Krasnikova, E.V. Kotova, E.P. Plotnikova, M.P. Zabugina, G.V. Vinogradov, V.E. Dreval, Z. Pelzbauer, Kompoz. Polim. Mater. **21**, 37 (1984)

N.P. Krasnikova, E.V. Kotova, G.V. Vinogradov, Z. Pelzbauer, J. Appl. Polym. Sci. **22**, 2081 (1978)

S. Krause, Macromolecules **13**, 1602 (1980)

J. Kressler, N. Higashida, T. Inoue, W. Heckmann, F. Seitz, Macromolecules **26**, 2090 (1993)

I.M. Krieger, G.N. Choi, *Proceedings of IX International Congress on Rheology*, Mexico, 1984; B. Mena, A. Garcia-Rejon, C. Rangel-Nafaile (eds.), *Advances in Rheology* (National Autonomous University, Mexico, 1984)

I.M. Krieger, T.J. Dougherty, Trans. Soc. Rheol. **3**, 137–152 (1959)

P. Kucharczyk, O. Otgonzu, T. Kitano, A. Gregorova, D. Kreuh, U. Cvelbar, V. Sedlarik, P. Saha, Polym. Plast. Technol. Eng. **51**, 1432–1442 (2012)

W. Kuhn, Kolloid Z. **132**, 84 (1953)

G. Kumar, R. Shyam, N. Sriram, N.R. Neelakantan, N. Subramanian, Polymer **34**, 3120 (1993)

J. Kwok, Minutes of *VAMAS TWP-PB meeting*, Berlin, 13 April 1987

F.P. La Mantia, D. Acierno, D. Curto, Rheol. Acta **21**, 4521 (1982)

F.P. La Mantia, D. Acierno, Plast. Rubber Process. Appl. **5**, 183 (1985); Polym. Eng. Sci. **25**, 279 (1985)

F.P. La Mantia, F. Cangialosi, U. Pedretti, A. Roggero, Eur. Poly. **29**, 671 (1994a)

F.P. La Mantia, D. Curto, D. Acierno, Acta Polym. **35**, 71 (1984)

F.P. La Mantia (ed.), *Thermotropic Liquid Crystal Polymer Blends* (Technomic Pub., Lancaster, 1993)

F.P. La Mantia, A. Valenza, D. Acierno, Polym. Bull. **15**, 381 (1986); Eur. Polym. J. **22**, 647 (1986)

F.P. La Mantia, A. Valenza, F. Scargiali, Polym. Eng. Sci. **34**, 799 (1994b)

F.P. La Mantia, A. Valenza, M. Paci, P.L. Magagnini, Rheol. Acta **28**, 417 (1989)

F.P. La Mantia, A. Valenza, M. Paci, P.L. Magagnini, Polym. Eng. Sci. **30**, 7 (1990)

C. Lacroix, M. Aressy, P.J. Carreau, Rheol. Acta **36**, 416–428 (1997)

C. Lacroix, M. Grmela, P.J. Carreau, J. Rheol. **42**, 41 (1998)

C. Lacroix, M. Bousmina, P.J. Carreau, B.D. Favis, A. Michel, Polymer **37**, 2939–2947 (1996)

R.G. Larson, G.H. Fredrickson, Macromolecules **20**, 1897 (1987)

R.G. Larson, Rheol. Acta **31**, 213, 497 (1992)

R.G. Larson, *The Structure and Rheology of Complex Fluids* (Oxford University Press on Demand, 1999)

H.M. Laun, H. Schuch, J. Rheol. **33**, 119 (1989)

L.G. Leal, Annu. Rev. Fluid Mech. **12**, 435 (1980)

H.M. Lee, O.O. Park, J. Rheol. **38**, 1405 (1994)

K.W. Lee, M.R. Kamal, P.K. Chan, Int. Polym. Process. **24**, 83–89 (2009)

K.-W.D. Lee, P.K. Chan, M.R. Kamal, J. Appl. Polym. Sci. **117**, 2651–2668 (2010)

S.M. Lee, C.H. Choi, B.K. Kim, Eur. Polym. J. **30**, 993 (1994)

S.Y. Lee, S.C. Kim, Polym. Eng. Sci. **37**, 463 (1997)

Y.K. Lee, Y.T. Jeong, K.C. Kim, H.M. Jeong, B.Y. Kim, Polym. Eng. Sci. **31**, 944 (1991)

L. Leibler, Macromolecules **13**, 1602 (1980)

A.I. Leonov, in *Progress in Heat and Mass Transfer*, ed. by W.R. Showalter (Pergamon, Oxford, 1972)

A.I. Leonov, J. Rheol. **34**, 155 (1990)

A.I. Leonov, J. Rheol. **38**, 1 (1994)

P. Lepoutre, M. Eng. Thesis, Department of Chemical Engineering, McGill University, 1989

W. Lerdwijitjarud, R.G. Larson, A. Sirivat, M.J. Solomon, J Rheol **47**, 37–58 (2003)

W. Lerdwijitjarud, A. Sirivat, R.G. Larson, J Rheol **48**, 843–862 (2004)

L. Li, T. Masuda, M. Takahashi, J. Rheol. **34**, 103 (1990)

X. Li, C. Pozrikidis, J. Fluid Mech. **341**, 165–194 (1997)

Z.-M. Li, L.-B. Li, K.-Z. Shen, W. Yang, R. Huang, M.-B. Yang, Macromol. Rapid. Commun. **25**, 553–558 (2004)

B.-R. Liang, J.L. White, J.E. Spruiell, B.C. Goswami, J. Appl. Polym. Sci. **28**, 2011 (1983)

K. Liang, J. Grebowicz, E. Valles, F.E. Karasz, W.J. McKnight, J. Polym. Sci. Part B Polym. Phys. **30**, 465 (1994)

S. Lim, J.L. White, Polym. Eng. Sci. **34**, 221 (1994)

C.-C. Lin, Polym. J. **11**, 185 (1979)

Y.G. Lin, H.H. Winter, Polym. Eng. Sci. **32**, 854 (1992)

J.T. Lindt, A.K. Ghosh, Polym. Eng. Sci. **32**, 1802 (1992)

Y.S. Lipatov, V.F. Shumsky, A.N. Gorbatenko, Y.N. Panov, L.S. Bolotnikova, J. Appl. Polym. Sci. **26**, 499 (1981)

T.Y. Liu, D.S. Soong, D. DeKee, Chem. Eng. Commun. **22**, 273 (1983)

G.W. Lohfink, M.R. Kamal, Polym. Eng. Sci. **33**, 1404 (1993)

G.W. Lohfink, Ph.D. Thesis, Chemical Engineering Department, McGill University, 1990

S. Lohmander, M. Rigdahl, Nord. Pulp Pap. Res. J. **15**, 231–236 (2000)

F.W. Lord, UK Pat. Appl. **51,292,** 1971

A. Luciani, M.F. Champagne, L.A. Utracki, Polym. Netw. Blends **6**, 41, 51 (1996)

A. Luciani, M.F. Champagne, L.A. Utracki, J. Polym. Sci. B Polym. Phys. Ed. **35**, 1393 (1997)

A. Luciani, Ph.D. Thesis, Univ. Pierre et Marie Curie, Paris VI, 1993

J. Lyngaae-Jørgensen, L.A. Utracki, Makromol. Chem. Macromol. Symp. **48/49**, 189 (1991)

J. Lyngaae-Jørgensen, in *Multiphase Polymers: Blends and Ionomers*, ed. by L.A. Utracki, R.A. Weiss. ACS Symposium Series, vol. 395 (American Chemical Society, Washington, DC, 1989)

J. Lyngaae-Jørgensen, in *Polymer Alloys III*, ed. by D. Klempner, K.C. Frisch (Plenum, New York, 1983)

J. Lyngaae-Jørgensen, in *Processing, Structure and Properties of Block Copolymers*, ed. by M.J. Folkes (Elsevier, London, 1985)

J. Lyngaae-Jorgensen, K. Lunde Rasmussen, E.A. Chtcherbakova, L.A. Utracki, Polym. Eng. Sci. **39**, 1060–1071 (1999)

J. Lyngaae-Jørgensen, K. Lunde Rasmussen, E.A. Chtcherbakova, L.A. Utracki, Polym. Eng. Sci. **39**, 1060 (1999)

J. Lyngaae-Jørgensen, K. Sondergaard, L.A. Utracki, A. Valenza, Polym. Netw. Blends **3**, 167 (1993)

J. Lyngaae-Jørgensen, L.D. Thomsen, K. Rasmussen, K. Sondergaard, F.E. Andersen, Intl. Polym. Process. **2**, 123 (1988)

P.L. Maffettone, M. Minale, J. Non-Newtonian Fluid Mech. **78**, 227–241 (1998)

P.L. Maffettone, F. Greco, J. Rheol. **48**, 83–100 (2004)

T.M. Malik, P.J. Carreau, N. Chapleau, Polym. Eng. Sci. **29**, 600 (1989)

S. Mani, M.F. Malone, H.H. Winter, J. Rheol. **36**, 1625 (1992)

G. Marin, Ph.D. Thesis, Universite de Pau, 1977

C.B. Martinez, M.C. Williams, J. Rheol. **24**, 421 (1980)

F.-D. Martischius, Rheol. Acta **21**, 311 (1982)

R.S. Marvin, in *Viscoelasticity - Phenomenological Aspects*, ed. by J.T. Bergen (Academic, New York, 1960)

R.O. Maschmeyer, C.T. Hill, Adv. Chem. **134**, 95 (1974)

R.O. Maschmeyer, C.T. Hill, Trans. Soc. Rheol. **21**, 183, 195 (1977)

T. Masuda, K. Kitagawa, T. Inoue, S. Onogi, Macromolecules **3**, 116 (1970)

T. Matsumoto, S. Yao, S. Onogi, J. Rheol. **30**, 509 (1986)

K. Matsuzaka, H. Jinnai, T. Koga, T. Hashimoto, Macromolecules **30**, 1146 (1997)

F.H.J. Maurer, J.H.M. Palmen, H.C. Booij, Rheol. Acta **24**, 243 (1985)

K.A. Mazich, S.H. Carr, J. Appl. Polym. Sci. **54**, 5511 (1983)

R.A. McAllister, AIChE J. **6**, 427 (1960)

R.K. McGeary, J. Am. Ceram. Soc. **44**, 513 (1961)

A. Mehta, A.I. Isayev, Polym. Eng. Sci. **31**, 963, 971 (1991)

D.J. Meir, J. Polym. Sci. Part C **26**, 81 (1969)

N. Mekhilef, P.J. Carreau, B.D. Favis, P. Martin, A. Ouhlal, J. Polym. Sci. Part B Polym. Phys. **38**, 1359–1368 (2000)

N.A. Memon, J. Appl. Polym. Sci. **54**, 1059 (1994)

R. Mertsch, B.A. Wolf, Ber. Bunsenges. Phys. Chem. **98**, 1275 (1994)

V.I. Metelkin, V.S. Blekht, Kolloid. Z. **46**, 476 (1984)

A.B.. Metzner, J. Rheol. **29**, 739 (1985)

R.E. Meyer (ed.), *Theory of Dispersed Multiphase Flow* (Academic, New York, 1983)

W. Michaeli, M. Cremer, R. Blum, Kunststoffe **83**, 992 (1993)

F. Mighri, A. Ajji, P.J. Carreau, J. Rheol. **41**, 1183 (1997)

F. Mighri, M.A. Huneault, J. Can, Chem. Eng. **80**, 1028–1035 (2002)

Y. Mikami, Nihon Reor. Gakk. **8**, 3, 137 (1980)

I.S. Miles, S. Rostami (eds.), *Multicomponent Polymer Systems* (Longman Sci. & Techn., Harlow, 1992)

J.V. Milewski, ACS, Div. Org. Coat. Plast. Chem. Prepr. **38**, 127 (1977)

J.V. Milewski, Ind. Eng. Chem. Prod. Res. Dev. **17**, 363 (1978)

J.V. Milewski, H.S. Katz, *Handbook of Reinforcements for Plastics* (van Nostrand Reinhold, New York, 1987)

J.V. Milewski, Ph.D. Thesis, Rutgers University, New Brunswick, 1973

R.L. Miller, R.V. Brooks, J.E. Briddell, Polym. Eng. Sci. **30**, 59 (1990)

W.J. Milliken, L.G. Leal, J. Non-Newtonian Fluid Mech. **40**, 355–379 (1991)

K. Min, Ph.D. thesis, University of Tennessee, Knoxville, 1984

K. Min, J.L. White, J.F. Fellers, Polym. Eng. Sci. **24**, 1327 (1984b)

M. Minale, P. Moldenaers, J. Mewis, Macromolecules **30**, 5470 (1997)

M. Minana-Perez, P. Jarry, M. Perez-Sanchez, M. Ramirez-Gouveia, J.L. Salager, J. Disp. Sci. Technol. **7**, 331 (1986)

Y. Minoura, M. Ueda, S. Mizunuma, M. Oba, J. Appl. Polym. Sci. **13**, 1625 (1969)

A. Mirzadeh, P.G. Lafleur, M.R. Kamal, C. Dubois, Polym. Eng. Sci. **50**, 2131–2142 (2010)

A. Mirzadeh, P. Lafleur, M. Kamal, C. Dubois, *Rubber Chemistry and Technology*. **86**, 521–537 (2013)

S.P. Mishra, B.L. Deopura, Rheol. Acta **23**, 189 (1984)

W.D. Mohr, R.L. Saxton, C.H. Jepson, Ind. Eng. Chem. **49**, 1857 (1957)

L.A. Mondy, H. Brenner, S.A. Altobelli, J.R. Abbott, A.L. Graham, J. Rheol. **38**, 444 (1994)

J.P. Montfort, Doctorat d'Etat, Universite de Pau, 1984

M. Mooney, J. Colloid Sci. **6**, 162 (1951)

J.F. Morris, Rheol. Acta **48**, 909–923 (2009)

M. Mours, M. Laun, F. Oosterlinck, I. Vinckier, P. Moldenaers, Chem. Eng. Technol. **26**, 740–744 (2003)

A.J. Muller, V. Balsamo, F. Da Silva, C.M. Rosales, A.E. Saez, Polym. Eng. Sci. **34**, 1455 (1994)

H. Munstedt, Polym. Eng. Sci. **21**, 259 (1981)

K.N. Murty, G.F. Modlen, Polym. Eng. Sci. **17**, 848 (1977)

A.T. Mutel, M.R. Kamal, in *Two-Phase Polymer Systems*, ed. by L.A. Utracki. Progress in Polymer Processing, vol. 2 (Hanser, Munich, 1991)

C. Nakason, P. Wannavilai, A. Kaesaman, J. Appl. Polym. Sci. **100**, 4729–4740 (2006)

A.I. Nakatani, H. Kim, Y. Takahashi, Y. Matsushita, A. Takano, B.J. Bauer, C.C. Han, J. Chem. Phys. **93**, 795 (1990)

J. Nancekivell, Canad. Plast. **43**(1), 28 (1985); **43**(9), 27

M.A. Nawab, S.G. Mason, Trans. Faraday Soc. **54**, 1712 (1958); J. Phys. Chem. **62**, 1248 (1958); J. Colloid Sci. **13**, 179 (1958)

E. Nazockdast, J.F. Morris, J. Fluid Mech. **713**, 420–452 (2012a)

E. Nazockdast, J.F. Morris, Soft. Matter. **8**, 4223–4234 (2012b)

N. Nemirovski, M. Narkis, R. Salovey, Polym. Adv. Technol. **4**, 589 (1993)

K.L. Ngai, D.J. Plazek, Macromolecules **23**, 4282 (1990)

X.Q. Nguyen, L.A. Utracki, U.S. Patent **5,451,106**, 19 Sep 1995, Appl. 08 Aug 1984, to National Research Council of Canada, Ottawa, Canada

L. Nicodemo, B. De Cindo, L. Nicolais, Polym. Eng. Sci **15**, 679 (1975)

L.E. Nielsen, *Polymer Rheology* (Dekker, New York, 1977)

K. Ninomiya, J.D. Ferry, J. Polym. Sci. Part A-2 **5**, 195 (1967)

M. Nishi, H. Watanabe, T. Kotaka, Nihon Reor. Gakk. **9**, 23 (1981)

T. Nishio, T. Sanada, K. Higashi, Sen-i Gakkaishi **48**, 446 (1992)

M.R. Nobile, D. Acierno, L. Incarnato, L. Nicolais, J. Rheol. **34**, 1181 (1990)

M.R. Nobile, E. Amendola, L. Nicolais, D. Acierno, C. Carfagna, Polym. Eng. Sci. **29**, 244 (1989)

J. Noolandi, Polym. Eng. Sci. **24**, 70 (1984)

N. O-Charoen, T. Hashimoto, Y.W. Leong, H. Hamada, Annu. Tech. Conf. Soc. Plast. Eng. **66**, 1808–1812 (2008)

E.U. Okoroafor, J.-P. Villemaire, J.-F. Agassant, Polymer **33**, 5264 (1992)

J.C. Oldroyd, Proc. R. Soc. Lond. **A218**, 122 (1953)

J.C. Oldroyd, Proc. R. Soc. Lond. **A232**, 567 (1955)

S. Onogi, T. Matsumoto, Polym. Eng. Rev. **1**, 45 (1981)

S. Onogi, T. Masuda, K. Koga, Polym. J. **1**, 542 (1970)

A. Onuki, K. Kawasaki (eds.), *Dynamics and Patterns in Complex Fluids* (Springer, New York, 1990)

A. Onuki, Phys. A **140**, 204 (1986)

A. Onuki, Europhys. Lett. **28**, 175 (1994)

A. Onuki, J. Phys. Condens. Matter **9**, 6119 (1997)

A. Onuki, Phys. Rev. A **35**, 5149–5155 (1987)

M. Oosterbroek, J. Mellema, J. Colloid Interface Sci. **84**, 14 (1981)

M. Oosterbroek, J.S. Lopulissa, J. Mellema, in *Rheology*, ed. by G. Astarita, G. Marrucci, L. Nicolais, vol. 2 (Plenum, New York, 1980)

M. Oosterbroek, J. Mellema, J.S. Lopulissa, J. Colloid Interface Sci. **84**, 27 (1981)

H. Orihara, T. Shibuya, T. Nagaya, S. Ujiie, J. Phys. Soc. Jpn. **75**, 063802/063801–063802/063804 (2006)

Y. Otsubo, Nihon Reor. Gakk. **22**, 75 (1994)

R.M. Ottenbrite, L.A. Utracki, S. Inoue (eds.), *Current Topics in Polymer Science* (Hanser, Munich, 1987)

J.M. Ottino, W.E. Ranz, C.W. Macosko, AIChE J. **27**, 565 (1981)

T. Ouhadi, R. Fayt, R. Jerome, P. Teyssie, J. Appl. Polym. Sci. **32**, 5647 (1986)

A.R. Padwa, Polym. Eng. Sci. **32**, 1703 (1992)

R. Pal, S.N. Bhattacharya, E. Rhodes, Canad. J. Chem. Eng. **64**, 3 (1986)

R. Pal, in *Encyclopedia of Emulsion Technology*, ed. by P. Becher (Marcel Dekker, New York, 1996)

R. Pal, J. Rheol. **36**, 1245 (1992)

R. Pal, J. Rheol. **41**, 141 (1997)

R. Pal, Food Hydrocoll. **22**, 428–438 (2008)

R. Pal, J. Colloid Interface Sci. **313**, 751–756 (2007)

J.F. Palierne, Rheol. Acta **29**, 204 (1990)

E. Paruta-Tuarez, P. Marchal, V. Sadtler, L. Choplin, Ind. Eng. Chem. Res. **50**, 10359–10365 (2011)

J.P. Pascault, V. Frèrejean, M. Taha, *Polymer Processing Society European Meeting*, Strasbourg, 29–31 Aug 1994

S.A. Patlazhan, J.T. Lindt, J. Rheol. **40**, 1095 (1996)

R. Patzold, Rheol. Acta **19**, 322 (1980)

D.R. Paul, J.W. Barlow, J. Macromol. Sci. Rev. Macromol. Chem. **C18**, 109 (1980)

X.-J. Peng, Y.-J. Huang, Y.-S. He, Y. Luo, Q. Yang, G.-X. Li, Gaodeng Xuexiao Huaxue Xuebao **32**, 2896–2901 (2011)

J. Peon, C. Dominguez, J.F. Vega, M. Aroca, J. Martinez-Salazar, J. Mater. Sci. **38**, 4757–4764 (2003)

T.J. Percorine, R.W. Herzberg, J.A. Manson, J. Mater. Sci. **25**, 3385 (1990)

C. Picart, J.-M. Piau, H. Gailliard, P. Carpentier, J. Rheol. **42**, 1 (1998)

A.P. Plochocki, in *Polymer Blends*, ed. by D.R. Paul, S. Newman (Academic, New York, 1978)

A.P. Plochocki, Polym. Eng. Sci. **23**, 618 (1983)

I.S. Polios, M. Soliman, C. Lee, S.P. Gido, K. Schmidt-Rohr, H.H. Winter, Macromolecules **30**, 4470 (1997)

A. Ponton, P. Clement, J.L. Grossiord, J. Rheol. **45**, 521–526 (2001)

P. Potschke, D.R. Paul, Polym. Rev. **43**, 87–141 (2003)

P. Prabodh, P. Stroeve, Break-up of model viscoelastic drops in uniform shear flow, Personal communication by P. Strove, Department of Chemical Engineering, University of California, 1991

W.M. Prest Jr., R.S. Porter, J. Polym. Sci. Part A-2 **10**, 1639 (1972); Inter-American Conf. Mater. Technol., Mexico (1972a)

D.C. Prieve, M.S. John, T.L. Koenig, J. Rheol. **29**, 639 (1985)

H.M. Princen, A.D. Kiss, J. Colloid Interface Sci. **112**, 427–437 (1986)

H.M. Princen, J. Colloid Interface Sci. **91**, 160 (1983)

H.M. Princen, J. Colloid Interface Sci. **105**, 150 (1985)

D. Quemada, P. Flaud, P.H. Jezequel, Chem. Eng. Commun. **32**, 61 (1985)

D. Quemada, C. Berli, Adv. Colloid Interface Sci. **98**, 51–85 (2002)

D. Quemada, Rheol. Acta **16**, 82–94 (1977)

M. Rajabian, C. Dubois, M. Grmela, Rheol. Acta **44**, 521–535 (2005)

J.D.F. Ramsay, P. Lindner, J. Chem. Soc. Faraday Trans. **89**, 4207–4214 (1993)

C. Rangel-Nafaile, A.B.. Metzner, K.F. Wissbrun, Macromolecules **17**, 1187 (1984)

L. Ratke, W.K. Thieringer, Acta Metal. **33**, 1793 (1985)

S. Ravati, B.D. Favis, Polymer **54**, 3271–3281 (2013)

L. Rayleigh, Proc. Lond. Math. Soc. **10**, 4 (1879); Proc. R. Soc. **29**, 71 (1879)

M.C. Ree, Ph.D. Thesis, University of Massachusetts, Amherst, 1987

D.A. Reinelt, J. Rheol. **37**, 1117 (1993)

M. Reiner, J. Rheol. **1**, 250 (1930)

M. Reiner, J. Rheol. **2**, 337 (1931)

Y.Y. Renardy, M. Renardy, V. Cristini, Eur. J. Mech. B Fluids **21**, 49–59 (2002)

N.M. Rezanova, M.V. Tsebrenko, Kompoz. Polym. Mater. **11**, 47 (1981)

J. Ritter, Appl. Polym. Symp. **15**, 239 (1971)

K.D. Roberts, M.Sc. Thesis, Washington University, St. Louis, 1973

C.M. Roland, G.G.A. Bohm, J. Polym. Sci. Polym. Phys. Ed. **22**, 79 (1984)

O.V. Romankevich, T.I. Zhila, S.E. Zabello, N.A. Sklyar, S.Y. Frenkel, Vysokomol. Soed. **A24**, 2282 (1982)

O.V. Romankevich, T.I. Zhila, N.A. Sklyar, S.E. Zabello, Khim. Tekhnol. Kiev **1**, 9 (1983)

J. Roovers, P.M. Toporowski, Macromolecules **25**, 1096 (1992)

R. Roscoe, J. Fluid Mech. **28**, 273 (1967)

W.B. Russel, in *Theory of Dispersed Multiphase Flow*, ed. by R.E. Meyer (Academic, New York, 1983)

Y. Saito, Nihon Reor. Gakk. **10**, 123, 128, 135 (1982)

J.L. Salager, M. Minana-Perez, J.M. Anderez, J.L. Grosso, C.I. Rojas, J. Disp. Sci. Technol. **4**, 161 (1983)

P. Sammut, L.A. Utracki, IUPAC *Working Party No. 4.2.1. Meeting*, Dusseldorf, 3–6 Nov 1986; *Rapport to VAMAS TWP-PB*, March 1986

P. Sammut, L.A. Utracki, *IUPAC W.P. No. 4.2.1. Meeting*, Montreal, 1–4 Nov 1987

T. Samurkas, M.G. Rogers, Polym. Eng. Sci. **32**, 1727 (1992)

A. Santamaria, M.E. Munoz, J.J. Pena, P. Remiro, Angew. Makromol. Chem. **134**, 63 (1985)

P. Sarazin, B.D. Favis, Biomacromolecules **4**, 1669–1679 (2003)

P. Sammut, L.A. Utracki, *NRCC/IMRI Symposium "Polyblends-'87"*, Boucherville, 28–29 April 1987; Polym. Eng. Sci. **27**, 359, 380, 1523 (1987)

C.F. Schmid, L.H. Switzer, D.J. Klingenberg, J. Rheol. **44**, 781–809 (2000)

L.R. Schmidt, J. Appl. Polym. Sci. **23**, 2463 (1979)

H.A. Schneider, M.J. Brekner, Polym. Bull. **14**, 173 (1985)

H.A. Schneider, J. Wirbser, New Polym. Mater. **2**, 149 (1990)

P. Scholz, D. Froelich, R. Muller, J. Rheol. **33**, 481 (1989)

W.R. Schowalter, C.E. Chaffey, H. Brenner, J. Colloid Interface Sci. **26**, 152 (1968)

W.J. Schrenk, K.J. Cleereman, T. Alfrey Jr., SPE Trans. **3**, 192 (1963)

C.E. Scott, C.W. Macosko, Polym. Bull. **26**, 341 (1991)

D.H. Sebastian, Y.-T. Chen, J. Elastom. Plast. **15**, 135 (1983)

G. Serpe, J. Jarrin, F. Dawans, Polym. Eng. Sci. **30**, 553 (1990)

S. Shahbikian, P.J. Carreau, M.-C. Heuzey, M.D. Ellul, H.P. Nadella, J. Cheng, P. Shirodkar, Polym. Eng. Sci. **51**, 2314–2327 (2011)

S. Shahbikian, *Phase Morphology Development and Rheological Behavior of Non-plasticized and Plasticized Thermoplastic Elastomer Blends* (Ecole Polytechnique, Montreal, 2010), p. 266

J. Sharma, N. Clarke, J. Phys. Chem. B **108**, 13220–13230 (2004)

P. Sherman, *Rheology of Emulsions* (Pergamon, Oxford, 1963)

P. Sherman, *Emulsion Science* (Academic, London, 1968)

D. Shi, G.-H. Hu, Z. Ke, R.K.Y. Li, J. Yin, Polymer **47**, 4659–4666 (2006)

Z.-H. Shi, L.A. Utracki, Polym. Eng. Sci. **32**, 1834 (1992)

C.K. Shih, Polym. Eng. Sci. **16**, 198 (1976)

C.K. Shih, in *Science and Technology of Polymer Processing*, ed. by N.P. Suh, N.-H. Sung (MIT Press, Cambridge, MA, 1979)

T. Shikata, D.S. Pearson, J. Rheol. **38**, 601 (1994)

A. Silberberg, W. Kuhn, Nature **170**, 450 (1952)

A. Silberberg, W. Kuhn, J. Polym. Sci. **13**, 21 (1954)

R. Simha, R.K. Jain, Polym. Eng. Sci. **24**, 1284 (1984)

R. Simha, T. Somcynsky, Macromolecules **2**, 342 (1969)

R. Simha, J. Appl. Phys. **23**, 1020 (1952)

A. Sirivat, S. Patako, S. Niamlang, W. Lerdwijitjarud, Phys. Fluids **23**, 013104/013101–013104/013112 (2011)

M.H.B. Skoby, J. Kops, R.A. Weiss, Polym. Eng. Sci. **31**, 954 (1991)

P. Smith, M. Hara, A. Eisenberg, in *Current Topics in Polymer Science*, ed. by R.M. Ottenbrite, L.A. Utracki, S. Inoue (Hanser, Munich, 1987)

M. Sobhanie, A.I. Isayev, Y. Fan, Rheol. Acta **36**, 66 (1997)

K. Søndergaard, A. Valenza, J. Lyngaae-Jørgensen, Polym. Netw. Blends **2**, 159 (1992)

W. Soontaranum, J.S. Higgins, T.D. Papathanasiou, J. Non-Newtonian Fluid Mech. **67**, 191–212 (1996)

C.S. Speed, Plast. Eng. **38**, 39 (1982)

R.S. Spencer, R.M. Wiley, J. Colloid Sci. **6**, 133 (1957)

T.W. Spriggs, Chem. Eng. Sci. **20**, 931 (1965)

R. Stadler, L.L. Freitas, V. Krieger, S. Klotz, Polymer **29**, 1643 (1988)

J.M. Starita, Soc. Rheol. Trans. **16**, 339 (1972)

S. Steinmann, W. Gronski, C. Friedrich, Polymer **42**, 6619–6629 (2001)

S. Steinmann, W. Gronski, C. Friedrich, Rheol. Acta **41**, 77–86 (2002)

R. Steller, D. Zuchowska, J. Appl. Polym. Sci. **41**, 1595 (1990)

H.A. Stone, L.G. Leal, J. Fluid Mech. **220**, 161–186 (1990)

L. Stradins, T.A. Osswald, Polym. Eng. Sci. **36**, 979 (1996)

T.A. Strivens, J. Colloid Interface Sci. **57**, 476 (1976)

P.M. Subramanian, V. Mehra, Polym. Eng. Sci. **27**, 663 (1987)

P.M. Subramanian, Polym. Eng. Sci. **25**, 483 (1985)

Y. Suetsugu, J.L. White, The influence of particle size and surface coating of calcium carbonate on the rheological properties of its suspensions in molten polystyrene, PATRA Report No. 186, June 1982

A.M. Sukhadia, D. Done, D.G. Baird, Polym. Eng. Sci. **30**, 519 (1990)

U. Sundararaj, C.W. Macosko, R.J. Rolando, Polym. Eng. Sci. **32**, 1814 (1992)

U. Sundararaj, C.W. Macosko, A. Nakayama, T. Inoue, Polym. Eng. Sci. **35**, 100 (1995)

P.M. Suquet, J. Mech. Phys. Solids **41**, 981–1002 (1993)

Y. Suzaka, U.S. Patent **4, 334, 783**, Jun 15 (1982), Appl. 21 Dec 1978, to Showa Denko, Kabushiki Kaisha, Oita, Japan

L.H. Switzer Iii, D.J. Klingenberg, J. Rheol. **47**, 759–778 (2003)

H. Takahashi, Y. Inoue, O. Kamigaito, K. Osaki, Kobunshi Ronbunshu **47**(7), 611–617 (1990)

Y. Takahashi, N. Kurashima, I. Noda, M. Doi, J. Rheol. **38**, 699 (1994)

V.B. Talstoguzov, A.I. Mzhel'sky, V.Y. Gulov, Colloid Polym. Sci. **252**, 124 (1974)

T. Tang, B. Huang, Polymer **35**, 281 (1994)

R.I. Tanner, J. Polym. Sci. A-2 **8**, 2067 (1970)

G.I. Taylor, Proc. R. Soc. Lond. **A138**, 41 (1932)

G.I. Taylor, Proc. R. Soc. Lond. **A146**, 501 (1934)

W. Thiele, in *Compounding and Processing for Performance*. Proceedings, POLYBLENDS-'95 and SPE RETEC, NRCC/IMI, Boucherville, 19–20 Oct 1995

D.G. Thomas, J. Colloid Sci. **20**, 267 (1965)

N. Tokita, Rubber Chem. Tech. **50**, 292 (1977)

M. Tomita, T.G.M. van de Ven, J. Colloid Interface Sci. **49**, 374 (1984)

M. Tomita, K. Takano, T.G.M. van de Ven, J. Colloid Interface Sci. **92**, 367 (1982)

S. Tomotika, Proc. R. Soc. Lond. **A150**, 322 (1935)

S. Tomotika, Proc. R. Soc. Lond. **A153**, 302 (1936)

D.A. Tree, A.J. McHugh, Intl. Polym. Process. **2**, 223 (1988)

B. Tremblay, J. Non-Newtonian Fluid Mech. **33**, 137 (1989)

B. Tremblay, Polym. Eng. Sci. **32**, 65 (1992)

M.V. Tsebrenko, M. Jakob, M.Y. Kuchinka, A.V. Yudin, G.V. Vinogradov, Int. J. Polym. Mat. **3**, 99 (1974)

M.V. Tsebrenko, Polym. Sci. USSR **20**, 108 (1978)

M.V. Tsebrenko, N.M. Rezanova, G.V. Vinogradov, Polym. Eng. Sci. **20**, 1023 (1980)

M.V. Tsebrenko, N.M. Rezanova, G.V. Vinogradov, Nov. Rheol. Polim. 11th Mater. Vses. Simp. Reol. **2**, 136 (1982)

M.V. Tsebrenko, A.V. Yudin, T.I. Ablazova, G.V. Vinogradov, Polymer **17**, 831 (1976)

C. Tsenoglou, J. Polym. Sci. Polym. Phys. Ed. **26**, 2329 (1988)

T. Uemura, W.L. Yew, H. Hamada, Seikei Kako **20**, 362–367 (2008)

L.A. Utracki, R.A. Weiss (eds.), *Multiphase Polymers: Blends and Ionomers*. ACS Symposium Series, vol. 395 (American Chemical Society, Washington, DC, 1989)

L.A. Utracki, The Rheology of Multiphase Systems, in *Rheological Fundamentals of Polymer Processing*, ed. by J.A. Covas, J.F. Agassant, A.C. Diogo, J. Vlachopoulos, K. Walters (Kluver Academic Publishers, Dordrecht, 1995)

L.A. Utracki, *Commercial Polymer Blends* (Chapman & Hall, London, 1998)

L.A. Utracki, *Polymer Alloys and Blends* (Hanser, Munich, 1989a)

L.A. Utracki, G.L. Bata, in *Polymer Alloys III*, ed. by D. Klempner, K.C. Frisch (Plenum, New York, 1982)

L.A. Utracki, B. Fisa, Polym. Comp. **3**, 193 (1982)

L.A. Utracki, J. Lara, Polym. Compos. **5**, 44 (1984)

L.A. Utracki, P. Sammut, *VAMAS TWP-PB Meeting*, Berlin, 13 April 1987

L.A. Utracki, P. Sammut, Polym. Eng. Sci. **28**, 1405 (1988)

L.A. Utracki, P. Sammut, Polym. Eng. Sci. **30**, 1019 (1990)

L.A. Utracki, P. Sammut, Polym. Netw. Blends **2**, 23, 85 (1992)

L.A. Utracki, B. Schlund, Polym. Eng. Sci. **27**, 367, 1512 (1987)

L.A. Utracki, Z.-H. Shi, Polym. Eng. Sci. **32**, 1824 (1992)

L.A. Utracki, T. Vu-Khanh, in *Multicomponent Polymer Systems*, ed. by I.S. Miles, S. Rostami (Longman Sci. & Techn., Harlow, 1992)

L.A. Utracki, G.L. Bata, V. Tan, M.R. Kamal, *Preprints of the 2nd World Congress of Chemical Engineering*, Montreal, 5 Oct 1981, Vol. 6, p. 428

L.A. Utracki, A.M. Catani, G.L. Bata, M.R. Kamal, V. Tan, J. Appl. Polym. Sci. **27**, 1913 (1982a)

L.A. Utracki, M.M. Dumoulin, P. Toma, Polym. Eng. Sci. **26**, 34 (1986)

L.A. Utracki (ed.), *Encyclopaedic Dictionary of Commercial Polymer Blends* (ChemTec Publishing, Toronto, Canada, 1994)

L.A. Utracki (ed.), *Two-Phase Polymer Systems*. Progress in Polymer Processing, vol. 2 (Hanser, Munich, 1991a)

L.A. Utracki, in *Current Topics in Polymer Science*, ed. by R.M. Ottenbrite, L.A. Utracki, S. Inoue (Hanser, Munich, 1987)

L.A. Utracki, in *Multiphase Polymers: Blends and Ionomers*, ed. by L.A. Utracki, R.A. Weiss. ACS Symposium Series, vol. 395 (American Chemical Society, Washington, DC, 1989b)

L.A. Utracki, in *Rheological Measurements*, ed. by A.A. Collyer, D.W. Clegg (Elsevier, London, 1988)

L.A. Utracki, J. Colloid Interface Sci. **42**, 185 (1973)

L.A. Utracki, *Proceedings of 74th AIChE Meeting*, Los Angeles, 15–18 Nov 1982

L.A. Utracki, ACS Polym. Prepr. **24**(2), 113 (1983); Canad. J. Chem. Eng. **61**, 753 (1983); Polym. Eng. Sci. **23**, 446 (1983)

L.A. Utracki, Polym-Plast. Technol. Eng. **22**, 27 (1984); Rubber Chem. Technol. **57**, 507 (1984)

L.A. Utracki, Polym. Eng. Sci. **25**, 655 (1985); Adv. Polym. Technol. **5**, 41 (1985)

L.A. Utracki, J. Rheol. **30**, 829 (1986)

L.A. Utracki, J. Rheol. **35**, 1615 (1991b)

L.A. Utracki, unpublished (1992)

L.A. Utracki, M.R. Kamal, N.M. Al-Bastaki, SPE-Techn. Pap. **30**, 417 (1984)

L.A. Utracki, M.R. Kamal, Z. Bakerdjian, J. Appl. Polym. Sci. **19**, 487 (1975)

E.B. Vadas, H.L. Goldsmith, S.G. Mason, J. Colloid Interface Sci. **43**, 630 (1973)

P. Vadhar, T. Kyu, Polym. Eng. Sci. **27**, 202 (1987)

A. Valenza, J. Lyngaae-Jørgensen, L.A. Utracki, P. Sammut, Polym. Netw. Blends **1**, 79 (1991)

W.E. Van Arsdale, J. Rheol. **26**, 477 (1982)

T.G.M. van de Ven, *Colloidal Hydrodynamics* (Academic, New York, 1989)

T.G.M. van de Ven, Polym. Compos. **6**, 209 (1985)

J.G.M. Van Gisbergen, W.F.L.M. Hoeben, H.E.H. Meijer, Polym. Eng. Sci. **31**, 1539 (1991)

H. Van Oene, J. Colloid Interf. Sci. **40**, 448 (1972)

S. Velankar, P. Van Puyvelde, J. Mewis, P. Moldenaers, J. Rheol. **45**, 1007–1019 (2001)

J. Vermant, M.J. Solomon, J. Phys. Condens. Matter **17**, R187 (2005)

J. Ville, P. Médéric, J. Huitric, T. Aubry, Polymer **53**, 1733–1740 (2012)

M. Vincent, J.F. Agassant, Polym. Compos. **7**, 76 (1986)

M. Vincent, J.F. Agassant, in *Two-Phase Polymer Systems*, ed. by L.A. Utracki. Progress in Polymer Processing, vol. 2 (Hanser, Munich, 1991)

M. Vincent, Dr. Eng. Thesis, Ecole Nationale Superieure des Mines de Paris, Sophia Antipolis, 1984

I. Vinckier, P. Moldenaers, J. Mewis, J. Rheol. **40**, 613 (1996)

I. Vinckier, P. Moldenaers, J. Mewis, J. Rheol. **41**, 705 (1997)

G.V. Vinogradov, N.P. Krasnikova, V.E. Dreval, E.V. Kotova, E.P. Plotnikova, Int. J. Polym. Mat. **9**, 187 (1982)

D. Vlassopoulos, A. Koumoutsakos, S.H. Anastasiadis, S.G. Hatzikiriakos, P. Englezos, J. Rheol. **41**, 739 (1997)

D. Vlassopoulos, Rheol. Acta **35**, 556 (1996)

N. Wakita, Polym. Eng. Sci. **33**, 781 (1993)

N. Walling, M.R. Kamal, Adv. Polym. Technol. **5**, 269 (1996)

N. Walling, M. Eng. Thesis, Chemical Engineering Department, McGill University, 1995

C.-y. Wang, Suzhou Daxue Xuebao, Gongkeban **25**, 19–21 (2005)

D. Wang, G. Sun, PMSE Prepr. **95**, 671–672 (2006)

K.J. Wang, J.L. Lee, J. Appl. Polym. Sci. **33**, 431 (1987)

Q.-J. Wang, H.-X. Huang, Z.-Y. Peng, Y.-F. Huang, Annu. Tech. Conf. Soc. Plast. Eng. **70**, 21–25 (2012)

J.L. White, L. Czarnecki, H. Tanaka, Rubber Chem. Technol. **5**, 823 (1980)

A. Wieckowski, F. Streg, Chem. Stosowana **1B**, 95 (1966)

C.R. Wildemuth, M.C. Williams, Rheol. Acta **23**, 627 (1984)

J.M. Willis, B.D. Favis, Polym. Eng. Sci. **28**, 1416 (1988)

C. Wisniewsky, G. Marin, P. Monge, Eur. Polym. J. **21**, 479 (1985)

B.A. Wolf, Makromol. Chem. Rapid Commun. **189**, 1613 (1980)

B.A. Wolf, Macromolecules **17**, 615 (1984)

D. Wu, N. Tang, D. Gu, W. Wen, Intern. Polym. Process. **5**, 47 (1990)

R. Wu, M.T. Shaw, R.A. Weiss, J. Rheol. **36**, 1605–1623 (1992)

S. Wu, J. Polym. Sci. Part B **25**, 557 (1987); Polym. Eng. Sci. **27**, 335 (1987); Polymer **28**, 1144 (1987)

M. Xanthos, M.W. Young, J.A. Biesenberger, Polym. Eng. Sci. **30**, 493 (1990)

P. Xing, M. Bousmina, D. Rodrigue, M.R. Kamal, Macromolecules **33**, 8020–8034 (2000)

K.V. Yakovlev, R.I. Zhitomirets, O.V. Romankevich, S.E. Zabello, A.V. Yudin, Khim. Tekhnol. Kiev **5**, 14 (1984)

U. Yalmazer, D.M. Kalyon, J. Rheol. **33**, 1197 (1991)

H.H. Yang, C.D. Han, J.-K. Kim, Polymer **35**, 1503 (1994)

H. Yang, H. Shibayama, R.S. Stein, N. Shimuzu, T. Hashimoto, Macromolecules **19**, 1667 (1986)

J. Yang, D. Shi, Y. Gao, Y. Song, J. Yin, J. Appl. Polym. Sci. **88**, 206–213 (2003)

I. Yaron, B. Gal-Or, Rheol. Acta **11**, 241–252 (1972)

Y.-C. Ye, F.P. La Mantia, A. Valenza, V. Citta, U. Pedretti, A. Roggero, Eur. Polym. J. **27**, 723 (1991)

T.W. Yoo, H.G. Yoon, S.J. Choi, M.S. Kim, Y.H. Kim, W.N. Kim, Macromol. Res. **18**, 583–588 (2010)

W. Yu, M. Bousmina, J. Rheol. **47**, 1011–1039 (2003)

W. Yu, C. Zhou, J. Rheol. **51**, 179–194 (2007)

W. Yu, M. Bousmina, C. Zhou, C.L. Tucker III, J Rheol **48**, 417–438 (2004)

W. Yu, R. Li, C. Zhou, Polymer **52**, 2693–2700 (2011)

W. Yu, C. Zhou, M. Bousmina, J Rheol **49**, 215–236 (2005)

A. Zaldua, E. Munoz, J.J. Pena, A. Santamaria, Polym. Eng. Sci. **32**, 43 (1992)

G.R. Zeichner, P.D. Patel, in *2nd World Congress on Chemical Engineering*, Montreal, 1981, Vol. 6, p. 333

A. Zkiek, W. Yu, M. Bousmina, M. Grmela, Rheol. Acta **43**, 333–341 (2004)

M. Zuo, Q. Zheng, Macromol. Chem. Phys. **207**, 1927–1937 (2006)

Morphology of Polymer Blends

8

Toshiaki Ougizawa and Takashi Inoue

Contents

T. Ougizawa (✉)
Department of Chemistry and Materials Science, Tokyo Institute of Technology, Meguro-ku, Tokyo, Japan
e-mail: tougizawa@op.titech.ac.jp

T. Inoue
Department of Polymer Science and Engineering, Yamagata University, Yonezawa, Japan
e-mail: tinoue@yz.yamagata-u.ac.jp

Abstract

In this chapter, as a guideline to control the phase separation morphology, the morphology formation mechanism is primarily explained. First the phase diagram and the phase separation mechanism are briefly explained to provide basic knowledge on controlling the morphology of polymer blends. Then, the effect of the shear flow on the phase diagram as a factor that influences the formation of the phase separation morphology is explained and the relation to the morphology control is shown. This is especially important in the polymer processing of polymer blends. Finally, as a control of the phase separation morphology using reactions, reaction-induced phase separation and reactive blending are explained. Because most polymer blends are immiscible, it is necessary to use some methods to obtain polymer blends that show good physical properties. Therefore, these are powerful tools for controlling the morphology in the polymer blends.

8.1   Introduction

It is not easy to satisfy the wide range of performance and function demanded of a material by using only one kind of polymer. Therefore, it is proper to satisfy these demands with polymer blends. Moreover, it is much easier to obtain a material that has the target characteristics by blending different polymers instead of designing and synthesizing really new polymers. Consequently, polymer blends which are composed of structurally and functionally different polymers have received much attention in terms of improving, e.g., mechanical, optical, and thermal properties, and numerous investigations have been done with these blends. However, most polymer blends are immiscible systems with dispersions of one polymer in the matrix of another, and it is not easy to improve their performance or function by simply mixing them. Hence, an effective control of the blend morphology is essential (Favis and Willis 1990; Bucknall 1977; Utracki 1982; Coran and Patel 1983).

The size level at which both polymers mix is very important, because it has a strong influence on the physical properties of the material. Whether a polymer blend that has mixed at the molecular level is better depends on its demanded performance. However, it is rare for a polymer blend to mix at a molecular level, because most polymer blends are immiscible and phase separation takes place. In addition, in the case where phase separation occurs, the physical properties greatly depend on the phase-separated morphology. Therefore, control of the phase-separated morphology is important. For example, the impact strength of polymer blends is generally controlled by the dispersed particle size, the ligament thickness, and the interfacial adhesion. If the morphology of polymer blends is altered by shear forces and the reaction during mixing, the material performance also changes. Thus, the morphology also greatly depends on how it is mixed.

In this chapter, morphology control using various mixing methods is described.

8.2   Phase Diagram and Phase Separation Mechanism

Generally, most polymer pairs of high molecular weight are immiscible in the range from glass transition temperature (T_{g}) to thermal decomposition temperature (T_{d}). It is difficult to mix polymers at a molecular level even for polymer pairs with similar structures, e.g., polyethylene (PE) and polypropylene (PP). To discuss the thermodynamics for the miscibility and the phase diagram of polymer blends, the Flory-Huggins equation has been widely used (Flory 1953),

$$\frac{\Delta G_M}{RT\,(V/V_{\mathrm{r}})} = \frac{\phi_1}{r_1}\ln\phi_1 + \frac{\phi_2}{r_2}\ln\phi_2 + \phi_1\phi_2\chi_{12} \tag{8.1}$$

where ΔG_M is the Gibbs free energy of mixing and R is the gas constant. V and V_{r} are the total and reference volumes, respectively. The first two terms on the right-hand side of Eq. 8.1 represent the combinatorial entropy of mixing and negative value, where ϕ_i is the volume fraction and r_i is the segment number of a polymer chain of component i. The third term contains the interaction parameter χ_{12}, which generally takes into account all contributions to the free energy that are not given by the combinatorial entropy. Using this Flory-Huggins equation, the miscibility of polymer blends can be described. In polymer blends, the combinatorial entropy of mixing the two polymers is a smaller negative than that of mixing two low molecular weight compounds, and the contribution to ΔG_M is very small. The miscibility tends to become better when ΔG_M decreases as χ_{12} becomes smaller. Therefore, pairs of dissimilar polymers are only miscible if there are favorable specific interactions between them leading to a negative contribution for ΔG_M.

   Miscible polymer blends can be classified into several categories. A blend that tends to phase-separate at low temperatures is termed an upper critical solution temperature (UCST) system, and one that separates at elevated temperatures is classified as a lower critical solution temperature (LCST) system. In addition, there are some pairs that are completely miscible and have both UCST and LCST characteristics. Figure 8.1a and b show the phase diagrams of a binary blend having LCST- and UCST-type phase behavior, respectively. The solid line is a "binodal line," which is a boundary between the one-phase and two-phase regions in the equilibrium state. The dashed line is called a "spinodal line," which satisfies the condition that the second derivative of the Gibbs free energy of mixing by composition is equal to zero ($\partial^2\Delta G/\partial\phi^2 = 0$). It is understood as a boundary that divides the style of the phase separation in a mixture, i.e., nucleation and growth (NG) type and spinodal decomposition (SD) type. The phase separation by NG takes place in the metastable region between the spinodal and the binodal lines on the phase diagram. SD occurs in the unstable region framed by the spinodal lines ($\partial^2\Delta G/\partial\phi^2 < 0$).

   In NG, a small particle (nucleus) with almost equilibrium concentration from the uniform solution is generated accidentally and grows gradually with time. There is no typical periodicity in the phase-separated morphology. Some domains having different sizes and positions are observed, as shown in Fig. 8.2a. In an SD process, on the other hand, a periodic fluctuation of the concentration in the system spontaneously

Fig. 8.1 LCST and UCST-type phase diagrams
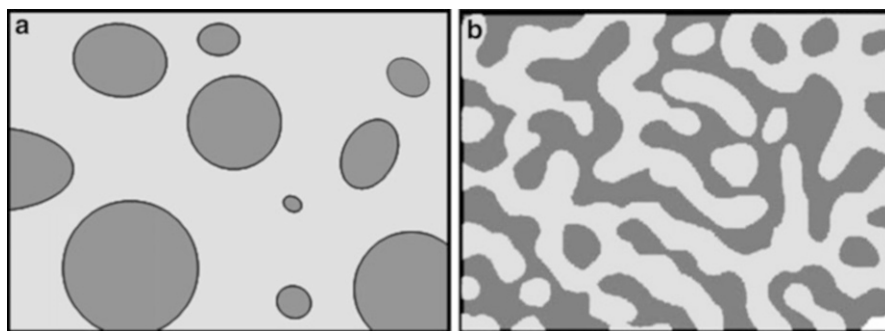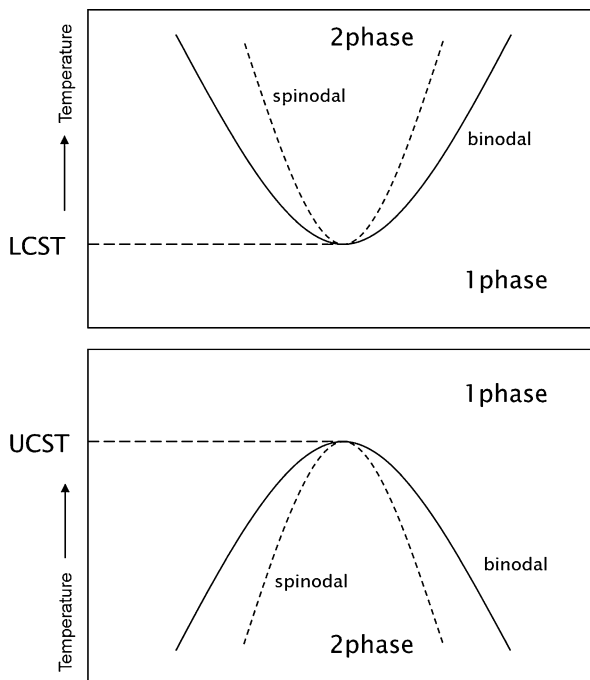
Fig. 8.2 Schematic phase-separated morphology induced by (**a**) NG and (**b**) SD mechanism

arises. Then, the fluctuation gradually increases and separates into a coexistence composition ϕ_{B1} and ϕ_{B2}. In SD, there is structural periodicity, and each phase connects mutually in three dimensions, as shown in Fig. 8.2b. Furthermore, a dissimilarity also exists in the diffusion of molecules between NG and SD. The diffusion takes place from low concentration to high concentration in the process of SD. This is the opposite direction for ordinary diffusion, which takes place in the NG mechanism (see Fig. 8.3, Cahn 1968).
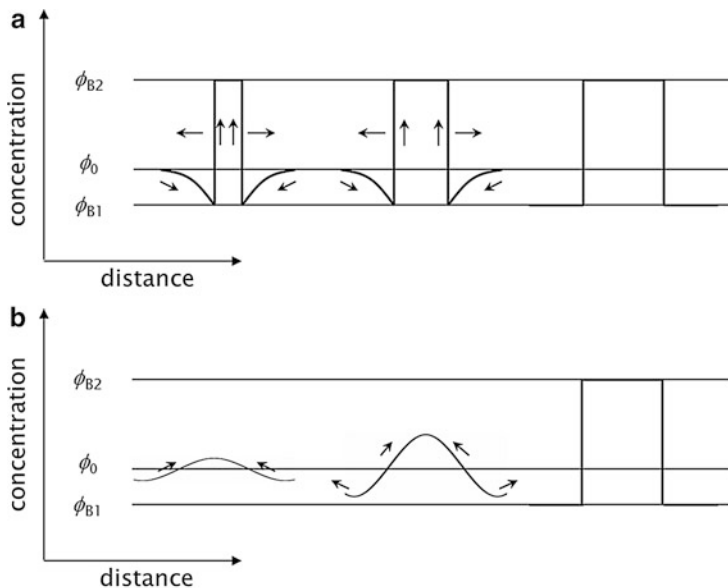
Fig. 8.3 Growth of concentration fluctuation in (**a**) NG and (**b**) SD mechanism

SD can be divided into three stages: the initial stage, middle stage, and late stage. In the initial stage (van Aartsen 1970; Binder and Stauffer 1973), the fluctuation of the concentration is gradually generated as a monochromatic wavelength and has a constant wavelength (Cahn 1965). A co-continuous morphology having the period distance Λ_m is formed as a consequence of the superimposed waves in various directions. The wavelength of the concentration fluctuation does not depend on time (constant), and the amplitude of the fluctuation increases exponentially. In the middle stage of SD, the periodic structure grows self-similarly, while the amplitude of the fluctuation increases gradually. In the late stage, the amplitude of the concentration fluctuation almost reaches the equilibrium concentration determined by the equilibrium composition of the blend, and then only the wavelength of the concentration fluctuation grows with self-similarity as time passes. Finally, the morphology with the dispersed particles phase (domain) in the continuous phase (matrix) is formed to reduce the interfacial tension at the late stage of SD. In this type of a system with dispersed particles, the domain size is also comparatively uniform, maintaining the regularity of the co-continuous morphology in the early stage. It can be said that the morphology after the SD is a characteristic structure.

8.3   Shear-Induced Phase Separation and Morphology

The effect of flow is of industrial relevance in the processing of polymer blends where high deformation rates are encountered, as in melt extrusion or injection molding.

Thus, the behavior of polymer blends in a flow field is of fundamental interest and is also technologically important, since deformation and related stresses are unavoidable in many processing steps. Recently, it has been reported that the shear flow can change the thermodynamic state of the system and perturb the phase diagram of the polymer mixtures, where it is now well established that the shear flow can shift the phase boundary a few degrees to higher or lower temperatures depending on the characterization of the blends under the shear (Mazich and Carr 1983; Lyngaae-Jorgensenn and Sondegaard 1987; Larbi et al. 1988; Katsaros et al. 1989; Nakatani et al. 1990; Kammer et al. 1991; Wu et al. 1991; Hindawi et al. 1992; Fernandez et al. 1995; Madbouly et al. 1999a). This also influences the morphologies that develop during polymer processing.

The effect of a simple shear flow on the phase behavior and morphology was investigated with the use of a parallel-plate apparatus (Fig. 8.4, Madbouly et al. 1999a) for some polymer mixtures: poly(methyl methacrylate) (PMMA)/poly(styrene-co-acrylonitrile) (SAN-29.5) and polystyrene (PS)/poly(vinyl methyl ether) (PVME), which have an LCST-type phase diagram; PS/PMMA, which has a UCST-type phase diagram; and polycarbonate (PC)/SAN and nylon4, 6(PA4,6)/poly(phenylene sulfide) (PPS), which are immiscible in the whole measurable region under the quiescent state.

8.3.1 PMMA/SAN-29.5 (AN:29.5 wt%) Mixture (LCST System)

This mixture phase-separates in the higher temperature region. Figure 8.5 shows the shear rate dependence of the cloud point at some compositions (Madbouly et al. 1999b). Since the cloud points increased monotonically for all of the measured compositions, only shear-induced mixing was observed. The shear flow can affect the phase behavior of the blend significantly; i.e., it suppresses the phase separation and enlarges the one-phase region of the polymer blend. Changes in the phase diagram of the polymer blends at different shear rates are represented in Fig. 8.6 (Madbouly et al. 1999b). The cloud points are affected by the values of the applied shear, as they gradually increase with shear rate values. Figure 8.7 represents the normalized shift in the cloud points $|\Delta T(\dot{\gamma})/T(0)| = |\{T(\dot{\gamma}) - T(0)\}/T(0)|$ versus shear rate $(\dot{\gamma})$ for different blend compositions. The following relation was given for the experimental data (Beysens and Gbadamassi 1979; Beysens and Perrot 1984):

$$|\Delta T(\dot{\gamma})/T(0)| = k\dot{\gamma}^n \tag{8.2}$$

where k and n are material constants that depend on composition. The experimental results can be fitted to Eq. 8.2 by using a nonlinear regression method. The constants k and n are used as fitting parameters. A good description of the data was obtained in Fig. 8.7, and Table 8.1 (Madbouly et al. 1999b) represents the values of the fitting parameters obtained from the regression. The values of the exponent n were almost constant regardless of the composition ratio of the blend, while the values of the prefactor k were greatly dependent on the composition of the
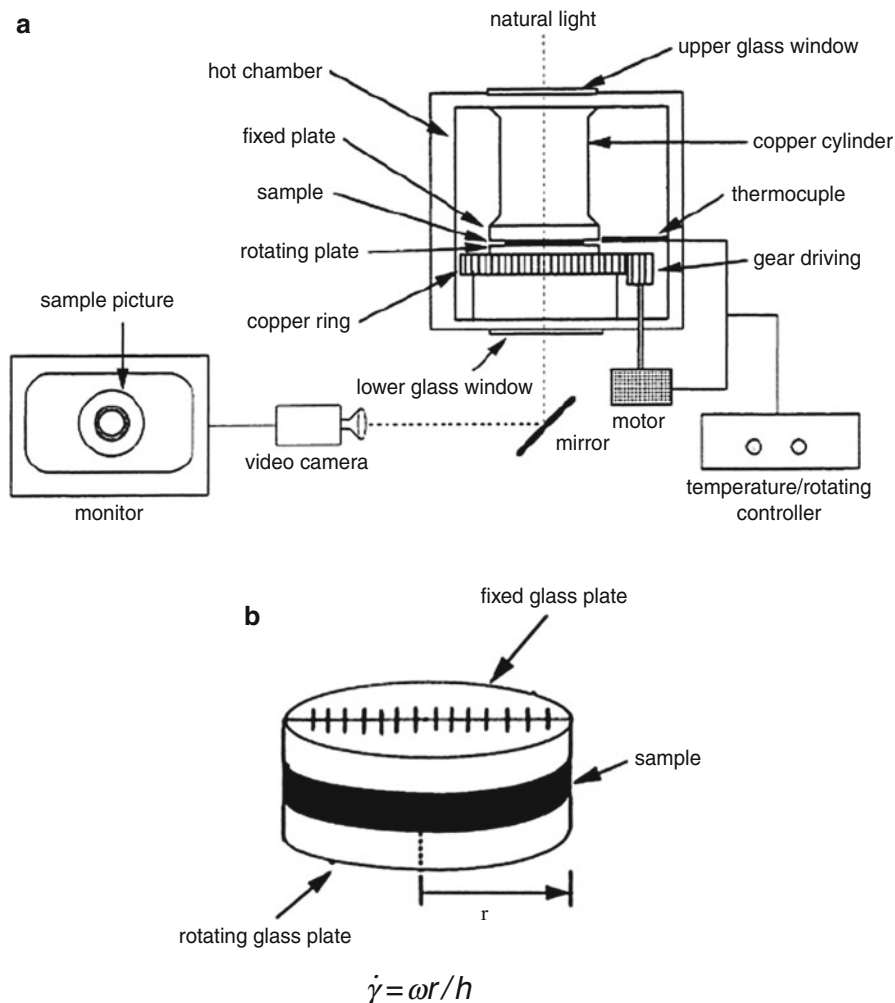
Fig. 8.4 Schematic representation of the shear apparatus used in this work: (**a**) general drawing; (**b**) sample between two parallel glass plates

blend. The value of k is a maximum for the critical composition (PMMA/ SAN $= 75/25$) and decreases on either side of this composition. This is attributed to the critical composition being more sensitive to the shear rate effect than the other compositions, as can be seen in Figs. 8.5 and 8.6. Note that Eq. 8.2 is applicable only at small shear rate values for this system ($\dot{\gamma} \leq 12\ \mathrm{s}^{-1}$) and deviated at higher shear rates. The cloud points become almost constant at higher shear rates, as shown in Fig. 8.5.

The phase-separated morphology under a flow field has also attracted considerable attention. The morphology of this system (PMMA/SAN $= 75/25$) was analyzed

Fig. 8.5 Shear rate
dependence of cloud points in
PMMA/SAN blends
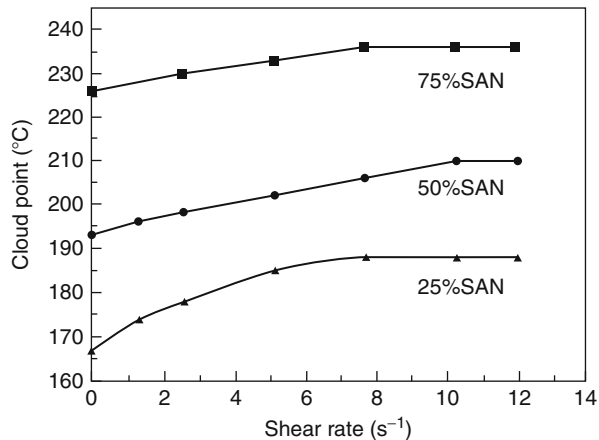
Fig. 8.6 Phase diagrams
at various shear rates of
PMMA/SAN blend. Phase
diagram does not change
more than $\dot{\gamma} = 12 \text{ s}^{-1}$
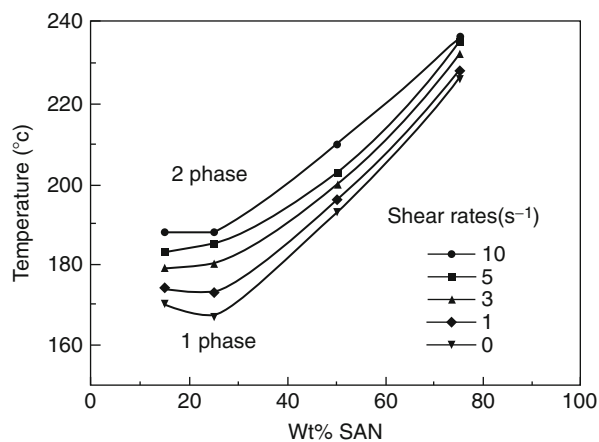
Fig. 8.7 Normalized shift in
the cloud point curve $\Delta T(\dot{\gamma})/$
$T(0)$ as a function of $\dot{\gamma}$ for
different compositions of the
PMMA/SAN blends
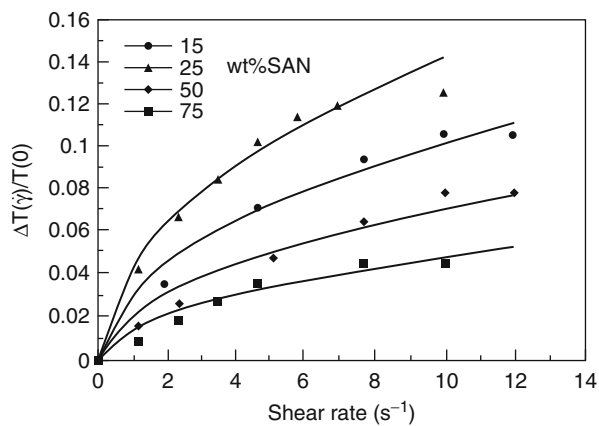
Table 8.1 Values of prefactor k and exponent n for different compositions of the PMMA/SAN blends

PMMA wt%	k	n
85	0.032	0.501
75	0.045	0.501
50	0.022	0.502
25	0.015	0.501
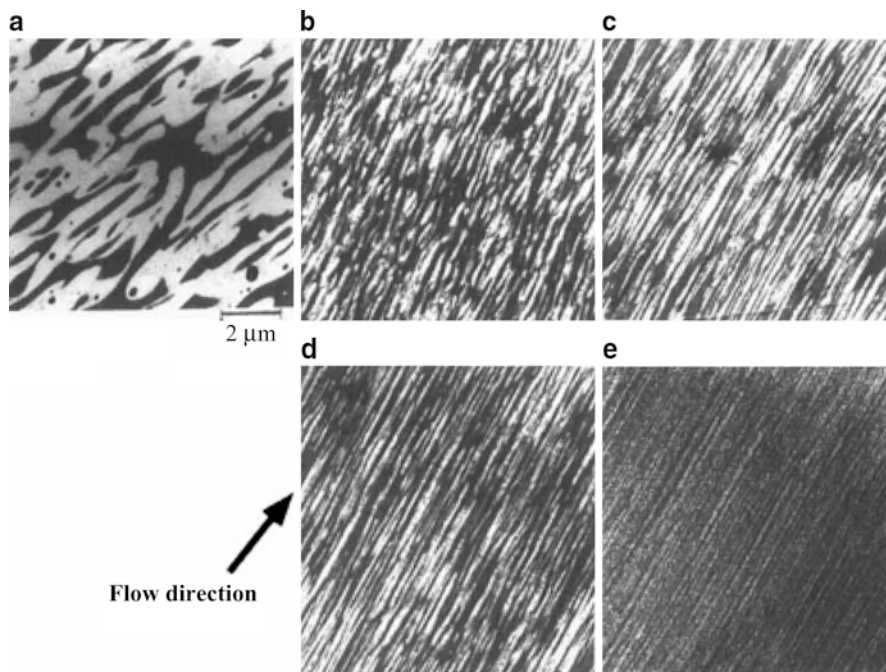
Fig. 8.8 TEM pictures of PMMNSAN (75/25) samples that were sheared at 185 °C (20 °C above their quiescent cloud point) at 0.5 rad/s for 3 min and then quenched in a water bath. Samples were then taken from different radial positions and consequently different shear rates: (**a**) $\dot{\gamma} \sim 0~\text{s}^{-1}$; (**b**) 1.17 s^{-1}; (**c**) 2.33 s^{-1}; (**d**) 4.7 s^{-1}; and (**e**) 7 s^{-1}

relative to the shear rate effect. The sheared sample was quickly quenched in a water bath just after the shear cessation, and the morphology was observed using a transmission electron microscope (TEM) in the sample, which was cut parallel to the flow direction. A typical observed morphology of the samples is shown in Fig. 8.8 (Madbouly et al. 1999b). The phase-separated morphology is clearly observed; the dark and bright regions correspond to SAN-rich and PMMA-rich phases, respectively. One can see a well-defined phase separation; a co-continuous two-phase morphology of the blend can be clearly observed at nearly zero shear rate. Under the shear flow, the two SAN-rich and PMMA-rich phases are elongated and highly oriented parallel to the flow direction. These TEM results indicate that the size and amplitude of the concentration fluctuations were strongly

Fig. 8.9 Phase diagrams at various shear rates of PS/PVME blend
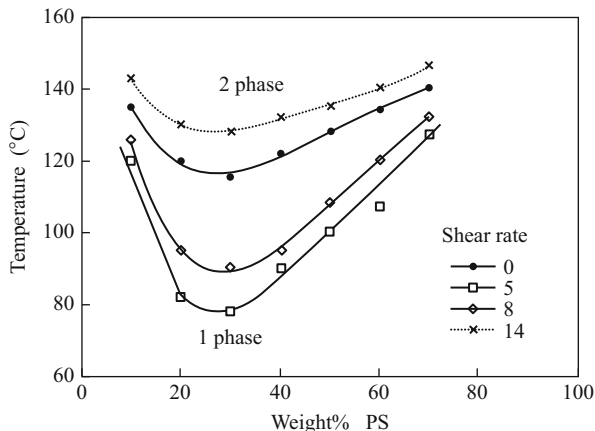
suppressed, as indicated by the decreasing intensity and contrast of the elongated phases. Lastly, no morphology was observed, which can be attributed to the shear-induced mixing of the polymer blend at the critical shear rate value ($10 \, \text{s}^{-1}$). The highly oriented phases are considered to be due to the nearly equal viscosity of SAN and PMMA. According to these results, it seems that macroscopic phase separation of the polymer blends cannot occur under the steady shear flow. With increasing shear rate, the macroscopic phase boundary is broken into pieces, generating smaller domains that can be elongated in the flow direction, resulting in a decrease in contrast (i.e., decreasing concentration fluctuations). Consequently, mixing of the unlike segments is enhanced.

8.3.2 PS/PVME Mixture (LCST System)

Changes of the cloud points on the shear rate in the PS/PVME system are shown in Fig. 8.9, which was measured by the same method as for the PMMA/SAN system (Madbouly et al. 1999a). This phase behavior is not simpler than that of the PMMA/SAN system. At low shear rates, the cloud point curve shifts to low temperature with increasing shear rate; i.e., the two-phase region becomes larger and a maximum decrease occurs when the applied shear rate value is around $5 \, \text{s}^{-1}$. Then the cloud point curve shifts to higher temperature with increasing shear rate up to $\dot{\gamma} = 14 \, \text{s}^{-1}$, at which point the cloud point curve is higher than that of the quiescent state. For larger shear rates than $\dot{\gamma} = 14 \, \text{s}^{-1}$, the cloud point curve does not change and becomes constant regardless of an increase in applied shear rate. This large effect of the shear rate on the miscibility behavior of this system is attributed to the large mismatch in the viscosity of the PS and PVME components: the bigger the mismatch in viscosity, the larger the effect of shear.

Based on this result, it appears that the shear flow can induce both phase demixing and mixing, as in the case of polymer solutions (Takebe et al. 1989). The fact that both were observed in the same blend suggests that two competing effects occur during

Fig. 8.10 Phase diagrams at various shear rates of PS/PMMA blend
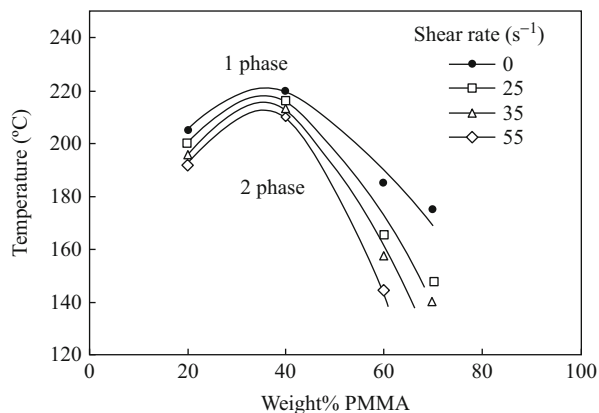
Table 8.2 Values of prefactor k and exponent n for different systems

System	k	n
Cyclohexane/Aniline[3,4]	$(5.9 \pm 0.66) \times 10^{-7}$	0.53 ± 0.03
Polymer solution (PS/PB/DOP)[10]	$(2.6 \pm 0.6) \times 10^{-3}$	0.5 ± 0.02
Oligomer mixture (PMMA/PS)	$0.0075 - 0.031$	0.5 ± 0.02
Polymer mixture (PMMA/SAN)	$0.015 - 0.045$	0.5 ± 0.02

flow. One of these effects tends to suppress growing spatial composition fluctuation, and this effect would tend to promote phase mixing. The other effect causes the growth of composition fluctuation with consequent phase demixing. This effect can be attributed to elastic deformation, which may act to enhance some concentration fluctuation, promoting the uphill diffusion that occurs in the phase separation, as has been reported by Helfand and Fredrickson (1989) and Onuki et al. (1989). Thus, the first effect could dominate at high shear rate and high temperature, while the second effect could dominate at low shear rate and low temperature.

8.3.3   PS/PMMA Mixture (UCST System)

This is an oligomer mixture (Mw (PS) = 2,500, Mw (PMMA) = 6,000), and the phase separation takes place in a lower temperature region (UCST-type phase diagram; Madbouly et al. 2001). Changes in the phase diagram of the blends at different shear rates are represented in Fig. 8.10. The cloud points decreased monotonically with the shear rate. Though the results were opposite to the case of PMMA/SAN, shear-induced mixing took place. The shear effect was found to be largely composition-dependent. The shear flow can suppress the phase separation and enlarge the single-phase region of the blend.

It is important to compare the effect of the shear flow on the phase behavior for different systems. Table 8.2 summarizes the values of the prefactor (k) and the

exponent (n) in Eq. 8.2 for the four different systems. The values of n are almost constant (0.5) in all cases, regardless of the type of system under shear. However, the values of k greatly depend on the system under consideration; the k values decrease from high molecular weight polymer blends (PMMA/SAN) to simple liquid mixtures. This may be attributed to the fact that the effect of shear on the cloud points is much more sensitive in the high molecular weight polymer blends and that the sensitivity decreases in the simple liquid mixtures. From this result one can say that the sensitivity of the cloud points to the effect of applied shear rate in the different systems moves with the same order as the prefactor value in the different cases, with a greater value of the prefactor giving greater sensitivity of the cloud points to the application of shear rate. These reported results are in good agreement with a renormalization group theory of Onuki and Kawasaki (Onuki and Kawasaki 1979a, b; Onuki et al. 1981), who predicated the following equation for small molecular systems:

$$|\Delta T(\dot{\gamma})/T(0)| = p\dot{\gamma}^{1/3v} \qquad (3)$$

where the prefactor p is given by

$$p = 0.0832\varepsilon\tau_\xi^{1/3v} \qquad (4)$$

and $\varepsilon = 4-d_s$ $1/3v = 0.5$ v is a universal constant which depends on the spatial dimensionality d_s τ_ξ is the characteristic relaxation time for the concentration fluctuations of the mixture. Equation 8.4 predicts that the larger the characteristic time (τ_ξ) for the concentration fluctuations, the larger the change of the cloud point will be. This general principle can also be applied to a polymeric system, since the relaxation time decreases from the high molecular weight polymer mixtures to the simple liquid mixtures and becomes very small. Therefore, the large difference in the prefactor value, which reflects the sensitivity of the different systems to the shear rate, is not surprising at all.

According to this experimental fact, one can say that the phase behavior of the blend under shear flow can be changed due to the difference in the relaxation time, which reflects the different sensitivities of the cloud point to change under the shear flow.

8.3.4 PC/SAN Mixture (Immiscible System)

The blend of bisphenol-A polycarbonate (PC) and acrylonitrile-butadiene-styrene (ABS) resin is a useful industrial material. One reason is that the miscibility between PC and poly(styrene-*co*-acrylonitrile) (SAN), which is a matrix of ABS resin, is not too bad, though it is immiscible. In particular, a blend of PC and SAN-25 with 25 wt% AN is useful, because the miscibility is the best in PC/SAN systems and the blend shows the lowest value of χ in the system (Li et al. 1999). The blend has been used without any compatibilizers. It would be expected that the
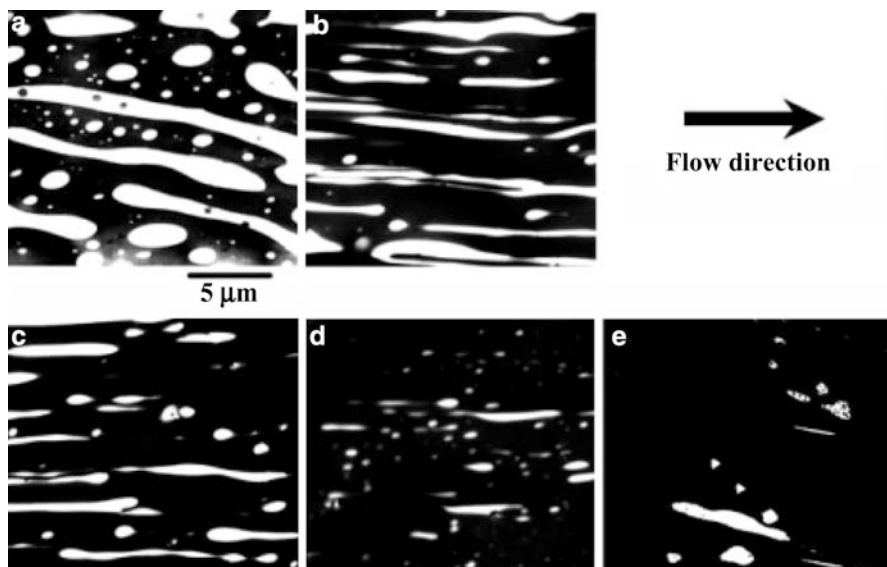
Fig. 8.11 TEM pictures of PC/SAN-25 = 70/30 samples that were sheared at 240 °C by different shear rates for 5 min and then quenched in water bath. Five pieces were then taken from different radial positions and consequently different shear rates (**a**) $\dot{\gamma} \approx 0$ s^{-1}; (**b**) 7.5 s^{-1}; (**c**) 15 s^{-1}; (**d**) 30 s^{-1} and (**e**) 90 s^{-1}

miscibility of the blend might be more enhanced under the shear flow. The two-phase morphology under a controlled shear condition has attracted considerable attention in recent years. For this reason, the effect of simple shear flow on the morphology and miscibility of the PC/SAN-25 blend was investigated. A typical morphological observation of the blend samples (PC/SAN-25 = 70/30) under different values of the shear rate at 240 °C is shown in Fig. 8.11 (Hanafy et al. 2004). The bright dispersed phase and dark matrix correspond to the SAN-rich (not stained) and PC-rich (stained by RuO$_4$) regions, respectively. It is apparent that a well-defined phase separation of the blend at nearly zero shear rate can be obtained. For the samples under the shear flow, particles oriented to the flow direction were formed, and the size decreased with the shear rate. These results of TEM observation indicate that the size and amplitude of the concentration fluctuations between the domains and the surrounding matrix were strongly suppressed as a result of decreasing the contrast of the elongated domains. According to these results, one can say that the miscibility of the PC/SAN-25 mixture is enhanced to a great extent under the shear flow; i.e., the shear suppresses the concentration fluctuations and enhances the miscibility between different polymers. However, no shear-induced one-phase morphology was detected even under higher shear rate values. We must state here that the morphology under higher shear rate values (higher than 30 s^{-1}) does not change very much; see, for example, that at 90 s^{-1} in Fig. 8.11e the morphology is almost similar to that at 30 s^{-1} in Fig. 8.11d. This may be attributed to the fact that the sample under a higher shear rate seems to be

Fig. 8.12 Shear rate
dependence of the total area
of SAN-rich phase
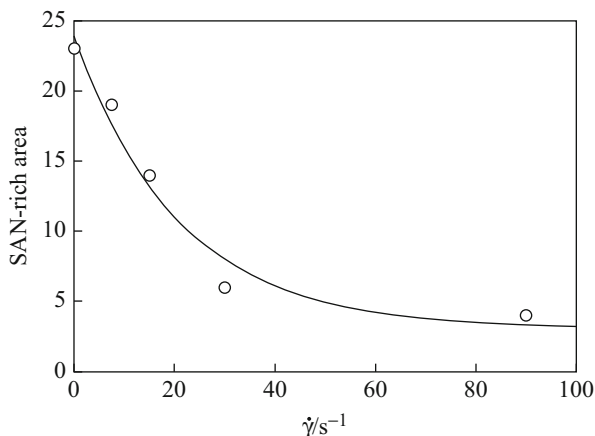
under a quasi-equilibrium condition. Based on this experimental fact, it is apparent
that the morphology might be controlled by two competitive factors. One is trying to
break up the domains into smaller ones, i.e., a shear-induced breakup of the dispersed
domains. The other tends to increase the rate of domain growth, i.e., a shear-induced
coalescence. The competition between the two factors is responsible for the
obtained morphology. Therefore, the breakup is not a unique phenomenon involved
during the shear flow, since coalescence of the dispersed particles also occurs, and the
finally obtained morphology is the result of these two opposite effects.

Figure 8.12 shows the total area of the individual particles of the SAN-rich
region as a function of the shear rate calculated from the image analysis of the
previous TEM images (Fig. 8.11). Obviously, the area of the dispersed domains
remarkably decreased with the shear rate and leveled off at high shear rates. As
mentioned above, this is due to a competition of particle breakup and coalescence
which may occur at high shear rate values.

Though the bisphenol-A PC is immiscible with SAN, as mentioned above, it was
reported that a blend of a PC copolymer (cPC) and SAN-23 had a miscible region
and showed an LCST-type phase diagram; see Fig. 8.13 (Okamoto et al. 1995). It
was understood that the miscibility with SAN was enhanced by using random
copolymer PC in comparison with the PC/SAN system. The LCST phase boundary
shifts to higher temperatures by shearing, as shown in the figure, and the miscible
region is enlarged, though the accurate amount is not clear quantitatively. The
kinetic results provided a plausible scenario for the development of a co-continuous
two-phase morphology in the melt-processed blend as follows. When the cold
pellets of both polymers are heated to above the glass transition temperature
(Tg) of the polymers in the extruder, the dissolution starts. Even after attaining
the spinodal temperature of the quiescent state (Ts = 223 °C) the dissolution occurs
continuously, since Ts can be elevated under the shear flow to above the barrel
temperature (260 °C), shown as a dotted line in the figure. The homogeneous melt is
extruded and quenched quickly in water. When the single-phase blend is heated
under high shear in an injection machine (at 290 °C) and injected into a cold mold,

Fig. 8.13 Phase diagram of cPC/SAN blend and processing conditions
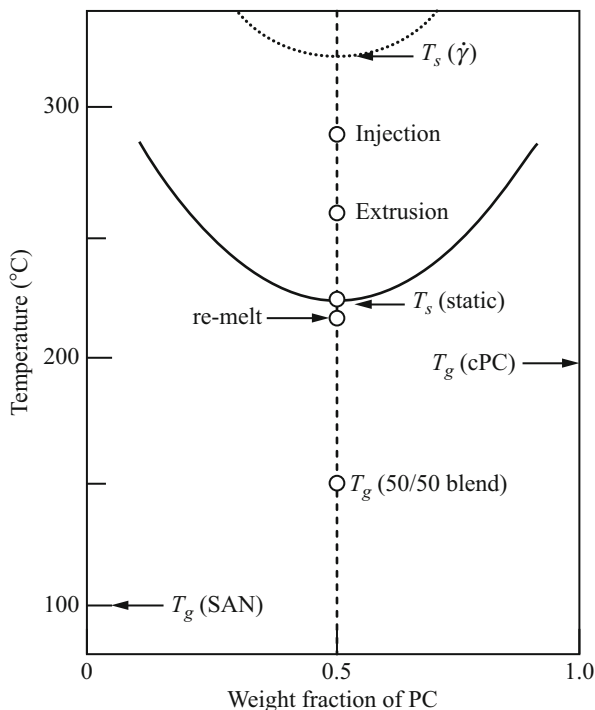
the polymer blend is thrust into the two-phase region from the single-phase region, since the phase boundary returns to the lower temperature of the quiescent state without shearing. Then the spinodal decomposition proceeds until the melt is cooled to Tg. The dissolution below Ts is negligible, and so the co-continuous morphology attained via the spinodal decomposition is frozen in the molded blend by vitrification near Tg. Thus, one can obtain the co-continuous morphology in the polymer blends by controlling the shear field.

Figure 8.14 shows a TEM picture of an injection molding sample in the bisphenol-A PC/ABS blend (Inoue 1996). The black particles are rubber in the ABS-rich region. When one draws the boundary line between the rubber particle-rich region (ABS-rich) and the rubber particle-poor region (PC-rich), a co-continuous morphology appears. This may show that the morphology formation occurs via spinodal decomposition after single-phase formation by shearing in the PC/ABS blend. It might be the reason why the PC/ABS blend shows nice physical properties. This morphology control is extremely interesting.

8.3.5   PA4,6/PPS Mixture (Immiscible System)

Both nylon 4,6 (PA4,6) and poly(phenylene sulfide) (PPS) are useful industrial materials and have a high melting temperature of the crystals ($T_m = 295$ °C and

Fig. 8.14 TEM picture of injection molding sample in PC/ABS (50/50). It is partitioned between overcrowdedness area (ABS-rich) of the rubber particle and white ground (PC-rich) by the line
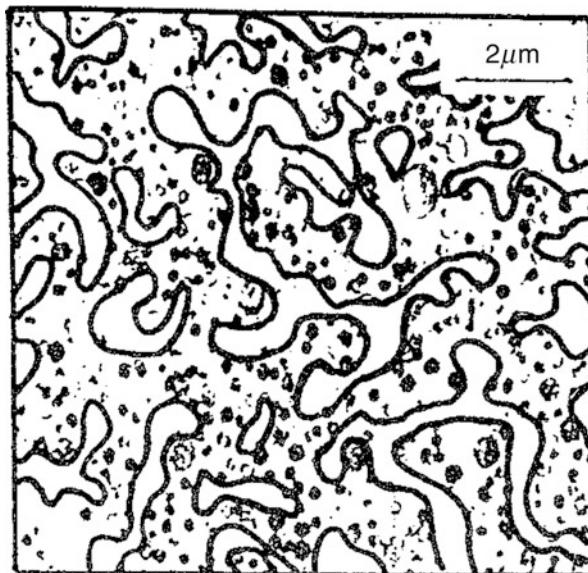
280 °C, respectively). Therefore, we expect them to have the advantage that their polymer blend can maintain high temperature properties. The polymer blend of PA4,6/PPS has been used industrially without any compatibilizers; nevertheless, the blend is immiscible. Thus, it is considered that the shear flow during processing plays an important role for the formation of the phase-separated morphology related to the appearance of desirable properties.

The phase diagram at a quiescent state was confirmed in a liquid state from the melting temperature of the crystal to 400 °C by the cloud point measurement (An et al. 2002). The specimens were opaque and two-phase for every composition and measurable temperature. This means that the blend of PA4,6/PPS is immiscible in all processable regions. However, the specimen of PA4,6/PPS (80/20) in the higher shear rate region became transparent at 310 °C. The shear rate in the boundary of the opaque-transparent region was calculated ($\dot{\gamma} = 150$ s^{-1}), and at higher shear rates than this value, the blend become miscible. This means that a shear-induced mixing took place in this blend. But a miscible region in other compositions could not be found. Figure 8.15 shows a phase diagram at $\dot{\gamma} = 150$ s^{-1} and $\dot{\gamma} = 189$ s^{-1}. A miscibility region (window) can open by the shear flow, though it is very narrow.

Figure 8.16a shows an optical micrograph of a PA4,6/PPS(80/20) specimen annealed at 310 °C for 10 min after the cessation of the shear flow, which was one phase under shear flow ($\dot{\gamma} > 150$ s^{-1}) at the same temperature. A regularly and co-continuously phase-separated structure appears. Figure 8.16b shows a light scattering profile exhibiting a peak due to the regular morphology. It seems that phase separation took place via spinodal decomposition from one phase state after the cessation of shear flow. Such a fine morphology in polymer blends often causes good physical properties.

Fig. 8.15 Phase diagram of PA4,6/PPS blend under simple shear flow. The lines of phase boundary at $\dot{\gamma} = 150\ \text{s}^{-1}$ and $\dot{\gamma} = 189\ \text{s}^{-1}$ are drawn arbitrarily because the shape of phase diagram is not clear at present
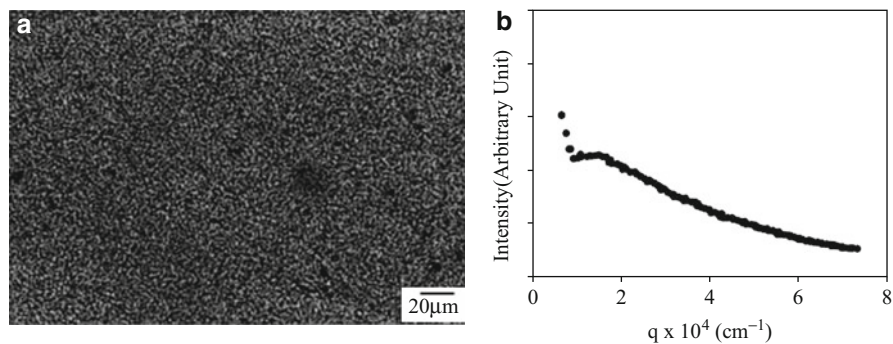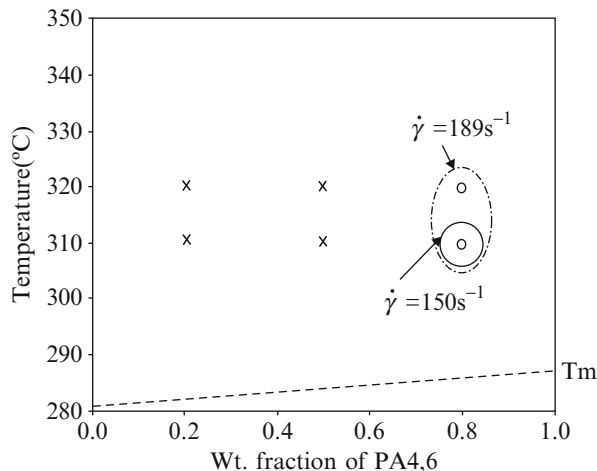
Fig. 8.16 (a) Optical micrograph of PA4,6/PPS (=80/20) blend annealed in hot chamber for 10 min at 310 °C after shear cessation. Co-continuous morphology appeared. (b) Light scattering profile of this sample

To conclude, the miscibility of the PA4,6/PPS blend changed with the shear flow, and a miscible region appeared. By using this phenomenon, a specimen with a fine morphology and good physical properties could be obtained.

8.4   Reaction-Induced Phase Separation

There are several methods used to mix polymers. Reaction-induced phase separation (RIPS) is one way to make useful polymer blends, and much research has been previously done on this topic (Visconti and Marchessault 1974; Manzione et al. 1981; Yamanaka and Inoue 1989, 1990; Yamanaka et al. 1989; Chen et al. 1994; Okada et al. 1995; Kojima et al. 1995; Inoue 1995). As explained before, many polymer blends are immiscible, and it is difficult to make them form a desirable
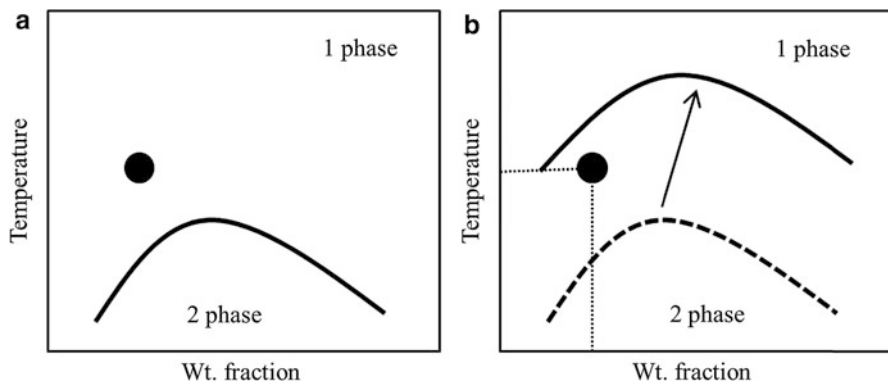
Fig. 8.17 Schematic representation of phase diagram in polymer blend with polymerization; (**a**) monomer/polymer blend before polymerization, (**b**) polymer/polymer blend after polymerization. *Solid circle* (●) represents polymerization condition

phase-separated morphology. RIPS occurs as a result of a curing reaction (c-RIPS) and polymerization of a monomer (p-RIPS) after one polymer is dissolved in another monomer forming a homogeneous solution initially. The phase separation is induced in the process of curing or polymerization of the monomer. Because the phase separation occurs from one phase state, it often occurs by the spinodal decomposition (SD) mechanism, and a regular phase-separated morphology is formed in the initial stage of the phase separation. Therefore, it is easy to obtain a material with a better performance. However, in RIPS, the obtained final morphology is remarkably different from that obtained by the usual phase separation of the binary polymer-polymer blends. Interest in the morphology of the blends obtained by RIPS has led to many research studies in this area.

Here the phase separation phenomenon by p-RIPS is explained by using the Flory-Huggins equation expressed by Eq. 8.1. Generally, if the interaction parameter χ_{12} is independent of the number of segments per chain, the miscibility during the polymerization is dominated by the number of segments in the combinatorial entropy terms on the right side of Eq. 8.1. That is, the larger the degree of polymerization, the narrower the miscible region becomes. Figure 8.17 shows the schematic representation of a UCST-type phase diagram in a blend: (a) the monomer/polymer blend before polymerization and (b) the polymer/polymer blend after polymerization. The solid circle in the phase diagram represents the position of the polymerization condition. When the degree of polymerization in a polymerized component is small, the system locates at the miscible state before the polymerization (Fig. 8.17a). The degree of polymerization becomes large as the polymerization proceeds, and the combinatorial entropy terms become negligible. Because the free energy of mixing becomes larger, the phase boundary shifts to the higher temperature with polymerization, as shown in Fig. 8.17b. Consequently, the system is thrust into a two-phase region from a one-phase region. Then, the phase separation occurs.

Fig. 8.18 TEM micrograph
of PMMA/EVAc(80/20)
blend polymerized at 60 °C
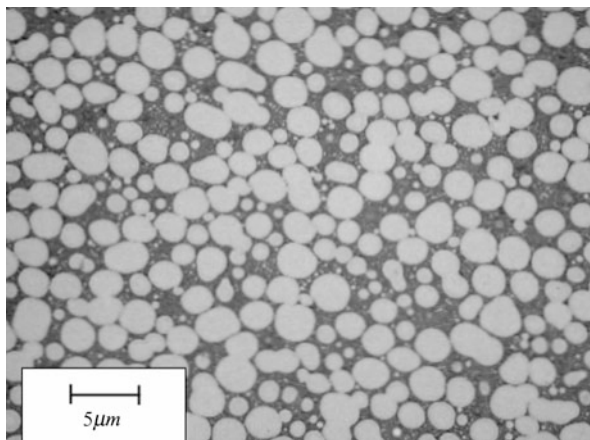
It has been reported that this phenomenon has been observed in the radical polymerization of methyl methacrylate (MMA) in the presence of poly(ethylene-*co*-vinyl acetate) (EVAc) (Chen et al. 1994). The MMA/EVAc blend shows a UCST phase diagram, and the shift of the phase diagram with polymerization of MMA is the same as that in Fig. 8.17. Figure 8.18 shows a TEM micrograph of the PMMA/EVAc (80/20) blend prepared by p-RIPS. The bright region is assigned to the polymerized PMMA region. The phase-separated structure shows a unique morphology in which the particles of the major component (PMMA) were dispersed in a matrix of the minor component (EVAc). Also, this blend prepared by polymerization shows a high impact strength. Figure 8.19 shows the notched Izod impact strength of PMMA/EVAc blends obtained by p-RIPS and melt-blending (Kojima et al. 1995). The blends obtained by polymerization show much higher impact strength than those by melt-blending. This result may be caused by the phase separation morphology in which the EVAc region with a rubbery property forms a matrix regardless of the minor component. This PMMA/EVAc blend obtained by polymerization is put to practical use because of its good physical properties.

As an example of c-RIPS, an epoxy/poly(ether sulfone) (PES) system with a phase diagram exhibiting an LCST behavior was demonstrated in Fig. 8.20 (Yamanaka and Inoue 1989). The binary mixture was first homogeneous at the curing temperature (below LCST). During the curing process, the system was thrust into a two-phase region by the LCST depression caused by increase of the molecular weight or the conversion, and the phase separation was expected to take place via SD. In this particular system, the progress of decomposition will eventually be suppressed by the vitrification, as shown by the approaching T_g line and by gelation in the epoxy-rich region. The morphology of the phase-separated structure in c-RIPS yields a variety of two-phase structures – interconnected globule structure, droplet structure with uniform domain size, and bimodal domain structure, depending on the relative rates of the chemical reaction and the phase separation (Yamanaka and Inoue 1989). Figure 8.21a shows a scanning electron

Fig. 8.19 Notched Izod impact strength of PMMA/EVA blend prepared by p-RIPS and melt blending
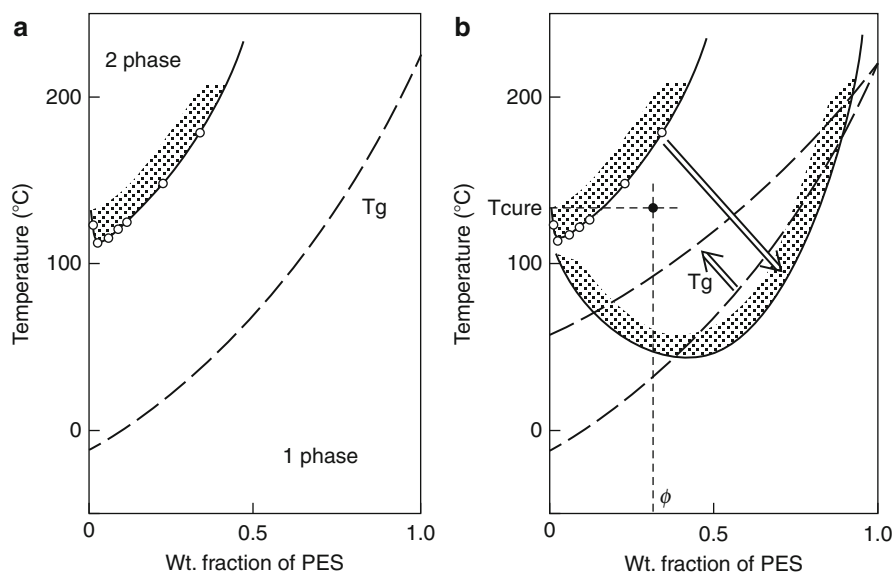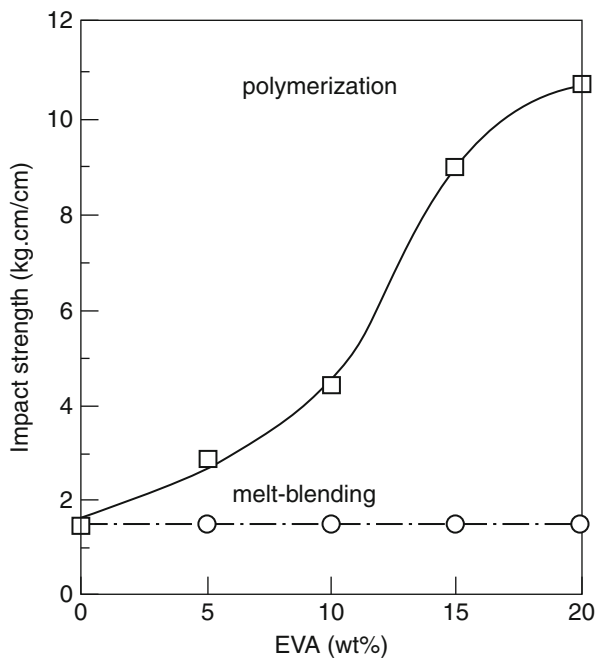
Fig. 8.20 (**a**) Phase diagram of epoxy oligomer/PES system. (**b**) Schematic representation of the variation of the phase diagram and Tg with curing. *Solid circle* (●) represents curing condition
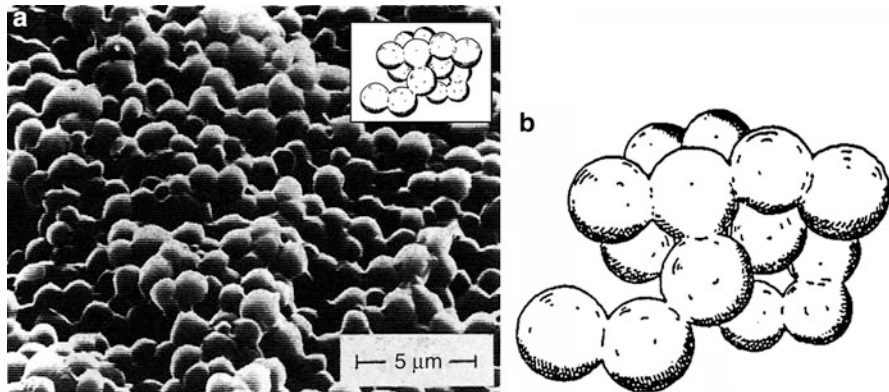
Fig. 8.21 SEM micrograph of cured resin epoxy/PES; PES 50 phr, 170 °C, 3 h
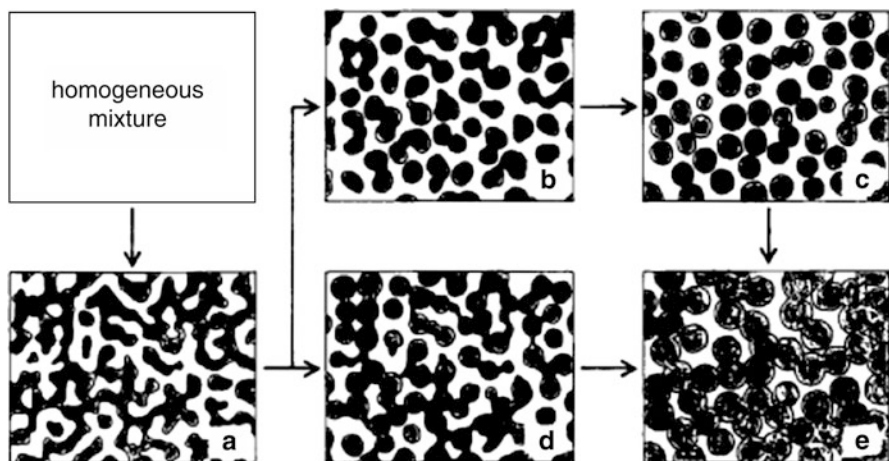
Fig. 8.22 Schematic representation of phase separation process resulting in connected-globule structure

microscope (SEM) micrograph for the cured resin in the epoxy/PES (100/50) system. Fine globules which are fairly uniform in size (a few micrometers) are seen. Furthermore, the particles seem to be connected to each other (Fig. 8.21b). This connected-globule structure implies a two-phase morphology of the interconnected spherical domains of the epoxy-rich phase of a major component dispersed regularly in a matrix of PES. This kind of morphology can never be obtained by mixing two polymers with an asymmetrical blend composition. The schematic representation of the changes in the phase separation structure is shown in Fig. 8.22 (Yamanaka and Inoue 1989). The dark region is assigned to the epoxy-rich region. During this curing reaction the homogeneous blend starts to phase-separate by SD (Fig. 8.22a). When the phase separation proceeds, the dispersed droplet-type
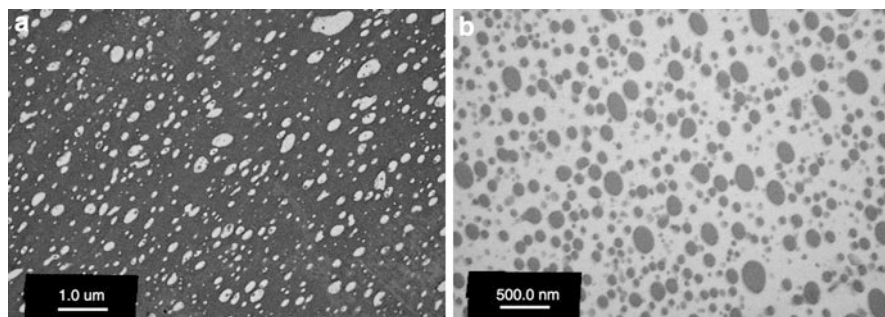
Fig. 8.23 TEM micrographs of the blends mixed by the mechanical blending at 200 °C for 5 min (**a**) PS/PMMA(80/20), (**b**) PMMA/PS(80/20)

morphology (Fig. 8.22b, c) or network morphology which is established with droplets (Fig. 8.22d) appears. The coarsening of domains then proceeds, eventually resulting in the connected-globule structure (Fig. 8.22e). The epoxy-rich region and PES-rich region form the domain and matrix, respectively. In polymer/polymer blend systems, generally the major component becomes the matrix while the minor component becomes the domain. However, in c-RIPS, the domain phase is formed by the cured component even if the cured component is major. This epoxy/PES system has good adhesive properties such as high peel strength because of this morphology.

Thus, the scenarios are plausible in the explanation of c-RIPS with the curing process. However, there was no explanation why the major component could form the domain in both of p-RIPS and c-RIPS. Also, so far the formation mechanism of the phase-separated morphology has apparently not been elucidated. Therefore, the following model experiments were carried out.

8.4.1 p-RIPS in PS/PMMA Systems

As a model blend of p-RIPS, the PS/PMMA systems were investigated. Both polymers are easily synthesized by radical polymerization from the monomer (Ono et al. 2008). This polymer blend is immiscible, but shows a small value of the positive interaction parameter, χ. The morphologies of the polymer blends mixed mechanically at 200 °C for 5 min are shown in Fig. 8.23a and b. The TEM micrographs are of PS/PMMA (80/20) and PMMA/PS (80/20), respectively. The darker regions correspond to the PS-rich phase and the brighter regions are associated with the PMMA-rich phase, because the phenyl group of PS is more stained by RuO_4. As shown in the figures, the minor component forms the domain in the major component matrix. In fact, in the case of PS/PMMA (80/20), PMMA, the minor component, was dispersed in the PS matrix as small domains after the mechanical melt blending. Phase inversion occurred in PMMA/PS (80/20) as a matter of course. The minor component of PS then formed many small domains. This phenomenon occurred predictably as is known in the field of polymer blends.

Fig. 8.24 TEM micrographs of the phase-separated structure of styrene/PMMA/AIBN(80/20/0.2) blend after polymerization at 80 °C in polymerization-induced phase separation

1.0 um
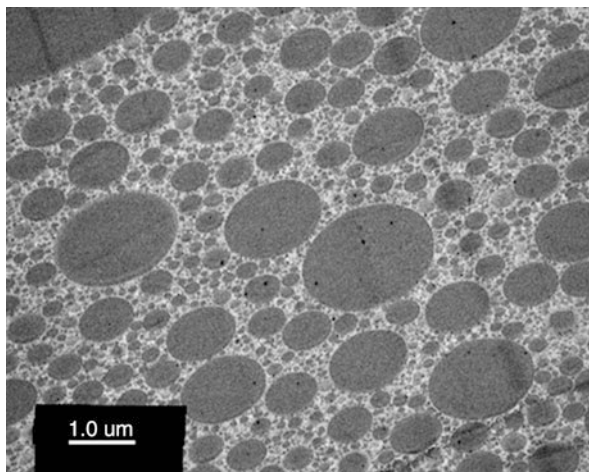
The final morphology of the binary blend prepared via p-RIPS is greatly different from that prepared via mechanical melt blending with the polymers, as stated above. The polymerized component tends to form the domains regardless of the varieties of monomer and reaction.

Here, not only styrene/PMMA (80/20) but also MMA/PS (80/20) could be prepared to observe the morphology obtained by p-RIPS. The process of the phase separation was observed by optical microscopy (OM) and light scattering (LS) measurements during the polymerization. The final morphology was observed by TEM, and image processing was carried out for the micrographs obtained by OM and TEM.

8.4.1.1 Styrene/PMMA Mixture

PMMA was dissolved in the styrene monomer with a radical initiator, α,α'-azobis (isobutyronitrile) (AIBN). Figure 8.24 shows the TEM micrograph for PS/PMMA/AIBN (80/20/0.2) after a polymerization of styrene completely finished at 80 °C. The brighter regions are associated with the PMMA-rich phase and the darker regions correspond to the PS-rich phase. According to this micrograph, the PS-rich phase formed the domains, although PS is the major component in this blend system, and the PMMA-rich phase formed the continuous phase in spite of being 20 wt% in content. This unique morphology can never be obtained by mechanical melt blending in binary polymers. As mentioned above, the minor component will form domains in mechanical melt blending. To confirm the particularity, the polymerized specimen was blended again by melt mixing. Of course, it was observed that the PMMA-rich phase of the minor component formed small domains in the PS-rich phase matrix of the major component, quite the same as in Fig. 8.23a. Furthermore, referring in detail to Fig. 8.24, there are several types of domains with different sizes, of which the larger domain is 10 μm and the smaller domain is 10 nm in diameter.

To investigate the formation process of the phase-separated morphology, the LS measurement and the observation by OM were carried out during the polymerization
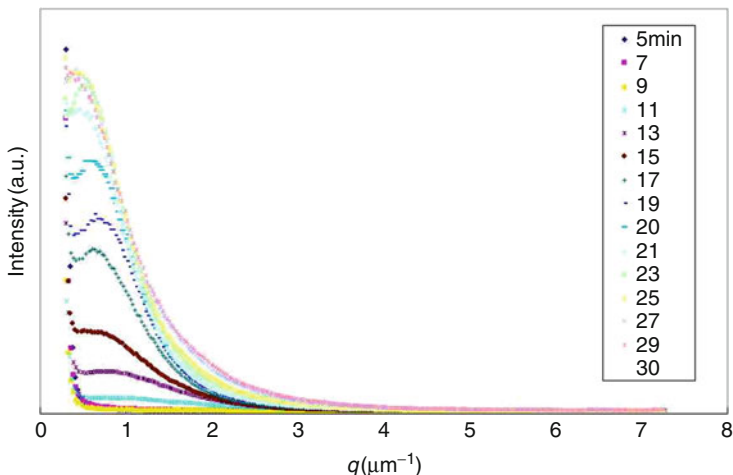
Fig. 8.25 Change of light scattering profiles in the process of the polymerization of sty/PMMA/AIBN (80/20/0.2) mixture at 80 °C

at 80 °C for a styrene/PMMA/AIBN (80/20/0.2) mixture. This mixture was homogeneous in solution between room temperature and the polymerization temperature (80 °C).

Figure 8.25 shows the time-resolved LS profiles during the process of the polymerization of the styrene/PMMA/AIBN (80/20/0.2) mixture at 80 °C. The scattering vector is defined by

$$q = \frac{4\pi}{\lambda} \sin \frac{\theta}{2} \tag{5}$$

where λ and θ are the wavelength of light in the medium and the scattering angle, respectively. The light scattering occurred slightly after a certain time lag of $\sim$9 min, then one peak started to appear at $q = 0.7$ μm^{-1} after 11 min. The peak implied the development of a regularly phase-separated morphology. From these profiles, one can estimate the periodic distance, Λ_m, in the phase-separated morphology using a Bragg equation and the scattering vector:

$$\Lambda_m = \frac{2\pi}{q} \tag{6}$$

The periodic distance was estimated to be 9 μm when the peak appeared first. However, this distance is too large for that in the initial stage of spinodal decomposition (SD) because the periodic distance in a typical SD is usually of submicron order in the case of polymer-solvent and polymer-polymer systems. This implies that this phase separation may not be occurring via SD. Therefore, an observation by OM was carried out to investigate the morphology at the early stage of the phase separation.

Figure 8.26 shows the optical micrographs observed at the various stages of polymerization at 80 °C. After about 8 min from the starting of polymerization of styrene monomer, the phase separation started to occur but with low contrast. A domain having a uniform particle size was generated at irregular positions like a morphology formed by the nucleation and growth (NG) mechanism. A co-continuous morphology was not observed in this blend system. Coarsening of the domains took place with time up to 15 min. In addition, the second phase separation was observed to occur in the matrix phase at 15 min. After that, collision and coalescence between the domains took place, and the two types of domains simultaneously coarsened with time. These optical micrographs indicated that the several phase separations took place in many stages in this blend system. Furthermore, it was confirmed that these step-by-step phase separations do not occur via SD-type but rather by NG-type processes.

The size distribution of domains in the phase-separated morphology in the picture of OM or TEM was estimated after threshold by image processing with the software Image J in order to investigate the change of the volume fraction and particle size with time. From this image analysis, the small domains generated at the initial stage (8 min) coarsened gradually, and then another phase separation was observed at 15 min with the advent of the bimodal distribution. Therefore, this indicates that the two phase separations occurred in steps in this system. Figure 8.27 shows the time dependence of particle diameter in a two-step phase separation. The smaller particle size generated in the second phase separation agreed with that of the domains generated in the first phase separation. Figure 8.28 shows the time dependence of the volume fraction of the polymerized major component, the PS-rich phase, by adding the values of each phase separation step. Because the area of the PS-rich region is almost 73 % of the TEM image of Fig. 8.24, which is a final morphology, it is considered that at least three steps of the phase separation occur.

It is possible to think about the phase separation in this system from the above discussion by looking at Fig. 8.29, which is the schematic diagram showing the triangle phase diagram of the styrene/PMMA/PS system at 80 °C. Since the PMMA content was fixed at 20 wt%, the initial binary solution of styrene/PMMA is indicated by the black filled circle. The polymerization process can be described by the arrow. Polymerization of styrene causes the solution to enter the two-phase region in which it separates into two phases, one rich in polymer PMMA and the other rich in generated polymer PS. The phase separation in the metastable region should proceed by the NG mechanism. Furthermore, the second phase separation took place in the PMMA-rich phase via NG. In this way, the several processes in the step-by-step phase separation are assumed to induce the unique phase-separated morphology. From this phase diagram, in the first phase separation, the PS-rich phase is minor and the PMMA-rich phase is major by the principle of leverage. The second phase separation occurs in the PMMA-rich phase, which is major, and it is repeated. Therefore, it is difficult for the domains to collide and coalesce with each other, and the coarsening of domains might be suppressed. As a result, the many PS-rich domains disperse in the matrix regardless of the major component until the polymerization finishes completely. Perhaps this is a reason why the PS which is a major component forms a domain.
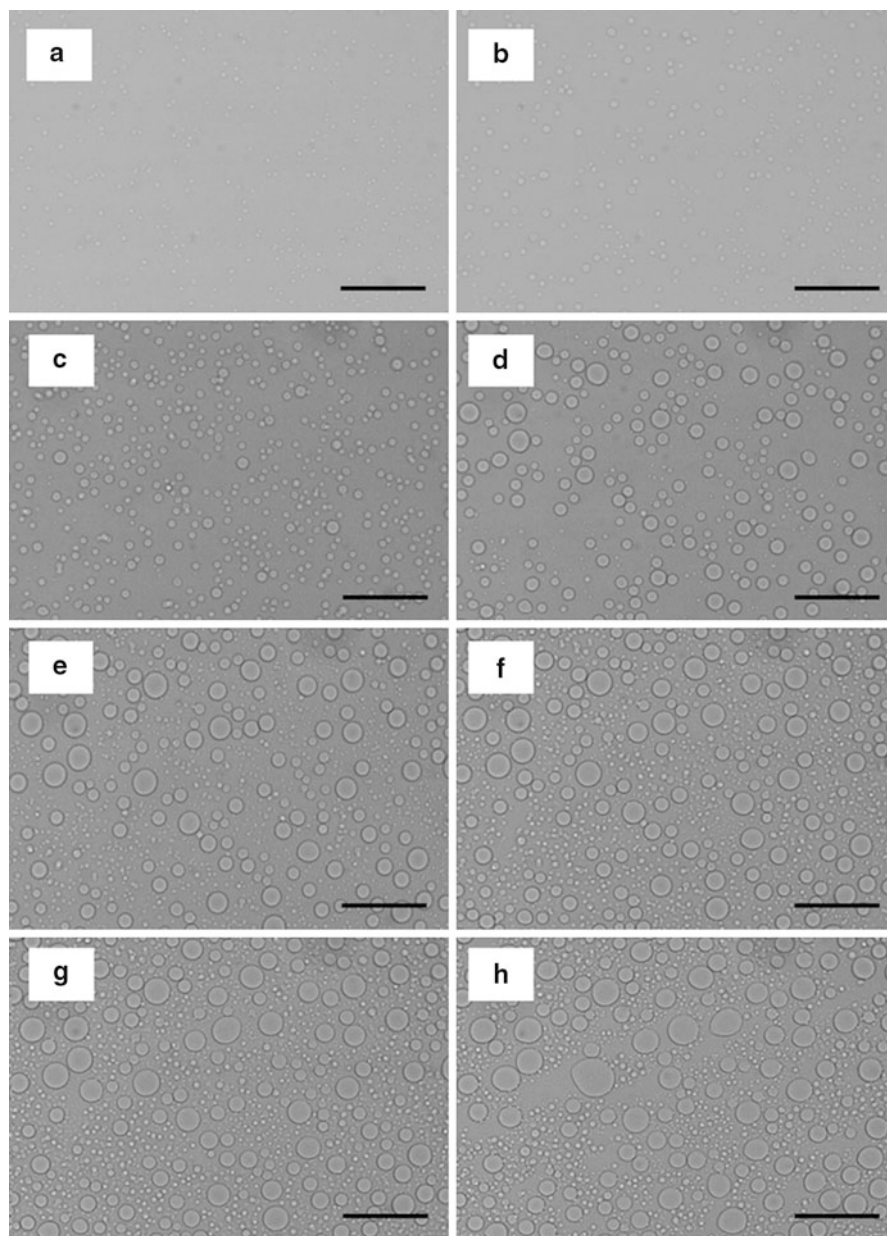
Fig. 8.26 Optical micrographs at various stages of polymerization of sty/PMMA/AIBN(80/20/ 0.2) at 80 °C. Scale bar: 50 μm (**a**) 8 min (**b**) 10 min (**c**) 13 min (**d**) 15 min (**e**) 20 min (**f**) 25 min (**g**) 30 min (**h**) 35 min

Fig. 8.27 Number-average particle diameter D_n vs time in sty/PMMA/AIBN(80/20/0.2) blend during polymerization at 80 °C. (●) Number-average particle diameter of PS-rich domains at 1st phase separation (■) at 2nd phase separation
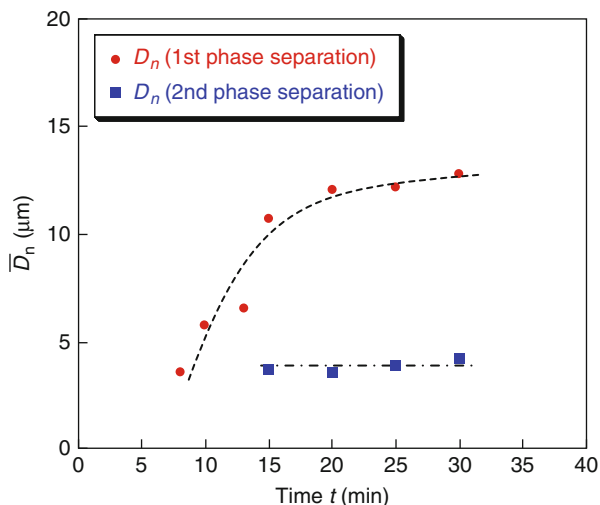
Fig. 8.28 Change of volume fraction of PS-rich domain in sty/PMMA/AIBN(80/20/0.2) blend during polymerization at 80 °C. (●) Volume fraction of PS-rich domains at 1st phase separation, (■) 1st & 2nd phase separation
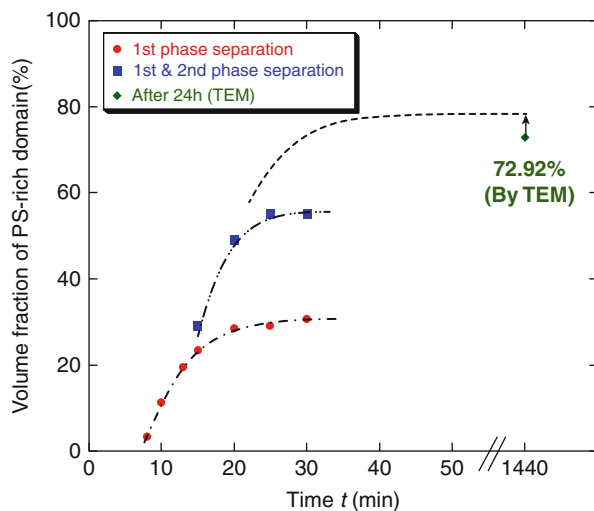
8.4.1.2 MMA/PS Mixture

Figure 8.30 shows a TEM micrograph for MMA/PS/AIBN (80/20/0.2) after polymerization of MMA completely finished at 80 °C. The brighter regions are associated with the PMMA-rich phase and the darker regions correspond to the PS-rich phase. According to this micrograph, the PMMA-rich phase formed the domains, although PMMA was a major component in this blend system, and the PS-rich phase formed the continuous matrix phase in spite of being 20 wt% content. This morphology is opposite to the morphology seen in the styrene/PMMA/AIBN (80/20/0.2) system as shown in Fig. 8.24.

Fig. 8.29 Triangle phase
diagram of styrene/PMMA/
PS system at 80 °C. Spinodal
and binodal curves are by
broken and *solid lines*,
respectively. *Arrow* indicates
the polymerization process
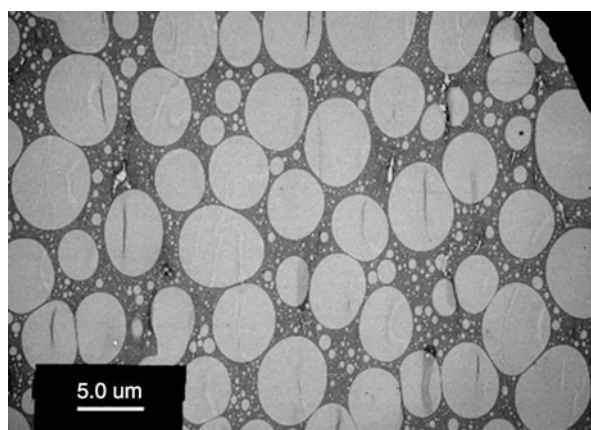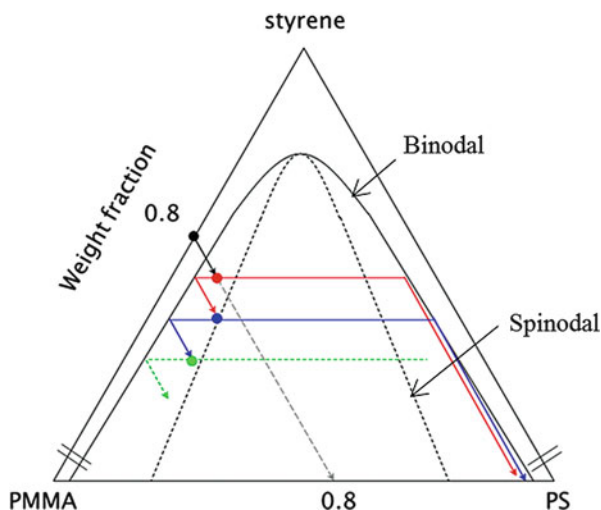
Fig. 8.30 TEM micrograph
of the phase-separated
structure of MMA/PS/AIBN
(80/20/0.2) blend after
polymerization at 80 °C in
p-RIPS

To investigate the formation process of the phase-separated morphology, the
measurement of LS and the observation by OM were carried out. Figure 8.31 shows
the time-resolved LS profiles during the process of the polymerization. The periodic
distance Λ_m was estimated to be about 2.1 μm. The position of the peak started to
shift toward a smaller angle as the polymerization progressed. The phenomenon
revealed the occurrence of coarsening of the periodic structure at the late stage of
the SD mechanism.

The change of the volume fraction of the PMMA-rich phase and the periodic
distance Λ_m of the co-continuous morphology versus time can be estimated
from the optical and TEM micrographs after threshold by the image processing
with the software Image J (see Fig. 8.32). The black region is associated with the
PMMA-rich phase. The pictures after the image processing clearly represent
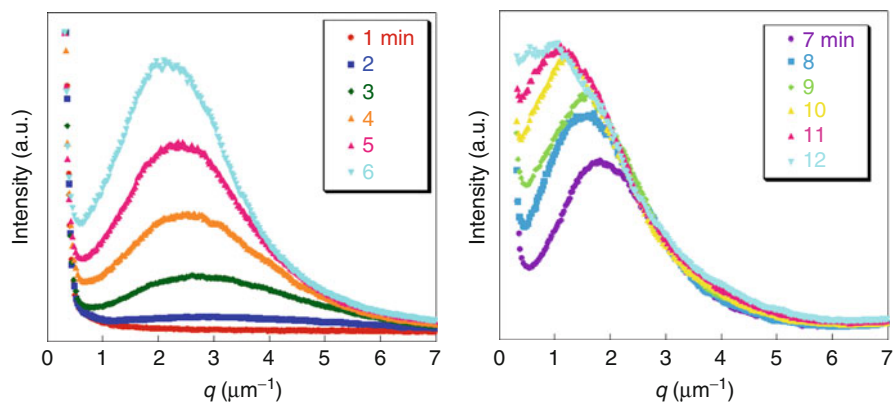
Fig. 8.31 Changes of light scattering profiles in the process of the polymerization of MMA/PS/AIBN (80/20/0.2) mixture at 80 °C
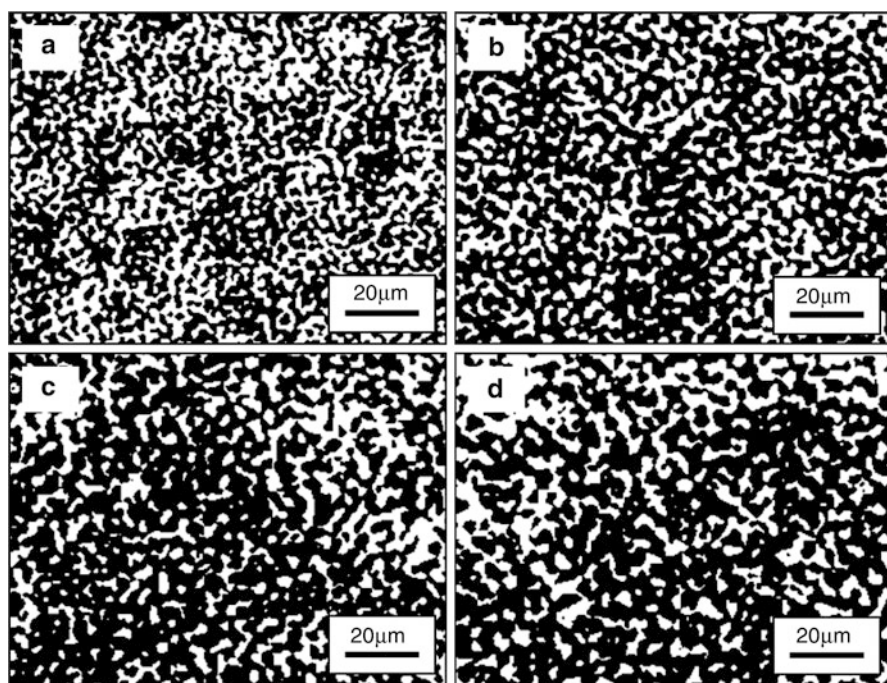
Fig. 8.32 Optical micrographs after image processing at various stages of polymerization of MMA/PS/AIBN(80/20/0.2) at 80 °C. (**a**) 10 min (**b**) 15 min (**c**) 20 min (**d**) 25 min

Fig. 8.33 Time dependence of volume fraction of PMMA-rich phase in MMA/PS/AIBN (80/20/0.2) blend during polymerization at 80 °C
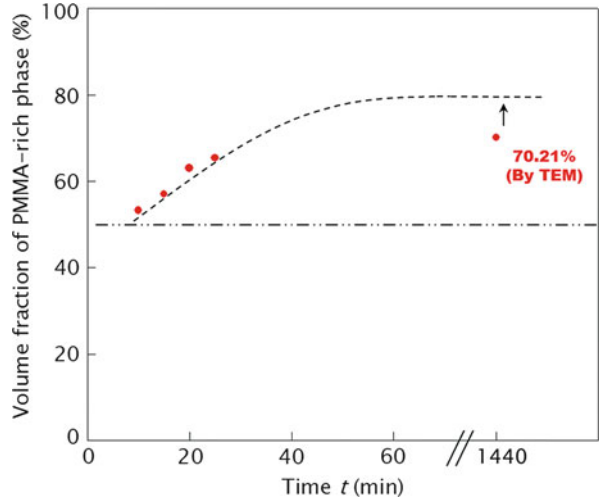
Fig. 8.34 Triangle phase diagram of MMA/PS/PMMA system at 80 °C. Spinodal and binodal curves are by *broken* and *solid lines*, respectively. *Arrow* indicates the polymerization process
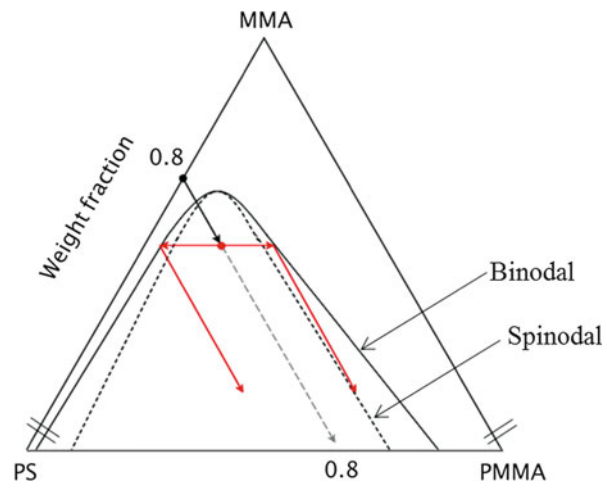
the co-continuous structure via the SD. Furthermore, the coarsening behavior of the periodic morphology was observed. This indicates that the volume fraction of the PMMA-rich phase increased gradually with time (Fig. 8.33). The volume fraction should approach 80 % of the mixing composition if the phase separates to pure PS and pure PMMA completely. However, it does not completely correspond because there are many small particles which were not recognized by the image processing, or perhaps the phases do not separate pure components.

It is possible to think about the phase separation in this system from the above discussion by looking at Fig. 8.34, which is the schematic diagram showing a triangle phase diagram of the MMA/PMMA/PS system at 80 °C. Since the PS weight fraction was fixed at 20 wt%, the initial binary solution of MMA/PS is

indicated by a black filled circle. The polymerization process can be described by the arrow. The binodal and spinodal lines shift to the PS-rich side in some measure, as shown in Fig. 8.34, because the MMA/PS/AIBN (90/10/0.225) system did not show phase separation after polymerization of MMA at 80 °C. However, we suppose that the blend system did not cause the phase separation and was frozen at the miscible state because the sample entered the two-phase region late during the process of polymerization which is a low mobility stage. From the above results, this phase separation took place in the spinodal region in the triangle phase diagram. Therefore, the volume fraction of the formed domain is supposed to be almost 50 % derived from the concentration fluctuation in the co-continuous morphology at the initial stage of SD. After that, the volume fraction of the PMMA-rich phase increases up to near 80 % that is the mixing composition. However, the PMMA-rich phase, which is the major component, forms domains in the late stage of the phase separation. Because the volume fraction of each phase in the initial stage of the phase separation should be almost even, one cannot explain this result as explained in the NG mechanism for styrene/PMMA/AIBN (80/20/0.2). Therefore, it is considered that the polymerization process induced the change of the coarsening mechanism and the formation of a unique morphology in p-RIPS.

Which phase wants to form domains after the co-continuity is lost? Considering that this unique morphology is never formed by conventional thermal-induced phase separation, it is thought that changes of some kind of physical properties induced by the polymerization cause it. There are changes in physical properties, such as viscoelasticity and volume shrinkage. The answer is not clear at present.

8.5 Reactive Blending

The reactive blending of immiscible polymers yields a block or graft copolymer at the interface. By an emulsifying effect of the in situ-formed copolymer, the dispersed particles can be reduced down to submicrometer size, and the interfacial adhesion can be improved. Then, the material properties are improved. It may be a commonly accepted story for compatibilization (Baker et al. 2001). In addition to the emulsifying effect, new interfacial behaviors of the in situ-formed copolymers have been found recently; such as pull-out and pull-in of copolymers by the external shear forces. These render a series of high-performance materials with new morphologies. Further, a new approach has been explored by combining many reactions, e.g., coupling and exchange reactions.

8.5.1 Coupling Reaction at Polymer-Polymer Interface

The first example of reactive blending is a system containing polyamide (PA-6) and polypropylene (PP) with a small amount of maleic anhydride (MAH) (Ide and Hasegawa 1974). A coupling reaction between the amino chain end of PA with MAH leads to the in situ formation of a PA-PP graft copolymer at the interface (see Fig. 8.35).

Fig. 8.35 Polymer-polymer
interface as the reaction site

X=MHA, $\diagdown_0$ Y=NH$_2$, COOH
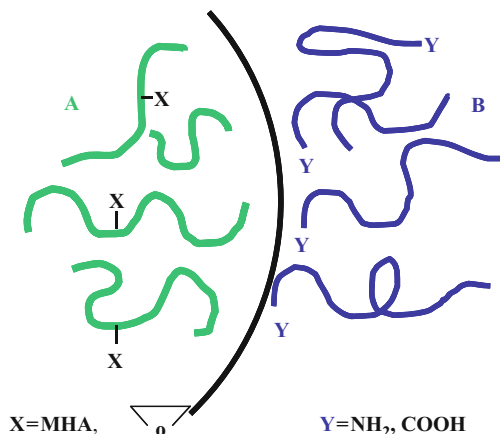
The coupling reaction proceeds very quickly, caused by concentrating the reactive
moieties (MAH, epoxide, NH$_2$, COOH, etc.) at the interface. The polymer chain end
generally prefers to locate at the interface, because such a chain conformation is more
probable, compared with the case where a mid-segment locates near the interface.
Then, the amino chain ends of PA may be concentrated at the interface. The MAH
unit is highly polar and is unstable in the non-polar PP-MAH phase, and it tends to
segregate at the interface to contact with the polar chain of PA. Thus, both reactive
sites may be concentrated near the interface to provide a favorable situation for the
coupling reaction.

This type of blending has been used to produce the "super-tough nylon" PA/poly
(phenylene ether) (PPE) alloy (Baker et al. 2001). Similar reactive blending of PPE
with poly(ethylene-*co*-glycidyl methacrylate) (EGMA) yields a high-temperature
engineering plastic with low dielectric loss and nice melt-processability (Furuta
et al. 2007). It can be classified as a super-engineering plastic, like poly(ether
sulfone) and poly(ether imide). A super-ductile alloy with excellent high-
temperature resistance was also developed by reactive blending of poly(butylene
terephthalate) (PBT) with EGMA (Hashima et al. 2008).

8.5.2   In situ-formed Copolymer as an Emulsifier

The in situ-formed copolymers locate at the interface to prevent coalescence of the
dispersed particles. The brush chains (the B chains of the in situ-formed A-B
copolymer; see Fig. 8.35) on the dispersed particles overlap when neighboring
particles approach each other. By the chain overlap, the conformational entropy
decreases to generate a repulsive interaction between the particles, which is different
from the electrostatic repulsion in low molecular weight systems (oil/water/soap).

The emulsifying effect of the in situ-formed copolymers allows a fine dispersion
to be achieved by reactive blending. The particle size during reactive blending of
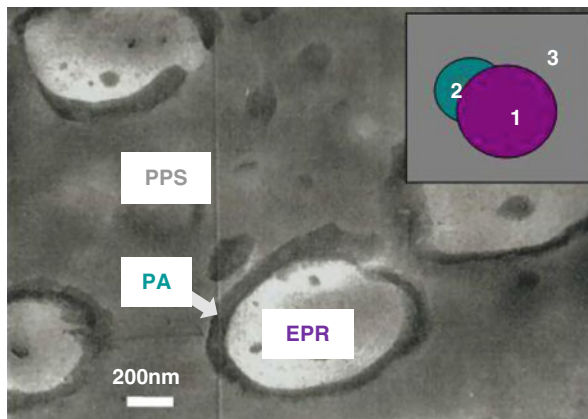
PA-6 and MAH-functionalized polystyrene (PS) decreased by two orders of magnitude, in comparison to the nonreactive PA-6/PS = 80/20 (Park et al. 1992). The change in the morphological parameters, such as the mean radius of dispersed particles and the specific interfacial area, with mixing time was quantitatively shown as a function of reaction time via light scattering analysis (Okamoto and Inoue 1993).

The in situ-formed copolymer reduces the interfacial tension. In ternary systems of a major component (3) and two minor components (1 and 2), as schematically shown in Fig. 8.36, component 2 spreads over the component 1 particles when the spreading coefficient S, determined by a balance between the interfacial tensions $\Gamma_{i/j}$, is positive. The S in a ternary system of EPR (ethylene-propylene rubber) (1)/PA(2)/PPS (poly(phenylene sulfide)) (3) defined by

$$S = \Gamma_{PPS/EPR} - \Gamma_{PA/EPR} - \Gamma_{PPS/PA}$$

can be positive when the value of $\Gamma_{PPS/PA}$ is reduced by the formation of an in situ-formed copolymer of PPS and PA. Then, PA shell-EPR core particles are dispersed in a PPS matrix, as shown in Fig. 8.36. The formation of the core-shell particles gives the ternary alloy high toughness, even when the surface-to-surface interparticle distance τ is fairly large ($\tau = 500$ nm) (An et al. 2001).

8.5.3   Pull-out of in situ-formed Copolymer

During reactive blending, the in situ-formed copolymers are sometimes pulled out from the interface and dispersed as micelles (domains) in the matrix, as shown in Fig. 8.37. The micelles are typically 20 nm in diameter (Ibuki et al. 1999). The pull-out does not occur at the static state; i.e., it is not caused by the interfacial instability of the highly crowded copolymers themselves. The pull-out takes place mechanically under the shear fields (Charoensirisomboon et al. 1999).

Fig. 8.37 Pull-out of in situ-formed block copolymer
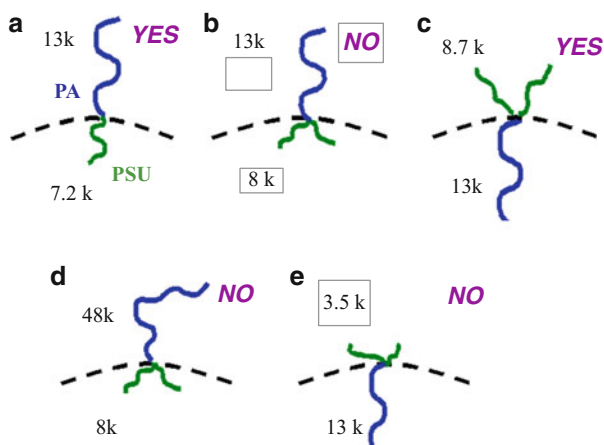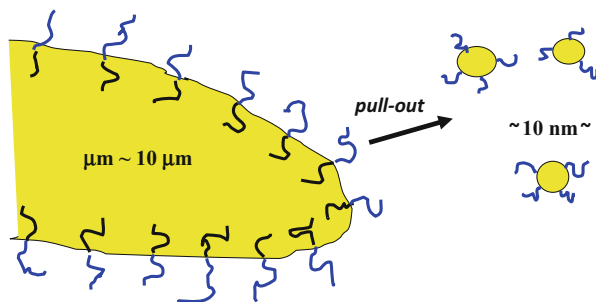
Fig. 8.38 In situ-formed copolymers are pulled out (YES) or not pulled out but stay at interface (NO), depending on the molecular architecture. Figures are number average molecular weight of component polymers

Whether pull-out occurs or not highly depends on the molecular architecture, as shown in Fig. 8.38 (Charoensirisomboon et al. 2000). A block copolymer with a linear structure is easily pulled out (YES, Fig. 8.38a). An in situ-formed graft copolymer with a trunk chain located in the dispersed particle (inverse-Y shape) is hardly pulled out and plays the role of emulsifier (NO, Fig. 8.38b). By contrast, a graft copolymer with a trunk chain in the matrix (Y shape) can be pulled out easily (Fig. 8.38c). An inverse-Y shaped graft copolymer is hardly pulled out, even in the case of a short trunk (Fig. 8.38d). A Y-shaped graft copolymer with a long anchoring chain is hardly pulled out (Fig. 8.38e). Following thermodynamic theory (equilibrium under quiescent conditions), an asymmetric copolymer is unstable at the interface. The results in Fig. 8.38 show that the external shear effect prevails over the thermodynamic effect.

Super-tough nylon is a case of the inverse-Y-type graft copolymer, which is hardly pulled out at all and stays at the interface to act as the emulsifier. It seems to be a clever and reasonable choice.

The pull-out occurs even at the very early stages of mixing in which the dispersed particles are large (∼10 μm). By continuing the mixing, the large particles shrink and the number of micelles increases. Eventually, the large particles
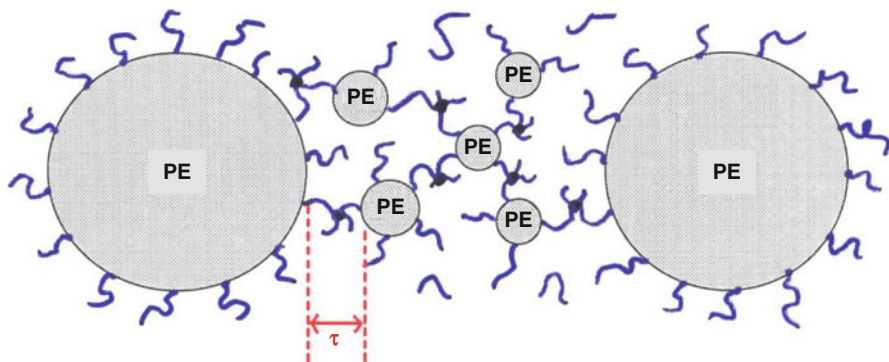
Fig. 8.39 Bimodal particle distribution by the pull-out of in situ-formed graft copolymer

disappear, leading to a pure copolymer domain system; that is, 100 % conversion is achieved. In other words, a solvent-free synthesis of the block or graft copolymer is realized by the dry process.

If the reactive blending is stopped at an intermediate stage, the micelles and the shrunken particles coexist and a bimodal particle distribution is realized, as shown in Fig. 8.39. In the case of Fig. 8.39, PA-6 was mixed with polyethylene (PE) modified with a small amount of MAH (0.1 wt%) and glycidyl methacrylate (3–12 wt%), at a 70/30 (PA/PE) blend ratio. The bimodal system can be easily crosslinked by electron beam irradiation at a low dose level, the same as that used for neat PE (Pan et al. 2002). The crosslinked PA/PE alloy shows good heat resistance in a lead-free solder test; thus, it may be applied in making construction parts with melt-down resistance in fires, e.g., a window frame.

8.5.4 Pull-in of in situ-formed Copolymer

As discussed in Fig. 8.38, an in situ-formed inverse-Y shaped copolymer is hardly pulled out of the matrix. However, "pull-out into the dispersed particles" (pull-in) takes place in reactive blending by the use of an extremely long (L/D = 100, L: screw length, D: screw diameter) twin screw extruder (Sato et al. 2007). Under the intensive shear fields in the extruder, the dispersed particles can be highly deformed, as shown in Fig. 8.40. The deformation to ellipsoids and the recovery to spherical particles would be repeated in the extruder, which implies that, from the shear fields in the dispersed particles, the in situ-formed graft copolymers would pull into the dispersed particles.

The pull-in leads to a fine "salami" morphology of 20 nm occlusion, as shown in Fig. 8.40. A PA/EGMA 70/30 alloy with a fine salami morphology showed ultra-high toughness (non-break under the Izod impact test) and a non-viscoelastic tensile property: the higher deformation rate leads to a lower modulus and a larger elongation at break (Sato et al. 2007). These results suggest a potential application in energy-absorbing car parts, designed to be friendly for both pedestrian and

Fig. 8.40 Pull-in of the in situ-formed inverse Y-type graft copolymer to form fine salami particle

20 nm PA domain

300 nm EGMA particle
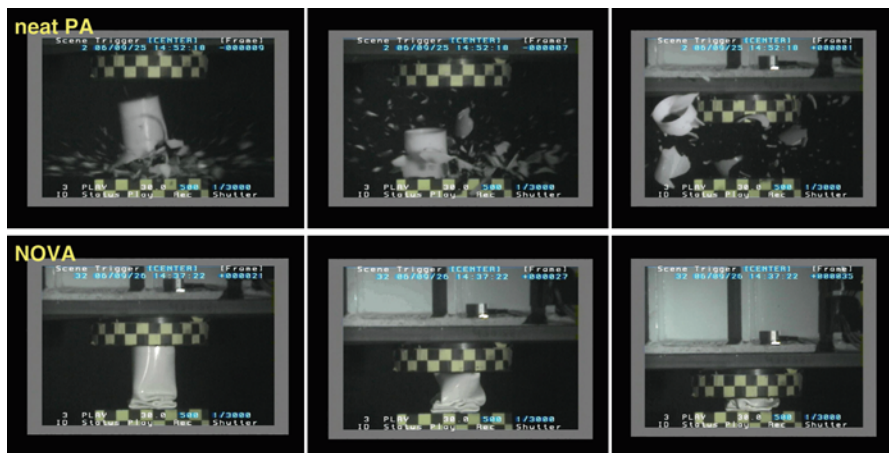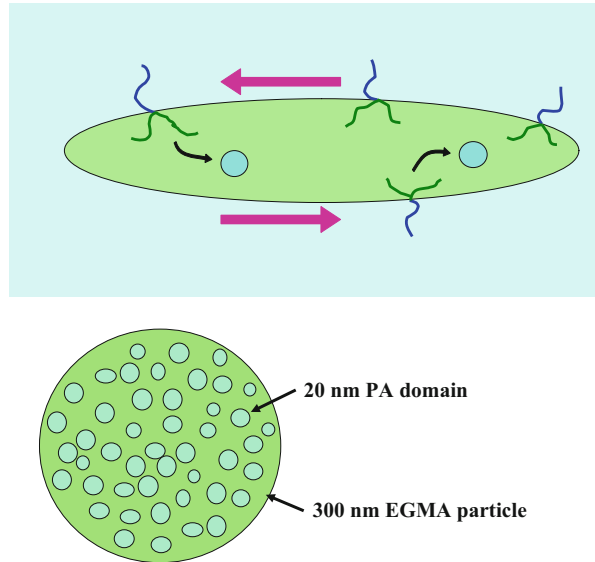
Fig. 8.41 Video images during the falling weight impact test for neat PA (*above*) and PA/EGMA alloy (*below*)

driver. Actually, the alloy showed super-ductile behavior in a high-speed crash test. The results of a high-speed falling weight impact test are shown in Fig. 8.41 (Inoue and Kobayashi 2011). A 193 kg weight fell from a 0.5 m height (impact speed = 11.2 km/h) on a pipe sample (50 mm diameter, 150 mm height, 2 mm thick). The neat PA crashes into tiny fragments immediately after the weight hits the pipe sample. The impact condition is so severe that this typical engineering
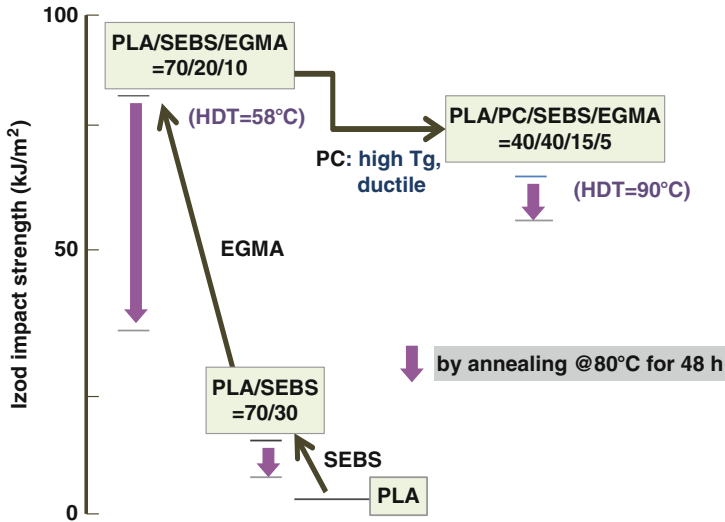
Fig. 8.42 Improvement of toughness, heat resistance (HDT), and ageing resistance of PLA

plastic, PA, breaks in a very brittle manner. However, even for such a severe impact test, the PA/EGMA alloy never breaks, but only deforms. It looks like a beer can and a rubber hose.

8.5.5 Blending by Combining Many Reactions

As shown in Fig. 8.42, the toughness of poly(lactic acid) (PLA) is improved by blending a hydrogenated styrene-butadiene-styrene block copolymer (polystyrene-*b*-poly(ethylene-co-butylene)-*b*-polystyrene; SEBS). By adding EGMA as the third component, the toughness can be improved further. However, the toughness of both binary and ternary alloys decreases by annealing at 80 °C for 48 h. By adding polycarbonate (PC) as the fourth component, the heat resistance is improved; i.e., the high toughness is maintained even after the annealing (Hashima et al. 2010). The four-component alloy may be classified as an engineering plastic, as shown in Fig. 8.43.

In the TEM micrographs of Fig. 8.44, the gray region is assigned to PC and the dark region to SEBS particles in which the microdomain structure of the block copolymer is seen. SEBS particles are covered by a thin layer of EGMA. The coupling reaction between PLA and EGMA may lead to a fine dispersion of SEBS-core/EGMA-shell particles. The right micrograph is a magnified one. A gray boundary is seen between the elongated PC particles and the PLA matrix. The boundary is assigned to a multi-block or random copolymer formed by an exchange reaction between PC and PLA. The copolymer is expected to enhance the interfacial adhesive strength.
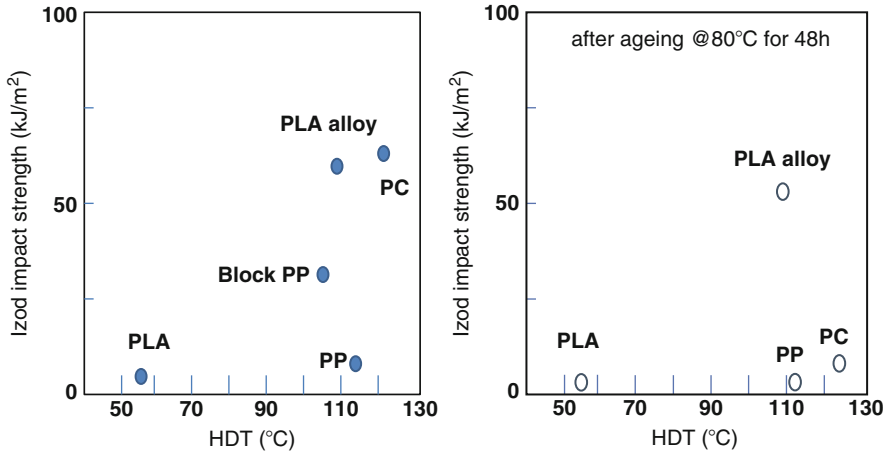
Fig. 8.43 PLA alloy on impact strength-HDT map, as compared with other plastics
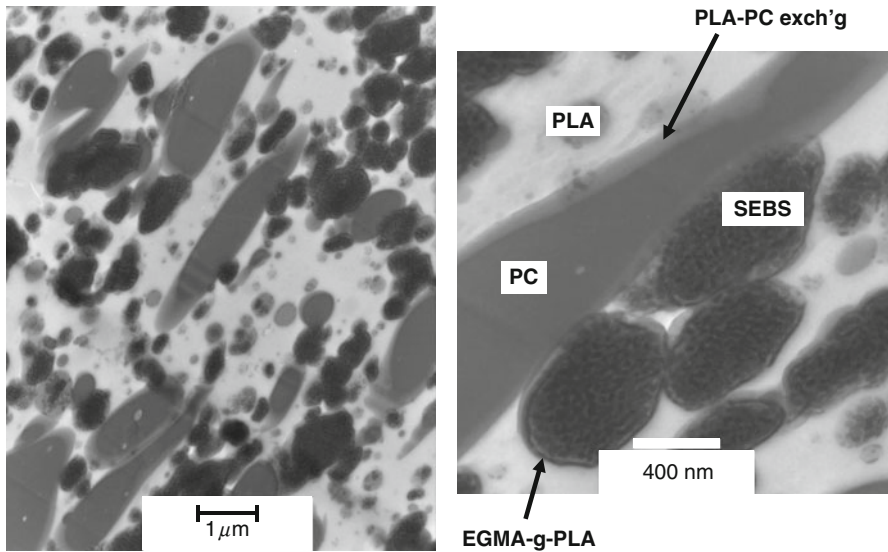
Fig. 8.44 TEM of four component PLA alloy

Thus, the morphology of the four-component alloy seems to be generated by combining two reactions: the coupling reaction between EGMA and PLA and the exchange reaction between PC and PLA.

A high-performance PP/PLA alloy is successfully developed by reactive blending with the aid of EGMA and organic peroxide (dicumyl peroxide, DCP),

Fig. 8.45 TEM of PLA/PP alloy
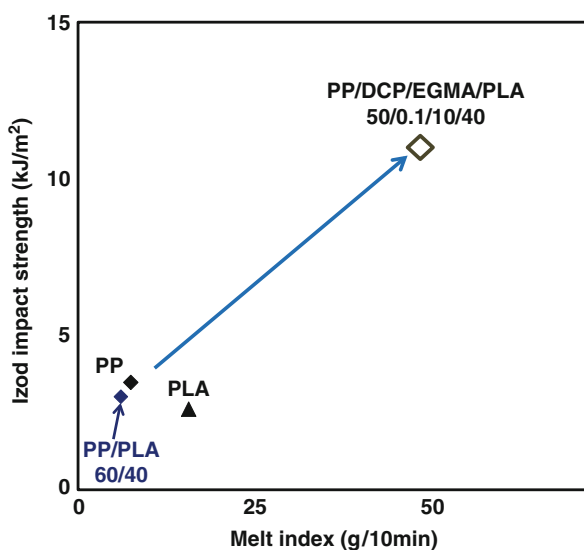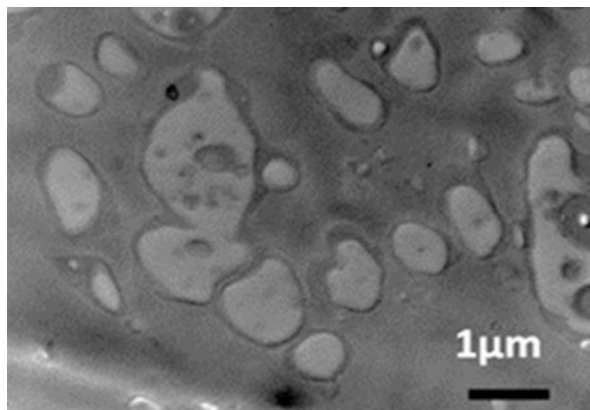
Fig. 8.46 Impact strength and fluidity of PLA/PP alloy

e.g., PP/DCP/EGMA/PLA = 50/0.1/10/40 (Ito et al. 2012). As shown in Fig. 8.45, PLA particles are coated with EGMA shell and dispersed in a PLA matrix. The rubber (EGMA) shell seems to help the cold drawing of the brittle occlusion (PLA) in the ductile matrix (PP) (Angola et al. 1988). It showed high Izod impact strength, large elongation at break (75 %), and nice fluidity (Fig. 8.46). The three reactions involved in this reactive blending, (1) coupling between the epoxide of EGMA and the carboxyl acid and/or hydroxyl chain ends of PLA, (2) chain scission of PP, and (3) radical grafting of PP onto EGMA, may generate a desirable morphology of fine particles of PLA-core/EGMA-shell, dispersed in a PP matrix of low viscosity (see Fig. 8.47).

Fig. 8.47 Chain scission of PP, PP-EGMA radical grafting, and EGMA-PLA coupling
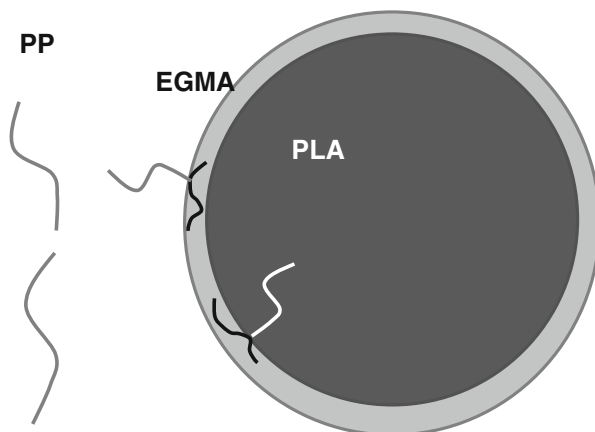
8.5.6 Blending with the aid of Reactive Plasticizer

It was quite difficult to develop a high-performance PP/PC blend. The difficulty is caused by the big differences in melt viscosity (the viscosity of PC is two decades higher than that of PP) and polarity (PP: non-polar vs. PC: polar). A new approach has been presented that uses a reactive plasticizer which is preferentially soluble with PC and polymerizable by organic peroxide (Matsumoto et al. 2012). As plasticizers, diallyl phthalate (DAP) and triallyl cyanurate (TAC) are used. For example, by adding 20 wt% of DAP, the melt viscosity of PC decreases to the same level of neat PP. By the reactive extrusion of PP/PC/plasticizer/dicumyl peroxide (e.g., 80/14/6/0.12 wt. ratio), a reaction-induced phase decomposition takes place in the dispersed PC particles to develop a regularly phase-separated nanostructure, and the graft copolymer of PP and polymerized plasticizer seems to be generated in situ at the interface. The extruded blend shows an excellent ductile behavior with ca. 500 %-elongation at break. TAC is shown to be more effective at elevating the heat resistance than DAP.

8.6 Concluding Remarks

Here, three important phenomena to control the phase separation morphology were explained: the phase diagram and the phase separation in a shear flow field, reaction-induced phase separation, and reactive blending.

Information about the phase diagram and the phase separation in the shear flow field is very important in polymer processing. For instance, it is important to know how the miscibility and the phase diagram change in a shear flow field. As shown in this chapter, the miscible area might extend by the shear flow, and there might be a case in which a two-phase region becomes a one-phase region. After the cessation of the shear flow, the miscible area reduces and the phase separation from the one-phase state might take place by spinodal decomposition. Control of the

phase-separated morphology using such a phenomenon must exist in other systems. Moreover, it may be that the physical properties are improved by increasing the adhesion between both separated phases due to the partial dissolution even if both polymers do not mix completely.

Reaction-induced phase separation is a very useful method because of a peculiar morphology in which the major component forms the domain and the minor component the matrix (occasionally a co-continuous morphology is formed). The utility value of this morphology is high. Because there are not very many miscible polymer blends, the method of controlling the morphology by using the phase separation from the one-phase state which is obtained by using the low molecular weight one as one component of polymer blend is useful. Therefore, another effect may be assumed to induce the phase separation and the unique morphology in RIPS. Regarding the change of physical properties by polymerization, it is known that volume shrinkage occurs in the process of polymerization from monomers to polymer. Considering that the polymerized component is sure to form domains in RIPS, this volume shrinkage is assumed to induce the unique morphology. Therefore, the shrinkage stress during polymerization may be assumed to affect the formation mechanism and also bring the differential in the coarsening mechanism.

Regarding the reactive blends, control of the molecules in the interfacial region is important, because they affect the morphology and the properties. The role of the in situ-formed copolymers is related to many phenomena. Therefore, the molecular design of the copolymer, including the type of copolymer, functional group, position of functional group, block length, and molecular weight, is important.

The formation of a phase separation morphology with crystallization is also important, though it was not described in this chapter.

The control of the phase separation morphology is just a key technology in polymer blends. In order to achieve good performance of the materials, it is important to handle the processing-morphology-properties relationship.

8.7　Cross-References

▶ Interphase and Compatibilization by Addition of a Compatibilizer
▶ Reactive Compatibilization
▶ Thermodynamics of Polymer Blends

Notation and Abbreviations

Notation

d_s　Spatial dimensionality
G_M　Free energy of mixing
q　Magnitude of scattering vector
R　Gas constant

r Number of segments in polymer chain
S Spreading coefficient
T_g Glass transition temperature
T_m Melting temperature of crystal
T_s Spinodal temperature
V Volume
$\Gamma_{i/j}$ Interfacial tension between i and j
$\dot{\gamma}$ Shear rate
θ scattering angle
Λ_m Periodic distance
λ Wavelength of light in the medium
τ Surface-to-surface interparticle distance
τ_ξ Characteristic relaxation time
ϕ_i Volume fraction of component i
χ_{12} Binary interaction parameter

Abbreviations

ABS Acrylonitrile-butadiene-styrene resin
AIBN α,α′-azobis(isobutyronitrile)
cPC PC copolymer
c-RIPS Curing reaction-induced phase separation
DAP Diallyl phthalate
DCP Dicumyl peroxide
EGMA Poly(ethylene-*co*-glycidyl methacrylate)
EPR Ethylene-propylene rubber
EVAc Poly(ethylene-*co*-vinyl acetate)
LCST Lower critical solution temperature
LS Light scattering
MAH Maleic anhydride
MMA Methyl methacrylate
NG Nucleation and growth
OM Optical microscope
PA4,6 Polyamide (nylon) 4,6
PA-6 Polyamide (nylon) 6
PBT Poly(butylene terephthalate)
PC Bisphenol-A polycarbonate
PE Polyethylene
PES Poly(ether sulfone)
PLA Poly(lactic acid)
PMMA Poly(methyl methacrylate)
PP polypropylene
PPE Poly(phenylene ether)

PVME Poly(vinyl methyl ether)
PPS Poly(phenylene sulfide)
p-RIPS Polymerization reaction-induced phase separation
PS Polystyrene
RIPS Reaction-induced phase separation
SAN Poly(styrene-*co*-acrylonitrile)
SD Spinodal decomposition
SEBS Hydrogenated styrene-butadiene-styrene copolymer
TAC Triallyl cyanurate
TEM Transmission electron microscope
UCST Upper critical solution temperature

References

J.-B. An, T. Ougizawa, T. Inoue, Y. Ishii, T. Yoshizaki, in *16th Polymer Processing Society, Abstract*. 2001, p. 21

J.-B. An, T. Suzuki, T. Ougizawa, T. Inoue, K. Mitamura, K. Kawanishi, J. Macromol. Sci. Phys. **B41**(407) (2002)

J.C. Angola, Y. Fujita, T. Sakai, T. Inoue, J. Polym. Sci. Phys. **26**, 807 (1988)

W. Baker, S. Scott, G.H. Hu (eds.), *Reactive Polymer Blending* (Hanser, Munich, 2001)

D. Beysens, M.J. Gbadamassi, Phys. Lett. (Paris) **40**, L565 (1979)

D. Beysens, F.J. Perrot, Phys. Lett. (Paris) **45**, L31 (1984)

K. Binder, D. Stauffer, Phys. Rev. Lett. **33**, 1006 (1973)

C.B. Bucknall, *Toughened Plastics* (Applied Science, London, 1977)

J.W. Cahn, J. Chem. Phys. **42**, 93 (1965)

J.W. Cahn, Trans. Met. Soc. AIME **242**, 166 (1968)

P. Charoensirisomboon, T. Chiba, S.I. Solomko, T. Inoue, Polymer **40**, 6803 (1999)

P. Charoensirisomboon, T. Inoue, M. Weber, Polymer **41**, 4483 (2000)

W. Chen, S. Kobayashi, T. Inoue, T. Ohnaga, T. Ougizawa, Polymer **35**, 4015 (1994)

A.Y. Coran, R. Patel, Rubber Chem. Technol. **56**, 1045 (1983)

B.D. Favis, J.M. Willis, J. Polym. Sci.: Polym. Phys. **28**, 2259 (1990)

J. Fernandez, J.S. Higgins, R. Horst, B. Wolf, Polymer **36**, 149 (1995)

D.J. Flory, *Principles of Polymer Chemistry* (Cornell University Press, Ithaca, 1953)

M. Furuta, Y. Koyama, T. Inoue, e-J. Soft Mater. **3**, 49 (2007)

G.M. Hanafy, S.A. Madbouly, T. Ougizawa, T. Inoue, Polymer **45**, 6879 (2004)

K. Hashima, K. Usui, L. Fu, T. Inoue, K. Fujimoto, K. Segawa, T. Abe, H. Kimura, Polym. Eng. Sci. **48**, 1207 (2008)

K. Hashima, S. Nishitsuji, T. Inoue, Polymer **51**, 3934 (2010)

E. Helfand, G.H. Fredrickson, Phys. Rev. Lett. **62**, 2468 (1989)

I.A. Hindawi, J.S. Higgins, R.A. Weiss, Polymer **33**, 2522 (1992)

J. Ibuki, P. Charoensirisomboon, T. Chiba, T. Ougizawa, T. Inoue, M. Weber, E. Koch, Polymer **40**, 647 (1999)

F. Ide, A. Hasegawa, J. Appl. Polym. Sci. **18**, 963 (1974)

T. Inoue, Prog. Polym. Sci. **20**, 119 (1995)

T. Inoue, J. Jpn. Soc. Polym. Process. **8**, 24 (1996)

T. Inoue, S. Kobayashi, Recent Res. Devel. Polym. Sci. **11**, 1 (2011)

I. Ito, M. Furuta, S. Nishituji, T. Inoue, in *28th Polymer Process Society*, Pattaya, Thailand, Dec 13 2012

H.W. Kammer, C. Kummerloewe, J. Kressler, J.P. Melior, Polymer **32**, 1488 (1991)

J. Katsaros, M. Malone, H. Winter, Polym. Eng. Sci. **29**, 1434 (1989)

T. Kojima, T. Ohnaga, T. Inoue, Polymer **36**, 2197 (1995)

F.B.C. Larbi, M.F. Malone, H.H. Winter, J.L. Halary, M.H. Leviet, L. Monnerie, Macromolecules **21**, 3534 (1988)

H. Li, Y. Yang, R. Fujitsuka, T. Ougizawa, T. Inoue, Polymer **40**, 927 (1999)

J. Lyngaae-Jorgensenn, K. Sondegaard, Polym. Eng. Sci. **27**, 351 (1987)

S.A. Madbouly, M. Ohmomo, T. Ougizawa, T. Inoue, Polymer **40**, 1465 (1999a)

S.A. Madbouly, T. Chiba, T. Ougizawa, T. Inoue, J. Macromol. Sci. Phys. B **38**, 79 (1999b)

S.A. Madbouly, T. Chiba, T. Ougizawa, T. Inoue, Polymer **42**, 1743 (2001)

L.T. Manzione, J.K. Gilliham, C.A. Mcpherson, J. Appl. Polym. Sci. **26**, 889 (1981)

K. Matsumoto, M. Nagai, K. Hamakawa, S. Nishitsuji, T. Inoue, J. Appl. Polym. Sci.(2012). doi:10.1002/App.38764

K. Mazich, S.H. Carr, J. Appl. Phys. **54**, 5511 (1983)

A.I. Nakatani, H. Kim, Y. Takahashi, Y. Matsushita, A. Takano, B.J. Bauer, C.C. Han, J. Chem. Phys. **93**, 795 (1990)

M. Okada, K. Fujimoto, T. Nose, Macromolecules **28**, 1795 (1995)

M. Okamoto, T. Inoue, Polym. Eng. Sci. **33**, 176 (1993)

M. Okamoto, K. Shiomi, T. Inoue, Polymer **36**, 87 (1995)

S. Ono, H. Isago, T. Ougizawa, Polym. Prep. Jpn **57**, 3122 (2008)

A. Onuki, K. Kawasaki, Ann. Phys. (N.Y.) **121**, 456 (1979a)

A. Onuki, K. Kawasaki, Phys. Lett. **72**, 233 (1979b)

A. Onuki, K. Yamazaki, K. Kawasaki, Ann. Phys. (N.Y.) **131**, 217 (1981)

A. Onuki, in *Taniguchi Conference on Polymer Research by Neutron Scattering*, Kyoto, Japan, Nov 1989

L. Pan, T. Inoue, H. Hayami, S. Nishikawa, Polymer **43**, 337 (2002)

L. Park, J.W. Barlow, D.R. Paul, J. Polym. Sci., Phys. Ed. **30**, 1021 (1992)

D. Sato, Y. Kadowaki, J. Ishibashi, S. Kobayashi, T. Inoue, e-J. Soft Mater. **3**, 9 (2007)

T. Takebe, R. Sawaoka, T. Hashimoto, J. Chem. Phys. **91**, 4369 (1989)

L.A. Utracki, Polym. Eng. Sci **22**, 1166 (1982)

J.J. van Aartsen, Eur. Polym. J. **6**, 919 (1970)

S. Visconti, R.H. Marchessault, Macromolecules **7**, 913 (1974)

R. Wu, M.T. Shaw, R.A. Weiss, Polym. Mater. Sci. Eng. **65**, 263 (1991)

K. Yamanaka, T. Inoue, Polymer **30**, 662 (1989)

K. Yamanaka, T. Inoue, J. Mater. Sci. **25**, 241 (1990)

K. Yamanaka, Y. Takagi, T. Inoue, Polymer, **30**, 1839 (1989)

Compounding Polymer Blends

9

Leszek A. Utracki, G. Z.-H. Shi, D. Rodrigue, and R. Gonzalez-Núñez

Contents

Leszek A. Utracki: deceased.

L.A. Utracki
National Research Council Canada, Industrial Materials Institute, Boucherville, QC, Canada
e-mail: leszek.utracki@cnrc-nrc.gc.ca

G.Z.-H. Shi
Industrial Materials Institute, National Research Council of Canada, Boucherville, QC, Canada

Rehau Inc, Leesburg, VA, USA
e-mail: gerard.shi@rehau-na.com

D. Rodrigue
Department of Chemical Engineering, Université Laval, Quebec, QC, Canada
e-mail: Denis.Rodrigue@gch.ulaval.ca

R. Gonzalez-Núñez
Department of Chemical Engineering, Universidad de Guadalajara, Guadalajara, Jalisco, Mexico
e-mail: rubenglz@cencar.udg.mx

Abstract

In processing polymer blends, equipment selection, conditions, and formulation are highly important to control the final morphology. In this chapter, a review of the fundamentals in mixing (laminar, chaotic, dispersive, and distributive) is given before presenting the main limitations/problems related to interfacial properties, coalescence, and measure of mixing quality. Then, different methods and equipments are presented for lab-scale and industrial applications. A special focus is made on reactive system and phase compatibilization to improve the properties of the final blends. Also, nonmechanical techniques (solutions) are presented.

9.1   Introduction

The cost of polymer alloys is mainly determined by the composition. By contrast, the profit that is based on the alloys' performance is controlled by the way the material is processed, i.e., by morphology and stability. The compounding process must ascertain that the alloy has the desired spectrum of the performance characteristics.

Undoubtedly, compounding is the most critical and difficult step in polymer blends' technology. It must combine the fundamental knowledge of thermodynamic and rheological material behavior, with engineering aspects of flow inside mixing devices. Furthermore, since nowadays about 90 % of blends are reactively compatibilized, good knowledge of polymer chemistry is also essential.

This chapter has four parts: fundamentals of polymer mixing, blending methods and equipment, nonmechanical methods of polymer blending, and reactive processing. The information is presented in a concise form, with tables of data and references to the source literature. Owing to the complex nature of the topic, interested readers are encouraged to consult other chapters in this book dedicated to specific topics that impact on the *Compounding of Polymer Blends* via compatibilization (▶ Chaps. 4, "Interphase and Compatibilization by Addition of a Compatibilizer" and ▶ 5, "Reactive Compatibilization") and rheology (▶ Chap. 7, "Rheology of Polymer Alloys and Blends").

9.2   **Fundamentals of Polymer Mixing**

According to English dictionaries, *mixing*, *blending*, *and compounding* are synonyms, indicating "an action to combine ingredients into one mass, so that the constituent parts are indistinguishable." However, in the plastic processing, these terms have different meanings: *mixing* indicates the physical act of homogenization (i.e., mixing of fractions), and *blending* usually indicates preparation of polymer blends or alloys, while *compounding* that of *a compound*, i.e., incorporation of additives into a polymeric matrix like antioxidants, lubricants, pigments, fillers, or reinforcements (Utracki 1994, 1998).

9.2.1   **The Reasons for Mixing**

Mixing is the most important operation in polymer processing. Uniformity of the molecular weight, degree of entanglement, temperature, and composition is the key to good plastics' performance. For example, fusion of rigid PVC formulation by heating, but without mechanical mixing, results in bad mechanical properties, poor thermal stability, and weatherability. Similarly, poor performance is obtained from compression molding of a dry blend of LLDPE reactor powder where low level of intermolecular entanglements result in low strength of molded parts.

Hydrodynamics recognize two kinds of a fluid motion: (1) laminar, in which the streamlines are smooth, and (2) turbulent, in which the motion is irregular or disorganized. These two types are separated by the critical value of the Reynolds number ($Re_{critical} \cong 2{,}000$ in a circular tube). The Reynolds number is defined as

$$\mathrm{Re} \equiv \mathrm{L}\overline{\mathrm{V}}\rho/\eta \tag{9.1}$$

where L is the channel size, $\overline{\mathrm{V}}$ is the flow velocity, ρ is the fluid density, and η is its viscosity. For a typical molten polymer with $\eta = 1$ kPa·s, $\rho = 10^3$ kg/m^3, flowing through a one centimeter channel in diameter (L $= 10^{-2}$ m), turbulence starts when the flow velocity exceeds the critical value of $\overline{\mathrm{V}} = 200$ km/s. Evidently, the turbulent flow is not to be expected for liquids with such a high viscosity; hence, molten polymers flow by laminar mechanism. (Note that the term "laminar" is used in two different connotations: to characterize the flow (as in laminar vs. turbulent) and that of mixing, "laminar mixing model," as described below.)

It is convenient to distinguish two types of flow: dispersive and distributive, schematically shown in Fig. 9.1.

The dispersive (or intensive) mixing involves *application of stress* (shear and elongation) that breaks domains of the dispersed phase to the desired size. The dispersed phase may be composed of liquid drops, gel particles of the matrix material, aggregates of filler particles, etc.

The distributive (or extensive) mixing involves homogenization of a fluid, accomplished by the *application of strain* (shear and elongation). Homogenization
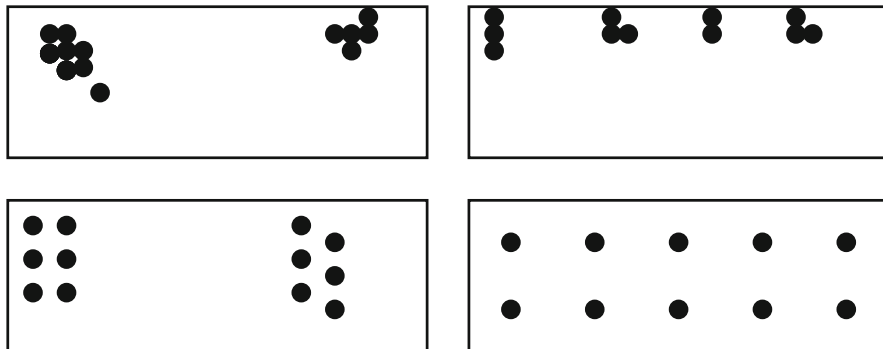
Fig. 9.1 Schematic representation of mixing (*top row*, *left* to *right*): bad dispersion and distribution; bad dispersion, but good distribution; (*bottom row*, *left* to *right*): good dispersion, but bad distribution, and good dispersion and distribution

may involve a single-phase fluid (i.e., homogenization of temperature), a miscible system (homogenization of concentration), or a multiphase system, blend or composite (homogenization of the dispersion).

Two other terms have also been used to describe mixing: the laminar and chaotic. In both types, the system is considered "passive," i.e., the rheological properties are identical and the interface is "invisible." Thus, flow-induced morphological changes do not affect the flow behavior, and the effects of flow and morphology are "decoupled." In real systems, the rheological and thermodynamic properties of two phases are different. In this case, the changes of morphology affect the flow, which in turn affect the morphology, and so on, until a steady state is reached and the effects are "coupled." Thus, laminar and chaotic mixing models are excellent to start with, but with the exception of special cases, they do not represent reality.

As indicated in Chap. ▶ 7, "Rheology of Polymer Alloys and Blends," the effects of flow on morphology have been described by micro-rheology. For highly diluted systems, a good agreement between experimental data and theoretical predictions has been reported. Furthermore, continuous efforts are made to incorporate the kinematics of the interface generation into the rheological description of the system (Doi and Ohta 1991; Grmela and Ait-Kadi 1994; Grmela et al. 1998; Lee and Park 1994; Roths et al. 2002; Keestra et al. 2003; Dressler and Edwards 2004; Das et al. 2005; Takahashi et al. 2007; Gu and Grmela 2008; Jelic et al. 2010).

9.2.2 Laminar Mixing

The following derivations for the laminar mixing are valid for the flow of passive mixtures. Neither the effects imposed by the interface nor those originating from the differences in the rheological properties of the fluid components

Table 9.1 Values of R for different types of deformation

Deformation	Elongation ratios	R	Comment
Plane elongation	$\lambda_x = \lambda_o;\ \lambda_y = 1/\lambda_o;\ \lambda_z = 1$	$\boldsymbol{\lambda_o}$	Regular, flow between rolls
Plane elongation	Averaging isotropic mixture	$\boldsymbol{\lambda_o/2}$	Random input orientation
Pure elongation	$\lambda_x = \lambda_o;\ \lambda_y = \lambda_z = \lambda_o^{-1/2}$	$\boldsymbol{\lambda_o^{1/2}}$	Uniaxial stretching
Pure elongation	$\lambda_x = \lambda_o;\ \lambda_y = \lambda_z = \lambda_o^{-1/2}$	$\boldsymbol{1/\lambda_o}$	Biaxial stretching
Simple shear	Expressed by shear strain, γ	$\boldsymbol{\gamma \cos \beta}$	Couette or Poiseuille flow

are taken into account. Thus, the laminar mixing (as presented below) provides the first approximation for the distributive (or homogenizing) mixing. The dispersive mixing has not been considered, and there is no need for it when there is no interface and the rheological properties of both fluids are the same (Edwards 1985).

9.2.2.1 Growth of the Interfacial Area

Laminar mixing depends on the strain tensor, which can be visualized as an ellipsoid formed upon straining a sphere. The strain magnitude is proportional to the relative size of the ellipsoidal axes while their relative positions to the orientational effects of the imposed flow. It can be shown that the interfacial area (A_o) will grow with the imposition of strain according to the relation (Erwin 1991):

$$R \equiv A/A_o = \left| \left\{ \left(\lambda_x \lambda_y \right)^2 + \lambda_y^2 \left(\lambda_z^2 - \lambda_x^2 \right) \cos^2\alpha + \lambda_x^2 \left(\lambda_z^2 - \lambda_y^2 \right) \cos^2\beta \right\}^{1/2} \right| \tag{9.2}$$

where λ_i ($i = x, y, z$) are the principal elongation ratios and α and β are the orientation angles. Depending on the type of deformation, the interfacial area ratio (R) takes on values listed in Table 9.1.

For example, the principal elongation ratios in simple shear can be expressed as

$$\begin{aligned}
\lambda_x &= \left[1 + \gamma^2/2 + (\gamma/2)(4 + \gamma^2)^{1/2} \right]^{1/2} \\
\lambda_y &= \left[1 + \gamma^2/2 - (\gamma/2)(4 + \gamma^2)^{1/2} \right]^{1/2} \\
\lambda_z &= 1
\end{aligned} \tag{9.3}$$

9.2.2.2 Energy of Mixing

It is important to be able to calculate how much energy is required to generate the same R in different flow fields, in particular in extension and in shear. The specific energy per unit volume (E) required to generate the aerial strain R in a passive liquid mixture with viscosity η for a time t_o is given by the following expressions (Erwin 1991):

Fig. 9.2 Energy
consumption as a function of
change of the interface area in
extensional (uniaxial, biaxial,
and plane strain) and simple
shear flows. The most
efficient is the biaxial stretch;
the worst (by a factor of
500,000!) is shear (after
Erwin 1991)

Mixing energy vs. interface growth for four types of flow
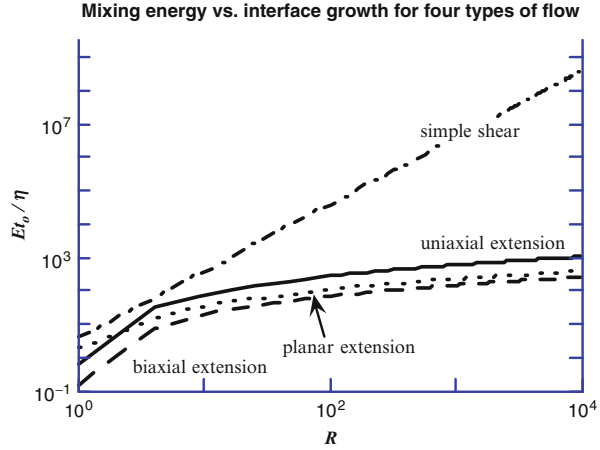
$$
\begin{aligned}
\text{Uniaxial extension}: \quad & E = (12\eta/t_o[\ln(5R/4)])^2 \\
\text{Biaxial extension}: \quad & E = (3\eta/t_o[\ln(5R/4)])^2 \\
\text{Planar extension}: \quad & E = (4\eta/t_o[\ln(2R)])^2 \\
\text{Simple shear}: \quad & E = (4\eta/t_o)R^2
\end{aligned}
\tag{9.4}
$$

These dependencies are shown in Fig. 9.2. Evidently, simple shear is inefficient for generation of a large interfacial area (for smaller deformations, $R \leq 10$, the inefficiency is not as dramatic). The inefficiency can be reduced if a large deformation is obtained not at once, but in a series of smaller deformation steps. The best formula is stretch–twist–fold, the second best is stretch-and-fold, and the third is stretch-and-randomize. Thus, to improve the mixing efficiency of the processing units that operate in the shear mode (like in a single-screw extruder), the flow should be interrupted and the flow lines randomized. For uniform shear strains of randomly oriented elements, the interfacial area increases linearly with strain, and when the process is repeated, the total increase of the interfacial area becomes proportional to the square of strain (γ^2), etc.:

$$
R_1 \cong \gamma/2 ; \quad R_2 \cong (\gamma/2)^2 ; \quad R_n \cong (\gamma/2)^n
\tag{9.5}
$$

The same approach may also be used to improve mixing in the extensional flow field. However, since the surface generation in extension is efficient to start with, the improvement is not as dramatic as that expected in shear.

The validity of Eq. 9.5 was experimentally confirmed using a specially designed mixer (Ng and Erwin 1981). Even if this device did not lend itself to be incorporated into a processing unit, the idea of the interrupted flow has been generally adopted by the designers of mixing equipment. The process would be even more efficient if the elements could be reoriented at 90° (biaxial stretching) or even 180° (folding and stretching). Several attempts have been made to incorporate these ideas into the extruders' design. Nowadays, this concept is successfully applied in so-called static mixers which are placed at the end of the screws in extruders.

Fig. 9.3 Kinematics of separation of two material points during laminar flow in the uniaxial elongation and in simple shear
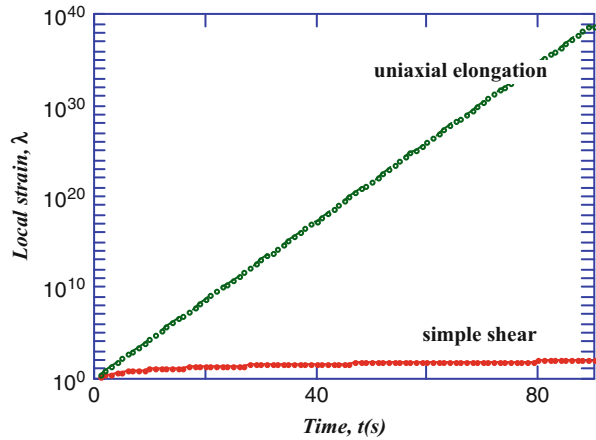
9.2.2.3 Kinematics of Mixing

The strain between two material points M and M′ can be expressed as

$$\lambda \equiv \|MM'\| / \|M_oM'_o\| \tag{9.6}$$

The kinematics of the deformation is described by the following set of differential equations (Poitou 1988):

$$dX/dt = u; \quad dm/dt = [grad\,u]\,m - ([\varepsilon]\,m \bullet m)\,m; \quad d\ln\lambda/dt = [\dot{\varepsilon}]\,m \bullet m \tag{9.7}$$

where **X** is the coordinate of M, **u** is the velocity field, [grad **u**] is the velocity gradient tensor, [ε] is their strain rate tensor, and **m** is the unit vector of **MM′**. Figure 9.3 presents the kinematics of strain evolution in simple shear and uniaxial elongation.

9.2.2.4 Laminar Mixing: A Summary

The elongational deformation provides more efficient mixing than shear. On all three accounts, the magnitude of the interface increase, the energy required for mixing, and the rate of spatial separation of two material points, significantly better mixing (frequently by several orders of magnitude) is expected for extensional than for shear flow.

The fundamental assumptions in all these derivations have been that the system is rheologically decoupled, that there is neither an "active" interface nor a significant difference between viscosity of the mixture components. In consequence, coalescence does not exist and the flowing materials always are stretched, deformed, and the degree of mixedness continuously improves. By contrast with immiscible polymer blends, the model does not take into account either the shear coalescence or the thermodynamic coarsening.

Thus, the laminar mixing provides good guidance for the distributive homogenization of idealized polymer mixtures. The conclusions that come from this model may be directly applied for mixing of homologous polymer blends, temperature homogenization of polymer melt, or to mixing different batches of the same resin.

9.2.3 Chaotic Mixing

The term *chaotic mixing* was introduced by Ottino (1989) to describe laminar, distributive mixing with continuous or periodic translation of cavity walls. The phenomenon is universal, observed in many diverse branches of science and technology from aerodynamics to geology (Ottino 1989; Rauwendaal 1994). This type of mixing can be observed even in a simple geometry as a result of interplay of at least two velocity fields, which can be generated by either applying two type of forces (heating and shearing), imposing two types of motion, or imposing a specific type of flow geometry.

To illustrate the principle, a "two-dimensional" cavity was constructed. The boxlike geometry had a transparent front wall and movable top and bottom neoprene walls. An insertion of rod-shaped, fluorescent tracer drop (with only a cross section visible) made it possible to follow the laminar mixing as a function of time for diverse sequences of the top and bottom wall translations. As shown in Fig. 9.4, periodic translations resulted in stretching, folding, and transporting the drop much more effectively than the regular, steady-state translation. At the same strain, the mixedness index, expressed as a ratio of the generated interface to the initial one, was significantly higher for the periodic translations than for the steady state.

The experiments also demonstrated presence of the "mixing islands," where very little mixing took place. In consequence, the chaotic mixing could be schematically represented by the streamline diagram comprising the elliptic points located in the center of the "blinking vortex" and a hyperbolic point. Little mixing takes place around the elliptic points surrounded by circulating streamlines, while extensive mixing takes place at the hyperbolic points where the streamlines
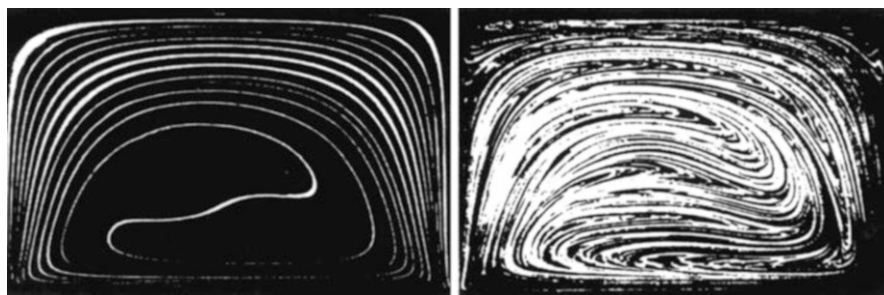
Fig. 9.4 Mixing in a 2D cavity with *upper* and *lower* neoprene walls. *Left*, effect of continuous motion of both walls and, *right*, that of discontinuous motion (1/2 *top*, then 1/2 *bottom*, etc.). In both tests, the total walls' displacement was the same (Leong and Ottino 1989)

(leading in opposite directions) cross-link. Thus, the principle of chaotic mixing involves a non-steady-state translation of the material by stretching and folding that creates horseshoe-shaped domains of the dispersed phases (Smale 1967; Leong and Ottino 1989; Ottino 1990, 1991). Formally, it was described as originating from a "blinking" vortex that is periodically displaced by imposed strain on different cavity walls (Aref 1983).

As in the case of laminar mixing, here also it is advantageous to start consideration with a passive system. Imposition of periodic motion causes the domains to stretch and fold. Several 2D flows were explored and mathematically treated. Of these, the cavity flow (with two moving walls) and the journal bearing flow were investigated. For example, in the first geometry, good stretch-and-fold mixing was observed for the periodic, interrupted shearing of the upper then lower wall (see Fig. 9.4).

Three-dimensional chaotic mixing was studied by Liu and Zambrunnen (1995). A cylindrical cavity of the journal bearing type was constructed. The cylinder diameter was 79.0 mm, the height of the cavity was 23.7 mm, and the offset of the shearing wall centers was 27.6 mm. The disks were alternatively rotated, each for half period. The cavity was used to generate fine fibrillar structures (aspect ratio of about 1,000) of PE in either EVAc or PS. The authors observed that owing to extensional flow the mixing process is insensitive to the viscosity ratio. The principles of chaotic mixing are well established, but the development of mixing devices based on them still awaits real commercialization at large scale.

9.2.4 Dispersive Mixing: Micro-rheology

This topic has been already presented in ▶ Chap. 7, "Rheology of Polymer Alloys and Blends." In the following section, only the aspects pertinent to mixing will be summarized (Utracki 1991, 1995).

It is important to recognize the advantages and the drawbacks of the micro-rheological approach. By contrast with the discussed above laminar mixing, the micro-rheology focuses on the physical differences between the two blends' components, the dispersed and the matrix fluids. Both the thermodynamic (expressed by the interfacial tension coefficient) and the rheological properties (expressed by the strain, stress, and the viscosity ratio) are important for the deformation and breakup of the dispersed phase. The drawbacks are numerous: assumptions of high dilution, low deformation rates, and that the systems are Newtonian. In spite of these, micro-rheology provides invaluable guidance for mixing of commercially interesting systems. For example, the use of these principles led to successful predictions of the blends' morphology evolution during flow in a twin-screw extruder (Utracki and Shi 1992; Huneault et al. 1995a).

9.2.4.1 Drop Deformability
When a neutrally buoyant, initially spherical droplet is suspended in another liquid and subjected to stress, it deforms into an ellipsoid and then breaks up into smaller

droplets. Taylor ([1932](#), [1934](#)) described the process (at low stress in a steady-state, uniform flow), using the following three dimensionless parameters: the viscosity ratio, the capillarity number, and the reduced time, respectively, defined as

$$\lambda \equiv \eta_d/\eta_m; \quad \kappa \equiv \sigma d/\nu_{12}; \quad t^* = t\dot{\gamma}/\kappa = \gamma/\kappa \tag{9.8}$$

where $\sigma = \dot{\gamma}\eta_m$ is the local stress; η_d and η_m are the dispersed phase and matrix viscosity, respectively; $\dot{\gamma}$ is the deformation rate; d is the droplet diameter; and ν_{12} is the interfacial tension coefficient.

During flow, the initially spherical drop deforms into a prolate ellipsoid with the long axis a_1 and two orthogonal short axes a_2. The drop deformability parameter (D) is a complex function. At low shear stress, it can be expressed as (Taylor [1934](#))

$$D_{shear} \equiv (a_1 - a_2)/(a_1 + a_2) = (\kappa/2)[(19\lambda + 16)/(16\lambda + 16)] \tag{9.9}$$

Since, for the full range of λ values from zero to infinity, the quantity in the square bracket in Eq. [9.9](#) ranges from 1.00 to 1.18, the drop deformability $D_{shear} \cong 0.55\,\kappa$. For highly viscous dispersed phase, i.e., $\lambda >> 1$, Taylor calculated that $D = 5/4\,\lambda$, but since the condition for drop break is $D \geq D_{crit} = 0.5$, this means that **shear flow can lead to drop breakage only when the viscosity ratio $\lambda < 3.8$** (Grace [1982](#)).

For the planar or the axisymmetric extensional flow, the theory predicts that the deformability is larger than in shear, respectively:

$$D_{planar} = 2D_{shear}; \quad D_{axisymmatric} = (3/2)D_{shear} \tag{9.10}$$

Cox ([1969](#)) derived the kinetic equation for the deformability of a drop in the planar flow:

$$D_{planar} = \kappa\left[(19\lambda + 16)/(16\lambda + 16)\right]\left[1 - \exp\left\{-(10\kappa/19\lambda)\,t^*_{planar}\right\} \right.$$
$$\text{where}: \quad t^*_{planar} \equiv (t\dot{\gamma}_{planar})\lambda/\kappa = \gamma_{planar}\lambda/\kappa \tag{11.11}$$

where γ_{planar} is the strain in planar flow and t^*_{planar} is the reduced time for planar deformation. It is worth noting that in the hyperbolic flow, the reduced time scale depends on the viscosity ratio. Unfortunately, Eq. [9.11](#) is valid only for small values of λ and κ. The exponential master curve is shown in Fig. [9.5](#). The effects of λ and κ on D are illustrated in Fig. [9.6](#).

The above relations are valid for Newtonian systems undergoing small, linear deformations, smaller than that which would lead to a breakup. As Fig. [9.4](#) indicates, in planar hyperbolic flow, about 10 units of strain is required to get into an equilibrium. In simple shear, $t^*_d \cong 25$ of the reduced time scale is required (Elemans et al. [1989](#)).

Fig. 9.5 Drop deformability
in a planar hyperbolic flow as
a function of total strain. The
dependence was calculated
from the Cox equation
(Eq. 9.11)

Exponential growth function for drops
in hyperbolic planar flow [Cox, 1969]
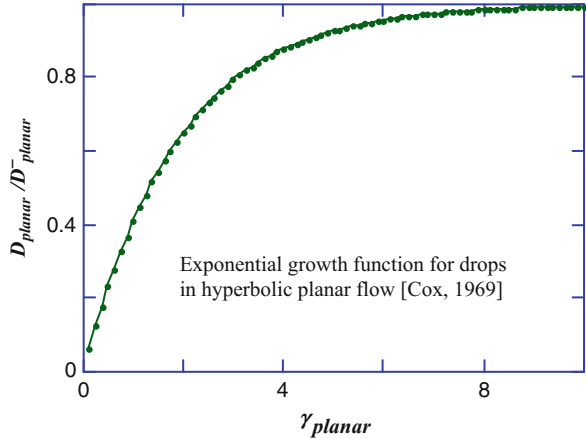
9.2.4.2 Drop Breakup

From the point of view of the drop deformation and breakup, there are four
regions of the reduced capillarity numbers $\kappa^* \equiv \kappa/\kappa_{cr}$, both in shear and elongation:

For	$\kappa^* < 0.1$,	Droplets do not deform
For	$0.1 < \kappa^* < 1$,	Droplets deform, but do not break
For	$1 < \kappa^* < 2$,	Droplets deform then split into two primary droplets
For	$\kappa^* > 2$,	Droplets deform into stable filaments

The critical capillary number (κ_{cr}) is defined as the minimum capillarity number
sufficient to cause breakup of a deformed drop. It is customary to plot κ_{cr} as
a function of λ. For simple shear and uniaxial extension flow, De Bruijn
et al. (1989) found the following dependence (see Table 9.2 and Fig. 9.7):

$$\log(\kappa_{cr}/2) = c_1 + c_2 \log\lambda + c_3 (\log\lambda)^2 + c_4/(\log\lambda + c_5) \qquad (11.12)$$

Similarly as κ_{cr}, also the critical time for drop breakup (t_b^*) varies with λ. When
values of the capillarity number and the reduced time are within the region of drop
breakup, the mechanism of breakup depends on the viscosity ratio (λ). In shear, four
regions have been identified:

For	$\lambda << 0.1$,	Small droplets are shed from sigmoidal drops: *tip streaming*
For	$0.1 < \lambda < 1$,	Drop breaks into two principal and odd number of satellite droplets
For	$1 < \lambda < 3.8$,	Drop deforms into fiber then disintegrates into small droplets
For	$\lambda > 3.8$,	Drop may deform, but does not break

9.2.4.3 Drop Fibrillation and Breakup

For $\kappa^* > 2$, drops deform affinely with the matrix into long fibers. When subse-
quently the deforming stress decreases, causing the reduced capillarity number to

Table 9.2 Constants for drop breakup in Newtonian systems

Flow	$1000c_1$	$1000c_2$	$1000c_3$	$1000c_4$	$1000c_5$
Shear	−506.0	−99.4	124.0	−115.0	−611.0
Elongational	−648.5	−24.42	22.21	−0.56	−6.45
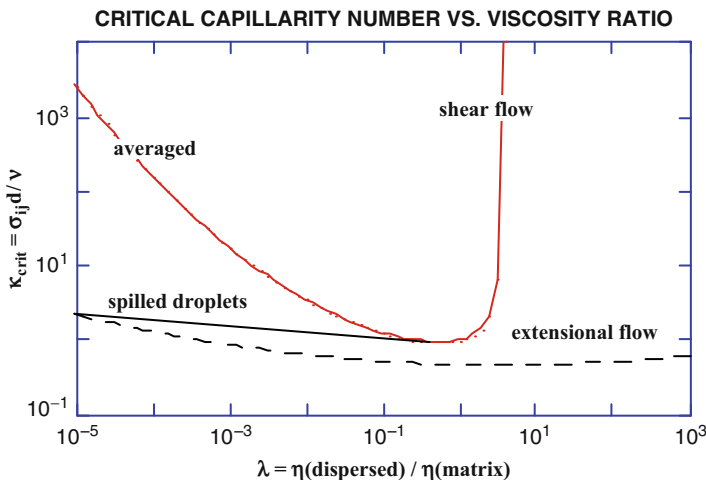
Fig. 9.7 Critical capillarity number for drop breakup in shear and extensional flow

fall below two ($\kappa^* < 2$), the fibers disintegrate under the influence of the interfacial tension (Tomotika 1935, 1936). The distortion amplitude α grows exponentially with time as

$$\alpha = \alpha_o \exp\{qt\} \qquad (11.13)$$

where α_o is the distortion at $t = 0$ and the growth rate parameter $q = \Omega(\Lambda, \lambda)(t^*/t)$, with $\Omega(\Lambda, \lambda)$ being a tabulated function of the distortion wavelength and the viscosity ratio. The thread breakup occurs when $\alpha = R \cong 0.81R_o$. The most serious obstacle for the quantitative use of Timotika's theory is the estimation of the initial distortion (α_o).

9.2.4.4 Micro-rheology of Viscoelastic Systems

The mechanisms governing deformation and breakup of drops in Newtonian liquid systems are relatively well understood. However, within the range of compounding and processing conditions, the molten polymers are viscoelastic liquids. In these systems, the shape of a droplet is determined not only by the dissipative (viscous) forces but also by the

pressure distribution around the droplet that originates from the elastic part of the stress tensor. Therefore, the characteristics of drop deformation and breakup in viscoelastic systems may be quite different from those in Newtonian ones. Some of the pertinent papers on the topic are listed in Table 9.3.

In summary, there is no theory capable to completely describe the deformability and breakup of viscoelastic drops in viscoelastic media or even one that provides explanation for the divergent observations. The complexity of the problem involves three-dimensionality, free surface, and nonstationary flow leading to complex constitutive equations. Furthermore, the role of fluid elasticity in the breakup process is still not well understood. In most experiments, the elasticity stabilized the deformed drops, thus making the dispersing process more difficult. However, there are also reports of the opposite effects. The micro-rheological behavior of two-phase liquid systems may provide but a general guidance for the drop deformation and breakup in polymer blends. For blends of industrial interest, the phenomenon is further complicated by higher concentration of the dispersed phase, as well as by the presence of numerous additives that affect the interfacial phenomena. The problem becomes even more complex for three-phase flows and for cases where surface active materials (surfactants, impurities, and particles) are present leading to Marangoni stresses and Pickering effect.

Nevertheless, one of the sources of confusion may originate from different types of liquids studied as large differences in deformability in convergent flow were observed for drop prepared from viscoelastic solutions or from Boger fluid (Bourry et al. 1999). Spiegelberg et al. (1996) have shown that a Boger fluid is strongly strain hardening. At Hencky strains larger than two, the elongational viscosity is larger than shear viscosity by three orders of magnitude. These high values of strain hardening may explain the large differences of deformability of two types of viscoelastic drops.

9.2.5 Distributive Mixing

Static mixers (SM), also called motionless mixers, operate on the principle of repetitive dividing of a flow channel into at least two new channels, reorienting them by 90° and dividing again. The flow is a pressure-driven, laminar shear. Mixing by SM is related to the numbers of striations (N_s) generated by a number of SM elements (n_e) and the number of divisions (new channels) engendered by each element (n_c):

$$N_s = n_c^{n_e} \tag{9.14}$$

Over 30 different SM designs have been commercialized (Rauwendaal 1986). Their efficiency is determined comparing (1) the length-to-diameter ratio

Table 9.3 Deformability of viscoelastic drop

Description	Reference
Higher κ_{crit} for viscoelastic system than for Newtonian drops	Gauthier et al. 1971
For Newtonian drops in viscoelastic fluid, elasticity of the medium stabilizes the drops	Flumerfelt 1972
$$\nu_{12} = \nu_{12}^o + (d_o/12)\big[(\sigma_{11} - \sigma_{22})_d - (\sigma_{11} - \sigma_{22})_m\big]$$ where ν^o_{12} is the interfacial tension in a quiescent polymer blend; d_o is the initial diameter of the dispersed drop; and the bracketed expressions are the first normal stress differences of the dispersed ($i = d$) and of the matrix ($i = m$) phase. For $(\sigma_{11} - \sigma_{22})_d > (\sigma_{11} - \sigma_{22})_m$, the above equation predicts that higher elasticity of the dispersed phase than that of the matrix causes the interfacial tension coefficient to increase, what leads to more stable drops. For $(\sigma_{11} - \sigma_{22})_d < (\sigma_{11} - \sigma_{22})_m$, it predicts that $0 < \nu_{12} < \nu^o_{12}$; thus the flow tends to enhance the dispersing process (flow compatibilization). However, as the shear stress increases, the above equation predicts a physically untenable condition: $\nu_{12} < 0$. To avoid this nonphysical situation, the system morphology changes from dispersed to lamellar	Van Oene 1978
Viscoelastic drops in either Newtonian or viscoelastic media were reported more stable (less deformable) than the Newtonian ones. The critical shear rate for droplet breakup was lower for $\lambda < 1$ than for $\lambda > 1$	Han and Funatsu 1978; Chin and Han 1979, 1980
Initially, disturbances grow more rapidly in viscoelastic filaments than in Newtonian ones, but at a later stage, there is stabilization, resulting from large extensional stresses (see Fig. 9.8). As a result, the time required to break the viscoelastic drop is longer than that for Newtonian. Formation of the satellite drops was found to be retarded by elasticity	Bousfield et al. 1986
Both the drop and the medium were viscoelastic. Drops did break during extrusion, even when $\lambda > 4$, but the mechanism is not clear	Wu 1987
In viscoelastic systems, κ_{crit} is always higher than in Newtonian: drop elasticity hinders drop breakup whatever the λ value	De Bruijn 1989
When $\lambda < 0.5$, the drop elasticity has stabilizing effect	Prabodh and Stroeve 1991
Predictive model for the morphology variation during simple shear flow under steady-state uniform shear field was developed. The model considers the balance between the rate of breakup and the rate of drop coalescence. The theory makes it possible to compute the drop aspect ratio ($p = a_1/a_2$), a parameter that was directly measured for PS/PMMA = 1:9 blends. Theoretically and experimentally, p vs. shear stress shows a sharp peak at the stresses corresponding to a transition from the Newtonian plateau to the power-law flow, i.e., to the onset of the elastic behavior (see Fig. 9.9)	Lyngaae-Jørgensen et al. 1993, 1999
Deformation of a single drop in a medium subjected to convergent flow was observed. Both liquids were of the Boger fluid type. For a given matrix, the drop deformability decreased with elasticity of the dispersed phase. For a given	Mighri et al. 1997

(*continued*)

Table 9.3 (continued)

Description	Reference
drop liquid, the drop deformability increased with the matrix elasticity. The following empirical equation was proposed: $$l_{d,E} = l_{d,N} - \Delta P(l_m - 1)$$ where l_d is the aspect ratio of the elastic (subscript E) or Newtonian (subscript N) drop, ΔP is a function of the elasticity ratio, and l_m is the matrix deformation expressed in Hencky terms	
The deformability of viscoelastic drops in a Newtonian matrix was studied in convergent slit flow. Both the experimental observations and the boundary element method computations were carried out. It was reported that deformation of Boger fluid drops was quite low: about 1/3 of that recorded for the deformability of a strongly shear-thinning, viscoelastic solution. The latter drops showed deformability similar to the ones observed for Newtonian drops of similar viscosities	Bourry et al. 1999
The steady-state deformation of isolated droplets decreases with increasing dispersed phase elasticity for the same imposed capillary number. A linear relationship between critical capillary number for droplet breakup (κ_{crit}) and dispersed-phase Weissenberg number (Wi_d) holds up to a value of Wi_d around unity, with a saturation at around $\kappa_{crit} = 0.95$ for high Wi_d	Lerdwijitjarud et al. 2002, 2004
In Newtonian fluids, drop deformation is dominated by the competition between interfacial tension and viscous forces due to flow. When the matrix is viscoelastic, however, drop deformation is suppressed when the Deborah number De is small, but increases with De for larger De	Yue et al. 2005
Viscoelastic effects alter the steady drop shape from being ellipsoidal to drop shapes with more blunt ends. The results reflect a balance between the direct tensile stress contribution of the viscoelastic fluid to the normal stress balance and modifications of the viscous (i.e., Newtonian) stress and pressure due to viscoelastic changes in the flow	Hsu and Leal 2009
The deformation of a viscoelastic drop suspended in a Newtonian fluid subjected to a steady shear is investigated using a front-tracking finite-difference method. The viscoelasticity is modeled using the Oldroyd-B constitutive equation. The drop shows slightly decreased alignment with the flow as viscoelasticity increases. κ_{crit} for drop breakup is observed to increase with De owing to the inhibitive effects of viscoelasticity	Aggarwal and Sarkar 2007
The breakup of confined droplets was studied systematically for systems with either interfacial or component viscoelasticity. κ_{crit} of Newtonian and compatibilized droplets showed a similar increase with increasing confinement ratio. However, a decrease in breakup length was observed in the compatibilized case, caused by the viscoelastic interface. Viscoelastic droplets experienced more stabilization by confinement compared to Newtonian droplets	Cardinaels et al. 2011

Fig. 9.8 Computed radius at the neck for disintegrating jet stream of Newtonian (*solid line*) and Maxwell fluid (*dashed line*) (Bousfield et al. 1986)
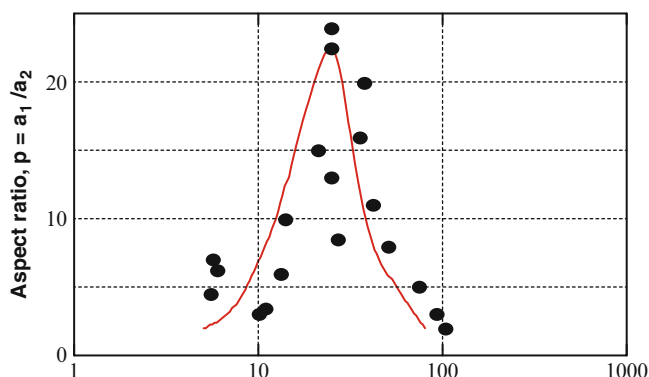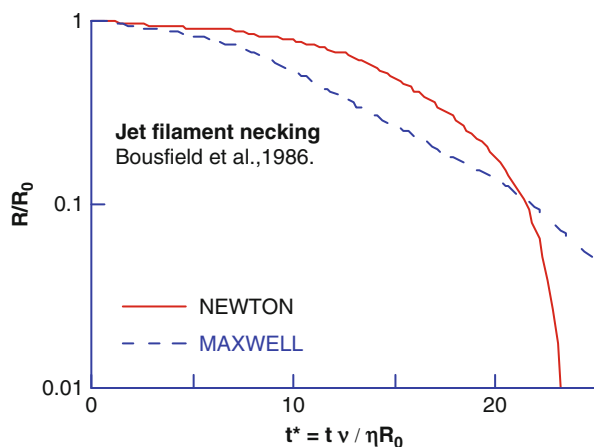
Fig. 9.9 Deformability of PS drops in PMMA during steady-state shear flow at 180 °C. The points are experimental; the line is to guide an eye (Lyngaae-Jørgensen et al. 1993)

(L/D proportional to n_e) required to produce the same degree of homogeneity; (2) the associated pressure drop, ΔP_{rel}; (3) the holdup volume, ΔV_{rel}; and (4) the relative dimensions of the device, D_{rel} and L_{rel}. The efficiency of SM also depends on the type of liquid. For example, Ross mixer was found better for pseudoplastic polymer melts, whereas Kenics mixer for Newtonian fluids (Ottino 1983). An example of comparative evaluation of 11 earlier commercial SM is presented in Table 9.4. Comparative studies have been published for the emulsification of low-viscosity liquids in turbulent flows (Theron and Le Sauze 2011) and for highly viscous liquids in laminar flows (Meijer et al. 2012). The most known SM producers, besides the ones presented in Table 9.4, are Chemineer, Euromixers, Koflo, Nordson, Parker, Statiflo, StaMixCo, Sulzer, and Westfall.

Table 9.4 Comparison of static mixers performance

Static mixer	L/D	ΔP_{rel}	ΔV_{rel}	D_{rel}	L_{rel}
Koch SMX	9	1.0	1.0	1.0	1.0
Koch SMXL	26	0.6	1.8	0.8	2.4
Koch SMV	18	2.3	4.6	1.3	2.7
Kenics	29	0.6	1.9	0.8	2.7
Etoflo HV	32	0.6	2.0	0.8	2.7
Komax	38	2.1	8.9	1.3	5.4
Lightnin	100	2.6	29.0	1.4	15.3
PMR	320	14.5	511.0	2.4	86.0
Toray	13	1.3	1.9	1.1	1.6
N-Form	29	1.4	4.5	1.1	3.6
Ross ISG	10	8.6	9.6	2.1	2.3

9.2.6 Mixing in Extensional Flow Field

The elongational flow field exists anywhere where the streamlines are not parallel. This type of deformation is quite common during the processing like in foaming, fiber spinning, film blowing, blow molding, biaxial and uniaxial stretching, and similar operations carried out downstream from the die (calendering). However, these operations have little to do with mixing.

It is extremely rare to find a mixer where the energy dissipated in extension is nearly as large as that in shear and mixing is overwhelmingly carried out in the shear field. Since the easiest method for the generation of extensional flow is by means of convergence and divergence, the attention will be focused on these types of deformations.

9.2.6.1 Orientation of Solid Particles

The extensional flow field has been used to generate orientation either in homopolymers or in filled or reinforced systems. The convergent flow results in high fiber alignment in the flow direction, whereas the diverging flow causes the fibers to align 90° to the major flow direction. Shearing reduces the alignment. The early theoretical studies of the elongational flows were carried out by Takserman-Krozer and Ziabicki (1963). Molden (1969) developed a geometrical theory that showed the extensional strain to be more effective than shear for fiber alignment. Several other theoretical descriptions of the chopped fibers orientation in flow have been proposed (Lockett et al. 1972; Johnson et al. 1972; Vincent and Agassant 1985). For example, Goettler used the convergent–divergent die geometry to orient fibers in the transverse direction, greatly improving pipes' hoop strength (Goettler 1970; Goettler and Lambright 1977; Lee and George 1978; Crowson et al. 1980; Goettler et al. 1981; Goettler and Shen 1983).

9.2.6.2 Convergent Flow of Viscoelastic Fluids

The fundamental studies of drop deformation in convergent–divergent geometry were carried out using either axisymmetric (Mighri et al. 1997) or slit geometry (Bourry et al. 1999) (see Table 9.3). The analysis of converging flow of viscoelastic fluids using nonlinear viscoelastic models was carried out by several authors. The work is summarized in Table 9.5.

9.2.6.3 Blending in Extensional Flow Field

The use of extensional flow field for mixing is relatively unexplored, while a growing number of reports show that mixing in extensional flow field is more efficient than in shear, especially for blends with higher viscosity ratio, $\lambda \geq 3.8$, where the shear field is unable to cause drop breakup (Grace et al. 1971).

Most of the works on mixing in the extensional flow field consider convergent flow of Newtonian liquids, flowing from a reservoir to a capillary (Tsebrenko et al. 1974, 1976; Ablazova et al. 1975; Krasnikova et al. 1978; Vinogradov et al. 1982; Han and Funatsu 1978; Chin and Han 1979, 1980; Han and Yu 1981; Han 1981). The following factors affecting the quality of blends were identified:
  (i) Diameter of the convergence, d_c
 (ii) The ratio of the reservoir-to-convergence diameters, usually expressed as the convergence ratio, $C \equiv d_r/d_c$
(iii) The capillary length-to-diameter ratio, $R \equiv L/d$
 (iv) The initial drop size, d
  (v) Extensional viscosity ratio, $\lambda_\varepsilon \equiv \eta_{\varepsilon d}/\eta_{\varepsilon m}$ (extensional viscosities of the dispersed phase and that of the matrix, $\eta_{\varepsilon d}$ and $\eta_{\varepsilon m}$, respectively, to be taken at the conditions existing during the mixing, i.e., extensional stress (σ_{11}), temperature (T), pressure (P), etc.)
 (vi) Absolute value of the elongational stress, σ_{11}
(vii) The number of passages through the convergence
    These factors affect both the dispersive and distributive mixings.
    Suzaka (1982) patented an extensional flow mixer, composed of a series of plates placed across the flow channel. A polymer blend was forced to pass through a series of convergent and divergent orifices (or c-d for short) that elongated the drops and dispersed them. All the circular orifices had the same size; i.e., the convergence ratio was constant. The mixer provided good mixing for some systems but not for others. Furthermore, the device could be optimized only by trial and error. Any change in the blend composition required repetitive testing, the process had to be interrupted, and the mixing plates changed. In consequence, the mixer has not been commercially explored.

9.2.6.4 Extensional Flow Mixer

During the last few years, there has been significant progress in the fundamental understanding of micro-rheology and its role for polymer blending. Flow visualizations of the Newtonian and non-Newtonian systems have been carried out (Mighri et al. 1996; Picot 1997; Bourry et al. 1999). The boundary element method (BEM)

Table 9.5 Convergent flow of viscoelastic systems

Description	Reference
Kaloni used the Oldroyd model and Schümmer a fourth-order fluid model, while Wissler a nonlinear Maxwell model. Employing the perturbation method, the authors observed that the inclusion of second-order perturbation terms (which bring in the non-Newtonian effects) predicted velocity profiles with superimposed secondary circulation patterns	Kaloni 1965; Schümmer 1967; Wissler 1971
Normal stresses of HDPE and PP flowing through a converging channel were measured. Near the die exit, the wall normal stress rapidly increased. Relationships were derived for the wall shear stress, normal stress difference at the channel wall, and the wall normal stress gradient in the flow through a converging channel and through a conical duct. Contrary to viscometric flows, in the converging flow field, the normal stress alone does not permit to determine the pressure gradient of viscoelastic fluids	Han 1973, 1974, 1975
Flow into either sharp-edged or tapered die was studied using stress-optical measurements. Distribution of shear stress and normal stress difference was obtained for PS melt: neither stresses nor velocities showed secondary motion	Han and Drexler 1973
Flow through converging–diverging tubes has been computed (velocity fields, pressure distribution, and wall stresses). The velocity profiles were measured using laser Doppler anemometry	Theodorou et al. 1984
Flow through an axisymmetric pipe, whose diameter was slowly varying in the axial direction, was theoretically described. A converging flow rheometer was developed	Williams and Javadpour 1980; Williams and Williams 1985
Converging and diverging dies produced flat, biaxially oriented extrudates. Relationships between the die geometry and product orientation were established	Mascia and Zhao 1991; Lohfink and Kamal 1993
Flow of multilayer viscoelastic fluids in converging channel slit die was analyzed. The neutral stability contours were altered in the channel flow. The effect of convergence on interfacial stability was similar to that of the elasticity. Channel convergence can be used to stabilize the interface at low depth ratios provided that shear-thinning effects are more dominant in more viscous layers	Su and Khomami 1992
The interface of PP/HDPE system can become unstable in both converging and diverging channels when the layer/depth ratio and disturbance wave number lie in a certain region	Khomami and Wilson 1995
Flow along the central axis of a converging conical channel was used to investigate the contribution of elasticity on drop using a Boger fluid. Drop deformation decreases with increasing elasticity. For elasticity ratio, $k' < 0.2$, the matrix elasticity has more effect on the drop deformation than drop elasticity. However, for $k' > 0.2$, drop deformation is more affected by drop elasticity	Mighri et al. 1997

Table 9.5 (continued)

Description	Reference
Flow in cylindrical, converging die with semi-hyperbolic shape was used to measure the elongational viscosity of polymer melts	Collier et al. 1998; Feigl et al. 2003
Droplets of polymer blends flowing through convergent channels undergo collisions and coalescence. Compared with methods using simple shear flow, the convergent flow pattern combines both shear and extensional flows	Miroshnikov et al. 2011

provided important information on the evolution of drop shape during the flow through c-d channel (Luciani et al. 1997; Khayat et al. 1996). This led to designing of a new extensional flow mixer (EFM) in which the blend is repeatedly exposed to extensional flow fields and semi-quiescent zones. The c-d channels are of progressively increasing intensity, with flow in the radial not axial direction. To reduce the pressure drop and to prevent blockage, slit restrictions are used (Nguyen and Utracki 1995; Utracki and Luciani 1997).

The EFM is a fully adjustable, general-purpose, motionless mixer. The mixing action is provided by the development of extensional flow field through the c-d geometry. It is primarily a dispersive mixer that should be attached to a pressure-generating device. It efficiently homogenizes different liquid systems, even these where the components' viscosity ratios are large. The mixer attached to a single-screw extruder provided comparable or better mixing than a twin-screw extruder with the so-called mixing screw geometry (Bourry et al. 1995; Utracki and Luciani 1996; Luciani and Utracki 1996). EFM has been used for polymer blending, incorporation of elastomers into resins, and dispersion of high-viscosity resins or "gel particles."

Figure 9.10 shows a cross section of the EFM. The molten polymer blend enters the EFM from an extruder through an adapter plate #1. The melt is distributed by the distributing plate #3 to six slits, located between the cone and the mounting ring of the part #3. Next, the melt enters the annular space inside the EFM body #5 where it is directed to the space limited by the upper (part #4) and lower (part #6) c-d plates. There it flows from the rim toward the center, undergoing the convergent and divergent deformations before sorting out through the central passage in the lower plate #6 and the central bore in the plate holder #7. The magnitude of the stresses is controlled by the pressure (generated by the extruder) and by the gap between the two c-d plates (parts #4 and 6). The latter is adjusted by turning the adjusting plate #8.

The pressure drop (ΔP) across the EFM was calculated using an expression proposed by Binding (1988). The pressure loss across the c-d plates (ΔP) was computed for a series of blends with either PE, PP, or PS as matrix. The result can be either expressed by the proportionality or given by a linear fit:

$$\begin{aligned}
\Delta P_{exp} &= (1.026 \pm 0.195)\Delta P_{calc}; \quad \text{or} \\
\Delta P_{exp} &= 0.0512 + 1.044\Delta P_{calc}, \quad R = 0.9772
\end{aligned} \quad (9.15)$$

The computations made it possible to separate the pressure losses into the extension and shear contributions (PE and PS), respectively. As evident
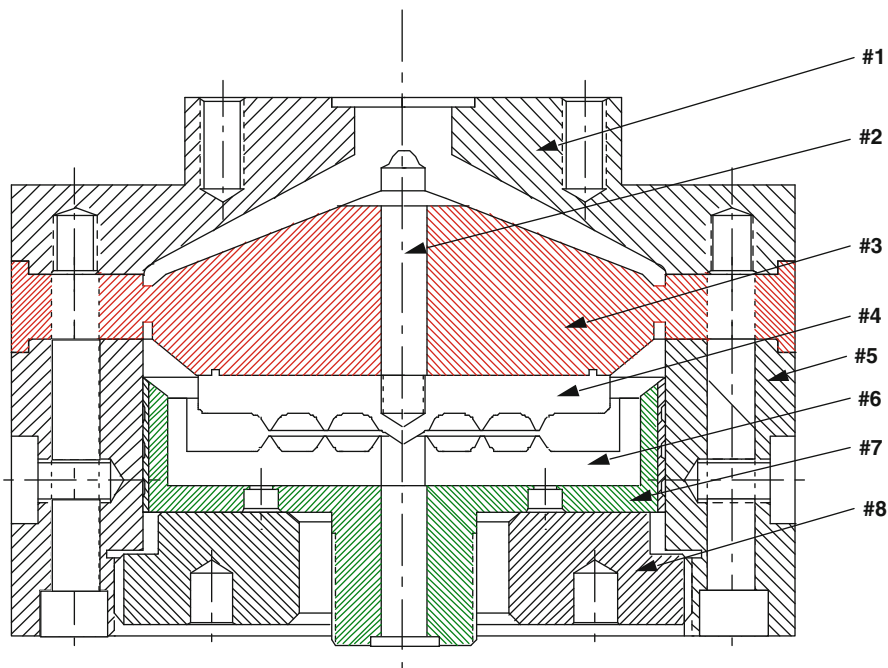
Fig. 9.10 Cross section of the extensional flow mixer (EFM) assembly. The numbered parts are described in the text

from Fig. 9.11, in EFM the pressure drop caused by elongation is larger than that by shear.

The performance of EFM attached to a single-screw extruder (SSE) was examined in reference to the results obtained using a corotating, intermeshing twin-screw extruder (TSE) equipped with the recommended-by-the-manufacturer high-dispersion screws. Four types of mixing were studied: dispersion of a viscous polymeric blend component in at least four times less viscous polymer matrix, impact modification of engineering resins, elimination of gel particles from reactor powders, and homogenization of new metallocene polyolefin mixtures having very large ratios of melt flow index. The results showed that compounding in SSE + EFM resulted in finer dispersion of HDPE in PS and vice versa than in a TSE. Similarly, the impact properties of EPR/PP blends prepared in SSE + EFM were better than of the same compositions mixed in TSE. The SSE + EFM mixing unit was also superior to TSE as far as dissolution of very high molecular weight fractions (polymeric gel particles) was concerned (Utracki and Luciani 1996; Luciani and Utracki 1996). The original EFM was commercialized in 1999, but an improved version was presented 1 year later reporting better gel elimination and more uniform morphology leading to higher blend strength (Song 2000). Then, numerical simulations (finite element methods) on shear-thinning (Carreau model)
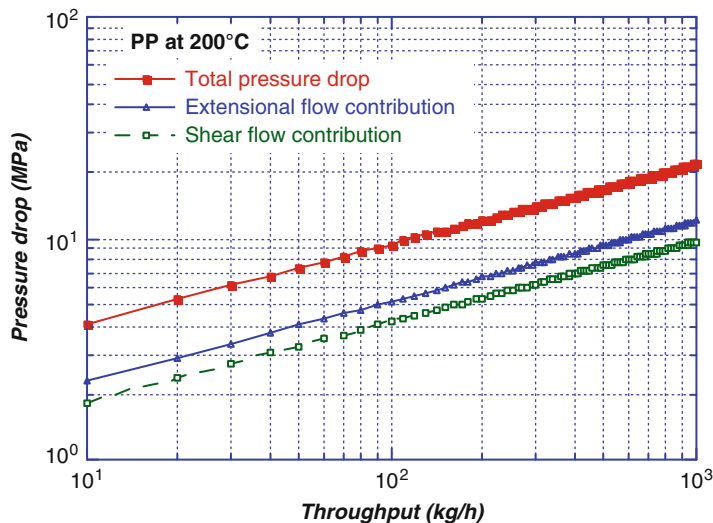
Fig. 9.11 Total pressure drop across the EFM c-d plates and its extensional and shear components vs. throughput of polypropylene, using a gap of one millimeter

and viscoelastic (Phan-Thien–Tanner model) fluids showed that possible stagnation regions in the c-d plates can be obtained for viscoelastic fluids. The size of the stagnation region increases for strain-thickening fluids, while it disappears when no elasticity is present (Tanoue and Iemoto 2003). Other versions, called EFM-3 and EFM-N, were shown to produce high-performance nano-composites based on PA-6 and PP with nanoclays (Cloisite C15A) due to increased dispersion and exfoliation (Tokihisa et al. 2006).

9.2.7 Interphase Properties

9.2.7.1 Importance of the Interfacial Tension Coefficient

At high dilution, the morphology of an immiscible blend is controlled by the viscosity ratio (λ), the capillarity number (κ), and the reduced time (t^*) as defined in Eq. 9.8. The interfacial and rheological properties enter into κ and t^*. As the concentration increases, the coalescence becomes increasingly important. This process is also controlled by the interphase properties.

Blending two immiscible polymers always creates a third phase called the interphase. In binary blends, thickness of this third phase (Δl) is inversely proportional to the interfacial tension coefficient (ν_{12}). When the blend approaches miscibility, ν_{12} approaches zero and Δl goes to infinity. Thus the interphase with its own set of characteristic parameters (viscoelasticity) may dominate the behavior of nearly miscible systems, as well as that of compatibilized blends. For further

details on this topic, see ▶ Chap. 4, "Interphase and Compatibilization by Addition of a Compatibilizer."

To modify the interphase properties, three strategies of compatibilization have been developed:

  (i) Addition of a small quantity of a third component that either is miscible with both phases (cosolvent), or it is a copolymer whose one part is miscible with one phase and another with the other phase (0.5–2 wt%, usually block-type or a graft one).
 (ii) Addition of a large quantity (less than 35 wt%) of a core-shell copolymer that behaves like a multipurpose compatibilizer-cum-impact modifier.
(iii) Reactive compatibilization designed to enhance domain interactions. The reactive blending may be employed to generate in situ the desired quantities of either block or graft copolymer(s) (see also in this book Chap. ▶ 5, "Reactive Compatibilization").

Different strategies lead to different alloys, having different sets of properties like addition of a small amount of block copolymer mainly affects the interfacial tension coefficient, thus the size of dispersion, but under normal circumstances, it only slightly affects the shear sensitivity of the blends' morphology or the solid-state behavior. Reactive compatibilization was found to produce thick interphase, which resulted in excellent stability during intense processing and good mechanical performance.

9.2.7.2 Theoretical Aspects of the Interface

The Helfand and Tagami (1971, 1972) model is based on self-consistent field that determines the configurational statistics of the macromolecules in the interfacial region. The interactions between the statistic segments of polymers A and B are determined by the thermodynamic binary interaction parameter (χ_{12}). The isothermal segmental density profile shown in Fig. 9.12, ρ_i (i = A or B), was calculated for infinitely long macromolecules, $M_w \to \infty$. The interfacial thickness (Δl_∞) and the interfacial tension coefficient (ν_∞) were expressed as

$$\Delta l_\infty = 2b/(6\chi_{12})^{1/2} \; ; \quad \nu_\infty = b\rho k_B T(\chi_{12}/6)^{1/2} \tag{9.16}$$

where b is a lattice parameter, k_B is the Boltzmann constant, and T is the absolute temperature. The Helfand–Tagami lattice theory predicted that (1) the product $\nu \Delta l|_\infty$ is independent of the thermodynamic binary interaction parameter, (2) the chain ends of both polymers concentrate at the interface, and (3) the low molecular weight components are repulsed to the interface.

Addition of a compatibilizer reduces ν_{12} to the level corresponding to the critical micelles concentration or CMC (Utracki and Shi 1992; Tang and Huang 1994). The radius of the dispersed drop (R) follows the same "titration curve" as the interfacial tension coefficient ν_{12}.

Segmental density profile across the interface
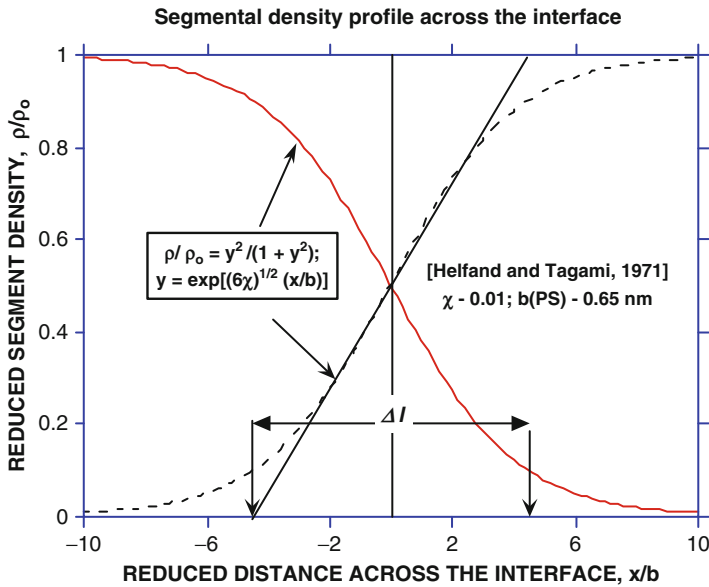
Fig. 9.12 Computed segmental density profile across the interface. The figure defines the interphase thickness Δl (after Helfand and Tagami 1971)

The amount of the interfacial agent required to saturate the interface (w_{cr}) per volume fraction of the dispersed phase (ϕ) can be expressed as (Paul 1978; Matos 1993)

$$w_{cr}/\phi = 3M/RN_{Av}\zeta \tag{9.17}$$

where M is the molecular weight, R is the radius of the dispersed drop, N_{Av} is the Avogadro number, and ζ is the area occupied by a copolymer molecule, taken either as a cross section of a copolymer chain (ca. 5 nm^2) or proportional to the square of the end-to-end distance of the copolymer chain, $\zeta = \langle r^2 \rangle/9$.

9.2.7.3 Calculations of the Interfacial Tension Coefficient

The interfacial tension coefficient can be calculated from the solubility parameters (δ) that comprises contributions from the dispersive, polar, and hydrogen bonding interactions. The following dependence was proposed (Luciani et al. 1996, 1997):

$$\nu_{12} = k(\rho RT)^{n-1} \left[\Theta(\delta_{1d} - \delta_{2d})^2 + (\delta_{1p} - \delta_{2p})^2 + (\delta_{1h} - \delta_{2h})^2 \right]^n \tag{9.18}$$

where k is a constant, $\Theta = 1$–4 is a parameter, and exponent n (depending on the adopted theoretical assumptions) $n = 1/2$–$3/2$. The expression $(\rho RT)^{n-1}$ is not sensitive to temperature. All available experimental values of ν_{12} were plotted as functions of the computed values for polymer blends, assuming that all factors have the same value, $\Theta_i = 1$ (see Fig. 9.13).
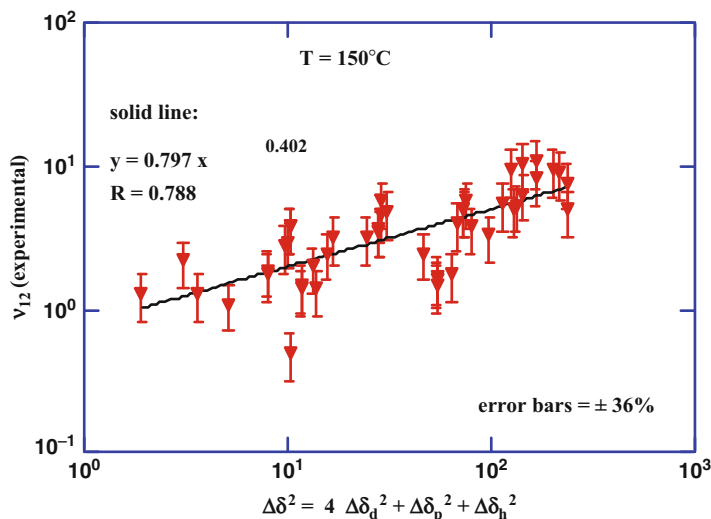
Fig. 9.13 Interfacial tension coefficient computed from the chain structure of the polymeric chains for 46 polymer blends vs. the computed solubility parameter difference (Luciani et al. 1996)

9.2.8 Coalescence

During mixing, the dispersed phase progressively breaks down until a minimum drop diameter, d, is reached. For Newtonian systems, the size of the smallest drop that can be broken can be calculated from the Taylor theory (see Eq. 9.9). However, many experimental studies (Tokita 1977; Roland and Bohm 1984; Plochocki et al. 1990; Willis et al. 1990, 1991; Favis et al. 1991) have shown that the final drop size is usually larger than predicted. For example, only when $\phi_d < \phi_o \approx 0.005$, the observed drop sizes approached the theoretical values (Elmendorp and Van der Vegt 1986). The source of the discrepancy is coalescence.

There are two types of coalescence mechanisms, the first being determined by the equilibrium thermodynamics and the second caused by flow. Thus, coalescence occurs in flowing as well as quiescent systems. To the latter type belongs the *Ostwald ripening*, characterized by the linear increase of the drop volume with time; i.e., $d^3 \sim t$. The process involves diffusion from smaller drops (high interfacial energy) to the larger ones. Flow modifies the rate of this process and the rate depends on the drop dynamic cross section, i.e., $d^n \sim t$, where $3/2 < n < 3$ (Ratke and Thieringer 1985).

Tokita (1977) suggested that the drop diameter in polymer blends originates from the two competitive processes: continuous breakup and coalescence of the dispersed particles. The equilibrium drop diameter should increase with concentration, number of drops, and the interfacial tension coefficient, but decrease with shear stress (σ_{12}). The dependence qualitatively agrees with experiments (Liang et al. 1983; White and Min 1985; Willis et al. 1991).

The coagulation time (t_c) of PVC lattices under steady-state shear flow followed the theoretical relation (Utracki 1973)

$$t_c \propto d^3 \phi_d^{-8/3} \dot{\gamma}^{-2} \qquad (9.19)$$

The coagulation rate was related to the projected area of the drop $d^* \propto \phi_d^{2/3}$. The relation separates the effects of the particle diameter, the concentration, and the rate of shear. When the other variables are constant, the coagulation time increases with particle diameter following the Ostwald ripening kinematics. It decreases with nearly a cube of concentration and with a square of the shear rate.

From Eq. 9.19, the rate of diameter change due to coalescence can be expressed as

$$(\mathrm{d}d/\mathrm{d}t)_{\text{coalescence}} \propto \dot{\gamma}\, \phi^{8/3}/d \qquad (9.20)$$

On the other hand, micro-rheology predicts that the rate of diameter change due to break is

$$(\mathrm{d}d/\mathrm{d}t)_{\text{break}} \propto \quad -\dot{\gamma}\, d/\kappa_{cr} t_b^* \qquad (9.21)$$

These two equations indicate which factors can be used to enhance either dispersion or coalescence. Clearly, the shear rate is expected to similarly affect coalescence and breakup. However, the flow-induced coalescence is a strong function of concentration, whereas the break is not; thus concentration may be used to discriminate between these two processes. Furthermore, the rate of break is proportional to d, whereas the coalescence is proportional to 1/d. Thus, coalescence is not expected to play a major role in the beginning of the dispersion process.

Equating Eqs. 9.20 and 9.21 leads to (Huneault et al. 1995a)

$$d_{eq} = d_{eq}^o + \left(6C\kappa_{cr} t_b^* \phi^{8/3}\right)^{1/2} \qquad (9.22)$$

where κ_{cr} is the critical capillary number for breakup, t_b^* is the time to break, ϕ is the volume fraction of the dispersed phase, d_{eq} is the equilibrium drop diameter, and d_{eq}^o is its value extrapolated to zero concentration (see Fig. 9.14).

9.2.9 Measures of Mixedness

As defined above, mixing is an operation that provides enhanced spatial homogeneity of a system. However, the homogeneity is not an absolute parameter. Depending on the scale of observation, one can always find domains belonging to a single component of the mixture. By definition, mixtures that show heterogeneity of composition on a scale not larger than the radius of gyration of a given polymeric chain are considered thermodynamically miscible. They may be considered as having the ultimate degree of mixedness.
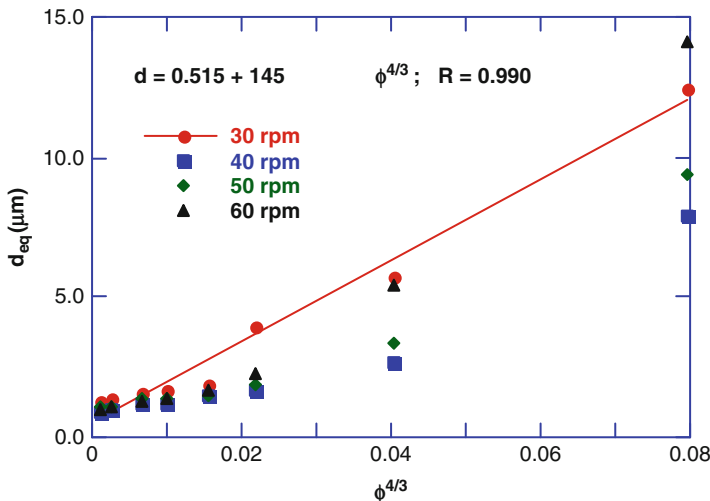
Fig. 9.14 Average equilibrium diameter of polyethylene dispersed in polystyrene matrix as a function of PE volume fraction. The data were obtained blending the resins in an internal mixer at 200 °C until an equilibrium drop size was obtained after 300 s

Assessment of the quality of a mixture, or mixedness, is difficult and time consuming. Since the performance of blends is controlled by the optimum degree of dispersion, as well as by other factors (compatibilization, adhesion in solid state, the level of degradation engendered during the blending, etc.), the mixedness must be considered a separated quantity, to be determined independently of the blends' performance.

In a binary mixture of two polymers, A and B, their local concentration (in weight fraction) can be expressed as $a(\mathbf{x}) + b(\mathbf{x}) = 1$ (where $\mathbf{x}$ denotes vectorial location). Similarly, the sum of the average compositions $a_{av} + b_{av} = 1$. For such a system, the mixedness can be described by the binary frequency function. For fine dispersions, variance of the composition and the intensity of segregation can be defined as (Hold 1991; Tucker 1991)

$$\text{Variance}: \quad \sigma_a^2 = \left\langle [a(x) - a_{av}]^2 \right\rangle$$
$$\text{Segregation intensity}: \quad I_s = \sigma_a^2 / a_{av} b_{av}$$
(9.23)

Since segregation is not uniform, it is important to know the scale of segregation in the mixture. The volume scale of segregation is defined as (Danckwerts 1953)

$$S_v = 2\pi \int_0^\infty \{R(r)/\sigma_a^2\} dr; \quad where: \quad R(r) \equiv \langle [a(x) - a_{av}][a(x + r) - a_{av}] \rangle$$

(9.24)

The segregation intensity varies between 0 and 1. For the mechanical mixtures of immiscible polymers, the parameter I_S is close to 1; thus other measures of mixedness must be found.

An excellent measure of mixedness is the *specific interfacial area*, or the interfacial area per unit volume of the mixture (A_V). For completely separated phases, $A_V = 1\ m^2/1\ m^3 = 1\ m^{-1}$. As the mixing progresses, the value of A_V increases. The larger is the value, better is the blend's mixedness. In laminar shear mixing A_V of randomly oriented elements depends on strain (γ):

$$A_v = 4\lim_{r\to o}(dR(r)/dr) = (A_{v,o}/2)\exp\{\gamma/2\} \qquad (9.25)$$

where $A_{v,o}$ is the initial interfacial area at strain $\gamma = 0$. It was estimated that for adequate laminar mixing, 18,000 strain units is required, which gives $A_v/A_{v,o} \to \infty$ (Hold 1991).

For layered or laminar mixtures, one can also define mixedness by the striation thickness (s) defined as 1/2 of the layer thickness. It can be shown that in these systems there is a simple relation: $A_V = 1/s$. Since in real blends there is a variety of striation thickness, s should be expressed by a volume distribution function.

Another excellent description of mixedness is the power spectrum, derived by Fourier transformation of the correlation function:

$$P(n) = \int_{-\infty}^{\infty} R(r)\exp\{-2\pi inr\}dr \cong 2\int_{-\infty}^{\infty} R(r)\cos(2\pi nr)\,dr \qquad (9.26)$$

where n is the wave vector. The power spectrum can be used to calculate the variance and the linear scale of segregation as

$$\sigma_a^2 = \int_{-\infty}^{\infty} P(n)dn; \qquad S_L = \int_{0}^{\infty} R(r)dr / \int_{-\infty}^{\infty} P(n)dn \qquad (9.27)$$

Although several image analysis techniques based on optical, electronic (SEM, TEM), and atomic (AFM, STM) microscopy have been developed to study the morphology of polymer blends, they are usually time consuming and need tedious sample preparation. Hyperspectral image analysis (UV-VIS-NIR) was shown to be a powerful tool to get rapid information as online and off-line measurements can be performed, but usually with lower resolution. For example, PS/LDPE blends were successfully analyzed via film blowing (Gosselin et al. 2009). These multivariate image analysis (MIA) is usually combined with principal component analysis (PCA) to extract two-dimensional information on composition, homogeneity via texture analysis (Gosselin et al. 2009), and crystallinity (Gosselin et al. 2008) and with some previous modeling/calibration mechanical properties (Gosselin et al. 2011).

9.2.10 Morphology Evolution During Processing

Blending is an economically viable, versatile method of manufacturing new materials with a wide range of properties (Utracki 1987, 1993; Rauwendaal 1986). The parameters most frequently targeted for the improvement by blending are stiffness, strength, processability, heat deflection temperature, and cost-to-performance ratio.

When designing a blend, first, the polymers and their approximate concentrations must be selected and then the most appropriate blend morphology for the envisaged application. For example, the need to improve impact properties implies that the minor phase ought to be dispersed as spherical droplets with micron or submicron diameter. On the other hand, if the material is to be used in vapor on solvent barrier applications, the minor phase should be dispersed in the form of relatively large, thin lamellas. The desired morphology is obtained by selecting the appropriate compatibilization and compounding/processing methods (Utracki 1993, 1998).

9.2.10.1 Sample Collection for the Morphology Characterization

Several methods have been proposed to follow the morphology evolution in an extruder. Ideally, the method should make it possible to instantaneously freeze the structure, without imparting changes due to stress, stress relaxation, or coalescence. The frozen structure may then be analyzed for the degree of fusion, crystallinity, composition, degree and type of dispersion, etc. Table 9.6 lists some of the more popular methods used for the characterization of morphology evolution during blending in an internal mixer, an extruder, or a special mixing device. Blends' morphology has been studied by several research teams: Elemans et al. (1988, 1990), Lindt et al. (1992), Utracki and Shi (1992), Huneault et al. (1995b), Delamare and Vergnes (1996), Cho and White (1996), etc.

There are numerous small single- or twin-screw extruders developed for the preparation of small quantity of blends and evaluation of their morphology. These are particularly useful for compatibilizer optimization. The SSE-type recirculating devices are well represented by mini-extruders, *Microtruder*™, having throughput ≥ 10 g/h (Luker and Leistritz 1996). Recirculating TSE with a sampling port in the bypass line was originally developed at DSM. Later, the unit was commercialized. Owing to the small size, its specimens can be rapidly quenched.

Following on the success of the extensional flow mixer (see Sect. 9.2.6.4), an extensional mini-mixer was designed. The device consists of two reciprocating pistons with a convergent–divergent, c-d, restriction between them. The material to be mixed is introduced to the mixing chamber, heated under vacuum until the desired temperature is reached. Next, it is forced repeatedly through the c-d restriction, by the action of the reciprocating pistons (Utracki 1996).

9.2.10.2 Modeling of the Morphology Evolution

Several attempts were made to develop mathematical models capable of describing the morphology evolution during blending in different model flows and compounding machines. These efforts are summarized in Table 9.7 and briefly discussed below under separated headings.

Table 9.6 Experimental methods for morphology characterization

Mixer	Description	Reference
SSE, now used also for TSE	The oldest and the most primitive method is the so-called carcass method, viz., stopping the motor, cooling the compound, and removing either screw(s) or a barrel to access the solidified resin. Due to the thermal inertia of the system, the minimum time for the solidification is about 15–20 min. During this period, extensive changes of blends' morphology may take place. The observed structure can hardly reflect the structure existing during the blending	Maddock 1959
TSE	Not much better is the dead-stop method and sliding out the barrel (Clextral BC 45 mm extruder). Three methods were described: 1. Cooling the barrel with water requires at least 5 min. 2. Sliding out the barrel and then cooling by sprinkling water on the melt still requires several minutes. 3. The best choice is to slide out the barrel and then to take molten samples from the hot screws and quench them in cold water. The methods 2 and 3 may affect the morphology. Significant differences of the average drop size were reported between samples collected using the three methods	de Loor et al. 1994, 1996; Delamare and Vergnes 1996
TSE	Similar to the sliding barrel is the method that uses a clamshell barrel. The morphology is quenched by either pouring a cooling liquid (ice water or liquid nitrogen) or quenching the specimens taken from various locations in a cooling medium. Opening the barrel causes deformation of the molten blend. Here, the time lag is 2–5 min. Prior cooling of the extruder and opening it after reheating the surface require a comparable time lag to the carcass method, 15–20 min. A Baker Perkins 50.8 mm and Werner & Pfleiderer up to 70 mm are popular TSE used for this method	Kalyon et al. 1988; Sundararaj et al. 1992
TSE	A quenching double-barrel clamshell section was designed and manufactured for a ZSK-30, to replace two barrel segments. The section played the same role as the regular barrel elements, but it had extra quenching channels for chilled water (4 °C). Once blending reached a steady state, the screw rotation and heating were stopped and the quenching unit was switched on. It took 4–6 s to quench the polymer near the barrel wall and about one minute to quench the position near the screw root. It was calculated that in the kneading disks, quenching took about 10 s. The advantage of this method is the ability to quench a blend at any location along the screw, within seconds without deforming the material	Bordereau et al. 1992; Shi et al. 1992

(continued)

Table 9.6 (continued)

Mixer	Description	Reference
TSE	TEX extruders with sampling nozzles along the barrel were introduced. The nozzles have been designed to follow the chemical reactions during the blending, but they can be used as well to follow the morphological changes. The disadvantage of the system is that the sampling barrel elements can be placed only at the locations where sufficient pressure is generated to force the melt through the nozzle. Furthermore, depending on the morphology and stresses in the nozzle, the blend morphology may be modified. The quenching time was estimated at 3–5 s	Nishio et al. 1990, 1992; Sanada et al. 1991; Sakai 1993
TSE	The most rapid method of quenching involves scooping the specimens directly from an operating extruder and quenching these in either ice water or liquid nitrogen. It takes ca. 1 s to quench the sample. Furthermore, scooping does not impose extensive changes of morphology. Its disadvantage rests with the limited number of sampling ports. Large differences of morphology were observed within the first few seconds after TSE screws were stopped	Huneault et al. 1995b
Special	A "dispersion tester" consists of a rotating drum with a milled grove, in which a stationary spreader was placed. The gap, clearance, drum speed, temperature, pressure on, and the shape of the spreader could be controlled. The specimen could be subjected to repeated passages, with the morphology analysis after each passage. The device was used to analyze the morphology generation of PS/LDPE blends with and without compatibilizing SEB di-block copolymer. The observed morphological changes are summarized in Fig. 9.15	Tadmor 1988; Kozlowski 1994
Mini-Max	The mixer is capable of mixing less than 1 g of the resin. The device has been reported to produce similar dispersions of reactive blends as those prepared in industrial mixers, TSE or internal mixer. It was found that Mini-Max makes it possible to pre-evaluate blends, especially those of polymers having low viscosity and elasticity	Maxwell 1972; Sundararaj et al. 1995
TSE	Morphology development of polymer blends was studied in TSE. Samples were cooled in liquid nitrogen immediately after being taken from the screws. Morphology develops faster in compatibilized blends than that in their uncompatibilized counterparts	Li and Sundararaj 2009

(*continued*)

Table 9.6 (continued)

Mixer	Description	Reference
Special mixer	A new laboratory-scale mixing device based on the geometry of Mackley's multipass rheometer. The flow in this mixer is characterized by a high contribution from elongational flow. Its efficiency for dispersive mixing is attributed to the combination of elongational flow in the convergent zone and shear flow in the die of the mixing element	Bouquey et al. 2010
TSE mixer	Morphological development of cross-linked blends was prepared both in an internal mixer and in a corotating TSE; despite the similar average apparent shear rate used in both mixing equipments, the intensive flow field inside the TSE resulted in a finer morphology in comparison to the internal mixer	Shahbikian et al. 2012

9.2.10.3 Morphology Evolution in Internal Mixers

A laboratory internal batch mixer was used by Shih et al. (1991, 1992) to simulate the progression of mixing in a compounding process of multicomponent polymer systems. A mixing bowl was modified with a glass window built into the front heating plate. A video picture taken through the glass window was recorded continuously. By using HDPE, PBT, and PAR, the authors distinguished four sequential characteristic states:

  I. Elastic solid pellets
 II. Deformable solid pellets
III. Transition material
    A. Fluid with suspended solid particles
    B. Fractured or semifluid material
    C. Doughlike material
IV. Viscoelastic fluid

The type of the transition material (No. III A, B, or C) mainly depends on the difference in the solid–liquid transition temperature of polymers. Furthermore, if the second polymer was crystalline, after melting, a phase inversion has been frequently observed.

For blends having widely different softening points (either melting point or glass transition temperature), the four stages were "shifted." Thus, the polymer having the lower softening temperature melted first and became matrix of a "highly filled composite." If the softening point and the concentration of the second polymer were high enough, the torque increased causing breakage of the shear pin in the mixer. In the extrusions, the consequences could be more serious. It was concluded that blends of polymers having widely different softening points should be fed consecutively, trying to match viscosities by judicious selection of the local temperature. Extensive studies of mixing in an internal mixer were carried out by Min and White (1985). The work combined the flow visualization with the modification of rotors and measurements of the pressure distribution. Detailed description of the blend morphology in an internal mixer is provided in a review chapter (Min 1994).

Fig. 9.15 Morphology evolution during flow in Tadmor's dispersion tester
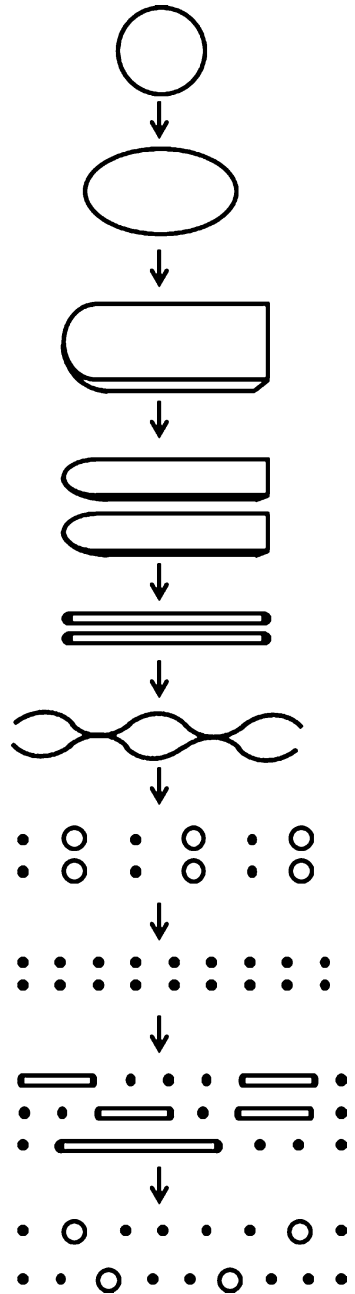
Table 9.7 Modeling of morphology evolution

Compounder	Modeling	References
Internal mixer	Flow visualization of blending elastomers and plastics	Min and White 1985
Internal mixer	Experimental studies of mixing in an internal mixer, after installing glass window in a mixing bowl	Shih et al. 1991, 1992
Rheometer	Experimental and theoretical study of drop elongation in a steady-state flow, at constant shear stresses.	Lyngaae-Jørgensen et al. 1991, 1993.
Single-screw extruder	Theoretical analysis of flow through a SSE using the "three-layer" model. Theoretical and experimental studies of the early stages of morphology development. Melting of two resins generated lamellas that during the flow through SSE were thinned out and then disintegrated into filament, which in turn broke into droplets	Lindt 1981; Gosh et al. 1991; Lindt and Ghosh 1992
Twin-screw extruder	Pressure flow model for Newtonian liquid in the pumping section	Vergnes et al. 1983, 1986
Twin-screw extruder	Flow of Newtonian fluids in kneading disk elements and (right- and left-handed) screw elements	Szydlowski et al. 1987
Twin-screw extruder	A simplified model was developed. It is based on the assumption that throughput is the same along the extruder as within the zone where the flights are full. Calculations of blend morphology evolution along an extruder and comparison with experimental data were published	Elemans et al. 1988, 1989, 1990
Twin-screw extruder	The groove model to describe the flow in axially open screw channels by introducing two parameters, dimensionless pressure gradient and dimensionless output	Potente et al. 1989
Twin-screw extruder	Dimensionless calculations of throughput and pressure gradients for flow of non-Newtonian fluids in screw and kneading disk elements of a modular intermeshing self-wiping corotating twin-screw extruder, as well as the temperature rise	Chen and White 1992, 1993
Twin-screw extruder	Experimental studies using Baker Perkins corotating TSE. During the melting stage, first sheets, then sheets with holes labeled "laces," and finally dispersed drops were observed	Sundararaj et al. 1992
Twin-screw extruder	Theoretical and experimental studies of morphology evolution during compounding of PS/PE blends. A quenching barrel section was designed for a corotating intermeshing TSE (W&P). A predictive model for morphology development was proposed	Bordereau et al. 1992; Utracki and Shi 1992; Utracki and Shi 1992, 1993

Table 9.7 (continued)

Compounder	Modeling	References
Twin-screw extruder	Morphology development along a corotating or counterrotating intermeshing TSE was observed. Different screw configurations were used. Increasing the number of kneading blocks enhanced the degree of dispersion	Lim and White 1993
Twin-screw extruder	Extension of the model developed by Shi and Utracki. Better fluid mechanics computations and micro-rheological drop fracture mechanisms were used. The model takes into account the coalescence	Huneault et al. 1995a
Corotating twin-screw extruder	Experimental work. Samples were scooped directly from the venting ports located between the melting and kneading block sections, as well as after the latter section. After melting, the dispersed phase consisted of fibers and droplets, both with diameters already below 10 μm. The kneading section (independently of its construction) further reduced the drop diameter by a factor of ten	Huneault et al. 1995b, 1996
Twin-screw extruder	Experimental and theoretical. Non-isothermal model with drop diameter computations based on micro-rheology and coalescence. Changes in polydispersity of sizes can also be computed	de Loor et al. 1994, 1996; Delamare and Vergnes 1996
Corotating twin-screw extruder (CORI)	A 3D modeling of flow was carried out by finite elements method. The flow profile, the backflow volume, pressure distribution, shear and elongation rates, and adiabatic T-gradient were computed for the conveying and kneading sections	Goffart et al. 1996; van der Wal et al. 1996
Co- or counterrotating twin-screw extruder	A 3D modeling of flow in full conveying screw elements of either a CORI or ICRR was reported. The flow velocity and stress fields were computed, as well as the residence time distribution. CORI was found to have better distributive mixing, whereas ICRR performed better as a dispersive mixer	Kajiwara et al. 1996
Twin-screw extruder	Experimental work using CORI. Blends of 10 and 30 wt% PS in HDPE were prepared either by feeding dry blended pellets or introducing molten PS to HDPE melt at different screw positions. The morphology was insensitive to the feeding method. The authors concluded that the blend morphology is determined by the melt mixing within the first 25 s	Bourry and Favis 1997

(continued)

Table 9.7 (continued)

Compounder	Modeling	References
Twin-screw extruder	Distributive mixing was experimentally measured during polymer melt blending along the length of a CORI. A mixing limited interfacial reaction between two reactive polymer tracers was used to gain direct evidence of the generation of interfacial area. Mixing in kneading blocks depended on the combination of the operating conditions and the stagger angle	Shearer and Tzoganakis 2001
Twin-screw extruder	In the melting section of CORI extruders, virtually all the degradation mechanisms that can essentially be distinguished, such as quasi-steady drop breakup, folding, end pinching, and decomposition through capillary instabilities, take place in parallel	Potente et al. 2001
Single-screw extruder	The evolution of the morphology of liquid–liquid systems along the axis of a single-screw extruder is predicted, from the onset of melting until the die outlet. The possibilities of stretching, breakup, and coalescence are taken into consideration. Melt flow was assumed as 2D (which is computationally advantageous), a simplified cross-channel helical pattern being adopted; full 3D analysis showed little difference in the results	Domingues et al. 2010
Twin-screw extruder	The melting and deformation mechanisms of polystyrene (PS) and polypropylene (PP) blends were investigated through online visualization of the corotating twin-screw extrusion process. A sliding barrel technique was used to perform online visualization using a glass window in the barrel. The axial temperature and pressure profiles along the screw channel were measured using the same sliding technique. The overall melting process was accelerated due to heating from viscous dissipation	Chen et al. 2004
Single-screw extruder, twin-screw extruder	A "screw pulling-out" technique was used to investigate polymer behavior along the screw axis in a single-screw extruder and an intermeshing counterrotating twin-screw extruder. In particular, solid conveying, melting positions, extent of starved character along the screw, and fully filled regions were observed	Wilczynski et al. 2012a, b

9.2.10.4 Blends' Morphology in a Single-Screw Extruder (SSE)

Lindt and Ghosh (1991, 1992) dealt with the early stages of blend morphology development in a SSE. According to the model, melting of two types of pellets having similar solid–liquid transition temperatures generates lamellas that during the flow through SSE progressively thin out and then disintegrate into filaments, which in turn break into droplets. Comparison between experimental data and theoretically simulated striation thickness of polymers in a SSE channel showed good agreement. Unfortunately, owing to theoretical difficulties, the model did not go beyond the lamellas thinning. The authors argued that the melting zone plays an important role during continuous blending of polymers. Within the residence time in the melting zone, the blend undergoes rapid morphological changes. Within a fraction of a second, the scale of mixing may decrease by several orders of magnitude.

9.2.10.5 Morphology Evolution in a Twin-Screw Extruder (TSE)

Twin-screw extruders are important tools for the plastic industry. Their principal advantages (over SSE) are better feeding and more positive conveying, self-wiping of the screws, short residence times, a narrow residence time distribution spectrum, better mixing, larger heat transfer area, an easier scale-up, and large output.

The predictive models of the morphology evolution during polymer blending in a TSE start with a description of the flow mechanics. The fundamental assumption is that there are "strong" and "weak" zones. Within the former, the screw elements are fully filled; there is a positive pressure, large deforming stresses, and usually material recirculation that offer a potential for modifications of the blends morphology. The "weak" zones are partially filled, made of mainly transport elements. Here the material is conveyed either at ambient pressure or under vacuum. The stresses are minimal. Within these regions, two mechanisms are expected (provided that the reduced time (t*) is sufficiently long): breakup of filaments by the Raleigh instability mechanism and coalescence. Table 9.7 summarizes the fluid mechanics models of flow through TSE. For a more detailed discussion on the early modeling of flow through co- or counterrotating TSE, see White (1990).

Utracki and Shi (1992) proposed the first model of the morphology changes in a corotating, intermeshing TSE, CORI. The model incorporated the microrheological dispersion mechanism, but coalescence was neglected. Its validity was evaluated comparing the predictions with the experimentally measured drop diameter at different axial positions in the twin-screw extruder. It was estimated that using the newly designed quenching barrel, the PS/PE blends were quenched within 7–10 s. The model well predicted the morphology evolution of these non-compatibilized blends but only to the last mixing block. In the assumed absence of coalescence, the model predicted continuous decrease of drop diameter, whereas the experiment indicated its stabilization. The second model refined these computations and introduced coalescence between drops (Huneault et al. 1995a). The model is fully predictive. Good agreement with experimental data was found (see Fig. 9.16).

PE-DROP DIAMETER vs. SCREW LENGTH

— Q5, N150 ●
— — Q5, N200 ◆
— · — · Q5, N250 ▼

d (μm)

Position along the screw, L (mm)

PS-DROP DIAMETER vs. SCREW LENGTH

d (μm)

— Q5, N150 ●
— — Q5, N200 ◆
— · — · Q5, N250 ▼

Position along the screw, L (mm)
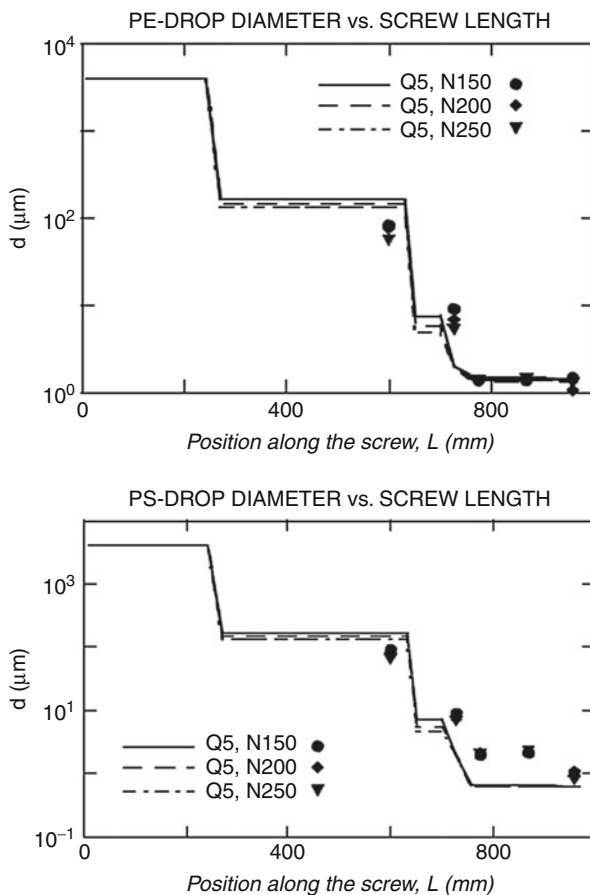
Some experiments were repeated using faster method for the samples' collection. The specimens were periodically "scooped" from open ports in the extruder and quenched in ice water. It was estimated that the quenching time was $t \leq 1$ s (Huneault et al. 1995b). Immediately after melting the dispersed phase consisted of fibers and droplets, both with diameters below 10 μm. The fibers were observed for $\phi \geq 0.02$ and were broken in the kneading section. The kneading blocks reduced the drop diameter to $d \cong 1$ μm. Its configuration had little influence on the resulting drop diameter. As the concentration increased, so did the final diameter of droplets, as well as the fiber content.

Evidently, in spite of the good agreement between the previous models and observations obtained after 7–10 s of the quenching time, the "incipient" blends' morphology is more complex than the models predicted. The morphology changes rapidly within the first few seconds after blending is stopped. This rapid variation of morphology would be particularly important for reactive blending. Furthermore, the morphology evolution during the melting stage may be

more important than initially assumed. During this stage, the viscosity ratio may vary by several orders of magnitude, both locally (stress and temperature gradients) and along the screw length. Furthermore, the coalescence affects not only the drops but fibrils as well.

Other types of morphological changes during blending in TSE were also observed (Sundararaj et al. 1992, 1995). The authors reported that both reactive and nonreactive blends in an extruder, internal mixer, or a miniature cup-and-rotor mixer show similar morphological features. Initially, during the melting, the polymers stretch into sheets and ribbons that first broke into fibers then into drops.

9.3   Blending Methods and Equipments

The term "processability" refers to the relative ease with which neat or compounded resin can be handled in production operation and equipment. In most cases, it is a synonym of a high throughput, low pressure at the die, and thus low viscosity. For the blending operations, another parameter is important: the energy consumed per mass or volume of the material, or the specific energy (E_{sp}). The polymer compounding or blending involves:

1. Preparation of ingredients (drying, sizing, heating, etc.)
2. Premixing (dry blending, homogenization, breakage of agglomerates, fluxing, etc.)
3. Melt mixing (usually with degassing)
4. Forming (granulation, pelletization, or dicing)

The most frequently applied operations are mixing, milling, extrusion, molding, and curing. The resin processability and the processability window are of main concern. Since they affect the material performance, their stability and control are of paramount importance.

9.3.1   Historical Evolution

Mixing is the oldest process. The first annular container with a spiked rotor (for rubber compounding) was developed in 1820 by Thomas Hancock. A more efficient, counterrotating twin shaft internal mixer with elliptical rotating disks was patented by Freyburger in 1876, while its sigma-blade versions 4 years later by Pfleiderer, and 40 years later by Banbury. These machines provided adequate mixing, but (owing to the batch mode) the production was slow and the performance erratic. An alternative was extrusion mixing.

Paul Troester started manufacturing single-screw extruders (SSE) in 1892, but it was only in 1935 that the first SSE for thermoplastics was introduced. Four years later, Paul Leistritz built electrically heated, air-cooled SSE, having L/D = 10, automatic temperature control, variable screw speed, and nitrided barrel. The machine is considered a prototype of the modern extruders. The SSE offered continuous processing capability, but it was notoriously poor as a mixer. Furthermore, under

the standard processing conditions, a significant nonuniformity in the shear history had resulted in large temperature differences of the melt, $\Delta T \cong 60\ °C$. To alleviate the problem, numerous types of mixing screws, mixing sections, or "add-ons" (inserted between the extruder barrel and the die) have been developed, for example:

1. Mixing screws: S-shaped kneader, Eagle mixing, turbine mixing, Cohen double wave, or Maillefer; screws with pin or blister ring and fluted or barrier screw, Dynamic Extensional Flow Mixer (DEFM), etc.
2. Mixing sections: Dulmage, Saxton, pineapple, Stratablend, and many others
3. Add-ons: Barmag add-on torpedo, *Staromix*™, Maddox, cavity transfer mixer (CTM), Twente Mixing Ring (TMR), the Extensional Flow Mixer (EFM), Dynamic Melt Mixer (DMX), and static or motionless mixers (SM) from Koch, Ross, or Kenics

Many of these devices were developed in parallel with the evolution of twin-screw extruders (TSE) in part to reduce the competitive advantage of TSE as far as their recognized capability for good mixing was concerned (Rauwendaal 1986; White 1990).

In 1937 Roberto Colombo and his associates developed an intermeshing, corotating TSE that during the early 1940s was used by I. G. Farbenindustrie for the continuous reactive extrusion of poly-ε-caprolactam. During the early 1940s, recognizing the need for improved compounding capability, Meskat and Erdmenger designed and manufactured intermeshing, corotating TSEs equipped with self-wiping corotating disks.

After the Second World War, the development of the TSE technology has been carried mainly in Germany and then in Japan. In 1959, Werner & Pfleiderer introduced ZSK – *Zwei Schnecken Kneter* – a CORI with segmented screws and barrel. The screws have been assembled from at least six different types of conveying and mixing elements. Japan Steel Works (JSW) started production of TSE in 1951. Thus, by the late 1950s, TSE technology has reached the end of the pioneering period: directions of the screw rotation, their intermeshing, principal left- and right-handed screw elements, and the kneading and mixing disks were designed, evaluated, and patented.

Over the years, significant improvement in the throughput capabilities was obtained by providing screws with higher "free volume," higher screw speeds (experimental machines operate at screw speeds exceeding 1,500 rpm), and higher torque. Several mixing elements as well as restrictors have also been introduced. However, probably the most significant is the progress in the construction of the intermeshing, counterrotating machines, ICRR. Several manufacturers offer TSEs in changeable configuration: CORI or ICRR, both capable of operating within similar ranges of the barrel lengths and screw speeds.

While developing either SSE or TSE machines for the mixing applications, the employed strategy was simple: when distributive mixing was required, the split-and-recombine flow stream was introduced; when dispersive mixing was needed, the high shear stress zones were incorporated. In spite of the recognized advantages of the extensional flow mixing, there has not been much effort to incorporate this concept into the processing equipment. The extensional flow mixer (EFM) is the only device that consciously utilizes the elongation flow for mixing.

Table 9.8 Melt mixing machines

No.	Machine	N	P	RTD	Feeding			Dispersive		Distributive	
					Powder	Filler	Sticky	As such	With additions	As such	With additions
1.	Internal mixer										
	Batch	+	−	−	+	+	+	+		+	
	Continuous	0	−	−	+	+	+	+		+	
2.	SSE	+	+	−	0	−	−	−	0	−	0
3.	TSE – CORI	++	0	+	+	+	0	+	+	0	+
	TSE – ICRR	+	+	+	+	0	+	+	+	−	0
	TSE – CRNI	+	−	−	+	+	+	−	0	−	0
4.	Special										
	Pin-barrel	+	0	0	0	−	+	+		+	
	Ko-Kneader	0	−	+	+	+	+	+		+	
	Planetary gear	−	−	+	0	−	−	++		0	
	Disk	+	+	+	0	0	−	0	+	0	+

Symbols: *N* high screw speed, *P* pressure generation, *RTD* residence time distribution, capability to be fed with difficult material, distributive and dispersive mixing without and with extra mixing elements or devices. *CORI* corotating intermeshing, *ICRR* intermeshing counterrotating, and *CRNI* counterrotating non-intermeshing. Evaluating symbols: + means good, 0 means acceptable, and − means poor

9.3.2 Melt Mixers

The melt mixers are either batch or continuous type. The former require lower investment cost but are more labor-intensive and have low output and poor batch-to-batch reproducibility. Developments in process control and automation eliminated some of these disadvantages (Utracki 1991). The continuous melt mixers comprise extruders, continuous shaft mixers, and specialty machines, and these will be discussed in the following part of this chapter. A brief overview of the melt mixing devices is given in Table 9.8.

9.3.2.1 Batch Mixers

Before the introduction of the intensive internal mixers, the mixing was accomplished on open mills which are slow and dirty processes requiring skilled operators. An efficient, counterrotating twin shaft internal mixer with elliptical rotating disks was patented by Freyburger, while its sigma-blade versions by Pfleiderer and by Banbury. The latter two inventors started the manufacturing companies, Werner & Pfleiderer (W&P) and Farrel Corporation, respectively. An important feature of these machines is that they are enclosed and pressurized, so that fine powders and additives would mix into the compound, not drifting away.

Batch mixing is not efficient for handling large capacities, but it is well suited for short-run operations (manufacture of color-concentrate

masterbatches) and products that have to have tailored identity. Because of the high stresses, an internal mixer can complete a cycle in minutes. The residence time, shear, and temperature can be controlled since all of these are of critical importance in the compounding of heat-sensitive materials or in alloying two materials of varying melt indices. Batch mixing also encourages close monitoring of formulations that combine expensive ingredients produced in small quantities.

Several basic designs of the internal batch-type mixers are available. The most popular are the laboratory mixers manufactured by Brabender or Haake and their homologues on the larger scale manufactured by Banbury or Moriyama dispersion mixers.

The laboratory machines are often used for the evaluation of compounds on a small scale, prior to production. The test requires a small amount of materials, short time, little efforts, and operational expense. The scale-up of the test results to production size is usually done through the "unit work" concept. The mixer makes it possible to assess the effects of changes in temperature, torque, and shear characteristics.

The most serious drawback of these internal mixers is the heat conduction by the mixing shafts. The mixer chamber is only heated from the outside and the shafts conduct the heat away from the molten polymers. During mixing at relatively low temperatures, a dynamic equilibrium may be reached as heat from the heaters is transferred to the melt, then the shafts conduct it to the internal drive system of the mixer. The dynamic equilibrium means that higher temperature is at the chamber wall and lower on the shafts' surface. However, for blending engineering or specialty polymers with high melting points, temperature drop across the chamber can be as large as $100\,^{\circ}\mathrm{C}$.

In the Readco High-Intensity Mixers, the agitators ascertain that the material is continuously moved in a circular pattern from one side of the chamber to the other, undergoing compression and expansion. At the same time, due to the helical angle of the agitators and the offset between the outer and inner agitators, the material is moved from one end of the mixing chamber to the other. The mixer is recognized for providing good dispersive mixing.

9.3.2.2 Continuous Mixers

Continuous mixing involves the continuous loading and unloading of components. When properly performed, mixing decreases the compositional variations to the desired level. Continuous operations have the advantage of providing a stable process. The power consumption is usually lower than in batch operations. The stresses are imposed systematically, either in the shear or in the shear-and-elongation mode of deformation. In spite of high capital costs and complex mixing, the continuous mixing is easy to justify on the basis of the production volume (mixers with throughputs up to 80 t/h are available) and quality.

The continuous mixers make it possible to control the feed rate, screw speed, temperature, as well as the discharge orifice setting and temperature. Machines can operate at high screw or shaft speeds require a short residence time. However, care must

be taken that high speeds will not lead either to excessive specific energy consumption or thermal decomposition of the resin. The continuous mixers require high capital investment but are easy to automate and robotize, have high output, and can be run with a statistical quality loop control (Kearney 1991; Canedo and Valsamis 1994).

Extruders

Extrusion is one of the most important forming methods in polymer processing. Virtually, all polymers go through an extruder at least once: compounding and pelletizing reactor powders. Furthermore, most forming operations involve extrusion: profiles, films, sheets, fibers, wire or paper coating, injection or blow molding, thermoforming, etc. More thermoplastics are converted into useful products by extrusion than by any other method.

The word "extrude" originates in the Latin words "ex" (out) and "trudere" (to thrust), and thus it closely described the process itself as shaping by forcing through an exit opening called the "die." In the nineteenth century, extruders were slow, thus rightly called "plodders." Extrusion is accomplished by a screw rotating in a cylindrical barrel. The feed to the extruder may be either solid or liquid. In the plastic industry, the solid-fed machines are called "plasticating extruders," while that fed by melt are known as "melt extruders."

There are three layers of the basic functions that extruder must perform:
- Primary: melting, pumping, and forming.
- Secondary: devolatilize and mix.
- Tertiary: conduct chemical reactions.
  Extruders are classified according to the principal element of their construction as:
- Single-, twin-, and multi-screw extruders
- Single-, twin-, multi-shaft compounders
- Gear or disk extruders like Maxwell melt-elasticity extruder, Tadmor's disk extruder, etc.
- Special extruders like Gelimat, Patfoort, etc.

In a plasticating extruder, the homopolymers, copolymers, or their blends are introduced at one end. As they advance along the extruder length, they are melted, homogenized, reacted, devolatilized, and transported either to a die (profile or blow molding) or into the mold cavity (injection molding). The extrusion that aims to produce pelletized material is conducted at higher screw speeds, using more intensive mixing than that aimed to manufacture the finished product. Hence, it is appropriate to distinguish the compounding extrusion and the forming extrusion.

The extruder operation is supported by an army of ancillary equipment. Their type and quality depend on the specific machine, type of operation, and material to be extruded. It is advantageous to divide this equipment into pre-extrusion and post-extrusion type. To the first category belong dryers, dry mixers, pre-compounders, solid and liquid feeders, etc. To the second group of post-extrusion equipment belong gear pumps, add-on mixers, dies, pelletizers, coolers or chillers, dewatering systems, sizing equipment, and many others.

Operation of an extruder is conducted considering the throughput (Q) vs. the pressure drop at the die (P) relation, schematically illustrated in Fig. 9.17.
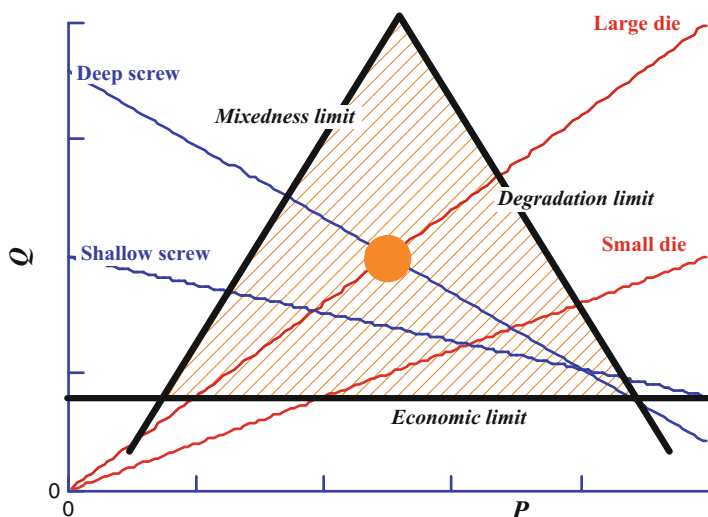
Fig. 9.17 The throughput (Q) vs. pressure drop at the die (P) dependence for a SSE. The operational triangle is defined by three limiting lines: the economy determined by the lowest acceptable value of Q, the mixing capability determined by the stresses (thus, by the screw speed, N, and P), and the degradability limit, also determined by N and P

Older SSEs have been equipped with minimum instrumentation: a pressure gauge at one point along the barrel (usually at the head) and a thermocouple in the hot melt region. For noncritical operations, the operator would record pressure, temperature, screw speed, and mass flow rates (typically determined by the sample weight–time method).

In operations requiring close tolerances of the extrudates, a greater degree of instrumentation and automation is employed. Usually, several pressure transducers and thermocouples along the barrel are used to ensure uniform extrusion and to control barrel and stock temperatures. Some designs may include thermocouple on the screw to monitor and control conveying flights. For specific applications, a closed-loop control may involve monitoring of composition, density, morphology, rheological performance, and other variables pertinent for the product. Standard methods of monitoring these variables may be used (radioisotopes, ultrasonics, rheological detectors, near and far infrared spectroscopy, mechanical testing, clarity scans, etc.).

Single-Screw Extruders (SSE)
The single-screw extruder is a relatively inexpensive machine for small- or medium-size production lines. For lines with the throughput exceeding 10 t/h, the capital costs of SSE and TSE are comparable. SSE that can produce 40 t/h can be custom-built by only few manufacturers. For example, in 1996 Berstorff demonstrated 600 mm machine for homogenization and degassing of LDPE at a throughput of 23 t/h. SSEs are characterized by a simple design, raggedness, and reliability, are easy to operate and maintain, and have favorable performance-to-cost ratio, and

theoretical description of their operation is well documented. On the other hand, they are difficult to scale-up and are notoriously poor mixers with broad residence time distribution and relatively long residence time (Hold 1982).

Over the years, SSEs have been made more versatile by introduction of special mixing screws, by using add-on mixing devices, by utilization of two or more extruders operating in tandem or as coextruders, etc. Refinements have been developed in feed preparation and feeding methods, including improved drying and premixing techniques, as well as downstream feeding of some formulation components (such as glass fibers).

The principal components of a single-screw extruder are illustrated in Fig. 9.18. The machine has a motor drive, a gear train, and a screw that is keyed into the gear-reducing train. The fluid layer between the screw flights and the barrel wall maintains the screw balanced and centered. Modern units are equipped with continuously variable speeds and electrically heated barrels. The barrel can be "zoned" according to the number of controllers or the heater bands. Depending on the application and type of service, the screw may be cored for heating or cooling.

The standard barrel (inside) diameter ranges from 12 to 600 mm. Larger extruders are available by special order. Standard screw has length-to-diameter ratio: L/D = 16–36, with $20 \leq$ L/D ≤ 24 being most common (feed length, 4–8D; transition length, 14–16D; and metering zone length, 6–10D). It has a single parallel flight, with pitch = 1D and pitch angle $\phi = 17.66°$. The flight width is usually about 0.1D; the channel depth in feed section is 0.1–0.15D. The channel depth ratio varies from less than 2 to 4. The compression ratio, CR, has been defined as a ratio of the screw flight volume at the entrance to that at the exit. The CR can be expressed as a function of the internal barrel diameter and external diameters of the screw as

$$
\begin{aligned}
CR &= \left[\left(\pi D_b^2/4 \right) - \left(\pi D_{s,feed}^2/4 \right) \right] / \left[\left(\pi D_b^2/4 \right) - \left(\pi D_{s,die}^2/4 \right) \right] \\
\therefore \ CR &= \left[\left(D_{s,feed} + H_1 \right)^2 - D_{s,feed}^2 \right] / \left[\left(D_{s,die} + H_1 \right)^2 - D_{s,die}^2 \right]
\end{aligned}
\tag{9.28}
$$

For the standard screw, CR varies from 1.5 (for rigid PVC) to 6 (for PA). The pressure generated at the die ranges from P = 70 to 200 MPa, or 10 to 30 kpsi. The rotational screw speed ranges from N = 20 (for rigid PVC) to 360 rpm (for PE).

There are three zones in the SSE: the solid conveying, the melting, and the melt conveying. In addition, there is the upstream (feeding) and downstream (cooling) zones. Owing to the importance of feeding to the extrusion process, it is appropriate to start with that zone.

Since SSE operates at the fully flooded conditions, the quality and throughput depend directly on the feed. **The feed zone** consists of a hopper or feed arrangement and a solid stock conveying region. Its purpose is to transfer a polymer from the feed hopper into the barrel, where it is initially compressed. This compression forces the air out from between the interstices of resin pellets or rubber chunks (air is expelled back through the hopper). It also breaks up lumps and polymer agglomerates, creating a more homogeneous feedstock that can be readily melted.
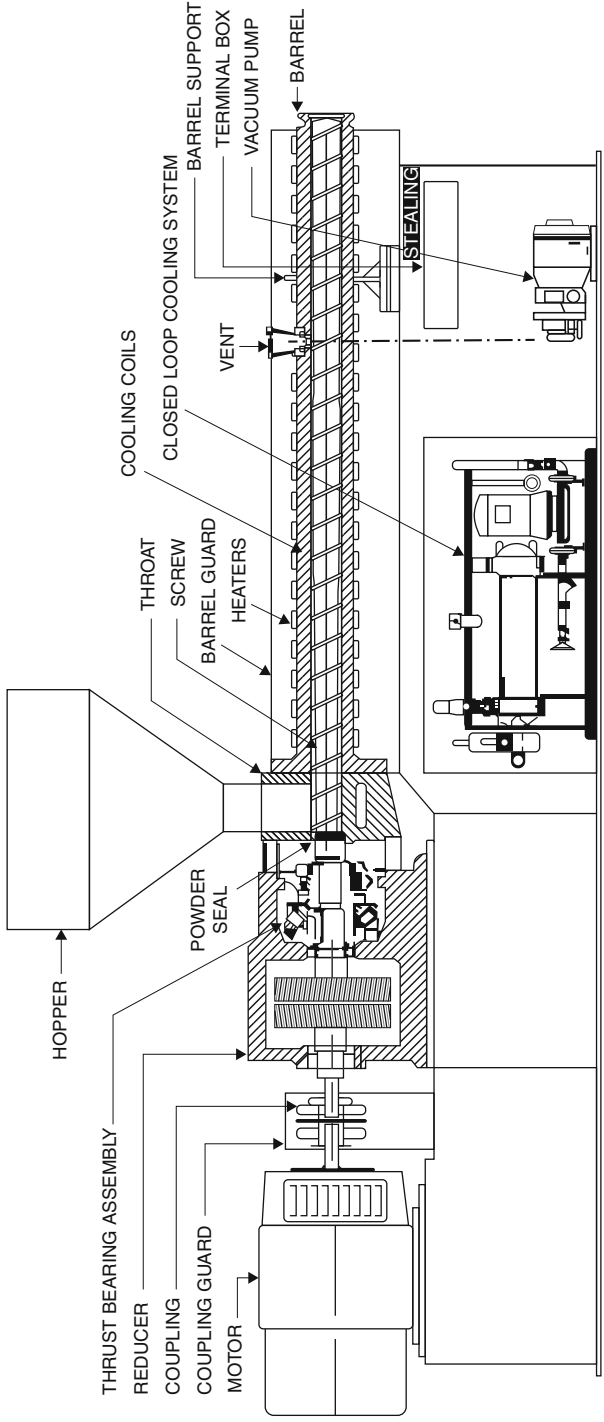
Fig. 9.18 Schematic representation of a single-screw extruder (SSE)

Flow in hoppers depends on their type (gravitational or forced), the bulk density of the material, the shape and location of the feed inlet (direct or tangential feed, straight or with a chamfer on the down-going side), as well as the type of screw and the barrel.

For good feeding, the flight volume in the feed zone must be as large as possible. Since the solids' conveying ability of an extruder depends on the ratio of the friction coefficients on the barrel and on the screw root, frequently grooved barrel (cooled by circulating cold water and thermally insulated from the rest of the barrel) is used in the feed zone. Its advantages are increased throughput, greater extrusion stability, and smaller effects of pressure variation at the die on the flow. For this, one pays by higher torque and pressure at the die and high wear and higher energy losses caused by the extra cooling.

The solid conveying zone begins at the feed inlet and extends to a point where the solid particles just begin to melt. The screw section is characterized by a deep flight between the root of the screw and the barrel wall. In most cases, the pitch (i.e., the screw length for a single turn of the screw flight) is 1D that means that the screw pitch angle is 17.66° (Darnell and Mol 1956). Here the solid bed is compressed and it moves forward as a plug. The flow causes the material to be compressed and to melt under the influence of frictional forces between the barrel surface and the solid plug. There are two important factors controlling these operations: the need to remove the entrapped air and to ascertain high friction coefficient on the barrel. Removal of air is an underrated activity that may seriously affect the performance of the extruder. Its importance depends on the type of feed as well as on the shape of the feed inlet. For powder feeding, a vacuum-assisted air removal may be required.

The melting zone follows the solid conveying zone. The purpose of this zone is to compress the solid bed and to provide intense friction between it and a barrel. Within this zone, the channel depth decreases, and the solid polymer coexists with its melt. In a SSE, this zone extends over a major part of the extruder: L(melt) = 10–14D. Melting is caused by the two principal forms of energy: the thermal, applied to the polymer by conduction from the external heaters through the barrel surface, and the mechanical converted to heat through friction and viscous dissipation. The friction coefficient of a polymer on the metal surface (f) depends of pressure (increasing P by a factor of 10 increases f by a factor of 3–4), temperature (for PE: $f = 0.6 - 0.002\ T°C$), and the sliding velocity. The effect of the friction coefficient ratio: f(barrel)/f(screw) is illustrated in Fig. 9.19. The conveying is controlled by the difference in the friction coefficient between the solid bed and either the barrel or the screw. It is important to maximize this difference.

Good balance of heating and shearing within this zone is crucial. For the heat-sensitive polymers such as PVC, too much shearing may cause degradation. For this reason, the frictional heat generation should be kept low by means of low screw rotational speed (N = 20–30 rpm). Good screw design should efficiently eliminate unmelted particles. Shallow screws and high pressure give better melting, but their throughput is relatively low and there are problems with scaling. Deep screws at
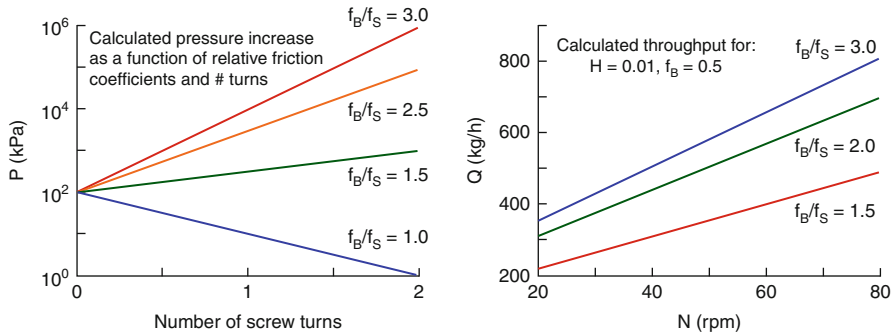
Fig. 9.19 Effects of the friction coefficient ratio on the pressure evolution within the feed zone (*left*) and on the throughput vs. screw speed (N)

low N provide better melt homogeneity and throughput stability at the cost of inefficient mixing. The best compromise seems to be high N and shallow screw.

The length of the melting zone should also take into account the type of feed as powder feeding requires a longer melting zone than pellets. However, vacuum-assisted removal of entrapped air significantly improves the melting rate and the melt homogeneity. The melting zone is particularly important for the generation of blends' morphology. The variation of temperature and high stresses encountered within this zone may profoundly affect the extrudate quality.

The melt conveying zone begins at the point where all solid particles are melted, and it extends to the outlet of the extruder; thus it encompasses the screen pack, the breaker plate, and the die. Once the resin is in the molten state, the extruder acts on it as a pump transferring and homogenizing the molten polymers and building up the pressure to the level required to force the material through a discharge nozzle or a die. SSE is capable of delivering up to 70 MPa or 10 kpsi of pressure.

In the classical approach to the mathematical modeling of flow through SSE, the screw and the barrel are unwound, the screw is assumed to be stationary, and the barrel moves over it at the correct gap height and the pitch angle, ϕ. Near the tip of the screw, there is the melt metering or the pumping zone, where the pressure builds up. In this region, the polymer melt is essentially homogenized and raised to the proper temperature for formation of the products.

Many types of screws have been developed. The screw configuration should be selected considering properties of the material being processed. A constant-pitch metering screw is usually employed in applications not requiring intensive mixing. Where mixing is important, for example, for color dispersion, a two-stage screw equipped with a letdown zone in the center of the screw is used. Mixing promoters can also be incorporated in the metering zone or near the tip of the screw (Gagliani 1991). Figure 9.20 shows two screws developed for improved dispersive mixing. All the material must pass through the narrow slit between the restriction and the barrel. To enter the slit, the material is exposed to an elongational flow field, while

Dray
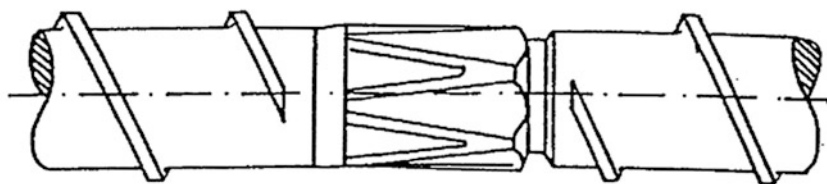
Blister ring
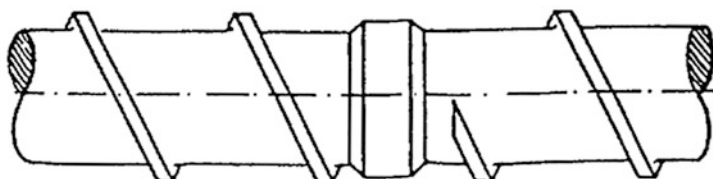
Fig. 11.20 Two SSE screws with restrictions designed to improve dispersive mixing

within the slit it is subjected to high shear stress. Many other screw modifications have been developed to enhance mixing. In some applications with two-stage screws, venting at the letdown section may be needed (Rauwendaal 1991, 2001).

The Buss Kneader is one of specialty SSE-type mixing extruders. The machine has relatively narrow residence time distribution and relatively low residence time. Here, the constant channel depth screw consists of interrupted flights and three rows of stationary pins in the barrel. During extrusion, the screw rotates and axially oscillates providing good self-wiping of the blades. This periodic reciprocation minimizes the material flow in one direction only. The intensive shearing strain is periodic and the gaps tend to reduce the effective shear stress. The large surface areas of exposed materials are a result of shear stresses generated by high torque. There is a good deal of distributive mixing during the high-stress dispersive process. The clamshell barrel design makes it easy to clean, service, analyze, and optimize the process. The machine is used for polymer blending, compounding of PVC formulations, preparation of engineering resins (with and without reinforcement), and extrusion of foodstuffs, carbon electrode pastes, etc. (Jakopin and Franz 1989; Anonymous 1989h).

By contrast with SSEs, the twin-screw extruders operate with partially filled screws. The polymers from a feeder are transported toward the pressure zone, usually created by a flow restrictor like a left-handed or reverse screw element. Under the pressure, the resins are compressed into a solid plug. The plug fractures and melts mainly by friction between the fragments of the initially compressed solid bed. The process is highly efficient. Its length can be as short as less than one diameter, $L \leq D$. There is evidence that melting in a TSE differently affects the generation of morphology than that in a SSE.

Twin-Screw Extruders (TSE)

Introduction to TSE

The first patent on the precursor of the TSE dates from 1869. However, the first commercial CORI for handling polymers was marketed 70 years later. Several intermeshing counterrotating twin-screw extruders (ICRR) were developed in the 1920–1930s. After the Second World War, the corotating, fully intermeshing TSE (CORI) started to dominate the field. Originally, CORI was developed for dewatering, devolatilization, and conduction of chemical reactions. The names of Meskat and Erdmenger are prominent on the early patent. The latter author is credited with designing the kneading blocks for the dispersive mixing, sometimes called "Erdmenger eggs." The prototype modular CORI was built by Werner & Pfleiderer (W&P) in 1955.

The non-intermeshing counterrotating TSE (CRNI) also dates from the 1920s when it was first designed by Ahnhudt for mixing and pumping rubbers and plastics. However, already in 1930, the Welding Engineers started to develop CRNI compounding extruders. In the 1950s, the company introduced a modular design. An excellent record of the TSE history is part of the monograph on the twin-screw extrusion (White 1990).

The TSE development work was completed by the mid-1950. The modular design of screws and barrel was universally accepted. The main types of screw elements (conveying forward, conveying backward, mixing, and neutral) were developed. Looking at the screw elements from dozens of TSE manufacturers, one must but note how similar they are. For example, the bilobal (egg-shaped) Erdmenger's mixing elements are universally popular. They provide high shear stress in the overflight (between the mixing element and the barrel) as well as in the direct intermeshing (between two mixing elements) regions. Many TSE manufacturers still insist that to control the dispersive-to-distributive mixing ratio, simply, the width of the mixing block should be used as a set of narrower blocks resulted in more distributive and less dispersive mixing.

TSEs are classified according to the following three categories:

Screw rotation	Intermeshing	Confinement
1. Corotating	A. Separated	a. Lengthwise closed or open (L-closed or L-open)
2. Counterrotating	B. Tangential	b. Crosswise closed or open (C-closed or C-open)
	C. Intermeshed	

In total, seven types of twin-screw extruders are on the market:
  I. **Counterrotating: not intermeshing (mostly tangential), L- and C-open (CRNI)**
 II. Counterrotating: partially intermeshing, L- and C-open (rare)
III. Counterrotating: partially intermeshing, L-open and C-closed (rare)
 IV. **Counterrotating: fully intermeshing, L- and C-closed (ICRR)**
  V. Corotating: not intermeshing, L- and C-open (rare)
 VI. Corotating: partially intermeshing, L- and C-open
VII. **Corotating: fully intermeshing screw, L-open and C-closed; disks, L- and C-open (CORI – the most popular)**

Table 9.9 Selected manufacturers of TSE

No.	TSE type	Manufacturer
1.	CORI – low-to-medium speed	Bandera, Colombo, Creusot–Loire, Ikegai, JSW
2.	CORI – high speed	APV, B&P Process Equipment, Betol, Berstorff, Clextral, Davis-Standard, Delaware Extruder, Egan, Ermefa, Farrel, ICMA San Giorgio, Ikegai, IKG, JSW, Kobe Steel, Leistritz, Mapré, Maris, Mitsubishi, OMC, Pomini, Reifenhäuser, Rockstedt–Farrel, Teledyne Readco, Theyson, Toshiba, Werner & Pfleiderer
3.	ICRR – parallel screws; high speed and long L/D	Amut SpA, Bandera, Battenfeld, Bausano, Clextral, Ermefa, Ikegai, JSW, KraussMaffei, Leistritz, Maplan, Mapré, Reinhäuser, Toshiba, Weber
4.	ICRR – conical (mainly for PVC profiles)	AGM, Anger, Cincinnati Milacron, Haake, JSW, Maplan, Mitsubishi, Toshiba, Weber
5.	CRNI – equal-length screws; high speed and short L/D	Bandera, Bausano, Bolling, Farrel, Davis-Standard, JSW, Kobe Steel, Leistritz, Pomini
6.	CRNI – non-equal screws	JSW, Welding Engineers

The three most popular types are indicated in bold. In Table 9.9 a partial list of TSE manufacturers is provided.

Whether the screws are open or closed lengthwise or crosswise, have a direct effect on the conveying capability, mixing, and the pressure buildup capacity of the system. For example, the non-intermeshing systems are open lengthwise and crosswise. Fully intermeshing, counterrotating systems can be closed lengthwise and crosswise. Here the material is locked in closed chambers (this is also the case for the screw pumps). The theoretically impossible systems are (i) lengthwise- and crosswise-closed CORI and (ii) lengthwise-open and crosswise-closed ICRR. Thus, CORIs are open lengthwise (normal screw flights are closed crosswise and staggered screw disks are open crosswise), while ICRR are lengthwise and crosswise closed.

A screw system lengthwise open has a passage from the inlet to the outlet of the apparatus. This means that material exchange can take place lengthwise along the channel. In a closed arrangement, the screw flights in the longitudinal direction are closed at intervals. It is important that the cross section of the screw channel be open in order for the material exchange to take place from one flight to the other in a direction normal to the screw channel. There is usually some leakage over the screw crests and through the areas required for the mechanical clearances.

The great advantage of TSEs stems from the modular design of barrel and screws. The manufacturers provide a diversity of the barrel elements (usually their length, L = 4D, sometimes 3D) that can be assembled in the configuration required for specific applications, viz.:
- Gland (or sealing) barrel
- Feeding barrel
- Standard-closed barrel

- Venting barrel
- Side feeder unit barrel
- Injection-sampling barrel
- Melt pressure barrel
- Mixing barrel, e.g., with hexagonal channel or profiled grooves
- Main gate barrel (a closing unit)

Similarly, the screws are assembled on shafts from selected elements. These are usually classified according to their functions into three categories: conveying, neutral (end or centering disks, screw tip), and mixing. There is again diversity of elements within each of these categories, the greatest being for the mixing type.

The conveying elements may differ in (1) the number of treads, (2) the helix angle or pitch, (3) the length, and (4) the thread direction (forward moving the material, or right handed, and back moving, or left handed). The elements are usually provided with a pitch angle of 14, 20, 28, and 42° and reversed −14 and −20°. As the pitch increases, the material is pumped faster, but at the same time, the dwell time and the conveying capability decrease. The conveying elements exercise very little shearing and mixing action of the transported material.

The mixing elements are available as individual elements or as their assemblies. There is a great diversity of these elements, for example:

- Perforated or slotted restrictor elements
- Compression elements
- Shearing elements
- Mixing turbines
- Multilobal elements (bilobal for CORI, tri- and hexa-lobal for ICRR)
- Polygon shifting elements
- Continuous mixing block
- Erdmenger's bi- or trilobal kneading blocks
- Low energy distributive vane mixers (usually the last elements before the screw tip, for homogenization of the melt within the highest pressure zone)
- Many others

The multielement kneading blocks are assembled of disks of different thickness (to adjust the ratio of dispersive-to-distributive mixing) and displacement angle (see Table 9.10). Blocks constructed from the same number of elements but of different thickness also behave differently. Wide disks provide much greater sharing action than the narrow ones; i.e., the former provide dispersive mixing while the latter the distributive one. As the disk thickness in the block decreases, its conveying capability increases.

Main Types of TSE

Out of the seven types of twin-screw extruders, the following three are of principal interest (in order of increasing commercial importance): **intermeshing counterrotating (ICRR), counterrotating non-intermeshing (CRNI)**, and **corotating intermeshing (CORI).**

Table 9.10 Effect of the twist angle on the performance of a block made of six Erdmenger's kneading disks

Angle (°)	Mixing	Shearing	Conveying
+30	Low	Low	High forward
+60	Medium	Medium	Medium forward
+90	High	High	Nil
−30	Highest	Highest	Medium backward

Table 9.11 Specifications JSW TEX TSE (Japan Steel Works, 2013)

Model	D (mm)	N (rpm)[a]	Torque (Nm)	Drive (kW)
30 α	32	2,500	401	22
44 αII	47	1,750	1,520	90
54 αII	58	1,450	2,863	185
65 αII	69	1,150	4,803	250
77 αII	82.5	950	8,235	450
90 αII	96.5	850	13,159	750
105 αII	113	710	21,169	1,500
120 αII	129.5	620	31,817	2,000
140 α	152	440	42,953	1,980
140 αII	152	440	51,544	2,375
160 α	174	300	64,277	2,000
160 αII	174	300	77,072	2,400
180 α	196	300	92,089	2,875
180 αII	196	300	110,507	3,450
200	218	270	115,338	3,250
200 αII	218	270	138,406	3,900
230 α	251	270	178,972	5,050
250 α	274	270	230,676	6,500
280 α	308	270	326,128	9,200
305 α	335	270	421,580	11,900
350 α	387	240	640,324	16,100
400 α	443	215	963,400	21,700

[a]Maximum speed reported

For many years, CORI has been the universal compounder of choice. It operated at higher screw speeds with longer barrel than ICRR, advantageous especially for the reactive processing. However, several manufacturers of these two types of extruders demonstrated that unbiased test results frequently show better performance of ICRR as far as the compound quality and the throughputs are concerned. Even at lower screw speed, ICRR frequently outperformed CORI. This resulted in interest in redesigning ICRR. Tables 9.11 and 9.12 list specifications from JSW and American Leistritz, respectively, for their standard machines that can be operated either as co- or as counterrotating, fully intermeshing TSE. Since these

Table 9.12 Specifications of ZSE MAXX TSE (American Leistritz, 2013)

Model	D (mm)	N (rpm)[a]	Torque (Nm)
ZSE-18	18.5	1,200	71
ZSE-27	28.3	1,200	304
ZSE-40	41.1	1,200	1,128
ZSE-50	51.2	1,200	2,144
ZSE-60	61.9	1,200	3,750
ZSE-75	77.5	1,200	7,324
ZSE-87	90.0	1,000	11,432
ZSE-110	113.7	600	22,982
ZSE-135	139.3	500	42,150
ZSE-180	178.8	400	91,460

[a]Maximum speed reported

manufacturers provide a diversity of processing equipment, they neither have a bias toward one of these types of machines, nor they pretend that one type can do all operations equally well as for certain applications CORI may be better than ICRR and vice versa. However, it is important to recognize the enlarged selection of the compounding equipment available on today's market.

Counterrotating Non-Intermeshing (CRNI)

Originally developed for natural rubbers, foodstuffs, and elastomers, at present these machines are used as a *stirred tank reactor* or a *twin-rotor continuous mixer*. Their bearings are exposed mainly to radial, not axial, forces. By using one screw longer than the other, one can separate the mixing and pumping functions.

In CRNI the material flow is based on a drag, not positive pumping. There is a low shear stress field, responsible for the absence of dispersive mixing. However, the interchange of material between the screws provides good distributive mixing. The chemical reaction proceeds on the continuously renewed surfaces, related to reorientation of the laminar flow patterns and the total strain. CRNI is well suited for the polymerization of miscible, low-viscosity systems, viz., polymerization of monomers, grafting, halogenation, and PP-*visbreaking* (degradation by the addition of organic peroxides). The main advantage of CRNI is long enough residence time, sufficient to complete slow reactions. The molecular weight of the generated polymer was found to be virtually independent of Q and N. Mild mixing during compounding prevents the mechanical degradation of elastomers as well as of crushing glass micro-balloons.

CRNI can offer larger outputs and more interchange of material between the two screws than the other type TSEs. These machines are frequently used for the preparation of composites with fibrous fillers. In general, the closer the clearances and intermeshing the more rapid the buildup of pressure. The narrower the lands and the larger the clearances between the screws, the greater the longitudinal mixing (Wood 1979, 1980).

Intermeshing Counterrotating (ICRR)

ICRR was developed as a positive displacement screw pump for viscous, difficult fluids (coal-oil, ceramic, or rubber compounds). This is the only TSE type that is fully, axially and radially, closed. The extrusion speed depends on the intermeshing geometry and the screw speed. The fully intermeshing ICRR has narrower distribution of residence times and better precision in controlling rapid reactions between liquid reagent and molten polymer than a CORI. The low-speed ICRRs have been used for PVC compounding and forming. At higher screw separations and speeds, the machines can be used for the incorporation of high-viscosity toughening elastomer. For example, ICRRs have been used for the reactive extrusion of ABS.

During the 1990s, there has been a significant progress in making ICRR fully competitive with the more popular CORI. This has been done by opening the calendering gap and moving the shearing action toward the barrel. While the older ICRR operated at the maximum screw speed of 150 rpm, the new ones can turn at least at 500 rpm without excessive gap pressure. For some applications, ICRR offers unique advantage of strong extensional flow field, able to disperse high-viscosity ingredients in a low-viscosity matrix.

Corotating Intermeshing (CORI)

These are the most popular and commercially important twin-screw extruders. The machines were originally developed in the 1860s for pumping stone paste. Their advantage arises from the movement of the intermeshing surfaces in opposite directions; thus the melt-free surface is continuously renewed and the screws clean each other. In addition, since at the intermeshing the material passes from one screw to the other (change of the drag direction), there is low probability that the material would go through the gap. Thus, there is no calendering pressure that may cause the screws to bend (a possibility for the ICRR machines). This in turn permits to use higher screw speeds and longer barrels. In 1938 CORI was used for the polymerization of butadiene and PA-6. The latter resin was commercialized by I. G. Farbenindustrie in 1939.

During the 1950s and 1960s, the design criteria for these extruders were:

1. Incorporation without degradation
2. High shear stress for dispersing
3. Homogenization of materials with different viscosity
4. Uniform stress and heat history
5. Precise control of mixing process

The present tendency in CORI development is to (1) maximize throughput from the given size machine by maximization of the *extruder free volume* or the OD/ID screw ratio, (2) provide capability to efficiently transmit the required amount of power into the material, and (3) increase the extruder speeds. The modern machines from Werner & Pfleiderer are supplied with OD/ID = 1.55, those from Berstorff with 1.74 (for reactive compounding and degassing). The latter company also developed several mixing elements (*turbo* or *gear mixers*) well suited for mixing resins with different viscosities. Smaller industrial CORI machines are available from JSW with the screw speed of $N \leq 1,500$ rpm. Similar speeds are also offered

by Werner & Pfleiderer. There is also talk in the industry of superfast extruders operating at 3,000 rpm. Maris increased free volume of their 58 mm extruder from 84 mL/D to 103 mL/D, an increase by 23 %. To make use of this extra throughput capability, the machines must have high torque capabilities.

Screws are available with 1, 2, or 3 screw flights; the first has the highest solid conveying capacity (used mainly for feeding powders). Two-flight screws have large free volume per unit length and low average shear rate. They are mainly used for processing temperature-sensitive materials. The three-flight screws are used when high shear stress is required. CORIs are efficient in alternating the direction of applied stresses, providing distributive mixing by lamellae folding, as well as controllable shearing (dispersing mixing). They are operated in starve-fed mode that demands high-performance feeders. The material transport mainly depends on drag flow, with only local contribution from the screw pumping in the so-called pressure zones. The maximum conveying is achieved when the screw pitch is equal to screw diameter. CORIs are used for compounding, polymerization, and devolatilization.

CORIs are the prime machines for polymer blending and reactive extrusion (Brown 1992). They have been used as reactors for the addition polymerization (polyacrylates, SAN, S-MMA, PA-6, POM, or TPU) and for the polycondensation (PA-66, polyarylates, PEST, PEI). Polymer grafting (polyolefin + silane, maleic anhydride, acetic anhydride, etc.) and mechanical and chemical degradation of polypropylene have also been carried out.

The reaction is usually conducted within the pressure zone (in a kneading block section). This section is followed by left-handed (reversed) elements that control the residence time within the pressurized section. Devolatilization (removal of the reaction by-products) is usually carried out immediately following the left-handed screw section. The *sliced screw mixing elements* provide gentler mixing than the kneading ones (now two-lobed, not three-lobed). There is a trend toward development of an *intelligent compounding plant*, where the polymerization, compounding, and shaping will be carried out in sequence.

Comparison of CORI and ICRR TSE Performance

There are several publications dealing with the comparison of efficiency of compounding, mixing, or reactive extruding in different types of extruders. Most of these studies suffer from the same aspect: the evaluated machines were not operated at a comparable level of performance efficiency. A summary of the reported observations is given in Tables 9.13 and 9.14.

Historically, the corotating geometry has been preferred by the plastic industry, as having more even distribution of stresses, providing easier control of compounding, and operating at higher screw speeds and throughputs. The counterrotating TSEs were known as the "calendering" extruders, with high stresses existing between the two screws and low stresses outside. In ICRR, owing to the high calendering pressures, the screws could rub against the barrel causing premature wear. Thus, shorter barrels, slower speeds, and large intermeshing gaps have been recommended. One of the advantages of these machines has been the presence

Table 9.13 Advantages and disadvantages of CORI- and ICRR-type TSE

Extruder	Advantages	Disadvantages
Corotating, intermeshing, CORI	Self-cleaning	Capital cost
	Dispersive and distributive mixing in transverse and longitudinal direction	Only residence times below about 10 min are economic
	Lower than in ICRR, uniform and controllable stress	Limited ranges of pressure and vacuum are available
	Good control of resin degradability	
	Local pressure control	
	High screw speeds and throughputs	
	Local high-vacuum possibilities	
	Double-walled barrel for rapid temperature changes	
	High specific energy input possible	
	Residence time up to one hour	
Counterrotating, intermeshing, ICRR	Self-cleaning	Transverse mixing is moderate
	High dispersive mixing in the shear and extension	Longitudinal mixing is poor
	It can accommodate multilobal mixing elements of the gear type with excellent dispersive mixing capabilities	Only residence times below 10 min are economic
	It has better specific energy than CORI	Limited screw speed
	It has narrower residence time distribution than CORI	Capital cost
	High local pressures possible	
	High local vacuum possible	
	Better devolatilization capability than CORI	
	High specific energy input possible	
	Shorter screws than in corotating	
	Easy separation of desired functions like mixing, devolatilization, chemical reaction, compounding, etc.	

of the elongational flow field within the calendering zone. The machines have been successfully used in numerous applications requiring high dispersive stresses.

There has been renewed interest in upgrading the TSE performance. This was spurred by the advances in the theory and methods of analysis of elemental contributions. The analysis resulted in modification of the screw profiles (higher free volume of the process), separation of screws that made it possible for CORI and ICRR to operate at the same screw speeds, as well as development of new mixing (or kneading) elements (American Leistritz 1996). The increased free volume (thus slender screw profile) resulted in lowering the average shear rate; thus the screw speeds needed to be increased, hence higher power/torque motors, which in turn

Table 9.14 Comments on CORI vs. ICRR performance

CORI	ICRR	Reference
Better control of shear and of mixing than in ICRR	Less efficient control of shear and of mixing than in CORI	Murray 1978
Broader distribution of residence times and slower melting and cleaning but better for dispersing glass fibers. For the same screw speed and throughput, higher melt temperature was obtained (an indication of not-optimized screw configuration)	Narrower distribution of residence times, better dispersing agglomerates of small particles, and faster cleaning time (of TiO_2 trace). Owing to periodic compression–depression effects, better devolatilization can be obtained	Sakai 1978; Sakai et al. 1988, 1992
Material transfer from one screw to another, axially open extruders. Melt is conveyed by frictional forces, allowing for partially filled melting zone	There is no transfer of material from one screw to another; closed C-shape chambers are developed. Melt flow is plug type. Materials see a wide range of pressures	Herrmann and Burkhardt 1981
Screws suspended in melt allow for high rotational speeds. In an axially open system, the pressure is controlled by purposely placed restrictions: either left-handed side screw, valves, or die. Material is compressed by the first screw and conveyed to the other. The melting process is similar to ICRR, but particle-to-particle rubbing makes it more efficient	Pressure within the calendar gap forces the screws to rub on the barrel. Low screw speeds must be used. Calendering gap problems are exacerbated in the feed region, leading to severe wear. The melting process is similar to that in single-screw extruders. Unmelted particles are observed in the discharge	Herrmann and Burkhardt 1981
Broader distribution of residence times, better distributive mixing, and better for blending	Better pumping capability, dispersion of small particles, and devolatilization	Rauwendaal 1981
Higher screw speed and output than the ICRR. Corotating extruders are especially suitable for reactive processing	Calendering leakage results in high lubrication pressure which in turn forces the screws apart, causing barrel abrasion. High calendering pressure causes mechanical degradation of polymers	White 1990
Polyethylene/polyamide-11 blend was compatibilized by radical copolymerization using diverse organic peroxides	The best performing material was obtained using corotating fully intermeshing machine	Lambla and Seadan 1993
At N = 400 rpm comparative blending produced lower throughput and poorer quality. Produced the same maximum lubricant concentration at different output. More aggregates than in ICRR	At N = 400 rpm comparative blending produced higher throughput at lower T and better quality. Higher maximum lubricant concentration achieved at higher power consumption	Thiele 1995
Final morphology is the same in both CORI and ICRR	Melts and mixes faster for a blend of HDPE and PS. Phase morphology develops faster along screw length	Cho and White 1996
For blends of PP with Al flakes, larger distribution of residence time due to backflow	ICRR has shorter residence time due to near plug flow	Shon et al. 1999

(*continued*)

Table 9.14 (continued)

CORI	ICRR	Reference
For blends of PP with glass fibers, fiber breakup is highly dependent on their feeding position and screw configuration	Same as CORI, but final fiber length is shorter	Shon and White 1999
For the polymerization of caprolactam, broadest residence time distribution. Conversion depends on residence time at low flow rate (1 kg/h) but almost independent at high flow rate	Lowest average residence time. Conversion change is highly dependent on residence time	Lee and White 2001
For blends of SEBS with graphite powder, CORI produced better mixedness. Volume resistivity is higher for the final composites	Similar maximum pressure for both configurations. Narrower residence time distribution	Erol and Kalyon 2005

improved the throughput. New kneading and mixing elements have been designed to improve either the distributive or dispersive mixing. To the first category belong the turbine-and-gear mixing elements (ZME, SME, or TME from Werner & Pfleiderer).

The intermeshing TSEs have self-cleaning screws. The material that adheres to the screw root may degrade and eventually fall off and be carried out with the product, showing up as contaminants (Wood 1979, 1980; Salden 1978). Self-cleaning action is achieved in both counterrotating and corotating screws, through an opposite roll-off or the wiping motion. The calendering flow does not take place in CORI, and a more efficient and uniform self-cleaning action is achieved.

In CORI the material is transferred from one screw to another in a tangential path (Salden 1978). Here, edges of one screw crest wipe the flanks of the other screw with a tangentially oriented, constant relative velocity. There is a high relative velocity and hence sufficiently high shear velocity to wipe the boundary layers.

In ICRR the roll-off process between the screw crest and screw root and between the screw flanks simulates the action of a calender. The necessary shear velocity required to wipe the boundary layers is proportionately lower because of the low relative velocity. Counterrotating screws require greater clearances between them since their mode of action is rather like a two-roll mill, passing material through the nip between them (Schoengood 1973). The material is drawn into the roller gap and is squeezed onto the surface. Consequently, ICRR has less efficient self-cleaning action.

The shear stresses and their distributions are higher in ICRR than in CORI. In the former it only depends on the screw pitch, while in the latter the shear stress distribution changes with the pitch angles, the throughput, and the screw speed. In addition, the flow pattern in these two types is different, with a higher radial flow in ICRR.

CORIs are used for the reactive processing, compounding of alloys and blends, color masterbatches, and fiber-reinforced composition. The quality of the

product critically depends on the selection of screws and their configuration. However, optimization of screw configuration and operating conditions remains an art.

TSEs are indispensable in several applications like reactive processing, high devolatilization, high additive loading, and/or intensive dispersive melt mixing. Furthermore, they are the preferred extruders for high throughput lines with the extrusion rates exceeding 10 t/h.

Table 9.13 summarizes the relative advantages and disadvantages of the intermeshing co- and counterrotating TSE (respectively, CORI and ICRR). A summary of published comments about the advantages and disadvantages of ICRR in comparison to CORI is provided in Table 9.14.

Comparison Between SSE and TSE Performance

Within TSE the shear and extensional stresses are generated by virtue of interactions between two screws. The degree to which this occurs depends on the relative direction of the screw rotation (co- or counterrotating), shapes of the screw elements, the degree to which they intermesh, and the rotational speed of the screws (Fisher 1958; Matthews 1962).

Conventional TSEs are claimed to be superior to SSE as compounders because they can provide (Adams 1974; Murray 1978; Wood 1979, 1980; White 1990):

1. Better feeding and more positive conveying characteristics
2. Shorter residence times and narrower residence time distribution
3. Improved kinetics and melt temperature control
4. High and controlled deformational stresses
5. Positive pumping action
6. Reduced melt slippage
7. Self-wiping action
8. Lower power consumption
9. Generation of high extrusion pressures with a short backup length

Table 9.15 summarizes these differences. The extrusion characteristics are given in Table 9.16.

TSEs have also drawbacks, the main being their cost. Owing to complex design of the screws and the thrust bearings these machines are more expensive than SSE (Prause 1967, 1968; Gras 1972). Furthermore, they are susceptible to quick overloading. The low bulk densities of preblends influence the throughput rate and the die pressure.

Mechanically, a major difference between SSE and TSE is the type of transport that takes place within the extruder. The material transport in the former is drag-induced: frictional drag in the solid conveying zone and viscous drag in the melt conveying zone. There are many materials with unfavorable frictional properties that cannot be fed into a SSE without getting into severe feeding problems. On the other hand, the transport in an intermeshing TSE is by positive displacement. Its degree depends on how well the flight of one screw closes the opposing channel of the other screw. The most positive displacement is obtained in a closely intermeshing, counterrotating geometry.

Table 9.15 Fundamental differences between single (SSE)- and twin-screw extruders (TSE)

Function	SSE	TSE
Degree of channel fill	Fully filled	Partially filled
Throughput (Q) is determined by:	Screw speed, N	Feed rate
Total strain	Independent of Q and N	Dependent on Q
Shear strain	Low	High, controllable
Material transport	By friction (drag flow)	Positive conveying
Material flow path	Smooth, regular thinning	Tortuous, diverse
Heat transport	Ineffective	Effective
Liquid and powder additives	Present problems	Do not present problems
High-viscosity additives	Impossible to disperse	Can be dispersed
Mixing capability	Poor	Good, adjustable
Extruder length for melting	Long	Very short
Extruder length for mixing	Long	Short
Advantages	Easy to make, inexpensive, theoretical description of its function well developed, a lot of experience	High flexibility (modular design), effective feeding, devolatilization, mixing, reactive processing
Disadvantages	Lack of flexibility, poor feeding characteristics, ineffective devolatilizer and mixer, not suitable for reactive processing	Difficult fabrication, cost up to 10x that of SSE, early stage of the theoretical analysis, poor back mixing (narrow residence time distribution), require accurate feeders

Another difference is the velocity profiles in these machines. In SSE these are well defined and fairly easy to describe. The situation in TSE is considerably more complex. The complex flow patterns have several advantages, such as good mixing and heat transfer, large melting capacity, good devolatilization capacity, and control over the stock temperatures. The theory of TSE is not nearly as well developed as that of SSE.

The extruders are assumed to be nominally "once through equipment." This implies that preblending, or bulk mixing, is essential for good mixing. In SSE that operates under the flooded conditions, feeding is often difficult and preblending

Table 9.16 Summary of extrusion characteristics for SSE and TSE

Function	Single screw	Twin screw	
		Counterrotating	Corotating
Flow mechanism	Continuous shear	Discrete c-sections, lengthwise and crosswise closed	Figure of eight; more uniform shear history for all flow elements
Stress field	Shear in the overflight and in the channel	High shear and elongation in the calendering gap, low in channels	Uniform stress field, mainly shear; convergent–divergent flow in mixing blocks
Conveying	Drag flow	Positive conveying	Less positive conveying
Pumping efficiency	Variable	Good, positive	Good
Die pressure	High	Low	Lowest
Die restriction	Often severe	Smaller effects	Smaller effects
L/D ratios	>20	16–40	Various
Compression	Decrease channel	Various designs	Various designs
Air entrapment	Possible	Possible, thus larger clearances	No
Screw speeds	20–100 rpm	500 rpm	Up to 1,500 rpm
Heating mode	High proportion by shear	Controllable low shear	Near-adiabatic
Residence time	Large spread-wide distribution	Narrow distribution, often easy to control	Wider distribution at high die pressures
Pressure in the gap	Low	High, thus possible wear	Low, effective self-wiping

may be necessary. In counterrotating tangential TSE, the degree of fill is low and feeding is relatively easy (provided that feeding devices have sufficient accuracy). Thus, uniform product quality is obtained by feeding separate streams either at the same or sequentially into various axial locations.

Most TSEs are of a modular design, having removable screw and barrel elements. The screw design can be altered by changing the sequence and type of the screw elements along the shaft. In this way, almost an infinite number of screw configurations can be put together. The modular design, therefore, creates great flexibility and allows careful optimization of screw and barrel geometry to each particular application. This flexibility is not available for SSE.

The modular design of TSE makes it possible to adjust the relative magnitude of the distributive and dispersive mixing. The shear stress in normal melt pumping SSE channels is not sufficient to provide adequate dispersive mixing. Similarly, the laminar flow through SSE channel is not sufficient to distribute the flow elements having different performance characteristics. Often, high shear stress mixing devices, such as modified screw, screw torpedoes, or external high energy planetary roller mixers, are required. For the distributive mixing, a static mixer may be inserted between the end of the extruder screw and the extrusion die.

The modern technology often requires that TSE performs a series of different functions. Owing to limitation of L/D, even these universal machines may profit from additional, external, either dispersive or distributive mixers. These devices are discussed in the following parts.

There are 12 criteria for the economic, high-quality compounding (Herrmann 1988):

1. Sound fundamental design principles of the compounding machine
2. Flexibility of operation
3. High screw torque
4. Appropriate selection of the screw elements
5. A balanced combination of the high-shear dispersive and low-shear distributive screw elements
6. Low pressure at the die
7. Reliability of components and parts
8. Long lifetime of parts
9. Reliable feeding/dosing equipment
10. Reliable granulation method
11. Automation of the process
12. Online quality inspection and closed-loop control

Flexibility and user friendliness are the key words for many extruders (easy-to-use control systems and displays, quick access for repair, and quick changeover). Several of the new machines feature segmented barrel, the ability to change screw-rotation direction, and the ability to be modified in place (to compound, to extrude a product, or to recycle plant scrap).

Other Mixing Devices

Planetary Roller Extruder

In these extruders, six or more evenly spaced planetary screws revolve around the circumference of the central or so-called "sun" screw. The planetary screws inter-mesh with the sun screw and the barrel. The planetary barrel section has helical grooves corresponding to the helical flights on the planetary screws. This section is usually a separate barrel with a flange-type connection to the feed barrel section.

In the first part of the machine, before the planetary screws, the material is processed as in a SSE. As the plasticated composition reaches the planetary section, it is exposed to intensive mixing by the rolling action between the planetary screws, the sun screw, and the barrel. The helical design of the barrel, sun screw, and planetary screws leads to a large surface area relative to the barrel length. The clearance between the planetary screws and the mating surfaces is about 1/4 mm. This allows thin layers of the compound to be exposed to large surface areas, resulting in effective devolatilization, heat exchange (thus good temperature control), and efficient mixing.

The planetary roller extruders are mostly used for processing heat-sensitive compounds like rigid or plasticized PVC formulations (Anders 1979; Collins 1987). The planetary roller section can also be used as an add-on mixer to SSE to

improve the mixing performance (Rust 1983; Huszman 1983). Degassing and addition of fillers or reinforcements into melt has also been carried out.

Multi-Screw Extruders (MSE)

Over the years, several extruder designs have been proposed using more than two screws. This concept is not new and has been around for over 40 years (Hanslik 1972). Nevertheless, several developments have been done over the years (Eckart et al. 2011). The main idea is to improve mixing and have better control on residence time and for process intensification, i.e., performing several tasks in a single step. These machines are also used for solvent removal (Gras 1972; Gras and Eise 1975). Flash devolatilization occurs in a flash dome attached to a barrel. The polymer solution is delivered under pressure and at temperature above the boiling point of the solvent. The solution is then expanded through a nozzle into the flash dome. The foamy material resulting from the flash devolatilization is then transported away by the four screws. In many cases, downstream vent sections are also used to further reduce solvent content. It is also reported that MSE (12 screws) have better control over elongational strains leading to better mixing efficiency (Loukus et al. 2004).

Disk Extruders

There are several extruders that do not use an Archimedean screw for transportation of materials, but still belong to the category of continuous extruders. These machines are sometimes referred to as screwless extruders. Usually they employ a disk or a drum. Most disk extruders are based on a viscous drag transport principle. To this category belong stepped disk extruders (Raleigh 1879; Westover 1962), drum extruders, spiral extruders (Ingen Housz 1975), disk pack extruder (Tadmor 1979, 1980; Tadmor et al. 1979, 1983; Hold et al. 1979; Valsamis 1983), and many others.

A disk pack (Tadmor and Gogos 1979) has the inherent capability of performing the elementary steps of plastic processing by combination of differently shaped rotating disks in a drumlike housing. The wiping action is provided by stationary channel blocks that cause the material to transfer from one disk-gap to another. Melting, laminar mixing, venting, and the pumping functions are all separated. Disk pack has been used for reactive processing, blending, compounding, mixing, and devolatilizing (Tadmor et al. 1983). The devolatilization capabilities are limited in comparison to TSE. The mixing capability and die pressure are influenced by:

1. Method of feeding
2. Disk diameter
3. Gap between disks
4. Shape and size of the feeding zone
5. Diameter and length of discharge
6. Hydraulic resistance of forming device
7. Viscoelastic properties of the melt
8. Shape of material particles

Elastic Melt Extruder (EME)

In EME the polymer is sheared between two plates, one stationary and one rotating. The extruder makes use of the viscoelastic properties of polymer melts. When a viscoelastic fluid is sheared, the normal stresses develop in the fluid, trying to push the shearing plates apart. Thus, leaving a hole in the center of the stationary plate makes it possible for the melt to flow continuously from the rim toward the center then out (Maxwell and Scalora 1959; Blyler 1966; Fritz 1968, 1971; Macosko and Starita 1971; Kocherov et al. 1973; Good et al. 1974).

The EME mixers have been used for mixing and extruding plastic formulations. Despite the relatively low pressures (0.3–0.7 MPa) in many applications (melt blending and incorporation of carbon fibers), EME was found superior to the screw-type extruders. The machines provide good mixing and melt homogenization at short residence time (for a unit with 150 mm disk diameter and a capacity of 25 kg/h, the average residence time is about 15 s). EME is two to three times smaller than screw-type extruders of similar capacities. The flow is laminar dispersive, preferentially generating co-continuous blend morphology leading to good performance (Thornton et al. 1980). Unfortunately, neither the original EME nor its modifications found a general acceptance in the plastic industry (Westover 1962; Frederix 1978; Michaux 1979).

Ram Extruders

The ram extruders are divided into (1) single-ram extruders that operate discontinuously (Berzen and Braun 1979; Zachariades et al. 1979; Sperati 1983) and (2) multi-ram extruders that offer a continuous flow of materials (Westover 1963; Yi and Fenner 1975).

FN-Plastifier

This is a short (L/D = 5) single-screw extruder, developed for polymer blending and recycling, with a three-start screw extended from the feed zone 2/3 over the screw length. The frontal part of the screw is smooth ending with a flat disk. The material is transported and partially fluxed by the grooved part of the screw and barrel. The pumping is assured by the normal stresses between the flat part of the screw end and the die (Maxwell–Scalora's EME principle). The short screw assures short (and narrow distribution) residence time. Large thrust bearing makes it possible to control the die gap, thus the magnitude of the normal stresses, hence morphology and performance (Frederix 1978; Michaux 1979; Anonymous 1981).

The extruder was developed by Patfoort and then licensed to Fabrique Nationale (FN) Herstal, SA (Patfoort 1976; Fabrique Nationale Herstal 1977). The machines were found to be particularly suitable for recycling commingled polymers from municipal waste streams. Under high stresses developed between the smooth part of the screw and the barrel, the free radicals were generated compatibilizing in situ the polymeric mixture. The usual product was of the "plastic wood" type. It had excellent mechanical performance characteristics. The FN plastificator was used for recycling by the city of Liege and other parts of Europe and then exported to China under the UNIDO program. However, FN discontinued manufacturing these machines.

Several other machines of this type have been developed since. They all involve intensive mechanical shearing that produces extensive chain scission. Recombination of the free radicals in situ generates sufficient concentration of copolymer, to compatibilize the system. The generated-under-high-stress, nonequilibrium morphology is then locked by quenching. Best performance has been observed for systems with co-continuous morphology.

Gelimat, K-mixer, and Homomicronizer

The residence time in the discussed above Patfoort's extruder is $7 < \tau < 25$ s (Patfoort 1976). The machine was originally designed for the extrusion of the thermally unstable resins, in particular PVC. For similar applications, Carlew Chemicals developed its *Gelimat*, latter renamed *K-mixer* (K- for the kinetic energy) (Crocker 1981). The mixer uses high-speed rotor with staggered blades mounted on a horizontal shaft at different angles. The number and position of the blades vary with the mixer size. The mixing is carried out at the blade tip velocity of 30–45 m/s. There is no external heating as the kinetic energy generated by the particles impacting on each other and the mixer elements produces sufficient heat to flux the material within 8–150 s. Once the material reaches the desired temperature, the infrared sensor activates the bottom doors of the chamber. The discharged dough can be either fed to a short screw extruder or passed between rolls and diced. The mixing is batch-type. However, with two *Gelimat* units each providing a load of plastified resin every 10 s or so, the downstream operation (calendering) is continuous.

When preparing polymer blends, the starting resins should have similar particle size and dimensions. There is an obvious advantage of using fine powders. The high stresses developed during the plastification are often sufficient to generate compatibilizing copolymers. Similarly like in the Patfoort extruder, here also good performance of antagonistically immiscible polymer blends was obtained.

Newplast developed a recycling process line that is based on a *homomicronizer* which is a machine similar to *Gelimat* or *K-mixer*. The unit has short, stubby radial blades attached to a horizontal shaft that rotates at high speeds, melting and homogenizing the postconsumer waste within 35–120 s. The blades are of two types, pushing the material away from the side walls toward the center of the cylindrical mixing chamber. The clearance between the blades and the chamber wall is 0.5–1.0 mm (Dubrulle D'Orhcel 1996; La Mantia et al. 1996).

Mixing or *Calendering* Rolls

The mixing rolls subject pastes and deformable solids to intense shear by passing them between smooth or corrugated metal rolls that revolve at different speeds. The principal design consists of two horizontal rolls or cylinders, arranged side by side and rotating toward each other at different speeds. The ratio of the peripheral roll speeds (known as the function ratio) ranges from 1 to 2, but it is usually about 1.2. The rolls' temperature is controlled by circulating oil. The higher friction ratio leads to greater heat generation. Friction, speed, sizes of the rolls, and gap between them influence the material temperature and the intensity of mixing.

Usually, the results obtained from one unit are specific to this machine and cannot be applied to a different one.

The material enters the mixing rolls in a form of lumps, powder, or friable laminates. As a result of rotation, adhesion, and friction, the material is entrained into the gap between the rolls, and upon discharge, it sticks to one of them. In batch mixing, the mass after loading passes through the gap between the rolls several times. In continuous mixing, the mass enters continuously from one side of the machine and passes between the rolls in rotational and forward motion along the unit's axis. The mixed material is continuously discharged in form of a narrow strip. Both the shearing action and entertainment of material into the gap are important to the mixing process and transporting the material through the unit.

Ribbon Blenders and Planetary Mixers

There are a number of design variations of this type of machines, with differences primarily in the agitator configuration. Ribbon blenders are essentially self-contained mixers best suited for batch or semicontinuous mixing. They are mainly used for preblending like dry mixing a composition. The continuous ribbon agitator is standard, with inner and outer ribbons that may be arranged for center or end discharge.

Planetary mixers are well suited for a wide range of liquid and solid applications. Double planetary mixers consist of two regularly shaped stirrer blades revolving around the tank on a central axis. Each blade also revolves on its own axis at approximately the speed of the central rotation. With each revolution on its own axis, the blade advances along the tank wall. This movement ensures good homogeneity of the material within a short time. Double planetary mixers have no packing glands or bearings within the product zone, thus cleaning between batches is relatively simple.

Emulsifiers and Blenders

Mixer emulsifiers are sometimes used as an alternative to slow-speed impeller mixing or high-pressure homogenization for a wide range of processing requirements. These mixers are normally used in dished or conical-bottom vessels.

Internal (Blade) Mixers

The internal mixers are used for kneading and mixing accompanied by either heating or cooling. The operation involves compressing the fluid mass, folding it over, and then compressing it again. The material is usually torn apart by high shear stresses engendered between the moving and stationary elements.

The mixing is performed using two Z-shaped blades rotating in opposite directions on parallel horizontal shafts. There is great variety of the commercially available blade designs, ranging from lightweight to heavyweight constructions. Selection of the specific design depends on the consistency of the mix. The size of the mixer is limited by the power input, batch weight, speed of mixing, materials of construction, and methods of mix discharge. Many machines are equipped with tilting facilities to discharge the batch while the blades are turning. The mixers require heavy-drive mechanisms and large motors.

The agitator blades in the sigma-blade mixer may be mounted so that their paths are either tangential or overlapping (intermeshing). In the tangential arrangement, the two blades rotate side by side with their circular paths of rotation not quite touching. The blades can have any relative speed because their paths of rotation do not overlap. In the overlapping arrangement, the paths of rotation overlap. Consequently here the blades must be designed and the speed of rotation adjusted so that the blades always clear each other. Many manufacturers provide double-arm mixers with interchangeable blades. Examples of materials handled by double-arm kneaders of the sigma-blade type are resins, putty, adhesives, baker's dough, and cellulose additives. Sigma-type agitator blades are best for general-purpose use.

Dispersion-Type Screw Mixers

Dispersion-type screw mixers are in an entirely separate class from the extruder designs described above. They are applicable to processing of either dry materials or moderately viscous pastes, creams, or lotions. These machines normally consist of a conical vessel equipped with a conical or inclined screw. There are either single- or twin-screw models that provide a gentle mixing action and thus are used for handling materials sensitive to attrition or fiber disintegration (one example is in dry cell battery manufacturing, where acetylene black has lacelike structure that easily breaks down).

The twin-screw design, in addition to the axial, orbital, and gravitational action offered by the single-screw design, provides intermixing between the two screws. Depending on the material properties, the mixing times can be 90 % faster than the single-screw system. The Combimixer employs two intersecting conical tanks with two orbiting spiral agitators. The axial and orbiting motions of the two agitators, along with the additional intermixing currants occurring through the juncture of the two tanks, provide for greater blending action than the single-screw mixer. Two motors and two gear boxes drive the smaller Combimixer. One set drives both screw flights axially and the other drives the two orbiting arms. For larger Combimixer units, separate motors are used for each screw flight and a single motor drives both orbiting arms.

Add-Ons

A need for better mixing in a SSE was already evident in the 1950s. Large effort was spent to redesign the screw by either changing the flow profile (mixing screws like Eagle, Chief, Meltstar, ODM, Pulsar, Stratablend, Toss-and-Rock, Stat-Dyn, etc.), adding mixing elements (pins, rectangles, or trapezoids), or modifying the screw tip. In the latter category, quite a long series of designs has been proposed: Axon, Dulmage, Egan, Maddox, pineapple, turbine, etc. These devices are parts of the extruder technology and have been well described (Manas-Zloczower and Tadmor 1994; Rauwendaal 1994).

By definition, an add-on device is an optional part to be attached to a standard SSE. While some of these use the extruder torque, the others can be used either as an attachment or stand-alone units with their own power (CTM or DMX mixers).

Barmag 3DD torpedo mixer is a forerunner of this category of mixers. The unit was designed to improve the temperature homogeneity of the film and fiber spinning extrusion lines. The device is made of a torpedo (to be attached to the tip of the SSE screw) and a sleeve (to be attached to the extruder barrel). Both the torpedo and the sleeve have slot-shaped grooves, arranged in rows (usually 12). Significant improvement of the melt homogeneity was reported by the manufacturer.

Cavity transfer mixer (or CTM) was designed at RAPRA as an add-on distributive mixer (Gale et al. 1982). The device is made of a torpedo (to be attached to the tip of the SSE screw) and a sleeve (to be attached to the extruder barrel). Both the torpedo and the sleeve have semispherical indentation. The number of rows of indentations must be selected to satisfy the mixing needs of the production line. The polymer flowing between them is sheared and split into different indentations. Furthermore, the extensional flows generated at the entrance and exit from the indentations introduce additional dispersive action. The flow through a simplified CTM was analyzed experimentally and by means of a fluid dynamics analysis package like FIDAP (Manas-Zloczower and Tadmor 1994; Wang and Manas-Zloczower 1996).

The University of Twente developed the mixing ring (or TMR). This device is made of three parts: smooth wall barrel extension, a torpedo with semispherical indentations (similar to these in CTM), and a perforated sleeve that goes between them. The sleeve provides shallow indentations. It slowly rotates between the torpedo and the barrel by the virtue of a drag flow. The flow in TMR is both dispersive and distributive. The advantage of TMR is its suitability to improve mixing in injection or blow molding machines (Housz 1989).

Another in this series of add-on mixing torpedoes is the Dynamic Melt Mixer, DMX. The device consists of a series of mixing modules inside a tubular housing. Two types of modules are available. Each module is made of two components: a stationary ring fixed to the sleeve and veined rotor keyed to an axial shaft either attached to the SSE screw or independently powered. Part of the rotor that does not enter the sleeve provides the cutting action across the flow lines that induces the distributive action. The primarily distributive one consists of a stator and a rotor (keyed to the central shaft) without the rolling semicylindrical lugs. As the rotating modules turn, they provide dispersive and distributive mixing (Miller 1996; Petren 1997).

An interesting distributive add-on mixer was proposed by Jurkowski et al. (1992). The mixer is made of a short barrel attached to the front of SSE. Within the barrel, there are several plates with channels directing the melt to flow from the rim toward the center and vice versa.

Other mixers, viz., the "static (or motionless) mixers," were discussed in Sect. 9.2.5, "Distributive Mixing," while the Extensional Flow Mixer (EFM) and the Dynamic Extensional Flow Mixer (DEFM) were described in Sect. 9.2.6.4, "Extensional Flow Mixer."

9.4   Nonmechanical Methods of Polymer Blending

9.4.1   Latex Blending

Historically, the preferred method of mixing was the latex blending. The early emulsion polymerization of rubbers (natural lattices or synthetic ones) and thermoplastic acrylates, methacrylates, and vinyls provided raw ingredients for the latex blending. A wide range of blends was described in the early I. G. Farbenindustrie patents. Later on, owing to the development of loop technology (Lanthier 1966), the method was revived by Shawinigan Chemicals.

The latex blends were used either directly, for example, as paints, adhesives, or sealants, or they were spray-dried or pelletized. Spray drying has been the most frequently used method. Since emulsion polymerization was able to produce either a fine dispersion (drop diameter d = 100–200 nm) of homo- or copolymer or alternatively large drop aggregates, comparable to those generated in suspension polymerization (d < 15 μm), the latex blending offered not only a wide range of compositions but also diverse morphologies. The principal disadvantage of the latex blending was high content of contaminants: emulsifiers, residuals of the initiators, chain transfers, stabilizers, etc.

9.4.2   Solvent and Spin Casting

There are several methods for the production of polymeric films (see Table 9.17). The oldest is calendering, but the most common methods are the film blowing and sheet extrusion. Others can be made by posttreating the extruded sheet like polyimide films (Sweeting 1971). Polymer films can also be polymerized onto a substrate from monomers in the vapor state or formed by the coalescence of polymer dispersions. However, several polymers cannot be formed without dissolving them.

Solvent casting is an important commercial technique utilized to fabricate thin layered films for diverse applications (Sweeting 1971). Most familiar is the solution casting of CA for photographic films having good dimensional stability, clarity, flexibility, and fracture resistance. The following advantages of solution-casting method (as compared to the melt process) have been given (Ricklin 1983):
- Higher quality (uniformity) and thinner film
- Freedom from pinholes and gel marks
- Purity and clarity
- Lack of residual stresses
- Possible to produce patterns or dull finishes

The solution-cast process consists of dissolution of the film ingredients in a suitable carrier that conveys the solution through a drier where the solvent is evaporated. The resulting film is removed from the substrate and wound into rolls. Solvents and scrap materials are reprocessed. As illustrated by examples in

Table 9.17 Methods for production of polymeric films

Process	Method
Film blowing or sheet extrusion	Continuous melt extrusion through a flat or circular die (PE, ionomers, PP, PS, PMMA, PEST, PA, etc.)
Calendering	Usually it follows the sheet extrusion. However, there are commercial lines where plastified polymer (semirigid PVC formulations) is directly fed to the calendar mill
Batch PVC plastisol or organosol casting	Plastisol and organosol casting process involves melting the polymer or polymeric mixture by an action of the temperature and presence of either a plasticizer or solvent
Continuous solvent casting	Extrusion of a solution through a flat die (CA, cellulose xanthate, PMMA, PVF, blends)
Batch in situ polymerization	Monomer casting, followed by controlled (co)polymerization (PMMA, epoxies)
Continuous in situ polymerization	Extrusion of Polymer-1 containing monomer of Polymer-2, followed by post reaction to Polymer 2 (polyimides, electrically conductive polymer blends, reactive blends) with cross-linked elastomers), etc.
Casting onto a substrate	Electrodeposition, plasma deposition, or dispersive deposition (vapor deposition of polyxylylene)

Table 9.18, the drying process can be used to manipulate the final film properties. Commercial solution casting is continuous (see Fig. 9.21) (Roberts 1967; Sittig 1967; Park 1969; Chow et al. 1976; Heffelfinger 1978; Ricklin 1983; Powers and Collier 1990).

The mathematical modeling of the process is complicated by the diffusivity dependence on composition. Low boiling solvents exhibit high diffusivity and usually are preferred, but for polymers with high T_g, high-boiling solvents may be more appropriate. The drying step is rate-limiting. An early mathematical model predicts the temperature and concentration profiles in the film during the drying (Collier 1981; Roehner 1982; Roehner and Collier 1983).

As indicated in Table 9.18, casting may induce orientation of the polymeric chains. The process is caused by the polymer movement induced by the solvent removal. Solvent removal from a solution constrained in two dimensions by a substrate results in one-dimensional thickness reduction. The orientation is caused by effectively stretching the polymer in the planar directions during thickness reduction. The resulting orientation depends on the evaporation rate. The competing rates for molecular relaxation and solvent removal are best considered using the Deborah number, defined as

$$De = \tau/t_{1/2} \qquad (11.29)$$

where τ is the polymer relaxation time and $t_{1/2}$ is the time required for the removal of one half of the solvent. For constrained processes with De $\gg$ 1, orientation occurs; for De $\ll$ 1, solvent removal results in only thickness reduction

Table 9.18 Examples of solution casting of polymers

Polymer	Solvent	Remarks, methods, and references
Poly(g-methyl-D-glutamate)	Chloroform, DCA, MC, FA, TCE	Solvent controls the degree of α- and ß-configuration or random coil contents in the film and its mechanical behavior and morphology. Rheovibron, stress–strain measurements, WAXS, SAXS, polarizing photomicrography, IR (Mohadger and Wilkes 1976)
Poly-2,5 (6) benzimidazole	Methane sulfonic acid, HCOOH/cresol	Solvent nature affects the morphologies of polymer films thus the extensibility and mechanical properties of films. DSC, Rheovibron viscoelastometer, WAXS (Wereta et al. 1978)
PS, PC, PVK	CH_3Cl benzene, THF	Casting aligns polymeric chains preferentially in the plane direction. DSC, optical anisotropy (Prest and Luca 1980)
Polyvinyl acetate	Methanol, acetone, chloroform	Mechanical properties of the films depended on the solvent and the time of exposure of film at each temperature; $CHCl_3$ was recommended. Mechanical tests (Olayemi and Adeyeye 1982)
PE, PC, PET, PS, i-PS, PVP, PMMA, PTFE PVAc, PVC	Toluene, CCl_4, $CHCl_3$, xylene, decalin, EtOH, H_2O, MeOH	The casting solvent has a pronounced influence upon the friction coefficient which may confer either ductile or brittle failure. "Good" solvent generally tends to promote brittle mode of failure with little temperature dependence. Friction measurements (Briscoe and Smith 1983)
PVC	MeOH, CHX, toluene, THF, decane, CS_2	The slowest evaporating solvent has the greatest effect on the surface properties; annealing above Tg reduces the surface porosity. Inverse gas chromatography, DSC (Wildman and Hsu 1984)
Ether polysulfone, PVDF	A high-water-affinity solvent	Swelling and the viscosity of the casting solution were controlled by addition of small amounts of partially miscible polymers. SEM, contact angle measurements (Stengaard 1988)

(Collier 1981). Birefringence measurements confirmed that drying conditions can affect the level of orientation in the films, but the techniques could not detect an orientation gradient developed across the thickness (Prest and Luca 1980).

Today, a great deal of literature is available on solution casting of polymers for applications like packaging, separation membranes, sensors, and fuel cells. A review on the subject is available (Guillen et al. 2011).

Solvent casting of polymer mixtures (usually with additives) may affect the density, porosity, mechanical properties, mode of failure, etc. These effects are
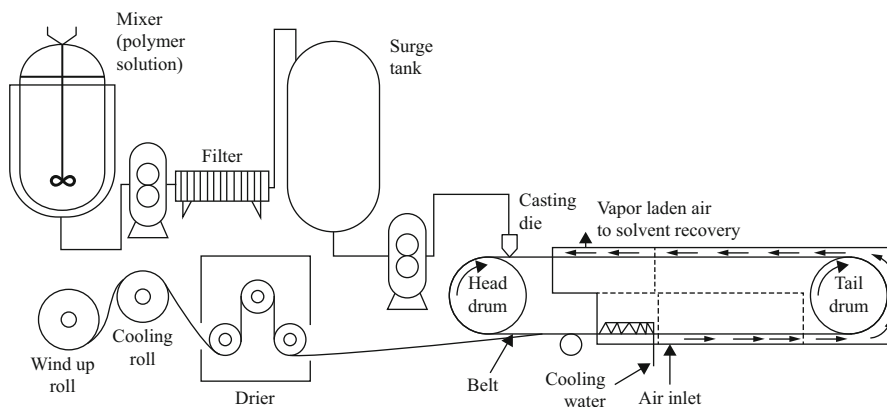
Fig. 9.21 The solution-casting process

particularly pronounced in films of immiscible polymers. Before discussing these effects, it is appropriate to consider the intermediate step like solvent casting of copolymers. Table 9.19 provides few examples.

For multicomponent systems, solution casting provides means for generating the desired degree and type of morphology. Profiting from the different (and controllable) rates of the phase separation and solvent evaporation, one may generate either co-continuity of phases (spinodal decomposition, SD) or dispersed structure (nucleation and growth or late stage of SD). The solvent casting offers additional flexibility in producing precisely what is needed. It is not necessary to use a single component solution. One frequently uses a mixture of solvents having different evaporation rates and different miscibility with the polymeric components. Furthermore, the films can be annealed, selected polymeric components extracted to form the desired size and shape of domains.

For example, it is possible to generate semipermeable membranes with well-controlled morphology, pore size, flux, and mechanical performance. The method is preferred for industrial preparation of semipermeable membranes from polymer blends (see Table 9.20).

Another method of morphology control in multicomponent polymeric systems is by the use of mixed solvents having different affinity to the polymeric components. When the non-solvent is less volatile than the good solvent, evaporation results in a two-phase structure.

When solvents are removed solely by evaporation, the membrane formation is known as a dry phase inversion process (Kesting 1985). When the phase separation and structure formation are achieved by immersion of a cast membrane in a quench medium, the process is known as a wet phase inversion process (Heffelfinger 1978). The latter process is used to prepare asymmetric membranes for either microfiltration (Roesink 1989), ultrafiltration (Michaels 1971), reverse

Table 9.19 Examples of solution casting of copolymers

Material	Solvent	Remarks, methods, and references
SBR	CHX, toluene, Et acetate, tetralin, cyclohexanone	Film properties depended on the evaporation rate, but there was no evaporation rate dependence when the casting solvent was CHX. Density measurements, Rheovibron dynamic viscoelastometer, TMA, SEM (Beamish and Hourston 1976; Beamish et al. 1977)
SEBS and SEPS	n-Heptane, cyclohexane, toluene	Spherical, cylindrical, and lamellar PS structures were obtained in the order of increasing solvent affinity to PS. Density, DSC, tensile test, dynamic viscoelastometer, SAXS (Séguéla and Prud'homme 1978)
SEBS	THF, CHCl$_3$, toluene, CHX, bromobutane, C$_6$H$_{14}$, C$_7$H$_{16}$	The complex modulus varied from 4.4 MPa (cast from low δ-solvents) to 205 MPa (cast from high δ-solvents); the area under the damping peak also depended on solvent. DMA, DSC (Cowie and McEwen 1979, 1980; Cowie et al. 1979)
SBS block copolymer	Toluene, CCl$_4$, EtAc, MEK	The solvent nature influenced film morphology. Position annihilation technique (Djermouni and Ache 1980)
Silicone-PC block copolymers	C$_6$H$_{14}$, methylene chloride	Casting from a homogeneous solution that favors the hard segments yielded better results than from mixed solvents from which PC blocks preferentially separated to form a discontinuous dispersion or network. Capillary viscometer, GPC, TMA, DMA (Maung et al. 1983)
Poly(styrene-b-butadiene-b-4-vinylpyridine)	THF, benzene, MEK, EtOH, MMA, nitromethane, hydroxyethyl methacrylate	A ball-in-a-box structure morphology was formed when the solvent for poly (4-vinylpyridine) is lost; a lamellar structure morphology was formed when solvents were equally distributed into the three phases; a random structure was formed when the solvent for one or two of the three block segments vaporizes faster than other solvent. SEM, Mechanical test (Arai et al. 1984)
PDMS-b-PS copolymers	CH$_3$Cl, Toluene, Cyclohexane	The interactions between the casting solvent and polymer affected the phase separation and the final morphology. DSC (Feng et al. 1988)
Ter-copolymer of acrylonitrile methyl methacrylate	Glycerol, water	An increase of glycol in the casting solution resulted in the formation of membranes with high pore density and small pore size, thus increasing the selectivity with respect to low molecular weight components. Selectivity of membrane, SEM, porosimetry (Petrov et al. 1991)

Table 9.19 (continued)

Material	Solvent	Remarks, methods, and references
Disulfonated poly (arylene ether sulfone) multiblock copolymer	N-methyl-2-pyrrolidone (NMP), dimethylacetamide (DMAC)	Morphology via transmission electron microscopy and small angle X-ray scattering showed that as the block length increased, the interionic-domain distance increased, with a subsequent increase in lamellar ordering and long-range continuity. SEM, TEM, rheology, mechanical properties (Lee et al. 2009)
Poly(lactic-co-glycolic) acid (PLGA)	dichloromethane	Infrared and Raman spectroscopy used to study composition and degradation of the copolymer films in a phosphate buffer solution. Mass loss, FTIR, Raman (Vey et al. 2011)

osmosis (Strathmann et al. 1971), or gas separation (Henis and Tripodi 1980; Van't Hoff 1988). Posttreatment may be necessary to prepare ultrathin asymmetric membranes for gas separation (Henis and Tripodi 1980; Zampini 1984; Zampini and Malon 1987; Murphy et al. 1989; Ekiner et al. 1989).

Membrane structures can also be formed by a microphase separation process in which the outermost region of the cast membrane undergoes phase separation induced by solvent evaporation, while the bulk of the structure is formed by solvent/non-solvent exchange during a quench step. This type of structure formation is defined as a dry/wet phase inversion process (Pinnau et al. 1990).

9.4.3 Special Methods

9.4.3.1 Freeze Drying

The freeze-drying of co-solutions of thermodynamically immiscible polymer pairs is a method of capturing kinetically the unlike molecules in molecular or "segmental" mixtures. PMMA/PVAc blends freeze-dried from co-solutions in benzene were reported homogeneous by dynamic-mechanical and dilatometric observations. They showed a single T_g intermediate between those of the pure polymers (Miyata and Hata 1970). Further dilatometric and differential calorimetric data corroborated the findings of homogeneity (Ichihara et al. 1971).

Berghmans and Overbergh (1977) found that freeze-drying of dilute solutions containing two miscible polymers produced a system with three glass transition temperatures, corresponding to the T_g's of both polymeric species and an intermediate T_g, characterizing their blend. A comparison of the density of freeze-dried and

Table 9.20 Solution casting of polymer blends

Material	Casting solvent	Remarks, methods, and references
Grafted block copolymer blends	Divers	The soluble polymer usually was the matrix with the other resins forming isolated domains. Physical properties and morphology (Merrett 1957; Inoue et al. 1960; Beecher et al. 1969; Kawai et al. 1971; Pedemonte et al. 1975; Kraus and Rollman 1976)
PMMA/PS/SA terpolymer blends	n-Butanol, toluene, CHCl$_3$, ethylene dichloride, ethanol	Good solvent produced tightly packed films, while poorer solvent yielded more porous ones. IGC, surface tension (Schreiber and Croucher 1980)
Poly(alkyl methacrylates), PS/BR	Methanol, toluene, DMF	The Tg of polymers varied because of residual solvent, possibly due to the plasticizing effect, and thermal history. DSC (Brostrom et al. 1980)
PC, PS, PC–PS blends, PC–PS copolymer	Dichloromethane, acetone	Blend properties were found to be a combination of these of the constituent homopolymers. Segmental motions of the PS chains in the copolymer were enhanced even though those chains were attached to more rigid PC chains. SEM, Rheovibron viscoelastometer, mechanical properties (Eastmond and Haraguchi 1983)
PS/poly(α-methyl styrene)	Toluene, cyclohexane, propylene glycol	Regions of miscibility and immiscibility as functions of a casting solvent and molecular weight for both components were established based on Tg consideration. DSC (Saeki et al. 1983)
PVC/NBR or EVAc; CR/NBR or EVAc; BR/SBR or IR; ABS/NBR or PMMA; PS/PMMA	THF	Faster rates of solvent evaporation yielded a smaller periodic distance in the modulated structure. The rate of phase separation was lower and the periodic distance of the modulated structure smaller as the blend ratio deviated from 50/50. **For high MW polymers, the system failed to phase-separate during fast casting**, resulting in a homogeneous blend without appreciable composition fluctuations. Light scattering (Inoue et al. 1985)
Perfluorinated Nafion ionomer/ PVDF blends	Dimethylformamide, dimethylacetamide, 1-Methyl-2-pyrrolidinone	The spherulitic crystalline morphology of PVDF showed strong dependence on the casting temperature and compositions. Mixed α- and γ-form crystals were obtained. DSC, SAXS, microscope, dielectric thermal analyzer (Kyu and Yang 1990)

Table 9.20 (continued)

Material	Casting solvent	Remarks, methods, and references
PC, PS, PPE, t-methyl PC	Dichloromethane	Casting induced distinct molecular order in the solid films; birefringence was influenced by the solvent type, the casting temperature, the surface energy of the substance, and the timing of the peel-off step; non-birefringence films could be produced by setting proper operating conditions. Birefringence (Machell et al. 1990)
PS, PMMA	Chloroform	Surface analysis showed an enrichment of the surface by PMMA (phase separation). The behavior is related to differences in solubility and dewetting of PMMA-rich domains by PS-rich phases. XPS, AFM (Ton-That et al. 2001)
PMMA, PVAc	Chloroform, toluene, tetrahydrofuran	FTIR analysis in transmission showed that residual solvent molecules can be trapped in the films and have an effect on transparency, absorption coefficient and refractive index, UV–Vis, reflection, and FTIR (Ahmed 2008)
PES, PI	N-dimethylacetamide, tetrahydrofuran	Different PES/PI ration and solution concentration showed that asymmetric thin films can be produced by process optimization (evaporation time). SEM, gas permeation (Madaeni et al. 2012)
PVDF, PMMA, PVP	N,N-dimethylformamide	For this ternary blend, PVDF was mainly found on the surface, and hydrophobicity and crystallinity were enhanced by PMMA/PVP addition SEM, WAXD, FTIR, DSC, and contact angle (Cheng et al. 2013)
P(VDF-TrFE), PEO	N,N-dimethylformamide	Differences in crystallization speed (sequential crystallization) results in a P(VDF-TrFE) fibrillar structure leading to two dynamic-mechanical relaxations. SEM, AFM, FTIR, DSC, TGA, DMA (Costa et al. 2013)

bulk PS has also led to the inference that freeze-drying from dilute solution leads to a system in which individual polymer chains are collapsed to globular particles rather than being intertwined (Miyamoto et al. 1970).

Schultz and Young (1980) prepared homogeneous blends of immiscible PMMA/PS blends by freezing and sublimation. The solutions containing 5 wt% of polymer

or polymer mixture were dissolved in naphthalene at 100 °C with a magnetic stirrer, under N_2 blanket. The hot solution was poured slowly into ice water undergoing high-speed stirring in a blender. After filtration on a sintered-glass filter, the naphthalene powder "solutions" were dried in an airstream for 24 h. The powders were then transferred to round-bottom flasks, and naphthalene was sublimed from the polymer blends at room temperature on a high-vacuum rack for 10 days. The first DSC scans showed single T_g for these blends, intermediate between those of the two polymers, while the second and the following ones showed two T_g's, corresponding to those of the two polymers.

9.4.3.2 Spray Drying

Spray drying is by definition the transformation of feed from a fluid state into a dried particulate form by spraying the feed into a hot drying medium (Masters 1985). This is an ideal process where the end product must comply with precise quality standards regarding particle size distribution, residual moisture content, bulk density, and particle shape. It involves the atomization of a liquid feedstock into a spray of droplets and contacting the droplets with hot air in a drying chamber. The sprays are produced by either rotary (wheel) or nozzle atomizers. Evaporation of solvent of matrix liquid from the droplets and formation of dry particles proceed under controlled temperature and air flow conditions.

The initial contact between spray droplets and drying air controls the evaporation rate and the product temperatures. The drying-chamber and air-disperser design must create a flow pattern that prevents deposition of partially dried product to the walls and the atomizer. There are three modes of contact:

1. Cocurrent: Drying air and particles move through the drying chamber in the same direction. On discharge, the product temperatures are lower than the exhaust air temperature. This is an ideal mode for drying heat-sensitive products.
2. Countercurrent: Drying air and particles move through the drying chamber in opposite directions. This mode is suitable for products that require a high degree of heating.
3. Mixed flow: Particle movement through the drying chamber experiences both cocurrent and countercurrent phases.

Spray drying has been used to prepare polymer blends from mixed lattices or cosolvent solutions.

9.5 Reactive Processing (Compatibilization)

Details of the reactive compatibilization are discussed in ▶ Chap. 5, "Reactive Compatibilization" of this book. For this reason, the following text is only concerned with the mechanical aspects of the process.

The term "reactive processing" is used to describe a polymer processing that involves chemical reactions. In principle, any processing operation can be conducted as a reactive process like reactive injection molding (RIM). However,

most often, the term refers to reactive extrusion and, in particular, to the reactive compatibilization of immiscible polymer blends, usually conducted in a TSE. During the last 50 years, the latter machines have been used a chemical reactor for the polymerization, depolymerization (chemical recycling), polymer modification, and compatibilization (Brown 1992; Xanthos 1992; Utracki 1989, 1991, 1994, 1997).

Four features make TSE particularly well suited as a reactor for highly viscous polymeric reactants (Thiele 1996):

1. An ability to compartmentalize the reactive mass into small melt pools, bounded by the screw flights and barrel walls, with short mass and heat transfer distances
2. The possibility of conducting a series of operations in a logical well-controlled sequence along the length of the extruder: melting, mixing, reacting, devolatilization, homogenization, and forming
3. The ability to provide the desired extent of the interface renewal that controls the overall reaction rate
4. The continuity of the process

For example, between 1966 and 1987, over 1,000 patents on reactive extrusion were granted to 200 companies. In order of decreasing number of patents, they were Asahi Chem., Bayer, Kabel Metal Gatehoff, BASF, Showa Electric, Mitsubishi Petrochem., Hitachi Cable, DuPont, Exxon, and many others (Utracki 1997).

9.5.1 The Use of Twin-Screw Extruders in Reactive Polymer Processing

TSEs have been used to prepare new families of engineering materials of high performance, polymers, and their blends. Polycondensation, free radical, and anionic and cationic polymerizations were conducted to obtain for PA, PEST, POM, styrenic, or acrylic resins. When the reaction is conducted in a low molecular weight liquid (solution or emulsion polymerization), usually devolatilization and compounding are carried out in a cascade second extruder. Functionalization and chemical modifications have been performed in TSE on virtually all polymers.

9.5.1.1 Advantages and Disadvantages of Reactive Processing

Reactive processing is a continuous, flexible process offering the technical and economic **advantages** vis-a-vis other reactors (Kamal and Ryan 1984; Sneller 1985; Tzoganakis 1989; Kowalski 1990):

- Low production volume, hence, small losses for equipment breakdown.
- Rapid and precise control of pressure and temperature; good heat exchange.
- Ability to introduce reactants and catalysts at the desired locations.
- Working with 100 % of reactant content, using rapidly renewed interface, which leads to higher reaction rates than those possible in batch processes.
- Self-cleaning system, hence, narrow and adjustable distribution of residence time.

- Good control of the residence time and residence time distribution; the residence time distribution is narrowest for ICRR, CORI, and then NIRT.
- Control of the reaction environment (airtight configuration or inert gasses).
- Ability to ascertain sequential high reaction rates.
- Capability of rapid removal of a large volume of volatiles.
- Controllable amount of dispersive and distributive mixing.
- Ability to disperse high-viscosity materials without a solvent.
- Ability to combine polymerization (or copolymerization), degassing, compounding, and forming, what results in overall more economic industrial process.
- Possibility of automation via the closed-loop control of product quality.
- Discharge through a forming die.
  The **disadvantages** of the reactive extrusion are:
- High initial capital investment.
- High cost of the reactions that require long residence times (reactions requiring residence time greater than 1 h are not acceptable).
- All the contaminants, inhibitors, and possible sources of side reactions must be removed or deactivated. This includes moisture, residual monomers, catalysts, etc.
- Difficulties in rapid removal of locally generated large heats of reaction.
- A need for high accuracy of ingredient addition and precise control of the process parameters.
- The reaction may need to be carried out under a blanket of dry, inert gas.
- Product quality is influenced by the residence time distribution.
- Run-out reaction usually leads to high-viscosity product; thus for safety reason high torque machines are needed with capability for rapid feed reduction and increase of temperature in the final barrel sections.
- The process must be closed-loop controlled, using either rheological (MFM), infrared, or ultrasonic sensors.
- The mathematical models of the reactive extrusion are in early stage of development.

The reactive processing is controlled on two levels: by selection of equipment, screw configuration, and ingredients and by the control of process variables. Depending on the type of reaction, the most appropriate TSE type must be selected and the appropriate steel alloy for the inner barrel and screw elements selected. Most manufacturers offer a selection of alloys with different resistance to abrasion and corrosion (to acids or halogens). Similarly, there is a variety of the control systems that must be considered knowing the number of sensor to be used and a need for protocolling. It is important that the metering system is selected to deliver the materials with the required precision and continuity. For liquid injections, the check valves that prevent freeze-off during the startup or shutdown should be used.

Reactive compatibilization requires good dispersive and distributive mixing of reactants and sufficient residence time for the reaction to take place. The introduced components should be immediately uniformly mixed. Thus, appropriate mixing screw elements (kneading, turbine, etc.) should be placed in the reaction zone of the

extruder where the reactants are introduced. Furthermore, adequate heat removal capabilities must be provided for the zone where the exothermic reaction takes place. It has been found that barrel cooling is not always adequate and screw (shaft) cooling has been used. Usually, the venting zone immediately follows the reaction one. Since in the venting zone the screw is only partially filled, between the two zones, there is a restriction of reversed screw elements, kneading element, check valve, or a throttling ring. Within the venting zone, multiple flight elements should be introduced to provide rapid surface renewal.

Owing to milder operating conditions, corotating TSE (CORI) has been preferred. However, the counterrotating TSEs (ICRR) are used with increasing frequency for polymerization of either polymethacrylates or polyurethanes. In the latter case, owing to higher pressures and stresses than those in CORI, the reaction must be controlled with greater precision. For example, during PBT modification with epoxy, the reaction started before the liquid was properly distributed in the melt, what resulted in poor quality products.

In conventional TSE, the residence time of up to 10 min can be achieved (Dreiblatt 1989). Special TSE systems for slow reactions have also been developed. For example, a TSE with a pre-reactor vessel may offer the residence time up to 45 min. However, the modern tendency goes in the opposite direction. TSEs are offered with the screw speed of up to 2,000 rpm (laboratory experiments are run at speeds of up to 3,000 rpm) that results in the residence time of the order of seconds. Hence, there is a rush to accelerate the reaction rates by catalysis, intensive mixing, as well as temperature and pressure.

The residence time distribution depends on the screw configuration, the throughput (or the degree of fill), and the screw speed. All three factors need to be optimized considering the rate of reaction, degradability of materials, and productivity.

9.5.1.2 Development of Reactive Compatibilization Process
Reactive processing combines fine polymer chemistry with polymer processing. Thus, development of the reactive compatibilization process involves:
1. Studies of chemical kinetics in glassware and internal batch mixers
2. Determination of the rheological and thermal parameters of the reaction ingredients and products
3. Mathematical modeling of the reactive processing
4. Reactive extrusion
5. Detailed evaluation of the properties of reaction products
6. Scale-up to industrial scale

9.5.1.3 Laboratory Equipment
To develop reactive compatibilization, the laboratory extruder should match the production unit. Thus, a TSE, either CORI or ICRR, with segmented barrel and screw should be used. The machine should have the screw diameter D ≥ 30 mm, with length-to-diameter ratio L/D ≥ 40. The extruder must provide an easy access to the reactive medium as well as the quenching capability with either screw or

barrel removal. It must be fully instrumented with temperature and pressure sensors all along the barrel. It should offer the possibility of working under dry inert atmosphere and have the capability of closed-loop control operation with an appropriate set of sensors. The machine should be equipped with a minimum of three feeders for solid and two for liquid ingredients. At least one vacuum system with cold trap is necessary.

The laboratory should have a drying facility for all components that are to be used (drying tower with closed resin transfer facility), as well as preblending facilities that can be operated under controlled temperature and atmosphere. The extrudate is usually granulated (thus, a need for the appropriate dies, cooling facility, and either granulator or pelletizer) and subsequently must be formed into suitable specimens and tested. Forming is usually done by injection molding into a standard, multi-cavity test mold.

The reactive extrusion is a process demanding precise operation by well-trained personnel. The knowledge of the extruder, compounding and mixing principles, design of screw and temperature profile, local residence time distribution, etc., is required. For optimization of the reactive extrusion, in- or online process monitoring, control, and data logging are recommended. This imposes further demands on the extruder operator.

9.5.1.4 Reactive Compatibilization Strategy

The experience indicates that the best results are obtained if:

1. The chemical reaction has low activation energy.
2. The required residence time is short ($t_{0.5} \leq 75$ s), what implies high reaction rates, and frequently catalysis.
3. The process can be simpler if the reaction is insensitive to moisture or oxygen.

The kinetics of the process should be studied on a model system in glassware. The kinetic parameters should be determined within the full range of the expected process parameters. Sensitivity of the reaction to moisture and oxygen should be examined. Next, the kinetics should be verified using polymeric ingredients. It is essential to know the lifetime of the activated sites. This determines the sequence and location of the reactant feeds. For example, if the radical is unstable, one may be better off feeding the peroxide and grafting monomer at the same location. Factors affecting group reactivity are listed in Table 9.21.

Since reactive compatibilization is carried out across the interface, the screws of the selected TSE must provide a suitable geometry for the mixing, mass, and heat transfer. The length of the reaction zone and the mixing intensity must ascertain sufficient mixing for the reactive groups to meet but without the accompanying mechanochemical degradation. It is essential that there is adequate devolatilization. The reaction by-products should be identified, removed, or rendered harmless (catalyst deactivation may be needed) (Dagli et al. 1994; Maier and Lambla 1995; Sundararaj et al. 1995; Hu et al. 1996a).

In principle, high melting point polymer should be fed and melted first, then the second polymer and liquid(s) should be added. After the reaction zone, the vacuum line should remove the volatile reactants (unreacted monomers) and by-products. Finally,

Table 9.21 Factors affecting group reactivity during reactive extrusion

Factor	Influence
Molecular weight	No influence of chain length onto which a functional group is attached was observed. Exceptions occur in stiff chain polymers
Neighboring groups	May increase or decrease group reactivity
Molecular configuration	Depending on chain configuration, the functional groups may co-interact which alters their reactivity
Electrostatic effect	Polarity of the reactive groups leads to repulsion or attraction effects
Accessibility	Stereo-barriers between functional groups
Supramolecular effect	Aggregation, associations, or clustering slows down the reaction, but the extent of these effects is difficult to predict
Mechanical shearing	Straining the macromolecules results in generation of stresses that may activate some bonds. Mechanically induced chain scission has been explored for grafting polymers and rubbers

just before the die, a filler (glass fiber) and unstable ingredients should be added. The reaction must be terminated when the product leaves the extruder. It is important that the process is well monitored and controlled (Broadhead et al. 1996; Gendron et al. 1996).

During the development stage, it is essential that samples are frequently taken from the extruder and analyzed for the extent of reaction as well as for the morphology and the key properties. The sampling methods are discussed in Sect. 11.2.1.2, "Morphology Evolution in an Extruder." It may also be profitable to verify the whole reactive compatibilization process by the carcass method.

The initial strategy formulated on the basis of chemical kinetics can serve as a starting point for the mathematical modeling of reactive extrusion. However, to ascertain successful strategy, mathematical "experiments" must be carried out, using realistic models of the process. To optimize the process parameters and the screw design, the model requires information on kinetics, rheology, and thermal properties (Menges and Bartilla 1987; Polance and Jayaraman 1995). The type of required rheological and thermal information depends on complexity of the model. The minimum rheological information is the shear viscosity as a function of the deformation rate, temperature, and the degree of conversion, $\eta = \eta(\dot{\gamma}, T, k)$. The minimum thermal information is the heat of reaction, transition temperatures of the ingredients and their enthalpies, as well as heat capacities and heat conductivity coefficients. The model must provide information on the sequence of extrusion steps like melting, homogenization of ingredients, chemical reaction, devolatilization, morphology, and performance.

The reactive extrusion should be optimized using a computer modeling procedure. The mathematical model of the reactive extrusion should combine three subroutines:

1. Pressure and temperature profile as a function of the degree of fill and screw length (Michaeli et al. 1991, 1993, 1995; Michaeli and Grefenstein 1996)
2. Rheology and chemical reaction (heat balance) as a function of screw length (Chen et al. 1996; Kye and White 1996; Hu et al. 1996b)
3. Variation of morphology along the screw length (De Loor et al. 1996)

An analytical model based on the energy balance in CORI was proposed. Anionic polymerization of ε-caprolactam in CORI was modeled, considering continuity of the process from one screw element to another. The model took into account the heat of reaction, viscous dissipation and heat transfer across the barrel. The calculations were performed for three different screw configurations comprising the transport and kneading elements. The predicted total conversion agreed with the experimental values within ± 3 % (Kye and White 1996).

Effects of the reactive processing are usually assessed either by analytical means or by their effects on morphology and performance. The analytical methods usually involve selective either extraction or destruction of one polymeric ingredient, followed by GPC, rheology, DSC, ^{13}CNMR, FTIR, and other analyses (Polance and Jayaraman 1995; Maier and Lambla 1995; Miyoshi et al. 1996; Kye and White 1996). The morphological studies should be conducted on several levels of magnification, from the optical to the transmission electron microscopy, TEM (Vesely 1996). For detailed discussion of the methods used to characterize the morphology, see ▶ Chap. 8, "Morphology of Polymer Blends".

Table 9.22 (see also literature reviews by Cassagnau et al. 2007; Raquez et al. 2008) lists examples reactive extrusion studies conducted in laboratory TSEs, whereas Table 9.23 provides examples for compatibilization (see also reviews by Feldman 2005; Karger-Kocsis et al. 2013). It is noteworthy that about 90 % of patents on polymer blends published during the last few years specify a TSE as the preferred compounder. Exceptions are blends formulated for oriented fibers and films (with LCP) that require high die pressure and thus are usually prepared in a SSE. Similarly, elastomeric blends of either PO or PVC are preferably prepared using one of the older methods like roll mill or Banbury mixer.

9.5.2 Scale-Up to Industrial Size

Scale-up is one of the most difficult engineering tasks. The main source of difficulty originates in the multifunctional capabilities of TSE. In addition to the primary functions of an extruder (solid conveying, melting, and pumping), TSE is used to mix, devolatilize, and more and more often conduct the chemical reactions. For these reasons, several schemes for the scale-up have been developed, each focusing on one particular process variable like constant specific energy (CSE), constant thermal conduction (CTC), constant residence time (CRT), etc. Usually, the CTC forms the lower, whereas the CRT the upper boundary.

The scale-up starts with optimization of the compounding conditions in a laboratory-scale TSE, having the screw diameter D ≤ 35 mm. Owing to the difference in thickness of the molten polymer between this and commercial size extruders (D ≥ 100 mm), it is advisable that the scale-up involves an intermediate stage, a midsize TSE with D ≥ 50 mm. The experience also showed that it is more difficult to scale up from 30 to 50 mm than from 50 to 200 mm TSE. Thus, the intermediary step may save a large amount of time, material, and the plant production capability.

Table 9.22 Examples of reactions conducted in laboratory TSEs

Process	TSE	Comment	Reference
PP peroxide degradation	CORI or SSE	Melt flow monitor (MFM) is needed	Xanthos 1992; Fritz and Stöhrer 1986
PA-6 polymerization	CORI or CRNI	Nitrogen blanket	Michaeli et al. 1991
Polyarylate synthesis	CRNI + SSE	Devolatilization using 3 vents	
TPU polymerization	CORI	T = 90–260 °C	
Radical polymerization of styrenics	CORI	3 CORI used	Illing 1970
Rubber polymerization	CORI	T = −5–100 °C	Sutter and Peuker 1977
PA toughening	CORI	T = 310 °C	Epstein 1979
MMA grafted onto EPR	CRNI		Staas 1981
PO-grafting	CORI, CRNI	N = 100 rpm	Binsack et al. 1981
PET/PA-6 + p-toluenosulfonic acid	CORI	Compatibilization of PA-6/PET	Pillion and Utracki 1984, 1987
Radical polymerization of MMA	ICRR	Kinetic studies	Stuber and Tirrel 1985
POM synthesis from trioxane	CORI	Conversion ≥ 90 %	Todd 1988
EVAc grafted with MA and styrene	CRNI + SSE	Study of the grafting parameters	Sakai et al. 1988
Continuous polymerization of PEI	Modified CORI	T = 25–400 °C	Schmidt et al. 1989
Cross-link: PE + CH2 = CH-Si(OR)3	CORI	Peroxide added	Ultsch and Fritz 1990
Reacting acrylic acid grafted PE with oxazoline-grafted PS	CORI	Controllable cross-link density	Curry and Andersen 1990
Vinyltrimethoxysilane-grafted PE	CORI	Moisture cross-linking	Ultsch and Fritz 1990
PS–PO blending	CORI	MFM monitoring	Curry and Andersen 1990
Imidization of MA-polymers	CORI	Plug-flow reactor	Hagberg 1992
Toughening of unsaturated polyesters	CORI	Incorporation of NBR by free radical grafting (DCPO)	Sakai et al. 1992
PS and S-I block copolymer anionic polymerization initiated with Bu-Li	CORI with nitrogen blanket	MW depends on initiator concentration not N	Michaeli et al. 1993
PA-6 with brominated isobutylene-methylstyrene elastomer	CORI	Compatibilization and dynamic vulcanization	Kuwamoto 1994
Peroxide-induced degradation of PP	ICRR	T = 180–240 °C, 3 screw configurations examined	Ebner and White 1994
Maleation of PP	CORI	T = 195–230 °C	Martinez et al. 1994

(*continued*)

Table 9.22 (continued)

Process	TSE	Comment	Reference
Peroxide-induced degradation and maleation of PP	ICRR and CORI	ICRR better for visbreaking, CORI for maleation	Kim and White 1995
Polyetheramine modification of PP	CORI	To enhance paintability	Clark 1995
Maleation of postconsumer plastics (HDPE, PET, PP, PVC)	CORI	Reactive blends compounded with fillers	Xanthos et al. 1995
PE grafting with GMA	CORI	Compatibilization of HDPE/PA-6	Wang et al. 1995
Reactive compatibilization of EVAc/EMAc/PP blends	CORI	Toughened PP had cross-linked EVAc/EMAc phase	De Loor et al. 1996
Mono-esterification of SMA using 1-octanol	CRNI	Accelerated reactivity caused by devolatilization	Chen et al. 1996
Reactive extrusion of PO blends	CORI	Peroxide modification	Kim 1996
Epoxy prepolymers with rubber	CORI	Carboxyl-terminated butadiene–acrylonitrile random copolymer	Taha et al. 1997
PP carboxylation via functionalized peroxide	ICRR	Grafting degree can be controlled by peroxide molecular weight	Assoun et al. 1998
PPS/LCP compatibilization	CORI	Compatibilization did not affect the fibrillar structure, but improved mechanical properties	Gopakumar et al. 1999
PS/starch graft copolymerization	ICRR	Two-step mechanism kinetics	de Graaf and Janssen 2000
Acrylic acid/glycidyl methacrylate grafting onto LDPE	CORI	TEMPO addition influences grafting degree and gel content	Yang et al. 2001
PP/EPDM compatibilization	ICRR	HAP better than peroxide to improve low temperature properties	Ludwig and Moore 2002
PBT/PA-6/EVA-g-MAH	CORI	Efficiency of EVA-g-MAH depends on the PBT/PA-6 ratio	Kim and Kim 2003
PS/epoxy-amine	CORI	Production and stabilization of the fibrillar structure helped via post-extrusion stretch	Fenouillot and Perier-Camby 2004
Polyamide–polyester block copolymers	CORI	Good control of the reaction via successive feeding strategies	Kim and White 2005
Modified PP with DCP/TMPTA	CORI	LCB-PP produced with better conversion at higher TMPTA concentration	Su and Huang 2009

(continued)

Table 9.22 (continued)

Process	TSE	Comment	Reference
L-lactide ring opening polymerization	CORI	Kinetics model based on Ludovic using axial dispersion and compartment model (series of ideal perfectly mixed and plug flow)	Banu et al. 2010
LCB-PP/HDPE/LLDPE produced via PP-g-MAH and EDA	CORI	Introduction of $scCO_2$ facilitates the reaction	Cao et al. 2011

In principle, good mathematical model that combines melting, fluid mechanics, morphology evolution, devolatilization, and chemical reactions should provide solid guidance for the scale-up. However, so far such a complex model has not been developed. In consequence, the methods are pragmatic and less formal. First, it must be decided which function is the most important and wherever possible, an appropriate mathematical model should be selected. At least three experiments must be conducted, both computer-type and extruder-type, using three sets of values like composition, throughput, and screw speed. For each composition, the nine specimens should be examined for the desired performance characteristics such as mechanical performance, permeability, solvent resistance, etc. Once the model is found to well describe the experiments, the exercise must be repeated for the larger diameter extruder, the model parameters readjusted, and the optimum screw configuration and the processing conditions computed and then experimentally verified.

Less formal method uses the power-law exponents. Here, the ratio of the screw diameters, $\delta = D_2/D_1 > 1$, is the principal variable. When scaling, the screw channel angle is to be kept constant, and the screw section length increased by δ. The channel depth is also increased as $H_2 = H_1 \delta^{0.92}$. If the ratio of heat transfer to throughput is assumed constant, then $Q_2 = Q_1 \delta^2$, and $N_2 = N_1/\delta$. On the other hand, if ESP is taken as constant, $Q_2 = Q_1 \delta^\alpha$, and $N_2 = N_1/\delta^\beta$, where the exponents $\alpha = 2.84-0.08/n$, and $\beta = -0.08(1 + 1/n)$, with n being the power-law exponent of the shear viscosity vs. rate of shear. Assuming CRT $N_2 = N_1$ and $Q_2 = Q_1 \delta^{2.92}$, the experimental data were found to closely follow the ESP = const. approximation (Potente 1985; Rauwendaal 1986).

For the applications where degassing is crucial, the degassing constant, K'', for specific TSE geometry must be established:

$$K'' = \left(Q/LN^{1/2}\right)\ln(\Delta c_o/\Delta c_f) \tag{11.30}$$

where Q is throughput, L is vent length, N is screw speed, and $\Delta c_o = c_o - c_{e,o}$, and $\Delta c_f = c_o - c_{e,f}$, c_o being the initial concentration of volatiles and c_e the equilibrium

Table 9.23 Examples of compatibilization in TSEs

Process	TSE	Comment	Reference
Free radical degradation of PO by addition of peroxides	CORI, ICRR, CRNI	Graftable monomer may also be added	McCullough and Bradford 1996
Reactive toughening of PC with functionalized TPOs	CORI	The blends may also contain PPE PPS, PEST, or acrylic	Khouri and Stoddard 1995
PPS modification by partial cross-linking with dinitro compounds	CORI	Fillers can also be added	Kohler and Sarabi 1995
Preparation of PC–PBT copolymers	CORI	Compatibilizer for PPE/PBT/SEBS blends	Chambers et al. 1995
Reactive blending of PPE/SBS with dioctylamine	CRNI	To improve resistance to loss of toughness upon thermal cycling	Richards and Pickett 1995
Reactive blending of epoxy triazine capped PPE with PBT/SBS	CORI	SEBS, (SB)$_n$ with epoxidized elastomer can be added	Yates 1995
Epoxidized PPE blended with grafted PO and SBS	TSE	PE or PP grafted with t-alkyl carbamate	Campbell and Presley 1995
PE/PB nonreactive blends	Leistritz TSE	Impact modification of PE	Sato 1995
Reactive toughening of PA	CORI	EEA or CHR containing glycidyl ether moiety	Nakajima 1994
PPE/PS/PO/SEBS blends	ICRR	Incorporation of PP and styrene-grafted PP	DeNicola and Guyer 1994
PA toughened by incorporation of solution-maleated SEBS	CORI	Blends can also be prepared in solution or using internal mixer	Gelles et al. 1994
Polyglutarimide/liquid crystal polyesters	CRNI	Other PEST or PC may also be added	Hallden-Abberton et al. 1994
PPE/PA blends improved by incorporation of a polysiloxane	TSE	Melt blending in TSE at 285 °C	Smits et al. 1994
POM with TPU, PA, PO, PEST	CORI	Ethylene-butylmethacrylate-glycidyl methacrylate added	Flexman 1994
PBT poly(styrene-co-methacrylic acid) blends	TSE	Impact modifier can be added	Yang and McCready 1994
PPE/HIPS/EPDM-SAN	TSE	Fillers (carbon black, mica, etc.) can also be added	Fujii and Ishikawa 1994
Poly(dimethylsiloxy-biphenylen epoxide) PBT blends	CORI	Improved flame retardancy and impact strength	Jordan and Webb 1994
Impact modification of PA	CORI	Acidified core-shell copolymers	Liu and Liwak 1994
PPE/PA compatibilized by addition of trimellitic anhydride acid chloride	CORI	T = 232–287 °C, N = 290 rpm	Aycock and Ting 1994

Table 9.23 (continued)

Process	TSE	Comment	Reference
HDPE/LDPE nonreactive blends	TSE	Improved low-T properties	Bohm et al. 1994
Syndiotactic PS, maleated PPE, and elastomer blends	TSE	Compounding at 300–350 °C	Okada and Masuyama 1994
Semicrystalline, semi-aromatic PA blended with polyesteramide	CORI	Extruded at T = 288 °C, N = 170–215 rpm	Goldwasser and Chen 1994
PAI/PPS/organic diisocyanate	TSE	T = 360 °C	Kawaki et al. 1994
Impact modification of POM by blending with TPU, pentaerythritol, and diphenylmethane-diisocyanate	CORI	T = 210 °C, residence time t = 1–2 min	Nagai et al. 1994
PPE/PA/SEBS blends compatibilized by addition of maleic anhydride	CORI	Blends compounded at T = 232–293 °C, N = 280 rpm	Lee 1994
Reactive blends of PPS with epoxy-functionalized polysiloxane	CORI	A dry blend extruded at T = 130–290 °C, vacuum devolatilization	Han 1994
PC/PEST/epoxidized PO/ABS	CORI	T = 270 °C, N = 250 rpm, vacuum devolatilization	Laughner 1994
Grafted PMP with glass fiber sized with carboxylic styrene–butadiene	CORI	T = 260–290 °C, N = 250 rpm	Hagenson et al. 1994
PP/PEST/PP-PEST graft copolymer	TSE	D = 45 mm, T = 280 °C, N = 200 rpm	Fujita et al. 1994
Recycled domestic or industrial plastics, reactively stabilized	TSE	T = 190 °C	Pauquet et al. 1994
PPS/PPE/PA/SEBS and acidified PO	TSE	D = 50 mm, T = 300 °C	Ishida and Kabaya 1994
PPE/PEST/ polystyrene–polycarbonate copolymer	CRNI	D = 20 mm, T = 120–266 °C, N = 400	Brown and Fewkes 1994
PC/acrylic multipolymer/grafted, unsaturated rubber	TSE	D = 30 mm, T = 232 °C, N = 100 rpm	Zimmerman et al. 1994
PEST/PA/EEA–GMA copolymer	TSE	T = 270 °C	Natarajan et al. 1994
Polyphthalamide/PP/carboxylated PO	CORI	D = 30, T = 285–320 °C, N_2	Paschke et al. 1994
PPE/maleated EPR/EVAc grafted with GMA/PA/PEST/4-functional epoxy resin/oleic acid amide	High-speed TSE	Maleation: D = 30 mm, L/D = 28, T = 230 °C, N = 60 rpm; compounding: D = 47 mm, T = 310 °C, N = 500 rpm	Nishio et al. 1994
Blends of semicrystalline PA (matrix) and amorphous PA (dispersed phase)	CORI	D = 30 mm, maleated EPR added	Schmid and Thullen 1994

(*continued*)

Table 9.23 (continued)

Process	TSE	Comment	Reference
PP/EPR/SEBS	CORI (tapered)	T = 246 °C, N = 350 rpm	deNicola and Conboy 1994
PC/PEST/amine-functionalized elastomer with maleated EPR	CORI	D = 34 mm, L/D = 40, T = 250–270 °C, N = 200–250 rpm	Akkapeddi and van Buskirk 1994
Blends of aliphatic and aromatic PAs with aliphatic polyester (PCL)	TSE	D = 30 mm, T = 285 °C	Hamada et al. 1994
Semi-aromatic PA blends with PC	CORI	D = 30 mm, T = 270 °C	Gambale et al. 1994
POM with core-shell copolymer	TSE	D = 30 mm, T = 200 °C	Sasaki et al. 1994
PET or PBT with 1 wt% sodium sulfonate groups, PE-ionomer, PBT	TSE	D = 30 mm, T = 245 °C, N = 80 rpm	Tajima et al. 1994
Polycycloolefin (PCO)/grafted PCO/grafted elastomer/PA	TSE	D = 30 mm, T = 260 °C	Moriya et al. 1994
PC/ABS containing hydroxyethyl methacrylate/flame retardant	CORI	D = 28 mm, T = 249 °C	Vilasagar and Rawlings 1994
Modified PPE reacted with terminal amino groups of PA + SEBS	TSE	Vacuum devolatilization, T = 290 °C	Kodaira et al. 1994
PET/PC/PEC/elastomer	TSE	T = 260–300 °C	Freitag et al. 1994
PPE/PA-6, PO, or PBT/maleic anhydride/SEBS	TSE	T = 230 °C, N = 250 rpm	Takagi et al. 1994
PA/PO/SEBS compatibilized by acidified SMA, SEBS-MA	Leistritz ICRR	L/D = 28, T = 249 °C	Chundury 1994
PPE/PO compatibilized by EAA	Leistritz TSE	T = 270 °C	Cottis and Natarajan 1994
PP/ionomer/EGMA/EPR	CORI	D = 28 mm, L/D = 28, T = 210 °C	Dawson 1993
PA/maleated EPR	TSE	D = 44 mm, T = 240–270 °C	Ohmae et al. 1991
PC/PP/acryloid	TSE	T = 255–295 °C	Liu 1985
PEI/PP	CORI	T = 304–322 °C	Giles and Schlich 1984
Reactive grafting and polymerization of vinyl acetate in PP/polyester blend	TSE	T = 105–210 °C	Waniczek et al. 1983
PP/PC blends with GMA	CORI	T = 250 °C, N = 100 rpm	Zhihui et al. 1997

(continued)

Table 9.23 (continued)

Process	TSE	Comment	Reference
Postconsumer PET/HDPE blends with SEBS	CORI	T = 250 °C, N = 100 rpm, L/D = 25	Iñiguez et al. 2000
ABS/PC blends with SBS	TSE	T = 230 °C, N = 306 rpm	Tasdemir 2004
PA-6/ABS blends with MAPP or bisphenol A	TSE	T = 240 °C, N = 30–40 rpm	Cheng et al. 2006
PA-6/HDPE or recycled PE blends with MAPE	CORI	T = 255 °C, N = 102 rpm, L/D = 13	Araujo et al. 2008
PP/ABS blends with MAPP	TSE	T = 220 °C, N = 100 rpm, L/D = 40	Lee et al. 2009
PC/HDPE blends with E-MA-GMA	CORI	T = 250 °C	Yin et al. 2010
Recycled PET/different PE grades with SEBS-g-MA	CORI	T = 245 °C, L/D = 48	Zhang et al. 2011

Table 9.24 Functional characteristics of TSE

Function	CORI		ICRR		CRNI
	Low N	High N	Low N	High N	
Throughput	+	++	+	+	++
Distributive mixing	+	++	+	+	++
Dispersive mixing	o	+	o	++	−
Devolatilization	o	+	+	++	+
Melting	+	+	+	++	+
Conveying	+	o	++	+	−
Self-wiping	+	++	+	o	−
High screw speed	−	++	o	+	++
Residence time distribution	+	o	++	+	o
Pressure development	+	o	++	+	o
Screw separation	−	+	o	o	+
Feed capacity	+	o	++	++	+

Note: − poor, o OK, + good, ++ excellent

value (initially with subscript o and finally with subscript f) (Hashimoto et al. 1993). From the scale-up strategy, Q and N are computed; then Eq. 9.30 is used to determine the required vent length and/or the pressure of the vacuum line (that controls the equilibrium values, $c_{e,o}$, and $c_{e,f}$).

In applications where mixing efficiency is most critical, the scaling should be based on the total induced strain (γ) and its value (optimized in the small TSE) should be preserved in the larger machine (Manas-Zloczower 1991).

9.6   Conclusion

This chapter was divided into four parts: fundamentals of mixing, blending methods and equipment, nonmechanical blending, and reactive blending.

The theory of mixing distinguishes the dispersive and distributive mixing, the former dependent on stress, while the latter on strain. Both types of mixing are more efficient in the extensional than in shear flow field. The extensional flows more economically generate large dispersing fields and induce larger strains. Independently of the flow field, the best mixing strategy is generation of a series of deformation and folding steps.

A majority of commercial polymer blends are melt-blended, mostly in TSE, less frequently in SSE, and rarely in batch mixer and other specialty mixing devices. Around 1999, about 94 % of all patents on polymer blends described blends preparation in a TSE, and this number has not changed much since. This is particularly significant, since to make the invention more attractive, many of the texts claim that the blend "may also be prepared by other methods like solution blending, in a batch and SSE mixer." The high percentage of TSE being used to develop blends corresponds to the recent estimates of these machines used in the engineering alloys' production, and some analysts put the number as high as 90 %. This dominance of TSE most likely stems from the growing use of the reactive blending. Since SSE is not well suited for conducting chemical reactions, the demands gravitate toward the twin-screw machines (an abbreviated comparison of the SSE and TSE performance was given in Tables 9.15 and 9.16). The TSE selection is based on the production requirements. A summary of the performance characteristics is given in Table 9.24 (Rauwendaal 1993).

The single-screw extruders are being used for the preparation of blends that either do not require compatibilization or are compatibilized by addition of nonreactive compatibilizers. For both applications, SSE is frequently supplemented by additional mixing devices like mixing screws, add-ons, extensional flow mixer, etc. To the first category of blends also belong these systems that are produced as filaments or fibers. It has been found that creation of a large interface (by stretching) reduces the need for compatibilization (when the viscosity ratio is large, it may be difficult to transfer stress to the non-compatibilized dispersed phase). To the second category of blends belong these systems that are compatibilized and at the same time impact modified by the addition of multicomponent core and shell additives. To the third group of blends belong systems based on either PO or PVC with a large amount of elastomer. These highly viscous systems are prepared on roll mills, in a Banbury-type mixer, or non-intermeshing twin-shaft continuous mixers.

When selecting the mixing strategy, one must consider the thermomechanical degradability of the blend ingredients (including the compatibilizer), the time scale of the relaxation processes, as well as the stress-induced coalescence. Some polymers like PP are sensitive to degradation. For this reason, better performance may be obtained from PP/EPR blends using low dispersing energy, just sufficient to adequately disperse the elastomer without inducing too extensive degradation of the matrix.

One of the most efficient mechanisms of mixing is development of fibrils that upon reduction of stress disintegrate by the capillarity mechanism into thousands of micro-droplets. This mechanism, well known in the Newtonian systems, seems to be less efficient in systems comprising highly elastic dispersed phase and low interfacial tension coefficient like in R-TPO systems. The loss of efficiency is related to, on the one hand, small interfacial energy and, on the other, long relaxation times. However, it must be stressed that dispersion of high-viscosity polymer into a less viscous matrix is greatly facilitated by the extensional flow field.

When selecting mixing devices, it is important to remember that the final degree of dispersion is related to dynamic equilibrium between the dispersive and coalescing mechanisms. With the exception of dispersed phase concentration, they both depend on the same parameters. Thus, the rate of drop diameter decrease during dispersing is $\partial d/\partial t = -k_1 \dot{\gamma} d$, whereas that of coalescing $\partial d/\partial t = k_2 \dot{\gamma} \phi^{8/3}/d$. Hence, the rate of shear similarly affects the dispersion as the coalescence process. For this reason, when all other parameters are constant, the drop diameter is often found to be insensitive to the screw speed. It has been even reported that, owing to generation of very large interface and/or shear degradation of a compatibilizer, an increase of the shear rate may cause the drop size to grow.

9.7   Cross-References

Abbreviations

ABS acrylonitrile-butadiene-styrene
AFM atomic force microscope
Al aluminum
BEM boundary elements method
CA cellulose acetate
CHO cyclohexanone
CHX cyclohexane
CMC critical micelles concentration
CORI corotating intermeshing TSE
CRNI counterrotating non-intermeshing TSE
CRT constant residence time

CSE constant specific energy
CTC constant thermal conduction
CTM cavity transfer mixer
DCA dichloroacetic acid
DCP dicumyl peroxide
DCPO dicumyl peroxide
DMA dynamic-mechanical analysis
DMAC dimethylacetamide
DMF dimethyl formamide
DMX dynamic melt mixer
DSC differential scanning calorimetry
EDA ethylenediamine
EFM extensional flow mixer
EME elastic melt extruder
EPDM ethylene-propylene-diene monomer
EPR ethylene-propylene rubber
ESP specific energy (kWh/kg)
EtAc ethyl acetate
EtOH ethanol
EVA ethylene vinyl acetate
FA formic acid
FCM Farrel continuous mixer
FTIR Fourier transform infrared spectroscopy
GMA glycidyl methacrylate
GPC gel permeation chromatography or size exclusion chromatography (SEC)
HAP hexa(allylamino)cyclotriphosphonitrile
HDPE high-density polyethylene
ICRR intermeshing counterrotating TSE
JSW Japan (Nippon) Steel Works
LCB long chain branching
LCP liquid crystalline polymer
LDPE low-density polyethylene
LLDPE linear low-density polyethylene
MA methyl acrylate
MAH maleic anhydride
MAPE maleic anhydride polyethylene
MAPP maleic anhydride polypropylene
MC methyl chloride
MEK methylethylketone
MeOH methanol
MFM melt flow monitor (measuring shear viscosity vs. shear rate)
MIA multivariate image analysis
MMA methyl methacrylate
MSE multi-screw extruder

MW molecular weight
MWD molecular weight distribution
NIR near infrared
NMP N-methyl-2-pyrrolidone
NMR nuclear magnetic resonance spectroscopy
PA polyamide (nylon)
PBT polybutylene terephthalate
PC polycarbonate
PCA principal component analysis
PEO polyethylene oxide
PES polyethersulfone
PET polyethylene terephthalate
PI polyimide
PLGA Poly(lactic-co-glycolic) acid
PMMA polymethylmethacrylate
PO polyolefin
POM polyoxymethylene
PP polypropylene
PPS polyphenylene sulfide
PS polystyrene
PVAc polyvinyl acetate
PVC polyvinyl chloride
PVDF polyvinylidene fluoride
P(VDF-TrFE) poly(vinylidenefluoride-co-trifluoroethylene)
PVP polyvinyl pyrrolidone
SAN styrene acrylonitrile
SBS styrene-butylene-stryrene
scCO$_2$ supercritical carbon dioxide
SD spinodal decomposition
SEB styrene–ethylene–butylene block copolymer
SEBS styrene–ethylene–butylene–styrene block copolymer
SEM scanning electron microscopy
SM static (motionless) mixer
SSE single-screw extruder
STM scanning tunneling microscope
TCE tetrachloroethane
TEM transmission electron microscopy
TEMPO 2,2,6,6-tetramethyl-1-piperidinyloxy
TGA thermogravimetric analysis
THF tetrahydrofuran
TMPTA trimethylolpropane triacrylate
TMR Twente mixing ring
TPO thermoplastic olefin

TPU   thermoplastic urethane
TSE   twin-screw extruder
UV   ultraviolet
VIS   visible
W&P   Werner and Pfleiderer
WAXD   wide angle X-ray scattering
XPS   X-ray photoelectron spectroscopy
ZSK   *Zwei Schnecken Kneter* (two-screw kneader)

Nomenclature

a   area occupied by a copolymer molecule
b   channel width in a rectangular flow channel
B   droplet width, or the smaller diameter of prolate ellipsoid
C, c_i   constants
C_L   screw center-to-center distance
D   deformability parameter
d   droplet diameter
d*   equilibrium droplet diameter
De   Deborah number
d_o   initial diameter of droplet
D_p   particle diffusion coefficient
dP/dz   pressure gradient
E   energy of mixing
e'   relative flight width $= e/(\pi D_s \sin\varphi)$
E_+   threshold energy of coagulation
E_{DK}   macroscopic bulk breaking energy
$\overline{F}_d, F_p$ correction shape factors
$\overline{h}$ mean channel depth
H   Hamaker constant of the system
h_c   critical separation distance
K''   degassing constant
k_B   Boltzmann constant
L   length of a drop
L   screw length, or vent length
L/D   length-to-diameter ratio (TSE barrels)
m   consistency index (power-law viscosity model)
n   power-law flow index, or number of particles
N   screw rotation speed
N_{av}   Avogadro's number
n_c   number of divisions in a static mixer
N_s   number of striations

p aspect ratio

P pressure

$\mathbf{p_r}$ probability that two particles that have collided result in coalescence

q sinusoidal distortion

$\mathbf{Q, Q_c}$ throughout, throughput capacity

R radius of a dispersed drop

R interfacial area ratio

Re Reynolds number

$\mathbf{R_i}$ interfacial area

T temperature

t time, or pitch

$\mathbf{t_b}$ necessary time for breakup of droplets

$\mathbf{t_b}^*$ dimensionless breakup time

$\mathbf{t_c}$ coalescence time

u velocity field

V free volume of the extruder

v velocity

$\mathbf{v_x}$ velocity in the x direction

$\mathbf{V_x/V}$ volume fraction of emulsion undergoing uniform shear

$\mathbf{\overline{V}}$ average flow velocity

x linear distance

$\mathbf{Wi_d}$ dispersed phase Weissenberg number

$\boldsymbol{\alpha}$ orientation or tip angle

$\boldsymbol{\alpha_i}$ breakup parameter

$\boldsymbol{\alpha_o}$ the distortion at t = 0

$\boldsymbol{\beta}$ orientation angle

$\boldsymbol{\chi_{12}}$ thermodynamic binary interaction parameter

$\boldsymbol{\delta}$ solubility parameter

$\boldsymbol{\Delta l_\infty}$ interphase thickness for MW $\rightarrow \infty$

$\boldsymbol{\Delta P}$ pressure drop

$[\dot{\boldsymbol{\varepsilon}}]$ velocity gradient tensor

$\boldsymbol{\phi_c}$ percolation threshold volume fraction

$\boldsymbol{\phi_d}$ volume fraction of dispersed phase

$\boldsymbol{\phi_m}$ maximum packing volume fraction

$\boldsymbol{\eta}$ viscosity

$\boldsymbol{\eta_d, \eta_m}$ viscosity of dispersed and matrix phase, respectively

$\boldsymbol{\gamma}$ shear rate

$\boldsymbol{\kappa}$ capillary (or Taylor) number

$\boldsymbol{\kappa_{crit}}$ critical capillary number

$\boldsymbol{\Lambda}$ distortion wavelength

$\boldsymbol{\lambda}$ viscosity ratio

$\boldsymbol{\nu_{12}}$ interfacial tension coefficient between phase 1 and 2

$\boldsymbol{\nu^\circ_{12}}$ interfacial tension in a quiescent polyblend

$\boldsymbol{\rho, \rho_d}$ density, droplet density

$\sigma_{11} - \sigma_{22}$ the first normal stress difference

σ_{12} shear stress

τ relaxation time

$\Omega(\Lambda, \lambda)$ Tomotika's tabulated function

References

T.I. Ablazova, M.B. Tsebrenko, A.B.. Yudin, G.V. Vinogradov, B.V. Yarlykov, J. Appl. Polym. Sci. **19**, 1781 (1975)

B.I. Adams, Soc. Plast. Eng. Reg. Tech. Conf. Paper, 13 March 1974

N. Aggarwal, K. Sarkar, J. Fluid Mech. **584**, 1 (2007)

R.M. Ahmed, Int. J. Polym. Mater. **57**, 969 (2008)

M.K. Akkapeddi, B. VanBuskirk, U.S. Patent 5,283,285, 01 Feb 1994, Appl. 05 Apr 1993, to AlliedSignal, Incorporated

American Leistritz Extruder Corporation, *Twin Screw Workshop*, Sommerville, NJ, Dec (1996)

D. Anders, Kunststoffe **69**, 194 (1979)

Anonymous, *Plast. Machin. Equip.*, **53**, June (1981)

Anonymous, *A No-nonsense Guide to Extrusion Systems for Continuous Compounding*, Welding Eng., Technical Bulletin (1989a)

Anonymous, *Bitruders BT*, Reifenhäuser Techn. Inf. Bull. No. 0/3.2-8903 (1989b)

Anonymous, *Compounding and Granulating Plant for PVC*, Berstorff Techn. Inf. (1989c)

Anonymous, *High Performance Twin-screw Compounding System*, Werner & Pfleiderer GmbH, Techn. Inf. Bull. Nos. 21E.8910A.1000, 05-098/2, 05-085/1, 05-100/2 (1989d)

Anonymous, *MPC/V, AP V Chemical Machinery*, Baker Perkins, Techn. Inf. (1989e)

Anonymous, *Planetary Roller Extruder*, Battenfeld Extrusiontechnik (1989f)

Anonymous, *Twin-screw Continuous Mixers*, ComacPlast, Techn. Inf. (1989g)

Anonymous, *Buss Kneader Lines*, Bulletin Nos. 0075, 2152, 2282, Buss A.-G., Basel (1989h)

K. Arai, C. Ueda-Mashima, T. Kotaka, K. Yoshimura, K. Murajama, Polymer **25**, 230 (1984)

J.R. Araujo, M.R. Vallim, M.A.S. Spinacé, M.A. De Paoli, J. Appl. Polym. Sci. **110**, 1310 (2008)

H. Aref, J. Fluid Mech. **143**, 1 (1983)

L. Assoun, S.C. Manning, R.B. Moore, Polymer **39**, 2571 (1998)

D.F. Aycock, S.P. Ting, U.S. Patent 5,331,060, 19 July 1994, Appl. 22 Feb 1993, 28 Dec 1990, 14 Sept 1990, 06 Nov 1987, 19 Sept 1985, to General Electric Company

I. Banu, J.P. Puaux, G. Bozga, I. Nagy, Macromol. Symp. **289**(108) (2010)

A. Beamish, D.L. Hourston, Polymer **17**, 577 (1976)

A. Beamish, R.A. Goldberg, D.L. Hourston, Polymer **18**, 49 (1977)

J.F. Beecher, L. Marker, R.D. Bradford, S.L. Aggarwal, J. Polym. Sci. A2 **26**, 117 (1969)

H. Berghmans, N. Overbergh, J. Polym. Sci. Polym. Phys. Ed. **15**, 1757 (1977)

J. Berzen, G. Braun, Kunststoffe **69**(2), 62 (1979)

D.M. Binding, J. Non-Newt. Fluid Mech. **27**, 173 (1988)

R. Binsack, D. Rempel, H. Korber, D. Neuray, U S. Patent 4,260,690, 1981 to Bayer A.-G.

L.L. Blyler, *Ph.D. thesis*, Princeton University 1966

L. Bohm, H.F. Enderle, H. Jastrow, U. S. Patent 5,338,589, 16 Aug 1994, Appl. 03 June 1992, to Hoechst A.-G.

V. Bordereau, Z.-H. Shi, P. Sammut, L.A. Utracki, M. Carrega, Polym. Eng. Sci. **32**, 1846 (1992)

M. Bouquey, C. Loux, R. Muller, G. Bouchet, J. Appl. Polym. Sci. **119**, 482 (2011)

D. Bourry, B.D. Favis, Polymer **39**, 1851 (1998)

D. Bourry, L.A. Utracki, A. Luciani, *Polyblends*-'95, NRCC/IMI Bi-annual symposium and SPE-RETEC on *Polymer Alloys and Blends*, Boucherville, QC, Canada, Oct (1995)

D. Bourry, F. Godbille, R.E. Khayat, A. Luciani, J. Picot, L.A. Utracki, Polym. Eng. Sci. **39**, 1072 (1999)

D.W. Bousfield, R. Keunings, G. Marucci, M.M. Denn, J. Non-Newt. Fluid Mech. **21**, 79 (1986)

B. Briscoe, A.C. Smith, J. Appl. Polym. Sci. **28**, 3827 (1983)

T.O. Broadhead, W.I. Patterson, J.M. Dealy, Polym. Eng. Sci. **36**, 2840 (1996)

L.R. Brostrom, D.L. Coleman, D.E. Gregonill, J.D. Andrade, Macromol. Chem. Rapid Commun. **1**, 341 (1980)

S.B. Brown, in *Reactive Extrusion: Principles and Practice*, ed. by M. Xanthos (Hanser, Munich, 1992)

S.B. Brown, E.J. Fewkes Jr., U.S. Patent 5,290,863, 01 Mar 1994, Appl. 31 Dec 1990, to General Electric Company

J.R. Campbell, J.R. Presley, U.S. Patent 5,380,796, 10 Jan 1995, Appl. 21 Jan 1994, to General Electric Company

E.L. Canedo, L.N. Valsamis, in *Mixing and Compounding of Polymers*, ed. by I. Manas-Zloczower, Z. Tadmor (Hanser, Munich, 1994)

K. Cao, Y. Li, Z.Q. Lu, S.L. Wu, Z.H. Chen, Z. Yao, Z.M. Huang, J. Appl. Polym. Sci. **121**, 3384 (2011)

R. Cardinaels, A. Vananroye, P. van Puyvelde, P. Moldenaers, Macromol. Mater. Eng. **296**, 214 (2011)

P. Cassagnau, V. Bounor-Legaré, F. Fenouillot, Int. Polym. Proc. **22**, 218 (2007)

G.R. Chambers, G.F. Smith, J.B. Yates III, U.S. Patent 5,384,359, 24 Jan 1995, Appl. 08 Nov 1989, to General Electric Company

Z. Chen, J.L. White, SPE ANTEC Tech. Pap. **38**, 1332 (1992); Int. Polym. Process **6**, 342 (1992); SPE ANTEC Tech. Pap. **39**, 3401 (1993)

L. Chen, G.-H. Hu, J.T. Lindt, Int. Polym. Proc. **11**, 329 (1996)

H. Chen, U. Sundararaj, K. Nandakumar, Polym. Eng. Sci. **44**, 1258 (2004)

F. Cheng, H. Li, W. Jiang, D. Chen, J. Macromol. Sci. **B45**, 557 (2006)

J. Cheng, J. Zhang, X. Wang, J. Appl. Polym. Sci. **127**, 3997 (2013)

H.B. Chin, C.D. Han, J. Rheol. **23**, 557 (1979); J. Rheol. **24**, 1 (1980)

J.W. Cho, J.L. White, Int. Polym. Proc. **11**, 21 (1996)

T.S. Chow, C.A. Liu, R.C. Penwell, J. Polym. Polym. Phys. Ed. **14**, 1311 (1976)

D. Chundury, U.S. Patent 5,278,231, 11 Jan 1994, Appl. 24 May 1990, Appl. 16 Sept 1992, to Ferro Corporation

R.J. Clark, SPE ANTEC Techn. Paper **41**, 3306 (1995)

J.R. Collier, J. Educ. Modul. Mat. Sci. Eng. **3**, 275 (1981)

J.R. Collier, O. Romanoschi, S. Petrovan, J. Appl. Polym. Sci. **69**, 2357 (1998)

S.H. Collins, *Plastics Compounding*, 29 Nov/Dec 1987

C.M. Costa, M.N. Tamaño Machiavello, J.L. Gomez Ribelles, S. Lanceros-Méndez, J. Mater. Sci. **48**, 3494 (2013)

S.G. Cottis, K.M. Natarajan, U.S. Patent 5,356,992, 18 Oct 1994, Appl. 26 Feb 1993, to Enichem America Incorporated

J.M.G. Cowie, I.L. McEwen, J. Macromol. Sci. Phys. Ed. **B16**, 611 (1979); Macromolecules, **13**, 169 (1980)

J.M.G. Cowie, D. Lath, I.J. McEwen, Macromolecules **12**, 52 (1979b)

R.G. Cox, J. Fluid Mech. **37**, 601 (1969)

Z. Crocker, U.S. Patent 4,272,474, 09 Jun 1981, to Carlew Chemicals

R.J. Crowson, M.J. Folkes, P.F. Bright, Polym. Eng. Sci. **20**, 925 (1980)

J. Curry, P. Andersen, SPE ANTEC Techn. Papers **36**, 1938 (1990)

S.S. Dagli, M. Xanthos, J.A. Biesenberger, Polym. Eng. Sci. **34**, 1720 (1994)

P.V. Danckwerts, Appl. Sci. Res. **A3**, 279 (1953)

W.H. Darnell, E.A.J. Mol, SPE J. **12**, 20 (1956)

R.L. Dawson, U.S. Patent 5,206,294, 27 Apr 1993, Appl. 06 Nov 1991, to E. I. du Pont de Nemours & Company

R.A. De Bruijn, Ph.D. thesis, Eindhoven University of Technology, 1989

R.A. De Graaf, P.B.M. Janssen, Polym. Eng. Sci. **40**, 2086 (2000)

A. De Loor, T. Cassagnau, A. Michel, B. Vergnes, Int. Polym. Proc. **9**, 211 (1994)

A. De Loor, P. Cassagnau, A. Michel, L. Delamare, B. Vergnes, Int. Polym. Proc. **11**, 139 (1996)

L. Delamare, B. Vergnes, Polym. Eng. Sci. **36**, 1685 (1996)

A.J. DeNicola Jr., M.R. Conboy, U.S. Patent 5,286,791, 15 Feb 1994, Appl. 29 May 1992, to Himont, Incorporated

A.J. DeNicola, R.A. Guyer, U.S. Patent 5,370,813, 06 Dec 1994, Appl. 25 Feb 1994, 26 Mar 1990, to Himont, Incorporated

B. Djermouni, H.J. Ache, Macromolecules **13**, 168 (1980)

M. Doi, T. Ohta, J. Chem. Phys. **95**, 1242 (1991)

N. Domingues, A. Gaspar-Cunha, J.A. Covas, Polym. Eng. Sci. **50**, 2195 (2010)

A. Dreiblatt, in *Encyclopedia of Polymer Science and Engineering*, ed. by J.I. Kroschwitz, vol. 15 (John Wiley and Sons, New York, 1989)

M. Dressler, B.J. Edwards, Rheol. Acta **43**, 257 (2004)

B. Dubrulle D'Orhcel, in *Recycling of PVC & Mixed Plastic Waste*, ed. by F.P. La Mantia (ChemTec, Toronto, 1996)

G.C. Eastmond, K. Haraguchi, Polymer **24**, 1171 (1983)

K. Ebner, J.L. White, Int. Polym. Proc. **9**, 233 (1994)

L. Eckart, W. Bambeister, M. Baumeister, G. Oedl, U.S. Patent US20110128812 A1, 02 June 2011, Appl. 27 May 2009, to British Telecommunications Public Limited Company and Bruckner Maschinenbau GmbH & Co KG

M.F. Edwards, in *Mixing in the Process Industries*, ed. by N. Harnby, M.F. Edwards, A.W. Nienow (Butterwords, London, 1985)

O.M. Ekiner, R.A. Hayes, P. Manos, U.S. Patent 4,863,496, 1989

P.H.M. Elemans, H.E.M. Meijer, Polym. Eng. Sci. **30**, 893 (1990)

P.H.M. Elemans, J.G.M. Van Gisbergen, H.E.M. Meijer, in *Integration of Fundamental Polymer Science and Technology – 2*, ed. by P.J. Lemstra, L.A. Kleintjens (Elsevier Applied Science, London, 1988)

P.H.M. Elemans, Ph.D. thesis, Eindhoven University of Technology, The Netherlands, 1989

P.H.M. Elemans, J.M. Janssen, H.E.M. Meijer, J. Rheol. **34**, 1311 (1990)

J.J. Elmendorp, Polym. Eng. Sci. **26**, 418 (1986)

J.J. Elmendorp, R.J. Maalcke, Polym. Eng. Sci. **25**, 1041 (1985)

J.J. Elmendorp, A.K. Van der Vegt, Polym. Eng. Sci. **26**, 1332 (1986)

J.J. Elmendorp, Ph.D. thesis, Delft University of Technology, The Netherlands, 1986

B.N. Epstein, U.S. Patent 4,174,358; 4,172,859, 1979 to DuPont

M. Erol, D.M. Kalyon, Int. Polym. Proc. **20**, 228 (2005)

L. Erwin, in *Mixing in Polymer Processing*, ed. by C. Rauwendaal (Marcel Dekker, New York, 1991)

Fabrique Nationale Herstal, S. A., Neth. Pat. Appl. **007,963**, 18 Sep 1977, Appl. 18 Sep (1975)

B.D. Favis, J. Appl. Polym. Sci. **39**, 285 (1990); Can. J. Chem. Eng. **69**, 619 (1991)

F. Feigl, F.X. Tanner, B.J. Edwards, J.R. Collier, J. Non-Newt. Fluid. Mech. **115**, 191 (2003)

D. Feldman, J. Macromol. Sci. **A42**, 587 (2005)

D. Feng, G.L. Wilkes, J.V. Crivello, Preprints 3rd Chemical Congress of North America, ACS Division of Polymeric Materials, Science and Engineering, Toronto, 6–10 June 1988, vol 58 (1988)

F. Fenouillot, H. Perier-Camby, Polym. Eng. Sci. **44**, 625 (2004)

E.G. Fisher, *Extrusion of Plastics, Plastics Institute Monograph* (Iliffe, London, 1958)

E.D. Flexman Jr., U.S. Patent 5,318,813, 07 June 1994, Appl. 25 Nov. 1991; U.S. Patent 5,344,882, 06 Sept 1994, Appl. 27 Jan. 1993, to E. I. du Pont de Nemours & Company

R.W. Flumerfelt, Ind. Eng. Chem. Fundam. **11**, 312 (1972)

H. Frederix, 5th Conference of the European Plastic Caoutch, Paris (1978)

D. Freitag, K.-J. Idel, G. Fengler, U. Grigo, J. Kirsch, U. Westeppe, U.S. Patent 5,310,793, 10 May 1994, Appl. 30 Jan 1990, 12 Feb 1993, Ger. Appl. 02 Feb. 1989, to Bayer A.-G.

H.G. Fritz, Kunststoftechnik **6**, 430 (1968)

H.-G. Fritz, B. Stöhrer, Int. Polym. Proc. **1**, 31 (1986)

H.G. Fritz, Ph. D. thesis, Stuttgart University, Germany, 1971

T. Fujii, M. Ishikawa, U.S. Patent 5,334,636, 02 Aug 1994, Appl. 26 Mar 1992, to Sumitomo Chemical Company, Limited

Y. Fujita, T. Kawamura, K. Yokoyama, K. Yokomizo, S. Toki, U.S. Patent 5,298,557, 29 Mar 1994, Appl. 01 Feb 1991, Jap. Appl. 02 Feb 1990, to Tonen Corporation

G. Gagliani, U.S. Patent 5,044,759, 3 Sep 1991, Appl. 21 Feb 1989

G.M. Gale, R.S. Hindmarch, Eur. Rubber J. **29** (1982)

R.J. Gambale, D.C. Clagett, L.M. Maresca, S.J. Shafer, U.S. Patent 5,280,088, 18 Jan 1994, Appl. 14 June 1990, 28 Feb 1986, 29 Jan 1988, 08 Nov 1989, to General Electric Company

F. Gauthier, H.L. Goldsmith, S.G. Mason, Rheol. Acta **10**, 344 (1971)

R. Gelles, W.P. Gergen, R.G. Lutz, M.J. Modic, U.S. Patent 5,371,141, 06 Dec 1994, Appl. 02 Apr 1992, Appl. 31 July 1985, to Shell International Research Maatschappij, BV

R. Gendron, L.E. Daigneault, M.M. Dumoulin, J. Dufour, Int. Plat. Eng. Technol. **2**, 55 (1996)

H.F. Giles Jr., W.R. Schlicht, U.S. Patent 4,430,484; 4,427,830, 24 Jan 1984, Appl. 18 Mar 1982, to General Electric Company

L.A. Goettler, A.J. Lambright (to Monsanto Company), U.S. Patent 4,056,591, 1977

L.A. Goettler, K.S. Shen, Rubber Chem. Technol. **56**, 619 (1983)

L.A. Goettler, 25th Annual Conference, Reinforced Plastics, Composites Division, Society for Plastics Industry Inc., Section 14-A, 1 (1970)

L.A. Goettler, A.J. Lambright, R.I. Leib, P.J. Dimauro, Rubber Chem. Technol. **54**, 277 (1981)

D. Goffart, D.J. van der Wal, E.M. Klomp, H.W. Hoogstraten, L.P.B.M. Janssen, L. Breysse, Y. Trolez, Polym. Eng. Sci. **36**, 901 (1996)

D.J. Goldwasser, A.T. Chen, U.S. Patent 5,321,099, 14 June 1994, Appl. 02 Jan 1992, to The Dow Chemical Company

P.A. Good, A.J. Chwartz, C.W. Macosko, AIChE J. **20**, 67 (1974)

T.G. Gopakumar, S. Ponrathnam, A. Lele, C.R. Rajan, A. Fradet, Polymer **40**, 357 (1999)

A.K. Gosh, S. Lorek, J.T. Lindt, SPE Techn. Paper **37**, 232 (1991)

R. Gosselin, D. Rodrigue, R. González Núñez, C. Duchesne, Can. J. Chem. Eng. **86**, 869 (2008)

R. Gosselin, D. Rodrigue, R. González Núñez, C. Duchesne, Ind. Eng. Chem. Res. **48**, 3033 (2009)

R. Gosselin, D. Rodrigue, C. Duchesne, Comp. Chem. Eng. **35**, 296 (2011)

H.P. Grace, Paper presented at the Third Engineering Foundation Research Conference on Mixing, Andover, 9–14 Aug 1971; Chem. Eng. Commun. **14**, 225 (1982)

D. Gras, Plast. Tech. **18**, 40 (1972)

D. Gras, K. Eise, SPE ANTEC Tech. Papers **21**, 386 (1975)

M. Grmela, A. Ait-Kadi, J. Non-Newt. Fluid Mech. **55**, 191 (1994)

M. Grmela, A. Ait-Kadi, L.A. Utracki, J. Non-Newt. Fluid Mech. **77**, 253 (1998)

J.F. Gu, M. Grmela, Phys. Rev. E **78**, 056302 (2008)

G.R. Guillen, Y. Pan, M. Li, E.M.V. Hoek, Ind. Eng. Chem. Res. **50**, 3798 (2011)

C.G. Hagberg, SPE ANTEC Techn. Papers **38**, 2 (1992)

M.J. Hagenson, H.F. Efner, E. Bourdeaux Jr., U.S. Patent 5,308,893, 03 May 1994, Appl. 26 Oct 1992, to Phillips Petroleum Company

M.P. Hallden-Abberton, N.M. Bortnick, W.J. Work, Can. Pat. 2,108,392, 23 Apr 1994; U.S. Patent 5,362,809, 08 Nov 1994, Appl. 22 Oct 1992, to Rohm & Haas Company

T. Hamada, S. Yakabe, A. Ito ,U.S. Patent 5,283,282, 01 Feb 1994, US Appl. 05 Dec 1988, 10 Dec 1991, Jap. Appl. 08 Dec 1987, to Asahi Kasei Kogyo Kabushiki Kaisha

C.D. Han, *Multiphase Flow in Polymer Processing* (Academic, New York, 1981)

C.D. Han, Amer. Inst. Chem. Eng. J. **19**, 649 (1973); Rheol. Acta **14**, 173, 182 (1975)

C.D. Han, L.H. Drexler, J. Appl. Polym. Sci. **17**, 2329 (1973)

C.D. Han, K. Funatsu, J. Rheol. **22**, 113 (1978)

C.Y. Han, U.S. Patent 5,324,796, 28 June 1994, Appl. 02 Dec 1992, to General Electric Company

C.D. Han, T.C. Yu, J. Appl. Polym. Sci. **15**, 1163 (1981)

W. Hanslik, U.S. Patent 3,640,669, 08 Feb 1972, Appl. 05 Nov 1969, to Dorplastex A.G.

N. Hashimoto, K. Kubota, K. Koike, T. Mihara, K. Kataoka, *JSW Technical review No. 14* (1993)

C.J. Heffelfinger, Polym. Eng. Sci. **18**, 1163 (1978)

E. Helfand, Y. Tagami, Polym. Lett. **9**, 741 (1971); J. Chem. Phys. **57**, 1812 (1971); J. Chem. Phys. **56**, 3592 (1972)

J.M.S. Henis, M.K. Tripodi, U.S. Patent 4,230,463 (1980); J. Memor. Sci. **8**, 233 (1981)

H.H. Herrmann, Kunststoffe **78**, 876 (1988)

H.H. Herrmann, U. Burkhardt, *Polymer Extrusion*, PRI Intl. Conf. 27 & 28 June, 1979, London; Adv. Plast. Technol. **1**, 1 (1981)

P. Hold, Adv. Polym. Technol. **2**, 197 (1982)

P. Hold, Theory and Practice of Polymer Mixing, in *Two-Phase Polymer System*, ed. by L.A. Utracki (Hanser, Munich, 1991)

P. Hold, Z. Tadmor, L. Valsamis, SPE ANTEC Tech. Papers **25**, 205 (1979)

I. Housz, Europ. Meet. Polym. Process. Soc., Kerkrade, Oct–Nov (1989)

A.S. Hsu, L.G. Leal, J. Non-Newt. Fluid Mech. **160**, 176 (2009)

G.-H. Hu, Y.-J. Sun, M. Lambla, Polym. Eng. Sci. **36**, 676 (1996a)

G.-H. Hu, L. Chen, J.T. Lindt, Int. Polym. Proc. **11**, 228 (1996b)

M.A. Huneault, Z.H. Shi, L.A. Utracki, Polym. Eng. Sci. **35**, 115 (1995a)

M.A. Huneault, M.F. Champagne, A. Luciani, J.-F. Hetu, L.A. Utracki, Polymer Processing Society, Stuttgart, Sept (1995b)

M.A. Huneault, M.F. Champagne, A. Luciani, Polym. Eng. Sci. **36**, 1685 (1996)

J. Huszman, Kunststoffe **73**, 347 (1983)

S. Ichihara, A. Komatsu, T. Hata, Polym. J. **2**, 640 (1971)

G. Illing, U.S. Patent 3,536,680 (1970) to Werner & Pfleiderer

J.F. Ingen Housz, Plastverarbeiter **10**, 1 (1975)

C.G. Iñiguez, E. Michel, V.M. Gonzalez-Romero, R. Gonzalez-Nuñez, Polym. Bull. **45**, 295 (2000)

T. Inoue, T. Soen, T. Hashimoto, H. Kawai, J. Polym. Sci.: Part A-2, **7**, 1283 (1960)

T. Inoue, T. Ougizawa, O. Yasuada, K. Miyasaka, Macromolecules **18**, 57 (1985)

H. Ishida, H. Kabaya, U.S. Patent 5,292,789, 08 Mar 1994, Appl. 15 May 1992, Jap. Appl. 16 May 1991, to GE Plastics Japan, Limited

S. Jakopin, P. Franz, Plast. South Africa, 32–46, April (1989)

A. Jelic, P. Ilg, C. Öttinger, Phys. Rev. E **81**, 011131 (2010)

A. F. Johnson, *National Physical Laboratory report, Division of Materials applications*, Report No. 26, Teddington (1972)

T.C. Jordan, J.L. Webb, U.S. Patent 5,334,672, 02 Aug 1994, 26 July 1991, 12 Aug 1992, to General Electric Company

B. Jurkowski, R. Urbanowicz, M. Szostak, Pol. Patent 168,449, 04 Sep 1992

T. Kajiwara, Y. Nagashima, Y. Nakano, K. Funatsu, Polym. Eng. Sci. **36**, 2142 (1996)

P.N. Kaloni, J. Phys. Soc. Japan **20**, 132, 610 (1965)

D.M. Kalyon, A.D. Gotsis, U. Yilmazer, C.G. Gogos, H. Sangani, B. Aral, C. Tsenoglou, Adv. Polym. Technol. **8**, 337 (1988a)

D.M. Kalyon, A. Gotsis, C. Gogos, C. Tsenoglou, SPE ANTEC Tech. Pap. **34**, 64 (1988b)

M.R. Kamal, M.E. Ryan, Adv. Polym. Technol. **4**, 323 (1984)

J. Kargar-Kocsis, L. Mészaros, T. Barany, J. Mater. Sci. **48**, 1 (2013)

H. Kawai, T. Soen, T. Inoue, T. Ono, T. Uchida, Memo. Fac. Eng., Kyoto University **33**, 383 (1971)

T. Kawaki, A. Amagai, M. Ishikawa, T. Yamada, Y. Hirai, H. Ban, U.S. Patent 5,321,097, 14 June 1994, Appl. 20 Dec 1990, to Mitsubishi Gas Chemical Company, Incorporated

M.R. Kearney, in *Mixing in Polymer Processing*, ed. by C. Rauwendaal (Marcel Dekker, New York, 1991)

B.J. Keestra, P.C.J. van Puyvelde, P.D. Anderson, H.E.H. Meijer, Phys. Fluids **15**, 2567 (2003)

R.E. Kesting, *Synthetic Polymeric Membranes: A Structural Perspective*, 2nd edn. (Wiley-Interscience, New York, 1985)

R.E. Khayat, A. Luciani, L.A. Utracki, Bound Elem **8**, 515 (1996)

K. Khomami, G.M. Wilson, J. Non-Newt. Fluid Mech. **58**, 47 (1995)

F.F. Khouri, G.J. Stoddard, U.S. Patent 5,391,616, 21 Feb 1995, Appl. 22 Dec 1993, to General Electric Co.

B.K. Kim, Korea Polym. J. **4**, 215 (1996)

B.J. Kim, J.L. White, Int. Polym. Proc. **10**, 213 (1995)

I. Kim, J.L. White, J. Appl. Polym. Sci. **96**, 1875 (2005)

V.L. Kocherov, Y.L. Lukach, E.A. Sporyagin, G.V. Vinogradov, Polym. Eng. Sci. **13**, 194 (1973)

T. Kodaira, H. Ishida, H. Kabaya, U.S. Patent 5,310,821, 10 May 1994, Appl. 11 Dec 1992, to GE Plastics Japan, Limited

B. Kohler, B. Sarabi, U.S. Patent 5,378,749, 01 Mar 1995, Appl. 09 Oct 1993, to Bayer A.-G.

R.C. Kowalski, SPE ANTEC Tech. Papers **36**, 1902 (1990)

M. Kozlowski, Polym. Netw. Blends **4**, 39 (1994)

N.P. Krasnikova, E.V. Kotova, G.V. Vinogradov, Z. Pelzbauer, J. Appl. Polym. Sci. **22**, 2081 (1978)

G. Kraus, K. Rollman, J. Polym. Sci., A2 **14**, 1133 (1976)

K. Kuwamoto, Int. Polym. Proc. **9**, 319 (1994)

H. Kye, J.L. White, Int. Polym. Proc. **11**, 129, 310 (1996)

T. Kyu, J.-C. Yang, Macromolecules **23**, 176 (1990)

F.P. La Mantia (ed.), *Recycling of PVC & Mixed Plastic Waste* (ChemTec, Toronto, 1996)

F.P. La Mantia, M. Marrone, B. Dubrulle D'Orhcel, Polym. Recyc. **2**, 3 (1996)

M. Lambla, M. Seadan, Polym. Eng. Sci. **32**, 1687 (1992); Makromol. Chem., Macromol. Symp. **69**, 99 (1993)

R. Lanthier, *Internal Report, Shawinigan Chemicals, Limited*, Sept (1966)

M.K. Laughner, U.S. Patent 5,189,091, 23 Feb 1993, Appl. 29 Nov 1990; U.S. Patent 5,308,894, 03 May 1994, Appl. 10 Mar 1992, to Dow Chemical Company

G.F. Lee Jr., U.S. Patent 5,324,782, 28 June 1994, Appl. 26 Oct 1992, to General Electric Company

W.K. Lee, H.H. George, Polym. Eng. Sci. **18**, 146 (1978)

H.M. Lee, O.O. Park, J. Rheol. **38**, 1405 (1994)

B.H. Lee, J.L. White, Int. Polym. Proc. **16**, 172 (2001)

W.K. Lee, Ph.D. thesis (Chemical Engineering), University Houston, Houston (1972)

M. Lee, J.K. Park, H.S. Lee, O. Lane, R.B. Moore, J.E. McGrath, D.G. Baird, Polymer **50**, 6129 (2009a)

H.G. Lee, Y.T. Sung, Y.K. Lee, W.N. Kim, H.G. Yoon, H.S. Lee, Macromol. Res. **17**, 417 (2009b)

C.W. Leong, J.M. Ottino, J. Fluid Mech. **209**, 463 (1989)

W. Lerdwijitjarud, A. Siriva, E.G. Larson, Polym. Eng. Sci. **42**, 798 (2002)

W. Lerdwijitjarud, A. Siriva, E.G. Larson, J. Rheol. **48**, 843 (2004)

H. Li, U. Sundararaj, Macromol. Chem. Phys. **210**, 852 (2009)

B. Liang, J.L. White, J.E. Spruiell, B.C. Goswami, J. Appl. Polym. Sci. **28**, 2011 (1983)

S. Lim, J.M. White, Int. Polym. Proc. **8**, 119 (1993)

J.T. Lindt, Polym. Eng. Sci. **21**, 1162 (1981)

J.T. Lindt, A.K. Ghosh, Polym. Eng. Sci. **32**, 1802 (1992)

P.Y. Liu, U.S. Patent 4,520,164, 28 May 1985, Appl. 22 Dec 1982, to General Electric Company

Y.H. Liu, D.A. Zambrunnen, SPE ANTEC Techn. Paper **41**, 3104 (1995)

W.L. Liu, S.M. Liwak, U.S. Patent 5,332,782, 26 July 1994, Appl. 26 Feb 1993, 01 May 1989, 27 Aug 1986, to Rohm & Haas Company

F.J. Lockett, *National Physical Laboratory Report, Division of Materials Applications*, Report No. 25, Teddington (1972)

G.W. Lohfink, M.R. Kamal, Polym. Eng. Sci. **33**, 1404 (1993)

J.E. Loukus, A.C. Halonen, M. Gupta, SPE ANTEC Tech. Pap. **50**, 133 (2004)

A. Luciani, L.A. Utracki, Int. Polym. Proc. **11**, 299 (1996)

A. Luciani, M.F. Champagne, L.A. Utracki, Polym. Networks Blends **6**, 41, 51 (1996); J. Polym. Sci. B, Polym. Phys. Ed. **35**, 1393 (1997)

A. Luciani, R.E. Khayat, L.A. Utracki, Eng. Anal. Bound. Elem. **19**, 279 (1997)

K. Luker, Leistritz Workshop 1996.12.02-06; Randcastle Extrusion System Microtruders, U.S. Patent 5,486,328

J. Lyngaae-Jørgensen, L.A. Utracki, Makromol. Chem. Macromol. Symp. **48/49**, 189 (1991)

J. Lyngaae-Jørgensen, K. Sondergaard, L.A. Utracki, A. Valenza, Polym. Netw. Blends **3**, 167 (1993)

J. Lyngaae-Jørgensen, K. Lunde Rasmussen, E.A. Chtcherbakova, L.A. Utracki, Polym. Eng. Sci. **39**, 1060 (1999)

C.W. Macosko, J.M. Starita, SPE J. **27**, 30 (1971)

S.S. Madaeni, A. Farhadian, V. Vatanpour, Adv. Polym. Tech. **31**, 298 (2012)

B.H. Maddock, SPE J. **5**, 383 (1959)

C. Maier, M. Lambla, Polym. Eng. Sci. **35**, 1197 (1995)

I. Manas-Zloczower, Mixing in high-intensity batch mixers, in *Mixing in Polymer Processing*, ed. by C. Rauwendaal (Marcel Dekker, New York, 1991)

I. Manas-Zloczower, Z. Tadmor (eds.), *Mixing and Compounding of Polymers* (Hanser, Munich, 1994)

J.M.G. Martinez, J. Taranco, O. Laguna, E.P. Collar, Int. Polym. Proc. **9**, 346 (1994)

L. Mascia, J. Zhao, Rheol. Acta **30**, 369 (1991)

K. Masters, *Spray Drying Handbook*, 4th edn. (John Wiley & Sons, New York, 1985)

M. Matos, Master thesis, École Polytechnique de Montréal (1993)

G.A.R. Matthews, in *Advances in PVC Compounding and Processing, Chapter 5*, ed. by M. Kaufman (Maclaren, London, 1962)

W. Maung, K.M. Chua, T.H. Ng, H.L. Williams, Polym. Eng. Sci. **23**, 439 (1983)

B. Maxwell, A.J. Scalora, Mod. Plast **37**, 107 (1959)

J.D. McCullough, J.F. Bradford, U.S. Patent 5,587,434, 24 Dec 1996, Appl. 13 Oct 1995, to Union Carbide Chemicals & Plastics Technology Corporation

H.E.H. Meijer, M.K. Singh, P.D. Anderson, Prog. Polym. Sci. **37**, 1333 (2012)

G. Menges, T. Bartilla, Polym. Eng. Sci. **27**, 1216 (1987)

F.M. Merrett, J. Polym. Sci. **24**, 294 (1957)

W. Michaeli, A. Grefenstein, Int. Polym. Proc. **11**, 121 (1996)

W. Michaeli, U. Berghaus, G. Speuser, Int. Polym. Proc. **6**, 163 (1991)

W. Michaeli, W. Frings, H. Höker, U. Berghaus, Int. Polym. Proc. **8**, 308 (1993a)

W. Michaeli, A. Grefensttein, W. Frings, Adv. Polym. Technol. **12**, 25 (1993b)

W. Michaeli, A. Grefenstein, U. Berghaus, Polym. Eng. Sci. **35**, 1485 (1995)

A.S. Michaels, U.S. Patent 3,615,024 (1971)

J. Michaux, *International Seminar Energy Conservation Research*, Brussels, 23–25 Oct 1979

F. Mighri, A. Ajji, P.J. Carreau, J. Rheol. **41**, 1183 (1997)

B. Miller, *Plastics World*, March, 14 (1996)

K. Min, in *Mixing and Compounding of Polymers*, ed. by I. Manas-Zloczower, Z. Tadmor (Hanser, Munich, 1994)

K. Min, J.L. White, Rubber Chem. Technol. **58**, 1024 (1985)

Y.P. Miroshnikov, A.K. Egorov, M.V. Egorova, J. Appl. Polym. Sci. **120**, 2724 (2011)

T. Miyamoto, K. Kodama, K. Shibitani, J. Polym. Sci., Part A-2 **8**, 2095 (1970)

S. Miyata, T. Hata, *Proceedings of the 5th Congress of Rheology* (1968), vol. 3 (University of Tokyo Press Tokyo 1970)

R. Miyoshi, N. Hashimoto, K. Koyanagi, Y. Sumihiro, T. Sakai, Int. Polym. Proc. **11**, 320 (1996)

Y. Mohadger, G.L. Wilkes, J. Polym. Sci., Polym. Phys. Ed. **14**, 963 (1976)

G.F. Molden, J. Mater. Sci. **4**, 283 (1969)

S. Moriya, A. Ishimoto, M. Takahashi, U.S. Patent 5,304,596, 19 Apr 1994, Appl. 23 May 1991, Jap. Appl. 25 May 1990, to Mitsui Petrochemical Industries, Limited

M.K. Murphy, E.R. Beaver, A.W. Rice, Paper presented at the *AIChE Spring National Meeting*, Houston, April (1989)

T.A. Murray, Plast. Tech. **24**(11), 83 (1978); **24**(12), 65 (1978)

S. Nagai, M. Hasegawa, H. Mimura, M. Kobayashi, U.S. Patent 5,326,846, 05 July 1994, Jap. Appl. 04 Apr 1992; U.S. Patent 5,292,824, 08 Mar 1994, Jap. Appl. 19 Mar 1992, to Mitsubishi Gas Chem.

N. Nakajima, U.S. Patent 5,376,712, 27 Dec 1994, Appl. 09 Sept 1993, to The University of Akron

K.M. Natarajan, P. Arjunan, D. Elwood, U.S. Patent 5,296,550, 22 Mar 1994, Appl. 01 Nov 1991, to Enichem S.p.A.

K.Y. Ng, L. Erwin, Polym. Eng. Sci. **21**, 212 (1981)

X.Q. Nguyen, L.A. Utracki, U. S. Patent 5,451,106, 19 Sept 1995, Appl. 08 Aug 1984, to National Research Council of Canada, Ottawa

T. Nishio, Y. Suzuki, K. Kojima, M. Kakugo, 7th Annual Meeting of Polymer Processing Society, Hamilton, 22–24 Apr 1991; Kobunshi Robunshu, **47**, 331 (1990)

T. Nishio, T. Sanada, K. Higashi, Sen-i Gakkaishi **48**, 446 (1992)

T. Nishio, T. Sanada, S. Hosoda, K. Nagaoka, T. Okada, U.S. Patent 5,162,433; 5,288,786, 22 Feb 1994; 5,304,593; 5,304,594, 19 Apr 1994, Appl. 30 Sept 1992, Jap. Appl. 30 Sept 1986, to Sumitomo Chemical Company, Limited

T. Ohmae, Y. Toyoshima, K. Mashita, N. Yamaguchi, J. Nambu, U.S. Patent 5,010,136, 23 Apr 1991, Appl. 09 Aug 1989, to Sumitomo Chemical Company, Limited

A. Okada, A. Masuyama, U.S. Patent 5,326,813, 05 July 1994, Appl. 10 Dec 1992, Jap. Appl. 10 Dec 1991, to Idemitsu Kosan Company, Limited

J.Y. Olayemi, A.A. Adeyeye, Polym. Test. **3**, 25 (1982)

J.M. Ottino, *The Kinematics of Mixing: Stretching, Chaos and Transport* (Cambridge University Press, Cambridge, 1989)

J.M. Ottino, AICHE J. **29**, 159 (1983); Ann. Rev. Fluid Mech. **22**, 207 (1990); Phys. Fluids **A3**(5), 1417 (1991)

W.R.R. Park, *Plastic Film Technology* (Van Nostrand Reinhold, New York, 1969)

E.E. Paschke, C.L. Myers, G.P. Desio, U.S. Patent 5,292,805, 08 Mar 1994; Japanese Patent 60 57,058, 01 Mar 1994, Appl. 29 May 1992, to Amoco Corporation

G.A.R. Patfoort, Belgian Patent 833,543, 18 Mar 1976, Appl. 18 Sep 1975

D.R. Paul, in *Polymer Blends*, ed. by D.R. Paul, S. Newman (Academic, New York, 1978)

J.-R. Pauquet, F. Sitek, R. Todesco, U.S. Patent 5,298,540, 29 Mar 1994, Appl. 25 Mar 1993, Appl. 27 Mar 1991, to Ciba-Geigy Corporation

E. Pedemonte, G. Dondcro, G. Alfonso, F. DeCandia, Polymer **16**, 531 (1975)

S.M. Petren, Personal communication (1997)

S. Petrov, A. Dimov, S. Petrova, P. Petkova, J. Membr. Sci. **64**, 183 (1991)

J.J. Picot, Private communication (1997)

L.Z. Pillion, L.A. Utracki, Polym. Eng. Sci. **24**, 1300 (1984); **27**, 984 (1987)

I. Pinnau, W.J. Koros, J. Appl. Polym. Sci. **43**, 1491 (1991)

I. Pinnau, J. Wind, K.-V. Peinmann, Ind. Eng. Chem. Res. **29**, 2028 (1990)

A.P. Plochocki, S.S. Dagli, R.D. Andrews, Polym. Eng. Sci. **30**, 741 (1990)

A. Poitou, Ph.D. thesis, École des Mines de, Paris, 1988

R. Polance, K. Jayaraman, Polym. Eng. Sci. **35**, 1535 (1995)

H. Potente, M. Koch, Int. Polym. Proc. **4**(4), 208 (1989)

H. Potente, *Scaling up of Twin-screw extruders*, Polymer Extrusion II (1985)

H. Potente, M. Bastian, K. Bergermann, M. Senge, G. Scheel, T. Winkelmann, Polym. Eng. Sci. **41**, 222 (2001)

G.W. Powers, J.R. Collier, Polym. Eng. Sci. **30**, 118 (1990)

P. Prabodh, P. Stroeve, "Break-up of model viscoelastic drops in uniform shear flow", personal communication by P. Strove, Department Chemical Engineering, University of California (1991)

J.J. Prause, Plast. Tech. **13**, 41 (1967); **14**, 52 (1968)

W.M. Prest Jr., D.L. Luca, J. Appl. Phys. **51**, 5170 (1980); Org. Coat. Plast. Chem. Prepr. **42**, 291 (1980)

J.M. Raquez, R. Narayan, P. Dubois, Macromol. Mater. Eng. **293**, 447 (2008)

L. Ratke, W.K. Thieringer, Acta Metal. **33**, 1793 (1985)

C. Rauwendaal, *Polymer Extrusion* (Hanser, Munich, 1986)

C. Rauwendaal (ed.), *Mixing in Polymer Processing* (Marcel Dekker, New York, 1991)

C. Rauwendaal, in *Mixing and Compounding of Polymers*, ed. by I. Manas-Zloczower, Z. Tadmor (Hanser, Munich, 1994)

C. Rauwendaal, *Polymer Extrusion*, 4th edn. (Hanser, Munich, 2001)

C. Rauwendaal, Polym. Eng. Sci. **21**, 1092 (1981); SPE ANTEC Techn. Paper, **32**, 968 (1986); JSW Techn. Report, **49**, 3 (1993)

L. Rayleigh, Proc. London Math. Soc. **10**, 4 (1879); Proc. Roy. Soc. **29**, 71 (1879)

W.D. Richards, J.E. Pickett, U.S. Patent 5,384,360, 24 Jan 1995, Appl. 20 Sept 1993, Appl. 12 Mar 1990, Appl. 17 Dec 1990, to General Electric Company

S. Ricklin, Plast. Eng. **39**, 29 (1983)

R.W. Roberts, Mod. Plast. **44**, 121 (1967)

R. Roehner, MS thesis, Ohio University, 1982

R. Roehner, J.R. Collier, *Proceedings of the AIChE 1983 National Meeting*, Washington, DC Nov (1983)

E. Roesink, Ph.D. thesis, Twente University, 1989

C.M. Roland, G.G.A. Bohm, J. Polym. Sci. Polym. Phys. Ed. **22**, 79 (1984)

T. Roths, C. Friedrich, M. Marth, J. Honerkamp, Rheol. Acta **41**, 211 (2002)

H. Rust, Kunststoffe **73**, 342 (1983)

S. Tomotika Proc. Roy. Soc. **A150**, 322 (1935); Proc. Roy. Soc. **A153**, 302 (1936)

S. Saeki, J.M.G. Cowie, I.J. McEwen, Polymer **24**, 60 (1983)

T. Sakai, Gose Jushi **29**, 7 (1978)

T. Sakai, Personal communication (1993)

T. Sakai, N. Hashimoto, N. Kobayashi, SPE ANTEC Techn. Paper, **33**, 146 (1987); Int. Polym. Proc. **7**, 116 (1992)

T. Sakai, K. Nakamura, S. Inoue, SPE ANTEC Techn. Paper **34**, 1853 (1988)

T. Sakai, N. Hashimoto, K. Kataoka, SPE ANTEC Techn. Paper **38**, 7 (1992)

D.M. Salden, *Melt Compounding and Compounding Machinery*, 1st Major Conference on Thermoplastic Compounding, PRI, London (1978)

T. Sanada, T. Ogihara, Y. Suzaki, T. Nishio, *PPS, European Meeting*, Palermo, 15–18 Sept 1991

I. Sasaki, T. Teraoka, J. Oshima, U.S. Patent 5,280,076, 18 Jan 1994, Appl. 21 Sept 1990, to Takeda Chemical Industries, Limited

K. Sato, U.S. Patent 5,403,889, 04 Apr 1995, Appl. 17 Nov 1993, Can. Appl. 26 Nov 1992, to Novacor Chemicals, Limited

E. Schmid, H. Thullen, U.S. Patent 5,288,799, 22 Feb 1994, Appl. 02 July 1992, Ger. Appl. 04 July 1991, to EMS-Inventa A.-G.

L.R. Schmidt, E.M. Lovgren, P.G. Meisner, Int. Polym. Proc. **4**, 270 (1989)

A.A. Schoengood, APEJ **29**(2), 21 (1973)

H.P. Schreiber, M.D. Croucher, J. Appl. Polym. Sci. **25**, 1961 (1980)

A.R. Schultz, A.L. Young, Macromolecules **13**, 663 (1980)

P. Schümmer, Rheol. Acta **6**, 192 (1967); Rheol. Acta **7**, 271 (1967)

R. Séguéla, R. Prud'homme, Macromolecules **11**, 1007 (1978)

S. Shahbikian, P.J. Carreau, M.-C. Heuzey, M.D. Ellul, J. Cheng, P. Shirodkar, H.P. Nadella, Polym. Eng. Sci. **52**, 309 (2012)

G. Shearer, C. Tzoganakis, Adv. Polym. Techn. **20**, 169 (2001)

Z.-H. Shi, L.A. Utracki, Polym. Eng. Sci. **32**, 1846 (1992); Proceedings of the Polymer Processing Society Annual Meeting, Manchester, April, 1993

Z.-H. Shi, P. Sammut, V. Bordereau, L.A. Utracki, SPE ANTEC Techn. Paper **38**, 1818 (1992)

C.-K. Shih, SPE ANTEC Tech. Pap. **37**, 99 (1991); Adv. Polym. Technol. **11**, 223 (1992)

C.-K. Shih, D.G. Tynan, D.A. Denelsbeck, Polym. Eng. Sci. **31**, 1670 (1991)

K. Shon, J.L. White, Polym. Eng. Sci. **39**, 1757 (1999)

K. Shon, D. Chang, J.L. White, Int. Polym. Proc. **14**, 44 (1999)

M. Sittig, *Plastic Films from Petroleum Raw Materials* (Noyes Development Corporation, New Jersey, 1967), p. 141

S. Smale, Bull. Am. Math. Soc. **73**, 747 (1967)

H.J.E. Smits, R. van der Meer, A.H.L. Groothuis, U.S. Patent 5,357,003, 18 Oct 1994, US Appl. 15 Nov 1989, to General Electric Company

J.A. Sneller, Mod. Plast. Int. **15**, 42 (1985)

W.N. Song, SPE ANTEC Techn. Paper **46**, 270 (2000)

C.A. Sperati, *Modern Plastics Encyclopedia* (McGraw-Hill, New York, 1983)

S.H. Spiegelberg, D.C. Ables, G.H. McKinley, J. Non-Newt. Fluid Mech. **64**, 229 (1996)

W.H. Staas, Eur. Pat. Appl. **33,220** (1981) to Rohm and Haas

F.F. Stengaard, J. Membr. Sci. **36**, 257 (1988)

H. Strathmann, P. Scheible, R.W. Baker, J. Appl. Polym. Sci. **15**, 811 (1971)

N.P. Stuber, M. Tirrel, Polym. Proc. Eng. **3**, 71 (1985)

F.H. Su, H.X. Huang, Adv. Polym. Technol. **28**, 16 (2009)

Y.-Y. Su, B. Khomami, J. Rheol. **36**(2), 357 (1992)

U. Sundararaj, C.W. Macosko, R.J. Rolando, H.T. Chan, Polym. Eng. Sci. **32**, 1814 (1992)

U. Sundararaj, C.W. Macosko, A. Nakayama, T. Inoue, Polym. Eng. Sci. **35**, 100 (1995)

H. Sutter, R. Peuker, U.S. Patent 4,058,654 (1977) to Bayer A.G.

Y. Suzaka, U.S. Patent 4,334,783, 15 Jun 1982, Appl. 21 Dec 1978, to Showa Denko, Kabushiki Kaisha, Oita

O.J. Sweeting, *The Science and Technology of Polymer Films, II* (John Wiley, New York, 1971)

W. Szydlowski, J.L. White, Adv. Polym. Technol. **7**, 177 (1987); Int. Polym. Proc. **2**, 143 (1988); J. Non-Newt. Fluid Mech. **28**, 29 (1988)

W. Szydlowski, R. Brzoskowski, J.L. White, Int. Polym. Proc. **1**, 207 (1987b)

Z. Tadmor, AICHE J. **34**, 1943 (1988)

Z. Tadmor, C.G. Gogos, *Principles of Polymer Processing* (Wiley, New York, 1979)

Z. Tadmor, U.S. Patent 4,142,805 (1979); 4,194,841 (1980)

Z. Tadmor, P. Hold, L. Valsamis, Plastics Engineering, 20–25 Nov 1979; SPE ANTEC Tech. Papers, **25**, 193 (1979)

Z. Tadmor, L.N. Valsamis, J.C. Yang, P.S. Mehta, O. Duran, J.C. Hinchcliffe, Polym. Eng. Rev. **3**, 29 (1983)

M. Taha, V. Perrut, A.A. Roche, J.P. Pascault, J. Appl. Polym. Sci. **65**, 2447 (1997)

Y. Tajima, K. Kawaguchi, T. Nakane, 5,300,572, 05 Apr 1994, US Appl. 12 June 1992, Jap. Appl. 14 June 1991, to Polyplastics Company, Limited

K. Takagi, Y. Kurasawa, K. Nishida, S. Ohi, K. Mori, T. Sato, T. Itou, U.S. Patent 5,310,776, 10 May 1994, Appl. 30 Apr 1993, Jap. Appl. 13 May 1992, to Mitsubishi Petrochemical Company, Limited

M. Takahashi, P.H.P. Macaubas, K. Okamoto, H. Jinnai, Y. Nishikawa, Polymer **48**, 2371 (2007)

R. Takserman-Krozer, A. Ziabicki, J. Polym. Sci. **1**, 491 (1963)

T. Tang, B. Huang, Polymer **35**, 281 (1994)

S. Tanoue, Y. Iemoto, Polym. Eng. Sci. **43**, 254 (2003)

M. Tasdemir, J. Appl. Polym. Sci. **93**, 2521 (2004)

G.I. Taylor, Proc. Roy. Soc. (London) **A138**, 41 (1932); Proc. Roy. Soc. (London) **A146**, 501 (1934)

G. Theodorou, D.P. Ly, D. Bellet, Rheol. Acta **23**, 266 (1984)

F. Theron, N. Le Sauze, Int. J. Multiph. Flow **37**, 488 (2011)

W. Thiele, in *Compounding and Processing for Performance*, Proceedings, POLYBLENDS-'95, NRCC/IMI, Boucherville, 19–20 Oct 1995

W. Thiele, *Plastics Formulating and Compounding*, 14 Nov/Dec 1996

B.A. Thornton, A. Villasenor, R.G. Maxwell, J. Appl. Polym. Sci. **25**, 653 (1980)

D.B. Todd, Polym. Proc. Eng. **6**, 15 (1988)

M. Tokihisa, K. Yakemoto, T. Sakai, L.A. Utracki, M. Sepehr, J. Li, Y. Simard, Polym. Eng. Sci. **46**, 1040 (2006)

N. Tokita, Rubber. Chem. Tech. **50**, 292 (1977)

C. Ton-That, A.G. Shard, D.O.H. Teare, R.H. Bradley, Polymer **42**, 1121 (2001)

M.V. Tsebrenko, M. Jakob, M.Y. Kuchinka, A.V. Yudin, G.V. Vinogradov, Int. J. Polym. Mater. **3**, 99 (1974)

M.V. Tsebrenko, A.V. Yudin, T.I. Ablazova, G.V. Vinogradov, Polymer **17**, 831 (1976)

C.L. Tucker III, Principles of Mixing Measurements, in *Mixing in Polymer Processing*, ed. by C. Rauwendaal (Marcel Dekker, New York, 1991)

C. Tzoganakis, Adv. Polym. Technol. **9**, 321 (1989)

S. Ultsch, H.-G. Fritz, Plast. Rubber Process Appl. **13**, 81 (1990)

L.A. Utracki, *Polymers and composites* (Oxford and IBH Publishers, New Delhi, 1987)

L.A. Utracki, *Polymer Alloys and Blends – Thermodynamics and Rheology* (Hanser, Munich, 1989)

L.A. Utracki, in *Two-Phase Polymer Systems*, ed. by L.A. Utracki (Hanser, Munich, 1991)

L.A. Utracki (ed.), *Encyclopaedic Dictionary of Commercial Polymer Blends* (ChemTec, Toronto, 1994)

L.A. Utracki, The Rheology of Multiphase Systems, in *Rheological Fundamentals of Polymer Processing*, ed. by J.A. Covas (Kluver, Dordrecht, 1995)

L.A. Utracki, *Commercial Polymer Blends* (Chapman and Hall, London, 1998)

L.A. Utracki, J. Coll. Interf. Sci. **42**, 185 (1973); Polym. Netw. Blends **1**, 61 (1991)

L.A. Utracki, A. Luciani, Int. Plast. Eng. Technol. **2**, 37 (1996)

L.A. Utracki, Z.-H. Shi, Polym. Eng. Sci. **32**, 1824 (1992)

L.A. Utracki, unpublished, (1996)

L.A. Utracki, in *Polymers and Composites; Recent Trends*, National Seminar organized by DST, Government of India (Oxford & IBH Publishers, New Delhi, 1989a)

L.A. Utracki, A. Luciani, "Extensional flow mixer", *Canadian Patent application*, 1997; to National Research Council of Canada, Ottawa

L. Valsamis, AIChE Meeting, Washington, DC, Oct (1983)

D.J. van der Wal, D. Goffart, E.M. Klomp, H.W. Hoogstraten, L.P.B.M. Janssen, Polym. Eng. Sci. **36**, 912 (1996)

H.J. Van Oene, J. Coll. Interf. Sci. **40**, 448 (1978)

J.A. Van't Hoff, Ph.D. thesis, Twente University, 1988

B. Vergnes, E. Wey, J.F. Agassant, Caoutchouc et Plastiques **633**, 81 (1983)

B. Vergnes, N. Bennani, C. Guichard, Int. Polym. Proc. **1**, 19 (1986)

D. Vesely, Polym. Eng. Sci. **36**, 1586 (1996)

E. Vey, C. Rodger, J. Booth, M. Claybourn, A.F. Miller, A. Saini, Polym. Degrad. Stabil. **96**, 1882 (2011)

S. Vilasagar, H.S. Rawlings, U.S. Patent 5,302,646, 12 Apr 1994, Appl. 28 Feb 1992, to General Electric Company

M. Vincent, J.F. Agassant, Rheol. Acta **24**, 603 (1985)

G.V. Vinogradov, N.P. Krasnikova, V.E. Dreval, E.V. Kotova, E.P. Plotnikova, Int. J. Polym. Mater. **9**, 187 (1982)

C. Wang, I. Manas-Zloczower, Int. Polym. Proc. **9**, 115 (1996)

H.-H. Wang, W.-C. Lee, D.-T. Su, W.-J. Cheng, B.-Y. Lin, SPE ANTEC Techn. Paper **41**, 2105 (1995)

H. Waniczek, C. Süling, C. Lindner, H. Bartl, U.S. Patent 4,395,517, 26 July 1983, Appl. 17 July 1981, to Bayer A.-G.

J.R.A. Wereta, M.T. Gehatia, D.R. Wiff, Polym. Eng. Sci. **18**, 204 (1978)

R.F. Westover, SPE J. **1**, 473 (1962); Mod. Plast. March (1963)

J.L. White, *Twin Screw Extruder Technology and Principles* (Hanser, Munich, 1990)

J.L. White, K. Min, Adv. Polym. Technol. **5**, 225 (1985)

K. Wilczynski, A. Lewandowski, K.J. Wilczynski, Polym. Eng. Sci. **52**, 449 (2012a)

K. Wilczynski, A. Lewandowski, K.J. Wilczynski, Polym. Eng. Sci. **52**, 1258 (2012b)

G.C. Wildman, S.-J. Raymond Hsu, J. Appl. Polym. Sci. **30**, 4385 (1984)

E.W. Williams, S.H. Javadpour, J. Non-Newt. Fluid Mech. **7**, 171 (1980)

P.R. Williams, R.W. Williams, J. Non-Newt. Fluid Mech. **19**, 53 (1985)

J.M. Willis, B.D. Favis, J. Lunt, Polym. Eng. Sci. **30**, 1073 (1990)

J.M. Willis, V. Caldas, B.D. Favis, J. Mater. Sci. **26**, 4742 (1991)

E.H. Wissler, Ind. Eng. Chem. Fundam. **10**, 411 (1971)

R. Wood, Plast. Rub. Int. **4**(5), 207 (1979); **5**(1), 25 (1980)

S. Wu, Polymer **26**, 1855 (1985); Polym. Eng. Sci. **27**, 335 (1987)

M. Xanthos (ed.), *Reactive Extrusion* (Hanser, Munich, 1992)

M. Xanthos, J. Grenci, S.H. Patel, A. Patel, C. Jackob, S. Dey, S.S. Dagli, Polym. Compos. **16**, 204 (1995)

L.S. Yang, R.J. McCready, U.S. Patent 5,340,875, 23 Aug 1994, Appl. 18 Feb 1993, Appl. 15 Aug 1991, to Arco Chemical Technology

J.B. Yates III, U.S. Patent 5,384,363, 24 Jan 1995, Appl. 11 June 1993, 28 Sept 1990, to General Electric Company

B. Yi, R.T. Fenner, Plast Polym. **43**, 224–228 (1975)

B. Yin, J. Lan, L.P. Li, M.B. Yang, Polym. Plast. Tech. Eng. **49**, 503 (2010)

P. Yue, J.J. Feng, C. Liu, J. Shen, J. Fluid Mech. **540**, 427 (2005)

A.E. Zachariades, M.P.C. Watts, T. Kanamoto, R.S. Porter, J. Polym. Sci. Polym. Lett. Ed. **17**, 485 (1979)

A. Zampini, U.S. Patent 4,484,935 (1984)

A. Zampini, R.F. Malon, U.S. Patent 4,652,283 (1987)

Y. Zhang, H. Zhang, W. Guo, C. Wu, Polym. Adv. Tech. **22**, 1851 (2011)

Y. Zhihui, Z. Xiaomin, Z. Yajie, Y. Jinghua, J. Appl. Polym. Sci. **63**, 1857 (1997)

D.D. Zimmerman, G. Vieiro, D.S. Pavlick, U.S. Patent 5,290,860, 01 Mar 1994, Appl. 12 Nov 1992, to Cyro Industries

Part II

Properties

Properties and Performance of Polymer Blends

10

S. F. Xavier

Contents

The Sect. 10.4, "Miscibility and Solubility" is authored by R. Arunima[1], V. P. Poornima[2], Sabu Thomas[1,2]

[1]Centre for Nanoscience and Nanotechnology

[2]School of Chemical Sciences, Mahatma Gandhi University, Priyadarshini Hills, Kottayam, Kerala-686560, India

S.F. Xavier
Parul Innovation Center, Parul Institute of Technology, Vadodara, Gujarat, India

Formerly at Research Center, Indian Petrochemicals Corporation Ltd., Vadodara, Gujarat, India
e-mail: dr.sfxavier@gmail.com; francis1951@yahoo.com

Abstract

This chapter presents an overview of properties and performance of
polymer blends. It is structured into nine sections dealing with aspects required
for assessing the performance of a polymer blend. These are mechanical prop-
erties comprising of both low-speed and high-speed popularly studied proper-
ties; chemical and solvent effects; thermal and thermodynamic properties;
flammability; electrical, optical, and sound transmission properties; and
some special test methods which assumed prominence recently because of
their utility.

Each section opens up with standard test methods such as ASTM, BS, DIN, and ISO for each property evaluation and is summarized. Since presentation of all test methods for each property is beyond the scope of this chapter, one popular test method is described in detail while others are discussed with reference to it. The factors controlling each property are also examined. Each section concludes with an outline of the state of the art pertinent to the aspect in focus. Definitions of all terms from each section are grouped together in Table 10.36.

Toughening plays an important role in designing polymer blends. Due emphasis has been given to this aspect by presenting the different methods of determining blend toughness, specially using ductile fracture mechanics; the mechanisms of toughening; and also the factors influencing toughness. Flammability aspect assumed a great deal of interest ever since the US Federal Trade Commission's (FTC) action in 1972. Commercial exploitation of a polymer blend is regulated, since then, by its flammability characteristics. A brief review on factors affecting flammability is presented, and a list of fire-retardant chemicals is provided in Table 10.37.

The recent advances in optical properties, sound transmission properties, and certain "special testing methods" are presented at the closing of the chapter. These "special test methods" are not yet matured into international test methods but, nevertheless, are popularly used for meeting the requirements of certain applications. Hence, awareness of these methods is considered to be essential. The chapter concludes with perspectives for the future developments.

10.1   Introduction

Modern technology thrusts challenging demands on the performance capabilities of materials, including polymers and their blends. A new approach to the science and technology of polymer blends has emerged recently, i.e., polymer blends by design rather than by availability. These polymeric materials must perform under strenuous mechanical, chemical, thermal, and electrical conditions imposed by the requirements of a specific application. Service in these applications usually involves several criteria to be fulfilled without a loss of economic advantage. Indeed, performance requirements of polymer blends are often at the limit of the properties that can be achieved. Moreover, these materials are expected to endure complex environmental conditions for extended time. All these factors stress the need for in-depth studies of the properties and performance of polymer blends.

There are three aspects to material properties and performance:
1. The origin – identification of the mechanisms responsible for given performance characteristics
2. Methods of determination – the most reliable way that the properties should be measured
3. The numerical values of the characteristic parameters of the material

In principle, the entire handbook is dedicated to discussion of these three aspects. For example, in ▶ Chap. 2, "Thermodynamics of Polymer Blends," the molecular aspects of polymer–polymer interactions, the methods of

characterization, as well as the numerical values of the thermodynamic parameters are given. Similarly, in ▶ Chap. 3, "Crystallization, Morphological Structure, and Melting of Polymer Blends," the three aspects vis-à-vis nucleation, melting, etc., are presented. In ▶ Chap. 7, "Rheology of Polymer alloys and Blends," flow, generation of flow-imposed lamellar morphology was discussed. This morphology has been used to control permeability through polymeric membranes.

Another important aspect of the material performance characteristics that is growing in significance is the balance of properties – for many applications it is not so important what is the value of a single parameter, but how well the material combines a number of characteristic properties. Take, for example, the use of polymer alloys for automobile fenders. Here the general requirements (viz., weight reduction, part consolidation, cost, design flexibility, increased impact, crashworthiness) translate into requirements for stiffness, strength, impact resistance, low coefficient of linear thermal expansion, weight reduction, chemical, corrosion and heat resistance, finish, oven paintability, and cost. These aspects are well presented in ▶ Chap. 15, "Applications of Polymer Blends."

The third aspect of the properties, the numerical values of measured parameters, represents enormous challenge to authors of a chapter such as this ▶ Chap. 12, "Broadband Dielectric Spectroscopy on Polymer Blends". The polymer blend industry produces well over 500 generic name blends, each in dozens of grades (Utracki 1994, 1998). Physically, it is impossible and practically useless to attempt reproducing the data sheets of these thousands of blends. Furthermore, the industry is dynamic, continuously adding and/or removing grades from the market. The modern source of the numerical information must also be active, changing along with the variability of materials, viz., the Internet. Most of the major resin producers' offer updated data sheets on the Internet, for example, www.allied.com, www.amoco.com, www.basf.com, www.dow.com, www.dupont.com, www.eastman.com, www.ge.com, www.hoechst.com, www.solutia.com, etc.

This chapter presents an overview of properties and performance of polymer blends, focusing on these aspects that are outside the main domain of the other chapters in this handbook. Such properties as mechanical, chemical, and solvent effects and thermal, flame retardancy, electrical, and optical properties are discussed. Further, the developments in sound transmission, certain special test methods in aroma barrier, permeability test for liquids, and environment stress cracking are included in the second edition of this handbook. In addition, the data is updated and upgraded. And, finally, the relevant and useful websites for additional information are also provided towards the end of this chapter.

The response of a polymer blend to tensile, compressive, and flexural stresses is examined in the initial section. Its rigidity, fatigue, and failure characteristics are also studied. The toughened polymers have enhanced the status of polymer blends, thus the toughening mechanisms have received considerable attention from researchers. The fracture mechanics approach of testing and the fascinating toughening mechanisms prevailing in these wonderful materials are also examined.

Insufficient chemical resistance of a blend at times leads to its rejection for use in an aggressive chemical environment, although it possesses an excellent combination

of mechanical properties. Thus, chemical and solvent effects on polymer blends are important factors that frequently determine blends' applicability. Attention has been given to chemical resistance of blends starting from the fundamental concept of the solubility parameters. Apart from the chemical and environmental restrictions, thermal resistance of a polymer blend is often a major criterion for its applicability. Thus, the thermal conductivity, heat capacity, and heat deflection temperature of polymeric materials are discussed in separate sections.

In this second edition of handbook, discussions regarding low-temperature brittle point, Vicat softening point, oxidative induction time, melt and crystallization parameters using DSC, and thermal degradation using TGA are added in order to bring around completion of comprehension on thermal properties of polymers and blends.

Flame resistance has become a legal requirement for commercial utilization of polymers and their blends in many applications. Innumerable test methods for flammability have been developed in different countries, and several books and handbooks are exclusively dealing with this subject. Discussion of the test methods that are *en vogue* in various countries is beyond the scope of this chapter; thus only the most popular test methods are discussed. The fire-retardant chemicals and their suppliers are tabulated in Table 10.37.

The use of polymer blends in electrical as well as electronic applications has been increasing rapidly. The electrical insulation properties of these materials cannot be ignored. Moreover, conducting polymers are likely to make an industrial breakthrough. These types of blends are also briefly discussed.

In addition, oxidative induction time, an exclusive test method popularly engaged in checking the suitability of an insulation material for cables, is added in the second edition.

Optical clarity has received considerable attention from the research community, as well as industry, especially, since transparent ABS was introduced to the market. Although success in this area has been limited, nevertheless this property is pertinent when considering blend suitability to a particular application. Few significant innovations have come up in photoluminescence and thermoluminescence, but the subject is, however, not mature enough to make a comprehensive story of the subject.

Some special test methods which have illuminated the applications of polymer blends are grouped together towards the end, viz., aroma barrier test, permeation test for liquids, and environmental stress cracking, which are special in nature but not really obtained the status of ASTM or BS methods. Nevertheless, they are used in industry as they meet the special application requirements of these wonderful materials. The chapter concludes with a discussion of these aspects.

10.2 Low-Speed Mechanical Properties

10.2.1 Tensile Strength, Tensile Modulus, and Elongation

The tensile stress–strain test is most widely used. Owing to the viscoelastic nature of polymers, the test is only a rough guide to how a polymer will behave in

Fig. 10.1 Material in tension
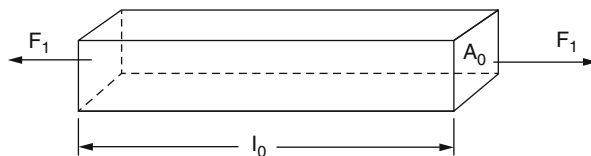
a finished product. Often, results of a single test conducted at one temperature and speed of testing are published. To get a clear understanding of a polymer, it is required to have the tests at several temperatures, rates of testing, and other conditions (Dukes 1966).

There is no universally accepted set of definitions with regard to the tensile tests. The terms listed in Appendix 2 have been taken from the widely accepted norms (ISO/DIS 527; **BS 2782 Methods 320A to F; ASTM D638-95).

The most frequently applied stress–strain measurements are made in tension by stretching the specimen as shown in Fig. 10.1. A tensile stress can thus be defined as

$$\sigma_1 \quad = \quad \frac{F_1}{A_o} \tag{10.1}$$

where σ_1 is the tensile stress, F_1 is the tensile force, and A_o the cross-sectional area of the specimen. If the tensile stress stretches the specimen to length l_1, the tensile strain, ε_1, is defined as

$$\varepsilon_1 \quad = \quad \frac{(l_1 - l_o)}{l_o} \quad = \quad \frac{kt}{l_o} \tag{10.2}$$

where l_o is the initial length of the specimen, k is the rate of extension, and t is the time. Continuing the stressing operation to the ultimate, i.e., measuring the force until the material breaks, tensile strength, known as the ultimate tensile stress:

$$\sigma \quad = \quad \frac{F}{A} \tag{10.3}$$

where F is the force at failure and A is the cross section at failure.

During the process of stretching, the specimen's dimensions orthogonal to the axis of applied force decrease, and thus the area of cross section decreases. For experimental convenience, however, tensile strengths are usually based on the original cross section (A_o) which is easily measured at the beginning of the experiment:

$$\text{Elongation at break } (\%) \quad = \quad 100 \; \frac{(l - l_o)}{l_o} \tag{10.4}$$

From the point of view of mechanical performance, four types of materials have been identified. They are best discussed in terms of the stress–strain dependence:

1. Brittle, showing proportionality between stress and strain up to the point of rupture. Here, the modulus, $E = \sigma/\varepsilon$, is constant, independent of strain, ε.

2. Semi-ductile, showing decreasing proportionality between stress and strain up to the point of rupture. Here, the modulus, $E = \sigma/\varepsilon$, decreases with strain, ε.
3. Ductile, initially showing similar relationship between stress and strain as the semi-ductile materials. However, these materials deform further, causing the stress pass through a maximum (yield). The rupture takes place at lower values than the yield stress.
4. Ductile with flow. These materials show still greater deformability than the typical ductile materials. Initially, the stress–strain dependence resembles that described for ductile resin, but before the rupture, there is a zone of deformation where the stress remains about constant. Within this zone there is "flow" of material that usually leads to molecular alignment and/or to changes to the crystalline structure (viz., deformation of polyolefins).

10.2.1.1 Methods of Measurement

Stress–strain measurements for polymer blends can be conducted in one of two modes: using a constant rate of loading or a constant rate of stretching. The first method is very often used in adhesives testing. The latter method is the most extensively employed in polymer and blend testing. In tensile testers, a sample is clamped between grips or jaws that are pulled apart at constant strain rates varying from 0.5 to 500 mm/min. The stress on the sample is monitored with the load cells ranging between 2 g and 5,000 kg or more. The elongation must avoid errors arising out of sample slippage from the grips. There are a variety of jaws that can hold different samples. A review of grip systems is presented in "Handbook of Plastics Test Methods" (Brown 1981). Jaw design and specimen shape and preparation are selected so as to minimize the introduction of extraneous stress or strain.

Tensile tests on different polymer blends employ specimens of different sizes. To conduct a tensile test, a specimen capable of being gripped at both ends is required. The basic types of dumbbell configurations and dimensions recommended by ISO are illustrated in Fig. 10.2. The American specifications differ only in number of dimensional details and are based essentially on imperial units. In case of rigid polymer blends (such as engineering blends), the specimen can be molded, machined on a lathe, or simply cut out from thin, flat sheets.

The dumbbell specimen with narrow waist (Fig. 10.2a) is generally preferred in testing rubbers and their blends with thermoplastics. The dumbbell specimen with broad waist (Fig. 10.2b) is used for polymers and blends exhibiting low-to-moderate elongation at break. Dog-bone test specimens (Fig. 10.2c) are used for polymer blends that do not allow any elongation measurement to be made. The parallel strip specimens (Fig. 10.2d) are used for reinforced thermoplastics or blends. In order to avoid the problem of sample fracturing near the grips, the end pieces of the grips are normally bonded.

10.2.1.2 Standard Test Methods for Tensile Properties

The standard test methods for tensile properties are listed in Table 10.1 and the recommended test speeds in Table 10.2.

Fig. 10.2 (**a**) Tensile test
specimen: Narrow-waisted
dumbbell (ISO/DIS 527
Type A). (**b**) Tensile test
specimen: Broad-waisted
dumbbell (ISO/DIS 527
Type B). (**c**) Tensile test
specimen: Dog-bone
dumbbell (ISO/DIS 527
Type C). (**d**) Tensile test
specimen: Parallel-sided strip
(ISO/DIS 527 Type D)
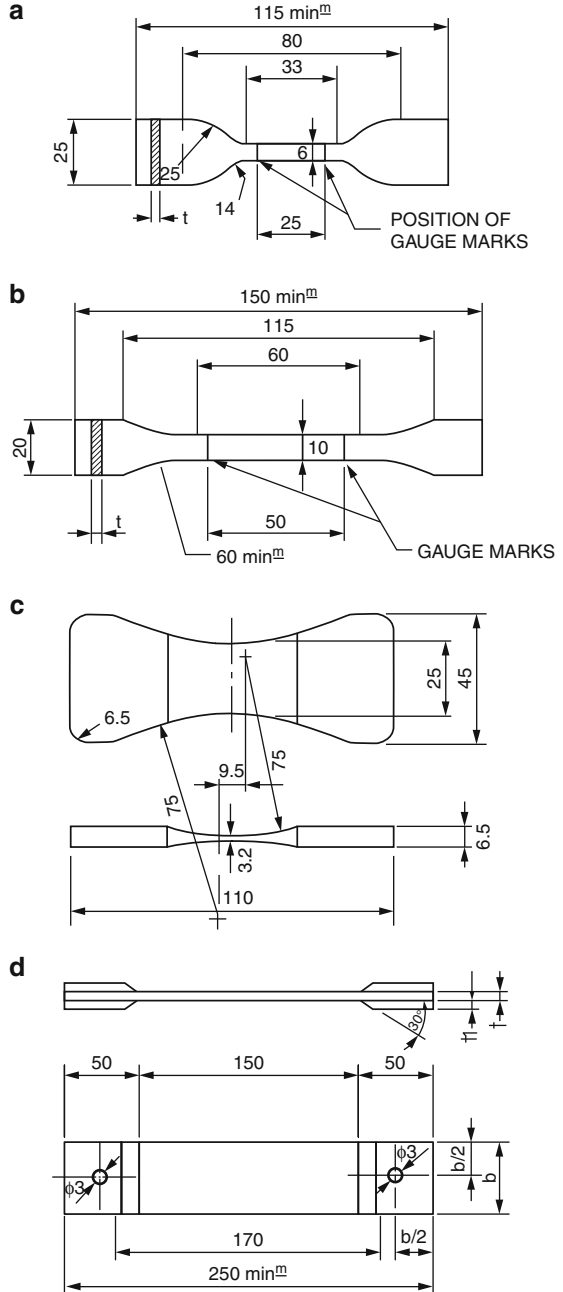
Table 10.1 Standard test methods for the determination of the tensile properties of polymers

Test method	Materials	Specimen	Test speeds
ISO R527	Plastics	1 mm thick	See Table 10.2
ISO R1184		<1 mm thick	
BS 2782			
Method 320A	Flexible plastic sheets blends, filled or reinforced	Stamped from sheets	500 mm/min
Method 320B	Composites	Injection molded	1, 5, 25, 50 and 100 mm/min
Method 320C	Rigid thermoplastic, thermosets	Machined from sheets	As in Method-A

Table 10.2 Recommended test speeds according to DIS 527 (ISO/DIS 527)

Speed A	1 mm/min	±50 %
Speed Al	2 mm/min	±20 %
Speed B	5 mm/min	±20 %
Speed C	10 mm/min	±20 %
Speed D[a]	20 or 25 mm/min	±10 %
Speed E	50 mm/min	±10 %
Speed F	100 mm/min	±10 %
Speed G[a]	200 or 250 mm/min	±10 %
Speed H	500 mm/min	±10 %

[a]Both the mentioned speeds are allowed because they are popularly used throughout the world

Measurements of "Apparent" Strain
The elongation of specimen is followed by using gauge marks and measuring the distance between them preferably continuously or by making use of clip-on type of extensometer. In the case of blends exhibiting strains in excess of 50 %, optical extensometers are to be used. The merits and demerits involved in different methods of strain measurements are discussed in detail elsewhere (Brown 1981).

Measurement of Modulus
The standard test methods calculate the tensile modulus by drawing a tangent to the initial linear part of the stress–strain curve and calculating the slope of the line. In cases where no clearly defined linear portion exists, the "secant modulus" should be determined.

10.2.2 Compressive Strength

Stress–strain curves developed during tensile, flexural, and compression tests may be quite different from each other. The moduli determined in compression are generally higher than those determined in tension. Flaws and submicroscopic cracks significantly influence the tensile properties of brittle polymeric materials.

However, they do not play such an important role in compression tests as the stresses tend to close the cracks rather than open them. Thus, while tension tests are more characteristic of the defects in the material, compression tests are indicators of the material content of the specimen used. The ratio of compressive strength to tensile strength in the case of polymers is in the range 1.5–4 (Dukes 1966).

10.2.2.1 Standard Methods for Compressive Tests

The standard methods for compressive tests are listed in Table 10.3. For example, the ISO Standard 604 allows four types of test specimens: (1) the right square prism, (2) the right rectangular prism, (3) the right cylinder, and (4) the right circular crown tube. The test specifies for each of these test specimens, the load-bearing surfaces be parallel to each other within 0.1 % of the height of the test piece.

10.2.2.2 Plane-Strain Compression Test

Williams and Ford developed "plane-strain compression test" which was initially applied to metals (Williams and Ford 1964). It was based on the fact that strain is easier to measure in compression test. The same test method may be used for polymer blends to obtain total deformation curves up to high levels of strain that may be encountered in engineering applications. Williams had further explained the application of this technique to polymers (Williams 1964).

10.2.3 Flexural Strength and Flexural Modulus

Flexural tests may be carried out in tensile or compression test machines. In standard tests, three-point bending test is preferred, although it develops maximum stress localized opposite the center point (support). If the material in this region is not representative of the whole, this may lead to some errors. Four-point test offers equal stress distribution over the whole of the span between the inner two supports (points) and gives more realistic results for polymer blends (Fig. 10.3). Expressions for the calculation of flexural strength and modulus for differently shaped specimens are given in Table 10.4.

Standard test methods for flexural properties are listed in Table 10.5. They may be carried out in tensile or compression test machines. Three-point bending is often used. Four-point test offers equal stress distribution over the whole of the span between the inner two supports (points), and it is preferred for polymer blends. The curvature of the bearing rods is also important as too sharply curved rods lead to fracture of the specimen.

10.2.4 Rigidity and Rockwell Hardness

"Hardness" is not a fundamental property. Its measurement is subjected to the effects of temperature, time, and other test variables. Hardness measurement of

Table 10.3 Standard test methods for compressive tests

No.	Test method	Specimen	Materials
1.	ISO 604 (1973)	(1) The right square prism, (2) the right rectangular prism, (3) the right cylinder, and (4) the right circular crown tube	The load-bearing faces are to be parallel to each other within 0.1 % of the test piece height
2.	British standard BS 2782, Method 345A		
	Type 1	For sheets of thickness not less than 12 mm	Thermoplastics, including polymer blends and thermosets
	Type 2	For sheets of thickness less than 12 mm (for sheets of thickness >12 mm, the test piece is machined only on one face so as to reduce the thickness to 12 mm)	Thermoplastics, including polymer blends, and thermosets
	Type 3	For casting and lamination resin systems without fibrous reinforcement	
	Type 4	Test pieces are identical to ISO 604	Neat resins
	Type 5	For flat injection-molded or compression-molded thin sheets materials	Glass fiber-reinforced laminates
3.	USA standards ASTM D695-10[a] The method is the same as in BS, but specimen dimensions differ	For a right prism the preferred dimensions are 12.7 mm square by 25.4 mm height	For rod slenderness ratio should be in the range 11–15:1
4.	German standards DIN 53454 (1971)	Similar to British Standards in the form as well as dimensions of test specimens	

[a]ASTM standard test methods are available on web: http://enterprise.astm.org/
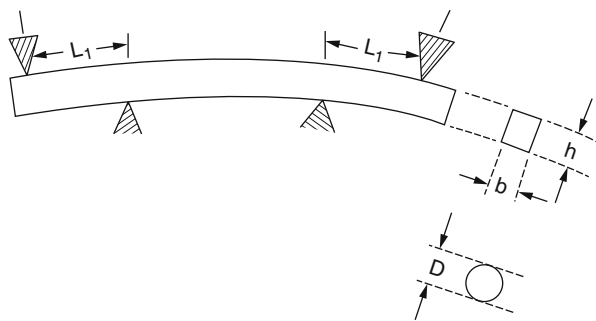
Fig. 10.3 Four point bending

Table 10.4 Expressions for calculation of flexural strength and modulus

No.	Geometry	Strength (MPa)	Modulus (MPa)	Comments
1.	**Four-point bending**			P = Load (N) at the moment of break
				P_Y = Maximum load (N) at yield or break
	ASTM D6109-97 (load span = 1/3 support span)	$S = PL/bd^2$	$E = 0.21\ L^3m/bd^3$	L = Support span (mm)
				B = Width of beam (mm)
				d = depth of beam (mm)
	ASTM D6272-98 (load span = 1/2 support span)	$S = 3PL/4bd^2$	$E = 0.17\ L^3m/bd^3$	m = slope of the secant (N/mm)
				For Unreinforced and reinforced plastics
2.	**Two-point bending**			For fiber-reinforced pultruded rods use ASTM D4476-97
	ASTM D790-99 (support span-to-depth ratio < 16:1)	$S = 3P_Y L/2bd^2$	$E = L^3m/4bd^3$	

plastics is similar to the traditional methods applied to metals. It usually employs a standard indenter (often a hardened steel ball), forcing it under known load into a flat surface of the plastic and then measuring the resultant degree of indentation.

Unlike other Rockwell scales, Rockwell R_α parameter correlates with the hardness as determined by ball indentation. Fett (1972) has shown that

$$H = \left[\frac{441.4}{(150\text{-}R_\alpha)}\right]^{1.23} \tag{10.5}$$

where H is the hardness by ball indentation and R_α is the Rockwell hardness parameter.

The standard test methods for determining Rockwell hardness are listed in Table 10.6, and the Rockwell scales are given in Table 10.7. For example, ISO 2039 employs a hardened steel ball, 5 mm diameter. The ball is pressed into the specimen under a specified load selected to give an indentation between 0.07 and 0.10 mm (Method A) or between 0.15 and 0.35 mm (Method B). The recommended thickness of the specimen is 4 mm and the suggested time of application of the load is 30 s before the depth reading is taken.

10.2.5 Fatigue Characteristics

Fatigue failure may occur when a specimen fractured into two parts was softened and/or its stiffness significantly reduced by thermal heating or cracking. Sometimes, for different reasons, a large number of cycles elapses from the first formation of microscopic cracks to complete fracture. In this case, the fatigue failure is

Table 10.5 Standard test methods for flexural properties

No.	Test method	Specimen	Material
1.	ISO standards	Standard test specimen dimensions: $80 \times 10 \pm 0.5 \times 4 \pm 0.2$ mm	For single-phase materials
	ISO 178	Length is 20 times the thickness and width is between l0 and 25 mm	For materials containing fillers
		Length is 20 times the thickness and width is between 20 and 50 mm	
2.	British standards BS 2782 Method 335A Method 336B	Identical to ISO 178.	
		It employs cantilever-bending mode. Standard test specimen (molded) dimensions are $70 \times 25.4 \times 1.5$ mm. A hole of diameter 2.0–2.02 mm is to be drilled centrally	
3.	USA standards ASTM[a] D790 Method I Procedure-A Procedure-B Method II Procedure A Procedure B	Three-point loading system	Procedure-A is for materials that fracture at small deflections
		Test specimen dimensions and rate of cross-head motion are to be selected based on support span-to-depth ratios ($1/d$ = 16 to 1, 32 to 1, 40 to 1 or 60 to 1)	
		Four-point loading system. Recommended test specimen dimensions and rate of crosshead motion are given based on support span-to depth ratios	Procedure-B is for materials that undergo large deflections
4.	German standards DIN 53452 DIN 53435	Similar to three-point loading for ISO 178 For four-point loading (using Dynstat apparatus)	

[a]ASTM standard test methods are available on web: http://enterprise.astm.org/

arbitrarily defined as having occurred when the specimen can no longer support the applied load within the deflection limits of the apparatus.

Plastics, including polymer blends, are relatively high damping and low thermal conductivity materials. Thus, repeated straining of an article leads to a temperature rise within and throughout its body. Rapid stress–strain cycling can significantly heat up the article and thereby induce thermal failure – the phenomenon is frequency dependent. Where the thermal effect is to be a minimized, much lower frequency, of the order of a few Hz, should be employed.

Fatigue data are usually presented in the form of S–N curves, in which stress amplitude S is plotted versus log N_f, where N_f is the number of cycles to fracture an unnotched specimen, either in bending or in tension. A typical example of such a curve is shown in Fig. 10.4. Here, the S–N curve for rubber-toughened PMMA provides the "endurance limit," which is defined as the lowest stress amplitude at which fracture occurs. In general, most S–N curves flatten out at $N_f = 10^7$. Rubber toughening, in the case of styrene polymers, is found to reduce fatigue resistance and causes a decrease in the endurance limit (Sauer and Chen 1983, 1984). This is due to promotion of crazing and reduction of stresses by the rubber particles. The cyclic loading then degrades the crazes into cracks.

Table 10.6 Standard test methods for determining Rockwell hardness

No.	Test method	Specimen	Indentation
1.	ISO standards: ISO 2039 Method A Method B Revised procedure follows that of ASTM D785-98.	4 mm thick specimen	Between 0.07 and 0.10 mm
			Between 0. 15 and 0.35 mm
			Time of load application is 30 s
2.	British standards	8 to 1 0 mm thickness	
	BS 2782	For "Softness Number"	
	Method 365A	As ISO 2039	
	Method 365D	As ASTM D2583-95	
	Method 1001	Measures Rockwell	
	Part 3 (Method 365C)	Hardness	
3.	USA standards ASTM D785-98[a]	Uses Rockwell hardness tester, and scales (see Table 10.7)	Minor load is applied for 10 s, then major load for 15 s; the hardness reading is taken off the scale 15 s after the major load is removed
	Procedure A Procedure B	6 mm thick specimen	Indentation is recorded 15 s after application of major load, but with minor load still on
4.	German standards DIN 53456	As in ISO 2039	Same as ISO 2039 except the major load must be selected from 49 N, 132 N, 358 N and 96IN, with a minor load of 9.81 N in all cases

[a]See: http://enterprise.astm.org/

Table 10.7 Rockwell scales (ASTM D785-98 (http://enterprise.astm.org/))

Rockwell hardness	Minor load (kg)	Major load (kg)	Indenter diameter	
			(in.)	(mm)
R	10	60	0.5000 ± 0.0001	12.7000 ± 0.0025
L	10	60	0.2500 ± 0.0001	6.3500 ± 0.0025
M	10	100	0.2500 ± 0.0001	6.3500 ± 0.0025
E	10	100	0.1250 ± 0.0001	3.1750 ± 0.0025
K	10	150	0.1250 ± 0.0001	3.1750 ± 0.0025

Fatigue-induced deformation mechanisms can be studied by measuring the volume changes. Another sensitive method is to monitor the hysteresis loops under tension–compression loading. This is illustrated in Fig. 10.5. All specimens initially show a small elliptical loop, indicating the viscoelastic response of the polymer (Bucknall and Stevens 1980; Sauer and Chen 1984; Bucknall and Marchetti 1983). Plots of tensile versus compressive loop area reflect the proportions of shear yielding and crazing. This method has been used to detect the onset of crazing in fatigue tests

Fig. 10.4 S-N curve for rubber-toughened PMMA (Bucknall 1988)
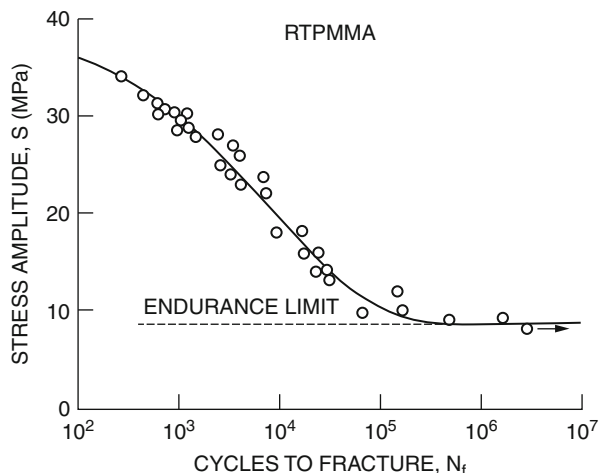
on ABS. Following the trend in metallurgy, fracture mechanics techniques are now widely used to study fatigue in polymers.

Standard test methods for fatigue testing are listed in Table 10.8. As an example, ASTM D671 makes use of the constant amplitude of force approach (Satake 1970). Two dumbbell-type test pieces, both of triangular form, are described. They are to be selected according to the thickness and stress range over which the measurements are to be made. The apparatus described operates only at a fixed frequency of 30 ± 5 % Hz.

10.2.6 Review of Low-Speed Mechanical Properties of Blends

The low-speed stress–strain dependence for PS and HIPS is shown in Fig. 10.6. These data well illustrate the change induced by incorporation of elastomeric particles into PS matrix. As shown, upon toughening, PS brittle behavior changes into ductile with flow.

The low-speed mechanical properties of polymer blends have been frequently used to discriminate between different formulations or methods of preparation. These tests have been often described in the literature. Examples of the results can be found in the references listed in Table 10.9. Measurements of tensile stress–strain behavior of polymer blends are essential (Borders et al. 1946; Satake 1970; Holden et al. 1969; Charrier and Ranchouse 1971). The rubber-modified polymer absorbs considerably more energy; thus higher extension to break can be achieved. By contrast, an addition of rigid resin to ductile polymer enhances the modulus and the heat deflection temperature. These effects are best determined measuring the stress–strain dependence.
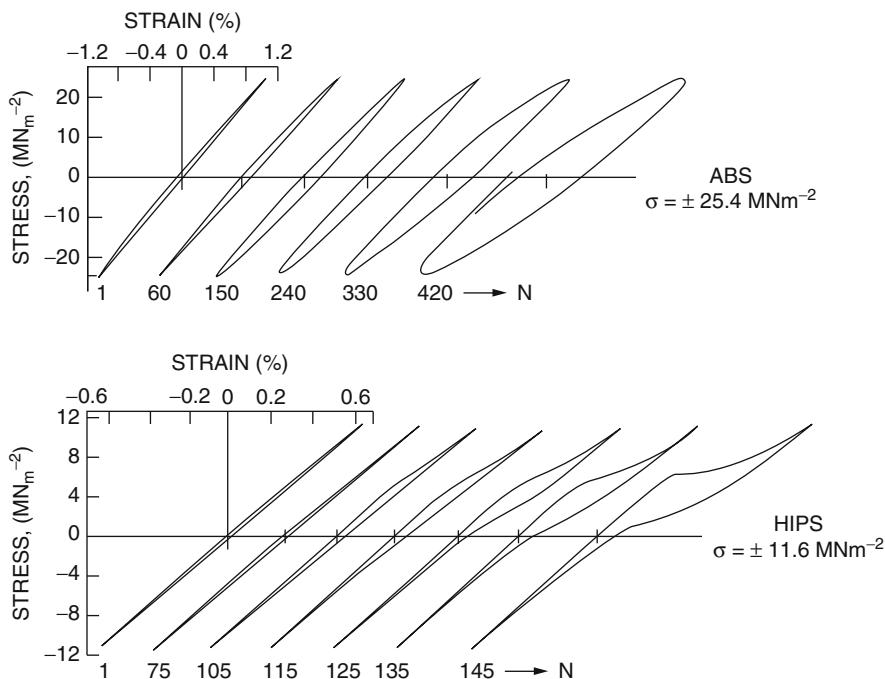
Fig. 10.5 Hysteresis loops developed during fatigue tests of ABS and HIPS (Bucknall 1988)

Table 10.8 Standard methods for fatigue testing

No.	Test method	Approach	Specimen	Frequency of testing
1.	USA standards ASTM D671-93[a]	Constant amplitude of force	Two specimens of triangular form with rectangular cross section	Fixed frequency of 30 Hz
2.	German standards DIN 53442	Constant amplitude of deformation	Dumbbell shaped (tensile dumbbell) test specimens	Variable frequency

[a]See: http://enterprise.astm.org/

10.3   High-Speed Mechanical Properties

The subject of impact strength of plastics has received considerable attention in official standards, material data sheets, and literature at large. The result of an impact test is basically no more than one point on the general curve of studying strength properties as a function of speed of testing. One advantage an impact test can offer is a ready measure of the actual energy required to break a test piece, which information can also be calculated from stress–strain diagrams in tensile or flexural tests with some effort.

Fig. 10.6 Tensile stress–strain curves for PS and HIPS (Bucknall 1988)
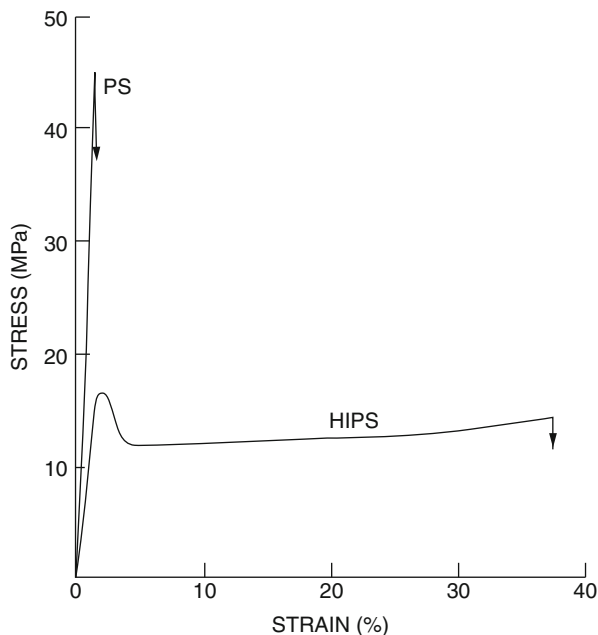
All materials tend to fracture if stressed severely enough. Some materials fracture more easily than others and are thereby said to be "brittle." Brittleness is the property of a material manifested by fracture without appreciable prior plastic deformation. In ductile fracture significant plastic flow occurs before fracture. Strain at fracture is more than a few per cent, unlike brittle fracture, and may be several hundred per cent. However, a sharp distinction cannot be made between brittle and ductile fracture since even in glassy materials some deformations take place. Further, a given material will fail in a brittle manner under some conditions and a ductile manner under other conditions. Thus, brittle fracture is favored by the low temperature and fast loading and when the state of stress approaches a uniform, i.e., triaxial or dilatational, state. Materials with low T_g are more likely to suffer ductile fracture, but the mode of fracture also depends on the fracture conditions. Furthermore, any structural feature that raises T_g, such as bulky side groups or cross-linking, promotes brittle fracture. In a given material fracture may undergo brittle/ductile transition, depending upon the testing temperature. At this transition temperature, the mode of fracture changes from brittle to ductile fracture (Kinloch and Young 1983).

10.3.1 Impact Strength

In many applications a satisfactory resistance to impact loading is an important performance requirement, and, indeed, impact toughness is often the deciding

Table 10.9 Sources for low-speed mechanical property data of polymer blends, Examples:

Blend	Test	Results	References
HIPS	Tensile stress–strain	See Fig. 10.6	Bucknall 1988
HDPE/PP	Tensile properties		Robertson and Paul 1973; Deanin and Sansone 1978; Greco et al. 1980; Dumoulin 1988
HDPE/PP/EPR		EPR acts as a compatibilizer	Nolley et al. 1980; Utracki 1995
HDPE/PP + two EPR's	Tensile properties for different compositions	Stress–strain curves, strength, modulus, yield stress, etc.	D'Orazio et al. 1983
PP/Cross-linked rubber		Tensile yield strength, tensile modulus etc.	Dao 1982
PC/SAN	Tensile properties of different compositions	Effect of blend composition on mechanical properties	Keitz, et al. 1984; Kurauchi and Ohta 1984; Koo et al. 1985; Weber and Schoeps 1985; Gregory et al. 1987; Chiang and Hwung 1987; Skochdopole et al. 1987; Quintens and Groeninckx 1990
PC/HDPE, PC/LDPE and PC/PS	Tensile properties	Mechanical properties of. immiscible/miscible blends	Kunori and Geil 1980
PC/ABS	Tensile properties	Tensile strength, modulus and elongation at break	Suarez et al. 1984; Chiang and Hwung 1987
PA/PE/ionomer	Mechanical properties	Reduction in particle size of dispersed phase	Fisa 1991; Fairley 1990; Fairley and Prud'homme 1987; Chuang and Han 1984, 1985; Macknight et al. 1985; Han and Chuang 1985
Polymers/blends	Fatigue behavior	Review of fatigue behavior	Takemori 1984; Radon 1980; Hertzberg and Manson 1980; Saur and Richardson 1980; Andrews 1969
Rubber-toughened PMMA	Fatigue behavior	Fig. 10.4	Bucknall 1988
Rubber-toughened PS	Fatigue behavior	Rubber toughening reduced the fatigue resistance and endurance limit	Sauer and Chen 1983, 1984
HDPE/LCP	Mechanical properties	Increased tensile strength, modulus and HDT. Decreased elongation at break, and impact strength	Yamaoka et al. 1989

(continued)

Table 10.9 (continued)

Blend	Test	Results	References
PP/LCP, PVC/LCP	Tensile and impact properties	Mechanical properties varied with interphase adhesion and orientation of LCP domains	Seppala et al. 1992; Lee 1988
PA-6/LCP	Mechanical properties	Changes in mechanical explained in terms of morphology	La Mantia et al. 1989
PA-12/LCP	Mechanical properties	Mechanical properties correlated with morphology	Kiss 1987; Ramanathan et al. 1987; Blizard and Baird 1986
Amorphous PA/LCP	Mechanical properties	Tensile strength and flexural modulus increased with increasing LCP content	Siegmann et al. 1985
PC/LCP	Tensile and other mechanical properties	Tensile properties improved	Isayev and Modic 1987; Kiss 1987; Weiss et al. 1989; Blizard and Baird 1986a, b; Malik et al. 1989; Blizard et al. 1990; Zhuang et al. 1988; Shin and Chung 1989
PET/LCP	Flexural properties	Flexural modulus increased with LCP content	Zhuang et al. 1988; Amano and Nakagawa 1987; Brostow et al. 1988; Joseph et al. 1984; Sukhadia et al. 1990; Seppala et al. 1992
PET/LCP, PBT/LCP	Tensile properties	PET-LCP copolymer as compatibilizer was used	Poli et al. 1996
PES/LCP	Flexural properties	Increasing LCP content increased modulus, but decreased strength	Kiss 1987; Cogswell et al. 1981; Yazaki et al. 1994
PPS/LCP	Tensile and impact properties	Mechanical properties depended on miscibility, LCP orientation, etc	Ramanathan et al. 1988; Seppala et al. 1992; Nobile et al. 1990
PSU/LCP	Mechanical properties		Nobile et al. 1990
PEI/LCP	Mechanical properties		Blizard et al. 1990; Nobile et al. 1990; Kiss 1987
PEEK/LCP	Tensile and impact properties	Properties varied with anisotropy due to LCP content	Kiss 1987; Cogswell 1981; Mehta and Isayev 1991
PP/Olefinic Elastomer	Mechanical properties and morphology	Elastomer enhanced the toughness of blends but reduced stiffness	Lotti et al. 2000

(continued)

Table 10.9 (continued)

Blend	Test	Results	References
EPR/PP, peroxide cross-linked	Tensile, elongation, elastic modulus, Izod, hardness, Vicat softening point, HDT	Microstructure (DSC, SEM) found to influence mechanical properties	Tasdemir and Topsakaloglu 2007
NBR and E-MA toughened PA6 nanocomposites	Tensile, Young's modulus	Finely dispersed nonreactive polar elastomers provided best balanced mechanical properties	Kelnar et al. 2006
PA6/4 % MMT/ SEBS-g-MA	Fracture toughness, tensile properties, impact properties	SEBS-g-MA enhanced fracture toughness of PA6/4 % MMT	Tjong and Bao 2005
PP/Elastomer; PP/Calcium carbonate	Toughness	PP toughness higher with elastomer compared to calcium carbonate	Zhang et al. 2004
NanoCaCO$_3$/PPE/ SBS	Toughness, impact strength	Synergistic toughening occurred with nanoCaCO$_3$ and SBS in PPE matrix	Chen et al. 2004
PP/EOR	Tensile, impact strength	EOR with high octane content and high molecular wt provide blends of high impact strength	Premphet and Paecharoenchai 2002
PA6/VLDPE, PA6/VLDPE-g-MA, PA6/VLDPE-g-DEM	Fracture toughness, impact strength	Compatibilized blends behaved different and better way	Lazzeri et al. 1999
PA6/LDPE-g-MAH	Tensile, flexural, Izod impact	Izod impact strength increased with LDPE-g-MAH was 20 %	Sandeep 2006
PA6/PP-g-ITA, PA6/HDPE-g-ITA, PA6/PP-g-(ITA-St), PA6/HDPE-g-(ITA-St)	Tensile, impact strength	Impact strength increased up to 70 % after using PP-g-ITA and HDPE-g-ITA as compatibilizer	Liu 2007
PA6/UHMWPE using HDPE-g-MAH as compatibilizer	Mechanical properties	HDPE-g-MA improved mechanical properties of blends	Zhao 2005
PA6/LDPE, PA6/LDPE using Na-EMAA as compatibilizer	Mechanical properties	Mechanical properties of compatibilized blends were improved	Canfora 2004; Lahor 2004; Pakeyangkoon 2005
Nano-PA6/ABS using POE-g-MA	Impact strength, HDT	Impact strength increased with addition of compatibilizer (POE-g-MA0)	Lai 2006

Table 10.9 (continued)

Blend	Test	Results	References
HDPE/PA6 + Electron Beam Irradiation	Mechanical properties	Mechanical properties of electron beam irradiated blends were improved	Lian 2004
PP/EPDM with Nano-SiO$_2$	Izod impact strength	Izod impact strength of ternary blends improved two to three times compared to binary blends	Hong et al. 2007
PTT/LCP(Vectra A950)	Mechanical properties	LCP improved tensile modulus, slightly reduced tensile strength and drastically reduced elongation compared to PTT	Pisitsak and Magaraphan 2009

factor in materials selection (Vincent 1971; Bucknall et al. 1972; Turner 1973; Bucknall 1977; Reed 1979; Kinloch and Young 1983; Savadori 1985; Brostow and Corneliussen 1986; Havriliak et al. 1996). For the past several decades, ductile grades of usually brittle polymers, such as PS, PMMA, PVC, or PA, have been used. The most widely used test for impact assessment is the notched Izod impact test. A single operator can run up to 150,000 tests in a year (Havriliak et al. 1996).

The test is also an important material or product specification for toughness – it is often one of few material constants specified as a product development objective. It appears that the earliest reference to the subject of impact testing was in 1734 by Swedenborg who wrote that iron bars were tested by throwing them against a sharp edge (Lethersich 1948). If the blow marks the bar without breaking any part of it, this was a sign of tenacity. Further, experimental and theoretical works pointed out the dependence of the resistance of metals on the test speed and notches. Two devices were introduced by Charpy (in 1901) and by Izod (in 1903) for analyzing the impact performance of materials (see Fig. 10.7). The impact resistance is evaluated in energy terms, i.e., by evaluating the difference between the potential energy before and after impact, the energy absorbed by the specimen during the impact process is obtained.

From the physical point of view, the Izod equipment is equivalent to that of Charpy. However, the main differences between the two are the clamping system, the notch, the hammer speed, and its weight. Charpy adopted the keyhole form of notch. At such an early stage in the history of impact testing, Charpy found that correlations between static and dynamic tests were obtainable provided a notched bar was used. In 1925, the Izod and Charpy tests were extended to plastic materials, and many results on plastics were published a year later (Werring 1926).

The growth of fracture mechanics has placed greater emphasis on tests that use sharply notched specimens. These results were found to provide more fundamental information. Instrumented impact testing is a recent development that provides information on force – deflection curves. In addition to these notched bar tests, extensive use of falling dart tests is also being made. However, interpretation of the

Fig. 10.7 Cantilever beam (Izod type) impact machine (ASTM D256)
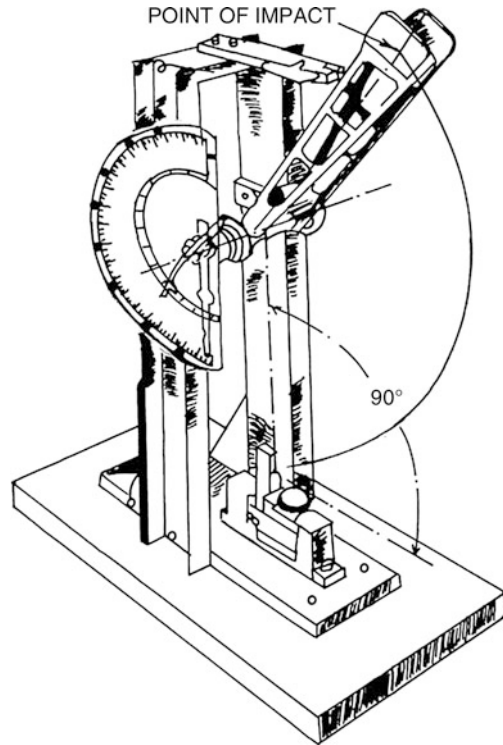
data from the latter is far from straightforward. The impact strength is not a fundamental material property. The results depend on the specimen geometry, test method, and the employed parameters. Thus, it is difficult to correlate the results obtained from different test techniques and extremely difficult to correlate the results from impact tests on specimens of the material to the impact performance of the manufactured article.

Correlation of results from one test to another for a given material becomes difficult because of different stress states of the specimen and the associated strain rates in different tests. In the tensile-impact test, the stress state is uniaxial and it measures the tensile property at a high strain rate. In Izod and Charpy tests, the presence of notch gives a triaxial state of stress. The falling-weight test is always in the forefront of high-speed testing for evaluating the strain rate sensitivity of materials. In this case, the stress is biaxial. Several attempts were made to relate fracture mechanics theories to impact test results (Brown 1973; Marshall et al. 1973; Plati and Williams 1975). The topic was also reviewed (Kinloch and Young 1983; Brostow and Corneliussen 1986).

10.3.1.1 Izod Impact

One of the most often used tests for impact assessment is the notched Izod impact test. The basic principle of the test is to allow a pendulum of known mass to fall

Fig. 10.8 Relationship of vise, specimen and striking edge to each other for Izod test methods A and C (ASTM D256)

STRIKING EDGE RADIUS
0.79 ± 0.12 MM.
(0.031 ± 0.005 IN.)

SPECIMEN

DEPTH

0.25 ± 0.12 MM RADIUS
(0.010 ± 0.005 IN.)

22.0 ± 0.05MM.
(0.866 ± 0.002 IN.)

FIXED
VISE
JAW

MOVE ABLE
VISE
JAW

C

D

PLANES C AND D MUST BE PARALLEL TO
WITHIN 0.025MM (0.001 IN.)
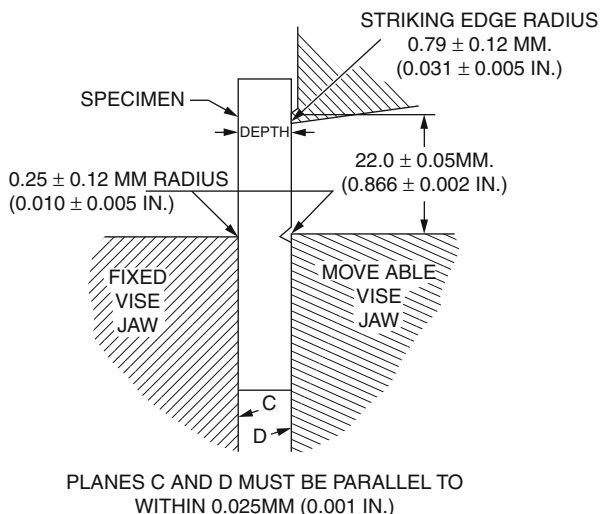
from a known height and strike a standard specimen at the lowest point of its swing, and to record the height to which the pendulum continues its swing (see Fig. 10.7). If the striking edge of the pendulum coincides with the center of the percussion of the pendulum, the bearings of the pendulum are frictionless, and there is no loss of energy to windage, then the product of the mass of the pendulum and the difference between the fall distance and the height it reaches after impacting the test specimen is the impact strength of the latter.

The test may be carried out on plane rectangular bars, but most often a carefully defined notch is molded or machined into the face to be struck (Fig. 10.8). The impact tests are often regarded as a means of assessing the resistance of a material to shock where notches or "stress raisers" generally are present. The ratio of impact strength of unnotched to that of notched specimen is sometimes regarded as a measure of the notch sensitivity of a material.

Despite the popularity of the test, it is still poorly understood in terms of generating an actual "material" property. The test reveals little about molecular dynamics and is not related to molecular structure. It is often criticized by fracture mechanics experts because of uncertainties about gauge length, complex state of stress, its dependence on thickness as well as a wide range of shear rates during the experiment, and the relationship of these factors to real situations (Havriliak 1996).

The test, nevertheless, does have several important features. First, it is accepted by a large technical audience and is in common use. Second, it is a reproducible test, mostly because of the work of the ASTM. Finally, the impact results for various materials are spread over two orders of magnitude. When this spread is compared with the signal-to-noise ratio, the material range is impressive. Attempts are made to set up this ubiquitous test method on a firm platform based on the principles of fracture mechanics.

Table 10.10 Standard test methods for the determination of Izod impact strength

No.	Test method	Impact energies	Test specimen	Notch
1.	ISO R180	1.0, 2.75, 5.5, 11.0 and 22.0 J	Four types permitted. Type 4 is preferred ($80 \pm 2 \times 10 \pm 0.2 \times 4 \pm 0.2$ mm)	Two types of cut notches allowed
2.	BS 2782 Method 306 A	1.36, 4.07 and 13.6 J	($63.5 \pm 2 \times 12.7 \pm 0.2 \times 12.7.0 \pm 0.3$ mm) or ($63.5 \pm 2 \times 12.7 \pm 0.2 \times 6.4 \pm 0.3$ mm)	Molded notch allowed in Type A. Cut notches allowed in Type B and C
3.	ASTM D 256-00	A range of pendulum energies from 2.710 to 21.680	Length: 63.50 mm (max.), 60.30 mm (min) Width: 12.7 mm (max), 3.00 mm (min). Breadth: 12.70 ± 0.15 mm	Cut notches allowed

Standard test methods for the determination of Izod impact strength are listed in Table 10.10. For example, ISO R180 normalizes the notch length. The velocity of the striker on impact has been standardized at 3.5 ± 10 % m/s with impact energies of 1.0, 2.75, 5.5, 11.0, and 22.0 J. Four types of test pieces are permitted.

10.3.1.2 Charpy Impact

The Charpy test is similar to the Izod impact test. In both the tests, flexural impact takes place by a pendulum (Fig. 10.9) striking a bar-shaped test piece (Fig. 10.10). However, as described before, there are quite significant differences between them, and no general correlation relating the data obtained from each have been developed.

Standard test methods for the determination of Charpy impact strength are listed in Table 10.11. For example, BS 2782 (Method 351A) uses a rectangular, notched or unnotched, bar supported at both ends in such a position that the pendulum strikes it in the center, directly behind the notch. The energy absorbed in the impact is read directly by means of a pointer from a scale calibrated to allow for frictional and windage errors. Three standard test pieces are defined – the preferred being $120 \times 15 \times 10$ mm with a span of 70 mm. The standard impact energies are 0.5, 1, 4, 15, and 50 J.

10.3.2 Fracture Mechanics

Griffith (1920) showed that brittle solid materials fail at lower strengths because of the presence of flaws acting as stress concentrators. The hypothesis has become the basis of "fracture mechanics," used to interpret the fracture of many solids, including polymers and their blends. The theoretical background is presented in standard texts (Kinloch and Young 1983; Williams 1984; Broek 1986; Brostow and Corneliussen 1986).

Linear elastic fracture mechanics (LEFM), which has grown out of the work of Griffith, provides the most satisfactory basis for characterizing the fracture process

Fig. 10.9 Simple beam
(Charpy-Type) impact
machine (ASTM D6110-97)
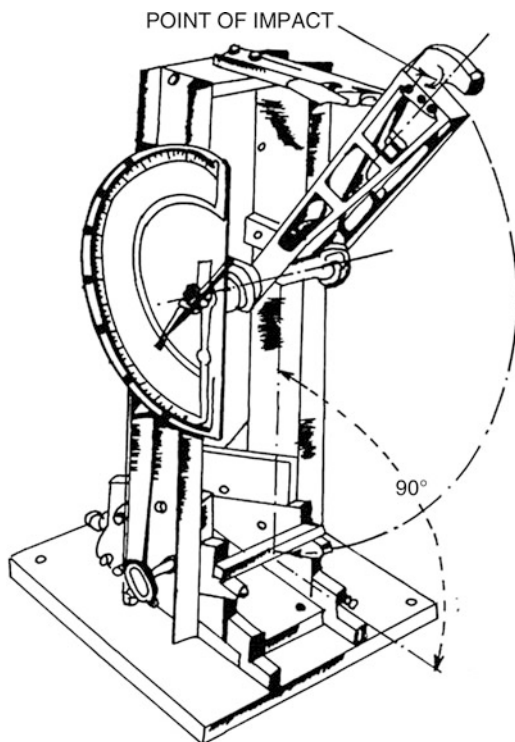
of polymer composites and multiphase polymers. It enables each of the factors contributing to fracture to be considered separately. Results obtained from the fracture mechanics analyses have thrown considerable light upon the behavior of polymers under tensile, impact, and fatigue loading. Unfortunately, the conditions of LEFM are very severe and require that the fracture process is nearly totally elastic. Only under such conditions the data can be used for large scale predictions. However, elastic behavior cannot always be obtained in a laboratory-scale test and some experimental or theoretical tools need to be available to help in predicting the brittleness of large-scale article. Furthermore, in case of rubber-toughened plastics, extensive yielding usually precedes fracture even in the presence of a sharp crack, so that LEFM techniques are Unsuitable.

A crack in a solid may be stressed in three different modes (Kinloch and Young 1983; Brostow and Corneliussen 1986). The cleavage or tensile-opening mode (Mode I) is technically the most important one since it is commonly encountered and usually results in failure. Two closely related approaches have been used (Williams 1984):

1. The first is an energy criterion that supposes that fracture takes place when sufficient energy is released (from the stress field) during crack growth to supply the energy requirements of the new fracture surfaces created (Orowan 1948).
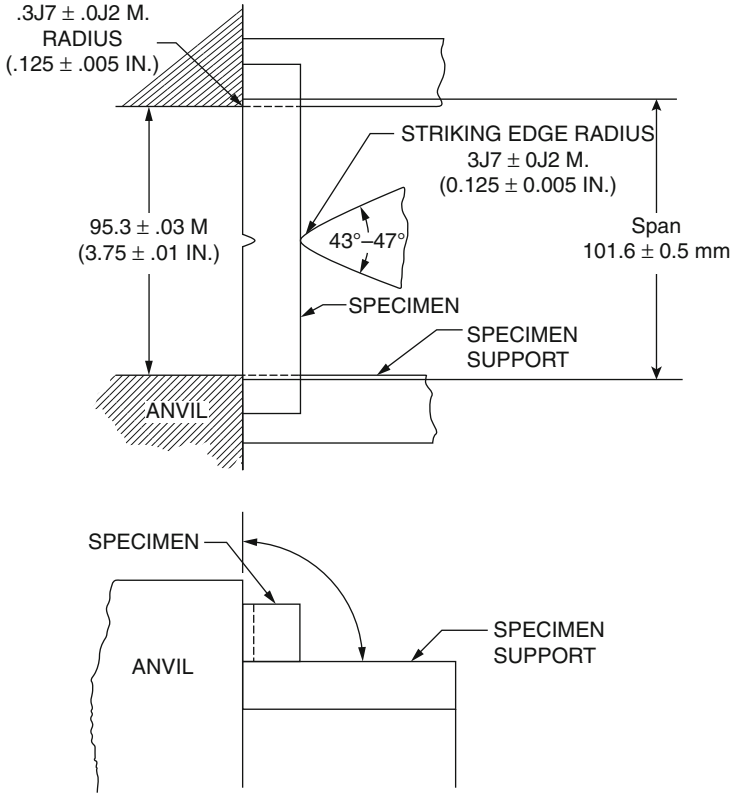
Fig. 10.10 Relationship of anvil, specimen and striking edge to each other for Charpy test method (ASTM D6110-97)

The fracture of a material is thereby characterized by the material property G_c known as the "strain energy release rate" or "fracture energy" (Kinloch and Young 1983; Brostow and Corneliussen 1986).

2. Rivlin and Thomas (1953) developed the second approach. They showed that the stress field around a sharp crack in an elastic material could be uniquely defined by a parameter known as the "stress intensity factor," K. When K reaches a critical value K_c (which is a material property often called the "fracture toughness"), fracture takes place.

The criterion for crack propagation is that $K_I > K_{Ic}$. For plane strain in Mode I, values of G_{Ic} and K_{Ic} are related:

$$K_{Ic}^2 = \frac{E\,G_{Ic}}{(1 - \nu^2)} \qquad (10.6)$$

where E is Young's modulus and ν is Poisson's ratio. In SI units, K_{Ic} is usually given in $MPa.m^{0.5}$ and G_{Ic} in $kJ\ m^{-2}$. To make valid fracture mechanics

Table 10.11 Standard test methods for the determination of Charpy impact strength

No.	Test method	Impact energies	Test specimen	Notch
1.	BS 2782, Method 351 A	0.5, 1, 4, 15, and 50 J	Preferred test dimensions are $120 \times 15 \times 10$ mm	Type A (standard), square section, 2 mm wide and one-third specimen thickness in depth. Type B and C are V-shaped with base radii 0.25 mm and 1.00 mm respectively. The depth of these notches is set to one-fifth thickness
2.	ISO R179	Two striking energy levels	Four types of test pieces are allowed. First three are as in British standards. Fourth type is 125 mm long by 13 mm square	Same notch types as above. Molded notches are permitted. Machined notches are preferred
3.	DIN 53453 (Similar to BS Method)	As in BS Method	As in BS Method	Type A as given in BS Method (Type B-and C are not specified)
4.	ASTM D6110-97	2.710 ± 0.135 J	$(127.00$ to $124.50) \times (12.70 \pm 0.15) \times (12.70$ to 3.00 mm)	The included angle of the notch is $45 \pm 1°$, with a radius of curvature at the apex of 0.25 ± 0.05 mm

[a]ASTM standard test methods are available on web: http://enterprise.astm.org/

measurements, it is necessary to ensure that specimen dimensions are large in comparison with the plastic zone surrounding the crack tip. For metals, according to ASTM E399,

$$(w - a), \ a, \ B \ > \ 2.5 \ \left(\frac{K_{Ic}}{\sigma_y} \right)^2 \qquad (10.7)$$

where w is the width of the specimen, a is the crack length, B is the thickness, and σ_y is the uniaxial yield stress of the specimen. In the case of polymer blends, it is preferable to experimentally determine the effects of specimen dimensions upon G_c and K_c rather than rely upon the applicability of the above conditions.

The main experimental problem is to prepare specimens in which the plane-strain/plane-stress conditions are satisfied (Williams 1984; Kinloch and Young 1983). Apparent toughness values of K_c and G_c are higher in thin specimens than in thick ones. Measurements on several rubber-toughened plastics have shown a decrease in K_{Ic} with increasing thickness, B. The minimum value of B required, in the case of HIPS, for a valid determination of K_{Ic} at 296 K appears to be about four times higher than that given by Eq. 10.7 (Yap et al. 1983). Unfortunately, there is no reliable criterion for crazing under plane strain, and therefore it is difficult to suggest an alternative to the standard approach that has been used successfully for metals.

The toughness observed for rubber-toughened plastics is determined by the mechanism of deformation created by the plane strain at the tip of a sharp crack. There are two factors to be considered:

1. The fall in yield stress that occurs in ductile polymers as the temperature increases or the strain rate reduces. This fall results in a plane-strain to plane-stress transition, as indicated in Eq. 10.7 and therefore an increase in fracture resistance.
2. The release of constraint that results from cavitation in the matrix or void formation in the rubber particles (Bucknall 1988; Young 1988).

Linear elastic fracture mechanics studies on toughened brittle plastics at room temperature concentrated on thermosetting resins, which have sufficiently high yield stresses to meet the requirements of Eq. 10.7. There has been increasing emphasis on ductile fracture mechanics in testing the toughened thermoplastics. An alternative approach is to determine the parameter, J_{Ic}, which is the quantity corresponding to G_{Ic} in linear elastic fracture mechanics, as discussed below.

10.3.3 Fracture Mechanics Testing

10.3.3.1 Determination of G_c

The ductile fracture mechanics is gaining importance in testing polymer blends, especially the toughened thermoplastics. Some of the types of specimen which have been used to study the failure of ductile polymers whose deformation is elastic (but nonlinear) are shown in Fig. 10.11 (Kinloch and Young 1983). Formulae have been developed to determine G_c for these specimens, and examples are given in Table 10.12. Again, the parameter defining the fracture process G_c, is a function of applied load, crack length, and geometrical factor (Young 1988). Typical values of G_c and K_c are listed in Table 10.13.

The problem of defining conditions for crack propagation becomes more difficult when the material is sufficiently ductile to form a large plastic zone at the crack tip. The problem is encountered particularly while testing rubber-modified plastics. Two ductile fracture criteria have been developed for metals, one based on crack-tip opening displacement (CTOD) and the other upon the energy line integral (J-integral) around the crack tip. The crack-opening displacement (COD) criterion has been applied to a number of polymers and blends, but the J-integral method is receiving more attention. Physically, COD is measured between the outer edges of the crack whereas CTOD is defined as the distance between two crack walls at the end of the fatigue crack. Thus, while COD is easy to measure, the determination of CTOD is not simple.

The CTOD δ is the relative displacement of the two fracture surfaces at the crack tip. Critical values of CTOD δ_c may be measured by means of a mechanical clip gauge or recorded photographically. Furthermore, a cine camera may be used to follow the crack initiation and propagation as in HIPS (at 293 K) (Ferguson et al. 1973). The authors reported that both LEFM and CTOD criteria were applicable at different stages of the fracture. On application of load to the specimen, the crack began to extend at a fixed value of K_I, to give a value of K_{Ic}, for crack initiation. Then, at the crack tip, began to form a stress-whitened yield zone. The load on the

Fig. 10.11 Schematic diagrams of various specimens used for fracture mechanics testing of flexible polymeric materials. P = Applied load (Young 1988)
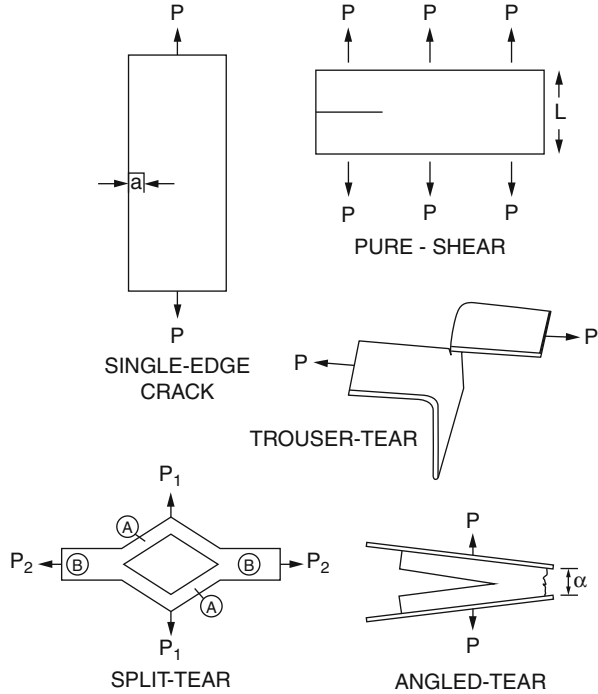
specimen continued to increase as both crack and yield zone extended, and a load maximum was observed at a fixed value of CTOD.

Precise determination of CTOD is often difficult. Furthermore, these measurements are unsuitable for use in design. For these reasons, models that enable CTOD to be calculated in terms of stresses have been developed (Dugdale 1960). In a wide plate with a central crack of length 2a with a narrow planar plastic zone of length L, extending from each of the crack tips, the applied stress σ is given by (Bucknall 1978)

$$\sigma = \frac{a}{(a+L)} = \cos\left(\frac{\pi\sigma}{2\,\sigma_y}\right) \tag{10.8}$$

The CTOD δ can be expressed as

$$\delta = \left[\frac{8\,\sigma_y\,a}{(\pi E)}\right]\ln\,\sec\,\left(\frac{\pi\sigma}{2\,\sigma_y}\right) \tag{10.9}$$

For small values of applied stress ($\sigma < 0.3\,\sigma_y$), the plastic zone size is small compared with the crack length and Eq. 10.9 can be simplified to read

Table 10.12 Expressions for G_C for fracture mechanics of crack growth in flexible polymers (Kinloch and Young 1983)

Geometry (see Fig. 10.11)	Expressions for G_C	Comments	References
Single-edge crack	$G_C = 2k_1 a W_C$	λ_c = extension ratio at onset of crack growth	Rivlin and Thomas 1953; Greensmith 1963; Lake 1979
	$k_1 = \pi \lambda_c^{-1/2}$	W_C = critical stored elastic strain energy density	
Pure shear	$G_c = l W_C$	l = initial length	Rivlin and Thomas 1953
Trouser tear	$G_C = (2P_C \lambda_C / b) - 2wW_C$ when $\lambda_C = 1$ $G_C = 2P_C/b$	P_C = load at onset of crack growth	Rivlin and Thomas 1953
		w = width of specimen arms	
		λ_C = critical extension ratio in arms	
		W_C = strain-energy density in arms	
		b = specimen thickness	
Split tear	$G_C = \frac{\lambda_C^A + \lambda_C^B}{2b}\left(\sqrt{P_{1C}^2 + P_{2C}^2} - P_{2C}\right)$	λ_C^A and λ_C^B are critical extension ratios in regions A and B respectively; P_1 and P_2 are loads respectively transverse and in the split direction	Lake 1979
Angled tear	$G_C = (2P_C/b)\sin(\alpha/2)$		Thomas 1960

Table 10.13 Typical values of the fracture energy G_c and the fracture toughness K_c. for various materials (Kinloch and Young 1983)

Material	Young's modulus E (GPa)	G_c (kJm^{-2})	K_C (MNm$^{-3/2}$)
Rubber	0.001	13	–
Polyethylene	0.15	20	–
Polystyrene	3.0	0.4	1.1
High-impact polystyrene	2.1	15.8	–
PMMA	2.5	0.5	1.1
Epoxy	2.8	0.1	0.5
Rubber-toughened epoxy	2.4	2.0	2.2
Glass-reinforced thermoset	7.0	7.0	7.0
Glass	70	0.007	0.7
Wood	2.1	0.12	0.5
Aluminum alloy	68	20	37
Steel mild	210	12	50
Steel alloy	210	107	150

$$\delta = \pi\sigma^2 \ \frac{a}{\left(E\sigma_y\right)} \tag{10.10}$$

Under these conditions, LEFM analysis is applicable to the specimen.

In the case of a brittle fracture in a wide and thick plate containing an edge crack of length a, the critical applied stress at fracture σ_c is related to the Young's modulus E, the Poisson's ratio ν, and the fracture surface energy G_{Ic}; the critical stress can be expressed from the Griffith equation as

$$\sigma_c^2 = \frac{E \ G_{Ic}}{\pi a \ (1 - \nu^2)} \tag{10.11}$$

From Eqs. 10.10 and 10.11, for plane-strain deformation,

$$G_{Ic} = \sigma_y \ \delta_c \ \left(1 - \nu^2\right) \tag{10.12}$$

Tests are conducted, in normal practice, on compact tension specimens rather than wide center-notched plates. Some allowance must be made for geometrical effects, including the finite width of the specimen, the difference between edge and center notches, and any rotations occurring at the grips.

In general, it is not possible to measure CTOD, but rather the crack-opening displacement (COD). The latter quantity can be determined at the outer end of the notch with a suitable clip gauge. Thus, for a notched three-point-bend specimen, it was shown that a "plastic hinge" can form around the tip of the crack (Brostow and Corneliussen 1986). If the center of rotation is known, the CTOD can be calculated from the measured COD. A standard has been published (BS 5762).

10.3.3.2 J-Integral Techniques
Single-Specimen Method
If there is extensive plasticity in a material under tension, it gives rise to a relatively large size of the crack-tip plastic zone, and solutions for elastic–plastic behavior are not readily available. J-integral provides a means of determining the energy release rate for such cases. This integral was applied to crack problems (Cherepynov 1967; Rice 1968). Rice showed that J-integral describes the flow of energy into the crack-tip region and that the dominant term in the description of stress and strain singularities at the crack tip could also be written in terms of J. He demonstrated that the value of J was independent of the integration path. In practice, J can be determined from changes in load displacement diagram with changes in crack length (ASTM E813). This method has been reviewed (Williams 1984; Landes and Begley 1979; Pascoe 1986). The J-integral is given by (Kinloch and Young 1983).
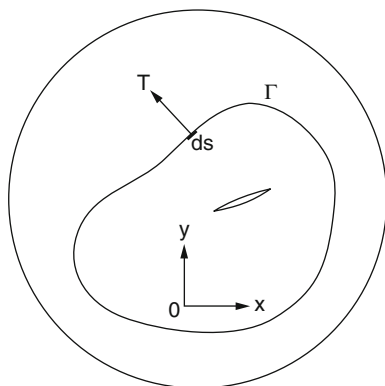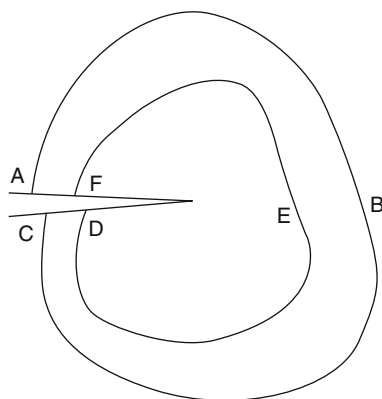
$$J = \int_{\Gamma} \left\{ Z\partial y - T\left(\frac{\partial u}{\partial x}\right) ds \right\} \tag{10.13}$$

where Γ is a closed contour in a stressed solid (Fig. 10.12), T is the tension vector perpendicular to the contour in an outward direction, u is the component of displacement of the contour in x-direction, ds is an element of the contour Γ, and Z is the strain energy (plastic and elastic) per unit volume.

In Fig. 10.13, a closed contour is taken as two curves surrounding the tip of the crack, one DEF inside the other ABC which are joined by two portions of the crack surface AF and CD. The integral around the contour is zero. Along the parts AF and CD which lie parallel to the x-axis and which have no normal stress on them, T = 0 and dy = 0. Therefore, the integral along ABC is equal and opposite in sign to that along DEF. For outward directed vectors, T, therefore, the integral is path independent. The J-integral method (ASTM E813) of

fracture toughness measurement has been applied to a variety of polymers (Theuer et al. 1988; Rimnac et al. 1988) and rubber-toughened polymers (Huang and Williams 1987; Huang 1988; Huang and Wang 1989; Hashemi and Williams 1985; Takemori and Narisawa 1989).

The multi-specimen J-integral technique (ASTM E813) also provides a method for determination of J_{Ic}, a measure of fracture toughness. A critical evaluation of ASTM E813-81 and E813-87 has been published (Narisawa and Takemori 1989; Huang and Wang 1989; Huang et al. 1990).

Multiple-Specimen Method

A major problem often encountered in the above described "single-specimen method" is that the crack growth measured from a side view may not be accurate, as the crack front may vary from the central region to the sides. A "multiple-specimen method" was developed to bypass this problem.

The method has been applied to numerous ductile polymeric materials (Begley and Landes 1972; Landes and Begley 1974). The critical J values obtained by using single-specimen method were greater than those obtained from the standard multiple-specimen method (Westerlind et al. 1991). Many workers have used the ASTM standards of E813-87 to characterize the fracture toughness of polymers (Chan and Williams 1981, 1983; Hashemi and Williams 1986; So and Broutman 1986; Huang and Williams 1987; Narisawa 1987; Rimnac et al. 1988; Narisawa and Takemori 1989; Huang and Williams 1990; Huang 1990; Moskala and Tant 1990).

Hysteresis Energy Method

When a pre-cracked specimen of a toughened polymer is under load, viscoelastic and inelastic micro-mechanisms such as crazing, cavitation, debonding, and shear yielding are expected to take place mainly around the crack tip. These micro-mechanisms occur during the process of crack-tip blunting (pre-crack) and during crack propagation. A portion of the storage energy is therefore consumed, and a relatively large crack-tip plastic zone is formed, which can be quantified by the corresponding hysteresis energy. For rubber-toughened polymeric materials, the crack tends to propagate within the plastic zone. A new J-integral method based on hysteresis properties of polymeric materials was proposed (Lee and Chang 1992; Lee et al. 1992).

In case of a cracked specimen, the material surrounding the crack tip can be divided into three parts: (1) the first plastic zone, (2) the second plastic zone, and (3) the elastic fracture surface (Lu et al. 1996). The specific energy balance equation for a cracked specimen can be expressed as

$$\left(\frac{1}{B}\right) \left(\frac{dU}{da} - \frac{dU_e}{da} - \frac{dU_k}{da}\right) = \left(\frac{1}{B}\right) \left(\frac{dU_p^{ppz}}{da} + \frac{dU_p^{spz}}{da}\right) + 2\gamma_s \quad (10.14)$$

where U is the input energy at different displacements, U_e is the elastic energy, U_k is the kinetic energy, U_p^{ppz} is the plastic energy for the primary plastic zone, U_p^{spz} is the

Fig. 10.14 Plots of critical J_{IC} value versus the strain rate (Lu et al. 1996)
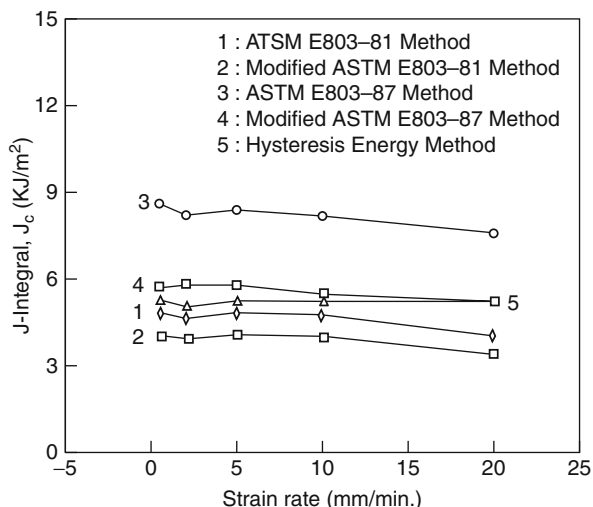
plastic energy for the secondary plastic zone, and γ_s is the fracture surface energy and a is the initial crack length. The energy dissipated of the system is given by

$$\left(\frac{1}{B}\right) \frac{d(HE)}{da} = \left(\frac{1}{B}\right) \left(\frac{dU_p^{ppz}}{da} + \frac{dU_p^{spz}}{da}\right) + 2\ \gamma_s \qquad (10.15)$$

where HE is the hysteresis energy.

This approach assumes that there is a region surrounding the crack tip with local energy dissipation. This arises from viscoelasticity, plasticity, and bond rupture and can be considered the characteristic of the fracture process. For polymers the characteristic of this localized energy dissipation is considered to be independent of geometries.

The J_{Ic} values obtained based on hysteresis energy method were close to these obtained using E813-81 method, but significantly lower than those from E813-87 method. Experimentally the hysteresis energy method is relatively simple, because the tedious measurement of crack growth length is not necessary. Figure 10.14 shows variations of J_c values for PC/ABS blends obtained using different J-integral methods – as shown, the spread is $\pm 40\ \%$ (Lu et al. 1996).

The J-integral by hysteresis energy method was applied to elastomer modified PC (Lee and Chang 1992; Lee et al. 1992), HIPS (Lee et al. 1992, 1993), ABS (Lu et al. 1995), PC/ABS blend (Lu and Chang 1995; Lu et al. 1996), and PC/PBT blend (Lu and Chang 1995).

Essential Work of Fracture Method

The theoretical analysis of J-integral is well established (Rice 1968; Begley and Landes 1972), and the experimental procedure is standardized (ASTM E813-89). However, some aspects of the method still remain controversial (Hashemi and

Williams 1986; Huang and Williams 1987, 1990; Narisawa and Takemori 1989, 1990; Swei et al. 1991). For example, the procedure for J–R curve construction restricts the application of the J-integral method to only static loading tests. J-integral method is usually difficult and expensive (Bramuzzo 1989). The specimen size required by the J-integral method makes it impossible to characterize the toughness of polymeric thin films. It is also well recognized that using a blunting line to define the critical value of J-integral may not be proper for some ductile polymers (Hashemi and Williams 1986; Narisawa and Takemori 1989). The J-integral analysis based mainly on metals is not fully appropriate to polymers. This is particularly true when the heterogeneous and toughened polymer blends are involved.

To overcome the above drawbacks, a new method based on "essential work of fracture" concept was introduced (Broberg 1971, 1975). In this method, it is proposed that when a cracked ductile solid, such as a toughened polymer blend, is loaded, the fracture process and the plastic deformation take place in two different regions, viz., the inner process zone and the outer plastic zone. Much of the fracture work during crack propagation, dissipated in the plastic zone, is not directly associated with the fracture process. Only that work that goes into the fracture process zone is a material constant. Hence, the total fracture work, W_f, should be separated into two parts, i.e., the essential work of fracture (i.e., the work required to create two new fracture surfaces, W_e) and a nonessential work of fracture (W_p):

$$W_f = W_e \;+\; W_p \tag{10.16}$$

W_e is essentially a surface energy, and for a given thickness it is proportional to ligament length ($l = W - a$), while W_p is a volume energy and proportional to l^2. Thus, the total fracture work is rewritten as

$$W_f = w_e tl \;+\; \beta w_p tl^2 \tag{10.17}$$

where w_e and w_p are the specific essential work of fracture and nonessential work of fracture (or specific plastic work), respectively; β is the plastic zone shape factor; while t, W, and a are thickness, width, and initial crack length, respectively. Then, the specific total fracture work, w_f, is

$$w_f = \frac{W_f}{tl} = w_e \;+\; \beta w_p l \tag{10.18}$$

There are two kinds of specific essential work of fracture available, according to the stress state of the ligament area, viz., plane-stress-specific essential work of fracture (w_e) and plane-strain-specific essential work of fracture (w_{Ic}) (Wu and Mai 1996).

The w_e can be obtained if l/t ratio is large enough to ensure plane-stress condition in the ligament area, and it is proved to be a material constant for a given sheet thickness (Mai and Cotterell 1986a, b; Mai et al. 1987; Mai and Powell 1991). With a reduction of l/t ratio, plastic constraint increases and the plane-stress/plane-strain fracture transition may occur at a certain l/t ratio. Theoretical analysis shows that the specific essential work of fracture method is equivalent to the J-integral method for all three fracture modes (Mai and Powell 1991; Mai 1993).

The essential work of fracture approach has been applied to characterize the fracture properties of toughened polymer blends, such as PBT/PC/IM (where IM is the impact modifier) and ABS/PC. It is successfully used to determine the fracture toughness of a ductile LLDPE film (Wu and Mai 1996), and single-edge and double-edge notched different polymeric films (Hashemi 1993; Hashemi and Yuan 1994; Chan and Williams 1994; Karger-Kocsis and Czigany 1996; Karger-Kocsis and Varga 1996). It is also applied to study the effect of specimen size, geometry, and rate of tests in case of PBT/PC blends (Hashemi 1997).

10.3.4 Mechanisms of Toughening

Early investigations of the fracture of solids assumed that fracture involved only the creation of new surfaces (Griffith 1920; Kinloch and Young 1983). However, since measured values of G_c were well in excess of the surface energy of the material, it was soon realized that significant amounts of energy were also dissipated through other processes such as localized plastic deformation in the vicinity of the crack (Kinloch and Young 1983). In general, two mechanisms are responsible for this plastic deformation in rigid polymers, namely, "crazing" (Kausch 1983; Kambour 1973) and "shear yielding" (Ward 1983). The two mechanisms are not mutually exclusive. Under certain conditions both operate simultaneously.

10.3.4.1 Crazing

Crazing is an important source of toughness in rubber-modified thermoplastics. A craze can be described as a layer of polymer a nanometer to a few micrometers thick, which has undergone plastic deformation approximately in the direction normal to the craze plane as a response to tension applied in this direction (Kambour 1986). Crazing occurs without lateral contraction. As a result, the polymer volume fraction in the craze is proportional to $1/\lambda$, where λ is the draw ratio in the craze. The reduction in density occurs on such a small scale that the refractive index is markedly reduced, which accounts for the reflectivity of the craze (Kramer 1983).

Several methods of studies have been developed. Osmium-staining technique, pioneered by Kato (1967), is one of the most successful methods for observing crazing in rubber-toughened plastics. It depends upon a reaction between osmium tetroxide, OsO_4, and double bonds in PBD and other unsaturated polymers. But, it is not suitable for saturated rubbers.

Ruthenium tetroxide, RuO_4, is more reactive staining agent that can be used to differentiate between rubber and matrix when the former is essentially saturated. For example, clean glass slides (50×10 mm) were dipped in 2 wt% solutions of polymer, and the solvent was subsequently evaporated under vacuum at 50 °C (323 K) for 24 h. The films were removed from the glass substrate by immersing the slides in distilled water and then lifting the floating film from the water surface onto copper microscope grids. A 0.5 wt% solution of RuO_4 in distilled deionized water was used for staining. The aqueous solution (golden yellow when fresh) was found to

be effective for a considerable time (up to 6 months if kept in a firmly sealed glass container in a freezer). Film-covered grids were vapor stained in a glass-covered dish (Trent et al. 1981, 1983). Transmission electron micrographs, TEM, can be taken to illustrate detailed morphological features (at an accelerating voltage of 80 KV).

Recently, methods have been developed to characterize the relative amount of crazing and non-crazing that occurs in rubber-toughened glassy polymers, using the invariant obtained from small-angle X-ray scattering (SAXS) analysis. SAXS not only overcomes the disadvantages of transmission electron microscopy (e.g., the use of ultrathin samples), but the use of high intensity synchrotron radiation permits in situ deformation studies (Paredes and Fischer 1979; Brown and Kramer 1981). The new method of SAXS analysis leads to quantification of the contribution from crazing and non-crazing to the total deformation (He et al. 1998).

10.3.4.2 Shear Yielding

Yielding is a mechanism, in which a thin layer of polymer deforms in shear at constant volume. It is characterized by regions of sheared polymer oriented approximately at $45°$ to the tensile or compression stress. Unlike crazing, shear flow is essentially a process continuous in space, i.e., one that may spread through a much greater volume fraction of the stressed body and thus consume much more energy in total. Shear yielding is much less sensitive to environmental effects. In short, shear deformation is better than crazing, but crazing is better than no deformation at all (Kambour 1986).

Shear bands are highly birefringent and are most clearly observed in transmitted polarized light (Bucknall 1977). They are also visible as reflecting planes in ordinary transmitted light at glancing incidence, owing to refractive index differences between the band and the adjacent undeformed polymer (Kramer 1974, 1975). Both crazing and shear yielding involve the absorption of energy, and most methods of toughening polymers involve modifying the polymer such that more crazing and shear yielding take place. The rubber-modified polymer absorbs considerably more energy in a tensile test because of its higher extension to break, which can be achieved only as a result of yielding in the matrix. The rubber particles play only a secondary role but, nevertheless, a vital one.

Firstly, they accelerate yielding by acting as stress concentrators initiating deformation in the matrix; secondly, they respond to the hydrostatic component of stress by cavitating and increasing in volume, thus allowing the strain in the matrix to increase; and thirdly, in their cavitated and extended state, they stabilize the yielded polymer by carrying a share of the applied stress (Bucknall 1988). All three functions appear to be necessary for effective toughening, although their relative importance varies, depending upon the mechanisms contributing to toughening, and the kinetics of deformation, which in turn depend upon the material and the type of loading. Various types of response of the rubber particles have been observed experimentally as the polymer yields. They include (a) debonding between rubber and matrix (Haward and Bucknall 1976), (b) cavitation within the particle (Breuer et al. 1977; Kinloch 1985; Yee and Pearson 1986), (c) craze like fibrillation of the rubber
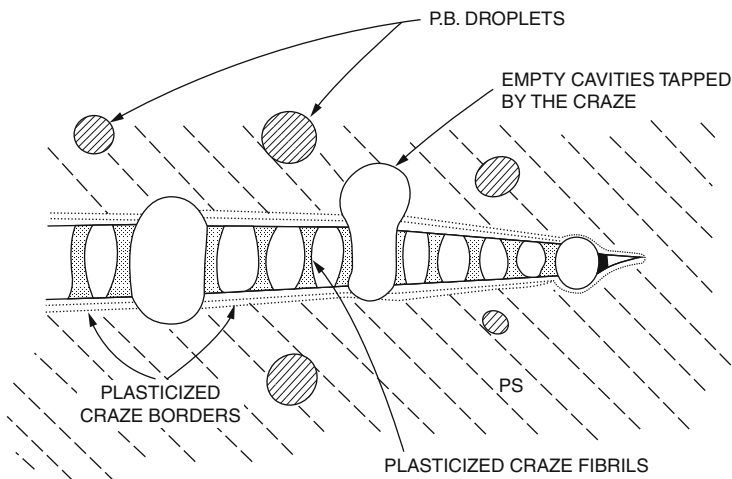
Fig. 10.15 Schematic rendering of craze moving in a field of encapsulated PB pools draining their content onto the craze surfaces when tapped by the advancing craze (Argon et al. 1990)

phase (Beahan et al. 1976; Donald and Kramer 1982), and (d) crazing within sub-inclusions (Seward 1970). Many polymers are toughened by blending or copolymerizing with a rubber (Kinloch and Young 1983; Bucknall 1977). This method of toughening is now well established for many thermoplastics, thermosets, and even adhesives.

10.3.4.3 Other Mechanisms

A new route for achieving a substantial lowering of stresses for craze growth without relying on potent craze initiators involves controlled local plasticization of a polymer by a low molecular weight diluent, distributed in a heterogeneous fashion throughout the material (Gebizlioglu et al. 1990; Argon and Cohen 1990). This mechanism is schematically shown in Fig. 10.15.

The advancing craze, nucleated from free surfaces or other occasional imperfections, cuts into the dispersed population of PB-2.76 K pools (which at this low molecular weight acts like a relatively low viscosity liquid) and drains the contents of these pools onto the surfaces of the craze. Although the solubility of the PB 2.76 K into PS under standard conditions of room temperature and atmospheric pressure is negligibly small (of the order of 4×10^{-3}), this should increase greatly in the presence of a negative pressure (Argon and Cohen 1990). The plasticization due to the increased sorption of the low molecular weight PB diluent into the craze surfaces is a highly interactive and complex process. The new mechanism offers considerable promise for practical industrial applications as only very small quantities of the plasticizing substance are needed, and thus subsidiary properties such as optical transparency and tensile modulus are less affected compared to the other methods of toughening.

Fig. 10.16 Influence of EPDM concentration on Izod impact strength of PPBC-EPDM blends
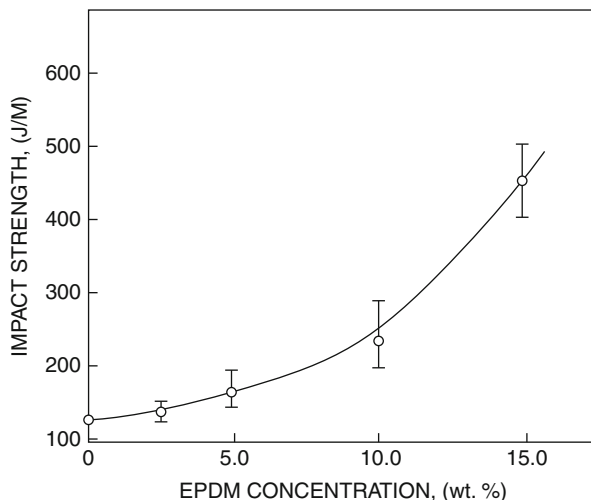
10.3.5 Factors Affecting Blend Toughness

Rubber toughening is the most often used method of improving the impact resistance of polymers (Bucknall 1977). The impact modified materials are usually the blends of a rigid matrix polymer with an elastomer. The composition of the constituents, their miscibility, and the morphology influence the deformation and failure mechanism in the blend. Particle size of the elastomer, its dispersion, and its adhesion with matrix are also the important factors determining the toughness.

10.3.5.1 Composition

The composition of individual constituents of a blend plays an important role in modifying the impact strength of the blend. The impact strength of polypropylene block copolymer (PPBC) blends with different concentrations of EPDM is shown in Fig. 10.16 (Xavier et al. 1994). Upon incorporation of the elastomer, the impact strength increases. EPDM was found to reduce the crystallinity of PPBC and significantly influence its failure mechanism. Both crazing and shear yielding were found to be responsible for the observed increase in impact strength. As shown in Fig. 10.16, above 10 wt% of EPDM, the increase in impact strength is more prominent. However, it was observed that such significant rise in impact strength adversely affected the other mechanical properties, such as flexural and tensile moduli of the blends.

In the case of PVC/ABS blend, the addition of ABS improved the impact strength of the blend (Sharma et al. 1988). At low concentrations of ABS, a small number of rubber particles (i.e., the butadiene particles in ABS) are insufficient to significantly improve the impact strength (Fig. 10.17). Increasing ABS concentration up to 50 wt% increased impact strength. The maximum impact strength obtained at the optimum blend composition is considerably higher than that of neat ABS itself. Since the particle size (Kulshreshtha et al. 1989) of the dispersed

Fig. 10.17 Influence of PVC/ABS blend composition on Izod impact strength
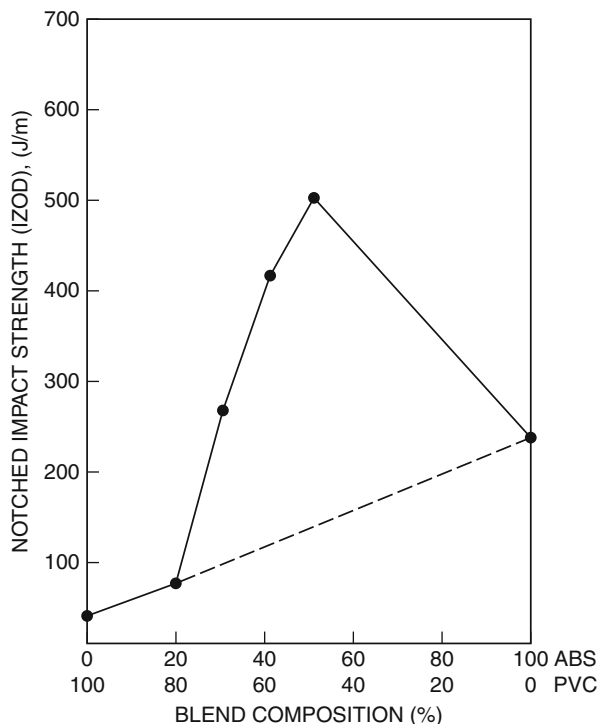
PBD (of ABS) phase is unlikely to change with blend composition, it is evident that there exists a critical volume fraction of rubber phase necessary for the maximum improvement in impact strength. When this critical concentration of rubber (or ABS) is exceeded, impact strength drops.

10.3.5.2 Morphology

The performance characteristics of a blend depend on its morphology, which in turn depends on the thermodynamic and rheological properties of the components (Plochocki 1983; Karger-Kocsis et al. 1984; Howe and Wolkowicz 1987; Wu 1987; Utracki 1989). However, due to nonequilibrium nature of the highly viscous polymer mixtures, often the processing conditions strongly influence the product morphology. The topic is discussed in the last part of Sect. 10.3.6: Low-Speed Mechanical Properties of Blends. Further details of the morphology-processing conditions can be found in ▶ Chap. 7, "Rheology of Polymer Alloys and Blends"; ▶ Chap. 8, "Morphology of Polymer Blends"; and ▶ Chap. 9, "Compounding Polymer Blends."

The properties of PPBC/EPDM blends strongly depend on the crystalline micromorphology of PPBC, as well as on the particle size and degree of dispersion of EPDM (Xavier et al. 1994). The DSC cooling thermograms indicated that the degree of crystallinity in PPBC decreased with increasing concentration of EPDM (Table 10.14 and Fig. 10.18).

Table 10.14 Crystallinity indices (A/m values) from DSC (Xavier et al. 1994)

No.	Blend	A/m (arbitrary units)
1.	PPBC (neat polymer)	232
2.	PPBC + EPDM (2.5 wt%)	216
3.	PPBC + EPDM (5.0 wt%)	208
4.	PPBC + EPDM (10.0 wt%)	206
5.	PPBC + EPDM (15.0 wt%)	197

Fig. 10.18 DSC thermograms recorded during cooling cycle for PPBC and its blends with EPDM (10 wt%)
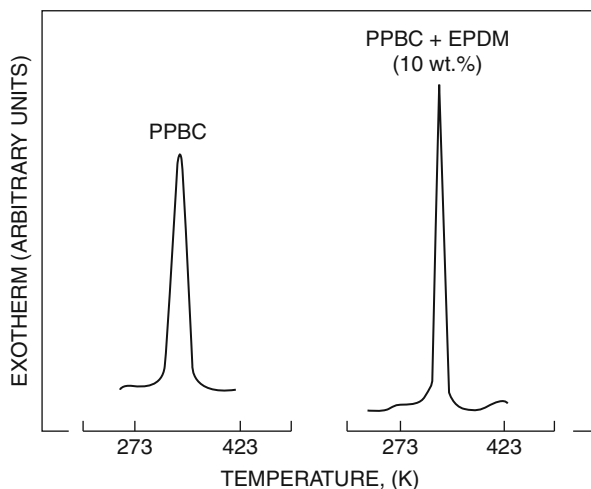
As observed under optical microscope with crossed polarizers, incorporation of up to 10 wt% EPDM into PPBC does not affect the nucleation density or ultimate size of PPBC spherulites (Fig. 10.19). The EPDM particles act as inert inclusions, constituting geometrical obstacles to the PPBC spherulites' growth, thus changing their morphology. Nevertheless, some interfacial interactions are observed in the case of a blend with 10 wt% EPDM. The spherulites of PPBC are found to nucleate from the interface with EPDM (Fig. 10.19c). This resembles the transcrystalline structure observed in several glass or carbon fibers reinforced, semicrystalline polymers, such as PP, PE, PA-6, etc. (Xavier 1991). Such a structure was considered an indication of good interfacial interaction between the two constituents.

The EPDM particles were found either to initiate crazes or to terminate them, depending on the interfacial bonding, the particle size, the concentration, and the interparticle distances. The variation of notched Izod impact strength of PPBC blends with different EPDM concentrations is shown in Fig. 10.16. The fracture surface of a blend with 10 wt% EPDM, as examined under SEM, is shown in Fig. 10.20. The hemispherical embeddings and hollows (representing the removed EPDM particles) are clearly visible on the fracture surface. The ribbonlike structures visible on the fractured surfaces are probably the micro-shear bands in the blends.
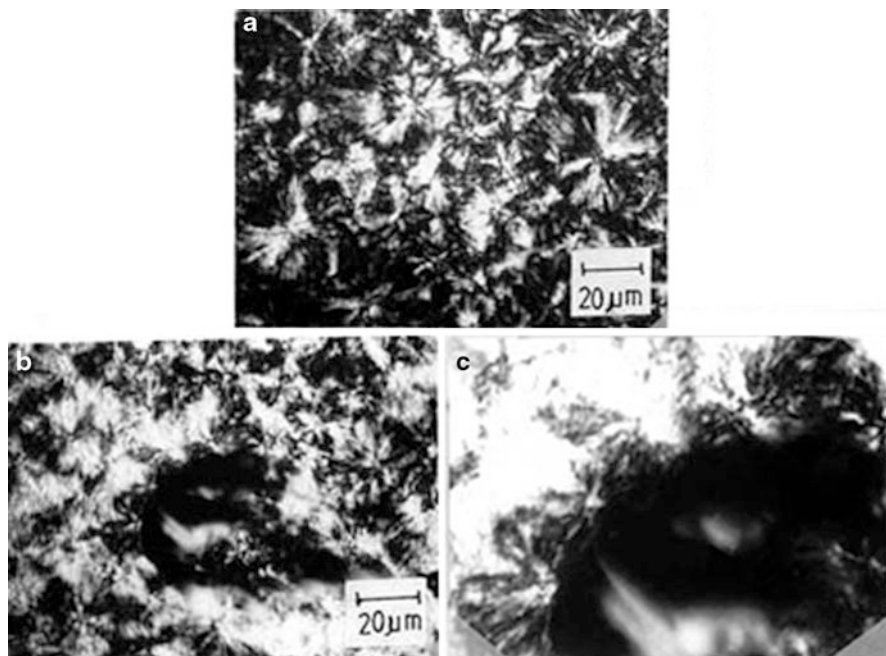
Fig. 10.19 Optical micrographs of (**a**) PPBS spherulites, (**b**) PPBC spherulites in the presence of EPDM and (**c**) PPBC spherulites nucleating from interface with EPDM
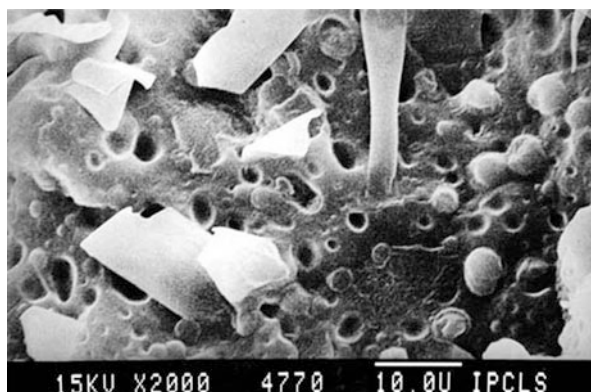
Fig. 10.20 SEM micrograph of PPBC + EPDM (10 wt%) blend fracture surface

Approximate ranges of the experimental techniques to study different blend morphologies are summarized in Table 10.15. See also ▶ Chap. 8, "Morphology of Polymer Blends" in this handbook.

10.3.5.3 Elastomer Particle Size

Elastomeric particle size plays a prominent role in controlling the toughening mechanisms of a polymer. It has been shown that particle size of an elastomer

Table 10.15 Approximate ranges of experimental techniques to study blend morphology of (1) interatomic; (2) molecular, spherulites; (3) Filler aggregates, compatibilized blends; (4) reinforcements, immiscible blends; (5) Voids (Utracki 1989)

Domain Size	1	2		3		4	5
Scale (μm)	10^{-4}	10^{-3}	10^{-2}	10^{-1}	10^{0}	10^{1}	10^{2}
Microscopy						Optical	
					SEM		
				TEM			
Spectroscopy		IR					
Thermal			DSC				
Mechanical			TMA				
Dielectric			DS				
Diffraction	WAXS						
			SAXS				
					SANS		
						Light	
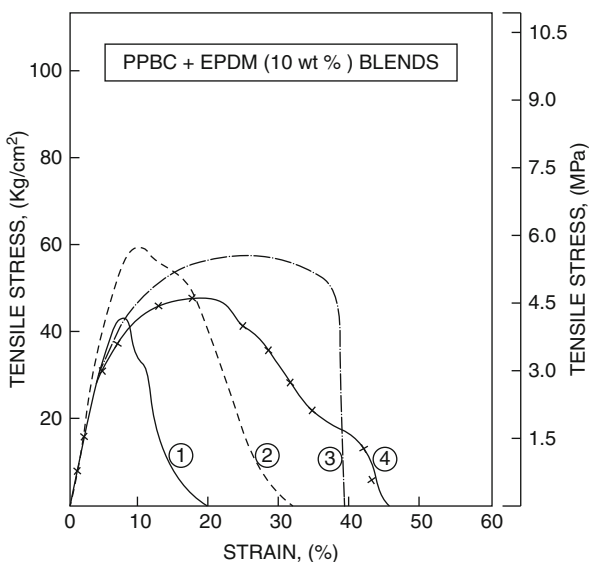
Fig. 10.21 Influence of EPDM particle size on tensile stress–strain curves of PPBC blends. EPDM particle sizes (*1*) 0.60 mm, (*2*) 3.45 mm, (*3*) 4.35 mm, (*4*) 5.50 mm

significantly influences the deformation and failure processes: small particles favor shear yielding, while coarser dispersions promote crazing (Jang et al. 1985). There is an optimal particle size resulting in maximum impact resistance (Speri and Patrick 1975; Stehling et al. 1981; Karger-Kocsis et al. 1981).

The tensile stress–strain curves of PPBC and its blends with EPDM of different particle sizes (for concentration equal 10 wt%) are shown in Fig. 10.21 (Xavier et al. 1994). The particle size of EPDM has considerably affected the post-yield behavior of the blends. Although the yield stress initially increases with reduction

Fig. 10.22 Influence of
EPDM particle size on
flexural modulus and Izod
impact strenght of PPBC/
EPDM (10 wt%)
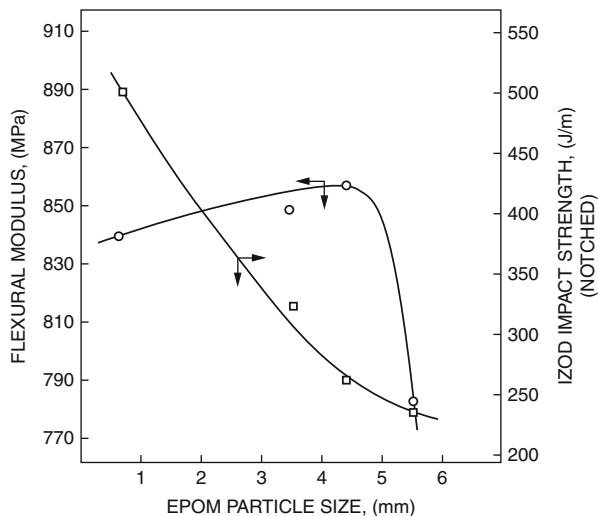
of EPDM particle size (from 4.35 to 3.45 μm), with further reduction of size
(to 0.60 μm), it decreases. Earlier studies of the tensile properties of heterogeneous
polymer blends have shown that Young's modulus poorly reflects morphological
changes (Pukanszky et al. 1989; Pukanszky and Tudos 1990). Accordingly, the
particle size dependence of Young's modulus is weak.

By contrast (see Fig. 10.22), in the case of PPBC blend with EPDM, the flexural
modulus was found to significantly decrease when large EPDM particles (d ≥ 4 mm)
were used. The notched Izod impact strength was strongly affected by the particle
size. As usually it is the case, reducing it caused the impact strength to increase. With
the reduction in EPDM particle size, the number of particles has increased and the
interparticle distance was reduced. Thus, multiple crazing in the blend was enhanced
further with increased number of rubber particles and also reduced particle size.

The shear yielding also is influenced with change in particle size resulting in
increased impact strength. The notched Izod impact fracture surfaces examined
under SEM are shown in Fig. 10.23. Change in EPDM particle size had significantly
changed the fracture morphology. The fibrous sheets like structures are probably the
micro-shear bands in the blends. The number of these bands increases with reduction
of the rubber particle size as the smallest particle (at constant loading) corresponds to
their maximum number. The formation and break down of the micro-shear bands
absorb enormous energy, and hence it increases the Izod impact strength.

Both principal fracture mechanisms, shear yielding and crazing, are influenced
by the particle size. In PPBC matrix, where spherical elastomeric particles are
chemically bonded, the energy absorption takes place mainly by deformation of the
matrix. In such systems, a large amount of shear yielding is to be expected. The
shear yielding becomes more prominent upon increasing the concentration of
EPDM as well as reduction of their particle size. The micro-shear bands in the
fracture surface (Fig. 10.23e) clearly support these expectations.
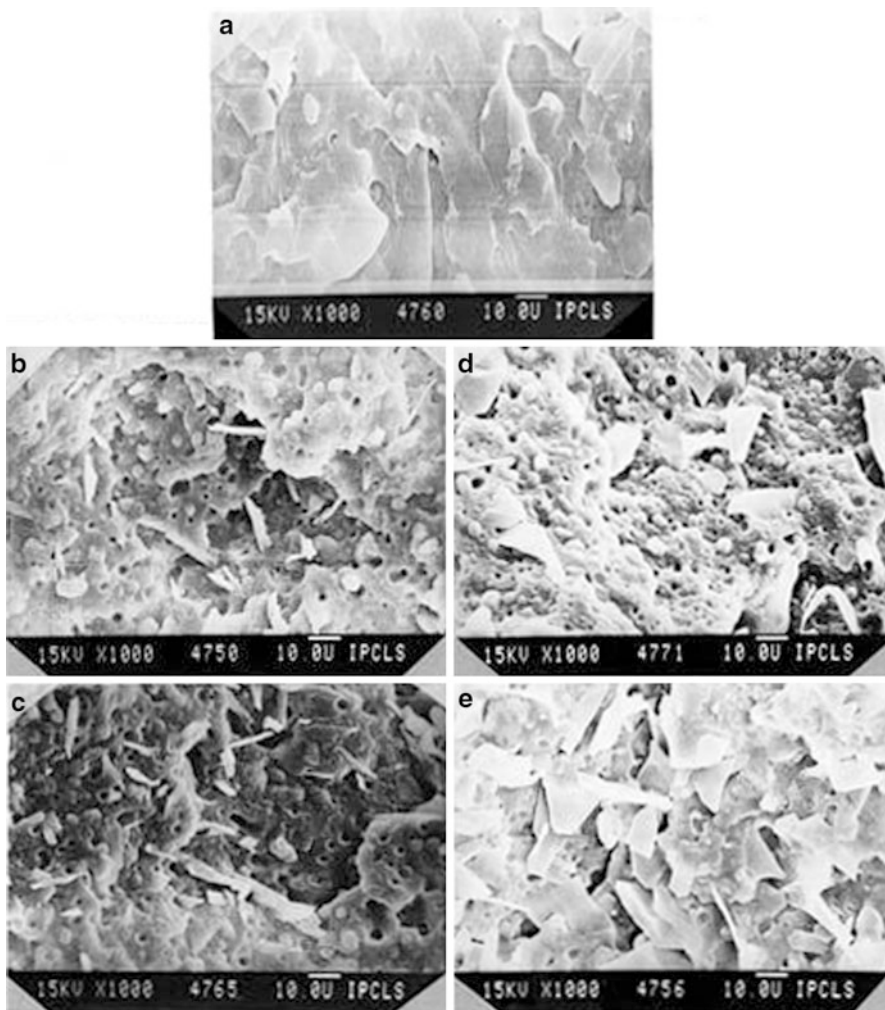
Fig. 10.23 SEM micrographs of the impact fracture surfaces of (**a**) PPBC and its blends with EPDM (10 wt%) with different (**b**) 5.50 mm, (**c**) 4.35 mm, (**d**) 3.45 mm and (**e**) 0.60 mm particle sizes

10.3.5.4 Miscibility

The notion of polymer miscibility implies intimate mixing on the segmental level. A miscible blend is expected to have a homogeneous composition throughout. The understanding of chemical principles in polymer miscibility is getting refined as a result of the appearance of several reviews and books on the topic (Krause 1972; Olabisi et al. 1979; Paul and Barlow 1980; Paul 1982; Ottenbrite et al. 1987; Utracki 1989). The level of molecular mixing existing in polymer blends that exhibit macroscopic properties indicative of single-phase behavior is commanding

considerable attention. More detailed information on this topic can be found in ► Chap. 2, "Thermodynamics of Polymer Blends" in this handbook.

The best commercial advantages of a polymer blend can best be summarized by the word "versatility" (Olabisi et al. 1979). Unfortunately, miscible polymer–polymer blends usually show additivity of the component polymers properties, thus their versatility is limited. Furthermore, like any other single-phase resin, for most applications miscible blends need to be toughened and/or reinforced. Thus, with the exception of PMMA/PVDF blends (primarily used for coatings), there are no miscible blends on the market. The interest in miscible polymer blends is for the purpose of compatibilization and judicious selection of the processing conditions that may lead to the spinodal decomposition-type morphology (see ► Chap. 8, "Morphology of Polymer Blends" in this handbook).

Immiscibility dominates polymer blends. It reveals itself as opacity, delamination, double glass transition, or combination of these properties. Most immiscible polymer blends require compatibilization and toughening.

Owing to low values of the combinatorial entropy mixing, miscibility in polymer–polymer systems requires the existence of strong specific interactions between the components, such as hydrogen bonding (Olabisi et al. 1979; Solc 1982; Walsh and Rostami 1985; Utracki 1989). The thermodynamic characterization of the interactions in miscible polymer blends has been the subject of extensive studies (Deshpande et al. 1974; Olabisi 1975; Mandal et al. 1989; Lezcano et al. 1992, 1995, 1996; Farooque and Deshpande 1992; Juana et al. 1994).

Based on the Huggins–Flory theory, the polymer–polymer interaction parameter, χ_{12}, has been used to describe interactions between the two components. As a consequence, this "parameter" takes into account the enthalpic and non-combinatorial entropy of mixing contributions. Calorimetry, differential scanning calorimetry (DSC), Fourier transform infrared spectroscopy (FTIR), inverse gas chromatography, microscopy, etc., are used to investigate the miscibility and morphology of the blends (Zhong and Guo 1998; Lezcano et al. 1998). Comprehensive surveys of miscible polymer systems along with various methods of miscibility determination have been published (Olabisi et al. 1979; Utracki 1989; Coleman et al. 1991).

10.3.5.5 Other Factors

Temperature strongly influences the impact behavior of toughened plastics. Charpy impact energy measurements at different temperatures in the case of HIPS containing various concentrations of PBD showed two transitions, at 233 and 273 K (Bucknall 1988). At these temperatures, the material exhibited transitions from brittle to semi-ductile and then to ductile.

Newman and Williams (1978) carried out sharp-notch Charpy tests for ABS at $193 \leq T(K) \leq 333$ and showed that linear elastic fracture mechanics was applicable only up to 233 K. Above 273 K, the energy absorbed in impact was proportional to the fracture area and correlated well with the volume of the whitened zone. Mixed behavior occurred at the intermediate temperatures. More detailed study of the notched Izod impact behavior of ABS was carried out using instrumented

tests (Rink et al. 1978). The authors found that the force at peak load, F_m, decreased slowly with increasing temperature from 133 to 353 K; increased by a factor of two between 193 and 273 K; and then decreased again.

Because of the oxidative degradation of the main-chain double bonds, the plastics toughened by diene-type elastomers (e.g., PBD or other rubbers) are susceptible to aging. The UV radiation breaks the chemical bonds, initiating chain reactions in which the polymer is attacked by the atmospheric oxygen, becoming cross-linked or chemically degraded. Embrittlement of the surface has a similar effect to the introduction of a sharp crack. The effects are clearly seen in Charpy and Izod impact tests. Although the subsurface polymer is unaffected by the aging, a crack initiated at the surface can accelerate throughout the degraded layer and cause low-energy fracture of the specimen (see ▶ Chap. 14, "Degradation, Stabilization, and Flammability of Polymer Blends").

Geometry of a toughened plastic specimen also influences the impact strength and its mode of failure. The specimen's length, width, and thickness may affect the fracture behavior. Whether the specimen is notched or not, as well as the dimensions of the notch, may also influence the impact behavior (Kinloch and Young 1983). As discussed above in Sect. 10.3.3, "Fracture Mechanics Testing" – it is important to determine the material parameters (the initiation and the propagation energies) using the specimen geometry that reduces the effects of geometry to an acceptable level.

10.4   Miscibility and Solubility

10.4.1 Miscibility in Polymer Blends

Since physical properties of polymer blends are influenced strongly by blending conditions and processes that, in turn, affect the level of mixing of the blends, there is a growing interest in studying the miscibility and phase behavior of polymer blends. The most important factor leading to miscibility in low molecular weight materials is the combinatorial entropy contribution which is very large compared to high molecular weight polymers. For miscibility to occur, ΔG_m must be smaller than 0.

The properties of polymer blends are determined mainly by the miscibility of the components and structure. The miscibility of polymer blends is generally believed to originate from the specific interactions between polymers. The miscibility has been widely used to describe multicomponent polymer blends whose behavior is similar to that expected of a single-phase system. Many attempts have been made for the understanding of the miscibility of polymer blends, in which the determination of the crystallization behavior and the thermodynamic interaction between polymers are of central importance. Usually thermodynamic miscibility and homogeneity can be attained when the free energy of mixing, ΔG_m, is negative. (A more detailed discussion is available in ▶ Chap. 2, "Thermodynamics of Polymer Blends.")

The term ΔG_H has been used to describe all types of specific interactions (hydrogen bonding, ion–ion, ion–dipole, charge transfer, electron interactions, etc.) that provide negative contribution to the free energy of mixing. The interactions of

the van der Waals type are accounted for by the $\chi'_{12}\phi_1\phi_2 \geq 0$ term with χ'_{12} given by Hildebrand's solubility parameter (Hildebrand 1964).

Hildebrand pointed out that the order of solubility of a given solute in a series of solvents is determined by the internal pressures of the solvents. Later, Scatchard introduced the concept of "cohesive energy density" into Hildebrand's theories. The solubility parameter is a numerical value that indicates the relative solvency behavior of a specific solvent. It is derived from the **cohesive energy density** of the solvent, which in turn is derived from the **heat of vaporization.** In 1936 Joel, H. Hildebrand proposed the square root of the cohesive energy density as a numerical value indicating the solvency behavior of a specific solvent:

$$\delta = \sqrt{c} = \left(\frac{\Delta H - RT}{V_m}\right)^{\frac{1}{2}} \tag{10.19}$$

Hildebrand and Scott and Scatchard proposed that the enthalpy of mixing is given by

$$\Delta H_m = V_{mix}\left[\left(\frac{\Delta E_1^V}{V_1}\right)^{\frac{1}{2}} - \left(\frac{\Delta E_2^V}{V_2}\right)^{\frac{1}{2}}\right]^2 \Phi_1\Phi_2 \tag{10.20}$$

where V_{mix} is the volume of the mixture, ΔE_i^V is the energy of vaporization of species i, V_i is the molar volume of species i, and Φ_i is the volume fraction of i in the mixture. ΔE_1^V, i is the energy change upon isothermal vaporization of the saturated liquid to the ideal gas state at infinite volume.

The heat of mixing must be smaller than the entropic term ΔGm for polymer–solvent miscibility ($\Delta Gm \leq 0$). Therefore, the difference in solubility parameters ($\partial_1 - \partial_2$) must be small for miscibility or dissolution over the entire volume fraction range (Grulke et al. 1999).

The effect of polymer–polymer interactions on the miscibility and macroscopic properties of PVC/PMMA, PVC/PS, and PMMA/PS blends were studied and the miscibility of the components was characterized by the Flory–Huggins interaction parameter or by quantities related to it by Fekete et al. (Fekete et al. 2005). The comparison of interaction parameters determined by different methods indicates that PVC and PMMA are nearly miscible, while PS is immiscible either with PMMA or with PVC at all compositions. Flory–Huggins interaction parameters calculated from equilibrium methanol uptake (χ'_{12}) are plotted as a function of composition in Fig. 10.24. The negative values obtained for the PVC/PMMA blends hint at complete miscibility, although χ'_{12} depends on composition which indicates limited miscibility. The positive interaction parameters determined for the PVC/PS and PMMA/PS blends suggest immiscibility.

The influence of chemicals and solvents on a polymer blend depends on the nature of solvent and the blend components, as well as on morphology of the blends. The chemical/solvent resistance of an amorphous polymer is improved by the presence of semicrystalline polymer(s). For the best solvent resistance, the latter

Fig. 10.24 Relationship between composition and the Flory–Huggins interaction parameter determined from equilibrium solvent uptake; (□) PVC/PMMA, (○) PMMA/PS, (Δ) PVC/PS; component 2: PMMA in PVC/PMMA, PS in PMMA/PS, and PVC/PS blends (Fekete et al. 2005)
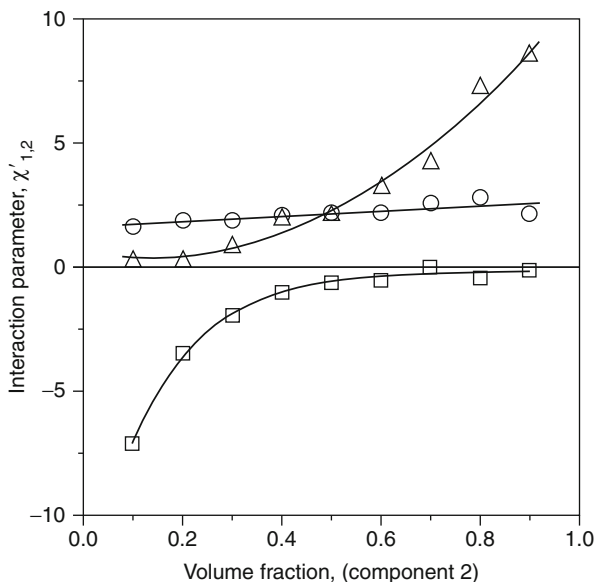
polymers should be the matrix. The semicrystalline polymers such as PA, POM, PBT, or PET contribute to the solvent and chemical resistance, high processability, and rigidity, while amorphous polymers (ABS, PC, and PSF) provide impact strength and elongation and often the cost reduction.

10.4.2 Solubility Parameter/Prediction of Miscibility

According to the solubility parameter approach at predicting compatibility, two polymers mix well if the difference in the pure component solubility parameter is small. In polymer systems where the interactions are dominated by the van der Waals forces, solubility is favored by chemical similarity of solvent and polymer. Molecular weight, chain branching, and cross-linking of individual polymers slightly influence the solubility parameter (for more details see ▶ Chap. 2, "Thermodynamics of Polymer Blends," Sect. 2.6.2.3).

For polymer molecules, the solubility parameter (δ) is best calculated using the table of molar attraction coefficients. Here, E is given as

$$\delta \; = \; e \; \Sigma \frac{E}{M} \tag{10.21}$$

where E is summed over the structural units of the polymer, M the "polymer" molecular weight, and "e" is the density.

In coating and in rubber industry, the solubility approach is used respectively to select the solvent or to study swelling of the cured rubber by solvents. The

approach was also useful in calculating the effects of pressure and temperature on free energy of mixing. However, the predictions with the Hildebrand solubility parameters are made in the absence of any specific interactions, especially hydrogen bonds. They also do not account for the effects of morphology (crystallinity) and cross-linking. In addition, there may be (non-ideal) changes with changes in temperature and, in many cases, with changes in concentration. Polymer blends with specific interaction include PMMA/PEO, PVAc/PEO, etc.

In a strict sense, the molecular interactions should be nonspecific, without forming associations or orientation, hence not of the hydrogen or polar type.

The solubility parameter approach is applicable to amorphous polymer systems. Highly crystalline polymers, viz., PE or PTFE, are insoluble at room temperature, but they obey the solubility principles at $T \geq 0.9\ T_m$, i.e., at temperatures not more than 10 % (in Kelvin) above their melting temperature.

The biggest drawback of the solubility parameter approach has been the omission of the specific and entropic interactions effects.

10.4.3 Binary Interaction Parameters

The binary interaction generally refers to the interactions between polymer–polymer and polymer–solvent. The nature of solvent–polymer interaction plays an important role in the miscibility of blends. Many thermodynamic properties of polymer solutions such as solubility, swelling behavior, etc., depend on the polymer–solvent interaction parameter (χ). The quantity was introduced by Flory and Huggins. Discussions of polymer miscibility usually start with Flory–Huggins equation for free energy of mixing of a blend (refer to ▶ Chap. 2, "Thermodynamics of Polymer Blends").

The Flory–Huggins theory is widely used still and has been successful, largely, in describing thermodynamics of polymer solutions.

It is also important to note that the Flory–Huggins is a mean-field theory (for the use of the formulation of the change in internal energy due to mixing).

The miscibility of ethylene–styrene copolymer blend was studied by the help of interaction parameters by Chen et al. (2001). They proposed that the interaction parameter for a blend of copolymers is a linear combination of the individual parameters. The nature of the polymer–solvent interaction plays an important role in deciding the influence of chemical and solvent effect on blends. For a compatible amorphous/crystalline blend, the Nishi–Wang equation (Nishi and Wang 1975) is commonly used to determine the polymer–polymer interaction parameter from the melting point depression experiments. Nishi and Wang equation is based on Flory–Huggins theory. The method involves a comparison of the equilibrium melting point of a neat semicrystalline polymer to that of the same polymer in blends of different compositions. For a binary mixture of two relatively high molecular weight polymers, one semicrystalline and one noncrystalline, Nishi and Wang showed that

Fig. 10.25 Nishi–Wang plot for semicrystalline PSMA14/PCL blends (Gouveia et al. 2011)

$$\frac{1}{T^0_{mb}} - \frac{1}{T^0_m} = -\frac{R V_{Bu}}{\Delta H^0_f V_{Au}} \ \chi_{AB} \phi^2_A \tag{10.22}$$
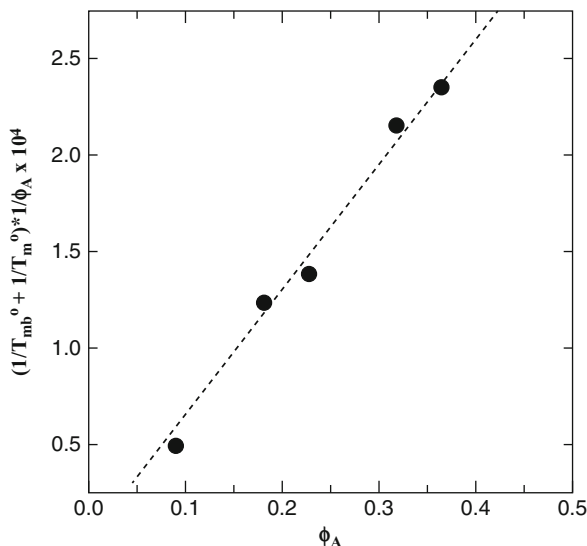
where T^0_m and T^0_{mb} are, respectively, the equilibrium melting points of the neat semicrystalline component and of the blend containing a volume fraction of amorphous component f. R is the universal gas constant, ΔH^0_f is the molar heat of fusion, V_{Au} and V are the molar volumes of the amorphous and crystalline units, respectively.

PSMA/PCL blends were analyzed by Gouveia et al. (2011) using Nishi–Wang equation. They plotted $(1/T^0_{mb} - 1/T^0_m)$ against ϕ^2_A and resulted in a straight line with slope proportional to χ_{AB} and zero y-intercept (Fig. 10.25).

10.4.4 Phase Separation Process

In polymer solutions and polymer blends, LCST, UCST, combined UCST and LCST, hourglass, and closed-loop shaped phase diagrams have been found experimentally. These five types of phase diagrams are the most commonly observed phase diagrams in polymer systems. An important role is played by temperature in the phase diagrams according to the equation:

$$T^* = \frac{d_1}{d_2} \tag{10.23}$$

Here d_1, d_2 are constant for a particular system. If the signs of d_1 and d_2 are opposite, then T^* is negative, and all miscibility gaps are of one type, for
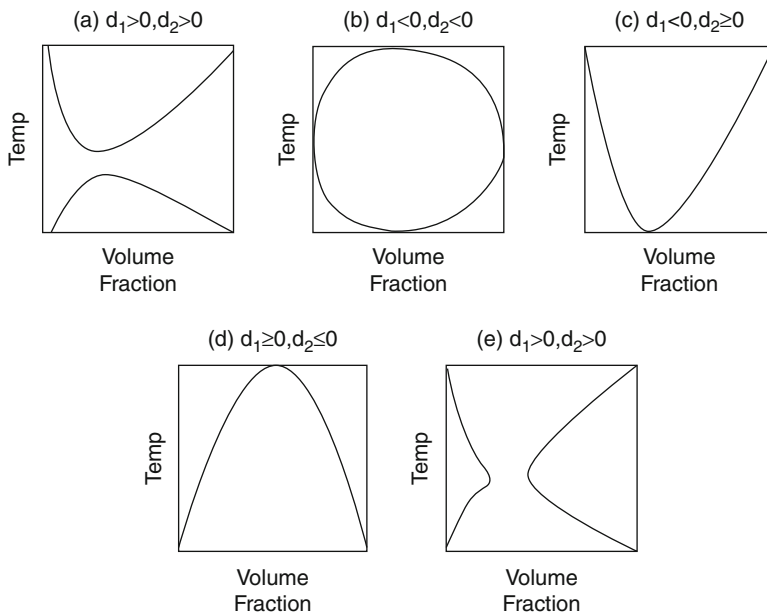
Fig. 10.26 Schematic illustration of types of possible polymer blend phase diagrams, for binary blends where additional complications that can be introduced by competing processes (such as crystallization of a component) are absent. The coefficients d_1 and d_2 refer to a general functional form (as a function of temperature and component volume fractions) of the binary interaction parameter that quantifies deviations from ideal mixing (Courtesy: *Online resources*)

$d_1 > 0$, $d_2 < 0$ yielding exclusively the UCST type. In the opposite case of $d_1 < 0$ and $d_2 > 0$, leading exclusively to the LCST type. However, in the remaining cases where both the coefficients possess the same sign, the temperature T^* is physically important – with $d_1 > 0$ and $d_2 > 0$ (LCST type) for $T > T^*$ but changes to (UCST type) for $T < T^*$, resulting in an hourglass type of phase diagram for lower molecular weights. Finally, for $d_1 < 0$ and $d_2 < 0$, the pattern is switched and the diagram has the form of a closed loop. A simple schematic representation is given above (Fig. 10.26).

Diblock copolymers formed from polystyrene covalently linked to poly(*n*-pentylmethacrylate), P(S-b-*n*PMA), which have only weak segmental interactions, are shown to exhibit closed-loop phase behavior over a narrow range of molecular weight.

Liquid–liquid phase separation of a miscible blend system can occur either during heating (LCST type) or during cooling (UCST type) (Fig. 10.27). A detailed discussion on phase diagrams is presented in ► Chap. 2, "Thermodynamics of Polymer Blends."

Phase separation in polymer solutions may proceed either by nucleation and growth (NG) or by spinodal decomposition (SD). Spinodal decomposition is also of interest from a more practical standpoint, as it provides a means of producing a very

Fig. 10.27 Phase diagram showing LCST and UCST behavior for polymer blends (Courtesy: *Online resources*)
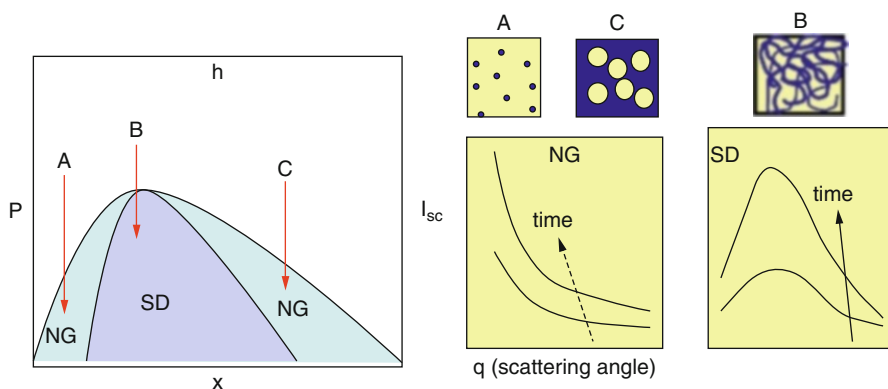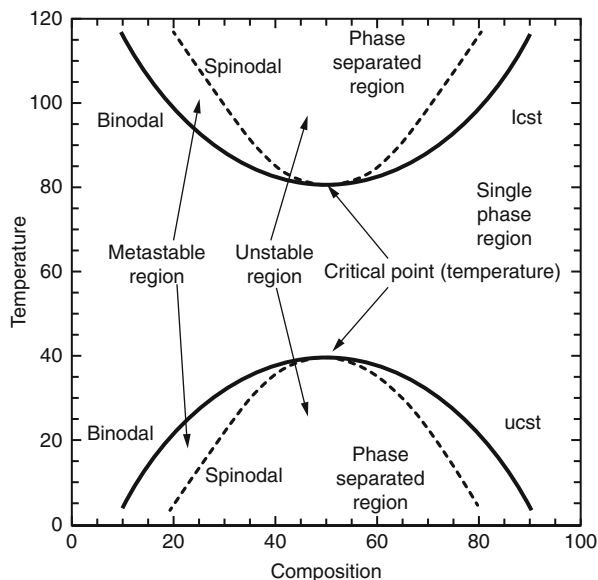
Fig. 10.28 Schematic illustration of the metastable (nucleation and growth) and unstable (spinodal decomposition) domains in polymer solutions and consequences of pressure quench at different polymer concentrations (Courtesy: *Online resources*)

finely dispersed microstructure that can significantly enhance the physical properties of the material. Nucleation and growth is the phase separation mechanism in the metastable regions which are schematically illustrated in Fig. 10.28 which shows the phase boundaries for a polymer solution in term of the miscibility pressures (or demixing pressures) at a given polymer concentration x.

A simple representation of the two mechanisms is given in Fig. 10.29.

The phase boundaries and the kinetics of phase separation of polymer blends are very rich areas of investigation, with, additionally, important technological applications.
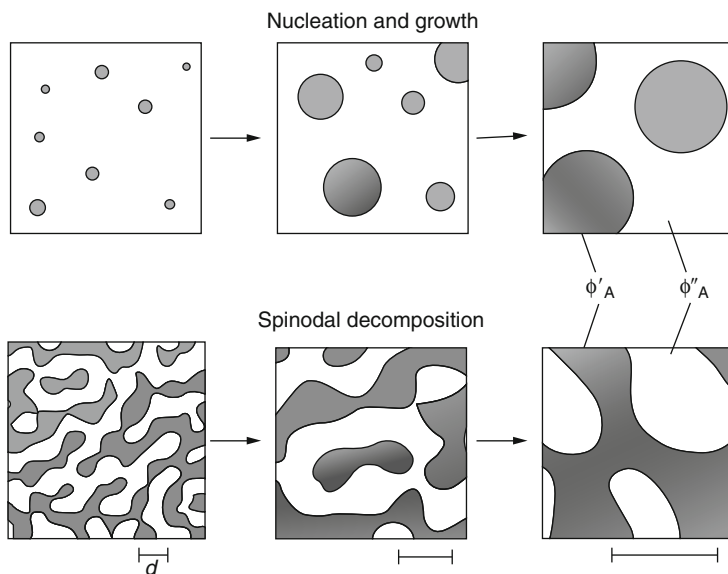
Fig. 10.29 Nucleation and growth and spinodal decomposition patterns in binary blends (Longjian Xue et al. 2012)

Figure 10.30 shows schematically the variation of the free energy of mixing, ΔG_m, with composition for a typical high molecular weight binary polymer blend and the corresponding phase diagram. The binodal denotes the limits of miscibility and is determined by the points of common tangent to the free energy curve, where the chemical potentials of the two coexisting phases will be equal. The spinodal denotes the limits of metastability of the system where the curvature changes from positive to negative and the second derivative of ΔG_m is zero. Inside the spinodal, the system is unstable to all concentration fluctuations and the blend spontaneously separates into coexisting phases via the process known as spinodal decomposition.

When mixing, most of the polymer mixtures get phase separated. Consider the example of polystyrene and polybutadiene. Mixing these two polymers results in an immiscible blend. When polystyrene is mixed with a small amount of polybutadiene, the two polymers will not blend; instead the polybutadiene will separate from the PS into little spherical blobs.

The determination of phase separation in partially miscible polymer blends by means of thermal analysis is often difficult because of the small demixing enthalpy and the slow rate of the diffusion-controlled process. Dreezen et al. (2001) studied the phase separation of PEO/PES and PEO/Aramid blends by optical microscopy, conventional DSC and MTDSC. The onset of phase separation from optical microscopy corresponds very well to the onset of a small stepwise increase in the MTDSC heat capacity (Fig. 10.31).

Phase separation process takes place in a number of ways. It may be thermally induced, reaction induced, crystallization induced, etc. Thermally induced phase

Fig. 10.30 Schematic showing the Gibbs free energy of mixing as a function of composition at a chosen temperature T_0 (*upper panel*). Given in the *lower panel* is the corresponding phase diagram showing the binodal (*outer, dark grey*) and spinodal (*inner, light grey*) curves; marked are the binodal and spinodal compositions at T_0 (B′, B″ and S′, S″) which are related to the features) (Courtesy: *Online resources*)
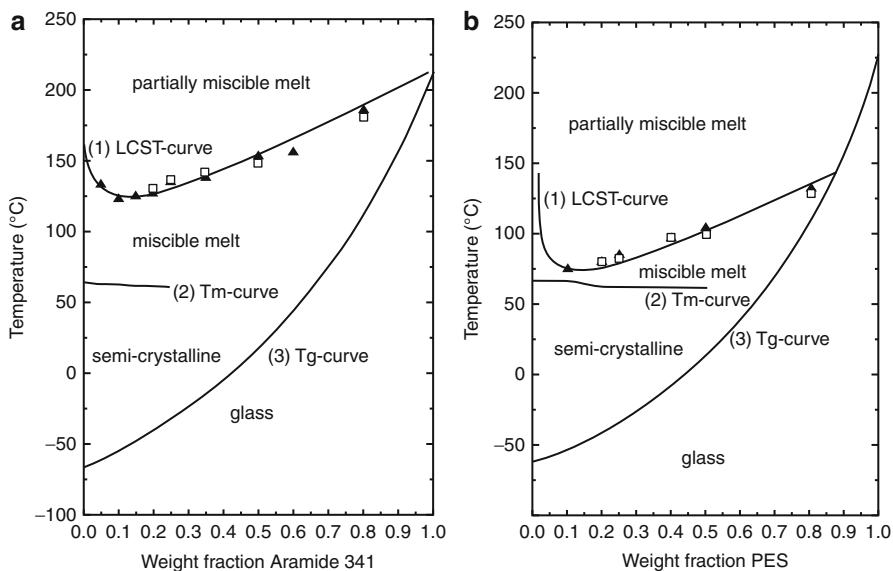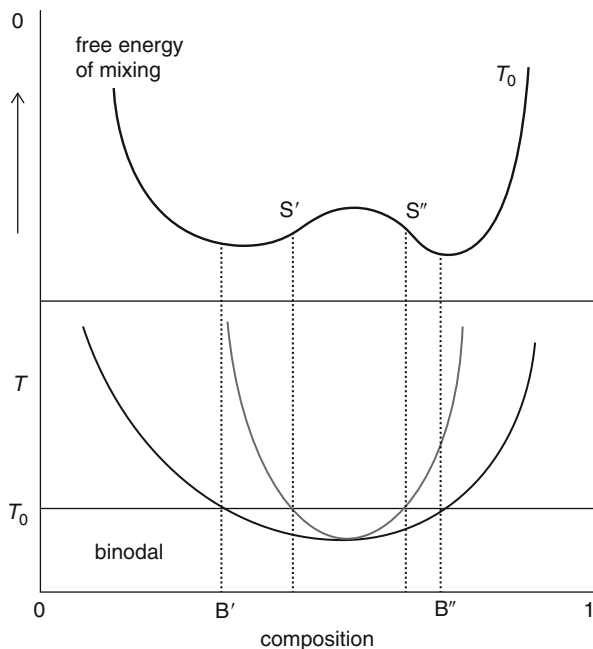
Fig. 10.31 Phase diagram of (**a**) PEO/Aramid and (**b**) PEO/PES blend system (▲) cloud point determined by optical microscopy, (□) onset of demixing obtained by modulated differential scanning calorimetry (Dreezen et al. 2001)

separation process is based on the phenomena that the solvent quality usually decreases when temperature is decreased. After demixing is induced, the solvent is removed by extraction, evaporation, or freeze-drying. The reaction-induced phase separation can be investigated by different observation techniques such as time-resolved small-angle light scattering (TRSALS), optical microscopy (OM), differential scanning calorimetry (DSC), digital image analysis (DIA), etc.

The phase separation process of blends has been studied by a number of researchers. Chaleat et al. investigated the phase separation of plasticized starch/PVA blends (Chaleat 2012) blends of vinylidene fluoride/trifluoroethylene copolymer and poly(1, 4-butylene adipate) was studied by Kap Jin Kim and Kyu (Kim and Kyu 1999). Fully biodegradable blends of poly(butylene succinate) and poly (butylene carbonate) and its phase behavior were studied by Wang (2012).

10.4.5 Factors Affecting Miscibility and Solubility

Miscibility can be influenced by various factors such as crystalline phase, intermolecular interaction, and reduction of surface tension.

10.4.5.1 Effect of Crystallinity

Growing numbers of commercial materials are blends of two or more polymers in which at least one of the components is a crystalline polymer. The crystallization in miscible blends is restricted to temperatures between the blend glass transition temperature and the equilibrium melting point, $T_{m,e}$, i.e., to the crystallization temperature, $T_c < T_{m,e}$. The difference, $D_c = T_{m,e} - T_c$, depends on the cooling rate and the nucleation process. There are three mechanisms of the crystallization nucleation (Utracki 1989):

1. Spontaneous, homogeneous nucleation – it rarely occurs in the supercooled homogeneous melt.
2. Orientation-induced nucleation, caused by alignment of macromolecules, e.g., in extensional flow field.
3. Heterogeneous nucleation on the surface of a foreign phase.

   In thermoplastic blends (2) and (3) are most important mechanisms.

   Miscible crystalline/amorphous polymer blends such as PLA/PVC blends have been widely investigated, and oriented crystallization has also been applied to some miscible crystalline/amorphous polymer blends. For miscible blends containing semicrystalline polymers, analysis of the melting point depression is widely used to estimate the Flory–Huggins interaction parameter (χ).

It has been known for more than a century that impurities reduce the melting point. This observation has been used to determine the molecular weight of the contaminant by Raoult. Nearly a hundred years later, this concept was used to calculate the thermodynamic binary interaction parameter χ_{12} from a melting point depression of a crystalline polymer in miscible blend with low concentration of another polymer. The relation is popularly used in the simplified form for very high molecular weight components (Nishi and Wang 1977):
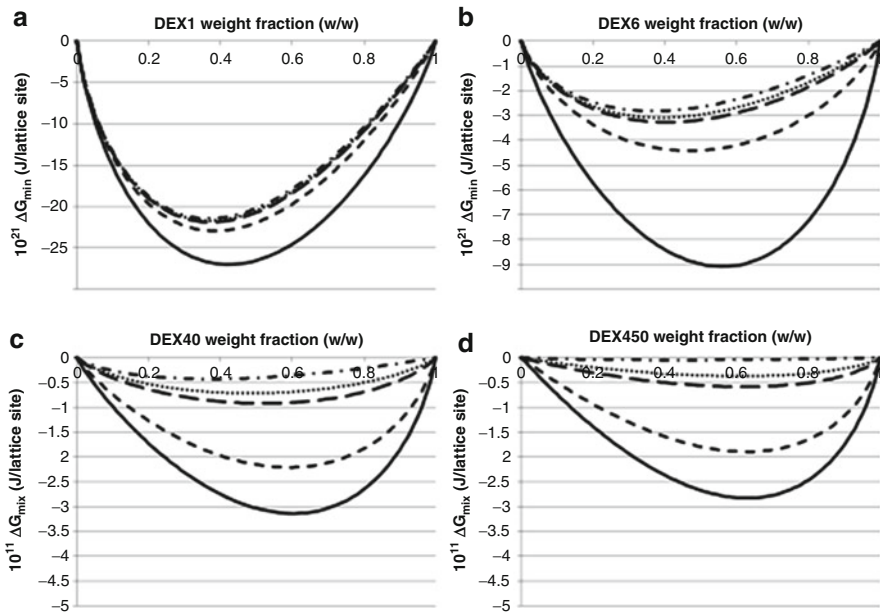
Fig. 10.32 Entropic part of the free energy of mixing per lattice site as a function of DEX weight fraction (w/w): (**a**) DEX1 systems, (**b**) DEX6 systems, (**c**) DEX40 systems, and (**d**) DEX450 systems. Key: PVP12 (*solid*), PVP 17 (*short dash*), PVP25 (*long dash*), PVP30 (*dotted*), and PVP90 (*dash-dot*) (van Eerdebbrugh et al. 2012)

$$\frac{T_m}{T_{m,n}} = 1 + \left(\frac{\chi_{12}\, RT}{V_1}\right) \left(\frac{V_2}{\Delta H_m}\right) \phi^2 \tag{10.24}$$

where T_m is the melting point of crystalline polymer in miscible blend, $T_{m,n}$ is melting point of crystals of neat polymer, V_i is molar volume, and ΔH_m is the heat of fusion. But the determination of the experimental melting points using DSC or optical microscopy and substituting those values in the above equation gives erroneous values for χ.

10.4.5.2 Effect of Molecular Weight

It is well known that polymer molecular weight is a key factor that influences miscibility. Thus, by changing molecular weights of the polymers, systems with variable miscibility characteristics but virtually constant chemical composition potentially can be obtained. Bernard Van and Lynne Taylor applied this to their study and they took dextran and Maltodextrin with PVP (van Eerdebbrugh et al. 2012). Depending on the molecular weights used to prepare DEX-PVP blends, miscibility can vary from completely miscible to virtually immiscible. The higher the combined polymer molecular weight, the lower the miscibility of the resultant blends (Fig. 10.32).

Fig. 10.33 Phase homogenization temperature of the PS/P4MS blend system of (I) PS Mw = 192,000, (II) 250,000 g/mol, both as a function of composition. UCST (*critical point*) is also indicated (Chang and Woo 2001)
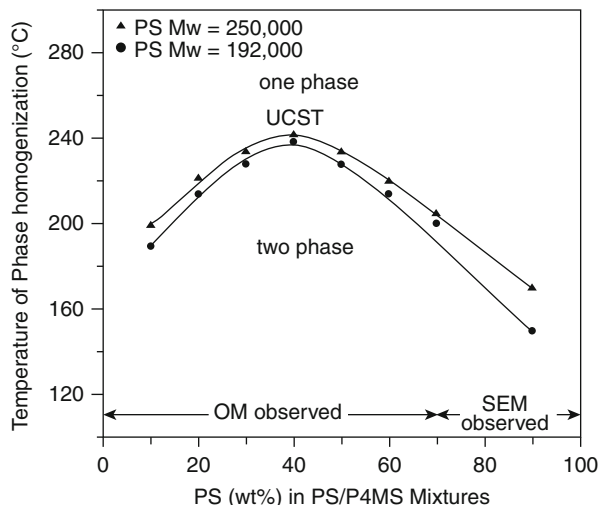
Polymer blends (like low molecular weight solvents) can exhibit miscibility or phase separation and various levels of mixing in between the extremes (e.g., partial miscibility). The most important factor leading to miscibility in low molecular weight materials is the combinatorial entropy contribution which is very large compared to high molecular weight polymers. This contribution is the reason that solvent–solvent mixtures offer a much broader range of miscibility than polymer–solvent combinations. The range of miscible combinations involving polymer–polymer mixtures is even much smaller. As an example compare the miscibility of hexane–ethanol mixtures with their high molecular weight analogs of polyolefins and poly(vinyl alcohol). The former is miscible, whereas the latter is highly immiscible.

Phase behavior of blends of polystyrene with poly(4-methylstyrene) has been studied by Chang and Woo (2001). Their study clearly indicates that an increase of molecular weight leads to a reduction in the entropic contribution to the Gibbs free energy of mixing, which is less favorable for miscibility (Fig. 10.33).

10.4.5.3 Effect of Copolymerization

In blends of random copolymers, or in blends of a polymer with random copolymer, the presence of repulsive forces among segments (other than specific interactions discussed before) may lead to miscibility (Wang et al. 2006). The effect of ethylene–styrene content on the miscibility and cocrystallization was studied extensively by Chen (2001). They showed that the miscibility of the system depends only on the comonomer content with composition expressed as weight fraction. Based on the experimental observations, they constructed a miscibility map for binary blends (Fig. 10.34).

The transition from miscibility to immiscibility occurs over a very small change in styrene content; which (difference from 9 to 11 wt%) is sufficient to change the system from miscible to immiscible for copolymers of this molecular weight.

Fig. 10.34 Miscibility map of ethylene–styrene copolymer blends (Chen 2001)
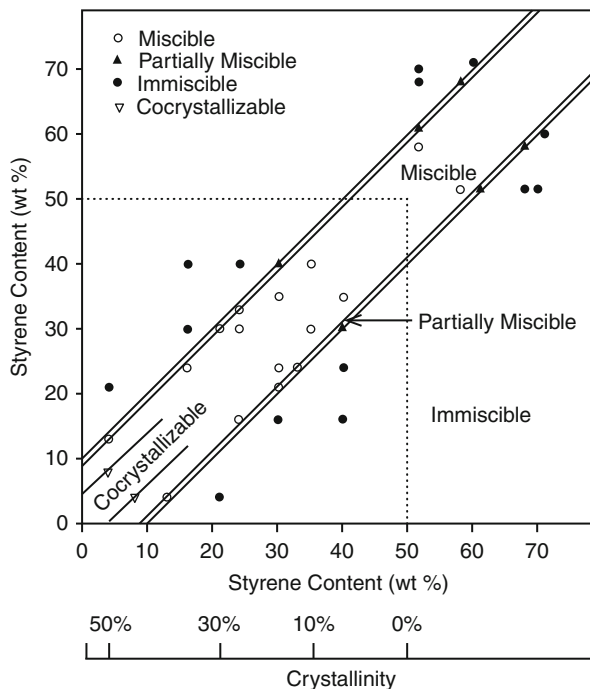
It has been found in the study of PVME and SBS triblock copolymer that solubility of PVME in PS block copolymer domains is larger than in PS homopolymer. This may indicate that the mixing enthalpy has an effect on the blend miscibility. The behavior has been attributed to the effect of PB segments in SBS. The phase equilibriums and miscibility in polymer blends containing random or block copolymer were reviewed. The solubility and miscibility of homopolymer/copolymer blends has been studied by Jiang and Xie (1991). They proposed that when increasing the amount of homopolymer A to the ordered state of block copolymer AB, initially the homopolymer will be dissolved in the microdomains of the block A of the copolymer until the solubility limit is reached beyond which macroscopic phase separation occurs. Results show that the solubility limit depends upon the relative lengths of the block copolymer and the corresponding homopolymer. The dependence of copolymer content on the miscibility of PMMA/SAN blend showed that the transition from miscibility to immiscibility increases with increase in AN copolymer content (Cameron 2002).

10.4.5.4 Effect of Solvents

The solvent effects on polymer blends can be estimated using the solubility parameter δ. The concept was originally used to characterize the strength of interactions in simple liquids, but later it was extended to polymer/polymer as well as polymer/solvent systems. Certain factors, such as structure, composition, and nature of the

Fig. 10.35 Tan δ of SF/PVA blend films cast from aqueous solution of various blend ratios: (**a**) 100/0, (**b**) 70/30, (**c**) 50/50, (**d**) 30/70, and (**e**) 0/100 (Um and Park 2007)
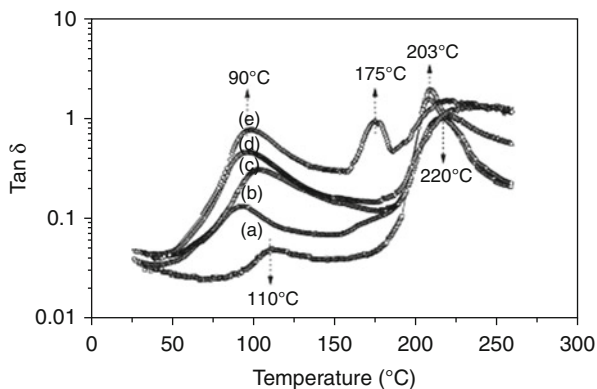
copolymer, influence the solvent effect. Chemical structure of polymers constituting the blend determines its solvent resistance. The polymers, having the backbone linkages involving oxygen, sulfur, and silicone exhibited enhanced chemical and solvent resistance. Thus, enhanced chemical and solvent resistance has been reported for polymer blends that comprise polymers with ether, thioether, oxymethylene linkages, siloxane and/or imide groups, fluorine, certain block polymers, etc.

The structure of repeat units of individual polymers constituting a blend and the nature of interactions between polymers in a blend are the factors that influence solubility characteristics of a blend. Thus, solubility is affected by cross-linking, hydrogen bonding, formation of donor–acceptor complexes, dipole–dipole interactions, ion–dipole interactions, ion–ion interactions, and segmental interactions.

The effect of casting solvent on the miscibility behavior of silk fibroin/PVF blends was investigated by Um et al. SF/PVA blend films cast from aqueous and formic acid solution. The β-sheet conformation of SF formed by formic acid casting was retained for all SF blends regardless of blend ratio. SF/PVA blends from aqueous solution exhibited a phase-separated morphology and immiscibility by SEM observation and DMTA (Dynamic Mechanical Thermal Analysis) measurement (Um and Park 2007) (Figs. 10.35 and 10.36).

Wu et al. (1997) used the DSC method to study the crystallization behavior of the PVAc/PEO blends using two solvents of chloroform and benzene. They observed that the crystallization of PEO was more suppressed in benzene (Fig. 10.37).

10.4.5.5 Effects of Compatibilizers and Interface Modification

A common method to enhance poor miscibility of two components in a blend is to add a third component to the blend that will have a favorable interaction with the precursor polymers. This third component, often termed a compatibilizer, is designed with the hope it will favorably affect the blend system by potentially changing a miscibility window, strengthening phase-separated domains, or by affecting the kinetics of phase separation thus causing a change in the phase-separated morphology.

A compatible blend is mixture of polymers with low repulsive forces between phases. Compatibilization is referred to any physical or chemical method that

Fig. 10.36 Tan δ of SF/PVA blend films cast from formic acid solution of various blend ratios: (**a**) 100/0, (**b**) 70/30, (**c**) 50/50, (**d**)30/70, and (**e**) 0/100 (Um and Park 2007)
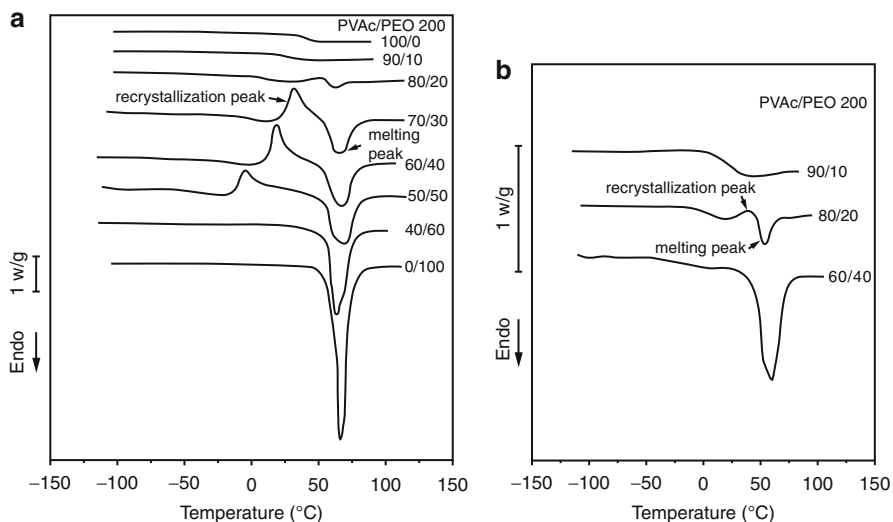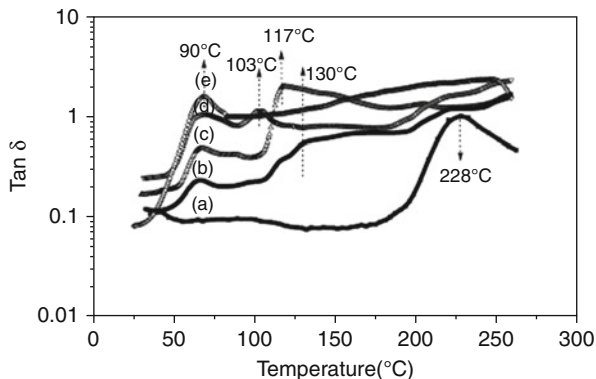
Fig. 10.37 DSC thermograms of (**a**) PVAc/PEO200 blends cast from chloroform and (**b**) benzene (Wu et al. 1997)

results in stabilization (prevention to separate) of polymer blends morphology and properties. Polymer blends are used to change impact or flex properties, chemical resistance, thermoformability, and printability, for example. Some properties of the compatibilized blend exceed that of either component alone. Compatibilizers act through a chemical reaction (reactive compatibilization) or through intermolecular forces of attraction such as van der Waals, hydrogen bonding, based on polarity of the materials (nonreactive compatibilization). In addition, a compatibilizer may function by more or less the same mechanism as a surfactant does to stabilize oil/water mixture, i.e., by being soluble in one or both major
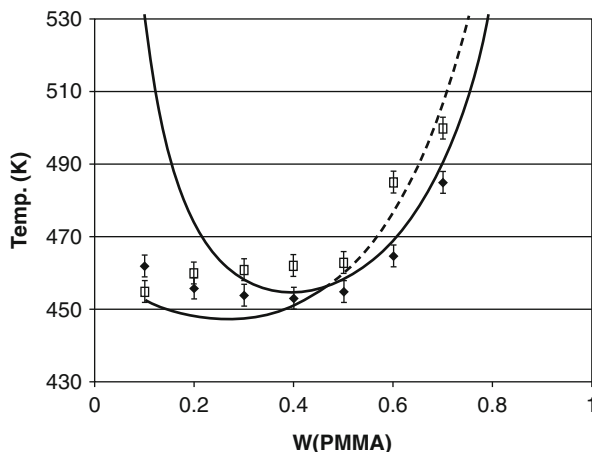
Fig. 10.38 Qualitative comparison between the theory and the experimental phase diagram (*cloud points*) for the PVA/PMMA polymer blend without fillers (*filled diamonds*) and with 10 wt% fumed silica (*open squares*). The *two curves* correspond to the spinodals calculated using equations. It is assumed that both PVA and PMMA had degrees of polymerization (N) 1,000 and that (øN) a + bT, with (a)-10.0, (b) 0.026374. Finally, assumed that (F) 0.65. For the filled system, we took nanoparticle loading of 14 vol%, with the dimensionless particle radius (R) 20 (corresponding to the ªrealº particle radius of 10 nm) (Ginzburg 2005)

components of the blend. One such mechanism is by attaching itself to one of the blend components through chemical grafting and leaving a polymeric "tail" that is soluble in the other component.

Most polymers are not miscible and those having closely similar solubility parameter values are likely to be compatible. Two incompatible polymers can be compatibilized by the presence of a third component, which results in a good improvement in the physical and mechanical properties of the blend. The effect of the polyacrylonitrile compatibilizer, on the miscibility and properties of NBR/SBR blends, has been studied by Darwish et al. (2005).

Nowadays, nanoparticles have been widely used as fillers and compatibilizers. They exert certain effect on the miscibility of blends. Ginzburg applied a simple theory to study the effect of nanoparticles on the miscibility of PVA/PMMA blends and compared theoretical and experimental results for the same system with fillers and without fillers (Ginzburg 2005) when nanoparticle radius is smaller than polymer radius of gyration, the addition of nanoparticles increases the critical value of χ_N and stabilizes the homogeneity (Fig. 10.38).

Phase separation of poly(methyl methacrylate)/poly(styrene-co-acrylonitrile) blends in the presence of silica nanoparticles was studied by rheological method by Jianping Gao (2012). Rheology is a frequently used method to determine the phase separation temperature. However, unlike the optical method which can show the phase-separated morphology directly, no visual information can be obtained from rheology (Fig. 10.39).

Fig. 10.39 The binodal phase diagram of PMMA/SAN (*solid circles*) and PMMA/SAN/SiO (*solid squares*) by combining the gel-like method and Cole–Cole plot. The spinodal points of PMMA/SAN (*hollow circles*) and PMMA/SAN/SiO (*hollow squares*) are also shown. The *lines* are drawn to guide the eyes (Gao 2012)
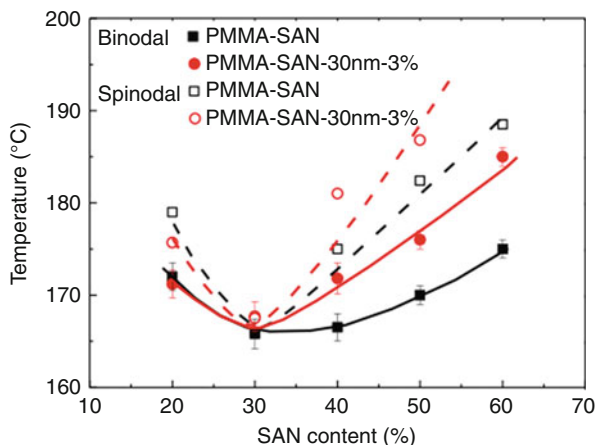
10.4.6 Standard Methods of Evaluation of Miscibility, Solubility, and Interaction Parameter

The miscibility behavior of the blends can be determined by various techniques. Glass transition temperature (T_g)-based analysis using differential scanning calorimetry, dynamic mechanical analysis, spectroscopic techniques such as Fourier transform infrared (FTIR) spectroscopy and solid-state nuclear magnetic resonance (NMR), fluorescence spectroscopy, scattering techniques such as small-angle light scattering (SALS) and small-angle X-ray scattering (SAXS), morphology determination by transmission electron microscopy (TEM), scanning electron microscopy (SEM), etc., are the commonly used techniques for the miscibility studies in polymer blends. Each method has its own standard and sensitivity. The specific method used to determine the solubility and miscibility behavior is inverse gas chromatography (IGC); the effect of crystallinity is studied by DSC. The optical microscopy is used to study the spherulitic superstructure of polymer crystals from the melt and explain the relationship between morphology and crystal growth rate. In addition, small-angle light scattering (SALS) and small-angle X-ray scattering (SAXS) are used to study the morphology of crystalline/amorphous polymer blends.

10.4.6.1 Glass Transition Temperature (T_g) Analysis

Thermal methods are useful to study modern polymeric material, usually blends or composites with complex morphologies that are crucial to determining their material properties. The miscibility of polymer blends is often assessed by the measurement of a single glass transition temperature (T_g) as a function of composition. Two T_gs in a DSC thermogram indicates a two-phase system, and a single composition-dependent T_g is often taken as evidence of the formation of a miscible blend.

The differential scanning calorimetry (DSC) is the thermal analysis mainly used to determine a first-order transition (melting) and a second-order endothermic transition (glass transition). DSC has been extensively used for the characterization

Fig. 10.40 DSC *curves* of
PCP–PVC blends of different
composition. (*a*)–(*g*)
represent T_g of the blends
(Saha 2001)
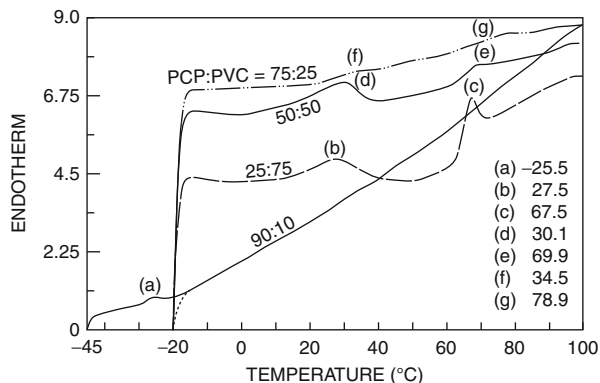
of interchange reactions. Experimentally, the least ambiguous criterion for polymer
miscibility is the detection of a single glass transition temperature (T_g), which is
intermediate between those corresponding to the two component polymers. Phase
separation is judged by the existence of two distinct glass transition temperatures.

The effect of transesterification on the miscibility of the PC–PET blends was
studied by Zheng et al. using DSC (Zheng 2004). The binary interaction energies of
completely miscible binary pairs that do not phase separate like PPO/PS are studied
by small-angle neutron scattering (SANS). The miscibility of PEOx and PVPh
blends was investigated by Wang et al. (2001) using FTIR, DSC, high-resolution
solid-state NMR, etc. Compatibility of PCP–PVC blends was studied by DSC by
Saha (2001). He concluded that the compatibility increases with increase in PCP
content (Fig. 10.40). The difference in peaks gradually decreases and at 90 % PCP
content merges into single peak.

The phase behavior of blends of TMOS and SAN was investigated by means of
optical cloud point measurements and DSC by Pfefferkorn et al. (2012). The blends
display partial miscibility with an upper critical solution temperature (UCST).
Moreover, the SAN/TMOS blends show pronounced miscibility-window behavior,
i.e., the UCST depends strongly on SAN copolymer composition.

DSC technique was used to study polybenzoxazine/poly(ε-caprolactone) blends
(Huang 2005), poly([2-oxo-1,3-dioxolan-4-yl]methyl vinyl ether-co-acrylonitrile)/
poly(vinyl chloride) blend (Ha et al. 2002), polypropylene/polyethylene binary
blends (Wong et al. 2002), etc.

DMA is another technique, which is widely used for the determination of
miscibility of polymer blends. Generally for an immiscible blend, the tanδ curves
show the presence of two damping peaks corresponding to the T_gs of individual
polymers. For a highly miscible blend, the curves show only a single peak in
between the transition temperatures of the component polymers, whereas broaden-
ing of the transition occurs in the case of partially miscible systems. In the case of
miscible or partially miscible blends, the T_gs are shifted to higher or lower tem-
peratures as a function of composition. Perera et al. (2001) studied the miscibility of
polyvinyl chloride (PVC)/nitrile butadiene rubber (NBR) and PVC/epoxidized

natural rubber (ENR) blends using DMA. The tanδ curve for PVC/NBR and PVC/ENR blends appeared in between the respective homopolymers, indicating miscibility. The tanδ peaks for the blends were broader than the two homopolymer curves due to some degree of dynamic heterogeneity in the blend. In other words, the blends appeared to be miscible but had a wide range of relaxation times as a result of molecular proximity of the unlike chains.

10.4.6.2 Microscopic Measurements

The liquid–liquid decomposition of a blend of polycarbonate(PC)/polyethylene oxide(PEO) taking place via spinodal decomposition has been studied by optical microscope (Tsuburaya 2004) in Fig. 10.41.

Phase separation may proceed either by nucleation or growth or by spinodal decomposition when the changes in the conditions take the solution into metastable or unstable domains, respectively. Kiran (2009) studied solutions of poly(ε-caprolactone) in acetone/carbon dioxide fluid mixtures.

The structural morphology of a blend is a product of compositional variations formed in the micro-/nanoscales. Atomic force microscopy produces high-resolution images of the sample topography by monitoring the physical displacement of a cantilever interacting with a sample surface. Phase separation is observable in immiscible or partially miscible blends. High-resolution imaging provides useful information pertaining to the domain size and morphological character.

10.4.6.3 Scattering Techniques

Various light-scattering and optical techniques have been investigated as potential candidates for characterization of multiphase polymeric materials. Kinetics of phase separation and dissolution (demixing) of polymer blends, stress whitening process, photon migration in polymer composites, etc., are examined using light-scattering techniques. A light-scattering theory known as the Rayleigh–Gans theory was developed to extend Rayleigh theory to particles that are not optically small. The correction method involves extrapolation techniques that extrapolate light-scattering intensity to zero-scattering angle. This correction technique is important for analyzing results on polymer solutions.

The assessment of miscibility and phase separation conditions is relatively easy and is carried out in many laboratories employing view cells that allow visual or optical observations as phase separation is accompanied by a change in the transmitted light intensity. The assessment of phase separation needs special techniques that allow measurement of the scattered light intensities as a function of the scattering angle and time.

A pattern like the following one is observed after the liquid–liquid phase boundary. The scattered light intensities become brighter in time at all angles (Fig. 10.42).

Direct information on the χ value between blends can be obtained from small-angle neutron scattering (SANS). SANS studies usually involve studies on multiple pairs of deuterated samples, so the effect of deuteration on the interaction parameter can be evaluated quantitatively. Light-scattering techniques can be used to determine the miscibility of PE blends by slowly cooling or heating the blend from the
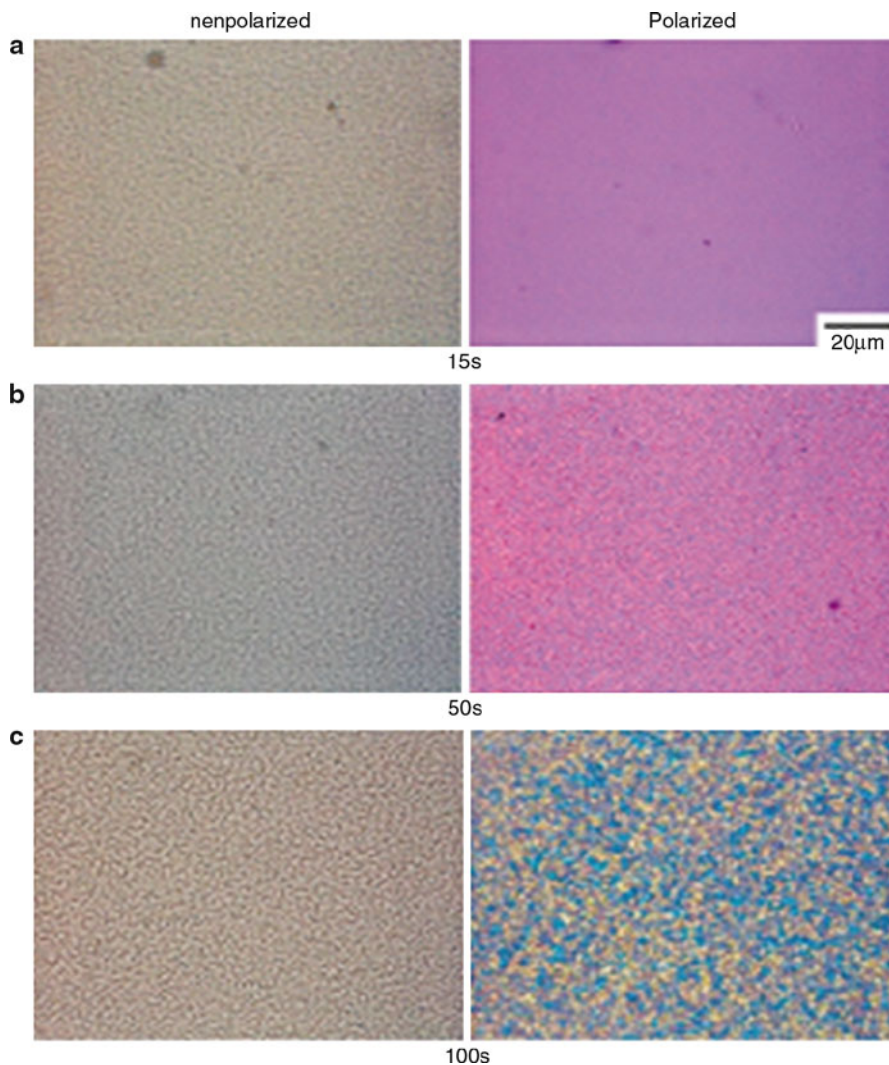
Fig. 10.41 Microscopic observation of the structural development in the 70/30 PC/HM-PEO blend during isothermal annealing at 180 °C. *Left*: unpolarized light. *Right*: polarized light (Tsuburaya 2004)

one-phase region. We can observe the cloud point at which the forward-scattered light intensity increases, indicating the onset of liquid–liquid phase separation.

Akpalu and Ping Peng (Akpalu et al. 2005) studied the melt miscibility of a commercial linear polyethylene and LLDPE system using SANS.

A similar technique called SAXS (small-angle X-ray scattering) is also used to study polymer blends. Small-angle X-ray scattering (SAXS) is a nondestructive scattering technique that records elastic scattering of X-rays at scattering angles
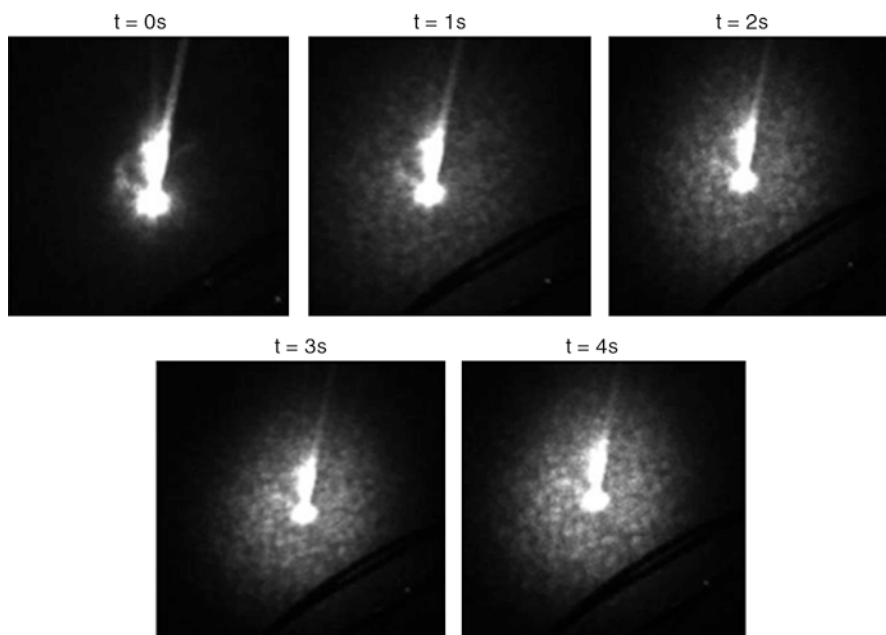
Fig. 10.42 Liquid–liquid phase boundary of blend observed in light-scattering experiment (Courtesy: *Online resources*)

close to the direction of the incident beam. SAXS, due to its q range, often proves useful to study the large structures in binary or ternary blends where one or more components crystallize. Mickiewicz studied extensively the application of SAXS with binary blends of four different high molecular weight poly(styrene-b-isoprene) diblock copolymers with a low molecular weight poly(styrene-b-isoprene-b-styrene) triblock copolymer (Mickiewicz et al. 2008).

Polymerization-induced binodal phase separation in rubber-modified epoxy system containing DGEBA and HTBN during curing was studied using time-resolved SANS. The following figure (Fig. 10.43) shows the pattern during polymerization-induced phase separation (PIPS). The PIPS at 160 °C is much higher (Zhang et al. 1999).

The quantitative analysis of the spectrum is also given. As the time passes from 9 to 11 min, the minimum appeared become closer to the second maxima and finally merged into one to give a broad peak, Fig. 10.44.

The phase separation behaviors of PMMA/SAN blends with and without fumed silica (SiO_2) have been investigated using time-resolved small-angle light-scattering and dynamic rheological measurements. It is found that the effect of SiO_2 on the phase separation behavior of PMMA/SAN blend obviously depends on the composition of the blend matrix (Du et al. 2013).

In the case of polymer blends, refractometric and viscometric methods are used to study the polymer–solvent and polymer–polymer miscibility. It is clear that
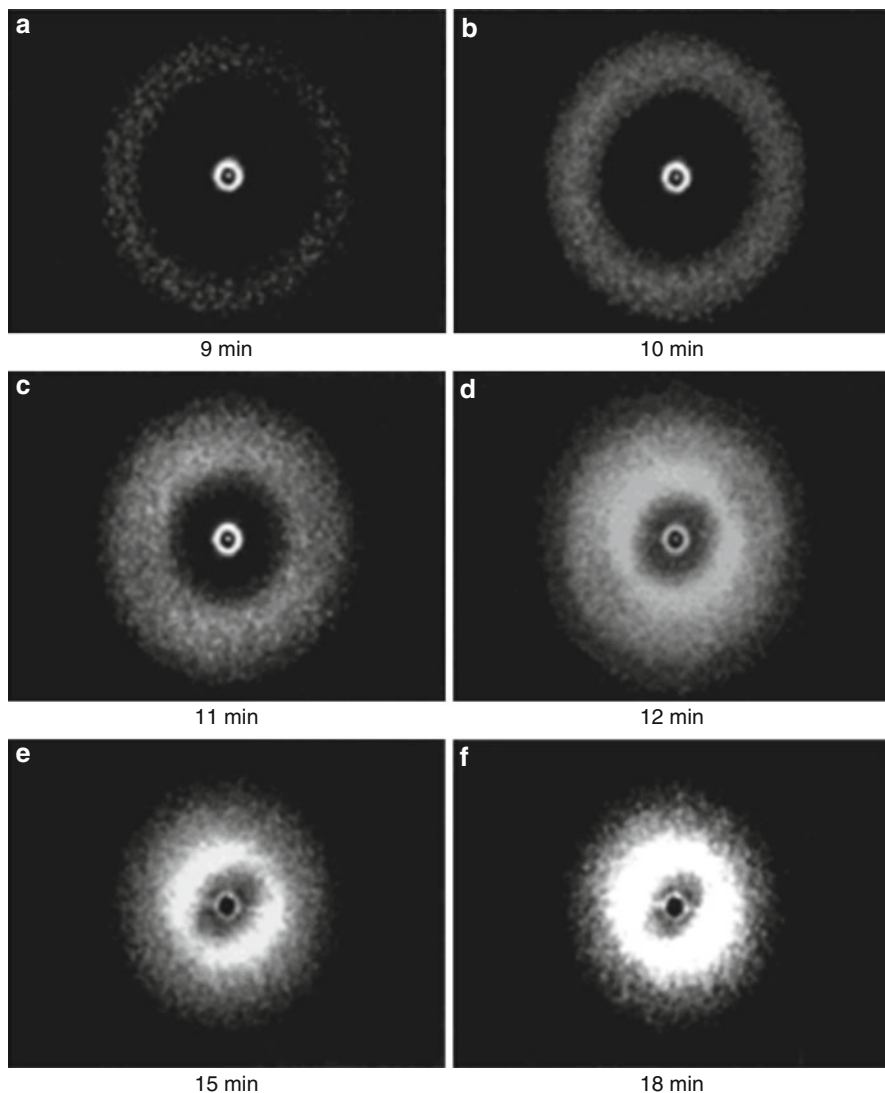
Fig. 10.43 Evolution of light-scattering pattern for the epoxy system cured at 160 °C. HTBN/E-51/MeTHPA/BDMA 5 40/90/70/0.056; (**a**) 9 min, (**b**) 10 min, (**c**) 11 min, (**d**) 12 min, (**e**) 15 min, (**f**) 18 min (Zhang et al. 1999)

behavior of viscosity and refractive index with blend composition is linear for the miscible blends and nonlinear for partially and immiscible blends.

Radhakrishnan and Venkatachalapathy (Radhakrishnan et al. 1996) used the X-ray diffraction to study the crystallization, the PMMA/PEO blends cast from three solvents. The solvent effect is demonstrated from the large differences in the crystallinity values.
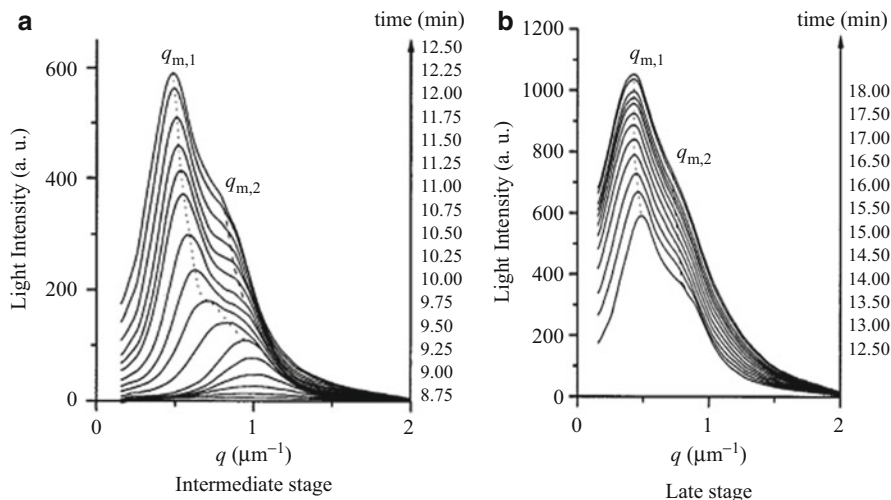
Fig. 10.44 Evolution of light-scattering profile for the epoxy system cured at 160 °C. HTBN/E-1/MeTHPA/BDMA 5 40/90/70/0.056; (**a**) intermediate stage, (**b**) late stage (Zhang et al. 1999)

10.4.6.4 Rheological Measurements

Rheological methods have been frequently used to study the phase separation behavior of partially miscible polymer blends. Rheology is generally sensitive to morphological changes during phase separation. Like optical methods rheological methods are not affected by the transparency of the blend. This method is strongly related to viscoelastic properties of the blend. It is said to have more resolution depending upon the applied oscillatory frequency. Rheological methods are used to get the phase diagram and to study the kinetics and mechanism of phase separation using some empirical rules.

The rheological properties of miscible blends under different temperatures can be obtained from some theoretical models. One such model is the double reptation self-concentration. The DRSC (double reptation self-concentration) model actually includes the temperature dependency and concentration dependency through a complex mixing rule given by the double reptation model and self-concentration model, which helps to exclude the complex contribution from miscible components under different temperatures in the experimental data and only illustrate the effect of the concentration fluctuation and interface formation. This model is applied to study PMMA/SMA (Wei 2011).

The frequency dependent apparent bimodal temperature is shown in Fig. 10.45. In this study, they showed that the storage modulus starts to deviate at the point of phase separation.

The rheological study was also done by Ceren Ozdilek et al. to investigate the thermally induced phase separation of PαMSAN/PMMA blends in presence of functionalized multiwall carbon nanotubes (Ozdilek 2011).

Fig. 10.45 Transition temperature as a function of oscillatory frequency during temperature ramp with a rate 1 °C/min. The triangle point at zero frequency is the transition temperature determined from isothermal frequency sweep (Wei et al. 2011)
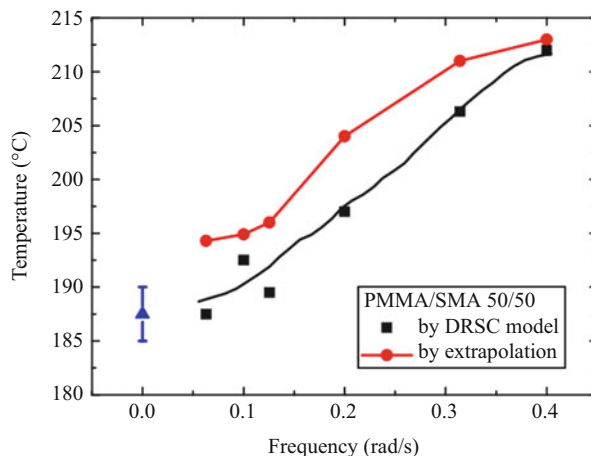
10.4.6.5 Inverse Gas Chromatography

Inverse gas chromatography (I_{GC}) has been proven to be useful for the characterization of polymer blends in terms of polymer–polymer interaction parameters, polymer–solute interaction parameters, solubility parameters, molar heat of sorption and mixing, melting point depression as an indicator of miscibility, contact energy parameters, and surface characterization. I_{GC} has the capability of glass transition temperatures as a function of relative humidity. The technique involves creating within a column a stationary phase of the solid material of interest and determining its different physicochemical properties. The glass transition and polymer–polymer interactions are also studied using I_{GC}. Using the T_g detection by I_{GC}, Aouak and Alarifi showed the ability of this technique to study and confirm the miscibility of PBMA/PEO blends (Aouak and Alarifi 2009). It is well known that miscible blends have only one T_g, while immiscible blends have two or more T_g. Retention diagrams are constructed by two probes (solutes): chloroform as a common solvent and heptanes as a common nonsolvent to PBMA and PEO.

The miscibility of binary mixtures of poly(ether imide) (Ultem^{TM}) and a copolyester of bisphenol-A with terephthalic and isophthalic acids (50/50) (Ardel^{TM}) in three compositions (25/50, 50/50, and 75/25) was studied by F. Cakar et al. (2012).

10.4.6.6 Spectroscopic Analysis

Infrared spectroscopy has been widely used to investigate specific interactions in polymer blends in which the miscibility driving force is hydrogen bonding between components. Possibility of hydrogen bonding between hydroxyl groups of PVPh and carbonyl groups of PLLA in the blends of poly(L-lactide) with poly(vinylphenol) was reported by Meaurio et al. (2005). The miscibility and formation of hydrogen bond in the PMMA/CAB blends were studied. The carbonyl frequency of pure PMMA at 1,750 cm^{-1} is reduced to 1,740 cm^{-1} in the 50/50 blend indicating the formation of hydrogen bonding between the component polymers which contribute to the
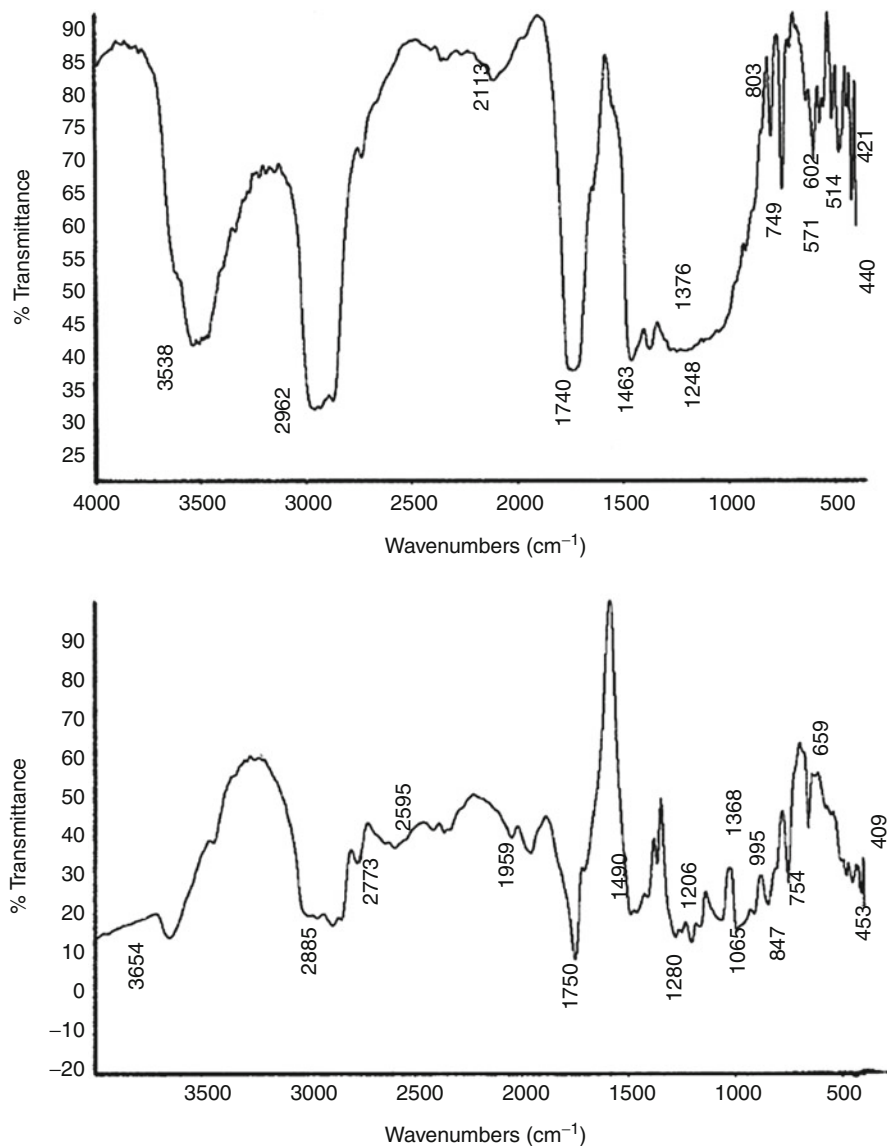
Fig. 10.46 FTIR spectra of Pure PMMA and blend of PMMA/CAB of 50/50 composition (Meaurio et al. 2005)

miscibility of the blends. The FTIR data (Fig. 10.46) also compliments the solution techniques (Selvakumar et al. 2008).

The complete miscibility of the PMMA/DGEBA epoxy blends was confirmed by FTIR spectroscopy by Ritzenthaler et al. Increasing the heating time does not induce any shift or modification of the O–CH$_3$ (2,850–2,950 cm^{-1}) and the
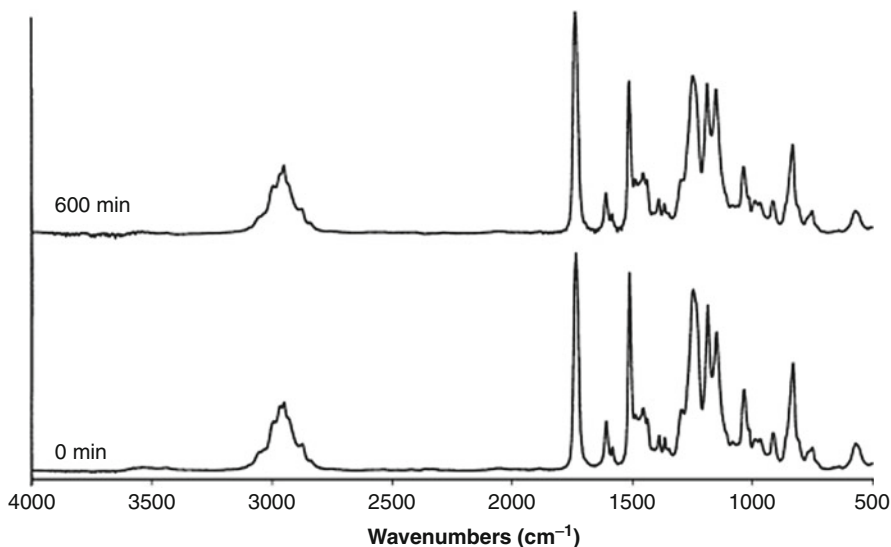
Fig. 10.47 FT-IR spectra of DGEBA 30 wt% PMMA blend at 135 °C (Ritzenthaler et al. 2000)

C = O (1,725 cm^{-1}) peaks of PMMA. The results also confirm that there is no specific interaction between the PMMA and the thermoset components during curing (Fig. 10.47) (Ritzenthaler, et al. 2000).

^{1}H NMR was used to characterize the structure of the reactive and physical blend products of poly(lactic acid) and poly(ε-caprolactone) system by Wang et al. (1998). The investigation of EVA reject/phenolic resin from cashew nut shell liquid (CNSL) blends, using combined NE techniques at solid state, showed the range of compatibility as well as the domain structure present in the microdomains (Martins et al. 1996). The miscibility of poly(styrene-*co*-vinylphenol) containing 5 % vinylphenol monomer units (MPS-5) with syndiotactic poly(methyl methacrylate) (PMMA-s) and with isotactic poly(methyl methacrylate) (PMMA-i) was studied with ^{13}C solid-state n.m.r. complemented with cloud point and differential scanning calorimetry measurements (Lei Jong et al. 1993).

10.4.7 Influence of Miscibility on Final Properties of Blends

In general, a miscible blend of two polymers is likely to have properties somewhere between those of the two unblended polymers. The relative miscibility of polymers controls their phase behavior, which is of crucial importance for final properties. Polymer–polymer miscibility depends on a variety of independent variables, viz., composition, molecular weight, temperature, pressure, etc.

Jong-Han Chun studied the synergistic effect of impact strength and miscibility in polycarbonate PC/ABS blends (Chun et al. 1991). Positive deviations of the modulus

Fig. 10.48 Horizontal shift factors for the pure components and the single-phase 20/80 PS/PVME blend at a reference temperature of 1 °C (Polios 1997)
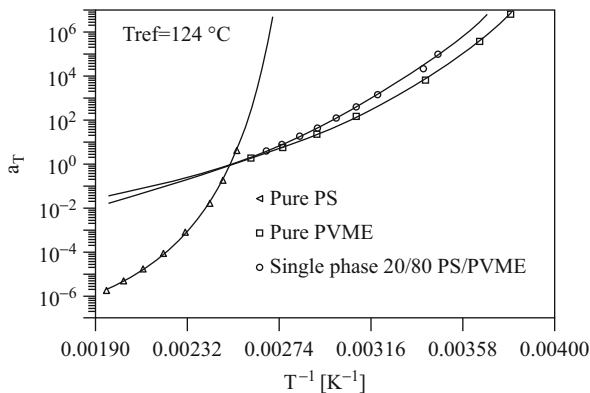
E_b and yield strength S of polymer blends consisting of partially miscible polymers are analyzed by combining models for miscible and immiscible blends by Jan Kolarík (2000). Several heterogeneous blends of partially miscible polymers, such as polycarbonate (PC)/poly(styrene-co-acrylonitrile) (PSAN) (Kolarik et al. 1997), poly(ether sulfone)/phenoxy (An et al. 1996a, b), and poly(ether-imide)/polyarylate, PC/poly(acrylonitrile-butadiene-styrene) (ABS), PC/PS, polyamide-6/ABS, and PC/poly(ether sulfone) (An et al. 1996) were found to show modulus E_b and/or yield strength S higher than predicted by the rule of mixing (additivity).

In the case of PS/PVME blends studied by Polis et al., the phase separation results initially in a large increase in the low-frequency complex moduli which is attributed to the highly interconnected PVME-rich and PS-rich phases, formed during the spinodal decomposition. The subsequent decrease is the result of the loss of interconnectivity between the two phases due to the breakup and coarsening of the phase-separated domains (Fig. 10.48) (Polios 1997).

The influence of miscibility on the transport properties of polymer electrolyte blends composed of a proton conductor and an insulator was investigated by Jeffrey, Gasa, Weiss, and Montgomery Shaw (2006). The proton conductive component in the blends was SPEKK, while the nonconductive component was either PEI or PES. The phase behavior of PEI–SPEKK blends was strongly influenced by the sulfonation level of the SPEKK. At low sulfonation levels (ion-exchange capacity (IEC) = 0.8 meq/g), the blends were miscible, while at a slightly higher level (IEC = 1.1 meq/g), they were only partially miscible, and for IEC = 1.4 meq/g, they were effectively immiscible over the entire composition range. The PES–SPEKK blends were miscible over the entire range of SPEKK IEC considered in this study (0.8–2.2 meq/g). Poly(ether ketone ketone) (PEKK) itself is a relatively new engineering thermoplastic that has high-temperature stability, excellent chemical and solvent resistance, and excellent mechanical properties. The effect of compatibilization on the miscibility and final effect on the mechanical properties of PA/PPO blend have been studied by Cao et al. (2011). They used graphite oxide as a compatibilizer. Figure 10.49 represents the stress behavior and tensile strength data of the uncompatibilized and GO sheet compatibilized blends. They observed that the tensile strength of the blends increased by 87 %.
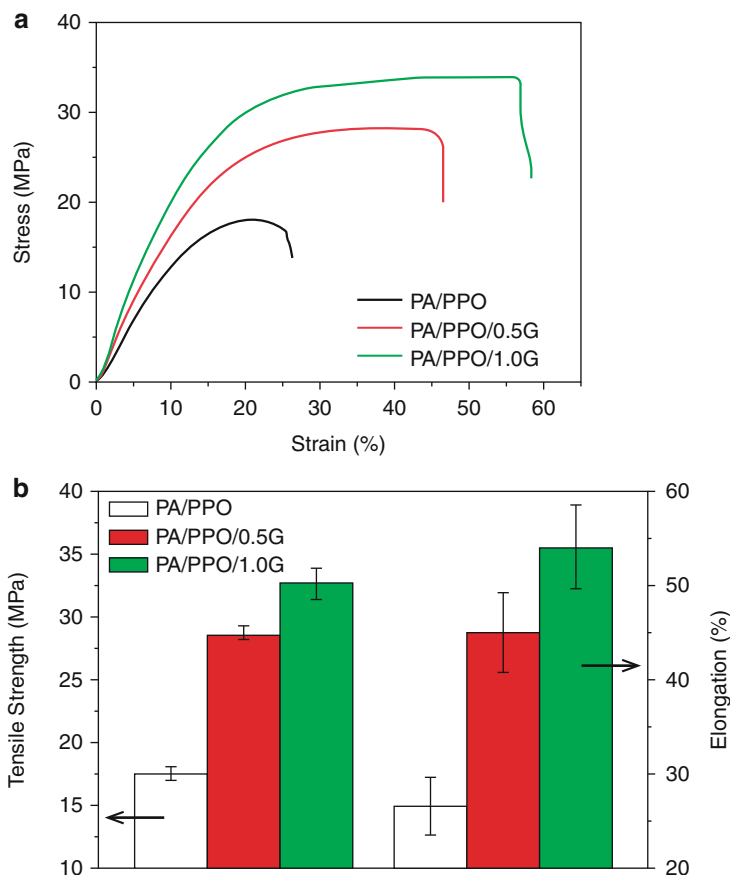
Fig. 10.49 (**a**) Stress–strain curve and (**b**) tensile strength and elongation data of uncompatibilized and GOS compatibilized PA/PPO blend (Cao et al. 2011)

10.5 Thermal Properties

10.5.1 Thermal Resistance (R)

For a flat slab, it is calculated as (ASTM C177)

$$R = A \ \frac{(T_1 - T_2)}{Q} \ = \ \frac{1}{\Gamma} \ = \ \frac{D}{\lambda} \tag{10.25}$$

where R = thermal resistance (Km^2W^{-1}), A = area measured on a selected isothermal surface (m^2), T_1 = temperature of warm surface of specimens (K), T_2 = temperature of cold surface of specimens (K), Q = heat flow rate (W), Γ = thermal conductance ($Wm^{-2} \ K^{-1}$), D = thickness of specimen measured

Table 10.16 Thermal conductivity units (Ives et al. 1971)

Units	Cal/(cm s °C)	W/(cm °C)	W/(m °C)	Kcal/(m h °C)	Btu in/(ft² h °F)
Cal cm/(cm² s °C) (or) cal/(cm s °C)	1	4.19	419	360	2900
J cm/(cm² s °C) (or) W/cm °C	0.230	1	100	86.0421	693
J cm/(m² s °C) (or) W/m °C	0.00239	0.01	1	0.860421	6.93
Kcal m/(m² h °C) (or) Kcal/m h °C	0.00278	0.0116	1.16	1	8.06
Btu in/ft² h °F	0.000345	0.00144	0.144	0.124	1

along a path normal to isothermal surfaces (m), and λ = thermal conductivity, (W/mK). The reciprocal of thermal resistance is known as thermal conductance, Γ.

10.5.2 Thermal Conductivity (λ)

Thermal conductivity of materials can only be defined for homogeneous materials, where the thickness is greater than that for which the apparent thermal resistivity of the material does not change by more than 2 % with further increase in thickness. The thermal resistance must be sufficiently independent of the area of the specimen, and for a flat slab specimen, the thermal resistance must be proportional to the thickness. When all these conditions are met,

$$\lambda = \frac{QD}{A}(T_1 - T_2) = \frac{D}{R} \qquad (10.26)$$

where the symbols are the same as in Eq. 10.25. The reciprocal of the thermal conductivity is called thermal resistivity (r).

The most common units for thermal conductivity are cal/cm °C and Btu in/ft² h°F. The SI unit for conductivity is W/mK. Since a variety of units has been in practice for thermal properties, the conversion factors are given in Table 10.16.

ASTM C177 and BS 874 recommend guarded plate method for materials of low conductivity. Two different types of guarded hot plate apparatus are described in ASTM C177. The low-temperature guarded hot plate is the most suitable method for determining the thermal conductivity of polymeric solid materials including foams. It is generally used for measurements where the temperature of the heating unit is not above 500 K. The second method is the high-temperature guarded hot plate which is ordinarily used for measurements where the heating unit temperature is greater than 550 K but less than 1,350 K. The schematic arrangement of the apparatus is shown in Fig. 10.50.

Three possible configurations to restrict edge heat flux are illustrated in Fig. 10.51. The apparatus consists of a heating unit, a cooling unit, and edge insulation. The heating and cooling units may be either round or square. The heating unit consists of a central metering section and a guard section.

Fig. 10.50 General features
of the metal surfaced hot plate
apparatus (ASTM C177)
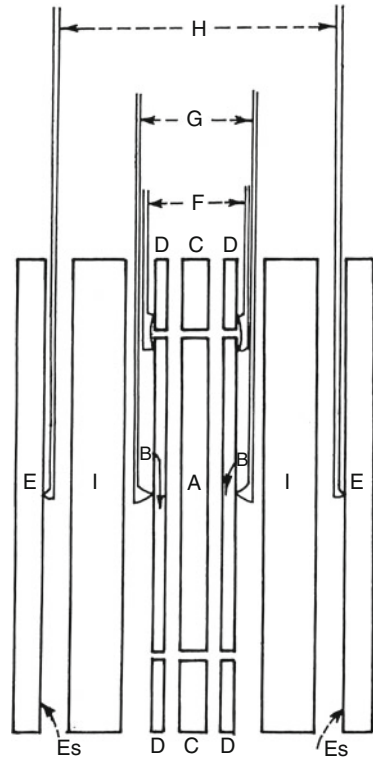
The metering section consists of a metering area heater and metering area surface
plates. The guard section consists of one or more guard heaters and the guard
surface plates. The working surfaces of the heating unit and cooling plates should
be smoothly finished to conform to a true plane.

The heating unit has a separation (or gap) not greater than 4 mm between the
surface plates of the metering area and the guard. Two specimens should be selected
from each sample with their surfaces made plane. The temperature difference
between the hot and cold surfaces of the specimens should be not less than 5 K
(De Ponte and Di Filippo 1974).

The central heat source and the guard should have independent power supplies.
The cold surface heaters are to be adjusted so that the temperature drops through the
two specimens do not differ by more than 1 %. To attain a correct value for
properties, the time required should be adjusted – its magnitude depends on
the specific apparatus, control system and its operation, the test temperatures,
the thermal diffusivity, and thickness of the specimens (Shirtliffe 1974). The con-
ductivity is calculated using the Eq. 10.26. The attainment of equilibrium is important,
especially for polymer blends that have low conductivity. The equilibrium times, for
example, for cellular materials, are in the order of hours or tens of hours. For this
reason, stable over long time period power supplies are necessary.

Fig. 10.51 Possible configurations to restrict edge heat loss or gain (ASTM C177)
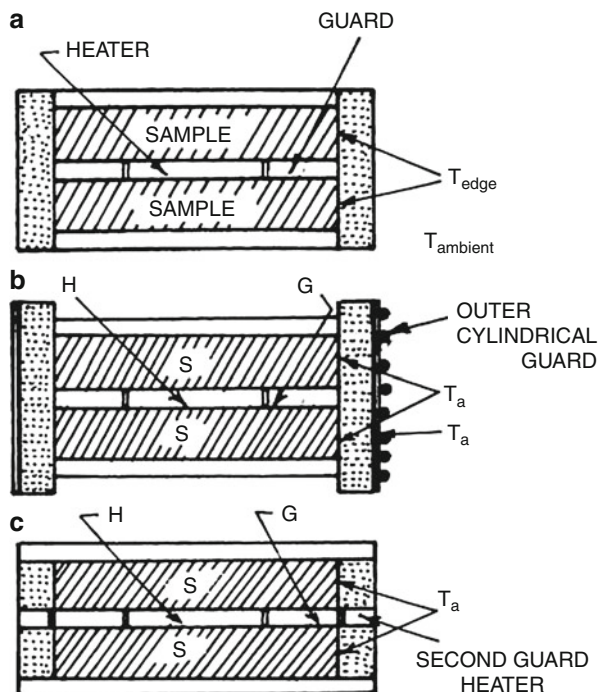
10.5.3 Heat Capacity

Specific heat of polymer blends is usually measured by differential thermal analysis (DTA) (Slade and Jenkins 1966) or differential scanning calorimetry (DSC) (Strella and Erhardt 1969; Richardson and Burrington 1974). DTA measures the difference in temperature between the sample and a standard for the same rate of heat input, while DSC compares the rate of heat inputs for the same rate of temperature rise. The results of DSC are easier to analyze as they give a direct measure of the rate of heat input.

Measurement of specific heat is made by heating a test specimen at a known and fixed rate (Blaine 1973). Once dynamic heating equilibrium of the specimen is reached, the heat flow is recorded as a function of temperature. This heat flow, normalized to specimen mass and heating rate, is directly proportional to the specimen's specific heat capacity.

In practice, two thermal experiments are required for each measurement. In the first, a baseline run is performed only on the empty pan and lid. In the second run, the test specimen is enclosed in the pan and lid. The specific heat capacity information is derived from the difference between the two resulting thermograms.

Heat flow calibration of the apparatus is also required. This is obtained by running baseline and experimental traces for a material whose specific heat capacity is well known. Sapphire is the calibration material of choice since it is easily available and its specific heat capacity is accurately known.

The relationship for calculation of specific heat capacity is given by

$$C_p \ = \ \frac{KEq}{m\beta} \tag{10.27}$$

where C_p is the specific heat capacity (J/kg K), E is the calibration coefficient (dimensionless), q is the heat flow (mW), β is the heating rate (K/min), m is the specimen mass (mg), and K (60,000) is the conversion constant. The calibration coefficient E is expressed as

$$E \ = \ \frac{C_p \ (lit)}{C_p \, (obs)} \tag{10.28}$$

where C_p (lit) is the reported literature value of specific heat capacity of the standard sample, while C_p (obs) is its experimentally observed value under the same conditions. The coefficient, E, is to be used for the determination of the unknown.

It is wise to calculate E for several temperatures over the region of interest – E should be constant. If it is not, particularly at low temperatures, it indicates that dynamic temperature equilibrium is not attained at the temperature and that the experimental temperature program needs to be started at a lower temperature. The overall accuracy of the method is found to be ± 5.5 %. Precision can be improved with large samples and higher heating rates, provided dynamic temperature equilibrium is achieved.

10.5.4 Heat Distortion Temperature (HDT)

ASTM D648 describes the determination of temperature of deflection under load for plastics and ebonite. ISO 75, BS 2782 Method 121 A and 121 B are equivalent. DIN 53461 is similarly related to the ISO method. Since these standards are similar, only the ASTM method will be described.

The heat distortion temperature (HDT), the deflection temperature under load (DTUL), or the softening temperature is a practical and important parameter of a polymeric material. They denote the upper temperature limit up to which the material can support a load for any appreciable time.

ASTM D648 provides a method for determining DTUL of plastics under flexural load. The method is applicable to molded and sheet materials available in thickness ≥ 3 mm, which are rigid at room temperature. The specimen is taken in the form of a rectangular bar with the load applied at its center to give maximum fiber stresses of 4.55 or 18.20 kPa (see below). The metal supports (rounded to a radius of mm) for the
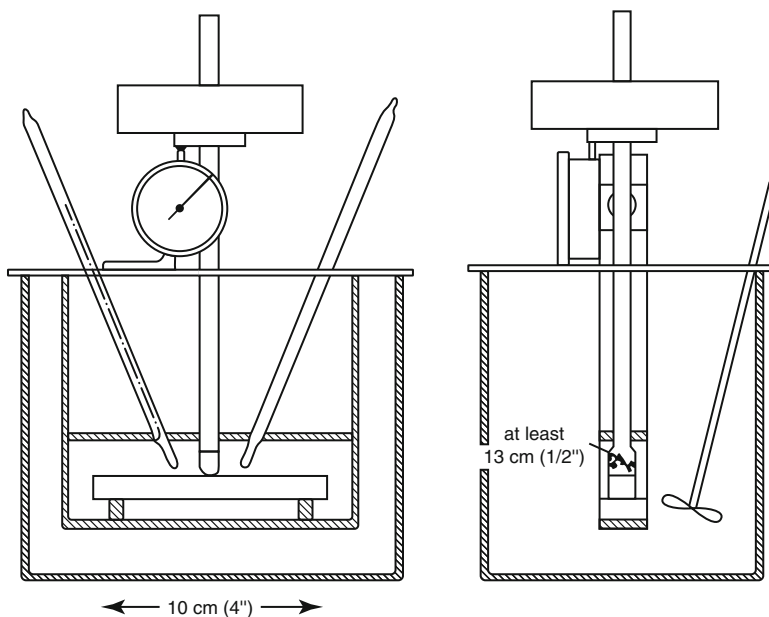
Fig. 10.52 Apparatus for heat deflection temperature test [ASTM D648]

specimen are provided 100 mm apart (see Fig. 10.52) allowing the load to be applied on top of the specimen vertically and midway between the supports. The specimen is immersed under load in a heat-transfer medium. The temperature is raised at 275 ± 0.2 K/min. The load applied on the specimen to obtain a maximum fiber stress of 18.20 kPa $\pm$ 2.5 % is calculated using the formula below:

$$P = \frac{2\,S\,b\,d^2}{3L} \tag{10.29}$$

where P is the load (N), S is the maximum fiber stress in the specimen (18.20 or 4.55 kPa), b is the width of specimen (m), d is the depth of specimen (m), and L (0.1) m is width of span between supports. The load of 18.20 kPa is usually used for rigid polymers (e.g., PS) while 4.55 kPa is used for softer crystalline materials that have $T_g < 298$ K (e.g., PE).

ASTM D1637 provides tensile HDT test for plastic sheets. In this test a load of 345 kPa is applied to a strip, and the temperature is increased at a rate of 2 K/min. The HDT in this case is defined as the temperature at which the elongation becomes 2 %.

ASTM D1525 provides a third type of the softening temperature test. A flat-ended needle of 1 mm circular cross section is pressed into a thick sheet of the polymer with a load of 1.0 kg. The polymer is heated at a rate of either 50 or 120 K/h. The Vicat softening temperature, which is explained in detail below, in Sect. 10.5.5, is the temperature at which the needle has penetrated the polymer to a depth of

Fig. 10.53 Variation of heat deflection temperature with PC/ABS blend composition (curves 1 and 2 are obtained with loads 4.6 and 18.2 kg.f/cm^2, respectively)
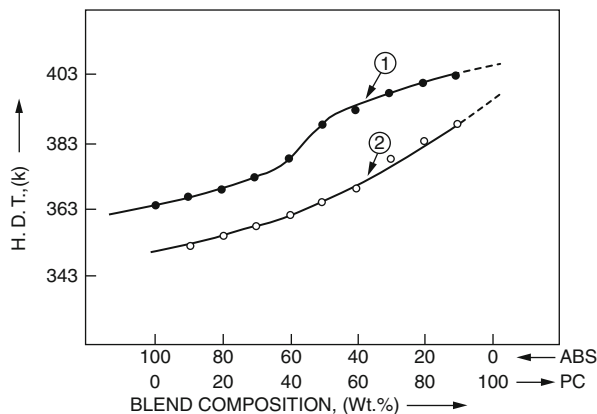
Table 10.17 Variation of HDT with talc concentration in PPCP-EPDM blend (Xavier et al. 1994)

Blend composition	Talc (wt%)	HDT (K)
Neat PPCP	0	353
PPCP + EPDM (10 wt%)	8	355
PPCP + EPDM (10 wt%)	10	356
PPCP + EPDM (10 wt%)	12	359
PPCP + EPDM (10 wt%)	15	360

1 mm. For such a depth of penetration, the material must be very soft; hence, the Vicat softening temperature is higher than other HDT data.

Heat deflection temperature is influenced by (i) blend composition, (ii) fillers/reinforcing agents, (iii) annealing, and (iv) applied stress:

- HDT of a blend is influenced by its composition. Figure 10.53 shows variation of HDT (measured according to ASTM D648) with PC/ABS blend composition (Xavier and Pendyala unpublished). The observed variation is caused by changes in flexural modulus, which is also shown.
- Inorganic fillers (e.g., talc, mica, or CaCO$_3$) or reinforcements (e.g., glass or carbon fibers) increase HDT of neat polymers or blends (Nielsen 1974; Xavier and Sharma 1986). Table 10.17 illustrates the influence of talc concentration on HDT for a blend.
- Annealing of a crystalline polymer, either neat or in a blend, increases the degree of crystallinity, changes the crystallite morphology, and relieves built-in stresses in the amorphous phase. Table 10.18 shows the gradual increase of HDT with annealing time. Flexural modulus also increases. Similar effects were reported for amorphous polymers such as PS (Nielsen 1974).
- Polymer HDT decreases with applied stress. The major cause of this effect is the decrease of modulus with temperature with the consequent greater deformation at the higher temperature for a given load. HDT occurs, by definition, at

Table 10.18 Effect of annealing time on HDT and flexural modulus of PPCP: EPDM (10 wt%) blend (HDT was tested at 4.55 kPa) (Sarcar 1989)

Test	Value obtained after annealing (h)		
	0	3	6
Heat deflection temperature (K)	330.0	343.0	349.4
Flexural modulus (MPa)	805.2	882.2	889.8

Table 10.19 HDT of some alloys with and without reinforcement for car body panels and bumpers (Moro et al. 1988)

No.	Blend	HDT (K); ASTM[a] tests at 455 kPa
1.	PPE/PA (NORYL GTX 900)	456
2.	PBT/Elastomer	348
3.	PBT/Elastomer, Glass Reinforced	421
4.	PP/Elastomer	333
5.	PP/Elastomer, Glass Reinforced	403
6.	PC/PBT	393

[a]ASTM D648-01; see: http://enterprise.astm.org/

a constant deformation. The deformation is proportional to the load and inversely proportional to the modulus. HDT values of some commercial polymer alloys are given in Table 10.19.

10.5.5 Vicat Softening Point

The effect of temperature on the mechanical properties of plastic materials has a fundamental role in the selection of materials. Unlike metals and ceramics, plastics are extremely sensitive to the slightest changes in temperature. The selection of plastics for applications under different temperatures is a complex task. The plastic material must be able to support a stress under operating conditions without getting distorted. The effect of temperature on geometrical stability and mechanical properties in general can be studied following different procedures and methods like at constant temperature or with a temperature ramp.

The Vicat softening temperature (VST) is standardized in ISO 306 and ASTM D 1525. It is very useful as a quality control or development tool (ASTM D1525-2009). (This test method is technically equivalent to ISO 306:1987(E)). The result is a measure of the temperature at which thermoplastics begin to rapidly soften. VST describes the temperature at which a circular indenter with a cross section of 1 mm^2 under a standardized loading of 10 N or 50 N penetrates exactly 1 mm into the specimen. VST was introduced to measurement technology as a substitute value for melting point. VST for some common polymers are presented in Table 10.20.

The apparatus for testing VST consists of a temperature regulated oil bath with a flat-ended needle penetrator so mounted as to register degree of penetration on

Table 10.20 Vicat softening temperatures for some common polymers

	(1 kg load)
Plastics	Measured value (K)
PS	375.5
ABS	375.3
PVC	365.0
PC	429.2
PE	400.3
PP	425.2

Source: Report by Japan Society for Testing Plastics (1972)

Table 10.21 Four different methods used for testing VST

	Load (N)	Heating Rate (K/h)
A50	10	50
B50	50	50
A120	10	120
B120	50	120

a gauge. A specimen is placed with the needle resting on it. The temperature of the bath (preheated to about 323 K lower than anticipated Vicat softening point) is raised at the rate of 323.0 K/h. or 393.0 K/h. The temperature at which the needle penetrates 1 mm is the Vicat softening point. For the Vicat A test, a load of 10 N is used. For the Vicat B test, the load is 50 N. The test conditions are summarized above in Table 10.21.

The test specimen must be between 3 and 6.5 mm thick and at least 10 mm in width and length. No more than three layers may be stacked to achieve minimum thickness.

Traditionally silicone oil has been the most popular medium for performing HDT and VST tests on polymers. They can be used safely only up to a maximum temperature of 553 K.

An alternative medium is required to test high-temperature polymers, such as PEEK, PEI, etc., as they have HDTs and VSTs higher than the temperature at which silicone oil can be used. "CEAST HV500," which utilizes an aluminum oxide fluidized bath, is used to perform a range of HDT and VST tests for both high- and low-temperature applications. Engaging "CEAST HV500" different grades of PEEK, PS, PC, PA, and PPS incorporated with 40 % glass fillers and PP with 15 % glass fillers were tested, at temperature ramps of 323 K/h and 393 K/h:

- VST is a measure of how much a plastic material would soften with increasing temperature. The higher the VST, the higher the temperature necessary for lamination and higher is the service temperature.
- Standard PVC card films (homopolymer) have a VST of 349 K. To achieve high VST values, special blends of PVC/ABS card films (0.25–0.8 mm thick) are engaged. High-VST (364 ± 2 K) cards are required in environments with high temperatures and stress. Applications include SIM (GSM) cards and pay TV cards.
- Apart from its practical applicability, VST is also used in studying the "miscibility" of polymer blends. Miscibility of PVC/PMMA blends was studied by determining

Table 10.22   Glass transition temperatures of some common polymers

Polymer family	Glass transition temperature	
	(°C) (Approx.)	(K) (Approx.)
PCTFE	120–215	393–488
PTFE	130	403
PS	100	373
PMMA	100	373
PVC	90	363
PET	70	343
PA(nylon)	50	323
ROOM TEMP.	20	293
POM	−15	258
PP	−20	253
PVDF	−45	228
PE-LD	−120 to −100	153–173

the VST of blends. The plot of VST against composition exhibited a continuous curve which revealed miscibility of the blend. This was further confirmed from the study of viscometry, DSC, and FTIR analysis of the blends (Kamira and Naima 2006).

- α-Methylstyrene-acrylonitrile copolymers (AMSAN) are highly compatible with PVC and have a high glass transition temperature. Trials with proportions of AMSAN in the blend confirmed that the Vicat temperature of the blends can be raised by adding this copolymer. For every 10 % by weight of AMSAN added, the Vicat temperature increased by approximately 4 °C (Gottschalk 2006).

10.5.6   Low-Temperature Brittle Point

For most materials low temperatures present a challenging environment and plastics are no exception. Most polymers at room temperature show their familiar properties of flexibility (a low Young's modulus) and high resistance to cracking, but when the temperature decreases, this can change rapidly and many common polymers become brittle with low failure stresses. Low temperatures can be more harmful to plastics than high temperatures. Catastrophic failures can occur if materials selection does not take account of the low-temperature properties of plastics.

Brittle fracture takes place by rapid crack propagation. For most brittle crystalline materials, crack propagation corresponds to the successive and repeated breaking of atomic bonds along specific crystallographic planes, known as cleavage. Cleavage is essentially a low-temperature phenomenon, which can be eliminated if a sufficiently high deformation temperature is used.

The actual value of glass transition temperature (T_g) for real polymers will vary greatly with the specific molecular structure of the base polymer, the molecular weight and the molecular weight distribution of the polymer, the additives incorporated into the mix, and a variety of other factors. Table 10.22 above gives some

typical values of T_g for some common polymers (but these should be regarded as indicative rather than definitive). Polymers that have a T_g greater than room temperature are in glassy state at room temperature, and examples of these are plastics such as PS, PMMA, and PET. These polymers tend to be brittle and easy to break at room temperature. PVC is in the glassy state at room temperature but is a special case because it can be easily modified to be rubbery by the addition of plasticizers (Zeus 2005).

The brittle point test developed by the Bell Telephone Laboratories is simple and sensitive. It is believed that this test may be used to study all cold-resistance problems where damage to the rubber itself and not increase in stiffness is the first consideration.

The "slow-bend brittle point test" does not have the same practical significance as the Bell Telephone Laboratories' brittle point test because most rubber articles which are exposed to low temperatures in service are required to withstand fairly rapid flexing. If the slow-bend brittle point test were used as a criterion of the cold resistance of these rubber articles, it might qualify the rubbers for a lower temperature than they could safely withstand in service (Morris et al. 1944).

ASTM D746-07 describes the Standard Test Method for Brittleness Temperature of Plastics and Elastomers by Impact. It employs three types of specimens. In this method the brittleness temperature is determined by immersing the specimens in a bath containing a heat transfer that is cooled, usually by liquid nitrogen, carbon dioxide, or powdered dry ice, to a predetermined temperature for a period of three minutes. The specimens are then impacted by a device having a striker of a specific geometry, under defined conditions of velocity, distance, and energy. The test temperatures are varied over a range and the brittleness point is defined as that at which 50 % of the specimens fail. This test provides for the evaluation of long term effects, such as crystallization, or the incompatibility of plasticizers incorporated in the material when subjected to subnormal temperatures (ASTM D746-07). This test, however, does not, necessarily, determine the lowest temperature at which the subject material may be used. The results may be used to predict the behavior of plastic and elastomeric materials at low temperatures.

ASTM D1329-08 offers Standard Test Method for Evaluating Rubber Property–Retraction at Lower Temperatures (TR Test). The other related Methods for Temperature Retraction (TR) Test are ISO 2921, BS 903-A29 (UK), and NF T4NF T46-032 (France). This test method describes a temperature-retraction procedure for rapid evaluation of crystallization effects and for comparing viscoelastic properties of rubber and rubberlike materials at low temperatures. This test method is useful when employed in conjunction with other low-temperature tests for selection of materials suitable for low-temperature service (ASTM D1329-08). This is more commonly known as a TR-10; this temperature-retraction test is considered by many within the rubber industry to be the most useful indicator of a material's low-temperature performance. In a nutshell, the TR-10 measures material resilience. Samples are frozen in a stretched state and then gradually warmed until they lose 10 % of this stretch (i.e., retract by 10 %). The results of such tests are believed to provide a good basis for evaluating the effects of crystallization and the impact of low

temperatures on viscoelastic properties. TR-10 results are generally thought to be consistent with the capabilities of most dynamic seals. Static seals can often function at 15 °F/8 °C/281 K below the TR-10 temperature (Hudson 2011).

ASTM D2137-11 provides Standard Test Methods for Rubber Property – Brittleness Point of Flexible Polymers and Coated Fabrics. Related Methods for Brittleness Point Test are ISO 812, DIN ISO 812 (Germany), and BS 903-A25 (UK). These test methods cover the determination of the lowest temperature at which rubber vulcanizates and rubber-coated fabrics will not exhibit fractures or coating cracks when subjected to specified impact conditions (ASTM D2137-11).

Unlike the changes that result from exposure to high temperatures, changes brought about by low-temperature exposure are generally not permanent and can often be reversed once heat returns. For example, extended exposure to low temperatures will increase an elastomer's hardness, but the material will soften again when the temperature rises. Perhaps the most important consideration related to low temperatures involves seals which must also work in a low-pressure environment. Unless the selected seal compound is sufficiently soft and resilient, the combination of low temperature and low service pressure can cause leakage and failure (Hudson 2011).

The brittle–ductile transition temperatures of some commercial polymers, blends, and composites are given in Table 10.23.

10.5.7 Melt and Crystallization Parameters (Using DSC)

Differential scanning calorimeter (DSC) can be used to ascertain melting point, degree of crystallinity, and glass transition temperature or for component quantification of polymeric materials. For some materials – such as crystalline polymers and certain organic chemicals –DSC is used to measure melting points and degree of crystallinity. For amorphous polymers, rubbers, and cross-linked thermoset materials, DSC also provides a fast and accurate measure of the glass transition temperature or the degree of cure.

In a DSC experiment, when a polymer is heated, as it reaches its melting temperature (T_m), the polymer crystals begin to melt. The polymer chains come out of their ordered arrangements and begin to move around. When the polymer crystals melt, they absorb heat in order to do so. Melting is a first-order transition. This means when polymer reaches its melting point, the polymer's temperature does not rise until the crystals melt off. This also means that the furnace has to put up additional heat into polymer in order to melt both the crystals and keep the temperature rising at the same rate as that of the reference pan. This extra heat flow during melting shows up as a large dip in DSC plot as heat is absorbed by the polymer. The temperature at the apex of the peak is taken as the point where the polymer is completely melted. And the area under the peak gives the heat of melting of the polymer. As energy is added to the polymer to make it melt, melting is considered as an endothermic transition (Daniels 1973; Turi 1981).

An understanding of the degree of crystallinity for a polymer is important since crystallinity affects physical properties such as storage modulus, density,

Table 10.23 Low-temperature brittle point of some rubbers (Lindsay 2010)

Properties	Ethylene propylene diene	Nitrile rubber	Poly-chloroprene	Natural rubber	Poly-isoprene	Styrene butadiene rubber	Butyl rubber	Polybutadiene
	EPDM	NBR	CR	NR	IR	SBR	IIR	BR
Tensile strength max, psi (MPa)	2,000 (13.8)	2,500 (17.3)	2,500 (17.3)	3,500 (24.1)	3,000 (20.7)	2,500 (17.3)	2,000 (13.8)	2,000 (13.8)
Low-Temperature brittle point, K	215	222	219	215	215	215	215	200

permeability, and melting point. And melting point in turn influences the processing temperature. While most of these manifestations of crystallinity can be measured, a direct measure of degree of crystallinity provides a fundamental property from which these other physical properties can be predicted.

Polymer crystallinity can be determined with DSC by quantifying the heat associated with melting (fusion) of the polymer. This heat is reported as "% crystallinity" by taking ratio against the heat of fusion for a 100 % crystalline sample of the same material or more commonly by taking ratio against a polymer of known crystallinity to obtain relative values.

If ΔHf is equal to area under the melting peak, then ΔHf is proportional to % crystallinity:

$$\% \text{ Crystallinity} = \left[\frac{\Delta Hf}{\Delta H^* f}\right] \times 100 \tag{10.30}$$

where ΔH^*f is ΔHf of 100 % crystalline polymer.

In case of polyethylene, $\Delta H^*f = 68.4$ cal/g;

In case of polypropylene, $\Delta H^*f = 209.3 \pm 29.9$ J/g.

(These values of ΔH^*f are reported to be widely varying from one laboratory to another for the same polymer.)

An empirical relationship between T_g and T_m of a polymer is given as follows: $T_g/T_m \sim 0.6$

(Here, T_g and Tm are to be taken in Kelvin).

When a semicrystalline polymer, such as polypropylene, cools from melt, the polymer chains begin to form crystals at foreign particles in the melt (Wunderlich 1990). The completely solidified PP part is typically about 60 % crystalline and 40 % amorphous. These crystals exhibit a peak melting temperature (via DSC) of about 438 K. When nucleating agents are incorporated into the PP, the number of sites where crystal growth can start is dramatically increased. This means that the part will crystallize more rapidly in the mold and will also achieve a higher final level of crystallinity. The faster crystallization rate results in faster setup in the mold, and reduced cycle times, while the higher crystallinity results in increased part stiffness.

Another side benefit that accompanies with the use of certain nucleants is improved clarity. Since clarity or transparency is evidently related to the crystalline structure of the polymer and the structure is determined by the conditions of crystallization, parameters characterizing crystallization must be also connected with the optical properties of a PP product. The peak temperature of crystallization (T_c) is one of the quantities often used for the characterization of the crystallization process and efficiency of nucleating agents. With increased crystallization temperature, the thickness of the lamellae increases well. Higher efficiency and concentration of nucleating agent lead to an increase of T_c (as determined by DSC) and decrease of the size of the spherulites.

Figure 10.54a and b illustrate the shift in T_c for polypropylene homopolymer with the addition of a nucleating agent.
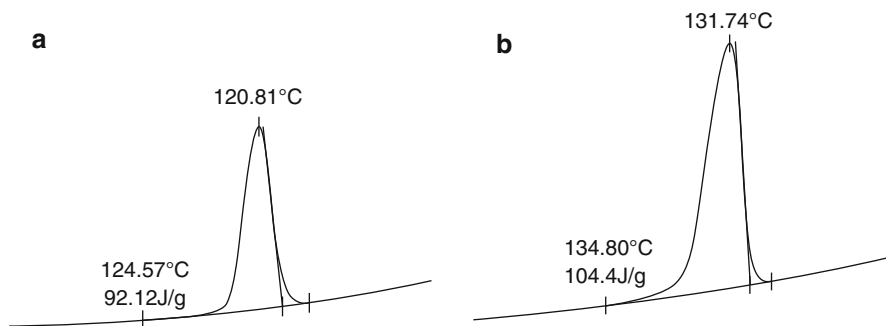
Fig. 10.54 Crystallization exotherm for (**a**) neat PP homopolymer and (**b**) PP with nucleating agent (Xavier 2002)

10.5.7.1 Crystallization of Polypropylene Homopolymer (PPHP)
Influence of Nucleating Agent, Millad-3988

Semicrystalline polymers, such as PPHP, display different microstructural features due to the factors like (i) the presence of various additives (Kopp et al. 1994), (ii) depending upon their processing history (Lotz 2003), and (iii) strain in solid (Butler and Donald 1997) as well as melt (Pople et al. 1999) phases. Many methods are being applied to modify the polymers in order to attain high-performance properties. Properties modification by incorporation of additives in polypropylene and its related polymers is observed to be particularly common.

In polypropylene, the crystallization results in large size spherulites, and hence inclusion of heterogeneous nucleating agents is often adopted to improve mechanical properties (Quande Gui and Weiping Zhu 2003) or to reduce optical haze (Gahleitner et al. 1996; Zhao and Dotson 2002). Hence, providing such heterogeneous nucleation is an essential consideration. Creation of various crystallographic phases, differed by the unit cells as well as by the spherulites, is known to be a result of the heterogeneous nucleation (Lotz 2003).

Nucleating efficiency is normally determined isothermally from crystallization half-time, by use of peak crystallization temperature of the nucleated system measured during cooling and compared with that of the neat polymer. The peak crystallization temperature technique is based on a single-point observation. Fillon et al. proposed alternate approach for the evaluation of nucleating efficiency using two dynamic reference points to understand the crystallization behavior of a polymer (Fillon et al. 1993). These two reference points include (i) polymer's crystallization temperature when crystallized normally and (ii) the same when polymer nucleated ideally.

In order to obtain an ideally nucleated polymer, it is heated to just above its melting point so that large number of residual crystal fragments exist in the melt and act as nuclei. This method is referred to as self-seeding or self-nucleation (Blundell 1966). Zhao et al. have evaluated crystallization behavior of propylene/ethylene copolymer by self-seeding approach (Zhao et al. 2001), which was found in good agreement with the earlier published DSC data (Laihonen et al. 1970, 1997).

Millad-3988 is a breakthrough "clarifying agent" for PP. Use of this additive in properly formulated and processed PP gives improved transparency, increased resin throughput, productivity gains, and enhanced physical properties.

DSC investigations were carried out (Fig. 10.55) using PPHP granules as well as fast cooled compression-molded sheets with three different concentrations of Millad-3988 (0.07, 0.14, and 0.21 wt%) in order to see whether the molding conditions would play a role and thus influence the DSC data in comparison to the data obtained using plant supplied granules. The properties of PPHP with different concentrations of Millad-3988 are shown in Table 10.24. From the Table 10.24, it is clear that T_m values for sections cut from the sheets were always less than their corresponding values obtained using granules. In fact, T_c also showed the same trend. The difference between T_m and T_c (i.e., $T_m - T_c$) gradually reduced with increasing concentration of Millad-3988. This behavior is more systematic in case of the sheets. However, T_{onset} which indicates the crystallization "onset" is found to be gradually enhanced with Millad-3988 concentration. The degree of crystallinity, as determined by X-ray diffraction, also gradually increased with increasing concentration of Millad-3988.

The crystallinity (%) of PPHP increases with increasing Millad-3988 concentration, which also influences the surface gloss of polymer sheets to increase (as observed in Haze meter measurements, not presented here). However, the transmission (%) (as measured by the Haze meter) does not undergo the same pattern of change. In fact the transmission (%) was found to be maximum for PPHP sheet with Millad-3988 concentration 0.07 wt% followed by the one with 0.14 and 0.21 wt%. It is interesting to note that the transmission (%) for neat PPHP (87.1 %) is not much different from that with maximum transmission (88.6 %) with Millad-3988 of 0.07 wt%.

10.5.8 Oxidative Induction Time

Oxidative induction time (OIT) provides an index useful in comparing the relative resistance to oxidation of a variety of hydrocarbon materials. The OIT procedure was first developed in 1975 by Gilroy and coworkers at Bell Laboratory as a test procedure to screen polyethylene insulation used in telephone wire and cable for its oxidation resistance. The method first became available as a Western Electric Specification and later as ASTM Test Method for Copper-Induced Oxidative Induction Time of Polyolefins. Polyolefin manufacturers quickly embraced the procedure and began to apply it to other applications including raw resins, finished pipes, wire and cable insulation, and, most recently, geosynthetic waste pit liners (ASTM D3895 2009).

The test consists of heating a specimen to an elevated temperature (often 200 °C) in a DSC. Once temperature equilibrium is established, the specimen atmosphere is changed from inert nitrogen to oxidizing air or oxygen. The time from first oxygen exposure until the onset of oxidation is taken as the OIT value. This general procedure is applied, for example, to polyethylene wire insulation, edible oils, lubricating oils and greases, and geosynthetic barriers. Most materials are tested to measure the
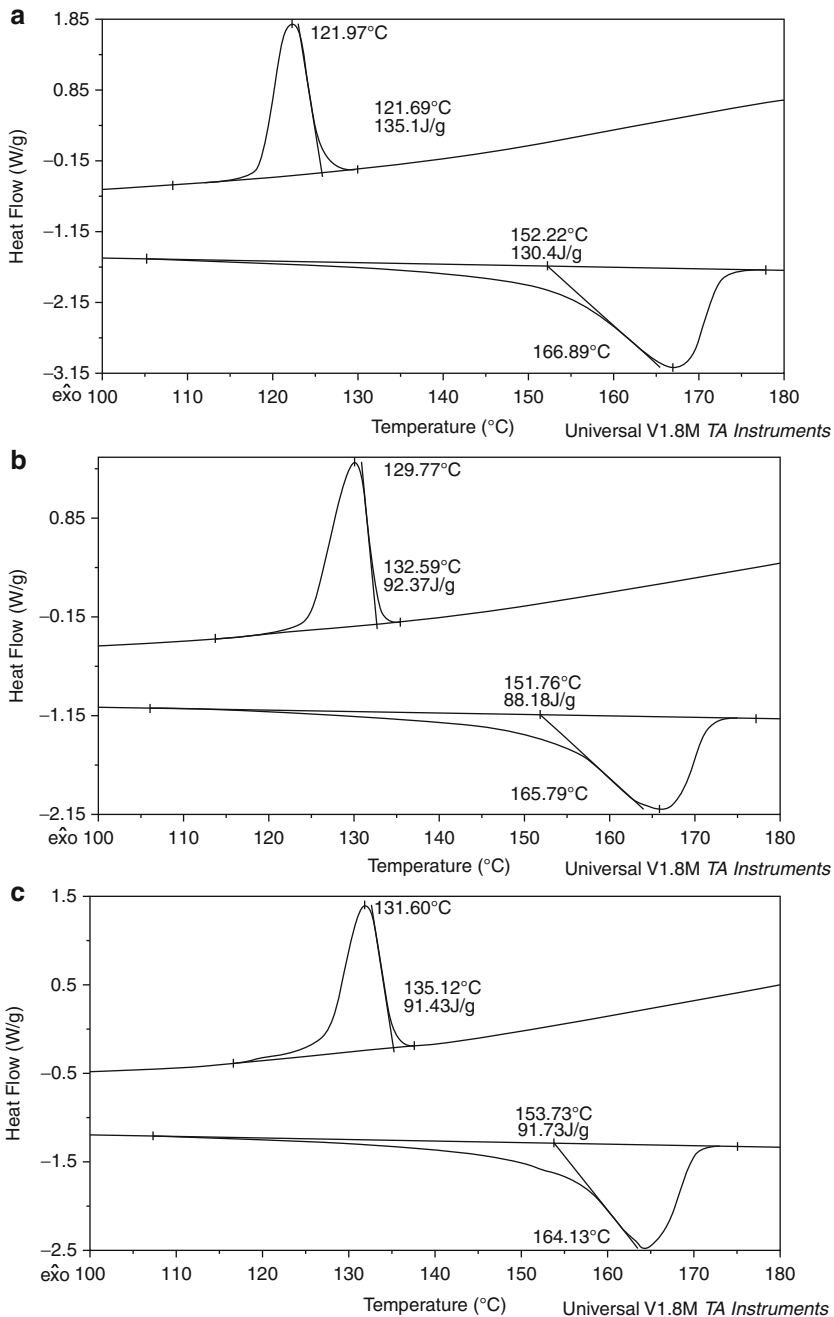
Fig. 10.55 DSC thermograms of PPHP + Millad-3988 at different concentrations (**a**) 0.07 wt%, (**b**) 0.14 wt%, and (**c**) 0.21 wt%, carried out using sections cut from ∼0.7 mm thick, fast cooled, compression-molded sheets (Pendyala et al. 2004)

Table 10.24 Properties of polypropylene homopolymer in presence of Millad-3988 (Pendyala et al. 2004)

	PPHP		PPHP + Millad (0.07 %)		PPHP + Millad (0.14 %)		PPHP + Millad (0.21 %)	
	granule	sheet	granule	sheet	granule	sheet	granule	sheet
Melting temp.* (Tm) °C	169.25	167.49	167.30	166.89	167.29	165.79	168.63	164.13
Cryst. temp.* (Tc) °C	120.81	122.11	123.76	121.97	130.59	129.77	131.74	131.60
$(T_m–T_c)$ (°C)	48.44	45.38	43.54	44.92	36.70	36.02	36.89	33.53
T_{onset} (°C)	124.57	125.70	129.75	125.69	136.16	132.59	137.39	135.12
Deg. of cryst.** (%)	–	38.20	–	38.60	–	39.90	–	40.60
Transmission*** (%)	–	87.10	–	88.60	–	88.35	–	86.50

* Tm and Tc were determined from DSC experiments.
** Degree of crystallinity was obtained from X-ray diffractions.
*** Transmission studies were carried out on Haze meter.

effectiveness of the antioxidant package added to improve lifetime, although a few materials (e.g., edible oils) are tested in their natural, non-fortified state.

The onset of oxidation is taken as the endpoint for the OIT measurement. Two means of determining the oxidation onset are in use (Blaine et al. 1997). The most common is the "extrapolated onset" in which the tangents are drawn at the point of maximum rate of oxidation and the baseline prior to oxidation (say 0.05 W/g). The endpoint for the OIT determination is taken at the point where the exothermic event crosses that threshold. If the oxidation exotherm is sharp, these two endpoint indicators produce similar results as seen in Fig. 10.56. However, some materials seem to have a multistaged oxidation, and the endpoint established by the two experimental procedures may be quite different as shown in Fig. 10.57 (Blaine et al. 1997). The selection of the method of determination of the OIT endpoint is the first parameter affecting the comparison of results from one laboratory to another. Apart from this, OIT values are influenced by temperature, oxygen flow rate, oxygen pressure, catalysts (sample pan materials), sample mass and form, and time, which will be discussed below.

10.5.8.1 Parameters Influencing OIT

OIT has been proved to be a useful diagnostic tool in assessing the extent of degradation in the polymer insulation of electric cables. Sample preparation and test conditions are parameters recognized to influence OIT results obtained by DSC. However, quantitative results on the variability of OIT as a function of these parameters have not been presented systematically in the literature.

Factors that influence OIT include test temperature, sample preparation, sample geometry, sample mass, particle size, thermogram interpretation, shelf life, heating rates to reach the isotherm, and oxygen flow. The influence of these parameters was investigated using a two level factorial design using HDPE samples (Rosa et al. 2000). Sample shape, amount of sample, and heating rate were the parameters that showed significant variability.

Fig. 10.56 Single stage
oxidation endpoint
determination (Xavier 2002)
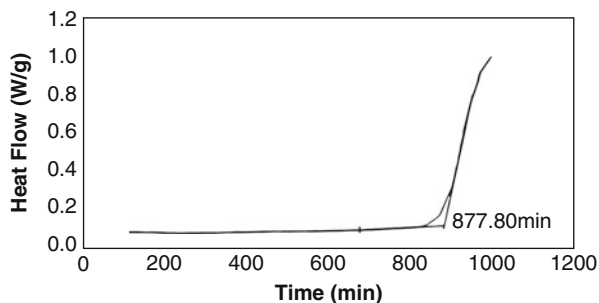
Fig. 10.57 Multistage
oxidation endpoint
determination (Xavier 2002)
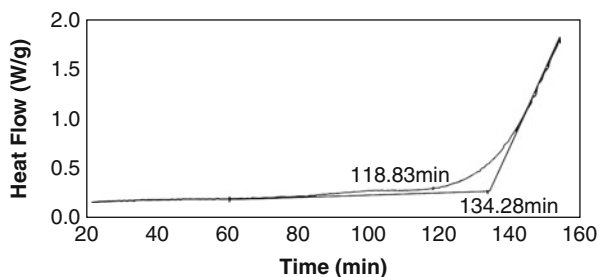
The effects of these parameters and cross-linking in polymer cable insulations, aged in radiation and thermal environments, were investigated. The results were then used to recommend standards for an OIT methodology suited for practical use, including the nuclear power industry. Techniques to estimate error in (O.I.T.) thermograms interpretation and reproducibility were also developed (Mason and Reynolds 1997).

A HDPE film, lightly stabilized with Irganox 1010 and a hindered phenol antioxidant, was proposed as a Standard Reference Material for OIT testing by Blain and Harris of TA Instruments, Inc. The mean OIT values, derived from nine interlaboratory studies and for a number of experimental conditions, were presented (Blaine et al. 1997). The material was found to be statistically homogeneous, a necessary condition for a reference material. The effects of temperature, oxygen pressure, and storage time on the proposed reference material were also explored. As a kinetic parameter, the OIT value appeared to be decreasing with time but in a well behaved and predictable manner. Because the material had been thoroughly tested in a wide variety of OIT conditions, it appeared to be the best available candidate and was offered for consideration as an OIT Reference Material (Blaine et al. 1997).

Oxidation is generally recognized as the key degradation mechanism regarding the long-term durability of HDPE geomembranes. For protection against oxidation during their service lifetime, antioxidants are added. A laboratory accelerated

aging program was conducted to assess the depletion of antioxidant from a Korean HDPE geomembrane subjected to air oven aging followed by incubation in acidic and alkaline buffer solutions at three different temperatures. The changes in OIT were monitored at selected time intervals. The results indicated that for samples subjected to oven aging incubation for 90 days, the OIT results showed that the geomembrane had enough antioxidants to ensure long-term oxidation stability. Immersion in the alkaline buffer solution was found to accelerate the antioxidant depletion rate relative to that observed in the acidic buffer solution. Greater depletion rates were recorded at higher temperature, indicating the temperature dependency of the depletion process. Conservative values of the depletion time ranged from 107 to 9 years depending on temperature and exposure condition. The estimated antioxidant depletion times were longest for exposure to acidic solutions and shortest for exposure to alkaline solutions (Jeon et al. 2008). These studies support the idea to use HDPE as a reference material for studying O.I.T.

10.5.8.2 O.I.T and O.O.T

Two different methods of studying O.I.T. are used in practice: dynamic and isothermal tests. In the dynamic technique, the sample is heated at a defined constant heating rate under oxidizing conditions until the reaction begins. The Oxidation Induction Temperature (O.I.T.) (also called Oxidation Onset Temperature (O.O.T.)) is the same as the extrapolated onset temperature of the exothermal DSC effect which occurs. In isothermal tests, the materials to be investigated are first heated under a protective gas and then held at a constant temperature for several minutes to establish equilibrium and subsequently exposed to an atmosphere of oxygen (or air). The time span from the first contact with oxygen until the beginning of oxidation is called the Oxidation Induction Time (OIT) (NETZSCH).

The procedure for the preparation, implementation, and evaluation of measurements is described in detail in national and international standards such as ASTM D3895 (polyethylene), DIN EN 728 (plastic pipelines), or ISO 11357-6 (plastics). Generally, either open crucibles or crucibles with multiple piercings in the lids are used. For polyolefins like PE or PP, a longer OIT allows one to conclude that the oxidation stability is better and the lifetime therefore longer.

10.5.8.3 OIT Measurements Using TGA

The measurement of OIT based on TGA was used for monitoring the re-stabilization of post-use LDPE samples, subjected to multiple extrusion cycles. This method has abilities and limitations as well which are discussed in literature (Kyriakou et al. 1999). The use of a re-stabilization system improved the oxidative stability of LDPE. A linear calibration curve correlating OIT values to the amount of re-stabilization system was obtained. Nevertheless, limitations concerning quantitative determinations appeared to exist, as a change in the behavior of re-stabilization system during subsequent re-melting cycles was observed.

10.5.8.4 TOIT: A New Method

OIT's oxidation condition is considered as very harsh especially in case of pure and irradiated polymers, particularly PP. PP undergoes pronounced molecular weight degradation in the course of processing and is prone to very fast oxidation and consequently very fast degradation, especially on samples submitted to previous aging and irradiation.

Lugao and his group had introduced a new procedure to determine OIT in non-stabilized, stabilized, irradiated, and nonirradiated PP. The new procedure was based on two main features: (1) starting the oxidation on melted samples at temperatures as low as possible and (2) oxidation under slow heating conditions. Since each sample has a set of two values of time and temperature, it is called as "temperature-dependent oxidative induction time." This new method is found to be reproducible, sensitive (to small changes in additive compositions), simple, and inexpensive (Lugao et al. 2002).

10.5.8.5 High Pressure OIT

A series of high pressure oxidative induction time measurements (HPOIT) were conducted on a PE geomembrane sheet in order to investigate the interaction of the pressure and temperature variables on the induction time. The experiments consisted of determining the HPOIT at constant cell volume employing a wide operational range of pressure and temperature values. The HPOIT test results were found to be inversely related to both variables, with temperature being the predominant factor (Tikuisis et al. 1985).

10.5.9 Thermal Degradation (Using TGA)

Thermogravimetry (or thermogravimetic analysis, TGA) is one of the oldest thermo-analytical procedures and has been used extensively in the study of polymeric systems. The technique involves monitoring the weight loss of the sample in a chosen atmosphere (usually nitrogen or air) as a function of temperature. It is a popular technique for the evaluation of the thermal decomposition kinetics of polymeric materials and hence provides information on thermal stability and shelf life. However, it is well known for its ability to provide information on the bulk composition of polymer compounds.

In the analysis of polymer compounds, the sample is initially heated in a nitrogen atmosphere. Heating under nitrogen ensures that no oxidation reactions take place. Additives are lost first, in order of decreasing volatility, and then the polymer fraction will undergo thermal degradation and volatilizes off. Once the entire polymer has thermally degraded, the species remaining in the TGA pan (which can include, carbon black, inorganic fillers and carbonaceous residue from the breakdown of the polymer) can be examined. This is achieved by changing the atmosphere to air and heating to around 1,273 K. Weight loss events can be
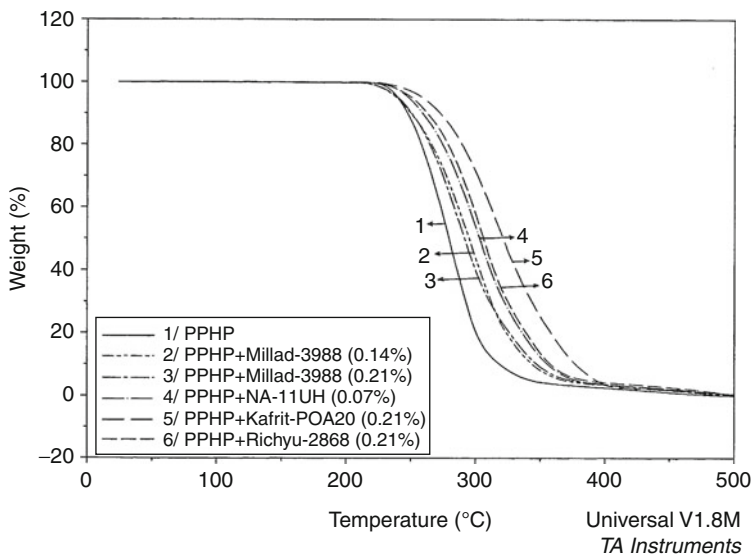
Fig. 10.58 TGA thermograms of ~0.7 mm thick compression-molded specimens of neat PPHP and its compositions with different nucleating agents carried out at a heating rate of 10 K/min in static air (Pendyala et al. 2004)

observed for the oxidation of carbonaceous residues and carbon black and the decomposition of inorganic fillers, such as calcium carbonate. At the end of the analysis an amount of stable inorganic residue will remain. This procedure will enable the amount of plasticizers, polymer, carbon black, and inorganic species to be quantified to an accuracy of at least ~0.5 %.

Although certain additives can be quantified by techniques such as solvent extraction and dry ashing, the advantage of TGA is that only 5–10 mg of sample is required. In recent years the benefits of coupling TGA instruments to either an infrared spectrometer or a mass spectrometer have been appreciated. This enables both qualitative and quantitative data to be obtained in a single analytical experiment. Here, how TGA can be used to evaluate different commercial nucleating agents by studying the thermal stability imparted to the polymer is illustrated below.

10.5.9.1 Thermal Degradation of Polypropylene Homopolymer (PPHP)

TGA of PPHP with and without commercial nucleating agents (Millad-3988 and three other selected nucleating agents) is shown as overlay in Fig. 10.58 and thermal characteristics are shown in Table 10.25. The thermal stability of a polymer is, generally, influenced by various factors such as bond strength, activation energy, cross-linking, presence of low molecular weight/volatile material and weak links, etc.

Table 10.25 Thermal characteristics of PPHP[a] and its compositions with different commercial nucleating agents (Pendyala et al. 2004)

	Composition	Decomposition temp. at K		T_{onset}		$T_{inflection}$	
		10 wt% loss	50 wt% loss	°C	K	°C	K
1	PPHP	247.00	288.20	219.96	492.96	279.01	552.01
2	PPHP + Millad-3988 (0.14 %)	249.70	309.92	213.43	486.43	297.68	570.68
3	PPHP + Millad-3988 (0.21 %)	250.10	303.24	215.00	488.00	297.68	570.68
4	PPHP + NA-11UH (0.07 %)	258.80	304.28	222.66	495.66	301.46	574.46
5	PPHP + Richyu-2868 (0.21 %)	262.60	297.40	221.28	494.28	276.09	549.09
6	PPHP + Kafrit-POA20 (0.21 %)	272.50	311.38	222.73	495.73	312.62	585.62

[a] ∼0.7 mm thick compression-molded sheets were used for analysis

The factors influencing thermal stability are to be considered prior to its evaluation. It is observed that the polymer may retain its "usefulness" when half of its strength is retained after one hour of exposure to a specified temperature and that the limit is reached with a weight loss of 10 wt% (Eirich and Mark 1961). This limit is based on many assumptions and it varies with the polymer. Polymer material's decomposition criterion is established by recording the temperatures: (a) at 10 % and 50 % decompositions and (b) at the maximum rate of decomposition (Mark and Gaylord 1971).

From Table 10.25, it is found that neat PPHP indicated loss of 10 % weight at 520 K. The incorporation of Millad-3988 in PPHP, in the concentration range of 0.14–0.21 wt%, showed a marginal increase in the temperatures for 10 % weight loss (∼523 K). However, PPHP in presence of the selected commercial nucleating agents (NA-11UH 0.07 %, Richyu-2868 0.21 %, and Kafrit-POA20, 0.21 %) exhibited significant increase in the temperatures (531.80–545.50 K) for 10 % weight loss. Similarly for the 50 % weight loss, PPHP degradation temperatures are found to be enhanced in the presence of Millad-3988 as well as the other selected nucleating agents. From their thermograms shown in Fig. 10.58, it is observed that the decomposition is occurring in single stage for PPHP and a similar behavior is observed in presence of Millad-3988 as well as the other selected commercial nucleating agents.

The onset of thermal decomposition, T_{onset}, of PPHP is found to be 492.96 K (Table 10.25). With the incorporation of commercial nucleating agents, it is observed Millad-3988, in the concentration range of 0.14–0.21 %, reduced the onset temperature of PPHP (∼5–7 K) while the other selected nucleating agents enhanced it and that enhancement is higher than that offered by PPHP with the incorporation of Millad-3988. $T_{inflection}$ temperatures, at which the rate of decomposition is maximum, for PPHP incorporated with Millad-3988 (555.54–570.68 K), are found to be higher than that of neat PPHP (552.01 K); among the selected three commercial nucleating agents, PPHP incorporated with NA-11UH (574.46 K), with Richyu-2868 (549.09 K), and with Kafrit-POA20 (585.62 K) indicated significant improvement in their thermal stability except Richyu-2868. It is observed that Kafrit-POA20 offered the highest improvement of thermal stability for PPHP

among the nucleating agents tried. From the above study, the commercial nucleating agents imparting thermal stability to PPHP is in the following order (Pendyala et al. 2004):

$$Kafrit - POA20(0.21\%) > NA - 11UH(0.07\%) > Millad - 3988\ (0.21\%) >$$
$$Millad - 3988(0.14\%) > Richyu - 2868(0.21\%).$$

10.5.10 Review of Blends' Thermal Properties

Owing to the absence of electronic effects in most polymers, heat conduction occurs as a result of lattice vibrations, similar to dielectrics. It is known that the thermal conductivity of an amorphous polymer increases to T_g with increasing temperature while it decreases above T_g (Godovsky 1992). Thermal conductivity is a fundamental and important factor in processing polymer blends (Agari 1992).

Influence of miscibility on thermal conductivity and diffusivity was studied (Agari 1993, Agari and Ueda 1994). In the blend of low molecular weight PS with coumarone–indene resin, which showed miscibility over all blend compositions, the thermal conductivity was approximately linearly dependent on composition (Agari 1993). Thermal conductivity, thermal diffusivity, and heat capacity of PMMA/PC blends were studied with respect to temperature and blend composition. The specific heat capacity of the two-phase 50/50 blend was larger than that of the one-phase blend. The thermal diffusivity and the conductivity of the 50/50 blend slightly decreased with the increase of temperature up to 450–460 K (LCST) and then decreased abruptly with increase of temperature (Agari et al. 1997).

Several investigators (Krause et al. 1982; Schultz and Young 1983; Rodriguez-Parada and Percec 1986) had used the specific heat increment (ΔC_p) to investigate the polymer–polymer miscibility by DSC.

The effect of molecular weight of PMMA on the miscibility of PMMA/PS blends was examined by studying the specific heat increment ΔC_p at T_g (Burns and Kim 1988). Using Couchman's equation, C_p for PMMA was calculated and was found to decrease with the composition of PS (Couchman 1978). The C_p for PS similarly decreased with PMMA composition. From these results the authors inferred that some of the PMMA dissolved in the PS phase and vice versa. Thus, the blends were found to be partially miscible. This result was found to be consistent with the polymer–polymer interaction parameter values. The authors also studied the PC/SAN blends miscibility by the thermal analysis (Kim and Burns 1988). The values of the specific heat increment ΔC_p at T_g for PC and SAN in PC/SAN blends were measured. For PC, C_p decreased linearly with addition of SAN. For SAN, C_p also linearly decreased with addition of PC. This suggested that some of the PC dissolved in the SAN-rich phase and *vice versa*.

Thermal studies have become important tools for understanding various basic phenomena in polymer blends and composites all over the world. The changes in crystallization kinetics of polymer blends in comparison to the

parent polymers involved the way a compatibilizing polymer interferes with the crystallization kinetics, and if a reinforcing filler or fiber is introduced into the same system, how the kinetics are getting affected is more a curious situation and it is not easy to make simple predictions without conducting experiments on DSC. The thermal stability of a blend after introducing a compatibilizer needs to be elucidated.

The literature available with such studies is also vast and also several books dedicated to thermal analysis alone are appearing time to time; hence, it is not possible to really justify such a presentation here. Nevertheless, some illustrative examples of such studies are given here in Table 10.26. The reader is advised to go through the desired literature.

10.6   Flammability

10.6.1 Standard Methods of Measurement

There are two types of tests, viz., burning and combustion toxicology tests. The burning tests aim at determining either the burning characteristics or the burning rate. The combustion toxicology tests aim at measuring the types and quantities of toxic gases that evolve during burning and smoldering of plastics and their effects on men and animals. A list of ASTM tests, the specimens, the purpose of each test, etc., is provided in Table 10.27.

Underwriters Laboratories (UL) provide Standards UL 94 Tests for Flammability of Plastic Materials for Parts in Devices and Appliances. The standard is important for classifying polymeric materials (including polymer blends and alloys) for the use in electrical applications. It is widely used and the results are reported in the literature and in company catalogues. However, the requirements are not applicable to polymeric materials used in building construction or finishing. The tests conducted under this standard are summarized below.

10.6.1.1 Horizontal Burning Test for Classifying Materials: 94 HB
The test uses small bar specimens: 127×12.7 mm. It is similar to ASTM D635. Materials classified under this test shall not have a burning rate exceeding either 38 or 75 mm/min over a 75 mm span, for specimen's thickness of, respectively, 12.7 or 3 mm. The materials must cease burning before reaching the 100 mm mark.

10.6.1.2 Vertical Burning Test for Classifying Materials: 94 V-0, V-1, V-2
The test specimen (127×12.7 mm, with maximum thickness 12.7 mm) is supported vertically by its upper end and is ignited at its lower end for 10 s by Bunsen/Tirril burner, in a draft-free area (see Fig. 10.59). If flaming or glowing combustion stops within 30 s after removal of the flame, the specimen is re-ignited for 10 s. The duration of the flame is again noted. In case the specimen drips flaming particles, they are allowed to fall into a layer of surgical cotton 0.3 m below the sample. The particles are considered significant if the cotton ignites.

Table 10.26 Sources for thermal properties data of polymer blends: examples

Blend	Test	Results	References
HDPE/NA6 with compatibilizers (i) KRATON FG1901X and (ii) KRATON FG1921X	Thermal analysis (DSC), heats of crystallization,	Compatibilizers changed the crystallization kinetics, softened NA6 phase and enhanced impact strength	Chandramouli and Jabarin 1995
PPCP blends with commercial elastomers/plastomers (EXACT 5371, ENR 7370, ENGAGE 8150, VERSIFY 2300, NORDEL IP 4760P, NORDEL IP 4770P, Chemtura EPDM IM 7565)	DSC, Delta heat of fusion, delta heat of crystallization, T_m, T_c	Charpy impact strength (notched) raised up to 70 kJ/m^2 in case of Engage-8150, Nordel-4760, Nordel-4770, and Chemtura EPDM IM 7565	Xavier 2008
LDPE/DCP	DSC, isothermal studies	Peroxide cross-linking reaction with LDPE studied	Ghasemi et al. 2005
PLLA/PDLLA biodegradable blends	DSC, Glass transition temperature, thermal degradation of blends, TGA	Miscibility of Poly-l-lactic acid (PLLA) and Poly-dl-lactic acid (PDLLA) was studied using DSC and thermal stability using TGA were studied.	Chen et al. 2003
Blends of corn starch with poly(ε-caprolactone), CA, PLA and ethylene-vinyl alcohol copolymer	DSC and TGA	Three degradation mechanisms were identified in the blends	Mano et al. 2003
LDPE/PA6 blends with ethylene-methacrylic acid copolymer Na salt ionomer as compatibilizer	Thermal stability of blends using TGA	TGA measurements demonstrated an improvement in thermal stability when ionomer was added	Lahor et al. 2004
Compatibilized LDPE/PA6 blends	Thermal stability of blends using TGA	Thermal stability of blends increases in the presence of Escor 5001	Yordanov and Minkova 2003
LDPE/PA6 blends using two different compatibilizers	Isothermal crystallization using DSC	Relative evaluation of compatibilizers used	Minkova et al. 2002
HDPE/PA6 blends with HDPE-g-MAH as a compatibilizer	Thermal properties were studied using TGA and DSC	Thermal behavior of in situ compatibilized blends was studied using TGA and DSC	Hsu et al. 2001
PA6/LDPE blends compatibilized using maleated hydrolyzed ethylene-vinyl acetate copolymer (EVALM)	Crystallinity was studied using DSC	EVALM affected the degree of crystallinity and Tg of PA6 phase	Luo et al. 2001

(continued)

Table 10.26 (continued)

Blend	Test	Results	References
NA6/HDPE blends with LDPE-g-GMA (glycidyl methacrylate) as compatibilizer	Crystallization temperature using, and melting point measurements using DSC	Increase in crystallization temperature and a reduction in melting point of nylon phase were observed with addition of the compatibilizers	Wang et al. 1995
PP nanocomposite toughened with poly (ethylene-co-octene) using PP-g-MAH (6 wt%) as compatibilizer	Thermal stability of the rubber-toughened PP nanocomposites was studied	Thermal stability was improved significantly with the addition of small amount of organoclay	Lim et al. 2006
Kinetics of thermal and thermo-oxidative degradation of PS, PE and PP	Thermal degradation of PS, PE, and PP was studied in N_2 and air environments	Activation energies were calculated as a function of extent of degradation	Peterson et al. 2001
LDPE/EPDM and HDPE/EPDM modified with LDPE-g-MAH reinforced with jute fibers	Thermal properties	Influence of compatibilizer on the thermal and mechanical properties of the blends was studied	Sarkhel and Choudhury 2008
PTT/LCP(Vectra A950)	Thermal properties using DSC and TGA	DSC studies revealed the blends are immiscible; and TGA investigations showed that the thermal stabilities of blends were improved	Pisitsak and Magaraphan 2009
XLPE and EPDM cables	OIT measurements using DSC	Assessing the extent of degradation in the polymer insulation of electric cables in nuclear power plants	Mason and Reynolds 1997
Irradiated and nonirradiated PP	Temperature dependant OIT as a new method	A new method more suitable in case irradiated and nonirradiated PP (and other polyolefins) was described	Lugao et al. 2002
Electrochemically aged PP with a dye added	Vicat softening point	Electrochemical aging results (in PP) in decrease in hardness and Vicat softening temperature while increase in water absorptivity and in size of spherulites was noticed	Gnatowski et al. 2010
Polyethylene compositions with improved Vicat softening point	Vicat softening point	A method of selecting materials for polyethylene with improved Vicat softening point has been disclosed	Davis 2008

(*continued*)

Table 10.26 (continued)

Blend	Test	Results	References
Thermal degradation kinetics of LLDPE and Silane cross-linked LLDPE	TGA was employed to study the degradation mechanisms	Silane cross-linked LLDPE was found to be thermally more stable compared to LLDPE	Zong et al. 2005
PE/MMT nanocomposites	Non-isothermal TG experiments	Char formation plays a key role in the mechanism of flame retardation for nanocomposites	Lomarkin et al. 2008
Glycerol modified linseed oil based polyurethane and cardanol based dye	Thermal stability of the blends was investigated using TGA, derivative thermogravimetry (DTG) and other methods	Glycerol modified linseed oil based polyurethane and cardanol based dye are highly cross-linked with high thermal stability and the rate of decomposition of polymer blends depends upon NCO/OH molar ratios and the nature of the dye	Achary et al. 2012
NR/BR rubber blends	Influences of preparation mode and elastomer ratio in blends on thermal degradation using TGA	Degradation of the blends takes place in two steps	Castro et al. 2007
Poly(ester urethane) and poly(ether sulfone) blends with or without poly(urethane sulfone) as a compatibilizer	Thermal degradation of blends using TGA	The presence of polysulfone caused a rise in thermal stability of the blends	Filip and Vlad 2004
Thermal stability of nine polymer systems	Thermal degradation of blends using TG-DTG-DTA etc	Thermal stability, degradation mechanism of organic systems in the presence of inorganic species	Muhammad 2013

Flammability ratings are based on the specimen behavior during the test, materials rated 94 V-0 being the most while those rated 94 V-2 being the least resistant to burning. Table 10.28 summarizes the test requirements.

10.6.1.3 Vertical Burning Test for Classifying Materials: 94 5 V

This test is more stringent than UL 94 V-0, V-1, and V-2. Here, 127 mm ignition flame is applied on specimen bars of dimensions 127×12.7 mm, with maximum thickness 12.7 mm. In Method A, a Tirril burner is positioned 20° from the vertical and the overall height of the flame is adjusted to 127 mm. The flame is applied for 5 s and removed for 5 s. The procedure is repeated five times. After the fifth removal of the flame, the duration of flaming and glowing, the distance the specimen burned, the

Table 10.27 Summary of ASTM test methods[a]

No	Test method	Specimen/sample	Purpose of the test	Comments
1.	ASTM D229-96 testing rigid sheet and plate materials used for electrical insulation	Flat sheet or plate form	Relative comparison of the ignition resistance of materials and the extent of burning	
2	ASTM D568 for rate of burning and/or extent of burning of flexible plastics in a vertical position	Flexible thin sheets or films	Relative comparison of rate of burning and/or extent and time of burning (of plastics)	Discontinued in 1991, not replaced
3.	ASTM D635-98 for rate of burning and/or extent of burning of self-supporting plastics in a horizontal position	Bars either molded or cut from sheets, plates, or panels	Relative comparison of average burning rate, average time of burning, and average extent of burning	This method combined with the best features of UL 94 resulted in writing of ASTM D3801
4.	ASTM D757 for incandescence resistance of rigid plastics in a horizontal position	Rigid plastic	Relative resistance to incandescent surface at $1,223 \pm 10$ K ($1,742 \pm 18$ °F)	Discontinued in 1966, no replacement
5.	ASTM D1433 for rate of burning of flexible thin plastic sheeting supported in a 45° incline	Flexible plastic in the form of film or thin sheeting	Relative rate of burning and/or extent and time of burning	Discontinued in 1987, replaced by D4549
6.	ASTM D1929-96 for ignition properties of plastics (Setchkin technique)		Determination of self-ignition, flash-ignition temperatures, and self-ignition by temporary glow	
7.	ASTM D2843-99 for density of smoke from the burning or decomposition of plastic		To measure smoke density across a 12 in. light path	For materials that excessively drip, auxiliary burner is used
8.	ASTM D2863-97 for measuring the minimum oxygen concentration to support candle-like combustion of plasticThe ratio $O_2/(O_2 + N_2)$ when multiplied by 100 is designated as the oxygen index (Imhof and Steuben 1974)	Various forms such as films, etc	To determine relative flammability of plastic by measuring the minimum concentration of oxygen in a flowing mixture of oxygen and nitrogen that will just support flaming combustion. The apparatus is shown in Fig. 10.60	Useful for determining the "Limiting Oxygen Index" of plastics. It has gone through several modifications

Table 10.27 (continued)

No	Test method	Specimen/sample	Purpose of the test	Comments
9.	ASTM D3014-99 for flame height, time of burning, and loss of weight of rigid cellular plastics in a vertical position	Rigid cellular plastics	Determining relative extent and time of burning	Revised to accommodate thermosets
10.	ASTM D3713 for measuring response of solid plastic to ignition by a small flame	A set of specimens of identical composition and geometry	To characterize the response of a plastic to a small flame of controlled intensity for quality control	Discontinued in 2000, no replacement
11.	ASTM D3801-96 for measuring the comparative extinguishing characteristics of solid plastics in a vertical position	Solid plastic material. A set of specimens with identical composition and geometry	Determination of comparative extinguishing characteristics	Combination of the best features of UL 94 and ASTM D635
12.	ASTM D3894 for evaluation of fire response of rigid cellular plastics using a small corner configuration	Rigid cellular plastic	Prediction of performance of a Factory Material Full-Scale Corner Wall Test	Discontinued in 1994 and not replaced
13.	ASTM D4100 for gravimetric determination of smoke particulates from combustion of plastic materials	Plastic material in a slab configuration	Gravimetric determination of smoke particulate matter produced from the pyrolysis of plastics	Discontinued in 1997 and not replaced
14.	ASTM E84-00 for surface burning characteristics of building materials	Any building material of dimensions 24 ft. × 20.25 in.	Determination of surface burning characteristics, e.g., of foam insulation	Suffers from several limitations. Also known as Steiner Tunnel Test
15.	ASTM E 119-00 methods of fire tests of building construction and materials	Full-size wall section	Determination of fire resistance of walls, floors, ceilings, roofs, etc	It is similar to UL 263 and NFPA 251
16.	ASTM E136-99 for behavior of materials in a vertical tube furnace at 705 °C	Building material test specimens of size 1.5 × 1.5 × 2 in.	Determination of combustion characteristics of building materials	
17.	ASTM E162-98 for surface flammability of materials using radiant heat energy source (Radiant Panel Test)	Specimen of dimensions 6 × 18 in.	Determination of flame spread index of a material	Intended for research and development only

[a]ASTM standard test methods are available on web: http://enterprise.astm.org/

Fig. 10.59 Test layout for classification in 94 V-0, 94 V-1 and 94 V-2 according to UL 94 (Troitzsch 1983)

SPECIMEN

BURNER

SURGICAL COTTON

(ca. 50•50•6.5)
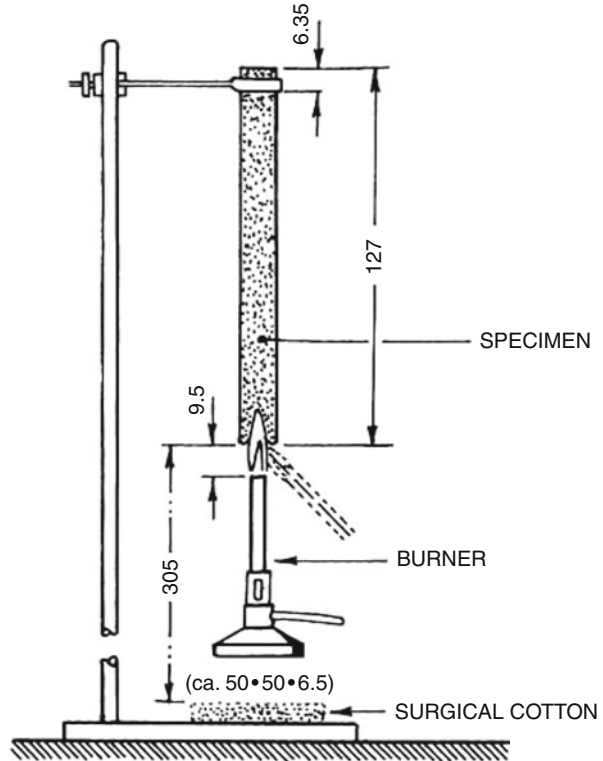
dripping of particles from the specimen (during the test), and deformation of physical strength of the specimen immediately after burning (and when cooled) are observed.

When the specimen shrinks, elongates, melts, etc., additional tests are carried out using test plaques (152 × 152 mm) under Method B. These tests are conducted in various positions both vertical and horizontal positions of the plaques with flame applied to different places in the plaques, using the procedure as in Method A. The observations focus on the same items as in Method A.

Materials are classified 94-5V when:

- No specimen burns with flaming and/or glowing combustion (after the fifth flame) for more than 60 s.
- None specimen drips particles.

10.6.1.4 Flame Spread Index Test Using Radiant Panels

This test is conducted in accordance with ASTM E162 mentioned in Table 10.28.

10.6.1.5 Vertical Burning Test for Classifying Materials: 94 VTM-0, VTM-1, or VTM-2

Some materials due to their thickness distort, shrink, or get consumed up to the holding clamp, when tested according to the methods described above.

Table 10.28 UL 94 vertical burning test for classifying very thin materials (Landrock 1983)

No.	Requirement	Classification		
		94 V-0 (most severe)	94 V-1 (intermediate)	94 V-2 (least severe)
1.	Total flaming combustion time for 10 ignitions, maximum (sec)	50	250	250
2.	Individual flaming time, maximum (sec)	10	30	30
3.	Glowing combustion time (sec)	30	60	60
4.	Flame drippings	None	None	Allowed if burns briefly
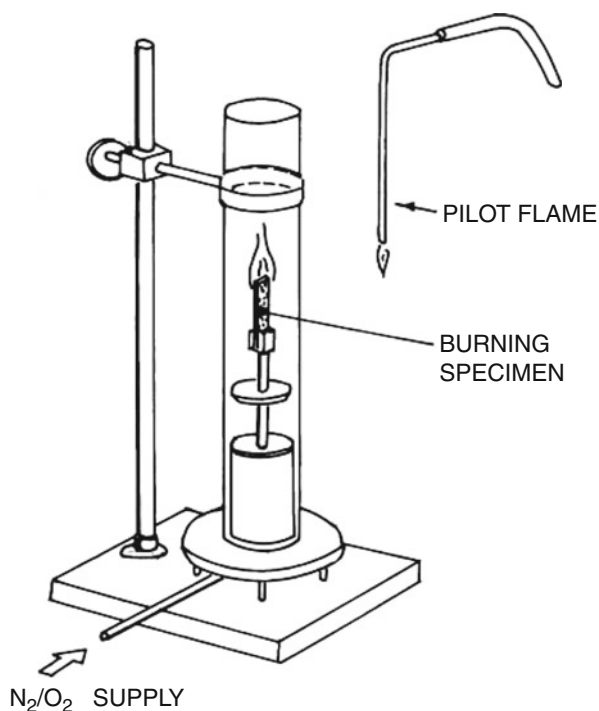
Fig. 10.60 Oxygen index apparatus [Troitzsch, 1983]

VTM means "very thin materials" – test specimens are cut to 200 × 50 mm dimension. Each specimen is supported from the upper 6 mm of its length, with the longitudinal axis vertical using a heavy spring clamp. The lower end of the specimen is placed 9.5 mm above the top of the Bunsen burner tube and 0.3 m above a horizontal layer of dry surgical cotton. The test flame is placed under the lower end of the test specimen for 3 s. Then the flame is taken away from the specimen and the duration of specimen flaming is noted. When flaming of the specimen ceases, the test flame is applied once again for 3 s and then withdrawn.

The deviation of flaming and glowing of the specimen is noted. In case the specimen drips molten or flaming material, the burner may be lighted to angle up to 45°. The following are observed after the removal of the flame:

- Duration of flaming after first flame application
- Duration of flaming after second flame application
- Duration of flaming plus glowing after second flame application
- Whether or not specimens burn up to 127 mm
- Whether or not specimens drip flaming particles that ignite the cotton

94 VTM-0 classifies materials under most severe conditions. Table 10.28 summarizes the test requirements.

10.6.1.6 UL 746A-78 Polymeric Materials' Short-Term Property Evaluations

Test procedures for seven major areas are given in this standard. They are all applied for the determination of resistance of polymeric materials to ignition from electrical sources. The individual tests are Resistance to Hot Wire Ignition, Resistance to High-Current Arc Ignition, Resistance to High-Voltage Arc Ignition, and Resistance to Hot-Bar Ignition.

10.6.1.7 UL 746B-79 Polymeric Material Long-Term Property Evaluations

This standard deals with long-term tests for the evaluation of materials and parts of end products. Along with UL 94, UL 746A, and UL 746C, these tests provide data regarding the physical, electrical, flammability, thermal, and other properties of the materials under consideration.

10.6.1.8 UL 746C-78 Polymeric Materials' Use in Electrical Equipment Evaluations

This is the test procedure, including flammability, for parts of polymeric materials used in electrical equipment. It provides a table of short-term and long-term properties to be considered during evaluation of polymeric materials used in electrical equipment.

10.6.1.9 UL 746D-80 Polymeric Materials' Fabricated Parts

This standard is for blends of polymers, copolymers, terpolymers, and alloys. It considers plastic parts that have been produced under a material identity control system. Molders/fabricators are required not to employ such additives/flame retardants that would adversely affect critical material properties. A detailed discussion on national and international fire protection regulations and test methods for plastics is presented by Troitzsch (1983).

10.6.1.10 ASTM D2863 Measuring the Minimum Oxygen Concentration

The method provides means for the determination of relative flammability of plastics by varying the oxygen to nitrogen concentration. The oxygen indexer is shown in Fig. 10.60.

10.6.2 Factors Affecting Flammability

Application of a heat source, such as flame, raises the temperature of polymer and ultimately causes it to burn. Burning of a solid polymer has been divided into four stages: (i) heating, (ii) decomposition, (iii) ignition, and (iv) combustion (Landrock 1983). In the first stage, a thermoplastic material softens or melts and begins to flow. The temperature at which it melts can have a significant effect. In the second stage, gases or the volatile fragments of degraded polymer are removed. The temperature and the rate at which this occurs depend on the thermal stability of polymer and the chemical reactions occurring under those conditions. Ignition takes place as the flammable gases combine at appropriate ratios with oxygen from the air.

Sustaining the burning depends on the transfer of sufficient heat from the flame to polymer, capable to maintain supply of flammable decomposition byproducts. Supply of oxygen is also essential. If decomposition of the polymer requires more heat than it is supplied by the flame, or if solid nonflammable residues coat the surface and insulate the remainder of the flammable part, a continuous propagating flame will not be obtained. Thus, the last stage of the burning sequence very much depends on the polymer characteristics. It may be correlated with such energy factors as cohesive energy, hydrogen bonding, heat of combustion, and dissociation energy (Einhorn 1972).

An interesting relationship between polymer structure and polymer flammability has been observed. Commercial polymers that possess aromatic groups in the main chain (e.g., PPE, PC, PSF, phenolic resins) undergo char-forming condensed-phase reactions – as a result they have low flammability. Higher oxygen index of PC and PPE was apparently related to their higher charring tendency in comparison to the aliphatic hydrocarbon-type polymers. The greater thermal stability of aromatic-type polymer backbone leads to a higher tendency for condensation into aromatic chars and, therefore, to the less flammable products (Fenimore and Martin 1966).

Van Krevelen had confirmed the empirical relationship between polymer structure, char formation, and polymer flammability. A mathematical formula was proposed that (based on structural units) allows calculation of the oxygen index and char residue values for a wide variety of hydrocarbon polymers. The very existence of such a relationship indicates that pyrolytic condensed-phase process is of primary importance in determining polymer flammability at least in the studied cases (Van Krevelen 1975).

A relationship between the polymer structure and its flammability was related to unsaturation for co-polyterephthalates and co-polycarbonates (Quinn 1977). This work is an excellent illustration of the importance of condensed-phase pyrolytic mechanisms upon polymer flammability.

10.6.3 Prevention Methods

Since a thorough review of fire-retardant methods is beyond the scope of this chapter, only a brief summary is given below. The readers interested in a more

detailed discussion are referred to pertinent reviews (Einhorn 1972; Hilado 1972, 1981; Vandersall 1971). Four general methods for reduction of polymer flammability have been identified (Kuryla and Papa 1978):

- A nonflammable coating that prevents the normal pyrolytic or combustion mechanism is either applied to the polymer surface or produced in the presence of a flame.
- Appropriate chemicals are incorporated during polymer processing. Their role is either to alter the rate of pyrolytic fuel generation or to inhibit the exothermic gas-phase reactions.
- Gas-phase flame reaction can be prevented by the generation of nonflammable gases, which dilute the fuel gases below the flammability limits.
- Incorporated solid components consume sufficient heat during pyrolytic decomposition that they sufficiently cool the substrate to a temperature below the ignition point.

In any given fire retardant, one or more above methods may be used. The effect of a fire retardant strongly depends on the basic chemical structure of the polymeric material. Owing to complexity of the processes and the experimental limitations, it is difficult to predict which mechanism is most important or operative for any system. A list of commercially available fire retardants is given in Appendix 2 (Table 10.37). These materials are classified as organic, inorganic, and reactive types. A fact to be kept in mind is that for blends or alloys, the fire retardancy behavior is usually between those of the base resins; for example, consider Arylon and Kydene (acrylic/PVC) (Landrock 1983).

10.6.4 Review of Fire Retardancy in Polymeric Materials

The concept of fire retardancy is remarkably old. The Greek historian, Herodotus, in 484–431 BC recorded that the Egyptians imparted fire resistance to wood by soaking it in a solution of alum (potassium aluminum sulfate) (Browne 1958). The Romans added vinegar to the alum for the same purpose. Vitruvius in the first century BC described the natural fire-retardant properties of the larch tree and some military applications of fire-retardant materials such as plaster of clay reinforced with hair (Vitruvius 1960). In 1638, Circa recorded that Italian theaters were painted with a mixture of clay and gypsum (potassium aluminum silicate and hydrated calcium sulfate) to protect them from fire. Wild was issued a British patent in 1735 for his process of treating wood with a mixture of alum, ferrous sulfate, and borax (sodium tetraborate decahydrate). And Gay-Lussac in 1821 showed that a solution of ammonium phosphate, ammonium chloride, and borax acts as a fire retardant for wood.

In all these processes the key ingredients are the elements from group III (B and Al) of the periodic table. Now, at the end of the twentieth century, with so much of research activity for better fire retardants, the most effective elements are still found in groups III (B and Al), V (N_2, P, and Sb), and VII (Cl and Br). Research efforts to find new and improved fire-retardant agents for synthetic polymers and their blends have been concentrated on the same three groups of the periodic table, with the same seven elements. The search is for new ways of incorporating them into polymers

(Chamberlain 1978). Certain compounds based on Ba (group II), Zn (group II B), and Sn (group IV) are claimed to be effective in some polymers, especially when used in conjunction with one or more of the seven key elements mentioned above.

The burning or non-burning characteristics of plastics have been given a great deal of attention by the scientific community. After the Federal Trade Commission (FTC) announced inquiry into flammability of plastics in October, 1972, the suppliers started more carefully to describe flammability of their products. ASTM and other standard developing groups have given considerable effort to develop more meaningful tests and have dropped or modified certain tests. Thus, ASTM D1692 was discontinued (Hendersinn 1977).

A theory that certain flame retardants vaporize and produce an effect by acting as free-radical chain stoppers to extinguish the flame or to inhibit the flame speed of the burning gases was proposed. It is based on extensive studies for 30–40 years (Kuryla and Papa 1978). The research efforts devoted to understand the mechanisms of combustion and inhibition for solid materials burning with a diffusion flame in an air environment have multiplied rapidly in the last two decades.

Polymer matrix-based nanocomposites have become a prominent area of current research and development. Exfoliated clay-based nanocomposites have dominated the polymer literature, but there are a large number of other significant areas of current and emerging interest. Increased flammability resistance has been noted as an important property enhancement involving nanoplatelet/nanofiber modification of polymeric matrices. The primary advantage noted with nanofiller incorporation is the reduction in the maximum heat release rate (determined by cone calorimetry) (Morgan 2006; Bourbigot et al. 2006). The majority of the flame retardant studies on nanofiller incorporation in polymers involve exfoliated clay. Studies involving PA6 (Dasari et al. 2007; Kashiwagi et al. 2004) and PP (Qin et al. 2005) yielded similar observations with reduced peak heat release rate but no change in the total heat release with exfoliated clay addition. The primary advantage for nanofiller addition for these tests generally involves reduction in the flame retardant additives that need to be incorporated to pass the specific test (Morgan 2006; Schartel et al. 2006; Nazare et al. 2006). This has been observed in various nanoparticle modified composites including exfoliated clay with halogen-based flame retardants/Sb_2O_3 (Zanetti et al. 2002) and EVA nanocomposites with magnesium hydroxide nanoparticles and microcapsulated red phosphorus (Lv and Liu 2007).

Studies involving carbon nanotubes have also shown decrease in the peak heat release rate with no change in the total heat release (Kashiwagi et al. 2002, 2005) with effectiveness equal to or better than exfoliated clay. The level of dispersion of the carbon nanotubes in the polymer matrix was shown to be an important variable (Kashiwagi et al. 2005). Upon combustion, the surface layer was enriched with a protective nanotube network providing a thermal and structural barrier to the combustion process. Continuity of the network was important to achieve optimum performance as very low levels of nanotube incorporation or poor dispersion did not allow a continuous surface network during the combustion process. It is noted that the incorporation of nanoclay and carbon nanotubes often results in slightly earlier

ignition than the unmodified polymer presumably due to the increased thermal conductivity. However, at the later stages of combustion, the reinforcement of the char layer provides a stable thermal barrier preventing regeneration of polymer at the surface available for rapid combustion (Paul and Robeson 2008).

Fire retardancy behavior of PP/PA66 blends compatibilized with PP-g-MAH and modified with untreated and treated nanoclays was studied (Kouini and Serier 2012). It was found that the intercalation, exfoliation of nanoclays of nanocomposites, and the flame retardancy properties were improved significantly. In addition a good balance of impact strength and flame retardancy was obtained for PP/PA66 nanocomposites in the presence of PP-g-MA compatibilizer. The presence of the clay led to an increase in the flammability time. In addition, the treatment made a more pronounced effect. A 23 % increase was observed only when 4 wt% nanoclay was added and a longer flammability time was noticed with treated clay. This was attributed to the stacking of nanoclay which created a physical protective barrier on the surface of the material. Similar behavior has been reported by earlier workers (Kocsis and Apostolov 2004).

Thermal insulating materials are required to protect structural components of space vehicles during the reentry stage, missile launching systems, and solid rocket motors. A series of review papers were published (Koo et al. 2006, 2007; Ho et al. 2007) on using polymeric composites as ablative thermal protection systems for a variety of military and aerospace applications. Thermal protection materials such as char-forming phenolics and carbon–carbon composites are used for spacecraft heat shields, rocket motor insulation, and rocket nozzle assembly materials. The TPU nanocomposites (TPUNs), with the addition of nanoclays and carbon nanofibers, are prepared, and properties such as density, specific heat capacity, thermal diffusivity, and thermal conductivity of the different TPUN compositions were determined. Cone calorimetry was employed to study the flammability properties of these TPUNs. These novel materials were proposed to replace Kevlar-filled EPDM rubber, the current state-of-the-art solid rocket motor internal insulation (Ho et al. 2010).

10.6.5 Data on Blends

The flame retardancy properties of some commercial polymer blends are given in Table 10.29.

10.7   Electrical Properties

10.7.1 Standard Methods of Measurement

10.7.1.1 Resistivity of Insulating Plastics
Measurements of insulating polymers or polymer blends are usually carried out using a sheet specimen in form of a disc or a square (ASTM D257).

Table 10.29 Data on blends

Blend (trade name, grade, and manufacturer)	UL 94 Flame class			Oxygen index ASTM D 2863-97
	HB rating (inch)	V-0 rating (inch)	5 VB rating (inch)	
PC/ABS **Cycoloy**, GEC	**0.060**	**0.060**	0.098	<**21.0**
ASA/PC **Geloy**, XP 1001, XP 2003, XP 4001, GEC	**0.063**	**0.130 V-1**	0.130 VA	–
PC/PBT **Xenoy**, 6120, 6240, 6123, 6370, 6620, 6380, GEC	**0.061**	–	–	–
PC/ABS **Bayblend**, Miles; FR 1439	–	0.062	–	**28**
FR 1440, FR 1441	–	0.062	–	**30**

Commercially available resistance meters can measure resistance in the range from 10^6 to 10^{15} Ω. In the case of plastics, the method can be applied if the resistance values are of the same order or lower than the volume resistance and if the volume resistivity is $>10^8$ Ω. Flat plate metal electrodes, preferably guarded (Fig. 10.61), are used for testing flexible and compressible materials (at room or elevated temperatures).

Voltmeter–Ammeter Method

The DC voltmeter and the DC amplifier (or electrometers to increase the sensitivity) are connected to the voltage source and the specimen. The applied voltage, V_x, is measured by a DC voltmeter. The current, I_x, is measured in terms of voltage drop across a standard resistance R_s. The voltage drop is amplified by the DC amplifier and read on an indicating meter as V_s. The resistance R_x or the conductance G_x is calculated as

$$R_x \;=\; \frac{1}{G_x} \;=\; \frac{V_x}{I_x} \;=\; \left(\frac{V_x}{V_s}\right) R_s \tag{10.31}$$

The time of electrification, unless otherwise specified, should be 60 s and the applied direct voltage $V_x = 500 \pm 5$ V.

Volume Resistivity or Conductivity

Measure the dimensions of the electrodes and width of the guard gap, g, accurately. Unless otherwise specified, the time of electrification should be 60 s and the applied direct voltage 500 ± 5 V. Volume resistivity is expressed as (Ω-cm)

$$\rho_v \;=\; \frac{A}{t R_v} \tag{10.32}$$

where A = the effective area of the measuring electrode (see Fig. 10.61), t = average thickness of the specimen, R_v = measured volume resistance in Ω.

Fig. 10.61 Top view and side view of flat plate guarded metal electrodes [ASTM D257]
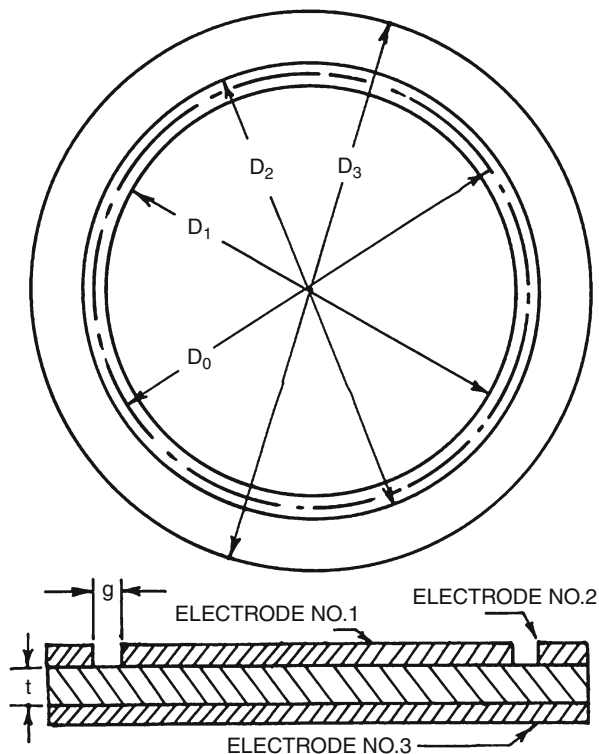
Volume conductivity is calculated as (S/cm)

$$\nu_v = \frac{t}{A G_v} \qquad (10.33)$$

where G_v = measured volume conductance in Siemens.

Surface Resistivity or Conductivity

The electrode dimensions and the distance between the electrodes, g, are to be measured accurately. The surface resistance or conductance between electrodes No. 1 and 2 is measured with a suitable device (Brown 1981). The time of electrification should be 60 s and the applied direct voltage shall be 500 ± 5 V.

Surface resistivity, per square cm is given by

$$\rho_s = \frac{P}{g R_s} \qquad (10.34)$$

where P is the effective perimeter of the guarded electrode (see Fig. 10.61), R_s is the measured surface resistance in Ω, and g is as indicated in Fig. 10.61. For specimens of square, rectangular, and tube forms, appropriate electrodes and mathematical relations are given in ASTM D257.

BS 4618 recommends preconditioning of the test specimens at not more than 1 % relative humidity (RH) for the study of effect of temperature. ASTM D257 covers resistivity measurements for insulating materials. Electrode sizes are not stipulated (round, square, and rectangular types are permitted). The gap between guard ring and center electrode is made approximately equal to twice the specimen thickness. The test voltage is usually 500 V applied for 60 s, as in the British test.

DIN 53482 uses methods similar to some of those in IEC 93, using silver or graphite painted electrodes for volume resistivity. A different electrode system was suggested for the measurements of surface and volume resistivity. A narrow guard gap of 1 mm makes it difficult to avoid short-circuiting the electrodes.

Power Factor and Permittivity

Measurements of dielectric constant and loss in polymeric solids and melts over a wide frequency range were described in detail elsewhere (Porter and Boyd 1972). An updated and detailed account of these topics may be found in ▶ Chap. 12, "Broadband Dielectric Spectroscopy on Polymer Blends" of this handbook (Andreas Schonhals 2014).

The measurement of power factor and permittivity and the related parameters such as dissipation factor, phase angle, etc., may need to be carried out over a wide range of frequencies from a few Hz to several tens of GHz. However, most measurements are made between 50 Hz and 100 MHz (Brown 1981).

Insulating materials, such as polymers and polymer blends, are used as dielectrics at commercial frequencies between approximately 50 Hz and 100 GHz. Two different techniques are adopted to study the dielectrics in two ranges, i.e., below and above 100 MHz. Dielectric measurements at ultralow frequencies are of some interest, as they reveal the basic structure of the material (McCrum et al. 1967). Bridge circuits are invariably employed for the measurements of power factor and permittivity.

The test specimen, whose dielectric constant and loss factor are to be measured, is cut or molded to a suitable shape and thickness determined by the material specifications or the test method. The thickness of the specimen must be accurately measured. The electrodes are selected, based on convenience and whether or not the specimen must be conditioned at high temperature and high relative humidity. The test specimen with its attached electrodes is placed in a suitable measuring cell, and its capacitance and a-c loss are measured using a suitable bridge. For routine work when either the highest accuracy is not required, or when neither terminal (of the specimen) is grounded, it is not necessary to place the solid specimen in a test cell.

In the Schering Bridge, one sets the ratio R_1/R_2 (range) and varies C_s and C_1 to obtain a balance (ASTM D150):

$$C_x = \left(\frac{R_1}{R_2}\right) C_s \qquad\qquad (10.35)$$

$$D_x = W.C_1R_1 \qquad\qquad (10.36)$$

The test method covers dielectric measurements from 1 Hz to several hundred MHz. It has few recommendations about the procedure or apparatus.

Size of the electrodes is not suggested and it is recommended that the guard gap should be as small as possible and the guard width should be at least twice the thickness of the specimen. An appendix is provided, which describes number of bridges and their circuits. The German standard for dielectric measurements is DIN 53483.

Dielectric Strength

Low-level conduction in insulating materials can originate in a variety of ways. Often it is attributed to impurities that provide small concentrations of charge carriers in the form of ions and/or electrons. At high fields, the electrodes may also inject new carriers into the polymer, causing the current to increase more rapidly with voltage. At very high fields, these and other processes inevitably lead to complete failure of the polymer as a dielectric. This localized, sudden, and catastrophic phenomenon is known as the dielectric breakdown (Ku and Liepins 1987). In many cases the dielectric breakdown or dielectric strength of a material can be the determining factor in the design of an apparatus in which it is to be used.

A method for determination of dielectric strength of solid electrical insulating materials at commercial power frequencies was developed (ASTM D149). The voltage can be applied at a fast uniform rate or step-by-step or at a slow rate of rise. At the dielectric breakdown voltage, an abrupt rupture through the specimen results in a visible puncture and decomposition of the material – the occurrence can be seen and heard. This form of breakdown is irreversible. Dielectric strength is calculated (in terms of KV/mm or V/mil) by noting the gradient at the highest voltage step at which breakdown did not occur. BS 2782 Method 201, deals with plastics breakdown voltage. Other British standards such as BS 3784, BS 3816, BS 3924, and BS 5102 directly invoke BS 2782.

10.7.2 Factors Affecting Electrical Properties

Factors such as improper mixing of polymer blends lead to variations in test specimens. Such compositional and/or structural changes from specimen to specimen often lead to widely divergent data.

10.7.2.1 Effect of Temperature

Resistivity depends on temperature – for nonmetallic materials it invariably decreases with T. Volume resistivity is markedly more sensitive to temperature than surface resistivity. In any measurement it is important to ensure that temperature is maintained constant during the test. Temperature fluctuations produce changes in measured current and lead to significant errors (Brown 1981; ASTM D257). In the case of power factor or permittivity determinations, the effects of temperature and frequency are interrelated. With nonpolar polymeric materials, the changes in properties with temperature and frequency are small, while with polar materials very large changes may take place.

10.7.2.2 Effect of Humidity

The insulation resistance of solid dielectric materials decreases with increasing humidity. Surface resistance is particularly sensitive to humidity changes. Insulation resistance or conductance is a function of both the volume and surface resistance or conductance of the specimen. Surface resistance changes almost instantaneously with a change of RH. Therefore, it is essential to maintain both T and RH within close limits during the conditioning and measuring of the specimens. In a humid environment, absorption of water into the volume of the insulating material as well as the formation of an ionized water film on the specimen surface takes place. These factors lead to significant rise in the insulating materials' permittivity and loss index. The process of dielectric breakdown in the case of neat polymers is not completely understood, and many unknowns are still remaining (Ku and Liepins 1987).

Still many uncertainties exist for polymer blends and alloys. However, it is clear that the chemical structure, the solid-state structure, degree of plasticization, the nature and concentration of filler, molecular weight and morphology of a polymer, etc., influence the electrical properties. For example, the dielectric breakdown of EVAc and its blends was studied in the low-temperature region (193 K) (Nagao et al. 1976, 1977). The dielectric breakdown voltage of EVAc and blends was found to rise with an increase in VAc content. This may be caused by increased electron scattering associated with the decrease of crystallinity and the increase of polar groups.

The process of polymer blending was used for improving the mechanical properties of electric wire insulation, as early as 1968 (Ku and Liepins 1987). In 1978, it was found that the use of a HDPE/LDPE blend enhanced the electrical treeing inception voltage (Nitta and Funayama 1978). This approach to electrical treeing inhibition and some of the experimental results on the use of SB/LDPE and HDPE/LDPE blends are given in Table 10.30 (Wu and Chen 1983).

10.7.3 Review of Blends' Electrical Properties

Most polymers have high electrical resistivity, are inexpensive in comparison to other known insulating materials, and are heat resistant and sufficiently durable. Owing to their sensitivity to oxidation and solvents, they are frequently blended to generate better electrical insulating alloys. In the past two decades, there has been serious effort to modify the electrical properties of polymers and their blends. The electrically conductive polymers can be broadly categorized as (i) electrostatic dissipating polymeric compositions and (ii) electrically conductive polymer blends. Utracki has reviewed evolution of these materials (Utracki 1998).

The electrostatic dissipating polymeric compositions (ESD) are developed to overcome problems related to the accumulation of surface charge and its rapid discharge leading to shocks, fire, explosions, damage to electronic components, etc. These compositions must provide surface resistivity $10^5 < R < 10^{12}$ (Ω cm).

Table 10.30 Effect of polymer blending on tree growth and length (Wu and Chen 1983)

Parameter	LDPE	SBR			HDPE		
Modifier wt%	100	10	20	30	10	15	20
Tl (min)	–	198	127	54	25	70	90
T2 (min)	300	100	200	230	156	170	160
T3 (min)	–	2,180	2,200	–	75	30	2,100
Tl + T2 + T3 (min)	2,300	2,478	2,527	2,284	250	270	2,350
Length §(μm)	1,300	300	600	1,400	450	500	400

T1, induction period for tree initiation in minutes; T2, growth period of the tree in minutes; T3, the saturation period of tree development in minutes; §, The length of the tree after saturation period

The early efforts to achieve the optimum surface resistivity, such as coating the polymeric parts with electrostatic dissipative materials, addition of either graphite, metal particles or fibers, incorporation of low molecular weight antistatic agents, etc., did not yield fruitful results (Kozlowski 1995). Antistatic properties are observed for materials having either -SH or –OH groups (e.g., phenolic, alcoholic, or acidic).

Since the mid-1980, the most frequently used ESD has been a copolymer of ethylene oxide and epichlorohydrin, EO-CHR. Many chemical companies (such as Borg-Warner, B.F. Goodrich, Asahi, and General Electric) came up with several ESD formulations containing EO-CHR for improving the electrostatic properties of PVC, CPC, PC, PEST, epoxy, phenolics, etc. (Federl and Kipouras 1986; Kipouras and Federl 1988; Yu 1988; Lee 1993; Shimamura and Suzuki 1991; Giles and Vilasagar 1994).

The second variety of materials, viz., electrically conducting polymer blends, ECPB, has been known since the early 1980s. These are prepared, in principle, by synthesis of the conducting polymer within the host or by simple blending (Billingham and Calvert 1989). Polyacetylene, PACE, blends were prepared by the polymerization of acetylene in LDPE films doped with Ziegler catalyst (Galvin and Wnek 1982, 1983; Galvin et al. 1984). PACE formed a particulate second phase with a size ranging from 60 to 200 nm. Addition of 7 % PACE LDPE increased the yield point of the latter resin from 7 to 10 MPa, but the extension to break was reduced. The effect was greater in blends produced by polymerization in solid PE.

Acetylene was polymerized in the presence of polybutadiene rubber, and the blends were investigated for their electrical conductivity (Rubner et al. 1983; Sichel and Rubner 1985). The electrical properties of these blends were explained in terms of the morphological features (Tripathy and Rubner 1984). In these investigations, a conductivity of 10 S/cm was achieved at PACE loadings above 30 %. Polymerization of acetylene in EPDM resulted in tough, conductive films (Lee and Jopson 1983, 1984). The conductivity of these films was found to be significantly enhanced by stretching.

Mechanical blending of various conducting polymers with thermoplastics was studied (Wessling and Volk 1987). These materials although processable showed low electrical conductivity ($<10^{-5}$ S/cm). They were prepared by blending an electrically

conductive polymer (such as polyacetylene or polypyrrole) with a polymer having strong anionic group (such as sulfonated PE, sulfonated SEBS, sulfonated PS, or sulfonated polyacrylamidomethylpropane) (Cross and Lines 1995).

Electrically conducting polymer blends are also produced by blending another conducting polymer (e.g., poly-3-octylthiophene) with a matrix polymer (e.g., PP, PVC, PS, PE, EVAc, PVC/ABS, etc.) introducing a dopant (e.g., iodine) (Kokkonen et al. 1994). Several strategies were adopted in preparing ECPBs. In one example, polyaniline was blended with dodecylbenzenesulfonic acid, mixed with PS, PE, or PP and then melt processed. In another case, polyaniline was mixed with protoning acid metallic salt. The conductive material was melt mixed with PE, PS, PP, or ABS (Karna et al. 1994a, b).

ECPBs were prepared by melt blending a matrix polymer (selected from between PE, PP, PB, PIB, PMP, EPR, CPE, CSR, PS, polyalkanes containing styrene, acryl, vinyl, or fluoroethyl groups and their blends) and an electrically conducting thermotropic liquid-crystal polymer, containing either ferric chloride or iodine as a dopant. The blend which could be manufactured into fibers and films was reported to have conductivity as 10^{-12}–10^2 S/cm (Ho and Levon 1995). Amine-terminated polyaniline was first grafted onto a thermoplastic polymer comprising a functional group capable of reacting with -NH$_2$, e.g., maleic anhydride. They were further compounded with polymers, fillers, and/or electrically conductive solids (Jongeling 1993). Blends of PVC with "doped" polyaniline and at least one other additive (e.g., impact modifier, plasticizer, acidic surfactant) were developed to give electrically conductive blends.

ECPBs were also prepared compounding polyaniline and a thermoplastic polymer (selected from PA-6, PA-66, PA-11, PA-12, PET, PC TPU, CPE, etc.) and 0–10 wt% carbon black (Kulkarni and Wessling 1992, 1993). Electrically conductive materials were prepared by dispersing pre-blends of aniline to sylate particles and poly(ethylene terephthalate glycol), PETG, and then diluting the pre-blend with PETG. The blends were useful for the manufacture of films, printing inks, and coatings, in shielding, antistatic, and adhesive applications (Shacklette et al. 1993). Curable blends, with good flame retardancy, comprising of fluorine-containing polycyanurates and a thermoplastic polymer (e.g., PSF, PPE, and PEEK) were patented by IBM in 1992. The filled materials were useful in several applications (fabrication of printed circuit boards, semiconductor chip carriers, metal-core boards, chip modules, and multilayer thin film circuits) (Ardakani et al. 1994).

Conducting polymer fibers were prepared by melt mixing and chemical coating on fibers. Different conductive materials were used in order to obtain conductive PP-based fibers with specific electrical and mechanical properties. The electrical conductivity and morphological characteristics of these fibers were investigated (Kim et al. 2004). The conductive fibers are intended for use in creating conductive yarns, conductive fabrics (which can be used as electromagnetic shields), and multifunctional textile structures for novel applications.

Melt-processed immiscible polymer blends of HIPS, LCP, and CB were prepared. Relationships between composition, electrical resistivity, and morphology of the blends produced by adopting different processing methods

were investigated. The LCP phase morphology in the blends was found sensitive to the processing conditions. An important role of the skin region in determining the resistivity of injection-molded samples was found. The study also revealed that shear rate effect on resistivity of capillary rheometer filaments might serve as a predictor of resistivity behavior in real processing procedures (Tchoudakov et al. 2004). Such studies are not frequent. In fact, processing–structure–property relationships in electrical properties of polymeric materials are rarely available.

A two-step method was used to prepare carbon nanotube (CNT)/(EVA)/(PE) and CNT/(PC)/PE composites. First, CNT–EVA and CNT–PC master batches were obtained by solution-phase processing, and second, the CNT master batches were melt mixed with PE. Phase morphological observations revealed decrease in the size of the dispersed particles in the composites (Li et al. 2007).

Pure polyaniline (PANI) and its blends with PVA and PEO were prepared by solution cast method. The blends were characterized by XRD, FTIR, and SEM techniques. The blends were prepared in order to combine the mechanical properties of PVA and PEO with conducting properties of PANI. It was found that the conductivity of pure PANI was more than PANI blends (Subrahmanyam et al. 2012).

Nunoshige et al. developed a novel low-dielectric-loss thermosetting material by blending poly(2-allyl-6-methylphenol-co-2,6-dimethylphenol) (Allyl-PPE) with 1,2-bis(vinylphenyl)ethane (BVPE). BVPE could be used effectively as a cross-linking agent for Allyl-PPE, decreasing the cured temperature to 523 K or lower. The cured products exhibited better thermal and thermomechanical properties. The effect of the composition of the blends on the dielectric constant and the dielectric loss were evaluated (Nunoshige et al. 2007).

Mao et al. had tuned the morphology to improve the electrical properties of graphene filled immiscible polymer blends. PS and PMMA blends filled with octadecylamine-functionalized graphene (GE-ODA) were fabricated to obtain conductive composites with a lower electrical percolation threshold. The dependence of the electrical properties of the composites on the morphology was examined by changing the proportion of PS and PMMA. The electrical conductivity of the composites was optimal when PS and PMMA phases formed a co-continuous structure. For the PS/PMMA blend (50 wt/50 wt), the composites exhibited an extremely low electrical percolation threshold (0.5 wt%) because of the formation of a perfect double percolated structure (Mao et al. 2012).

Advances in nano-material research have opened the door for transparent conductive materials, each with unique properties. These include CNTs, graphene, metal nanowires, and printable metal grids. Transparent electrodes are necessary components in many modern devices such as touch screens, LCDs, OLEDs, and solar cells, all of which are growing in demand. Traditionally, this role has been well served by doped metal oxides, such as indium tin oxide. A review exploring these innovations in transparent conductors and the emerging trends is presented recently (Hecht et al. 2011). Electrical conductivity in PS nanocomposites with ultralow graphene level was found to enhance significantly (Qi et al. 2011).

10.7.4 Data on Blends

Electrical properties of selected commercial polymer blends are listed in Table 10.31.

10.8   Optical Properties

10.8.1 Methods of Measurement

10.8.1.1 Haze and Luminous Transmittance
ASTM D1003 provides two methods for measuring light transmittance and haze in planar sections of transparent plastics. The method making use of a hazemeter is briefly described.

A spherical hazemeter, which is pivotable about a vertical axis through the entrance port (where the specimen is placed), is shown in Fig. 10.62. In the normal position the collimated incident light passes straight through the sphere, leaving through the exit port, which is closed by an absorbent light trap. When light is scattered either by the instrument alone or by the specimen and the instrument (when the specimen is loaded), it is reflected from the region around the edge of the exit port and finally collected by the photocell after multiple reflections from the highly reflecting walls of the sphere.

When the integrating sphere is rotated slightly so that the incident light hits the opposite highly reflecting wall of the sphere adjacent to the exit port, the measurements with and without a specimen give a measure of the total transmittance. The total transmittance, T_t, is given by

$$T_t \quad = \quad \frac{T_2}{T_1} \tag{10.37}$$

where T_2 = the total light transmitted by the specimen and T_1 = the incident light without the specimen. Diffuse transmittance, T_d, and % of haze are calculated as

$$T_d \quad = \quad \frac{\left[T_4 - T_3 \left(\frac{T_2}{T_1 I} \right) \right]}{T_1} \tag{10.38}$$

$$\text{Haze} \ (\%) \quad = \quad 100 \ \left(\frac{T_d}{T_t} \right) \tag{10.39}$$

where T_4 = light scattered by instrument and specimen and T_3 = light scattered by instrument (without specimen). BS 2782 Method 515 A is the British equivalent, which deals with only haze of films.

10.8.1.2 Refractive Index
When a ray of light passes from one isotropic medium into another, the sinus of the angle of incidence makes a constant ratio to the sinus of the angle of refraction (both

Table 10.31 Data on some commercial polymer blends (Martino 1994)

No.	BLEND (trade name, composition, and manufacturer)	Volume resistivity (ohm-m) ASTM D257-99	Surface resistivity (ohm) ASTM D257-99	Dielectric strength oil, 0.125″; V/mil (3.2 mm; kV/mm) ASTM D149-97	Dielectric constant (100 Hz), ASTM D150-98	Dissipation factor (100 Hz), ASTM D150-98
1.	CYCOLOY C2950 (PC/ABS) GE Thermoplastics	1.0E15		495 (19.3)	3.0	0.0049
2.	GELOY GY1220(ASA/PVC) GE Thermoplastics	1.4E12	1.0E15–1.8E15	476 (19)–490 (17) (in air)	3.4–3.5	0.0007–0.0021
3.	XENOY-2230, 2735, 5220, 5230, 5720 (PC/PBT) GEC	2.1E14–9.5E14		705 (28)–1,096 (43) (in air)	2.93–3.60	0.001–0.002
4.	**MAKROBLEND**					
	(PC/PET) UT 1018	>2.6E13		396	3.06 (1 MHz)	0.014 (1 MHz)
	UT 400 and UT 403 MILES	>7.4E13		406	3.10 (1 MHz)	0.009 (1 MHz)
5.	**BAYBLEND**(PC/ABS) MILES					
	T45MN, T65MN, T44, T64	>1.0E14	>1.0E14	600		0.007 (1 MHz)
	T85MN, T84	>1.0E14	>1.0E14	600		0.008 (1 MHz)

Note: ASTM standard test methods are available on web: http://enterprise.astm.org/
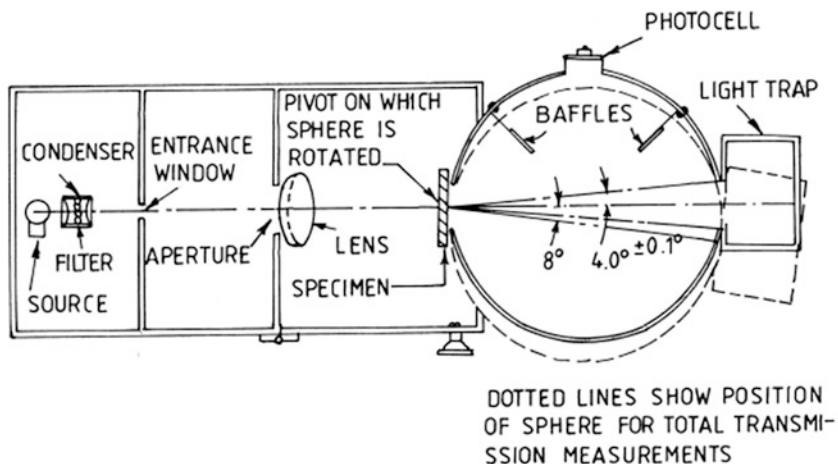
Fig. 10.62 Pivotable-sphere hazemeter [ASTM D1003]

measured with respect to the normal) for all angles of incidence. This dimensionless ratio, while dependent on the wavelength of the light and temperature, characterizes the two media concerned.

ASTM D542 describes two methods, viz., (i) refractometric and (ii) microscopic, for the measurement of refractive index of transparent organic plastics. Both the methods require optically homogeneous specimens of uniform index. The ASTM recommends that refractometric method is to be preferred wherever possible, since it is capable of providing results with greater precision (up to four significant figures). The microscopic method depends on operator's skill, and it yields results accurate up to only three significant figures.

For the refractometric method, the apparatus consists of an Abbe refractometer, a suitable source of white light and a small quantity of suitable contacting liquid. The test specimen for refractometer method should be 12.7×6.3 mm, with one flat face and one perpendicular surface. The two surfaces (preferably polished) shall intersect along a sharp line (without a rounded edge). The test specimen is attached to the prism of the refractometer with a drop of liquid of refractive index higher than the test specimen by at least 0.01, and it should not soften or dissolve the specimen. ASTM D542 suggests a list of liquids for a variety of plastics. Measurements are to be carried out at specified conditions, 296 ± 2 K and 50 ± 5 % RH. Temperature is to be accurately controlled. For maximum accuracy, sodium D lines are recommended.

ISO R489 suggests two methods based on Abbe refractometer and the Becke line methods. It does not recommend any specimen conditioning procedure prior to the test. DIN 53491 provides practical details relevant to refractometer measurements. It recommends test temperature as 293 ± 5 K, like ISO R489. For maximum accuracy it suggests the use of sodium light. All these methods provide lists of liquids suitable for different plastics.
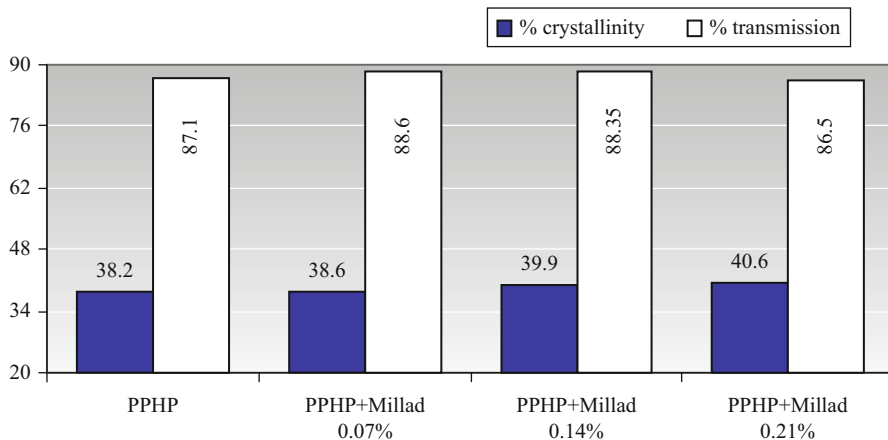
Fig. 10.63 Transmission (%) determined using Haze Meter and crystallinity (%) measured using X-ray diffraction are shown for polypropylene homopolymer mixed with different concentrations (0.07 wt%, 0.14 wt%, and 0.21 wt%) of Millad-3988 (Pendyala et al. 2004)

10.8.2 Transparency in Polypropylene

The degree of crystallinity and regularity of crystallite size have noticeable effects on properties of bulk isotactic polypropylene (PP). Clarity is commonly obtained in PP in two ways. First, resins with lower crystallinity will be clearer than those with higher, but a minimum level of crystallinity is necessary to provide the required strength, stiffness, and resistance to softening at elevated temperature expected of the PP. Second, certain nucleating agents greatly improve the clarity of PP by producing very small crystals in the polymers. These smaller crystals are below the size which scatters visible light that produces haze. Crystallinity vis-à-vis transmission in polypropylene homopolymer with different concentrations of Millad-3988 is illustrated in Fig. 10.63 (Pendyala et al. 2004).

Isotactic polypropylene can crystallize into three different forms: (i) α-phase, (ii) β-phase, and (iii) γ-phase. These spherulites satisfy two requirements to scatter light – they are larger than the wavelength of light and they have a refractive index different from that of the amorphous region. The refractive indices of the crystalline and amorphous regions of a polymer cannot be changed. So, in order to improve clarity, the average spherulites' size must be reduced. Since a spherulite grows until it meets another, their size is dependent on the number of nucleation sites (nucleation density) within the crystallizing polymer.

PP with improved clarity was commercialized in the 1980s by incorporating sorbitol-based clarifying agents by Milliken Chemical Co. and others (Carroll 1984). In PP, the crystallization results in large size spherulites, and hence inclusion of heterogeneous nucleating agents is often adopted to improve mechanical properties (Quande Gui and Weiping Zhu 2003) or to reduce optical haze (Sterzynski et al. 1994; Mannion 1994; Gahleitner et al. 1996; Amos et al. 1999; Zhao and Dotson 2002).

Hence, providing such heterogeneous nucleation is an essential consideration. Creation of various crystallographic phases, differed by the unit cells as well as by the spherulites, is known to be a result of the heterogeneous nucleation (Varga 1992; Lotz 1998).

10.8.3 Review of Blends' Optical Properties

Lack of transparency is a significant drawback in the commercially important toughened polymers such as HIPS or ABS (Manson and Sperling 1981). Transparency in these materials is lost due to the light scattering at the interface between the phases. The degree of light scattering (turbidity) was found to be a function of the amount of dispersed phase present, its particle size, the ratio of refractive indices of the phases, and the wavelength of light. In typical polymer pairs, at a given dispersed phase level, the maximum turbidity was observed in the range of particle sizes considered to be necessary for good impact strength (Conaghan and Rosen 1972). If the refractive indices are matched at a particular temperature, small particle sizes greatly increase the temperature range over which scattering is minimized. In other words, a clear blend can be obtained if both phases have identical refractive indices, regardless of the details of the phase morphology (Rosen 1967). Thus, for example, clarity in ABS and toughened acrylics was achieved by matching refractive indices of the continuous and dispersed phases (Gesner 1967). Impact modifiers for PVC that can impart toughness as well as clarity were described by several workers (Petrich 1972; Souder and Larson 1966; Ryan and Crochowski 1969; Ryan 1972).

Formation of transparent blend films cast from solutions of PVC and (PC-PDMS)$_n$ multiblock copolymer has created concern (Gorelova et al. 1992). The finding is interesting because the refractive indices of PVC, PC, and PDMS are different, and consequently, transparency of the blend films may suggest miscibility of their constituents, despite the fact that PVC is immiscible with PC and PDMS (Krause 1978). In other words, these blends are pseudo-miscible and their transparency is caused by the very small size of the dispersed block copolymer phase. PVC was also found to form transparent blends with other multiblock copolymers (Papkov et al. 1995). Several examples of the formation of transparent blends were reported. The constituents of these blends are homopolymers of various chemical compositions and flexibility, viz., PS, PMMA, and PVC, and the multiblock copolymers are PC-PDMS, PSF-PDMS, PSF-PB, and polytetramethylene oxide-PB (Papkov et al. 1998). For copolymers and homopolymers of various chemical structures, the composition range for each type of block copolymer, within which the formation of transparent blend film takes place, is relatively narrow.

The phenomenon appears to be similar to the so-called miscibility window in some blends with random copolymers (ten Brinke et al. 1983). Micro phase separation and the evolution of the multiblock copolymer phase in the form of small-sized particles (up to 100 nm in diameter) is the physical basis of their transparency. Thus, these transparent blends are considered microheterogeneous

systems (Papkov et al. 1998). Detailed theoretical and experimental investigations are required to understand details of this phenomenon (Sikora and Karasz 1993).

Blends of transparent polymers are generally hazy. However, transparency is required in many products. The miscible blends, PET/PBT, maintain transparency in almost all cases regardless of the blending ratio, whereas some immiscible blends become hazy. The reason for this haze is the number and size of the dispersed particles. Differences in the refractive indices of various polymers also have a large influence on haze. Stretching makes even the transparent blends hazy, because stretching increases the size of the dispersed particles in the sheet plane and also the difference in the anisotropic refractive indices of the matrix and the dispersed phase is increased by stretching, which is in agreement with the theory of light scattering (Maruhashi and Iida 2001).

The effect of added nanoclays to the morphological characteristics and the macroscopic properties in a blend of isotactic PP and PEO was examined. It was shown that strong interactions between the surfactant used for clay modification and the binary matrix effectively controlled the spatial organization of the suspended polymer droplets. The incorporation of a small amount of organically modified nanoclay induced a dramatic transformation from an opaque to a transparent system (Kelarakis and Yoon 2008).

Several blends of polymers that varied concentrations of PMMA and polyimides based on 2,20-bis(3,4-dicarboxyphenyl)hexafluoropropane dianhydride (6FDA) were prepared in film form by solution casting and using various solvents. The miscibility of the blended films was studied. DSC thermograms revealed two T_gs for specimens using THF as a solvent, indicating immiscibility; on the other hand, samples using methyl chloride and cyclohexanone showed a single T_g, indicating miscibility between the two polymers. The transmittance for 6FDA-6FpDA/PMMA had a value of about 85 % (according to ASTM D1003), in the visual light range. However, 6FDA–6FpDA:DABA 2:1/PMMA showed a low transmittance below wavelengths of 550 nm. For haze, all of the films were clear with values of less than 1 % (Im et al. 2009).

In a separate study immiscible blends were rendered transparent. The components of the immiscible blends were having refractive indices which differ by about 0.006 to about −0.0006. The small difference in the refractive indices enabled the incorporation of regrind into the polymer composition to produce transparent shaped articles (Gilliam et al. 2011; Cliffton et al. 2012).

Interesting advances are taking place in biopolymers with regard to optical transparency. An opaque polylactide/poly(ethylene-co-vinyl alcohol) (PLA/EVOH 90/10 w/w) blend was made transparent by reactive compatibilization. In the presence of a multifunctional epoxy compound and zinc stearate, the dispersed domain size of EVOH in the blend and its distribution decreased significantly. Consequently, the light transmission at 700 nm increased from 9.3 % to 83.5 % for the compatibilized sample. A significant difference in the transparency of the samples can also be confirmed by naked eye (Zhang et al. 2013). In a separate study, binary blends composed of biomass-based cellulose acetate propionate (CAP) and poly(epichloro-hydrin) (PECH) were studied. As a result of the interdiffusion, leading to fine

morphology, the blends exhibited high level of optical transparency although the individual pure components had different refractive index. Furthermore, the mechanical toughness of CAP was considerably improved by blending PECH. This will have a great impact on industries because the blend technique widens the application of CAP (Yamaguchi and Masuzava 2013).

10.9 Sound Transmission Properties

Sound retardant (acoustical) assemblies are one of the most commonly used in commercial building. An acoustical assembly is an acoustical door or window that maintains its basic operating function and is at the same time designed to be a significant barrier to the passage of sound. It is called an acoustical assembly because an entire system is involved. A sound retardant assembly encompasses not just the door or window itself but all the components around it. The wall, the frame which surrounds the door, the door itself, the hardware components, and finally the sealing system, whereby the passage of noise is minimized, all combine to create an acoustical assembly.

Sound ratings are typically based off the sound transmission class (STC) scale system, Table 10.32. This single rating system enables a designer to match up architectural products that when combined will create an STC rating for the entire assembly controlling the noise and vibration in room, office, or even an entire building.

10.9.1 Method of Measurement

The preferred method for determining the STC rating of a product is a test called the ASTM E-90, "Standard Method for Laboratory Measurement of Airborne Sound Transmission," which is summarized here below.

ASTM E90-09 provides a method covering the laboratory measurement of airborne sound transmission loss of building partitions such as walls of all kinds, operable partitions, floor–ceiling assemblies, doors, windows, roofs, panels, and other space-dividing elements (ASTM E90 2009). Laboratories are designed so the test specimen constitutes the primary sound transmission path between the two test rooms, and so approximately diffuse sound fields exist in the rooms.

Sound transmission loss refers to the response of specimens exposed to a diffuse incident sound field. The test results are therefore most directly relevant to the performance of similar specimens exposed to similar sound fields. They provide, however, a useful general measure of performance for the variety of sound fields to which a partition or element may typically be exposed. In laboratories designed to satisfy the requirements of this test method, the intent is that only significant path for sound transmission between the rooms is through the test specimen. Laboratories are designed so the test specimen constitutes the primary sound transmission path between the two test rooms and so approximately diffuse sound fields exist in the rooms.

This standard does not purport to address all of the safety concerns.

Table 10.32 Sound transmission class (ZERO International 2001)

Sound Transmission Class (STC) Table		
STC	Performance	Description
50–60	Excellent	Loud sounds heard faintly or not at all
40–50	Very good	Loud speech heard faintly. But not understood
35–40	Good	Loud speech heard but hardly intelligible
30–35	Fair	Loud speech understood fairly well.
25–30	Poor	Normal speech understood easily and distinctly
20–25	Very poor	Low speech audible

It is important to know the sound transmission loss of walls and floors in order to be able to compare different constructions, to calculate acoustic privacy between apartments or noise levels from outdoor sources such as road traffic, and to engineer optimum solutions to noise control problems. Laboratory measurements can be made for many different types of partitions, but it is impractical to test every possible design, and so it is necessary to have reliable methods for predicting the sound transmission loss of typical building constructions.

There are various methods for predicting the sound transmission loss of walls and floors that can be used by noise control engineers. It is important to know how accurate these methods are for typical constructions used in building acoustics (Ballagh 2004). As the standard grows in experience over the years, it reveals the complex variables that must be addressed in order to equalize the conditions that have a potential to affect results.

10.9.2 Factors Affecting Sound Transmission

During an ASTM E-90 test, a test specimen is mounted between a room containing an isolated source of noise and a receiving room. Sound transmission loss, the difference between the sound level in the source room and the receiving room, is measured at specific sound frequencies and used to arrive at the STC rating. The higher the STC rating calculated, the quieter it is in the receiving room.

When sound waves come in contact with a boundary obstacle, such as a wall or door, a portion of the sound wave energy is reflected, a portion is transmitted through the obstacle, and the rest is absorbed by the obstacle. One of the standard methods of measuring the effective sound absorption coefficient of an acoustical material is by finding its effect on the reverberation time, or decay rate, of the sound pressure level in the sound chamber. The total sound absorption in the receiving room is required to determine the noise reduction of the specimen being tested. The key here is to rule out the absorption of sound waves within the chamber that may be attributed to the door being tested.

Because the ASTM standard does not provide a resolution for measuring and standardizing absorption levels from one laboratory to the next, the same product tested in laboratories with different absorption levels can result in different STC ratings. Another variable that the standard does not currently address is the difference between a door and a partition. While the standard makes a provision that a door must be cycled (opened and shut) a number of times, prior to commencing the test, the operating force or the pressure required to release a tightly sealed door is not addressed.

STC values are used to define the performance requirements for achieving a specified reduction in sound transmission from a source room to a receiving room. The STC rating of an installed door also determines how much noise reduction is possible between a given source room and receiving room.

10.9.2.1 Salient Features of Sound Transmission

- Sound waves travel through any opening with very little loss. While the amount of air flowing through a gap increases in proportion with the size of the gap.
- A tiny hole transmits almost as much sound as a much larger gap. For example, a one square inch hole in 100 square feet of gypsum board partition can transmit as much sound as the rest of the partition. Air paths through gaps, cracks, or holes pose serious problems.
- Air trapped in a "sound lock" between a pair of doors, or between layered sets of seals in a gasket, is one of the best sound absorbers.
- It is important to understand that STC values are not proportionate units of measurement. To achieve increasingly higher levels of sound control, each 10 dB increment requires ten times as much improvement as the one before. While door openings rated in the range from STC of 30 to STC of 40 are common, achieving STC of 50 and higher ratings is extraordinarily difficult.
- Acoustical performance depends upon wall design, its thickness and weight, and ultimately cost. Frequently it is not possible to optimize one factor without seriously compromising the others.

10.9.3 Review of Blends in Noise Reduction

Noise has become an environmental issue, and legislation on noise regulation is under review and being drafted in industrialized countries, especially those in Europe. The reduction of noise from machinery, automobiles, and appliances has been studied extensively (Tokairin and Kitada 2005; Zhang et al. 2007; Jiang et al. 2007; Mazeaud and Galland 2007). The techniques using sound absorption and insulation materials to reduce ambient noise have received much attention in this area of research (Zhou et al. 2006; ASTM E413-10).

Traffic noise, which falls within the frequency range of 250 and 4,000 Hz (Lapcik 1998), has been a huge headache for the public, and the common practice to deal with it is to build concrete noise barriers along roads and highways.

The study done by American Acoustical and Insulation Materials Association (1974) showed that these concrete barriers are of very high acoustic reflectivity (95 % and above) and of low sound absorption. This means that concrete barriers are not effective in controlling and reducing traffic noise (Campbell 2000).

In recent years, some notable progress has been made in making non-concrete barriers. It has been reported that a section of polycarbonate noise wall was built in 1996 near Culver City Park in Los Angeles, California, USA. The polycarbonate noise reduction panels are developed by Quilite International (QUILITE Noise Barriers 1997). A jet engine testing shelter was installed by using Lexan (polycarbonate) plastic manufactured by General Electric (Anderson 1997).

Another development is a noise barrier system developed by Carsonite International based in the city of Early Branch, South Carolina, USA, and those noise barriers are lightweight hollow panels made of tongue-and-groove planks of reinforced composite material filled with crumbed tire rubber. A few sections of Carsonite noise barriers have been built in Long Beach, California. Traditional noise barriers have a flat surface. Now new designs are experimenting with nonflat surface textures (Watts and Morgan 1997).

Placing noise reducers on the top of highway noise barriers is another way that aims to reduce traffic noise (Shono et al. 1994). Numerical and/or analytical studies have also been reported on the estimate of noise reduction effect (Alfredson 1990; Tanaka et al. 1990).

These, abovementioned, noise barriers exhibit a much better performance than concrete with sound absorption and transmission loss. But noise reduction is not the only criterion dominating the decision to construct noise barriers. There are other crucial criteria, and they include (1) cost-effectiveness, (2) technology maturity, (3) durability, (4) low cost and convenience in installation, (5) low cost and convenience in maintenance and repair, and (6) aesthetics. Concrete noise barriers meet those criteria very much (Kay et al. 2000). Crumb rubber blends aiming at the application in noise reduction are also developed and are found to yield encouraging results (Han et al. 2008).

The sound insulation efficiency of ABS/carbon nanotube (CNT) composites was increased with an increase in the amount of CNT. Since the sound insulation of ABS/CNT composite was improved with higher stiffness due to CNT, it might be concluded that stiffness is one of principal factors influencing the improvement of transmission loss of polymer/CNT composites (Lee et al. 2008).

Particle boards (PB) from jute stick (JS), date palm leaf, and their blends offered higher sound transmission loss, higher thermal insulation, and lower swelling compared to plywood. Increase of JS in blend with date palm leaf increased sound loss as well as thermal insulation. Sound loss increased with increase in thickness of PB. Relationship between sound loss and thickness is found to be nonlinear. Sound loss reached maximum at board thickness of 19 mm for PB (Ghosh et al. 2010).

Noise inside a motor vehicle arises from various sources. External sources include rain and wind impacting on the vehicle body panels, and internal sources

include the engine of the vehicle. Vibration of the body panels, such as the bonnet, the roof, and door panels, is the source of considerable noise inside the vehicle. Attempts have been made to damp vibration of the body panels and hence reduce the noise inside the vehicle, by attaching layers of damping material to the surfaces of the panels. One traditional method has been to attach press-formed fibrous composite sheets. However, these sheets are prone to rotting when damp, as the material is not water resistant and is very difficult to clean.

More recently, viscoelastic materials have been used. One such material is a copolymer comprising ethylene, vinyl acetate, and acrylic and/or methacrylic acid. Another proposal has been to apply a viscoelastic adhesive composition comprising a polyepoxide, a polyether amine, a hetrocyclic amine, and a phenol, which is said to be useful as a damping material. A yet further proposal has been to use composite comprising an elastomeric butyl polymer sheet bonded to a thin layer of non-elastomeric material on the surface. Furthermore they are not particularly useful in preventing transmission of noise from other sources. Multilayered acoustic tiles for suppressing noise and also reducing its transmission were developed (Gunasekara and Alwis 2004; Bourcier et al. 2009). Improved materials that will not only effectively damp the vibration of the body panels but will also reduce sound transmission through the body panels would be a great advance in the art of vehicle sound proofing which is still evolving.

10.10 Special Test Methods

10.10.1 Aroma Barrier Test

Until the first half of the twentieth century, perishable food articles of daily life, such as meat or cheese, and also non-food articles like detergents or soap were mostly sold in shops and did not use packaging or were just wrapped in paper or cardboard. Glass and metal were the only packaging materials providing high barrier for the few applications which required long shelf life.

Modern lifestyle with self-service supermarkets, plus worldwide and year-round availability of all articles, would not be possible without adequate packaging of those articles. Processing, preservation, and distribution of those articles have created not only a huge growth of traditional packaging materials, e.g., glass, metal, and paper, but also the development of new packaging concepts, especially flexible packaging with plastic materials, for better economy, convenience of packaging, and quick transportation (Kemmer et al. 2008).

The food industry has long depended upon reliable, impermeable packaging materials such as glass and metal. Both suppliers and food manufacturers focus research efforts into lighter-weight, flexible, and semirigid packages, which are typical qualities of plastics. While parameters such as functionality, recyclability, and cost are critical characteristics, the lack of complete impermeability and inertness in these polymer materials can have important effects. Due to their size

and nature, the aroma compounds will interact with packaging materials often consisting of lipophilic hydrocarbons (Johansson 1996).

10.10.1.1 Factors Influencing Aroma Barrier Test

An aroma is a chemical substance sensed by the taste and/or the smell defined by parameters such as its volatility, its polarity, and its aromatic value. The aromas must be protected throughout the retail chain until its use. The conservation of these aromatic contents is mainly based on the packaging (Risch 2000).

Aroma compounds interact with the polymer matrix, leading to polymer structural changes. Plastic packages are made up of polymers that form a matrix of crystalline and amorphous regions, which contain submicroscopic voids. Aromas permeate through packaging by first being adsorbed onto the package's surfaces, diffusing through the voids (absorption), and, without a barrier material, desorbed to the package's exterior. A sorption–diffusion mechanism is thus applied.

The mass transfer phenomenon, commonly described by the sorption, the migration, and the permeation can be determined by three parameters: S, the solubility coefficient; D, the diffusion coefficient; and P, the permeability coefficient. When diffusion is Fickian and sorption follows Henry's law, the relationship $P = DS$ can be used (ASTM F 1769-97).

Literature and knowledge on mass transfer of aroma compounds are few and no standard procedure is recommended. Methods developed for aroma compounds permeability measurements are commonly approached by isostatic or quasi-isostatic methods and depend on the physical state (vapor or liquid) of the aroma compounds (Piringer and Baner 2000).

Aroma barrier is somewhat analogous to flavor barrier. Food products must be protected from outside aromas in the distribution chain, grocery store, and home. Other food and non-food products such as garlic, agricultural chemicals, pesticides, insecticides, or perfumes can be highly aromatic. The desire is to retain the aroma in the package and not let it escape into the surrounding environment (Eval Americas 2007).

Numerous apparatus have been designed, to different degrees of success, to obtain information regarding aroma permeability of packaging films in a reasonable time frame. Experimental setup for studying the permeability through polymeric films is presented in Fig. 10.64 (Vähä-Nissi et al. 2008).

Sensory evaluations of some common aromas packaged in a variety of film structures are presented in Table 10.33. And comparison of permeation rate of different film structures for some common aromas is shown in Table 10.34.

The area of "flavor" and "aroma" barrier is receiving growing attention in the field of plastics packaging. The permeation of flavors is difficult to measure quantitatively because they contain many components. Many times, only a simple component of a flavor is measured if a quantitative value must be determined. Gas chromatography and mass spectrophotometric (GC/MS) techniques have been developed that allow the analysis of complex flavors. However, in most cases, the use of organoleptic testing provides reliable and pertinent data at a greatly reduced cost.

As with flavor permeation, aroma permeation can be determined by sensory evaluation or gas chromatography.

Fig. 10.64 Permeation device with *1*, GC; *2*, test cell; *3*, test cell oven and sample transfer oven (Vähä-Nissi et al. 2008)
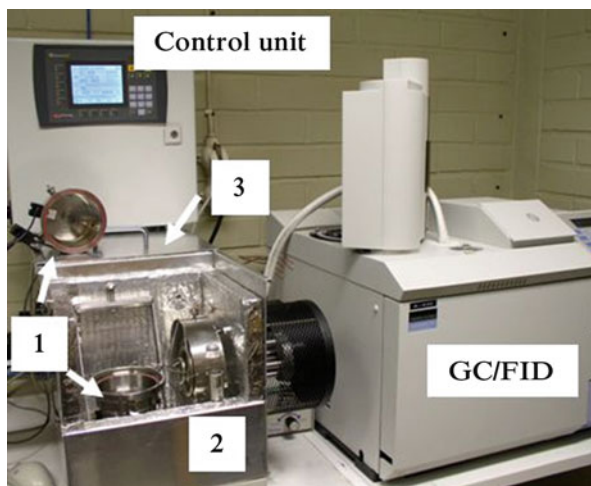
Table 10.33 Results of sensory evaluations for various aromas packaged in a variety of film structures. The numbers represent the time it takes the aroma to permeate the package at room temperature (Eval Americas 2007)

Aroma permeation						
PVDC						
Structure thickness (μ)	LDPE (50)	OPP/PE (20/50)	PET/PE (20/50)	Nylon (15)	F Series/ PE (15/50)	EF-XL/PE (15/50)
Orange essence	1	2	3	2	4	5
Strawberry essence	2	2	3	2	3	3
Curry powder	2	3	2	2	3	3
Garlic powder	2	2	2	2	3	3
Coffee powder	2	3	3	3	5	5
Linalol	1	3	3	4	5	5
Geraniol	1	3	3	4	5	5
Prenyl Benzoate	1	2	2	3	5	5
Methyl ionone	2	3	3	3	5	5

Key: 1: <1 h, 2: <1 day, 3: <1 week, 4: <2 weeks, 5: <2 weeks

Diffusion (D) and Permeability (P) Coefficients

For different aroma/synthetic material couples, the results of the D and P obtained by the HS-GC/MS and gravimetric methods are compared in the literature (Table 10.35).

D and P for the Limonene/LDPE Couple in Function of Relative Humidity

In view of the previous results, the study of the influence of the relative humidity on the mass transfer of an aroma through a packaging material was realized for the couple limonene/LDPE (Maki and Stevens 2002).

Table 10.34 Comparison of permeation rate of various film structures for common aromas (Eval Americas 2007)

Aroma permeation					
Days to Leakage					
Film construction	Thickness (mils)	Vanillin (Vanilla)	Menthol (Peppermint)	Piperonal (Heliotropin)	Camphor
PET/F Series/ PE	0.5/0.6/2.0	15	25	27	>30
OPP/F Series/ PE	0.7/0.6/2.0	30	>30	27	>30
PET/F Series	0.5/0.6	>30	>30	30	>30
ON/F Series	0.6/0.6	2	>30	27	30
PET/PE	0.5/2.0	2	16	5	>30
ON/PE	0.6/2.0	2	20	5	28
PVDC ct'd PET/PE	0.6/2.0	7	>30	6	30
PVDC ct'd/ OPP/PE	0.7/2.0	6	2	1	13
PVDC ct'd PET	0.9	5	6	1	7

Values in the table above indicate the number of days until leakage through the package is detected. The greater the values, higher the fragrance preservation

Table 10.35 Comparison of the diffusion and permeability coefficients of the HS-GC-MS and gravimetric methods for different relative humidity for the limonene/LDPE couple (Martine and Louvier 2010)

Method	Coefficient at 23 °C	20 % r.h.	50 % r.h.	90 % r.h.
HS-GC/MS	Mean diffusion (**D**) (cm^2/s)	5.34×10^{-9}	7.03×10^{-9}	5.23×10^{-9}
	Permeability (**P**) (g.μm/m2.d.Pa)	14 (n = 3)	20 (n = 7)	7 (n = 3)
		9 → 18	14 → 35	6 → 8
Gravimetry	Mean permeability (**P**) (g.μm/m^2.d.Pa)	13 (n = 3)	26 (n = 3)	13 (n = 3)
		13	26 → 27	12 → 15

Notice that D and P are lower for 20 % and 90 % relative humidity compared with those for a relative humidity of 50 % whatever the analytical methods used

10.10.1.2 Examples of Polymers as Barrier Films
Nylon 6
Nylon 6 is a good barrier material for nonpolar to slightly polar solvents and smaller organic molecules and a very good barrier to bulky aroma molecules of low to intermediate polarity. For some nonpolar materials, its barrier even exceeds that of EVOH, whereas EVOH has slight advantages for molecules of intermediate polarity. Only for highly polar migrants, as methanol or isopropanol, the barrier of nylon 6 is clearly lower than that of EVOH – a situation well known from oxygen and carbon dioxide permeation.

Due to its moderate price, good processability, and high mechanical and thermal properties, it is found to be a suitable material for packaging of many aroma-containing materials, such as menthol-flavored toothpaste. In case of detergent refill pouches, it further prevents contamination of the environment by the aroma migrating out of the package, an effect that may be undesirable when too many different flavors come together. Another application PA6 that is frequently used for is barrier layer in blow-molded containers as are used for packaging herbicides or pesticides with cyclohexane, xylene, or methyl ethyl ketone solution. Here, nylon provides another advantage over EVOH: nylon 6 may be processed as inner, sealing layer, thereby providing a continuous barrier layer in the container. EVOH however needs to be processed as a core layer, with a PE inner layer which is then in contact to the solvent and also forms the seal. This seal will then be a weak spot in the container for both migration and mechanical strength.

Cyclic Olefin Copolymer (COC)

COC has better aroma barrier than polyethylene and is found to reduce aroma/flavor loss from food when it is utilized as a barrier layer in food packaging. COC is also found to reduce the transmission of objectionable odors to surrounding areas and has utility in disposable food storage bags. Low extractables in COC reduce the possibility of generating an "off-taste" in water or susceptible foods when used as a contact layer or just under a seal layer in packaging (Jester et al. 2005).

10.10.2 Permeability Test for Liquids

There has been a trend to use more plastic-based packaging materials for different applications such as replacements for metal and glass containers. This situation has stimulated the industry to provide new and more efficient barrier solutions. A number of different technologies are being developed and are making their way into the market. Melt processable thermoplastic blends which allow injection molding, blow molding, thermoforming, and other conventional techniques to be applied for making products that are impermeable for diesel, petrol, and other organic liquids while possessing high-performance properties, even after recycling, are being focused.

Following the success story of the plastic bumpers, for automobiles, which commercially replaced the heavy metallic bumpers, the plastic fuel tanks are making inroads to replace metallic fuel tanks. The plastic tanks offer weight reduction, freedom from corrosion, and ease of fabrication.

The principal performance property required for HDPE blend (with polyamide-6) is the reduced permeability for diesel; hence, the morphology of the blends in the final product is extremely important. The morphology of the binary blends and the influence of different compatibilizers in different concentrations were also investigated using scanning electron microscope (SEM). Here, for morphology

studies, the injection-molded flexural bars were allowed to soak in liquid nitrogen and were fractured quickly after taking them out. The fractured surfaces were carefully cut and were studied under SEM, after making their surfaces conducting by depositing gold vapors in an ion sputtering unit.

The blends disclosed dispersed domains of polyamide within a continuous phase of HDPE. Since HDPE and polyamide are incompatible, use of a compatibilizer is essential. There are three main factors governing compatibilization and interfacial interactions, viz., reduction of the interfacial tension, increased interfacial adhesion, and achievement of a viscosity ratio conducive to efficient dispersion.

10.10.2.1 Factors Influencing Permeability Test

Permeation is a mass transport phenomenon in which molecules transfer through the polymer from one environment to another through diffusive processes. Mass transport proceeds through a combination of three factors in case of polymers. They are (1) dissolution of molecules in polymer (following absorption at the surface), (2) diffusion of molecules through the material, and (3) desorption from the surface of the material (Crank and Park 1968; Kumins and Kwei 1968).

In case of polymers, mass transport of small molecules can take place, as there is intrinsic porosity in the polymer matrix. Even solid homogeneous polymers are likely to be porous to some degree owing to defects, inclusions and different phases, which leave pores, voids, and crazes capable of accommodating small molecules. For molecules to undergo transport within a polymer, they must dissolve in the solid polymer. If the molecules do not dissolve, in the polymer, then diffusion is irrelevant. The basic mechanism for diffusion is occupation of the free volume between the polymer chains. Dissolution is a thermodynamic process, where the solubility is determined by enthalpy change on dissolution of the molecule in the polymer matrix and the volume available. And diffusion is the net transport of matter in a system, which acts to nullify the potential differences in order to bring in a state of equilibrium. Here, the rate of diffusion is proportional to the concentration gradient of the diffusant.

The factors, which influence the permeability or mass transport, are the following: chemical composition of the polymer matrix and its free volume. In fact, crystallinity, molecular orientation, and physical aging in turn influence the free volume of a polymer matrix. In addition, porosity and voids, like free volume, offer sites into which molecules can absorb and are far less of a barrier to transport than solid polymer. Temperature also affects permeability and diffusion properties of small molecules in polymers. With increased temperature, the mobility of molecular chains (in polymer) increases and thermal expansion leads to reduced density; therefore, the free volume in the system will increase. External tensile stress applied is expected to increase free volume and open up internal voids or crazes, providing additional sites into which molecules can absorb. Of course, there may be unquantified internal residual stresses, arising from processing, present in the polymers. It is well established that the properties of materials

Fig. 10.65 HDPE–
polyamide-6 (20 wt%) blend.
Injection-molded flexural bar
in the skin zone as viewed
under SEM (Xavier and
Pendyala 2008)

near the interphase are different from those of the bulk material. Thus, the
diffusion properties in the interfacial region are likely to be different from those
of the bulk material.

10.10.2.2 Permeability and Polymer Blend Morphology
Morphology of HDPE-Polyamide-6 Compatibilized Blends
PE and PA-6 are incompatible with an unstable morphology when blended. To stabilize
PE/PA-6 blends, many compatibilizers have been used (Yeh et al. 1995; Chen et al.
1988; Kouloori et al. 1997; Gadekar et al. 1998; Raval et al. 1991; Willis and Favis
1988; Halldén et al. 2001), e.g., copolymers or adducts of maleic anhydride (Chen
et al. 1988; Gadekar et al. 1998), acrylate copolymers such as poly(ethylene-*g*-butyl
acrylate) (Raval et al. 1991) and ethylene/methacrylic acid/isobutyl acrylate terpoly-
mer (Willis and Favis 1988), poly(ethylene-*g*-ethylene oxide) and poly(ethylene-
co-acrylic acid) (Halldén, and Wesslen 1996; Serpe et al. 1988), and succinic anhydride
functional groups (Padwa 1992; Sánchez-Valdes et al. 1998; Kudva et al. 1999; Kelar
and Jurkowski 2000; Pan et al. 2001; Jurkowski et al. 2002; Filippi et al. 2002).

The morphology of the cryogenic fracture surfaces of HDPE blends with
polyamide-6 (PA-6) are presented in Figs. 10.65 and 10.66. PA-6 distributed in
a matrix of HDPE is clearly visible in Fig. 10.65. Here, as no compatibilizer was
engaged, the protruding strips of PA-6 do not show any interaction with the matrix
material. But when a compatibilizer, ethylene-methacrylic acid copolymer, was
engaged, the fracture morphology has altered (Fig. 10.66) and the PA-6 dispersion
is rather more uniform and does not show such protruding strips. The dispersion of
PA-6 (35 wt%) as viewed from optical microscope (Fig. 10.67) also exhibits good
dispersion of the same (Xavier and Pendyala 2008).

Morphology of HDPE-Polyamide-66 Compatibilized Blends
Poor interfacial interactions between polyamide-66 and matrix material are respon-
sible for considerable pulling out of the dispersed phase as revealed in Fig. 10.68.

Fig. 10.66 HDPE–
polyamide-6 (20 wt%) blend
with compatibilizer
ethylene–methacrylic acid
copolymer neutralized with
metal ions (5 wt%). Injection-
molded flexural bar in the skin
zone as viewed under SEM
(Xavier and Pendyala 2008)
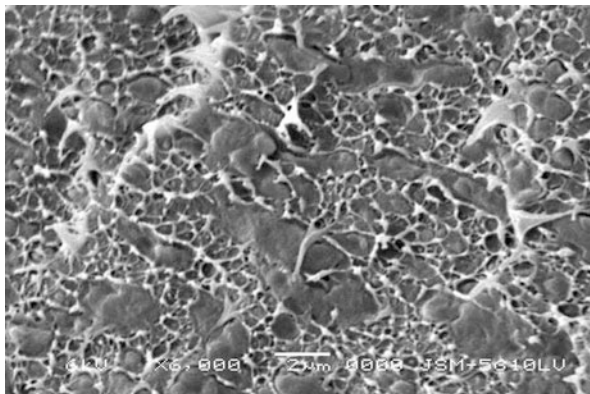
Fig. 10.67 Optical
micrograph of
HDPE–polyamide-6
(35 wt%) at 20X with
polarizers crossed.
Microtomed section of
injection-molded flexural bar
in the core region (Xavier and
Pendyala 2008)
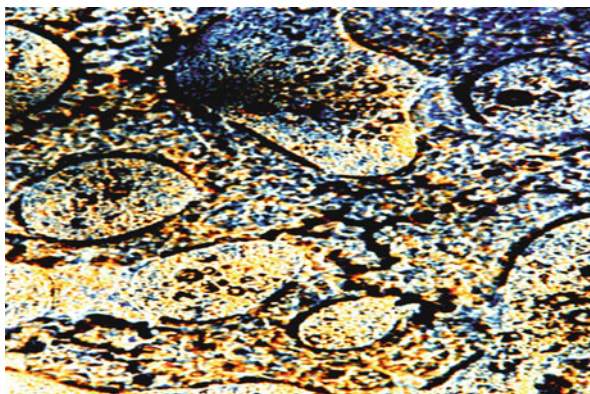
Fig. 10.68 HDPE–
polyamide-66 (30 wt%)
blend. Injection-molded
flexural bar in the core zone as
viewed under SEM (Joshi
et al. 2005)

Fig. 10.69 HDPE–polyamide-66 (23.75 wt%) with compatibilizer ethylene–methacrylic acid copolymer neutralized with metal ions (5 wt%). Injection-molded flexural bar in the core zone as viewed under SEM (Joshi et al. 2005)
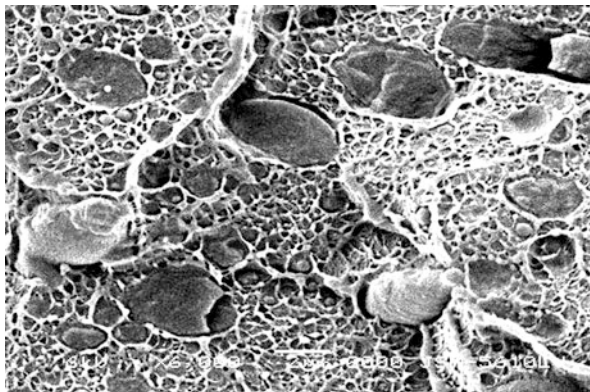
Fig. 10.70 Lamellar morphology in fractured bottle wall of HDPE–polyamide-6 compatibilized blend with good barrier properties for diesel as viewed under SEM (Xavier and Pendyala 2008)
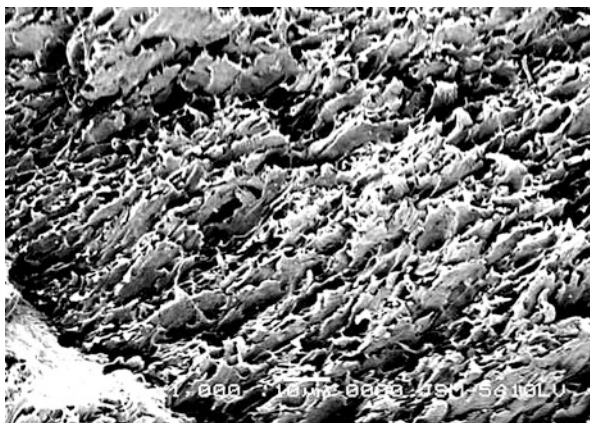
String and bead type of morphology is observed at many locations. However, as compatibilizer ethylene–methacrylic acid copolymer is introduced, the fracture has taken place in flat plane and no protrusions of polyamide-66 are observed (Joshi et al. 2005). The presence of the compatibilizer has altered the fracture propagation mechanism (Fig. 10.69).

The blow-molded bottle of HDPE blend with polyamide-6, after testing for permeability of diesel, was also tested for its morphology, using SEM. The bottle wall was cut into strips and the strip was fractured after soaking in liquid nitrogen. The morphology of the fractured surface revealed lamellae formed by the dispersed phase and oriented in the melt flow direction, parallel to the wall surface of the bottle (Fig. 10.70). These lamellae are responsible for restricting the permeation of diesel through the bottle. The wall of the bottle as well as the bottom of the cylindrical-shaped bottle was cut, and morphology
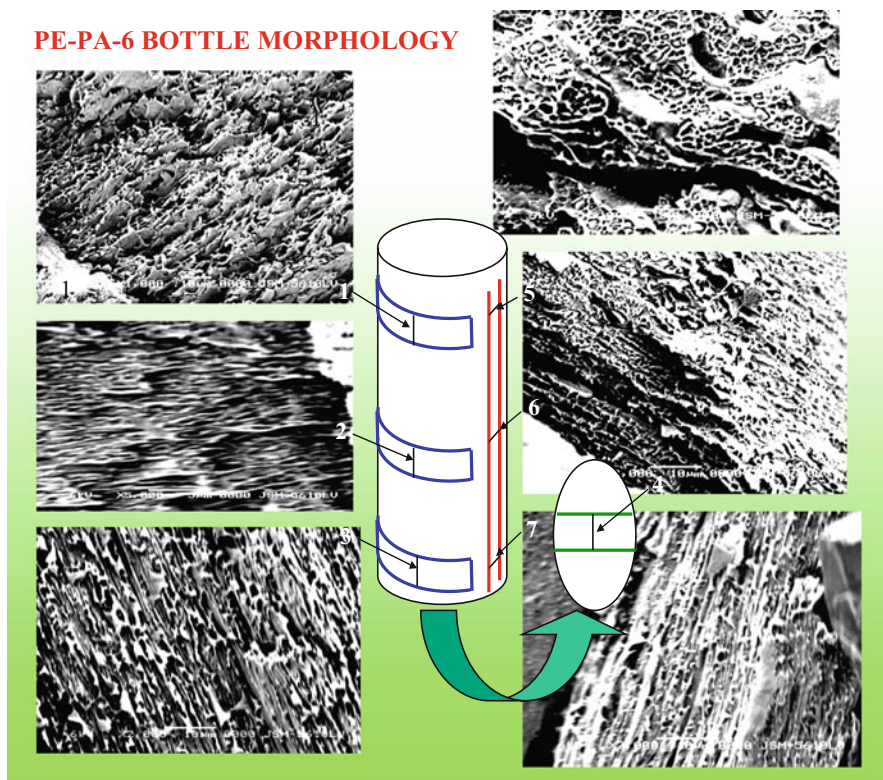
Fig. 10.71 PE–PA-6 bottle wall morphologies at different locations (Xavier and Pendyala 2008)

was studied at different locations. The lamellar morphology (as viewed in Fig. 10.70) was found to be present at all the locations of the bottle investigated (Fig. 10.71).

10.10.2.3 Permeability Tests for Diesel and Petrol

Permeation tests by pouring liquids in bottles and monitoring the weights of the bottles with regard to time have been practiced in many laboratories (Armstrong 1968a, b; Mesrobian et al. 1968; Subramanian 1983, 1984, 1985, 1987; Jen-Taut 1997; Xavier and Pendyala 2008).

Bottles of 250 ml capacity were prepared out of the dried granules of HDPE as well as compatibilized blend (with PA-6) having high mechanical properties; preferably with high notched Izod impact strength along with suitable melt flow characteristics. The injection molding was carried out in a Windsor Machine, SP-110, in a temperature range, 513–573 K, with injection pressure, 50–60 kg/cm^2, locking pressure around 70 t, injection time, 4.0–6.0 s, and cooling time, 5.0–7.0 s.
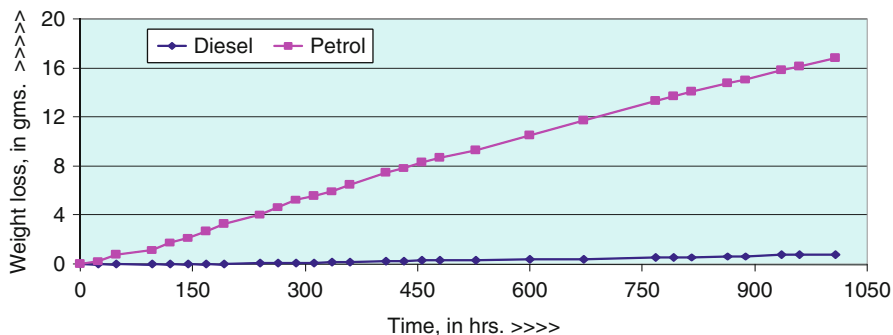
Fig. 10.72 Weight loss in bottles filled with Petrol and Diesel with regard to time in hours. Each point on the graph is an average weight of three bottles kept under investigation (Xavier and Pendyala 2008)

Diesel, as well as petrol, was poured separately into bottles of neat HDPE (control) and the selected blend bottles, at least three bottles for each case, covered with aluminum foil using a silicone sealant that cured at room temperature. It was further covered with molded plastic lid and was sealed with the same sealant. After the adhesive is cured, diesel/petrol permeation is tested and recorded at regular intervals by measuring the weight of each bottle.

Bottles with Petrol had shown a loss of 7 wt% in 25 days (600 h). Bottles filled with diesel had shown a marginal loss of 0.2 wt% in 25 days (600 h) or a weight loss of 0.8 g in about 1,000 h. See Fig. 10.72 (Xavier and Pendyala 2008).

10.10.3 Environmental Stress Cracking

Environmental stress cracking (ESC) in plastics means the failure of the plastic involved at about room temperature due to continuously acting external and/or internal stresses in the presence of surface-active substances (known as stress-cracking agents), which are normally liquids, such as alcohols, soaps, dyes, and agents containing moisture (Scheirs 2000; Wright 1996; Lagaron and Dixon 1998; Lagaron et al. 1999). ESC is a major problem in the long-term service behavior of plastic products. It can lead to quite expensive failures during warehouse storage, shipping, or during long-time applications. ESC of polymers is analogous to the stress corrosion problem in metals. It takes place after a certain period of time: the lower the stress, the longer the durability.

ESC occurs, in general, in amorphous polymers such as PC, PMMA, PS, PVC, SAN, and ABS as well as in semicrystalline thermoplastics like PE, PP, PA, and PB (Wright 1996). Amorphous polymers exhibit a higher tendency for this type of failure because their loose structure facilitates fluid permeation into the polymer. Amorphous polymers show enhanced sensitivity to ESC at temperatures close to

Fig. 10.73 Bent Strip ESCR Test (ASTM D1693-12)

"C" Shaped Bracket

IGEPAL® Solution

10 Notched Test Specimen in C Shaped Bracket
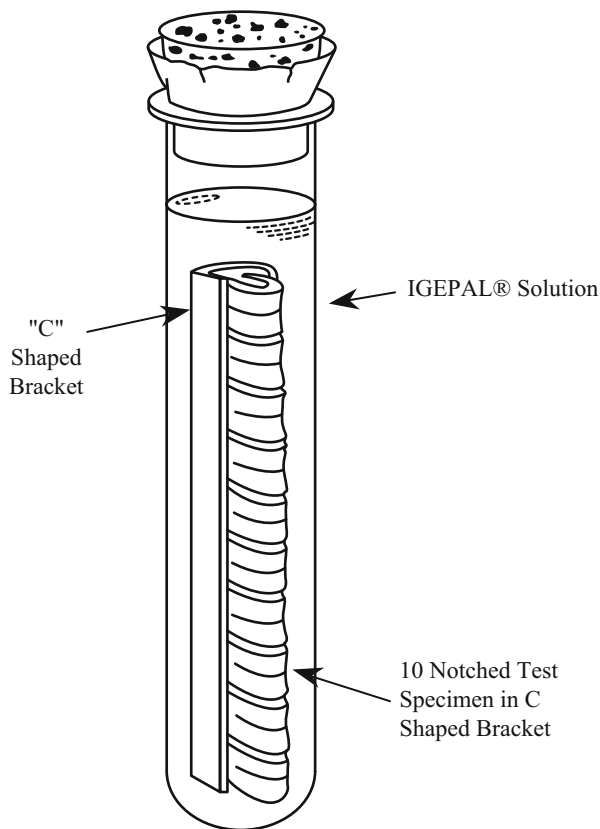
their T_g values due to the increased free volume as T_g is approached, which facilitates fluid permeation into the polymer. The solvent then becomes locally dissolved and promotes crazing which is a fore runner for cracking. Several molecular mechanisms have been proposed to explain ESC over the past few years (Lagaron et al. 2000). Lustiger and Ishikawa have proposed "interlamellar failure" as the controlling mechanism of ESC (Lustiger and Ishikawa 1991).

10.10.3.1 Test Methods for ESC
ASTM D 1693: Bent Strip ESC Test
This is a well-known original ESC test developed by Bell Labs in the late 1940s. Ten rectangular-shaped specimens are cut from a molded plaque prepared using standard methods. A controlled notch is cut horizontally across each specimen, which serves as a crack initiation point. The specimens are bent and inserted into a "C"-shaped bracket, creating a stress in the specimen. A diagram of this test method is shown in Fig. 10.73. The specimens and bracket are inserted into a tube filled with Igepal® solution. The tube is then placed into a heated environment

and monitored for cracking (failures). Solution concentration, environment temperature, and sample dimensions vary with the test condition mentioned in the method.

The various test conditions suggested in the method introduce different stresses and strains and allow testing of different polymers and still obtain results in a timely manner.

ASTM D 1693 is not used popularly, today, for it is not sufficiently aggressive towards modern resins. This test is a constant strain test, but polyethylene, like many polymers, relaxes when strained. This stress relaxation allows testing to run without failure for very long time periods ($>$1,500 h), even under severe conditions of temperature and *Igepal*[®] concentrations.

ASTM F 1248: Notched Pipe Ring ESCR Test

This method has been used in the United States for many years to measure ESC on finished pipe up to 12 in. diameter that is notched using a razor blade in a special notching device.

ASTM D 5397-99 Standard Test Method for Evaluation of Stress Crack Resistance of Polyolefin Geomembranes Using Notched Constant Tensile Load Test

This test is typically used in the United States to test Geomembrane materials. But other PE materials, including some pipe resins, have been tested to gauge slow crack growth performance. Typical test conditions are 50 °C in a 10 % *Igepal*[®] *solution*, and the applied load is 30 % of the sample's yield stress. The depth of the notch is 20 % of the thickness of the sample (ASTM D 5397-99).

The Full Notch Creep Test (FNCT)

This method is being accepted throughout Europe as the standard method to test PE pipe grade materials that exhibit very high environment stress crack resistance (ESCR) values. The FNCT test has been preferred in Europe, as it leads to shorter failure times, due to its particular specimen design and to the presence of a surface-active environment.

ASTM F 1473: The Polyethylene Notch Tensile (PENT) Test (Constant Load)

The PENT test is being used in the United States to test PE pipe grade materials that exhibit high ESCR values (ASTM F1473-11). A parallel test method is also being developed in Europe under the ISO protocol. Typical test conditions are 80 °C air and 2.4 MPa stress.

ISO 13479: Notch Pipe Pressure Test

This method is accepted as the standard method to test PE pipes throughout Europe. The specific performance levels are detailed in the respective pipe standards (i.e., ISO 4427 for water and ISO 4437 for gas). Typically a minimum of 165 h is set for PE pipe materials.

10.10.3.2 Factors Influencing ESC

The ESC behavior of a polymer is strongly influenced by (a) the concentration of the stress-cracking agent (liquid chemical), (b) exposure temperature, (c) exposure time, and, most of all, (d) the level of strain on/in the polymer.

The absorption of a stress-cracking agent into a micro-yielded or stress-dilated zone of a polymer ultimately leads to ESC. This process locally reduces yield strength of the polymer and leads to fracture. The fracture may be either ductile or brittle depending on stress and time considerations. Diffusion of detergent molecules into the polymer due to stress might result in increased chain mobility and therefore in a reduction of the activation energy (plasticizing effect) of the deformation process (Lagaron et al. 1999). Stress-cracking agents act to lower the cohesive forces which maintain the tie molecules in the crystallites, thus facilitating their "pullout" and disentanglement from the lamellae (Scheirs 2000). The stress-cracking agents accelerate the brittle-failure process. Any stress-cracking agent will lubricate the tie molecules and that will facilitate their pullout from the lamellae.

The effect of temperature is complex. It has been shown that the higher the test environment temperature, the faster the ESC onset. The transition to brittle behavior is accelerated to shorter times by increasing temperature, cyclic loading, dilational stress, and stress concentrations. Localized concentration of the stress due to local geometrical features as notches, voids, and inclusions will increase the stress and modify the nature of the stress field. Craze initiation is accelerated by stress fields with high dilational stress and retarded under hydrostatic pressure (Wright 1996).

In addition, there are critical polymer properties and variables which affect ESCR significantly. The higher the molar mass the longer the polymer chains, which results in more tie molecules and increased ESCR (Huang and Brown 1988). ESCR is directly influenced by the type, length, and complexity of chain branching. For polyethylenes, density is a convenient, if not wholly accurate, measure of short chain branching. As a general rule of thumb, as branching increases, so does ESCR. Thus, as density decreases, ESCR generally increases. ESCR appears to be particularly sensitive to subtle variations in crystal structure and thus to differences in short chain branching. ESCR decreases with increasing the degree of crystallinity (Huang and Brown 1988; Lagaron et al. 1998). Higher comonomer content and longer comonomer short chain branches (higher α–olefins) provide better ESCR of LLDPE (Lustiger 1998; Soares et al. 2000). Increased pigment content usually decreases the ESCR (Kendall and Sherliker 1980; Lustiger 1986). The thermal history of the material and the processing conditions are also important factors for the ESCR behavior of the polymers (Roe and Gieniewski 1975; Lu and Brown 1987; Wang et al. 2003).

10.10.3.3 ESC in Polymers and Blends: Examples
Polycarbonate
Polycarbonate is tough, strong, high-performance amorphous engineering thermoplastic which is finding widespread use in industry. It has applications where high

impact resistance and its ability to maintain its shape and size even under great stresses over a wide range of temperatures are desired. It is an ideal engineering plastic since it can be injection molded or extruded. Due to its excellent properties, it is often used in the appliance industry for vacuum cleaner bases, cord hooks, impellers and blender, and food processor housings. Motorcycle windshields, police shields, and headlight covers are other typical high stress applications that use polycarbonate.

A detailed investigation of environmental stress cracking was conducted with both monoethanolamine and surfactants. The detailed investigation (Faulkner 1985) included determinations of cracking strains for polycarbonate upon exposure to the fluid's components and several nonionic surfactants. Critical strain determinations for polycarbonate exposed to the liquid components indicate that both monoethanolamine and surfactants are stress-cracking agents for polycarbonate. Cracking strains were also determined for a polycarbonate/acrylic blend upon exposure to the same fluid and were shown to be significantly greater than those obtained for pure polycarbonate. However, both the materials stress crack in splash tests. Plastics with even moderate amounts of designed-in stress are at risk under prolonged exposure to certain chemicals, which makes design and manufacturing of such parts a challenge (Krishna and Berg 2011).

The synergistic effects of photodegradation on ESC of PC were also investigated. Injection-molded samples were exposed to the ultraviolet light for various times in the laboratory prior to solvent contact. The bars were then stressed with two different loads in a tensile testing machine under the presence of ethanol. During this period, the stress relaxation was monitored, and, after unloading, the ultimate properties were evaluated. The results indicated that ethanol causes significant modification in PC, with extensive surface crazing as well as reduction in mechanical properties. The synergist action of photodegradation and stress cracking in PC may be a consequence of the chemical changes caused by oxidation (Timoteo et al. 2008).

High-Density Polyethylene
Considering the fact that the slow crack resistance of polyethylene is usually assessed by tedious and time-consuming testing methods performed on the notched samples in contact with specific fluids, the findings of Kurelec et al. offer a possibility to assess the information on slow crack propagation in much simpler and faster way (Kurelec et al. 2005; Jansen 2004). It is shown that the average strain hardening slope <G> correlates with the data obtained by a classical accelerated ESCR test. The results provide experimental evidence for the existence of the unique strain–stress–strain rate surface by offering a simple way to predict long-term performance. The resistance to slow crack propagation in polyethylene can be predicted from a simple tensile measurement performed at 80 °C and for different types of polyethylene homopolymers and copolymers the slope of a tensile curve above its natural draw ratio (i.e., strain hardening) correlates well with the measured stress crack resistance.

The investigations confirm that the slow crack resistance in polyethylene is determined by the failure of the fibrils within the craze, which is shown to be determined by the strain hardening of a tensile curve. A material with a strong strain hardening will reduce the strain rate and consequently the time to failure will be strongly increased (ASTM D2561-12).

Polymethyl Methacrylate (PMMA)

The deterioration of polymer properties by ESC has been studied for several decades. But the actual mechanism is not certainly established (Hansen 2002). It is believed that in the presence of the stress, the active fluid causes local plasticization that generates crazes and eventually catastrophic cracks. The ultimate result in many cases is brittle fracture, even in normal ductile polymers like polyethylene, ABS, and polycarbonate. Since failure by ESC can be induced by environmental fluids like cleaning agents and lubricants and the mechanical stress can be the residual (molded-in) stresses, it was considered to be a "silent killer" (Sepe 1999).

The effects of environmental stress cracking in injection-molded PMMA samples were studied by Sousa et al. They used both γ-radiation and ethanol as stress-cracking agents. The combination of gamma degradation and the contact with ethanol intensifies the action of stress-cracking in PMMA (Sousa 2007).

Alex and Janice studied the resistance to crack and craze growth in PC and PMMA in the presence of several surface-active solvents including a component of the universal chemical warfare decontaminant, DS2 (Alex and Janice 1989). A static dead weight-loading apparatus is used for experimentation, and LEFM is used to interpret craze initiation and crack propagation via compact tension specimens. Results reflect relationships based on solubility parameters of the solvents and the polymers.

Acrylonitrile Butadiene Styrene (ABS)

The evaluation of the resistance of plastics to ESC is very important in material selection. ABS is widely used in a variety of fields owing to favorable cost/performance ratio. The advantages of ABS are its luster and resistance to impact. ABS is, therefore, used mainly for housings of appliances. However, ABS is vulnerable to certain chemical agents such as organic solvents and surfactants (Faulkner 1984; Woshinis 1994). ESC of ABS caused by a nonionic surfactant was investigated by creep tests and edge crack tension (ECT) tests. It was found that the results of the creep tests performed in the nonionic surfactant were very different from those conducted in air. The results showed that the change in the mechanism of fracture was attributable to the change of morphology at the crack tip (Kawaguchi et al. 2002).

An investigation was carried out by Wang et al. to determine the appropriate values of strain to be exerted in the test for environmental stress cracking of different kinds of polymeric materials (Wang et al. 2003). It was found that for

the brittle plastics the elastic region on the stress–strain curve is the best selection; for toughened plastics the strain should be selected in the plastic region; for polycarbonate, which can crack easily in a chemical medium, a strain below the yield point is Suitable.

10.10.3.4 Predicting ESC

The phenomenon of ESC has been known for several decades. And many researchers have been focusing their attention in understanding the phenomenon. However, research has not yet enabled prediction of this type of failure for all environments and for every type of polymer. Some scenarios are well known and documented and are able to be predicted. But there is no complete or comprehensive reference for all combinations of stress, polymer, and environment. The rate of ESC is dependent on many factors including the polymer's chemical structure, bonding, crystallinity, surface roughness, molecular weight, and residual stress. It also depends on the liquid reagent's chemical nature and concentration, the temperature of the system and the strain rate. Theoretical studies with computer-assisted modeling and practical confirmations may enable researchers to predict ESC with reasonable accuracy. And one may look forward for such attempts in research in years to come.

10.11 Outlook on the Future of Polymer Blends

This chapter is focused on the characteristic properties of polymer blends. Their measurements have reached a mature stage, both in terms of necessary theories and the methods of testing. However, efforts made in enhancing one property are often mitigated by the loss of another property. Intensive study of interrelations between processing, microstructure, and properties would certainly enable one to have a good control on performance of an ultimate product. Looking at the likely advances in understanding of these materials and their integration with developing technology, polymer blends will continue to receive increasing acceptance for a variety of applications.

10.12 Cross-References

Notations and Abbreviations Used

ABS Poly(acrylonitrile-co-butadiene styrene)
ASTM American Standard Test Method
BS British Standard
CAB Cellulose acetate butyrate
DGEBA Diglycidyl ether of bisphenol A
DSC Differential scanning calorimetry
ENR Epoxidized natural rubber
EVA Ethylene-co-vinylacetate
EPDM Ethylene propylene diene monomer
ESC Environmental stress cracking
HDT Heat deflection/distortion temperature
HDPE High-density polyethylene
HIPS High-impact polystyrene
HTBN Hydroxyl terminated poly(butadiene/acrylonitrile)
IGC Inverse gas chromatography
LCST Lower critical solution temperature
LEFM Linear elastic fracture mechanics
LLDPE Linear low-density polyethylene
OIT Oxidative induction time
PA-6 Polyamide-6
PA-66 Polyamide-66
PBMA Poly(butyl methacrylate)
PBT Polybutylene terephthalate
PC Polycarbonate
PCL Poly(ε-caprolactone)
PE Polyethylene
PEEK Polyether ether ketone

PEI Polyetherimide
PEO Polyethylene oxide
PEOx Poly(ethyl oxazoline)
PES Polyethylene sulphide
PET Poly ethylene terephthalate
PLLA Poly(L-lactic acid)
PMMA Poly(methyl methacrylate)
POM Polyoxymethylene
PPBC Polypropylene block copolymer
PPHP Polypropylene homopolymer
PPS Polyphenylene sulphide
PPO Polyphenylene oxide
PS Poly styrene
PSMA Poly(styrene-*co*-maleic anhydride)
PTFE Poly tetra fluoro ethylene
PTT Poly(trimethylene terephthalate)
PVAc Polyvinyl acetate
PVB Polyvinyl butyral
PVC Polyvinyl chloride
PVDF Polyvinylidene fluoride
PVME Poly(vinyl methyl ether)
PVP Polyvinyl pyrrolidone
PVPh Poly(4-vinylphenol)
SAN Poly(styrene-co-acrylonitrile)
SANS Small-angle neutron scattering
SAXS Small-angle X-ray scattering
SF Silk fibroin
SMA Styrene-co-maleic anhydride
SPEEK Sulfonated poly(ether ether ketone)
TGA Thermogravimetric analyzer
TMOS Tetramethyl bisphenol A oligosulfones
UCST Upper critical solution temperature

Appendix 1

See Table 10.36.

Appendix 2

See Table 10.37.

Table 10.36 Definition of terms used in this chapter

Autoignition	Ignition caused solely by heat without application of a flame (also called self-ignition)
Autoignition temperature	The minimum temperature to which a substance must be heated, without application of a flame, in order to cause that substance to ignite
Burning behavior	The physical and chemical changes that take place when materials, products, or structures burn and/or exposed to fire
Char	Carbonaceous material formed by pyrolysis or incomplete combustion (ASTM E 176-81a)
Chemical resistance	The ability of a material to resist chemical attack (the attack is dependent on the method of test and its severity and is measured by determining the changes in physical properties (ASTM 1982)
Combustion	Reaction of a substance with oxygen with release of heat, generally accompanied by flaming and/or emission of smoke. Any chemical process that produces light and heat, either as glow or flame
Decomposition temperature	This is the temperature range associated with the decomposition of the polymer in the presence of oxygen
Dielectric breakdown voltage	The voltage at which electrical failure or breakdown of a dielectric occurs when energized between two electrodes under prescribed test conditions
Dielectric constant	For a given configuration of electrodes, the ratio of the capacitance with the material as the dielectric to the capacitance with vacuum
Dielectric strength	The average voltage gradient at which electric breakdown occurs under specific conditions of test
Dissipation factor	The ratio of the loss index to its relative permittivity, the tangent of its loss angle, δ or the cotangent of its phase angle, Θ
Elongation	The strain produced in the test specimen by a tensile stress, expressed as a percentage with respect to the gauge length
Elongation at break	The percentage elongation produced in the gauge length of the test specimen at the break point
Elongation at yield	The percentage elongation produced in the gauge length of the test specimen at the yield stress
Fatigue	The process of progressive localized permanent structural change occurring in a material subjected to conditions that produce fluctuating stresses and strains at some point or points that may culminate in cracks, complete fracture, or thermal softening after sufficient number of fluctuations (Borders et al. 1946)
Fatigue crack growth rate	Crack extension caused by constant amplitude fatigue loading and expressed in terms of crack extension per cycle of fatigue, da/dN (Borders et al. 1946)
Fire	A process of combustion characterized by the emission of heat, accompanied by smoke and/or flame (Mark et al. 1975)
Fire resistance	The property of a material or an assembly to withstand fire or give protection from it

(continued)

Table 10.36 (continued)

Fire retardant (flame retardant)	The quality of a substance of suppressing, reducing, or delaying markedly the combustion of certain materials. A fire retardant causes a material to resist burning when exposed to a high-energy source (Sanders 1978)
Flexural deflection	The distance over which the top or the bottom surface of the test piece at mid-span has deviated during flexure from its original position
Flexural stress (at conventional deflection)	The flexural stress at a deflection equal to 1.5 times the thickness of the test piece
Flexural stress at maximum load	The flexural stress developed when the load reaches the first maximum
Flexural stress at rupture	The flexural stress developed at the moment of rupture
Fracture	A break in the mechanical continuity of a material caused by stress exceeding the strength of the material, including joints and faults
Fracture toughness	A conventional fracture mechanics strength parameter indicating the resistance of a material to crack extension
Gauge length	The original length between two marks on the test piece over which the change in length is determined
Haze	Percentage of transmitted light that passes through the specimen deviates from the incident beam by forward scattering (ASTM D 1003)
Haze reflection	The scattering of reflected light in directions near that of specular reflection by a specimen having a glossy surface
Haze transmission	The scattering of light within a specimen or at its surface responsible for the cloudy appearance of objects observed through the specimen
Homogeneous specimen	A specimen in which every geometrically identical portion has the same apparent thermal conductivity
Impact strength	The property to resist physical breakdown when subjected to a rapidly increasing applied force (ASTM Standard Definitions 1982)
Layered specimen	A specimen that if sliced parallel to the faces has one or more slices with a significantly different apparent thermal conductivity than the other slices
Limiting oxygen index (LOI)	This is a measure of the minimum concentration of oxygen in an oxygen–nitrogen atmosphere that is necessary to support a flame for at least 3 min under specified test conditions (Mark et al. 1975)
Refraction	Change in the direction of propagation of radiation determined by change in the velocity of propagation in passing from one medium to another
Refractive index	The ratio of the velocity of light (of specified wavelength) in air to its velocity in the substance under examination
Rockwell hardness	A number derived from the net increase in the depth of impression as the load on a penetrator is increased from a fixed minor load to a major load and then returned to the minor load (ASTM D 785)

(continued)

Table 10.36 (continued)

Secant modulus	The ratio of stress to strain, in general, at any given point on the stress–strain curve
Smoldering	Combustion of a solid without flame. The combustion of a material without light being visible and generally evidenced by smoke and an increase in temperature (ASTM E 176-81a)
Specific heat	The heat capacity, C, per unit mass or per unit volume; usually the term refers to mass specific heat (Brown 1981)
Strain	The change in length per unit original length of the measured gauge length of the test specimen. It is expressed as a dimensionless ratio
Surface resistance (R_s)	Resistance between two electrodes that are on the surface of a specimen is the ratio of the direct voltage applied to the electrodes to that portion of the current between them which is primarily in a thin layer of moisture or other semiconducting material that may be deposited on the surface
Surface resistivity	The ratio of the potential gradient parallel to the current along its surface to the current per unit width of the surface
Tensile modulus (also elastic modulus in tension or Young's modulus)	The ratio of tensile stress to corresponding strain below the proportional limit. Many polymers/blends do not obey Hooke's law through out the elastic range but deviate therefrom even at stresses well below the yield stress. However, stress–strain curves almost always show a linear region at low stresses, and a straight line drawn tangent to this portion of the curve permits calculation of tensile modulus
Tensile strength (nominal)	The maximum tensile stress (nominal) sustained by a test piece during a tension test
Tensile stress (nominal)	The tensile force per unit area of the original cross section within the gauge length carried by the test piece at any given moment. The standard unit is mega-Pascal (MPa = MN/m)
Tensile stress at break	The tensile stress at which break of the test specimen occurs
Tensile stress at yield	The tensile stress at which the first marked inflection of the stress–strain curve occurs. Where any increase in strain occurs without any increase in stress, this point is taken as the tensile stress at yield or yield stress
Thermal conductance, (Γ)	The reciprocal of thermal resistance
Thermal Conductivity, (λ)	The heat flux per unit temperature gradient in the direction perpendicular to an isothermal surface, under steady-state conditions
Thermal resistance, R	The temperature difference required to produce a unit of heat flux through the specimens under steady state conditions (ASTM C 177)
Thermal resistivity (r)	The reciprocal of the thermal conductivity
Toughness	That property of a material by virtue of which it can absorb work

<div align="right">(continued)</div>

Table 10.36 (continued)

Toxicity	The amount of a substance that produces detrimental effects in an animal. It is expressed as a dose divided by the body weight of the animal, i.e., in mg/kg (Chamberlain 1978)
Transmittance (of light)	That fraction of the incident light of a given wavelength which is not reflected or absorbed, but passes through a substance
Volume resistance, (R_v)	The volume resistance between two electrodes that are in contact with or embedded in a specimen is the ratio of the direct voltage applied to the electrodes to that portion of the current between them that is distributed through the volume of the specimen (ASTM Standard Definitions 1982)
Volume resistivity	The volume resistance (in ohm-cm) between opposite faces of one centimeter cube of the material

Table 10.37 Principal flame retardants, their trade names, and suppliers (Agranoff 1993)

No.	Name	Recommended for	Supplier	Trade name
A. Organic				
1.	Phosphate esters	A, CA, CAB, CN, E, EC, N, P, PE, PP, PS, PVA, PVC, UF, UR	Akzo, Harwick	Lindol, Phosflex TPP 362, 370, 387, 390, 710
			Albright and Wilson	Pliabrac TCP, TXP, 521, 519, 524.
			FMC	Kronitex 50, 100, 200, 3600, 100B, 20OB; TCP, TXP25
			Monsanto	Santicizer 141, 143, 148, 154, TPPa
2.	Decabromodiphenyl oxide	ABS, A, E, P, PET, PE, PP, PS, PVA, UF, UR, PBT, N, (EPDM)	Ameribrom	FR-1210
			Elf Atochem	Thermoguard 505
			Ethyl	Saytex 102E
			Great Lakes Chem.	Great Lakes DE – 83R
3.	Tricresyl phosphate	A, CN, E, EC, PET, PS, PVA, PVC	Akzo, Harwick	Lindol, Lindol XP Plus
			Albright and Wilson	Pilabrac TCP
			FMC	Kronitex TCP
			Miles	Disflamoll TKP
4.	Tributyl phosphate	CA, CAB, CN, EC, PVC	Akzo, Harwick	Phosflex 4
			Albright and Wilson	Albrite TBPO
			FMC	TBP
			Focus Chem.	TEP
5.	Tributoxy ethyl phosphate	A, CA, CAB	Akzo, Harwick.	Phosflex TBEP
			Albright and Wilson	Amgard TBEP
			FMC	KP-140
			Focus Chem.	TBEP

(*continued*)

Table 10.37 (continued)

No.	Name	Recommended for	Supplier	Trade name
6.	Halogenated hydrocarbons	A, E, EC, N, PVA, PVC, UF	Argus	Flexchlor, CPP, FLX
			Elf Atochem	Electrofine S-70
			Dover	Chlorez, Paroil
			Ferro	Kloro series
			Harwick	Plastichlor, CPW100
			Occidental	Chlorowax
7.	Trioctyl phosphate	PVC	Albright and Wilson	Amgard TOF
			FMC	TOF
			Miles	Disflamoli TOF
			Rhone-Poulenc	TOF
8.	Triphenyl phosphate	CA, CAB, CN, PVA, PVC	Akzo	Phosflex TPP
			FMC	Kronitex TPP
			Miles	Disflamoli TP
9.	Halogenated organic phosphate	A, CA, CAB, CN	Akzo	Fyrol CEF, DMMP, EFF 38, 25, 6, FR2, PCF 99, 51
			Albright and Wilson	Antiblaze 78, 80, 100, 125, 150, 175, 190
			Great Lakes Chem.	Firemaster 836, 642, HP 36
10.	Halogenated organics	ABS, A, CA, E, EC, N, PET, PA, PE, PP, PS, PVA, PVC, UR, UF, (PBT, EVA, TPR)	Argus	Flexchlor CPF, FLX, Fyarestor 100, 102, 205, 104
			Elf Atochem	Electrofine S-70 and Thermoguard XS 70T
			Dover	Chlorez and Paroil
			Ferro	Kloro-check series
			Harwick	Plastichlor, CPW 100
			Occidental	Chlorowax and Dechlorane Plus
			Quantum, USI.	Spectratech
			Stanchem.	Cereclor 42, 545, 562, 70
11.	Nonhalogenated organics	PE, PP, UF, UR, PBT, EVA, TPU, PET	Great Lakes Chem.	NH-1511, CN-1197
			Hoechst Celanese	Exolit IFR
			Monsanto	Spin-Flam MF-82
			3-V Chem.	Plastisan B
12.	Chlorinated paraffin	ABS, A, CA, E, EC, N, PET, PS, PVA, PVC, UF, UR	Elf Atochem	Electroline S-70, Thermoguard XS-70-T
			Argus	Flexchlor CPF, FLX
			Dover	Chlorez solids and Paroli liquids
			Ferro	Keil CW Series.
			Harwick	Plastichlor Series, CPW 100

(*continued*)

Table 10.37 (continued)

No.	Name	Recommended for	Supplier	Trade name
			Occidental	Chlorowax
			Quantum USI	Spectratech
13.	Chlorinated hydrocarbon	ABS, A, CA, E, EC, N, PET, PS, PVA, PVC, UF, UR (Polybutylene)	Elf Atochem	Electrofine S-70, Thermoguard XS-70-T
			Argus	Flexchlor, CPF, FLX
			Dover	Chlorez solids and Paroli liquids
			Ferro	Kloro 6001
			Harwick	Plastichlor series CPW 100
			Occidental	Chlorowax
			Stanchem	Cereclor 42, 545, 552, 70
14.	Brominated organic	ABSI E, PC, PA, PS (PBT, PET)	Ameribrom	FR-1034, FR-1025, FR-913
			Argus	Fycerestor series
			Elf Atochem	Thermoguard 200 series, BBH 44, Pyronil series
			Dover	DD 8426, DD 8133, DD 8207, DG 8410
			Ethyl	Saytex: BN-451, BCL-462, BT-93, BT-93 W, 120, 8010
			FMC	Kronitex PB-460, PB-370
			Ferro	Bromoklor 50/70 Pyro-chek
			Great Lakes Chem.	BC-52, BC-58, FF-680, PE-68, PO-64P, DP-45, FR-756, FB-72, PDBS-10 and 80
			Quantum, USI	Spectratech
			Santech	Santechem 17-184
15.	Chlorinated organics	ABS, A, CA, CAB, CN, E, EC, N, P, PET, PE, PP, PS, PVA, PVC, UF, UR	Akzo	Fyrol PCF, CEF, Fr-2, 38
			Albright and Wilson	Antiblaze 80, 100, 125, 150, 175, 195
			Argus	Flexchlor, CPF, FLX
			Elf Atochem.	Electrofine S-70, Thermoguard XS-70-T
			Ferro	Kloro 3000, 3100
			Dover	Chlorez solid and Paroil liquids
			Harwick	Plastichlor series, CPW 100
			Occidental	Chlorwax, Dechlorane Plus
			Quantum, USI	Spectratech
B. Inorganic additives				
1.	Alumina trihydrate	ABS, A, E, N, P, PC, PET, PE, PP, PS, PVA, PVC, UF, UR	Alcan	H, FRF, SF and UF series
			Alcoa	C-series, Hydral series
			AluChem.	AC-series
			Climax	Hydrax ATH series

(continued)

Table 10.37 (continued)

No.	Name	Recommended for	Supplier	Trade name
			Custom Grinders	Polyfil series Custom grinds
			Franklin Industrial	H-series Custom grinds of hydrate and carbonate
			Georgia Marble	KC-series
			R. J. Marshall	A-100 series, A-200 series
			Solem, Harwick	SB-series surface-modified aluminas. Micral series
2.	Antimony oxide	ABS, A, CA, CAB, CN, E, EC, N, P, PC, PET, PE, PP, PS, PVA, PVC, UF, UR	Amspec	Amstar HP, KR-High and LTS-Low Tint
			Anzon	TMS, Oncor 75 RA and 55, TMS-HP Trutint 50 Microfine, Trutint 80
			Asarco	Very high, high, and low tint, ultra pure
			Elf Atochem.	Thermoguard S.L., CPA, Low Dust Series, Antimony Halogen Series
			Harwick, Laurel Ind.	Fire shield H-L and Ultrafine grades; LSFR, Pentoxide TP2, TPL
			Miljac	Regular, Red and White, Treated
			Quantum, USI	Spectratech
			Holtrachem	Montana high tint, low tint, Micropure treated blends
3.	Antimony oxide dispersions	ABS, A, CA, CAB, CN, E, EC, N, P, PC, PET, PE, PP, PS,PVA, PVC, UF, UR	Amspec	Amsperse
			Anzon	Environstrand, Fyrebloc
			Elf Atochem	Thermoguard S, L, NF
			Holtrachem.	Montana DIDP treated, high, low, tints, Micro pure
4.	Magnesium hydroxide	ABS, A, E, P, PE, PP, PS, PVC, UF, UR (TPE, EPR, EVA)	Aluchem	ACM-MW, ACM-MH 93
			Climax	Hydramax HM-B8, HM-B8S, HM-C9, HM-C9S
			D. J. Enterprises	ACM-MW, ACM-MH93
			Solem	Zerogen
5.	Organic–inorganic additive	ABS, A, CA, CAB, CN, E, R, EC, N, P, PC, PA, PE, PP, PS, PVA, PVC, UFF, UFR.(EVA, PBT, SAN, TPE)	Anzon	F.R.C. Enviro- strands, Fyrebloc
			D. J. Enterprises	Micro P, Sillum 200, PL-200, Q/P
6.	Sodium antimonate	ABS, A, CN, E, N, PET, PE, PP, PS, PVC, UFF, UFR	Amspec.	S. A. 100
			Anzon	Pyrobloc SAP
			Elf Atochem	Thermoguard FR
			Holtrachem	Montana

Table 10.37 (continued)

No.	Name	Recommended for	Supplier	Trade name
7.	Tin compounds	ABS, El N, P, PC, PA, PET, PE, PP, PS, PVA, PVC, UFF, UFR	Alcan	Flamtard H.S
8.	Zinc Borate	ABS, A, E, N, P, PC, PET, PE, PP, PS, PVA, PVC, UFF, UFR	Climax	ZB-112, 325, 237, 233, 467
			Harwick	Firebrake ZB,
			U.S – Borax	Zb-Fine, Fire brake 500, Fire brake 415
Reactive types				
1.	Tribromoneopentyl alcohol	A, CA, CN, PET, UFF, UFR	Ameribrom	FR-513
2.	Di-(polyoxyethylene) hydromethyl phosphonate	CN, P, PET, UFF, UFR	Akzo	Victastab HMP
3.	Tribromophenyl maleimide	ABS, PE, PP, PS	Ameribrom	FR-1033
4.	Dibromoneopentyl glycol	A, CA, E, PET, UFF, UFR	Ameribrom Ethyl	FR-522 / FR-1138
5.	Tetrabromobisp henol A	ABS, E, P, PC, PET, UFF, UFR	Ameribrom Ethyl	1524 Saytex RB-100
			Great Lakes Chem.	Great Lakes BA-59P
6.	Ethylene oxide adduct of TBBPA	ABS, E, PET, UFF, UFR	Ameribrom	FR-1525
7.	Phosphorus-containing polyol	E, P, UFF, UFR	Albright and Wilson	Vircol 82
8.	Tetrachlorophthalic anhydride	E, P, PET, UFR	Monsanto	Tetrathal
9.	Hexa-chloro cyclopentadiene	CA, CAB, CN, EC	Velsicol	PCL

Note: A = acrylic; CA = cellulose acetate; CAB = cellulose acetate butyrate; CN = cellulose nitrate; E = epoxy; EC = ethyl cellulose; N = nitrile; P = phenolic; PC = polycarbonate; PA = polyamide; PE = polyethylene; PET = polyester, thermoset; PP = polypropylene; PS = polystyrene; PVA = polyvinyl acetate; PVC = polyvinyl chloride; UFF = urethane flexible foam; UFR = urethane rigid foam

References

P.G.R. Achary, N. Mohanty, B.N. Guru, N.C. Pal, J. Chem. Pharm. Res. **4**, 1475 (2012)

Y. Agari, A. Ueda, J. Polym. Sci. Polym. Phys. Ed. **32**, 59 (1994)

Y. Agari, A. Ueda, S. Nagai, J. Appl. Polym. Sci. **45**, 1957 (1992)

Y. Agari, A. Ueda, S. Nagai, J. Appl. Polym. Sci. **47**, 331 (1993)

Y. Agari, A. Ueda, Y. Omura, S. Nagai, Polymer **38**, 801 (1997)

J. Agranoff (ed.), *Modern plastics encyclopedia* (McGraw-Hill, New York, 1993)

Y.A. Akpalu, P. Ping, Mater Manuf Process **23**, 269 (2005)

R.J. Alfredson, *Vibration and Noise-Measurement Prediction and Control* (Melbourne, 1990), pp. 16–19. Preprints of Papers, Barton, ACT: Institution of Engineers, Australia

M. Amano, K. Nakagawa, Polymer **28**, 263 (1987)

S.E. Amos, K.E. Nielson, C. McRoberts, M.A. Wicki, U.S. Patent 5,981,636 to 3M Innovative Properties Company, 1999

L. An, Z. Wang, D. Yu, J. Jing, Y. Jiang, R. Ma, X. Kou, J. Appl. Polym. Sci. **59**, 1843 (1996a)

L. An, Z. Wang, D. Yu, J. Jing, Y. Jiang, R. Ma, X. Kou, Angew. Makromol. Chem. **243**, 1 (1996b)

K.M. Anderson, Wall J. **31**, 5 (1997)

E.H. Andrews, in *Testing of Polymers*, ed. by W.E. Brown, vol. 4 (Wiley-Interscience, New York, 1969), p. 237

T. Aouak, A.S. Alarifi, J. Saudi Chem. Soc. **13**, 227 (2009)

A.A. Ardakani, J.T. Gotro, J.C. Hedrick, K. Papathomas, N.M. Patel, J.M. Show, A. Vichleck, European Patent Applications, 581,314, 2 Feb 1994; Jpn. Pat., 6,107,958, 19 Apr, Appl. 31 July 1992, to IBM Corp.

A.S. Argon, R.E. Cohen, in *Advances in Polymer Science 91/92*, ed. by H.H. Kausch (Springer, Berlin, 1990)

R.G. Armstrong, US Patent 3,373,222, 1968a

R.G. Armstrong, US Patent 3,373,223, 1968b

ASTM F 1769-97, *Standard Test Method for Measurement of Diffusivity, Solubility, and Permeability of Organic Vapor Barriers Using a Flame Ionization Detector* (Philadelphia, 1997)

ASTM C177-93, *Steady-State Thermal Transmission Properties by Means of the Guarded Hot Plate* (Philadelphia, 1993)

ASTM D1003-92, *Standard Test Method for Haze and Luminous Transmittance of Transparent Plastics* (Philadelphia, 1992)

ASTM D1329-08, *Standard Test Method for Evaluating Rubber Property – Retraction at Lower Temperatures (TR Test)* (Philadelphia, 2008)

ASTM D149-93, *Standard Test Method for Dielectric Breakdown Voltage and Dielectric Strength of Solid Electrical Insulating Materials at commercial Power Frequencies* (Philadelphia, 1993)

ASTM D150-93, *Standard Test Methods for A–C Loss Characteristics and Permittivity (Dielectric Constant) of Solid Electrical Insulating Materials* (Philadelphia, 1993)

ASTM D1525-09, *Standard Test Method for Vicat Softening Temperature of Plastics* (Philadelphia, 2009)

ASTM D1525-91, *Test for Vicat Softening Point of Plastics* (Philadelphia, 1992)

ASTM D1637-61, *Test for Tensile Heat Distortion Temperature of Plastic Sheeting* (Philadelphia, 1970; discontinued in 1990)

ASTM D1693-12, *Standard Test Method for Environmental Stress-Cracking of Ethylene Plastics* (Philadelphia, 2012)

ASTM D2137-11, *Standard Test Methods for Rubber Property – Brittleness Point of Flexible Polymers and Coated Fabrics* (Philadelphia, 2011)

ASTM D256-00, *Impact Resistance of Plastics and Electrical Insulating Materials* (Philadelphia, 1993)

ASTM D2561-12, *Standard Test Method for Environmental Stress-Crack Resistance of Blow-Molded Polyethylene Containers* (Philadelphia, 2012)

ASTM D257-93, *Standard Test Method for D–C Resistance or Conductance of Insulating Materials* (Philadelphia, 1993)

ASTM D2583-95, *Standard Test Method for Indentation Hardness of Rigid Plastics by Means of a Barcol Impressor* (Philadelphia, 1996)

ASTM D3895-09, *Standard Test Method for Oxidative-Induction Time of Polyolefins by Differential Scanning Calorimetry* (American Society for Testing and Materials, Philadelphia, 2009)

ASTM D542-90, *Standard Test Methods for Index of Refraction of Transparent Organic Plastics* (Philadelphia, 1990)

ASTM D635-91, *Test Method for Rate of Burning and/or Extent of Burning of self-supporting Plastics in a Horizontal Position* (Philadelphia, 1991)

ASTM D638-95, *Standard Test Method for Tensile Properties of Plastics* (Philadelphia, 1996)

ASTM D648-82, *Deflection Temperature of Plastics Under Flexural Load* (Philadelphia, 1988)

ASTM D671-93, *Flexural Fatigue of Plastics by Constant Amplitude of Force* (Philadelphia, 1993)

ASTM D695-91, *Compressive Properties of Rigid Plastics* (Philadelphia, 1992)

ASTM D746-07, *Standard Test Method for Brittleness Temperature of Plastics and Elastomers by Impact* (Philadelphia, 2007)

ASTM D785-93, *Rockwell Hardness of Plastics and Electrical Insulating Materials* (Philadelphia, 1993)

ASTM D790-92, *Flexural Properties of Plastics and Electrical Insulating Materials* (Philadelphia, 1992)

ASTM E162-94, *Method for Surface Flammability of Materials Using a Radiant Heat Energy Source* (Philadelphia, 1994)

ASTM E399-90, *Standard Test Method for Plane-Strain Fracture Toughness of Metallic Materials* (Philadelphia, 1991)

ASTM E413-10, *Standard Classification for Rating Sound Insulation* (Phildelpheia, 2010)

ASTM E813, *Standard Test Method for J_{IC}, A Measure of Fracture Toughness*, in 1997 was replaced by E1737, which in turn was discontinued in 1998, Annual Book of ASTM Standards, Part 10 (American Society for Testing and Materials, Philadelphia, 1981)

ASTM E813-89, *Standard Test Method for J_c, a Measure of Fracture Toughness* (Philadelphia, 1990)

ASTM E90-09, *Standard Method for Laboratory Measurement of Airborne Sound Transmission* (Philadelphia, 2009)

ASTM F1473-11, *Standard Test Method for Notch Tensile Test to Measure the Resistance to Slow Crack Growth of Polyethylene Pipes and Resins* (Philadelphia, 2011)

ASTM, *Standard Definitions, Compilation of* (Philadelphia, 1982)

K.O. Ballagh, in *The 33rd International Congress and Exposition on Noise Control Engineering*, August 22–25 (Prague, 2004)

P. Beahan, A. Thomas, M. Bevis, J. Mater. Sci. **11**, 1207 (1976)

J.A. Begley, J.D. Landes, *ASTM STP 514* (1972)

N.C. Billingham, P.D. Calvert, Adv. Polym. Sci., 90 (Springer, Berlin, 1989)

R.L. Blaine, E-53865, Brief #88, *Du Pont Thermal Analysis Technical Literature* (Wilmington, DE, 1973)

R.L. Blaine, C.J. Lundgren, M.B. Harris, in *Oxidative Induction Time – A Review of DSC Experimental Effects*, ed. by A.T. Riga, G.H. Patterson, ASTM STP 1326 (American Society for Testing and Materials, Philadelphia, 1997)

K.G. Blizard, D.G. Baird, Polym. News **12**, 44 (1986a)

K.G. Blizard, D.G. Baird, SPE Techn. Pap. **44**, 311 (1986b)

K.G. Blizard, D.G. Baird, Polym. Eng. Sci. **27**, 653 (1987)

K.G. Blizard, C. Federici, O. Federico, L. Chhapoy, Polym. Eng. Sci. **30**, 1442 (1990)

D.J. Blundell, A. Keller, A.J. Kovacs, J. Polym. Sci. Part B Polym. Lett. **4**, 481 (1966)

A.M. Borders, R.D. Juve, L.D. Hess, Ind. Eng. Chem. **38**, 955 (1946)

S. Bourbigot, S. Duquesne, C. Jama, Macromol. Symp. **233**, 180 (2006)

D.P. Bourcier, J.J. D'Errico, J-P. Etienne, G. Matis, V.J. Yacovone, U.S. Patent Pub. No. US 2009/0286046 A1, 2009

M. Bramuzzo, Polym. Eng. Sci. **29**, 1077 (1989)

H. Breuer, F. Haaf, J. Stabenow, J. Macromol. Sci. Phys. B. **14**, 387 (1977)

K.B. Broberg, J. Mech. Phys. Solids **19**, 407 (1971)

K.B. Broberg, J. Mech. Phys. Solids **23**, 215 (1975)

D. Broek, *Elementary Engineering Fracture Mechanics*, 4th edn. (Nijhoff, Dordrecht, 1986)

W. Brostow, R.D. Corneliussen (eds.), *Failure of Plastics* (Hanser, Munich, 1986)

W. Brostow, R.S. Dziemianowicz, J. Romanski, W. Werber, Polym. Eng. Sci. **28**, 785 (1988)

H.R. Brown, J. Mater. Sci. **8**, 941 (1973)

R.P. Brown (ed.), *Handbook of Plastics Test Methods* (George Godwin, London, 1981)

H.R. Brown, E.J. Kramer, J. Macromol. Sci. Phys. **19B**, 487 (1981)

F.L. Browne, *Theories of the Combustion of Wood and its Control*, Report No. 2136, Forest Products Laboratory, Forest Service (U.S. Department Agriculture, Madison, Wisconsin, 1958)

BS 2782 Method 1001, *Measurement of Hardness by Means of a Barcol Impressor* (London, 1977).

BS 2782 Method 306A, *Impact Strength (Pendulum Method)* (London, 1970)

BS 2782 Method 365A, *Determination of Softness Number of Flexible Plastics Materials* (London, 1976)

BS 2782 Method 365D, *Determination of Hardness by Ball Indentation Method* (London, 1978)

BS 2782, *Methods of Testing Plastics* (London, 1970)

BS 2782, Method 335A, *Determination of Flexural Properties of Rigid Plastics* (London, 1978)

BS 2782, Method 336B, *Determination of Deflection in Bend Under an Applied Force* (London, 1978)

BS 2782, Method 345A, *Determination of Compressive Properties by Deformation at Constant Rate* (London, 1979)

BS 2782, Method 351A, *Determination of Charpy Impact Resistance of Rigid Plastics and Ebonite* (London, 1977)

BS 2782, Method 515A, *Haze of Film* (London, 1970)

BS 2782, Methods 121A and 121B, *Determination of Temperature of Deflection under a Specified Bending Stress of Plastics and Ebonite* (London, 1976)

BS 2782, Methods 320 A to F, *Plastics-Tensile Strength, Elongation and Elastic Modulus* (London, 1976)

BS 3784, *Polytetrafluoroethylene Sheet* (London, 1973)

BS 3816, *Cast Epoxide Resin Insulating Material for Electrical Applications at Power Frequencies* (London, 1964)

BS 3924, *Specification for Pressure Sensitive Adhesive Tapes for Electrical Insulating Purposes* (London, 1978)

BS 4618, *Recommendations for the Presentation of Plastics Design Data. Part 2. Electrical Properties, Section 2. 3 Volume Resistivity; Section 2. 4 Surface Resistivity* (London, 1975)

BS 5102, *Phenolic Resin Bonded Paper Laminated Sheets for Electrical Applications* (London, 1974)

BS 5762, *Methods for Crack Opening Displacement Testing* (British Standards Institution, London, 1979)

BS 874, *Methods for Determining Thermal Insulating Properties* (London, 1973)

C.B. Bucknall, *Toughened Plastics* (Applied Science Publishers, London, 1977)

C.B. Bucknall, in *Comprehensive Polymer Science*, ed. by C. Booth, C. Price, vol. 2 (Pergamon Press, New York, 1988)

C.B. Bucknall, A. Marchetti, J. Appl. Polym. Sci. **28**, 2689 (1983)

C.B. Bucknall, W.W. Stevens, J. Mater. Sci. **15**, 2950 (1980)

C.B. Bucknall, K.V. Gotham, P.I. Vincent, in *Polymer Science*, ed. by A.D. Jenkings (North-Holland, Amsterdam, 1972)

C.B. Bucknall, in *Advances in Polymer Science*, vol. 27 Ed. J. D. Ferry (Springer, New York, 1978)

C.M. Burns, W.N. Kim, Polym. Eng. Sci. **28**, 1362 (1988)

M.F. Butler, A.M. Donald, J. Mater. Sci. **32**, 3675 (1997)

F. Cakar, O. Cankurtaran, F. Karaman, Chromatographia **75**, 1157 (2012)

N. Cameron, Eur. Polym. J. **38**, 597 (2002)

K. Campbell, Wall J. **41**, 12 (2000)

L. Canfora, S. Fillippi, F.P. La Mantia, Polym. Eng. Sci. **44**, 1732 (2004)

Y. Cao, J. Zhang, J. Feng, P. Wu, www.acsnano.org (2011)

C.C. Carroll, *Modern Plastics* (1984)

D.F. Castro, R.C.R. Nunes, L.L.Y. Visconte, G.M. Silva, Int. J. Polym. Mater. Polym. Biomater. **56**, 1127 (2007)

C.M. Chaleat, Polym. Degrad. Stabil. **97**, 1930 (2012)

D.L. Chamberlain, in *Flame Retardancy in Polymeric Materials*, ed. by W.C. Kuryla, A.J. Papa, vol. 4 (Marcel Dekker, New York, 1978)

M.K.V. Chan, J.G. Williams, Polym. Eng. Sci **21**, 1019 (1981)

M.K.V. Chan, J.G. Williams, Polym. Eng. Sci. **19**, 145 (1983)

W.Y.F. Chan, J.G. Williams, Polymer **35**, 1666 (1994)

K. Chandramouli, S.A. Jabarin, Adv. Polym. Tech. **14**, 35 (1995), Published Online: 8 Apr 2003

L.L. Chang, E.M. Woo, Macromol. Chem. Phys. **5**, 202 (2001)

J.-M. Charrier, R.J.P. Ranchouse, Polym. Eng. Sci. **11**, 381 (1971)

H.Y. Chen, Polymer **42**, 7819 (2001)

C.C. Chen, E. Fontan, K. Min, J.L. White, Polym. Eng. Sci **28**, 69 (1988)

C.C. Chen, J.Y. Chueh, H. Tseng, H.M. Huang, S.Y. Lee, Biomaterials **24**, 1167 (2003)

J. Chen, G. Wang, X. Zeng, H. Zhao, D. Cao, J. Yun, C.K. Tan, J. Appl. Polym. Sci. **94**, 796 (2004)

C.P. Cherepynov, Appl. Math. Mech. **31**, 503 (1967)

W.-Y. Chiang, D.-S. Hwung, Polym. Eng. Sci. **27**, 632 (1987)

H.K. Chuang, C.D. Han, Adv. Chem. Ser. **206**, 171 (1984)

H.K. Chuang, C.D. Han, J. Appl. Polym. Sci. **30**, 2457 (1985)

J.H. Chun, S. Ki-Maeng, K.S. Suh, J. Mater. Sci. **26**, 5347 (1991)

M.D. Cliffton, S.A. Gilliam, W.R. Hale, T.J. Pecorini, M.E. Rogers, M.D. Shelby, M.E. Stewart, U.S. Patent 8,133,417, 13 Mar 2012, Appl. 29 Apr 2011, to Eastman Chem. Co.

F.N. Cogswell, B.P. Griffin, J.B. Rose, Eur. Pat. Appl. **30**, 417 (1981)

M.M. Coleman, J.T. Graf, P.C. Painter, *Specific Interactions and the Miscibility of Polymer Blends* (Technomic, Lancaster, 1991)

B.F. Conaghan, S.L. Rosen, Polym. Eng. Sci. **12**, 134 (1972)

P.R. Couchman, Macromolecules **11**, 1156 (1978)

J. Crank, G.S. Park, in *Diffusion of Polymers*, ed. by J. Crank, G.S. Park (Academic, New York, 1968). Chapter 1

M.G. Cross, R. Lines, U.S. Patent 5,378,402, 3 Jan 1995, Appl. 21 July 1983, Br. Appl. 2 Aug 1982, to Raychem Ltd.

T. Daniels, *Thermal Analysis* (Kogan Page, London, 1973)

K.C. Dao, J. Appl. Polym. Sci. **27**, 4799 (1982)

N.A. Darwish, A.B.. Shehata, A.A. Abd El-Megeed, S.F. Halim, A. Mounir, Polym. Plast. Tech. Eng. **44**, 1297 (2005)

A. Dasari, Z.Z. Yu, Y.W. Mai, S. Liu, Nanotechnology **18**, 445602 (2007)

D.S. Davis, U.S. Patent 7,439,306, 2008 to ExxonMobil Chemical Patents Inc.

F. De Ponte, P. Di Filippo, *Design Criteria for Guarded Hot Plate Apparatus, Heat Transmission Measurements in Thermal Insulations* (ASTM STP 544, Am. Soc. Testing Mats., Philadelphia, 1974)

R.D. Deanin, M.F. Sansone, Polym. Symp. **19**, 211 (1978)

D.D. Deshpande, D. Patterson, H.P. Schreiber, C.S. Su, Macromolecules **7**, 530 (1974)

DIN 53435, *Testing of Plastics Determination of Flexural Properties and Impact Resistance with Dynstat Test Specimens* (1977)

DIN 53442, *Testing of Plastics: Fatigue Test in the Field of Bending Strain of Flat Specimens* (1975)

DIN 53452, *Testing of Plastics Bending Test* (1977)

DIN 53453, *Testing of Plastics; Determination of Impact Resistance* (1975)

DIN 53454, *Testing of Plastics Compression Test* (1971)

DIN 53456, *Testing of Plastics Indentation Hardness* (1979)

DIN 53461, *Testing of Plastics-Determination of Temperature of Deflection Under Load According to ISO 75* (1979)

DIN 53482, *Methods for Determination of Electrical Resistance Values* (1967)

DIN 53483, *Determination of Dielectric Properties* (1969)

DIN 53491, *Testing of Plastics Determination of Refractive Index and Dispersion* (1955)

A.M. Donald, E.J. Kramer, J. Mater. Sci. **17**, 1765 (1982)

L. D'orazio, R. Greco, E. Martuscelli, G. Ragosta, Polym. Eng. Sci. **23**, 489 (1983)

G. Dreezen, G. Groeninck, S. Swier, B. Van Mele, Polymer **42**, 1449 (2001)

M. Du, Q. Wu, M. Zuo, Q. Zheng, Eur. Polym. J. http://dx.doi.org/10.1016/j.eurpolymj.2013.06.006 (2013)

D.S. Dugdale, J. Mech. Phys. Solids **8**, 100 (1960)

W.H. Dukes, *Unresolved Problems in Brittle Material Design*, U.S. Govt. Report, AD 654119 (1966)

M.M. Dumoulin, Ph.D. Thesis, Ecole Polytech., Montreal 1988

I.N. Einhorn, in *Fire Retardance in Polymeric Materials*, ed. by I. Skeist. Reviews in Polymer Technology, vol. 1 (Marcel Dekker, New York, 1972), pp. 113–184

F.R. Eirich, H.F. Mark, *Thermal Degradation of Polymers*. Monograph No. 13 (Society of Chemical Industry, London, 1961), p. 43

Eval Americas, Technical Bulletin No. 190, *Flavor and Aroma Barrier Properties of EVAL Resins* (2007); www.evalca.com

G. Fairley, R.E. Prud'homme, Polym. Eng. Sci. **27**, 1495 (1987)

G. Fairley, Ph. D Thesis, Laval University, Quebec 1990

A.M. Farooque, D.D. Deshpande, Polymer **33**, 5005 (1992)

D.L. Faulkner, Polym. Eng. Sci. **24**, 1174 (1984)

D. Faulkner, *Environmental Stress Cracking of Polycarbonate and a Polycarbonate/Acrylic Blend by Windshield Washer Fluids*. SAE Technical Paper 851628 (1985). doi:10.4271/851628

A.R. Federl, G. Kipouras, U.S. Patent 4,588,773, 13 May 1986, Appl. 21 Dec 1984, to Borg-Warner Chemicals Inc.

E. Fekete, E. Foldes, B. Pukanszky, Eur. Polym. J. **41**, 727 (2005)

C.P. Fenimore, F.J. Martin, Mod. Plast. **44**, 141 (1966)

R.J. Ferguson, G.P. Marshall, J.G. Williams, Polymer **14**, 451 (1973)

T. Fett, Mater. Prüfung **14**, 151 (1972)

D. Filip, S. Vlad, High Perform. Polym. **16**, 101 (2004)

S. Filippi, V. Chiono, G. Polacco, M. Paci, L. Minkova, P. Magagnini, Macromol. Chem. Phys. **203**, 1512 (2002)

B. Fillon, J.C. Williams, B. Lotz, A. Thierry, J. Polym. Sci. Polym. Phys. Ed. **31**, 1383 (1993)

B. Fisa, SPE Techn. Pap. **37**, 1135 (1991)

R. Gadekar, A. Kulkarni, J.P. Jog, J. Appl. Polym. Sci. **69**, 161 (1998)

M. Gahleitner, J. Wolfschwenger, C. Bachner, K. Bernreitner, W. Neissl, J. Appl. Polym. Sci. **61**, 649 (1996)

M.E. Galvin, G.E. Wnek, Polym. Commun. **23**, 795 (1982)

M.E. Galvin, G.E. Wnek, J. Polym. Sci. Chem. **21**, 2727 (1983)

M.E. Galvin, G.F. Dandreaux, G.E. Wnek, Am. Chem. Soc. Ser. **242**, 40 (1984)

J. Gao, Polymer **53**, 1772 (2012)

O.S. Gebizlioglu, H.W. Beckham, A.S. Argon, R.E. Cohen, H.R. Brown, Macromolecules **23**, 3968–3975 (1990)

B.D. Gesner, J. Appl. Polym. Sci. **11**, 2499 (1967)

I. Ghasemi, H.K. Rasmussen, P. Szabo, J. Morshedian, Iranian Polym. J. **14**, 715 (2005)

S.K. Ghosh, S. Sengupta, M. Naskar, J. Sci. Indus. Res. **69**, 396 (2010)

B.S. Giles, S. Vilasagar, European Patent Applications 596,704, 11 May 1994, Appl. 2 Nov 1993, U.S. Appl. 4 Nov 1992, to GE Co.

S.A. Gilliam, W.R. Hale, T.J. Pecorini, M.D. Shelby, U.S. Patent 7,968,164, 28 June 2011, Appl. 27 Feb 2006, to Eastman Chem. Co.

V.V. Ginzburg, Macromolecules **38**, 2362 (2005)

A. Gnatowski, J. Wawrzyniak, T. Jaruga, Arch. Mater. Sci. Eng. **41**, 37 (2010)

Y.K. Godovsky, *Thermophysical Properties of Polymers* (Springer, New York, 1992)

M.M. Gorelova, A.J. Pertsin, V.Y. Levin, L.I. Makarova, L.V. Filimonova, J. Appl. Polym. Sci. **45**, 2075 (1992)

A. Gottschalk, M. Breulmann, E. Fetter, K. Kretschmer, M. Bastian, Kunststoffe Int. **7**, (2006)

Gouveia, Rev. Latin Am. Metal. Mat. **31**(1), 26 (2011)

R. Greco, G. Mucciariello, G. Rogasta, E. Martuscelli, J. Mater. Sci. **15**, 845 (1980)

H.W. Greensmith, J. Appl. Polym. Sci. **7**, 993 (1963)

B.L. Gregory, A. Siegmann, J. Im, E. Bear, J. Mater. Sci. **22**, 532 (1987)

A.A. Griffith, Philos. Trans. R. Soc. London Ser. A. **221**, 163 (1920)

E.A. Grulke, J. Brandrup, E.H. Immergut (eds), *Polymer Handbook*, 4th edn. Wiley, New York (1999), p. 675

D.A. Gunasekara, M.D. Alwis, U.S. Patent App. Pub. No. 2004/0168853, 2004

C.S. Ha, W.J. Cho, Polym. Test. **21**, 123 (2002)

Å. Halldén, B. Wesslén, J. Appl. Polym. Sci. **60**, 2495 (1996)

Å. Halldén, M.J. Deriss, B. Wesslén, Polymer **42**, 8743 (2001)

C.D. Han, H.K. Chuang, J. Appl. Polym. Sci. **30**, 2431 (1985)

Z. Han, L. Chunsheng, T. Kombe, Mater. Struct. **41**, 383 (2008)

C.M. Hansen, Polym. Stab. Degrad. **77**, 43 (2002)

S. Hashemi, J. Mater. Sci. **20**, 229 (1993a)

S. Hashemi, J. Plast. Rubber Compos. Proc. Appl. **20**, 229 (1993b)

S. Hashemi, Polym. Eng. Sci. **37**, 912 (1997)

S. Hashemi, J.G. Williams, Polym. Eng. Sci. **26**, 760 (1985)

S. Hashemi, J.G. Williams, Polymer **27**, 85 (1986)

S. Hashemi, Z. Yuan, J. Plast. Rubber Compos. Proc. Appl. **21**, 151 (1994)

S. Havriliak Jr., C.A. Cruz Jr., S.E. Slavin, Polym. Eng. Sci. **36**, 2327 (1996)

R.N. Haward, C.B. Bucknall, Pure Appl. Chem. **46**, 227 (1976)

C. He, A.M. Donald, M.F. Butler, O. Diat, Polymer **39**, 659 (1998)

D.S. Hecht, L. Hu, G. Irvin, Adv. Mater. 23, 1482 (2011). (doi:10.1002/adma.201003188. Epub 2011 Feb 15)

R. Hendersinn, Fire retardancy (survey), in *Encyclopedia of Polymer Science and Technology*, ed. by N.B. Bikales, vol. 2 (Wiley-Interscience, New York, 1977), pp. 270–339. Supplement

R.W. Hertzberg, J.A. Manson, *Fracture of Engineering Plastics* (Academic, New York, 1980)

C.J. Hilado, Chem. Tech. **2**, 32 (1972)

C.J. Hilado, J. Combustion Toxicol. **8**, 121 (1981)

J.H. Hildebrand, R.L. Scott, *The Solubility of Non-Electrolytes* (Dover, New York, 1964)

K.-S. Ho, K. Levon, U.S. Patent 5,391,622, 21 Feb 1995, Appl. 3 May 1994, U.S. Appl. 20 May 1992, to Neste Oy

D.W.K. Ho, J.H. Koo, M.C. Bruns, O.A. Ezekoye, in *Proceedings of the 43rd AIAA/ASME/SAE/ASEE Joint Propulsion Conference*, 8, 7524, AIAA, Reston, (2007), AIAA Paper 2007–5773

W.K. Ho, J.H. Koo, O.A. Ezekoye, J. Nanomater. 2010 (2010), Article ID 583234, 11 pp. doi:10.1155/2010/583234

G. Holden, E.T. Bishop, N.R. Legge, J. Polym. Sci. **C26**, 37 (1969)

Y. Hong, X. Zhang, C. Qu, B. Li, L. Zhang, Q. Zhang, Q. Fu, Polymer **48**, 860 (2007)

D.V. Howe, M.D. Wolkowicz, Polym. Eng. Sci. **27**, 1582 (1987)

A.J. Hsieh, J.J. Vanselow, U.S. Army Materials Technology Laboratory Watertown, Massachusetts 02172-0001 AMCMS Code 612105.H840011, SLCMT-EMP, Report No.: MTL TR 89-12, (1989)

H. Hsu, D.-J. Lin, L.-P. Cheng, J.-T. Yeh, K.-N. Chen, J. Polym. Res. **8**, 209 (2001)

D.D. Huang, Polym. Mater. Sci. Eng. **63**, 578 (1990)

J.M. Huang, Polymer **46**, 8068 (2005)

Y. Huang, N. Brown, J. Mater. Sci. **23**, 3648 (1988)

J.C. Huang, M.S. Wang, Adv. Polym. Technol. **9**, 239 (1989)

D.D. Huang, J.G. Williams, J. Mater. Sci. **22**, 2503 (1987)

D.D. Huang, J.G. Williams, Polym. Eng. Sci. **30**, 1341 (1990)

D.D. Huang, in *Proceedings, Seventh International Conference on Deformation, Yield and Fracture of Polymers* (The Plastics and Rubber Institute, London, 1988)

R.L. Hudson, *The ChemGuide App*. 2011 info@rlhudson.com

H. Im, H. Kim, J. Kim, Mater. Trans. **50**, 1730 (2009)

L.G. Imhof, K.C. Steuben, Polym. Eng. Sci. **13**, 146 (1974)

ZERO International, Website: www.zerointernational.com, (2001)

A.I. Isayev, M.J. Modic, Polym. Comp. **8**, 158 (1987)

ISO 2039, *Plastics and Ebonite Determination of Hardness by Ball Indentation Method* (Switzerland, 1973)

ISO 178, *Plastics Determination of Flexural Properties of Rigid Plastics* (Switzerland, 1975)

ISO 604, *Plastics Determination of Compressive Properties* (Switzerland, 1973)

ISO 75, *Plastics and Ebonite Determination of the Temperature of Deflection Under Load* (Switzerland, 1974)

ISO R1184, *Plastics-Determination of Tensile Properties of Films* (Switzerland, 1970)

ISO R179, *Determination of the Charpy Impact Resistance of Rigid Plastics* (Switzerland, 1961)

ISO R180, *Determination of the Izod Impact Resistance of Rigid Plastics* (Switzerland, 1961)

ISO R489, *Plastics, Determination of the Refractive Index of Transparent Plastics* (Switzerland, 1966)

ISO/DIS 527, *Plastics-Determination of Tensile Properties* (Switzerland, 1968)

G.C. Ives, J.A. Mead, M.M. Riley, *Handbook of Plastics Test Methods* (Butterworth Group, London, 1971)

B.Z. Jang, D.R. Uhlmann, J.B. Van der Sande, J. Appl. Polym. Sci. **30**, 2485 (1985a)

B.Z. Jang, D.R. Uhlmann, J.B. Van der Sande, Polym. Eng. Sci. **25**, 643 (1985b)

J.A. Jansen, Adv. Mater. Process., June 2004, 50–53

G. Jeffrey, M.S. Weiss, J. Polym. Sci. Part B Polym. Phys. **44**, 2253 (2006)

Y. Jen-Taut, C.–.C. Fan-Chiang, S.-S. Yang, J. Appl. Polym. Sci. **64**, 1531 (1997)

H.-Y. Jeon, A. Bouazza, K.-Y. Lee, Polym. Test **27**, 434 (2008)

R. Jester, et al. *2005 PLACE Conference*, Las Vegas, Nevada, September 27–29, (2005)

M. Jiang, H. Xie, Prog. Polym. Sci. **16**, 977 (1991)

Y.Y. Jiang, S. Yoshimura, R. Imai, H. Katsura, T. Yoshida, C. Kato, J. Fluid. Struct **23**, 531 (2007)

F. Johansson, *Food and Packaging Interactions Affecting Food Quality*, Doctoral Dissertation and SIK-Rapport no. 628, (Chalmers University of Technology, Gothenburgh, 1996)

L. Jong, E.M. Pearce, T.K. Kwei, Polymer **34**, 48 (1993)

T.J.M. Jongeling, European Patent Applications 538,939, 28 Apr 1993 Appl. 21 Oct 1991, to DSM NV

E.G. Joseph, G.L. Wilkes, D.G. Baird, Polym. Prepr. **25**, 94 (1984)

C. Joshi, S. Dabke, V.N.S. Pendyala, K.V. Rao, S.F. Xavier, *Chemcon-2005* (Department of Chem. Engg., I.I.T., Delhi, 2005)

R. Juana, A. Etxberria, M. Cortazar, J.J. Iruin, Macromolecules **27**, 1395 (1994)

B. Jurkowski, Y.A. Olkhov, K. Kelar, O.M. Olkhova, Eur. Polym. J. **38**, 1229 (2002)

R.P. Kambour, Polym. Sci. Macromol. Rev. **7**, 1 (1973)

R.P. Kambour, in *Encyclopedia of Polymer Science and Engineering*, ed. by H.F. Mark, N.M. Bikales, C.G. Overberger, G. Menges, J.I. Kroschwitz (Wiley, New York, 1986), p. 299

A. Kamira, B.-B. Naima, Polym. Test. **25**, 1101 (2006)

J. Karger-Kocsis, T. Czigany, Polymer **37**, 2433 (1996)

J. Karger-Kocsis, J. Varga, J. Appl. Polym. Sci. **62**, 291 (1996)

J. Karger-Kocsis, A. Kallo, V.N. Kuleznev, Plaste Kautsch **28**, 629 (1981)

J. Karger-Kocsis, A. Kallo, V.N. Kuleznev, Polymer **25**, 279 (1984)

T. Karna, J. Laakso, K. Levon, E. Savolainen, U.S. Patent 5,346,649, 13 Sep 1994a, US Appl. 4 Dec 1992, Fin. Appl. 5 Dec 1991, to Neste Oy

T. Karna, J. Laakso, T. Niemi, H. Ruohonen, E. Savolainen, H. Lindstrona, E. Virtanon, O. Ikkale, A. Andreatta, U.S. Patent 5,340,499, 23 Aug 1994b, US Appl. 11 Aug 1992, to Neste Oy

T. Kashiwagi, E. Grulke, J. Hilding, R. Harris, W. Awad, J. Douglas, Macromol. Rapid. Commun. **23**, 761 (2002)

T. Kashiwagi, R.H. Harris Jr., X. Zhang, R.M. Briber, B.H. Cipriano, S.R. Raghavan, Polymer **45**, 881 (2004)

T. Kashiwagi, F. Du, K.I. Winey, K.M. Groth, J.R. Shields, S.P. Bellayer, Polymer **46**, 471 (2005)

K. Kato, Kolloid-Z. Z. Polym. **220**, 24 (1967a)

K. Kato, Polym. Eng. Sci. **7**, 38 (1967b)

H.H. Kausch, (ed.), Adv. Polym. Sci. **52/53** (Springer, Berlin, 1983)

H.D. Kay, S.M. Morgan, S.N. Bodapati, Wall J. **41**, 24 (2000)

J.D. Keitz, J.W. Barlow, D.R. Paul, J. Appl. Polym. Sci. **29**, 3131 (1984)

K. Kelar, B. Jurkowski, Polymer **41**, 1055 (2000)

A. Kelarakis, K. Yoon, Eur. Polym. J. **44**, 3941 (2008)

I. Kelnar, J. Kotek, L. Kapralkova, J. Hromadkova, J. Kratochvil, J. Appl. Polym. Sci. **100**, 1571 (2006)

D. Kemmer, S. Smolic, R. Franz1, V. Coma, *Poster presentation at the 4th International Symposium on Food Packaging*, Prague, November 19–21 (2008)

K. Kendall, F.R. Sherliker, Brit. Polym. J. **12**, 111 (1980)

W.N. Kim, C.M. Burns, Polym. Eng. Sci. **28**, 1115 (1988)

K.J. Kim, T. Kyu, Polymer **40**, 6125 (1999)

B. Kim, V. Koncar, E. Devaux, AUTEX Res. J. **4**, 9 (2004)

A.J. Kinloch, in *Polymer Blends and Mixtures*, ed. by D.J. Walsh, J.S. Higgins, A. Maconnachie (Nijhoff, Dordrecht, 1985)

A.J. Kinloch, R.J. Young, *Fracture Behavior of Polymers* (Applied Science Publishers, New York, 1983)

G. Kipouras, A.R. Federl, U.S. Patent 4,755,716, 4 Oct 1988, Appl. 12 May 1986, to Borg-Warner Chemicals Inc.

E. Kiran, J. Supercritical Fluid. **47**, 466 (2009)

G. Kiss, Polym. Eng. Sci. **27**, 410 (1987)

J. Kocsis, A.A. Apostolov, J. Appl. Polym. Sci. **91**, 175 (2004)

T. Kokkonen, T. Karna, J. Laakso, P. Nuholm, J.-E. Sterholm, H. Stubb, U.S. Patent 5,279,769, 18 Jan 1994, US Appl. 2 Dec 1991, Fin. Appl. 30 Mar 1990, to Neste Oy

J. Kolařík, J. Macromol. Sci. Part B Phys. **39**, 53 (2000)

J. Kolarik, G.C. Locati, L. Fambri, A. Penati, Polym. Netw. Blend. **7**, 103 (1997)

K. Koo, T. Inoue, K. Miyasaka, Polym. Eng. Sci. **25**, 741 (1985)

J.H. Koo, D.W.H. Ho, O.A. Ezekoye, in *Proceedings of the 42nd AIAA/ASME/ SAE/ASEE Joint Propulsion Conference*, 8, 5895, AIAA, Reston, (2006), AIAA Paper 2006-4936

J.H. Koo, D.W.H. Ho, M.C. Bruns, O.A. Ezekoye, in *Proceedings of the AIAA/ASME/ASCE/AHS/ ASC Structures, Structural Dynamics and Materials Conference*, 5136–5175, AIAA, Reston, (2007), AIAA Paper 2007–2131

S. Kopp, J.C. Wittmann, B. Lotz, Polymer **35**, 908 (1994)

B. Kouini, A. Serier, Mater. Design **34**, 313 (2012)

E.G. Kouloori, A.X. Georgaki, J.K. Kallitsis, Polymer **38**, 4185 (1997)

M. Kozlowski, Polym. Netw. Blend. **5**, 163 (1995)

E.J. Kramer, J. Macromol. Sci. Phys. **B10**, 191 (1974)

E.J. Kramer, J. Polym. Sci. Phys. **13**, 509 (1975)

E.J. Kramer, in *Crazing in Polymers, Advances in Polymer Science*, ed. by H.H. Kausch, vol. 52/53 (Springer, Berlin, 1983)

S. Krause, J. Macromol. Sci. Revs. Macromol. Chem. **C7**, 251 (1972)

S. Krause, in *Polymer Blends*, ed. by D.R. Paul, S. Newman, vol. 1 (Academic, New York, 1978). Chapter 2

S. Krause, M. Iskandar, M. Iqbal, Macromolecules **15**, 105 (1982)

A. Krishna, E. Berg, *Stress Cracking of Polycarbonate Exposed to Sunscreen* (Delphi Automotive LLP, 2011-01-0037, 2011)

C.C. Ku, R. Liepins, *Electrical Properties of Polymers, Chemical Principles* (Hanser, Munich, 1987)

R.A. Kudva, H. Keskkula, D.R. Paul, Polymer **40**, 6003 (1999)

V.G. Kulkarni, B. Wessling, European Patent Applications 497,514, 5 Aug 1992, U.S. Appl 31 Jan 1991. U.S. Patent 5,290, 483, 2 Mar 1994, Appl. 22 June 1993

V.G. Kulkarni, B. Wessling, European Patent Applications 536, 915, 14 Apr 1993, U.S. Appl. 8 Oct 1991, to Americhem Inc.

A.K. Kulshreshtha, G.C. Pandey, S.F. Xavier, J.S. Anand, Eur. Polym. J. **25**, 925 (1989)

C.A. Kumins, T.K. Kwei, in *Diffusion of Polymers*, ed. by J. Crank, G.S. Park (Academic, New York, 1968). Chapter 4

T. Kunori, P.H. Geil, J. Macromol. Sci. Phys. **B18**, 93–135 (1980)

T. Kurauchi, T. Ohta, J. Mater. Sci. **19**, 1699 (1984)

L. Kureleca, M. Teeuwenb, H. Schoffeleersb, R. Deblieckb, Polymer **46**, 6369 (2005)

W.C. Kuryla, A.J. Papa (eds.), *Flame Retardancy of Polymeric Materials*, vol. 4 (Marcel Dekker, New York, 1978)

S.A. Kyriakou, M. Statherpoulos, G.K. Parissakis, C.D. Papaspyrides, C.N. Kartalis, Polym. Degrad. Stab. **66**, 49 (1999)

F.P. La Mantia, A. Valenza, M. Paci, P.L. Magagnini, J. Appl. Polym. Sci. **38**, 583 (1989)

J. Lagaron, N.M. Dixon, B.J. Kip, Macromolecules **31**, 5845 (1998)

J. Lagaron, J. Pastor, B. Kip, Polymer **40**, 1629 (1999)

J. Lagaron, G. Capaccio, L.J. Rose, B.J. Kip, J. Appl. Polym. Sci. **77**, 283 (2000)

A. Lahor, M. Nithitanakul, B.P. Grady, Eur. Polym. J. **40**, 2409 (2004)

S.-M. Lai, Y.-C. Liao, T.-W. Chaen, J. Appl. Polym. Sci. **100**, 1364 (2006)

S. Laihonen, U.W. Gedde, P.E. Werner, M. Westdahl, P. Jääskeläinen, G.J. Lake, *Conference Proceedings of the Physical Institute. The Yield Deformation and Fracture of Polymers* (Cambridge, 1970)

S. Laihonen, U.W. Gedde, P.E. Werner, J. Martinez-Salazar, Polymer **38**, 361 (1997)

G.J. Lake, P.B. Lindley, A.G. Thomas, in *Fracture*, ed. by L. Averbach (Chapman & Hall, London, 1979)

J.D. Landes, J.A. Begley, in *Post-Yield Fracture Mechanics*, ed. by D.G.H. Latzko (Applied Science Pubishers, London, 1979)

A.H. Landrock (ed.), *Handbook of Plastics Flammability and Combustion Toxicology* (Noyes Pub, New Jersey, 1983)

L. Lapcik Jr., in *Proceedings of Fifth International Conference on Composites Engineering* (Chicago, 1998), pp. 515–521

A. Lazzeri, M. Malanima, M. Pracella, J. Appl. Polym. Sci. **74**, 3455 (1999)

B.-L. Lee, Polym. Eng. Sci. **28**, 1107 (1988)

C.B. Lee, F.C. Chang, Polym. Eng. Sci. **32**, 792 (1992)

K.I. Lee, H. Jopson, Makromol. Chem. Rapid Commun. **4**, 375 (1983)

K.I. Lee, H. Jopson, Am. Chem. Soc. Symp. Ser. **242**, 39 (1984)

B.L. Lee, U.S. Patent 5,237,009, 17 Aug 1993, Appl. 24 Apr 1991, to B.F. Goodrich Co.

C.B. Lee, M.L. Lu, F.C. Chang, J. Chinese Inst. Chem. Eng. **23**, 305 (1992a)

C.B. Lee, M.L. Lu, F.C. Chang, Polym. Mater. Sci. Eng. **64**, 510 (1992b)

C.B. Lee, M.L. Lu, F.C. Chang, J. Appl. Polym. Sci. **47**, 1867 (1993)

J.-C. Lee, Y.-S. Hong, R.-G. Nan, M.-K. Jang, C.S. Lee, S.-H. Ahn, Y.-J. Kang, J. Mech. Sci. Technol. **22**, 1468 (2008)

J.D. Lendes, J.A. Begley, ASTM STP **560**, 170 (1974)

W. Lethersich, *Technical Report L/T 186 – Impact Testing Critical Resume* (British Electrical and Allied Industries Research Association, London, 1948)

E.G. Lezcano, C. Salom Coll, M.G. Prolongo, Macromolecules **25**, 6849 (1992)

E.G. Lezcano, M.G. Prolongo, C. Salom Coll, Polymer **36**, 565 (1995)

E.G. Lezcano, C. Salom Coll, M.G. Prolongo, Polymer **37**, 3603 (1996)

E.G. Lezcano, R. de Arellano, M.G. Prolongo, C. Salom Coll, Polymer **39**, 1583 (1998)

Z.-M. Li, S.-N. Li, X.-B. Xu, Polym-Plast. Tech. Eng. **46**, 129 (2007)

T. Lian, W. Xu, P. Liu, H. Ren, Polym. Plast. Tech. Eng. **43**, 31 (2004)

J.W. Lim, A. Hassan, A.R. Rahmat, M.U. Wahit, Polym. Intnl. **55**, 204 (2006)

Lindsay Rubber Products, Best *Type of Rubber* (2010)

Liu, X., Jiang, Z., and Zhu, W., *e-Polymers* (2007) Europ. Polym. Fed., CODEN: EPOLCI J. 7, 675 (1999)

S.M. Lomarkin, I.L. Dubnikova, A.N. Shchegolikhin, G.E. Zaikov, R. Kozlowski, G.-M. Kim, G.H. Michler, J. Therm. Anal. Calorim. **94**, 719 (2008)

C. Lotti, A.C. Carlos, V.C. Sebastiao, Mater. Res. **3**, 1 (2000)

B. Lotz, Polymer **39**, 4562 (1998)

B. Lotz, J. Macromol. Sci. Part B-Phys. **41**, 685 (2003)

X. Lu, N. Brown, Polymer **28**, 1505 (1987)

M.L. Lu, F.C. Chang, Polymer **36**, 2541–4639 (1995)

M.L. Lu, C.B. Lee, F.C. Chang, Polym. Eng. Sci. **35**, 1433 (1995)

M.L. Lu, K.C. Chiou, F.C. Chang, Polym. Eng. Sci. **36**, 2289 (1996)

A.B. Lugao, E.C.L. Cardoso, B. Hutzler, L.D.B. Machado, R.N. Conceicao, Radiat. Phys. Chem. **63**, 489 (2002)

A. Lustiger, Environmental stress cracking: the phenomenon and its utility, in *Failure of Plastics*, ed. by W. Brostow, R. Corneliussen (Hanser, Munich, 1986), pp. 305–329

A. Lustiger, N.J. Ishikawa, J. Polym. Sci. Polym. Phys. **29**, 1047 (1991)

A. Lustiger, Understanding Environmental Stress Cracking in Polyethylene, in *Medical Plastics: Degradation, Resistance & Failure Analysis* ed. R.C. Portnoy (SPE, Plastic Design Library, Rice RC, Tritsch DE, 1998), pp. 66–71

J.P. Lv, W.H. Liu, J. Appl. Polym. Sci. **105**, 333 (2007)

W.J. MacKnight, R.W. Lenz, P.V. Musto, R.J. Somani, Polym. Eng. Sci. **25**, 1124 (1985)

Y.W. Mai, Int. J. Mech. Sci. **35**, 995 (1993)

Y.W. Mai, B. Cotterell, Int. J. Fract. **32**, 105 (1986a)

Y.W. Mai, B. Cotterell, Int. J. Fract. **30**, R37 (1986b)

Y.W. Mai, P. Powell, J. Polym. Sci. Part B. Polym. Phys. **29**, 785 (1991)

Y.W. Mai, B. Cotterell, R. Horlyck, G. Vigna, Polym. Eng. Sci. **27**, 804 (1987)

D. Maki, M. Stevens, *Calculation of Effective Diffusion and Solubility Coefficients in Non-Fickian Materials*, in TAPPI 2002 PLACE Conference, p. 5 (2002)

T.M. Malik, P.J. Carreau, N. Chapleau, Polym. Eng. Sci. **29**, 600 (1989)

B.M. Mandal, C. Bhattacharya, S.N. Bhattacharya, J. Macromol. Sci. Chem. A, **26**, 175 (1989)

M.J. Mannion, U.S. Patent 5,310,950, 1994 to Milliken Research Corporation

J.F. Mano, D. Koniarova, R.L. Reis, J. Mater. Sci. Mater. Medic. **14**, 127 (2003)

J.A. Manson, L.H. Sperling, *Polymer Blends and Composites* (Plenum Press, New York, 1981)

C. Mao, Y. Zhu, W. Jiang, ACS Appl. Mater. Interfaces **24**, 5281 (2012). doi:10.1021/am301230q. Epub 2012 Sep 18

H.F. Mark, N.G. Gaylord (eds.), *Encyclopedia of Polymer Science and Technology*, vol. 14 (Interscience Publishers, New York, 1971), p. 24

H.F. Mark, S.M. Atlas, S.W. Shalaby, E.M. Pearce, in *Flame-Retardant Polymeric Materials*, ed. by M. Lewin, S.M. Atlas, E.M. Pearce (Plenum Press, New York, 1975)

G.P. Marshall, J.G. Williams, C.E. Turner, J. Mater. Sci. **8**, 949 (1973)

E. Martine, D. Louvier, *HEIG-VD/LEC, Analytical Method for the Determination of the Aroma Permeation Through Packaging Materials* (Switzerland, 2010)

R.J. Martino, (ed.), *Modern Plastics Encyclopedia '93*, (McGraw-Hill, New York, 1994)

M.A. Martins, C.G. Mothe, Polym. Test. **15**, 91 (1996)

Y. Maruhashi, S. Iida, Polym. Eng. Sci. 41, 1987 (2001), Article first published online: 7 APR 2004. doi:10.1002/pen.10895

L.R. Mason, A.B.. Reynolds, J. Appl. Polym. Sci. **66**, 1691 (1997)

B. Mazeaud, M.A. Galland, Mech. Syst. Signal Process. **21**, 2880 (2007)

N.G. McCrum, B.E. Read, G. Williams, *Anelastic and Dielectric Effects in Polymeric Solids* (Wiley, London, 1967)

E. Meaurio, E. Zuza, J.R. Sarasua, Macromolecules **38**, 1207 (2005)

A. Mehta, A.I. Isayev, Polym. Eng. Sci. **31**, 971 (1991)

R.B. Mesrobian, P.E. Hinsdale, O.F. Sellers, A. Domas, U.S. Patent 3,373,224, 1968

R.A. Mickiewicz, E. Ntoukas, A. Avgeropoulos, E.L. Thomas, Macromolecules **41**, 5785 (2008)

L. Minkova, H. Yordanov, S. Filippi, Polymer **43**, 6195 (2002)

M-j. Luo, Y-x. Lu, Q-q. Chen, Z. Deng, D-q. Chen, W-b. Xie, L. M-j. Fu, Gaofenzi Cailiao Kexue Yu Gongcheng **17**, 71–79 (2001)

A.B.. Morgan, Polym. Adv. Technol. **17**, 206 (2006)

A. Moro, A. Chiolle, L. Credali, G. Foschcini, Makromol. Chem. Macromol Symp. **16**, 137 (1988)

R.E. Morris, R.R. James, T.A. Werkenthin, Rubber Chem. Tech. **17**, 92 (1944)

E.J. Moskala, M.R. Tant, Polym. Mater. Sci. Eng. **63**, 63 (1990)

A. Muhammad, Ph.D. Thesis, Mechanistic Studies Of Thermal Behavior Of Certain Polymeric Systems With Additives, Bahauddin Zakariya University, Multan, 01 Apr 2013

M. Nagao, G. Sawa, M. Ied, Trans. Inst. Elect. Eng. Japan **96-A**, 605 (1976)

M. Nagao, S. Toyoshima, G. Sawa, M. Ieda, Trans. Inst. Elect. Eng. Japan **97-A**, 617 (1977)

L. Narisawa, Polym. Eng. Sci. **27**, 41 (1987)

I. Narisawa, M.T. Takemori, Polym. Eng. Sci. **29**, 671 (1989)

I. Narisawa, M.T. Takemori, Polym. Eng. Sci. **30**, 1345 (1990)

S. Nazare, B.K. Kandola, A.R. Horrocks, Polym. Adv. Technol. **17**, 294 (2006)

NETZSCH, G:\O I T\Determination of the Oxidation Induction Time or Temperature O_I_T_ and O_O_T_ – NETZSCH Analyzing & Testing.mht

L.V. Newmann, J.G. Williams, Polym. Eng. Sci. **18**, 893 (1978)

L.E. Nielsen, *Mechanical Properties of Polymers and Composites*, vol. 2 (Marcel Dekker, New York, 1974)

T. Nishi, T.T. Wang, Macromolecules **8**, 909 (1975)

T. Nishi, T.T. Wang, Macromolecules **10**, 421 (1977)

Y. Nitta, M. Funayama, IEEE Trans. Electr. Insul. **EI-13**, 130 (1978)

M.R. Nobile, D. Acierno, L. Incarnato, E. Amendola, L. Nicolais, C. Carfagna, J. Appl. Polym. Sci. **41**, 2723 (1990)

QUILITE Noise Barriers, *QUILITE International* (California, 1997)

E. Nolley, J.W. Barlow, D.R. Paul, Polym. Eng. Sci. **20**, 364 (1980)

J. Nunoshige, H. Akahoshi, Y. Liao, S. Horiuchi, Y. Shibasaki, M. Ueda, Polym. J. **39**, 828 (2007). doi:10.1295/polymj.PJ2006280

O. Olabisi, Macromolecules **8**, 316 (1975)

O. Olabisi, L.E. Robeson, M.T. Shaw, *Polymer-Polymer Miscibility* (Academic, New York, 1979)

E. Orowan, Rep. Prog. Phys. **12**, 185 (1948)

R.M. Ottenbrite, L.A. Utracki, S. Inoue (eds.), *Rheology and Polymer Processing, Multiphase Systems*. Current Topics in Polymer Science, vol. 2 (Hanser, Munich, 1987)

C. Ozdilek, Polymer **52**, 4480 (2011)

A.R. Padwa, Polym. Eng. Sci. **32**(22), 1703 (1992)

P. Pakeyangkoon, M. Nithiitanakul, B.P Grady, *World Congress of Chemical Engineering, 7th*, Glasgow, UK, July 10–14, (2005)

L. Pan, T. Chiba, T. Inoue, Polymer **42**, 8825 (2001)

V.S. Papakov, G.G. Nikiforova, I.M. Raygorodsky, I.P. Storozhuk, J. Polym. Sci. **37B**, 428 (1995)

V.S. Papakov, G.G. Nikiforova, V.G. Nikolsky, I.A. Krasotkina, E.S. Obolonkova, Polymer **39**, 631 (1998)

E. Paredes, E.W. Fischer, Macromol. Chemie **180**, 2707 (1979)

K.J. Pascoe, in *Failure of Plastics*, ed. by W. Brostow, R.D. Corneliussen (Hanser, Munich, 1986). Chapter 7

D.R. Paul, J.W. Barlow, J. Macromol. Sci. -Rev. Macromol. Chem. **C18**, 109 (1980)

D.R. Paul, L.M. Robeson, Polymer **49**, 3187 (2008)

D.R. Paul, in *Polymer Compatibility and Incompatibility Principles and Practice*, vol. 2, ed. by K. Solc, MMI Press Symposium Series (1982)

V.N.S. Pendyala, K.V. Rao, S.F. Xavier, A.K. Kulshreshtha, *Evaluation of Commercial Nucleating Agents' Efficiency in Polypropylene Homopolymer*, R.I.L., Report No. RD/MSG/153, Feb 21, (2004)

J.D. Peterson, S. Vyazovkin, C.A. Wight, Macromol. Chem. Phys. **202**, 775 (2001)

R.P. Petrich, *Impact Reinforcement of Polyvinylchloride*, presented at SPE RETEC meeting, Cleveland, 7 March 1972

D. Pfefferkorn, Eur. Polym. J. **48**, 200 (2012)

O.-G. Piringer, A.L. Baner, in *Plastic Packaging Materials for Food: Barrier Function, Mass Transport, Quality Assurance, and Legislation* (Wiley-VCH, 2000), p. 576

P. Pisitsak, R. Magaraphan, Polym. Test. **28**, 116 (2009)

E. Plati, J.G. Williams, Polym. Eng. Sci. **15**, 470 (1975)

A.P. Plochocki, Polym. Eng. Sci. **23**, 618 (1983)

G. Poli, M. Paci, P. Magagnini, R. Scaffaro, F.P. La Mantia, Polym. Eng. Sci. **36**, 1244 (1996)

I. Polios, Macromolecules **30**, 4470 (1997)

J.A. Pople, G.R. Mitchell, S.J. Sutton, A.S. Vaughan, C.K. Chai, Polymer **40**, 2769 (1999)

C.H. Porter, R.H. Boyd, in *Dielectric Properties of Polymers*, ed. by F.E. Karasz (Plenum Press, New York, 1972)

K. Premphet, W. Paecharoenchai, J. Appl. Polym. Sci. **85**, 2412 (2002)

B. Pukanszky, F. Tudos, Makromol. Chem., Macromol. Symp. **38**, 221 (1990)

B. Pukanszky, F. Tudos, A. Kallo, G. Bodor, Polymer **30**, 1399–1407 (1989)

X.Y. Qi, D. Yan, Z. Jiang, Y.K. Cao, Z.Z. Yu, F. Yavari, N. Koratkar, ACS Appl. Mater. Interfaces **3**, 3130 (2011). doi:10.1021/am200628c. Epub 2011 July 20

H. Qin, S. Zhang, C. Zhao, G. Hu, M. Yang, Polymer **46**, 8386 (2005)

Z.X. Quande Gui, G.D. Weiping Zhu, J. Appl. Polym. Sci. **88**, 297 (2003)

C.B. Quinn, J. Polym. Sci. Polym. Chem. **15**, 2587 (1977)

D. Quintens, G. Groeninckx, Polym. Eng. Sci. **30**, 1474 (1990)

S. Radhakrishnan, P.D. Venkatachalapathy, Polymer **37**, 3749 (1996)

J.C. Radon, Int. J. Fracture **16**, 533 (1980)

R. Ramanathan, K. Blizard, D. Baird, SPE Techn. Papers **33**, 1399 (1987)

R. Ramanathan, K. Blizard, D. Baird, SPE Techn. Papers **34**, 1123 (1988)

H. Raval, S. Devi, Y.P. Singh, M.H. Mehta, Polymer **32**, 493 (1991)

P.E. Reed, in *Developments in Polymer Fracture*, ed. by E.H. Andrews (Applied Science Publishers, London, 1979)

J.R. Rice, in *Fracture, An Advanced Treatise*, ed. by H. Liebowitz, vol. 2 (Academic, New York, 1968)

M.J. Richardson, P. Burrington, J. Thermal Anal. **6**, 345 (1974)

C.M. Rimnac, T.M. Wright, R.W. Klein, Polym. Eng. Sci. **28**, 1586 (1988)

M. Rink, T. Ricco, W. Lubert, A. Pavan, J. Appl. Polym. Sci. **22**, 429 (1978)

S.J. Risch, *ACS Symposium series-756* (2000), p. 94

S. Ritzenthaler, E. Girard-Reydet, J.P. Pascault, Polymer **41**, 6375 (2000)

R.S. Rivlin, A.G. Thomas, J. Polym. Sci. **10**, 291 (1953)

R.E. Robertson, D.R. Paul, J. Appl. Polym. Sci. **17**, 2579 (1973)

J.M. Rodriguez-Parada, V. Percec, J. Polym. Sci., (A) Polym. Chem. **24**, 579 (1986a)

J.M. Rodriguez-Parada, V. Percec, Macromolecules **19**, 55 (1986b)

R.J. Roe, C. Gieniewski, Polym. Eng. Sci. **15**, 421 (1975)

D.S. Rosa, J. Sarti, L.H.I. Mei, M.M. Filho, S. Silveira, Polym. Test. **19**, 523 (2000)

S.L. Rosen, Polym. Eng. Sci. **7**, 115 (1967)

M.R. Rubner, S.K. Tripathy, J. George Jr., P. Chlewa, Macromolecules **16**, 870 (1983)

C.F. Ryan, U.S. Patent 3,678,133, 1972

C.F. Ryan, R.J. Crochowski, U.S. Patent 3,426,101, 1969

S.F. Xavier, V.N.S. Pendyala, Unpublished results

S. Saha, Eur. Polym. J. **37**, 2513 (2001)

S. Sánchez-Valdes, I.Y. Flores, R. de Valle LF, O.S. Rodriguez-Fernandez, F. Orona-Villarreal, M.L. Quintanilla, Polym. Eng. Sci. **38**(1), 127 (1998)

K. Sandeep, B.V. Ramanaiah, A.R. Ray, Polym.-Plast Tech. Eng. **45**, 1039 (2006)

M.J. Sanders, *Flame Retardants Special Report*, Chem. Eng. News, 56, 22–28 (Apr 24) 1978

M.C. Sarkar, M. Tech., Dissertation, Delhi College of Engineering, Delhi, 1989

G. Sarkhel, A. Choudhury, J. Appl. Polym. Sci. **108**, 3442 (2008)

K. Satake, J. Appl. Polym. Sci. **14**, 1007 (1970)

J.A. Sauer, C.C. Chen, in *Crazing in Polymers*, ed. by H.H. Kausch (Springer, Heidelberg, 1983)

J.A. Sauer, C.C. Chen, Polym. Eng. Sci. **24**, 786 (1984)

J.A. Sauer, G.C. Richardson, Int. J. Fract. **16**, 499 (1980)

A. Savadori, Mater. Technik **4**, 212 (1985)

B. Schartel, M. Bartholmai, U. Knoll, Polym. Adv. Technol. **17**, 772 (2006)

J. Scheirs, *Compositional and Failure Analysis of Polymers* (Wiley, Chichester, 2000)

A.R. Schultz, A.L. Young, J. Appl. Polym. Sci. **28**, 1677 (1983)

B. Selvakumar, Ind. J. Chem. Tech. **15**, 547 (2008)

M.C. Senake Perera, U.S. Ishiaku, Z.A. Mohd. Ishak, Eur. Polym. J. **37**, 167 (2001)

M. Sepe, Stress cracking: how to avoid this silent killer (part 1). *IMM Magazine*, (1999)

J. Seppala, M. Heino, C. Kapanen, J. Appl. Polym. Sci. **44**, 1051 (1992)

G. Serpe, J. Jarrin, F. Dawans, Polym. Eng. Sci. **28**(21), 1416 (1988)

R.J. Seward, J. Appl. Polym. Sci. **14**, 852 (1970)

L.W. Shacklette, G.G. Miller, C.C. Han, R.L. Elsenbaumer, PCT Int. Appl., WO 93 024,555, 9 Dec 1993, Appl. 3 June 1992, to Allied Signal Inc.

S.D. Sharma, B.Tech. Dissertation, University of Calcutta, Calcutta, 1988

Y.N. Sharma, J.S. Anand, A.K. Kulshreshtha, S.F. Xavier, S. Chakrapani, Int. J. Polym. Mater. **12**, 165 (1988b)

K. Shimamura, Y. Suzuki, Jpn. Patent 0,324,153, 1 Feb 1991, to Asahi Chemical Co. Ltd.

B.Y. Shin, I.J. Chung, Polym. J. **21**, 851 (1989)

C.J. Shirtliffe, *Heat Transmission Measurements in Thermal Insulation* (ASTM STP 544, Am. Soc. Testing Mats., Philadelphia, 1974)

Y. Shono, Y. Yoshida, K. Yamamoto, in *Proceedings of the Japan Society of Civil Engineers* (Tokyo, 1994), pp. 81–89

E.K. Sichel, M.F. Rubner, J. Polym. Sci. Phys. **23**, 1616–1629 (1985)

A. Siegmann, A. Dagan, S. Kenig, Polymer **26**, 1325 (1985)

A. Sikora, F.E. Karasz, Macromolecules **26**, 3438 (1993)

R.E. Skochdopole, C.R. Finch, J. Marshall, Polym. Eng. Sci. **27**, 627 (1987)

P.E. Slade Jr., L.T. Jenkins (eds.), *Techniques and Methods of Polymer Evaluation*. Thermal Analysis, vol. 1 (Dekker, New York, 1966)

P.K. So, L.J. Broutman, Polym. Eng. Sci. **26**, 1173 (1986)

J. Soares, R. Abbott, J. Kim, J. Polym. Sci. Polym. Phys. **38**, 1267 (2000)

K.C. Šolc (ed.), *Polymer Compatibility and Incompatibility* (Harwood Academic, New York, 1982)

L.C. Souder, B.E. Larson, U.S. Patent 3,251,904, 1966

A.R. Sousa, E.S. Arau'jo, A.L. Carvalho, M.S. Rabello, J.R. White, Polym. Degrad. Stab. **92**, 1465 (2007)

W.M. Speri, G.R. Patrick, Polym. Eng. Sci. **15**, 668 (1975)

F.C. Stehling, T. Huff, C.S. Speed, G. Wissler, J. Appl. Polym. Sci. **26**, 2693 (1981)

T. Sterzynski, M. Lambla, H. Crozier, M. Thomas, Adv. Polym. Technol. **3**, 25 (1994)

S. Strella, P.F. Erhardt, J. Appl. Polym. Sci. **13**, 1373 (1969)

H. Suarez, J.W. Barlow, D.R. Paul, J. Appl. Polym. Sci. **29**, 3253 (1984)

A.R. Subrahmanyam, V. Geetha, A. Kumar, A. Alakanandana, J. Siva Kumar, Int. J. Mater. Sci. **2**, 27 (2012)

P.M. Subramanian, Polym. Eng. Sci. **25**, 483 (1985)

P.M. Subramanian, Polym. Eng. Sci. **27**, 663 (1987)

P.M. Subramanian, U.S. Patent 4,410,482, 1983

P.M. Subramanian, U.S. Patent 4,444,817, 1984

A.M. Sukhadia, D. Done, D.G. Baird, Polym. Eng. Sci. **30**, 519 (1990)

H. Swei, B. Crist, S.H. Carr, Polymer **32**, 1140 (1991)

T. Kawaguchi, H. Nishimura, F. Miwa, K. Abe, T. Kuriyama, I. Narisawa, *Environmental Stress Cracking (ESC) of ABS*, Web Page, 6/21/2002

M.T. Takemori, Ann. Rev. Mater. Sci. **14**, 171 (1984)

M.T. Takemori, I. Narisawa, in *Advances in Fracture Research*, ed. by K. Salama (Pergamon Press, New York, 1989)

T. Tanaka, T. Masuda, T. Yoshimura, S. Noguchi, R&D, Research Develop (Kobe Steel, Ltd) **40**, 53 (1990)

M. Tasdemir, M. Topsakaloglu, J. Appl. Polym. Sci. **104**, 3895 (2007)

R. Tchoudakov, M. Narkis, A. Siegmann, Polym. Eng. Sci. **44**, 528 (2004)

G. ten Brinke, R.E. Karsz, W.J. MacKnight, Macromolecules **16**, 1827 (1983)

T. Theuer, A. Cornee, J. Krey, K. Friedrich, in *Proceedings, 7th International Conference on Deformation, Yield and Fracture of Polymers* (The Plastics and Rubber Institute, London, 1988)

A.G. Thomas, J. Appl. Polym. Sci. **3**, 168 (1960)

T. Tikuisis, P. Lam, M. Cossar, *High Pressure Oxidative Induction Time Analysis By Differential Scanning Calorimetry* (TA Instruments Inc., TA085, 1985)

G.A.V. Timoteo, G.J.M. Fechine, M.S. Rabello, Stress cracking and photodegradation behavior of polycarbonate. Polym. Eng. Sci. **48**, 2003–2010 (2008)

S.C. Tjong, S.P. Bao, J. Polym. Sci. Part B. Polym. Phys. **43**, 585 (2005)

T. Tokairin, T. Kitada, Environ. Monit. Assess. **105**, 121 (2005)

J.S. Trent, J.I. Scheinbeim, P.R. Couchman, J. Polym. Sci. Polym. Lett. Ed. **19**, 315 (1981)

J.S. Trent, J.I. Scheinbeim, P.R. Couchman, Macromolecules **16**, 589 (1983)

S.K. Tripathy, M.F. Rubner, Am. Chem. Soc. Symp. Ser. **242**, 38 (1984)

J. Troitzsch, *International Plastics Flammability Handbook* (Hanser, Münich, 1983)

M. Tsuburaya, H. Saito, Polymer **45**, 1027 (2004)

E.A. Turi, *Thermal Characterization of Polymeric Materials* (Academic, New York, 1981)

S. Turner, *Mechanical Testing of Plastics* (The Butterworth Group, London, 1973). ASTM D 638-95 *Standard Test Method for Tensile Properties of Plastics* (Philadelphia, 1996)

I.C. Um, Y.H. Park, Fib. Polym. **8**, 6 (2007)

L.A. Utracki, *Polymer Alloys and Blends, Thermodynamics and Rheology* (Hanser, Munich, 1989)

L.A. Utracki (ed.), *Encyclopaedic Dictionary of Commercial Polymer Blends* (ChemTec Pub, Toronto, 1994)

L.A. Utracki, in *Polypropylene: Structure, Blends, and Composites*, ed. by J. Karger-Kocsis (Chapman & Hall, London, 1995)

L.A. Utracki, *Commercial Polymer Blends* (Chapman & Hall, London, 1998)

M. Vähä-Nissi, T. Hjelt, M. Jokio, R. Kokkonen, J. Kukkonen, A. Mikkelson, Packag. Technol. 4464 Sci. 425 (2008)

B. van Eerdebbrugh, L.S. Taylor, Pharm. Res. **29**, 2754 (2012)

D.W. Van Krevelen, Polymer **16**, 615 (1975)

H.L. Vandersall, J. Fire Flammability **2**, 97 (1971)

J. Varga, J. Mater. Sci. **27**, 2557 (1992)

P.I. Vincent, *Impact Tests and Service Performance of Thermoplastics* (Plastics Institute, London, 1971)

Vitruvius, *The Ten Books on Architecture* (M.H. Morgann, Tr.) (Dover, New York, 1960). (Original Pub., Howard University Press, 1914)

D.J. Walsh, S. Rostami, *Advances in Polymer Science*, vol. 72 (Springer, Berlin, 1985)

Wang, Polym.Test. **31**, 39 (2012)

J. Wang, S. Velankar, Rheol. Acta **45**, 741 (2006)

L. Wang, W. Ma, R.A. Gross, S.P. McCarthy, Polym. Degr. Stab. **57**, 161 (1998)

J. Wang, M.K. Cheung, Y. Mi, Polymer **42**, 2077 (2001)

H.T. Wang, B.R. Pan, Q.G. Du, Y.Q. Li, Polym. Test. **22**, 125 (2003)

H-H. Wang, W-C. Lee, D-T. Su, W-J. Cheng, B-Y. Lin, *Annual Technical Conference-Society of Plastics Engineers*, 53rd **2**, 2105 (1995); Pub., Society of Plastics Engineers

I.M. Ward, *Mechanical Properties of Solid Polymers*, 2nd edn. (Wiley, New York, 1983)
G.R. Watts, P.A. Morgan, Noise Vib Worldw **49**, 18 (1997)
G. Weber, J. Schoeps, Angew. Makromol. Chemie **136**, 45 (1985)
Y. Wei, R. Li, C. Zhou, Polymer **52**, 2693 (2011)
R.A. Weiss, N. Chung, A. Kohli, Polym. Eng. Sci. **29**, 573 (1989)
W.W. Werring, Proc. ASTM II **26**, 634 (1926)
B. Wessling, H. Volk, Synth. Met. **18**, 671 (1987)
B.S. Westerlind, J.A. Carlsson, Y.M. Andersson, J. Mater. Sci. **26**, 2630 (1991)
J.G. Williams, Trans. Plast. Inst. **35**, 505 (1964)
J.G. Williams, *Fracture Mechanics of Polymers* (Ellis Horwood, Chichester, 1984)
J.G. Williams, H. Ford, J. Mech. Eng. Sci. **6**, 405 (1964)
J.M. Willis, B.D. Favis, Polym. Eng. Sci. **28**, 1416 (1988)
L. Wong, Polym. Test. **21**, 691 (2002)
W.A. Woshinis, D.C. Wright, Advan. Mat. Proc. **12**, 39 (1994)
D. Wright, *Environmental Stress Cracking of Plastics* (RAPRA Technology, Shawbury, 1996)
S. Wu, Polym. Eng. Sci. **27**, 335 (1987)
J. Wu, S. Chen, J. Xian Jiao Tong Univ. **17**, 79 (1983)
J. Wu, Y.W. Mai, Polym. Eng. Sci. **36**, 2275 (1996)
W.B. Wu, W.Y. Chiu, W.B. Liauwu, J. Appl. Polym. Sci. **64**, 411 (1997)
B. Wunderlich, *Thermal Analysis*, (Academic, New York, 1990)
S.F. Xavier, in *Two Phase Polymer Systems*, ed. by L.A. Utracki (Hanser Pub, Munich, 1991)
S.F. Xavier, Y.N. Sharma, Polym. Comp. **7**, 42 (1986)
S.F. Xavier, *Thermal Analysis in Polymer Science* presented in 'Work-Shop on Thermal Analysis' (Vadodara, 2002)
S.F. Xavier, V.N.S. Pendyala, I.S. Bhardwaj, in *Encyclopaedic Dictionary of Commercial Polymer Blends*, ed. by L.A. Utracki (ChemTec Publishing, Toronto, 1994)
S.F. Xavier, V.N.S. Pendyala, *Impermeable Polyolefin Blends for Storing Diesel, other Organic Liquids and an Improved Process for the Preparation Thereof* (RIL Technical Report, Vadodara, 2008)
S.F. Xavier, *RIL Management Information Report, Key Result Area* (India, 2008)
L. Xue et al., Progr. Polym. Sci. **37**, 564 (2012)
M. Yamaguchi, K. Masuzava, *Transparent Polymer Blends Composed of Cellulose Acetate Propionate and Poly(epichlorohydrin)*, ResearchGate, 2013, (2013researchgate.net)
K. Yamaoka, T. Harada, K. Tomari, S. Tonogai, S. Nagai, *The Fifth Annual Meeting, PPS*, April 11–14, Kyoto, Japan (1989)
O.F. Yap, W.W. Mai, B. Cotterell, J. Mat. Sci. **18**, 657 (1983)
F. Yazaki, A. Kohara, R. Yosomiya, Polym. Eng. Sci. **34**, 1129 (1994)
A.F. Yee, R.A. Pearson, J. Mater. Sci. **21**, 2462–2475 (1986)
J.T. Yeh, C.C. Fanchiang, M.F. Cho, Poly. Bull. **35**, 371 (1995)
H. Yordanov, L. Minkova, Europ. Polym. J. **39**, 951 (2003)
R.J. Young, in *Comprehensive Polymer Science*, ed. by C. Colin Booth, C. Price, vol. 2 (Pergamon Press, New York, 1988)
S.H.P. Yu, European Patent Applications 282,985, 21 Sept 1988;Jpn. Patent 63 314,261, 22 Dec 1988; U.S. Appl. 20 Mar 1987, to B.F. Goodrich Co.
M. Zanetti, G. Camino, D. Canavese, A.B.. Morgan, F.J. Lamelas, C.A. Wilkie, Chem. Mater. **14**, 189 (2002)
Zeus Industrial Products, Inc., Technical White Paper, *Low Temperature Properties of Polymers*, 2005, http://www.zeusinc.com
J. Zhang, H. Zhang, Y. Yang, J. Appl. Polym. Sci. **72**, 59 (1999)
L. Zhang, C. Li, R. Huang, J. Polym. Sci. Part B. Polym. Phys. **42**, 1656 (2004)
Y. Zhang, L. Wang, Y. Gao, J. Chen, X. Shi, Med. Eng. Phys. **29**, 699 (2007)
W. Zhang, Z. Gui, C. Lu, S. Cheng, D. Cai, Y. Gao, Mater. Lett. **92**, 68 (2013)
Z. Zhao, H. Ma, Suliao **34**, 57–100 (2005)

Y. Zhao, A.S. Vaughan, S.J. Sutton, S.G. Swingler, Polymer **42**, l6599 (2001)
X.E. Zhao, D.L. Dotson, U.S. Patent 6,465,551 to Milliken & Co, 2002
S. Zheng, K. Nie, Q. Guo, Thermochim. Acta **419**, 267 (2004)
Z. Zhong, Q. Guo, Polymer **39**, 517 (1998)
H. Zhou, B. Li, G.S. Huang, Mater. Lett. **60**, 3451 (2006)
P. Zhuang, T. Kyu, J.L. White, Polym. Eng. Sci. **28**, 1095 (1988)
R. Zong, Z. Wang, N. Liu, Y. Hu, G. Liao, J. Appl. Polym. Sci. **98**, 1172 (2005)

Sources of Additional Information

International Patent Office Sites
European Patent Office: http://ep.espacenet.com/
Indian Patent Office: al_2007.htm: http://www.patentoffice.nic.in/ipr/patent/journal_archieve/journal_2007/patent_journal
Japanese Patent Office: http://ipdl.inpit.go.jp/homepg_e.ipdl (Select PAJ – Patent Abstract of Japan)
USPTO Patent Office: http://www.uspto.gov/ptft/index.html
World Intellectual Property Office (WIPO): http://www.wipo.int/pctdb/en
Free Online Patent Databases
Freepatentsonline: http://www.freepatentsonline.com
Freshpatents: http://www.freshpatents.com
Google Patent Search: http://www.google.com/patents
Patentstorm: http://www.patentstorm.us/, www.patentstorm.us/
Free Open Literature Databases
http://scholar.google.com
www.alltheweb.com
www.research.com
www.vivisimo.com

Mechanical Properties of Polymer Blends

11

Z. Bartczak and A. Galeski

Contents

Z. Bartczak (✉) • A. Galeski
Department of Polymer Physics, Centre of Molecular and Macromolecular Studies Polish
Academy of Sciences, Lodz, Poland
e-mail: bartczak@cbmm.lodz.pl; andgal@cbmm.lodz.pl

Abstract

Mechanical properties of polymer blends, including strength and toughness, are described in terms of morphology, resulting texture, and elementary deformation mechanisms and cavitation. Basic principles of toughening of blends based on glassy, crystalline, and thermoset polymers are described. Toughening strategies involving crazing, cavitation, crystal plasticity, and other micromechanisms involving energy dissipation are presented. Cavitation during deformation arising from mechanical mismatch between differently oriented stacks of lamellae in a semicrystalline polymer, decohesion at interfaces, as well as internal rubber cavitation contribute to the toughness by activation of other mechanisms of plastic deformation of the surrounding matter. Internal cavitation, although augmenting the toughness, greatly reduces the strength of the material. Micromechanisms that are engaged in rubber-toughened blends were characterized with significant attention. Matrix and dispersed-phase properties, as well as interfacial effects, were considered in the interpretation of structure–property relationship for incompatible and partially compatible polymer blends. The dispersion of the second component of the blend and its influence on stress concentrations around inclusions were discussed. The concept of easy deformation paths connected with interparticle distances and shear orientation was considered.

The function of the interfaces, including compatibilizers, in plastic response of polymer blends, is also analyzed.

11.1 Introduction

In polymer blends, the structure is more complicated than in homopolymers because usually there are three structure components: dispersed phase, continuous phase, and interface. Strong bonding between blend components assures that the applied force is transmitted into the dispersed inclusions. Therefore, modification of blends by introducing compatibilizers is a common practice. Compatibilized blends differ from blends of incompatible polymers, apart from more discrete dispersion of a minor component, mainly by the structure and properties of the interface between components. Usually, the achieved toughness of well compatibilized blends allows for their large plastic deformation. There are several simultaneous and synergistic phenomena which give a contribution to toughening of polymer blends. The important factors are the recovery of macromolecular chain mobility at interfaces connected with the change in morphology of interfacial layers and the shift of the brittle-to-ductile transition to a lower temperature. The modification of interfaces often removes the additional relaxation processes which can appear in the system containing unmodified interfaces. Therefore, the limitations to the mobility of kinetics elements at interfaces due to interactions between the inclusions and the matrix are also removed.

Nowadays plain homopolymers are rarely used. Instead, the use of polymer blends dominates in many applications. There are a great variety of blends, including a broad range of materials of a matrix as well as dispersed phase. They differ in compatibility of components, incompatibility, partial miscibility, and inclusion size and shape. A range of micromechanisms including crazing, shear yielding, cavitation of various kinds, and plasticity of polymer crystal are engaged in deformation of polymer blends. Dependencies on temperature, deformation rate, concentration of components, molecular characteristics of components, and other factors influence the brittle-to-ductile transition, morphology, and phase structure. Therefore, this chapter was divided into subsections in which the behavior and mechanical properties of most important cases, related phenomena, and features of mechanical performance of polymer blends are discussed.

11.2   Plastic Deformation and Damage Mechanisms in Polymers

There are a large variety of mechanical responses of solid polymers. The range spans from brittle fracture through highly ductile behavior to rubber elasticity. Deformation processes of both glassy and semicrystalline polymers have been extensively explored in the past. For an overview of these numerous studies, see, e.g., Argon 2013; Balta-Calleja and Michler 2005; Haward and Young 1997; Michler and Balta-Calleja 2012. Above the elastic region, deformation of polymers is usually nonhomogeneous, especially when observed in the microscale. This is not only the case of polymers with clear heterogeneous morphology, such as semicrystalline polymers, block copolymers, or phase-separated polymer blends but also of homogeneous materials as amorphous glassy polymers. Plastic deformation and/or fracture mechanisms start to operate locally above the elasticity limit. Depending on the polymer molecular characteristics, such as chain flexibility and chain entanglement density, as well as test conditions (specimen geometry, loading mode, strain rate, temperature), three types of heterogeneous deformation are observed in the microscale: crazes, shear bands, and shear deformation zones (Michler and Balta-Calleja 2012). Among parameters controlling deformation, under standardized testing conditions, the molecular characteristics of the polymer remain the predominant parameter affecting the deformation mechanism.

Crazes are crack-like sharply localized bands of plastically deformed material, initiated when an applied tensile stress causes microvoids to nucleate at points of high stress concentrations that are created by surface scratches, flaws, cracks, dust particles, or other heterogeneities (Bucknall 1977; Haward and Young 1997; Kinloch and Young 1983). In homogeneous glassy polymers, crazes are usually initiated from microscopic surface flaws or embedded heterogeneities, like dust particles. Dust is difficult to avoid in processing (injection molding, extrusion) because it begins with pellets that become statically charged and attract airborne particles. Typical surface defects are small random scratches introduced during processing, machining, and handling. When these flaws are removed, e.g., by

cautious polishing, there is a marked increase in the critical stress of craze initiation, sometimes to the point at which tensile shear yielding and ductile drawing are initiated in relatively brittle polymers such as PMMA and PS (Argon and Hannoosh 1977). Crazes form in planes normal to the direction of maximum (tensile) principal stress and consist of highly oriented polymer fibrils of approximately 5–15 nm in diameter, stretched out in the direction of loading, and separated by elongated nanovoids. Crazes develop and propagate by two processes: by craze tip advance that allows fibrils to be generated and by craze width growth. In contrast to crack, the craze (which is, in fact, a highly localized yielded region, consisting of a system of alternating oriented polymer fibrils and voids) is capable of transmitting load. However, crazes are frequent precursors of brittle fracture since with the growth of the craze the most elongated fibrils break, which usually leads to the development of microcrack in the center of the craze. Due to the presence of voids, deformation of crazes is dilatational – the volume increases markedly with strain (Haward and Young 1997; Kausch 1983, 1990).

On the other hand, the shear bands and deformation zones are the result of shear processes and do not contain voids so that deformation advances at nearly constant volume. Shear bands can be either localized or diffuse, but even for very localized bands, their interface with bulk material is much thicker than for crazes. Thick bands and deformation zones are usually made of coalescing micro-shear bands.

The basic mechanisms involved in plastic deformation of glassy polymers are crazing and shear yielding (Argon 2013; Bucknall 1977; Haward and Young 1997; Kausch 1983, 1990; Michler and Balta-Calleja 2012), giving rise to the formation of crazes or shear bands and zones, respectively. For polymer crystals, plastic shear is realized through crystallographic mechanisms, primarily by crystallographic slips along and transverses to the chain direction, which are supported by the shear in interlamellar amorphous layers (Argon 2013; Bartczak and Galeski 2010; Oleinik 2003). Their collective activity gives rise to the formation of shear bands or deformation zones, similar to shear yielding in glassy amorphous polymers.

Crazing requires the presence of dilatational component in the stress tensor and may be inhibited by hydrostatic pressure. On the other hand, it is enhanced by the presence of triaxial tensile stress (Kinloch and Young 1983). Unfortunately, such a stress state exists ahead of large flaws or notches in relative thick specimens (plane-strain conditions). Therefore, the presence of sharp cracks, notches, or defects in thick specimens will favor craze initiation leading to brittle fracture, which is opposite to a bulk shear yielding mechanism that leads usually to ductile behavior.

Even the most brittle polymers demonstrate some localized plastic deformation – in front of the crack tip, there exists a small plastic zone where stretching of chains, chain scission, and crack propagation appear in a small volume. The size of that plastic zone is too small to manifest in macroscopic plastic yielding and the crack propagates in a brittle manner. The relative low energy absorbed by the sample on its fracture is almost entirely that dissipated inside the small plastic zone.

11.2.1 Brittle and Pseudoductile Polymers

Under given experimental conditions, chemically different polymers behave differently. For example, in tensile test at a low rate polystyrene tends to craze and is brittle while polycarbonate tends to yield and shows ductile behavior. Based on that, polymers are classified frequently as brittle or pseudoductile (i.e., generally showing a ductile behavior but changing to brittle at more severe conditions, e.g., at a lower temperature). According to this classification, brittle polymers (e.g., PS or PMMA) tend to fail by crazing, have low crack initiation energy (low unnotched toughness), and low crack propagation energy (low notched toughness). Pseudoductile polymers (e.g., PC, PET, PA, or PE) tend to fail by yielding, have high energy of crack initiation (high unnotched toughness), and relatively low energy of crack propagation (notch sensitivity, low notched toughness). The brittle or ductile response depends not only on the polymer itself but also on many extrinsic variables as specimen geometry, loading mode, and test conditions, so frequently the same polymer may either craze (i.e., be brittle) or yield (ductile) depending on external conditions. Argon (Argon et al. 2000; Argon and Cohen 2003) argued that with the exception of only a small class of pure metals, all other solids, including all solid polymers, should be actually classified as intrinsically brittle. Intrinsically brittle polymers only can change their response from brittle to ductile at certain specific experimental conditions (see Sect. 11.4.2.3).

11.2.2 Basic Mechanisms of Deformation

The brittle or ductile behavior of polymer and the preferred mechanisms of deformation and failure are controlled principally by two molecular parameters – the entanglement density and chain flexibility, determining an initiation stress for crazing or shear yielding, respectively. Depending on these parameters, one of the two basic deformation mechanisms (crazing or shear yielding) is selected as the dominating mechanism, so they occur separately in most cases. However, they also can be active simultaneously at different proportion in some polymer systems. Moreover, even a small change in the test conditions can result in a change from shear yielding to crazing or reverse. Crazing and shear yielding are considered to be independent processes, and the mechanism that at given experimental conditions requires the lower stress is activated first and becomes the dominant deformation mechanism that leads ultimately to the failure of the material.

11.2.2.1 Crazing and Entanglement Density

Crazes, in contrast to cracks, are load-bearing features owing to highly stretched fibrils connecting the walls of what would otherwise be a crack. Multiple crazes are actually the main source of ductility in amorphous polymers modified by blending with elastomers. However, crazes have also a big drawback as they frequently appear precursors of brittle fracture. This is due to high localization of deformation in crazes – large plastic deformation and related local energy absorption are highly

localized and confined to a very small volume of the material. Craze can be considered as a thin layer of polymer in which elastic and plastic deformation in the direction of principal tensile stress has occurred without lateral contraction. The lack of lateral contraction is due to voids created between fibrils. These voids can constitute up to approximately 50–75% of the volume of the craze (Haward and Young 1997). The thickness of a craze at the tip is below 10 nm, while a body of the mature craze is much thicker, by 2–4 orders of magnitude. Such significant thickening of the craze proceeds mainly by involving more bulk polymer at the interface into the plastic deformation zone due to strain hardening of the craze matter. This keeps molecular stretch and the void content quite uniform within the craze.

In the literature, there are many theories and models describing nucleation, initiation, and growth of crazes. They were discussed in several reviews, see, e.g., Argon (2013), Donald (1997), Kausch (1983, 1990), Michler and Balta-Calleja (2012). A craze is nucleated by an event of local plastic deformation by shear occurring in the vicinity of a defect and leading to the buildup of significant lateral stresses. This is followed by nucleation of nanovoids, relieving the triaxial constraints, and then by growth of these voids and strain hardening of polymer nanofibrils between voids as molecular orientation advances (Kramer 1983). The nanovoid nucleation stage is considered as a critical one. In highly entangled polymers, the load is distributed over different entanglements and different chains, and, as a consequence, the probability of breaking chains and void formation is lower. It is thus expected that a high entanglement density is unfavorable for craze initiation. Once a craze is initiated, it must grow both in width and length. The general mechanism of craze tip advance has been known to be meniscus instability process (Argon and Salama 1977). Kramer and Berger (1990) derived a detailed model of the craze growth. The craze will grow only when the deformation energy associated with the applied stress is larger than the surface energy needed to create a new surface. This surface energy per unit area of the void surface (Γ) is (Kramer and Berger 1990)

$$\Gamma = \gamma + \frac{1}{4} d_e v_e U_{ch} \tag{11.1}$$

where γ is the van der Waals surface energy, d_e is the entanglement mesh size, v_e is the entanglement density and U_{ch} is the bond energy of the polymer chain. The second term is the energy cost of elimination of entanglements crossing the interface, for example, by chain scission. It appears weighty – in PS of relatively low entanglement density ($v_e \sim 3 \times 10^{25}$ m^{-3}) is about equal to the van der Waals term, both being around 0.04 J/m^2. Increasing the entanglement density of the molecular network leads to a significant increase in Γ and, therefore, to an increase of the craze initiation stress. For PC, which has v_e higher by one order of magnitude than PS ($v_e \sim 3 \times 10^{26}$ m^{-3}), the additional contribution to Γ is 0.2 J/m^2, and consequently much higher stress would be required to initiate a craze. This explains why polymers of high entanglement density, as PC, often deform without crazes but readily form shear bands, instead. The dependence of the craze initiation stress on

Fig. 11.1 Dependence of the craze initiation stress σ_e on the entanglement density v_e for various polymers and their miscible blends (From Wu (1990); reproduced with permission of Wiley)
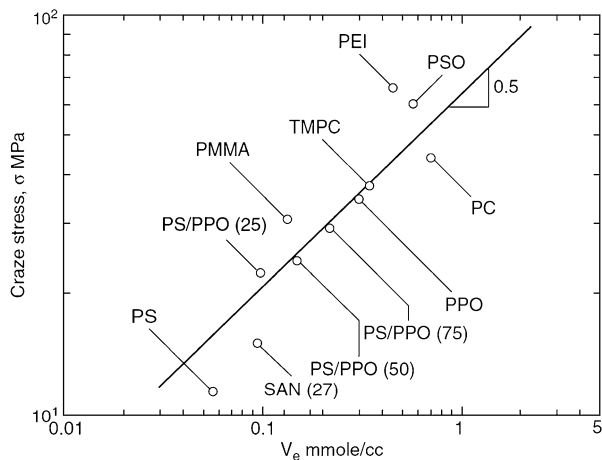
entanglement density was confirmed by experimental data (Wu 1990, 1992). The following relationship holds for the stress of craze initiation σ_{craze} and the entanglement density v_e:

$$\sigma_{craze} \propto f_z v_e^{1/2} \tag{11.2}$$

where f_z is a parameter related to the free volume, reflecting the effects of the physical aging on the crazing stress. Craze initiation stress appears weakly dependent on temperature. A low entanglement density should result in low stress σ_{craze}, thus favoring crazing – see Fig. 11.1, illustrating the relationship of σ_{craze} and entanglement density v_e, for a series of homopolymers and miscible blends of polystyrene (PS) and polyphenylene oxide (PPO), obtained by Wu (1990, 1992). Crazing is initiated at very low stress in PS, which demonstrates the low entanglement density. Blending of PS with PPO results in a notable increase of entanglement density and hence the resistance to crazing – much higher stress is needed to initiate crazing in PPO-rich blends (e.g., in the blend containing 75 wt.% PPO) than in plain PS. On the other hand, polymers exhibiting high entanglement density, as. e.g., PC, tend to deform by shear yielding rather than crazing.

Brittle polymers, such as PS and PMMA, developing crazes at low strains below 1 %, can absorb a greater amount of energy if crazing involves a larger volume of the sample. This can be achieved by increasing the number of the crazes upon deformation due to appropriate structure modification, e.g., by introducing rubber particles. The resultant greatly increased the concentration of crazes is referred to as multiple crazing, which is now acknowledged to be the principal mechanism by which glassy crazable polymers modified with elastomer particles accommodate deformation (Bucknall 1977, 1997, 2000). The multiple crazing mechanism was demonstrated operational and highly effective in high-impact polystyrene (HIPS), ABS copolymer, rubber-toughened PMMA, and other similar systems (Bucknall 1977).

Fig. 11.2 Multiple crazing in HIPS: TEM micrograph of the ultrathin section of HIPS with salami particles of rubber and crazes at early stage of deformation. *Arrow* indicates tensile direction. Scale bar 1 μm (From Heckmann et al. (2005); reproduced with permission of Taylor and Francis)
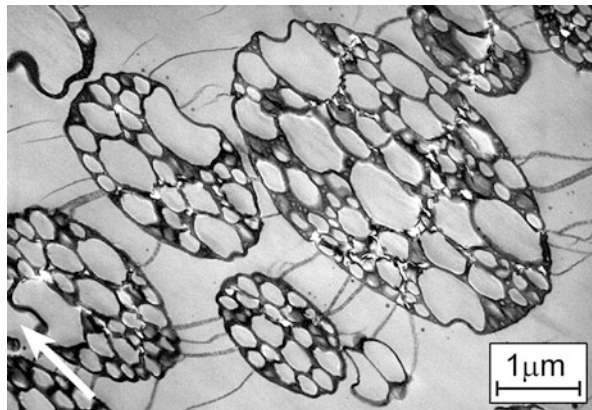
The occurrence of multiple crazing was evidenced by optical and electron microscopy (Bucknall 1977; Michler and Balta-Calleja 2012) and by real-time small-angle X-ray scattering (Bubeck et al. 1991). In glassy polymers modified with elastomer particles (commonly called rubber-toughened polymers), the numerous crazes were found to be initiated near the equator of the cavitating rubber particle due to high stress concentration there (Bubeck et al. 1991; Bucknall 1977). Initiation of numerous crazes at rubber particles involves a relatively large volume of the glassy matrix into deformation, all dissipating energy, which results in a significant increase of toughness. Multiple crazing phenomenon is illustrated in Fig. 11.2.

11.2.2.2 Shear Yielding and Chain Flexibility

Bucknall (2000) depicted shear yielding as the process by which most of the ductile polymeric materials accommodate high strains. Shear yielding involves a displacement of matter during the deformation (molecules sliding past each other). In contrast to crazing, there is no change in the volume or density associated with shear yielding. As cohesion is not lost, no voids are created by shear yielding. Opposite to crazing, shear yielding is strongly temperature dependent. The dependence of the yield stress on temperature and strain rate can be described by the Eyring-type equation (Bauwens 1967; Roetling 1965). In this approach, a positive correlation is expected between chain mobility, yielding, and toughness. That correlation was verified experimentally by Wu (1990, 1992), who found dependence of the reduced normalized yield stress on chain stiffness, which can be defined by the following parameter:

$$C_\infty = \lim_{n \to \infty} \left(R_o^2 / n_v l^2 \right) \qquad (11.3)$$

where $R_o{}^2$ is the mean-square end-to-end distance of an unperturbed chain, n_v is the number of statistical skeletal units, and l^2 is the mean-square length of a statistical unit. Rigid chains. such as liquid crystalline polymers. will have a high C_∞,

Fig. 11.3 Normalized reduced yield stress $\sigma_{yr} = \sigma_y/[\delta^2(Tg - T)]$ versus characteristic chain stiffness, C_∞ (From Wu (1990); reproduced with permission of Wiley)
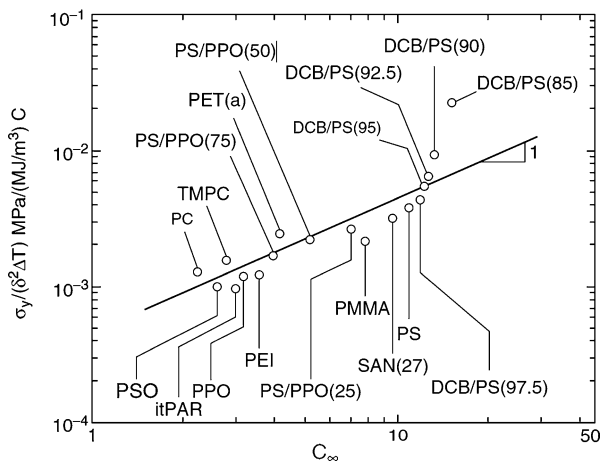
whereas flexible polymers, as, e.g., polyethylene, will demonstrate low values of C_∞. According to Wu (1990) C_∞ and v_e can be related by the equation:

$$v_e = \frac{\rho_a}{3M_v C_\infty^2} \tag{11.4}$$

where M_v is the molecular mass of a statistical skeletal unit and ρ_a is the density of an amorphous polymer.

The stress initiating the shear yielding σ_y depends strongly on temperature and is additionally proportional to two parameters: $\Delta T = T_g - T$ and to δ^2, where T_g and T are the glass transition temperature and the temperature of the test, respectively, while δ denotes the cohesive energy density. The reduced normalized yield stress was defined by:

$$\sigma_{yr} = \sigma_y/\left[\delta^2\left(T_g - T\right)\right] \tag{11.5}$$

The denominator $\delta^2(T_g - T)$ accounts actually for the interchain effects (friction between chains) on the yield stress. Thus, the reduced yield stress defined above by Eq. 11.5 should be only a function of an intrachain property, characterized by the chain stiffness (Wu 1990, 1992):

$$\sigma_{yr} \propto f_y C_\infty \tag{11.6}$$

where f_y is a parameter related to the free volume, reflecting the effects of the physical aging. The above relation implies that the higher the chain stiffness, the lower its mobility and, therefore, the higher the reduced normalized yield stress. Figure 11.3 presents a plot of σ_{yr} as a function of the stiffness ratio, C_∞, constructed by Wu (1992) for a series of polymers and miscible blends. This experimental dependence, confirmed for a number of glassy polymers, shows that the yield

initiation stress increases with increasing chain stiffness of the polymer and that the reduced yield stress for polymers that are known ductile is lower than for those known brittle, as, e.g., PC and PS, respectively. Chains of PC exhibit low stiffness, $C_\infty = 2.4$ (Wu 1992), and PC prefers to deform by shear yielding while PS demonstrates a high chain stiffness, $C_\infty = 10.8$, which results in a high initiation stress for shear yielding. As a consequence PS appears vulnerable to crazing, which can be initiated at stress lower than that needed for initiation of shear yielding.

11.2.2.3 Molecular Criterion for Craze/Yield Behavior from Chain Structure Parameters

The competition between crazing and shear yielding determines which mode of fracture will predominate, so that the transition between crazing (which leads to brittle behavior) and shear yielding deformation mechanism (leading to ductility) is one of the key phenomena for toughness modification. Shear yielding wins the competition with crazing when the yield initiation stress is simply lower than the stress needed for initiation of crazing. The combination of Eqs. 11.2, 11.4, 11.5, and 11.6 leads to the following relationship that expresses the molecular criterion for dominant deformation mode (Wu 1990, 1992):

$$\frac{\sigma_z}{\sigma_{yr}} \propto \frac{v_e^{1/2}}{C_\infty} \left[= \left(\frac{\rho_a}{3M_v} \right)^{1/2} C_\infty^{-2} = \left(\frac{3M_v}{\rho_a} \right)^{1/2} v_e \right] \qquad (11.7)$$

Henkee and Kramer (1984) evidenced the entanglement density to be a critical parameter determining whether the polymer will tend to deform by crazing or by shear yielding. A low entanglement density favors crazing, while the entanglement density rising above the critical value (roughly $v_e \sim 0.15$ mmol/cm^3 (Wu 1992)) results in a change from crazing to shear yielding. On the other hand, the flexibility of chains in thermoplastic polymers seems also to be likely an important parameter for this crazing/shear yielding transition, because when the pseudoductile polymer is cooled down below the temperature of its secondary relaxation process, it becomes brittle despite that entanglement density does not change at this temperature. Taking into account both entanglement density and chain stiffness parameters, the following classification was proposed:

1. Brittle polymers, for which $v_e < \sim 0.15$ mmol/cm^3 and $C_\infty > \sim 7.5$. They fracture by a dominant crazing mechanism and additionally exhibit a low crack initiation energy and a low crack propagation energy (resulting in low, both unnotched and notched, toughness). Examples are PS or PMMA.
2. Pseudoductile polymers, when $v_e > \sim 0.15$ mmol/cm^3 and $C_\infty < \sim 7.5$. They tend to deform by shear yielding mechanism prior to failure. They usually demonstrate a high crack initiation energy (resulting in high unnotched toughness) and a low crack propagation energy (low notched toughness). Examples are PC, polyesters (PBT, PET), or polyamides (PA6, PA6,6).

3. Intermediate class ($v_e \sim 0.15$ mmol/cm^3 and $C_\infty \sim 7.5$) demonstrating combined crazing/shear yielding deformation habit. Examples are some grades of PMMA, PVC, and POM.

   According to the Eq. 11.7 both v_e and C_∞ provide a consistent prediction of the deformation behavior. It seems, however, that the entanglement density v_e can be considered as the primary parameter which controls the crazing behavior, whereas the chain stiffness parameter C_∞ is predominant in controlling the shear yielding behavior.

11.2.3 Plastic Deformation of Semicrystalline Polymers

There are three, currently recognized, principal modes of deformation of the amorphous material in semicrystalline polymers: interlamellar slip, interlamellar separation, and lamellae stack rotation (Argon 2013; Bowden and Young 1971; Butler et al. 1998; Haudin 1982; Oleinik 2003). Interlamellar slip involves shear of the amorphous phase between lamellae. It is relatively easy mechanism of deformation for the material above T$_g$. The elastic part of the deformation can be nearly entirely attributed to the reversible interlamellar slip. Interlamellar separation is induced by a component of tension or compression perpendicular to the lamellar surface. This type of deformation is difficult since a change in the lamellae separation should be accompanied by a transverse contraction and the deformation must involve a change in volume. Stacks of lamellae are embedded in the amorphous matrix, and the stacks are free to rotate under the stress. When the possibility of further deformation of the amorphous phase is exhausted, the deformation of crystalline materials sets in. Any additional deformation of the amorphous phase requires a change in the crystalline lamellae. Crystalline component of polymeric materials is deformed by crystallographic mechanisms, mostly crystallographic slips (Bowden and Young 1974; Lin and Argon 1994; Oleinik 2003). The concept was initially proposed by Peterson (1966, 1968) and developed by Shadrake and Guiu (1976) and Young (1974, 1988): an emission of dislocations from the edges of the lamellae across their narrow faces and their travel across crystals via crystallographic slip mechanism. Many of such subtle slips contribute to a macroscopic strain. Much evidence for the correctness of that mechanism was found in the past (Kazmierczak et al. 2005; Lin and Argon 1994; Seguela 2007; Wilhelm et al. 2004; Young 1988). The model of thermal nucleation of screw dislocations (Peterson 1966, 1968; Young 1974, 1988) was demonstrated to account fairly well for the plastic behavior of many crystalline polymers (Argon et al. 2005; Brooks and Mukhtar 2000; Crist et al. 1989; Darras and Seguela 1993; Seguela 2002). Dislocation theory predicts the correct order of magnitude of the yield stress (O'Kane et al. 1995).

   It is commonly believed that the function of the amorphous phase, above the glass transition temperature, in yielding during tensile deformation of semicrystalline polymers is relatively small and is limited to transfer the stress between adjacent crystals (Seguela and Darras 1994). The stress is transmitted through

such elements as tie molecules, entanglements, etc., called "the tie-molecule fraction," An increase of the yield stress was observed with the increase in the tie-molecule fraction. Men et al. (2003) established that tie molecules are of lesser importance with respect to the deformation, while the entangled chains in amorphous phase play a decisive role.

Since all stress is transferred to crystals via amorphous layers, the amorphous phase appears nevertheless essential for load bearing of semicrystalline polymers, including yielding. Amorphous phase must be stressed at yield with a stress similar to plastically deformed crystals. On the other hand, when the stress in the amorphous phase exceeds its cohesive strength, it undergoes cavitation. Cavitation occurs in semicrystalline polymers, usually in tension. A triaxial local stress, contributing to negative pressure, is necessary for cavitation. If the plastic strength of crystals is low, then with an increase of the stress, it is easier to activate dislocation mechanisms of plastic deformation of lamellae rather than to disrupt the amorphous phase or the interface and create a cavity. In such a case, the deformation can proceed without cavitation. Opposite is the case when the breaking of an amorphous phase is easier than plastic deformation of crystals. Then cavities are generated in the amorphous phase during deformation prior to crystal yielding. However, the formation of voids changes rapidly the local stress state and by this can promote deformation of crystals. There are some ways of modification relations between strength of crystals and amorphous phase. First, it is by controlling the perfection, sizes, and number of crystals by crystallization process. Second, any modification of the amorphous component should result in changes of the material response to loading. Recently it was demonstrated that the amorphous phase can be subjected to various modifications without changing crystalline phase and morphology. Those modifications can greatly influence the yielding and deformation of semicrystalline polymers (Rozanski and Galeski 2013). The amorphous phase may be modified by removing of a low molecular weight fraction to increase its strength or by filling the free volume space with low molecular additives.

Many polymers cavitate during deformation at certain experimental conditions. The polymer morphology seems crucial for cavitation. It seems that the cavitation is generally easier in those semicrystalline polymers which are characterized by higher crystallinity and thicker, less defected crystals. However, it is difficult to separate the influence of crystallinity and crystal perfection. There is a kind of competition between two possible processes: cavitation of anamorphous phase and plastic deformation of crystals. If the crystals are defected and therefore become less resistant to plastic deformation, then their plastic deformation becomes relatively easy while the strength of the amorphous phase prevents for its cavitation. Conversely, if the crystals are thick and demonstrate a reduced number of defects giving rise to dislocations, the breaking of the amorphous phase may become easier and will occur first, prior to crystal yielding. Annealing causes some limited changes of crystal structure, including an increase of their thickness and perfection; however, it may cause also a significant change to amorphous phase and modify its cavitation ability. Average molecular weight and molecular weight distribution of polymers may also drastically change the yield cavitation stress (Kennedy et al. 1994). Also,

the deformation rate is an important factor: yields stress increases with deformation rate, and it becomes easier to initiate cavitation in the amorphous phase. Similar effect is due to lowering the temperature. If the cavitation occurs first, before significant deformation of crystals, then the stress at the apparent yield point is defined by cavitation, rather than by crystal plasticity.

Based on the facts presented above, the plastic deformation behavior of semi-crystalline polymer materials and the structural changes accompanying the deformation of such materials are controlled by the properties of both crystalline and amorphous phases.

The most significant contribution to toughness comes from the plastic deformation of a material, which is a complex phenomenon involving both the crystalline and amorphous phases. As discussed in Sect. 11.2, the ability to an extensive plastic deformation, called ductility, requires an adequate flexibility of polymer chain segments in order to ensure the plastic flow on a molecular level. It is long known that the macromolecular chain mobility is a critical factor deciding on either brittle or ductile behavior of a polymer (Ferry 1970; Galeski 2002). The increase in the yield stress of an amorphous polymer with a decrease of the temperature is caused by a decrease of chain mobility, and vice versa, the yield stress can serve as a qualitative measure of macromolecular mobility. It was shown that the temperature and strain rate dependencies of the yield stress are described in terms of relaxation processes, similarly as in linear viscoelasticity. Also, the kinetic elements taking part in yielding and viscoelastic response of a polymer are similar: segments of chains, part of crystallites, and fragments of an amorphous phase. On the other hand, in semicrystalline polymers tested above their glass transition temperature, the yield stress is determined by the stress required for crystal deformation and not by the amorphous phase, provided that there is no cavitation. The behavior of crystals differs from that of the amorphous phase because the possibilities of motion of macromolecular chains within the crystals are subjected to severe constraints. Since the mobility of kinetic elements taking part in plastic deformation (mobile dislocations in crystals and shear strain carriers in amorphous phase) is lower at a lower temperature, the energy dissipated increases and can lead to local rise of temperature and produce deformation instability. The rate of plastic deformation increases drastically in such local plastic events referred sometimes as micronecks, and the material may fracture quickly hereafter. At a higher temperature the mobility of kinetic elements is higher, so less energy is dissipated and the local temperature increase is smaller. As a result, the deformation zone is stable and tends to extend to the whole gauge length of the sample. The material shows then a tough behavior.

The necessary condition for high plastic deformation is the possibility of motions of kinetic elements in a time scale as it follows from the deformation rate. The relaxation times and the activation energies are the parameters describing the kinetics of the conformation motions of macromolecules and larger elements taking part in the deformation.

Both massive voiding and shear yielding dissipate energy; however, shear yielding is often favored over voiding, especially under uniaxial stress, elevated

temperature, or slow deformation. Shear yielding dissipates the energy more efficiently (Horst and Spoormaker 1996).

The deformation of polymeric materials starts usually at scratches, notches, or internal defects because they are sources of local stress concentration, frequently well above the applied stress. Toughening of polymeric materials is based on the activation of such plastic deformation mechanisms which are activated at a stress lower than that required for triggering the action of surface and internal defects. Consequently, one of the important means of toughening appears to be a significant lowering of the yield stress of the material.

11.3   Blends

The comprehensive introduction to polymer blends is given in ▶ Chap. 1, "Polymer Blends: Introduction," while ▶ Chaps. 5, "Reactive Compatibilization," ▶ 8, "Morphology of Polymer Blends," ▶ 10, "Properties and Performance of Polymer Blends," ▶ 18, "Polyethylenes and Their Blends," and ▶ 21, "Miscible Polymer Blends" of this handbook are devoted to various aspects and detailed description of the formulation, structure, and morphology of polymer blends. Here, the attention will be briefly turned to such features of polymer blends that directly influence or determine their mechanical properties. In polymer blends, the structure is more complicated than in homopolymers because usually they have three components: dispersed phase, continuous phase, and interface. The interface has a finite thickness; hence it is the third component of the system. Applied force is transmitted onto the dispersed inclusions from the matrix via the interface. Therefore, the properties of the interface play a vital role in force transmission and overall behavior of a blend. Strong bonding between blend components prevents for slip between a matrix and inclusions, while weak adhesion is not efficient in stress transfer, but it may cause a certain amount of friction and may originate decohesion. Modification of blends by introducing compatibilizers is a common practice; therefore, the third component is *explicit* present in blends. It follows then that when considering mechanical properties, the polymer blends should be considered as the systems containing at least three components and with complicated interactions among them.

Compatibilized blends differ from blends of incompatible polymers, apart from more discrete dispersion of a minor component, mainly by the structure and properties of the interface between components. Usually, the achieved toughness of well compatibilized blends allows for their large plastic deformation. In plain crystalline polymers, the elementary mechanisms of plastic deformation are crystallographic slips. However, in simple drawing, the cavitation obscures the real crystallographic mechanisms. The origin of cavitation is the mechanical misfit between stacks of crystalline lamellae. In polymer blends, the interfaces between components are the other source of cavitation. Cavitation creates new internal surfaces; however, the energy dissipated for the formation of cavities is rather low. It is not so for the energy needed for the reorganization of the surrounding matter to accommodate cavities.

These and other considerations concerning mechanical properties of polymer blends will be presented in the forthcoming sections. The survey of existing data and applications shows that the main purpose of polymer modification by blending with other polymers is to modify their mechanical performance and primarily increase toughness. Therefore, in the forthcoming sections we will focus on issues related to polymer toughening which can be achieved by blending with other polymers, mainly those demonstrating elastomeric properties. That method of toughness modification is known under the name of "rubber toughening," because of rather historical reasons. Nowadays it is well established that the toughness can be successfully improved by thoughtful blending not only with classic rubbers but also with various other elastomers, selected other polymers, ready-to-mix polymer particles with core–shell morphology, and even mineral filler particles.

11.3.1 Low Strain Rate Deformation of Polymer Blends

Blending of a polymer with other immiscible polymers can lead to a substantial improvement of drawability and impact strength without a reduction in T_g. Blends of miscible polymers show a single glass transition at a temperature that is in between glass transitions of components. The position of glass transition of a miscible blend on a temperature scale determines its mechanical properties.

When the material is subjected to loading, it responds with deformation. Polymeric materials exhibit two types of mechanical response in elasticity range: in a glassy state the energy is stored as free energy, while in a rubbery state, the energy is stored as a change of macromolecular chain configurational entropy. The first type of elasticity is called energy elasticity and the second entropy elasticity or just rubber elasticity. The physical response of polymeric materials to a small strain or stress is then different because of different sources and different temperature and pressure dependencies. The first is a characteristic of glassy polymers and all inorganic and organic crystals and arises from interatomic and intermolecular interactions, while the second is a characteristic of polymers in a rubbery state and amorphous phase of crystalline polymers and is created by reversible shear and relaxation processes. The latter are specific for different polymers and determine their viscoelastic properties. Similar characteristics of elastic reaction to a small strain or stress concern polymer blends and their components. When a blend is composed of immiscible or partially miscible polymers, most of the free energy of deformation is stored in its matrix, less in dispersed inclusions. For miscible blends, the elastic response depends on their glass transition temperature. The rule of linearity between strain and stress was discovered by Hooke in the seventeenth century, and uniaxial strain or stress experiments can be described as below:

$$\sigma = E_o\varepsilon \tag{11.8}$$

where σ stands for stress, while ε for strain. The elastic constant E_o is called Young's modulus and it should be always defined at zero strain or zero stress;

Fig. 11.4 Typical stress–strain curves for polypropylene blended with ethylene-propylene rubber (EPDM) at different rubber concentrations. Strain rate $10^{-2}\,s^{-1}$, room temperature. The plot illustrates the relation of modulus and strain presented in Eq. 11.9 (From Gaymans (2000); reproduced with permission of Wiley)
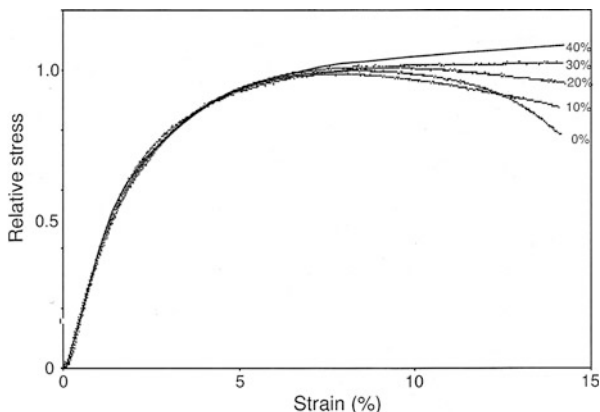
hence it is called the tangent modulus. As the strain increases, the stress–strain relationship becomes gradually nonlinear. It was shown by Rose for metals (Rose et al. 1983) that the elastic response is modified by bulk decohesion arising from binding energy in the material in the following form:

$$\sigma = E_o \varepsilon \exp(-\alpha\varepsilon) \tag{11.9}$$

where α is a nonzero constant related to uniaxial decohesion strain. Equation 11.9 suggests that the tangent modulus progressively decreases with increasing tensile uniaxial strain (Argon 2013). However, for uniaxial compression, the modulus tends to monotonically increase. Equation 11.9 can be transformed to modulus dependence on ε as follows:

$$E(\varepsilon) = \frac{d\sigma}{d\varepsilon} = E_o (1 - \alpha\varepsilon) \exp(-\alpha\varepsilon) \tag{11.10}$$

Similar relations apply for polymers and polymer blends except that the binding energy for polymeric material is lower than for metals and nonlinearity of modulus is even more pronounced.

From Eq. 11.10, it is seen that the modulus decreases with increasing strain from the initial value of E_o eventually to 0, for strain of $1/\alpha$. The stress reaches then a maximum which is called yield stress, and the processes responsible for the phenomenon are called yielding (Fig. 11.4).

From the above discussion, it follows that most isotropic materials including polymeric materials behave for small strains in a very similar way all according to Eq. 11.10, differing only in a single parameter α. However, yielding in polymeric materials is reached due to other factors that come to play at slightly larger strain and not exhibiting yielding at strain $1/\alpha$ which is related to the binding energy and bulk decohesion as defined by Rose et al. (1983).

11.3.2 Yielding

Yielding in polymer blends is a very complicated event and is usually composed of several micromechanisms that are activated at various stages of deformation depending on the deformation rate, the temperature, deformation mode, and blend morphology.

In glassy homogeneous polymer blends below T_g, their internal morphology plays only a secondary role, in contrast to the temperature, which is the major parameter governing the yielding, especially in compression, shear, and hardness measurements.

One of the few compatible polymer blends in a large concentration range is polystyrene–polyphenylene oxide system (PS/PPO) (Yee 1976). In tension, with increasing PPO content, the deformation habit changes from the formation of crazes, as in PS to homogeneous deformation bands and shear bands, characteristic for PPO (Berger 1990); *see* also the data of Figs. 11.1 and 11.3. There are other partially compatible blends, for instance, SAN/PMMA blends, when the acrylonitrile content in SAN is about 10–30 % (Fowler et al. 1987; Suess et al. 1987). Other examples are amorphous quenched blends of PMMA and polyvinylidene fluoride (PVDF), which are compatible at high temperatures (Nasef and Saidi 2006; Neuber and Schneider 2001). The blend PMMA/PVDF shows a remarkable agreement with the additivity rule of the two components for the yielding in microhardness measurements (Martinez-Salazar et al. 1991). The yielding behavior of the blend material is well correlated with glass transition temperature resulting from the equation of glass transition superposition of Gordon and Taylor (1952).

Immiscible blends have nonhomogeneous morphology and their tensile deformation at yield is much more complicated than miscible systems. There are several mechanisms that are activated at various stages of deformation depending on the deformation rate, the temperature, glass transition temperature of the components, deformation mode, and blend morphology.

Bubeck et al. (1991) showed that in high-impact polystyrene (HIPS), there are crazing and cavitation engaged. The complex mechanism of plastic deformation in the blends leading to improvement of ductility and toughness was revealed. They used real-time X-ray measurements during tensile deformation HIPS samples to show that cavitation of the rubber particles actually precedes crazing of the matrix under tensile impact conditions. Cavities formed within the rubber particles can thus be identified as nuclei for a craze growth, which occurs through the meniscus instability mechanism proposed by Argon and Salama (1977).

Another example of rubber-modified glassy polymer was given by the study of polylactide blends (Kowalczyk and Piorkowska 2012). Blending polylactide (PLA) with poly(1,4-*cis*-isoprene), which is immiscible with PLA, can lead to a substantial improvement of drawability and impact strength without a decrease in Tg. In contrast to HIPS reported by Bubeck et al. (1991), the rubbery particles initiated crazing in PLA matrix at the early stages of deformation. Crazing was accompanied by cavitation inside rubber particles, which further

Fig. 11.5 The tensile stress–strain curves of the two-phase PC/PMMA blends, obtained at room temperature. The plots illustrate a stepwise transition of yielding by crazing characteristic of PMMA, to shear banding, characteristic of PC (From Kyu et al. (1991); reprinted with permission of Hanser Verlag)
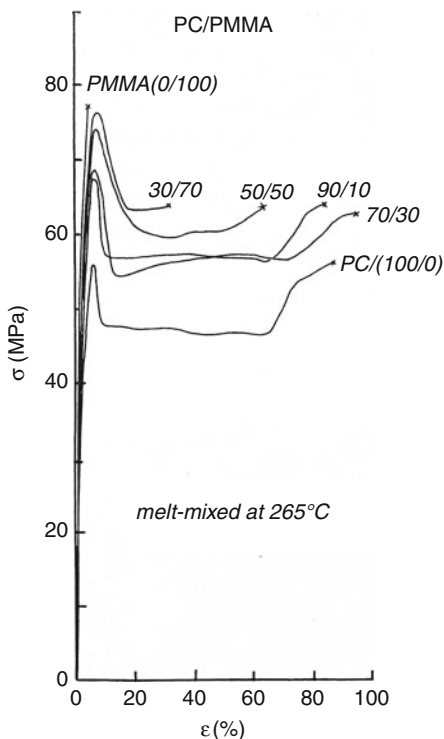
promoted shear deformation of PLA. All three elementary mechanisms acting in the sequence appeared responsible for surprisingly efficient toughening of PLA by blending with a small amount of poly (1,4-*cis*-isoprene) – a major component of natural rubber. In comparison, plain PLA not containing rubber particles deforms initially via crazing, stronger at higher deformation rate and lower temperature, and then shortly undergoes shear banding. Separate cavitation is not then observed. The yield stress depends on the deformation rate and temperature; however, yielding is triggered and then controlled by the micromechanism of deformation which is activated first, at the lowest stress under given experimental conditions, selected from crazing, shear yielding or cavitation.

In Fig. 11.5, the stress–strain plots are depicted for a series of two-phase PC/PMMA blends with various concentrations. The phase-separated morphology was obtained by melt mixing. The position of the yield point on the stress–strain curves illustrates the stepwise transition of micromechanism of tensile deformation, characteristic of PMMA, which is crazing, to the mechanism of deformation, characteristic of PC – shear yielding.

As an example, the tensile deformation of polycarbonate/polyethylene blends is similar for a range of concentrations except for the magnitude of the yield stresses (Yee 1977). In this blend polycarbonate matrix undergoes strong yield shearing, and the decisive factor is the shear resistance of polycarbonate.

11.3.3 Necking

Crazes always tend to be perpendicular to the tensile deformation direction. They are typical dilatational zones of deformation. Since most of deformation is located in fibrils spanning the edges of a craze, a polymeric material is elongated, but its transversal size is not much changed. Hence, the neck is not formed. Cavitation usually helps to generate crazes and also does not cause formation of a neck. Necking is always associated with shearing and formation of shear bands whenever they are formed as a basic micromechanism of deformation or when they are triggered by crazes or cavities.

The way in which polymer blends change the shape upon deformation is not very different from other polymeric materials. The decisive role is played by micromechanisms triggered or stimulated by the presence of other components of the blend. The other key parameters are the temperature and strain rate. One may induce or inhibit shear banding by changing those process parameters and in that way control necking.

11.4   Toughening

11.4.1 Overview

The toughness is the property of resisting a fracture by absorbing and dissipating energy during deformation prior to ultimate fracture (Bucknall 1997). Strength, on the other hand, is the ability of the material to resist high stresses. Strengthening is usually achieved by suppression of plastic deformation mechanisms, sometimes to the extent that the material becomes brittle under normal loading conditions. On the contrary, high toughness can be obtained by promotion of plastic deformation, although most frequently at some tolerated loss of stiffness, strength, and creep resistance. Some reduction of stiffness, as in the case of rubber toughening, is acceptable if accompanied by substantial increase of toughness. A simple measure of toughness is the area below the stress–strain curve. Three typical cases are illustrated in Fig. 11.6: (1) very high strength by avoiding all defects and suppressing of plastic deformation (e.g., highly oriented fibers); (2) very high elongation at break, but low stiffness and strength, obtained by significant softening of the material (e.g., by plasticization); and (3) good stiffness and strength with a higher elongation, which can be obtained only due to widespread plastic deformation. The optimum case in toughening is, of course, the combination of relatively high value of stiffness, strength, and possibly high ultimate strain (curve (3) of Fig. 11.6). This requires some suppression of large, critical defects producing high stress concentrations leading to brittle fracture and promotion of extensive plastic deformation proceeding in large volume of the material, initiated at relatively high yield stress in numerous small, localized yield events. Plastic deformation must be stabilized by strain hardening to prevent excessive strain localization and premature crack propagation.
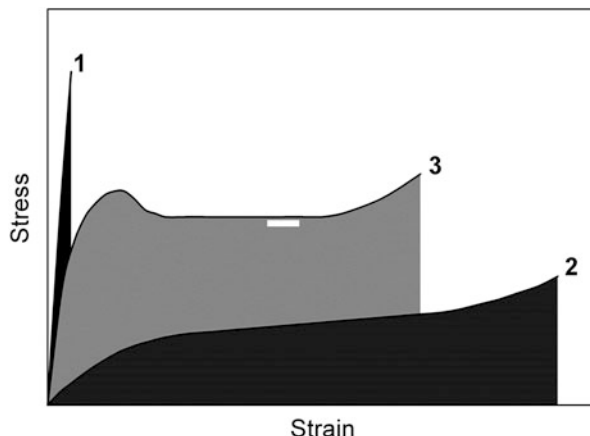
    Retaining strength and increasing plastic deformation are generally opposed
requirements and are very hard to achieve simultaneously. In fact, the most popular
and efficient practice of toughening by modification with elastomers (rubbers)
suffers a drawback of a notable, sometimes serious, decrease in stiffness and
strength of modified material due to relatively large content of a soft rubber
(5–25 wt.%) (Bucknall 1977).

    Toughness is one of the most complex mechanical properties. As it is greatly
influenced by many morphological as well as micromechanical parameters, it is
very difficult to control. Toughening can be realized by a particular morphology
that permits lots of small local yielding events simultaneously in the entire volume
of the material. This practically cannot be achieved in a homogeneous morphology,
but only in heterogeneous one with specific morphology (e.g., small particles
dispersed in the matrix) modifying the structure and structure-related
micromechanical properties of the polymer at various scale levels. These modifi-
cations stimulate a large number of local plastic yielding and deformation processes
on a nano- and microscale, all absorbing energy. They appear together in a large
volume of the loaded material and result in large total energy absorption.

    While many polymers can dissipate considerable amounts of energy through
plastic deformation and appear tough at low deformation rate, they became brittle in
the presence of notches and in high-rate impact loading. Therefore, toughening
should be aimed not only to improve drawability at low rates but primarily to
enhance the fracture resistance at impact conditions, especially in the most severe
case when a notch is present in a thick sample. Consequently, the most
frequent basis for assessment of toughening is the notched Izod (or Charpy) impact
strength, determined in standardized impact tests of Izod or Charpy. This notched
impact strength indicates the energy dissipated during impact fracture of
relatively thick notched sample (according to the ISO 180 international standard
of the Izod test, sample thickness must be greater than 3.2 mm and the striker
speed v = 3.5 m/s).

11.4.2 Basic Principles of Toughening

11.4.2.1 Competition Between Plastic Deformation and a Terminal Process of Fracture

The toughness is administered by a competition between plastic deformation and a terminal process of fracture. The fracture is ultimately governed by stress and strain concentrations due to various structure imperfections like sharp notches, cracks, and other critical sized flaws or heterogeneities. Most commercial products made of polymers contain such imperfections. When the material is loaded, stresses become concentrated there, which results in high concentrations of strain and increase of the strain rate, all leading to very high localization of the deformation process. This localization can be high enough to trigger a brittle fracture. On the other hand, at some instances smaller, not critical, stress concentrations help also effectively to initiate the desired plastic deformation. Therefore, all these flaws and structure imperfections should be controlled precisely in quantity and size below critical in order to govern the fracture processes that limit material toughness. However, such a careful and precise control or management of the structure (flaws, imperfections) and surface (notches, scratches) of a product would be too difficult and expensive to be a practical solution for toughening, so that other measures to promote plastic deformation are necessary.

11.4.2.2 Intrinsic Brittleness

Argon (Argon et al. 2000; Argon and Cohen 2003) reasoned that with the exception of only a small class of pure metals, perhaps all other solids, including all unoriented solid polymers, are intrinsically brittle solids in the definition of Kelly et al. (1967) and will demonstrate brittle behavior at low temperatures and/or high strain rates, where a crack can propagate with little resistance, particularly in the presence of crack-like flaws and notches. While many polymers may appear quite tough at room temperature under low or moderate deformation rates, they became brittle at lower temperatures, in the presence of notches and in high-rate impact loading. Intrinsic brittleness denotes here that, in an otherwise flaw-free and homogeneous material, local tensile stress at the atomically sharp crack tip reaches the decohesion strength before local shear stresses concentrated at that crack tip initiate plastic flow (Kelly et al. 1967). Consequently, even the complete elimination of any notches, flaws, and other imperfection from the sample will not bring transformation of intrinsically brittle material to intrinsically ductile one, so that the approach seems of limited use for toughening. However, as already noted, intrinsically brittle polymers actually can exhibit a transition from brittle to ductile behavior at certain experimental conditions, e.g., higher temperature or lower deformation rate. That brittle-to-ductile transition is a crucial phenomenon in considering the toughness of polymers.

11.4.2.3 Brittle–Ductile Transition in Fracture

Stress–strain data collected for many rigid polymers deformed at various conditions revealed stronger dependence of the yield strength σ_y on temperature and strain rate

Fig. 11.7 Schematic
representation of brittle-to-
ductile transition in fracture
(Davidenkov plot)
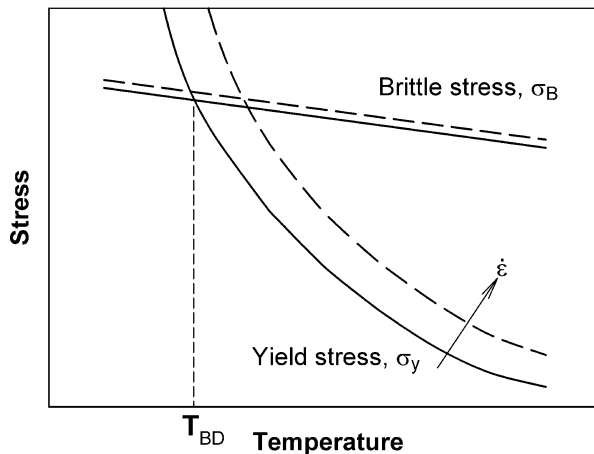
than that of brittle fracture strength σ_B (Vincent 1971): the yield stress σ_y decreases
faster with increasing temperature T (typically by a factor of 10 between $-180°$C
and room temperature) than the brittle stress (decrease only by factor of less than 2).
The competition between the energy-absorbing plastic behavior characterized by
the yield strength, having significant temperature and strain rate dependence, and
the relatively temperature-independent brittle strength, governed by microstructural
flaws or extrinsic imperfections, is illustrated schematically in Fig. 11.7 in terms of
the well-known Ludwig–Davidenkov–Orowan criterion (Orowan 1949). This dia-
gram, generic to intrinsically brittle solids, shows that for a given strain rate, there
should be a transition from brittle to ductile behavior at a particular temperature
T_{BD}, defined by the intersection of both curves – when increasing the test temper-
ature above T_{BD}, the yield strength becomes lower than the brittle stress, $\sigma_y < \sigma_B$,
and the material changes its behavior from brittle to ductile. The dotted lines
represent a higher strain rate resulting in a shift to higher stress values and,
consequently, a shift of the brittle-to-ductile transition to a higher temperature
(Vincent 1971). The brittle-to-ductile transition temperature is very sensitive to
change in material parameters and test conditions, including specimen shape and
size, temperature, or the deformation rate. For example, while the brittle strength
relates to a tensile stress, the yield behavior responds only to a critical level of the
effective (deviatoric) stress, σ_e. In the presence of sharp notches or other flaws,
individual normal stress components can be substantially augmented by negative
pressure, while the effective stress producing plastic flow remains equal to σ_e. This
will result in a marked increase of the brittle-to-ductile transition temperature, as is
well known in the notch impact testing.

11.4.2.4 Strategies and Options for Toughening

One of the possibilities to obtain tough polymeric materials is of course synthesis of
new polymers, which would appear to be intrinsically ductile instead of intrinsically
brittle. However, this is perhaps fundamentally impossible, or at least such attempts

are not economically justified. Analysis of the Davidenkov plot of Fig. 11.7 demonstrates that the only possibility of improving toughness of an intrinsically brittle rigid polymer is then by moving the brittle-to-ductile transition temperature well below the temperature range of the expected application of that material. This can be done either by an increase of the brittle strength, without altering plastic deformation mechanisms, or by reduction of the yield strength which makes plastic deformation easier. The first alternative can be realized through careful modification in both synthesis technology and processing to exclude critical sized flaws and extrinsic imperfections, as, e.g., dust particles. When such structural imperfections are well controlled in quantity and size and are limited to only subcritical size comparing to the size of the imperfections that control ultimate stress σ_B, the brittle strength can increase above the level of the initial yield strength. As a consequence, such polymer sample will tend to deform plastically. Once plastic deformation is initiated, it will result in molecular alignment due to advancing deformation and in neutralization of some of the effects of small imperfections still present in the structure which can eventually elevate, even substantially, the fracture toughness across the extension direction. This approach is always an option, but often is either not possible or technologically not profitable (Argon and Cohen 2003; Lin and Argon 1994). In such a case, the only practical choice left is to decrease the global plastic resistance of the modified polymeric material and shift in this way the brittle-to-ductile transition temperature T_{BD} to a lower temperature, below the temperature range of the expected applications. As a result, toughness of the material can be improved, even substantially, but inevitably in expense of some loss of its strength, and perhaps also stiffness and creep resistance. However, that sacrifice of stiffness and strength is often tolerable. Actually most of the approaches to toughening have followed this route, which when wisely practiced can be very effective (Argon 2013; Argon and Cohen 2003).

The other general rule in polymer toughening is to take advantage of the deformation mechanisms already operating in a particular polymer and only stimulate its response to loading to procure an extensive deformation and therefore large energy dissipation. In many approaches to polymer toughening, it has been assumed that incorporation of compliant rubber particles might impart toughness to a brittle polymer by a notion arising from the simple rule of mixtures, i.e., hoping that very flexible rubber could alleviate the brittleness of the matrix. However, in nearly every instance, when such practices are adopted, the beneficial effect of improved toughness actually does not arise from the added modifier directly, but rather through its indirect stimulation of very effective matrix response (Argon 2013), such as, multiple crazing in glassy polymers, providing widespread dilatational plasticity or an extensive plastic deformation promoted by significantly lowered plastic resistance due to conversion of a continuous solid material into porous (cellular) solid as a result of particle internal cavitation or debonding at the particle–matrix interface. This transition not only relieves volumetric strain but also greatly modifies the yield conditions for the matrix material and facilitates extensive yielding and plastic deformation of the matrix. Another example is cavitation-induced modification of the stress state allowing deformation of

preferentially oriented crystals within ligaments of the semicrystalline matrix between particles, the orientation of which had been induced by the presence of matrix–particle interfaces or by processing.

Glassy Polymers

Glassy polymers are frequently capable of dissipating locally significant amounts of energy per unit volume through viscoelastic–plastic flow, most frequently, highly localized either in crazes or thin shear bands. Bucknall (2000) estimated for crazable polymers, like polystyrene, that locally, within the craze or thin deformation zone, energy absorption per unit volume of a glassy polymer is high, on the order of 100 MJ/m^3! However, the amount of the material involved in the deformation is very limited, roughly to the thickness of the craze, i.e., single micrometers, and fracture is, therefore, essentially brittle. Such a small amount of material involved in the process of energy absorption through the plastic deformation occurring within a craze is too small to give the material a satisfactory fracture resistance and toughness. The problem is the acutest when the specimen or structure contains sharp notches, surface scratches, cracks, voids, or other structural imperfections that could cause a severe localization of the deformation, frequently so strong to end up with the brittle-like fracture, even due to a single craze. Therefore, strategies of toughening should be directed primarily towards maximizing the volume of the material participating in such deformation by multiplication of deformation events like crazes or deformation bands. Concurrently, some reduction of overall deformation resistance is needed to ease craze nucleation or initiate yielding as well as to avoid premature fracture of crazes, since failure in crazable polymers is caused by fracture of the craze matter. Many effective procedures have been advanced to reach toughening by the reduction of overall deformation resistance to promote new crazes and avoid premature craze fracture (Argon 2013; Bucknall 1977, 2000; Kausch 1983, 1990; Michler and Balta-Calleja 2012).

There are several methods known to improve the toughness of glassy polymers, e.g., by co-polymerization, by mixing with another miscible polymer, or by incorporation of a second phase through the blending process, like particles of other thermoplastic polymers or rubbers, fine particles of inorganic materials, or even very small voids. By dispersion of particles of the second phase, the energy dissipating deformation processes that are native to the matrix (either crazing or shear yielding) can be notably intensified and stabilized. The selection of the active deformation mechanisms depends primarily on the details of the matrix chemistry, and the modification by incorporation of the second phase usually does not alter it.

For glassy brittle polymers prone to crazing, such as PS or PMMA, apart from blending with non-crazable polymers miscible with them in order to alter the entanglement density and hence increase the craze flow stress above the distortional plastic resistance (Wellinghoff and Beaer 1978), the majority of approaches to their toughening were based on the incorporation of compliant heterogeneities, like soft spherical elastomer particles. Such particles appeared very effective in increasing the craze concentration by promotion of craze nucleation at lowered overall plastic resistance, as, e.g., in high-impact polystyrene (HIPS) or ABS. The rubbery

particles not only initiate crazes but also participate in their stabilization and act as craze terminators. This approach to toughening has been well developed practically and was described in many fine books and reviews (Argon 2013; Balta-Calleja and Michler 2005; Bucknall 1977, 1997, 2000; Collyer 1994; Kinloch and Young 1983; Michler and Balta-Calleja 2012). Very similar methods of toughness modification by incorporation of rubber particles are also widely used for toughening of semiductile glassy polymers that tend to deform by shear yielding. A further approach to additional toughening of crazable polymers by lowering the craze resistance through "plasticization-on demand" by low molecular weight diluent accelerating craze plasticity, which was prepackaged in inclusions, was also explored (Brown et al. 1989; Gebizlioglu et al. 1990). This method while appearing quite effective in certain ranges turns ineffective at high strain rates, mainly due to limitations of the stress-enhanced processes of case II diffusion which govern the local plasticization process (Argon et al. 1999; Piorkowska et al. 1993; Qin et al. 1999).

Thermoset Polymers

Epoxies and other thermoset resins are used widely as matrix materials in composites reinforced with long and short fibers as well as with fine particles and in other bulk applications. Therefore, the problem of alleviating their brittleness has attracted much attention. Incorporation of soft compliant particles into epoxies, in order to achieve a toughening effect similar to HIPS, has basically failed (Sultan and McGarry 1973) because of elementary reasons that these thermosets demonstrate notably in high plastic resistances due to cross-linking, which leads to a dense and robust molecular network. Consequently, they do not form crazes as PS or other glassy polymers do. Nevertheless, incorporation of well dispersed, small and compliant particles has demonstrated to be effective in promoting cavitation of particles under stress localized in planar zones (Sue 1992; Sue and Yee 1996) which give rise to craze-like dilatational bands similar to those observed on crazing of glassy polymers (Lazzeri and Bucknall 1995), a response similar to the cavitational craze process found in spherical-domain block copolymers (Schwier et al. 1985). It was also shown that use of rigid particulate fillers can also be quite effective through the crack pinning mechanism (Shaw 1994).

Semicrystalline Polymers

Many semicrystalline polymers, such as high-density polyethylene (HDPE), polypropylene (PP), polyacetals (POM), or polyamides (PA), are generally known to be quite tough at usual conditions of deformation, i.e., away from low temperatures and at moderate rates. Unfortunately, they also appear notch brittle, particularly under impact loading and at low temperatures. These and other semicrystalline polymers have been, however, successfully toughened by incorporation of elastomeric particles which, when present at certain conditions, triggered an extensive plastic deformation of the semicrystalline matrix through common crystallographic slip and interlamellar shear mechanisms. The primary function of rubbery particles here is again to bring about reduction of plastic resistance of the matrix, based on the same deformation mechanism as these are active already in the plain polymer.

Much of the recent work has been concerned on toughening of polyamides (Borggreve and Gaymans 1989; Borggreve et al. 1987; Dijkstra et al. 1994a; Gaymans 1994, 2000; Muratoglu et al. 1995a, c, d; Wilbrink et al. 2001; Wu 1985, 1988). These studies highlighted the correlation between toughness improvement and the critical interparticle distance, found in such blends. This interparticle distance was tried to relate mechanistically to a specific form of preferential "edge-on" orientation of lamellar crystals around particles that was shown to reduce markedly the overall plastic resistance of the polymer matrix (Muratoglu et al. 1995a, c, d). It was postulated that such a preferential local orientation could be obtained at the matrix–particle interfaces, not only for rubbery particles but also for other particles, including stiff particles of a mineral filler (Bartczak et al. 1999a, b, c). Considerable work was carried out on isotactic polypropylene (iPP) using both elastomeric particles (Jiang et al. 2000; Martuscelli et al. 1996; Liang and Li 2000; Liu et al. 2013; Nitta et al. 1998, 2005) and mineral filler (Chan et al. 2002; Cioni and Lazzeri 2010; Gong et al. 2006; Lazzeri et al. 2004; Thio et al. 2002; Zuiderduin et al. 2003; Dubnikova et al. 2004; Lin et al. 2010; Weon et al. 2006). Toughening of high-density polyethylene with both elastomeric and stiff particles was also studied extensively (Bartczak et al. 1999b, c; Deshmane et al. 2007; Yuan et al. 2009), and the effect of the critical interparticle distance was explored here, too.

11.4.3 Rubber Toughening

The invention of rubber toughening is one of the milestones in the history of the plastic industry (Bucknall 1977). In the late 1940s, high-impact polystyrene (HIPS) and acrylonitrile-butadiene-styrene (ABS) were developed by compounding butadiene rubber into PS or SAN, respectively. Both HIPS and SAN demonstrate a heterophase morphology with compliant micron-sized particles dispersed in the rigid matrix. The success of these products has led not only to the formulation of their improved grades, but also to the idea that the principle of rubber toughening could be applied to all other types of plastics, not only to crazable glassy polymers. Since then modification of polymers by blending them with other polymers, mostly compliant elastomers, to create a continuous matrix-dispersed inclusion morphology, commonly referred to as rubber toughening (due to rather historical reasons), has been successfully applied to many amorphous polymers such as PS, SAN, or PC (Hourston and Lane 1994; Parker et al. 1990), as well as to semicrystalline ones, including polyamides (Abate et al. 1992; Billon and Haudin 1997; Borggreve and Gaymans 1988, 1989; Borggreve et al. 1987, 1988, 1989a, b, Bucknall et al. 1989; Cimmino et al. 1986; Dijkstra and Gaymans 1994a, b; Dijkstra et al. 1994a, b; Epstein 1979; Flexman 1979; Gaymans 1994, 2000; Gaymans et al. 1990; Gaymans and Dijkstra 1990; Gaymans and van der Werff 1994; Gonzales-Montiel et al. 1995a, b, c; Hobbs et al. 1983; Janik et al. 1995; Kayano et al. 1997; Lu et al. 1993, 1995, 1996; Majumdar et al. 1994a, b, c, d, e; Margolina and Wu 1988; Muratoglu et al. 1995c, d; Okada et al. 2000; Oshinski et al. 1992a, b, 1996a, b, c, d;

Ramsteiner and Heckmann 1985; Scott and Macosko 1995; Takeda et al. 1992; Takeda and Paul 1992; Wilbrink et al. 2001; Wu 1983, 1985, 1987, 1988, 1989), polypropylene (Gensler et al. 2000; Harrats and Groeninckx 2005; Jang et al. 1984, 1985; Jiang et al. 2000, 2004b; Liang and Li 2000; Liu et al. 2013; Martuscelli et al. 1996; Nitta et al. 1998, 2005; Tiwari and Paul 2011; Utracki and Dumoulin 1995; van Der Wal et al. 1998), polyacetal (Flexman 1988; Kloos 1985; Xie et al. 1997), and thermoplastic polyesters such as polyethylene terephthalate and polybutylene terephthalate (Abu-Isa et al. 1996; Arostegui and Nazabal 2003; Brady et al. 1994; Cecere et al. 1990; Hage et al. 1997; Hale et al. 1999a, b, c, d, e; Hert 1992; Hosti-Miettinen et al. 1995; Hourston and Lane 1994; Hourston et al. 1991, 1995; Kanai et al. 1994; Kang et al. 1997; Laurienzo et al. 1989; Loyens and Groeninckx 2002, 2003; Mouzakis et al. 2001; Neuray and Ott 1981; Okamoto et al. 1994; Park et al. 2000; Penco et al. 1995; Polato 1985; Sanchez-Solis et al. 2000; Tanrattanakul et al. 1997). Rubber-modified polyamide 6,6 was the first marketed super-tough engineering blend (Epstein 1979; Flexman 1979; Wu 1987) with more than tenfold improvement in toughness when compared to the pristine parent polymer. Brittle thermosets like epoxies have also been toughened by blending with elastomers (Shaw 1994; Yee et al. 2000).

It has been established that the fracture toughness could be increased significantly by adding a relative small amount (usually from 5 to 25 wt.%) of a suitable elastomer to the thermoplastic matrix. Optimum particle size appropriate to toughen satisfactorily a rigid polymer varies, depending on properties of the host polymer (matrix), primarily on its inherent fracture mechanism, but is commonly within the range of 0.1–5 μm. As a general rule, brittle glassy matrices that tend to craze benefit more from large rubber particles size, typically between 2 and 3 μm. On the other hand, matrices that can absorb energy via shear yielding are effectively toughened with relatively small particles, on the order of 0.5 μm or less. Very fine particles, as, e.g., those smaller than 0.05 μm in blends based on polyamide, do not take part in toughening process (Gaymans et al. 1990; Oshinski et al. 1992a, 1996b), since they need higher stress to cavitate. The immiscibility and phase separation appear very important as a rubber dissolving in the matrix acts merely as a plasticizer, which reduces the glass transition temperature and hence seriously affects the stiffness but with only limited influence on toughness. Optimum commercial rubber-toughened glassy polymers (phase-separated blends), such as HIPS and ABS, demonstrate toughness about one order higher than the unmodified matrix material (PS, SAN). Similar, impressive results were obtained for elastomer-toughened semicrystalline polymers. Toughness of several glassy and semicrystalline polymers toughened by elastomers is given in Table 11.1.

The most important feature of rubber toughening is that the fracture of the toughened polymer is substantially postponed – material becomes ductile and undergoes extensive plastic deformation, usually according to the same mechanism as the pristine parent polymer, prior to reaching the failure limit – at the expense of a limited, yet usually tolerated reduction of stiffness, yield strength, and creep resistance (Bucknall 1977; Kinloch and Young 1983). This change from brittle to ductile behavior is possible due to the reduction of the overall plastic resistance of

Table 11.1 Toughness of selected polymers and their blends with rubbers

Matrix polymer	Predominant fracture mechanism	Typical notched Izod impact strength (J/m)	Polymer–rubber blend fracture mechanism	Optimum rubber diameter (μm)	Typical notched Izod impact strength of the blend (J/m)
PS	Crazing	21	Crazing	2.5	130
SAN	Crazing	16	Crazing and yielding	0.75	780
PMMA	Crazing	16	Crazing and yielding	0.25	80
POM	Yielding	110	Yielding	<0.5	910
PP	Yielding	20–40	Yielding	0.1–0.4	500–700
PA	Yielding	40–60	Yielding	0.1–0.4	1100

the matrix material below the brittle fracture strength. The desired changes in the deformation behavior and the balance of properties are achieved by a suitable dispersion of the soft elastomer or rubber in the polymer matrix, in the form of small spherical inclusions (particles). The dispersed particles can have a form of homogeneous or heterogeneous particles (as, e.g., "salami" particles in HIPS or core–shell particles (Cruz-Ramos 2000)).

It has been established that the use of phase-separated, well-dispersed elastomer with a suitable particle size allows to bring a large volume of the matrix into the process of plastic deformation, resulting in absorption of a significant amount of energy. Concurrently, rubbery particles frequently help to limit the growth and breakdown of voids and crazes and prevent in this way an initiation of a crack and premature failure. A number of quite different mechanisms of such toughening have been proposed in the past, but all of these rely on a dispersion of elastomer particles within a glassy or semicrystalline matrix. These have included energy absorption directly by rubber particles (Buchdahl and Nielsen 1950; Merz et al. 1956), energy dissipation upon rubber cavitation, or debonding at rubber–matrix interface (Sultan and McGarry 1973), matrix crazing (Bucknall 1977, 2000) or shear yielding (Newman 1978) or a combination of both (Bucknall 1977, 2000). The early hypothesis attributed toughness enhancement to dissipation of energy in the elastomeric phase either directly (Buchdahl and Nielsen 1950) or by the effect of bridging cracks by rubber particles (Merz et al. 1956). The amount of energy absorbed at impact was attributed to the sum of the energy to fracture the rigid matrix and the work to break the elastomeric particles encountered on the crack path. This hypothesis was dismissed soon since it was estimated that the total energy associated with the rubber deformation and break can account for only a small fraction of the observed enhanced impact energy (Bucknall 1978). Consequently, this mechanism can play only a minor role in toughening of rigid polymers. In the late 1960s Schmitt (1968) and Kesskulla (1970) proposed that the rubber particles can not only deflect or terminate cracks but can also act as stress concentrators, which efficiently initiate crazes in their very surroundings. Microscopic examination of deformed HIPS revealed formation of numerous crazes at

interfaces of rubber particles in their equatorial regions, which confirmed that hypothesis (Bucknall and Smith 1965). The role of rubber particles as stress concentrators, able to initiate extensive crazing, turned out crucial for toughening of the matrix. Bucknall proposed the mechanism of toughening by the so-called multiple crazing (Bucknall 1977), which became the basis of many toughening approaches developed later. It has been established and widely accepted that the deformation process involving crazing is initiated at surface of numerous elastomer particles, simultaneously in many sites of the matrix (Bucknall 1977, 2000; Collyer 1994). The primary function of elastomer particles is to modify the stress field in the surrounding matrix (stress concentrations, relief of the triaxial stress state upon cavitation), which can promote a widespread deformation of the matrix (Bucknall 2000). In rubber-modified crazable polymers, crazes are initiated under an applied tensile stress at points of maximum principal strain, which is typically near the equator of rubber particles (where maximum concentration of the stress is observed), and propagate outwards, normal to the direction of maximum tensile stress, although deviations may occur because of an interaction between the neighboring particle stress fields (Kinloch and Young 1983) (cf. Fig. 11.2). Craze propagation is terminated when another particle is encountered by a craze, which prevents the growth of very long crazes. As a result, a large number of small crazes are produced in polymer modified with rubber particles, in contrast to a small number of large crazes formed in the same polymer in the absence of elastomer. This mechanism is effective enough for absorption of large amounts of energy, which results in a substantial enhancement of impact strength of the material. Similar scenario of initiation of widespread plastic deformation at rubber particles (at points of maximum shear stress) holds also when the dominating deformation mechanism of the matrix is shear yielding rather than crazing.

The addition of rubber particles promotes energy absorption through the initiation of crazing or local yielding phenomena in the proximity of numerous particles, followed by an extensive plastic deformation that involves quite a large volume fraction of the sample. Such a toughening mechanism can be described by the following sequence (Bucknall 1977, 1997; Kim and Michler 1998b; Michler 2005; Michler and Balta-Calleja 2012):

1. **Stress concentration:** Tensile elastic deformation results in the generation of stress concentrations around the modifier particles, due to different stiffness of particles from the matrix. The stress concentration leads to the development of a triaxial stress in the rubber particles as well as in their surrounding within matrix.

2. **Voids formation:** Due to the stress concentration and/or thermal stress, a higher triaxial or hydrostatic stress builds up inside particles and gives rise to nano- or microvoids formation through cavitation inside particles or debonding at the particle–matrix interface which substantially modifies the local stress state (e.g., partially relieves triaxial stress in front of the crack tip) and matrix response to the stress (through a change of the sensitivity of the yield stress to mean stress). Due to void formation the volume strain is released and constraints imposed earlier by incompressible rubber particle on a neighboring matrix are relieved.

All of this can reduce the sensitivity of the material towards crazing and promote shear yielding.

3. **Local yielding:** Initiation of local yielding of the matrix occurs in the points of the highest stress concentrations, usually around the equatorial zone of a particle (plastic strain softening). The mechanism of that local yielding of the matrix can be either multiple crazing (fibrillated or homogeneous crazes), extensive shear yielding, or some combination of both. In semicrystalline matrices, local shear yielding proceeds by shear of crystals (crystal plasticity involving primarily crystallographic slip mechanisms) and amorphous layers (interlamellar shear) (Argon 2013; Oleinik 2003). If the shear yielding mechanism is active, then weak shear bands become to develop in the matrix between the voided/debonded particles at an angle of around $45°$ to the direction of the maximum principal tensile stress, simultaneously with continuous growth of voids.

4. **Extensive deformation stabilized by strain hardening** of the yield zone, mostly due to increasing matrix deformation, although stretching of the rubber phase to high strains can make a significant contribution to this, especially when the rubber is well bonded to the matrix and its content is high. The strain hardening stabilizes deformation process and prevents its localization which could result in a generation of crack and premature fracture. This stabilization is especially important when multiple crazing is the dominating mechanism of deformation. In specimens containing sharp notches or cracks, rubber particles can cause also crack tip blunting and consequently crack stop.

The selection of the dominant deformation mechanism in the matrix depends not only on the properties of this matrix material but also on the test temperature, strain rate, as well as the size, shape, and internal morphology of the rubber particles (Bucknall 1977, 1997, 2000; Michler 2005; Michler and Balta-Calleja 2012; Michler and Starke 1996). The properties of the matrix material, defined by its chemical structure and composition, determine not only the type of the local yield zones and plastic deformation mechanisms active but also the critical parameters for toughening. In amorphous polymers which tend to form fibrillated crazes upon deformation, the particle diameter, D, is of primary importance. Several authors postulated that in some other amorphous and semicrystalline polymers with the dominant formation of dilatational shear bands or extensive shear yielding, the other critical parameter can be the interparticle distance (ID) (the thickness of the matrix ligaments between particles) rather than the particle diameter.

11.4.3.1 Stress Concentrations

Particles dispersed in the matrix (as elastomer or other polymer inclusions in polymer blends or block copolymers, filler particles in composites, impurities) similarly to small voids initiate stress concentrations in loaded material due to the difference in stiffness between particle and the matrix. These stress concentrations are highly localized – they decrease rapidly with distance from particle or void (as r^{-3}), and at a distance of particle radius (R = D/2), the stress concentration almost disappears (see Fig. 11.8a). The intensity of stress concentration at the particle–matrix interface depends on the properties of both materials, as shear

Fig. 11.8 (a) Stress components in the equatorial plane of the rubber particle under the remote tensile stress of σ_1 and the change of the tensile stress $\sigma_{\delta\delta}$ with the distance r from the interface. (**b**) Stress concentrations overlap between the close particles when the interparticle distance is about 2D (*left*) and D/2 (*right*) (Drawn after Michler and Balta-Calleja (2012))
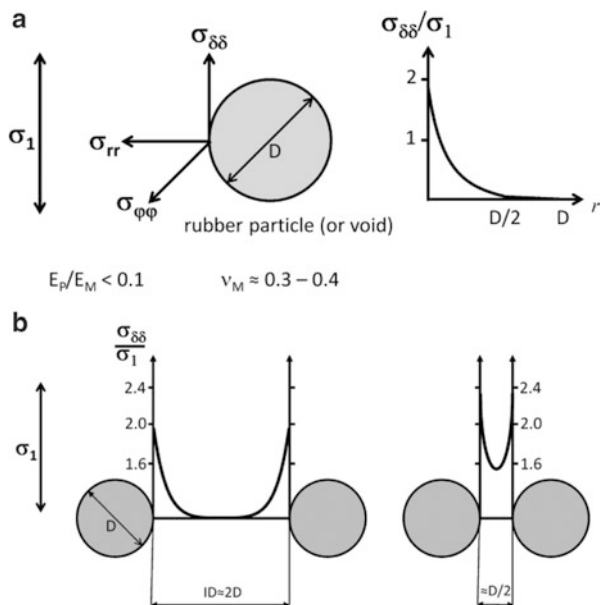
moduli and Poisson's ratio of the particle and the matrix, respectively, while it does not depend on the particle diameter D. The elastic stress concentration at rubber particle–rigid matrix interface depends mainly on the ratio of the moduli of rubber and matrix G_R/G_M and reaches the maximum value of slightly above than 2 for $G_R/G_M < 0.001$ and is already near 2 for $G_R/G_M = 0.1$ (Oxborough and Bowden 1974). This indicates that $G_R/G_M < 0.1$ is practically enough for high stress concentrations that can lead to effective toughening. However, the absolute size of the stress concentration region increases with increasing particle diameter D – the size of the equatorial stress concentration zone is approximately D/2. An initiation of the local deformation (e.g., through initiation of crazes) should be the most effective, when the size of the stress concentration region correlates with the typical size of the plastic zone (note that typical craze thickness in PS is in the range $0.2 - 1\ \mu m$ and the most effective rubber particles in HIPS appear to be of similar size). If the particle diameter decreases, then the size of the stress concentration zone and also the size of initiated plastic zone decrease, too. The minimum size of the deformation zone, which is double the thickness of the typical transition layer between the plastically deformed material and its undeformed surrounding, determines roughly the smallest effective particle radius for craze initiation. The small rubber particles are, therefore, unable to initiate any plastic deformation of the matrix by crazing, although, as will be discussed in Sect. 11.5, it may appear effective in the promotion of the shear yielding.

The stress concentration fields of the neighboring particles overlap when the interparticle distance ID becomes small, approximately below the particle diameter. Rough estimations, assuming regular packing of uniform particles in cubic lattice,

demonstrate that average interparticle distance ID decreases to around D at the rubber volume concentration of $\phi \approx 10$ vol.% and to D/2 at $\phi \approx 15$ vol.% (Michler and Balta-Calleja 2012). The resultant stress field between particles can be estimated by simple superposition of stress concentration field of isolated particles, as illustrated in Fig. 11.8b. Due to that superposition the stress concentration at the equatorial plane of particles which are placed close enough (ID < D/2) is higher than for isolated particles, and the stress concentrations extend over the entire cross section of the matrix interparticle ligament.

An inevitable side effect of compliant elastomeric particles (or voids) dispersed in rigid polymer matrix is a reduction of the yield stress of the material. As a first approximation the Ishai–Cohen effective area model (Ishai and Cohen 1968), considering a unit cube with a spherical particle of radius R at its center, can be used for estimation of the reduction of the yield stress:

$$\frac{\sigma_y(\phi)}{\sigma_y(0)} = 1 - \pi R^2 = 1 - \pi \left(\frac{3\phi}{4\pi}\right)^{2/3} = 1 - 1.21\phi^{2/3} \qquad (11.11)$$

where $\sigma_y(\phi)$ is the yield stress of a blend containing a volume fraction ϕ of voids or compliant inclusions with the radius R, and $\sigma_y(0)$ is the yield stress of the pristine matrix. Another dependence was found experimentally for rubber-toughened PMMA deformed in compression (cavitation inhibited) (Gloagen et al. 1993):

$$\frac{\sigma_y(\phi)}{\sigma_y(0)} = 1 - 1.375\phi \qquad (11.12)$$

Although different, both Eqs. 11.11 and 11.12 demonstrate a clear dependence of the yield stress on volume fraction alone. The above equations apply to uniform distribution of particles. Significantly higher local stress concentrations, leading to a deeper reduction of the yield stress, and higher toughness can be expected when the rubber particles are not dispersed uniformly but form a pseudo-network morphology (Bucknall 2000).

When shear modulus of a rubber is much smaller than that of the matrix ($G_R/G_M < 0.1$), the high stress concentrations around rubber particles can additionally cause a significant increase of the deformation rate (Bucknall 2000), in addition to modification of the stress state reducing locally the yield stress.

At temperature below glass transition temperature of the elastomer, its modulus becomes similar to that of the matrix, i.e., $G_R/G_M \approx 1$. As a consequence, stress concentrations weaken substantially, and rubber particles are not able any more to reduce the yield stress enough to produce significant toughening. Additionally, the stress required to cavitate a particle that becomes glassy increases dramatically, which practically stops any internal cavitation of particles and also leads to the disappearance of the toughening effect. In impact tests, like Charpy or Izod, the minimum temperature at which any toughening can be observed is usually about 10 K higher than the actual T_g (Bergen 1968) due to relatively slow relaxation and
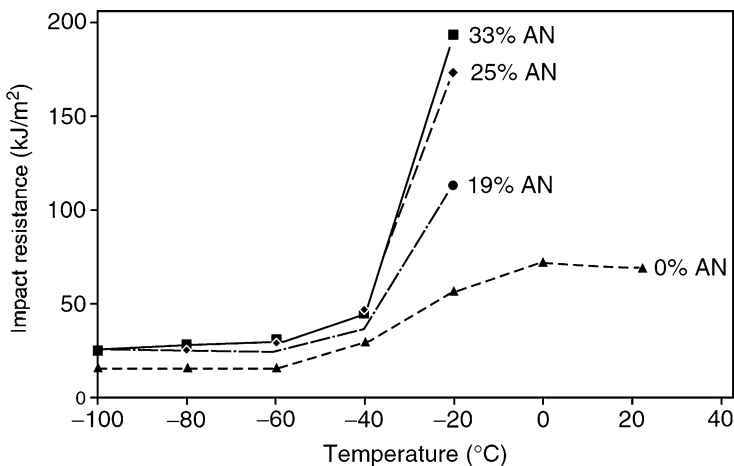
Fig. 11.9 Impact resistance of SAN of various compositions blended with PBA/SAN core-shell particle impact modifier (From Heckmann et al. (2005); reproduced with permission of Taylor and Francis)

high deformation rate. The effect is illustrated in Fig. 11.9 for different SAN copolymers toughened by blending with core–shell particles containing the poly (butylacrylate) (PBA) rubber core. One can observe here that toughness of the blends is enhanced only above the glass transition temperature of the rubber phase, which is below –40 °C, independently on properties of the matrix (the differences in toughening efficiency with changing composition of the matrix observed above T_g of the rubber are related primarily to the agglomeration habits of particles) (Heckmann et al. 2005).

In contrast to soft rubber particles, the stiff particles dispersed in a softer matrix (particles of stiff polymer or particulate filler, $G_R/G_M \geq 1$) respond on tensile loading with the concentration of the tensile stress in the polar regions ($\sigma_r/\sigma_o \approx 1.8$) and compressive stresses around particle equator. If the adhesion between the matrix and particles is poor, the concentration of tensile stress at the particle–matrix interface can result in debonding and formation of voids in polar region of particles. These voids become the source of new stress concentrations, similar to that around isolated void or rubber particle. Further elastic or plastic stretching of the matrix can lead to the expansion of these polar voids towards the equator and their eventual merging. This produces a single relatively large and elongated void around the particle. The voids created by debonding initiate stress concentrations, advantageous for matrix yield and deformation around the void equator. More frequently, however, due to other factors, the stiff particles debonded from the matrix initiate crack and followed by brittle fracture rather than yielding of the matrix.

In addition to the stress concentrations upon loading, which arise from a difference in stiffness of the matrix and elastomeric modifier, there are thermal stresses generated around particles due to the difference in thermal expansion

coefficient of the matrix and the elastomer. Upon cooling after melt processing, both the matrix and modifier phase contract, but with a different degree, which results in compressive or tensile radial stresses at particle–matrix interfaces. Elastomers shrink on cooling more than a glassy matrix, so that the tensile thermal stresses are produced, while, for stiff mineral fillers, which show expansion coefficient lower than the matrix, thermal stresses are compressive.

The thermal tensile stress developed in spherical rubber particle in the radial direction can be determined from the following relation (Beck et al. 1968):

$$\sigma_{rr} = \frac{2(\alpha_R - \alpha_M)E_R E_M \Delta T}{6(1 - 2v_R)E_R + 3E_M(1 - v_M)} \tag{11.13}$$

where α is coefficient of thermal expansion, v is Poisson's ratio, E is the Young's modulus, and the subscripts M and R refer to the matrix and rubber, respectively. It can be noted that similarly to intensity of stress concentrations, thermal stresses do not depend on the particle diameter. They depend strongly on Poisson's ratio, especially when the v_R approaches the value 0.5. Thermal stresses of 1.3 MPa and 9.6 MPa can be estimated for a glassy matrix, like PS, and rubber particles with the Poisson's ratio of $v_R = 0.49$ and 0.499, respectively (Michler and Balta-Calleja 2012). The thermal tensile stresses acting at a rubber particle–matrix interface together with the radial component of stress concentrations can induce debonding at interface when particles show poor interfacial strength. For well-bonded particles, an isotropic tension (negative hydrostatic pressure), which is produced inside particle, leads to their increased volume dilatation. This results in an increase of free volume and hence easier initiation of cavitation as well as reduction of the glass transition temperature. A significant reduction of T_g by 12–19 $^\circ$C was observed experimentally for polybutadiene inclusions dispersed in polystyrene (Bates et al. 1983).

Thermal stresses generated in the matrix around rubber particles have a radial tensile component and tangential compressive components. These tangential components reduce the effective stress concentration in the equatorial zone of the rubber particle.

11.4.3.2 Particle Cavitation

Rubber particle cavitation, i.e., formation of holes inside of rubber inclusions, is one of the most important ways in which toughened polymer can respond to tensile stress. Although recognized already in 1970s, this phenomenon was initially believed to be merely a secondary process, triggered by extensive shear yielding or crazing of the surrounding matrix, and not significant for toughening. With increasing experimental evidence, that opinion has gradually changed and there has been a growing understanding and acceptance of cavitation importance. Now it is widely accepted that cavitation within rubber particles is, in fact, a decisive step in toughening (Argon 2013; Argon and Cohen 2003; Bucknall 2000, 2007a, b; Bucknall and Paul 2009, 2013; Michler and Balta-Calleja 2012). Although

cavitation itself involves little energy absorption, it allows for the subsequent enhanced, sometimes massive, deformation of the matrix, which appears the primary source of the energy absorption.

In the middle of thick sample or in front of the crack tip, the stress state is triaxial (plane-strain conditions). It occurs also in front of the notch in Izod and Charpy notched samples. Such a stress state makes plastic deformation more difficult than the biaxial stress under plane-stress conditions and favors brittle fracture as the surrounding stressed material resists the lateral contraction which is needed to maintain a constant volume on deformation. The rubber particles respond to a high level of triaxial stresses produced by near plane-strain conditions with cavitation or sometimes with debonding, if the rubber–matrix interfacial adhesion is low. Both processes create voids either inside rubber particles or at their interfaces, respectively. Cavitation manifests with the easily observed stress whitening in the deformation zone (Ban et al. 1988; Gaymans et al. 1990). The volume strain experiments demonstrated that rubber cavitation begins at low strains (2–6 %) (Borggreve et al. 1989a; Bucknall et al. 1989) under triaxial stress when the matrix material is still in the elastic region.

The stress needed to initiate cavitation of an elastomer particle is a function of the cohesive energy density of that elastomer, chain entanglements, and presence of any inhomogeneities inside the elastomer particle (as, e.g., precavities, small crystallites, or foreign impurities) (Gent 1990; Kramer 1983; Wu 1989). The number of entanglements depends on the molecular weight and its distribution of the elastomer. Cavitation becomes easier for lower molecular weight and narrows its distribution (Brown and Ward 1983). Any defect or heterogeneity, if present inside the elastomer particle, can result in a significant reduction of the cavitation stress of that particle. The cavitation stress decreases further with an increasing inhomogeneity (defect) size to the micron-scale length (Gent 1990). However, it is frequently observed that rubber particles dispersed in the matrix, even those much smaller than 1 μm, cavitate quite easily under dilatational stress. This implies that there must be another mechanism for nucleation of nanovoids and cavitation, which is independent on the presence of occasional micron-scale defects and is inherent in the behavior of rubbers themselves, perhaps at the level of individual chain segments. Bucknall reasoned that since resistance to dilatation in rubbers arises almost entirely from weak van der Waals interactions, and shear occurs easily, it could be expected that under high triaxial tensile stresses, the distribution of polymer chains within the expanded volume of the elastomer become unstable, giving rise to nucleation of the nanovoid (Bucknall 1997). Calculations of Lazzeri and Bucknall (1993) and Bucknall et al. (1994) confirmed that hypothesis and demonstrated that even for particles as small as 0.2 μm in diameter, the energy barrier for cavitation is quite low and can be overcome easily with the aid of thermal energy.

Impact tests of pre-cavitated samples of rubber-toughened Nylon (pre-cavitation obtained by a slight tensile pre-straining at low deformation rate) demonstrated their impact behavior very similar to samples without initial cavities (Gaymans 1994). Similar results were reported by Dasari et al. (2010) for polypropylene and PP/CaCO$_3$ nanocomposites pre-cavitated during processing. They observed that the

voids in both plain iPP and composite acted in a similar way as the cavitating rubber particles in rubber-toughened polymer systems; i.e., the preexistent voids expanded at the early stage of the PP matrix deformation and subsequently triggered large plastic deformation of the surrounding matrix in the form of isolated and domain-like deformation zones (Dasari et al. 2010). The above findings demonstrate that the cavitation process itself, although crucial for toughening, is not a major energy-absorbing mechanism. It is rather the plastic deformation of the matrix, which follows the cavitation step.

Upon formation of voids, the constraints imposed on the matrix are locally eased, and the triaxiality of the stress is relieved, at least partially, around each cavitated elastomer particle ahead the notch or the running crack (Bucknall 1977; Donald 1994; Kinloch and Young 1983). Due to a notable reduction of constraints, the stress state around these particles, especially within thin matrix ligaments between neighboring cavitated particles, can be converted from a triaxial to a nearly biaxial one (plane-stress conditions). When the stress concentrations are present around voided particles (they actually become even slightly stronger than prior to internal particle cavitation), the change of the stress distribution from plane-strain to plane-stress conditions might be advanced enough to depress locally the yield strength and initiate plastic deformation. Shear yielding is favored by plane-stress, whereas crazing is preferred under plane-strain conditions (constraints reduced, yet not fully dismissed). Therefore, the primary effect of cavitation is usually an enhancement of shear yielding mechanism in the matrix (Bucknall 2000; Bucknall et al. 1989). Formation of cavities results in local decrease in the hydrostatic stress component and a corresponding increase in the deviatoric (shear) component, and a higher stress concentration factor (Bucknall et al. 1989). Another important result of cavitation is conversion of the material from a continuous solid to the porous (cellular) structure, which demonstrates modified sensitivity to the mean stress on yielding. Consequently, the matrix can yield easier, even at the plane-strain conditions ahead of the notch. This feature will be discussed further in Sect. 11.5.3.

Once the rubber particles have cavitated, the surrounding matrix is free to yield and stretch in a way it was previously impossible. The deforming shell of the matrix enclosing cavitated particle extends biaxially, which increases the volume of the cavitated particle. If the particle is isolated, that deformation of the adjacent matrix is limited by constraints imposed by yet undeformed surroundings. However, if particles are closely spaced, the thin matrix ligaments between them may become yielded fully across, which results in extensive plastic deformation in large volume of the sample and evolution of the shape of the cavitated rubber particle from spherical to ellipsoidal or sausage-like shape, elongated in the direction of local principal stretch due to high extension of the matrix ligaments around particle (Muratoglu et al. 1995d), as illustrated in Fig. 11.10.

It is sometimes suggested that rubber particles lose completely their ability to sustain a stress once they have cavitated. This is actually not true except only for a very few cases. First exception is when voids are formed along particle–matrix interfaces due to debonding (poor adhesion). Transfer of stress between the matrix

Fig. 11.10 SEM micrographs of cavitated tensile sample of polyamide 6,6 modified with 19 wt.% EPDM rubber: (**a**) stress-whitened zone outside the neck region and (**b**) stress-whitened zone inside the neck region. The scale bar represents 5 μm (From Muratoglu et al. (1995d); reproduced with permission of Elsevier)
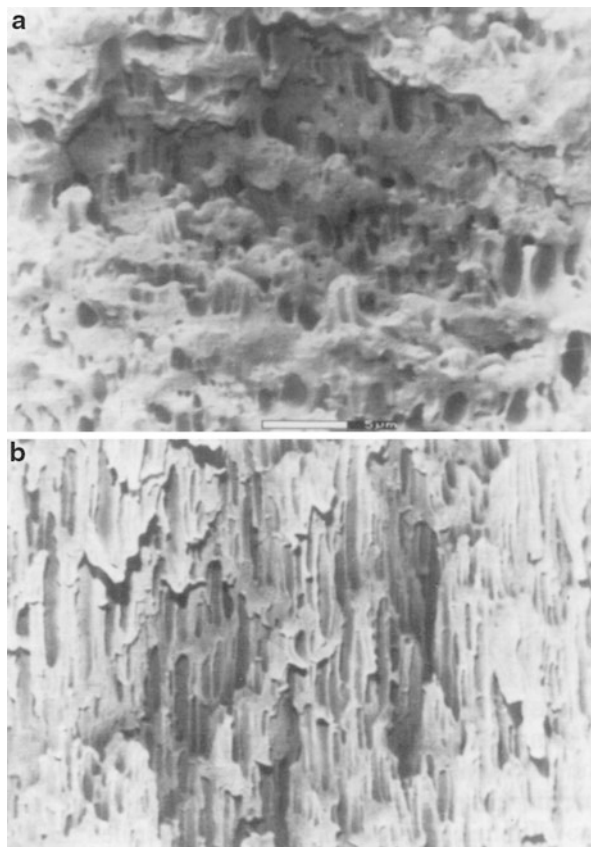
and such debonded particles is very limited. The other case is when crazes formed away from rubber particle intercept it upon their growth. In such a case, a significant lateral contraction must accompany elongation of the particle in the applied stress direction. As this contraction proceeds, debonding at the particle/craze interface occurs, and the void is created. This void grows then under increasing load, which can lead to premature craze breakdown and subsequent crack initiation.

For homogeneous rubber particles with high interfacial strength (strong adhesion) to the matrix, their cavitation results in the formation of the void in the center of the particle. When a void is formed, the rubber particle transforms into a continuous thick spherical shell around the void, in which the stress and strain are no longer uniform. As the void grows, the rubber shell is expanded by biaxial tension. The strain is distributed in this shell nonuniformly: the inner face of the shell must deform most, close to the ultimate stretch, which results in substantial strain hardening, whereas the outer layer, contacting the matrix, deforms much less. The expanding rubber shell bonded to the matrix can transmit load and also contribute to strain hardening of the entire material with an advance deformation of the matrix and the rubber, initiated by its cavitation. However, further expansion

of the void can lead eventually to the rupture of the most strained rubber segments in the inner layer close to the void, and consequently the entire shell can fail by progressive tearing (Bucknall 2000).

In all cases, a premature rupture of the rubber will restrict extensive deformation of the matrix as it leads to the formation of voids larger than critical, resulting in fast crack initiation and propagation. When rubber rupture occurs later, after some advance of matrix deformation, the orientation-induced hardening of the matrix can alleviate to some extent the effect of such flaws and the material is allowed to deform further.

Frequently fibrils are formed inside the rubber particle, especially in cross-linked or heterogeneous particles, as, e.g., particles with stiffer sub-inclusions or core–shell morphology. These fibrils, anchored both sides at particle–matrix interfaces or bridging a particle stiff core/inclusion with the matrix matter at the interface, are clearly load-bearing elements of the structure, which make a major contribution to the strain hardening. The fibrillar morphology of cavitated particle is the most effective for stress transfer and contribution in strain hardening that prevents premature fracture since stress and strain across fibrils are uniform and can be high, simultaneously in all fibrils. The experimental evidence indicated that the stress in the fibrils formed in core–shell particle reached much more than 30 MPa (Starke et al. 1997). Bucknall (1997) claimed that a low-level cross-linking of the rubber is desirable for homogeneous rubber particles, as it allows a still early cavitation of the particles and high strains by fibrillation, while the fibrils would have high strength. Excessive cross-linking, also that caused by photodegradation effect (e.g., in outdoor applications), can lead, however, to a marked reduction or even loss of the impact strength due to stiffening of the rubber and impediment of cavitation.

Various morphologies of cavitating rubber particles were considered by Kim and Michler (Kim and Michler 1998a, b). Depending on the original morphology of the particle (homogeneous, heterogeneous with inclusions, core–shell) and adhesion between particle and the matrix, which can be modified broadly by addition of various compatibilizers, different modes of cavitation or debonding can be observed: from single-site cavity in the center of a homogeneous inclusion, through multiple internal cavitation, to multiple cavitation with formation of fibrils in the shell of the core–shell particle or around debonding particle which had been moderately bound to the matrix, cf. Fig. 11.11. The most favorite situation is when rubber forms fibrils rather than a single smooth shell around cavity since contrary to a single shell around void, fibrils are strained uniformly and therefore can transmit higher stress and participate effectively in strain hardening (in a similar manner as fibrils in a craze), which stabilizes advancing deformation of the matrix and prevents premature initiation of a crack. The presence of fibrils controls also the size of the microvoids and prevents expansion of the void to the overcritical size which could quickly end up in crack formation.

Observations of rubber cavitation and growth of the voids offer an additional explanation for the enhanced shear yielding of the matrix (Donald and Kramer 1982). The presence of many closely packed particles which can cavitate enables
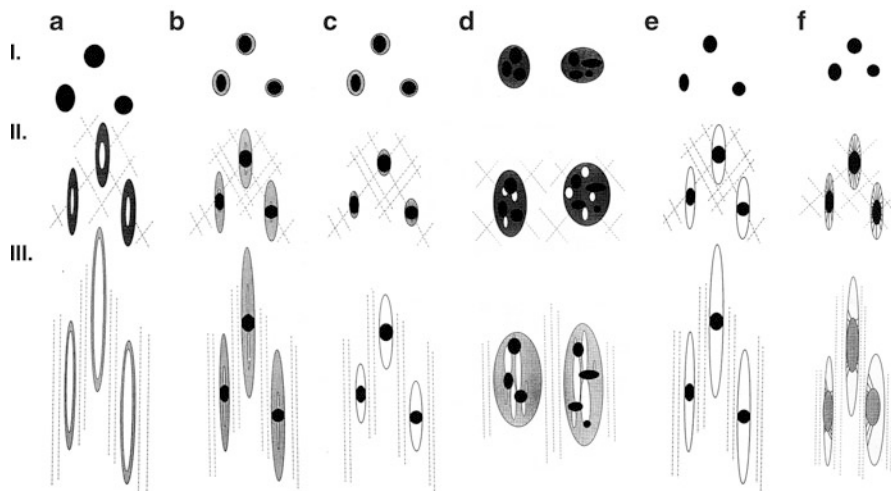
Fig. 11.11 Various morphologies produced by cavitation and debonding: (**a**) single cavitation in homogeneous particles (e.g., PA/BA blend); (**b**) single cavitation in heterogeneous particles (blend PP/ethylene–propylene block copolymer with low content of ethylene); (**c**) fibrilized cavitation (PP/PA/SEBS-g-MA blend); (**d**) multiple cavitation in heterogeneous particles (PP/LLDPE/SEBS-g-MA blend); (**e**) single debonding (PP/ethylene–propylene random copolymer blend); and (**f**) fibrilized debonding at the interface (PP/EPDM blend). *I* – initial morphology, *II* – low strain, *III* – high strain (Adapted from Kim and Michler (1998b); with permission of Elsevier)

relief of the local buildup of hydrostatic tension produced by localized shear process (proceeding at constant volume). Thus, possibly soon after initiation of cavitation and the development of some initial shear yielding, the constrained conditions might be fully relieved by expansion of numerous cavities distributed densely over the process zone, which changes the structure of the material into cellular, in which thin cell walls are under plane-stress, so that even the relatively thick bulk specimens may behave as if the matrix were everywhere under plane-stress conditions. Shear deformation occurs more readily under biaxial rather than at triaxial stress state, and cavitation of the rubber particles therefore favors local shear yielding deformation. However, if the matrix does not shear readily, but like polystyrene is far more prone to crazing, then this mechanism is not available and rubber cavitation followed by expansion of created voids is more damaging.

11.4.4 Core–Shell Particles

A very effective way of toughening is the use of core–shell particles instead of homogeneous rubber particles. The core–shell particles were commercially introduced as PVC impact modifiers in 1958 and since that time, their use has continuously expanded into new toughening applications, which now include a wide variety of engineering polymers (Cruz-Ramos 2000). In contrast to other impact

modifiers, as homogeneous rubber particles, which are most frequently formed by high shear forces during blending of a molten matrix polymer with an elastomer, the core–shell particles are preformed by emulsion polymerization prior to mixing with the host polymer. This makes a major difference between core–shell particles and other types of impact modifiers: the size and size distribution of core–shell particles are set during the synthesis process and continue the same after they are introduced and dispersed in a matrix of a host polymer, whereas elastomer particles formed in the blending process have the final size depending heavily on processing conditions.

The typical architecture of core–shell particles consists of a soft core, made up of a rubbery polymer, surrounded by relatively thin shell of rigid polymer that is grafted to the core. The core in commercial materials is usually a cross-linked rubber based on poly(butyl acrylate) (PBA), poly(butyl acrylate-co-styrene), or poly(butadiene-*co*-styrene). It provides the soft second phase that induces toughening similarly to homogeneous rubber particles in conventional blends. The shell of the particles consists of a polymer that is chemically grafted onto the core and generally is much stiffer since it has a much higher glass transition temperature than rubber of the core. Typical polymers used for a shell in commercial products are homo- and copolymers of PMMA and styrene–acrylonitrile copolymers (SAN) (Cruz-Ramos 2000). Two basic functions of the shell are (1) to prevent adhering of particles from one to another during the drying after emulsion polymerization process and (2) to provide a good dispersion and compatibility of particles with the matrix of the host polymer – the shell gives the particle a layer that physically binds the rubber core to the surrounding matrix and prevents particle coalescence upon blending.

There are several advantages on the use of core–shell particles as impact modifiers. The main is a relatively easy control of the matrix–particle morphology of the final blend. The particles, preformed prior to blending, have defined size and narrow size distribution, and dispersing them within the matrix does not alter these, independently on the processing conditions. Good and uniform particle dispersion can be achieved relatively easy. The shell, grafted to the rubbery core, provides usually sufficient bonding between particles and the matrix. Due to versatility of the emulsion polymerization, the particles of various sizes can be produced and selected for blend formulation according to particular demands. All this allows for a relative easy modification and fine-tuning of the impact strength and other mechanical properties of the material. Furthermore, the small size with a narrow size distribution and the uniform spatial distribution in the matrix make possible formulation of transparent impact-modified blends. The mechanism of the toughness improvement is the same as in the case of materials modified by homogeneous rubber particles, although cavities in core–shell particles are frequently stabilized by the core–shell structure, and this prevents coalescence of voids of neighboring particles, in which coalescence would lead to critical flaw and crack initiation (Michler and Bucknall 2001).

Another type of the core–shell particles is by multilayer particles that consist of a glassy core, a thin intermediate rubber layer, and an outer glassy shell (Lovell and
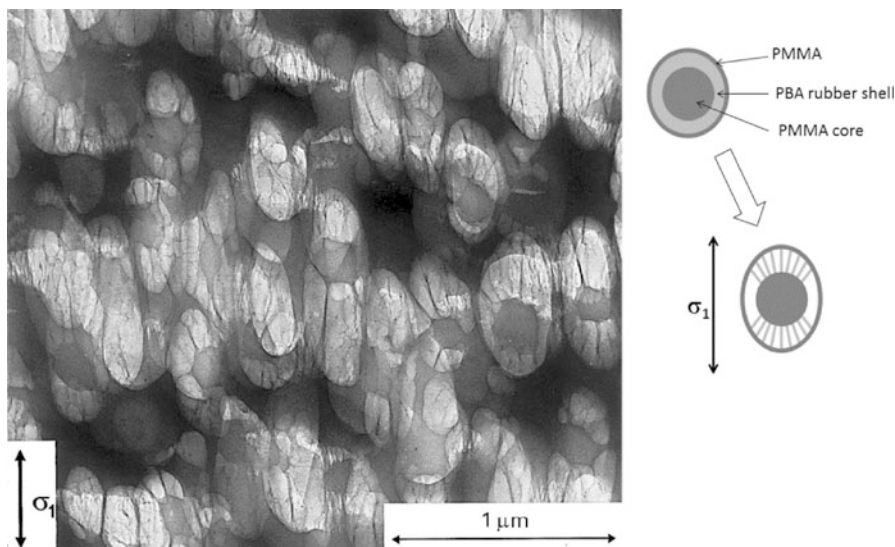
Fig. 11.12 TEM micrograph of fibrillar cavitation of the core–shell multilayer particle in the SAN/PBA blend; tension direction vertical (From Starke et al. (1997); reproduced with permission of Springer)

El-Aaser 1997; Michler and Bucknall 2001; Shah 1988; Starke et al. 1997). An example is the particle with the core of cross-linked PMMA, ca. 180 nm in diameter, poly(butyl acrylate-*co*-styrene) (PBA) rubber shell of approx. 40 nm thickness, and an additional outer thin-grafted PMMA shell added for improved bonding with the matrix (Michler and Bucknall 2001; Starke et al. 1997). The overall particle diameter was approximately 260 nm. Compounding of particles with SAN results in acrylonitrile–styrene–acrylate copolymer. Due to rigid core and relative low amount of the rubber, such multilayer particles with rigid core allow for better balance between toughness and stiffness of the final toughened material. The other extremely important benefit is that cavitation of such particles proceeds via nucleation of many small nanovoids in thin intermediate rubber shell. With subsequent expansion of these voids, a quite regular fibrillar morphology develops within the rubber shell with elongated fibrils anchored well to the rigid core and the outer shell (rubber had been grafted to both core and the outer shell). The morphology of cavitated particles is shown in Fig. 11.12.

As discussed in the previous section, such extended fibrils are effective load-bearing elements of the structure, which make a major contribution to strain hardening. Multiple cavitation and formation of fibrils results in uniform stress and strain distribution in these fibrils, which prevents their premature fracture, stabilizes cavities, and allows for effective stress transfer across the rubber shell. All of this brings a significant contribution of particles in strain hardening and stabilization of the matrix material extensive deformation. The stretching of fibrils is very similar to drawing of fibrils from the walls of a craze and generates

substantial stress, which can be estimated even above 100 MPa at room temperature for highly elongated fibrils (Michler and Balta-Calleja 2012). The experimental evidence indicated the stress in the fibrils formed in core–shell particle exceeded well 30 MPa (Starke et al. 1997). Such a high stress transmitted to the hard polymer core can be high enough to involve its yielding, which if happen would provide an additional effective mechanism of energy absorption upon impact. The plastic deformation of the core of particles was indeed observed by Michler and Bucknall (2001).

Taking all above into account, the multilayer core–shell particles seem to be suited very well for toughening of rigid polymers, as they provide a relatively good balance between toughness and stiffness of the impact-modified material, in contrast to modification with homogenous rubber inclusions, which frequently leads to unacceptable deep reduction of stiffness of toughened material. However, to get full benefit of potential of modification with core–shell particles, these particles must be carefully designed (with respect to particle composition, layer thickness, overall diameter, selection, or adequate chemical modification of the outer layer to ensure good adhesion to the matrix) and custom made for a particular blend and its application.

It is well known that the particle size needed to toughen a rigid polymer depends on inherent fracture mechanism of the matrix. In general, brittle glassy matrices that tend to craze benefit more from large rubber particles, of diameter exceeding 1 μm. Smaller particles, below 0.5 μm diameter, are, in turn, effective in toughening matrices in which shear yielding is a main deformation mechanism. Since typical core–shell particles have a diameter well below 1 μm (usually in the range of 0.25–0.5 μm), they are used most frequently for toughening of non-crazable polymers, in which shear yielding is a dominant deformation mechanism. Core–shell particles were used as effective impact modifier in many polymers, including PC (Kayano et al. 1996; Lovell and El-Aaser 1997), PMMA (He et al. 1998; Laatsch et al. 1998; Lovell and El-Aaser 1997; Lovell et al. 1993; Shah 1988; Vazquez et al. 1996), PVC (Lutz and Dunkelberger 1992), PA (Aerdts et al. 1997; Kesskula and Paul 1994; Majumdar et al. 1994d), PBT, and PET (Brady et al. 1994; Hage et al. 1997). Preparation of larger particles by emulsion polymerization to be used for toughening of crazable polymers, like PS, received also some amount of attention (Cruz-Ramos 2000).

11.4.5 Rigid Particles (Fillers)

The idea of toughening with rigid particles instead of soft rubber particles has attracted great attention because incorporation of rigid particles would contribute to a greatly enhanced stiffness of the modified material in addition to possible toughness improvement, while modification with elastomers always leads to an inevitable reduction in modulus. The rigid particles can be either particles of a particulate filler or particles of another polymer, stiffer than the matrix polymer. The possibility of simultaneous enhancement of both toughness and stiffness would be a significant advantage of rigid particles over traditional rubber toughening.

   Stiff particles dispersed in the polymer matrix increase its modulus, and if there is strong adhesion between particles, they can also increase the yield strength. However, in the case of low or missing interfacial strength, debonding appears on loading readily while still in the elastic region as stiff particles are unable to deform to any significant degree. The microvoids created around particles due to debonding should not form immediately upon application of stress as this may reduce the elastic modulus. Ideally, debonding should occur at stress only slightly lower than the yield of the pristine matrix. As it is often the case, it prevents any increase of the yield strength of the system, unwanted for toughening. The microvoids created at interfaces act as stress concentrators, like cavitated elastomer particles. Widespread particle debonding in the deformation zone close to notch root or fracture surface transforms this zone into a porous solid and helps to relieve plastic constraints imposed earlier on the matrix by rigid and hardly deformable particles (Bartczak et al. 1999b, c; Muratoglu et al. 1995a, d; Thio et al. 2002; Tzika et al. 2000; Wilbrink et al. 2001) and make yield easier due to modification of yield sensitivity to the mean stress. The related change in the stress state can initiate local yielding process and consequently lead to an improved toughness. This however can be achieved only in the case of small, semi-equiaxed, and homogeneously distributed particles, since large particles create large voids when debonding, with the disadvantage of void coalescence and formation of cracks of overcritical length. On the other hand, very small particles, well dispersed in the matrix, require high mean stress for debonding, while agglomerates of such very small particles, which are difficult to destroy in processing, can rupture easily on loading and produce sharp cracks reaching quickly the critical length (Kim and Michler 1998a, b; Michler 2005; Michler and Balta-Calleja 2012). Clustering of rigid particles can also result in the formation of quite large unbounded inclusions, which, similarly to very large particles, upon separating from the matrix, can act as supercritical flaws that trigger a brittle response (Argon and Cohen 2003).

   In the case of filler particles in shape of fibers or platelets (as, e.g., organoclays), oriented randomly, the distribution of voids created at their interfaces on loading can be not homogeneous enough to produce a uniform porous structure needed for successful toughening. Therefore, toughening with anisotropic rigid particles seems more difficult than with semi-equiaxed ones.

   It has been suggested (Bucknall 1978; Kinloch and Young 1983; Lavengood et al. 1973) that rigid particulate fillers might be used to increase the toughness of brittle glassy polymers by initiating multiple crazing. Under an applied stress, rigid particles do induce tensile stress concentrations in the matrix and debond from the matrix readily, which generate stress concentrations sufficient to initiate crazing, yet near the particle poles rather than the equator, as it was for rubber particles. On the other hand, due to limited adhesion between the rigid particulate filler and the matrix, the filler particles do not appear particularly as effective craze or crack terminators. To act as efficient terminators, the second phase has to be adequately bonded, while rigid particles when called to do this job may have already become debonded from the matrix. Consequently, rigid particles of particulate fillers debonding from the matrix prior to yield point demonstrate low ability to act as
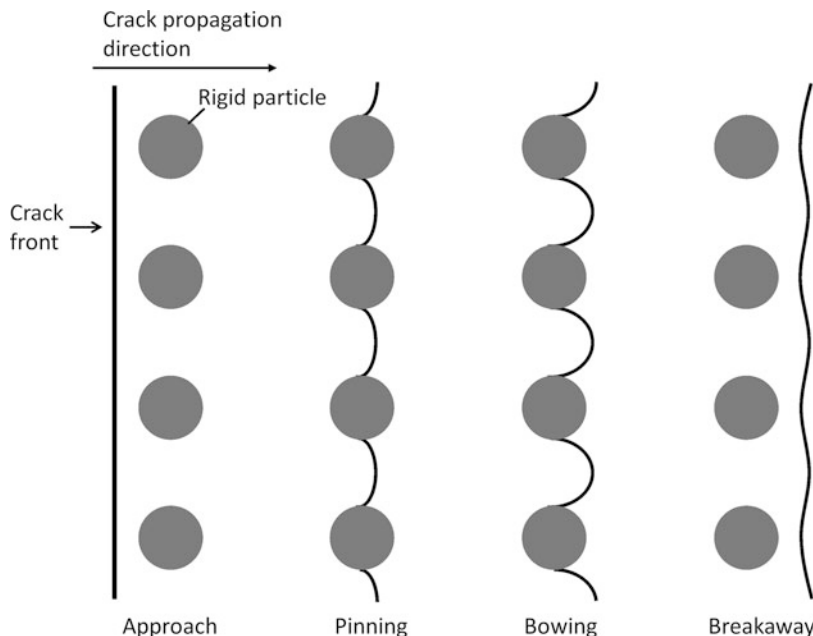
Fig. 11.13 Schematic representation of the crack pinning mechanism (Drawn after Kinloch and Young (1983))

effective craze and crack terminators, which results in much poorer toughening performance when compared with well-bonded rubber particles.

Several investigations have demonstrated that incorporation of particulate fillers such as silica or alumina trihydrate can improve the toughness of thermosets, like cross-linked epoxies (Shaw 1994). The mechanism considered responsible for an increase of impact resistance is different than that of rubber particles effective in promoting cavitation under stress localized in planar zones (Sue 1992; Sue and Yee 1996), giving rise to craze-like dilatational bands (Lazzeri and Bucknall 1995). Particles of filler are expected to impose stress concentrations in epoxy matrix due to a substantial modulus difference between particle and the matrix. However, this is usually not considered as significant. Instead, a mechanism based essentially on the impeding characteristics of the particles was proposed (Evans 1972; Green et al. 1979; Lange 1970). The mechanism, called the crack pinning mechanism (Lange 1970), postulates that a propagating crack front, when encountering an inhomogeneity, as, e.g., well-bonded filler particle, becomes temporarily pinned at that point. An increase in load increases the degree of bowing between pinning points caused by adjacent particles, resulting in both a new fracture surface and an increase in the length of the crack front, as illustrated schematically in Fig. 11.13. These processes will absorb some amount of energy and therefore lead to an increase of the fracture toughness of the resin. Although incorporation of the filler can lead to a noticeable toughness improvement, this is generally much smaller than

Fig. 11.14 TEM micrograph of polyethylene thin film with a particle of CaCO$_3$ (seen as a continuous *black* region in the left-hand side). Crystalline lamellae seen as *black ribbons* when oriented edge on against interface (From Chacko et al. (1982); reproduced with permission of Wiley)
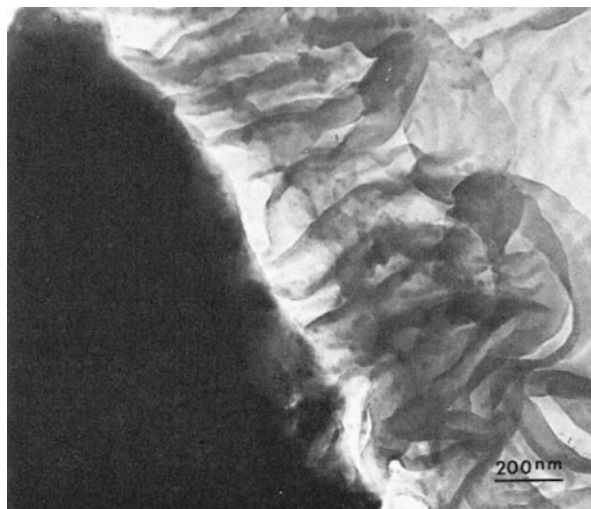
that obtained with cavitating elastomer particles. Thus, in the direct comparison, rubber modification would prevail, although a substantial stiffness increase accompanying toughness enhancement is a major advantage of rigid particle toughening and this method may be preferred for some applications.

Another possibility of improvement of impact strength with rigid particles was demonstrated for notch-sensitive semicrystalline polymers, like polyamides, polyethylene, or polypropylene. Many studies investigating toughening of polyamides with elastomer particles (Borggreve and Gaymans 1989; Borggreve et al. 1987; Dijkstra et al. 1994a; Gaymans 1994, 2000; Muratoglu et al. 1995a, c, d; Wilbrink et al. 2001; Wu 1985, 1988) emphasized the correlation between toughening and the critical interparticle distance. This distance was correlated with a specific form of preferential crystal orientation around particles (with crystalline lamellae oriented locally edge on with respect to the particle–matrix interface and with the low energy/low plastic shear resistance (001) crystallographic plane oriented parallel to that interface). Such an orientation was shown by Muratoglu et al. (Bartczak et al. 1999a, b, c; Muratoglu et al. 1995a, c, d) to reduce markedly the plastic resistance of the layer of polymer matrix around the particle due to possibility of activation of the easiest crystallographic slip system, (001) [010] of polyamide crystals (Lin and Argon 1992). Bartczak et al. (1999a, b, c) postulated that such a preferential local orientation can be obtained at the matrix–particle interfaces, not only in the system consisting of PA matrix and rubbery particles but also for other polymers and particles, including stiff particles of other polymers or mineral fillers. They demonstrated it for polyethylene modified with various elastomers and CaCO$_3$ particles of various sizes. Figure 11.14 presents the TEM micrograph illustrating an oriented layer formed in polyethylene around the particle of CaCO$_3$.

Bartczak et al. (1999a) proposed that the driving force for such a unique crystal orientation around particle is the secondary nucleation at the interface, enhanced

due to the difference in interfacial energy when lamella grows in bulk and in the edge-on contact with the substrate, here the particle surface. This energy difference results in faster growth of those lamellae which maintain contact with particle surface and are oriented edge on, and consequently in the formation of the preferred crystal orientation in a thin layer around particle. Thickness of this specially oriented layer of reduced shear plastic resistance is defined for a given polymer, while independent on the type and size of particles. It was determined approximately 150 nm for Nylon 6 (Muratoglu et al. 1995a) and around 300–400 nm for HDPE (Bartczak et al. 1999a). When the interparticle distance in the blend is reduced below double the oriented layer thickness (300 nm for PA or 800 nmm for PE, respectively), the matrix ligaments consist almost entirely of the oriented material of low plastic shear resistance. They create then easy deformation paths, which percolate the sample. Upon sample loading and particle debonding, the stress concentrations induced by microvoids initiate easily the plastic deformation of crystals within these ligaments just relieved from constraints by debonding of neighboring particles, massive formation of microvoids, and then conversion of the material within deformation zone into a cellular solid. Deformation of ligaments results in an extensive plastic deformation in a large volume of the sample and high energy absorption, exactly the same as in the case of toughening with cavitating rubber particles. It was demonstrated experimentally that a big jump of impact resistance (approximately one order of magnitude) occurred in blends of PE with various elastomers and PE filled with stiff $CaCO_3$ particles, in all systems for the same critical interparticle ligament thickness of approximately 800 nm (Bartczak et al. 1999b, c), which indicates that the same toughening mechanism has to be activated for rubber and rigid particle toughening.

Toughening with rigid particles has two significant advantages over rubber toughening: (a) First, it leads to simultaneous improvement of both toughness and stiffness, in contrast to rubber toughening, which always reduces material stiffness, as illustrated in Fig. 11.15. (b) The other benefit of toughening with rigid particles is its insensitivity to the test temperature (again in contrast to their rubber toughened counterparts). As mentioned earlier, in Sect. 11.4.3.1 at temperature below T_g of the elastomer used for toughening, the stress required to cavitate a particle which became glassy increases dramatically. This practically stops any internal particle cavitation and leads to disappearance of the toughening effect (rubber is usually well bonded and cannot debond from the matrix). In impact tests, the minimum temperature at which any toughening can be observed is usually even about 10 °C higher than actual T_g (Bergen 1968). This is not the case of rigid particles toughening as it relies on particle debonding which does not depend on temperature dramatically. As a result, semicrystalline polymers toughened with rigid particles remain tough in a wide range of temperatures down to around T_g of the matrix polymer (Bartczak et al. 1999c) – cf. Fig. 11.16. Therefore, for polymers with matrices of low glass transition temperature, toughening with stiff fillers has a clear advantages over rubber modification.

There are several prerequisites for successful toughening with rigid particles: particles must be small enough and with narrow size distribution in order to prevent
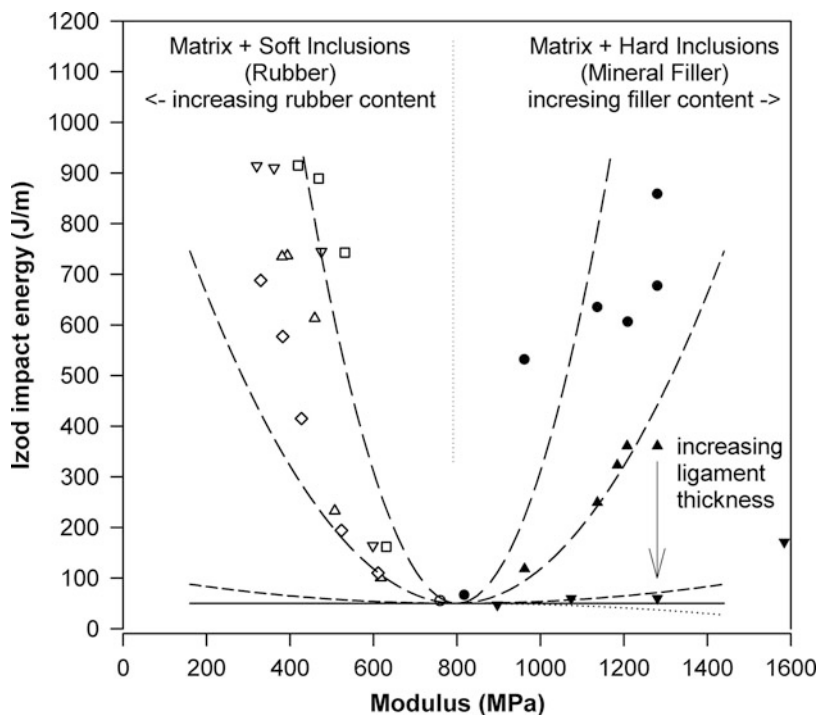
Fig. 11.15 Schematic plot of possible routes of toughening of semicrystalline polymers with soft particles (e.g., rubber, *left* branch) and hard particles (e.g., mineral filler, *right* branch) (From Bartczak et al. (1999c); reproduced with permission of Elsevier)

crack initiation at the microvoids of overcritical size formed around large particles due to their debonding, and particle dispersion must very good and their spatial distribution uniform to avoid clustering and to obtain an optimum interparticle distance, below the critical, set by matrix properties. The aspect ratio of particles should be close to unity to avoid very high stress concentrations (Zuiderduin et al. 2003). Moreover, adhesion between filler and the matrix must be kept as low as possible to allow easy particle debonding prior to matrix yielding. However, as the debonding stress increases with decreasing particle diameter, the filler particles cannot be too small since very small particles will not debond prior to the matrix yield and the mechanism will not work. Another negative consequence of very small particles is their tendency to form agglomerates or clusters. The composite suffers severely from clustering of rigid particles into quite large unbounded inclusions, which upon separating from the matrix often act as super-critical flaws, triggering a brittle response (Argon and Cohen 2003). Loose agglomerates can also rupture across, giving rise to the development of a sharp crack, cf. Fig. 11.17.

   All above show that there is only a limited range of average size and size distribution of particles to be used for toughening; moreover, particles must have
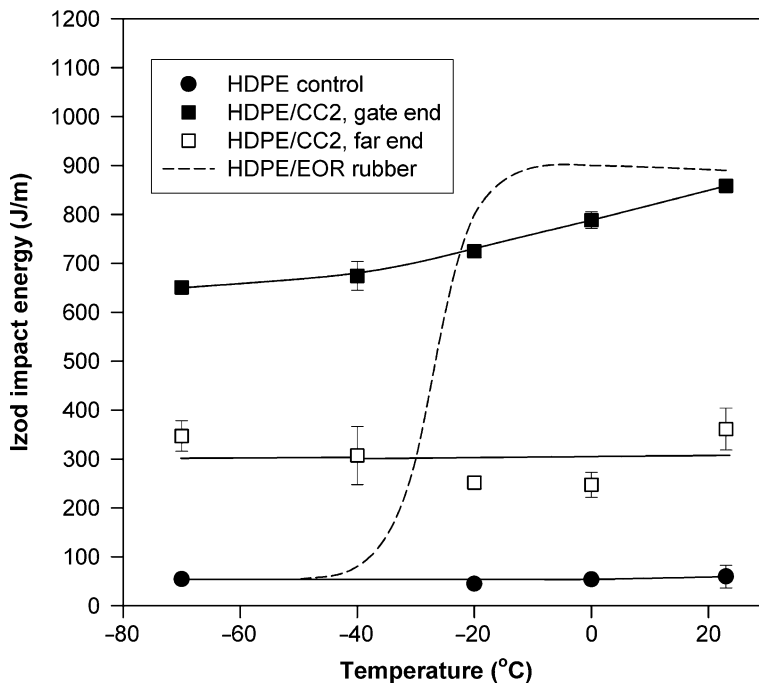
Fig. 11.16 The dependence of notched Izod impact energy on temperature for the HDPE/CaCO₃ (80:20vol./vol.) and HDPE/ethylene–octene rubber (78:22 vol./vol.) blends (From Bartczak et al. (1999c); reproduced with permission of Elsevier)

an appropriate surface treatment that promotes good dispersion but at the same time highly reduces or completely eliminates adhesion to the matrix. Furthermore, there is a strong need of optimum processing protocol, utilizing very high shear forces in order to obtain a very good and uniform particle dispersion, which is essential for toughening effect. A nonuniform dispersion causes some ligaments may become too thick to do deform easily. Particle clustering often results in supercritical flaws. All these effects can lead to material embrittlement instead of expected toughening. The method of toughening with rigid particles, with its potential and strong limitations, was analyzed in detail by Argon and Cohen (Argon and Cohen 2003).

Successful toughening with rigid particles, mainly of CaCO₃, was reported for high-density polyethylene (Badran et al. 1982; Bartczak et al. 1999b, c; Deshmane et al. 2007; Fu et al. 1993; Lazzeri et al. 2005; Lei and Zhou 2000; Liu et al. 2002; Wang et al. 1997; Yuan et al. 2009), polypropylene (Bartczak 2002; Chan et al. 2002; Cioni and Lazzeri 2010; Gong et al. 2006; Kamal et al. 2012; Lazzeri et al. 2004; Lin et al. 2008, 2010, 2012; Thio et al. 2002; Weon et al. 2006; Yang et al. 2006, 2007, 2009; Zuiderduin et al. 2003), Nylon 6 (Ou et al. 1998; Wilbrink et al. 2001), POM (Bartczak 2002), and aliphatic polyketone (Zuiderduin et al. 2006). On the other hand, a need of fulfillment of all severe preconditions mentioned above makes toughening with rigid particles very difficult, which in turn
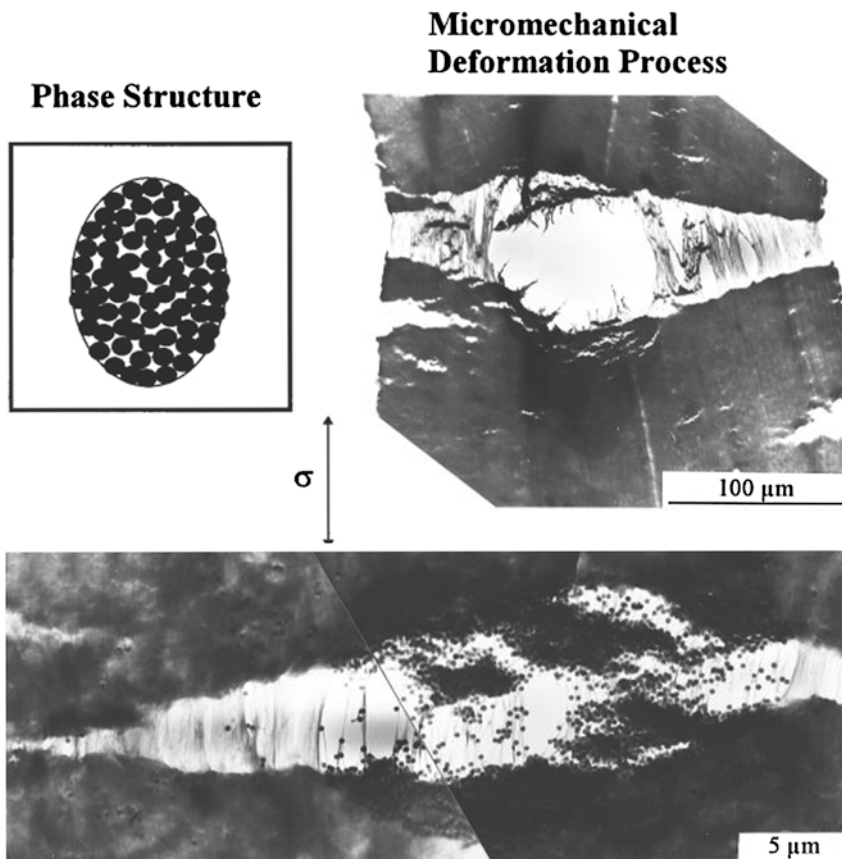
Fig. 11.17 Characteristic deformation structure depending on the phase structure of PP filled with SiO$_2$ particles demonstrating tendency to agglomeration (From Kim and Michler (1998a); reproduced with permission of Elsevier)

makes often the modification with rubbery particles more attractive in industrial practice.

The described above toughening mechanism of semicrystalline polymers proposed by Muratoglu was criticized by Hwang et al. (2006) who, on the basis of computer simulation, suggested that the observed preferred orientation of crystals which led to toughness improvement of studied samples might result from, or be significantly amplified by, oriented crystallization induced by shear during sample injection molding, possibly much enhanced within interparticle ligaments, rather than by interfacial energy differences postulated by Bartczak et al. (1999a, b, c). It was also questioned on other grounds by Bucknall and Paul (2009, 2013), who remarked inconsistency of the Muratoglu's hypothesis with recent work by Huang et al. which shows that the impact behavior of 80/20 rubber-toughened blends based on the amorphous polyamide (Zytel 330) is very similar to that of 80/20 blends

based on semicrystalline PA6 (Huang et al. 2006a, b; Huang and Paul 2006), which may suggest that crystalline structure and morphology of the matrix are inessential for toughening with particles.

11.5 Plastic Deformation Mechanisms in Toughened Polymer Blends

11.5.1 Overview of Micromechanical Behavior

As it was already discussed in Sect. 11.4.3, the modification of a rigid thermoplastic polymer with rubber particles promotes energy absorption through the initiation of local yielding in the close proximity of particles, followed by the extensive deformation involving large volume of the sample owing to dense arrangement of rubber particles. This deformation mechanism can be described by the following sequence (Bucknall 1977, 1997; Kim and Michler 1998b; Michler 2005; Michler and Balta-Calleja 2012):

- Buildup of stress concentrations around particles and negative pressure inside
- Generation of microvoids due to cavitation or debonding of rubber particles that alters the stress state in the surrounding and modifies matrix response by reducing locally the yield stress
- Initiation of local yielding by an accessible mechanism (crazing, shear yielding)
- Extensive plastic deformation stabilized by strain hardening, resulting in large energy absorption

The dominant mechanism of deformation depends mainly on the type and properties of the matrix polymer, but can vary also with the test temperature, the strain rate, and the morphology, shape, and size of the modifier particles (Bucknall 1977, 1997, 2000; Michler 2005; Michler and Balta-Calleja 2012; Michler and Starke 1996). Properties of the matrix determine not only the type of the local yield zones but also the critical parameters for toughening. In amorphous polymers with the dominant formation of crazes, the particle diameter, D, is of primary importance, while in some other amorphous and in semicrystalline polymers with the dominant formation of dilatational shear bands or intense shear yielding, the interparticle distance ID, i.e., the thickness of the matrix ligaments between particles, seems to be also an important parameter influencing the efficiency of toughening. This parameter can be adjusted by various combinations of modifier particle volume fraction and particle size.

It is now widely appreciated that independently on the actual mechanism of plastic deformation dominating the matrix response and brought about by modification with rubber particles, the critical step in toughening is generation of microvoids, common for all toughening mechanisms (Argon 2013; Argon and Cohen 2003; Bucknall 2000, 2007a, b; Bucknall and Paul 2009, 2013; Michler and Balta-Calleja 2012), not only in rubber toughening but also in toughening with rigid particles (Argon 2013). Cavitating or debonding particles facilitate the development of voids and then activation of dilatational yielding in the deformation zone

close to the fracture surface. The primary role of cavitating/debonding particles is to alter the stress state in the surrounding matrix. Such a change enables matrix to yield at moderate stress, even under plane-strain conditions (see Sect. 11.5.4) which initiate an extensive plastic deformation of the matrix (Bucknall 2000). This is possible because generation of microvoids by closely spaced cavitating/debonding particles converts the material in the deformation zone from continuous solid into a porous (cellular) solid, which is generally the most effective way to reduce plastic resistance of the material (Argon and Cohen 2003).

Depending on matrix characteristics and test conditions, its deformation, which has been triggered by the formation of microvoids, can proceed according to several mechanisms, including multiple crazing, shear yielding, or combination of both, or crystal plasticity mechanisms supported by shear of interlamellar amorphous layers, if the material is semicrystalline. It is not completely clear whether cavitation of rubber particles is the necessary precondition for multiple crazing. It seems that the triaxial stress at equatorial regions of rubber particles induced by stress concentrations may be alone sufficient to induce crazes. However, cavitation increases additionally the stress concentration (as the ratio of moduli of cavity and the surrounding, determining the stress concentration, falls to 0) and this must enhance craze initiation. Therefore, cavitation increases the efficiency of toughening by multiple crazing and perhaps allows to obtain the desired effect at lower rubber content. On the other hand, particle cavitation must certainly occur in order to induce the shear yielding of the matrix – prior to cavitation the extrinsic constraints and those imposed on the matrix deformation by well-bonded rubber particles do not allow for dilatation (as rubber is nearly incompressible), which in turn highly restricts deformation by shear, especially when sample is thick or in front of the notch or crack tip. The microvoids developed by cavitation help to alleviate these constraints and convert the stress state within interparticle ligaments from plane-strain towards plane-stress conditions, which corresponds to an increase in the shear component and thereby to reduction of the yield strength. Additionally, as the volume strain is released, the material sensitivity towards crazing is reduced. All of this might facilitate shear yielding in ligaments between particles, much less constrained now.

11.5.2 Criteria of Rubber Particle Cavitation

As discussed in the previous section, cavitation of rubber particles is practically necessary for toughening. In this section, some conditions important for cavitation to occur will be discussed.

The criteria for cavitation in polymers modified with rubbers were modeled by Lazzeri and Bucknall (Bucknall et al. 1994; Lazzeri and Bucknall 1993, 1995). They are based on energy release rate principles similar to those used in fracture mechanics. Void nucleation and expansion in elastomer particles are accompanied by the formation of a new surface, significant stretching of the surrounding layers of elastomer, and the stress relaxation in the adjacent matrix. All of these are driven by

the release of energy stored both in the particle itself and in the surrounding rigid matrix material. The model was simplified and did not account for any additional effects resulting in an energy barrier restricting void formation. The essential condition for void growth is that the volumetric strain energy release rate dU/dr must be greater than the rate at which energy is absorbed in increasing the surface area and stretching the adjacent layers of rubber. Considering the blend as an assembly of small volume elements, each consisting of a spherical elastomer particle of radius R which is surrounded by a rigid elastic shell of the outer radius Q (particle volume fraction is $\Phi_p = R^3/Q^3$), the total energy released upon cavitation can be calculated from the difference of potential energy of that element prior to and after cavitation (Lazzeri and Bucknall 1993). The simplified example in which a rubber particle of radius R is held at a fixed volume strain ε_v and forms a single void of radius r_{vd} can be described with the following equation:

$$U_p(r_{vd}) = \frac{2}{3}\pi R^3 K_R\left(\varepsilon_v - \frac{r_{vd}^3}{R^3}\right)^2 + 4\pi r_{vd}^2 \Gamma_r + 4\pi r_{vd}^3 G_R f(\lambda_f) \qquad (11.14)$$

where $U_p(r_{vd})$ is the potential energy of the rubber particle; r_{vd} is the radius of the cavity in the center of the particle; ε_v is the current volume strain of the particle, including the void; R is the radius of the particle; G_R, K_R are the shear and bulk moduli of the rubber; Γ_r is surface energy of that rubber; and λ_f is the extension ratio of the rubber at fracture in biaxial tension. The function $f(\lambda_f)$, which typically has a value close to 1, represents energy lost in tearing the thin layer of rubber that is very close to the expanding void surface, where $\lambda > \lambda_f \approx 10$.

Calculations based on this model demonstrated that the main parameter controlling cavitation is the size of rubber particles – the critical volume strain at cavitation, $\varepsilon_v(cav)$, increases as the particle size is decreased, principally because the strain energy release rate depends on the size of the local volume element. The model predicts that when the shear modulus of the rubber is small, the relationship between logarithms of critical volume strain at cavitation $\varepsilon_v(cav)$ and the particle diameter D should be approximately linear (Bucknall 1997, 2000), which, in fact, was confirmed by experimental data of PVC blends reported by Dompas et al. (1994a). They demonstrated that a decrease of particle size caused an increase of critical strain to a maximum value $\varepsilon_v(cav) = 0.0128$, where the specimens did not cavitate any longer and yielded before any cavitation happened. The observed dependence of $\log(\varepsilon_v(cav))$ on $\log(D)$ was almost linear and could be fitted with a straight line calculated with Eq. 11.14, although an upward shift in experimental $\varepsilon_v(cav)$ was seen, related most probably to several simplifying assumptions used for model formulation (Bucknall 2000). There are strong indications that similar relationships between D and $\varepsilon_v(cav)$ to the described above, predicted by Eq. 11.14, apply to other polymer blends containing soft rubber particles ($G_R \approx 0.1$ MPa) (Bucknall and Paul 2009). Apart from size, the other important factors which affect cavitation are the surface energy Γ_r (energy needed to create a new surface inside the rubber particle) and the shear modulus of the rubber G_R,
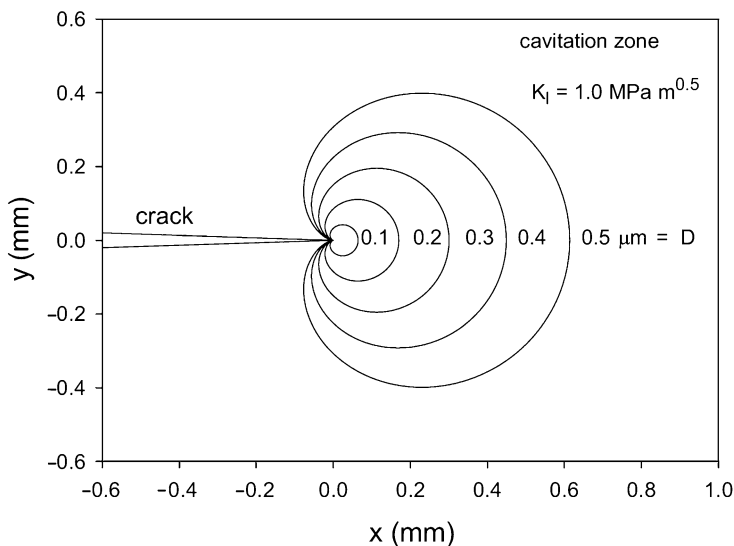
Fig. 11.18 Map of cavitated zone in plane-strain region, showing dependence of zone boundary on the particle diameter when $K_I = 1$ MPa m$^{0.5}$. Critical mean stresses calculated with bulk modulus K = 3GPa and data of Dompas et al. (Dompas and Groeninckx 1994) (From Bucknall and Paul (2009); reproduced with permission of Elsevier)

determining the work done in biaxial extension of the rubber shell upon void expansion. On the other hand, any additional energy barrier restricting formation of cavities, which was not taken into account in model calculations, would additionally increase critical volume strain and corresponding stress.

Figure 11.18 illustrates the effects of particle size on cavitation around a crack tip, calculated by Bucknall and Paul (2009) using Eq. 11.14 with $K_I = 1.0$ MPam$^{1/2}$ and ε_v(cav) from the line fitting the data of Dompas et al. (1994a). For fine particles the cavitated zone is very small, yet with increasing particle diameter, D, this zone expands distinctly outwards from the crack tip. Such behavior helps to explain observations that very small particles are not effective in toughening (Gaymans et al. 1990; Oshinski et al. 1992a, 1996b), which was usually interpreted as a result of an inability of very fine particle to cavitate. The results of calculations of Bucknall and Paul presented in Fig. 11.18 show that the difference in efficiency of toughening by fine and large particles can be explained without making an assumption that very small particles are unable to cavitate. According to these authors, problems arise simply because critical volume strain ε_v(cav) and stress are very high for fine particles, which limits noticeably the size of the cavitated yielded zone, which raises the probability of brittle fracture. In the limit, ε_v(cav) becomes so high that the void-free blend would yield under plane-strain conditions at the very high shear stress, still before reaching the particle cavitation stress. However, as the stress needed for craze nucleation is lower than the stress needed for shear yielding and so reached first, a craze will develop from the notch tip instead of shear zone

Fig. 11.19 Energy curves for a cavitating rubber particle, calculated using Eq. 11.14 in blends with D = 0.3 μm, Γ_r = 35 mJ/m^2, and ε_v = 0.255 %, showing the effect of varying rubber particle concentration at a critical particle size. Energy in aJ (atto-Joule; 1 aJ = 10^{-18} J) (From Bucknall and Paul (2013); reproduced with permission of Elsevier)
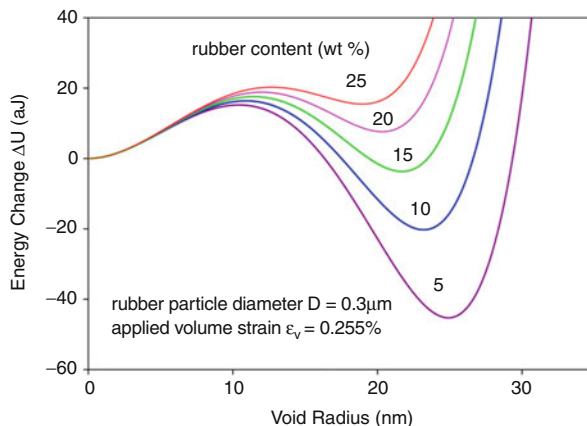
and a crack will be initiated before a significant amount of energy has been absorbed in ductile deformation by shear (Bucknall and Paul 2009). For a typical blend (Young's modulus E = 2 GPa and Poisson's ratio of v = 0.4), a stress intensity factor K_{IC} of 1.0 MPam$^{1/2}$ corresponds to a fracture surface energy G_{IC} = 420 J/m^2, which is sufficient to form and rupture a single mature craze. By contrast, increasing D (above about 0.03 μm (Bucknall and Paul 2009)) enables the particles to cavitate before reaching the yield point and consequently reduces the shear yield stress, which at this stage becomes a function of the volume fraction of cavitated particles (see Sect. 11.5.4).

Further calculations made by Bucknall and Paul (2013) illustrate additionally the influence of rubber concentration on cavitation, which is shown in Fig. 11.19. This figure compares curves of calculated energy change upon cavitation for blends containing various weight fractions of rubber particles, all with diameters of D = 0.3 μm. A fixed applied strain ε_v = 0.255 % was chosen for illustrating the sensitivity of the energy balance to the change in rubber content. It is clear in this example that blends containing up to 15 wt.% of rubber can cavitate at the specified applied volume strain but blends with 20 % or 25 wt.% rubber cannot, as there is no net energy fall: $\Delta U = U_p(r_{vd}) - U_p(0) > 0$. For these high rubber concentrations, the volume strain ε_v has to be increased in order to induce cavitation. Taking into account that increasing rubber concentration reduces the yield stress, the volume strain required for cavitation of such particles could be not reached before the yield point. This may indicate that the range of particle size ready to cavitate narrows with increasing rubber content.

Summarizing, the extent of cavitation and hence the level of toughness which can be achieved depend mainly on the particle size, although also partially on rubber concentration and its properties, as, e.g., shear modulus or surface energy, as well as on test conditions (especially temperature and strain rate). Cavitation resistance increases when either the shear modulus or the surface energy of the rubber is increased, similarly to the effect of reduced particle size. Most notably, increasing the shear modulus of the rubber phase due to cross-linking, change of

chemical composition, or simply reduction of the test temperature increases critical volume strain for cavitation $\varepsilon_v(cav)$, which eventually results in a reduction, sometimes dramatic, of fracture resistance of the blend (Gaymans 2000). The same shear modulus term accounts also for the brittle–ductile transition observed in many toughened polymers near T_g of the rubber phase (already discussed in Sect. 11.4.3.1), where G_R changes dramatically.

11.5.3 Shear Yielding

Analysis of the stress field and deformation behavior in front of the tip of sharp notch or crack allows to calculate principal stresses and estimates the size of the plastic zone ahead of the crack tip. Under assumption that the material near the crack tip is an elastic–plastic continuum, the radius of the plastic zone on the crack plane can be expressed, according to Irwin (1964):

$$r_p = \frac{1}{2\pi}\left(\frac{K_I}{m_p\sigma_{1y}}\right)^2 \tag{11.15}$$

where K_I is the stress intensity factor, σ_{1y} is the first principal stress at yield, and m_p is the plastic constraint factor, which reflects the amount of constraint on the developing plastic zone, created by the surrounding elastic material. This increases the stress necessary for the yield to occur above that needed in uniaxial tension, i.e.,

$$m_p = \frac{\sigma_e}{\sigma_y} \tag{11.16}$$

where σ_e and σ_y are the effective yield stress and the yield stress in uniaxial tension, respectively. The value of m_p depends upon the stress state around the crack tip. The value of $m_p = 1$ is for plane-stress conditions ($\sigma_3 = 0$), while according to Irwin and Paris (1971), the increased constraints in plane strain (where $\sigma_3 = v(\sigma_1 + \sigma_2)$ to the first approximation may be represented by assuming $m_p = \sqrt{3}$, which implies that the stress needed to yield in plane strain is higher than in uniaxial tension: σ_e (plane strain)$=\sqrt{3}\ \sigma_y$; thus, the radius of the plastic zone in plane strain is only one third or perhaps even less than that of plane stress. Another approach predicts the relation $m_p = 1/(1 - 2v)$, which for typical rigid polymer with the Poisson's ratio of $v = 0.4$ results in the size of the plastic zone under plane strain smaller than under plane stress by a factor of 25 (Bucknall and Paul 2009). The yield envelopes calculated for 80:20 PA6/rubber blend under the plane-stress and plane-strain conditions using the pressure-dependent von Mises criterion are shown in Fig. 11.20 (Bucknall and Paul 2009). The calculated sizes are probably underestimated because of simplified calculations, which have not allowed for stress redistribution sizes of real plastic zone in similar materials to be about double those shown in Fig. 11.20. Nevertheless, even after necessary adjustments, it appears clearly that the size of the yield
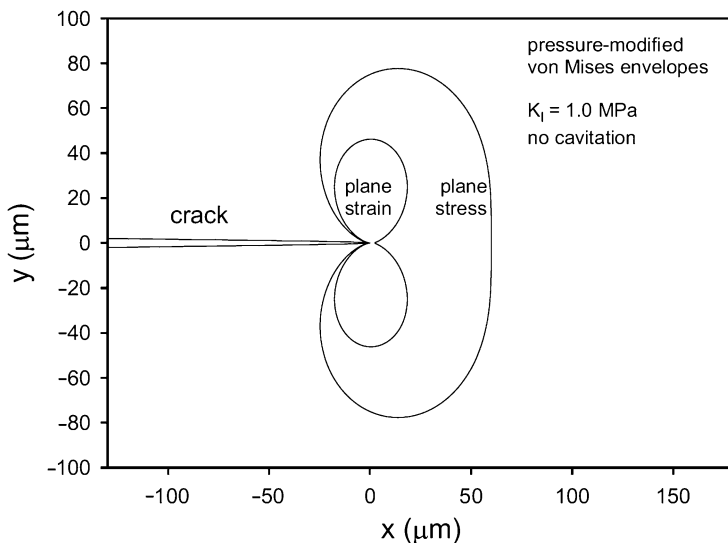
Fig. 11.20 Pressure-dependent von Mises yield envelopes under plane-stress and plane-strain condition of loading, calculated with $K_I = 1.0$ MPa m$^{0.5}$, for void-free 80:20 PA6/rubber blend with Poisson's ratio $v = 0.4$ and pressure coefficient $\mu = 0.36$ (From Bucknall and Paul (2009); reproduced with permission of Elsevier)

zone under plane strain is too small to enable a notched specimen to overcome its susceptibility to brittle fracture (Bucknall and Paul 2009).

Since a blend containing high concentration of cavitated rubber particles becomes cellular solid (porous) rather than continuous material, Eq. 11.15 does not apply to it any longer and any analysis of the plastic zone size must be based on yield criteria appropriate for the porous solid. Free from the constraints of continuum mechanics, the cavitated plastic zones formed in polymer blends are able to increase substantially in radius even under plane-strain conditions (Bucknall and Paul 2009).

The commonly used criterion for shear yielding in cavity-free rigid polymers is a pressure-modified von Mises criterion (Ward 1983):

$$\sigma_e \geq \sigma_{y0} + \mu P = \sigma_{y0} - \mu \sigma_m \qquad (11.17)$$

where σ_e is the effective stress, σ_{y0} is the yield stress in pure shear ($\sigma_m = 0$), μ is the pressure coefficient, P is pressure, and σ_m is the mean stress. The effective stress σ_e is given by

$$\sigma_e = \sqrt{\frac{(\sigma_1 - \sigma_2)^2 + (\sigma_2 - \sigma_3)^2 + (\sigma_3 - \sigma_1)^2}{2}} \qquad (11.18)$$

and the mean stress σ_m is defined as follows:

$$\sigma_m = -P = \frac{\sigma_1 + \sigma_2 + \sigma_3}{3} = K\,\varepsilon_v \tag{11.19}$$

where K is bulk modulus and ε_v is the volume strain. Typical values of K at room temperature are 3.5 GPa for a glassy polymer and 2.0 GPa for a rubber.

The presence of voids increases markedly the pressure sensitivity of the material. Gurson (1977a, b) modified the von Mises criterion to be used for porous solid that contains well-distributed small voids. He applied a continuum treatment to a cavitated ductile material containing a volume fraction Φ_{vd} of voids and obtained the following yield criterion:

$$\sigma_e \geq \sigma_{yt}\sqrt{1 - 2\Phi_{vd}\cosh\left(\frac{3\sigma_m}{2\sigma_{yt}}\right) + \Phi_{vd}^2} \tag{11.20}$$

where σ_{yt} is tensile yield stress of the rigid polymer matrix and Φ_{vd} is the volume fraction of voids. His analysis leads to the conclusion that yielding occurs through the formation of dilatation bands, which allows the original voids to expand as plastic flow proceeds in the intervening ligaments between voids.

By further modification of this approach to account for pressure sensitivity of the initial material, Bucknall and Paul (2009) obtained the following equation for pressure-sensitive material containing small voids, which can be applied to the description of a polymer blend in which all rubber particles have already fully cavitated:

$$\sigma_e \geq (\sigma_{yo} - \mu\sigma_m)\sqrt{1 - 2\Phi_{vd}\cosh\left(\frac{1.5\sigma_m}{\sigma_{yo} - \mu\sigma_m}\right) + \Phi_{vd}^2} \tag{11.21}$$

where $\sigma_{yt} = \sigma_{y0} - \mu\sigma_m$ is tensile yield stress of the rigid polymer matrix (pressure sensitive) and Φ_{vd} is the volume fraction of voids. For pure shear conditions ($\sigma_m = 0$), the above Eq. 11.21 reduces to the simple rule of mixtures:

$$\sigma_e = \sigma_{y0}(\Phi_{vd}) = \sigma_{y0}(0)(1 - \Phi_{vd}) \tag{11.22}$$

It was postulated (Bucknall and Paul 2009) that the same equation can be used also for the approximation of yield in pure shear of rubber-toughened blends, which contain only void-free rubber particles or the combination of cavitated and void-free particles with the total volume fraction of intact and cavitated particles ϕ replacing Φ_{vd} (pure shear):

$$\sigma_e = \sigma_{y0}(0)\,(1 - \phi) \tag{11.23}$$

Of course, this equation cannot be considered as a universal relationship, applicable also to other deformation modes. Other dependencies of the yield stress
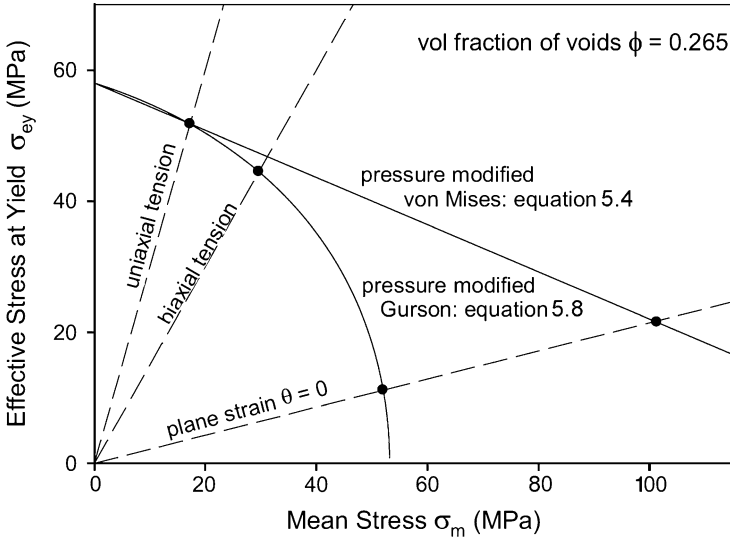
Fig. 11.21 Comparison between pressure-modified von Mises criterion for a void-free blend (Eq. 11.17 with $\mu = 0.36$) and the pressure-modified Gurson criterion for the same blend, now fully cavitated (Eq. 11.21) (From Bucknall and Paul (2009); reproduced with permission of Elsevier)

on concentration were presented in Sect. 11.4.3.1 (Eqs. 11.11 and 11.12) for uniaxial tension and compression and can be also considered in the context here. Both predict, however, a direct dependence of the yield stress on concentration as the Eq. 11.23 above.

Figure 11.21 illustrates the application of criteria of Eqs. 11.17 and 11.21 to shear yielding at the crack tip in a model blend of rigid polymer with 20 wt.% of soft rubber ($\phi = 0.265$) prior and after cavitation of the rubber particles, respectively. The plot was constructed by Bucknall and Paul (2009) with data of dry PA6 ($\nu = 0.4$, $\mu = 0.265$, $\sigma_{yt} = 70$ MPa) used for the matrix. Tensile stress of PA6 matrix $\sigma_{yt} = 70$ MPa corresponds to yield stress in pure shear of $\sigma_{yo} = 78.4$ MPa. Blending with the soft rubber reduces those to $\sigma_{yt} = 51.5$ MPa and $\sigma_{y0} = 57.6$ MPa, respectively. Under plane strain, the construction line meets the pressure-modified von Mises curve (calculated with Eq. 11.17 at a mean stress of $\sigma_m = 100.4$ MPa where $\sigma_1 = \sigma_2 = 107.6$ MPa and $\sigma_3 = \nu(\sigma_1 + \sigma_2) = 86.0$ MPa) and $\sigma_e = 21.5$ MPa). This shows that pressure sensitivity helps to alleviate the adverse effects of notch tip constraint on shear yielding. The lower curve in Fig. 11.21 calculated for the same blend but with all rubber particles cavitated (Eq. 11.21) demonstrates a significant departure from the curve of non-cavitated blend, but practically only in the plane-strain conditions. This means that differences between voids and well-bonded soft particles become prominent only when the material is subjected to large dilatational stresses as in the presence of triaxial stress (plane strain). The curve calculated for the fully cavitated blend intersects the plane-strain construction line at $\sigma_m = 52.1$ MPa and $\sigma_e = 11.1$ MPa (corresponding to the stress state of

$\sigma_1 = \sigma_2 = 55.8$ MPa, and $\sigma_3 = 44.7$ MPa), i.e., well below the yield stress for the same blend with non-cavitated, continuous rubber particles.

The results presented in Fig. 11.21 are very meaningful as they clarify some of the key issues concerning the contribution of void formation to toughness in polymer blends. It appears that the cavitation is extremely important in notched specimens because it allows the blend to yield under plane-strain conditions at still moderate stresses due to increased sensitivity to the mean stress. It implies that this modification of yielding does not result from eliminating geometrical constraints and converting a state of plane-strain to plane-stress state, as it has been frequently postulated in the past (Bucknall and Paul 2009).

Cavitation enables the plastic zone, including the plane-strain region in front of the notch or crack tip, to react to dilatational stresses by expansion in volume and an increase in radius. To get the maximum toughness, two conditions must be satisfied: a widespread cavitation ahead of the crack tip and extensive involvement of the matrix in plastic deformation. To engage the matrix fully in an energy absorption through deformation, shear yielding should be the dominant mechanism of deformation. The chains must be long enough to prevent premature failure and allow accommodation of high strain. Moreover, in most cases, participation of the rubber phase in the strain-hardening mechanism is also required. To achieve this, the rubber should be strongly bonded to the matrix and to any internal sub-inclusions, when particles have heterogeneous morphology. This implies that the formation of voids through internal cavitation, especially multiple, resulting in formation of fibrils inside particle, is more efficient in toughening than particle debonding, as internal cavitation allows for higher load transfer into particle and hence better stabilization of deformation owing participation of the elastomer phase in strain hardening. The range of cavitation and thereby the level of achieved toughness depends primarily on the particle size and additionally on the degree of cross-linking of the rubber phase, surface energy, and test conditions (temperature and strain rate).

11.5.4 Dilatation Bands

The mechanism for rubber toughening in non-crazing polymers has been explained by Lazzeri and Bucknall (1993, 1995, 2000) who demonstrated that rubber particles can facilitate formation of microvoids and activate dilatation yielding in the deformed zone close to the fracture surface. They concluded that yielding in the blend sample occurs through the formation of dilatation bands, containing cavitated rubber particles, which allows the original voids to expand as plastic flow develops in the band and to relieve the dilatational stress. There is broad evidence that rubber particle cavitation in several different polymers is indeed concentrated within band-like zones of high shear strain (Lazzeri and Bucknall 1995; Sue 1992). Similar cavitated yield zones have been reported in the literature concerning metals, where they have been referred to as "dilatation bands." Such dilatation bands form because when an element of material is restrained in two dimensions, the only

Fig. 11.22 (**a**) Transmission electron micrograph of an 0s0₄-stained ultrathin section from a fractured Charpy specimen of rubber-toughened PA6, showing a dilatation band. (**b**) Sketch showing the location of band in the broken Charpy bar and the strains within the band (From Lazzeri and Bucknall (1995); reproduced with permission of Elsevier)
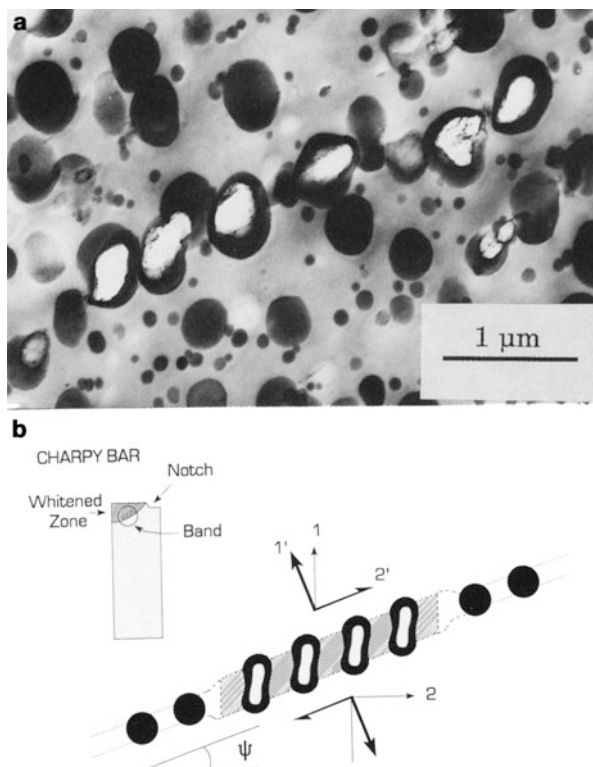
modes of deformation compatible with the imposed constraints are simple shear parallel to the plane and volume dilatation normal to it. The presence of both results in formation of a dilatation band, as illustrated in Fig. 11.22.

The inclination angle Ψ of the band to the principal tensile axis depends on the sensitivity of the yield stress to the mean stress (pressure) – cf. Eq. 11.17. The following equation was obtained (Lazzeri and Bucknall 1993):

$$\cos 2\Psi = -\frac{2\mu}{3}\frac{(\sigma_o - \mu\sigma_m)}{(\sigma_1 - \sigma_2)} \tag{11.24}$$

where Ψ is the inclination angle of the band, μ = pressure sensitivity coefficient, $\sigma_m = -P$ is the mean stress, and σ_1 and σ_2 are principal stresses in the deformation plane. For anisotropic material not sensitive to pressure, $\mu = 0$, and containing no voids, the angle between the principal tensile axis and the normal to the band is $\Psi = 45°$. For polymers, in which yielding depends on pressure, Ψ is about $38°$. Introduction of voids into the shear bands through cavitation increases significantly the pressure dependence (see the Sect. 11.5.3) and leads to further reduction in Ψ, so that dilatation bands respond to stress by both increasing thickness and

undergoing shear in a plane. The inclination angle eventually falls to zero when the void volume fraction reaches 0.53 (Lazzeri and Bucknall 1993). This rotation of the band plane reduces resistance to crack tip opening; at the crack tip plane, $\Theta = 0^\circ$, yielding occurs entirely in response to tensile stresses applied normal to the bands, which in that respect may resemble crazes. Some examples of craze-like cavitated shear bands have been reported for rubber-toughened epoxy by Sue (1992).

11.5.5 Crazing

Multiple crazing is the basic deformation mechanism of all disperse systems with an amorphous brittle matrix prone to crazing, including rubber-toughened grades of PS, SAN, PMMA, and related glassy polymers. On the other hand, it does not seem to play a significant role in the process of energy absorption in the blends based on ductile glassy polymers (such as PC), semicrystalline polymers, or thermosetting resins. In the above mentioned blends of amorphous brittle polymers, the matrix is a brittle thermoplastic, which tends to form crazes at strains between 0.3 % and 1 % and fractures shortly afterwards. Although macroscopically brittle, these polymers appear ductile on the length scale below 1 μm, within a single craze, and would absorb a considerable amount of energy if this ductility could be extended over a large volume of the material. Multiple crazing, first observed in HIPS, is an extensive crazing in which individual crazes are nucleated by numerous rubber particles dispersed in the matrix. Those rubber particles are also able to terminate crazes. As a result, large number of short crazes is developed in the material, which engages much more of its volume in plastic deformation events, and consequently notably higher energy dissipation is observed.

The soft rubber particles dispersed in glassy matrix act as stress concentrators (see Sect. 11.4.3.1) and like microscopic surface scratches can constitute the sites of effective craze initiation. Bubeck et al. (1991) used real-time X-ray measurements on HIPS to show that crazing of the matrix under tensile impact conditions is actually preceded by cavitation of the rubber particles. Cavities formed within the rubber particles can thus be seen as the real nuclei for the craze growth, which occurs through the meniscus instability mechanism proposed by Argon and Salama (1977). Cavitated particles initiate crazes in the immediate matrix adjacent to their equatorial regions. The crazes propagate then outwards through the matrix perpendicularly to the direction of principal tensile stress until termination by other rubber particle encountered along the propagation path. This produces secondary cavitation within encountered particle and crazing around. At higher rubber concentration (above approximately 15 vol.%), the stress concentration fields of neighboring particles overlap, which results in stress concentrations higher than around isolated particles. In such interparticle zones, broader crazes and craze bands develop roughly perpendicularly to the principal tensile stress and propagate from one particle to the other, cf. Fig. 11.8 in Sect. 11.4.3.

One of the serious difficulties in developing a quantitative description of toughening with elastomer particles is the lack of a suitable criterion for craze initiation.

Several criteria were developed in the past by Sternstein and Ongchin (1969), Oxborough and Bowden (1973), and Argon and Hannoosh (Argon 2011; Argon and Hannoosh 1977) suffer from serious flaws (Bucknall 2007a). Recently Bucknall (2007a, b) demonstrated that the craze initiation can be considered as a frustrated fracture process which actually falls within the scope of linear elastic fracture mechanics (LEFM); therefore, the Griffith equation, modified accordingly, can be regarded as an appropriate criterion for craze initiation. It is evidenced that rubber particles can be effective craze initiation sites, e.g., microscopic surface scratches. In order to act as craze initiators, the elastomer particle must cavitate internally first to form rubber-reinforced spherical holes, in which the rubber provides significant reinforcement, but only when it becomes highly strained. Such a behavior pattern was confirmed experimentally (Bubeck et al. 1991). Using LEFM approach and treating cavitated rubber particles as isolated spherical voids embedded in a homogeneous matrix, the following equation of the critical stress for craze initiation by cavitated particle can be formulated:

$$\sigma_{1craze} = \sqrt{\frac{\pi E G_{\text{craze}}}{2(1 - v^2) D}} \qquad (13.25)$$

where σ_{1craze} is the critical tensile stress for craze initiation, E is the matrix Young's modulus, G_{craze} is the energy absorbed in forming unit area of a new craze, and D is the diameter of the cavitated particle. Typically, in well-prepared tensile specimens of glassy crazable polymer (plain, not modified), the critical stress $\sigma_{1craze} \approx 20$–50 MPa. It can be estimated that G_{craze} is small, between 0.1 and 1 J/m^2.

Equation 11.25 becomes inaccurate with increasing rubber concentration, ϕ, and the average stress in the matrix raising much above the applied tensile stress σ_1. A simple solution might be to apply the rule of mixtures and assume the crazing stress is proportional to $(1 - \phi)$. However, comparison with experimental data demonstrates that this method leads to a substantial overestimation of the yield stress for HIPS blends, where multiple crazing is the dominant mechanism of deformation. Bucknall and Paul (2013) found that much better fitting the data, for both HIPS (Bucknall et al. 1986) and ABS (Ricco et al. 1985), can be obtained by using the effective area model proposed by Ishai and Cohen (1968), who assumed that cracks and shear bands tend to follow paths of minimum resistance through heterogeneous or porous solids and formulated the dependence of stress on rubber concentration (cf. Eq. 11.11 in Sect. 11.4.3.1). Applying this model to materials in which multiple crazing is the dominant mechanism, the critical tensile stress can be obtained:

$$\sigma_{1craze}(\phi) = \left(1 - \pi \left(\frac{3\phi}{4\pi}\right)^{\frac{2}{3}}\right) \sigma_{1craze}(0) = \left(1 - 1.21\phi^{\frac{2}{3}}\right) \sqrt{\frac{\pi E G_{\text{craze}}}{2(1 - v^2) D}} \quad (11.26)$$

where $\sigma_{1craze}(\phi)$ is the stress at which crazes propagate and thicken in a blend containing volume fraction ϕ of rubber particles, and $\sigma_{1craze}(0)$ is the limiting crazing stress at very low rubber contents.
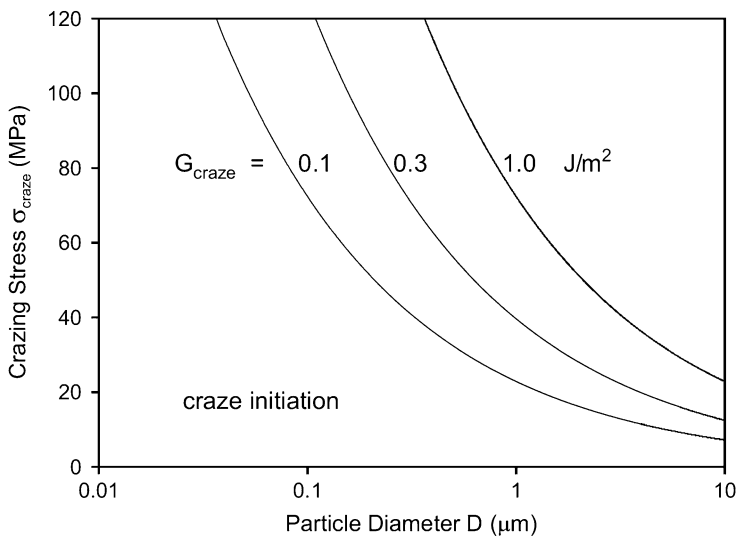
Fig. 11.23 Critical tensile stress for craze initiation as a function of (cavitated) rubber particle diameter, calculated using Eq. 11.26 with three different values of G_{craze}, the specific energy of craze initiation (From Bucknall and Paul (2009); reproduced with permission of Elsevier)

Equations 11.25 and 11.26 predict the proportionality of the critical craze initiation stress on the inverse square root of the particle diameter. It allows to estimate that σ_{1craze} decreases with increasing particle diameter from above 100 MPa to the level of below 20 MPa for large particles, exceeding 1 μm in diameter (typical values of E = 2.8GPa and v = 0.4 assumed for calculation) (Bucknall and Paul 2009); see Fig. 11.23 illustrating strong dependence of the critical stress for craze formation on particle size. That size dependence implies that for particles which are large enough, σ_{craze} must eventually decrease below the shear yield stress of the fully cavitated blend, which becomes independent of D after complete cavitation of particles (cf. Sect. 11.5.3). In this way, crazing can emerge as the dominating mechanism for large particles, in contrast to smaller particles which upon cavitation will initiate preferably the shear yielding in the same matrix. The process begins with primary cavitation of larger particles, which then initiate crazes that propagate outwards. These can induce secondary cavitation and crazing in other particles encountered by a propagating craze. Such a picture is supported by experimental evidence that in many blends tested at impact conditions, crazing is accompanied by dilatational shear yielding and that increasing particle size suppresses shear yielding while promoting crazing as an active mechanism (Bucknall 1977; Bucknall and Paul 2009). The exception is HIPS, which demonstrates almost no signs of ductility under tensile load.

Crazing is a mechanism of plastic deformation that is extremely localized. Even when the number of crazes in the sample is substantially increased, as in the case of multiple crazing in rubber-toughened blends, their early stages of development

engage much less of the matrix volume into plastic deformation than the shear yielding mechanism. Therefore, less energy is usually dissipated in crazing, and toughness improvement may appear below that demanded. Moreover, crazes, if have not been stabilized sufficiently, can quickly degrade to cracks, which inevitably leads to a premature failure. As a result, toughness of the blend which responds to load with crazing is usually lower compared to the blend responding with shear yielding. This explains the appearance of an upper ductile–brittle transition (see section "Rubber Concentration" and Figs. 11.26 and 11.27), observed for some blends, in which toughness falls down as the particle diameter increases. This transition is presumably a result of the change of active deformation mechanism from shear yielding, which is promoted by smaller particles, to crazing which is related to large particles present in the blend.

For effective performance of multiple crazing as the toughening mechanism, the craze growth must be controlled and stabilized. Crazes can be stabilized efficiently by rubber particles, provided these particles can transmit loads and consequently participate in strain hardening of the blend. The particles, especially large ones, tend to cavitate prior to craze initiation and their ability to transmit load depends strongly on their morphology after cavitation. From this point of view, the worst case is when particles are weakly bonded to the matrix and tend to debond from the matrix rather than cavitate internally. Debonding prevents any stress transfer from the matrix into the particles, which then cannot participate in the strain-hardening process and therefore are not able to stabilize craze. As a result, such material with particles debonded usually fractures shortly after craze initiation in nearly brittle fashion. The homogeneous particles, which are well bonded to the matrix, tend to cavitate internally in a single site and form a single void which is surrounded by the continuous rubber shell. Their ability to transfer stress is much higher than debonded particles, but participation in strain hardening is moderate, as the continuous rubber shell does not deform uniformly and eventually fails by progressive tearing with advance of the strain (Bucknall 2000). As a result, cracks can develop relatively early, and toughening effect may be unsatisfactory, especially when particles are large, e.g., few microns in diameter (which is just the optimum size for craze initiation). The most advantageous situation is when the particles are not only bonded well to the matrix but show additionally heterogeneous structure: either contain harder sub-inclusions dispersed inside or have a core–shell morphology. When the internal sub-inclusions or the core is bonded well with the surrounding rubbery phase, then cavitation is frequently followed by a stable fibrillation of the rubber. These fibrils, strongly bonded both to the core or sub-inclusion and to the surrounding matrix matter, can deform uniformly by stretching to high strains, close to the ultimate stretch of the rubber. This enables an effective participation of rubber in strain hardening which greatly helps to stabilize crazes. Consequently, properly formulated and balanced blends made with heterogeneous particles, which are ready to cavitate and form internal fibrils and thereby able to stabilize crazes, show frequently quite large elongations to break, sometimes up to above 50 %, and can even demonstrate a super-tough behavior at impact conditions.

11.5.6 Structure–Property Relationships

Important factors were found to affect the fracture behavior. These can be divided into three main groups related to:

- Matrix material:
  - Molecular weight
  - Entanglement density
  - Ability to crystallization and crystallinity
- Dispersed-phase material:
  - The type of the elastomer
  - Rubber modulus
  - Interfacial bonding
  - Concentration
  - Particle size/interparticle distance
- Sample and test parameters:
  - Sample shape and dimensions
  - Test method (deformation mode, presence of notch)
  - Test speed
  - Test temperature

Below, a short description of these parameters related to the properties of the matrix and the modifier dispersed in the matrix is presented. Sample and test parameters will be not addressed here.

11.5.6.1 Matrix Properties

Toughening of the polymer blend depends on the deformation mechanisms that dominate mechanical response of the host polymer (matrix), where most of energy is dissipated during deformation and fracture. These mechanisms are determined generally by the chemical structure of that polymer, including the repeat unit, chain architecture, molecular weight, and its distribution. Apart from crystal plasticity governing deformation of polymer crystals, the main deformation processes in polymers are shearing and crazing. Each of these mechanisms allows for different level of toughening, also because the starting level, i.e., the toughness of the pristine host polymer, is very different for brittle crazable polymers and quasi-ductile polymers which tend to deform by shear yielding. The selection of the active deformation mechanisms depends principally on details of the matrix chemistry (Bucknall 1977). As already discussed in Sect. 11.2, if the chains of the matrix polymer demonstrate low entanglement density and are stiff under the test conditions, like in PS, then crazing is promoted in tensile loading. On the other hand, if the chains are much more flexible and demonstrate higher entanglement density, then the shear deformation initiated by shear yielding is the dominant mechanism, as, e.g., in PC or PVC deformed at room temperature. These polymers exhibit secondary relaxation processes below their glass transition temperature. These relaxation transitions indicate some limited segmental mobility of the chain backbone which become allowed at temperature range between the lower, secondary relaxation and the glass transition temperature. These localized main-chain motions

facilitate parts of the macromolecules to slide past each other and initiate shear deformation when material is loaded. As a consequence, these polymers can exhibit ductile behavior already below their glass transition temperature. Temperature of the secondary relaxation determines then the brittle–ductile transition temperature (Kausch 1987). On the other hand, some of stiff glassy polymers like PS or SAN lack this type of secondary relaxation process below their T_g and consequently are not able to shear at the desired scale and deform at room temperature preferentially by crazing, instead. If this energy dissipating craze mechanism is not stabilized properly, e.g., by dispersed rubber particles, it leads shortly to crack formation and brittle fracture. PMMA, with a mobility of the side groups beginning near room temperature and also mobility of parts of the main chain slightly above room temperature (as indicated by the secondary relaxation process at 50°C), appears at room temperature to be in the intermediate range and can deform by shear yielding, by crazing, or by both mechanisms simultaneously, depending on particulate test conditions. Generally, crazing seems to dominate in tension at low temperatures and/or at high deformation rates, when the molecules have very limited time to rearrange under the stress, and also at conditions of triaxial tensile stress. In contrast to these situations resulting in brittleness, when enough time is given for possible chain rearrangement (e.g., at higher temperature, above the secondary relaxation temperature, and/or at low deformation rates), the polymer tends to yield in shear.

The details of the matrix chemistry determine not only the stiffness of the chain but also the tendency to form entanglements. Again, as discussed in Sect. 11.2, the density of chain entanglements, generally related to chain stiffness (cf. Eq. 11.4), influences markedly the choice of the deformation mechanism: low entanglement density promotes crazing, while polymers exhibiting high entanglement density tend to deform by shear yielding. Both the chain stiffness and entanglement density are intrinsic properties of the chains and therefore are difficult to modify by physical methods without interfering chain chemistry. The entanglement density can be increased, and thus vulnerability to crazing reduced, practically only by blending a polymer with another polymer, which is fully miscible with it and demonstrates higher flexibility. That blending leads to the formation of the uniform network consisting of stiff and flexible chains, and characterized by increased overall entanglement density. Such modification is possible for only a few polymer pairs that demonstrate complete miscibility, as, e.g., PS and PPO (cf. Fig. 11.1).

Polymers that deform preferentially by crazing demonstrate usually low fracture toughness. This toughness can be enhanced quite substantially by a suitable modification, e.g., by adding an elastomer, but the resulting toughness of the modified material, although much increased compared to the pristine polymer, can be still lower than the toughness of many quasi-ductile polymers that tend to deform by shear yielding rather than crazing. These quasi-ductile polymers, in general, demonstrate significantly higher initial toughness than brittle, crazable polymers and usually are also much more receptive for toughening. As a result, super-tough materials can be formulated on the basis of those polymers easier than using crazable polymers. Generally speaking, when a broad range of thermoplastic matrix

Fig. 11.24 Brittle-to-ductile transition temperature as a function of matrix molecular weight, 30 wt.% PP-CaCO$_3$ composites (From Zuiderduin et al. (2003); reproduced with permission of Elsevier)
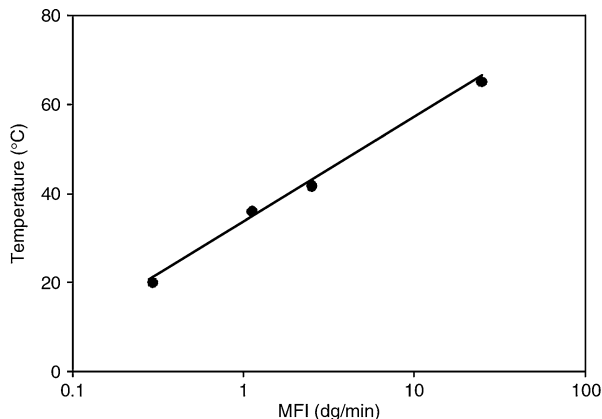
polymers are examined, the observation is that the toughest rubber-modified materials will be those which possess the toughest matrices (Bucknall 1977).

Besides the stiffness of the chain and entanglement density, the molecular weight appears also an important factor (Kausch 1991) as it influences the properties of the molecular network, important for an initiation and development of both crazing and shear yielding. Moreover, polymers of high molecular weight demonstrate usually an increased fracture stress relative to the yield stress and the brittle-to-ductile transition shifted to a lower temperature. This relationship can be illustrated by an example of semicrystalline polypropylene (here modified with rigid particles) shown in Fig. 11.24. It can be observed there that an increasing molecular weight, depicted by decreasing melt flow index (MFI), results in the shift of the brittle–ductile transition towards lower temperature (Zuiderduin et al. 2003). Similar dependence of T_{BD} on molecular weight was observed also in various blends with elastomers (Dijkstra and Gaymans 1994b; Oshinski et al. 1996a, b, d; van Der Wal et al. 1998).

The chemical structure of the polymer, including the structure of the repeat unit, chain architecture, and molecular weight determine also the ability of the polymer to crystallization. The presence of crystalline phase influences deeply the toughness of the polymer as well as deformation mechanisms governing it, as the polymer crystals are allowed to absorb energy upon their deformation according to typical mechanisms of crystal plasticity. Moreover, they can facilitate additional relaxation modes of the amorphous phase which can simplify shear yielding of the amorphous component. The crystalline regions in semicrystalline polymers constitute the physical cross-links that stabilize and hold material together, particularly above its glass transition temperature. Above T_g, the modulus and the yield strength increase with increasing crystallinity of the matrix (Ward 1983). Below T_g, the effect of crystallinity on the modulus and yield strength is much smaller as the number of crystalline cross-links is small compared to the number of frozen (immobilized) entanglements, which act now similarly to permanent cross-links. Increasing crystallinity has a strong negative effect on the brittle-to-ductile transition, causing an increase of T_{BD} (van Der Wal et al. 1998).

The yield stress in a semicrystalline polymer increases with increasing crystallinity as well as with increasing lamellar thickness, which, in turn, is controlled by the temperature at which crystallization had occurred (Kazmierczak et al. 2005; Sirotkin and Brooks 2001; Ward 1983). Moreover, crystallization leads frequently to an increase of the entanglement density in the amorphous phase, as most of the entanglements were not resolved by crystallization but merely swept into amorphous interlamellar regions (Strobl 1997), especially when the molecular weight of polymer is high. For obtaining high toughness, the crystallinity level must be carefully balanced, since too high crystallinity can constrain excessively deformation of the amorphous component, which would manifest in an increase of T_{BD} and eventually lead to material embrittlement. On the other hand, the balance of all properties is of practical interest. Usually, it is demanded to have high ductility combined with a possibly high modulus and high yield strength. A highly crystalline polymer, demonstrating relative high modulus but being more brittle than its low crystallinity counterpart, can be successfully modified to obtain material that exhibits low temperature ductility by adding more rubber. In practice, the best balance of properties is obtained just with highly crystalline grades. As blending with a second polymer can in some cases modify significantly crystallization kinetic of the matrix as well as the resultant lamellar thickness and degree of crystallinity (Bartczak et al. 1995), this factor must be also taken into account when selecting the type and grade of the rubber to be used for toughening of a particular polymer. Also the processing conditions, especially the cooling rate, must be controlled to prevent an excessively high crystallinity. However, these effects are minor as compared to others, as, e.g., those related to the rubber content or its average particle size.

11.5.6.2 Dispersed-Phase Parameters
The Type of Elastomers
The function of the dispersed-phase material that in most instances is an elastomer is to induce an adequate toughening mechanism in order to shift the T_{BD} temperature down and increase notably the toughness of the material above T_{BD}. Therefore, it is expected that the choice of the elastomer type is important. It appears that the type of rubber may have a little influence on the notched Izod impact strength in the tough region, but give a strong effect on the temperature of brittle-to-ductile transition, T_{BD}, as it was observed by Borggreve et al. (1989b) in PA6 blended with various elastomers (Fig. 11.25).

A good correlation between T_{BD} and the modulus of an elastomer was found by Gaymans et al. (1990) in PA6 modified with olefinic rubbers: T_{BD} decreases steadily with rubber modulus (all at constant rubber concentration and average particle size). The volume strain experiments (Borggreve et al. 1989a; Bucknall et al. 1989) demonstrated that the blends with the highest impact resistance cavitated most easily. The correlation of T_{BD} and modulus is possibly due to both the cavitational stress and the tensile modulus being related to the cohesive energy density of the elastomer.

The type and grade of elastomer, through its chemical composition, molecular weight, and viscosity, determine miscibility with the matrix, the state of dispersion,

Fig. 11.25 Temperature of brittle–tough transition as a function of the weight-average particle size for blends of PA6 and 10 wt.% rubber, with different types of rubbers: ■, EPDM; +, EPR; ×, LDPE; ▲, Keltaflex®; ●, polyester TPE (From Borggreve et al. (1989b); reproduced with permission of Elsevier)
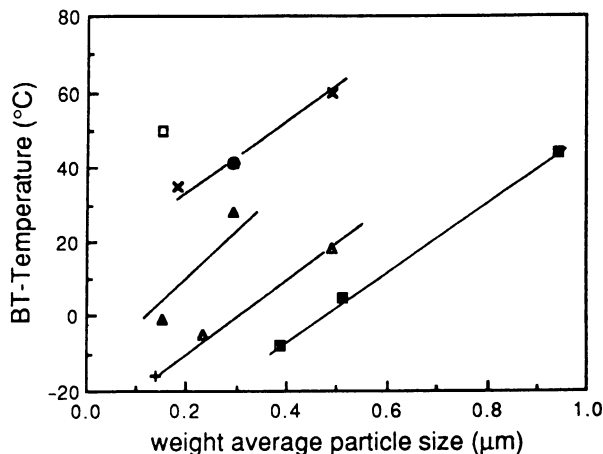
and the interfacial strength between rubber particles and the matrix, which in turn influence profoundly the impact behavior of the blend. The toughening effect is additionally dependent on the glass transition temperature of the rubber, as below T_g the cavitation stress increases drastically, so that rubber particles do not cavitate and consequently are not able to activate any toughening mechanism.

There are a great variety of elastomers applied to improve toughness of engineering polymers, including polyisoprene, butadiene elastomers (e.g., polybutadiene, styrene–butadiene, or butadiene–acrylonitrile copolymers), olefinic elastomers (e.g., ethylene–propylene, ethylene–octene-1 copolymers), styrene-butadiene-styrene (SBS), or styrene–ethylene–butene-1–styrene (SEBS) block copolymers, ionomers, polyurethanes, and many others, also functionalized with various groups, like maleic anhydride (MA) or glycidyl methacrylate (GMA), used for reactive extrusion. Elastomers used as toughness modifiers for various engineering polymers were reviewed, e.g., by Kesskula and Paul (1994). As an example, in Table 11.2 a survey of elastomers and compatibilization techniques tested for polyamides is presented (Akkapeddi 2001). Due to the polar nature of polyamides and apolar nature of elastomers, obtaining a very small rubber particles (0.2–0.4 μm in diameter) and their good dispersion, necessary for toughening of polyamides, is not easy and usually requires an adequate compatibilization, mainly through a reactive blending process, in order to produce blends containing appropriate small rubber particles.

Rubber Modulus

Because of very low stiffness, the rubber dispersed in the rigid matrix causes a decrease of the modulus and the yield strength of the blend. An extent of reduction depends, however, on the concentration of the rubber, rather than on its type or elastic properties (provided rubber is not highly cross-linked), since modulus of practically all elastomers above their glass transition is very much lower than modulus of the rigid matrix.

Table 11.2 Some common reactive rubbers and tougheners for polyamides (From Akkapeddi 2001)

Reactive rubber/toughener	Functionality	Reactivity	Other features
Maleic anhydride grafted ("maleated"), ethylene–propylene rubber (m-EPR)	Anhydride 0.3–0.9 % MA	High reactivity with the amine (NH_2) end group of PA	Amorphous rubber, low T_g leads to high-impact toughness down to –40 °C
Maleated, styrene–ethylene/butylene–styrene block copolymer rubber (m-SEBS)	Anhydride 0.5–2 % MA	High reactivity with the amine (NH_2) end group of PA	Amorphous rubber, low T_g leads to high-impact toughness down to –40 °C
Ethylene–ethyl acrylate–maleic anhydride (E-EA-MA) terpolymer	Anhydride 0.3–3 % MA	High reactivity with the amine (NH_2) end group of PA	Moderate T_g limits low-temperature toughness
Zinc neutralized, ethylene–methacrylic acid copolymer ionomer (E-MAA, Zn)	Zinc carboxylate, carboxylic acid	Low reactivity with amine but good polar interaction of Zn with amide and amine groups (interfacial complexation)	T_g and hardness limit low-temperature toughness; good solvent resistance
Zinc neutralized, ethylene–butyl acrylate–methacrylic acid terpolymer ionomer (E-BA-MAA, Zn)	Zinc carboxylate, carboxylic acid	Same as above	Low T_g and high-impact modification efficiency
Ethylene–glycidyl methacrylate copolymer (E-GMA)	Epoxide 3–8 % GMA	Moderate high reactivity with carboxyl group of PA	T_g and hardness limit achievable toughness; cross-linking tendency
Ethylene–ethyl acrylate–glycidyl methacrylate terpolymer (E-EA-GMA)	Epoxide 1–8 % GMA	Moderate high reactivity with carboxyl group of PA	Lower T_g, better impact; high viscosity
Acrylate core–shell rubber, functionalized	Carboxyl	Low reactivity with amine	Small rubber particle (<0.5 μm) aggregation
Ethylene–acrylic acid copolymers (E-AA)	Carboxyl	Low reactivity with amine	Not rubbery enough; modest impacts
Ethylene–ethyl acrylate or butyl acrylate copolymers (E-EA or E-BA)	Ester	No reactivity with amine	No impact improvement. Used only as codiluent

The stiffness of the rubber relative to the matrix determines the intensity of stress concentrations around rubber particles upon sample loading prior to their cavitation, as discussed in Sect. 11.4.3.1. The stress concentrations at the particle surface reach values very close to 2 already when G_R/G_M goes below 0.1 and are only slightly higher when G_R/G_M decreases below 0.01. That ratio of the moduli $G_R/G_M < 0.1$ facilitating high level of stress concentrations is easily reached for most of the rubber–matrix pairs at temperatures above T_g of the rubber. The situation changes when temperature decreases below T_g: the stress concentrations

diminish and additionally the stress required to induce cavitation in a glassy now particles increases dramatically, which practically inhibits any internal cavitation of particles and leads to the termination of the rubber toughening effect. Under impact loading conditions, the modulus is increased additionally due to high deformation rate and, therefore, the ductile-to-brittle transition is shifted to the "impact brittle point," which is about $10^{\circ}C$ above T_g (Bergen 1968). The impact strength can decrease then even below the level of unmodified material (see Sect. 11.4.3.1).

The modulus of the rubber can be increased notably also by cross-linking, either intentional or induced by material aging. It has long been known that some cross-linking is necessary to preserve the structure of the particles and avoid their coalescence at further stages of material processing (compression molding, injection molding, etc.). Bucknall (1977) reasoned that light cross-linking of the rubber, which does not increase significantly its modulus, is desirable also for other reasons: as during impact loading the rubber cavitates and then undergoes high strains, the light cross-linking would allow the rubber to reach high strains by fibrillation rather than of expansion of the shell around a single void in the center of the particle, and the fibrils would then participate more effectively in stabilization of the matrix deformation by strain hardening and help to avoid a premature fracture. On the other hand, excessive cross-linking impairs fracture resistance, notably by reducing notched impact strength. High levels of cross-linking shift T_g of the rubber highly upwards. Moreover, it results in a dense molecular network leading to a significant increase of the cavitation stress and serious reduction of the ultimate stretch. Therefore, a decrease of toughness of the blend with increasing cross-link density of the rubber can be expected: a heavy cross-linking should suppress substantially cavitation of rubber particles, and as a consequence, the impact strength would decrease either. Experimental results for PA6/SBS blends with different degree of rubber cross-linking, obtained by Suo et al. (1993), supported this view. The same, sometimes even dramatic, decrease of the impact strength can be a result of an excessive cross-linking which has occurred unwanted on improper processing or when material was exposed to prolonged sunshine during its outdoor use. It is known that HIPS and ABS can embrittle seriously if they have been processed too long or at too high temperatures, which leads to excessive thermal cross-linking of the rubbery phase. Embrittlement was also observed if the rubbery phase in the particles were intentionally cross-linked, either chemically or by radiation (Steenbrink et al. 1998; Suo et al. 1993). Similarly, these and other rubber-modified materials are known to turn brittle after long exposure to UV light or sunshine.

Structure of the Rubber Particles

Internal structure of the rubber particles is very important from the point of view of both initiation and stabilization of the matrix deformation. Generally, three types of rubber particles are used for toughening. In HIPS and solution ABS, salami particles obtained during polymerization process are preferred. These particles contain much occluded matrix so that the particles are sufficiently large for initiating crazing, while the rubber content is relatively low, which limits the

decrease of Young's modulus. The crazes are initiated near the equatorial region of the rubber particles, perpendicular to the tensile stress direction, as shown in Fig. 11.8. In this region, the normal stress component of the stress tensor is the highest.

Core–shell particles are used frequently with transparent polymer matrices. In this type of particle, the core is very often formed from a material similar or identical to the matrix and is covered with a relatively thin rubbery shell, which is grafted with an outer second shell of the polymer identical to the matrix. If the thickness of the rubber shell is small compared to the wavelength of light, then light scattering is reduced, and the final blend maintains some transparency (Heckmann et al. 2005). Due to the rigid core and relative low amount of the rubber, such multilayer particles with rigid core facilitate also a fairly good balance between toughness and stiffness of the toughened material. Core–shell particles are obtained by emulsion polymerization and their size as well as size distribution can be controlled precisely in a certain range, so that particles of the optimum size can be prepared for a particular blend. The only problem, rather minor, during compounding of such particles with the matrix polymer is in obtaining a good dispersion and avoiding agglomerates in the final blend. The other very important benefit of core–shell particles is that the cavitation of such particles proceeds usually via nucleation of many small nanovoids in the rubber intermediate shell (Michler and Bucknall 2001). With subsequent expansion of these voids, a fibrillar morphology develops easily within the rubber shell with many elongated fibrils very well bonded to a rigid core and the outer shell (cf. Fig. 11.12). Stress and strain are distributed uniformly in these fibrils, which prevents their premature fracture, stabilizes cavities, and allows for effective stress transfer across the rubber shell and eventually leads to a significant contribution of particles in strain hardening and stabilization of material extensive deformation. Consequently, a high impact strength can be reached (see Sect. 11.4.4).

The last group of rubber particles constitutes particles obtained by dispersion of an elastomer in the matrix by blending of molten polymers in the extruder. The size of particles and the state of dispersion depend on rheological properties of both constituents of the blend as well as parameters of the mixing process. Frequently, to obtain a blend with rubber particles of desired size and satisfactory dispersion, reactive rubbers or other components (e.g., compatibilizers) must be added to the blend. If the elastomer used was thermoplastic, then the small crystallites formed inside particles on cooling constitute heterogeneities that can act as nucleation sites for multiple nanovoids within particles. Such a multiple cavitation is followed by formation of fibrils rather than a single rubber shell, which fibrils then can participate effectively in strain hardening and stabilization of the deformation process. Rubber fibrillization on cavitation usually fosters enhanced impact strength. The same effect of fibrillization can be obtained also by using block copolymers in which small sub-inclusions can be formed inside the particles. Grafting particles to the matrix by using functionalized rubbers in the reactive extrusion process or using adequate compatibilizers can control the size and interfacial strength of the rubber particles.

Interfacial Effects

A low interfacial energy between components of the blend is essential for obtaining a fine elastomer particle dispersion, which in turn is necessary for effective toughening. This condition is relevant not only for dispersing of bulk rubber by melt blending but also for dispersing aggregated core–shell particles or rigid particles during compounding. A low interfacial tension can be obtained either by careful selection of a rubber suitable for modification of a given rigid polymer or through a grafting reaction at the interface or by adding selected third polymeric component as compatibilizer. Grafting at the interface or using compatibilizers reduces interfacial tension while increases the adhesion (interfacial strength) between elastomer particles and the matrix.

Wu (1985) studied the PA-EPR rubber blends with different levels of adhesion between components, prepared by reactive melt extrusion. He found that the minimum interfacial strength needed for toughening was around 10^3 J/m^2, which is about the tearing stress of a rubber. This level of an interfacial strength can be obtained already by van der Waals bonding (Gaymans 2000). When interfacial strength becomes higher, due to, e.g., compatibilization or grafting at interface, the rubber particles in the blend tend to fail by internal cavitation. Lower interfacial strength (weaker bonding) is usually not desirable since particle debonding at interfaces rather than internal cavitation can take place. Debonding is less favorable than cavitation since there is no stress transfer from the matrix to the debonded particles so that these particles practically do not deform and hence do not participate in the strain hardening as the deformation of the matrix in the plastic zone advances. Voids created by debonding, not stabilized by stretching rubber, may become quickly crack initiators that would lead to premature fracture resulting in relative low impact strength.

Borggreve and Gaymans (1989) studied the PA-EPR blends, in which the amount of maleic anhydride grafted on the rubber, used to bond rubber and the matrix, varied in the range of 0.1–0.7 wt.%. These blends had different particle size for a given PA/rubber composition but exhibited identical relationship between T_{BD} and average particle size. Thus, the interfacial strength, seriously modified by chemical bonding of the rubber and PA chains through MA groups, appeared to control the dispersion process and the final size of the rubber particles, but did not influence the impact behavior at the constant particle size, because in all blends studied, toughening was related to the same mechanism of particle cavitation initiating extensive shear deformation of the matrix. These results demonstrate the actual role of grafting and use of compatibilizers – their primary function is to reduce the average particle size to the desired level effective for toughening, and not to increase interfacial adhesion between particles and the matrix. The process of reactive compounding, during which rubber particles are formed by shear forces and grafted to the matrix, appears relatively simple and effective method of preparation of tough blends with controlled particle sizes.

The modification of the interfacial tension influences the particle size obtained in the blend, but does not influence yield stress and modulus, which both depend on rubber concentration rather than on particle size (Borggreve et al. 1987).

Rubber Concentration

Rubber concentration in the blend is a very important factor in deformation and fracture of all rubber-toughened polymer blends. The impact strength of ductile polymers was found to increase as a function of rubber content (Gaymans 1994; Harrats and Groeninckx 2005). The brittle–ductile transition, which is a crucial parameter in toughened polymers, shifts towards lower temperature as the rubber content is increased (Argon et al. 2000; Bucknall 1977; Michler and Balta-Calleja 2012). Unfortunately, this comes at a price of an inevitable reduction of the material stiffness (lowered modulus) and the yield strength. When the material is loaded, the particles of soft compliant rubber transfer the load to the stiffer matrix, thence set up stress concentrations and reduce in this way the modulus and the yield stress, as already discussed in Sect. 11.4.3.1. The reduction of the modulus or yield strength can be described with the simple theoretical "effective area" model of Ishai and Cohen (Ishai and Cohen 1968) (cf. Eq. 11.11) or with the empirical dependence found by Gloagen et al. (1993) for rubber-toughened PMMA:

$$\sigma_y(\phi) = (1 - 1.375\phi)\,\sigma_y(0) \qquad (11.27)$$

Both relationships show a dependence of the yield strength solely on the rubber volume concentration. The same holds for the modulus. It can be concluded then that in order to get an acceptable balance between toughness and stiffness of the modified material, the rubber content cannot be too high. The other reason for reducing the rubber content in the blend is related to the problems which may arise with appropriate rubber dispersion and particle size. When a bulk elastomer is dispersed in the matrix by high shear forces upon the melt compounding, a low rubber concentration is advantageous from the point of view of particle size and size distribution. Concentrations higher than 25–30 vol.% usually result in coalescence of inclusions already formed and consequently in an increase of the final average particle size and broad distribution of particle size, which in most cases appears negative for toughening. Similarly, when the ready particles of the core–shell type are used, their high concentration can bring on serious problems related to their dispersion, and particle agglomerates can survive the compounding process, which is also detrimental for toughening. Therefore, in most of the commercial formulations, the rubber concentration is kept usually rather low, in the range from 5 % to 20 % of the elastomer phase. Working within this concentration range usually allows to obtain a blend with sufficiently small rubber particles that are dispersed well enough in the matrix, which results in a tough material, while the unavoidable deterioration of its stiffness and yield strength is still at an acceptable level.

Particle Size and Interparticle Distance

It has been already well established that the impact resistance of rubber-toughened blends depends strongly not only on a concentration but also on size and size distribution of the rubber particles (Bucknall 1977). Generally, small particles (average diameter in the range 0.2–0.4 μm) are the most efficient in toughening

Fig. 11.26 Impact strength of PA-6/EPR blends as a function of particle size (26 vol.% of EPR rubber; notched Izod impact test at 20 °C): the different symbols refer to different manufacturing methods (From Gaymans (1994); reproduced with permission of Springer)
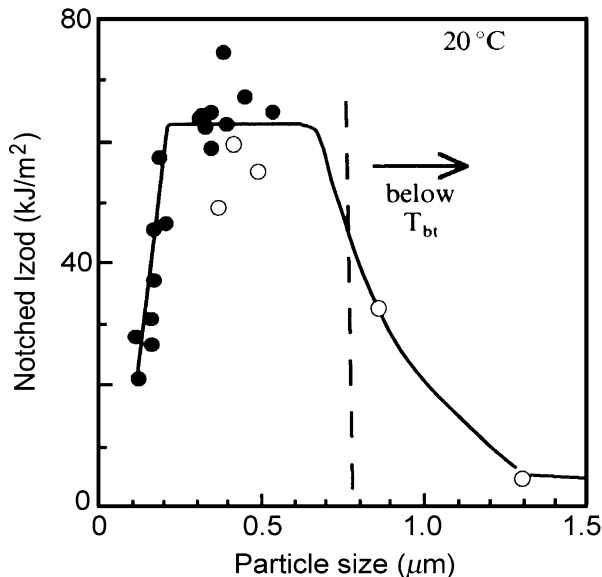
of these polymers for which shear yielding is the dominating mechanism of deformation and energy absorption. Significantly larger particles (D = 2–3 μm) appear, in turn, more effective when multiple crazing is the main mechanism of deformation.

It is now commonly recognized that the rubber particles play two major roles in the toughening of polymers: they generate a local stress concentrations (Bucknall 1977, 2000; Kausch 1983; Kausch 1987, 1990; Kinloch and Young 1983), and secondly, they modify the yield conditions for the matrix by altering significantly the stress state around cavitated particles and by increasing sensitivity of the yield to the mean stress, through transformation of the once continuous solid material into the porous (cellular) due to either particle cavitation or debonding (Bucknall and Paul 2009, 2013). The particles themselves should not initiate any fracture process; therefore, they should be sufficiently small to avoid excessive growth of voids up to the size of the critical flaw that can already cause crack initiation. On the other hand, in order to promote a necessary cavitation, they cannot be too small either (Bucknall 2000, 2007b; Bucknall and Paul 2009; Dompas and Groeninckx 1994; Lazzeri and Bucknall 1993). Numerous studies confirmed that for a given blend composition, optimum (high) toughness can be obtained only in certain, limited range of particle size. This size window was frequently found to be quite narrow. This feature can be illustrated by the results obtained for PA6/EPR blends of the constant overall compositions (26 vol.% of the rubber), in which the average particle size of the rubber was adjusted by variation in processing method or conditions, reported by Gaymans, Borggreve, and coworkers (Borggreve and Gaymans 1989; Borggreve et al. 1987, 1988, 1989a, b; Gaymans 2000; Gaymans et al. 1990) and presented in Fig. 11.26. They included in their study the blends with
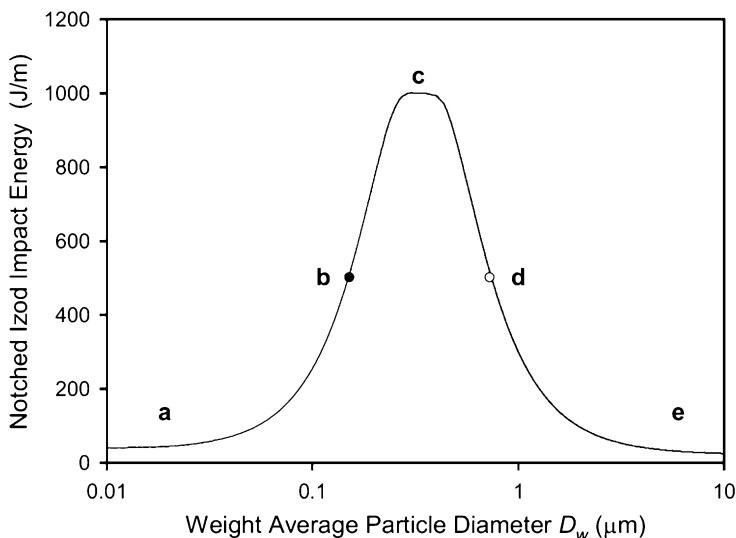
Fig. 11.27 Relationship between particle size and impact behavior for a typical "super-tough" thermoplastic blend. Points *b* and *d* mark *lower* (●) and *upper* (o) ductile–brittle transitions. Schematic representation based broadly on data of Huang et al. (2006a) for a series of 80/20 rubber-toughened PA6 blends (From Bucknall and Paul (2009); reproduced with permission of Elsevier)

large, medium, but also very small particles and performed impact tests at various temperatures. The obtained results demonstrated that these PA6/EPR blends exhibited both a lower and an upper ductile–brittle (DB) transition with respect to the particle size and that the upper critical particle size appeared temperature dependent, varying continuously from 0.5 μm at T = −10 °C to 1.5 μm at T = 50 °C as found in blends containing 20 wt.% (26 vol.%) of grafted EPDM rubber. Further extensive work has confirmed the existence of a minimum particle size for effective toughening in other semicrystalline as well as amorphous blends containing a variety of different elastomers (Dompas and Groenickx 1994; Dompas et al. 1994a, b; Huang et al. 2006a, b; Majumdar et al. 1994d; Okada et al. 2000; Oshinski et al. 1996c). There is now a substantial collection of papers which evidenced the effects of particle size on impact behavior in a wide range of polyamide (Borggreve and Gaymans 1989; Borggreve et al. 1987, 1989a, b; Gaymans 1994, 2000; Gaymans et al. 1990; Hobbs et al. 1983; Majumdar et al. 1994a, b, c, d, e; Oshinski et al. 1992a, b, 1996c; Takeda and Paul 1992; Wu 1983, 1985), polyesters (Gaymans 2000; Hage et al. 1997, 1999a, b, c, d, e), and polypropylene blends (Jang et al. 1984, 1985; Jiang et al. 2000, 2004a, b; Liang and Li 2000).

On the basis of numerous experimental data, Bucknall and Paul (2009) have proposed a model general curve illustrating the dependence of impact strength on average particle size. That curve, shown in Fig. 11.27, was drawn to follow the

results obtained for a representative "super-tough" rubber-toughened PA6 blend (Huang et al. 2006a). Similar curves can be obtained with appropriate scaling for other rubber-toughened blends as well. As illustrated in Fig. 11.27, moving beyond the preferred size range (around the optimum marked by **c**) in either direction results in a ductile–brittle transition, where **b** and **d**, respectively, mark the lower and upper transitions. These points define lower and upper critical particle sizes.

In his pioneering work, Wu (1985) studied PA6,6 blends with 10–25 % of grafted polyolefin rubber and average particle sizes varying from 0.3 to 3.0 μm. He observed in these blends a ductile-to-brittle transition similar to that shown in section **c–e** of Fig. 11.27, as expected. He also found the critical average particle size D_{crit} increasing systematically with rubber content (see Fig. 11.28a), which seems against the prediction of the model curve in Fig. 11.27, which shows also a lower critical particle size while does not predict any dependence on the rubber concentration. This behavior is probably because only blends with particles larger than 0.3 μm were studied, i.e., still above the expected lower DB transition. The intriguing observation was, however, that when plotting impact strength against the calculated average interparticle distance ID, a single critical value, ID_{crit} was found. This critical interparticle distance was independent on rubber concentration and appeared to control exclusively the upper ductile–brittle transition, cf. Fig. 11.28b. On this basis, Wu concluded that the average particle size is not the primary parameter controlling the impact resistance. He proposed then to use the interparticle distance ID instead, which, in his opinion, is the principal parameter. The interparticle distance ID, which was defined as the distance between surfaces of two adjacent rubber particles, referred later to as the matrix ligament thickness is, according to Wu, the crucial morphological parameter which governs the toughening efficiency in rubber-modified blends.

Making two simplifying assumptions that all particles have the same diameter D and are packed in a regular array, Wu derived the following expression for ID (Wu 1992):

$$ID = D\left[k\left(\frac{\pi}{6\phi}\right)^{\frac{1}{3}} - 1\right] \tag{11.28}$$

where D is the particle diameter and k is a parameter dependent on lattice packing arrangement, with $k = 1$ for simple cubic lattice and $k = 1.12$ for face-centered cubic (fcc) or hexagonal closed packing (hcp). Margolina and Wu have introduced the term "matrix ligament thickness" to describe ID, in order to shift the focus from the rubber particles to the matrix material (Margolina and Wu 1988). To explain the dependence of BD transition on ligament thickness, they use the percolation concept (Margolina and Wu 1988; Wu 1992). If the particles cavitating internally are close enough, then the zones of yielded matrix around both particles come into contact, so that the thin matrix ligaments between particles become fully yielded across. For small ID, these ligaments become interconnected, and the yielding process percolates across the specimen, stimulating its ductile
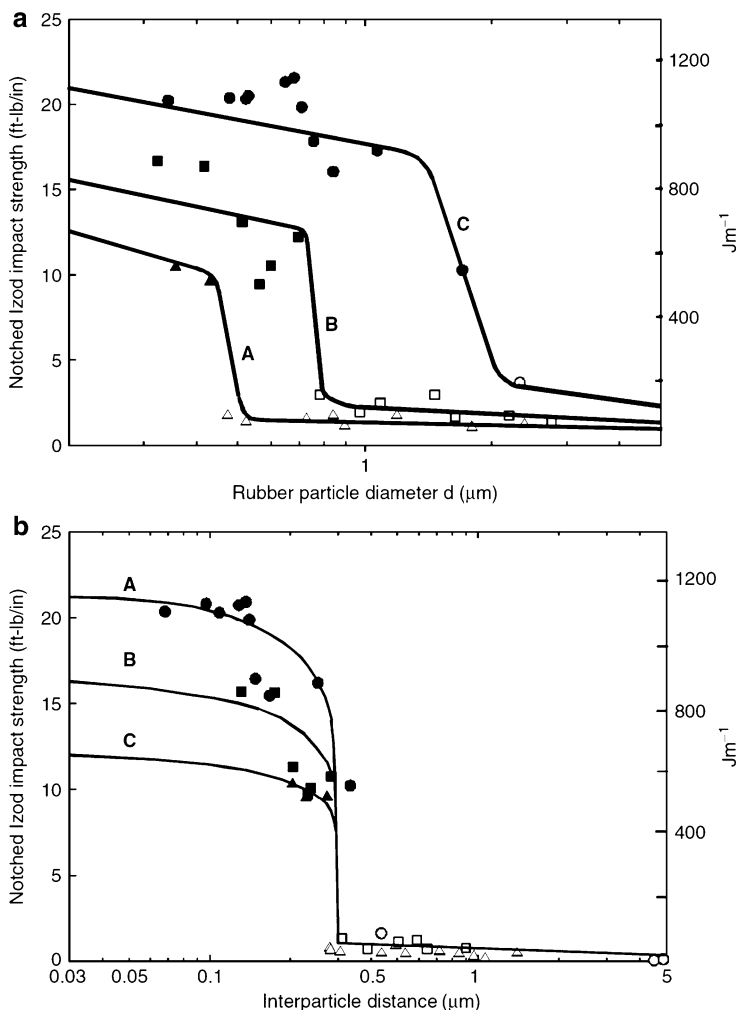
Fig. 11.28 (**a**) Notched Izod impact strength versus rubber particle diameter in PA 6,6/reactive rubber blends (curve A, 10 wt.% rubber; curve B, 15 wt.%; curve C, 20 wt.% rubber). (**b**) The same Izod impact strength data plotted versus interparticle distance (From Wu (1985); reproduced with permission of Elsevier)

deformation behavior. This occurs when the thickness of the matrix ligaments falls below the critical thickness. Such a state can be achieved for a given rubber volume fraction by decreasing the particle size and enhancing their dispersion. These ideas have been elaborated over the years by other researchers (Jiang et al. 2000, 2004a, 2008; Liu et al. 1998a, b, 1999; Sjoerdsma 1989).

To explain the observed effect of the interparticle distance, Wu proposed first that a strong overlap of the stress fields around particles induces shear yielding in PA6,6 matrix, turning the blend ductile. Later, however, Wu recognized

Fig. 11.29 TEM micrograph of PA6 modified with EPDM-g-MA. The sample was negatively stained with phosphotungstic acid. The *dark lines* are the amorphous regions and the *white lines* are the lamellae. The rubber particles are not stained and appear white. The scale bars represents 100 nm (From Muratoglu et al. (1995d); reproduced with permission of Elsevier)
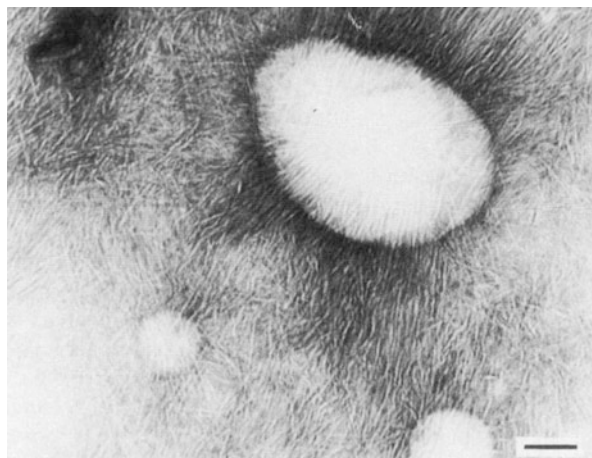
deficiencies of this model, since the local stress level depends on the ratio of the center-to-center distance ($L = D + ID$) to the diameter of the particle, L/D (Wu 1988). This ratio scales to volume fraction of particles and remains constant at a given volume fraction regardless of particle size, so that according to the stress field overlap model, toughening should be unaffected by the presence of large particles at any given L/D ratio. This, however, does not agree with the experimental results which demonstrate that small particles are certainly more effective in toughening than large ones (Borggreve et al. 1987; Bucknall and Paul 2009). A second proposed model was based on the transformation of the matrix material from a state of plane-strain to plane-stress when the volume fraction of cavitating rubber particles increases and the interparticle distance reduces below the critical size. This approach also fails because it attributes the embrittlement directly to the presence of high triaxial stresses. Those triaxial stresses in interparticle ligaments can be affected only by changing the geometrical ratios, but these ratios actually remain constant for a given volume fraction of the particles irrespective of their size.

To explain the sense of the ligament thickness parameter in semicrystalline polymers, Muratoglu et al. (1995d) proposed a model based on an specifically oriented crystalline layer of limited thickness ($\sim$0.15 μm for PA6,6 matrix) which forms upon matrix crystallization and extends radially from the surface of each rubber particle (Muratoglu et al. 1995a, b, c, d). This approach considered that in a tough blend where the rubber particles are closer than double the thickness of the oriented layer ($\sim$0.3 μm for PA6,6), the crystalline structure within the entire cross section of the interparticle ligament is well and specifically oriented. Crystalline lamellae oriented perpendicularly to the rubber–matrix interface were evidenced by TEM. Such a morphology surely induces a real anisotropy within the interparticle ligament zones, cf. Fig. 11.29. In these anisotropic zones, a considerable fraction of crystals is oriented with hydrogen-bonded (001) plane that appears as the plane of the easiest crystallographic slip, parallel to the rubber–matrix interface in the

interparticle ligament. As a result, the plastic shear resistance of ligaments is significantly reduced as compared to the isotropic matrix. Due to percolation effect, the entire deformation zone can deform extensively at the reduced stress, which eventually results in a super-tough material response. This approach was supported by microscopic observations of morphological features in the stress-whitened plastic process zones of tensile and Izod impact specimens, confirming the important role of the local orientation within ligaments. Similar local orientation behavior, leading to much enhanced impact strength, was postulated also for blends of polyethylene with various rubbers as well as those with stiff particles of $CaCO_3$ mineral filler (Bartczak et al. 1999a, b, c). In the latter case, debonding of stiff particles played the same role as rubber cavitation for yield initiation. Bucknall and Paul (2009) remarked critically that "the hypothesis of Muratoglu is not consistent with the strong relationship observed by Gaymans and co-workers (Borggreve and Gaymans 1989; Borggreve et al. 1988, 1989a, b; Gaymans 2000) between critical particle size and temperature, nor with recent work by Huang et al. which shows that the impact behavior of 80/20 rubber-toughened blends based on the amorphous polyamide Zytel 330 is very similar to that of 80/20 blends based on PA-6" (Huang et al. 2006a, b; Huang and Paul 2006).

Corte and Leibler (Corte et al. 2005; Corte and Leibler 2007) compared the characteristic lengths and deformation processes involved in toughening. On this basis they tried to explain a critical ligament thickness governing toughening of semicrystalline polymers by the existence of a characteristic confinement length that is governing the fracture behavior. They envisaged fracture of a semicrystalline polymer as a process in which a great number of very small nano- or submicron-sized cracks open in poorly cohesive amorphous layers and accumulate in the semicrystalline material long before its final rupture. A brittle fracture eventually occurs when these submicron cracks coalesce to form a flaw bigger than critical which happens at certain critical concentration, ρ^*, estimated on the order of 10^{14}–10^{16} cm^{-3} for semicrystalline polymers. This critical concentration implies the existence of a critical distance between nano- and submicron cracks $\xi^* \propto \rho^{*-1/3}$, estimated on the order of 100 nm. Analyzing the stress and strain state across the interparticle matrix ligament between cavitated particles, Corte and Leibler predicted that a small zone near particle equator should begin to yield due to high stress concentrations. Such yielded zones around neighboring particles would confine the elastically strained central part of the ligament between these particles. Now, if the width of this central part of the ligament is larger than the critical distance between nano- and microcracks ξ^* characteristic for a given polymer, then the discussed confinement by yielded zones does not affect crack coalescence, and a brittle fracture can propagate as in unmodified polymer. However, if this distance is smaller than ξ^*, the confinement can appear strong enough to shield interactions between microcracks and inhibit their coalescence. As a consequence, a brittle fracture does not develop. Instead, a plastic deformation can be activated, resulting in enhanced toughness. According to this approach, material becomes tough when the initial ligament thickness ID is smaller than a critical confinement length ID_{crit}, given by the equation (Corte and Leibler 2007):

$$\mathrm{ID}_{\mathrm{crit}} = \xi^* + \mathrm{D}\left(\frac{C\sigma_B}{\sigma_y}\right)^2 \tag{11.29}$$

where ξ^* is the critical distance between microcracks; D is the particle diameter; σ_B and σ_y are fracture and shear yield stress, respectively; and C is a dimensionless parameter depending on the ability of particles to release the stress and on the criterion for brittle stress. This equation suggests that $\mathrm{ID}_{\mathrm{crit}}$ depends not only on the matrix characteristics given by the critical distance ξ^*, σ_B, and σ_y but also directly on the particle diameter D. This model was applied to an interpretation of experimental data of polyamide-based blends and to demonstrate how the critical confinement length depends on material properties, temperature, and processing history. The model revealed an initially unexpected particle size effect: the critical interparticle distance $\mathrm{ID}_{\mathrm{crit}}$ varied linearly with the particle diameter and inversely with the square of the shear yield stress (Eq. 11.29). These findings demonstrate according to Bucknall and Paul that there is practically no advantage in using ID instead of D as a basis for comparisons of toughness data, especially as D is easier to measure experimentally, and ID is usually estimated indirectly (Bucknall and Paul 2009).

Bucknall and Paul (2009, 2013) reviewed and commented on the deficiencies of the interparticle spacing concept. They finally concluded that "there are sound reasons for abandoning the concept of interparticle spacing altogether. The alternative is to base all discussions of impact behavior on the size and volume fraction of rubber particles, which are known to affect fracture resistance in all polymer blends. From this perspective, any correlations involving interparticle spacings should be regarded as purely fortuitous" (Bucknall and Paul 2009). Consequently, they proposed an alternative approach, based on a new model for deformation and fracture of blends under the constraints imposed on the notch tip in Izod or Charpy specimens. This model is based on three stress criteria, which define critical conditions for rubber particle cavitation, dilational shear yielding, and craze initiation, respectively, described already in Sects. 11.5.2, 11.5.3, 11.5.4, and 11.5.5. The three criteria were used together with stress field equations to determine limits within which each of these mechanism can be activated in the notched or sample, and find in this way the sequence in which the various criteria are satisfied in a developing plane-strain deformation zone. This allowed to identify the mechanisms that govern fracture toughness under specific loading conditions in notched impact tests and to predict the relationships between rubber particle diameter and the impact strength.

Void formation plays a key role in this description of rubber toughening. At initial deformation stage, prior to rubber particle cavitation, very high constraints are imposed on the shear yielding in the plane-strain region of the notched sample, and therefore the local stress in the yield zone can increase rapidly up to the point of initiation of brittle fracture from the notch tip, which happens before any significant plastic deformation and energy dissipation has taken place. In order to obtain higher toughness, the blend must be capable of activating a widespread cavitation at

stresses still below the level required to generate shear yielding in a fully constrained, void-free material, the level of which under plane-strain conditions ahead of notch tip appears very high. This is possible only if the blend contains particles of average size above the critical minimum size (which is about 0.03 µm in blends of polyamides with elastomers). On the other hand, large particles tend to induce crazing upon the early stages of the test which leads to premature failure of the plastic zone and much lower energy absorption. Therefore, large particles, especially above approximately 1 µm in diameter, are not desirable. It appears that for many high-performance blends, the optimum particle size is about 0.3 µm.

The basic relationships between deformation behavior and the particle size are presented in Fig. 11.30. These plots were prepared by Bucknall and Paul to summarize their model of particle size dependence (Bucknall and Paul 2009, 2013). They indicate the ranges of the particle size in which the phenomena of particle cavitation, matrix shear yielding, and crazing, in sequence, control the maximum stress which can be supported by the blend under the plane-strain conditions, as, e.g., in notched impact tests. The basis for comparison is the critical major principal stress, σ_{1c}, which is an important parameter, controlling both the radius of the plastic zone and its susceptibility to fracture. Using this parameter enables to compare the critical stresses for cavitation, shear yielding, and craze initiation directly by means of a simple two-dimensional plot of σ_{1c} against log(D), although, in fact, cavitation is governed by the mean stress (pressure), shear yielding by the pressure-modified effective shear stress, and craze initiation by the applied tensile stress. For purposes of illustration, the plots in Fig. 11.30 are based on calculations done for a virtual series of idealized blends of dry PA6 with 20 wt.% of an olefin rubber which can be regarded as a representative case. Very similar charts can be calculated for other materials and/or test conditions as well.

Figure 11.30a shows how competition between the various deformation mechanisms affects the yield stress. The solid line denotes σ_{1c}, the critical value of σ_1 at the onset of shear yield, whether before (the first straight section, calculated with Eq. 11.17) or after cavitation. The cavitation stress curve was calculated with Eq. 11.14 scaled accordingly to fit experimental data of the real PA6/rubber blend. Finally, the craze initiation stress curve, similar to those shown in Fig. 11.23, was calculated with Eq. 11.25.

Under plane-strain loading conditions, the stresses (σ_1, σ_2, σ_3) on the crack plane are equal to ($\sigma,\sigma, 2v\sigma$). The highest calculated value of σ_{1c} is about 108 MPa, which corresponds to shear yielding of the void-free PA/rubber blend – cf. Fig. 11.21,which illustrates shear yielding of the non-cavitated blend under plane strain taking place when the mean stress $\sigma_m = 100$ MPa and the effective stress $\sigma_e = 21.5$ MPa, i.e., when stresses on the crack plane reach 108,108, 87 MPa. If the particles are very small, D < 0.03 µm, the cavitation stresses are higher than this σ_{1y}, so that the rubber does not cavitate, and constraints on shear yielding remain very high in the plane-strain region ahead of the notch. Yielding in a confined region close to the notch tip could take place
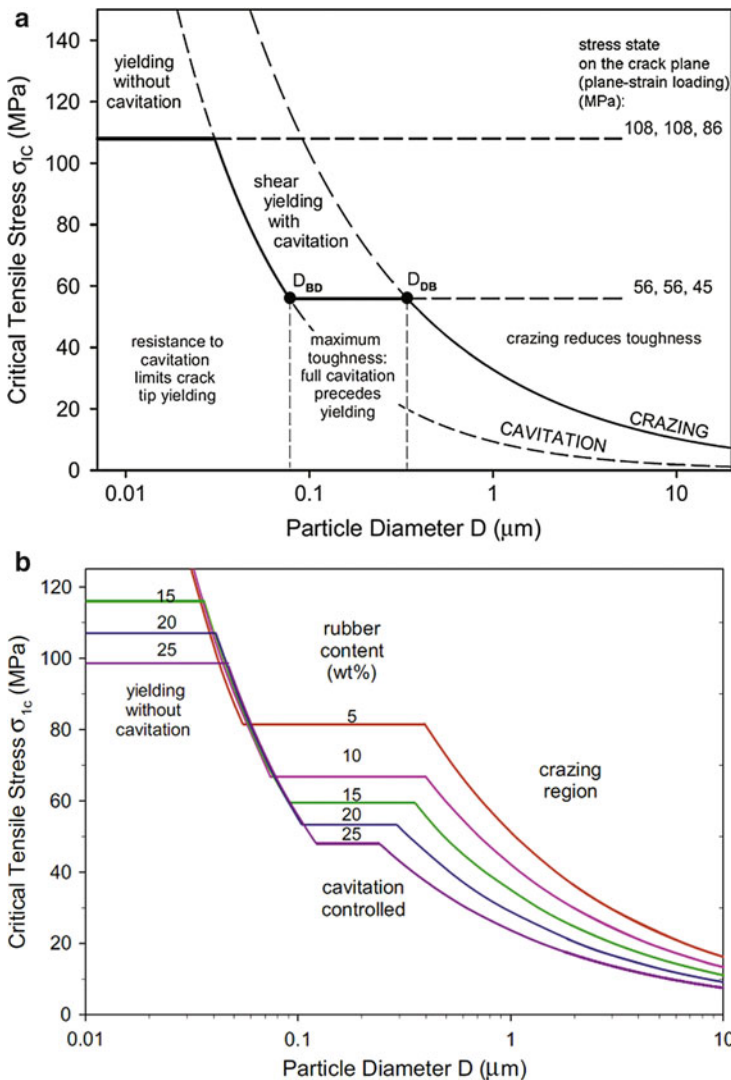
Fig. 11.30 (**a**) Critical stress map for PA6/rubber blends containing 20 % by weight (26.5 % by volume) of a lightly cross-linked olefin rubber, showing dependence of the critical major principal stress, on particle diameter. Craze line is calculated using Eq. 11.25 with E = 2.8 GPa and G_{craze} = 0.2 J/m^2. Shear yield stresses are calculated using Eq. 11.17, with pressure coefficient $\mu = 0.36$. *Solid line* defines critical stress for shear yielding, both with and without prior cavitation. Note that crazing and shear yielding can take place simultaneously in tough specimens containing relatively large particles (Adopted from Bucknall and Paul (2009); with permission of Elsevier). (**b**) Critical stress map for PA6/rubber blends containing various concentrations of rubber particles, showing the onset of rubber particle cavitation, shear yielding of cavitated blend, and crazing initiated by large particles (From Bucknall and Paul (2013); reproduced with permission of Elsevier)

without void formation, albeit at extremely high stresses (108,108, 87 MPa). Stresses of this magnitude do not develop in standard Izod or Charpy notched bars with rounded notch. Instead, local stresses increase quickly to the point of initiation of crack from the notch, leading to brittle fracture before reaching the high yield stress. By contrast, using the particle with size increasing above 0.03 μm enables the blend to cavitate before any fracture appears. Cavitation stress decreases with size, which causes a drop of the shear yield stress, down to $\sigma_{1c} = 56$ MPa (yield of the porous blend created by cavitation) at D ≈ 0.07 μm and to a significant increase of fracture toughness due to advancing plastic deformation. For even larger particles, the cavitation stress decreases below the shear yield stress of the fully cavitated blend; thus, the shear yield stress at plane strain is no longer a function of particle size. Consequently, an extensive dilatation shear yielding follows particle cavitation. This is the super-tough region, where K_I exceeds 3.5 MPam$^{0.5}$, and the radius of the plastic zone $r_p > 1$ mm. This dilatational shear yielding remains the dominating deformation mechanism until D ≈ 0.35 μm, the onset of the ductile–brittle transition, which occurs when the craze initiation curve crosses the line representing the shear yield. This crossing means that larger particles are likely to initiate crazes before the blend reaches its yield stress. Initiation and then propagation of crazes leads soon to failure of the plastic zone. As a result, impact strengths of the blend is reduced again. Summarizing, this chart explains the two brittle–ductile transitions, the lower brittle-to-ductile transition at $D_{BD} \approx 0.03$–0.08 μm, determined by the transition from brittle fracture in the absence of cavitation to dilatational shear yielding prompted by cavitation, and the upper ductile-to-brittle transition at $D_{DB} \approx 0.35$ μm, which is determined by the change from cavitation/yielding to crazing response. The optimum toughness is reached in the range of activity of cavitation and shear yielding, roughly at particle sizes between 0.1 and 0.3 μm.

Figure 11.30b is variant of Fig. 11.30a that illustrates the expected influence of the rubber concentration. It can be seen that critical stresses for yielding and for crazing tend to decrease with increasing concentration, but the same pattern of particle size dependence, discussed above, is valid for all composition. On the other hand, the range of particle size for which a super-tough behavior may be expected, limited by the upper ductile–brittle transition (transition from dilatational yield to crazing), drifts down with ϕ, which results in narrowing the size range optimum for toughening. What is more important, the yield stress goes down with increasing ϕ, which significantly reduces the probability of premature failure before the yield zone has fully developed. It must be noted, however, that once a high level of toughness has been achieved, any further increase of the rubber concentration becomes useless since the small expansion of the yield zone at the expense of a stronger reduction in the yield stress, so that total dissipated energy gradually decreases (Bucknall and Paul 2013).

The plots presented in Figs. 11.30a,b should be considered as diagrams which might appear useful in the interpretation of the notched impact toughness data, rather than a tool for predicting fracture resistance of any actual blend.

11.6   Concluding Remarks

Modification of polymers by blending with other polymers is known as an effective and economically justified method of enhancing their mechanical performance. Apart from modification of mechanical properties at low deformation rates, the most important target is the enhancement of toughness, especially at high deformation rates, including notched impact conditions.

Most of the amorphous glassy polymers tend to fracture in a brittle manner. Semicrystalline polymers, when unnotched, often fracture in a ductile manner, yet in the presence of a notch or other defects become brittle. Both amorphous and semicrystalline polymers can be made tougher by modification with particles of elastomers and in selected cases also with particles of other polymers or even stiff fillers. The change from brittle to ductile behavior is realized by promoting the deformation mechanism, either crazing or shear yielding, whichever is characteristic for a given polymer when in pristine form, in order to facilitate an extensive plastic deformation in possibly large volume of the sample that allows to dissipate large amounts of energy. The primary function of the particles is to cavitate (either internally or by debonding) and thereby produce changes in the local stress state in their adjacent vicinity that can facilitate the plastic response of the matrix. More importantly, cavitation transforms a continuous solid material into porous one, which demonstrates much higher sensitivity of the yield stress to the mean stress. This feature is crucial, especially in notched specimens, because it enables the blend to yield at moderate stresses still under plane-strain conditions found in front of the notch or crack tip. Recent studies indicate that the elimination of geometrical constraints and raising the state of plane-stress is not the primary role of cavitation, as some researchers have suggested in the past. Cavitation itself absorbs energy, but this is only a small fraction of the total fracture energy. The vast part of the impact energy is dissipated due to plastic deformation. Cavitation of the particles is, however, prerequisite for the enhanced ductile deformation.

The key to tough or super-tough impact behavior is the development of large and stable plastic zone, initially at the notch tip and then ahead of the propagating crack. One way of achieving this goal is to prepare the blend with high rubber contents (>25 % by volume), optimum particle sizes, and relatively low yield stresses. However, the high rubber content results also in a notably reduced material stiffness and therefore most frequently is not desirable. On the other hand, moderate yield stresses, obtained with the lower content of the rubber, and optimum particle sizes alone do not guarantee good toughening. Other material-related factors, including matrix chemistry and molecular weight, adhesion between particles and matrix, morphology of rubber particle shear modulus, and other properties of the rubber phase, are equally important in determining the total amount of energy absorbed and must be all taken into consideration when significant toughness improvement is demanded.

Average particle diameter of the rubber, D, and its volume fraction, ϕ, are among the most essential factors affecting the toughness of polymer blends. The concentration of the rubber must be well balanced in order to obtain material with

stiffness and strength, which are inevitably reduced, yet are still within acceptable limits. The optimum concentration of elastomer appears to be in the range from 5 to 20 wt.%. Regardless of the actual concentration, the average size of the rubber particles, together with its distribution, is the most important parameter. It is well known that there is an optimum range of particle sizes for which tough response in many systems may be expected, which is roughly from 0.1 to 0.5 μm for the majority of the blends, in which the shear yielding is the principal energy-absorbing deformation mechanism. To obtain tough materials on the basis of crazable polymers, larger particles, usually 2–3 μm in diameter, are necessary.

11.7   Cross-References

Notations and Abbreviations

Symbols

C_∞ Chain stiffness parameter
D Particle diameter
D_{BD}, D_{DB} Diameter of particle for brittle–ductile and ductile–brittle transition
d_e Entanglement mesh size
DB Ductile–brittle transition
E, E_M Young's modulus, modulus of the matrix
E_R Young's modulus of the rubber particle
f_z Function of the free volume accounting for the effect of the physical aging on crazing stress
f_y Function of the free volume accounting for the effect of the physical aging on yieldstress
G_{craze} Energy absorbed in formation of unit area of a craze
G_{IC} Fracture surface energy
G_M Shear modulus of the matrix
G_R Shear modulus of the rubber particle

ID Interparticle distance (matrix ligament thickness)

ID$_{crit}$ Critical interparticle distance

K Bulk modulus

K$_I$ Stress intensity factor

l^2 Mean-square length of a statistical unit of the chain

M$_v$ Molecular mass of a statistical skeletal unit

m_p Plastic constraint factor

n_v Number of statistical skeletal units in the chain

P Pressure

$R_o{}^2$ Mean-square end-to-end distance of an unperturbed chain

R Radius of the particle

r_p Radius of the plastic zone

r_{vd} Radius of the void

T$_{BD}$ Temperature of brittle–ductile transition

T$_g$ Temperature of glass transition

U_{ch} Bond energy of polymer chain

U_p Potential energy of the rubber particle

α Coefficient of thermal expansion

δ Cohesive energy density

ε_v Volume strain

ϕ Volume concentration of the rubber in the blend

Φ_p Volume fraction of particles

Φ_{vd} Volume fraction of voids

Ψ Inclination angle of the dilatation band

Γ Surface energy of the craze

Γ_r Surface energy of rubber particle

γ Van der Waals surface energy

λ_f Extension ratio of the rubber at fracture

ν_e Entanglement density

ν Poisson's ratio

μ Pressure sensitivity coefficient

ρ_a Density of amorphous polymer

ρ^* Critical concentration of submicron-sized cracks

ξ^* Critical distance between submicron cracks

σ_1 Applied tensile stress

σ_{1c} Critical major tensile stress

σ_{craze} Craze initiation stress

σ_{1craze} Critical tensile stress for craze initiation

σ_B Fracture strength

σ_e Effective (deviatoric) yield stress

σ_m Mean stress

σ_y Yield stress

σ_{y0} Yield stress in pure shear

σ_{yt} Yield stress in tension

Abbreviations

ABS Acrylonitrile–butadiene–styrene copolymer
EPDM Ethylene–propylene–diene terpolymer
EPR Ethylene–propylene copolymer
GMA Glycidyl methacrylate
HDPE High-density polyethylene
HIPS High-impact polystyrene
MA Maleic anhydride
PA Polyamide
PBA Poly(butyl acrylate)
PBT Poly(butylene terephthalate)
PC Polycarbonate
PE Polyethylene
PET Poly(ethylene terephthalate)
PMMA Poly(methyl methacrylate)
POM Polyoxymethylene
PP Polypropylene
PPO Poly(phenylene oxide)
PS Polystyrene
PVDF Polyvinylidene fluoride
PVC Poly(vinyl chloride)
SAN Styrene–acrylonitrile copolymer
SBS Styrene-butadiene-styrene block copolymer
SEBS Styrene–ethylene–butene-1–styrene block copolymer

References

M. Abate, V. Di Liello, E. Martuscelli, P. Musto, G. Ragosta, G. Scarinzi, Polymer **33**, 2940–2948 (1992)

I.A. Abu-Isa, C.B. Jaynes, J.F. O'Gara, J. Appl. Polym. Sci. **59**, 1957–1971 (1996)

A.M. Aerdts, G. Groenickx, H.F. Zirkzee, H.A.M. van Aert, J.M. Geurts, Polymer **38**, 4247–4252 (1997)

K. Akkapeddi, Rubber toughening of polyamides by reactive blending, in *Reactive Polymer Blending*, ed. by W. Baker, C. Scott, G.-H. Hu (Hanser Publishers, Munich, 2001), pp. 207–253

A.S. Argon, Polymer **52**, 2319–2327 (2011)

A.S. Argon, *The Physics of Deformation and Fracture of Polymers* (Cambridge University Press, Cambridge, 2013)

A.S. Argon, R.E. Cohen, Polymer **44**, 6013–6032 (2003)

A.S. Argon, J.G. Hannoosh, Philos. Mag. **36**, 1195–1216 (1977)

A.S. Argon, M.M. Salama, Philos. Mag. **36**, 1217–1234 (1977)

A.S. Argon, R.E. Cohen, A.C. Patel, Polymer **40**, 6991–7012 (1999)

A.S. Argon, Z. Bartczak, R.E. Cohen, O.K. Muratoglu, Novel mechanism of toughening semi -crystalline polymers, in *Toughening of Plastics: Advances in Modelling and Experiments*, ed. by R.A. Pearson, H.-J. Sue, A.F. Yee. ACS Symposium Series, vol. 759 (Oxford University Press, London, 2000), pp. 98–124

A.S. Argon, A. Galeski, T. Kazmierczak, Polymer **46**, 11798–11805 (2005)

A. Arostegui, J. Nazabal, Polymer **44**, 5227–5237 (2003)

B.M. Badran, A. Galeski, M. Kryszewski, J. Appl. Polym. Sci. **27**, 3669–3681 (1982)

F.J. Balta-Calleja, G.H. Michler (eds.), *Mechanical Properties of Polymers Based on Nano-Structure and Morphology* (Taylor and Francis, Boca Raton, 2005)

L.L. Ban, M.J. Doyle, M.M. Disko, G.R. Smith, Polym. Commun. **29**, 163–165 (1988)

Z. Bartczak, J. Macromol. Sci. Phys. **B41**, 1205–1229 (2002)

Z. Bartczak, A. Galeski, Macromol. Symp. **294**, 67–90 (2010)

Z. Bartczak, E. Martuscelli, A. Galeski, Primary spherulite nucleation in polypropylene-based blends, in *Polypropylene. Structure, Blends and Composites*, ed. by J. Karger-Kocsis. Copolymers and Blends, vol. 2 (Chapman and Hall, London, 1995), pp. 25–49

Z. Bartczak, A.S. Argon, R.E. Cohen, T. Kowalewski, Polymer **40**, 2367–2380 (1999a)

Z. Bartczak, A.S. Argon, R.E. Cohen, M. Weinberg, Polymer **40**, 2331–2346 (1999b)

Z. Bartczak, A.S. Argon, R.E. Cohen, M. Weinberg, Polymer **40**, 2347–2365 (1999c)

F.S. Bates, R.E. Cohen, A.S. Argon, Macromolecules **16**, 1108–1114 (1983)

J.-C. Bauwens, J. Polym. Sci **A2 5**, 1145–1156 (1967)

R.S. Beck, S. Gratch, S. Newman, K.C. Rusch, J. Polym. Sci. Part B Polym. Lett. **6**, 707–709 (1968)

R.L. Bergen, Appl. Polym. Symp. **7**, 41–51 (1968)

L.L. Berger, Macromolecules **23**, 2926–2934 (1990)

N. Billon, J.M. Haudin, Polym. Eng. Sci. **37**, 1761–1769 (1997)

R.J.M. Borggreve, R.J. Gaymans, Polymer **29**, 1441–1446 (1988)

R.J.M. Borggreve, R.J. Gaymans, Polymer **30**, 63–70 (1989)

R.J.M. Borggreve, R.J. Gaymans, J. Schuijer, J.F. Ingen-Housz, Polymer **28**, 1489–1496 (1987)

R.J.M. Borggreve, R.J. Gaymans, A.R. Luttmer, Macrolol. Symp. **16**, 195–207 (1988)

R.J.M. Borggreve, R.J. Gaymans, H.M. Eichenwald, Polymer **30**, 78–83 (1989a)

R.J.M. Borggreve, R.J. Gaymans, J. Schuijer, Polymer **30**, 71–77 (1989b)

P.B. Bowden, R.J. Young, Nature **229**, 23–25 (1971)

P.B. Bowden, R.J. Young, J. Mater. Sci. **9**, 2034–2051 (1974)

A.J. Brady, H. Kesskula, D.R. Paul, Polymer **35**, 3665–3672 (1994)

N.W.J. Brooks, M. Mukhtar, Polymer **41**, 1475–1480 (2000)

N. Brown, I.M. Ward, J. Mater. Sci. **18**, 1405–1420 (1983)

H.R. Brown, A.S. Argon, R.E. Cohen, O.S. Gebizlioglu, E.J. Kramer, Macromolecules **22**, 1002–1004 (1989)

R.A. Bubeck, D.J. Buckley, E.J. Kramer, H. Brown, J. Mater. Sci. **26**, 6249–6259 (1991)

R. Buchdahl, E. Nielsen, J. Appl. Phys. **21**, 482–487 (1950)

C.B. Bucknall, *Toughened Plastics* (Applied Science Publishers, London, 1977)

C.B. Bucknall, Adv. Polym. Sci. **27**, 121–148 (1978)

C.B. Bucknall, Rubber toughening, in *The Physics of Glassy Polymers*, ed. by R.N. Haward, R.J. Young, 2nd edn. (Chapman and Hall, London, 1997), pp. 363–412

C.B. Bucknall, Deformation mechanisms in rubber-toughened polymers, in *Polymer Blends, Vol. 2: Performance*, ed. by D.R. Paul, C.B. Bucknall (Wiley-Interscience, New York, 2000), pp. 83–117

C.B. Bucknall, Polymer **48**, 1030–1041 (2007a)

C.B. Bucknall, J. Polym. Sci. Part B Polym. Phys. **45**, 1399–1409 (2007b)

C.B. Bucknall, D.R. Paul, Polymer **50**, 5539–5548 (2009)

C.B. Bucknall, D.R. Paul, Polymer **54**, 320–329 (2013)

C.B. Bucknall, R.R. Smith, Polymer **6**, 437–446 (1965)

C.B. Bucknall, P. Davies, I.K. Partridge, J. Mater. Sci. **21**, 307–313 (1986)

C.B. Bucknall, P.S. Heather, A. Lazzeri, J. Mater. Sci. **24**, 2255–2261 (1989)

C.B. Bucknall, A. Karpodinis, X.C. Zhang, J. Mater. Sci. **29**, 3377–3383 (1994)

M.F. Butler, A.M. Donald, A.J. Ryan, Polymer **39**, 39–52 (1998)

A. Cecere, R. Greco, G. Ragosta, G. Scarinzi, Polymer **31**, 1239–1244 (1990)

V.P. Chacko, K.E. Karasz, R.J. Ferris, E.L. Thomas, J. Polym. Sci. B **20**, 2177 (1982)

C.M. Chan, J. Wu, J.X. Li, Y.K. Cheung, Polymer **43**, 2981–2992 (2002)

S. Cimmino, F. Coppola, L. D'Orazio, R. Greco, G. Maglio, M. Malinconico, C. Mancarella, E. Martuscelli, Polymer **27**, 1874–1884 (1986)

B. Cioni, A. Lazzeri, Compos. Interfac. **17**, 533–549 (2010)

A.A. Collyer (ed.), *Rubber Toughened Engineering Plastics* (Chapmann and Hall, London, 1994)

L. Corte, L. Leibler, Macromolecules **40**, 5606–5611 (2007)

L. Corte, B. Beaumeb, L. Leiblerer, Polymer **46**, 2748–2757 (2005)

B. Crist, C.J. Fisher, P.R. Howard, Macromolecules **22**, 1709–1718 (1989)

C.A. Cruz-Ramos, Core-shell impact modifiers, in *Polymer Blends, Vol. 2: Performance*, ed. by D.R. Paul, C.B. Bucknall (Wiley-Interscience, New York, 2000), pp. 137–176

O. Darras, R. Seguela, J. Polym. Sci. B **31**, 759–766 (1993)

A. Dasari, Q.-X. Zhang, Z.-Z. Yu, Y.-W. Mai, Macromolecules **43**, 5734–5739 (2010)

C. Deshmane, Q. Yuan, R.D.K. Misra, Mater. Sci. Eng. A **452–453**, 592–601 (2007)

K. Dijkstra, R.J. Gaymans, J. Mater. Sci. **29**, 3231–3238 (1994a)

K. Dijkstra, R.J. Gaymans, Polymer **35**, 332–335 (1994b)

K. Dijkstra, J. ter Laak, R.J. Gaymans, Polymer **35**, 315–322 (1994a)

K. Dijkstra, H. Wevers, R.J. Gaymans, Polymer **35**, 323–331 (1994b)

D. Dompas, G. Groeninckx, Polymer **35**, 4743–4749 (1994)

D. Dompas, G. Groeninckx, M. Isogawa, T. Hasegawa, M. Kadokura, Polymer **35**, 4750–4759 (1994a)

D. Dompas, G. Groeninckx, M. Isogawa, T. Hasegawa, M. Kadokura, Polymer **35**, 4760–4765 (1994b)

A.M. Donald, Failure mechanisms in polymeric materials, in *Rubber Toughened Engineering Plastics*, ed. by A.A. Collyer (Chapmann and Hall, London, 1994), pp. 1–28

A.M. Donald, Crazing, in *The Physics of Glassy Polymers*, ed. by R.N. Haward, R.J. Young, 2nd edn. (Chapman and Hall, London, 1997), pp. 295–341

A.M. Donald, E.J. Kramer, J. Mater. Sci. **17**, 1765 (1982)

I.L. Dubnikova, S.M. Berezina, A.V. Antonov, J. Appl. Polym. Sci. **94**, 1917–1926 (2004)

B. N. Epstein, U.S. Patent 4,174,358, 1979 (to du Pont)

A.G. Evans, Philos. Mag. **26**, 1327–1344 (1972)

J.D. Ferry, *Viscoelastic Properties of Polymers*, 2nd edn. (Wiley, New York, 1970)

E.A. Flexman, Polym. Eng. Sci. **19**, 564–571 (1979)

E.A. Flexman, ACS Polym. Prep. **29**, 189–190 (1988)

M.E. Fowler, J.W. Barlow, D.R. Paul, Polymer **28**, 1177–1184 (1987)

Q. Fu, G. Wang, J. Shen, J. Appl. Potym. Sci. **49**, 673–677 (1993)

A. Galeski, e-Polymers art. no. 026, 1–28 (2002)

R.J. Gaymans, Toughened polyamides, in *Rubber Toughened Engineering Plastics*, ed. by A.A. Collyer (Chapmann and Hall, London, 1994), pp. 210–242

R.J. Gaymans, Toughening of semicrystalline thermoplastics, in *Polymer Blends, Vol. 2: Performance*, ed. by D.R. Paul, C.B. Bucknall (Wiley-Interscience, New York, 2000), pp. 177–224

R.J. Gaymans, K. Dijkstra, Polymer **31**, 971–971 (1990)

R.J. Gaymans, J.W. van der Werff, Polymer **35**, 3658–3664 (1994)

R.J. Gaymans, R.J.M. Borggreve, A.J. Oostenbrink, Makromol. Chem. Macromol. Symp. **38**, 125–136 (1990)

O.S. Gebizlioglu, H.W. Beckham, A.S. Argon, R.E. Cohen, H.R. Brown, Macromolecules **23**, 3968–3974 (1990)

R. Gensler, C.J.G. Plummer, C. Grein, H.-H. Kausch, Polymer **41**, 3809–3819 (2000)

A.N. Gent, Rubber Chem. Techn. **63**, 49–53 (1990)

J.M. Gloagen, P. Steer, P. Gallliard, C. Wrotecki, J.M. Lefebvre, Polym. Eng. Sci. **33**, 748–753 (1993)

G. Gong, B.H. Xie, W. Yang, Z.M. Li, S.M. Lai, M.B. Yang, Polym. Test. **25**, 98–106 (2006)

A. Gonzales-Montiel, H. Kesskula, D.R. Paul, Polymer **36**, 4587–4603 (1995a)

A. Gonzales-Montiel, H. Kesskula, D.R. Paul, Polymer **36**, 4605–4620 (1995b)

A. Gonzales-Montiel, H. Kesskula, D.R. Paul, Polymer **36**, 4621–4637 (1995c)

M. Gordon, J.S. Taylor, J. Appl. Chem. **2**, 493–500 (1952)

D.J. Green, P.S. Nicholson, J.D. Emberg, J. Mater. Sci. **14**, 1657–1661 (1979)

A.L. Gurson, J. Eng. Mater. Technol. Trans. ASME **99**, 2–15 (1977a)

A.L. Gurson, in *CF 4 Fracture 1977, Waterloo, Canada, Vol. 2A*, ed. by D.M.R. Taplin (Pergamon Press, Oxford, 1977b), p. 357

E. Hage, H. Kesskula, D.R. Paul, Polymer **38**, 3237–3250 (1997)

W.R. Hale, H. Keskkula, D.R. Paul, Polymer **40**, 365–377 (1999a)

W.R. Hale, H. Keskkula, D.R. Paul, Polymer **40**, 3665–3676 (1999b)

W.R. Hale, H. Keskkula, D.R. Paul, Polymer **40**, 3353–3365 (1999c)

W.R. Hale, J.H. Lee, H. Keskkula, D.R. Paul, Polymer **40**, 3621–3629 (1999d)

W.R. Hale, L.A. Pessan, H. Keskkula, D.R. Paul, Polymer **40**, 4237–4250 (1999e)

C. Harrats, G. Groeninckx, Deformation mechanisms and toughness of rubber and rigid filler modified semicrystalline polymers, in *Mechanical Properties of Polymers based on Nano-Structure and Morphology*, ed. by F.J. Balta Calleja, G.H. Michler (Taylor and Francis, London, 2005), pp. 481–546

J.M. Haudin, Plastic deformation of semicrystalline polymers, in *Plastic Deformation of Amorphous and Semi-crystalline Materials*, ed. by B. Escaig, C. G'Sell (Les Editions de Physique, Paris, 1982), p. 291

R.N. Haward, R.J. Young (eds.), *The Physics of Glassy Polymers*, 2nd edn. (Chapman and Hall, London, 1997)

C. He, A.M. Donald, M.F. Butler, Macromolecules **31**, 158–164 (1998)

W. Heckmann, G.E. McKee, F. Ramsteiner, Structure-property relationship in rubber modified amorphous thermoplastic polymers, in *Mechanical Properties of Polymers Based on Nano-Structure and Morphology*, ed. by F.J. Balta-Calleja, G.H. Michler (Taylor and Francis, London, 2005), pp. 429–479

C.S. Henkee, E.J. Kramer, J. Polym. Sci. B **22**, 721–737 (1984)

M. Hert, Angew. Makromol. Chem. **196**, 89–99 (1992)

S.Y. Hobbs, R.C. Bopp, V.H. Watkins, Polym. Eng. Sci. **23**, 380–389 (1983)

J.J. Horst, J.L. Spoormaker, Polym. Eng. Sci. **36**, 2718–2726 (1996)

R.M. Hosti-Miettinen, M.T. Heino, J.V. Sappala, J. Appl. Polym. Sci. **57**, 573–586 (1995)

D.J. Hourston, S. Lane, Toughened polyesters and polycarbonates, in *Rubber Toughened Engineering Plastics*, ed. by A.A. Collyer (Chapmann and Hall, London, 1994), pp. 243–265

D.J. Hourston, S. Lane, H.X. Zhang, Polymer **32**, 2215–2220 (1991)

D.J. Hourston, S. Lane, H.X. Zhang, Polymer **36**, 3051–3054 (1995)

J.J. Huang, D.R. Paul, Polymer **47**, 3505–3519 (2006)

J.J. Huang, H. Keskkula, D.R. Paul, Polymer **47**, 639–651 (2006a)

J.J. Huang, H. Keskkula, D.R. Paul, Polymer **47**, 624–638 (2006b)

W.R. Hwang, G.W.M. Peters, M.A. Hulsen, H.E.H. Meijer, Macromolecules **39**, 8389–8398 (2006)

G.R. Irwin, Appl. Mater. Res.. **3**, 65–71 (1964)

G.R. Irwin, P.C. Paris, in *Fracture, an Advanced Treatise*, ed. by H. Liebowitz, vol. 3 (Academic, New York, 1971), p. 13

O. Ishai, L.J. Cohen, J. Compos. Mater. **2**, 302–315 (1968)

B.Z. Jang, D.R. Uhlmann, J.B. Vander Sande, J. Appl. Polym. Sci. **29**, 3409–3420 (1984)

B.Z. Jang, D.R. Uhlmann, J.B. Vander Sande, Polym. Eng. Sci. **25**, 643–651 (1985)

H. Janik, R.J. Gaymans, K. Dijkstra, Polymer **36**, 4203–4208 (1995)

W. Jiang, S.C. Tjong, R.K.Y. Li, Polymer **41**, 3479–3482 (2000)

W. Jiang, D. Yu, B. Jiang, Polymer **45**, 6427–6430 (2004a)

W. Jiang, D.H. Yu, L.J. An, B.Z. Jiang, J. Polym. Sci. B **42**, 1433–1440 (2004b)

W. Jiang, Y.X. Hu, J.H. Yin, J. Polym. Sci. B **46**, 766–769 (2008)

M. Kamal, C.S. Sharma, P. Upadhyaya, V. Verma, K.N. Pandey, V. Kumar, D.D. Agrawal, J. Appl. Polym. Sci. **124**, 2649–2656 (2012)

H. Kanai, A. Auerbach, A. Sullivan, J. Appl. Polym. Sci. **53**, 527–541 (1994)

T.-K. Kang, Y. kim, G. kim, W.-J. Chp, C.-S. Ha, Polym. Eng. Sci. **37**, 603–614 (1997)

H.H. Kausch (ed.), *Crazing in Polymers*. Advances in Polymer Science, vol. 52/53 (Springer, Berlin, 1983)

H.H. Kausch, *Polymer Fracture* (Springer, Berlin, 1987)

H.H. Kausch (ed.), *Crazing in Polymers, Vol. II*. Advances in Polymer Science, vol. 91/92 (Springer, Berlin, 1990)

H.H. Kausch, Macromol. Chem. Macromol. Symp. **41**, 1–8 (1991)

Y. Kayano, H. Kesskula, D.R. Paul, Polymer **37**, 4505–4518 (1996)

Y. Kayano, H. Kesskula, D.R. Paul, Polymer **38**, 1885–1902 (1997)

T. Kazmierczak, A. Galeski, A.S. Argon, Polymer **46**, 8926–8936 (2005)

A. Kelly, W.R. Tyson, A.H. Cottrell, Philos. Mag. **15**, 567–586 (1967)

M.A. Kennedy, A.J. Peacock, L. Mandelkern, Macromolecules **27**, 5297–5310 (1994)

H. Kesskula, Appl. Polym. Symp. **15**, 51–78 (1970)

H. Kesskula, D.R. Paul, Toughening agents for engineering polymers, in *Rubber Toughened Engineering Plastics*, ed. by A.A. Collyer (Chapmann and Hall, London, 1994), pp. 136–164

G.-M. Kim, G.H. Michler, Polymer **39**, 5689–5697 (1998a)

G.-M. Kim, G.H. Michler, Polymer **39**, 5699–5703 (1998b)

A.J. Kinloch, R.J. Young, *Fracture Behaviour of Polymers* (Applied Science Publishers, London, 1983)

F. Kloos, Angew. Makromol. Chem. **133**, 1–24 (1985)

M. Kowalczyk, E. Piorkowska, J. Appl. Polym. Sci. **124**, 4579–4589 (2012)

E.J. Kramer, Microscopic and molecular fundamentals of crazing, in *Crazing in Polymers*, ed. by H.H. Kausch. Advances in Polymer Science, vol. 52/53 (Springer, Berlin, 1983), pp. 1–56

E.J. Kramer, L.L. Berger, Fundamental processes of craze growth and fracture, in *Crazing in Polymers, Vol. II*, ed. by H.H. Kausch. Advances in Polymer Science, vol. 91/92 (Springer, Berlin, 1990), pp. 1–68

T. Kyu, J.M. Saldanka, M.J. Kiesel, Toughness enhancement in polycarbonate/polymethyl-methacrylate blend via phase separation, in *Two-Phase Polymer Systems*, ed. by L.A. Utracki (Hanser Publishers, Munich, 1991), pp. 259–275

J. Laatsch, G.-M. Kim, G.H. Michler, T. Arndt, T. Sufke, Polym. Adv. Technol. **9**, 716–720 (1998)

F.F. Lange, Philos. Mag. **22**, 983–992 (1970)

P. Laurienzo, M. Malinconico, E. Martuscelli, G. Volpe, Polymer **30**, 835–841 (1989)

R.E. Lavengood, L. Nicolais, M. Narkis, J. Appl. Polym. Sci. **17**, 1173–1185 (1973)

A. Lazzeri, C.B. Bucknall, J. Mater. Sci. **28**, 6799–6808 (1993)

A. Lazzeri, C.B. Bucknall, Polymer **36**, 2895–2902 (1995)

A. Lazzeri, C.B. Bucknall, Recent development in the modelling of dilatational yielding, in *Toughening Plastics, Advances in Modeling and Experiments*, ed. by R.A. Pearson, H.J. Sue, A.F. Yee. ACS Symposium Series, vol. 759 (ACS, Washington, DC, 2000), p. 14

A. Lazzeri, Y.S. Thio, R.E. Cohen, J. Appl. Polym. Sci. **91**, 925–935 (2004)

A. Lazzeri, S.M. Zebarjad, M. Pracella, K. Cavalier, R. Rosa, Polymer **46**, 827–844 (2005)

J. Lei, R. Zhou, Polym. Eng. Sci. **40**, 1529 (2000)

J.Z. Liang, R.K.U. Li, J. Appl. Polym. Sci. **77**, 409–417 (2000)

L. Lin, A.S. Argon, Macromolecules **25**, 4011–4024 (1992)

L. Lin, A.S. Argon, J. Mater. Sci. **29**, 294–323 (1994)

Y. Lin, H. Chen, C.M. Chan, J. Wu, Macromolecules **41**, 9204–9213 (2008)

Y. Lin, H. Chen, C.-M. Chan, J. Wu, Polymer **51**, 3277–3284 (2010)

Y. Lin, H.B. Chen, C.M. Chan, J.S. Wu, J. Appl. Polym. Sci. **124**, 77–86 (2012)

Z.H. Liu, R.K.Y. Li, S.C. Tjong, Z.N. Qi, F.S. Wang, C.L. Choy, Polymer **39**, 4433–4436 (1998a)

Z.H. Liu, X.D. Zhang, X.G. Zhu, Z.N. Qi, F.S. Wang, R.K.Y. Li, C.L. Choy, Polymer **39**, 5047–5052 (1998b)

Z.H. Liu, R.K.Y. Li, S.C. Tjong, C.L. Choy, X.G. Zhu, Z.N. Qi, Polymer **40**, 2903–2915 (1999)

Z.H. Liu, K.W. Kwok, R.K.Y. Li, C.L. Choy, Polymer **43**, 2501–2506 (2002)

G. Liu, X. Zhang, Y. Liu, X. Li, H. Chen, K. Walton, G. Marchand, D. Wang, Polymer **54**, 1440–1447 (2013)

P.A. Lovell, M.S. El-Aaser (eds.), *Emulsion Polymerization and Emulsion Polymers* (Wiley, Chichester, 1997)

P.A. Lovell, J. McDonald, D.E.J. Saunders, R.J. Young, Polymer **34**, 61–69 (1993)

W. Loyens, G. Groeninckx, Polymer **43**, 5679–5691 (2002)

W. Loyens, G. Groeninckx, Polymer **44**, 4929–4941 (2003)

M. Lu, H. Kesskula, D.R. Paul, Polymer **34**, 1874–1885 (1993)

M. Lu, H. Kesskula, D.R. Paul, J. Appl. Polym. Sci. **58**, 1175–1188 (1995)

M. Lu, H. Kesskula, D.R. Paul, J. Appl. Polym. Sci. **59**, 1467–1477 (1996)

J.T. Lutz, D. Dunkelberger (eds.), *Impact Modifiers for PVC. The History and Practice* (Wiley, New York, 1992)

B. Majumdar, H. Kesskula, D.R. Paul, Polymer **35**, 4263–4279 (1994a)

B. Majumdar, H. Kesskula, D.R. Paul, J. Polym. Sci. B **32**, 2127–2133 (1994b)

B. Majumdar, H. Kesskula, D.R. Paul, Polymer **35**, 5468–5477 (1994c)

B. Majumdar, H. Kesskula, D.R. Paul, Polymer **35**, 1386–1398 (1994d)

B. Majumdar, H. Kesskula, D.R. Paul, Polymer **35**, 5453–5467 (1994e)

A. Margolina, S.H. Wu, Polymer **29**, 2170–2173 (1988)

J. Martinez-Salazar, J.C.C. Camara, F.J.B. Balta-Calleja, J. Mater. Sci. **26**, 2579–2582 (1991)

E. Martuscelli, P. Musto, G. Ragosta (eds.), *Advanced Routes for Polymer Toughening* (Elsevier, Amsterdam, 1996)

Y. Men, J. Riegel, G. Strobl, Phys. Rev. Lett. **91**, 95502-95501–95502-95504 (2003)

E.H. Merz, G.C. Claver, M. Baer, J. Polym. Sci. **22**, 325–341 (1956)

G.H. Michler, Micromechanical mechanisms of toughness enhancement in nanostructured amorphous and semicrystalline polymers, in *Mechanical Properties of Polymers Based on Nano-Structure and Morphology*, ed. by F.J. Balta Calleja, G.H. Michler (Taylor and Francis, London, 2005), pp. 375–428

G.H. Michler, F.J. Balta-Calleja, *Nano- and Micromechanics of Polymers* (Carl Hanser, Munich, 2012)

G.H. Michler, C.B. Bucknall, Plastics Rubber Compos. **30**, 110–115 (2001)

G.H. Michler, J.U. Starke, Investigation of micromechanical and failure mechanisms of toughened thermoplastics using electron microscopy, in *Toughened Plastics II: Novel Approaches in Science and Engineering*, ed. by C.K. Riew, A.J. Kinloch (American Chemical Society, Washington, DC, 1996), pp. 251–277

D.E. Mouzakis, N. Papke, J.S. Wu, J. Kerger-Korcsis, J. Appl. Polym. Sci. **79**, 842–852 (2001)

O.K. Muratoglu, A.S. Argon, R.E. Cohen, Polymer **36**, 2143–2152 (1995a)

O. K. Muratoglu, A. S. Argon, R. E. Cohen, M. Weinberg, Polymer **36**, 4787–4795 (1995b)

O.K. Muratoglu, A.S. Argon, R.E. Cohen, M. Weinberg, Polymer **36**, 4771–4786 (1995c)

O.K. Muratoglu, A.S. Argon, R.E. Cohen, M. Weinberg, Polymer **36**, 921–930 (1995d)

M.M. Nasef, H. Saidi, Mater. Chem. Phys. **99**, 361–369 (2006)

R. Neuber, H.A. Schneider, Polymer **42**, 8085–8091 (2001)

D. Neuray, K.-H. Ott, Angew. Makromol. Chem. **98**, 213–224 (1981)

S. Newman, in *Polymer Blends*, ed. by D.R. Paul, S. Newman, vol. 2 (Academic, New York, 1978), pp. 63–89

K.H. Nitta, K. Okamoto, M. Yamaguchi, Polymer **39**, 53–58 (1998)

K.H. Nitta, Y.-W. Shin, H. Hashiguchi, S. Tanimoto, M. Terano, Polymer **46**, 965–975 (2005)

W.J. O'Kane, R.J. Young, A.J. Ryan, J. Macromol. Sci. Phys. B **34**, 427–458 (1995)

O. Okada, H. Keskkula, D.R. Paul, Polymer **41**, 8061–8074 (2000)

K. Okamoto, K. Shiomi, T. Inoue, Polymer **35**, 4618–4622 (1994)

E.F. Oleinik, Polym. Sci. C **45**, 17–117 (2003)

E. Orowan, Rep. Prog. Phys. **12**, 185–232 (1949)

A.J. Oshinski, H. Kesskula, D.R. Paul, Polymer **33**, 268–283 (1992a)

A.J. Oshinski, H. Kesskula, D.R. Paul, Polymer **33**, 284–293 (1992b)

A.J. Oshinski, H. Keskkula, D.R. Paul, Polymer **37**, 4891–4907 (1996a)

A.J. Oshinski, H. Keskkula, D.R. Paul, Polymer **37**, 4919–4928 (1996b)

A.J. Oshinski, H. Keskkula, D.R. Paul, J. Appl. Polym. Sci. **61**, 623–640 (1996c)

A.J. Oshinski, H. Kesskula, D.R. Paul, Polymer **37**, 4909–4918 (1996d)

Y.C. Ou, F. Yang, Z.-Z. Yu, J. Polym. Sci. B **36**, 789–795 (1998)

R.J. Oxborough, P.B. Bowden, Philos. Mag. **28**, 547–559 (1973)

R.J. Oxborough, P.B. Bowden, Philos. Mag. **30**, 171–184 (1974)

J.-G. Park, D.-H. Kim, K.-D. Suh, J. Appl. Polym. Sci. **78**, 2227–2233 (2000)

D.S. Parker, H.J. Sue, J. Huang, A.F. Yee, Polymer **31**, 2267–2277 (1990)

M. Penco, M.A. Pastorino, E. Ochiello, F. Garbassi, R. Braglia, G. Gianotta, J. Appl. Polym. Sci. **57**, 329–334 (1995)

J.M. Peterson, J. Appl. Phys. **37**, 4047–4050 (1966)

J.M. Peterson, J. Appl. Phys. **39**, 4920–4928 (1968)

E. Piorkowska, A.S. Argon, R.E. Cohen, Polymer **34**, 4435–4444 (1993)

F. Polato, J. Mater. Sci. **20**, 1455–1465 (1985)

J. Qin, A.S. Argon, R.E. Cohen, J. Appl. Polym. Sci. **71**, 2319–2328 (1999)

F. Ramsteiner, W. Heckmann, Polym. Commun. **26**, 199–200 (1985)

T. Ricco, M. Rink, S. Caporusso, A. Pavan, An analysis of fracture initiation and crack growth in ABS resins, in *Toughening of Plastics II*, ed. by C.B. Bucknall (Plastics & Rubber Institute, London, 1985), pp. 27/21–27/29

J.A. Roetling, Polymer **6**, 311–317 (1965)

J.H. Rose, J.R. Smith, J. Ferrante, Phys. Rev. **28**, 1835–1845 (1983)

A. Rozanski, A. Galeski, Int. J. Plast. **41**, 14–19 (2013)

A. Sanchez-Solis, M.R. Estrada, J. Cruz, O. Manero, Polym. Eng. Sci. **40**, 1216–1225 (2000)

J.A. Schmitt, J. Appl. Polym. Sci. **12**, 533–546 (1968)

C.E. Schwier, A.S. Argon, R.E. Cohen, Philos. Mag. A **52**, 581–603 (1985)

C.E. Scott, C.W. Macosko, Int. Polym. Process. **10**, 36–45 (1995)

R. Seguela, J. Polym. Sci. B **40**, 593–601 (2002)

R. Seguela, O. Darras, J. Mater. Sci. **29**, 5342–5352 (1994)

R. Seguela, e-Polymers art. no. 032 (2007)

L.G. Shadrake, F. Guiu, Philos. Mag. **34**, 565–581 (1976)

N. Shah, J. Mater. Sci. **23**, 3623–3629 (1988)

S.J. Shaw, Rubber modified epoxy resins, in *Rubber Toughened Engineering Plastics*, ed. by A.A. Collyer (Chapmann and Hall, London, 1994), pp. 165–209

R.O. Sirotkin, N.W. Brooks, Polymer **42**, 3791–3797 (2001)

S.D. Sjoerdsma, Polymer **30**, 106–108 (1989)

J.U. Starke, R. Godehardt, G.H. Michler, C.B. Bucknall, J. Mater. Sci. **32**, 1855–1860 (1997)

A.C. Steenbrink, V.M. Litvinov, R.J. Gaymans, Polymer **39**, 4817–4825 (1998)

S.S. Sternstein, L. Ongchin, Polym. Preprint. Am. Chem. Soc. Div. Polym. Chem. **10**, 1117 (1969)

G. Strobl, *The Physics of Polymers. Concepts for Understanding Their Structures and Behavior* (Springer, New York, 1997)

H.-J. Sue, J. Mater. Sci. **27**, 3098–3107 (1992)

H.-J. Sue, A.F. Yee, Polym. Eng. Sci. **36**, 2320–2326 (1996)

M. Suess, J. Kressler, H.W. Kammer, Polymer **28**, 957–960 (1987)

J.N. Sultan, F.J. McGarry, Polym. Eng. Sci. **13**, 29–34 (1973)

Y. Suo, S.S. Hwang, K.U. Kim, J. Lee, S.I. Hong, Polymer **34**, 1667–1676 (1993)

Y. Takeda, D.R. Paul, J. Polym. Sci. B **30**, 1273–1284 (1992)

Y. Takeda, H. Kesskula, D.R. Paul, Polymer **33**, 3394–3407 (1992)

V. Tanrattanakul, A. Hiltner, E. Baer, W.G. Perkins, F.L. Massey, A. Moet, Polymer **38**, 2191–2200 (1997)

Y.S. Thio, A.S. Argon, R.E. Cohen, M. Weinberg, Polymer **43**, 3661–3674 (2002)

R.R. Tiwari, D.R. Paul, Polymer **52**, 5595–5605 (2011)

P.A. Tzika, M.C. Boyce, D.M. Parks, J. Mech. Phys. Solids **48**, 1893–1929 (2000)

L.A. Utracki, M.M. Dumoulin, Polypropylene alloys and blends with thermoplastics, in *Polypropylene: Structure, Blends and Composites*, ed. by J. Karger-Kocsis, vol. 2 (Chapman & Hall, London, 1995)

A. van Der Wal, J.J. Mulder, J. Oderkerk, R.J. Gaymans, Polymer **39**, 6781–6787 (1998)

F. Vazquez, M. Schneider, T. Pith, M. Lambla, Polym. Int. **41**, 1–12 (1996)

P. Vincent (ed.), *Mechanical Properties of Polymers* (Wiley Interscience, New York, 1971)

Y. Wang, J. Lu, G.J. Wang, J. Appl. Polym. Sci. **64**, 1275–1281 (1997)

I.M. Ward, *Mechanical Properties of Solid Polymers* (Wiley, New York, 1983)

S.T. Wellinghoff, E. Beaer, J. Appl. Polym. Sci. **22**, 2025–2045 (1978)

J.-I. Weon, K.-T. Gam, W.-J. Boo, H.-J. Sue, C.-M. Chan, J. Appl. Polym. Sci. **99**, 3070–3076 (2006)

M.W.L. Wilbrink, A.S. Argon, R.E. Cohen, M. Weinberg, Polymer **42**, 10155–10180 (2001)

H. Wilhelm, A. Paris, E. Schafler, S. Bernstorff, J. Bonarski, T. Ungar, J. Mater. Sci. Eng. A **387–389**, 1018–1022 (2004)

S. Wu, J. Polym. Sci. B **21**, 699–716 (1983)

S. Wu, Polymer **26**, 1855–1863 (1985)

S. Wu, Polym. Eng. Sci. **27**, 335–343 (1987)

S. Wu, J. Appl. Polym. Sci. **35**, 549–561 (1988)

S. Wu, J. Polym. Sci. B Polym. Phys. Ed. **27**, 723–741 (1989)

S. Wu, Polym. Eng. Sci. **30**, 753–761 (1990)

S. Wu, Polym. Int. **29**, 229–247 (1992)

H.Q. Xie, D.S. Feng, J.S. Guo, J. Appl. Polym. Sci. **64**, 329–335 (1997)

K. Yang, Q. Yang, G.X. Li, Y.J. Sun, D.C. Feng, Polym. Compos. **27**, 443–450 (2006)

K. Yang et al., Polym. Eng. Sci. **47**, 95–102 (2007)

A.F. Yee, J. Mater. Sci. **12**, 757–765 (1977)

A. F. Yee, Polymer Prepr. **17** (1976)

A.F. Yee, J. Du, M.D. Thouless, Toughening of epoxies, in *Polymer Blends, Vol. 2: Performance*, ed. by D.R. Paul, C.B. Bucknall (Wiley-Interscience, New York, 2000), pp. 225–268

R.J. Young, Philos. Mag. **30**, 85–94 (1974)

R.J. Young, Mater. Forum. **11**, 210–216 (1988)

Q. Yuan, J.S. Shah, K.J. Bertrand, R.D.K. Misra, Macromol. Mater. Eng. **294**, 141 (2009)

W.C.J. Zuiderduin, C. Westzaan, J. Huetink, R.J. Gaymans, Polymer **44**, 261–275 (2003)

W.C.J. Zuiderduin, J. Huetink, R.J. Gaymans, Polymer **47**, 5880–5887 (2006)

Broadband Dielectric Spectroscopy on Polymer Blends

12

Huajie Yin and Andreas Schönhals

Contents

Abstract

In this chapter broadband dielectric spectroscopy (BDS) is employed to polymeric blend systems. In its modern form BDS can cover an extraordinary broad frequency range from 10^{-4} to 10^{12} Hz. Therefore, molecular and collective dipolar fluctuations, charge transport, and polarization effects at inner phase boundaries can be investigated in detail including its temperature dependence.

H. Yin • A. Schönhals (✉)
BAM Federal Institute for Materials Research and Testing, Berlin, Germany
e-mail: huajie.yin@bam.de; Andreas.Schoenhals@bam.de

In the first part of the chapter, the theoretical basics of dielectric spectroscopy are briefly introduced covering both static and dynamic aspects. This section is followed by short description of the various experimental techniques to cover this broad frequency range. To provide the knowledge to understand the dielectric behavior of polymeric blend systems, the dielectric features of amorphous homopolymers are discussed in some detail. This concerns an introduction of the most important relaxation processes observed for these polymers (localized fluctuations, segmental dynamics related to the dynamic glass transition, chain relaxation), a brief introduction to the conductivity of disordered systems as well as polarization effects at phase boundaries. Theoretical models for each process are shortly discussed. In the last paragraph the dielectric behavior of polymer blends is reviewed where special attention is paid to binary systems for the sake of simplicity. In detail the dielectric behavior of binary miscible blends is described. The two most important experimental facts like the broadening of the dielectric relaxation spectra and the dynamic heterogeneity of the segmental dynamics are addressed in depth. Appropriate theoretical approaches like the temperature-driven concentration fluctuation model and the self-concentration idea are introduced.

12.1 Introduction

It was proved by many investigations that broadband dielectric spectroscopy (BDS) is a powerful technique to investigate the properties of polymeric systems (see, for instance, references McCrum et al. 1967; Hedvig 1977; Karasz 1972; Blythe 1979; Williams 1979, 1989, 1993; Runt and Fitzgerald 1997; Adachi and Kotaka 1993; Riande and Diaz-Calleja 2004; Kremer and Schönhals 2003; and references therein). This is mainly due to the fact that an extremely broad dynamical range from the millihertz to the terahertz region can be covered by dielectric spectroscopy in its modern form. A quite recent discussion of the basics and applications of this method can be found in reference Kremer and Schönhals (2003). This broad frequency range of BDS enables one to investigate motional processes which can take place in polymers on quite different length scales (localized fluctuations, segmental dynamics, and motions of the whole chain) by this method in broad range of frequencies and temperatures. This includes furthermore that the molecular motions in the different states of a polymeric material (i.e., the glassy or rubbery state) can be studied in detail from both points of view of basic and applied research. Moreover, the different motional processes as well as charge transport processes depend on the morphology of the system under consideration. Therefore, information on the structural state of the polymeric system under investigation can be indirectly extracted using molecular mobility and/or charge transport as probe for structure.

These considerations are absolutely relevant also for polymeric blends which have received much attention because materials with tailor-made and desired properties can be designed by the combination of polymers with different

properties. Therefore, the purpose of this chapter is to discuss the dielectric properties of polymers with special attention to polymeric blends. The motivation is both scientific and technological.

The literature about dielectric relaxation is rich. For instance, there are several recent reviews available for that field (Simon and Schönhals 2003; Runt 1997; Floudas et al. 2011; Colmenero and Arbe 2007). For instance, by application of dielectric spectroscopy to polymeric blends, the phase behavior of a system can be probed or the degree of miscibility of the blend components in the different phases can be discussed and estimated. This concerns also the question of the dynamic heterogeneity in miscible blend systems or confinement effects in dynamically asymmetric polymer blends (Colmenero and Arbe 2007).

The chapter is organized as follows. In the first part broadband dielectric spectroscopy is introduced. A brief review of the theoretical background of dielectric spectroscopy is provided. This will include the basics of dielectric spectroscopy, dielectric measurement techniques, and also data analysis. This section is followed by a discussion of the dielectric behavior of homopolymers to provide the basics to understand the dielectric properties of blends. In the second part of the chapter, the dielectric behavior of polymeric blends is reviewed where both miscible and immiscible systems are discussed. The chapter is restricted to binary systems.

12.2 Broadband Dielectric Spectroscopy

12.2.1 Fundamentals

Broadband dielectric spectroscopy deals with the interaction of electromagnetic fields with matter. The fundamental relationship between the electric field $\vec{E}$, the magnetic field strength $\vec{H}$, the dielectric displacement $\vec{D}$, the magnetic induction $\vec{B}$, the current density $\vec{j}$, and the density of charges ρ is given by the Maxwell equations (Maxwell 1865, 1868). In the linear case, this means for small electric field strengths, $\vec{D}$ can be expressed by

$$\vec{D} = \varepsilon^* \varepsilon_0 \, \vec{E} , \tag{12.1}$$

where ε_0 is the dielectric permittivity of vacuum ($\varepsilon_0 = 8.854 \ 10^{-12}$ As V^{-1} m^{-1}). The material properties are characterized by the complex dielectric function or dielectric permittivity ε^*. ε^* is time (or frequency) dependent if time-dependent processes take place within the sample. The molecular origin of the time dependence of ε^* will be discussed later during the course of this chapter.

In general, time-dependent processes within a material lead to a difference of the time dependencies of the outer electric field $\vec{E}$ (t) and the resulting dielectric

displacement $\vec{D}$ (t). In the simple case of a periodical field $E(t) = E_0 \exp(-i\,\omega\,t)$ (ω-radial frequency, $\omega = 2\pi f$, f-technical frequency, $i = \sqrt{-1}$ – imaginary unit) in the stationary state, the difference in the time dependence of $\vec{E}$ (t) and $\vec{D}$ (t) is a phase shift which can be described by the complex dielectric function

$$\varepsilon^*(\omega) = \varepsilon'(\omega) - i\varepsilon''(\omega), \tag{12.2}$$

where $\varepsilon'(\omega)$ is the real part and $\varepsilon''(\omega)$ the imaginary part of the complex dielectric function.

Equation 12.1 contains contribution to the dielectric displacement coming from the vacuum. The polarization $\vec{P}$ describes the dielectric displacement which originates from the response only of a material to an external field. It is defined as

$$\vec{P} = \vec{D} - \vec{D}_0 = (\varepsilon^* - 1)\,\varepsilon_0\ \vec{E} = \chi^*\varepsilon_0\ \vec{E}\ \text{ with } \chi^* = (\varepsilon^* - 1), \tag{12.3}$$

where χ^* is the dielectric susceptibility of the material under the influence of an outer electric field. For higher field strengths ($>10^6$ V/m, this order of magnitude will be valid for the most conventional polymeric systems), nonlinear effects may take place which can be described by a Taylor expansion of $\vec{P}$ with regard to $\vec{E}$ (t) where only odd powers will contribute. The corresponding coefficients are called hyperpolarizabilities. For more details, see, for instance, reference Schönhals and Kremer (2003c).

Analogous to Eq. 12.1, Ohm's law

$$\vec{j} = \sigma^* \vec{E} \tag{12.4}$$

gives the relationship between the electric field and the current density $\vec{j}$ (Ohm's law) where $\sigma^*(\omega) = \sigma'(\omega) + i\,\sigma''(\omega)$ is the complex conductivity where σ' and σ'' are the corresponding real and imaginary parts, respectively. In the case of absent magnetic fields, the current density and the time derivative of the dielectric displacement are equivalent quantities. It holds

$$\sigma^* = i\,\omega\,\varepsilon_0\,\varepsilon^*. \tag{12.5}$$

The time dependence of the dielectric properties of a material (expressed by ε^* or σ^*) under study can have different molecular origins. Resonance phenomena are due to atomic or molecular vibrations and can be analyzed by optical spectroscopy. The discussion of these processes is out of the scope of this chapter. Relaxation phenomena are related to molecular fluctuations of dipoles due to molecules or parts of them in a potential landscape. Moreover, drift motion of mobile charge carriers (electrons, ions, or charged defects) causes conductive contributions to the dielectric response. Moreover, the blocking of carriers at internal and external interfaces introduces further time-dependent processes which are known as Maxwell/Wagner/Sillars (Wagner 1914; Sillars 1937) or electrode polarization (see, for instance, Serghei et al. 2009).

Because $\vec{D}$ and $\vec{E}$ are vectors, $\varepsilon^*(\omega)$ and σ^* are in general tensors. This becomes important for anisotropic systems like liquid crystalline (Williams 1979) or crystalline materials. For the sake of simplicity, the tensorial character of the dielectric properties is neglected in the further discussion of this chapter.

In the following this chapter is organized as follows. In the first part the essential points of electrostatics are reviewed. That means the dielectric properties are discussed at an infinite time after an application of an outer electric field. In the second part, using the frame of linear response theory, the formalism of time-dependent dielectric processes is developed.

12.2.2 Electrostatics

12.2.2.1 Dipole Moments

The molecular origins of a macroscopic polarization P are dipole moments p_i. Hence, for molecules and/or particles in a volume V, the polarization can be calculated to

$$\vec{P} = \frac{1}{V}\sum \vec{p}_i, \tag{12.6}$$

where i counts all dipole moments in the system. Generally, a dipole moment is created if the electric centers of gravity of positive and negative charges do not collapse. In the simplest case a dipole moment is obtained if a positive and a negative charge q are separated by a distance. Then the dipole moment is $p = q * d$. This picture can be generalized to any distribution of charges (Schönhals and Kremer 2003c).

The microscopic dipole moments can have a permanent or an induced character. In the latter case the dipole moment is induced by the outer electric field itself which distorts a neutral distribution of charges. An example of induced polarization is the electronic polarization where the negative electron cloud of an atom (molecule) is shifted with respect to the positive nucleus. This process takes place at a time constant of 10^{-12} s because of the low mass of the electrons. A further example is atomic polarization which has a comparable time scale. Induced polarization effects can be abstracted in the induced polarization P_∞.

For molecules with a permanent dipole moment μ, charge separation is given by the structure of the chemical compound. Hence, for a system containing only one kind of dipoles, Eq. 12.6 simplifies to

$$\vec{P} = \frac{1}{V}\sum \vec{\mu}_i + \vec{P}_\infty = \frac{N}{V}\left\langle \vec{\mu} \right\rangle + \vec{P}_\infty, \tag{12.7}$$

where N denotes the whole number of dipoles in the system and $<\vec{\mu}>$ the mean dipole moment. If the system contains different kinds of dipoles, one has to sum up over all kinds. This is especially true for polymeric systems where dipole moments

can be related to molecular groups, to segments (repeating unit), or to the chain itself (Schönhals 2003). This will be discussed later during the course of this paragraph.

Permanent dipole moments can be oriented by an electric field. This is called orientation polarization. To calculate the mean dipole moment $<\vec{\mu}>$ under the influence of an electric field, several assumptions must be made. Generally, inertia effects contribute only to P_∞ because of the short time scale involved. Assuming further that the electric field at the locus of the dipole is equal to the outer electric field and that the dipoles do not interact with each other (isolated dipoles), then the mean dipole moment can be calculated in the framework of the Debye approach (Debye 1929). Under these assumptions the mean dipole moment is due to a counterbalance of the thermal energy k_BT (Boltzmann constant) and the interaction energy W of a dipole with the electric field given by $W = -\vec{\mu} \cdot \vec{E}$. Employing Boltzmann statistics and further reconsidering that the electrical interaction energy is small compared to the thermal energy, one obtains (Schönhals and Kremer 2003c)

$$\left\langle \vec{\mu} \right\rangle = \frac{\mu^2}{3\,k_B\,T}\ \vec{E}. \qquad (12.8)$$

The polarization can be calculated by inserting Eq. 12.8 into Eq. 12.7:

$$\vec{P} = \frac{\mu^2}{3\,k_B\,T}\ \frac{N}{V}\ \vec{E}. \qquad (14.9)$$

The change in the dielectric permittivity due to orientation polarization can be obtained by combining Eqs. 12.3 and 12.9. It holds

$$\Delta\varepsilon = \varepsilon_S - \varepsilon_\infty = \frac{1}{3\,\varepsilon_0}\,\frac{\mu^2}{k_B\,T}\,\frac{N}{V}, \qquad (12.10)$$

where $\varepsilon_S = \lim_{\omega\to 0} \varepsilon'(\omega)$. $\varepsilon_\infty = \lim_{\omega\to\infty} \varepsilon'(\omega)$ covers all contributions to the dielectric function which are due to induced polarization P_∞. In the following $\Delta\varepsilon$ is also called dielectric strength.

The fact that the electric field at the dipole is not exactly the same as the applied one results in shielding effects. These internal field effects were treated historically by Lorentz (1879), Clausius (1879), and Massotti (1847). A more general approach was developed by Onsager (1938) introducing the reaction field. Within this approach Eq. 12.10 is modified to

$$\varepsilon_S - \varepsilon_\infty = \frac{1}{3\varepsilon_0}F\frac{\mu^2}{k_B\,T}\,\frac{N}{V} \ \text{with} \ F = \frac{\varepsilon_S(\varepsilon_\infty + 2)^2}{3\,(2\varepsilon_S + \varepsilon_\infty)}. \qquad (12.11)$$

In general the Onsager factor F is an unspecific correction. A more detailed discussion can be found in reference Böttcher (1973).

In difference to the Onsager factor F, the interaction of dipoles plays an important role in condensed systems. This is especially true also for polymeric materials. Specific interactions between molecules and segments in the case of polymers can be caused, for instance, by hydrogen bonding, steric interactions, etc., and can lead to associations of molecules or segments.

The problem of the interaction of dipoles was treated by Kirkwood (1939, 1940, 1946) and Fröhlich (1958). Starting point is the statistical mechanics (Böttcher 1973; Landau and Lifschitz 1979) where the contribution of the orientation polarization to the dielectric permittivity is expressed by

$$\varepsilon_S - \varepsilon_\infty = \frac{1}{3\,k_B\,T\,\varepsilon_0}\,\frac{<\vec{P}(0)\;\vec{P}(0)>}{V} = \frac{1}{3\,k_B\,T\,\varepsilon_0}\,\frac{<\sum_i \vec{\mu}_i(0) \sum_j \vec{\mu}_j(0)>}{V},$$

(12.12)

where $<\vec{P}(0)\;\vec{P}(0)>$ is the static correlation function of polarization (dipole) fluctuations. The symbol (0) refers to an arbitrary time, for instance, $t = 0$. In the further consideration it is dropped for brevity. The brackets denote averaging which has to be carried out over the whole system considering all interactions. For complex systems including polymers, Eq. 12.12 is extremely difficult to analyze. Therefore, a correlation factor g was introduced by

$$g = \frac{<\sum_i \mu_i \sum_j \mu_j>}{N\mu^2} = 1 + \frac{<\sum_i \sum_{i<j} \mu_i \mu_j>}{N\mu^2} = \frac{\mu_{Interact.}^2}{\mu^2},$$

(12.13)

where μ^2 is the mean square dipole moment for noninteracting, isolated dipoles which can be measured, for instance, in diluted solutions. The value of g can be smaller or greater than 1 depending on the case if the segments have the tendency to orient antiparallel or parallel due to specific interaction as discussed above.

The calculation of g by Eq. 12.13 involves the same difficulties as estimations according to Eq. 12.12. Therefore, Kirkwood and Fröhlich (Kirkwood 1939, 1940, 1946; Fröhlich 1958) suggested to treat a given number of dipoles exactly where the remaining molecules/segments were considered like in the Onsager approach as an infinite continuum where the dielectric behavior is characterized by ε_S. Within this approach one obtains

$$\varepsilon_S - \varepsilon_\infty = \frac{1}{3\varepsilon_0}\,F\,g\,\frac{\mu^2}{k_B T}\,\frac{N}{V}.$$

(12.14)

In the simplest case only the nearest neighbors of a selected test dipole are considered. For that case g can be approximated by

$$g = 1 + z < \cos \Psi >, \tag{12.15}$$

where z is the coordination number and ψ is the angle between the test dipole and a neighbor (Böttcher 1973).

12.2.2.2 Dipole Moments of Polymers

For a macromolecule the polarization can be written as

$$\vec{P} = \frac{1}{V} \sum_{\text{chain}} \sum_{\text{repeating unit}} \vec{\mu}_i, \tag{12.16}$$

where $\vec{\mu}_i$ is the dipole moment of the repeating unit i. In difference to low-molecular-weight compounds where the dipole moment can be well represented by a rigid vector for long-chain molecules, there are different possibilities for the orientation of a molecular dipole vector with respect to the polymer backbone. A corresponding nomenclature was developed by Stockmayer (1967) (Stockmayer and Burke 1969). A macromolecule where the dipole moment is oriented parallel to the backbone is called type-A polymer. For these systems the dielectric strength is proportional to the mean square end-to-end vector of the chain (Adachi and Kotaka 1993). For type-B polymers the dipole moment is rigidly attached perpendicular to the chain skeleton. Therefore, for the dipole moment $\vec{P}_B$ of a type-B polymer $< \vec{P}_B \cdot \vec{r} > = 0$ holds, where $\vec{r}$ is the end-to-end vector of the chain, there is no correlation between the dipole moment and the chain contour (no long-range correlations of the dipole moments of different repeating units). Most of the synthetic polymers are of type B. Although there is no polymer which is solely of type-A, there are several examples of macromolecules like *cis*-1,4-polyisoprene (Adachi and Kotaka 1993) having components of the dipole moment parallel and perpendicular to the chain. These polymers are also called type-A or type-AB polymers. A more detailed discussion is given by Adachi (Adachi and Kotaka 1993).

Macromolecules having a flexible side chain carrying a dipole moment are called to be of type C (Block 1979). A typical example are poly(n-alkyl methacrylate)s. This definition is only appropriate under the condition that the side chain can fluctuate on a shorter time scale than the segmental dynamics of the macromolecule. Otherwise the polymer is of type B.

For a type-B polymer, the mean square dipole moment can be expressed by

$$<\mu^2> = \sum_{i=1}^{N} |\vec{\mu}_i|^2 + 2 \sum_{i=1}^{N} \sum_{j<i} |\vec{\mu}_i| \, |\vec{\mu}_j| < \cos \gamma_{ij} >, \tag{12.17}$$

where γ_{ij} is the angle between bonds i and j. $| \vec{\mu} | = m$ denotes the norm of the dipole moment perpendicular to the chain. $< \cos \gamma_{ij} > = 0$ holds for the freely joined

chain model (for definition see Flory (1989)). For real chains also short-range intramolecular correlations ($<\cos \gamma_{ij}> \neq 0$) contribute to the mean square dipole moment which can be described by the intramolecular dipolar correlation coefficient g_{intra} defined as

$$g_{intra} = \frac{<\mu^2>}{\sum\limits_{i=1}^{N} m_i^2} = 1 + 2 \sum\limits_{i=1}^{N} \sum\limits_{j<i} <\cos \gamma_{ij}>. \tag{12.18}$$

g_{intra} can be regarded as the Kirkwood/Fröhlich correlation factor for an isolated chain and is a measure for the correlations between dipole moments of neighbored repeating units. Calculations of g_{intra} were started by Debye and Bueche (1951). The rotational isomeric state model (Flory 1989; Volkenstein 1963) can be used to make more detailed estimations. A discussion can be found elsewhere (Riande and Saiz 1992).

12.2.3 Time-Dependent Dielectric Processes

For small electric field strength, the dielectric relaxation can be described in the framework of the linear response theory (Landau and Lifschitz 1979). The relevant materials equation which links the time-dependent polarization P(t) with the time-dependent electric field E(t) is given by (Schönhals and Kremer 2003c)

$$P(t) = P_\infty + \varepsilon_0 \int\limits_{-\infty}^{t} \varepsilon(t - t') \frac{dE(t')}{dt'} dt', \tag{12.19}$$

where P_∞ is the polarization for infinite time covering all contributions from induced polarization and $\varepsilon(t)$ is the time-dependent dielectric function. $\varepsilon(t)$ can be directly measured as response of the system caused by a steplike change of the outer electric field as it is shown in Fig. 12.1.

If the time dependence of the outer electric field is periodically $E^*(\omega) = E_0 \exp(-i\omega t)$, in the stationary case, Eq. 12.19 becomes

$$P^*(\omega) = \varepsilon_0 (\varepsilon^*(\omega) - 1) E^*(\omega), \tag{12.20}$$

where $\varepsilon^*(\omega)$ is the complex dielectric function defined above (see Eq. 12.2). The relationship between $P^*(\omega)$ and $E^*(\omega)$ on the one hand side and $\varepsilon'(\omega)$ and $\varepsilon''(\omega)$ on the other side is sketched in Fig. 12.2. The tangent of the phase angle δ (see Fig. 12.2) is given by

Fig. 12.1 Schematic relationship between the time dependence of the electric field ΔE (*upper panel*), the polarization P(t), and the time-dependent dielectric relaxation function ε(t) (*lower panel*). For the sake of simplicity, the vector sign is omitted in the figure
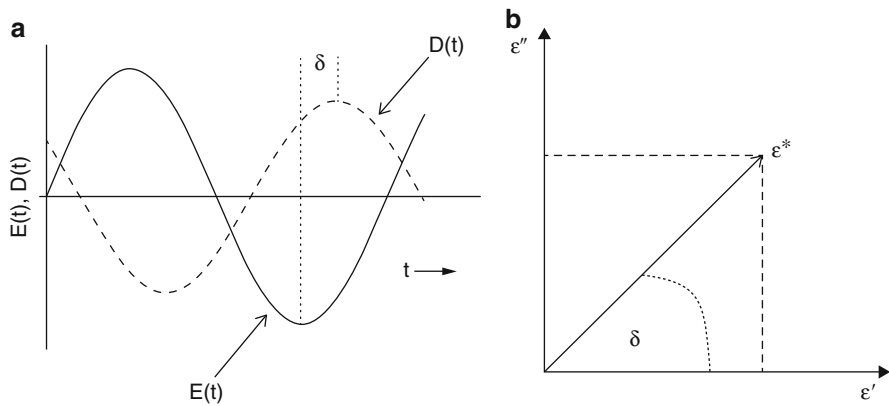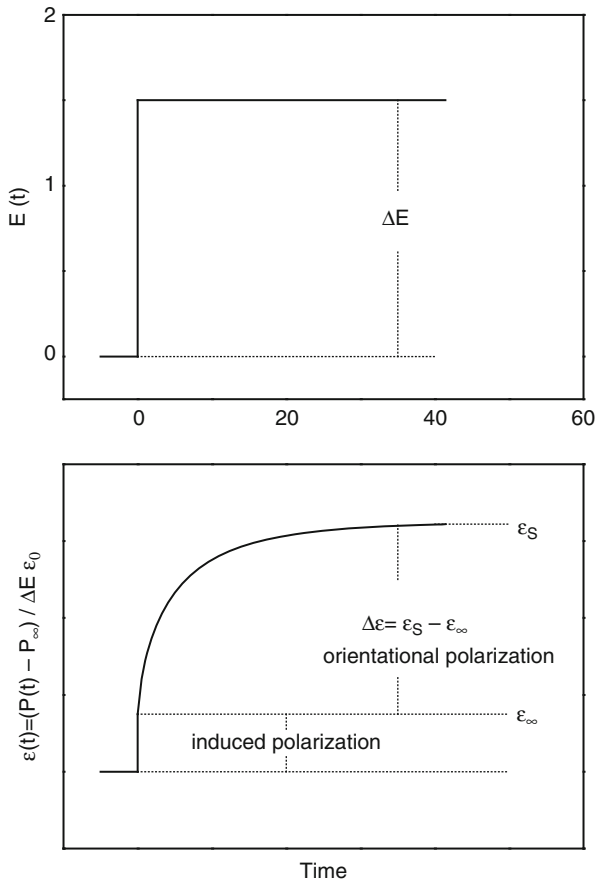
Fig. 12.2 (**a**) Phase shift between the electric field and dielectric displacement. (**b**) Relation between the complex dielectric function, its real part ε' and imaginary part ε'' as well as the phase angle δ

$$\tan \delta = \frac{\varepsilon''}{\varepsilon'}. \tag{12.21}$$

For scientific studies, however, the dielectric properties should be characterized by $\varepsilon'(\omega)$ and $\varepsilon''(\omega)$ since they have a defined physical significance. In electrical engineering, the reciprocal value of $\tan \delta$ is termed the merit factor $Q = 1/\tan\delta$.

Equation 12.22 further provides the relationship between the time-dependent dielectric function $\varepsilon(t)$ and the complex dielectric function $\varepsilon^*(\omega)$:

$$\varepsilon^*(\omega) = \varepsilon'(\omega) - i\varepsilon''(\omega) = \varepsilon_\infty - \int_0^\infty \frac{d\varepsilon(t)}{dt} \exp(-i\omega t)\, dt. \tag{12.22}$$

The time dependence of the dielectric response can be due to different processes like the fluctuations of dipoles (relaxation processes), the drift motion of charge carriers (conduction processes), and the blocking of charge carriers at interfaces (Maxwell/Wagner/Sillars polarization). In the following subchapters these effects will be discussed from a theoretical point of view.

12.2.3.1 Dielectric Relaxation

Relaxation processes are due to molecular fluctuations of dipoles. For this case Eq. 12.12 can be generalized to time-dependent processes defining a correlation function $\Phi(\tau)$ by

$$\Phi(\tau) = \frac{<\Delta P(\tau)\,\Delta P(0)>}{<\Delta P^2>} \sim \frac{<\sum_i \vec{\mu}_i(0) \sum_j \vec{\mu}_j(\tau)>}{<\sum_i \mu_i \sum_j \mu_j>}, \tag{12.23}$$

where τ denotes a time variable. It holds $\Phi(0) = 1$ and $\Phi(\tau\rightarrow\infty) = 0$. Like Eq. 12.12 $\Phi(\tau)$ can be related to the fluctuations of microscopic dipole moments (right part of Eq. 12.23). For more details see references Williams (1979) and Schönhals and Kremer (2003). Equation 12.23 is difficult to handle from a microscopic point of view.

From a macroscopic point of view, the simplest approach to calculate the time dependence of the dielectric behavior is to assume that the change in polarization is proportional to its actual value (Debye 1929; Fröhlich 1958)

$$\frac{dP(t)}{dt} = -\frac{1}{\tau_D} P(t), \tag{12.24}$$

where τ_D is a characteristic relaxation time. The solution of this first-order differential equation leads to an exponential decay for $\Phi(\tau)$:

Fig. 12.3 Frequency
dependence of the real part ε'
and imaginary part ε'' of the
complex dielectric function
according to the Debye
function
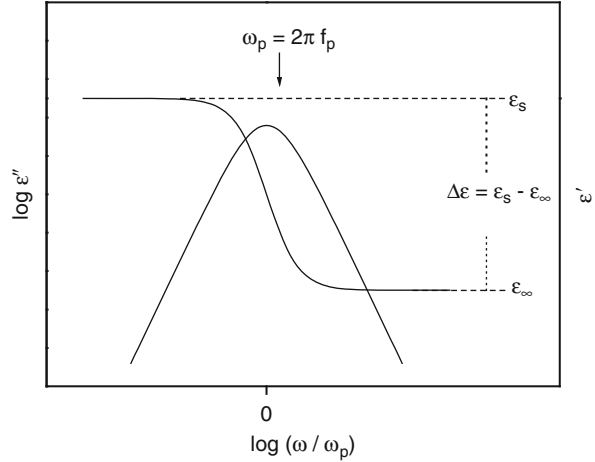
$$P(t) \sim \varepsilon(t) \sim \Phi(\tau) = \exp\left[-\frac{t}{\tau_D}\right]. \tag{12.25}$$

According to Eq. 12.22 for the complex dielectric function, one obtains

$$\varepsilon^*(\omega) = \varepsilon_\infty + \frac{\Delta\varepsilon}{1 + i\omega\tau_D}; \ \varepsilon' = \varepsilon_\infty + \frac{\Delta\varepsilon}{1 + (\omega\tau_D)^2}; \ \varepsilon'' = \frac{\Delta\varepsilon\,\omega\tau_D}{1 + (\omega\tau_D)^2}. \tag{12.26}$$

Equation 12.26 is known as Debye equation. Figure 12.3 gives the frequency
dependence of the real and imaginary (loss) part of the Debye function. ε' shows
a steplike decay with increasing frequency where ε'' presents a symmetric peak
with a maximum $\omega_p = 2\pi f_p = 1/\tau_p$ and a half width of 1.14 decades. The Debye
equation can be justified by different molecular models like in the framework of
a simple double potential model or the rotational diffusion approach.

For polymeric systems in the most cases, the measured dielectric loss is much
broader and in addition the loss peak is asymmetric. This is called non-Debye or
nonideal relaxation behavior. Formally such a non-Debye-like behavior can be
described by a supposition of Debye functions

$$\varepsilon^*(\omega) - \varepsilon_\infty = \Delta\varepsilon \int_{-\infty}^{\infty} \frac{L(\tau)}{1 + i\omega\tau} d\ln\tau \qquad \int_{-\infty}^{\infty} L(\tau)\,d\ln\tau = 1, \tag{12.27}$$

where $L(\tau)$ is the dielectric relaxation time distribution. A modeling of a dielectric
relaxation process by Eq. 12.27 does not mean automatically that the underlying
molecular processes can be interpreted in terms of Eq. 12.26.

There were several attempts to generalize the Debye function like the Cole/Cole formula (Cole and Cole 1941) (symmetric broadened relaxation function), the Cole/Davidson equation (Davidson and Cole 1950, 1951), or the Fuoss/Kirkwood model (asymmetric broadened relaxation function) (Fuoss and Kirkwood 1941). The most general formula is the model function of Havriliak and Negami (HN function) (Havriliak and Negami 1966, 1967; Havriliak 1997) which reads

$$\varepsilon^*_{HN}(\omega) = \varepsilon_\infty + \frac{\Delta\varepsilon}{\left(1 + (i\omega\tau_{HN})^\beta\right)^\gamma}. \tag{12.28}$$

In Eq. 12.28 β and γ ($0 < \beta$, $\beta\gamma \leq 1$) are fractional shape parameters which describe the symmetric and asymmetric broadening of the complex dielectric function. τ_{HN} is characteristic relaxation time. The maximum position of the dielectric loss depends on the shape parameters according to (Diaz-Calleja 2000; Boersema et al. 1998; Schröter et al. 1998)

$$\omega_p = \frac{1}{\tau_{HN}} \left[\sin \frac{\beta\pi}{2 + 2\gamma}\right]^{\frac{1}{\beta}} \left[\sin \frac{\beta\gamma\pi}{2 + 2\gamma}\right]^{\frac{-1}{\beta}}. \tag{12.29}$$

The separation into real and loss part yield to

$$\varepsilon'(\omega) - \varepsilon_\infty = \Delta\varepsilon\, r(\omega) \cos(\gamma\Psi(\omega)); \quad \varepsilon'' = \Delta\varepsilon\, r(\omega) \sin(\gamma\Psi(\omega)) \tag{12.30}$$

with

$$r(\omega) = \left[1 + 2(\omega\tau_{HN})^\beta \ \cos\left(\frac{\beta\pi}{2}\right) + (\omega\tau_{HN})^{2\beta}\right]^{\frac{-\gamma}{2}} \tag{12.30a}$$

and

$$\psi(\omega) = \arctan\left[\frac{\sin\left(\frac{\beta\pi}{2}\right)}{(\omega\tau_{HN})^{-\beta} + \cos\left(\frac{\beta\pi}{2}\right)}\right]. \tag{12.30b}$$

Figure 12.4 compares the calculated dielectric loss for the Debye and the HN function for different shape parameters.

From the experimental point of view, all relevant parameters like the relaxation rate (or time), the dielectric strength, and the shape parameters can be estimated by fitting the HN function to the data (for details see references Schlosser and Schönhals 1989; Schönhals and Kremer 2003). As an example Fig. 12.5 gives the dielectric loss for poly(vinyl acetate) at the dynamic glass transition versus frequency at a temperature of T = 335.6 K. Only the HN function is able to describe the data correctly.
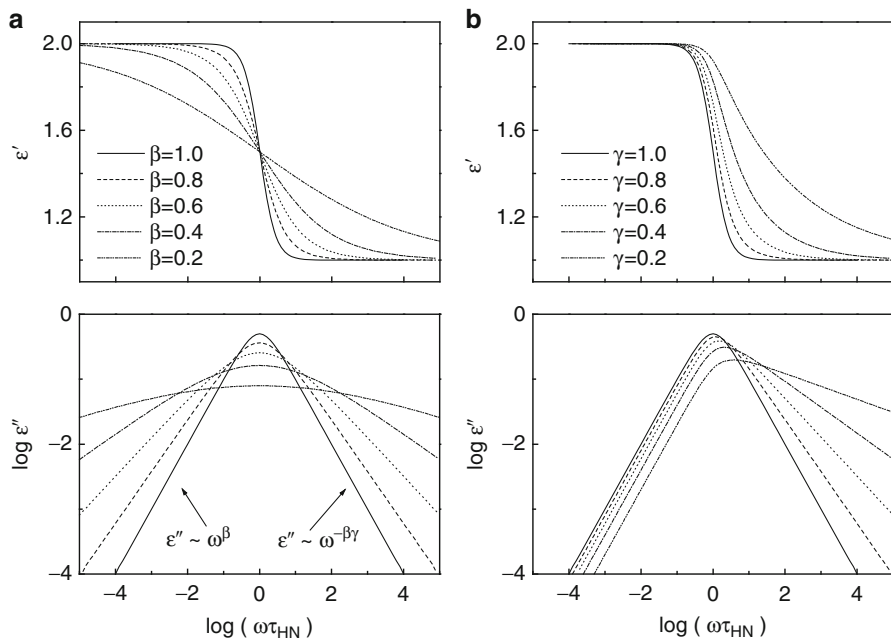
Fig. 12.4 Complex dielectric function according to the Havriliak/Negami function ($\tau_{HN} = 1$ s, $\Delta\varepsilon = 1$, $\varepsilon_\infty = 1$): (**a**) γ fixed to $\gamma = 1$, β varied. (**b**) β fixed to $\beta = 1$, γ varied

Fig. 12.5 Dielectric loss of poly(vinyl acetate) versus frequency at T = 335.6 K. The *dashed line* is a fit of the HN equation to the data including a conductivity contribution. The *solid line* represents the relaxational contribution according to the HN function. The *dashed-dotted line* represents the Debye function
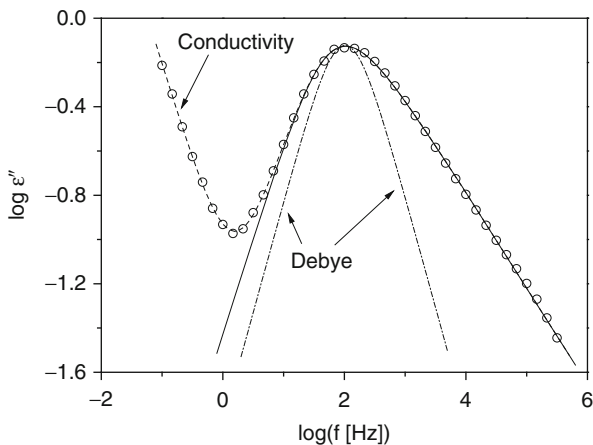
12.2.3.2 Electrical Conduction

Equation 12.5 gives the relationship between the complex dielectric function and the complex conductivity. For semiconducting disordered materials like conducting polymers, the frequency dependence of the real part of the complex conductivity

$\sigma'(\omega)$ displays a kind of similar behavior (Dyre and Schroder 2000). (1) At temperatures where charge transport is enabled, $\sigma'(\omega)$ has a plateau σ_0 for frequencies ω smaller than a given crossover frequency ω_c. (2) For frequencies $\omega > \omega_c$ a gradual dispersion sets in the form of a power law $\sigma'(\omega) \sim \omega^s$, with $0.5 \leq s \leq 1$. The parameter s increases with decreasing temperature and increasing frequency. (3) In a good approximation a time-temperature superposition can be assumed by scaling the normalized conductivity $\sigma'(\omega)/\sigma'(0)$ with respect to a normalized frequency ω/ω_c. (4) Between $\sigma'(0)$ and ω_c the Barton-Nakajima-Namikawa (BNN) relationship $\sigma'(0) \sim \omega_c$ holds (Barton 1966; Nakajima 1971; Namikawa 1975).

A variety of models exist to explain these similarities on a microscopic level. The simplest of them is the random free energy barrier model developed by Dyre (1988). In this model hopping is assumed to be basic mechanism for conduction where hopping takes place over spatially varying energy barriers. Within the continuous time random walk approximation (Montroll and Weiss 1965), this model results in

$$\sigma^*(\omega) = \sigma(0) \left[\frac{i\omega\tau_e}{\ln(1 + i\omega\tau_e)} \right], \tag{12.31}$$

where $1/\tau_e$ is the attempt frequency to overcome the highest energy barrier determining the DC conductivity $\sigma(0)$. For the real $\sigma'(\omega)$ and imaginary part $\sigma''(\omega)$,

$$\sigma'(\omega) = \frac{\sigma(0)\,\omega\tau_e \arctan(\omega\tau_e)}{0.25\ln^2\left(1 + \omega^2\tau_e^2\right) + \arctan(\omega\tau_e)} \tag{12.32}$$

$$\sigma''(\omega) = \frac{\sigma(0)\,\omega\tau_e \ln(1 + \omega\tau_e)}{0.25\ln^2\left(1 + \omega^2\tau_e^2\right) + \arctan(\omega\tau_e)} \tag{12.33}$$

is delivered. For the exponent s one obtains $s = 1 - 2/\ln(\omega\tau_e)$ (Dyre 1988).

12.2.3.3 Interfacial Polarization

Interfacial polarization or Maxwell/Wagner/Sillars (MWS) polarization (Wagner 1914; Sillars 1937) is a phenomenon that is characteristic for phase-separated or multiphase systems like immiscible polymer blends. Precondition for the observation of a MWS polarization is that the different phases have nonidentical properties. As a result of this, for instance, accumulation of charges takes place at the interfaces of the different phases. Steeman and van Turnhout (2003) published a compilation concerning polymeric materials including polymer blends.

MWS polarization gives rise to a dielectric behavior that can be very difficult to be distinguished from dipole relaxation. All properties of the process related to MWS polarization like its position, its strength, and its shape depend strongly on

the complex permittivity, the geometry and conductivity of the dispersed phase, as well as the dielectric properties of the matrix. As an example, a dispersed phase is considered having the complex dielectric function $\varepsilon_f^*(\omega)$ with the volume fraction ϕ_f where the matrix exhibits a complex dielectric permittivity $\varepsilon_M^*(\omega)$. In a mean field approach, the complex dielectric function $\varepsilon_C^*(\omega)$ of the heterogeneous system can be calculated to (Steeman and van Turnhout 2003)

$$\varepsilon_C^*(\omega) = \varepsilon_M^*(\omega) \frac{\left[n\varepsilon_f^*(\omega) + (1-n)\varepsilon_M^*(\omega) \right] + (1-n)\left[\varepsilon_f^*(\omega) - \varepsilon_M^*(\omega)\phi_f \right]}{\left[n\varepsilon_f^*(\omega) + (1-n)\varepsilon_M^*(\omega) \right] - n\left[\varepsilon_f^*(\omega) - \varepsilon_M^*(\omega)\phi_f \right]}. \quad (12.34)$$

n $(0 \leq n \leq 1)$ is the shape factor of the dispersed phase in the direction of the electric field lines. For spheres the values n in three directions (a, b, c) are identical with $n_a = n_b = n_c = 1/3$. For rodlike phase $0 \leq n \leq 1/3$ holds with the limiting case of a needle $n_a = 0$ and $n_b = n_c = 1/2$. For a platelike particle $n_a = 1$ and $n_b = n_c = 0$ holds. For more details see reference van Beek (1967).

Considering these equations one has to keep in mind that the morphology of phase-separated polymer systems is often more complex or even not well defined. This makes a quantitative modeling quite difficult.

12.2.4 Dielectric Instrumentation

The complex dielectric function $\varepsilon^*(f)$ can be measured in the extremely broad frequency regime from 10^{-3} to 10^{12} Hz. To do so different methods based on different physical principles must be combined. A detailed overview can be found elsewhere (Kremer and Schönhals 2003).

For lower frequencies (10^{-3}–10^7 Hz), the sample is modeled as a parallel or serial circuit of an ideal capacitor and an ohmic resistor. The spatial extent of the sample on the distribution of the electric field is neglected. This is called lumped circuit approximation. For frequencies higher than 100 kHz, firstly, parasitic impedances caused by cables, connectors, etc., become important. Secondly, the wavelength of the electromagnetic field decreases to the order of magnitude of the sample dimension. This means the geometrical dimensions of the sample capacitor become more and more important limiting the application of the lumped circuit methods to about 10 MHz. For higher frequencies the so-called distributed circuit approach has to be applied. By the application of both waveguide and cavity techniques, complex propagation factor (in reflection or transmission) can be measured from which the complex dielectric function can be deduced in the frequency range from 10^7 to 10^{11} Hz. For even higher frequencies quasi-optical setups and Fourier transformation techniques can be employed. A detailed discussion of these methods is beyond the scope of this chapter.

The complex dielectric function is related to the complex capacity C* of a capacitor filled with a polymeric material under study by

$$\varepsilon^*(\omega) = \frac{C^*(\omega)}{C_0} = \frac{J^*(\omega)}{i\,\omega\,\varepsilon_0\,E^*(\omega)} = \frac{1}{i\,\omega\,Z^*(\omega)\,C_0}, \qquad (12.35)$$

where C_0 is the (geometrical) capacitance of the unfilled sample capacitor. For a periodical field in the linear range with the angular frequency ω, the complex dielectric function can be expressed by measuring the complex impedance $Z^*(\omega)$ of the sample where $J^*(\omega)$ is the complex current density. Different experimental setups (Kremer and Schönhals 2003) like Fourier correlation analysis in combination with dielectric converters (10^{-6}–10^7 Hz) (Pugh and Ryan 1979; Schaumburg 1994, 1999), impedance analysis (10^1–10^7 Hz), RF reflectometry (10^6–10^9 Hz) (Böhmer et al 1989; Jiang et al. 1993), and network analysis (10^7–10^{11} Hz) (Collin 1966; Hewlett Packard 1985; Pelster 1995) are employed. In the following selected methods which have implications on polymeric blend systems are described in more detail.

12.2.4.1 Fourier Correlation Analysis in Combination with Dielectric Converters

The principle of the Fourier correlation analysis is given in Fig. 12.6. A generator provides a sinusoidal voltage $U_1(t)$ with angular frequency ω which causes a current $I_S(t)$ through the sample having an impedance $Z_S^*(\omega)$. The resistor R converts $I_S(t)$ into a voltage $U_2(t)$. Both voltages $U_1(t)$ and $U_2(t)$ are analyzed with respect to their amplitude and phase with regard to the base frequency ω by Fourier analysis. Technically this is carried out by employing two phase sensitive correlators providing the complex voltages $U_1^*(\omega)$ and $U_2^*(\omega)$. Hence, the sample impedance is given according to Ohm's law by

$$Z_S^*(\omega) = \frac{U_S^*(\omega)}{I_S^*(\omega)} = R\left(\frac{U_1^*(\omega)}{U_2^*(\omega)} - 1\right) \qquad (12.36a)$$

where for $U_j^*(\omega) = U_j'(\omega) + i\,U_j''(\omega)$ (j = 1,2),
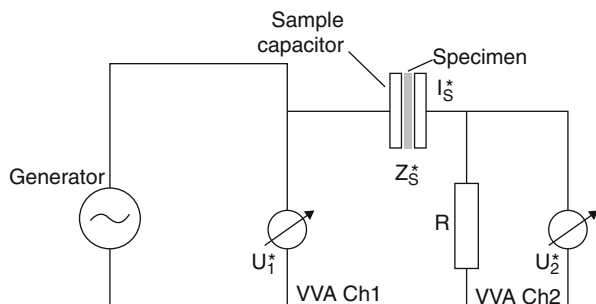
Fig. 12.6 Circuit diagram of Fourier correlation analysis (*VVA* vector voltage analyzer)

Fig. 12.7 Circuit diagram of Fourier correlation analysis with a dielectric converter for the low-frequency range and a variable reference impedance $Z_R^*(\omega)$ (*VVA* vector voltage analyzer)
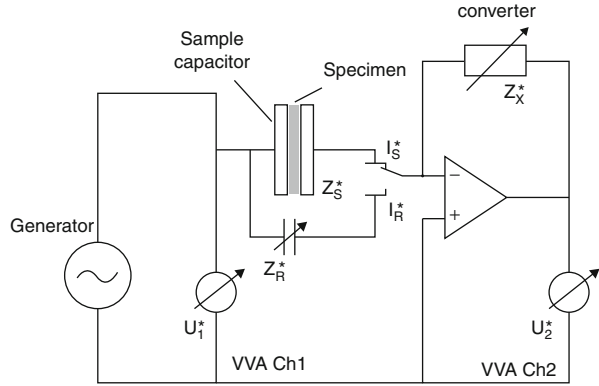
$$U_j'(\omega) = \frac{1}{NT} \int_0^{NT} U_j(t) \sin(\omega t)\, dt \quad \text{and} \tag{12.36b}$$

$$U_j''(\omega) = \frac{1}{NT} \int_0^{NT} U_j(t) \cos(\omega t)\, dt \tag{12.36c}$$

holds. N is the number of cycles with duration $T = 2\pi/\omega$, $U_S^*(\omega)$ is the complex voltage at the sample, and $I_S^*(\omega)$ is the complex current through the sample. Technically the Fourier analysis is done by frequency response analyzers or lock-in amplifiers which are state-of-the-art equipments. Digital components like filters are employed.

A fixed resistor R especially for low frequencies f suffers several limitations. Therefore, the resistor R is replaced by an amplifier with a variable gain according to Fig. 12.7. This results in a variable impedance $Z_X^*(\omega)$ which can be adjusted to the impedance of the sample $Z_S^*(\omega)$. For the sample impedance, then

$$Z_S^*(\omega) = \frac{U_{1S}^*(\omega)}{I_S^*(\omega)} = -\frac{U_{1S}^*(\omega)}{U_{2S}^*(\omega)} Z_X^*(\omega) \tag{12.37}$$

holds. The accurateness in the determination of $Z_S^*(\omega)$ is limited by phase and amplitude errors in the amplifier and correlators as well as by the contribution of the cables. These errors can be minimized by measuring a known impedance $Z_R^*(\omega)$ under the same condition as the sample. Analogous to Eq. 12.37

$$Z_R^*(\omega) = \frac{U_{1R}^*(\omega)}{I_R^*(\omega)} = -\frac{U_{1R}^*(\omega)}{U_{2R}^*(\omega)} Z_X^*(\omega) \tag{12.38a}$$

holds. By combining Eqs. 12.37 and 12.38a, one obtains for the impedance of the sample

Fig. 12.8 Circuit diagram of an impedance bridge
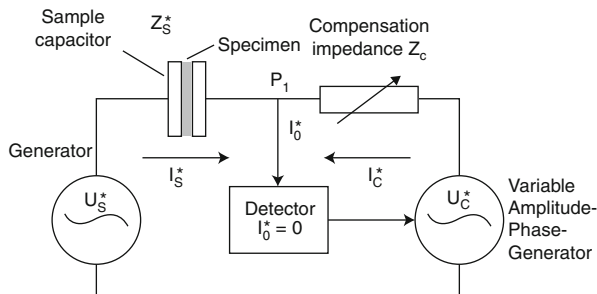
$$Z_S^*(\omega) = \frac{U_{1S}^*(\omega)}{U_{2S}^*(\omega)} \frac{U_{2R}^*(\omega)}{U_{1R}^*(\omega)} Z_R^*(\omega). \tag{12.38b}$$

12.2.4.2 Impedance Bridges

In principle impedance bridges are the extensions of the Wheatstone resistance bridge to complex resistances (impedances). Historically one has to consider the Schering bridge or the bridge according to Giebe und Zickner (see, for instance, McCrum et al. 1967).

The principle of modern impedance bridges is given in Fig. 12.8. In the sample branch a generator generates the sinusoidal voltage $U_S^*(\omega)$ with an angular frequency ω. This voltage causes a current $I_S^*(\omega)$ through the sample with the impedance $Z_S^*(\omega)$ at point P1. In the comparison branch a second generator generates a voltage which can be varied with regard to both its phase and its amplitude. This voltage is adjusted in that way that it drives a current $I_C^*(\omega)$ through a compensation impedance $Z_C^*(\omega)$ which is equal to $-I_S^*(\omega)$. Hence, in the balanced state at P1 $I_0^* = I_S^* - I_C^* = 0$ is valid and for the sample impedance

$$Z_S^*(\omega) = \frac{U_S^*(\omega)}{I_S^*(\omega)} = -\frac{U_S^*(\omega)}{U_C^*(\omega)} Z_C^*(\omega) \tag{12.39}$$

is obtained.

12.2.4.3 High-Frequency Methods

For frequencies higher than 10^6 Hz, the electromagnetic waves have to be guided in coaxial waveguides because the use of cables will lead to parasitic losses mainly due to inductivities. Moreover, standing waves may arise at frequencies higher than 10^7 Hz. A modern approach to measure the dielectric properties in the frequency range from 10^6 to 10^9 Hz is coaxial reflectometry (Böhmer et al. 1989; Jiang et al. 1993; Agilent Technologies 2000). By this approach the sample is modeled as a part of the inner conductor of a coaxial short. The principle of this technique is illustrated in Fig. 12.9. The impedance of the specimen is estimated from a complex reflection coefficient Γ^* defined by the ratio of the complex voltages of the incident (U_{Inc}^*) and reflected (U_{Ref}^*) waves:
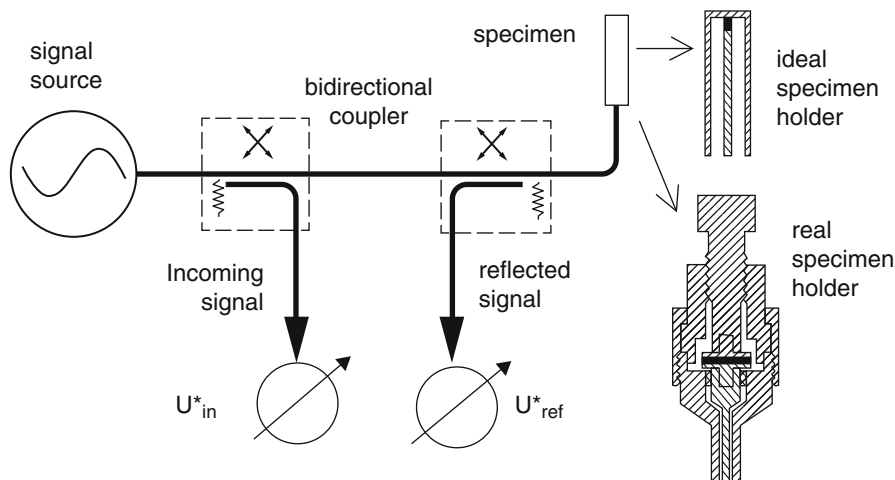
Fig. 12.9 Scheme of a coaxial line reflectometer with sample head

$$\Gamma^* = \Gamma_x - i\,\Gamma_y = \frac{U^*_{Ref}}{U^*_{Inc}} \quad Z^* = Z_0\,\frac{1 + \Gamma^*}{1 - \Gamma^*}. \tag{12.40}$$

Z_0 is the wave resistance of the coaxial line.

To derive Eq. 12.40 ideal coaxial lines have to be assumed which is not the case in practice. Therefore, calibration procedures have to be applied. First, the influence of the measuring cell has to be obtained and considered during the calculation of the sample impedance. Second, the direction-dependent resistance of the line has to be measured by a second calibration procedure because it cannot be obtained by an equivalent circuit diagram.

At frequencies above 1 GHz, network analysis might be applied where both the reflected and the transmission of the signal through the sample are analyzed with respect to phase and amplitude (Kremer and Schönhals 2003).

An example for a broadband dielectric measurement is given in Fig. 12.10, where the dielectric loss versus frequency is given for poly(propylene glycol) ($M = 200\ \mathrm{g\ mol^{-1}}$). The data were obtained by a combination of Fourier correlation analysis and coaxial line reflectometry.

12.2.4.4 Thermostimulated Currents

The dielectric properties of a polymeric system can be also investigated in the temperature domain by the method of thermally stimulated currents (TSC) developed by Bucci et al. (1966). This method was broadly applied to polymers by van Turnhout (1975), Lacabanne (Larvergne and Lacabanne 1993), and Teyssedre (Teyssedre et al. 1997) (see also the references given therein). In principle the method is based on the temperature dependence of the relaxation times and the fact that a given value of the relaxation time corresponds to an experimental time scale

Fig. 12.10 Dielectric loss ε'' versus frequency for poly (propylene glycol) (M = 2,000 g mol^{-1}) at the given temperatures. The peak at lower frequencies corresponds to the normal mode process, whereas the peak at higher frequencies is due to the α-relaxation. The data were obtained by a combination of Fourier correlation analysis and coaxial line reflectometry
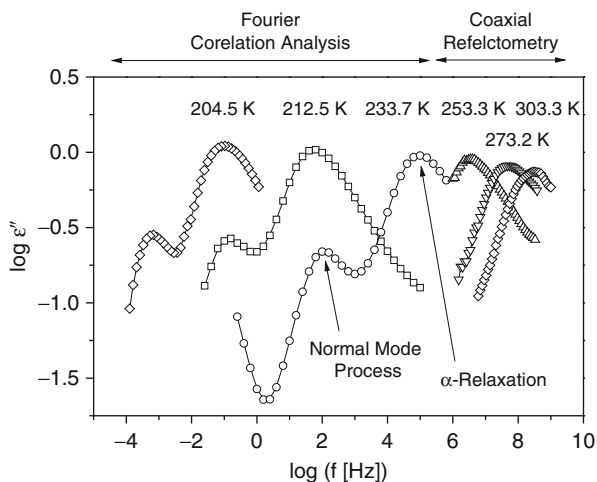
(heating rate) at a certain temperature. In the simplest approach assuming a Debye-like response (see Eq. 12.24), the sample is polarized by a field E_P for a given time at a polarization temperature T_P. After that, the sample is cooled down to a temperature T_S with applied electric field. T_S should be low enough that $\tau(T_S)$ is long enough to prevent any depolarization of the sample at the experimental time scale. The frozen-in polarization P_0 is estimated to $P_0 = \frac{N\mu^2}{3k_B T_P V} E_P$. A subsequent heating of the specimen with a heating rate $\kappa = dT/dt$ leads to a depolarization current or depolarization current density J(T). By measuring the current density as function of time, a peak is observed when groups or segments become mobile and frozen-in polarization can be released. According to Eq. 12.24 the temperature dependence of the polarization can be described theoretically by

$$P(T) = P_0 \exp\left(-\int_{T_S}^{T} \frac{dT'}{\kappa \tau(T')}\right). \tag{12.41}$$

Experimentally the temperature dependence of the polarization can be obtained by integrating J(T) between T and a temperature T_f at which J(T) becomes zero:

$$P(T) = \frac{1}{\kappa} \int_{T}^{T_f} J(T') \, dT'. \tag{12.42}$$

Depending on the heating rate, a TSD measurement corresponds to a conventional dielectric measurement carried out at a low frequency of 10^{-4}

to 10^{-3} Hz. For this reason a TSC curve can be also directly compared to a corresponding differential scanning calorimetry (DSC) measurement.

A relaxation time can be calculated from the measurements according to (Teyssedre et al. 1997)

$$\tau(T) = -\frac{P(T)}{dP/dT} \tag{12.43}$$

without any further hypothesis.

In addition to these general considerations, methods have been developed considering also a distribution of relaxation times based on partial heating techniques or the fractional depolarization approach (Teyssedre et al. 1997).

Because currents can be measured with a high accuracy, the TCS method is a quick and sensitive method to investigate the dielectric properties of polymers. But it should be noted that, for instance, in the glass transition range, the data depends on the experimental conditions like heating and cooling rates which make the quantitative analysis of these measurements more difficult (Kubon et al. 1988; Schrader and Schönhals 1989).

The application of the TSC method to miscible blends is discussed below (see Sect. 12.4.2). Some further discussion can be found in references Vanderschueren et al. (1980), Topic et al. (1987), Migahed and Fahmy (1994), Topic and Veksli (1993), Sauer et al. (1997), Sauer and Hsiao (1993), and Sauer et al. (1992).

12.3 Dielectric Relaxation of Amorphous Homopolymers

In the following section the essential properties of amorphous polymer systems in the bulk will be discussed briefly. In general, for dense polymers one has to consider that the fluctuations of segments or whole chains are influenced not only by intramolecular but also by intermolecular correlations. In order to calculate the mean square dipole moment (see Eq. 12.16) or the corresponding correlation function, one has to sum up over all chains in the system (Schönhals 2003).

The most amorphous polymers have two relaxation regions. At low temperature (or high frequencies) a so-called β-relaxation is observed as a broad peak in the dielectric loss. At higher temperatures or lower frequencies than the β-process, the α-relaxation is observed which is also called principal relaxation or dynamic glass transition. For type-A polymers (see Sect. 12.2.2.2) having a component of the dipole in the direction of the chain backbone at frequencies lower than that of the α-relaxation, a further dielectric active process is observed which is called α'- or normal mode relaxation related to the overall chain dynamics. As an example for the last two processes, Fig. 12.10 depicts the dielectric loss for poly(propylene glycol) (M = 2,000 g mol^{-1}) as a type-A polymer in the frequency range from 10^{-4} to 10^9 Hz. The relaxation processes are indicated as peaks in the dielectric loss. The process at higher frequencies is the α-relaxation which is related to the dynamic

Fig. 12.11 Dielectric loss versus frequency for the β-relaxation of polycarbonate. At a temperature of T = 198.2 K. The *solid line* is a fit of two HN functions to the data where the *dashed* and the *dashed-dotted lines* represent the individual contribution (The figure was adopted from reference Yin et al. (2012))
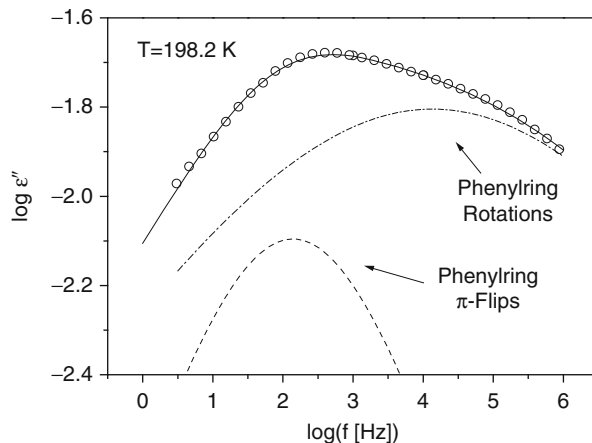
glass transition, whereas the peak at lower frequencies corresponds to the normal mode process. In the following the characteristic properties of the β-, α-, and the normal mode relaxation of amorphous polymers are briefly discussed. Apart from these processes amorphous polymers can also exhibit further dielectrically active relaxation processes.

12.3.1 β-Relaxation

There is a general agreement that the dielectric β-relaxation of amorphous polymers arises from localized rotational fluctuations of the dipole vector. There are two different approaches to discuss the β-relaxation on a molecular level. At the one hand side, Heijboer (1978) developed a nomenclature for the molecular mechanisms which can be responsible for this process. According to this picture, fluctuations of localized parts of the main chain and the rotational fluctuations of side groups or parts of them can be discussed. There are studies on model systems which seem to support this approach (Buerger and Boyd 1989; Katana et al. 1993; Corezzi et al. 1999; Tetsutani et al. 1982a, b). Moreover, detailed investigations on poly(n-alkyl methacrylate)s in dependence on the length of the alkyl side chain seem to favor this idea also (Tetsutani et al. 1982a, b; Gomes Ribelles and Diaz Calleja 1985; Garwe et al. 1996; Zeeb et al. 1997). Regarding the latter class of materials, one has to keep in mind that the relaxation behavior of the poly(n-alkyl methacrylate)s is quite unusual compared to other polymers. Also a degeneration of the calorimetric glass transition with increasing length of the side chains (Hempel et al. 1996) and indications for a nanophase separation (Beiner and Huth 2003) are detected. Moreover, the β-peak can consist of different relaxation processes. This is demonstrated by Fig. 12.11 where the β-peak of poly(bisphenol A carbonate) is deconvoluted in to two processes (Yin et al. 2012) in agreement also with the literature (Alegría et al. 2006; Arrese-Igor et al. 2008).

The second approach to assign the β-relaxation on a molecular level was outlined by Goldstein and Johari (1970; Johari 1973). In their approach the β-relaxation is a generic feature of the glass transition and the amorphous state. The main argument is that such β-relaxation processes could be observed besides for polymeric systems for a great variety of glass-forming materials like low-molecular-weight glass-forming liquids and rigid molecular glasses (Johari 1973). Also for polymers in which the dipoles are rigidly attached to the main chain, the dielectric β-relaxation was well known. Recently the β-relaxation is intensively discussed because it is supposed that the investigation of this process can help to understand the nature of the dynamic glass transition which is a topical problem of soft matter physics (Anderson 1995; Angell 1995). As a general conclusion one can state that the β-relaxation can be of intra- and/or intermolecular nature.

In the following the properties of the β-relaxation are briefly given in terms of its relaxation rate, its dielectric strength, and the shape of the relaxation function.

12.3.1.1 Relaxation Rate $f_{p,\beta}$

In general the temperature dependence of the relaxation rate of the β-relaxation follows the Arrhenius equation:

$$f_{p,\beta} = f_{\infty\beta} \exp\left[-\frac{E_A}{k_B T}\right]. \tag{12.44}$$

$f_{p\infty}$ is the preexponential factor which should be in the order of 10^{12}–10^{13} Hz. The activation energy E_A depends on both the internal rotational barriers and the environment of a fluctuating unit. Typical values for E_A are 20–50 kJ mol^{-1}.

12.3.1.2 Dielectric Strength $\Delta\varepsilon_\beta$

For most of the polymers for the relaxation strength of the β-relaxation, $\Delta\varepsilon_\beta << \Delta\varepsilon_\alpha$ holds. Here $\Delta\varepsilon_\alpha$ is the dielectric strength of the α-relaxation. This is true for such polymers like polycarbonate (Katana et al. 1993), poly(vinyl chloride) (Matsuo et al. 1965; Colmenero et al. 1993), poly(propylene glycol) (Schönhals and Kremer 1994), or poly(chloroprene) (Matsuo et al. 1965), just to mention a few. This is also the case for semicrystalline polymers poly(ethylene terephthalate) (Coburn and Boyd 1986; Hofmann et al. 1993) or poly(ethylene 2,6 naphthalene dicarboxylate) (Hardy et al. 2001). For some polymers containing flexible side groups like poly(n-alkyl acrylate)s (Kremer et al. 1992; Williams and Watts 1971), $\Delta\varepsilon_\beta \leq \Delta\varepsilon_\alpha$ is valid. The exceptions of these rules are the poly(n-alkyl methacrylate)s for which $\Delta\varepsilon_\beta > \Delta\varepsilon_\alpha$ is measured (McCrum et al. 1967; Garwe et al. 1996; Williams and Edwards 1966; Sasabe and Saito 1968). Untill now the molecular reason for this behavior is not clear. NMR measurements show that the motions of the main and the side chain are coupled (Kulik et al. 1994). This might be a molecular reason for this exception.

12.3.1.3 Shape of the Relaxation Function

The peak related to the β-relaxation is rather broad and symmetric. Using the half-height width of the loss peak, it can be four to six decades wide. With increasing temperature, the width of the β-peak decreases. Quite often the width of the β-relaxation is modeled by both a distribution of the activation energy and the preexponential factor (in the sense of Eq. 12.27) which might be related to a distribution of molecular environments of the relaxing dipole. In most cases it is difficult to extract information on the basic mechanisms of molecular motion. In other cases the broadness of the β-peak can be also due to the overlapping of different relaxation processes as demonstrated for polycarbonate (see Fig. 12.11).

12.3.2 α-Relaxation (Dynamic Glass Transition)

Untill today the dynamic glass transition (α-relaxation) which is related to the thermal glass transition is a topical problem of soft matter research (Anderson 1995; Angell 1995; Schönhals and Kremer 2012). For polymers the dynamic glass transition is related to segmental dynamics which is related to conformational changes. These changes are not independent from each other and many degrees of freedom are involved in such a process. A variety of models have been developed for such a process. Examples for such models are the Shatzki crankshaft (Shatzki 1962) and the so-called three-bond motion (Valeur et al. 1975a, b) which are critically discussed in reference Hall and Helfand (1982). Today, the understanding of the segmental dynamics in an isolated chain is based on ideas of Helfand et al. (Hall and Helfand 1982) and/or Skolnik et al. (Skolnik and Yaris 1982). They describe the segmental motion as a damped diffusion of conformational states along the chain. A conformational transition can occur spontaneously and isolated, but due to the disturbed bond lengths and also the angles, the probability that in a neighbored segment also a conformational transition will take place is enhanced. For this reason a conformational state seems to diffuse along the backbone. At some point this process will stop because of the fact that the probability for a conformation change in a neighbored segment is smaller than one. This means not each conformational change in a segment will lead automatically to a conformational transition in the neighbored unit. So the diffusion of conformational states along the chain is damped.

The model developed for isolated chains in solutions should be also applied in the dense state. But for bulk systems besides the intermolecular interactions, also the intramolecular interactions have to be taken into account. This can be done, for instance, by considering a test segment which fluctuates in the environment of other fluctuating segments (Schönhals and Schlosser 1989).

12.3.2.1 Relaxation Rate $f_{p,\alpha}$

It is well known that the temperature dependence of the relaxation rate of the α-relaxation does not follow the Arrhenius law. Very often close to the thermal

glass transition temperature T_g, it can be described by the Vogel/Fulcher/Tammann/Hesse (VFT) formula (Vogel 1921; Fulcher 1925; Tammann and Hesse 1926):

$$\log f_{p\alpha} = \log f_{\infty\alpha} - \frac{A}{T - T_0}. \tag{12.45}$$

$\log f_{\alpha\infty}$ ($f_{\alpha\infty} \approx 10^{10}$–$10^{12}$ Hz) and A are constants where T_0 is the so-called Vogel temperature which is found to be 30–70 K below T_g. Empirically and also by temperature-modulated DSC (Schick 2012), it was shown that the glass transition temperature corresponds to relaxation rates of 10^{-3}–10^{-2} Hz. Therefore, a dielectric glass transition temperature T_g^{Diel} can be defined by $T_g^{Diel} = T$ ($f_{p\alpha} \approx 10^{-3}...10^{-2}$ Hz).

An analogous representation for the temperature dependence of the relaxation rate of the α-relaxation is the Williams/Landel/Ferry (WLF) relation (Ferry 1980):

$$\log a_T(T) = \log \frac{f_{p\alpha}(T)}{f_{p\alpha}(T_{Ref})} = -\frac{C_1(T - T_{Ref})}{C_2 + T - T_{Ref}}, \tag{12.46}$$

where $a_T(T)$ is the so-called shift factor, T_{Ref} is a reference temperature and $f_{p\alpha}(T_{Ref})$ is the relaxation rate at this temperature. C_1 and $C_2 = T_{Ref} - T_0$ are the WLF parameters. Equations 12.45 and 12.46 are mathematically equivalent. Moreover, it has been discussed that the WLF parameters should have universal material-independent values if $T_{Ref} = T_g$ is chosen (Ferry 1980). However, it was found experimentally that these estimates are only rough approximations.

$a_T(T)$ is often used to construct master curves in the framework of the time-temperature superposition (TTS) principle (Ferry 1980).

The VFT equation can be used to describe the temperature dependence of the relaxation rate close to the glass transition temperature. For higher temperatures ($T = T_g + 80 \ldots 100$ K) deviations are observed. It is discussed in the literature whether the data at higher temperature have to be described by a second VFT law with different parameters or by an Arrhenius equation.

There are several models to understand the strong temperature dependence of the relaxation rate of the dynamic glass transition. Besides mode coupling theory (see, for instance, Götze 2009), one of them is the free volume approach discussed in detail in reference Schönhals and Kremer (2012). The cooperativity approach was pioneered by Adam and Gibbs (1965). They introduced the cooperatively rearranging region (CRR) which is defined as the smallest volume which can change its configuration independently from the neighboring regions. If z(T) is the number of segments per CRR, the relaxation rate can be expressed as

$$\frac{1}{\tau} \sim f_p \sim \exp\left(-\frac{z(T)\,\Delta E}{k_B\,T}\right) \sim \exp\left(-\frac{s^*\Delta E}{k_B\,T\,S_C}\right) \sim \exp\left(-\frac{C}{T\,S_C}\right). \qquad (14.47)$$

ΔE is a free energy barrier for a conformational change of a segment, S_C is the total configurational entropy, and s^* is the configurational entropy related to such a rearrangement. The right-hand part of Eq. 12.47 corresponds to the original formulation of Adam and Gibbs theory (Adam and Gibbs 1965). The configurational entropy S_C can be related to the change of the specific heat capacity Δc_p at T_g by

$$S_c(T) = \int_{T_2}^{T} \frac{\Delta c_p}{T}\, dT. \qquad (12.48)$$

With $T_2 = T_0$ and $\Delta c_p \sim 1/T$, the VFT equation is obtained. At the Vogel temperature the configurational entropy vanishes, $z(T)$ diverges like $z(T) \sim (T - T_0)^{-1}$, but no information about the absolute size of a CRR can be obtained. The approach of Adam and Gibbs was extended by Donth (1992, 2001) to obtain the size of a CRR. Within a fluctuation model a formula was developed which allows to calculate a correlation length ξ (or volume V_{CRR}) from the height of the step in c_p and the temperature fluctuation δT of a CRR at T_g as

$$\xi^3 = V_{CRR} = \frac{k_B\, T_g^2 \Delta\left(1/c_p\right)}{\rho\,\delta T^2}, \qquad (12.49)$$

where ρ is the density and $\Delta(1/c_p)$ the step of the reciprocal specific heat capacity at the glass transition where $c_V \approx c_p$ was assumed. δT can be extracted experimentally from the width of the glass transition (Donth 1982; Schneider et al. 1981; Donth et al. 2001a, b). Within that approach the size of a CRR was estimated for several polymers to be in the range of 1 to 3 nm in accord with the above estimation. This corresponds to 10–200 segments (Hempel et al. 2000; Beiner et al. 1998b; Kahle et al. 1997).

12.3.2.2 Dielectric strength $\Delta\varepsilon_\alpha$

Generally, for the α-relaxation $\Delta\varepsilon_\alpha$ decreases with increasing temperature. This seems in accord with Eq. 12.11, but the experimental results show that the dependence is much stronger than predicted. Especially close to T_g the increase of $\Delta\varepsilon_\alpha$ with decreasing temperature is quite strong. It is clear that this increase of $\Delta\varepsilon_\alpha$ with decreasing temperature cannot be explained by the increase of the density with decreasing temperature. Also its modeling by a temperature-dependent g-factor remains formal because g was introduced to describe static correlations between dipoles like association. Apart from polymer a similar temperature dependence of $\Delta\varepsilon_\alpha$ was also observed for low-molecular-weight glass-forming materials (Schönhals 2001). It can be argued that this temperature dependence results from

Fig. 12.12 Dielectric loss versus temperature at fixed frequency of 10^4 Hz for *cis*-1,4-polyisoprene. The molecular weights are as follows: *circles*, 1,400 g mol^{-1}; *squares*, 3,830 g mol^{-1}; and *triangles*, 8,400 g mol^{-1}. *Lines* are guides for the eyes (The figure was adapted from Schönhals (1993))
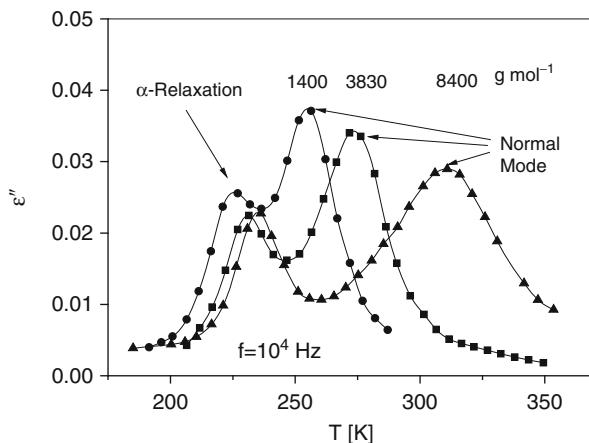
an increasing influence of (intermolecular) cross-correlation terms to μ^2 with decreasing temperature. In other words the reorientation of a test dipole is influenced increasingly by its environment with decreasing temperature. This is in agreement with the cooperativity approach to the glass transition as discussed above.

12.3.2.3 Shape of the Relaxation Function

In general the α-process shows in the frequency domain a broad (the width ranges from two up to six decades depending on structure) and asymmetric peak. Generally, it is assumed that in contradiction to the β-process, the shape of the relaxation function of the dynamic glass transition is not related to a distribution of relaxation times due to local spatial heterogeneities. Rather this broad, asymmetric loss peak is an intrinsic feature of the dynamics of glass-forming systems.

12.3.3 Normal Mode Process

A dielectric normal mode process is observed only for polymers having a dipole moment in parallel to the chain backbone, the so-called type-A polymers like *cis*-1,4-polyisoprene or poly(propylene glycol). The resulting dipole moment is proportional to the end-to-end vector of the chain. Therefore, the normal mode relaxation is directly related to the overall chain dynamics. Figure 12.10 shows that the corresponding relaxation rate $f_{p,n}$ is always located at frequencies lower than that characteristic for the α-relaxation. $f_{p,n}$ depends strongly on the molecular weight of the polymer chain. Figure 12.12 shows the dielectric loss versus temperature at a fixed frequency for *cis*-1,4-polyisoprene for different molecular weights. While the low-temperature (high-frequency) α-relaxation shows only a weak dependence on the molecular weight M, the high-temperature peak caused by the normal mode process depends strongly on M.

Fig. 12.13 Relaxation rate versus inverse temperature for poly(propylene glycol) (M = 4,000 g/mol): *stars*, β-relaxation; *spheres*, α-relaxation; *squares*, normal mode relaxation. The *dashed line* is a fit of the Arrhenius equation to the data of the β-relaxation. The *solid lines* are fits of the VFT equation to the corresponding data
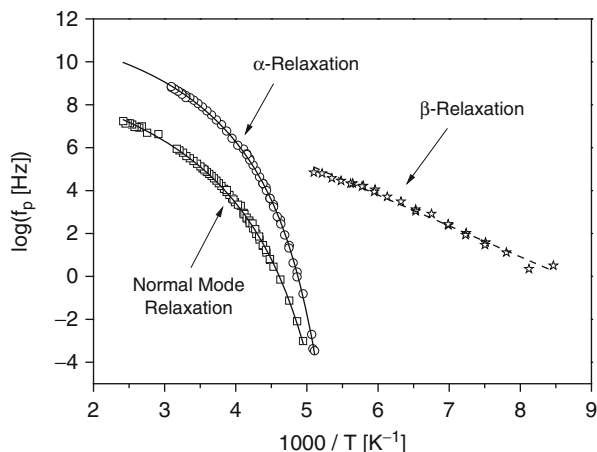
The temperature dependence of the relaxation rate for the normal mode process follows in a wide temperature range the VFT equation but with different parameters than for the α-relaxation.

For chains with a low molecular weight (unentangled case), the Rouse theory (Adachi and Kotaka 1993; Rouse 1953) can be employed to describe it because excluded volume effects and hydrodynamic interactions are screened out (de Gennes 1979).

For higher molecular weights (entangled case), in principle the reputation theory (de Gennes 1979; Doi and Edwards 1986) and its generalization (contour length fluctuations and/or constrained release) have to be used (Milner and McLeish 1998; Likhtman and McLeish 2002; Liu et al. 2006; Zamponi et al. 2006; Chávez and Saalwächter 2010). A more detailed discussion of the normal mode process is beyond this chapter. The reader is referred to the relevant literature (Adachi and Kotaka 1993; Schönhals 1993; Gainaru and Böhmer 2009; Abou Elfadl et al. 2010).

To conclude this section Fig. 12.13 gives the relaxation map where the relaxation rates for the different processes are plotted versus inverse temperature for poly (propylene glycol) with a molecular weight of 4,000 g mol^{-1}. While the temperature dependence of the β-relaxation follows the Arrhenius equation, the relaxation rates for both the α-process and the normal mode process are curved when plotted 1/T.

12.4   Dielectric Relaxation of Polymer Blends

12.4.1 General Consideration

The blend miscibility is governed by the free energy of mixing:

$$\Delta G_M = \Delta H_M - T\Delta S_M, \qquad (12.50)$$

where ΔG_M is the change in the Gibbs free energy of mixing. ΔH_M and ΔS_M denote the excess enthalpy and the mixing entropy. Mixing will take place for $\Delta G_M < 0$.

For polymers the contribution of the entropy of mixing ΔS_M to the free enthalpy of mixing ΔG_M is small. According to the lattice model of Flory/Huggins (Sperling 1986), ΔG_M is assumed to be

$$\Delta G_M = -k_B T \Delta S_M + \kappa \Phi_1 \Phi_2. \tag{12.51}$$

Here Φ_i are the volume fractions, N_i are the degrees of polymerization, and κ denotes the Flory/Huggins interaction parameter. For the entropy of mixing ΔS_M,

$$\Delta S_M = -\left[\frac{\Phi_1}{N_1}\ln\Phi_1 + \frac{\Phi_2}{N_2}\ln\Phi_2\right] \tag{12.52}$$

is assumed. Based on the principle of thermodynamics, the conditions for miscibility, the critical (solution) temperature for phase separation T_C, or the binodals can be calculated from Eqs. 12.51 and 12.52. In general the Flory/Huggins theory can be used to describe systems with an upper critical solution temperature. This means at temperatures above T_C, the two components are miscible on a molecular level, whereas below T_C phase separation occurs. The composition of these phases follows the binodal. That means even in the phase-separated state, a certain degree of mixing (depending on κ and on N_i) is observed which leads to a component 1 and to a component 2 rich phase. Systems with a lower critical solution temperature cannot be described by the Flory/Huggins theory.

Because for most systems the entropy of mixing is small, attractive interactions between both components are needed to obtain a homogeneous mixed state. In the opposite case miscible polymer blends for which $\kappa \approx 0$ (no or weak interactions) are called athermal blends.

In general the β-, the α-, and even the normal mode process will be modified in the case of miscible blends or in systems with partial miscibility. Only for completely phase-separated materials (as the limiting case), the relaxational characteristic of both compounds is fully maintained. The most sensitive process with regard to blending is the α-relaxation. Figure 12.14a shows the expected relaxation map for a miscible system. From the theoretical point of view, a single α-process should be observed which is located – depending on the composition – in between the traces obtained for each component. There are several models like the Flory/Fox or the Gordon/Taylor equation for the dependence of the glass transition temperature on the composition for a homogeneous blend which can be found in standard textbooks of polymer science (Sperling 1986; Strobl 1996). For more theoretical discussion see, for instance, reference Lu and Weiss (1992). A recent comparison is given in reference Brostow et al. (2008). Discussions in the frame of the self-concentration model (for a detailed discussion see below) are given in Lodge and McLeish (2000). This concerns also the Brekner equation (Brekner et al. 1988).

For a phase-separated blend with a partial miscibility, two α-processes will be observed where the location of both processes depends on the composition of both

Fig. 12.14 Schematic representation (relaxation map) of the temperature dependence of the rate of the α-relaxation for a binary polymeric blend: (**a**) theoretical expectation for a molecular miscible blend. (**b**) A blend with a partial miscibility of the two components
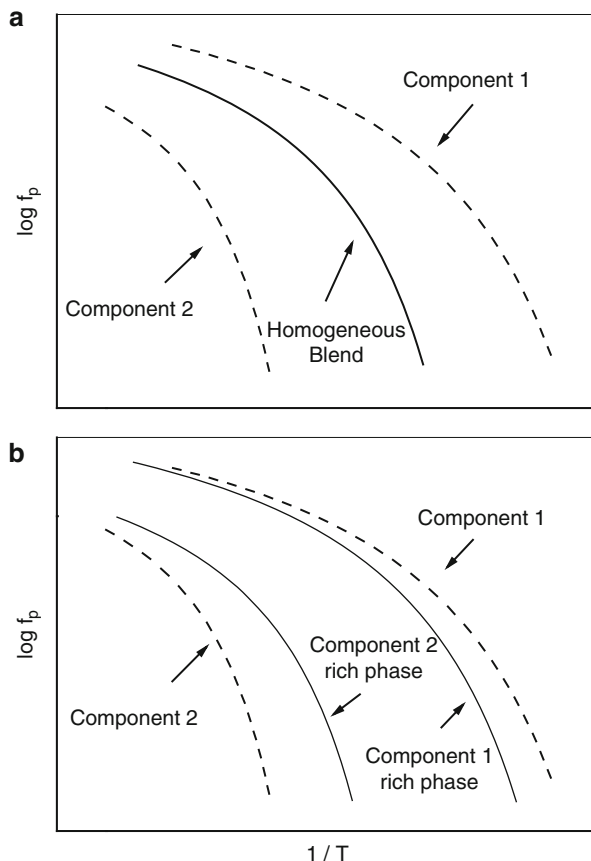
phases (see Fig. 12.14b). Therefore, dielectric spectroscopy is expected to provide valuable information on the local fluctuations of concentrations and on the local miscibility.

Therefore, dielectric spectroscopy can be used to detect and to define criteria of miscibility on a molecular level (Zetsche et al. 1990) by studying the dynamic glass transition. Moreover, both components of a blend will have different polarities in general. One component can be dielectrically more visible than the other one. In the limiting case one component can be dielectrically invisible (Zetsche et al. 1990). Extending this idea by blending a type-A and a type-B polymer, the overall chain dynamics can be studied only for the polymer of type A employing dielectric spectroscopy. Taking advantage from the fact that the chain dynamics of type-B polymer is dielectrically invisible, one can raise the question how the chain motion of the type-A polymer is influenced by the second component. The normal mode relaxation senses a larger length scale than the segmental one, so information about composition fluctuations on different length scales can be deduced. This was discussed, for instance, for blends of polybutadiene and *cis*-1,4-polyisoprene

(Adachi and Kotaka 1993; Adachi et al. 1995; Poh et al. 1996), polystyrene and *cis*-1,4-polyisoprene (Se et al. 1997), *cis*-1,4-polyisoprene and poly(vinyl ethylene) (PVE) (Hirose et al. 2003), or poly(n-butyl acrylate) and poly(propylene glycol) (Hayakawa and Adachi 2000a, b).

Concerning the localized β-relaxation, it was found if the interaction of the two components are weak (athermal blends) the effect of blending on this relaxation process is small (see, for instance, Schartel and Wendorff 1995; Pathmanathan et al. 1986; Cendoya et al. 1999; Urakawa et al. 2001; Dionissio et al. 2000). These dielectric results are also in agreement with quasielastic neutron scattering investigations (Arbe et al. 1999) and are probably a consequence of the rather small length scale (localized fluctuations) of motions involved in these processes. This is further discussed also in reference Fischer et al. (1985).

12.4.2 Miscible Polymeric Blends

12.4.2.1 Dynamic Glass Transition: Experimental

There is a considerable large literature body concerning the dielectric relaxation of binary polymer blends especially in the temperature range of the dynamic glass transition (see, for instance, Floudas et al. 2011; Colmenero and Arbe 2007; Zetsche et al. 1990; Adachi et al. 1995; Poh et al. 1996; Se et al. 1997; Hirose et al. 2003; Schartel and Wendorff 1995; Dionissio et al. 2000; Arbe et al. 1999; Wetton et al. 1978; Alexandrovich et al. 1980; Miura et al. 2001; Rellick and Runt 1986a, b, 1988; Angeli and Runt 1990; Alvarez et al. 1997; Hoffman et al. 2002; Cangialosi et al. 2005, 2006; Alegria et al. 2002; Leroy et al. 2002, 2003; Lorthioir et al. 2003; Schwartz et al. 2007a, b; Jin et al. 2004; Ngai and Roland 2004; Watanabe et al. 1991, 1996; Urakawa et al. 1993a, b, 2006; Katana et al. 1995, 1993, 1992; Zetsche and Fischer 1994; Karatasos et al. 1998; Sy and Mijovic 2000; Roland et al. 2006; Zhang et al. 2005; Mpoukouvalas et al. 2005; Pathak et al. 1999; Krygier et al. 2005).

Broadening of the Relaxation Spectrum

It is known for a long time (Wetton et al. 1978) that the relaxation function measured for a miscible blend is considerably broadened compared to the spectra of the pure polymers (Colmenero and Arbe 2007). To be more precise the broadening is more or less symmetric. As an example this is shown for a miscible blend of polystyrene (PS) and poly(vinyl methylether) (PVME) in Fig. 12.15 (Colmenero and Arbe 2007; Katana et al. 1992; Zetsche and Fischer 1994). Compared to PVME the dipole moment of PS is weak, and therefore, the contribution of PS to the dielectric loss of the blend is negligible. In other words the fluctuations of PVME are selectively monitored by dielectric spectroscopy, whereas the fluctuations of the PS segments are dielectrically invisible. For the blend (see Fig. 12.15b), the loss peak is much broader than that for the single component PVME (see Fig. 12.15a). Moreover, the loss peak narrows as temperature increases. For the PVME/PS blend system, it was proven by a combination

Fig. 12.15 Dielectric loss for the PVME/PS blend at a composition of 65 % PVME/35 % PS. (**a**) Dielectric loss versus frequency for pure PVME: (T = 253 K, 258 K, 263 K, 268 K, 278 K, 288 K, 298 K, 308 K, 328 K, 348 K). (**b**) Dielectric loss versus frequency for PVME/PS blend: (T = 263 K, 273 K, 283 K, 293 K, 308 K, 318 K, 338 K, 368 K) (Data were taken from reference Cendoya et al. (1999))
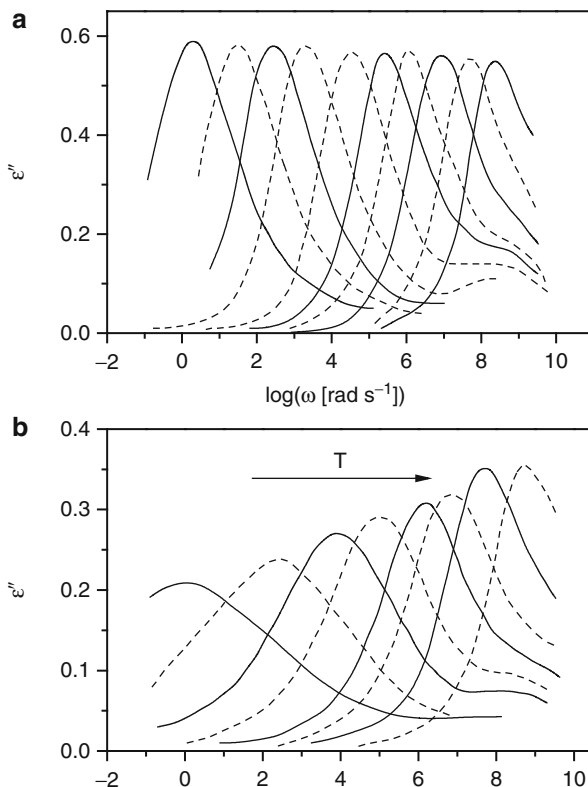
of dielectric, NMR, and quasielastic neutron scattering investigations using deuterated polystyrene that the shape of the relaxation function is similar to that of the corresponding homopolymer at high temperatures (Colmenero and Arbe 2007).

The broadening of the dielectric spectra for miscible polymer blends is not only observed for the PS/PVME system. This further demonstrated by Fig. 12.16 where the normalized dielectric loss is plotted for a blend poly(ethylene-co-vinyl acetate) (EVA70, 70 % vinyl acetate) with poly(vinyl chloride) (PVC). With increasing concentration of PVC in the blend, the loss peak systematically broadens in comparison to that of both components (Rellick and Runt 1988).

The broadening of the dielectric spectra has to be considered as an intrinsic feature of the dielectric properties of miscible blends. Moreover, the broadening of the α-relaxation increases with the difference of the glass transition temperatures.

A phenomenological treatment is most simple if one component is dielectrically more or less invisible as it is the case for polystyrene. In this case the broadening of the loss peak can be described by a distribution function $\widetilde{c}$ in the sense of Eq. 12.27:

Fig. 12.16 Normalized
dielectric loss versus
normalized frequency for the
blend system
EVA70/PVC. Parameter is
the concentration of EVA70
in the blend as indicated.
Lines are guides for the eyes
(Data were taken from
reference Rellick and Runt
(1986b))
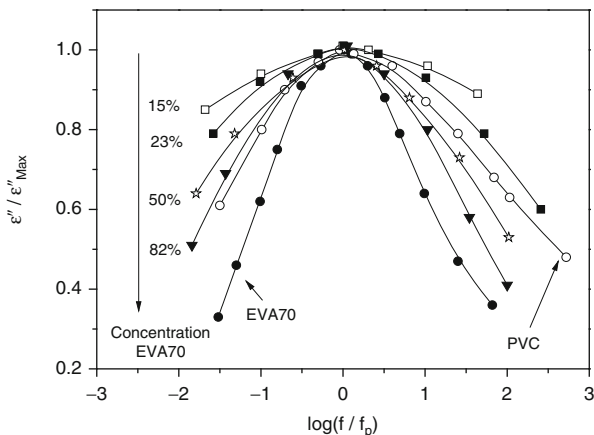
$$\varepsilon''_{\text{Blend}}(\omega) = \int_0^\infty \widetilde{c}(\tau)\, \varepsilon''_{\text{Vis}}(\omega\tau)\, d\tau. \tag{12.53}$$

$\varepsilon''_{\text{Vis}}(\omega)$ is the relaxation function of the dielectrically visible component of the blend. Clearly $\widetilde{c}$ should be related to the molecular structure of the miscible blend. Equation 12.53 is derived under the assumption that the "live time" of $\widetilde{c}$ is much longer than the longest relaxation time for the α-relaxation. Often $\widetilde{c}$ is assigned on a molecular level to temperature-driven composition fluctuations (Katana et al. 1995; Zetsche and Fischer 1994) which will be discussed in detail later.

Adachi et al. (Hayakawa and Adachi 2000b) suggest the following formula for the complex dielectric function of a miscible blend:

$$\varepsilon*_{\text{Blend}}(\omega) = \Phi_1 \varepsilon*_1 \left(\frac{\zeta_{\text{Blend}}}{\zeta_1}\omega \right) + \Phi_2 \varepsilon*_2 \left(\frac{\zeta_{\text{Blend}}}{\zeta_2}\omega \right), \tag{12.54}$$

where $\varepsilon*_i$ are the complex dielectric function of pure components and ζ_i the corresponding monomeric friction coefficients (for definition see Ferry 1980; Sperling 1986; Strobl 1996). This formula is firstly based on the idea that the dipole moment of the mixture is a weighted sum of the dipole moments of each component. Secondly, the segmental mobility in the blend can be described by a common friction coefficient ζ_{Blend}. According to this assumption the segmental relaxation time τ_i for the pure component i has to be changed to $\tau_i \frac{\zeta_{\text{Blend}}}{\zeta_i}$. For the friction coefficient of the blend ζ_{Blend},

$$\ln \zeta_{\text{Blend}} = \Phi_1 \ln \zeta_1 + \Phi_2 \ln \zeta_2 + k\Phi_1\Phi_2 \tag{12.55}$$

was suggested. k is a parameter which characterizes the interaction between the two components. Please note that the k parameter can be different from the Flory/Huggins interaction parameter. This model can also qualitatively describe experimental results (Hayakawa and Adachi 2000a, b).

Fig. 12.17 Dielectric loss versus frequency at 270 K for the PVE/PI blend at a composition of 50 % PVE/50 % PI. *Circles*, pure PVE; *squares*, pure PI; *stars*, blend PVE/PI. *Lines* are estimated contributions of the dynamic glass transition (Data were taken from reference Arbe et al. (1999))
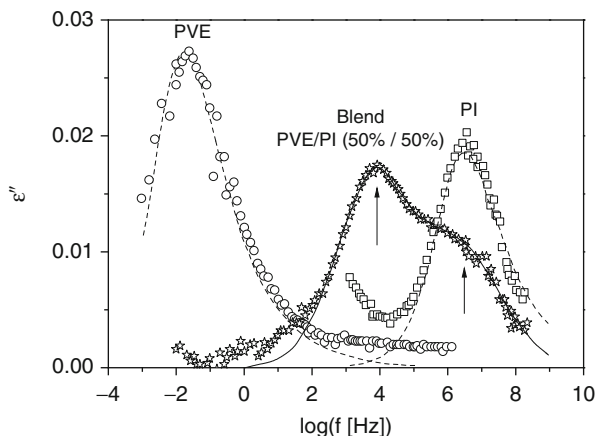
Dynamic Heterogeneity

For the simple theoretical approach outlined in Fig. 12.14a, one should expect that for a blend which is fully miscible on a molecular level, only a single relaxation process with a single average relaxation rate (or time) should be observed. In other words this would correspond to a single average $<T_g>$ measured by DSC. Figure 12.17 gives the dielectric spectra of poly(vinyl ether) (PVE) and *cis*-1,4-polyisoprene (PI) together with results for the blend PVE/PI (50 %/50 %) according to reference Arbe et al. (1999). For the PVE/PI system both components are dielectrically visible. For the blend a two peak structure is observed. It is worth to point out that this double peak structure is observed independently of the already discussed broadening of the α-relaxation peak. That was proven by quasielastic neutron scattering investigations where both components of the blend were selectively deuterated (Hoffman et al. 2000). This effect observed for a variety of miscible binary polymer blends and is called "dynamic heterogeneity."

Further evidence for the dynamical heterogeneity in miscible polymer blend was provided by a combination of DSC and TSC measurements. While DSC is sensitive to the molecular dynamics of the whole blend, TSC monitors selectively the molecular fluctuations of the polar component. Figure 12.18 compares the temperature dependence of specific heat capacity with that of the depolarization current for the blend system PVME/PS (Leroy et al. 2002). For the polar component PVME, the peak in the TSC curve collapses with the midpoint of the steplike change of the specific heat capacity usually taken as thermal glass transition temperature. This indicates that both methods sense the same process which is the molecular fluctuation of PVME segments responsible for the glass transition. For the blend a broad DSC trace is observed but with a single step in the specific heat capacity indicating miscibility. In difference to the thermal data, the TSC peak is observed at essential lower temperatures. This means the effective ("local") $T_{g,eff}$ due to the polar PVME segments is observed at much lower temperatures than the overall T_g ($<T_g>$) of the blend and proves that an $T_{g,eff}$ different from $<T_g>$ exists (Leroy et al. 2002).

Fig. 12.18 Comparison of DSC and TSC measurements for pure PVME (*dashed lines*) and a PVME/PS (*solid lines*) at a composition of 50 % PVME/50 % PS. *Dotted vertical lines* indicate the glass transition temperatures (Data were taken from reference Leroy et al. (2002))
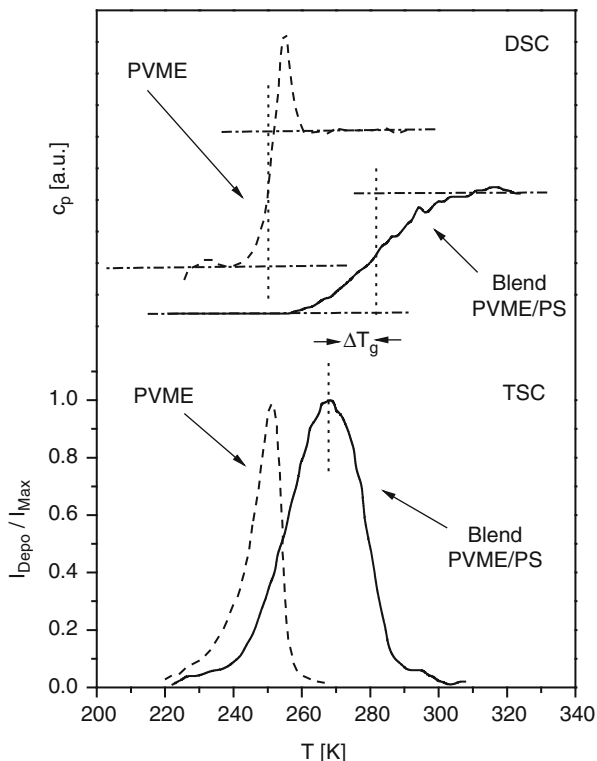
In reference Leroy et al. (2002), this was investigated for three different blend systems. Also Lodge and coworkers evidenced the existence of two different glass transitions in miscible blends by DSC measurements alone (Lodge et al. 2006) or by a combination of DSC and TSC investigations (Herrera et al. 2005). A similar conclusion was provided by a combination of dielectric spectroscopy with adiabatic calorimetry (Sakaguchi et al. 2005) or employing temperature-modulated DSC (Miwa et al. 2005). Results provided in reference Schwartz et al. 2007b can be discussed in the same direction. In conclusion, besides the broadening of the relaxation spectrum, the dynamic heterogeneity must be considered as the second main feature of the (dielectric) properties of miscible blends.

Kirkwood/Fröhlich Correlation Factor

In Sect. 12.2.2.1 the Kirkwood/Fröhlich correlation factor g as a measure of static correlations between dipoles is introduced and discussed (see Eq. 12.14). It seems to be an interesting question in which way g is changed in miscible blends. Data are provided, for instance, in references Wetton et al. (1978), Alexandrovich et al. (1980), and Malik and Prud'homme (1984) using Eq. 12.14. As a result it was observed that the g parameter is only weakly affected by blending

(Alexandrovich et al. 1980; Rellick and Runt 1986b) in the whole considered concentration range. This means the conformation of segments was not significantly changed in the blend. Runt et al. (Rellick and Runt 1986b) derived an equation to assess the effect on blending on the g-factor relative to the unblended state:

$$g_{Blend} = 9\varepsilon_0 k_B T \, \frac{\frac{\Delta\varepsilon \, (2\varepsilon_s + \varepsilon_\infty)}{n\,\varepsilon_S}}{g_1 n_1 \mu_1^2 \left(\varepsilon_\infty^1 + 2\right)^2 + g_2 n_2 \mu_2^2 \left(\varepsilon_\infty^2 + 2\right)^2}, \qquad (12.56)$$

where subscript i indicates the component, n the overall dipole density in the blend, and n_i the mole fraction of the component i in the blend. The numerator is the effective squared dipole moment in the blend where the denominator was obtained by a linear combination of the dielectric properties of the blend. Then g_{Blend} is a measure of the polarization of the blend with respect to an unblended environment (Rellick and Runt 1986b; Angeli and Runt 1989).

12.4.2.2 Dynamic Glass Transition: Theoretical Models

Most researchers will agree that the molecular fluctuations of a segment i of a polymer "A" in binary blend are controlled by the local composition ϕ_i in some volume around that segment. This local concentration which is different from the macroscopic blend composition will give rise to a relaxation time τ_i which is different from the mean relaxation time. In general we have a distribution of different environments having different compositions ϕ_i which will lead to a distribution of relaxation times and hence results in a broadening in the loss curve. A further consequence of this distribution at a segment i is a distribution of local T_g.

One approach to model this effect is based on the coupling scheme of Ngai et al. (Roland and Ngai 1991, 1992a, b). In this scheme a so-called coupling parameter determines the shape of the relaxation function. In its application to blends, the local concentrations ϕ_i lead to a distribution of the coupling parameter which will consequently cause a broadening of the relaxation function.

Besides the coupling model two other groups of model have been developed during the last 15 years: the model of "temperature-driven composition fluctuations" at the one side and the idea of "self-concentration" on the other side.

Temperature-Driven Concentration Fluctuations (TCF)

The idea of temperature-driven concentration or composition fluctuation traces back to Karazs et al. (Wetton et al. 1978). One of the first models was developed by Fischer et al. (Katana et al. 1995; Zetsche and Fischer 1994). This work was further extended in several directions by Kumar and Colby et al. (Salaniwal et al. 2002; Kamath et al. 2003a, b, 1999; Kumar et al. 1996, 1999; Kant et al. 2003).

The temperature-driven concentration fluctuation approach is based on the following assumptions (see Fig. 12.19):

Fig. 12.19 Scheme of the temperature-driven concentration fluctuation approach to binary miscible blends
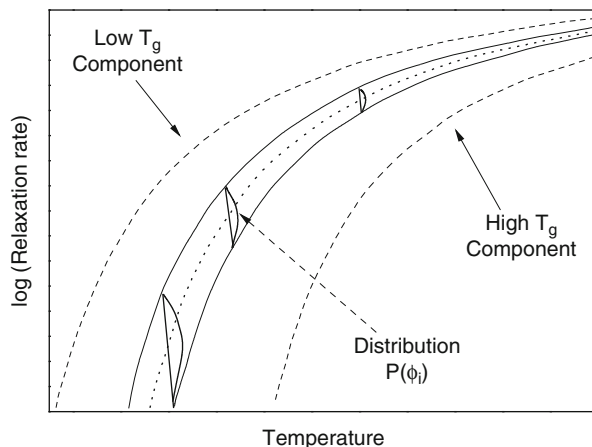
1. The sample is divided into i subcells of the volume V having a composition ϕ_i and thus a local glass transition temperature $T_g^i(\phi_i)$.
2. A distribution $P(\phi_i)$ of the composition ϕ_i is introduced. This will lead to a distribution of relaxation times and also a distribution of the local glass transition temperatures $T_g^i(\phi_i)$. In the approach by Fischer et al. (Katana et al. 1995; Zetsche and Fischer 1994), $P(\phi_i)$ was assumed to be Gaussian with a variance $<(\delta\phi)^2>$. In this model $<(\delta\phi)^2>$ is the only adjustable parameter. Extending this model non-Gaussian distributions have been also discussed, for instance, by Kumar (Kumar et al. 1996).
3. The system is incompressible which means that density fluctuations do not exist.
4. The lifetime of the composition fluctuations is much longer than the longest relaxation time for the α-relaxation.

One open point in the discussion untill now is the size of the volume V. Usually it is assumed that V is related to the cooperatively rearranging region (CRR, $V \sim V_{CRR}$, see discussions above) characteristic for the glass transition. It can be estimated taking advantage from the fact that for a Gaussian distribution $P(\phi_i)$ V should be inversely proportional to $< (\delta\phi)^2 >$ ($V \sim < (\delta\phi)^2 >^{-1}$). A quantification can be done by assuming the CRR to be spherical and relating $<(\delta\phi)^2>$ to the static structure factor S(Q) in the same way as it was proposed by Ruland for density fluctuations (Ruland 1957). This approach is based on the random phase approximation (de Gennes 1979). In reference Katana et al. (1995), a comparison is made between the values estimated from that approach and the V_{CRR} calculated from the fluctuation approach by Donth (see Eq. 12.49). The data are in the same order of magnitude but do not agree quantitatively.

The TCF models are able to describe the broadening of the relaxation function as temperature approaches the average glass transition temperature $<T_g>$. It can be also seen from Fig. 12.19 that the extra-broadening due to blending decreases with increasing temperature. The main problem of that approach is the fact that these

models have no explanation for the heterogeneous behavior. Moreover, the estimated length scales for glass transition $\xi \sim V_{CRR}^{1/3}$ grow too strongly as temperature decreases towards $<T_g>$ and can become larger than 10–20 nm. This is much too large than expected for the glass transition. A more detailed discussion can be found, for instance, in reference Colmenero and Arbe (2007).

Self-Concentration Models (SC)

The idea of self-concentration in polymer blends was mainly developed by Lodge and McLeish (2000) based also on earlier works of Kornfield et al. (Chung et al. 1994a, b). For reviews in relation to dielectric spectroscopy, see, for instance, references Colmenero and Arbe (2007) and Maranas (2007). The basic idea is that due to chain connectivity the average composition in local environment around any selected segment is enriched in the same kind of segments (correlation hole effect). In consequence this will lead to different average relaxation times for the segment of the two components in the blend and hence each component will sense its own glass transition temperature which is of course composition dependent. For this reason the self-concentration can account for the heterogeneity effects in the dynamic of polymer blends.

In the formulation of Lodge and McLeish (2000) (LM model) for a binary blend with the components i (i = 1,2), the effective concentration is

$$\phi_{eff}^i = \phi_{self}^i + \left(1 - \phi_{self}^i\right) < \phi > , \qquad (12.57)$$

where $<\phi>$ is the overall macroscopic composition of the blend. Because of the chain connectivity, the relevant intramolecular length scale to estimate the self-concentration is the Kuhn segment length l_k (Strobl 1996) which is only weakly temperature dependent. The self-concentration can be estimated from the volume fraction due to monomers in a volume spanned by the Kuhn length $(V_k \sim l_k^3)$ as

$$\phi_{self} = \frac{C_\infty M_0}{k \rho N_A V_K}, \qquad (12.58)$$

where C_∞ is the characteristic ratio, ρ density, M_0 the molar mass of the repeating unit, N_A Avogadro number, and k counts the number of backbone per repeating unit. The effective glass transition temperature is defined as

$$T_{g,eff}^i = <T_g> \left(\phi = \phi_{eff}^i\right). \qquad (12.59)$$

Besides the self-concentration the Lodge and McLeish model assumes further that the composition of the volume V is similar to the macroscopic one. Basically this means that one distribution of relaxation times (or T_g) is involved. The LM model treats in contradiction to the TCF approach only mean values. But it is interesting to note that also self-concentration effects decreases with increasing temperature.
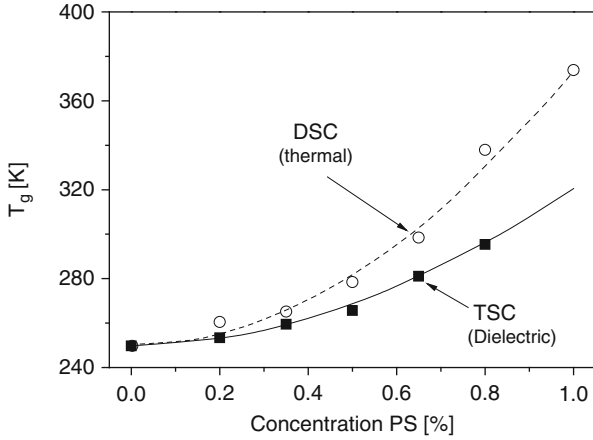
Fig. 12.20 Glass transition temperatures for the blend system PVME/PS versus the concentration of PS. The *open spheres* are data measured by DSC indicating the macroscopic T_g of the sample. The *solid squares* are data measured by TSC for the dielectrically visible component PVME. The *dashed line* is a fit of the Brekner equation to the DCS data. The *solid line* corresponds to the prediction of the LM model according to Eq. 12.61 (Data were taken from reference Rellick and Runt (1986))

In Fig. 12.20 the DSC and TSC data for the blend system PVME/PS discussed in Fig. 12.18 are analyzed in the framework of the LM model (for details see reference Leroy et al. 2002). The glass transition temperature of the blend measured by DSC is described by the Brekner formula (Brekner et al. 1988):

$$T_g(\phi^2) = T_g^1 + \left(T_g^2 - T_g^1\right)\left[(1 + K_1)\phi^2 - (K_1 + K_2)(\phi^2)^2 + K_2(\phi^2)^3\right].$$
(12.60)

ϕ^2 is the blend concentration of the polymer with the higher T_g value, and T_g^i (i = 1,2) are the glass transition temperatures of the pure polymers. K_1 and K_2 are fitting constants. By combining Eqs. 12.57, 12.59, and 12.60 according to Lodge and McLeish (2000), the glass transition temperature for the individual components can be estimated. For the component with the higher T_g^2, one obtains

$$T_{g,\,eff}^2(\phi^2) = T_g^1 + \left(T_g^2 - T_g^1\right)\left[(1 + K_1)\phi_{eff}^2 - (K_1 + K_2)(\phi_{eff}^2)^2 + K_2(\phi_{eff}^2)^3\right].$$
(12.61)

An analogous equation can be obtained for T_g^1. For details see reference Leroy et al. (2002). Figure 12.20 reveals a remarkably good agreement between the experimental data and the predictions of the LM model.
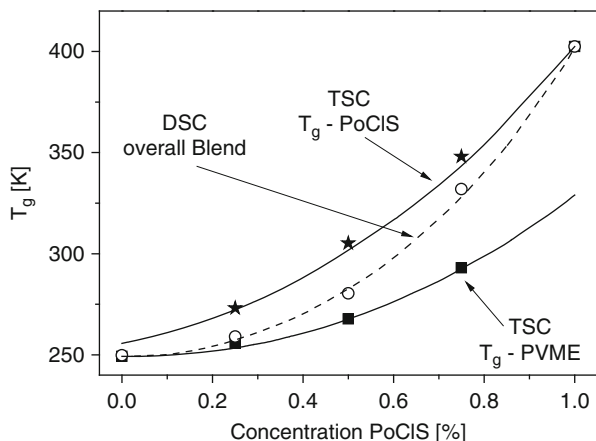
Fig. 12.21 Glass transition temperatures for the blend system PVME/PoClS versus the concentration of PoClS. The *open spheres* are data measured by DSC indicating the macroscopic T_g of the sample. The *solid squares* are data measured by TSC for PVME, whereas the stars are TSC data measured for PoClS. The *dashed line* is a fit of the Brekner equation to the DCS data. The *solid line* corresponds to the prediction of the LM model for both the low and the high glass transition temperature component (Data were taken from reference Leroy et al. (2002))

The same approach was also applied by Colmenero et al. to poly (vinyl methylether) blended with poly(o-chlorostyrene) (PoClS) (Leroy et al. 2002). The difference to the PVME/PS is that in the case of PVME/PoClS system, both components are polar and therefore dielectrically visible. Figure 12.21 shows the results for this system also obtained by a combination of DSC and TSC investigations. Again a good agreement with the LM model is obtained.

The self-concentration model by Lodge and McLeish can be also employed to describe the relaxation map of a miscible blend system. In reference Mpoukouvalas and Floudas (2008), Floudas et al. report dielectric data for the miscible blend poly (methyl methacrylate) (PMMA) and poly(ethylene oxide) (PEO) (see Fig. 12.22). As expected, with increasing concentration of PEO the relaxation rates shifts to lower temperatures. The data can be modeled by assuming the Vogel temperature T_0 in the VFT equation (see Eq. 12.45) to be dependent on the effective concentration according to Eq. 12.57:

$$-\log f_p^i = \log \tau^i(\phi_{eff}, T) = \log \tau_\infty^i + \frac{A^i}{T - T_0^i(\phi_{eff})}, \qquad (12.62)$$

where A^i and τ_∞^i are the VFT parameters for the two components. In this approach only the Vogel temperature depends on composition according to
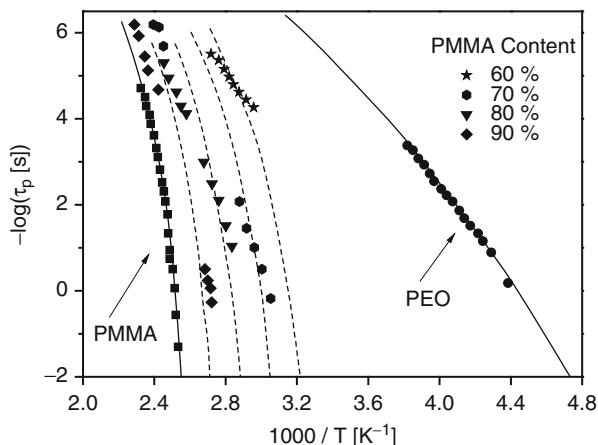
Fig. 12.22 Temperature dependence of the relaxation times of the segmental dynamics (α-relaxation) for the blend system PMMA/PEO at the indicated concentrations: *solid squares*, PMMA; *solid circles*, PEO. The *solid lines* correspond to fits of the VFT equation to the data of the pure polymers. The *dashed lines* are due to fits of the LM model with the Kuhn lengths for PMMA as adjustable parameter ($l_k = 1.62$ nm, theoretical value 1.38 nm) (Data were taken from reference Mpoukouvalas and Floudas (2008). The concentration dependence of the whole blend was described by the Fox/Flory equations. For details see also reference Mpoukouvalas and Floudas (2008))

$$T_0^i(\phi_{eff}) = T_0^i + \left[T_g^i(\phi_{eff}) - T_g^i \right], \tag{12.63}$$

where T_0^i are the Vogel temperatures of the pure polymers and $T_0^i(\phi_{eff})$ the value of the Vogel temperature for the polymer i in the blend. As Fig. 12.22 shows this approach can reasonably describe the segmental dynamics of PMMA in the blend PMMA/PEO under the condition that l_k is adjusted to 1.62 nm which is larger than the theoretical value of 1.38 nm (Mpoukouvalas and Floudas 2008). This means, the self-concentration approach covers some intrinsic features of the molecular dynamics in polymer blends. A better agreement can be obtained by adjusting l_k for each blend composition.

As discussed above the self-concentration idea is able to describe one essential experimental fact of the molecular dynamics of polymer blends, the dynamic heterogeneity. But nevertheless there are some strong problems of this approach which are discussed in detail in reference Colmenero and Arbe (2007). Here only the main arguments are summarized:

1. The most important drawback of the self-concentration approach is the fact that the model cannot describe the broadening of the relaxation function induced by blending. Attempts to combine the self-concentration idea with that of temperature-driven composition fluctuations are discussed, for instance, in reference Leroy et al. (2003) and more recently in Shenogin et al. (2007).

2. In the original version of the LM model, ϕ_{self}^i is assumed to be independent of temperature that is found in some cases. But in other cases the data can be only described allowing ϕ_{self}^i to be temperature dependent. This concerns also the relevant length scale ξ, which is in the LM approach the Kuhn length known to be only weakly temperature dependent. Experimentally it was motivated that ξ could be dependent on temperature (Colmenero and Arbe 2007) as well as on pressure (Mpoukouvalas and Floudas 2008). This length scale can be also dependent on the composition and the components (Lutz et al. 2005; He et al. 2003).

Combination of the Self-Concentration Approach with the Adam/Gibbs Theory

In the framework of the Adam and Gibbs theory, the temperature-dependent size of a CRR is related to the spatial extent of cooperative segmental fluctuations at the dynamic glass transition. For polymer blends the effect of chain connectivity depends on temperature and can be less or more pronounced. Therefore, the assumption of a temperature-dependent CRR has some consequences for the relevant length scale responsible for glassy dynamics. Recently the approach of self-concentration was combined with the theory of Adam and Gibbs to the glass transition (Cangialosi et al. 2005). Two essential assumptions are made. Firstly, the systems should behave athermal – this means that thermodynamic quantities are additive according to the composition. Secondly, both the configurational entropy S_C and the constant C (see Eq. 12.47) are assumed to be depend on the effective concentration according to Eq. 12.57:

$$S_C^{1/Blend} = \phi_{eff}^1 S_C^1 + \left(1 - \phi_{eff}^1\right)S_C^2; \quad C^{1/Blend} = \phi_{eff}^1 C^1 + \left(1 - \phi_{eff}^1\right)C^2. \quad (12.64)$$

It is worth to note that $S_C^{1/Blend}$ and $C^{1/Blend}$ are related to a region (radius r_C) centered around a segment of the polymer 1 relevant to the dynamics of the α-relaxation. (Similar equations can be written down for polymer 2).

Depending on the value of r_C with respect to the Kuhn length l_k, the self-concentration can be estimated using simple geometrical arguments to

$$\phi_{self} = \frac{l_k l_P}{2\pi r_C^2} \quad \text{for } r_C < l_k \quad \text{and} \quad \phi_{self} = \frac{3l_P}{2\pi r_C} \quad \text{for } r_C > l_k. \quad (12.65)$$

l_P is a packing density. In the Adam/Gibbs approach, the number of correlated segments is proportional to S_C^{-1}. Therefore, r_C can be related to the configurational entropy by $r_C = \alpha S_C^{-1/3}$ where α is a constant which can be obtained in principle by fitting experimental data. With that the self-concentration can be expressed by the configurational entropy:
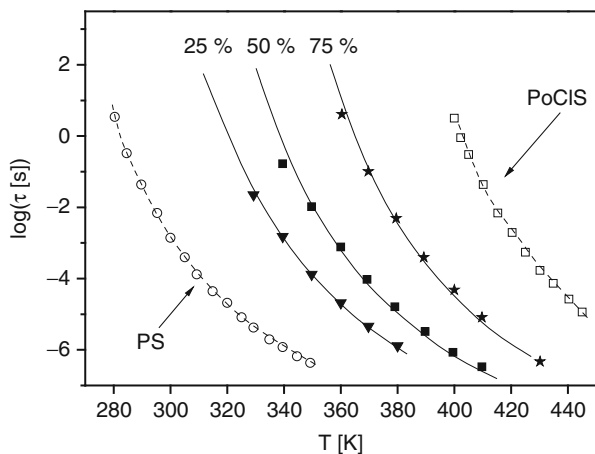
Fig. 12.23 Relaxation time versus temperature for the blend system PS/PoClS: *open circles*, pure PS (molecular weight 700 g/mol); *triangles*, 25 % PoClS; *squares*, 50 % PoClS; *stars*, 75 % PoClS; *open squares*, pure PoClS. The *solid lines* are fits of the combined Adam/Gibbs – self-concentration approach as described in the text. The *dashed lines* are fits of the Adam and Gibbs model to the data of the pure components. For details see reference (Data were taken from reference Cangialosi et al. (2005))

$$\phi_{\text{self}} = \frac{l_k \, l_P}{2\pi \, \alpha^2} S_C^{2/3} \quad \text{for } r_C < l_k \quad \text{and} \quad \phi_{\text{self}} = \frac{3 l_p}{2\pi \, \alpha} S_C^{1/3} \text{ for } r_C > l_k. \tag{12.66}$$

To apply this approach to experimental data, several further assumptions have to be made: (1) the prefactor for the temperature dependence of the relaxation times or rates of the blends is similar to that of the pure components, (2) the configurational entropy S_C is expressed by the excess entropy $S_C \sim S_{\text{Ex}} = S^{\text{Melt}} - S^{\text{Crys}}$ where Eq. 12.64 applies also for S_{Ex}, and (3) the contribution of the vibrations to the excess entropy is similar for the two components in the blend. Under these assumptions the temperature dependence of the relaxation times for the blends can be described for several systems. This is demonstrated in Fig. 12.23 for the blend system PS/PoClS (Cangialosi et al. 2005).

This approach was further extended in reference Cangialosi et al. (2007) to estimate the absolute size of a CRR. Therefore, the parameter α has to be obtained quantitatively. As a result for a variety of polymers, the size of a CRR was found to be between 1 nm and 3 nm at the glass transition. These numbers are in agreement with the fluctuation approach by Donth (Donth et al. 2001b; Hempel et al. 2000; Beiner et al. 1998; Kahle et al. 1997) as well as with more recent theories using approximations of higher order correlation functions (Berthier et al. 2005; Dalle-Ferrier et al. 2007).

Fig. 12.24 Scheme of the dynamics of dynamic asymmetric blends
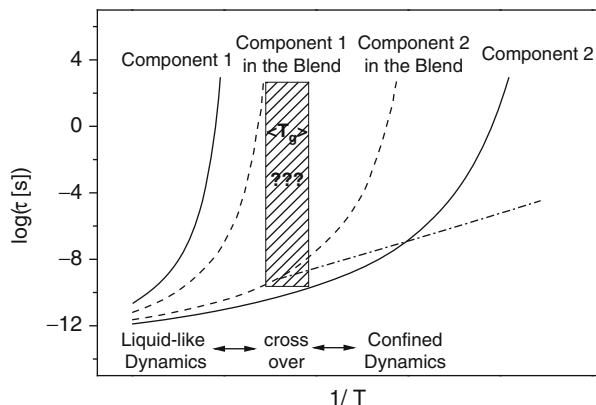
12.4.2.3 Dynamically Asymmetric Polymer Blends: Confinement Effects

Besides the dynamic heterogeneity discussed above, binary miscible polymer blends can be considered as dynamically asymmetric if the two components have a large difference in the glass transition temperatures. Usually the dynamic asymmetry is defined by $\Delta = \tau^{1/Blend}/\tau^{2/Blend}$ where $\tau^{i/Blend}$ is the relaxation time of the component i in the blend and 1 is the polymer with the higher glass transition temperature (Colmenero and Arbe 2007). It becomes clear from Fig. 12.19 that the dynamic asymmetry decreases with increasing temperature.

Figure 12.24 gives schematically the relaxation map for the α-relaxation of a polymer blend where the two components have a large difference in their glass transition temperatures. The solid lines indicate the behavior of the pure polymers where the dashed lines correspond to the heterogeneous dynamics of miscible blends which can be estimated by the LM model. It becomes clear from Fig. 12.24 that the dynamic asymmetry Δ is small and both blend components behave as expected. With decreasing temperature Δ increases strongly and the segmental dynamics of the polymer 1 (component in the blend with the higher T_g) slows more and more down. This will have some implications onto the dynamics of the component 2 having a lower T_g. These segments have to fluctuate in a kind of more and more frozen environment built by the segments of the component 1 which will act as a rigid confinement. As it is known for low-molecular-weight glass formers and polymers confined to nanoporous glasses (Zorn et al. 2002; Schönhals et al. 2005), polymer segments embed between liquid crystalline structures (Turky et al. 2012), as well as water intercalated in the intergalleries of clays (Swenson et al. 2001) or in pores (Gallo 2000), such a confinement will lead to a crossover from a VFT behavior at high-temperature behavior to an Arrhenius-like dependence at low temperatures because of the fact that the molecular fluctuations become localized due to the confinement relative to that what is expected for the confined state. According to Fig. 12.24 this is also expected for dynamically asymmetric blends.

Fig. 12.25 Result for the dynamic asymmetric blend PS/PVME at a composition 80 %/20 %. *Lower panel*: *solid spheres*, dielectric data; *dashed line*, temperature dependence of the relaxation times expected for PVME in the blend; *solid lines* indicate the temperature dependence of the relaxation times for the pure components. *Upper panel*: temperature dependence of the heat capacity measured by DSC (All data were taken from reference Cendoya et al. (1999))
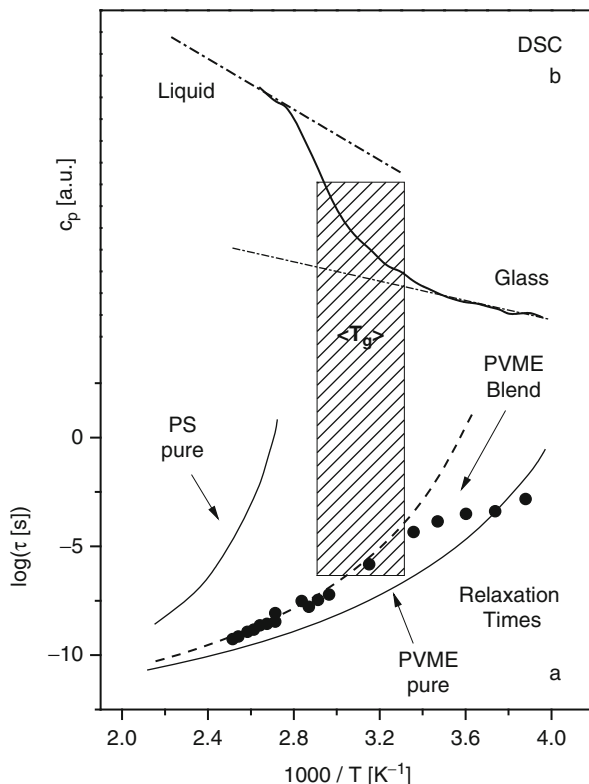
Figure 12.25a shows dielectric results for the blend system PVME (T_g = 249 K)/PS (T_g = 373 K) at a composition of 20 % PVME/80 % PS which is rich in the component with the higher T_g PS (see reference Cendoya et al. 1999). Due to the low dipole moment of PS, it is dielectrically invisible in the blend and only the segmental dynamics of the low T_g component PVME is dielectrically monitored. It is evident from Fig. 12.25a that the temperature dependence of the PVME segments in the blend is curved and follows the VFT equation. In the broad range of the glass transition of the whole blend measured by DSC (see Fig. 12.25b), this VFT temperature dependence crosses over to an Arrhenius-like behavior which is fully developed at even lower temperatures. Because of the fact that the blend is rich in PS, the DSC measurement monitors mainly the glass transition of polystyrene. This fact implies that the crossover in the temperature dependence of PVME is really due to the freezing of the PS segments. In the same temperature range also characteristic deviations in the temperature dependence of the forward scattering intensity S(Q→0) obtained from small angle neutron scattering from the predictions of the random phase approximation are observed for the same system (Koizumi 2004). These deviations are consistent with the formation of a gel-like structure due to the freezing of the PS segments.

Similar results have been also reported by Adachi et al. (Urakawa et al. 2002) for PVME/PS, for the blend PMMA/PEO (Maranas 2007), or for blends of PVDF/PMMA (Sy and Mijovic 2000). Besides dielectric spectroscopy quasielastic neutron scattering is found to be quite useful to investigate the molecular dynamics of dynamic asymmetric polymer blends because spatial information is provided by this technique (see, for instance, Tyagi et al. 2006, 2007). For a more detailed discussion, the reader is referred to the literature (Colmenero and Arbe 2007).

Besides of the segmental dynamics also the chain dynamics in blends is affected by the dynamical asymmetry (Brodeck et al. 2010). Recently a generalized Langevin approach was presented to calculate the chain (Rouse dynamics) for dynamically asymmetric blends (Colmenero 2013). A further discussion is beyond the scope of this chapter.

12.4.2.4 Dielectric Relaxation of Blends Under Pressure

Besides temperature pressure is an important quantity. Moreover, from the applicative point of view, pressure has a direct implication in processing. From the point of basic research, the properties and the thermodynamics of polymer blends are often discussed assuming incompressibility (properties are unaffected of pressure) like in the random phase approximation (de Gennes 1979; Binder 1994) or in the approach of temperature-driven concentration fluctuations (Katana et al. 1995). The effect of pressure on the dielectric properties of blends has been intensively discussed by Floudas et al. (Floudas et al. 2011; Floudas 2003) and is also reviewed in reference Roland et al. (2005). On the one hand as a general result, the assumption of incompressibility seems to be in contradiction to the results obtained by dielectric spectroscopy under pressure (Floudas et al. 2011) as it was also found by other methods in reference Beiner et al. (1998a). Moreover, pressure can increase or decrease miscibility. But one has also to consider that the number of dielectric relaxation studies under pressure is quite limited and different (partly contradictory) results have been found (see discussion in reference Roland et al. 2005). From the experimental point of view, this indicates that the influence of pressure on the molecular dynamics is complex and that more experimental studies should be carried out. Theoretical approaches have been pioneered by Rabeony et al. (Rabeony et al. 1998), by Kumar (Kumar 2000), and by Lipson et al. (lattice-based equation of state) (Lipson et al. 2003, 1998; Tambasco et al. 2006). Recently Colmenero et al. (Schwartz et al. 2007) combined the approach of Adam and Gibbs with the idea of self-concentration as described above by considering also pressure. For the PVME/PS blend system, this approach can describe the temperature dependence of the dielectric relaxation times measured under the different pressures (Schwartz et al. 2007).

12.4.3 Immiscible Blends

Immiscible blends are inhomogeneous systems. For dielectric spectroscopy this fact – like for semicrystalline polymers – has several implications: Firstly,

appropriate mixing rules for the dielectric permittivity have to be applied. For a completely phase-separated structure and if the two components having approximately the same dipole moment in the most simplest case, one can write for the dielectric function of the blend to

$$\varepsilon*_{Blend}(\omega) = \Phi_1 \varepsilon_i^*(\omega) + \Phi_2 \varepsilon_2^*(\omega). \qquad (12.67)$$

However, in most cases a limited miscibility (depending on N_i and κ) (see Eq. 12.52) is observed leading to two phases enriched in one component which can be described by a concentration C_i. In principle the concepts developed in Sect. 12.4.2 can be employed to model the dielectric properties of each phase. In principle by analyzing the frequency position of the α-relaxation and its dielectric strength, the unknown concentration of each component can be estimated assuming appropriate mixing rules. In practical work this can be difficult. Of special interest is again the case where one component is dielectrically invisible as also discussed in Sect. 12.4.2.

12.4.3.1 Blends with a Semicrystalline Component

Miscible blends where one component of the blend is a semicrystalline polymer and the other one are typical examples for two or more phase systems. In such a system in the amorphous state, both components are miscible, whereas the crystallites appear as a second phase. As a first fact of course, the crystallinity measured, for instance, by DSC or by wide angle X-ray diffraction might be changed by blending. This further implies that the volume fraction of dipoles in the amorphous phase which can become mobile at the glass transition will decrease with increasing crystallinity. This will result in a decrease in the dielectric relaxation strengths. Secondly, the frequency (or temperature) position of the glass transition will shift to lower frequencies (higher temperatures) with increasing crystallinity.

Even for semicrystalline homopolymers it is well-known fact that its morphology cannot be described by a simple two-phase model. A characteristic feature of semicrystalline homopolymers is the so-called rigid amorphous fraction (RAF) (Wunderlich 2003). The RAF is phase which is amorphous in structure but immobilized at the dynamic glass transition of the amorphous phase. Therefore, the steplike change of the heat capacity at the glass transition is smaller than expected. Probably the RAF is located between the crystals and the mobile amorphous regions. Besides DSC the rigid amorphous phase can be also investigated by dielectric spectroscopy (Schlosser and Schönhals 1989; Huo and Cebe 1992a, b, 1993; Cebe and Huo 1994; Kalika and Krishnaswamy 1993). Like for the thermal measurements, the dielectric strength is found to be smaller than expected.

For miscible blends an even more complex behavior is observed as discussed in reference Runt et al. (1991) with regard to interphases. As discussed (Runt et al. 1991) interphases can be consists on the one hand side of segments of the

Fig. 12.26 Temperature dependence of dielectric tan δ at a frequency of 2 kHz for melt crystallized PCL/PVC blends at the indicated concentrations (Data were taken from reference Runt et al. (1991))
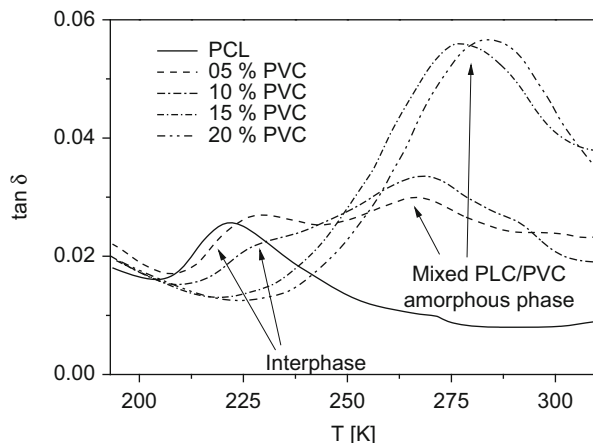
semicrystalline polymer. Examples for that are blends of poly(vinylidene fluoride) with PMMA or blends of poly(ethylene oxide) also with PMMA. On the other side the interphase can contain segments of both polymers. This is, for instance, the case for blends of poly(butylene terephthalate) with polyarylate or poly(ε-carpolactone) (PLA) mixed with poly(vinyl chloride). As an example for the latter system, Fig. 12.26 depicts the temperature dependence of tan δ for the blend system PLA/PVC at a frequency of 2 kHz. Two relaxation processes are indicated by peaks in tan δ. The process located at lower temperatures is assigned to the discussed interphase where the peak at higher temperatures is related to the segmental fluctuations in the blended PLA/PVC amorphous phase. The interphase process shifts a bit to higher temperatures with increasing concentration of PVC. For concentration greater than 15 % of PVC, the interphase peak disappears.

The discussed situation can become even more complex for cases where a variety of different morphologies have been observed like for blends of polyimides (Hudson et al. 1992; Sauer and Hsiao 1993; Hsiao und Sauer 1993; Li and Kim 1997). This includes the observation of multiple glass transitions (Bristow and Kalika 1997). In this connection one has to note that the existence of a given morphology will depend on the thermal history of a sample like for instance crystallization rates.

12.4.3.2 Interfacial Polarization

Due to the phase-separated structure of immiscible polymer blends including phase boundaries in the corresponding dielectric spectra, Maxwell/Wagner polarization process can be observed especially at low frequencies. As discussed in Sect. 12.2.3.3, the theoretical equations are complex and hard to solve. For certain model systems like inclusion in poly(carbonate filled) with poly(ethylene oxide) (Hayward et al. 1992), it could be shown that for low concentrations the most important quantities are the volume fraction, the geometry of the dispersed phase

(expressed by the shape factor n), and its conductivity as well as the permittivity of the matrix. Also for model systems it was early shown that the shape factor n extracted from the dielectric measurements is in good agreement with the observed morphology using electron microscopy (Steeman et al. 1994). This suggests that from a careful analysis of the dielectric spectra, quantitative conclusions about the morphology of immiscible polymeric blends can be drawn. That also includes the detection of the first stages of a phase-separated structure (Dionisio et al. 1996). Higher concentrations of the dispersed phase were considered, for instance, in reference Banhegyi (1986, 1991).

The most complete theoretical treatment of Maxwell/Wagner polarization process in polymer blends was done by Steeman and coworkers (Steeman and van Turnhout 2003) especially also for higher concentrations of the dispersed phase and multicomponent polymer blends (Steeman et al. 1994; Steeman and Maurer 1990, 1992). Quantitative conclusions about the phase structure of the different systems can be drawn including the modeling also of interfaces. This has also some impact on blend compatibilization by grafted copolymers (Eklind et al. 1997).

12.5   Conclusions

Broadband dielectric spectroscopy is a powerful method to investigate the molecular dynamics of polymeric blend systems. This is particularly due to the fact that an extraordinary broad dynamic range can be covered by this technique in its modern form. Different dielectric active processes can be observed in this extended frequency range like relaxation processes due to the fluctuation of molecular dipole moments, charge transport related to the drift motion of charge carriers, or polarization effects due to the presence of both interfaces and interphases. In this chapter broadband dielectric spectroscopy is discussed in relationship to polymer blends where mainly binary blends are considered. The impact of blending on the different relaxation processes is discussed where special attention is paid on the dynamic glass transition related to segmental dynamics. The main features of miscible binary polymeric blends like broadening of the relaxation function as well as dynamic heterogeneity are discussed in detail. The experimental results are related to theoretical approaches like temperature-driven concentration fluctuations and the self-concentration phenomenon characteristic for chain molecules. Immiscible polymeric blends are briefly reviewed.

12.6   Cross-References

▶ Applications of Polymer Blends
▶ Mechanical Properties of Polymer Blends
▶ Miscible Polymer Blends
▶ Morphology of Polymer Blends
▶ Thermodynamics of Polymer Blends

List of Important Symbols and Abbreviations

a_T Shift factor
C Concentration
C_1, C_2 Parameters of the WLF equation
D Dielectric displacement
E Electric field strength
E_A, ΔE Activation energy, barrier heights
f Frequency
f_i Relaxation rate at maximal loss, $i = \beta, \alpha, n$
$f_{\infty i}$ Preexponential factor, $i = \beta, \alpha, n$
Φ_i Volume fraction
ϕ_i Weight fraction
g, g_{intra} Dipolar correlation coefficients
ΔG_M Free energy of mixing
Γ^* Reflection coefficient
I, J Current, Current density
k_B Boltzmann constant, $k_B = 1.380662 \ 10^{-23}$ J K^{-1}; $k_B = R/N_A$
M, M_W Molecular weight, weight average
N_A Avogadro number ($N_A = 6.022 \ 10^{23}$ mol^{-1})
R Gas constant R $= 8.314$ kJ mol^{-1}
S_C Configurational entropy
ΔS_M Mixing entropy
σ^*, σ', σ' Complex conductivity, real and imaginary part
T Temperature
T_0 Vogel temperature, ideal glass transition temperature
T_g Glass transition temperature
$\tan \delta$ Dielectric loss tangent
β, γ Shape parameter of the HN function
ε_0 Permittivity of vacuum ($\varepsilon_0 = 8.854 \ 10^{-12}$ As V^{-1} m^{-1})
ε^*, ε', ε' Complex dielectric function, real and imaginary part
$\Delta \varepsilon_i$ Dielectric relaxation strength, $i = \beta, \alpha, n$,
ζ Monomeric friction coefficient
ξ Correlation length
κ Flory/Huggins interaction parameter
μ Dipole moment
ω Angular frequency ($\omega = 2*\pi*f$)
τ Relaxation time
τ_{HN} Relaxation time of the HN function
τ_e Time constant for conduction
PEO   Poly(ethylene oxide)
PI   *Cis*-1,4-Polyisorene
PMMA   Poly(methyl methacrylate)
PPG   Poly(propylene glycol)
PS   Polystyrene

PVAC Poly(vinyl acetate)

PVME Poly(vinyl methylether)

PoClS Poly(o-chlorostyrene)

PVC Poly(vinyl chloride)

U Voltage, different meanings

$\mathbf{Z_S^*(\omega); Z_R^*(\omega)}$ Sample impedance; Reference impedance

$<\ldots>$ Correlation function; Averaged quantities

References

A. Abou Elfadl, R. Kahlau, A. Herrmann, V.N. Novikov, E.A. Rössler, Macromolecules **43**, 3340 (2010)

K. Adachi, T. Kotaka, Prog. Polym. Sci. **18**, 585 (1993)

K. Adachi, T. Wada, T. Kawamoto, T. Kotaka, Macromolecules **28**, 3588 (1995)

G. Adam, J.H. Gibbs, J. Chem. Phys. **43**, 139 (1965)

Agilent Technologies, Agilent PN 4291–1: New technologies for wide impedance range measurements to 1.8 GHz (2000)

A. Alegria, D. Gomez, J. Colmenero, Macromolecules **35**, 2030 (2002)

A. Alegría, O. Mitxelena, J. Colmenero, Macromolecules **39**, 2691 (2006)

P.S. Alexandrovich, F.E. Karasz, W.J. MacKnight, J. Macromol. Sci. Phys. B. **7**, 501 (1980)

F. Alvarez, A. Alegria, J. Colmenero, Macromolecules **30**, 597 (1997)

P.W. Anderson, Science **267**, 1615 (1995)

S.R. Angeli, J. Runt, J. Contemp. Top. Polym. Sci. **6**, 289 (1989)

S.R. Angeli, J. Runt, ACS Polym. Preprints **31**, 286 (1990)

C.A. Angell, Science **267**, 1924 (1995)

A. Arbe, A. Alegria, J. Colmenero, S. Hoffmann, L. Willner, D. Richter, Macromolecules **32**, 7572 (1999)

S. Arrese-Igor, O. Mitxelena, A. Arbe, A. Alegría, J. Colmenero, B. Frick, Phys. Rev. E. **78**, 021801 (2008)

G. Banhegyi, Colloid Polym. Sci. **264**, 1030 (1986)

G. Banhegyi, Polym. Plast. Technol. Eng. **30**, 183 (1991)

J.L. Barton, Verres Refract **20**, 328 (1966)

M. Beiner, H. Huth, Nat. Mater. **2**, 595 (2003)

M. Beiner, G. Fytas, G. Meier, S.K. Kumar, Phys. Rev. Lett. **81**, 594 (1998a)

M. Beiner, S. Kahle, E. Hempel, K. Schröter, E.J. Donth, Macromolecules **31**, 2460 (1998b)

L. Berthier, G. Biroli, J.-P. Bouchaud, L. Cipelletti, D. El Masri, D. L'Hôte, F. Ladieu, M. Pierno, Science **310**, 1797 (2005)

K. Binder, Adv. Polym. Sci. **112**, 181 (1994)

H. Block, Adv. Polym. Sci. **33**, 94 (1979)

A.R. Blythe, *Electrical Properties of Polymers* (Cambridge University Press, Cambridge, 1979)

A. Boersema, J. van Turnhout, M. Wübbenhorst, Macromolecules **31**, 7453 (1998)

R. Böhmer, M. Maglione, P. Lunkenheimer, A. Loidl, J. Appl. Phys. **65**, 901 (1989)

C.J.F. Böttcher, in *Theory of Electric Polarization*. Dielectrics in Static Fields, vol. I (Elsevier, Amsterdam/Oxford/New York, 1973)

M.J. Brekner, H.A. Schneider, H.J. Cantow, Polymer **29**, 78 (1988)

J.F. Bristow, D.S. Kalika, Polymer **38**, 287 (1997)

M. Brodeck, F. Alvarez, A. Moreno, J. Colmenero, D. Richter, Macromolecules **43**, 3036 (2010)

W. Brostow, R. Chiu, I.M. Kalogeras, A. Vassilikou-Dova, Mater. Lett. **62**, 3152 (2008)

C. Bucci, R. Fieschi, G. Guidgi, Phys. Rev. **148**, 816 (1966)

D.E. Buerger, R.H. Boyd, Macromolecules **22**, 2649 (1989)

D. Cangialosi, G.A. Schwartz, A. Alegria, J. Colmenero, J. Chem. Phys. **123**, 144908 (2005)

D. Cangialosi, A. Alegria, J. Colmenero, Macromolecules **39**, 7149 (2006)

D. Cangialosi, A. Alegria, J. Colmenero, Phys. Rev. E. **76**, 011514 (2007)

P. Cebe, P. Huo, Thermochim. Acta. **238**, 229 (1994)

I. Cendoya, A. Alegria, J.M. Alberti, J. Colmenero, H. Grimm, D. Richter, B. Frick, Macromolecules **32**, 4065 (1999)

F.V. Chávez, K. Saalwächter, Phys. Rev. Lett. **104**, 198305 (2010)

G.-C. Chung, J.A. Kornfield, S.D. Smith, Macromolecules **27**, 5729 (1994a)

G.-C. Chung, J.A. Kornfield, S.D. Smith, Macromolecules **27**, 964 (1994b)

R. Clausius, *Die mechanische Wärmelehre*, vol. II (Vieweg und Sohn, Braunschweig, 1879)

J. Coburn, R.H. Boyd, Macromolecules **19**, 2238 (1986)

K.S. Cole, R.H. Cole, J. Chem. Phys. **9**, 341 (1941)

R.E. Collin, *Foundations for Microwave Engineering*, 2nd edn. (McGraw-Hill, New York, 1966)

J. Colmenero, Macromolecules **46**, 5363 (2013)

J. Colmenero, A. Arbe, Soft Matter **3**, 1474 (2007)

J. Colmenero, A. Arbe, A. Alegria, Phys. A. **201**, 447 (1993)

S. Corezzi, E. Campani, A.P. Rolla, S. Capaccioli, D. Fioretto, J. Chem. **111**, 9343 (1999)

C. Dalle-Ferrier, C. Thibierge, C. Alba-Simionesco, L. Berthier, G. Biroli, J.-P. Bouchaud, F. Ladieu, D. L'Hôte, G. Tarjus, Phys. Rev. E. **76**, 041510 (2007)

D.W. Davidson, R.H. Cole, J. Chem. Phys. **18**, 1417 (1950)

D.W. Davidson, R.H. Cole, J. Chem. Phys. **19**, 1484 (1951)

P.G. de Gennes, *Scaling Concepts in Polymer Physics* (Cornell University Press, Ithaca New York, 1979)

P. Debye, *Polar Molecules, Chemical Catalog*, reprinted by (Dover, New York, 1929)

P. Debye, F. Bueche, J. Chem. Phys. **7**, 589 (1951)

R. Diaz-Calleja, Macromolecules **33**, 8924 (2000)

M.C.S. Dionisio, J.J.M. Ramos, A.C. Fernandes, J. Appl. Polym. Sci. **60**, 903 (1996)

M. Dionissio, A.C. Fernandes, J.F. Mano, N. Correia, R.C. Sousa, Macromolecules **33**, 1002 (2000)

M. Doi, S.F. Edwards, *The Theory of Polymer Dynamics* (Clarendon, Oxford, 1986)

E.J. Donth, J. Non-Cryst. Solids. **53**, 325 (1982)

E.J. Donth, *Relaxation and Thermodynamics in Polymers, Glass Transition* (Akademie Verlag, Berlin, 1992)

E.J. Donth, *The Glass Transition: Relaxation Dynamics in Liquids and Disordered Materials* (Springer, Berlin, 2001)

E.J. Donth, E. Hempel, C. Schick, J. Phys. Cond. Mat. **12**, L281 (2001a)

E.J. Donth, H. Huth, M. Beiner, J. Phys. Cond. Mat. **13**, L451 (2001b)

J.C. Dyre, J. Appl. Phys. **64**, 2456 (1988)

J.C. Dyre, T.B. Schroder, Rev. Mod. Phys. **72**, 873 (2000)

H. Eklind, F.H.J. Maurer, P.A.M. Steeman, Polymer **38**, 1047 (1997)

J.D. Ferry, *Viscoelastic Properties of Polymers*, 3rd edn. (Wiley, New York, 1980)

E.W. Fischer, G.P. Hellmann, H.W. Spiess, F.J. Horth, U. Ecarius, B. Wehrle, Macromol. Chem. Macromol. Chem. Phys. **S12**, 189 (1985)

J.P. Flory, *Statistical Mechanics of Chain Molecules* (Hanser Verlag, München, 1989)

G. Floudas, Effect of pressure on the dielectric spectra of polymeric systems (Chapter 8), in *Broadband Dielectric Spectroscopy*, ed. by F. Kremer, A. Schönhals (Springer, Berlin, 2003)

G. Floudas, M. Paluch, A. Grzybowski, K.L. Ngai, *Pressure Effects on Polymer Blends in Molecular Dynamics of Glass-forming Systems* (Springer, Berlin, 2011)

H. Fröhlich, *Theory of Dielectric* (Oxford University Press, London, 1958)

G.S. Fulcher, J. Am. Ceram. Soc. **8**, 339 (1925)

R.M. Fuoss, J.G. Kirkwood, J. Am. Chem. Soc. **63**, 385 (1941)

G. Schaumburg Dielectric Newsletter of Novocontrol, issue March (1994)

G. Schaumburg Dielectric Newsletter of Novocontrol, issue May (1999)

C. Gainaru, R. Böhmer, Macromolecules **42**, 7616 (2009)

P. Gallo, Phys. Chem. Chem. Phys. **2**, 1607 (2000)

F. Garwe, A. Schönhals, M. Beiner, K. Schröter, E. Donth, Macromolecules **29**, 247 (1996)

J.L. Gomes Ribelles, R.J. Diaz Calleja, J. Polym. Sci. Polym. Polym. Phys. Ed. **23**, 1297 (1985)

W. Götze, *Complex Dynamics of Glass-forming Liquids – A Mode-Coupling Theory* (Oxford University Press, Oxford, 2009)

C. Hall, E. Helfand, J. Chem. Phys. **77**, 3275 (1982)

L. Hardy, I. Stevenson, G. Boiteux, G. Seytre, A. Schönhals, Polymer **42**, 5679 (2001)

S.J. Havriliak, *Dielectric and Mechanical Relaxations in Materials* (Hanser Publishers, Munich, 1997)

S. Havriliak, S. Negami, J. Polym. Sci. Part C **16**, 99 (1966)

S. Havriliak, S. Negami, Polymer **8**, 161 (1967)

T. Hayakawa, K. Adachi, Macromolecules **33**, 6834 (2000a)

T. Hayakawa, K. Adachi, Macromolecules **33**, 6840 (2000b)

D. Hayward, R.A. Pethrick, T. Siriwittayakorn, Macromolecules **25**, 1480 (1992)

Y.Y. He, T.R. Lutz, M.D. Ediger, J. Chem. Phys. **119**, 9956 (2003)

P. Hedvig, *Dielectric Spectroscopy of Polymers* (Adam Hilger, Bristol, 1977)

J. Heijboer, in *Moelecular Basis of Transition and Relaxation*, ed. by D.J. Meier (Gordon and Breach Science Publishers, New York, 1978)

E. Hempel, M. Beiner, T. Renner, E. Donth, Acta. Polym. **47**, 525 (1996)

E. Hempel, G. Hempel, A. Hensel, C. Schick, E.J. Donth, J. Phys. Chem. B **104**, 2460 (2000)

D. Herrera, J.C. Zamora, A. Bello, M. Grimau, E. Laredo, A.J. Müller, T.P. Lodge, Macromolecules **38**, 5109 (2005)

Hewlett Packard Product Note 8510-3 (1985) Measuring the dielectric constant of solids with the HP8510 network analyzer

Y. Hirose, O. Urakawa, K. Adachi, Macromolecules **36**, 3699 (2003)

S. Hoffman, L. Willner, D. Richter, A. Arbe, J. Colmenero, B. Farago, Phys. Rev. Lett. **85**, 772 (2000)

S. Hoffman, D. Richter, A. Arbe, J. Colmenero, B. Farago, Appl. Phys. A. **74**, S442 (2002)

A. Hofmann, F. Kremer, E.W. Fischer, Phys. A. **201**, 106 (1993)

B.S. Hsiao, B.B. Sauer, J. Polym. Sci. Polym. Phys. Ed. **31**, 901 (1993)

S.D. Hudson, D.D. Davis, A.J. Lovinger, Macromolecules **25**, 1759 (1992)

P. Huo, P. Cebe, J. Polym. Sci. Phys. Ed. **30**, 239 (1992a)

P. Huo, P. Cebe, Macromolecules **25**, 902 (1992b)

P. Huo, P. Cebe, Polymer **34**, 696 (1993)

G.Q. Jiang, W.H. Wong, E.Y. Raskovida, W.G. Clark, W.A. Hines, J. Sanny, Rev. Sci. Instrum. **64**, 1614 (1993)

X. Jin, S. Zhang, J. Runt, Macromolecules **37**, 8110 (2004)

G.P. Johari, J. Chem. Phys. **28**, 1766 (1973)

G.P. Johari, M.J. Goldstein, J. Chem. Phys. **53**, 2372 (1970)

S. Kahle, J. Korus, E. Hempel, R. Unger, S. Höring, K. Schröter, E.J. Donth, Macromolecules **30**, 7214 (1997)

D.S. Kalika, R.K. Krishnaswamy, Macromolecules **26**, 4252 (1993)

S. Kamath, R.H. Colby, S.K. Kumar, K. Karatasos, G. Floudas, G. Fytas, J.E.L. Roovers, J. Chem. Phys. **111**, 6121 (1999)

S. Kamath, R.H. Colby, S.K. Kumar, Macromolecules **36**, 8567 (2003a)

S. Kamath, R.H. Colby, S.K. Kumar, Phys. Rev. E. **67**, 010801 (R) (2003b)

R. Kant, S.K. Kumar, R.H. Colby, Macromolecules **36**, 10087 (2003)

F.E. Karasz (ed.), *Dielectric Properties of Polymers* (Plenum, New York, 1972)

K. Karatasos, G. Valaachos, D. Vlassopoulos, G. Fytas, G. Meier, A. Du Chesne, J. Chem. Phys. **108**, 5997 (1998)

G. Katana, A. Zetsche, F. Kremer, E.W. Fischer, ACS Polym. Preprints **33**, 122 (1992)

G. Katana, F. Kremer, E.W. Fischer, R. Plaetscke, Macromolecules **26**, 3075 (1993)

G. Katana, E.W. Fischer, T. Hack, V. Abetz, F. Kremer, Macromolecules **28**, 2714 (1995)

J.G. Kirkwood, J. Chem. Phys. **58**, 911 (1939)

J.G. Kirkwood, Ann. NY Acad. Sci. **40**, 315 (1940)

J.G. Kirkwood, Trans. Faraday Soc. **42A**, 7 (1946)

S. Koizumi, J. Polym. Sci. Polym. Phys. Ed. **42**, 3148 (2004)

F. Kremer, A. Schönhals, *Broadband Dielectric Spectroscopy* (Springer, Berlin, 2003)

F. Kremer, A. Schönhals, Broadband dielectric measurement techniques (Chapter 2), in *Broadband Dielectric Spectroscopy*, ed. by F. Kremer, A. Schönhals (Springer, Berlin, 2003b), pp. 35–58

F. Kremer, A. Hofmann, E.W. Fischer, ACS-Polym. Preprints **33**, 96 (1992)

E. Krygier, G. Lin, J. Mendes, G. Mukandela, D. Azar, A.A. Jones, J.A. Pathak, R.H. Colby, S. Kumar, G. Floudas, R. Krishnamoorti, R. Faust, Macromolecules **38**, 7721 (2005)

U. Kubon, R. Schilling, J.H. Wendof, Colloid Polym. Sci. **266**, 123 (1988)

A.S. Kulik, H.W. Beckham, K. Schmidt-Rohr, D. Radloff, U. Pawelzik, C. Boeffel, H.W. Spiess, Macromolecules **27**, 4746 (1994)

S.K. Kumar, Macromolecules **33**, 5285 (2000)

S.K. Kumar, R.H. Colby, S.H. Anastasiadis, G. Fytas, J. Chem. Phys. **105**, 3777 (1996)

L.K.H. van Beek Dielectric behavior of heterogeneous systems, in *Progress in Dielectrics*, vol. 7, ed. by J.B. Birks (Heywood, 1967), pp. 69–114

L.D. Landau, E.M. Lifschitz, *Statistical Physics*. Textbook of Theoretical Physics, vol. V (Akademie-Verlag, Berlin, 1979)

C. Larvergne, C. Lacabanne, IEEE Elec. Insul. Mag. **9**, 5 (1993)

E. Leroy, A. Alegria, J. Colmenero, Macromolecules **35**, 5587 (2002)

E. Leroy, A. Alegria, J. Colmenero, Macromolecules **36**, 7280 (2003)

H.S. Li, W. Kim, Polymer **38**, 2657 (1997)

A.E. Likhtman, T.C.B. McLeish, Macromolecules **35**, 6332 (2002)

J.E.M. Lipson, Macrom. Theory Simul. **7**, 263 (1998)

J.E.M. Lipson, M. Tambasco, K.A. Willets, J.S. Higgins, Macromolecules **36**, 2977 (2003)

C.-Y. Liu, R. Keunings, C.D. Bailly, Phys. Rev. Lett. **97**, 246001 (2006)

T.P. Lodge, T.C.B. McLeish, Macromolecules **33**, 5278 (2000)

T.P. Lodge, E.R. Wood, J.C. Haley, J. Polym. Sci. Polym. Phys. Ed. **44**, 756 (2006)

H.A. Lorentz, Ann. Phys. **9**, 641 (1879)

C. Lorthioir, A. Alegria, J. Colmenero, Phys. Rev. E. **86**, 031805 (2003)

X. Lu, R.A. Weiss, Macromolecules **25**, 3242 (1992)

T.R. Lutz, Y.Y. He, M.D. Ediger, Macromolecules **38**, 9826 (2005)

T. Malik, R.E. Prud'homme, Polym. Eng. Sci. **24**, 144 (1984)

J. Maranas, Curr. Opin. Colloid Interface Sci. **12**, 29 (2007)

P.F. Massotti, Bibl. Univ. Modena **6**, 193 (1847)

M. Matsuo, Y. Ishida, K. Yamafuji, M. Takayanagi, F. Irie, Kolloid-Z und Z für Polymere **201**, 7 (1965)

J.C. Maxwell, Phil. Trans. **155**, 459 (1865)

J.C. Maxwell, Phil. Trans. **158**, 643 (1868)

N.G. McCrum, B.E. Read, G. Williams, *Anelastic and Dielectric Effects in Polymeric Solids* (Wiley, New York, 1967) (reprinted by Dover Publications 1991)

D. Migahed, T. Fahmy, Polymer **35**, 1688 (1994)

S.T. Milner, T.C.B. McLeish, Phys. Rev. Lett. **81**, 725 (1998)

N. Miura, W. MacKnight, S. Matsuoka, F.E. Karasz, Polymer **40**, 6129 (2001)

Y. Miwa, K. Usami, M. Yamamoto, T. Sakaguchi, M. Sakai, S. Shimada, Macromolecules **38**, 2355 (2005)

E. Montroll, G.H. Weiss, J. Math. Phys. **6**, 167 (1965)

K. Mpoukouvalas, G. Floudas, Macromolecules **41**, 1552 (2008)

K. Mpoukouvalas, G. Floudas, S. Zhang, J. Runt, Macromolecules **38**, 552 (2005)

T. Nakajima, *Annual Report, Conference on Electrical Insulation and Dielectric Phenomena* (National Academy of Sciences, Washington, DC, 1971)

H. Namikawa, J. Non-Cryst. Solids **18**, 173 (1975)

K.L. Ngai, C.M. Roland, Macromolecules **37**, 2817 (2004)

L. Onsager, J. Am. Chem. Soc. **58**, 1486 (1938)

J.A. Pathak, R.H. Colby, G. Floudas, R. Jerome, Macromolecules **32**, 2353 (1999)

K. Pathmanathan, G.P. Johari, J.P. Faivre, L. Monnerie, J. Polym. Sci. **24**, 1587 (1986)

R. Pelster, IEEE Trans. Microw. Theory Tech. **43**, 1494 (1995)

B.T. Poh, K. Adachi, T. Kotaka, Macromolecules **29**, 6317 (1996)

J. Pugh, T. Ryan, IEE Conf. Dielectric Mater. Meas. Appl. **177**, 404 (1979)

M. Rabeony, D.J. Lohse, R.T. Garnert, S.J. Ham, W.W. Graessley, K.B. Migler, Macromolecules **31**, 6511 (1998)

G.S. Rellick, J. Runt, J. Polym. Sci. Polym. Phys. Ed. **24**, 279 (1986a)

G.S. Rellick, J. Runt, J. Polym. Sci. Polym. Phys. Ed. **24**, 313 (1986b)

G.S. Rellick, J. Runt, J. Polym. Sci. Polym. Phys. Ed. **26**, 1425 (1988)

E. Riande, R. Diaz-Calleja, *Electrical Properties of Polymers* (Marcel Dekker, New York, 2004)

E. Riande, E. Saiz, *Dipole Moments and Birefringence of Polymers* (Prentice Hall, Englewood Cliffs, 1992)

C.M. Roland, K. Ngai, Macromolecules **24**, 2261 (1991)

C.M. Roland, K. Ngai, J. Rheol. Acta. **36**, 1691 (1992a)

C.M. Roland, K. Ngai, Macromolecules **25**, 363 (1992b)

C.M. Roland, S. Hensel-Bielowka, M. Paluch, R. Casalini, Rep. Prog. Phys. **68**, 1405 (2005)

C.M. Roland, K.J. MacGrath, R. Cassalini, Macromolecules **39**, 3581 (2006)

P.E. Rouse, J. Chem. Phys. **21**, 1272 (1953)

W. Ruland, Prog. Colloid Polym. Sci. **57**, 192 (1957)

J.P. Runt, Dielectric studies of polymer blends, in *Dielectric Spectroscopy of Polymeric Materials*, ed. by J.P. Runt, J.J. Fitzgerald (ACS-books, Washington, DC, 1997), pp. 283–302

J.P. Runt, J.J. Fitzgerald (eds.), *Dielectric Spectroscopy of Polymeric Materials* (American Chemical Society, Washington, DC, 1997)

J. Runt, C.A. Barron, Z.-F. Zhang, S.K. Kumar, Macromolecules **24**, 3466 (1991)

T. Sakaguchi, N. Taniguchi, O. Urakawa, K. Adachi, Macromolecules **38**, 422 (2005)

S. Salaniwal, R. Kant, R.H. Colby, S.K. Kumar, Macromolecules **35**, 9211 (2002)

H. Sasabe, S. Saito, J. Polym. Sci. Part A-2 **6**, 1401 (1968)

B.B. Sauer, B.S. Hsiao, J. Polym. Sci. Poly. Phys. Ed. **31**, 917 (1993)

B.B. Sauer, P. Avakian, G.M. Cohen, Polymer **33**, 2666 (1992)

B.B. Sauer, P. Avakian, E.A. Flexman, M. Keating, B.S. Hsiao, R.K. Verma, J. Polym. Sci. Polym. Phys. Ed. **35**, 2121 (1997)

B. Schartel, J.H. Wendorff, Polymer **36**, 899 (1995)

C. Schick, Calorimetry (Chapter 2.31), in *Polymer Science: A Comprehensive Reference*, vol. 2, ed. by K. Matyjaszewski, M. Möller (Elsevier, Amsterdam, 2012), pp. 793–823

E. Schlosser, A. Schönhals, Colloid Polym. Sci. **267**, 963 (1989)

K. Schneider, A. Schönhals, E.J. Donth, Acta Polym. **32**, 471 (1981)

A. Schönhals, Macromolecules **26**, 1309 (1993)

A. Schönhals, Europhys. Lett. **56**, 815 (2001)

A. Schönhals, Molecular dynamics in Polymeric model systems (Chapter 7), in *Broadband Dielectric Spectroscopy*, ed. by F. Kremer, A. Schönhals (Springer, Berlin, 2003)

A. Schönhals, F. Kremer, J. Non-cryst. Solids **172–174**, 336 (1994)

A. Schönhals, F. Kremer, Analysis of dielectric spectra (Chapter 3), in *Broadband Dielectric Spectroscopy*, ed. by F. Kremer, A. Schönhals (Springer, Berlin, 2003a), pp. 59–98

A. Schönhals, F. Kremer, Theory of dielectric relaxation (Chapter 1), in *Broadband Dielectric Spectroscopy*, ed. by F. Kremer, A. Schönhals (Springer, Berlin, 2003c)

A. Schönhals, E. Schlosser, Colloid Polym. Sci. **267**, 125 (1989)

A. Schönhals, H. Goering, C. Schick, B. Frick, R. Zorn, J. Non-cryst. Solids **351**, 2668 (2005)

A. Schönhals, F. Kremer, Amorphous polymers (Chapter 1.08), in *Polymer Science: A Comprehensive Reference*, vol. 1, ed. by K. Matyjaszewski, M. Möller (Elsevier, Amsterdam, 2012), pp. 201–226

S. Schrader, A. Schönhals, Prog. Colloid Polym. Sci. **80**, 93 (1989)

K. Schröter, R. Unger, S. Reissig, F. Garwe, S. Kahle, M. Beiner, E. Donth, Macromolecules **31**, 8966 (1998)

G.A. Schwartz, A. Alegria, J. Colmenero, J. Chem. Phys. **127**, 154907 (2007a)

G.A. Schwartz, J. Colmenero, A. Alegria, Macromolecules **40**, 3246 (2007b)

K. Se, O. Takayanagi, K. Adachi, Macromolecules **30**, 4877 (1997)

A. Serghei, M. Tress, J.R. Sangoro, F. Kremer, Phys. Rev. B **80**, 184301 (2009)

T.F. Shatzki, J. Polym. Sci. **57**, 496 (1962)

S. Shenogin, R. Kant, R.H. Colby, S.K. Kumar, Macromolecules **40**, 5767 (2007)

R.W. Sillars, J. Inst. Elect. Eng. **80**, 378 (1937)

G.P. Simon, A. Schönhals, Dielectric relaxation and thermal stimulated currents, in *Polymer Characterization Techniques and Their Application to Blends*, ed. by G.P. Simon (Oxford University Press, Oxford/New York, 2003), pp. 96–131

J. Skolnik, R. Yaris, Macromolecules **15**, 1041 (1982)

L.H. Sperling, *Introduction to Physical Polymer Science* (Wiley, New York, 1986)

P.A.M. Steeman, F.H.J. Maurer, Colloid Polym. Sci. **268**, 315 (1990)

P.A.M. Steeman, F.H.J. Maurer, Colloid Polym. Sci. **270**, 1069 (1992)

P.A.M. Steeman, J. van Turnhout, Dielectric properties of inhomogeneous media (Chapter 13), in *Broadband Dielectric Spectroscopy*, ed. by F. Kremer, A. Schönhals (Springer, Berlin, 2003), pp. 495–522

P.A.M. Steeman, F.H.J. Maurer, J. van Turnhout, Polym. Eng. Sci. **34**, 697 (1994)

W.H. Stockmayer, Pure Appl. Chem. **15**, 539 (1967)

W.H. Stockmayer, J.J. Burke, Macromolecules **2**, 647 (1969)

G.R. Strobl, *The Physics of Polymers* (Springer, Heidelberg, 1996)

J. Swenson, R. Bergman, S. Longeville, J. Chem. Phys. **115**, 1299 (2001)

J.W. Sy, J. Mijovic, Macromolecules **33**, 933 (2000)

M. Tambasco, J.E.M. Lipson, J.S. Higgins, Macromolecules **39**, 4860 (2006)

G. Tammann, W. Hesse, Z. Anorg. Allg. Chem. **156**, 245 (1926)

T. Tetsutani, M. Kakizaki, T. Hideshima, Polym. J. **14**, 305 (1982a)

T. Tetsutani, M. Kakizaki, T. Hideshima, Polym. J. **14**, 471 (1982b)

G. Teyssedre, S. Mezghani, A. Bernes, C. Lacabanne, in *Thermally Stimulated Currents of Polymers in Dielectric Spectroscopy of Polymeric Materials*, ed. by J. Runt, J.J. Fitzgerald (ACS, Washington, DC, 1997), pp. 227–258

M. Topic, Z. Veksli, Polymer **34**, 2118 (1993)

M. Topic, A. Mogus-Milankovic, Z. Katovic, Polymer **28**, 33 (1987)

G. Turky, D. Wolff, A. Schönhals, Macromol. Chem. Phys. **22**, 2420 (2012)

M. Tyagi, A. Arbe, J. Colmenero, B. Frick, J.R. Stewart, Macromolecules **39**, 3007 (2006)

M. Tyagi, A. Arbe, A. Alegria, J. Colmenero, B. Frick, Macromolecules **40**, 4568 (2007)

O. Urakawa, K. Adachi, T. Kotaka, Macromolecules **26**, 2036 (1993a)

O. Urakawa, K. Adachi, T. Kotaka, Macromolecules **26**, 2042 (1993b)

O. Urakawa, Y. Fuse, H. Hori, Q. Tran-Cong, O. Yano, Polymer **42**, 765 (2001)

O. Urakawa, T. Sugihara, K. Adachi, Polym. Appl. (Japan) **51**, 10 (2002)

O. Urakawa, T. Ujii, K. Adachi, J. Non-cryst. Solids **352**, 5042 (2006)

B. Valeur, J.P. Jarry, F. Geny, J. Monnerie, J. Polym. Sci. Polym, Polym. Phys. Ed. **13**, 667 (1975a)

B. Valeur, J. Monnerie, J.P. Jarry, J. Polym. Sci. Polym. Phys. Ed. **13**, 675 (1975b)

J. van Turnhout, *Thermally Stimulated Discharge of Polymer Electrets* (Elevier, Amsterdam, 1975)

J. Vanderschueren, M. Landang, J.M. Heuschen, Macromolecules **13**, 973 (1980)

H. Vogel, Phys. Z. **22**, 645 (1921)

M.V. Volkenstein, *Configurational Statistics of Polymeric Chains* (Wiley Interscience, New York, 1963)

R.W. Wagner, Arch. Elektrotech. **2**, 371 (1914)

H. Watanabe, M. Yamazaki, H. Yoshida, K. Adachi, T. Kotaka, Macromolecules **24**, 5365 (1991)

H. Watanabe, O. Urakawa, H. Yamada, M.-L. Yao, Macromolecules **29**, 755 (1996)

R.E. Wetton, W.J. MacKnight, J.R. Fried, F.E. Karasz, Macromolecules **11**, 158 (1978)

G. Williams, Adv. Polym. Sci. **33**, 60 (1979)

G. Williams, D.A. Edwards, Trans. Faraday Soc. **62**, 1329 (1966)

G. Williams, D.C. Watts, Trans. Faraday Soc. **67**, 2793 (1971)

G. Williams, in *Comprehensive Polymer Science*, vol. II, ed. by G. Allen, J.C. Bevington (Pergamon Press, Oxford, 1989)

G. Williams, in *Structure and Properties of Polymers*, ed. by E.L. Thomas. Materials Science & Technology Series, vol. 12 (Wiley and Sons, Hoboken, New Jersey, 1993), p. 471

B. Wunderlich, Prog. Polym. Sci. **28**, 383 (2003)

H. Yin, S. Napolitano, A. Schönhals, Macromolecules **45**, 1652 (2012)

M. Zamponi, A. Wischnewski, M. Monkenbusch, L. Willner, D. Richter, A.E. Likhtman, G. Kali, B. Farago, Phys. Rev. Lett. **96**, 238302 (2006)

S. Zeeb, S. Höring, F. Garwe, M. Beiner, A. Schönhals, K. Schröter, E. Donth, Polymer **38**, 4011 (1997)

A. Zetsche, E.W. Fischer, Acta Polym. **45**, 168 (1994)

A. Zetsche, F. Kremer, H. Jung, Polymer **31**, 1883 (1990)

S. Zhang, X. Jin, P.C. Painter, J. Runt, Macromolecules **38**, 6216 (2005)

R. Zorn, L. Hartmann, B. Frick, D. Richter, Kremer F **307**, 547 (2002)

Physical Aging of Polymer Blends

13

J. M. G. Cowie and V. Arrighi

Contents

Abstract

The selection of polymers and polymer blends for use as specific materials requires the consideration of how these will withstand the environmental

---

J. M. G. Cowie: Deceased.

J.M.G. Cowie • V. Arrighi (✉)
Institute of Chemical Sciences, School of Engineering and Physical Sciences, Heriot-Watt University, Edinburgh, Scotland, UK
e-mail: V.Arrighi@hw.ac.uk

conditions to which these will be subjected. The long-term stability of a polymer will depend on its aging characteristics both physical and chemical.

Physical aging is the term used to describe the observed changes in properties of glassy materials as a function of storage time, at a temperature below the glass transition, T_g. This phenomenon is important mainly when the materials have a substantial amorphous content. For these materials, a quench from above T_g into the glassy state introduces a nonequilibrium structure which, on annealing at constant temperature, approaches an equilibrium state via small-scale relaxation processes in the glassy state. The aging process can be detected through the time evolution of thermodynamic properties such as the specific volume or enthalpy or mechanical methods such as creep, stress-relaxation, and dynamic mechanical measurements. Here, the fundamental principles of physical aging will be described, and models that quantitatively describe the aging process are briefly described.

Physical aging effects have practical implications and need to be considered when assessing the long-term stability of polymers and polymer–polymer mixtures. This chapter focuses on a discussion of the effect of blending on physical aging and gives a review of the different experimental methods that can be used to compare aging rates in blends to those of the individual components.

13.1   Introduction

The long-term stability of polymeric materials is a matter of considerable importance, both to materials scientists and to engineers. Two types of aging occur that result in changes in the properties of polymers: chemical and physical. Chemical aging normally leads to modification of the polymer chain and may involve chain scission, oxidation, dehalogenation, loss of pendant groups, hydrolysis, and cross-linking, all of which are nonreversible chemical reactions. Physical aging is a manifestation of small-scale relaxation processes that take place predominantly in the amorphous regions of a glassy polymer, causing volume contraction and densification of the sample. Thus, while both are time and temperature dependent, the chemical aging results in an alteration of the chemistry of the polymer and usually leads to degradation with a concurrent deterioration of the properties (e.g., discoloration, embrittlement, loss of tensile strength). This type of aging will not be considered here.

During physical aging more subtle changes take place which do not involve chemical modification: the polymer structure remains unchanged, but the local packing of the chains alters due to the slow structural relaxation of the glass. This leads to dimensional changes and alteration of physical properties such as density, brittleness, tensile strength, and the glass transition temperature, T_g. Unlike chemical aging, physical aging is a reversible process.

In practice, aging tends to render the material more brittle and this may impair any long-term applications. A wide range of materials may be affected by physical aging and extensive studies have been carried out on homopolymers and copolymers. Contrary to this, less attention has been devoted to physical aging of polymer

blends, and there are still important aspects of the aging process, e.g., the role of intermolecular interactions that are not fully understood. This is somewhat surprising given the commercial importance of polymer blends, but it is likely related to our incomplete understanding of the molecular processes that govern physical aging even in the case of relatively simple homopolymers. Extending our current knowledge to complex systems such as blends, composites, and nanocomposites is not trivial. However, a detailed knowledge of the glassy state of polymeric materials is necessary if we are to measure and model the aging process and then use the results to design more stable materials.

In the following sections, aging data for blend systems will be reviewed.

13.2   Thermodynamics of the Glass Transition

Polymers behave as liquids as long as temperature changes occur at a slower rate than that required by the molecules to readjust to their new equilibrium condition. As the annealing temperature, T_a, approaches T_g [i.e., as $(T_g - T_a)$ increases], the aging process slows down. A temperature is eventually reached at which the characteristic rate of motion is too slow compared to the rate of temperature changes: molecular conformations are fixed, and the material is no longer able to attain structural equilibrium, i.e., it behaves as a glass.

Below T_g the glass that is formed is not in equilibrium with its surroundings, and, on annealing at a given temperature, T_a, there will be a driving force to reduce excess thermodynamic quantities such as volume and enthalpy to their equilibrium values at that temperature. The continuous, slow, relaxation of the glass from the initial nonequilibrium state toward a final thermodynamic equilibrium state produces time-dependent changes in the physical properties of the polymer. This slow structural reorganization of the glass is termed *physical aging*.

Chain mobility is rather limited below T_g and so structural changes can only result from limited segmental relaxation processes. Therefore, it is believed that aging should occur within a limited temperature range, $T_\beta < T < T_g$, where T_β is the temperature of the first secondary relaxation process that can take place in the glassy state (Struik 1978). This restricted temperature range is disputed (Johari 1982; McCrum 1992), and it is believed that aging is a phenomenon affecting all viscoelastic relaxation processes.

13.3   Experimental Determination of Aging

As the annealing temperatures T_a drop further away from T_g, the aging process slows down and the time scales involved become quite long. Consequently many studies are carried out under thermally accelerated conditions. The relaxation of the enthalpy and volume of the glass are convenient parameters to follow when monitoring the physical aging process, as are the time-dependent small strain mechanical properties. Spectroscopic and scattering methods can also be employed

in some cases. A brief description of the techniques is given in the following sections. A more comprehensive review has been given by Hutchinson (Hutchinson 1992).

13.4   Enthalpy Relaxation

Calorimetry has been one of the most commonly used techniques to follow the enthalpic relaxation during aging. Measurements are readily carried out at temperatures below T_g using a differential scanning calorimeter (DSC), a convenient and widely available instrument.

To obtain meaningful results, it is important to define a reproducible thermal history for the sample. The principles underpinning the measurements are summarized in the schematic diagrams of Fig. 13.1a, b. The first step is to ensure that the influence of any previous thermal history is erased by annealing the sample at a temperature in excess of $T_g + 50\ °C$, i.e., at the point A in Fig. 13.1. The polymer is then cooled from the melt at temperature T_2, (A), at a rate q_1, into the glass at temperature T_a, (B). The distance of the sample from its "equilibrium state" at T_a will depend on the rate of cooling of the sample, and so this thermal treatment should remain unchanged for all measurements that are to be compared. Annealing the sample at temperature T_a, for a specified time t_a, results in an enthalpy loss $H_B - H_C$ (along the lines B-C), the extent of which depends on the magnitude of t_a. When measurements are carried out using DSC, the sample is then quenched from T_a after t_a, and on reheating the polymer at a rate q_2, the enthalpy overshoots the equilibrium curve, as shown in Fig. 13.1 by an amount proportional to that lost during the aging process. This is represented by the line (C-A). The enthalpy difference $(H_B - H_C)$ is then given by

$$(H_B - H_C) = \Delta H(t_a, T_a) = \int_{T\alpha}^{T\beta} \left\{ C_p(\text{aged}) - C_p(\text{unaged}) \right\} dT \qquad (13.1)$$

and it is equivalent to the area (A-B) in Fig. 13.2.

As DSC measures the specific heat, C_p, and $C_p = (\partial H / \partial T)_p$, the enthalpy change can be obtained by integration of the DSC curves. From a practical point of view, the aging temperatures T_a are normally close to T_g because the greater $(T_g - T_a)$, the slower the aging processes become and the time scales for the relaxation events are too long for accurate measurement. It is necessary to carry out accelerated aging at temperatures close to T_g, so that measurements can be made over periods of a few hours up to several days at the most.

The majority of models developed to describe the physical aging process are based on the idea of free volume in the polymer. Some only attempt to model the

Fig. 13.1 (**a**) Schematic diagram of the time–temperature profile used in enthalpy relaxation experiments and (**b**) schematic representation of cooling, aging, and heating cycles using the time–temperature profile in (**a**)
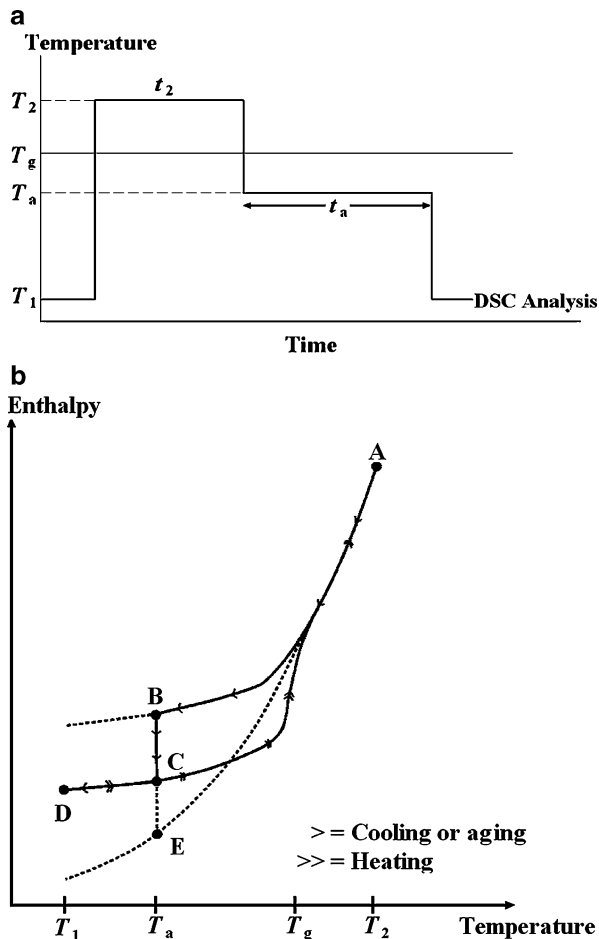
observed behavior, while others take a more holistic approach and try to understand the relationship between the molecular relaxation events and the distribution of free volume in the sample.

13.4.1 The Multiparameter Phenomenological Models

A number of theoretical treatments have been developed that attempt to model the aging process in organic and inorganic glasses. Notable examples are the phenomenological models of Narayanaswamy (1971), Moynihan et al. (1976), Hodge et al. (Hodge and Berens 1981; Hodge and Berens 1982; Hodge and Huvard 1983), Gomez-Ribelles and Monleon-Pradas (1995), and Gomez-Ribelles et al. (1995).

Fig. 13.2 Schematic diagram of DSC curves for an aged (full line) and unaged (broken line) polymer sample (top diagram) before and after (bottom diagram) subtraction
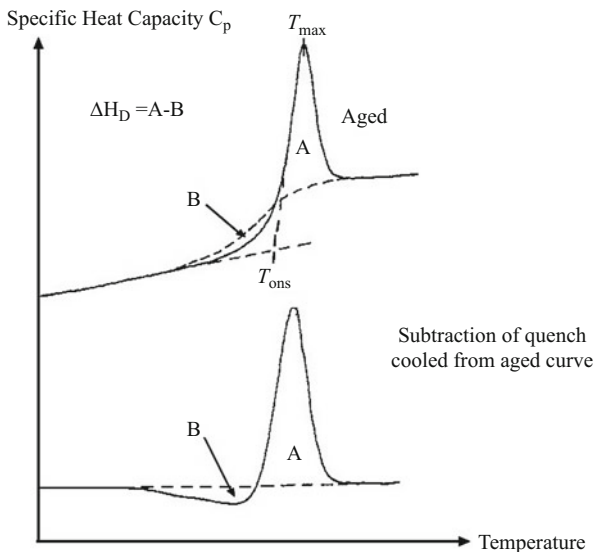
As the relaxation processes in the glassy state and glass transition region are non-exponential and nonlinear, the theories must take account of the thermal history of glass formation and the asymmetry of the relaxations, which depend on how the system departs from equilibrium.

To account for the nonlinearity of the relaxation use is made of the convenient concept of a "fictive" temperature, T_f, first proposed by Tool (1946). This is defined as the temperature at which the nonequilibrium value of a macroscopic property of the system would be an equilibrium one. As shown in Fig. 13.3, the enthalpy difference $H(T_2) - H(T)$ can be expressed in one of the two equivalent ways:

$$H(T_2) - H(T) = \int_T^{T_2} \left\{ C_p\left(T'\right) \right\} dT' \tag{13.2}$$

$$H(T_2) - H(T) = \int_T^{T_f} \left\{ C_{p,\,\text{glass}}\left(T'\right) \right\} dT + \int_{T_f}^{T_2} \left\{ C_{p,\,\text{liquid}}\left(T'\right) \right\} dT' \tag{13.3}$$

where T' is a dummy variable. Equating the two terms and rearranging leads finally to

$$\int_T^{T_f} \left\{ C_p\left(T'\right) - C_{p,\,\text{glass}}\left(T'\right) \right\} dT - \int_{T_f}^{T_2} \left\{ C_{p,\,\text{liquid}}\left(T'\right) - C_p\left(T'\right) \right\} dT' = 0 \tag{13.4}$$

From this a normalized heat capacity can be formulated in terms of experimental quantities as

Fig. 13.3 Representation of how the fictive temperature is defined (Reproduced with permission from Cowie and Ferguson (1993))
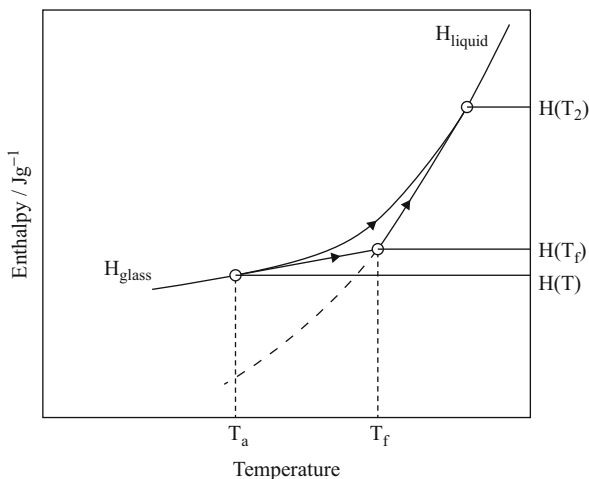
When the heat capacities of the glass and the liquid are defined by linear functions of temperature, the value of T_f can be calculated from numerical integration of the DSC curves to obtain $H(T_2) - H(T)$.

The concept was developed further by Narayanaswamy (1971) and Moynihan et al. (1976) who treated the kinetics of the aging processes by describing the relaxation toward an equilibrium state in terms of a nonequilibrium decay function. As this depended on the departure from equilibrium, the kinetics are also nonlinear. To allow for this, the average relaxation time, τ, was made a function of both temperature and structure and expressed as

$$\tau\left(T, T_f\right) = \tau_o \exp\left[\frac{x\Delta h^*}{RT} + \frac{(1-x)\Delta h^*}{RT_f}\right] \tag{13.6}$$

where τ_o is the relaxation time at equilibrium ($T_f = T$) at high temperatures, x is the structural or nonlinearity parameter which defines the relative contribution of structure and temperature to the relaxation time ($0 < x \leq 1$), and Δh^* is the effective activation energy for the relaxation processes, assumed to display an Arrhenius temperature dependence.

Equation 13.6 is referred to as the Tool–Narayanaswamy–Moynihan (TNM) equation to acknowledge the contributions of different authors to the theoretical model. Both Δh^* and x have no clear physical meaning. However, in their treatment of the glassy state, Gibbs and DiMarzio (1958) (GD) postulated that a second thermodynamic transition T_2 existed below T_g at which the configurational entropy S_c is zero. The concept of a temperature at which $S_c = 0$ was introduced by

Kauzmann in 1948 and further developed in the Adam–Gibbs theory (Adam and Gibbs 1965), which introduces the idea of a "cooperative rearranging region," where the configurational entropy changes may occur without affecting the surrounding. At T_2 only one-chain configuration is possible; thus $S_c = 0$. Hodge (1987) used the GD theory to show that $x = (T_f'/T_2)$ where T_f' is the value of the fictive temperature in the glass and T_2 is the "equilibrium" T_g.

As discussed previously, the annealing of the glass at the aging temperature T_a results in a relaxation of the enthalpy toward the equilibrium value ΔH_∞. The relaxation function, $\phi(t)$, describes the progression of a system to equilibrium and is defined by

$$\phi(t) = \frac{\Delta H_t - \Delta H_\infty}{\Delta H_0 - \Delta H_\infty} \tag{13.7}$$

where ΔH_0, ΔH_t, and ΔH_∞ are the enthalpy values at the initial time, at time t, and at equilibrium, respectively.

The relaxation function, $\phi(t)$, can also be expressed in terms of a semiempirical function introduced originally by Kohlrausch (1897) and revived by Williams and Watts (1970), abbreviated as the KWW equation:

$$\phi(t) = \exp\left[-\left(\frac{t}{\tau}\right)^\beta\right] \tag{13.8}$$

Equation 13.8 expresses the non-exponentiality of the recovery process during isothermal aging in terms of the parameter β which is related to the breadth of the distribution of relaxation times and has values $0 < \beta < 1$. A value of $\beta = 1$ would imply an infinitely sharp distribution with only one relaxation time. The latter parameter is represented by τ and the effects of physical aging are then analyzed in terms of β and τ. Equation 13.8 has been shown to describe the relaxation process well for small temperature jumps, but it is reported to fail for temperature jumps higher than 1 K. As a result, the relaxation function does not scale linearly with the extent of the departure from equilibrium meaning that the responses cannot be superimposed to form a single master curve by a linear transformation in time.

Gomez-Ribelles and Monleon-Pradas (1995) and Gomez-Ribelles et al. (1995) did not use the fictive temperature, but considered instead the temporal evolution of the configurational entropy, S_c. This provides an improved correlation between the theory and experimental heat capacity data during aging, allowing for the direct use of C_p from experiment without having to normalize the data and removing the restriction of having to calculate the limiting C_p of a fully aged glassy polymer from a linear extrapolation of the liquid C_p curve. In other words the authors recognized that because of the physical restrictions imposed by chain entanglements and inefficient chain packing, the glass may be unable to attain the limiting value derived from a simple linear extrapolation procedure. This concept had been adopted earlier by Cowie and Ferguson (1986, 1989).

Alternative analytical methods are the KAHR isothermal single relaxation time model (Kovacs et al. 1979) and the peak shifting technique (Hutchinson 1992).

13.4.2 Predictive Models for Long-Term Aging

The Petrie–Marshall (P-M) (Petrie and Marshall 1975) or the Cowie–Ferguson (C-F) (1986, 1989) models have been developed in order to facilitate predictions of long-term aging. In both, the enthalpy lost on aging is given by

$$\Delta H(t_a, T_a) = \Delta H(\infty, T_a)[1 - \phi(t_a)] \tag{13.9}$$

where the P-M approach uses Eq. 13.9 to define $\phi(t_a)$ with $\beta = 1$, but C-F express this relaxation function as

$$\phi(t_a) = \exp\left[-\left(\frac{t}{t_c}\right)^{\beta}\right] \tag{13.10}$$

where t_c is a characteristic time, such that $t_a = t_c$ when the polymer glass has aged to 63.2 % of the fully aged glass. The method of determining $\Delta H(\infty, T_a)$ also differs. In the P-M model, this is estimated by a linear extrapolation of the heat capacity (liquid) into the glassy state. The relaxation time is then related to the departure from equilibrium of the enthalpy (δH) by

$$\frac{1}{\tau} = \frac{1}{t_a}\ln\left[1 - \frac{\Delta H(t_a, T_a)}{\Delta H(\infty, T_a)}\right] \tag{13.11}$$

where $\delta H = \Delta H(\infty, T_a) - \Delta H(t_a, T_a)$.

The C-F approach treats $\Delta H(\infty, T_a)$ as an adjustable parameter as it is considered that the linear C_p extrapolation is inaccurate. The data are analyzed by curve fitting plots of $\Delta H(t_a, T_a)$ against log t_a, to assess the thermodynamic aspects from the $\Delta H(\infty, T_a)$ parameter, and the kinetic aspects, embodied in $\phi(t_a)$, both of which are obtainable from this approach. Also considered in the C-F approach is the prediction of t_e, which is the time to reach 99.9 % of the thermodynamic equilibrium state of the infinitely aged glass, from accelerated aging experiments.

The C-F model has been extensively used to compare the aging behavior of polymer blends to that of the corresponding homopolymers, because of its simplicity. However, it should be noted that this model does not adequately describe all of the phenomenology associated with the glass transition, namely, its nonlinear character. The consequences of this when describing the physical aging process have been recently discussed in the literature (Li and Simon 2006; Hutchinson and Kumar 2002).

13.4.3 Molecular Models

The majority of the models developed are based on the idea that significant free volume exists in the glass state of a polymer. Some only attempt to model the consequences of the reduction in this free volume during aging, while others try to understand the relationship between the molecular relaxation processes which are responsible for the change in free volume, and the distribution of this free volume in the aging sample. The latter approach is much more desirable if a deeper understanding of the glassy state is to be achieved. This philosophy underpins the approach of Simha, Robertson, and coworkers.

Simha et al. have used the "hole" theory of Simha–Somcynsky (S-S) (Simha and Somcynsky 1969) as a starting point to develop further the idea of free volume. In their vacant cells or "holes" in a polymer lattice constitute the free volume arising from inefficient chain packing. An equation of state was developed to calculate the fraction of occupied lattice sites and hence the fractional free volume.

This approach has been expanded by Robertson (1979) who examined the relationship between molecular relaxation events that occur via small, simple trans, and gauche conformational changes in the chains and the free volume distribution. The former are assumed to be coupled with the free volume environment which will also be subject to thermal fluctuations.

Making use of these ideas and the S-S theory, Robertson and coworkers (Robertson et al. 1984) have described the structural relaxation in terms of the free volume reduction via the diffusion of vacant holes, in response to molecular relaxation events along the polymer chains. Other models have been proposed by Ngai (1979) and Kubat et al. (1999, 2000).

In the coupling model of Ngai (1979), account is made for the influence of the strength of molecular relaxation on the relaxation times. It was suggested that a "primary relaxing species," such as an α-relaxation, can be described by a time-independent relaxation state $W_o = \tau_o^{-1}$. However, this can be affected by low energy excitations in the glass which modifies W_o to a time-dependent rate $W(t)$. This leads to an expression for a coupled relaxation time:

$$\tau^* = \left[(1-n)\,\omega_c^n\,\tau_o \right]^{\frac{1}{(1-n)}} \tag{13.12}$$

where ω_c is a critical frequency and $(1-n)$ is the equivalent of β in the KWW function. As n depends on temperature and structure, it may vary during the relaxation process. This means that the system is no longer considered to be thermorheologically simple.

A coupling model has also been developed by Kubat et al. (1999, 2000). In it, the authors proposed that, while single relaxation events are most likely to occur, a cluster of these relaxations can also take place. Thus, in addition to single elementary transitions, double, triple, and higher transitions may occur with decreasing relaxation times ($\tau, \tau/2, \tau/3, \ldots$). While the available free volume still

imposes a limitation on the motion of the molecular units, the authors assumed that the activation energy of one unit will facilitate the simultaneous molecular rearrangement of other units in the vicinity of the first. Calculation of the size of the distribution of these clusters shows that the simple relaxing units are the most numerous and that the clustering tendency decreases with time.

13.4.4 Enthalpic Relaxation in Polymer Blends

The phenomenon of physical aging in polymers has received considerable attention, but relative few studies of physical aging in polymer/polymer mixtures have appeared in the literature. Most of these have made use of differential scanning calorimetry and enthalpic data to assess physical aging behavior in blends. Tables 13.1 and 13.2 provide a list of the most important systems investigated to date.

13.4.5 Aging as a Means of Detecting Phase Behavior

One of the most commonly used criteria for establishing the phase behavior in amorphous binary polymer blends is the presence of one or more T_gs. If the blend is one phase, a single T_g lying between the values for each component is detected and characterizes the mixture. If the blend is two phase, then two T_gs are observed close to or matching those of the two components.

It was initially believed that thermoanalytical methods such as DSC could not to be used to study blend systems whose constituent polymers had T_gs in close proximity to each other, namely, 10–20 degrees apart, due to the difficulty of discriminating between the presence of one or two T_gs at normal scan rates. However, both Bosma et al. (1988) and Jorda and Wilkes (1988) demonstrated that the use of isothermal aging experiments could overcome this problem. These authors argued that in a homogeneous, one-phase, blend, the kinetics of the aging process would be an average representing the blend and as such would exhibit only one enthalpy recovery peak. Early enthalpy relaxation studies of poly(methyl methacrylate) (PMMA)/poly(styrene-co-acrylonitrile) (SAN) blends carried out by Naito et al. (1978) had confirmed this point as a single endothermic aging peak was observed for the 50/50 blend and the pure components. In this case, no measurable changes on the magnitude of the enthalpy relaxation peak after blending were detected and the authors concluded that this was a result of a weak interaction between the two polymers.

Isothermal aging experiments have been used to determine phase behavior in several systems. Blends of poly(vinyl chloride), PVC, ($T_g = 80$ °C) and poly (isopropyl methacrylate), PiPMA, ($T_g = 82.5$ °C), are believed to be immiscible, but because of the closeness of the T_g values, this is difficult to confirm. A 50/50 blend was annealed first at 195 °C, to erase previous thermal history, then quenched to 60 °C, i.e., ($T_g - T_a$) ~20 °C, and aged for various times t_a (Bosma et al. 1988).

Table 13.1 Physical aging in polymer–polymer blends: qualitative treatment

Polymer	Technique	References
ABS/BPAPC	Mech	Maurer et al. 1985
ABS/BPAPC	DSC, FTIR	Tang and Lee-Sullivan 2008
Aromatic polyamides	DSC	Ellis 1990
BPAPC/SAN	DSC	Belloch et al. 1999
Nylon 6,6/PPE	Mech	Laverty 1988
PB/SBR	DSC	Shi et al. 2013
PEMA/Nylon 6	DSC	Estelles et al. 1993
PMMA/SAN	DSC	Naito et al. 1978
PMMA/SAN	DSC	Mijovic et al. 1989
PMMA/SAN	Dil, DSC, Mech	Robertson and Wilkes 2001
PMMA/SAN	DSC	Cowie and Ferguson 1991
PMMA/SAN	Mech	Cowie et al. 1998
PMMA/PEG	PALS, Mech	Robertson and Wilkes 2000
IPN (PMMA/PU)	DSC	Sartor et al. 1994
IPN (PMMA/PMA)	DSC	Ribelles et al. 2003
PLA/Starch	DSC, Mech	Acioli-Moura and Sun 2008
Poly(lactide) blends	DSC	Jorda and Wilkes 1988
PS/P(2-VP)	DSC	ten Brinke and Grooten 1989
PSF/CPSF	DSC	Lau et al. 1993
PVC/PiPMA	DSC	ten Brinke and Grooten 1989; Bosma et al. 1988
PVC/PMMA	DSC	Bosma et al. 1988
PPE/PVME	PALS, Mech	Chang et al. 1997
PS/PPO	Dil, DSC, Mech	Chang et al. 1997
PEEK/PPS	Mech	Guo and Bradshaw 2007
PVP/PVAc	PALS	Cowie et al. 2001
PVP/P(VAc-co-VA)	PALS	Cowie et al. 2001
iPMMA/PEO	Dil, ESR	Shimada and Isogai 1996
PMMA/PEO	Dil, DSC, Mech	Vernel et al. 1999
PMMA/PEO	PALS	Wästlund 1997
PMMA/PEO	Dil	Slobodian et al. 2004
PMMA/PEO	Dil, DSC	Slobodian et al. 2006a
PMMA/PEO	Dil, DSC	Slobodian et al. 2006b
PMMA/CCS-PS	DSC, Termomech	Spoljaric et al. 2011
PS/NR	Mech	Asaletha et al. 2008
PS/PU	Mech	Babkina et al. 2012
PEO/PPO	DSC	Morales and Acosta 1995
Polymide blends	DSC	Goodwin 1999
Polyimide/PEI	DSC	Campbell et al. 1997
PC/AIM[a]	Mech	Tan et al. 2005

[a]AIM: acrylic impact modifier

Table 13.2 Physical aging in blends: quantitative treatment

Blend system	Technique	Model	References
BPAPC/ABS	Mech	KWW	Haghighi-Yazdi and Lee-Sullivan 2013
BPAPC/PMMA	DSC	TNM	Penco et al. 2007
PEEK/PEI	DSC	KWW	Hay 1992
PES/Epoxy	DSC	C-F	Breach et al. 1992
PES/Epoxy	DSC	C-F	Hay 1992
PMMA/PVDF	E(t)	KWW	Mijovic et al. 1991
PMMA/SAN	DSC	Hodge	Mijovic et al. 1990
PMMA/SAN	DSC	Hodge	Mijovic and Ho 1993
PMMA/SAN	Mech	KWW	Mijovic et al. 1991
PS/PVME	DSC	C-F	Cowie and Ferguson 1989
PS/PPO	DSC	TNM	Oudhuis and ten Brinke 1992
PS/PPO	DSC	G-M	Cowie et al. 1999
PS/PPO	Mech	KWW	Mijovic et al. 1991
PHS/PVME	DSC, PALS	C-F	Arrighi et al. 2006
PHS/PMMA	DSC	C-F	Cowie et al. 2005
PMMA/SMA	DSC	C-F	Cameron et al. 2001
PMMA/SAN	DSC	G-M	Cameron et al. 2002
PMMA/PEO	Dil, DSC, Mech	TNM	Vernel et al. 1999
PEO/PPO	DSC	C-F	Morales and Acosta 1995
Epoxy/PES	DSC	C-F	Jong and Yu 1997
sPS/aPS	DSC	C-F	Hong et al. 1998

CCS-PS core cross-linked star PS

The thermograms shown in Fig. 13.4a demonstrate clearly the development of two distinct enthalpy recovery peaks that increase with increasing aging time t_a. Good separation of the peak maxima is obtained as T_{max} tends to increase with aging time for both components but at different rates. This indicates that phase separation has occurred and the enthalpy recovery peaks are characteristic of each distinct phase in the mixture. A miscible blend of PVC and atactic PMMA was also treated in a similar fashion, but only one enthalpy recovery peak could be detected (Fig. 13.4b) indicating a single-phase system.

This work was extended by Grooten and ten Brinke (1989) to include the immiscible blend of polystyrene, PS, with poly(2-vinyl pyridine), P2VP. The authors concluded that the most appropriate range of aging temperature for this type of experiment was T_g to $\sim (T_g - 20\ °C)$. The same method was applied to distinguish the two-phase nature of PS-P2VP diblock copolymers (ten Brinke and Grooten 1989).

The sensitivity of this method was demonstrated by Jorda and Wilkes (1988) who showed, after aging, that blends of racemic polylactide and its optically active L-form were two phase, a convincing demonstration that two stereo-regular forms of a polymer may be immiscible.
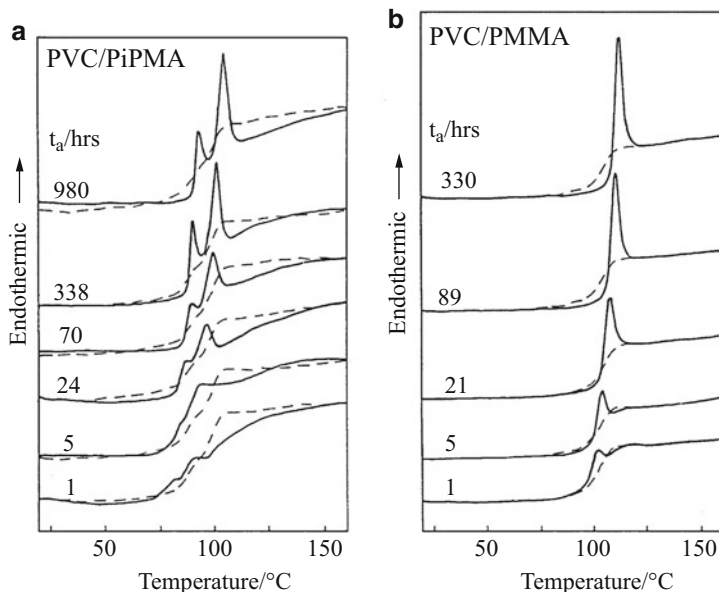
Fig. 13.4 (**a**) DSC thermograms for aged polymer blends (**a**) poly(vinyl chloride)//poly(isopropyl methacrylate), immiscible blend, aged at a temperature of 60 °C, and (**b**) poly(vinyl chloride)//poly(methyl methacrylate), miscible blend, aged at 80 °C. Time of aging, t_a in hours, is shown alongside each curve. Broken lines represent the unaged samples for comparison (Adapted from Bosma et al. (1988))

It was noted that it is the difference in the enthalpy relaxation of the single components that is crucial when investigating polymer–polymer miscibility. As pointed out by ten Brinke et al. (1994), the ability to distinguish between one- and two-phase systems as the T_g values approach one another depends on the effective aging times, t_{eff}:

$$t_{eff} = \frac{t_a}{\tau} \tag{13.13}$$

Since the relaxation time τ is related to x, $\Delta E,^*$ and τ_o (Eq. 13.6), even if the two blend components have a similar T_g, when these kinetic parameters differ so will the enthalpy relaxation at T_a.

Analysis of the kinetics of the recovery process in terms of T_{max}, T_{on} (see Fig. 13.2) provides a further means to quantitatively assess phase behavior (Ellis 1990; Hong et al. 1998). The structural dependence of these parameters has made it possible to investigate the phase behavior of blends containing aromatic polyamides (Ellis 1990). Despite the similarity in structure of the blend components and therefore the close proximity of the glass transition temperatures, Ellis was able to confirm the immiscibility behavior predicted using the mean field binary interaction model (ten Brinke et al. 1983; Paul and Barlow 1984).

Fig. 13.5 Curves of calorimetric overshoots at various T_a for a PB/SBR blend (at 0.5 volume fraction). Inset: amplitudes of peaks as a function of aging temperature (Reproduced with permission from Shi et al. 2013)
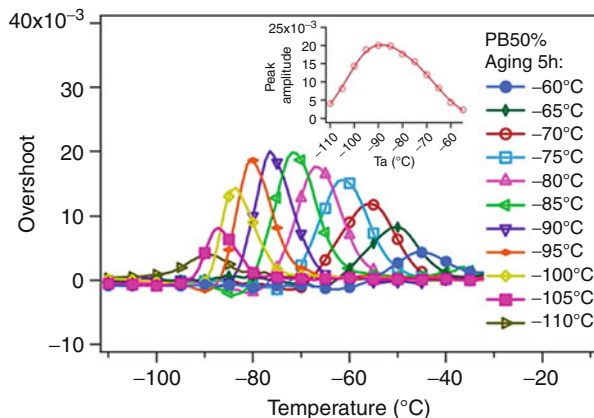
The effect of annealing temperature on aging has been well demonstrated by Shi et al. (2013) who investigated blends of polybutadiene (PB) and styrene butadiene rubber (SBR). Starting from the idea that a blend can be viewed as an ensemble of different domains each exhibiting its own glass transition, these authors carried out a range of annealing experiments and showed that annealing affects only a region of the relaxation spectrum, specifically the one that has a relaxation time close to the annealing time at T_a. This is shown in Fig. 13.5 where a 50/50 PB/SBR blend's response to annealing is plotted. The assumption that annealing at a given T_a is selective toward the blend's response was confirmed by consecutively annealing samples at very different temperatures and observing that this results in two distinct annealing peaks. Interestingly, the envelope of all contributions determined by the aging experiments was exploited to predict quantitatively the viscoelastic spectrum of the PB/SBR blends.

Similar effects have been observed in interpenetrating networks (IPN) characterized by an exceptionally wide distribution of relaxation times, with $\beta \rightarrow 0$. For example, the DSC traces of an IPN consisting of 25 % polyurethane and 75 % PMMA measured by Sartor et al. (1994) did not provide evidence of a step-like change that could be attributed to the T_g. However, aging experiments revealed aging peaks with onset close to the aging temperature, an effect that was attributed to the existence of a very broad distribution of relaxation times.

13.4.6 Enthalpy Relaxation: Quantitative Treatment

The first comprehensive study of physical aging in a miscible blend system using enthalpy relaxation was reported by Cowie and Ferguson (1989) who followed the enthalpic relaxation in a series of blends of PS and poly(vinyl methyl ether), PVME. Comparison of the blend behavior with that of the two components by analyzing the data on the basis of both the P-M and C-F models led to the conclusions that the blends aged more slowly than PVME when aging was carried

Table 13.3 Physical aging parameters derived from Petrie model for PS/PVME blends (Cowie and Ferguson 1989)

wt% PVME	ln (A/min^{-1})	E$_H$/kJ mol^{-1}	C/g J^{-1}
0	366.6	1,192	2.92
50	388.2	929	4.08
100	192.3	407	1.14

Table 13.4 Physical aging parameters derived from C-F model for PS/PVME blends (Cowie and Ferguson 1989)

System	T_a/K	$T_g - T_a$/K	ΔH_∞ (T_a)/J g^{-1}	$\log_{10}(t_c$/min)	β	$\log_{10}(t_e$/min)
PVME	250.0	5.6	1.08	1.23	0.91	2.15
	247.5	8.1	2.43	1.77	0.51	3.41
	245.0	10.6	2.83	1.82	0.66	3.09
	240.0	15.6	3.24	2.44	0.50	4.12
	235.0	20.6	3.77	2.84	0.62	4.20
PS/PVME[a]	270.0	11.8	1.08	2.15	0.449	3.83
	265.0	16.8	1.39	2.46	0.316	5.12
	260.0	21.8	1.65	2.47	0.373	4.72
	255.0	26.8	1.88	2.74	0.412	4.77
	250.0	31.8	2.09	3.25	0.364	5.56
PS	367.0	10.1	1.97	1.90	0.39	79.2
	363.5	13.6	2.14	2.12	0.41	80.3
	360.0	17.1	2.71	2.85	0.30	82.9

[a]50 wt% PVME

out at a comparable temperature below T_g; hence the component with the lower T_g, i.e., the more mobile component in the blend, PVME, was responsible for most of the aging effects seen in this blend (see Tables 13.3 and 13.4). The PS component did not appear to contribute significantly to the total aging because the relaxation processes were much slower than PVME at the aging temperature. This suggests that even though the blend can be regarded as a miscible, one-phase system, the components can largely relax independently although the relative rates of each will be influenced by the second component. In the PS/PVME blends, the T_gs of the two components are quite different and the blends can be regarded as comprising a flexible polymer (PVME) mixed with a relatively stiff polymer (PS), a situation which is not favored thermodynamically. It is interesting to note that if an even more rigid analogue poly(α-methyl styrene) replaces PS in the blend, a two-phase system is obtained.

The PS/PVME blend is unlikely to be representative of a typical miscible system; its glass transition region is quite broad, spanning up to 23 K. Thus, aging close to the enthalpic T_g might impinge on the onset region of the glass transition process, and this may result in accelerated aging of the more flexible component. As shown in Fig. 13.6, these conclusions are supported by a comparison of the C-F parameters of a 50/50 wt% blend and those of the pure polymers. In the case of
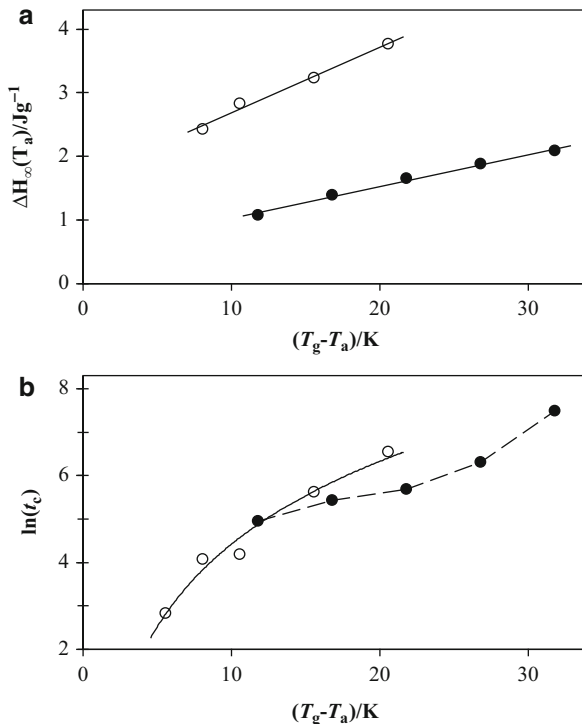
random mixing, one may expect ΔH_∞ for a blend to have intermediate values
between those of the two pure components. This is not the case for this system and
in fact ΔH_∞ for the blend lies below the PVME values (Fig. 13.6).

However, an alternative explanation may be found in the "Sequential Aging
Theory" proposed by Chai and McCrum (1980). The authors postulated that at
a given T_a and t_a, the viscoelastic elements with relaxation times equivalent to t_a
will be aging, but that elements with $\tau < t_a$ will already have reached equilibrium
and those with $\tau > t_a$ will not yet have begun to move toward equilibrium. Thus, in
the PVME/PS case, the more flexible PVME, which at T_a will also be closer to its
own T_g, will possess more elements with shorter relaxation times than the
PS. Consequently the PVME relaxation spectrum will tend to move more rapidly
toward equilibrium than the PS and so would age more rapidly. In fact this blend is
known to be dynamically heterogeneous in the molten state (Zhang et al. 2004) with
the PVME relaxing much faster (by ca. three decades) than the PS segments at
temperature close to the blend T_g.

Values of the β parameter (Table 13.4) are relatively large for PVME com-
pared to those measured for the blend and PS. This suggests that, while aging is
dominated by the faster PVME component, blending causes a broadening of the
distribution of relaxation times. The dielectric studies of PS/PVME blends of
Roland and Ngai (1992) indicate that the coupling parameter n defined by

Eq. 13.12 is 0.67 in a blend (60 % PVME content) substantially larger than $n = 0.56$ for PVME. Bearing in mind the relationship between coupling and β parameter, the aging behavior seems to follow the dynamic changes arising from the distribution of environments experienced by the relaxing units in a blend. As shown by data in Table 13.4, the degree of intermolecular coupling of the PVME segments substantially increased in the blend (average $n = 0.41$ for PVME vs. average $n = 0.60$ for the blend).

The work of Oudhuis and ten Brinke (1992) on the aging of blends of PS with poly(2,6-dimethyl-1,4-phenylene oxide), PPO, provides an interesting comparison with the PS/PVME system. In PS/PPO blends, both components are relatively rigid, although there is still about 100 °C difference between the T_g values. While the amount of enthalpy relaxation observed in these blends was lower than that for either component, there was no evidence for faster relaxation by the component with the lower T_g, viz., PS (Table 13.5). This observation has been confirmed by Cowie and Elliot (1990). Oudhuis and ten Brinke suggested that since the enthalpic definition of T_g was used as proposed by Cowie and Ferguson (1989) and the blend showed a broad glass transition region covering about 23 °C, the use of the onset T_g instead of the mid-range temperature might be a more accurate reference for selection of the aging temperatures. This would partially overcome some of the problems associated with accelerated aging studies where the precise location of T_g for a weakly miscible blend may be difficult to define.

Blends of PMMA and poly(styrene-*stat*-acrylonitrile), SAN, have been studied by several authors (Naito et al. 1978; Mijovic et al. 1989; Mijovic et al. 1990; Cowie et al. 1991; Cowie et al. 1998; Robertson and Wilkes 2001). Mijovic et al. have investigated blends of PMMA with a commercial SAN sample containing 25 wt% AN, using enthalpy (Mijovic et al. 1989) and stress-relaxation (Mijovic et al. 1990) measurements. Data are shown in Tables 13.5 and 13.6. The authors observed, in common with all other workers, that aging is faster at higher temperatures. No comparison was made with the component polymers, but it was observed that blends rich in SAN relaxed faster than PMMA- rich blends. The aging times used in that work were no more than 150 min.

A more comprehensive study of this system has been carried out by Cowie and Ferguson (1991) who studied a series of blends with SAN compositions spanning the miscibility window, i.e., from 13.3 to 30 wt% AN, using enthalpy and stress relaxation. In agreement with findings of Mijovic et al. (1989), temperature was reported to affect the enthalpic relaxation behavior: at $(T_g - T_a) = 10$ °C blends were found to relax faster than either of the components, but aging was intermediate to both components at $(T_g - T_a) = 20$ °C. Examples of $\Delta H(t_a, T_a)$ versus log t_a plots are shown in Fig. 13.7 together with fits obtained using the P-M and C-F models. It is evident that the C-F model provides a better estimate of the long-term aging effects, whereas overestimates of the time taken to reach equilibrium are made when using the P-M model. The parameters derived from each analysis are shown in Table 13.6 for PMMA/SAN (26.6 wt% AN) at $T_a = (T_g - 10\ °C)$.

Several models are available to quantitatively describe the aging process and practically all of these have been applied to blends as indicated in Table 13.2.

Table 13.5 Enthalpy relaxation in blends of PS/PPO and SAN/PMMA analyzed using the Hodge model (N-parameters)

Blend	w_2	ln (A/s)	$\Delta h^*/R$, kK	x	β	T_r/K	References
SAN/PMMA[a]	100	−328.9	125.0	0.221	0.48	380.05	Mijovic et al. 1989
	80	−358.5	134.7	0.137	0.46	375.73	Mijovic et al. 1989
	60	−370.8	138.6	0.147	0.42	373.79	Mijovic et al. 1989
	40	−392.6	146.2	0.253	0.35	372.39	Mijovic et al. 1989
	20	−377.6	140.3	0.227	0.35	371.56	Mijovic et al. 1989
	0	−359.8	132.2	0.338	0.26	367.43	Mijovic et al. 1989
PS/PPO[b]	0	−288.1	140	0.37	0.58	485.94	Oudhuis and ten Brinke 1992
	50	−316.6	135	0.33	0.56	426.41	Oudhuis and ten Brinke 1992
	100	−328.8	126	0.28	0.57	383.21	Oudhuis and ten Brinke 1992

w_2 = weight % first homopolymer component in blend
[a]Values for unaged
[b]Values for $t_a = 120$ min

Table 13.6 Aging parameters calculated from the C-F and P-M analysis of data obtained from PMMA, SAN (26.6 wt% AN), and their (50/50) blend PMMA/SAN at $T_a = (T_g - 10$ K)

Polymer	C-F model				P-M model	
	$\Delta H(\infty)$	$\log t_c$	β	$\log t_e$	$\Delta H(\infty)$	$\log t_e$
PMMA	0.820	1.780	0.290	4.678	2.381	11.479
SAN (26.6 wt% AN)	2.365	1.864	0.422	3.853	3.386	4.697
PMMA/SAN (50/50)	1.766	1.678	0.498	3.362	4.142	6.008

For example, Cameron et al. (2002) have employed the G-M model (Gomez-Ribelles and Monleon-Padras 1995) to describe the aging in blends of PMMA and SAN copolymers. The temperature dependence of the equilibrium relaxation time, τ^{eq}, that can be extracted from the enthalpic data is particularly informative. As shown in Fig. 13.8, log τ^{eq} versus $T_{g,100}/T$ (where $T_{g,100}$ is the temperature at which the relaxation time in equilibrium is 100 s) blends that are far from the upper limit of miscibility (i.e., containing SAN13 and SAN17) have nearly identical behavior, whereas PMMA/SAN26 has a significantly lower slope. This has been attributed to microheterogeneity and the blend being close to the miscibility limit. This is reflected in a distribution of glass transition temperatures, broader than in pure polymers. Such an effect which is evident in the enthalpy relaxation studies cannot be observed by conventional DSC measurements, nor does it manifest itself in the enthalpic aging data which display a single aging peak (Fig. 13.8).

The G-M theoretical approach has also been used to reproduce the enthalpic relaxation of PS/PPO blends, and in agreement with other studies, the results show that the distribution of relaxation times is broader in the blends than in the individual components (Brunacci et al. 1997a, b). Considering the Angell (1991) concept of "fragile-strong" classification of materials, this suggests that blends are "stronger" than the individual components.

a $\Delta H\,(t_a, T_a)\,/\,\mathrm{Jg}^{-1}$

b $\Delta H\,(t_a, T_a)\,/\,\mathrm{Jg}^{-1}$

c $\Delta H\,(t_a, T_a)\,/\,\mathrm{Jg}^{-1}$
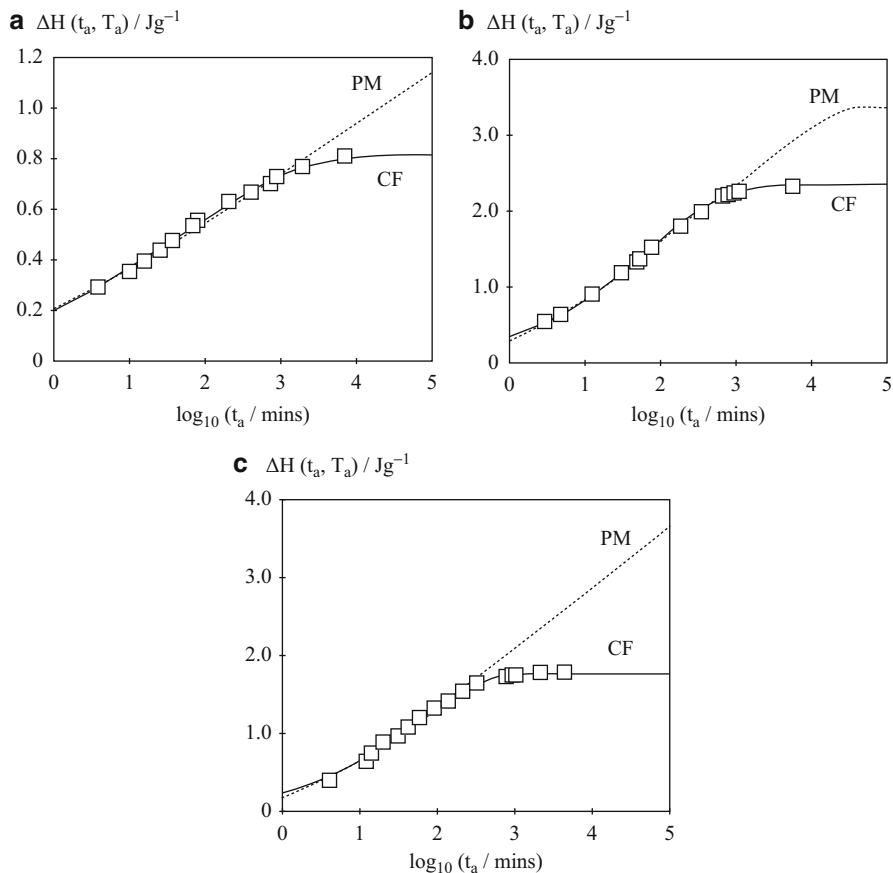
Fig. 13.7 Comparison of the experimental enthalpy change on aging for t_a minutes for (**a**) PMMA, (**b**) SAN containing 26.6 wt% AN, and (**c**) a 50/50 blend of these two polymers, with the theoretical curves derived from the Petrie–Marshall (P-M) and Cowie–Ferguson (C-F) models (Adapted from Cowie et al. (1991))

Enthalpy relaxation studies have also been used to assess the aging of polyether ether ketone blends with polyetherimide, PEEK/PEI = 50/50 (Hay 1992). The preparation of the blend produced an amorphous system with T_g ~215 °C, but crystallization of the PEEK occurred after raising the temperature above T_g. Data could only be collected in the temperature range T_g to ($T_g - 50$) and no aging could be detected at temperatures below 150 °C (Table 13.7). The enthalpic relaxation data were analyzed using the C-F model and fits yielded values of β = 0.4, intermediate between those of the pure polymers. It was noted that values of β were higher than those obtained from dielectric relaxation measurements (0.1–0.22). This technique probes the dipole relaxation spectrum, and the lower

Fig. 13.8 Temperature dependence of the equilibrium relaxation times, τ^{eq} from the G-M model, calculated for PMMA (•), SAN13 (▲), SAN17 (X), SAN26 (■), and SAN30 (▼) (Reproduced with permission from Cameron et al. (2002))
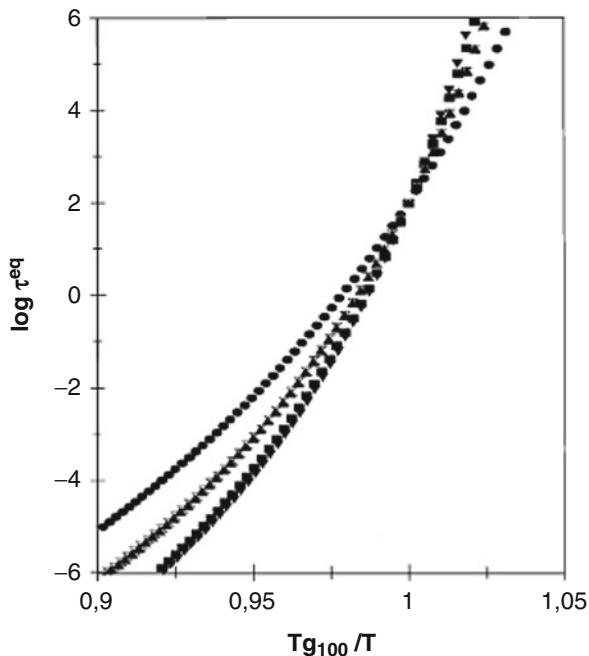
Table 13.7 C-F parameters extracted from enthalpy relaxation data of PEEK/PEI blends (Hay 1992)

wt% PEEK	T_a/K	$\Delta H\infty(T_a)$/J g^{-1}	$\log_{10}(t_c$/min)	β
0	457–482	Not given	Not given	0.35
50	429–445	Not given	Not given	0.40
100	389–410	Not given	Not given	0.55–0.60

values of the shape parameter could be a result of heterogeneity at the molecular level caused by the crystallization of the PEEK component.

Polyethersulfone, PES, can be blended with epoxy resins in certain combinations that do not lead to phase-separated systems, and Breach et al. (1992) have investigated the aging characteristics of Epikote 828 (Shell) and Victrex 5003P. Comparison of aged and unaged samples allowed the enthalpy relaxation to be calculated from the peak areas. Data in Table 13.8 show once that the blends age at a faster rate than the components and that this increases with increasing PES content. In this case, β also increases and these effects can be explained by considering that the incorporation of PES loosen the epoxy resin network thereby increasing the free volume. As this would change the size distribution of the free volume "holes," the presence of larger holes would accelerate the relaxation process and narrow the relaxation time distribution.

Table 13.8 C-F parameters extracted from enthalpy relaxation data of epoxy resin blends with polyethersulfone (Breach et al. 1992)

Blend	T_a/K	$T_g - T_a$/K	$\Delta H\infty(T_a)$/J g^{-1}	$\log_{10}(t_c$/min)	β	$\log_{10}(t_e$/min)
E828DDS/PES[a] 0	453.2	…	3.35	3.672	0.26	6.900
E828DDS/PES 20	453.2	…	3.13	3.515	0.36	5.846
E828DDS/PES 30	453.2	…	2.52	2.881	0.52	4.495

[a]Epikote 828 resin (Shell) cured with 4,4′-diaminodiphenylsulphone (DDS) and blended with polyethersulphone (Victrex 5003P)

It follows from the discussion so far that the kinetics of the structural relaxation in miscible polymer blends can show significant differences with respect to the pure components. Aging experiments on well-investigated blend systems, such as PS/PVME and PS/PPO, suggest that blending causes a reduction of the enthalpic changes compared to the pure components, at similar undercoolings. However, blending may affect the rate of aging in different ways, depending on the specific system under study, even for systems having equally large differences between the T_gs of the components (as is the case for PS/PVME and PS/PPO). One possible reason for this is that blends may display different levels of microheterogeneity and therefore unequal distribution of relaxation times. In some cases, the presence of secondary relaxations (e.g., β process) may need to be considered as it will be discussed later, PMMA/SAN blends (Robertson and Wilkes 2001).

One would also expect polymer–polymer interactions to play a major role in the physical aging process, particularly when the blend components can interact strongly, e.g., via hydrogen bonding. To date, very few studies have considered the effect of hydrogen bonding and other secondary interactions on the physical aging of polymer blends. The most investigated systems are blends of poly (4-hydroxystyrene) (PHS) with PVME (Arrighi et al. 2006) and PMMA (Cowie et al. 2005). The hydroxyl group in PHS can act as a proton donor and acceptor, forming self-associated hydrogen bonds between either two PHS repeat units of the same chain (intra-chains) or two adjacent ones (interchain). When blended with a proton acceptor such as PVME or PMMA, intermolecular hydrogen bonds are formed with PHS through the ether or carbonyl linkages of PVME and PMMA, respectively. The presence of strong interactions leads to a considerable increase in glass transition temperature of the PS/PVME blends compared to that of pure PVME. The presence of intermolecular hydrogen bonds retards the aging process as shown in Fig. 13.9 where the average relaxation time, $\langle t_c \rangle$ for the KWW distribution:

$$\langle t_c \rangle = t_c \ \Gamma(1 + 1/\beta) \tag{13.14}$$

of blends and pure polymers are compared.

The rate of aging of PHS is comparable to that of PVME and PS/PVME, thus indicating that, at similar undercoolings, the presence of inter- and intra-H-bonding has little effect on the aging rate of the pure polymer.

Fig. 13.9 Average
relaxation times as a function
of $(T_g - T_a)$ for the
PHS/PVME blends: (△)
(81/19); (×) (33/67); (◇)
(59/41); and for (□) PVME;
(+) PHS and (•) PS/PVME
(Replotted from data reported
by Arrighi et al. (2006))
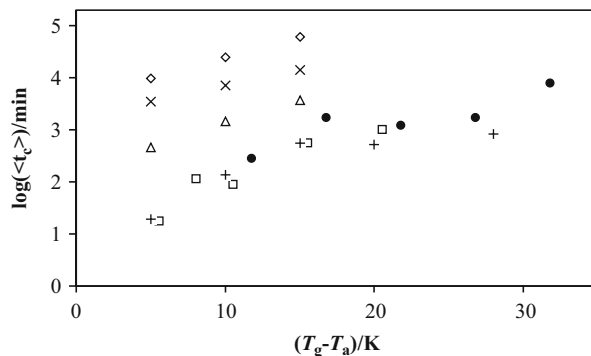
However, intermolecular hydrogen bonding between PHS and PVME strongly affects the enthalpic relaxation (Fig. 13.9). PALS measurements have indicated that at an optimum 59:41 mol% PHS/PVME composition, the free volume is at a minimum compared to the pure components. As illustrated in Fig. 13.9, this blend aged more slowly than any of the other systems investigated, suggesting that an optimum strength of the interaction is realized at approximately equimolar composition. At compositions where intermolecular hydroxyl–ether interactions are greatest, the C-F enthalpy parameters for PHS/PVME blends were found to be higher than those of the PHS/PMMA blends, reflecting the higher strength of the former interactions compared to the hydroxyl–carbonyl interactions.

The effect of hydrogen bond strength on physical aging has also been examined, but it was noted that differences in aging behavior could not simply be accounted for by the strength of the hydrogen bonding (Cowie et al. 2005). Other factors such as structural differences between the polymeric components are likely to affect the aging properties, and this makes it difficult to establish a simple structure–property relationship in hydrogen-bonded blends.

13.5   Volume Relaxation

During physical aging, short-chain segments relax into the free volume available, and this causes reduction in the total volume upon aging results of the relaxation of short chain, a process that leads to improved chain packing and a denser material. Dilatometry can be used to monitor the time dependence of the volume change on aging. The material is either cooled from an equilibrium state above (T_g) to the aging temperature T_a (down-jump) and the isothermal volume contraction (*volume relaxation*) is measured (Greiner and Schwarzl 1984) or the sample is heated in the glassy state (up-jump) in which case an expansion follows (Adachi and Kotaka 1982).

The simplest volume recovery experiment is the down-jump. Volumetric data collected at a series of aging temperatures are normalized in order to examine the relative departure from equilibrium δ which is defined as

$$\delta = \frac{V - V_\infty}{V_\infty} \qquad (13.15)$$

where V represents the volume at a specific aging time and V_∞ is the equilibrium volume. Volume relaxation can be quantitatively described in terms of the volume relaxation rate, b_V (Struik 1978):

$$b_V = -\frac{1}{V} \frac{dV}{d\log t_a} \qquad (13.16)$$

which is valid for isothermal volume relaxation following a fast quench (or down-jump) into the glassy state from the equilibrium liquid state. This parameter can be used to follow changes with blend composition and aging temperature (Robertson and Wilkes 2000, 2001). One should note that the volume changes during isothermal volume recovery are small, typically of the order of 1 % or less, and require high precision measurements.

Compared to aging studies using enthalpy relaxation, very few reports have appeared in the literature where volume changes have been exploited to monitor aging in polymer–polymer mixtures. For PS/PPO blends, negative deviations from simple additivity have been observed, for small undercoolings which seem to disappear upon aging at temperatures deep in the glassy state (Robertson and Wilkes 2000). To verify whether this behavior was to be attributed to concentration fluctuations and the breadth of the glass transition as suggested by Oudhuis and ten Brinke (1992), Robertson and Wilkes (2000) scaled the volume relaxation rates by the onset temperature, T_{onset} and T_g, and found similar trends. Therefore, the authors concluded that the volume data provided no evidence of concentration fluctuations being responsible for the trends in volume relaxation rate. Measurements of specific volume suggested that the blends have better packing in the glassy state compared to expected values based on the densities of the pure polymers. The existence of interactions between the PS and PPO components was considered to be the more likely cause of the observed slower aging of the blends.

To assess how the presence of specific interactions affects the physical aging behavior, Robertson and Wilkes carried out volume relaxation measurements on PMMA/SAN blends as a function of blend composition (Robertson and Wilkes 2001). In this system, there are no attractive interactions between the components, and miscibility is a result of the so-called copolymer repulsion effect. The dependence of the volume relaxation rate on blend composition was found to be consistent with the enthalpic measurements of Mijovic et al. (1989) on the same system: both values of volume and enthalpy relaxation rates were intermediate for the blends compared to the pure components and composition dependent except for $T_g - 45\,^\circ\text{C}$. In contrast to the PS/PPO system that displayed deviations from simple additivity, PMMA/SAN showed a linear dependence of b_V upon blend composition. As discussed by Robertson and Wilkes (2000, 2001), the volume relaxation properties of these blend systems are related to the different density, secondary relaxation, and fragility characteristics of PMMA/SAN and PS/PPO.

Fig. 13.10 Relaxed enthalpy versus relaxed volume for blends PMMA (○) and PMMA/PEO blends with (△) 3 vol%, (□)6 vol%, (◇)10 vol%, and (▽)14 vol% of PEO (Reproduced with permission from (Slobodian et al. 2006)
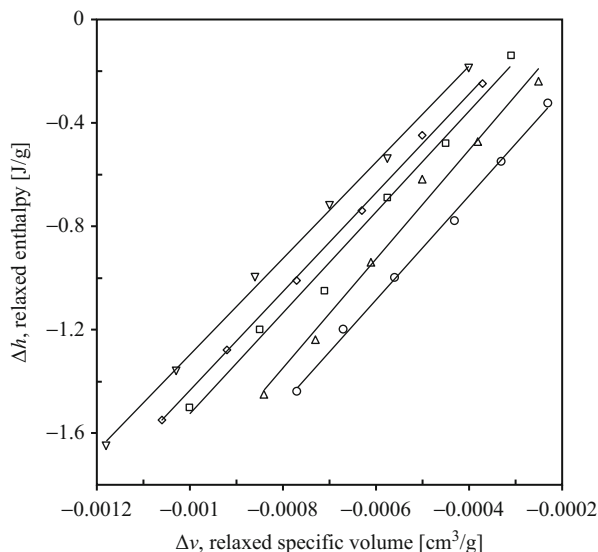
One of the blends whose aging properties have been extensively studied is PMMA/PEO (Shimada and Isogai 1996; Vernel et al. 1999; Slobodian et al. 2006a, b; Riha et al. 2007). The blend consists of a fully amorphous polymer (PMMA) and a crystallizable component (PEO). Miscibility in the melt state occurs when the PMMA content is above 70–80 %, but phase separation in the glassy state has been reported as indicated by the appearance of heterogeneous structures with domain sizes of 20–70 nm.

Slobodian et al. (2004) have shown that addition of PEO to atactic PMMA causes a significant increase in volume relaxation rate. For example, annealing at about 28 degrees below T_g causes β_V to increase by approximately 37 % when the blend contains 14 vol% PEO, compared to pure PMMA. Further studies by Slobodian et al. have provided insight into the relationship between enthalpy and volume relaxation in PMMA/PEO (Slobodian et al. 2004, 2006). These authors found that both volume and enthalpy changes, following a temperature down-jump of 15 degrees, varied linearly with the logarithm of annealing time for all miscible PMMA/PEO blends containing up to 14 vol% PEO. As shown in Fig. 13.10, the measured volume and enthalpy changes are linearly related to each other. These graphs were used to calculate an aging bulk modulus K_a defined as the slope of the relaxed enthalpy versus volume curves, i.e., $(dh/dv)_T$, whose dimensions equal those of a modulus. Values of K_a (2 GPa) are similar in magnitude to the bulk modulus and therefore consistent with the inverse of the isothermal compressibility.

13.6   Mechanical Relaxation

The effect of thermal and chemical aging on the mechanical properties of polymers including blends is of primary concern to assess the service lifetime and long-term

Fig. 13.11 Schematic representation of temperature, strain, and stress program for a single aging time test (Reproduced with permission from reference (Bernatz et al. 1999)
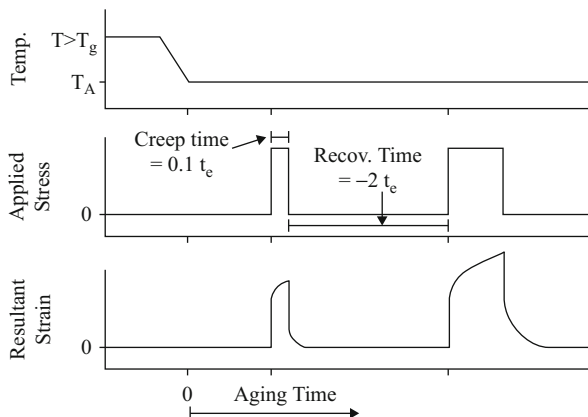
performance of these materials (Sanchez 2007; McKenna 2012). Since the visco-elastic relaxation spectrum shifts to longer times as aging progresses, aging can be followed using stress-relaxation, creep, or volume relaxation measurements. It has been shown that momentary creep curves have a universal shape and a master curve can be constructed using either time–aging time (t–t_a) or time–temperature (t–T) superposition (Kovacs et al. 1979; Struik 1978).

A schematic representation of a creep experiment is given in Fig. 13.11. Similar to enthalpic relaxation measurements, in a creep test the sample is quenched from above T_g to the annealing temperature T_a. A series of short (typically less than 10 % of the aging time t_a) load–unload tests are performed. As shown in Fig. 13.11, the applied stress, σ_o, is constant and the time-dependent response, the strain, is measured following both load and unload steps. Because times t_e during which creep response is measured are kept deliberately short, the creep response gives a "snapshot" of the viscoelastic properties of the material at a particular aging time.

The momentary creep compliance, $D(t)$, can be calculated:

$$D(t) = \frac{\varepsilon(t) - \varepsilon_{\text{unload}}(t)}{\sigma_o} \qquad (13.17)$$

where ε is the measured strain value and $\varepsilon_{\text{unload}}(t)$ is the extrapolated strain from the previous unload step. The momentary creep compliance curves can be described in terms of the KWW function using a relationship originally proposed by Struik (1978):

$$D(t) = D_o e^{(t/\tau)^{\beta}} \qquad (13.18)$$

where D_o is the compliance at zero time, τ is the relaxation time, and β is the usual shape parameter. Stress-relaxation measurements are carried out in a similar way,

but in this case small strains rather than small stresses are applied to the specimen. The stress-relaxation modulus can be expressed in a manner similar to Eq. 13.18:

$$G(t) = G_o \exp\left[-\left(\frac{t}{\tau}\right)^{\beta}\right] \tag{15.19}$$

where G_o and $G(t)$ are the stress-relaxation moduli at zero time and time t, respectively. Hence a relaxation function can be defined as $\phi(t) = G(t)/G_o$.

Momentary creep or stress-relaxation curves usually have a universal shape: a master curve can be constructed using either time–aging time $(t–t_a)$ or time–temperature $(t–T)$ superposition. A small vertical shift is sometime needed to overlap the data. Both time–temperature and time–aging time superposition are a feature of systems displaying structural–rheological simplicity; superposition rests on the idea of a constant distribution of relaxation times. Thus, provided that the measuring time is short compared to the relaxation or retardation times, the aging process can be studied effectively. For small values of an applied deformation, the shift factors needed to superimpose the isothermal data depend on aging time according to

$$\mu = \frac{d(\log \tau)}{d(\log t_a)} \tag{13.20}$$

where $\log \tau$ is the shift along the logarithmic relaxation time necessary to superimpose compliance or modulus data determined at increasing aging times, t_a. It follows that the shift factor μ can be viewed as a measure of the rate of aging and can be used to predict long-term behavior.

Mechanical relaxation techniques have been used to investigate aging in single component systems and blends. Measurements of the effect of aging on the viscoelastic properties of PMMA/SAN blends have been reported by different research groups. For example, Ho et al. (1991) have carried out short-term stress-relaxation tests on blends of PMMA/SAN and PS/PPO. By analyzing their data using the KWW equation, they were able to show that the stress-relaxation time, τ, depended on blend composition according to

$$\ln \tau = A + C_T \ln\left(T_g - T_a\right) + C_t \ln t_a \tag{13.21}$$

where A is a function of the weight fraction of one of the components in the blend, while C_T and C_t are adjustable temperature and time coefficients, respectively. Fitting parameters for PMMA/SAN and PS/PPO are reported in Table 13.9. Values of the shape parameter β were found to be centered within a narrow range around 0.41. While this, as well as many other reports, suggests β does not vary significantly during aging, there is not common agreement. In fact, by analogy to other relaxations, one might expect β to be an increasing function of $(T_g - T_a)$, reaching a plateau at temperatures well below the glass transition.

Table 13.9 Stress-relaxation parameters from Eq. 13.21 for PMMA/SAN and PMMA/SAN blends (Mijovic et al. 1990; Ho et al. 1991)

System	w_2[a]	C_w	C_T	C_t	References
PMMA/SAN	0	−6.68	3.325	1.013	Mijovic et al. 1990
	20	−7.02	3.325	1.013	Mijovic et al. 1990
	40	−7.25	3.325	1.013	Mijovic et al. 1990
	60	−7.49	3.325	1.013	Mijovic et al. 1990
	80	−7.65	3.325	1.013	Mijovic et al. 1990
	100	−7.72	3.325	1.013	Mijovic et al. 1990
PS/PPO	0	−8.08	3.61	0.357	Ho et al. 1991
	20	−10.34	4.24	0.683	Ho et al. 1991
	40	−14.55	5.15	0.885	Ho et al. 1991
	60	−14.35	5.15	0.936	Ho et al. 1991
	80	−10.42	4.31	0.838	Ho et al. 1991
	100	−8.07	3.68	0.849	Ho et al. 1991

Note: $C_t = \partial(\ln \tau)/\partial(\ln t_a) = \mu$
[a]w_2 = weight % first homopolymer component in blend

In some cases, when one blend component is in excess of the other, the aging of the blend appears to match that of the major component. Stress-relaxation measurements carried out by Cowie et al. (1998) have shown that the aging rate of a (50/50) PMMA/SAN blend was similar to that of PMMA rather than being intermediate between the two components. This was attributed to the PMMA component being more responsive to the mechanical stresses than SAN, a conclusion that is consistent with spectroscopic measurements of stressed blends indicating that PMMA is more oriented than the SAN component (Oultache et al. 1994).

Chang et al. have compared the stress-relaxation behavior of three miscible blend systems, PS/PPO, PS/PVME, and PMMA/PEO (Chang et al. 1997), for compositions in which one of the components was always in excess. For PS/PPO and PS/PVME, the stress-relaxation rates were found to be faster for the blends in comparison with PS alone, whereas the opposite was true for a PMMA/PEO blend when compared with pure PMMA. Two main effects were discussed: packing density and concentration fluctuations. It was noted that for PS/PPO and PS/PVME, addition of the second component leads to a decrease in the packing density of the blend but this is not the case for PMMA/PEO. Concentration fluctuations in the blend, detected via changes in width of the stress-relaxation time distribution, may also be responsible for differences in mechanical response, and their contribution appeared to be particularly significant in the PS/PVME system.

While the creep and stress-relaxation data of many pure polymers and blends have been reported to obey time–aging time superposition, failure to achieve this has been observed in some cases. For example, Robertson et al. have questioned the applicability of time–aging time superposition to the creep data of PMMA and PMMA/SAN blends (Robertson and Wilkes 2001). These authors argued that

apparent failure to produce a fully superimposed master curve by horizontal and vertical shifting of the creep data was due to overlapping, for the PMMA component, of primary and secondary mechanical relaxations. Thus, when two distinct relaxation processes overlap in the time and temperature regions of the mechanical measurements, the system is expected to display thermorheological complexity.

An attempt to correlate the results of enthalpic and viscoelastic measurements was made by Mijovic and Ho (1993) who reported comparable enthalpy and stress-relaxation times. This suggests that it should be possible to establish correlations between calorimetric and viscoelastic changes during aging, despite the fundamental difference between these two types of measurements. However, one should note that these are empirical correlations and should be tested for each system. Differences in response between enthalpic and mechanical tests have been often observed. For example, Brunacci et al. (1997a, b; 1998) noted that free volume arguments were not sufficient to explain discrepancies between enthalpic and mechanical data of polystyrene and substituted polystyrenes and suggested that dipole interactions while not affecting enthalpic aging could become active during mechanical relaxation.

Novel mechanical tests are being developed and shown to be useful tools to investigate thermal and structural relaxation. These include the modulated-temperature–thermomechanometry technique (mT-TM) which has been recently employed to investigate blends of core cross-linked (CCS) PS and PMMA (Spoljaric et al. 2011) and nanomechanical thermal analysis. By using silicon microcantilever deflection measurements, the latter technique can provide a measure of temperature-dependent thermal stresses and therefore investigate the influence of physical aging (Yun et al. 2011).

13.7   Positron Annihilation Lifetime Spectroscopy

The decrease in volume that accompanies the physical aging process can be related to a change of the distribution of free volume holes. Since the size and concentration of free volume holes in amorphous polymers is closely linked to the thermal expansion, direct measurements of the free volume can be used to monitor the aging processes.

Positron Annihilation Lifetime Spectroscopy (PALS) provides a measure of free volume "holes" or "voids," free volume, and free volume distribution, at an atomic scale. The technique exploits the fact that the positively charged positron (e^+), the antiparticle to the electron, preferentially samples regions of low positive charge density. When injected in a polymer matrix, thermalized positrons can combine with an electron to form a bound state, known as positronium (Ps). This species can only exist in a void and it rapidly annihilates on contact with the electron cloud of a molecule. For polymer studies using PALS, it is ortho-positronium (oPs, a triplet state) which is of interest. The oPs spin exchanges with electrons of opposite spin on the walls of the cavity and it is annihilated. Thus, the oPs lifetime, τ_3, gives a measure of the mean free volume cavity radius, whereas the relative intensity of

the oPs component, I_3, can be related to the number of cavities. A semiempirical equation has been derived that correlates τ_3 with the cavity radius, r (Eldrup et al. 1981):

$$\tau_3 = \frac{1}{2}\left[1 - \frac{r}{r + \Delta r} + \frac{1}{2\pi}\sin\left(\frac{2\pi r}{r + \Delta r}\right)\right]^{-1} \qquad (13.22)$$

which was obtained by using a spherical potential of radius r_o with an electron layer of thickness $(r - r_0) = 1.656$ Å.

As aging tends to be accompanied by changes in the packing density of the system, PALS can provide a qualitative estimate of the free volume in the system and its changes due to blending. For PS/PPO blends, PALS measurements were found to be in qualitative with stress-relaxation data. As discussed in the previous sections, Chang et al. (1997) found that PS/PPO and PS/PVME blends were less dense than PS, while PMMA/PEO was denser than PMMA, thereby making chain relaxation easier in the former and more difficult in the latter, a result that could explain the stress-relaxation behavior.

PALS has been used to examine the effect of intermolecular interactions on aging in copolymers and blends. The technique has proven to be particularly useful when attempting to correlate physical aging data of a series of hydrogen-bonded blends (Cowie et al. 2001; McGonigle et al. 2005). The PALS data of blends of poly (vinylacetate-*co*-vinylalcohol) (PVAc-*co*-VA) with poly(vinylpyrrolidone) (PVP) have revealed a particularly interesting behavior. As discussed by Cowie et al. (2001), for this system, low levels of hydrogen bonding give rise to open structures with increased free volume, but as the hydrogen bond concentration increases, a dramatic "collapse" in the free volume is observed (Fig. 13.12). This dramatic change which should greatly affect the physical aging properties has not been observed for similar blends with strong interactions between components.

13.8   Phase-Separated Blends

The behavior of the two-phase systems is complex and responses on aging can be affected by the thermal history and aging temperature. This is well illustrated by a series of investigations, the two-phase blend of acrylonitrile–butadiene–styrene copolymer (ABS, $T_g = 110$ °C) and polycarbonate of bisphenol-A (BPAPC, $T_g = 151$ °C). Due to the phase-separated structure of the blend, two enthalpy recovery peaks are detected by enthalpy relaxation and attributed to the two components (Tang and Lee-Sullivan 2008). However, aging appears to have little effect on the ABS component even at temperatures close to the ABS glass transition.

Using stress relaxation, Maurer et al. (1985) have observed four regimes of behavior for BPAPC/ABS blends. Below 70 °C both time–temperature and time–ta superpositions were possible, because the two components had similar aging
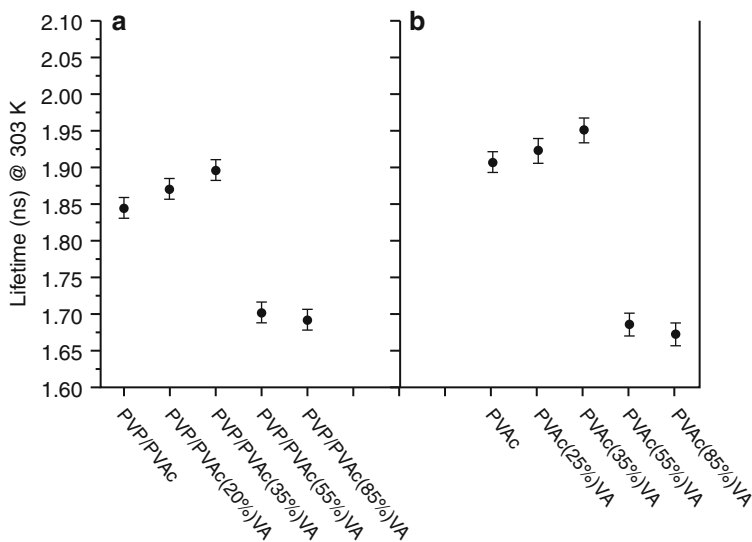
Fig. 13.12 Positron annihilation lifetimes at 303 K for poly(vinylacetate-*co*-vinylalcohol) (PVAc-*co*-VOH) copolymers (**b**) and blends of these copolymers with poly(vinylpyrrolidone) (PVP) (Reproduced with permission from Cowie et al. (2001))

rates, μ. Between 70 °C and 100 °C, only time–ta superposition was achieved. However, close to the T_g of the ABS component, and between the T_gs of both components, neither were valid. While Eq. 13.19 has been used by other workers, Booij and Palmen (1978) proposed a modified form:

$$G(t) = G_o \left(\frac{t}{\tau}\right)^\alpha \exp\left[-\left(\frac{t}{\tau}\right)^\beta\right] \qquad (13.23)$$

where β was kept constant to 0.4 (although this might be structure dependent) and α was normally a very small number. Equation 13.23 was used to analyze the ABS/PC blend data.

Aging may affect the mechanical performance of both miscible and phase-separated blends. For example, polycarbonate has been found to lose its toughness when aged at temperatures below T_g. This has been recently confirmed by Suzuki et al. (2012) who showed that the Izod impact strength decreased suddenly in the very early stage of physical aging and suggested that annealing may trigger a ductile-to-brittle transition in BPAPC.

Impact modifiers are often added to BPAPC to counteract this effect (Cheng et al. 1992; Tan et al. 2005) and a few studies have been conducted to investigate the effect of thermal annealing on the mechanical performance of BPAPC. For example, blends of BPAPC with several core–shell methacrylate–butadiene–styrene impact modifiers have been studied after aging at 125 °C, 130 °C, and 135 °C (Cheng et al. 1992).

Although changes in impact strength, tensile strength, dynamic mechanical response, and fracture morphology were complicated by the simultaneous chemical degradation of the samples when aged in air, it was reported that the modifiers did slow down the sample embrittlement caused by physical aging. More recent studies have shown that when blending BPAPC with a hydrogenated styrene–butadiene–styrene block copolymer (SEBS), aging of the polycarbonate component proceeded at the same rate as in the pure polymer, but the Izod impact strength did not decrease. This thermal aging resistance was attributed to the negative pressure effect of the SEBS particles leading to enhanced local segment dynamics of BPAPC (Suzuki et al. 2012).

As shown by the early work of Cheng et al. (1992), both chemical and physical effects may be responsible for changes in mechanical properties during aging. In this respect the work of Haghighi-Yazdi·and Lee-Sullivan (2013) has highlighted the competing effects of physical aging and moisture absorption on the stress-relaxation behavior of a BPAPC/ABS blends subjected to both thermal and hygrothermal aging. Short-term tests were carried out and master curves generated by applying time–t_a and time–moisture superposition. The relaxation times were found to increase in the order $\tau_{\text{thermally aged}} > \tau_{\text{hygrothermally aged}} > \tau_{\text{unaged}}$, for the same temperature levels. The authors concluded that relaxation was more affected by physical aging than absorbed moisture effects, meaning that the former provides the dominant mechanism affecting the relaxation behavior of this blend even in the presence of relatively high levels of absorbed moisture.

13.9   Summary and Conclusions

Physical aging is a universal phenomenon displayed by amorphous glasses, including blends and composites. As discussed in this chapter, aging over an extended time period results in changes in many physical properties and strongly affects the performance of polymeric materials. A great deal of effort has been expended by both theoreticians and experimentalists in attempting to understand the phenomenon and provide a sound theoretical description of the vitreous state and the aging process.

On a simplistic level, one might expect that the physical aging properties of blends could be predicted from those of the constituent polymers on an additive basis. This is clearly not the case and examination of the available data suggests that several other factors can influence the response of a blend to thermal annealing.

In weakly interacting systems, the differences in chain stiffness, reflected in the T_g values, can determine the aging characteristics of a blend. This can be quite variable, however, and, at our present level of knowledge, each blend needs to be viewed as a unique system with its own unique aging behavior. This is determined by a combination of the relative flexibility of the component polymers and the extent and strength of the intermolecular interactions between them.

Recent investigations show considerable changes in the rate of aging for blends where there is significant intermolecular H-bonding. For these systems, it may be

argued that molecular relaxation processes are either impeded or retarded due to formation of the reversible cross-links originating from the hydrogen-bonded network structure. Comparable results have been obtained in some heterogeneous nanocomposites, particularly in systems where the additive can interact with the polymer through secondary bonding. Generally, materials that are stabilized by effective intermolecular interactions appear to show reduced physical aging effects, and their properties are less likely to alter significantly over time.

13.10 Cross-References

▶ Applications of Polymer Blends
▶ Broadband Dielectric Spectroscopy on Polymer Blends
▶ Commercial Polymer Blends
▶ Degradation, Stabilization, and Flammability of Polymer Blends
▶ Mechanical Properties of Polymer Blends
▶ Miscible Polymer Blends

Abbreviations

General and Chemical

ABS Acrylonitrile–butadiene–styrene
AIM Acrylic Impact Modifier
AN Acrylonitrile
BPAPC Bisphenol-A polycarbonate
CCS-PS Core cross-linked star PS
CPSF Carboxylated polysulfone
C-F Cowie–Ferguson model
Dil Dilatometry
DSC Differential scanning calorimetry
FTIR Fourier-transform infrared spectroscopy
GD Gibbs and Di Marzio theory
G-M Gomez-Ribelles and Monleon-Padras model
HS 4-Hydroxystyrene
IPN Interpenetrating network
KWW Kohlrausch, Williams, and Watts function
Mech Mechanical
NR Natural rubber
PALS Positronium annihilation lifetime spectroscopy
PB Polybutadiene
PEEK Polyether ether ketone
PEG Polyethylene glycol
PEI Polyether imide

PEMA Poly(ethyl methacrylate)
PEO Polyethylene oxide
PES Poly(ether sulfone)
PHS Poly(hydroxy styrene)
PiPMA Poly(isopropyl methacrylate)
PLA Poly(lactic acid)
PMA Polymethacrylate
PMMA Poly(methyl methacrylate)
PPO Poly(*p*-phenylene oxide) or poly(2,6-dimethyl-1,4-phenylene ether) (PPE)
PPS Polyphenylene sulfide
PS Polystyrene (atactic)
PSF Polysulfone
P-M Petrie–Marshall model
PU Polyurethane
PVAc Polyvinyl acetate
PVC Polyvinyl chloride
PVDF Polyvinylidenefluoride
PVME Poly(vinyl methyl ether)
P2VP Poly(2-vinylpyridine)
PVP Poly(N-vinyl pyrrolidone)
SAN Poly(styrene-*stat*-acrylonitrile)
S Styrene
SBR Styrene butadiene rubber
SEBS Hydrogenated styrene–butadiene–styrene block copolymer
SMA Styrene-*co*-maleic anhydride
S-S Theory of Simha–Somcynsky
TNM Tool–Narayanaswamy–Moynihan model
VA Vinyl alcohol
VAc Vinyl acetate

Notations

Notation Roman Letters
A Fitting constant
b_V Volume relaxation rate
C_p Heat capacity
C_T Adjustable temperature coefficient
C_t Adjustable time coefficient
ΔC_p Heat capacity change
D_o Creep compliance at zero time
$D(t)$ Creep compliance at time t
E_o Modulus at zero time
$E(t)$ Modulus at time t

G_o Stress-relaxation moduli at zero time
$G(t)$ Stress-relaxation moduli at time t
H Enthalpy
$H(\infty)$ Equilibrium enthalpy value
ΔH Enthalpy change
Δh^* Effective activation energy
e^+ Positively charged positron
I_3 Relative intensity of the oPs component
oPs Ortho-positronium
Ps Positronium
q Cooling rate
r Cavity radius
R Gas constant
S_c Configurational entropy
t Time
T Temperature
t_a Annealing time
T_a Annealing temperature
t_c Characteristic time
T_f Fictive temperature
T_g Glass transition temperature
V Specific volume
V_∞ Specific volume at equilibrium, at temperature T
x Structural parameter

Notation Greek Letters

β Parameter of KWW function
β_T Isothermal compressibility
δ Departure from equilibrium
ε Strain
$\phi(t)$ Relaxation function
σ Stress
μ Shift factor
τ Relaxation time
τ_3 oPs lifetime
τ_o Equilibrium relaxation time
ω_c Critical frequency

References

R. Acioli-Moura, X.S. Sun, Polym. Eng. Sci. **48**, 829 (2008)
K. Adachi, T. Kotaka, Polym. J. **14**, 959 (1982)

G. Adam, J.H. Gibbs, J. Chem. Phys. **43**, 139 (1965)

C.A. Angell, J. Non Cryst. Solids **131**, 13 (1991)

V. Arrighi, J.M.G. Cowie, R. Ferguson, I.J. McEwen, E.-A. McGonigle, R.A. Pethrick, E. Princi, Polym. Int. **55**, 749 (2006)

R. Asaletha, P. Bindu, I. Aravind, A.P. Meera, S.V. Valsaraj, W.M. Yang, S.J. Thomas, Appl. Polym. Sci. **108**, 904 (2008)

N.V. Babkina, L.F. Kosyanchuk, T.T. Todosiichuk, N.V. Kozak, G.Y. Menzheres, G.M. Nesterenko, Polym. Sci. A **54**, 125 (2012)

G.P. Belloch, M. S. Sanchez, J. L. G. Ribelles, M. M. Pradas, J. M. M. Duenas, P. Pissis, Polym Eng Sci **39**, 688 (1999)

K.M. Bernatz, L. Giri, S.L. Simon, D.J. Plazek, J. Chem. Phys. **111**, 2235 (1999)

H.C. Booij, J.H.M. Palmen, Polym. Eng. Sci. **18**, 78 (1978)

M. Bosma, G. ten Brinke, T.S. Ellis, Macromolecules **21**, 1464 (1988)

C.D. Breach, M.J. Folkes, J.M. Barton, Polymer **33**, 3080 (1992)

A. Brunacci, J.M.G. Cowie, R. Ferguson, I.J. McEwen, Polymer **38**, 865 (1997a)

A. Brunacci, J.M.G. Cowie, R. Ferguson, I.J. McEwen, Polymer **35**, 3263 (1997b)

A. Brunacci, J.M.G. Cowie, I.J. McEwen, J. Chem. Soc. Faraday Trans. **94**, 1105 (1998)

N.R. Cameron, J.M.G. Cowie, R. Ferguson, I. McEwan, Polymer **42**, 6991 (2001)

N. Cameron, J.M.G. Cowie, R. Ferguson, J.L.G. Ribelles, J.M. Estelles, Eur. Polym. J. **38**, 597 (2002)

J.A. Campbell, A.A. Goodwin, F.W. Mercer, V. Reddy, High Perform. Polymers **9**, 263 (1997)

C.K. Chai, N.G. McCrum, Polymer **21**, 706 (1980)

G.-W. Chang, A.M. Jamieson, Z. Yu, J.D. McGervey, J. Appl. Polym. Sci. **63**, 483 (1997)

T.W. Cheng, H. Keskkula, D.R. Paul, J. Appl. Polym. Sci. **45**, 531 (1992)

J.M.G. Cowie, R. Ferguson, Polym. Commun. **27**, 258 (1986)

J.M.G. Cowie, S. Elliott, R. Ferguson, R. Simha, Polym. Commun. **28**, 298 (1987)

J.M.G. Cowie, R. Ferguson, Macromolecules **22**, 2312 (1989)

J.M.G. Cowie, S. Elliot, Internal publication, Heriot-Watt University, Edinburgh (1990)

J.M.G. Cowie, R. Ferguson, Paper presented at IUPAC, Montreal (1991)

J.M.G. Cowie, R. Ferguson, Polymer **34**, 2135 (1993)

J.M.G. Cowie, I.J. McEwen, S. Matsuda, J. Chem. Soc. Faraday Trans. **94**, 3481 (1998)

J.M.G. Cowie, S. Harris, J.L. Gomez Ribelles, J.M. Meseguer, F. Romero, C. Torregrosa, Macromolecules **32**, 4430 (1999)

J.M.G. Cowie, I. McEwan, I.J. McEwen, R.A. Pethrick, Macromolecules **34**, 7071 (2001)

J.M.G. Cowie, V. Arrighi, E.-A. McGonigle, Macromol. Chem. Phys. **206**, 767 (2005)

M. Eldrup, D. Lightbody, J.N. Sherwood, Chem. Phys. **63**, 51 (1981)

T.S. Ellis, Macromolecules **23**, 1494 (1990)

J.M. Estelles, J.L.G. Ribelles, M.M. Pradas, Polymer **34**, 3837 (1993)

J.H. Gibbs, J. Di Marzio, Chem. Phys. **28**, 373 (1958)

R. Greiner, F.R. Schwarzl, Rheol. Acta **23**, 378 (1984)

J.L. Gomez-Ribelles, M. Monleon-Pradas, Macromolecules **28**, 5867 (1995)

J.L. Gomez-Ribelles, M. Monleon, A. Vidaurre, F. Romero, J. Estelles, J.M. Mesegner, Macromolecules **28**, 5878 (1995)

A.A. Goodwin, J. Appl. Polym. Sci. **72**, 543 (1999)

R. Grooten, G. ten Brinke, Macromolecules **22**, 1761 (1989)

Y.L. Guo, R.D. Bradshaw, Mech. Time-Depend. Mater. **11**, 61 (2007)

M. Haghighi-Yazdi, P. Lee-Sullivan, Mech. Time-Depend. Mater. **17**, 171 (2013)

J.N. Hay, Prog. Colloid Polym. Sci. **87**, 74 (1992)

T. Ho, J. Mijovic, C. Lee, Polymer **32**, 619 (1991)

I.M. Hodge, A.R. Berens, Macromolecules **14**, 1599 (1981)

I.M. Hodge, A.R. Berens, Macromolecules **15**, 762 (1982)

I.M. Hodge, G.S. Huvard, Macromolecules **16**, 371 (1983)

I.M. Hodge, Macromolecules **20**, 2897 (1987)

B.K. Hong, W.H. Jo, J. Kim, Polymer **39**, 3753 (1998)

J.M. Hutchinson, Prog. Coll. Polym. Sci. **87**, 69 (1992)

J.M. Hutchinson, P. Kumar, Thermochim. Acta **391**, 197 (2002)

G.P. Johari, J. Chem. Phys. **77**, 4619 (1982)

S.R. Jong, T.L. Yu, J. Polym. Sci. Part B Polym. Phys. **35**, 69 (1997)

R. Jorda, G.L. Wilkes, Polym. Bull. **20**, 479 (1988)

R. Kohlrausch, Pogg. Ann. **12**, 393 (1897)

A.J. Kovacs, J.J. Aklonis, J.M. Hutchinson, A.R. Ramos, J. Polym. Sci. Polym. Phys. Ed. **17**, 1079 (1979)

M.J. Kubát, P. Ríha, R.W. Rychwalski, S. Uggla, Mech. Time-Depend. Mater. **3**, 31 (1999)

M.J. Kubát, P. Riha, R.W. Rychwalski, J. Kubat, Europhys. Lett. **50**, 507 (2000)

W.W.Y. Lau, Y.G. Jiang, P.P.K. Tan, Polym. Int. **31**, 163 (1993)

J.J. Laverty, Polym. Eng. Sci. **28**(6), 360 (1988)

Q. Li, S.L. Simon, Polymer **47**, 4781 (2006)

F.H.J. Maurer, J.H.M. Palmen, H.C. Booij, Rheol. Acta. **24**, 243 (1985)

N.G. McCrum, Plast. Rubb. Comp. Proc. Appl. **18**, 181 (1992)

E.-A. McGonigle, J.M.G. Cowie, V. Arrighi, R.A. Pethrick, J. Mater. Sci. **40**, 1869 (2005)

G.B. McKenna, Physical aging in glasses and composites, in *Long-Term Durability of Polymeric Matrix Composites*, ed. by K.V. Pochiraju, G.P. Tandon, G.A. Schoeppner (Springer, New York, 2012), pp. 237–31

J. Mijovic, T. Ho, T.K. Kwei, Polym. Eng. Sci. **29**, 1604 (1989)

J. Mijovic, S.T. Devine, T. Ho, J. Appl. Polym. Sci. **39**, 1133 (1990)

J. Mijovic, T. Ho, C. Lee, Polymer **32**, 619 (1991)

J. Mijovic, T. Ho, Polymer **34**, 3865 (1993)

E. Morales, J.L. Acosta, Polym. J. **27**, 226 (1995)

C.T. Moynihan, P.B. Macedo, C.J. Montrose, P.K. Gupta, M.A. DeBolt, J.F. Dill, B.E. Dom, P.W. Drake, A.J. Easteal, P.B. Elterman, R.P. Moeller, H. Sasabe, J.A. Wilder, Ann. N.Y. Acad. Sci. **279**, 15 (1976)

K. Naito, G.E. Johnson, D.L. Allara, T.K. Kwei, Macromolecules **11**, 1260 (1978)

K.L. Ngai, Comments Solid State Phys. **9**, 127 (1979)

O.S. Narayanaswamy, J. Am. Ceram. Soc. **54**, 491 (1971)

E.F. Oleinik, Polym. J. **19**, 105 (1987)

A.A.C.N. Oudhuis, G. ten Brinke, Macromolecules **25**, 698 (1992)

A.K. Oultache, Y. Zhao, B. Jasse, L. Monnerie, Polymer **35**, 681 (1994)

D.R. Paul, J.W. Barlow, Polymer **25**, 287 (1984)

M. Penco, L. Sartore, S. Della Sciucca, Polym. Eng. Sci. **47**, 218 (2007)

S.E.B. Petrie, A.S. Marshall, J. Appl. Phys. **46**, 4223 (1975)

J.L.G. Ribelles, J.M.M. Duenas, C.T. Cabanilles, M.M. Pradas, J. Phys. Cond. Matter **15**, S1149 (2003)

P. Riha, J. Hadac, P. Slobodian, P. Saha, R.W. Rychwalski, J. Kubat, Polymer **48**, 7356 (2007)

R.E. Robertson, J. Polym. Sci. Polym. Phys. Ed. **17**, 597 (1979)

R.E. Robertson, R. Simha, J.G. Curro, Macromolecules **17**, 911 (1984)

C.G. Robertson, G.L. Wilkes, Polymer **41**, 9191 (2000)

C.G. Robertson, G.L. Wilkes, Polymer **42**, 1581 (2001)

C.M. Roland, K.L. Ngai, Macromolecules **25**, 363 (1992)

E.M.S. Sanchez, Polym. Test. **26**, 378 (2007)

G. Sartor, E. Mayer, G.P.J. Johari, Polym. Sci. Polym. Phys. **32**, 683 (1994)

P. Shi, R. Schach, E. Munch, H. Montes, F. Lequeux, Macromolecules **46**, 3611 (2013)

S. Shimada, O. Isogai, Polym. J. **28**, 655 (1996)

R. Simha, T. Somcynsky, Macromolecules **2**, 342 (1969)

P. Slobodian, A. Lengalova, P. Saha, Polym. J. **36**, 176 (2004)

P. Slobodian, P. Riha, R.W. Rychwalski, I. Emri, P. Saha, J. Kubat, Eur. Polym. J. **42**, 2824 (2006a)

P. Slobodian, J. Vernel, V. Pelisek, P. Saha, P. Riha, R.W. Rychwalski, J. Kubat, I. Emri, Mech. Time-Depend. Mater. **10**, 1 (2006b)

S. Spoljaric, A. Genovese, T.K. Goh, A. Blencowe, G.G. Qiac, R.A. Shanks, Macromol. Chem. Phys. **212**, 1677 (2011)

L.C.E. Struik, *Physical Aging in Amorphous Polymers and Other Materials* (Elsevier, Amsterdam, 1978)

S. Suzuki, S. Nishitsuji, T. Inoue, Polym. Eng. Sci. **52**, 1958 (2012)

Z.Y. Tan, S.L. Sun, X.F. Xu, C. Zhou, Y.H. Ao, H.X. Zhang, J. Polym. Sci. Polym. Phys. **43**, 2715 (2005)

J.K.Y. Tang, P. Lee-Sullivan, J. Appl. Polym. Sci. **110**, 97 (2008)

G. ten Brinke, R. Grooten, Colloid Polym. Sci. **267**, 992 (1989)

G. ten Brinke, G., Karasz, F. E., MacKnight, W. J. Macromolecules. **16**, 1827 (1983)

G. ten Brinke, L. Oudhuis, L., T. S. Ellis, Thermochmica Acta. **238**, 75 (1994)

A.Q. Tool, J. Am. Ceram. Soc. **29**, 240 (1946)

J. Vernel, R.W. Rychwalski, V. Pelisek, P. Saha, M.K. Schmidt, F.H.J. Maurer, Thermochim. Acta **342**, 115 (1999)

G. Williams, D.C. Watts, Trans. Faraday Soc. **66**, 80 (1970)

M. Yun, N. Jung, C. Yim, S. Jeon, Polymer **52**, 4136 (2011)

S.H. Zhang, X. Jin, P.C. Painter, J. Runt, Polymer **45**, 3933 (2004)

Degradation, Stabilization, and Flammability of Polymer Blends

14

Zvonimir Matusinovic and Charles A. Wilkie

Contents

Abstract

The thermal degradation and fire retardancy of polymer blends is covered in this chapter. Blends of PVC, polystyrenes, polyolefins, and polyamides are covered. The component parts of the blend may have the same stability as does its homopolymer or it may be less or more thermally stable. In some cases the relative amounts of the polymers may cause a change from a less thermally

Z. Matusinovic (✉)
Faculty of Chemical Engineering and Technology, University of Zagreb, Zagreb, Croatia
e-mail: zmatus23@gmail.com

C.A. Wilkie
Department of Chemistry and Fire Retardant Research Facility, Marquette University, Milwaukee, WI, USA
e-mail: charles.wilkie@marquetteu.edu

stable polymer to one which is more thermally stable. Thus, one can only determine through experimentation how making a blend will affect the thermal stability of its constituent parts.

14.1   Introduction

It has been generally accepted that new polymers are not always necessary to meet the need for new materials. Blending of existing commodity or engineering polymers often can be implemented more rapidly and can be a less expensive alternative than the development of new polymers (Koning et al. 1998).

Polymer blending has a developed scientific basis (Folkes and Hope 1993; Utracki 1997), and the impressive increase in commercialization of blends is one of the most prominent and rapidly growing features of the contemporary polymer industry. Polymer blends are intimate mixtures of different commercially available polymers with no covalent bonds between individual component polymers (La Mantia 1994). They can be formed by melt mixing or solution blending and/or by coprecipitation or co-coagulation of systems arising from polymerization of a monomer in a latex medium. Properties of the resulting materials may be tailored to meet requirements of customers or expectations of specific new applications with satisfactory balance of a wide range of material properties and costs (La Mantia 1992). In most cases, each component polymer contributes in a specific manner to the overall property profile. The final materials are mostly characterized by combinations of the useful properties of the components of the polymer blend, superior to those of single polymers. Synergy in material properties is obtained (Koning et al. 1998; Utracki 1997; La Mantia 1992).

Blending substantially improves the properties of commodity plastics, such as polyolefins, styrenics, or poly(vinyl chloride) (PVC). Encouraging commercial results were obtained with blends containing engineering and specialty plastics, such as polyamides (PA), polycarbonates (PC), poly(phenylene oxide) (PPO), or electroconducting polymers, like polyaniline, polythiophene, polypyrrole, or polyacetylene. The main goal of blending is modification of mechanical properties, improvement of impact strength at low temperatures, in particular abrasion resistance and improvement of processability (Billingham et al. 1997). Moreover, blending of recycled and virgin plastics is a promising technique in plastic waste management.

Important material properties are miscibility and compatibility of component polymers. Polymer blends may be homogeneous or heterogeneous on a microscopic scale, but should not exhibit any obvious inhomogeneity on the macroscopic scale (Fox and Allen 1991). The terms "compatible" or "incompatible" refer to the degree of intimacy in blends. A blend that is heterogeneous on the macroscopic level and exhibits symptoms of polymer segregation is considered incompatible. Heterogeneous blends appear in a variety of morphologies. These include most frequently dispersion of one polymer in the matrix of the other and/or a co-continuous two-phase morphology (Koning et al. 1998). The blend morphology and character of interfaces influence co-reactivity in degrading blends.

A low degree of compatibility is a serious problem encountered in polymer blends. Consequently, there is a strong effort to enhance compatibility by using additives (compatibilizers). They reduce the dimensions of dispersed particles and prevent undesirable processes such as separation of phases, delamination, agglomeration or skinning, and ultimate physical failure (Koning et al. 1998; Bonner and Hope 1993). While compatibilizers certainly contribute to the material properties of polymer blends, they are also an impurity and could have a negative influence on the lifetime of blends, which has probably been underestimated (Pospisil et al. 1999).

Unfortunately, all polymers, including polymer blends, undergo degradation, and thus the purpose of this chapter is to address this degradation.

14.2   General Aspects of Polymer Degradation

The term degradation of polymers must include all changes in both the chemical structure and physical properties of polymers which occur due to external chemical or physical action and will lead to materials with properties, both chemical and physical, that are different from those of the starting material (La Mantia 1994). Usually this means poorer properties. Organic polymers can be changed by the environment, due to both chemical reaction and physical stresses (heat, mechanical forces, radiation). According to the lifetime stages of polymers, these may be classified as melt degradation, long-term heat aging, and weathering. Thermomechanical, thermal, catalytic, and radiation-induced oxidations and environmental biodegradation may be involved (Pospisil and Klemchuk 1990).

In addition to the regular structure of a polymer, there may also be low amounts of polymeric inhomogeneities (e.g., unsaturation, oxygenated structures, weak links) and non-polymeric impurities, including metallic contaminants and photoactive pigments, and each of these may be affected by various degradation processes (Pospisil et al. 1998). The concentration of active impurities (catalysts or sensitizers) increases over the polymer lifetime. The knowledge of degradation mechanisms of homopolymers and copolymers is helpful only to some extent in elucidation of the degradation of polymer blends as individual components of a blend may behave rather differently from their behavior as isolated polymers (La Mantia 1992; Wypych 1992). This may affect the degradation resistance of the blend in a positive or a negative manner. Consequently, the degradation behavior of blends is not predictable without experimentation (La Mantia 1992), due to co-reaction phenomena at the interfaces of the blended polymers, controlled by morphology. The processes are complicated by the reactivity of compatibilizers (Chiantore et al. 1998). The heterogeneous character of the system, reaction in the bulk and at the boundaries of individual phases, and involvement of macromolecular and low-molecular-weight degradation products, increase the complexity of reactions in blends (La Mantia 1992, 1994; Chiantore et al. 1998; McNeill 1977; McNeill et al. 1978). Thus, improvements of mechanical properties by blending are sometimes at the expense of stability (Chiantore et al. 1998). Structural changes,

due to aging, produce an effect on various physical properties. The practical service lifetime of blends in general and blends containing recycled materials can be different in terms of resistance to degradation. Accordingly, performance characteristics of blends are of major commercial importance.

14.3 Thermal Degradation

The processes described in this part proceed in polymer blends stressed in an inert atmosphere by a single agent – heat. The effect of thermal degradation on blends containing vinyls, styrenics, polyolefins, acrylics, and rubber elastomeric blends are herein described. Most of the experimental data were obtained by dynamic or isothermal differential scanning calorimetry (DSC) and thermogravimetry (TG) or thermal volatilization analysis (TVA). Infrared (IR) and nuclear magnetic resonance (NMR) spectrometry, chromatographic methods, and conductometric measurements were used for analysis of volatile and condensable products of thermolysis. Interactions are observed between the components in the polymer bulk with low-molecular-weight molecules or free-radical products, arising by thermolysis of any of the component polymers and migrating across the phase boundaries from one polymer to another (McNeill et al. 1978; McNeil 1989). Ultimately, the products of thermolysis either trigger degradation of the blend (destabilizing effect) or act as stabilizing species for any of the component polymers (Wypych 1992; McNeil 1989). The final effect may depend on the ratio of components or the temperature. Systems where the ultimate degradation rates are reduced or the decomposition temperatures of all component polymers are shifted to higher values have the optimum behavior. The thermal behavior of polymer blends shows some similarities with graft copolymers, but differs from those of random copolymers (McNeill 1977).

14.4 Vinyl Blends

14.4.1 PVC

Much attention has been paid to blends containing PVC. Blending with other polymers improves the properties of this commodity polymer and increases possible applications (Braun and Böhringer 1989). Knowledge of the thermal behavior of different blends containing PVC is of commercial importance.

Thermal dehydrochlorination of unstabilized PVC occurs at about 100 °C and is also an undesired process in stabilized PVC at processing temperatures (180/200 °C) (Braun 1981). Dehydrochlorination accounts for the formation of conjugated double bonds (Scheme 14.1) and leads to allylic activation in degrading PVC. Hydrogen atoms of the methylene group in the allylic moiety are able to form hydrogen bonds with functional groups (e.g., $>C=O$) in the component of the blend (Lizymol et al. 1997). Sequences of conjugated double bonds may participate in PVC cross-linking (McNeil 1989).
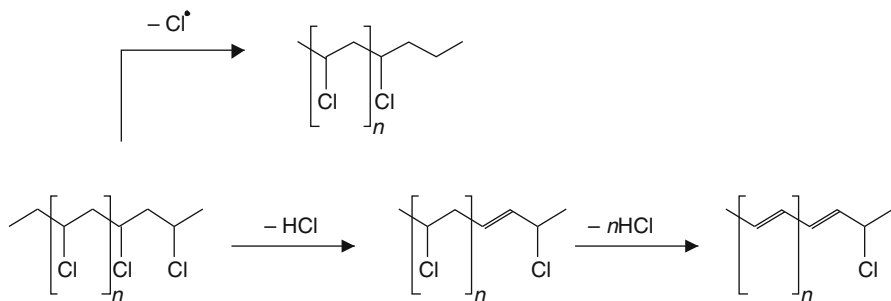
Scheme 14.1 Degradation of PVC

The low thermal stability of PVC requires effective stabilization (Braun 1981). It was realized that performance of tin stabilizers was enhanced in some blends of PVC in comparison with pure PVC (Braun and Böhringer 1989).

A detailed elucidation of dehydrochlorination rates of PVC blends with HIPS containing 16 % non-grafted PS, poly(styrene-*co*-acrylonitrile) (SAN), and acrylonitrile–butadiene–styrene terpolymer (ABS) containing 27 % non-grafted SAN in inert atmosphere at 180 °C revealed accelerated degradaon of the PVC component (Braun et al. 1994).

14.4.2 PVC/PMMA

The influence of PMMA in the PVC matrix on the thermal stability of blends has been investigated by dynamic TGA (Ahmad et al. 2008). The thermal degradation of PVC proceeds in two distinct stages in an inert atmosphere (Owen 1984; Ahmad and Mahmood 1996; Marongiu et al. 2003). In the first stage, the most abundant volatile product is HCl. At low temperature molecular dehydrochlorination plays a fundamental role, whereas at higher temperature a radical mechanism becomes relevant. The initiation reaction can involve $C-C$, $C-H$, and $C-Cl$ bond cleavage, the last being the weakest and consequently the most probable initiation step. The $Cl^{\cdot}$ radicals can initially abstract a H atom from a repeating unit and form HCl. The HCl further catalyzes the degradation process releasing more HCl with the formation of polyenes.

The typical species involved in the first degradation stage are H_2, Cl_2, and HCl. After the loss of HCl, the allylic chlorine is more reactive, and its unzipping leads to the polyene linkage; the conjugated structure is stabilized by resonance. The decomposition temperature in the first step of dehydrochlorination, which starts around 220 °C, increases as the heating rates increases (Ahmad et al. 2008).

The polyene linkages above 360 °C may undergo aromatization through intermolecular cyclization leading to volatile aromatics, e.g., benzene, naphthalene, and anthracene, or through intermolecular cross-linking reaction leading to alkyl aromatics and char above 500 °C.

As the heating rate increases, the thermal decomposition temperature of the second step of degradation also increases (Ahmad et al. 2008), since there is less time available for the degradation. The fraction of residue at 600 °C also increases at high heating rates. In the cyclization process taking place around 450 °C, the polyene linkages not only cyclize but cross-link as well (Nagi et al. 1980; Varma and Sharma 2003). The cross-linked structure, however, decomposes with difficulty (Yanborisov et al. 2003) as seen by the mass retained in the thermograms.

The details of the PMMA degradation process have been studied by Manring (Manring 1988, 1991; Manring et al. 1989) and Kashiwagi (Kashiwagi et al. 1986). PMMA generally degrades by end-chain scission at 360 °C and by random scission around 400 °C giving monomer as the product. Random scission produces both primary and tertiary radicals. The tertiary radical degrades by unzipping to give monomer and a new tertiary radical. The primary radical may form a methallyl-terminated species which leads to a new tertiary radical. The detailed analysis and DTA show that a part of PMMA begins to degrade around 140 °C. Nearly 2 % weight loss is evident from the TGA curves. In the second degradation stage, which starts around 220 °C, nearly 3 % weight loss occurs. PMMA polymerized by free-radical polymerization may contain some head-to-head linkages and early decomposition, which takes place around 140–150 °C, is due to breakage at these linkages as the bond dissociation energy of such bonds is less than the C–C bonds, mainly due to steric and inductive effects of vicinal ester groups. The second degradation stage, which occurs around 230–255 °C, is likely due to the unsaturated chain ends resulting from the termination by disproportionation. The thermal decomposition in both the first and second stage results in a weight loss of nearly 4–5 %; the main degradation process involving random scission starts in the third stage around 360 °C (Ahmad et al. 2008). Thermal decomposition temperatures in all cases increase with an increase in the heating rates, though with higher heating rates the initial step is not that visible (Ahmad et al. 2008).

The thermal degradation of PVC/PMMA blends containing between 2.5 and 20 wt% PMMA in PVC were studied at various heating rates (Ahmad et al. 2008). For 10 wt% PMMA in PVC at 2.5 °C min^{-1}, the first degradation step, which in pristine PVC is at 280 °C, increases to 300 °C. At 20 wt% PMMA content, the first degradation is at 287 °C. The thermal decomposition temperature increases with higher heating rates in all cases. Blends with 10 wt% PMMA again show the maximum increase from 319 °C in case of pure PVC to 352 °C, whereas at higher PMMA content it decreases, but always remains above the thermal decomposition temperature of pristine PVC. More mass is retained above 600 °C in blends containing 10 wt% PMMA. The relative decrease of the thermal decomposition temperature with higher content (15 wt% or more) of PMMA in blends was less in the case of higher heating rates. The thermal decomposition temperature in the second degradation step in PVC also increases and shows a maximum value for 10 wt% PMMA in PVC; the decrease is larger compared to the first decomposition step (Ahmad et al. 2008).

The PMMA/PVC blends, as observed through SEM studies, seem heterogeneous, particularly at higher PMMA content where the two polymers may

predominantly degrade in their phase-separated regions. However, they may give rise to some cross products formed by small radicals or molecules migrating across the phase boundaries. The reaction of a macroradical of one component with the macroradical of the other component may take place at the phase boundaries, but there is more probability for the reaction of a microradical of one polymer with the macroradical of the other. As shown already, some weak links in PMMA, e.g., head-to-head linkages, decompose earlier, at 140–200 °C. These will produce primary radicals, which then can further degrade. Free radicals thus produced may combine with macroradicals of the matrix. This can act as a catch or block for further unzipping in PVC. The first degradation step, the dehydrochlorination process in PVC, is therefore delayed as the chain is stabilized. It was observed through dehydrochlorination and UV–Vis spectroscopic studies that the size of polyene linkage in PVC increases with heating in the presence of a destabilizer such as metal chlorides (Manzoor et al. 1996; Khan and Ahmad 1996), whereas Aouachria and Belhaneche-Bensemra have recently observed relatively shorter polyene linkages produced in degradation of rigid and plasticized PVC/PMMA blends (Aouachria and Belhaneche-Bensemra 2006). This observation supports a mechanism where the reaction of free radicals produced in PMMA degradation combine with the unzipping PVC chain, thus stabilizing it.

In PMMA, random degradation occurs around the same temperature where the second stage of degradation of PVC begins. The combination of the free radicals from both components may produce some cross-linked structures, which are slightly more difficult to degrade. This is evident by the larger amount of weight retained above 600 °C with blends having 10 wt% PMMA in the PVC matrix (Ahmad et al. 2008). The slight decrease in the thermal degradation temperatures at higher concentration of PMMA, 15 % or more, seems due to phase aggregation tendencies of the components in blends, which is confirmed by SEM micrographs. This may result in less interaction between the degrading products from the two polymers thus reducing the mutual stabilization.

The activation energies for the thermal decomposition of PVC and its various blends with different concentrations of PMMA can be calculated using dynamic TGA data obtained at different heating rates and methods by Flynn, Friedman, and Ozawa (Flynn and Wall 1983; Friedman 1965; Ozawa and Bull 1965). The apparent activation energy of decomposition for pure PVC is 138.8 kJ mol^{-1}. Bockhorn et al. (Bockhorn et al. 1999) have discussed the mechanism and kinetics of thermal decomposition of PVC and reported the value of activation energy of the first step to be 140 kJ mol^{-1}, which agrees with the value obtained in the work of Ahmad et al., who showed that the activation energy of the degradation in blends varies with an increase in the PMMA content. The activation energy increases for up to 10 wt% of PMMA in the matrix and then falls sharply. The maximum value of activation energy measured in these blends is 149.9 kJ mol^{-1}. The higher value of activation energy for the blends confirms the stability of all the blends as compared to the pure polymer, however, the optimum amount of PMMA was found to be 10 % by weight in PVC.

14.4.3 PVC/CPE

Chlorinated polyethylene (CPE) is a commonly used impact modifier of PVC, and its compatibility depends upon the chlorine content and the distribution of the chlorine atoms on the polyethylene (PE) backbone. As the chlorine content in CPE increases, first the regularity of the polyethylene structure breaks up, reducing and then eliminating crystallinity, then converting a rigid polymer into a flexible, rubbery material. When the rubbery phase is semi-compatible with PVC, it disperses as small discrete domains in the PVC matrix and serves as an impact modifier for rigid PVC. A continuous increase in the chlorine content of CPE increases its polarity, making it more miscible in PVC and can improve melt processability. At high concentrations of chlorine, it can act as a polymeric plasticizer. In all these functions, the saturated structure of CPE makes it more weather resistant than butadiene polymers, and its high molecular weight makes it a much more permanent plasticizer than the conventional liquid monomeric ones (Deanin and Chuang 1987). CPE with 36 % chlorine is the optimum composition for obtaining the necessary features of impact, processing, and strength (Walsh and Higgis 1985). The morphology of the polymer blend has a significant effect on the impact behavior of the material. At a concentration less than 13 mass % CPE in the PVC/CPE blend, PVC is the continuous phase, while CPE is the noncontinuous phase. Increasing the CPE concentration above 13 mass % reverses the phase distribution (Chen et al. 1995).

It is well established that blending may greatly influence the thermal stability of the individual polymers (McNeil 1977; McNeil and Gorman 1991; Goh 1993). Under degradation conditions, considerable interactions may occur between components in the blend and/or their degradation products. The type of interaction will depend on the degree of miscibility of the components, as well as on their ratio in the blend.

Differential scanning calorimetry results showed that amorphous PVC and partly crystalline CPE are immiscible for all the investigated compositions of the blends in the temperature range 30–150 °C, that is, PVC/CPE blends are heterogeneous, and the glass transitions of both PVC (83 °C) and CPE (115 °C) are observed (Klarić et al. 2000). The TGA curves at higher heating rates (5, 10, 20, and 40 °C) are shifted to higher temperatures. Both pure polymers undergo two degradation steps. In the first stage, the dehydrochlorination of the polymer occurs, and in the second, the degradation of the dehydrochlorinated residue and the formation of compounds of low molecular mass take place. The maximal rate of PVC dehydrochlorination is about six times greater than the maximal rate of CPE. Dehydrochlorination of PVC occurs with a peak temperature between 250 °C and 290 °C, while in CPE this is at about 330 °C. The maximal rate of PVC dehydrochlorination in the blends decreases by one-half for each 20 % addition of CPE, and the corresponding peak temperature is shifted to higher values.

When the experimental TG curves of the blend were compared with the curves predicted on the basis of the TG curves of the unblended components (Fig. 14.1), the additivity rule indicates interactions in the blends (Goh 1993; Moscala and Lee 1989). Klarić et al. found that in the heterogeneous blend, PVC/CPE 50/50,

Fig. 14.1 TGA curves for (*1*) PVC, (*2*) CPE, (*3*) PVC/CPE 50/50 blend, and (*4*) predicted TGA curve for PVC/CPE 50/50 blend; heating rate 2.5 °C min^{-1} (Reproduced with permission from John Wiley and Sons, from I. Klarić, N. Stipanelov-Vrandečić, U. Roje, J. App. Polym. Sci. **78**, 166 (2000))
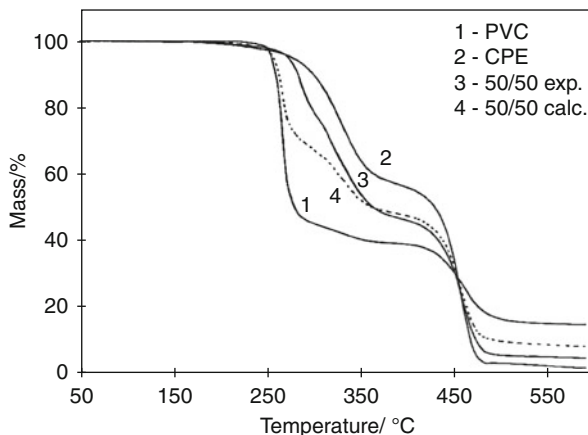
interactions do occur between the polymers. In the temperature range about 240–370 °C (the first degradation step), the blend is more stable than calculated according to the additivity rule. For example, at 300 °C, the blend has lost approximately 10 % mass less than predicted. At temperatures over 370 °C, the blend shows less stability. The values $\Delta\alpha = (\alpha_{exp} - \alpha_{calc})/\alpha_{calc}$ were also calculated (Kovačić et al. 1993) for all blend compositions at a heating rate 2.5 °C min (Moscala and Lee 1989). The PVC/CPE blends are thermally more stable in the temperature range for which $\alpha_{calc} > \alpha_{exp}$, that is, $\Delta\alpha < 0$. If $\Delta\alpha > 0$, the PVC/CPE blends are less stable than would be predicted from the behavior of the pure polymers (Fig. 14.2).

The main degradation reaction of PVC at moderate temperatures is dehydrochlorination, which is also the dominant reaction in CPE degradation. While dehydrochlorination of PVC is an autocatalytic reaction, the dehydrochlorination of CPE is statistical (Jimenez 1993; Stoeva et al. 2000).

The addition of heat stabilizers improves the thermal stability of polymers. One group of commercially available PVC heat stabilizers are Ca/Zn stabilizers. According to the Frye–Horst mechanism (Thomas 1993), the zinc fatty acid salt reacts with PVC by an esterifying displacement of chlorine. Stabilization arises from substitution of labile chlorine atoms with more stable carboxylate groups (Scheme 14.2):

The progressive dehydrochlorination reaction is prevented in this way, but the zinc chloride, produced as a result of the esterification reaction, will cause further rapid degradation. This problem is solved by the synergistic effect of combining alkaline earth (Ca) carboxylates with the covalent metal carboxylates. Alkaline earth carboxylates undergo ester exchange reactions with covalent metal chlorides, regenerating the covalent metal carboxylates:

$$ZnCl_2 + Ca(OOCR)_2 \rightarrow Zn(OOCR)_2 + CaCl_2$$
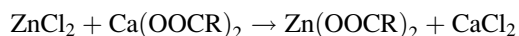
Alkaline earth chlorides do not promote dehydroxylation, thus the alkaline earth carboxylates are not primary stabilizers of PVC resin but serve to

Fig. 14.2 Dependence of the interaction $\Delta\alpha$ on the degradation temperature for PVC/CPE blends of different compositions; heating rate 2.5 °C min^{-1} (Reproduced with permission from John Wiley and Sons, from I. Klarić, N. Stipanelov-Vrandečić, U. Roje, J. App. Polym. Sci. **78**, 166 (2000))

$$Zn(OOCR)_2 + {\sim}CHC{-}CH{=}CH{\sim} \rightarrow ClZn(OOCR) + {\sim}\overset{\overset{\displaystyle OOCR}{|}}{CH}{-}CH{=}CH{\sim}$$

$$ClZn(OOCR) + {\sim}CHC{-}CH{=}CH{\sim} \rightarrow ZnCl_2 + {\sim}\overset{\overset{\displaystyle OOCR}{|}}{CH}{-}CH{=}CH{\sim}$$
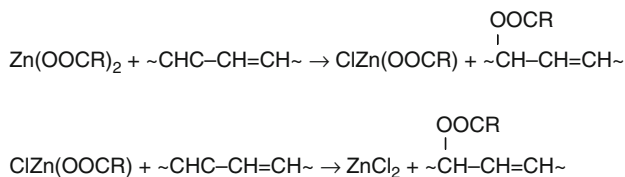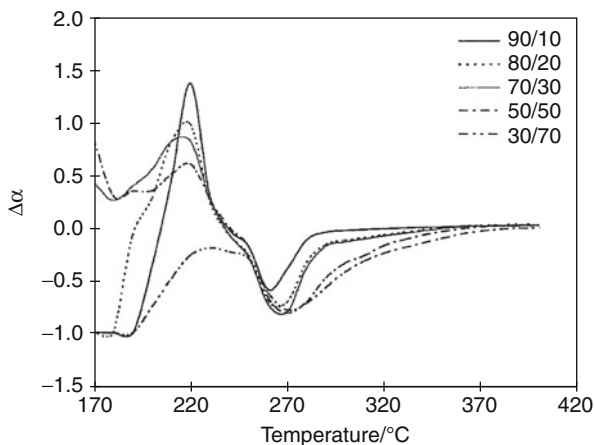
Scheme 14.2   Stabilization of PVC by Zinc Carboxylates

regenerate the active stabilizer and remove the potentially destructive effect of the covalent metal chloride.

Thermal degradation of stabilized and unstabilized PVC/CPE was studied by Stipanelov Vrandečić et al. (Stipanelov Vrandečić et al. 2001). Dynamic TGA was performed for the thermal degradation of PVC/CPE blends between 50 °C and 600 °C at a heating rate 2.5 °C min^{-1}. It was found that the thermal degradation of the "pure" unstabilized and stabilized polymers, as well as the PVC/CPE blends, occurs in two degradation steps: dehydroclorination of PVC or/and CPE and the degradation of the dehydrochlorinated residues.

The maximum rate of autocatalytic PVC dehydrochlorination is considerably higher than the maximum rate of statistical dehydrochlorination of CPE, and it decreases as the ratio of CPE increases from 0 % to 50 %. In the PVC/CPE 30/70 blend, the maximum dehydrochlorination rate of CPE is higher than that of PVC. In the second degradation step, the dehydrochlorination rate of CPE is the highest, but it is lowered by increasing the ratio of PVC in the blends.

In the first degradation step of the stabilized PVC/CPE blends, there are two maxima in the TGA curves for 90/10 and 80/20 blends, while for other blends those maxima become one. By comparing the DTG curves of the stabilized and unstabilized blends, it can be concluded that the Ca/Zn stabilizer

increases the maximum dehydrochlorination rate of "pure" PVC and decreases the corresponding rate of "pure" CPE.

Although they are chemically similar, CPE has superior thermal stability to PVC, which can be explained by difference in microregularity of the corresponding polymer chains. The mutual location of the monomer segments in PVC corresponds to "head-to-tail" pattern. PVC releases HCl more readily on dehydrochlorination, since the chloroallylic fragments of the relatively weak C–Cl bond are formed. CPE has non-regular location of chlorine atoms along the polymer chain associated with certain "blockwise" structures involving "head-to-tail," "tail-to-tail," and other patterns of connection of the chain segments. The dehydrochlorination results in the formation of "vinyl" structure of much stronger C–Cl bonds. The degradation of CPE with the same chlorine content in PVC occurs more slowly than that of PVC; dehydrochlorination of CPE is slow random HCl elimination as opposed to the rapid dehydrochlorination of PVC (Stoeva et al. 2000).

In immiscible polymer blends, one polymer is dispersed in the form of domains in the continuous phase of the other. The degree of dispersion depends upon the mixing ability of the polymers, which decreases with an increase in concentration of the other polymer in the blend. Therefore, the quantity of domains and the degree of dispersion in PVC/CPE blends determine the progress of the degradation. The evolved HCl partially lags in the bulk sample, due to inefficient diffusion and, consequentially, has a catalytic effect on dehydorchlorination at low level of dehydrochlorination, as well as on the secondary reactions of polyene residues (Mahmood and Quadeer 1994).

To evaluate the thermal stability of the blends, the characteristics of the first degradation step were determined from the TGA and DTG curves: the onset temperature, $T_1(o)$ (the intersection of the extrapolated baseline with the inflection tangent); the temperature at the maximum rate of PVC degradation, $T_1(m)$; the degree of conversion at the corresponding maximum rate, $\alpha_1(m)$; and the mass loss at the end of the first degradation step, Δm_1.

The $T_1(o)$ and $T_1(m)$ of unstabilized blends shift towards higher values with increasing CPE ratio. With the addition of stabilizer, the blends containing up to 30 % CPE have higher $T_1(o)$ than the corresponding unstabilized blends, the addition of stabilizer does not change the $T_1(o)$ of the blend with 50 % of CPE, while in the 30/70 and 0/100 blends, it decreases. The temperature $T_1(m)$, at which the dehydrochlorination rate of stabilized blends is maximum, is higher than for the corresponding unstabilized blends, with the exception of the 0/100 blend.

The conversion value $\alpha_1(m)$, at the maximum dehydrochlorination rate of PVC, is 19–20 % for 100/0, 90/0, and 80/20 blends. With an additional increase in the CPE content, $\alpha_1(m)$ decreases, and for the 30/70 blend it amounts to 9 %, though it is 25 % for the "pure" CPE. The maximum dehydrochlorination rates of stabilized PVC/CPE blends are achieved at higher conversion in comparison with unstabilized blends, with the exception of the 0/100 blend.

During degradation of either unstabilized or stabilized blends, the Δm_1 mass losses depend on the blend composition, and, by increasing the amount of CPE in the blend, Δm_1 decreases. The values of Δm_1 for stabilized blends are somewhat

lower than for the corresponding unstabilized blends. In the investigated temperature range, the unstabilized PVC loses 61 % of its mass in the first degradation step. This mass loss is a bit higher than the stoichiometric quantity of chlorine contained in PVC and corresponds to total PVC dehydrochlorination. The difference of several percent is attributed to the formation of benzene (Jimenez 1993; McNeill et al. 1995). The mass loss of 43 % of the unstabilized CPE in the first degradation step is also a bit higher than the chlorine content in CPE, so the dehydrochlorination of CPE is total. At the end of the first degradation step, the stabilized PVC and stabilized CPE have lost 60 % and 42 %, respectively.

To estimate the thermal stability of unstabilized and stabilized blends, besides the abovementioned indicators, temperatures $T_{1\%}$ and $T_{5\%}$, at which the mass loss (conversion) of 1 and 5 % was achieved, are determined. The $T_1(o)$ temperature is considered to be an inadequate indicator of thermal stability as it depends on experimental conditions during recording of the TG curve. The $T_{1\%}$ temperatures of stabilized blends are, on average, about 20 % lower than the $T_{1\%}$ of unstabilized blends of the same composition. The $T_{5\%}$ temperatures for the stabilized blends containing up to 20 % of CPE are higher than the $T_{5\%}$ of unstabilized blends; for the blends with 30 % of modifier, these temperatures are equal. For the stabilized blends with 50 % and 70 % of modifier, $T_{5\%}$ is lower than for the corresponding unstabilized blends. The increase of mass ratio of CPE in the stabilized blends has a destabilizing effect. The destructive effect of $ZnCl_2$ seems to be the probable explanation for this behavior (Prospect Dow CPE Resins for Impact Modification of Rigid PVC. Dow Chemical 1993).

The thermal stability of a particular polymer in the blend depends on possible interactions of the blend components and their degradation products. In immiscible blends, as PVC/CPE, the type of interaction depends on the ratio of the components in the blend and their mixing ability. The interactions of PVC and CPE are confirmed by comparison of experimental TGA curves and TGA curves calculated using the additivity rule. In the temperature range which corresponds to the first degradation step (240–370 °C), PVC/CPE blends were more stable than was calculated (Klarić et al. 2000).

14.4.4 PVC/PS

Polystyrene (PS) is considered an excellent polymer suitable for various commercial and domestic applications. PVC and PS stand second and third in the world, respectively, as far as the consumption of polymers is concerned. The structure and composition of various products formed during the degradation process and their mutual interactions in the ultimate degradation mechanism depends on the compatibility of polymeric components in the blends. PS/PVC blends with different compositions have been prepared (Ahmad et al. 2007) in the forms of film and powder. Thermal degradation was studied at various heating rates in an inert atmosphere. Pure PS degrades in one step between 300 °C and 400 °C, producing monomer, dimer (2,4-diphenyl-1-butene), trimer(2,4,6-triphenyl-1-hexane),

benzene, and toluene as volatile products (Faravelli et al. 2001; Ohtani et al. 1990; Kruse et al. 2002; Swistek et al. 1996) and a residue above 430 °C which may consist of some condensed products. The thermal decomposition temperatures at different heating rates were obtained from the DTG curves. The thermal decomposition temperature of PS increases at higher heating rates, due to less exposure to heat as the degradation time is reduced. At low heating rates, some cross-linked products are evident at temperature around 400–500 °C, but at higher heating rates the volatile products may not have sufficient time in the matrix to react.

A small weight loss, 1–1.5 %, occurs around 200 °C in all blends, which is likely due to the presence of moisture or residual solvent. The TDT of the blends increases as the amount of PVC increases in the blend then it slightly decreases for higher amounts of PVC. At this heating rate, the mutual stabilizing effect of these polymers is higher for relatively low PVC loadings, which may be due to more interfacial interaction due to homogenous distribution compared to the higher PVC loadings.

Two different concentrations of PVC, i.e., 2.5 and 20 wt% in PS, were examined at 2.5 °C min^{-1} heating rate. Only one DTA peak at 378 °C is observed, showing that the thermal degradation temperature of PS has increased from 352 °C to 378 °C. But with higher PVC amounts (20 wt%), three DTA peaks are observed, and it seems that the phase-separated PVC component decomposes earlier than PS. The first degradation step in high PVC content blends is the dehydrochlorination reaction in the temperature range of 280–350 °C. The second DTA peak at 370 °C is due to PS degradation. In these blends, the first-step degradation of PVC is not affected by PS, whereas the degradation of PS is affected by the degraded components of PVC. The third DTA peak around 500 °C is due to second-step degradation of PVC where the polyene sequence formed as a result of dehydrochlorination further splits up into small polyene linkages ultimately giving volatile aromatic products. Blends with high PVC loading degrade predominantly within their phase-separated regions. As the phase boundaries, where mutual interactions occur, are dominant in the blends with lower PVC loading, a higher stabilization effect is observed. From the DMTA and SEM studies, there is a tendency towards phase aggregation (leading ultimately to phase separation) with higher PVC content in the matrix. The SEM micrographs of the films with prolonged heating also show that at higher temperature this tendency further increases due to the viscous properties of the polymer matrix. The slow heating rate (and thus longer heating times) increases the phase aggregation tendencies in blends in particular with higher PVC contents. The interfacial interaction between the polymeric components with 20 wt% PVC in PS therefore is greatly reduced with a tendency for the polymer to degrade independently which causes a smaller increase in TDT as compared to lower amounts of PVC in the matrix.

For higher heating rates, the increase in the concentration of PVC has a different effect on the TGA curves than at low heating rates (Ahmad et al. 2007). The thermal decomposition temperature of the blends with higher PVC contents shows a continuous increase in contrast to that observed for low heating rates. When the polymer blends are degraded at higher heating rates (giving less time for

degradation), phase segregation, which depends upon diffusion, does not takes place to the same extent as in case of low heating rates.

The degradation reactions involved in PS include random scission (which reduces the molecular weight of the polymer), depolymerization (which yields monomer), intramolecular transfer reaction (which produces dimer, trimer, etc.), and intermolecular transfer reaction which reduces the molecular weight of the polymer. The initial degradation products from PVC are Cl radicals and HCl (Owen 1984; Ahmad and Mahmood 1996). The structure and composition of PVC and PS and the interaction of various products formed may give rise to some cross products formed from the radicals or molecules which migrate across these phase boundaries and can play an important role in the degradation of blends.

In such blends, the loading of PVC in the blend cannot impose diffusion restrictions on PS to reduce the possibility of PS degradation by intramolecular reaction. It has already been shown in programmed-heating experiments on the degradation of PS using thin films (McNeill and Mohammed 1972) that the production of styrene is delayed by as much as 60 °C. The matrix in this can be considered as a two-dimensional structure, and this was interpreted due to reduction of intermolecular transfer reaction in PS which gives rise to more active centers. Interference with the intermolecular transfer process in PS due to the presence of PVC may also possibly be one factor affecting PS stability.

It is expected that the Cl radical produced from the degradation of PVC (Scheme 14.3) can either combine with a tertiary hydrogen atom from PS or abstract hydrogen from PVC to produce HCl. The macroradical produced when the abstraction is from PS can combine with the radical from PVC, leading to cross-linking, thus mutually annihilating free radicals; zip elimination of the polymer chain stops and requires renewed initiation. The PVC chain, however, may also continue unzipping due to further abstraction of hydrogen by chlorine or by the catalytic action of HCl producing double bonds which can cross-link with PS products. When TGA curves were compared in the temperature range 400–500 °C, it was found that cross-linked products are formed through the cross-reaction.

Flammability of PVC/PS blends were investigated by cone calorimetry (Yao and Wilkie 2001). Cone calorimetry is the most effective method for the laboratory evaluation of the fire performance of polymers. The parameters obtained are total heat released (THR); average specific extinction area (ASEA), a measure of smoke; average mass loss rate (AMLR); and the time to ignition (t_{ig}); the most important is the heat release rate (HRR) and especially its peak value (PHRR) which gives information about the size of the fire and can be viewed as the "driving force" of the fire. Although there is modulation of the 90/10 PVC/PS curve, which may be caused by the action of HCl on the combustion of PS, the trend for the blends is similar to that of virgin PVC. As a matter of fact, the extinction area (total smoke) shows very similar values for PVC and 90/10 PVC/PS. If one excludes the specific extinction area contributed by PS, one finds that PVC in 90/10 PVC/PS is not significantly different from pure PVC. This conclusion holds true for most of the cone parameters. Because the specific extinction area is related to the production of aromatic
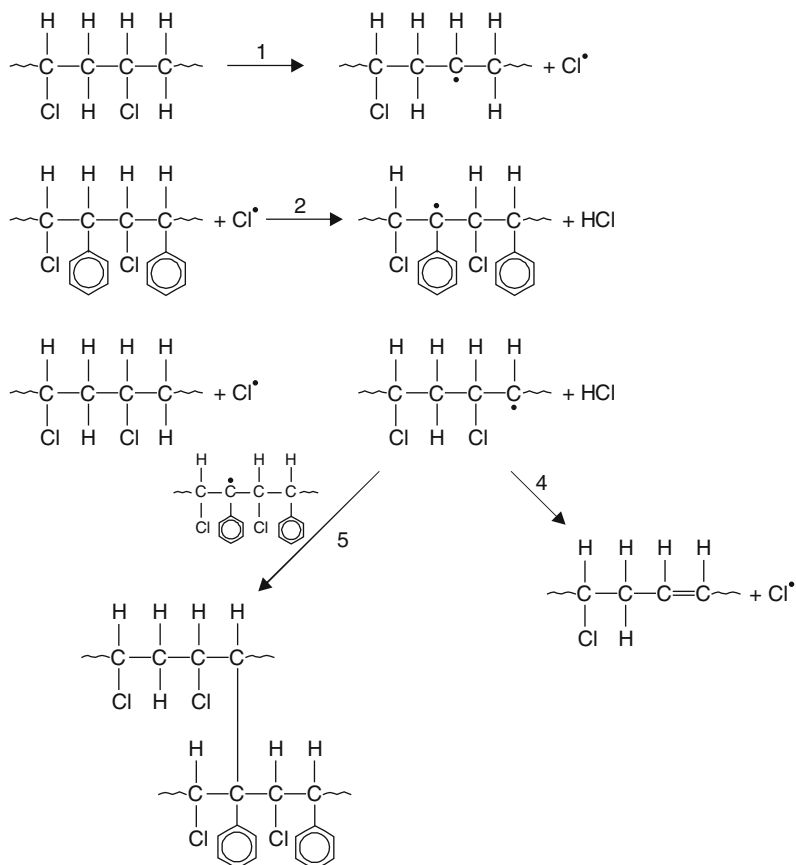
Scheme 14.3 Cross-linked products formed for PVC/PS blends

compounds, which, in the case of PVC, are produced by the intra- or intermolecular cyclization of polyenes, the similarity in the curves and values indicates that the combustion of PVC is unaffected by the presence of PS, which means that there is a little chemical interaction between PVC and PS.

14.5 Polyolefin Blends

Polyolefins are synthetic polymers of olefinic monomers. They may be classified based on their monomeric unit and chain structures as ethylene-based polyolefins (contain mostly ethylene units), propylene-based polyolefins (contain mostly propylene units), higher polyolefins (contain mostly higher olefin units), and polyolefin elastomers (Gahleitner 2001).

Ethylene-based polyolefins are normally produced either under low pressure conditions using transition metal catalysts resulting in predominantly linear chain

structure or under high pressure conditions using oxygen or peroxide initiators resulting in predominantly branched chain structures of various densities and crystallinities.

Propylene-based polyolefins are normally produced with transition metal catalysts resulting in linear chain structures with stereospecific arrangement of the propylene units or special stereoblock structures from a single-site catalyst. Higher polyolefins are normally produced using transition metal catalysts resulting in linear and stereospecific chain structures. Polyolefin elastomers, based mainly on a combination of ethylene and propylene, may be produced using metal or single-site catalysts with or without the inclusion of dienes (for cross-linking) and are mostly amorphous with high molecular weights and heterogeneous phase structures. A given polyolefin may be a homopolymer, copolymer, or terpolymer depending on the number of monomers used in making the polyolefin, crystalline, or amorphous depending on their chain conformation, configuration, and processing conditions.

Polyolefin homopolymers, copolymers, and terpolymers are foundation materials for polyolefin blends. They may be obtained via radical or ionic chain growth polymerization of alkenes using conventional free radicals (e.g., from peroxides) and organometallic complexes (Ziegler–Natta and metallocenes) catalyst systems. Polyolefin polymerization technologies and novel catalyst systems have enabled the rapid development of polyolefins with a wide range of molecular chain structures, morphologies, properties, and particle size and shape. Polyolefin homopolymers include polyethylene (PE), polypropylene (PP), polybutene-1 (PB), polymethylpentene-1 (PMP), and higher polyolefins. PE and PP are the largest by amount produced yearly by the global polyolefin companies. PE comes in various forms differing in chain structures, crystallinities, and densities. These are high-density polyethylene (HDPE), low-density polyethylene (LDPE), linear low-density polyethylene (LLDPE), ultralow-density polyethylene (ULDPE), and ultrahigh-molecular-weight polyethylene (UHMWPE). PP and higher polyolefins come in three stereospecific forms of varying densities: isotactic, syndiotactic, and atactic forms.

14.5.1 PP/PE

Although both polyethylene and polypropylene have similarities in properties (Brydson 1975), the two polymers are immiscible and incompatible in general. The terms "immiscible" and "incompatible" have been adopted here in line with the definition by Utracki (Utracki 1989), where immiscible is defined thermodynamically as the case when the Gibbs free energy of mixing ΔG_m is greater than 0, whereas incompatible means that the blend gives properties inferior to those of both the original constituents or neat polymers. Addition of a small amount of polyethylene or ethylene–propylene copolymer to polypropylene improves the impact performance of polypropylene (Brydson 1975; Utracki 1989), whereas the addition of a small amount of polypropylene to polyethylene enhances the

transparency of solid polyethylene (Last 1959), at the expense of environmental stress cracking resistance.

The effects of an organoclay and alumina trihydrate (ATH) and/or magnesium dihydroxide (MDH) on the fire retardancy of a ethylene–vinyl acetate (EVA) and low-density polyethylene (LDPE) blend were assessed by TGA and the cone calorimeter (Zhang et al. 2009).

The profiles of the polymer blend (PB) and polymer blend/nanoclay (PB/NC) in nitrogen are similar; both curves show two-step thermal degradation depicting two-stage degradation processes. The first step occurs between 300 °C and 400 °C and likely corresponds to the loss of acetic acid (Camino et al. 2000; Allen et al. 2000), while the second step involves the thermal decomposition of the resulting backbone by further radical scission (Beyer 2001). The presence of nanoclay accelerates the deacetylation of EVA (Zhang et al. 2009, 2001). On the other hand, the inclusion of a flame retardant reduces the onset degradation temperature to around 200–350 °C due to liberation of water in the flame retardant (Beyer 2001); ATH gives the greatest shift, since it has lower thermal stability, compared with magnesium dihydroxide. The second weight loss step is also affected by the presence of the clay; the onset of the second weight loss step for PB/NC is lower compared to PB, possibly related to a catalytic cracking of polymer induced by the clay (Zhang et al. 2009), in agreement with results reported in the literature for PE and PP (Manos et al. 2001; Tartaglione et al. 2008). Interestingly, this effect is particularly significant for PB/NC/ATH compared with PB/ATH and for PB/NC/MH compared with PB/MH.

When heated in air, the same two main weight loss stages are found, although the profiles of the weight loss curves are more complex due to the presence of oxygen, which promotes additional degradation pathways compared to the degradation in inert atmosphere. The presence of nanoclay promotes thermo-oxidative stabilization of PB, resulting in an overall decreased weight loss, whereas light destabilization is observed for PB/NC/ATH compared to PB/ATH, and no significant differences are seen for PB/NC/MH compared with PB/MH. The onset temperatures of PB/NC are slightly lower than those of PB, whereas those of the Fire Retardant Clay Materials (FRCMs) are significantly lower due to release of water at lower temperatures. In particular, PB/ATH and PB/NC/ATH reduce the onset temperature by more than 50 °C. In both nitrogen and air, PB pyrolyzes completely whereas about 4 % (in nitrogen) and 6 % (in air) residues were found for PB/NC, which are approximately the same as its initial concentration of 5 %, implying that NC remains after pyrolysis. It should be noted that the residual inorganic clay results from degradation of the organic compatibilizer of the organoclay, which reduces the initial weight of clay from 5 % to 4 %. For the FRCMs, it is worth noting that the final residues are slightly lower (4–7 %) than the theoretical ones calculated from the weight loss contributions of the individual components in the formulation. This may reflect an experimental error resulting from compounding of very highly filled formulations, but chemical interactions between the polymers and the hydroxide to produce a higher amount of volatile products cannot be excluded at this stage.

Once the PB ignited, extensive bubbling was observed having the appearance of liquid-like foam. The other formulations behave more like solids with only minor bubbling but with large deformations. No cracks were found for PB/NC and ATH-containing materials, whereas cracks were found for MH-containing materials. At heat fluxes below 40 kW m^{-2}, deformation (especially severe for PB/NC/ ATH and PB/NC/MH) caused the samples to move towards the igniter. This upward movement has two effects on the test results: (i) it causes the actual imposed heat flux to be higher than the nominal one, affecting the accuracy of the test results (Schartel and Hull 2007; Babrauskas 1992) and (ii) in some cases the experiment had to be stopped prior to ignition to avoid contact between the igniter and the sample. No ignition (within 10 min) was observed for all the formulations at 15 kW m^{-2}, and for PB/NC/ATH and PB/NP/MH, no ignition occurred at 20 and 30 kW m^{-2}. At low heat fluxes (15 and 20 kW m^{-2}), a carbonaceous layer was observed to form on the surface prior to ignition, which poses uncertainties in measuring the ignition time (there are relatively large differences between the measurements in duplicated tests). At higher heat fluxes (30 kW m^{-2} and above), the ignition times of the PB and PB/NC are similar, indicating again that NC does not alter the thermal properties of polymers. In contrast, all the FRCMs (ATH or MH) increase the ignition time. This should not be considered contradictory to the TGA results that the FRCMs decrease the onset degradation temperature, because (i) the water released from the FRs hinders ignition and (ii) ATH or MH is completely transformed into oxides (endothermic reaction) before ignition during heating, and therefore the temperature of the substrate is lowered, increasing the ignition time (Bourbigot et al. 1999).

The results at other heat fluxes show similar patterns. Although PB/NC has the same first peak HRR as the PB, the second peak for the PB is completely removed by the addition of 5 wt% nanoclay. This may be attributed to a surface layer formed during pyrolysis of nanocomposites, reducing the transfer of heat into unpyrolyzed material and increasing the surface radiation heat loss (Kashiwagi et al. 2004a, b; Wilkie 2002; Zanetti et al. 2001). For the FRCMs, the reduction is more substantial; even the first peak HRR is reduced by a factor of 2–3 compared to the PB with PB/NC/ATH achieving the lowest HRR. However, one should note that the reduction of the HRR by the FRCM is also due to the fact that there is less polymer in the FRCMs. Comparing the results of PB/ATH to PB/NC/ATH and PB/MH to PB/NC/ MH indicates that the effect of NC is not significant, and there is no clear indication of a synergistic effect between NC and FRs.

Since the HRR is proportional to the mass loss rate (MLR) (the proportionality factor is the heat of combustion), the MLR results have similar trends as the HRR.

The effective heat of combustion (EHC) is calculated as the ratio of the total heat released over the total mass loss (for the FRCMs, the mass loss of water (35 % for ATH and 32 for MH) was subtracted from the total mass loss). The average value for the PB is about 32 kJ g^{-1}, which is similar to the one reported for pure EVA by Lyon (Lyon and Janssens 2005). PB/NC has a similar but slightly lower value, implying that though it takes longer for PB/NC to burn, it burns completely. As for the FRCMs, the EHC is actually higher than the PB and PB/NC. To explain this,

it must be noted that the combustion efficiency of EVA (Lyon and Janssens 2005) is only about 0.8, and the water released due to degradation of FRs appears to assist combustion by increasing the mixing efficiency, as commonly used in combustion engines.

The mass loss (%) is essentially the same in the TGA and the cone. For the FRCMs, there are some differences between the residual weights obtained and the theoretical values, and these differences might also relate to the higher EHC discussed above.

As observed very recently (Shah and Paul 2006; Cervantes et al. 2007; Leszczynska et al. 2007), the products of the degradation of the organic modifier may interact with the matrix, and their solubility in the matrix would play a vital role in the process. In particular, the α-olefins produced by the Hoffman reaction, due to their affinity with the polyolefin phase, will disperse quickly into polyethylene (Frankowski et al. 2007). Likely, this diffusion is slower when the affinity is lower, as for PA6. In this latter case, as already observed for another system (Frankowski et al. 2007), the final effect would be a sort of swelling of the tactoid caused by the permanence of the degradation products between the clay layers. This was confirmed in separate investigations (Scaffaro et al. 2008) performed on PA6 and HDPE nanocomposites (5 % clay, extruded under the same conditions as the other blends). The interlayer distance in the clay is 3.15 nm, while in PA6 it is 3.57 nm and in HDPE it is 2.54 nm; a significant degradation of the clay modifier occurs during preparation.

In the HDPE phase, the reduction of the interlayer distance can be explained by a rapid diffusion of the degradation products from the clay galleries towards the HDPE phase and, as a consequence, the collapse of the tactoid and the reduction of the interlayer distance.

In addition, the slight increase of the interlayer distance in the PA6 phase can be ascribed, beyond some intercalation of the polymer, also to the permanence of the degradation products in the clay galleries. In this case, these products are less prone to diffuse into the PA6 matrix, and the final effect is the expansion of the tactoids.

Of course, the interactions of the degradation products with the matrix can contribute, together with the decrease of the crystalline fraction, to the decrease of the mechanical properties.

14.6   Styrenic Blends

The thermal degradation of polystyrene proceeds by a random scission process (Cullis and Hirschler 1981); the production of benzene, toluene, styrene, and styrene oligomers begins at about 350 °C (Suzuki and Wilkie 1995). A graft copolymer has been produced by the addition of acrylonitrile onto polystyrene using an anionic copolymerization process (Xue and Wilkie 1997a, b). In order to offer thermal protection by a graft copolymerization process, it is necessary that the graft layer degrades first and forms a char which can protect the underlying layer. From a TGA/FTIR study, the first product one observes is ammonia which arises

from the degradation of polyacrylonitrile. For virgin polyacrylonitrile, ammonia evolution begins at about 290 °C, while in this graft copolymer ammonia evolution does not commence until 350 °C, and the evolution of aromatics, which is the signature of polystyrene degradation, does not begin until 420 °C which is 70 °C higher than in virgin polystyrene. Both graft copolymers and blends of polystyrene with polyacrylonitrile show similar behavior. There are two observations of significance here: the degradation of polystyrene begins at higher temperature and the degradation of acrylonitrile begins at higher temperature; each of these will be examined separately.

The higher temperature for the evolution of aromatics indicates enhanced thermal stability for the graft copolymer (Wilkie 1999). Since the graft layer does degrade initially, it will form a char layer, i.e., a thermal barrier, which protects the underlying polystyrene. A similar degradation pathway is seen in blends, which implies that it is not necessary that the char be formed at the surface of the polymer, it is just important that char be formed. From TGA/FTIR, the graft copolymerization of acrylonitrile onto polystyrene does enhance the thermal stability of polystyrene. While from cone calorimetry, this is not observed, and the graft copolymer and the blends have a lower thermal stability than virgin polystyrene. This leads to an apparent contradiction. The graft copolymerization of sodium methacrylate onto ABS, SBS, and K-resin gives a good correlation between TGA/FTIR studies in an inert atmosphere and cone calorimetric studies in air, while for poly(styrene-graft-acrylonitrile) there is no correlation. The difference is due to the kind of graft layer. When the graft layer is inorganic, it cannot burn and one would not expect a difference between nitrogen and air; this is the case for the graft copolymerization of sodium methacrylate. When the graft layer is largely carbonific, it must burn, and a correlation between studies in air and in an inert atmosphere may not be observed.

In order to understand why the presence of polystyrene should raise the temperature at which polyacrylonitrile begins to degrade, a detailed investigation of the degradation of polyacrylonitrile, PAN (Xue et al. 1997), was undertaken. It was realized that TGA/FTIR studies do not enable a complete understanding of a degradation pathway, and the solid residues which are produced in the course of the thermolysis were also examined. The solid residues were obtained at temperatures which corresponded to some change in the TGA curve or the appearance of the infrared spectrum of gaseous products and at other temperatures based upon these results. The solids were characterized both by elemental analysis and by infrared spectroscopy. From the analysis of the solid residues, one can determine that PAN undergoes a cyclization reaction without any mass loss and that the loss of ammonia occurs from this cyclized product. A complete degradation pathway has been mapped out for PAN based on these results. Cyclization occurs through the ends groups of the PAN chain, and this is then followed by tautomerization and aromatization with the elimination of ammonia and hydrogen.

The application of this degradation pathway to poly(styrene-graft-acrylonitrile) permits one to understand the stabilization of the acrylonitrile fragments in the graft copolymer. Degradation of PAN is initiated at the chain ends; the graft copolymer is prepared via an anionic route so the chain ends will be saturated and will not contain

functionalities, and thus the initiation of cyclization will be more difficult and the degradation will occur at higher temperatures.

The above leads one to believe that a material which gives an inorganic char should be more efficacious than an organic char. Accordingly, other monomers which have the potential for graft copolymerization have been examined; these include sodium styrenesulfonate, sodium vinylsulfonate, vinylsulfonic acid, and vinylphosphonic acid (Jiang et al. 1999). All of these materials show a significant volume expansion during degradation. This intumescent behavior may be of advantage for the stabilization of some polymers. One of the more significant observations in this study is that the TGA curve is essentially the same in either air or an inert atmosphere. As noted above, this is likely due to the production of a largely inorganic residue and lends further credence to the assertion made above on the nature of the residue.

14.6.1 Acrylonitrile–Butadiene–Styrene (ABS)

Acrylonitrile–butadiene–styrene terpolymer (ABS), as well as its fiber reinforced composites and blends, is a very important and widely used engineering material. The demand for and production of this family of materials increase year by year; however, there is only little work on the thermal degradation of ABS terpolymer (Dong et al. 2001; Luda di Cortemiglia et al. 1985; Suzuki and Wilkie 1995).

A thermal degradation process was performed upon ABS by heating ABS (200 mg) to 350 °C at the rate of 50 °C min^{-1} and keeping it at 350 °C (Dong et al. 2001). The evolution of butadiene commenced at 340 °C and styrene at 350 °C, while the evolution of monomeric acrylonitrile began at 400 °C. The evolution of volatile substances, butadiene and aromatics, e.g., styrene and benzene, is observed throughout the process. The residue dissolves in tetrahydrofuran (THF); no cross-linked product was formed throughout the whole process, but the resulting solution darkened as the reaction time increased.

The ABS residues were investigated by GPC; the average molecular weight of ABS decreases rapidly. The molecular weight distribution curve suggests that larger fragments of ABS chains are generated due to random scission. The low-molecular-weight peaks are attributed to a combination of monomers (butadiene, styrene) and small molecular weight oligomers (dimer, trimer) due to specific scission, i.e., end-chain scission. However, most of monomers volatilized, therefore the peaks for monomers in GPC curve are not strong but detectable. No evidence for repolymerization or cross-linking reaction was observed. Apparently, the nonvolatile degradation product contains monomers, oligomers (dimer, trimer), and larger fragments of ABS chain. The results suggest that both random and specific scissions occur during the degradation procedure of ABS at 350 °C.

From the infrared spectra of the nonvolatiles residues, one learns that aromatics increase and nitrile decreases and new bands corresponding to C=C and C=N appear (Fochler et al. 1985; Conley 1972) (C=C stretching, 1,590–1,670 cm^{-1}; C=N stretching, 1,580–1,620 cm^{-1}). Some nitrile groups are converted as a result

of the cyclization reaction. Furthermore, coloration as the reaction proceeds confirms that conjugation increases. Extensive work concerning thermal degradation behavior of polyacrylonitrile has demonstrated that new structures result from the polymerization or oligomerization of sequences of adjacent nitrile groups by a radical process (Grassie and Scott 1985; Coleman and Sivy 1981; Grassie and McGuchan 1970; Xue et al. 1997). However, acrylonitrile is only one component of ABS, so the conjugated nitrile sequence is of very short length and linked by unchanged segments, which is one of the reasons why the residues are soluble in THF. Some spectra exhibit absorption in the 1,680–1,750 cm^{-1} region. This group of peaks is generally assigned to a composite absorbance in which aldehydes (1,735 cm^{-1}) and ketones (1,720 cm^{-1}) are the main species formed during the early stages of degradation, but carboxylic acids (1,710 cm^{-1}) predominate in the later stages. Undoubtedly, oxygen in the air participated in the thermal degradation reaction at high temperature and led to the formation of the carbonyl groups. In fact, ABS is particularly sensitive to oxidation due to the presence of polybutadiene which is an oxidation sensitizer and leads to the formation of carboxylic acids (Grassie and Scott 1985). Additionally, it is reasonable that the formation of carboxylic acids can also result from the oxidation of some (isolated) nitrile groups.

Specific microstructural aspects of a polymer often facilitate thermal oxidation. In the case of ABS, hydrogen abstraction by oxygen is thermodynamically favorable due to the presence of tertiary substituted carbon atoms in the PB phase. The presence of sufficient thermal energy activates hydrogen abstraction to initiate oxidation and accelerates the overall process of degradation. After periods of exposure to heat and oxygen, the mechanical properties of ABS, impact strength and elongation to break, deteriorate as a consequence of polymer degradation, inducing premature failure (Wolkowicz and Gaggar 1981). The literature cites various explanations for the degradation of ABS due to heat aging. Several researchers state that thermo-oxidative degradation of ABS is confined to the rubbery PB phase, while others propose that property degradation is due to a combination of physical aging in the SAN phase and oxidation of the PB phase (Gesner 1965; Shimada and Kabuki 1968; Wyzgoski 1976; Salman 1991). Shimada and Kabuki (Shimada and Kabuki 1968) proposed that thermo-oxidative degradation occurs in the rubber phase of unstabilized ABS film, leading to the formation of hydroperoxides. Degradation was thought to occur by hydrogen abstraction from the carbon next to the *trans*-1,4 and *trans*-1,2 unsaturations in the PB phase, producing hydroperoxide radicals. The rate of this reaction was said to follow Arrhenius-type kinetics, with rate constants and reaction orders determined from the formation rate of carbonyl and hydroxyl products, as monitored by Fourier transform infrared (FTIR) spectroscopy. In contrast, Wyzgoski (Wyzgoski 1976) states that annealing ABS below the glass transition temperature (T_g) of its SAN phase (physical aging) produces molecular conformations which embrittle the polymer, significantly decreasing tensile elongation properties. Below its glass transition temperature, the SAN microstructure adopts an energetically unfavorable state driving towards equilibrium via molecular motion (Simha et al. 1984). The transformation between a glass and an amorphous polymer involves a kinetic

process of polymer molecular mobility. By providing thermal energy during the physical aging (annealing) process, a glass tends to equilibrate its polymer micro-structure (Wyzgoski 1976; Qi et al. 1993). When heating annealed polymers, as the temperature increases towards T_g, the rate of the kinetic process is retarded in comparison to unannealed polymers (Simha et al. 1984), and thus, in comparison, the rate of change in tan δ decreases as T_g is approached. On a macro level, this physical aging process increases stiffness and yield stress – in fact, yield stress is increased above craze stress such that brittle fracture is favored over yielding.

If one compares the degradation of ABS with that of its constituent parts (Suzuki and Wilkie 1995), one notes that the evolution of butadiene begins 50 °C higher for ABS than for PBD. Grafting SAN onto PBD stabilizes the PBD structure. Since SAN is directly bonded to butadiene units, the liberation of butadiene should be less facile. In SAN, the evolution of aromatics is first noted at 370 °C while in ABS, aromatics are first seen at lower temperature, 350 °C. These results are the same as reported by Camino (Luda di Cortemiglia et al. 1985). Apparently SAN is destabilized by the presence of butadiene. The formation of acrylonitrile is not reported by Camino; in SAN, it is first observed at 405 °C, and in ABS the evolution of acrylonitrile begins at about 400 °C. Since the thermocouple is not directly at the sample, these are considered to be the same temperature.

The degradation of ABS may be considered to be essentially the same as that of its constituents. It begins in the butadiene region of the polymer then proceeds to the SAN portion. The presence of SAN stabilizes the PBD while SAN is destabilized by the presence of PBD. Less acrylonitrile is obtained from ABS than from SAN. The amount of residue that is produced is directly related to the butadiene content of the sample.

The common flame retardants for ABS are halogen-containing compounds. Bromine-containing compounds such as decabromodiphenyl oxide (DB), tetrabro-mobisphenol (TBBPA), and 1,2-bis(2,4,6-tribromophenoxy)ethane (BTBPOE) have been regarded as very good flame retardants for ABS resin (Brebu et al. 2004).

The first halogenated flame retardant examined, aiming at the reduction of nanocomposite ignitability, was DB combined with antimony trioxide (AO). Metal oxides, such as AO, are added to halogenated compounds as synergists, since their interaction contributes to flame retardancy probably through the gener-ation of antimony halides (Mack 2004; Levchik and Weil 2000). The DB–AO system was employed by Hu and his colleagues (Wang et al. 2004) to prepare flame-retardant ABS/OMMT nanocomposites which could be rated by the UL94 protocol. Accordingly, the same type of clay (5 wt%) was well dispersed in ABS along with 15 wt% DB and 3 wt% AO using a twin-roll mill, and the fire properties of the resulting mixture were thoroughly studied. In contrast to neat ABS and its nanocomposite, the sample containing both the clay filler and the flame-retardant system obtained a V-0 rating and an increased LOI value (27.5 vol.%). Further-more, the performance in cone calorimeter was greatly improved, 78 % reduction in PHRR of the flame-retarded nanocomposite relative to pure ABS.

The challenge to enhance the thermal stability of ABS nanocomposites along with their resistance to ignite was faced by Ma et al. (Ma et al. 2006), substituting

DB with a brominated epoxy resin (BER). BER is a high molecular weight gas-phase flame retardant with 53 wt% bromine content based on tetrabromobisphenol A, which is commonly used in ABS or PC/ABS blends with AO as synergist. With small amount of the halogenated compound (12 wt% BER + 4wt%AO), the LOI of ABS containing 2 wt% clay increased from 20.5 to 31.4 vol.%, which is far beyond 24 vol.%, the LOI value usually required for a material to obtain a V-0 rating (Weil et al. 1992).). The combustion process and the synergistic effect of clay and BER–AO are presented schematically in Fig. 14.3. Similar to the OMMT–DB–AO system, the synergy between OMMT–BER–AO derived from silicates forming barriers that hindered BER pyrolysis and reactions between BER–AO at lower temperatures. Consequently, continuous flame retardancy in the vapor phase could be attained throughout combustion. Moreover, it was suggested that the alkylammonium cations residing in the interlayer decomposed, at around 200 °C, to fragments which could volatilize and expand clay layers promoting dispersion. Exfoliated structures, exhibiting better barrier properties than their intercalated analogues, could efficiently delay mass and heat transport. On the other hand, the reaction between the surfactant decomposition products and DB–AO, occurring at high temperatures, resulted in the formation of radical scavengers.

Although halogen-containing flame retardants show remarkable efficiency, they lead to environmental problems by generating great quantities of toxic and corrosive fumes during combustion which restricts their application. Organic phosphates, halogen-free flame retardants, are known to be good candidates to replace halogens. Among the various phosphorus-based flame retardants, triphenyl phosphate (TPP) (Kim et al. 2003; Lee et al. 2002; Costa et al. 1998) and tetra-2,6-dimethylphenyl resorcinol diphosphate (DMP-RDP) (Lee et al. 2003) are employed as the flame retardants for ABS resin with various novolac phenol resins (NP) and epoxy compounds (EP). TPP/NP, TPP/EP, and DMP-RDP/NP mixtures are effective in enhancing the thermal stability of ABS. TPP itself generates phosphoric acid during thermal degradation, and the reaction among phosphoric acids takes place and leads to pyrophosphoric acid, which acts as heat transfer barrier in the condensed phase (Green 2000; Hastie and McBee 1975). However, the evaporation temperatures of TPP and its analogues are lower than the processing temperature of ABS, which lead to TPP and its analogues partially decomposing/evaporating during processing (Costa et al. 1998). To utilize the mixtures of TPP with other polymers in order to overcome evaporation, mixtures of TPP with novolac phenols are the most intensively studied, and the evaporation of TPP is effectively suppressed due to the interaction between TPP and phenol, elevating the evaporation temperature of TPP (Costa et al. 1998; Fyfe et al. 1983; Chetan et al. 1993; Jackson and Conley 1964; Boscoletto et al. 1994). Polycondensates are produced from rearrangements of phenol formaldehyde in the main thermal degradation routes, and they act as char-forming agents and flame-retarding effects are observed (Costa et al. 1997; Jackson and Conley 1964; Morterra and Low 1985; Serio et al. 1991; Jha et al. 1989; Peters et al. 1980). On the other hand, the epoxide ring can be converted into carboxylic acid during thermal oxidation (Malinovski 1965). Consequently, enhancement in thermal stabilization may be expected if
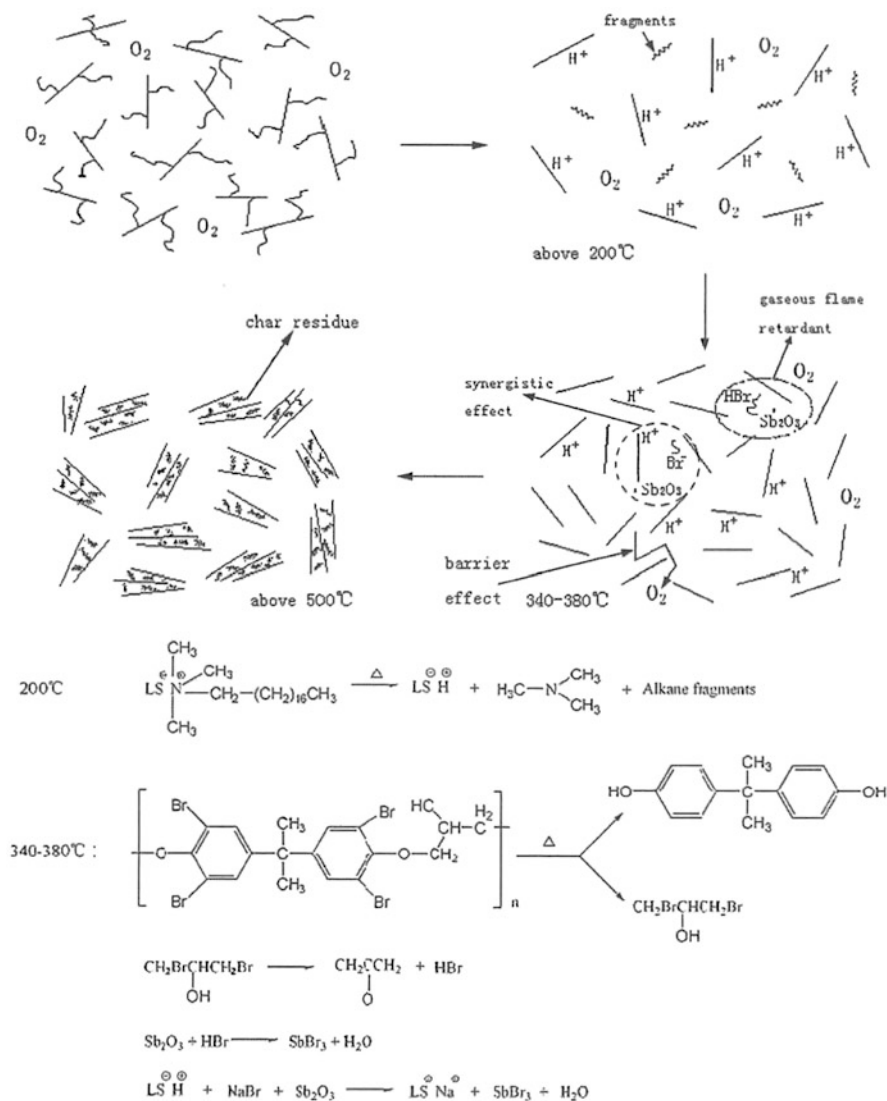
Fig. 14.3 Schematic presentation of the synergistic effects between clay and BER–AO incorporated in ABS (Reproduced with permission from Elsevier, from H. Ma, Z. Fang, L. Tong, Polym. Degrad. Stab. **91**, 1972 (2006))

reaction between TPP and the generated carboxylic acids can take place during thermal oxidation. Mixtures of TPP and epoxy were incorporated into ABS and investigated to determine if there is any synergistic effect of epoxy addition on the thermal stability of ABS (Lee et al. 2002). The initial weight loss observed at 200–400 °C, which is mainly caused by TPP evaporation, is greatly reduced for the

compound containing epoxy resin. TGA results (Lee et al. 2002) show that epoxy resin delays evaporation of TPP in the initial thermal degradation, and, during further thermal degradation, more thermally stable char is formed through some reaction, which is not clear at this time, between TPP and epoxy resin. However, the earlier results are enough to claim that epoxy can be a very efficient synergistic co-flame retardant for ABS. Furthermore, most phosphorus-based flame retardants used for ABS are liquids, which are not convenient to use in the manufacturing of flame-retarded products.

Intumescent flame retardants (IFR) that contains phosphorus are also used in halogen-free flame-retardant systems. Most reported IFRs are mixtures of the three ingredients, an acid source, a polyol, and a nitrogen-containing compound (Halpern et al. 1984). Since processing of ABS resin requires that the additives withstand temperatures in excess of 200 °C, the commonly used intumescent system, ammonium polyphosphate, pentaerythritol, and melamine, which do not have sufficient thermal stability, cannot be incorporated into ABS resin under normal processing conditions; they are usually used in polyolefins.

A phosphorous–nitrogen-containing intumescent flame retardant, poly (diaminodiphenyl methane spirocyclic pentaerythritol bisphosphonate) (PDSPB), was synthesized and investigated by TGA and DTG. Only one step decomposition around 350–500 °C is found for pure ABS under nitrogen, leaving negligible char above 500 °C. Both T_{onset} and T_{max} in TGA curve of PDSPB in N_2 are lower than those of ABS resin, which means PDSPB degrades early. For ABS/PDSPB samples, T_{onset} of PDSPB-containing samples is lower than that of the pristine material, due to the earlier degradation of PDSPB; however, T_{max} of the major degradation step increases for the PDSPB-containing samples, indicating the thermal-enhancing effect of PDSPB. The amount of residue improves greatly with the increase of PDSPB addition.

TGA and DTG thermograms showed that the addition of PDSPB reduces the initial degradation temperature but enhances the thermal stability at high temperature. There must be a difference between the initial degradation temperature of the polymer and the intumescent flame retardant, since phosphoric and polyphosphoric acids have to be produced in the beginning of combustion to accelerate esterification and carbonization (but the T_{onset} of flame retardants should not be lower than the processing temperature) (Wang 2005).

The LOI value of ABS resin is 19.1 indicating its inherent flammability. As the amount of PDSPB increases, the LOI increases, indicating that the flame retardancy of the treated ABS composites is improved; at the same time, there is less tendency for dripping. PDSPB is an effective flame retardant for ABS resin.

Pure ABS resin burns rapidly after ignition and a sharp PHRR appears at 930 kW m^{-2}. In the case of the ABS/PDSPB system, both the PHRR and average HRR are reduced significantly. The PHRR is reduced by 52 % and 58 % for ABS/20 % PDSPB and ABS/30 % PDSPB samples, respectively, relative to pure ABS resin. The THR is reduced by 25 % and 33 % for the two PDSPB contained samples. The reduction of PHRR and THR becomes smaller as the PDSPB concentration increases. The reduction of PHRR indicates that a cohesive char

layer is formed during combustion which acts as an insulating barrier between the fire and ABS resin. Meanwhile, the ASEA and AMLR are also reduced. However, the ignition time of ABS/PDSPB samples is lower than that of pure ABS. This may be due to the earlier decomposition of PDSPB, producing some small volatile molecules. PDSPB cannot only reduce the HRR but also can suppress the emission of smoke.

A novel intumescent flame-retardant (IFR) system composed of a phosphorous–nitrogen (PSPTR)-containing spiro triazine structure and phenol formaldehyde resin (PF) was investigated by Hu et al. (Hu et al. 2012).

PSPTR shows four weight loss stages. The first stage is due to the scission of the methoxy group around 222 °C, while the second at around 290 °C is due to the pyrolysis of the P–N bond. The third is attributed to the decomposition of P–O–C and the triazine structure at around 337 °C (Chen and Jiao 2008). Meanwhile, a new substance, 2,4-diamino-1,3,5-triazine polyphosphate, is formed in this step. N-2-(4-amino-1,3,5-triazin-2-yl)-1,3,5-triazine-2,4-diamine polyphosphonate and ammonium polyphosphate groups could be formed from 2,4-diamino-1,3,5-triazine polyphosphate at high temperature. The last stage is attributed to the cracking of N-2-(4-amino-1,3,5-triazin-2-yl)-1,3,5-triazine-2,4-diamine polyphosphonate forming a complex P–N mixture at around 506 °C. Two simple thermal degradation processes are found in PF. The first weight loss stage is due to the condensation reaction at around 360 °C and the formation of diphenyl ether linkages (Costa et al. 1997). The diphenyl ether linkages will generate a polyaromatic system at about 450 °C. The second stage can be assigned to the thermal degradation of the polyaromatic system at around 548 °C.

What is more, the IFR has a high-residue char of 50.2 wt% at 700 °C and three weight loss stages. The first degradation stage occurs at 200−420 °C, which is the most important stage for intumescent char formation. The formation of polyphosphoric acid could catalyze PF to form diphenyl ether linkages. The second weight loss stage around 420–510 °C can be attributed to the thermal decomposition of the diphenyl ether linkages which leads to the formation of the polyaromatic system at high temperature. The third step around 546 °C is attributed to the thermal degradation of the polyaromatic system. In addition, a new DTG peak is observed at 420–510 °C, which does not appear in the DTG curve of either PSPTR or PF. It is thought that polyphosphoric acid, formed from PSPTR, can react with PF to form more diphenyl ether linkages during the heating process. The thermal decomposition of a large amount of diphenyl ether linkages at 420−510 °C will help in the formation of the char which can improve the flame retardancy of ABS. The catalytic char formation is also the reason for the observed synergistic flame-retardant action of PSPTR and PF. Furthermore, pure ABS starts to decompose at 383 °C and has a negligible char (1.6 wt%) at 700 °C. The onsets of degradation (5 wt% mass loss) of the PSPTR and PF occur at about 249 °C and 216 °C, which are lower than pure ABS resin, but higher residues, 40.3 wt% and 42.6 wt% at 700 °C, respectively, are obtained. The addition of IFR decreases the onset of degradation but enhances the thermal stability at high temperature. The char yield of the composite can reach 16.4 wt% at 700 °C. This could be the result of the

thermal degradation of PSPTR and PF at the lower temperature and formation of intact char layer which can protect the remaining polymer from heat and limit the access of oxygen to the polymer.

It was found that a possible synergistic chemical interaction may occur between PSPTR and PF during the thermal process. In order to investigate this further, the calculated and experimental TG curves of IFR system (PSPTR/PF = 1:1, wt %) were compared. It is unambiguously found that the char residue yield is higher than the calculated value above 346 °C and an improvement of 8.8 wt% at 700 °C is noted, indicating PF plays a synergistic role in the thermal degradation and acts as carbon source to participate in the formation of char. This result is favorable for the protection of the inner polymeric material from fire and oxygen.

14.6.1.1 Polyamides

Polyamides are a very attractive class of engineering polymers, used for numerous engineering applications because of their excellent tensile properties, chemical and abrasion resistance, high melting point, and fatigue resistance. However, polyamides are very notch sensitive and brittle at low temperatures (Keskkula and Paul 1995; Flexman 1979; Gayman 1994). Blends of polyamide with rubber have been extensively studied in order to obtain new materials with good impact properties (Van Duin and Borggreve 1997; Wu 1987, 1988; Borggreve et al. 1987, 1989; Oshinski et al. 1992, 1996; Cimmino et al. 1984, 1986; D'Orazio et al. 1988; Modic and Pottick 1993; Lu et al. 1995). Some requirements to achieve toughening include (i) an appropriate range of rubber particle size and interparticle distance and (ii) a uniform distribution of the rubber particles. Both requisites can be obtained by controlling the level of interfacial adhesion between the phases (Lu et al. 1995). To fulfill those requirements, existing rubbers can be chemically and/or physically modified prior to blending with polyamide. Maleated rubbers are a successful example of these modifications. The maleic anhydride (MA) groups can react with polyamide amine end group and form a graft copolymer at the rubber–matrix interface, reducing interfacial tension and retarding particle coalescence during mixing (Scheme 14.4). The resulting particles have suitable sizes uniformly distributed for effective toughening (Van Duin and Borggreve 1997; Wu 1987, 1988; Borggreve et al. 1987, 1989).

For non-functionalized rubbers, addition of a compatibilizer can be an alternative to improve toughness (Oshinski et al. 1992, 1996; Cimmino et al. 1984, 1986; D'Orazio et al. 1988; Modic and Pottick 1993; Lu et al. 1995), because it can react with one phase and physically interact with the other improving the adhesion between the rubber and polyamide phases.

Investigation of an effective method to compatibilize rubber–polyamide blends has been carried out (Carone et al. 2000). The rubber particles are formed from natural rubber (NR) and the matrix is polyamide 6. Compatibilization occurs by adding MA to the rubber in a roll mill at room temperature, prior to blending with polyamide 6. During processing at high temperature (240 °C), two different reactions can occur (Subramaniam 1986; Pinazzi et al. 1962, 1963; Nakayama 1973; Le Bras and Compagnon 1947). The first is the grafting of the MA

Maleic Anhydride (MA)
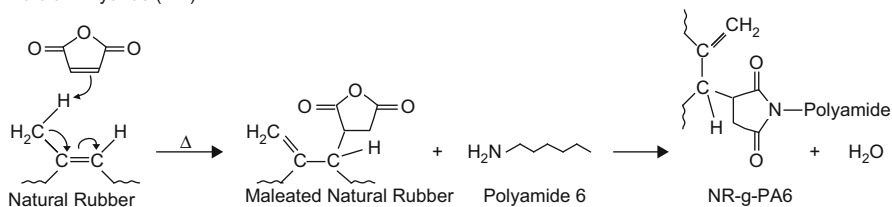
Scheme 14.4 Possible reactions between MA, NR, and PA6

onto NR chains as shown in Scheme 14.4. This reaction occurs only at temperatures above 200 °C, even in the absence of any free-radical initiator. Addition of peroxides increases the efficiency; however, a high degree of reticulation can be obtained (Subramaniam 1986). The other possible reaction is the formation of the graft copolymer between NR and polyamide 6 (NR-g-PA6), through the reaction between already maleated NR and polyamide. The question of interest in this work is whether this graft copolymer (NR-g-PA6) was generated during processing.

All of the polyamide-containing materials showed a weight loss of approximately 3 wt% at around 100 °C due to loss of water, and MA-containing materials showed weight loss due to free MA anhydride sublimation at approximately 200 °C. Natural rubber (with or without MA) showed weight loss due to degradation at around 400 °C, whereas all polyamide-containing materials showed weight loss at higher temperatures (around 500 °C).

It is interesting to note that after polymer degradation (above 500 °C), only MA-containing materials showed residual material up to 800 °C. This evidence indicates that reactions take place during processing and cause the formation of both gel and graft copolymer. Gel material is formed during processing of NR with MA as can be seen in the literature (Subramaniam 1986; Pinazzi et al. 1962, 1963; Nakayama 1973; Le Bras and Compagnon 1947). In the blend of polyamide 6/(NR 3 wt% MA), rubber reticulation also takes place; however, the 15 wt% rubber blend showed the same residual mass as neat NR with 3 wt% MA. This allows one to conclude that besides rubber cross-linking, the NR-g-PA6 graft copolymer is also formed, since the same amount of residual material was obtained.

It was shown that incorporating APP in PA6 enables the fire properties of interest to be obtained. Moreover, using PA6 as a carbonization agent in association with APP was shown to be successful in polypropylene (PP) (Bourbigot and Le Bras 2000). However, the stability of the APP/PA6 blends obtained by direct mixing of APP in melted PA6 is low: migration of the mineral (Le Bras et al. 2000) occurs during solidification of the melt and over time in the solid. The use of an interfacial agent is required. EVA compounds, which are known to be very efficient interfacial agents (Davis et al. 2001; Liu and Baker 1992), have been used as compatibilizers in the intumescent PP/APP/PA6 system. It was shown using oxygen consumption calorimetry that using EVA19 as a compatibilizer in the PP/APP/PA6 intumescent system gives fire properties of interest (Almeras et al. 2002a).

In addition, using the cone calorimeter a sharp reduction in the mass loss rate is demonstrated compared with pure PP (Almeras et al. 2002b). The virgin polymer degrades rapidly within 150 s whereas the PP/APP/PA6/EVA19 intumescent blend shows an initially reduced mass loss rate, which rapidly decreases, corresponding to the development of the intumescent structure. After 300 s, the second step of degradation is observed, which corresponds to the degradation of the protective shield.

From TGA in both air and nitrogen, PP degradation involves the scission of the polymer chain and occurs between 250 °C and 400 °C in air and 300 °C and 440 °C in nitrogen.

The mechanisms of thermal and thermo-oxidative degradations of PA6 were investigated by Dabrowski et al. (Dabrowski et al. 2000). In air, the major stage of weight loss occurs between 310 °C and 440 °C and is assigned to the main-chain breakdown, releasing water, ammonia, and carbon oxides. Above 460 °C, a charred residue (aromatic structure) stable up to 800 °C is formed. In nitrogen, the major stage of weight loss (about 90 wt%) occurs above 400 °C and may be assigned to the main-chain breakdown releasing water, ammonia, carbon monoxide and dioxide, and hydrocarbon fragments (Bourbigot et al. 1993), leading to the formation of a charred residue (about 3 wt%).

The thermal and thermo-oxidative degradations of APP have been reported (Hornsby et al. 1996; Camino et al. 1984; Zhang et al. 1993); they are similar and consist of two steps. The degradation begins around 300 °C with the elimination of NH_3, leading to the formation of a highly cross-linked polyphosphoric acid, whereas the second step above 550 °C corresponds to polyphosphoric acid evaporation and/or dehydration to P_4O_{10} which sublimes.

Incorporating APP in PA6 leads to the destabilization of PA6. Indeed the (APP/PA6) blend begins to degrade at a temperature 50 °C lower than virgin PA6. This can be explained by the attack induced by the phosphoric acid species (formed from the degradation of APP; Camino et al. 1985) on alkylamide bonds of PA6, which leads to the formation of a phosphate ester and primary amide chain ends and then elimination of ε-caprolactam (Levchik et al. 1992). A residue (about 35 wt% in air and about 25 wt% in nitrogen) with a low degradation rate between 400 °C and 500 °C in nitrogen and between 400 °C and 550 °C in air is then formed. Its degradation in air around 600 °C (in nitrogen around 550 °C) leads to the formation of a stable 2 wt% residue (10 wt% in nitrogen).

The thermo-oxidative degradation and the pyrolysis of the intumescent blend PP/PA6/APP/EVA19 occur in a three-step process. In air, the first step occurs at about 250 °C, and a carbonaceous material is formed in the temperature range 300–430 °C. Its degradation rate is low in the temperature range 410–540 °C. Finally, it degrades rapidly in the higher temperature range to give a residue about 4 wt% at 800 °C.

In nitrogen, the first stage (about 20 wt%) loss occurs at about 300 °C. Then the major weight loss takes place leading, above 500 °C, to the formation of a carbonaceous residue with a low degradation rate.

Oxygen plays a major role in the degradation process of the intumescent blend (as already put forward for the APP/PA6 blend). In particular, it must be noted that an oxidative atmosphere favors the charring process, increasing the residual weight after the second step from about 17 to 30 wt%. It is assumed that the two first steps correspond to the reaction between APP and PA6 and to the PP degradation. However, the order in which these steps occur is controversial.

14.7   Conclusions

Polymer blends, like all organic polymers, will undergo degradation by a variety of processes, including thermal degradation, photolytic degradation, biodegradation, and mechanical degradation. In this chapter, only thermal degradation and its close relative, fire retardancy, are covered. The starting point for the degradation of a blend is always the degradation of the constituent parts of the blend. In some cases, the components have an unchanged thermal stability, while in other cases they may be either more or less stable. One cannot predict how the stability may change, and it also can depend upon the relative amounts.

14.8   Cross-References to This Book

▶ Reactive Compatibilization
▶ Morphology of Polymer Blends
▶ Physical Aging of Polymer Blends
▶ Polymer Blends: Introduction
▶ Properties and Performance of Polymer Blends

Notations and Abbreviations

ABS Acrylonitrile–butadiene–styrene terpolymer
AMLR Average mass loss rate
AO Antimony oxide
ASEA Average specific extinction area
ATH Aluminum trihydroxide – $Al(OH)_3$
BER Brominated epoxy resin
BTBPOE 1,2-bis(2,4,6-tribromophenoxy)ethane
CPE Chlorinated polyethylene
DB Decabromodiphenyl ether
DMP-RDP Tetra-2,6-dimethylphenyl resorcinol diphosphate
DSC Differential scanning calorimetry

DTA Differential thermal analysis
EHC Effective heat of combustion
EP Epoxy resin
EVA Ethylene–vinyl acetate copolymer
FR Fire retardant
FRCM Fire-retardant clay material
GPC Gel permeation chromatography
HDPE High-density PE
HRR Heat release rate
IFR Intumescent fire retardant
IR Infrared spectroscopy
LDPE Low-density PE
LLDPE Linear low-density PE
LOI Limiting oxygen index
MH Magnesium hydroxide – $Mg(OH)_2$
MMT Montmorillonite
NC Nanoclay
NMR Nuclear magnetic resonance
NP Novolac phenol resins
OMMT Organically modified MMT
PA Polyamide
PAN Polyacrylonitrile
PB Polybutene-1
PC Polycarbonate
PE Polyethylene
PHRR Peak heat release rate
PMMA Poly(methyl methacrylate)
PMP Polymethylpentene
PP Polypropylene
PPO Poly(phenylene oxide)
PVC Poly(vinyl chloride)
RDP Resorcinol diphosphate
SAN Styrene–acrylonitrile copolymer
SEM Scanning electron microscopy
TBBPA Tetrabromobisphenol A
TDT Thermal decomposition temperature
TG Thermogravimetric analysis
TGA Thermogravimetric analysis
THR Total heat released
t_{ig} Time to ignition
TPP Triphenyl phosphate
TVA Thermal volatilization analysis
UHMWPE Ultrahigh-molecular-weight PE
ULDPE Ultralow-density PE

References

Z. Ahmad, F. Mahmood, Polym. J. **28**, 951 (1996)

Z. Ahmad, N.A. Al-Awadi, F. Al-Sagheer, Polym. Degr. Stab. **92**, 1025 (2007)

Z. Ahmad, N.A. Al-Awadi, F. Al-Sagheer, Polym. Degr. Stab **93**, 456 (2008)

N.S. Allen, M. Edge, M. Rodriguez, C.M. Liauw, E. Fontan, Polym. Degrad. Stab. **68**(3), 363 (2000)

X. Almeras, F. Dabrowski, M. Le Bras, R. Delobel, S. Bourbigot, G. Marosi, P. Anna, Polym. Degrad. Stab **77**, 315 (2002a)

X. Almeras, F. Dabrowski, M. Le Bras, F. Poutch, S. Bourbigot, G. Marosi, Polym. Degrad. Stab **77**, 305 (2002b)

K. Aouachria, N. Belhaneche-Bensemra, Polym. Degrad. Stab. **91**, 504 (2006)

V. Babrauskas, in *Heat Release in Fires*, ed. by V. Babrauskas, S. Grayson (Elsevier Applied Science, London, 1992)

G. Beyer, Fire Mater. **25**, 193 (2001)

N.C. Billingham, O.J. Hoad, F. Chenard, D.J. Whiteman, Macromol. Symp. **115**, 204 (1997)

H. Bockhorn, A. Hornung, U. Hornung, J. Anal. Appl. Pyrolysis **50**, 77 (1999)

J.G. Bonner, P.S. Hope, in *Polymer Blends and Alloys*, ed. by M.J. Folkes, P.S. Hope (Chapman and Hall, London, 1993)

R.J.M. Borggreve, R.J. Gaymans, J. Schuijer, J.F. Ingen Housz, Polymer **28**, 1489 (1987)

R.J.M. Borggreve, R.J. Gaymans, H.M. Enchenwald, Polymer **30**, 78 (1989)

A.B.. Boscoletto, M. Checchin, M. Tavan, G. Camino, L. Costa, M.P. Luda, J. Appl. Polym. Sci. **53**, 121 (1994)

S. Bourbigot, R. Delobel, M. Le Bras, D. Normand, J. Chim. Phys. **90**, 1909 (1993)

S. Bourbigot, M. Le Bras, R. Leeuwendal, K.K. Shen, D. Schubert, Polym. Degrad. Stab. **64**, 419 (1999)

S. Bourbigot, M. Le Bras, S. Bourbigot, M. Le Bras, in *International Plastics Flammability Handbook*, ed. by J. Troitzsch, S. Bourbigot, M. Le Bras (Hanser, New York, 2000)

D. Braun, Pure Appl. Chem. **53**, 549 (1981)

D. Braun, B. Böhringer, Makromol. Chem. Macromol. Symp. **29**, 73 (1989)

D. Braun, B. Böhringer, N.E.M. Fisher, Angew. Makromol. Chem **216**, 1 (1994)

M. Brebu, T. Bhaskai, K. Murai, A. Muto, Y. Sakata, M.A. Uddin, Chemosphere **56**(1), 433 (2004)

J.A. Brydson, *Plastic Materials* (Newnes-Butterworths, London, 1975)

G. Camino, L. Costa, L. Trossarrelli, Polym. Degrad. Stab. **6**, 243 (1984)

G. Camino, L. Costa, L. Trossarelli, Polym. Degrad. Stab. **12**, 203 (1985)

G. Camino, R. Sgobbi, A. Zaopo, S. Colombier, C. Scelza, Fire Mater. **24**, 85 (2000)

E. Carone Jr., U. Kopcak, M.C. Goncalves, S.P. Nunes, Polymer **41**, 5929 (2000)

J.M. Cervantes, J.V. Cauich-Rodriguez, H. Vazquez-Torres, L.F. Garfias-Mesias, D.R. Paul, Thermochim. Acta. **457**, 92 (2007)

X.L. Chen, C.M. Jiao, Polym. Degrad. Stab. **93**(12), 2222 (2008)

C.H. Chen, R.D. Wesson, J.R. Collier, Y.W. Lo, J. Appl. Polym. Sci. **58**, 1087 (1995)

M.S. Chetan, R.S. Ghadro, C.R. Rajan, V.G. Gunjikar, J. Ponrathnam, J. Appl. Polym. Sci. **50**, 685 (1993)

O. Chiantore, L. Trosarelli, M. Lazzari, Polymer **39**, 2777 (1998)

S. Cimmino, L. D'Orazio, R. Greco, G. Maglio, M. Malinconico, C. Mancarella, E. Martuscelli, R. Palumbo, G. Ragosta, Polym. Eng. Sci. **24**, 49 (1984)

S. Cimmino, F. Coppola, L. D'Orazio, R. Greco, G. Maglio, M. Malinconico, C. Mancarella, E. Martuscelli, G. Ragosta, Polymer **27**, 1874 (1986)

M.M. Coleman, G.T. Sivy, Carbon **19**, 123 (1981)

R.T. Conley, *Infrared Spectroscopy*, 2nd edn. (Allyn and Bacon, Boston, 1972)

L. Costa, L. Rossi di Montelera, G. Camino, E.D. Weil, E.M. Pearce, Polym. Degrad. Stab **56**, 23 (1997)

L. Costa, L.R.D. Montelera, G. Camino, E.D. Weil, E.M. Pearce, J. Appl. Polym. Sci. **68**(7), 1067 (1998)

C.F. Cullis, M.M. Hirschler, *The Combustion of Organic Polymers* (Clarendon, Oxford, 1981)

L. D'Orazio, C. Mancarella, E. Martuscelli, J. Mater. Sci. **33**, 161 (1988)

F. Dabrowski, S. Bourbigot, R. Delobel, M. Le Bras, Eur. Polym. J. **36**, 273 (2000)

R.D. Davis, W.L. Jarrett, L.J. Mathias, Polymer **42**, 2621 (2001)

R.D. Deanin, W.L. Chuang, J. Vinyl Technol. **9**, 60 (1987)

D. Dong, S. Tasaka, S. Aikawa, S. Kamiya, N. Inagaki, Y. Inoue, Polym. Degrad. Stab. **73**, 319 (2001)

T. Faravelli, M. Pinciroli, F. Pisano, J. Anal. Appl. Pyrolysis **60**, 103 (2001)

E.A. Flexman Jr., Polym. Eng. Sci. **19**, 654 (1979)

J.H. Flynn, L.A. Wall, J. Therm. Anal. **27**, 95 (1983)

H.S. Fochler, J.R. Mooney, L.E. Ball, R.D. Boyer, J.G. Grasseli, Spectrochim. Acta **41 A**, 271 (1985)

M.J. Folkes, P.S. Hope (eds.), *Polymer Blends and Alloys* (Chapman and Hall, London, 1993)

D.Q. Fox, R.B. Allen, D.Q. Fox, R.B. Allen, D.Q. Fox, R.B. Allen, in *High Performance Polymers and Composites*, ed. by J.I. Kroschwitz (Wiley, New York, 1991)

D.J. Frankowski, M.D. Capracotta, J.D. Martin, S.A. Khan, R.J. Spontak, Chem. Mater. **19**, 2757 (2007)

H.L. Friedman, J. Polym. Sci. **6**, 183 (1965)

C.A. Fyfe, M.S. Mckinnon, A. Rudin, W.J. Tchir, Macromolecules **16**, 1216 (1983)

M. Gahleitner, Prog. Polym. Sci. **26**, 895 (2001)

R.J. Gayman, in *Rubber Toughened Engineering Plastics*, ed. by A.A. Collyer (Chapman and Hall, London, 1994)

B.D. Gesner, J. Appl. Polym. Sci. **9**, 3701 (1965)

S.H. Goh, Thermochim. Acta. **215**, 291 (1993)

N. Grassie, R. McGuchan, Eur. Polym. J. **6**, 1277 (1970)

N. Grassie, G. Scott, *Polymer Degradation and Stabilization* (University Press, Cambridge, 1985)

J. Green, in *Fire Retardancy of Polymeric Materials*, ed. by A.F. Grand, C.A. Wilkie (Marcel Dekker, New York, 2000)

Y. Halpern, D.M. Mott, R.H. Nlswander, Ind. Eng. Chem. Prod. Res. Dev. **23**(2), 233 (1984)

J.W. Hastie, C.L. McBee, National Bureau of Standards IR (1975)

P. Hornsby, J. Wang, R. Rothon, G. Jackson, G. Wilkinson, K. Cossick, Polym. Degrad. Stab. **51**, 235 (1996)

X. Hu, Y. Guo, L. Chen, X. Wang, L. Li, Y. Wang, Polym. Degrad. Stab. **97**, 1772 (2012)

W.M. Jackson, R.T. Conley, J. Appl. Polym. Sci. **8**, 2163 (1964)

V. Jha, A.K. Banthia, A. Paul, J. Therm. Anal. **35**, 1229 (1989)

D.D. Jiang, Q. Yao, M.A. McKinney, C.A. Wilkie, Polym. Degrad. Stab. **63**, 423 (1999)

A. Jimenez, J. Appl. Polym. Sci. **50**(9), 1565 (1993)

T. Kashiwagi, A. Inaba, J.E. Brown, K. Hatada, T. Kitayama, E. Masuda, Macromolecules **19**, 2160 (1986)

T. Kashiwagi, E. Grulke, J. Hilding, K. Groth, R. Harris, K. Butler, J. Shields, S. Kharchenko, J. Douglas, Polymer **45**, 4227 (2004a)

T. Kashiwagi, R.H. Harris Jr., X. Zhang, R.M. Briber, B.H. Cipriano, S.R. Raghavan, W.H. Awad, J.R. Shields, Polymer **45**, 881 (2004b)

H. Keskkula, D.R. Paul, in *Nylon Plastics Handbook*, ed. by M.I. Kohan (Hanser, Munich, 1995)

W. Khan, Z. Ahmad, Polym. Degrad. Stab. **53**, 243 (1996)

J. Kim, K. Lee, J. Bae, J. Yang, S. Hong, Polym. Degrad. Stab. **79**(1), 201 (2003)

I. Klarić, N. Stipanelov-Vrandečić, U. Roje, J. App. Polym. Sci. **78**, 166 (2000)

C. Koning, M. van Duin, C. Pagnulle, R. Jerome, Prog. Polym. Sci. **23**, 707 (1998)

T. Kovačić, I. Klarić, A. Nardelli, B. Barić, Polym. Degrad. Stab. **40**, 91 (1993)

T.M. Kruse, O.S. Woo, H.W. Wong, S.S. Khan, L.J. Broadbelt, Macromolecules **35**, 7830 (2002)

F.P. La Mantia, in *Handbook of Polymer Degradation*, ed. by S. Halim Hamid, M.B. Amin, A.G. Maadhah (Marcel Dekker, New York, 1992)

F.P. La Mantia, Angew. Makromolek. Chem. **216**, 45 (1994)

A.G.M. Last, J. Polym. Sci. **39**, 543 (1959)

J. Le Bras, P. Compagnon, Rubber Chem. Technol. **20**, 938 (1947)

M. Le Bras, S. Bourbigot, E. Felix, F. Pouille, C. Siat, M. Traisnel, Polymer **41**, 5283 (2000)

K. Lee, J. Kim, J. Bae, J. Yang, S. Hong, H.K. Kim, Polymer **43**(8), 2249 (2002)

K. Lee, K. Yoon, J. Kim, J. Bae, J. Yang, S. Hong, Polym. Degrad. Stab. **81**(1), 173 (2003)

A. Leszczynska, J. Njuguna, K. Pielichowski, J.R. Banerjee, Thermochim. Acta. **454**, 1 (2007)

S.V. Levchik, E.D. Weil, Polym. Int. **49**, 1033 (2000)

S.V. Levchik, L. Costa, G. Camino, Polym. Degrad. Stab. **36**, 229 (1992)

N.C. Liu, W.E. Baker, Adv. Polym. Tech. **11**, 249 (1992)

P.P. Lizymol, S. Thomas, M. Jayabalan, Polym. Int. **44**, 23 (1997)

M. Lu, H. Keskkula, D.R. Paul, J. Appl. Polym. Sci. **58**, 1175 (1995)

M.P. Luda di Cortemiglia, G. Camino, L. Costa, M. Guaita, Thermochim. Acta. **93**, 187 (1985)

R.R. Lyon, M.L. Janssens, *Polymer Flammability* (Office of Aviation Research, Washington, DC, 2005)

H. Ma, Z. Fang, L. Tong, Polym. Degrad. Stab. **91**, 1972 (2006)

A.G. Mack, Flame retardants, halogenated, in *Kirk-Othmer Encyclopedia of Chemical Technology*, ed. by A. Seidel, vol. 11 (Wiley, Hoboken, 2004)

F. Mahmood, R. Quadeer, J. Therm. Anal. **42**, 1167 (1994)

M.F. Malinovski, *Epoxies and Their Derivatives* (Israel Programme for Scientific Translations, Jerusalem, 1965)

T. Manos, I.Y. Yusof, N. Papayannakos, N.H. Gangas, Ind. Eng. Chem. Res. **40**, 2220 (2001)

L.E. Manring, Macromolecules **21**, 528 (1988)

L.E. Manring, Macromolecules **24**, 3304 (1991)

L.E. Manring, D.Y. Sogah, G.M. Cohen, Macromolecules **22**, 4654 (1989)

W. Manzoor, S.M. Yousaf, Z. Ahmad, Polym. Degrad. Stab. **51**, 295 (1996)

A. Marongiu, T. Faravelli, G. Bozzano, M. Dente, E.J. Ranzi, Anal. Appl. Pyro. **70**, 519 (2003)

I.C. McNeil, in *Developments in Polymer Degradation*, ed. by N. Grassie (Elsevier, London, 1977)

I.C. McNeil, in *Comprehensive Polymer Science*, ed. by G.C. Eastmond, A. Ledwith, S. Russo, P. Sigwalt, vol. 6 (Pergamon, Oxford, 1989)

I.C. McNeil, J.G. Gorman, Polym. Degrad. Stab. **40**, 205 (1991)

I.C. McNeill, in *Developments in Polymer Degradation*, ed. by N. Grassie, vol. 1 (Applied Science Publishers, London, 1977)

I.C. McNeill, M.A.J. Mohammed, Eur. Polym. J. **8**, 975 (1972)

I.C. McNeill, N. Grassie, J.N.R. Samson, A. Jamieson, T.J. Straiton, Macromol. Sci. Part A **12**, 503 (1978)

I.C. McNeill, L. Memeta, W.J. Cole, Polym. Degrad. Stab. **49**, 181 (1995)

M.J. Modic, L.A. Pottick, Polym. Eng. Sci. **33**, 819 (1993)

C. Morterra, M.J.D. Low, Carbon **23**, 525 (1985)

E.J. Moscala, D.W. Lee, Polym. Degrad. Stab. **25**, 11 (1989)

T.T. Nagi, B. Ivan, B. Tyi, T. Kelen, F. Tudos, Polym. Bull. **3**(11), 1436 (1980)

Y. Nakayama, British Patent 1,332,050 (Kansai Paint Co.), 1973

H. Ohtani, T. Yuyama, S. Tsuge, B. Plage, H.R. Schulten, Eur. Polym. J. **26**(8), 893 (1990)

A.J. Oshinski, H. Keskkula, D.R. Paul, Polymer **33**, 268 (1992)

A.J. Oshinski, H. Keskkula, D.R. Paul, Polymer **37**, 4891 (1996)

E.D. Owen (ed.), *Degradation and Stabilization of PVC* (Elsevier, New York, 1984)

T. Ozawa, Bull. Chem. Soc. Jpn. **38**, 1881 (1965)

E.N. Peters, A.B.. Furtek, D.L. Steinberk, D.T. Kwiatkowski, J. Fire Retard. Chem. **7**, 69 (1980)

C. Pinazzi, R. Cheritat, R. Pautrat, Rev. Gen. Caoultch. **39**, 1951 (1962)

C. Pinazzi, J.C. Danjard, R. Pautrat, Rubber Chem. Technol. **36**, 282 (1963)

J. Pospisil, P.P. Klemchuk, in *Oxidation Inhibition in Organic Materials*, ed. by J. Pospisil, P.P. Klemchuk (CRC Press, Boca Raton, 1990)

J. Pospisil, Z. Horak, Z. Krulis, S. Nešpurek, Macromol. Symp. **135**, 247 (1998)

J. Pospisil, Z. Horak, Z. Krulis, S. Nešpurek, S. Kuroda, Polym. Degrad. Stab. **65**, 405 (1999)

Prospect Dow CPE Resins for Impact Modification of Rigid PVC. Dow Chemical 1993.

Z.N. Qi, Z.H. Wan, Y.P. Chen, Polym. Test. **12**, 185 (1993)

S.R. Salman, Polym. Plastics Techn. Eng. **30**(4), 343 (1991)

R. Scaffaro, M.C. Mistretta, F.P. La Mantia, Polym. Degrad. Stab. **93**, 1267 (2008)

B. Schartel, T.R. Hull, Fire Mater. **31**, 327 (2007)

M.A. Serio, S. Charpenay, R. Bassilakis, P.R. Solomon, ACS Div. Fuel Chem. **36**, 66 (1991)

R.K. Shah, D.R. Paul, Polymer **47**, 4075 (2006)

J. Shimada, K. Kabuki, J. Appl. Polym. Sci. **12**, 665 (1968)

R. Simha, J.G. Curro, R.E. Robertson, Polym. Eng. Sci. **24**(14), 1071 (1984)

N. Stipanelov-Vrandečić, I. Klarić, U. Roje, Polym. Degrad. Stab. **74**, 203 (2001)

S. Stoeva, K. Gurova, M. Zagorcheva, Polym. Degrad. Stab. **67**, 117 (2000)

A. Subramaniam, in *Encyclopedia of Polymer Science and Engineering*, ed. by H.F. Mark, N.M. Bikales, C.G. Overberger, G. Menges, J.I. Kroschwitz (Wiley, New York, 1986)

M. Suzuki, C.A. Wilkie, Polym. Deg. Stab. **47**, 217 (1995)

M. Swistek, G. Ngyen, D.J. Nicole, Anal. Appl. Pyrolysis **37**, 15 (1996)

G. Tartaglione, D. Tabuani, G. Camino, M. Moisio, Compos. Sci. Technol. **68**, 451 (2008)

N.L. Thomas, Plast. Rub. Compos. Proc. Appl. **19**(5), 263 (1993)

L.A. Utracki, *Polymer Alloys and Blends-Thermodynamics and Rheology* (Hanser, New York, 1989)

L.A. Utracki (ed.), *Polymer Blends Handbook* (Chem(Tec Publ), Toronto, 1997)

M. Van Duin, R.J.M. Borggreve, in *Reactive Modifiers for Polymers*, ed. by S. Al-Malaika (Blackie Academic and Professional, London, 1997)

I.K. Varma, K.K. Sharma, Angew. Makromol. Chem. **79**(1), 147 (2003)

J.Q. Wang (ed.), *Foundation and Application of Non-halogen Flame Retardant Polymer* (Science Publisher, Beijing, 2005)

S. Wang, Y. Hu, R. Zong, Y. Tang, Z. Chen, W. Fan, Appl. Clay Sci. **25**, 49 (2004)

E.D. Weil, M.M. Hirschler, N.G. Patel, S. Shaki, Fire Mater. **16**, 159 (1992)

C.A. Wilkie, Polym. Degrad. Stab. **66**, 301 (1999)

C.A. Wilkie, Recent advances in fire retardancy of polymer-clay nanocomposites, in *Proceedings of the 13th Annual BCC Conference on Flame Retardancy*, Stanford, 2002

M.D. Wolkowicz, S.K. Gaggar, Polym. Eng. Sci. **21**(9), 571 (1981)

S. Wu, Polym. Engng. Sci. **27**, 335 (1987)

S.J. Wu, Appl. Polym. Sci. **35**, 549 (1988)

J. Wypych, Polym. Networks Blends **2**, 53 (1992)

M.G. Wyzgoski, Polym. Eng. Sci. **16**(4), 265 (1976)

T.J. Xue, C.A. Wilkie, J. Polym. Sci., Part A: Polym. Chem **35**, 1275 (1997a)

T.J. Xue, C.A. Wilkie, Polym. Degrad. Stab **56**, 109 (1997b)

T.J. Xue, M.A. McKinney, C.A. Wilkie, Polym. Degrad. Stab. **58**, 193 (1997)

V.M. Yanborisov, K.S. Minsker, G.E. Zaikov, Plast. Massy. **3**, 33 (2003)

Q. Yao, C.A. Wilkie, J. Vinyl Addit. Technol. **7**, 26 (2001)

M. Zanetti, G. Camino, R. Thomann, R. Mulhaupt, Polymer **42**, 4501 (2001)

J. Zhang, R. Horrocks, M.E. Hall, Fire Mater. **18**, 307 (1993)

J. Zhang, J. Hereid, M. Hagen, D. Bakirtzis, M.A. Delichatsios, A. Fina, A. Casrovinci, G. Camino, F. Samyn, S. Bourbigot, Fire Safety J. **44**, 504 (2009)

Part III

Applications

Applications of Polymer Blends

<div style="text-align:right">

15

</div>

Lloyd A. Goettler and James J. Scobbo

Contents

Lloyd A. Goettler: retired

L.A. Goettler (✉)
Department of Polymer Engineering, The University of Akron, Akron, OH, USA
e-mail: lagoett@uakron.edu

J.J. Scobbo
SABIC-Innovative Plastics, Mount Vernon, IN, USA
e-mail: jim.scobbo@sabic-ip.com

Abstract

This chapter builds on the information contained on the same subject in Chap. 13 of the first edition of the *Polymer Blends Handbook* by providing an overview of current applications of polymer blends and alloys with an outlook towards developing areas. A dual approach employed herein to portray the field covers both a description of polymer blend technologies directed toward solving application issues related to societal megatrends, as well as the generic performance/ testing specifications required for products in broad areas of commerce amenable to polymer blend applications.

15.1 Introduction

The blending and alloying of polymers is an important component of approaches for providing materials to address sustainable solutions to global needs, such as those associated with population growth and aging, urbanization, climate change, and energy demand. For example, according to Roland Hingmann of BASF Advanced Materials and Systems Research in an address to the Polymer Engineering Department of The University of Akron on March 20, 2013, the earth's current population of seven billion will increase to nine billion by the year 2050, 50 % more energy will be needed by 2030, 67 % of the world population will live in cities by 2025, and there will be 1.2 billion cars on the roads by only 2020. These megatrends open up opportunities for new polymeric products to address needs for lightweight vehicles, renewable and biodegradable materials in packaging and other applications, energy efficiency, safety, lifestyle comforts, medical instruments and supplies, and components for the food industry.

Polymers are ideal materials to meet developing societal needs due to their broad performance profiles, economical shape forming ability and generally low density. They thus can provide valuable properties in a cost-effective manner. The blending and alloying of various types of polymers, along with the compounding in of other ingredients such as fillers, plasticizers, stabilizers, colorants and reinforcements, extend their reach by providing a means to economically generate polymer systems with broader performance spectra than possible from individual polymer components.

While some commercial blends are marketed for wide-ranging applications deriving from their generally beneficial mechanical, electrical, thermal, chemical, or flow properties, as the technology matures, it focuses more on new blends and alloys having unique or critical properties or property mixes for specific applications. Other wide-ranging applications comprise the major subject matter of this chapter.

The chapter is organized by two complementary views of polymer blend applications. In Part 1, the focus is placed on describing important and emerging polymer blend technologies and their fit in applications that help solve issues related to current megatrends. In Part 2, the focus is placed on specific application areas, where requirements are described independent of blend system. This "outside-in" approach from market needs to performance requirements not only will be applicable to polymer blends on the market today but can aid in the design of new blend systems, which may incorporate the technologies highlighted in Part 1.

It is hoped that the approach outlined above provides a fresh view on polymer blend applications that builds on, and complements the presentation on the same subject in Chap. 13 of the first edition of the Polymer Blends Handbook.

15.2   Part 1: Polymer Blend Developments for Developing Opportunities

There are some newer application areas and polymer blend products targeted to fit those new opportunities. The latter include such combinations as PVC and PS blended with PP, HDPE, and each other; metallocene-polymerized nanoscale blends of polyolefins with more polar polymer partners; and, for high-temperature/high-performance applications, PPS blended with PSF, PEI, and polyamides as well as blends incorporating poly(aryl ketones), polyimides, and poly(amide-imides) (Thomas et al. 2006).

While the polyketone terpolymer derived from carbon monoxide, ethylene, and propylene is economical with some attractive properties, such as heat, chemical, permeation, and abrasion resistance, it suffers from low-impact strength. One cost-effective approach to overcoming this shortcoming and upgrading its performance profile for automotive applications such as wheel covers, wheel caps, fuel filter necks, fuel tanks, fuel tubes, center fascias, door handles, roof rack covers, gears, junction boxes, connectors, and seat backs, as well as electric/electronic components and durable household items involves blending with polyamides including a rubber modification (Lee et al. 2013).

Isotactic polypropylene can be blended with its random copolymers to enhance toughness. This can be accomplished without loss of stiffness and impact strength by nucleating beta form crystallization for applications such as in cables, pipes, and fittings (Machl et al. 2012).

Transparent blends having good properties can be made from suitable formulations containing sufficiently compatible components that the phase domains remain too small to scatter light (Hong et al. 2012).

The superior properties of semi-crystalline thermoplastics make them desirable for high-performance applications. While they can be suitably molded, their low elongational viscosity at forming temperature makes for difficult sheet processing such as by thermoforming. This limitation can be overcome by blending with other polymers, such as ABS, or by inducing cross-linking, e.g., by exposure to high-energy radiation (Seefried et al. 2012).

Improved impact strength with lower melt viscosity for better processability can be obtained by blending a thermoplastic polyester such as PTT with an ethylene copolymer. Including a nucleating agent increases crystallinity and impact strength (Talkowski et al. 2012).

Co-continuous blend structures find industrial application in selective, reverse osmosis and ion exchange membranes requiring specific functional properties. For example, PA/polyester blends could be appropriate for hydrophilic microporous separation and filtration membranes when the phases form a co-continuous structure with domain sizes ranging from 0.01 to 10.0 μm (Harrats and Makhlef 2006a).

15.2.1 Polymer Blends from Renewable Resources for Biodegradable Applications

The usage of naturally sourced polymers has increased in recent years in response to environmental threats, such as expanding landfills and carbon dioxide emissions, along with the rising prices of hydrocarbon raw materials. Three types of polymers considered to be derived from renewable resources are truly natural polymers (e.g., natural rubber, starch, protein, and cellulose), polymers synthesized from natural monomers (e.g., polylactic acid), and those produced by microbial fermentation (the PHA polyhydroxyalkanoates). The limiting properties of some natural polymers having a generally hydrophilic nature (including brittleness, narrow processing window, low heat resistance, and rapid degradation rate especially in wet environments) and the generally high cost of biosynthesis make blending of these with commodity synthetic polymers or other types of renewably resourced polymers attractive. It is preferable to limit blend components to biodegradable polymers in order to preserve full biodegradability. For example, 1,4-transpolyisoprene can be blended with gelatinized starch for food packaging or biomedical applications. Natural rubber can be dispersed in a blend with thermoplastic starch to reduce brittleness. Blends of cellulose and water-soluble starch can be formulated over a range of properties for applications in bone cements, drug delivery carriers, and tissue scaffolds (Yu et al. 2006).

Degradable aliphatic polyesters include both PLA and the PHAs. PLA, being biodegradable and compostable with low toxicity and high mechanical properties, is becoming a strong alternative to conventional plastic packaging materials in specialized markets. But it has insufficient thermal stability for many potential applications and is high in cost. Biodegradation in landfills can be enhanced by blending such biodegradable polyesters with starch and a transesterification catalyst (Changping 2012).

Poly(3-hydroxybutyrate) (PHB) as well as the more general class of PHAs produced by bacterial fermentation, being both biodegradable and biocompatible, are ideally suitable as materials for tissue engineering. The PHA biodegradable polyesters, however, tend to be brittle and thermally unstable in their neat state. Blending with other biopolymers can alleviate these problems along with reducing production cost. The PLA and PHB polymers can be blended together to provide a range of physical properties with improved processability. PLA can also be blended with starch to reduce its cost while maintaining biodegradable properties. Since these materials are thermodynamically incompatible due to the PLA being relatively hydrophobic and the natural starch polymer hydrophilic, various additives are required as compatibilizers.

Chitosan, a natural polymer derived from chitin, has application in edible coatings or films for packaging foodstuffs, but its use is limited by its high sensitivity to moisture. Its ability to form a water barrier can be improved by blending with a more hydrophobic polymer also derived from natural resources, such as PLA. Blends of starch with PCL can be reinforced with nanoscale platelets derived from smectic clay to significantly increase film ductility and barrier properties.

Despite the likely loss of some biodegradability, "green" materials of growing interest for environmental protection are nevertheless blended with synthetic polymers to manipulate their degradation rate and boost their relatively poor mechanical, physical, and formability properties. The shortcomings of the common bio-renewable resin polylactic acid can be addressed through blending of its D- and L-isomers along with poly(ethylene–alkyl acrylate–glycidyl methacrylate) terpolymer to improve heat resistance, impact strength, and tensile strength for applications in automotive parts (Hong and Han 2013). A balanced PLA/PC alloy (compatibilized blend) is still environmentally friendly with improved appearance, weldability, impact strength, and heat resistance over neat PLA (Chung et al. 2012). Similarly to the methyl methacrylate-butadiene-styrene terpolymer used for PC toughening, PLA can be blended with soft polyolefins or with a bio-based impact modifier to improve its toughness, flexibility, and processability. Enhanced mechanical strength and heat resistance may be achievable by blending with harder polyolefin resins like PP for applications in vehicles and building construction, as well as for films and heat-shrinkable labels (Ikeda and Taniguchi 2012; Hong and Han 2012). Compatibilization would be required.

Bio-based PHAs (polyhydroxyalkanoates) show improved mechanical and environmental performance over PVC. Since some versions may be miscible with PVC, it is possible to produce blends that have superior plasticization, impact strength, and processability. Acting as a plasticizer in the PVC, the PHA provides low migration and extractability, volatile loss, and staining. Toughness can exceed that afforded by traditional MBS core/shell impact modifiers without compromising transparency or UV stability (Anon 2013a).

Synthetic and natural biodegradable polymers may be difficult to process, as the high required molding temperature requirements may lead to degradation. Blending with a pliable synthetic resin as a continuous phase allows forming under the more gentle conditions characteristic of the additive without losing the character of the renewable component (Wang et al. 2012). Thus, PLA blended with PP can be extrusion cast or injection molded (Li et al. 2012).

15.2.2 Electrically Conducting Polymer Blends

Expensive conductive polymers can be blended with a commodity polymer major phase to produce a more economical and easily processed blend. The materials may be either both thermoplastic (e.g., PES), or one may be a thermoset (e.g., a phenolic). Another approach employs blending a rubber phase (EPR or urethane) with a commodity thermoplastic resin like PP, LDPE, or even polyesters or polyamides, to form a co-continuous phase structure in which incorporated carbon black resides either at the interface or within one of the phases. A similar approach, incorporating, for example, PC and PET along with an impact modifier, could be employed to produce conductive automotive body parts that are amenable to electrostatic painting (Harrats and Makhilef 2006b).

The increased electrical conductivity achieved by incorporating carbon nanotubes (CNTs) into a polymer would find application, for example, in the cathodes of lithium-ion batteries. Improved static charge dissipation could be achieved at lower CNT loadings than those conventionally used for carbon black in electrical component enclosures, thus avoiding detrimental filler effects on other properties. Furthermore, confining the incorporation to one phase, probably that having a continuous morphology, in an incompatible blend would concentrate the inclusions, leading to more efficient usage. Carbon black present at the interface in PS/PE blends provides a percolation threshold at 0.4 wt% (Thomas et al. 2006).

15.2.3 Molecular Composites

Blends of liquid-crystalline or other rigid-rod polymers, such as polybenzoxazoles, usually in a non-thermotropic high-performance plastic matrix, comprise this category of self-reinforced materials if they are molecularly dispersed in the host polymer. The dispersed network polymer would act as a reinforcement to enhance the load-bearing properties of the continuous polymer, which would in turn produce toughness by relieving stresses and could even provide a self-healing capability. A larger microfibrillar network phase structure produced, for example, when LCPs are blended with PPS would also provide synergistic properties suitable for automotive applications (Harrats and Makhilef 2006c).

15.2.4 Hard Phase–Soft Phase Polymer Blends: Thermoplastic Elastomers

Thermoplastic elastomers (TPEs) combine the physical properties of vulcanized rubber with the ease and economy of conventional thermoplastic processing. They are also well suited to reprocessing and recycling and minimize toxicity issues. Many types of thermoplastic elastomers are polymer blends comprising a thermoplastic continuous phase in combination with a discontinuous vulcanized or unvulcanized elastomeric phase, which in the latter case could also be co-continuous.

Global demand for all TPEs is forecasted to grow 6.3 % annually to 5.6 million metric tons by the year 2015. Since many applications (around 30 %) of these materials fall in the automotive sector, where they are replacing metal, conventional rubber and, for trim and interior applications, traditional thermoplastics like PVC and ABS, this improved growth rate can be attributed to recovery of motor vehicle production in the western world as well as its continuing emphasis on weight reduction. There is about a 60 % weight reduction for each metal part replaced with a polymer or its composite. Projected fuel savings due to reduced weight according to new fuel standards in year 2025 would amount to $1.7 trillion. New applications supplanting more traditional materials are also prevalent, for example, in appliances and housewares, especially in developing countries. Entirely new applications are appearing in medical products and packaging, though

these are currently of small volume. Some traditional application areas, such as footwear, however, are beginning to mature. Over the longer term, TPE demand will shift from the West to developing regions around the globe (Anon 2011).

The wide range of hardness properties achievable through blend compounding allows a wealth of specific applications across a wide spectrum of industries, including (Rader et al. 1986):

Appliances: boots, bumpers, casters, couplings, diaphragms, feet, gaskets, gears, grommets, handles, hose, seals, tubing, and wheels

Underhood automotive: air ducts, bushings, cable covers, hose, protective boots, shock mounts, tubing

Building/construction: door seals, drain seals, glazing seals, cover bases, pipe gaskets, plumbing fixtures, roof flashing, weather stripping

Electronic and electrical: battery blankets, flexible cord, coil cord, wire/cable insulation and jacketing, pad membranes, mining cable, motor shaft mounts, splicing tape, terminal plugs, transformer housings

Machinery and tools: bumpers, casters, rollers, welding hose connectors, welding rod handles, wheels, step pads

Medical devices: closures, gaskets, stoppers, plunger tips

Sporting goods: bat grips, rifle stock cushions, scuba diving equipment, ski pole handles.

"Super-TPVs" are replacing higher-cost thermoset rubbers in underhood, appliance, and industrial molded parts subject to higher temperatures and aggressive environments, for example, truck air-brake hoses and ignition-coil boots. Examples include cross-linked silicone rubber enveloped by a polyamide or TPU continuous phase. These can find application in consumer goods such as communication and medical devices that require high-temperature resistance, low-temperature flexibility, abrasion resistance, weathering resistance, colorability, and soft touch along with easy processability and bondability. A moderate performing cousin of conventional EPDM–PP TPVs at only moderately increased cost uses a styrenic rubber (SBR or hydrogenated styrenic block copolymer) for improved compression set, oil resistance, and adhesion that postures these materials for overmolded grips, seals, bellows, tubing, and diaphragms. A modified ethylene–acrylate rubber in combination with a polyamide or copolyester matrix exhibits superior oil resistance at elevated temperature, as needed in CVJ and spark plug boots as well as other underhood seals, hose, and ducting where temperatures are increasing due to stricter electrical and vapor-emission standards (Leaversuch 2004).

High-performance thermoplastic vulcanizates (TPVs), such as a dynamically vulcanized polyacrylate thermoset elastomer particulate dispersed in a continuous thermoplastic polyamide matrix, have more recently been finding greater under-the-hood automotive applications due to their improved heat and oil resistance. The presence of polar components would also allow adhesion to condensation polymer in-mold substrates to form soft overlays. This technology allows reduction of part complexity in previously multiple-component pieces, for example, high-temperature air intake and turbo engine ducts, by forming soft overmolded cuffs on a polyamide or copolyester core (Harber et al. 2005). Polyamide-bondable TPV

alloys now available in various colors over a range of hardness grades are said to offer thermal resistance up to 135 °C, excellent chemical resistance and better compression set than comparable styrenic-based TPEs (Anon 2013b).

Film and sheeting applications for soft TPV grades include surgical drapes, dental dams, and elastic tapes for wound care in the medical and healthcare arena; waist band tapes for clothing; and elastic geomembranes in building and construction (Mapleston 2007).

Hard grades of thermoplastic elastomers such as thermoplastic vulcanizates find applications as living hinges (useful in electronic products, toys, tools, and cases).

15.2.5 Reinforced Blends

15.2.5.1 Fiber-Reinforced Hard–Hard Polymer Blends

A synergistic interaction between the properties generated by polymer blending and polymer reinforcement with either micro- or nanoscale inclusions can be realized by introducing the reinforcing agents into a preformed blend of two hard plastics or into one or both of the components of the blend prior to the blending operation. The resulting reinforced blend shows higher toughness than either the unreinforced blend or fiber reinforcement of one of the plastic components acting alone, due to enhanced cavitation followed by local shear deformation and ductility.

A prime example is the glass fiber reinforcement of blends of ABS with notch-sensitive polymers such as polyamide or polycarbonate (Nair et al. 1997). The toughness of the reinforced blend can be greater than that of a corresponding polymer composite formed either with polymer of the blend or even with them in the neat state, as evidenced by the critical J-integral toughness parameter. Even the unreinforced blend can be tougher than either neat polymer component, but unlike the case for the reinforced blend, there could be a region of embrittlement. In that range, the reinforced blend would be tougher than its corresponding unreinforced composition. Such materials could find use in structural applications where additional toughness is required without loss of rigidity.

15.2.5.2 Nanocomposite Blends

Blends can also be reinforced with nanoscale inclusions, primarily for stiffening, as elongation to break usually suffers. However, that does not have to be the case. The identity of the phase containing the nanoparticle as well as its continuity in the blend are of prime importance to property development in the blend, as found for PP–EPDM blends reinforced with montmorillonite clay (Lee and Goettler 2004).

Besides mechanical performance, the introduction of nanoclay to the proper location and with the proper phase morphology can also be utilized to enhance the permeation properties of polymer blends in barrier film applications. The high aspect ratio and platelike shape of impermeable montmorillonite inclusions allow them to disrupt the diffusion of permeants through a polymer, thereby increasing the tortuosity of the path through the film and reducing its permeability. The component polymers comprising blends are often selected for reasons other than

their inherent permeability, for example, for mechanical integrity or sealability. In the case of a polymer blend, the nanoclay can be situated at a higher concentration in one phase of a selected polymer pair to maximize the overall barrier resistance of the blend. For example, it could augment the phase of least permeation resistance in order to diminish its deleterious effect on the overall permeability of the blend.

Adding nanoclay to the polar polyamide phase of a PA/PE blend will reduce its water vapor transmission rate significantly, even when the polyamide phase is discontinuous. Such nanoscale reinforcement can also operate by changing the phase morphology of the blend, through changes to the relative viscosity levels of the two polymer phases. The polyamide phase of the above example could be changed from being co-continuous with the polyethylene to becoming discontinuous, where its high water vapor permeability would be far less deleterious, through inclusion of nanoclay (Bhuva and Goettler 2014).

15.2.6 Recycling of Post-consumer and Postindustrial Waste

Recycling is critical to extending the life cycle of polymeric products and diminishing environmental impact by reducing waste, thereby allowing cost reduction. Automotive vehicles are a prime example of increased recycling requirements that envelop the entire package. These include polymer components, which must either all be of similar nature, separated, or compatibilized to form useful alloys.

Another, though older, example of alloying in recycling is compounding post-consumer nylon carpet (including the backing) with coupling agent to produce a compatibilized blend containing major components of nylon and polypropylene and having competitive properties to polypropylene. Its mechanical performance could be upgraded by adding fiberglass and/or rubber to allow partial nylon or polypropylene replacement in automotive applications (Hagberg and Dickerson 1996).

Polystyrene, including foams, can be recycled without degradation by blending with virgin polystyrene to improve tensile strength. Alternately, styrene monomer can be added and polymerized in situ, resulting in improved melt flow (Grossetete et al. 2012).

Nanoscale inclusions, such as nanoclays and nanopowders, could upgrade if not compatibilize mixed plastic post-consumer and postindustrial recycle streams to improve their processability, mechanical properties, thermal resistance, and stability.

15.3   Part 2: Application Areas for Polymer Blends

15.3.1 Healthcare

15.3.1.1 Recent Trends
The healthcare industry has seen rapid expansion in recent years with growth in virtually all segments. These segments include a breadth of applications from IV therapy, drug delivery, and surgical instruments to monitoring, diagnostics, and medical lighting. Within these applications, some trends include a need for higher

autoclave temperatures as well as enhanced compatibility with proteins and blood. Additionally, large part processing is becoming more critical. The regulatory and compliance arena is seeing constant change to stricter standards.

15.3.1.2 Performance Requirements

As autoclave temperatures increase, so do the needs for materials to be used in a wide variety of sterilization environments including gamma, E-beam, and ethylene oxide sterilization. In terms of more general physical properties, color and clarity are critical for visual identification of contents, and for this reason, blend systems which are typically opaque, are not a fit. However, requirements for impact resistance, extreme temperature resistance (both high and low), and good dimensional stability and creep resistance are frequently applicable to blends. Secondary operations and processing are also important and include capability for ultrasonic welding, adhesive and solvent compatibility, high flow for complex part geometries, and thin-wall moldability.

Chemical compatibility/resistance is of particular importance to medical applications. Disinfectants represent one class of chemicals that includes Betadine™, glutaraldehyde-based disinfectants, sodium hypochlorite solution (5 %), ethyl alcohol, isopropyl alcohol, hydrogen peroxide (3 %), and ammonium chloride-based disinfectant. Additionally, resistance to methyl ethyl ketone, saline solution, lipid-based compounds, and fatty acids is important.

15.3.1.3 Regulatory and Compliance Requirements

Generally speaking, applications that contain power supplies or that are electrical in nature require flame retardance in compliance with Underwriters Laboratory standards and test protocols that include UL-94 HB, V2, V1, V0, 5VA, and 5VB ratings. Environmental standards require no bromine or chlorine in accordance with TCO-99 and Blue Angel.

Biocompatibility involves adherence to ISO 10993 "Biological Evaluation of Medical Devices" or USP Class VI standards, hemocompatibility, platelet retention, and reduced protein binding. Moreover, food contact standards are typically applied to healthcare applications. The US Food and Drug Administration oversees adherence to the standards of the US Food, Drug, and Cosmetics Act. In Europe, the European Union Directive 2002/72/EC is applicable.

End-of-use requirements have evolved and the healthcare industry is not an exception to the newer standards. These include Waste Electrical and Electronic Equipment (WEEE) Directive 1002/96/EC that is in place in the European Union. In this standard, OEMs are required to be responsible for collection and treatment of materials at end of life.

15.3.1.4 Specific Applications

One of the more significant segments in the healthcare industry involves the handling and management of fluids. This segment includes blood handling during surgery, general blood collection and blood oxygenation. The segment also includes membrane and filter applications such as leukocyte filters, arterial filters, and kidney dialysis. In addition to blood handling, intravenous (IV) and

gastrointestinal fluid delivery systems often involve bottles, bags, pumps, and tubes. Blood handling typically requires clarity and transparency, but applications such as IV fluid handling are more applicable to blend systems that have impact resistance and chemical resistance. Polyester blends and PC/ABS blends have seen penetration into some of these applications.

There are additional applications with similar requirements which can be a fit for PPE/PS blends. Clinical diagnostics and labware applications such as connectors, fittings, and filtration housings require radiation/autoclave sterilizability and chemical resistance.

One of the application segments that is commonly associated with polymer blends is that of surgical instruments. As surgical techniques have proliferated, so has the need for increasingly specialized instruments. The drive toward minimally invasive surgeries has created the need for miniaturization, which in turn drives the need for smaller components with sufficient strength and durability. Access devices that are appropriate for polymer blends include trocars, retractors, and speculums. Hand instruments include staplers and forceps. Thermal ablation and electrosurgical techniques require powered instruments.

Drug delivery is a growing area of healthcare technology. Needleless injection techniques and inhalation are specific modes of delivery that are fueling this growth, driven largely by elevated requirements for patient comfort. As with blood handling applications, biocompatibility and sterilizability are key requirements. However, impact and wear resistance are also important. Some of the blends used in these applications include PC/PBT and PC/ABS.

Sleep therapy and respiratory care represent an additional class of applications in healthcare. Respirators, ventilators, and positive-pressure devices to allow airways to function properly are specific examples and require biocompatibilty. Respiratory masks and valves require chemical resistance and impact performance. PC-based blends are commonly used in applications in this space.

There are also many healthcare applications that have a more indirect connection to the patient. Medical trays that are used to transport, store, and sterilize surgical instruments require autoclave sterilizability, chemical resistance, and biocompatibility. Additionally, good mechanical performance such as high-impact resistance, as well as colorability, is required. PPE/PS blends are frequently positioned for these applications where this combination of properties is needed. Polymer blends provide other significant benefit in these applications. Many other materials in use such as metals or fiberglass have a significant deficiency relative to polymer blends since repeated use can cause creation of metallic, resin, and glass particles.

Monitoring, imaging, and medical lighting represent a broad set of applications that can range from relatively small component parts in blood glucose meter and pulse oximeters to large luminaire housings in a surgical theater and stationary equipment such as CT, MRI, and PET imaging machines. These applications require flame retardance and may require EMI/RFI shielding. Resistance to cleaners and chemicals may also be required. Impact and high-temperature performance are additional needs for lighting. Blend systems positioned for these applications include PPE/PS, PC/ABS, and ASA.

A series of thermoplastic vulcanizate elastomers available in a wide range of hardness values and displaying low compression set, high fatigue resistance, and long flex life along with good high-temperature and abrasion resistance are targeted for medical applications like syringe stoppers, peristaltic tubes, collection and drainage tubes, caps, plugs, seals, handles, valves, diaphragms, and vial gaskets. Their advantage is high purity and resilience with easy processability, offering high design freedom and recyclability. They are certified to pass ISO 10993-5 and are non-hygroscopic. Their lower oxygen permeability imparted by dynamic vulcanzation makes them well suited for vial seals and gaskets. They can be sterilized in steam, autoclave, or gamma radiation processes (Anon 2013c).

In tissue engineering, two biodegradable polymers can be blended to form a scaffold with a co-continuous structure, perhaps in the presence of an active drug to be dispensed by controlled release into the body. For example, hydroxyapatite can be combined with PLA and PMMA via melt extrusion processing to form a tissue scaffold or alternately be used in prosthetics. Blends of PP with SBR or SEBS can also be formulated to achieve the necessary body weight support and movement for the latter application (Harrats and Makhilef 2006a).

15.3.2 Aerospace

15.3.2.1 Recent Trends
Trends in the aerospace industry parallel those in the overall transportation-related market segments. Lighter weight for decreased fuel consumption and enhanced safety are trends that immediately come to mind. In addition to these, reduced cabin noise, and reduction of maintenance/extension of lifetime are important as well.

15.3.2.2 Performance Requirements
One of the most critical attributes of polymer blends in the aerospace segment is related to how the material performs in a fire. An industry standard test utilizes the Ohio State University heat release methodology as described in ASTM E906 as well as FAR25.853. In this test, the rate of heat and smoke release are calculated per unit area of exposed surface. Heat release is dependent on the mode of ignition, gas phase, or point ignition. This is a common test in the development of new materials. Smoke release is determined by the measured change in transmitted light caused by combustion products. Flammability can be evaluated for vertical burn performance according to Boeing standard BSS7330 and $60°$ flammability according to FAR25.853. In addition to flame and smoke generation behavior, the potential generation of toxic components is also a concern. Some tested for toxicity, which include BSS7239, Airbus standard ABD0031, and Bombardier standard SMP800C. Commonly measured combustion by-products include HF, HCl, NOx, SO2, HCN, and CO. Halogen-free flame retardant technology is an additional attribute that is desired for these applications.

15.3.2.3 Specific Applications

Traditional injection molding allows significant design flexibility and can allow for part consolidation and simplicity in aerospace interiors. Applications including arm and foot rests, overhead bins, tray arms, and structural supports all require weight reduction relative to traditional materials; high modulus and strength; aesthetic appeal; as well as flame, smoke, and toxicity compliance. Applications for lavatories and galleys require many of the attributes already mentioned but add requirements for chemical resistance and low moisture uptake.

There are many applications for opaque materials based on thermoforming. These include signage, window covers, seat components including seat backs, and semi-structural panels. Film products include safety labels commonly seen on seat backs.

Melt-spun or solvent-spun fibers can be converted into fabrics for use in textile applications. These can include wall coverings, kick-panels, and seating.

Foams, honeycomb structures, and composites are all viable routes to utilizing polymer blends to reduce weight. Many of the structural components in aircraft utilize composite and/or honeycomb structures as a way to reduce weight, reduce noise, and provide design flexibility relative to thermoset pre-preg-based systems.

15.3.3 Consumer Electronics

15.3.3.1 Recent Trends

Several trends are clearly evident in consumer electronics. Firstly, miniaturization continues to drive much of the portable electronics segment. As size and weight decrease for mobile phones, for example, the need for higher flow blends that maintain stiffness and ductility are important. Furthermore, as the industry moves to higher power processors, batteries with greater capacity, and the consolidation of functions into a single device, the need for higher-temperature capability becomes more critical. Aesthetics have become an element of branding, where specific colors and/or effects have become part of the OEM's marketing efforts.

In addition to the trends mentioned above, wireless technology is expanding. Radio frequency interference and electromagnetic interference attenuation are becoming more important attributes. This can be achieved through conductive filler technology. Electrostatic discharge behavior can also be achieved.

Radio frequency identification (RFID) is growing rapidly in multiple end use segments such as transportation, security, and asset/inventory management. Polymer blends can be used in the housings, internals, and plastic films containing passive tags.

Flame retardance is another critical attribute. As the industry continues to evolve, Underwriters Laboratory recognition continues to be essential. In addition to this, China Compulsory Compliance (CCC) is becoming more important due to the growth of the consumer electronics industry in the Pacific region. The China Quality Certification Center is responsible for defining products to meet CCC as well as managing the process to apply for registration.

15.3.3.2 Specific Applications

The display industry has evolved considerably over recent years. Just over a decade ago, most displays were based on cathode ray tube (CRT) technology. Liquid-crystal display (LCD) technology was just starting to displace CRTs and was based on cold-cathode fluorescent (CCFL) tube light sources. Plasma displays were also competing strongly, but have since taken a minor role relative to LCD. The LCD technology has also evolved, with light emitting diode (LED) light sources replacing CCFL in the interest of lower-energy usage, lower environmental impact, and reduced heat generation.

For display enclosures, WEEE/RoHS (Restriction of Hazardous Substance) standards have driven blend formulations to avoid flame retardants that contain chlorine and/or bromine. Given the move toward flat panel displays, the overall amount of plastic components has decreased relative to CRTs for similar sized displays. However, as the size of the average display increased, so does the opportunity for polymer blends in bezels, stands, and display backs.

Bezels are demanding in terms of aesthetic performance. High gloss, scratch resistance, and molded-in colors to replace painted surfaces are important. Also, films for in-mold decoration (IMD) can be used. For display backs, high strength and modulus are needed to replace metals, as well as EMI shielding. Speaker components benefit from sound and vibration absorption and moveable stands benefit from abrasion and wear resistance. Within the display, the deflection yoke application of CRTs has been supplanted by LCD components, such as the back-light frame, which typically requires high flow for thin-wall molding.

Beyond the display space, there are several other consumer segments that are seeing the trends noted earlier. For portable devices like mobile phones, the housings needed allow design flexibility such that the phones can be smaller and lighter which means thin-wall moldability is important while maintaining good surface aesthetics. ABS/polycarbonate blends impart lightweight and impact/chemical resistance along with good processing for molded cases incorporating portable electronics such as cell phones. Soft elastoplastics can also be molded against and bonded to the hard blend for gripping and aesthetics.

In laptop and desktop computers, internal components need good heat dissipation and static/shock protection. For housings, good aesthetics and mechanical robustness to drops and impacts are key. Home entertainment and networking are similar to the above. For printers and scanners, moving parts are involved, so for gear applications, wear resistance and lubricity are critical.

15.3.4 Electrical

15.3.4.1 Recent Trends

Electrical applications are experiencing increasingly strict standards. European standards such as EN, which are maintained largely by the European Committee for Standardization (CEN), are replacing other national standards as well as IEC (International Electrotechnical Commission).

Environmental trends are having an impact on electrical applications. Waste legislation includes WEEE (Waste of Electrical and Electronic Equipment) directive 2002/96/EC which holds producers responsible for collection and recovery of materials at end of life. Additionally, materials that contain bromine-based flame retardants must be removed from the waste and handled separately. In restrictions on use of hazardous substances (ROHS) directive 2002/95/EC, the use of various hazardous materials is restricted. These include lead, mercury, cadmium, hexavalent chromium, polybrominated biphenyls, and polybrominated diphenyl ether. Since the introduction of Blue Angel in Germany in 1978, several other eco-labels have been implemented. These include TCO (Sweden), Nordic Swan, Milieukeur (Netherlands), and the EU Ecolabel. The general purpose of these labels is to provide consumers with information relating to the environmental impact of the products they purchase.

15.3.4.2 Performance Requirements

Flammability testing is perhaps the most common requirement for materials that go into electrical applications. Underwriters Laboratories (UL) UL94 test standard is typically used to evaluate the material performance in molded test bars, which is not to be confused with application testing. It is equivalent to EN60695-11-10 and EN60695-11-20. There are several possible ratings for this test for materials used in enclosures, structural parts, and insulators. These include the horizontal burn test (HB), the vertical burn test (V0, V1, V2), as well as 5VA and 5VB ratings. Another standard, the glow wire test (GWT) is widely used in Europe (EN60695-2010,11,12,13) in conjunction with the needle flame test (9EN60695-11-5). Temperatures in the glow wire test can vary from $650\,^{\circ}\text{C}$ up to $960\,^{\circ}\text{C}$. Limited oxygen index (LOI, ISO 4589) is a measure of the minimum amount of oxygen that will support combustion. A higher LOI indicates a greater threshold for burning, i.e., a LOI greater than 21 % indicates the material will not burn in atmospheric conditions.

Another test that is critical for electrical applications is the comparative tracking index (CTI, UL746A, and IEC 60112). This test is used to determine the breakdown voltage of an insulating material. The voltage at which a conductive path, or breakdown due to carbonization, is quantified. Performance level categories (PLC) correlate inversely with the tracking voltage.

Flammability and electrical performance are the two categories of performance most unique to electrical application, which is not to say that other common performance criteria such as thermal, mechanical, and weathering behavior are unimportant.

The overall trend for enclosures is toward materials that have low-temperature performance, UV resistance, chemical resistance, and contain non-halogen flame retardants. Housing for fuse boxes typically requires good impact and tracking resistance, as well as consistent electrical performance in humid conditions. Power tool housings, on the other hand, require good impact and chemical resistance. Common UL electrical tests for this segment are covered under UL746C and include hot wire ignition, high-current arc ignition, and comparative tracking index tests.

Materials for plugs and sockets for household purposes are tested in accordance with IEC60884. For industrial plugs and sockets, standard EN60309 applies. Low-voltage connecting devices for household circuits are covered by EN 60998. Many of these applications also require weatherability and enhanced UV stability.

Conduit and installations are tested in accordance to IEC 60614 and EN 61386-1 as well as flame testing and glow wire. Applications for channels and pipes require extrudability.

Switchers and breakers require resistance to tracking, arcing, and elevated temperatures. For circuit breakers, high temperatures of 200 °C and high forces can be experienced.

The connectors segment is broad. Each subsegment has a rather unique set of requirements. Automotive connectors, for example, require chemical resistance and high heat. Flexible hinge connectors require high melt flow for small parts in intricate geometries, good chemical resistance, and exceptional ductility and elongation. In large connectors, good dimensional stability, warp resistance, and heat resistance or chemical resistance are vital. Fiber-optic connectors are particularly demanding for dimensional stability, where low CTE is critical.

Flammability requirements are stringent for electrical meters and are covered by EN 62053. Capacitor housings require good thermal resistance and dimensional stability. Additionally, both meters and capacitor housings are frequently laser marked, so materials that are compatible with laser marking processes have an advantage. Materials for transformers and insulation systems are tested in accordance with UL 1446 and EN 60085.

15.3.4.3 Specific Applications

One of the largest segments within the electrical application space is for lighting. Depending on the specific application, various degrees of heat performance and impact resistance may be required. EN 60598 covers requirements for flammability CTI and GWT.

For light reflectors, inherent reflectivity (i.e., 90 % or more) or ability to be metalized are important. For lamp holders, either fluorescent or incandescent, materials are categorized according to the temperature class of the holder according to EN 60238.

Other applications in the lighting segment include housings, which require high heat distortion temperature and weatherability. Examples of housings include street lamps which require mechanical strength and lightweight, spotlights, emergency lights, and traffic lights.

Recent demands for energy efficiency, longer life, and decreased environmental issues related to waste have created tremendous growth in the LED lighting segment. This growth is further fueled by increasing legislation mandating the phaseout of more traditional lighting such as incandescent bulbs. In general, materials going into LED applications require flame resistance without halogen or phosphorous and heat and impact resistance and may require direct metallization, reflectivity, thermal conductivity, and electrical conductivity.

Even though LEDs produce light more efficiently relative to incandescent bulbs, they must still convert input energy into heat. The lifetime of an LED is determined, in part, by its ability to manage heat. Blends with enhanced thermal conductivity can provide an advance over traditional heat sinks such as aluminum due to the design flexibility afforded by injection molding. Also, for housings and reflectors, high heat distortion and continuous use temperature are important.

Enhanced thermal conductivity useful in advanced packaging of electronic components could be achieved through selective dispersion of conductive high aspect ratio nanofillers into a polymer blend where they could segregate to form self-assembled conducting pathways. Mechanical properties could similarly benefit (Xu et al. 2013).

15.3.5 Automotive

15.3.5.1 Recent Trends

Lightweighting, fuel efficiency, reduction of emissions, enhanced safety, green sourcing, and recycling are a few of the more recent needs articulated by today's consumers that have translated directly into the design of plastic parts for automotive applications.

Thus, alloys employing plastics compatibilized to PP, which could be derived from recycled interior scrap, would be attractive. Properties could be enhanced as needed by further blending with virgin polymer or through reinforcement with micro- or nanoscale fillers.

Plastics find increasing use in "mobility" applications for weight savings (especially important in the new electric cars that need extended range between charging of their heavy batteries), increased durability, and improved appearance. Automotive plastics payload is expected to increase from 15 % today to 25 % by 2020. Both bodywork and interior component applications will benefit. Blending is an important route to providing property balances needed for these applications (Anon 2013d). For example, heat distortion and impact resistance are enhanced in blends of PVC with polyester or TPU with ABS for automotive applications (Harrats and Makhilef 2006c).

15.3.5.2 Exterior Automotive

Rigid–rigid blends of notch-sensitive plastics with ABS or PPO, like the commercial Noryl GTX™ blend of PA66 and PPO, are superior to rubber-toughened counterparts of the single components in their retention of stiffness and high-temperature performance. The GTX™ 979 blend of PA with a modified PPO makes an ideal replacement for steel in exterior body panels such as fenders. It provides good impact strength along with sufficient electrical conductivity for electrostatic painting. The Pulse GX PC/ABS blend targets interior automotive applications, for which it is optimally formulated to provide sufficient heat resistance along with low-temperature ductility to meet safety requirements (Toensmeier 2012).

One recent application for exterior body panels utilizes a hybrid polymer blend composite technology. It is currently being positioned for large horizontal body panels such as roof modules, hoods, and deck lids [IXIS®, Azdel, Inc]. The composite structure can comprise blends of PC/Polyester with unidirectional glass fiber orientation of 0/90 and 90/0, with a core of chopped glass mat-reinforced thermoplastic. The structure can be formed using aluminum tooling, which provides reduced capital cost relative to tooling to stamp steel body panels.

For some time, the designers of vertical body panel polymer blends have sought to achieve high modulus without sacrificing impact and toughness, with the greatest possible dimensional stability and ability to withstand temperatures of paint bake ovens [PC/ABS]. For painted body panels, it is critical for the material to withstand automotive online paint oven temperatures, which can be in excess of 200 °C. PA/PPE is suited for these extremes. For off-line painting, where the temperature requirements are significantly less, PC/PBT and PC/ABS can be used. Additionally, PC/PBT is commonly used for paint-free applications where in-mold color capability is leveraged. Fender and tailgate applications also see the use of PA/PPE and PC/PBT.

Film technology has been developed that makes use of a multilayer coextruded structure comprising a highly weatherable, glossy transparent surface layer above a colorable blend substrate layer [LEXAN ™ SLX]. Such a structure was designed to avoid the use of paint altogether by using an in-mold decoration process, whereby the multilayer film replaces the traditional clear coat and color coat layers of paint systems. Coextruded films are thermoformed into the shape of the final part and are subsequently back molded to create a roof module structure. Benefits of this technology include system cost reduction, lower emissions, and reduced weight when compared to steel roof structures.

15.3.5.3 Underhood and Powertrain

As automobiles become more reliant on microprocessors and electrical power, the application of polymer blends to housings for electronic components continues to increase. Key requirements for these applications can include electromagnetic shielding and electrostatic discharge.

For the foreseeable future, the automobile industry will continue to manufacture at least a portion of the overall car build with internal combustion engines. Fuel system components require extreme chemical resistance and heat resistance, while providing a balance of mechanical performance that includes such properties as dimensional stability, impact, and stiffness.

Gears require wear resistance and lubricity. Brackets for engines and gear boxes require toughness and stiffness across a wide range of temperatures.

15.3.5.4 Interior Trim/Accessories

EPDM–PP thermoplastic vulcanizates (TPVs) provide cost-effective durable sealing performance, with resistance to UV light, ozone, heat, and chemical

exposure. Being about 30 % lighter than traditional thermoset rubber formulations for weight savings and fuel economy, they can be used to produce weatherseal systems with aging resistance, balanced hardness, good extrudability, and low coefficient of friction, allowing the glass to slide easily. Moreover, part consolidation can be achieved through tri-extrusion processes that combine the lip, foot, and slip coat components of the glass run channel sealing system (Anon 2013e).

An application outside of packaging for nanoscale platelets to impart barrier resistance to a polymer blend is in preventing undesirable small molecule (plasticizer) migration to the surface. As in all applications, the clay particles should be dispersed to the highest degree possible without losing aspect ratio, even if it means only including them in one phase of the blend.

In some instances, existing polymer blends or alloys could be replaced by higher performance or less expensive neat polymers. LEXAN™ FST 3403 copolymer with high resistance to flame, smoke, and toxicity can augment or replace PC/ABS polymer blends in automotive seat back shells and side covers. It delivers high flow properties for injection molding of large parts with excellent appearance and impact strength, in compliance with new European safety standards (Anon 2012).

15.3.5.5 Automotive Safety

Within the last decade, pedestrian impact requirements have begun to play a visible role in automotive design. The front and hood portion of cars has effectively grown in volume to allow for deformable zones to absorb impact from pedestrians based on lower leg, upper leg, torso, and head impacts.

The front fascia serves multiple functions which are obvious by visual inspection. These include aesthetics, aerodynamics, and to house functional elements such as fog lights and air inlets. What is not obvious is the energy absorber systems that sit behind the fascia. Material properties such as impact strength and flexural modulus must be considered over a wide range of ambient temperatures. When these properties are combined with part design, an overall system can be produced that is light and space efficient and allows for macroscopic deformation to allow vehicles to meet FMVSS, CMVSS, IIHS, and ECE 42 requirements.

Polymer blends can play a role in airbag systems. Robust airbag deployment at down to $-40\,°C$ is critical to avoid material fragmentation. Frontal impact requirements include FMVSS201/208, CMVSS 201/208, ECE R49, and TRIAS 47.

15.3.5.6 Automotive Lighting

As automotive lighting systems become more advanced, there is an overall trend toward solid state lighting. There are two applications, in particular, that are well suited to polymer blends. These include bezels and reflectors. As with other injection molding applications, use of blends as bezel materials allows for part consolidation, lightweight, and design freedom. For reflectors, extreme heat performance at temperatures up to $230\,°C$ is required. Additionally, direct metallization is required.

15.3.5.7 Tires

Blends of two or more unsaturated elastomers (rubber–rubber blends) have traditionally found application in various components of the commercial and automotive tire. Specific applications are (Hess et al. 1993):

Component	Blend in passenger tires	Blend in commercial tires
Tread	SBR–BR	NR–BR or SBR–BR
Belt	NR	NR
Carcass	NR–SBR–BR	NR–BR
Sidewall	NR–BR or NR–SBR	NR–BR
Liner	NR–SBR–IIR	NR–IIR

Blends of saturated with unsaturated rubbers, e.g., EPDM–NR and BIMS–NR, find application in the tire sidewall, where the saturated component could aid in environmental resistance. Compatibilization is likely required to form a stable blend morphology from such dissimilar components.

Now dynamically vulcanized rubber–plastic blends are poised to enter the realm of automobile tires. A TPV comprising a PA thermoplastic phase with isobutylene-co-*p*-methylstyrene (BIMSM) rubber can be used as an innerliner, outperforming either historical butyl rubber or the more classical halobutyl and its blend with natural rubber. These and future developments are targeting down-gauging of the barrier film thickness to simultaneously reduce both tire weight and reduced air permeation. A five-to-tenfold reduction in the latter is claimed to be feasible along with improved tire performance (Tsou 2007).

15.3.6 Miscellaneous Applications

15.3.6.1 Packaging

A blend of HDPE and thermoplastic starch finds application in blow-molded bottles, especially for cosmetics, pharmaceuticals, and household chemicals due to its high permeation barrier and chemical resistance while enhancing sustainability due to significantly reduced greenhouse gas emissions during manufacture. Produced by extrusion blending with excess water to convert the starch to a thermoplastic form, the compound containing a minor dispersed starch phase can be employed in various layered combinations with HDPE depending on the application and contacting substances (Anderson 2012).

Blends of rubber modified SMA and PBT could be used to produce ductile blow-molded containers suitable for low-temperature environments (Harrats and Makhlef 2006c).

The numerous parameters defining polymer blends provide flexibility for tailoring their permeability for numerous applications as barrier films in the packaging, automotive, and medical industries through control of morphology and component

interactions. Newer high barrier components for such applications include liquid-crystalline polymers, ethylene–carbon monoxide-based copolymers, and syndiotactic polystyrene.

Co-continuous blends, e.g., of thermoplastic polyester with hydrogenated block copolymers can exhibit gas permeation barrier properties with good chemical, water, and heat resistance (Harrats and Makhilef 2006c). The degree of mixing becomes a critical parameter defining blend permeation performance when the barrier polymer is in a discontinuous morphology (Fetell 1985). Experimentally, essentially equal synergistic permeation decrease occurs with increase of barrier resin content in biaxially oriented blended versus coextruded films, both of which outperform the linear change characteristic of the cast blend (Watanabe 1986).

15.3.6.2 Fluid Engineering

One specialized application area for polymer blends involves water contact for such parts as water meters, pump housings, covers, and impellers. Traditionally, these parts have been manufactured using metal, but corrosion has been a long-standing issue that polymer blends can mitigate. At the top of the list of requirements is hydrolytic stability, where property retention after long exposure is needed. Low water absorption is another relatively obvious requirement which translates into dimensional stability. Since many of these applications are pressurized, high burst strength is needed. High modulus at elevated temperature may be required for hot water applications. Chemical resistance could be important, depending on the particular fluid in contact with the parts. Additionally, for components in contact with drinking water, NSF 61 compliance is needed.

15.3.6.3 Motorcycle and Scooter

Many of the requirements for motorcycles and scooters mirror those of the automotive industry. Metal replacement for lightweighting has become more important not only as a means to improve fuel efficiency but also for better handling and performance. Paint elimination is another benefit of using polymer blends. Through molded-in color, aesthetic needs can be met while eliminating the paint processes that add cost and can emit volatile organic compounds. In-mold decoration technology can also be applied to injection molded parts and provide enhanced manufacturing efficiency by eliminating or reducing the need for masking and point and/or decal application. Conductive plastics enable no-prime painting and can therefore reduce VOC emission and provide simpler operations.

15.4 Outlook: Evolution of Polymer Blends

The blending and alloying of new and existing polymer components is expected to continue adding value to the ongoing creation and development of polymer technologies. Prime focus among the application areas delineated in the above sections would be in those providing greatest impact on current societal concerns, such as sustainability via recycling, energy conservation, and green/renewable resourcing.

Indeed, while the market niche for bio-based polymers today is still less than 1 %, and only 3 % of that derive from new synthetic materials, the overall growth rate is about 13 % per year (Smith 2013). Drivers include consumer concerns and demands, as well as environmental, political, and economic considerations. Significant productivity increases in historical and projected corn yields will help to provide agricultural feedstock to fuel some of these developments.

Opportunities exist for multicomponent polymer systems utilizing new polymers and/or production/forming technologies in unique sophisticated applications, such as smart and high-performance materials for medical, aerospace, and military applications. Highway infrastructure and military needs for heavy-load bridges are being addressed by new developments in plastic lumber comprising blends of HDPE with either PS or reclaimed automotive bumper scrap (Giordano 2013).

Even conventional polymer blends can find new or expanded applications under evolving codes and performance requirements. For example, white roofing membranes of PP/EPR thermoplastic olefin elastomer having high reflectance result in reduced cooling costs (Giordano 2013), while blending polystyrene for foam insulation with an olefinic polymer can enhance its elastic strength and toughness against fracture during installation.

15.5   Summary

This chapter has reviewed applications for polymer blends from the dual perspectives of material development and application requirements. It indicates the viability of various types of polymer blends for current markets and emerging opportunities.

15.6   Cross-References

▶ Commercial Polymer Blends
▶ High Performance Polymer Alloys and Blends for Special Applications
▶ Mechanical Properties of Polymer Blends
▶ Polyethylenes and Their Blends
▶ Polymer Blends Containing "Nanoparticles"
▶ Properties and Performance of Polymer Blends
▶ Recycling Polymer Blends

Notations and Abbreviations

Polymers

ABS   Acrylonitrile–butadiene–styrene terpolymer
ASA   Acrylonitrile–styrene–acrylate terpolymer

BIMS   Brominated isobutylene-co-methylstyrene rubber
BIMSM   Brominated isobutylene-co-methylstyrene monomer terpolymer rubber
BR   Butadiene rubber
EPDM   Ethylene–propylene–diene–monomer rubber
EPR   Ethylene–propylene rubber
HDPE   High-density polyethylene
IIR   Butyl rubber
LCP   Liquid-crystalline polymer
LDPE   Low-density polyethylene
MBS   Methylmethacrylate–butadiene–styrene terpolymer
NR   Natural rubber
PA   Polyamide (nylon)
PA66   Polyamide 66 (nylon 66)
PBT   Polybutylene terephthalate
PC   Polycarbonate
PCL   Poly-caprolactone
PE   Polyethylene
PEI   Polyether imide
PES   Polyether sulfide
PET   Polyethylene terephthalate
PHA   Polyhydroxy alkanoate
PHB   Polyhydroxy butyrate
PLA   Poly-lactic acid
PMMA   Polymethyl methacrylate
PP   Polypropylene
PPE   Polyphenylene ether
PPO   Polyphenylene oxide
PPS   Polyphenylene sulfide
PS   Polystyrene
PSF   Polysulfone
PTT   Polytrimethylene terephthalate
PVC   Polyvinyl chloride
SBR   Styrene–butadiene rubber
SEBS   Styrene–ethylene–butylene–styrene block copolymer
SMA   Styrene–maleic anhydride
TPE   Thermoplastic elastomer
TPU   Thermoplastic urethane
TPV   Thermoplastic vulcanizate

Chemicals

CO   Carbon monoxide
HCl   Hydrochloric acid
HCN   Hydrogen cyanide

HF Hydrofluoric acid
NOx Nitrogen oxides
SO$_2$ Sulfur dioxide

Organizations

ASTM American Society for Testing Materials
IEC International Electrotechnical Commission
IIHS Insurance Institute for Highway Safety
ISO International Standards Organization
NSF National Sanitation Foundation (now NSF International)
UL Underwriters Laboratory
WEEE Waste Electrical and Electronic Equipment regulations

Technology/Testing

CCC China Compulsory Compliance
CCFL Cold-cathode fluorescence
CMVSS Canada Motor Vehicle Safety Standards
CNT Carbon nanotube
CRT Cathode ray tube
CTE Coefficient of thermal expansion
CT Computed tomography
CTI Comparative Tracking Index
CVJ Constant velocity joint
ECE Economic Commission for Europe
EMI Electromagnetic interference
FMVSS Federal Motor Vehicle Safety Standards
GWT Glow wire test
HB Horizontal burn
IMD In-mold decoration
IV Intravenous
LCD Liquid-crystal display
LOI Limiting oxygen index
MRI Magnetic resonance imaging
OEM Original equipment manufacturer
PET Positron emission tomography
PLC Performance level category
RFI Radio frequency interference
RFID Radio frequency identification
ROHS Restriction on use of hazardous substances
TRIAS Test Requirements and Instructions for Automotive Standards
UV Ultraviolet radiation

VB Vertical burn
VOC Volatile organic compound

Trademarks

BETADINE Purdue Products L.P.
GTX SABIC
LEXAN SABIC
NORYL GTXSABIC
IXIS Azdel

References

G.J. Anderson, Plast. Eng. **68**(6), 48–50 (2012)

Anon., Rubber World **245**(2), 8 (2011)

Anon., Plast. Eng. **68**(10), 45 (2012)

Anon, Plast. Eng. **69**(1), 43 (2013a)

Anon., Rubber World. **248**(1), 52 (2013b)

Anon., Plast. Eng. **69**(3), 51 (2013c); **68**(10), 27 (2012)

Anon., Plast. Eng. **69**(1), 42 (2013d)

Anon., Rubber World. **248**(1), 49 (2013e)

N. Bhuva, L.A. Goettler, Polym. Eng. Sci. (to appear May 2014)

C. Changping, U.S. Patent 8,232,348, 31 Jul 2012, to Biograde (Hong Kong)

Y.-M. Chung, C.-D. Jung, Y.-J. Lee, J.-W. Pack, Y.-C. Kwon, H.-T. Lee, J.-K. Cho, U.S. Patent 8,232,343, 31 Jul 2012, to Cheil Industries

A.I. Fetell (Petroleum Packaging Council, Miami Beach, 1985)

G. Giordano, Plast. Eng. **69**(6), 4–12 (2013)

C. Grossetete, D. W. Knoeppel, J. M. Sosa, S. Steagall, C. Corleto, U.S. Patent 8,242,212, 14 Aug 2012, to Fina Technology

C.G. Hagberg, J.L. Dickerson, Plast. Formul. Compd 33–36 (1996)

S.C. Harber, B.J. Cail, C.M. Smith, Rubber World **233**(1), 36 (2005)

C. Harrats, N. Makhilef, Predictions, generation and practical applications, in *Micro- and Nano-structured Multiphase Polymer Blend Systems*, ed. by C. Harrats, S. Thomas, G. Groeninckx (Taylor and Francis, Boca Raton, 2006a), p. 122

C. Harrats, N. Makhilef, Predictions, generation and practical applications, in *Micro- and Nano-structured Multiphase Polymer Blend Systems*, ed. by C. Harrats, S. Thomas, G. Groeninckx (Taylor and Francis, Boca Raton, 2006b), p. 123

C. Harrats, N. Makhilef, Predictions, generation and practical applications, in *Micro- and Nanostructured Multiphase Polymer Blend Systems*, ed. by C. Harrats, S. Thomas, G. Groeninckx (Taylor and Francis, Boca Raton, 2006c), p. 124

W.M. Hess, C.R. Herd, P.C. Vergari, Rubber Chem. Technol. **66**, 329 (1993)

C.H. Hong, D.S. Han, U.S. Patent 8,211,966, 03 Jul 2012, to Hyundai Motor

J.K. Hong, B.D. Lee, Y.S. Jin, H.S. Park, H.R. Sun, U.S. Patent 8,232,349, 31 Jul 2012, to Cheil Industries

C.H. Hong, D.S. Han, U.S. Patent 8,378,027, 19 Feb 2013, to Hyundai Motor

M. Ikeda, K. Taniguchi, U.S. Patent 8,304,048, 06 Nov 2012, to Mitsubishi Plastics

R. Leaversuch, Super-TPVs. Plast. Technol. **50**(8), 56–61 (2004)

K.Y. Lee, L.A. Goettler, Polym. Eng. Sci. **44**(6), 1103–1111 (2004)

C.S. Lee, M.H. Lee, B.H. Park, S.H. Lee, J.H. Kim, S.K. Yoon, B.G. Kang, U.S. Patent 8,378,023 19 Feb 2013, to Hyundai Motor, Desco, and Hyosung

F. Li, T.J. Coffy, M. Daumerie, U.S. Patent 8,268,913, 18 Sep 2012, to Fina Technology

D. Machl, B. Malm, F. Ruemer, K. Bernreitner, U.S. Patent 8,304,049, 06 Nov 2012, to Borealis Technology

P. Mapleston, Plast. Eng. **63**(8), 22–26 (2007)

S.V. Nair, S.-C. Wong, L.A. Goettler, J. Mat. Sci. **32**(20), 5335–5346 (1997)

C.P. Rader, J. R. Richwine, E. P. Tam, G. E. O'Connor, Santoprene thermoplastic elastomer processability and product applications. International rubber and plastic exhibition and conference for Asia, Singapore, 1986

A. Seefried, M. Fuchs, D. Drummer, Plast. Eng. **68**(10), 14 (2012)

P.B. Smith, Plast. Eng. **69**(6), 44–48 (2013)

C.J. Talkowski, K. Hausmann, D.J. Walsh, U.S. Patent 8,242,209, 14 Aug 2012, to du Pont

S. Thomas, C. Harrats, G. Groeninckx, State of the art, challenges and future prospects, in *Micro- and Nano-Structured Multiphase Polymer Blend Systems*, ed. by C. Harrats, S. Thomas, G. Groeninckx (Taylor and Francis, Boca Raton, 2006), pp. 28–33

P. Toensmeier, Plast. Eng. **68**(7), 16–22 (2012)

A.H. Tsou, Rubber World **236**(6), 17–21 (2007)

J.H. Wang, G.J. Wideman, B. Shi, S.A. Funk, U.S. Patent 8,283,006, 09 Oct 2012, to Kimberly-Clark Worldwide

H. Watanabe, Ryder conference on plastic beverage containers, 1986

W. Xu, J. Xu, Z.S. Gonen-Williams, G.D. Cooper, U.S. Patent 8,344,053, 01 Jan 2013, to Pixelligent Technologies

L. Yu, K. Dean, L. Li, Prog. Polym. Sci. **31**, 576–602 (2006)

High Performance Polymer Alloys and Blends for Special Applications

16

Mark T. DeMeuse

Contents

Abstract

This chapter discusses blends that are based on the use of high performance polymers. Both miscible and immiscible mixtures of such polymers are discussed and advantages that are provided by both types of blends are highlighted. It is pointed out that due primarily to the molecular conformation of high performance polymers the criteria for obtaining miscible mixtures of these type of polymers are different than for more flexible type polymers

M.T. DeMeuse
MTD Polymer Consulting, Charlotte, NC, USA
e-mail: kumquats88@aol.com

and the influence of the entropic energy of mixing is emphasized. The continued need for in-depth structure–property studies of blends that contain high performance polymers is stressed so that a better understanding of the molecular features that lead to miscibility can be obtained. In addition, the requirement of improved theoretical models that explicitly consider the molecular conformation of the two polymers in a mixture is discussed in detail.

16.1   Introduction to High Performance Polymers

Polymer blends are being used in an increasing number of applications. Industrial sectors that range from the automotive to the aircraft industry have material requirements for specific applications that can be satisfied by blends. In fact, for some time, research in blends has been one of the biggest areas of polymer research, both in the industrial and academic world.

Recently, requirements for materials in certain areas have become increasingly severe. Temperatures that are in excess of 200 °C for times of hundreds of hours have become typical stated requirements for some materials. Particularly severe in this regard are needs for the aircraft industry where high service temperatures for long periods of time are often normal.

One approach to meet those performance requirements is to synthesize totally new polymers. Another method to tailor the properties of materials is through the blending of two polymers. In that particular approach, the goal is to highlight the positive features of both materials in the mixture while attempting to reduce or even eliminate the negative features.

This chapter will address various aspects of high temperature polymers and highlight the advantages of producing blends that involve those polymers. For purposes of these discussions, a high temperature polymer is generally defined as a material that has a service temperature in the neighborhood of 175 °C. This definition is obviously somewhat arbitrary in nature and is largely governed by the fact this is the temperature range that is specified in many high performance applications. Similarly, high temperature polymer blends are defined by the same use temperature. It should be noted that amorphous polymers that have a service temperature of 175 °C in general have glass transition temperatures or T_g's in the range of about 200 °C, approximately 25 °C higher than the actual service temperature. On the other hand, semicrystalline polymers have service temperatures that are largely defined by their melting points or T_m's.

Most high temperature polymers are amorphous in nature but several are semicrystalline. In the case of semicrystalline polymers, polymers with melting points that are less than about 400 °C are desirable. Above that temperature, degradation becomes significant and can become a competitive process with the melting.

16.2   Historical Development of High Performance Polymers (HPP)

16.2.1 Single-Phase, Single Component HPP

Much of the developmental work that has been done on high performance polymers has been based on needs of various branches of the U.S. federal government. An example of one such polymer is poly (benzimidazole) or PBI, the chemical structure of which is shown in Fig. 16.1. In the late 1950s, Carl Marvel first synthesized PBI while studying the creation of high-temperature stable polymers for the U.S. Air Force (Vogel and Marvel 1961). In 1961, PBI was further developed by Marvel and Herward Vogel, correctly anticipating that the polymer would have exceptional thermal and oxidative stability. In 1963, NASA and the Air Force Materials Laboratory sponsored considerable work with PBI for aerospace and defense applications as a non-flammable and thermally stable textile fiber.

After the tragedy of Apollo 1, NASA intensified its focus on advanced fire-resistant materials and one of the first alternatives considered was PBI. NASA contracted with Celanese Corporation to develop a line of PBI textiles for use in space suits and vehicles. Heat and flame resistant PBI fabric based on the fiber for high-temperature applications was developed. The fibers developed from the PBI polymer showed a number of highly desirable features, such as inflammability, no melting point, and retention of both strength and flexibility after exposure to flames. The stiff fibers also maintained their integrity when exposed to high temperatures and were mildew, abrasion and chemical resistant.

Poly (etheretherketone) or PEEK, the structure of which is shown in Fig. 16.2, was originally developed primarily for composite applications. It is produced by the step-growth polymerization process of dialkylation of bisphenolate salts. PEEK is a semicrystalline thermoplastic with excellent mechanical and chemical resistance properties that are retained at high temperatures. It has a glass transition temperature or T_g at about 143 °C and melts around 343 °C. It is highly resistant to thermal

Fig. 16.1 Chemical structure of PBI polymer
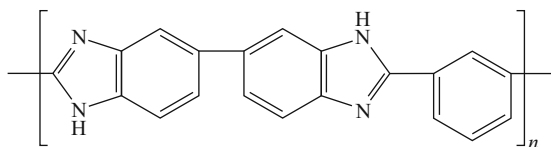
Fig. 16.2 Chemical structure of PEEK
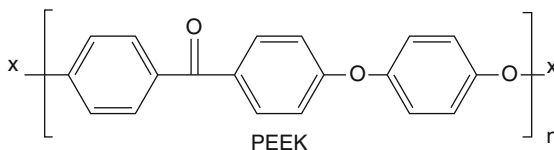
Fig. 16.3 General chemical
structure of polyimides
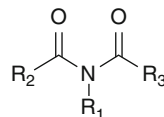
degradation as well as attack by both organic and aqueous environments. Due to its
robustness, PEEK is also used in demanding applications such as bearings, piston
parts and pumps. Also, it is considered an advanced biomaterial used in medical
implants.

Liquid crystal polymers or LCP's are a class of aromatic polyester polymers.
They are present in melted/liquid or solid form (Callister 2007). Processing of
LCP's from liquid-crystal phases, or mesophases, gives rise to fibers and injection
molded materials having high mechanical properties as a results of the self-
reinforcing properties that are derived from the macromolecular orientation that
is present in the mesophase. They can be melt-processed on conventional equip-
ment at high speeds with excellent replication of mold details. The high ease of
forming of LCP's is an important competitive advantage against other plastics,
partially offsetting high raw material costs.

Typically, LCP's have a high mechanical strength at high temperature, extreme
chemical resistance, inherent flame retardancy, and good weather ability features.
They come in a variety of forms from sinterable high temperature compounds to
injection moldable formulations. Due to their various properties, LCP's are useful
for electrical and mechanical parts, food containers, and other applications that
require chemical inertness and high strength. They are particularly attractive for
microwave frequency electronic uses due to their low relative dielectric constants,
low dissipation features, and commercial availability of laminates.

Polyimides have the general chemical structure that is shown in Fig. 16.3. They
have been in mass production since 1955. Typical monomers used in their produc-
tion include pyromelitic dianhyride and 4,4′-oxydianiline. Polyimides can be either
thermoplastic or thermosetting in nature.

Polyimide materials are lightweight, flexible, and resistant to heat and
chemicals. Due to these properties, they are often used in the electronics industry
as flexible cables, as insulating film on magnet wire and in medical tubing appli-
cations. The semiconductor industry uses polyimides as a high temperature adhe-
sive material. Molded polyimide parts and laminates have very good heat resistance
that facilitates their use as bushings, bearings, sockets or constructive parts in
demanding applications. A further use of polyimide resin is as an insulating and
passivation layer in the manufacturing of digital semiconductors. The polyimides
have excellent elongation and tensile strength, which aids in the adhesion between
the polyimide layers or between the polyimide layer and the deposited metal layer.
The minimum interaction between the gold film and the polyimide film, coupled
with the high temperature stability of the polyimide film, leads to a system that
provides reliable insulation when subjected to various types of environmental
stresses.

There are other high performance polymers, such as polysulfone (PSF) and polyphenylene sulfide (PPS) that will briefly be discussed later in regards to blends. This section of the chapter is certainly not meant to be an exhaustive review of high performance blends. In fact, a single book (DeMeuse 2014) has already been devoted to that topic in detail. It has been the purpose of this brief historical review to provide some information on the classes of polymers that will be the main topics of discussion in the blends results that are later described.

16.2.2 Miscible Blends

There have been several miscible high temperature polymer pairs that have been identified in both the patent and open literature. The term thermodynamics invariably brings to mind miscibility. The aim of this section is to discuss the thermodynamic features of polymer blends and highlight studies that have focused on a determination of the features that lead to miscibility.

Since most high temperature polymers contain some form of heterocyclic units, they often have some restricted motion in their backbone. It is exactly that restricted motion that often leads to the high glass transition temperature that is observed in high temperature polymers, such as polyimides. Thus, most high temperature polymers can be regarded as rigid, or at least, semi-rigid in overall molecular conformation. An adequate theoretical model is still to be developed for the mixing of such polymers that have a molecular conformation between random coils and rigid rods.

It should be noted that there have been attempts to produce molecular modeling results and simulations of high temperature polymer blends. The most extensive of these efforts was published by Jacobson et al. (1992). Those workers used a short chain molecular model that incorporates the effects of both inter- and intra-molecular interactions. Using that model, estimates of the net interaction energies for a series of high temperature polymer blends were calculated and used to predict miscibility. The results were in general agreement with experiments and were used to focus the direction of additional experimental work.

Several of the polymer pairs that have been found to be miscible have been formed in solution and cast films have been produced. However, when processing of this same mixture is attempted in the melt state, immiscibility often results. These results suggest that the blends phase separate when heated above their glass transition temperature. Also, kinetic factors along with thermodynamic effects seem to be relevant for the observed miscibility. The general role of the solvent needs to be better understood in the overall scheme of the miscibility that is observed. It may be that the presence of the solvent produces a kinetically favorable situation for miscibility but, upon attainment of thermodynamic equilibrium, that situation no longer exists. One of the challenges for many of the systems that will be discussed is to broaden the temperature range between the blend glass transition temperature and its phase separation temperature. Such an
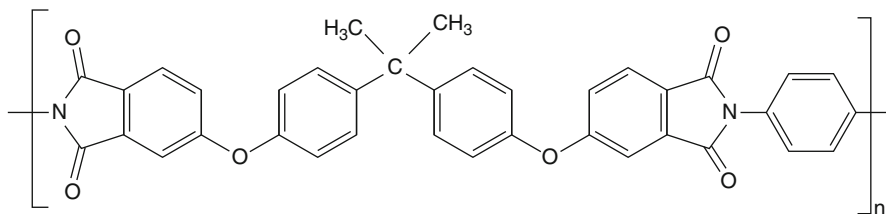
Fig. 16.4 Chemical structure of Ultem polyetherimide

effect will allow for the initially miscible blends to be processed in the melt state, thus eliminating the need for processing and handling of solvents in the fabrication of products from the blends.

PBI is one of the most highly studied high temperature polymers in miscible blends. The fundamental reason for the observation of miscibility in PBI-based systems is the presence of the N-H functional group that can interact with the functional groups which are present on the backbone of other polymers. Thus, miscibility in these type of systems is an example of a specific interaction that leads to a negative enthalpy of mixing, a requirement for forming miscible mixtures.

The most extensively studied PBI blend system that has been studied is PBI blended with a polyetherimide originally available from GE, Ultem (Takekoshi 1980). The chemical structure of Ultem is shown in Fig. 16.4.

The early work on that blend system lead to the phase diagram shown in Fig. 16.5.

That figure shows that a melt processing window exists for blends that contain in excess of 75 % PBI. In this case, a processing window is defined as those temperatures between T_g and the blend phase separation temperature. For a 85/15 PBI/Ultem blend ratio, the glass transition temperature is about 400 °C and the processing window is 25 °C.

Infrared (IR) studies of these blends showed that hydrogen bonding exists between the N-H groups of PBI and the carbonyl groups of the Ultem (Guerra et al. 1988) and that the hydrogen bonding relaxes during the thermal treatment phase separation (Musto et al. 1991; Choe et al. 1990). In subsequent studies (Foldes et al. 2000), a direct relationship was determined to exist between the strength of the hyrdogen bonding of the two component polymers, the glass transition temperature of the blends and the solvent diffusion rate of both water and 1,2,4-trichlorobenzene. These latter studies concluded that there is partial miscibility between the two polymers and that phase inversion occurs between 0.4 and 0.6 Ultem content.

The phase behavior observed with the PBI/Ultem blends is to be contrasted with the phase separation that was observed in blends of PBI with another polyimide, XU218 from Ciba Geigy (Choe et al. 1991). That system showed phase separation only above 400 °C. The actual phase separation temperatures are determined by the blend composition. Thus, the phase behavior that is observed in PBI/polyimide blends is dependent both on the type of polyimide and the thermal history of the blends.

Fig. 16.5 Phase separation diagram for PBI/Ultem blends

$$-CF_3-C-CF_3-$$
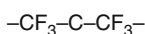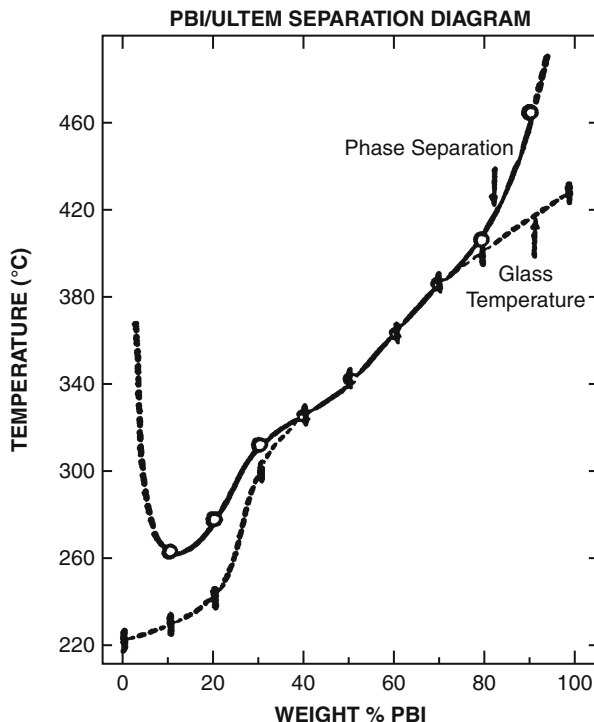
Fig. 16.6 6F chemical moiety

In further investigations of PBI blends, Jaffe et al. (1992a, b) showed that PBI is miscible with certain polyimides that contain the hexafluoroisopropylidene or 6F moiety, shown in Fig. 16.6. The miscibility and phase behavior in these blend systems is dependent on the $-CF_3-C-CF_3$ content and the overall structure of the polyimide. In addition, the amount of the 6F chemical group affects the T_g of the polyimide itself as well as the T_g of any miscible blends.

Those initial studies of blends of PBI with various polyimides were subsequently extended to include other polymers. For example, it was shown that PBI and polysulfone form immiscible mixtures (Chung et al. 1993). However, it was later shown (Deimede et al. 2000a) that the introduction of functional groups, such as sulfonate groups, into the polysulfone polymer chain resulted in the formation of miscible blends with PBI. It was shown that the sulfonation level as well as the blend composition controls the observed miscibility. FT-IR analysis confirmed the presence of specific interactions between the PBI N-H group and the sulfonate groups on the polysulfone.

There are other high temperature polymers that have been shown to form miscible mixtures as well. Several polyimides (PI's) have already been discussed in blends with PBI. Other miscible PI blends have been reported with PEEK (Kong et al. 1998), polyethersulfone (Liang et al. 1992) and sulfonated PEEK (Karcha and Porter 1989). Although the mechanism for miscibility of PBI/PI mixtures was demonstrated to be related to hydrogen bonding between the chains of the two components, the mechanism for miscibility of these other systems was not so clear.

In order to better understand miscibility in polyimide-based systems, Sun et al. (1991) prepared pairs of polyimide blends with different molecular structures by two ways, mixing of the polyamic acid precursors with subsequent imidization and direct solution mixing of the polyimides. Dynamic mechanical analysis (DMA) techniques showed that all of the blends prepared in the two different ways were miscible, as evidenced by the existence of only one T_g for all of the blends. It was proposed that the miscibility of these polyimide/polyimide blends is a result of the strong intermolecular charge-transfer interaction between the chains of the blend components.

Another polymer that has been investigated in several miscible polymer blends is polysulfone (PSF). Blends made from polyamide 11 (PA11) and sulfonated polysulfone (SPSF) were prepared by solution casting from dimethyl formamide (DMF) (Deimede et al. 2000b). In that work, differential scanning calorimetry (DSC) showed a melting point depression of the equilibrium melting point of the PA11. With lower degrees of sulfonation, less interaction between the two polymers was observed. FT-IR and FT-Raman spectroscopic techniques were used to confirm the nature of the specific interactions involved.

In EP07708077A3 (Dabou et al. 1996), gas separation polymer membranes were prepared from mixtures of a polysulfone, Udel P-1700 and an aromatic polyimide, Matrimid 5218. The two polymers were proven to be completely miscible as confirmed by optical microscopy, glass transition temperature values and spectroscopy analysis of the prepared mixtures. This complete miscibility allowed for the preparation of both symmetric and asymmetric blend membranes in any proportion from 1 to 99 wt% of polysulfone and polyimide. The blend membranes showed significant permeability improvements, compared to the pure polyimides, with a minor change in the selectivity. Blend membranes were also considerably more resistant to plasticization compared with pure polyimides. This work showed the use of polysulfone-polyimide polymer blends for the preparation of gas separation membranes for applications in the separation of industrial gases.

In another development focused on membranes, miscibility in blends of polysulfone with poly (1-vinylpyrrolidone-co-styrene) (P (VP-S)) copolymers containing various amounts of 1-vinylpyrrolidone (VP) was examined (Kim et al. 2002). Copolymers that contained VP from 68 to 88 wt% were used in that work and were found to be miscible with polysulfone. On the other hand, polysulfone blends with P (VP-S) copolymers containing 65 wt% VP and those with the P (VP-S) copolymers containing 90 wt% VP showed two Tg's, indicating that phase separation had occurred. In terms of membrane performance, the solute rejection examined with membranes made from miscible blends was similar to that

of a pure polysulfone membrane while the solute rejection examined with the membranes fabricated from the immiscible blends was lower than that of polysulfone membranes.

Overall, then, the high temperature polymer blends that have been discussed thus far display some type of well-defined specific interaction that leads to the observed miscibility. In the case of PBI blends, it is hydrogen bonding that occurs through the N-H group that is present in the PBI backbone. For PI blends, there appears to be a charge-transfer interaction that leads to miscibility in mixtures. In both cases, it is clearly the enthalpic part of the free energy of mixing that leads to miscible blends.

Such is not the case in blends of two liquid crystal polymers or LCP's that were first extensively studied by DeMeuse and Jaffe. In their initial study (DeMeuse and Jaffe 1988), they examined blends of LCP's that contain copolymers of *p*-hydroxybenzoic acid (HBA) and 6-hydroxy-2-naphthoic acid (HNA) of different copolymer ratios. It was surmised that miscibility in the melt state depended on the difference in copolymer ratios between the two component polymers. However, miscibility in the solid state seemed to be present for all blends that were studied. This is an interesting contrast to the systems previously mentioned because there is no obvious enthalpic interaction that is occurring between the two blend components.

In further studies by these same workers (DeMeuse and Jaffe 1989, 1990), efforts were extended to include LCP's that contained other monomers such as terephthalic acid (TA) and hydroquinone (HQ). In some cases, miscible systems were defined (DeMeuse and Jaffe 1989) and sometimes immiscible blends were observed (DeMeuse and Jaffe 1990). For all cases, however, there was not a well-defined specific interaction that could be ascribed to the observed miscibility. It appears that the entropy of mixing is important in defining miscibility in these type of blend systems.

Thus, we have two different types of behavior in blends of high temperature polymers. The first situation is exemplified by the PBI blends in which specific interactions through the N-H group of the PBI are responsible for the observed miscibility. The other situation is displayed by the mixtures of two LCP's in which entropic effects are important for the miscibility. These types of behavior are the extreme case of behavior. This also suggests that there are blend systems of high temperature polymers in which both enthalpic and entropic effects should be important factors in the miscibility.

This concept was explored by Lee and DiBenedetto (1992) who introduced a second LCP as a compatibilizing agent in order to improve the interfacial adhesion and dispersion between components of incompatible LCP/thermoplastic blends. The primary reason that the LCP and thermoplastic polymers are immiscible is due to molecular conformation differences or entropy effects. The concept for using a second LCP in such blends is that the two LCP's will be miscible due to entropy effects and the second LCP and the thermoplastic polymer will adhere due to specific interactions. The LCP coupling agent used in this work was a copolymer of PET and HBA known as PHB60. Blends of an LCP with both polycarbonate (PC) and PET were prepared with and without the addition of the second LCP

coupling phase. Morphological evidence indicated that the LCP reinforcing phase in the ternary systems exhibited improved adhesion and dispersion on a much finer scale than in binary blends that were produced using the same processing conditions.

This approach was further explored by Hakemi (2000) who prepared blends that contain both a wholly aromatic and an aromatic-aliphatic LCP that are miscible with each other. The ultimate goal of this approach was to develop multi-component blends that have components of thermoplastics. The miscible LCP blends could be useful as reinforcing agents for the thermoplastic matrix polymer and, due to the fact that the LCP's contain some of the components of the thermoplastic polymer, there is expected to be improved adhesion between the LCP portion and the matrix portion of the mixture. This is another example of an attempt to balance the phase separation that is inherent in high temperature polymer blends due to molecular conformation differences by strengthening the enthalpic interaction between the two polymers.

Before leaving the topic of LCP/LCP blends, one additional point needs to be stressed. Low molecular weight liquid crystals (LMWLC's) of the same mesophasic class often show miscibility (Gray and Windsor 1974). On the other hand, TLCP's that form the same mesophase, usually nematic, do not necessarily exhibit complete miscibility. Thus, in order to be able to implement the ideas of the last several paragraphs, caution must be exercised in choosing the two LCP's to form the miscible blend.

16.2.3 Immiscible Blends Based on HPP

This section of the chapter will focus on two applications of immiscible blends that contain high performance polymers. The first will be on the use of LCP's as processing aids and reinforcements of thermoplastics. There has been a great deal of both open literature and patents devoted to that topic. The second focus area will be on the use of polysulfone to enhance the fracture toughness of other thermoplastics. In that case, immiscibility is the desired phase structure for the observed effect.

In LCP/thermoplastic type blends, the size, shape and distribution of the LCP phase depends on many factors such as the blend composition, the processing conditions, the viscosity ratio of the component polymers at the shear rate that is being used in the processing, and the rheological features of the thermoplastic matrix polymer. This observation is prevalent in the work of Acierno et al. (1987) who demonstrated that different morphologies could be observed in the same LCP/polycarbonate blend simply by varying the processing temperature. The observed morphological differences were attributed solely to different viscosity ratios at the different processing temperatures.

Several reports have appeared in the literature which discuss the lowering of the viscosity of a thermoplastic polymer with the addition of a small amount of an LCP component. These studies have been performed on a variety of polymers

including polyamide (Siegmann et al. 1985), poly(etherimide) (Swaninathan and Isayev 1987), poly(ethersulfone) (James et al. 1987; Froix and Park 1984a; Froix et al. 1984b) and polycarbonate (Isayev and Modic 1987a; Malik et al. 1989; Kohli et al. 1989). All of the studies have reported a lowering of the viscosity of the traditional thermoplastic polymer with the addition of various small amounts of an LCP. The results are interpreted as being due to a lubricating effect of the LCP on the melt. This is due to the fact that the groups of LCP molecules, called domains, slide past each other.

This lowering of the melt viscosity allows the LCP to act as a processing aid for the conventional thermoplastic. Cogswell et al. (1983, 1984a, b) concluded that, in order for this effect to be realized, the temperature range at which the conventional polymers are melt-processed should overlap the temperature range in which the LCP forms an anisotropic melt. In that work, as in the other previously reported studies, the melts had lower viscosities than the pure thermoplastic polymer and, therefore, the processing temperature would be lower. The advantages of the subsequent reduction in the processing temperatures include reduced energy consumption and less degradation of polymers that are sensitive to high temperatures. Also, a lowering of the melt viscosity allows for easier filling of large and complex molds in injection molding applications.

The other principal effect that has been observed in blends of LCP's with thermoplastic polymers is the utilization of the LCP as a reinforcement for the more flexible polymer. A detailed discussion of the mechanical properties that are obtained will be provided later in this chapter. Here, just a brief introduction to the topic is made.

In numerous studies reported in the literature (Chung 1987a, b; Weiss et al. 1987a, b, c, d; Kiss 1987; Blizzard and Baird 1987; Weiss et al. 1988, 1990; Kohli et al. 1989; Wellmann et al. 1980; Nehme et al. 1988; Joseph et al. 1984; Ramanathan et al. 1987; Amano and Nakagawa 1987a, b), improved mechanical properties in blends that contain LCP's have been reported. Most of those studies have attempted to explain the changes in properties in terms of the morphology of the LCP domains in the blends. The most widely used experimental technique to study the blend morphology has been scanning electron microscopy or SEM.

One of the main drawbacks of using LCP's as a reinforcement is the poor adhesion to the matrix polymer. This lack of adhesion between two immiscible polymers is a quite general phenomenon and appears to be a concern for many blends that contain LCP's. A unique approach to address that problem has been proposed by Akkapeddi et al. (1986). They suggested blending thermoplastic oligomers and isotropic polymers in the presence of a particulate material such as talc or silica. The purpose of the particulate is twofold. First, it appears to reduce the phase separation between the thermotropic oligomer and the matrix polymer. Second, its presence helps improve the dispersion of the oligomer in the polymer. The final blend has an increased tensile modulus, tensile strength and abrasion resistance compared to blends in which the particulate was not used.

The second topic to be discussed is the use of polysulfone in blends with other thermoplastics as a way to increase the material toughness. The same technology

can be applied to thermoset polymer matrices. It will be discussed later in a section on semi-interpenetrating networks.

Kohlman and Petrie (1995) produced blends of 5 %, 10 % and 20 % by weight of polysulfone in polycarbonate by melt blending. The average impact strength and the percent of ductile failures decreased with increasing amount of polysulfone. The ballistic testing results that were reported showed a linear relationship exists between the percent of polysulfone in the blend and the critical velocity for complete penetration.

In a similar study, Garcia et al. (2004) produced blends of polysulfone with a liquid crystalline copolyester, Rodrun 5000, by processing methods of direct injection molding and extrusion followed by subsequent injection molding. The blends were immiscible and showed two pure polymer phases. There is an improvement in the notched impact strength of the polysulfone with the addition of small amounts of LCP that indicates a reduction in its notch sensitivity. The behavior of the tensile strength was close to linear with respect to the blend composition, except a 20/80 blend that showed synergistic behavior. This combination of behaviors is reminiscent of what has been observed previously in rubber-toughened blends.

Ramiro et al. (2004) studied the behavior of injection molded specimens based on blends of poly (ether imide) (PEI) and polysulfone. The impact strength was higher than that of the poly (ether imide) alone. On the other hand, the tensile strength and elongation at break were almost additive. The reported behavior is indicative of rubber-modified blends.

In terms of optimizing the fracture toughness enhancements that have been observed with these blends, immiscibility of the two polymers is the desired phase structure. However, control of the phase separation is required to be able to take full advantage of the observed effects. In other words, there is more to the effect than simply blending the two polymers together but an understanding of the mixing parameters on the resulting blend morphology needs to be obtained. More discussion of this point will be provided later in the Recommendation section of this Chapter.

16.2.4 Molecular Composites

Abe and Flory (1978) and Flory (1978) first proposed the concept of molecular composites that are systems based on the mixing of a rigid rod polymer and a random coil polymer, vastly different molecular conformations. The theoretical prediction was made that phase separation is easily induced in such mixtures. The predicted phase separation is based solely on entropic effects that arise from the conformation differences of the two component polymers.

Initial experimental work on molecular composites focused on attempting to kinetically delay the phase separation with a desirable morphology before the thermodynamics leads to complete immiscibility of the two polymers in the

mixture. Most of this initial work was performed as part of a program sponsored by the United States Air Force. For example, poly(*p*-phenylene terephtalamide) (PPTA) and poly(*p*-phenylene benzobisthiazole) (PBT) were successfully dispersed in a polyamide 66 matrix (Takayanagi et al. 1978, 1983; Takayanagi 1983; Takayanagi and Gotta 1985; Hwang and Wiff 1986). Kyu et al. (1989) reported that there are specific interactions present in a PPTA and polyamide six system and that phase separation can be thermally induced in molecular composites based on those two polymers. Thermally induced phase separation has also been observed in the PBT/PA six system when the melting temperature of the PA component is reached. Finally, Moore and Mathias (1986) reported a unique method for the preparation of molecular composites using an in-situ polymerization in which the anion of the PPTA molecule was used as the initiator for the anionic polymerization of acrylamide in the formation of a PA three matrix.

In order to improve the adhesion between the two components in the molecular composite, ionic bonds were utilized to produce miscibility (Parker et al. 1996a, b; Eisenbach et al. 1994; Weiss et al. 1992). Ionic bonds are stronger and more thermally stable than hydrogen bonds and, thus, are deemed to be more effective at promoting miscibility. Those initial studies focused primarily on molecular composites that were cast from solution.

One of the major challenges for this approach is the identification of a proper solvent that can be used. In addition, the majority of the solvents that are suitable are quite corrosive in nature. That fact, as well as the control of the phase separation and, hence, the final properties have largely limited widespread industrial development of these materials.

Recently, studies have also focused on the development of melt-processable molecular composites. Such mixtures were produced by dispersing a rigid rod polymer, such as ionic versions of Kevlar, poly(*p*-phenylene terephthalamide) (PPTA), in a matrix of a flexible coil polymer such as poly(4-vinyl pyridine) (PVP) (Hara and Parker 1992; Parker and Hara 1997a, b). Relatively low additions of a PPTA anion, that contains the ionic groups directly attached to the backbone chains, in the PVP matrix led to miscibility and to a good dispersion of the rigid rods in the matrix. These miscibility effects were attributed to the presence of ionic interactions between the ionic groups of the modified PPTA and the polar groups of the vinyl pyridine units.

This work represents another attempt of overcoming the inherent phase separation in mixtures of polymers of vastly different molecular conformations through the use of specific molecular interactions. That seems to be an effective approach for interrupting the phase separation. The general application to the development of specific high temperature blends is still to be realized, however. Also, it needs to be better understood how the chemical modifications of the rigid rod component in a molecular composite to increase molecular interactions alters its molecular conformation, if at all, towards more of a semi-rigid polymer. This could also contribute to enhanced miscibility with other high temperature polymers.

16.3   Properties and Performance of High Performance Polymers

16.3.1 Miscible HPP Blends

One of the properties that is affected by the production of miscible blends is the glass transition temperature or T_g. The T_g of miscible blends has been modeled using several different approaches in the literature (Wood 1958; Couchman and Karasz 1978). The simplest of these is the Flory-Fox equation:

$$T_{gBlend} = w_1 T_{g1} + w_2 T_{g2} \tag{16.1}$$

in which w_1 is the weight fraction of component 1 in the blend, T_{g1} is the glass transition temperature of component 1 and w_2 and T_{g2} are the same respective parameters for component 2 in the blend. Equation 16.1 predicts a monotonic change in a blend T_g between the respective T_g values of the two blend component values. It should be noted that Eq. 16.1 predicts an increase in the T_g when a higher T_g polymer is mixed with a lower T_g material.

The free volume of thermoplastic miscible blends has also been determined as a function of blend composition (Zhou et al. 2003; Campbell et al. 1997; Roland and Ngai 1991). Those studies have shown that the degree of blend miscibility alters the free volume behavior as a function of blend composition. On the other hand, Hsieh et al. (2000) have studied a number of blends containing only thermotropic liquid crystalline polymers TLCP's as the only components. That work showed that regardless of their various miscibilities, TLCP blends tend to display smaller, fewer free volume sites than expected from a weighted average. This observation has been ascribed to the intrinsic affinity of nematic TLCP's.

These observations are relevant to the work of Kenig et al. (1991) who studied blends containing two wholly aromatic, naphthalene-based liquid crystalline polymers. They observed synergistic behavior in the tensile and flexural properties of injection-molded specimens. A detailed analysis indicated that in the composition range where synergistic effects are observed in mechanical properties, only one glass transition temperature is detected. This suggests that miscibility is desirable for obtaining the maximum properties in these blend systems.

A similar synergistic effect in the physical properties of blends was observed by Cho et al. (2000) who studies novel blends of nitro-substituted poly(benzimidazole) ($NO_2 - PBI$) and poly(etherimide) (PEI) in a cosolvent. The blends possess tractable processability owing to the enhanced solubility of $NO_2 - PBI$. Miscilbility was observed and attributed to hydrogen bonding between the N-H groups of the NO_2-PBI and the carbonyl groups in the PEI.

These two examples, then represent cases of synergies being observed in the mechanical properties of miscible blends. These effects are likely due to improved packing of the polymer chains, as observed in the case of LCP/LCP blends.

Also, hydrogen bonding, as observed in PBI-based blends, is also expected to lead to efficient packing of the blend components. This improved packing effect leads to enhanced physical properties.

16.3.2 Immiscible Blends Based on HPP's

Often times, the performance of immiscible blends is worse than that of either of the component polymers. This is true of the strength and modulus of the immiscible polymer blends. In terms of temperature performance, it is largely dictated by the temperature behavior of the lower T_g component. This is because, in the case of immiscible blends, the T_g's of the two component polymers are observed at the same location as in the case of the unblended materials.

One exception to the above mentioned trend in physical properties of immiscible blends is in the utilization of liquid crystal polymers as a reinforcement for a more flexible thermoplastic polymer. The fact that LCP's can act as reinforcing agents in a blend has led some workers to model the mechanical behavior of the blends using theories of composites. Thus, Dutta et al. (1990) showed that the moduli values of highly drawn melts that contain liquid crystal polymers can be treated effectively by a simple rule of mixtures. That is, the modulus of a blend is given by

$$M_{Blend} = v_1 M_1 + v_2 M_2 \qquad (16.2)$$

where v_1 and v_2 are the volume fraction of the two components in the blend and M_1 and M_2 are the corresponding modulus values of the two polymers. These same workers showed that the moduli values of samples in which the LCP forms spherical particles can be treated using an inverse rule of mixtures.

The biggest technical issue that has prevented more widespread use of these type of blends is the lack of adhesion between the LCP and the matrix polymer. Additional work needs to be focused on solving that problem before the full potential of these blends can be realized. Effective ways to compatibilize the two polymers in the immiscible blends need to be further developed.

Another blend that consists of two immiscible polymers and has attracted recent attention is Victrex T (Victrex website 2013), which is a mixture of PBI and PEEK. The melt processability of the blend could bring the heat performance that is provided by PBI to a broader range of applications. In the blend, PBI gains processability but gives up some of its physical properties. PEEK boosts its strength, hardness and resistance to wear and creep. The blend's coefficient of thermal expansion approaches that of PBI, among the lowest of all commercial polymers.

One of the most important features of Victrex T is its heat resistance. It retains excellent mechanical properties up to 300 °C, 40 °C higher than glass-filled PEEK alone. Unfilled Victrex T has about three times the flexural modulus of conventional unfilled PEEK at 250 °C. It does even better when filled with either glass or

chopped carbon fiber. The blend is used in markets where PEEK does not quite meet the temperature targets. These markets include molded bearings, bushings and anything that faces mechanical loads and aggressive temperatures and chemicals.

16.3.3 Molecular Composites, Theory and Examples

Much of the theory behind molecular composites has already been elaborated in Sect. 16.2.4 of this chapter. Briefly, the idea is to disperse a rigid rod polymer into a more flexible random coil polymer to use the reinforcing effect of the rigid rod to increase the mechanical properties of the random coil matrix component. It is expected that the reinforcing effect that is observed will be dependent on the level of dispersion that is achieved for the rigid rod. This section of the chapter will focus explicitly on the mechanical properties that are achieved in molecular composite materials.

The early work on properties of molecular composites was done by Hwang et al. (1983a, b). They performed experimental studies of solution processing of films based on poly(p-phenylene benzobisthiazole) with both poly(2,5 (6′) benz-imidazole (ABPBI) and poly(2,5 (6′) benzothiazole) (ABPBT). The films were shown to possess very high modulus and strength values, which improve upon heat treatment. The uniaxial modulus of highly oriented molecular composites was shown to follow the linear rule of mixtures.

Tsou et al. (1996) prepared molecular composites by dispersing rigid-rod molecules of ionically-modified poly(p-phenylene terephtalamide) in a polar poly (4-vinyl pyridine) (PVP) matrix. The mechanical properties of the molecular composite were found to increase with concentration and to attain maximum values at about 5 wt% of the PPTA anion. When specific interactions are not present, as in composites with non-anionic PPTA, the properties are significantly reduced compared to those of the PPTA anion/PVP composites.

The mechanical properties of molecular composites have also been analyzed theoretically. A theory by Halpin and Tsai relates the composite modulus to the individual moduli of the components (Halpin and Tsai 1973; Halpin and Kardos 1976). In the limiting case where the reinforcing fiber aspect ratio approaches infinity, the composite modulus and tensile strength are predicted to follow a linear rule of mixtures. That is, the composite properties are a linear function of the fiber and the matrix properties and volume fraction. This ultimate rule of mixture reinforcement behavior was achieved for composites of PBT in aromatic, heterocyclic matrix polymers (Krause et al. 1986, 1988; Hwang et al. 1983) and work was also done to achieve that same effect with thermoplastic matrix materials (Wickcliffe 1986; Tsai and Arnold 1982).

16.3.4 Thermoplastic Blends with Liquid Crystal Polymers

An introduction to these types of blends has already been briefly provided in previous sections of this chapter. They have been categorized in the literature as

self-reinforced polymer composites. This section will specifically focus on the physical properties of these materials and the factors that affect the attainment of those property profiles.

A number of studies have considered the effect of LCP concentration on the mechanical properties and morphology of blends. Ko and Wilkes (Ko et al. 1989) reported that the modulus of blends of HNA/HBA and PET increased only at high LCP content of 80 % and higher. However, when this same LCP was blended with an amorphous polyamide, the mechanical properties increased monotonically with increasing LCP content (Zheng et al. 2003). For blends of another LCP with PET, Bhattacharya et al. (1987) found that the initial modulus and tenacity of melt-spun fibers increased with increasing LCP content, while elongation to break decreased. As the LCP content was increased, the fiber mode of failure changed from brittle to ductile.

Zhuang et al. (1988) found that adding small amounts of 40 PET/60 PHB to PET, PC or PS increased the modulus and tensile strength of compression molded films, extrudates, and melt spun filaments. Froix and Park (1984) also showed that the mechanical properties of PC were improved by incorporation of melt-processable, wholly aromatic liquid crystalline polyesters. Amano and Nakagawa (1987) studied the drawing behavior of blends of PET and a 40 PET/60 PHB copolyester using conventional and microwave heating methods. The optimum drawing tension, drawing temperature, and draw ratio for attaining an optimum modulus decreased with increasing LCP concentration.

Isayev and Modic (1987b) reported that injection molded and extruded blends of an HBA/HNA LCP and PC containing greater than 25 wt% LCP had spherical LCP domains dispersed in the PC matrix. However, blends with 10 % LCP had a fibrillar morphology. Pracella et al. (1987) reported a similar observation when they examined the morphology of blends of PBT with another LCP. The fracture surfaces of blends that contain up to 50 wt% LCP revealed the presence of rod-like structures of the LCP component oriented perpendicular to the fracture plane. For blends that contain more than 50 wt% LCP, the morphology was homogeneous and LCP domains were not observed.

Skin/core morphologies are common in blends of LCP's and thermoplastic polymers and they play a significant role in defining the properties of both extruded and injection molded samples. Usually, LCP's in the skin have a higher degree of orientation than in the core when the blends are extruded or injection molded (Husman et al. 1980; Hedmark et al. 1989; Lee 1988). Baird et al. (Baird and Mehta 1989; Baird and Sukhadia 1993) observed a skin/core morphology in blends of PA 66 with HBA/HNA and 40 PET/60 PHB and 20 PET/80 HBA copolyesters. More LCP fibers were present in the skin than in the core for both systems. Isayev and Swaninathan (1994) also reported shell-core structure in the fracture surfaces of injection molded blends of HNA/HBA liquid crystalline copolyesters and poly (etherimide).

In summary, then, a suitable processing history that includes extensional flow can yield a reinforcing, microfibrillar morphology of the dispersed LCP phase. Modulus values that are similar to those of short glass fiber-reinforced plastics can

be achieved. One major issue with these blends is poor interface adhesion, which limits the overall strength of the material. It is also quite difficult to prepare samples that possess other than a unidirectional microfibrillar orientation. This currently limits the applications of these blends to those requiring high mechanical anisotropy. Future work in this area needs to be focused on addressing these issues.

16.3.5 Semi-Interpenetrating Networks

The idea behind semi-interpenetrating networks (semi-IPN's) is to combine the processabiity of thermoplastics with the high temperature performance of crosslinked thermosetting materials. Such mixtures should possess the desirable features of both types of materials. The majority of semi-IPN's contain continuous phases and the components are immiscible at the molecular level.

St. Clair et al. (Hanky and St. Clair 1985; Egli et al. 1986) used the concept of sequential semi-IPN's to produce two unique IPN's that are based on acetylene-terminated imide oligomers and thermoplastic polyimides, particularly a material designated LARC-TPI. Pater and others (Pater and Morgan 1988; Pater 1988; Pater and Morgan 1988) used the concept of simultaneous semi-IPN's to make materials that are based on PMR-15 mixed with such materials as LARC-TPI, NR-150B2 and thermid 600 polyimides. Other examples of semi-IPN's that fit into the category of high temperature materials include thermoplastic modified bismaleimides (BMI). As one example, BMI has been mixed with condensation poly (aryl ether ketone) oligomers (Steiner et al. 1987). The observed miscibility that is based on thermoplastic BMI's was found to be further improved when a BMI and a thermoplastic, both prepared from aromatic diamines were blended (Arnold et al. 1988; Olabishi et al. 1979).

It is well recognized that phase separation is a necessary condition for improving the fracture toughness in thermoplastic-modified thermosetting matrixes (Bucknall and Partridge 1983; Hay et al. 1996). For a particular thermoplastic-modified thermosetting matrix, two primary properties control the final morphology and, hence, ultimate properties of the mixtures: thermodynamics and the kinetics of phase separation during the curing process itself. Both of these factors can be modified by changing the thermoplastic content in the mixture and/or by varying the cure conditions.

Martinez et al. (2000) performed such a study of polysulfone-modified diaminodiphenylmethane-cured diglycidyl ether of bisphenol-A epoxy mixtures. The immiscibility for the mixtures was proven for various polysulfone contents and as a function of the curing conditions that were used. It was found that the control of the generated morphologies can be performed only by varying the processing temperature. For a particular thermoplastic amount, it was discovered that immiscibility lowers the rigidity and strength but increases the fracture toughness of the mixtures. The properties, including the fracture toughness, are also dependent upon the percentage of thermoplastic and the subsequent morphology. The higher values of fracture toughness are achieved for a bicontinuous morphology.

Fig. 16.7 Chemical structure
of bisphenol A dicyanate
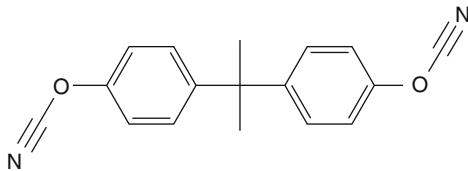
Hwang et al. (1997) have investigated mixtures of polysulfone with bisphenol A dicyanate, the structure of which is shown in Fig. 16.7.

When mixtures with less than 10 wt% were cured isothermally, they were phase separated due to a nucleation and growth mechanism. On the other hand, with more than 20 wt% polysulfone, the blends were phase separated by spinodal decomposition. These different mechanisms are important because in thermoset/thermoplastic blending, the fracture toughness is determined by the morphology that is formed as a consequence of the phase separation.

Those studies were extended to include the addition of an organic montmorillonite nanoscale filler to the polysulfone/dicyanate mixture (Mondragon et al. 2006). The primary reason for the introduction of the filler is the significant improvement in properties that can be obtained at low clay contents. The exfoliated configuration for the clay is of particular interest in that regard because it maximizes the interactions, making the entire surface of the clay layers available for interactions with the polymer matrix. This should lead to dramatic changes in both mechanical and physical properties.

In the quoted study, it was found that the polysulfone was initially miscible with the cyanate prepolymer and phase separates into spherical domains during the course of the cyanate polymerization process. The flexural modulus was not significantly modified by the thermoplastic/organoclay addition. On the other hand, the fracture toughness was slightly improved with the addition of polysulfone and clay to the cyanate.

All of these studies highlight the importance of obtaining the proper morphology in the polysulfone/thermoset mixtures in order to maximize the fracture toughness improvement that is observed. The mixtures often begin as miscible blends and upon curing of the thermoset component, phase separation occurs. It is control of the phase separation process that ultimately leads to the attainment of a particular physical property profile. Variables that can affect the phase separation process include the mixture composition as well as the curing temperature of the thermoset component in the mixture. Amont the blend composition variables, the molecular weight of the two components is very significant due to its effect on the overall mixture viscosity, an important factor in controlling the phase separation kinetics.

These conclusions imply that fundamental studies of the phase separation process in polysulfone/thermoset mixtures are needed to better understand the kinetics of the situation. General conclusions about the range of variables that allow for the development of a desirable morphology compared to others are needed to be able to take full advantage of the fracture toughness enhancements

that have been observed in polysulfone/thermoset mixtures. It is through such an understanding that the optimum polysulfone/thermoset mixtures can be defined and developed.

Variables that should be examined include the molecular weights of the two component materials, both the thermoplastic and thermoset component. It should be defined if these both affect the overall mixture viscosity in similar ways, or if it is not the overall viscosity that affects the phase separation kinetics but how that overall viscosity is indeed obtained. These studies should be performed on a single chemical system as a function of the curing temperature and a complete understanding of the resultant morphologies should be obtained. Having obtained that basic understanding on a single system, the goal is to apply that knowledge to be able to design other systems. That way, systems with particular and specific property profiles can be designed and fabricated.

16.4   Summary, Outlook and Conclusions

Much of the work that has been done up to this point on high temperature polymer blends is the definition of miscible blend polymer pairs and an understanding of the features that lead to that miscibility. The development of miscible blends often leads to the ability to tailor the properties, including the T_g of mixtures. Such a tailoring is an alternative to the development of entirely new polymeric materials with the desired property profile. One of the advantages of the blend approach is that it is generally faster and less expensive than the synthesis and scale-up of an entirely new polymer. The downside of the blend approach is that it is difficult to define miscible pairs and miscibility is often the situation that is not observed with polymer mixtures.

As has already been discussed earlier in this chapter, one of the most common ways to achieve miscibility in high temperature polymer blends is through the introduction of specific interactions between the two components in the mixture. This is not surprising, as this is also an often-used approach to develop miscibility in other types of blend systems as well. The one exception to this pattern is the case of blends of two liquid crystal polymers in which miscibility has been determined in systems in which there is no well-defined specific interaction. In those systems, miscibility appears to occur based primarily on similarities in molecular conformation between the two blend components. These results suggest that entropic effects play a significant role in defining the phase behavior of mixtures that contain high performance polymers.

This phenomenon is most clearly displayed in molecular composites, mixtures of rigid rods and random coils. In those systems, phase separation has been theoretically predicted and experimentally verified, based solely on the molecular conformation differences of the two polymers in the mixture. Thus, immiscibility can be observed without the implicit consideration of enthalpic interactions. In fact, one of the approaches that has been examined in the published literature to delay or interrupt phase separation in molecular composite systems is to provide favorable

specific interactions between the two polymer components to use favorable enthalpic interactions to overcome the inherent entropic molecular differences.

An area of work that needs to be further explored is a better quantitative definition of the interplay between the enthalpy and entropy energies of mixing for blends of high temperature polymers. As just discussed, molecular composites are largely controlled in their phase behavior by entropic effects while in the case of random coil/random coil mixing, enthalpy is assumed to dominate the situation. These observations, when taken together, imply that there are certain molecular conformations of polymer mixtures for which both the enthalpic and entropic portions of the free energy of mixing are significant. This region of behavior falls under the category of semi-rigid polymers, for which many high temperature polymers fall. This suggests that the class of high temperature polymers offers the possibility to manipulate the phase behavior of mixtures through a balance of the polymer conformation and interactions between the component materials.

Better theoretical models need to be developed that explicitly incorporate the conformational features of the polymers in a mixture. Such models need to deal with behaviors that range from the limits of rigid rods to random coils in a systematic way. In particular, semi-rigid polymers, that are common to high temperature polymers, need to be studied. In addition to the conformation of the two polymers, an explicit way of incorporating specific enthalpic interactions needs to be defined. The development of the proposed model will allow for a theoretical examination of the relative importance of entropic and enthalpic effects to the phase behavior and miscibility.

From an experimental perspective, systematic structure–property relationship studies of high performance polymer blends are needed to completely define the polymer features that lead to miscible mixtures. One of the primary focuses of those studies should be continued quantification of the molecular features, both entropic and enthalpic in nature, responsible for miscibility. Such quantitative input can, then, be used as information in theoretical developments. The entire process should be regarded as highly iterative in nature in the sense that theoretical predictions can be made, tested experimentally, and the results of the experimental work should lead to revised models that can make additional predictions.

In the case of immiscible blends, additional understanding needs to be obtained of the effect of various processing conditions on the final blend morphology. This is true of not only mixtures in which both components are thermoplastic in nature but also of semi-interpenetrating blends that are mixtures of thermoset materials with thermoplastic polymers. It is especially true of blends that are based on liquid crystal polymer with more traditional thermoplastic polymers. For example, different mechanical property profiles have been observed in such blends through changes in the processing conditions. Additional efforts need to be completed in that area to completely understand the effect of the different processing temperatures and conditions on the blend morphology and final properties. Much of the work that has appeared in the published literature has largely been of a trial-and-error variety. While many interesting property enhancements have been observed in numerous of those studies, a full realization of the benefits has still not been

obtained. Systematic studies are needed to take full advantage of the unique features that are provided by these types of mixtures.

Many of the features of high performance polymer blends that have been highlighted as requiring additional work are quite similar in nature to issues that need to be addressed with polymer blends in general. However, one of the somewhat unique features that high performance polymers have is the fact that many of them have molecular conformations that can be described as semi-rigid in nature. That feature modifies the miscibility criteria for mixtures that contain such polymers from usual random coil mixing. Since miscibility or at least some form of compatibility is generally believed to influence the physical properties of polymer mixtures, it can be inferred that the molecular conformation of high performance polymers has a direct bearing on the performance that is observed in blends.

Since many of the applications for high performance polymer blends are specialized in nature, these mixtures can often command a premium price. Due to that fact, efforts can be expended to optimize the performance to meet specific requirements. Sometimes that optimization can be done through the incorporation of chemical functionalities to take advantage of specific interactions. The overall key is to be able to define polymer features that allow for the attainment of the ever-increasing needs for high performance polymers and blends made from them.

16.5   Cross-References

▶ Miscible Polymer Blends
▶ Properties and Performance of Polymer Blends
▶ Thermodynamics of Polymer Blends

Notations and Abbreviations

6F Hexafluoroisopropylidene
ABPBI Poly (2,5 (6′) benzimidazole)
ABPBT Poly(2, 5 (6′) benzothiazole)
BMI Bismaleimide
DMA Dynamic mechanical analysis
DMF Dimethyl formamide
DSC Differential scanning calorimetry
HBA p-Hydroxybenzoic acid
HNA 6-Hydroxy-2-napthoic acid
HPP High performance polymer
HQ Hydroquinone
IPN Interpenetrating network
IR Infrared
LCP Liquid crystal polymer
LMWLC Low molecular weight liquid crystal

M_1 Modulus of component 1
M_2 Modulus of component 2
M_{blend} Modulus of blend
$NO_2 - PBI$ Nitro-substituted poly (benzimidazole)
PA11 Polyamide 11
PBI Poly (benzimidazole)
PBT Poly (*p*-phenylene benzobisthiazole)
PC Polycarbonate
PEEK Poly (etheretherketone)
PEI Poly (etherimide)
PET Poly (ethylene terephthalate)
PI Polyimide
PPS Poly (phenylene sulfide)
PPTA Poly (*p*-phenylene terephthalamide)
PS Polystyrene
PSF Polysulfone
PVP Poly (4-vinyl pyridine)
SEM Scanning electron microscopy
SPSF Sulfonated polysulfone
TA Terephthalic acid
T_g Glass transition temperature
T_{g1} Glass transition temperature of component 1
T_{g2} Glass transition temperature of component 2
T_{gblend} Glass transition temperature of blend
TLCP Thermotropic liquid crystal polymer
T_m Melting temperature
v_1 Volume fraction of component 1
v_2 Volume fraction of component 2
VP-S 1-Vinyl pyrrolidone-co-styrene
w_1 Weight fraction of component 1
w_2 Weight fraction of component 2

References

A. Abe, P.J. Flory, Macromolecules **11**, 1122 (1978)
D. Acierno, E. Amandola, C. Cartagna, L. Nicolais, R. Noblile, Mol. Cryst. Liq. Cryst. **153**, 533 (1987)
M.K. Akkapeddi, T. DeBona, H.L. Li, D.C. Prevorsek, U.S. Patent 4,611,025, 1986
M. Amano, K. Nagawa, Polymer **28**, 263 (1987)
M. Ammo, K. Nakagawa, Polymer **28**, 275 (1987)
C.A. Arnold, D. Chen, Y.P. Chen, J.D. Graybeal, R.H. Bott, T. Yoon, B.E. McGrath, J.E. McGrath, Polym. Mater. Sci. Eng. **59**, 534 (1988)
D.G. Baird, R. Mehta, *Processing Behavior of Blends of Liquid Crystalline Polymers* (PPS Summer Meeting, Amherst, 1989)
D.G. Baird, A.M. Sukhadia, U.S. Patent 5,225,488, 1993
S.K. Bhattacharya, A. Tandokar, A. Misra, Molec. Cryst. Liq. Cryst. **153**, 501 (1987)

K.G. Blizzard, D.G. Baird, Polym. Eng. Sci. **27**, 653 (1987)

C.B. Bucknall, I. Partridge, Polymer **24**, 639 (1983)

W.D. Callister, *Materials Science and Engineering – An Introduction* (2007), pp. 557–558

J.A. Campbell, Y.A. Goodwin, M.S. Ardi, G.P. Simon, C.J.T. Landry-Colton, Macromol. Symp. **118**(1), 383 (1997)

J. Cho, M.S. Park, J.H. Choi, B.C. Li, S.S. Han, W.S. Lyoo, J. Polym. Sci. Part B: Polym. Phys. **39**(15), 1778 (2000)

S. Choe, F.E. Karasz, W.J. MacKnight, in *Contemporary Topics in Polymer Science, Multiphase Macromolecular Systems*, ed. by W.M. Culbertson (Plenum, New York, 1990)

S. Choe, W.J. MacKnight, F.E. Karasz, in *Polyimides: Materials, Chemistry, etc.*, ed. by C. Feger, M.M. Khojaseth, J.E. McGrath (1991)

T. Chung, Plast. Eng. **43**, 39 (1987a)

T. Chung, Proc. Ann. Tech. Conf. Soc. Plast. Eng. **33**, 1404 (1987b)

T.S. Chung, M. Glick, E. Powers, Polym. Eng. Sci. **33**(16), 1042 (1993)

F.N. Cogswell, B.P. Griffin, J.B. Rose, U.S. Patent 4,386,174, 1983

F.N. Cogswell, B.P. Griffin, J.B. Rose, U.S. Patent 4,433,083, 1984

F.N. Cogswell, B.P. Griffin, J.B. Rose, U.S. Patent 4,438,236, 1984

P.R. Couchman, F.E. Karasz, Macromolecules **11**, 117 (1978)

X.S. Dabou et al., EP0778077A3, Filed, Dec. 5, 1996

V. Deimede, G.A. Voyiatzsis, J.K. Kallitsis, L. Qingfeng, N.J. Bjerrum, Macromolecules **24**(33), 7609 (2000a)

V. Deimede, K.V. Frajou, J.K. Kallitsis, G.A. Voyiatzis, Polymer **26**(41), 9095 (2000b)

M.T. DeMeuse, *High Temperature Polymer Blends* (Woodhead Publishing, Cambridge, 2014)

M.T. DeMeuse, M. Jaffe, Mol. Cryst. Liq. Cryst. **157**, 535 (1988)

M.T. DeMeuse, M. Jaffe, Polym. Prepr. **30**, 540 (1989)

M.T. DeMeuse, M. Jaffe, in *Liquid Crystalline Polymers*, ed. by R.A. Weiss, C.K. Ober. ACS Symposium Series, vols 435, 439 (1990)

D. Dutta, H. Fruitwala, A. Kohli, R.A. Weiss, Polym. Eng. Sci. **30**(17), 1005 (1990)

A.H. Egli, L.L. King, T. St. Clair, in *18th International SAMPE Technical Conference*, October 1986

C.D. Eisenbach, J. Hoffmann, W.J. MacKnight, Macromolecules **27**, 3162 (1994)

P.J. Flory, Macromolecules **11**, 1138 (1978)

E. Foldes, E. Fekete, F.E. Karasz, B. Pukasnszky, Polymer **41**, 975 (2000)

M.F. Froix, M. Park, U.S. Patent 4,460,735, 1984

M.F. Froix, M. Park, N. Trouw, U.S. Patent 4,460,736, 1984

M. Garcia, J.I. Equiazabal, J. Nazabal, Polym. Int. **53**(3), 272 (2004)

G.W. Gray, P.A. Windsor, *Liquid Crystals and Plastic Crystals*, vol. 1 (Halsted, New York, 1974), p. 20

G. Guerra, S. Choe, D.J. Williams, F.E. Karasz, W.J. MacKnight, Macromolecules **21**, 231 (1988)

H. Hakemi, Polymer **41**, 6145 (2000)

J.C. Halpin, J.L. Kardos, Polym. Eng. Sci. **6**(5), 344 (1976)

J.C. Halpin, S.W. Tsai, *Environmental Factors in Composite Materials Design*, AFML-TR-67-423 (1973)

A.O. Hanky, T. St. Clair, SAMPE J., July/Aug., 40 (1985)

M. Hara, G. Parker, Polymer **33**, 4650 (1992)

J.N. Hay, B. Woodfine, M. Davies, High Perform. Polym. **8**, 35 (1996)

P.G. Hedmark, J. Manuel Rego Lopez, M. Westdahl, P.E. Werner, J.F. Janssom, U.F. Gedde, Polym. Eng. Sci. **28**, 1248 (1989)

T.T. Hsieh, C. Tiu, G.P. Simon, Polymer **41**(12), 4737 (2000)

G. Husman, T. Helminiak, M. Wellman, W. Adams, D. Wiff, C. Benner, ACS Symp. Ser. EMS **132**, 203 (1980)

W.F. Hwang, D.R. Wiff, C.L. Benner, T.E. Helminiak, J. Macromol. Sci. Phys. **B22**, 231 (1983a)

W.F. Hwang, D.R. Wiff, C. Verschoore, G.E. Price, T.E. Helminiak, W.W. Adams, Polym. Eng. Sci. **23**(14), 784 (1983b)

W.F. Hwang, D.R. Wiff, U.S. Patent 4,631,318, 1986

J.W. Hwang, S.D. Park, K. Cho, J.K. Kim, C.E. Park, T.S. Oh, Polymer **38**(8), 1835 (1997)

A.I. Isayev, M.J. Modic, Polym. Compos. **8**, 158 (1987a)

A. Isayev, M. Modic, Polym. Compos. **8**, 269 (1987b)

A. Isayev, S. Swaninathan, European Patent EP 0291323, A2 (1994)

S.H. Jacobson, D.J. Gordon, G.V. Nelson, A. Balazs, Adv. Mater. **4**(3) (1992)

M. Jaffe, E. Chenevey, W. Cooper, M. Glick, M.I. Haider, J. Rafalko, Makromol. Chem. Macromol. Symp. **53**(1), 163 (1992a)

M. Jaffe et al., Polym. Eng. Sci. **32**(17), 1236 (1992b)

S.G. James, A.M. Donald, W.A. MacDonald, Mol. Cryst. Liq. Cryst. **153**, 491 (1987)

E.G. Joseph, G.L. Wilkes, D.G. Baird, ACS Polym. Prepr. **25**(2), 94 (1984)

R.J. Karcha, R.S. Porter, J. Polym. Sci. Part B: Polym. Phys. **27**, 2153 (1989)

S. Kenig, M.T. DeMeuse, M. Jaffe, Polym. Adv. Technol. **2**, 25 (1991)

J.H. KIm, J.E. Yoo, C.K. Kim, Macromol. Res. **101**(4), 209 (2002)

G. Kiss, Polym. Eng. Sci. **27**, 410 (1987)

C.U. Ko, G.L. Wilkes, C.P. Wong, J. Appl. Polym. Sci. **37**(11), 3063 (1989)

A. Kohli, N. Chung, R.A. Weiss, Polym. Eng. Sci. **29**, 573 (1989)

W.G. Kohlman, S.P. Petrie, Adv. Polym. Technol. **14**(2), 111 (1995)

Y. Kong, H. Tang, L. Dong, F. Teng, Z. feng, J. Polym. Sci. Part B: Polym. Phys. **36**(13), 2267 (1998)

S.J. Krause, T.B. Haddock, G.E. Price, P.G. Lenhert, J.F. O'brien, T.E. Helminiak, W.W. Adams, J. Polym. Sci. Part B: Polym. Phys. **24**(9), 1991 (1986)

S.J. Krause, T.B. Haddock, G.E. Price, W.W. Adams, Polymer **29**(2), 195 (1988)

T. Kyu, T.I. Chen, H.S. Park, J. White, J. Appl. Polym. Sci. **37**, 201 (1989)

B. Lee, SPE ANTEC Tech. Pap. **34**, 1088 (1988)

C.W. Lee, A.T. DiBendetto, Polym. Eng. Sci. **32**, 400 (1992)

K. Liang, J. Grabowicz, E. Valles, F.E. Karasz, W.J. MacKnight, J. Polym. Sci. Part B: Polym. Phys. **30**(5), 465 (1992)

T.M. Malik, P.J. Carreau, N. Chapleau, Polym. Eng. Sci. **29**, 600 (1989)

I. Martinez, M.D. Martin, A. Eceiza, P. Oyangurea, I. Mondragon, Polymer **41**, 1027 (2000)

I. Mondragon, L. Salar, A. Nohales, C.I. Vallo, C.M. Gomez, Polymer **47**, 3401 (2006)

D.R. Moore, L.J. Mathias, J. Appl. Polym. Sci. **32**, 6299 (1986)

P. Musto, F.E. Karasz, W.J. MacKnight, Macromolecules **24**, 4762 (1991)

O.A. Nehme, C.A. Gabriel, R.J. Farris, E.L. Thomas, M.F. Malone, J. Appl. Polym. Sci. **35**, 1955 (1988)

O. Olabishi, L. Robeson, M.T. Shaw, *Polymer-Polymer Miscibility* (Academic, New York, 1979)

G. Parker, M. Hara, Polymer **38**, 2701 (1997a)

G. Parker, M. Hara, Polymer **38**, 2773 (1997b)

G. Parker, W. Chen, L. Tsou, M. Hara, ACS Symp. Ser. **54**, 632 (1996a)

G. Parker, W. Chen, M. Hara, Polym. Mater. Sci. Eng. **72**, 534 (1996b)

R. Pater, C. Morgan, SPE ANTEC Proc. 1639 (1988)

R. Pater, Presented at the RETEC technical conference, Los Angeles, November 1988

R. Pater, C.D. Morgan, SAMPE J. **24**(5) (1988)

M. Pracella, E. Chiellini, G. Galli, D. Dainelli, Molec. Cryst. Liq. Cryst. **153**, 525 (1987)

K.A. Ramanathan, K.G. Blizzard, D.G. Baird, Proc. Ann. Tech. Conf. Soc. Plast. Eng. **33**, 1399 (1987)

J. Ramiro, J.I. Equiazabal, J. Nazabal, J. Appl. Polym. Sci. **93**(5), 2913 (2004)

C.M. Roland, K.L. Ngai, Macromolecules **24**, 2261 (1991)

A. Siegmann, A. Dagan, S. Kenig, Polymer **26**, 1325 (1985)

P.A. Steiner, J.M. Browne, M.T. Blainand McKillen, SAMPE J. March/April (1987)

Z. Sun, H. Li, Y. Zhang, M. Ding, Z. Feng, Polym. Bull. **26**, 557 (1991)

S. Swaninathan, A.I. Isayev, Proc. ACS Div. Polym. Mater. **57**, 330 (1987)

M. Takayanagi, Pure Appl. Chem. **55**, 819 (1983)

M. Takayanagi, K. Gotta, Polym. Bull. **13**, 35 (1985)

M. Takayanagi, T. Ogata, M. Morikawa, T. Kai, J. Macromol. Sci. Phys. **B17**(4), 176 (1978)

M. Takayanagi, T. Ogata, M. Morikawa, T. Kai, J. Macromol, Sci. Phys. **B22**, 231 (1983)

T. Takekoshi et al., J. Polym. Sci., Polym. Chem. Ed. **18**, 3069 (1980)

T.T. Tsai, F.E. Arnold, Polym. Prepr. ACS Div. Polym. Chem. **23**(1), 1 (1982)

L. Tsou, G. Parker, W. Chen, M. Hara, Liquid crystalline polymer systems. ACS Symp. Ser. **632**, 54 (1996)

Victrex website, T series brochure (2013)

H. Vogel, C.S. Marvel, J. Polym. Sci. **50**, 511 (1961)

R.A. Weiss, W. Huh, L. NIcolais, Polym. Eng. Sci. **27**, 684 (1987a)

R.A. Weiss, W. Huh, L. Nicolais, in *International Conference on Emerging Technologies in Materials*, AIChe, August, 1987

R.A. Weiss, W. Huh, L. Nicolais, A. Kohli, in *International Conference on Liquid Crystal Polymers*, Bordeaux, 1987

R.A. Weiss, W. Huh, L. Nicolais, P. Yanisko, Proc. Reg. Tech. Soc. Plast. Eng. **267** (1987)

R.A. Weiss, W. Huh, L. NIcolais, in *High Modulus Polymers*, ed. by A.E. Zacharides, R.S. Porter (Marcel Dekker, New York, 1988)

R.A. Weiss, A. Koli, N.S. Chung, D. Dutta, Unpublished results (1990)

R.A. Weiss, L. Shao, R.D. Lundberg, Macromolecules **25**, 6370 (1992)

N. Wellmann et al., ACS organic ocat. Plast. Chem. **43**, 783 (1980)

S.M. Wickcliffe, AFWAL-TR-86-4126 (1986)

L.A. Wood, J. Polym. Sci. **28**, 319 (1958)

X. Zheng, J. Zhang, J. He, J. Appl. Polym. Sci. **87**(9), 1952 (2003)

Q. Zhou, L. Zhang, M. Zhang, B. Wang, S. Wang, Polymer **44**(5), 1733 (2003)

P. Zhuang, T. Kyu, J.L. White, SPE Antec. Tech. Pap. **34**, 1237 (1988)

Polymer Blends Containing "Nanoparticles"

17

D. R. Paul and R. R. Tiwari

Contents

Abstract

This chapter discusses the role of various nanoparticles in immiscible polymer blends for control of the size of the dispersed polymer phase particles, phase inversion and rheological behavior, impact strength, and mechanical performance. Various issues such as the effect of nanoparticle dimensions on the polymer particle size and properties, blending sequence, location of nanoparticles in the blend components, mechanism behind improvement in

D.R. Paul (✉) • R.R. Tiwari
Department of Chemical Engineering and Texas Materials Institute, The University of Texas at Austin, Austin, TX, USA
e-mail: drp@che.utexas.edu; rajkirantiwari@gmail.com; rtiwari@che.utexas.edu

properties, individual effect of various fillers on the blend properties, and future trends are also discussed in detail. Since the literature on polymer nanocomposites is vast and the utilization of nanoparticles in blends has significantly increased in recent years, this chapter is designed to review the current state of knowledge in this area. To do so, various examples of polymer blends and nanofillers relevant to the abovementioned factors are discussed.

17.1 Introduction

Polymer blends potentially offer materials with an attractive combination or balance of properties often not available in a single polymer; however, most polymer pairs are thermodynamically immiscible, and they often exhibit an unstable phase morphology during melt processing resulting in poor mechanical performance (Barlow and Paul 1981; Wu 1982; Brown 1989; Utracki 1989; Folkes and Hope 1993; Utracki 1998; Paul and Bucknall 2000a, b; Robeson 2007). There are significant numbers of polymer–polymer pairs, in spite of being immiscible, that can still provide a useful combination of properties desired for various commercial application purposes. The immiscibility arises from the fact that the mixing between the segments of two polymers is energetically unfavorable and the entropy of mixing is too small to achieve sufficient driving force for miscibility (Paul 1996). Incompatibility is caused to some extent by nonpolarity, low interfacial adhesion, specific group interactions, and molecular weight differences between two polymers (Tiwari and Paul 2011a). The thermodynamics of polymer mixing is well known and thoroughly reviewed in various scientific reports on polymer blends (Paul and Barlow 1980; Barlow and Paul 1981; Anastasiadis et al. 1988; Utracki 1989; Sundararaj and Macosko 1995; Paul 1996; Utracki 1998; Paul and Bucknall 2000a; Ophir et al. 2009).

The addition of copolymers that have block or graft segments chemically identical to the respective phases of immiscible polymers is commonly used to improve adhesion between polymer pairs, and since they solve the problem of "mechanical incompatibility" in blends, they are generally referred to as "compatibilizers" (Paul 1996). The appropriate selection of a compatibilizer can promote a stable and fine distribution of the dispersed phase within the matrix by reducing the interfacial tension between the blend components. The addition of functional groups to the minor phase that can react chemically with the major phase may form block or graft structures that can retard the coalescence of the dispersed phase by steric interaction and improve adhesion between immiscible polymer pairs; this approach is referred to as "reactive compatibilization" (Wu 1985, 1987; Oshinski et al. 1992a, b; Sundararaj and Macosko 1995; Oshinski et al. 1996a, b, c; Majumdar et al. 1997; Wildes et al. 1999; Paul and Bucknall 2000a, b). The purpose of using either approach is to obtain a fine and stable morphology along with improvement in the properties of the blend. However, the application of block copolymers or in situ reactive processing is sometimes not

a viable option, and there is a need to look for alternate routes that can lead to compatibilization of polymer blends.

In the last three decades, polymer composites based on nanofillers have shown remarkable improvements in material properties usually achieved at low filler content. Such composites are referred to as "nanocomposites." Nanocomposites are particle-filled polymer matrices where at least one dimension of the dispersed particles is in the nanometer range (Giannelis 1996; LeBaron 1999; Ray and Okamoto 2003; Paul and Robeson 2008). Among various nanofillers, layered silicate-based nanocomposites have attracted great interest from industry and academia because they often exhibit remarkable improvement in material properties when compared to the bulk polymer phase or conventional micro- and macro-composites. These improvements can include high moduli, increased tensile strength and heat resistance, decreased gas permeability and flammability, and increased biodegradability of biodegradable polymers (Giannelis 1996; Giannelis et al. 1999; Gilman 1999; Lagaly 1999; LeBaron 1999; Alexandre and Dubois 2000; Ishida et al. 2000; Bharadwaj 2001; Schmidt et al. 2002; Ray and Okamoto 2003; Jordan et al. 2005; Zeng et al. 2005; Okada and Usuki 2006; Tjong 2006; Crosby and Lee 2007; Goettler et al. 2007; Pavlidou and Papaspyrides 2008). Today, efforts are being conducted globally, using almost all types of known polymers.

In the past few years, the number of studies involving the use of organoclays to reduce dispersed phase particle size in immiscible blends has increased significantly (Li et al. 2002; Chow et al. 2003; Gelfer et al. 2003; Wang et al. 2003; Chow et al. 2004; Khatua et al. 2004; Lee and Kim 2004; Li and Shimizu 2004; Mehta et al. 2004; Ray et al. 2004; Gahleitner et al. 2005; González et al. 2005; Lee et al. 2005; Mishra et al. 2005; Austin and Kontopoulou 2006; González et al. 2006a, b; Hong et al. 2006b; Kelnar et al. 2006; Lai et al. 2006; Lee et al. 2006a; Si et al. 2006; Wu et al. 2006; Xu et al. 2006b; Kelnar et al. 2007; Kim et al. 2007b; Ray et al. 2007; Vo and Giannelis 2007; Zou et al. 2007; González et al. 2008; Kelnar et al. 2008; Kim et al. 2008; Rosales et al. 2008; Kelnar et al. 2009; Martin et al. 2009; As'habi et al. 2010; Moghbelli et al. 2010; Yoo et al. 2010a, b; Tiwari and Paul 2011a, b, c; Ojijo et al. 2012; Tiwari et al. 2012; Tiwari and Paul 2012; Vuluga et al. 2012; Tiwari et al. 2013); however, very few studies have focused on the usefulness of this strategy to achieve a balance of properties required for commercial applications. In immiscible polymer blends, organoclays have been shown to effectively reduce the dispersed phase particle size by locating either at the domain interface or in the continuous phase. When clay particles are completely dispersed in the matrix phase, it is believed that montmorillonite, MMT, particles act as a barrier to coalescence of the dispersed phase leading to a decrease in the dispersed phase particle size.

The presence of clay particles at the interface in a blend can occur when the interfacial energies are appropriate, and this will result in improved interfacial adhesion between the two polymer phases and a decrease in the dispersed phase domain size. The final morphology in the blend is also affected by the viscosity ratio of the dispersed and continuous phases and has been known to significantly

influence the deformability and breakup of droplets and might affect phase conti-
nuity. Hence, apart from the compatibilization and barrier effects of clay, any
change in the viscosity ratio also influences the final blend morphology (Khatua
et al. 2004; Vo and Giannelis 2007; Filippone et al. 2010b; Tiwari and Paul 2011b).
Similarly, kinetic effects during mixing affect the final filler dispersion and its
location in the polymer blend in addition to equilibrium effects expected from
a surface energy analysis (Yoo et al. 2010b; Tiwari and Paul 2011a). Nonetheless,
the presence of clay in blends can result in property trade-offs, e.g., stiffness
increases while toughness decreases which limits their use when both properties
are required. An optimum performance in blends can be achieved with proper
selection of materials and design of experiments (Chow et al. 2003; Gelfer
et al. 2003; Chow et al. 2004; Mehta et al. 2004; Kelnar et al. 2006, 2007, 2008;
Filippone et al. 2010a; Yoo et al. 2010b; Chen and Evans 2011; Martín et al. 2011;
Tiwari and Paul 2011a, b, c, 2012).

The decrease in the dispersed phase particle size using organoclay can be quite
beneficial in rubber toughening of rigid thermoplastics since elastomer particle
size is critical for improving toughness (Majumdar et al. 1994a, b; Oshinski
et al. 1996a, b, c; Majumdar et al. 1997; Zhou et al. 2005; Ahn and Paul 2006;
Huang et al. 2006b; Tiwari and Paul 2011b, c; Tiwari et al. 2012). Similarly, the
presence of organoclay in the blend can provide a stable morphology upon
annealing; however, the location of organoclay in the polymer blend has
a significant role on stability during annealing (Khatua et al. 2004; Moghbelli
et al. 2010; Tiwari and Paul 2011a). The major objective of this chapter is to
provide some understanding on the role of organoclay on the dispersed phase
particle size and their effects on the mechanical performance of immiscible poly-
mer blends. The effects of polymer properties such as molecular weight, rheology,
and clay content on the dispersed phase particle size and mechanical performance
are discussed in detail with several examples of polymer blends of commercial
interest. The effect of other nanofillers on the blend properties is also highlighted;
however, the major portion of this chapter is devoted to the role of organoclay filler
on the blend morphology and properties.

17.2   Role of Organoclay in Immiscible Polymer Blends

17.2.1 Polypropylene (PP)–Polystyrene (PS) Blends

Polypropylene (PP) and polystyrene (PS) are important commodity polymers;
however, blends of PP and PS are immiscible and several reports describe the use
of commercial block copolymers such as styrene–butadiene–styrene (SBS),
styrene–ethylene–butadiene–styrene (SEBS), styrene–ethylene–propylene (SEP),
and styrene–isoprene–styrene (SIS) as nonreactive compatibilizers to achieve
a finer morphology and improved performance in their blends (Bartlett
et al. 1981; Radonjič et al. 1998; Hlavatá et al. 1999; Raghu et al. 2003). However,
the block copolymers may tend to form micelles due to their high molecular weight

rather than residing at the interface, and often the synthesis of desirable block copolymers makes them rather expensive (Hung et al. 2008). On the other hand, organoclays are relatively cheap and easy to modify and, therefore, provide an economical route to prepare compatibilized polymer blends.

Wang et al. (2003) has observed a significant decrease in the dispersed phase PS particle size when clay is present in the dispersed PS phase and at the interface in the PP/PS (70/30) blend. The PS particle size decreased from ∼3 μm for PP/PS blend to ∼1 μm with the addition of ∼10 wt% organoclay in the blend. This was attributed to the decrease in coalescence of PS particles due to increase in viscosity ratio of blend components and enhanced compatibility due to intercalation of PP and PS chains in clay galleries. Later Zhu et al. (2008a, b) showed that the location of clay can be switched from one phase to another in PP/PS blends by tailoring the polarity of PP with the addition of PP grafted maleic anhydride, PP-g-MA, or by addition of sulfonate groups to PS; this promotes migration of clay particles from less polar to high-polarity blend components due to increased interfacial interactions between clay and the more polar component of PP/PS blends. It has been also proposed that organoclay platelets act like a "knife" thereby reducing dispersed PS domain size due to shear stress generated during mixing (Zhu et al. 2008a). Ray et al. (2004) observed higher mechanical properties for blends of PP-g-MA/PS/ C20A compared to PP/PS/C20A blends due to the better compatibilization effect of clay in the presence of polar anhydride groups. Although the literature on blend nanocomposites is growing, there is a lack of systematic and in-depth studies to better understand the effects of clay on the morphology development, their stability, and property improvements.

Recently, Tiwari and Paul (2011a) carried out detailed studies on the effect of PP viscosity on the dispersed phase particle size, stability of dispersed phase morphology upon annealing, phase inversion behavior, and changes in the mechanical properties of PP/PP-g-MA/MMT/PS nanocomposites prepared with different molecular weight grades of PP. PP-g-MA was added to PP to facilitate dispersion of organoclay in the nonpolar PP; moreover, it also provides better reinforcement effect when PP forms the continuous phase.

The location of clay particles in blend nanocomposites has a significant effect on the blend properties; hence, it is important to elucidate the location of clay particles in the blend. Figure 17.1 shows the dispersed phase morphology for PP/PP-g-MA/ MMT/PS nanocomposites before and after phase inversion. At 30 wt% PS in a PP/PP-g-MA/MMT/PS blend where PS forms the dispersed phase, the MMT particles are located in the PP matrix as well as at the PP/PS interface which confirms the decrease in the interfacial adhesion between PP and PS in the presence of clay. The PS particles are circular in low molecular weight PP (L-PP)- and medium molecular weight PP (M-PP)-based PP/PP-g-MA/MMT/PS nanocomposites and become elongated in the high molecular weight PP (H-PP)-based nanocomposites due to the high shear stress exerted by the H-PP on the dispersed phase during injection molding. To confirm the injection molding effects on the PS particle shape in H-PP blends, Tiwari and Paul showed TEM images of extruded H-PP blends with and without MMT and observed that PS particles are
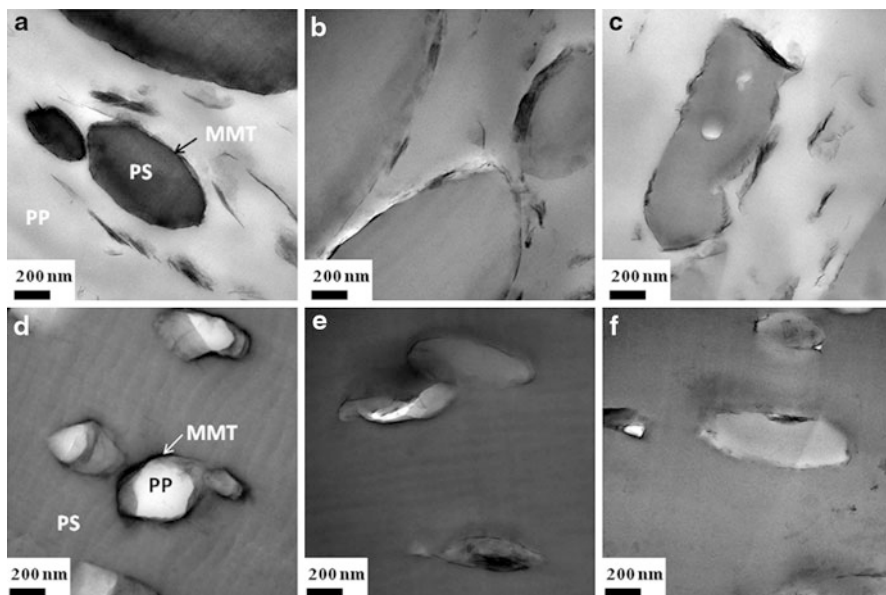
Fig. 17.1 TEM micrographs showing the location of the MMT particles in PP/PP-g-MA/MMT/
PS blends containing 30 wt% PS (*top row*) and 90 wt% PS (*bottom row*). The blends were prepared
with different molecular weight grades of PP: L-PP (**a** and **d**), M-PP (**b** and **e**), and H-PP (**c** and **f**).
Images were taken from the core and viewed perpendicular to the flow direction (FD) (Tiwari and
Paul 2011a)

globular in shape as opposed to the elongated morphology seen for injection-
molded specimens. Such molding effects arise from the various flow fields gener-
ated during the mold filling process in addition to the effect of the matrix viscosity.
Moldenaers and coworkers have also observed elongated PS particles in blends of
high molecular weight PP and PS (Omonov et al. 2007). Above the phase inversion
composition, i.e., for 90 wt% PS in PP/PP-g-MA/MMT/PS blends, PP particles are
dispersed in the PS matrix and MMT particles are still located in the PP phase as
well at the interface (see Fig. 17.1d–f).

Figure 17.2 shows the combined effects of PS composition and PP viscosity
(influenced by the PP molecular weight and presence of clay) on the dispersed
phase particle size and co-continuous region of blends with and without MMT. The
dispersed phase particle size is significantly reduced in the presence of organoclay;
this decrease is more prominent when clay is present in the continuous PP phase and
envelope PS particles, i.e., below 50 wt% of PS in a PP/PP-g-MA/MMT/PS blend.
The effect of PP viscosity on the PS particle size is less prominent in the presence of
MMT compared to blends without MMT. At higher PS compositions, i.e., above
phase inversion, the PP viscosity has negligible effect on the dispersed PP particle
size. The increase in PS particle size with increased PS composition in the
blend results from the higher rate of coalescence during mixing finally resulting
in formation of co-continuous structures followed by phase inversion

Fig. 17.2 Effect of PS
content and PP melt viscosity
on the dispersed phase
particle size for (**a**) blends
without MMT and (**b**) blends
with MMT. PS is the
dispersed phase when the PS
content is below 50 wt%
while the matrix is PP/PP-g-
MA or PP/PP-g-MA/
MMT. The wt% MMT is
based on the MMT content in
PP/PP-g-MA/MMT. The
dashed line represents the
co-continuous region as
observed from TEM images
for blends prepared with
various grades of PP. The
L-PP, M-PP, and H-PP
represent low, medium, and
high molecular weight grades
of PP, respectively (Tiwari
and Paul 2011a)
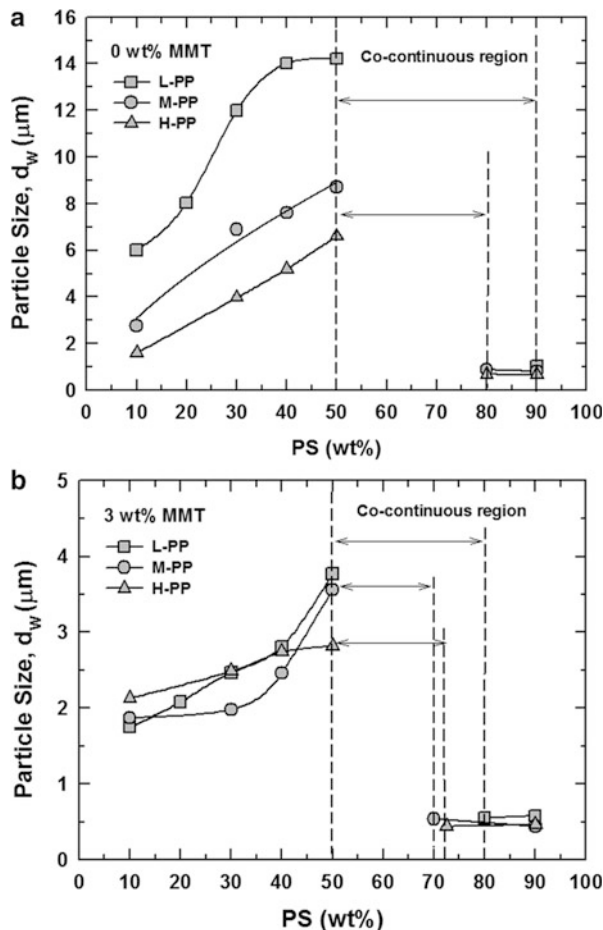
(Fortelný and Živný 1995; Sundararaj and Macosko 1995; Wildes et al. 1999; Paul
and Bucknall 2000a). The phase inversion composition can be predicted based on
the empirical model developed by Paul and Barlow as given by $\phi_1/\phi_2 = \eta_1/\eta_2$
where ϕ and η represent volume fraction and viscosity of polymer components in
blend (Paul and Barlow 1980). According to this relation, the phase inversion
composition ϕ_1 decreases as the viscosity ratio η_1/η_2 decreases; the blends with
PS and PP/PP-g-MA/MMT show phase inversion at lower PS contents than blends
without MMT as the viscosity ratio of PS phase to PP phase decreases in the
presence of MMT (Tiwari and Paul 2011a). The onset of co-continuity did not
change when clay is present in the major PP phase, whereas the presence of clay in
the dispersed phase has been known to increase the co-continuity as observed in
HDPE/PA 6/MMT blends where organoclay is present in the dispersed PA 6 phase
(Filippone et al. 2008, 2010b).

17.2.1.1 Effects of MMT and Matrix Molecular Weight on Dispersed Phase Particle Size

The final morphology of a blend is a result of competing effects of droplet breakup and coalescence during blending that depends on several factors including the viscosity ratio of the dispersed phase to matrix phase (Barlow and Paul 1981; Favis and Chalifoux 1987; Wu 1987; Sundararaj et al. 1992; Sundararaj and Macosko 1995). The lower ratio defines the higher matrix viscosity which increases the breakup of dispersed particles due to high shear stresses and reduces the dispersed phase particle size in the blend. The high matrix viscosity also creates a more immobile interface thereby reducing coalescence of dispersed particles. It has been reported for PP/PP-g-MA/MMT/PS blend nanocomposites that for nearly similar viscosity ratios of the dispersed to continuous phase, i.e., for $\eta_{PS}/\eta_{(L-PP/PP-g-MA/MMT)} = 2.75$ and $\eta_{PS}/\eta_{(M-PP/PP-g-MA)} = 2.56$, the PS particle size in the L-PP-based blend with MMT is 2.47 μm compared to PS particle size of 6.9 μm observed for M-PP-based blends without MMT. Similarly, in H-PP-based blends containing 30 wt% PS, although the viscosity ratio of two phases did not change much with the addition of MMT, the PS particle size is reduced from 3.82 μm for the blend without MMT to 2.49 μm for a blend with MMT (Tiwari and Paul 2011a). This suggests that although rheology is a factor in decreasing particle size of dispersed phase, the decrease in coalescence of PS particles in the presence of MMT is an additional factor which helps to reduce the PS particle size to a much greater extent in blends with MMT than in blends without MMT.

17.2.1.2 Effect of MMT on Dispersed Phase Morphology Stability

For incompatible blends a low shear processing can lead to the coalescence of the dispersed phase particles and reduce their performance. An increase in the phase stability in the melt state extends the possibility of commercial applications for blends at high temperatures. Not many studies have explored the effect of annealing on dispersed phase particle size and shape in blends with organoclay (Khatua et al. 2004; Moghbelli et al. 2010; Tiwari and Paul 2011a). It is expected that polymer blends compatibilized with organoclay should lead to a more stable morphology; however, the location of organoclay in such blends can have a significant effect on the morphology stability. Well-dispersed clay particles in the continuous phase of immiscible blends can lead to improved phase stability of dispersed particles in the melt state as seen for the PA 6/ethylene–propylene rubber (EPR) (80/20) blends where organoclay resides in the PA 6 continuous phase. A poor stability of the dispersed phase in the melt is observed when MMT particles are located in the dispersed PS phase in PP/PS (70/30) blends (Khatua et al. 2004). The clay particles located in the continuous phase and at the interface in immiscible blends can also lead to significant improvement in phase stability upon annealing. Figures 17.3 and 17.4 show the morphology of dispersed PS particles in PP/PP-g-MA/PS blends with and without MMT after being subjected to annealing in a quiescent state at 210 °C for 2 h (Tiwari and Paul 2011a). The phase stability is significantly higher in blends with MMT compared to blends without MMT where the PS particle sizes increased by ∼10 times for the H-PP/PP-g-MA/PS blend.
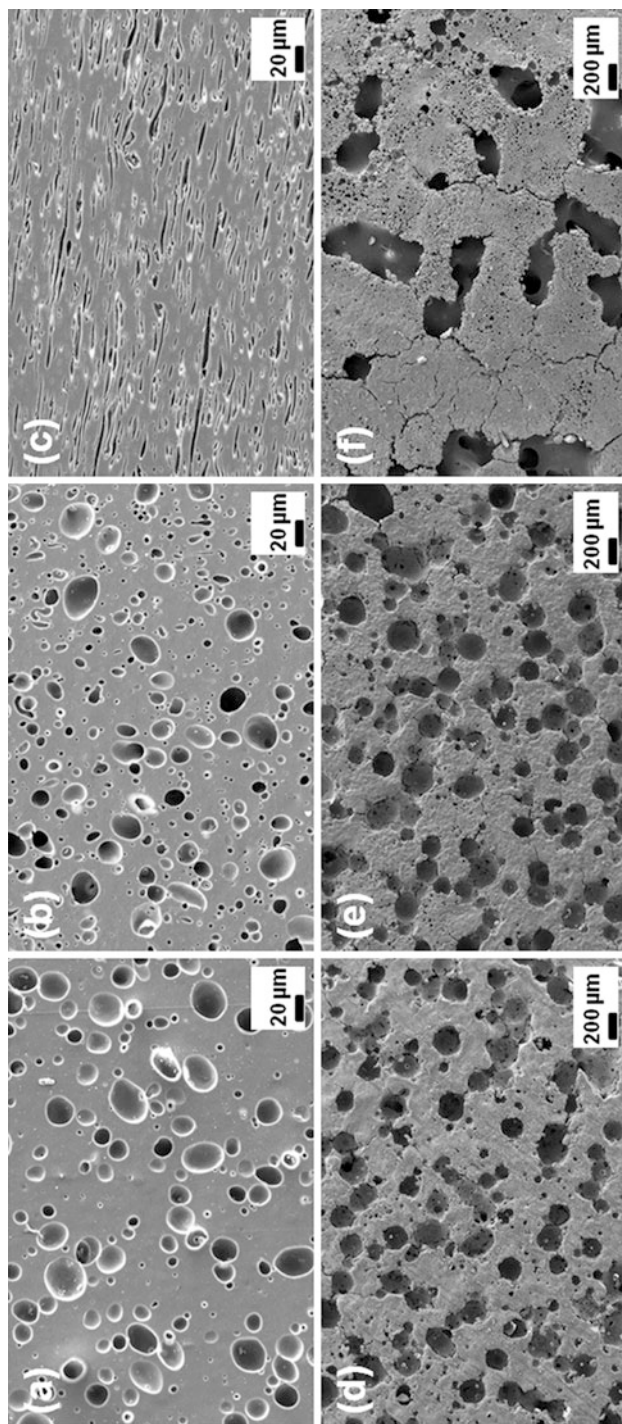
Fig. 17.3 SEM images of PP/PP-g-MA/PS blends containing 30 wt% PS. *Top row* shows images for as-molded samples, while the *bottom row* shows images for annealed samples at 210 °C for 2 h. The blends were prepared with different PP grades: L-PP (**a** and **d**), M-PP (**b** and **e**), and H-PP (**c** and **f**) (Tiwari and Paul 2011a)
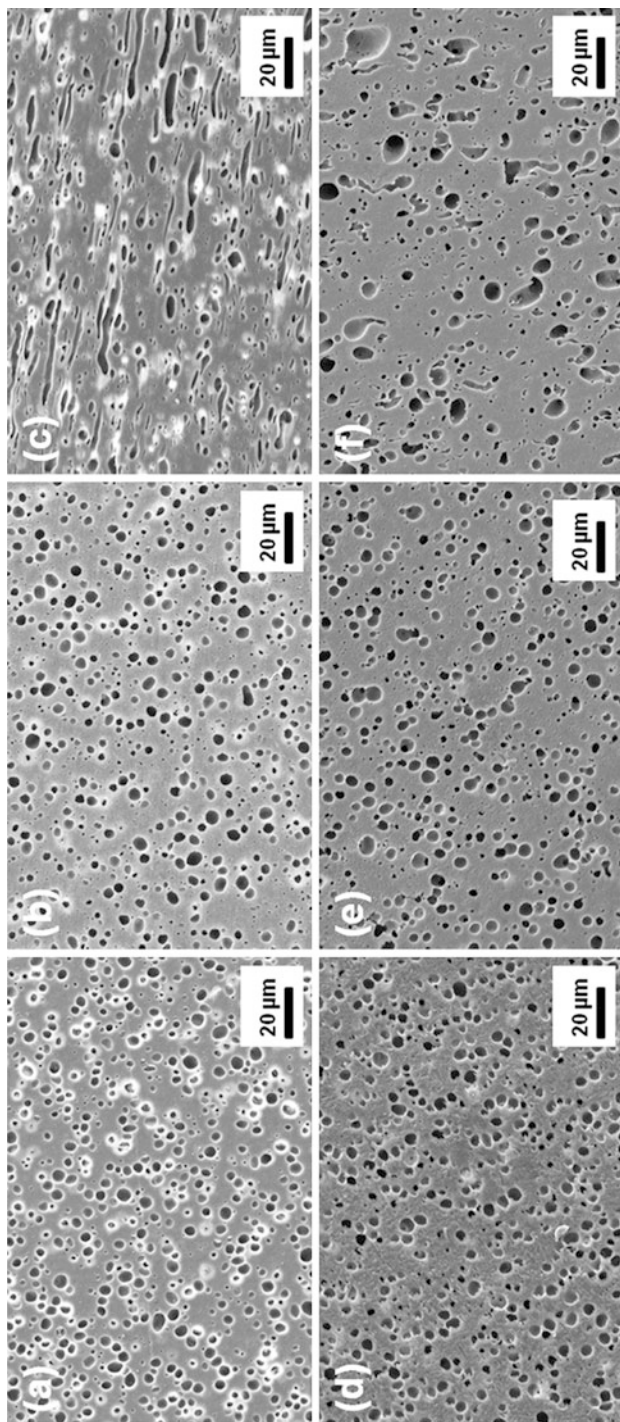
Fig. 17.4 SEM images of PP/PP-g-MA/MMT/PS blends containing 30 wt% PS. *Top row* shows images for as-molded samples, while *bottom row* shows images for annealed samples at 210 °C for 2 h. The blends were prepared with different PP grades: L-PP (**a** and **d**), M-PP (**b** and **e**), and H-PP (**c** and **f**) (Tiwari and Paul 2011a)

Table 17.1 Viscosity ratio and weight average PS particle size ($\overline{d}_w$) in PP/PP-g-MA/PS blends with and without MMT. The PS composition in blend is 30 wt% (Data taken from Tiwari and Paul 2011a)

Matrix	MMT wt% in matrix[a]	η_d/η_c[b]	$\overline{d}_w$(μm) As molded	After 2 h in melt at 210 °C
L-PP[c]	0	4.25	12.0	60.5
	3	2.75	2.47	2.66
M-PP[c]	0	2.56	6.9	72.3
	3	1.87	1.98	2.38
H-PP[c]	0	1.24	3.82	44.5
	3	0.97	2.49	2.71

[a]The PP/PP-g-MA or PP/PP-g-MA/MMT was used as a matrix to prepare blends at 30 wt% PS. The MMT wt% is based on MMT content in PP/PP-g-MA/MMT. The PP-g-MA/organoclay ratio is 1.0
[b]η_d is viscosity of dispersed phase PS; η_c is the viscosity of continuous phase PP/PP-g-MA (0 wt% MMT) and PP/PP-g-MA/MMT (3 wt% MMT). The viscosity ratio for the two phases is assumed for blends where PS forms the dispersed phase
[c]The various PP represent viscosities for PP/PP-g-MA (0 wt% MMT) and PP/PP-g-MA/MMT (3 wt% MMT)

The presence of MMT at the interface and in the PP matrix for PP/PP-g-MA/MMT/PS blends has a significant effect on morphology stability. The presence of clay at the interface effectively acts as a compatibilizer leading to smaller dispersed phase particles and morphology stability in the quiescent melt (Moghbelli et al. 2010; Tiwari and Paul 2011a). The increase in dispersed phase stability in the melt state for blends with clay correlates well with the stable morphology observed for reactive-compatibilized PP and amino-terminated PS blend (Omonov et al. 2007). Table 17.1 shows changes in PS particle size after annealing PP/PP-g-MA/PS and PP/PP-g-MA/MMT/PS blends.

17.2.2 Polypropylene (PP)–Elastomer Blends

Polypropylene is a semicrystalline thermoplastic with major application in diverse areas due to its excellent processability, low density, high thermal stability, good chemical resistance, and low cost; however, its low impact properties limit many practical applications (Karian 2003; Holden and Hansen 2004). Elastomers such as EPR, ethylene–propylene–diene terpolymer (EPDM), and SEBS have been used to improve toughness of PP (Yang et al. 1984; Chou et al. 1988a, b; Mighri et al. 2001; Bassani and Pessan 2002; Yazdani-Pedram et al. 2003; Abreu et al. 2005; Öksüz and Eroğlu 2005; Matsuda et al. 2006; Naderi et al. 2008; Bai et al. 2009). However, the recent development of metallocene catalyst technology has led to new ethylene-co-octene copolymer rubbers (EOR) with controlled levels of chain branching, narrow molecular weight distribution (MWD) that provides improved rheological properties, such as better shear thinning behavior, melt elasticity, and melt processability; EOR materials have shown better efficiency of impact modification of

Fig. 17.5 Comparison of
relative modulus as a function
of filler content formed from
melt mixing with MMT and
with talc (Lee et al. 2005)
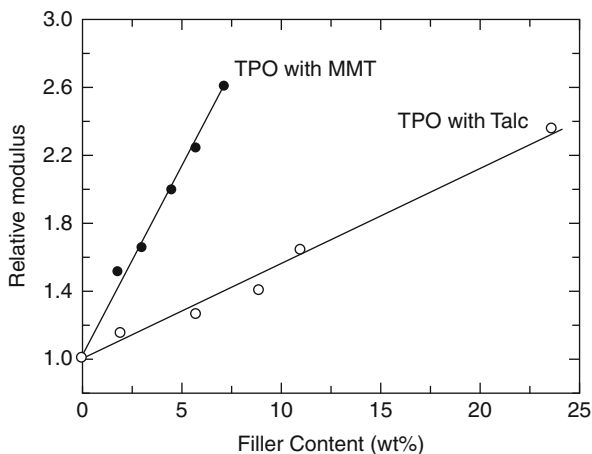
PP compared to other elastomers (Reddy and Sivaram 1995; Bensason et al. 1996;
Carriere and Silvis 1997; Keating and Lee 1999; Da Silva et al. 2000a, b; Premphet
and Horanont 2000; Da Silva et al. 2001; Marquardt et al. 2001; Premphet and
Paecharoenchai 2001; Yu 2001; Da Silva et al. 2002; Ling et al. 2002; McNally
et al. 2002; Premphet and Paecharoenchai 2002; Prieto et al. 2002; Qiu et al. 2002;
Zhang et al. 2002; Rabinovitch et al. 2003; Yang et al. 2003; Arzondo et al. 2004;
Ono et al. 2005; Lim et al. 2006; Meng et al. 2006; Xu et al. 2006a; Lee et al. 2007;
Fasce et al. 2008; Svoboda et al. 2009; Zhu et al. 2009). Such blends of polyolefin
with elastomers are referred to as a "thermoplastic olefin" or TPO.

   Toughness of PP is usually obtained at the cost of stiffness due to the presence of
the soft elastomer particles; however, a major issue for some applications is to
achieve an optimum balance of stiffness and toughness. To address this issue,
conventional fillers such as calcium carbonate ($CaCO_3$), talc, short glass fiber, or
kaolin are generally added to PP/elastomer blends to improve their stiffness;
however, due to the low aspect ratio of conventional fillers, large loadings are
required to significantly increase stiffness which can result in poor processability,
lower ductility, and rough surface finish of the final product (Stamhuis 1984,
1988a, b; Pukánszky et al. 1990; Kolařík and Jančář 1992; Schaefer et al. 1993;
Premphet and Horanont 2000; Lee et al. 2005; Ma et al. 2010). Replacing such
fillers with high-aspect-ratio nanofillers such as organoclays could potentially
alleviate these issues, assuming good levels of clay dispersion can be achieved.
As seen in Fig. 17.5, the addition of ∼5 wt% MMT in TPO provides an equivalent
improvement in modulus as 20 wt% of talc (Lee et al. 2005, 2006a).

   TPO can be prepared either by melt mixing PP and elastomer in an extruder or by
copolymerization of olefins in a series of reactors to give a blocklike structure. The
reactor-made TPO produces a fine and stable morphology due to controlled reaction
parameters; however, they have an elastomer composition fixed by the polymeri-
zation process. On the other hand, extruder-made TPOs provide wide flexibility in

terms of changing material composition and properties to explore and understand their effects on elastomer phase morphology and mechanical performance (Carriere and Silvis 1997; Da Silva et al. 2000b; Premphet and Paecharoenchai 2002; Lee et al. 2005, 2006a; Lim et al. 2006; Tiwari and Paul 2011b, c; Tiwari et al. 2012; Tiwari and Paul 2012; Tiwari et al. 2013). This also forms a convenient route for formulating TPOs in terms of particle size control and properties based on end use applications. The purpose here is to focus on the role of organoclay to achieve a good balance of stiffness and toughness in extruder-made TPO nanocomposites. Deshmane et al. (2007) reported up to 10 % increases in the room temperature impact strength for reactor-made TPO nanocomposite with 4 wt% clay. On the contrary, Mehta et al. (2004) observed a decrease in the notched impact strength with clay content for TPO nanocomposites prepared from commercial TPO having 30 wt% EPR. Later, Paul and coworkers reported extensive work on the extruder-made TPO nanocomposites and systematically studied the effect of the molecular weight of PP, melt flow index of elastomers, elastomer octene content, and MMT content on the elastomer particle shape and size, toughness, ductile–brittle transition temperature, and thermal expansion behavior (Lee et al. 2005, 2006a; Tiwari and Paul 2011b, c; Tiwari et al. 2012; Tiwari and Paul 2012; Tiwari et al. 2013). The understanding of the role of nanofillers on blend morphology and properties is still evolving; however, the following provides a summary of the current state of this approach.

17.2.2.1 Effect of PP-g-MA Content

The nonpolar nature of PP is an impediment to a high level of dispersion of organoclays unlike polar polyamide nanocomposites, wherein clay can be efficiently exfoliated using appropriate melt processing techniques (Fornes et al. 2001). Addition of small amounts of PP-g-MA to a PP matrix can increase polarity of PP leading to improved affinity for the silicate surface to achieve better dispersion of the MMT particles in the PP matrix and, as a consequence, improved stiffness of PP nanocomposites can be obtained (Hasegawa et al. 2000; Nam et al. 2001; Okamoto et al. 2001; Reichert et al. 2001; Marchant and Jayaraman 2002; Zhang et al. 2003). Increasing PP-g-MA content in the PP results in significant improvement in the level of exfoliation of MMT particles in a PP matrix which in turn increases the stiffness and the thermal expansion behavior of PP/PP-g-MA/MMT nanocomposites (Kim et al. 2007a). The addition of an elastomer to PP nanocomposites can lead to "super-tough" materials at elastomer contents of ∼30 wt% and 3 wt% MMT as seen in Fig. 17.6. The masterbatch used here contains an equal amount of PP-g-MA and organoclay. The addition of PP-g-MA to the PP matrix facilitates the dispersion of MMT particles which in turn decreases elastomer particle size by retarding coalescence and, then, leading to increased toughness (Lee et al. 2005). Figure 17.7 shows the weight average elastomer particle size decreases from 2.8 μm for PP/EOR blend without MMT to 0.8 μm in the presence of 7 wt% MMT at 30 wt% elastomer content. The impact strength does not change much with further increase in MMT content beyond the onset from the brittle–ductile transition (Lee et al. 2005). In another study, the effect of

Fig. 17.6 Effect of MMT
and elastomer contents on
notched impact strength of
PP/elastomer/masterbatch
nanocomposites containing
various amounts of
elastomers. The masterbatch
contains equal amount of
PP-g-MA and organoclay
(Lee et al. 2005)
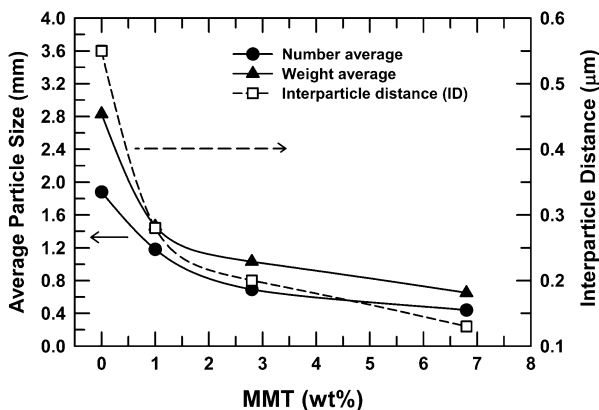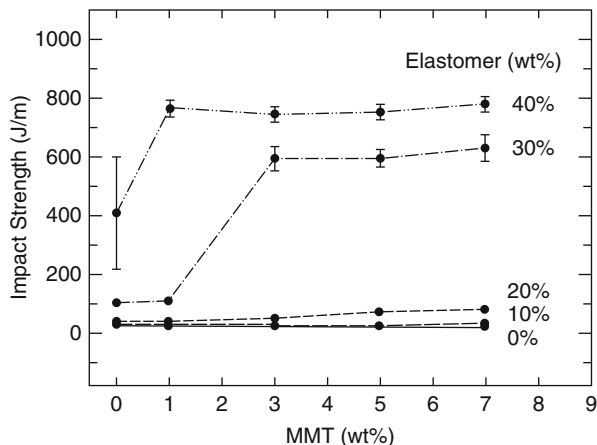
Fig. 17.7 The effect of MMT levels on the number and weight average apparent elastomer particle sizes (filled symbols) and interparticle distance (open symbol) of PP/elastomer/masterbatch nanocomposites containing 30 wt% elastomer. The masterbatch contains equal amount of PP-g-MA and organoclay (Lee et al. 2005)

PP-g-MA/organoclay ratio and MMT content on the toughness of extruder-made PP/PP-g-MA/MMT/EOR nanocomposites was determined by Tiwari et al. (2012). The elastomer content in this work was fixed at 30 wt% following the work done by Lee et al. (2005) where elastomer content >30 wt% showed a decrease in the tensile properties. Figure 17.8 shows the effect of MMT content and PP-g-MA/organoclay ratio on the notched impact strength of PP/PP-g-MA/MMT/EOR nanocomposites. A sharp brittle–ductile transition is observed in the presence of PP-g-MA in the nanocomposite; the onset of the transition shifts to lower MMT contents along with an increase in the plateau impact strength as the PP-g-MA/organoclay ratio is

Fig. 17.8 Notched impact strength of PP/PP-g-MA/ MMT/EOR nanocomposites. (**a**) Effect of MMT content and PP-g-MA/organoclay ratio, (**b**) effect of elastomer particle size (Tiwari et al. 2012)
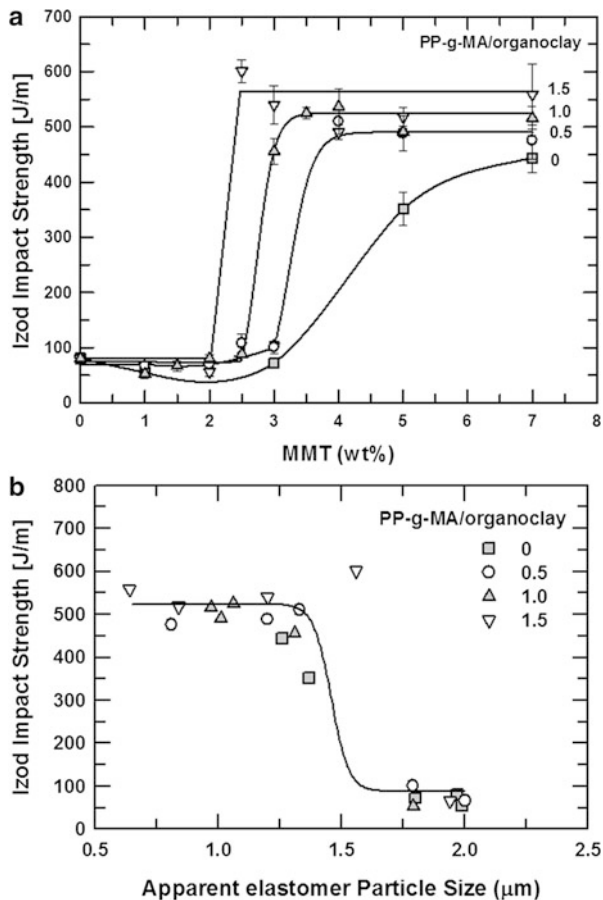
increased. In the case of reactor-made "super-tough" TPO, the impact strength decreases with the addition of the PP-g-MA and MMT; the ductile–brittle failure is more prominent at a PP-g-MA/organoclay ratio of 2.0 as reported by Kim et al. (2007b). This reduced impact strength results from the decreased matrix ductility of reactor-made TPO in the presence of MMT; however, other factors such as differences in the TPO preparation methods (extrusion vs. reactor-made), molecular weight of PP and elastomer, matrix crystallinity, and elastomer type can also affect the performance of reactor-made TPO nanocomposites. The plot of elastomer particle size versus impact strength for extruder-made PP/PP-g-MA/ MMT/EOR nanocomposites shows the onset of toughness occurs at ∼1.6 μm followed by a plateau at lower elastomer particle size down to ∼0.6 μm (see Fig. 17.8b). The elastomer particle size at onset is specific to the matrix molecular weight, elastomer type, and content and can be easily tailored by varying these properties which is discussed in detail in next section. Except for impact strength,

the extruder-made and reactor-made TPO nanocomposites show similar trends in other properties where filler effects are dominant; such nanocomposites show increases in stiffness and yield strength and decrease in elongation at break as the MMT dispersion and MMT content are increased (Lee et al. 2005, 2006a; Kim et al. 2007b, 2008; Tiwari et al. 2012).

17.2.2.2 Effect of PP Molecular Weight and Elastomer MFI

The matrix molecular weight has a significant effect on the mechanical properties and toughness of elastomer-toughened blends; this is due to inherent ductility of the matrix and its response to toughening for different elastomers (Bucknall 1977; Wu 1985, 1987; Dijkstra and Gaymans 1994; Dijkstra et al. 1994; Majumdar et al. 1994a; Oshinski et al. 1996a, b; van der Wal et al. 1998, 1999). Tiwari and Paul (2011c) reported the effects of PP molecular weight, elastomer type, and MMT content on the elastomer particle size and toughness. Tables 17.2 and 17.3 lists the properties and designations of various PP and EOR used to prepare PP/PP-g-MA/MMT/EOR nanocomposites reported in this section. The elastomers designated as EOR 8150 and EOR 8150N are the same grade of Engage® 8150; however, based on the rheological measurements, EOR 8150N is reported to have high molecular weight than EOR 8150. PP/PP-g-MA/MMT/EOR nanocomposites were prepared with different molecular weight grades of PP and elastomer MFI at a fixed elastomer content of 30 wt% and PP-g-MA/organoclay ratio of 1.0. As seen in Fig. 17.9, the MMT particles in PP/PP-g-MA/MMT/EOR nanocomposites are exclusively located in the PP phase, irrespective of the PP molecular weight. The dark domains are the elastomer phase stained with ruthenium tetroxide.

The decrease in the elastomer particle size of PP/PP-g-MA/MMT/EOR nanocomposites is believed to result from the "barrier" effect of clay which retards the coalescence of elastomer particles. The dispersion of MMT particles has a significant effect on the extent of decrease in coalescence of dispersed phase; hence, it is important to understand the dispersion behavior of MMT particles as a function of matrix molecular weight. It is known that in partially exfoliated nanocomposites, the MMT particles are mostly skewed and randomly distributed in the low molecular weight matrix but become more well dispersed and aligned in the flow direction as the molecular weight of the matrix increases. The increased shear viscosity associated with increased molecular weight of the matrix improves MMT dispersion and aligns the particles along the flow direction (Fornes et al. 2001; Tiwari and Paul 2011a, b). Figure 17.10 shows the aspect ratio of the MMT particles as a function of elastomer MFI and octene content for PP/PP-g-MA/MMT/EOR nanocomposites prepared with various molecular weight grades of PP at a fixed MMT content of 5 wt%. A maximum MMT aspect ratio is observed for nanocomposites containing elastomers with MFI in the range of 0.5–1.0. For a given elastomer MFI, the aspect ratio of MMT ranks in the order: H-PP > M-PP > L-PP. The difference in the octene content of elastomers does not affect the aspect ratio of MMT particles in PP/PP-g-MA/MMT/EOR nanocomposites, even though they are reported to have different viscosities (see Table 17.3).

Table 17.2 Properties and designations of polypropylene (Tiwari and Paul 2011b)

Grade	Designation[a]	MFI g/10 min at 190 °C/2.16 kg	Viscosity (Pa. s) η_0	$\eta_{at250\ rad/s}$	ΔH_{fusion} (J/g^{-1})[b]	$T_m(°C)$[b]	Izod impact (J/m)	Tensile modulus (GPa)	Yield strength (MPa)	Elongation at break (%)
Pro-fax PH020	L-PP	24	820	130	104	163	27 ± 4	1.38 ± 0.08	28 ± 0.1	>200
Pro-fax 6301	M-PP	6.3	3250	235	95.3	164	33 ± 4	1.35 ± 0.07	27 ± 0.02	>200
Pro-fax 6523	H-PP	2.1	7510	360	96.2	163	45 ± 3	1.17 ± 0.04	26 ± 0.2	>200
Polybond 3200	PP-g-MA	110	–	–	–	–	–	–	–	–

[a]The L-PP, M-PP, and H-PP designate the low, medium, and high molecular weight PP grade, respectively
[b]D.S.C. measurements at heating and cooling rate of 10 °C/min

Table 17.3 Properties and designations of elastomers (Tiwari and Paul 2011b)

Grade[a]	Designation[b]	MFI g/10 min at 190 °C/ 2.16 kg	Viscosity (Pa.s)		T_g (°C)[c]	T_m (°C)[c]	χ_c (%)[c]
			η_0	$\eta_{at250rad/s}$			
Engage 8200	EOR 8200	5.0	1740	505	−54	60	13.8
Engage 8100	EOR 8100	1.1	10820	1160	−56	59	12.6
Engage 8150	EOR 8150	0.5	19860	1490	−56	55	13.7
Engage 8150	EOR 8150N	0.25	69070	1980	−54	44	12.6
Exact 8201	EOR 8201	1.15	12810	830	−46	74	27.0

[a]The octene contents in Engage® and Exact® grades are ∼39 wt% and ∼28 wt% respectively
[b]EOR8150 is from an original batch of Engage from DuPont Dow Elastomer, while EOR 8150N (N = new) was purchased later from Dow Chemical through a distributor
[c]DSC measurements at heating and cooling rate of 10 °C/min
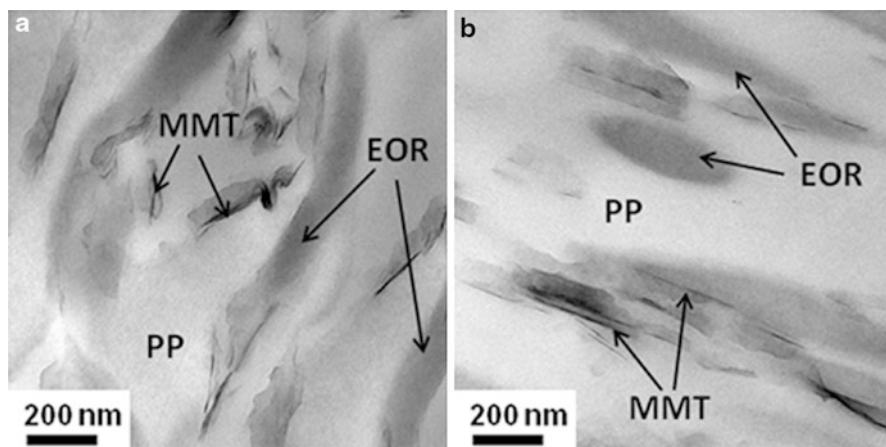
Fig. 17.9 TEM micrographs of PP/PP-g-MA/MMT/EOR 8100 nanocomposite prepared from L-PP (**a**) and H-PP (**b**) showing the location of the elastomer and the MMT particles. The elastomer content is 30 wt% and MMT content is 5 wt% based on total nanocomposite. All images viewed parallel to TD; clay particles are oriented parallel to FD (Tiwari and Paul 2011b)

The effect of MMT content and PP molecular weight on the elastomer morphology in PP/PP-g-MA/MMT/EOR nanocomposites is shown in Fig. 17.11. The elastomer particles are large with a mixture of spherical and elongated shapes in L-PP/EOR blend or mostly spherical shapes in the H-PP/EOR blend without MMT and become small and mostly elongated in the presence of MMT in both L-PP- and H-PP-based nanocomposites. The nonspherical nature of elastomer particles is

Fig. 17.10 The effect of elastomer MFI on MMT particle aspect ratio of PP/PP-g-MA/MMT/EOR nanocomposite prepared from various molecular weight PP. *Gray-* and *black-* filled symbol represents nanocomposites containing elastomers having 39 and 28 wt% octene content, respectively. The EOR and MMT content is based on the total nanocomposite weight (Tiwari and Paul 2011b)
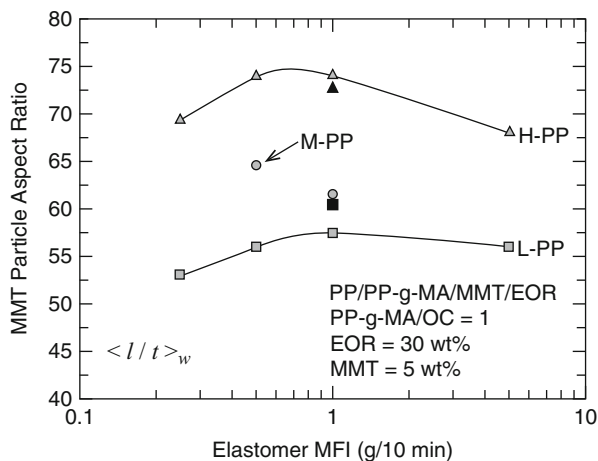
related to the deformation that occurs during injection molding, whereas a decrease in the elastomer particle size and an increase in elastomer particle density are observed as the molecular weight of PP and MMT content increases. This is related to the effects of increased PP viscosity caused by MMT and the "barrier" effect of clay that retards the coalescence of elastomer particles as explained in various reports on blend nanocomposites (Gelfer et al. 2003; Khatua et al. 2004; Lee et al. 2005; Vo and Giannelis 2007; Yoo et al. 2010a, b). The percent decrease in the elastomer particle size in the presence of clay is higher for nanocomposites prepared from L-PP; however, the nanocomposites based on H-PP always have a smaller elastomer particle size than L-PP. For example, in the case of PP/PP-g-MA/MMT/EOR 8100 nanocomposites, L-PP is reported to be more effective in reducing elastomer particle size by 59 % at 3 wt% MMT compared to 41 % for M-PP and 16 % for H-PP-based nanocomposites at 3 wt% MMT; however, the elastomer particle size for L-PP nanocomposites is higher than the H-PP-based nanocomposite at any fixed MMT content, and this trend is the same for other elastomers (Tiwari and Paul 2011b, c, 2012). The elastomer with an MFI in the range of 0.5–1.0 gives maximum decrease in the elastomer particle size in PP/PP-g-MA/MMT/EOR nanocomposites irrespective of the PP molecular weight. The effect of elastomer MFI range on the properties cannot be generalized for blends of elastomer with other thermoplastics and may depend on several factors such as interaction between matrix and elastomer in addition to the viscosity ratio of elastomer to matrix.

17.2.2.3 Correlation Between Impact Strength and Elastomer Particle Size

Notched impact specimens fail in three different modes based on the ability to absorb impact energy: a hinged break for tough samples, a complete break into two pieces for brittle samples, and a mixed mode, either a hinged or a complete break, for samples near the ductile–brittle transition composition. These three failure
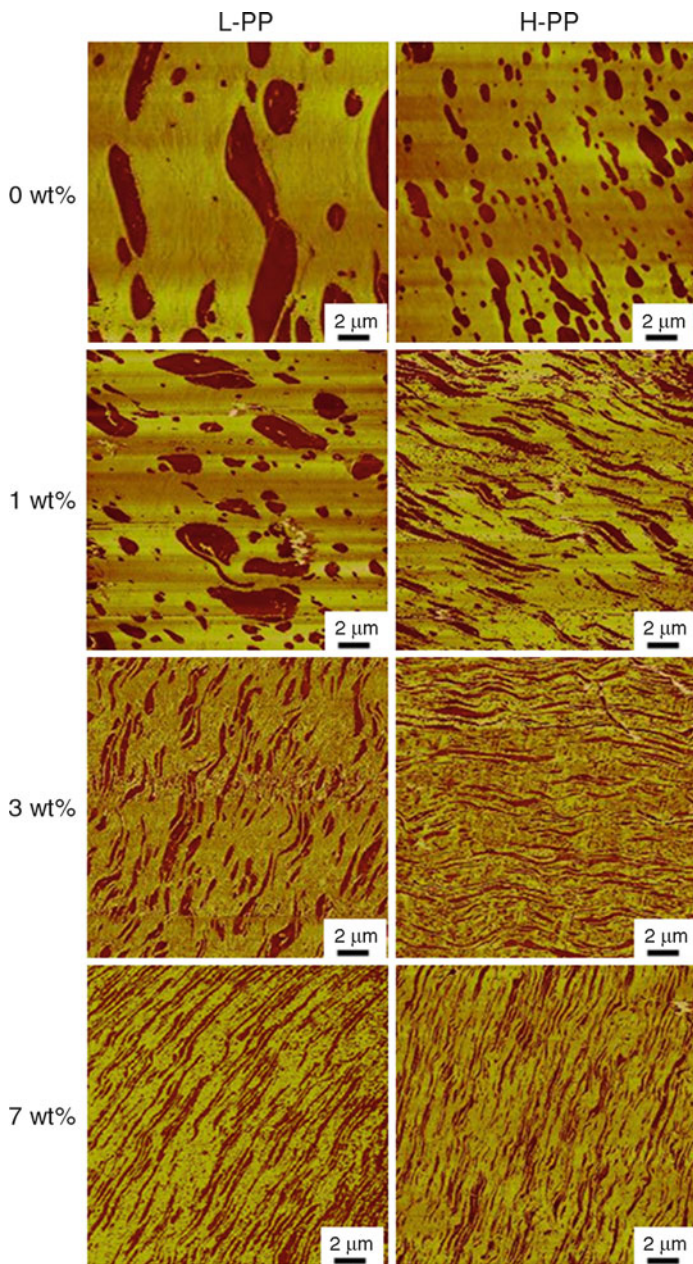
Fig. 17.11 AFM images of PP/PP-g-MA/MMT/EOR nanocomposites showing elastomer particle morphology as a function of MMT content and PP molecular weight grade. The PP-g-MA/organoclay ratio is 1.0 and elastomer content is 30 wt%. All images were taken from the core of the injection-molded sample and viewed parallel to TD; elastomer particles are oriented parallel to FD (Tiwari and Paul 2011b)
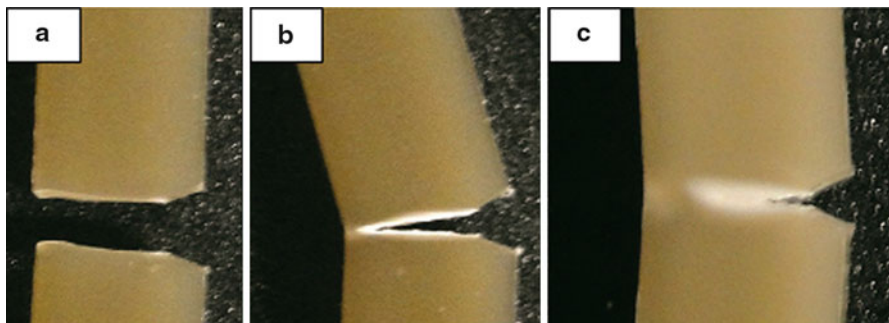
Fig. 17.12 Image representing failure modes in impact specimen. (**a**) A complete break into two pieces for brittle sample, (**b**) a mixed mode with hinged or a complete break for samples near brittle–ductile transition, and (**c**) a hinged break for tough samples (Tiwari and Paul 2011c)

modes for elastomer-toughened PP nanocomposites are shown in Fig. 17.12 (Tiwari and Paul 2012). Paul and coworkers have reported that elastomers with MFI in the range of 0.5–1.0 provide maximum improvement in the toughness in the case of L-PP/PP-g-MA/MMT/EOR nanocomposites. However, the effect of elastomer MFI becomes less significant as the PP molecular weight is increased, i.e., in the H-PP-based system; all nanocomposites maintain super-toughness, and no significant change in the impact strength is observed with MMT content and elastomer MFI (Tiwari and Paul 2011c). Figure 17.13 shows the effects of elastomer MFI and MMT content on the impact strength of extruder-made TPO nanocomposites prepared from different molecular weight grades of PP.

The elastomer particle size and size distribution plus elastomer content significantly affect the toughness of elastomer/thermoplastic blends (Oshinski et al. 1996a, b, c; Majumdar et al. 1997; Huang et al. 2006b; Bucknall and Paul 2009; Tiwari and Paul 2011b, c, 2012). It has been observed that small particles (weight average particle diameter, $\overline{d}_w \sim 0.2 - 0.4$ μm) provide toughness when shear yielding dominates the toughening mechanism, whereas larger particles ($\overline{d}_w \sim 2 - 3$ μm) are more effective when crazes contribute to energy absorption. It is also known that for most elastomer-toughened thermoplastics, the maximum toughness is restricted to a limited range of particle sizes, which is often quite narrow (Oshinski et al. 1996a, b, c; Majumdar et al. 1997; Huang et al. 2004, 2006a, b; Huang and Paul 2006; Bucknall and Paul 2009; Tiwari and Paul 2011b, c, 2012). It is believed that any deviation beyond the preferred range in either direction results in a ductile–brittle transition, as illustrated in Fig. 17.14, where b and d respectively mark the midpoints of the lower and upper transitions and thus define critical particle sizes. The curve represents the elastomer particle size for the blend of PA 6 and reactive-compatibilized elastomer; however, with appropriate scaling of particle size and peak height, similar curves could be drawn for almost any well-made rubber-toughened polymer blend provided elastomer particle size with lowest limit are obtained (Bucknall and Paul 2009). Not much is known about the elastomer particle size limits on the toughening of PP/elastomer blends and

Fig. 17.13 Effect of the
MMT content on the notched
impact strength of PP/PP-g-
MA/MMT/EOR
nanocomposites prepared
from (**a**) L-PP and (**b**) H-PP.
Elastomer content is 30 wt%
and PP-g-MA/organoclay
ratio is 1.0 (Tiwari and Paul
2011c)
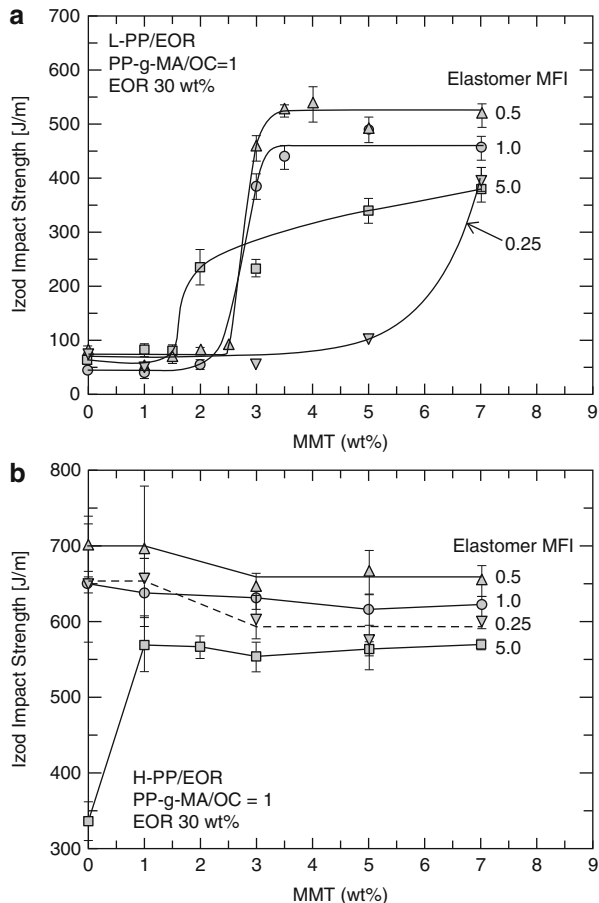
nanocomposites (Jiang et al. 1995; Liang and Li 2000). The results on the effect
of various parameters such as PP molecular weight, elastomer and MMT content
on the elastomer particle size, and toughness in extruder-made TPO
nanocomposites can provide knowledge about elastomer particle size limits in
elastomer-toughened PP.

Figure 17.15 shows the effect of elastomer particle sizes on the room tempera-
ture impact strength for blends and nanocomposites prepared by varying elastomer
MFI and MMT content for L-PP, M-PP, and H-PP nanocomposites. The general
behavior is that the critical elastomer particle size below which the nanocomposite
shows tough behavior appears to decrease as the PP molecular weight increases; the
H-PP materials did not show any critical elastomer particle size irrespective of
elastomer octene content. The nanocomposites based on elastomers with high
octene content have higher impact strength, and the onset of toughness occurs at
a larger elastomer particle size compared to nanocomposites based on elastomers
with low octene content (see Fig. 17.15a). This relates to the higher crystallinity and
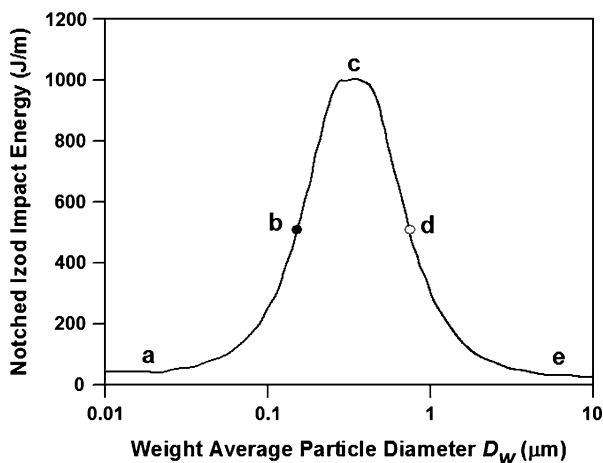
Fig. 17.14 Relationship between particle size and impact behavior for a typical "super-tough" thermoplastic blend. Points b and d mark *lower* (●) and *upper* (○) ductile–brittle transitions. Schematic representation based broadly on data of Huang et al. (2006b) for a series of 80/20 RTPA6 blends (Bucknall and Paul 2009)

higher modulus of the low octene content elastomer which limits its tendency to undergo cavitation desired for toughness; however, this effect of elastomer crystallinity and modulus on the onset of toughness and impact strength diminishes with the increase in the PP molecular weight especially for H-PP-based nanocomposite. Tiwari and Paul (2011c) have observed that for nearly similar elastomer particle sizes, the impact strength varies in the order H-PP > M-PP > L-PP indicating PP molecular weight has a significant effect on the toughness of PP/PP-g-MA/MMT/EOR nanocomposites other than elastomer particle size. The effect of matrix molecular weight on the toughness as seen in elastomer-toughened blends without MMT seems to be valid in the case of a matrix with clay particles (Bucknall 1977; Wu 1985, 1987; Dijkstra and Gaymans 1994; Dijkstra et al. 1994; Majumdar et al. 1994a; Oshinski et al. 1996a, b; van der Wal et al. 1998, 1999; Liang and Li 2000).

17.2.2.4 Toughening Mechanism and Ductile–Brittle (D-B) Transition Temperature

The ductile–brittle (D-B) transition temperature provides information about the performance limit below which the material fails in a brittle manner. The D-B transition temperature is generally defined as the midpoint in the steplike change in impact strength recorded as a function of temperature. The matrix and elastomer properties and elastomer particle size have a significant effect on the D-B transition temperature. Although, the understanding of the role of elastomer particle size and shape in the toughening process is still evolving, the two toughening mechanisms prominent in elastomer-toughened blends are (1) the stress concentration effect of

Fig. 17.15 Effect of the weight average apparent elastomer particle size on the notched impact strength of PP/PP-g-MA/MMT/EOR nanocomposites prepared from (**a**) L-PP, (**b**) M-PP, (**c**) H-PP, and elastomers with different MFI. Elastomer content is 30 wt% and PP-g-MA/organoclay ratio is 1.0 (Tiwari and Paul 2011c)
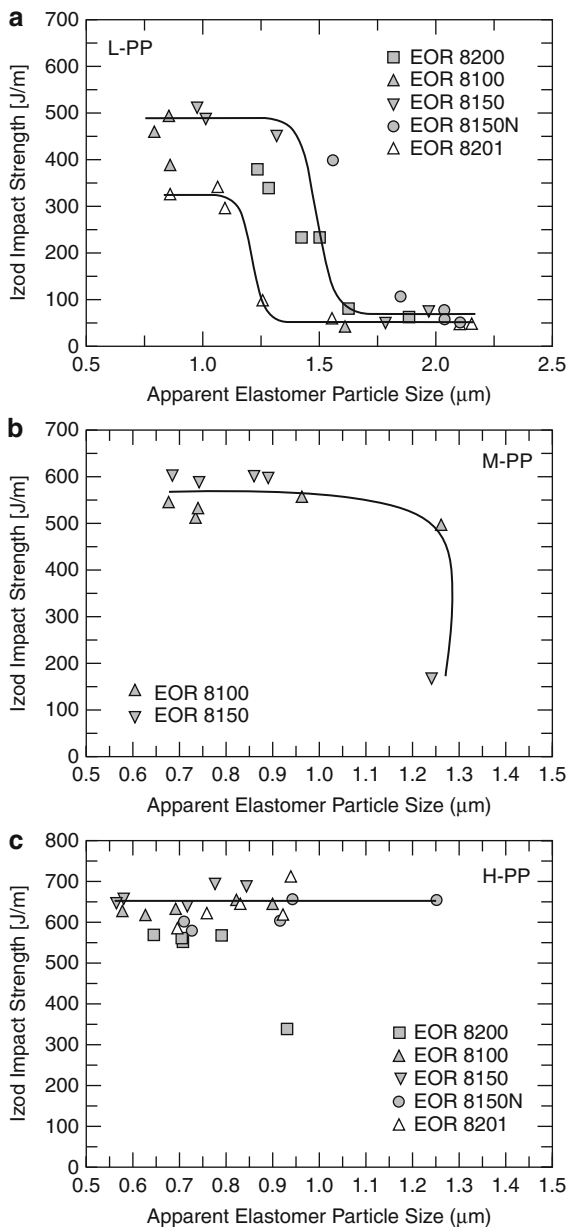
the low modulus elastomer particles in a more rigid matrix to initiate and terminate crazes and (2) rubber particle cavitation thereby relieving triaxial stress leading to shear yielding of pseudo-ductile matrices such as PP and nylon (Goodier 1933; Oxborough and Bowden 1974; Epstein 1979a, b; Lazzeri and Bucknall 1993;

Fig. 17.16 Modulus ratio of PP or PP/PP-g-MA/MMT and the elastomer as a function of temperature. The total MMT content in the PP/PP-g-MA/MMT is equivalent to 3 wt% MMT in the PP/PP-g-MA/MMT/EOR nanocomposites. Note that MMT is exclusively located in the PP phase in TPO nanocomposites (Tiwari and Paul 2012)
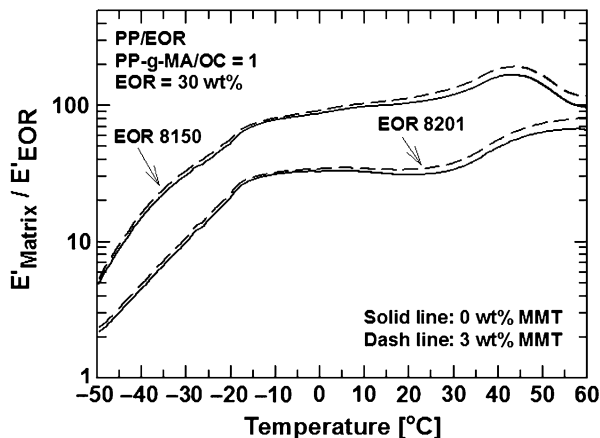
Bucknall et al. 1994; Dompas and Groeninckx 1994; Liang and Li 2000). The elastomer properties such as elastomer glass transition temperature, T_g, and modulus also put limits on the D-B transition temperature since it ceases to be elastomeric below T_g thereby reducing the stress concentration and the ability to undergo cavitation which are the important aspects of the toughening mechanism. The temperature at which the ratio of matrix to elastomer moduli falls below about 10 provides an empirical lower limit for the D-B transition temperature for rubber-toughened materials based on prior observations for rubber-toughened blends (Keskkula and Paul 1995; Oshinski et al. 1996c; Tiwari and Paul 2012).

According to Lim et al. (2007, 2010), cavitation of elastomer particles followed by extensive shear yielding of PA 6 matrix accompanied by delamination of intercalated clay particles is a major cause of toughening in PA 6/elastomer/MMT nanocomposites. The delamination of clay particles in the matrix is an additional contributing factor to the toughening; however, no crazing was observed in the PA 6 matrix unlike in PA 6/EOR grafted maleic anhydride (EOR-g-MA) blends as reported by Huang and Paul (2006). More fundamental studies are required to elucidate toughening mechanisms in other elastomer-containing nanocomposites.

Figure 17.16 shows the modulus ratio of PP or PP/PP-g-MA/MMT and the elastomer as a function of temperature for PP/PP-g-MA/MMT/EOR nanocomposites. As seen in Fig. 17.16, the empirical matrix to elastomer modulus ratio of 10 when used as a criteria to define the lower limit of D-B transition temperature is obtained at approx. $-44\,°C$ and approx. $-30\,°C$ for nanocomposites containing elastomers with 39 wt% octene content and 28 wt% octene content, respectively. These temperatures are significantly lower than the lowest D-B temperatures observed with these elastomers, viz., $-17.5\,°C$ and $0\,°C$, respectively (Tiwari and Paul 2012). It is known that the elastomer properties, such as T_g and modulus, set the lower limit for the D-B temperature; however, elastomer particle

Fig. 17.17 Effect of MMT content (**a**) and weight average apparent elastomer particle size (**b**) on the ductile–brittle transition temperature of PP/PP-g-MA/ MMT/EOR 8100 nanocomposites prepared from three different molecular weight grades of PP. Elastomer content is 30 wt% and PP-g-MA/ organoclay ratio is 1.0 (Tiwari and Paul 2012)
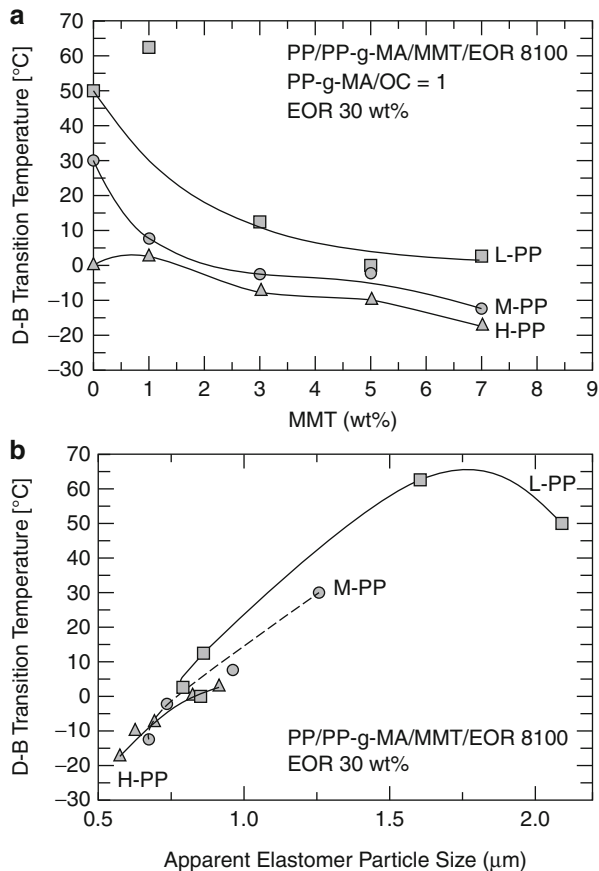
size must be optimized to approach such a limit. The presence of MMT particles in the PP matrix might alter the applicability of this empirical rule of thumb based on the modulus ratio.

In the elastomer particle size range where toughness is expected, the D-B transition temperature is known to decrease with increased matrix molecular weight; however, little is known about this behavior in the presence of clay. In a recent study on the effect of PP molecular weight and elastomer MFI on the properties of extruder-made TPO nanocomposites, a significant drop in the D-B transition temperature is reported for the nanocomposites (Tiwari and Paul 2012). As seen in Fig. 17.17, the D-B transition temperature decreases with increased MMT content of PP/PP-g-MA/MMT/EOR nanocomposites. At a fixed MMT content, the D-B transition temperature decreases with increased PP molecular weight. The D-B transition temperature generally correlates with elastomer particle size with a smaller effect of PP molecular weight in the order of H-PP < M-PP < L-PP, and the trend becomes less significant for elastomer particle sizes smaller than ∼0.75 μm. The increase in the PP molecular weight reduces the

Fig. 17.18 Effect of elastomer MFI on the ductile–brittle transition temperature of (**a**) PP/EOR blend and (**b**) PP/PP-g-MA/MMT/EOR nanocomposites. *Gray*- and *black*-filled symbol represents nanocomposites containing elastomers having 39 and 28 wt% octene content, respectively. The total MMT content in the nanocomposites is 5 wt%. Elastomer content is 30 wt% and PP-g-MA/organoclay ratio is 1.0 (Tiwari and Paul 2012)
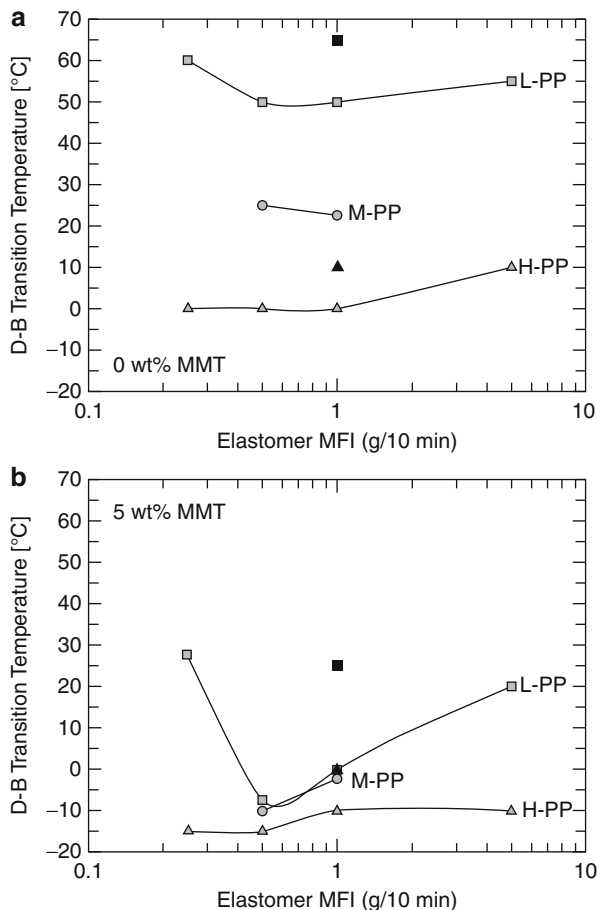
D-B transition temperature, and the effect of elastomer MFI on the D-B transition temperature becomes less prominent with the increased PP molecular weight as seen in Fig. 17.18. The nanocomposites based on the high-octene-content elastomer (~39 wt%) also lead to a lower D-B transition temperature compared with nanocomposites based on the elastomer with low octene content (~28 wt%). The toughening mechanism was not explored for this system; a more detailed study in this area would further enhance the understanding of the role of organoclay in elastomer-toughened nanocomposites with partially exfoliated clay particles.

17.2.2.5 Thermal Expansion Behavior

Recently, polymers have found a significant utilization in the automotive industry mainly due to their low density, ease of processing and molding into desired parts, and the ability to tailor properties based on the end application (Garcés et al. 2000; Hussain and Gorga 2006; Okada and Usuki 2006; Goettler et al. 2007). Among these, thermoplastic olefins are widely used due to their high toughness and low

Fig. 17.19 Typical thermal
expansion behavior of
PP/elastomer/masterbatch
nanocomposites during the
first and second heating runs;
in this example, the
composition is 30 wt%
elastomer and ∼3 wt%
MMT. The masterbatch
contains equal amount of
PP-g-MA and organoclay
(Lee et al. 2006a)
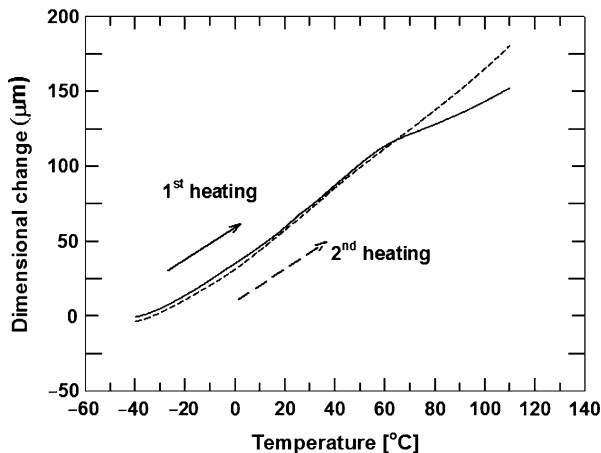
density. However, most polymers have significantly higher coefficients of linear
thermal expansion (CTE) than most metals within a temperature range suitable for
application purposes. For example, the CTE for PP is $\sim 10^{-4}$ mm/mm $^\circ$C compared
to CTE for metals $\sim 10^{-5}$ mm/mm $^\circ$C; this limits utilization of lightweight plastic
parts in various automotive applications (Kim et al. 2008). Layered silicates have
high modulus and low CTE; therefore, well-dispersed and appropriately oriented
clay particles can significantly reduce the CTE of thermoplastic olefins by simple
mechanical restraints imposed on expansion of the soft elastomer particles. More-
over, the small absolute size of filler particles gives a better surface finish of the
final product than that expected for conventional composites based on talc or glass
fibers. The nonuniform shape of the elastomer particle in the blend can lead to
anisotropic thermal expansion behavior; this issue is more complicated upon
addition of filler as the thermal expansion behavior is strongly influenced by the
nature of dispersion and orientation of the filler (Ono et al. 2005; Lee et al. 2006a;
Kim et al. 2008). Yoon et al. (2002) observed anisotropic thermal expansion
behavior in the flow direction (FD) and transverse direction (TD) of injection-
molded nanocomposite specimens; the CTE in the FD is significantly lower than
that in the TD due to the lower degree of alignment of the exfoliated clay platelets in
the TD compared to the FD as indicated by TEM images. Their work evaluates the
effect of angle of orientation of clay platelet and MMT dispersion on CTE in
various orthogonal directions of the injection-molded specimen.

Figure 17.19 shows typical thermal expansion behavior of a PP/PP-g-MA/MMT/
elastomer nanocomposite from the first and second heating; the thermal expansion
is a nonlinear function of temperature when viewed over the wide range of −40 $^\circ$C
to 125 $^\circ$C; hence, CTE is reported in the temperature range of 0–30 $^\circ$C so it can be
related to the mechanical properties determined at room temperature (Lee
et al. 2006a). For both extruder-made and reactor-made TPO nanocomposites, the
CTE along the FD and the TD decreases, whereas CTE along the normal direction
(ND) increases as the MMT content is increased. The increase in CTE in the ND is

related to the reduced thermal expansion in the FD and the TD in the presence of MMT. However, it is interesting to note from Fig. 17.20 that the initial CTE for the PP/EOR blend in the ND is higher than in the FD and the TD. This is ascribed to effects of elastomer shape and size plus elastomer deformation in the flow direction along with the polymer crystallite orientation (Lee et al. 2006a; Kim et al. 2008). The differences among CTE in the FD, TD, and ND are related to the anisotropic dispersion of MMT and elastomer in the injection-molded specimen. The MMT particles in TPO nanocomposites are more aligned in the FD than in the TD which results in more mechanical constraint imposed in the elastomer particles in the FD than in TD resulting into larger decrease in the CTE along FD than TD. Tiwari et al. (2011b, 2013) showed AFM images of elastomer particles in three orthogonal directions of injection-molded specimen of PP/PP-g-MA/MMT/ EOR nanocomposites and projected elastomer particle as a prolate ellipsoid as seen in Fig. 17.21.

17.2.3 Polyamide Blend Nanocomposites

17.2.3.1 Elastomer Particle Size, Impact Strength, and Fracture Behavior

Polyamides are widely used commercially due to their high stiffness and strength, excellent chemical resistance, low coefficient of friction, and toughness. However, their poor low-temperature impact strength and extreme sensitivity to notch failure put limits on some applications (Keskkula and Paul 1995). Rubber toughening of polyamides has been extensively studied where the effect of elastomer type and elastomer content and nature of reactive/functionalized groups on the elastomer morphology and elastomer particle size and toughness has been reported (Wu 1985, 1987; Oshinski et al. 1996a, b, c; Majumdar et al. 1997; Yu et al. 1998; Huang et al. 2004; Okada et al. 2004; Huang et al. 2006a, b; Huang and Paul 2006). Due to the amine end group of polyamides, they can react with elastomers functionalized with anhydride, acid, or other functional groups, and this grafting leads to reduced elastomer particle size along with improvement in the notched impact strength and a lower ductile–brittle transition temperature (Oshinski et al. 1996a, b, c).

Blends of semicrystalline and amorphous polyamides with the reactive and nonreactive elastomers and with other thermoplastics have been extensively studied in the polymer blend nanocomposite literature (Chow et al. 2003, 2004; Khatua et al. 2004; Li and Shimizu 2004; Chiu et al. 2005; Dasari et al. 2005; González et al. 2005; Kelnar et al. 2005; Lai et al. 2005; Li and Shimizu 2005; Tjong and Bao 2005; Ahn and Paul 2006; González et al. 2006a, b; Kelnar et al. 2006; Lai et al. 2006; Wahit et al. 2006c; Wahit et al. 2006a, b; Kelnar et al. 2007; Lim et al. 2007; Vo and Giannelis 2007; Filippone et al. 2008; Goitisolo et al. 2008; González et al. 2008; Kelnar et al. 2008, 2009; As'habi et al. 2010; Filippone et al. 2010a, b; Lim et al. 2010; Motamedi and Bagheri 2010; Yang et al. 2010; Yoo et al. 2010a, b; González et al. 2012). The polar nature of polyamide facilitates dispersion of clay particles in it while the location of the clay particles at the
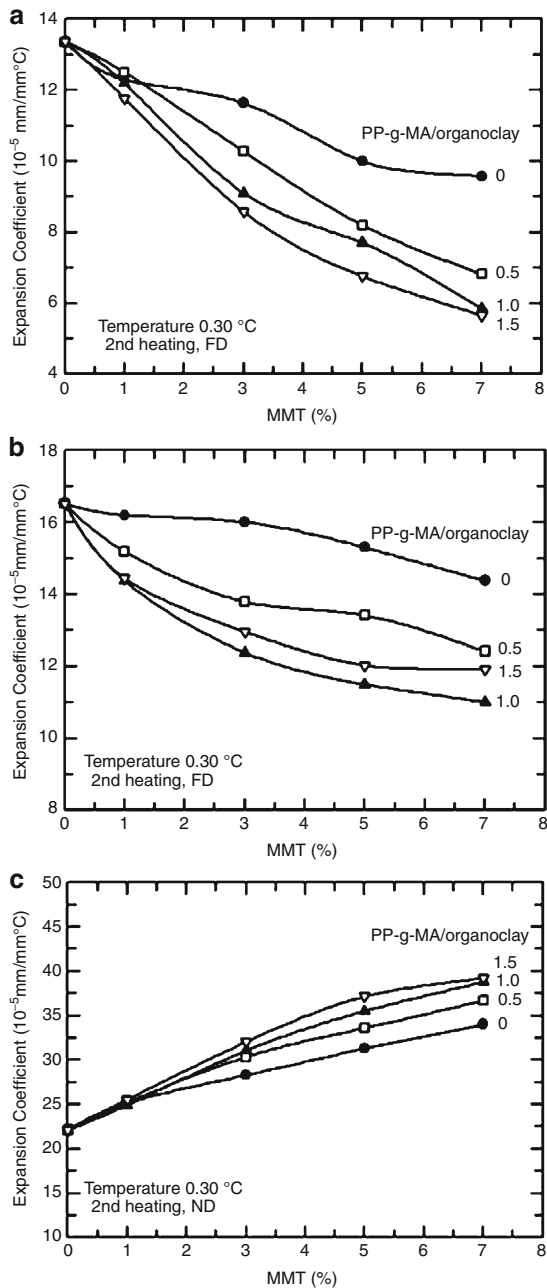
Fig. 17.20 (continued)
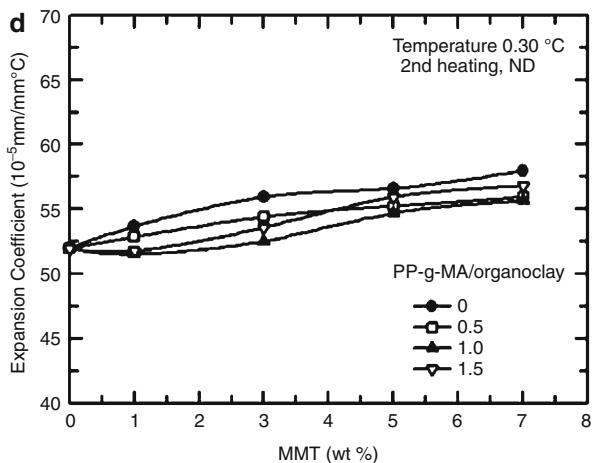
Fig. 17.20 Coefficient of linear thermal expansion (CTE) for PP/PP-g-MA/MMT/EOR nanocomposites as a function of MMT content for (**a**) FD, (**b**) TD, (**c**) ND, and (**d**) bulk expansion coefficients (Tiwari et al. 2013)
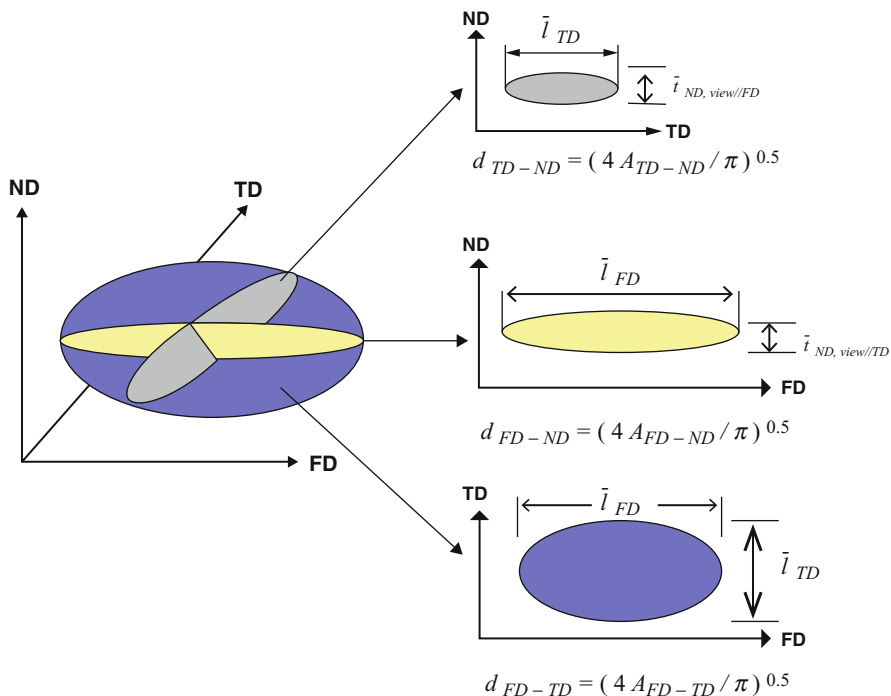
Fig. 17.21 Illustration of elastomer phase morphology of PP/PP-g-MA/MMT/EOR nanocomposites based on the AFM imaging in three orthogonal directions of the injection-molded Izod bar (Tiwari et al. 2013)

interface depends largely on the interfacial interaction of clay with other blend components. Khatua et al. (2004) reported significant decreases in the elastomer particle size with the addition of clay in PA 6/EPR (80/20) blend; the elastomer particle sizes in blend nanocomposites were similar to those obtained for PA 6/EPR grafted maleic anhydride (EPR-g-MA) (80/20) blend. The presence of clay particles in the PA 6 matrix retards the coalescence of EPR particles and thereby reduces their size similar to steric stabilization by maleated EPR; moreover, the EPR particles are more stable upon annealing when clay is present in the PA 6 phase. On the contrary, when clay particles are located exclusively in the dispersed phase, they can transform matrix-domain morphology into a co-continuous structure as observed for blends of polyamide with acrylonitrile–butadiene–styrene (ABS), polyphenylene oxide (PPO), low-density polyethylene (LDPE), and high-density polyethylene (HDPE) (Li and Shimizu 2004, 2005; Filippone et al. 2008; Filippone et al. 2010a; Filippone et al. 2010b). The increase in the viscosity ratio of dispersed to continuous phase with the addition of clay promotes co-continuity at lower dispersed phase content in these blends. The co-continuous morphology leads to the better combination of properties; hence, there is considerable interest in understanding the effect of nanoparticles in promoting co-continuity and their properties (Sundararaj and Macosko 1995; Pötschke and Paul 2003a; Pötschke and Paul 2003b; Li and Shimizu 2004, 2005; Wu et al. 2006; Ray et al. 2007; Zou et al. 2007; Filippone et al. 2008; Filippone et al. 2010a, b). Figure 17.22 shows TEM images and a schematic of co-continuous blend morphology observed for PA 6/ABS (40/60) nanocomposites where the clay particles are exclusively located in the dispersed PA 6 phase. The thermomechanical properties such as storage modulus are reported to increase by 205 % at 180 °C with the addition of 4 wt% clay in the blend. The co-continuous blend morphology becomes more finer as the clay content is increased (Li and Shimizu 2004, 2005).

Unlike PP/elastomer blends, a decrease in the elastomer size does not always lead to the increase in the impact strength of polyamide/elastomer blend containing organoclays. Figure 17.23 shows the effect of elastomer particle size on the notched impact strength for amorphous polyamide (a-PA) blends based on EOR and EOR-g-MA. The elastomer content in the blend is 20 wt%. The impact strength for a-PA/EOR-g-MA (80/20) blend reduced from 1,000 J/m for blend without clay to 20 J/m in the presence of 7 wt% MMT even though the elastomer particle sizes were within the range where toughness is expected. In the case of the a-PA/EOR (80/20) blend, the elastomer particle size decreased from 2 to 0.3 μm with addition of clay; however, no improvement in toughness was observed. The high T_g of a-PA and highly exfoliated clay particles makes a-PA brittle enough to contribute to the toughening mechanism. In general, for polyamide/maleated elastomer nanocomposites, the elastomer particle size either slightly increased or did not change with the addition of clay; this has been ascribed to the chemical interactions between the maleic anhydride group of the elastomer and the surfactant of the organoclay that may hinder the compatibilizing effect of elastomer resulting in a higher elastomer particle size as reported in Table 17.4 (González et al. 2006a).
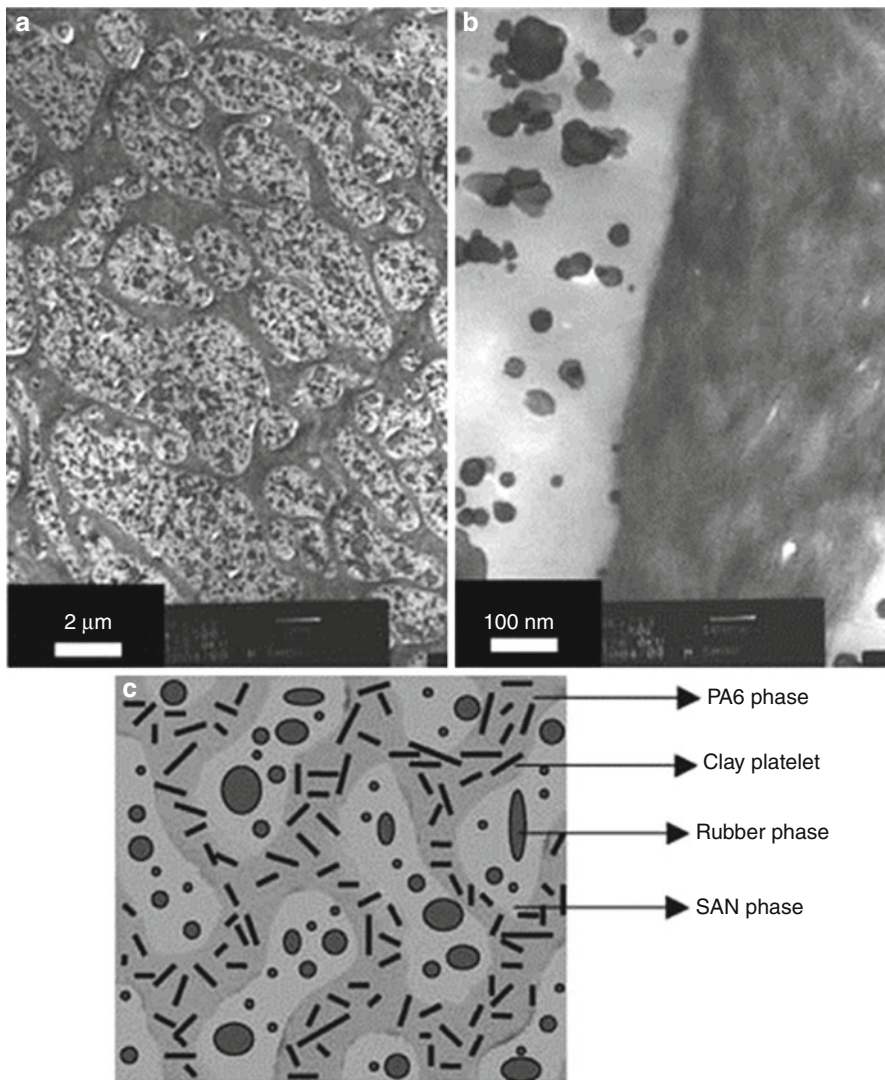
Fig. 17.22 TEM micrographs of ABS/PA6 nanocomposite with 4 % clay. (**a**) Low-magnification image, (**b**) high-magnification image, (**c**) schematic diagram for the co-continuous ABS/PA6 blend nanocomposite. The *white* part is the SAN phase, the *gray* part is the PA6 phase, the *black* particles are the butadiene rubber phase, and the *dark line* in the PA phase is the organoclay platelet in (**a**) and (**b**) (Li and Shimizu 2005)

In another study on PA 6/MMT/EPR-g-MA blend nanocomposites where clay particles are exclusively located in the PA 6 phase, the impact strength was reported to decrease as the MMT content in the blend increases; a significant improvement in the toughness was observed for 25 parts per hundred (pph) of elastomer content in

Fig. 17.23 Effect of weight average elastomer particle sizes on the notched impact strength of a-PA/elastomer blend (80/20) nanocomposites containing (**a**) EOR and (**b**) EOR-*g*-MA. Data for a-PA/EOR (−*g*-MA) blend without organoclay are from Huang et al. (2006b) (Yoo et al. 2010a)
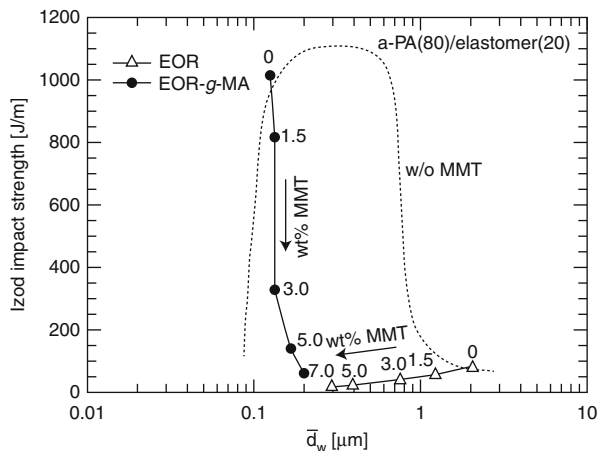
Table 17.4 Weight average dispersed elastomer particle size ($\overline{d}_w$) in PA 6/SEBS-g-MA blend nanocomposites as a function of maleic anhydride (MA) content in SEBS-g-MA. The elastomer content in blend is 15 wt% (González et al. 2006b)

MA content in SEBS-g-MA (wt%)	$\overline{d}_w$ (μm)	
	Blend	Nanocomposite
0.5	0.52	0.94
1	0.23	0.71
1.5	0.08	0.36

the blend nanocomposites. The D-B transition temperature increased with the addition of clay at fixed elastomer content and further decreased with the addition of elastomer at fixed MMT content (Ahn and Paul 2006). The toughening mechanism for PA 6-based blend nanocomposites has not been extensively studied; however, it is reported that the toughening in elastomer-containing PA 6 nanocomposites arises from the cavitation of elastomer particles followed by extensive shear yielding of PA 6 matrix accompanied by delamination of intercalated clay particles (Lim et al. 2010). However, no crazing was observed within the matrix as previously observed in the case of PA 6/EOR-g-MA blend without clay (Huang and Paul 2006). Figure 17.24 shows the TEM images of the fractured surface of the PA 6/EOR-g-MA/MMT nanocomposites at various distances from the crack tip location (Lim et al. 2010). As seen in Fig. 17.24a, the voids are due to the delamination of the intercalated clay stacks at ∼100 μm away from the crack tip location in schematic. At position (b), i.e., closer to the crack tip, the elastomer particles have undergone significant cavitation even in the presence of organoclay in the PA 6 matrix followed by the extensive shear yielding of the PA 6 observed around the crack tip as seen from extensive deformation and coalescence of the elastomer particles at position (c). The voids generated by delamination of clay
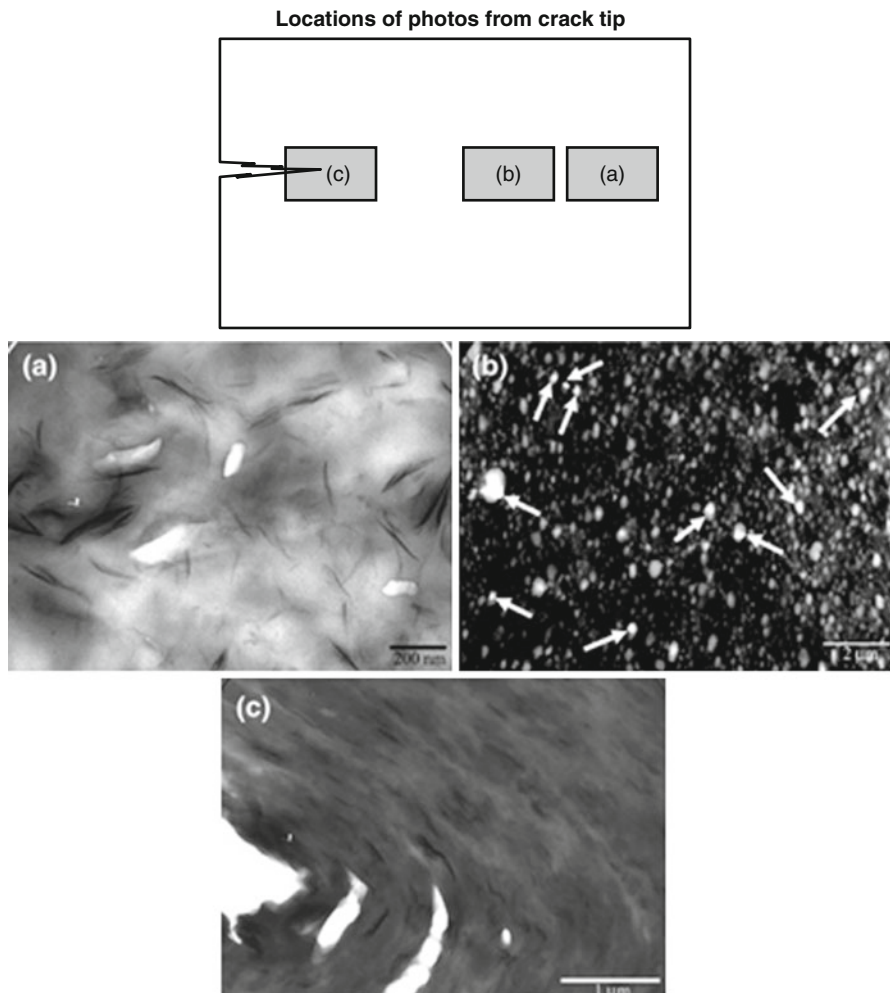
Fig. 17.24 TEM micrographs of nylon 6/organoclay/EOR-g-MA (76/4/20) ternary nanocomposite showing (**a**) submicron and nano-voids which are associated with intra-gallery delamination of some organoclay layers (note that the section is not selectively stained in order to clearly reveal delaminations of clay layers), (**b**) cavitation of EOR-g-MA particles which preferentially starts from the larger particles as indicated by *arrows*, and (**c**) extensive matrix shear yielding at the arrested crack tip which in turn causes the EOR-g-MA particles and delaminated clay layers to collapse within the matrix. A schematic of the arrested crack tip illustrating different locations from where TEM micrographs (**a–c**) were taken is also shown. Note that the schematic is not to scale (Lim et al. 2010)

stacks are arrested and do not turn into micro-cracks; this contributes to toughening. More studies in this area including toughening mechanisms on other elastomer-toughened blend nanocomposites are required to further elucidate toughening mechanisms in blends with nanoparticles.

It is clear from the literature that PA 6/maleated elastomer/MMT nanocomposites show a decrease in the impact strength in the presence of clay compared to the pure blend; this decrease in the impact strength depends on several factors including clay content, elastomer type, location of clay in blend, and crystallinity of the matrix and elastomer in the presence of MMT. No clear understanding about this behavior is available; perhaps the low impact strength arises from the high aspect ratio of clay particles in the polyamide matrix that reduces their ability to contribute to toughening.

Kelnar et al. (2005, 2006, 2007) reported on morphology and properties of PA 6 nanocomposites prepared with various reactive and nonreactive elastomers and various organoclays. They concluded that in the PA 6/elastomer blend nanocomposites having nonreactive elastomer, the "core-shell" structures where clay particles form a shell around the elastomer particles provide improvement in the toughness. Later it was reported that combination of two clays where the elastomer is pre-blended with a less polar clay followed by blending the elastomer nanocomposite with PA 6 and more polar clay provides high reinforcement, better compatibilization, and favorable "core-shell" structure with balance of toughness and mechanical properties (Kelnar et al. 2007). This is an interesting observation that departs from usual behavior since the clay particles in a soft elastomer particle should reduce their ability to undergo cavitation; hence, further studies are needed to gain a better understanding about the practical applicability of this approach. Observations on other blends containing clay are listed in Table 17.5.

17.2.3.2 Effect of Blending Sequence

The mixing sequence is known to have a significant effect on the elastomer particle size, toughness, and mechanical properties of blends; in the case of blend nanocomposites, this can affect the dispersion and location of clay particles in the blend and dispersed phase particle size (Li et al. 2002; Dasari et al. 2005; García-López et al. 2007; Vo and Giannelis 2007; Wang et al. 2007; Gallego et al. 2008; González et al. 2008; Yoo et al. 2010b; Zhai et al. 2010; Chen and Evans 2011). Vo and Giannelis (2007) compared the effect of two organoclays, Cloisite® 30B and Cloisite® 20A, and simultaneous and sequential extrusions on the properties of polyvinylidene fluoride (PVDF)/PA 6 (30/70) blends. They demonstrated that the blend containing Cloisite® 30B prepared by simultaneous extrusion had good dispersion of organoclay, lower PVDF domain size, and exhibited the best mechanical properties. The majority of organoclay is dispersed in the PA 6 matrix, and some of the organoclays were observed at the PVDF/PA 6 interface. In another report on blending PA 66 with Cloisite® 30B, followed by mixing with SEBS-*g*-MA, led to maximum notched impact strength (Dasari et al. 2005). In the case of PA 6/EPDM-*g*-MA/organoclay nanocomposites, blending sequence had less influence on the mechanical properties, and simultaneous blending was selected as the simplest way to prepare nanocomposites. A two-step blending approach where the polyamide is mixed with organoclay followed by blending with elastomer leads to higher notched impact strength (Dasari et al. 2005; García-López et al. 2007) although other mixing routes such as blending the polyamide and elastomer

Table 17.5 Observations on immiscible polymer blends containing organoclays

Blend	Composition/content	Filler	Filler location	Observations	Reference
PA 6/ABS	40/60	Cloisite® 30B	PA 6 phase	Morphology changes from dispersed phase to co-continuous structure in the presence of organoclay. Co-continuity leads to significant improvement in dynamic storage modulus of the nanocomposites compared to pure blend	Li and Shimizu 2004, 2005
Nylon 6/EPR	80/20	Cloisite® 20A	Nylon 6 phase	Decrease in the dispersed elastomer particle size in the presence of clay and increase in the phase stability of elastomer particles on annealing	Khatua et al. 2004
PA 6/EOR-g-MA	90/10	Cloisite® 30B	PA 6 and EOR-g-MA phases	Tensile modulus and strength increased while elongation at break and impact strength decreased in the presence of MMT	Chiu et al. 2005
PP/EPDM/PP-g-MA	25 wt% PP	Cloisite® 20A	EPDM	Improvement in the tensile modulus and strength and decrease in the elongation at break in the presence of organoclay. Addition of PP-g-MA leads to a higher improvement in the properties compared to nanocomposites without PP-g-MA	Mishra et al. 2005
Nylon 66/SEBS-g-MA	84/16	Cloisite® 30B	Nylon 66 phase	Flexural modulus and strength increases while impact strength decreases in the presence of organoclay	Dasari et al. 2005

(continued)

Table 17.5 (continued)

Blend	Composition/content	Filler	Filler location	Observations	Reference
PA 6/elastomer Elastomers: EPR-g-MA, SBS-g-MA, VP701, EPR, E-MA-GMA, PE-GMA, PP-g-MA	95/5	Cloisite® 30B	PA 6 phase	Reactive elastomers, mainly EPR-g-MA and SBS-g-MA, result in better improvement in toughness compared to other elastomers. A tensile property increases in the presence of organoclay	Kelnar et al. 2005, 2006
Nylon 6/EPR-g-MA	EPR-g-MA: 0–25 wt%	Cloisite® 30B	Nylon 6 phase	Impact strength increased with the addition of elastomer at a fixed MMT content. Ductile–brittle transition temperature decreased with the addition of elastomer and with the decrease in the MMT content	Ahn and Paul 2006
PBT/HDPE	PBT: 1 to 90 wt%	Nanofil® 919	PBT phase and interface based on blend composition	The MMT particles located at the blend interface reduce the interfacial tension between blend components. The addition of organoclay also increases the thermal stabilization of blend morphology	Hong et al. 2006a, b
PPS/PA 66	60/40	OMMT	PA 66 phase	Morphology changes from dispersed phase to co-continuous and lamellar structure with the addition of clay. Tensile strength and impact strength increased with clay content. Increase in anti-wear property	Zou et al. 2007
PVDF/nylon 6	30/70	Cloisite® 30B	Nylon 6 and interface	Improvement in the tensile modulus, strength, and elongation at break of blend in the presence of organoclay	Vo and Giannelis 2007
PVDF/nylon 6	30/70	Cloisite® 20A	Interface		

HDPE/PA 6	75/25	Cloisite® 15A	PA 6 phase	Formation of co-continuous structure in the presence of MMT in PA 6 phase. Increase in the tensile modulus and strength and slight decrease in the elongation at break observed in the presence of clay	Filippone et al. 2008
PA 6/SEBS-g-MA	70/30	Nanomer® I.30TC	PA 6 phase	Modulus and yield strength increases and tensile ductility decreases with the increase in clay content. Higher rubber content is required to achieve toughness as clay content increases	González et al. 2008
Nylon 66/PP/PP-g-MA	70/20/10	OMMT	Nylon 66 phase and interface	Increase in the tensile modulus and strength and the flexural modulus and strength. Impact strength decreases with the addition of clay	Yang et al. 2010
PP/PP-g-MA/PS	70/30	Cloisite® 20A	PP/PP-g-MA phase and interface	Improvement in the phase stability, tensile modulus, and strength in the presence of clay	Tiwari and Paul 2011a
PP/PP-g-MA/EOR	70/30	Cloisite® 20A	PP/PP-g-MA phase	Improvement in the toughness, modulus, and yield strength in the presence of clay. CTE decreases in the presence of clay. CTE decreases in the FD and the TD in the presence of clay	Tiwari et al. 2012, 2013
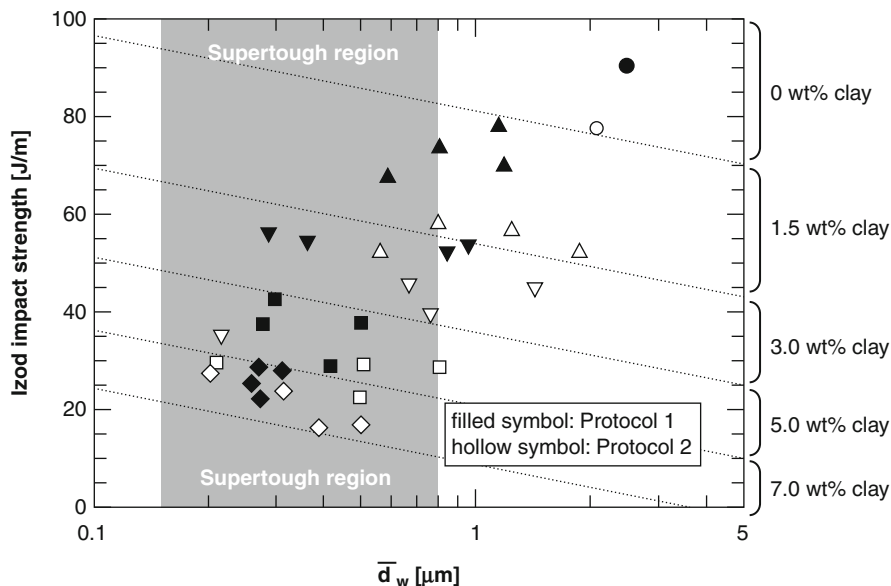
Fig. 17.25 Effect of weight average elastomer particle sizes on the Izod impact strength of a-PA/ EOR (80/20) blends. The shadowed part refers to the "super-tough region" from Huang et al. (2006b) (Yoo et al. 2010b)

followed by mixing with organoclay have also resulted into high toughness and high ductility of nanocomposites (González et al. 2008). Wahit et al. (2006a) reported a three-step mixing for PA 6/PP/PP-g-MA/MMT/EOR nanocomposites where PP/PP-g-MA/EOR and PA 6/MMT were blended separately and then mixed together; this blend resulted in significant improvement in toughness compared to other mixing routes such as simultaneous mixing. Recently Yoo et al. (2010b) demonstrated that the mixing protocol where organoclay is first blended with a-PA followed by mixing a-PA nanocomposite with EOR results in much lower elasto- mer particle size and slightly better mechanical properties compared to an approach where a-PA/EOR/MMT masterbatch is further diluted with a-PA to give a ternary nanocomposite. Irrespective of the mixing sequence, the elastomer particle sizes were similar and in the range where "super-toughness" is expected for a-PA/EOR blends; however, all blends break in a brittle manner on impact test. Increased elastomer content does not lead to any improvement in the notched impact strength. Figure 17.25 shows a plot of impact strength as a function of weight average elastomer particle size. The shaded area shows the optimum elastomer particle size within the range of 0.15–0.8 μm that leads to super-toughness as observed for a-PA/EOR-g-MA (80/20) blends, whereas the a-PA/EOR/MMT blends with elas- tomer particle sizes in the shaded area ("super-tough" region) do not exhibit improved toughness. In fact, the toughness decreases as the elastomer particles become smaller in the presence of MMT. This is correlated to the increased stress

level of the nanocomposite as observed from the decrease in the extent of plastic deformation; however, the extent of plastic deformation as determined by elongation at break and area under the stress–strain or force–displacement curve does not always correlate well with the impact strength as has also been pointed out in various reports (Bucknall and Paul 2009; Yoo et al. 2010a; Tiwari and Paul 2011c). In fact, the toughening response is a complex process where yield strength, viscoelastic behavior, and other matrix effects in addition to blend morphology all play some role (Huang et al. 2006b; Yoo et al. 2010a).

17.3   Role of Other Nanofillers in Immiscible Polymer Blends

17.3.1   Polymer Blends Containing Nanometals (Metal and Metal Oxides)

The stabilization of immiscible polymer blends by nanoparticles at the blend interface can be considered similar to stabilization of low-viscosity emulsions by colloidal particles as in "Pickering emulsions" (Ramsden 1903; Pickering 1907). There have been several reports on the effect of the use of solid particles for stabilization of the morphology of immiscible polymer blends (Tambe and Sharma 1994; Yan and Masliyah 1995; Midmore 1998; Binks and Lumsdon 1999; Lagaly et al. 1999; Binks and Lumsdon 2000; Karim et al. 2000; Binks and Kirkland 2002; Aveyard et al. 2003; Vermant et al. 2004; Binks et al. 2005; Thareja and Velankar 2006; Elias et al. 2008b). The addition of fumed silica in a polydimethylsiloxane (PDMS)/polyisobutylene (PIB) (70/30) blend has resulted in decreased coalescence of PIB particles leading to a more stable blend morphology as reported by Vermant et al. (2004). Later a "particle bridging" mechanism was proposed for this blend based on the gel-like behavior observed at the low frequency (Thareja and Velankar 2006). In a separate study on the effect of hydrophilic and hydrophobic silica on the morphology of PP/PS (70/30) blend, both types of silica gave a similar decrease in the PS particle size from 3 μm in a blend without silica to 1 μm in a blend with silica (Elias et al. 2007). The hydrophilic silica is located exclusively in the PS phase, while hydrophobic silica is located in the PP phase and at the PP/PS interface. The effect of mixing protocols such as pre-blending silica with PP followed by mixing PP/silica with PS or simultaneously mixing PP, PS, and silica does not affect the final location of the silica particles based on the interfacial interactions although kinetic issues may preclude obtaining an equilibrium state for silica particles in the blend. The hydrophilic silica in the PS dispersed phase stabilizes morphology due to reduction in interfacial tension, whereas hydrophobic silica in PP matrix stabilizes the morphology by reducing coalescence of dispersed PS particles. The migration of nanoparticles from one phase to another is known to be affected by the interfacial interactions between the polymers and the filler along with kinetic effects (see Table 17.6) (Fowler et al. 1989; Cheng et al. 1992; Elias et al. 2007, 2008a). In the case of PP/EVA/silica nanocomposites, a significant drop in the dispersed EVA particle size is observed with the addition of 3 wt% silica in blend.

Table 17.6 Estimate of the equilibrium localization of fillers in polymer blends by calculation of a wetting coefficient, ω_a, from Young's equation. Here, 1 and 2 are two polymer components in blend and p represents solid filler

Young's equation	$\omega_a < -1$	$-1 < \omega_a < 1$	$\omega_a > 1$
$\omega_a = \frac{\gamma_{1p} - \gamma_{2p}}{\gamma_{12}}$	Filler p will reside in phase 1	Filler p will reside at interface	Filler p will reside in phase 2

When silica is pre-blended with PP, the hydrophilic silica particles migrate from the PP to the EVA phase on mixing. The effective interfacial tension determined using the Palierne model showed a decrease in the interfacial tension between PP and EVA in the presence of hydrophilic silica; however, a similar drop in the EVA particle size in the presence of hydrophobic silica indicated that decrease in interfacial tension alone is not responsible for the reduction in EVA size; other effects such as viscosity and structure of different phases should be considered to predict the final blend morphology of such systems (Elias et al. 2008b). In another study on PP/PS/silica nanocomposites, the addition of nanosilica particles showed a significant drop in the dispersed PS particle size when silica particles are located at the PP/PS interface; however, with the increase of mixing time, silica particles migrate back to the PP phase from the interface resulting in increased PS particle size. It was concluded that the compatibilization in PP/PS blends by nanosilica particles is controlled by kinetics rather than thermodynamics (Zhang et al. 2004). Observations on various blends containing nanoparticles are also reported in Table 17.7.

As discussed earlier in Sect. 17.2.3.2, blending sequence has a significant effect on the final dispersion of nanoparticles in the blend components, dispersed phase particle size, and impact behavior. A two-step processing method, wherein elastomer and filler is blended first and then mixed with PP or PP-g-MA, led to significant improvement in the toughness of PP (or PP-g-MA)/EPDM (80/20)/silica nanocomposites containing hydrophilic silica (Yang et al. 2006, 2007). The migration of hydrophilic silica from the elastomer phase to PP (or PP-g-MA) phase forms a filler-network-like structure wherein a large amount of silica particles agglomerate around EPDM particles and resides in the PP (or PP-g-MA) matrix as seen in SEM images of PP (or PP-g-MA)/EPDM/silica nanocomposites (see Fig. 17.26). The relative impact strength of PP/EPDM/silica or PP-g-MA/EPDM/silica nanocomposites prepared using nanosilica is increased by 1.6 and 2.7 times respectively in the presence of 5 wt% silica as seen in Fig. 17.27. The remarkable increase in the impact strength is attributed to the overlap of the stress volume between EPDM and silica particles due to the formation of the silica particles network around EPDM particles.

Kontopoulou and coworkers reported that addition of nanosilica to a PP/PP-g-MA/EOR (50/50) co-continuous blend resulted in refinement of the co-continuous structure followed by formation of dispersed elongated elastomer particles as the silica content is increased. This leads to improvement in the toughness with silica content as seen in Fig. 17.28 (Lee et al. 2010). Moreover, the dispersed elastomer

Table 17.7 Observations on immiscible polymer blends containing various nanoparticles

Blend	Composition/content	Filler	Filler location	Observations	Reference
LCP/PP	30/70	Hydrophobic nanosilica	PP phase	Morphology revealed deformation of LCP particles in the presence of nanosilica due to increase in the matrix viscosity and higher shear rates, resulting in a larger aspect ratio of the LCP particles	Lee et al. 2006b
PP/SBS	92/8	Nano-$CaCO_3$	PP phase	$CaCO_3$ particles located in the PP phase reduce SBS particle size resulting in a higher toughness, flexural modulus, and tensile strength of the nanocomposites. On contrary, the addition of micro-$CaCO_3$ particles into SBS/PP blends reduces toughness	Yu et al. 2007a
PP/PS	70/30	Aerosil® A200 (hydrophilic nanosilica)	PS phase	Decrease in the interfacial tension and dispersed PS particle size in the presence of nanosilica	Elias et al. 2007
PP/PS	70/30	Aerosil® R805 (hydrophobic nanosilica)	PP phase and interface	Hydrophilic silica resides in EPDM phase and forms aggregate, whereas hydrophobic silica is located in EPDM phase and at the interface	
PP/EPDM	EPDM: 10–50 wt%	nanosilica	Hydrophilic silica resides in EPDM phase and forms aggregate, whereas hydrophobic silica is located in EPDM phase and at the interface	The strain recovery profile for nanocomposites improved in the presence of nanosilica in blend; the addition of hydrophobic silica showed improvement in instantaneous and long-term strain recoveries compared to double-step recovery profile observed for	Martin et al. 2009

Table 17.7 (continued)

Blend	Composition/ content	Filler	Filler location	Observations	Reference
				hydrophilic silica resulting in poor elastic properties	
PLLA/PS	PS: 20–80 vol%	Hydrophilic nanosilica	PLLA phase	The coalescence rate is reduced and morphology stability of blend improved in the presence of silica. The incorporation of hydrophilic silica resulted in broad co-continuous PS/PLLA blends and refinement of morphology	Zhang et al. 2012
PP/PP-g-MA/ EOR	EOR: 30–50 wt%	Nanosilica	PP/PP-g-MA phase	The presence of nanosilica in PP/PP-g-MA phase significantly reduces dispersed phase EOR particle size and improved phase stability on annealing. The reinforcing effect of silica resulted in higher tensile and flexural strength and modulus, whereas impact strength did not change	Lee et al. 2012
PS/PA 6	PA 6: 20–40 wt%	Titanium dioxide (TiO$_2$)	PA 6 phase	TiO$_2$ particles are preferentially located in the PA 6 phase and reduce the coalescence of the dispersed phase; however, phase transformation was observed on annealing. At higher content, the nanoparticles agglomerate in the dispersed phase which reduces formation of co-continuous phase but slightly increases PA 6 domain size	Cai et al. 2012

PA 6/ABS	ABS: 0–100 wt%	Hydrophobic nanosilica	At interface when ABS forms the dispersed phase. In ABS phase when ABS is a continuous phase	The change in matrix and dispersed phase viscosity ratio shifts the phase inversion at higher ABS composition in the presence of nanosilica. The phase inversion composition was determined by various characterization techniques such as DSC, DMA, rheological behavior, and solvent extraction method	Liu et al. 2013
PA6/PP	80/20	Hydrophobic and hydrophilic nanosilica	Hydrophilic silica resides in PA 6 phase, whereas hydrophobic silica is located in PP phase and at the interface	Significant decrease in the PP particle size is observed when silica is located at the interface. Tensile modulus and yield strength increase in the presence of silica irrespective of the silica polarity; however, nanocomposites based on the hydrophobic silica showed higher elongation at break compared to pure blend	Laoutid et al. 2013
LLDPE/EVA	75/25	Hydrophobic nanosilica	LLDPE, EVA, and interface	The addition of nanosilica resulted in an increase in the tensile modulus, strength, and elongation at break; maximum improvement was observed at 10 wt% silica content. Interestingly, elongation at break did not decrease significantly in the presence of nanosilica	Heidary et al. 2013
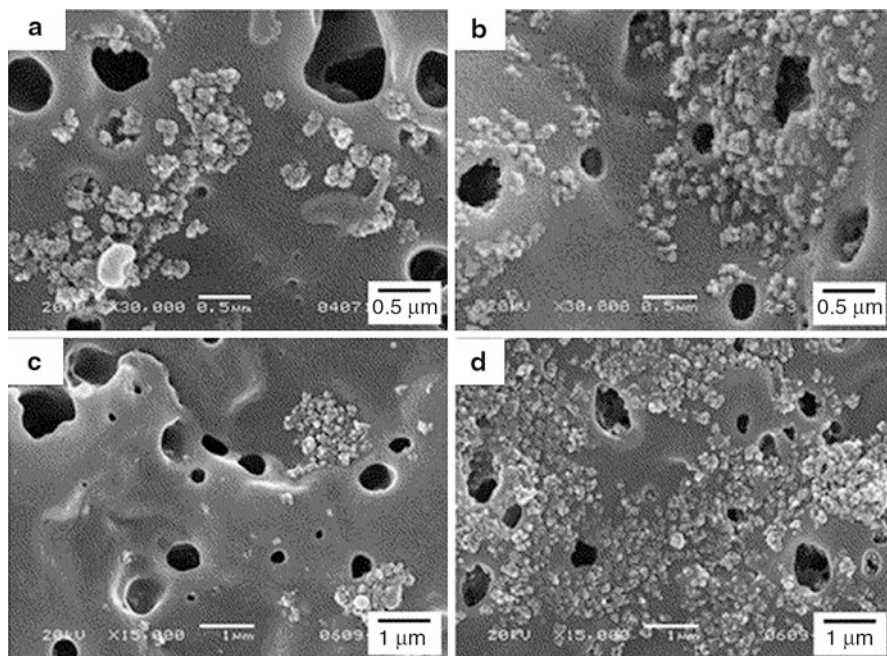
Fig. 17.26 SEM images of PP/EPDM/SiO$_2$ ((80/20/3) (**a** and **b**) and PP-g-MA/EPDM/SiO$_2$ (80/20/3) (**c** and **d**) ternary composites prepared using hydrophilic silica: (**a** and **c**) one-step simultaneous mixing and (**b** and **d**) two-step mixing (elastomer and the filler were mixed by means of a two-roll mill at room temperature for 10 min to get masterbatch first, and then the masterbatch was melt blended with pure PP or PP-g-MA) (Yang et al. 2007)

phase is much more stable when silica is present in the continuous phase compared to the blend without silica. The silica particles localized in the PP matrix also provides a reinforcement effect leading to increased tensile and flexural modulus and yield strength. The addition of nanoparticles into a thermoplastic olefin is similar to what has been observed for clay-containing blends; however, the relative increase in the properties especially impact strength of PP/EOR blend is significantly higher for clay-containing nanocomposites. The efficiency of spherical particles as a barrier to coalescence is much smaller than organoclay due to their low aspect ratio and poor dispersion compared to MMT particles. In another approach where either PP-g-MA was added or the silica was functionalized to improve dispersion in the PP matrix of PP/EOR (70/30) blend, the impact strength did not change much with the addition of silica although mechanical properties were found to increase (Liu and Kontopoulou 2006; Bailly and Kontopoulou 2009). The effect of silica on toughness improvement is more effective at higher elastomer contents in PP/EOR blends.

The addition of nanoparticles to an immiscible blend greatly influences the viscosity ratio of the dispersed to continuous phase which in turn changes the phase inversion composition. When hydrophobic silica particles were added to
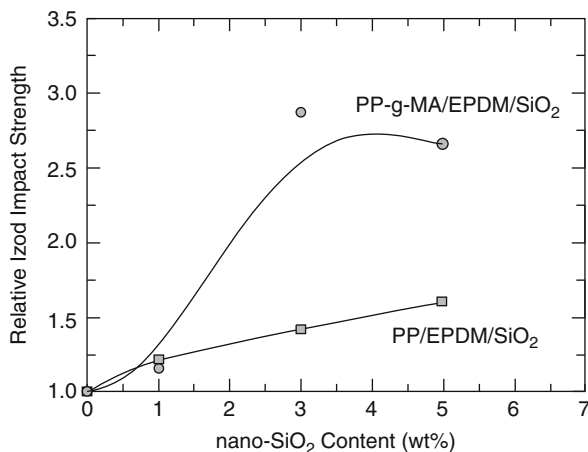
Fig. 17.27 Relative impact strength for PP/EPDM/SiO$_2$ and PP-g-MA/EPDM/SiO$_2$ nanocomposites as a function of SiO$_2$ content for composites prepared using hydrophilic silica and two-step processing method in which the elastomer and the filler were mixed by means of a two-roll mill at room temperature for 10 min to get masterbatch first and then the masterbatch was melt blended with pure PP. The weight ratio of PP/EPDM or PP-g-MA/EPDM was fixed at 80/20. Data taken from Yang et al. (2006, 2007)
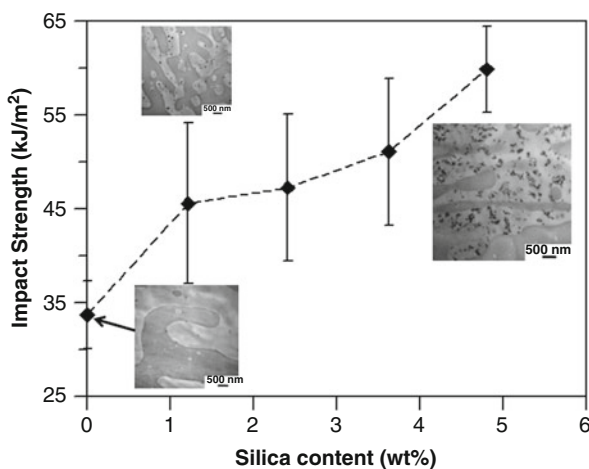
Fig. 17.28 Notched Izod impact strength for (PP/PP-g-MA 90/10)/EOR (50/50) blend as a function of silica content. Error bars represent the standard deviation. TEM images in inset show change in blend morphology from co-continuous structure to elongated dispersed elastomer particles in the presence of silica. Dark domains represent the stained elastomer phase (Lee et al. 2010)

PA 6/ABS blends, the phase inversion was observed to shift towards higher ABS content due to increase in the viscosity ratio of ABS/PA 6 resulting from migration of silica particles from PA 6/ABS interface to ABS phase at higher ABS compositions in the blend (Liu et al. 2013).

Ou and Li (2009) showed that the dispersed PA 6 particle size was reduced from 4 to 1 μm in PP/PP-g-MA/PA 6 (70/30) blends with addition of 2 wt% functionalized TiO_2 nanoparticles. The addition of PP-g-MA did not influence blend morphology but significantly improved dispersion of TiO_2 nanoparticles in the PA 6 matrix as observed from much finer and uniform distribution of PA 6 particle size. In the case of HDPE/EVA/$CaCO_3$ blend obtained from HDPE/$CaCO_3$ masterbatch, the EVA particles encapsulate the $CaCO_3$ nanoparticles along with separate dispersion of $CaCO_3$ nanoparticles observed in an HDPE matrix. A surface energy analysis predicts the complete encapsulation of $CaCO_3$ by EVA due to lower interfacial tension (γ) of EVA/$CaCO_3$ than HDPE/$CaCO_3$; however, kinetic effects preclude the complete encapsulation of $CaCO_3$ by EVA as also observed in several other blends (see Table 17.6) (Fowler et al. 1989; Cheng et al. 1992; Yoo et al. 2010a; Ali et al. 2011; Tiwari and Paul 2011a). In addition to thermodynamic factors, kinetic factors almost always have some effect on the final blend morphology, location, and distribution of filler in blend nanocomposites.

17.3.2 Polymer Blends Containing Carbon Nanotubes (CNTs)

Addition of CNTs to polymers has been shown to improve electrical conductivity and mechanical properties of the polymer matrix (Pötschke et al. 2003; Ruan et al. 2003; Gorga and Cohen 2004; Meincke et al. 2004; Pötschke et al. 2004; Coleman et al. 2006; Dondero and Gorga 2006; Moniruzzaman and Winey 2006; Zou et al. 2006; Pötschke et al. 2007; Zhang and Zhang 2007; Zhao et al. 2007; Li and Shimizu 2008; Pötschke et al. 2008; Bose et al. 2009; Dasari et al. 2009; Liu et al. 2009; Wu et al. 2009; Grady 2010; Liu et al. 2010; Spitalsky et al. 2010; Baudouin et al. 2011; Li et al. 2011; Tao et al. 2011; Zonder et al. 2011; Göldel et al. 2012; Shi et al. 2012; Wode et al. 2012; Xiang et al. 2012; Chen et al. 2013); however, strong van der Waals interaction between nanotubes inhibits their dispersion in the polymer leading to a weak percolation network and low mechanical properties (Breuer and Sundararaj 2004; Zhao et al. 2007; Pötschke et al. 2008; Grady 2010; Spitalsky et al. 2010; Li et al. 2011; Tao et al. 2011). The covalent and non-covalent modifications of nanotube surfaces have been utilized to improve CNT dispersion in the polymer matrix (Breuer and Sundararaj 2004; Moniruzzaman and Winey 2006). Apart from improvement in the chemical affinity of CNTs for the polymer, the various modification strategies also assist in effective processing to form polymer–CNT nanocomposites with enhanced mechanical and electrical properties (see Table 17.8). The addition of CNTs into immiscible polymer blends results in higher electrical conductivity compared to single polymer filled with nanotubes at the same loading (Gorga and Cohen 2004; Meincke et al. 2004; Pötschke et al. 2004; Moniruzzaman and Winey 2006;

Table 17.8 Observations on immiscible polymer blends containing carbon nanotubes

Blend	Composition/ content	Filler	Filler location	Observations	Reference
PA 6/ABS	45/55	MWCNT masterbatch	PA 6 phase	Co-continuous structure. Tensile modulus increases, while elongation at break and impact strength decrease with the addition of CNT. The onset of electrical conductivity was observed at 2–3 wt% CNT	Meincke et al. 2004
PPS/PA66	60/40	Acid-treated MWCNT	PA 66 phase	At low content, CNTs are dispersed evenly in PA 66 phase and blend exhibits co-continuous structure. At high loading, the CNTs aggregate to give dispersed PA 66 phase	Zou et al. 2006
PVDF/PA6	50/50	MWCNT	PA 6 phase	Improvement in electrical conductivity, modulus, and ductility	Li and Shimizu 2008
PCL/PLA	70/30	MWCNT and carboxylic MWCNT	PCL phase and interface	Unfunctionalized MWCNT is located exclusively in the PCL phase, while carboxylic MWCNT is located in the PCL phase and at the interface. The reinforcing and compatibilization effect of nanotubes results in a higher improvement in electrical conductivity and mechanical properties compared to pure blend. Improved phase stability and lower rheological and electrical conductivity percolation threshold were observed	Wu et al. 2009
PA 6/PP	20/80 and 50/50	MWCNT	PA 6 phase	In PA6/PP (20/80) blend nanocomposites, nanotubes are dispersed in the PA6 phase and form the conductive network resulting in a higher electrical conductivity than the PA6/PP (50/50) nanocomposites	Zhang et al. 2009

(continued)

Table 17.8 (continued)

Blend	Composition/content	Filler	Filler location	Observations	Reference
PP/EVA	80/20 and 64/40	Acid-treated MWCNT	Mostly in EVA phase and tend to migrate in PP phase at higher CNT loading leading to bridge effect	The formation of co-continuous morphology results in significant improvement in the electrical conductivity and fracture toughness compared to disperse phase structure in the presence of nanotubes. A "dual-network structure" of MWCNTs and EVA phase exists in PP/EVA (60/40) system which accounts for the largely improved fracture toughness of the composites as opposed to "single-network" structure observed in PP/EVA (80/20) blend	Liu et al. 2009
PC/SAN	60/40	C150HP MWCNT	PC phase	Irrespective of mixing protocols, even for pre-dispersing the nanotubes in SAN, all CNTs are located in the PC phase. The formation of double percolation network resulted in lower electrical resistivity	Göldel et al. 2009
EA/PA 6/12	90/10	Nanocyl®-7000	Interface	Increase in the phase stability	Baudouin et al. 2011
PE/PA6	PA 6: 20–37 wt%	MWCNT	PA 6 phase	Co-continuous structures were obtained by blending PE with PA6-CNT masterbatch. Nanocomposites showed solvent resistance, improvement in tensile modulus, and increase in the tensile strength as the PA 6 and CNT content increase	Périé et al. 2012
PA 6/ABS	70/30 and 50/50	MWCNT	PA 6 phase	ABS particle size decreased from 22 μm to ~2–4 μm in the presence of MWCNT in PA6/ABS (70/30 wt) blends. PA6/ABS (50/50 wt) blends show refinement of	Liu et al. 2012

				co-continuous morphology in the presence of MWCNT. Significant improvement in the yield strength and flexural modulus was obtained for both blends in the presence of MWCNTs, irrespective of the blend morphology	
PP/PS	70/30 and 50/50	Nanocyl NC 7000	PS phase and interface	Improvement in electrical conductivity and onset of thermal degradation in the presence of nanotubes. In all cases, nanocomposites prepared from PP masterbatch and having co-continuous structure have shown higher improvement in properties	Hwang et al. 2012
PPC/PLA	70/30	MWCNT	PPC	MWCNT is located in the PPC phase due to the lower interfacial tension between PPC and nanotubes. Blend nanocomposites exhibit higher electrical conductivity than homopolymer nanocomposites, whereas blend properties are in between those of PPC and PLA nanocomposites	Park et al. 2012
PET/LDPE	LDPE 0–100 wt %	Nanocyl NC7000	PET phase and interface at higher CNT loadings	Increase in the electrical conductivity observed for co-continuous structure and when PET forms the continuous phase	Cardinaud and McNally 2013
PC/SAN	90/10	Nanocyl NC7000	SAN phase	Significant increase in the electrical conductivity with lower percolation threshold observed at 0.18 wt% MWCNT. Thermal and dynamic properties of nanocomposites are higher in the presence of CNT	Maiti et al. 2013

Zou et al. 2006; Bose et al. 2007; Pötschke et al. 2007; Li and Shimizu 2008; Pötschke et al. 2008; Liu et al. 2009; Wu et al. 2009; Baudouin et al. 2010b; Liu et al. 2010; Li et al. 2011; Xiang et al. 2011; Zonder et al. 2011; Shi et al. 2012; Xiang et al. 2012; Chen et al. 2013). The concept of a double percolation network, observed for carbon black-filled polymer blends, where conducting carbon black filler is located in one of the polymer phases or at the interface, reduces the percolation threshold composition and provides higher electrical conductivity; this has also been observed in blends containing CNTs depending on the location of the nanotubes in the blend and its morphology (Sumita et al. 1991; Gubbels et al. 1995; Zhang et al. 1998).

Pötschke and coworkers have shown that electrical conductivity in co-continuous blends of polycarbonate (PC) and high-density polyethylene (HDPE) is significantly higher in the presence of multiwalled carbon nanotubes (MWCNTs). The MWCNTs are located in the PC phase and at the PC/HDPE interface; this results in a stable blend morphology and broad co-continuous region. Increased mixing time leads to attrition of the nanotubes and a decrease in conductivity (Pötschke et al. 2003, 2004). In another blend of PC-2 wt% MWCNT and PP-3 wt% MMT, the nanotubes are located in the PC phase while MMT particles migrate from the PP phase to the PP/PC interface and encapsulate the PC-2 wt% MWCNT. This hinders the migration of MWCNTs into the nonconductive PE phase and results in higher conductivity values for this blend compared to a PC-2 wt% MWCNT/HDPE blend without MMT (Pötschke et al. 2007). In the case of polyamide 12 (PA12)/HDPE/MWCNT blend nanocomposites prepared from three different mixing procedures, it was reported that when nanotubes are located at the interface surrounding the dispersed HDPE particles, the electrical resistivity decreases by at least four orders of magnitude. The formation of surface and volume percolating networks, where the CNTs envelope HDPE particles and interconnect through the interphase to the few CNTs dispersed throughout the volume of the PA phase, leads to a significant decrease in the electrical resistivity (Zonder et al. 2011).

The presence of CNTs at the interface alters the region of co-continuous morphology and can lead to improvement in electrical conductivity at much lower CNT content (Meincke et al. 2004; Bose et al. 2007, 2009). The CNTs have a tendency to preferentially locate in the more polar component of immiscible blends as seen from the location of the nanotubes in the polyamide phase of PVDF/ PA 66, PA 6/ABS, and PPS/PA 66 blends when nanotubes are pre-blended with the polyamide matrix (Meincke et al. 2004; Zou et al. 2006; Li and Shimizu 2008; Zonder et al. 2011). It is reported that nanotubes are likely to migrate from the less polar to the more polar polymer phase even when the differences between the surface energies of the two are small. Bailly and coworkers reported that nanotubes are located at the interface and envelope the minor polyamide phase in blends with ethylene–acrylate (EA) copolymers resulting in a more stable blend morphology and narrow particle size distribution (Baudouin et al. 2010a, b, 2011; Tao et al. 2011). The presence of nanotubes at the interface significantly reduces the coalescence of dispersed phase droplets as seen in other nanoparticles containing
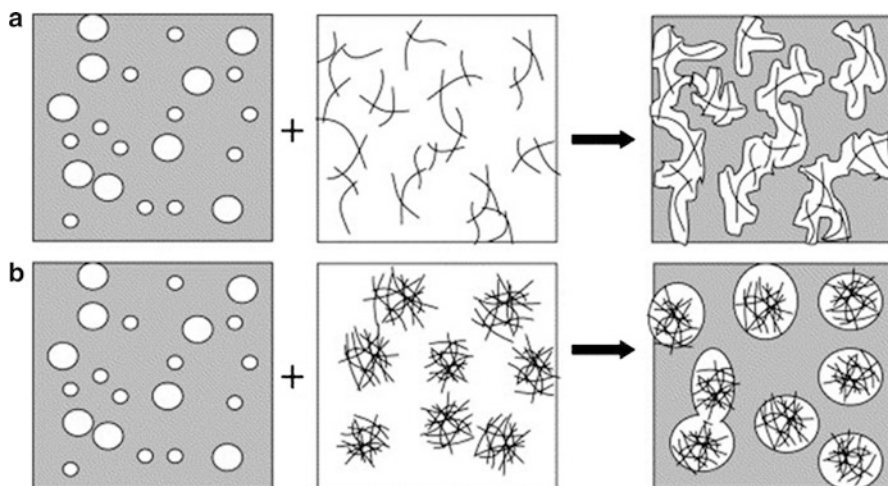
Fig. 17.29 Schematic representation of the PPS/PA66 (60/40 w/w)/MWCNT nanocomposites morphology changing: (**a**) low load MWCNTs (<0.5 phr) disperse evenly and form a percolating network, and (**b**) high load MWCNTs (>0.5 phr) aggregate like clews (Zou et al. 2006)

blends (Elias et al. 2007; Tiwari and Paul 2011a). Carbon nanotubes behave similar to other nanoparticles in immiscible blends, i.e., they promote co-continuity when completely located in the dispersed phase; however, at higher concentrations they tend to aggregate and can transform a co-continuous structure into a dispersed phase morphology (Zou et al. 2006). Figure 17.29 schematically shows the change from co-continuous to dispersed morphology as a function of nanotube content in poly (*p*-phenylene sulfide) (PPS)/polyamide 66 blends.

The addition of nanoparticles in immiscible blends leads to stabilization of blend morphology and a decrease in the dispersed phase particle size; the smaller dispersed phase particle size, particularly for elastomers, can lead to improvement in toughness of the blend. The decrease in the dispersed phase particle size is influenced by the filler dimension, their dispersion, and interfacial interactions with different polymer phases in blend. In a few studies on polymer–CNT nanocomposites, it is reported that good orientation and dispersion of nanotubes are required for improvement in tensile toughness. The nanotubes oriented in the flow direction can act as a bridge to crazes and cracks in tensile specimens resulting in a higher strain at break; moreover, the higher load-carrying capacity of nanotubes and ability to undergo deformation may also contribute to the improvement in ductility (Qian et al. 2000; Zhao et al. 2007; Liu et al. 2009; Li et al. 2011). Liu et al. (2009) reported a significant increase in the toughness of PP/EVA (60/40) blend nanocomposites from 102 to 632 J/m in the presence of 2 wt% MWCNT in the blend. The toughness is observed for co-continuous morphology where nanotubes are located at the interface and form a bridge between the two phases resulting in "super-tough" blends. The functionalization of CNT is important for

Fig. 17.30 Schematic
representation shows (**a**) the
selective distribution of
FMWCNTs at the interface
between phase A and phase
B and (**b**) the crack
propagation along the
interface plane
(Chen et al. 2013)
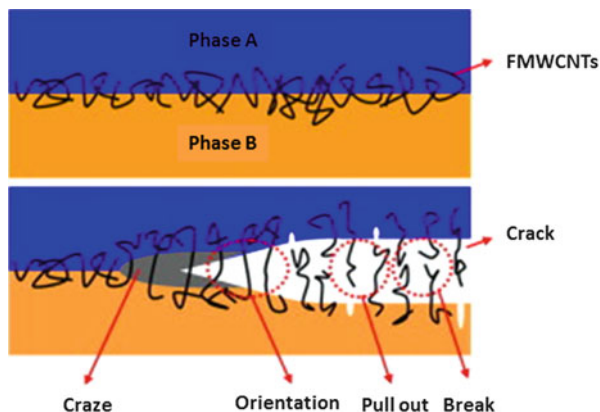
improving dispersion; however, some functionalization processes such as acid
treatment reduce the length of CNT with some loss of bridging effect (Liu
et al. 2009, 2010). Figure 17.30 shows the schematic of the possible fracture
mechanism of immiscible polymer blends containing functionalized MWCNTs at
the interface. Under the load, the initiation of a crack first occurs at the interface
because of the smaller entanglement density compared with the bulk polymer
which is followed by crazing of the polymer usually observed at the crack tip due
to high stress concentration. Crazing is also known to cause brittle fracture; it is
usually related to the fibrillation and the volume expansion of polymer, contributing
to the major part of energy dissipation (Bucknall 1977). When MWCNTs are
selectively distributed at the interface, the fibrillation of polymer chain segments
promotes the orientation of nanotubes perpendicularly to the interface plane and
facilitates further energy absorption. During initiation and propagation of cracks
along the interface, some nanotubes are oriented and few are pulled out of the
matrix. The oriented nanotubes that bridge the crack face prevent further propaga-
tion. Specifically when the interfacial adhesion between the CNT and polymer
matrix is strong enough, one can also see the breakage of MWCNTs; however, this
favors the energy absorption during the fracture process (Qian et al. 2000; Gorga
and Cohen 2004; Zhang and Zhang 2007; Zhao et al. 2007; Chen et al. 2013). The
co-continuous morphology has been extensively studied for CNT-containing blends
and has shown significant improvement in electrical conductivity and toughness
with double percolation effects (Bose et al. 2009; Liu et al. 2009, 2010; Xiang
et al. 2011). The various mixing sequences such as pre-blending versus simulta-
neous mixing, functionalization of carbon nanotubes, mixing time, and blend
composition all have a significant effect on the overall improvement of properties.
Although, CNTs are not as efficient for size reduction as MMT, CNTs are stiffer
and stronger plus their high aspect ratio and tubular structure provide a better load-
bearing capacity compared to other fillers provided there is an adequate interfacial
interaction.

17.4   Rheology of Blend Nanocomposites

The melt rheological behavior provides fundamental insights about the flow properties of materials and is important to optimize processing conditions for polymers, their blends, and composites. In the case of polymer blends, the flow behavior is much more complex and influenced by several factors such as composition, the viscoelastic properties of the blend components, and their interfacial interactions. The presence of solid filler particles in the blend further complicates the interpretation of the rheological behavior. The melt rheology of blends in the presence of nanoparticles such as organoclays, silica, and carbon nanotubes has been extensively studied to understand their effect on the interfacial interactions between the blend components, blend morphology, and phase inversion composition (Kontopoulou et al. 2003; Vermant et al. 2004; Austin and Kontopoulou 2006; Thareja and Velankar 2006; Elias et al. 2007; Vermant et al. 2007; Elias et al. 2008b; Pötschke et al. 2008; Vermant et al. 2008; Bailly and Kontopoulou 2009; Madivala et al. 2009a, b; Lee et al. 2010; Tiwari and Paul 2011a; Zonder et al. 2011; Liu et al. 2013).

17.4.1 Blends Containing Silica

Vermant et al. (2004) reported the rheological behavior of PDMS/PIB (70/30) blends in the presence of silica and observed no change in the G' behavior for the blend nanocomposite samples pre-sheared at various shear rates before rheological measurements. This confirmed the stable morphology of the blend in the presence of silica; moreover, the change in the interfacial properties obtained by fitting experimental data to the Palierne model also confirmed the compatibilizing effect of silica resulting in decreased coalescence of PIB particles. The general use of the Palierne model in immiscible blends is to determine the volume average dispersed particle radius, R, from the dynamic modulus provided the interfacial tension values are readily available from an independent measurement. However, for filled polymer blends, the interfacial tension is not usually known and cannot be determined by any direct method. Vermant et al. (2004) found that fitting the Palierne model to the experimental data for filled polymer blends is difficult even after introducing additional fitting parameters; therefore, they used the ratio R/γ_{12} (volume average dispersed particle radius over interfacial tension) in the Palierne model to avoid any ambiguity concerning the interfacial tension. The ratio R/γ_{12} was calculated from the following relation (Palierne 1990; Vermant et al. 2004):

$$\tau = \frac{R\eta}{4\gamma_{12}} \frac{(19p+16)(2p+3-2\phi(p-1))}{10(p+1)-2\phi(5p+2)} \tag{17.1}$$

where η is the viscosity of the matrix phase, p is the viscosity ratio, ϕ is the volume fraction of the dispersed phase, and τ is the dispersed phase relaxation time obtained from the crossover frequency between $G'(\omega)$ and $G''(\omega)$. Cassagnau and coworkers

have observed that the peaks corresponding to relaxation processes are complicated and difficult to follow; in some cases the dispersed phase relaxation time may be similar to one of the matrices which can lead to inaccurate determination of relaxation time (Elias et al. 2008b; Fenouillot et al. 2009). It was suggested that the ratio R/γ_{12} can be easily determined by isolating the dispersed phase contribution from the complex relaxation modulus using a modified Palierne model equation:

$$G'_{\text{Palierne}} = G^*_{\text{Composition}} + G^*_{\text{Dispersed}} \tag{17.2}$$

where $G^*_{\text{Composition}}$ is the complex shear modulus of the blend without any interfacial effects and $G^*_{\text{Dispersed}}$ captures the interfacial effects. The storage part of complex shear modulus, G', for a blend of two viscoelastic fluids can be expressed as follows:

$$G'_{\text{Palierne}}\left(\gamma_{12}, G^*_m, G^*_d\right) = G'_{\text{Palierne}}\left(0, G^*_m, G^*_d\right) + G'_{\text{Palierne}}\left(\gamma_{12}, \eta^*_m, \eta^*_d\right) \tag{17.3}$$

where G^* and η are the complex modulus and Newtonian viscosity, respectively, and subscripts m and d represent the matrix and dispersed phase, respectively. From the above equations, Eqs. 17.2 and 17.3, the contribution of the dispersed phase relaxation, which only depends on the interfacial tension, γ, can be easily determined by subtracting the composition effects to the experimental data of G^*. The modified approach was used to determine the effective interfacial tension between PP/EVA (80/20) blends in the presence of silica, and it was observed that the effective interfacial tension decreased from 0.75 to 0.25 mN/m when the silica particles are located in the dispersed phase. (Elias et al. 2008b).

17.4.2 Blends Containing MMT

In clay-based polymer nanocomposites, a part of the enhancement of rheological properties is due to the formation of percolated networks of clay platelets. Figure 17.31 shows the storage modulus, G', plots as a function of frequency, ω, for PP/PP-g-MA/MMT/EOR nanocomposites containing different amount of MMT and various PP-g-MA/organoclay ratios. As seen in Fig. 17.31, a significant increase in the storage modulus is observed with the addition of MMT ≥ 3 wt% at fixed PP-g-MA/organoclay ratio of 1.0. Similar effects are seen with increasing PP-g-MA/organoclay ratio ≥ 0.5 at a fixed MMT content of 5 wt%. The decrease in the G' slope in the terminal zone ($\omega < 1$ rad/s) with increasing MMT and PP-g-MA/ organoclay ratios is due to the formation of a percolated network of clay particles resulting in solid-like behavior of nanocomposites at low frequency. The formation of a percolation network is facilitated either by increasing the number of clay stacks with increase in the amount of clay at fixed PP-g-MA content or by increasing the degree of exfoliation of clay platelets with increase of PP-g-MA content at fixed
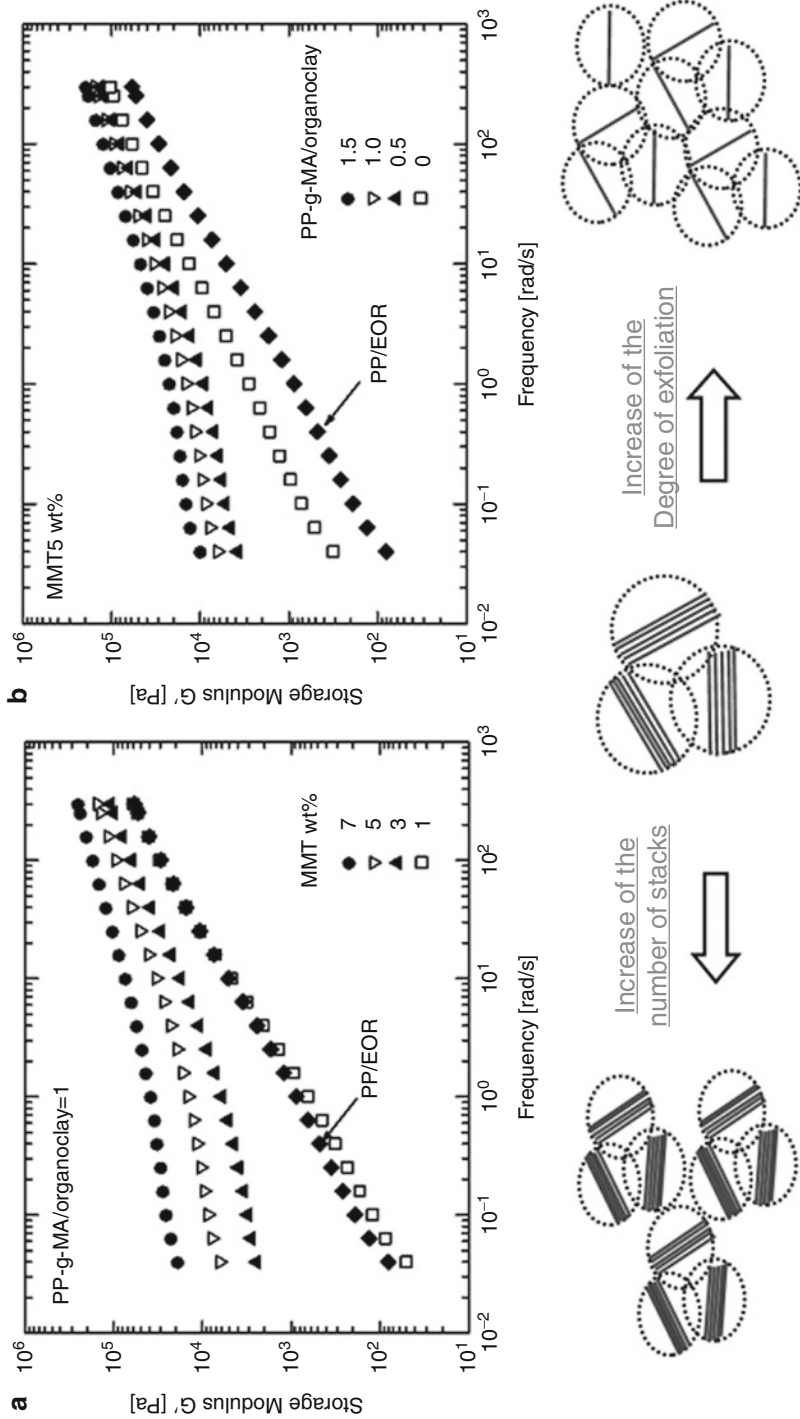
Fig. 17.31 Storage modulus of PP/PP-g-MA/MMT/EOR nanocomposites (**a**) as a function of MMT content at fixed PP-g-MA/organoclay ratio of 1.0 and (**b**) as a function of PP-g-MA content at fixed MMT content of 5 wt%. All measurements were done at 190 °C (Tiwari et al. 2012)

clay content as seen in schematic in Fig. 17.31. However, it is difficult to distinguish the effect of the minor phase on the rheological behavior from that of clay platelets in blend nanocomposites. To address this issue quantitatively, Paul and coworkers used a modified Carreau-Yasuda model to separate out effects of addition of elastomer in PP/PP-g-MA/MMT nanocomposites using the following relation:

$$\eta(\omega) = \frac{\sigma_0}{\omega} + \eta_0 [1 + (\lambda\omega)^a]^{\frac{(n-1)}{a}} \qquad (17.4)$$

where σ_0 is the melt yield stress, η_0 is the zero shear viscosity, λ is the time constant, a is the Yasuda parameter, and n is the power law index (Lertwimolnun and Vergnes 2005; Kim et al. 2007a). This approach is more appropriate for the systems where clay particles are exclusively located in the matrix phase such as in the case of PP/PP-g-MA/MMT/EOR nanocomposites (Tiwari and Paul 2011b). The melt yield stresses and terminal zone slope for PP/PP-g-MA/MMT and PP/PP-g-MA/MMT/EOR nanocomposites obtained from the best fit of the experimental data are compared in Fig. 17.32a, b. The melt yield stress increases with increase in the MMT content and with PP-g-MA/organoclay ratio; however, the PP/PP-g-MA/MMT/EOR nanocomposites have a higher value than for the PP/PP-g-MA/MMT nanocomposites and show a sharp increase beyond 3 wt% MMT and with increased PP-g-MA/organoclay ratio. The terminal slope of G' versus ω or $(d \ln G'/d \ln \omega)_{\omega \to 0}$ decreases with increasing MMT content and PP-g-MA/organoclay ratios due to the presence of MMT particles forming a percolated network leading to a solid-like behavior. This is because the elastomer phase in PP/PP-g-MA/MMT nanocomposite suppresses the dispersion of MMT particles and forms a percolated network at lower MMT content.

17.4.3 Blends Containing CNTs

Pötschke et al. (2002) first reported rheological behavior of polycarbonate (PC)/CNT nanocomposites prepared by diluting a masterbatch containing 15 wt% MWCNT using a twin-screw extruder. They observed significant increase in the low-frequency melt viscosity for nanocomposites having greater than 2 wt% MWCNT. The non-Newtonian behavior was ascribed to the rheological threshold obtained at lower CNT loading due to its high aspect ratio which also correlates well with the electrical conductivity percolation threshold observed between 1 and 2 wt% nanotubes in blend. Several later papers have described correlation between the percolation threshold obtained from the rheological behavior and the electrical properties for immiscible blend containing carbon nanotubes (Gubbels et al. 1995; Li and Shimizu 2008; Bose et al. 2009; Tao et al. 2011; Wode et al. 2012). Zonder et al. (2011) studied the effect of three different mixing procedures on the rheological behavior of polyamide 12 (PA12)/HDPE blends containing 0.75 wt% MWCNT. The addition of carbon nanotubes resulted in higher dynamic storage modulus, G', values for all blend nanocomposites, irrespective of the blend

Fig. 17.32 Comparison of melt yield stress and terminal slope of G′ for PP/PP-g-MA/MMT/EOR and PP/PP-g-MA/MMT nanocomposites as a function of (**a**) MMT content and (**b**) PP-g-MA/organoclay ratio. Data for PP/PP-g-MA/MMT taken from Kim et al. (2007a) (Tiwari et al. 2012)
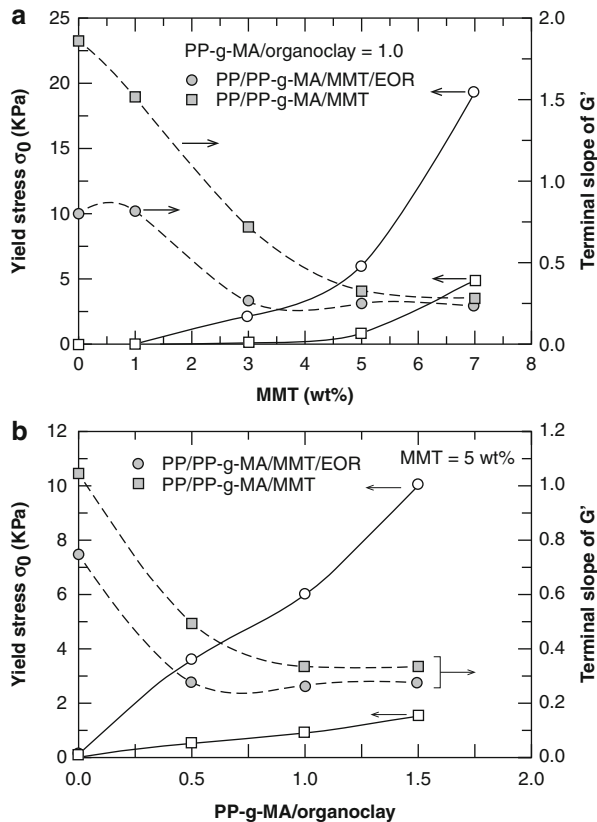
compositions; however, the effect of blending sequence was evident in PA12/HDPE (75/25) and PA12/HDPE (25/75) blend nanocomposites. In the case where PA 12 forms the continuous phase, the G' is significantly higher than the pure blend and shows a solid-like behavior at low frequency; this is attributed to the well-dispersed CNTs in the PA 12 matrix and formation of network structure. Among various blending sequences, the PA 12/HDPE (75/25) nanocomposite prepared from HDPE masterbatch has a slightly higher G' value in the low-frequency region as well as decreased frequency dependence compared to nanocomposites obtained from simultaneous mixing and PA 12 masterbatch. Based on SEM images, it was suggested that the kinetic parameters such as higher HDPE viscosity than PA 12 trap some nanotubes at the interface during migration from HDPE to PA 12 phase which delays relaxation of the dispersed HDPE particles. As carbon nanotubes do not have a significant effect on the rheology of HDPE, it is assumed that the nanotubes at the interface promote blend elasticity by either increasing the compatibility between HDPE and PA 12 or affecting the interfacial relaxation processes. The location of CNTs in blend is influenced by the mixing protocol and has a significant effect on the blend morphology, rheology, percolation threshold, and electrical conductivity.

17.5 Mechanical Properties of Blend Nanocomposites

The mechanical properties of blends are important factors for performance in most applications. The addition of high modulus fillers into polymers always increases the tensile modulus; however, tensile strength is very dependent on the interfacial adhesion between blend components (Bigg 1987; Ward and Sweeney 2013). Nonetheless, the addition of solid fillers reduces the elongation at break in nanocomposites. Figure 17.33 shows the effect of PP molecular weight and PS composition on the tensile modulus for PP/PP-g-MA/MMT/PS blend with and without MMT. The addition of PS to PP/PP-g-MA or PP/PP-g-MA/MMT substantially increases the modulus although the PP molecular weight has little effect on blend modulus. The addition of MMT increases blend modulus with the greatest increase observed at low PS contents <30 wt%. The contribution of MMT on blend modulus decreases as the PS content increases due to the increasing PS contribution to the blend modulus. The tensile modulus also increases with the increase in the MMT content at fixed PS composition in blend; however, no significant difference observed among PP with different molecular weight grades (Tiwari and Paul 2011a). The tensile strength at yield was usually found to increase for elastomer-toughened blends such as thermoplastic olefin nanocomposites (Tiwari et al. 2012). Kontopoulou and coworkers also observed increases in blend modulus and decreases in the elongation at break with the addition of nanosilica in PP/EOR blend nanocomposites containing 10–30 wt% of elastomer and 0–5 wt% silica content (Liu and Kontopoulou 2006). Meincke et al. (2004) reported significant increases in the modulus of PA 6/ABS blends in the presence of carbon nanotubes; however, the elongation at break and notched impact strength for the nanocomposites were lower than for the pure blend. The improvement in modulus was higher for blends containing carbon nanotubes than those containing carbon black. In another study on HDPE/PA 6/MWCNT (80/20/2) blend prepared from functionalized MWCNT, the blend nanocomposites prepared from a HDPE/MWCNT masterbatch showed excellent tensile strength and toughness simultaneously. The nanotubes migrate from the HDPE phase to the HDPE/PA 6 interface and provide a nano-bridge effect that prevents crack initiation and propagation along the interfaces and results in higher ductility of blend. Other blending sequences, where nanocomposites were obtained from a PA 6 masterbatch with the nanotubes located in the PA 6 phase, resulted in lower improvement in properties (Xiang et al. 2011). Though nanoparticles seem to provide reinforcement effects in blends, tensile strength or elongation at break may or may not be similarly improved. There is interest in modeling tensile modulus of blends and nanocomposites and to correlate the experimental data with composite models (Brune and Bicerano 2002; Fornes and Paul 2003; Chavarria and Paul 2004; Sheng et al. 2004; Stretz et al. 2005; Kim et al. 2007a; Shah et al. 2007; Clifford and Wan 2010; Wang et al. 2010). Paul and coworkers successfully used the Halpin–Tsai and Mori–Tanaka composite theories to predict the modulus trends for polymer nanocomposites (Hill 1965; Wu 1966; Halpin 1969; Mori and Tanaka 1973; Halpin and Kardos 1976; Fornes and Paul 2003; Chavarria and Paul 2004;

Fig. 17.33 (**a**) Tensile modulus for blends with and without MMT at various PS compositions and (**b**) effect of MMT content on tensile modulus of blends prepared with different molecular weight grades of PP having 30 wt% PS. The MMT wt% is based on the PP/PP-g-MA/MMT phase in blend (Tiwari and Paul 2011a)
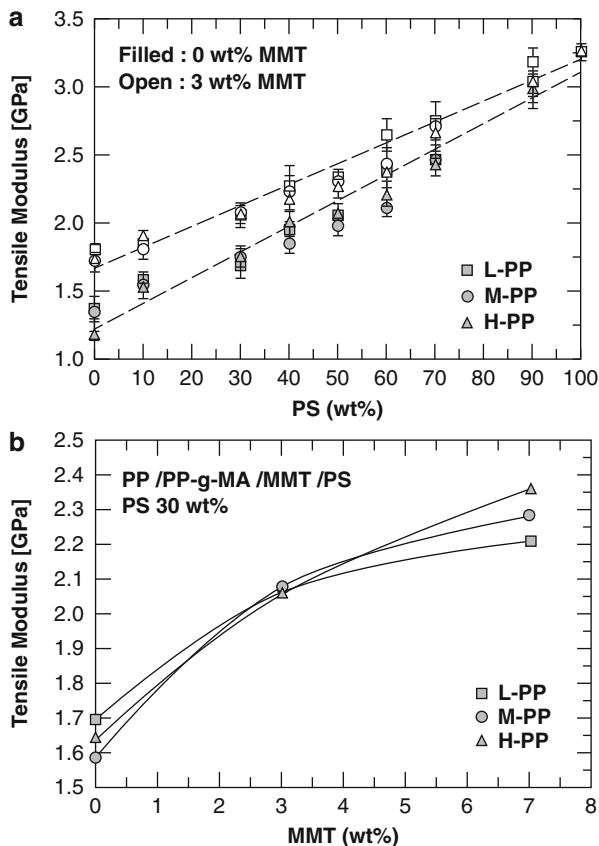
Shah et al. 2007; Spencer et al. 2010). They have also modified the Mori–Tanaka model using a two-population approach to predict modulus of ternary systems such as polymer blend nanocomposites and polymer composites containing two different fillers. More details can be found in papers describing the extensive modeling work by Paul and coworkers (Spencer and Paul 2011; Yoo et al. 2011; Tiwari et al. 2012). Other composite models such as the Christensen model has been also used to predict modulus of PS/PP/PP-g-MA/MMT nanocomposites where PP particles form the dispersed phase (Istrate et al. 2012).

17.6   Future Trends

Polymer blends containing nanoparticles provide a route to balance the properties when prepared using an appropriate mixing protocol. Nonetheless, the improvement in the blend properties is very specific to the blend components and type of nanoparticle. For example, organoclays and silica reduce elongation at break, while functionalized carbon nanotubes have been shown to increase the tensile ductility

of blends in tensile tests (Liu and Kontopoulou 2006; Tiwari and Paul 2011a; Xiang et al. 2011). On the other hand, organoclay is much more beneficial in reducing dispersed phase particle size compared to other nanoparticles (Liu and Kontopoulou 2006; Elias et al. 2007; Kelnar et al. 2007; Vo and Giannelis 2007; Elias et al. 2008b; Fenouillot et al. 2009; Wu et al. 2009; Baudouin et al. 2011; Tiwari and Paul 2011a). The combination of two nanofillers such as MMT and CNTs in (PC/CNT)/(HDPE/MMT) blend has shown significant improvement in electrical conductivity than nanotube alone (Pötschke et al. 2007). Although there have been very few reports on utilization of multiple nanofillers in polymer blends, this concept is more frequently used in polymer nanocomposites (Liu and Grunlan 2007; Rattanasom et al. 2007; Yu et al. 2007b; Sumfleth et al. 2008; Tang et al. 2008; Wang et al. 2009). Polymer blend nanocomposites can offer a balance of properties such as combination of toughness and stiffness, increase in electrical conductivity, lightweight, and increased weatherability. The combination of high-aspect-ratio clay particles and conductive carbon nanotubes can provide improvement in toughness and electrical conductivity of elastomer-toughened thermoplastics. Recently, graphene has gained significant interest as a next-generation nanofiller for polymer nanocomposites due to the advantages of lower mass density compared to clay and, low cost and comparable mechanical properties, electrical and thermally conductivity than carbon nanotubes. However, there are challenges and difficulties associated with the production of high quality exfoliated monolayer graphene, poor dispersion of graphene in the polymer matrix, impurities and damaged edges after reduction of graphene oxide. The addition of graphene into a polymer matrix results in higher improvement in mechanical properties such as tensile modulus and strength and higher electrical conductivity depending on surface modification of graphene and processing method (Jang and Zhamu 2008; Kim et al. 2010; Li and Zhong 2011; Potts et al. 2011). The combination of graphene with carbon fibers has also been utilized to improve network formation; this resulted in higher electrical conductivity at low concentration of fillers (King et al. 2008). The application of graphene as a compatibilizer in PA 6/PPO blend showed a decrease in dispersed PPO particle size by an order of magnitude (Cao et al. 2011). Based on the exceptional properties of graphene it is expected to be the next-generation high performance material; however, many challenges exist in fundamental understanding and applicability to produce nanocomposites with excellent properties. More efforts to understand the effect of graphene on the dispersed particle size, blend morphology and stability, and mechanical properties are required to enhance knowledge and find new avenues for application of graphene in immiscible polymer blends.

17.7 Conclusions

This chapter discusses the role of nanofillers as a compatibilizer for immiscible blends when located at the blend interface or as an aid to reduce coalescence of dispersed particles when located in the continuous phase of blends. The presence of

a nanofiller in a blend can lead to significant decreases in the dispersed phase particle size; however, the extent of the decrease in size depends on the dimension of the filler, the state of dispersion, and location in blend. The nanofiller located in the minor component of blend results in an increase of dispersed phase particle size. The reinforcement effect of nanofiller provides higher mechanical properties in comparison to a pure blend; moreover, the dispersed particle size distribution is narrow, and a stable blend morphology can be observed during thermal annealing. In many blend nanocomposites, it was reported that kinetic effects contribute to the location of the filler in the blend in addition to that predicted from a surface energy analysis. In general, addition of a nanofiller increases tensile modulus and strength while elongation at break is usually mostly reduced; however, functionalized nanotubes have shown improvement in tensile ductility in some cases.

In the majority of papers, only a few compositions are studied, and details on the phase inversion behavior in the presence of nanofiller and its content, morphology stability, and possible application of those materials are not provided. The most promising advantage of using nanofillers is improvement in toughness and stiffness as observed for several elastomer-containing blends; however, this depends largely on the polymer blend system, interfacial interactions between polymer and filler, type of filler, and its location in the blend components. The presence of nanofiller in a soft elastomer particle can also act as stress concentrator reducing toughness; however, in elastomer-containing polyamide nanocomposites, the presence of organoclay in the elastomer and polyamide phase has shown improvement in toughness and other mechanical properties. The commercial viability of such approaches remains to be determined.

The extent of nanofiller dispersion and matrix properties have a significant effect on the overall blend properties, for example, highly exfoliated MMT particles in the polyamide matrix can make it brittle, whereas partially exfoliated clay particles in extruder-made thermoplastic olefin nanocomposites can lead to significant improvements in impact strength depending on the PP molecular weight and elastomer MFI.

The nanofillers discussed in this chapter have their own unique properties, e.g., organoclays with high surface area and platelet-like structure are more beneficial in reducing dispersed phase particle size compared to spherical nanosilica or tubular carbon nanotubes. However, addition of nanosilica in co-continuous blends can convert this structure into a dispersed phase structure with a stable morphology, whereas carbon nanotubes provide higher electrical conductivity in the blend and can improve tensile ductility acting as bridge to arrest propagation of cracks and crazes. The utilization of two fillers to encapsulate one of the phases to restrict migration of other filler and to promote network structure has also shown significant improvement in the electrical conductivity of blend nanocomposites.

Other than the thermodynamic effects, the mixing time can significantly affect the equilibrium location of filler; in fact, the additional processing time can even lead to migration of filler particles from its equilibrium position as predicted from the surface energy analysis. Future work on polymer blends containing nanoparticles should combine the basic and applied research that has been done

to date with additional considerations of the processing issues and experimental designs to prepare materials with better combinations of properties for commercial applications. The combination of experiments, computational modeling, and theory can be a powerful tool for optimizing properties of commercially valuable polymer blends. This chapter should provide a platform for building knowledge about fundamental issues and applications.

17.8   Cross-References

▶ Applications of Polymer Blends
▶ Commercial Polymer Blends
▶ Compounding Polymer Blends
▶ Interphase and Compatibilization by Addition of a Compatibilizer
▶ Mechanical Properties of Polymer Blends
▶ Morphology of Polymer Blends
▶ Polymer Blends: Introduction
▶ Properties and Performance of Polymer Blends
▶ Rheology of Polymer Alloys and Blends
▶ Thermodynamics of Polymer Blends

Nomenclature

ABS Acrylonitrile–butadiene–styrene
AFM Atomic force microscopy
a-PA Amorphous polyamide
CaCO$_3$ Calcium carbonate
CNT Carbon nanotube
CTE Coefficient of linear thermal expansion
D-B Ductile–brittle
EA Ethylene–acrylate copolymer
E-MA-GMA Ethylene–methyl acrylate–glycidyl methacrylate copolymer
EOR Ethylene–octene rubber
EOR-g-MA Ethylene–octene rubber grafted maleic anhydride
EPDM Ethylene–propylene–diene terpolymer
EPDM-g-MA Ethylene–propylene–diene grafted maleic anhydride
EPR Ethylene–propylene rubber
EPR-g-MA Ethylene–propylene rubber grafted maleic anhydride
EVA Ethylene–vinyl acetate copolymer
FD Flow direction
HDPE High-density polyethylene
H-PP High molecular weight polypropylene
LCP Liquid crystalline polymer

LDPE Low-density polyethylene
LLDPE Linear low-density polyethylene
L-PP Low molecular weight polypropylene
MA Maleic anhydride
MFI Melt flow index
MMT Montmorillonite
M-PP Medium molecular weight polypropylene
MWCNT Multiwalled carbon nanotube
MWD Molecular weight distribution
ND Normal direction
OMMT Organically modified montmorillonite
PA Polyamide
PA 6 Polyamide 6
PA 66 Polyamide 66
PBT Polybutylene terephthalate
PC Polycarbonate
PCL Poly (ε-caprolactone)
PDMS Polydimethylsiloxane
PE Polyethylene
PE-GMA Ethylene–glycidyl methacrylate
PET Poly (ethylene terephthalate)
PIB Polyisobutylene
PLA Polylactide
PLLA Poly (L-lactide)
PP Polypropylene
PPC Poly (propylene carbonate)
PP-g-MA Polypropylene grafted maleic anhydride
pph Parts per hundred
PPO Polyphenylene oxide
PPS Poly (*p*-phenylene sulfide)
PS Polystyrene
PVDF Polyvinylidene fluoride
SAN Poly (styrene acrylonitrile)
SBS Styrene–butadiene–styrene
SEBS Styrene–ethylene–butylene–styrene
SEBS-g-MA SEBS grafted maleic anhydride
SEM Scanning electron microscope
SEP Styrene–ethylene–propylene
SiO$_2$ Silica
SIS Styrene–isoprene–styrene
TD Transverse direction
TEM Transmission electron microscope
TiO$_2$ Titanium dioxide
TPO Thermoplastic olefin

VA Vinyl acetate
VP 701 Vulcanized butadiene–styrene rubber
a Yasuda parameter
$\bar{d}_w$ Weight average particle size
G′, G″, G* Storage, loss and complex shear modulus, respectively
h Hour
m Meter
min Minute
N Newton
n Power law index
nm Nanometer
p Viscosity ratio of dispersed to continuous phase
R Volume average dispersed particle radius
T_g Glass transition temperature
T_m Melting temperature
wt% Weight percent
γ Interfacial tension
η Shear viscosity
η_0 Zero shear viscosity
η_1, η_2 Viscosity of phase 1 and 2 respectively
η_d, η_m Viscosity of dispersed and matrix phase respectively
λ Time constant
μm Micrometer
σ_0 Melt yield stress
τ Relaxation time
ϕ Volume fraction
χ_c Percent crystallinity
ω Frequency
ω_a Wetting coefficient

References

F.O.M.S. Abreu, M.M.C. Forte, S.A. Liberman, J. Appl. Polym. Sci. **95**, 254 (2005)
Y.C. Ahn, D.R. Paul, Polymer **47**, 2830 (2006)
M. Alexandre, P. Dubois, Mater. Sci. Eng. **R28**, 1 (2000)
I. Ali, R. Elleithy, S.M. Al-Zahrani, M.E. Ali Mohsin, Polym. Bull. **67**, 1961 (2011)
S.H. Anastasiadis, I. Gancarz, J.T. Koberstein, Macromolecules **21**, 2980 (1988)
L.M. Arzondo, N. Pino, J.M. Carella, J.M. Pastor, J.C. Merino, J. Póveda, C. Alonso, Polym. Eng. Sci. **44**, 2110 (2004)
L. As'habi, S.H. Jafari, H.A. Khonakdar, B. Baghaei, J. Polym. Res. **18**, 197 (2010)
J.R. Austin, M. Kontopoulou, Polym. Eng. Sci. **46**, 1491 (2006)
R. Aveyard, B.P. Binks, J.H. Clint, Adv. Colloid Interface Sci. **100–102**, 503 (2003)
H. Bai, Y. Wang, B. Song, T. Huang, L. Han, J. Polym. Sci. Pt. B: Polym. Phys. **47**, 46 (2009)
M. Bailly, M. Kontopoulou, Polymer **50**, 2472 (2009)
J.W. Barlow, D.R. Paul, Annu. Rev. Mater. Sci. **11**, 299 (1981)

D.W. Bartlett, D.R. Paul, J.W. Barlow, Mod. Plast. **58**, 60 (1981)

A. Bassani, L.A. Pessan, J. Appl. Polym. Sci. **86**, 3466 (2002)

A.C. Baudouin, J. Devaux, C. Bailly, Polymer **51**, 1341 (2010a)

A.C. Baudouin, C. Bailly, J. Devaux, Polym. Degrad. Stab. **95**, 389 (2010b)

A.C. Baudouin, D. Auhl, F. Tao, J. Devaux, C. Bailly, Polymer **52**, 149 (2011)

S. Bensason, J. Minick, A. Moet, S. Chum, A. Hiltner, E. Baer, J. Polym. Sci. Pt. B: Polym. Phys. **34**, 1301 (1996)

R.K. Bharadwaj, Macromolecules **34**, 9189 (2001)

D.M. Bigg, Polym. Compos. **8**, 115 (1987)

B.P. Binks, M. Kirkland, Phys. Chem. Chem. Phys. **4**, 3727 (2002)

B.P. Binks, S.O. Lumsdon, Phys. Chem. Chem. Phys. **1**, 3007 (1999)

B.P. Binks, S.O. Lumsdon, Langmuir **16**, 8622 (2000)

B.P. Binks, J. Philip, J.A. Rodrigues, Langmuir **21**, 3296 (2005)

S. Bose, A.R. Bhattacharyya, P.V. Kodgire, A. Misra, Polymer **48**, 356 (2007)

S. Bose, A.R. Bhattacharyya, A.R. Kulkarni, P. Pötschke, Compos. Sci. Technol. **69**, 365 (2009)

O. Breuer, U. Sundararaj, Polym. Compos. **25**, 630 (2004)

H.R. Brown, Macromolecules **22**, 2859 (1989)

D.A. Brune, J. Bicerano, Polymer **43**, 369 (2002)

C.B. Bucknall, *Toughened plastics* (Applied Science Publishers, London, 1977)

C.B. Bucknall, D.R. Paul, Polymer **50**, 5539 (2009)

C.B. Bucknall, A. Karpodinis, X.C. Zhang, J. Mater. Sci. **29**, 3377 (1994)

X. Cai, B. Li, Y. Pan, G. Wu, Polymer **53**, 259 (2012)

Y. Cao, J. Zhang, J. Feng, P. Wu, ACS Nano **5**, 5920 (2011)

R. Cardinaud, T. McNally, Eur. Polym. J. **49**, 1287 (2013)

C.J. Carriere, H.C. Silvis, J. Appl. Polym. Sci. **66**, 1175 (1997)

F. Chavarria, D.R. Paul, Polymer **45**, 8501 (2004)

B. Chen, J.R.G. Evans, J. Polym. Sci. Pt. B: Polym. Phys. **49**, 443 (2011)

J. Chen, Y.-Y. Shi, J.-H. Yang, N. Zhang, T. Huang, Y. Wang, Polymer **54**, 464 (2013)

T.W. Cheng, H. Keskkula, D.R. Paul, Polymer **33**, 1606 (1992)

F.-C. Chiu, S.-M. Lai, Y.-L. Chen, T.-H. Lee, Polymer **46**, 11600 (2005)

C.J. Chou, K. Vijayan, D. Kirby, A. Hiltner, E. Baer, J. Mater. Sci. **23**, 2521 (1988a)

C.J. Chou, K. Vijayan, D. Kirby, A. Hiltner, E. Baer, J. Mater. Sci. **23**, 2533 (1988b)

W.S. Chow, Z.A. Mohd Ishak, J. Karger-Kocsis, A.A. Apostolov, U.S. Ishiaku, Polymer **44**, 7427 (2003)

W.S. Chow, Z.A.M. Ishak, U.S. Ishiaku, J. Karger-Kocsis, A.A. Apostolov, J. Appl. Polym. Sci. **91**, 175 (2004)

M.J. Clifford, T. Wan, Polymer **51**, 535 (2010)

J.N. Coleman, U. Khan, W.J. Blau, Y.K. Gun'ko, Carbon **44**, 1624 (2006)

A.J. Crosby, J.Y. Lee, Polym. Rev. **47**, 217 (2007)

A.L.N. Da Silva, M.C.G. Rocha, F.M.B. Coutinho, R. Bretas, C. Scuracchio, Polym. Test. **19**, 363 (2000a)

A.L.N. Da Silva, M.C.G. Rocha, F.M.B. Coutinho, R. Bretas, C. Scuracchio, J. Appl. Polym. Sci. **75**, 692 (2000b)

A.L.N. Da Silva, M.C.G. Rocha, F.M.B. Coutinho, R.E.S. Bretas, C. Scuracchio, J. Appl. Polym. Sci. **79**, 1634 (2001)

A.L.N. Da Silva, M.C.G. Rocha, F.M.B. Coutinho, R.E.S. Bretas, M. Farah, Polym. Test. **21**, 647 (2002)

A. Dasari, Z.-Z. Yu, Y.-W. Mai, Polymer **46**, 5986 (2005)

A. Dasari, Z.-Z. Yu, Y.-W. Mai, Polymer **50**, 4112 (2009)

C. Deshmane, Q. Yuan, R.D.K. Misra, Mater. Sci. Eng. A **460–461**, 277 (2007)

K. Dijkstra, R.J. Gaymans, Polymer **35**, 332 (1994)

K. Dijkstra, H.H. Wevers, R.J. Gaymans, Polymer **35**, 323 (1994)

D. Dompas, G. Groeninckx, Polymer **35**, 4743 (1994)

W.E. Dondero, R.E. Gorga, J. Polym. Sci. Pt. B: Polym. Phys. **44**, 864 (2006)

L. Elias, F. Fenouillot, J.C. Majesté, P. Cassagnau, Polymer **48**, 6029 (2007)

L. Elias, F. Fenouillot, J.C. Majesté, G. Martin, P. Cassagnau, J. Polym. Sci. Pt. B: Polym. Phys. **46**, 1976 (2008a)

L. Elias, F. Fenouillot, J.C. Majesté, P. Alcouffe, P. Cassagnau, Polymer **49**, 4378 (2008b)

B.N. Epstein, U.S. Patent 4,174,358, 1979a, to DuPont

B.N. Epstein, U.S. Patent 4,172,859, 1979b, to DuPont

L.A. Fasce, V. Pettarin, C. Marano, M. Rink, P.M. Frontini, Polym. Eng. Sci. **48**, 1414 (2008)

B.D. Favis, J.P. Chalifoux, Polym. Eng. Sci. **27**, 1591 (1987)

F. Fenouillot, P. Cassagnau, J.C. Majesté, Polymer **50**, 1333 (2009)

G. Filippone, N.T. Dintcheva, D. Acierno, F.P. La Mantia, Polymer **49**, 1312 (2008)

G. Filippone, N.T. Dintcheva, F.P. La Mantia, D. Acierno, J. Polym. Sci. Pt. B: Polym. Phys. **48**, 600 (2010a)

G. Filippone, N.T. Dintcheva, F.P. La Mantia, D. Acierno, Polymer **51**, 3956 (2010b)

M.J. Folkes, P.S. Hope, *Polymer blends and alloys* (Chapman and Hall, London, 1993)

T.D. Fornes, D.R. Paul, Polymer **44**, 4993 (2003)

T.D. Fornes, P.J. Yoon, H. Keskkula, D.R. Paul, Polymer **42**, 09929 (2001)

I. Fortelný, A. Živný, Polymer **36**, 4113 (1995)

M.E. Fowler, H. Keskkula, D.R. Paul, J. Appl. Polym. Sci. **37**, 225 (1989)

M. Gahleitner, B. Kretzschmar, G.V. Vliet, J. Devaux, D. Pospiech, K. Bernreitner, E. Ingolic, Rheol. Acta **45**, 322 (2005)

R. Gallego, D. García-López, S. López-Quintana, I. Gobernado-Mitre, J.C. Merino, J.M. Pastor, J. Appl. Polym. Sci. **109**, 1556 (2008)

J.M. Garcés, D.J. Moll, J. Bicerano, R. Fibiger, D.G. McLeod, Adv. Mater. **12**, 1835 (2000)

D. García-López, S. López-Quintana, I. Gobernado-Mitre, J.C. Merino, J.M. Pastor, Polym. Eng. Sci. **47**, 1033 (2007)

M.Y. Gelfer, H.H. Song, L. Liu, B.S. Hsiao, B. Chu, M. Rafailovich, M. Si, V. Zaitsev, J. Polym. Sci. Pt. B: Polym. Phys. **41**, 44 (2003)

E.P. Giannelis, Adv. Mater. **8**, 29 (1996)

E.P. Giannelis, R. Krishnamoorti, E. Manias, Adv. Polym. Sci. **138**, 107 (1999)

J. Gilman, Appl. Clay. Sci. **15**, 31 (1999)

L.A. Goettler, K.Y. Lee, H. Thakkar, Polym. Rev. **47**, 291 (2007)

I. Goitisolo, J.I. Eguiazábal, J. Nazábal, Eur. Polym. J. **44**, 1978 (2008)

A. Göldel, G. Kasaliwal, P. Pötschke, Macromol. Rapid Commun. **30**, 423 (2009)

A. Göldel, G.R. Kasaliwal, P. Pötschke, G. Heinrich, Polymer **53**, 411 (2012)

I. González, J.I. Eguiazábal, J. Nazábal, J. Polym. Sci. Pt. B: Polym. Phys. **43**, 3611 (2005)

I. González, J.I. Eguiazábal, J. Nazábal, Eur. Polym. J. **42**, 2905 (2006a)

I. González, J.I. Eguiazábal, J. Nazábal, Compos. Sci. Technol. **66**, 1833 (2006b)

I. González, J.I. Eguiazábal, J. Nazábal, Eur. Polym. J. **44**, 287 (2008)

I. González, J.I. Eguiazábal, J. Nazábal, Polym. J. **44**, 294 (2012)

J.N. Goodier, Trans. Am. Soc. Mech. Eng. **55**, 39 (1933)

R.E. Gorga, R.E. Cohen, J. Polym. Sci. Pt. B: Polym. Phys. **42**, 2690 (2004)

B.P. Grady, Macromol. Rapid Commun. **31**, 247 (2010)

F. Gubbels, S. Blacher, E. Vanlathem, R. Jerome, R. Deltour, F. Brouers, P. Teyssie, Macromolecules **28**, 1559 (1995)

J.C. Halpin, J. Compos. Mater. **3**, 732 (1969)

J.C. Halpin, J.L. Kardos, Polym. Eng. Sci. **16**, 344 (1976)

N. Hasegawa, H. Okamoto, M. Kawasumi, M. Kato, A. Tsukigase, A. Usuki, Macromol. Mater. Eng. **280–281**, 76 (2000)

M. Heidary, S.H. Jafari, H.A. Khonakdar, U. Wagenknecht, G. Heinrich, R. Boldt, J. Appl. Polym. Sci. **127**, 1172 (2013)

R. Hill, J. Mech. Phys. Solid **13**, 213 (1965)

D. Hlavatá, Z. Horák, J. Hromádková, F. Lednický, A. Pleska, J. Polym. Sci. Pt. B: Polym. Phys. **37**, 1647 (1999)

G. Holden, D.R. Hansen, Applications of thermoplastic elastomers, in *Thermoplastic elastomers*, ed. by G. Holden, H.R. Kricheldorf, R.P. Quirk, 3rd edn. (Hanser Publishers, Munich, 2004)

J.S. Hong, Y.K. Kim, K.H. Ahn, S.J. Lee, C. Kim, Rheol. Acta **46**, 469 (2006a)

J.S. Hong, H. Namkung, K.H. Ahn, S.J. Lee, C. Kim, Polymer **47**, 3967 (2006b)

J.J. Huang, D.R. Paul, Polymer **47**, 3505 (2006)

J.J. Huang, H. Keskkula, D.R. Paul, Polymer **45**, 4203 (2004)

J.J. Huang, H. Keskkula, D.R. Paul, Polymer **47**, 624 (2006a)

J.J. Huang, H. Keskkula, D.R. Paul, Polymer **47**, 639 (2006b)

C.-J. Hung, H.-Y. Chuang, F.-C. Chang, J. Appl. Polym. Sci. **107**, 831 (2008)

F. Hussain, R.E. Gorga, J. Compos. Mater. **40**, 1511 (2006)

T.Y. Hwang, Y. Yoo, J.W. Lee, Rheol. Acta **51**, 623 (2012)

H. Ishida, S. Campbell, J. Blackwell, Chem. Mater. **12**, 1260 (2000)

O.M. Istrate, M.A. Gunning, C.L. Higginbotham, B. Chen, J. Polym. Sci. Pt. B: Polym. Phys. **50**, 431 (2012)

B.Z. Jang, A. Zhamu, J. Mater. Sci. **43**, 5092 (2008)

W. Jiang, H. Liang, J. Zhang, D. He, B. Jiang, J. Appl. Polym. Sci. **58**, 537 (1995)

J. Jordan, K.I. Jacob, R. Tannenbaum, M.A. Sharaf, I. Jasiuk, Mater. Sci. Eng. A **393**, 1 (2005)

H.G. Karian, *Handbook of polypropylene and polypropylene composites*, 2nd edn. (Marcel Dekker, New York, 2003)

A. Karim, D.W. Liu, J.F. Douglas, A.I. Nakatani, E.J. Amis, Polymer **41**, 8455 (2000)

M. Keating, I.-H. Lee, J. Macromol. Sci. Phys. **38**, 379 (1999)

I. Kelnar, J. Kotek, L. Kaprálková, B.S. Munteanu, J. Appl. Polym. Sci. **96**, 288 (2005)

I. Kelnar, J. Kotek, L. Kaprálková, J. Hromádková, J. Kratochvíl, J. Appl. Polym. Sci. **100**, 1571 (2006)

I. Kelnar, V. Khunová, J. Kotek, L. Kaprálková, Polymer **48**, 5332 (2007)

I. Kelnar, J. Rotrekl, J. Kotek, L. Kaprálková, Polym. Int. **57**, 1281 (2008)

I. Kelnar, J. Rotrekl, J. Kotek, L. Kaprálková, J. Hromádková, Eur. Polym. J. **45**, 2760 (2009)

H. Keskkula, D.R. Paul, Toughened nylons, in *Nylon plastics handbook*, ed. by I.M. Kohan (Hansner Publishers, Munich, 1995)

B.B. Khatua, D.J. Lee, H.Y. Kim, J.K. Kim, Macromolecules **37**, 2454 (2004)

D.H. Kim, P.D. Fasulo, W.R. Rodgers, D.R. Paul, Polymer **48**, 5308 (2007a)

D.H. Kim, P.D. Fasulo, W.R. Rodgers, D.R. Paul, Polymer **48**, 5960 (2007b)

D.H. Kim, P.D. Fasulo, W.R. Rodgers, D.R. Paul, Polymer **49**, 2492 (2008)

J. Kim, L.J. Cote, F. Kim, W. Yuan, K.R. Shull, J. Huang, J. Am. Chem. Soc. **132**, 8180 (2010)

J.A. King, R.A. Hauser, A.M. Tomson, I.M. Wescoat, J.M. Keith, J. Compos. Mater. **42**, 91 (2008)

J. Kolařík, J. Jančář, Polymer **33**, 4961 (1992)

M. Kontopoulou, W. Wang, T.G. Gopakumar, C. Cheung, Polymer **44**, 7495 (2003)

G. Lagaly, Appl. Clay Sci. **15**, 1 (1999)

G. Lagaly, M. Reese, S. Abend, Appl. Clay Sci. **14**, 83 (1999)

S.-M. Lai, Y.-C. Liao, T.-W. Chen, Polym. Eng. Sci. **45**, 1461 (2005)

S.-M. Lai, Y.-C. Liao, T.-W. Chen, J. Appl. Polym. Sci. **100**, 1364 (2006)

F. Laoutid, D. François, Y. Paint, L. Bonnaud, P. Dubois, Macromol. Mater. Eng. **298**, 328 (2013)

A. Lazzeri, C.B. Bucknall, J. Mater. Sci. **28**, 6799 (1993)

P. LeBaron, Appl. Clay Sci. **15**, 11 (1999)

S.-S. Lee, J. Kim, J. Polym. Sci. Pt. B: Polym. Phys. **42**, 246 (2004)

H.-S. Lee, P.D. Fasulo, W.R. Rodgers, D.R. Paul, Polymer **46**, 11673 (2005)

H.-S. Lee, P.D. Fasulo, W.R. Rodgers, D.R. Paul, Polymer **47**, 3528 (2006a)

M. Lee, X. Hu, L. Li, Acta Mater. **54**, 3359 (2006b)

H.-Y. Lee, D.H. Kim, Y. Son, J. Appl. Polym. Sci. **103**, 1133 (2007)

S.H. Lee, M. Kontopoulou, C.B. Park, Polymer **51**, 1147 (2010)

S.H. Lee, M. Bailly, M. Kontopoulou, Macromol. Mater. Eng. **297**, 95 (2012)

W. Lertwimolnun, B. Vergnes, Polymer **46**, 3462 (2005)

Y. Li, H. Shimizu, Polymer **45**, 7381 (2004)

Y. Li, H. Shimizu, Macromol. Rapid Commun. **26**, 710 (2005)

Y. Li, H. Shimizu, Macromolecules **41**, 5339 (2008)

B. Li, W.-H. Zhong, J. Mater. Sci. **46**, 5595 (2011)

X. Li, H.-M. Park, J.-O. Lee, C.-S. Ha, Polym. Eng. Sci. **42**, 2156 (2002)

C. Li, H. Deng, K. Wang, Q. Zhang, F. Chen, Q. Fu, J. Appl. Polym. Sci. **121**, 2104 (2011)

J.Z. Liang, R.K.Y. Li, J. Appl. Polym. Sci. **77**, 409 (2000)

J.W. Lim, A. Hassan, A.R. Rahmat, M.U. Wahit, J. Appl. Polym. Sci. **99**, 3441 (2006)

S.-H. Lim, A. Dasari, Z.-Z. Yu, Y.-W. Mai, S. Liu, M.S. Yong, Compos. Sci. Technol. **67**, 2914 (2007)

S.-H. Lim, A. Dasari, G.-T. Wang, Z.-Z. Yu, Y.-W. Mai, Q. Yuan, S. Liu, M.S. Yong, Compos. Part B: Eng. **41**, 67 (2010)

Z. Ling, H. Rui, L. Liangbin, W. Gang, J. Appl. Polym. Sci. **83**, 1870 (2002)

L. Liu, J.C. Grunlan, Adv. Funct. Mater. **17**, 2343 (2007)

Y. Liu, M. Kontopoulou, Polymer **47**, 7731 (2006)

L. Liu, Y. Wang, Y. Li, J. Wu, Z. Zhou, C. Jiang, Polymer **50**, 3072 (2009)

L. Liu, H. Wu, Y. Wang, J. Wu, Y. Peng, F. Xiang, J. Zhang, J. Polym. Sci. Pt. B: Polym. Phys. **48**, 1882 (2010)

X.-Q. Liu, W. Yang, B.-H. Xie, M.-B. Yang, Mater. Des. **34**, 355 (2012)

X.-Q. Liu, R.-Y. Bao, Z.-Y. Liu, W. Yang, B.-H. Xie, M.-B. Yang, Polym. Test. **32**, 141 (2013)

Q. Ma, X. Su, P.C. Tibbenham, X. Lai, Z. Lin, Polym. Plast. Tech. Eng. **49**, 121 (2010)

B. Madivala, J. Fransaer, J. Vermant, Langmuir **25**, 2718 (2009a)

B. Madivala, S. Vandebril, J. Fransaer, J. Vermant, Soft Matter **5**, 1717 (2009b)

S. Maiti, S. Suin, N.K. Shrivastava, B.B. Khatua, Synth. Met. **165**, 40 (2013)

B. Majumdar, H. Keskkula, D.R. Paul, Polymer **35**, 1386 (1994a)

B. Majumdar, H. Keskkula, D.R. Paul, N.G. Harvey, Polymer **35**, 4263 (1994b)

B. Majumdar, D.R. Paul, A.J. Oshinski, Polymer **38**, 1787 (1997)

D. Marchant, K. Jayaraman, Ind. Eng. Chem. Res. **41**, 6402 (2002)

J. Marquardt, R. Thomann, Y. Thomann, J. Heinemann, R. Mülhaupt, Macromolecules **34**, 8669 (2001)

G. Martin, C. Barres, P. Sonntag, N. Garois, P. Cassagnau, Mater. Chem. Phys. **113**, 889 (2009)

Z. Martín, I. Jiménez, M.A. Gómez-Fatou, M. West, A.P. Hitchcock, Macromolecules **44**, 2179 (2011)

Y. Matsuda, M. Hara, T. Mano, K. Okamoto, M. Ishikawa, Polym. Eng. Sci. **46**, 29 (2006)

T. McNally, P. McShane, G.M. Nally, W.R. Murphy, M. Cook, A. Miller, Polymer **43**, 3785 (2002)

S. Mehta, F.M. Mirabella, K. Rufener, A. Bafna, J. Appl. Polym. Sci. **92**, 928 (2004)

O. Meincke, D. Kaempfer, H. Weickmann, C. Friedrich, M. Vathauer, H. Warth, Polymer **45**, 739 (2004)

K. Meng, X. Dong, X. Zhang, C. Zhang, C.C. Han, Macromol. Rapid Commun. **27**, 1677 (2006)

B.R. Midmore, Colloids Surf. A. **132**, 257 (1998)

F. Mighri, M.A. Huneault, A. Ajji, G.H. Ko, F. Watanabe, J. Appl. Polym. Sci. **82**, 2113 (2001)

J.K. Mishra, K.-J. Hwang, C.-S. Ha, Polymer **46**, 1995 (2005)

E. Moghbelli, H.-J. Sue, S. Jain, Polymer **51**, 4231 (2010)

M. Moniruzzaman, K.I. Winey, Macromolecules **39**, 5194 (2006)

T. Mori, K. Tanaka, Acta Metall. **21**, 571 (1973)

P. Motamedi, R. Bagheri, Mater. Des. **31**, 1776 (2010)

G. Naderi, P.G. Lafleur, C. Dubois, Polym. Compos. **29**, 1301 (2008)

P.H. Nam, P. Maiti, M. Okamoto, T. Kotaka, N. Hasegawa, A. Usuki, Polymer **42**, 9633 (2001)

V. Ojijo, S.S. Ray, R. Sadiku, ACS Appl. Mater. Inter. **4**, 2395 (2012)

A. Okada, A. Usuki, Macromol. Mater. Eng. **291**, 1449 (2006)

O. Okada, H. Keskkula, D.R. Paul, J. Polym. Sci. Part B: Polym. Phys. **42**, 1739 (2004)

M. Okamoto, P.H. Nam, P. Maiti, T. Kotaka, N. Hasegawa, A. Usuki, Nano Lett. **1**, 295 (2001)

M. Öksüz, M. Eroğlu, J. Appl. Polym. Sci. **98**, 1445 (2005)

T.S. Omonov, C. Harrats, G. Groeninckx, P. Moldenaers, Polymer **48**, 5289 (2007)

M. Ono, J. Washiyama, K. Nakajima, T. Nishi, Polymer **46**, 4899 (2005)

A. Ophir, L. Zonder, P.F. Rios, Polym. Eng. Sci. **49**, 1168 (2009)

A.J. Oshinski, H. Keskkula, D.R. Paul, Polymer **33**, 268 (1992a)

A.J. Oshinski, H. Keskkula, D.R. Paul, Polymer **33**, 284 (1992b)

A.J. Oshinski, H. Keskkula, D.R. Paul, Polymer **37**, 4891 (1996a)

A.J. Oshinski, H. Keskkula, D.R. Paul, Polymer **37**, 4909 (1996b)

A.J. Oshinski, H. Keskkula, D.R. Paul, Polymer **37**, 4919 (1996c)

B. Ou, D. Li, Polym. Bull. **63**, 441 (2009)

R.J. Oxborough, P.B. Bowden, Philos. Mag. **30**, 171 (1974)

J.F. Palierne, Rheol. Acta **29**, 204 (1990)

D.H. Park, T.G. Kan, Y.K. Lee, W.N. Kim, J. Mater. Sci. **48**, 481 (2012)

D.R. Paul, Polymer blends containing styrene/hydrogenated butadiene block copolymers: solubilization and compatibilization, in *Thermoplastic elastomers*, ed. by G. Holden, N.R. Legge, R.P. Quirk, H.E. Schroeder, 2nd edn. (Hanser Publishers, Munich, 1996)

D.R. Paul, J.W. Barlow, J. Macromol. Sci. Polym. Rev. **18**, 109 (1980)

D.R. Paul, C.B. Bucknall, *Polymer blends. volume 1: formulation*, 2nd edn. (Wiley, New York, 2000a)

D.R. Paul, C.B. Bucknall, *Polymer blends. volume 2: performance*, 2nd edn. (Wiley, New York, 2000b)

D.R. Paul, L.M. Robeson, Polymer **49**, 3187 (2008)

S. Pavlidou, C.D. Papaspyrides, Prog. Polym. Sci. **33**, 1119 (2008)

T. Périé, A.-C. Brosse, S. Tencé-Girault, L. Leibler, Polymer **53**, 984 (2012)

S.U. Pickering, J. Chem. Soc. Trans. **91**, 2001 (1907)

P. Pötschke, D.R. Paul, J. Macromol. Sci. Polym. Rev. **43**, 87 (2003a)

P. Pötschke, D.R. Paul, Macromol. Symp. **198**, 69 (2003b)

P. Pötschke, T.D. Fornes, D.R. Paul, Polymer **43**, 3247 (2002)

P. Pötschke, A.R. Bhattacharyya, A. Janke, Polymer **44**, 8061 (2003)

P. Pötschke, A.R. Bhattacharyya, A. Janke, Carbon **42**, 965 (2004)

P. Pötschke, B. Kretzschmar, A. Janke, Compos. Sci. Technol. **67**, 855 (2007)

P. Pötschke, S. Pegel, M. Claes, D. Bonduel, Macromol. Rapid Commun. **29**, 244 (2008)

J.R. Potts, D.R. Dreyer, C.W. Bielawski, R.S. Ruoff, Polymer **52**, 5 (2011)

K. Premphet, P. Horanont, Polymer **41**, 9283 (2000)

K. Premphet, W. Paecharoenchai, J. Appl. Polym. Sci. **82**, 2140 (2001)

K. Premphet, W. Paecharoenchai, J. Appl. Polym. Sci. **85**, 2412 (2002)

Ó. Prieto, J.M. Pereña, R. Benavente, M.L. Cerrada, E. Pérez, Macromol. Chem. Phys. **203**, 1844 (2002)

B. Pukánszky, F. Tüdős, J. Kolařik, F. Lednický, Polym. Compos. **11**, 98 (1990)

D. Qian, E.C. Dickey, R. Andrews, T. Rantell, Appl. Phys. Lett. **76**, 2868 (2000)

G. Qiu, F. Raue, G.W. Ehrenstein, J. Elastom. Plast. **34**, 295 (2002)

E.B. Rabinovitch, J.W. Summers, G. Smith, J. Vinyl Addit. Technol. **9**, 90 (2003)

G. Radonjič, V. Musil, I. Šmit, J. Appl. Polym. Sci. **69**, 2625 (1998)

P. Raghu, C.K. Nere, R.N. Jagtap, J. Appl. Polym. Sci. **88**, 266 (2003)

W. Ramsden, Proc. R. Soc. Lond. Ser. A **72**, 156 (1903)

N. Rattanasom, T. Saowapark, C. Deeprasertkul, Polym. Test. **26**, 369 (2007)

S.S. Ray, M. Okamoto, Prog. Polym. Sci. **28**, 1539 (2003)

S.S. Ray, S. Pouliot, M. Bousmina, L.A. Utracki, Polymer **45**, 8403 (2004)

S.S. Ray, J. Bandyopadhyay, M. Bousmina, Macromol. Mater. Eng. **292**, 729 (2007)

S. Reddy, S. Sivaram, Prog. Polym. Sci. **20**, 309 (1995)

P. Reichert, B. Hoffmann, T. Bock, R. Thomann, R. Mülhaupt, C. Friedrich, Macromol. Rapid Commun. **22**, 519 (2001)

L.M. Robeson, *Polymer blends: a comprehensive review* (Hanser Publishers, Munich, 2007)

C. Rosales, V. Contreras, M. Matos, R. Perera, N. Villarreal, D. García-López, J.M. Pastor, J. Nanosci. Nanotechnol. **8**, 1762 (2008)

S.L. Ruan, P. Gao, X.G. Yang, T.X. Yu, Polymer **44**, 5643 (2003)

K.U. Schaefer, A. Theisen, M. Hess, R. Kosfeld, Polym. Eng. Sci. **33**, 1009 (1993)

D. Schmidt, D. Shah, E.P. Giannelis, Curr. Opin. Solid State Mater. Sci. **6**, 205 (2002)

R.K. Shah, D.H. Kim, D.R. Paul, Polymer **48**, 1047 (2007)

N. Sheng, M.C. Boyce, D.M. Parks, G.C. Rutledge, J.I. Abes, R.E. Cohen, Polymer **45**, 487 (2004)

Y. Shi, Y. Li, F. Xiang, T. Huang, C. Chen, Y. Peng, Y. Wang, Polym. Adv. Technol. **23**, 783 (2012)

M. Si, T. Araki, H. Ade, A.L.D. Kilcoyne, R. Fisher, J.C. Sokolov, M.H. Rafailovich, Macromolecules **39**, 4793 (2006)

M.W. Spencer, D.R. Paul, Polymer **52**, 4910 (2011)

M.W. Spencer, L. Cui, Y. Yoo, D.R. Paul, Polymer **51**, 1056 (2010)

Z. Spitalsky, D. Tasis, K. Papagelis, C. Galiotis, Prog. Polym. Sci. **35**, 357 (2010)

J.E. Stamhuis, Polym. Compos. **5**, 202 (1984)

J.E. Stamhuis, Polym. Compos. **9**, 72 (1988a)

J.E. Stamhuis, Polym. Compos. **9**, 280 (1988b)

H.A. Stretz, D.R. Paul, P.E. Cassidy, Polymer **46**, 3818 (2005)

J. Sumfleth, L.A.S.D.A. Prado, M. Sriyai, K. Schulte, Polymer **49**, 5105 (2008)

M. Sumita, K. Sakata, S. Asai, K. Miyasaka, H. Nakagawa, Polym. Bull. **25**, 265 (1991)

U. Sundararaj, C.W. Macosko, Macromolecules **28**, 2647 (1995)

U. Sundararaj, C.W. Macosko, R.J. Rolando, H.T. Chan, Polym. Eng. Sci. **32**, 1814 (1992)

P. Svoboda, D. Svobodova, P. Slobodian, T. Ougizawa, T. Inoue, Eur. Polym. J. **45**, 1485 (2009)

D.E. Tambe, M.M. Sharma, Adv. Colloid Interface Sci. **52**, 1 (1994)

C. Tang, L. Xiang, J. Su, K. Wang, C. Yang, Q. Zhang, Q. Fu, J. Phys. Chem. B **112**, 3876 (2008)

F. Tao, B. Nysten, A.C. Baudouin, J.-M. Thomassin, D. Vuluga, C. Detrembleur, C. Bailly, Polymer **52**, 4798 (2011)

P. Thareja, S. Velankar, Rheol. Acta **46**, 405 (2006)

R.R. Tiwari, D.R. Paul, Polymer **52**, 1141 (2011a)

R.R. Tiwari, D.R. Paul, Polymer **52**, 4955 (2011b)

R.R. Tiwari, D.R. Paul, Polymer **52**, 5595 (2011c)

R.R. Tiwari, D.R. Paul, Polymer **53**, 823 (2012)

R.R. Tiwari, D.L. Hunter, D.R. Paul, J. Polym. Sci. Pt. B: Polym. Phys. **50**, 1577 (2012)

R.R. Tiwari, D.L. Hunter, D.R. Paul, J. Polym. Sci. Pt. B: Polym. Phys. **51**, 952 (2013)

S.C. Tjong, Mater. Sci. Eng. R **53**, 73 (2006)

S.C. Tjong, S.P. Bao, J. Polym. Sci. Pt. B: Polym. Phys. **43**, 585 (2005)

L.A. Utracki, *Polymer alloys and blends* (Hanser Publishers, Munich, 1989)

L.A. Utracki, *Commercial polymer blends* (Chapman and Hall, London, 1998)

A. van der Wal, J.J. Mulder, J. Oderkerk, R.J. Gaymans, Polymer **39**, 6781 (1998)

A. van der Wal, R. Nijhof, R.J. Gaymans, Polymer **40**, 6031 (1999)

J. Vermant, G. Cioccolo, K. Golapan Nair, P. Moldenaers, Rheol. Acta **43**, 529 (2004)

J. Vermant, S. Ceccia, M.K. Dolgovskij, P.L. Maffettone, C.W. Macosko, J. Rheol. **51**, 429 (2007)

J. Vermant, S. Vandebril, C. Dewitte, P. Moldenaers, Rheol. Acta **47**, 835 (2008)

L.T. Vo, E.P. Giannelis, Macromolecules **40**, 8271 (2007)

Z. Vuluga, D.M. Panaitescu, C. Radovici, C. Nicolae, M.D. Iorga, Polym. Bull. **69**, 1073 (2012)

M.U. Wahit, A. Hassan, A.R. Rahmat, Z.A.M. Ishak, J. Elastom. Plast. **38**, 231 (2006a)

M.U. Wahit, A. Hassan, A.R. Rahmat, J.W. Lim, Z.A.M. Ishak, J. Reinf. Plast. Compos. **25**, 933 (2006b)

M.U. Wahit, A. Hassan, Z.A. Mohd Ishak, A.R. Rahmat, N. Othman, Polym. J. **38**, 767 (2006c)

Y. Wang, Q. Zhang, Q. Fu, Macromol. Rapid Commun. **24**, 231 (2003)

K. Wang, C. Wang, J. Li, J. Su, Q. Zhang, R. Du, Q. Fu, Polymer **48**, 2144 (2007)

Z. Wang, X. Meng, J. Li, X. Du, S. Li, Z. Jiang, T. Tang, J. Phys. Chem. C **113**, 8058 (2009)

J.F. Wang, J.K. Carson, M.F. North, D.J. Cleland, Polym. Eng. Sci. **50**, 643 (2010)

I.M. Ward, J. Sweeney, *Mechanical properties of solid polymers*, 3rd edn. (Wiley, Chichester, 2013)

G. Wildes, H. Keskkula, D.R. Paul, Polymer **40**, 5609 (1999)

F. Wode, L. Tzounis, M. Kirsten, M. Constantinou, P. Georgopanos, S. Rangou, N.E. Zafeiropoulos, A. Avgeropoulos, M. Stamm, Polymer **53**, 4438 (2012)

T.T. Wu, Int. J. Solid Struct. **2**, 1 (1966)

S. Wu, *Polymer interface and adhesion* (Marcel Dekker, New York, 1982)

S. Wu, Polymer **26**, 1855 (1985)

S. Wu, Polym. Eng. Sci. **27**, 335 (1987)

D. Wu, C. Zhou, M. Zhang, J. Appl. Polym. Sci. **102**, 3628 (2006)

D. Wu, Y. Zhang, M. Zhang, W. Yu, Biomacromolecules **10**, 417 (2009)

F. Xiang, J. Wu, L. Liu, T. Huang, Y. Wang, C. Chen, Y. Peng, C. Jiang, Z. Zhou, Polym. Adv. Technol. **22**, 2533 (2011)

F. Xiang, Y. Shi, X. Li, T. Huang, C. Chen, Y. Peng, Y. Wang, Eur. Polym. J. **48**, 350 (2012)

X. Xu, X. Yan, T. Zhu, C. Zhang, J. Sheng, Polym. Bull. **58**, 465 (2006a)

Y. Xu, W.J. Brittain, R.A. Vaia, G. Price, Polymer **47**, 4564 (2006b)

N. Yan, J.H. Masliyah, Colloids Surf. A. **96**, 229 (1995)

D. Yang, B. Zhang, Y. Yang, Z. Fang, G. Sun, Z. Feng, Polym. Eng. Sci. **24**, 612 (1984)

J. Yang, Y. Zhang, Y. Zhang, Polymer **44**, 5047 (2003)

H. Yang, Q. Zhang, M. Guo, C. Wang, R. Du, Q. Fu, Polymer **47**, 2106 (2006)

H. Yang, X. Zhang, C. Qu, B. Li, L. Zhang, Q. Zhang, Q. Fu, Polymer **48**, 860 (2007)

Q.-Q. Yang, Z.-X. Guo, J. Yu, J. Appl. Polym. Sci. **115**, 3697 (2010)

M. Yazdani-Pedram, R. Quijada, M.A. López-Manchado, Macromol. Mater. Eng. **288**, 875 (2003)

Y. Yoo, L. Cui, P.J. Yoon, D.R. Paul, Macromolecules **43**, 615 (2010a)

Y. Yoo, R.R. Tiwari, Y.-T. Yoo, D.R. Paul, Polymer **51**, 4907 (2010b)

Y. Yoo, M.W. Spencer, D.R. Paul, Polymer **52**, 180 (2011)

P.J. Yoon, T.D. Fornes, D.R. Paul, Polymer **43**, 6727 (2002)

T.C. Yu, Polym. Eng. Sci. **41**, 656 (2001)

Z.-Z. Yu, Y.-C. Ou, G.-H. Hu, J. Appl. Polym. Sci. **69**, 1711 (1998)

J. Yu, G. Wang, J. Chen, X. Zeng, W. Wang, Polym. Eng. Sci. **47**, 201 (2007a)

T. Yu, J. Lin, J. Xu, T. Chen, S. Lin, X. Tian, Compos. Sci. Technol. **67**, 3219 (2007b)

Q.H. Zeng, A.B.. Yu, G.Q.M. Lu, D.R. Paul, J. Nanosci. Nanotechnol. **5**, 1574 (2005)

W. Zhai, S.N. Leung, L. Wang, H.E. Naguib, C.B. Park, J. Appl. Polym. Sci., **116**, 1994 (2010)

H. Zhang, Z. Zhang, Eur. Polym. J. **43**, 3197 (2007)

M.Q. Zhang, G. Yu, H.M. Zeng, H.B. Zhang, Y.H. Hou, Macromolecules **31**, 6724 (1998)

X. Zhang, F. Xie, Z. Pen, Y. Zhang, Y. Zhang, W. Zhou, Eur. Polym. J. **38**, 1 (2002)

Q. Zhang, Y. Wang, Q. Fu, J. Polym. Sci. Pt. B: Polym. Phys. **41**, 1 (2003)

Q. Zhang, H. Yang, Q. Fu, Polymer **45**, 1913 (2004)

L. Zhang, C. Wan, Y. Zhang, Compos. Sci. Technol. **69**, 2212 (2009)

M. Zhang, Y. Huang, M. Kong, H. Zhu, G. Chen, Q. Yang, J. Mater. Sci. **47**, 1339 (2012)

P. Zhao, K. Wang, H. Yang, Q. Zhang, R. Du, Q. Fu, Polymer **48**, 5688 (2007)

C.Z. Zhou, T. Liu, T.-T. Lin, X.-H. Zhan, Z.-K. Chen, Polymer **46**, 10952 (2005)

Y. Zhu, H.-Y. Ma, L.-F. Tong, Z.-P. Fang, J. Zhejiang Univ. Sci. B **9**, 1614 (2008a)

Y. Zhu, Y. Xu, L. Tong, Z. Xu, Z. Fang, J. Appl. Polym. Sci. **110**, 3130 (2008b)

L. Zhu, X. Xu, N. Ye, N. Song, J. Sheng, Polym. Compos. **31**, 105 (2009)

L. Zonder, A. Ophir, S. Kenig, S. McCarthy, Polymer **52**, 5085 (2011)

H. Zou, K. Wang, Q. Zhang, Q. Fu, Polymer **47**, 7821 (2006)

H. Zou, N. Ning, R. Su, Q. Zhang, Q. Fu, J. Appl. Polym. Sci. **106**, 2238 (2007)

Polyethylenes and Their Blends

18

Leszek A. Utracki

Contents

L.A. Utracki
National Research Council Canada, Industrial Materials Institute, Boucherville, QC, Canada
e-mail: leszek.utracki@cnrc-nrc.gc.ca

Abstract

Several books offer information on various aspects of polyolefin (PO) synthesis, technology, performance, as well as on the preparation, fundamentals, and degradability and recyclates of polymer alloys and blends (PAB) [Utracki and Weiss, *Multiphase Polymers: Blends and Ionomers.* ACS Symposium Series, vol. 395 (Washington, DC, 1989); Utracki *Polymer Alloys and Blends* (Hanser, Munich, 1989); J. Rheol. **35**(8), 1615–1637, 1991; *Encyclopaedic Dictionary of Commercial Polymer Blends* (Chem Tec Pub., Toronto, 1994); Makromol. Chem. Macromol. Symp. **118**, 335–345, 1997, *Commercial Polymer Blends* (Chapman & Hall, London, 1998); Zweifel, *Stabilization of Polymeric Materials* (Springer, Berlin, 1998); Moeller, *Progress in Polymer Degradation and Stability Research* (Nova Sci. Publ., New York, 2008); Anand (ed.), *National Seminar on Emerging Trends in Plastic Recycling Technologies and Waste Management* (Goa, India, 1995); *Recycling and Plastics Waste Management, Proceedings of National Seminar* (CIPET, Chennai, 1997); Akovali et al., *Reprocessing of Commingled Polymers and Recycling of Polymer Blends.* NATO ASI, vol. 351 (Kluwer, Dordrecht, 1998)]. There are also encyclopedic editions on PAB, e.g., Utracki [*Encyclopaedic Dictionary of Commercial Polymer Blends* (Chem Tec Pub., Toronto, 1994, 2013); Isayev (*Encyclopedia of Polymer Blends* (Wiley-VCH, Weinheim, 2010–2014)].

The first patent on PAB was granted to Parkes in 1846 for two natural polymers co-vulcanized during blending in the presence of CS_2, i.e., a natural rubber (NR = amorphous *cis*-polyisoprene, IR) with gutta-percha (GP = semi-crystalline *trans*-polyisoprene, IR). Thus, rubber PAB predates that of synthetic polymers by ca. 80 years (PMA/PVAc 1929). Notably, while the early plastics were bio-based, their usage fell to <5 wt% nowadays slowly recovering from the absolute dominance of synthetic, petroleum-based plastics.

PO is a part of the commodity resin category, where the continuous use temperature (CUT) $\leq 75\ ^{\circ}C$. Specifically, to this category belong polyethylenes (PE), polypropylenes (PP), styrenics (PS), acrylics (PMMA), and vinyls, such as poly(vinyl chloride) (PVC). The relative importance of commodity resin is evident from the data displayed in Fig. 18.1.

In the 1900s, world plastic production was about 30 kt, increasing to 300 Mt
by the year 2010. Figure 18.1 shows the growth after 1960, extrapolated
to 2020. Accordingly to Pardos Marketing [Pardos Marketing] plastic
consumption is dominated by the commodity resins to the extent that the total
consumption of plastics on the plot is indistinguishable from that of commodity
resin. Notably, within the commodity resin category, PE contribution is
45–55 wt%.

The 75th anniversary of the invention of the first commercial PE seemed to be
an appropriate occasion for summarizing in a (relatively) short chapter the
factors that create such a vast spectrum of materials often having unexpected
properties. Considering the character of the Polymer Blends Handbook – 2
(PBH-2), the Chapter provides concise, fundamental information in a historical
perspective, starting with single PE resins before addressing PE blends. It also
offers extensive tabulated data, useful for readers.

The chapter is divided into 19 parts, including classification of PE resin, their
discovery and historical evolution, and methods and equipment of PE charac-
terization, and then PE blends preceded by greatly abbreviated fundamentals
and followed by description of various mixtures. In view of the importance of
miscibility for processability and performance of PE blends, this aspect is
particularly stressed.

18.1   Introduction: 75 Years of Polyethylenes and Their Blends

Polyethylene (PE) is a product of ethene polymerization in a radical, anionic-
addition, ion-coordination, or cationic-addition reaction. These reactions
result in polyethylenes having different composition, molecular weight (MW)
branching type (short and long, SCB and LCB), branching distribution (SCBD),

and density (ρ) dependent on the structure regularity, thus crystallinity. Accordingly, PE is classified as:

- Cross-linked polyethylene (PEX or XLPE)
- High-density cross-linked polyethylene (HDXLPE)
- High-density polyethylene (HDPE)
- High-molecular-weight polyethylene (HMWPE)
- Linear low-density polyethylene (LLDPE)
- Low-density polyethylene (LDPE)
- Medium-density polyethylene (MDPE)
- Ultrahigh-molecular-weight polyethylene (UHMWPE)
- Ultralow-density polyethylene (ULDPE)
- Ultralow-molecular-weight polyethylene (ULMWPE or PE-WAX)
- Very low density polyethylene (VLDPE)

Process ability and properties of PE blends depend on the composition, the molecular structure, and the MW. The typical values of density, melting temperature, and crystallinity are listed in Table 18.1; there is a linear relation:

$$T_{\mathrm{m}}(^{\circ}C) = 171.9 + 1763 \cdot \log(\rho); r^2 = 0.925.$$

The first highly crystalline polymethylenes, $(CH_2)_n$ (melting point, $T_{\mathrm{m}} = 137\,^{\circ}\mathrm{C}$), were obtained fortuitously by thermal decomposition of diazomethane. In 1930, Carothers and his colleagues at du Pont de Nemours produced polydispersed polymethylenes by condensation of decamethylene bromide: $(CH_2)_{10}Br_2 + Na = H(CH_2)_nH$. After fractionation, the polymerization degrees were determined as $n = 40, 50, 60, 70, \ldots$. At about the same time, at IG Farbenindustrie, the polymerization of ethylene in the presence of BF was carried out under high pressure (Hofmann and Otto 1931).

Industrial polymerization or copolymerization of olefins started in 1936, thus a year after the Faraday Society meeting where Fawcett described Perrin's discovery of ethylene polymerization, dismissed by Herman Mark who stated that *ethylene does not polymerize* (Kennedy 1986). During the elapsed, 75 years or so, ethylene polymerization went through several stages, incorporating new technologies without abandoning the old ones:

1935–1936: Free radical polymerization of ethylene solution at high temperature $T > 180\,^{\circ}\mathrm{C}$ and pressure $P = 120$–300 MPa, facilitated by the presence of oxygen or peroxides producing **LDPE**.

1950: Catalytic polymerization of ethylene under mild conditions, e.g., $T = 100$–$250\,^{\circ}\mathrm{C}$ and $P = 1$–8 MPa, in the presence of a metal oxide, e.g., Cr_2O_3 or NiO on carbon black and Mo_2O_3 or $CoMoO_4$ on alumina; product **LLDPE** or **HDPE**.

1953: Disclosure of the Ziegler catalyst, used for industrial production of **HDPE** since 1954–1955. The Ziegler–Natta (Z-N) catalyst is mainly a binary mixture of a titanium halide and an organoaluminum compound producing mainly LLDPE copolymer with a broad MW distribution (MWD). Academic and industrial modifications of the Z-N catalyst started right away, e.g., by Elston in DuPont

Table 18.1   Typical range of PE properties

Acronym	Density range ρ (g mL^{-1})	Melting range point, T_m (°C)	Crystallinity range X (wt%)	Year of introduction
LDPE	0.910–0.940	100–115	40–60	1935
HDPE	0.940–0.965	125–135	65–80	1955
LLDPE	0.915–0.940	110–125	40–80	1975
VLDPE	0.885–0.910	100–120	25–40	1983

Canada who developed *Sclaire* catalyst based on vanadium (V) instead of titanium (Ti). A majority of commercial polyolefins (POs) are still produced with heterogeneous, multi-sited, modified Z-N catalysts, e.g., TiCl$_4$ on MgCl$_2$ support.

1975: Discovery of the metallocene catalyst by Kaminsky and Sinn. The catalyst is composed of a metallocene (Cp$_2$MCl$_2$, i.e., it has two Cp (cyclopentadienyl) ligands; M is Zr, Ti, or Hf) and a linear or cyclic methylaluminoxane (MAO) – both soluble in organic solvents. The metallocene polymers are produced under mild polymerization conditions (e.g., $T = 100$ °C and $P = 1$ MPa), producing **m-LLDPE** with narrow MWD and homogeneously distributed short-chain branches (SCB). The mono-Cp catalysts are known as single sited or pseudo metallocene.

1997: Beginning of the post-metallocene catalysis – the new ones often have imine ligand, but not Cp. They are characterized by high activity, a possibility of adjusting polymer MW and MWD as well as copolymerization of olefins with polar monomeric and macromeric species. A wide spectrum of catalysts based on light and heavy transition metals have been published in open literature and patents. There are also several types of catalysts with intermediate structure – pseudo metallocene with a post-metallocene imine ligand. Unfortunately, the product shows poor thermal stability and is not ready for commercialization.

More details on the historical evolution of PE and PE blend technology are tabulated in Appendix and Nomenclature.

18.2   Types of PE

18.2.1 LDPE

LDPE has a high degree of short-chain branching (SCB) and long-chain branching (LCB), which reduce macromolecular crystallization. Thus, since the intermolecular forces are weaker, so is the modulus and strength, accompanied by increased ductility. LDPE is a product of free radical polymerization. Owing to the LCB, molten LDPE in extensional flow shows the strain-hardening effects, which stabilize the bubble during the film-blowing operation. In consequence, LDPE is frequently used in PO blends for easing process ability of, e.g., LLDPE.

LDPE is being manufactured using either an autoclave reactor (AR as in ICI process) or a tubular reactor (TR process of IG Farbenindustrie, now BASF). The high-strength tubes are $L = 0.5–2$ km long with inner/outer diameters ID/OD = 70/180 mm; thus, L/OD = 3,000–11,000. Since the operating conditions in AR and TR are different ($T = 180–330$ and 140–340 °C and $P = 100–250$ and 200–350 MPa, respectively), the polymers have different properties.

18.2.2 HDPE

HDPE has a low degree of branching and thus higher crystallinity, modulus, and tensile strength. HDPE has been produced in several catalytic processes, viz., Zletz used molybdena-alumina, Hogan and Banks claimed CrO_3 on silica, and Ziegler et al. employed $TiCl_4$ with trialkyl aluminum (e.g., triethyl: $AlEt_3$). The lack of branching is ensured by the catalyst and reaction conditions. HDPE is produced either in suspension, gas phase, solution, or their combinations, using a variety of reactor type and polymerization media, viz., a continuously stirred tank (CSTR), loop, reactor, or fluidized bed reactor (FBR). There are single and multi-reactor production lines; there is a diversity of hydrocarbon solvents or suspending liquids and of catalysts and operating conditions, which leads to great performance diversity of HDPE available on the market.

18.2.3 UHMWPE

UHMWPE is HDPE with MW = 3.1–5.67 Mg mol^{-1}. The high molecular weight makes it tough and less crystalline than the lower-MW HDPE (e.g., $\rho = 930–935$ kg m^{-3}). UHMWPE can be made using any catalyst, but Ziegler type is common. Because of its outstanding toughness and its cut, wear, and chemical resistance, UHMWPE is used for moving machine parts, bearings, gears, artificial joints, edge protection on ice rinks, and butchers' chopping boards. More recently, through gel spinning and stretching, UHMWPE has been formed into highly oriented crystalline fibers, which under the trade names Spectra™ and Dyneema™ compete and complement aramids in bulletproof vests and helmets used in implants for hip and knee replacements.

18.2.4 LLDPE

LLDPE is a substantially linear polymer with numerous short branches, primarily made by copolymerization of ethylene (C_2) with short-chain alpha-olefins (e.g., 1-butene, 1-hexene, or 1-octene, i.e., C_4, C_6, or C_8). LLDPE is more difficult to process than LDPE, but it has higher modulus, strength, impact, and puncture resistance than LDPE and better environmental stress cracking resistance (ESCR). Thinner films of LLDPE replace those of LDPE in packaging applications.

Table 18.2 Operating conditions for the production of LLDPE in the solution and gas-phase reactors

Process	Solution	Gas-phase
Operating temperature (T °C)	>100	80–105
Operating pressure (MPa)	2–20	0.7–2
Polymer content in reactor (wt%)	10–30	(not applicable)
Residence time in reactor (min)	5–30	60–180
Hydrocarbon solvent	C_6–C_9	C_5–C_7
Comonomer	C_3, C_{10}	C_4, C_6
Catalyst	Z-N or metallocene	Ziegler or metallocene
Ref.	CA Pat. 660,869	U.S. Patent 4,302,566

The work on Z-N-type catalysts in DuPont Canada in Kingston resulted in a low-pressure solution technology, *SCLAIRTECH™*, based on a new coordination catalyst (Elston 1972, filed 1968). The process made it possible to copolymerize C_2 with 10–20 mol% of C_4, C_6, or C_8 olefins. The *SCLAIRTECH™* provides greater variety of PE properties than the standard Z-N-type process, ranging from HDPE to that of LLDPE. The density and crystallinity depend on the type, amount, and sequence of placement of a comonomer. Owing to excellent performance parameters, these resins are used for films and fibers as well as for gas pipelines. A full-scale production facility near Sarnia, ON, was built in the early 1960s (Lank and Williams 1982).

In 1968, Union Carbide introduced the gas-phase FBR low-pressure *UNIPOL™* process. The first large-volume production unit started in 1970 in Sweden and later in the USA and 13 other countries. Initially the *UNIPOL™* process used Z-N catalyst and after 1980 the metallocene single-site catalyst. In the early 1990s LLDPE constituted 25 % of the world production of PEs (Fraser et al. 1997; Univation Technol. 2007). A summary of conditions used in the solution- and gas-phase processes is presented in Table 18.2.

The conventional Z-N–LLDPE contains a major fraction of a "copolymer" with the desired MW, a large PE "homopolymer" fraction with broad molecular weight distribution (MWD) and a small amount of a very low density copolymer. Such heterogeneity leads to several problems: (1) organoleptic caused by the low-MW wax; (2) suboptimal impact strengths caused by the crystallinity of the homopolymer fraction; and (3) processability – the resins were difficult to process on LDPE lines. The development of the *m*-LLDPE resins has mitigated these disadvantages (Huang et al. 2002). However, the *m*-LLDPE has narrow MWD again causing processability problems, usually solved by blending (Brown et al. 2009; U.S. Patent **6777509**, 2004).

Numerous articles and patents were published on diverse methods of **LLDPE** blending with other POs and elastomers, e.g., *m*-LLDPE, LDPE variety of ethylene copolymers, thermoplastic elastomers, TPO, EPDM, EPR, EVAc, maleated polypropylene, and PP-MA (Haas and Raviola 1982; Hughes 1982; Cowan 1983; Jager et al. 1983; Turtle 1983; Fukui et al. 1983; Haas 1983; Hert 1983).

Fig. 18.2 Melting point
versus density dependencies
for LLDPE prepared using
Ziegler–Natta multi-site and
a single-site metallocene
catalyst
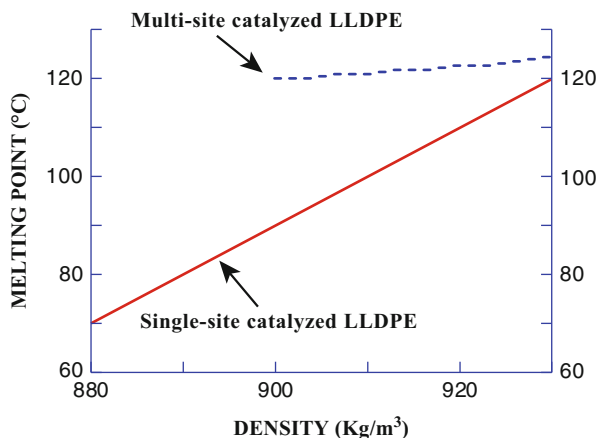
18.2.4.1 m-LLDPE

The metallocene-type LLDPE (*m*-LLDPE) has been produced using the **single-site metallocene catalysts**. This technology started the production of high-quality PO, with controlled MW, MWD, comonomer placement, and density or crystallinity. As shown in Fig. 18.2, there is a significant difference in the melting point versus composition dependence for LLDPE and m-LLDPE. The difference originates in the regularity of the comonomers' placement, which controls the size of the crystallizing chain segments. Such regularity may be obtained using metallocene, but not Z-N catalysts.

In 1975, Mitsui Petrochemicals introduced metallocene *TAFMER*™ polyolefins, the m-LLDPO, with strictly controlled comonomer distribution. The resins had rather low MW. Eight years later, Polysar disclosed bimetallic metallocene alumoxane catalyst used in polymerization of olefins into elastomeric ethylene-α-olefin copolymer or ethylene-α-olefin-*non* conjugated diolefin (Davis 1994). Also in 1983, Exxon Chemical filed a patent application (granted 11 years later!) for polymerization of C_2 in the presence or absence of a comonomer into PE of controlled MW and density. The metallocene catalysts were cyclopentadienyl derivatives (Cp) of the general formula: R′s(Cp)$_2$MQ [M is a metal from Group 4b, 5b, or 6b (preferably Zr); R′ is a C_1–C_4 radical; Q is an alkylidene radical]. The catalyst was used in combination with alumoxanes (Welborn and Ewen 1994). Four years later, Exxon with Mitsui Petrochem. jointly developed *Exxpol*™ – a single-site metallocene catalyst for PO (co)polymerization in a solution, gas, or slurry phase. The metallocene catalyst had *at least one* substituted Cp ring facilitating production of PEs with less regular structure, beneficial for process ability (Jejelowo 1994). *Exxpol*™ from Exxon–Mitsui and *INSITE*™ from Dow showed better process ability, clarity, and mechanical properties than those obtained using Z-N catalysts. The first commercial metallocene-made PE was introduced by Exxon in 1991 as a *Plastomer*™ (Leaversuch 1991; Lai et al. 1993, 1994).

18.2.4.2 MDPE

MDPE can be produced by chromium/silica, Z-N, or metallocene catalysts. The polymer has good shock and drop resistance properties; it is less notch sensitive and has higher stress cracking resistance than HDPE. It is typically used in gas pipes and fittings, sacks, shrink film, packaging film, carrier bags, and screw closures.

18.2.4.3 VLDPE and ULDPE

In the 1980s, new catalysts $Mg_rAl_sTi_t(OR)_uCl_v$ (the subscripts are positive integers) were developed for gas-phase or solution polymerization at $T = 70–11\,°C$ and $P = 0.5–2\,MPa$ (Cady 1987) for the production of **VLDPE** with density of $\rho = 900–915\,kg\,m^{-3}$ and its homologue, **ULDPE** ($\rho = 855–900\,kg\,m^{-3}$). The latter copolymer was commercialized by Mitsui Toatsu in 1986 and has low crystallinity and $T_m = 40–85\,°C$. As a result, it shows properties intermediate between those of PE and an elastomer (Kim et al. 1992). The VLDPE and ULDPE are substantially linear metallocene copolymers of C_2 with α-olefins (e.g., $C_{4–8}$).

With development of VLDPE and ULDPE, the distinction between thermoplastic PE and olefinic rubbers became less apparent. By 1992, *Exact™ PE*, a VLDPE made using metallocene or "single-site" catalyst, was introduced by Exxon Chem. The main use of ULDPE is in blends of LDPE, HDPE, or PP (Utracki 1989b; Kohyama and Yamada 1991; Leaversuch 1992). While the extent of blending varies from one country to the next, the general advantages of blending are widely recognized. Blends with PP have attracted much commercial interest (Utracki and Dumoulin 1995). Since these polymers are immiscible (see Fig. 18.3), copolymers such as EPR or EPDM are frequently used. Compatibilization can also be achieved by reactive blending, "dynamic vulcanization," or post-blending cross-linking using peroxides, electron beam, or γ-radiation. Both factors, the reactive compatibilization and irradiation, lower the crystallinity. Thus, the micromorphological character of PP/PE blends can be controlled by composition, presence of the nucleating agents, type of compatibilizer, and thermal or radiative treatment (Nadkarni and Jog 1991).

18.2.4.4 PEX

PEX is a medium- to high-density PE containing cross-links. Cross-linking reduces its flow and increases the continuous use temperature (CUT) and chemical resistance. Because tubes made of the material can be expanded to fit over a metal nipple and then slowly return to its original shape, forming a permanent, watertight connection PEX is used in potable water plumbing systems.

In summary, as presented in Table 18.3, the current world production of PEs is close to 100 million metric tons (equivalent to a sphere with 1.3 km diameter), with ca. 45 % of this mass being HDPE, than LLDPE and the old LDPE keeping about 20 % of the market.
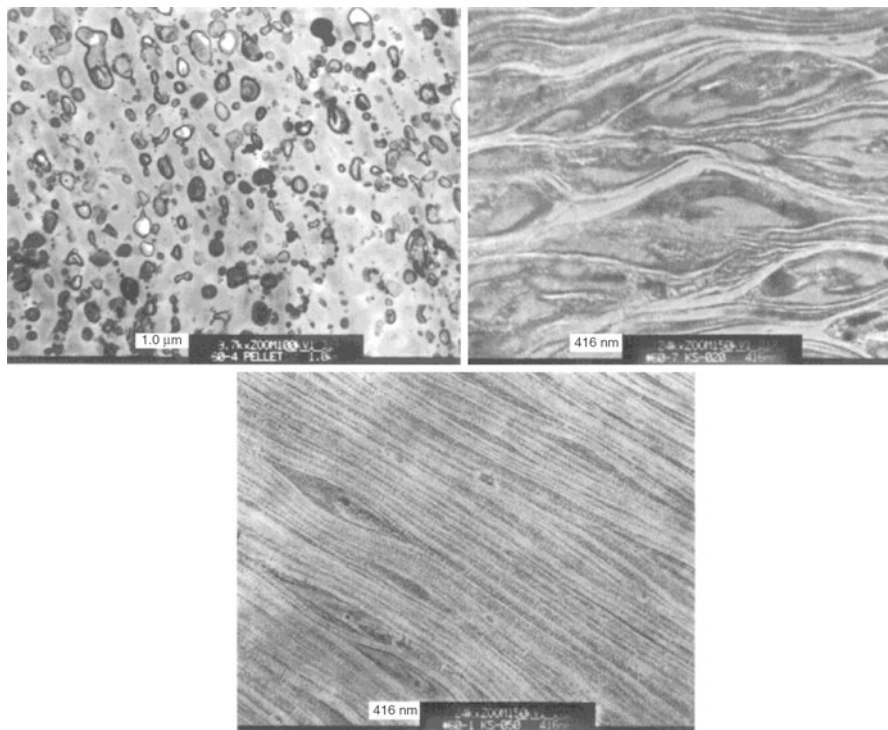
Fig. 18.3 PP with 65 wt% elastomer (from the LHS): morphology in pellets, in blown film, and in blown film in PP copolymerized with 3 mol% C_2 – effect of compatibilization (Montell Impact Copolymer Polypropylene, commercial information 2012)

Table 18.3 PE production/consumption in four regions 2008–2015

Region	LDPE (%PE)	HDPE (%PE)	LLDPE (%PE)	Total (Mton)
Asia Pacific	19	47	34	42.0
South and Central America	20	44	36	14.6
North America	18	44	38	20.8
Europe	34.4	49.7	15.9	22.1

18.3 PE Discovery and Evolution

18.3.1 High-Pressure Polymerization of LDPE

In March 1933, as a part of ICI studies of high-pressure reactions, Fawcett and Gibson observed the formation of a waxy white powder (later identified as polymethylene) in a reactor filled with C_2 and benzaldehyde T $\approx$ 170 °C and $P = 190$ MPa. It took 2 years for Perrin and Swallow to establish that polymerization was radical, initiated

by traces of O_2 or peroxide. The discovery was presented during the 1935 meeting of the Faraday Society (Kennedy 1986). A year later, a provisional British patent was filed. It described polymerization of ethylene at $T = 100$–$300\ ^\circ$C and $P = 50$–300 MPa into polymers with density $\rho = 910$–920 kg m^{-3} and melting point $T_m = 115\ ^\circ$C. In 1937, the first *Telcothene*™, a blend of PE and polyisobutylene (PIB), was produced for submarine cables, and in 1939, a large plant with 100 t year^{-1} capacity started the production of *Alketh*™ (Seymour and Cheng 1985; Ballard 1986). The following year a tenfold larger plant was commissioned.

The LDPE technology continues evolving. In the USA, the first PE was produced by Union Carbide in a tubular reactor in 1940. The ICI-developed **LDPE** technology was licensed to du Pont de Nemours, Arco, Eastman, and several other companies. Configurational studies indicated the presence of two types of branching: LCB and SCB, caused by intermolecular and intramolecular hydrogen transfer, respectively; LCB depends on the monomer/polymer ratio and mainly affects melt flow, whereas SCB is related to the polymerization temperature via formation of a 6-member ring that forms a C_4 pendant group, which influences the solid-state properties, viz., crystallinity and density ($\rho = 0.89$–0.97 g mL^{-1}). On the weight basis, the estimated branching density for LCB and SCB is, respectively, 8–10 and ≤ 50 per macromolecule (Roedel 1953).

18.3.2 Early Stage of Catalysis

In 1951, the first patent for low-pressure ($P = 1$–10 MPa) catalytic polymerization of ethylene into **HDPE** ($\rho = 920$–980 kg m^{-3}) was deposited by Standard Oil of Indiana (Zletz 1954; Nowlin 1985). The document described formation of a rubbery polymer with high MW. Similar discovery was announced by Phillips Petroleum Co. (Hogan and Banks 1955) and then by Ziegler et al. (1960, 1966). In 1953, Karl Ziegler, using a catalyst based on transition metal compounds suspended in organic solvent, polymerized ethylene at pressures slightly above ambient into linear HDPE, as well as propylene and butylene to isotactic polymers, PP and *i*-PB. Similar discoveries were published by Giulio Natta, who focused on the ability of the new catalyst to produce stereospecific poly-α-olefins. In 1963, Ziegler and Natta shared the Nobel Prize in chemistry. The organometallic compounds (e.g., $AlEt_3 + TiCl_4$) are known as the Z-N catalysts.

Z-N catalysts are based either on $TiCl_4$, VCl_5, or $CoCl_3$ mixed with $Al(C_2H_5)_3$ or $Al(C_2H_5)_2Cl$ in an inert solvent. Both the crystalline solid and highly colored supernatant solution can initiate polymerization, but only the former leads to stereospecific polymer. The crystalline catalyst has many active sites initiating different reactions – e.g., four types postulated by Floyd et al. (1987, 1990). Thus, the Z-N catalysts lead to polymers with a wide range of polydispersity, composition, and limited stereospecificity.

In 1954 Hoechst was the first manufacturer of HDPE by Ziegler process, followed by Hüls, Rührchemie, Montecatini, Shell, Mitsui, Dow, Esso, Gulf, Hercules, Koppers, Monsanto, and Union Carbide. In 1957, Hercules introduced

the Z-N-catalyzed **UHMWPE**. The industrial production of HDPE using Phillips technology started in 1956, which by that date was already licensed to nine companies in seven countries.

The comonomer distribution between LLDPE molecules produced using a multi-sited catalyst is not random. Their distribution is heterogeneous, where the copolymer molecules do not have the same ethylene/comonomer ratio. These copolymers are differentiated for the type of the degree of heterogeneity and the MW-dependent ethylene/comonomer ratio. In the heterogeneous copolymer type I, the ethylene/comonomer ratio is independent of MW; individual macromolecules have comonomer content above or below the average. Heterogeneous copolymers type II and III have the ethylene/comonomer ratio increasing and decreasing with MW, respectively. Combinations of types I, II, and III are also possible (Elston 1965, 1972).

This situation observed in Z-N PE may be compared to the homogeneous metallocene copolymers in which not only the comonomer is randomly distributed within a given macromolecule, but also all the copolymer molecules have the same ethylene/comonomer ratio. Homogeneous copolymers of narrow MWD exhibit a reduced haze in films, higher impact strength, reduced tendency toward delamination, and better (than heterogeneous ones) balance of physical properties in the machine (MD) and transverse (TD) direction of the blown films. It is interesting that blends of these two LLDPE types, heterogeneous and homogeneous, lead to films with improved impact and tensile properties (Chum et al. 1998, 2006).

18.3.3 Metallocene Catalysts

To improve selectivity of the catalyst, two routes were taken: (i) additives have been used to "poison" some of the sites, e.g., by injection of H_2 (Vanderberg 1962), and (ii) ligands have been incorporated forcing the monomer to a unique molecular orientation when approaching the active site. The latter strategy resulted in development of new class of metallocene catalysts discovered in 1976 by Kaminsky and Sinn for a slurry process. A metallocene or sandwich compound consists of two cyclopentadienyl anions ($Cp = C_5H_5^-$) bound to a metal (M) in the oxidation state II. The compounds are usually miscible in organic solvents.

Metallocene catalysts have well-defined single catalytic site and well-understood molecular structures consisting of a transition metal atom sandwiched between ring structures to form a sterically hindered site (Thayer 1995). The oligomeric co-catalyst is alumoxane, $[Al(CH_3)-O]_n$. The stereoselective catalytic sites polymerize almost any monomers into a polymer with well-defined MW and MWD, comonomer distribution and content, and tacticity. The two Cp rings may not be identical. Monocyclopentadienyl structures also exist in which one ring has been replaced by a heteroatom (often N). The transition metal, M, usually is from Group 4b (Zr, Ti, Hf). For example, the Dow Chem. *INSITE*™ metallocene catalyst contains $[C_5Me_4(SiMe_2N\text{-}Bu)]TiMe_2$ (where C_5Me_4 is a tetramethylcyclopentadienyl group), with two co-catalysts tris(pentafluorophenyl)borane and modified

methylaluminoxanes (ratios: B:Ti = 2:1; Al:Ti = 4:1), all soluble in saturated hydrocarbons, C_{8-10}.

Metallocene polymers, ranging from crystalline to elastomeric, have been commercialized since the early 1990s. They show increased impact strength and toughness, better melt characteristics because of the control over molecular structure, and improved film clarity. Most early applications have been in specialty markets where value-added and higher-priced polymers may compete.

In the USA Exxon Chemical and Dow Plastics were the leaders in the metallocene technology. While Exxon explored both mono- and bis-cyclopentadienyl metallocenes, Dow focused on "constrained geometry catalysts" based on Ti-monocyclopentadienyl metallocenes. Exxon first produced metallocene-based polymers with its *Exxpol* catalysts in 1991. Dow uses its *INSITE* technology to make ethylene–octene copolymers, introduced in 1993. Copolymers with up to 20 wt% octene are sold as *AFFINITY* "plastomers," competing with specialty polymers in packaging, medical devices, and other applications. Dow, producing its own catalyst, considers that it leads to the uniform introduction of comonomers and long-chain branches that improve processability of otherwise linear polymers.

In 1995, Exxon received a patent and conducted successful test runs of a new m-LLDPE technology using the super-condensed mode (SCM) process, which allows for the operation of gas-phase reactors with higher levels of liquids, increasing plant productivity by 60–200 % at half of the plant cost (Univation Technologies 2008; Sirohi and Ramanathan 1998). There have been other engineering developments where loop reactors or multi-reactors have been used in sequence for the production of copolymers with desired composition and performance. These technologies eventually resulted in the production of multilayered PE particles, which resemble the earlier acrylic resins produced in emulsion or suspension processes and broadly used as compatibilizers in a variety of polymer blends (Utracki 1997a, b). Thus, it is of no surprise that the number of patents in PE technology is large (Dow has been issued over 100 US patents related to *INSITE* technology, NOVA Chem. 120 CA patents, etc.) and litigations provide a rich feeding ground.

18.3.4 Post-metallocene Catalysis

The beginning of the post-metallocene catalysis dates back to 1997; the new catalysts most often have imine instead of Cp ligand. They are characterized by high activity, possibility of adjusting polymer MW and MWD, as well as copolymerization of olefins with polar monomeric and macromeric species. A wide spectrum of catalysts based on light and heavy transition metals were patented and published in open literature. There are also several types of catalysts with intermediate structure – pseudo metallocene with a post-metallocene imine ligand. More recent post-metallocene catalysts use M-complexes (Sc, La) and ligands containing O, N, P, and S activated by MAO. Pd(II) and Ni(II) R-diimine catalysts (DuPont's Versipol™) are also used for copolymerization of C_2 with a variety of

functionalized olefins. Notably, they do not need a co-catalyst/activator (Brookhart et al. 1983, 2007).

During the last 10 years, Mitsui Chem. has been developing new, single-site, post-metallocene catalysts capable of modifying polymer molecular structure. Large enhancement of catalyst activity was found for Zr salts complexed with two phenoxyimine ligands (Mitsui and Fujita 2001). The authors showed that under mild polymerization conditions, certain salicylaldimine complexes of M Group IV lead to higher activity than that of metallocenes (Makio et al. 2002, 2011). The highest activity exhibited by a Zr-FI catalyst reached a catalyst turnover frequency (TOF) of 64,900 s^{-1} atm^{-1}, thus two orders of magnitude greater than that seen with Cp_2ZrCl_2 under the same conditions. At 50 °C, the Ti-based FI catalysts with fluorinated ligands produce, at high-rate, living, monodispersed, high MWPEs ($M_w/M_n < 1.2$, $M_n > 400$ kg mol^{-1}). The maximum TOF, 24,500 min^{-1} atm^{-1}, is three orders of magnitude greater than those for known living ethylene polymerization catalysts. The versatility of the FI catalysts leads to new polymers which are difficult or impossible to prepare using the metallocene technology. For example, it is possible to prepare low-molecular-weight ($M_v \sim 1$ kg mol^{-1}) PE or EPR with olefinic end groups, UHMWPE or EPR, high-molecular-weight poly(1-hexene) with atactic structures including frequent regions of monodispersed poly(ethylene-*co*-propylene) with various propylene contents, and a number of polyolefin block copolymers [e.g., polyethylene-*b*-poly(ethylene-*co*-propylene), syndio-polypropylene-*b*-poly(ethylene-*co*-propylene), polyethylene-*b*-poly(ethylene-*co*-propylene)-*b*-syndio-polypropylene].

One of the numerous advantages of the FI catalysis is its capability for producing nearly monodispersed, low-MWPE with a variety of functional end groups (Sainath et al. 2009), which may be converted into a salt and oxidized into an epoxy or an amino-terminated group (Matoishi et al. 2011). However, so far there is little commercial interest for these new materials. On the one hand, this may originate in the continuously growing number of new catalysts that have higher productivity and versatility but on another caused by inadequate thermal stability of the system and the current global economic problems (Ittel et al. 2000).

18.4 Characterization of Polyethylenes (PEs)

18.4.1 Standard Test Methods

As with any other polymer, PE needs to be tested using standard methods, tailored to the needs, viz., determination of MW, chemical structure; morphology; and thermal, mechanical, and dielectric properties. During a century of testing, the methods and equipment have been developed, which although expensive make the task relatively simple. For example, MW is determined using the size exclusion chromatography (SEC, previously known as gel permeation chromatography, GPC; Striegel 2004), the chemical analysis is performed using a Fourier transform infrared spectroscopy (FT-IR), and stereospecificity of macromolecule by the

nuclear magnetic resonance (NMR) in a number of its versions, e.g., using ^{1}H or ^{13}C NMR, determining dyads (r, m), triads (mm, rm + mr, rr), and/or higher order n-ads. The other methods include X-ray powder diffraction (XRD) and secondary ion mass spectrometry (SIMS).

These standard tests are used for PE, but mostly these are part of special procedures capable of distinguishing a wide variety of polymer and copolymer structures unknown in other polymers.

18.4.2 Specific Methods of PE Characterization

There are several levels of macromolecular structures belonging to:
- Configuration, the intrinsic structure that cannot be changed without breaking a bond
- Conformation, imposed by stress, σ; strain, γ; pressure, P; or temperature, T
- Micromorphology discussed in terms of submicron-sized crystalline unit cells
    Thus, macromolecular **Configuration** belongs to the sub-nanometer structures such as:
- Chain tacticity of tertiary carbon macromolecules
- Head-to-head, head-to-tail, and tail-to-tail configuration in polyvinyls
- *Trans* (the planar zigzag) versus *gauche* ($\alpha = 120°$) configuration
- *Cis* and *trans* isomerism and 1,2- versus 1,4-addition of dienes
- Branching (short and long)
- Copolymerization (short sequence: *co*, *stat*, *ran*, *alt*; long sequence: block, graft, star, star-block; networks: *cross*, *inter*, etc.)
- Ladder, planar, dendromeric, and other macromolecular structures
- Isomerism that can be changed only by bond breakage
    Conformation (*scale* 1–30 nm) – kinetic arrangements of chain elements in space, engendered by rotation about bonds, e.g., from *trans* to *gauche* position or vice versa, e.g., random coils, helices, and folded chains. Conformation depends on internal and external forces, e.g., interactions, σ, γ, P, and T, as well as on the route used for its creation (thermodynamically nonequilibrium structures).

Micromorphology (*submicron* scale) is related to vitrification and crystallinity, viz., crystalline unit cell shape and size; lamellae type, shape, and size; and stress-induced shish-kebab crystals. Dramatic changes of micromorphology may be introduced by gel spinning of UHMWPE [*Dyneema*® (DSM); *Spectra*® (Honeywell)] or UHMWPP [Innegra®, Innegra Technologies] high-performance fabrics used in ballistic composite applications.

As discussed above, the diverse polymerization methods primarily affect **configuration**. One needs to know how changes in catalyst, monomer composition, or reaction variables affect the intrinsic nature of the macromolecules, thus the final performance of the resin.

18.4.2.1 Temperature Rising Elution Fractionation, TREF
Invented in the late 1970s the TREF is a method for fractionating semicrystalline polymers from solution according to composition and microstructure. In TREF the

polymer is dissolved at elevated temperature and then slowly cooled to crystallize on regular-shaped column support. In the following step, the sample is eluted by fresh solvent at successively rising temperature intervals, collecting and analyzing the fractions, which then are injected into a SEC determining MW and MWD of each slice of the PE melting point. Initially, the homebuilt instruments and experimental procedures varied from one laboratory to the next, but since the late 1990s the commercial systems are available (Wild 1990). TREF is usually classified as preparative and analytical (respectively, p-TREF and a-TREF) (Wijga et al. 1960).

Preparative Temperature Rising Elution Fractionation, p-TREF

In the **p-TREF** mode, ca. 1–5 g of polymer is dissolved and loaded onto column packing (e.g., 1.4 kg of sea sand), then cooled to room temperature (RT). Next, the crystallized polymer is eluted at successively higher T. For example, extraction over $T = 30\text{--}150\,^\circ\text{C}$ divided into 10–15 T-steps (Shirayama et al. 1965). After these preliminary tests a large-scale, robust, and continuous system was developed for unsupervised operation (Wild et al. 1971, 1982). The instrument consisted of a stainless steel column L/D = 0.60/0.12 m packed with Chromosorb-P support onto which 4 g of polymer was crystallized by slow cooling (2 K h^{-1}) from a hot xylene solution in a T-programmed oil bath. A variety of PEs followed a linear dependence between the elution T and the degree of SCB (Usami et al. 1986; Kelusky et al. 1987). Hazlitt and Moldovan (1989) described an automated TREF system capable of a semi-preparative fractionation of 0.5 g of LLDPE. The cooling rate of 2.5 K h^{-1} was used and the column was packed with steel shot (0.57 × 0.57 mm) for improved heat transfer.

Ramachandran et al. (2011) measured the structure and branch content of LLDPE using a small-angle neutron scattering (SANS). The scaling approach quantified SCB and LCB content in polymers concurrently, thereby illustrating the distribution of these branches within the fractions. Additionally, new quantities such as the average LCB length and hyperbranch content were measured providing further insight into the structure. LLDPE used in this study was fractionated using p-TREF. For commercial LLDPE these results evidenced LCB, which could be attributed to post-reaction processes. TREF has been particularly useful in analyzing Z-N–LLDPE, recovering 98 % of the eluted polymer. The main advantage of p-TREF is that it provides also samples for external analysis, by DSC, IR, SEC, ^{13}C NMR, SANS, etc.

Analytical Temperature Rising Elution Fractionation, a-TREF

The **a-TREF** was developed later than p-TREF with instrumentation "borrowed" from SEC. However, because of the nature of fractionation in TREF, the sample preparation is different and some device is needed for controlling the cooling and heating cycles. Furthermore, a calibration is needed for the plot of the elution T versus SCB, which requires different standards than those used for SEC calibration.

Wild and Ryle (1977) described a-TREF that used solvent reservoir, degasser, pump, and detectors (e.g., refractive index, RI). PE was crystallized by slow cooling a solution of 0.2 g in 5 mL TCB on Chromosorb-P packing. TREF was performed at

a flow rate of 6 mL min^{-1} and a rate of *T*-rise of 8 K h^{-1}. The RI response and the separation *T* were recorded continuously. A calibration curve of methyl content versus elution *T* was obtained using p-TREF fractions of LDPE and LLDPE. This information was transformed into comonomer content (e.g., mol% of C$_8$) versus elution time; as shown in Fig. 18.4, the semilogarithmic plot is linear. Over the years TREF system was refined by reducing the column and sample size, the *T*-programmed gas chromatography oven was replaced with an oil bath, and the detector was also replaced by multiple ones (e.g., FTIR and ^{13}C NMR, while polymer concentration was measured by IR) with better sensitivity and baseline stability (Knobeloch and Wild 1984).

Not only PEs but also their blends have been successfully analyzed (e.g., LDPE with LLDPE dissolved in α-chloronaphthalene) (Kelusky et al. 1987).

TREF/SEC (GPC)

During the 1980s a-TREF/SEC evolved into an integrated system, where p-TREF provided fractions for a wide range of subsequent testing, e.g., SEC, ^{13}C-NMR, XRD, DSC, solution viscosity, and FT-IR (Nakano and Goto 1981; Hazlitt and Moldovan 1989). For example, Usami et al. (1986) studied the mechanism of SCB distribution (SCBD) in LLDPEs, using TREF, SEC, ^{13}C-NMR, DSC, and FTIR measurements. They examined six LLDPEs (polymerized using Z-N-type catalyst in gas, slurry, bulk, and solution) and one LDPE. They concluded that Z-N-type polymers had a bimodal SCBD from two types of active sites in Ti-based heterogeneous Z-N catalysts; one produced an alternating copolymer, while the other a random one. The former sites lead to higher SCB concentration peak of the bimodal SCBD and lower MW, while the latter an opposite: lower SCB concentration peak and higher MW. An example of TREF/SEC results is displayed in Fig. 18.5 (Vadlamudi et al. 2009).

Mirabella and Ford (1987) studied the molecular structure of a series of commercial C$_{2+4}$ Z-N–LLDPE copolymers (with ca. 7 wt% of *n*-butene) and compared it to that of LDPE and HDPE. The tests determined SCB, LCB, MW, MWD, and the melting behavior of LLDPE – the latter strikingly different from that of LDPE and HDPE. In commercial LLDPE, the SCB content decreased with increasing MW. The LLDPEs had relatively narrow MWD ($M_w/M_n = 4.0 \pm 0.5$) and no LCB.

Fig. 18.5 Inter- and intramolecular branching distribution of tailored LLDPEs; two side views and surface contours of the averaged 3D bivariate (MW-1-hexene content) distribution from SEC and TREF corresponding to M and T effects. The profile on the *right* corresponds to 180° rotation over the *vertical axis* of the *left*-hand-side profile (Vadlamudi et al. 2009)
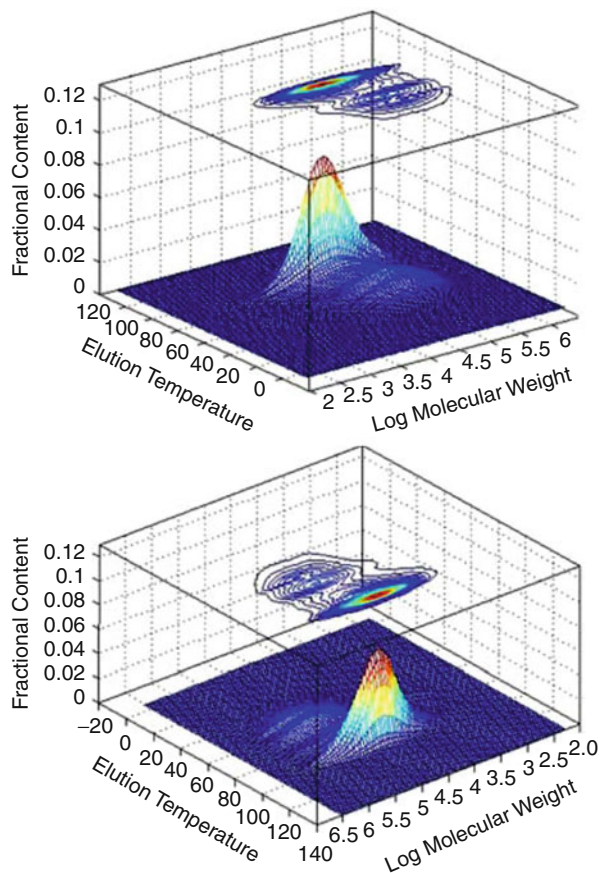
The broad and multimodal SCBD was responsible for the unique melting and crystallization behavior, in commercial LLDPEs decreasing with increasing MW.

Hosoda (1988) also studied Z-N–LLDPE. The MW and MWD were determined using SEC with a refractometer and LALLS. The SCB was calculated from FT-IR spectra, while SAXS provided information on the crystalline lamellar thickness. ^{13}C NMR spectra of LLDPE solutions in *o*-dichlorobenzene (ODCB)/perdeuteriobenzene provided the triad sequence distribution, average sequence length, and run number in ethylene/*n*-butene copolymer. There are many ways to display the plethora of results, but the most interesting is the global cross-plot of MWD and composition; the authors called this "the bird's-eye view" presented in Fig. 18.6.

The first fully automatic 3D-SEC/TREF system was described by Yau and Gillespie (2001). The instrument was based on the Waters 150C SEC, and in addition to RI detector, it had IR, viscometer, and dual-angle light scattering (LSc). With the autosampling facility, it run 16 samples with 4 h/sample test time. During the following years, the instrument underwent modifications (Yau 2007)

Fig. 18.6 "Bird's-eye view" of LLDPE;^{13}C NMR signal intensity versus SCB and MW for commercial Z-N–LLDPE (Hosoda 1988)
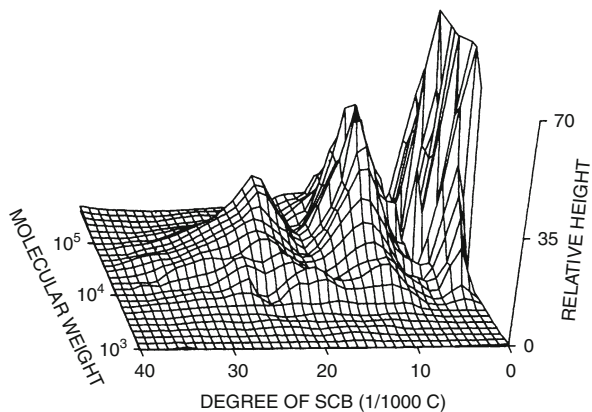
that widened the applicability of the 3D-SEC/TREF, providing MW, MWD, SCB, LCB, and LCB distribution.

The company Polymer Char (Valencia, Spain) was created for developing fully automated PO characterization instruments. The first device, commercialized and patented in 1994, was the ***CRYSTAF***, crystallization analysis fractionation, for the fast measurement of the chemical composition distribution (CCD) in PE, PP, copolymers, and blends. Next came the SEC (with a quadruple detector system) and then SEC/a-TREF and p-TREF instruments. The first commercial, fully automated cross-fractionating SEC/TREF apparatus for microstructure characterization of POs was described by Ortin et al. (2007). The instrument yields a bivariate distribution CCD by TREF fractionation and then SEC fraction analysis in a single run. A schematic diagram of this new cross-fractionation instrument is shown in Fig. 18.7.

TREF/FT-IR Method

Another approach to characterization of PO was explored by Mahdavi and Nook (2008) and by Zhang (2009). In both cases, TREF and FT-IR were used for analyzing a series of different polymers or copolymers, e.g., LDPE, HDPE, LLDPE and C_{2+8} copolymers, PE, eicosane (C_{20}), ethylene–vinyl acetate copolymer (EVAc), PS, PS-*g*-EVAc, ethylene–methyl acrylate (EMA), respectively. In both articles a p-TREF was used, FT-IR furnishing the information on polymer concentration and composition. However, while Mahdavi and Nook carried out extensive, external testing, Zhang used the CRYSTAF–TREF 200+ connecting the FT-IR spectrometer to MW detectors. Both teams stressed the benefits of the FT-IR detectors.

LDPE, HDPE, and LLDPE films have similar structures, differing primarily by SCB. In consequence, it is possible to distinguish between LDPE, HDPE, and LLDPE from their FTIR spectra. Butyl branches were determined using the –CH_3 rocking band at 894.5 cm^{-1}. The amount of unsaturation was measured after bromination. The branch distribution and melting endotherm of each fraction were analyzed with ATR FT-IR and DSC. The results indicated that the SCB frequency decreased and the crystallinity increased as a function of an increasing
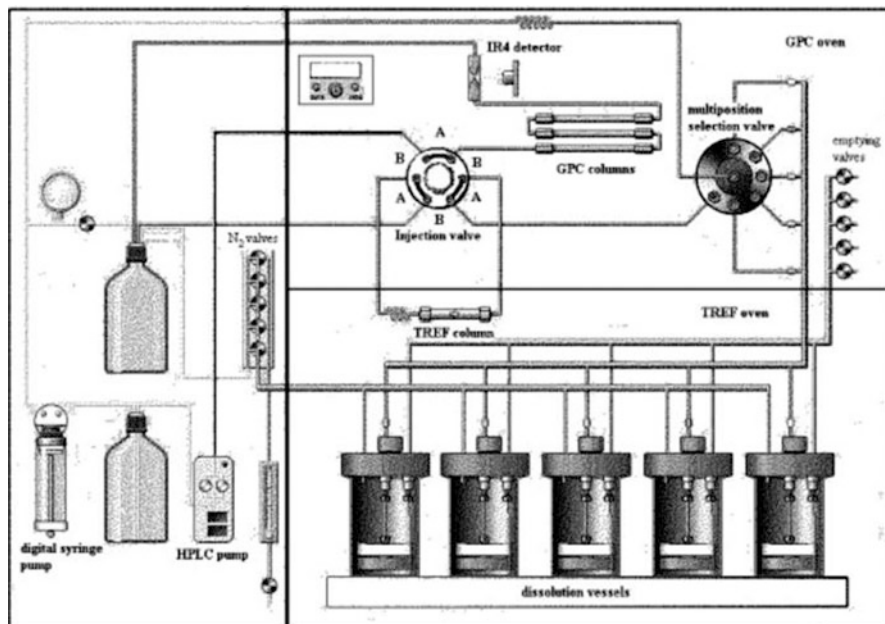
Fig. 18.7 Cross-fractionation SEC/TREF; injection valve shown in "load" position A; "inject" position marked as B (Ortin et al. 2007)

TREF elution T. Low-T fractions had tails related to waxy moieties in LDPE. The melting point of the fractions increased with increasing elution T, and the endotherms were sharper for high-*T* fractions indicating thicker lamellae and/or more perfect crystals.

18.4.2.2 Crystallization Analysis Fractionation, CRYSTAF

CRYSTAF is a process for the analysis of composition distribution in semicrystalline polymers, determination of the branching distribution in PE, or tacticity in PP. Similarly like **TREF**, CRYSTAF is a separation method that fractionates species of differing crystallizability by slow cooling of a polymer solution (Monrabal 1993, 1994; Monrabal et al. 2007; Monrabal and del Hierro 2011). The method was developed as a process that speeds analysis of CCD in POs (Ortín et al. 2010). It shares with TREF the same fundamentals on separation according to crystallizability, but fractionation takes place during crystallization instead of dissolution. The analysis is carried out in stirred crystallization vessels without support, by monitoring the polymer solution concentration while decreasing *T*. Aliquots of the solution are filtered (through an internal filter inside the vessel) and the supernatant liquid analyzed by a concentration detector. The process resembles a stepwise fractionation by precipitation, except that here attention is paid to the polymer that remains in solution instead to the precipitate. The automated instrument (shown in Fig. 18.8) has been available since 1994.

Fig. 18.8 (*left*) Schematic diagram of an automated TREF–CRYSTAF apparatus and (*right*) chromatographs of a bimodal LLDPE resin as detected by TREF and CRYSTAF
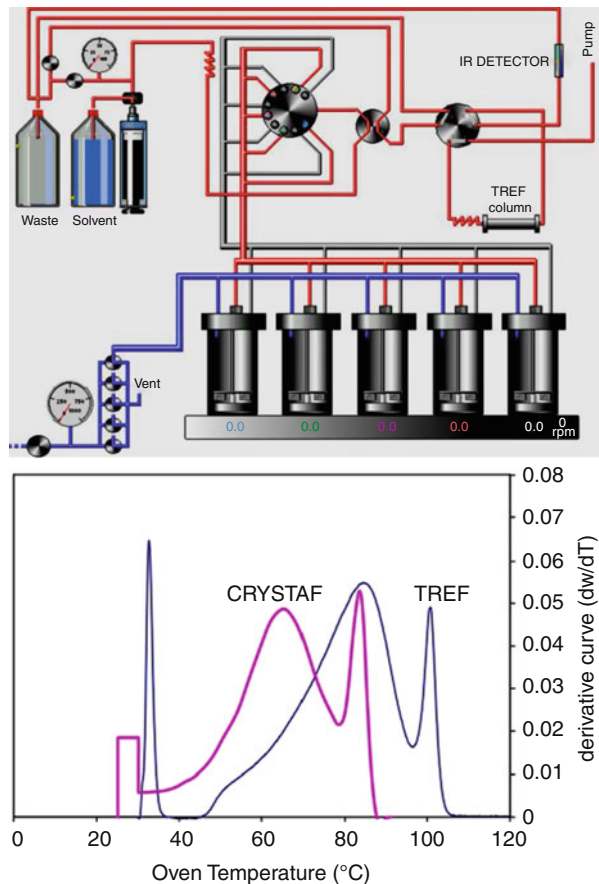
Dry samples are placed in the crystallization vessels, dissolved, crystallized, and sampled. The polymer concentration is measured by an FT-IR at increasing T. The instrument may be converted into a CRYSTAF–TREF system capable of running both types of measurements in the same hardware. Each method provides complementary information on the CCD in some complex resins.

As shown by a red curve in Fig. 18.8 (right), the CRYSTAF chromatograph starts at T just below T_m, and upon cooling first, the most crystalline fraction precipitates. The fractionation continues as T decreases crystallizing the macromolecules with increasing branch content. The last data point, at the lowest T, represents highly branched or amorphous polymer, i.e., the fraction which would not crystallize. The first derivative of this curve corresponds to the CCD and is similar in shape to the one obtained in TREF with a T shifted by about 16 °C; the shift originates in the difference between the crystallization and dissolution T. The CRYSTAF method has been often reviewed (Hamielec and Soares 1996; Soares et al. 1998; Soares and Hamielec 1999; Pasch et al. 2000; Monrabal 2000, 2011;

Gownder 2001; Anantawaraskul et al. 2005; Monrabal et al. 2007; Suriya et al. 2011; Monrabal and del Hierro 2011).

The latter reviews also provide information on the next-generation method, the crystallization elution fractionation, CEF. The experiments are performed in a modified Polymer Char TREF instrument. The instrument incorporates an autosampler for 70 vials of 10 mL. The dissolved samples are injected with the pump flow into the column head, and the dynamic crystallization process begins at a set cooling rate and crystallization flow. As the crystallization ends, the oven starts the heating program and flow is adapted to the elution flow passing through the column to a dual wavelength IR detector, so concentration and composition may be measured. A dual capillary viscometer was added for measuring the composition – MW dependence. Thus, the same instrument may be programmed to run TREF, dynamic crystallization, or CEF. Analysis of complex PO takes about half an hour.

However, in the normal growth pattern, the technology becomes progressively more complex. New catalysts, new multi-catalyst/multi-reactor processes, blending of various PO and additives result in complex structures, especially in terms of CCD, severely complicating their characterization. Certain combinations of POs may result in ambivalent results if only TREF or CRYSTAF is used. To obtain unequivocal results for complex PP or PE copolymer or blend, both TREF and CRYSTAF should be conducted.

18.4.2.3 Recent Alternatives: HTLC, CFC

During the last few years, other methods for PO microstructure analysis have been proposed. Of these, the high-temperature liquid chromatography (HTLC) is the most promising. Using two sets of columns, one may fractionate the polymer according to composition (TREF part) and then MW (SEC part) or vice versa.

Petro et al. (2005) were one of the pioneers of the multidimensional liquid chromatography (LC) for characterization of polymers. The multidimensional LC comprises several HPLC subsystem separated into subcomponents. For characterization of a single polymer, the sample is injected into a first dimension HPLC, separating the polymer into fractions, optionally using flow-through detectors (e.g., mass, universal concentration, light-scattering detector), and then injecting the sampled portions into a second dimension HPLC unit. The role of these subcomponents is detection during a flow through. Generally, the first dimension HPLC subsystem can be adapted for distinguishing between chemical composition and/or structural variations of polymer sample components (e.g., reverse-phase chromatography, mobile-phase compositional gradient elution chromatography, or mobile-phase T-gradient elution chromatography), while the second HPLC subsystem is preferably for MWD with a universal concentration or mass detector, such as an evaporative light-scattering detector (ELSD). Furthermore, a third, fourth, or higher dimension HPLC subsystem may be added, such as liquid chromatography, gas

chromatography, electrophoretic chromatography, flow-field fractionation, flow injection analysis, or mass spectrometry. The methods and instruments described in the invention are useful for:

- Characterizing individual polymer samples or their libraries
- Polymer fingerprinting – determining both compositional/structural characteristics and molecular size/molecular weight characteristics
- An effective scale-up of a polymerization process, in a microscale or nanoscale format

HPLC more rapidly separates PO copolymers or blends than conventional TREF or CRYSTAF. The new PL XT-220 rapid screening HPLC system enables one to perform isocratic and gradient separations at $T = 30$–$220\ ^{\circ}C$ with rapid switching between up to six different columns, each with different solvents (Pasch et al. 2009).

One of the advantages of the HPLC is its ability for analyzing crystalline and amorphous POs (Van Damme et al. 2011). The recent patent describes a method and apparatus for chromatography of a PO using a flowing solution through an LC with graphitic carbon stationary phase for determining the monomer-to-comonomer ratio of a PO copolymer. The strategy is to use SEC for determining MW and MWD and HPLC for assessing the chemical composition. Thus, the HPLC determines composition of a C_{2+3} copolymer in steps: (a) flowing a solution into contact with an LC comprising graphitic carbon and (b) introducing a solution of the copolymer into the liquid mobile phase so that the copolymer emerges in the effluent stream with a retention factor that varies as a function of the monomer-to-comonomer ratio in copolymer. Brief reviews of new methods for PO analysis that include SEC, HPLC with evaporative light-scattering detector, FTIR, and ^{1}H-NMR spectroscopy are available (Heinz and Pasch 2005; Macko and Pasch 2009; Roy et al. 2010; Dolle et al. 2011).

Another recent alternative to TREF/SEC is the cross-fractionation chromatography (CFC), described by Ortín et al. (2010). The instrument is based on a high-resolution a-TREF combined with a dedicated SEC column oven and equipped with five vessels for sample preparation. Polymer detection is made through an IR4 detector for maximum sensitivity and long-term baseline stability. A sample placed in a stainless steel vessel is dissolved at $T = 140$–$160\ ^{\circ}C$ with stirring. The instrument loads the polymer solution into the TREF column where it crystallizes and then as T increases elutes in fractions (or "slices"). Next, the solution is transmitted to the SEC columns, which provide the MWD of each fraction. The relative area of the individual chromatograms reflects the compositional heterogeneity, while their retention time and shape relate to MW. However, the procedure must be optimized for the sample size. CFC was found desirable for analyzing blends of m- LLDPE having different densities and MW. The full CCD $\times$ MWD was determined in 12 h by elution 24 TREF fractions into the SEC columns. The bivariate distribution (intensity vs. MW and T) may be displayed in a 3D plot.

18.4.2.4 LCB Index (LCBI) and Slice LCB Index (SLCBI)

The LCB indices provide a measure of LCB as a function of a fraction (slice) of the MWD. Two indices are involved, an average LCB index (LCBI = $\langle g ' \rangle_{avg}$) of the entire sample and the slice LCB index (SLCBI = g'_i); these are defined in Eq. 18.1:

$$\frac{\langle g' \rangle_{\mathrm{avg}} = \sum_{i=1}^{n} C_i [\eta_i]}{\sum_{i=1}^{n} C_i [kM_i^a]} = \frac{\sum_{i=1}^{n} C_i [\eta_i]}{kM_v^a \sum_{i=1}^{n} C_i}$$

$$g'_i = \frac{[\eta]_i}{kM_v^a}$$

$$(21.1)$$

Here the index "i" refers to a retention volume slice, C_i is the polymer concentration measured by SEC for the slice i, M_i is MW determined by light-scattering analysis at retention volume slice i, and $[\eta_i]$ is the intrinsic viscosity determined by viscometry of slice i. The constants k and a are the Mark–Houwink coefficients for a linear polymer of the same chemical composition; M_v is the viscosity-average MW (Lue and Kwalk 2005).

The portion of a composition having a particular MW range and a particular SLCBI may be expressed in terms of wt% calculated from the SEC measurements. Its value should be 100 wt% at zero retention volume and zero after the polymer composition has fully eluted. For various applications, the SLCBI should be determined for a specific MW, e.g., $M_w = 100$ or 300 kg mol^{-1}. An example of the SLCBI plot is presented in Fig. 18.9. Here PE-1 represents the most common behavior. Its blends with PE-2 are expected to be advantageous with good transparency and mechanical performance resulting from strong interactions between phases.

18.4.2.5 Summary and Conclusions for POs

From the chemical point of view, POs are simple materials composed of C and H. However, the configuration diversity of even the simplest polymethylene results in a spectrum of properties. The situation becomes more complex for polymers of the general formula $(C_nH_{2n})_{DP}$ where $n \geq 3$ and the degree of polymerization, DP, is large. The next level of complexity is encountered with blends and copolymers, e.g., poly(ethylene-*co-n*-olefin) or poly(propylene-*co-n*-olefin). However, today the ultimate challenge for characterization is found in POs obtained during multi-catalyst/multi-reactor/multi-monomer polymerization processes.

Fortunately, as the complexity of macromolecules increases, the precision and sophistication of instruments designed for their characterization improve. The analytical and preparative fractionating columns of GPC used in the 1950s are transformed into automatic multicolumn, multi-detector, high-temperature SEC. Similar advance is observed for TREF and CRYSTAF, now fused into CFC. At the same time, new methods are being developed for faster and more precise characterization by means of the multi-detector liquid chromatography, HTLC or HPLC.

Fig. 18.9 Slice long-chain branching index (SLCBI) as a function of a slice MW determined by SEC for two polymers in a favorable blend (Lue and Kwalk 2005)
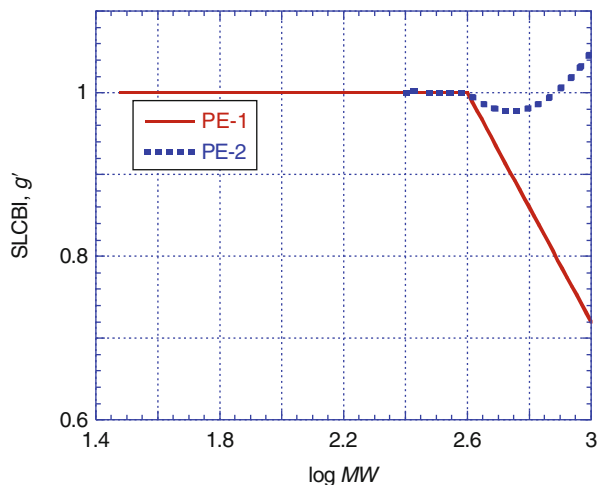
Various mathematical models have been proposed for TREF and CRYSTAF, but none predicts crystallization and co-crystallization effects during the fractionation with sufficient precision. Thus, for the accurate determination of semicrystalline copolymer microstructure, one should use the two optimized complementary methods: TREF and CRYSTAF.

18.5 Polyethylene Blends

PE mixtures constitute an important part of commercial blends. The information in Appendix, Table 18.12, suggests five major steps in the production of commercial PE, which result in different types of PE, commercially available at present, viz., **1935** – LDPE with LCB; **1950** – LLDPE or HDPE catalyzed by, e.g., Cr_2O_3, NiO, Mo_2O_3, or CoO; **1953** – the Ziegler–Natta (Z-N) catalysis for HDPE, UHMWPE, and LLDPE with a broad MWD and heterogeneous comonomer placement; **1975** – the metallocene catalysis producing narrow MWD and homogeneously distributed SCB; and **1997** – post-metallocene catalysis that leads to PE copolymers with adjustable MW and MWD as well as copolymerization of olefins with polar monomers and macromers.

As a consequence, before 1953, the only possible blends were those of LDPE with other polymers than PO or with elastomers (e.g., chlorosulfonated polyethylene rubber, CSR; chlorinated butyl rubber, CBR; ethylene/propylene/diene copolymers, EPR, EPDM; thermoplastic olefinic elastomer TPE, TPO). However, in addition to the original autoclave polymerization, already in 1938, a tubular reactor was introduced and its product had different properties than that from the autoclave. Also varying the reaction condition affected the degree of short- and long-chain branching in LDPE; thus, blending different LDPEs offered a way for optimizing the resin to specific applications.

The first LDPE/HDPE blends were patented by du Pont de Nemours before Z-N polymers became available (Roedel 1961). The blend comprised an experimental HDPE ($\rho = 0.939$–1.096 g mL^{-1}; $T_m \approx 120$ °C) obtained by polymerizing C_2 in its own medium at $T \approx 0$ °C and $P \approx 31$ MPa, using, e.g., a hydroxy-cyclohexyl-L-hydroperoxide catalyzed by ferrous chloride tetrahydrate. The blend showed 50 % moisture permeability of that by LDPE. In 1958 Phillips Petroleum patented PE/PE blends, either cross-linked in electron accelerator or not (Canterino and Martinovich 1963; Nelson 1964). Mitsubishi disclosed PO blends comprising vinyl–trimethoxysilane-grafted polyolefin (PP, LDPE, EPR, or EVAc) and ethylene–acryloyloxy tetramethylpiperidine copolymer. These water-cross-linkable resins were used for the manufacture of weather-resistant cross-linked PO pipes in outdoor applications (Ohnishi and Fukuda 1993). Thermally reversible cross-links (based on ionic interaction between maleated- and glycidyl methacrylate-grafted polyolefins) were also proposed (Okada 1994; Okada and Masuyama 1994).

Starting in the early 1950s, development of LDPE with LLDPE was the principal aim of the Z-N period for the film-blowing applications. It was patented by all major PE manufacturers, viz., du Pont de Nemours and DuPont of Canada Ltd., Phillips Petroleum, Celanese, and Esso. Some blends were cross-linked chemically or in electron beam. Incorporation of as little as 5 wt% of LDPE significantly improved the strain-hardening behavior of LLDPE, thus greatly improving process ability and performance (e.g., the heat sealability, puncture resistance, tensile and optical properties). However, in some cases for >35 % LLDPE in LDPE modification of film-blowing line was needed. Blends of broad MWD LLDPE/LLDPE also were advantageous (Utracki 1998).

During this initial period, blending was dominated by mechanical compounding involving:

- Preparation of ingredients (drying, sizing, heating, etc.)
- Premixing (dry blending, homogenization, breakage of agglomerates, fluxing, etc.)
- Melt mixing (usually with degassing)
- Forming, e.g., granulation, pelletization, or dicing

Mixing is the oldest process developed for rubbers by Hancock in 1820. The development of several types of mixers (including sigma blade internal mixers and twin-screw extruders, TSEs) may be traced to it. The single-screw extruder (SSE), inherited by the plastics industry from macaroni manufacturers in 1892, is good for continuous squeezing out a material, but not for mixing it. In 1939 Leistritz built an electrically heated, air-cooled SSE, having L/D = 10, automatic temperature control, variable screw speed, and nitride barrel, which underwent a rapid growth in L/D as well as modifications to improve its homogenization capability. Several types of mixing screws, mixing elements, and "add-ons" have been developed. The complex nature of the process was slowly unraveled, leading to educated attempts in maximalization of the elongational flow, as well as balancing the dispersive and distributive mixing in linear or chaotic flows. Many of these devices were developed in parallel with the evolution of TSE that ended by the late 1950s (Utracki and Shi Gerard 2002).

However, already by mid-1950s advantages of reactor mixing started to be explored. Hoechst patented a slurry cascade process for the polymerization of HDPE in a CSTR, capable of using different reaction conditions and/or monomer composition. The tubular, loop, or FBR also offered such possibilities – these became fashionable before the 1960s. An advantage of reactor blending was the countless possibilities of compatibilization and adjustment of the blend performance characteristics for large-scale applications. On the negative side was the loss of opportunities for smaller compounders and manufacturers for fine tuning the blend performance for specific applications.

The compounding technology of PE blends has been expanded by the need for the addition of fillers, reinforcements, and nanoparticles, the latter treated as inorganic macromolecules that require compatibilization and dispersion. The reactive compatibilization in a TSE developed by the end of the 1980s revitalizing the academic and industrial interest in the mechanical compounding of blends.

18.6   Essentials of Polymer Blending

The essentials or the fundamental knowledge that offers understanding why the blends behave as they do is being discussed in several chapters of this book, namely, ▶ Chap. 2, "Thermodynamics of Polymer Blends"; ▶ Chaps. 3, "Crystallization, Micro- and Nano-structure, and Melting Behavior of Polymer Blends" and ▶ 8, "Morphology of Polymer Blends"; ▶ Chap. 4, "Interphase and Compatibilization by Addition of a Compatibilizer"; ▶ Chap. 5, "Reactive Compatibilization"; ▶ Chap. 7, "Rheology of Polymer Alloys and Blends"; ▶ Chap. 9, "Compounding Polymer Blends"; ▶ Chaps. 13, "Physical Aging of Polymer Blends" and ▶ 14, "Degradation, Stabilization, and Flammability of Polymer Blends"; and ▶ Chap. 21, "Recycling Polymer Blends". The aim of writing the following pages is to focus on what is unique and essential for the PE/PE blends, referring to the broader perspectives presented in these chapters. The unique aspects of the PO blends are the great range of molecular configurations combined with small entropy and enthalpy of mixing, which taken together made prediction of blend performance particularly difficult.

18.6.1 Miscibility of Polyethylene Blends

18.6.1.1 Introductory Notes
Several methods have been used for detecting PE_1/PE_2 phase behaviors, i.e.:
- *Nondirect*, e.g., DSC, XRD, light scattering (LS), atomic force microscopy (AFM), electron and optical microscopy, and rheology
- *Direct*, for example, SANS, small-angle light scattering (SALS), or nuclear reaction analysis such as direct excitation exchange NMR (Akpalu and Peng 2008; Wachowicz et al. 2009)

As discussed in ► Chap. 2, "Thermodynamics of Polymer Blends" of this handbook, miscibility of polymer blends is usually presented as an isobaric phase diagram with the lower or upper critical solution temperature, T_c = LCST or UCST (see Fig. 2.15). Most PE/PE blends show UCST, while LCST occurs more frequently in other blends. There is a significant difference in the rate of phase separation and the generated morphology when a single-phase blend is "quenched" into either the metastable or spinodal regions. The phase separation within the metastable region occurs via nucleation and growth (NG) resembling crystallization – NG leads to polydispersed drop sizes. Since phase separation within the spinodal region follows the spinodal decomposition mechanism (SD), these blends may not need compatibilization. Furthermore, the SD blends most efficiently combine the advantageous properties of both polymers, for example, high modulus of one component with high elongation at break of another.

For proper understanding of the immiscible blends, it is important to take into account the interphase. In binary blends, the interphase thickness is inversely proportional to the interfacial tension coefficient, v_{12}; thus, the poorer the miscibility, the larger the interfacial tension coefficient and the smaller the interphase thickness, Δl. The latter variable ranges from $\Delta l \approx$ 2–65 nm, the former for uncompatibilized, highly immiscible systems, and the latter for reactively compatibilized polymer alloys. Owing to the thermodynamic forces, the polymeric chain ends and the low-molecular-weight components concentrate within the interphase. Thus, in binary blends this third region is characterized by low entanglement density, low viscosity, and poor interphasial adhesion. These drawbacks must be alleviated by compatibilization.

Miscible polymer blend is defined as a polymer mixture homogeneous down to the molecular level, in which the domain size is comparable to macromolecular dimension, associated with the negative value of the Gibbs free energy and heat of mixing, $\Delta G_m \approx \Delta H_m \leq 0$, and positive second derivative: $\partial^2 \Delta G_m / \partial \phi^2 > 0$. One may also ask at what dispersed drop size, d_d, the blend may be declared thermodynamically miscible; the answer based on NMR seems to be $d_d \leq 2$ nm (Utracki 2002). Often a small configurational difference leads to immiscibility, e.g., LLDPE prepared with Ti-based catalyst is immiscible with another one based on V catalyst. Even more strangely, a single LLDPE produced with multisided Z-N catalyst may show phase separation of fractions produced at different catalytic sites.

While miscibility of the low-MW substances is driven by entropy, in polymer blends it is the enthalpy that dominates the phase behavior. In PE/PE blends the absence of the specific interactions and small entropic effects lead to precarious miscibility. In any PO blend including PE_1 and PE_2, a mixture is composed mostly of –CH_2– groups with few –CH_3 end groups. Evidently, the intermolecular interactions between them are weak and immiscibility dominates the behavior. The PE_1/PE_2 blends with different type chain structure are usually immiscible. The immiscibility is not limited to the resins with different comonomers. For example, two LLDPEs, both being C_{2+6} copolymers polymerized using Z-N-type catalyst, but one

based on Ti, the other on V, are immiscible (Utracki and Schlund 1987b, d; Schlund and Utracki 1987c, e). By contrast, some LLDPEs, especially those containing a small amount of C_4 comonomer, show limited miscibility with the linear HDPE.

The PE immiscibility refers to the molten as well as to the solid state. Note that the small changes in molecular structure lead to difference in T_m, what affects a sequence of crystallizations of different blend components. Thus, in most cases the spherulites of one PE (having higher T_m) are encapsulated by those of the other PE. Co-crystallization of two PEs into single-type isomorphic cells rarely has been observed (Utracki 1989a, 1991).

18.6.1.2 Mean-Field Approach

During the years 1992–1998, numerous publications emerged from Prof. Graessley's laboratory. The model PEs with different structures (see Fig. 18.10) were commercial (e.g., HDPE or PP) or from laboratory (e.g., hydrogenation/deuteration of diolefins, anionic reaction for PIB, Z-N catalysis using a V-based catalyst in C_6 for poly (ethylene-*co*-α-olefin) or later a metallocene catalyst. The thermodynamic properties of numerous PO blends were extracted from the pressure–volume–temperature (PVT) data (Walsh et al. 1992; Krishnamoorti et al. 1996) or from SANS results (Krishnamoorti et al. 1994, 1995; Graessley et al. 1994, 1995; Reichart et al. 1997; Alamo et al. 1997).

Several mean-field theories have been developed for predicting liquid/liquid thermodynamic behavior (Huggins 1941; Flory 1941; Simha and Somcynsky (S-S) 1969; Koningsveld 1985; Koningsveld and Kleintjens 1985; Koningsveld et al. 1987; Dee and Walsh (D-W) 1988). These theories were found useful in explaining some basic behavior of solutions and blends, e.g., decreasing miscibility with increasing MW, as well as they identified the driving force for miscibility in a given system For example, S-S and D-W equations of state (eos) were fitted to the *PVT* data of blends (Walsh et al. 1992; Park et al. 1999; Utracki and Simha 2001; Moulinié and Utracki 2010).

Assuming the validity of the corresponding states principle, the eos is expressed in reduced variable form, where the reducing parameters, $P*$, $T*$, and $V*$, depend on the two Lennard–Jones potential parameters: $\varepsilon*$ and $v*$:

$$\left. \begin{array}{l} \widetilde{P} = P/P* \rightarrow \quad P* = zq\varepsilon*/(sv*) \\ \widetilde{T} = T/T* \rightarrow \quad T* = zq\varepsilon*/(Rc) \\ \widetilde{V} = V/V* \rightarrow \quad V* = v*/M_s \end{array} \right\} \quad (P*V*/T*)M_s = Rc/s \qquad (18.2)$$

Here $\varepsilon*$ and $v*$ are measures of the maximum attraction energy and the segmental repulsion volume, respectively, $qz = s(z - 2) + 2$, $v*$ a specific volume for a molar segmental mass M_s, $R = 8.314462$ [JK^{-1} mol^{-1}] is the universal gas constant, and $z = 12$ is the lattice coordination number. The data analyzed by Walsh et al. (1992) were based on the mixtures of commercial HDPE, PP, and EPR copolymers containing
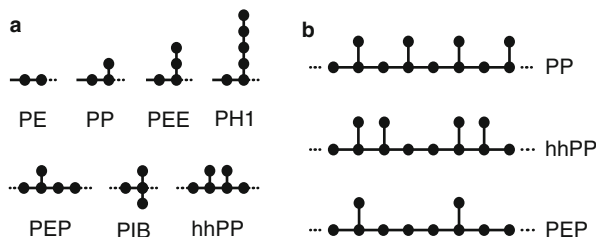
Fig. 18.10 (**a**) United atom group models for monomers of PE, PP, poly(ethyl ethylene) (PEE), poly(hexene-1) (PH1), poly(ethylene propylene) (PEP), PIB, and head-to-head PP (hhPP). *Circles* designate CH_n groups, *solid lines* represent C–C bonds inside the monomer, and *dotted lines* indicate the C–C bonds linking the monomer to its neighbors along the chain. (**b**) United atom models of iPP, hhPP, and PEP homopolymer chains constructed by linking monomers of (**a**) (Freed and Dudowicz 2005)

16, 24, 43, and 77 wt% C_2, etc. Miscibility and shape of the phase separation curves, i.e., LCST or UCST, were estimated from the magnitude of P^* and T^*.

Besides eos, the statistical thermodynamic theories also predict variations of the reduced cohesive energy density, $\widetilde{CED}$; solubility parameter, δ; and the internal pressure, $\widetilde{p}_i$:

$$\widetilde{CED} = \widetilde{U}/\widetilde{V} = \left(y/2\widetilde{V}\right)\left[AQ^4 - 2BQ^2\right] \Rightarrow \delta = \sqrt{CED}$$

$$= \sqrt{\widetilde{CED}} \times P^* \left(\partial \widetilde{U}/\partial \widetilde{V}\right)_{\widetilde{T}} = \widetilde{p}_i$$

$$= -\frac{1}{2}\left[3AQ^4 - 2BQ^2\right]\left(\partial y/\partial \widetilde{V}\right) + \left(2y/\widetilde{T}\right)\left[AQ^4 - BQ^2\right] \qquad (18.3)$$

Here, U is the internal energy of the system, y is the occupied volume fraction, and $A = 1.011$ and $B = 1.2045$ are the cell constants. The dependencies originally written for a single-component liquid are readily extended to binary systems (Moulinié and Utracki 2010):

$$\langle P^* \rangle = qz\langle \varepsilon^* \rangle/(\langle s \rangle \langle v^* \rangle); \quad \langle T^* \rangle = qz\langle \varepsilon^* \rangle/R\langle c \rangle; \quad \langle V^* \rangle = \langle v^* \rangle/\langle M_o \rangle$$

$$\langle P^* \rangle \langle V^* \rangle/R\langle T^* \rangle = (\langle c \rangle/\langle s \rangle)(1/\langle M_o \rangle)$$

$$\langle c \rangle = \sum_i c_i x_i; \quad \langle s \rangle = \sum_i s_i x_i; \quad \langle M_o \rangle = \sum_i M_{si} s_i x_i / \sum_i s_i x_i \qquad (18.4)$$

$$\langle \varepsilon^* \rangle \langle v^* \rangle^m = \sum_{i,k} X_i X_k \varepsilon_{i,k}^* \left(v_{i,k}^*\right)^m; \quad m = 2,4$$

where the two values of m reflect the volumetric Lennard–Jones (L-J) 6–12 potential. From Eqs. 18.1 and 18.3 the pairs of L-J parameters were computed for HDPE, PP, and EPR with variable C_2 content (data Walsh et al. 1992). Simplified molecular configuration of these macromolecules is presented in Fig. 18.11.

Fig. 18.11 The L-J potential parameters, ε^* and v^*, versus ethylene content (Data Walsh et al. 1992). Since in miscible systems they are proportional to each other, the lack of proportionality at high C_2 content may indicate phase separation
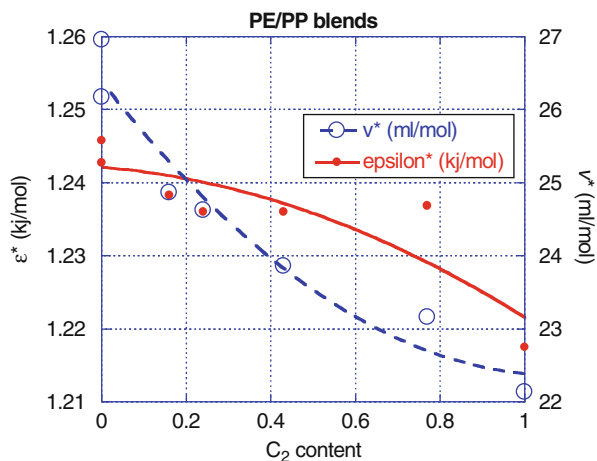
Fig. 18.12 The H-F binary interaction parameter, χ, for head-to-head blend with PIB as functions of temperatures (*solid circles* are for 1/T(K), open for T °C) (Data Krishnamoorti et al. 1996). The parameters calculated from SANS results
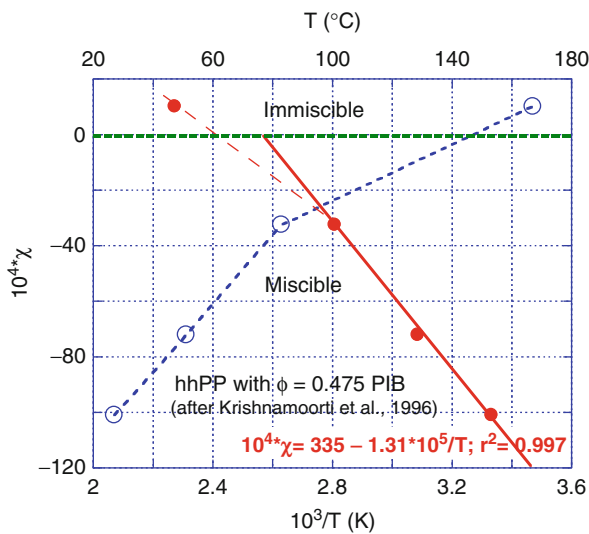
The calculation results are presented as ε^* and v^* versus ethylene content, C_2 in Fig. 18.12. It has been observed that for single-phase liquids, single component, solution, or miscible blend, the L-J potential parameters are linearly related, e.g., for molten polystyrenes (PS) the following dependence was found (Utracki 2005):

$$\varepsilon* = a_0 + a_1 v*; \quad a_0 = 13.44; \quad a_1 = 0.455; \quad r = 0.952 \qquad (18.5)$$

The data in Fig. 18.11 show an anomaly – there is a common trend for neat polymers and blends containing up to about 25 wt% of C_2, but due to phase separation, at higher C_2 content, the trend is not followed.

For SANS measurements of thermodynamic interactions in binary PO blends, one component should be deuterated. This was done starting with partially unsaturated samples and catalytically hydrogenating or deuterating them in solution. The specimens were prepared by solution blending of one hydrogenated and one deuterated polymer such as polybutylene (PB), thus HPB and DPB, respectively. The measurements were performed at $T = 27$–$167\ ^{\circ}C$ (one-phase region) (Balsara et al. 1992). In these experiments not only molecular configuration, but also non-negligible isotope effect had to be taken into effect. The data were interpreted using the Huggins–Flory (H-F) incompressible random phase approximation into ΔG_m for binary liquids (Krishnamoorti et al. 1994a, b, 1995; Graessley et al. 1994, 1995; Alamo et al. 1997):

$$\Delta G_m/RT = \phi_i \ln \phi_i/V_i + \phi_j \ln \phi_j/V_j + X_{ij}(T)\phi_i\phi_j$$
$$\chi_{ij}(T) = v_o X_{ij}(T)/RT \cong v_o(\delta_1 - \delta_2)^2/RT \tag{18.6}$$

where δ_i and δ_j are volume fractions and V_i and V_j are the volumes per monomeric unit. The interaction energy density X_{ij} is proportional to the H-F binary interaction parameter, χ_{ij}, and an arbitrary reference volume, v_o, which for blends was calculated following the square-average Berthelot rule:

$$v_o = \left(v_{oi}v_{oj}\right)^{1/2}$$

An example of calculations is shown in Fig. 18.12 as the Huggins–Flory binary interaction parameter, χ versus temperature (SANS data from Krishnamoorti et al. 1996). The extrapolated Arrhenius dependence suggests that the system is miscible up to about $118\ ^{\circ}C$.

The H-F Eq. 18.6 has two parts: the ϕ-dependent configurational entropy derived from the lattice model without free volume and the enthalpic part taken from the Hildebrand's theory of regular solutions (Shinoda 1978; Reichart et al. 1997; Maranas et al. 1998). More recent version of Eq. 18.6 was used for the interpretation of SANS data, and it will be discussed in reference to the lattice cluster theory (LCT) (Freed and Dudowicz 2005).

For a series of polyethylene–hexene (PEH $= C_{2+6}$) and polyethylene–butene (PEB $= C_{2+4}$) blends, Krishnamoorti et al. (1994b) proposed a four-parameter empirical expression:

$$\chi_{12}(\phi,T) = \beta_{12}(T) + \gamma_{12}(T)/\phi_1\phi_2$$
$$\beta_{12}(T) = A_\beta/T + B_\beta; \quad \gamma_{12}(T) = A_\gamma/T + B_\gamma \tag{18.7}$$

Accordingly, plotting $\chi_{12}(\phi, T)\phi_1\phi_2$ versus $\phi_1\phi_2$ should linearize the dependence. Plot of β_{12} and γ_{12} parameters versus $1/T$ should also be linear; the parameters are positive, indicating UCST-type phase separation. Having the numerical values of d_i for individual PO structure elements, in principle, the miscibility of two polymers could be predicted from their difference: $(\delta - \delta)^2$. A similar linear increase of $\chi_{12}(\phi, T)$ with decrease of T was reported for most PO blends, although
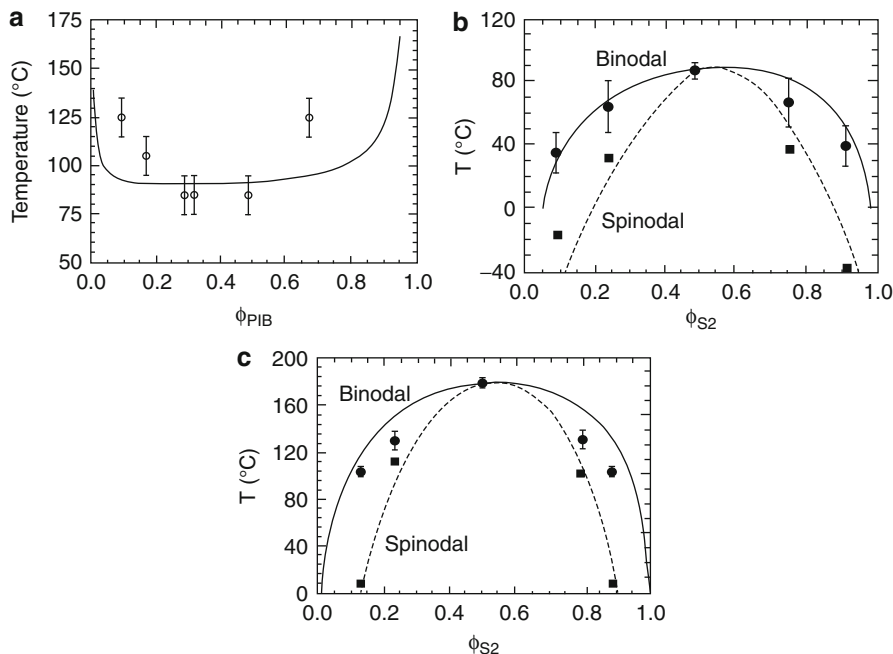
Fig. 18.13 (**a**) Phase diagram for PIB/H66B blends based on a quenching-calorimetry procedure. The LCST spinodal curve was calculated using X(T) for PIB/D66A blends (Krishnamoorti et al. 1995). (**b**) Calculated and experimental UCST binodal and spinodal for *H66/D52*. The calculations were based on SANS data in the single-phase region (Krishnamoorti et al. 1994). (**c**) Calculated and experimental UCST binodal and spinodal for *H52/D*66. The calculated and experiment results were obtained as in Fig. 18.11b (Krishnamoorti et al. 1994)

in some cases LCST type or only a part of phase separation curve was observed (Krishnamoorti et al. 1994b, 1995; Graessley et al. 1994, 1995; Alamo et al. 1997). Examples are displayed in Fig. 21.13.

The PE–PE interactions originate in induced dipole moment, which makes them highly sensitive to configurational changes. For example, they show strong deviation from the behavior predicted by the copolymer theory. Empirically the immiscibility was found related to the comonomer content and the difference in the branch length, the latter well correlating with δ. PE blends are homogeneous when the branch content is low, but they phase separate when there are ≥ 8 branches/100 backbone carbons. For sufficiently high MW, phase segregation may also be caused by the H^1/D^2 isotope effects. However, several blend types showed behavior inconsistent with this explanation (Graessley et al. 1995).

Reichart et al. (1998) studied blends of metallocene statistical copolymers of C_2 with a range of propylene, 1-butene, 1-hexene, or 1-octene content, i.e., C_{2+3}, C_{2+4}, C_{2+6}, and C_{2+8} ($M_w/M_n \approx 2$). As expected, the new data scattered less than those for the Z-N copolymers, confirming the validity of the earlier observations. Thus, the interaction parameters obeyed Hildebrand's assumption as being controlled by

Fig. 18.14 Isothermal, relative solubility parameters of C_{2+3}, C_{2+4}, C_{2+6}, and C_{2+8} versus comonomer content at $T = 118\ °C$, $142\ °C$, $167\ °C$, and $196\ °C$. The effect of deuteration was removed. The data are displaced vertically from those at $118\ °C$ by 0.3, 0.6, and 0.9 (Data: Reichart et al. 1998)
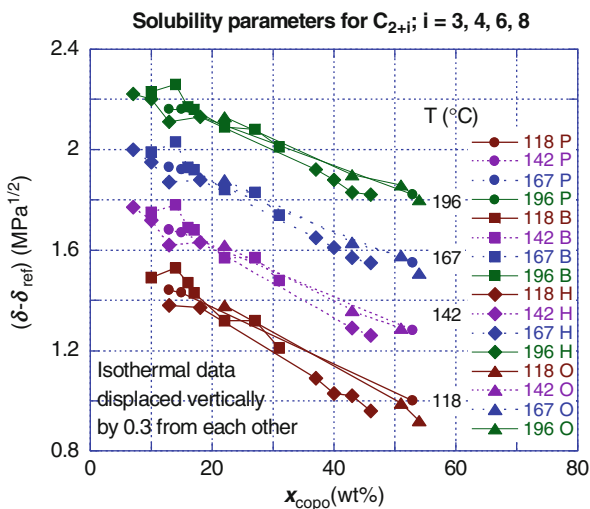
Table 18.4 Solubility parameter $(\delta - \delta_{ref})^{1/2} = A–B\ x$ (Reichart et al. 1998)

T (°C)	A	B	r_2
118	1.634	0.0134	0.948
142	1.553	0.0117	0.949
167	1.485	0.0108	0.952
196	1.409	0.0097	0.945

the enthalpy, viz., the solubility formalism. As shown in Fig. 18.14, the isothermal values of $(\delta - \delta_{ref})^{1/2}$ linearly depend on x, the α-olefin comonomer content and T, thus are independent of SCB. The parameter δ_{ref} takes into account the two reference states for the hydrogenated and deuterated polymers (Table 18.4).

Furthermore, the illustrated dependence is the same as found earlier for model copolymers with different SCBD, indicating that variations in comonomer distribution have little effect on solubility.

The data displayed in Fig. 18.14 indicate that the interaction strength parameter, X, decreases as T increases. Rabeony et al. (1998) observed that the intermolecular interactions are only a function of density for UCST blends far from a critical point, i.e., the free volume: $X(P, T) = X(\rho)$. Within the range $T = 60–200\ °C$ and $P \leq 200\ MPa$, a good superposition of data on a single curve was obtained for the UCST blends and poorer ones for LCST. Increasing density increased X in UCST and decreased it in LCST, thus making the blend less miscible in the first and more soluble in the second case. The effects of T and P on miscibility may be predicted from the free volume changes. For LCST blends, the density-predicted trends are correct, but here the interactions depend on T and P in a more complex way.

The older mean-field theories are often based on the lattice model of ill-defined a priori size and shape, neglecting variability of monomer structures in PO copolymers and blends. Several newer approaches have been proposed, viz., the polymer reference interaction site model (PRISM) (Schweizer and Curro 1989, 1997), the Monte Carlo (MC) simulations (Sariban and Binder 1987; Müller and Binder 1995; Weinhold et al. 1995; Escobedo and de Pablo 1999), the continuum field theory (CFT) (Fredrickson et al. 1994), or an analytical lattice models (Dudowicz and Freed 1991). The latter model leads to relatively simple mathematical expressions, which offer an insight into basic thermodynamics, but again do not predict how monomer structure affects blend miscibility.

Chen et al. (2000, 2002) studied phase behavior of binary blends of linear and branched poly(ethyl-ethylene), PEE. The branched PEE_{br} had 54 arms ($M_A = 13.7$ kg mol^{-1}) attached randomly to a saturated hydrocarbon backbone ($M_B = 10$ kg mol^{-1}). Blends of this compound with two linear PEE_{lin} ($M_L = 60$ and 220 kg mol^{-1}) were investigated by SANS. Blends containing high-MW linear polymer phase separated, whereas the ones with lower MW were miscible at all concentrations. The first publication provided experimental details and compared the LCST phase diagram with theory (Fredrickson et al. 1994; Fredrickson and Liu 1995). The theory assumed Gaussian statistics and did not account for a disparity between the statistical segment lengths of linear and branched polymers. Thus, for correct prediction of the phase diagram, two average statistical segment lengths had to be assumed: 0.57 and 0.76 nm for the linear and branched polymer, respectively.

The second publication examined miscibility of two series of poly(ethylene-*r*-ethyl-ethylene), PEE *xx* polymers with different percentages (*xx*) of ethyl–ethylene (EE) repeat units.

- *The first series* consisted of comb/linear blends in which the first component was a heavily branched comb polymer (B90) containing 90 % EE and an average of 62 long branches with $M_w = 5.5$ kg mol^{-1} attached to a backbone with $M_w = 10.0$ kg mol^{-1}. The comb polymer was blended with six linear PEExx copolymers, all of which had $M_w = 60$ kg mol^{-1} and EE content ranging from 55 % to 90 % (coded L55–L90).
- The second series consisted of linear/linear blends; the first component, with $M_w = 220$ kg mol^{-1} and 90 % EE, coded L90A, and the second components were the same as in the first series of linear polymers ($M_w = 60$ kg mol^{-1} and L55–L90). The investigated concentration was 50 wt%, except for the blend of branched B90 and linear L90 (both components had 90 % EE), for which 25/75 and 75/25 concentrations were also examined.

The blends of linear PEE90 ($M_w = 220$ kg mol^{-1}, 50 wt%) formed single phase with linear $M_w = 60$ kg mol^{-1} PEE83 and PEE78 but phase separated from PEE73, PEE68, and PEE55. However, a PEE90 comb polymer ($M_w = 350$ kg mol^{-1}) was miscible with linear PEE90 but phase separated in all blends with linear PEE_{xx} random copolymers. The results showed that phase behavior in PO blends depends on (1) differences in SCB, which produce enthalpic contributions, and (2) LCB contributing

excess entropy of mixing. Both effects increase the interaction parameter; thus, each one may induce phase separation between linear and branched PO. Furthermore, the LCB significantly narrows the miscibility window of the studied blends. The results were interpreted using CFT (Fredrickson et al. 1994; Fredrickson and Liu 1995) as the only theory directly predicting the LCB effects on PO blend miscibility. The field theory was developed from the random phase approximation (RPA) and H-F theories that focus on the importance of the excess entropy arising from long-range effects.

18.6.1.3 Effects of Molecular Structures

Freed et al. developed the lattice cluster theory (LCT) specifically to account for diversity of segmental structures, affecting blend miscibility, viz., the critical point $[T_c, \phi_c]$, chain swelling $[T_\Theta]$, as well as the scale and intensity of composition fluctuations (Freed and Bawendi 1989; Foreman and Freed 1997; Freed and Dudowicz 1998, 2005; Dudowicz et al. 2002). As an example, several monomeric and polymeric structures are shown in Fig. 18.15, and LCT predictions of the phase behavior the authors are discussed in details.

The simplified LCT (SLCT) expresses the free energy of mixing, ΔF^{mix}, of a high-MW binary homopolymer blend at incompressible limit, as (Freed and Dudowicz 1998)

$$\frac{\Delta F^{\text{mix}}}{N_1 kT} = \frac{\phi}{M_1}\ln\phi + \frac{1-\phi}{M_2}\ln(1-\phi) + \phi(1-\phi)\{\Delta\}$$

$$\{\Delta\} \equiv \frac{(r_1 - r_2)^2}{z_2} + \frac{\varepsilon}{kT}\left\{\frac{z-2}{4} - [p_1(1-\phi) + p_2\phi]\right\}$$

$$-\phi(1-\phi)\left(\frac{\varepsilon}{kT}\right)^2\left[\frac{z+2}{4} + r_1(1-\phi) + r_2\phi\right] \quad r_\alpha = \frac{N_\alpha^{(2)}}{M_\alpha} = 1 + \frac{s_\alpha^{(tri)}}{s_\alpha} + 3\frac{s_\alpha^{(tetra)}}{s_\alpha}$$

$$\tag{18.8}$$

Here ϕ and N_1 are the volume fraction and number of united atom groups, z is the lattice coordination number, and $\varepsilon = \varepsilon_{11} + \varepsilon_{22} - 2\varepsilon_{12}$ is the blend exchange energy. The parameter N_α^i expresses the number of dissimilar sets of i sequential bonds in α-chain. The only coefficients in Eq. 18.8 (see Table 18.5) are the ratios of $r_\alpha = N_\alpha^{(2)}/M_\alpha$ and $p_\alpha = N_\alpha^{(3)}/M_\alpha$ where M_α is the number of united atom groups in polymer α, which may be represented in terms of the respective numbers $s_\alpha^{(tri)}$ and $s_\alpha^{(tetra)}$ of tri- and tetrafunctional united atom groups, a monomer of species α.

The first two terms on the right-hand side of Eq. 18.8 represent the H-F configurational entropy, while the noncombinatorial entropy contribution is given by $\phi(1-\phi)[(r_1 - r_2)/z]^2$; the latter originates from the local correlations associated with the packing of monomers with different sizes and shapes.

The theory is based on an extended lattice model where monomers have molecular structures illustrated in Fig. 18.15. Individual groups [CH_n; $n = 0$–3] occupy single lattice sites, and the bonds between united atom groups correspond to the
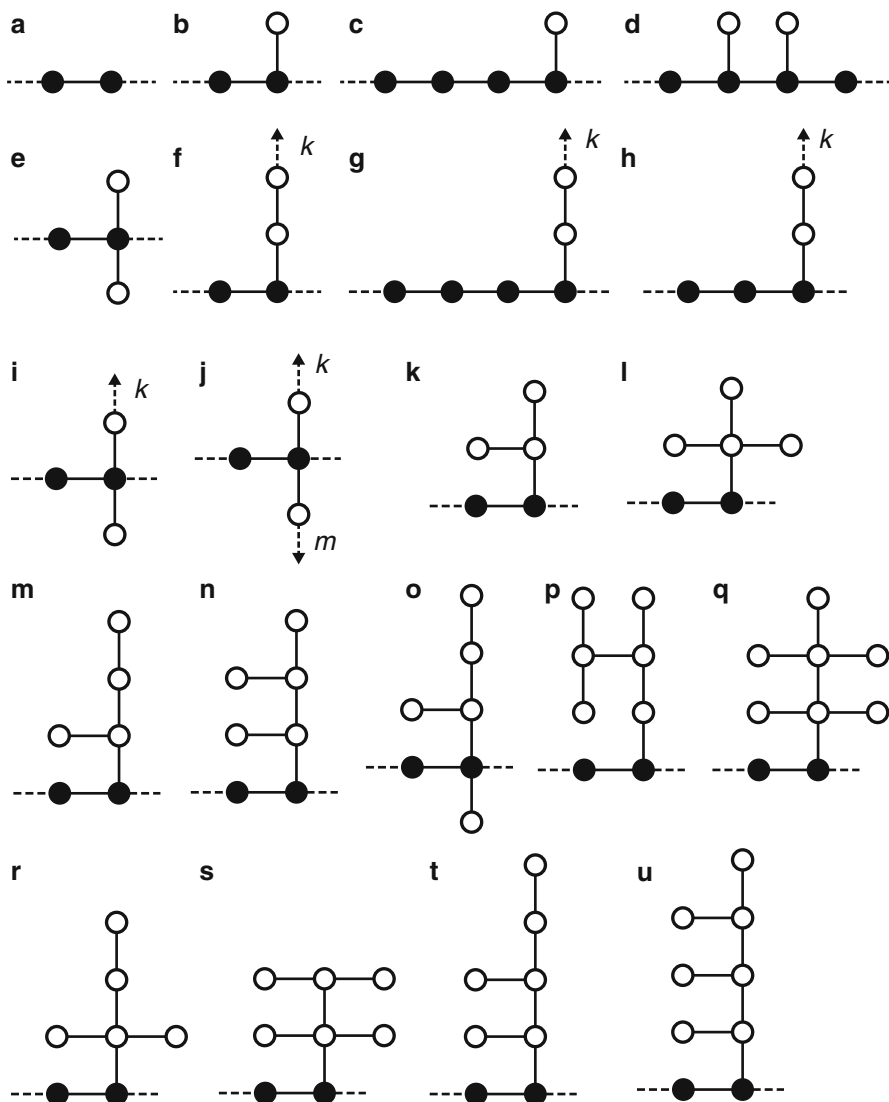
Fig. 18.15 Structural models of united atom monomers whose structural parameters r_α and p_α are listed in Table 21.5. *Filled circles* denote monomer portions lying on the chain backbone, while *open circles* represent those belonging to the side groups. *Dashed horizontal lines* designate the bonds to neighboring monomers, and vertical lines with *arrows* and *symbols k* (or *m*) indicate that a given monomer has *k* (or *m*) united atom side group connected units (Freed and Dudowicz 1998, 2005)

C–C bonds in the actual molecules. The LCT is an analytical molecular-based theory for the statistical thermodynamics of molten polymers, associated with recognizing the degree to which the distinct chemical structures of the individual monomers are relevant. LCT also incorporates free volume and uses the nonrandom

Table 18.5 Geometrical coefficients r r and p r for various polymers whose united atom monomer structure models are depicted in Fig. 18.12 (Freed and Dudowicz 1998)

Monomer structure in Fig. 18.12	r_α	p_α
a	2/2	2/2
b	4/3	4/3
c	6/5	6/5
d	4/3	9/6
e	7/4	6/4
f[a]	$(3 + k)/(2 + k)$	$(4 + k)/(2 + k)$
g[a]	$(5 + k)/(4 + k)$	$(6 + k)/(4 + k)$
h[a]	$(4 + k)/(3 + k)$	$(5 + k)/(3 + k)$
i[a]	$(6 + k)/(3 + k)$	$(7 + k)/(3 + k)$
j[b]	$(5 + k + m)/(2 + k + m)$	$(8 + k + m)/(2 + k + m)$
k	7/5	8/5
l	5/3	5/3
m	16/9	19/9
n	4/3	5/3
o	10/7	12/7
p	9/7	14/7
q	11/8	12/8
r	11/7	13/7
s	13/8	16/9
t	11/8	14/8
u	13/9	16/9

[a]Valid for $k \geq 2$
[b]Valid for $k \geq 2$ and $m \geq 2$

mixing principle. The theory went through several modification and simplifications, making it easy to use in comparison to MC or PRISM (Freed and Dudowicz 1996).

LCT has been applied to binary blends with variable SCB (Freed and Dudowicz 1996), predicting miscibility and interfacial properties of PO blends (Dudowicz and Freed 1996), to copolymers (Dudowicz and Freed 1997, 1998) and other systems. However, the most important is the discovery of four classes of critical behavior (Freed and Dudowicz 2005). The classification comes from data recalculated via SLCT binary interaction parameter, χ_{SANS}, calculated from the SANS data:

$$\chi_{SANS}/C = a + (b + c\phi)/T;$$
where
$$a = [(r_1 - r_2)/z]^2;$$
$$b = (\varepsilon/k)[(z - 2)/2 - (2p_1 - p_2)/z]; \qquad (18.9)$$
$$c = 3\varepsilon(p_1 - p_2)/kz$$

The classification is based on Eq. 18.9 parameters (a, b, c) presented in Table 18.6.

Table 18.6 Four classes of PO blends (After Dudowicz et al. 2002; Freed and Dudowicz 2005)

Parameters	Class I $a=0,$ $b>0$	Class II $a\neq 0,$ $b>0$	Class III $a\neq 0,$ $b<0, c=0$	Class IV $a\neq 0,$ $b<0, c\neq 0$
$\phi_c = \phi_c^{(1)}$	$\equiv \left(\frac{M_2}{M+M_2}\right)^{1/2}$	$\approx \phi_c$	$\phi_c^{(1)}$	$\sim M^{-1/2}$
T_c	$\sim M$	$\sim \frac{M}{1-2aMM_2\left(M^{1/2}+M_2^{1/2}\right)}$	$=\lvert b\rvert/a$	$=\lvert b\rvert/a$
ξ_o	$\sim M^{1/2}$	$\sim \left\{\frac{M}{1-2aMM_2\left(M^{1/2}+M_2^{1/2}\right)}\right\}^{1/2}$	Constant	$\sim M^{1/4}$
Gi	$\sim M^{-1}$	$\sim \frac{M^{-1}}{1-2aMM_2\left(M^{1/2}+M_2^{1/2}\right)}$	$\sim M^{-2}$	$\sim M^{-1/2}$
$\delta T_\theta^{(1)}$	$\sim \frac{M+2(MM_2)^{1/2}}{M_2}$	$\sim [1-2aM_2]^{-1}$	$\sim M^{-1}$	c/b
$\delta T_\theta^{(2)}$	$\sim 1+2(M_2/M)^{1/2}$	$\sim [1-2aM_2]^{-1}$	$\sim M^{-1}$	$\sim M^{-1/2}$
L or U CT	UCST	UCST	LCST	LCST
Examples	PPE/PEE; PP/PE; PE/PIB; PE/P2B; PE/PEP	PH1/PEP	PPE/PEP; PE/PEP	PIB/PEP

The critical point coordinates for LCST or UCST are (ϕ_c, T_c); ξ_o is the correlation length amplitude at ϕ_c; Gi is the Ginsburg number, which estimates the crossover from mean-field- to Ising-type behavior; $\delta T_\theta^{(i)} \equiv (T_\theta^{(i)} - T_c)/T_c$.

The phase diagrams of PO-type random copolymers may be more complex than those for homopolymers with different, but uniform, molecular structure. Thus, similar to SLCT, but simplified further, is the basic lattice cluster theory (BLCT). The version was developed for the random copolymers or random and block copolymer systems.

The preliminary work involved binary blends of ethylene/norbornene random copolymers studied by ^{13}C NMR spectroscopy. The miscibility was observed for norbornene content >50 % where the microstructure changes due to side group crowding. The SLCT computations indicate that the chain stiffness significantly affects miscibility – the entropic contribution to χ seems to be the controlling factor. Experimental miscibility diagrams agreed reasonably well with LCT predictions (Delfolie et al. 1999).

The BLCT is based on Flory–Huggins random copolymer theory with two significant improvements: (I) description of the polymer–polymer interactions in terms of the united atom groups and (II) addition of entropic contributions to the interaction parameter χ_{ij} (Dudowicz and Freed 1997, 2000b). The Helmholtz free energy of mixing in BLCT formalism is given by:

$$\frac{\Delta F^{\text{mix}}}{kT} = \frac{\phi}{M_1}\ln\phi + \frac{1-\phi}{M_2}\ln(1-\phi) + \phi^2\chi_{11} + (1-\phi)^2\,\chi_{22} + \phi(1-\phi)\chi_{12}$$
$$M_1 = n_A s_A + n_B s_B; \quad M_2 = n_C s_C + n_D s_D$$

$$(18.10)$$

With the interaction parameters

Fig. 18.16 Computed LCT phase boundaries for PPxPEE1-*x*/PEE blends (at $P = 0.1$ MPa) with the same polymerization indices $N_1 = N_2 = 320$ but different compositions x of the random copolymer. The *solid lines* indicate the spinodal for the PP/PEE system (Dudowicz and Freed 1997, 2000b)
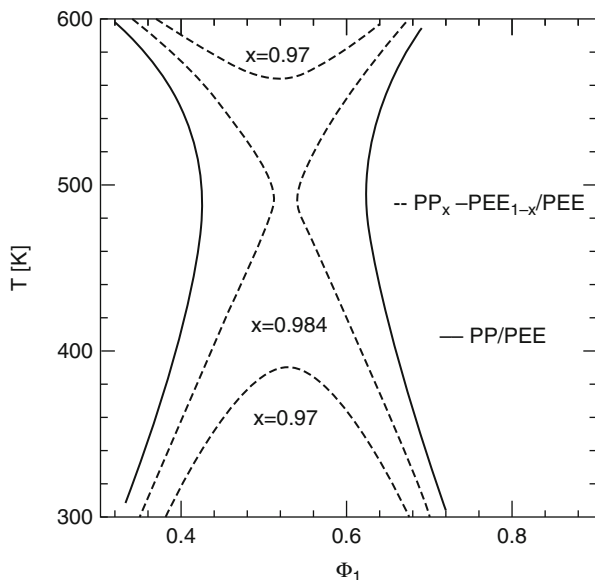
$$\chi_{11} = -\frac{z}{2}\left[\frac{\varepsilon_{AA}}{kT}m_A^2 + \frac{\varepsilon_{BB}}{kT}m_B^2 + 2\frac{\varepsilon_{AB}}{kT}m_A m_B\right] - \frac{r_1^2}{z^2}$$

$$\chi_{22} = -\frac{z}{2}\left[\frac{\varepsilon_{CC}}{kT}m_C^2 + \frac{\varepsilon_{DD}}{kT}m_D^2 + 2\frac{\varepsilon_{CD}}{kT}m_C m_D\right] - \frac{r_2^2}{z^2} \qquad (18.11)$$

$$\chi_{12} = -\frac{z}{2}\left[\frac{\varepsilon_{AC}}{kT}m_A m_C + \frac{\varepsilon_{AD}}{kT}m_A m_D + \frac{\varepsilon_{BC}}{kT}m_B m_C + \frac{\varepsilon_{BD}}{kT}m_B m_D\right] - \frac{2r_1 r_2}{z^2}$$

where ε_{ij}(i, j = A, B, C, D) are nearest-neighbor van der Waals attractive energies between groups of atoms. The effects of chain stiffness and side groups and steric interaction have been incorporated into the basic lattice cluster theory, BLCT. Defining s_i as the occupancy number, the compositional fractions may be expressed as

$$\frac{n_A s_A}{M_1} = m_A = 1 - m_B = \frac{x s_A}{x s_A + (1 - x)s_B}$$

$$\frac{n_C s_C}{M_2} = m_C = 1 - m_D = \frac{x s_C}{x s_C + (1 - x)s_D} \qquad (18.12)$$

An example of computed phase boundaries for homopolymer/copolymers is presented in Fig. 18.16.

18.6.1.4 Assessing Miscibility from the Flow Behavior

The PO_1/PO_2 blend miscibility depends on the degree of difference of their chain structures and concentration. As a rule, different PE types are immiscible with each other. However, since for controlling PO properties a small amount of

comonomer may be incorporated, without detailed information, it is impossible to predict if a given resin grade will be miscible with another PO or not. For example, for controlling crystallinity of HDPE, it usually contains a small amount of C_3 or C_4 comonomer. It was reported that some LLDPEs (containing a small amount of C_4) have limited miscibility with HDPE (Kotani et al. 1990; Taka et al. 1990).

Generally, it is difficult to judge if a PO blend is miscible or not. Because of small difference between the refractive indices (RI), the melt turbidity is often absent during or after the phase separation. When crystallized, co-crystals may form under specific set of the thermodynamic and kinetic conditions, e.g., co-crystallization is possible when the components are isomorphic or miscible in the amorphous and crystalline phase (Olabisi et al. 1979).

Two principles have been used for detecting miscibility by rheological means:
- Molecular polydispersity effect on a rheological function – assuming miscibility one may compute what effect incorporation of another polymer should have, compare with the experimental data, and draw conclusion. The following functions have been examined:
- Coordinates of the Gross frequency relaxation spectrum maximum (see below).
- Deviation from the log-additivity, $\log \eta_{blend} = \sum w_i \log \eta_i$, etc.
- Cross-point coordinates (G_x, w_x), where $G_x \equiv G' = G''$
- Free volume gradient of viscosity: $a_1 \equiv d \ln h/d(1/h)$
- Initial slope of the stress growth function: $m = 1/n$
- The power-law exponent, n, etc.
- Effect of the inherent nature of the two-phase flow
- Deformability of the dispersed phase leads to behavior not observed for single phase
- Extrudate swell parameter, $B = D/D_o$
- Strain (form) recovery, γ_r
- Yield stress, σ_y

Gross frequency relaxation spectrum, $H_G(\tau)$, leads to (Utracki and Schlund 1987)

$$\widetilde{H}_G \equiv H_G/\eta_o = (2/\pi)r^{-m_2} \sin(m_2\theta); \quad \text{but}: \int_{-\infty}^{\infty} \widetilde{H}_G d\ln\omega = 1 \qquad (18.13)$$

Here the two equation parameters, r and θ, are defined in terms of the Carreau–Yasuda equation (Carreau 1968, 1972; Yasuda 1979, 1981):

$$(\eta - \eta_\infty)/(\eta_o - \eta_\infty) = [1 + (\tau\dot{\gamma})^{m_1}]^{-m_2} \qquad (18.14)$$

Since the integral over the reduced Gross frequency spectrum equals zero-shear viscosity, η_o, the coordinates of the maximum, ω_{max}; $\widetilde{H}_{G,max}$, are related to MW

Fig. 18.17 The five types of
the viscosity/concentration
dependence in polymer blend
(Utracki 1991)
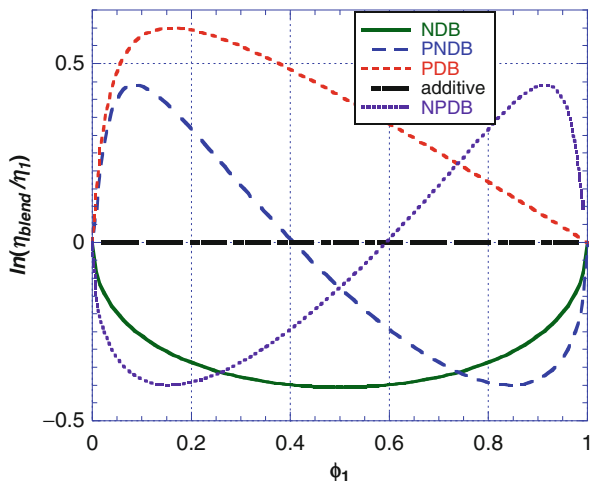
and MWD, respectively. In miscible blends, the general relation between the relaxation spectrum of a mixture and its composition follows the third order blending rule:

$$H_G(\tau) = \sum w_{ijk} H_{Gijk}(t/\tau_{ijk}) \quad \Rightarrow \quad H_G(\omega) = \sum w_i H_{Gi}(\omega) \qquad (18.15)$$

The second dependence is valid when all fractions are either entangled or not. Thus, $H_G(\tau)$ of a miscible blend is a linear combination of the component relaxation spectra and their weight fractions, w_i; *ergo* deviation from linearity in plots of log H_G versus M_w/M_n and log w_{max} versus log η_o indicates immiscibility.

Another approach to miscibility effect on flow is through analysis of the constant stress viscosity–concentration dependence. For solutions of small molecules, the log-additivity rule is most often found:

$$\log\eta_{blend} = \sum_i w_i \log\eta_i \qquad (18.16)$$

However, for polymer blends the situation is more complex as four additional forms of this dependence have been identified, namely, negatively deviating blends (NDB), positively deviating blends (PDB), and combination of these two, i.e., PNDB and NPDB (see Fig. 18.17).

It is interesting that for perfectly miscible low-MW paraffins (Utracki 1983) as well as for HDPE (Bai et al. 2010) blends, a PDB was observed. The effect originates in a more efficient packing of different size statistical segments, which leads to a reduction of free volume and increase of viscosity.

In the case of noncompatibilized blends, the chain ends and low-molecular-weight additives migrate to the interphase, providing a low-viscosity lubricating

layer in shear flow, which results in the NDB behavior (Utracki 1989a). It has been shown that steady-state flow of immiscible polymer blends is governed by (Utracki 1991; Bousmina et al. 1999)

$$
\begin{aligned}
&\ln\eta_{\text{blend}} = \ln\eta_{\text{layers}} + \Delta\ln\eta_{\text{emulsion}} \\
&1/\eta_{\text{layers}} = (\phi_A/\eta_A) + (\phi_B/\eta_B) + k\sqrt{\phi_A\phi_B}; \quad k \propto (\eta_i\Delta l)^{-1} \\
&\Delta\ln\eta_{\text{emulsion}} = \eta_{\max}\left\{1 - \left[(\phi_1 - \phi_{1I})^2/(\phi_1\phi_{2I}^2 + \phi_2\phi_{1I}^2)\right]\right\}
\end{aligned}
\tag{18.17}
$$

In the second relation in Eq. 18.17, the k-parameter is inversely proportional to the thickness of the interphase, Δl, and the interphase viscosity, η_i. Thus, a large negative deviation from the additivity is a sign for the interlayer slip, hence immiscibility. However, the slip may be eliminated by compatibilization, which results in the yield stress at low stress level and PDB. In such a case, tests at higher stresses may show a progressive change of the viscosity–concentration curve from PDB to deepening NDB. Equation 18.17 (in its initial form) was found to follow well the η_o versus ϕ dependence for immiscible m- LLDPE/LDPE blends (Liu et al. 2002). Blends with the viscosity ratio $\lambda \equiv (\eta_1/\eta_2)_{\sigma = \text{cont}} > 3.8$ behave like suspensions – the viscous drops are nondeformable and these emulsions are expected to follow a PDB behavior, at least up to the phase inversion volume fraction, ϕ_I.

Hussein and his colleagues studied miscibility of various types of the PE_1/PE_2 blends following their melt rheology and crystallization. The authors assumed that for miscible blends the rheological behavior linearly changes with composition, while the PDB or NDB is an evidence of immiscibility by the emulsion or interlayer slip mechanism, respectively. However, the rheological response also is related to the system free volume content (v), and addition of branched polymer with lower v increases the rheological signal, even if the system is miscible. However, phase separation that leads to emulsion-like system, indeed, increases the departure from linearity (additivity). Table 21.7 summarizes results of these publications. The data suggest that (1) the PE/PE miscibility depends on MW; (2) blends with m-LLDPE are more miscible than those with Z-N–LLDPE, i.e., the regularity of branch placement along the main chain is more important than branch content; (3) increasing the branch length from C_4 to C_8 increases miscibility of LLDPE with LDPE; and (4) decreasing SCB enhances miscibility with HDPE.

In 1987 Utracki and Schlund characterized a series of ten Z-N–LLDPEs, LDPE, and their LLDPE/LDPE blends (Utracki and Schlund 1987; Schlund and Utracki 1987a, b). Properties of the ten experimental resins are listed in Table 18.8. Since for full evaluation of performance a large quantity of material was needed, the blends were compounded in a corotating twin-screw extruder (TSE), using commercial LPX-30, LLDPE-10 (both Z-N–LLDPE), and LDPE-102. Two series of blends were prepared: Series I of LPX-30 with LLDPE-10 and Series II of LPX-30 with LDPE-102. The miscibility was judged from the location of the Gross relaxation spectra maximum (Eqs. 18.12, 18.13, and 18.14). Two dependencies for the

Table 18.7 Miscibility at 190 °C of LLDPE with LDPE or HDPE

Polymer 1	Type 2	SBC/LCB 3	M_w 4	MWD 5	CODE 6	Ref. 7
LLDPE	C_6, m-	1.4/0	102	2.1	LLD-1m	Hussein et al. 2003
LLDPE	C_6, m-	3.2/0	97	2.0	LLD-2m	Hussein et al. 2003
LLDPE	C_6, Z-N	1.7/0	107	4.0	LLD-1Z	Hussein et al. 2003
LDPE	–	BC = 1.1	100	4.1	LD-1	Hussein et al. 2003
LLDPE	C_4, m-	1.4/0	108	2.0	LLD-3m	Hussein 2003
LLDPE	C_4, m-	4.2/0	125	1.8	LLD-4m	Hussein 2003
LLDPE	C_4, Z-N	1.3/0	118	3.1	LLD-2Z	Hussein 2003
HDPE	–	BC = 0	102	6.7	HD-1	Hussein 2003
LDPE	–	0.9/0.3-	100	1.2	LD-2	Hameed and Hussein 2004
LDPE	–	1.9/0	101	6.7	LD-3	Hameed and Hussein 2004
HDPE	–	BC = 0	116	6.5	HD-2	Hameed and Hussein 2004
LLDPE	C_4, Z-N	1.5/0	51	3.5	LLD-3Z	Hussein and Williams 2004b
LLDPE	C_4, Z-N	2.2/0	105	3.6	LLD-4Z	Hussein and Williams 2004b
LLDPE	C_8, Z-N	1.5/0	106	6.2	LLD-5Z	Hussein and Williams 2004b
LDPE	–	BC = 2.3	72	5.4	LD-4	Hussein and Williams 2004a
LDPE	–	BC = 2.2	99	6.4	LD-5	Hussein and Williams 2004b, c
LLDPE	C_8, m-	1.1/0	77	2.0	LLD-5m	Hussein and Williams 2004c
LLDPE	C_8, m-	3.0/0	69	2.7	LLD-6m	Hussein and Williams 2004b
LLDPE	C_8, Z-N	1.3/0	102	5.0	LLD-6Z	Hussein and Williams 2004b
LLDPE	C_8, Z-N	3.5/0	106	6.1	LLD-7Z	Hussein and Williams 2004b
Miscible	LLD-3m and LLD-4m with HD-1; LD-2 with HD-2; LLD-3Z with LD-4; LLD-6m with LD-5					
Partially miscible	LLD-1Z with LD-1 for ϕ(LD-1) $\leq$ 0.1; LLD-4Z with LD-5 for ϕ(LD-5) $\leq$ 0.1; LLD-5Z with LD-5 for ϕ(LD-5) $\leq$ 0.2					
Immiscible	LLD-1m and LLD-2m with LD-1; LLD-2Z with LD-1 (interlayer slip); LD-3 with HD-2; LLD-5m, LLD-6Z, and LLD-7Z with LD-5					

Column 2. Comonomer: butene, hexene, or octene (C_4–C_8); Column 3. BC stands for branch content; short- and long-branch content/100-BCA, or their sum, BC; Column 4. M_w is in kg mol^{-1}; Column 5. MWD = M_w/M_n; Column 7. References

Table 18.8 Z-N–LLDPEs used in Utracki and Schlund (1987) studies of PEs and their blends

Polymer	Manufacturer	Comonomer	MI (dg min^{-1})	ρ (g L^{-1})	M_n	M_w	M_w/M_n
LLDPE-1	Exxon	Butene	0.5	0.918	44 ± 13	150 ± 4	3.4
LLDPE-2	Exxon	Butene	0.7	0.926	47 ± 8	142 ± 2	3.0
LLDPE-3	Exxon	Butene	0.8	0.920	16 ± 1	111 ± 4	6.9
LLDPE-4	Exxon	Butene	1.0	0.918	40 ± 9	134 ± 2	3.4
LLDPE-5	Exxon	Hexene	1.0	0.918	34 ± 3	135 ± 2	4.0
LLDPE-6	Exxon	Hexene	0.8	0.927	40 ± 6	144 ± 2	3.6
LLDPE-7	Dow	Octene	1.0	0.920	30 ± 3	127 ± 2	4.2
LLDPE-8	Exxon	Hexene	0.04	0.946	23 ± 1	256 ± 14	11.1
LLDPE-9	Exxon	Hexene	0.07	0.946	21 ± 2	232 ± 6	11.0
LLDPE-10	Exxon	Hexene	0.3	0.955	17 ± 1	180 ± 2	10.6
LPX-30	Exxon	Butene	1.0	0.918	41 ± 2	133 ± 6	3.2
LDPE	Exxon	(none)	6.5	0.922	16 ± 1	64 ± 2	4.1

M_n and M_w are in kg mol^{-1}; LLDPE-8, LLDPE-9, and LLDPE-10 have bimodal MW distribution
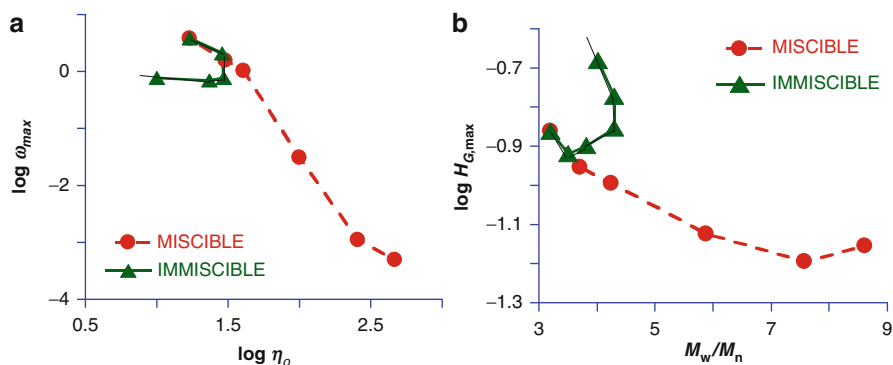
Fig. 18.18 (**a**) Correlation between the abscissas of relaxation spectrum maximum and the zero-shear viscosity for PE/PE Series-I (miscible LPX-30/LLDPE-10) and Series-II (immiscible LPX-30/LDPE). (**b**) Correlation between the ordinate of relaxation spectrum maximum and the polydispersity factor M_w/M_n for PE/PE Series-I (miscible LPX-30/LLDPE-10) and Series-II (immiscible LPX-30/LDPE)

two series of PE blends are shown in Fig. 18.18a, b. Evidently, Series I is miscible, while Series II is not. The conclusions were confirmed by measuring the extrudate swell. In immiscible LPX-30/LDPE blends, the strain recovery of elongated droplets created disproportionately large extrudate swell, $B = d/d_o$ (Utracki and Schlund 1987; Schlund and Utracki 1987).

Good historical review on the *Characterization and Optimization of Polyethylene Blends* is a part of the PhD thesis (Cran 2004). Zhao and Choi (2006) reviewed miscibility of PE blends in three parts: (1) miscibility inferred from indirect methods, (2) interaction parameters, and (3) molecular simulation. Unfortunately, only selected binary blends of HDPE, LDPE, Z-N–LLDPE, and m-LLDPE, from ca. 1990 to 2000, are discussed. The authors postulate that the branch content, BC, of the two components determines miscibility, while MW, MWD, and branch length are secondary. However, the presence of a few long-chain branches could induce immiscibility in the blends.

18.6.2 Rheology

Rheology may be used for detecting miscibility or for changing it – there is a reciprocal interaction between the flow and equilibrium thermodynamics. The simple and elegant way for expressing it is by using the Gibbs energy of mixing of a flowing system and then computing the binodal and spinodal curves:

$$\Delta G_{\dot{\gamma}} = \Delta G_{\mathrm{m}} + \Delta E_{\dot{\gamma}} = \Delta G_{\mathrm{m}} + E_{\dot{\gamma}} - \sum_i \phi_i E_i$$

$$\text{binodal:} \quad \left(\partial \Delta G_{\dot{\gamma}} / \partial \phi_i\right)_{P,T,n_j}^{\text{phase}-1} = \left(\partial \Delta G_{\dot{\gamma}} / \partial \phi_i\right)_{P,T,n_j}^{\text{phase}-2} \qquad (18.17)$$

$$\text{spinodal:} \quad \left(\partial^2 \Delta G_{\dot{\gamma}} / \partial \phi_1^2\right)_{P,T} = 0$$

Thus, the problem is reduced to selection of expressions for ΔG_{m} and $E_{\dot{\gamma}}$ followed by an appropriate algebra. An example of results is displayed in Fig. 18.19 for a blend that is being shear homogenized (Soontaranun et al. 1996). However, this behavior is not universal as the different topographies of PE result in either thermorheological simplicity (linear- and short-chain-branched PE) or two different types of thermorheological complexity, i.e., LCB-mPE has a temperature-dependent spectrum, whereas LDPE complexity requires a modulus shift (Resch et al. 2011). Equation 18.17 suggests that homogenization and demixing depend on the sign of the derivative: $(\partial^2 E_s / \partial \phi^2)$. If its value is negative, the homogenization is to be expected; if it is positive, shear demixing is to be expected.

At low concentration of a second polymer, blends have dispersed-phase morphology of a matrix and discrete second phase. As the concentration increases, at the percolation threshold volume fraction of the dispersed phase, $\phi_{\mathrm{c}} \cong 0.16$, the blends' structure changes into co-continuous. Maximum co-continuity is achieved at the phase inversion concentration, ϕ_{I}. The morphology as well as the level of stress leads to different viscosity–composition dependencies. The deformation and dispersion processes are best described by microrheology, using the three dimensionless parameters: the viscosity ratio (λ), the capillarity number (κ), and the reduced time (t^*), respectively (Taylor 1932):

Fig. 18.19 Computed spinodals at constant shear rates, $\dot{\gamma} = 0.01 - 1.0$ s^{-1}, for a shear homogenizing blend (Soontaranun et al. 1996)
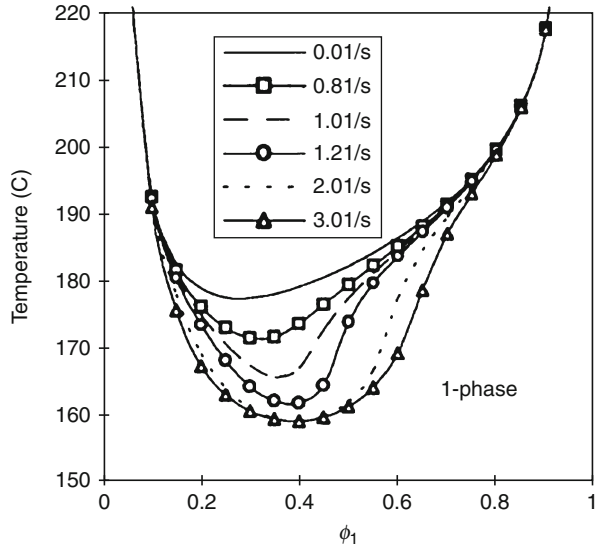
$$\lambda \equiv \eta_{\text{dispersed}}/\eta_{\text{matrix}}; \quad \kappa \equiv \sigma_{ij}d/v_{12}; \quad t^* \equiv t\dot{\gamma}/\kappa \qquad (18.18)$$

where $\eta_{\text{dispersed}}$ and η_{matrix} are the dispersed phase and matrix viscosity, respectively, σ_{ij} is the local stress, $\dot{\gamma}$ is the deformation rate, d is the droplet diameter, and v_{12} is the interfacial tension coefficient. The equilibrium deformation is reached at the reduced time, $t_d^* \simeq 25$, whereas the break at $t_b^* \simeq 160$. Thus, the dispersion process is controlled by the type of flow field, the viscosity ratio (at a given stress), the interfacial tension coefficient, as well as the duration of deformation.

At concentration, $\phi_2 \geq 0.005$, the dynamic process of dispersion is paralleled by coalescence. The dynamic equilibrium morphology is a net result of the dispersive and coalescing processes. The dynamic coagulation rate is related to the projected area of the drop, $d* \propto \phi_2^{2/3}$. Thus, during the shear flow, the rates of the diameter change may be expressed as

$$\left.\begin{array}{l} (dd/dt)_{\text{coalescence}} \propto \dot{\gamma}\phi^{8/3}/d \\ (dd/dt)_{\text{break}} \propto -\dot{\gamma}d/\kappa_{cr}t_b^* \end{array}\right\} \qquad (18.19)$$

According to these equations, the shear rate is expected to affect similarly coalescence and breakup; thus, increasing or decreasing $\dot{\gamma}$ should only slightly affect the degree of dispersion. However, the flow-induced coalescence depends on concentration, whereas the break is independent of ϕ. Thus, concentration discriminates these two processes. Also, the rate of break is proportional to d, whereas the coalescence is proportional to $1/d$. Thus, coalescence is not expected to play a major role at the beginning of the dispersion process when the drops are large – importance of this process increases with the progress of dispersion.

Droplet growth dynamics have been studied, experimentally and theoretically, by Vinckier et al. (1998). The diluted blends had $\lambda \approx 1$. The experiment started by

pre-shearing the material at a high rate to create small droplets. Then, the shear rate was reduced, and droplet coalescence was followed as a function of time under shear (Vinckier et al. 1998). Thus, by selecting appropriate test conditions, one may study dynamics of coalescence and the breakup processes (Vinckier et al. 1998; Tucker and Moldenaers 2002).

Results of recent experimental and theoretical studies of PP blends with a series of C_{2+8} m-LLDPE η_o (200 °C) = 0.7, 1.4, and 7.3 kPa s followed a modified Lee and Park equation. Good fit to the stress growth viscosity was obtained and indicated that shearing at low rate of $\dot{\gamma} = 0.1$ s^{-1} for about 30 min reduced the interfacial area by 88 %, 48 %, and 42 %, respectively; hence, the most viscous blend coalesces the easiest.

Increasing concentration of the minor phase changes the blends' morphology from drop dispersion to increasingly interconnected structures. At the phase inversion volume fraction, ϕ_I, the distinction between the dispersed and matrix phases vanishes – the morphology becomes co-continuous. It has been observed that the onset of continuity in polymer blends occurs at the volume fraction of the dispersed phase: $\phi_{onset} = 0.19 \pm 0.09$, i.e., near the percolation threshold concentration, $\phi_{perc} = 0.156$ (Lyngaae-Jørgensen and Utracki 1991). The co-continuity may result in several desirable properties, for example, synergism between rigid and ductile blend components that leads to materials with advantageous combination of high modulus and high impact strength.

The predictive relation for the volume fraction at phase inversion, $\phi_{1I} = 1 - \phi_{2I}$, is given by the following dependence:

$$\lambda = [(\phi_m - \phi_{2I})/(\phi_m - \phi_{1I})]^{[\eta]\phi_m} \tag{18.20}$$

where ϕ_m is the maximum packing volume fraction: $\phi_m = 1 - \phi_{perc}$. Equation 18.20 postulates that at the phase inversion, the two nominal blends, polymer-1 in polymer-2 and polymer-2 in polymer-1, have the same *relative* viscosity. For immiscible polymer blends the two equation constants, $[\eta] = 1.9$; $\phi_m = 0.84$, provided good description of data (Utracki 1991).

The percolation threshold near $\phi_p \approx 0.2$ is evident in several plots of η_o versus ϕ, of LDPE/branched PE (Peón et al. 2003), LDPE/HDPE (Sarkhel et al. 2006), or melt strength of LDPE/LLDPE (Field et al. 1999; Ho et al. 2002). The latter authors noted that for film-blowing bubble stability, miscibility and melt strength in elongation are important. For good process ability of LLDPE, ≥20 wt% of LDPE was required.

The miscible blends of LDPE/m-LLDPE often follow the Friedman and Porter (1975) equation:

$$\eta_{o,\,blend} = \left[\sum w_i(\eta_{oi})^{1/3.4}\right]^{3.4} \tag{18.21}$$

Schlund and Utracki (1987) carried out extensive rheological studies on two series of PE blends both containing LLDPE (C_{2+4} with $M_w/M_n = 3.22$) polymerized with Cr catalyst. Series I was its blend with LLDPE (C_{2+6} with $M_w/M_n = 8.94$) polymerized with Ti catalyst, while Series II contained LDPE ($M_w/M_n = 4.00$);

Series I was found miscible, Series II immiscible. In the second series the percolation concentration in plots of η_o or extrudate swell versus ϕ was hardly detectable but dramatically evident in the plot of the T and P coefficient, a. The latter was determined by plotting η_o as a function of the free volume fraction, f (Utracki 2011):

$$\log\eta_{\sigma=const} = a_o + a_1/[f + a] \tag{18.22}$$

The effect may be related to variation of the interphasial area and the excess free volume.

18.6.3 Compatibilization of Polyolefins

Only in rare cases (mixtures with $\phi_2 < 0.1$ or compositions near the phase inversion) the compatibilization may not be necessary. However, even in these cases it has beneficial effects on the performance. The compatibilization must (1) reduce the interfacial tension and facilitate dispersion, (2) stabilize the generated morphology against modification during the subsequent processing steps, and (3) enhance adhesion between the polymers' domains, facilitating the stress transfer, hence improving the mechanical properties of the product. Details of compatibilization are provided in ▶ Chaps. 4, "Interphase and Compatibilization by Addition of a Compatibilizer" and ▶ 5, "Reactive Compatibilization" of this handbook.

In essence, the compatibilization is a control of the interface of two immiscible PO phases, i.e., the interphase. In the simplest case, this is accompanied by partial dissolution of parts of the compatibilizer in the two phases. However, too much compatibilizer or using too high MW may form micelles then mesophases that reduce the blend performance. A compatibilizer must be designed by taking the thermodynamic and kinetic parameters into account.

In the case of PO blends, compatibilization most frequently aims for improved ductility and/or transparency. The Z-N–LLDPE obtained using multi-sited catalyst constitutes a specific case – the homopolymer may have phase-separated morphology that requires compatibilization. It has been known that addition of 5–20 wt% LDPE needs to be used for improved performance. However, explanation for this is rather recent (Robledo et al. 2009). The relaxation spectrum of the blend may be decomposed into three components: (1) Z-N–LLDPE matrix, (2) LDPE dispersed drops, and (3) a thick interphase with its own viscoelastic properties, obtained by interaction between the high-MW linear fraction of the LLDPE and the low-MW linear LDPE macromolecules.

Four methods of compatibilization have been used with PO blends:
- Addition of a compatibilizer: either a small amount (0.5–4 wt%) of tailored copolymer, a multipurpose compatibilizer-*cum*-impact modifier, or a cosolvent. Here, the elastomeric polymers or copolymers are primarily used (see Appendix, Table 18.11).
- Reactor compatibilization, wherein sequential steps PO-1, compatibilizer, and PO-2 are polymerized with the same or different catalyst (see Appendix, Table 18.11).

- Reactive compatibilization in a compounder that generates the desired quantity of either block or graft copolymers, which form chemical bonds across the interphase.
- Physical compatibilization that generates fine, nonequilibrium morphology and locks it by nucleated crystallization. The process may be carried out in the molten or solid state.
  Several types of reactive compatibilization have been used:
- Chain cleavage and recombination that lead to formation of random copolymers
- Reactions involving chain end groups of both polymers, forming of block copolymers
- Reactions between chain end of one polymer and side group forming graft copolymers
- Covalent grafting and cross-linking that result in high-MW copolymers
- Ionic bonding

During these reactions, the copolymers are produced at the interface. The method is superior to that of compatibilizer addition. Since TSEs are operated with short residence time, to complete the reactive compatibilization, one must use either high concentration of reactive groups, highly reactive functional groups, or efficient catalyst; hence, it is required that:

- There is sufficient mixing to achieve the desired dispersion.
- Reactive functionalities will form covalent or ionic bonds.
- The reactants are capable reacting across the interphase.
- The reaction rate is high.
- The formed bonds are stable.

18.6.4 Compounding Polymer Blends

The shear flow is inefficient for dispersing one polymer in another if they significantly differ in viscosity, especially for $\lambda \geq 3.8$. The elongational field is more proficient and rapid. It exists anywhere where the streamlines are not parallel. In elongational flow:

- The magnitude of interfacial area increases more rapidly than in shear.
- The rate of spatial separation between drops is higher.
- The energy consumption is reduced.
- The temperature is more stable (no shear heating).

Mighri and Huneault (2001, 2002) reported interesting differences in drop deformation and breakup during the Couette flow at increasing stress, between Newtonian and viscoelastic drops (see Fig. 18.20). While Newtonian drops elongated as κ (see Eq. 18.18) increased, the viscoelastic ones elongated only up to a critical value, characteristic of the system. Next, as the stress increased further, the deformed drops began to contract in the flow direction, thus elongating in perpendicular to the flow direction. This deformation increased with shear stress until breakup. Such a behavior is related to the normal forces present at high deformation rates in viscoelastic systems such as the investigated EPR/PP one. In Couette flow,
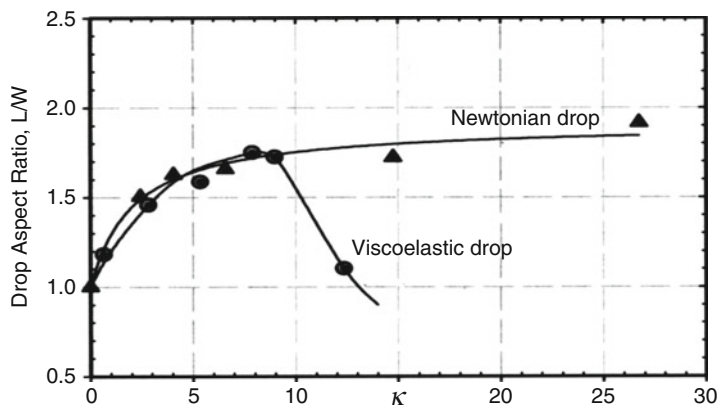
Fig. 18.20 Contrasted deformability of Newtonian and viscoelastic drops – 2D drop length-to-width versus the capillarity number (Mighri and Huneault 2001)

the breakup of these viscoelastic drops was initiated by a flow disturbance, caused by a stress gradient across the flow gap, when drop ends are in different planes, experiencing different shear stress. Other dispersion mechanisms, e.g., erosion, have also been observed for the viscoelastic, but not for Newtonian systems. Comparing the stress tensors of shear with elongational flows, it is evident that the reported problems associated with the deformation-opposing normal forces in shear are absent in elongation.

A single-screw extruder (SSE) operates on the principle of laminar shear flow. The lamellas of each polymer are thinned down along the screw length without folding. If the screw is long enough (for a given system), eventually the lamellas may break into fibers and these disintegrate into drops (Lindt and Ghosh 1992). To improve the mixing capabilities of SSEs, diverse mixing screws and add-on devices have been developed. The motionless mixers (MM) operate on the principle of splitting the flow stream into channels, reorienting and dividing them. The devices are quite efficient as distributive mixers, but they do not provide the dispersive function. The extensional flow mixer (EFM) has strong, controllable dispersive capabilities (Nguyen and Utracki 1995; Bourry et al. 1995; Luciani and Utracki 1996, 1997). The results demonstrated better blending performance of the SSE + EFM system than that of a twin-screw extruder, TSE.

In order of importance the polymer blending aims at producing materials with improved toughness, strength, rigidity, process ability, and heat deflection temperature (HDT) and with reduced permeability. Designing a blend for specific performance means that its morphology must be optimized. Furthermore, different properties require different morphologies, viz., for toughness, the elastomeric component should be dispersed as spherical drops with micron or submicron diameter, while for the reduction of permeability, the minor phase should be in form of relatively large drops, $d \cong 50 \ \mu m$, that during the biaxial stretching (e.g., while blow molding of containers) could be deformed into thin lamellas,

etc. Thus, selecting suitable compounding method is important. For example, under comparable conditions, uncompatibilized PE/PS blends emerging from SSE, TSE, and SSE + EFM showed the number average diameter, $d_n \cong 650$, 1.6, and 1.2 μm, respectively.

There are several mathematical models that attempt describing the variations of blend morphology during compounding in a TSE (Utracki and Shi 1992; Shi and Utracki 1992; Bordereau et al. 1992; Huneault et al. 1995; Delamare and Vergnes 1996). They require the following inputs: screw configuration, extrusion conditions, and polymer properties. Usually, the pressure profile and local strains in the extruder are first computed, and then, using this information, the average drop size along the screw is calculated from the microrheological rules supplemented by the coalescence kinetics. Due to the very rapid change of blends' morphology during the first instant after the mixing is stopped, there are some doubts regarding the accuracy of the models. Certainly, they may describe well the morphological changes, but even quenching the specimens within a second does not guarantee that the observation represents the true state present during mixing.

18.6.5 Polyolefin Degradation and Stabilization

Polyolefins are susceptible to several degradative mechanisms, out of which thermo-oxidative and thermomechanical are dominant. The PO stability depends on macromolecular configuration and it follows the order: HDPE > LLDPE > LDPE > i-PP. Chemiluminescence, FT-IR, mechanical properties, and thermogravimetry have been used for detecting and quantifying degradations (Cran 2004).

Degradation occurs during compounding, forming, and lifetime of an article; thus, stabilizers are needed. However, since these substances are expensive, they are added in a quantity just sufficient to protect the polymer during the first compounding, forming, and serving cycle – to be recycled, the polymer must be restabilized as:

- Degradative processes may have changed macromolecular structure.
- Different residual stabilizers may be present. It was observed that when recycling resins from different sources, these stabilizers may co-react, into inert compounds.
- The new additives should not react antagonistically with old ones,

In the following text, the principles of degradation and methods of stabilization will be discussed, first in the context of melt compounding and forming, then concerning the postforming processes (Herbs et al. 1997; Zweifel 1998). An excellent review of degradation of polymer blends was published by La Mantia (1992).

18.6.5.1 Degradation and Stabilization During Processing

Compounding and forming are carried out in the melt, at higher T and P and in intensive shear field. Owing to the enhanced chain mobility in the molten phase, the degradation processes are rapid. The compounding and/or melt forming of commodity plastics requires heating them to the processing temperature, $T_{process} = 175-300\,°C$,

for several minutes at a time. In the absence of stabilizers, this may lead to severe reduction of MW, thus performance. Depending on the type of polymer and processing conditions, one or several degradation mechanisms may take place (Klemchuk 1997; Zweifel 1998):

- Thermo-oxidative degradation of macromolecules in the presence of oxygen (O_2). The process is catalyzed by metals and metal ions, accelerated by heat and shear.
- Auto-oxidation – an autocatalytic free radical degradation in the presence of O_2. It affects polymers during aging; thus, it is controlled by diffusion of O_2 in solid state.
- Mechanochemical degradation caused by high stresses during mixing, blending, compounding, or processing. It results in chain scission and generation of free macroradicals. The process leads to the thermo-oxidative degradation as described above. Depending on the relative concentration of the tertiary carbons, the macroradicals terminated by different mechanism reduces or increases MW.

In principle, since compounding and forming are carried out in an enclosed heated space, e.g., in an extruder, they are conducted in the absence of oxygen and destructive radiation, which dominate the postforming degradation. For addition polymers, the thermo-oxidative and mechanochemical degradations are most important. These processes are mostly radical, but in the presence of specific catalysts, they may ionically decompose. During storage, PO chains slowly react with ambient oxygen forming peroxy, hydroperoxy, or peroxy-acid groups (the auto-oxidation). When heated, these decompose into free radicals that start the degradative chain reactions (Bateman 1954). Their rate is related to unsaturation, viz., the time to failure at 100 °C was 10,000, 500, 69, and 15 h, respectively, for PP, HIPS, SBR, and BR.

In a stress field, macromolecules are susceptible to bond breakage. This process also generates free radicals that lead to the degradative chain reactions. In POs, the free radical chain reactions lead to chain scission, grafting, or double-bond formation. Proportions of these structures depend on the concentration of tertiary carbon atoms. Thus, chain scission dominates degradation of PP, whereas grafting and cross-linking occur in HDPE. The LLDPEs, with copolymeric structures, show more complex behavior caused by the presence of all three reactions. Since chain scission statistically affects the longest chains, it reduces MW and narrows MWD. The opposite is true for the chain branching. The easiest method of identification of the prevailing mechanism is to use the dynamic mechanical test at low frequency. The time-dependent variation of the storage and loss moduli gives independent information about, respectively, grafting and chain scission (Schlund and Utracki 1987a).

As shown in Table 18.9, to be effective, stabilization should involve addition of several agents active within a specific stage of the degradation process, viz., initiation, propagation, or termination. Thus, it is important to use a cocktail of properly formulated stabilizers that is optimized to inhibit degradation of a specific polymer type.

Table 18.9 Stabilization strategies (Gätcher and Müller 1989; Zweifel 1998)

| Examples of stabilizers | Degradation | |
	Thermo- and auto-oxidative	Photooxidative
Complexing agent: N,N'-bis(o-hydroxybenzyl) oxalyl dihydrazide	Metal deactivation	(Not applicable)
UV absorbers: hydroxybenzophenones, triazoles, triazines, oxanilides, etc.	(Not applicable)	Absorb UV portion of sunlight
Quencher: Ni chelates	(Not applicable)	Deactivate excited chromophores
Hydroperoxide decomposers: phosphites and phosphonites, organosulfur compounds	Reacts with peroxides	Reacts with peroxides
Radical scavengers hydroxylamines, benzofuranone derivatives, etc.	Reacts with free radicals	Reacts with free radicals
H-donors: hindered phenols, secondary and sterically hindered aromatic amines, etc.	Reacts with macroradicals	Reacts with macroradicals

To stabilize POs against degradation during the melt processing, antioxidants (e.g., hindered phenols, sulfide esters, organic phosphites, secondary aromatic amines, and hindered amines), peroxide decomposers (usually a phosphite), and frequently acid acceptors (e.g., calcium stearate) are used. For special applications, metal deactivators may be needed.

The following rules were formulated regarding stabilization of recyclates:

- Antioxidants, hydroperoxide decomposers, and processing stabilizers should be added in quantity required by the process and service time under given exposure.
- Light stabilizers should be added depending on the foreseen storage conditions, applications, and service lifetime.

It is important to recognize that additives suitable for one type of resin may have detrimental effects on another and/or on their additives. Furthermore, the stabilizing systems of one polymer type may neutralize the system of another polymer. For example, to stabilize postconsumer waste (PCW), 55–75 wt% PO, 5–25 wt% PS, 5–15 wt% PVC, and 0–10 wt% other thermoplastics, 0.1–0.5 wt% of a stabilizer mixture was added. The mixture comprised a sterically hindered phenol [pentaerythritol ester] and tris(2,4-di-tert-butylphenyl) phosphite at a ratio of 5:1–1:5. For other compositions of PCW, different stabilizers, viz., thiopropionic acid, benzophenones, oxalides, benzotriazoles, HALS, and/or CaO, may have to be used (Pauquet et al. 1994).

18.6.5.2 Post-processing Degradation and Stabilization

During the life-span of the polymeric products, they are exposed to a wide range of degradative influences. Besides the previously mentioned oxidative and hydrolytic processes, the photodegradation, thermal aging, physical aging, as well as biodegradation may be present.

The photooxidation takes place when UV irradiation causes formation of free radicals that in turn absorb oxygen molecules. Most double-bond structures in

rubbers and aromatics readily absorb photo energy at 200–360 nm. Hydroperoxides are powerful chromophores for PO with tertiary carbon.

As shown in Table 18.9, stabilization against photooxidative degradation is accomplished by adding similar mixture of additives as that used for the thermo-oxidative degradation. The main difference is replacement of a metal deactivator by UV absorbers with high extinction coefficient in the range of 300–400 nm (e.g., hydroxy benzophenones, triazoles, triazines, oxanilides) and quenchers (e.g., Ni chelates). In principle, UV absorbers act as transformers, converting the high photo energy into heat. However, they are also being consumed in reactions with perox-ides; hence, they must be protected against oxidation, e.g., by phenolic antioxi-dants. Similarly, quenchers deactivate the excited chromophores by energy transfer, but they also enter into other stabilizing reactions, e.g., decomposing hydroxy peroxides, thus slowly are consumed during the service time.

18.6.5.3 Effect of Reprocessing on Performance

Figure 18.21a, b illustrates the extent to which the judicious stabilization is able to protect PO resins and their blends from the thermo- or photodegradation. As they indicate, the recyclates even after five extrusions show performance within 10 % approximating that of a virgin material. Similar behavior is expected for strongly immiscible polymer blends, under the condition that the recyclates will be re-compatibilized to recover the original morphology.

It is noteworthy that additives used for one type of resin may have detrimental effects on another resin and/or on its additives. This was dramatically shown by blending several grades of PA-6 with POs produced by different manufacturers – the aim was to determine the interfacial properties of PA/PO blends (Luciani et al. 1997). Mixing a PA with a PO containing phosphite stabilizer resulted in a rigid membrane formed at the interface through reaction between $-NH_2$ end groups of PA and phosphite acidic functionality. The membrane increased melt viscosity and decreased the degree of dispersion. The detrimental effects are most likely in the presence of heat and light stabilizers.

To recycle polymer blends it is important to regenerate the morphology and to restabilize the ingredients. Thus, it is necessary to provide adequate mixing, re-compatibilize and restabilize the blend. Frequently, the recycled blends should be impact modified. There are two reasons for this: (i) contamination of the composition by other polymers and (ii) degradation of the usually less stable compatibilizers and impact modifiers.

Useful properties of mixed resins can be obtained without compatibilization when:

- Recycling commingled resins of the same chemical species, e.g., recycled resin with virgin resin, LLDPE with LDPE, and m-PO with ZN-PO.
- Components are nearly miscible with each other, e.g., Z-N–LLDPE with some PP or *m*-LLDPE, and HDPE with some LLDPE.
- Content of the dispersed phase does not exceed 5–15 vol%.
- Blends have co-continuous morphology.
- Materials developed for aesthetic, not structural reasons, viz., compositions showing nacreous or wood-grain effect.

Fig. 18.21 (**a**) Effects of addition of Irganox B225 (1:1 blend of Irganox 101 and Irgafos 168) on repetitively extruded (up to five times) HDPE. The stabilizer was added in the amount of 0, 0.05, and 0.20 wt% (After Herbst et al. 1997). (**b**) Stabilization effects of HALS on a virgin and recycled LLDPE/LDPE blends with and without carbon black (CB) (After Herbst et al. 1997)
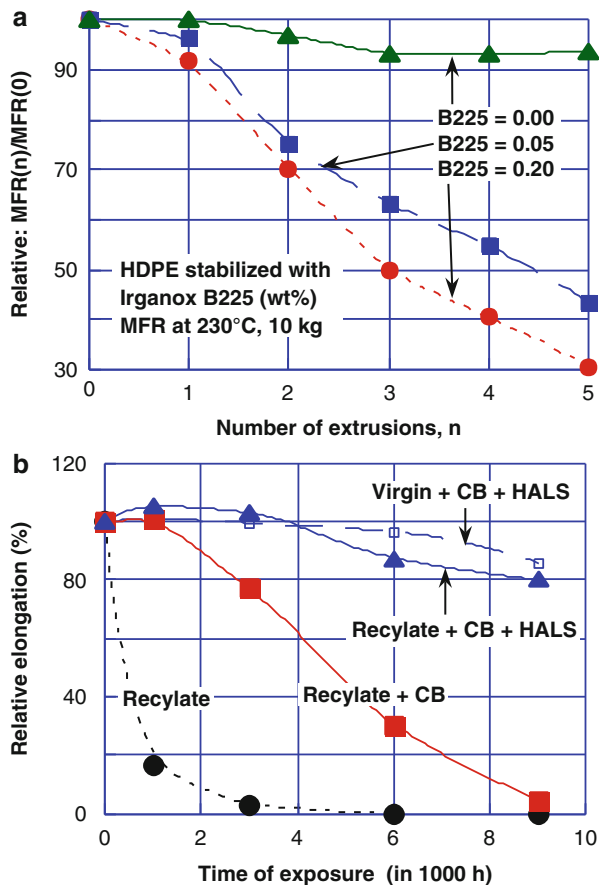
It is seldom recognized that mixing two PE resins from different sources constitutes blending with all what this term implies. Polyethylenes prepared using different catalysts or containing different comonomers are mostly immiscible. Furthermore, miscible blends that have widely different molecular weights are difficult to homogenize – frequently surface of the manufactured article is coarse due to "fish eyes" or gel particles being left behind after inadequate compounding. Incorporation of virgin PE to recycled one is frequently done to improve performance (La Mantia 1997; Zahavich and Vlachopoulos 1997). The incorporation must be done according to the standard rules of blending: adequate blending, compatibilizing, and stabilizing. For the miscible or well-compatibilized blends, the modulus (E) and yield stress (σ_y) are additive, whereas the maximum strain at break (ε_b) follows the inverse additivity rule:
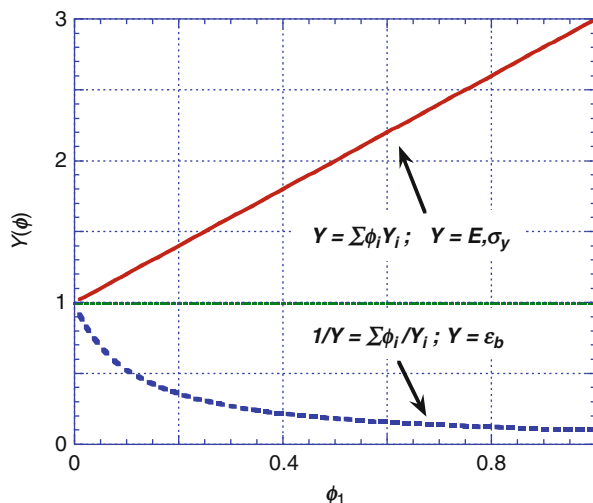
$$Y = \sum_i \phi_i Y_i \bigg|_{Y=E,\,\sigma_y} \quad ; \quad \frac{1}{\varepsilon_b} = \sum_i \frac{\phi_i}{\varepsilon_{bi}} \qquad (18.23)$$

where ϕ_i is the volume fraction of polymer i. The dependencies are illustrated in Fig. 18.20.

There are diverse factors that make blends to disobey these rules. It has been frequently observed that blending two semicrystalline resins (e.g., HDPE/PP) enhances the heterogeneous nucleation which leads to higher crystallinity and finer crystals. As a result, blends' stress and modulus show a positive deviation from additivity – considered synergism. For example, for augmenting heterogeneous nucleation of LDPE and/or LLDPE with 2–60 wt% recycled HDPE, the mixture was compounded with 0.1–1.5 wt% ZnO and 0.1–2 wt% glycerol monostearate. The resulting blends could be foamed, extruded, molded, or cast to form films having up to 100 % higher elongation and 50–90 % increase in transverse film strength over LDPE alone. The products were used for packaging (Lee 1995) (Fig. 18.22).

On the opposite side is the antagonism observed in the elongation at break. This dependence originates in reduced adhesion between phases. Numerous mechanisms are responsible for it. For example, in the PE/PP blends, there is a phase separation – any low-molecular-weight impurity migrates to the interphase lowering its viscosity and reducing the strength. This may be seen using an acoustic microscope – coarse PP crystals in PE/PP blends are virtually rattling inside the matrix – there is a physical void around them. The void is created by the change of

density on crystallization. Materials having such micromorphology will have reduced maximum elongation, below the level predicted by Eq. 18.23.

Blends of two or more POs were recycled in the solid state at the processing temperature, T_p, such that $T_{m1} < T_p < T_{m2}$ (T_{m1}s are the softening points of the blends' components, provided that $T_{m1}–T_{m2} > 20$ °C). The components were PE, PP, PS, and polydienes – virgin, recycled, or mixed. The preferred POs were PE and PP, and preferred blends were those containing at least one PE, particularly a substantially linear ethylene polymer (Lai and Edmondson 1995). Reground PP from automotive interior parts was contaminated with up to 15 wt% of POM. At present, there is about 16 kg of PP per 1 kg of POM, the latter used for clips, fasteners, door-lock buttons, pivots, grilles, seat-belt buckles, etc. Presence of POM facilitated processability, and it had little effect on the tensile strength of recycled PP, and it improved modulus by ca. 12 % (Naitove 1996).

18.7   PE/PE Blends by Type

Historically, there were four major inventions in PE manufacture, i.e., LDPE, HDPE, Z–N–LLDPE (and Cr–LLDPE), and *m*-LLDPE. Blending them resulted in six categories: (1) LDPE/HDPE, (2) LDPE/Z–N–LLDPE, (3) LDPE/*m*-LLDPE, (4) HDPE/Z–N–LLDPE, (5) HDPE/*m*-LLDPE, and (6) Z–N–LLDPE/*m*-LLDPE. However, in reality, many modern blends are multicomponent as the "homopolymers" are frequently modified by small amount of comonomer. Numerous resin grades for specific application may be blends, e.g., Z–N–LLDPE with a small amount of LDPE that promotes strain hardening in elongational flow, essential for the film formation and wire coating or foaming. Thus, saying that there are six categories of binary blends is a simplification.

The following text will present these categories of PO blends and then it will attempt identifying characteristic properties and applicability of each. Avoiding duplication, the patent information to these blends will remain in Appendix, Table 18.11. The PE/PE blends have been reviewed (Utracki 1989a, b; Hamid and Atiqullah 1995; Utracki 1997; Cran 2004; Zhao and Choi 2006; Isayev 2011).

18.7.1 LDPE/HDPE Blends

Because miscibility of two PE resins depends on the degree of difference of their chain structures, HDPE blends with LLDPE are not expected to form single-phase melt or co-crystallize. However, since for controlling density HDPE may contain C_3 or C_4 comonomer, some HDPE blends with LDPE showed limited miscibility.

Depending on MW, molten LDPE/HDPE blends phase separate, but on rapid cooling, they may crystallize into single-type crystals with single T_m. The structure is not at the thermodynamic equilibrium since slow cooling leads to separated peaks for LDPE and HDPE (sometimes with an intermediate residual peak). The phase separation in LDPE/HDPE blends mainly depends on the MW of the HDPE

component. The immiscibility of LDPE/HDPE blends is often reflected in poor mechanical properties. Here, compatibilization and processing are the keys to success.

In 1977 Idemitsu Petrochemicals announced that immiscible blends of LDPE with HDPE, with EPDM, or with an atactic polypropylene, aPP, are suitable for the production of soft, thin films, with improved properties for packaging (Sakane et al. 1979). Similar blends, LDPE with HDPE, PP, and EP block copolymer, were proposed by Shin-Kobe Electric Machinery (1984) for films with good modulus, tear strength, and no sagging behavior. Also, Showa Denko (1983) found that immiscible, but lightly compatibilized, blends of LDPE with either HDPE or MDPE are suitable for films with uniform thickness and anisotropic tensile strength.

Hoechst disclosed blends having a bimodal MWD, comprising 50–80 wt% HDPE blended with either LLDPE or LDPE. The alloys were found suitable for molding or extrusion of tubes, pipes, and other articles requiring high stress crack resistance (Boehm et al. 1992). While most LDPE/HDPE blends were found immiscible, some reports stress that they formed homogeneous melt and could be quenched into co-crystals with a single T_m. There are two other variables that need a thought – the degree of LCB in LDPE and MW of both polymers (Zhao and Choi 2006).

18.7.2 LDPE/Z-N–LLDPE Blends

Miscibility is identified as an existence of a single phase; thus, the term refers to liquid systems: solutions and melts (some authors treat co-crystallization as a solid-state miscibility). Most polymer blends available on the market are immiscible, but with adequate interactions across the interphase. For example, by 1980 ca. 42 % film producers used immiscible LLDPE/LDPE blends, where LLDPE improved modulus and strength and LDPE enhanced processability and ductility. Properties of LLDPE/LDPE blends have been described in several publications (Utracki and Schlund 1986, 1987; Schlund and Utracki 1987; Zahavich and Vlachopoulos 1997). Blends of LLDPE with PP were also studied (Dumoulin et al. 1987, 1988, 1991; Dumoulin and Utracki 1990). Similarly, blends of PE with PC were described (Utracki and Sammut 1989, 1990b).

Blending Z-N–LLDPE with LDPE is widely established as a means for improving various properties of LDPE, and the commercial importance, melt behavior, and performance of LDPE/LLDPE film blends are well documented. While most blends of this type are reported miscible, the phase separation has been reported for some blends in the molten and semicrystalline state; in the latter case, two crystal populations were observed by DSC and TEM. Increasing the SCB from C_4 to C_8 promoted miscibility (Hussein et al. 2003; Hussein and Williams 2004b). However, the last statement contradicts the observation of LDPE/m-LLDPE (Fang et al. 2005). Furthermore, reduction of LLDPE MW improves miscibility (Hussein and Williams 2004a. Zhao and Choi (2006) concluded that miscibility of LDPE blended with Z-N–LLDPE or m-LLDPE is determined by LCB. The difference in branch content is the major factor, while those in MW, MWD, and SCB are secondary.

Shear and elongational data of LDPE/LLDPE blends have been reported, indicating thermorheological complex behavior. In unidirectional shear or elongational flow, the linear range of viscoelastic deformation is reduced and the terminal relaxation times are shifted toward that of LDPE (Wagner et al. 2004). Significantly, the strain-hardening (SH) behavior of LLDPE/LDPE blends entirely originates in LDPE. The nonlinear strain does not depend on the composition for blends with LDPE but rather on the SH of LDPE. Such a behavior may be understood by assuming the existence of two phases in the blends: the first containing highly branched low-MW chains from both polymers and the second composed of the high MW of both polyethylenes.

Several LDPE/Z-N–LLDPE blends have been found to be miscible in the melt and when cooled quickly do not segregate into separate crystalline phases, while slow cooling results in the formation of independent crystalline phases. It was suggested that the addition of HDPE to immiscible LDPE/LLDPE blends may induce full miscibility of the resulting ternary blend (Lee and Denn 2000). Blending Z-N–LLDPE with LDPE may improve processability, toughness, impact strength, optical clarity, environmental stress cracking resistance, as well as resistance to thermal embrittlement and increased tear resistance.

The blends comprising LDPE with Z-N–LLDPE have improved stiffness and abrasion resistance and reduced water vapor permeability. Celanese patent application from 1961 stressed the improvement of LLDPE processability (Wissbrun et al. 1962, 1965). In a contemporary DuPont application, 10–50 wt% LLDPE was blended with LDPE to obtain materials suitable for the use as heat-shrinkable films (Golike 1962). Since LLDPE differs from LDPE by the presence of short side groups introduced as a part of the comonomer unit and by the absence of long-chain branching, there have been several attempts to create the latter chain structure by addition of radicals to molten LLDPE, expecting that these will graft on some LLDPE macromolecules converting part of the resin into LDPE-like polymer. These long-branched molecules would be simultaneously blended with unmodified LLDPE macromolecules creating an intimate PE/PE blend possessing all the superior characteristics of the LLDPE/LDPE blend. The main problem associated with this technology was the difficulty in controlling uniformity of product. The small quantity of peroxides tended to form pockets of degraded resins that contaminated the product. In 1971, Exxon Research and Engineering disclosed reactive grafting of PE or PP. The extruder was modified for separately feeding the polymer and grafting the monomer and peroxide (Steinkamp and Grail 1976).

In 1979, the *UNIPOL*™ process for gas-phase production of LLDPE was introduced by the Union Carbide Corp. Since the new resins were difficult to process on the lines designed for LDPE, by 1982 several patents were issued for improvement of LLDPE processability by blending it with other polyolefins, viz., LDPE, PP, and olefinic rubbers. Ethylene copolymers, rubbers, EPDM, EVAc, maleated polypropylene, EPR, etc., have also been used (Cowan 1983; Turtle 1983; Fukui et al. 1983; Haas 1983; Hert 1983). Thus, blends LLDPE/LDPE were found miscible at low LDPE contents, then immiscible at high LDPE. Addition of HDPE as cosolvent resulted in miscible tertiary blends (Lee and Denn 2000).

In Societé Chimique des Charbonnages patent application of 1982, Z-N–LLDPE was blended with 2–25 wt% LDPE for the manufacture of films with large difference of tensile strength in the machine and transverse direction (Hert 1983). The reversed compositions were disclosed in Japan the following year. Thus, LDPE was blended with LLDPE at ratios varying from 100:20 to 100:90. The alloys were reported useful for the production of packaging films (Asahi Chem. Ind. 1985). A 1984 patent from Mobil Oil described LLDPE blends with 10–45 wt% LDPE, PP, or EPR copolymer with a high propylene content, 2–15 wt% EPR. The blends had high modulus and excellent clarity (Bahl et al. 1985). LLDPE was grafted with dimethylamino ethyl methacrylate, t-butyl amino ethyl methacrylate, vinyl pyridine, or allyl urea. The copolymers were used as reactive components for PO alloys with acidified polymers, viz., maleated LLDPE or PP (Baker and Simmons 1991). In 1992, Euro-Matic developed blends comprising Z-N–LLDPE with LDPE at a ratio of about 3:10. These resins were used for blow molding hollow balls containing pressurized air and consisting of two hemispheres welded to form a ball with a wall thickness of 0.5–1.8 mm (Moss and Modigh 1994).

Delgadillo-Velázquez et al. (2008a) studied the thermorheological effect of LCB for a number of LLDPE/LDPE. A C_{2+6} Z-N–LLDPE was blended with four LDPEs having the zero-shear viscosity at 150 °C, $\eta_o = 8, 44, 73$, and 132 kPa s. The LDPE content in blends was 1, 5, 10, 20, 50, and 75 wt%. The elongational behavior of the blends was studied using a Sentmanat extensional rheometer (SER). The blends showed strain hardening at all LDPE concentrations including 1 wt%. It is noteworthy that at LDPE < 20 wt% the effects of its addition were non-detectable in the shear field. Above that concentration, a positive deviation behavior (PDB) from log-additivity rule was observed, in the whole range of temperatures. The DSC showed three peaks at high LDPE contents that may be taken as an evidence of some co-crystallization.

In the recent patent application (Mavridis 2011), blends of Z-N–LLDPE with 0.3–0.8 wt% of high-MW LDPE (MW ≥ 100 kg mol^{-1}; MI = 0.1–0.6 dg min^{-1}; $\rho = 0.91$–0.94 g mL^{-1}) were described. The LLDPE ($\rho = 0.915$–0.940 g mL^{-1}; MI = 0.2–10 dg min^{-1}) must have the slice LCB index, $LCBI \geq 0.96$, in any portion of the composition: C_{2+n}, where $n = 2$–12, preferably 4 or 6. Blown films of these LLDPE/LDPE blends exhibited an enhanced balance of properties and high transparency (haze of a 2.5 μm film was <15 %).

Blends of 95–15 wt% Z-N–LLDPE (or preferably m-LLDPE) with m-VLDPE were patented by Univation Technology (German et al. 2006). The linear and without long-chain branching m-VLDPE had $\rho < 916$ kg m^{-3} and MI = 5 dg min^{-1}, while LLDPE had $\rho = 916$–940 kg m^{-3} and MI = 0.5–20 dg min^{-1}. The blends were formed into blown and cast film for packaging and liquid containers and for surface protection during manufacturing or transportation.

In a Phillips application, two Z-N type polymers were blended; 10–80 wt% of low-MW LLDPE [$\rho \geq 940$ kg m^{-3}, MI > 25 dg min^{-1}, and $M_w/M_n = 2$–12] with 20–90 wt% of a high-MW LLDPE [$\rho \leq 955$ kg m^{-3}, MI = 2–10 dg min^{-1}, and $M_w/M_n = 2$–10]. The blends with MI > 0.05 dg min^{-1} showed excellent film processability and improved transparency (Coutant and Martin 1995). The best performing blends with high transparency were probably miscible.

18.7.3 LDPE/m-LLDPE Blends

In 1977 Phillips Petroleum Co. developed blends of Z-N–LLDPE using C_{2+4} and C_{2+6} copolymers which were disclosed as suitable for pipe extrusion (Larsen 1982). The same year, Mobil Oil announced reactor blends of PE (copolymer of C_{2+4} and/or C_{2+6}) for production of blown films that exhibited improved MD/TD tear balance. The latter materials were produced in a multistage, gas-phase, fluidized bed polymerization process with in situ blending. The resulted bimodal MWD resins had 0.35 to about 0.75 wt% of a higher-MW component (Ali et al. 1994).

In 1992 the 3 M disclosed blends that comprised 100 parts VLDPE [*Flexomer* or *Attane* 80–95 mol% ethylene and 5 mol% C_{4-8} comonomer(s)] and 15–600 parts m-LLDPE [*DOWLEX* ethylene copolymer with 2–8 mol% C_8]. The blends showed excellent processability. Formed into 10–300 μm thick films, they were used for transdermal drug delivery devices as single-layer backings. The films were clear, colorless, transparent to visible light, and sealable at relatively low temperature. They were permeable to O_2, stable to various common components of transdermal delivery devices, strong, and comfortable and did not absorb significant amounts of common elements of transdermal carriers (Godbey and Martin 1993, 1994).

An early study of LDPE/m-LLDPE indicated immiscibility accompanied by good interactions that at constant loading of ≤ 25 wt% LLDPE resulted in additivity of the mechanical properties. The latter resin was DOWLEX 2045, a C_{2+8} m-LLDPE copolymer. Rapid quenching resulted in formation of two phases and slow cooling produced an additional third peak (Müller et al. 1992). In a contemporary patent application from W. R. Grace, improved heat-shrinkable PE films were described. These comprised single-site catalyzed copolymer of C_2 with C_{3-8} alpha-olefin and m-LLDPE with $\rho \geq 900 \, kg \, m^{-3}$ and blended with another polymer of C_2 and a C_{3-8} alpha-olefin and a second comonomer (e.g., vinyl acetate, alkyl acrylate, CO, butadiene, styrene, acrylic acid, and a metal salt of an acrylic acid) or an α-olefin homopolymer. These films had improved shrinkability, impact resistance, and optical properties as compared to homogeneous copolymers. The blends were found useful for manufacturing packaging films (Babrowicz et al. 1994).

Blends of PE with PP are immiscible; thus, for enhancement of the interphasial interaction, copolymerization has been used (Da Silva et al 2000, 2001). For example, m-LLDPE was blended with ethylene–propylene–butene-1 terpolymer (*ter*-PP: 2.9/92.4/4.7 wt%). Even in the presence of immiscibility, the enhancement of interactions at 20 wt% of *ter*-PP sufficiently improved processability and performance to warrant commercial interest (Cho et al. 1997).

Replacing Z-N–LLDPE by m-LLDPE in blends with LDPE resulted in an improvement of film properties. This may originate from improved miscibility, which in turn depends on the MW of m-LLDPE, branch content (BC), and composition distribution (CD) (Hussein et al. 2003; Hussein and Williams 2004). In addition to the improved physicomechanical properties, the processability of m-LLDPE blends with LDPE is better than that of Z-N–LLDPE. LDPE/ m-LLDPE blends with the same MI as those with Z-N–LLDPE are inherently tougher; thus, they may be thinner for the equivalent mechanical properties in

plastic bags. However, the miscibility difference depends on branch content (BC). Thus, at the same MW and MWD but low-BC (14.4 CH_3/1,000 C), Z-N–LLDPE/ LDPE blends are more miscible than m-LLDPE/LDPE, whereas at a *high-BC* = 32.2 CH_3/1,000 C the situation was reversed. The high-BC m-LLDPE blends with LDPE were partially miscible with phase separation for LDPE-rich blends.

Exxon Chem. (Stehling et al. 1995) disclosed blends of linear ethylene interpolymer that comprised m-LLDPE and VLDPE (Appendix, Table 18.12). The polymers prepared using metallocene catalyst had narrow MWD, M_w/M_n = 1–3, and a narrow chemical composition distribution (CCD), expressed by its index, CDBI > 50 %, and measured by TREF. The components could have the same MW but different BC, the same BC but different MW, or BC that increase with MW. The blends had either M_w/M_n > 3 or CDBI < 50 % or both these inequalities. They could be multimodal in respect to MW and/or BC. They were generally free of components having both a higher average MW and a lower average BC than other blend components and have a density of ρ = 910–940 kg m^{-3}. The blends could be coextruded or compounded with other polymers for additional improvement of processability and of performance (Stehling et al. 1995). Similar blends of either Z-N type or metallocene VLDPE with SCB were blended with LDPE (Chen et al. 2001). The blends of C_{2+4} m-VLDPE1 with LDPEs showed co-crystallization, thus at least a partial melt miscibility at all compositions. However, blends of VLDPE1 with C_{2+8} m-VLDPE2 co-crystallized at ≤50 % VLDPE2 content, whereas blends of VLDPE2 with C_{2+8} Z-N–VLDPE3 co-crystallized at ≥50 % of VLDPE2. Notably, miscibility and morphology of these blends showed little MW dependence; only the distribution of branches along the chains was important.

In 1994 Exxon Chemical deposited EP application for blends that included (a) the base polymer derived from C_2 and optionally an α-olefin having MI = 1–5; (b) from 1 to 45 % by weight of (a) + (b) of a second polymer co-crystallizable with (a) and derived from C_2 and at least one olefinically unsaturated comonomer having MI = 0.5–4.5 units below that of (a) and which responds rapidly to cross-linking. The materials were developed for use as shaped coatings or wire and cable insulation (Wong and Varrall 1994). Many other patents followed from Exxon for blends, e.g., m-LLDPE, VLDPE, or LDPE, having melt index, MI = 0.1–10, 10–30 wt% of a secondary co-crystallizable C_{2+n} copolymer, e.g., LLDPE, VLDPE, or LDPE, having MI ≥ 80 % lower than that of the first polymer, and moisture cross-linking additives (e.g., a silane, a silanol condensation catalyst, and a free radical initiator) were disclosed (Wong and Varrall 1994; Datta et al. 2006).

Hameed and Hussein (2002) blended m-LLDPE (C_{2+4} and C_{2+6}; low and high MW) with LDPE. The miscibility was investigated by indirect rheological methods. Assuming that for miscible blends the rheological behavior should be additive, the authors noted that MW has a strong effect on miscibility, but not on the concentration behavior, i.e., initial addition of m-LLDPE to LDPE formed immiscible system, while in reversed situation single phase remained. The immiscibility was observed for blends comprising >20 wt% m-LLDPE. Pérez et al. (2005) observed that immiscibility of m-LLDPE (SCB = 10.5/1,000 C) with LDPE takes place only

for 52.5 wt% of the latter component. Curiously, m-LLDPE copolymerized with C_4 and C_6 comonomers showed similar immiscibility with LDPE.

The next publication in this series focused on the immiscibility of C_{2+6} LLDPE prepared either with Z-N or metallocene catalyst, having variable BC and CD with LDPE or HDPE (Hussein 2003; Hussein et al. 2003). The effect of CD on miscibility was judged by comparing blend of Z-N–LLDPE with m-LLDPE – for the same MW and similar BC, better miscibility was observed for the former than for the latter system. Similarly, a high-BC m-LLDPE (32.2 CH_3/1,000 C) was more miscible with LDPE than a low-BC m-LLDPE (14.4 CH_3/1,000 C) of similar MW and MWD. In blends with HDPE, the composition distribution (CD) had no effect on miscibility, but increase of SCB resulted in a phase separation. These conclusions were confirmed in a later publication on C_{2+4} Z-N–LLDPE blends with LDPE (Hussein and Williams 2004a, b). In particular, while low-MW C_{2+8} Z-N–LLDPE was miscible with LDPE, the miscibility of high-M_w Z-N–LLDPE with LDPE was limited to blends with >50 wt% Z-N–LLDPE. However, increasing the branch length in Z-N–LLDPE from C_4 to C_8 increased miscibility with LDPE.

Fang et al. (2005) studied the thermal and rheological properties of two types of m-LLDPEs, two LDPEs, and their blends. The C_{2+6} m-LLDPE-1 was immiscible, whereas the C_{2+8} m-LLDPE-2 was miscible with the LDPEs, indicating that increasing the length of SCB in m-LLDPEs promoted miscibility with LDPE. The Palierne (1990, 1991) emulsion model provided good predictions of the linear viscoelastic behavior for both miscible and immiscible blends. The low-frequency data showed an influence of the interfacial tension on the elastic modulus of the blends for the immiscible blends.

18.7.4 HDPE/Z-N–LLDPE or Cr–LLDPE Blends

In 1981, Showa Denko announced that blown films from HDPE blends with 50–55 wt% Z-N–LLDPE have improved strength and transparency over those of neat HDPE (Showa Denko 1983). The industrial interests in these systems grew over the years. For example, while blends of LDPE and HDPE slowly cooled from the melt formed separate crystalline phases, those of HDPE with LLDPE may co-crystallize – the presence of these single crystals may indicate miscibility. The phase separation in HDPE/Z-N–LLDPE or HDPE/m-LLDPE blends has been frequently reported, but some blends of this type are miscible in the melt and solid states. MD simulation by Choi (2000) suggests that miscibility of HDPE with C_{2+4}–LLDPE depends on BC – the computed critical level for phase separation was 4 SCB/100 C. This finding is consistent with the SANS data on model polymers (Alamo et al. 1997). The latter authors reported that HDPE blends with hydrogenated/deuterated polybutadiene are miscible at all concentrations when the branch content is low, SCB <4 for $M_w = 100$ kg mol^{-1}, but immiscible for SCB $\geq$ 8 branches/100 C. However, in blends of HDPE with ULDPE, miscibility (or partial miscibility) was observed only at low ULDPE content, when blends of m-LLDPE with m-HDPE are fully miscible in the molten and crystalline state (Guimares et al. 2003).

The tensile, flexural, and impact properties of HDPE/LLDPE blends significantly deviate from the rule of mixtures, especially at HDPE/LLDPE $\approx$ 1; this effect has been attributed to the blend amorphous phase. Thus, the resistance to slow crack growth (SCG) of LLDPE blended with HDPE may be higher by 30–50 % than that of neat LLDPE. On the opposite concentration range, addition of 10 wt% LLDPE to HDPE yields tough blend without unduly affecting other tensile properties. In blends of film-grade m-LLDPE/HDPE, addition of ca. 25 % m-LLDPE improves the tear resistance and film stiffness compared with films made entirely from HDPE. The use of m-LLDPE in blends with flame-retarded HDPE improves processability and impact resistance compared to blends using conventional Z-N–LLDPE. Films blown from binary blends of HDPE with 50–55 wt% LLDPE showed improved strength and transparency over that of neat HDPE. In the following patents, the company disclosed immiscible blends of LDPE with either HDPE or MDPE. These were well suited for films with uniform thickness and anisotropic tensile strength (Showa Denko 1981, 1983).

Phillips Petroleum patented PE blends prepared by dry powder blending followed by compounding in an internal mixer or an extruder. The two PEs were 30–70 wt HDPE, narrow MWD LLDPE, and 30–70 wt% HDPE, having significantly different MW (Bailey and Whitte 1984). The former was Z-N–LLDPE [Ti catalyst; $\rho \leq 955$ kg m^{-3}, MI = 0.1–50 g/10 min, and M_w/M_n = 2–10], while the second comprised low-MW HDPE [Cr catalyst; $\rho \geq 955$ kg m^{-3}, MI = 25–400 g/10 min, and M_w/M_n = 2–35]. The blends were used for the produced pipes, films, and bottles with good mechanical properties and environmental stress crack resistance, ESCR.

Phillips disclosed blends comprising 1–30 wt% LDPE [ρ = 910–930 kg m^{-3}, MI = 6 dg min^{-1}] blended with 99–70 wt% Cr-catalyzed LLDPE [ρ = 910–940 kg m^{-3}, MI < 1 dg min^{-1}, M_w/M_n > 6]. The blends had synergistic increase of tear strength and reduction of haze (Benham et al. 1995). Similar effects were also reported for LLDPE blends with 10–40 wt% of an ethylene–vinyl acetate copolymer, EVAc [ρ = 920–945 kg m^{-3}, MI = 6–10 dg min^{-1}, and 10–20 wt% VAc]. The materials had good processability and high tear strength and transparency (Benham and McDaniel 1994). In 1991, Hoechst disclosed blends having a bimodal MWD. The materials comprised 50–80 wt% HDPE blended with either Z-N–LLDPE or LDPE. The alloys were found suitable for molding or extrusion of tubes, pipes, and other articles requiring high ESCR (Böhm et al. 1994).

Blends of HDPE with an elastomeric C_{2+8} Z-N–LLDPE (SCB = 25 mol% of C_8 and LCB) are partially miscible under quiescent conditions, but under sheared conditions, they develop complex morphologies composed of fine globular interconnected domains, probably originating from coarsening after SD (Tabtiang et al. 2001). Thus, miscibility of these blends is enhanced by flow, and after its cessation parallel liquid–liquid and solid–liquid phases separate. The process leads to the formation of an interpenetrating morphology comprising amorphous PE and copolymer and crystalline PE.

Solvay patented blends comprising (A) high-density copolymer, C_{2+n}, where n = 4–10 ($\rho \geq 950$ kg m^{-3}, MI$_5$ = 0.05–2 dg min^{-1}; α-olefin content 0.15–1 mol%),

with (B) 42 wt% of another copolymer, C_{2+m}, where $m = 4$ or 6 ($\rho \geq 969$ kg m^{-3}, MI$_2 \geq 100$ dg min^{-1}, and $M_w/M_n > 4$ copolymerized with 0.8 mol % of C_4 or C_6 alpha-olefin) (Mattioli et al. 2002). The copolymers were synthesized using two "in-series" suspension polymerization reactors: (I) in a first reactor, at 40 °C, the C_2 was polymerized in a medium comprising a diluent, H_2, a catalyst based on Ti or Zr and a co-catalyst (MAO), to form 53–63 wt% of the component (A); (II) the product from the first reactor was introduced into the second reactor and C_{2+n}, $n = 4$–10, α-olefin was added, and the remaining part of the patented system [37–47 wt% copolymer (B)] was formed. The blends were used for the production of pipes with improved creep resistance while maintaining other mechanical properties (e.g., resistance to crack growth). This is one of many patents for the production of partially miscible blends, where polymerization controls composition and configuration of macromolecules producing optimized resin grades.

Exxon patented blends of high-MW HDPE with 20–50 wt% of Z-N–LLDPE or m-LLDPE (Mehta et al. 1994). The HDPE had $\rho > 0.94$ g mL^{-1} and MI$_2 < 0.1$ dg min^{-1} and LLDPE $\rho = 0.90$–0.93 g mL^{-1} and MI$_2 = 0.5$–5 dg min^{-1}. The LLDPEs were C_{2+6} copolymers for films with dart drop impact strength >500 g. The blends with improved resistance to environmental stress cracking (ESC) were used for the production of medium-density pipes or geomembranes [U.S. Patent 6,649,698 to Equistar Chem.]. Simulating blends of HDPE with LLDPE having three LCBs and up to 40, C_4 SCB suggested that about 3/100 C is needed for phase separation (Fan et al. 2002).

18.7.5 HDPE/m-LLDPE Blends

Phillips Petroleum applied for patents for HDPE/m-LLDPE blends with improved processability. These comprised 30–70 wt% low-MW HDPE [Cr catalyst, $\rho \geq 955$ kg m^{-3}, MI $= 25$–400 g/10 min, and $M_w/M_n = 2$–35], and 30–70 wt% high-MW LLDPE [Ti catalyst, $\rho \leq 955$ kg m^{-3}, MI $= 0.1$–50 g/10 min, and $M_w/M_n = 2$–10]. The blends were used for pipes, films, and bottles with enhanced mechanical properties and ESCR. In another patent 5–40 wt% low-MW HDPE [Ti catalyst, $\rho \geq 955$ kg m^{-3}, MI ≥ 25 dg min^{-1}, and $M_w/M_n = 2$–8], blended with 60–95 wt% high-MW HDPE [Cr catalyst, $\rho \geq 93$ kg m^{-3}, MI $= 1.5$–15 dg min^{-1}, and $M_w/M_n = 6$–100], yielded blends with MI $= 0.05$ dg min^{-1} and excellent ESCR (Martin et al. 1994). In another document, 10–80 wt% low-MW LLDPE [$\rho \geq 940$ kg m^{-3}, MI > 25 dg min^{-1}, and $M_w/M_n = 2$–12] was blended with 20–90 wt% of a high-MW LLDPE [$\rho \leq 955$ kg m^{-3}, MI $= 2$–10 dg min^{-1}, and $M_w/M_n = 2$–10]. The blends were reported to have MI > 0.05 dg min^{-1} and improved optical properties (Coutant and Martin 1995).

ExxonMobil patented blends of 60–95 wt% linear m-VLDPE ($\rho = 0.916$ g mL^{-1}; 5–15 wt% comonomer C_3–C_{12}; $M_w/M_n = 2$–3, bimodal, produced in the gas phase using di-Cp metallocene catalyst) with HDPE ($\rho \geq 0.940$ g mL^{-1}) have shown that blown and cast films may be downgauged by up to 30 % for similar performance to those of conventional films (Halle 1999; German et al. 2004).

Three Z-N-type HDPEs from BP (M_w = 62, 137 and 292 kg mol^{-1}) were blended with C_{2+8} m-LLDPE from Dow (narrow MWD, different MW and C_8 content) (Stephens et al. 2003). Miscibility very much depended on the C_8 comonomer content, for 5.3 mol% of C_8 being miscible, but immiscible (with UCST) for 8.5 and 12.3 mol% C_8. After extracting the solubility parameters, the authors concluded that miscibility of low-MW fraction of HDPE with broad MWD is significantly higher than that of the high ones.

Hameed and Hussein (2007) studied blends of m-LLDPE with HDPE varying the MW and branch content (BC) in m-LLDPE. No influence of MW on miscibility was observed for polymers with low BC ($\approx$2/100 C). However, at high-BC levels (ca. 4/100 C) MW did affect miscibility of m-LLDPE/HDPE blends. Low-MW m-LLDPE/HDPE blends were miscible at all compositions, while high-MW phase segregated into layered morphology. The HDPE-rich blends co-crystallized, whereas m-LLDPE-rich phase showed separate crystallization. Mechanical properties of these blends strongly depended on blend miscibility and properties of components. It is noteworthy that the high-BC pairs had poor mechanical properties, caused by weak interphase.

The effect of MW on phase separation was discussed for one branched LLDPE blended with linear PE of different MW (Hill 1994). While at high MW there was a region of phase-separated blends, at low MW the system was fully miscible. The effect of branch length on the miscibility of HDPE blended with C_{2+8} m-LLDPE was studied by Shin et al. (2008). The m-LLDPE had variable C_8 content (21–45 wt%) which apparently did not affect miscibility. At the same composition and MW, the miscibility of HDPE with C_{2+8} m-LLDPE was slightly better than that with C_{2+4} m-LLDPE. The results suggested phase separation leading to UCST.

In 2009, Equistar Chemicals obtained patent protection for thick blend films manufactured from HDPE (ρ > 0.955 g mL^{-1}, MI$_2$ < 1.0 dg min^{-1}) blended with m-LLDPE (ρ = 0.900–925 g mL^{-1}, MI$_2$ < 5.0 dg min^{-1}). The films 50–200 μm thick had the tear strength in the machine direction (MD) >20 % than that of a film with the same modulus prepared from a neat HDPE (Mavridis 2009).

Blends of ZN-HDPE with metallocene or single-site catalyzed hyperbranched LLDPEs (m-LLDPE branching content 7.2 wt% and HbPE with comonomer content 17.8 wt%, respectively) were prepared by dissolving the ingredients in xylene at 130 °C (Poltimäe et al. 2011). Next, the mixtures were cooled in liquid N_2 and freeze-dried under vacuum. The double melting peaks in DSC endotherms were observed in all blends, indicating separate crystallization of the two polymers. However, limited degree of co-crystallization was detected in the LLDPE/HbPE blends and HDPE/HbPE blend rich in HbPE component.

18.7.6 Z-N–LLDPE/m-LLDPE Blends

For facilitating film blowing of Z-N–LLDPE, the polymer may be blended with LDPE, known for its strong SH behavior. However, on conventional process lines, films from neat LLDPE are also being produced, but with considerable difficulties. Generally,

film-grade m-LLDPE is easier to process than Z-N–LLDPEs with the added benefit of better physicomechanical and optical properties. Blending Z-N–LLDPE with m-LLDPE having different comonomer may result in phase separation (controlled by branch content and branch type) and a reduction of the mechanical properties.

Intuitively, the two LLDPE types are structurally sufficiently different that immiscibility might be expected. The experimental data published by Rana et al. (2000) for blends of C_{2+8} Z-N- and metallocene-type LLDPE seem to confirm the expectation. The authors studied rheological and morphological behaviors of three binary blends of C_{2+8} with different melt index (MI), density, and comonomer contents (SCB) of the kind used for film blowing. In these blends, one component was made using a Z-N and the other a metallocene catalyst. The miscibility depended on the value of the MI, density, and SCB. When the latter was similar, then the melt viscosity was a weight average, expected for a miscible blend. The microtomed surface prepared during fast or slow cooling indicated separate crystallization of the two components, regardless of the density, MI, and SEC. The Z-N–LLDPEs had larger spherulites and ring space than those of the m-LLDPEs, independently of the cooling rate. The melt rheology was reflected in the mechanical and film properties. The blend miscible in the molten state showed linearity in the mechanical properties, whereas the immiscible blends showed positive or negative deviation from linearity, usually associated with the type of morphology and the interphasial interactions.

In 1992, Phillips Petroleum applied for patent protection of blends comprising melt-blended high- and low-MW LLDPE, having the melt viscosity (at 100 s^{-1}) of, respectively, $\eta > 5$ and $\eta < 0.3$ kPa s. The polymers were blended in two stages: first the high-MW polymer was blended with a small amount of the low-MW one, and then an additional low-MW polymer was incorporated in a second stage to form the final blend. The materials had good processability and excellent physical properties. The process provided improved resins for the production of films with low fish-eye content, for blow molding, extrusion of pipes, wire coating, and injection or rotational molding (Coutant 1994).

Two (C_{2+6} and C_{2+8}) Z-N–LLDPEs and two m-LLDPEs (C_{2+4} and C_{2+8}), η_o ranging from 11 to 34 kPas, were blended with a single LDPE (Delgadillo-Velázquez et al. 2008b). The focus was on the effects of the LLDPE manufacture and the effects of LCB. It was found that m-LLDPE is more compatible with LDPE at all concentrations as compared to blends with Z-N polymer. The elongational flow was a sensitive tool capable for detecting subtle changes in PE macrostructure, e.g., low levels of LCB. DSC indicated that in solid state m-LLDPEs are miscible with an LDPE. These results have not been confirmed by Robledo et al. (2009), who also compared Z-N type (C_{2+8}) and m-LLDPE (C_{2+6}) in blends with 5 and 15 wt% LDPE. Blends with m-LLDPE were thermorheologically complex showing immiscibility, while those with Z-N–LLDPE obeyed the time–temperature superposition principles (t-TSP), but exhibiting a linear viscoelastic response, characteristic for immiscible systems with a sharp interface. The broad linear response in the Z-N-type

blends may be related to strong interactions between the high-MW fraction of the LLDPE and the low-MW chains of the LDPE phase, forming a thick interface with its own viscoelastic properties. The interphase may play a key role in extensional properties, orientation phenomena, the final microstructure, and system performance.

Frederix et al. 2010 studied the properties of three series of polymers: high-density ethylene/hexene Z-N–LLDPE (HD), C_{2+8} m-LLDPE (LL), and C_{2+8} m-ULDPE (UL). The blends LL/HD, UL/HD, and UL/LL comprised about 0, 25, 50, 75, and 100 wt% of each polymer. The crystallinity of melt-compounded blends was 77 %, 46 %, and 16 %, for the HD, LL, and UL, respectively. The zero-shear viscosity (η_o) indicated immiscibility of the three binary series over the whole composition range. For most blends, the temperature shift of the crystallization (T_c) and melting (T_m) peaks from those of neat copolymers indicated partial miscibility in the crystalline or the amorphous region. In some cases, the presence of intermediate endotherm and exotherm between the two main peaks of the melting and crystallization traces, respectively, indicated hybrid crystals. A marked positive deviation of the upper T_c from the linear mixing rule was observed for the three systems. A nucleating effect from the interface of the phase-separated domains promoted early crystallization in the upper T_c phase. The SAXS data reveal electron density fluctuations at a much larger scale than that of the semicrystalline structure, demonstrating the occurrence of micro-phase separation in the melt prior to crystallization. Solubility of low-T_m chain species in the amorphous layers of the high-T_m phase was also evident. AFM and DMTA support micro-phase separation in the three systems.

Cycloolefin copolymer (COC) is an amorphous, clear metallocene product of norbornene and ethylene with a spectrum of attractive performance characteristics. Thus, COC (MFI at 190 °C and 2.16 kg = 1.7 dg min^{-1}, $\rho = 1{,}020$ kg m^{-3}) was blended with C_{2+6} LLDPE (MFI at 190 °C and 2.16 kg = 3.2 dg min^{-1}, $\rho = 920$ kg m^{-3}). The mechanical properties of the blends indicate immiscibility, despite the increased LLDPE crystallinity. The presence of COC improved the thermo-oxidative stability. Quasi-static tensile tests showed that increasing fraction of COC in the blends accounts for an enhancement of the elastic modulus and a decrease in the strain at break, while tensile strength passes through a minimum. A significant reduction of the creep compliance of LLDPE could be achieved only for the COC fractions exceeding 20 wt% (Dorigato et al. 2010).

18.8   Conclusions and Outlook

18.8.1 Future Trends in PE Synthesis

The future activities in PE synthesis are expected to have three aspects:
1. Improve activities of the metallocene catalytic systems, e.g., by developing (1) bulky, weakly coordinating co-catalysts (perfluorophenylborate, boranes)

and (2) more efficient MAO-activated catalyst and (3) by reducing the amount of MAO required for the activation (Kaminsky 2012).

2. Continue the development toward commercialization of the new class of post-metallocene catalysts based on transition metal (Ti, Zr, Hf, V, ...) complexes without Cp, but with imino-carboxylate and imino-amido ligands and sometimes with a neutral Lewis acid acting as a co-catalyst (Makio and Fujita 2009; Makio et al. 2011; Ivanchev et al. 2012). These systems are capable efficiently polymerized monomers containing polar group. Furthermore, different reactions are possible, e.g., anionic polymerization, ring-opening polymerization, or polycondensation.

3. Polymeric nanocomposites (PNC) are relatively new materials on the market with an array of interesting properties and applications (Utracki 2004; Kaminsky et al. 2006; Compton and Nguyen 2010). There are many types of nanoparticles (historically starting with layered clay), but the common problem originating from the nature of nano-size is the dispersibility – on the nanoscale the Lennard–Jones forces form aggregates, which are difficult to break. One method that has been used for dispersing clay in polyamide matrix was the addition of clay to monomer and polymerization of the suspension (Okada et al. 1988). Evolution of PE synthesis, especially the metallocene and post-metallocene catalysts, offers a new and potentially highly efficient route to new materials with a wide range of properties generated not only by the nanoparticles but also the PE structures that dispersed and coated those (Kaminsky et al. 2006).

18.8.2 Future of Commercial PE Blends

- The key to the equilibrium phase behavior of the PE/PE blends is that in the molten state – upon solidification the polymers crystallize or vitrify. Both of these states are affected by kinetics and aging. Molten blends are either miscible or immiscible with UCST or LCST after the phase separation via SD or NG mechanism. Extensive experimental studies of blended model polymers have been published.

- The early theories of phase separation are of the mean-field, cell, or cell-hole lattice (statistical thermodynamics) type. The theory takes into account the configurational entropic and enthalpic contributions, but since these are weak, the effects on miscibility are not as predictable as that for other PO blends. Nevertheless, the enthalpy as a difference of the solubility parameters well correlate with the experimental data being independent on SCBD and SCB if SCB $<$ 5/100 C. This observation is unexpected, since the miscibility was reportedly controlled by entropy, e.g., chain stiffening led to phase separation.

- The newer theoretical models attempt incorporating the model macromolecular chain structures using either mathematical modeling via MC, molecular

dynamics (MD), PRISM, CFT, etc. Evidently, another possibility is an analytical approach where the configurational elements are identified taking into account MW, SCB, and LCB and their concentration and distribution. This has been done by Freed and Dudowicz, who formulated the lattice cluster theory (LCT) in its full, basic (BLCT), and simplified (SLCT) versions. The latter approach identified four classes of PE blends, defined by structure and led to two UCST and two LCST classes.

18.9   Cross-References

▶ Compounding Polymer Blends
▶ Crystallization, Micro- and Nano-structure, and Melting Behavior of Polymer Blends
▶ Degradation, Stabilization, and Flammability of Polymer Blends
▶ Interphase and Compatibilization by Addition of a Compatibilizer
▶ Morphology of Polymer Blends
▶ Physical Aging of Polymer Blends
▶ Reactive Compatibilization
▶ Recycling Polymer Blends
▶ Rheology of Polymer Alloys and Blends
▶ Thermodynamics of Polymer Blends

Nomenclature

^{13}CNMR   Carbon-13 nuclear magnetic resonance
^{1}HNMR   Hydrogen nuclear magnetic resonance
ABC   Alloying–blending–compounding
ABS   Acrylonitrile butadiene styrene
AE   Aminoethyl
AGR   Annual growth rate
An   9-Anthryl
APME   Association of Plastics Manufacturers in Europe
AR   Autoclave reactor
ATBN   Amine-terminated butadiene nitrile liquid rubber
ATR   Attenuated total reflection (in FT-IR)
a-TREF   Analytical temperature rising elution fractionation
BAF   Tetrakis[3,5-bis(trifluoromethyl)phenyl]borate
BC   Branch content
BLCT   Basic lattice cluster theory (LCT)
bPET   Branched polyethylene terephthalate
BR   Polybutadiene, butadiene rubber

Bu   Butyl

Bz   Benzyl

C_{2+i}   Abbreviated notation for poly(ethylene-*co*- *i*-olefin); $i = 3, 4, 6, 8, \ldots$.

CA   Cellulose acetate

CBR   Chlorinated butyl rubber

CCD   Chemical composition distribution (or charge-coupled detector)

CED   Cohesive energy density

CEF   Crystallization elution fractionation

CFC   Cross-fractionation chromatography

CFT   Continuum field theory

CGC   Constrained geometry catalyst

CHX   Cyclohexyl

CMC   Critical micelles concentration

CO   Carbon monoxide

COD   1,5-Cyclooctadiene

COPO   Poly(carbon monoxide-co-polyolefin), a linear, alternating terpolymer

CORI   Corotating, fully intermeshing TSE

Cp   Cyclopentadienyl

$Cp = C_5H_5{}^-$ Cyclopentadienyl anion$^-$

CPE   Chlorinated polyethylene

CR   Chloroprene, or neoprene, rubber

CRNI   Counterrotating, non-intermeshing TSE

CSR   Chlorosulfonated polyethylene rubber

CSTR   Continuously stirred tank reactor

CTM   Cavity transfer mixer

CUT   Continuous use temperature

DAB   1,4-Diazabutadiene

DIPP   2,6-Diisopropylphenyl

DR   Drawdown ratio

DSC   Differential scanning calorimetry

D-W   Dee and Walsh theory

EAA   Ethylene acrylic acid copolymer or "carboxylated PE"

EBA   Ethylene butyl acrylate copolymer

EEA   Elastomeric copolymer from ethylene and ethyl acrylate

EFM   Extensional flow mixer

EGMA   Ethylene-glycidyl methacrylate copolymer

ELSD   Evaporative light-scattering detector

EMA   Ethylene-maleic anhydride copolymer

EMAc   Copolymer from ethylene and methacrylic acid

EPDM   Ethylene-propylene-diene terpolymer

EPR   Ethylene-propylene rubber

EPR-MA   Maleated ethylene-propylene rubber (EPR)

EPS   Polystyrene foam; expanded PS

Et   Ethyl ($C_2H_5{}^-$)

EVAc   Copolymer from ethylene and vinyl acetate
EVAc-MA   Copolymer from ethylene, vinyl acetate, and methacrylic acid
EVAL   Copolymer of ethylene and vinyl alcohol
FBR   Fluidized bed reactor
FOA   Fluorinated octyl acrylate
FT-IR   Fourier transform infrared (spectroscopy)
GF   Glass fiber or glass fiber-reinforced plastic
Gi   The Ginsburg number
GMA   Glycidyl methacrylate
GPC   Gel [permeation chromatography (see SEC)
HALS   Hindered amine light stabilizer
HAS   Hindered amine stabilizer
HBA   Hydroxybenzoic acid
HDPE   High-density polyethylene
HDPE-MA   Maleated high-density polyethylene
HDXLPE   High-density cross-linked polyethylene
hhPP   Head-to-head polypropylene
HIPS   High impact polystyrene
HMWPE   High-molecular-weight polyethylene
HNA   Hydroxy naphthoic acid
HTLC   High-temperature liquid chromatography
Hx   Hexyl
ICRR   Intermeshing, counterrotating TSE
ID and OD   Inner and outer pipe diameters
Ind   Indentyl
i-**PB**   Isotactic polybutylene
i- **PP**   Isotactic polypropylene
LA   Lactic acid
LC   Liquid chromatography
LCB   Long-chain branching
LCBPE   Long-chain branched PE
LCP   Liquid crystalline polymer
LCST   Lower critical solution temperature
LCT   Lattice cluster theory
LDPE   Low-density polyethylene
L-J   Lennard–Jones (theory, potential, parameters)
LLDPE   Linear low-density polyethylene
M   Transition metal in a catalyst
MA   Methyl acrylate
MAH   Maleic anhydride
MAO   Methylaluminoxane
MBS   Copolymer from methyl-methacrylate-*co*-butadiene-*co*-styrene
MC   Monte Carlo simulation
MD   Machine direction

MDPE   Medium-density polyethylene

Me   Methyl (CH_3-)

Mes   Mesityl

MFR   Melt flow rate

m-**LLDPE**   Metallocene LLDPE

m-LLDPO   Metallocene PO

MM   Motionless mixer

M_n, M_w Number, weight average molecular weight

MW   Molecular weight

M_w/M_n Molecular polydispersity index, MWD

MWD   Molecular weight distribution usually expressed as M_w/M_n

Nb   Norbornyl

NDB   Negatively deviating blends

NG   Nucleation and growth mechanism

NIR   Near-infrared (spectroscopy)

NMR   Nuclear magnetic resonance

Np   Naphthyl

NPDB   Negatively–positively deviating blends

NR   Natural rubber

ODCB   *o*-Dichlorobenzene

OM   Optical microscopy

P(HB-b-I-S)   Block copolymer of hydrogenated butadiene, isoprene, and styrene

P(S-b-MMA)   Block copolymer of styrene and methyl methacrylate

PA   Polyamide

PA-46   Poly(tetramethylene adipamide)

PA-6   Poly-ε-caprolactam

PA-66   Poly(hexamethylene diamine-adipic acid), polyhexamethylene-adipamide

PA-6IT6   Poly(caprolactam-*co*-hexamethylene diamine-isophthalic/terephthalic acids)

PA-mXD6   Poly(*m*-xylylenediamine -adipic acid-*co*-caprolactam)

PAr   Polyarylate

PARA   Aromatic (mainly amorphous) polyamide

PB1   Poly(butene-1)

PB2   Poly(butene-2)

PBD   Polybutadiene

PBMA   *Polybutyl* methacrylate

PBSA   Poly(polybutylene succinate-*co*-adipate)

PBT   Polybutylene terephthalate

PC   Polycarbonate of bisphenol-A

PCL   Poly-ε-caprolactone

PCW   Postconsumer waste

PD   Polydispersity, M_w/M_n

PDB   Positively deviating blends

PE Polyethylene
PEA Polyetheramide
PEB = C$_{2+4}$ Poly(ethylene butylene)
PEE Poly(ethylene propylene)
PEEI Polyesteretherimide
PEEK Polyetheretherketone
PEE *xx* Poly(ethylene-*r*-ethyl-ethylene); random copolymer with *xx*% of ethyl–ethylene (EE) units
PEG Polyethylene glycol
PEH=C$_{2+6}$ Polyethylene–hexene
PEI Polyetherimide
PEi≡C$_{2+I}$ Poly(ethylene-*co*-α-olefin), PEi≡C$_{2+I}$; *i* = 3–8
PEN Poly(ethylene 2,6-naphthalene dicarboxylate), or polyethylene naphthalate
PEP=C$_{2+3}$ Poly(ethylene butylene)
PEP Poly(ethylene propylene)
PEST Thermoplastic polyesters such as PET, PBT, and PEN
PET Polyethylene terephthalate
PETG Polyethylene terephthalate glycol; copolymer
PEtI Polyethyleneimine
PEX Cross-linked polyethylene
PGI Polyglutarimide
Ph Phenyl
PH1 Poly(hexene-1)
PHB Polyhydroxybutyrate
PHBA Poly(β-hydroxybutyric acid)
PHBV Poly(hydroxybutyrate-*co*-valerate)
Phenoxy Polyhydroxyether of bisphenol-A
PHV Poly(hydroxy valerate)
***p*$_i$** Internal pressure
PI Polyimide
PIB Polyisobutylene
PIB Polyisobutylene
PLA Polylactic acid
PMA Polymethylacrylate
PMMA Polymethylmethacrylate
PMP Poly-4-methyl-1-pentene, also TPX
PNDB Positively–negatively deviating blends
PO Polyolefin
POM Polyoxymethylene
PP, *i*-PP Isotactic polypropylene (*a*- PP – atactic; *s*-PP – syndiotactic)
PPA Polyphthalamide (also polypropyleneadipate)
PPE Poly(propylene ethylene)
PPE Polyphenylene ether

PPG   Polypropylene glycol
PP-MA   Maleated polypropylene
PPS   Polyphenylene sulfide
Pr   Propyl
PRISM   Polymer reference interaction site model
PS   Polystyrene
PSF   Polysulfone
PS-g-EPR   Styrene-grafted EPR
PS-g-EVAc   Styrene-grafted EVAc
PS-g-PP   Styrene-grafted PP
p-TREF   Preparative temperature rising elution fractionation
PVAc   Polyvinyl acetate
PVAl   Polyvinyl alcohol
PVC   Polyvinyl chloride
PVDC   Polyvinylidene chloride
PVDF   Polyvinylidene fluoride
PVF   Polyvinyl fluoride
PVME   Polyvinylmethylether
PVP   Polyvinyl pyridine
PVT   Pressure-volume-temperature
py   Pyridyl
QC   Quality control
RI   Refractive index
RPA   Random phase approximation
R-TPO   Reactor-blended thermoplastic olefinic elastomer
SAN   Styrene acrylonitrile
SANS   Small-angle neutron scattering
SAXS   Small-angle X-ray scattering
SB   Styrene–butadiene copolymer
SBR   Styrene–butadiene elastomer
SBS   Styrene–butadiene–styrene three-block copolymer
SCB   Short-chain branching
SCBD   Distribution of SCB
SCM   Super-condensed mode of *m*-LLDPE production
SD   Spinodal decomposition mechanism
SEBS   Styrene–ethylene/butene–styrene three-block copolymer
SEBS-MA   Maleated SEBS
SEC   Size exclusion chromatography
SEM   Scanning electron microscopy
SH   Strain hardening
SIMS   Secondary ion mass spectrometry
SIS   Styrene–isoprene–styrene three-block copolymer
SLTC   Simplified lattice cluster theory (LCT)
SMA   Styrene–maleic anhydride

SMMA   Styrene–methyl methacrylate block copolymer
sPS   Syndiotactic polystyrene
S-S   Simha and Somcynsky cell-hole theory
SSE   Single-screw extruder
SSSE   Solid-state shear extrusion
TD   Transverse direction
TEM   Transmission electron microscopy
T_{g} Glass transition temperature
THF   Tetrahydrofuran
TIBA   *tri*-Isobutyl aluminum
T_{m} (°C)   Melting temperature
TMA   *tri*-Methyl aluminum
TMS   Trimethylsilyl
TO   Turnovers, number of moles of monomer polymerized per mole of metal in the catalyst
TOF   Catalyst turnover frequency
TPE   Thermoplastic elastomer
TPO   Thermoplastic olefinic elastomer
TPU   Thermoplastic urethanes
TPV   Thermoplastic vulcanizate
TR   Tubular reactor
TREF   Temperature rising elution fractionation
TSE   Twin-screw extruder
t-TSP   Time–temperature superposition (also: t-T)
UCST   Upper critical solution temperature
UHMWPE   Ultrahigh-molecular-weight polyethylene (over 3 Mg mol^{-1})
ULDPE   Ultralow-density polyethylene
UV   Ultraviolet light spectroscopy (irradiation)
UV-Vis   Ultraviolet–visible light spectroscopy
VCH   Vinyl cyclohexane
VLDPE   Very low density PE
XLPE   Cross-linked polyethylene
XRD   X-ray powder diffraction
Z-N   Ziegler–Natta catalyst
Z-N–LLDPE   Ziegler–Natta-catalyzed LLDPE
ZN-LLDPO   Ziegler–Natta-catalyzed PO
ΔG_{m} Gibbs free energy and heat of mixing
δ Solubility parameter
ρ Polymer density

Appendix

See Tables 18.10, 18.11, and 18.12

Table 18.10 Chronology of polyolefin technology

Date	Event	Inventor/company	Comment	Reference
1898	Polymethylene obtained by thermal decomposition of diazomethane with $T_m = 128\ ^\circ C$	Hans von Pechmann. In 1953, Kantor and Osthoff produced UHMWPE from diazomethane + BF_3	White, waxy powder in 1898, while UHMWPE (MW = 3,000 kg mol^{-1}) in 1953 had $T_m = 132\ ^\circ C$	R.A.V. Raff, J.B. Allison, *Polyethylene* (Interscience Publication, New York, 1956); Germ. Pat. Appl., B25064 (1955). http://en.wikipedia.org/wiki/Polyethylene#History
1933	PE obtained at $P = 120$–300 MPa and $T = 140$–180 °C from a mixture of ethylene (C_2), benzaldehyde, and oxygen. The early ICI design utilized stirred autoclave reactors	Eric W. Fawcett and Reginald O. Gibson at the ICI Works in Northwich, England	White, waxy powder, due to contamination by O_2; the reaction was irreproducible. The first PE patents were registered by ICI in 1936	http://archive.thisischeshire.co.uk/2006/8/23/275808.html; E.W. Fawcett, R.O. Gibson, M.H. Perrin, J.G. Patton, E.G. Williams, British Patent 471,590 (1937)
1935	ALKATHENE, the high-pressure polyethylene (HPPE) or low-density PE (LDPE: $\rho = 915$–940 kg m^{-3}); polymerization in an autoclave with benzoyl peroxide and hydroxyperoxide Three years later IG Farben (BASF), introduced a tubular reactor technology	M. Perrin and W. R. D Manning at ICI. In 1933 invented the autoclave polymerization of LDPE, commercialized by ICI in 1938	Commercial production of ALKATHENE beginning in 1938 for submarine telegraph and then later the radar cables. The technology transferred to the USA delegation in 1941	Poly – The All Star Plastic, Popular Mechanics, pg 126, July 1949; S.W. Bigger, P.J. Watkins, M.A. Raymond, S.S. Verenich, J. Schei, Characterization of oligomeric by-products produced during the high-pressure polymerization of ethylene, Eur. Polym. J. **32**(4), 487–492 (1996); http://www.chemsystems.com/about/cs/news/items/PERP%200809_1_LDPE.cfm
1938	High-pressure tubular reactor for the continuous production of LDPE (Lupolen). Tubes 0.5–1.6 km long, with ID = 70 mm, and OD/ID ≈ 2.6 were made of high-strength steel	IG Farbenindustrie, now BASF – Ludwigshafen engineers developed a new high-pressure reactor	The first tubular reactor was invented by IG Farbenindustrie in 1938, but commercial production started after the WWII in 1953	http://www.basf.com/group/corporate/en/about-basf/history/1925–1944/index; High pressure equipment for LDPE plants, http://www.uhde-hpt.com/index

Year				References
1943	Union Carbide Corp. (UCC) commercialized in 1943 a LDPE process in a tubular reactor. Sumitomo also patented (U.S. Patent 4168355) ethylene copolymerization in reactor with ID = 19 mm and L = 190 m at P > 100 MPa. At present (2012) tubular reactors dominate the LDPE production. Length-to-diameter of tubular reactors = 250/1.0–12,000/1.0	LLDPEs from tubular or cascade loop reactor have fewer LCB and broader MWD than autoclave products. Modeling of an industrial slurry-phase olefin catalytic polymerization of two loop reactors in series was carried out by U. Thessaloniki and Total Petrochemicals	The slurry copolymerization of ethylene with other olefins uses a Z-N catalyst, an organometallic, and H_2 as MW regulator in two or more reaction zones producing PE with broad MWD and $\rho < 0.945$ g mL^{-1}. A mathematical model accounts for the effects of T and P, rates of catalyst addition, monomers and diluent, on MW, MWD, and viscosity	J.C. Swallow, in *Polythene*, ed. by A. Renfrew and P. Morgan, 2nd ed. (Interscience, New York, 1960), pp. 1–10; T.Y. Xie, K.B. McAuley, J.C.C. Hsu, D.W. Bacon, Gas-phase ethylene polymerization, Ind. Eng. Chem. Res. **33**, 449–479 (1994). CA Patent 1162700A of 21 Feb 1984 to Sumitomo Chem.; V. Touloupides et al., Modeling and simulation of an industrial slurry-phase catalytic olefin polymerization reactor series, Chem. Eng. Sci., **65**, 3208–3222 (2010)
1944	Further research on LDPE and large-scale commercial production licensed by ICI	Bakelite Corporation at Sabine, TX and Du Pont at Charleston, WV	Insulation for ultra- and superhigh (UHF and SHF, respectively)coaxial cables of radar sets	Poly – The All Star Plastic Popular Mechanics, pg 126, July 1949
1948	Radiative cross-linking LDPE produced dimensionally and thermally stable material different from the original LDPE	M. Dole, Argonne Natl. Lab. (ANL)	The radiative cross-linking was followed by UV (G. Oster et al.) and then by chemical with peroxides (Scott)	M. Dole, J. Macromol. Sci., Chem. **A15**, 1403 (1981); G. Oster et al. J. Polym. Sci. **34**, 671 (1959); H.G. Scott, U.S. Patent 3,646,155, 1972
1949	Oligomerization of ethylene by LiAlH4 (the Aufbau or buildup reaction). The work was followed by oligomerization of ethylene by catalytic activity of AlEt3	At ambient P and $T \approx 170$ °C, K. Ziegler (Kaiser Wilhelm Institute) dimerized ethylene to butene-1, propylene to 2-methyl-1-pentene, and butene-1 to 2-ethyl-1-hexene	Ziegler presentation in 1952 on the Aufbau reaction started collaboration with Natta. The 2-methyl-1-pentene was the starting material for industrial synthesis of isoprene, while the 2-ethyl-1-hexene opened up the way to terephthalic acid	K. Ziegler, A forty years' stroll through the realms of organometallic chemistry, Adv. Organometal. Chem. **6**, 1–17 (1968); L. Cerruiti, Hyle, Intl. J. Philos. Chem. **5**, 3–41 (1999); G. Wilke, Angew. Chem. Int. Ed. **42**, 5000–5008 (2003)

Table 18.10 (continued)

Date	Event	Inventor/company	Comment	Reference
1951	HDPE $\rho = 0.96$ polymerized at $T = 230–270\ °C$, $P = 4 – 8$ MPa, with NiO on activated carbon, Mo_2O_3 or $CoMoO_4$ on alumina, activated by electropositive metals, e.g., Na or Li. Producing HDPE with $\rho = 0.96\ g\ mL^{-1}$	Standard Oil Co., E. Field, M. Feller, U.S. Patent 2,691,647, 12 Oct 1954, filed 06 Dec 1952; A. Zletz, U.S. Patent 2,692,257; 2,780,617, priority 1951	Zletz recorded the polymerization to PO on 21 July 1950; the reaction was conducted in benzene solution initially with H_2 as an activator	Edmund Field, Morris Feller, Promoted Molybdenum-Alumina Catalysts in Ethylene Polymerization, Ind. Eng. Chem., 49, 1883–1884 (1957); A. Zletz, Ethylene polymerization with conditioned alumina-molybdenum catalysts, U.S. Patent 2,692,257, 19 Oct 1954
1951	Catalytic polymerization in gas phase or in a slurry at mild $T = 70–100\ °C$, $P = 3–4$ MPa (later $T = 40–260\ °C$, $P = 0.7–4.8$ MPa) into LLDPE (with hexene): $\rho = 0.93–0.97\ g\ mL^{-1}$. By the late 1956, the system also produced HDPE in the Phillips double-loop reactor	Marlex, disclosed by J. P. Hogan and R. Banks, Phillips Petroleum Co. slurry process. The PE was recovered from slurry by flashing off the diluent. Phillips catalyst is less expensive and easier to work with than Z-N	The first catalyst: Cr_2O_3 on amorphous SiO_2 or Al_2O_3 (at $T = 230–800\ °C$, with H_2) was discovered when dimerizing C_2. Second was a Cr compound with Ti, Ga, and/or Sn oxide. A 1998 patent significantly enhanced Phillips catalyst with $AlEt_3$ on SiO_2 as a base for partially reduced bis-triphenyl silyl-Cr	J.P. Hogan, R.L. Banks, U.S. Patents 2,825,721 of 04 Mar 1958, by others: 2927915; 2,939,892; 3,087,917; 3,351,623; 3,622,521; 3,635,840; 3,676,417; 4,376,851; 4,342,854 and British Patent 853,414 to Phillips Petroleum Co.; H.L. Hsieh, Catal. Rev.: Sci. Eng. **26**, 631–651 (1984); Arduini et al., CA Patent 2,192,722 of 06 Dec 1998, to NOVA Chem
1952	The authors correlated properties of LDPE with molecular structure, characterized by long- and short- chain branching (LCB and SCB, respectively) and the molecular weight (MW)	In 1944, Roedel from DuPont postulated formation of SCB via intramolecular chain transfer, which reduced crystallinity, density, modulus, and solubility	The elongation at break, Vicat temperature, and hardness are controlled by both density and MW, while melt viscoelasticity by LCB and MW	See a series of five articles on: The Molecular Structure of Polyethylene from DuPont (by Roedel, Bryant and Voter, Billmeyer, Beasley, and by Sperati et al.) in, J. Am Chem Soc. **75**, 6110–6133 (1953)

Year				References
1953	Popular catalyst for HDPE, LLDPE, and i-PP. Polymerization at $P \leq 5$ MPa, $T \leq 90$ °C, $M_w = 1–10$ kg mol^{-1}., then to UHMWPE with $M_w \geq 1{,}000$ kg mol^{-1}. Development of Ziegler catalyst was precipitated by observed catalytic reaction caused by Ni, followed by systematic examination of other metal for their effects on reaction. These identified Ti, Zr, Hf, etc., are good candidates for the polymerization catalysts	Karl Ziegler and Erhard Holzkamp from Kaiser Wilhelm Institute. Starting in the mid-1960s a series of patents was issued for the second generation of Z-N catalyst. It was later found that addition of Mg compound tenfold increased the catalyst activity	Ziegler–Natta (Z-N) catalyst with oxides or hydroxides of a metal from groups IVB, VB, and VIB with AlEt$_3$. For example, TiCl$_4$ activated by Al(C$_2$H$_5$)$_3$ or Al (C$_2$H$_5$)$_2$Cl in a hydrocarbon medium. PE density: $\rho = 0.88–0.96$ g mL^{-1}. By 1984, at least 32 companies applied for patents on Z-N catalyst	K. Ziegler, H. Breil, E. Holzkamp, H. Martin, DE 973,626, 1953; U.S. 3,257,332 of 21 June 1966; K. Ziegler, Angew. Chem. **67**, 541–547 (1955); L. Cerruti, Hyle, Intl J. Philos. Chem. **5**, 3–41(1999); H.L. Hsieh, Catal. Rev. Sci. Eng. **26**(3–4), 631–651 (1984); S. Sivaram, Ind. Eng. Chem., Prod. Res. Dev. **16**, 121 (1977); Catalyst composition for polymerization of olefins, U.S. Patent 4292200 of 29 Sept 1981 to Solvay and Cie; T.E. Nowlin, Prog. Polym. Sci. **11**, 29–55 (1985)
1954	New catalyst for polymerization of ethylene, which contains Ti + 2 and complexing and reducing agents for controlling MW	A W Anderson from DuPont suggested a coordination catalyst: TiCl$_4$ with phenyl–Mg–Br in, e.g., cyclohexane (CHX)	The new catalyst polymerized C$_2$ at ambient T and P to polymers with density ranging from about $\rho = 0.92$ to 0.98 g mL^{-1}	A.W. Anderson, U.S. Patent 2,905,645 of 22 Sept 1959 (filed 16 Aug 1954) to E. I. du Pont de Nemours & Co., Wilmington, Del
1954/ 1955	Hoechst (reincorporated in 1952 from IG Farben after WWII) started production of HDPE in a slurry cascade process involving two CSTRs, capable of forming either low- or high-MWD HDPE	Farbwerke Hoechst AG produced Hostalen at low pressure using Ziegler catalyst. The HDPE had high crystallinity, $X = 65–85$ %, and $T_m = 130$ °C	Since 1960, GUR® ultrahigh-molecular-weight polyethylene (UHMWPE) has been manufactured by Ruhrchemie. In 1988, the company merged with Hoechst AG and in 1999 with Celanese AG, forming Ticona	A.G. Hoechst. http://www.referenceforbusiness.com/history2/22/Hoechst-A-G; R.A.V. Raff, J.B. Allison, *Polyethylene* (Interscience Publication, New York, 1956)

(continued)

Table 18.10 (continued)

Date	Event	Inventor/company	Comment	Reference
1955	The use of H_2 for controlling MW during polymerization of C_2 improved the Ziegler process and PE performance	E. J. Vandenberg of Hercules Powder	The method was claimed applicable to any $CH_2=C(RR_1)$ monomer or comonomer, especially C_2 or C_3	E.J. Vandenberg, U.S. Patent 3,051,690 of 28 Aug 1962 to Hercules Powder; Chem. Eng. News, **40**(36a), 25–26 (1962)
1955	The catalyst polymerizing mono-α-olefinic monomers (e.g., propylene). The catalyst [$TiCl_4$ + $AlEt_3$] was deposited on neutral support such as TiO_2	Guyer from Esso. The patent describes composition developed by Ziegler, but his name is not mentioned	The catalyst on solid support was dispersed in n-heptane then propylene added. The reaction was carried out at ambient P and $T = 20$–$150\,°C$	Walter R.F. Guyer, Polymerization catalyst, U.S. Patent 3,008,943 of 14 Nov 1961 (filed 01 Dec 1955) to Esso Res. & Eng. Co.
1955	Natta et al. used Ziegler catalyst for polymerization of propylene to i-PP. U.S. Patent of 1973 describes i-PP consisting of head-to-tail connected propylene units, having $M_v \geq 20\ kg\ mol^{-1}$, and being crystalline due to steric arrangement along the main macromolecular chain. The authors discovered the principles of the regio- and stereospecific polymerization of 1-alkenes, e.g., propylene into i-PP, s-PP, or a-PP	Giulio Natta et al.; Politecnico – Milano, patents assigned to Montecatini Edison SpA. The Z-N catalysts are based on Natta et al. U.S. Patent 3,715,344 and Kaminsky et al. DE Patent 3,240,382 of 1984	Z-N catalyst is based on transition M (Groups 3–8) and organometallic (Groups 1, 2, and 13), for example, Cp_2ZrCl_2 + MAO. The modern Z-N catalysts are either (1) $MgCl_2$ supporting $TiCl_3$ complex or (2) bridged complex of Ti, Zr, or Hf. More recent post-metallocene catalysts use an M-complex (Sc, La) and ligands containing O, N, P, and S activated by MAO	G. Natta, Angew. Chem. **68**, 869–887 (1956); G. Natta, Angew. Chem. **76**, 553–566 (1964); G. Natta, G. Mazzanti, P. Longi, F. Bernardini, Chim. Ind. **41**, 519–526 (1959); G. Natta, P. Pino, G. Mazzanti, U.S. Patent 3,715,344 of 06 Feb 1973, to Montecatini Edison SpA.; http://en.wikipedia.org/wiki/Ziegler%E2%80%93Natta_catalyst; J. Schmidt, T. Risse, H. Hamann, H.-J. Freund, J. Chem. Phys. **116**, 10861 (2002)

Year				
1955	Homogeneous catalysis using Z-N catalyst in a hydrocarbon (toluene), Cp_2TiCl_2 with an Al-alkyl compound, $Al(C_2H_5)_3$ – i Cli: $(C_5H_5)_2Ti(C_2H_5)Cl/Al(C_2H_5)Cl_2$	Breslow for Hercules Powder Co. Owing to low activity the system was not used	Polymerization of C_2 at $-10 < T\,°C < 100$, at nearly ambient P in the presence of 0.01–0.5 mol% of oxygen. Kinetics was described 15 years later	S. Breslow David, Polymerization of ethylene, U.S. Patent 2,827,446, of 18 Mar 1958 (filed 27 Sept 1955), to Hercules Powder Co.; Breslow and Newburg, J. Am. Chem. Soc. **79**, 5072 (1957); 81 (1959) 81; K.R. Meyer, Dissertation, TH München, 1969
1955	Commercialization of UHMWPE, $M_w = 0.2$–4 Mg mol^{-1}, $\rho = 0.925$ g mL^{-1}, produced using Ziegler catalyst, later metallocene	Ruhrchemie AG (now Ticona), also Mitsui, Braskem	Gel spun into high-performance ballistic fibers such as Dynema (1970) by DSM	S.M. Kurtz, *The UHMWPE Handbook: Ultra-high Molecular Weight Polyethylene in Total Joint Replacement* (Academic, 2004)
1956	Another disclosure based on modified Ziegler catalyst for either isomerization of hydrocarbons or olefin polymerization in the presence of subhalide of Ti or Zr	Thomas from Sun Oil Co. Polymerization was carried out at $T = 60$–80 °C and $P = 517$ kPa	A 2 wt% of $TiCl_4$ was deposited on γ-alumina. Reaction with H_2 at 300 °C reduces Ti + 4 to Ti + 2 or Ti + 3, which catalyzed polymerization in the presence of $Al(alkyl)_3$	C.L. Thomas, Gamma alumina supported titanium and zirconium subhalides polymerization catalysts and preparation thereof, U.S. Patent 3153634 of 20 Oct 1964 to Sun Oil Co.
1956	New polymerization catalyst for ethylene was prepared by slurring ethylaluminum sesquibromide, $Al_2Br_3Et_3$, with ethylhexyl titanate in *n*-heptane	Hagenieyer and Edwards to Eastman Kodak Co. The catalyst, activated by C_2, was used for polymerizing or copolymerizing olefins	The polymerization took place in a slurry reactor using hydrocarbon as the suspending medium at near ambient T and P	H.J. Hagenieyer Jr., B. Edwards Marvin, U.S. Patent 3067183 of 04 Dec 1962 (filed 15 Oct 1956), to Eastman Kodak Co.
1957	Fluidized bed reactor for polymerization of ethylene with Phillips Cr[VI] catalyst on SiO_2/	Dye from Phillips Petroleum Co. disclosed a gas-phase polymerization of HDPE. The	Ethylene + catalyst are fed to the lower part of the 3-segmented vertical reactor, passing through a reaction zone to cyclone	R.F. Dye, U.S. Patent 3023203 of 27 Feb 1962 (filed 16 Aug 1957), to Phillips Petroleum Co.;

Table 18.10 (continued)

Date	Event	Inventor/company	Comment	Reference
	Al_2O_3 supports at $T = 75$–100 °C and $P = 2$–3 MPa. HDPE from the Phillips catalyst had the highest crystallinity ($X = 90$–95 %) and density $\rho = 0.92$–0.96 g mL^{-1}	UNIPOL patent was originally deposited 14 Mar 1975 by UCC. The PE powder was removed from the fluidized bed reactor (FBR) and gas returned back to it	separating solids from remaining gases. The residence time in FBR was 3–5 h and conversion 97–99 % at 75 % lower energy cost than that in CSTR	A.R. Miller, U.S. Patent 4003712, 18 Jan 1977, to Phillips Petroleum Co; F.J. Karol, G.L. Goeke, B.E. Wagner, W.A. Fraser, R.J. Jorgensen, N. Friis, U.S. Patent 4302566 of 24 Nov 1981 & 4,621,952 of Nov 11 Nov 1986 to Union Carbide Corporation (UCC)
1957	Hercules Powder started production of HDPE (HITAX) in Parlin, NJ, in the presence of Karl Ziegler, whose catalyst the company has licensed	The first plant for the production of HDPE in the USA	Ziegler was the Institute Director and Manager of the organization for the patents defense; in 1956–1999, 149 infringements and objections had to be warded off	"Karl Ziegler," by GDCh &Max-Planck-Institut of 08 May 2008 honours his achievements in the field of organometallic catalysis and chemistry; http://www.kofo.mpg.de/media/2/D1105213/0478051227/Festschrift_e.pdf
1959	The first LLDPE (Sclaire resins) was produced by DuPont Canada Ltd. in a solution process using Z-N vanadium (V) catalyst: $VO(O\text{-}n\,\text{butyl})_2$ Cl, and Al $(Et)_{1.5}Cl_{1.5}$. The comonomer was $C_{4\text{–}20}$, with the Al/V ratio increasing with comonomer MW from 5:1 to 12:1	Elston from DuPont Canada Ltd. patented Advanced SCLAIRTECH technology with a single-site catalyst, which produced a bimodal ethylene–hexene copolymer for films or injection moldings	The Advanced SCLAIRTECH process uses two CSTR with CHX as a solvent and metallocene catalyst at $T = 160$–220 °C and $P = 3$–34 MPa. Process advantage is the heat recovery. The patent for the first time uses the homogeneity index, HI calculated from T_m	Clayton Trevor Elston. Process for preparation of homogenous random partly crystalline copolymers of ethylene with other $\tilde{\alpha}$ olefins, U.S. Patent 3645992 of 29 Feb 1972; CA Patent 703704 of 09 Feb 1965 to Du Pont of Canada Ltd.); D. Malpass, *Introduction to Industrial Polyethylene* (Wiley, 2010); J. Gray, Prog. Rubber Plast. Technol. 1(1), 1–12 (1985)

1960	The patent describes catalyst for polymerization of unsaturated monomers, such as C_2 or C_3. Conversion $\geq 99.5\%$ was achieved with 0.0005 g Ti per 1 g of $CoBr_2$	W. A. Hewett for Shell Oil Co.	The catalyst has small crystals of metal salts. The metals with atomic weight 24–209 are claimed, e.g., Co or Mg dihalide, deposited on $TiCl_4$ with $AlEt_3$ or $AlClEt_2$ as activator	W.A. Hewett, Catalysts and their preparation, U.S. Patent 3,238,146 of 01 Mar 1966 (filed 21 Mar 1960) to Shell Oil Co.
1963	Solution polymerization of ethylene was described in the CA patent of 1963. The reaction uses a Z-N-type catalyst, viz., $CpMLX_n$ [$M = Ti$, Hf, or Zr; $L =$ heteroligand; $X =$ activable ligand; $n = 2$ for Ti] with an ionic activator [$Ph_3CB(C_6F_6)_4$]. Gillis, Zboril, and Hughson developed a heat-treated (at 180–250 °C) catalyst for solution copolymerization of C_2 with C_{3-12} at 105–320 °C. The catalyst was TiX_4 VOX_3 ($X =$ Cl or Br) and AlR_nX_{3-n} ($R =$ phenyl or alkyl; $n = 2$ or 3). The catalyst mixture was heated to 180–250 °C and then cooled to $T < 150$ °C. Next, the extra VOX_3 (not heat treated) was added	A. W. Anderson, E. L. Fallwell, and J. M. Bruce to du Pont de Nemours; Vaclav G. Zboril to DuPont Canada and Gillis, Zboril, and Hughson; Zboril and Brown to Novacor Chem. (International)	The catalyst comprises a Group IVB–VIB transition metal and an organometallic compound of a metal belonging to Groups I–IIIA. A preferred polymerization copolymerization method of C_2 with C_{3-20} is the high-T "solution" process, where the monomer and polymer are soluble in the reaction medium. The Gillis et al. catalyst showed superior activity to catalysts in which additional VOX_3 was not added or added at temperatures above 150 °C. The catalyst was activated with $AlEt_2Cl$ or Al-siloxane compound at the atomic ratio: $Al/(Ti + V) = 0.8–7.0/1$ and $V/Ti = 0.15–4.0/1$	Arthur W. Anderson, Ernest L. Fallwell, John M. Bruce, Jr., CA Patent 660869 of 09 Apr 1963 to E.I. du Pont De Nemours and Co.; V.G. Zboril, U.S. Patent 4,430,488, of 1984, priority 1980 to Du Pont Canada Inc.; D.J. Gillis, V.G. Zboril, M.C. Hughson, U.S. Patent 5,492,876, of 20 Feb 1996 to Novacor Chem. (International); V.G. Zboril, S.J. Brown, U.S. Patent 5,589,555, of 31 Dec 1996 to Novacor Chem.; S. Brown, X. Gao, R. Spence, E. Von Haken, Q. Wang, P. Zoricak, CA Patent 2228802 of 25 Apr 2006 (Filed 19980) to Novacor Chem

(continued)

Table 18.10 (continued)

Date	Event	Inventor/company	Comment	Reference
1967	Catalyst [based on cyclopentadienyl-Cr + 2 and adsorbed on dehydroxylated SiO_2] was granted in 1973. Owing to catalyst heterogeneity, polydispersity of HDPE resulted in improved processability	Karapinka et al. to UCC. The chromocene catalyst on aluminum phosphate support was similar to that of Phillips Petroleum Co., invented by Hogan and Banks	The system shows high activity, but differs from Ti- and V-based catalysts as they produce HDPE with broad MWD. The catalyst contains active sites with different geometries and activities	G.L. Karapinka, U.S. Patent 3709853 of 09 Jan 1973, to UCC; F.J. Karol, G.L. Karapinka, C. Wu, A.W. Dow, R.N. Johnson, W.L.J. Carrick, Polym. Sci. Part A-1 **10**, 2621–2637 (1972); F.J. Karol, C. Wu, W.T. Reichle, N.J. Maraschin, J. Catal. **60**, 68–76 (1979)
1968	Catalysts for polymerizing ethylene and its mixtures with α-olefins are obtained by mixing a hydride or an organometallic compound of a metal belonging to Groups I–III with $TiCl_4$ with an anhydrous $MgCl_2$ or $ZnVCl_2$. Other catalyst is (1) a compound of Ti, V, or Zr and (2) a complex, e.g., $MCl_{2p}AlRCl_{2p}AlCl_3$ [M = Ba, Ca, Mg or M_n; $R = C_1–C_{20}$; $n = 1–4$; $p \leq 1$; M/transition metal atomic ratio = 0.1–50]	A. Mayr, P. Galli, E. Susa, G. DiDrusco, E. Giachetti, from Montecatini Edison SpA	Catalyst was prepared by ball milling $MgCl_2$ with $TiCl_4$, dispersed in n-heptane with $Al(C_4H_9)_3$ at $T = 75$ °C. C_2 and H_2 were introduced and for 2 h the polymerization was carried out at 1 MPa; PE yield ranged from 50 to 590 kg/1 g of Ti	Adolfo Mayr, Paolo Galli, Ermanno Susa, Giovanni Di Drusco, Ettore Giachetti,CA 906981 of 08 Aug 1972; CA 910891 of 26 Sept 1972; CA 923483 of 27 Apr 1973; CA 949542 18 June 1974; CA 991620, CA 991621 & CA 991628 of 22 June 1976; CA 1076544 29 Apr 1980; U.S. Patent 4298718 of 03 Nov 1981 (priority 25 Nov 1968) to Montecatini Edison/Montedison SpA. (Italy)
1971	Dow deposited a patent on the use of two reactors, primary and auxiliary, for the solution polymerization of C_2 with C_3 into impact-modified HDPE + EPR	John H. Mitchell from Dow Chem. Co.	Ziegler catalyst was a mixture of $TiCl_4$ + $AlEt_3$ (see U.S. Patent 3,051,690 to Hercules or U.S. Patent 3,257,332 to K. Ziegler)	J.H. Mitchell, U.S. Patent 3,914,342 of 21 Oct 1975 (priority 13 July 1971) to Dow Chem. Co.

Year				References
1971	Henrici-Olive and Olive from Monsanto Research S. A. postulated that ligands in Z-N catalysts may lead to specific structures of macromolecules. The possible reasons:	(1) Due to steric factors the stability of olefin-to-M complex decreases with olefin size; (2) the bond between ligand and M is unstable	(3) The ligand influence takes place through σ- and π-electrons, i.e., more electronegative ligand, weaker M–R bond and more reactive; (4) bulky ligands enhance stereospecific polymerization	G. Henrici-Olive, S. Olive, Angew. Chem., Int. Ed. Engl. **10**, 105 (1971)
1972	Gas-phase polymerization of ethylene and α-olefins using a dual-reactor process: the CSTR for the preparation of pre-polymer and FBR for the polymerization step	The Naphtachimie continuous two-stage process uses in series a stirred tank and fluidized bed reactors (FBR)	The process after amalgamation was adopted by BP Chemicals for the production of HDPE and LLDPE	R. Dormenval, L. Havaa, P. Mangin, Process for dry polymerization of olefins, U.S. Patent 3922322, 25 Nov 1975, priority 17 Nov 1972, to Naphtachimie France
1973	Addition of a small amount of water to the Z-N soluble catalyst: (Cp_2TiCl_2) with $AlEt_3$–iCli greatly increased the catalyst activity	Reichert and Meyer, TU Munich, studied kinetics of polymerization as function of the Al/Ti ratio	At Al/Ti > 1 excess of Al acts as a deactivator, while for Al/Ti < 1 the polymerization has the "living" character	K.H. Reichert, K.R. Meyer, Makromol. Chem. **169**, 163 (1973); K. Meyer, K.H. Reichert, Angew. Makromol. Chem. **12**, 175 (1970); K.H. Reichert, Angew. Makromol. Chem. **13**, 177 (1970)
1973	Multiple reactors for controlling MWD of HDPE (in parallel or in cascade with different feeds) have been known in the plastics industry as described in a patent DE 656,469 (1938) or U.S. Patent 2363951 (priority 1937) for PS or PVC production. The "Advanced Cascade Process (ACP)" with three reactors in cascade is an	Hoechst's slurry Hostalenis produced via advanced cascade process (ACP), which uses three CSTR in a cascade, enabling the production of multimodal HDPE and/or LLDPE (with butene) resins in butane. For example, the first CSTR is alimented with C_2, the second with C_2 and C_4, and	ICI patented polymerization or copolymerization of ethylene using transition metal complex (preferably Z-N catalyst on support) at $P = 30$–100 MPa and $T = 100$ °C in pentane. Multi-reactor with different feeds and/or conditions or a tubular reactor with different reaction zones may be used. Several other LDPE manufacturers (e.g., DuPont, Mitsui)	L.L Bohm, in *Progress and Development of Catalytic Olefin Polymerization*, ed. by T. Sano, T. Uozumi, H. Nakatani, M. Terano (Technol. Edu. Pub., Tokyo, 2000); R.R. Cooper, K.S. Whiteley, U.S. Patent 4,133,944 of 09 Jan 1979 to ICI; K. Kawai, K. Mashita, K. Hanji, H. Takao, CA 1162700 A, 21 Feb

(continued)

Table 18.10 (continued)

Date	Event	Inventor/company	Comment	Reference
	extension of the 1954 Hostalen bimodal process technology for the production of multimodal HDPE	the third with C_2 and a small amount of C_4	modified the ICI HP process by introducing non-peroxide catalysts	1984 to Sumitomo Chem.; N. Platzer, Ind. Eng. Chem. **62**, 6–20 (1970); A.W. Anderson, G.S. Stamatoff, U.S. Patent 4,076,698, 28 Feb 1978 to du Pont; T. Shiomura, Y. Kinoshita, Y. Kokue, U.S. Patent 4,128,607, 05 Dec 1978 to Mitsui
1975	Discovery that addition of H_2O into metallocene homogeneous catalyst, Cp_2MCl_2 (M = Zr, Ti, Hf) + AlR_3 at a molar ratio of H_2O to $Al(CH_3)_3 \approx 1:1$, results in formation of the methylaluminoxane (MAO) soluble in organics: R_2AlO $[RAlO]_nAlR_2$. In comparison to Z-N the m-type catalyst activity is higher by a factor of 10–100. The linear or branched oligomeric MAO is particularly an efficient co-catalyst for Cp_2ZrCl_2. Diverse metallocenes have been described, e.g., in U.S. Patents 4752597, 5017714, Europe Patents A320762, A416815, A537686, A669340, 0485823, 0549900, 0576970. Furthermore, in U.S. Patent 5403942, R.-J. Becker,	Walter Kaminsky and Hansjörg Sinn (Univ. Hamburg) discovered the key beneficial role of moist MAO for a metallocene-catalyzed polymerization of olefins, cycloolefins, dienes, styrenes, etc. The discovery was followed by numerous patents on the modification/improvements, e.g., L. H. Slaugh and G. W. Schoenthal, U.S. Patent 4665047 of 12 May 1987 to Shell; H. W. Turner, U.S. Patent 4752597 of 21 June 1988, to Exxon; F.R.W.P. Wild, L. Zsolnai, G. Huttner, H. H. Brintzinger, ansa-Metallocene Derivatives: IV, J. Organometal. Chem., 232, 233–247 (1982); Angew. Chem., 107, 1255 (1995); etc.	Accidental contamination of $AlEt_3$ by water greatly increased Z-N catalytic activity and led to the development of diverse metallocene catalysts. By contrast, with earlier catalysts, the metallocene copolymers have well-defined structure, a single active polymerization center leading to high polymerization efficiency (1 kg polymer per 1 g catalyst), narrow MWD, and uniform properties. Metallocenes show better thermal stability, facile incorporation, high α-olefins even at high concentration (plastomers), and control of stereostructure. Most frequently, the active part of Z-N catalyst is a zirconocene cation	W. Kaminsky, in *History of Polyolefins*, ed. by R.B. Seymour, T. Cheng (1986), pp. 257–270; J. Polym. Sci. Part A: Polym. Chem., **42**, 3911–3921 (2004); Metallocene catalyzed polymerization, RAPRA Rev. Rep. **10**(7) (1999). The initial patent [DE 3007725 of 29 Feb 1980] was abandoned once learned about earlier work by Reichert and Meyer (1973); H.W. Sinn, W.O. Kaminsky, H.-J.C. Vollmer, R.O.H.H. Woldt, U.S. Patent 4404344 of 1983 to BASF; W. Kaminsky, H. Hahnsen, K. Kulper, R. Woldt, U.S. Patent 4542199 of 17 Sept 1985, to Hoechst; B.A. Harrington, M.G. Williams, Rubber World **230**, 20–26 (2004); P.C. Möhring,

Year			References
	S. Gurtzgen, and R. Schrader detail preparation of MAO by addition of H_2O to a solution of AlR_3 in an inert solvent, using a mixing nozzle and a static mixer		N.J. Coville, J. Organometal. Chem. **479**, 1–29 (1994); R.-J. Becker, S. Gurtzgen, R. Schrader, U.S. Patent 5403942 of 04 Apr 1995 (filed 16 Mar 1994), toWitco GmbH
1977	Discovery of MAO by W. Kaminsky group and identification of its structure as linear or cyclic, [-Al(Me)-O-]$_{10-15}$, were crucial for the increase of catalyst activity, by a factor of 10,000 or more. Thus, the expensive MAO plays a key role in metallocene catalysis	Metallocenes (esp. zirconocenes) treated with MAO polymerize up to 21 kg PE/(mmol Zr h). The C_2H_4 mer insertion time into a growing chain is about 10 μs. Two types of MAO have been used as co-catalysts: MAO (1) and MAO (2) prepared in the ratio $Al/H_2O = 2$ and 3. The complexes, zirconocene/MAO, belong to the most active catalysts. The active site consists of Zr and 6–20 Al atoms	H. Sinn, W. Kaminsky, Adv. Organomet. Chem. **18**, 99 (1980); W. Kaminsky, RAPRA Rev. Rep. **10**(7) (1999); J. Justino, Polym. Intl. **44**, 407–412 (1997); W Kaminsky, Metallocenes, in *Ullmann's Encyclopedia*, Ind. Chem. **22**, 685–601 (2006)
1977	CdF Chimie modified the standard high-P radical polymerization for LDPE by using N_2 and H_2O [N_2 caused phase separation; water improved dissipating reaction heat]. These modifications reduced the reaction conditions to $P = 30–80$ MPa and $T = 150–300$ °C. Z-N catalyst at high T caused an ionic radical	The reaction took place in a multi-zone CSTR, in the presence of up to 28 wt% N_2 and some H_2O. Demixing caused by N_2 reduced LCB and increased unsaturation. H_2O increases MW and LCB and reduces unsaturation. The presence of comonomers (e.g., C_4, C_6, or C_8) improved the reaction stability. LDPE density was controlled by comonomer content, while MWD by H_2 concentration. H_2O improved conversion up to the saturation concentration. Retrofitting the ICI system reduced the LDPE production cost by 15–20 %	D. Constantin, J.P. Machon, Eur. Polym. J. **14**, 703–708 (1978); D. Constantin, M. Hert, J.P. Machon, Europ. Polym. J. **17**, 115–120, (1981); D. Constantin, M. Hert, J.-P. Machon, Structure of polyethylene produced at high pressure by simultaneous ionic and radical mechanisms, Makromol. Chem. **179**, 1581–1591 (1978)

(continued)

Table 18.10 (continued)

Date	Event	Inventor/company	Comment	Reference
1978	UNIPOL gas-phase polymerization in a fluidized bed reactor was introduced by Union Carbide Corp. (UCC). Expected capacity 450 kt year^{-1} for copolymerization of C_2 with C_{3-8} comonomers	The novel technology is a combination of gas- and slurry-phase reactions at $P = 0.7-2.1$ MPa and $T = 100$ °C	Cascaded processes are suitable for bimodal Spherilene PE from LyondellBasell (Covezzi 1995; Galli 1995) and Borstar PE from Borealis and Borouge (Avela et al. 1998)	Anon., Low pressure LDPE, Mod. Plast. **56**, 42–43 (1979); Anon., New route to low density polyethylene, Chem. Eng., 80–85 (1979); U.S. Patent 4,363,904 of 14 Dec 1982 to UCC
1981	A solution copolymerization of C_2 with C_{3-12} at $T = 105-320$ °C for the preparation of high-MW LLDPE. The catalyst was obtained by solution mixing $TiCl_4$ or $VOCl_3$ and $AlEt_3$ at $T < 30$ °C, heating to $T = 150-300$ °C for 10–600 s, then injecting to a solution of AlR_nX_{3-n}, [R = alkyl, cycloalkyl, or aryl having 1–20 carbons, $n = 1, 1.5, 2,$ or 3 and X is Cl or Br	Hamilton and Zboril from DuPont Canada Inc. The solvent (hexane, heptane, octane, methylcyclohexane, hydrogenated naphtha, but preferably CHX), used in the preparation of the catalyst was the same as that used in the polymerization process	The coordination catalyst was fed to the reactor containing hydrocarbon solvent and appropriate monomers. Polymerization was carried out at $T = 105-310$ °C. The catalyst was deactivated and either left in the obtained LLDPE ($\rho = 0.915-0.965$ g mL^{-1}) or the solution was passed through a bed of activated alumina or bauxite to remove at least a part of the deactivated catalyst residues	M.A. Hamilton, V.G. Zboril, Process for the preparation of polymers of α-olefins at high temperatures, CA 1171065 of 17 July 1984 (filed 06 Jan 1981, expired 17 July 2001); M.A. Hamilton, V.G. Zboril, U.S. Patent 4431784 of 14 Feb 1984 (filed in 1981) to Du Pont Canada Inc.
1982	$C_2 + C_8$ type LLDPE with density of $\rho = 0.927$ g mL^{-1}	DuPont Canada	Replacing $C_2 + C_4$ type films with the $C_2 + C_8$ type permitted rotomolding downgauging by 30 %	R. Martino, Mod. Plast. 126–128 (1984)
1984	Ansa-metallocene complexes have been studied for olefin polymerization, e.g., polymerizing i-PP with an ansa-titanocene. The bridged ligands change the catalysts and the polymer structures, also affecting MW and MWD	Kaminsky et al.; see also reviews by Möhring and Coville (1994) and by Wang (2006)	Catalysts with metal from Group 3 [Coord. Chem. Rev. **248**, 397–410 (2004)] or 4 [J. Organomet. Chem. **542**, 191–204 (1997)] have been studied. (N.b., ansa = a bridge between two functional ligands)	W. Kaminsky, J. Polym. Sci. Part A: Polym. Chem. **42**, 3911–3921 (2004); P.C. Möhring, N.J. Coville, J. Organometal. Chem. **479**, 1–29 (1994); B. Wang, Coord. Chem. Rev. **250**, 242–258 (2006)

1985	Deposition of Dow modification of Z-N catalyst incorporating $MgCl_2$. Numerous versions of the new catalyst are listed	William M. Coleman from Dow Chem Co.	Improved Ziegler–Natta catalysts with $MgCl_2$, Ti, and V compounds producing narrow MWD PE copolymers	W.M. Coleman III, U.S. Patent 4,612,300 of 16 Sept 1986 (deposited 06 June 1985) to The Dow Chemical Company
1985	A solution copolymerization of C_2 with C_{3-12} at $T = 105$–$320\ ^\circ C$ into high-MW LLDPE comprised feeding monomers, a catalyst, and a hydrocarbon solvent to a reactor, polymerizing the monomers, recovering the polymer, and deactivating the catalyst by injecting H_2O followed by desalination. The coordination catalyst was obtained combining (i) a solution of AlR_nX_{3-n} (R = alkyl C_{1-20}; $n = 1, 1.5, 2$, or 3, and X = halogen) with a solution of $TiCl_4$ and $VOCl_3$ at $T < 30\ ^\circ C$, heating to $T = 150$–$300\ ^\circ C$ for $t = 5$ s to 60 min, and adding $VOCl_3$	Zboril and Müllhaupt from DuPont Canada Inc. modified the Hamilton and Zboril polymerization process [U.S. Patent 4431784 of 14 Feb 1984]. Polymerization was carried out in CHX at $T = 105$–$320\ ^\circ C$ and $P = 0.1$ MPa. The improvement comes from the second component of the catalyst, primarily from aluminoxanes. High catalyst activity and acceptable polymer color were reported	The second catalyst component was a solution of an aluminoxane in a hydrocarbon solvent, selected from between aluminoxanes: (i) linear, $R'AlO$ $(R'AlO)_m$–AlR'_2 [where R' is C_{1-20} alkyl and cycloalkyl and $m = 0$ or an integer], and (ii) cyclic, $$\left[(R2''AL\!-\!O) \right]$$ $R'' = C_{1-20}$ (alkyl or cycloalkyl), the atomic ratio of $Al/(Ti + V)$ in the second component $= 0.9$–10. The organoaluminum was mixed with the Ti and V at a ratio of $Al/(Ti + V) = 0.2$–2.0	V.G. Zboril, R. Müllhaupt, Solution process for the preparation of polymers of alpha-olefins, U.S. Patent 4769428 of 06 Sept 1988, (filed in 16 Oct 1986, priority 1985) to Du Pont Canada Inc.
1986	The transition metal in a Z-N-type catalyst was prepared by reacting Mg(alkoxide)$_2$ with $TiCl_4$ and an organoaluminum compound: $AlR_{3-n}X_n$ (R = organo group, $n = 0$–2)	E. I. Band and W. E. Summers, III for Stauffer Chem. Co. Isotacticity of the PP obtained using the new catalyst was 95 % pure	Mg(2-butoxyethoxy)$_2$ $(Z\!-\!(CH_2)_n\!-\!O)\!-\!Mg\!-\!(O(CH_2)_m\!-\!OR_2)$ (where $m, n = 1$–12) is soluble in hydrocarbons, such as heptane or toluene for the synthesis of i-PP at 70 °C and $P = 0.7$ MPa	E.I. Band, W.E. Summers III, Transition metal catalyst component containing magnesium alkoxy alkoxides, U.S. Patent 4698323 of 06 Oct 1987 (filed 29 Sept 1986), to Stauffer Chem. Co.
1986	Metallocene/MAO catalysts (e.g., Z-N type) are soluble, thus unsuitable for the gas- or slurry-	In the 1980s a series of patents (e.g., from Exxon Chem) disclosed methods of supporting	The U.S. Patent 6720396 lists >50 patents on the catalyst supporting methods and offers detailed discussion on their	H.C. Welborn Jr., U.S. Patent 4701432 of 20 Oct 1987 (filed 1986); J.A.M. Canich,

(continued)

Table 18.10 (continued)

Date	Event	Inventor/company	Comment	Reference
	phase processes. Adsorption on a solid support (silica, alumina, MAO, etc.) with or without organosilicon spacers transforms these systems into heterogeneous catalysts for the solvent-less polymerization	catalyst of Groups IV and III, aiming at increased activity, reduction of the amount of co-catalyst, and increasing MW of the resulting polymer	properties. The main application for the new catalytic systems has been for the gas-phase or slurry copolymerization of C_2 with higher α-olefins. High catalyst activity ($\leq$36 kg PE/mmol Zr h) has been noted	G.F. Licciardi, U.S. Patent 5057475 of 13 Sept 1990, both to Exxon Chemical; Kao et al., U.S. Patent 6136747 of 24 Oct 2000, to UCC; S.L. Bell, A.G. Vadagama, U.S. Patent 6720396 of 13 Apr 2004, to Univation Technol.; G.G. Hacky, Chem. Rev. **100**, 1347–1376 (2000); M.C. Haag et al., J. Mol. Catal. A: Chem. **197**, 223–232 (2003)
1989	Soluble in hydrocarbons chiral catalyst Et(bisindenyl)ZrCl$_2$/ MOA copolymerized cyclopentene with ethylene at $T = -10$–20 °C	Kaminsky and Spiehl incorporated up to 10 mol% of cyclopentene monomeric units into cycloolefin copolymers (COC)	The technology was transferred to Ticona (now TOPAS Advanced Polymers), which in 2000 started production of C_2 with norbornene as TOPAS COC	W. Kaminsky, R. Spiehl, Copolymerization of cycloalkenes with ethylene in presence of chiral zirconocene catalysts, Makromol. Chem., **190**, 515–526 (1989)
1990	Catalysts with a cyclopentadienyl group based on transition metals of group IVB (Zr, Hf, Ti) with a co-catalyst, e.g., alumoxane	J. A. M. Canich from Exxon Chem.	Polymerization of C_{3-20} (esp. propylene) into crystalline poly(α-olefins) in solution, slurry, gas, or bulk phase	Jo Ann M. Canich, U.S. Patent 5,026,798 of 25 June 1991 (deposited 13 Sept 1990) to Exxon Chemical Patents Inc.
1990	A monocyclopentadienyl metal complex, CpMX$_n^+$ A$^-$ (M is metal of Groups 3–10), is a Z-N-type catalyst for olefin polymerization	Stevens and Neithamer from Dow Chem. Co. $\mathrm{Cp^*{-}M^{+}}$ with $Z{-}Y$, $(X)_n$, A^-	In the preferred compounds M = Zr or Ti, while Z = SiR$_2$N(R*); n = 1 or 2; X = alkyl or aryl; Y = N- or P-containing group; A = non-coordinating Bronsted anion	J.C. Stevens, D.R. Neithamer, Metal complex compounds, U.S. Patent 5064802 of 12 Nov 1991 (deposited 03 July 1990) to The Dow Chemical Co.

1991	First commercialization of metallocene PE based on Kaminski (1976) $ZrCl_2Cp_2$ catalyst	Exxpol® technology by ExxonMobil to produce Exact® PE via gas phase	Metallocene: mPE (Enable™) and mPP (Exceed™, Vistamaxx™) propylene-based elastomers	http://www.exxonmobilchemical.com/Chem-English/about/news-releases.aspx
1991	A coordination catalyst was prepared by (i) mixing a solution of AlR_nX_{3-n} [R = phenyl or C_{1-4} radical, X = Cl, or Br and n = 2 or 3; e.g., $AlEt_2Cl$] in a solvent, with a solution of TiX_4 and VOX_3 at $T < 30$ °C and heating the mixture to T = 180–250 °C for t = 15–300 s [the atomic ratio of $Al/(Ti + V)$ = 0.2–3.0:1 and V/Ti = 0.05:1–1.5:1]; (ii) cooling the solution to $T < 150$ °C; and (iii) adding a solution of VOX_3 thus increasing the V-content to $\geq$10 at.%. Combine the cold solution with that of (a) AlR_nX_{3-n} and (b) $R''_3SiO(R''_2SiO)_mAlR''_2$ [where R'' is a C_{1-6} alkyl radical and m = 0–4, e.g., $EtMe_2SiOMe_2SiOAlEt_2$]. In the coordination catalyst $Al/(Ti +$ V) = 0.8–7.0:1; and V/Ti = 0.15–4.0:1	Gillis, Zboril, Hughson, Hamilton, Russell, Harbourne, Müllhaupt, Hughson from DuPont Canada Inc. and/or Novacor Chem. (International) This is the next level of Z-N catalyst modification for solution copolymerization of C_2 with C_{3-12}: See U.S. Patents 4431784, 4769428	A solution polymerization for high-MW LLDPE uses a coordination catalyst at T = 105–320 °C. The catalyst was heat treated at 180–250 °C, then cooled to a $T < 150$ °C. Additional VOX_3 was added and catalyst activated with an Al compound. The catalyst had greater activity than the one without additional VOX_3 or with that added at $T >$ 150 °C. After reaction, the catalyst was deactivated using, e.g., tri-i-propanol amine, acids, salts, or alcohols. After deactivation, the polymer solution might be passed through a bed of activated alumina or bauxite to remove part or the catalyst residues. LLDPE was pelletized with an antioxidant	D.J. Gillis, V.G. Zboril, M.C. Hughson, Solution process for the preparation of polymers of a-olefins, CA 2081887 of 07 Aug 2001, filed 05 Apr 1991; A. Hamilton Michael, G. Russell Charles, A. Harbourne David, M. Rolf, G. Zboril Vaclav, CA 1220189 of 07 Apr 1987 (filed 03 July 1983); Zboril Vaclav G. and Müllhaupt Rolf.,CA 1257863 of 25 July 1989 (filed 17 Oct 1985); Gillis Daniel John, Zboril Vaclav George.Hughson Millard Clifford, CA 2081887 of 07 Aug 2001 (filed 05 Apr 1991); U.S. Patent 5492876 of 20 Feb 1996 (filed 01 Feb 1994, priority 1991) to Du Pont Canada Inc. or to Novacor Chemicals (International) S.A.

Table 18.10 (continued)

Date	Event	Inventor/company	Comment	Reference
1991	New coordination catalyst is (i) a mixture of MgR^1_2 and AlR^2_3 [R^1 and $R^2 = C_{1-10}$ alkyls]; (ii) TiX_4 at the molar ratio Mg: Ti $= 4$:1–8:1, that of halide: Mg $= 1.9$:1–2.6:1; and Mg: Al $= 1.0$:0.1–1.0:0.4. The CHX solutions were mixed for 5 s at $T = 30\,°C$ and heated to $T < 300\,°C$ for 5–60 s and then to $T = 170$ to $220\,°C$ for 10–120 s. The catalyst activator was $AlEt_3$ mixed with an $R''OH$, $R'' = C_{2-8}$ alkyl radical, e.g., t-butyl alcohol (molar ratio of 0.05:1–1: 1). The precursor comprised a VOX_3 at a ratio V: Ti $= 1$:6–4: 1	Brown, Ungar, and Zboril, from Novacor Chem. (International) This is the next modification of Z-N catalyst for solution copolymerization of C_2 with C_{3-12}. See U.S. Patents 4431784, 4769428, 5492876	LLDPE was polymerized in solution with a coordination catalyst at $T = 180$–$320\,°C$ and $P = 4$–20 MPa. The new modification relates to a method for activating Z-N coordination catalysts using an alkoxy aluminum alkyl compound prepared by mixing an alcohol and alkyl aluminum. The activator retains its activity and is easy to prepare simplifying the polymerization process. Small amount of H_2 may be used for MW control (see Elston CA Patent 703704 of 1965 to DuPont of Canada Ltd.)	S.J. Brown, R.K. Ungar, V.G. Zboril, Activation of catalyst in ethylene polymerization at high temperatures, CA 2119737 of 03 June 2003 (filed 25 July 1992), to Du Pont Canada Inc. (Canada); U.S. Patent 5519098 of 21 May 1996 (filed 12 Oct 1994, priority 1991) to Novacor Chemicals (International)
1991	A coordination catalyst was prepared at $T < 30\,°C$: (i) a mixture of MgR^1_2 and AlR^2_3 [R^1 and $R^2 = C_1$–C_{10} alkyl radicals], (ii) a reactive halide, and (iii) $TiCl_4$; molar ratios: halide, Mg $= 2.2$–10 2.4; Mg:Ti $= 5$; and Al:Ti $= 0.9$. The catalyst activator was prepared by mixing	Zboril and Brown, from Novacor Chemicals (International) S.A. This is the next level modification of Z-N catalyst for solution copolymerization of C_2 with C_{3-12}. See U.S. Patents 4431784, 4769428, 5492876, and 5519098. The technology described in these patents was	A solution copolymerization of C_2 with C_{3-12} into high-MW LLDPE was carried out using a coordination catalyst at $T = 105$–$320\,°C$ and $P = 4$–20 MPa in a tubular reactor or in a system of reactors each operating under different conditions, in an inert solvent at $T > 105\,°C$. The catalyst was activated with a solution of aluminum alkyl and alkoxy aluminum	V.G. Zboril, S.J. Brown, Control of a solution process for polymerization of ethylene, U.S. Patent 5589555 of 31 Dec 1996 (priority 1991) to Novacor Chemicals (International); CA 2119738 of 18 July 206 (PCT filed 25 Sept 1992) to Du Pont Canada Inc.;J.C.-K. Huang,

Year				References
	at $T < 30$ °C of AlR_3 ($R = C_{2-8}$) alkyl radical with an R_4OH alkyl alcohol ($R_4 = C_1$–C_{20} alkyl radical in a ratio of alcohol: $Al = 0.1$–1. The catalyst was injected, then polymerization carried at $T = 230$ °C, $P = 7.5$ MPa. The catalyst was deactivated and the PE recovered	vital for the future production of PO articles, viz., shrink and cast films described in the U.S. Patents 6340532 and 6713189	alkyl in inert solvent. The process was controlled by adjusting the ratio of AlR_nX_{3-n} to $AlR'_mOR''_{3-m}$, where each of R, R' and R'', is C_{1-20} alkyl or aryl; X is halogen, $n = 2$–3 and $m = 0$–3	P.A. Sipos, L.T. Kale, P.R. Thomas, J.A. Auger, Shrink films, U.S. Patent 6340532 of 22 Jan 2002 (filed 31 Jan 2001); K.W. Ho, N.D.J. Aubee, Cast films, U.S. Patent 6713189 of 30 Apr 2004 (filed 09 Dec 2002, priority 2001), to Nova Chemicals (International) S.A.
1992	Introduction of PE based on the proprietary INSITE® "constrained geometry catalyst"	Dow announces the solution-based process for AFFINITY® PE	When a lower seal initiation T is needed in fast packaging line, AFFINITY™ should be used instead of DOWLEX™ PE, Attane™ ULDPE, or Elite™ EPE resins	http://dowplastics.custhelp.com/app/answers/detail/a_id/8023/~/affinity---resin-selection; A. Wood, Dow plans metallocene PE plant in Argentina, Chem. Week **158**, 23 (1996)
1992	Reactor blends are prepared during polymerization. The strategy has been often explored in syntheses of multimodal PE compositions for the blown film with MD/TD tear balance and good processability. In bimodal blend, the optimum was usually found between 35 and 75 wt% of the higher-MW component	Reactor blending during the slurry polymerization with a catalyst, $TiCl_4$/pentanol on MgO/acetic acid, and treated with tri-*n*-hexyl-aluminum solution, gave two PE fractions with different MW. Borealis generated multimodal resins for optical cables using slurry-/gas-phase reaction with Z-N catalyst with $MgCl_2$	Ahmed H. Ali, John T. T. Hsieh, Keith J. Kauffman, Yury V. Kissin, S. Christine Ong, Giyapuram N. Prasad, Ann L. Pruden, Sandra D. Schregenberger, to Mobil Oil Co.; Ruth Dammert, Eeva-Leena Heino, Tarja Korvenoja, Hans-Bertil Martinsson, to Borealis	Ali et al. (1994); Ruth Dammert, Eeva-Leena Heino, Tarja Korvenoja, Hans-Bertil Martinsson, U.S. Patent 6185349 of 06 Feb 2001 (filed 1999) to Borealis Polymer Oy
1995	The 3rd-generation Z-N catalyst was evaluated in the Fritz-Haber-Institut der Max-Planck-Gesellschaft, Berlin. The proposed strategy was that by Magni and Somorjai. It was	Schmidt et al. prepared well-ordered $MgCl_2$ film, which only absorbed $TiCl_4$ when activated by electron or ion bombardment. Ti^{3+} was detected after severe bombardment of $MgCl_2$ layers	Interaction with aluminum alkyl leads to the formation of the active catalyst with ethyl radicals formed from trimethylaluminum in an abstraction process: $TiCl_4$/surface + $AlMe_3$ → Me-$TiCl_3$/surface + $AlMe_2Cl$; Me-$TiCl_3$/	J. Schmidt, T. Risse, H. Hamann, and H.-J. Freund, J. Chem. Phys. **116**, 10861 (2002); H.S. Cho, W. Y Lee, J. Mol. Catal. A: Chem. **191**, 155–165 (2003); E. Magni,

(continued)

Table 18.10 (continued)

Date	Event	Inventor/company	Comment	Reference
	a δ-TiCl$_3$ supported on activated MgCl$_2$ in the presence of AlEt$_3$. The new catalyst showed 50-fold higher catalytic activity		surface $\rightarrow$ TiCl$_3$/surface + Me; Me + Me$_3$Al $\rightarrow$ C$_2$H$_5$ + AlH(Me)$_2$	G.A. Somor, Catal. Lett. **35**, 205–214 (1995)
1995	Multizone circulating reactor (MZCR) disclosed by Montel Technology is a modified FBR polymerizing olefins in 2-tubular polymerization zones, to which one or more α-olefins are fed in the presence of catalyst, e.g., TiCl$_4$+ MgCl$_2$ 3EtOH, described in U.S. Patent 4399054 of 1983 to Montedison SpA	Govoni, Rinaldi, Covezzi, and Galli, modified the UNIPOL FBR forming a vertical closed-loop reactor. The PE particles circulated through a fast fluidization riser then densified, under gravity flowing through a downer again to enter the raiser, etc.	The catalyst was the reaction product of a Ti compound and MgCl$_2$ in the form of spherical particles with a diameter of 1–100 μm. The high-productivity gas-phase polymerization in MZCR gave multilayered particles with designed chemical composition and MWD	G. Govoni, R. Rinaldi, M. Covezzi, P. Galli, U.S. Patent 5698642 of 16 Dec 1997 (filed 19 July 1996), to Montel Technology Co. ; M. Covezzi, G. Mei, Chem. Eng. Sci. **56**, 4059–4067 (2001); F. Lona, J App. Polym. Sci. **93**, 1053–1059 (2004). M. Ferraris, F. Rosati, S. Parodi, E. Giannetti, G. Motroni, E. Albizzati, U.S. Patent 4399054 of 16 Aug 1983 to Montedison SpA
1995	The polymerization catalysts were Ni and Pd diimines. Variations of P, T, and ligands changed the PE structure from branched and amorphous to a linear and semicrystalline, HDPE. Copolymerization of ethylene with functionalized comonomers was found feasible	Brookhart from UNC and his colleagues from DuPont. The catalyst has (1) highly electrophilic, cationic Pd and Ni metal centers; (2) sterically bulky R-diimine ligands; and (3) non-coordinating counterions	Brookhart et al. reported on Pd(II) and Ni (II) R-diimine catalysts (DuPont's Versipol™ catalyst) for copolymerization of C$_2$, R-olefins, cycloolefin, and functionalized olefins. This post-metallocene catalyst does not need co-catalyst/activator, such as MAO	L.K. Johnson, C.K. Kilian, M. Brookhart, J. Am. Chem. Soc. **117**, 6414 (1995); S.D. Ittel, L.K. Johnson, M. Brookhart, Chem. Rev. **100**, 1169–1203 (2000); WO Pat. Appl. 9623010, 03 Apr 1995; U.S. Pats. 5866663, 02 Feb 1999; 5880241, 03 May 1999; 5880323, 09 Mar 1999; 5886224, 23 Mar 1999; 5891963, 06 Apr 1999 all to DuPont
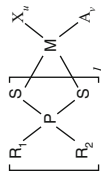
1995	The dithiophosphinate catalyst precursor capable of complexing with M = Cr, Ti, Ni, Zr, Hf, V, W, and Mo was initially used for oligomerization of α-olefins	Somogyvari, Creed, Nicola, Sanger, Law, Cavell, from the University of Alberta. The invention started a long-term search for a proprietary catalyst (based on phosphinimine), capable of olefin polymerization	The invention relates to oligomerization of α-olefins in the presence of a catalyst precursor having a dithiophosphinate and heterobifunctional ligands with a phosphine and imine or a similar center, in the presence of an $AlR_{3-n}X_n$ activator	F. Somogyvari Arpad, C.B. Lorraine, N.A. Pietro, S.A. Rodney, L.D. John, C.R. George, CA 2357805 of 04 Feb 2003 (filed 21 May 1996, priority 1995); U.S. Patent 5,557,023 of 17 Sept 1996 (filed 1995) to University of Alberta
1996	In 1959 Elston patented solution polymerization of LLDPE at $T = 160-220\,°C$ and $P = 3-34$ MPa. At lower T polymer could precipitate, thus changing into a suspension polymerization	Zboril, Kiel, Karnik, Burke, Foy, Iatrou, (Nova Chem.) patented a method of premixing cold reactants with a portion of hot reacting solution before injecting it to the main reactor without causing undue precipitation of the warmer reactor contents and changing the reaction mechanism	The chemical reactor has an intensive micro-mixing zone and a less intensively mixed principal reactor, with a re-circulation loop to exchange reactants between the two. The reactor is suitable for bulk, mass, and solution reactions with a cold feed stream, i.e., mixing a liquid at $T = 20-200\,°C$ with viscous solution at $110-300\,°C$	Z.V. George, K.D. Edward, K. Umesh, CA 2193431 of 19 June 1998 (filed 1996), to Nova Chem. Ltd. (Canada); A.L. Burke, E.C. Foy, J. Iatrou, U. Karnik, D. Edward Kiel, V. George Zboril, U.S. Patent 6024483 of 15 Feb 2000 (priority 27 Mar 1997); U.S. Patent 6319996 of 20 Nov 2001 (filed 12 Nov 1999) to Nova Chemical (International) S.A.
1996	Post-metallocene FI catalyst for PE copolymerization: (1) it may produce functionalized olefinic copolymers; (2) it is	Kawai, Kitahara, Fujita, Japanese Patent 1996, 325283, and Japanese Patent 1996, 325315;	Salicylaldimine complexes (phenoxyimine) of Group 4 metals show substantially higher activity than the metallocenes	M. Mitani, J. Saito, S. Ishii, Y. Nakayama, H. Makio, N. Matsukawa, S. Matsui, J. Mohri, R. Furuyama, H. Terao,

(continued)

Table 18.10 (continued)

Date	Event	Inventor/company	Comment	Reference
	characterized by high catalyst activity; and (3) It is capable of controlling polymer microstructure (tacticity)	U.S. Patent 7,053,159; 7,393,907, of 2006 (priority 2000), to Mitsui		H. Bando, H. Tanaka, T. Fujita, Chem. Rec. **4**, 137 (2004); Makio et al. (2011)
1997	The single-site post-metallocene catalyst for solution polymerization (e.g., in toluene) of olefins or conjugated dienes is based on bis-phenoxyimine ligand of a transition metal from Groups 3–11, e.g., Ti, Zr, Hf, V, Nb, and Ta. The co-catalyst is an organometallic compound, e.g., a methylaluminoxane (MAO), added to initiate polymerization. The reaction was conducted at 25 °C, for 30 min in an ethylene gas atmosphere at normal pressure, and then terminated with a small amount of butanol; polymer was precipitated with MeOH, acidified with HCl, filtered, and dried at 80 °C. In the FI catalyst with MAO and a variety of R-groups, the activity ranged from 0.4 to 6,552 kg-PE/(mmol Zr h)	Fujita, Tohi, Mitani, Matsui, Saito, Nitabaru, Sugi, Makio, and Tsutsui, from Mitsui Chemicals, Inc. Post-metallocene catalysts are more varied than metallocene. These are using a wide variety of M from Ti to Cu. Also ligands have diverse structures. Thus, close to M radicals R^1 and R^2 control the reaction. They are structurally and electronically flexible showing dependent on M electron-receptive or electron-donating properties. Ivanchev et al. discussed another group of binuclear phenoxyimine Ti catalysts	The invention describes new type of catalyst with excellent polymerization activities (PAC). Depending on M, ligand, co-catalyst, and polymerization conditions, the PAC ranges from 0.003 to 7,200 kg polymer/(mmol M h), thus within 7 orders of magnitude. The new catalyst has a formula: $M = Zr$; $m = 1–3$; R^1 to R^5 = hydrocarbon; R^6 and X = halogen	T. Fujita, Y. Tohi, M. Mitani, S. Matsui, J. Saito, M. Nitabaru, K. Sugi, H. Makio, T. Tsutsui, Olefin polymerization catalysts, transition metal compounds, processes for olefin polymerization, and α-olefin/conjugated diene copolymers, U.S. Patent 6,309,997 B1, 30 Oct 2001, to Mitsui Chem.; Makio et al. (2011); S.S. Ivanchev, A.V. Yakimansky, N.I. Ivancheva, I.I. Oleinik, G.A. Tolstikov, Ethylene polymerization using catalysts based on binuclear phenoxyimine titanium halide complexes, Europ. Polym. J. **48**,191–199 (2012)

Year	Inventors / Assignee	Description	Polymerization details	Patents
1997	D. W. Stephan, J. C. Stewart, D. G. Harrison, S. J. Brown, J. W. Swabey, Q. Wang, from Nova Chem. (International)	Catalyst useful in slurry- or gas-phase olefin polymerizations comprises an organometallic complex (a Group 4 metal with a cyclopentadienyl and phosphinimine ligands) on a solid particulate support. The complex + an activator (e.g., aluminoxane) create excellent catalyst. One hr polymerization at $T = 90\,°C$ and $P = 1.38$ MPa gave PAC = 57 kg/(mmol Ti h)	By contrast, with the Fujita et al. patent, this one is for a solution polymerization of C_2 copolymers at $T > 80\,°C$, with the catalyst system comprising unbridged Group 4 metals with 3 ligands: a monocyclopentadienyl, a phosphinimine ≥ 1 uni-negative, activation reactive ligand. Polymerization at $T = 160\,°C$ gave PAC = 1 kg/(mmol Ti h)	D.W. Stephan, J. C. Stewart, D. G. Harrison, U.S. Patent 5965677 of 12 Oct 1999 (filed 29 Oct 1997); CA Patent 2210131 of 02 Aug 2005; D. W. Stephan, J. C. Stewart, S. J. Brown, J. W. Swabey, Q. Wang, U.S. Patent 6063879 of 16 May 2000 (priority 1997); CA Patent 2206944 of 29 Aug 2006 (filed 30 May 1997), to Nova Chem
1998	Brown, Gao, Jeremic, Koch, McKay, von Haken Spence, Wang, Zoricak, Xu, to Nova Chemicals, Ltd.	The new catalyst comprises (A) an organometallic complex and (B) an activator. The complex $A = M(PI, H, L_n)$, where $M = Ti, Zr, Hf$; $PI =$ phosphinimine; $H =$ hetero-; $L =$ activable ligands, with (depending on the valency) $n = 1$–3. The activator is methylaluminoxane, MAO. In patent (1) none of the three ligands are Cp. In patent (2) two valencies of P are hetero-substituted and Cp replaces hetero-ligand H	In patent (1) solution polymerization was conducted in CHX at $T = 160\,°C$ and $P = 1$ MPa, either in a solution batch reactor (SBR) or in a continuous reactor. Concentration of catalyst and activator was 200 and 210 μmol L^{-1}, respectively. The activity was ≤ 12 kg PE per 1 g of M. According to patent (2) the reaction was conducted at $T = 160\,°C$ and $P = 10$ MPa. The activity was ≤ 303 kg PE per 1 g of M	(1) St.J. Brown, Xiaoliang Gao, Q. Wang, P. Zoricak, R.E. von Haken Spence, Wei Xu CA 2243775 of 12 June 2007 (filed 21 July 1998); U.S. Patent 6147172 of 14 Nov 2000, priority 21 July 1998; (2) R.E. von Haken Spence, L. Koch, D. Jeremic, S.J. Brown, CA 2254841 of 06 Feb 2007 (filed 26 Nov 1998); U.S. Patent 6234950 of 22 May 2001, priority 15 Nov 1998, all to Nova Chemicals, Ltd., or Nova Chemicals (Intl.) S.A.

(continued)

Table 18.10 (continued)

Date	Event	Inventor/company	Comment	Reference
1998	PE having $M_w/M_n > 8$ was obtained in a multistage copolymerization of C_2, with C_{3-10} α-olefins, catalytically in one or more reactors. The catalyst comprises (a) solid product of $MgCl_2 + ZrCl_4$, (b) $AlMe_2Cl$, and (c) $AlEt_3$, molar ratio $(b)/(c) < 10$. Then, optionally, activating the pre-catalyst and polymerizing the monomer(s)	T. Dall'Occo, G. Baruzzi, C. J. Schaverien from Basell Technology Co. The catalyst comprises Ti, Zr, or V; $MgCl_2$; an alkyl Al compound; and optionally an electron donor compound, e.g., alkyl, cycloalkyl, or aryl esters of polycarboxylic acids (phthalic or succinic)	Multistage polymerization for the preparation of broad MWD PE uses the same catalyst, but in several reactors with different concentration of H_2. Such a procedure leads to a large amount of "bad" oligomers. Basell's new Zr catalysts, without H_2, produce low-MWPE of narrow MWD, without these undesirable oligomers	T. Dall'Occo, G. Baruzzi, C.J. Schaverien, U.S. Patent 6,479,609 of 12 Nov 2002 (priority 09 Mar 1998); T. Dall'occo, G. Baruzzi, D. Brita, M. Sacchetti, Catalyst for the polymerization of olefins, CA 2382009 of 22 Mar 2001 (filed 29 Aug 2000; priority 1999) to Basell Technology Company BV
1998	A catalyst for slurry- or gas-phase olefin polymerizations comprises an organometallic complex of a Group 4 metal (unbridged and having a Cp, a phosphinimine, and an activable ligands) and co-deposited ionic activator [e.g., triphenylcarbenium tetrakis (pentafluorophenyl) boron] on a metal oxide support pretreated	Brown, Ciupa, Chisholm, Ciupa, Jeremic, McKay, to Nova Chemicals (International) S.A. The productivity of the new catalyst was about 6 kg PE/(1 g catalyst h), leaving <1 ppm of Ti in PE, thus PAC > 48 kg PE/(mmol Ti hr)	In these patents the catalyst support was SiO_2 and hydrotalcite: $(Mg_{1-x} Al_x(OH)_2)_n + An\text{-}x/n\ m\ H_2O$ [$x = 0\text{--}0.5$; $m > 0$, A = anion with $n = 2$ or 3]. For eliminating the surface –OH, the particles (size <5 μm) were treated with alumoxanes and trialkyl aluminum [Al $(C_{2, 4, 6})_3$]. The activator was MAO. The product had $\rho = 0.910\text{--}0.935$ g mL^{-1} and ≥30 wt% C_{4-8} comonomer. Polymerization in a stirred, gas-phase	(1) M. Ian, J. Dusan, B.S. John, Process for preparing supported olefin polymerization catalyst, CA 2228923 of 06 Aug 1999 (filed 06 Feb 1998), to NOVA Chem. Ltd.; U.S. Patent Appl. 2002/0010078 A1, (filed: 04 Apr 2001, priority 06 Feb 1998); (2) M. Ian, C. Alison, C.P. Scott, Heterogeneous metallocene catalyst, CA
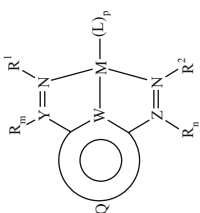
				References
	with, e.g., an aluminum alkyl. The catalyst, R_3-P = N-M(Cp)-L_2, had M = Ti, Zr, or Hf and fivefold substituted Cp, phosphinimine, and two univalent ligands, e.g., Cl. The phosphinimine ligand was tri-(tertiary butyl) phosphine-imine	reactor used a NaCl seedbed, at $T = 100\ °C$ and $P = 1.4$ MPa, and showed the catalyst activity PAC $\leq$ 220 to 360 kg PE/(mmol Ti h)		2237231 of 08 Aug 2006 (filed 08 Aug 1998); U.S. Patent 6235671 of 22 May 2001 (filed 14 Apr 1999, priority 08 May 1998), all to Nova Chemicals, Ltd., or Nova Chemicals (International) S.A.
1998	The disclosures in U.S. Patents 5519098 and 5589555 describe modification of the Novacor Z-N catalysts. Patent (1) describes new, based on Ti, V and a low amount of Al and Mg catalyst used for copolymerization of olefins. The molar ratio Mg/Al = 4.0:1–8.0:1 and Mg/(Ti + V) = 4.0:1–8.0:1. Its novel preparation method increased the polymer MW at high-T polymerization. Patent (2) provides Z-N catalyst having molar ratios Mg/Al = 4.0:1–5.5:1 and Mg/Ti = 4.0:1–5.5:1	Jaber and Brown, from Nova Chemicals (International) S.A. A solution copolymerization of $C_2 \geq 40$ wt% with C_{3-12} into high-MW LLDPE was described. Using the new coordination catalyst, the reaction was carried out at $T = 105$–$320\ °C$ and $P = 4$–20 MPa	The new catalyst comprises (i) a mixture of an alkyl aluminum $Al^1(R^1)_3$, and Mg $(R^2)_2$, where $R^1 = C_{1-4}$ and $R^2 = C_{1-4}$ alkyl radicals in a molar ratio Mg/Al^1 = 6:1–8:1; (ii) a halide R^3Cl where $R^3 = C_{1-4}$ alkyl radicals; (iii) $TiCl_4$; (iv) $VOCl_3$ (Ti/V = 90:10–75:25; and (v) $(R^4)_2Al^2OR_5$ where R^4 and $R^5 = C_{1-4}$ with molar ratios Mg/(Ti + V) = 6.0:1–8.0:1; Al^1/(Ti + V) = 1:1–1.5:1; halide/Mg = 1.9:1–2.3:1; and Al^2/(Ti + V) = 3.0:1–4:1	(1) I. Jaber, S.J. Brown, Mixed titanium–vanadium catalysts for solution ethylene polymerization, U.S. Patent 6084042 of 04 July 2000 (filed 29 June 1998); CA 2271680 of 24 Nov 2009; (2) I. Jaber, Low aluminum and magnesium Z-N solution catalysts, U.S. Patent 6130300 of 10 Oct 2000 (filed 27 Jan 1999, priority 12 Mar 1998); CA 2232099, of 08 Aug 2006, to Nova Chemicals (International) S.A.

(continued)
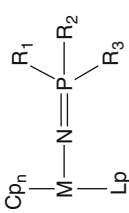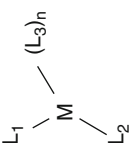
Table 18.10 (continued)

Date	Event	Inventor/company	Comment	Reference
1998	A dual-reactor process for a solution copolymerization of C_2 uses two different catalysts in the two reactors: (A) catalyst with a phosphinimine ligand in the first and (B) Z-N catalyst in the second. Alternatively, in the two reactors the polymerization may be carried out at different T and P. The reaction is relatively easy to control, producing LLDPE with desired MWD for the molded goods or films. Resulting LLDPE has excellent processability, balance of dart impact and tear strength, and excellent optical properties	Brown, Chisholm, JaberJeremic, McKay, Wang, to Nova Chemical (International) S.A. or NOVA Chem. LTD. (Canada) The produced LLDPE had M_w = 66–234 kg mol^{-1} and MWD = 2–21. As disclosed in patent (3) the polymerization in a dual reactor may also be carried out in a slurry process, when the polymer is no longer soluble in the solvent	Copolymerization of C_2 with C_{3-12} α-olefins, in cyclohexane, starts in a reactor (A) at T = 80–200 °C and P = 3.4–55.2 MPa with a catalyst (M = Ti, having a phosphinimine ligand) and its co-catalyst. The copolymerization continues in a second stirred reactor (B) at a higher T in the presence of a Z-N catalyst comprising a transition metal (e.g., Ti + V) and a co-catalyst: Al $(X')_a(OR)_b(R)_c$ where X' = halide; OR = alkoxy or aryloxy group; R is a hydrocarbyl; and a, b, and c are each 0, 1, 2, and 3 with the proviso that $a + b + c$ = 3 and $b + c \geq 1$	(1) I. Jaber, S.J. Brown, CA 2247703 of 17 Apr 2007 (filed 22 Sept 1998), U.S. Patent 6277931 of 2001 Aug 21 (filed 1999 Aug 30); (2) S.J. Brown, CA 2245375 of 15 Aug 2006 (filed 19 Aug 1998); U.S. Patent 6372864 of 16 Apr 2002 (filed 2000 Oct 31); (3) M. Ian, J. Dusan, W. Qinyan, P. Scott Chisholm, CA 2254512 of 12 Jan 2008 (filed 25 Nov 1998); U.S. Patent 6235853 B1 of 22 May 2001 (filed 15 Nov 1999), all to Nova Chemical (International) S.A. or Nova Chemicals Ltd. (Canada)
1999	MAO such as RAl-O (R-AlO)$_m$AlR$_2$ [R = C$_{1-20}$ hydrocarbyl] may contain residual Al(alkyl)$_3$ poisoning the catalysts. Its treatment with carbohydrates such as monosaccharides or polysaccharides (e.g., cellulose, starch, or sugar) significantly improves the catalyst activity	Hoang, Jeremic, Kearns, McLaren Coulter, Donaldson, to NOVA Chemicals (International) S.A. (CH)	In the U.S. Patent 4431788 of 14 Feb 1984, Kaminsky mentioned olefin polymerization with a transition metal catalyst and starch + Al(alkyl)3. The NOVA patents report that addition of cellulose enhanced productivity by 20 % increasing to 32 % if the cellulose + Al (alkyl)3 was filtered out	P.P. Minh Hoang, D. Jeremic, J.R. Kearns, I.M. Coulter, R.D. Donaldson, "Sweet" MAO, U.S. Patent 6750170 B2 of 15 June 2004 (filed 04 Dec 2001); U.S. Patent 6340771 B1 of 22 Jan 2002 (filed 22 Dec 1999), to NOVA Chemicals (International) S.A. (CH)

| 1999 | A supported catalyst for the polymerization of olefins has ≥ 2 catalysts with different propagation and/or termination constants. Each has ≥ 1 phosphinimine ligand described by Stephan et al. in 1997 [CA Patents 2210131 and 2206944; U.S. Patents 5965677 and 6063879]. The polymer shows a broad MWD. Catalysts according to this invention have a surprising, desirable H_2 response | McKay Ian; Ciupa Alison; Hall Barbara Christine, to NOVA Chemicals Solution polymerization in pentane (C_5) or hexane (C_6). The mixed catalyst had high activity. The mixed catalysts, phosphinimine + Z-N, provided LLDPE with a broad MWD | At RT SiO_2 and $Al(Et)_3$ were introduced to reactor filled with solvent (C_5), C_5 was removed at 70 °C, and a suspension of Bu_2Mg and $Al(Et)3$ in hexane was injected. After stirring for 2 h the solvent was flushed off, t-BuCl + $TiCl_4$ in C_5 added. Reaction at $T = 90$ °C and $P = 1.4$ MPa gave LLDPE with MWD ≈ 2.5, nearly unaffected by H_2. PAC ≤ 342 kg PE/(mmol Ti h) | M. Ian; C. Alison; H.B. Christine, Mixed Phosphinimine Catalyst, CA 2278042 of 16 Dec 2008 (filed 19 July 1999); U.S. Patent 6235672 B1 of 22 May 2001 (filed 14 July 2000, priority 19 July 1999) to NOVA Chemicals Corp. (Canada) or Nova Chemical (International) S.A. |
| 1999 | The C_{2-12} α-olefins might be copolymerized into LLDPE having suitable MW and SCB in the presence of a tridentate complex of a Groups 8–10 "late" metal. The new catalyst evolved from the cited above U.S. Patents 5557023 and 5589555. Its formula is shown in the right column | Xu, Wang, Wurz, to NOVA Chemicals here M = Fe Co, Ni or, Pd; R = H or hydrocarbyl; W = O, N, S, or B; Y and Z = P; L = Cl, alkyl, or alkoxy | Slurry or solution polymerization was carried out in toluene in the presence of MAO at $P = 2$ MPa for $t = 10$–30 min and $T = 50$ and 140–160 ° C. Polymerization was terminated by adding MeOH. Polymer properties from the slurry and solution processes were comparable (excerpting the rate). The average values were $M_w = 470$–976 kg mol^{-1}, $T_m = 134 \pm 1$ °C, MWD = 1.7–2.6, PAC = 0.3–0.9 kg PE/(mmol cat*h). The results were affected by the catalyst, comonomer type, and content (s) | Wei Xu, Qinyan Wang, Ryan Paul Wurz, Group 8, 9 or 10 transition metal catalyst for olefin polymerization, U.S. Patent 6239237 B1 of 29 May 2001 (filed 22 Apr 1999); CA 2303767 of 02 Mar 2010 (filed 06 Apr 2000, to Nova Chemicals (International) S.A. or Nova Chemicals Corp. (Canada) |

Table 18.10 (continued)

Date	Event	Inventor/company	Comment	Reference
1999	New organometallic complexes with Group 4 transition metals (Ti, Zr, Hf) have a phosphinimine and two or more cyclopentadienyl ligands. Some of these exhibit unusual NMR behavior. Well-defined crystals of the inventive complexes have been isolated and analyzed by X-ray crystallography. They behave as active polymerization catalysts, producing 62 kg of polymer per 1 mmol of Ti, which is more than obtained with their metallocene analogs	Spence, Brown, Wurz, Jeremic, Stephan, to NOVA Chemicals Cp_n / $M-N=P$ with R_1, R_2, R_3 / Lp	The organometallic complex of interest is shown left with $M = Ti$; each Cp is an indenyl; each of R_1, R_2, and R_3 is an alkyl (e.g., $t\text{-}C_4$) bonded to P; $n = 2$ or 3; $n + p = 3$; and when $p = 1$, L is monoanionic ligand. The gas-phase copolymerization of C_{2-10} in the presence of the catalyst with a supported activator at $P = 0.1\text{–}2.0$ MPa and $T = 60\text{–}130\,^{\circ}\text{C}$. The process may be conducted in the presence of a hydrocarbon diluent or solvent	R.E. von Haken Spence, S.J. Brown, R.P. Wurz, D. Jeremic, D.W. Stephan, Hydrocarbyl phosphinimine/cyclopentadienyl complexes of group IV metals and preparation thereof, CA 2282070 of 09 Dec 2008 (filed 10 Sept 1999); U.S. Patent 6440890 of 27 Aug 2002 (filed 06 Sept 2000, priority 10 Sept 1999) to NOVA Chemicals Corporation (Canada) or NOVA Chemicals (International) S.A.
2001	A catalyst system for olefin polymerization comprises SiO_2 treated with H_2SO_4 Deposited on sulfated SiO_2 aluminoxane (MAO) and Deposited an organometallic complex. The latter has the structure shown right. Ligands	Gao, Chisholm, Kowalchuk, Donaldson (Nova Chemicals Corp.) L_1 / M — $(L_3)_n$ / L_2 $M = Ti$, Zr, or Hf	Gas-phase polymerization was conducted at $T = 80\text{–}90\,^{\circ}\text{C}$ and $P = 1.4$ MPa. A seedbed of dry NaCl was used. A tri-isobutyl aluminum (TIBAL) was used as a poison scavenger. Some copolymerizations were studied by injecting hexene into the reactor. After addition of the scavenger, C_2 was used to push the catalyst system into the reactor. The supported catalyst activity was PAC ≤ 276 kg PE/(mmol Ti h)	Xiaoliang Gao, P.S. Chisholm, M.G. Kowalchuk, R.D. Donaldson, Catalyst for olefin polymerization, U.S. Patent 6734266 of 11 May 2004 (filed 13 Feb 2002, 23 Feb 2001); CA 2338094 of 15 Sept 2009 (filed 23 Feb 2001), to NOVA Chemicals (International) S.A. or NOVA Chemicals Corporation (Canada)

Year				
	L_{1-3} are, respectively cyclopentadienyl, heteroatom (e.g., phosphinimine) and activable (e.g., halide or methyl). The catalyst is used in slurry or a gas-phase process			
2001	The phosphinimine catalyst comprises (1) $(Cp)_a M(PI)_b (L)_c$ [PI = phosphinimine; Cp = indenyl, cyclopentadienyl, fluorenyl (substituted or not); L = H or halogen, a C_{1-10} hydrocarbyl, alkoxy, or aryl oxide; M = Ti, Zr, or Hf; and $a = b = 1$; $c = 1$ or 2 and $a + b + c =$ the valence of M]; (2) an activator, e.g., a salt of tetrakis (pentafluorophenyl) borate; and (3) at least one $Al(Me)_3$ with a methylaluminoxane, MAO	Brown, Swabey, Dobbin, (NOVA Chemicals Corp.)	Continuous solution polymerization of C_{2-20} with a phosphinimine catalyst and a boron activator [at $T = 170{-}250$ °C, $P = 10{-}40$ MPa in the presence of $Al(C_{1, 2, or 4})_3$] leads to PE having a relatively broad MWD, $\rho = 0.910{-}0.935$ g mL^{-1} and good processability. The PE is suitable for the preparation of blown or cast films, blow-molded parts, extruded goods, and injection-molded products	S.J. Brown, J.W. Swabey, C.J.B. Dobbin, Solution polymerization process catalyzed by a phosphinimine catalyst, CA 2347410 of 08 Sept 2009 (filed 11 May 2001); U.S. Patent 6,777,509 B2 of 17 Aug 2004 (filed 17 Apr 2002, priority 11 May 2001), to NOVA Chemicals Corporation (Canada) or Nova Chemicals (International) S.A (CH)
2001	The invention provides a Z-N catalyst for solution polymerization of olefins in the presence of low Al and Mg content	Jaber I. (Nova Chemicals Corp.) used Ph_3SiOH, $Al(Et)3$ or $Al (O-Et)3$, at a molar ratios: Si: Ti = 0.25:1–4:1; Al:Ti = 1	The catalysts are effective for the solution polymerization of olefins at $T = 180{-}250$ °C. $TiCl_4$ and $Mg(Et, But)$ at a ratio Mg:Ti = 5	J. Isam, CA 2365718 abandoned 18 Dec 2009 (filed 18 Dec 2001; U.S. Patent 6878658 of 12 Apr 2005 (filed 09 Dec 2002, Nova Chemicals Corporation (Canada)
2004	Multizone tubular reactor for C_2 polymerization at $P = 12{-}20$ MPa. The reactor length was $L = 1.87$ km and inner	The LDPE reactor had three zones: preheating, primary and secondary reactions, and injection ports: 2 or 3 for C_2 and 3 or 4 for	The low- (140–160), mid- (160–190), and high-$T = 190{-}250$ °C initiators were, respectively, t-butyl peroxy pivalate	Jin-Suk Lee, Byoung-Yong Chung, Myung-Jae Lee, Kun Lo: Method of ethylene polymerization, U.S. Patent Appl.

(continued)

Table 18.10 (continued)

Date	Event	Inventor/company	Comment	Reference
	diameter ID = 40–60 mm. The resulting LDPE had $\rho \approx 0.925$ g mL^{-1}, MI = 1–2 g/10 min, and polydispersity index 10–17	catalyst. As T increased different peroxides were injected	(TBPV), TBP-octanoate (TBPO), and di-TBP (DTBP)	20060149004, Publ. 2006-07-06, Priority 19 Nov 2004, to Samsung Total Petrochem
2004	Priority date of Borealis patent for the Advanced Cascade Process (Hostalen ACP) using the Z-N Avant Z-501 or Avant Z-509 catalysts	M. Baeckman, W. Gustafsson, E. Van Praet, R. Van Marion, U.S. Patent Appl. 2009/0252910 to Borealis	Three reactors in series with Z-N catalyst on MgCl$_2$ support #1 a polymerizing low-MW HDPE, #2 a midrange C$_2$ + C$_4$ copolymer, and #3 the high-MW copolymer	J. Schut, Plastics Eng. Blog, posted 30 June 2010; Baeckman et al., Multimodal PE composition, U.S. Patent Appl. 2009/0252910 of 08 Oct 2009, to Borealis Technology Oy
2005	The new co-catalyst comprises (A1) MAO; (A2) an Al-alkyl, Al (R)$_a$(OR$_1$)$_b$X$_c$ [R and R$_1$ = C$_{1-10}$ hydrocarbyl; X is a halide; and $a + b + c = 3$ and A2 < AlJ; and (A3) a halogenated phenol (hPl). The alkyl in A2 is C$_{1, 2 \text{ or } 4}$. The ratio of A2/Al = 0.1/1–0.5/1. 6. The catalyst system, (A) a CpTi [NP(t-Bu)$_3$]Cl$_2$ and (B) the co-catalyst, is suitable for olefin polymerization	Jaber, Swabey, Gao, Carter, Baar, to NOVA Chem. The modified MAO where R = Me ≡ C$_1$ and R$_1$ is C$_{2-8}$: $$\left[\underset{\mid}{\overset{R}{}} -(Al-O)- \right]_x \left[\underset{\mid}{\overset{R^1}{}} -(Al-O)- \right]_Y$$	The halogenated phenol, e.g., pentafluorophenol, C$_6$F$_5$OH, permits the substitution of a portion of the expensive MAO with inexpensive Al(alkyl)$_3$. This co-catalyst is most frequently used with an organometallics having ≥1 PI ligand. The copolymerization of C$_2$ with C$_{3-10}$ may be carried out at $T = 30$–$280\,^\circ$C and $P = 14$–22 MPa in a dual-reactor system	I. Jaber, J.W. Swabey, X. Gao, C.A. Garret Carter, C.R. Baar, Modified (MAO + aluminum alkyl), CA 2503461, filed 01 Apr 2005; U.S. Patent Appl. 2006/0223960 A1, Published 05 Oct 2006 (filed 28 Feb 2006 (priority 01 Apr 2005), to NOVA Chemicals Corporation(Canada) or NOVA Chemicals (International) S.A.
2006	For a gas- or slurry-phase reaction, the catalyst should be adsorbed on porous particles	McKay, Jeremic, Jacobsen, Mastroianni to NOVA Chemicals	A supported catalyst for olefin polymerization comprises an ionic activator, an organometallic catalyst, and	I. McKay, D. Jeremic, G.B. Jacobsen, S. Mastroianni, Supported polymerization

(e.g., SiO$_2$) then added an activator system: (1) a cation capable of reacting with a metallocene and forming a transition metal complex active for the polymerization of α-olefins; (2) a compatible anion having up to 100 non-hydrogen atoms and containing at least one substituent comprising a moiety having an active hydrogen; and a CpM(PI)L$_n$ complex where M = Ti, Zr, or Hf; three ligands: Cp = substituted η-5; PI = phosphinimine; L = activable; n = 1 or 2	(International) S.A; Ineos Europe Ltd. MAO such as RAlO (R-AlO)$_m$AlR$_2$ [where R = C$_{1-20}$ hydrocarbyl] may contain residual Al(alkyl)3 poisoning the catalysts. Its treatment with carbohydrates such as monosaccharides or polysaccharides (e.g., cellulose, starch, or sugar) significantly improves the activity	a support material. The selected activator must contain an active hydrogen moiety. The organometallic catalyst is characterized by having a phosphinimine ligand and a substituted cyclopentadienyl ligand having 7–30 carbon atoms. The supported catalyst exhibits excellent activity in gas-phase olefin polymerizations and may be used under substantially "non-fouling" polymerization	catalysts, CA 2587230, filed 02 May 2007 (priority 30 May 2006), to NOVA ChemicalsCorp. (Canada); INEOS Europe Ltd.; U.S. Patent Appl. 2008/0045406 A1 of 21 Feb 2008; now U.S. Patent 7863213 of 04 Jan 2011 (filed 07 May 2007), to NOVA Chemicals (International) S.A; INEOS Europe Ltd
2008 Pro-catalyst for olefin polymerization was prepared: (a) reacting MgRaRb (Ra and Rb = C$_{1-8}$ hydrocarbyl) with a source of active chlorine (HCl, isopropyl chloride, and tertiary butyl chloride) at T = 30–80 °C; (b) adding a soluble Hf$_4$ compound (e.g., tri-benzyl-HfCl) for the molar ratio Hf/Mg = 1/10–1/100; (c) adding a TiCl$_n$(OR)$_m$ (n = 2–4 and n + m = 4, preferably TiCl$_4$); Mg/Ti = 5/1–10/1; (d) adding an electron donor and then a second increment of TiCl$_4$	Wang, Zoricak, and Ronne-Newman, from NOVA Chem. Corp In olefin polymerization the pro-catalyst must be combined with an organoaluminum co-catalyst, such as a methylaluminoxane (MAO). The polymerization takes place at T = 160–250 °C and P = 14–22 MPa	An Mg–Ti olefin polymerization pro-catalyst was prepared by reacting a di-organo-magnesium (DOM) with a source of active chlorine in the amount insufficient to completely convert the DOM to MgCl$_2$, removing unreacted DOM, adding Hf + 4 species to the washed MgCl$_2$ support, then depositing Ti$_4$ species on the supported Hf. The new pro-catalyst is highly active in the solution polymerization of olefins when combined with a co-catalyst	Q. Wang, P. Zoricak, J.R. Newman, Magnesium-Titanium-Hafnium for high temperature polymerization, CA 2629550; U.S. Patent Appl. 2009/0264282 A1 of 08 Aug 2009, priority 21 Apr 2008, to NOVA Chem. Corp

Table 18.10 (continued)

Date	Event	Inventor/company	Comment	Reference
2009	Two catalysts, based on Cr and Fe on $MgCl_2/AlEt_n(OEt)_{3-n}$, were used for C_2 polymerization	(DSM) Fe catalyst had $3\times$ lower activity than that based on Cr, but it produced $15\times$ higher MW	Mixtures of the two catalysts resulted in bimodal distribution of PE MW and good processability and performance	N. Kukalyekar, L. Balzano, G.W.M. Peters, S. Rastogi, J.C. Chadwick, Macromol. React. Eng., **3**, 448–454 (2009)
2009	Chevron Phillips developed a single-reactor bimodal HDPE technology using a dual metallocene catalyst with Elf Atochem solid super acid (SSA), which consists of a support for a solid catalyst component, formed from a porous mineral oxide, modified to carry on the surface, Al and/or Mg Lewis acid sites	The modified metallocene catalyst can also create broad MWD bimodal or multimodal HDPE in a single Phillips loop reactor. Catalyst activity ≤ 11.7 kg PE/mmol Zr	Patents on SSA activator/co-catalyst are Thierry Saudemont, Roger Spitz, Jean-Pierre Broyer, Jean Malinge, Nathalie Verdel, activator solid support for metallocene catalysts, U.S. Patent 6239059 of 29 Mar 2001 (filed 02 Oct 1998, priority 02 Oct 1997) to Elf Atochem, S.A.	Qing Yang, K.C. Jayaratne, M.D. Jensen, M.P. McDaniel, J.L. Martin, M.G. Thorn, J.T. Lanier, T.R. Crain, U.S. Patent 7619047 of 17 Nov 2009 (filed 22 Feb 2006); U.S. Pat. Appl. 20110201770 of 18 Aug 2011 to Chevron Phillips Chemical Company, LP
2012	Control of long-chain branching (LCB) of HDPE was obtained by using a modified Phillips chromium on silica catalyst. The analysis by SEC-MALS (SEC coupled to multiangle light scattering) shows that LCBs are concentrated in the molecular weight peaks	Schwerdtfeger, Ding, Masino, Martin, Yu, from Chevron Phillips	The modified catalyst can control production of LCB increasing its frequency to >40/106 C atoms. This improves processability and melt strength, reduces sag, prevents pipe ovality, improves shear thinning, and reduces extrudate swelling	Eric Schwerdtfeger, Plastics Engineering Blog, Posted on 07 Feb 2012; E. Ding, A.P. Masino, J.L. Martin, Y. Yu, U.S. Patent Appl. 20120077665 of 29 Mar 2012, to Chevron Phillips Chemical Company LP

Table 18.11 Evolution of polyolefin blends

Year	Development	References
1937	This first patent on the use of rubber for toughening polyolefins disclosed an addition of rubber "as a softening agent" to "saturated, linear hydrocarbons of the linear type." The MW of rubber was greater than that of paraffin, e. g., MW = 0.8–500 kg mol^{-1}	P.J. Gaylor, Standard Oil Development Co., French Patent 812,490, 11 May 1937
1942	High-pressure LDPE was blended with cyclorubber, to give compounds useful for bonding PE to metal	C.L. Child, R.B.F.F. Clarke, B.J. Habgood, British Patent 544,359, 09 Apr 1942
1951	Discovery of isotactic PP was immediately followed by search for low-T impact improvement, initially by blending with either LDPE or elastomers, later by copolymerizing with ethylene and dienes into EPR and EPDM	J.P. Hogan, R.L. Banks, U.S. Pat. Appl., 333,576, filed 27 Jan 1953, to Phillips Petroleum Co.
1955	The first LDPE/HDPE blends were patented by du Pont de Nemours. Incorporation of 20 wt% HDPE (ρ = 0.939–1.096 g mL^{-1}; $T_m \approx 120\,^{\circ}$C) into LDPE reduced its moisture permeability by 50 %	M.J. Roedel, U.S. Patent 2983704 of 09 May 1961, filed 13 Oct 1959, to du Pont de Nemours (priority 1955)
1958	5–120 parts of LDPE were blended with chlorosulfonated polyethylene, CSR, cured or not (with tribasic lead maleate). The blends found were used as smooth, non-tacky, tough films or coatings for natural or synthetic rubbers	V.C. Boger, A.G. Thomas, U.S. Patent 2854425, filed 30 Sept 1958, to B. F. Goodrich Co.
1958	PP was blended with 5–50 parts of chlorinated butyl rubber, CBR, in the presence of a non-peroxide curative (e.g., oxides or sulfides of Zn, Cd, Mn, Fe, or Pb) on a roll mill at 138–157 °C. The dynamic vulcanization resulted in materials useful for high tensile strength applications	A.M. Gessler, W.H. Haslett Jr., U.S. Patent 3037954, 05 June 1962, Appl. 15 Dec 1958, to Esso Research & Engineering Co.
1958	To improve the low-temperature flexibility of PP, it was blended with 5–20 wt% polyisobutylene (PIB). The Montecatini patent was the first one on the low-temperature modification of PP. The Esso patent used butyl rubber, BR, the Sun Oil document, 5–50 wt% PE (MW = 1.6 Mg mol^{-1} for high impact strength and low brittleness temperature). BASF patent described the use of narrow MWD PIB (0.5–40 wt%)	F. Ranalli, Italian Patent 583501, 14 Oct 1958, to Montecatini; Schramm, K., U.S. Patent 2939860, 07 June 1960; Esso Res. and Eng.; British Patent 893540, 11 Apr 1962; Sun Oil, British Patent 952089, 11 Mar 1964; H. Merkel, G. Cramer, German Patent 1145791, 21 Mar 1963, to BASF
1958	Phillips Petroleum blended LDPE with LLDPE for improved stiffness, abrasion resistance, and reduced H$_2$O vapor permeability. The most important was the gage reduction by 15–30 % for the plastic bags, sacks, and stretch films	P.J. Canterino, R.J. Martinovich, U.S. Patent 3086958, 23 Apr 1963, Appl. 1958; W.M. Nelson, Belgiam Patent 647,311, 29 Oct 1964, Appl. 1963, to Phillips Petrol.; W. R. Grace and Co., British Patent 904,985, 05 Sept 1962; Wissbrun et al. (1962, 1965); Golike (1962); R.M. Lillis, C. van Thomas,
	In the DuPont Canada patent deposited in 1961, 10–50 wt% HDPE (a copolymer of C$_2$ and C$_4$) was blended with LDPE or its copolymers for generating films of high clarity and stiffness were heat shrinkable. The improved film may be manufactured by blending of	

Table 18.11 (continued)

Year	Development	References
	polymers of density $\rho = 0.950$–0.965 and MI < 10, with ≤ 30 % of LDPE (MI $= 0.1$–10, $\rho = 0.910$–0.945 g mL^{-1}). Wissburn et al. in the 1965 Celanese patent particularly stressed improved processability	U.S. Patent 3998914 of 21 Dec 1976, to du Pont of Canada; J. Nancekivell, Canad. Plast. 27–30 (1982); 18–20 (1984); 27–32 (1985)
	In 1983 Union Carbide Corporation, UCC, started selling LLDPE/LDPE blends for check-stand sacks	
1958	Low-density polyethylene (LDPE) was blended with polyisobutylene, 25–40 wt% (PIB), and a copolymer of styrene and isobutylene, 0–10 wt% (PSIB), for the use as transparent, impermeable, shrink-wrap packaging films. In the Phillips patent, LLDPE was blended with PIB to manufacture grocery bags. In the BASF patent, a pre-blend comprising 60 wt% PIB and LDPE was granulated and subsequently compounded with LDPE	J.R. Briggs, R.G. Newburg, R.E. Clayton, U.S. Patent 2,854,435, 30 Sep 1958, to Esso Res. and Eng.; R.J. Martinovitch, R.P. March, U.S. Patent 3,074,616, 22 Jan 1963, Appl. 1959, to Phillips Petroleum; H. Dietrich, German Patent 1,288,293, 30 Jan 1969, Appl. 1961, to BASF A.-G.
1958	The first patent on polyamide/polyolefin, PA/PO, blends comprised 10–80 wt% of either PA-6 or PA-66 with either LDPE or PP. The resins, used to produce sheets, films, fibers, or bottles, reported showing excellent processability, good printability, and low permeability	R.B. Mesrobian, C.J. Ammondson, British Patent 889,354, 14 Feb 1962, Appl. 1958, to Continental Can Co., Inc.
1959	Partially cross-linked polyethylene (by either peroxides or irradiation), XLPE, was blended with polybutadiene, 5–40 wt% BR, to improve resistance to cut at elevated temperatures and elongation. The blends were found suitable for wire coating	Q.P. Cole, U.S. Patent 2,912,410, 10 Nov 1959, to General Electric Co.
1959	Polyethylene, PE, blended with immiscible polymers (e.g., PVC, PIB, PS) was compatibilized by addition of graft copolymer (e.g., styrene or vinyl acetate grafted on PE)	Houillières du Bassin-du-Nord et du Pas-de-Calais and Ethylene-Plastique, French Patent 1,193,104, 30 Oct 1959
1959	Polypropylene, PP, was blended with 5–20 wt% elastomers [styrene–butadiene, SBR, or butadiene–acrylonitrile, NBR] to produce materials useful for blow molding of bottles, free from brittleness and stress cracking. In a later patent, EPR, BP, and PIB, with a dicarboxylic acid anhydride, were used	Shell International Research Maatschappij N. V., British Patent 873,227; 933,727, 14 Aug 1963, Appl. 27 Aug 1959; Belgian Patent 611,727, 19 June 1962, Appl. 21 Dec 1960
1959	For improved processability and mechanical properties of polyethylene, HDPE or LLDPE, it was blended with elastomeric polyethylene–polypropylene copolymer, EPR. For further enhancement of properties, either polypropylene, PP, or polybutene, PB, could also be added. In ICI patent, HDPE was blended with 30–60 wt% EPR for improved processability and impact strength	L. Corbellini, German Patent 1,137,859, 11 Oct 1962, Appl. 1959, to Montecatini; J.W. Crawford, W.G. Oakes, British Patent 941,083, 06 Nov 1963; German Patent 1,217,608, 16 May 1966, to Imperial Chemical Industries Ltd.
1960	These are the first patents on polypropylene, PP, blended with ethylene–propylene rubbers, 10–60 wt% EPR, for improved low-temperature impact strength.	W.M. Schilling, U.S. Patent 3200173, 10 Aug 1966, Appl. 1960; British Patent 975,877,

(*continued*)

Table 18.11 (continued)

Year	Development	References
	In Esso patent, PP was blended with varying amount of polyisobutylene, PIB, and polyethylene, LDPE, to give marked improvement in tear strength and impact. In the Shell patent, reactor powder blending of PP with 0.1–10 wt% EPR (2–25 wt% ethylene) was disclosed. In Farbwerke Hoechst patent, PP was blended with 5–70 wt% LLDPE, for good mechanical properties at low temperature	18 Nov 1964, to Hercules Powder; British Patent 950,551, 26 Feb 1964; G.A. Short, U.S. Patent 3,354,239, 21 Nov 1967, to Shell Oil Co.; R. Holzer, K. Mehnert, German Patent 1,145,792, 21 Mar 1963, Appl. 23 Jan 1960, to Hoechst A.-G.
1960	PE, PP, and their homologues were blended with ethylene–vinyl acetate, EVAc, and cured with free radicals into products showing desired impact strength and modulus. The blends were used for manufacturing of fibers, films, or moldings	Monsanto Co., British Patent 967,334, 19 Aug 1964, Appl. 27 Apr 1960
1960	Blends of PE with 0.1–50 wt% of copolyamides (e.g., LDPE with 5 wt% PE–PA-6 copolymer) showed higher gloss, transparency, and elasticity; lower stress corrosion; and reduced permeability	H. Craubner, G. Illing, A. Hrugesch, German Patent 1,138,922, 31 Oct 1962, Appl. 1960, to Badische Anilin und Soda-Fabrik A.-G.
1960	Mechanical properties of polyolefins, PO, were improved by blending them with 0.5–50 wt% polycarbonate, PC. For example, LLDPE + 5 wt% PC showed improved impact strength, modulus, hardness, and HDT	H. Peters, F. Schuelde, German Patent 1,146,251, 28 Mar 1963, Appl. 22 Jan 1960, to Farbwerke Hoechst A.-G.
1960	To improve dyeability, flexibility, and toughness of isotactic polypropylene, PP, it was compounded in a Banbury-type mixer with ethylene–vinyl acetate, 7 wt% EVAc. Several other ethylene copolymers were also used. In Miliprint patent, EVAc or ethylene–ethyl acrylate copolymer, 18–32 wt% EVAc or EEA, was found to improve impact strength, elongation, and low brittleness temperature of PP. In Firestone patent, linear polybutadiene, BR, was used. The Mitsubishi patent disclosed improvements of PP impact strength properties by blending it with 0.5–25 wt% ethylene–aliphatic esters, e.g., EVAc	Holladay, H. P., Salyer, I. O., U.S. Patent 3433573, 18 Mar 1969, Appl. 1960, to Monsanto; Miller, A., Reddeman, N. G., Belgian Patent 620,703, 14 Nov 1962, to Miliprint; Reid, R. J., Conard, W. R., Belgian Patent 617,870, 21 Nov 1962, to Firestone; Sakata, R., Kuroda, T., Masuda, K., Nakayama, Y., Tanaka, M., Japanese Patent 003,964, 13 Feb 1968, to Mitsubishi Petrochem
1961	High-density polyethylene, HDPE, was blended with 15 wt% EPR. The blend had good impact resistance	A.-G. Farbwerke Hoechst, Belgian Patent 589,358; 612,855, 19 July 1962, Appl. 19 Jan 1961
1961	HDPE, LDPE, or LLDPE, blended with styrene–acrylonitrile copolymer, 2–6 wt% SAN, showed improved crack resistance. Furthermore, a synergistic behavior was observed when 0.1–1 wt% 2,4,6-tri-alkyl phenol was also added. In Esso patent, the mechanical properties of PE were improved by blending it with 5–25 wt% copolymers of mono- and diolefins, EPDM	A.L. Jankens, Belgian Patent 625,004, 20 May 1963, Appl. 24 Nov 1961, to Dow Chemical Co.; Prillieux, M., Delbende, P., Moulin, M., French Patent 1,289,580, 06 Apr 1962, Appl. 1961, to Esso Standard S. A.

<div align="right">(continued)</div>

Table 18.11 (continued)

Year	Development	References
1961	Blending two chlorinated LLDPEs, CPEs containing 40 or 70 wt% Cl, yielded materials with good moldability, impact resistance, and thermal stability	A.-G. Farbwerke Hoechst, Belgian Patent 621,775, 27 Feb 1963, Appl. 1961
1961	Polypropylene, PP, was blended (without compatibilizer) with 20–40 wt% LLDPE, for improved impact resistance and low brittleness temperature	Esso Research & Engineering Co., British Patent 934,640, 21 Aug 1963, Appl. 13 Feb 1961
1961	These are the first patents on PP/PE/EPR blends. Polypropylene/polyethylene, PP/PE, blends were compatibilized by addition of EPR. The resulting blends showed improved low-temperature brittle point and Izod impact strength. In UCC patent, 50–96 wt% was blended with 2–25 wt% PE and 2–25 EPR and/or PIB	L.S. Rayner, J.A. Bond, M. Clark, R.E. Nott, British Patent 958,079, 13 May 1964 Appl. 1961; British Patent 1,026,254, 1966, to ICI; J.P. Lehane Jr., U.S. Patent 3137672, 16 Jan 1964, to Hercules Powder; W.M. Jayne Jr., U.S. Patent 3256367, 14 June 1966to UCC.
1962	LDPE, or its copolymers blended with poly-1-butene, PB, showed improved processability and resistance to environmental stress cracking	A. Rudin, H.P. Schreiber, French Patent 1,349,823, 17 Jan 1964, Appl. 23 Mar 1962, to Canadian Industries Ltd.
1963	Isotactic PP was blended with 3–50 wt% syndiotactic PP, sPP. The blends had excellent impact strength at low T and freedom from surface crazing upon repeated flexing	D.D. Emrick, U.S. Patent 3268627, 23 Aug 1966, Appl. 16 May 1963, to Standard Oil Co.
1963	Polypropylene, PP, was compatibilized with polyethylene, PE, by grafting PP with a basic monomer and PE with an acidic monomer, then blending the modified polymers. Thus, PP was modified with dimethylamino ethyl methacrylate while PE with methacrylic acid. These were blended in 1:1 ratio to result in high-performing alloys	R. Langworth, U.S. Patent 3299176, 17 Jan 1967, Appl. 24 June 1963, to E. I. du Pont de Nemours & Co.
1963	Impact properties of HDPE, LDPE, or LLDPE were improved by blending them with EPDM and PP or polybutene, PB	H.P. Schreiber, British Patent 1,037,819; 1,037,820, 03 Aug 1966, Appl. 1963, to Canadian Industries Ltd.
1963	LDPE and PP were blended with 1–10 wt% polyoxymethylene, POM, for improved melt flow, processability, and extrudate appearance	A. Rudin, H.P. Schreiber, Canadian Patent 688,416; 688,578, 09 June 1964, Appl. 18 May 1963, to Canadian Industries Ltd.
1964	Polyethylene, 10–81 wt% LDPE, was blended with butyl rubber, 15–50 wt% BR, and ethylene–vinyl acetate copolymer, 4–40 wt% EVAc, for cold molding of sealing gaskets	R.J. Ceresa, N.E. Davenport, T.L. Trudgian, British Patent 1,112,024, 01 May 1968, Appl. 1964, to W. R. Grace and Co.
1965	PP was blended with polybutadiene, 5–15 wt% PB, and linear PE, 2–15 wt% LLDPE or HDPE. Good balance of properties was reported	I. Aijima, H. Sakurai, T. Koseki, Japanese Patent 011,539, 27 May 1969, Appl. 09 July 1965, to Asahi Chemical Industry Co., Ltd.

(continued)

Table 18.11 (continued)

Year	Development	References
1966	PE was blended with ethylene–methacrylic acid copolymer, 80 wt% ionomer, and ethylene–vinyl acetate, 10 wt% EVAc, for films with high toughness, stiffness, and impact resistance	M.C.K. Willott, British Patent 1,118,545, 03 July 1968, Appl. 1966, to Imperial Chemical Industries, Ltd.
1966	To improve the low-temperature impact strength of PP, it was blended with a small amount of HDPE and ethylene–propylene block copolymer, EP	Asahi Chemical Industry Co., Ltd., British Patent 1,154,447, 11 June 1969, Appl. 02 Feb 1966
1967	For improved stress crack resistance, PE was blended with 1–95 wt% styrene–butadiene, SBR, or p-methylstyrene–isoprene block copolymer	S. Minekawa, K. Yamaguchi, K. Toyomoto, E. Fujimoto, Y. Takeuchi, Japanese Patent 016,429, 06 May 1971, to Asahi Chem. Ind. Co., Ltd.
1968	Polyolefin, PP or PE, blended with polyvinyl alcohol, 2 wt% PVAl, showed good mechanical, hygroscopic, and antistatic properties. The blends were formed into films, fibers, and tubes or used for coatings	S. Minekawa, K. Yamaguchi, K. Toyomoto, E. Fujimoto, Y. Takeuchi, Japanese Patent 008,585, 12 Sept 1969, to Asahi Chem. Ind. Co., Ltd.
1968	Polymer alloys were prepared by blending PE or its copolymer with lactams, then polymerizing the latter. For example, ethylene–vinyl pyrrolidinone copolymer, EVP, was blended with ε-caprolactam for molding application	R.W. Hill, R.P. Anderson, S.V. Scroggins, U.S. Patent 3,539,662, 10 Nov 1970, Appl. 12 July 1968, to Gulf Research and Development Co.
1968	Polyolefins, PP or HDPE, were blended with amorphous ethylene copolymer, 5–100 EVAc, and 1–80 parts of either polyoxymethylene, POM; polymethylmethacrylate, PMMA; polystyrene, PS; or styrene–methyl methacrylate copolymer, SMM, (as well as inorganic fillers) to extrude into paperlike films	S. Yamamoto, S. Honda, H. Shimizu, Japanese Patent 043,468; 043,469; 043,470, 23 Dec 1971, Appl. 26 Jan 1968, to Sekisui Chemical Co., Ltd.
1968	PP/PE blends were compatibilized by addition of EPR. The resulting materials showed improved low-temperature impact strength	H.J. Leugering, H. Schaum, South African Patent 004,328, 08 Jan 1970, to Farbwerke Hoechst A.-G.
1968	PP or PE was blended with EPR and ethylene–acetoxybicycloheptene copolymer, to increase impact and tensile strength, as well as brittle resistance. In the later patent, PP and EPR were separately dissolved then blended, precipitated, and processed. The blends showed fine, uniform dispersion of the rubber phase, resulting in superior mechanical properties	K. Shirayama, K. Iketa, Japanese Patent 021,303; 021,305, 16 June 1971, Appl. 23 Feb 1968; M. Asada, T. Tokumaru, S. Saito, M. Saeki, H. Ueda, Japanese Patent 008,145, 08 Mar 1972, to Sumitomo Chem. Co.
1969	PE was blended with <15 wt% EPDM, to give resistance to corona discharge. The blends were used as insulating materials for high-voltage cables	H. Matsubara, Japanese Patent 030,095, 05 Aug 1972, Appl. 29 May 1969, to Sumitomo Electric Ind., Ltd.
1969	PP or poly(pentene-co-propylene) was reactor blended with ethylene–butene, or ethylene–pentene, copolymer. The product was melt blended with PP for improved	I. Yamazaki, T. Fujimaki, Japanese Patent 007,627, 03 Mar 1970, Appl. 24 Dec 1969;

(*continued*)

Table 18.11 (continued)

Year	Development	References
	performance. In the second patent, EPR was blended with PP. The alloys showed good mechanical properties. In the Sumitomo patent, for improved impact strength, PP was blended with 5–30 wt% of either polyhexene or polyoctene	007,141, 29 Feb 1972, Appl. 26 Nov 1969, to Showa Denko; K. Shirayama, S. Shiga, H. Watanabe, Japanese Patent 008,370, 10 Mar 1972, Appl. 25 Feb 1969, to Sumitomo Chem
1969	Polypropylene, >70 wt% PP, was blended with ≥5 wt% ethylene–vinyl acetate–vinyl chloride copolymer, EVAc and HDPE, to give materials with low-temperature impact resistance	M. Kojima, M. Tanahashi, Japanese Patent 014,710, 02 May 1972, Appl. 05 Nov 1969, to Chisso Co., Ltd.
1970	LDPE was blended with PIB in an SSE at the shear rates 600,000 s^{-1}, for 34 μs. No thermal degradation was observed. The PIB drop size was 2–5 μm	F. Urban, O. Buchner, K. Steigerwald, K.H. Fauth, H. Gehrig, German Patent 2,028,751, 16 Dec 1971, Appl. 11 June 1970, to BASF A.-G.
1970	PP was blended with hydrogenated styrene–butadiene or styrene–isoprene block copolymer, 6–8 wt%. The alloys were used for the manufacturing of materials with good transparency and impact strength	L.M. Porter, German Patent 2,156,681, 18 May 1972, Appl. 16 Nov 1970, to Shell International Research Maatschappij N. V.
1971	Blends comprising 40–20 wt% polyolefin, PE or PP, with 60–80 wt% of ethylene–propylene–dicyclopentadiene = 47.5:47.5:5 or ethylene–propylene–ethylidene–norbornene = 61:35:4 were disclosed. The blends were masticated and partially cross-linked with peroxides or sulfur, keeping the gel content at 45–96 %. The product could be shaped into articles with good properties without vulcanization. The material may be reprocessed	W.K. Fischer, South African Patent 72 00,388, 23 Aug 1972, U.S. Ref., RE 32,028; W.K. Fischer, U.S. Patent 3806558, 23 Mar 1974, Appl. 12 Aug 1971, to Uniroyal Inc.
1971	Reactive grafting of polyolefins, PE or PP, was disclosed. The extruder was modified for feeding the polymer, the monomer to be grafted and a peroxide. As an example, PP was grafted with acrylic acid	Steinkamp and Grail (1976)
1972	Good mechanical properties were reported for PP or PE blends with chlorosulfonated polyethylene, 4.5 wt% CSR, and filled with a large amount of CaSO$_4$	K. Shikata, K. Okamura, S. Nakamura, Japanese Patent 097,946, 13 Dec 1973, to Tokuyama Soda Co.
1972	LLDPE was blended with atactic polypropylene, 0.1–5 wt% aPP. Blown and stretched films showed large anisotropy in tensile strength and elongation, making them useful for packaging	K. Nakamura, T. Kimura, H. Tsunoda, Japanese Patent 083,174, 06 Nov 1973, Appl. 10 Feb 1972, to Sanyo Pulp Co., Ltd.
1972	UCC discovered the very low density polyethylene, VLDPE, and ultralow-density polyethylene, ULDPE, as copolymers of C$_2$ with α-olefin (C$_{4-8}$) having high SCBD, ρ = 0.860–0.915 g mL^{-1} and T_m = 60–90 °C. UCC used the 2nd-generation Z-N	Levine and F.J. Karol, U.S. Patent 4011382 of 08 Mar 1977 priority 1975, to UCC; E. Berger et al., U.S. Patent 4292200 of 29 Sept 1981, priority

(*continued*)

Table 18.11 (continued)

Year	Development	References
	catalyst with MgO. The VLDPE (comonomer C_{3-8} = 6 wt%) with $\rho < 0.91$ g mL^{-1} and modulus $E <$ 140 MPa was produced in a fluidized bed at $T =$ 10–80 °C and $P < 7$ MPa, in a mixture of gases (C_2, C_{3-8}, molar ratio = 1: 0.35–1:8 and 3–5 mol% H$_2$), with a catalyst system comprising a precursor. For PE with $\rho < 0.86$–0.9 g mL^{-1} reaction $T < 60$ °C and $P < 2.5$ MPa are needed. VLDPE has higher α-olefin content than LLDPE	1972, to Solvay and Co.; A. Delbouille et al., U.S. Patent 4250284 of 10 Feb 1981 priority 1969, to Solvay; E.R. Smith, U.S. Patent 5032463 of 16 July 1991, priority 1988, to Viskase; Fujii et al., U.S. Patent 5110870, of 05 May 1992, priority 1989, to Mitsubishi Kasei; Farley et al., U.S. Patent 6,932,592, 23 Aug 2005, to ExxonMobil; Lustig et al., U.S. Patents 5439717, 08 Aug 1995, 5256351 of 1993-10-26, priority 1985, to Viskase; Karol et al., EP 0120,503, of 11 Oct 1984 priority 1983, to UCC; L.M.J. van Assldonk, S.J. Brown, U.S. Patent Appl., 2011/0144289 of 16 June 2011, to Nova Chemhttp://www.novachem.com/researchtech/docs/2010-19.pdf; S. Sivaram, Second Generation Ziegler Polyolefin processes, Ind. Eng. Chem. Prod. Res. Dev. **16**(2), 121–127 (1977); Anonym. VLDPE – a new class of polyethylene, Plast. Rubber **11**(2), 34–36 (1986)
	These linear elastomers are produced by coordination polymerization using a Phillips or Z-N catalyst at low P and T. Here belongs Mxsten XLDPE from Eastman Chem. and Attane ULDPE from Dow. The first metallocene-catalyzed VLDPE was a hexene copolymer with $\rho = 0.912$ g mL^{-1}, made in the UNIPOL gas-phase process with Z-N catalyst and introduced by ExxonMobil as Exceed metallocene VLDPE. The resin has outstanding sealing properties (hot tack and seal strength) compared with ZN-VLDPE. The solution polymerization in a hydrocarbon usually is carried out in a continuously stirred tank reactor (CSTR), at $T = 160$–300 °C and $P = 2.5$–10 MPa with the residence time of 1–5 min [Dow in 1992 and UCC in 1984]	
	The resins are used for geotextile, hose and tubing, ice and frozen food bags, food packaging and stretch wrap, as well as impact modifiers for blending with other polymers. VLDPE has high flexibility, toughness, sealing, and softness	
1973	PE was blended with ≤35 wt% PP; ≤15 wt% polydimethylsiloxane, PDMS; and 5–35 wt% PPE, PA-6, PC, PET, or Phenoxy. The blends were used for injection molding of products with good processability, high rigidity and impact strength, and long life under sterilization in boiling water or irradiation	A. Plochocki, T. Bek, J. Bojarski, L. Czarnecki, L. Grabiec, J. Kepka, P. Machowski, Polish Patents 097,228, 30 Dec 1978; 100,160, 17 Apr 1979; 100,669, 15 May 1979, Appl. 21 Dec 1973, to Institut Chem. Ind.
1973	HDPE was blended with 50 wt% PP, having matched melt flow index, to give good flowability, weld-line strength, surface quality, and low-temperature impact strength	D. Moorwessel, R. Glasser, G. Pfirrmann, German Patents 2,306,892; 2,306,893, 22 Aug 1974, Appl. 13 Feb 1973, to BASF A.-G.
1974	PP (70–90 wt%) was reactor blended with 8–25 wt% PE and 2–10 wt% EPR for high impact strength down to −60 °C. R-TPO had good hardness and is distinguished by a melt index, MFI 230/5, lower than that of the PP contained therein but higher by the coefficient 1.3–7.0 than that of a PP prepared in the presence of the same catalyst as the molding composition having the same RS	H. Strametz, H.J. Leuering, K. Rust, M. Engelmann, Ger. Offen, 2,417,093, 06 Nov 1975; U.S. Patent 3998911, of 21 Dec 1976, Appl. 07 Apr 1975, Priority 08 Aug 1974, to Hoechst A.-G.

(*continued*)

Table 18.11 (continued)

Year	Development	References
1975	PP was blended with ethylene-5-ethylidene-2-norbornene-propylene copolymer, EPDM, having a high ethylene length index (ELI), to give moldings with good tensile strength. In the following patent, EPDM was blended with LDPE. The blends exhibited superior tensile strength, significantly better than that predicted from additivity. The polymers were blended on a two-roll mill. The thermoplastic polymer blends are useful to prepare molded products, tubing, liners, and like products	P.T. Stricharczuk, German Patent 2,644,644, 07 Apr 1977, Appl. 06 Oct 1975; C.J. Carman, M. Batiuk, R.M. Herman, U.S. Patent 4046840, 06 Sept 1977, Appl. 23 Feb 1976, to B. F. Goodrich Co.
1975	Homogeneous blends of immiscible polymers can be prepared in a high-stress, low residence time extruder (e.g., Patfoort extruder sold by FN). Thus, LLDPE was blended with PS to give blends with good mechanical properties	G.A.R. Patfoort, Belgian Patent 833,543, 18 Mar 1976,; Fabrique Nationale Herstal, Neth. Pat. Appl. 007,963, 18 Sept 1977, Appl. 18 Sept 1975
1976	In a series of patents, the dynamic vulcanization of PP was disclosed. Thus, 60 wt% PP was blended with butyl rubber, BR; elastomeric ethylene–vinyl acetate, 35–85 wt% EVAc, with polyolefins, PE or PP; chlorosulfonated polyethylene rubber, $\geq$50 wt% CSM, with polyolefins, PE or PP; or EPDM, with PP. The blends showed excellent toughness, elongation, and impact strength and a wide range of Shore hardness and dimensional stability. In the latter patent, a PO was compatibilized with an elastomeric block copolymer, NBR. The compatibilization nearly doubled the blend tensile strength and increased its elongation at break by a factor of 4	A.Y. Coran, R. Patel, German Patent 2,757,430, 06 July 1978; U.S. Patent 4130534; A.Y. Coran, B. Das, R. Patel, U.S. Patent 4130535, 19 Dec 1978, Appl. 27 Dec 1976; A.Y. Coran, R. Patel, U.S. Patent 4141878, 27 Feb 1979, Appl. 14 Apr 1977; German Patent 2,805,930, 17 Aug 1978, Appl. 14 Aug 1977; Europ. Pat. Appl., 036,279, 23 Sept 1981; U.S. Patent 4355139, 1982, Appl. 10 Mar 1980, to Monsanto Co.
1976	PP/LDPE blends were compatibilized by addition of 2–22 wt% EPR. Blending was done in two stages, curing EPR before the second portion of PP was added. The resulting materials had good mechanical, low-temperature impact and optical properties	T. Huff, U.S. Patent 4087485, 02 May 1978, Appl. 1976, to Exxon Research & Engineering Co.
1976	To improve modulus of HDPE, it was blended with a graft copolymer of HDPE with vinyl or vinylidene monomer (e.g., styrene)	H. Yui, T. Kakizaki, H. Sano, Japanese Patent 014,752, 09 Feb 1978, Appl. 27 July 1976, to Mitsubishi Petrochem. Co., Ltd.
1977	Soft, thin films, with improved cuttability, suitable for packaging materials, were prepared by blending a mixture of LDPE and HDPE, with EPDM or atactic polypropylene, aPP	S. Sakane, K. Minato, M. Takashige, Japanese Patent 000,052, 5 Jan 1979, Appl. 03 June 1977, to Idemitsu Petrochem. Co., Ltd.
1977	PE blends, suitable for extrusion of pipes, were obtained by blending two types of LLDPE, one with C_4 and the other with C_6 comonomer. The blend also contained carbon black, CB	O.E. Larsen, Canadean Patent 1,120,630, 23 Mar 1982, Appl. 12 Oct 1977, to Phillips Petroleum Co.

(*continued*)

Table 18.11 (continued)

Year	Development	References
1977	PP blends with 5–20 wt% LDPE and 1–15 wt% EPR showed excellent transparency and mechanical properties. Similarly, in Daicel patent PP was blended with 15–85 wt% ABS and 0.5 wt% CPE (or low-molecular-weight PS) as a compatibilizer (?). EPR patented blends of 10–60 wt% PP with EPR block copolymer and a peroxide-containing polyolefin copolymer to give a masterbatch that subsequently was blended with 60 wt% EPDM and to give elastomeric alloy with excellent mechanical properties	T. Oita, T. Hara, R. Samejima, K. Tanabe, Japanese Patent 108,146, 20 Sept 1978, Appl. 03 Mar 1977, to Sumitomo Chem.; M. Kamosaki, S. Tokuhara, M. Kita, N. Nakashima, Japanese Patents 146,748; 146,753, 20 Dec 1978, Appl. 27 May 1977, to Daicel Ltd.; A. Yamamoto, M. Shiraishi, S. Nakayama, Y. Tsurugi, H. Nakanishi, Japanese Patent 001,386, 08 Jan 1979, Appl. 07 June 1977, to EP Rubber Co., Ltd.
1979	PP was sequentially blended with EPR, then with PE. The blend showed co-continuous morphology resulting in excellent impact and mechanical properties, superior to those observed for blends with a particulate dispersion	T. Huff, Europ. Pat. Appl., 015,066, 03 Sept 1980, Appl. 31 Jan 1979, to Exxon Res. Eng. Co.
1979	A 60 wt% PP was blended with polyamide, 20 wt% PA-6 or PA-66, and glass fibers, 20 wt% GF, for superior tensile and impact strength	Asahi Fiber Glass Co., Ltd., Japanese Patent 030,451, 27 Mar 1981, Appl. 23 Aug 1979
1979	Polyethylene, 70 wt% PE; polyamide, 20 wt% PA-66; and 3 wt% of ethylene–fumaric acid graft copolymer were mixed to reduce moisture permeation and to improve impact strength. In 1982 DuPont introduced PA/PO blends, Selar™, to be used as additive to polyolefin to reduce permeability	P.M. Subramanian, Europ. Pat. Appl., 015,556, 17 Sept 1980, Appl. 06 Mar 1979, to E. I. du Pont de Nemours; "Selar™ Barrier Resins," Bulletins E73971, E73973, E73974 by du Pont
1979	PE was grafted with 0.1–5 wt% maleic anhydride and blended with 1–50 wt% EPDM. The blend showed excellent adhesion to polar materials	A. Honkanen, M. Arina, R. Holstii, Finnish Patent 064,805, 30 Sept 1983, Appl. 10 Dec 1979, to Neste Oy
1979	PP was blended with 5 wt% PDMS for improved processability, impact strength, and elasticity	U. Grigo, L. Morbitzer, K. Arlt, R. Binsack, J. Marten, German Patent 2,905,357, 21 Aug 1980, Appl. 13 Feb 1979, to Bayer A.-G.
1979	A patent on reactor-blended thermoplastic olefinic elastomer, R-TPO, was disclosed. Thus, PE was polymerized in the presence of an active catalyst and an already polymerized olefinic copolymer (e.g., ethylene-co-1-butene) or the sequence was reversed. The blend had superior resistance to environment stress cracking, and the blown film showed few fish eyes	Y. Morita, N. Kashiwa, Europ. Pat. Appl., 022,376, 14 Jan 1981, Appl. 09 July 1979, to Mitsui Petrochemical Industries, Ltd.

(*continued*)

Table 18.11 (continued)

Year	Development	References
1980	In 1979 UNIPOL™ process for gas-phase production of LLDPE was introduced by the UCC. Since the new resins were difficult to process on the LDPE processing lines, several patents were issued for LLDPE blends with, e.g., LDPE or PP, which had better processability In 1982 a number of patent applications for blends of LLDPE, with other polyolefins, co-polyolefins, and olefinic elastomers, for example, ethylene copolymers and thermoplastic elastomers (e.g., TPO, EPDM, EPR, EVAc, PP-MA,), have been filed	A. Haas, F. Raviola, EP Appl. 042,743, 13 Jan 1982; A. Haas, French Patent 2,526,803, 18 Nov 1983; M. Hert, French Patent 2,528,055, 09.121983, to Soc. Chim. Charbon., SA; P.M. Hughes, EP Appl. 045,455, 10 Feb 1982, Appl. 1980, to Shell Oil; M.A. Cowan, EP Appl. 095,299, 30 Nov 1983, to Intercont. Plast.; K.C. Janac, R.C. Puydak, D.R. Hazelton, EP., Appl., 092,318, 26 Oct 1983, Appl. 26 Mar 1982, to Exxon Res. & Eng. Co.; B.L. Turtle, EP Appl. 095,253, 30 Nov 1983, to BP; O. Fukui, Y. Inuizawa, S. Hinenoya, Y. Takasaki, French Patent 2,522,331, 02 Sept 1983, to Ube
1980	To improve its low-temperature impact strength, polyethylene, PE, was blended on a roll mill with polybutadiene rubber, 10 wt% PB	E.G. Kent, U.S. Patent 4,423,181, 27 Dec 1983, Appl. 10 Mar 1980, to Polysar Ltd.
1981	Polyethylene, 50–95 wt% HDPE, was blended with LLDPE for improvement of film strength and transparency	Showa Denko (1983)
1981	Polyethylene, PE, was blended with neoprene rubber at a ratio 1:1. The blends were irradiated by electron beam for improved tensile strength and other mechanical properties	A.Y. Coran, R. Patel, U.S. Patent 4,348,266, 07 Sep 1982, Appl. 02 Apr 1981, to Monsanto
1981	Polypropylene, 100 parts PP, blended with 8–25 parts of amorphous ethylene–propylene copolymer, EPR, and 2–10 parts crystalline EPR showed improved impact strength. In the Idemitsu patent, PP was blended with maleated LDPE, EVAc, and inorganic filler, to give blends with good melt strength and rigidity	P. Galli, M. Spataro, Europ. Pat. Appl., 077,532, 27 Apr 1983, Appl. 14 Oct 1981, to Montedison; Idemitsu Petrochemical Co., Japanese Patent 096,640, 08 June 1983, Appl. 04 Dec 1981
1982	Semicrystalline ethylene–propylene copolymer, EP, was blended with amorphous EP and inorganic filler. The blends had good processability, mechanical properties, and impact strength. In the Mitsubishi patent, crystalline EP was blended with styrene–isoprene block copolymer, 5–30 wt% SIS, and polystyrene, 3–5 wt% PS, to give good paintability	Ube Industries, Japanese Patent 162,652, 27 Sep 1983, Appl. 23 Mar 1982; Japanese Patent 168,648; 168,649, 05 Oct 1983, Appl. 30 Mar 1982; Mitsubishi Petrochem. Co., Ltd., Japanese Patent 213,039, 10 Dec 1983, Appl. 04 June 1982
1982	Polypropylene, 94 wt% PP, was blended with chlorinated polyethylene, 6 wt% CPE. The blends had good processability and gave moldings with good mechanical properties	R. Newe, E. Lange, H. Hoffmann, K. Wetzel, East German Patent 207,381, 29 Feb 1984, Appl. 05 Apr 1982, to VEB Chemiekombinat Bitterfeld

(continued)

Table 18.11 (continued)

Year	Development	References
1982	Polypropylene, 50–90 wt% PP, and/or ethylene–propylene block copolymer, EP, was blended with talc having particle size $d = 5$–20 μm. The materials had high impact strength. In the following patent, PP was blended with 5–40 wt% styrene-grafted chlorinated polyethylene, CPE, to give high modulus and impact resistance	Chisso Corp., Japanese Patent 036,149, 28 Feb 1984, Appl. 24 Aug 1982; Japanese Patent 213,038, 10 Dec 1983, Appl. 03 June 1982
1982	Polypropylene, 35 wt% PP, was blended with polyisobutylene, 50 wt% PIB, and ethylene–vinyl acetate copolymer, 15 wt% EVAc, to give alloys useful for films, moldings, and extrusions	C.B. Shulman, Europ. Pat. Appl., 116,783, 29 Aug 1984, Appl. 27 Dec 1982, to Exxon Research and Eng. Co.
1982	Polyethylene, PE, blends from LDPE, HDPE, and MDPE were found suitable for manufacturing films with uniform thickness and anisotropic tensile strength	K.K. Showa Denko, Japanese Patent 157,837, 20 Sep 1983, Appl. 15 Mar 1982; Japanese Patent 176,234, 15 Oct 1983, Appl. 09 Apr 1982
1982	Linear low-density polyethylene, LLDPE, was blended with 2–25 wt% LDPE to give films with large difference of the tensile strength in the machine and transverse direction	M. Hert, French Patent 2,528,054, 09 Dec 1983, Appl. 03 June 1982, to Societé Chim. des Charbonnages S. A.
1982	Low-density polyethylene, LDPE, was blended with 1–40 wt% poly(2-ethyl-2-oxazoline), PEOX. The blends had excellent adhesion to substrates, e.g., thermoplastic polyesters, viz., PET	S.M. Hoenig, D.P. Flores, S.P. Ginter, U.S. Patent 4,474,928, 02 Oct 1984, Appl. 28 June 1982, to Dow Chemical Co.
1982	Ethylene polymer blends are prepared by mechanical blending of dry powders or compounding in an internal mixer, a compounder or (preferably) combining the two methods. The two polymers are high-density, narrow MWD LLDPE and HDPE, significantly differing in MW. PE films with superior tear strength with <30 wt% LDPE and >70 wt% Cr-type LLDPE with $M_w/M_n > 6$. Bailey, Whitte, Coutant Martin, and Benham et al. to Phillips Petroleum Co; Cobler et al. to Dow Chem. Co. (mixing on the blow line); Harris to Media Plus. Blends of a high-MW ethylene–α-olefin copolymer, a low-MW PE with narrow MWD, and low levels of LCB for films with good ESCAR are useful for the manufacture of films, pipes and wire coating	Bailey and Whitte (1984), Coutant and Martin (1995), Benham and McDaniel (1994), Benham et al. (1995); U.S. Patent 5,681,523, 28 Oct 1997, to Dow Chem. Co.; U.S. Patent 6822051, 23 Nov 2004, to Media Plus, Inc.
1982	Low-density polyethylene, LDPE, was blended with HDPE, PP, and EP block copolymer, to give films with good modulus, tear strength, and sagging	Shin-Kobe Electric Machinery Co., Ltd. (1984)
1983	Low-density polyethylene, LDPE, blended with linear low-density polyethylene in a ratio 100:20–90 gave alloys useful for production packaging films	Asahi Chemical industry Co., Ltd. (1985)
1984	Linear low-density polyethylene, LLDPE, was blended with low-density polyethylene, 10–45 wt% LDPE; polypropylene, PP; and/or ethylene–propylene copolymer [with a high propylene content], 2–15 wt% EPR. The blends had high modulus and clarity	Bahl et al. (1985)

(*continued*)

Table 18.11 (continued)

Year	Development	References
1985	Polyethylene, PE, blended with 10–40 wt% ethylene–vinyl carboxylate or an acrylate copolymer exhibited notched Izod impact strength more than three times larger than that of functional group-free PE	T.O. Broadhed, Europ. Pat. Appl., 209,294, 21 Jan 1987, Appl. 15 July 1985; to Du Pont Canada, Inc.
1985	Polyolefin blends with good compatibility comprised 100 parts PO and 0.1–100 parts polytransoctanamer, PTO. For example, PP with 9 wt% PTO showed about 5x higher impact strength at $T = -40$–23 °C than PP alone	M. Kita, K. Hashimoto, Japanese Patent 131,043, 13 June 1987, Appl. 04 Dec 1985, to Daicel Huels Ltd.
1987	Transparent-, impact-, and "blush"-resistant blends were obtained by compounding linear low-density polyethylene, LLDPE, with hydrogenated styrene–butadiene block copolymer, SEBS	G. Holden, D.R. Hansen, Europ. Pat. Appl., 308,001, 22 Mar 1989, Appl. 1987, to Shell Int. Res. Maatschappij BV.
1987	Polypropylene, PP, blended with polyoctadecene, POD, was found to show temperature-sensitive transparency (thermochromic blends)	S. Tanaka, J. Sakai, T. Fukao, K. Wakatsuki, K. Wakamatsu, Europ. Pat. Appl., 285,414, 05 Oct 1988, Appl. 1987, to Sumitomo Chemical Co., Ltd.
1989	Polypropylene, PP, reactor blends were obtained with high yield using a chiral metallocene catalyst and an aluminoxane. The preferred blends comprised 60–95 wt% of a crystalline isotactic PP homo- or copolymer produced in the first stage and (the second stage) random copolymer ethylene–propylene (and another 1-olefin), as well as a partly crystalline polymer of the second 1-olefin. The moldable blends showed good flow properties and a very good low-temperature impact strength	M. Schreck, A. Winter, V. Dolle, H. Kondoch, M. Antberg, J. Rohrmann, U.S. Patent 5,322,902, 21 June 1994, Appl. 21 Dec 1989, U.S. Appl. 19 Dec 1990, to Hoechst Aktiengesellschaft
1990	Three-component polypropylene, 1–99 wt% PP, blends comprised 1. either acidified PP, its mixture with PP, or a mixture of PP with carboxylic acid-modified EPR; 2. 99–1 wt% of maleated polymer [e.g., poly(methyl methacrylate-co-styrene-co-MA]; and 3. epoxy group-containing copolymer [e.g., 0.1–300 phr of ethylene–methyl methacrylate–glycidyl methacrylate = 65-15-20 or ethylene–vinyl acetate–glycidyl methacrylate = 85-5-10]. The blends were used to mold car bumpers and fenders, with good stiffness and low-temperature impact resistance	H. Abe, T. Fujii, M. Yamamoto, S. Date, U.S. Patent 5,278,233, 11 Jan 1994, Appl. 14 June 1990, U.S. Appl. 12 June 1991, to Sumitomo Chemical Co., Ltd.
1990	Polypropylene (PP) was blended with ethylene-co-vinyl alcohol (EVAL) and maleated polypropylene (PP-MA). The blends were extruded through a sheeting die that engendered overlapping layers of EVAL. Their presence reduced permeability by gases or liquids through the PP wall	M.R. Kamal, G. Lohfink, L. Arghyris, S. Hozhabr-Ghelichi, PCT Int. Appl., 006,837, 30 Apr 1992, Appl. 16 Oct 1990, to McGill University

(continued)

Table 18.11 (continued)

Year	Development	References
1990	Linear low-density polyethylene, LLDPE, was blended with very low density polyethylene, VLDPE. The polymers prepared using metallocene catalyst had narrow molecular weight distribution, $M_w/M_n = 1–3$. Blending resulted in resins having the density $\rho = 910–940$ kg m^{-3}	Stehling et al. (1995)
1991	Polyolefin blends with density of $\rho = 930–940$ kg m^{-3} at 23 °C and MFI(90/2.16) = 0.05–1.0 dg min^{-1} comprised high-density polyethylene, 50–80 wt% HDPE [polymerized in two stages, with a broad bimodal molecular mass distribution, $\rho = 940–960$ kg m^{-3} and MFI(90/2.16) = 0.01–0.5 dg min^{-1}], and linear low-density polyethylene, 20–50 wt% LLDPE [$\rho = 910–925$ kg m^{-3} and MFI (90/2.16) = 0.5–2.0 dg min^{-1}]. The blends were used for forming tubes and pipes with high stress crack resistance	Boehm et al. (1992); U.S. Patent 5,338,589, 16 Aug 1994, U.S. Appl. 03 June 1992, German Appl. 05 June 1991, to Hoechst Aktiengesellschaft
1991	Linear low-density polyethylene, LLDPE, was graft modified by incorporation of basic groups from, e.g., dimethylamino ethyl methacrylate, t-butylamino ethyl methacrylate, vinyl pyridine, or allyl urea. These copolymers were then used as reactive components for alloys with acidified polymers, viz., maleated polyolefins	Baker and Simmons (1991)
1991	Linear low-density polyethylene, LLDPE, was blended with low-density polyethylene, LDPE, at a ratio of about 0.3. The blends were used for blow molding hollow balls containing pressurized air and consisting of two hemispheres welded to form a ball with a wall thickness $t = 0.5–1.8$ mm	Moss and Modigh (1994)
1991	Blends comprising 30–70 wt% low-molecular-weight (MW) polyethylene, DPE [made using a chromium catalyst, having density $\rho \geq 955$ kg m^{-3}, MI = 25–400 g/10 min, and $M_w/M_n = 2–35$], and 30–70 wt% high-MW ethylene copolymer, LLDPE [made using a titanium catalyst, having $\rho \leq 955$ kg m^{-3}, MI = 0.1–50 g/10 min, and $M_w/M_n = 2–10$], showed improved processability. The blends were used to produce pipes, films, and bottles with enhanced mechanical properties as well as the environmental stress crack resistance, ESCR. In the following patent 5–40 wt% low-MW HDPE [made using a titanium catalyst, with density $\rho \geq 955$ kg m^{-3}, MI ≥ 25 dg min^{-1}, and $M_w/M_n = 2–8$] blended with 60–95 wt% high-MW HDPE [from chromium catalyst, with density $\rho \geq 930$ kg m^{-3}, MI = 1.5–15 dg min^{-1}, and $M_w/M_n = 6–100$] yielded blends with MI = 0.05 dg min^{-1} and ESCR. In the last patent	Martin et al. (1994), Coutant and Martin (1995), Appl. 16 Apr 1993, Appl. 18 Sep 1991, to Phillips Petroleum Company

Table 18.11 (continued)

Year	Development	References
	10–80 wt% low-MW LLDPE [$\rho \geq 940$ kg m^{-3}, MI > 25 dg min^{-1}, and $M_w/M_n = 2$–12] was blended with 20–90 wt% of a high-MW LLDPE [$\rho \leq 955$ kg m^{-3}, MI = 2–10 dg min^{-1}, and $M_w/M_n = 2$–10]. The blends had MI > 0.05 dg min^{-1} and had improved optical properties	
1991	Polyethylene, PE Rigidex™ or Innovex™, was blended with liquid crystal polyester, 0.01–5 wt% LCP, to give materials with good melt processability, low viscosity, and reduction of the specific energy during compounding	P.T. Alder, J.G. Dolden, D.G. Othen, PCT Int. Appl., 008,231, 29 Apr 1993, Appl. 22 Oct 1991, to British Petroleum Co.
1991	Compositions comprised 10–80 wt% low-MW polyethylene, HDPE [$\rho \geq 940$ kg m^{-3}], and 20–90 wt% high-MW ethylene–hexene copolymer, LLDPE [$\rho \leq 955$ kg m^{-3}]. The blends had a MFI > 0.05 g/10 min. The blend showed improved optical and physical properties, resulting in better blow-molded products	W.R. Coutant, J.L. Martin, Eur. Pat. Appl., 533,160, 24 Mar 1993; Norwegian Patent 9203,598, 19 Mar 1993; Hungarian Patent T62,631, 28 May 1993; Japanese Patent 5,194,796, 03 Aug 1993, Appl. 18 Sep 1991, to Phillips Petroleum Co.
1991	Ethylene–propylene copolymer (EPR, EPDM, or their mixture with $T_m = 35$–55 °C) was blended with ethylene copolymer (very low density polyethylene VLDPE with density 885 kg m^{-3} and $T_m = 65$–90 °C), PP or PP block copolymers, and 0–7 phr talc. The blend showed excellent moldability, surface appearance, and hardness, as well as good impact resistance	T. Nishio, T. Nomura, N. Kawamura, H. Sato, A. Uchikawa, I. Tsutsumi, Y. Goto, Europ. Pat. Appl., 519,725, 23 Dec 1992, Appl. 21 June 1991, to Mitsubishi Petrochemical Co.
1991	N,N-diethylaminoethyl-, lycidyl methacrylate, or acrylic acid chloride was used	N. Koyama, M. Usui, H. Furuhashi, S. Ueki, U.S. Patent 5,382,634, 17 Jan 1995, Appl. 25 Apr 1994, Jap. Appl. 15 Mar 1991, to Tonen Corporation
1991	Polymer alloys comprised 20–30 wt% PP, 25–35 wt% uncross-linked elastomeric ethylene-propylene-1,4-hexadiene, EPDM (60–80 wt% ethylene), 30–50 wt% ionomer, and 2–3 wt% ethylene/n-butyl acrylate/glycidyl methacrylate, EBA-GMA. The blends were used in applications where a wide temperature range and abrasive conditions were encountered	R.L. Dawson, U.S. Patent 5,206,294, 27 Apr 1993, Appl. 6 Nov 1991, to E. I. du Pont de Nemours & Co.
1991	Deposition of patent on the constrained geometry catalyst technology (CGCT) based on the transition metals, M = Ti, Zr, Hf. The resulting PO is substantially linear. The preferred composition comprises 10–95 wt% of homogeneously branched linear α-olefin copolymer ($\rho = 0.930$–0.965 g mL^{-1}, MWD = 1.8–2.8, single T_m)	S.-Y. Lai, J.R. Wilson, G.W. Knight, J.C. Stevens, P.-W. S. Chum, Elastic substantially linear olefin polymers, CA 2120766 of 08 July 2008 (filed 15 Oct 1993; priority 15 Oct 1991); U.S. Patent 5,272,236 of

Table 18.11 (continued)

Year	Development	References
	and 5–90 wt% of heterogeneously branched C_2C_8 copolymer ($\rho = 0.935$ g mL^{-1})	21 Dec 1993 (deposited 15 Oct 1991); P.-W.S. Chum, R.P. Markovich, G.W. Knight, Shih-Yaw Lai, Fabricated articles made from ethylene polymer blends, CA 2160705 of 22 Aug 2006 (filed 190 Apr 1994; priority 28 Apr 1993); Ethylene polymer film made from ethylene polymer blends, U.S. Patent 5847053 of 08 Dec 1998 (filed 11 Apr 1997; priority 15 Oct 1991), to The Dow Chemical Company
	Lai, Wilson, Knight, Stevens, Chum, Markovich, to the Dow Chemical Company	
	The SCBDI = wt% of macromolecules having a comonomer content within 50 % of the median total molar comonomer content, calculated from TREF (temperature rising elution fractionation) data. The elastic, substantially linear C_2–C_8 copolymer has $0.01 \leq$ LCB/1000C ≤ 3, $M_w/M_n = 1.5$–2.5, $2 \leq$ SCB (CH$_3$/1000C) ≤ 30), and short-chain branch distribution index: SCBDI > 50 %. The homogeneously branched copolymer may be produced as described in C. T. Elston (DuPont Canada Ltd.) patent. Films produced from the bimodal MWD new copolymers show good impact and tensile properties	
1991	Polypropylene, 50 wt% PP, was blended with a linear low-density polyethylene, 10–50 wt% LLDPE, and a low-molecular-weight ethylene–butene plastomer (a compatibilizer). The blends were useful for melt-spun or melt-blown fibers or fabrics. In the following patent heat sealable at 100 °C, blends were disclosed. They comprised 30–70 wt% ethylene–alpha-olefin copolymer prepared using a metallocene catalyst, VLDPE or plastomer [with density $\rho = 880$–915 kg m^{-3}, MI = 1.5–7.5 dg min^{-1}, $M_w/M_n \leq 3.0$, $T_m = 60$–100 °C], and 70–30 wt% propylene–alpha-olefin random copolymer [with 88–100 mol% propylene]. The blends showed good processability, resistance to tearing, and tensile strength. They were useful for manufacturing packaging films, tubes, trays, etc.	K.W. Bartz, L.P. Land, A.K. Mehta, A.A. Montagna, PCT Int. Appl., WO 06,169 A1, 01 Apr 1993, Appl. 16 Sep 1991; A.K. Mehta, M.C. Chen, U.S. Patent 5,358,792, 25 Oct 1994, Appl. 22 Feb 1991, 23 Apr 1993, to Exxon Chem. Co.
1991	Polypropylene, 55–90 wt% PP, was blended with poly (1-butene), PB, as a dispersed phase and optionally with up to 10 wt% of low-MW poly(α-olefin-co-ethylene) plastomer compatibilizer. The blends were useful for manufacturing fibers and nonwovens, with good "hand" and tensile strength	K.W. Bartz, J.C. Floyd, P. Meka, F.C. Stehling, PCT Int. Appl., WO 006,168, 01 Apr 1993, Appl. 16 Sep 1991, to Exxon Chemical Patents, Inc.
1991	Semicrystalline polyolefin blends and method of their preparation were described. The blends were reported to show enhanced inter-spherulitic and interlamellar strength. The first polymer should have higher crystallinity and crystallization temperature than the second. Thus, 50–99.9 wt% PP was blended with ethylene–α-olefin copolymers, either a stereo block polypropylene or an ethylene–propylene copolymer, EPR	A. Lustiger, Can. Pat. Appl., 2,083,664, 21 June 1993, Appl. 20 Dec 1991, to Exxon Research and Engineering Co.

<div align="right">(continued)</div>

Table 18.11 (continued)

Year	Development	References
1991	Vinyl-trimethoxysilane-grafted polyolefin, PO (e.g., PP, LDPE, EPR, or EVAc), was blended with and ethylene–acryloyloxytetramethylpiperidine. The water-cross-linkable blends were found useful for manufacturing weather-resistant cross-linked polyolefin pipes for outdoor applications	S. Ohnishi, T. Fukuda, Eur. Pat. Appl., 548,565, 30 June 1993, Appl. 12 Dec 1991, to Mitsubishi Yuka Industrial Products Corp.
1991	Blends comprised 1–70 wt% of either metallocene polypropylene, PP, or a copolymer of propylene with ≤10 mol% ethylene or C_2–C_{20} α-olefin that has $M_w/M_n \leq 3$ and 30–99 wt% of a similar copolymer but with $M_w/M_n = 3.5$–10. The blends were used for films having excellent low-temperature heat sealability and blocking resistance	T. Fujita, T. Sugano, H. Mizuno, H. Uchino, U.S. Patent 5,331,054, 19 July 1994, Appl. 19 Oct 1992, Jap. Appl. 21 Oct 1991, to Mitsubishi Petrochemical Co., Ltd.
1991	Radiation-resistant, heat-sealable polypropylene, PP, blends (softer and tougher than similar ones) comprised 1–99 wt% mesomorphous PP or its copolymer, ethylene–vinyl acetate (EVAc) and/or ethylene–acrylic acid copolymer (EAA) and polybutene (PB). For example, films were prepared by blending, extruding, and then quenching. The resins were useful for manufacturing medical goods, tapes, ostomy bags, packaging materials, drug delivery patch, medical type, etc.	D.L. Wilfong, R.J. Rolando, Eur. Pat. Appl., 547,834, 23 June 1993, Appl. 18 Dec 1991, to Minnesota Mining and Mfg. Co.
1992	Polyolefin, 100 parts PO [PE, PP, or EPR], was grafted with 0.01–20 parts of the monomers' mixture [consisting of 5–50 mol% of glycidyl (meth)acrylate and 95–50 mol% of acrylamide, vinylpyrrolidone, acrylic acid esters, and/or methacrylic acid esters]. Grafted PO was used as modifier for engineering plastics or as adhesion improver for filled plastics	T. Teraya, S. Kikuchi, K. Yokoyama, Y. Fujita, Japanese Patents 61 45,260, 61 45,261, 24 May 1994; Eur. Pat. Appl., 596,654, 11 May 1994, Appl. 28 Oct 1993, JP Appl. 30 Oct 1992, to Tonen Corp.
1992	Heterogeneous ion exchange materials contained 44–55 wt% of an ion exchange resin dispersed within a blend of LLDPE and HDPE (having $MW > 200$ kg mol^{-1}.) The maximum density of LLDPE, and minimum density of HDPE, was approximately 940 kg m^{-3}. The ion exchange material was selected from between anionic, cationic, and amphoteric ion exchange resins and their mixtures	A. Giuffrida, U.S. Patent 5,346,924, 13 Sep 1994, Appl. 23 Sep 1992, to IP Holding Company
1992	Linear low-density polyethylene, LLDPE, was blended with starch and at least one ionic compound (in such amount that the concentration of anions and cations was between 0.002 and 5 mol kg^{-1}) to produce high-frequency sealable articles. The starch could also contain ≤50 wt% of a plasticizer. The alloys could be processed by calendering, extrusion, etc., to produce multilayer films or sheets weldable or sealable by induction heating at high frequency, useful in packaging, paper making, etc. The presence of the starch improved the long-term biodeterioration of the materials	C. Dehennau, T. Depireux, I. Claeys, Eur. Pat. Appl., 587,216, 16 Mar 1994; Japanese Patent 62 07,046, 26 July 1994, Appl. 01 Sep 1992, to Solvay et Cie.

Table 18.11 (continued)

Year	Development	References
1992	Polymer blends comprised melt-blended high- and low-molecular-weight polyethylenes, PE, having the viscosity (at $100\,\mathrm{s}^{-1}$) of, respectively, $\eta > 5$ and $\eta < 0.3$ kPas. The two polymers were blended at two stages: first the high-molecular-weight polymer was blended with a small amount of the other polymer, and then an additional low-molecular-weight resin was incorporated. The blends showed good processability and excellent properties. They were used for production of films with low fish-eye content, blow molding, pipes, wire coating, and injection or rotational molding	Coutant (1994)
1992	Reactor blends of high-density polyethylene, HDPE with butene and/or hexene, were produced in a multistage, gas-phase, fluidized bed polymerization, where blending occurred in situ. The resulted bimodal molecular weight distribution resin had 35–75 wt% of the higher-molecular-weight component. The blown films had improved MD/TD tear balance	Ali et al. (1994); Dammert et al., U.S. Patent 6,185,349 of 06 Feb 2001 (filed 1999) to Borealis Polymer Oy
	PE blends were prepared during polymerization. This strategy has been widely implemented in syntheses of multimodal PE compositions. The blown film showed MD/TD tear balance. The bimodal blend contained 0.35–0.75 weight fraction of a higher-MW component. Ali A.H. et al. to Mobil Oil Co.; Dammert et al. to Borealis. Catalyst: $TiCl_4$/pentanol deposited on MgO/acetic acid and then treated with tri-n-hexyl-aluminum solution. Reactor blending during the slurry polymerization gave two PE fractions with different MW. Borealis generated multimodal resins for optical cables using slurry-/gas-phase reaction with Z-N catalyst with $MgCl_2$	
1992	Polyolefin blends with improved barrier properties comprised 85–99.5 wt% of a polyolefin (e.g., high-density polyethylene, HDPE) with 0.5–15 wt% of high-nitrile polymer (e.g., an acrylonitrile–butadiene copolymer). The alloys were found useful for molding plastic bottles, automobile gasoline tanks, and other containers having limited or restricted permeability to gases, vapors, or organic liquids. These materials also showed good chemical resistance, strength, and processability	G.P. Coffey, E.S. Perec, N.W. Standish, L. Melamud, J. Smola, Eur. Pat. Appl., 586,066, 09 Mar 1994; Japanese Patent 61 57,837, 07 June 1994, Appl. 23 July 1992, to Standard Oil Co.
1992	Blends comprising very low density polyethylene, 100 parts VLDPE [80–95 mol wt% ethylene and C_4–C_8 comonomer(s)], and linear low density polyethylene, 15–600 parts LLDPE (ethylene copolymer with 2–8 mol% octene), showed excellent processability. They were formed into 10–300 μm thick sheets, useful for transdermal drug delivery devices as single-layer backings. They were clear, colorless, transparent,	Godbey and Martin (1993, 1994)

<div align="right">(continued)</div>

Table 18.11 (continued)

Year	Development	References
	permeable to oxygen, stable to various common components of transdermal delivery devices, strong, comfortable, and not absorbing significant amounts of elements of transdermal carriers. Sheets made from the blends could be heat sealed at a low temperature	
1992	Heat-shrinkable film comprised single-site catalyzed copolymer of ethylene and a 3–8C alpha-olefin, LLDPE with $\rho \geq 900$ kg m^{-3} blended with another polymer of ethylene and a 3–8C alpha-olefin and a second comonomer [e.g., vinyl acetate, alkyl acrylate, CO, butadiene, styrene, acrylic acid, and a metal salt of an acrylic acid], or an alpha-olefin homopolymer. The films had improved shrinkability, impact resistance, and optical properties as compared to prior art and were used in packaging	Babrowicz et al. (1994)
1992	Polyolefin blends formulated for heat seamable roof sheeting comprised 25–95 wt% of amorphous PO having <1 wt% crystallinity (<60–61 wt% ethylene, dicyclopentadiene, and/or ethylidene norbornene); 5–75 wt% of a crystalline polymer, i.e., PE, PP, poly(ethylene-co-propylene), poly(ethylene-b-octene), or poly(ethylene-b-butene), having 2–65 wt% crystallinity; 20–300 phr of a (non) reinforcing filler; and 20–150 phr of either paraffinic oil, naphthenic oil, and/or wax. The materials exhibited good adhesion. Neither an adhesive nor curing was necessary	J.A. Davis, J.K. Valaitis, Eur. Pat. Appl., 564,961, 13 Oct 1993; Canadian Patent 2,093,397, 07 Oct 1993; U.S. Patent 5,286,798, 15 Feb 1994; Japanese Patent 60 65,434, 08 Mar 1994, Appl. 06 Apr 1992, to Bridgestone/Firestone, Inc.
1992	Blends comprising cycloolefin polymer, 0–95 wt% PCO; polyethylene, 0–95 wt% PE; and 0.1–99 wt% block copolymer(s) were prepared for moldings with outstanding properties, viz., improved melt viscosity, elongation at break, impact strength, toughness, hardness, and modulus. The block copolymers of ethylene (or propylene) and norbornene blocks were obtained in the presence of aluminoxane and a metallocene catalyst, resulting in $M_w/M_n \leq 2$	U. Epple, M.-J. Brekner, U.S. Patent 5,359,001, 25 Oct 1994, Appl. 20 Apr 1993, Ger. Appl. 22 Apr 1992, to Hoechst A.-G.
1992	Blends included 70–90 wt% of a polymer derived from ethylene and at least one higher alpha-olefin (e.g., LLDPE, VLDPE, or LDPE having MI = 0.1–10), 10–30 wt% of an auxiliary co-crystallizable polymer derived from ethylene and at least one olefinic comonomer (e.g., LLDPE, VLDPE, or LDPE having MI $\geq$ 80 %, below that of the first polymer), and moisture cross-linking additives including a silane, a silanol condensation catalyst, and a free radical initiator. Cross-linking was rapid; thus, the moisture-curing step subsequent to extrusion of an electrical cable	Wong and Varrall (1994)

Table 18.11 (continued)

Year	Development	References
	was short. The blends could contain processing aid (fluorinated polymer and/or polyethylene with high MI) and 5–70 wt% filler. They were used for shaped coatings and cable coating	
1992	Polyethylene blends having toughness and elastic recovery comparable to those of plasticized PVC comprised $\geq$50 wt% of a copolymer of ethylene and either butene or hexene [LLDPE, $\rho = 880$–915 kg m^{-3}, MI $\leq$ 1 dg min^{-1}, long-chain branching =0.5–1.5 long chains/1,000C, $M_{\mathrm{w}} \geq 200$ kg mol^{-1}]; $\geq$5 wt% of a copolymer of ethylene and either vinyl acetate or ethyl acrylate, EVAc or EEA; and 5–30 wt% liquid hydrocarbon oil. The blends showed essentially no yield point and behavior similar to that of cross-linked materials, although they were not cross-linked (strain recovery). They were found competitive with plasticized PVC in terms of both physical properties and economics	M.R. Rifi, U.S. Patent 5,326,602, 05 July 1994, Appl. 01 Dec 1992, to Union Carbide Chemicals & Plastics Technology Corporation
1992	Linear low-density polyethylene, 90–99 wt% LLDPE, was blended with polymethylmethacrylate, 10–11 wt% PMMA, and optionally a compatibilizing copolymer, viz., SEBS, EPR, ethylene–styrene block copolymer, ES. The blends were found to produce blown films with improved tear in the machine direction, modulus, and impact strength	D.V. Dobreski, J.J. Donaldson, U.S. Patent 5,290,866, 01 Mar 1994, Appl. 16 Apr 1992, to Mobil Oil Corp.
1992	Continuous process for the preparation of polyisobutylene, PIB, blends with at least one other polymer, e.g., polyolefin, PO, was described. PIB was continuously polymerized in ethylene. The resin was fed to a degassing extruder where it was mixed with PO, fillers, and/or additives. The process was used for the preparation of blends in a simpler and more cost-effective manner than that of prior art	H. Gropper, E. Kolk, K.H. Fauth, G. Isbarn, G. Scherer, German Patent 4,319,181, 27 Jan 1994; French Patent 2,694,010, 28 Jan 1994, Appl. 22 July 1992, to BASF A.-G.
1992	Thermoplastic rubber blends with good adhesion to reinforcing agents comprised 10–100 wt% polyolefin grafted with polar monomers (e.g., 27–75 wt% PP grafted with vinyl acetate, acrylic acid, methacrylic and itaconic acid, or maleic acid anhydride) and elastomer(s) (EPDM, NBR, or BR) that could be dynamically cross-linked by peroxide, silane, or sulfur. The blends may also contain 0.3–2.5 wt% plasticizer, fillers, pigments, processing aids, and flame retardants. They showed bondability to solids, especially after application of high temperature and pressure, thus were used for the production of conveyor belts, hoses and V-belts	S. Luepfert, F. Roethemeyer, E. Maeder, Eur. Pat. Appl., 580076, 26 Jan 1994; German Patent 4,223,984, 27 Jan 1994, Appl. 21 July 1992, to Continental A.-G.

Table 18.11 (continued)

Year	Development	References
1992	Polyolefin compositions with improved toughness, flexibility, and high clarity were prepared by blending 90–95 wt% setereoregular polymer or copolymer of 4-methyl-1-pentene, PMP, with polybutene, PB, having $M_n < 500$	M.J. Hagenson, H.F. Efner, L.C. Hasselbring, W.H. Beever, Eur. Pat. Appl., 556,843, 25 Aug 1993, Appl. 20 Feb 1992, to Phillips Petroleum Co.
1992	Polyolefin (PO = PP, HDPE, EPR, or PMP) was blended with an impact modifier, 0.1–5 wt% colorant and/or 5–50 wt% of opacifiers, and a styrene–diolefin block copolymer, grafted with 1–6 mol% of acrylic acid, maleic anhydride, or sulfonate functionality (SEBS, SEPS, radial SEB, or SEP). To improve scratch resistance the blend contained 100–3,000 ppm Zn stearate and 16–22C fatty acid amide. The alloys were injection molded into parts showing impact, scratch, and abrasion resistance. They were used to manufacture interior trim for vehicles and in other applications where a scratch- and scuff-resistant plastic material is required	J. O'Leary, S. Musgrave, PCT Int. Appl., WO 93 21,269, 28 Oct 1993; Australian Patent 93 36,840, 10 Oct 1993; Australian Patent 93 40,363, 18 Nov 1993, Appl. 09 Apr 1992, to ICI Australia Operations Proprietary Ltd.
1992	To prepare polyolefin blends, PO (e.g., EVAc, PE, PP, EPR), with vinyl polymers, 10–200 parts of vinyl monomer [e.g., (meth)acrylates, styrenics, vinyl chloride, glycidyl methacrylate, maleic anhydride, acrylonitrile, divinylbenzene] and 0.01–4.0 parts of a free radical initiator were used to impregnate 100 parts of PO particles at $T = 20$–130 °C. After 50–99 wt% of the monomer was absorbed, the particles were dispersed in water and the free radical polymerization initiated. Good adhesion between the components in the extruded or molded articles was achieved	T. Vestberg, I. Lehtiniemi, U.S. Patent 5,300,578, 05 Apr 1994, U.S. Appl. 27 Jan 1993, Fin. Appl. 27 Jan 1992, to Neste Oy
1992	Polyolefin, PO, blends with copolymers of vinyl acetate and acrylate esters, EVAc (20–40 wt% VAc), were extruded into films, weldable by high-frequency currents. It replaced PVC flexible films, e.g., in inflatable goods. For example, 400 μm PVC film, inflated to 100 m bars, after 13 days, had lost 72 wt% of the pressure, while the new blends (15 wt% VAc in the blend) of 200 μm film lost 50 wt% in 19 days	G. Benatre, French Patent 2,688,511, 17 Sep 1993, Appl. 13 Mar 1992
1992	Polyolefin, PO, molding compositions, suitable for the use in automotive application, comprised polyolefin wax [$M_w = 1$–50 kg mol^{-1}, $M_w/M_n = 1.8$–4.0, and $T_m = 120$–160 °C] and 1–80 wt% of either a PO [$M_w \geq 100$, $M_w/M_n = 1.8$–4.0, and $T_m = 120$–160 °C], an olefinic copolymer derived from at least two different olefins [$M_w \geq 100$, $M_w/M_n = 1.98$–4.0, and $T_m = 90$–160 °C], or an elastomer with $T_g < -20$ °C. The blends could be impact modified by incorporation of a copolymer. They were molded, extruded, or blow molded into articles showing high modulus, hardness, scratch resistance, and low shrinkage	B. Bachmann, A. Winter, European Patent 563,818, 6 Oct 1993, Appl. 31 Mar 1992, to Hoechst A.-G.

<div align="right">(continued)</div>

Table 18.11 (continued)

Year	Development	References
1992	Blends of PE (selected from VLDPE and/or LLDPE), with 13–17 wt% ethylene–butene plastomer copolymer [Mitsui's TAFMER™, $\rho < 900\,\mathrm{kg\,m^{-3}}$, $T_\mathrm{m} = 55$–$85\,^{\circ}\mathrm{C}$], and 35–50 wt% ethylene–vinyl acetate copolymer, EVAc, were used for film blowing, useful as packaging materials for foods. The film had shrink properties in MD and TD similar to those of EVAc film and plastic orientation properties similar to those of VLDPE films. In the U.S. Patent the biaxially oriented heat-shrinkable multilayer stretch film comprising 65–80 wt% VLDPE and a plastomer was reported useful as poultry wrap	B.L. Wilhoit, European Patent 562,493, 29 Sep 1993; Ralph, D. J., U.S. Patent 5,279,872, 18 Jan 1994, Appl. 17 Feb 1993, Appl. 23 Mar 1992, to Viskase Corp.
1992	Polyolefin, PO [of ethylene, propylene, butylene, 4-methylpentene, and their copolymers with 1-alkenes, vinyls, (meth)acrylates – preferably PP], was grafted at a ratio 1:9–4:1 with 1–20 wt% of (meth)acrylic acid and ≥ 30 wt% of styrene and/or alkyl- and/or halo-substituted styrene, methacrylic ester, and 0–60 % of other comonomers [e.g., vinyl aromatic, ester], at least some of the acid units of methacrylic acid and/or acrylic acid bearing a charge and being associated with non-polymeric counterions [e.g., 90 % methyl methacrylate, 5 % butyl acrylate, and 5 % methacrylic acid with either Ca^{2+} or Mg^{2+}. The ionomer could be blended with PO either during or after manufacturing. The blends were extruded either directly or after pelletization. They exhibited high sag resistance without increased viscosity. PP fibers could be used for strapping, netting, slit tape, rope, twine, bags, carpet backing, foamed ribbons, upholstery, rugs, pond liners, awnings, swimming pool covers, tarpaulins, bristles, sutures, nonwoven fabrics, bedsheets, bandages, diaper liners, etc.	R.G. Hamilton, M.T. McCarty, Eur. Pat. Appl., 589,659, 30 Mar 1994; U.S. Patent 5,319,031, 07 June 1994; Candian Patent 2,106,344, 25 Mar 1994; British Patent 93 03,861, 31 May 1994; Japanese Patent 62 012,048, 02 Aug 1994, Appl. 24 Sep 1992, to Rohm and Haas Co.
1992	Polyolefin blends comprised 25–95 wt% of a crystalline random copolymer, EPR1 (of propylene with ethylene and/or an alpha-olefin), and 5–75 wt% of a mixture consisting of PE and EPR2. The density of EPR1 was about equal that of the mixture. The blends had good transparency and impact resistance even at low temperatures and were used to manufacture food containers, medical, packaging films, etc.	G. Cecchin, R. Ghisellini, D. Malucelli, European Patent 557,953, 01 Sep 1993, Appl. 24 Feb 1992, to Himont, Inc.
1992	Nonwoven textile materials comprised fibers obtained from a blend of 5–95 wt% propylene, PP (or propylene/ ethylene copolymer with ≤ 10 wt% ethylene, EPR), and 95–5 % polyolefin, PO, selected from EPDM, EPR, LLDPE, etc. The materials have been used in disposable personal hygiene products or protective clothing. The products showed improved strength, drapability, softness, and bonding performance	K. Ogale, M.E. Strasinic, Eur. Pat. Appl., 598,224, 25 May 1994, Appl. 15 Oct 1993; Canadian Patent 2,108,819, 01 May 1994; Japanese Patent 62 00,093, 19 July 1994; U.S. Patent 5,346,756, 13 Sep 1994, Appl. 30 Oct 1992, to Himont Inc.
1992	Polypropylene, PP, was blended with a random crystalline terpolymer of 96–85 wt% propylene, 1.5–5.0 wt% ethylene, and 2.5–10 wt% 4–8C alpha-	L. Clementini, A.F. Galambos, G. Lesca, K. Ogale, L. Spagnoli, M.E. Starsinic, L. Giuseppe,

<div align="right">(continued)</div>

Table 18.11 (continued)

Year	Development	References
	olefin. The blends were used to manufacture strands of multiple monofilaments or staple fibers with high resiliency and shrinkage, for pile fabric, textiles, geotextiles, or carpets. The carpet yarn had a twist retention of over 30 %, shrinkage on heat setting at 143 °C of at least 15 %, and uniform shrinkage	European Patent 552,810, 28 July 1993, Appl. 29 May 1992, to Himont Inc.
1992	Blends comprising polypropylene, 50–97 wt% PP [or a PP block copolymer with ethylene block], and 50–53 wt % of an ethylene/4–18C alpha-olefin copolymer [α-olefin content = 10–60 wt%, $\rho \leq 913$ kg m^{-3} obtained by using a metallocene catalyst and aluminoxane] were found useful as automobile trims and trims of electrical instruments. They showed high moldability, improved impact resistance at room and low temperature, and balance of rigidity and impact resistance	K. Shichijo, Eur. Pat. Appl., 593,221, 20 Apr 1994; Japanese Patent 61 92,500, 12 July 1994, Appl. 15 Oct 1992, to Mitsubishi Petrochemical Co., Ltd.
1992	A multilayer film comprised polypropylene, PP [or PP copolymer with 20–40 wt% hydrocarbon resin], in the core; outer layers from PP, LLDPE, PB, or their blends with 4–15 wt% PP; and the intermediate layers from polyolefin-based carboxylic acid or maleic anhydride. An oxygen barrier layer from EVAL, PVDC, PEST, or PA could also be used. The films were biaxially oriented at ratios of 3:1–8:1. They had low moisture transmission rate, toughness, abrasion resistance, good clarity and gloss, suitable as moisture barrier packaging for food, pharmaceuticals, and electronics	P.S. Gautam, Eur. Pat. Appl., 588,667, 23 Mar 1994, Appl. 20 Sep 1993; Br. Pat. Appl., 93 03,823, 22 Mar 1994; Australian Patent 93 47,378, 24 Mar 1994; Canadian Patent 2,106,258, 19 Mar 1994; Japanese Patent 61 98,826, 19 July 1994, U.S. Appl. 18 Sep 1992, to W. R. Grace & Co.
1992	Ternary blends contained 87–96 wt% LLDPE (with either butene-1, hexene-1, or octene-1), 1–10 wt% isotactic polybutene, 1–10 wt% PS, and 0.01–10 wt% color and anti-blocking agents. The blends exhibited improved process efficiency in terms of extruder amps/ rpm ratio, while the terpolymer substantially retained the inherent strength of the LLDPE. The compositions were used for blown films and for the manufacture of waste bags	S.P. Evans, P.P. Shirodkar, US 5,258,463, 02 Nov 1993, Appl., 24 Aug 1992, to Mobil Oil Corporation
1992	Semicrystalline polyolefin blends were prepared by mixing two different random copolymers of propene with 4–10C alpha-olefin at a ratio from 1:3–1:1. The first copolymer contained 1–10 wt% of C$_{4–10}$ alpha-olefin (1-butene, 1-pentene, 1-hexene, 1-octene, and 4-methyl-1-pentene), whereas the second 15–40 wt% of the same comonomer. The mixing was carried out in reactors, polymerizing the monomers in the presence of stereospecific catalysts supports on active magnesium dihalides, in at least two sequential stages. The resulting R-TPOs showed limited	G. Cecchin, F. Guglielmi, European Patent 560,326, 15 Sep 1993, Appl. 10 Mar 1992, to Himont Inc.

(*continued*)

Table 18.11 (continued)

Year	Development	References
	solubility in xylene, low heat-sealing temperature, and high melting point and were used for the production of heat-sealable laminated mono- or bi-oriented films suitable for the food industry	
1992	PE blends were prepared during polymerization. This strategy has been widely implemented in syntheses of multimodal PE compositions. The blown film showed MD/TD tear balance. The bimodal blend contained 0.35–0.75 weight fraction of a higher-MW component	Ali et al. (1994); Dammert et al., U.S. Patent 6,185,349 of 06 Feb 2001 (filed 1999) to Borealis Polymer Oy
	Ali A.H. et al. to Mobil Oil Co.; Dammert et al. to Borealis. Catalyst: $TiCl_4$/pentanol deposited on MgO/acetic acid and then treated with tri-n-hexyl-aluminum solution	
	Reactor blending during the slurry polymerization gave two PE fractions with different MW. Borealis generated multimodal resins for optical cables using slurry-/gas-phase reaction with Z-N catalyst with $MgCl_2$	
1993	Polyethylene blends comprised a low-density polyethylene, ≤60 wt% either LDPE or LLDPE; postconsumer recycled high-density polyethylene, 4–30 wt% HDPE; and an effective amount of a compatibilizer comprising 0.1–1.5 wt% ZnO and 0.1–2 wt% of glycerol monostearate. The blends could also contain 5–30 pph of a blowing agent. The blends were used to make aesthetically appealing foamed products for use as cushioning materials or as packaging films	S.-T. Lee, U.S. Patent 5,428,093, 27 June 1995, Appl. 05 Nov 1993, to Sealed Air Corporation
2003	Polymer blends (mechanical) comprised (A) 35–85 wt% Z-N i-PP ($T_m > 130\,°C$) and (B) 30–70 wt% metallocene α-olefin-co-PP with crystallizable α-olefin sequences [narrow MWD, composition distribution single T_m]. The blends showed improved processing, unexpected compatibility, single T_m, and increased tensile strength	S. Datta, C. Cozewith, P. Ravishankar, E.J. Stachowski, Elastic blends comprising crystalline polymer and crystallizable polymers of propylene, U.S. Patent 6867260 of 15 Mar 2005 (filed 22 Apr 2004; priority 29 June 1999, U.S. Patent 6642316); Datta et al. (2006)
	Datta, Cozewith, Ravishankar, Stachowski, Gadkari to ExxonMobil Chemical Patents, Inc.	
	The (A) component is either i-PP with <10 wt% comonomer, while (B) is preferably crystallizable C_2–C_3 copolymer. Blends were mechanically mixed	
	ExxonMobil developed poly(propylene-co-ethylene) Vistamaxx™ post-metallocene resin. The polymerization procedure for the blend component is described in U.S. Patents 5198401 of 30 Mar 1993 and 5057475 of 15 Oct 1991; catalyst system of enhanced productivity, 5153157 of 06 Oct 1992, to Exxon Chem	
2004	The copolymers of the blend were prepared using (a) a silyl chromate catalyst, $(R_{10})3Si-O-CrO_2-O-Si(R_{10})_3$ wherein $R_{10} = C_{1-10}$ alkyl, and (b) a phosphinimine catalyst, $(L)_n$-M-$(PI)_m(X)_p$ where M = Ti, Hf, or Zr;	Kazakov Alexei, Yim Gary, Polyolefin blends and pipe, CA 2508436, filed 26 May 2005; U.S. Patent 7,309,741 of (filed

(*continued*)

Table 18.11 (continued)

Year	Development	References
	PI = phosphinimine ligand; ligand L = Cp, indenyl, or fluorenyl; X = Cl or C_{1-4} alkyls; $m = n = 1$; and $p = 2$. A catalyst activator includes alumoxanes (e.g., MAO) with a molar ratio of Al:M = 50:1–250:1 and ionic boron-containing activators. Kazakov and Yim, to NOVA Chemicals	01 June 2004); U.S. Patent Appl. 2008/0090040A1 (filed 14 Nov 2007, priority 01 June 2004) now U.S. Patent 7696281 of 13 Apr 2010 to NOVA CHEMICALS CORPORATION (Canada) or NOVA Chemicals (International) S.A.
	The invention describes PE blends of a low-MW HDPE made using a Z-N-type or Cr-based catalyst and a high-MW m-LLDPE made using a Group 4 single-site-type catalyst. The blends are suitable for the manufacture of pipes, tested according to ASTM D 2837 or ISO 9080	
	A polyolefin blend comprises (a) 30–80 wt% of a low-MW copolymer [85–99.5 wt% of C_2 and 0.05–15 wt% of C_{4-8} α-olefin, $\rho = 0.953$–0.965 g mL^{-1}, and MFR (2.16 kg 190 °C) = 0.1–20.0 g/10 min] and (b) 70–20 wt% of a high-MW copolymer [85–99.9 wt% of C_2 and from 15 to 0.1 wt% of C_{4-8} α-olefin, $\rho = 0.915$–0.940 g mL^{-1}, and an MFR (21.6 kg 190 °C) = 0.05–5.0 g/10 min]. The selected resins were blended in a compounder and then extruded as pipes	The ionic activators are disclosed in, e.g., U.S. Patents: by James C. Stevens, David R. Neithamer, 5132380 of 21 July 1992 (filed 12 Sept 1991), to Dow Chem. Co.; and by Howard W. Turner, Gregory G. Hlatky, Richard R. Eckman, 5198401 of 30 Mar 1993 (filed 30.07 1991) to Exxon Chemical Patents Inc.
2009	Solution polymerization of HDPE ($\rho = 0.890$–0.970 g mL^{-1}) takes place in ≥2 reactors. The process (a) provides a first C_2 and C_{4-10} feed to ≥1 continuously stirred tank reactor (CSTR) in the presence of a catalyst, producing a first PE component; (b) the second (tubular) reactor (TR) is fed with the first PE solution, enriched by preheated $T \geq 100$ °C monomer(s) and solvent. The weight ratio of the additional solvent to C_2 = 20/1–0.1/1, and the additional C_2 = 1–50 wt% of the C_2 added to CSTR	L.M.J. Van Asseldonk, S.J. Brown, Multi reactor process, CA 2,688,217 of 11 June 2011 (filed 11 Dec 2009); US 8,101,693 B2 of 24 Jan 2012 (filed 06 Dec 2010; priority 2009) to NOVA Chemicals (International) S.A.
	Asseldonk and Brown, from NOVA Chemicals (International) S.A.	
	This document describes a process with one CSTR and one TR, but a single STR may also be used – in the former case a catalyst should be injected to each reactor. While the main catalyst is Z-N type, use of a single-site one may offer additional advantages blending homogeneously and heterogeneously branched chains	
	This multi-reactor system used for copolymerization of C_2 with higher α-olefins comprises a CSTR connected in series to a tubular reactor (TR). The latter receives a polymer solution from the CSTR. Polymerization in TR improves efficiency, by reducing the amount of energy required to recover the polymer and residual comonomer from the solution. The use of preheated C_2 in TR mitigates the contaminating gel problems (fouling TR and creating "fish eyes" on film) and reduces hexane extractables	

Table 18.12 Patented polyolefin blends

Year	Development	References
1937	This first patent on the use of rubber for toughening polyolefins disclosed addition of rubber "as a softening agent" to "saturated, linear hydrocarbons of the linear type, the mean molecular weight of which is greater than that of paraffin, e.g., between 800 and 500,000"	P.J. Gaylor, Standard Oil Development Co., French Patent 812,490, 11 May 1937
1942	High-pressure, low-density polyethylene, LDPE, was blended with cyclorubber, to give compounds useful for bonding polyethylene to metal	C.L. Child, R.B.F.F. Clarke, B.J. Habgood, British Patent 544,359, 09 Apr 1942
1951	Discovery of isotactic polypropylene, PP, was immediately followed by search for low-temperature impact improvement, initially by blending with either polyethylenes or elastomers, later by copolymerizing with ethylene and dienes into EPR and EPDM	J.P. Hogan, R.L. Banks, U.S. Pat. Appl., 333,576, filed 27 Jan 1953, to Phillips Petroleum Co.
1958	Low-density polyethylene, 5–120 parts LDPE, was blended with chlorosulfonated polyethylene, 100 parts CSR, with or without curing agent (tribasic lead maleate). The blends found were used as smooth, non-tacky, tough films or coatings for natural or synthetic rubbers	V.C. Boger, A.G. Thomas, U.S. Patent 2854425, filed 30 Sept 1958, to B. F. Goodrich Co.
1958	Polypropylene, PP, was blended with 5–50 parts of chlorinated butyl rubber, CBR, in the presence of a non-peroxide curative (e.g., oxides or sulfides of Zn, Cd, Mn, Fe, or Pb) on a roll mill at 138–157 °C. The dynamic vulcanization resulted in materials useful for high tensile strength applications	A.M. Gessler, W.H. Haslett Jr., U.S. Patent 3037954, 05 June 1962, Appl. 15 Dec 1958, to Esso Research & Engineering Co.
1958	To improve the low-temperature flexibility of polypropylene, PP, it was blended with polyisobutylene, 5–20 wt% PIB. The Montecatini patent was the first one on the low-temperature modification of PP. In the Esso patent, butyl rubber, BR, was incorporated. In the Sun Oil patent, 50–95 wt% PP (MW = 4 Mg mol^{-1}) was blended with PE (MW = 1.6 Mg mol^{-1}) for high impact strength and low brittleness temperature. In BASF patent 0.5–40 wt% PIB (with narrow molecular weight distribution) was used	F. Ranalli, Italian Patent 583,501, 14 Oct 1958, to Montecatini S. G.; K. Schramm, U.S. Patent 2,939,860, 07 June 1960; Esso Res. & Eng. Co., British Patent 893,540, 11 Apr 1962, Appl. 1960; Sun Oil Co., British Patent 952,089, 11 Mar 1964, Appl. 9 Aug 1960; H. Merkel, G. Cramer, German Patent 1,145,791, 21 Mar 1963, Appl. 1961, to BASF A.-G.
1958	First polyethylene–polyethylene, PE/PE, blends were patented; both cross-linked (using electron accelerators) and uncross-linked components were disclosed. In Phillips patent, low-density polyethylene, LDPE, was blended with linear low-density polyethylene, LLDPE, for improved stiffness and abrasion resistance and reduced water vapor permeability. In the Celanese patent, improvement of processability was particularly stressed. In the DuPont patent, 10–50 wt% LLDPE was used with LDPE or its copolymers for generating heat-shrinkable films	P.J. Canterino, R. J. Martinovich, U.S. Patent 3,086,958, 23 Apr 1963, Appl. 1958; W.M. Nelson, Belgian Patent 647,311, 29 Oct 1964, Appl. 1963, to Phillips Petroleum; W. R. Grace & Co., British Patent 904,985, 05 Sep 1962, Appl. 1960; Wissbrun et al. (1962, 1965), Appl. 1961, to Celanese; Golike, R. C., Belgian Patent 619,351, 27 Dec 1962, Appl. 1961, to du Pont de Nemours

Table 18.12 (continued)

Year	Development	References
1958	The first PE/PE blends were patented by du Pont de Nemours, Phillips, Celanese, and DuPont of Canada Ltd. The first were LDPE/HDPE blends, but later LLDPE/LDPE blending dominated the film-blowing application. Even a small amount of LDPE significantly improved LLDPE processability as well as the heat sealing, puncture resistance, tensile, and optical properties. However, for >35 % LLDPE in LDPE modification of film-blowing line was needed. Also LLDPE/LLDPE blends with broad MWD showed improved processability and performance	M. J. Roedel, U.S. Patent 2983704 of 09 May 1961 to du Pont de Nemours (priority 1955); P. J. Canterino, R. J. Martinovich, U.S. Patent 3,086,958, 23 Apr 1963, Appl. 1958; Nelson. W. M., Belgian Patent 647,311, 29 Oct 1964, Appl. 1963, to Phillips Petrol.; W. R. Grace and Co., British Patent 904,985, 05 Sept 1962, Appl. 1960; K. F. Wissbrun, R. H. Ball, P. J. Rossello, Belgian Patent 614,282, 22 Aug 1962; British Patent 994,376, 10 June 1965, Appl. 1961, to Celanese; R. C. Golike, Belgian Patent 619,351, 27 Dec 1962 (filed 1961); R. M. Lillis, C. van Thomas, U.S. Patent 3998914 of 21 Dec 1976 (filed in 1974), to du Pont of Canada Ltd; J. Nancekivell, Canad. Plast., May 1982, 27–30, ibid., Sept 1985, 27–32; L. A. Utracki, Commercial Polymer Blends, 658 pg., Chapman and Hall, London (1998); Anon., Canad. Plast., March 1984, 18–20
	The first PE/PE blends were disclosed by Phillips Petroleum in 1958. In the patent, LDPE was blended with LLDPE for improved stiffness and abrasion resistance and reduced H2O vapor permeability. The most important was the gage reduction by 15–30 % for plastic bags, sacks, and stretch films. By 1980 ca. 42 % of film producers used immiscible LLDPE/LDPE blends. The PE miscibility refers to the molten and solid states	
	In the DuPont patent of 1961, 10–50 wt% LLDPE was used with LDPE or its copolymers for generating heat-shrinkable films. In the 1965 Celanese patent, improvement of processability was particularly stressed. The 1976 DuPont Canada patent specified density of the two components as ρ = 0.950–0.965 and 0.910–0.945 g ml^{-1}, the MI = 0.1–10 with less than 30 wt% of LDPE. In 1983 UCC started selling LLDPE/LDPE blends for check-stand sacks	
	Most PE blends are immiscible, e.g., LLDPEs C$_{2+6}$ prepared with Ti-based catalyst are immiscible with one based on V catalyst	
1958	Low-density polyethylene, LDPE, was blended with polyisobutylene, 25–40 wt% PIB, and a copolymer of styrene and isobutylene, 0–10 wt% PSIB, for the use as transparent, impermeable, shrink-wrap packaging films. In the Phillips patent, LLDPE was blended with PIB to manufacture grocery bags. In the BASF patent, a pre-blend comprising 60 wt% PIB and LDPE was granulated and subsequently compounded with LDPE	J. R. Briggs, R. G. Newburg, R. E. Clayton, U.S. Patent 2,854,435, 30 Sep 1958, to Esso Res. and Eng.; R. J. Martinovitch, R. P. March, U.S. Patent 3,074,616, 22 Jan 1963, Appl. 1959, to Phillips Petroleum; H. Dietrich, German Patent 1,288,293, 30 Jan 1969, Appl. 1961, to BASF A.-G.
1958	The first patent on polyamide/polyolefin, PA/PO, blends comprised 10–80 wt% of either PA-6 or PA-66 with either LDPE or PP. The resins, used to produce sheets, films, fibers, or bottles, were claimed to show excellent processability, good printability, and low permeability	R. B. Mesrobian, C. J. Ammondson, British Patent 889,354, 14 Feb 1962, Appl. 1958, to Continental Can Co., Inc.

(*continued*)

Table 18.12 (continued)

Year	Development	References
1959	Partially cross-linked polyethylene (by either peroxides or irradiation), XLPE, was blended with polybutadiene, 5–40 wt% BR, to improve resistance to cut at elevated temperatures and elongation. The blends were found suitable for wire coating	Q. P. Cole, U.S. Patent 2,912,410, 10 Nov 1959, to General Electric Co.
1959	Polyethylene, PE, blended with immiscible polymers (e.g., PVC, PIB, PS) was compatibilized by addition of graft copolymer (e.g., styrene or vinyl acetate grafted on PE)	Houillières du Bassin-du-Nord et du Pas-de-Calais and Ethylene-Plastique, French Patent 1,193,104, 30 Oct 1959
1959	Polypropylene, PP, was blended with 5–20 wt% elastomer [styrene–butadiene, SBR, or butadiene–acrylonitrile, NBR] to produce materials useful for blow molding of bottles, free from brittleness and stress cracking. In the later patent, EPR, BP, and PIB, with a dicarboxylic acid anhydride, were used	Shell International Research Maatschappij N. V., British Patent 873,227; 933,727, 14 Aug 1963, Appl. 27 Aug 1959; Belgian Patent 611,727, 19 June, 1962, Appl. 21 Dec 1960
1959	For improved processability and mechanical properties of polyethylene, HDPE or LLDPE, it was blended with elastomeric polyethylene–polypropylene copolymer, EPR. For further enhancement of properties, either polypropylene, PP, or polybutene, PB, could also be added. In ICI patent, HDPE was blended with 30–60 wt% EPR for improved processability and impact strength	L. Corbellini, German Patent 1,137,859, 11 Oct 1962, Appl. 1959, to Montecatini SG.; J. W. Crawford, W. G. Oakes, British Patent 941,083, 06 Nov 1963; German Patent 1,217,608, 16 May 1966, Appl. 1961, to Imperial Chemical Industries Ltd.
1960	These are the first patents on polypropylene, PP, blended with ethylene–propylene rubbers, 10–60 wt % EPR, for improvement of the low-temperature impact strength. In Esso patent, PP was blended with varying amount of polyisobutylene, PIB, and polyethylene, LDPE, to give marked improvement in tear strength and impact. In Shell patent, reactor powder blending of PP with 0.1–10 wt% EPR (2–25 wt% ethylene) was disclosed. In Farbwerke Hoechst patent, PP was blended with 5–70 wt% LLDPE, for good mechanical properties at low temperature	W. M. Schilling, U.S. Patent 3,200,173, 10 Aug 1966, Appl. 1960; British Patent 975,877, 18 Nov 1964, Appl. 1962, to Hercules Powder; Esso Res. and Eng., British Patent 950,551, 26 Feb 1964, Appl. 21 Aug 1961; G. A. Short, U.S. Patent 3,354,239, 21 Nov 1967, Appl. 1962, to Shell Oil Co.; R. Holzer, K. Mehnert, German Patent 1,145,792, 21 Mar 1963, Appl. 23 Jan 1960, to Hoechst A.-G.
1960	Polyethylene, PE; polypropylene, PP; and their homologues were blended with ethylene–vinyl acetate, EVAc, copolymer and cured with free radicals into products showing desired impact strength and modulus. The blends were used for manufacturing of fibers, films, or moldings	Monsanto Co., British Patent 967,334, 19 Aug 1964, Appl. 27 Apr 1960
1960	Blends of polyethylene, PE, with 0.1–50 wt% of copolyamides (e.g., LDPE with 5 wt% PE–PA-6 copolymer) showed higher gloss, transparency, and elasticity; lower stress corrosion; and reduced permeability	H. Craubner, G. Illing, A. Hrugesch, German Patent 1,138,922, 31 Oct 1962, Appl. 1960, to Badische Anilin und Soda-Fabrik A.-G.

(*continued*)

Table 18.12 (continued)

Year	Development	References
1960	Mechanical properties of polyolefins were improved by blending them with 0.5–50 wt% polycarbonate, PC. For example, LLDPE + 5 wt% PC showed improved impact strength, modulus, hardness, and HDT	H. Peters, F. Schuelde, German Patent 1,146,251, 28 Mar 1963, Appl. 22 Jan 1960, to Farbwerke Hoechst A.-G.
1960	To improve dyeability, flexibility, and toughness of isotactic polypropylene, PP, it was compounded in a Banbury-type mixer with ethylene–vinyl acetate, 7 wt% EVAc. Several other ethylene copolymers were also used. In Miliprint patent, EVAc or ethylene–ethyl acrylate copolymer, 18–32 wt% EVAc or EEA, was found to improved impact strength, elongation, and low brittleness temperature of PP. In Firestone patent, linear polybutadiene, BR, was used. The Mitsubishi patent disclosed improvements of PP impact strength properties by blending it with 0.5–25 wt% ethylene–aliphatic esters, e.g., EVAc	H. P. Holladay, I. O. Salyer, U.S. Patent 3,433,573, 18 Mar 1969, Appl. 1960, to Monsanto; A. Miller, N. G. Reddeman, Belgian Patent 620,703, 14 Nov 1962, Appl. 27 July 1961, to Miliprint; R. J. Reid, W. R. Conard, Belgian Patent 617,870, 21 Nov 1962, Appl. 19 May 1961, to Firestone; R. Sakata, T. Kuroda, K. Masuda, Y. Nakayama, M. Tanaka, Japanese Patent 003,964, 13 Feb 1968, Appl. 1964, to Mitsubishi Petrochem
1961	High-density polyethylene, HDPE, was blended with 15 wt% ethylene–propylene copolymer, EPR. The blend had good impact resistance	Farbwerke Hoechst A.-G., Belgian Patent 589,358; 612,855, 19 Jul. 1962, Appl. 19 Jan 1961
1961	Polyethylenes, HDPE, LDPE, or LLDPE, blended with styrene–acrylonitrile copolymer, 2–6 wt% SAN, showed improved crack resistance. Furthermore, a synergistic behavior was observed when 0.1–1 wt% 2,4,6-tri-alkyl phenol was also added. In Esso patent, the mechanical properties of PE were improved by blending it with 5–25 wt% copolymers of mono- and diolefins, EPDM	A., L. Jankens, Belgian Patent 625,004, 20 May 1963, Appl. 24 Nov 1961, to Dow Chemical Co.; M. Prillieux, P. Delbende, M. Moulin, French Patent 1,289,580, 06 Apr 1962, Appl. 1961, to Esso Standard S. A.
1961	Blending two chlorinated LLDPEs, CPEs with 40 and 70 wt% Cl, resulted in materials with good moldability, impact resistance, and thermal stability	A.-G. Farbwerke Hoechst, Belgian Patent 621,775, 27 Feb 1963, Appl. 1961
1961	Polypropylene, PP, was blended (without compatibilizer) with a linear low-density polyethylene, 20–40 wt% LLDPE, for improved impact resistance and low brittleness temperature	Esso Research & Engineering Co., British Patent 934,640, 21 Aug 1963, Appl. 13 Feb 1961
1961	These are the first patents on PP/PE/EPR blends. Polypropylene/polyethylene, PP/PE, blends were compatibilized by addition of ethylene–propylene copolymer, EPR. The resulting blends showed improved low-temperature brittle point and Izod impact strength. In UCC patent, 50–96 wt% was blended with 2–25 wt% PE and 2–25 EPR and/or PIB	L. S. Rayner, J. A. Bond, M. Clark, R. E. Nott, British Patent 958,079, 13 May 1964 Appl. 1961; British Patent 1,026,254, 1966, to ICI; J. P. Lehane, Jr., U.S. Patent 3,137,672, 16 Jun. 1964, Appl. 1962, to Hercules Powder; W. M. Jayne, Jr., U.S. Patent 3,256,367, 14 June 1966, Appl. 1962, to Union Carbide Corp.

(continued)

Table 18.12 (continued)

Year	Development	References
1962	Polyethylene, LDPE, or its copolymers when blended with poly-1-butene, PB, showed improved processability and resistance to environmental stress cracking	A. Rudin, H. P. Schreiber, French Patent 1,349,823, 17 Jan 1964, Appl. 23 Mar 1962, to Canadian Industries Ltd.
1963	Isotactic polypropylene, PP, was blended with syndiotactic polypropylene, 3–50 wt% sPP. The blends showed excellent impact strength at low temperature and freedom from surface crazing upon repeated flexing	D. D. Emrick, U.S. Patent 3,268,627, 23 Aug 1966, Appl. 16 May 1963, to Standard Oil Co.
1963	Polypropylene, PP, was compatibilized with polyethylene, PE, by grafting PP with a basic monomer and PE with an acidic monomer, then blending the modified polymers. Thus, PP was modified with dimethylamino ethyl methacrylate while PE with methacrylic acid. These were blended in 1:1 ratio to result in high-performing alloys	R. Langworth, U.S. Patent 3,299,176, 17 Jan 1967, Appl. 24 June 1963, to E. I. du Pont de Nemours & Co.
1963	Impact properties of polyethylenes, HDPE, LDPE, or LLDPE, were improved by blending them with ethylene–propylene–diene terpolymer, EPDM, and with polypropylene PP, or polybutene, PB	H. P. Schreiber, British Patent 1,037,819; 1,037,820, 03 Aug 1966, Appl. 1963, to Canadian Industries Ltd.
1963	Polyethylene, LDPE, or polypropylene, PP, were blended with 1–10 wt% polyoxymethylene, POM, for improved melt flow properties, processability, and extrudate appearance	A. Rudin, H. P. Schreiber, Canadean Patent 688,416; 688,578, 09 June 1964, Appl. 18 May 1963, to Canadian Industries Ltd.
1964	Polyethylene, 10–81 wt% LDPE, was blended with butyl rubber, 15–50 wt% BR, and ethylene–vinyl acetate copolymer, 4–40 wt% EVAc, for cold molding of sealing gaskets	R. J. Ceresa, N. E. Davenport, T. L. Trudgian, British Patent 1,112,024, 01 May 1968, Appl. 1964, to W. R. Grace and Co.
1965	Polypropylene, PP, was blended with polybutadiene, 5–15 wt% PB, and linear polyethylene, 2–15 wt% LLDPE or HDPE. Good balance of properties was claimed	I. Aijima, H. Sakurai, T. Koseki, Japanese Patent 011,539, 27 May 1969, Appl. 09 July 1965, to Asahi Chemical Industry Co., Ltd.
1966	Polyethylene, PE, was blended with ethylene–methacrylic acid copolymer, 80 wt% ionomer, and ethylene–vinyl acetate, 10 wt% EVAc, to give films with high toughness, stiffness, and impact resistance	M. C. K. Willott, British Patent 1,118,545, 03 July 1968, Appl. 1966, to Imperial Chemical Industries, Ltd.
1966	To improve the low-temperature impact strength of polypropylene, PP, it was blended with a small amount of polyethylene, HDPE, and ethylene–propylene block copolymer, EP	Asahi Chemical Industry Co., Ltd., British Patent 1,154,447, 11 June 1969, Appl. 02 Feb 1966
1967	Polyethylene, PE, was blended with 1–95 wt% styrene–butadiene or p-methylstyrene–isoprene block copolymer, to improve stress crack resistance	S. Minekawa, K. Yamaguchi, K. Toyomoto, E. Fujimoto, Y. Takeuchi, Japanese Patent 016,429, 06 May 1971, Appl. 15 Mar 1967, to Asahi Chemical Ind. Co., Ltd.

(*continued*)

Table 18.12 (continued)

Year	Development	References
1968	Polyolefin, PP or PE, blended with polyvinyl alcohol, 2 wt% PVAl, showed good mechanical, hygroscopic, and antistatic properties, for the manufacturing of films, fibers, tubes, and coatings	S. Minekawa, K. Yamaguchi, K. Toyomoto, E. Fujimoto, Y. Takeuchi, Japanese Patent 008,585, 12 Sep 1969, Appl. 25 Jan 1968, to Asahi Chemical Ind. Co., Ltd.
1968	Polymer alloys were prepared by blending polyethylene, PE, or its copolymers with lactams, then polymerizing these. For example, ethylene–vinyl pyrrolidinone copolymer, EVP, was blended with ε-caprolactam for molding application	R. W. Hill, R. P. Anderson, S. V. Scroggins, U.S. Patent 3,539,662, 10 Nov 1970, Appl. 12 July 1968, to Gulf Research and Development Co.
1968	Polyolefins, PP or HDPE, were blended with amorphous ethylene copolymer, 5–100 EVAc, and 1–80 parts of either polyoxymethylene, POM; polymethylmethacrylate, PMMA; polystyrene, PS; or styrene–methyl methacrylate copolymer, SMM (as well as inorganic fillers) to extrude into paperlike films	S. Yamamoto, S. Honda, H. Shimizu, Japanese Patent 043,468; 043,469; 043,470, 23 Dec 1971, Appl. 26 Jan 1968, to Sekisui Chemical Co., Ltd.
1968	Polypropylene/polyethylene, PP/PE, blends were compatibilized by addition of ethylene–propylene block copolymer, EPR. The resulting blends showed improved low-temperature impact strength	H. J. Leugering, H. Schaum, South African Patent 004,328, 08 Jan 1970, Appl. 1968, to Farbwerke Hoechst A.-G.
1968	Polypropylene, PP, or polyethylene, PE, was blended with ethylene–propylene copolymer, EPR, and ethylene–acetoxybicycloheptene copolymer, to increase impact and tensile strength, as well as brittle resistance. In the later patent, PP and EPR were separately dissolved then blended, precipitated, and processed. The blends showed fine, uniform dispersion of the rubber phase, resulting in superior mechanical properties	K. Shirayama, K. Iketa, Japanese Patent 021,303; 021,305, 16 June 1971, Appl. 23 Feb 1968; M. Asada, T. Tokumaru, S. Saito, M. Saeki, H. Ueda, Japanese Patent 008,145, 08 Mar 1972, Appl. 1 Nov 1968, to Sumitomo Chemical Co., Ltd.
1969	Polyethylene, PE, was blended with <15 wt% EPDM, to give resistance to corona discharge. The blends were used as insulating materials for high-voltage cables	H. Matsubara, Japanese Patent 030,095, 05 Aug 1972, Appl. 29 May 1969, to Sumitomo Electric Ind., Ltd.
1969	Polypropylene, PP, or poly (pentene-co-propylene) was reactor blended with ethylene–butene or ethylene–pentene copolymer. The product was melt blended with PP to give material with improved performance. In the second patent, ethylene–propylene copolymer, EPR, was blended with PP. The alloys showed good mechanical properties. In the Sumitomo patent, to improve impact strength, PP was blended with 5–30 wt% of either polyhexene or polyoctene	I. Yamazaki, T. Fujimaki, Japanese Patent 007,627, 03 Mar 1970, Appl. 24 Dec 1969; 007,141, 29 Feb 1972, Appl. 26 Nov 1969, to Showa Denko; K. Shirayama, S. Shiga, H. Watanabe, Japanese Patent 008,370, 10 Mar 1972, Appl. 25 Feb 1969, to Sumitomo Chem
1969	Polypropylene, >70 wt% PP, was blended with ≥5 wt% ethylene–vinyl acetate–vinyl chloride copolymer, ethylene–vinyl acetate copolymer, and HDPE, to give materials with low-temperature impact resistance	M. Kojima, M. Tanahashi, Japanese Patent 014,710, 02 May 1972, Appl. 05 Nov 1969, to Chisso Co., Ltd.

<div align="right">(continued)</div>

Table 18.12 (continued)

Year	Development	References
1970	Polyethylene, LDPE, was blended with polyisobutylene, PIB, in a single-screw extruder at the shear rates 600,000 s^{-1}, for 34 μs. No thermal degradation was observed. The PIB drop size was 2–5 μm	F. Urban, O. Buchner, K. Steigerwald, K. H. Fauth, H. Gehrig, German Patent 2,028,751, 16 Dec 1971, Appl. 11 June 1970, to BASF A.-G.
1970	Polypropylene, PP, was blended with hydrogenated styrene–butadiene or styrene–isoprene block copolymer, 6–8 wt%. The alloys were used for manufacturing of materials with good transparency and impact strength	L. M. Porter, German Patent 2,156,681, 18 May 1972, Appl. 16 Nov 1970, to Shell International Research Maatschappij N. V.
1971	Blends comprising 40–20 wt% polyolefin, PE or PP, with 60–80 wt% of ethylene–propylene–dicyclopentadiene = 47.5:47.5:5 or ethylene–propylene–ethylidene–norbornene = 61:35:4 were disclosed. The blends were masticated and partially cross-linked with peroxides or sulfur, keeping the gel content at 45–96 %. They could be shaped into articles with good properties without vulcanization	W. K. Fischer, South African Patent 72 00,388, 23 Aug 1972, U.S. Ref., RE 32,028, U.S. Patent 3,806,558, Appl. 12 Aug 1971, to Uniroyal Inc.
1971	Reactive grafting of polyolefins, polyethylenes (PE), or polypropylenes (PP) was disclosed. The extruder was modified, allowing to feed polymer, grafting monomer and peroxide. As an example, PP was grafted with acrylic acid	R. A. Steinkamp, T. J. Grail, U.S. Patent 3,953,655, 27 Apr 1976, Appl. 09 Apr 1971, to Exxon Research and Engineering Co.
1972	Polyolefins, PP or PE, blended with chlorosulfonated polyethylene, 4.5 wt% CSR, and filled with large amount of CaSO4 showed good mechanical properties	K. Shikata, K. Okamura, S. Nakamura, Japanese Patent 097,946, 13 Dec 1973, Appl. 28 Mar 1972, to Tokuyama Soda Co., Ltd.
1972	Polyethylene, LLDPE, was blended with atactic polypropylene, 0.1–5 wt% aPP. Blown and stretched films showed large anisotropy in tensile strength and elongation, making them useful for packaging	K. Nakamura, T. Kimura, H. Tsunoda, Japanese Patent 083,174, 06 Nov 1973, Appl. 10 Feb 1972, to Sanyo Pulp Co., Ltd.
1972	In 1975 Union Carbide Corp. (UCC) discovered the very low density polyethylene (VLDPE) or "ultralow-density polyethylene" (ULDPE), i.e., copolymers of C$_2$ with α-olefin (C$_{4-8}$) having ρ = 0.860–0.915 g ml^{-1}. VLDPE has higher α-olefin content than that in LLDPEs. These linear elastomers are produced by coordination polymerization using a Phillips or Z-N catalyst at low P and T. Here belong Mxsten XLDPE from Eastman Chem. and Attane ULDPE from Dow. The first metallocene-catalyzed VLDPE was a hexene copolymer ρ = 0.912 g ml^{-1} introduced by ExxonMobil as Exceed 1012CA, made in the UNIPOL gas-phase process. Exceed (m-VLDPE) has outstanding sealing properties (hot tack and seal strength) compared with Z-N VLDPEs VLDPE has low crystallinity (X = 7–30 %) densities ρ = 0.875–0.915 g ml^{-1} and melting point,	I. J. Levine, F. J. Karol, U.S. Patent 4,011,382 of 08 Mar 1977 priority 1975, to UCC; E. Berger et al., U.S. Patent 4,292,200 of 29 Sept 1981, priority 1972, to Solvay & Co.; A. Delbouille et al., U.S. Patent 4,250,284 of 10 Feb 1981 priority 1969, to Solvay & co.; E. R. Smith, U.S. Patent 5,032,463 of 16 July 1991, priority 1988, to Viskase Corp.; T. Fujii et al., U.S. Patent 5,110.870, of 05 May 1992, priority 1989, to Mitsubishi Kasei; Farley et al., U.S. Patent 6,932,592, 23 Aug 2005, priority 2001, to ExxonMobil; S. Lustig et al., U.S. Patent 5439717, 08 Aug 1995,

Table 18.12 (continued)

Year	Development	References
	T_m = 60–90 °C. It is a linear copolymer, with high SCB, made by copolymerization of C_2 with alpha-olefins (e.g. C_8), initially using a Phillips or Z-N-type catalyst and then metallocene one. VLDPEs are used for geotextile, hose and tubing, ice and frozen food bags, food packaging and stretch wrap, as well as impact modifiers for blending with other polymers. VLDPE shows the physical properties of LLDPE, high flexibility, toughness, sealing, and softness	priority i985, and U.S. Patent 5256351 of 1993-10-26, priority 1985, to Viskase Corp.; Karol et al., EP 0120,503 (WO 84/03888), of 11 Oct 1984 priority 1983, to UCC; L. M. J. van Assldonk, S. J. Brown, U.S. Patent Appl., 2011/ 0144289 0f 16 June 2011, filed 2010, to Nova Chem. http://www. novachem.com/researchtech/docs/ 2010-19.pdf; S. Sivaram, Second generation ziegler polyolefin processes, Ind. Eng. Chem.. Prod. Res. Dev., **16**(2):121–127 (1977); Anonym. VLDPE – a new class of polyethylene, Plast. Rubber **11**(2):34–36 (1986)
	The solution polymerization in a hydrocarbon usually is carried out in a continuously stirred tank reactor (CSTR), at T = 160–300 °C and P = 2.5–10 MPa with residence time of 1–5 min. In 1991 Exxon introduced the first metallocene VLDPE (Exceed 1012CA, ρ = 0.912 g ml^{-1} based on Z-N catalyst), followed by Dow in 1992 and UCC in 1984. UCC used the 2nd-generation Z-N catalyst with MgO. The VLDPE (comonomer C_{3-8} = 6 wt%) with ρ < 0.91 g ml^{-1} and modulus E < 140 MPa was produced in a fluidized bed at T = 10–80 °C and P < 7 MPa, in a mixture of gases (C_2, C_{3-8}, molar ratio = 1:0.35–1:8 and 3–5 mol % H2), with a catalyst system comprising a precursor. For PE with ρ < 0.86–0.9 g ml^{-1} reaction T < 60 °C and P < 2.5 MPa are needed	
1973	Polyethylene, PE, was blended with ≤35 wt% polypropylene, PP; ≤15 wt% polydimethylsiloxane, PDMS; and 5–35 wt% PPE, PA-6, PC, PET, or Phenoxy. The blends were used for injection molding of products with good processability, rigidity, impact strength, and long life under sterilization in boiling water or by irradiation	A. Plochocki, T. Bek, J. Bojarski, L. Czarnecki, L. Grabiec, J. Kepka, P. Machowski, Polish Patent 097,228, 30 Dec 1978; Polish Patent 100,160, 17 Apr 1979, Appl. 21 Dec 1973; Polish Patent 100,669, 15 May 1979, Appl. 21 Dec 1973, to Inst. Chem. Ind.
1973	High-density polyethylene, HDPE, was blended with 50 wt% polypropylene, PP, having matched melt flow index, to give good flowability, weld-line strength, surface quality, and low-temperature impact strength	D. Moorwessel, R. Glasser, G. Pfirrmann, German Patent 2,306,892; 2,306,893, 22 Aug 1974, Appl. 13 Feb 1973, to BASF A.-G.
1974	Polypropylene, PP, was reactor blended with polyethylene, PE, and ethylene–propylene copolymer, EPR, to give high impact strength R-TPO, especially at low temperature	H. Strametz, H. J. Leuering, K. Rust, M. Engelmann, German Offence 2,417,093, 06 Nov 1975, Appl. 1974, to Hoechst A.-G.
1975	Polypropylene, PP, was blended with ethylene-5-ethylidene-2-norbornene-propylene copolymer, EPDM, to give moldings with good tensile strength. In the following patent, EPDM was blended with LDPE to give unexpectedly high tensile strength	P. T. Stricharczuk, German Patent 2,644,644, 07 Apr 1977, Appl. 06 Oct 1975; C. J. Carman, M. Batiuk, R. M. Herman, U.S. Patent 4,046,840, 06 Sep 1977, Appl. 23 Feb 1976, to B. F. Goodrich Co.

<div align="right">(continued)</div>

Table 18.12 (continued)

Year	Development	References
1975	Homogeneous blends of immiscible polymers can be prepared in a high-stress, low residence time extruder (later labeled Patfoort extruder and sold by FN). Thus, LLDPE was blended with PS to give blends with good mechanical properties	G. A. R. Patfoort, Belgian Patent 833,543, 18 Mar 1976, Appl. 18 Sep 1975; Fabrique Nationale Herstal, Netherland Patent Appl. 007,963, 18 Sep 1977, Appl. 18 Sep 1975
1976	In a series of patents, dynamic vulcanization of polypropylene, PP, was disclosed. Thus, 60 wt% PP was blended with butyl rubber, BR; elastomeric ethylene–vinyl acetate, 35–85 wt% EVAc, with polyolefins, PE or PP; chlorosulfonated polyethylene rubber, ≥50 wt% CSM, with polyolefins, PE or PP; or ethylene–propylene–diene, EPDM, with PP. The blends showed excellent toughness, elongation, impact strength, a wide range of Shore hardness, and dimensional stability. In the latter patent, a compatibilizing block copolymer was disclosed of NBR with polyolefins, e.g., PP. Compatibilization nearly doubled the blend tensile strength and increased its elongation at break by a factor of 4	A. Y. Coran, R. Patel, German Patent 2,757,430, 06 July 1978; U.S. Patent 4,130,534; A. Y. Coran, B. Das, R. Patel, U.S. Patent 4,130,535, 19 Dec 1978, Appl. 27 Dec 1976; A. Y. Coran, R. Patel, U.S. Patent 4,141,878, 27 Feb 1979, Appl. 14 Apr 1977; German Patent 2,805,930, 17 Aug 1978, Appl. 14 Feb 1977; European Patent Appl., 036,279, 23 Sep 1981; U.S. Patent 4,355,139, 1982, Appl. 10 Mar 1980, to Monsanto Co.
1976	Polypropylene/polyethylene, PP/LDPE, blends were compatibilized by addition of 2–22 wt% EPR. Blending was done in two stages, curing EPR before the second part of PP was added. The resulting materials had good mechanical, low-temperature impact, and optical properties	T. Huff, U.S. Patent 4,087,485, 02 May 1978, Appl. 1976, to Exxon Research & Engineering Co.
1976	To improve modulus of high-density polyethylene, HDPE, it was blended with a graft copolymer of HDPE with vinyl or vinylidene monomer (e.g., styrene)	H. Yui, T. Kakizaki, H. Sano, Japanese Patent 014,752, 09 Feb 1978, Appl. 27 July 1976, to Mitsubishi Petrochemical Co., Ltd.
1977	Soft, thin films, with improved cuttability, suitable for packaging materials, were prepared by blending polyethylene, a mixture of LDPE and HDPE, with EPDM or atactic polypropylene, aPP	S. Sakane, K. Minato, M. Takashige, Japanese Patent 000,052, 5 Jan 1979, Appl. 03 June 1977, to Idemitsu Petrochemical Co., Ltd.
1977	Polyethylene blends, suitable for extrusion of pipes, were obtained by blending two different types of linear low-density polyethylenes, LLDPE, one with butene and the other hexene comonomer. The blend also contained carbon black, CB	O. E. Larsen, Canadian Patent 1,120,630, 23 Mar 1982, Appl. 12 Oct 1977, to Phillips Petroleum Co.
1977	Polypropylene, PP, blends with low-density polyethylene, 5–20 wt% LDPE, and ethylene–propylene copolymer, 1–15 wt% EPR showed excellent transparency and mechanical properties	T. Oita, T. Hara, R. Samejima, K. Tanabe, Japanese Patent 108,146, 20 Sep 1978, Appl. 03 Mar 1977, to Sumitomo Chemical Co., Ltd.
1977	Polypropylene, PP, was blended with 15–85 wt% ABS and 0.5 wt% CPE (or low-molecular-weight PS) as a compatibilizer	M. Kamosaki, S. Tokuhara, M. Kita, N. Nakashima, Japanese Patent 146,748; 146,753, 20 Dec 1978, Appl. 27 May 1977, to Daicel Ltd.

(*continued*)

Table 18.12 (continued)

Year	Development	References
1977	Polypropylene, 10–60 wt% PP, was blended with ethylene–propylene block copolymer, EPR, and a peroxide-containing polyolefin copolymer to give a masterbatch that subsequently was blended with 60 wt% EPDM, to give elastomeric alloy with excellent mechanical properties	A. Yamamoto, M. Shiraishi, S. Nakayama, Y. Tsurugi, H. Nakanishi, Japanese Patent 001,386, 08 Jan 1979, Appl. 07 June 1977, to Japan, EP Rubber Co., Ltd.
1979	Polypropylene, PP, was sequentially blended with EPR, then with PE. The blend showed co-continuous morphology resulting in excellent impact and mechanical properties, superior to those observed for blends with a particulate dispersion	T. Huff, European Patent Appl., 015,066, 03 Sep 1980, Appl. 31 Jan 1979, to Exxon Research and Engineering Co.
1979	Polypropylene, 60 wt% PP, was blended with polyamide, 20 wt% PA-6 or PA-66, and glass fibers, 20 wt% GF, for superior tensile and impact strength	Asahi Fiber Glass Co., Ltd., Japanese Patent 030,451, 27 Mar 1981, Appl. 23 Aug 1979
1979	Polyethylene, 70 wt% PE; polyamide, 20 wt% PA-66; and 3 wt% of ethylene–fumaric acid graft copolymer were mixed to reduce moisture permeation and to improve impact strength. In 1982 DuPont introduced PA/PO blends, Selar™, to be used as additive to polyolefin to reduce permeability	P. M. Subramanian, European Patent Appl., 015,556, 17 Sep 1980, Appl. 06 Mar 1979, to E. I. du Pont de Nemours & Co.; "Selar™ Barrier Resins," Bulletins E73971, E73973, E73974 by du Pont
1979	Polyethylene, PE, was grafted with 0.1–5 wt% maleic anhydride and blended with 1–50 wt% EPDM. The blend showed excellent adhesion to polar materials	A. Honkanen, M. Arina, R. Holstii, Finnish Patent 064,805, 30 Sep 1983, Appl. 10 Dec 1979, to Neste Oy
1979	Polypropylene, PP, was blended with 5 wt% PDMS for improvement of processability, impact strength, and elasticity	U. Grigo, L. Morbitzer, K. Arlt, R. Binsack, J. Marten, German Patent 2,905,357, 21 Aug 1980, Appl. 13 Feb 1979, to Bayer A.-G.
1979	The first patent on reactor-blended thermoplastic olefinic elastomer, R-TPO, was disclosed. Thus, polyethylene, PE, was polymerized in the presence of an active catalyst and an already polymerized olefinic copolymer (e.g., ethylene-1-butene copolymer) or the sequence was reversed. The blend had superior resistance to environment stress cracking, and the blown film showed fewer fish eyes	Y. Morita, N. Kashiwa, European Patent Appl., 022,376, 14 Jan 1981, Appl. 09 July 1979, to Mitsui Petrochemical Industries, Ltd.
1980	In 1979 UNIPOL™ process for gas-phase production of the "linear low-density polyethylene," LLDPE, was introduced by the Union Carbide Corp. Since the new resins were difficult to process on the processing lines designed for the low-density (high pressure) polyethylenes, LDPE, soon several patents were	A. Haas, F. Raviola, European Patent Appl. 042,743, 13 Jan 1982, to Soc. Chim. Charbon.; P. M. Hughes, European Patent Appl., 045,455, 10 Feb 1982, Appl. 1980, to Shell Oil Co.; Cowan, M. A,

<div align="right">(continued)</div>

Table 18.12 (continued)

Year	Development	References
	issued for LLDPE blends with other polyolefins, e.g., LDPE or PP	European Patent Appl. 095,299, 30 Nov 1983, to Intercont. Plast., Inc.; K. C. Janac, R. C. Puydak, D. R. Hazelton, European Patent Appl., 092,318, 26 Oct 1983, Appl. 26 Mar 1982, to Exxon Res. & Eng. Company; B. L. Turtle, European Patent Appl. 095,253, 30 Nov 1983, to British Petroleum Co.; O. Fukui, Y. Inuizawa, S. Hinenoya, Y. Takasaki, French Patent 2,522,331, 02 Sep 1983, to Ube Industries, Ltd.; A. Haas, French Patent 2,526,803, 18 Nov 1983; M. Hert, French Patent 2,528,055, 09 Dec 1983, to Soc. Chim. Charbon., SA
	In 1982 numeroU.S. Patentent applications for blends of linear low-density polyethylenes, LLDPE, with other polyolefins, co-polyolefins, and olefinic elastomers have been filed. For example, ethylene copolymers, thermoplastic elastomers (TPO), EPDM, EPR, EVAc, maleated polypropylene, and PP-MA have been used	
1980	To improve its low-temperature impact strength, polyethylene, PE, was blended on a roll mill with polybutadiene rubber, 10 wt% PB	E. G. Kent, U.S. Patent 4,423,181, 27 Dec 1983, Appl. 10 Mar 1980, to Polysar Ltd.
1981	Polyethylene, 50–95 wt% HDPE, was blended with LLDPE for improvement of film strength and transparency	K. K. Showa Denko, Japanese Patent 059,242, 08 Apr 1983, Appl. 05 Oct 1981
1981	Polyethylene, PE, was blended with neoprene rubber at a ratio 1:1. The blends were irradiated by electron beam for improved tensile strength and other mechanical properties	A. Y. Coran, R. Patel, U.S. Patent 4,348,266, 07 Sep 1982, Appl. 02 Apr 1981, to Monsanto
1981	Polypropylene, 100 parts PP, blended with 8–25 parts of amorphous ethylene–propylene copolymer, EPR, and 2–10 parts crystalline EPR showed improved impact strength. In the Idemitsu patent, PP was blended with maleated LDPE, EVAc, and inorganic filler, to give blends with good melt strength and rigidity	P. Galli, M. Spataro, European Patent Appl., 077,532, 27 Apr 1983, Appl. 14 Oct 1981, to Montedison S.p.A.; Idemitsu Petrochemical Co., Ltd., Japanese Patent 096,640, 08 June 1983, Appl. 04 Dec 1981
1982	Semicrystalline ethylene–propylene copolymer, EP, was blended with amorphous EP and inorganic filler. The blends had good processability, mechanical properties, and impact strength. In the Mitsubishi patent, crystalline EP was blended with styrene–isoprene block copolymer, 5–30 wt% SIS, and polystyrene, 3–5 wt% PS, to give good paintability	Ube Industries, Ltd., Japanese Patent 162,652, 27 Sep 1983, Appl. 23 Mar 1982; Japanese Patent 168,648; 168,649, 05 Oct 1983, Appl. 30 Mar 1982; Mitsubishi Petrochem. Co., Ltd., Japanese Patent 213,039, 10 Dec 1983, Appl. 04 June 1982
1982	Polypropylene, 94 wt% PP, was blended with chlorinated polyethylene, 6 wt% CPE. The blends had good processability and gave moldings with good mechanical properties	R. Newe, E. Lange, H. Hoffmann, K. Wetzel, East German Patent 207,381, 29 Feb 1984, Appl. 05 Apr 1982, to VEB Chemiekombinat Bitterfeld

(continued)

Table 18.12 (continued)

Year	Development	References
1982	Polypropylene, 50–90 wt% PP, and/or ethylene–propylene block copolymer, EP, was blended with talc having particle size $d = 5$–20 μm. The materials had high impact strength. In the following patent, PP was blended with 5–40 wt% styrene-grafted chlorinated polyethylene, CPE, to give high modulus and impact resistance	Chisso Corp., Japanese Patent 036,149, 28 Feb 1984, Appl. 24 Aug 1982; Japanese Patent 213,038, 10 Dec 1983, Appl. 03 June 1982
1982	Polypropylene, 35 wt% PP, was blended with polyisobutylene, 50 wt% PIB, and ethylene–vinyl acetate copolymer, 15 wt% EVAc, to give alloys useful for films, moldings, and extrusions	C. B. Shulman, European Patent Appl., 116,783, 29 Aug 1984, Appl. 27 Dec 1982, to Exxon Research and Eng. Co.
1982	Polyethylene, PE, blends from LDPE, HDPE, and MDPE were found suitable for manufacturing films with uniform thickness and anisotropic tensile strength	K. K. Showa Denko, Japanese Patent 157,837, 20 Sep 1983, Appl. 15 Mar 1982; Japanese Patent 176,234, 15 Oct 1983, Appl. 09 Apr 1982
1982	Linear low-density polyethylene, LLDPE, was blended with 2–25 wt% LDPE to give films with large difference of the tensile strength in the machine and transverse direction	M. Hert, French Patent 2,528,054, 09 Dec 1983, Appl. 03 June 1982, to Societé Chim. des Charbonnages S. A.
1982	Low-density polyethylene, LDPE, was blended with 1–40 wt% poly(2-ethyl-2-oxazoline), PEOX. The blends had excellent adhesion to substrates, e.g., thermoplastic polyesters, viz., PET	S. M. Hoenig, D. P. Flores, S. P. Ginter, U.S. Patent 4,474,928, 02 Oct 1984, Appl. 28 June 1982, to Dow Chemical Co.
1982	Ethylene polymer blends are prepared by mechanical blending of dry powders or compounding in an internal mixer or a compounding extruder or (preferably) combining the two methods. Bailey, Whitte, Coutant, and Martin, to Phillips Petroleum Co; Cobler et al. to Dow Chem. Co. (mixing on the blow line); Harris to Media Plus, Inc. Blends of a high-MW ethylene–α-olefin copolymer and a low-MWPE with narrow MWD and low levels of LCB for films with good ESCAR are useful for the manufacture of films, pipes, and wire coating	F. W. Bailey, W. M. Whitte, Ethylene polymer blends, U.S. Patents. 4,461,873 (24 July 1984, filed 22 June 1982); 4,547,551 (15 Oct 1985); 5,380,803 (10 Jan 1995), all to Phillips Petroleum Co.; U.S. Patent 5,681,523 (28 Oct 1997), to Dow Chem. Co.;U.S. Patent 6822051 (23 Nov 2004), to Media Plus, Inc.
1982	Low-density polyethylene, LDPE, was blended with HDPE, PP, and EP block copolymer, to give films with good modulus, tear strength, and sagging	Shin-Kobe Electric Machinery Co., Ltd., Japanese Patent 096,156, 02 June 1984, Appl. 24 Nov 1982
1983	Low-density polyethylene, LDPE, blended with linear low-density polyethylene in a ratio 100:20–90 gave alloys useful for production packaging films	Asahi Chemical industry Co., Ltd., Japanese Patent 044,540, 09 Mar 1985, Appl. 19 Aug 1983
1984	Linear low-density polyethylene, LLDPE, was blended with low-density polyethylene, 10–45 wt% LDPE; polypropylene, PP; and/or ethylene–propylene copolymer [with a high propylene content], 2–15 wt% EPR. The blends had high modulus and clarity	S. K. Bahl, P. J. Canterino, R. Shaw, British Patent 2,152,515, 07 Aug 1985, Appl. 04 Jan 1984, to Mobil Oil Corp.
1985	Polyethylene, PE, blended with 10–40 wt% ethylene–vinyl carboxylate or an acrylate copolymer exhibited notched Izod impact strength more than three times larger than that of functional group-free PE	T. O. Broadhed, European Patent Appl., 209,294, 21 Jan 1987, Appl. 15 July 1985; to Du Pont Canada, Inc.

(*continued*)

Table 18.12 (continued)

Year	Development	References
1985	Polyolefin blends with good compatibility comprised 100 parts PO and 0.1–100 parts polytransoctanamer, PTO. For example, PP with 9 wt% PTO showed about 5× higher impact strength at $T = -40$–23 °C than PP alone	M. Kita, K. Hashimoto, Japanese Patent 131,043, 13 June 1987, Appl. 04 Dec 1985, to Daicel Huels Ltd.
1987	Transparent-, impact-, and "blush"-resistant blends were obtained by compounding linear low-density polyethylene, LLDPE, with hydrogenated styrene–butadiene block copolymer, SEBS	G. Holden, D. R. Hansen, European Patent Appl., 308,001, 22 Mar 1989, Appl. 1987, to Shell Int. Res. Maatschappij BV
1987	Polypropylene, PP, blended with polyoctadecene, POD, was found to show temperature-sensitive transparency (thermochromic blends)	S. Tanaka, J. Sakai, T. Fukao, K. Wakatsuki, K. Wakamatsu, European Patent Appl., 285,414, 05 Oct 1988, Appl. 1987, to Sumitomo Chemical Co., Ltd.
1989	Polypropylene, PP, reactor blends were obtained with high yield using a chiral metallocene catalyst and an aluminoxane. The preferred blends comprised 60–95 wt% of a crystalline isotactic PP homo- or copolymer produced in the first stage and (the second stage) random copolymer ethylene–propylene (and another 1-olefin), as well as a partly crystalline polymer of the second 1-olefin. The moldable blends showed good flow properties and a very good low-temperature impact strength	M. Schreck, A. Winter, V. Dolle, H. Kondoch, M. Antberg, J. Rohrmann, U.S. Patent 5,322,902, 21 June 1994, Appl. 21 Dec 1989, US Appl. 19 Dec 1990, to Hoechst Aktiengesellschaft
1990	Three-component polypropylene, 1–99 wt% PP, blends comprised 1. either acidified PP, its mixture with PP, or a mixture of PP with carboxylic acid-modified EPR; 2. 99–1 wt% of maleated polymer [e.g., poly(methyl methacrylate-*co*-styrene-*co*-MA]; and 3. epoxy group-containing copolymer [e.g., 0.1–300 phr of ethylene–methyl methacrylate–glycidyl methacrylate = 65-15-20 or ethylene–vinyl acetate–glycidyl methacrylate = 85-5-10]. The blends were used to mold car bumpers and fenders, with good stiffness and low-temperature impact resistance	H. Abe, T. Fujii, M. Yamamoto, S. Date, U.S. Patent 5,278,233, 11 Jan 1994, Appl. 14 June 1990, US Appl. 12 June 1991, to Sumitomo Chemical Co., Ltd.
1990	Polypropylene, PP, was blended with ethylene-*co*-vinyl alcohol, EVAL, and maleated polypropylene, PP-MA. The blends were extruded through a sheeting die that engendered overlapping layers of EVAL. Their presence reduced permeability by gases or liquids through the PP wall	M. R. Kamal, G. Lohfink, L. Arghyris, S. Hozhabr-Ghelichi, PCT Int. Appl., 006,837, 30 Apr 1992, Appl. 16 Oct 1990, to McGill University
1990	Linear low-density polyethylene, LLDPE, was blended with very low density polyethylene, VLDPE. The polymers prepared using metallocene catalyst had narrow molecular weight distribution, $M_w/M_n = 1$–3. Blending resulted in resins having the density $\rho = 910$–940 kg m^{-3}	F. C. Stehling, C. S. Speed, C. H. Welborn, Jr., U.S. Patent 5,382,630; 5,382,631, 17 Jan 1995, Appl. 04 Feb 1993, 25 May 1990, to Exxon Chemical Patents, Inc.

(*continued*)

Table 18.12 (continued)

Year	Development	References
1991	Polyolefin blends with density of ρ = 930–940 kg m^{-3} at 23 °C and MFI(90/2.16) = 0.05–1.0 dg min^{-1} comprised high-density polyethylene, 50–80 wt% HDPE [polymerized in two stages, with a broad bimodal molecular mass distribution, ρ = 940–960 kg m^{-3}, and MFI(90/2.16) = 0.01–0.5 dg min^{-1}], and linear low-density polyethylene, 20–50 wt% LLDPE [ρ = 910–925 kg m^{-3} and MFI(90/2.16) = 0.5–2.0 dg min^{-1}]. The blends were used for forming tubes and pipes with high stress crack resistance	L. Boehm, H. F. Enderle, H. Jastrow, European Patent Appl., 517,222, 09 Dec 1992; U.S. Patent 5,338,589, 16 Aug 1994, US Appl. 03 June 1992, German Appl. 05 June 1991, to Hoechst Aktiengesellschaft
1991	Linear low-density polyethylene, LLDPE, was graft modified by incorporation of basic groups from, e.g., dimethylamino ethyl methacrylate, t-butylamino ethyl methacrylate, vinyl pyridine, or allyl urea. These copolymers were then used as reactive components for alloys with acidified polymers, viz., maleated polyolefins	W. E. Baker, A. H. Simmons, Canadian Patent Appl., 2,028,784, 16 May 1991, Appl. 29 Oct 1990, to Queen's University at Kingston
1991	Linear low-density polyethylene, LLDPE, was blended with low-density polyethylene, LDPE, at a ratio of about 0.3. The blends were used for blow molding hollow balls containing pressurized air and consisting of two hemispheres welded to form a ball with a wall thickness t = 0.5–1.8 mm	H. Moss, J. G. Modigh, U.S. Patent 5,320,887, 14 June 1994, Appl. 04 Mar 1993, GB Appl. 27 Feb 1992, to Euro-matic Ltd.
1991	Blends comprising 30–70 wt% low-molecular-weight (MW) polyethylene, HDPE [made using a chromium catalyst, having density $\rho \geq$ 955 kg m^{-3}, MI = 25–400 g/10 min, and M$_w$/M$_n$ = 2–35], and 30–70 wt% high-MW ethylene copolymer, LLDPE [made using a titanium catalyst, having $\rho \leq$ 955 kg m^{-3}, MI = 0.1–50 g/10 min, and M$_w$/M$_n$ = 2–10], showed improved processability. The blends were used to produce pipes, films, and bottles with enhanced mechanical properties as well as the environmental stress crack resistance, ESCR. In the following patent 5–40 wt% low-MW HDPE [made using a titanium catalyst, with density $\rho \geq$ 955 kg m^{-3}, $MI \geq$ 25 dg min^{-1}, and M$_w$/M$_n$ = 2–8] blended with 60–95 wt% high-MW HDPE [from chromium catalyst, with density $\rho \geq$ 930 kg m^{-3}, MI = 1.5–15 dg min^{-1}, and M$_w$/M$_n$ = 6–100] yielded blends with MI = 0.05 dg min^{-1} and ESCR. In the last patent 10–80 wt% low-MW LLDPE [$\rho \geq$ 940 kg m^{-3}, $MI >$ 25 dg min^{-1}, and M$_w$/M$_n$ = 2–12] was blended with	J. L. Martin, M. B. Welch, W. R. Coutant, M. P. McDaniel, U.S. Patent 5,306,775, 26 Apr 1994, Appl. 16 Apr 1993; U.S. Patent 5,319,029, 07 June 1994, Appl. 16 Apr 1993; W. R. Coutant, J. L. Martin, U.S. Patent 5,380,803, 10 Jan 1995, Appl. 16 Apr 1993, Appl. 18 Sep 1991, to Phillips Petroleum Company

(*continued*)

Table 18.12 (continued)

Year	Development	References
	20–90 wt% of a high-MW LLDPE [$\rho \leq 955$ kg m^{-3}, $MI = 2$–10 dg min^{-1}, and M$_w$/M$_n = 2$–10]. The blends had $MI > 0.05$ dg min^{-1} and had improved optical properties	
1991	Polyethylene, PE Rigidex™ or Innovex™, was blended with liquid crystal polyester, 0.01–5 wt% LCP, to give materials with good melt processability, low viscosity, and reduction of the specific energy during compounding	P. T. Alder, J. G. Dolden, D. G. Othen, PCT Int. Appl., 008,231, 29 Apr 1993, Appl. 22 Oct 1991, to British Petroleum Co.
1991	Compositions comprised 10–80 wt% low-MW polyethylene, HDPE [$\rho \geq 940$ kg m^{-3}], and 20–90 wt% high-MW ethylene–hexene copolymer, LLDPE [$\rho \leq 955$ kg m^{-3}]. The blends had a MFI $>$ 0.05 g/10 min. The blend showed improved optical and physical properties, resulting in better blow-molded products	W. R. Coutant, J. L. Martin, European Patent Appl., 533,160, 24 Mar 1993; Norwegian Patent 9203,598, 19 Mar 1993; Hungarian Patent T62,631, 28 May 1993; Japanese Patent 5,194,796, 03 Aug 1993, Appl. 18 Sep 1991, to Phillips Petroleum Co.
1991	Ethylene–propylene copolymer (EPR, EPDM, or their mixture with $T_m = 35$–$55\ ^\circ$C) was blended with ethylene copolymer (very low density polyethylene VLDPE with density 885 kg m^{-3} and $T_m = 65$–$90\ ^\circ$C), PP or PP block copolymers, and 0–7 phr talc. The blend showed excellent moldability, surface appearance, and hardness, as well as good impact resistance	T. Nishio, T. Nomura, N. Kawamura, H. Sato, A. Uchikawa, I. Tsutsumi, Y. Goto, European Patent Appl., 519,725, 23 Dec 1992, Appl. 21 June 1991, to Mitsubishi Petrochemical Co.
1991	"Living" polypropylene, PP, or ethylene–propylene random copolymer, EPR [prepared in the presence of a catalyst consisting of an organic aluminum and a vanadium compound], was modified by reacting the terminal groups with a (meth)acrylic derivative to give a substantially monodispersed copolymer, suitable for further compounding and blending. Vinyl-, allyl-, trimethylsiloxyethyl-, 2-trimethylsiloxypropyl-, N, N-dimethylaminoethyl-, N, N-diethylaminoethyl-, glycidyl methacrylate, or acrylic acid chloride were used	N. Koyama, M. Usui, H. Furuhashi S. Ueki, U.S. Patent 5,382,634, 17 Jan 1995, Appl. 25 Apr 1994, Japanese Appl. 15 Mar 1991, to Tonen Corporation
1991	Polymer alloys comprised 20–30 wt% PP; 25–35 wt% uncross-linked elastomeric ethylene-propylene-1,4-hexadiene, EPDM (60–80 wt% ethylene); 30–50 wt% ionomer; and 2–3 wt% ethylene/n-butyl acrylate/glycidyl methacrylate, EBA-GMA. The blends were used in applications where a wide temperature range and abrasive conditions were encountered	R. L. Dawson, U.S. Patent 5,206,294, 27 Apr 1993, Appl. 6 Nov 1991, to E. I. du Pont de Nemours & Co.
1991	Deposition of patent on the constrained geometry catalyst technology (CGCT) based on the transition metals, M = Ti, Zr, Hf. The resulting PO is substantially linear. The preferred composition comprises 10–95 wt	S.-Y. Lai, J. R. Wilson, G. W. Knight, J. C. Stevens, P.-W. S. Chum, Elastic substantially linear olefin polymers, CA 2120766 of

(*continued*)

Table 18.12 (continued)

Year	Development	References
	% of homogeneously branched linear α-olefin copolymer (ρ = 0.930–0.965 g ml^{-1}, MWD = 1.8–2.8, single T_m) and 5–90 wt% of heterogeneously branched C_2C_8 copolymer (ρ = 0.935 g ml^{-1})	08 July 2008 (filed 15 Oct 1993; priority 15 Oct 1991); U.S. Patent, 5,272,236 of 21 Dec 1993 (deposited 15 Oct 1991); P.-W. Steve Chum, R. P. Markovich, G. W. Knight, S.-Y. Lai, Fabricated articles made from ethylene polymer blends, CA 2160705 of 22 Aug 2006 (filed 190 Apr 1994; priority 28 Apr 1993); Ethylene polymer film made from ethylene polymer blends, U.S. Patent 5847053 of 08 Dec 1998 (filed 11 Apr 1997; priority 15 Oct 1991), to The Dow Chemical Company
	Lai, Wilson, Knight, Stevens, Chum, Markovich, to the Dow Chemical Company	
	The SCBDI = wt% of macromolecules having a comonomer content within 50 % of the median total molar comonomer content, calculated from TREF (temperature rising elution fractionation) data. The elastic, substantially linear C_2–C_8 copolymer has 0.01 ≤ LCB/1000C ≤ 3, M_w/M_n = 1.5–2.5, 2 ≤ SCB (CH3/1000C) ≤ 30), and short-chain branch distribution index: SCBDI > 50 %. The homogeneously branched copolymer may be produced as described in C. T. Elston (DuPont Canada Ltd.) patent. Films produced from the bimodal MWD new copolymers show good impact and tensile properties	
1991	Polypropylene, 50 wt% PP, was blended with a linear low-density polyethylene, 10–50 wt% LLDPE, and a low-molecular-weight ethylene–butene plastomer (a compatibilizer). The blends were useful for melt-spun or melt-blown fibers or fabrics. In the following patent heat sealable at 100 °C blends were disclosed. They comprised 30–70 wt% ethylene–alpha-olefin copolymer prepared using a metallocene catalyst, VLDPE or plastomer [with density ρ = 880–915 kg m^{-3}, MI = 1.5–7.5 dg min^{-1}, M_w/M_n ≤ 3.0, T_m = 60–100 °C], and 70–30 wt% propylene–alpha-olefin random copolymer [with 88–100 mol% propylene]. The blends showed good processability, resistance to tearing, and tensile strength. They were useful for manufacturing packaging films, tubes, trays, etc.	K. W. Bartz, L. P. Land, A. K. Mehta, A. A. Montagna, PCT Int. Appl., WO 06,169 A1, 01 Apr 1993, Appl. 16 Sep 1991; A. K. Mehta, M. C. Chen, U.S. Patent 5,358,792, 25 Oct 1994, Appl. 22 Feb 1991, 23 Apr 1993, to Exxon Chem. Co.
1991	Polypropylene, 55–90 wt% PP, was blended with poly (1-butene), PB, as a dispersed phase and optionally with up to 10 wt% of low-MW poly(α-olefin-co-ethylene) plastomer compatibilizer. The blends were useful for manufacturing fibers and nonwovens, with good "hand" and tensile strength	K. W. Bartz, J. C. Floyd, P. Meka, and F. C. Stehling, PCT Int. Appl., WO 006,168, 01 Apr 1993, Appl. 16 Sep 1991, to Exxon Chemical Patents, Inc.
1991	Semicrystalline polyolefin blends and method of their preparation were described. The blends were reported to show enhanced inter-spherulitic and interlamellar strength. The first polymer should have higher crystallinity and crystallization temperature than the second. Thus, 50–99.9 wt% PP was blended with ethylene–α-olefin copolymers, either a stereo block polypropylene or an ethylene–propylene copolymer, EPR	A. Lustiger, Canadian Patent Appl., 2,083,664, 21 June 1993, Appl. 20 Dec 1991, to Exxon Research and Engineering Co.

<div align="right">(continued)</div>

Table 18.12 (continued)

Year	Development	References
1991	Vinyl-trimethoxysilane-grafted polyolefin, PO (e.g., PP, LDPE, EPR, or EVAc), was blended with and ethylene–acryloyloxytetramethylpiperidine. The water-cross-linkable blends were found useful for manufacturing weather-resistant cross-linked polyolefin pipes for outdoor applications	S. Ohnishi, T. Fukuda, European Patent Appl., 548,565, 30 June 1993, Appl. 12 Dec 1991, to Mitsubishi Yuka Industrial Products Corp.
1991	Blends comprised 1–70 wt% of either metallocene polypropylene, PP, or a copolymer of propylene with ≤ 10 mol% ethylene or C_2–C_{20} α-olefin that has $M_w/M_n \leq 3$ and 30–99 wt% of a similar copolymer but with $M_w/M_n = 3.5$–10. The blends were used for films having excellent low-temperature heat sealability and blocking resistance	T. Fujita, T. Sugano, H. Mizuno, H. Uchino, U.S. Patent 5,331,054, 19 July 1994, Appl. 19 Oct 1992, Jap. Appl. 21 Oct 1991, to Mitsubishi Petrochemical Co., Ltd.
1991	Radiation-resistant, heat-sealable, polypropylene, PP, blends (softer and tougher than similar ones) comprised 1–99 wt% mesomorphous PP or its copolymer, ethylene–vinyl acetate, EVAc, and/or ethylene–acrylic acid copolymer, EAA, and polybutene, PB. For example, films were prepared by blending, extruding, and then quenching. The resins were useful for manufacturing medical goods, tapes, ostomy bags, packaging materials, drug delivery patch, medical type, etc.	D. L. Wilfong, R. J. Rolando, European Patent Appl., 547,834, 23 June 1993, Appl. 18 Dec 1991, to Minnesota Mining and Mfg. Co.
1992	Polyolefin, 100 parts PO [PE, PP, or EPR], was grafted with 0.01–20 parts of the monomers' mixture [consisting of 5–50 mol% of glycidyl (meth) acrylate and 95–50 mol% of acrylamide, vinylpyrrolidone, acrylic acid esters, and/or methacrylic acid esters]. Grafted PO was used as modifier for engineering plastics or as adhesion improver for filled plastics	T. Teraya, S. Kikuchi, K. Yokoyama, Y. Fujita, Japanese Patents 61 45,260, 61 45,261, 24 May 1994; European Patent Appl., 596,654, 11 May 1994, Appl. 28 Oct 1993, JP Appl. 30 Oct 1992, to Tonen Corp.
1992	Heterogeneous ion exchange materials contained 44–55 wt% of an ion exchange resin dispersed within a blend of LLDPE and HDPE (having $MW > 200$ kg mol^{-1}.) The maximum density of LLDPE, and minimum density of HDPE, was approximately 940 kg m^{-3}. The ion exchange material was selected from between anionic, cationic, and amphoteric ion exchange resins and their mixtures	A. Giuffrida, U.S. Patent 5,346,924, 13 Sep 1994, Appl. 23 Sep 1992, to IP Holding Company
1992	Linear low-density polyethylene, LLDPE, was blended with starch and at least one ionic compound (in such amount that the concentration of anions and cations was between 0.002 and 5 mol kg^{-1}) to produce high-frequency sealable articles. The starch could also contain ≤ 50 wt% of a plasticizer. The alloys could be processed by calendering,	C. Dehennau, T. Depireux, I. Claeys, European Patent Appl., 587,216, 16 Mar 1994; Japanese Patent 62 07,046, 26 July 1994, Appl. 01 Sep 1992, to Solvay et Cie.

(*continued*)

Table 18.12 (continued)

Year	Development	References
	extrusion, etc., to produce multilayer films or sheets weldable or sealable by induction heating at high frequency, useful in packaging, paper making, etc. The presence of the starch improved the long-term biodeterioration of the materials	
1992	Polymer blends comprised melt-blended high- and low-molecular-weight polyethylenes, PE, having the viscosity (at $100\ s^{-1}$) of, respectively, $\eta > 5$ and $\eta < 0.3\ k\ Pa\ s$. The two polymers were blended at two stages, first the high-molecular-weight polymer was blended with a small amount of the other polymer, and then an additional low-molecular-weight resin was incorporated. The blends showed good processability and excellent properties. They were used for production of films with low fish-eye content, blow molding, pipes, wire coating, as well as for injection or rotational molding	W. R. Coutant, European Patent Appl., 588,147, 23 Mar 1994; Can. Pat., 2,099,750, 02 Mar 1994; Japanese Patent 61 82,756, 05 July 1994, Appl. 01 Sep 1992, to Phillips Petroleum Co.
1992	Reactor blends of high-density polyethylene, HDPE with butene and/or hexene, were produced in a multistage, gas-phase, fluidized bed polymerization, where blending occurred in situ. The resulted bimodal molecular weight distribution resin had 35–75 wt% of the higher-molecular-weight component. The blown films had improved MD/TD tear balance	A. H. Ali, J. T. T. Hsieh, K. J. Kauffman, Y. V. Kissin, S. C. Ong, G. N. Prasad, A. L. Pruden, S. D. Schregenberger, U.S. Patent 5,284,613, 08 Feb 1994, Appl. 04 Sep 1992, to Mobil Oil Corporation
1992	Polyolefin blends with improved barrier properties comprised 85–99.5 wt% of a polyolefin (e.g., high-density polyethylene, HDPE) with 0.5–15 wt% of high-nitrile polymer (e.g., an acrylonitrile butadiene copolymer). The alloys were found useful for molding plastic bottles, automobile gasoline tanks, and other containers having limited or restricted permeability to gases, vapors, or organic liquids. These materials also showed good chemical resistance, strength, and processability	G. P. Coffey, E. S. Perec, N. W. Standish, L. Melamud, J. Smola, European Patent Appl., 586,066, 09 Mar 1994; Japanese Patent 61 57,837, 07 June 1994, Appl. 23 July 1992, to Standard Oil Co.
1992	Blends comprising very low density polyethylene, 100 parts VLDPE [80–95 mol wt% ethylene and C_4–C_8 comonomer(s)], and linear low-density polyethylene, 15–600 parts LLDPE (ethylene copolymer with 2–8 mol% octene), showed excellent processability. They were formed into 10–300 μm thick sheets, useful for transdermal drug delivery devices as single-layer backings. They were clear, colorless, transparent, permeable to oxygen, stable to various common components of transdermal delivery devices, strong, comfortable, and not absorbing significant amounts of elements of transdermal carriers. Sheets made from the blends could be heat sealed at a low temperature	K. J. Godbey, P. G. Martin, PCT Int. Appl., WO 94 03,539, 17 Feb 1994; U.S. Patent 5,264,219, 23 Nov 1993, Appl. 07 Aug 1992, to Minnesota Mining and Mfg. Co.

<div align="right">(continued)</div>

Table 18.12 (continued)

Year	Development	References
1992	Heat-shrinkable film comprised single-site catalyzed copolymer of ethylene and a C_{3-8} alpha-olefin, LLDPE with $\rho \geq 900$ kg m^{-3} blended with another polymer of ethylene and a C_{3-8} alpha-olefin and a second comonomer [e.g., vinyl acetate, alkyl acrylate, CO, butadiene, styrene, acrylic acid, and a metal salt of an acrylic acid], or an alpha-olefin homopolymer. The heat-shrinkable films had improved shrinkability, impact resistance, and optical properties compared to prior art and were used in packaging	R. Babrowicz, B. C. Childress, K. R. Ahlgren, G. P. Shah, European Patent Appl., 597,502, 18 May 1994, Appl. 13 Nov 1992, to W. R. Grace and Co.
1992	Polyolefin blends formulated for heat seamable roof sheeting comprised 25–95 wt% of amorphous PO having <1 wt% crystallinity (<60–61 wt% ethylene, dicyclopentadiene, and/or ethylidene norbornene); 5–75 wt% of a crystalline polymer, i.e., PE, PP, poly (ethylene-*co*-propylene), poly(ethylene-b-octene), or poly(ethylene-b-butene), having 2–65 wt% crystallinity; 20–300 phr of a (non)reinforcing filler; and 20–150 phr of either paraffinic oil, naphthenic oil, and/or wax. The materials exhibited good adhesion. Neither an adhesive nor curing was necessary	J. A. Davis, J. K. Valaitis, European Patent Appl., 564,961, 13 Oct 1993; Can Pat., 2,093,397, 07 Oct 1993; U.S. Patent 5,286,798, 15 Feb 1994; Japanese Patent 60 65,434, 08 Mar 1994, Appl. 06 Apr 1992, to Bridgestone/ Firestone, Inc.
1992	Blends comprising cycloolefin polymer, 0–95 wt% PCO; polyethylene, 0–95 wt% PE; and 0.1–99 wt% block copolymer(s) were prepared for moldings with outstanding properties, viz., improved melt viscosity, elongation at break, impact strength, toughness, hardness, and modulus. The block copolymers of ethylene (or propylene) and norbornene blocks were obtained in the presence of aluminoxane and a metallocene catalyst, resulting in $M_w/M_n \leq 2$	U. Epple, M. -J. Brekner, U.S. Patent 5,359,001, 25 Oct 1994, Appl. 20 Apr 1993, Ger. Appl. 22 Apr 1992, to Hoechst A.-G.
1992	Blends included 70–90 wt% of a polymer derived from ethylene and at least one higher alpha-olefin (e.g., LLDPE, VLDPE, or LDPE having MI = 0.1–10), 10–30 wt% of an auxiliary co-crystallizable polymer, derived from ethylene and at least one olefinic comonomer (e.g., LLDPE, VLDPE, or LDPE having MI $\geq$ 80 %, below that of the first polymer), and moisture cross-linking additives including a silane, a silanol condensation catalyst, and a free radical initiator. Cross-linking was rapid; thus, the moisture-curing step subsequent to extrusion of an electrical cable was short. The blends could contain processing aid (fluorinated polymer and/or a polyethylene with high MI) and 5–70 wt% filler. They were used for shaped coatings and cable coating	W. K. Wong, D. C. Varrall, European Patent Appl., 584,927, 02 Mar 1994, Appl. 24 July 1992, to Exxon Chemical Patents Inc.
1992	Polyethylene blends having toughness and elastic recovery comparable to those of plasticized PVC comprised $\geq$50 wt% of a copolymer of ethylene and either butene or hexene [LLDPE,	M. R. Rifi, U.S. Patent 5,326,602, 05 July 1994, Appl. 01 Dec 1992, to Union Carbide Chemicals & Plastics Technology Corporation

(*continued*)

Table 18.12 (continued)

Year	Development	References
	ρ = 880–915 kg m^{-3}, MI $\leq$ 1 dg min^{-1}, long-chain branching = 0.5–1.5 long chains/1,000C, M$_w \geq$ 200 kg mol^{-1}]; $\geq$5 wt% of a copolymer of ethylene and either vinyl acetate or ethyl acrylate, EVAc or EEA; and 5–30 wt% liquid hydrocarbon oil. The blends showed essentially no yield point and behavior similar to that of cross-linked materials, although they were not cross-linked (strain recovery). They were found competitive with plasticized PVC in terms of both physical properties and economics	
1992	Linear low-density polyethylene, 90–99 wt% LLDPE, was blended with polymethylmethacrylate, 10–11 wt% PMMA, and optionally a compatibilizing copolymer, viz., SEBS, EPR, ethylene–styrene block copolymer, ES. The blends were found to produce blown films with improved tear in the machine direction, modulus, and impact strength	D. V. Dobreski, J. J. Donaldson, U.S. Patent 5,290,866, 01 Mar 1994, Appl. 16 Apr 1992, to Mobil Oil Corp.
1992	Continuous process for the preparation of polyisobutylene, PIB, blends with at least one other polymer, e.g., polyolefin, PO, was described. PIB was continuously polymerized in ethylene. The resin was fed to a degassing extruder where it was mixed with PO, fillers, and/or additives. The process was used for the preparation of blends in a simpler and more cost-effective manner than that of prior art	H. Gropper, E. Kolk, K. H. Fauth, G. Isbarn, G. Scherer, German Patent 4,319,181, 27 Jan 1994; French Patent 2,694,010, 28 Jan 1994, Appl. 22 July 1992, to BASF A.-G.
1992	Thermoplastic rubber blends with good adhesion to reinforcing agents comprised 10–100 wt% polyolefin grafted with polar monomers (e.g., 27–75 wt% PP grafted with vinyl acetate, acrylic acid, methacrylic and itaconic acid, or maleic acid anhydride) and elastomer(s) (EPDM, NBR, or BR) that could be dynamically cross-linked by peroxide, silane, or sulfur. The blends may also contain 0.3–2.5 wt% plasticizer, fillers, pigments, processing aids, and flame retardants. They showed bondability to solids, especially after application of high temperature and pressure, thus were used for the production of conveyor belts, hoses and V-belts	S. Luepfert, F. Roethemeyer, E. Maeder, European Patent Appl., 580076, 26 Jan 1994; German Patent 4,223,984, 27 Jan 1994, Appl. 21 July 1992, to Continental A.-G.
1992	Polyolefin compositions with improved toughness, flexibility, and high clarity were prepared by blending 90–95 wt% setereoregular polymer or copolymer of 4-methyl-1-pentene, PMP, with polybutene, PB, having M$_n$ < 500	M. J. Hagenson, H. F. Efner, L. C. Hasselbring, W. H. Beever, European Patent Appl., 556,843, 25 Aug 1993, Appl. 20 Feb 1992, to Phillips Petroleum Co.
1992	Polyolefin (PO = PP, HDPE, EPR, or PMP) was blended with an impact modifier, 0.1–5 wt% colorant and/or 5–50 wt% of opacifiers, and a styrene–diolefin block copolymer, grafted with 1–6 mol% of acrylic	J. O'Leary, S. Musgrave, PCT Int. Appl., WO 93 21,269, 28 Oct 1993; Australian Patent 93 36,840, 10 Oct 1993; Australian Patent 93

(*continued*)

Table 18.12 (continued)

Year	Development	References
	acid, maleic anhydride, or sulfonate functionality (SEBS, SEPS, radial SEB, or SEP). To improve scratch resistance the blend contained 100–3,000 ppm Zn–stearate and C_{16-22} fatty acid amide. The alloys were injection molded into parts showing impact, scratch, and abrasion resistance. They were used to manufacture interior trim for vehicles and in other applications where a scratch- and scuff-resistant plastic material is required	40,363, 18 Nov 1993, Appl. 09 Apr 1992, to ICI Australia Operations Proprietary Ltd.
1992	To prepare polyolefin blends, PO (e.g., EVAc, PE, PP, EPR), with vinyl polymers, 10–200 parts of vinyl monomer [e.g., (meth)acrylates, styrenics, vinyl chloride, glycidyl methacrylate, maleic anhydride, acrylonitrile, divinylbenzene] and 0.01–4.0 parts of a free radical initiator were used to impregnate 100 parts of PO particles at $T = 20–130\,°C$. After 50–99 wt% of the monomer was absorbed, the particles were dispersed in water and the free radical polymerization initiated. Good adhesion between the components in the extruded or molded articles was achieved	T. Vestberg, I. Lehtiniemi, U.S. Patent 5,300,578, 05 Apr 1994, U.S. Appl. 27 Jan 1993, Finnish Appl. 27 Jan 1992, to Neste Oy
1992	Polyolefins, PO, blends with copolymers of vinyl acetate and acrylate esters, EVAc (20–40 wt% VAc), were extruded into films, weldable by high-frequency currents. It replaced PVC flexible films, e.g., in inflatable goods. For example, 400 µm PVC film, inflated to 100 mbars, after 13 days, had lost 72 wt% of the pressure, while the new blends (15 wt% VAc in the blend) of 200 µm film lost 50 wt% in 19 days	G. Benatre, French Patent 2,688,511, 17 Sep 1993, Appl. 13 Mar 1992
1992	Polyolefin, PO, molding compositions, suitable for the use in automotive application, comprised polyolefin wax [$M_w = 1–50\ kg\ mol^{-1}$, $M_w/M_n = 1.8–4.0$, and $T_m = 120–160\,°C$] and 1–80 wt% of either a PO [$M_w \geq 100$, $M_w/M_n = 1.8–4.0$, and $T_m = 120–160\,°C$], an olefinic copolymer derived from at least two different olefins [$M_w \geq 100$, $M_w/M_n = 1.98–4.0$, and $T_m = 90–160\,°C$], or an elastomer with $T_g < -20\,°C$. The blends could be impact modified by incorporation of a copolymer. They were molded, extruded, or blow molded into articles showing high modulus, hardness, scratch resistance, and low shrinkage	B. Bachmann, A. Winter, European Patent 563,818, 6 Oct 1993, Appl. 31 Mar 1992, to Hoechst A.-G.
1992	Blends of PE (selected from VLDPE and/or LLDPE), with 13–17 wt% ethylene–butene plastomer copolymer [Mitsui's TAFMER™, $\rho < 900\ kg\ m^{-3}$, $T_m = 55–85\,°C$], and 35–50 wt% ethylene–vinyl acetate copolymer, EVAc, were used for film blowing, useful as packaging materials for foods. The film had shrink properties in MD and TD similar to those of EVAc film and plastic orientation properties similar to	B. L. Wilhoit, European Patent 562,493, 29 Sep 1993; D. J. Ralph, U.S. Patent 5,279,872, 18 Jan 1994, Appl. 17 Feb 1993, Appl. 23 Mar 1992, to Viskase Corp.

<div align="right">(continued)</div>

Table 18.12 (continued)

Year	Development	References
	those of VLDPE films. In the U.S. Patent the biaxially oriented heat-shrinkable multilayer stretch film comprising 65–80 wt% VLDPE and a plastomer was reported useful as poultry wrap	
1992	Polyolefin, PO [of ethylene, propylene, butylene, 4-methylpentene, and their copolymers with 1-alkenes, vinyls, (meth)acrylates – preferably PP], was grafted at a ratio 1:9–4:1 with 1–20 wt% of (meth)acrylic acid and $\geq$30 wt% of styrene and/or alkyl- and/or halo-substituted styrene, methacrylic ester, and 0–60 % of other comonomers [e.g., vinyl aromatic, ester], at least some of the acid units of methacrylic acid and/or acrylic acid bearing a charge and being associated with non-polymeric counterions [e.g., 90 % methyl methacrylate, 5 % butyl acrylate, and 5 % methacrylic acid with either Ca^{2+} or Mg^{2+}. The ionomer could be blended with PO either during or after manufacturing. The blends were extruded either directly or after pelletization. They exhibited high sag resistance without increased viscosity. PP fibers could be used for strapping, netting, slit tape, rope, twine, bags, carpet backing, foamed ribbons, upholstery, rugs, pond liners, awnings, swimming pool covers, tarpaulins, bristles, sutures, nonwoven fabrics, bedsheets, bandages, diaper liners, etc.	R. G. Hamilton, M. T. McCarty, European Patent Appl., 589,659, 30 Mar 1994; U.S. Patent 5,319,031, 07 June 1994; Canadian Patent 2,106,344, 25 Mar 1994; British Patent 93 03,861, 31 May 1994; Japanese Patent 62 012,048, 02 Aug 1994, Appl. 24 Sep 1992, to Rohm and Haas Co.
1992	Polyolefin blends comprised 25–95 wt% of a crystalline random copolymer, EPR1 (of propylene with ethylene and/or an alpha-olefin), and 5–75 wt% of a mixture consisting of PE and EPR2. The density of EPR1 was about equal that of the mixture. The blends had good transparency and impact resistance even at low temperatures and were used to manufacture food containers, medical, packaging films, etc.	G. Cecchin, R. Ghisellini, D. Malucelli, European Patent 557,953, 01 Sep 1993, Appl. 24 Feb 1992, to Himont, Inc.
1992	Nonwoven textile materials comprised fibers obtained from a blend of 5–95 wt% propylene, PP (or propylene/ethylene copolymer with $\leq$10 wt% ethylene, EPR), and 95–95 % polyolefin, PO, selected from EPDM, EPR, LLDPE, etc. The materials have been used in disposable personal hygiene products or protective clothing. The products showed improved strength, drapability, softness, and bonding performance	K. Ogale, M. E. Strasinic, European Patent Appl., 598,224, 25 May 1994, Appl. 15 Oct 1993; Canadian Patent 2,108,819, 01 May 1994; Japanese Patent 62 00,093, 19 July 1994; U.S. Patent 5,346,756, 13 Sep 1994, Appl. 30 Oct 1992, to Himont Inc.
1992	Polypropylene, PP, was blended with a random crystalline terpolymer of 96–85 wt% propylene, 1.5–5.0 wt% ethylene, and 2.5–10 wt% $C_{4–8}$ alpha-olefin. The blends were used to manufacture strands of multiple monofilaments or staple fibers with high resiliency and shrinkage, for pile fabric,	L. Clementini, A. F. Galambos, G. Lesca, K. Ogale, L. Spagnoli, M. E. Starsinic, L. Giuseppe, European Patent 552,810, 28 July 1993, Appl. 29 May 1992, to Himont Inc.

(*continued*)

Table 18.12 (continued)

Year	Development	References
	textiles, geotextiles, or carpets. The carpet yarn had a twist retention of over 30 %, shrinkage on heat setting at 143 °C of at least 15 %, and uniform shrinkage	
1992	Blends comprising polypropylene, 50–97 wt% PP [or a PP block copolymer with ethylene block], and 50–53 wt% of an ethylene/C_{4-18} alpha-olefin copolymer [α-olefin content t = 10–60 wt%, $\rho \leq$ 913 kg m^{-3} obtained by using a metallocene catalyst and aluminoxane] were found useful as automobile trims and trims of electrical instruments. They showed high moldability, improved impact resistance at room and low temperature, and balance of rigidity and impact resistance	K. Shichijo, European Patent Appl., 593,221, 20 Apr 1994; Japanese Patent 61 92,500, 12 July 1994, Appl. 15 Oct 1992, to Mitsubishi Petrochemical Co., Ltd.
1992	A multilayer film comprised polypropylene, PP [or PP copolymer with 20–40 wt% hydrocarbon resin], in the core; outer layers from PP, LLDPE, PB, or their blends with 4–15 wt% PP; and the intermediate layers from polyolefin-based carboxylic acid or maleic anhydride. An oxygen barrier layer from EVOH, PVDC, PEST, or PA could also be used. The films were biaxially oriented at ratios of 3:1–8:1. They had low moisture transmission rate, toughness, abrasion resistance, good clarity, and gloss, suitable as moisture barrier packagings for food, pharmaceuticals, and electronics	P. S. Gautam, European Patent Appl., 588,667, 23 Mar 1994, Appl. 20 Sep 1993; British Patent Appl., 93 03,823, 22 Mar 1994; Australian Patent 93 47,378, 24 Mar 1994; Ca. Pat., 2,106,258, 19 Mar 1994; Japanese Patent 61 98,826, 19 July 1994, US Appl. 18 Sep 1992, to W. R. Grace & Co.
1992	Ternary blends contained 87–96 wt% LLDPE (with either butene-1, hexene-1, or octene-1), 1–10 wt% isotactic polybutene, 1–10 wt% PS, and 0.01–10 wt% color and anti-blocking agents. The blends exhibited improved process efficiency in terms of extruder amps/rpm ratio, while the terpolymer substantially retained the inherent strength of the LLDPE. The compositions were used for blown films and for the manufacture of waste bags	S. P. Evans, P. P. Shirodkar, US 5,258,463, 02 Nov 1993, Appl., 24 Aug 1992, to Mobil Oil Corporation
1992	Semicrystalline polyolefin blends were prepared by mixing two different random copolymers of propene with C_{4-10} alpha-olefin at a ratio from 1:3 to 1:1. The first copolymer contained 1–10 wt% of C_{4-10} alpha-olefin (1-butene, 1-pentene, 1-hexene, 1-octene, and 4-methyl-1-pentene), whereas the second 15–40 wt% of the same comonomer. The mixing was carried out in reactors, polymerizing the monomers in the presence of stereospecific catalysts supports on active magnesium dihalides, in at least two sequential stages. The resulting R-TPOs	G. Cecchin, F. Guglielmi, European Patent 560,326, 15 Sep 1993, Appl. 10 Mar 1992, to Himont Inc.

(continued)

Table 18.12 (continued)

Year	Development	References
	showed limited solubility in xylene, low heat-sealing temperature, and high melting point and were used for the production of heat-sealable laminated mono- or bi-oriented films suitable for the food industry	
1992	PE blends were prepared during polymerization. This strategy has been widely implemented in syntheses of multimodal PE compositions. The blown film showed MD/TD tear balance. The bimodal blend contained 0.35–0.75 weight fraction of a higher-MW component.	A. H. Ali, J. T. T. Hsieh, K. J. Kauffman, Y. V. Kissin, S. Christine Ong, G. N. Prasad, A. L. Pruden, S. D. Schregenberger, Producing blown film and blends from bimodal high density high molecular weight film resin using magnesium oxide supported Ziegler catalyst, U.S. Patent 5,284,613 of 08 Feb 1994 (filed 1992) to Mobil Oil Co.; Dammert et al., U.S. Patent 6,185,349 of 06 Feb 2001 (filed 1999) to Borealis Polymer Oy
	Ali A.H. et al. to Mobil Oil Co.; Dammert et al. to Borealis. Catalyst: $TiCl_4$/pentanol deposited on MgO/acetic acid and then treated with tri-n-hexyl-aluminum solution	
	Reactor blending during the slurry polymerization gave two PE fractions with different MW. Borealis generated multimodal resins for optical cables using slurry-/gas-phase reaction with Z-N catalyst with $MgCl_2$	
1993	Polyethylene blends comprised a low-density polyethylene, ≤60 wt% either LDPE or LLDPE; postconsumer recycled high-density polyethylene, 4–30 wt% HDPE; and an effective amount of a compatibilizer comprising 0.1–1.5 wt% ZnO and 0.1–2 wt% of glycerol monostearate. The blends could also contain 5–30 pph of a blowing agent. The blends were used to make aesthetically appealing foamed products for use as cushioning materials or as packaging films	S.-T. Lee, U.S. Patent 5,428,093, 27 June 1995, Appl. 05 Nov 1993, to Sealed Air Corporation
2003	Polymer blends (mechanical) comprised (A) 35–85 wt% Z-N i-PP ($T_m > 130$ °C) and (B) 30–70 wt% metallocene α-olefin-*co*-PP with crystallizable α-olefin sequences [narrow MWD, composition distribution single T_m]. The blends showed improved processing, unexpected compatibility, single T_m, and increased tensile strength	S. Datta, C. Cozewith, P. Ravishankar, E. J. Stachowski, Elastic blends comprising crystalline polymer and crystallizable polymers of propylene, U.S. Patent 6867260 of 15 Mar 2005 (filed 22 Apr 2004; priority 29 June 1999, U.S. Patent 6642316); Sudhin Datta, Avinash C. Gadkari, Charles Cozewith, Alpha-olefin/propylene copolymers and their use, U.S. Patent 6982310 of 03 Jan 2006 (filed 06 May 2005; priority 03 July 2003, USPat. 6635715) to ExxonMobil Chemical Patents, Inc.
	Datta, Cozewith, Ravishankar, Stachowski, Gadkari to ExxonMobil Chemical Patents, Inc.	
	The (A) component is either i-PP with <10 wt% comonomer, while (B) is preferably crystallizable C_2–C_3 copolymer. Blends were mechanically mixed	
	ExxonMobil developed poly(propylene-*co*-ethylene) Vistamaxx™ post-metallocene resin. The polymerization procedure for the blend component is described in U.S. Patents. 5198401 of 30 Mar 1993 and 5057475 of 15 Oct 1991; catalyst system of enhanced productivity, 5153157 of 06 Oct 1992, to Exxon Chem	

Table 18.12 (continued)

Year	Development	References
2004	The copolymers of the blend were prepared using (a) a silyl chromate catalyst, $(R10)_3$Si-O-CrO$_2$-O-Si$(R10)_3$ wherein R10 = C_{1-10} alkyl, and (b) a phosphinimine catalyst, $(L)_n$-M-$(PI)_m(X)_p$ where M = Ti, Hf, or Zr; PI = phosphinimine ligand; ligand L = Cp, indenyl, or fluorenyl; X = Cl or C_{1-4} alkyls; $m = n = 1$; and $p = 2$. A catalyst activator includes alumoxanes (e.g., MAO) with a molar ratio of Al:M = 50:1–250:1 and ionic boron-containing activators. Kazakov and Yim, to NOVA Chemicals	K. Alexei, Y. Gary, Polyolefin blends and pipe, CA 2508436, filed 26 May 2005; U.S. Patent 7,309,741 of (filed 01 June 2004); U.S. Patent Appl. 2008/0090040A1 (filed 14 Nov 2007, priority 01 June 2004) now, U.S. Patent 7696281of 13 Apr 2010 to NOVA CHEMICALS CORPORATION (Canada) or NOVA Chemicals (International) S.A.
	The invention describes PE blends of a low-MW HDPE made using a Z-N type or Cr-based catalyst and a high-MW m-LLDPE made using a Group 4 single-site-type catalyst. The blends are suitable for the manufacture of pipes, tested according to ASTM D 2837 or ISO 9080	The ionic activators are disclosed in, e.g., J. C. Stevens, D. R. Neithamer, U.S. Patents 5132380 of 21 July 1992 (filed 12 Sept 1991); to Dow Chem. Co.; H. W. Turner, G. G. Hlatky, R. R. Eckman, 5198401 of 30 Mar 1993 (filed 30.07 1991) to Exxon Chemical Patents Inc.
	A polyolefin blend comprises (a) 30–80 wt% of a low-MW copolymer [85–99.5 wt% of C_2 and 0.05–15 wt% of C_{4-8} α-olefin, $\rho = 0.953$–0.965 g mL^{-1}, and MFR (2.16 kg 190 °C) = 0.1–20.0 g/10 min] and (b) 70–20 wt% of a high-MW copolymer [85–99.9 wt% of C_2 and from 15 to 0.1 wt% of C_{4-8} α-olefin, $\rho = 0.915$–0.940 g mL^{-1}, and an MFR (21.6 kg 190 °C) = 0.05–5.0 g/10 min]. The selected resins were blended in a compounder and then extruded as pipes	
2009	Solution polymerization of HDPE ($\rho = 0.890$–0.970 g mL^{-1}) takes place in ≥ 2 reactors. The process (a) provides a first C_2 and C_{4-10} feed to ≥ 1 continuously stirred tank reactor (CSTR) in the presence of a catalyst, producing a first PE component; (b) the second (tubular) reactor (TR) is fed with the first PE solution, enriched by preheated $T \geq 100$ °C monomer(s) and solvent. The weight ratio of the additional solvent to C_2 = 20/1–0.1/1 and the additional C_2 = 1–50 wt% of the C_2 added to CSTR	Lauwrence Martin Jozef Van Asseldonk, Stephen John Brown, Multi reactor process, CA 2,688,217 of 11 June 2011 (filed 11 Dec 2009); US 8,101,693 B2 of 24 Jan 2012 (filed 06 Dec 2010; priority 2009) to NOVA Chemicals (International) S.A.
	Asseldonk and Brown, from NOVA Chemicals (International) S.A.	
	This document describes a process with one CSTR and one TR, but a single STR may also be used – in the former case a catalyst should be injected to each reactor. While the main catalyst is Z-N type, use of a single-site one may offer additional advantages blending homogeneously and heterogeneously branched chains	

<div align="right">(continued)</div>

Table 18.12 (continued)

Year	Development	References
	This multi-reactor system used for copolymerization of C_2 with higher α-olefins comprises a CSTR connected in series to a tubular reactor (TR). The latter receives a polymer solution from the CSTR. Polymerization in TR improves efficiency, by reducing the amount of energy required to recover the polymer and residual comonomer from the solution. The use of preheated C_2 in TR mitigates the contaminating gel problems (fouling TR and creating "fish eyes" on film) and reduces hexane extractables	

References

J.M. Aime, G. Mention, A. Thouzeau, U.S. Patents 4,873,270, Oct 10, 1989, Appl. 9 Feb 1988, to Charbonnages De France

A. Ajji, L.A. Utracki, Polym. Eng. Sci. **36**, 1574 (1996); Prog. Rubber Plast. Technol. **13**, 153 (1997)

G. Akovali, T.T. Torun, Properties of blends prepared from surface-modified low-density polyethylene and poly(vinyl chloride). Polym. Int. **42**, 307 (1997)

G. Akovali, C.A. Bernardo, J. Leidner, L.A. Utracki, M. Xanthos (eds.), *Reprocessing of Commingled Polymers and Recycling of Polymer Blends*. NATO ASI, vol. 351 (Kluwer, Dordrecht, 1998)

Y.A. Akpalu, P. Peng, Probing the melt miscibility of a commercial polyethylene blend by small-angle light scattering. Mater. Manuf. Process. **23**, 269–276 (2008)

R.G. Alamo, W.W. Graessley, R. Krishnamoorti, D.J. Lohse, J.D. Londono, L. Mandelkern, F.C. Stehling, G.D. Wignall, Small angle neutron scattering investigations of melt miscibility and phase segregation in blends of linear and branched polyethylenes as a function of the branch content. Macromolecules **30**(3), 561–566 (1997)

A.-C. Albertson, in *Handbook of Polymer Degradation*, ed. by S.H. Hamid, M.B. Amin, A.G. Maadhah (Marcel Dekker, New York, 1992)

A.H. Ali, J.T.T. Hsieh, K.J. Kauffman, Y.V. Kissin, S. Christine Ong, G.N. Prasad, A.L. Pruden, S.D. Schregenberger, Producing blown film and blends from bimodal high density high molecular weight film resin using magnesium oxide supported Ziegler catalyst, U.S. Patent 5,284,613 of 08 Feb 1994 (filed 1992) to Mobil Oil Co.

J.S. Anand, ed., *National Seminar on Emerging Trends in Plastic Recycling Technologies and Waste Management* (Goa, 1995)

J. S. Anand, ed., *Recycling and Plastics Waste Management*. Proceedings of National Seminar (CIPET, Chennai, 1997; Prints India, Chennai, 1997)

S. Anantawaraskul, J.B.P. Soares, M. Paula, P. Wood-Adams, Fractionation of semicrystalline polymers by crystallization analysis fractionation and temperature rising elution fractionation. Adv. Polym. Sci. **182**, 1–54 (2005)

S.H. Anastasiadis, Interfacial tension of immiscible polymer blends, Ph.D. thesis, University of Princeton, 1988

A.L. Andrady, J.E. Pegram, S. Nakatsuka, Studies on enhanced degradable plastics: 1. The geographic variability in outdoor lifetimes of enhanced photodegradable polyethylenes. J. Environ. Polym. Degrad. **1**, 31–43 (1993a)

A.L. Andrady, J.E. Pegram, Y. Tropsha, Changes in carbonyl index and average molecular weight on embrittlement of enhanced-photodegradable polyethylenes. J. Environ. Polym. Degrad. **1**, 171–179 (1993b)

S.R. Angeli, Canadian Patent 2,059,914, 28 Aug 1992, Appl. 28 Aug 1992, U.S. Appl. 27 Feb 1991, to General Electric Company

Anonymous, *PLASTIC WASTES – Disposal and Recycling, Past, Present and Future in Japan* (Plastic Waste Management Institute, Tokyo, 1991)

Anonymous, Plast. Technol. **41**(1), 12 (1995)

Anonymous, Plast. Rub. Wkly. Sep. 6, p. 7 (1996a)

Anonymous, Recycl. Today (12), 34 (1996b)

Anonymous, Information system on plastics waste management in Western Europe – European overview, Association of Plastics Manufacturers in Europe (APME) (1997a)

Anonymous, Plast. Technol. **43**(4), 64 (1997b)

Asahi Chemical Industry Co., Ltd., Japanese Patent 044,540, 09 Mar 1985, Appl. 19 Aug 1983

R. Babrowicz, B.C. Childress, K.R. Ahlgren, G.P. Shah, Eur. Pat. Appl., 597,502, 18 May 1994, Appl. 13 Nov 1992, to W. R. Grace and Co.

S.K. Bahl, P.J. Canterino, R. Shaw, British Patent 2,152,515, 07 Aug 1985, Appl. 04 Jan 1984, to Mobil Oil Corp.

L. Bai, Y.-M. Li, W. Yang, M.-B. Yang, Rheological behavior and mechanical properties of high-density polyethylene blends with different molecular weights. J. Appl. Polym. Sci. **118**, 1356–1363 (2010)

F.W. Bailey, W.M. Whitte, Ethylene polymer blends, U.S. Patents 4,461,873, 24 July 1984, filed 22 June 1982; 4,547,551, 15 Oct 1985

W.E. Baker, A.H. Simmons, Ca. Pat. Appl., 2,028,784, 16 May 1991, Appl. 29 Oct 1990, to Queen's University at Kingston

D.G.H. Ballard, The discovery of polyethylene and its effect on the evolution of polymer science, in *History of Polyolefins*, ed. by R.B. Seymour, T. Cheng (D. Reidel, Dordrecht, 1986)

D.G.H. Ballard, A.J.P. Buckmann, PCT Int. Appl., 93 17,064, 02 Sep 1993, Appl. 28 Feb 1992, to Zeneca Limited

N.P. Balsara, L.J. Fetters, N. Hadjichristidis, D.J. Lohse, C.C. Han, W.W. Graessley, R. Krishnamoorti, Thermodynamic interactions in model polyolefin blends obtained by small-angle neutron scattering. Macromolecules **25**(23), 6137–6147 (1992)

E. Bamberger, F. Tschirner, Ber. Dtsch. Chem. Ges. **31**, 1524 (1898)

C. Bastioli, in *The Wiley Encyclopaedia of Packaging Technology*, ed. by A.L. Brody, K.S. Marsh, 2nd edn. (Wiley, New York, 1997); NATO-ASI Frontiers in the Science and Technology of Polymer Recycling, Antalya, 16–27 June 1997

C. Bastioli, V. Bellotti, L. Del Giudice, G. Gilli, J. Environ. Polym. Degrad. **1**, 181 (1992a)

C. Bastioli, V. Bellotti, G.F. Del Tredici, R. Lombi, A. Montino, R. Ponti, Intl. Pat. Appl., WO 92/19,680, 1992b

C. Bastioli, V. Bellotti, A. Rallis, Microstructure and melt flow behavior of a starch-based polymer. Rheol. Acta **33**, 307–316 (1993)

C. Bastioli, V. Bellotti, M. Camia, L. Del Giudice, A. Rallis, in *Biodegradable Plastics and Polymers*, ed. by Y. Doi, K. Fukuda. Proceedings of the III International Scientific Workshop on Biodegradable Plastics and Polymers, Osaka, 9–11 Nov 1993 (Elsevier, Amsterdam, 1994)

L. Bateman, Olefin oxidation. Q. Rev. Chem. Soc. **8**, 147–167 (1954)

BCC (Business Communications Co.), Norwalk, CT, News Releases of 11, 24 Feb 1997

S.L. Bell, A.G. Vadagama, Polymerization process, U.S. Patent 6720396 of 13 Apr 2004, to Univation Technol

E.A. Benham, M.P. McDaniel U.S. Patent 5,344,884 06 Sept 1994

E.A. Benham, F.W. Bailey, J.D. Webmeyer, M.P. McDaniel 5378764 of 03 Jan 1995, all to Phillips Petroleum Co.

C.L. Beyler, M.M. Hirschler, Thermal decomposition of polymers (Chap. 7), in *The SFPE handbook Fire Protection Engineering*, ed. by P.J. DiNenno, D. Drysdale, C.L. Beyler, W.D. Walton, 3rd edn. (NFPA, Quincy, 2002)

C.A.B.. Bjoerkengren, E.S. Joensson, Swedish Patent 413,031, 31 Mar 1980, Appl. 05 Mar 1979, to Aktiebolag Akerlund och Rausing

L. Boehm, H.F. Enderle, H. Jastrow, Europ. Pat. Appl., 517,222, 09 Dec 1992

L. Böhm, H.-F. Enderle, H. Jarstrow, Polyethylene molding composition, U.S. Patent 5338589 of 16 Aug 1994, priority 03 June 1992, to Hoechst Aktiengesellschaft

V. Bordereau, Z.-H. Shi, L.A. Utracki, P. Sammut, M. Carrega, Development of polymer blend morphology during compounding in a twin screw extruder. Part 3: experimental procedures and preliminary results. Polym. Eng. Sci. **32**(24), 1846–1856 (1992)

D. Bourry, L.A. Utracki, A. Luciani, *The Extensional Flow Mixer (EFM)*. Polyblends-'95, NRCC/IMI Bi-annual Symposium and SPE-RETEC on Polymer Alloys and Blends, Boucherville, 19–20 Oct 1995

M. Bousmina, J.F. Palierne, L.A. Utracki, Modeling of polymer blends' behavior during capillary flow. Polym. Eng. Sci. **39**(6), 1049–1059 (1999)

M. Brookhart, M.L.H. Green, Carbon-hydrogen-transition metal bonds. J. Organomet. Chem. **250**, 395–408 (1983)

M. Brookhart, M.L.H. Green, G. Parkin, Agostic interactions in transition metal compounds. Proc. Natl. Acad. Sci. U. S. A. **104**(17), 6908–6914 (2007)

S.J. Brown, J.W. Swabey, C.J.B. Dobbin, Solution polymerization process catalyzed by a phosphinimine catalyst, CA 2347410 of 08 Sept 2009 (filed 11 May 2001); U.S. Patent 6,777,509 B2 of 17 Aug 2004 (filed 17 Apr 2002, priority 11 May 2001), to NOVA Chemicals Corporation (Canada) or Nova Chemicals (International) S.A (CH)

F. Buehler, E. Schmid, H.J. Schultze, European Patent Application 536,679, 14 Apr 1993, Appl. 08 Oct 1991; U.S. Patents 5,346,936, 13 Sep 1994, Appl. 15 June 1992, Ger. Appl. 17 June 1991; P. Meier, German Patent 4,139,468, 03 June 1993, Appl. 29 Nov 1991, to Ems-Inventa Aktiengesellschaft

P.J. Canterino, R.J. Martinovich, Blends of high pressure type polyethylene with cracked highly crystalline 1-olefin polymers, U.S. Patents 3,086,958, 23 April 1963, filed 17 Nov 1958, to Phillips Petroleum Co.

P.J. Carreau, Rheological equation from molecular network theories. Trans. Soc. Rheol. **16**, 99–127 (1972)

P.J. Carreau, Ph.D. thesis, University of Wisconsin, Madison, 1968

G.M. Chapman, R.H. Downie, U.S. Patents 5,352,716, 04 Oct 1994, Appl. 16 Dec 1992, to Ecostar International, L. P.

Y.Y. Chen, T.P. Lodge, F.S. Bates, Entropically driven phase separation of highly branched/linear polyolefin blends. J. Polym. Sci. B: Polym. Phys. **38**, 2965–2975 (2000)

F. Chen, R. Shanks, G. Amarasinghe, Miscibility behavior of metallocene polyethylene blends. J. Appl. Polym. Sci. **81**, 2227–2236 (2001)

Y.Y. Chen, T.P. Lodge, F.S. Bates, Influence of long-chain branching on the miscibility of poly (ethylene-*r*-ethyl-ethylene) blends with different microstructures. J. Polym. Sci. B: Polym. Phys. **40**, 466–477 (2002)

K. Cho, T.-K. Ahn, B.H. Lee, S. Chor, Miscibility and processability in linear low density polyethylene and ethylene-propylene-butene-1 terpolymer binary blends. J. Appl. Polym. Sci. **63**, 1265–1274 (1997)

P. Choi, Molecular dynamics studies of the thermodynamics of HDPE/butene-based LLDPE blends. Polymer **41**, 8741–8747 (2000)

P.-W.S. Chum, R.P. Markovich, G.W. Knight, S.-Y. Lai, Ethylene polymer film made from ethylene polymer blends, U.S. Patent 5847053 of 08 Dec 1998 (filed 11 April 1997) to Dow Chem. Co.

P.-W.S. Chum, R.P. Markovich, G.W. Knight, S.-Y. Lai, Fabricated articles made from ethylene polymer blends, CA 2160705 of 22 Aug 2006 (filed 19 April 1994); Ethylene polymer film

made from ethylene polymer blends, U.S. Patent 5847053 of 08 Dec 1998 (filed 11 April 1997) to Dow Chem. Co.

Chuo Chemical Co., Japanese Patent Application 146,953, 1992

O.C. Compton, S.-B.T. Nguyen, Graphene oxide, highly reduced graphene oxide, and graphene: versatile building blocks for carbon-based materials. Small **6**(6), 711–723 (2010)

W.R. Coutant, European Patent Application 588,147, 23 Mar 1994; Canadian Patent 2,099,750, 02 Mar 1994; Japanese Patent 61 82,756, 05 July 1994, Appl. 01 Sep 1992, to Phillips Petroleum Co.

W.R. Coutant, J.L. Martin U.S. Patent 5,380,803, 10 Jan 1995

M.A. Cowan, European Patent Application 095,299, 30 Nov 1983, to Intercontinental Plast., Inc.

M.J. Cran, Characterization and optimization of polyethylene blends, Ph.D. thesis, School of Molecular Sciences, Victoria University, Australia, 2004

A.L.N. Da Silva, M.C.G. Rocha, F.M.B. Coutinho, R.E.S. Bretas, C. Scuracchio, Rheological, mechanical, thermal, and morphological properties of polypropylene/ethylene-octene copolymer blends. J. Appl. Polym. Sci. **75**, 692–704 (2000)

A.L.N. Da Silva, M.C.G. Rocha, F.M.B. Coutinho, R.E.S. Bretas, C. Scuracchio, Rheological and thermal properties of binary blends of polypropylene and poly(ethylene-co-1-octene). J. Appl. Polym. Sci. **79**, 1634–1639 (2001)

S. Datta, A.C. Gadkari, C. Cozewith, Alpha-olefin/propylene copolymers and their use, U.S. Patent 6982310 of 03 Jan 2006 (filed 06 May 2005; priority 03 July 2003, U.S. Patent 6635715) to ExxonMobil Chemical Patents, Inc.

S.C. Davis, U.S. Patents 5,372,980, 13 Dec 1994, Appl. 03 June 1993, to Polysar

G.T. Dee, D.J. Walsh, Equations of state for polymer liquids. Macromolecules **21**, 811–815 (1988); A modified cell model equation of state for polymer liquids, Macromolecules **21**, 815–817 (1988)

C. Dehennau, T. Depireux, I. Claeys, European Patent Application 587,216, 16 Mar 1994; Japanese Patent 62 07,046, 26 July 1994, Appl. 01 Sep 1992, to Solvay et Cie

I. Delaby, B. Ernst, Y. Germain, R. Muller, J. Rheol. **38**, 1705 (1994)

L. Delamare, B. Vergnes, Computation of the morphological changes of a polymer blend along a twin-screw extruder. Polym. Eng. Sci. **36**(12), 1685–1693 (1996)

C. Delfolie, L.C. Dickinson, K.F. Freed, J. Dudowicz, W.J. MacKnight, Molecular factors affecting the miscibility behavior of cycloolefin copolymers. Macromolecules **32**(23), 7781–7789 (1999)

O. Delgadillo-Velázquez, S.G. Hatzikiriakos, M. Sentmanat, Thermorheological properties of LLDPE/LDPE blends. Rheol. Acta **47**, 19–31 (2008a)

O. Delgadillo-Velázquez, S.G. Hatzikiriakos, M. Sentmanat, Thermorheological properties of LLDPE/LDPE blends: effects of production technology of LLDPE. J. Polym. Sci. B: Polym. Phys. **46**, 1669–1683 (2008b)

V. Dolle et al., Macromol. Chem. Phys. **212**, 959–970 (2011)

B. Dubrulle D'Orhcel, *Recycling PVC and Mixed Plastics* (ChemTec, Toronto, 1996)

J. Dudowicz, K.F. Freed, Effect of monomer structure and compressibility on the properties of multicomponent polymer blends and solutions: 1. Lattice cluster theory of compressible systems. Macromolecules **24**(18), 5076–5095 (1991)

J. Dudowicz, K.F. Freed, Pressure dependence of polymer fluids: application of the lattice cluster theory. Macromolecules **28**(19), 6625–6641 (1995)

J. Dudowicz, K.F. Freed, Influence of monomer structure and interaction asymmetries on the miscibility and interfacial properties of polyolefin blends. Macromolecules **29**(27), 8960–8972 (1996)

J. Dudowicz, K.F. Freed, Energetically driven asymmetries in random copolymer miscibilities and their pressure dependence. Macromolecules **30**(18), 5506–5519 (1997)

J. Dudowicz, K.F. Freed, Molecular influences on miscibility patterns in random copolymer/homopolymer binary blends. Macromolecules **30**(15), 5094–5104 (1998)

J. Dudowicz, K.F. Freed, Explanation for the inversion of an UCST phase diagram to a LCST diagram in binary polybutadiene blends. Macromolecules **33**(26), 9777–9781 (2000a)

J. Dudowicz, K.F. Freed, Lattice cluster theory for pedestrian. 2. Random copolymer systems. Macromolecules **33**(9), 3467–3477 (2000b)

J. Dudowicz, M.S. Freed, K.F. Freed, Effect of monomer structure and compressibility on the properties of multicomponent polymer blends and solutions: 2. Application to binary blends. Macromolecules **24**(18), 5096–5111 (1991)

J. Dudowicz, K.F. Freed, J.F. Douglas, Modification of the phase stability of polymer blends by diblock copolymer additives. Macromolecules **28**(7), 2276–2287 (1995)

J. Dudowicz, K.F. Freed, J.F. Douglas, Beyond Flory-Huggins theory: new classes of blend miscibility associated with monomer structural asymmetry. Phys. Rev. Lett. **88**(9), 955031–955034 (2002a)

J. Dudowicz, K.F. Freed, J.F. Douglas, New patterns of polymer blend miscibility associated with monomer shape and size asymmetry. J. Chem. Phys. **116**(22), 9983–9996 (2002b)

J.R.M. Duhaime, W.E. Baker, Plast. Rubber Compos. Process. Appl. **15**, 87 (1991)

M.M. Dumoulin, L.A. Utracki, Time-temperature superposition for polyethylene/polypropylene blends (Chap. 8), in *Rheology and Polymer Processing*, ed. by A.A. Collyer, L.A. Utracki (Elsevier, Barking, 1990)

M.M. Dumoulin, L.A. Utracki, P.J. Carreau, Polym. Eng. Sci. **27**, 1627 (1987)

M.M. Dumoulin, L.A. Utracki, P.J. Carreau, Rheol. Acta Suppl. **26**, 215 (1988)

M.M. Dumoulin, L.A. Utracki, P.J. Carreau, Melt rheology and morphology of linear low density polyethylene/polypropylene blends (Chap. 7), in *Two Phase Polymer Systems*, ed. by L.A. Utracki. Progress in Polymer Processing Series (Hanser, Munich, 1991), pp. 185–212

P.H.M. Elemans, Ph.D. thesis, Technische Universiteit Eindhoven, 1989

C.T. Elston, Process for preparation of homogenous random partly crystalline copolymers of ethylene with other α-olefins, U.S. Patent 3645992 of 29 Feb 1972; CA Patent 703704 of 09 Feb 1965 to Du Pont of Canada Ltd.

L. Erwin, in *Mixing in Polymer Processing*, ed. by C. Rauwendaal (Marcel Dekker, New York, 1991)

F.A. Escobedo, J.J. de Pablo, On the scaling of the upper critical solution temperature of binary polymer blends with chain length. Macromolecules **32**, 900 (1999)

S.A. Fabrique Nationale Herstal, Netherland Patent Application 007,963, 18 Sep 1977, Appl. 18 Sep 1975

Z.J. Fan, M.C. Williams, P. Choi, A molecular study of the effects of branching characteristics of LDPE on its miscibility with HDPE. Polymer **43**, 1497–1502 (2002)

Y. Fang, P.J. Carreau, P.G. Lafleur, Thermal and rheological properties of m-LLDPE/LDPE Blends. Polym. Eng. Sci. **45**, 1254–1264 (2005)

R. Fayt, R. Jérôme, P. Teyssié, Makromol. Chem. **187**, 837 (1986)

R. Feigenbaum, Recycl. Today **35**(12), 70 (1997)

G.J. Field, P. Micic, S.N. Bhattacharya, Melt strength and film bubble instability of LLDPE/LDPE blends. Polym. Int. **48**, 461–466 (1999)

P.J. Flory, J. Chem. Phys. **9**, 660 (1941); Discuss. Faraday Soc. **49**, 7 (1970)

S. Floyd, T. Heiskanen, T.W. Taylor, G.E. Mann, W.H. Ray, J. Appl. Polym. Sci. **33**, 1021 (1987)

S. Floyd, T. Heiskanen, T.W. Taylor, G.E. Mann, W.H. Ray, J. Appl. Polym. Sci. **41**, 1933 (1990)

K.W. Foreman, K.F. Freed, Influence of stiffness, monomer structure, and energetic asymmetries on polymer blend miscibilities: applications to polyolefins. Macromolecules **30**(23), 7279–7295 (1997)

Fraser et al. 1997

C. Frederix, J.M. Lefebvre, C. Rochas, R. Séguéla, G. Stoclet, Binary blends of linear ethylene copolymers over a wide crystallinity range: rheology, crystallization, melting and structure properties. Polymer **51**, 2903–2917 (2010)

G.H. Fredrickson, A.J. Liu, Design of miscible polyolefin copolymer blends. J. Polym. Sci. B: Polym. Phys. **33**, 1203–1212 (1995)

G.H. Fredrickson, A.J. Liu, F.S. Bates, Entropic corrections to the Flory-Huggins theory of polymer blends: architectural and conformational effects. Macromolecules **27**, 2503–2511 (1994)

K.F. Freed, M.G. Bawendi, Lattice theories of polymeric fluids. J. Phys. Chem. **93**, 2194–2203 (1989)

K.F. Freed, J. Dudowicz, A lattice-model molecular theory for the properties of polymer blends. Trends Polym. Sci. **3**(8), 248–255 (1995)

K.F. Freed, J. Dudowicz, Influence of short chain branching on the miscibility of binary polymer blends: application to polyolefin mixtures. Macromolecules **29**(2), 625–636 (1996)

K.F. Freed, J. Dudowicz, Lattice cluster theory for pedestrians: the incompressible limit and the miscibility of polyolefin blends. Macromolecules **31**(19), 6681–6690 (1998)

K.F. Freed, J. Dudowicz, Influence of monomer molecular structure on the miscibility of polymer blends. Adv. Polym. Sci. **183**, 63–126 (2005)

K.F. Freed, J. Dudowicz, K.W. Foreman, Molecular mechanisms for disparate miscibilities of poly (propylene) and head-to-head poly(propylene) with other polyolefins. J. Chem. Phys. **108**(18), 7881–7886 (1998)

E.M. Friedman, R.S. Porter, Polymer viscosity-molecular weight distribution correlation via blending: for high molecular weight poly(dimethyl siloxanes) and for polystyrene. Trans. Soc. Rheol. **19**, 493 (1975)

Fukui et al. 1983

R. Gätcher, H. Müller, *Kunststoff-Additive*. Plastics Additives Handbook, vol. 3 (Hanser, Munich, 1989)

P.M. German, J.M. Farley, R.W. Halle, G. Panagopoulous, Polyethylene blends, European Patent Office (EPO) Patent EP1373404, 02 April 2004, Appl. 22 June 2001, to ExxonMobil Chem. Pats.

K.J. Godbey, P.G. Martin, U.S. Patent 5,264,219, 23 Nov 1993, Appl. 07 Aug 1992, to Minnesota Mining and Mfg. Co.

K.J. Godbey, P.G. Martin, PCT Int. Appl., WO 94 03,539, 17 Feb 1994

L.A. Goettler, Polym. Compos. **5**, 60 (1984)

R.C. Golike, Belgian Patent 619,351, 27 Dec 1962

A. Golovoy, M.F. Cheung, K.R. Carduner, M.J. Rokosz, Polym. Eng. Sci. **29**, 1226 (1989)

V. Gorianov, H.A. Butlerov, Ann. Rev. Mar. Sci. **169**, 146 (1873)

M. Gownder, Branching of LLDPE as studied by crystallization-fractionation and its effect on mechanical properties of films. J. Plast. Film Sheet. **17**, 53–61 (2001)

W.W. Graessley, R. Krishnamoorti, N.P. Balsara, R.J. Butera, L.J. Fetters, D.J. Lohse, D.N. Schulz, J.A. Sissano, Thermodynamics of mixing for blends of model ethylene-butene copolymers. Macromolecules **27**(14), 3896–3901 (1994)

W.W. Graessley, R. Krishnamoorti, G.C. Reichart, N.P. Balsara, L.J. Fetters, D.J. Lohse, Regular and irregular mixing in blends of saturated hydrocarbon polymers. Macromolecules **28**(4), 1260–1270 (1995)

J. Grande, Mod. Plast. Int. (7), 26 (1996)

N. Grassie, ed., *Developments in Polymer Degradation*. Applied Science (London, 1982, 1998)

G.J.L. Griffin, U.S. Patents 4,016,117, 1977

G.J.L. Griffin, *Polyethylenes 1933–1983* (Plastics & Rubber Institute, 1983)

E. Grünschloss, *Polymer Processing Society European Meeting*, Stuttgart, 26–28 Sept 1995

F. Gugumus, *Kunststoff-Additive*. Plastics Additives Handbook, vol. 3 (Hanser, Munich, 1989)

J.E. Guillet, in *Polymer Science and Technology*, ed. by J.E. Guillet, vol. 3 (1973), pp. 1–26

G.G. Gusavage, T.A. Hessen, T.R. Hardy, H.G. Schirmer, S.R. Flye, U.S. Patents 5,118,561, June 1992, Appl. 01 Oct 1990; U.S. Patents 5,330,596, 19 July 1994, Appl. 13 May 1992

W. Gutowski, *Controlled Interfaces in Composite Materials* (Elsevier, New York, 1990)

A. Guttag, U.S. Patents 5,120,089, 1992, Appl. 28 Feb 1990; U.S. Patents 5,346,929, 13 Sep 1994, Appl. 18 Mar 1992

H.H. Lank, E.L. Williams, *The Du Pont Canada History* (Du Pont Canada, Incorporated, 1982)

A. Haas, French Patent Application 2,526,803, 18 Nov 1983, Appl. 14 May 1982, to Societé Chimique des Charbonnages, S. A.

A. Haas, F. Raviola, European Patent Application 042,743, 13 Jan 1982, to Societé Chimique des Charbonnages S. A.

R.W. Halle, *Downgauge Paper Overwrap Films Using m-LLDPE Blends, TAPPI Corrugated Container Division's Conference*, Chicago, 2–5 Nov 1999. http://www.tappi.org/content/events/10PLACE/papers/halle.pdf

T. Hameed, I.A. Hussein, Effect of short chain branching of LDPE on its miscibility with linear HDPE. Macromol. Mater. Eng. **289**(2), 198–203 (2004)

T. Hameed, I.A. Hussein, Melt miscibility and solid-state properties of metallocene LLDPE blends with HDPE: influence of MM of LLDPE, J. Cent. South Univ. Technol. s1−0183−05 (2007)

S.H. Hamid, M. Atiqullah, J. M. S.: Rev. Macromol. Chem. Phys. **C35**, 495 (1995)

S.H. Hamid, M.B. Amin, A.G. Maadhah (eds.), *Handbook of Polymer Degradation* (Marcel Dekker, New York, 1992)

A.E. Hamielec, J.B.P. Soares, Polymerization reaction engineering – metallocene catalysts. Prog. Polym. Sci. **21**, 651–706 (1996)

G.H. Hartley, J.E. Guillet, Macromolecules **1**, 165 (1968)

L.G. Hazlitt, D.G. Moldovan, High temperature continuous viscometry coupled with analytic temperature rising elution fractionation for evaluating crystalline and semi-crystalline polymers, U.S. Patent 4,798,081 of 22 Dec 1989, filed 17 Jan 1989, to Dow Chem. Co.

C. Heinz, H. Pasch, Polymer **46**, 12040 (2005)

E. Helfand, A.M. Sapse, J. Chem. Phys. **62**, 1327 (1975)

E. Helfand, Y. Tagami, J. Polym. Sci. Polym. Lett. **9**, 741 (1971)

E. Helfand, Z.R. Wasserman, Macromolecules **9**, 879 (1976)

H. Herbst, K. Hoffmann, R. Pfaendner, F. Sitek, *Quality Improvement of Recycled Plastics Through Additive (Stabilizers)*. National Seminar on Emerging Trends in Plastic Recycling Technologies and Waste Management, Goa, 27–28 May 1995.

H. Herbst, K. Hoffmann, R. Pfaendner, H. Zweifel, *Upgrading of Recyclates – The Solution for High Value Applications: Restabilization and Repair*. NATO-ASI Frontiers in the Science and Technology of Polymer Recycling, Antalya, 16–27 June 1997. NATO ASI Series, E351 73–103 (Kluwer, Lampertheim, 1997, 1998)

M. Hert, French Patent 2,528,054, 09 Dec 1983, Appl. 03 June 1982, to Societé Chimique des Charbonnages, S. A.

M.J. Hill, Liquid-liquid phase separation in binary blends of a branched polyethylene with linear polyethylenes of differing molecular weight. Polymer **35**(9), 1991–1993 (1994)

E. Hinderman, Dissertation, Zürich, 1897

K. Ho, L. Kale, S. Montgomery, Melt strength of linear low-density polyethylene/low-density polyethylene blends. J. Appl. Polym. Sci. **85**, 1408–1418 (2002)

G.H. Hofmann, U.S. Patents 5,352,735, 04 Oct 1994, Appl. 19 Aug 1993, Appl. 23 July 1991, to E. I. du Pont de Nemours & Company

F. Hofmann, M. Otto, U.S. Patents 1,811,130, 23 June 1931, to I. G. Farbenindustrie Aktiengesellschaft

J.P. Hogan, R.L. Banks, Belgian Patent 530,617, Jan 24 1955; U.S. Patent Application 333,576, 27 Jan 1953, to Phillips Petroleum Company

J.P. Hogan, R.L. Banks, in *History of Polyolefins*, ed. by R.B. Seymour, T. Cheng (D. Reidel, Dordrecht, 1985)

G. Holden, L.H. Gouw, European Patent Application 004,685, 17 Oct 1979, Appl. 30 Mar 1978, to Shell International Research Maatschappij B. V.

P.A. Holmes, A.B.. Newton, F.M. Willmouth, European Patent Application 052,460, 26 May 1982, Appl. 18 Nov 1980, to Imperial Chemical Industries

S. Hosoda, Structural distribution of linear low-density polyethylene. Polym. J. **20**(5), 383–397 (1988)

D.J. Hourston, *Degradation of Plastics and Polymers*, ed. by J.A. Brysdon, This article is a revision of the 3rd edition, vol. 2 (Elsevier, 2010), pp. 18:53–18:77

H.-W. Hsu, S.-C. Liuo, S.-F. Jiang, J.-H. Chen, H.-M. Lin, H.-D. Hwu, M.-L. Chen, M.-S. Lee, T. Hu, U.S. Patents 5,308,897, 14 Jan 1994, Appl. 03 May 1993, to Industrial Technology Research Institute, Taiwan

J.C.-K. Huang, P.A. Sipos, L.T. Kale, P.R. Thomas, J.A. Auger, Shrink films, U.S. Patent 6340532 of 22 Jan 2002 (filed 31 Jan 2001) to Nova Chem. Intl.

B. Huckestein, *Plastics Recycling – Today and the Future*. Proceedings Polymer Processing Society European Meeting, Stuttgart, 26–28 Sep 1995

M.L. Huggins, J. Chem. Phys. **9**, 440 (1941)

P.M. Hughes, European Patent Application 045,455, 10 Feb 1982, Appl. 1980, to Shell Oil Company

M.A. Huneault, Z.-H. Shi, L.A. Utracki, Development of polymer blend morphology during compounding in a twin screw extruder. Part IV: a new computational model with coalescence. Polym. Eng. Sci. **35**(1), 115–127 (1995)

I.A. Hussein, Influence of composition distribution and branch content on the miscibility of m-LLDPE and HDPE blends: rheological investigation. Macromolecules **36**, 2024–2031 (2003)

I.A. Hussein, M.C. Williams, Rheological study of heterogeneities in melt blends of ZN-LLDPE and LDPE: influence of M_w and comonomer type, and implications for miscibility. Rheol. Acta **43**, 602–614 (2004a)

I.A. Hussein, M.C. Williams, Rheological study of the influence of branch content on the miscibility of octene m-LLDPE and ZN-LLDPE in LDPE. Polym. Eng. Sci. **44**, 660–672 (2004b)

I.A. Hussein, T. Hameed, B.F. Abu Sharkh, K. Mezghani, Miscibility of hexene-LLDPE and LDPE blends: influence of branch content and composition distribution. Polymer **44**, 4665–4672 (2003)

V.N. Ipatiev, O. Rutala, Polymerisation des Äthylens bei hoher Temperatur und Druck in Gegenwart von Katalysatoren. Ber. Dtsch. Chem. Ges. **46**, 1748–1755 (1913)

A.I. Isayev, ed., *Encyclopedia of Polymer Blends*, 5 vols. (Wiley-VCH, Weinheim, 2010–2014). ISBN-10:3-527-31928-X; ISBN-13:978-3-527-31928-2 (2010–2014)

S.D. Ittel, L.K. Johnson, M. Brookhart, Late-metal catalysts for ethylene homo- and copolymerization. Chem. Rev. **100**, 1169–1203 (2000); K.P. Bryliakov, Post-metallocene catalysis for olefin polymerization, Russian Chem. Rev. **76**(3), 253–277 (2007)

S.S. Ivanchev, A.V. Yakimansky, N.I. Ivancheva, I.I. Oleinik, G.A. Tolstikov, Ethylene polymerization using catalysts based on binuclear phenoxyimine titanium halide complexes. Europ. Polym. J. **48**, 191–199 (2012)

H. Jager, E.J. Vorenkamp, G. Challa, LCST behaviour in blends of PMMA with PVC. Polym. Commun. **24**(10), 290–292 (1983)

M.O. Jejelowo, U.S. Patents 5,359,015, 25 Oct 1994, Appl. 01 Feb 1994, 07 Nov 1991, to Exxon Chemical Patents, Incorporated

W. Kaminsky, Discovery of methylaluminoxane as cocatalyst for olefin polymerization. Macromolecules **45**, 3289–3297 (2012)

W. Kaminsky, A. Funck, K. Wiemann, Nanocomposites by in situ polymerization of olefins with metallocene catalysts. Macromol. Symp. **239**, 1–6 (2006)

E.C. Kelusky, C.T. Elston, R.E. Murray, Characterizing polyethylene-based blends with temperature rising elution fractionation (TREF) techniques. Polym. Eng. Sci. **27**(20), 1562–1571 (1987)

C. Kennedy, *ICI, the company that changed our lives* (Hutchinson Limited, London, 1986)

K. Khait, SPE Techn. Pap. **40**, 1752 (1994); **41**, 2066 (1995)

K. Khait, *Recycling of Post-consumer Plastic Waste via New Solid-State Shear Extrusion Pulverization Process*. Proceedings Polymer Processing Society and American Institute of Chemical Engineers Joint Meeting, Chicago, 11–14 Nov 1996

G.B. Kharas, S.P. Nemphos, European Patent Application 515,203, 25 Nov 1992, Appl. 24 May 1991, to Novacor Chemicals

B.K. Kim, M.S. Kim, H.M. Jeong, K.J. Kim, J.K. Jang, Angew. Makromol. Chem. **194**, 91 (1992)

M. Knights, Plast. Technol. **42**(8), 34 (1996)

M. Knights, Plast. Technol. **43**(12), 24 (1997)

D.C. Knobeloch, L. Wild, SPE Polyolefins IV Conf. Prepr. 427 (1984)

R. Koningsveld, The influence of polymolecularity on thermodynamic properties of macromolecular systems. Polym. Eng. Sci. **25**(17), 1118–1119 (1985)

R. Koningsveld, L.A. Kleintjens, Liquid-liquid phase equilibria, in *Polymer Blends*, NATO ASI Series, Series E: Applied Sciences, vol. 89 (1985), pp. 89–115

R. Koningsveld, L.A. Kleintjens, A.M. Leblans-Vinck, Mean-field lattice equations of state. 1. Possible molecular basis for empirical parameters. J. Phys. Chem. **91**, 6423–6428 (1987)

L. Koskan, Ind. Bioprocess. (5), 1 (1992)

T. Kotani, T. Taka, Y. Saito, High density polyethylene type transparent film and process for production thereof, U.S. Patent 4,954,391 of 04 Sept 1990, priority 1986, to Showa Denim Kabushiki Kaisha

S. Kozo, I. Sumio, U.S. Patents 4,132,633, 02 Jan 1979, Appl. 14 Mar 1975, to Mitsui Mining & Smelting Co.

R. Krishnamoorti, W.W. Graessley, N.P. Balsara, D.J. Lohse, Structural origin of thermodynamic interactions in blends of saturated hydrocarbon polymers. Macromolecules **27**(11), 3073–3081 (1994a)

R. Krishnamoorti, W.W. Graessley, N.P. Balsara, D.J. Lohse, The compositional dependence of thermodynamic interactions in blends of model polyolefins. J. Chem. Phys. **100**(5), 3894–3904 (1994b)

R. Krishnamoorti, W.W. Graessley, L.J. Fetters, R.T. Garner, D.J. Lohse, Anomalous mixing behavior of polyisobutylene with other polyolefins. Macromolecules **28**(4), 1252–1259 (1995)

R. Krishnamoorti, W.W. Graessley, G.T. Dee, D.J. Walsh, L.J. Fetters, D.J. Lohse, Pure component properties and mixing behavior in polyolefin blends. Macromolecules **29**(1), 367–376 (1996)

E.E. La Fleur, R.M. Amici, W.J. Work, U.S. Patents 5,189,097; 5,322,892, 21 June 1994, Appl. 25 Nov 1992, Appl. 07 Dec 1990, Appl. 22 Oct 1991, to Rohm & Haas Company

F.P. La Mantia, Degradation of polymer blends, in *Handbook of Polymer Degradation*, ed. by S.H. Hamid, M.B. Amin, A.G. Maadhah (Marcel Dekker, New York, 1992)

F.P. La Mantia, *Reprocessing of Poly(vinyl chloride), Polycarbonate and Polyethyleneterephthalate*. NATO-ASI Frontiers in the Science and Technology of Polymer Recycling, Antalya, 16–27 June 1997. NATO ASI Series, E351 249–270 (Kluwer, Lampertheim, 1997, 1998)

F.P. La Mantia, M. Marrone, B. Dubrulle D'Orhcel, Polym. Recycl. **2**, 3 (1996)

C.H. Lai, J.M. Brady, European Patent Application 582,383, 09 Feb 1994; Canadian Patent 2,099,924, 17 Jan 1994, Appl. 16 July 1992, to Rohm & Haas Company

S.-Y. Lai, M.S. Edmondson, Polyolefin blends and their solid state processing, U.S. Patents 5,408,004, 18 April 1995, Appl. 17 Aug 1993, to Dow Chem. Co.

S.-Y. Lai, S. Land, J.R. Wilson, G.W. Knight, J.C. Stevens, P.-W. Chum, U.S. Patents 5,272,236, 21 Dec 1993, Appl. 15 Oct 1991, to Dow Chemical Company

S.-Y. Lai, S. Land, J.R. Wilson, G.W. Knight, and J.C. Stevens, U.S. Patents 5,278,272, 11 Jan 1994, Appl. 02 Sep 1992, to Dow Chemical Company

X.-Y. Lai, D.-F. Zhao, F. Lai, U.S. Patents 5,344,895, 06 Sep 1994, Appl. 01 Apr 1993, to University of Massachusetts Lowell

O.E. Larsen, Canadian Patent 1,120,630, 23 Mar 1982, Appl. 12 Oct 1977, to Phillips Petroleum Co.

H.M. Laun, H. Schuch, J. Rheol. **33**, 119 (1989)

J.J. Laverty, R.L. Bullach, T.S. Ellis, T.E. Mcminn, Polym. Recycl. **2**(3), 159 (1996)

R.D. Leaversuch, Mod. Plast. **63**(4), 108 (1986)

R.D. Leaversuch, Mod. Plast. **68**(10), 46 (1991)

R.D. Leaversuch, Mod. Plast. Intl. **22**(7), 34 (1992); **23**(10), 37, 56 (1993)

S.-T. Lee, Polyethylene blend compositions and methods for making same, U.S. Patents 5,428,093, 27 June 1995, Appl. 05 Nov 1993, to Sealed Air Corporation

H.S. Lee, M.M. Denn, Blends of linear and branched polyethylenes. Polym. Eng. Sci. **40**(5), 1132–1142 (2000)

L. Leibler, Macromolecules **13**, 1602 (1980); Makromol. Chem., Macromol, Symp. **16**, 1 (1988)

J. Leidner, *PLASTIC WASTE, Recovery of Economic Value* (Marcel Dekker, New York, 1981)

J. Leidner, *NATO-ASI Frontiers in the Science and Technology of Polymer Recycling*, Antalya, 16–27 June 1997

R.W. Lenz, Adv. Polym. Sci. **107**, 1 (1993)

M. Lieberman, U.S. Patents 5,424,013, 13 June 1995, Appl. 09 Aug 1993

M. Lifschitz, J. Dudowicz, K.F. Freed, Limits of validity for mean field description of compressible binary polymer blends. J. Chem. Phys. **100**(5), 3957–3978 (1994)

J.T. Lindt, A.K. Ghosh, Fluid mechanics of the formation of polymer blends. 1. Formation of lamellar structures. Polym. Eng. Sci. **32**, 1802 (1992)

C. Liu, J. Wang, J. He, Rheological and thermal properties of m-LLDPE blends with m-HDPE and LDPE. Polymer **43**(13), 3811–3818 (2002)

A. Luciani, L.A. Utracki, The extensional flow mixer, EFM. Int. Polym. Process. **11**, 299–309 (1996)

A. Luciani, M.F. Champagne, L.A. Utracki, Interfacial tension determination by retraction of ellipsoidal drops. J. Polym. Sci. B. Polym. Phys. Ed. **35**(9), 1393–1403 (1997)

C.-T. Lue, T.H. Kwalk, Low haze high strength polyethylene compositions, U.S. Patent 6870010 B1, of 22 Mar 2005, filed 01 Dec 2003, to Univation Technologies, LLC

J. Lyngaae-Jørgensen, L.A. Utracki, Dual phase continuity in polymer blends. Makromol. Chem. Macromol. Symp. **48/49**, 189–209 (1991)

J. Lyngaae-Jørgensen, K. Søndergaard, L.A. Utracki, A. Valenza, Formation of ellipsoidal drops in simple shear flow: transient behavior. Poly. Netw. Blends **3**(4), 167–181 (1993)

A. Maani, M.-C. Heuzey, P.J. Carreau, Coalescence in thermoplastic olefin (TPO) blends under shear flow. Rheol. Acta **50**, 881–895 (2011)

T. Macko, H. Pasch, Macromolecules **42**, 6063 (2009)

V.J. Maddever, in *Handbook of Polymer Degradation*, ed. by S.H. Hamid, M.B. Amin, A.G. Maadhah (Marcel Dekker, New York, 1992)

S.L. Madorsky, *Thermal Degradation of Organic Polymers* (Wiley, New York, 1964)

H. Mahdavi, M.E. Nook, Characterization and microstructure study of low-density polyethylene by Fourier transform infrared spectroscopy and temperature rising elution fractionation. J. Appl. Polym. Sci. **109**, 3492–3501 (2008)

H. Makio, T. Fujita, Development and application of FI catalysts for olefin polymerization: unique catalysis and distinctive polymer formation. Acc. Chem. Res. **42**(10), 1532–1544 (2009)

H. Makio, H. Terao, A. Iwashita, T. Fujita, FI catalysts for olefin polymerization – a comprehensive treatment. Chem. Rev. **111**, 2363–2449 (2011)

L. Manolis-Sherman, Plast. Technol. 27 (1996); Plast. Rubber Wkly. 12 (1996)

J.K. Maranas, M. Mondello, G.S. Grest, S.K. Kumar, P.G. Debenedetti, W.W. Graessley, Liquid structure, thermodynamics, and mixing behavior of saturated hydrocarbon polymers. 1. Cohesive energy density and internal pressure. Macromolecules **31**(20), 6991–6997 (1998)

J.L. Martin, M.B. Welch, W.R. Coutant, M.P. McDaniel, U.S. Patent 5,306,775, 26 Apr 1994, Appl. 16 Apr 1993; 5,319,029, 07 June 1994, Appl. 16 Apr 1993

S.K. Mathur, in *Recycling and Plastics Waste Management*, ed. by J.S. Anand (CIPET, Chennai, 1997)

K. Matoishi, K. Nakai, N. Nagai, H. Terao, T. Fujita, Value-added olefin-based materials originating from FI catalysis: production of vinyl- and Al-terminated PEs, end-functionalized PEs, and PE/polyethylene glycol hybrid materials. Catal. Today **164**, 2–8 (2011). doi:10.1016/j.cattod.2010.11.078

S. Matsui, T. Fujita, FI catalysts: super active new ethylene polymerization catalysts. Catal. Today **66**(1), 63–73 (2001)

H. Mavridis, Films of polyethylene blends, U.S. Patent 201110160403 A1, 30 June 2011, to Equistar Chemicals LP

P. Meier, German Patent 4,139,468, 03 June 1993, Appl. 29 Nov 1991, to EMS-Inventa Aktiengesellschaft

G. Menges, IUPAC Pure Appl. Chem. **68**, 1809 (1996)

F. Mighri, M.A. Huneault, Visualization of dispersion of model fluids in a transparent Couette flow cell. J. Rheol. **45**(3), 783–797 (2001)

F. Mighri, M.A. Huneault, Drop deformation and breakup mechanisms in viscoelastic model fluid systems and polymer blends. Canad. J. Chem. Eng. **80**, 1028–1035 (2002)

F.M. Mirabella, E.A. Ford, Characterization of linear low-density polyethylene: cross-fractionation according to copolymer composition and molecular weight. J. Polym. Sci. B: Polym. Phys. **25**(4), 777–790 (1987)

H.W. Moeller (ed.), *Progress in Polymer Degradation and Stability Research* (Nova Science, New York, 2008)

B. Monrabal, Crystallization analysis fractionization, U.S. Patent 5222390 of 29 June 1993, filed 20 Sep 1991 to Dow Chem. Co.

B. Monrabal, Crystallization analysis fractionation: a new technique for the analysis of branching distribution in polyolefins. J. Appl. Polym. Sci. **52**(4), 491–499 (1994)

B. Monrabal, Temperature rising elution fractionation and crystallization analysis fractionation, in *Encyclopedia of Analytical Chemistry*, ed. by B. Monrabal, R.A. Meyers (Wiley, New York, 2000)

B. Monrabal, Method for separating and purifying crystallisable organic compounds, U.S. Patent 8071714 of 06 Dec 2011, priority 15 Mar 2006, to Polymer Characterization, S.A.

B. Monrabal, P. del Hierro, Characterization of polypropylene-polyethylene blends by temperature rising elution and crystallization analysis fractionation. Anal. Bioanal. Chem. **399**, 1557–1561 (2011)

B. Monrabal, J. Sancho-Tello, N. Maya, L. Romero, Crystallization elution fractionation. A new separation process for polyolefin resins, in *Encyclopedia of analytical chemistry*, ed. by R.A. Meyers (Wiley, New York, 2000), pp. 71–79

B. Monrabal, J. Sancho-Tello, N. Mayo, L. Romero, Crystallization elution fractionation. A new separation process for polyolefin resins. Macromol. Symp. **257**, 71–79 (2007)

S.J. Monte, Polyblends – '97. NRCC/IMI Bi-annual Symposium and SPE-RETEC on Polymer Blends, Alloys and Filled Systems, Boucherville, 9–10 Oct 1997

Montell Impact Copolymer Polypropylene Commercial Information, https://polymers. lyondellbasell.com/portal/site/basell/menuitem.81bd1022b7c8ec5bbaabbd10e5548a0c/?VCM ChannelID=71f6746516cf4110VgnVCM100000646f3c14____&productQueryText=&filter Type=resin&resin=7&market=&region= (2012)

D.R. Morrow, T.J. Nosker, K.E. VanNess, R.W. Renfree, U.S. Patents 5,298,214, 29 Mar 1994, Appl. 30 Oct 1990, to Rutgers State University

H. Moss, J.G. Modigh, U.S. Patent 5,320,887, 14 June 1994, Appl. 04 Mar 1993, GB Appl. 27 Feb 1992, to Euro-matic Ltd.

P. Moulinié, L.A. Utracki, Equations of state and free volume content (Chap. 6), in *Polymer Physics*, ed. by L.A. Utracki, A.M. Jamieson (Wiley, New York, 2010)

M. Müller, K. Binder, Computer simulation of asymmetric polymer mixtures. Macromolecules **28**, 1825–1834 (1995)

A.J. Müller, V. Balsamo, C.M. Rosales, On the miscibility and mechanical compatibility of low density and linear low density polyethylene blends. Polym. Netw. Blends **2**(4), 215–223 (1992)

W.G. Munk, Ger. Offen. 4,204,083 A1, 04 Mar 1993, Appl. 09 Aug 1991, to Nordmann Rassmann GmbH & Company

L.C. Muschiatti, B.A. Smillie, U.S. Patents 5,391,582, 21 Feb 1995, Appl. 19 Mar 1994, to du Pont

V.M. Nadkarni, J.P. Jog, Crystallization behavior of polymer blends, in *Two-Phase Polymer Systems*, ed. by L.A. Utracki (Hanser, Munich, 1991)

M. Naitove, PP/acetal blends are recyclable. Plast. Technol. **42**(4), 53 (1996)

S. Nakano, Y. Goto, J. Appl. Polym. Sci. **26**, 4217 (1981)

W.M. Nelson, Belgian Patent 647,311, 29 Oct 1964, filed 1963, to Phillips Petroleum Co.

X.Q. Nguyen, L.A. Utracki, Extensional flow mixer, U.S. Patent 5,451,106, 19 Sept 1995, Appl. 08 Aug 1984, Canadian Patent Application, 1994; to National Research Council Canada

E. Nies, A. Stroeks, R. Simha, R.K. Jain, Colloid Polym. Sci. **268**, 731 (1990)

T. Nishio, T. Sanada, K. Higashi, Sen-i Gakkaishi **48**, 446 (1992)

J. Noolandi, Polym. Eng. Sci. **24**, 70 (1984)

T.E. Nowlin, Low pressure manufacture of polyethylene. Prog. Polym. Sci. **11**, 29–55 (1985)

S. Ohnishi, T. Fukuda, European Patent Application 548,565, 30 June 1993, Appl. 12 Dec 1991, to Mitsubishi Yuka Industrial Products Corp.

A. Okada, U.S. Patents 5,352,727, 04 Oct 1994, Appl. 09 Sep 1993, Jap. Appl. 10 Sep 1992, to Idemitsu Kosan

A. Okada, A. Masuyama, U.S. Patents 5,326,813, 05 July 1994, Appl. 10 Dec 1992, Jap. Appl. 10 Dec 1991, to Idemitsu Kosan Compan

A. Okada, A. Fukushima, M. Kawasumi, S. Inagaki, A. Usuki, S. Sugiyama, T. Kurauchi, O. Kamigaito, U.S. Patent 4739007 (1988, priority 1985), Toyota Chuo Kenkyuusho

O. Olabisi, L.M. Robeson, M.Y. Shaw, *Polymer-Polymer Miscibility* (Academic, New York, 1979)

A. Ortin et al., Macromol. Symp. **257**, 13 (2007)

A. Ortín, B. Monrabal, P. del Hierro, Polymer Char Application Notebook of 01 Sept 2010

F.H. Otey, U.S. Patents 4,133,784, 1979

F.H. Otey, in *Starch: Chemistry and Technology*, ed. by R.L. Whistler, J.N. BeMillr, E.F. Paschall, 2nd edn. (Academic, New York, 1984)

J.M. Ottino, *The Kinematics of Mixing: Stretching, Chaos and Transport* (Cambridge University Press, Cambridge, 1989)

E.D. Owen (ed.), *Degradation and Stabilization of PVC* (Elsevier, New York, 1984)

J.F. Palierne, Linear rheology of viscoelastic emulsions with interfacial tension. Rheol. Acta **29**, 204–214 (1990); Erratum, Rheol. Acta **30**, 497 (1991)

J. Pan, W.J.D. Shaw, Microstruct. Sci. **20**, 351 (1993); **21**, 95 (1994)

Pardos Marketting. http://www.pardos-marketing.com/paper_g04.htm

J. Park, M. Hong, H. Kim, A new equation of state based on Hole theory: mixtures. Fluid Phase Equilib. **161**, 265–270 (1999)

Parkes Alexander of Birmingham, Artist in the County of Warwick, British Patent 1,147, 25 Mar 1846; 1,313, 07 Nov 1865

H. Pasch, R. Brüll, U. Wahner, B. Monrabal, Analysis of complex polymers by MALDI-TOF mass spectrometry. Macromol. Mater. Eng. **279**, 46–51 (2000)

H. Pasch et al., Macromol. Symp. **282**, 71–80 (2009)

G.A.R. Patfoort, Belgian Patent 833,543, 18 Mar 1976

J.-R. Pauquet, F. Sitek, R. Todesco, Process for stabilizing recycled mixed plastics, U.S. Patents 5,298,540, 29 Mar 1994, Appl. 25 Mar 1992, priority 27 Mar 1991, to Ciba-Geigy Corp.

J. Peón, C. Domínguez, J.F. Vega, M. Aroca, J. Martínez-Salazar, Viscoelastic behaviour of metallocene-catalysed polyethylene and low density polyethylene blends: use of the double reptation and Palierne viscoelastic models. J. Mater. Sci. **38**, 4757–4764 (2003)

R. Pérez, E. Rojo, M. Fernández, V. Leal, P. Lafuente, A. Santamaría, Basic and applied rheology of m-LLDPE/LDPE blends: miscibility and processing features. Polymer **46**, 8045–8053 (2005)

R.J. Petcavich, U.S. Patents 5,367,003, 22 Nov 1994, Appl. 18 June 1992, 23 Apr 1991

M. Petro, S.H. Nguyen, E.D. Carlson, Methods for characterization of polymers using multi-dimensional liquid chromatography with parallel second-dimension, U.S. Patent 6,855,258 of 15 Feb 2005, filed 28 Aug 2002, to Symyx Technologies

Plast. Rubber Wkly. (9), 9 (1996)

A. Poitou, Ph.D. thesis, École des Mines de Paris, 1988

R.S. Porter, L.-H. Wang, Polymer **33**, 2019 (1992)

J. Preiss, U.S. Patents 5,566,889, 22 Oct 1996, Appl. 20 May 1993, to Montell Inc.

M. Rabeony, D.J. Lohse, R.T. Garner, S.J. Han, W.W. Graessley, K.B. Migler, Effect of pressure on polymer blend miscibility: a temperature-pressure superposition. Macromolecules **31**(19), 6511–6514 (1998)

H.-J. Radusch, J. Ding, NATO-ASI Frontiers in the Science and Technology of Polymer Recycling, Antalya, 16–27 June 1997

R. Ramachandran et al., Polymer **52**, 2661–2666 (2011)

B.A. Ramsay, I. Saracova, J.A. Ramsay, R.H. Marchessault, Appl. Environ. Microbiol. **57**, 625 (1991)

D. Rana, H.L. Kim, K. Hanjin, J. Rhee, K. Cho, T. Woo, B.H. Lee, S. Choe, Blends of ethylene 1-octene copolymer synthesized by Ziegler–Natta and metallocene catalysts. II. Rheology and morphological behaviors. J. Appl. Polym. Sci. **76**, 1950–1964 (2000)

O.P. Ratra, in *Recycling and Plastics Waste Management*, ed. by J.S. Anand. CIPET National Seminar, 24–26 Sept 1997

C. Rauwendaal, *Polymer Extrusion* (Hanser, Munich, 1986)

G.C. Reichart, W.W. Graessley, R.A. Register, R. Krishnamoorti, D.J. Lohse, Measurement of thermodynamic interactions in ternary polymer blends by small-angle neutron scattering. Macromolecules **30**(11), 3363–3368 (1997)

G.C. Reichart, W.W. Graessley, R.A. Register, D.J. Lohse, Thermodynamics of mixing for statistical copolymers of ethylene and α-olefins. Macromolecules **31**(22), 7886–7894 (1998)

J.A. Resch, U. Keßner, F.J. Stadler, Thermorheological behavior of polyethylene: a sensitive probe to molecular structure. Rheol. Acta **50**, 559–575 (2011)

W.D. Richards, J.F. Kelly, European Patent Application 491,187, 24 June 1992; U.S. Patents 5,324,769, 28 June 1994, Appl. 25 Oct 1993, Appl. 12 Mar 1990, Appl. 17 Dec 1990, to General Electric

W.D. Richards, J.E. Pickett, U.S. Patents 5,384,360, 24 Jan 1995, Appl. 20 Sep 1993, Appl. 12 Mar 1990, Appl. 17 Dec 1990, to General Electric Company

W.D. Richards, D.M. White, European Patent Application 592,144, 13 Apr 1994; Japanese Patent 62 07,049, 26 July 1994, Appl. 07 Oct 1992, to General Electric Company

R.-E. Riemann, H.-J. Cantow, C. Friedrich, Polym. Bull. **36**, 637 (1996)

W. Ritter, R. Bergner, M. Schäfer, Ger. Offen. 4,121,111 A1, 07 Jan 1993, Appl. 26 June 1991, to Henkel K.-G.a.A.

N. Robledo, J.F. Vega, J. Nieto, J. Martínez-Salazar, The role of the interface in melt linear viscoelastic properties of LLDPE/LDPE blends: effect of the molecular architecture of the matrix. J. Appl. Polym. Sci. **114**, 420–429 (2009)

M.J. Roedel, The molecular structure of polyethylene. I. Chain branching in polyethylene during polymerization. J. Am. Chem. Soc. **75**(24), 6110–6112 (1953)

M.J. Roedel, Blends of high density and low density ethylene polymers and films thereof, U.-S. Patent 2983704 of 09 May 1961, priority 28 April 1955 to du Pont de Nemours

A. Roy et al., Macromolecules **43**, 3710–3720 (2010)

A.V.S. Sainath, M. Isokawa, M. Suzuki, S. Ishii, S. Matsuura, N. Nagai, T. Fujita, Synthesis and characteristics of succinic anhydride and disodium succinate-terminated low molecular weight polyethylenes. Macromolecules **42**, 4356–4358 (2009). doi:10.1021/ma900858e

S. Sakane, K. Minato, M. Takashige, Japanese Patent 000,052, 05 Jan 1979, Appl. 03 June 1977, to Idemitsu Petrochemical Co.

A. Sariban, K. Binder, Critical properties of the Flory-Huggins lattice model of polymer mixtures. J. Chem. Phys. **86**, 5859–5873 (1987)

G. Sarkhel, A. Banerjee, P. Bhattacharya, Rheological and mechanical properties of LDPE/HDPE blends. Polym. Plast. Technol. Eng. **45**(6), 713–718 (2006)

B. Schlund, L.A. Utracki, Linear low density polyethylenes and their blends: linear low density polyethylenes and their blends. Part 1: molecular characterization. Polym. Eng. Sci. **27**(5), 359–366 (1987a)

B. Schlund, L.A. Utracki, Linear low density polyethylenes and their blends: linear low density polyethylenes and their blends. Part 3: extensional flow of LLDPE's. Polym. Eng. Sci. **27**(5), 380–386 (1987b)

B. Schlund, L.A. Utracki, Linear low density polyethylenes and their blends. Part 5: extensional flow of LLDPE blends. Polym. Eng. Sci. **27**(20), 1523–1529 (1987c)

J.H. Schut, Plast. World (12), 29 (1996)

K.S. Schweizer, J.G. Curro, PRISM theory of the structure, thermodynamics, and phase transitions of polymer liquids and alloys. Adv. Polym. Sci. **116**, 320–377 (1994)

K.S. Schweizer, J.G. Curro, Integral equation theories of the structure, thermodynamics, and phase transitions of polymer fluids. Adv. Chem. Phys. **98**, 1–142 (1997)

R.B. Seymour, T. Cheng (eds.), *History of Polyolefins* (D. Reidel, Dordrecht, 1985); *Advances in Polyolefins*. ACS Symposium, Miami Beach Spring 1985 (Plenum, New York, 1987)

W.J.D. Shaw, Canadian Patent Application 2,071,707, 20 Dec 1993, Appl. 19 June 1992, to University (of Calgary) Technologies International, Incorporated

W.J.D. Shaw, J. Pan, M.A. Gowler, *Proceedings of Second International Conference on Structural Applications of Mechanical Alloying*, Vancouver, 20–22 Sept 1993

L.M. Sherman, Plast. Technol. **42**(3), 27 (1996)

L.M. Sherman, Plast. Technol. **43**(12), 35 (1997)

Z.-H. Shi, L.A. Utracki, Development of polymer blend morphology during compounding in a twin screw extruder. Part 2: theoretical prediction on morphology development during extrusion. Polym. Eng. Sci. **32**(24), 1834–1845 (1992); in *Proceedings of the Canadian Society of Chemical Engineering Annual Meeting*, Toronto, Oct 1992

Z.-H. Shi, P. Sammut, V. Bordereau, L.A. Utracki, Morphological study of polyethylene/ polystyrene blending in a twin – screw extruder. SPE Techn. Pap. **38**, 1818–1821 (1992)

C.-K. Shih, D.G. Tynan, D.A. Denelsbeck, Polym. Eng. Sci. **31**, 1670 (1991)

S.-Y.A. Shin, L.C. Simona, J.B.P. Soares, G. Scholz, Polyethylene–clay hybrid nanocomposites: in situ polymerization using bifunctional organic modifiers. Polymer **44**, 5317–5321 (2003)

K. Shin, N.B. Uk, J. Bang, J.Y. Jho, Melt-state miscibility of poly(ethylene-*co*-1-octene) and linear polyethylene. J. Appl. Polym. Sci. **107**, 2584–2587 (2008)

Shin-Kobe Electric Machinery Co., Ltd., Japanese Patent 096,156, 02 June 1984, Appl. 24 Nov 1982

K. Shinoda, *Principles of Solutions and Solubility* (Marcel Dekker, New York, 1978)

K. Shirayama et al., J. Polym. Sci. **A3**, 907 (1965)

K.K. Showa Denko, Japanese Patent 059,242, 08 Apr 1983, Appl. 05 Oct 1981

R. Simha, T. Somcynsky, On the statistical thermodynamics of spherical and chain molecule fluids. Macromolecules **2**, 342–350 (1969); T. Somcynsky, R. Simha, J Appl. Phys. **42**, 4545–4548 (1971)

A. Sirohi, S. Ramanathan, Design issues in converting to super-condensed mode operation for polyethylene. Presented at AIChE Spring 98 Meeting, New Orleans, 1998

F.A. Sitek, Mod. Plast. Int. **10**, 74 (1993)

J.B.P. Soares, A.E. Hamielec, Temperature rising elution fractionation, in *Modern Techniques for Polymer Characterization*, ed. by R. A. Pethrick, J.V. Dawkins (Wiley, New York/Chichester, 1999)

J.B.P. Soares, B. Monrabal, J. Nieto, B.J. Javier, Crystallization analysis fractionation (CRYSTAF) of poly(ethylene-*co*-1-octene) made with single-site-type catalysts: a mathematical model for the dependence of composition distribution on molecular weight. Macromol. Chem. Phys. **199**, 1917–1926 (1998)

W. Soontaranun, J.S. Higgins, T.D. Papathanasiou, Shear flow and the phase behaviour of polymer blends. Fluid Phase Equilib. **121**, 273–292 (1996)

F.C. Stehling, C.S. Speed, C.H. Welborn Jr., U.S. Patent 5,382,630; 5,382,631, 17 Jan 1995, Appl. 04 Feb 1993, 25 May 1990, to Exxon Chemical Patents, Inc.

R.A. Steinkamp, T.J. Grail, U.S. Patent 3953655, 27 Apr 1976, Appl. 09 Apr 1971, to Exxon Research and Engineering Co.

C.H. Stephens, A. Hiltner, E. Baer, Phase behavior of partially miscible blends of linear and branched polyethylenes. Macromolecules **36**(8), 2733–2741 (2003)

A.M. Striegel, ed., *Multiple Detection in Size-Exclusion Chromatography*. ACS Symposium Series, vol. 893 (2004)

J.P. Sullivan, M.B. Hoyt, U.S. Patents 5,565,158, 15 Oct 1996, Appl. 16 Nov 1994, to BASF Corporation

K. Suriya, S. Anantawaraskul, J.B.P. Soares, Cocrystallization of ethylene/1-octene copolymer blends during crystallization analysis fractionation and crystallization elution fractionation. J. Polym. Sci. B: Polym. Phys. **49**, 678–684 (2011)

A. Tabtiang, B. Parchana, R.A. Venables, T. Inoue, Melt-flow-induced phase morphologies of a high-density polyethylene/poly(ethylene-*co*-1-octene) blend. J. Polym. Sci. B: Polym. Phys. **39**, 380–389 (2001)

Z. Tadmor, P. Hold, L. Valsamis, SPE Techn. Pap. **25**, 193 (1979)

T. Taka, K. Shishido, T. Ohkubo, Low temperature heat shrinkable film, U.S. Patent 4913977 of 03 April 1990, priority 1984, to Showa Denim Kabushiki Kaisha

E. Takiyama, T. Fujimaki, in *Biodegradable Plastics and Polymers*, ed. Y. Doi, K. Fukuda. Proceedings of the III International Scientific Workshop on Biodegradable Plastics and Polymers, Osaka, 9–11 Nov 1993 (Elsevier, Amsterdam, 1994)

T. Tang, B. Huang, Polymer **35**, 281 (1994)

B. Tekkanat, H. Faust, B.L. McKinney, European Patent Application 533,304, 24 Mar 1993; U.S. Patents 5,280,066, 18 Jan 1994, Appl. 18 Sep 1991, to Johnson Service Company, Globe-Union Inc.

A.M. Thayer, Metallocene catalysts initiate new era in polymer synthesis, Chem. Eng. News (Sept 11 1995)

R. Timmermann, R. Dujardin, P. Orth, E. Ostlinning, H. Schulte, R. Dhein, E. Grigat, European Patent Application 583,595, 23 Feb 1994; Japanese Patent 61 92,570, 12 July 1994, Appl. 20 July 1992, to Bayer

I. Tomka, Ger. Offen. 4,116,404, 19 Nov 1992, Appl. 18 May 1991; I. Tomka, J. Meissner, R. Menard, Ger. Offen. 4,134,190, 22 Apr 1993, Appl. 16 Oct 1991

H. Tompa, *Polymer Solutions* (Butterworths, London, 1956)

C.L. Tucker, P. Moldenaers, Microstructural evolution in polymer blends. Annu. Rev. Fluid Mech. **34**, 177–210 (2002)

B.L. Turtle, European Patent Application 095,253, 30 Nov 1983, to British Petroleum Company

Univation Technologies, LLC, Capacity expansion technology, 05–2008, © 2003–2008

T. Usami, Y. Gotoh, S. Takayama, Generation mechanism of short-chain branching distribution in linear low-density polyethylenes. Macromolecules **19**(11), 2722–2726 (1986)

L.A. Utracki, Pressure dependence of Newtonian viscosity. Polym. Eng. Sci. **23**, 446–452 (1983)

L.A. Utracki, *Polymer Alloys and Blends* (Hanser, Munich, 1989a) [Japanese translation Tokyo Kagaku Dozin, Tokyo (1991)]

L.A. Utracki, Melt flow of polyethylene blends, in *Multiphase Polymers: Blends and Ionomers*, ed. L A. Utracki, R.A. Weiss. ACS Symposium Series, vol. 395 (Washington, DC, 1989b)

L.A. Utracki, On the viscosity – concentration dependence of immiscible polymer blends. J. Rheol. **35**(8), 1615–1637 (1991)

L.A. Utracki (ed.), *Encyclopaedic Dictionary of Commercial Polymer Blends* (ChemTec Pub, Toronto, 1994)

L.A. Utracki, The rheology of multiphase systems, in *Rheological Fundamentals of Polymer Processing*, ed. by J.A. Covas, J.F. Agassant, A.C. Diogo, J. Vlachopoulos, K. Walters (Kluwer, Dordrecht, 1995)

L.A. Utracki, Polyolefin alloys and blends. Makromol. Chem. Macromol. Symp. **118**, 335–345 (1997a)

L.A. Utracki, *Commercial Polymer Blends* (Chapman & Hall, London, 1997b)

L.A. Utracki, Polymer blend's technology for plastics recycling, in *Frontiers in the Science and Technology of Polymer Recycling*, ed. by G. Akovali, C.A. Bernardo, J. Leidner, L.A. Utracki, M. Xanthos. Proceedings of the NATO Advanced Study Institute on Frontiers in the Science and Technology of Polymer Recycling, Antalya, 16–27 June 1997, vol. E351 (Kluwer, Dordrecht, 1997c)

L.A. Utracki, *Commercial Polymer Blends* (Chapman & Hall, London, 1998)

L.A. Utracki, Thermodynamics of polymer blends (Chap. 2), in *Polymer Blends Handbook* (Kluwer, Dordrecht, 2002)

L.A. Utracki, *Clay-Containing Polymeric Nanocomposites*. Monograph (RAPRA, Shrewsbury, 2004), p. 786

L.A. Utracki, Pressure-volume-temperature dependencies of polystyrenes. Polymer **46**, 11548–11556 (2005)

L.A. Utracki, Rheology of polymer blends (Chap. 2), in *Encyclopedia of Polymer Blends*, ed. by A. Isayev, vol. 2 (Wiley-VCH, Weinheim, 2011)

L.A. Utracki, M.M. Dumoulin, Polypropylene alloys and blends with thermoplastics, in *Polypropylene: Structure, Blends and Composites*, ed. by J. Karger-Kocsis, vol. 2 (Elsevier, Barking, 1994), pp. 50–94

L.A. Utracki, A. Luciani, Int. Plast. Eng. Technol. **2**, 37 (1996); "Extensional flow mixer", Canadian Patent application, 1997; to National Research Council of Canada, Ottawa, Canada

L.A. Utracki, P. Sammut, Dynamic mechanical and capillary flow behavior of LLDPE/PC blends. SPE Techn. Pap. **35**, 1205–1208 (1989)

L.A. Utracki, P. Sammut, On the uniaxial extensional flow of polystyrene/polyethylene blends. Polym. Eng. Sci. **30**(17), 1019–1026 (1990a)

L.A. Utracki, P. Sammut, Rheology of polycarbonate/linear low density polyethylene blends. Polym. Eng. Sci. **30**(17), 1027–1040 (1990b)

L.A. Utracki, P. Sammut, Rheological response of polyamide/polypropylene blends. Part 2: extensional flow. Polym. Netw. Blends **2**(1), 85–93 (1992)

L.A. Utracki, B. Schlund, Molecular characterization of linear low density polyethylenes. SPE Techn. Pap. **32**, 737–740 (1986)

L.A. Utracki, B. Schlund, Linear low density polyethylenes and their blends. Part 2: shear flow of LLDPE's. Polym. Eng. Sci. **27**(5), 367–379 (1987a)

L.A. Utracki, B. Schlund, Linear low density polyethylenes and their blends. Part 4: shear flow of LLDPE blends. Polym. Eng. Sci. **27**(20), 1512–1522 (1987b)

L.A. Utracki, B. Schlund, Shear flow of linear low density polyethylenes and their blends. SPE Techn. Pap. **33**, 1002–1005 (1987c)

L.A. Utracki, Z.-H. Shi, Development of polymer blend morphology during compounding in a twin screw extruder. Part 1: droplet dispersion and coalescence – a review. Polym. Eng. Sci. **32**(24), 1824–1833 (1992)

L.A. Utracki, Z.H. Shi Gerard, Compounding polymer blends (Chap. 9), in *Polymer Blends Handbook*, ed. by L.A. Utracki (Kluwer, Dordrecht, 2002)

L.A. Utracki, R. Simha, Analytical representation of solutions to lattice-hole theory. Macromol. Theory Simul. **10**(1), 17–24 (2001)

L.A. Utracki, R.A. Weiss, eds., *Multiphase Polymers: Blends and Ionomers*. ACS Symposium Series, vol. 395 (Washington, DC, 1989)

Vadlamudi et al., J. Therm. Anal. Calorim. (2009)

U.R. Vaidya, M. Bhattacharya, U.S. Patents 5,321,064, 14 June 1994, Appl. 12 May 1992, to Regents of the University of Minnesota, Minneapolis

A. Valenza, J. Lyngaae-Jørgensen, L.A. Utracki, P. Sammut, Polym. Netw. Blends **1**, 79 (1991)

F. Van Damme, J.W. Lyons, W.L. Winniford, A.W. Degroot, M.D. Miller, Chromatography of polyolefin polymers, U.S. Patent 8,076,147 B2 of 13 Dec 2011, filed 13 Dec 2011, priority 15 Apr 2010, to Dow Global Technologies LLC

Vanderberg 1962

D. Vesely, Polym. Eng. Sci. **36**, 1586 (1996)

T.A. Vilgis, J. Noolandi, Makromol. Chem. Makromol. Symp. **16**, 225 (1988)

I. Vinckier, P. Moldenaers, A.M. Terracciano, N. Grizzuti, Droplet size evolution during coalescence in semiconcentrated model blends. AIChE J. **44**(4), 951–958 (1998)

D.L. Visioli, V. Brodie III, U.S. Patents 5,350,788, 27 Sep 1994, Appl. 11 Mar 1993, to du Pont

H. von Pechman, Ber. Dtsch. Chem. Ges. **31**, 2440 (1898)

M. Wachowicz, L. Gill, J.L. White, Polyolefin blend miscibility: polarization transfer versus direct excitation exchange NMR. Macromolecules **42**, 553–555 (2009)

M.H. Wagner, S. Kheirandish, M. Yamaguchi, Quantitative analysis of melt elongational behavior of LLDPE/LDPE blends. Rheol. Acta **44**(2), 198–218 (2004)

D.J. Walsh, W.W. Graessley, S. Datta, D.J. Lohse, L.J. Fetters, Equations of state and predictions of miscibility for hydrocarbon polymers. Macromolecules **25**(20), 5236–5240 (1992)

A. Webb, A.W. Carlson, T.J. Galvin, PCT Int. Appl., 001,733, 06 Feb 1992, Appl. 1990, to ICI Americas, Incorporated

J.D. Weinhold, S.K. Kumar, C. Singh, K.S. Schweizer, J. Chem. Phys. **103**, 9460–9474 (1995)

J.L. White, *Twin screw extruder technology and principles* (Hanser, Munich, 1990)

P.W.O. Wijga, J. Van Schooten, J. Boe, The fractionation of polypropylene. Makromol. Chem. **36**, 115–132 (1960)

L. Wild, Adv. Polym. Sci. **98**, 1–47 (1990)

L. Wild, T. Ryle, ACS Polym. Prepr. **18**, 182 (1977)

L. Wild et al., J. Polym. Sci. **A-2**(9), 2137 (1971)

L. Wild et al., J. Polym. Sci. Polym. Phys. Ed. **20**, 441 (1982)

J.L. Willett, U.S. Patents 5,087,650, 11 Feb 1992, Appl. 1990, to Fully Comp. Plastics, Inc.

K.F. Wissbrun, R.H. Ball, P.J. Rossello, Belgian Patent 614,282, 22 Aug 1962

K.F. Wissbrun, R.H. Ball, P.J. Rossello, British Patent 994,376, 10 June 1965, to Celanese

J.E. Wolak, J.L. White, Factors that allow polyolefins to form miscible blends: polyisobutylene and head-to-head polypropylene. Macromolecules **38**(25), 10466–10471 (2005)

W.K. Wong, D.C. Varrall, Eur. Pat. Appl., 584,927, 02 Mar 1994, Appl. 24 July 1992, to Exxon Chemical Patents Inc.

M. Xanthos, A. Patel, S.K. Dey, S.S. Dagli, C. Jacob, T.J. Nosker, R.W. Renfree, SPE Techn. Pap. **38**, 596 (1992)

M. Xanthos, J. Grenci, S.H. Patel, A. Patel, C. Jacob, S. Dey, S.S. Dagli, Polym. Compos. **16**, 204 (1995)

M. Xanthos, S.K. Dey, D.H. Sebastian, *Proceedings Polymer Processing Society and American Institute of Chemical Engineers Joint Meeting*, Chicago, 11–14 Nov 1996

K. Yasuda, Investigation of the analogies between viscometric and linear viscoelastic properties of polystyrene fluids, Ph.D. thesis, Massachusetts Institute of Technology, Cambridge, MA, 1979

K. Yasuda, R.C. Armstrong, R.E. Cohen, Shear flow properties of concentrated solutions of linear and star branched polystyrene. Rheol. Acta **20**, 163–178 (1981)

W.W. Yau, Polyolefin microstructure characterization using 3D-GPC-TREF. Macromol. Symp. **257**, 29 (2007)

W.W. Yau, D. Gillespie, New approaches using MW-sensitive detectors in GPC-TREF for polyolefin characterization. Polymer **42**, 8947–8958 (2001)

H. Yoon, Y. Feng, Y. Qiu, C.C. Han, J. Polym. Sci. Polym. Phys. Ed. **32**, 1485 (1994)

K. Yoshikawa, N. Ofuji, M. Imaizumi, Y. Moteki, T. Fujimaki, Polymer **37**, 1281 (1996)

T. Yoshitake, T. Tasaka, R. Sato, Japanese Patent 050,254; 050,264, 08 May 1978, Appl. 18 Oct 1976, to Kuraray Co.

S. Yukioka, T. Inoue, Polymer **35**, 1182 (1994)

A.T.P. Zahavich, J. Vlachopoulos, *Reprocessing of Polyolefins: Changes in Rheology and Reprocessing Case Studies*. NATO-ASI Frontiers in the Science and Technology of Polymer Recycling, Antalya Turkey, 16–27 June 1997. NATO ASI Series, E351 271–298 (Kluwer, Lampertheim, 1997, 1998)

Z. Zhang, Use of FT-IR spectrometry for on-line detection in temperature rising elution fractionation. Macromol. Symp. **282**, 111–127 (2009)

L. Zhao, P. Choi, A review of the miscibility of polyethylene blends. Mater. Manuf. Process. **21**(2), 135–142 (2006)

K. Ziegler, H. Breil, H. Martin, E. Hozkamp, Ger. Offen. 973,626, 14 Apr 1960, Appl. 17 Nov 1953; U.S. Patents 3,257,332, 21 June 1966, Appl. 15 Nov 1954, to K. Ziegler

A. Zletz, U.S. Patents 2,692,257, 19 Oct 1954, Appl. 28 Apr 1951, to Standard Oil of Indiana

H. Zweifel, *Recycling of Polymers for Reuse, Recovery Experiences, Trends and Case Studies*, NATO-ASI on Polymer Recycling, Antalya 16–27 June 1997

H. Zweifel, *Stabilization of polymeric materials* (Springer, Berlin, 1998)

Commercial Polymer Blends

19

M. K. Akkapeddi

Contents

M.K. Akkapeddi: retired

M.K. Akkapeddi
York, PA, USA
e-mail: kakkapeddi@mysite.com

Abstract

In this chapter, an overview of the commercially important polymer blends is presented with a particular emphasis on the rationale for their commercial development, the compatibilization principles, their key mechanical properties, and their current applications and markets. To facilitate the discussion, the commercial polymer blends have been classified as follows into 13 major groups depending on the type of the resin family they are based on.

  (i) Polyolefin blends
 (ii) Styrenic blends
(iii) Vinyl resin blends
 (iv) Acrylic blends
 (v) Elastomeric blends
 (vi) Polyamide blends
(vii) Polycarbonate blends
(viii) Poly(oxymethylene) blends
 (ix) Polyphenyleneether blends
 (x) Thermoplastic polyester blends
 (xi) Specialty polymer blends
(xii) Thermoset blend systems
(xiii) Biodegradable polymer blends

Within each major category, the individual polymer blends of industrial significance have been described with relevant data. Since the discussion is limited only to those blends that are actually produced and used on a commercial scale, the relevant cost and performance factors that contribute to the commercial viability and success of various types of blends have been outlined.

In comparing the different blends, the specific advantages of each type, as well as any potential overlap in performance with other types of blends have also been discussed. The fundamental advantage of polymer blends, viz., their ability to combine cost-effectively the unique features individual resins, is particularly illustrated in the discussion of crystalline/amorphous polymer blends such as the polyamide and the polyester blends. Key to the success of many commercial blends, however, is the selection of intrinsically complementing systems or the development of effective compatibilization methods. The use of reactive compatibilization techniques in commercial polymer blends has also been illustrated under the appropriate sections such as the polyamide blends.

In many commercial blends, rubber toughening plays an important and integral part of the blend design. Combining high impact strength with other useful properties such as heat and solvent resistance can significantly enhance the commercial value of a blend. Hence, the nature of the impact modifiers used and the role of morphology on properties have been discussed under the appropriate cases of commercial blends. The chapter concludes with an outline of the potential trends in the commercial polymer development.

19.1 Introduction

Synthetic polymers represent an ubiquitous class of raw materials that are used in a wide spectrum of applications ranging from textiles, packaging, construction, automotive, industrial, electrical, and electronic equipments to appliances, toys, and various other consumer goods affecting our everyday life. Thus, polymers play an important major role in the global economy. The current global overall consumption of polymers used as plastics (i.e., excluding the textile fibers) is about 280 million metric tons/year (280 Mt/year) with a growth rate of 4–5 % (Reseau-plasturgie 2012). Among these, the commodity thermoplastics consisting of polyolefins (PE and PP), PVC, styrenics, PET bottle resins together represent ≥85 % of the total volume (Figs. 19.1 and 19.2). The higher-performance, value-added engineering thermoplastic resins such as ABS, PC, PMMA, POM, polyamides, PBT, and others represent about 10 % of the total market volume of thermoplastics with an annual global consumption of >20 million tons (Fig. 19.3). Polymer blends are a subgroup of such engineering plastics, with an estimated global consumption of over 2 Mt/year. The historical origin and development of polymer blends technology has been reviewed in another chapter of this handbook, viz., ▶ Chap. 1, "Polymer Blends: Introduction." In this chapter, only the various types of commercially significant polymer blend families will be discussed in detail.

The primary motivation for the commercial development of polymer blends has been to adjust the cost-performance balance and tailor-make products for specific end-use applications. Thus the commercial growth of polymer blends in the last several decades outpaced the growth rate of existing polymers by at least 2 %. The demand for polymers and the polymer blends will continue to increase as the global economy continues to grow. Several key factors contribute to the commercial success and continued interest in the polymer blends, such as those listed below:

1. The blending of commercially available polymers is a more cost-effective method of developing a new product that meets the specific customer or market requirements, as opposed to developing a totally new polymer which generally involves higher research and development costs and more importantly, prohibitively higher capital costs for the plant.
2. Polymer blends can fill the cost-performance gaps in the existing commercial polymers. Several properties can be uniquely combined in a blend that a single resin often cannot provide. In some cases, synergistic improvements in properties such as toughness and heat resistance are achievable.
3. Polymer blending can be done at a relatively low cost using an extruder. Production of new polymers, on the other hand, requires capital-intensive plants and reactors that must operate on a reasonably large scale for reasons of economics.
4. The flexibility of extruder blending enables custom production of different blends in a wide range of production volumes. Polymerization plants are generally not as flexible and not economical for small-volume production.
5. Polymer blends provide an avenue for diversifying and expanding the product line for resin producers and suppliers, without significant investment risks.

Fig. 19.1 Global consumption of thermoplastics (ca. 230 Mt/year) (Reseau-plasturgie 2012)
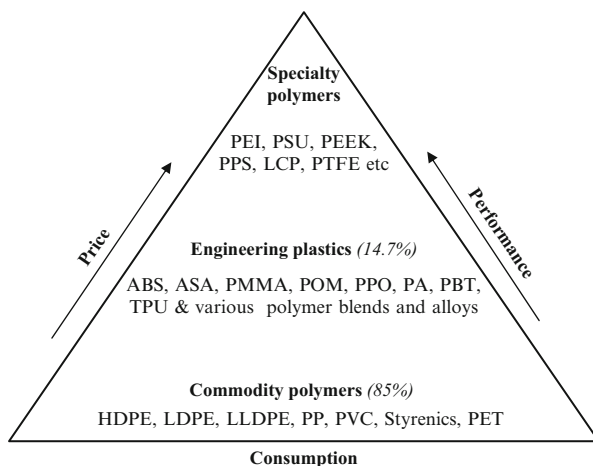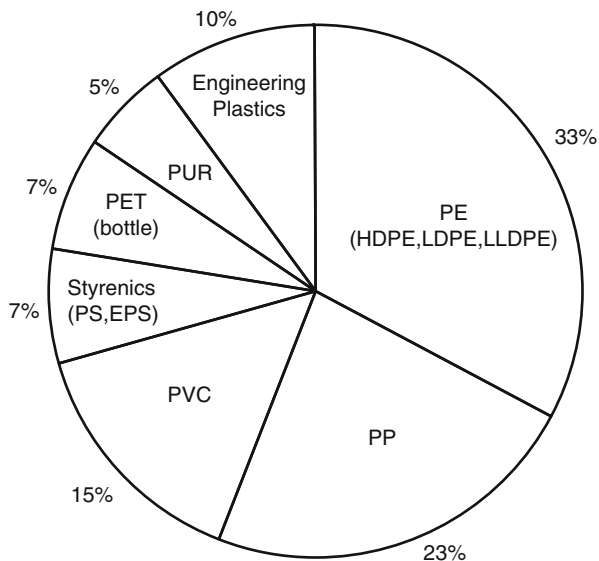
Fig. 19.2 Price/Performance profile of commercial thermoplastic polymers

6. Blends can be formulated, optimized, and commercialized generally at a much faster rate (from concept to commercialization) than new polymers, provided there are no major technical hurdles for the compatibility development between the components.

7. The development of an effective compatibilization technology, whenever it is needed, allows the resin supplier to establish a proprietary and competitively advantageous position. Effective compatibilization is also essential for polymer blend fabricated product's mechanical strength, toughness, and long- term durability during its intended service life.

8. Blends offer a useful, economic means of upgrading recycled or off-specification polymers.

Fig. 19.3 Global
consumption of engineering
thermoplastics (>20 Mt/year,
in 2012)
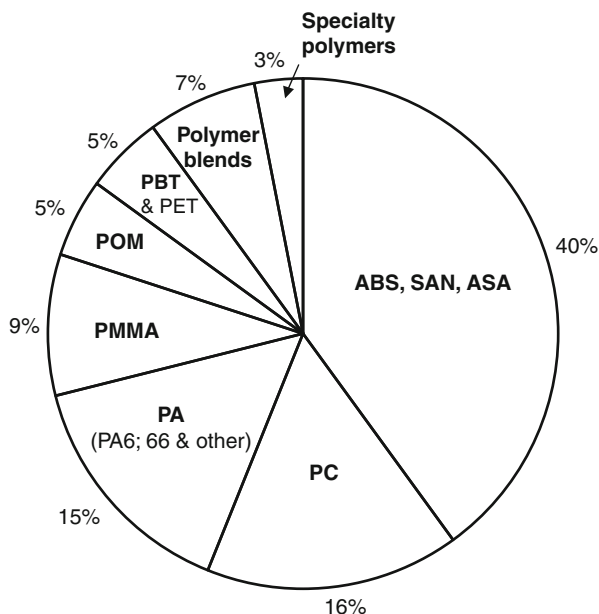
The terms "polymer blends" and "polymer alloys" have already been defined in the other chapters of this handbook, viz., ▶ Chap. 1, "Polymer Blends: Introduction" and ▶ Chap. 2, "Thermodynamics of Polymer Blends." In the trade literature, these terms have often been used interchangeably. In the context of current discussion, only the term "polymer blends" will be employed most of the time, except specifying, where possible, the origin of the technological compatibility between the components in each type of blend. Table 19.1 lists the commercially available polymer blends according to their primary structural categories indicated in Fig. 19.1.

19.1.1 Compatibilization Mechanisms in Commercial Polymer Blends

To be useful, most commercial polymer blends are either designed or selected to have some degree of the technological compatibility between the components to resist delamination and loss in ductility. Compatibility is defined here as the ability for the polymer components to coexist either as molecularly miscible or as morphologically distinct phases, but interfacially stabilized, without a tendency for delamination.

The compatibility in polymer blends can result from any of the following mechanisms:

1. Thermodynamic miscibility between the components such as in the case of polystyrene (PS) and poly(2,6-dimethyl 1,4-phenylene ether) (PPE) blends.
2. Partial miscibility at segmental level between the blend components, even when they are phase separated, imparting a low interfacial tension and an adequate

Table 19.1 Commercial polymer blends

Blend	Producer	Trade name	Compatibilization mechanism[a]	Blend type
Elastomeric polyolefin blends				
PP/EPDM	ExxonMobil Teknor Apex	Santoprene® Sarlink 3000®	None[b]; Dynamic vulcanization[c]	Crystalline/amorphous
PP/NBR	ExxonMobil	Geolast®	Grafting/Dynamic vulcanization	Crystalline/amorphous
PP/EPDM/NBR	Japan Synthetic Rubber	Dynaflex P®	Grafting/Dynamic vulcanization	Crystalline/amorphous
PP/PBD	ExxonMobil Teknor Apex	Vyram® Sarlink 1000®	None; Dynamic vulcanization	Crystalline/amorphous
PP/Butyl	Teknor Apex ExxonMobil	Sarlink 2000® TPE-3000® Trefsin®	None; Dynamic vulcanization	Crystalline/amorphous
Ethylene terpolymer/PVC	Advanced Polymer Alloys	Alcryn®	Partial miscibility[d]	Amorphous/amorphous
Thermoplastic polyolefin blends (TPOs)				
PP/EP or EPDM	ExxonMobil; LyondellBasell; Spartech; Schulman Total; Mitsubishi Petrochem. and others		None	Crystalline/amorphous
Styrenic blends				
ABS blends				
ABS/PC	Styrolution Sabic Bayer Daicel Polymer	Novodur® Cycoloy® Bayblend® Novolly® S	Partial miscibility Partial miscibility	Amorphous/amorphous
ABS/PBT	Daicel Polymer	Novolly® B	–	
ABS/PA	Styrolution Daicel Polymer	Terblend® N Novolly® A	Grafting	Amorphous/crystalline
ABS/PVC	Spartech Kydex LLC	Royalite® R59 Kydex® 430	Partial miscibility	Amorphous/amorphous
ABS/SMI	Denka (Japan)	Malecca K®	Partial miscibility	Amorphous/amorphous
ASA blends				
ASA/PC	Styrolution	Luran® SC	Partial miscibility	
ASA/PA	Styrolution	Terblend® S	Graft-coupling	
Vinyl blends				
PVC/PMMA PVC/Acrylic blend	Spartech Kydex LLC	Royalite® R52 Kydex® 100	Partial miscibility	Amorphous/amorphous

<div align="right">(<i>continued</i>)</div>

Table 19.1 (continued)

Blend	Producer	Trade name	Compatibilization mechanism[a]	Blend type
PVC/Nitrile rubber	Showa Denka Lanxess Minnesota Rubber and Plastics/Quadion	Denka LCS® Krynac® 567A,B	Miscibility occurs with NBR containing >25 % AN	Amorphous/ amorphous
PVC/polyurethane	AlphaGary	Vythene®	None	Amorphous/ amorphous
Acrylic blends				
PMMA/acrylic rubber MMA-SAN terpolymer/acrylic rubber	Arkema-Altuglass Evonik Industries	Plexiglas® Cyrolite®, XT®	Miscibility Miscibility	Amorphous/ amorphous
MMA-SAN terpolymer/ Polycarbonate	Evonik Industries	Cyrex®	Patial miscibility	Amorphous/ amorphous
PMMA/PVC	Kydex LLC	Kydex®	Partial miscibility	Amorphous/ amorphous
Elastomeric blends				
EPDM/PP	ExxonMobil Teknor Apex	Santoprene® Sarlink®	Dynamic vulcanization	Amorphous/ amorphous
NBR/PP	ExxonMobil Teknor Apex	Geolast® Sarlink®	Dynamic vulcanization	Amorphous/ amorphous
Butyl rubber/PP	Teknor Apex	Trefsin®	Dynamic vulcanization	Amorphous/ amorphous
PBD/PP	Teknor Apex	Vyram®	Dynamic vulcanization	Amorphous/ amorphous
Polyamide blends				
PA/ABS	Syrolution	Terblend® N	Graft-coupling[e]	Crystalline/ amorphous
PA/Acrylic rubber	DuPont	Zytel® FN	Grafting/ controlled cross-linking	Crystalline/ amorphous
PA/Elastomer	DuPont BASF EMS	Zytel® ST801,FN Ultramid® 8350, 8351, 8254 A28, BT40X	Graft-coupling Polar interactions[f]	Crystalline/ amorphous
PA/Polypropylene	Techmer Lehvoss	Luvotech® J75	Graft-coupling	Crystalline/ crystalline
PA/Polyarylate	Unitika	X-9		Crystalline/ amorphous
PA/PBD with Co (oxygen scavenger)	Honeywell	Aegis® OX	Reactive compatibilizer	Crystalline/ amorphous

Table 19.1 (continued)

Blend	Producer	Trade name	Compatibilization mechanism[a]	Blend type
PPE blends				
PPE/HIPS	Sabic	Noryl®	Miscibility	Amorphous/amorphous
PPE/PA66 (and 6)	Sabic BASF	Noryl® GTX Ultranyl®	Graft-coupling	Crystalline/amorphous
PPE/PP	Sabic	Noryl® PPX	Compatibilizer	Crystalline/amorphous
Polycarbonate blends				
PC/ABS	Styron	Pulse®	Partial miscibility	Amorphous/amorphous
PC/ASA	BASF	Terblend® S	Partial miscibility	Amorphous/amorphous
PC/MMA-SAN terpol.	Evonik industries	Cyrex®	Partial miscibility	Amorphous/amorphous
PC/PBT/acrylic rubber PC/PET/acrylic rubber	Sabic Bayer Romira	Xenoy® Makroblend® Romiloy®	Partial miscibility	Amorphous/crystalline
PC/PET/acrylic rubber	Sabic Bayer	Xenoy® Makroblend®	Partial miscibility	Amorphous/crystalline
Polyester blends				
PBT/PET	Sabic Celanese/Ticona	Valox® Celanex®	Miscibility	Crystalline/crystalline
PBT/Elastomer	Sabic	Valox®	–	Crystalline/amorphous
PBT/ASA	BASF	Ultradur® S	PC additive (?)	Crystalline/amorphous
PBT/PC/Elastomer	Sabic	Xenoy®	Partial miscibility	Crystalline/amorphous
PBT/PPE				Crystalline/amorphous
PET/Oxygen scavenger blends				
PET/PET-b-PBD with Co catalyst	ColorMatrix/Polyone	Amosorb®	Compatibiizer	
PET/PA-MXD6 with Co catalyst	Constar Invista M&G	Monoxbar® Polyshield® Poliprotect®	None Sulfoisophthalate Compatibilizer	Crystalline/crystalline
PET/PTMG-PET	Invista; PET bottle producers	Oxyclear®	Self-compatibilized	
Specialty polymer blends				
Polyarylate/PET	Unitika	U-8000	Partial miscibility	Crystalline/amorphous
Polyarylate/PA6	Unitika	U-AX-1500	Partial miscibility	Crystalline/amorphous

Table 19.1 (continued)

Blend	Producer	Trade name	Compatibilization mechanism[a]	Blend type
Polyetherimide/PC	Sabic	Ultem® 9085	Partial miscibility	Amorphous/amorphous
Polyetherimide/PCE, Polycarbonate ester	Sabic	Ultem® AX100	Partial miscibility	Amorphous/amorphous
Polyphenylsulfone/Polysulfone	Solvay Plastics	Acudel®	Miscibility	Amorphous/amorphous
PTFE/PFA	Dupont	Teflon® 855G	None	Crystalline/crystalline
PEEK/PBI	Boedeker Plastics	Celazole® T	Partial miscibility?	Crystalline/amorphous

[a]Compatibilization mechanisms are defined here as the underlying principles responsible for the blend's desirable properties, delamination resistance and morphology stability. Compatibility may originate from inherent miscibility, partial miscibility or low interfacial tension between the components or through a chemical means, such as reactive graft-coupling or addition of interfacial agent
[b]No compatibilizer is used. Low interfacial tension between the components is responsible for the inherent compatibility in these systems
[c]The dispersed phase is selectively cross-linked via dynamic vulcanization to stabilize the blend morphology
[d]Partial miscibility between the components leads to self-compatibilization even though these systems are phase separated. Experimentally, these blends exhibit two T_g's, but different from each of the pure components due to a small amount of mutual miscibility
[e]Grafting involves direct chemical reaction between the components during melt mixing, generating a graft copolymer as the compatibilizer
[f]Ionic or chelate complex interactions between the components at the interface, may lead to compatibilization

    level of interfacial adhesion, e.g., in ABS/polycarbonate, PBT/polycarbonate, PVC/nitrile rubber blends.
3. Compatibilizing effects of interfacial agents such as block or graft copolymers that reduce the interfacial tension, stabilize the morphology, and strengthen adhesion at the interface.

    Although complete miscibility between polymers is generally rare, when this does happen, it provides a unique opportunity to custom tailor the blend properties by simply adjusting the blend ratio. The immense commercial success of PPE blends with high-impact polystyrene (HIPS) is primarily attributed to the miscibility between PPE and PS, that enabled one to combine the low cost and easy processability features of HIPS with the high-performance (high heat resistance and strength) features of PPE. There was also some synergistic improvement of the toughness due to the improved ductility of the blend matrix resulting in improved rubber toughening efficiency. Simple melt mixing in extruder-type compounding equipment is adequate to make an alloy from such miscible polymers.

    Even in the phase-separated blends, where some degree of partial miscibility or compatibility exists between the components, simple melt blending in an intensive

shear mixer is adequate for making well-dispersed, reasonably stable blend products with useful combination of properties, e.g., in polypropylene/ethylene-propylene rubber blends or ABS/polycarbonate blends. The self-compatibilizing nature of these blends stems from the partial miscibility and the mutual interpenetration of the individual component's polymer chains at the interface. Slight modifications of the polymer backbone are often employed, particularly in the case of styrenic and ABS resins to induce partial miscibility with other resins.

Compatibilization of the highly immiscible commercial polymer pairs has thus far been a technically more challenging task for the polymer technologists in the industry to make cost-effective, high-performance polymer blend products. Significant progress has, however, been made in recent years in utilizing compatibilizers based on graft or block copolymer or other interfacial agents that effectively reduce the interfacial tension between the components to achieve useful levels of ductility and delamination resistance, while at the same time stabilizing the morphology against processing effects. Interfacial compatibilization in commercial polymer blends is generally achieved through reactive extrusion in which the block or graft copolymer compatibilizer is generated in situ at the interface. The end groups or pendant groups in some commercial polymers such as polyamides (amine or carboxyl), polyesters (carboxyl or hydroxyl), and styrene-maleic anhydride copolymers (anhydride group) are useful for this purpose. In most other cases, the polymer backbones must appropriately be modified to include reactive functionalities by graft reactions with small molecules (e.g., maleation of polyolefins with maleic anhydride) or through copolymerization techniques.

The recent advances in reactive extrusion technology, involving reactive modification of polymers and/or reactive blending to form graft or block copolymer compatibilized blends in an extruder, have resulted in several successful commercial blends of otherwise highly immiscible polymer pairs, such as polyamide/olefinic elastomer, polyamide/polyolefin, and polyamide/PPE blends. In many cases, the reactive modification of the base polymers and the subsequent reactive blending can be combined into a one-step, sequential operation in a twin-screw extruder, making this an economically attractive process. Reactive compatibilization is still a growing technology aimed at the development of useful blends from otherwise highly immiscible polymers, and particularly those from crystalline polymers. Specific examples of reactive modification and reactive blending will be discussed later, in individual cases. Further details on compatibilization can be found in the other chapters of this book, viz., ▶ Chap. 4, "Interphase and Compatibilization by Addition of a Compatibilizer" and ▶ Chap. 5, "Reactive Compatibilization."

19.1.2 Rationale for Polymer Blends

Commercial polymer blends belong to one of the following three categories:
1. Blends of amorphous/amorphous polymers
2. Blends of crystalline/amorphous polymers
3. Blends of crystalline/crystalline polymers

While the specific advantages of each type of the blends will be discussed later in detail for the individual cases, the general motivations for making commercial polymer blends may be any of the following factors:

- Lower cost
- Improved dimensional stability
- Improved heat resistance
- Improved processability
- Improved toughness
- Improved weatherability
- Improved solvent resistance
- Improved flame resistance
- Improved moisture resistance
- Improved esthetics and appearance, etc.

Many commercial polymer blends often include an elastomer, to improve the impact strength of the blend under conditions of stress concentration (notched Izod impact strength) and to lower the ductile-brittle transition temperature of the blend. The elastomeric dispersions are judiciously employed either in the matrix phase, in the dispersed polymer phase, or in both phases, depending upon the requirement and the fracture behavior of the blend. As a general rule, the more brittle component in a given polymer blend has a greater need for rubber toughening.

However, an overwhelming factor in determining the impact strength of an immiscible or partially miscible blend is the degree and efficiency of interfacial compatibilization that either is inherent in or has been designed into the blend system. If the interfacial adhesion or compatibilization is poor, the elastomer dispersion alone will not improve the toughness. Further details on the role of compatibilization and rubber toughening effects in polymer blends will be discussed later with specific commercial examples. Combining a high level of impact strength with a high level of heat resistance and/or chemical resistance has been the primary thrust of most commercial polymer blends (Figs. 19.4 and 19.5).

19.1.3 Polymer Blend Processing

Most commercial polymer blends are produced by melt-mixing in continuous compounding equipment such as single-screw or twin-screw extruders and kneader-extruders. Twin-screw extruders are now well established and widely used for polymer blends manufacturing because of their great versatility and production efficiency. Owing to their segmented barrel and screw designs, twin-screw extruders offer the advantage of multiple processing zones. The degree of shear mixing, residence time, and the temperature in each of these zones can be varied at will by simply changing the order and/or the type of the screw elements and kneading blocks, and using separately controlled heaters.

Currently, there are three common types of twin-screw extruders (TSE) available for thermoplastic polymer compounding, viz.,
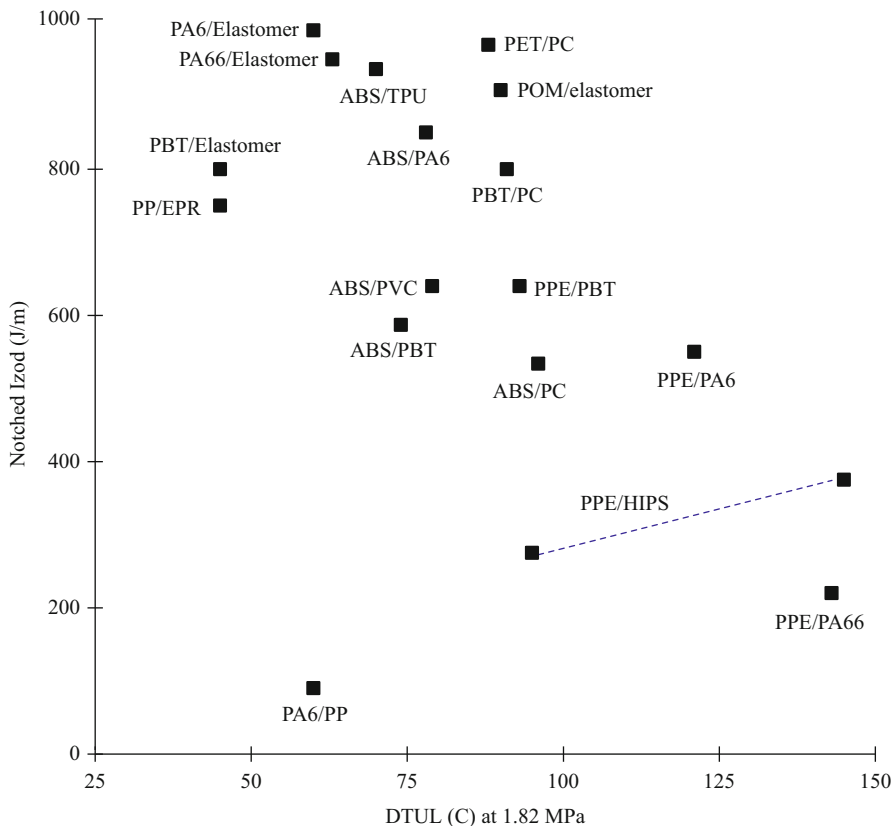
Fig. 19.4 Notched Izod vs. DTUL (°C at 1.8 MPa) of some commercial polymer blends

(1) Intermeshing corotating TSE
(2) Intermeshing counterrotating TSE
(3) Nonintermeshing counterrotating TSE

Among these, the intermeshing corotating twin-screw extruder is the most common type of equipment used by the polymer blends manufacturers. The barrels and screws of all commercial intermeshing corotating TSEs have modular designs allowing the processor to rearrange the barrel and screw components in different configurations to suit the processing needs of different polymer blends. In these modular designs, the desired screw configuration for a given polymer blend processing is obtained by assembling the various screw elements, viz., the conveying, kneading, and mixing elements in a desired manner to achieve consistent blend products.

The corotating twin-screw extruders also offer the choice of multiple ports for liquid injection, venting, and downstream feeding purposes. For example, the twin-screw extruder can be readily adapted to combine both the polymer modification and polymer-polymer grafting steps of a reactive blending process into a single-pass, multistage reactive extrusion process.
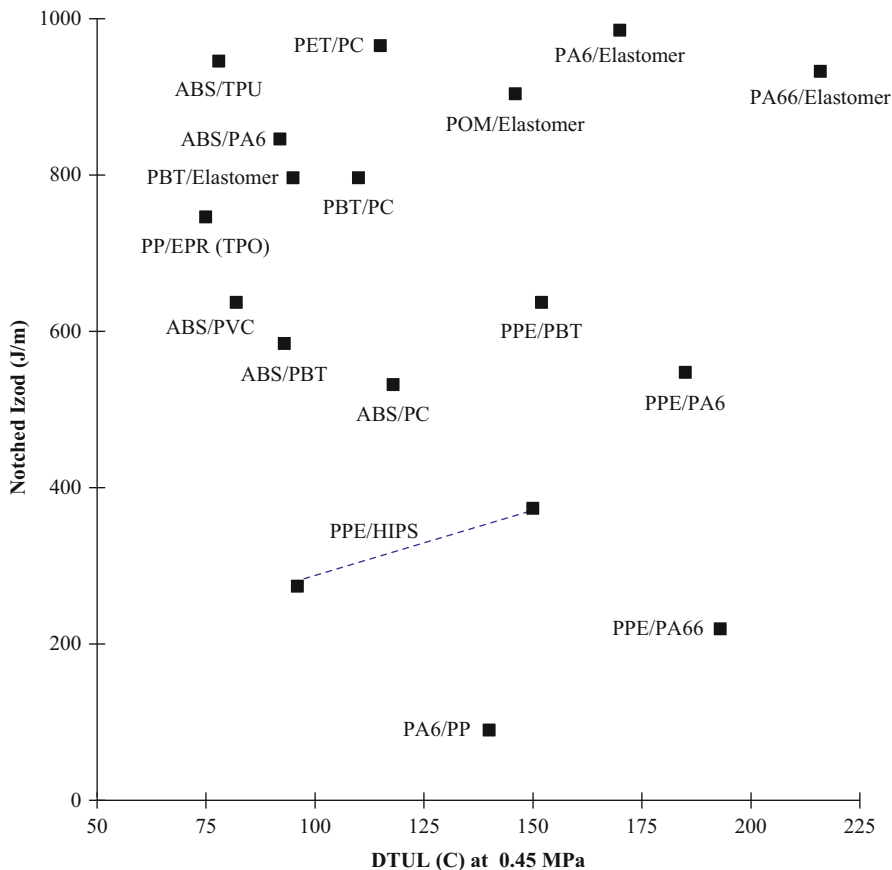
Fig. 19.5 Notched Izod vs. DTUL (°C at 0.45 MPa) of some commercial polymer blends

The polymer that needs to be functionalized is fed at the throat of a corotating twin-screw extruder and melt-mixed with a suitable grafting agent and catalyst in the initial zones. After vacuum venting to remove the unreacted and volatile materials, the "functionalized polymer" melt is then mixed with the second polymer and other components (impact modifier, fillers, additives, etc.) added through the downstream feed ports. The temperature and the shearing conditions in these latter zones of the extruder are controlled to promote intimate mixings. Polymer-polymer grafting, compatibilization, and the morphology development in the blend occur at this stage of extrusion. Thus all the sequences of the complex blending process can be accomplished in an economically viable one-step, extruder process.

Many commercial blends are often not as complex as above and can be made by simple melt-blending without a compatibilizer because of partial miscibility between the components. However, even in these cases, good intimate mixing (dispersive and distributive) between the components is necessary to ascertain a morphologically stable, good-quality product. Although twin-screw extruders are now invariably

preferred for polymer blending, many of the older plants also use the single-screw extruders, with mixing devices, for the reason of their low capital costs. There are many detailed reviews available regarding the theory and practice of twin-screw extruders and their mixing mechanisms in polymer processing (Chung 2000; Manas-Zloczower 2009; Hyun et al. 2011). Further discussion on the extruder compounding processes relevant to polymer blend manufacturing can also be found in another chapter of this handbook, viz., ▶ Chap. 9, "Compounding Polymer Blends."

Although commercial twin-screw extruders can be as large as 300 mm in size, capable of compounding up to 40 t/h, the actual type and size of the equipment used depend on the type of the polymer blend and the production volume. Normally, for engineering polymer blends, twin-screw extruders of about D = 90 mm size (L/D ≅ 30–40) and capable of compounding at 700–1,000 kg/h, are used. For blending PVC or elastomer blends, other types of compounding equipment are used; e.g., Farrell continuous mixer (FCM), Buss cokneader, or a batch mixer, such as Banbury, have also been used.

The technological details on commercial polymer blends are kept proprietary by the manufacturers, particularly with respect to the exact compositions of the commercial grades and the processes used to make them. Even when the patent literature is available for a given type of polymer blend, often one cannot infer the actual compositions and processes used for the commercial blends. Hence, in reviewing the technology of commercial polymer blends, certain assumptions and generalizations have to be made regarding the compositional effects on the properties of some commercial blends, where the literature information is lacking. However, in the following sections, all relevant technological principles behind the various commercial blends have been outlined along with a discussion of their key properties, differentiating values and applications based on a reasonable evaluation of the literature available to date.

19.2 Polyolefin Blends

Polyolefins (PO) constitute the largest single group among all the commercial thermoplastics, amounting to >50 % of the global volume of all commercial polymers. The polyolefin family comprises of (a) polyethylenes of various types, viz., high-density polyethylene (HDPE), low-density polyethylene (LDPE), linear low-density polyethylene (LLDPE); (b) polypropylene (PP) homopolymer and PP-b-E/P block copolymers; (c) ethylene-propylene rubbers (d) ethylene-octene copolymer and other polyolefin elastomers (POEs) (e) ethylene copolymers with other comonomers such as ethyl acrylate, acrylic/methacrylic acid, and the ionomers; (f) specialty polyolefins such as poly(4-methyl,1-pentene), poly(1-butene), etc. Among these, HDPE, LDPE, and LLDPE and polypropylene (PP) are the four most widely used polyolefins amounting to a current global consumption of >125 million metric tons (Nexant 2012). Polyethylenes together represent about 60 % and polypropylenes about 40 % of the global market share for polyolefins.

Because of the wide range of properties available within POs, generally there has not been any major need to blend polyolefins with other types of polymers.

Furthermore, the immiscibility of the commodity polyolefins with other types of polymers has also been a major reason for the lack of commercial interest in such blends, although with the advent of reactive modification and grafting chemistry, significant progress has been made in compatibilizing such dissimilar polymer systems as PA/PO blends (Ide and Hasegawa 1974; Epstein 1979; Hobbs et al. 1983).

Blending within the family of polyolefins has, however, been more common (Plochocki 1978). Although they are usually immiscible with each other, there exists some degree of mutual compatibility between them. The similarity of their hydrocarbon backbones and the closeness of their solubility parameters, although not adequate for miscibility, account for a relatively low degree of interfacial tension. For example, the solubility parameters of polyethylene, polyisobutylene, ethylene-propylene rubber, and polypropylene are estimated to be 16.0, 16.4, 16.5, and 17.0 $J^{1/2}$ $cm^{3/2}$ respectively, all very close to each other (VanKrevelen 1990). Similarly, the interfacial tension coefficients between PE or PP and EP-elastomers are quite small (typically ca. 0.1 MN/m) (Shih 1990; Wu 1989). Hence, polyolefin blends have been made since the early days of polyolefin commercialization via a simple melt mixing, without a compatibilizer.

The crystalline polyolefin homopolymers (HDPE and PP) have often been blended with low-modulus/elastomeric polyolefins such as LDPE, EP-rubber, in order to improve the toughness. Hence, toughened POs have been known for a long time commercially. Most of the toughened PO blends are simple mixtures of POs and olefinic elastomers melt blended in an extruder without a compatibilizer. However, recent advances in polymerization technology have allowed the production of toughened polypropylenes ("Impact PP"), through a sequential polymerization of ethylene-propylene copolymer in the PP matrix leading to blends with some block or graft copolymer exhibiting improved modulus/toughness balance (Galli and Haylock 1991).

19.2.1 Blends Based on Polyethylenes (HDPE, LDPE, LLDPE Based Blends)

HDPE, LDPE, and LLDPE are the three main types of commercial polyethylenes with a combined global consumption of >80 Mt/year. HDPE is a strictly linear homopolymer while LDPE is a long-branched homopolymer because of the different methods of polymerization. LLDPE, on the other hand, is a linear ethylene copolymer with small amounts of α-olefin comonomers such as butene, hexene, or octene. Traditionally, polyethylenes are classified according to the densities. The density of polyethylene decreases as the branching and/or comonomer content increases. The crystallinity and the properties associated with crystallinity, such as stiffness, strength, and chemical resistance, progressively decrease from HDPE to LDPE/LLDPE to POE grades.

Among the different types of polyethylene listed in Table 19.2, the HDPE is the most crystalline form with a reasonably high stiffness and strength. Hence, it is widely used in the injection molding, blow-molding, extrusion, and film applications. LDPE and LLDPE polymers, on the other hand, are the softer and tougher grades of

Table 19.2 The key features of commercial polyethylene homopolymers and copolymers

	HDPE	LDPE	LLDPE	Plastomer	PE elastomers (POE)
Comonomer (wt%)	None	None (branched)	2–5	10–25	>25
Density	0.94–0.97	0.91–0.92	0.91–0.92	0.87–0.91	0.85–0.87
Crystallinity	High	; Decreasing ⟶			
Modulus	High	; Decreasing ⟶			
Toughness at low temp.	Moderate	; Increasing ⟶			

polyethylene and hence are used primarily ($\geq$80 %) in the film applications. Because of the continuous nature of the film extrusion process, it is more amenable for blending different types of polyolefins to achieve specific improvements in the processability and properties of the desired film products. Some examples of commercial polyethylene blends will be discussed in the following section. A more detailed discussion on the polyethylene blends may also be found in another chapter of this handbook, viz., ▶ Chap. 18, "Polyethylenes and Their Blends."

19.2.1.1 Toughened HDPE (HDPE/LLDPE and HDPE/Olefinic Elastomer Blends)

HDPE is a highly crystalline polymer with a good combination of stiffness, strength, toughness, and chemical resistance. Hence, it is widely used in a variety of blow-molded rigid containers, pipe and profile applications, as well as film applications. However, for the automotive and miscellaneous outdoor and environmental applications, the low-temperature impact toughness and notch-sensitivity of HDPE often needed some improvement. Similarly, for the heavy-duty film applications such as in industrial bagging, agricultural, and geomembrane applications, improvement in toughness, puncture resistance, and environmental stress crack resistance was also needed. Hence, blending of low-modulus/rubbery modifiers has been used for a long time to achieve the above-described toughness in HDPE.

Blending of an elastomeric polyolefin such as polyisobutylene was used early on, to improve the dart impact and tear strength of the HDPE films (Anonymous 1974). Some commercial grades of HDPE utilized this rubber toughening technology (Haartman et al. 1970). With the advent of high melt-flow LLDPE resins and the lower-modulus/rubbery ethylene-α-olefin copolymers (plastomers and polyolefin elastomers-POEs), it is now more common to use these for toughening of HDPE, instead of the traditional rubbers, due to their improved processability and cost.

Thus, blends of HDPE with up to 30 % LLDPE have been considered for producing thinner-gauge films with improved tear strengths and toughness (Forger 1982; Kosoff 1987; Ogah and Afikuwa 2012). Blending LLDPE lowers the modulus and improves the tear strength of HDPE films (Fig. 19.6). In addition, the melt-processability and heat-sealability properties are also improved. Likewise, blending of LLDPE in LDPE is also used to improve the film processability and properties. More recently, polyolefin elastomers (POE) have been used in HDPE blends to significantly improve the low-temperature toughness of HDPE
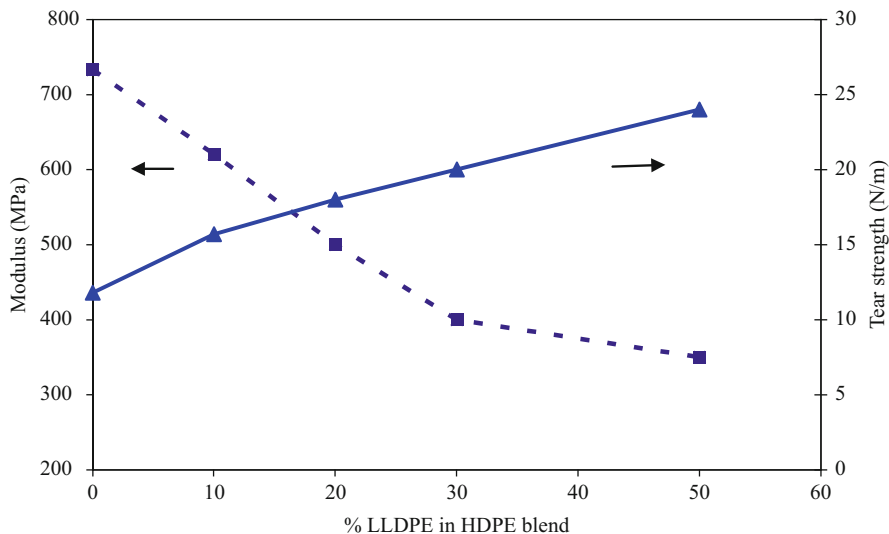
Fig. 19.6 Effect of LLDPE on the modulus and tear strength of HDPE blend films
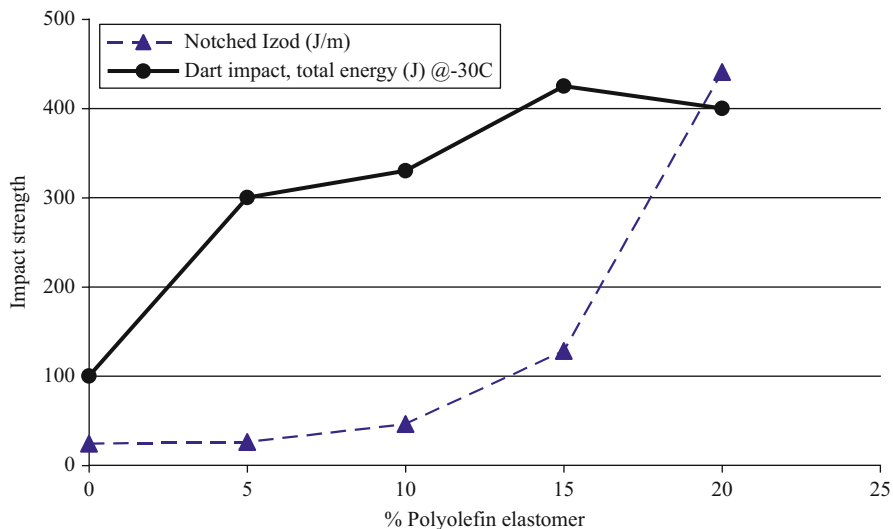
Fig. 19.7 Effect of POE content on the impact strength of HDPE-POE blends

(Anonymous 2006a). Typically, 5–20 wt% POE is blended in HDPE to achieve the desired low-temperature toughness (Fig. 19.7).

Commercially, the melt blending of an impact modifier in HDPE can be done simply during the extrusion process used for making the blown film or blow-molded rigid containers or in the extrusion of pipes and ducts. Ideally, such low-temperature

impact-resistant HDPE blends are particularly useful in many commercial applications such as in automotive underhood, industrial liquid/gas pipes, pipe fittings, and pipes for water transportation, geomembranes for environmental and waste-water management, agricultural and industrial packaging films, etc.

19.2.1.2 HDPE/Ionomer Blends

Commercial ionomers are ethylene-methacrylic acid copolymers and terpolymers in which the carboxylic acid moiety is partially neutralized with sodium or zinc, to promote interchain ionic bonding. Ionomers exhibit excellent low-temperature toughness, chemical resistance, and adhesion. However, they lack in stiffness and heat resistance. Hence, ionomer blends with polyolefins such as polyethylene have been developed which, upon reinforcing with suitable fillers, seem to give a unique combination of high strength, excellent low-temperature toughness, and moderate stiffness and heat resistance (Surlyn® HP, DuPont). Key to this technology appears to be the selection of a suitable surfactant that must be added in small amounts (0.3 %) to aid the dispersibility of glass fibers, yet retain high toughness (Murphy 1986).

The blend is reported to have an interpenetrating network (IPN)-type morphology, with the ionomer as the continuous phase. An unusual feature of this blend is the high notched Izod impact strength of >1,000 J/m at 23 °C and >760 J/m at −29 °C, even in the presence of 15 % of chopped glass fiber. In the absence of the surfactant additive, the blend with the same level of glass fiber showed somewhat poorer impact properties, e.g., notched Izod of <500 J/m at −29 °C and elongation at break of <3 %. In the presence of the surfactant additive, an ionomer/polyolefin blend reinforced with 15 % glass (Surlyn® HP) exhibits a flexural modulus of 1,600 MPa, a high notched Izod of >1,000 J/m and a moderate DTUL of 82 °C (at 0.45 MPa). These properties were claimed to be good enough to enable this blend to compete with the impact-modified polyamides in some applications.

19.2.1.3 HDPE/Polystyrene Blends

A blend of PS in HDPE (interpenetrating network) was commercially sold for some time, as expandable beads (Arcel®, ARCO; Neopolen® S, BASF) for making cellular foams (Kossoff 1987). Although PS and polyethylene are immiscible, closed-cell foams made from this immiscible pair appear to combine the rigidity of PS with the solvent resistance and abrasion resistance of HDPE. Hydrogenated styrene-butadiene-styrene block copolymers are known to compatibilize the PE/PS blends. However, these no longer seem to be commercially used.

19.2.1.4 Polyethylene/Polyamide Blends

A graft copolymer-compatibilized blend of PA-66-PA-6 (75/25) copolymer with HDPE was commercially offered as a barrier resin for making permeation-resistant solvent containers (Selar® RB, DuPont) (Subramanian 1984). Before melt blending with the PA, the PE backbone was modified by grafting with such reagents as maleic anhydride (Steinkamp 1976). A graft-coupling reaction between the PA and the maleated polyethylene, involving an amine/anhydride addition reaction, leads

to the graft copolymer formation at the interface, which reduces the interfacial tension and stabilizes the PA dispersion in the HDPE matrix.

By proper choice of the molecular weight, melt rheology of the PA, and processing conditions, a platelet-like dispersion of the PA in HDPE matrix could be achieved (Subramanian 1985). Since PA is a good barrier to hydrocarbons and many organic solvents, the platelets in HDPE provide the desired permeation resistance to solvents that HDPE lacks. On the other hand, polyethylene matrix provides the toughness, moisture resistance, and low cost advantages compared to PA. The blend was designated as a "laminar barrier" blend.

The PA/PE "grafted blend" was offered commercially as a concentrate (Selar$^{®}$ RB) to be melt blended with HDPE to a final PA/HDPE ratio of ca. 15/85 for subsequent blow molding into containers such as gasoline tanks, solvent containers, etc. This laminar barrier blend of HDPE and PA was reported to provide up to 100-fold improvement in the barrier to permeation of such organic solvents as toluene, relative to pure HDPE, or a similar blend composition containing PA as a uniform spherical dispersion.

The HDPE/PA laminar barrier blend technology has not been commercially utilized. A potential problem could be the high sensitivity of the morphology to the process conditions, which could lead to a lack of reproducibility in achieving the desired platelet morphology. The advent of coextrusion blow molding thwarted the blend's market penetration. Coextrusion assures a more uniform barrier layer of PA that can be relied upon for permeation resistance. Other techniques such as surface fluorination of polyethylene and SiOx coating, to improve the resistance to permeation of oxygen and solvents, are also commercially competing technologies.

19.2.1.5 HDPE/PET Blends

Blends of post-consumer recycled HDPE (from milk bottles) and post-consumer recycled PET (from soda bottles) were investigated for their potential utility (Akkapeddi 1992; Dagli and Kamdar 1994). The blend is highly immiscible and some level of compatibilization could be achieved by the use of functionalized polyethylenes such as ethylene-glycidyl methacrylate (E-GMA copolymer) or maleic anhydride-grafted polyethylene (MAnh.-g-HDPE) as reactive comptatibilizers. However, the blends lacked enough performance benefits to be commercially useful.

19.2.2 Polyolefin Blends Based on Polypropylene

19.2.2.1 Impact-Modified Polypropylene (PP/EPR Blends)

Polypropylene is a very large-volume thermoplastic with a current annual global consumption of over 62 Mt (Ceresana 2012). It is used in a variety of applications such as fibers, films, and molded parts. Commercial polypropylene homopolymer is produced by the stereospecific polymerization of propylene in the presence of Ziegler-Natta-type catalysts, which gives an isotactic polymer of high crystallinity. Due to this crystallinity and a reasonably high melting point (165 °C), isotactic polypropylene exhibits a useful combination of properties such as good stiffness,

strength, heat, and solvent resistance. The hydrocarbon nature of the backbone imparts it excellent hydrolytic and dimensional stability. In addition to these properties, polypropylene's low density, 900 kg/m^3, and relatively low cost makes it an attractive candidate for many applications and often competing with even the higher-priced engineering thermoplastics.

The crystallinity of isotactic polypropylene homopolymer, PP, however, leads to its well-known brittle behavior at low temperatures or when impacted under conditions of stress concentration, i.e., in the presence of sharp notches. For example, the low-temperature drop weight (Gardner) impact strength of unmodified PP is typically <2 J (at −30 °C) and its notched Izod impact strength is <40 J/m at room temperature, both significantly lower than that of polyethylene. This brittleness of polypropylene is related to the spherulitic morphology and the intrinsic tendency of PP for crazing followed by unstable craze growth and crack propagation under conditions of stress concentration and/or low temperatures (Kinloch and Young 1983; Friedrich 1983).

Commercial impact-modified PPs were developed during the early 1970s by melt blending about 5–25 wt% ethylene-propylene rubbers (EP or EPDM) with the polypropylene homopolymer via extruder compounding (Holzar 1966). Some LDPE or HDPE is often used to assist the dispensability of the EP rubber and enhance the impact/modulus balance of the product (D'Orazio et al. 1982). For the toughening of PP, EP rubbers meet the normal criteria for impact modifiers. Toughening of rigid polymers generally requires the formation of fine rubber dispersions with good adhesion to the matrix and thus providing multiple sites for crazing and localized shear yielding as mechanisms for the impact energy dissipation. Although not miscible, there exists a reasonable level of compatibility between EP rubbers and the polypropylene matrix due to their similarity in the hydrocarbon-type structures and the closeness of solubility parameters which leads to low interfacial tension and an adequate level of interfacial adhesion (Krause 1972). Hence, a small particle size dispersion of EP rubber is readily achievable by adjusting the molecular weights and melt viscosity ratio of EPR to PP and through the proper choice of mixing conditions (Yeh and Bisley 1985; Rifi et al. 1987). The control of the rubber-phase morphology in polypropylene is also dependent on the rubber composition (ethylene/propylene ratio), crystallinity, compounding and processing methods, as well as rheological properties. A slight cross-linking of EPDM rubber leads to better morphology stability during high-shear flow conditions such as injection molding (Dao 1982, 1984).

Commercial impact-modified PPs based on such blends exhibit excellent notched Izod impact strengths ranging from 80 to 800 J/m and moduli ranging from 1,000 to 1,700 MPa. Because of the large number of commercial suppliers and grades, no attempt will be made to describe the properties of any specific types of commercial impact-modified PP blends, except to generalize the trends in the impact/modulus behavior with respect to the content and the nature of the EPR.

In general, for best impact modification, the ethylene-propylene copolymer must have >30 % propylene and show essentially no crystallinity (Rifi et al. 1987). The size and distribution of the EP rubber particles in the polypropylene matrix depend on the molecular weights and the melt viscosity ratio between the two polymers, as

Fig. 19.8 Typical behavior of the effect of EPR content on the modulus and the low temperature impact strengths of PP/EPR blends (adapted from Rifi et.al. 1987)
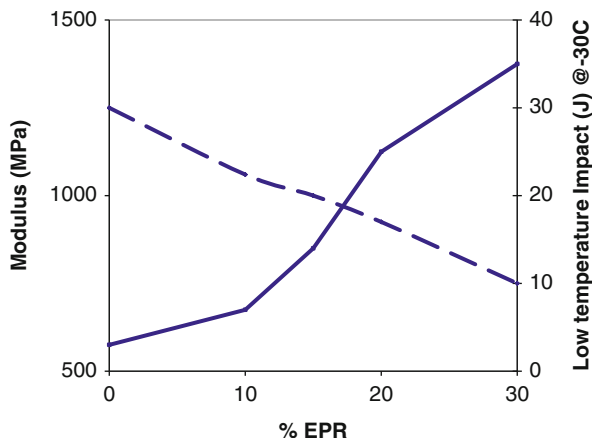
well as the mixing conditions (Speri and Patrick 1975; Jang et al. 1985). Particle size must be <3 μm and preferably be <1 μm for optimum impact strengths. Melt index ratio of PP/EPR, MI ≅ 10–60, was found to give acceptable dispersion size. The volume fraction and the particle size distribution of the rubber dispersion affect the modulus, impact strength, and melt flow of the blend significantly.

Although historically, commercial impact modified PP has been produced by extruder compounding, more recent advances made in the catalyst and polymerization technology allowed the production of these blends via an "in situ" process in the reactors (Rifi et al. 1987; Galli and Haylock 1991). By using a "super-active" catalyst and a gas phase, fluidized-bed reactor technology, the ethylene/propylene copolymer is allowed to polymerize and grow within the polypropylene homopolymer particle, polymerized earlier in the same reactor without isolation. The reactor technology could be tailored to produce a wide choice of products ranging from impact-modified polypropylene to thermoplastic elastomer-type PP/EPR blends (TPOs) by a judicious choice of the reaction conditions and the component feed ratios. The particle size of EPR in reactor TPOs is reported to be much smaller and hence more efficient in impact modification.

Impact vs. modulus balance of the extruder-compounded blends of PP/EPR is illustrated in Fig. 19.8. While the flexural modulus values are comparable, the low-temperature impact strength of the reactor-made PP/EPR blend products is usually better than that of extruder-made blends.

Conventional extruder compounding process for making impact-modified PP and thermoplastic polyolefin blends (TPOs) is still widely used to date, particularly by the independent compounders because of the versatility of this process for making a variety of specialized products having a wide range of performance characteristics. Compounding additive packages for improved heat stability, weatherability, and paintability is readily feasible in the extruder blending process. Colors, pigments, and fillers can also be blended in during the compounding of the PP/EPR blends.

Impact-modified polypropylene is used for injection molding automotive, consumer, and appliance parts. For example, the medium-impact PP is widely used for automotive interior trim. High-impact PP is used for battery cases, fenders, and truck liners. Impact PP is also used extensively in the houseware and appliance markets.

19.2.2.2 Thermoplastic Polyolefin Blends (TPOs)

Thermoplastic polyolefin (TPO) is a generic name that refers to polyolefin blends usually consisting of some fraction of polypropylene (PP), polyethylene (PE) or polypropylene block copolymer (PP-b-EP or "BCPP"), and a thermoplastic olefinic rubber, with or without a mineral reinforcing filler such as talc or wollastonite. Common rubbers include ethylene propylene rubber (EPR), EPDM rubber, ethylene-octene (EO) copolymer rubber, ethylene-butadiene (EB), and styrene-ethylene-butadiene-styrene (SEBS) block copolymer rubbers. Currently, there are a great variety of commercial polypropylene homopolymers, PP block copolymers, and olefinic rubbers available to make a wide range of TPO blends with densities ranging from 0.92 to 1.1.

Thermoplastic polyolefin blends (TPOs) can have properties ranging from flexible elastomers to tough rigid materials, each specifically formulated in a melt compounding process, to meet the needs of a particular application (Srinivasan 1991; Spencer 1990). The rigid or semirigid TPOs are essentially not much different from the impact-modified polypropylenes, except that higher levels of EP rubber are used during compounding of TPO to achieve additional low-temperature impact strength and minor levels of reinforcing fillers are added for additional stiffness. Such compounded TPOs generally contain 20–40 % elastomer, such as EPDM or POE (typical is 35 % EPDM or POE) in a conventional or impact polypropylene.

Generally, the TPOs are produced by extruder compounding processes in which the polypropylene resin is blended with an ethylene copolymer rubber (EPR or other polyolefin elastomers or POEs), along with a desired level of reinforcing fillers. The components are blended together at 210–270 °C under high shear using a twin-screw extruder or a continuous mixer.

The specific composition of the TPO blend produced depends on the balance of flexural modulus (stiffness) and impact toughness (drop impact and notched Izod) properties needed to meet the target performance specifications. In the formulation of TPO blends, the polypropylene is used normally as the major component, i.e., as the matrix phase, to provide the needed rigidity and thermal stability, while the elastomer dispersion provides the low-temperature impact toughness. A minor amount of a mineral filler such as talc provides additional stiffness and dimensional stability to the TPO. Hence, the levels of elastomer and mineral filler modifiers are carefully adjusted to achieve the desired balance of properties in the TPO.

The following is typical rigid TPO blend composition (Hemphill et al. 2005):

- 60–65 % Polypropylene – generally an impact copolymer or homopolymer
- 25–30 % Elastomer (EPR, EPDM or POE)
- 10 % Talc + small amounts of other additives

The small amount of other additives include heat stabilizers, UV stabilizers, mold-release agents/lubricants, paint-adhesion promoters, mar and scratch-resistance improving additive, etc.

In contrast to the rigid TPOs described above, low-modulus/flexible grades of TPO blends are also produced commercially. In flexible TPOs, the rubber content can be as high as 60 %, and in some cases, the dispersed rubber may also be partially cross-linked during the mixing without losing the thermoplastic character of the matrix. However, the latter type of "dynamically vulcanized" elastomeric alloys or thermoplastic vulcanizate rubbers (TPVs) are considered as a separate class of elastomeric materials and hence will be discussed under elastomer blends. On the other hand, the "soft" TPO blends discussed here contain a low-modulus olefin copolymer elastomer as the major component with some polypropylene added to impart melt processability.

Typically, a soft TPO would be composed of (a) 60 wt% of an olefinic elastomer of high melt strength, (b) 30 wt% PP homopolymer or impact PP copolymer and (c) 10 wt% of mineral filler.

The commercially important rigid and semirigid TPOs may have flexural moduli upto 2,000 MPa and service temperatures ranging from -40 °C to 130 °C. These TPOs are noted for their excellent toughness, high notched Izod impact strengths, and reasonable level of chemical resistance. The largest market for TPO is in the automotive area because of the material's low cost, low specific gravity, low temperature toughness, and weatherability. The rigid type of TPOs are extensively used for injection-molded automotive interior or exterior fascia which target high ductility at -30 °C and high part rigidity. Such paintable TPOs or those with molded-in colors are used for bumper fascias, grilles, air dams, side moldings, etc. Typical properties of TPO grades used in automotive applications are illustrated in Table 19.3. As may be noted, in these TPOs, the balance between the stiffness and toughness depends on the type and level of rubber and the level of mineral filler (usually the talc) used in the blend. The current annual consumption of TPO blends in the transportation market segment alone is >1.5 million metric tons. Lower cost and recyclability are the primary reasons for the rapid growth of TPOs in the automotive bumper applications, relative to SMC, PURIM, and steel.

TPO blends with added UV stabilizers are used in outdoor applications such as in roofing. Such TPOs are also used in a wide variety of exterior and interior structural parts such as in tractor, truck, and recreational vehicles, lawn and garden equipment, snowmobile body panels, industrial equipment and fan shrouds, etc. The low-modulus, soft TPO blends can be extruded into sheets and thermoformed for use in automotive interior skins that are competitive with products like vinyl, leather, and thermoplastic urethanes (TPUs). Advances in the development of specialty high melt strength elastomers that complement the rheology-modified polypropylenes are now enabling the formulation of high melt strength TPOs, extending their use in new thermoforming, profile extrusion, and blow molding applications (Weaver et al. 2006).

Table 19.3 Typical properties of some commercial TPOs used in automotive applications

Property	ASTM	Units	Compounded TPO		Reactor TPO
					Adflex®
			Daplen® EE015U	Daplen® EE109AE	KE051P
			Borealis	Borealis	LyondellBasell
	Filler level (%) →		10	20	None
Specific gravity	D792		0.94	1.04	0.89
Flexural modulus	D790	MPa (kpsi)	1,150 (167)	1,500 (218)	820 (119)
Tensile strength at yield	D638	MPa (kpsi)	16.5 (2.4)	17 (2.5)	17 (2.5)
Elongation at break	D638	%	100	70	500
Charpy impact, notched, at 23 °C	ISO179	kJ/m² (ft-lb/in.)	50 (24)	40 (19)	NB
Charpy impact, notched, at −20 °C			7 (3.3)	6 (2.9)	–
HDT at 0.45 MPa	D648	C	89	92	80
Key applications			Automotive exterior, bumper fascias, trim	Automotive exterior bumper fascias, trim	Automotive interior panels

Until recently, all compounded TPOs were based on PP/EP rubber blends. However, the new metallocene catalyst-based polyolefin elastomers (POEs) are now steadily displacing the EPR and EPDM rubber modifiers in the TPO blends due to the ease of handling and the overall lower cost of POEs. The evolution of the use of POEs in TPO blends will be discussed in the next section.

19.2.2.3 Polyolefin Elastomer (POE)-Based TPO Blends

The development of novel metallocene catalyst systems for polyolefin polymerizations represents a true technological breakthrough with very wide ramifications in the plastics industry (Wigotsky 1995; Schut 1996; Zamora and Miller 1997). As the latest-generation catalysts, the metallocenes differ from the traditional Ziegler-Natta catalysts in that they have well-defined single catalytic sites and well-understood molecular structures. Typically, they consist of a transition metal such as zirconium sandwiched between suitably substituted cyclopentadienyl ring structures to form a sterically hindered or "constrained geometry" metal catalyst site. With these new generations of catalysts, a wide variety of monomers can be polymerized or copolymerized in high efficiency but more importantly, various parameters such as comonomer distribution, polymer molecular weight, molecular weight distribution, molecular architecture, stereospecificity, degree of linearity, or branching can be independently and precisely controlled.

While the range of the new metallocene-based polymers includes such specialty polymers as cyclo-olefin copolymers (COC), syndiotactic polystyrene, ethylene/styrene copolymers, which are still in the developmental stage, commercially, the most prominent candidates are the ethylene/α-olefin copolymers such as ethylene/butylene or hexene copolymers (Exxon's Exact®) or ethylene/1-octene copolymers (Dow's Engage® and Affinity®). Depending on the comonomer content, these copolymers have been classified as plastomers or elastomers. At comonomer levels of >25 %, the copolymers exhibit the characteristics of thermoplastic elastomers such as high softness, toughness, flexibility, and resilience and hence been referred to as polyolefin elastomers (POE). Compositionally, these POEs usually contain 65 % ethylene and 35 % octene-1, hexene-1, or butene-1 as comonomers.

As a result of the controlled long-chain branching in otherwise linear polymers, the processability of these resins is claimed to be significantly enhanced compared to the standard LLDPE and EP rubber materials. Environmental stress crack resistance of metallocene polyolefin is also claimed to be significantly better. A wide range of densities (0.86–0.93), flexural modulus (10–100 MPa), melting points (60–120 °C), and melt flow index (0.5–125) is available in the commercial metallocene-based ethylene copolymers.

Thermoplastic polyolefin (TPO) blends of metallocene-based polyolefin elastomers (POE) with polypropylenes have gained commercial significance because of the improved melt flow and toughness compared to the conventional TPOs based on EPR or EPDM blends made with high melt-flow PP (Toensmeier 1994). In comparative tests with 70/30 PP/elastomer blends, the blends with POE maintained ductile behavior at −29 °C even with high melt flow index PP (MFI = 35), while the corresponding EPR-based blends were brittle with PP of MFI = 20. In addition, they showed improved knit-line strengths.

Because of their high shear-thinning and melt elasticity, plastomers and POEs disperse well in the PP matrix yielding fine elastomer domain dispersions leading to the better properties. POEs are easier to handle as they are available in pellet form, whereas EPDM is typically baled and needs additional equipment for feeding into the extruder compounding process. POEs also offer improved melt flow in TPO blends compared to EP copolymer-type elastomers. Currently, POEs account for about a third of the elastomer volume used in the compounded TPOs.

19.2.2.4 In-reactor TPO Blends Based on Polypropylenes

An in-reactor TPO may be defined as a reactor-produced polypropylene copolymer (PP-b-E/P), containing between 22 % and 55 % ethylene-propylene copolymer blocks. Small amounts of other comonomers, such as octene-1 or butene-1, may also be present so as to provide unique functionality. In-reactor propylene block copolymers containing less than 20 % ethylene are fairly hard and are usually classified as impact polypropylenes. Reactor-made polymers containing >50 % ethylene are soft and also have relatively poor elastomeric properties – these are classified as plastomers.

In-reactor TPOs are made in special polypropylene reactors, and they are designed to be cost- competitive to some extent against the compounded TPOs.

Table 19.4 Comparison of key features of reactor vs. compounded TPOs

TPO	Method	Advantages	Disadvantages
Compounded TPO	Extruder compounding of PP, elastomer, filler and additives	Flexible sourcing to optimize for lower cost and wider range of products	Compounding capital
Reactor TPO	• Reactor TPOs made by sequential copolymerization of PP and EP copolymer • Compounding with fillers and additives needed	• Excellent dispersion • Lower need for rubber than compounded TPO • Improved melt-flow	• Need special catalyst and reactor technologies • Somewhat higher cost • Reactor elastomer may not be quite as efficient as compounded TPO for low temperature toughness

However, in situ TPOs with high elastomer content are difficult to produce, and high levels of other additives, such as fillers and especially colorants such as carbon black, must still be done by compounding. In-reactor TPOs are used to reduce cost and increase the end-use value in those cases where the TPO does not need to be compounded prior to fabrication. In-reactor TPOs are mostly used in the automotive applications such as bumpers, interior impact trim, under-the-hood cladding, wire harness, weather strip, etc.

Some flexible grades of in-reactor TPOs ("r-TPO"), trademarked as Hifax®, are commercially produced by Lyondell-Basell using their Catalloy® process technology. Due to the higher levels of rubber dispersion in PP, these soft r-TPOs exhibit high toughness, flexibility, moisture barrier properties, and environmental stress-crack resistance and hence used in roofing and geomembrane applications. Typically, these flexible reactor TPOs exhibit a low modulus of ≤ 80 MPa, Shore A hardness of <90, a tensile elongation at break of >800 %, and a brittleness temperature of < -70 °C. They are widely used in geomembrane applications for (i) waste management- municipal solid waste landfill caps, wastewater treatment reservoirs; (ii) water containment in aquaculture ponds, decorative and golf course pond liners, and in (iii) water conveyance for canal liners, storage reservoirs, storm water ponds, tunnel liners, etc. The relative advantages and disadvantages of reactor vs. compounded TPOs are shown in Table 19.4.

19.2.2.5 Thermoplastic- Elastomeric Blends(TPEs) Based on Polypropylene

Thermoplastic elastomer blends comprising fully cured elastomer dispersions in a matrix of thermoplastic polyolefin such as PP have been commercial for some time. These blends have been made by the technology of dynamic vulcanization (Speri and Patrick 1975). The process consists of melt mixing and dispersing a high volume fraction of an elastomer such as EPDM rubber or nitrile rubber (NBR) into a thermoplastic matrix such as PP, using a compatibilizer if necessary, and then selectively cross-linking the dispersed elastomer during the extrusion, with specific curing agents. The resulting elastomeric blends display the typical properties of

cured rubbers such as high elastic recovery, low compression or tension set, yet process like thermoplastics, due to the presence of PP thermoplastic matrix. Commercial, elastomeric polyolefin blends produced by the dynamic vulcanization include EPDM/polypropylene blend (Santoprene®); Nitrile/polypropylene blend (Geolast®); Butyl rubber/polypropylene (Trefsin®). The technology of these blends will be discussed under the "Elastomeric Blends" heading.

Thermoplastic vulcanizates (TPVs) typically contain 60–70 % EPDM and 30–40 % impact polypropylene. These products contain a low level of cross-links, but they are true thermoplastic materials. TPVs have superior strength, high-temperature mechanical properties, hot oil and solvent resistance, and better compression set than partially cured material. These materials are almost always "dynamically cured," which refers to the process whereby the rubber phase is vulcanized during melt mixing with the molten non-cross-linked plastic.

TPVs have many of the elastomeric properties of vulcanized rubbers and yet can be molded or extruded using conventional thermoplastic fabrication equipment. They derive their properties from a unique physical network of seemingly incompatible structures, which coexist through chemical bonding. These structures can generically be referred to as soft-block and hard-block components. The soft blocks are amorphous, rubber-like elastomer components. The hard blocks, which are crystalline with their melting point above room temperature, form domains that prevent plastic deformation and provide tensile strength at normal-use temperature. TPVs can exhibit a range of properties because of the different types of hard and soft blocks, ratio of blocks, degree of polymer linearity, crystallinity, and cross-linking. Properties can be further changed by coblending and compounding with other vulcanized rubber components.

TPV market is primarily in automotive sealing where TPVs are displacing EPDM in less demanding (e.g., static) molded window seals. However, compression set remains an issue in more demanding (e.g., dynamic) applications such as door seals. TPVs are also increasingly used in overmolding on engineering plastics to achieve soft-touch tactile feel to the molded parts.

19.2.2.6 Reactor-Made Polypropylene/Nonolefinic Polymer Alloys

A new class of "reactor-made" alloys or "in situ" graft copolymer compatibilized blends of polypropylene with other amorphous, nonolefinic polymers have been commercially introduced by Montell recently under the trade name of Hivalloy® (DiNicola 1994). The commercial Hivalloy G series consisting of polypropylene/polystyrene alloys were first launched on a pilot scale in mid-1994 and later fully commercialized in 1996. Their Hivalloy W series are developmental grades of polypropylene/acrylic alloys, while the Hivalloy T series are experimental grades of polypropylene/styrene-maleic anhydride (SMA) copolymer alloys. All these reactor-made PP alloys are produced by Montell's proprietary "Catalloy" or "reactor granule" technology (Galli and Haylock 1991; Galli et al. 1994), which is a multistage, multimonomer polymerization process.

The fundamental basis for the reactor granule technology starts with the formation of a highly porous polypropylene particle first by the polymerization of propylene

monomer using a "super-active," third-generation, Ziegler-Natta initiator system which consists of a $MgCl_2$-supported, electron donor-modified $TiCl_4/AlR_3$ catalyst in a very high surface area, spherical particle shape ("Spheripol" process). A unique feature of this catalyst system is the high uniform porosity that is maintained during the polymerization in the growing PP particles. As the polymerization takes place, a growing skin of PP polymer is formed from the active sites on the surface of the expanding initiator particle. Proper control of the morphological structure of the initiator particles and the polymerization process results in the formation of highly porous PP granules.

These highly porous PP granules or beads are then used as the "reactor bed" for subsequent polymerization of one or more nonolefinic monomers such as styrene and methyl methacrylate. Since the latter polymerization is generally free radical, it results in the simultaneous formation of the nonolefinic polymer as well as its graft copolymer with PP uniformly distributed in micron-scale domains within the individual PP granules. This "in situ" generated graft copolymer then effectively compatibilizes and stabilizes the PP blend morphology during subsequent melt processing such as injection molding. The blends exhibit typical multiphase morphology behavior with the nonolefinic polymer generally forming the fine dispersed phase in the continuous PP matrix phase (DeNicola 1992). The PP matrix may contain additional rubber particle (EPR-type) dispersions for impact toughening of the blend.

The mechanical properties of these reactor-made alloys offer a balance of stiffness and toughness not generally attainable through the simple melt blending of the same polymer systems, primarily due to the effective graft copolymer compatibilization and good interfacial adhesion between the component phases. The Hivalloy reactor blends have been positioned by Montell to compete against ABS alloys and other low-end engineering resins based on at least some of the comparable properties, better chemical resistance, and a lower specific gravity. The higher T_g of the amorphous, nonolefinic polymer dispersion (PS, Acrylic, SMA) is expected to reinforce the PP matrix yielding a somewhat higher stiffness, strength, and heat distortion temperature, while the high crystalline melting point, ductility, chemical resistance, and high melt flow characteristics of PP are maintained. The following is a summary of the properties and applications of the two reactor-made alloys, viz., PP/PS and PP/acrylic polymer alloys.

Reactor-Made, Polypropylene/Polystyrene (PP/PS) Alloys

A series of reactor alloys of PP and PS were developed in the mid-1990s by former Montell (now part of LyondelBasell) under the Hivalloy G trade name, in the unreinforced, rubber–toughened, and glass-reinforced forms. These reactor-made Hivalloy-grade PP/PS and PP/PMMA alloys are no longer available. The lack of a cost-performance balance was the probable business reason for their discontinuance. Nevertheless, for the purpose of comparison with other PP blends such as TPOs, the typical properties of PP/PS and PP/PMMA are illustrated in Table 19.5. A key feature of these PP/PS alloys was claimed to be the impact strength/stiffness envelope that reportedly exceeded the performance of conventional PP and approached in some aspects with those of other engineering resins such as acetals,

Table 19.5 Properties of some "reactor-made" PP/PS and PP/PMMA alloys

Property	ASTM	Units	PP/PS	PP/PS/EP	PP/PMMA
Density	D792	kg/m³	0.94	0.92	0.95
Mold shrinkage	D955	%	1.3	1.2	1.4
Water absorption, 24 h	D570	%	<0.2	<0.2	<0.05
Flexural modulus	D790A	MPa (kpsi)	1,520 (220)	1,200 (170)	1,380 (200)
Flexural strength	D790A	MPa (kpsi)	43 (6.2)	33 (4.8)	39 (5.7)
Tensile strength at yield	D638	MPa (kpsi)	33 (4.8)	27 (3.9)	30 (4.3)
Elongation at break	D638	%	45	200	180
Notched Izod, at 23 °C	D256	J/m (ft-lb/in.)	135 (2.5)	No break	160 (3.0)
Instrumented impact	D3763	J (ft-lb)			
Total energy, at 23 °C			36 (27)	40	44 (32)
Total energy, at −20 °C				47	
Heat deflection temp.	D648	°C			
at 0.45 MPa			93	88	90
at 1.82 MPa			60	55	57

PC/ABS, PC/PBT. Depending on the PS content in the blend, the flexural modulus and DTUL increased predictably above that of PP while maintaining a high level of ductility and ultimate elongation. The notched Izod impact toughness could be raised to a "no-break" level particularly with the incorporation of some ethylene-propylene (EP) or styrene-ethylene/butylene-styrene block copolymer (SEBS) rubber modifiers. Compounding varying levels of glass fibers and reinforcing mineral fillers provided the desired balance of stiffness and toughness in these PP/PS alloys. The reinforced grades showed improved stiffness and creep resistance compared to PP alone to be able compete against reinforced polyamides and polyesters, particularly in applications that do not require high-temperature performance. Typical applications explored with these PP/PS alloys included automotive bumper beams, pillars, sporting and recreational equipment, sledge hammer handles, and other consumer tools and appliance components. The lighter weight to stiffness and toughness balance of these alloys was claimed to be a key advantage compared to the PC alloys.

Reactor-Made, Polypropylene/Acrylic Polymer (PP/PMMA) Alloys
A series of reactor alloys based on polypropylene and methyl methacrylate copolymer were briefly commercialized in the mid-1990s by Montell (now LyondelBasell), under the Hivalloy brand, but later discontinued. Nevertheless, the typical properties of such an alloy are shown in Table 19.5. These alloys were claimed to exhibit excellent weatherability, surface appearance, and colorability in addition to a good stiffness/toughness combination. In comparative SAE J1960 exterior weathering tests, PP/acrylic alloy showed superior color and gloss retention compared to ASA and PC/PBT (Sherman 1997; Hivalloy Data sheets 1997). The UV resistance of the blend must originate from the acrylic polymer, which may be enriched on the surface of the part. The attractive refractive index of the blend also makes it easy to color with molded-in colors.

Typical applications explored with the PP/acrylic polymer reactor alloys included automotive exterior mirror housings, interior trim and handles, truck wheel fenders, marine/outdoor recreational equipment, building and construction applications such as the outer layer for siding, etc. The apparent good weatherability, colorability, and mechanical properties of these alloys were believed to be good enough to compete against the well-established engineering resins such as ABS, ASA, PC/ABS, and PC/PBT. However, the lack of a cost-performance balance caused the commercial discontinuation of these PP/acrylic alloys.

19.3   Styrenic Blends

Styrenic resins, a family of commercially significant polymers and copolymers derived from styrene, rank among the major volume polymeric materials used, with an annual global consumption of nearly 26 Mt (Nexant 2012). Their low cost, ease of processability, and good balance of properties account for widespread use. Commercial styrenic thermoplastic resins may be classified into the following types:

1. Polystyrene (PS) and high-impact polystyrene (HIPS)
2. Styrene-acrylonitrile copolymer (SAN) and its impact-modified versions, viz., ABS (polybutadiene rubber grafted SAN), ASA (acrylate rubber grafted SAN), AES (EPDM rubber grafted SAN)
3. Styrene-maleic anhydride copolymer (SMA) and terpolymers with methyl methacrylate (SMA-MMA) and acrylonitrile (SMA-AN)
4. Styrene-methyl methacrylate copolymer (S-MMA)
5. Styrene-butadiene block copolymers [di, tri, and radial block $(S-B)_n$]

Among these, polystyrene is the lowest cost, most widely used commodity-type resin with an annualized global consumption of nearly 11 Mt in 2011 (Orhon 2012). This is followed by SAN, SMA, S-MMA, and the other specialty styrenic copolymers. All the styrenic resins are basically amorphous polymers with reasonably high glass transition temperatures ranging from about 100 °C to 130 °C, and heat distortion temperatures ranging from about 80 °C to 120 °C, depending upon the comonomer and impact modifier content. Because of the commodity nature of styrenic resin business, generally, there is less motivation to make blends via a compounding route which adds cost and sacrifices clarity. Improvements in styrenic resin properties such as strength, toughness, heat, and chemical resistance are generally made through copolymerizations (with acrylonitrile or methylmethacrylate) and in situ rubber-grafting techniques directly in the reactors.

Although the unmodified styrenics, viz., polystyrene, SAN, SMA, SMMA copolymers, exhibit good clarity, strength, and rigidity, they are invariably brittle for many applications. Hence, the rubber-modified styrenics such as HIPS and ABS, which combine a good level of impact strength with moderate heat resistance, have become more widely accepted in many molding and extrusion applications. Structurally, HIPS and ABS may themselves be considered as blends, since they contain ≥5 % polybutadiene rubber as a discrete phase, dispersed as 0.1–5 μm-size

particles in the matrix of polystyrene or SAN copolymer (Echte 1989). However, the rubber phase in these resins is incorporated during the free radical polymerization of styrene or S-AN monomer mixture via a mass, suspension, or emulsion polymerization process that results in the graft-coupling of the rubber phase to the matrix phase. In the context of the current discussion on blends, HIPS and ABS are not considered as blends, but more as impact-modified resin systems made in a reactor, although several grades of ABS are produced routinely by captively melt blending with SAN to adjust the rubber levels to the desired property specifications. However, HIPS and ABS are themselves used as base resins for blending with other thermoplastic resins to make new blends with desired combinations of properties.

The general motivation for blending styrenic resins with other polymers, particularly with the higher-priced, high-T_g, amorphous engineering resins such as polycarbonate, or polyphenylene ether, is primarily to lower the cost and improve the processability of the latter resins. The main reason for blending styrenic resins with crystalline polymers such as PA6 and PBT is to improve the solvent and chemical resistance which the styrenics lack.

19.3.1 Polystyrene and High-Impact Polystyrene (HIPS)-Based Blends

Because of its inherent brittleness, polystyrene homopolymer itself has limited application in blends. However, its impact-modified version, viz., HIPS, is more widely used. HIPS itself is a reactor-made multiphase system with 5–13 % polybutadiene ("cis"-rich) dispersed as discrete particles in the polystyrene phase, with an optimum particle size of mean diameter of 2.5 μm. The rubber in HIPS is chemically grafted to some extent to the polystyrene. The effective volume of the rubber dispersion is actually increased through the occlusion of some polystyrene. To optimize the impact strength, the rubber particle size ($\geq$2.5 μm) and the distribution is normally controlled by the agitation and the proper choice of other process conditions during the polymerization. The property improvements in HIPS, viz., increased impact strength and ductility, are accompanied by the loss in clarity and a decrease in the tensile strength and modulus compared to the unmodified polystyrene.

19.3.1.1 Blends of Polystyrene with S-B Block Copolymers (PS/SBC Blends)

Styrene-butadiene block copolymers (SBC) with a high (70–85 %) styrene content are commercially produced and marketed as transparent, stiff, and tough thermoplastic resins under the trade names of Styrolux® (Styrolution), K-Resin® (Chevron-Phillips), Finaclear® (Total petrochemical), and Clearene® (Denka-Kaguku). Unlike other more elastomeric types of styrene-butadiene block copolymers, the rigid SBC resins contain only $\leq$25 % polybutadiene rubber content. Structurally, these SBC polymers are composed of polystyrene (S) and polybutadiene (B) blocks, linked together in an unsymmetrical star-block [(S-B)$_x$] structure.

This star-block architecture results from the unique, sequential anionic polymerization and coupling process used. Due to the high styrene content of these resins, the polystyrene blocks form the major matrix phase, thus retaining high rigidity and DTUL while the PBD blocks form the minor dispersed phase leading to a high level of ductility and toughness, e.g., high tensile elongation to break of up to 300 %. Because of the extremely fine lamellar morphology of PBD dispersions ($<0.1\ \mu m$), the SBC resins retain a high level of clarity (Koller 1998). Due to their ease of processing and low density (1.01 g/cc), ca. 20–30 % lower than competing high clarity resins like polycarbonate, the SBC resins are cost-competitive in many clear thermoforming applications.

Since the SBC resins cost about twice as much as general-purpose polystyrene, there has been a significant motivation for blending SBC and polystyrene to lower the cost of the final SBC product without sacrificing the clarity, ductility, and impact toughness. Currently, 80 % of SBC resin used is in the form of blends with polystyrene. In most of the thermoforming clear packaging applications of SBC, the cost of the product is lowered by blending about 30–40 wt% of the lower-cost polystyrene, without sacrificing the clarity and toughness. The best blend ratio for an application is primarily determined by part design. Since biaxial orientation during the forming process increases part toughness, shallow draw parts like lids require higher SBC content than do deep-draw parts such as disposable cups. In practice, in most of the SBC/PS blended parts, the SBC content is usually in the 40–80 % range. The effect of PS/SBC blend ratio on two key properties, viz., the tensile elongation at break (a measure of ductility) and % transmission (a measure of transparency) is illustrated in Fig. 19.9.

Commercially, the SBC and PS melt blending is done directly by the fabricators during the sheet extrusion thermoforming or extrusion blow molding processes (Traugott 1985; Salay 1991). Such SBC/PS blends are widely used in various thermoforming (60 %), injection molding (20 %), films (8 %), and blow molding (7 %) applications. SBC/PS blends are very commonly used in the thermoforming clear packaging for food-service, medical packaging markets such as in the thermoformed clear yogurt containers, drinking cups, plates, tubs, trays, pharmaceutical bottles, shrink labels and blister packaging, etc. Injection molding applications include toys, hinged boxes, cases for electronic equipments, appliance parts, medical devices, etc.

Another promising area of growth is for SBC blends with higher-performing styrenics such as styrene-methyl methacrylate (SMMA) and SAN, in order to "down-engineer" applications currently in higher-cost PC, acrylic, or clear ABS. Potential uses include molded appliance parts and medical devices and extruded graphic display profiles.

19.3.1.2 Polystyrene or HIPS Blends with Poly(phenylene ether) (PPE/HIPS Blends)

Blends of polyphenylene ether (PPE, also known as PPO[®]) with HIPS are, by far, the most successful of all the commercial blends. General Electric company, which originally introduced this blend commercially in 1964 under the trade name Noryl[®], has since sold all their Plastics business to Sabic. Noryl[®] resins are now
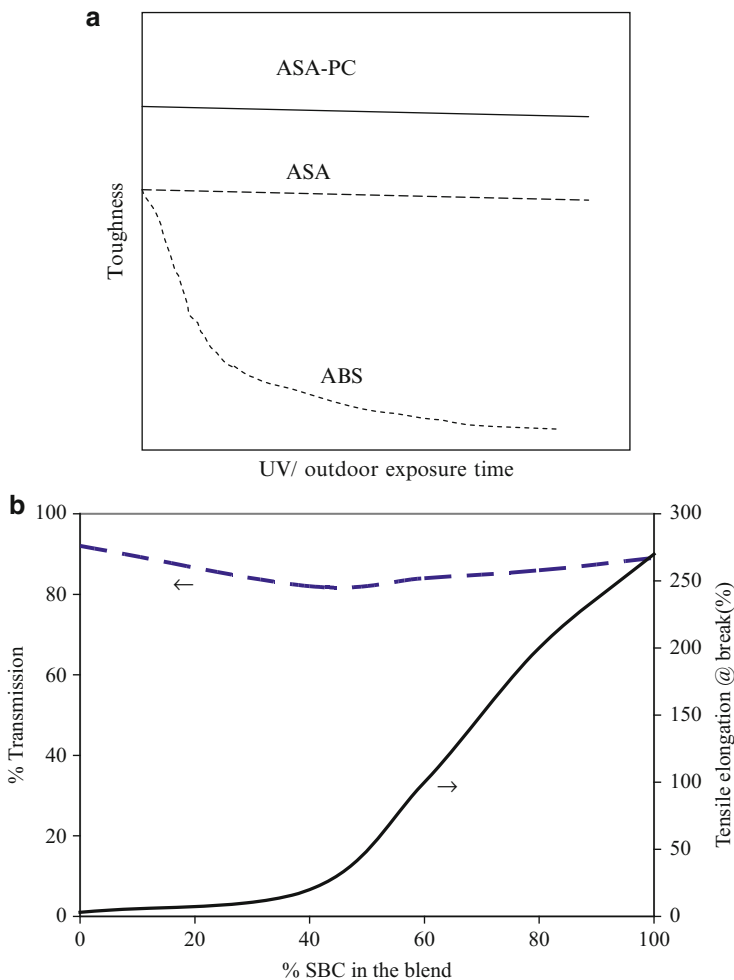
Fig. 19.9 (**a**) Schematic representation of the weatherability of ASA & ASA-PC vs ABS (**b**) Effect styrene-butadiene copolymer (*SBC*) in polystyrene/SBC blends on the transparency and tensile elongation at break (Anonymous 2006)

commercially produced and marketed by Sabic, although there are also other producers of such blends in Europe and Asia.

PPE is the acronym used for poly (2,6-dimethyl 1,4-phenylene ether), a high-T_g (205–210 °C) polymer produced by the oxidative coupling polymerization of 2,6-dimethyl phenol (Hay 1959, 1976). Sometimes, a minor amount of 2,3,6 trimethyl phenol is used as comonomer. Although PPE exhibits a good level of ductility and toughness along with a high heat distortion temperature, its high softening temperature and high melt viscosity precluded it from being used as a commercial molding resin, by itself. However, the discovery that blending PPE

with high-impact styrene could lead to improved processability and impact properties resulted in the successful commercialization of these blends (Cizek 1968). By simply adjusting the blend ratio, a wide spectrum of blend products with the desired combinations of DTUL, impact strength, processability, and cost balance could be produced. This versatility of tailor-making the blends for various levels of performance led to their rapid commercial success.

Key to this success, however, was the observed miscibility between the PPE and the PS phases resulting in a single-phase matrix with a single glass transition temperature that can be varied at will with the blend ratio. This thermodynamic miscibility between PPE and PS was established by various characterization techniques, viz., glass transition temperature (Schulz and Gendron 1972; Fried et al. 1978), electron microscopy (Kambour et al. 1980), small-angle X-ray scattering and calorimetric methods (Weeks et al. 1977), the latter showing a negative heat of mixing over the entire composition range. The presence of polybutadiene rubber particle dispersions in such a homogeneous matrix was found to lead to significant synergistic enhancement of the toughness of the blend, due to both the crazing and shear yield mechanisms of toughening (Bucknall 1977; Yee 1977). The particle size and the amount of rubber, however, affect the impact, modulus, and tensile properties of the blend.

Commercial PPE/HIPS blends may span a wide range of blend ratios, i.e., a PPE/HIPS blend ratio of about 25/75 to 60/40. Typical properties of commercial PPE/HIPS blends with varying PPE content are shown in Table 19.6. As expected, with increasing PPE content, the heat distortion temperature can vary from 90 °C to about 150 °C, because of the increasing T_g in these miscible blends. The melt rheology and flow characteristics again depend predominantly on the ratio of PPE to HIPS, with the molecular weights of PPE and HIPS also playing an important role (Schmidt 1979; Priest and Porter 1972). All the blends exhibit good ductility and impact strength. The notched Izod values range from 250 to 500 J/m. The rubber particles in HIPS contribute to the enhanced toughness of the blend. Since PPE is inherently more ductile than polystyrene, the efficiency of rubber toughening increases as the PPE content in the blend increases. Shear yielding process also contributes to the overall toughening effect, in addition to the usual craze-toughening mechanism. In blends containing ≥50 % PPE, shear yielding is the dominant mode of energy dissipation (Yee 1977). Unlike the case of polystyrene, the blend needs smaller-size (≤2 μm) rubber particles for optimum impact strength properties (Bucknall 1972). For higher impact strength, additional blending of styrene-butadiene-styrene (S-B-S) block copolymer-type elastomers and their hydrogenated derivatives, S-EB-S, are often employed. The ratio of PPE to PS in the blends can be determined from the ratio of the IR peaks at 854 and 700 cm^{-1}, respectively (White and Hallgreen 1983). The rubber particle size is determined by transmission electron microscopy using osmium tetroxide staining (Bucknall 1977).

Most of the PPE/HIPS blends are utilized by the injection molding process, although blow molding and extrusion/thermoforming applications are also increasingly practiced. Low moisture absorption and the good melt stability of PPE/HIPS blends along with their broad range of melt viscosities enable the fabricators a wide

Table 19.6 Typical properties of some commercial PPE/HIPS blends

Property	ASTM	Units	Noryl® SPN410	Noryl® SPN420	Noryl® 731	Noryl® PX1391
					Sabic	
Density	D792	kg/m³	1,060	1,070	1,060	1,070
Flexural modulus	D790	MPa (kpsi)	1,830 (265)	2,240 (325)	2,420 (346)	2,440 (354)
Flexural strength	D790	MPa (kpsi)	55 (8)	72 (10.4)	90 (13)	110 (15.9)
Tensile strength at yield	D638	MPa (kpsi)	35 (5.1)	44 (6.4)	58 (8.3)	68 (9.9)
Elongation at break	D638	%	82	60	28	25
Notched Izod impact, at 23 °C	D256	J/m (ft-lb/in.)	373 (7)	293 (5.5)	213 (4)	224 (4.2)
Notched Izod impact, at −40 °C	D256	J/m (ft-lb/in.)	186 (3.5)		133 (2.5)	133 (2.5)
HDT at 1.82 MPa	D648	°C	98	110	126	153
PPE content			Increasing			

choice of processing conditions. PPE/HIPS blends are used in a wide range of applications in the automotive, business equipment, appliance, electrical/electronic, and industrial markets. The automotive applications include instrument panel frames, interior trim, glove boxes, fuse boxes, connectors, wheel covers, mirror housings, etc. Flame-retarded grades are used for business machine housings, which are also often foamed to reduce the specific gravity and blow molded to reduce processing costs. Appliance parts and housings include those for refrigerators, washers, dryers, dishwashers, power tools, etc. The blends exhibit extremely low moisture absorption and good electrical properties suitable for electrical and electronic applications such as TV cabinets, connectors, electrical junction boxes, housings, relays, and bobbins.

The low moisture absorption and excellent hydrolysis resistance of PPE/HIPS blends coupled with their high dimensional stability makes them suitable for water meters and pump housings, plumbing parts, and a variety of fluid handling equipment parts. Some perceived building and construction applications include roofing panels, insulation, flooring substrates, etc. The high heat distortion temperature of PPE/HIPS led to its evaluation in microwave packaging. In applications requiring clarity, a blend of PPE and crystal PS containing no polybutadiene (Noryl® TN300, Sabic) is also offered commercially. Trays and packages that can be safely heated in microwave ovens have been made from such blends.

19.3.2 ABS Blends

Among the styrenic resins, acrylonitrile-butadiene-styrene (ABS) resins enjoy a unique position of being considered as engineering thermoplastics due to their outstanding high-impact strength performance over a wide temperature range coupled with good stiffness, and moderate heat and chemical resistance. ABS resins have now established globally to be the largest-volume (36 %) among all engineering thermoplastic resins used today. The current global production capacity of ABS resin is estimated to be nearly 10 Mt/year (NCPS 2011).

ABS resins are composed mainly of styrene (over 50 %) and varying amounts of acrylonitrile comonomer in the SAN polymer backbone and polybutadiene as a chemically grafted rubber dispersion. While the styrene units provide the rigidity and ease of processability, the acrylonitrile units contribute to the chemical resistance and heat stability. The polybutadiene rubber particles in ABS provide the toughness and impact strength. Structurally, ABS itself is a two-phase polymer blend system with the dispersed polybutadiene rubber phase (0.1–1 μm) embedded in a continuous matrix of SAN copolymer. Thus, the composition of ABS resins can vary widely, allowing the production of several grades tailored for different end-use applications.

ABS is commercially produced by the free radical polymerization of styrene/ acrylonitrile monomer mixture (usually 3:1 wt. ratio) in the presence of polybutadiene (of high "cis" content), which is added as a solution (ca. 10 %) in the mass polymerization process or as a latex seed during the emulsion polymerization

(30–60 % rubber) (Ku 1985). The emulsion-grade ABS is usually blended with virgin SAN copolymer to produce an ABS with a desired level of rubber (10–25 %). The impact strength, modulus, tensile strength, processability, and surface gloss of ABS depend on the rubber content and its particle size and distribution that is determined by the polymerization process and its conditions. The high-rubber ABS (25–50 % rubber) grades can be made only by emulsion process, and such resins (e.g., "Blendex" grades from Sabic) are often used for compounding with other thermoplastic resins such as polyvinylchloride (PVC) for impact modification (Dotson and Niznik 1991). The bulk polymerization process (continuous or suspension) produces low-gloss, medium-impact grades of ABS.

Due to its large scale of production and relatively low cost, ABS bridges the gap between the commodity plastics and the higher-priced engineering thermoplastics such as polycarbonate. Large-volume applications for ABS include appliance parts (including electrical/electronic) and automotive/transportation uses. A growing portion of ABS resins is now used in polymer blends. While the standard ABS resins inherently have a wide range of useful engineering properties, it is possible to extend and improve these properties further for certain niche applications via blending with other polymers. For example, blending with PVC can improve the flame retardancy of ABS at a low cost. Blending with higher-T_g, engineering resins such as polycarbonate and polysulfone can improve the heat distortion temperatures. On the other hand, use of ABS in blends with other resins can bring the advantages of low cost, improved impact strength, and processability. These will be discussed with the following examples of blends.

19.3.2.1 ABS/PVC Blends

Incorporation of 10–40 wt% ABS into PVC improves its impact strength, processability, and hot tear strength. Commercially, ABS/PVC blends are available from several sources, but more often, these blends are made in situ by the fabricators of sheet or profile extrusions. High-rubber, low-modulus grades of ABS made by emulsion polymerization are often used for the impact modification of PVC. Because of the thermal degradation problem of PVC, blending is done typically in Banbury-type mixers. The blend exhibits significantly improved notched Izod impact strength ($\geq 1,000$ J/m) over PVC. Although PVC is immiscible with ABS, the interfacial tension between the SAN phase and PVC is low enough to allow enough compatibility. The rubber particles, of course, are responsible for the enhancement of toughness. The primary application of this type of ABS/PVC blend, particularly in Western Europe, is in the manufacture of foil for vacuum thermoforming automotive and mass-transit interiors. The fabricators blend the powders of PVC and ABS and use the blend captively for the foil manufacture. Similar blends of PVC with MBS and ASA as impact modifiers are also used. These will be discussed in another section of this chapter entitled "PVC/Impact Modifier Blends" (Sect. 19.4.1).

Precompounded blends of ABS and PVC have also been commercially available for molding and extrusion applications as low-cost alternatives to flame-retarded grades of ABS and PPE/HIPS blends. Commercial ABS/PVC blends offer

Table 19.7 Properties of some commercial, styrenic resin/PVC blends

Property	ASTM	Units	ABS/PVC Cycovin KAF Goodrich	ABS/PVC Kaneka Enplex Kanegafuchi	ASA/PVC Geloy GY1220 Sabic
Density	D792	kg/m^3	1,200	1,200	1,200
Flexural modulus	D790	MPa (kpsi)	2,310 (330)	2,740 (390)	2,140 (310)
Flexural strength	D790	MPa (kpsi)	67 (9.6)	61 (8.7)	60 (8.5)
Tensile strength, yield	D638	MPa (kpsi)	40 (5.8)	44 (6.3)	46 (6.6)
Elongation at break	D638	%	20	20	25
Rockwell hardness	D785		R100	R105	R96
Notched Izod at 23 °C	D256	J/m (ft-lb/in.)	570 (10)	201 (3.7)	1,080 (20)
HDT at 1.82 MPa	D648	C	79	71	76
Flammability rating	UL94		V-0	V-0	V-0

high-impact strength coupled with flame-retardant characteristics (self-extinguishing, V-O ratings of UL-94) at a reasonable cost (Table 19.7). Such ABS/PVC blends have been used in appliance and business machine housings, TV cabinets, electrical and electronic component manufacture. Although the low cost, flame retardancy advantages of ABS/PVC blend are attractive, the thermal instability of PVC poses processing problems requiring careful control of processing conditions and temperature. In the injection molding markets, the processing disadvantages of ABS/PVC blend are limiting its growth, while improved versions of flame-retardant grades of ABS, ABS/PC, and PPE/HIPS blends are steadily gaining competitive advantage due to their superior processability.

19.3.2.2 ABS-Polycarbonate Blends

Blends of ABS and polycarbonate (PC) were first commercially introduced in the 1960s (McDougle 1967; Grabowski 1964). After an initial sluggish growth, these blends have now gained increased acceptance by resin fabricators and end users. Currently, ca. 1 Mt/year of ABS/PC blends are produced globally (Reseauplasturgie 2012). There are many suppliers of ABS/PC blends, primarily by those who produce the polycarbonate and/or ABS.

ABS/PC blend is an essentially immiscible blend (Echte 1989; Suarez and Barlow 1984; Kim and Burns 1988) with three distinct phases, viz., the PC phase, the SAN copolymer phase, and the grafted polybutadiene rubber phase dispersed within the SAN phase (as in the ABS to begin with). Depending upon the blend ratio, the continuous phase can either be the ABS (or more correctly, the SAN phase) or the PC phase. In spite of the immiscible nature, the blends exhibit good toughness, particularly in the region of 30–65 vol% PC (Weber and Page 1986). A primary reason for the good properties and delamination resistance in ABS/PC blends is partial miscibility between the PC and SAN phases, which leads to low interfacial tension and high interfacial adhesion, particularly when the SAN contains ≥25 % acrylonitrile (Keitz et al. 1984). The partial miscibility between PC and SAN has been demonstrated by the small yet finite increases in

Table 19.8 Properties of some commercial ABS/polycarbonate blends vs. neat polycarbonate

Property	ASTM	Units	ABS/PC			PC
			Cycoloy EHA	Bayblend T65	Pulse 710	Lexan 141
			Sabic	Bayer	Styron	Sabic
Density	D792	kg/m^3	1,090	1,120	1,120	1,200
Mold shrinkage	D955	%	0.5	0.6	0.6	0.6
Flexural modulus	D790	MPa (kpsi)	2,550 (370)	2,100 (305)	2,412 (350)	2,300 (340)
Flexural strength	D790	MPa (kpsi)		75 (10.9)	83 (12)	97 (14)
Tensile strength at yield	D638	MPa (kpsi)	45 (6.6)	50 (7.2)	48 (7)	60 (9)
Tensile strength at break	D638	MPa (kpsi)		45 (6.5)	45 (6.5)	70 (10)
Elongation at break	D638	%	40	80	60	130
Rockwell hardness	D785		R111	R118	R110	R118
Notched Izod at 23 °C	D256	J/m (ft-lb/in.)	370 (6.9)	534 (10)	534 (10)	694 (13)
Notched Izod at −29 °C	D256	J/m (ft-lb/in.)	320 (6)	481 (9)	250 (4.6)	320 (6)
Instr. impact, energy at 23 °C	D3763	J (ft-lb)	47 (35)	45 (33)	57 (42)	62 (46)
Instr. impact, energy at −29 °C	D3763	J (ft.lb)	47 (35)	40 (30)	57 (42)	
HDT at 1.82 MPa	D648	C	95	104	102	130
Clarity			Opaque	Opaque	Opaque	Clear

the T_g of SAN phase and similar decreases in the T_g of PC phase (Kim and Burns 1988; Morbitzer et al. 1985). The polymer-polymer interaction parameter for this blend was calculated to be slightly positive ($\chi_{12} = 0.03$). Some interpenetration of the chains at the phase boundary is responsible for the increase in the interfacial strength.

Properties of ABS/PC blend depend on the blend ratio. Blends containing major amounts of ABS (e.g., Cycoloy EHA) show improvements in DTUL and tensile properties relative to ABS but not in the notched Izod impact strength (Table 19.8). But as the polycarbonate level in the blend increases (particularly at PC ≥ 50 %), the notched Izod impact strength improves significantly, even at low temperatures. The ductile-brittle transition temperature in the latter blends is shifted to significantly lower temperature (Weber and Paige 1985), even compared to polycarbonate alone. The high dimensional stability, the excellent impact toughness at low temperatures, low gloss, and easy processability features of ABS/PC blends have led to their application in automotive interior instrument panels and, more recently, in exterior body panels, wheel covers, etc. ABS/PC is also used in business machine housings, snow throwers, snowmobiles, and other such equipment housings. A continued high growth rate (ca. 10 %) is expected for the ABS/PC blends because of their balance of high impact and heat resistance properties and moderate cost.

19.3.2.3 ABS/Polyamide Blends

Blends of ABS with commercial polyamides such as PA6 and PA66 are highly incompatible due to their dissimilar polarity, and accordingly, simple blends of ABS and PA exhibit poor delamination resistance with no practical value. Hence, several different approaches for compatibilization of the ABS-PA blends were investigated in the literature. In one approach, ABS was modified by copolymerization with acrylamide to improve the compatibility between ABS and PA-6, presumably through hydrogen bonding interaction (Grant et al. 1988).

In another approach, the SAN backbone of ABS was modified through copolymerization with maleic anhydride. This modification introduced controlled amounts of an anhydride functionality on ABS, which upon subsequent melt blending with a PA reacts to form a graft copolymer of SAN and PA at the interface (Eq. 19.1).

wwwwww NH₂   +   Maleic anhydride-SAN copolymer   →   PA-SAN graft copolymer
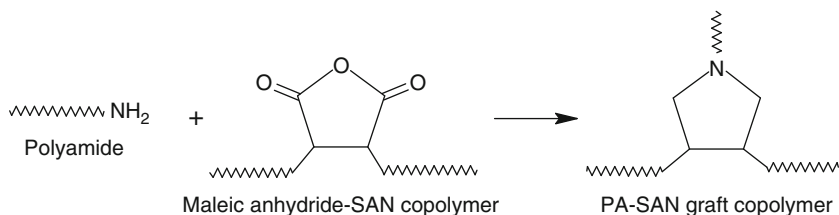
Polyamide

Equation 19.1 Polyamide graft coupling reaction with maleic anhydride modified SAN or ABS

The above graft-coupling reaction effectively compatibilizes the blend by reducing the interfacial tension and improving the interfacial adhesion leading to high impact strength. Such ABS-PA blends were initially commercialized in the 1990s by Monsanto under the trade name of Triax® 1000, utilizing the reactive compatibilizers (Lavengood 1987). Currently, these ABS/PA blends are commercially offered by Ineos ABS under the trade name of Triax® and by Styrolution under the trade name Terblend® N.

In another compatibilization technique, commercial ABS was directly modified by reactive extrusion with fumaric acid, without the need for copolymerization in a reactor, and the resulting "maleated ABS" was blended with a small amount of maleated EP rubbers followed by final PA6 blending, to make very high-impact ABS/PA6 blends (Akkapeddi et al. 1990). It was found that for maximizing the impact strength in the 50/50 ABS/PA6 blends, the ABS optimally had to contain about 25 % PBD rubber and about 5 % maleated EP rubber additionally preblended. Since polyamides are crystalline with high melting points and solvent resistance, it is desirable to keep the PA as the continuous phase and ABS as the dispersed phase in the blends. However, the ABS/PA blends tend to form cocontinuous morphology, which becomes somewhat finer and more stabilized with the compatibilization (Jafaria et al. 2002). Typically, such compatibilized, commercial ABS/PA blends (Terblend N, Styrolution) exhibit good solvent resistance coupled with high impact strengths and heat resistance (Table 19.9).

Some applications pursued for the ABS/Polyamide blends are: unpainted automotive interior parts, center consoles, steering wheel covers, air inlet systems,

Table 19.9 Comparison of commercial, ABS blends with amorphous vs. crystalline polymers

Property	ASTM	Units	ABS/PVC Cycovin K25 Goodrich	ABS/PC Pulse 710 Styron	ABS/TPU Prevail 3150	ABS/PA Terblend N Styrolution	ABS/PBT Verolloy Plastx world
Density	D792	kg/m^3	1,200	1,120	1,090	1,070	1,180
Flexural modulus	D790	MPa (kpsi)	2,310 (330)	2,412 (350)	1,034 (150)	1,800	2,210 (320)
Flexural strength	D790	MPa (kpsi)	67 (9.6)	83 (12)		62	79.3 (11.5)
Tensile strength at yield	D638	MPa (kpsi)	40 (5.8)	48 (7)	28 (4)	43	51.7 (7.5)
Elongation at break	D638	%	20	60	180	30	100
Notched Izod, at 23 °C	D256	J/m (ft-lb/in.)	640 (12)	534 (10)	NB	65 (kJ/m^2) 31 (ft.lb/in^2)	750 (14)
Notched Izod, at −29 °C	D256	J/m (ft-lb/in.)		481 (9)	374 (7)	15 (kJ/m^2) 7 (ft.lb/in^2)	
Drop weight impact							
at 23 °C		J (ft-lb)		57 (42)	52 (38)	–	–
at −29 °C		J (ft-lb)		57 (42)	64 (48)	–	–
HDT at 0.45 MPa	D648	C	83	118	78	85	
HDT at 1.82 MPa			79	102	63	65	96
Chemical resistance			Fair	Fair	Good	Excellent	Excellent

helmets, equipment housings, etc. ABS/PA blends have not developed a significant market growth presumably because they are unable to compete with the more widely established PPE/PA blends or ABS/PC blends to offer any tangible cost-performance benefits.

19.3.2.4 ABS/PBT Blends

The primary motivation to blend ABS with PBT was to combine the property advantages of crystalline PBT such as its high solvent and chemical resistance, high melting point, and ease of thin-wall injection moldabilty with the excellent impact toughness, stiffness balance of ABS. However, the high incompatibility of PBT and ABS required a suitable means of compatibilization. Various reactive compatibilization methods were investigated such as by using a maleic anhydride-grafted ABS or an epoxide-functionalized polymer such as a glycidyl methacrylate copolymer or epoxidized styrene-butadiene copolymer as reactive compatibilizers (Akkapeddi 1992; Ohtsuka 1995). Commercial ABS/PBT blends were developed (Novalloy®, Daicel; Verolloy®, Plastxworld) using such reactive compatibilization,

compounding techniques. Thin-wall moldability, high surface gloss, and chemical resistance are the key attributes of ABS-PBT blends useful in appliance parts and equipment housings. ABS/PBT blends have still not established any commercial significance.

19.3.2.5 ABS/Thermoplastic Polyurethane Blends (ABS/TPU)

Commercial ABS/TPU blends contain thermoplastic polyurethane elastomer (TPU) as the main blend component. The blends were first introduced in 1990 by Dow Chemical Co., under the trade name Prevail®. These blends characteristically exhibited low modulus (340–1,000 MPa) and high impact strength at low temperatures, e.g., notched Izod values of 370–1,500 J/m at $-29\ ^\circ C$. The TPU component of the blend imparts high toughness and also allows paintability without a primer. ABS component imparts heat resistance (for paint ovens) and good tensile strength in the blend. The blend was projected to be useful for automotive soft bumper fascias, but faced stiff competition from TPOs. Typical properties of ABS/TPU blends are shown in Table 19.9.

19.3.3 Acrylic-Styrene-Acrylonitrile (ASA) Terpolymer-Based Blends

Acrylic-Styrene-Acrylonitrile (ASA) resins, commercialized initially by BASF and subsequently by Styrolution and others, are normally produced by the graft copolymerization of styrene-acrylonitrile copolymer (SAN) onto an acrylic rubber (usually polybutylacrylate) via emulsion polymerization. The properties of ASA polymers are similar to those of ABS, exhibiting high impact strength, but unlike ABS, the ASA resins exhibit outstanding weatherability, lasting for a substantially longer service life than ABS. The polybutadiene (PBD) rubber in ABS is known to be prone to oxidative degradation reaction (Eq. 19.2) by the combined effect of atmospheric oxygen and solar radiation.

$$\text{\textbf{www}}\ CH_2CH=CHCH_2\ \text{\textbf{www}} \xrightarrow[\text{UV}]{O_2} \text{\textbf{www}}\ CH_2CH=CHCH\ \text{\textbf{www}} \longrightarrow \text{Chain scission}$$

PBD   oxidized PBD   OOH
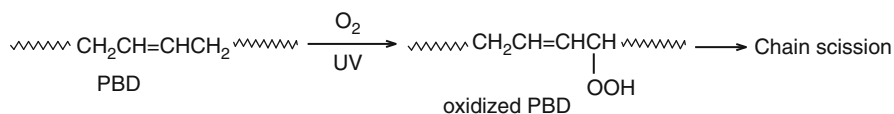
Equation 19.2 Oxidative chain scission reaction in polybutadiene phase of ABS

Because of the above oxidative chain scission reaction in PBD phase, ABS gradually loses its impact strength upon exposure to sunlight. The ASA polymers, on the other hand, retain their impact strength and toughness even after prolonged outdoor/UV exposure, significantly better than ABS, due to the presence of the weatherable acrylic elastomer phase, which replaces the unstable PBD phase. The outdoor/UV resistance of ASA and ASA-PC blend vs. ABS is schematically illustrated in Fig. 19.9a.

Hence, ASA and ASA blends are primarily used in the automotive/ transportation, recreational and agricultural vehicle parts requiring long outdoor

weather durability. Typical automotive exterior applications are: mirror housings, radiator grills, center pillar trims, window frames, cowl vent grills, fairings, and lamp housings. Pigmented ASA and ASA blends replace metal, coated, or painted ABS, or SMC materials in exterior parts of many types of vehicles.

ASA resins are generally produced as powders for easy blending with other resins such as PVC. ASA is also supplied as pellets for extrusion or injection molding applications. Compared to ABS, the ASA resins are relatively more expensive, hence used only for specialty applications requiring their very high outdoor weatherability and aging resistance. The following are some of the commercial ASA blends that are gaining increasing uses:

19.3.3.1 ASA/PVC Blends

Most of the ASA produced is used for blending with a lower-cost PVC resin by the end users. The fabricator blends powders of ASA and PVC in the desired ratio using conventional PVC processing equipment. The blend has been used in profile extrusions and coextrusions. Applications for ASA/PVC blend included siding, mobile home skirts, window profiles, vending machine trim, automotive exterior trim, etc. The blend has significantly better impact strength, heat distortion temperature, and color retention than PVC. The blend seems to have some cost advantage over neat ASA. Typical properties of ASA/PVC blends are described in Table 19.10.

19.3.3.2 ASA/PC Blends

In order to take advantage of the high impact strength of polycarbonate and outstanding weatherability of ASA resins, blends of ASA and PC have been developed commercially for exterior automotive applications. Some commercial grades of ASA/PC blends are Geloy® XP4025 from Sabic, Luran® SCKR2801 from Styrolution, Astoloy™ PC/ASA401 from Marplex. Blending polycarbonate with ASA enhances the notched impact strength and DTUL, while maintaining the weatherability, property-retention characteristics of ASA. Black and pigment-colored parts, such as automotive mirror housings, trim, cowl vents, grilles, etc., are some of the key applications for this blend. Typical properties of ASA/PC blend are shown in Table 19.10. In the commercial market, such ASA/PC blends have to compete with the painted or plated ABS/PC blends. However, the overall cost saving by pre-colorability without primer or paint and long-term durability factors will favor the ASA/PC blends in the exterior automotive, transportation, and outdoor equipment applications.

19.3.3.3 ASA/PA Blends

The primary rationale for developing the ASA/polyamide blends is to combine the high UV resistance of ASA resins with high heat and solvent resistance properties of the common semicrystalline polyamides such as PA6. The compatibilization of the ASA/PA6 blends uses the same technical approach as for the ABS/PA6 blends, viz., the use of a maleic anhydride-modified (copolymerized) SAN copolymer as a polyamide-reactive compatibilizer as discussed before under the ABS/PA blends

Table 19.10 Properties of some commercial ASA blends

Property	ASTM	Units	ASA/PVC Geloy 1220[a] Sabic	ASA/PC Geloy XP4025 Sabic	Luran SC KR2861 Styrolution	ASA/PA Terblend S NM-31 Styrolution
Physical						
Density	D792	kg/m³	1,200	1,140	1,150	1,070
Mold shrinkage	D955	%		0.5–0.7	0.45	
Mechanical						
Flexural modulus	D790	MPa (kpsi)	2,140 (310)	2,580 (374)	2,250 (320)	2,000 (286)
Flexural strength	D790	MPa (kpsi)	60 (8.5)	88 (12.7)	61 (11.2)	65 (9.3)
Tensile strength at yield	D638	MPa (kpsi)	46 (6.6)	58 (8.5)	53 (7.5)	50 (7.1)
Elongation at break	D638	%	25	25	>50	25
Impact						
Izod impact, notched at 23 °C	D256	J/m (ft-lb/in.)	1,080 (20)	170 (3.2)	610 (11)	65 (kJ/m²)
Thermal						
HDT at 1.82 MPa	D648	C	76	90	106	65
Chemical resistance			Moderate	Moderate	Moderate	Excellent
UV/weatherability			Excellent	Excellent	Excellent	Moderate

[a]Commercial status unknown

section (Sect. 19.3.2.3). Some commercial grades of ASA/PA blends currently available are: Terblend® S (Styrolution), Romiloy® 3020 (Romira GmBH). Key features of the ASA/PA blends are reportedly (a) enhanced UV resistance and color fastness (b) good melt flow for high surface quality appearance and (c) high impact strength. ASA/PA blends are still at an early stage of commercial growth. Since the corresponding ABS/PA blends were commercially known for a longer period of time and yet have not grown in significant volume of applications, it is likely that the growth of ASA/PA may be similarly limited. However, the substantially superior weatherability, color fastness, and chemical resistance of the ASA/PA blends may gain them a more favorable market growth in applications such as unpainted automotive interior parts, trim, outdoor equipment housings.

19.3.4 Styrene-Maleic Anhydride (SMA) Copolymer-Based Blends

Commercial SMA resins (Xiran®, Polyscope Polymers) are amorphous, random copolymers of styrene and maleic anhydride (8–30 %) that exhibit higher glass transition temperatures (20–60 °C higher) and higher heat distortion temperatures than polystyrene. The SMA resins were originally commercialized under the trade name of Dylark® by ARCO and by Nova chemicals but later on discontinued.

Table 19.11 Properties of commercial SMA/elastomer blends (impact modified SMA resins)

Property	Test method	Units	SMA/ Elastomer Xiran® SM200 Polyscope	SMA/ Elastomer Xiran® SM400 Polyscope
Density	ISO1183	kg/m^3	1,070	1,050
Mold shrinkage		%	0.7	0.5–0.6
Water absorption, 24 h		%	0.2	0.2
Flexural modulus	ISO 178	MPa (kpsi)	2,200 (330)	2,000 (286)
Tensile strength at break	ISO 527	MPa (kpsi)	32 (4.6)	30 (4.3)
Elongation at break	ISO 527	%	18	10
Notched Izod impact, at 23 °C	ISO 180/A	kJ/m^2 (ft-lb/in.)	14 (6.6)	15
Notched Izod impact, at −40 °C			7 (3.3)	10
HDT at 1.82 MPa	ISO 75	C	100	85
Vicat softening point	ISO 306	C	120	110

Currently, the high-molecular weight injection molding and extrusion-grade SMA resins are available only from Polyscope. The maleic anhydride comonomer imparts rigidity to the styrenic backbone raising its T_g by 2 °C with each 1 wt% increase in the maleic anhydride content. In addition, the maleic anhydride comonomer imparts higher polarity to the styrenic backbone and hence, increasing the modulus, strength, solvent resistance, and adhesion to reinforcing fillers and glass fibers (Wambach 1991). Hence, glass-reinforced SMA resins with high stiffness and strength have been used in many applications. The polarity and the reactivity of the SMA resins have also been utilized for the compatibilization of other polymer blends.

Unmodified SMA resins are quite brittle, like the PS, and hence they are invariably toughened by incorporating suitable rubber dispersions, either by grafting of a polybutadiene rubber during the polymerizations in a manner similar to the HIPS technology, or by blending with styrene-butadiene multiblock copolymer-type elastomers. Rubber-toughened SMA resins (Table 19.11) exhibit somewhat higher heat distortion temperatures than HIPS or ABS, yet have an equivalent toughness. Hence, such elastomer-modified SMA copolymers have found niche application in automotive interior instrument panels, headliners, and in some equipment-housing applications.

Terpolymers of SMA containing small amounts of methyl methacrylate comonomer were found to exhibit good miscibility with SAN (Hall 1982); hence, this technology was used to develop blends of SMA-MMA terpolymers with ABS. These blends exhibited higher DTUL/impact balance compared to ABS (Table 19.10) and reportedly offered processing and cost advantages over PPE/HIPS and ABS/PC blends (Kossoff 1987). However, these SMA blends are now no longer commercial. Similarly, SMA copolymers and terpolymers have also

been used for blending with PVC to improve the heat distortion temperature and processability of PVC. These blends contained a rubbery component for impact modification that is usually a high-rubber ABS or an acrylate core-shell rubber such as MBS. For improved weatherability, acrylic rubber-modified PVC has been used for blending with SMA. These SMA/PVC blends are no longer commercial, because they could not compete with the flame-retarded ABS resins in the business machine housing market.

A commercial blend of SMA and polycarbonate (Arloy®) was offered formerly by ARCO, but later discontinued. The polarity of SMA copolymer may account for the good compatibility between the two resins. The blend contained the polybutadiene rubber normally used in SMA resins for impact strength. It exhibited properties comparable to ABS/PC blend but with no cost advantage. In general, because of the lack of a competitive advantage of SMA compared to ABS in polymer blends, very few blends of SMA could be commercialized. The impact-modified SMA resins are the only commercial SMA blends known today (Table 19.11).

19.4   Vinyl Resin Blends

Poly(vinyl chloride) (PVC) is commercially the most significant member of the family of vinyl resins. The other important members of this group are chlorinated-PVC (CPVC) and poly(vinylidene chloride) (PVDC). PVC is one of the most widely used, commodity-type thermoplastics with an annual consumption of nearly 5 Mt/year in the USA. The excellent versatility of PVC is attributed to its blending capability with a variety of plasticizers, additives, and fillers to yield products ranging from very flexible to very rigid types. In addition, PVC has a low-cost advantage and a reasonably good balance of properties, which include (a) general inertness to many chemicals and aqueous fluids, (b) good dimensional stability, (c) good electrical properties, (d) inherent flame resistance, and (e) good weatherability. These attributes led to its widespread use in building construction, wire/cable, and packaging markets.

PVC, however, suffers from an inherent susceptibility to thermal degradation and hence must invariably be processed with heat stabilizers and careful control of processing temperature. The other important drawbacks of PVC are its brittleness in the absence of a plasticizer (low-notched Izod impact strength) and its low heat distortion temperature (ca. 60 °C) originating from its low glass transition temperature and essentially amorphous character. Hence, the primary motivations for blending PVC with other polymers in rigid applications have been to improve its impact strength (notched Izod), DTUL, and processability. In flexible, plasticizer-free (free from low-molecular-type materials) applications, PVC is blended with low-modulus polymeric modifiers known as flexibilizing modifiers or as polymeric plasticizers. For impact modification of rigid PVC, suitable rubbery impact modifiers are blended. The impact-modified and flexibilized PVC blends together constitute a major fraction of PVC used commercially.

Compounding mixtures of PVC, rubber, or flexibilizing modifiers is usually done by a two-step process involving dry blending followed by melt compounding.

Dry blends are usually made in conventional equipment, such as ribbon blenders and high-speed Henschel mixers. Proper mixing conditions are used to avoid excessive heat generation or agglomeration. For melt compounding, intensive mixing with heat and shear is used to compound PVC and the modifiers. Banbury or continuous mixers such as Buss kneaders, and high-shear twin-screw extruders are generally used for achieving a well-mixed PVC blend product.

19.4.1 PVC/Impact Modifier Blends

In rigid PVC applications (pipes, building, and construction), PVC is compounded with typically 5–15 wt% of the rubber-containing impact modifiers, to improve the notched Izod impact strength without sacrificing tensile strength and modulus. Various commercial impact modifiers effective in toughening the PVC are illustrated in Table 19.12. These are generally core-shell-type rubbers with a controlled particle size, rubbery core (polybutadiene, styrene-butadiene rubber, or poly-n-butylacrylate) grafted to a styrene-acrylonitrile (SAN) or styrene-methyl methacrylate (S-MMA) copolymer or polymethylmethacrylate as a rigid outer shell. These are made by emulsion polymerization of the corresponding monomers using a premade rubber latex as seed or core. The shell (rigid polymer) content in the methacrylate-butadiene-styrene-type (MBS) and the all-acrylic-type core rubbers is usually 20–30 % as compared to 30–50 % SAN in "high rubber" ABS.

The toughening effect of ABS, MBS, and acrylic modifiers is undoubtedly due to the controlled particle size of the elastomer phase (Shaw 1982; Shur and Ranby 1976; Walsh and McKeown 1990). For high impact strength, the particle size should be >0.1 μm but <1 μm. The good degree of compatibility or miscibility between PVC and PMMA or SAN phase also plays an important role in the toughening effect. Hence, a notched Izod impact strength of >1,000 J/m is readily achieved with these impact modifiers. ABS, MBS, and acrylic impact modifiers are available as powders and are usually blended with PVC powder in high-shear intensive mixers prior to fabrication of sheet or profile extrusion (Forger 1977). Precompounded grades of PVC are also sold commercially by all the major producers of PVC. When the particle size of the core-shell rubber is >0.2 μm, the toughened PVC is opaque. The ductile-brittle transition temperature shifts to lower temperature as the rubber particle size is decreased (Hassan and Haworth 2006).

Clear impact modifiers for PVC are controlled particle size grades of MBS, i.e., acrylic core shell rubber ABS. They offer the impact strength improvement as well as maintenance of sufficient optical clarity in the PVC blend. These impact modifiers are designed to match the refractive index of PVC. Controlled particle size (100–300 nm) and sufficient compatibility or solubility of the rigid SAN, S-MMA, or PMMA phase with the PVC account for the clarity of the blends. Some grades of MBS have been designed to have cluster-like structures (Saito 1973), in which the individual rubber particles of very small diameter (50–70 μm) are held together by a styrene-methylmethacrylate graft copolymer or terpolymer. When blended with PVC, these rubber particles are small enough to offer transparency to the blend, but

Table 19.12 Effect of various types of commercial impact modifiers for rigid PVC

Modifier	Advantages	Notched Izod (J/m) at various impact modifier levels (%) →			
		0	3	5	12
"High rubber" ABS (PBD $\geq$ 50 %)	Impact, processability	53	69	203	972
Methacrylate-butadiene-styrene ("MBS") (PMMA-g-SBR)	Clarity, impact and processability	53	64	240	1,335
Acrylate core-shell rubbers (PMMA-g-BuA)	Weatherability, clarity, impact, processability	53	69	192	1,041
Chlorinated polyethylene (CPE)	Weatherability, impact	54	90	235	1,225

the clusters of these particles in PVC matrix are large enough to cause craze toughening. Typical applications for clear impact-modified PVC blends are in clear, calendered sheets or films for packaging and for making blown bottles. Acrylic impact modifiers based on poly(n-butyl acrylate) or poly(2-ethyl hexyl acrylate) rubbery cores offer improved weatherability to PVC due to their saturated backbone. These blends are used for outdoor applications such as siding, window profiles, etc.

Chlorinated polyethylene (CPE) flexibilizes and toughens PVC more by a miscibility mechanism, especially when the chlorine content is >42 % (Donbe and Walsh 1979). However, partial miscibility occurring at chlorine levels of 36 % leads to higher toughening effects. CPE offers also weatherability advantage, which is the major reason for its commercial use. When CPEs are used as impact modifiers, they provide excellent toughness-weatherability balance for the entire range of rigid PVC applications, including vinyl siding, fence, window profiles, and pipes.

19.4.2 PVC/Polymeric, Flexibility Modifier Blends

The use of low-molecular weight plasticizers, such as dioctyl phthalate, to flexibilize PVC has been known and commercially practiced for a long time. Almost 90 % of current liquid plasticizer market is for PVC alone. The plasticizers work via molecular miscibility with PVC, thus lowering the PVC's T_g from ca. 80 °C to well below room temperature. The modulus of PVC is lowered from a high of about 3,000 Mpa to <100 Mpa with the addition of 30–40 wt% plasticizers, thus making it flexible enough for a wide range of applications. The transformation of rigid PVC into high-impact, rigid PVC and flexible PVCs and their key features are illustrated in Table 19.13.

Flexible PVC compounds incorporating the phthalate plasticizers have been used for a long time now in a wide range of tubing, hoses, films, wire, and cable jacketing applications in automotive, building, consumer, and health-care markets. However, the recent controversy over the migratability of phthalate ester

Table 19.13 Key features of various types of commercial PVCs

	Rigid PVC	Rigid, high impact PVC	Semi-rigid PVC	Flexible PVC
Modification	Unmodified	Rubber/impact modifiers	Low plasticizer (std. or polymeric)	High plasticizer (std. or polymeric)
Modulus (Mpa)	>3,000	2,400–2,700	100–1,000	10–100
T_g (°C)	85	80 (matrix)	≤0	<0 to −50
Ductile-brittle transition (°C)	60	0	0 to −20	−20 to −50
Elongation at break (%)	10	100–300	150–360	300 to >500
Notched Izod (J/m)	53	960	NB	NB
Key applications	Siding, pipes	Pipes, ducts, oil/chemical tanks	Films, sheets	Hoses, tubing, jacketing

plasticizers and their potential health concerns have spurred intense investigation into the use of various low-modulus, PVC-compatible polymers as potential "polymeric plasticizer alternatives" to the conventional low-molecular weight plasticizers for PVC (Robeson 1989; Brookman 1989). The high-molecular weight, polymeric plasticizers provide greater permanency than the liquid plasticizers, in maintaining the PVC flexibility, since they are not likely to leach out of the PVC during the service life of the part.

Hence, several types of low-modulus, rubbery polymeric modifiers are now used commercially for blending with PVC in order to make flexible PVC products. Most often, the blending is done directly during the fabrication of the flexible PVC product such as extruded sheet, tubing, or jacketing. These flexibilizing polymeric modifiers for PVC include the ethylene-vinyl acetate copolymers and terpolymers, nitrile rubbers (NBR), chlorinated polyethylenes (CPE), polyolefin elastomers (POE), TPU elastomers, etc. Some commercial flexibilizing modifiers and their key features are given in Table 19.14.

19.4.2.1 PVC/Nitrile Rubber Blends

Historically, nitrile rubber (NBR) blends with PVC were one of the earliest examples of any commercial polymer blends, dating as far back as 1946. In the rubber-rich PVC/NBR blends, PVC was added more as an ozone-resistant additive. In the thermoplastically processable PVC/NBR blends, the NBR was used to flexibilize PVC just enough to be used for "soft" goods, wire jacketing, hoses, gaskets, and seals. When the NBR contains >25 % acrylonitrile, it becomes highly miscible with PVC, and at ≤20 % acrylonitrile level, it is still compatible due to partial miscibility (Matsuo et al. 1969). PVC/NBR alloys are commercially produced (TeknorApex and others) and used in various automotive, industrial, and construction hoses, jacketing, seals, weather stripping, etc., where oil-resistance and low-temperature flexibility is important.

Table 19.14 Various modifiers for PVC flexibilization, their key features and benefits

Modifier	T_g (°C)	Miscibility with PVC	Benefits	Applications
Ethylene-vinylacetate copolymer	−20	Partial	Low-cost flexibilizer	Window profiles, films, cable jacketing
Ethylene-vinyl acetate-carbon monoxide terpolymer (E-VA-CO)	−32	High	Effective flexibilizer	Roofing membranes
			Low smoke generation	Geomembranes
Ethylene-butyl acrylate-carbon monoxide terpol. (E-BA-CO)	−54	High	Best flexibilizer for low temp. (−20 °C) flexibility and weatherability.	Roofing membranes
				Geomembranes
Chlorinated PE (30–40 % Cl)	−16	Partial	Chemical resistance + flexibility	Calendered PVC liners and roofing membranes
Polyolefin elastomers (POE)	−16	Immiscible	Low-density/cost, good toughness, processability	Hoses, tubing, seals and gaskets, boots
Thermoplastic polyurethane (TPU)	−30	Low	Chemical resistance	Shoe soles and heels, gaskets, seals, tubing
			Low temp. toughness	
High-nitrile NBR (45 % AN)	−14	High	Oil resistance, flexibility at low temperatures	Cable jacketing, hoses, tubing, belting, seals, gaskets, shoe soles, etc.
Low-nitrile NBR (20 % AN)	−48	Low		

19.4.2.2 PVC/E-VA-CO or E-BA-CO Terpolymer Blends

From a cost-performance balance point of view, the ethylene-vinyl acetate (EVA) copolymers and subsequently, the more effective ethylene-vinyl acetate-carbon monoxide (E-VA-CO) terpolymers have gained increasing use as "polymeric plasticizers" for PVC. Low cost and good weatherability of these PVC/EVA modifier blends permitted their use in window profiles, roofing, cable jacketing, and other outdoor applications. Although ethylene-vinyl acetate copolymer with 65–75 % vinyl acetate content is quite miscible with PVC exhibiting a single T_g for the blend (Hammer 1971; Ranby 1975; Rellick and Runt 1985), such EVA copolymers were quite difficult to process with PVC. EVA copolymers with ≤45 % vinyl acetate showed only a limited degree of partial miscibility with PVC, basically forming two-phase blends. Although commercial EVA copolymers with 25–30 % vinyl acetate can be used for flexibilizing PVC, their effectiveness is limited by their lack of adequate miscibility with PVC.

However, more recently, the ethylene-vinyl acetate-carbon monoxide (E-VA-CO) terpolymers (T_g = −32 °C), offering a more complete miscibility with PVC, because of the polar keto groups in the terpolymer structure, have replaced the EVA copolymers for flexibilizing the PVC. The E-VA-CO/PVC blends exhibit a single T_g behavior, indicating the complete miscibility (McConnell et al. 2004). Thus, the E-VA-CO terpolymer is more effective as a miscible, polymeric plasticizer for effectively lowering the T_g of PVC to make it more flexible.

Hence, commercial E-VA-CO terpolymers (Elvalloy® 741 and 742, DuPont) are now the more preferred and more commonly used flexibilizing modifiers in PVC blends. For an even better low-temperature flexibility in PVC blends, ethylene-n-butyl acrylate-carbon monoxide (E-BA-CO) (Evalloy® HP, Dupont) is used. The advantage of E-BA-CO terpolymer is its lower T_g (-52 °C). PVC/E-VA-CO blends and PVC/E-BA-CO blends are particularly used in roofing membrane and geomembrane application.

19.4.2.3 PVC/Chlorinated Polyethylene (CPE) Blends

Chlorinated polyethylene (CPE) has been in commercial use for a long time as an impact modifier to rigid PVC to achieve a combination of good impact resistance, ductility, and weatherability for use in the entire range of standard rigid PVC applications, including vinyl siding, fence, window profiles, and pipes. CPE has been used in these semirigid/high-impact PVC applications primarily due to its excellent weatherability. CPE has also been used to replace part of the plasticizer in flexible PVC compounds. However, for complete replacement of low-MW plasticizers, CPE lacks complete miscibility in PVC. Compatibility in the immiscible PVC/CPE blends is only due to a partial miscibility, which occurs only when the Cl content in CPE is >42 % (Donbe and Walsh 1979). Hence, for flexible applications, PVC/CPE blends are not flexible enough unless some plasticizer is included. CPE by itself with a small amount of PVC added as a reinforcement is often used for outdoor flexible roofing membrane applications.

19.4.2.4 PVC/POE Blends

The recent proliferation of metallocene-based polyolefins and polyolefin elastomers have gained their popularity owing to their density, cost, and ease of processability. PVC/POE blends have therefore been investigated as flexible PVC compounds. However, these blends are thermodynamically immiscible and needed suitable compatibilizers such as the chlorinated polyethylenes (Eastman and Dadmun 2002). Since they are not miscible, POEs do not lower the PVC modulus sufficiently unless some plasticizer or a compatible elastomer such as EPE is also added. Commercially, some PVC/POE alloys are offered by TeknorApex under Flexalloy® trade name with a shore A hardness 40–60 and brittle points down to -50 °C. They are claimed to have excellent low-temperature toughness, flexibility, compression set-resistance, and oil resistance. Suitable applications include automotive hoses, seals, gaskets, wire jacketing, etc.

19.4.2.5 PVC/TPU Blends

Many TPU elastomers are compatible with PVC exhibiting only a single T_g, in between that of TPU and PVC, indicating some level of miscibility. Because of the heat sensitivity of PVC, only very soft TPUs (i.e., high soft-segment, low-melting grades) can be melt blended with PVC. Typically, 40–50 % TPU is blended. The key advantage of TPU in the blend is wear and abrasion resistance and low-temperature toughness. The oil resistance of PVC is also improved. However, TPU is relatively more expensive as a blend candidate for PVC. Some plasticizer

may also be used to tailor-make desired softness. A 70/30 blend of PVC/TPU is as flexible as conventional plasticized PVC but with substantially better abrasion resistance and toughness at low temperatures. Commercially, PVC-TPU blends are available or formulated with varying Shore A hardness from various compounders (e.g., Apex® product line from TeknorApex). Specialty niche applications for PVC-TPU blends include shoe soles and heels, gaskets, seals, and tubing.

19.4.3 PVC/Styrenic Blends

Styrenic resins have been blended with some PVC primarily to achieve some degree of flame-retardant characteristics and cost benefits in the styrenic resins. ABS, SMA, and rubber-modified SMA, SMA-MMA copolymers have been used commercially for blending with PVC. These have been discussed under the styrenic blends and illustrated in Table 19.7.

19.4.4 PVC/PMMA Blends

PVC blends with poly(methyl methacrylate) (PMMA) have been commercialized (e.g., Kydex®, Kleerdex Co.) as extruded sheets for thermoforming applications such as chairs, seats, trays, etc. Ease of thermoformability, toughness, resistance to cleaning solvents, and the flame retardancy characteristics of the blends have been the primary features leading to its use. The good level of compatibility between PMMA and PVC is mainly responsible for the toughness characteristics of the blend (Walsh and Cheng 1984; Tremblay and Prud'homme 1984; Jager et al. 1983). Notched Izod impact strength of >600 J/m has been reported, although it is likely that some acrylic rubber modifier may have been used. The inherent flame retardancy and low smoke-generation characteristics of PVC/PMMA blends meet the aircraft fire safety standards. This factor coupled with the low cost, high toughness, and easy processing features of the blend led to its use in aircraft components such as toilet shrouds, floor pans, air diffusers, emergency respirator enclosures, etc.

19.5 Acrylic Blends

Commercial acrylic resins comprise a broad array of polymers and copolymers derived from esters of acrylic acid and methacrylic acid. They range from the homopolymer of methyl methacrylate to a variety of copolymers including both the thermoplastic and thermoset type and ranging from hard and stiff types to soft and elastomeric types. The most common of the thermoplastic acrylic resins are the poly(methyl methacrylate) homopolymer (PMMA) and the copolymers containing predominantly methyl methacrylate but with small amounts of methyl or ethyl acrylate, acrylonitrile, or styrene comonomers added for improved toughness.

The commercial PMMA-based acrylic resins are rigid, amorphous polymers (T_g's ranging from 85 °C to 105 °C) particularly noted for their exceptional clarity and UV resistance. They are therefore widely used for glazing, extruded sheet and thermoforming applications, as well as in several molding applications in which these properties are well utilized.

Since most of the applications of the PMMA-type acrylic resins are based on their high degree of transparency and UV resistance characteristics, there has been very little commercial motivation or interest in developing any significant types of acrylic blends. This is understandable because unless there is complete, molecular-level miscibility between the components, it is not possible to maintain a high-degree clarity in the blends. Nevertheless, several examples of commercial blends of acrylic resins are known. These will be discussed under separate headings.

19.5.1 Impact-Modified Acrylic Resins

Since the homopolymer PMMA as well as the MMA-rich copolymers are quite brittle, exhibiting low elongation to break (≤5 %) and low notched Izod impact strength (typically ≤15 J/m), there was a need to blend suitable impact modifiers that would improve the ductility and impact strength of these resins without sacrificing the transparency, rigidity, and weatherability characteristics.

Two general types of impact-modified acrylic resins have been developed commercially, viz., (a) weatherable, impact-modified, transparent acrylic resins for outdoor use in signs and automobiles; (b) nonweatherable impact-modified, transparent acrylic resins for medical and food packaging applications. The weatherable grades of acrylics are made by blending "all acrylic" core-shell rubbers, viz., PMMA-grafted, cross-linked poly(n-butyl acrylate)-type rubbers (Paraloid®, Rohm Haas). The nonweatherable grades are made by blending poly (methyl methacrylate)-g-butadiene/styrene ("MBS")-type core-shell rubbers. In both cases, due to the small particle size of these core-shell rubbers (≤100 nm) and the miscibility of the shell (PMMA) with the PMMA matrix, the refractive index could be matched and the transparency could be completely maintained. The rubber particles were found to promote localized shear banding in the matrix and hence, the ductility and toughness of the matrix improves (Hooley et al. 1981; Bucknall et al. 1984; Wrotecki et al. 1991).

Commercial impact-modified acrylic resins (Table 19.15) exhibit five- to tenfold improvement in the notched Izod impact strength and the ultimate tensile elongation compared to the neat PMMA resin. These impact-modified acrylics are usually blended captively by the manufacturers of the acrylic resins. The base resin in a typical weatherable grade (Plexiglas DR, Rohm and Haas) could be a methyl methacrylate copolymer with ethylacrylate and styrene, while the rubber additive (ca. 10 %) could be an emulsion-polymerized, PMMA-grafted, cross-linked poly (n-butylacrylate) rubber of controlled particle size (≤200 nm). The nonweatherable impact-modified acrylic (XT, CYRO) typically consists of a MMA/S/AN copolymer with MBS (ca. 10 %) rubber particle dispersions.

Table 19.15 Commercial acrylic polymer blends vs. acrylic polymer

Property	ASTM	Units	PMMA/core-shell rubber blend	PMMA/PVC blend	PMMA/PC blend	PMMA/PLA blend	PMMA
			XT 375	Solarkote® PB/PVC	Cyrex 200-8000	Plexiglas® Rnew PRD-1042	Plexiglas® V045
			Evonik	Arkema	Evonik	Arkema	Arkema
Density	D792	kg/m³	1,120	1,340	1,150		1,190
Mold shrinkage	D955	%	0.7		0.4–0.8		0.4
Flexural modulus	D790	MPa (kpsi)	2,400 (350)	2,400 (350)	2,400 (350)		3,160 (450)
Flexural strength	D790	MPa (kpsi)	76 (11)	73 (10.5)	86 (12.5)		120 (17)
Tensile modulus	D638	MPa (kpsi)		2,168 (310)		1,830 (260)	3,160 (450)
Tensile strength at yield	D638	MPa (kpsi)	48 (7)	42 (6.1)	61 (8.8)	34 (4.9)	72 (10.2)
Elongation at break	D638	%	28	45	58	14	5
Rockwell hardness	D785		M45	M30	M46	M85	M96
Notched Izod at 23 °C	D256	J/m (ft-lb/in.)	107 (2)		1,600 (30)	127 (2.4)	12 (0.2)
Notched Izod at 0 °C	D256	J/m (ft-lb/in.)	85 (1.6)		213 (4)	–	
HDT at 1.82 MPa	D648	C	86	70	101	66	92
Light transmission	D1003	%	86	Opaque	Opaque	87	92

Generally, the weatherable impact-modified acrylic resin has better color and transparency retention than the nonweatherable grade but the latter shows better toughness. The weatherable grades are used for making outdoor signs, automotive headlight lenses, lighting fixtures, glazing, etc. The nonweatherable, high-impact acrylics are used for medical devices, medical and food packaging, refrigerator trays, etc. Polycarbonate is a competitive threat to the impact-modified acrylic resin markets.

19.5.2 Acrylic/PVC Blends

Since PVC is known to be quite miscible with PMMA (miscibility with an LCST behavior) (Jager et al. 1983) and is also low in cost, some blends of PVC and PMMA have been used in sheet extrusion and thermoforming applications.

However, the acrylic PVC compositions commercially used invariably contain an acrylic core-shell rubber (PMMA-g-n-BuA or MBS-type) to get high toughness, with some PMMA, to reduce the cost/impact performance balance. The role of PVC in these blends is primarily to reduce the cost and impart some degree of flame-retardancy to the acrylic resin. The acrylics definitely help in the processability of PVC. These blends have already been discussed under PVC heading.

19.5.3 Acrylic/PVDF Blends

Poly(vinylidene fluoride) (PVDF) is increasingly used in outdoor applications such as architectural coatings, due to its outstanding chemical and UV resistance and long-lasting weatherability performance. However, the chemical inertness of PVDF prevents good adhesion to substrates and makes it difficult to disperse pigments. Furthermore, the high cost of PVDF makes it indispensable to blend a second polymer component to optimize the performance of PVDF materials. The most widely used class of polymers for blending with PVDF is acrylic resin, such as poly (methyl methacrylate) (PMMA) and its copolymers. Acrylics have good compatibility with PVDF providing clarity coupled with good heat resistance and weatherability. Typically, 30 % acrylic polymer is blended in PVDF architectural coatings (Wood et al. 2005).

PVDF is known to form thermodynamically miscible blends with PMMA exhibiting a single T_g, an indication of a single-phase behavior (Bernstein et al. 1977; Mijovic et al. 1982). The homogeneous PVDF-PMMA blend does not phase-separate until above the lower critical solution temperature (LCST) of around 300 °C. Upon cooling to below the melting temperature at 178 °C, PVDF does tend to crystallize to some degree however, from the homogeneous blend (Bernstein et al. 1977; Wang and Nashi 1977). The melt-cooled solid blend contains some PVDF crystallites, and the remaining PVDF plus the acrylic form a second amorphous, miscible alloy phase. This unique combination of crystalline and amorphous phases gives PVDF-PMMA coatings many of their superior properties, such as flexibility combined with solvent resistance.

A commercial PVDF/PMMA blend film (Fluorex® A, Rexham Corp.) is produced captively by solvent-casting for use in specialty film applications, such as a protective and decorative film overlaminated for automotive parts. It is laminated to metal, followed by fabrication (stamping, rolling) into automotive parts such as rocker panels, hubcaps, pillar posts, door edge guards, etc. The role of PVDF in this blend is to offer chemical resistance coupled with weather resistance.

19.5.4 Acrylic/PC Blends

PMMA/polycarbonate (50/50) blends prepared by melt-mixing are mostly immiscible, exhibiting two glass transition temperatures in DSC, one at the normal T_g of PMMA (ca. 105 °C) and the other for PC at about 8 °C below $\boldsymbol{T_g}$

of **PC** (i.e., 142 °C vs. 150 °C), indicative of, at best, only a small degree of partial miscibility (Chiou 1987). Because of this phase-separated morphology, PMMA-PC blends made by the usual melt compounding techniques are understandably opaque and exhibit lower impact toughness than polycarbonate. However, the impact toughness of PMMA/PC blends were substantially improved by blending a PMMA-grafted EPDM rubber as compatibilizing toughener (Zimmerman 1992). Using such a compatibilizer toughening technology, Cyro Industries (now part of Evonik industries) commercially developed a family of opaque, high-impact, PMMA-PC alloys under the trade name of Cyrex®. The key advantage of Cyrex® PMMA-PC blends is the substantially higher notched Izod impact strength (two to three times higher) than that of PC or ABS/PC, with comparable modulus, strength, and hardness properties. Key properties of a commercial high-impact, PMMA/PC blend are shown in Table 19.15.

Key applications for Cyrex® PC-PMMA alloys include the following markets:
  (i) Appliances
 (ii) Toys
(iii) Furniture
 (iv) Automotive components
  (v) Protective casings
 (vi) Housings for personal electronic devices
(vii) Medical equipment

19.5.5 Acrylic/PLA Blends

Polymethyl methacrylate (PMMA) has been found to form miscible alloys with polylactic acid (PLA), a bio-based, biodegradable polyester (Eguiburu et al. 1998; Zhang et al. 2002). Miscibility also means that PMMA and PLA can be blended at any ratio, keeping the transparency high. Blending of PLA into PMMA improves the ductility and solvent resistance of PMMA while maintaining good transparency. The processability and melt flow characteristics are also improved to allow the molding of more complex and intricate PMMA parts. Blending of PMMA in PLA elevates the heat resistance, hydrolysis, and UV-resistance of PLA.

Some commercial PMMA/PLA blends containing 25–35 % PLA have been recently introduced by Arkema as "Plexiglas® Rnew Biopolymer Alloys" (Naitove 2012). The primary motivation to develop these PMMA blends is the desire to reduce the carbon footprint by incorporating bio-based polymers. By blending >25 % PLA into PMMA, a "bio-based" certification is achievable while simultaneously improving the toughness, solvent-resistance, and processability of PMMA. Transparency is retained due to the mutual miscibility of the two polymers. Properties of a transparent grade of PMMA/PLA blend (Plexiglas® Rnew PRD-1042, Arkema) are included in Table 19.15. Target applications for such transparent PMMA/PLA blends, with improved impact and chemical resistance, appear to be primarily in medical equipment markets.

19.6   Elastomeric Blends

The blending of different types of rubbers and then curing into the final fabricated parts such as automotive tires has long been known in the rubber industry and will not be discussed here. This discussion will deal with the commercial blends containing a high volume fraction of a rubbery polymer and minor amounts of a rigid, amorphous, or crystalline thermoplastic. A major motivation for developing such blends was to combine the elastomeric character of the rubber component with the melt processability of the thermoplastic. Hence, blending has been an alternative and somewhat lower-cost approach to making thermoplastic elastomers compared to the block copolymer approach.

Vulcanized rubbers are distinguished by their characteristically low modulus, high extensibility, and high elastic recovery, i.e., by their ability to return to the original dimensions after stretching to high strain levels and then releasing the applied stress. The elasticity behavior in vulcanized rubbers is related to the cross-linking between the polymer chains. However, in the thermoplastic elastomers, the elasticity originates from the pseudo-cross-links formed by the rigid phase, which is either the hard segment of the block copolymer or the rigid inclusion having high gloss transition temperature, or crystalline polymer phase blended into the elastomer as a fine dispersion.

Blends of metallocene polyolefin elastomer/plastomer materials compounded with EPDM (typically 70/30) are finding several extrusion applications such as flexible hoses, cords, and wire jacketing because of much higher extrusion rates and better heat aging characteristics than EPDM (Sherman 1997). Blends of POEs with ethylene-vinyl acetate copolymers are used as cushioning in sports shoes because of improved resiliency and durability. Blends of POE with PVC are employed in some extruded profiles for refrigerator gaskets, window and garage door seals. Other applications of POE blends include soft-touch handles for handheld tools and for automotive noise, vibration, and harshness (NVH) dampening. As the metallocene olefin copolymers become increasingly more cost-effective, the application of their corresponding blends are expected to proliferate.

19.6.1 Nitrile Rubber/PVC Blends

Blends of butadiene-acrylonitrile copolymer rubber (nitrile rubber or NBR) and PVC are among the oldest known examples of commercial elastomer/thermoplastic blends. The shortage of natural rubber during World War II stimulated research in the USA on the compounding and modification of synthetic polymers to produce rubber-like materials. An outcome of this research was the commercial introduction of NBR/PVC blends by B.F. Goodrich in 1947 under the trade name of Geon® Polyblends (Pittenger and Cohan 1947). The blend showed improved ozone resistance and melt processability compared to the nitrile rubber (Table 19.16).

Table 19.16 Typical properties of nitrile rubber/PVC blends vs. nitrile rubber

Property	NBR/PVC (70/30)	NBR/PVC (55/45)	NBR
Hardness (Shore A)	73	82	63
Modulus (MPa) at 100 %	4.6	7.5	2
at 300 % elongation	12	13.5	10
Tensile strength (MPa)	17	15.8	22
Elongation at break (%)	530	460	600
Compression set (%) (22 h, 100 °C)	48	64	37

Butadiene-acrylonitrile copolymer rubbers containing >25 % acrylonitrile exhibit good miscibility with PVC as evidenced by single T_g behavior of the blend (Zakrzewski 1973; Matsuo et al. 1969), although high-resolution electron microscopy indicated some degree of microheterogeneity with a very fine dispersion size (<10 nm) (Matsuo 1968). This high degree of miscibility, or partial miscibility, between the components accounts for the blend's high compatibility and improved mechanical properties. Commercial nitrile rubber/PVC blends are used in both nonvulcanized and vulcanized forms. A descriptive list of commercially available nitrile rubber/PVC blends can be found under a variety of trademarks in the Nitrile Elastomers section of "The Blue Book, Materials, Compounding Ingredients and Machinery for Rubber," published annually by Bill Communications, Inc. Nitrile rubbers are known for their oil and chemical resistance, and addition of PVC improves the ozone resistance. Use of carboxylated NBR is believed to obviate the necessity of vulcanization. Nitrile rubber/PVC blends have reached a mature stage in their commercial usage. They face increasing competition from other thermoplastic elastomers such as the dynamically vulcanized blends of PP/EPDM and PP/NBR (Santoprene® and Geolast® grades).

19.6.2 Thermoplastic Dynamically Vulcanized Elastomer Blends (TPV Blends)

Another class of thermoplastic elastomer blends, which has gained significant commercial growth in recent years, is the "dynamically vulcanized" or a fully cured elastomer blended in a thermoplastic matrix (Coran 1987). Dynamically vulcanized alloys are produced by melt blending a high volume fraction of an elastomer with a thermoplastic in a high-intensity mixer, with a compatibilizer if necessary, such that a fine dispersion of the elastomer is achieved. The elastomer is then fully cured during the melt mixing through the use of selective cross-linking agents. Since the elastomer is fully cured, the blend achieves a high rubber elasticity character, but since the thermoplastic still remains as an uncross-linked matrix, the blend can be melt processed like a thermoplastic. In order to distinguish from the

simple blends of an elastomer and thermoplastic, the dynamically vulcanized blends have previously been classified as "elastomeric thermoplastic alloys" (ETA), (Wallace 1992) but currently more commonly referred to as the "thermoplastic vulanizates" (TPVs).

Dynamically vulcanized, elastomeric thermoplastic alloys or TPVs display properties as good as or even better than the block copolymers, viz., a high degree of rubber elasticity yet good melt processability. The main advantages of the thermoplastic vulcanizate elastomer blends over the uncured thermoplastic/elastomer blends are

- Improved resistance to compression or tension set
- Improved tensile strength, elongation, and resiliency
- Improved flexural fatigue resistance
- Improved chemical resistance
- Better morphology stability during melt processing
- Improved melt processability and recyclability (regrind reusability)

   The dynamically vulcanized blends are melt-processable elastomers, which can be processed by conventional injection molding, blow molding, and extrusion techniques. Some key factors affecting the performance of a TPV are

   - The degree of cross-linking of the rubber phase. A high level of cross-linking offers more rubbery elasticity and low compression set in the product.
   - The degree of fineness of the rubber dispersion in the thermoplastic matrix. The rubber domains must be in 1–2 μm range, although they may be interconnected.
   - The thermodynamic compatibility between the rubber and matrix polymers. A high inherent compatibility needs no compatibilizer, but those with low inherent compatibility (e.g., NBR rubber/PP) will need compatibilizers to stabilize the interface and improve interfacial adhesion strength.

Examples of commercially important TPV alloys include the dynamically vulcanized blends of PP with high volume fractions of EPDM (Santoprene®) and similarly, the PP/polybutadiene rubber blend (Vyram®), PP/nitrile rubber blend (Geolast®), and PP/butyl rubber (Trefsin®), all of which were initially sold by Advanced Elastomer Systems, which is now owned by Exxon. Among these, the dynamically vulcanized EPDM/PP blend (Santoprene®) has enjoyed the most commercial success and market growth, due to its outstanding properties, ease of processability, and relatively low cost. Hence currently, Exxon and other TPE suppliers have a major focus only on the Santoprene®-type EPDM/PP-based TPV blends. Commercially, another member of the dynamically cured elastomeric thermoplastic alloys, which is gaining some interest, is the blend of PVC with a cross-linked ethylene copolymer (Alcryn®, DuPont). The current global consumption of thermoplastic dynamically vulcanized elastomeric alloys is >100 kt/year, with the EPDM/PP blend (Santoprene®) assuming the dominant (>90 %) market share. Some important applications of the commercial thermoplastic vulcanizate (TPV) blends are

- Automotive seals and weather stripping for windows, hoods, trunks, doors, sun roofs, handle gaskets, window spacers, window guides, lock seals, windshield

wiper pivot seals. The automotive window seal/door weather stripping alone is a high-volume application. Other automotive uses include protective boots, jacketing, hoses, grommets, etc.

- Building and architectural applications also include window-glazing gaskets and weather seals in which TPVs offer the advantages of dimensional stability, low compression set, sealing out the noise, wind, and water, while providing long-term UV resistance.
- Other nonautomotive applications include office equipment, household appliances, toys, products requiring the use of boots, bushings, seals, tubing, and other rubber articles.
- Electrical wire-jacketing applications for use in automotive, construction, industrial, appliance, and many other segments.
- Soft-touch overmolding applications in kitchen appliances and tools (e.g., knife handles), handheld power tools, consumer electronics, etc.

19.6.2.1 Thermoplastic, Dynamically Vulcanized EPDM Rubber/PP Blends

Owing to adequate levels of compatibility between polypropylene and ethylene-propylene copolymers, simple blends of these two polymers have been known for a long time. Impact-modified polypropylene blends containing up to 30 % EPR have already been discussed under polyolefin blends. Blends containing high contents of an uncured or partially cured EPDM in polypropylene have been known (Kresge 1978). However, the advantage of fully cured EPDM/PP blends made by selective cross-linking of the rubber phase during the melt mixing has not been commercially realized until recently (Santoprene®, Exxon; Sarlink®, Teknor Apex). The technology (Coran et al. 1978; Coran and Patel 1980) involved an accelerated sulfur cure of the EPDM rubber ($\geq$70 %) in the presence of minor amounts of polypropylene ($\leq$30 %) while melt compounding under high-shear mixing conditions. The curing agents typically consisted of zinc oxide (5 phr), sulfur (2 phr), tetramethylthiuram disulfide (1 phr), and 2-benzothiazolyl disulfide (0.5 phr). The particle size of cured EPDM dispersions was typically <2 μm, but interconnected to look like a cocontinuous morphology.

Increasing the crosslink density of the elastomer dispersion results in improvements of the strength and tension set of the blend. The difference between the earlier commercial grades of partially cured EPDM/PP blends (TPR, Uniroyal) and the more recent commercial grades of completely cured EPDM/PP blends is in the improved elastomeric properties, viz., reduced compression and tension set and improved flexural fatigue. More important, the chemical resistance and resistance to oil swelling is improved. Typical properties of commercial EPDM/PP TPV blends (Santoprene® and Sarlink®) are shown in Table 19.17.

Nearly all of the EPDM/PP-based TPV's growth has been at the expense of thermosetting rubbers due to this TPV's low cost, easier melt processability,

Table 19.17 Key properties of some typical TPVs based on PP/elastomer blends

Properties	ASTM	PP/EPDM Santoprene® 101-73 ExxonMobil	PP/EPDM Sarlink® 4175 TeknorApex	PP/NBR Geolast® ExxonMobil	PP/ Butyl Trefsin®
Specific gravity (g/cc)	D792	0.97	0.96	1.0	1.2
Shore hardness	D2240	78A	72A	70A	70A
100 % modulus (MPa)	D412	3.6	3.4	3.3	5.2
Tensile strength at break (MPa)	D412	8.8	8.1	6.2	7.6
Elongation at break (%)	D412	490	527	265	250
Tear strength (KN/m)	D624	27	39	33	26
Compression set (%), 70 °C, 22 h	D395B	28	22	29	52
Brittlness temp. (°C)	D746	−60		−40	−60
Oil swell (vol%), 70 h at 100 °C		32		10	

Key attributes: melt processability, rubber elasticity, low compression set, low brittleness temperature

and recyclability. Much of this growth has been in automotive applications such as window and door glazing seals, weather stripping, boots and bellows for steering and suspension, seat belt sleeves, and air induction system ducts. The EPDM/PP-based TPV is also used for window glazing and weather seals in building industry, electrical wire jacketing, and for various soft-touch overmolding applications.

19.6.2.2 Thermoplastic, Dynamically Vulcanized, Nitrile Rubber/PP Blends

The oil resistance and chemical resistance of nitrile rubber (NBR) is generally superior to that of EPDM rubbers. However, the ozone resistance of NBR is poor. The highly polar nature of acrylonitrile comonomer causes high incompatibility between NBR and polypropylene when melt-blended. Hence, the stability of NBR dispersions in PP matrix is relatively poor. Reactive compatibilization technology could be used to improve the blend morphology stability (Coran and Patel 1983). It consisted of blending a small amount of a low-molecular weight amine-terminated butadiene-acrylonitrile copolymer (ATBN, B.F. Goodrich) with the high-molecular weight NBR and a small amount of maleic anhydride-grafted polypropylene (maleated PP) with the high-molecular weight polypropylene and then intimately mixing all the components together. A graft-coupling reaction takes place between the ATBN and maleated PP, and the resulting poly(butadiene/acrylonitrile)-g-polypropylene copolymer compatibilizes the NBR/PP blend.

Typically, a 50/50 blend of nitrile rubber and polypropylene is melt mixed with 5 % maleated PP and 1 % ATBN respectively and then cured with $SnCl_2$ (0.5 %). The resistance to hot oil swell (72 h, 100 °C) of NBR/PP blend was found to be significantly better than that of EPDM/PP blend. Typical properties of the commercial dynamically cured NBR/PP TPV (Geolast®) are compared with other PP-based TPVs in Table 19.16. Commercial applications for this TPV were targeted for automotive seals and gaskets in the oil, fuel, and brake systems. However, this blend has not been as commercially successful as the Santoprene®-type PP/EPDM-based TPV.

19.6.2.3 Thermoplastic, Dynamically Vulcanized Butyl Rubber/PP Blends

The dynamically cured, butyl rubber/polypropylene blends were first developed by Gessler et al. using phenolic-type cross-linking agents. Commercial dynamic vulcanizates are based on halobutyl rubbers and polypropylene cured by zinc oxide-type curatives (Hazelton and Puydak 1987; Kay and Ouhadi 1991; Anonymous 1988). The blend containing a high volume fraction of butyl rubber dispersion in PP exhibits good thermoplastic elastomers with (a) low moisture permeability (b) high vibration damping (c) good heat, UV, and solvent resistance. However, excepting in a few niche medical applications, this TPV has no competitive advantage over Santoprene®-type PP/EPDM-TPV.

19.6.3 Thermoplastic Vulcanizates (TPV) of PVC/Ethylene Terpolymer Blends

Blends of ethylene-butyl acrylate-carbon monoxide (E-BA-CO) terpolymers with PVC, which have been dynamically vulcanized into highly elastomeric yet thermoplastically processable blends, have been available commercially (Alcryn®, DuPont). The principle behind this technology appears to be the selection of proper types of low-T_g, ethylene-acrylate-CO terpolymers, which exhibit high degrees of miscibility with PVC and which can selectively be cross-linked in situ, during the melt mixing with specific curing agents (Loomis and Statz 1986). It has been known that PVC forms miscible or partially miscible blends with certain types of ethylene copolymers such as ethylene-vinyl acetate (EVAc), ethylene-methyl acrylate (EMA), and ethylene-butyl acrylate (EBA) copolymers (Krause 1989). The degree of miscibility depends on the structure of ethylene copolymers. For example, when the vinyl acetate content in EVAc is high (e.g., >65 wt%), the copolymer forms completely miscible blends with PVC (Hammer 1971; Rellick and Runt 1985). At lower levels, the blends are partially miscible. Similarly, ethylene-methyl acrylate and ethylene-butyl acrylate copolymers form miscible to partially miscible blends with PVC (Kalfouglou 1983).

However, ethylene terpolymers containing keto groups, such as the ethylene-butyl acrylate-carbon monoxide (E-BA-CO) terpolymers, exhibit complete miscibility with PVC due to the compatibilizing nature of the polar keto groups. Furthermore, these keto groups in the E-BA-CO terpolymers are useful as a reactive functionality in facilitating the free-radical-induced cross-linking of the ethylene terpolymer rubbers. This concept was applied to a dynamic vulcanization process in a twin-screw extruder to achieve high-volume fraction dispersions of cured E-BA-CO terpolymer rubbers in the thermoplastic matrix of PVC. This technology was initially developed by DuPont in the late 1980s to produce their commercial Alcryn® thermoplastic vulcanizate (TPV) elastomer alloys, also known as "melt processable rubbers" (Alcry® MPR). From the available patent information, these TPVs are blends of PVC with ethylene-n-butylacrylate-carbon monoxide (E-BA-CO) terpolymer systems in which the elastomeric ethylene terpolymer was cross-linked selectively through the use of a combination of peroxide and bis-maleimide-type free-radical cross-linking agents (Loomis and Statz 1986).

In a typical formulation, an ethylene-n-butylacrylate-carbon monoxide (60/30/10) terpolymer (60 wt%) is melt compounded in a twin-screw extruder with PVC (30 wt%) along with an optional, nonvolatile plasticizer such as trioctyl trimellitate (10 wt%) such that the ethylene terpolymer dispersion was cured in situ during the mixing by catalytic amounts of a suitable peroxide (0.3 %) and a bismaleimide crosslink promoter (0.2 %). It is believed that the initial homogeneous miscible melt blend later forms the "micro" phase-separated rubber domains as the selective rubber cross-linking progresses. Currently, such TPV blends are commercially sold as Alcryn® melt-processable rubbers by Advanced Polymer Alloys division of Ferro.

These commercial TPVs composed of E-BA-CO terpolymer/PVC blends can be processed by conventional melt fabrication processes such as profile extrusion, extrusion coating, milling and calendering of sheets, injection, and/or compression molding. The typical properties of a commercial grade of ethylene terpolymer and PVC (Alcryn®) are shown in Table 19.18 as compared to other elastomeric TPVs.

Some key advantages of the ethylene terpolymer/PVC blend-based TPV (Alcryn®) are
- Excellent rubber-like elasticity with high strain recovery
- Excellent low-temperature toughness
- Outstanding weatherability and ozone resistance
- High chemical resistance to oils
- High abrasion resistance
- Melt processability and recyclability

Commercial Alcryn® TPVs are used in various automotive seals and gaskets, weather stripping, noise and vibration dampening, tubing, hoses, wire jacketing, fabric coating, pond linings, soft-touch overmolding, and a variety of other extruded and molded goods applications. These TPVs continue to compete against other lower-cost TPVs using their better low-temperature toughness, oil and

Table 19.18 Comparison of the acrylate rubber based TPV blends vs. PP/EPDM blend based TPVs

Property	PA6/Acrylate rubber TPV (Zeotherm® 100-70)	PVC/E-BA-CO terpolymer TPV (Alcryn® 2070)	PP/EPDM-TPV (Santoprene® 101-73)
Density (kg/m^3)	1,150	1,200	980
Shore hardness	75A	68A	70A
100 % modulus (MPa)	5	4	3.6
Tensile strength (MPa)	8	8.6	7.6
Elongation at break (%)	200	400	470
Compression set (%) at 24 °C	–	16	11
Compression set (%) at 125 °C	60	62	37
Brittleness temperature (°C)	−40	−85	−65
Hot oil resistance	Excellent	Good	Moderate
Weatherability	Good	Excellent	Good
Heat aging resistance	Excellent (upto 150 °C)	Moderate (<100 °C)	Good (to 120 °C)
Melting temperature (°C)	220	<120	165

chemical resistance, abrasion resistance, and weatherability as marketing advantages. The growing ecological concerns about PVC and chlorinated polymers in general may limit the market growth of these TPVs.

19.6.4 Thermoplastic Vulcanizates (TPV) of PA6/Acrylic Rubber Blends

Polyamides such as PA6 are engineering thermoplastics with high heat and solvent resistance properties and hence make ideal thermoplastic matrix candidates of choice to make high-performance TPVs with dynamically vulcanized rubber blends. Although nylon blends with low rubber content have been known for a long time as impact-modified nylons, as discussed under Sect. 19.7.1, elastomeric TPV blends of polyamide with high rubber content (≥ 60 %) have not been commercially available until recently. Because of their higher thermal and chemical resistance performance, the polyamide-based TPVs have often been called super-TPVs (Leaversuch 2004).

Currently, a PA6-acrylic rubber-based TPV blend is commercialized by Zeon Chemical under the trade name of "Zeotherm®." Zeotherm is composed predominantly of a heat- and oil-resistant polyacrylate (ACM) elastomer, which has been dynamically vulcanized and well dispersed in a polyamide (PA6) thermoplastic matrix. Based on the patent literature (Aonuma et al. 1991),

the technology is based on blending a mixture of functionalized polyacrylate rubbers such as an epoxy functional, ethyl acrylate-glycidyl methacrylate copolymer and a carboxyl functional, ethyl acrylate-methacrylic acid copolymer. During the melt blending with nylon, the two mutually miscible acrylate rubbers cross-link with each other via the carboxyl-epoxy reaction (Eq. 19.3).

$$\text{Acrylate rubber with carboxy groups} + \text{Acrylate rubber with epoxy groups} \longrightarrow \text{COOCH}_2\text{CHOH} \longrightarrow \text{Cross-linked acrylate rubber}$$

| Acrylate rubber with carboxy groups | Acrylate rubber with epoxy groups | Cross-linked acrylate rubber |
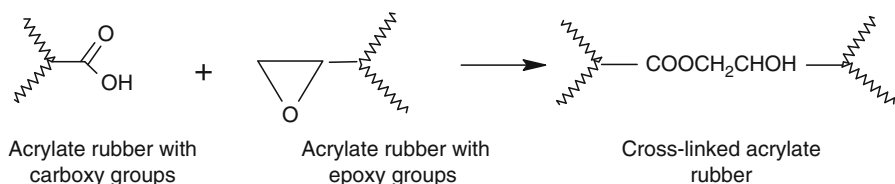
Equation 19.3 Graft-coupling cross-linking reactions in functional acrylate rubber blends

The above selective cross-linking of acrylate rubbers in a polyamide thermoplastic matrix leads to a PA-acrylate rubber-blend TPV with the melt-processing advantages of the PA and the high-performance properties of a thermoset acrylate rubber. The PA matrix provides the high heat resistance and solvent resistance while the cross-linked polyacrylate provides the rubber elasticity coupled with its own excellent weatherability and oil resistance properties to the TPV.

The key properties of commercial PA6-acrylate rubber TPV (Zeotherm®) are shown in Table 19.18. Based on the properties and the available commercial literature, the key advantages of the PA6/acrylate rubber TPVs (Zeotherm®) vs. other TPVs may be summarized as follows:

- Higher heat resistance, i.e., higher property retention in hot air
- Spike temperature resistance to 175 °C; long-term use heat resistance to 150 °C
- Higher chemical resistance (to hot, aggressive automotive fluids)
- Improved weatherability
- Superior overmolding adhesion to rigid nylon parts (nylon-nylon compatibility)
- Low-temperature performance to −40 °C

Hence, from above properties, the PA/acrylate rubber TPV is particularly suited to various automotive under-the-hood applications where high heat and fluid resistance is needed such as in automotive boots (CVJ, rack, and pinion), noise/vibration dampening components, dynamic seals, dust covers, underbody/e-coat plugs, grommets, clean air-intake ducts, transmission oil cooler hose, and so on. The nonautomotive applications take advantage of its better overmolding adhesion to nylons to make soft-touch, nylon parts such as power tool handles, overmolded clips, fasteners, and connectors.

Among the various other types of PA-TPVs investigated in the literature, PA/EPDM rubber-based TPV is interesting. As will be discussed in more detail, under impact-modified polyamides section (Sect. 19.7.1.1), binary blends of PA6 of EPDM rubbers can be compatibilized via reactive extrusion

techniques using maleic anhydride EPDM rubbers. At the high rubber loading ($\geq$60 %) needed to make a PA-matrix-based thermoplastic elastomer, it was found that phase inversion or formation of cocontinuous morphology occurs (Oderkerk 2002). However, by lightly cross-linking the EP rubber with a peroxide in a dynamic vulcanization process, even at 60 wt% EPDM rubber content in the PA blend, the rubber was kept as fine-domain dispersed phase. However, although the morphology stability was achieved, the TPV has not yet achieved desired rubber elastic recovery properties due perhaps to the inefficient cross-linking. Currently, the commercial PA6/acrylate rubber TPV (Zeotherm®) meets several of the high-performance TPV application targets and is likely to enjoy further growth in the automotive under-the-hood application segment.

19.6.5 Thermoplastic Vulcanizates (TPV) of PA6/Silicone Rubber Blends

Dynamically vulcanized silicone rubber-polyamide blends with a high volume fraction of the in situ cross-linked silicone rubber dispersions in a polyamide matrix was developed by Dow Corning as a thermoplastic silicone vulcanizate (Brewer et al. 2003). This technology is based on a selective, catalyzed cross-linking reaction (Eq. 19.4) between a hydride-functional polydimethyl siloxane and a vinyl-functional polydimethyl siloxane rubber during the extruder compounding with PA as shown below. In addition, the interface between the highly incompatible silicone rubber and PA in the blend was stabilized by the addition of a small amount of another silicone polymer, which had a PA-reactive, epoxy-functional group.

$$-Si\text{-}H \quad + \quad H_2C = CH\text{-}Si \quad \longrightarrow \quad SiCH_2CH_2Si$$

crosslinked silicone rubber

$$COOH \quad + \quad \overset{\triangle}{\underset{O}{}} \text{epoxy silicone} \quad \longrightarrow \quad COOCH_2CHOH$$

Polyamide end group   epoxy silicone   PA-silicone graft copolymer at the interface
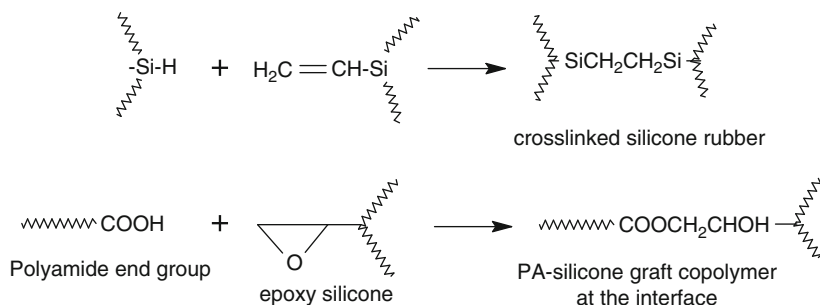
Equation 19.4 Selective cross-linking reactions in PA6/Silicone rubber TPVs

Commercially, a polyamide (PA6)-based thermoplastic silicone vulcanizate is currently commercialized by Multibase, a Dow Corning company under the trade name TPSiV® 1180-50D. It has been evaluated for automotive brake hose

applications because of its resistance to hot brake-fluids (to 150 °C). In addition, this PA-silicone TPV is reported to have excellent long-term resistance to automotive transmission fluids and regular fuels. However, the high cost of silicones may limit the use of such PA-silicone rubber blends in the automotive market. The commercial status of PA-based thermoplastic silicone vulcanizates is still at an early stage.

19.7 Polyamide Blends

Commercial polyamides, frequently referred to as nylons, are crystalline engineering thermoplastics exhibiting high-performance characteristics such as high melting points, high mechanical strength, ductility, and excellent resistance to solvents, fatigue, and abrasion. Nylon is a generic term used for all synthetic polyamides in which the recurring amide groups (−CONH−) are part of the main polymer chain. These amide groups impart strong hydrogen bonding capability and crystallinity in the polyamides, PA, which account for their outstanding solvent resistance and mechanical properties.

Commercial polyamides are generally of two types: (a) those derived from diamines and dicarboxylic acids and (b) those derived from amino acids or lactams as monomers. The major characteristics of these two types of polyamides are similar since these are determined largely by the hydrogen bonding structure of the amide groups. However, within these two types, a wide variety of polyamides are known, varying in their melting points and moisture absorption characteristics, depending on their structure. Among these, PA-66, a polyamide made by polycondensation of hexamethylene diamine and adipic acid, and PA-6, a polyamide made by the ring-opening polymerization of caprolactam, are the two major nylon-engineering thermoplastics produced commercially. Because of their widespread use in fibers, plastics, and films, both PA-66 and PA-6 are produced on a large scale with an estimated total volume globally to be >7 Mt/year. About 60 % of the global PA6 and 66 consumption is in fiber applications, and the remaining 40 % production volume is used in the engineering plastics and film applications (Nexant 2009). PA66 is predominantly used in the injection molding market while the PA6 is used in both the injection molding and the extrusion markets such as cable jacketing and packaging films because of its wider window of melt processability.

There are a number of other specialty polyamides produced from a combination of other diamines and dicarboxylic acids and/or lactams of varying number of carbon atoms. PA-11 and PA-12 with 11 and 12 methylene units between each repeat amide group are relatively low-melting point (170 °C), but exhibit excellent ductility and moisture resistance. Among the more recent class of polyamides are the high-melting (ca. 300 °C) PA-4,6 and PA-6T copolymers with 6 or 66 or 6T monomer units, known as polyphthalamide (PPA) nylons.

Table 19.19 Effect of various polymer blend components on the properties of polyamides

Polymer blend component	Reasons for blending	Compatibilization method
Elastomers (functionalized EP rubber, acrylate rubber, etc.)	Improve PA's notched Izod impact	Graft-coupling reaction
	Shift the ductile brittle transition in PA to lower temperatures	
Ethylene copolymer ionomers	Improve toughness	Polar interaction
	Lower modulus/increase flexibility	
Polyolefins (LDPE, PP)	Lower cost	Graft-coupling reaction
	Improved dimensional stability with humidity	
ABS	High toughness and strength	Graft-coupling reaction
	Reduce moisture sensitivity (better strength and stiffness retention)	
Polyphenylene ether	Improve DTUL (at 1.8 MPa), unfilled	Graft-coupling reaction
	Improve strength and creep resistance	
	Reduce moisture sensitivity (better strength and stiffness retention)	
Silicone IPN	Improve lubricity and wear	None (IPN cured in situ)
	Reduce shrinkage and warp	
High T_g, amorphous PA or a barrier PA (PA6I/6T, MXD6)	Improve the oxygen barrier of PA at high humidity levels	None (miscibility)
Oxidizable polymers (such as PBD) with cobalt catalyst	Oxygen scavenging (active barrier), i.e., achieve near-zero O_2 permeation	grafting

Because of the high level of crystallinity and high melting points, all PAs generally exhibit high heat distortion temperature at low loads even in unfilled form, and when reinforced with glass fibers, definitely exhibit high heat distortion temperatures at high loads. Most of the commercial polyamides exhibit a common set of property advantages attributable to their crystalline nature and hydrogen bonding character. The main advantages offered by the crystalline polyamides (PA-6, PA-66) in blends with other polymers, are: excellent solvent resistance (e.g., gasoline, oils, paint solvents, etc.), heat resistance, and melt flow characteristics. On the other hand, the primary motivation to blend other thermoplastic polymers with polyamides is for reducing the moisture sensitivity of PA and improving its dimensional stability and toughness. Some of the more important polymer candidates commercially used for blending with polyamides and the major reasons for blending them are listed in Tables 19.19 and 19.20.

Because of their highly polar and hydrogen-bonded structure of the backbone, as a general rule, polyamides are immiscible with most of the commercially known polymer systems. In addition, the high degree of interfacial tension (Wu 1989) between polyamides and other classes of polymers leads to highly phase-separated

Table 19.20 Relative performance rating of polyamides compared to the other key thermoplastic polymers, commercially used for blending with the polyamides

	Polyamides (PA6, PA66, PPA)	Rubbers (EPR, SEBS, PE-ionomers)	PP	ABS	PPE
Melting/softening temperature	High	Low	Moderate	Moderate	Very high
Glass transition temperature	Low	Very low	Low	Moderate	High
Melt processability	Excellent	Excellent	Excellent	Excellent	Poor
Moisture absorption	High	None	None	Low	None
Moisture sensitivity (properties, dimensions)	High	None	None	None	None
Drop weight impact strength	High	Very high	Moderate	High	Moderate
Notched Izod impact	Low	Very high	Low	High	Low
Tensile strength	High (dry) Moderate (wet)	Low	Moderate	Moderate	High
Creep resistance	Good	Low	Low	Moderate	Excellent
Solvent resistance					
Hydrocarbons, oils	Excellent	Poor	Moderate	Moderate	Poor
Paint solvents (MEK, toluene)	Excellent	Moderate	Moderate	Moderate	Poor
Alcohols, glycols	Poor	Excellent	Excellent	Excellent	Excellent
Hydrolysis resistance (in acidic or basic aq. fluids)	Poor	Excellent	Excellent	Moderate	Excellent

blends with poor delamination resistance. Hence, simple blends of PA with other commercial polymers generally do not have any practical value. Significant progress has been made over the last several decades for developing techniques for compatibilizing polyamide blends, particularly utilizing the reactivity of polyamide end groups in forming ionic or covalently linked bonds with other polymers at the blend interface. Several commercial blends are based on such reactive compatibilization technology.

The graft copolymer compatibilization technique requires the other polymer component to be already "functionalized," i.e., modified with functionalities such as anhydride or epoxide groups, which are reactive toward the amine or carboxyl end groups of PA respectively. During the melt blending, the reaction between the functionalized polymers and polyamides leads to graft copolymer formation at the interface, which is essential for the compatibilization and stabilization of the blend against delamination. Such a graft copolymer compatibilization mechanism in reactive blending is illustrated for PA/rubber blends in Fig. 19.10 and Eq. 19.5.
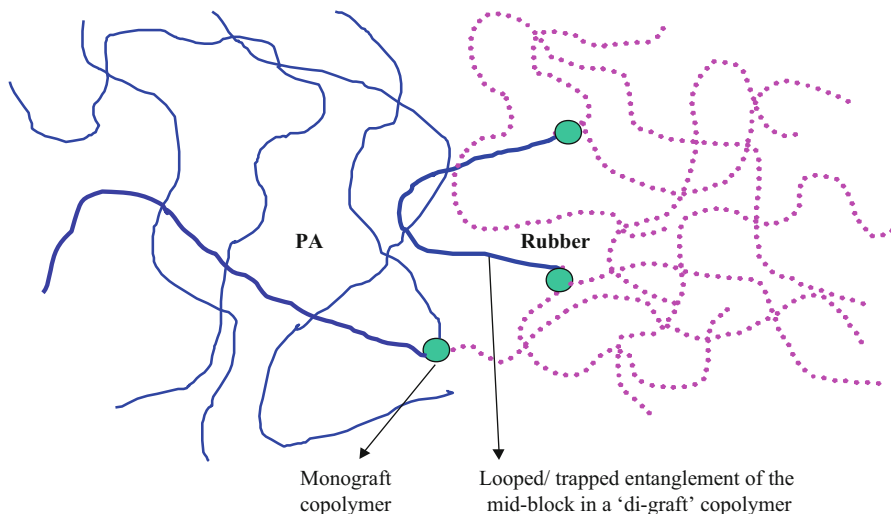
Fig. 19.10 Schematic illustration of interfacial graft copolymers in polyamide/reactive rubber blends (Note: Balanced end group PA (1-amine/chain) forms a mono-graft copolymer. A "diamine" terminated PA forms di-graft copolymers. The latter can lead to entanglement at interface. Both graft copolymers stabilize and strengthen the blend interface)
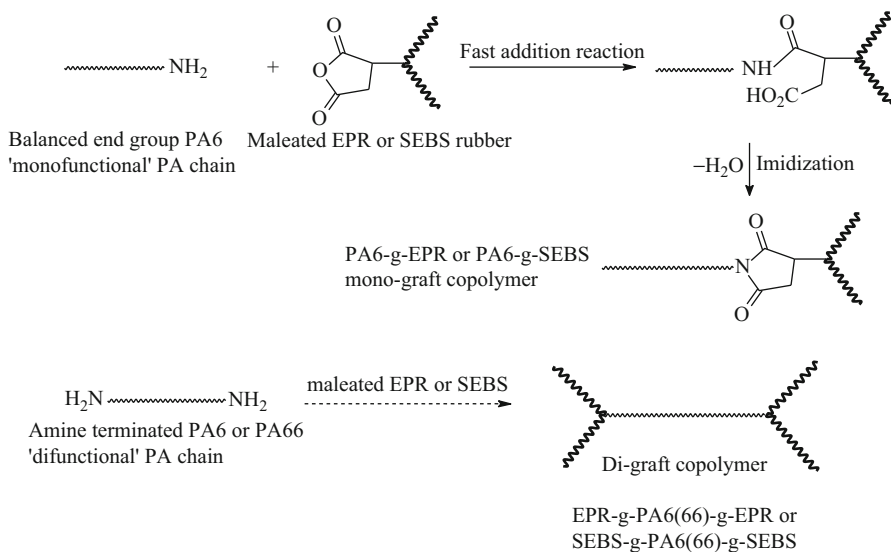
Equation 19.5 Melt-phase reactions during the blending of polyamides with maleated EP or SEBS rubbers

19.7.1 Polyamide/Elastomer Blends

19.7.1.1 Impact-Modified Polyamides

Commercial polyamides such as PA-6 and PA-66 are generally regarded as tough and ductile materials since they exhibit high tensile elongation to break and high drop weight impact strengths. They become even tougher after equilibration with ambient humidity, due to the plasticization effect of the absorbed water. However, under conditions of stress concentration such as in the presence of sharp notches or cracks, polyamides exhibit brittle failure. This property, commonly evaluated as notched Izod or Charpy impact tests, indicates that unmodified polyamides exhibit relatively low energies for crack propagation. To overcome this deficiency, polyamides have been blended with several types of impact modifiers that are typically elastomeric or low-modulus-type olefinic polymers. However, the inherent immiscibility of polyamides with all other polymers and particularly with the olefinic rubbers necessitated the development of proper compatibilization techniques to reduce the interfacial tension and improve the dispensability of the rubber for effective impact modification.

The technology for impact modification of polyamides has evolved significantly over a period of many years through the improved methods of compatibilization and particularly through reactive blending techniques (Kray and Bellet 1968; Murch 1974; Epstein 1979; Mason and Tuller 1983). Commercially, several "impact modifier" polymers are available for blending with polyamides to achieve the desired level of impact modification in polyamides. These include (a) reactive elastomers such as maleic anhydride-grafted ("maleated") EPDM, EPR, or styrene-ethylene/butylene-styrene block copolymer rubbers, and (b) functional ethylene copolymers such as ethylene-ethyl acrylate, ethylene-acrylic acid, ethylene-ethylacrylate-maleic anhydride and ethylene-methacrylic acid ionomers. Table 19.21 lists some of these impact modifiers and their relative features, mechanisms, and efficiencies for PA-impact modification. The reactive toughening chemistry, the relative efficiency of tougheners, and the role of nylon end groups has been extensively studied with particular emphasis on PA6 (Akkapeddi 2001).

Compatibilization of an olefinic rubber dispersion in a polyamide melt blend is achievable through a direct chemical coupling reaction between the polymers at the interface such as through the addition reaction between the amine end groups of polyamide and the anhydride functionality of a maleated EP rubber (Schemes I and II). The graft copolymer formed in situ via this reaction during the melt blending process effectively compatibilizes the blend by reducing the interfacial tension and increasing the adhesion at the phase boundary. Due to the graft copolymer's capability to act as an interfacial agent, the dispersibility of the rubber in the polyamide matrix improves considerably, resulting in well-stabilized, small (≤ 1 μm), rubber particle dispersions and thereby substantially increasing the toughness.

The commercially successful "super-tough" nylon (e.g., Zytel® ST801, DuPont') is based on a reactive blending technology using PA-66 and a maleated (m-) EPDM rubber (Epstein 1979). The resulting PA-66/m-EPDM blend exhibits

Table 19.21 Some common reactive rubber and other types of impact modifiers used for melt-blending and impact modification of polyamides

Reactive rubber/ toughener	Functionality	Reactivity	Other features
Maleic anhydride grafted ("maleated"), ethylene-propylene rubber (m-EPR)	Anhydride (0.3–0.9 % MA)	High reactivity with the amine (NH$_2$) end group of PA	Amorphous rubber, low T$_g$ leads to high impact toughness down to −40 °C
Maleated, styrene-ethylene/butylene-styrene block copolymers (m-SEBS)	Anhydride (0.5–2 % MA)	High reactivity with the amine (NH$_2$) end group of PA	Amorphous rubber, low T$_g$ leads to high impact toughness down to −40 °C
Ethylene-ethyl acrylate-maleic anhydride (E-EA-MA) terpolymer	Anhydride (0.3–3 % MA)	High reactivity with the amine (NH$_2$) end group of PA	Moderate T$_g$ limits the low temp. toughness
Zinc neutralized, ethylene-methacrylic acid copolymer "ionomer"	Zinc carboxylate	Low reactivity with amine but good polar interaction of Zn with amide and amine groups (interfacial complexation)	T$_g$ not low enough, limits low temp. toughness; Good solvent resistance
Zinc neutralized, ethylene-butyl acrylate methacrylic acid terpolymer "ionomer"	Zinc carboxylate	Same as above	Lower T$_g$, higher impact modification efficiency
Ethylene-glycidyl methacrylate copolymer (E-GMA)	Epoxide (3–8 % GMA)	Moderate reactivity with carboxyl group of PA	T$_g$ and hardness limit the achievable toughness; Cross-linking tendency
Etlylene-ethyl acrylate-glycidyl methacrylate terpolymer (E-EA-GMA)	Epoxide (1–8 % GMA)	Moderate reactivity with carboxyl group of PA	Viscosity too high
Ethylene-ethylacrylate or butyl acrylate copolymers	Ester	No reactivity with amine end group of nylon	Do not improve impact but useful as flexibilizers

an excellent notched Izod impact strength ($\geq$900 J/m) that is remarkably insensitive to part thickness and notch radius. Impact modification of PA-6 has also been achieved by blending with such ethylene copolymers as ethylene-ethylacrylate, ethylene-acrylic acid and ethylene-methacrylic acid copolymer, particularly their zinc carboxylate salts commonly known as ionomers. It is believed that favorable, associative interactions involving some type of complexation between the amine end groups of polyamide and the zinc carboxylate groups of the ionomer are responsible for the high compatibility and toughening efficiency of ionomers. Some commercial impact-modified PA-6 blends (Capron® 8253 and 8350, 8351, BASF) are based on such "ethylene copolymer ionomer" tougheners (Mason and Tuller 1983).

There are several other routes to compatibilizing polyamide/elastomer blends for the purpose of impact modification such as through the use of anhydride-modified ABS rubbers (Baer 1988), anhydride-modified S-EB-S block (Gelles et al. 1988)

Fig. 19.11 Morphology of typical polyamide/impact modifier blends – TEM., Phosphotungstic acid stain, *top*: PA-6/ethylene copolymer/ionomer blend (21,000X); *bottom*: PA-6/maleated EPR blend (30,000X) (Akkapeddi 2001)
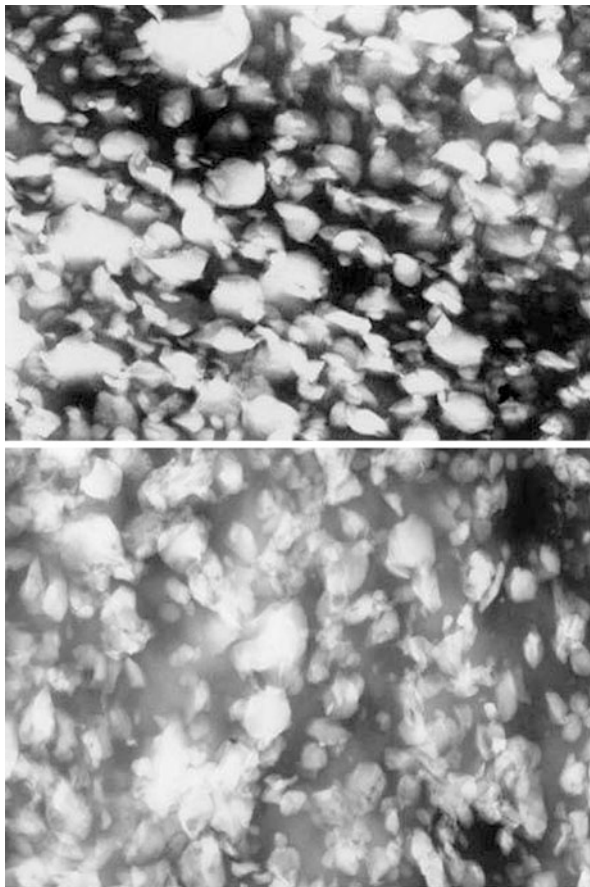
copolymers, carboxylated core-shell rubbers (MBS or acrylic type) (Liu 1988), and acylcaprolactam-grafted EP rubbers (Akkapeddi et al. 1989). Among these, the more common impact modifiers for PA6 are (a) ethylene-copolymer/terpolymer-based Zn ionomers (b) maleated EPR (c) maleated E-EB-S rubbers.

The outstanding impact toughness of the commercial impact-modified polyamides is attributed to the small particle size of rubber dispersion and their good degree of adhesion to the polyamide matrix. In all of these blends, the rubber particle size is >1,000-fold smaller than would be obtained with a typical unmodified EPR phase even under intensive mixing. Typical morphologies of compatibilized PA-elastomer blends is shown in Fig. 19.11.

The toughening mechanism is believed to involve the internal cavitation and debonding of the rubber, which induces localized shear yielding of the polyamide matrix as the primary energy dissipation processes (Borggreve and Gaymans 1989; Ramsteiner and Heckmann 1985; Borggreve et al. 1988) occurring during the impact deformation. Rubber particle size, distribution, and interparticle distance (Wu 1988) are some of the key parameters that have been correlated to the impact

Table 19.22 Properties of some commercial impact modified polyamides (PA/elastomer blends)

| Property | ASTM | Units | PA66/Elastomer | | PA6/ Elastomer | PPA/ elastomer |
| | | | Zytel 408 | Zytel ST801 | Ultramid 8351 | Amodel AT1001 |
			Du Pont		BASF	Solvay
Density	D792	kg/m^3	1,090	1,080	1,070	1,100
Flexural modulus	D790	MPa (kpsi)	1,960 (285)	1,690 (245)	1,800 (240)	2,210 (316)
Flexural strength	D790	MPa (kpsi)	80 (12)	68 (9.8)	65 (9.5)	96.5 (13.8)
Tensile strength at yield	D638	MPa (kpsi)	62 (9)	52 (7.5)	55 (8)	62 (8.9)
Elongation at break	D638	%	80	40	200	30
Rockwell hardness	D785		R115	R112	R82	
Notched Izod at 23 °C	D256	J/m (ft-lb/in.)	240	937 (17)	990 (18)	1,100 (20.7)
Notched Izod at −40 °C	D256	J/m (ft-lb/in.)		220 (4)	265 (5)	750 (14)
Drop weight impact, 23 °C	D3029	J (ft-lb)		170 (125)	200 (150)	
HDT at 1.8 MPa	D648	C	73	71	60	120
at 0.45 MPa	D648	C	230	216	170	
Melting temperature		C	260	260	220	310
Chemical resistance			← Excellent →			

The key attributes of high impact PA/elastomer blends from above are:
• High notched impact strength with good stiffness and strength
• High heat resistance with high melt/softening temperatures
• High chemical resistance

toughness. The ductile-brittle transition of the polyamide blend is shifted to low temperature, both by choosing a low-T_g rubber, as well as controlling the rubber particle size (≤ 1 μm) and volume fraction. At an equivalent content of the compatibilized rubber, PA-6 tends to show higher impact strength at low temperatures than PA-66.

Commercial impact-modified polyamides typically contain 10–25 % of the reactive or compatible elastomer to maximize the toughening efficiency while retaining a high level of tensile strength and DTUL. Commercial impact-modified PA blends (Table 19.22) indeed offer a unique combination of high notched Izod impact and drop weight impact strengths, coupled with a good balance of modulus, tensile strength, heat, solvent, and abrasion resistance characteristics. These properties are suitable for many engineering and metal replacement applications. Because of their wide range of melt flow characteristics, impact-modified polyamides can be processed by injection molding, extrusion, and blow molding techniques. Currently, the impact-modified nylons enjoy the largest market share among all the commercial nylon blends. Some key applications for the elastomer-toughened polyamides (including glass fiber reinforced) are

(a) Automotive applications such as push-pull cables, clips, fasteners, seat belt restraints, gas cap covers, cooling system shrouds, emission control canisters, oil pans, steering column stone shields, fan blades, blow molded air ducts, resonators, etc.

(b) Nonautomotive applications such as elevator buckets, lawn and garden equipment components, power tool housings, outdoor/sports and recreational equipment such as helmets, hockey masks, golf ball covers, snow boards, ski bindings, snow mobiles, etc.

19.7.1.2 Flexible, Polyamide/Elastomer Blends

Some PA66- or PA6-based blends containing a combination of different types of impact modifiers and elastomers have been specifically designed to achieve low modulus, flexible polyamide blends for extrusion applications such as tubing, hoses, and other profiles. These formulations were developed to compete with other higher-cost PA-11 and PA-12 resins, which are extensively used in specialty extrusion applications. Generally, these flexible blends contain higher levels of these elastomers or impact-modifying polymers than the impact-modified polyamides. Often, the PA/rubber blends are used in combination with some plasticizers to achieve a flexible, low-modulus blend product that still retains much of the polyamide advantages, viz., heat and solvent resistance, particularly permeation resistance to such automotive fluids as gasoline, fluorocarbon-based refrigerants. These blends are often formulated to suit a specific customer or application requirement.

In some commercial, semirigid/flexible nylon formulations, an unextracted PA6 resin, which can contain up to 8 % caprolactam monomer, is used since the residual monomer can serve as a low-cost, built-in, internal plasticizer for PA6. Low-modulus, PA6/ethylene-copolymer blends (e.g., Ultramid® 8254) containing such low-cost nylon formulations are commercial (Table 19.23) as extrusion-grade nylons. They are used in automotive under-the-hood applications such as convoluted tubing, emission tubing, etc.

Another extrusion-grade polyamide blend is a reactively compatibilized PA6/polyolefin (PP or LDPE) alloy with some additional olefinic elastomer present for lowering the modulus (Jacquemet et al. 2000). Such low-modulus PA blends (Orgalloy® LT series, Arkema) have been qualified for use in automotive under-the-hood air-intake systems such as clean air tubes and ducts. Low density, high chemical resistance to oil and greases, heat-age resistance, fatigue, and vibration resistance have been the main criteria for the selection of this blend in automotive air-intake duct applications.

The demand for polyamide-based flexible polymer blends, particularly those "free from plasticizers," seems to be increasing. Flexible polyamide blends (Saltman and Varnell 1988; Saltman 1992) containing <50 % PA-6 or PA-66 and >50 % acrylic elastomers have been commercialized by DuPont (Zytel® FN) as a plasticizer-free, low-modulus composition with good low-temperature toughness, resistance to thermal-aging and solvents (particularly to fluorocarbon refrigerants) (Table 19.23). Although flexible polyamide blends contain <50 % polyamide,

Table 19.23 Properties of commercial, low-modulus, semi-flexible PA6/elastomer blends

Property	ISO	Units	PA66/ Elastomer Zytel FN718 Du Pont	PA6/ Elastomer Ultramid 8254 BASF	PA6/polyolefin/ elastomer Orgalloy LT4060 Arkema
Density	1183	kg/m^3	1,040	1,070	1,040
Flexural modulus	178	MPa (kpsi)	1,050 (152)	750 (107)	500 (72.5)
Tensile strength at break	527	MPa (kpsi)	40 (5.8)	34 (4.9)	30 (4.3)
Tensile strain at break	527	%	125	>100	380
Notched Izod at 23 °C	180/1A	kJ/m^2	NB	NB	NB
Notched Izod at −40 °C	180/1A	kJ/m^2	20	6	
HDT at 1.8 MPa	75	C	50	47	
HDT at 0.45 MPa	75	C	80	124	60
Melting temperature		C	263	220	220

The key attributes of semi-flexible PA6/elastomer blends are:
• Low modulus, low hardness
• High elongation at break and high notched impact resistance
• High melt/softening temperatures

the PA phase is continuous, and the major elastomeric phase (>50 %) is kept as dispersion. It is believed that the morphology was controlled by modifying the viscosity of the elastomer phase during the blending through controlled and selective grafting reactions. By using two mutually compatible, coreactive elastomers, a high viscosity ratio between the elastomer and polyamide phases can be maintained preventing phase inversion even when the total volume fraction of elastomer phase is higher than that of polyamide.

For example, by using an ethylene-butylacrylate-methacrylic acid ionomer (P_1) in combination with an ethylene-butylacrylate-glycidyl methacrylate (E-BA-GMA) terpolymer (P_2), a grafting or cross-linking reaction between the two elastomers via the carboxyl/epoxide addition reaction (Eq. 19.6) is expected to take place during the melt blending with the polyamide.
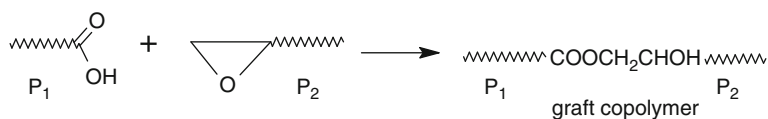
Equation 19.6 Graft-coupling reactions in polyamide blends with a mixture of epoxy and carboxy functional elastomer blends

The above interpolymer reaction would cause an increase in the melt viscosity of the elastomer phase relative to polyamide, thus preventing a phase inversion

(Saltman 1992; Ohme 1991). At the same time, the compatibility between the ionomer and polyamide as well as some degree of reactive compatibilization between E-BA-GMA and polyamide leads to the stabilization of the dispersions. The key advantage of this stabilized, high-rubber blend dispersion morphology of PA appears to translate into a significant improvement of impact strength and elongation at break, after heat-aging at 150 °C for 14 days. Because of the saturated and polar nature of the rubber and the continuous matrix of polyamide, the blend retains solvent resistance (including refrigerants) and long-term heat-aging resistance. Typical applications are automotive air conditioning hoses, ducts, and air-intake systems.

19.7.2 Polyamide/Polypropylene Blends

Polyamide and polypropylene are both crystalline polymers but are significantly different in their structure and polarity. Hence, they are immiscible. The primary motivations for blending polypropylene with polyamide appear to be based on some cost advantages and some improvements in dimensional stability in the presence of moisture. Although compatibilization of polyamide and polypropylene via grafting with a maleic anhydride-modified polypropylene was known for a long time (Ide and Hasegawa 1974), commercial interest in such polyamide/polypropylene blends has not developed until recently (Girard 1990; Moody 1992).

It is known that polypropylene can be modified by a free radical-catalyzed grafting reaction with maleic anhydride (maleation) in the melt phase under extruder processing conditions The process involves some chain degradation that must be controlled by the amount of peroxide used and the temperature and mixing conditions used. Typically, about 0.5 % maleic anhydride can be grafted to PP. Similarly, other unsaturated anhydrides can be used to modify PP. Melt blending of PA-6 (or 66) with such an anhydride-functionalized polypropylene causes a graft copolymer reaction between the polyamide and PP at the interface, which subsequently compatibilizes the blend.

Some commercial polyamide/polypropylene blends (Orgalloy®, Arkema; Dexlon®, D&S Int.) were developed a few years ago. Some of the PA/PP blend grades have now been discontinued. The advantages of polyamide/PP blends vs. other polyamide blends have not been clearly established commercially. Since both the polyamide and PP are crystalline polymers, one would expect the usual notch sensitivity and brittleness under impact loading conditions, despite the compatibilization. Accordingly, the earlier grades of PA6/PP blends showed about the same low notched Izod impact strengths as the individual components. However, the recent metallocene-based reactor-made impact-PP offered the potential for higher notched Izod impact strength in the polyamide/PP blends. Table 19.24 shows some PA6/PP blend properties. These current commercial-grade PA/PP blends seem to exhibit a desirable level of impact strength.

Polyamide/PP blends exhibit significantly slower rate of moisture absorption compared to the polyamides due to the presence of the moisture-resistant

Table 19.24 Typical properties of commercial PA6/PP blends vs. PP

Property	ISO	Units	PA6/PP Schulablend® PA/PP A. Schulman	Orgalloy® RS6000 Arkema	PP Profax® 6523 LyondellBasell
Density	1183	kg/m³	1,010	1,040	900
Flexural modulus	178	MPa		2,000	
Tensile modulus	525	MPa	1,800		1,610
Tensile strength at yield	527	MPa	50	50	30
Tensile strain at yield,	527	%	5	4	12
Tensile strain at break				220	200
Charpy impact, at 23 °C	179	kJ/m²	11	20	6.3
Charpy impact at −30 °C	179	,, ,,	6	14	1.2
HDT at 0.45 MPa	75	C	119	140	84
Chemical resistance			high		moderate

The key attributes of PA/PP blends relative to PP are (a) higher impact and tensile, strength (b) higher heat resistance due to higher melt temperatures and (c) higher chemical resistance

polypropylene phase. The morphology of typical commercial PA/PP blends shows nylon as the continuous phase and polypropylene as the dispersed phase. The blend's improved moisture-dimensional stability over polyamide has led to some applications in automotive, lawn, and power tool markets, particularly using the 30 % glass-fiber reinforced form of the PA6/PP blend.

19.7.3 Polyamide/ABS Blends

As indicated in Table 19.19, the advantages of blending ABS with PA are primarily to improve the impact strength and moisture resistance. Since ABS is an amorphous polymer, its heat resistance is limited by the T_g of the SAN phase, thus the blend would be expected to exhibit lower heat resistance than polyamide. However, by keeping the polyamide as a continuous phase and ABS as the dispersion, blends with high softening point (due to the high melting point of polyamide), high HDT can be achieved. In addition, a polyamide matrix would be advantageous for maintaining solvent resistance in the blend.

Simple blends of ABS and PA are highly immiscible and hence are of little practical value. Compatibilization of ABS with polyamide was accomplished by several methods, most of which involve structural modification of ABS. In one approach, ABS was modified by copolymerization with acrylamide, during the preparation of ABS by the standard emulsion polymerization. The introduction of polar acrylamide units on the SAN backbone of ABS in sufficient concentration caused compatibilization with PA-6 when melt blended, presumably due to favorable hydrogen bonding interactions (Grant 1985).

In another approach, a small amount of maleic anhydride was copolymerized with styrene and acrylonitrile during the preparation of ABS by emulsion polymerization. The "anhydride modified" ABS was then melt blended with polyamide to form a compatibilized ABS/PA blend (Lavengood et al. 1986, 1987; Howe and Wolkowicz 1987). Obviously, a reaction between the anhydride functionality of ABS and the amine end group of polyamide leads to an in situ graft copolymer responsible for compatibilizing this blend. The erstwhile Monsanto's ABS/PA blends sold under the Triax® trade name (now marketed by Ineos ABS of USA) are believed to be based on this reactive compatibilization technology. The polybutadiene rubber content of the ABS used in this blend technology was about 40 %, significantly higher than the standard-grade ABS (10–20 % PBD). Because of the high rubber content and the compatibilization chemistry, the blends exhibited excellent notched Izod impact strengths of >850 J/m at room temperature.

Standard-grade ABS (20 % PBD) could also be directly modified by grafting an anhydride functionality via reactive extrusion with maleic anhydride in the presence of a trace amount of peroxide initiator (Akkapeddi et al. 1990). Such an "extruder-maleated ABS" upon subsequent melt blending with an amine terminated PA-6, gave a compatibilized ABS/PA-6 blend with significantly improved impact strength (Fig. 19.12) and a fine dispersion morphology (Fig. 19.13). Undoubtedly, the chemical coupling between the phases via the amine/anhydride reaction is responsible for the observed compatibilization. A small amount (5 wt%) of maleated EP rubber preblended with the maleated ABS led to substantial improvement in the notched Izod impact strength of the final ABS/PA-6 blend. It was postulated that migration of the maleated EPR to the vicinity of SAN/PA-6 boundary and subsequent graft copolymer reaction with nylon led to substantial toughening of the interphase region (Akkapeddi et al. 1993).

Currently, ABS/PA blends are commercially available primarily from Styrolution under the trade name of Terblend® N and Ineos ABS under the trade name of Triax®. In general, ABS/PA blends exhibit excellent notched Izod impact ($\geq$850 J/m or >65 KJ/m^2)) at room temperature (Table 19.9). These impact properties are equivalent to those of impact-modified polyamide (Table 19.22). However, the DTULs (0.45 MPa) of ABS/PA blends are relatively low compared to those of impact-modified nylons. The key difference being that in ABS/polyamide blends, due to the significant level of ABS, a substantial drop in the modulus occurs at the T_g of ABS (SAN), and hence the blend exhibits lower DTUL at 0.45 MPa than the impact-modified polyamide. The latter blends are polyamide-rich ($\geq$75 %) elastomer blends and hence maintain a higher level of heat resistance due to the higher level of the crystalline PA phase.

Commercial ABS/PA blends compete for the same type of applications as the impact-modified polyamides, primarily in areas where impact strength and chemical resistance are required. Presumably due to their lower heat resistance and slightly inferior low-temperature notched Izod impact strengths, their market growth has been somewhat slower than that of impact-modified polyamide. However, ABS/PA blends exhibit somewhat better dimensional stability and lower warpage characteristics than impact-modified polyamide, which led to some applications.

Fig. 19.12 Instrumented
Impact behavior of
ABS/PA-6 (50/50) blends;
top: uncompatibilized blend,
bottom: compatibilized blend
(Akkapeddi 1993)
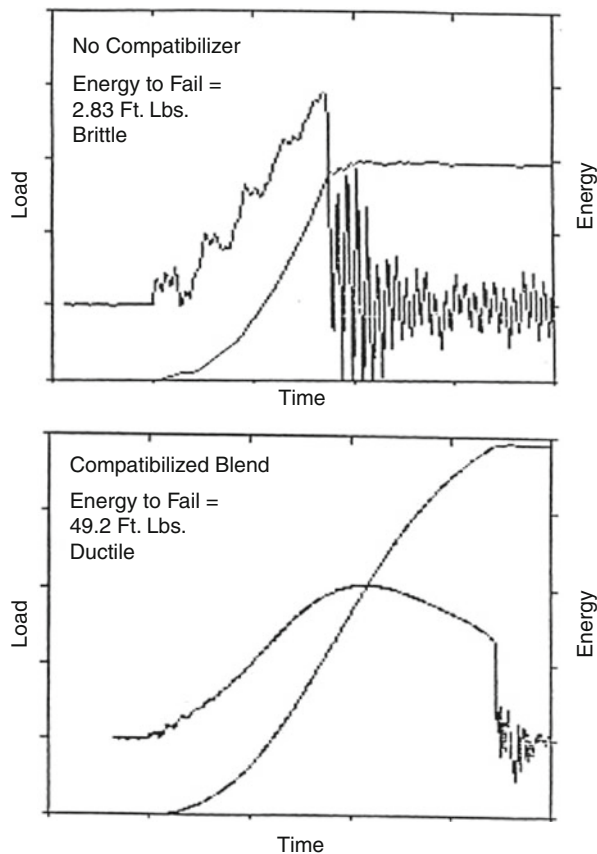
19.7.4 PPE/Polyamide Blends

Poly (2,6-dimethyl-1,4-phenylene ether) PPE is a high-T_g, amorphous polymer
(Hay 1976). It was originally developed by General Electric Co. which until
recently has been the sole producer of this polymer (Hay 1967). PPE is generally
of homopolymer type, although a copolymer with minor amounts of 2,3,6 trimethyl
phenol is also produced. Although PPE exhibits high mechanical strength, DTUL,
and ductility, it is generally difficult to process as a molding resin due to its high
softening temperature ($T \geq 300$ °C), high melt viscosity and tendency for thermo-
oxidative degradation at the high melt processing temperatures (330 °C). The
discovery that PPE can form highly compatible (miscible) blends with polystyrene
led to the development of PPE/HIPS blends (Cizek 1969) that have been the
commercially most successful to date. The properties of PPE/HIPS blends are
suitable for many applications. However, they lack adequate chemical resistance.
    In order to improve chemical resistance, blends of PPE with crystalline polymers
such as polyamides have been the subject of much investigation. Simple blends of

Fig. 19.13 Morphology of
ABS/PA-6 blends (TEM,
phosphotungstic acid); *Top*:
Uncompatibilized blend
(5,000X), *bottom*:
Compatibilized blend
(10,000X) (Akkapeddi 1993)
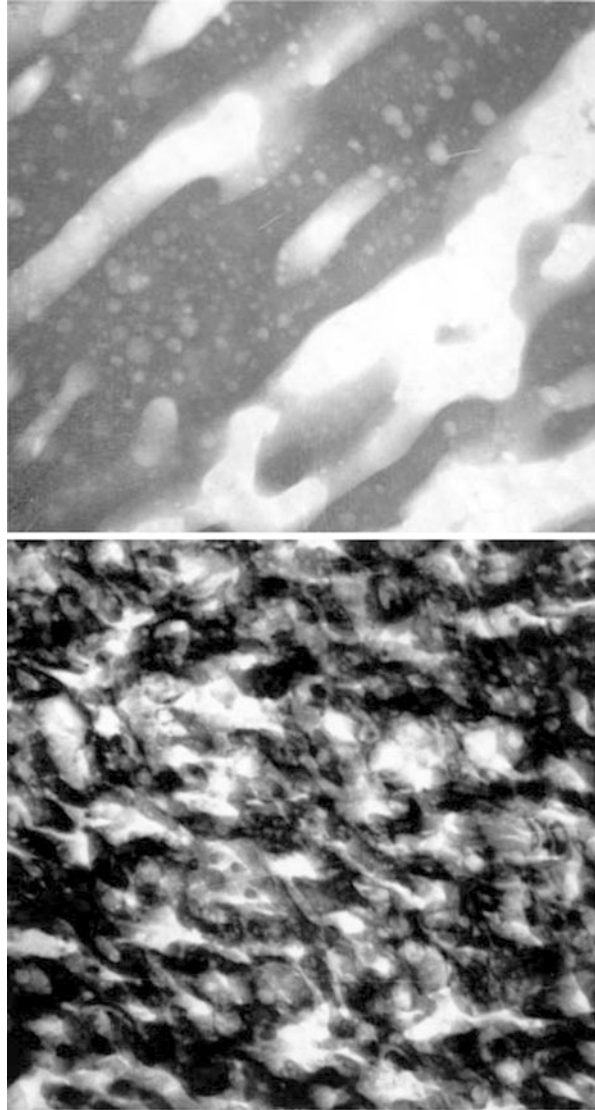
PPE and polyamides are highly incompatible, generally leading to brittle and readily delaminating products of low value. Hence, considerable attention was paid in recent years to develop the technology for effective compatibilization and impact modification of these blends. The exact compositions, the nature of grafting agents or compatibilizers used, and the impact modifiers used in commercial PPE/PA blends are kept proprietary, although many patents have been issued.

Research efforts have been focused largely on the methods of improving the compatibility between PPE and polyamides. Several compatibilizer additives were

claimed in the early patent literature (Ueno and Maruyama 1982), which included the use of liquid diene rubbers, epoxies, and unsaturated compounds containing acid, anhydride, amino, imino, or hydroxyl groups. Since polyamides have reactive end groups (amine and carboxyl), it is quite conceivable that the compatibilizing additives may react first with polyamide if all the components are blended together all at once, inhibiting any actual coupling reaction between PPE and polyamide. The latter is more desirable for the effective compatibilization of the blend. Hence, subsequent investigators focused first on the functionalization of PPE with a grafting agent such that suitable functional groups are attached to the PPE backbone (Jalbert and Grant 1987; Akkapeddi et al. 1988). Although functionalization of PPE is possible through solution-phase end-capping reaction with trimellitic anhydride acid chloride (Aycock and Ting 1986), one would prefer to use melt-phase grafting reactions via reactive extrusion techniques for reasons of economics.

Melt-phase reactions of PPE with unsaturated functional reagents such as maleic anhydride, fumaric acid, acrylic acid, and their derivatives, glycidyl methacrylate, and other unsaturated compounds were investigated. This functionalization reaction could be done in extruders, and the functionalized PPE could be isolated and characterized. The functionalization step introduced a reactive functional group on the PPE chain that upon subsequent melt blending with polyamide would react with the amine or carboxyl end groups of nylon forming a graft copolymer of PPE and polyamide at the interface. Since the block and graft copolymers are the best interfacial agents for a blend, the dispensability of PPE in polyamide improves due to decreased interfacial tension, and consequently, the tensile properties (strength, elongation) and toughness of the blend improve considerably. The structure of maleated PPE and the characterization of the graft copolymer was reported (Glans and Akkapeddi 1991; Akkapeddi 1993; Campbell et al. 1990).

Functionalization of PPE with maleic anhydride or fumaric acid could be done by melt blending (ca. 300 °C) in an extruder. This anhydride-functionalized PPE could either be isolated and reextruded with PA-6 or melt blended in a single-pass through downstream addition of the polyamide in a twin-screw extruder. In either case, prefunctionalization of PPE is a necessary and an important step in order to optimize the selective grafting reaction between PPE and polyamide and prevent any premature reaction between polyamide and the maleic anhydride or fumaric acid. The graft-coupling reaction itself is an addition reaction between the amine end group of polyamide and the anhydride group of the functionalized PPE. It was also found that the compatibilization efficiency increased when a PA6 polymer rich in the amine end groups ("amine terminated polyamide") was used (Akkapeddi 1992, 1993). The tensile elongation to break increased considerably, as did also the melt viscosity, the latter indicative of increased polymer-polymer grafting reaction (Fig. 19.14). Typical morphology illustrations obtained by transmission electron microscopy of uncompatibilized vs. reactively compatibilized PPE/PA-6 blend indicated a substantially finer dispersion of PPE in the PA-6 matrix in the compatibilized blend as shown in Fig. 19.15.

Fig. 19.14 Effect of blending amine terminated PA-6 on the tensile elongation and melt flow behavior of reactively compatibilized PPE/PA-6/m-EPR (50/40/10) blends (Akkapeddi et al. 1993)
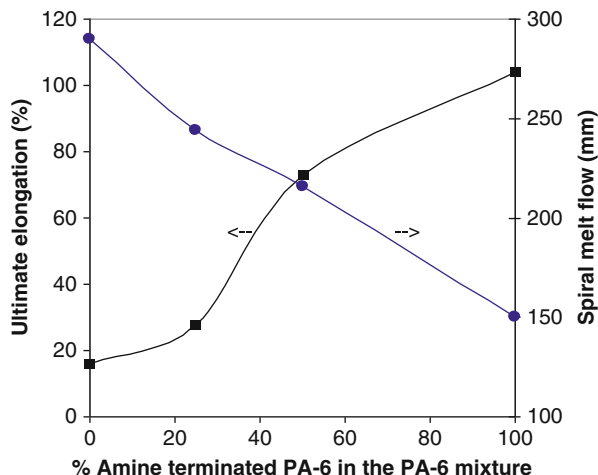
The heat distortion temperature of the PPE/PA blend at high load (1.8 MPa) increases with the amount of PPE in the blend (Fig. 19.16) (Akkapeddi, unpublished results). However, because of the crystallinity of the polyamide matrix, the heat distortion temperature at low load (0.4 MPa) is relatively less sensitive to the PPE content and is largely determined by the polyamide. This is one significant difference between blends of crystalline/amorphous polymers (PA-6/PPE) vs. blends of amorphous/amorphous (PS/PPE) polymers. In the PPE/polyamide blends, the crystalline PA phase is invariably the continuous phase, because of the large melt viscosity difference between PPE and PA.

Although the binary blends of PPE and polyamides exhibit good ductility (tensile elongation and drop weight impact) after the reactive compatibilization, the notched Izod impact strengths are still relatively low. This is to be expected since the individual resin components, viz., PA-6 (or PA-66) and PPE, exhibit low notched Izod impact strengths (<70 J/m). Hence, commercial PPE/PA blends invariably include an impact modifier component, the exact composition and content of which is kept varied from grade to grade. Commercial impact-modified PPE/PA blends exhibit notched Izod impact strengths ranging from 175 to 700 J/m at room temperature. They also differ in their ductile-brittle transitions and low-temperature impact strength behavior.

The type of nylon used (PA-6 or PA-66 or copolymer type), its end group concentrations and molecular weight, and more importantly, the nature of the rubber modifier used (compatible or reactive type), its content, and manner in which it is added determine the efficiency of notched Izod impact strength improvement and the low-temperature ductility. Hydrogenated styrene-butadiene-styrene block copolymer (S-EB-S) rubbers have been used as impact modifiers in PPE/PA-66 blends (Grant et al. 1988) since they are expected to be compatible and readily dispersible in the PPE phase. Preblending a functionalized rubber (such as a maleic anhydride-modified EP rubber) into the functionalized PPE, followed by melt blending with the polyamide, was found to give a better impact strength

Fig. 19.15 Morphology of PPE/PA-6 (60/40) blends (TEM, phosphotungstic acid stain); *Top*: Uncompatibilized blend (10,000X), *Bottom*: Compatibilized blend (20,000X)
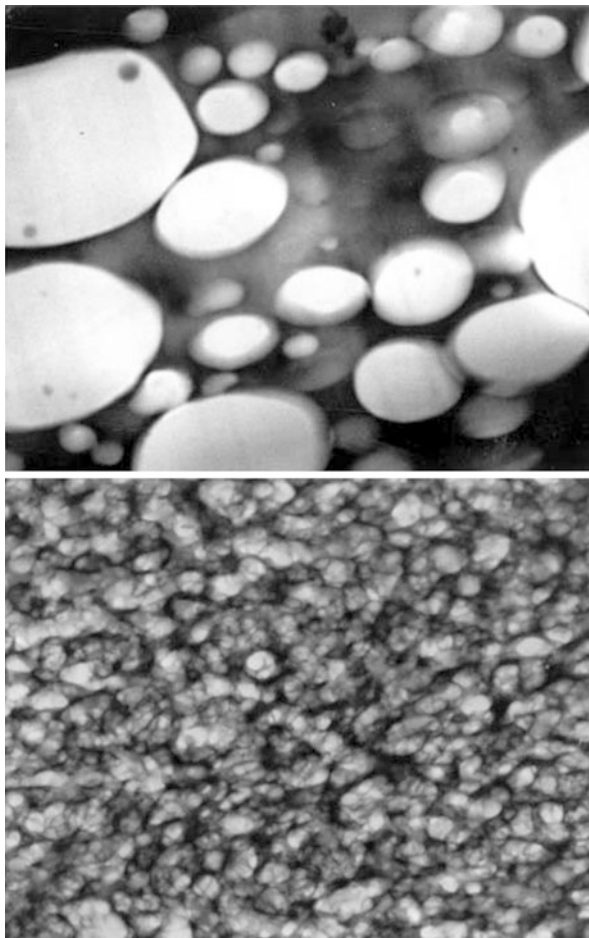
improvement in PPE/PA-6 blends than when the rubber was blended simultaneously with the nylon (Akkapeddi et al. 1988, 1992). An impact-modified PPE/PA blend developed by Hüls in Europe contained polyoctenylene as impact modifier (Doescher et al. 1988).

Commercial PPE/polyamide blends typically contain 40–60 % polyamide and 0–10 % of the impact modifier, each grade being formulated for specific types of applications. Typical properties of some commercial unfilled PPE/PA blends are illustrated in Table 19.25. In general, PPE/polyamide blends offer a unique combination of high heat resistance (DTUL and continuous use temperatures), high impact strength, hygrothermal dimensional stability, and ease of processability. In addition, the blends exhibit better chemical resistance compared to other high-heat, amorphous engineering resins such as PPE/HIPS blend and polycarbonate (Table 19.26). Most of the commercial PPE/PA blends are based either on PA-66, that gives a somewhat higher heat resistance to the blend or PA-6, that gives
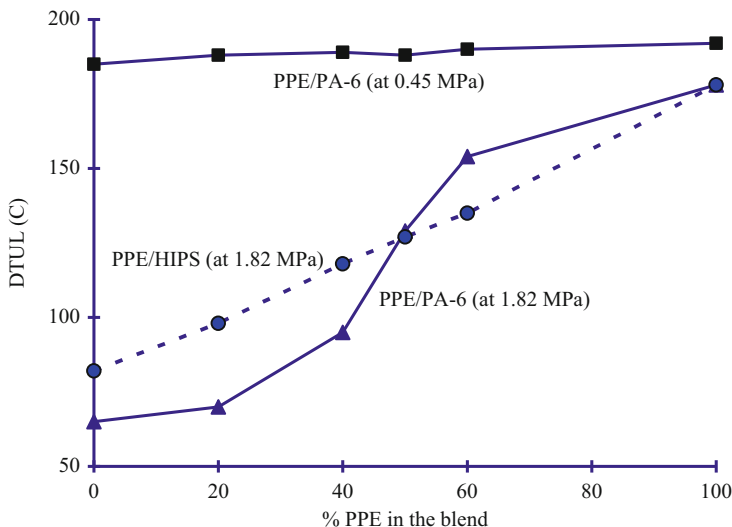
Fig. 19.16 Effect of PPE content on the DTUL of PPE/PA-6 blend vs. PPE/HIPS blend

Table 19.25 Properties of some commercial PPE/Polyamide blends

			PPE/PA66		PPE/PA6
			Noryl® GTX914	Noryl® GTX944	Noryl® GTX626
Property	ASTM	Units	Sabic		
Density	D792	kg/m³	1,100	1,080	1,090
Flexural modulus	D790	MPa (kpsi)	1,900 (282)	1,900 (282)	2,270 (329)
Flexural strength	D790	MPa (kpsi)	80 (11.6)	75 (10.8)	95 (13.8)
Tensile strength at yield	D638	MPa (kpsi)	55 (7.9)	50 (7.2)	56 (8.9)
Elongation at break	D638	%	100	50	83
Izod impact, notched, at 23 °C	D256	J/m (ft-lb/in.)	280 (5.2)	680 (12.7)	336 (6.3)
Izod impact, notched, at −30 °C	D256	J/m (ft-lb/in.)	120 (2.2)	280 (5.2)	122 (2.3)
Instrument impact energy at 23 °C	D3763	J (ft-lb)	60 (44)	55 (40)	31 (23)
HDT at 0.45 MPa	D648	C	180	185	179

somewhat higher impact strength at any given blend ratio. Although other specialty polyamides such as PA-12 and PA-4,6 have also been investigated in PPE blends, they have not gained any commercial interest due to their higher cost. The cost of PPE/PA6 or PPE/PA66 blends can be further lowered by the addition of some polystyrene or HIPS into the PPE phase, taking advantage of their mutual miscibility. However, this results in some sacrifice in DTUL, but gives improved melt flow useful for thin-wall parts.

Table 19.26 Comparison of chemical resistance of PA6, PPE/PA6, PPE/HIPS-% change in properties[a]

	PA-6		PPE/PA-6		PPE/HIPS	
Solvent	Y.S.	E_b	Y.S.	E_b	Y.S.	E_b
Water	−40	200	0	0	0	−30
Antifreeze (50 % aqueous glycol)	−20	200	0	0	0	−70
Gasoline	0	200	0	100	Stress	Cracked
Gasohol (15 % MeOH)	−50	300	−50	0	Dissolved	
Brake fluid	0	21	10	−25	−80	−100
Transmission fluid	0	−25	0	0	Stress	Cracked
Power steering fluid	0	−50	0	0	Stress	Cracked
Motor oil	10	−50	0	0	Stress	Cracked
Trichloroethylene	0	200	−70	100	Dissolved	

[a]3 mm thick tensile bars tested after 1 week immersion in various solvents; % change in properties, increase (+) or decrease (−) relative to initial.; Y.S. Yield Stress, E_b elongation at break (Akkapeddi et al. 2002)

19.7.4.1 Applications of PPE-Polyamide Blends

Because of their unique combination of chemical resistance, stiffness, and impact resistance properties, PPE/PA blends have found many automotive exterior applications such as in body panels and trim. Typically, PPE/PA blends are used in such exterior automotive parts as the fenders, quarter panels, tail gates, hatchbacks, grilles, tank flaps, wheel covers, and mirror housings. Because of their high heat and chemical resistance, parts made from of PPE/PA blends can be painted "online," attached to the metal frame in the existing automotive paint oven temperatures of ca. 180–200 °C. The parts retain good toughness required in these applications. Conductive grades of PPE/PA blends are used for cost-effective production of large automotive body panels, which can be electrostatically painted online without a primer.

Glass fiber-reinforced PPE/PA blends designed to meet varying demands of stiffness, impact, and heat resistance properties are used in automotive under-the-hood applications such as engine control modules, cooling system parts, power distribution boxes, connectors, lamp sockets, etc. Other applications include lawn and garden tractor hoods, pumps, water meter housings, etc.

19.7.5 Polyamide/Polycarbonate Blends

Polycarbonate has been blended with commercial polyamides (PA-66 and PA-6), in order to improve its poor solvent resistance while maintaining a reasonable level of heat resistance and toughness. However, simple blends of polycarbonate and polyamides were highly incompatible and hence not useful. Several different additives such as phenoxy resins, polyester amide elastomers in combination with maleated polyolefins, polyetheramide block copolymers, and polyamide-polyacrylate block copolymers have been used as potential compatibilizers and impact modifiers.

However, even such compatibilized PA/PC blends could not be successfully commercialized, perhaps due to a lack of a cost-performance advantage over other PA blends.

A developmental grade of PA/PC blend (formerly known as Dexcarb®, now discontinued) was claimed to have a high notched Izod impact strength comparable to that of impact-modified polyamides and polycarbonate. From available patent literature, such blends utilized a polyether-amide and a maleated polypropylene or EPR as the compatibilizing/impact-modifying additives (Perron 1988). Polyamide/polycarbonate blends had only a very limited evaluation in exterior automotive applications such as bumper beams. Their dimensional stability and resistance to paint solvents and automotive fluids may have been some of the reasons for their consideration. However, PA/PC blends were commercially discontinued, due to the competition from PA66/PPE blends, which offered better heat resistance and toughness at a comparable cost.

19.7.6 Polyamide/Silicone Blends

A blend of a thermoplastic polyamide (PA-6 or PA-66) and 5–25 wt% of a cross-linkable silicone, which forms a semi-interpenetrating network (semi-IPN) upon curing, was offered commercially for a brief period in the 1980s under the trade name of Rimplast® (Petrarch, div. of Hüls) (Arkles 1985). These blends were produced by extruding the polyamide with a vinyl-terminated, polydimethyl-siloxane and silicone hydride-terminated dimethyl siloxane in the presence of a platinum catalyst. The siloxanes react with one another forming cured silicone thermoset in the thermoplastic matrix phase of the polyamide. At the low concentrations of 5–10 % silicone, the blend was reported to retain much of its thermoplasticity and processability. This silicone semi-IPN reportedly improved the lubricity, wear, and biocompatibility of polyamide as well as reducing the shrinkage and warpage, although with some sacrifice in strength and elongation.

More recently, a dynamically vulcanized silicone rubber-nylon blend with a high concentration of the cross-linked silicone dispersion in a nylon matrix was developed by Dow Corning as a thermoplastic silicone vulcanizate (Brewer et al. 2003). This technology is also based on the selective, catalyzed cross-linking reaction between a hydride-functional polydimethyl siloxane and a vinyl-functional polydimethyl siloxane rubber during the extruder compounding with nylon as discussed before under the polyamide-silicone rubber thermoplastic vulcanizate section. The interface between the silicone rubber and nylon in the blend was compatbilized by the addition of a small amount of another silicone polymer, which had a nylon-reactive, epoxy-functional group.

Commercially, polyamide (PA6)-based thermoplastic silicone vulcanizates are commercialized by Multibase, a Dow Corning company under the trade name TPSiV® 1180-50D. It was evaluated for automotive brake hose application because of its hot brake fluid resistance (to 150 °C). The high cost of silicones may limit the use of such nylon blends only to specialty niche applications.

19.7.7 Polyamide/Polyamide Blends

Blends of PA-6,6 with some aliphatic-aromatic polyamides of higher T_g such as poly (hexamethylene isophthalamide) (PA-6,I) have been evaluated as fibers, in order to achieve improved modulus and heat resistance in PA-66 tire yarn and consequently reduce the tire flat-spotting tendency (Zimmerman et al. 1973). Although the rate of amide interchange in these polyamide/polyamide blends was found to be quite slow (<3 % interchange based on the aromatic polyamide), the formation of some block copolymer was not ruled out. Nevertheless, the observed improvements in the modulus and T_g were primarily attributable to some degree of compatibility or miscibility between the components of the blend. There have been several other research investigations on the compatibility and phase behavior of polyamide/polyamide blends (e.g., Takyanagi et al. 1980; Ellis 1990; Hirakawa et al. 1985). However, there are no commercially significant polyamide/polyamide blends developed to-date for the injection molding market, although recently, there has been some commercial interest in the packaging films market segment particularly for the blends of PA-6 with aliphatic-aromatic polyamides exhibiting sufficiently good oxygen barrier properties suitable for food packaging applications.

Certain types of aliphatic-aromatic random copolyamides such as those derived from the polymerization of (a) hexamethylene diamine and isophthalic/terephthalic acids (6I/6T) or (b) m-xylylenediamine, isophthalic/terephthalic acids, and caprolactam (MXDI/T,6) exhibit high glass transition temperature, amorphous character, and a high barrier to oxygen permeation (Akkapeddi and Gervasi 1989). The oxygen barrier property of these amorphous polyamides is retained even under high humidities because of their high T_g's. In contrast, semicrystalline polyamides such as PA-6 and PA-66 characteristically exhibit low T_g (ca. 50 °C) that becomes even lower after moisture absorption. As a consequence, the permeability of oxygen in PA-6 and PA-66 increases with humidity. There are several commercial semiaromatic, amorphous polyamides that exhibit good oxygen barrier properties, suitable for packaging applications, e.g., Selar® PA (duPont), Novamid® (Mitsubishi Chemical), Grivory® HB (EMS).

To improve the oxygen barrier properties of PA-6 (and PA-66), high T_g, barrier-type amorphous polyamides such as PA-6I/6T (Selar® PA) have been blended (Krizan et al. 1989; Blatz 1989). These blends exhibit improved barrier to oxygen permeation particularly at high relative humidity (Fig. 19.17), presumably due to a good degree of miscibility. Commercially, PA-6 blends with various amorphous PA grades (such as Selar® PA or Grivory® G21) are used by various packaging film fabricators who melt-blend and fabricate these blend films directly for various food packaging applications. Similar blends of poly(m-xylylene adipamide) (MXD6) with PA-6 have also been used as barrier films. PA-MXD6, produced by Mitsuibishi Gas Chemical Co, is a high oxygen barrier resin particularly useful in multilayer coextrusions (Harada 1988) and blends. In the blends of MXD6 with aliphatic polyamides, interchange reactions may play a role during melt-mixing, particularly at long residence time (Takeda and Paul 1992). However, under the

Fig. 19.17 Oxygen
permeability and water vapor
transmission rate (*WVTR*) in
PA6/amorphous PA6I/6T
blends at 95%RH (Adapted
from Anonymous 2005)
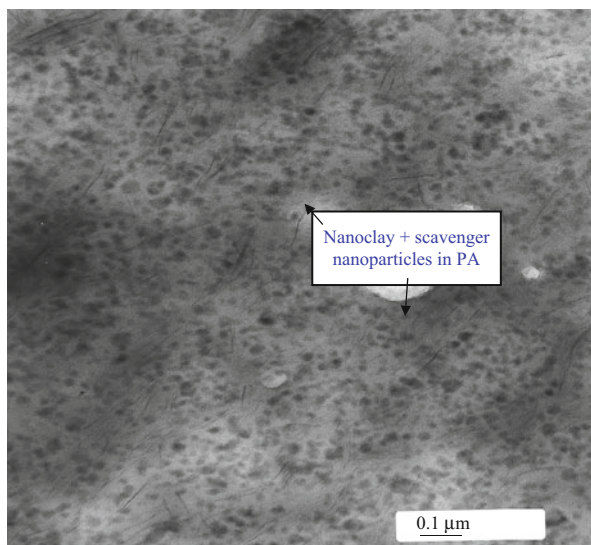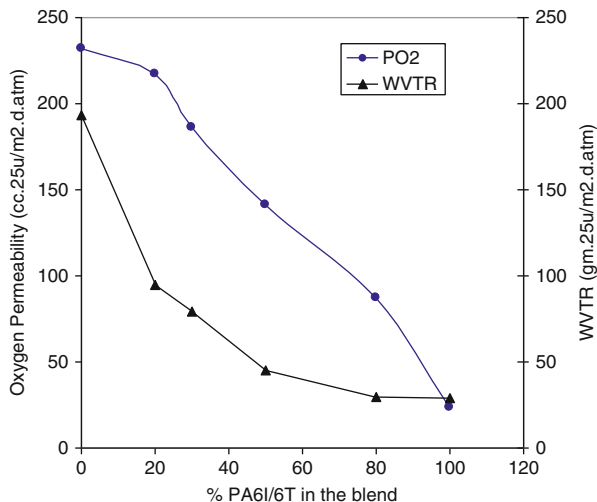
Fig. 19.18 Morphology of
PA6-nanocomposite-PA6I/6T
blend with nanoscale oxygen
scavenger dispersions
(Akkapeddi et al. 2004)

normal commercial melt compounding and extrusion throughput rates, interchange
reactions are minimal and good miscible blend products can be obtained.

More recently, polyamide blend compositions exhibiting high oxygen scaveng-
ing barrier properties have been developed for particular use in multilayer barrier
PET bottles (Akkapeddi et al. 2004). According to the published patents, these
blend compositions contain PA6 or PA6-nanocomposite (ca. 2 % nanoclay)
blended with an amorphous nylon such as PA6I/6T, along with small amounts of
functionalized polybutadiene (PBD) and cobalt catalyst serving as the oxygen
scavengers. The resulting polyamide blend exhibited high oxygen scavenging

barrier while retaining a high degree of clarity because of the morphology with extremely fine, "nanoscale" dispersions of the clay platelets and the oxygen scavenger particles (Fig. 19.18). The nanoclay platelets act as the passive barrier, and the nanoscale dispersion of the PBD provides the oxygen scavenging ("active" barrier) properties to the PA blend. Such barrier PA blends have been commercialized as barrier resins (Aegis® OX, Honeywell), for use in coinjection stretch blow molded multilayer PET bottles with enhanced shelf-life for packaging juices, beer, and other oxygen-sensitive food and beverages.

19.8 Polycarbonate Blends

Commercial polycarbonate is an amorphous engineering thermoplastic characterized by a high glass transition temperature (ca. 150 °C) and an excellent balance of properties such as high toughness, clarity, heat resistance, dimensional stability, and good electrical and ignition-resistance characteristics. Because of this outstanding combination of properties, polycarbonate has become one of the most successful of engineering thermoplastics.

Standard polycarbonate, (PC), is made from bisphenol A and phosgene via an interfacial polymerization process. The polymer backbone has an aromatic polycarbonate structure with a recurring carbonate moiety, which uniquely accounts for the outstanding toughness of the polycarbonate, and the rigid aromatic unit contributes to its high glass transition temperature. Although a large number of applications of polycarbonate have been based on its unique combination of high impact strength, heat resistance, and clarity, there are still a few property deficiencies in the neat polymer, which can be overcome by blending with other polymers or additives. Some deficiencies of polycarbonate are

- High notch sensitivity and part thickness sensitivity in impact strength (Fig. 19.19).
- Lack of an adequate low-temperature notched Izod impact strength.
- Lack of an adequate solvent resistance and stress crack resistance.
- Limited long-term hydrolytic stability at elevated temperatures.
- High melt viscosity compared to crystalline engineering polymers such as PA-6, PBT.

Hence, the development of polycarbonate blends was primarily market driven, with a motivation to extend the applications of polycarbonate into areas where improved chemical resistance and processability are required while still retaining high impact strength. The rationale for the development of commercial PC blends is summarized in Table 19.27. Comparison of the properties of various polycarbonate blends is shown in more detail in Table 19.28. In the development of all these commercial polycarbonate blends, one common goal was to maintain a very high level of impact strength while improving the notch sensitivity of impact, chemical, or solvent resistance properties and the cost balance.

Fig. 19.19 Effect of sample thickness on the notched impact strength of unmodified (I) vs. impact Modified (II) Polycarbonate (Adapted from Freitag et al. 1985)
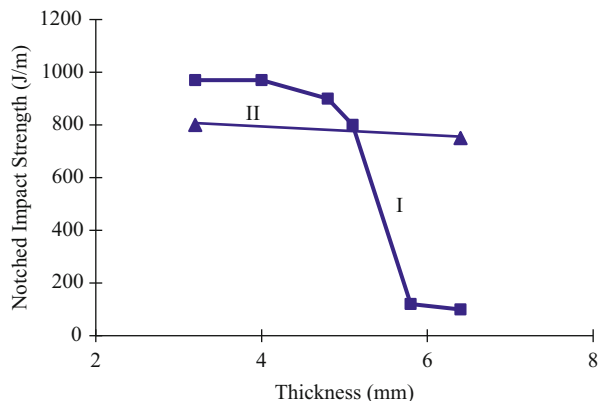
Table 19.27 Rationale for the development of various commercial polycarbonate blends

Polycarbonate blend	Rationale for blending
Impact modified PC (blends with rubber)	Improve notch sensitivity
	Improve low temperature toughness
	Improve thermal-aging resistance
PC/ABS blend	Improve low temperature toughness
	Improve processability
	Lower cost
PC/ASA blends	Improve the weatherability
PBT/PC, PET/PC	Improve solvent resistance
	Improve the processability
PEI/PC	Lower the cost of PEI
	Improve the processability of PEI

19.8.1 Impact-Modified Polycarbonates

Although polycarbonate is exceptional among engineering resins in exhibiting an outstanding level of toughness, its ductile-brittle transition depends on the temperature, notch sharpness, sample thickness, and thermal aging effects. A sharp ductile-brittle transition (Carhart 1985) for polycarbonate occurs at 0–10 °C, hence its notched Izod impact strength at low temperatures is low, e.g., ≤100 J/m at −30 °C. Another important deficiency of polycarbonate is the sensitivity of its notched impact strength to part thickness and notch radius. The notched Izod impact strength of polycarbonate is reduced from 900 to about 100 J/m when the thickness is increased from 3.2 to 6.4 mm (Jones 1985) These effects are due to the changes in the deformation behavior at the crack tip from shear yielding (plane stress) to crazing and unstable crack propagation. By blending small amounts of elastomeric or low-modulus polymers, the impact

Table 19.28 Comparison of different types of commercial polycarbonate blends

Property	ISO	Units	PC/ elastomer Makrolon 1837 Bayer	PC/ABS Bayblend T85	PC/PBT/ elastomer Makroblend KU2-7912	PC/PET/ elastomer Makroblend DP7645
Density	1183	kg/m^3	1,190	1,150	1,200	1,200
Flexural modulus	178	MPa	2,000	2,300	2,000	2,100
Flexural strength	178	MPa	86	90	70	75
Tensile strength at yield	527	MPa	58	55	50	50
Strain at break	527	%	120	>50	>50	>50
Izod impact, notched at 23 °C	180-A	kJ/m^2	70	48	60	50
Izod impact, notched at −30 °C	180-A	kJ/m^2	60	38	45	23
Puncture energy at 23 °C	6603-2	J	50	46	47	
Puncture energy at −30 °C	6603-2	J	55	52	58	
HDT at 0.45 MPa	75	C	134	127	84	
HDT at 1.82 MPa	75	C	121	109	100	94
Vicat softening point	306	C	143	131	120	133
Solvent resistance			Increasing —————————————————→			

strength of polycarbonate could be readily improved, largely by modifying the crack tip plastic deformation.

Polycarbonate modified with small amounts of low-density polyethylene (ca. 5 %) was found to exhibit a substantially improved notched Izod (>500 J/m) in thick sections (6.4 mm) (Dobkowski 1988; Dobrescu and Cobzaru 1978; Gardlund 1984). Some early grades of commercial impact-modified grades of PC were based on this technology (Freitag et al. 1985). However, it is now believed that the current commercial, nontransparent, impact-modified polycarbonates are made by blending small amounts of a low-T$_g$, elastomeric impact modifier such as the core-shell rubbers, viz., PMMA-g-SBR (MBS), PMMA-g-n-butylacrylate (acrylic core-shell) types, all composed of ≤0.1 μm cross-linked rubbery core particles. These modifiers improve both the thick-section (6.4 mm) and low-temperature notched Izod impact properties of polycarbonate (Witman 1981; Neuray and Ott 1981; Bussink et al. 1977) as illustrated in Figs. 19.19 and 19.20. Impact-modified polycarbonates also show better retention of impact strength with heat-aging. However, such impact-modified polycarbonate grades are opaque.

In order to improve the low-temperature notched impact strength of polycarbonate while still maintaining the transparency, new polycarbonate-poly(dimethyl siloxane) block copolymers were developed (Maruvada et al. 2005). These PC-siloxane block copolymers were transparent as long as the siloxane block length was kept short (<10 units), so that fine siloxane rubber domains (10–40 nm) were
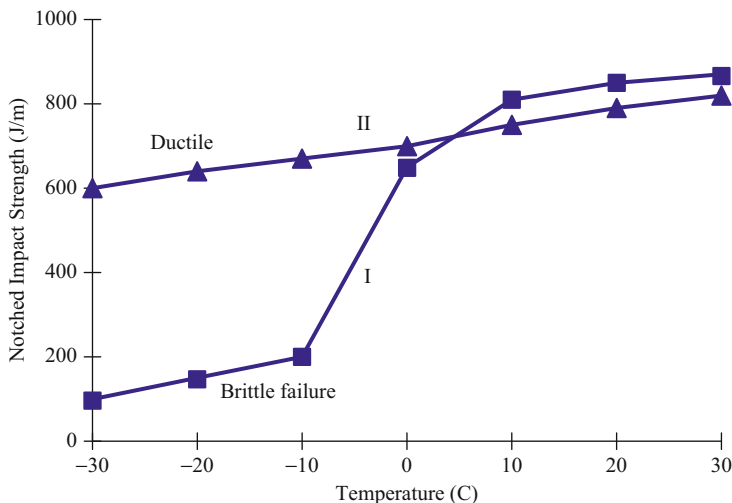
Fig. 19.20 Low temperature Impact Strength of unmodified (I) vs. Impact Modified (II) Polycarbonate (Adapted from Freitag et al. 1985)

achieved. Such a PC-siloxane copolymer exhibited high notched Izod impact retention (>600 J/m) down to −50 °C due to the toughening effect of the small siloxane rubber particles. Transparent blends of such a PC-siloxane copolymer with a standard PC also showed improvement in notched impact as well as some hydrolytic/thermal aging resistance. Some key properties of such commercial impact-modified polycarbonates are shown in Table 19.29.

Commercial impact-modified (elastomer-blended) polycarbonates are used for protective headgear, sporting goods, and bobbins for textile industry. Flame-retarded, impact PC blends are used in electronic and electrical equipment housings requiring high toughness. Impact-modified PC has to compete with the lower-cost ABS/PC blends as well as the more chemical-resistant, high-impact, PBT/PC, PET/PC blends, which will be discussed in the following sections.

19.8.2 ABS/Polycarbonate Blends

Since their introduction in 1967, ABS/polycarbonate blends (Grabowski 1964) have enjoyed a dramatic growth in market volume. They are by far the largest-volume polycarbonate blends used with the current global consumption of almost 1 Mt/year (Reseau-plasturgie 2012). The growth rate of ABS/PC blends is estimated to be about 10 %, somewhat faster than that of polycarbonate or ABS. The major reason for the success of ABS/PC blends is their overall better cost/performance balance relative to PC and impact-modified PC. Particularly noteworthy is their unique, synergistic improvement in the low-temperature notched impact strength (Morbitzer et al. 1983), which is better than the individual

Table 19.29 Properties of commercial impact modified polycarbonate vs. neat polycarbonate

Property	ISO	Units	PC/Elastomer Makrolon 1837 Bayer	PC copolymer Lexan EXL 1120T Sabic	PC Makrolon 2800 Bayer
Density	1183-1	kg/m^3	1,190	1,190	1,200
Flexural modulus	178	MPa	2,000	2,140	2,350
Flexural strength	178	MPa	86	89	96
Tensile strength at yield	527	MPa	58	57	65
Strain at break	527	%	120	119	125
Izod impact, notched at 23 °C	180-A	kJ/m^2	70	65	85
Izod impact, notched at −30 °C	180-A	kJ/m^2	60		16
Izod impact, notched at 23 °C	ASTM D256	J/m		710	908
Izod impact, notched at −30 °C	ASTM D256	J/m		609	117
Puncture energy at 23 °C	6603-2	J	50		60
Puncture energy at −30 °C	6603-2	J	55		65
HDT at 0.45 MPa	75	C	134		138
HDT at 1.82 MPa	75		121	116	131
Vicat softening point	306	C	143	138	157
Light transmission	13468	%	Opaque	82	89

components (Fig. 19.21). The partial miscibility between the SAN and the polycarbonate phases, the intrinsic ductility of polycarbonate matrix, and the presence of small particle size polybutadiene dispersions are the key factors contributing to the overall low-temperature toughness of the blend.

A discussion of the ABS/PC blends comparing with other ABS blends may be found under the ABS blends section (Sect. 19.3.2). The properties of the ABS/PC blends, primarily the DTUL and impact strength, are determined by the ratio of ABS to polycarbonate. The morphology is also dictated by the blend ratio. In blends containing ≥50 % polycarbonate, the continuous phase is formed by the polycarbonate with ABS as the dispersed phase. The rubber particles are primarily located in the SAN phase. Typical properties of some of the commercial ABS/PC blends have already been discussed under the ABS blends section (Sect. 19.3.2) and illustrated in Tables 19.8, 19.9, and 19.28. The blends containing higher levels of polycarbonate exhibit better low-temperature impact strengths.

ABS/PC blends are used in a variety of automotive components such as instrument panels, flaps for glove compartments, dashboards, cladding for steering wheel columns, ventilation ports, spoilers, wheel covers, and protective side trims. Flame-retardant ABS/PC blends are used in office equipment and business machine housings. Chlorine or bromine-free flame-retardant ABS/PC compositions contain organophosphate/PTFE powder dispersions (Freitag et al. 1991). ABS/PC blends have been used in automotive exterior body panels first in the GM's former Saturn

Fig. 19.21 Ductile-brittle transition in ABS/PC blend vs. ABS and PC (Adapted from Freitag et al. 1985)
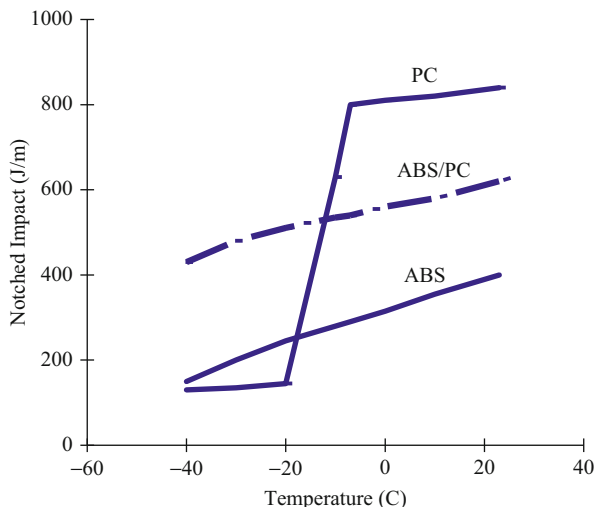
models. The assembly line for this car was equipped to handle the new waterborne paint systems, which cure at lower temperatures than the normal "E-coat" paint ovens. Due to their excellent low-temperature toughness, dimensional stability, and cost advantages, ABS/PC blends are replacing some of the PPE/HIPS applications and are also competing against some polyamide applications. However, they cannot compete with the impact-modified polyamides and the PPE/PA blends in all those applications, which require higher heat and chemical resistance such as automotive fuel emission canisters, fasteners, connectors, and exterior parts like fenders, etc.

19.8.3 Thermoplastic Polyester/PC Blends (PBT/PC, PET/PC, PCTG/PC)

The second most important class of commercial polycarbonate blends is derived by blending with commercial thermoplastic polyesters such as polybutylene terephthalate (PBT) and polyethylene terephthalate (PET). Both PBT and PET are crystallizable polymers and hence offer the expected chemical resistance advantages of the crystalline polymers in blends with polycarbonate. Among the thermoplastic polyester/polycarbonate blends, the PBT/PC blend has the major commercial volume, followed by the PET/PC blend. A copolymer of 1,4-cyclohexanedimethanol, ethylene glycol, and terephthalic acid (PCTG) forms a miscible blend with polycarbonate. PCTG/PC blend was earlier offered by Eastman (Ektar®) for specialty applications, but it is no longer commercial.

A commercial PBT/polycarbonate blend (Xenoy®) was first introduced in 1980 by General Electric when it initially enjoyed a fast growth in automotive applications, particularly for rigid bumper fascias. The blend was developed to meet the low-temperature impact strength, dimensional stability, and paintability requirements of the rigid bumper fascias (Bertolucci and Delaney 1983), which accounted

Table 19.30 Typical properties of some commercial PBT/PC and PET/PC blends

Property	ASTM	Units	PBT/PC Xenoy 1102 Sabic	PBT/PC Makroblend KU2-7912 Bayer	PET/PC Makroblend DP7645 Bayer	PET/PC Xenoy X2202 Sabic
Density	D792	kg/m^3	1,200	1,200	1,200	
Flexural modulus	D790	MPa (kpsi)	1,964 (285)	2,000 (290)	2,100 (305)	2,360 (342)
Flexural STRENGTH	D790	MPa (kpsi)	82 (11.9)	70 (10.1)	75 (10.9)	86 (12.5)
Tensile strength	D638	MPa (kpsi)	54 (7.9)	50 (7.2)	50 (7.2)	58 (8.4)
Elongation at break	D638	%	150	>50	>50	105
Izod impact, notched at 23 °C	D256	J/m (ft-lb/in.)	800 (15)	60 (kJ/m^2)	50 (kJ/m^2)	500 (9.3)
Izod impact, notched at −40 °C			640 (13)	45 (kJ/m^2)	23 (kJ/m^2)	–
Drop weight impact at 23 °C	D3029	J (ft-lb)	54 (40)	46 (34)	–	59 (44)
HDT at 0.45 MPa	D648	C	110	100	94	131
HDT at 1.82 MPa	D648	C	91	84	–	107

for the bulk of the market for this blend during the 1980s and 1990s. With the advent of low-cost TPOs successfully dominating the bumper cover market today, the growth for PBT-PC blends has been somewhat slowed down. The development of commercial PET/PC blends also followed shortly after the initial success of PBT/PC blends. Currently, some commercial blends of both PBT/PC and PET/PC types are available, and their properties are shown in Table 19.30.

All the commercial PBT/PC and PET/PC blends also contain typically 10–20 wt% of an additional elastomeric impact modifier. The exact nature and the content of the impact modifier is kept proprietary and often forms the basis for a particular blend patent. Typically, core-shell rubbers such as poly(methyl methacrylate)-grafted butadiene-styrene rubber (MBS) or an all acrylic core-shell rubber such as poly (MMA-g-n-BuA) are used (Nakamura et al. 1975; Chung et al. 1985). ABS (with high polybutadiene content ≥50 %) or ASA rubber (≥50 % acrylate rubber) have also been used. The presence of such a rubber component is definitely needed to obtain high notched Izod impact strengths (≥500 J/m) in these blends.

The binary blends of polycarbonate with poly(butylene terephthalate) (PBT/PC) or poly(ethylene terephthalate) (PET/PC) are now known to be essentially phase-separated blend systems exhibiting two glass transition temperatures in each case, one for the polycarbonate-rich phase and another for the polyester-rich phase (Murff et al. 1984; Huang and Wang 1986; Wahrmund et al. 1978). The evaluation of the amorphous phase miscibility in these blends was often complicated by the potential of a transesterification reaction between the two polymers during the melt blending, which may in principle lead to a block copolymer and eventually to

a random copolymer with a single-phase, single glass transition temperature behavior (Deveaux et al. 1982; Hobbs et al. 1987; Porter and Wang 1992). Sometimes, different conclusions have appeared in the literature regarding the phase behavior of PET/PC and PBT/PC blends, because different methods were used to prepare the blends.

19.8.3.1 Poly(butylene terephthalate)/Polycarbonate Blends (PBT/PC)

Early investigations of the melt blends of PBT and PC showed two glass transition temperatures indicative of two amorphous phases (Murff et al. 1984). However, the T_g's did not correspond to those of pure components, and in addition, there was a slight depression in the melting point of PBT. A melt-phase reaction was hypothesized to take place. Subsequent studies showed that the melt-phase transesterification reaction between PBT and PC can indeed take place, at these high temperatures (T $\geq$ 260 °C), as followed by NMR spectral changes as a function of melt residence time (Deveaux et al. 1982). The presence of titanium catalyst normally present in PBT also catalyzed this reaction.

Although NMR and IR techniques were used in characterizing these interchange reactions, these techniques are often insufficient to detect small changes in the structure that occurs when only one or few interchanges per chain take place. For example, NMR can detect only gross structural changes that take place after long reaction times ($\geq$30 min at 250 °C). Blends made by solution technique or by normal extruder melt blending process under short residence time exhibited a two-phase structure (Hanrahan et al. 1985; Dekkers et al. 1990). However, the T_g of the PC phase in the melt-blended product was usually lower (by 20 °C) than the PC phase of solution-blended product or neat PC. This was attributed to the effect of a small, although not readily detectable, level of interchange reaction in the melt-blended product.

The transesterification reactions in PBT/PC melt blends could be suppressed by using organophosphites and phosphonates, which probably function by deactivating the titanium or antimony type polymerization catalyst residues present in PBT (Golovoy et al. 1989). Even in the presence of phosphite stabilizers, PBT/PC blends showed dual-phase behavior. However, a partial miscibility was evident since the T_g of PC phase was still reduced from the normal 150 °C to about 140 °C. This partial miscibility between PBT and PC even in the absence of an exchange reaction is responsible for the good compatibility and interfacial strength of the blend.

19.8.3.2 Poly(ethylene terephthalate)/Polycarbonate Blend (PET/PC)

Early work on the PET/PC blends indicated that in blends containing >70 % PET, PC was miscible, and in blends with <70 % PET, the components separated into two phases. Subsequent investigations concluded that the blend was essentially immiscible over the entire composition range. The transesterification reaction between PET and PC in the melt phase was found to be slower than in the case of PBT at 270 °C. However, when the reaction does occur, the newly formed ethylene carbonate linkages, $-CH_2-CH_2O-CO-O-$ in the polymer chain appear to degrade more rapidly than the butylene carbonate units generated with PBT. The divergent

conclusions in the literature on the phase behavior of PET/PC blend are undoubtedly caused by the differing degrees of transesterification reaction occurring under the conditions of melt mixing (temperature, time) and the amount of catalyst residues (Goddard et al. 1986).

Under the normal extrusion blending conditions, PET/PC blend forms a two-phase blend morphology. The melt residence times are short enough such that the interchange reaction does not occur, and the PC can be quantitatively extracted out with methylene chloride. From the observed glass transitions of the PET-rich phase and PC-rich phase, measured by DSC or DMA, the blend can be classified as partially miscible with an estimated interaction parameter of slightly positive ($\chi_{12} \simeq 0.04$). From the measured T_g's, it appears that more PET dissolves in PC phase than PC does in the PET-rich phase (Kim and Burns 1990). Nevertheless, the existence of a partial miscibility, even in the absence of transesterification, accounts for the self-compatibilization effect in the blend. Mutual interpenetration of the components at the phase boundary accounts for the high interfacial strength.

The binary blends of PET/PC and PBT/PC exhibit good ductility and tensile strengths, but the notched Izod impact strengths are still low at all the blend compositions containing $\leq$80 % PC. This is a significant difference from ABS/PC blends, in which the grafted polybutadiene rubber particles of ABS phase contribute to the toughness at all the ABS/PC blend ratios. Hence, commercial PBT/PC and PET/PC blends, by necessity, include a proper level of an effective impact modifier, usually a core-shell rubber of small particle size, such as MBS, ABS, etc. It has been shown that during the melt blending, these rubber particles preferentially migrate to the PC phase due to the known compatibility of the PMMA or SAN component of these rubbers (shell structure) with the polycarbonate (Dekkers et al. 1990). Hence, the blend morphology indicates that the rubber particles are predominantly located in the PC phase (Fig. 19.22).

Commercial PBT/PC and PET/PC blends contain about 15–20 % of such core-shell rubber impact modifiers for maximum toughness, i.e., notched Izod impact strengths of typically $\geq$700 J/m, which is maintained even at low temperature (Table 19.30). The ratio of PBT/PC or PET/PC is usually kept between 50/50 and 40/60 to optimize the ductility in the blend, while still maintaining a continuous or cocontinuous phase of the polyester. A continuous phase of PBT or PET with PC as dispersed phase would be preferred for solvent resistance.

The crystallization of PBT and PET in these blends is somewhat suppressed by the partial miscibility of the PC. However, since PBT crystallizes intrinsically faster than PET, blends of PBT and polycarbonate after injection molding show a crystalline PBT phase in their morphology. Injection-molded PET/PC blends, on the other hand, generally lead to an essentially amorphous PET phase. Short-term annealing at elevated temperatures (120–150 °C) causes this PET phase to crystallize and leads to some loss in ductility especially when the polycarbonate content in the blend is $\leq$30 % (Akkapeddi et al., unpublished results).

Long-term thermal aging of PBT/PC blends is known to lead to severe embrittlement (Bertillson et al. 1988). Phase segregation, secondary crystallization, and changes in the amorphous phase free volume with aging are some of the key factors

Fig. 19.22 Morphology of PET/PC/MBS core-shell elastomer (40/40/20) blends – TEM; RuO4 stain; 15,000X (Akkapeddi et al. 1993)
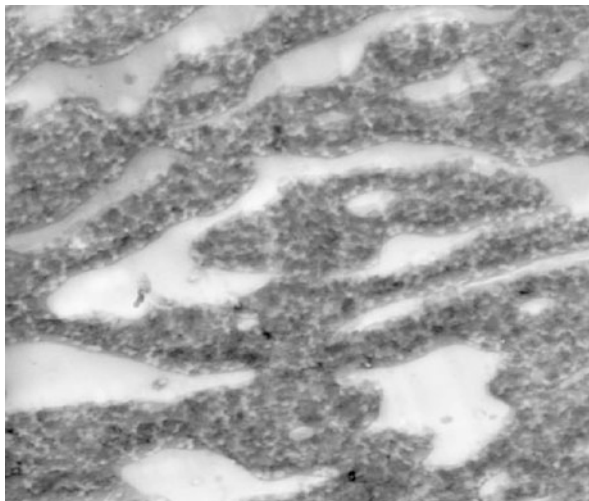
attributable to the embrittlement phenomenon. Embrittlement of PET/PC blends upon heat-aging is even more likely to occur due to the more brittle nature of crystalline PET phase. Recent work has focused on the use of reactive rubber tougheners to improve the embrittlement resistance of PET/PC blends upon heat-aging (Akkapeddi and Mason 1991; Akkapeddi et al. 1993).

The excellent low-temperature toughness and solvent resistance of PBT/PC and PET/PC blends have found good application in automotive exterior parts such as bumper beams and fascias (mainly PBT/PC), air dams, rocker panels, wheel covers, and mirror housings. Nonautomotive applications included instrument housings, lawn-mower chutes, snow blower components, etc. With the increasing competition from low-cost paintable thermoplastic polyolefins (TPO's) in the automotive bumper and fascia markets, further growth for PBT/PC and PET/PC blends may be limited in this area. Hence, these blends must find other applications where their dimensional stability, chemical resistance, high toughness, and moderate DTUL ($T \leq 100\ °C$) are well suitable.

19.8.3.3 PCTG/PC Blends

The commercial copolyester derived from 1,4-cyclohexane dimethanol, ethylene glycol, and terephthalic acid (PCTG, Ektar® DN003, Eastman Kodak) is an amorphous polymer exhibiting excellent toughness (notched Izod impact strength of ≥ 800 J/m), high clarity, and good chemical resistance characteristics. However, it has a relatively low glass transition temperature (ca. 85 °C) and a low heat distortion temperature (ca. 66 °C at 1.8 MPa).

Hence, a blend of PCTG and polycarbonate was developed, which maintained the high toughness of both components (notched Izod import strength ≥ 800 J/m), yet had a useful combination of DTUL (ca. 95 °C) and chemical resistance. More importantly, the blend maintained a high degree of clarity because of the thermodynamic miscibility between the PCTG and polycarbonate, although some

transesterification cannot be ruled out. The miscibility was confirmed by a single-T_g, single-phase behavior of the blend (Mohn et al. 1979; Smith et al. 1981). Such PCTG/PC blends were commercialized as Ektar® DA series by Eastman, but they are no longer available.

19.8.4 Polycarbonate/ASA Blends

ASA polymers are similar to ABS except that the polybutadiene rubber dispersion in the SAN copolymer matrix is substituted by the more weatherable acrylic-rubber dispersion, as the cross-linked n-butyl acrylate rubber particles grafted with SAN copolymer. Since the withdrawal of EPDM-g-SAN copolymer (formerly AES, Rovel® from Dow) from the market, ASA and ASA blends have assumed increased commercial significance for many outdoor, weatherable applications. The weatherability advantages of ASA can be extended into the polycarbonate blends (Sakano et al. 1980) as long as sufficient ASA is used in the blend (≥ 50 %). The compatibility between ASA and PC follows the same fundamental mechanism as in the ABS/PC blends, viz., the partial miscibility of SAN in PC, which compatibilizes and stabilizes the interface against delamination. Hence, ASA/PC blends uniquely combine high notched Izod impact strengths (>500 J/m) with better UV resistance and weatherability than ABS.

Some current commercial grades of ASA/PC blends include Geloy® XP4025 from Sabic, Luran® SCKR2801 from Styrolution, and Astoloy™ PC/ASA401 from Marplex. The properties of ASA/PC blends have already been discussed under ASA blends section in Table 19.10. The two outstanding advantages of ASA/PC blends are (a) high impact strength down to $-20\ °C$ and (b) high outdoor weatherability. Hence, commercial ASA/PC blends find niche applications in exterior automotive parts such as cowl vents, grills, mirror housings, trim, etc., where the parts can be pigmented (black or color) instead of being painted, unlike the case of ABS/PC. The market for ASA/PC blends is likely to grow because it can compete and replace painted or plated ABS/PC blends. The cost saving due to pre-colorability without the need for primer and paint and overall durability of ASA/PC blends will favor their increased use in exterior automotive/transportation and outdoor equipment applications.

19.8.5 Miscellaneous Other Polycarbonate Blends

19.8.5.1 Specialty Styrenic/PC Blends

Blends of polycarbonate with other specialty styrenic resins such as styrene-maleic anhydride (SMA), styrene-methyl methacrylate (S-MMA) resins were investigated primarily to upgrade the performance of these styrenic resins with regard to their impact strength and to some extent DTUL improvement. A developmental SMA/PC blend (former Arloy®, Arco) contained SMA grafted with polybutadiene as the impact modifier. The properties of SMA/PC blend were similar to ABS/PC blend with comparable impact strength (>500 J/m). However, it was discontinued

from the market due to unfavorable economics relative to ABS/PC blend. The partial miscibility between the SMA and polycarbonate may account for the compatibility of this blend.

Similarly, a developmental S-MMA/PC blend (erstwhile Novacor® SD from Nova Chemical) was reported to have better surface finish and scratch resistance than PC/polyester blends and an equivalent level of impact toughness. It is believed that these formulations also include some acrylic rubber (core-shell type) for impact modification. One would expect a sufficient level of partial miscibility for self-compatibilization between the styrene-methyl methacrylate copolymer (S-MMA) and the polycarbonate, especially at high MMA content of the copolymer, since the binary blends of PMMA and PC are known to be miscible.

19.8.5.2 Polyamide/PC blends

Unlike the thermoplastic polyesters (PBT and PET), the commercial polyamides such as PA-6 or PA-66 are strongly hydrogen-bonded polymers and hence highly immiscible with polycarbonate. Simple blends of polyamide and polycarbonate delaminate readily, as expected, unless a suitable compatibilizer is used. Because of the lack of an efficient compatibilization technique, blends of PA-6 (or PA-66) with polycarbonate have not been successfully commercialized, although there are several patents claiming some improvement in properties. Several years ago, there was an attempt to commercialize a polyamide/polycarbonate blend (former Dexcarb®, Dexter Corp.). According to their patent, the blend was compatibilized by using a combination of a polyesteramide elastomer and a maleated olefinic polymer, such as maleated polypropylene or EP rubber (Perron 1984, 1988). However, the efficiency of compatibilization is questionable, since the added components are not known to be miscible or compatible with the polycarbonate. At the present time, there are no commercially significant polyamide/PC blends.

19.8.5.3 Polyetherimide/PC Blends (PEI/PC)

Polyetherimide (PEI, Ultem®, Sabic) is a high-performance engineering thermoplastic with high heat distortion temperature (>200 °C), high mechanical strength, and inherent flame-retardancy characteristics. Blends of polyetherimide with polycarbonate were primarily developed to lower the cost of the PEI while retaining a high level of heat resistance to be used as thermoformable sheets and as molding compounds. The blend was reported to have about the same impact strength as the polyetherimide, (Mellinger et al. 1985). However, the DTUL and chemical resistance of the blend is better than that of polycarbonate.

Extrusion-grade PEI/PC blend was developed for aircraft applications to meet the federal aviation standards for low flammability, smoke, and toxic gas generation (Skeist 1991). PEI/PC thermoformable sheet has been used for the fabrication of transport aircraft window housings, air ducts, consoles, and other components. PEI/PC sheet is also used as high-temperature paint mask in the automotive industry. PEI/PC molding compounds were also evaluated for microwaveable cookware. However, due to the high cost of PEI, commercially, the blends of PEI and PC have not achieved any significant penetration in the injection molding market.

19.9   Polyoxymethylene Blends

Polyoxymethylene polymers, POM, commonly known as polyacetals or "acetal" resins, are linear thermoplastic polymers containing predominantly the $-CH_2-O-$ repeat unit in their backbone. There are two types of acetal resins available commercially: (1) homopolymers made by the polymerization of formaldehyde, followed by endcapping, (2) copolymers derived from the ring-opening polymerization of trioxane (a cyclic trimer of formaldehyde) and a small amount of a comonomer such as ethylene oxide. Acetal resins are highly crystalline polymers with melting points of 160–175 °C and heat distortion temperatures of 110–125 °C at 1.82 MPa, unfilled. Due to highly crystalline nature, POM resins exhibit excellent rigidity, hardness, and resistance to creep, fatigue, and chemical attack. They also exhibit low wear and friction, high dimensional stability, and good electrical properties. Because of their excellent mechanical properties and moderate cost, acetal resins are among the more widely used engineering resins with an estimated current global consumption of over 370 kt/year.

Owing to their high crystallinity, POM resins are not miscible with any of the commercially available polymers. Unmodified POM resins tend to be brittle, particularly when notched. Due to their lack of reactivity, POMs are generally not amenable to any chemical modification by post-reactions with grafting agents. Hence, there are very few commercial blends based on POM resins, with the exception of impact-modified POMs that are simple blends containing elastomeric/impact modifiers. In order to improve the notched Izod impact strength, several types of impact modifiers have been employed, which included core-shell rubbers of acrylic-type (Kusumgar 1987) poly(methyl methacrylate)-g-styrene/butadiene (Schuett et al. 1986) or poly(methyl methacrylate)-g-polybutadiene type (Burg et al. 1985). Some commercial medium-impact grades with notched Izod impact strengths of 100–150 J/m, may contain such impact modifiers.

A commercial grade of high-impact (notched Izod > 900 J/m) POM resin (Delrin® 100 ST, DuPont) is believed to be a blend of POM with ≥30 wt% of a thermoplastic poly(ester-urethane) elastomer derived from poly(1,4-butane adipate) diol and methylene-bis-(4,4′-diphenyl diisocyanate) (MDI) (Flexman 1989). This blend is reported to have a cocontinuous or semi-interpenetrating network of the elastomer in a matrix of the polyacetal (Flexman et al. 1990). The toughening effect in such a blend of IPN-type morphology was interpreted to occur partly through a rubber band mechanism by which the fracture energy is absorbed. The bands of rubbery domains were believed to span the crack and participate in the deformation process.

Typical properties of commercial impact-modified POM resins are shown in Table 19.31. With the increase in the impact strength of these blends, there is a corresponding decrease in the modulus, strength, and DTUL relative to the neat POM resin. Impact-modified POM blends are still low volume in usage relative to unmodified POM. About 80 % of the impact-modified POMs are used in the automotive area in typical applications such as electrical switches, fuel system components, gears, and hardware. Industrial applications include cams, gears, valves, impellers, pumps, and a variety of plumbing and appliance parts.

Table 19.31 Properties of some commercial polyoxymethylene/impact modifier blends

Blend type			POM/TPU	POM/RUBBER	POM
			Delrin 100ST	Ultraform N2640X	Delrin 500
	ASTM				
Property	Test	Units	Dupont	BASF	
Density	D792	kg/m^3	1,340	1,360	1,420
Flexural modulus	D790	MPa (kpsi)	1,240 (180)	1,690 (240)	2,880 (410)
Flexural strength	D790	MPa (kpsi)	40 (5.8)		100 (14.3)
Tensile strength at yield	D638	MPa (kpsi)	45 (6.5)	48 (6.8)	70 (10)
Elongation at break	D638	%	260	70	40
Izod impact, notched at 23 °C	D256	J/m (ft-lb/in.)	908 (17)	152 (2.8)	76 (1.4)
HDT at 0.45 MPa	D648	C	145	155	172
at 1.82 MPa	D648	C	90	85	136
Coefficient of thermal expansion	D676	m/m/C	1.2E-04	1.9E-04	1.0E-04

19.10 Polyphenylene Ether (PPE) Blends

PPE is the generic name for the homopolymer, poly(2,6-dimethyl,1,4-phenylene ether) derived from the oxidative coupling polymerization of 2,6-dimethyl phenol (Hay 1976). Developed in the early 1960s by GE, the polymer had many desirable properties such as a high T_g (205 °C) and DTUL (174 °C at 1.8 MPa), high strength and dimensional stability, moisture and hydrolysis resistance, and inherent flame retardancy. However, because its extremely high melt viscosity dictated melt-processing temperatures of well above 300 °C, at which the polymer tends to degrade or cross-link in the presence of air, its use as a molding resin by itself was severely limited. Commercially, all the PPE that is produced is alloyed with other polymers such as high-impact polystyrene (HIPS), nylons, and polypropylene to produce processable, cost-effective blends, which compete with other engineering thermoplastics in various applications. Currently, the only global producer of PPE homopolymer (trademarked as PPO[®]) and the major producer of the PPE alloys and blends (trademarked as Noryl[®]) is SABIC Innovative Plastics.

A major motivation for blending PPE with other thermoplastic polymers has been to take advantage of PPE's high heat performance and combine with useful melt processability of the other thermoplastic polymer. The average PPE content in commercial PPE alloys is about 45 %. Several PPE blends were investigated prompted by the initial success of PPE/polystyrene blends. Table 19.31 compares the key properties of the various types of commercial PPE blends.

19.10.1 PPE/High-Impact Polystyrene (HIPS) Blends

Since the early discovery of miscibility between the low-cost polystyrene and PPE, several commercial grades of PPE/HIPS have been developed, which offer a wide choice of heat resistance (DTUL), impact strength, and melt processability (Cizek 1969; Fried et al. 1978). This versatility of PPE/HIPS blends led to their unparalleled commercial success, accounting for nearly 50 % of market volume of all engineering polymers commercial blends. PPE/HIPS blends filled the price-performance gap between the styrenic resins (HIPS, ABS) and the engineering resins such as polycarbonate, polyarylate, and polysulfones. The technology of PPE/HIPS blends has already been discussed previously under the styrenic blends section (Sect. 19.3), and the typical blend properties are shown in Tables 19.6 and 19.32.

19.10.2 PPE/Polyamide Blends

Commercial PPE/PA blends were developed by the motivation to combine the high heat resistance characteristics of PPE with the chemical resistance characteristics of the crystalline polyamide polymers (PA-66 and PA-6). Because of the inherent incompatibility between PPE and polyamides, suitable methods of compatibilization and toughening have not been developed until recently. The technology of compatibilized, impact-modified PPE/PA blends have already been discussed under polyamide blends section (Sect. 19.7). Commercial PPE/PA blends are based primarily on the lower-cost polyamide (PA6 and PA66) and most often include a rubbery impact modifier as the third blend component, added for a desired level of toughness (Tables 19.25 and 19.32).

The unique difference between PPE/PA blends and PPE/HIPS blends is illustrated by (a) the differences in DTUL at 0.45 MPa and the DTUL at 1.82 MPa in glass-reinforced compositions (b) the difference in their relative sensitivity or resistance to chemicals, e.g., some common solvents and automotive fluids (Table 19.26). These differences arise from the facts that (a) polyamide is a crystalline polymer unlike HIPS, which is amorphous and (b) due to the large melt viscosity difference between polyamide and PPE at the normal blend ratios, the polyamide forms the continuous phase. Hence, in the molded parts, the polyamide surface offers resistance to solvent permeation and high softening temperature. In PPE/HIPS blends due to the single-phase amorphous character of the matrix, the solvent resistance is limited, and the heat resistance is limited by the T_g of the blend. Because of these differences, PPE/PA blends have found significant application niches.

19.10.3 PPE/Polyester Blends

Thermoplastic polyesters, PET, and PBT also offer the advantages of easy melt processability and good solvent resistance owing to their semicrystalline nature.

Table 19.32 Commercial PPE blends

Blend type ➜			PPE/HIPS	PPE/PA-6,6	PPE/PP
	ASTM		Noryl®	Noryl®	Noryl®
Property	Test Method	Units	731 Sabic	GTX910 Sabic	PPX7110 Sabic
Physical					
Specific gravity	D792		1.06	1.1	0.97
Mold shrinkage	D955	%	0.6	1.4	0.8–1.2
Water absorption, 24 h	D570	%	0.07	0.5	–
Water absorption at saturation		%	–	2.8	None
Mechanical					
Flexural modulus	D790	MPa (kpsi)	2,530 (360)	2,135 (310)	1,550 (224)
Flexural strength	D790	MPa (kpsi)	95 (13.5)	76 (11)	51 (7.4)
Tensile strength at yield	D638	MPa (kpsi)	60 (8.6)	60 (8.6)	35 (5.1)
Elongation at break	D638	%	60	60	195
Impact					
Izod impact, notched	D256	J/m (ft-lb/in.)			
at 23 °C			270 (5)	220 (4)	437 (8.2)
at −30 °C			130 (2.5)	137 (2.5)	149 (2.8)
Thermal					
Heat deflection temp	D648	C			
at 0.45 MPa			137	193	113
at 1.82 MPa			129	143	77
Vicat softening point	D1525	C	140	232	138
Chemical resistance			Poor	Excellent	Good

Key features: Combination of high heat resistance, dimensional stability, and toughness with an adequate level of chemical resistance

In addition, PET and PBT are relatively moisture insensitive under ambient conditions, unlike the polyamides (PA-6 and PA-66), which can absorb significant levels of moisture. Moisture absorption in polyamides leads to significant growth in dimensions and loss in modulus and strength. Although PPE/PA blends exhibit lower moisture absorption than the standard polyamides, they are still not suitable for some exterior automotive applications such as vertical door panels and many electrical and electronic applications, which require stringent moisture resistance and dimensional stability.

Several research investigations were made to compatibilize PET or PBT with PPE both by reactive and nonreactive routes of compatibilization (Brown et al. 1990, 1991; Akkapeddi and VanBuskirk 1992). Compatibilized binary blends of PPE/polyesters still lacked adequate toughness and invariably required the addition of rubbery impact modifiers (reactive or compatible type) and polycarbonate. The addition of polycarbonate suppresses the crystallization of the PET or PBT phase, due to its partial miscibility and therefore contributes to the overall toughness. It was reported that polycarbonate encapsulated the PPE dispersions in

the PBT matrix and consequently improved the compatibility of the blend (Hobbs et al. 1992). The addition of PC to PPE/PET or PBT blends causes some decrease in heat resistance. Although a developmental grade of PPE/PBT blend (Gemax®, GEC) was announced many years ago, currently, there are no commercially significant PPE/PBT blends available.

19.10.4 PPE/Polypropylene Blends

Several approaches to compatibilizing PPE blends with commercial polyolefins (polypropylene, etc.) have been reported in the literature (Lee 1990; Kirkpatrick et al. 1989). Simultaneous compatibilization and impact modification of PPE/polypropylene blends was achieved by choosing selected types of styrene-ethylene/butylene-styrene block copolymers and PPE resin of low molecular weight (Akkapeddi and VanBuskirk 1992). A family of PPE/polypropylene alloys were commercially launched by G.E. in 2001, under the Noryl® PPX trade name, and these are now sold by Sabic. Typical properties of a commercial PPE/PP blend are shown in Table 19.32. These PPE/PP blends are claimed to offer a balance of cost and performance between the TPOs and other higher-cost engineering thermoplastics such as nylons, modified PET, and PBT resins. Basically, the PPE/PP blends offer a balance of key properties: stiffness, toughness, chemical, and heat resistance.

The high-impact, unfilled PPE/PP blends (Noryl® PPX) are marketed for automotive bumper fascias. Compared with TPOs used in bumper fascias, PPE/PP blend offers both higher heat resistance and about 50 % higher stiffness for the same level of toughness. High stiffness and high flow of PPE/PP blend can allow for thinner walls and faster molding cycles. In addition, the scratch resistance and creep resistance are also superior. These factors coupled with a low density makes the PPE/PP cost-competitive to TPOs for bumper fascia application.

The scratch resistance of polypropylene was improved by blending 20 wt% PPE/HIPS blend (Noryl® PX0844) as a modifier and 5 % styrene-ethylene/propylene diblock copolymer (Kraton® G) as a compatibilizer (Sue 2001, 2002). It appears that the fracture energy dissipation in the PP matrix occurs by craze promotion around the dispersed particles of PPE/HIPS blend and thus preventing crack formation, while the compatibilizer promoted the PP/PPE interfacial adhesion.

Glass-filled PPE/PP blends are targeted for automotive uses, as well as power-tool housings, pump housings, heat exchanger housings, and food-handling trays. Glass-filled PPE/PP blends seem to offer a combination of good chemical resistance and excellent dimensional stability with zero moisture growth, an advantage over nylon, particularly in fluid-handling components such as pump and heat exchanger housings where precise assembly is required, especially in contact with hot water. Glass-filled PPE/PP blends claim good heat resistance of up to 110 °C continuous use, and up to 130 °C peak exposure. Glass-reinforced PPE/PP blend is claimed to

offer good surface quality in power tools and good nonstick properties in industrial food-handling trays.

In the automotive area, short glass fiber-filled PPE/PP blends are used for front-end modules, seat backs, load decks, and underhood parts. PPE-PP blends were also evaluated as a thermoplastic matrix for continuous glass-mat reinforced composites. GM's Chevy Volt concept electric car featured light-weight, compression-molded thermoplastic composite hood and door panels, the core of each panel being made from low-density glass mat (Azdel) reinforced Noryl® PPX grade PPE/PP blend (EV world 2007).

19.10.5 Miscellaneous PPE Blends

19.10.5.1 PPE-PPS Blends

Blends of PPE and PPS (Noryl® GTX APS8740, Sabic; Xyron® DG141, Asahi Kasei) are commercially available as glass fiber-reinforced, high-performance engineering resins (Gabrielle 1992). PPS is a brittle semicrystalline polymer with high heat and chemical resistance and is, of course, incompatible with PPE. However, in the PPS/PPE blend, the semicrystalline PPS forms the matrix phase with the more ductile PPE as the dispersed phase. Hence, the addition of the amorphous PPE can improve the ductility of PPS somewhat, while retaining its high-performance properties in the glass fiber-reinforced form. GF-reinforced PPS-PPE blend exhibits high heat resistance (HDT at 1.8 MPa of ca. 230 °C), flame retardancy, and conductivity permitting electrostatic painting or powder coating. Applications of GF-reinforced PPS/PPE blends will be similar to those of standard GF-PPS resins in electrical/electronic and industrial markets, except that the presence of PPE in PPS matrix reduces the part warpage and improves the toughness.

19.10.5.2 PPE-Epoxy Blends

PPE was also blended with some commercial epoxy resins (Chao et al. 1993) to improve the dielectric properties (lower the dielectric constant), toughness, and moisture resistance of the cured thermoset. These formulations with fiberglass reinforcements were used for the printed circuit boards and other electronic applications. In one formulation of epoxy resin (Epon 825, Shell) cured with aluminum alkoxide, incorporation of 30 % PPE increased the tensile elongation at break for the epoxy thermoset from <2 % to 17 %. The HDT was increased from 60 °C to 195 °C. The dissolution of PPE in the epoxy raised its viscosity from 0.2 to 400 Pa.s. (Anonymous 1991).

19.11 Thermoplastic Polyester Blends

Poly(ethylene terephthalate) (PET) and poly(butylene terephthalate) (PBT) are two of the most important members of a family of commercial thermoplastic polyesters.

Other members of this family include specialty polyesters such as PET copolymers (PETG) and poly(1,4-cyclohexanedimethylene terephthalate) (PCT). Commercially important PET and PBT resins are known for their high crystalline melting points (265 °C and 225 °C), good mechanical properties, and solvent resistance characteristics. Among all polyesters, PET is the largest-volume commercial polyester with an estimated global consumption of over 40 Mt/year in fiber applications alone and nearly 25 Mt/year in the injection stretch-blow-molded iPET bottles and containers applications (Nexant/Chemsystems 2007). In the context of textile fibers, PET is referred to by its common name, "polyester," whereas the acronym "PET" is used in relation to the bottles and thermoformed packaging and film markets.

Due to the slow rate of crystallization, unfilled PET resin is generally not used in the conventional injection molding, engineering plastics applications. However, a large volume of neat PET resin is almost exclusively used in the injection stretch-blow molding market for the production of clear PET bottles and containers, which are widely used in the food, beverage, and consumer packaging markets. The commercial success of the PET bottles in replacing the glass bottles is largely due to the unique combination of light weight, clarity, toughness, and good gas barrier (i.e., barrier to O_2 and CO_2) properties coupled with the recyclability.

The dramatic growth in the use of PET in the soft-drink, beverage, and food packaging markets has indeed spurred considerable activity in the recycling of PET. Hence, PET is a relatively low-cost polymer not only because of large-scale production economics but also due to its availability as a recycled material, thus providing a cost incentive for blending with other polymers. Nevertheless, only a few cases of PET blends are actually used commercially in the conventional injection molding markets again because of the slow crystallization rate of PET as compared to PBT or PBT blends. Most of these commercial PET blends used in injection molding market are made either with PBT or polycarbonate, in combination with impact modifiers and/or reinforcing fillers, in which the role of PET is to improve the surface aesthetics and ductility of the molded part. These engineering plastic-grade PET blends will be discussed in a later section.

In the rigid packaging/PET bottle market, there has been some interest in recent years, to blend small amounts of other barrier polymers ("passive" barrier type) or more importantly, "oxygen scavenger" ("active" barrier type) polymers, to improve the barrier performance of PET. Such commercially important PET-oxygen scavenger blends used as barrier PET containers in the food and beverage packaging markets will also be discussed in a later section.

Poly(butylene terephthalate) (PBT) is produced in a much smaller volume than PET. However, PBT is more widely accepted as an injection-moldable engineering plastic in the large automotive and electronic markets due to its faster crystallization rate (Pratt and Hobbs 1976). Hence, PBT is more commonly employed in the formulation of blends also. PBT has generally been preferred over PET in the engineering plastics arena because of its superior processability, faster crystallization rate, shorter molding cycles, and better properties (DTUL/impact balance) in the molded parts, particularly in the unfilled form. Nevertheless, PET is also used to

a limited extent in glass or mineral reinforced forms admixed with nucleators and crystallization promoters.

The primary motivations for blending a crystalline thermoplastic polyester such as PBT with other polymers are: (a) to improve the solvent resistance and processability of amorphous polymers such as PC, styrenics, PPE, etc.; (b) to reduce the mold shrinkage of the thermoplastic polyesters associated with their crystallization; (c) to increase the DTUL of the unfilled polyesters; and (d) to improve toughness.

The largest-volume polyester blend sold commercially is the PBT/polycarbonate blend. PET/PC blend is also gaining some commercial importance because it is almost similar to PBT/PC blend in properties and moldability but has some cost advantages. Unlike the neat, unfilled PET that is difficult to injection-mold due to its slow crystallization rate (long mold cycle times with hot molds and amorphous parts with cold molds), PET/PC blends can be molded readily using the normal hot molds (ca. 80–100 °C) and fast mold cycles. The presence of PC helps retain high stiffness and strength in the part at the mold temperatures, to enable the demolding of distortion-free parts. The properties and applications of PET/PC blends have already been discussed under the polycarbonate blend section (Sect. 19.8). Other commercial blends of PET and PBT are discussed below.

19.11.1 PBT/PET Blends

These blends take advantage of the low cost of PET and the rapid crystallization rate of PBT. Despite their large difference in the crystallization rates, PET and PBT form stable blends without the need for compatibilizing agents. This was attributed to the amorphous phase miscibility between the two components (Escala and Stein 1979; Mondragon et al. 1989). X-ray, DSC, and IR studies indicated that the two components form separate crystalline phases and a single amorphous phase with a single T_g. Some transesterification was detected in the melt by NMR, especially at long melt residence times ($\geq$6 min) (Mondragon et al. 1989). The extent of transesterification under the fast extruder blending operation is however expected to be low.

Commercial grades of PET/PBT blends are generally glass fiber-reinforced (15–30 wt%). Compared to the glass-reinforced PBT and PET, the heat distortion temperatures of the blends at 264 psi are actually lower indicating the lower level of net crystallinity in the blend, an effect possibly caused either by miscibility or transesterification. The primary reason for developing these blends appears to be the improvement of surface appearance and gloss in the injection-molded parts compared to those made from the individual resins. There is also some cost advantage over PBT.

PBT/PET blends are used for making visible parts of both large and small appliances that need the appeal of smooth and glossy surface along with high stiffness, strength, and DTUL. There are also other electrical and automotive applications. Compared to the neat PBT molding resins, the market for the blend is still relatively small.

19.11.2 PBT/Elastomer Blends

Unmodified PBT is a fairly ductile material exhibiting high elongation at break, even after crystallization. However, as to be expected of all rigid semicrystalline polymers, molded parts of PBT show low notched Izod impact strength indicating that under conditions of stress concentration, the resistance to unstable crack propagation is low. Impact modification of PBT was investigated through the use of several elastomeric modifiers. Commercial PBT/elastomer blends are of two types, viz., (a) high impact strength type, (b) low-modulus, highly flexible types.

Commercial impact-modified PBT grades generally contain 20–30 wt% of controlled particle size (<0.3 μm), core-shell rubber modifiers (Neuray and Ott 1981; Farnham and Goldman 1978; Binsack 1985). Typical impact modifiers are: PMMA-g-SBR (MBS), PMMA-g-poly(n-BuA) (acrylic core-shell rubbers), SAN-g-PBD (high rubber ABS), or SAN-g-poly(n-BuA) (high rubber ASA). Commercial impact-modified PBT grades (Table 19.33) exhibit notched Izod impact strengths in excess of 500 J/m, while retaining a good level of modulus, strength, and DTUL. In these blends, the dispersed rubber particles promote multiple sites for crazing and shear yielding in the PBT matrix, thus providing mechanisms for energy dissipation during impact deformation and hence offering resistance to crack propagation (Hourston et al. 1991).

A commercial blend of PBT with a high-rubber ABS as impact modifier (Pocan S1506, Bayer) has been used in Europe for automotive bumpers, mirror housings, and other exterior parts (Kossoff et al. 1987). The blend was reported to exhibit good heat sag resistance at 135 °C and maintain high notched Izod impact strength >700 J/m even at −29 °C (Table 19.33). Substitution of ABS with ASA (SAN-grafted to cross-linked poly(n-butylacrylate) rubber particles) gives a more weatherable, impact-modified PBT (Ultradur KR4071, BASF). Similarly, a commercial PBT blend containing 25 wt% of MBS-type impact modifier (Vandar® 2100, Ticona) has been used in such exterior automotive applications as under-body rivets, fuel-line clips, etc.

PBT/elastomer blends display a unique combination of high impact strength, dimensional stability (due to their non-hygroscopic nature), excellent resistance to automotive fluids such as gasoline, oils, paint solvent, aqueous salt solutions, and good heat resistance. In addition, their easy processability (low melt viscosities) lends themselves to the fabrication of both small and large parts. High mold shrinkage and tendency to warp are some of the drawbacks resulting from the crystallization, which need to be addressed by proper tools and molding process designs.

19.11.3 PBT/Copoly(ether-ester) Elastomer Blends

Commercial copoly(ether-ester) elastomers (e.g., Hytrel®, DuPont; Riteflex®, Celanese) are segmented block copolymers containing a polyether soft segment such as poly(tetramethylene oxide) and a hard segment that is chemically identical

Table 19.33 Properties of typical, commercial PBT/elastomer blends

Property	ASTM	Units	Vandar® 2100 (Ticona)	Toray PBT 5207X11 (Toray)	Pocan® S1506 (Lanxess)
Density	D792	kg/m^3	1,230	1,200	1,200
Mold shrinkage	D955	%	1.8	2.6	1.8
Flexural modulus	D790	MPa (kpsi)	1,800 (260)	1,660 (235)	1,600 (220)
Flexural strength	D790	MPa (kpsi)	60 (8.7)	54 (7.8)	55 (7.9)
Tensile strength at yield	D638	MPa (kpsi)	40 (5.8)	37 (5.3)	35 (5.1)
Elongation at break	D638	%	>50	250	>50
Notched Izod at 23 °C	D256	J/m (ft.lb/in.)	NB	770 (14)	>900 (18)
HDT at 0.45 MPa	D648	C	110		100
HDT at 1.82 MPa	D648	C	50	50	55

to poly(butylene terephthalate). When the soft segment is ≥50 %, these block copolymers exhibit high degrees of rubbery elasticity, yet they process like thermoplastics and hence appropriately are called thermoplastic elastomers (Adams and Hoeschele 1987).

Because the hard segments crystallize like PBT, these thermoplastic elastomers exhibit high heat resistance with Vicat softening points typically in the range of about 180 °C. The hard segment crystallinity also imparts a good level of solvent resistance in these materials. The low T_g of the soft segment is responsible for the flexibility, resilience, and low-temperature toughness characteristics. Although the poly(ether-ester) block copolymers have been used in many niche applications requiring high-performance thermoplastic elastomer characteristics, their high cost has been a drawback in extending to larger volume applications.

To reduce the cost, these elastomers have been diluted with some PBT homopolymer. Because of the chemical similarity between the hard segment of the copoly(ether-ester) elastomers and the PBT, they form fairly compatible blends. When the hard segment content in the copoly(ether-ester) is >80 wt%, it was found to be completely miscible with PBT, showing a single T_g, amorphous phase and cocrystallization of the PBT segments of the elastomer with PBT homopolymer. As the hard segment content was lowered to ≤60 %, the blend exhibited incomplete miscibility, with two T_g's for two amorphous phases and also two separate crystalline phases (Runt et al. 1989). Nevertheless, a partial miscibility was indicated due to changes in the T_g observed in DSC and dielectric relaxation spectra. The partial miscibility and low interfacial tension between the phases makes the blend very compatible.

Commercial PBT/copoly(ether-ester) blends are generally richer (≥50 %) in the copoly(ether-ester) elastomer content. These blends originally designed for the automotive, flexible bumper fascia market (Bexloy® V, DuPont) appear to be no longer

commercial. They exhibited low moduli ($\leq$800 MPa), high elongation, and toughness needed for bumper application. The purpose of PBT in the blend was to lower the cost and improve the heat sag resistance required for paint oven capability. PBT/copoly (ether-ester) elastomer blend-molded parts also exhibited excellent surface finish and good paint adhesion without the need for primers. Because of the excellent surface esthetics of the blend, molded-in colors were also used to reduce the painting costs. Lower levels ($\leq$20 %) of copoly(ether-ester) elastomers have also been blended with PBT to make high impact strength molding resins (Celanex® grades, Celanese).

19.11.4 Impact-Modified Polyesters (Glass Fiber-Reinforced)

PET/elastomer blends have not been commercialized in the unfilled form, due to the slow rate of crystallization of PET. Unfilled PET and PET/elastomer blends are not easy to injection-mold under normal mold temperatures (ca. 80–100 °C) in fast molding cycles. The parts tend to stick to the mold and distort. Use of cold molds allows molding of amorphous PET parts (1–2 mm) lacking heat resistance (DTUL). Upon annealing at elevated temperatures (ca. 150 °C), one can develop crystallinity in PET parts, but they become brittle even in the presence of a modifier. Lack of proper adhesion between the rubber and the PET after crystallization, in general, seems to be the reason for this embrittlement.

Use of reactive tougheners such as ethylene-glycidyl methacrylate copolymers (Iida et al. 1981) and ethylene-n-butyl methacrylate-glycidyl methacrylate terpolymer (Deyrup 1988) leads to significantly improved toughness, which is retained even after annealing (Akkapeddi and VanBuskirk 1993). However, at present, no commercial PET/elastomer blends are offered in the unfilled form. The compositions such as those described above may be nucleated and glass-filled. An ethylene copolymer rubber-modified, glass-filled PET (Rynite® SST) with improved notched Izod impact strength and elongation is commercially available. A glass-filled PBT, impact modified with SAN-g-poly(n-BuA) core-shell rubbers (ASA), is also available commercially (Ultrablend® S, BASF). Because of the superior weatherability of ASA rubber vs. other rubbers such as ABS, MBS, etc., the PBT/ASA blend is likely to find applications in the exterior automotive applications. Mirror housings, door handles, roof racks are typical exterior, automotive applications.

Some grades of glass/mineral-reinforced, impact-modified PET molding resins have also been developed specifically for automotive exterior body panel applications (Bexloy® K, DuPont). This specific formulation was reported to withstand automotive on-line "E-coat" paint oven temperatures (ca. 200 °C) as well as give low warpage and smooth surface finish in the molded parts. A combination of glass fiber or glass beads and/or mica is believed to be used for reinforcement. The impact modifier is more likely a reactive toughener of the ethylene-n-butylacrylate glycidyl methacrylate terpolymer type or an ionomeric-type ethylene-butylacrylate-methacrylic acid terpolymer.

19.11.5 PET/Oxygen-Scavenging Polymer Blends

An oxygen-scavenging polymer, by definition, is a polymer that is capable of reacting with the oxygen from air, under ambient conditions and at a controlled rate. When used as an integral layer or as a blend in a PET container, an oxygen-scavenging polymer can intercept and scavenge the oxygen that permeates through the walls of the container, thus providing a sufficiently long-lasting, oxygen barrier performance to be useful for extending the shelf-life of the packaging. An alternate technology, normally referred to as "oxygen absorbers," is usually based on inorganic materials such as iron powders or ascorbate salts, for use as sachets or closure liners to scavenge the headspace oxygen in a package (Brody et al. 2001). These will not be discussed here. The barrier enhancement achieved with the oxygen-scavenging polymers is referred to as "active barrier" in contrast to the "passive" diffusional barrier achieved by blending with common oxygen barrier resins. The barrier performance of PET blends with active vs. passive barrier polymers is schematically illustrated in Fig. 19.23.

It may be noted that at low barrier resin loading, a PET/passive barrier resin blend can give only a marginal improvement in the oxygen barrier performance, while the PET/oxygen scavenging resin blend can provide a more substantially improved oxygen barrier. Commercial oxygen-scavenging polymers contain oxidizable functional groups (R) such as those shown below, react with oxygen under ambient conditions in the presence of a cobalt catalyst, to impart high barrier performance in PET blends. The oxygen scavenger lasts until its concentration is depleted, resulting in substantial shelf-life extension in the PET containers.

$$\underline{\text{Functional group (R)}} \qquad \underline{\text{Relative oxidizability}}$$

Allylic ($-CH=CHCH_2-$)

Benzylic ($-Ar-CH_2-$)   Increasing oxidizability ↑

Alkylene ether ($-CH_2-CH_2-O-$)

Oxygen scavenging reaction (Cobalt catalyzed oxidation):

$$R\text{-}H + O_2 \rightarrow ROOH$$

Oxygen scavenging rate and capacity $\propto [RH]$

Commercially, the enhanced oxygen barrier PET containers containing the oxygen-scavenging polymers are gaining increased importance, not only for extending the shelf life of standard PET bottles, but more importantly in gaining a larger market share and opportunity in replacing the glass containers traditionally used for packaging oxygen-sensitive foods such tomato-based pasta sauces, salsas, etc., and beverages such as beer and wines. The level of oxygen barrier and the desired shelf life in these containers varies with the type of foods and beverages.

Basically, a high barrier to oxygen ingress in PET containers is needed not only to prevent the microbial growth and spoilage of the food, but also to preserve the quality of taste, aroma, color, and nutritional values such as Vitamin C, all of which are

Fig. 19.23 Schematics of typical O_2 permeability rates (*top*) and the net oxygen ingress in bottles made from PET-O_2 scavenger blends
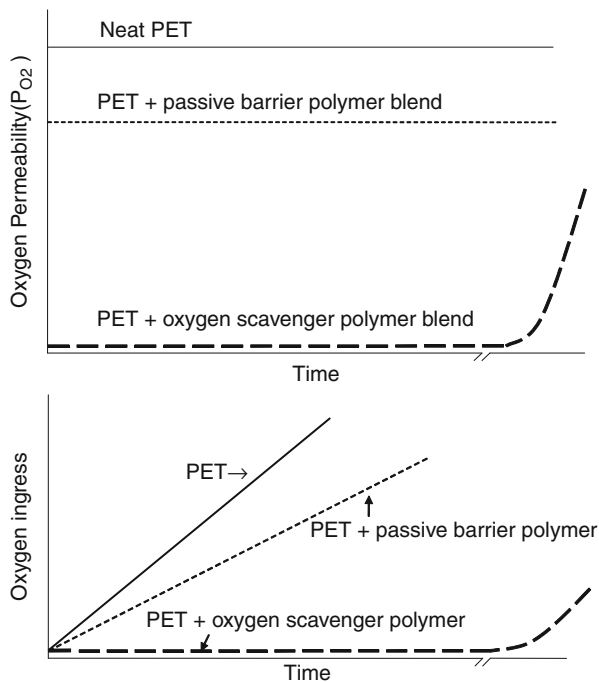
susceptible to oxidative degradation. For most of the oxygen-sensitive food and beverage products such as tomato-based products, juices, and wines, the total oxygen ingress must be $<5–10$ ppm over the desired shelf-life period of 2 years in a barrier PET container, to prevent browning and deterioration of product taste and quality. For beer, <1 ppm oxygen ingress and >85 % CO_2 retention is needed over the desired shelf life of 6 months. Hence, there is a significant market-driven technical motivation to develop PET-oxygen-scavenger polymer blends to make barrier PET containers. The main advantages of the barrier PET vs. glass containers are

- PET bottles are lighter in weight and more shatter-proof than glass.
- PET bottles are >60 % more energy-efficient than glass bottles.
- PET bottles require less oil to produce than glass bottles.
- PET bottles help in fuel savings in transportation, due to their lower weight.
- PET bottles generate 60 % less atmospheric emissions compared to glass.
- PET bottles generate 70 % less solid waste by weight compared to glass.

The commercially important oxygen-scavenging polymer systems useful for blending with PET are based on oxidizable olefinic polymers such as a polybutadiene block or graft copolymers, oxidizable polyamides, such as PA-MXD6, or oxidizable aliphatic polyether copolymers such as PTMG-b-PET. For the purpose of oxygen scavenging in PET bottles, these oxidizable polymers are always used in combination with a cobalt salt as catalyst, at a level of 50–200 ppm of cobalt.

Table 19.34 Some commercial oxygen scavenger polymers used in barrier PET containers

Oxygen-scavenger system	Oxidizable polymer	Catalyst	Compatibilizer
Amosorb® (*ColorMatrix Corp.*)	PBD-PET block copolymer	Co^{2+}	Block copolymer
Oxbar®, Monoxbar® (*Constar*)	PA-MXD6	Co^{2+}	–
Polyshield® (*Invista*)	PA-MXD6	Co^{2+}	Sulfoisophthalate
Poliprotect® (*M&G corp.*)	PA-MXD6		Sulfoisophthalate
Aegis® OX (*Honeywell*)	PBD-g-PA6 + PA6I/6T blend	Co^{2+}	Graft copolymer
Oxyclear® (*Invista, Indorama*)	PTMG-PET block copolymer	Co^{2+}	Block copolymer

Typically, these oxygen-scavenging polymers are used either as barrier layers in multilayer PET bottles or as blends in monolayer PET bottles. However, the mono-layer PET bottles are preferred because of the lower equipment cost and easier processing compared to the relatively more complex and more expensive coinjection molding processes. There is already a large, globally well-established manufacturing capacity and know-how for making monolayer PET bottles. Hence, there is an economical motivation to make barrier PET blends for monolayer bottles. However, the oxygen scavenger polymers used in these monolayer barrier PET bottles must meet the regulatory requirements for direct food contact safety, not only for the components of the blend but also for the products of oxidation resulting from the oxygen-scavenging reaction. These oxidation byproducts must in principle be nonmigratable or meet the safety threshold limits. Commercial oxygen-scavenging polymers have been designed to meet these requirements and obtain the FDA approvals. Some commercial oxygen-scavenger polymer systems used in the enhanced oxygen barrier PET container applications are listed in Table 19.34.

19.11.5.1 PET/PBD-b-PET Oxygen-Scavenging Blends

Polybutadiene-PET block copolymers (PBD-b-PET) containing about 10 wt% PBD blocks have been developed by a reactive extrusion process via a transesterification reaction between PET and hydroxyterminated polybuadienes using a cobalt salt as a transesterification catalyst (Tibbitt et al. 2007). Such a PBD-b-PET copolymer containing preblended cobalt catalyst is sold commercially as Amosorb® DFC (ColorMatrix USA) resin, for use as an oxygenscavenger concentrate for blending with PET to make enhanced barrier PET bottles.

Typically, this PBD-b-PET copolymer-based oxygen scavenger concentrate is used at 2–5 wt% to blend with PET, to make injection stretch blow-molded bottles with improved oxygen barrier. Such PET/PBD-b-PET blend-based bottles are now commercially used for packaging oxygen-sensitive beverages such as juices, green teas, and wines. These bottles exhibit 6–12 month shelf-life, a two to threefold improvement over the shelf-life of standard PET bottles. However, because of the high reactivity of the allylic groups in PBD, the oxygen-scavenging activity of these bottles can decrease somewhat with the empty bottle storage time. Hence, the PET/PBD-b-PET blend-based bottles must be filled preferably fresh as molded to fully utilize the oxygen-scavenging capacity.

The oxygen-scavenging capacity and consequently the achievable oxygen barrier shelf-life increases steadily with the PBD-b-PET content in the blend. However, due to the inherent phase separation of PBD blocks in PET matrix, the PET blend bottles tend to exhibit some haze particularly at high loading of the PBD-b-PET copolymer. The PBD domains in the PET block copolymers reportedly range from 100 to 1,000 nm, the predominant number of these PBD particles being below 300 nm (Cahill and Chen 2000). The morphology stability of these PBD domains in the PET blend can be attributed to the interfacial compatibilization offered by the covalently bound PBD-PET block copolymer in the PET matrix. Control of bottle clarity or haze will therefore be influenced by the control of the PBD morphology (domain size and distribution) in these PET blends, particularly after the orientation in the bottle.

A blend of PBD-b-PET, PA-MXD6, and cobalt catalyst is also sold under the trade name Amosorb® SolO2 as an oxygen scavenger for blending with PET. Such ternary PET blends can exhibit improved oxygen and CO_2 barrier, suitable for packaging some carbonated beverages.

19.11.5.2 PET/PA-MXD6 Oxygen-Scavenging Blends

Poly(m-xylene adipamide) (PA-MXD6) has gained considerable interest in recent years as a thermoplastic barrier packaging resin. The excellent gas barrier (O_2 and CO_2) properties (ca. 20× improvement over PET), orientability, and melt-processability at as high as the PET processing temperatures, made PA-MXD6 attractive for commercial use in making barrier PET containers of both the multilayer type and the monolayer PET/PA-MXD6 blend type. However, in order to be cost-effective, the PA-MXD6 content in these PET containers is generally limited to $\leq$5 wt%.

PA-MXD6 is also an oxidizable polyamide because of the reactive benzylic groups in its structure. The oxidizability or oxygen-scavenging property of PA-MXD6 was first recognized for its utility in making high oxygen barrier PET containers (Cochran et al. 1981). It was demonstrated that in the presence of a cobalt catalyst, blending as little as 1–4 wt% PA-MXD6 in PET caused an efficient scavenging of the oxygen permeating into the PET bottles, resulting in near-zero O_2 permeability for a considerable period of time (Fig. 19.21). However, the PA-MXD6-Cobalt catalyst-based oxygen scavenger system was initially commercialized in multilayer, barrier PET bottles as Oxbar® (Constar international), SurShot® CPTX-312 (Graham Packaging Co.) systems.

Such multilayer PET containers of three- and five-layer types, containing thin layers of neat PA-MXD6, both as a passive barrier and as an active barrier/oxygen-scavenging type in combination with cobalt catalyst are currently used to some extent in the packaging of oxygen-sensitive beverages (juices, beer, and wines) and some tomato-based food products such as ketchups. However, because of the cost of multilayer coinjection equipment, there has been a significant interest in recent years for developing monolayer barrier PET containers based on PET/PA-MXD6 blends. Hence, several commercial barrier PET technologies were developed for monolayer containers based on PET/PA-MXD6/cobalt catalyst blends, such as Monoxbar® (Constar International), Polyshield® (Invista Corp.), Poliprotect® (M&G USA Corp.), as outlined in Table 19.34.

For optimum barrier performance in PET/MXD6 blends, one needs at least 3–5 wt% PA-MXD6, but even at these low levels, the bottle clarity is invariably compromised due to the inherent incompatibility between the two polymers. The compatibilization in PET/PA-MXD6 blends was found to be somewhat improved by incorporating a small amount of sodium or lithium 5-sulfoisophthalate (SIPA) comonomer units in the PET, thereby reducing the polyamide particle size and reducing the haze in the bottles (Liu et al. 2011; Heater et al. 2007). Without a compatibilizer, the blend morphology consisted of relatively large spherical or ellipsoidal polyamide particles of ca. 2 μm dispersed in the PET matrix. The addition of ca. 0.5 % mol% SIPA to the PET phase reduced the MXD6 particle size to 0.3 μm (Prattipati et al. 2006; Ozen, et al. 2010). It is known from earlier literature that sulfonated ionomers exhibit favorable interaction with nylons via a sulfonate anion-amide complexation mechanism (Feng et al. 1996).

The PET/PA-MXD6 blend-based bottles are relatively more stable and can exhibit longer barrier shelf-life (>1 year) compared to the PBD-b-PET blend-based bottles. Although the bottles exhibit some haze at high PA-MXD6 levels (>5 %), suitable colorants and tints have been employed to mask the haze for use in carbonated and/or oxygen-sensitive beverages such as beers and wines. The market application for PET/PA-MXD6 blends in monolayer PET bottles and jars is still at an early growth stage.

19.11.5.3 PET/PTMG-b-PET Oxygen-Scavenging Blends

Polyethers such as poly(tetramethylene oxide) {PTMO or poly(THF)} are known to be prone to oxidation in air, although not as reactive as polybutadienes. Blends of PET with polyether diols such as poly(tetramethylene oxide)glycol (PTMG) as well as copolymerized polyether-polyester resins were investigated for potential oxygen-scavenging properties, using a cobalt catalyst and photoinitiators (Cyr et al. 2002). Subsequently, some PTMG-PET block copolyether-esters with high PTMG content (ca. 50 wt%) were made via an inreactor copolycondensation process in the presence of a cobalt salt, and the resulting copolyether-ester was evaluated for oxygen-scavenging properties (Chen et al. 2009; Roodvoets 2012). Commercially, a PTMG-b-PET copolyester is marketed as an oxygen scavenger concentrate (Oxyclear® 3500, Invista/Indorama) for use in blending with PET, to make injection stretch-blow molded, oxygen-scavenging PET bottles. Because of the tendency for phase separation of the polyether blocks in the PET, good mixing during the blending and injection molding is critical to get a uniform scavenger dispersion and reduce the bottle haze. Commercial development of this blend is still at an early stage.

19.12 Specialty Polymer Blends

In the plastics industry, specialty polymers are generally considered as high-performance, high-priced resins whose current market volume is still relatively

low compared to the more widely used engineering thermoplastics and commodity thermoplastics. Specialty polymers may be of two types, viz., (a) high-T_g, amorphous engineering thermoplastics such as polysulfones, polyarylates, polyetherimide, polyamideimide, polyimides; (b) high-melting, crystalline thermoplastics such as polyphenylene sulfide, liquid-crystalline polyesters (LCP's), polyetherketones (PEEK, PEK). Both categories of polymers can be classified as high-temperature polymers with long-term service capability at $T \geq 150$ °C and more often at $T \geq 200$ °C, as defined by the U.L. temperature index; i.e., temperature at which ≥ 50 % tensile strength is retained after 10,000 h of heat-aging. A common structural feature of all these high-temperature polymers is their essentially all aromatic backbone structures.

The high-temperature specialty polymers possess certain common property advantages such as (i) high T_g and/or T_m, (ii) inherent flame retardancy, (iii) high thermo-oxidative stability, (iv) high continuous-use temperatures, (v) high mechanical rigidity and strengths, (vi) high dimensional stability (to moisture and temperature) and creep resistance.

The crystalline polymers such as PPS, LCP, PEEK offer the additional advantages of high solvent resistance. Due to the inherently high cost of the specialty polymers, very few blends have been developed for commercial applications. The only driving force for the development of even the few blends of specialty polymers has been the desire to reduce the cost of the base resins by blending with lower-cost engineering plastics, although this invariably results in a lower performance. Some commercially significant specialty polymer blends will be discussed in the following section. The reader may also refer to another chapter of this handbook, viz., ▶ Chap. 16, "High Performance Polymer Alloys and Blends for Special Applications."

19.12.1 Polysulfone Blends

Polysulfones are aromatic high-T_g, amorphous polymers having the rigid aromatic sulfone linkages in the recurring units of their backbone. The three commercially significant polysulfone resins are (1) Polysulfone (PSU; Udel®, Solvay; Ultrason® S, BASF), (2) Polyphenylsulfone (PPSU, Radel® R, Solvay), and (3) Polyethersulfone (PESU-Veradel®, Solvay; PES-Ultrason E, BASF). All are transparent, high-T_g, amorphous ductile engineering resins. The T_g of PSU is 185°CC while that of PPSU and PES are 230 °C and 220 °C respectively. Due to its relatively lower cost, PSU enjoys the major market share by volume (>70 %). Poly(phenyl sulfone) (PPSU) is the highest-performance sulfone with not only a higher T_g (230 °C) but a much better notched impact strength than the more notch-sensitive PSU and PES polysulfones.

Owing to their high T_g and the hydrolytic resistance of the aromatic sulfone backbone structure, polysulfones display reliable long-term performance in hot water and steam even under autoclave conditions. Unlike the other high-T_g, transparent polymers, such as polycarbonate (PC), polycarbonate-ester (PCE), and polyetherimides (PEI), the sulfone polymers are not prone to crazing and failure

Table 19.35 Key properties of a commercial polyphenyl sulfone/polysulfone blend

Property	ASTM	Unit	PPSU/PSU blend (Acudel® Solvay)	PPSU (Radel®, Solvay)
Tensile strength at yield	D-638	MPa	77	69.6
Elongation at break (%)	D-638		50	60
Flexural modulus	D-790	MPa	2,760	2,410
Flexural strength	D-790	MPa	108	91
Notched Izod	D-256	J/m	110	690
HDT at 1.8 MPa	D-648	C	197	207
Transparency			No	Yes
Chlorine resistance			Yes	Yes

in long-term exposure to hot water. Hence, the polysulfones are used in niche specialty applications such as steam-sterilizable medical, dental, and surgical devices, sterilization, and food service trays, hot water/plumbing parts. The inherent flame retardancy and low smoke generation of polysulfones makes them also suitable for aircraft interior applications.

These unique combinations of transparency, hydrolytic, and heat resistance of polysulfones would be lost if other polymers are blended. Hence, there has been very little commercial incentive for blends of polysulfone. Nevertheless, in the early days of polysulfone commercialization, some blends with ABS and PET were developed primarily to lower the cost but also to improve selected properties such as plateability or chemical resistance. A PSU/ABS blend (Mindel® A) was commercially offered for some time but is now no longer available. Additives such as phenoxy resins, styrene-maleic anhydride copolymers have been claimed to improve the compatibility and weld-line strength of the PSU/ABS blends (Robeson 1985). The blend was evaluated for selected appliance, plumbing, and sterilizable equipment plated parts. This blend lacked the heat resistance needed for the vapor phase solderability in electronic applications.

Polysulfone was also blended with PET for the purposes of cost reduction and improvement in solvent stress-crack resistance. The blend was developed in the glass-reinforced forms for applications in electrical and electronic markets (Mindel® B, Amoco). However, the DTUL, flexural strength, and impact strength of this PSU/PET blend were inferior to those of PET at comparable levels of glass reinforcement and hence no longer offered.

Currently, the only commercially available polysulfone blend is a polyphenylsulfone/polysulfone blend (Acudel® PPSU/PSU, Solvay) (Table 19.35). It offers a cost and processing advantage over neat PPSU, while retaining good resistance to hot chlorinated water, useful in plumbing system components such as ball valves, connectors, and housings. The blend is opaque (immiscible) and has a lower notched Izod than PPSU but is more cost-effective.

19.12.2 Polyarylate Blends

Commercial polyarylate is an aromatic polyester of high glass transition temperature (ca. 180 °C) derived from bisphenol A and a mixture of terephthalic and isophthalic acids. It is a transparent, rigid, and tough thermoplastic of high heat distortion temperature (174 °C). Polyarylates face competition from the more established polycarbonate and its higher heat analogs, viz., polyester carbonates, as well as the polysulfone that is superior in hydraulic stability. Although polyarylate has been commercially available for many years, its market growth has been slow due to its high cost/performance balance. Nevertheless, polyarylate's transparency, UV/weather resistance, and high heat distortion temperature properties have found specialty niche applications in automotive taillights, reflectors, etc. Polyarylates have also been used in electrical/electronic connector applications. However, the production volume of polyarylates is still very low. Relatively few blends of polyarylate have been commercialized because blending other polymers results in the loss of the clarity and DTUL advantages of the polyarylate. Currently, the only commercial blend of polyarylate appears to be a blend with polyamide (U-polymer AX-1500, Unitika).

Polyarylate/PET blends prepared by solution or melt blending under short residence times at $T \leq 280$ °C with or without an added ester interchange inhibitor such as triphenylphosphite are essentially phase-separated, exhibiting two glass transition temperatures, one each for a PET phase and a polyarylate-rich phase. From the observed glass transition temperatures, one can conclude that it is a partially miscible blend in which more PET dissolves in the polyarylate phase than polyarylate does in PET. The interaction parameter has been estimated to be slightly positive ($\chi_{12} \cong 0.1$) (Chung and Akkapeddi 1993). The miscibility between polyarylate and PET may be further driven by transesterification reaction within the melt phase (Robeson 1985; Equiazabal et al. 1991). Although polyarylate-PET blends were briefly commercialized (U8000, Unitika; Ardel D-240, Amoco), they are no longer available.

More recently, a polyarylate-polyamide blend with improved chemical, stress-crack resistance is commercially offered (AX1500, Unitika). Due to the inherent immiscibility of polyarylate with polyamide, the blend is opaque and the notched Izod impact is somewhat sacrificed (Table 19.36). Compatibility in polyarylate-PA6 blends could be achieved through addition of ≤ 10 % of a reactive ethylene copolymer such as ethylene-glycidyl methacrylate copolymer (Okamoto et al. 1989).

19.12.3 Polyetherimide Blends

Commercial polyetherimide (PEI; Ultem®, Sabic) is a transparent, amorphous, high-performance engineering thermoplastic with its repeat unit structure containing both the rigid aromatic imide units and the slightly more flexible

Table 19.36 Key properties of a commercial polyarylate/polyamide blend

Property	ASTM	Units	Polyarylate (U100, Unitika)	Polyarylate/PA66 (AX1500, Unitika)
Tensile strength at yield	D-638	MPa	69	72
Elongation at break (%)	D-638		60	50
Flexural modulus	D-790	Mpa	2,100	2,600
Notched Izod	D-256	J/m	225	78
HDT at 1.8 MPa	D-648	°C	175	
Transparency			Yes	No

aromatic ether units. Owing to the unique structure of its backbone, polyetherimide exhibits high glass transition temperature ($T_g \simeq 215\ °C$), high mechanical strength and rigidity, yet with a good degree of ductility and melt processability. Its highly aromatic backbone structure also imparts an inherent flame retardancy and low smoke generation characteristics in the polymer. Recently, a new transparent, polyetherimidesulfone (PEIS) copolymer (Ultem® XH6050) with a higher glass transition temperature ($T_g = 247\ °C$) and enhanced hydrolysis-resistance has been developed. Because of the high thermal and mechanical performance characteristics, PEI and PEI copolymers find specialty niche applications in the aerospace, automotive under-the-hood, electronic, food-service, and medical equipment markets.

Very few blends of PEI have been commercialized because blending a lower-cost polymer invariably compromises the transparency and high-performance properties of the neat PEI resin.

Blends of PEI with polycarbonate (PC) form phase-separated morphologies (Chun et al. 1996). Nevertheless, some PEI/PC blends (Ultem® LTX) exhibiting improved melt flow and toughness were commercialized in the 1990s, but now seemed to be discontinued. PEI blended with some PC is used as thermoformable sheets (Ultem® 1668, Sabic) for aircraft interior applications, to meet the processability and the low flammability and low smoke generation requirements.

More recently, blends of PEI with a polycarbonate-ester (PCE) have been introduced by Sabic as Ultem® ATX series (Table 19.37). It was found that the modification of standard bisphenol-A polycarbonate with some resorcinol terephthalate/isophthalate moieties gave a polycarbonate-ester copolymer, which had a surprising miscibility with PEI (Gallucci 2005, 2008). The key advantages of the PEI/PCE blend are (a) high notched impact toughness (b) high melt flow for thin-wall molding (c) metallizability without primer (d) heat-resistance (e) transparency (f) flame-retardant properties. PEI/PCE blend is used in various automotive, aerospace, electrical/electronic components, food-service, and medical equipment applications.

Several years ago, PEI/PET blends with high (>75 %) PEI content and those with very low (<10 %) PEI content were found to exhibit clarity and single-T_g

Table 19.37 Properties of some commercial PEI blends

Property	ASTM	Units	PEI/PC Ultem® LTX100A* Sabic	PEI/PCE Ultem® ATX100 Sabic	PEI/PET Ultem® U-1285 Sabic	PEI/PPSU Ultem® HU1004 Sabic
Specific gravity	D792		1.31	1.21	1.29	1.27
Mold shrinkage	D955	%	0.7	0.5–0.7	–	0.07
Flexural modulus	D790	MPa (kpsi)	2,900 (420)	2,530 (367)	3,420 (495)	3,370 (480)
Tensile strength at yield	D638	MPa (kpsi)	93 (13.5)	68 (9.9)	108 (15.7)	106 (15)
Elongation at break	D638	%	90	80	–	60
HDT at 1.82 MPa (264 psi)	D648	C	185	157	160	210
Transparency			No	Yes	Yes	Yes

behavior indicative of miscible blends while other blend ratios from 75/25 to 10/90 showed phase separation behavior (White et al. 1979). An ~85:15 PEI:PET blend was commercialized by GE as Ultem® 1285, but this seems to be no longer available. In a more recent reinvestigation, the use of a lower-molecular weight (0.56 IV vs. 0.84 IV) PET was found to increase the miscibility window in these blends to enable the blending of up to 40 % PET without sacrificing the high modulus, strength, and ductility of PEI and yet retain some transparency (Gallucci 2011). These blends are still not commercial.

To meet the demands in the health care and medical device markets, new transparent PEI blends with improved hydrolysis resistance under the autoclave, steam sterilization conditions, were developed (Sanner 2011). Based on the known superior hydrolytic stability of the sulfone resins and the published patent literature (Kailasam et al. 2009), it is very likely that these clear, hydrolysis-resistant blends are the compatibilized blends of PEI and polyphenylsulfone (PPSU).

It was reported earlier that PEI and PPSU formed a clear "miscible" blend with a single T_g observed by DSC and DMA (Ramiro et al. 2006). However, they could not ascertain the absence of a dispersed phase. This was because the refractive indices of the two components were too close to be differentiated. Later, it was found that the clarity in these blends is likely a result of small domain size of the dispersed phase (<0.5 μm) as determined by TEM (Kailasam et al. 2009). These PEI/PPSU blends are hydrolysis-resistant– capable of >1,000 steam autoclave cycles at 134 °C, while still retaining good ductility, toughness, and transparency (Sanner 2011).

Polyetherimide was also found to be miscible with polyether-ether-ketone (PEEK) exhibiting a single T_g (Chen 1992). Since PEEK is a high-melting, crystalline polymer, the blend should be useful in film and composite applications, but no commercial applications are known to date.

19.12.4 Polyphenylenesulfide (PPS) Blends

Polyphenylenesulfide (PPS) is an aromatic semicrystalline polymer with a recurring sulfide linkage in the backbone. Due to the highly aromatic nature of its structure, PPS is inherently flame-retardant and also exhibits an outstanding level of chemical resistance. PPS is high-melting ($T_m = 285\ °C$), yet its low melt viscosity allows easy processing and high loading of glass or mineral fillers. Since unfilled PPS is too brittle to be used by itself, PPS is generally compounded with reinforcing fillers. Glass-reinforced PPS exhibits high heat distortion temperature (HDT $\cong 265\ °C$) and high continuous use temperature (U.L. index of ca. 200 °C).

Owing to its unique combination of properties, PPS is experiencing a recent growth in the market interest with several producers and suppliers entering this business. Although current worldwide consumption of PPS is still relatively low, a steadily improving cost and supply position of PPS may increase its usage in the future. Since most PPS is used in the glass or mineral reinforced form, blending other polymers generally has no benefits. In addition, the chemical inertness of PPS and the crystallization tendency do not promote any degree of compatibility with other polymers.

Among the few commercial blends of PPS currently being used is the blend of PPS with PTFE. However, in these formulations, PTFE is simply added as a lubricating filler and may not be considered as a blend. These products (Dianippon Ink, Japan) are used for making low-friction gears (for floppy disc drives), bearings, relays, and other moving parts.

Since a major weakness of PPS is its brittleness, some attempts have been made to improve its toughness by blending with other suitable polymers. A commercial impact-modified PPS (Toray) is believed to consist of a blend of PPS with ethylene-glycidylmethacrylate polymer. A grafting reaction is expected to occur if the PPS has active end groups such as –SH or $–S^-Na^+$, which can in principle react with the epoxy group of the ethylene/GMA copolymer.

A PPS blend with liquid crystalline polyesters (LCP) is offered commercially in 40 % glass-filled form (Vectra® V140, Hoechst-Celanese). Since this blend would be considered more as a modified LCP, it will be discussed under the LCP blends section (Sect. 19.12.5). There has been some commercial development activity in the blends of PPS with PPE, in which the PPE is claimed to improve the ductility of PPS, e.g., with an elongation at break of 8 % in a 40 % glass fiber-reinforced blend (Gabriele 1992). The contribution of high ductility, high DTUL of 270 °C, and good processability (low mold shrinkage, warpage, and flash) appears to make this blend to be a significant improvement over glass-filled PPS.

19.12.5 Liquid Crystalline Polyester Blends

Liquid crystalline polyesters (LCP's) are interesting polymers, exhibiting inherently high mechanical strength and modulus due to a high degree of self-orientation; very few commercial blends of LCP are commercial. LCP blends

Table 19.38 Typical properties of commercial LCP/PPS blend (GF-reinforced)

Density (kg/m^3)	1,670
Flexural modulus (MPa)	16,550
Flexural strength (MPa)	248
Tensile strength (MPa)	165
Elongation at break (%)	1.4
DTUL (°C,1.8 MPa)	265
Dielectric constant at 1 kHz	3.7
Dielectric strength (kV/mm)	23.6

have been investigated by many researchers, but their high cost has precluded the successful commercialization of any such blends. The only commercial blends of LCP appear to be those with PPS (Vectra® V140 and V143XL). The liquid crystalline polyester used in this blend is a copolyester of p-hydroxybenzoic acid and 2-hydroxy-6-naphthoic acid. The melting point of this LCP and of PPS closely match, i.e., $T_m = 285–290$ °C. Since there is no compatibility or grafting reaction between the two components, LCP/PPS blend is considered to be a simple mechanical blend. The purpose of blending PPS seems to be simply to lower the cost of LCP without sacrificing the high heat distortion temperature and high melt flow.

In the commercial LCP/PPS blends, it is very likely that due to its low melt viscosity, LCP forms the continuous phase, while PPS may simply be present as a dispersed filler along with the glass fibers. The commercial LCP-PPS blends (Vectra® V140 and Vectra® V143XL, Celanese) are used in electrical, electronic, and industrial components such as connectors, bobbins, housings, switches, breakers, and sensors and other high-tolerance, thin-walled parts. Compared to PPS, the blend offers better flow with no flash into thin-wall part molds at lower injection pressures and lower mold temperatures. Compared to LCP, the blend offers higher weld-line strength and lower warpage. The blends are compatible with lead-free solder and seem to retain the physical and mechanical properties of both the LCP and PPS. Some typical properties of commercial LCP-PPS blend are shown in Table 19.38.

19.12.6 Polyimide Blends

High-performance polyimides (Vespel®, Dupont) and polyamide-imide (Torlon®, Amoco) molding compounds are often mixed with ca. 10 % polytetrafluoroethylene (PTFE) to fabricate a variety of low-friction bearings, bushings, and seals used in automotive, aerospace, and industrial markets. The role of PTFE in these formations is simply to function as a lubricating filler. Hence, these may not be considered as real blends. The PTFE particles are inert and not bonded to the polyimide matrix in the molded part. Because of this heterogeneity, higher amounts of PTFE cannot be tolerated in the polyimide compounds, due to undesirable loss in tensile strength.

19.13 Thermoset Blend Systems

Thermoset systems are, by definition, three-dimensional polymer networks formed by thermal radiation or catalyst-induced polymerization and cross-linking (curing) chemical reactions between multifunctional monomers and/or oligomeric prepolymers. Most often, the thermosetting resin formulation itself consists of a blend of different monomers and prepolymers along with curing agents and other additives. Since a thermosetting resin solidifies upon curing and cannot be remelted or reprocessed, it is necessary to mix all the required ingredients including the reinforcing fillers or fibers, modifiers, stabilizers, and additives during the initial monomeric or prepolymer stage before being fabricated into the final shape by curing. The mixing is facilitated by the low viscosity of the monomer, prepolymer system.

The global thermoset resins market is expected to reach as high as 95 million metric tons by 2016 (Axis Research Mind report 2012). Excluding the alkyd resins, which are used primarily in the coatings, commercially important major types of thermoset resins, along with their relative % market share, estimated from literature (Fosdyke and Starr 2002), can be categorized as follows: Polyurethanes (31 %), Phenolics (18 %), Amino resins (18 %), Unsaturated polyesters (12 %), Epoxies and other specialty/high performance thermosets (12 %), such as silicones, polyimides, bismaleimides (BMI), cyanate ester thermosets, etc.

Commercial thermoset resins offer a range of high heat performance with high glass transition temperatures ranging from 150 °C to >300 °C. When used in conjunction with glass fiber reinforcements and inorganic fillers, the thermoset resin composites invariably offer high heat distortion temperatures (200 °C to >300 °C), high modulus (>20 GPa), and strength (>20 MPa) properties. However, depending on the molecular rigidity of the structural units and the cross-link density, the conventional thermosets exhibit a high tendency for brittleness as generally indicated by their low tensile elongations at break.

Hence, a common goal for making thermoset blends is to improve their toughness without sacrificing their thermal and rigidity characteristics. Additional motivations for thermoset blends are to seek property improvements such as increased heat resistance, moisture resistance, dielectric properties via a cost-effective blending of materials. Figure 19.24 illustrates the typical commercial thermoset types and their blends, comparing their glass transition temperatures with the tensile strains at break, as a relative measure of toughness. As may be seen from Fig. 19.24, the commercial high-performance thermoset blends tend to bridge the gap between the thermal performance, toughness, and cost-effectiveness of the individual components.

A major application for high-performance thermosets and their blends is for making the copper clad laminates (CCL) used in fabricating integrated circuit boards in microelectronic industry. High-performance CCL (HPCCL), which can translate information by high frequency and high speed, has been gaining prominence due to the increased demands from the market. HPCCL must be fabricated by using high-performance resin matrix, with high thermal stability, low dielectric constant and dielectric loss over a wide range of frequency, and easy processability characteristics
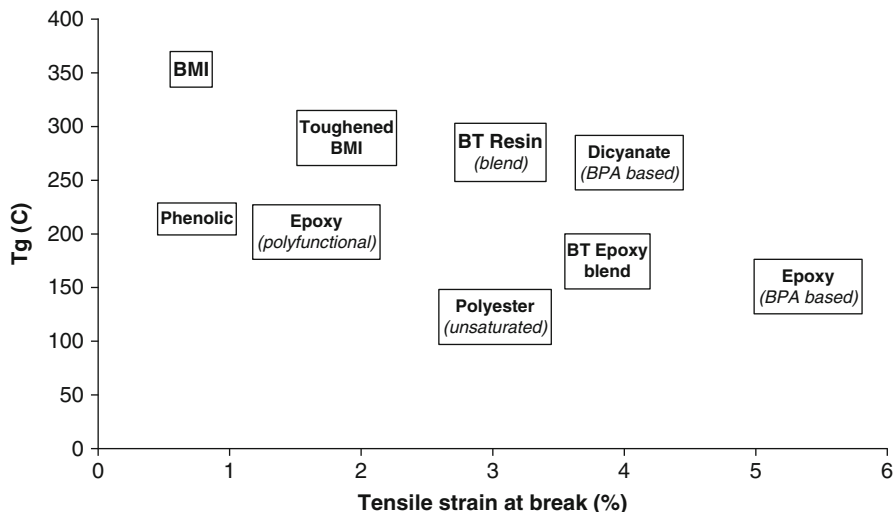
Fig. 19.24 T_g vs. Tensile strain at break (%) of various commercial thermosets

at an acceptable price. Hence, there is a strong motivation to modify thermoset polymers via a blend approach to achieve the proper balance of properties and cost.

Many commercial thermosets are often used as complex mixtures of several coreacting monomers and prepolymers, specifically formulated to suit a given end-use application. For example, in coating and adhesive applications, often mixtures of different epoxies, differing in chemical structure and/or molecular weights, are used as required. Even two different thermosetting monomers may be mixed such as in the case of single-package epoxyphenolic molding compounds (Fry et al. 1985). However, even these hybrid thermoset systems are not usually considered as blends. Since the molecular weights of the epoxy and novolaks are low and during curing they become integral parts of the polymer network through coreaction, the system may be called a coreacted or cocured thermoset. Although it is sometimes hard to distinguish some thermoset blends from the coreacting thermosets, thermoset blends can be ideally classified as (a) Thermoset-thermoset blends and interpenetrating networks (IPN's), (b). Rubber-modified thermosets, and (c) Thermoset-thermoplastic blends and semi-IPNs.

An interpenetrating network (IPN) is defined as a combination of two polymer networks, at least one of which is in the presence of the other. The distinction between interpenetrating network and blend may often be based on morphology and the degree of phase separation. If there is a sufficient degree of molecular interaction, the phase separation tendency is suppressed, and a true molecularly or morphologically uniform interpenetrating network can be achieved. Very few systems can form truly homogeneous blend networks and, in reality, some microheterogeneity is invariably observed. Compatible IPNs generally form <5 nm size domains, and incompatible IPNs or blends form domain size >30 nm.

19.13.1 Thermoset/Thermoset Blends

As previously mentioned, several commercial hybrid thermosets are known to be coreacting thermosets; i.e., when the mixture of two different thermosetting monomers or prepolymers is cured, there is a simultaneous graft or coreaction between the components along with the cross-linking reactions. These systems may therefore be considered as copolymerizing thermosets and not as true blends. Examples of such systems are: phenolic novolak/epoxy resin, melamine prepolymer/epoxy resin, carboxyl-terminated unsaturated polyester/epoxy thermosets. The graft or copolymer network reaction involves the reaction between the phenolic $-OH$ or an amine or a carboxyl and the epoxide group.

In a majority of cases, the thermoset/thermoset blends are actually formulated by the fabricator or the end user during the fabrication and processing of such materials as composite prepregs, printed circuit boards, laminates, and adhesives. The formulations and compositions are often kept proprietary and are designed to meet their own individual requirements. The following are some commercially important high-performance thermoset/thermoset blend examples:

- Epoxy/Cyanate ester thermoset blends
- BMI/Cyanate ester thermoset blends
- Epoxy and bismaleimide (BMI) cocured thermosets known as "BT-Epoxy" resins

19.13.1.1 Epoxy/Cyanate Ester Thermoset Blends

Epoxy thermosets are widely used in numerous formulations and forms in the composites applications, particularly in the aircraft-aerospace industry. Epoxy resins are indeed considered the workhorse of the modern day composites. Most of the common epoxies (90 %) are based on bisphenol-A diglycidyl ether, a cross-linkable diepoxide monomer (e.g., Epon™828, Momentive Specialty Chem.). Multifunctional epoxies (Epon™ HPT and SU-8, Momentive) leading to higher cross-link density and higher temperature capability are used in advanced composites. Epoxy resins are used not only in composites for military and civilian aircraft-aerospace but also in such commercial applications as epoxy-reinforced concrete. Glass fiber or carbon fiber-reinforced epoxies are used in building and bridge structures in construction industry and in the printed circuit boards in microelectronic industry. The epoxy formulations used in composites are often modified with toughening or flame-retardant additives. Similarly, to improve moisture resistance and electrical properties, while retaining heat resistance, epoxies are modified by cocuring with other thermosetting resins such as dicyanate esters (Nair et al. 2001).

Aromatic cyanate esters cross-link by catalyst or thermally induced cyclotrimerization to form a cross-linked network of triazine ethers. Cross-linked cyanate ester systems typically exhibit higher glass transition temperatures ($T_g \geq 250\ °C$), lower moisture absorption, and lower dielectric constants than the standard epoxy systems, yet retaining an equivalent level of toughness and elongation at break. Hence, the cyanate esters are considered as high-performance thermosets. Several types of thermosetting cyanate esters are available commercially (AroCy®,Ciba-Geigy; BT-2000/Mitsubishi), and the most common among these is the bisphenol

A dicyanate ester. Due to their high cost, cyanate esters are not used as widely as epoxies but are now being used as blend candidates for improving the properties of epoxy and BMI thermoset resins in composites.

Thus, several properties of the common bisphenol A-diglycidyl ether-based epoxy thermosets can be improved by cocuring with a commercial bisphenol A-dicyanate ester, and the blend is more cost-effective than the cyanate ester alone. Such epoxy/cyanate ester thermoset blends exhibit improvements in processability, toughness, hot-wet performance, and low dielectric properties.

Epoxy/cyanate ester thermoset blend–based composites have low dielectric constant desirable for advanced radomes, microwave antennas, and stealth aircraft composite applications. Other applications include its use in copper clad laminates, semiconductor devices, and fire-resistant aircraft structural composites.

19.13.1.2 Bismaleimide/Cyanate Ester Thermoset Blends

Bismaleimide (BMI) resins are a relatively young class of thermosetting polymers gaining increased acceptance in high-performance composite industry because of their high T_g ($\geq$300 °C) and high retention of physical and electrical properties in hot-wet environment. Typically, bismaleimides are difunctional monomers containing a rigid aromatic unit with two terminal maleimide groups capable of catalyst or thermally induced polymerization resulting in a highly cross-linked rigid thermoset. BMIs bridge the temperature performance gap between epoxies and the high-temperature polyimides. They exhibit epoxy-like processing characteristics, but unlike the polyimides, they cure by an addition, rather than a condensation polymerization reaction. Thus, they avoid the off-gassing issues of polyimides, ensuring high hygrothermal performance.

Commercial bismaleimide thermoset resins are based on aromatic bismaleimides such as 4,4'-bismaleimidodiphenylmethane (Compimid® MDAB, Evonik). Compimid® MDAB, also known in literature as "MDA-BMI" is derived from the condensation reaction between 4,4'-methylene dianiline (MDA) and maleic anhydride, both relatively low-cost monomers. The MDA-BMI is often used as a eutectic mixture with other BMIs such as TDA-BMI, to reduce its melting point for improved impregnation and tackiness in the glass and carbon-fiber-based composite prepregs.

BMI thermosets can be processed basically like the epoxy (177 °C) cure but followed by an elevated temperature post-cure (232 °C), to achieve superior properties. Upon the thermal curing, BMI forms a highly cross-linked rigid thermoset matrix with very high T_g (>300 °C), allowing the continuous use temperatures of upto 250 °C. Such BMI thermosets adequately compete with the high-temperature, multifunctional epoxy-based thermosets in composite applications, primarily due to their better performance and cost advantages. BMI composites are used in electrical printed circuit boards, structural aircraft/aerospace composites, composites for pipes, and other structures for use at high temperature and chemical environments. In these applications, the BMI resin offers high heat resistance, stiffness, and strength but a relatively low elongation at break (<1 %). Hence, BMI needs suitable toughening modifiers to improve its damage tolerance in composites.

For the toughening purposes, BMI monomers have been mixed with different types of coreactive comonomers such as O,O′-diallyl bisphenol A ("DABA" or Compimid® TM124, Evonik) or 4,4′ Bis(2-propenyl phenoxy) benzophenone ("PPB" or Compimid® TM123, Technochemie), to achieve BMI thermoset composites with improved damage tolerance, with unchanged or even enhanced thermal performance. Such a toughened BMI formulation was developed by Cytec as Cycom® 5250-4 ($T_g = 285$ °C; Elongation to break = 4.8 %), for use in advanced carbon-fiber composites in aerospace industry (Boydy et al. 2001). Cycom 5250-4-based BMI composites have been successfully used in Raptor F-22 fighter jets for U.S. Air Force for many years. In addition to such a comonomer approach, the blending of other ductile thermoplastic or thermoset polymers have also been extensively investigated for toughening the BMI composites (Stenzenberger 2006).

Among the candidates to blend with BMI, cyanate esters have the unique advantage of very good processability, low dielectric constant, and adequate toughness with almost a comparable thermal performance of BMI resins (Fig. 19.23). Hence, an obvious approach to combine high thermal stability and easy processability is to blend the two resins. Blends of commercial BMI mixture (i.e., Compimide-353, Evonik) and the commercial bisphenol A dicyanate (AroCy B-30) have been evaluated for high-performance composites (Barton 1996). Such hybrid BMI/cyanate ester blend resins have been commercially available as "BT resins" and the corresponding prepregs and copper clad laminates from Mitsubishi gas chemical. Obviously, the acronym "BT" stands for the bismaleimide-triazine resin blend system. The blend ratio may vary depending on the application. Currently, the BT resins are the most preferred raw materials for making high-speed signal processing, complex high-count multilayer integrated circuit boards used in the tablet computers, motherboards for internet routers, servers, and IC tester devices. The low dielectric constant of the blend is ideal for the high-speed, multilayer circuit boards. The presence of the cross-linked triazine ether network in the matrix of bismaleimide cross-linked network is believed to improve the toughness, reduce the moisture sensitivity, and improve the dielectric properties without a sacrifice in heat resistance.

19.13.1.3 BT-Epoxy Thermoset Blend System

Commercial BT-epoxy resins and laminates (e.g., BT epoxy G200®, Isola group; Nelco® N5000) belong to a growing class of preferred thermoset resins currently used in the printed circuit boards (PCBs) industry. It is a mixture of a standard epoxy resin, a low-cost raw material for PCBs, and the high-temperature BT resins. BT resin itself is a mixture of bismaleimide and cyanate ester as discussed under BMI/cyanate ester blend section. Hence, BT/epoxy may be considered as a ternary blend-based thermoset. The purpose of blending epoxy is simply to lower the cost and improve the toughness of BT resin, while the latter provides the high T_g and low dielectric loss properties retained over a wide temperature range. BT resin also offers excellent electrical insulation resistance even after moisture absorption. BT resin costs about $1.5\times$ that of epoxy, and hence a blend of BT resin and epoxy is more cost-effective and popular in PWB/PCB laminate industry.

The cure reaction for BT-epoxy system occurs similar to epoxy at 180 °C. followed by a post-cure at a higher temperature (upto 250 °C). The cure is catalyzed by strongly basic molecules like Dabco (diazabicyclooctane) and 4-DMAP (4-dimethylaminopyridine). The resulting thermoset products have higher glass transition temperatures of 180–260 °C range and lower dielectric constant (Dk) and dissipation factor (Df) than standard epoxy thermosets. These properties make these materials very attractive and cost-effective enough for use in mass-produced, high-speed printed circuit boards.

19.13.2 Thermoset/Thermoplastic Blends

19.13.2.1 Low-Profile/Low-Shrinkage Polymeric Additives for Unsaturated Polyesters

Unsaturated polyester-based thermosets account for ≥ 70 % of the total global volume of all the glass fiber-reinforced thermosetting composites currently used (Atkins 1978; Majumdar 2008).

Commercial unsaturated polyester thermosets are derived from the polycondensation of glycols such as propylene glycol and maleic anhydride with some phthalic anhydride added to form prepolymers of ca. 800–5,000 number average molecular weight and a controlled degree of unsaturation (ca. 4–20 C=C groups/chain). Such an unsaturated polyester prepolymer is further mixed with styrene as comonomer (ca. 40 %) and then polymerized and cross-linked ("cured") via the use of a preoxyester-type free radical initiator and heat to achieve the final cross-linked thermoset product. Invariably, significant amounts of glass fiber reinforcements and inorganic fillers are also added to the polyester prepolymer-styrene mixture prior to the curing to increase the stiffness, strength, and the impact properties of the thermoset product.

Such glass fiber-reinforced composites based on the unsaturated polyester thermosets are usually fabricated as sheet molding compounds (SMC) and bulk molding compounds (BMC). These are widely used in various metal replacement applications because of their cost-effectiveness, rigidity, light weight, and corrosion resistance properties particularly useful in transportation (cars and trucks), construction, pipe, and tank applications. Automotive and truck body panel and structural component applications of SMC include doors, hatchbacks, hoods, front grilles, etc. Some nonautomotive applications of SMC and BMC include sanitaryware (bathtubs, shower stalls, sinks), appliances, business machine, and electrical components.

Typically, in an SMC composition, chopped glass fiber roving (18–75 mm long) is used, and its content can vary from about 20–40 wt%. In a BMC composition, shorter glass fiber (6–12 mm. long) is used at 15–20 wt%. In both the SMC and BMC compositions, about 40–60 wt% of an inorganic filler such as calcium carbonate (3 μm) is additionally used, primarily to lower the cost of the composites but also to improve the flame retardancy and other physical properties.

In the SMC process, typically the unsaturated polyester resin with styrene monomer along with the fillers, glass fibers, catalyst, and other additives are mixed together

and cast into a sheet sandwiched by polyethylene film. The sheet is then cured at 150 °C by compression molding in a heated, matched-die mold to the required part shapes such as automotive exterior body panels. The SMC composite parts fabricated from reinforced polyester thermosets exhibit excellent rigidity, strength, and toughness. However, the high shrinkage associated with the polymerization and crosslinking of the unsaturated polyester-styrene monomer-curing matrix can cause the following potential defects in the final thermoset composite part:

- Warpage of molded parts preventing the molding of close tolerances.
- Depressions ("sink marks") on the part surface where the ribs or bosses are located.
- Rough, wavy surfaces resulting in a poor surface appearance of the part.

Hence, for parts requiring close tolerance and surface appearance such as automotive body panels, unsaturated polyester-based SMC composites could not be used for a long time, until it was found that blending of suitable high-molecular weight thermoplastic polymers to the formulations helped reduce the shrinkage and produce smooth surfaces (Atkins 1993). Such thermoplastic polymer additives for shrinkage control can be divided into two separate performance categories:

(a) The low-profile additives, which allow an excellent reproduction of the mold surface to give a smooth class "A" surface (<0.05 % to zero shrinkage).
(b) The low-shrink additives, which do not reproduce the mold surface, but reduce the shrinkage moderately and more easily allow internal pigmentability than the low-profile additives.

Some thermoplastic polymers commercially used as the low-profile, low-shrink additives to SMC and BMC composites are

Low-profile additives:
Polycaprolactone (Norsolook® A70091, CCP composites)
Thermoplastic polyurethanes (Neulon® 520, Ashland resins)
Polyvinyl acetate -PVAc (Neulon® T, Ashland; Vinnapas® UW, Wacker Chemie)
Carboxylated PVAc, (Vinnapas® C, Wacker Chemie)

Low-shrink additives:
Polyethylene powders (Microthene® F Lyodell-Basell)
Impact polystyrene (Stypol® AIP, CCP composites)
Poly(methyl methacrylate) (Aropol® Q, Ashland resins)

A typical low-profile SMC recipe consists of ca. 10 % unsaturated polyester, 10 % styrene, 4 % thermoplastic additive, 50 % calcium carbonate, 25 % glass fiber ($>$25 mm) along with 1 % zinc stearate, 0.2 % peroxide catalyst, and small amounts of other additives as needed.

A typical BMC recipe consists of ca. 13 % unsaturated polyester, 12 % styrene, 4 % thermoplastic additive, 55 % calcium carbonate, 15 % glass fiber (6 mm) along with 0.3 % peroxide catalyst, 1 % zinc stearate, and small amounts of other additives as needed.

Among all the thermoplastic additives for SMC and BMC composites, poly (vinyl acetate) was found to be the most effective low-profile, shrinkage-control

Table 19.39 Effect of various polymer additives on the shrinkage of unsaturated polyester SMC

Polymer additive	Linear shrinkage (%)
None	0.5
Polyethylene	0.2
Polystyrene	0.2
Impact polystyrene	0.12
PMMA	0.1
Poly(vinylacetate)	0

additive (Atkins 1998). In general, the relative effectiveness of various polymer additives for shrinkage control in the unsaturated polyester thermoset composites may be summarized as in Table 19.39.

Currently, with the polyvinyl acetate additives, SMC composites can be fabricated at high mold temperatures with zero shrinkage and zero expansion. The resulting parts exhibit excellent, class "A" surface smoothness and dimensional stability without warpage. In addition to this "zero shrink" effect, certain high-temperature SMC processes require effective thickening for easy handling of the composite and good glass-fiber distribution during molding. In such cases, the carboxylated polyvinyl acetates are used in combination with magnesium oxide as the thickening agent and shrinkage control additive for the unsaturated polyester SMC.

It is believed that during the curing of the above type of mixture, the thermo-plastic polymer, which is initially dissolved, becomes phase separated by the reaction-induced spinodal decomposition. The fine domains of the phase-separated thermoplastic then counteract the curing shrinkage in the matrix by thermal expansion and stress relief via microvoid formation mechanisms (Montagne 2005). Thus, a primary requirement for the low-profile polymer additive appears to be that it must be amorphous with a low to moderate T_g and fairly soluble or dispersible in the resin matrix initially, but capable of phase separation during the polymerization to counteract the polymerization shrinkage stresses via thermal expansion and microvoiding. Almost all of the class-A surface SMC composites used currently in the automotive industry are based on the polyvinyl acetate-type low-profile, low-shrinkage additives blended into the unsaturated polyester-styrene-based thermoset recipe.

19.13.2.2 PPE/Epoxy Blends

Poly(2,6-dimethyl 1,4-phenylene ether) (PPE) is a high-T_g (215 °C) ductile polymer with a low dielectric constant and extremely low moisture absorption. Epoxy thermosets exhibit a very good combination of useful properties such as good adhesion, low shrinkage, high electrical resistivity, and good thermal properties. The brittleness and the moisture sensitivity of epoxies can be improved by blending a thermoplastic additive such as PPE. In addition, since PPE has a high T_g, the thermal properties are not sacrificed, but improved. Furthermore, the dielectric constant is lowered. Such blends have been used in glass cloth-reinforced composites form for laminates and printed circuit boards.

In a typical formulation of epoxy resin (Epon 825, Shell) cured with aluminum alkoxide, incorporation of 30 % PPE increased the elongation at break from <2 % to >17 %. The heat distortion temperature increased from 160 °C to 195 °C. The dissolution of PPE in epoxy formulation raised its viscosity at 200 °C from 0.2 to 4 Pa.s. (Anonymous 1991).

19.13.2.3 Thermoplastic/Silicone Semi-IPNs

Although the dynamically vulcanized blends such as EPDM/PP (Santoprene®) and NBR/PP (Geolast®) have sometimes been referred to in the literature as semi-IPNs, we considered them as blends of cross-linked elastomer dispersions in a thermoplastic matrix and as such treated them under the elastomer blends. There is yet another class of thermoplastic/thermoset blend system in which a minor amount of the cross-linkable monomer(s) is allowed to polymerize in the thermoplastic matrix forming a loose network. Examples of such systems are silicone semi-IPNs in thermoplastics that have been recently commercialized (Rimplast®, Petrarch, div. of Hüls) (Anonymous 1983).

The silicone semi-IPNs consist of mixing a hydride-containing silicone prepolymer and a vinyl-functionalized silicone polymer into a thermoplastic matrix such as PA, PBT, thermoplastic polyurethane (TPU), or styrene-ethylene/butylene-styrene (S-EB-S) block copolymer elastomer. The two silicone prepolymers coreact in the thermoplastic matrix during melt extrusion and injection molding to form a partially cross-linked network within the thermoplastic matrix.

The cross-linking reaction may be catalyzed by a small amount of suitable organometallic catalysts. The blends typically contain ca. 5–20 % silicone. Injection-molded or extruded parts are further heat-treated to complete the curing reactions. There is, of course, a significant level of phase separation. In the thermoplastic molding compounds such as glass-filled PA and PBT, addition of the silicone semi-IPN in small amounts (ca. 5–10 %) is reported to reduce the mold shrinkage, improve mold release, and increase wear and friction resistance. Polyamide-silicone blends have already been discussed under PA blends section (Sect. 19.7).

Elastomeric silicone IPN with TPU and S-EB-S thermoplastic elastomer matrices have found some medical applications (Carew and Deisher 1989). The silicone contributes to the excellent release characteristics and to the biocompatibility. Typical applications include medical tubing, catheters, implants, diaphragms, seals, gaskets, etc. The commercial volume for silicone IPNs is, however, still very small.

19.13.3 Rubber-Toughened Thermosets

Most commercial rigid thermosets of high T_g exhibit brittleness and low tensile elongation because of the inherent nature of cross-linked network structures. Addition of rubbery dispersions into the thermoset matrix should improve the ductility and impact strength of the matrix by promoting the absorption of strain energy through multiple crazing and shear deformation sites in the matrix.

Table 19.40 Reactive oligomeric rubbers used in commercial toughened epoxy thermosets

Oligomeric elastomer	Reactive functionality
Polypropylene glycol diglycidyl ether (Riew et al. 1976)	Epoxide end groups
Polyaminoamides (condensation products of polyamines and "dimer" acids) (McAdams 1985)	Amine groups
Liquid polysulfides (McAdams 1985)	Thiol groups
Aliphatic polyesters (Drake 1983)	Carboxyl and −OH groups
Liquids, butadiene-acrylonitrile copolymers (Hycar® ATBN or CTBN) (McGerry 1968; Drake 1975)	Amine or carboxyl end groups

However, dispersion of high-molecular weight rubbers into the monomeric or prepolymer mixtures of the thermosetting resin matrix is usually difficult due to a viscosity mismatch and a lack of solubility or compatibility.

Hence, a low-molecular weight, reactive elastomer is normally used for impact modification of thermosets. The low molecular weight of the rubbery prepolymer aids its easy dissolution or dispensability in the thermosetting resin. The reactive functionality couples the rubber covalently to the growing polymer network during the curing reaction. Hence, the rubber-toughened thermosets may also be considered as coreacted thermosets and not true blends.

Rubber-toughened epoxy resins are the well-known examples of impact-modified thermosets utilizing reactive rubbery prepolymers. Epoxy resins can be toughened or flexibilized by any one of the several types of oligomeric reactive elastomers listed in Table 19.40.

These oligomeric reactive rubbers coreact with the epoxy resins through their corresponding reactive end groups, thus incorporating rubbery blocks into the cross-linked epoxy network. For impact modification, usually 10 wt% of the reactive rubber is used. For flexibilizing the thermoset, higher levels (up to 50 %) are needed. The type and the amount of the oligomeric rubber used depends upon the degree of toughness and flexibility required in the product. The rubbery segments must phase separate after curing into discrete domains for effective impact modification without sacrificing the glass transition temperature or heat resistance of the matrix. Generally, 1–5 μm-size rubber particles promote craze formation while shear deformation is promoted by rubber particles of <0.5 μm. Systems possessing both small and large particles, i.e., bimodal distribution, provide maximum toughness (Riew et al. 1976). Elastomer-modified epoxy resins are primarily used in composites, structural adhesives, and electronics applications.

19.13.4 Miscible Thermoplastic-Toughened Thermoset Blends

Rubber toughening of thermosets can lead to a significant increase in toughness, but this method usually leads to a decrease in the material's stiffness and strength,

which may be undesirable in many applications. The blending of a ductile, thermoplastic polymer that initially dissolves in a thermosetting formulation but subsequently either remains mostly dissolved or has an incipient microphase separation during the curing of the matrix is an alternative approach for toughening the thermoset polymers.

For example, incorporation of 10–20 % polycaprolactone (PCL) in a vinyl ester thermosetting matrix significantly improved the fracture toughness and impact properties while retaining stiffness and thermal properties (Ollier et al. 2012). The interaction between PCL and vinyl ester was strong enough to prevent phase separation as indicated by SEM of the cured blend.

Another interesting case of a thermoplastic-toughened thermoset is the "thermally mendable" thermoset/thermoplastic blend. The principle behind this type of thermoset blend consists of the use of a polymerization-induced phase separation technique to fabricate a "biphasic" blend with a so-called "bricks and mortar" morphology structure in which (a) the major "load-bearing" phase is the cross-linked thermoset providing high stiffness and strength needed for the structural functions and (b) the minor thermoplastic phase provides a "healing" function, upon a short thermal exposure, to repair any crack damage and restore the blend's mechanical integrity.

An example of the "thermally mendable" thermoset blend is the epoxy/polycaprolactone (PCL) blend (Luo et al. 2009). The initially miscible blend composed of 15 wt% PCL undergoes a polymerization-induced phase separation during the cross-linking of the epoxy, yielding a biphasic morphology in which the epoxy phase exists as tightly interconnected spheres ("bricks") interpenetrated with a percolating PCL matrix ("mortar"). The fully cured material is stiff and strong. In the event of an impact or stress-induced damage in the part made from this material, the damage can be thermally mendable with a short heat exposure. A heat-induced "bleeding" behavior of the PCL phase causes a wicking of the molten PCL into the crack or microcrack, thus bridging the crack gap. Upon cooling, the recrystallized PCL in the crack gap is capable of load bearing and thus repairing the crack damage and restoring a significant portion of the initial mechanical strength. Interest in the development of such thermally mendable thermoset-thermoplastic blends continues as they have significant commercial potential.

19.14 Biodegradable Polymer Blends

The generally accepted definition of the term "biopolymer" covers polymers that belong to the following two main categories:

(1) Bio-based polymers, i.e., polymers produced from natural, renewable feedstocks such as the plants and biomass in general. Bio-based polymers are not necessarily biodegradable and quite often include conventional plastic types

such as PE, PET except that they are made from bio-based monomer feed-stocks. The main motivation to use such bio-based polymers is the environmental benefit of reduced carbon dioxide emission.

(2) Biodegradable polymers, i.e., polymers which can be degraded by microorganisms present in the normal soil or composting conditions and must be completely metabolized into CO_2, water, energy, and biomass. Biodegradable polymers can be of three subtypes:

(i) Natural biodegradable polymers such as starch, cellulose, soya protein.

(ii) Biodegradable polymers made from bio-based raw materials,
e.g., Polylactic acid (PLA), Polyhydroxybutyric acid (PHA)

(iii) Biodegradable polymers made from petrochemical raw materials,
e.g., Polycaprolactone (PCL), Polybutylene adipate-*co*-terephthalate (PBAT), Polybutylene succinate (PBS); Polybutylene succinate-*co*-adipate (PBSA)

In general, the growing environmental concerns and the increased consumer awareness of the harmful environmental effects of conventional plastic products is driving the growth of both the bio-based polymers and the biodegradable polymers. However, the public opinion and new legislations are particularly driving toward the development of environment-friendly, fully biodegradable and compostable plastic products. For this purpose, various biodegradable polymers have been developed in recent years (Vroman 2009). Although full biodegradability and compostability are not always readily achievable in thick-wall, injection-molded products, certain plastic wastes from food packaging films and foamed articles, disposable fabrics and agricultural films can be readily managed by the proper use of biodegradable plastics technology.

The demand for consumer products that are truly biodegradable has led to national and international "Definitions and Standards of Biodegradability." Regulatory bodies, such as ASTM (USA) and ISO (international), CEN (Europe), JAS (Japan), have all published such standards and issued logos that certify to meet these standards. Although the definitions, test methods, and certification requirements differ, the following are some common features:

1. A biodegradable polymer in an active composting environment must sufficiently fragment and/or disintegrate so that it completely passes through specifically sized sieve screens within a time frame comparable to kraft paper degradation.
2. In a time frame comparable to kraft paper, usually 6 months, the biodegradable polymer must be completely reduced to carbon dioxide, water, energy, and biomass, in an active composting environment.
3. No toxic residues or toxic monomers should be produced by the composting process.
4. The compost containing the biodegraded polymers must support plant growth.

Hence, the current commercial focus has been on is on the development and application of biodegradable polymers to meet the above biodegradation

Table 19.41 Key properties of commercial biodegradable polyesters

Property	PLA Ingeo® 2003 (NatureWorks)	PCL CAPA® 6800 (Perstorp)	PBSA Bionolle® 3000 (Showa)	PBAT Ecoflex® (BASF)
Melting point (°C)	152	65	93	110–115
T_g (°C)	58	−60	−45	−30
Modulus (MPa)	3,600	190	320	95
Elongation at break (%)	6	800	900	>500
Physical nature	*Rigid and brittle*	*Soft and flexible*	*Soft and flexible*	*Soft and flexible*
Biodegradation	←――――――――――― *Complete* ―――――――――――→			

and compostability standards. The market thrust is primarily in the food packaging/food-service markets (films, thermoformed containers, disposable cups, cutlery, etc.), sanitary and disposable fabrics, agriculture/horticulture film markets. Biodegradable polyesters are commercially the most important class of biodegradable polymers (Table 19.41). To achieve faster compostability and better cost benefits, biodegradable polyesters are also used as blends with starch. These blends generally fulfill the range of mechanical properties and compostability requirements in these markets. Although the biodegradable polyesters and starch have also been individually blended with nonbiodegradable conventional polymers such as polyethylene and polypropylene, such "hybrid blends" do not meet the true biodegradability standards and hence will not be discussed. Only the commercially significant, truly biodegradable or compostable polymer blends will be discussed in this chapter.

Among the biodegradable polyesters summarized in Table 19.41, poly(lactic acid) (PLA) has historically received the most commercial attention. The PLA monomer ("lactide") is derived from the low-cost corn starch, and a large-capacity plant has already been built by Natureworks LLC. PLA polymer has mechanical properties somewhat similar to those of polystyrene, and as such it can be used in similar applications. However, its inherent brittleness, low elongation at break, and low impact strength limit a more widespread use of PLA. On the other hand, the more recently developed biodegradable, "aromatic-aliphatic" copolyester "PBAT" (Eastar Bio®, Eastman; Ecoflex®, BASF) is based on conventional petrochemical-based monomers (Haile et al. 2002). Similarly, an aliphatic polyester "PBS" and a copolyester "PBSA" (Bionolle®, Showa Denko) have become available recently as biodegradable polymers. All of these new biodegradable polyesters are soft and flexible with physical properties and processability features similar to LDPE. Hence, these are quite suitable for extruded films and fabrics. Although all these polyesters are fully biodegradable in accordance with ASTM and ISO standards, their rates of biodegradation can be further enhanced for faster compostability. This can be accomplished by blending some thermoplastic starch.

19.14.1 Starch/Biodegradable Polyester Blends

Starch is an inexpensive biodegradable polymer obtained from the abundant renewable plant resources such as corn, wheat, and potato harvests. Natural starch is a complex structure of highly crystalline amylopectin and lesscrystalline amylose polysaccharides, which degrade thermally without melting. Formation of a thermoplastic starch requires the disruption of supramolecular structure and melting of starch crystals with the aid of water (gelatinization) followed by the stabilization of amorphous amylose with other plasticizers or complexing agents. Starch can thus be modified (plasticized and destructurized) with a combination of water, glycerol, polyethylene glycol, or polyvinyl alcohol-type additives for thermoplastic processability (Shanks et al. 2012).

Although such a thermoplastic starch alone can be processed like a traditional plastic, its sensitivity to humidity makes it unsuitable for most applications. Hence, the thermoplastic starch is primarily used in blends with other polymers (Imre and Pukanszky 2013). Blending of a thermoplastic starch with the commercial biodegradable polyesters not only reduces their cost, but also increases their rate of biodegradation for faster compostability. The first commercial example of such a biodegradable polyester/starch blend is the Novamont's Mater-Bi® Z, which is a blend of polycaprolactone (PCL) and thermoplastic starch (Bastioli 1998). More recent examples include Showa-Denko's Bionelle™- Starcla™ series, which are ternary blends of biodegradable polyesters PBSA and PLA with some thermoplastic starch. The composition and mechanical properties of these blends have been balanced to be in the range of LDPE and HDPE for blown film packaging applications while maintaining full biodegradability and compostability.

19.14.2 PLA Blends with Other Biodegradable Polyesters

The other major type of commercial biodegradable polymer blends are the binary and ternary combinations of biodegradable polyester PLA with other synthetic biodegradable polyesters such as the PBAT and PBS, listed in Table 19.41. BASF's Ecovio® series consists of such PLA/PBAT blends. Since PLA is brittle, blending some PBAT improves the toughness and puncture resistance that is needed in rigid and semirigid packaging of thermoformed and foamed structures. On the other hand, PBAT is too soft, and blending of some PLA improves its stiffness and strength while lowering the cost. In all cases, the blends retain full biodegradability and compostability. Some commercial bidegradable polyester blends are listed in Table 19.42, along with their targeted applications. The key properties of some commercial biodegradable polyester blends, used in packaging and agricultural films, are shown in Table 19.43. It is apparent that these biodegradable polymer blends have the processability and properties comparable to LDPE, particularly suitable for film applications, but also have the great environmental benefit of being completely biodegradable and compostable.

Table 19.42 Some commercial types of biodegradable polymer blends

Biodegradable polymer blend	Commercial grades	Key applications
I. Starch/biodegradable polyesters PBSA, PBAT, PLA, etc. – Binary and ternary blends	Mater-Bi®, Novamont Bionolle® Starcla, Showa Biograde®, Biograde Terraloy®, Teknor Apex Compostables®, Cereplast	*Food packaging*: Films, bags, containers, cutlery, etc.
		Agricultural films: Seed mats, ground cover/mulch, erosion control films, etc.
II. PLA blends with other biodegradable polyesters-PBAT, PBSA	Ecovio®, BASF Bio-Flex®, FKuR	*Food packaging*: Films, bags, containers, rigid foam pkg., paper board coating
		Agricultural films: as above

Table 19.43 Key properties of some commercial biodegradable polymer blends

Property	PCL/Starch Mater-By® Z (Novamont)	PLA/PBATEcovio® F (BASF)	PBSA/PLA/Starch Bionelle Starcla™ (Showa Denko)	LDPE
Melting point (C)	65	110–140	93	110
Tensile strength (MPa)	31	35	20	26
Tensile modulus (MPa)	185	750	690	260
Elongation at break (%)	800	300	–	300
Water permeability	High	High	High	Low
Compostability	←——————— yes ———————→			No

19.14.3 Bio-based, Biodegradable PLA/PBS Blends

Recently, NatureWorks, announced the plans to produce PLA blends with bio-based PBS under its Ingeo trade name, in a joint venture with BioAmber (Anonymous 2012). As already discussed before, PBS is a biodegradable polyester made from succinic acid and butane diol (BDO), both normally petrochemical-based. However, BioAmber currently produces bio-based succinic acid by a fermentation process from wheat starch. They also plan to make bio-based BDO from the bio-based succinic acid, thus making a completely bio-based PBS. Unlike pure PLA, which is stiff and brittle like polystyrene, pure PBS is more ductile like polyethylene. Hence, PLA/PBS blends exhibit good flexibility, toughness, and heat resistance, resembling PP and HIPS. Two developmental, thermoforming, and injection grades are available. The injection molding grade (Ingeo AW 300D) is aimed at tableware used with hot foods and drinks. The thermoforming grade (Ingeo AW 240D) is targeted for food-service ware such as

Table 19.44 Key properties of bio-based, biodegradable PLA/PBS blends

	Injection moldable PLA/PBS (*Ingeo*® *AW300*)	Thermoformable PLA/PBS (*Ingeo*® *AW240D*)
Specific gravity	1.34	1.48
Flexural modulus (MPa)	2,485	1,670
Notched Izod, (J/m)	34	–
Vicat softening point, °C	107	105

hot and cold drink cup lids, vending cups, trays, plates, and bowls. Both are opaque materials meeting the FDA requirements. Both these bio-based polymer blends are completely biodegradable and meet the industrial composting standards (Table 19.44).

19.15 Conclusions and Future Trends

Polymer blends will continue to play a significant role in the commercial development and application of plastic materials because of their desirable overall cost/performance balance and their ability to fill the performance gaps between existing single resins. In many cases, polymer blends have provided unique combinations of properties and processability advantages not available in single resins. While further growth in commercial polymer blends will undoubtedly be strongly driven by global economic conditions and economic growth rates, specific market needs and applications, there are also several technological factors, which can drive and sustain this growth. Although the general global economic slowdown in 2009 caused a negative effect on the polymer blends and alloys market growth, it is now on the upswing again since 2012, mainly due to the high growth of the electronics applications and a recovery in the automotive markets.

In the near future, electronic housing and computer-related applications appear to be the main development areas for polymer blends, especially for polycarbonate blends. The electronic housing industry, including housings for information technology-related products such as personal computers, tablets, etc., will be the major growth driver for the polymer blends and alloys market globally. It is expected that bio-based and biodegradable polymer blends will also have a growth potential since increasing environmental concerns and government regulations are driving the demand for sustainable products that can be used for engineering applications.

Polymer blend manufacturers continue to identify new application areas for polymer blends by working closely with the customers to identify the niche opportunities. Hence, engineering design and application developments are currently the major thrust areas in polymer blends. Engineering polymer blends tend to be more expensive than commodity polymers, due to higher processing and material costs. Hence, for high-volume applications like automotive, there is

a continuing trend to move toward modified commodity polymers like long glass fiber-reinforced PP or ABS. These polymers often offer nearly the same performance as polymer blends. Thus, it is necessary to identify niche applications in which commodity polymers cannot replace polymer blends.

The following key factors will likely influence the future growth of commercial polymer blends:

1. Use of low-cost recycled polymer feedstocks of acceptable quality.
2. New compatibilization/reactive alloying strategies for immiscible polymer blends, which fulfill the desired economic, safety, and productivity targets.
3. Improved technology for obtaining reproducible and stable morphologies under commercial extrusion and molding conditions, ensuring blend product quality and reliability.
4. Novel melt-blending technologies such as "chaotic advection mixing" process to make structured morphologies (e.g., micro- or nanolayered) containing blend products.
5. Better understanding of the correlations between rheology, morphology, and mechanical properties to help optimize polymer blend design.
6. Development of efficient toughening technology (impact strength, fracture toughness, and ductile/brittle transition temperature) without sacrificing flexural modulus, strength, and HDT of the blend products.
7. Improving the long-term service life and performance of polymer blends (thermal aging and embrittlement resistance, creep and fatigue resistance, weatherability, and so on).
8. Developing cost-effective processing (compounding and post-fabrication) technology.
9. Improving the recyclability and reprocessability aspects of polymer blends, particularly with respect to the retention of properties after multiple processing histories, to increase the efficiency of regrind reuse.
10. Development of cost-effective technology for polymer blends that can continue to bridge the performance gaps between the commodity, engineering, and specialty polymers.
11. Development of nanocomposite polymer blends to achieve higher levels of stiffness/strength and toughness balance while retaining a low specific gravity desirable for making light-weight parts for the transportation industry.
12. Bio-based and biodegradable polymer blends technology will be a major growth area, as growing environmental awareness and government regulations fuel the demand for sustainable products that can be used for engineering applications.

19.16　Cross-References

▶ Applications of Polymer Blends
▶ Compounding Polymer Blends
▶ High Performance Polymer Alloys and Blends for Special Applications
▶ Interphase and Compatibilization by Addition of a Compatibilizer

Notations and Abbreviations

ABS   Acrylonitrile-*co*-butadiene-*co*-styrene polymer
AES   Acrylonitrile-*co*-ethylene/propylene-*co*-styrene polymer
ASA   Acrylonitrile-*co*-styrene-*co*-acrylate polymer
BMC   Bulk molding compound
BMI   Bismaleimide
DMA   Dynamic mechanical analyzer
DSC   Differential scanning calorimeter
DTUL   Distortion temperature under load
EPDM   Ethylene-*co*-propylene-*co*-diene terpolymer rubber
EPR   Ethylene propylene copolymer rubber
EVA   Ethylene-vinylacetate copolymer
EVOH   Ethylene vinyl alcohol copolymer
HDPE   High density polyethylene
HDT   Heat distortion temperature
HIPS   High impact polystyrene
IPN   Interpenetrating network
LCP   Liquid crystal polyester
LCST   Lower critical solution temperature
LDPE   Low density polyethylene
LLDPE   Linear low density polyethylene
MBS   Methyl methacrylate-butadiene-styrene terpolymer rubber
Mt   Million metric tons
NBR   Acrylonitrile-*co*-butadiene rubber
PA   Polyamide
PBAT   Poly(butylene adipate-*co*-terephthalate)
PBD   Polybutadiene
PBS   Poly(butylene succinate)
PBT   Poly(butylene terephthalate)
PC   Polycarbonate
PCL   Polycaprolactone
PCTG   Poly (cyclohexane dimethanol-*co*-ethylene glycol terephthalate)
PEI   Polyetherimide
PET   Poly(ethylene terephthalate)
PHB   Poly(hydroxybutyric acid)
PLA   Poly(lactic acid)
PMMA   Poly(methyl methacrylate)
POE   Polyolefin elastomer
POM   Polyoxymethylene

PP   Polypropylene
PPA   Polyphthalamide
PPE   Poly(phenylene ether)
PPS   Poly(phenylene sulfide)
PPSU   Poly(phenyl sulfone)
PSU   Polysulfone
PVC   Poly(vinyl chloride)
SAN   Styrene-acrylonitrile copolymer
SBC   Styrene-butadiene block copolymer
SBR   Styrene-butadiene rubber
SEBS   Styrene-ethylene/butane-styrene block copolymer
SMA   Styrene-maleic anhydride copolymer
SMMA   Styrene-*co*-methyl methacrylate polymer
TPE   Thermoplastic elastomer
TPO   Thermoplastic polyolefin
TPU   Thermoplastic polyurethane
TPV   Thermoplastic vulcanizate

References

R.K. Adams, G.K. Hoeschele, in *Thermoplastic Elastomers*, ed. by N.R. Legge, G. Holden, H.E. Schroeder (Hanser, Münich, 1987)

M.K. Akkapeddi, B. VanBuskirk, A.C. Brown, PCT Int. Appl., W088/08433, 3 Nov 1988, Appl. 24 Aug 1987; U.S. Patent 5,162,440, 10 Nov 1992, Appl. 24 Apr 1987, to AlliedSignal Inc.

M.K. Akkapeddi, J.A. Gervasi, U.S. Patent 4,826,955, 2 May 1989, Appl. 21 Jan 1988 to AlliedSignal Inc.

M.K, Akkapeddi, J.C. Haylock, J.A. Gervasi, U.S. Patent 4,847,322, 11 July 1989, Appl. 22 Oct 1987 to AlliedSignal Inc.

M.K. Akkapeddi, C.D. Mason, PCT Int. Appl., WO91/15545, 17 Oct 1991, Appl. 26 Feb 1991 to AlliedSignal Inc.

M.K. Akkapeddi, T.J. Kraft, B. VanBuskirk, U.S. Patent 5,115,018, 19 May 1992 to AlliedSignal Inc.

M.K. Akkapeddi, B. VanBuskirk, Adv. Polym. Technol. **11**(4), 263 (1992); Polym. Prepr. **33**(2), 602 (1992); *Proceedings of the Polymer Processing Society, 9th Annual Meeting*, Manchester, 1993

M.K. Akkapeddi, B. VanBuskirk, Polym. Mater. Sci. Eng. **67**, 317 (1992)

M.K. Akkapeddi, C.D. Mason, B. VanBuskirk, Polym. Prepr. **34**(2), 848 (1993a)

M.K. Akkapeddi, B. VanBuskirk, J.H. Glans, in *Advances in Polymer Blends and Alloys Technology*, ed. by K. Finlayson, vol. 4 (Technomic Publishing, Lancaster, 1993b)

M.K. Akkapeddi, B. VanBuskirk, T. Kraft, U.S. Patent 4,902,749, 20 Feb 1990, Appl. 24 Aug 1987; U.S. Patent 5,1115,018, 9 May 1992, Appl. 24 Aug 1987; U.S. Patent 5,210,134, 11 May 1993, Appl. 24 Aug 1987, to AlliedSignal Inc.

K. Akkapeddi, Rubber toughening of polyamides by reactive blending, Chap. 8, in *Reactive Polymer Blending*, ed. by W. Baker, C. Scott, G.H. Hu (Hanser, Munich, 2001), pp. 207–253

M.K. Akkapeddi, B. VanBuskirk, P. Gallantly, Unpublished results

M.K. Akkapeddi et al., U.S. Pat. 6,410,156; U.S. Pat. 6,423,776 (2002)

M.K. Akkapeddi et al., ANTEC'03 SPE Conference Tech. Papers *61*, 3845 (2003)

M.K. Akkapeddi et al., E.P. Socci, T.J. Kraft, U.S. Pat. 6,756,444 (2004)

Anonymous, Product Literature on Vistanex® Polyisobutylene, Exxon Chem. Co. (1974)

Anonymous, Mod. Plast. **60**(2), 12 (1983)

Anonymous, Product Literature on Trefsin® Thermoplastic Elastomer, Exxon Chem., Co. (1988)

Anonymous, Selar® PA 3426 Product Literature, DuPont Co. (1989)

Anonymous, Preliminary Product Literature on Blendex® HPP PPO® Modifier resins, General Electric Co. (1991)

Anonymous, Preliminary Literature on Capron® AB, AlliedSignal (1992)

Anonymous, Mod. Plast. **70**(1), 83 (1993)

Anonymous, Technical information-Plastics modification, Engage® Polyolefin elastomers, Dow Chem. Co. (2006a)

Anonymous, Styrolux® Styrene-butadiene copolymer (SBC)- mechanical and optical properties, BASF chem. brochure (2006b)

Anonymous, Plast. Technol., April 2012, p.13

M. Aonuma, T. Suzuki, I. Isomura, K. Nishimura, U.S. Patent 4,996,264, issued 26 Feb 1991 to Nippon Zeon

B.C. Arkles, U.S. Patent 4,500,688, 19 Feb 1985, Appl. 20 Apr 1982, to Petrarch Systems

K.E. Atkins, in *Polymer Blends*, ed. by D.R. Paul, S. Newman, vol. 2 (Academic, New York, 1978)

K.E. Atkins, in *Sheet Molding Compounds: Science and Technology*, ed. by H.G. Kia (Hanser, NewYork, 1993), Chap. 4

K.E. Atkins, in *Plastic Additives, an A-Z Reference*, ed. by G. Pritchard (Chapman Hall, NewYork, 1998), p. 442

D.F. Aycock, S.P. Ting, U.S. Patent 4,600,741, 15 July 1986, Appl. 27 Sept 1984, to General Electric Co.

M. Baer, U.S. Patent 4,707,513, 17 Nov 1987, Appl. 11 Mar 1986, to Monsanto Co.

C. Bastioli, Polym. Degrad. Stab. **59**, 263 (1998)

R.E. Bernstein, C.A. Crua, D.R. Paul, J.W. Barlow, Macromolecules **10**, 681–686 (1977)

R.E. Bernstein, C.A. Cruz, D.R. Paul, J.W. Barlow, Macromolecules **10**, 681 (1997)

H. Bertillson, B. Franzen, J. Kubat, Plast. Rubber Process. Appl. **10**, 137 (1988)

M.D. Bertolucci, D.E. Delaney, SPE Tech. Pap **29**, 23 (1983)

R. Binsack, T. Goldman, Ger. Patent 3,336,499, 25 Apr 1985, App. 7 Oct 1983, to Bayer A. G.

M. Biron, O. Marichal, *Thermoplastics and Thermoplastic Composites*, 2nd edn. (Elsevier, Oxford, U.K.) p. 31 (2013)

E.M. Boldebuck, U.S. Patent 3,063,872, 13 Nov 1962; App. 15 Feb 1960, to General Electric Co.

R.J.M. Borggreve, R.J. Gaymans, A.R. Luther, Makromol. Chem. Macromol. Symp. **16**, 195 (1988)

R.J.M. Borggreve, R.J. Gaymans, Polym. Commun. **30**, 71 (1989)

R.S. Brookman, Overview of blends and alloys for flexible PVc, in *PVC Blends, Alloys and Graft Polymers Conference Proceedings* (Atlanta, GA, 10th–12th Oct. 1898), p. 7–18

A.L. Brody, E.R. Strupinsky, L.R. Kline, Oxygen scavenger systems, in *Active Packaging for Food Applications* (Technomic Publishing, Pennsylvania, 2001)

S.B. Brown, D. McFay, J.B. Yates, G.F. Lee, U.S. Patent 4,978,715, 18 Dec 1990, Appl. 15 Aug 1988, to General Electric Co.

S.B. Brown, J.R. Campbell, T.J. Shea, U.S. Patent 5,039,742, 13 Aug 1991, Appl. 30 Oct 1989, to General Electric Co.

C.B. Bucknall, *Toughened Plastics* (Applied Science Publishers, London, 1977)

C.B. Bucknall, D. Clayton, W.E. Keast, J. Mater. Sci. **7**, 1443 (1973)

C.B. Bucknall, I.K. Partridge, M.V. Ward, J. Mater. Sci. **19**, 2064 (1984)

K. Burg, H. Chedron, F. Kloos, H. Schlaf, Eur. Patent App. 156,285, 2 Oct 1985, Appl. 19 March 1985; U.S. Patent 5,047,470, 10 Sept 1991, Appl. 20 May 1988

L.R. Burke, J.M. Newcombe, Plast. Eng., April 1982, p. 35

J. Bussink, J. DeMunck, C. Van Abeleen, U.S. Patent 4,122,131, 24 Oct 1978; App. 11 Sept 1977, to General Electric Co.

P.J. Cahill, S.Y. Chen, U.S. Patent 6,083,585, 4 July 2000 to B. P. Amoco Corp.

J.R. Campbell, S.Y. Hobbs, T.J. Shea, V.H. Watkins, Polym. Eng. Sci. **30**, 1056 (1990)

R. Carew, R. Deisler, in *Proceedings of the Compalloy '89* (Schotland Business Research, Princeton, 1989)

R.O. Carhart, in *Engineering Thermoplastics*, ed. by J.M. Margolis (Marcel Dekker, New York, 1985)

Ceresana Brochure, *Market Study: Polypropylene*, 2nd edn (2012), http://www.ceresana.com/en/market-studies/plastics/polypropylene

H.S. Chao, R.E. Colborn, J.R. Presley, J.M. Whalen, M.J. Davis, J.E. Tracy, E.F. Chu, U.S. Patent 5,213,886, 25 May 1993, Appl. 17 Feb 1989, to General Electric Co.

H. Chen, R. Porter, Polym. Eng. Sci. **32**, 1870 (1992)

Y. Chen, Q. Sun, J. Drbohlav, Int. Patent. Appl. Pub. WO 2009/032560, 12 March 2009, to Invista Technologies.

C.I. Chung, *Extrusion of Polymers: Theory and Practice* (Hanser, 2000)

J.C. Chung, M.K. Akkapeddi, Polym. Prepr. **34**(1), 614 (1993)

J.Y. Chung, D. Neuray, M. Witman, U.S. Patent 4,554,314, 19 Nov 1985, Appl. 14 Nov 1984, to Mobay Co.

E.P. Cizek, U.S. Patent 3,383,435, 14 May 1968, Appl. 6 Jan 1965, to General Electric Co.

A.Y. Coran, in *Thermoplastic Elastomers*, ed. by N.R. Legge, G. Holden, H.E. Schroeder (Hanser, Münich, 1987)

A.Y. Coran, R. Patel, Rubber Chem. Technol. **53**, 781 (1980)

A.Y. Coran, R. Patel, U.S. Patent 4,355,139, 29 Oct 1982, Appl. 22 June 1981, to Monsanto Co.

A.Y. Coran, R. Patel, Rubber Chem. Technol. **56**, 1045 (1983)

A.Y. Coran, B. Das, R. Patel, U.S. Patent 4,130,535, 19 Dec 1978, Appl. 30 Apr 1978 to Monsanto Co.

M.J. Cyr, H. Clauberg, M.E. Stewart, S.N. Falling, M.E. Rogers, U.S. Patent 6,455,620 24 Sept 2002 to Eastman Chemical Co.

S. Dagli, K. Kamdar, Polym. Eng. Sci. **34**, 709 (1994)

L. D'orazio, R. Greco, C. Mancarella, E. Martucelli, G. Ragosta, C. Silvester, Polym. Eng. Sci. **22**, 536 (1982)

K.C. Dao, J. Appl. Polym. Sci. **27**, 4799 (1982)

K.C. Dao, Polymer **25**, 1527 (1984)

M.E.J. Dekkers, S.Y. Hobbs, I. Bruker, V.H. Watkins, Polym. Eng. Sci. **30**, 1628 (1990)

A. DeNicola, K. Okamoto, M. Van Cleuvenbergen, Proceed. Compalloy Europe, 95 (1992)

A. DeNicola, Hivalloy Resin technology: reactor produced polyolefin alloys, in *2nd Annual North America Symposium on "Recent Advances in Polymer Blends Alloys*, Hilton Head, 1994

J. Deveaux, P. Goddard, J.P. Mercier, J. Polym. Sci. Poly. Phys. Ed. **20**, 1881 (1982)

E.J. Deyrup, U.S. Patent 4,352,904, 5 Oct 1982, Appl. 5 Jan 1979 to DuPont Co.

E.J. Deyrup, U.S. Patent 4,753,980, 28 June 1988, Appl. 14 Nov 1986, to DuPont Co.

F. Dobkowski, Polymer **25**, 110 (1988)

V. Dobrescu, V. Cobzaru, J. Polym. Sci. Polym. Symp. **64**, 27 (1978)

M. Doescher, H. Jadamus, U.S. Patent 4,760,115, 26 July 1988, Appl. 30 March 1987, to Hüls A. G.

C.P. Donbe, D.J. Walsh, Polymer **20**, 1115 (1979)

S. Dotson, G. Niznik, *Modern Plastics Encyclopedia* (McGraw Hill, New York, 1991), p. 175

R.S. Drake, A.R. Siebert, SAMPE Q **6**, p. 1 (1975)

R.S. Drake, D.R. Egan, W.T. Murphy, ACS Symp. Ser. **221**, 1 (1983)

E.A. Eastman, M.D. Dadmun, Polymer **43**, 6707–6717 (2002)

A. Echte, *Rubber Toughened Plastics* (ACS Monograph, Washington, DC, 1989)

J.L. Eguiburu, J.J. Iruin, M.J. Fernandez-Berridi, J. Roman, Polymer **39**, 6891 (1998)

T.S. Ellis, Polym. Eng. Sci. **30**, 998 (1990)

B.N. Epstein, U.S. Patent 4,174,358, 13 Nov 1979, App. 11 Apr 1977, to DuPont Co.

J. Equiazabal, M. Cortazar, J. Irwin, J. Appl. Polym. Sci. **42**, 489 (1991)

A. Escala, R.S. Stein, Adv. Chem. Ser. **176**, 455 (1979)

T.R. Evans, D.D. Mosier, Plast. Eng. **17** (1991)

S.B. Farnham, T. Goldman, U.S. Patent 4,096,202, 20 June 1978, Appl. 9 June 1976, to Rohm and Haas Co.

Y. Feng, A. Schmidt, R.A. Weiss, Macromolecules **29**, 3909 (1996)

E.A. Flexman, D.D. Huang, H.L. Snyder, Polym. Prepr. **31**(2), 189 (1990)

E.A. Flexman, U.S. Patent 4,804,716, 24 Feb 1989; App. 21 July 1987, to DuPont Co.

G.R. Forger, Mater. Eng. **85**, 44 (1977)

G.R. Forger, Plast. World **40**, 28 (1982)

D. Freitag, V. Grigo, P.R. Muller, W. Nouvertne, in *Encyclopedia of Polymer Science and Technology*, ed. by H.F. Mark, N. Bikales, C.G. Overberger, G. Menges, vol. 11 (Wiley, New York, 1985), p. 706

D. Freitag, G. Fengler, L. Morbitzer, Angew. Chem. Int. Ed. **30**, 1598 (1991)

J.R. Fried, F.E. Karasz, W.J. McKnight, Macromolecules **11**, 150 (1978)

K. Friedrich, Crazing in polymers, in *Advances in Polymer Science*, ed. by H.H. Kausch, vol. 52/53 (Springer, Berlin, 1983)

J.S. Fry, C.N. Merriam, W.H. Boyd, in *Applied Polymer Science*, ed. by R.W. Tess, G.W. Poehlain, ACS Symp. Ser. **285**, 1141 (1985)

M. Gabrielle, Plast. Technol., 59 (1992)

P. Galli, J.C. Haylock, E. Albizzati, A.J. DeNicola, *High Performance Polyolefins* (IUPAC, Akron, 1994)

P. Galli, J.C. Haylock, Prog. Polym. Sci. **16**, 443 (1991)

R.R. Gallucci, M.A. Sanner, P. Sybert, SPE-ANTEC Tech. Conf., 2508 (2005)

R.R. Gallucci, A. Sanner, A. May, SPE ANTEC Tech. Conf., 1278 (2008)

R.R. Gallucci, M.A. Sanner, SPE ANTEC Tech. Conf., 2741 (2011)

Z.G. Gardlund, in *Polymer Blends and Composites in Multiphase Systems*, ed. by C.D. Han, Adv. Chem. Ser., **206** (ACS, Washington, DC, 1984)

B. Gelles, M. Modic, J. Kirkpatrick, SPE Tech. Pap. **34**, 513 (1988)

J. Girard, Eng. Plast. **3**, 51 (1990)

J.H. Glans, M.K. Akkapeddi, Macromolecules **24**, 383 (1991)

P. Goddard, J.M. Dekoninck, V. Pevlesaver, J. Deveaux, J. Polym. Sci. Polym. Chem. **24**, 3315 (1986)

T.S. Grabowski, U.S. Patent 3,130,177, 21 Apr 1964 to Borg-Warner Co.

T.S. Grant, C.L. Meyers, U.S. Patent 4,496,690, 29 Jan 1985, Appl. 3 June 1983, to Borg-Warner Co.

T.S. Grant, R.L. Jalbert, D. Whalen, U.S. Patent 4,732,935, 22 March 1988; App. 6 Dec 1985, to Borg-Warner

B. F. Greek, *C & EN*, June 10, 39 (1991)

P.F. Haartman, C.L. Eddy, G.P. Koo, SPE. J. **26**(5), 62 (1970a)

P.F. Haartman, C.L. Eddy, G.P. Koo, Rubber World **163**, 59 (1970b)

W.A. Haile, M.E. Tincher, F.W. Williams, Tappi INJ Summer 2002

W.J. Hall, A.C.S. Div. Org. Coat. Plast. Prepr., **47**, 298 (1982)

C.F. Hammer, Macromolecules **4**, 69 (1971)

B.D. Hanrahan, S.R. Angeli, J. Runt, Polym. Bull. **14**, 399 (1985)

A. Hassan, B. Haworth, J. Mater. Process. Technol. **172**, 341 (2006)

A.S. Hay, Polym. Eng. Sci. **16**, 1 (1976)

A.S. Hay, U.S. Patent 3,306,874, 18 Feb 1967, Appl. 24 July 1962, to General Electric Co.

A.S. Hay, J. Am. Chem. Soc. **81**, 6335 (1959)

D.R. Hazelton, R.C. Puydak, U.S. Patent 4,639,487, 27 Jan 1987, Appl. 11 July 1984, to Exxon Co.

P.L. Heater, G.A. Elliott, U.S. Patent App.Pub. US2007/0082157, 12 Apr 2007 to M&G U.S.A.

J.L. Hecht, T.M. Ford, SPE Tech. Pap. **31**, 777 (1985)

J.J. Hemphill et al., Expanding the product portfolio of ethylene elastomers – ENGAGE™ polyolefin elastomers for large volume TPO applications, in *Proceedings of the SPE-Automotive TPO Global Conference*, October 10–12, 2005, Sterling Heights, MI, USA

S. Hirakawa, M. Haraguchi, M. Yasinawa, Rep. Progr. Polym. Phys. Jpn. **28**, 171 (1985)

S.Y. Hobbs, R.C. Bopp, V.H. Watkins, Polym. Eng. Sci. **23**, 380 (1983)

S.Y. Hobbs, M.E.J. Dekkers, V.H. Watkins, Polym. Bull. **17**, 341 (1987)

S.Y. Hobbs, T. Stanley, O. Phansteil, Polym. Prepr. **33**(2), 614 (1992)

C.J. Hooley, D.R. Moore, M. Whale, Plast. Rubber Process Appl. **345**, 1 (1981)

D.J. Hourston, S. Lane, H.S. Zhang, Polymer **32**, 2215 (1991)

D.V. Howe, M.D.J. Wolkowicz, Polym. Eng. Sci. **27**, 1582 (1987)

Z. Huang, L. Wang, Makromol. Rapid Commun. **7**, 255 (1986)

K.S. Hyun, C.G. Gogos, M.H. Kim, Extrusion technology for manufacturing polymer blends, in *Encyclopedia of Polymer Blends*, vol. 2 (Wiley-VCH, Weinheim, 2011)

F. Ide, A. Hasegawa, J. Appl. Polym. Sci. **18**, 963 (1974)

Encyclopedia of Polymer Blends, vol. 2, Chap. 5, ed. by A.I. Isayev (Wiley-VCH, Weinheim, 2011), pp. 207–259

B. Imre, B. Pukanskzy, Eur. Polym. J. (2013; Article in press @ http://dx.doi.org/10.1016/j.eurpolymj.2013.01.019)

S.H. Jafaria, P. Potschkea, M. Stephana, H. Warth, H. Alberts, Polymer **43**, 6985 (2002)

H. Iida, K. Kometani, M. Yanagi, U.S. Patent 4,284,540, 18 Aug 1981; App. 16 Apr 1980, to Toray Co.

H. Jager, E.J. Vorenkamp, G. Challa, Polym. Commun. **24**, 290 (1983)

R.L. Jalbert, T.S. Grant, U.S. Patent 4,654,405, 31 March 1987; App. 5 Dec 1985, to Borg-Warner Co.

B.Z. Jang, D.R. Uhlman, J. VanderSande, Polym. Eng. Sci. **25**, 643 (1985)

A.A. Jones, Macromolecules **18**, 902 (1985)

G. Kailasam, R. Gallucci, M.A. Sanner, U.S. Patent App., 2009/0018242, 15 Jan 2009 to G.E.

N.K. Kalfouglou, Angew. Makromol. Chem. **118**, 19 (1983)

R.P. Kambour, R.C. Bopp, A. Maconnachie, W.J. McKnight, Polymer **21**, 133 (1980)

P.J. Kay, T. Ouhadi, J. Elastom. Plast. **23**, 282 (1991)

J.D. Keitz, J.W. Barlow, D.R. Paul, J. App. Polym. Sci. **29**, 3131 (1984)

W.N. Kim, C.M. Burns, Polym. Eng. Sci. **28**, 1115 (1988)

W.N. Kim, C.M. Burns, J. Polym. Sci. Polym. Phys. **28**, 1409 (1990)

A.J. Kinloch, R.J. Young, *Fracture Behavior of Polymers* (Applied Science Publishers, New York, 1983)

K. Kircher, Kunststoffe **80**, 1113 (1990)

J. Kirkpatrick, M. Modic, D. Gilmore, in *Proceedings of the Compalloy '89* (Schotland Business Research, Princeton, 1989)

K. Knoll, N. Niesner, Macromol. Symp. **132**, 231 (1998)

R.M. Kossoff, "Future of Plastics Alloys" – III, international strategic plastics reports (R. M. Kossoff Associates, New York, 1987)

G.P. Kozielski, Plast. Technol., 73 (1988)

S.M. Krause, Compatible polymers, Chap. VI, in *Polymer Handbook*, ed. by J. Brandrup, E.H. Immergut (Wiley, New York, 1989), p. 347

S. Krause, Macromol. J. Sci. Rev. Macromol. Chem. **C-7**, 251 (1972)

R.J. Kray, R.J. Bellet, U.S. Patent 3,388,186, 11 June 1968, Appl. 2 March 1965, to Allied Chemical Co.

E.N. Kresge, in *Polymer Blends*, ed. by D.R. Paul, S. Newman, vol. 2 (Academic, New York, 1978)

T.D. Krizan, J.C. Coburn, P.S. Blatz, Polym. Prepr. **30**, 9 (1989)

P.L. Ku, Adv. Polym. Technol. **8**(3), 201 (1985)

R. Kusumgar, U.S. Patent 4,713,414, 15 Dec 1987, Appl. 16 July 1986, to Celanese Co.

L. Landers, J. Schmitt, J. Terenzi, U.S. Patent 3,354,238, 21 Nov 1967, Appl. 20 Dec 1966, to American Cyanamid Corp.

R.E. Lavengood, F.M. Silver, *SPE RETEC '87*, 266 (1987a)

R.E. Lavengood, F.M. Silver, *SPE Tech. Pap*. **33**, 1369 (1987b)

R.E. Lavengood, A.F. Harris, A.R. Padwa, Europ. Patent Appl. 202,214, 20 Nov 1986, Appl. 9 May 1986, to Monsanto Co.

R.E. Lavengood, R. Patel, A.R. Padwa, U.S. Patent 4,777,211, 11 Oct 1988; App. 9 July 1986, to Monsanto Co.

G.F. Lee Jr., U.S. Patent 4,972,021, 20 Nov 1990, Appl. 14 Sept 1988, to General Electric Co.

Y.C. Lee, Q. Trementozzi, U.S. Patent 4,305,869, 15 Dec 1981; App. 17 Dec 1979, to Monsanto Co.

R. Legras, C. Bailley, M. Daumerie, J. Dekoninck, J. Mercier, V. Zichy, E. Nield, Polymer **25**, 835 (1984)

H.M. Li, A.H. Wong, *MMI Press Symposium Series*, vol. 2 (Harwood Academic, New York, 1982)

P. Liu, D. Overton, U.S. Patent 4,532,282, July 1985, Appl. 16 March 1983, to General Electric Co.

W.L. Liu, Ger. Patent 3,728,685, 10 March 1988, Appl. 27 Aug 1987, to Rohm and Haas Co.

Z. Liu, S. Mehta, X. Huang, D.A. Schiraldi, U.S. Patent 7,919,159, 5 Apr 2011 to Invista.

G.L. Loomis, R.J. Statz, U.S. Patent 4,613,533, Sept 1986, App. July 1982, to DuPont Co.

W.A. Mack, Mod. Plast. **48**(8), 62 (1971)

I. Manas-Zloczower (ed.), *Mixing and Compounding of Polymers* (Hanser, Munich, 2009)

C.D. Mason, H.W. Tuller, U.S. Patent 4,404,325, 13 Sept 1983, Appl. 11 May 1981 to AlliedSignal Inc.

M. Matsuo, Jpn. Plast. **2**, 6 (1968)

M. Matsuo, C. Nozaki, Y. Jyo, Polym. Eng. Sci. **9**, 197 (1969)

L.V. McAdams, J. Gamon, in *Encyclopedia of Polymer Science and Technology*, ed. by H.F. Mark, N. Bikales, C.G. Overberger, G. Menges, vol. 6 (Wiley, New York, 1985), p. 363

D.C. McConnell, G.M. McNally, W.R. Murphy, Dev. Chem. Eng. Miner. Process. **12**, 37 (2004)

S.M. McDougle, SPE Tech. Pap. **13**, 596 (1967)

F.J. McGarry, A.M. Willner, Research Report RJ-68-8 (School of Eng., M.I.T., Cambridge, MA, 1968)

G.A. Mellinger, H.F. Giles Jr., F. Holub, W.R. Schlich, U.S. Patent 4,548,997, 22 Oct 1985, App. 22 May 1984, to General Electric Co.

J. Mijovic, H.L. Luo, C.D. Han, Polym. Eng. Sci. **22**, 234 (1982)

R.N. Mohn, D.R. Paul, J.W. Barlow, C.A. Cruz, J. Appl. Polym. Sci. **23**, 575 (1979)

I. Mondragon, M. Gartelumindi, J. Nazabal, Polym. Eng. Sci. **28**, 1126 (1989)

B.W. Moody, SPE Tech. Pap. **50**, 1416 (1992)

L. Morbitzer, H.J. Kress, C. Lindner, K.H. Ott, Angew. Makromol. Chem. **132** (1983)

L.E. Murch, U.S. Patent 3,845,163, 29 Oct 1974; App. 24 Jan 1966, to DuPont Co.

S.R. Murff, J.W. Barlow, D.R. Paul, J. Appl. Polym. Sci. **29**, 3231 (1984)

C.V. Murphy, SPE Tech. Pap. **31**, 73 (1986)

M. Naitove, Conference report: bioplastics are breaking out of their green niche, Plastics Technology, Apr 2012

Y. Nakamura, R. Hasegawa, H. Kubota, U.S. Patent 3,864,428, 4 Feb 1975, App. 27 Aug 1973, to Teijin Ltd.

T.R. Nassar, D.R. Paul, J.W. Barlow, J. Appl. Polym. Sci. **23**, 85 (1979)

D. Neuray, K.H. Ott, Angew. Makromol. Chem. **98**, 123 (1981)

Nexant/Chemsystems online news article "PET suffering from over supply" (2007), www.chemsystems.com

Nexant/Chemsystems, "Nylon 6 and Nylon 66" PERP07/08S6 Report Abstract (2009)

Nexant/Chemsystems Online news article on 'Polyolefins (2012)', www.chemsystems.com

Y. Ohtsuka, EP 0658603 A2, 21 June 1995 to Daicel Chemical Industries

T. Okamoto, K. Yasue, T. Marutani, Y. Fukushima, U.S. Patent 4804707, 14 Feb 1989 to Unitika Ltd.

A.O. Ogah, J.L. Afikuwa, Int. J. Eng. Manag. Sci. **3**(2), 85 (2012)

I. Ozen, G. Bozoklu, C. Dalgicdir, Y. Orcun, E. Unsal, M. Cakmak, Y. Menceloglu, Eur. Polym. J. **46**, 226 (2010)

P.J. Perron, Adv. Polym. Technol. **6**, 79 (1984)

P.J. Perron, U.S. Patent 4,782,114, 1 Nov 1988, Appl. 3 Oct 1986, to Dexter Corp.

E. Pittenger, G. Cohan, Mod. Plast. **25**(1), 81 (1947a)

E. Pittenger, G. Cohan, Rubber Age **61**, 563 (1947b)

A.P. Plochocki, Polyolefin blends, Chap. 21, in *Polymer Blends*, ed. by D.R. Paul, S. Newman, vol. 2 (Academic Press, New York, 1978), p. 223

R.S. Porter, L.H. Wang, Polymer **33**, 2019 (1992)

V. Prattipati, Y. Hu, S. Bandi, S. Mehta, D.A. Schiraldi, A. Hiltner, E. Baer, J. Appl. Polym. Sci. **99**, 225 (2006)

C.F. Pratt, S.Y. Hobbs, Polymer **17**, 12 (1976)

W.M. Priest, R.S. Porter, J. Polym. Sci. Polym. Chem. **10**, 1639 (1972)

F. Ramsteiner, W. Heckmann, Polym. Commun. **26**, 199 (1985)

G.G. Ranby, J. Polym. Sci. Polym. Symp. **51**, 89 (1975)

G.S. Rellick, J. Runt, Proc. ACS PSME **52**, 331 (1985)

Reseau-plasturgie netzworke kunsoffetechnologie Conference- Bayer presentation on "Plastics industry and its role on our society", Fribourg, Apr 2012

C.K. Riew, E.H. Rowe, A.R. Siefert, ACS Adv. Chem. Ser. **154**, 326 (1976)

M.R. Rifi, H.K. Fieker, D.A. Walker, Mod Plast. **62**(2), 62 (1987)

L.M. Robeson, J. Appl. Polym. Sci. **30**, 4081 (1985)

L.M. Robeson, U.S. Patent 4,532,288, 30 July 1985; App. 29 Jan 1982, to Union Carbide Co.

L.M. Robeson, Miscible polymer blends containing poly (vinyl chloride), In *PVC Blends, Alloys and Graft Polymers Conference Proceedings* (Atlanta, GA; October 10–12, 1989), p. 134

M. Roodvoets, F. Embs, U.S. Patent App.Pub. US2012/02114935, 23 Aug 2012, to Invista, N. A.

J. Runt, D. Lei, L.M. Martynowicz, D.M. Brezny, M. Mayo, Macromolecules **22**, 3908 (1989)

K. Saito, High Polym. Jpn. **22**, 463 (1973)

H. Sakano, M. Kodama, T. Shoji, I. Yoshida, U.S. Patent 4,228,051, 14 Oct 1980, Appl. 31 July 1979 to Sumitomo Chem., Co.

J. Salay, D.J. Dougherty, *Modern Plastics Encyclopedia* (McGraw Hill, New York, 1992), p. 94

R. Saltman, B. Varnell, SPE Tech. Pap. **34**, 1725 (1988)

R. Saltman, U.S. Patent 5,091,478, 25 Feb 1992; App. 21 May 1990, to DuPont Co.

M.A. Sanner, R.R. Gallucci, SPE ANTEC Tech. Conf., 2684 (2011)

L.R. Schmidt, J. Appl. Polym. Sci. **23**, 2463 (1979)

W. Schuett, E. McKee, A. Hilt, H. Gorissen, G. Heinz, Ger. Patent 3,441,547, 15 May 1986, App. 14 Nov 1984, to BASF Co.

A.R. Schulz, B.M. Gendron, J. Appl. Polym. Sci. **16**, 461 (1972)

H.H. Schut, Plast. Technol. **39**(3), 29 (1993)

J.H. Schut, Plast. Technol. **38**(7), 31 (1992)

J.H. Schut, Plast. World, 41 (1996)

R. Shanks, I. Kong, Thermoplastic starch, Chap.6, in *Thermoplastic Elastomers*, ed. by A. El-Sonbati (2012), http://www.intechopen.com/books/thermoplasticelastomers/thermoplastic-starch

M.T. Shaw, Polym. Eng. Sci. **22**, 115 (1992)

L. Sherman, Plast. Technol., 17 (1997)

C.K. Shih, in *Proceedings of the Compalloy* (Schotland Business Research, Princeton, 1990)

Y.J. Shur, B.G. Ranby, J. Appl. Polym. Sci. **20**, 3721 (1976)

W.A. Smith, J.W. Barlow, D.R. Paul, J. Appl. Polym. Sci. **26**, 4223 (1981)

L.R. Spencer, *Modern Plastics Encyclopedia* (McGraw Hill, New York, 1991), p. 128

W.M. Speri, G.R. Patrick, Polym. Eng. Sci. **15**, 668 (1975)

SRI, *Report on Compounding of Engineering Thermoplastics* (SRI International, Menlo Park, 1992a)

SRI, *Report on World Petrochemicals* (SRI International, Menlo Park, 1992b)

S. Srinivasan, *Modern Plastics Encyclopedia* (McGraw Hill, New York, 1992), p. 103

R.A. Steinkamp, U.S. Patent 3,953,655, 27 Apr 1976; App. 9 Apr 1971, to Exxon Co.

H. Suarez, J.W. Barlow, J. Appl. Polym. Sci. **29**, 3253 (1984)

P.M. Subramanian, U.S. Patent 4,444,817, 24 Apr 1984, App. 29 Sept 1982, to DuPont. Co.

P.M. Subramanian, Polym. Eng. Sci. **25**, 483 (1985)

M. Takayanagi, T. Ogata, M. Morikawa, T. Kai, J. Macromol. Sci. Phys. **B17**, 591 (1980)

Y. Takeda, D.R. Paul, Polymer **33**, 3899 (1992)

J.M. Tibbitt, P.J. Cahill, G.E. Rotter, D.P. Sinclair, G.T. Brooks, R.T. Behrend, U.S. Patent 7,214,415, 8 May 2007 to B. P. Corporation North America Inc.

T.D. Traugott, in *Encyclopedia of Polymer Science and Technology*, ed. by H.F. Mark, N. Bikales, C.G. Overberger, G. Menges, vol. 16, 2nd edn. (Wiley, New York, 1985), p. 83

C. Tremblay, R.E. Prud'homme, J. Polym. Sci. Polym. Phys. **22**, 1857 (1984)

K. Ueno, T. Maruyama, U.S. Patent 4,315,086, 9 Feb 1982, App. 16 July 1980, to Sumitomo Chemical Co.

L.A. Utracki, *Commercial Polymer Blends* (Chapman and Hall, London, 1998)

D.W. VanKrevelen, *Properties of Polymers*, 3rd edn. (Elsevier, Amsterdam, 1990)

I. Vrooman, L. Tighzert, Materials **2**, 307 (2009)

D.C. Wahrmund, D.R. Paul, J.W. Barlow, J. Polym. Sci. **22**, 2155 (1978)

J.G. Wallace, *Modern Plastics Encyclopedia* (McGraw Hill, New York, 1992), p. 100

T.T. Wang, T. Nashi, Macromolecules **10**, 421–425 (1977)

D.G. Walsh, J.G. McKeown, Polymer, **21**, 1220, 1335 (1980)

D.J. Walsh, G.L. Cheng, Polymer **25**, 495 (1984)

L.B. Weaver et al., Novel ethylene/alpha-olefin copolymers-polyproylene blends for thermoforming, blow molding and extruded profiles, in *Proceedings of SPE Polyolefins 2006*, Houston, 2006

A. Wambach, *Modern Plastics Encyclopedia* (McGraw Hill, New York, 1992), p. 95

G.A. Weber, J. Schoeps, Angew. Makromol. Chem. **136**, 45 (1985)

C.A. Weber, W. Paige, U.S. Patent 4,624,986, 25 Nov 1986, Appl. 7 Aug 1984, to Dow Chemical Co.

N.E. Weeks, F.E. Karasz, W.J. McKnight, J. Appl. Phys. **48**, 4068 (1977)

W. Wenig, T. Schoeller, Angew. Makromol. Chem. **130**, 155 (1985)

D.M. White, J.E. Hallgreen, J. Polym. Sci. Polym. Chem. **21**, 2921 (1983)

D. White, R. Matthews, U.S. Patent 4,141,927 (1979) to G.E.

V. Wigotsky, Plast. Eng., 15 (1995)

M.W. Witman, Eur. Patent Appl. (05) 0036127, 23 Sept 1981, Appl. 4 March 1981 to Mobay Chemical Co.

K. Wood, A. Tanaka, M. Zheng, D. Garcia, 70% PVDF coatings for highly weatherable architectural coatings. Atofina Chem. Tech. Paper (2005) www.arkema-inc.com/pdf/techpoly/kurtpaper.pdf

S. Wu, in *Polymer Handbook*, Chap. VI, 3rd edn, ed. by J. Brandrup, E.H. Immergut (Wiley, New York, 1989)

S. Wu, Polymer **26**, 1855 (1985)

S. Wu, J. Appl. Polym. Sci. **35**, 549 (1988)

A.F. Yee, Polym. Eng. Sci. **17**, 213 (1977)

A.F. Yee, Proceedings of the International Conference on Toughening of Plastics – II, London (1985).

P.-L. Yeh, A.W. Bisley, Plast. Rubber Process. Appl. **5**, 249 (1985)

G.A. Zakrzewski, Polymer **14**, 347 (1973)

M.P. Zamora, T. Miller, Plast. Eng., 75 (1997)

G. Zhang, J. Zhang, S. Wang, D. Shen, J. Polym. Sci. Polym. Phys. **41**, 23 (2002)

J. Zimmerman, E.M. Pearce, I.K. Miller, J.A. Muzzio, I.G. Epstein, E.A. Hosegood, J. Appl. Polym. Sci. **17**, 849 (1973)

Recycling Polymer Blends

20

Francesco Paolo La Mantia and Roberto Scaffaro

Contents

Abstract

Starting with the second half of the 1970s, polymer recycling was extensively adopted to reuse plastics otherwise destined for landfills with the goal to avoid the consequent net loss of money and energy. The simple idea to reintroduce scraps or post-consumer plastics in the processing lines actually revealed complications because even adding the recycled polymer to the same virgin material often led to secondary materials due to differences in the molecular weight, branching, and difference of density. The situation appeared more complicated in the recycling of commingled plastics. In this case, the chemical nature and

F.P. La Mantia (✉) • R. Scaffaro
Department of Civil, Environment, Aerospace and Materials Engineering, University of Palermo, Palermo, Italy
e-mail: francescopaolo.lamantia@unipa.it; francescopaolo.lamantia@gmail.com; roberto.scaffaro@unipa.it

structures of the different components produce secondary materials with poor properties, thus inhibiting any possible practical application. Nevertheless, enforcement of the law about mandatory collection of post-consumer plastic and the repeated economic crises pushed toward the implementation of recycling of polymer blends in industrial processes, especially if the same processing equipments/methods used for virgin materials can be adopted. In this chapter a review of the recycling technologies of plastic blends is presented. In particular, the mechanical recycling of single polymers in the same virgin materials (the so-called "homopolymer" blends), typical in the on-site reuse of industrial scraps, and, in another section, the strategies that can be pursued to recycle directly a stream of commingled post-consumer plastics to obtain secondary materials with properties suitable for practical applications are analyzed.

20.1 General Introduction

It is commonly accepted that material recycling is a consequence of the strong environmental movement that arose throughout the world in the second half of the 1970s. Actually, especially before the advent of the industrial age in the nineteenth century, a payback way to get raw materials was just recycling and reuse. With the rapid growth of mass-production industrial activities in the twentieth century – particularly during the economic boom of the 1960s – and the optimization of the processes, it was very cheap to produce items and it appeared much more economically advantageous to throw away old objects replacing them with brand-new ones. In the following, the repeated energy crises and the growth of an environmental consciousness for the invading and pollutant landfills induced industries to reconsider the throw-away politic toward a greener recycling one. Beyond metal, paper, glass, or other fine chemicals used in processes (catalysts, solvents), particular attention was paid to plastic recycling as plastic waste, probably much more than other materials, invaded and saturated landfills representing a net loss of money in terms of energy and raw materials (Andrews and Subramanian 1992; La Mantia 1993b; Brandrup et al. 1995; Scheirs 1998; La Mantia 2002).

The initial enthusiasm about the possibility to reprocess plastic waste, thus recovering the added value of the material, was frozen by the decrease – sometime dramatic – of the overall properties/performance of reprocessed plastic. Moreover, even adding recycled polymers to the same virgin material often leads to forms of incompatibility between the two, because of several reasons such as different molecular weights or branching levels, different size/shape of the scraps, different apparent density, and different crystallinity.

Of course, the situation is more complicated in the recycling of commingled plastics, like those coming from post-consumer household items or of polymer blends. In this case, in fact, the different chemical natures and structures of the multicomponent stream make it, in some cases, impossible to get materials that can

be still used for practical applications. Nevertheless, after an initial resistance both on the industrial and on the consumers' side, plastic recycling volumes are generally increasing from year to year, as a result of the implementation and optimization of processes and additives carried out by academia in conjugation with industrial needs, thus making recycled materials economically convenient and with performances fully accepted by the end users. The way to recycling is also accelerated by law enforcement on the mandatory collection of post-consumer plastics and about minimum amounts of recycled materials to be used to produce brand-new items.

From a technical–industrial point of view, recycling is generally referred to as a series of processing operations to obtain secondary materials that can be used to produce the same or different articles. It is evident that, when the segregation level in a mix of different plastic is high, the recycling operation will be simpler than in mixtures in which the single components coexist together. Moreover, while the preventive separation of commingled plastic is generally recommended to get secondary materials with better final properties, in some cases it is not possible or it is not economically advantageous to perform this kind of pretreatment.

This chapter will analyze the application of mechanical recycling technologies to polymer blends, describing the use of recycled materials as a blend's second component or the direct recycling of mixed plastic waste.

20.2   Basic Concepts on Plastic Recycling

Plastic recycling is a general procedure related to processing both for basic theoretical aspects and for applications. In particular, getting monomers from a waste polymer is, of course, a form of recycling (chemical recycling) as well as is incineration (in this case the energy is "recycled"). When discussing plastic recycling issues, people implicitly refer to mechanical recycling, i.e., to a class of processes able to transform waste into secondary materials. Usually, one of more steps of recycling occurs in the melt using equipment and know-how of the parent polymers forming the waste stream. The plastics targeted by mechanical recycling can be conveniently divided into two main categories:

– Mixed plastic from post-consumer mass household applications
– Industrial plastic scraps and post-consumer other than mass household

The first class includes films and sheets for packaging, thermoformed trays, bottles and jars, cookware plastic bags, and other accessories, generally single use or with a short life. Polyolefins and polyesters cover almost all the uses while polyamides are less represented. The second category refers to medium- to long-life articles such as car bumpers and interiors, furniture, and appliances. However in all the cases, it is more correct to look at the plastic recycling as a process regarding blends. The recyclates are materials with properties different from the original virgin polymers; even adding a recycled polymer to its corresponding parent – for instance, in the primary recycling of industrial scraps – generates a new material with new properties, often showing an antagonist effect between the two

components. This feature requires the use of specific additives (compatibilizers, surfactants, coupling agents) to overcome this problem and get a material valid for the preparation of brand-new articles. This is more evident when reprocessing together different polymers such that, without an adequate compatibilizing system, a new material is obtained with very poor properties and often unusable for further applications.

Another important role is played by the degradation of plastic both prior to recycling and during recycling operations. This issue is, of course, even more dramatic for polymer blends (La Mantia 1992). During their first forming process, plastics undergo thermo-mechanical degradation, and during their lifetime they are degraded by the combined effect of humidity, UV light, chemical oxidation, and other environmental factors. Degradation effects are generally more intense in multiphase polymeric systems with obvious consequences on the properties of the secondary materials. To counterbalance the negative effect of degradation occurring during the first processing, the lifetime, and the second processing, it is necessary to add stabilizing systems and, in some cases, change the processing conditions with respect to those adopted for the parent polymers. In fact, beyond a simple chain scission causing the decrease of the molecular weight, degradation may induce other relevant changes in the molecular weight distribution, in the formation of short- and long-chain branches, in the chemical composition (appearance of oxygenated groups or unsaturations). When these changes are important, only milder processing conditions and appropriate additives will allow one to obtain good secondary materials.

In the recycling of polymer blends, another important issue is the difference of the melting points of the different components. Of course, the reprocessing temperature must be set as high as necessary to process the highest melting point material, but this temperature can be too high for lower melting point materials, with a sharp increase of the degradation rate, which is difficult to manage.

The problems of recycled materials do not end with processing. Compatibilizers and stabilizers are necessary to obtain secondary materials with adequate properties, but they must also protect the new objects made from secondary materials from environmental degradation during the second life of plastic. Similar to what occurs during processing, recycled plastics are often "weaker" if compared with the virgin components. As a consequence, the additive system must take into account not only the accelerated thermal and thermo-oxidative degradation typical of plastic reprocessing, but also the higher sensitivity of the secondary materials to environmental degradation.

Another important need when recycling mixed plastic is to ensure adequate mixing. In fact, while in single polymer processing or reprocessing this is not a relevant parameter, in multiphase systems having a fine dispersion of the different phases, it is critical to achieve good final properties. Increasing the mixing speed, of course, will cause an increase of cost but also an intensification of mechanical degradation processes. Therefore, the compatibilizing system, the stabilizing additives, and the processing conditions must be strictly integrated and designed for a successful recycling operation.

A possible answer to these issues could be the preventive separation of the different plastics prior to processing. Actually, since recycling has attracted the interest of industry, the separation processes are becoming more numerous and efficient achieving almost total segregation of the different plastic fractions. However, despite the improvement of the effectiveness of the pretreatment steps, there is still the possibility to find other polymers as contaminants in a main stream, and even at those low amounts, they can disturb the regularity of the recycling operation.

In some situations, the recycled plastic is voluntarily added to a virgin material to form a sort of hybrid virgin-recycled blend. This practice is common for recycling of plastic scraps forming homopolymer (also known as monopolymer) virgin recycling blends, but when applied to heteropolymer virgin-recycled blends, it is possible to obtain good materials, thereby widening the possible uses of plastic wastes.

The above considerations indicate that recycling is far from being close to a final optimization typical of mature processes. Knowing the processing–properties–structure relationships, essential in polymer science, is much more complex in plastic recycling where the number of variables is higher and rarely the streams can be considered composed by a single material. In the same direction, the investigation of the behavior of recycled commingled plastics is particularly attractive both from a scientific and from an industrial point of view as a comprehensive method regarding the reuse of mixed post-consumer objects would imply lower costs and easier waste collection.

20.3   Recycling of Commingled Plastics

20.3.1 With a Compatibilizing Method

While a generic stream of mixed plastics may have a variable composition both in the kind and in the amount of each single component, municipal waste streams consist of three types of polyethylenes (HDPE, LLDPE, LDPE), PET, and, in lower amounts, PP, PVC, PS, and polyamides. In this case, the processing temperature of the whole stream must be as high as that necessary for melting the PET and PP fractions with the consequent need to protect other thermosensitive fractions like PVC, PS, and the polyethylenes. Of course, an appropriate compatibilizer must be used to improve the phase adhesion and dispersion between all these polymers that form highly incompatible systems. One of the first materials used as general compatibilizing agent was chlorinated polyethylene (Paul et al. 1972, 1973a; Park et al. 1996a) followed by several other polymers modified with carboxyl or other polar groups, styrene block copolymers (Paul et al. 1973a; Nosker et al. 1990; La Mantia 1992b, 1993b; Hope et al. 1994; Xanthos et al. 1994, 1995), or maleated polymers (Martinez et al. 2008). The main effect of adding such compatibilizers is a general improvement of the mechanical properties and especially of impact strength and elongation at break. Even if the effects of PVC degradation were

difficult to control with the typical yellowing of the recycled materials, UV irradiation prior to processing was found helpful in forming more compatible blends due to the formation of oxygenated groups that generated in situ compatibilizer copolymers by reactive processing (Martinez et al. 2008).

In another study (Equiza et al. 2007) SEBS/EPR and SBR/EPR were used as binary compatibilizing systems of a mixed PE/PP/PS/HIPS stream. In the same study, beyond the effect of the presence of the compatibilizers, the important effect of the processing conditions in relationship with the final properties was also investigated. It was found that the best parameters set for the whole system are 190 °C, 14 min processing, and 3.5 % of SEBS/EPR. This was found to be more effective than using SBR/EPR. The mechanical properties are better in the presence of the compatibilizing system as well as the morphology that was modeled as a couple of two co-continuous phases containing PE/PP and PE/PS with a small amount of a secondary PP/PS phase. The morphological results were consistent with the PE/PP/PS theoretical ternary phase diagram with the compatibilizer granting good adhesion between the different phases. A similar system composed by HDPE/PP/PS/PVC commingled waste, with HDPE as major phase, was melt reprocessed in the presence of CPE, SEP, or a mix of the two as compatibilizing agents (Ha et al. 2000). The tensile strength was found slightly decreased, but CPE, SEP, or their combination caused an evident increase of the impact strength. The best morphology in terms of adhesion was shown by the CPE/SEP-added blends, while the SEP-containing ones showed the highest values of impact strength. Interestingly, the elongation at break of the recycled materials did not change by the addition of any of those compatibilizers. CPE was also found to be an effective compatibilizer for post-consumer HDPE/PVC blends (Park et al. 1996a) that show improved interfacial adhesion and superior ultimate stress if compared with uncompatibilized blends. Moreover, EPDM and EPM were successfully used in the recycling of LDPE/PP blends (Bertin and Robin 2002; Fortelny et al. 1996, 2002; Nedkov et al. 2008). These additives have a sharp positive effect on properties such as microhardness, elongation at break, and impact strength and show even better properties when PE-g-MB graft copolymer or liquid PB or PB-MA was used. The first reprocessing is usually protected by the presence of residual antioxidants, while further processing may induce significant changes in the blend (Santos et al. 2001). Adding EVA copolymer to the blend allowed increasing the maximum tolerated PP concentration in order to keep unaltered the impact strength of a recycled LLDPE/LDPE/PP blend.

In other situations, it can be decided to add no compatibilizers/modifier considering the natural chemical affinity of the two components. This is the case of PC/PBT blends that were aged and then reprocessed at 275 °C (Sanchez 2007). The recycled materials showed a significant increase of the elongation at break, while reprocessing did not affect the modulus and the tensile stress despite the likely occurring chain scissions due to thermal degradation. A similar approach was chosen for recycling PC/ABS blends (Reig et al. 2007). In particular, the effect of the different variables was studied using a statistical model applied to an injection molding processing. ABS was kept as a major phase, while PC was added

up to 10 % in order to simulate the presence of this second polymer as contaminant of the main ABS stream. It was found that amounts of PC added as small as 5 % do not imply significant change in the optimum processing conditions compared with 100 % ABS, while at higher PC content the change becomes significant. PC/ABS blends are often found as post-consumer plastic from dismantled cars. PA and PMMA, with the latter coming from taillight, can be present as minor phase/contaminants (Liu and Bertilsson 2000). The use of impact modifiers provides the mixture with better impact properties than any of their individual components. However, PA is highly incompatible with the other polymers – especially if filled with glass fibers – and should be either sorted out of the stream or compatibilized with maleated derivatives such as SEBS-g-MA (Liu et al. 2002; Liu and Bertilsson 1997) that are specifically appropriate to increase the compatibility between ABS and PA6. In any case, the use of maleated rubber led to an increase of the impact strength of the recycled materials. For this system, the use of antioxidants or metal deactivators during the melt reprocessing does not help the recyclates to show better mechanical properties.

If recycling mixed plastic waste can be complicated, when cross-linked fractions are present, the complication level can drastically increase. Attempts were made to recycle mixed plastic waste containing ground tire rubber and post-consumer films from greenhouses (essentially LDPE, LLDPE, and small amounts of EVA and additives) (Scaffaro et al. 2005). In this case, mixed film/rubber blends with different compositions were extruded at high temperatures (up to 300 °C) to induce the chemical de-structuration of the rubber cross-links and at high processing speed (up to 300 rpm). The blends show fairly good properties provided that low GTR concentration (no more than 25 %) and high processing temperature are adopted. However, some good mechanical performances of the blends must be attributed to a sort of filler-like effect due to the partial carbonization of the rubber phase. This approach for treating cross-linked rubbers was followed by several other authors (Grigoryeva et al. 2005; Sonnier et al. 2007; Mészáros et al. 2012; Montagna and Santana 2012; Gugliemotti et al. 2012; Karger-Kocsis et al. 2013) with good results in terms of morphology and mechanical performance. Polyurethane foams are also cross-linked systems that are difficult to reprocess. Blends of PU foam-backed PVC sheets for soundproof applications were reprocessed to obtain materials to be used as PCV plasticizers or modifiers (Grigoryeva et al. 2005). The process occurs in an extruder, where the PU–PVC grains are de-structured, partially destroying the PU phase and preserving the PVC backbone. Monoethanolamine and potassium acetate at temperature of up to 200 °C were used as destructing agents for PU, while the protection of PVC was ensured by the residual stabilizers contained in it. Similar to the recycling of the cross-linked rubber, it was found that the processing temperature plays a vital role in the compatibility of the two components, with an increment of the PU segments mobility and of their compatibility with PVC segments.

A promising technique to obtain good secondary materials from mixed plastic with modifier-free processes is to change the micromorphology of the blend. HDPE/PET blends where recycled in the presence of a stabilizer aiming to get

a particular new morphology without adding other modifiers or compatibilizers (Jiang et al. 2007). More in detail, PET and HDPE were first processed by extrusion with a top temperature of 270 °C and then they were hot-stretched in the molten state to promote the formation of microfibrillar PET within the HDPE main phase and immediately quenched to freeze this morphology. After this stage, they were further processed to get the final object and in this phase the initially aligned PET fibrils formed a random network losing the orientation but keeping the fibrillar shape. The materials prepared in this way showed higher yield stress and unchanged modulus, while in the conventionally reprocessed material these values are lower. Another study (Yam Kit et al. 1998) investigated the optimization of the processing conditions and particularly on the blending temperature, demonstrating that when it is in the range 235–265 °C, modulus and tensile stress have a maximum, while the impact strength is the lowest. In particular, an interesting correlation between the processing temperature and the domain sizes was found which decrease significantly when the temperature is higher. However, when processing PET/polyolefins blends, the use of a compatibilizer always leads to better properties. Several studies on recycled PET/HDPE blends (Ballauri et al. 1993; Pawlak et al. 2002a, b, 57A; Pluta et al. 2001; Park et al. 1996b) demonstrated, in fact, that compatibilizer such as SEBS-g-MA, HDPE-g-MA, or EGMA up to 10 phr led to a dramatic improvement of the morphology and to an increase of the ductility and of the impact strength. Beyond the compatibility, in some cases, e.g., PP/PET, the necessary high processing temperature for PET and the thermosensitivity of PP may cause a dramatic loss of properties of the secondary materials. Multilayer PP/PET/silicon oxide (SiOx) films used for gas barrier applications were reprocessed with and without PP-g-MA as compatibilizer (Wyser et al. 2000). The recycling operation consisted in two steps: (i) extrusion at moderate temperature (maximum 245 °C in the melting zone) followed by cooling and pelletization and (ii) injection molding with a top temperature of 260 °C. While SiOx particles, even if they changed dimension due to the reprocessing steps, did not affect the mechanical behavior of the recyclates, the effect of compatibilizer was dramatic. The tensile strength as a function of the compatibilizer content is reported in Fig. 20.1. It can be clearly seen that at low compatibilizer amounts the effects are negligible, while at higher contents (5–10 %) the tensile strength sharply increases to values up to ten times those measured for the uncompatibilized blend.

The reason for this behavior may be found in the morphological changes induced by the compatibilizer. At low PP-g-MA content, there is only a decrease of the PET phase domains with respect to the uncompatibilized PP/PET blends, Fig. 20.2a–c. At concentrations of compatibilizer as high as 5–10 %, beyond a further reduction of the PET particle size, the increase of adhesion between the two phases can be observed, Fig. 20.2d, e. This adhesion is supposed to be responsible for the propagation of the cracks through the phases rather than around the particle edges with consequent increase of the ultimate stress. Further increasing the PP-g-MA concentration to 20 % weakens the interface, with the cracks that go again around the particle edges and not across them.

Fig. 20.1 Strength of the recycled PP/PET/SiOx as a function of the compatibilizer content (Taken from Y. Wyser, Y. Leterrier, J.-A.E. Månson, Effect of inclusion and blending on the mechanical performance of recycled multilayer PP/PETSiOx films, J. Appl. Polym. Sci. **78**, 910 (2000); Fig. 6. Copyright © 2000 John Wiley & Sons, Inc. Reproduced with permission)
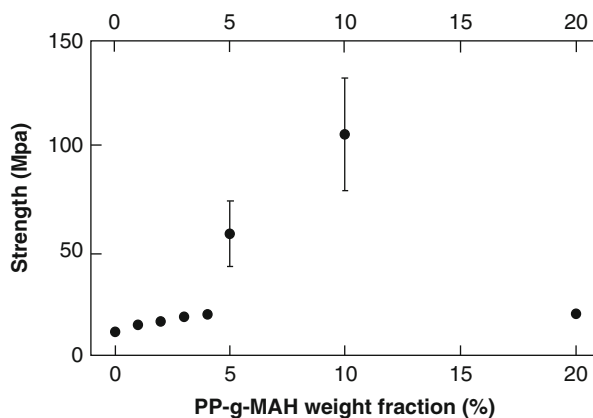
This example makes clear how determinant is the knowledge of the relationships between processing–properties–structure and morphology to control the final performance of the secondary materials. Also PP/PA blends suffer the same thermal incompatibility and need an adequate compatibilizing system that, however, may not be sufficient to grant good properties to the secondary material. In fact, when using PP-g-MA or PP-g-AA copolymers as compatibilizer for that blend, an improvement of the mechanical performance is observed. However, when the blend is reprocessed several times, the degradation effects prevail over compatibilization and a decrease of the ultimate properties occurs (La Mantia and Capizzi 2001). A SEBS-based compatibilizer (SEBS-g-MA) was used for the compatibilization of post-consumer PP/PA blends coming from packaging (Kim et al. 2007). Different from the previous systems, the SEBS rubber contains a reactive functional group (maleic anhydride) that is able to produce, during processing, copolymers with the PA fraction thus enhancing the adhesion between the phases. The morphology was found significantly improved in terms of phase adhesion and dispersion with an increase of impact strength of about three times with respect to the uncompatibilized blend. This effect is correlated with the concurrent improved adhesion to the rubbery state of SEBS-g-MA rather than other maleated compatibilizers (PP-g-MA, PE-g-MA) or neat SEBS, which did not induce significant change of this property.

Reprocessing was found to be effective also in PP/EPDM blends (Lee et al. 2012). In this case, the rubber particles in the PP matrix are progressively smaller with positive influence on the mechanical properties. Moreover, the interfacial tension, estimated by using Palierne and Choi–Schowalter models, was lower in multiple processed materials.

In the same line of recycling plastic waste without the aid of compatibilizers, the family of homogenization and solid-state pulverization processes can be found (Daren 1998; Dubrulle D'Orhcel 1993; La Mantia et al. 1996; Khait et al. 1999; Khait et al. 2001) essentially based on the fractionation of plastic waste into fine particles and formation of cross-polymers induced by shear activated reactions that
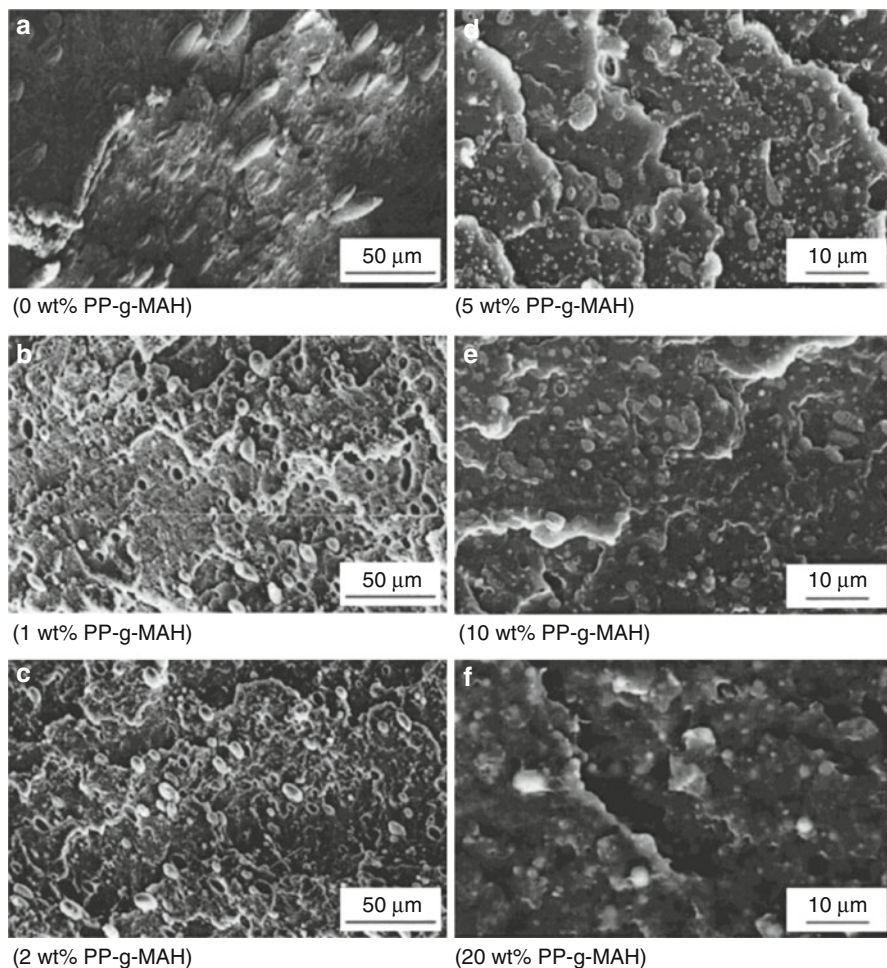
Fig. 20.2 Morphology of the rupture surface of the reprocessed PP/PET/SiOx material at various compatibilizer weight fractions: (**a**) 0 %; (**b**) 1 %; (**c**) 2 %; (**d**) 5 %; (**e**) 10 %; (**f**) 20 % (Taken from Y. Wyser, Y. Leterrier, J.-A.E. Månson, Effect of inclusion and blending on the mechanical performance of recycled multilayer PP/PETSiOx films, J. Appl. Polym. Sci. **78**, 910 (2000); Fig. 7. Copyright © 2000 John Wiley & Sons, Inc.)

create a self-compatibilized blend as output. One of these processes, by Newplast, is based on mechanochemical reactions that break mixed-waste polymer backbones at thermodynamically weak points (S–S, O–O bonds), double bonds, cross-links, and entanglement points. The commingled plastic waste is initially shredded and rid of eventual metal fractions and then fed to the homomicronizer – a steel chamber containing a high-speed mechanical rotor with blades – in which the residence time is about 1 min. The resulting alloy is extruded, filtered, degassed, cooled, and pelletized, ready to be used as secondary material. The recycled material shows an
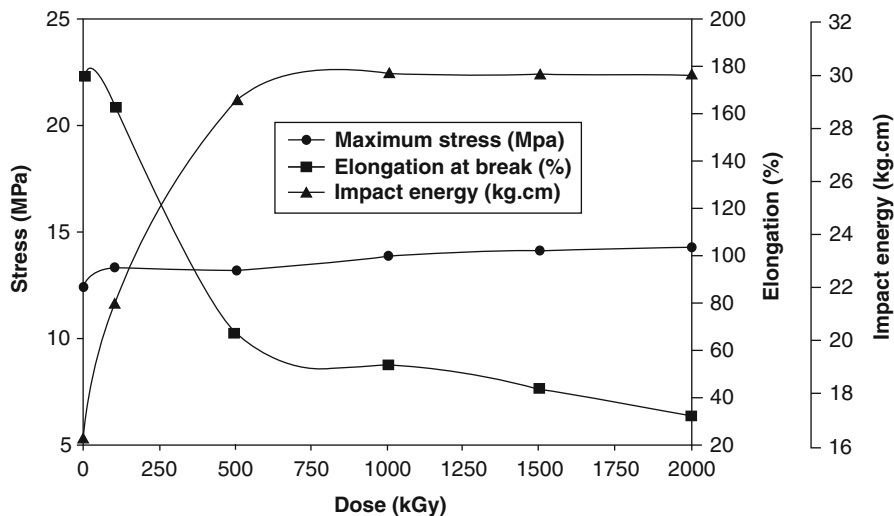
Fig. 20.3 Tensile strength, elongation at break and impact energy as a function of the dose (Reprinted from J.C.M. Suarez, E.B. Mano, Characterization of degradation on gamma-irradiated recycled polyethylene blends by scanning electron microscopy, Polym. Degrad. Stab. **72**, 217 (2001); Fig. 1 with permission of Elsevier. Copyright © 2001 Elsevier)

unprecedented ductility (elongation at break may be 33 % higher than virgin HDPE) and tensile strength together with a fine morphology with small particle dimensions and very high adhesion. Other versions of this kind of technology consider the use of additives to obtain even better performing materials (Mital 1996).

LDPE/HDPE recycled blends, despite the similar chemical structure, show a pronounced incompatibility strongly dependent on which one of the two is the major phase (Laguna et al. 1989), thus needing compatibilizing agents like CPE or EVA to improve the interface adhesion (Laguna et al. 1988). An alternative additive-free method to increase the compatibility between two incompatible phases is the use of gamma irradiation. It was found that increasing the irradiation dose causes a net increase of impact strength, Fig. 20.3, which levels off beyond 1,000 kGy, a moderate increase of the ultimate stress, and a decrease of the elongation at break (Suarez and Mano 2001; Patel and Keller 1975; Aslaniam et al. 1987; Moad and Windzor 1998; Suarez et al. 1999; Suarez and Mano 2000; Suarez et al. 2000a, b). An increment of the mechanical properties was observed in postirradiated GTR/LDPE blends, especially when EVA is added to the system (Mészáros et al. 2012). The mixed plastics were melt processed and then irradiated to obtain the final material that shows mechanical performance generally better than that nonirradiated and even better when high amounts of EVA (up to 30 %) are added.

Another interesting approach to recycling is the upturn of the concept of recycling from downcycling (i.e., a process that yields materials with generically
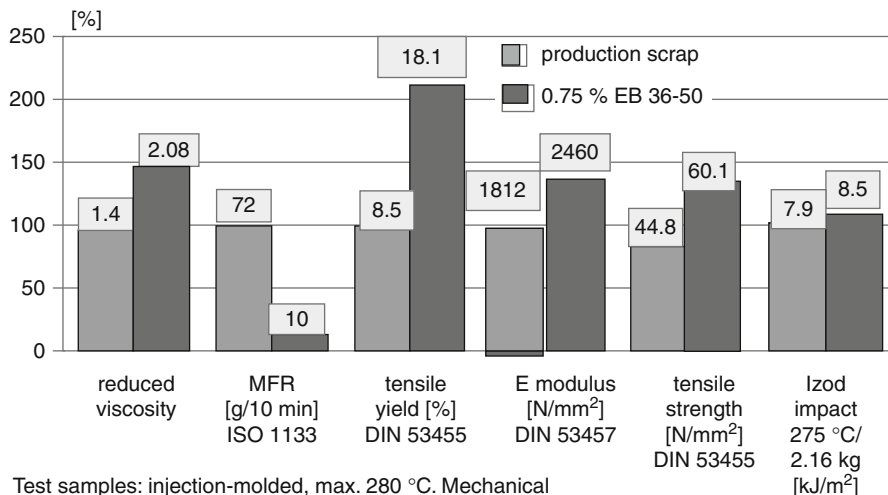
Fig. 20.4 Improvement of molecular and mechanical properties of reclaimed PA66 by using a repairing stabilizer (Taken from R. Pfaendner, H. Herbst, K. Hoffmann, Innovative concept for the upgrading of recyclates by restabilization and repair molecules, Macromol. Symp. **135**, 97 (1998); Fig. 10 with permission of Elsevier. Copyright © 1998 Elsevier)

inferior properties) to upcycling (La Mantia 2004) and the possible totally closed loop of reuse of plastic waste (La Mantia 2010). In this sense, the use of appropriate additives (stabilizers, compatibilizers, impact modifiers, etc.) can be intended as repair and enhancement of the properties rather than limiting their loss. One of the first attempts in this direction was carried out in the late 1990s (Pospisil et al. 1995; Pfaendner et al. 1995; Pfaendner et al. 1996, 1998) with the use of nitroxyl-based stabilizers that acted as repairing agent for chain scission with significant positive effects on several polymeric materials such as HDPE, LDPE, ABS, and PA66 and blends such as PE/PP, PE/PA6, and PBT/PC or composites containing carbon black. In Fig. 20.4 the improvement of some molecular and mechanical properties by using a repairing additive is evident (Pfaendner et al. 1998).

These concepts were taken back later in some studies regarding the rebuilding of post-consumer polyethylene (Scaffaro et al. 2009; Scaffaro et al. 2006; Chaudhary et al. 2007) in which nitroxyl-based compounds were used as radical generator, in conjugation with peroxides or other coupling agents (e.g., EGMA), observing an upgrading of the properties of the reclaimed materials in terms of rupture properties and of impact and tear resistance. The same approach was used in the recycling of post-consumer polyethylene blends coming from pipes (PCP), stabilized with CGX CR946, an hydroxylamine derivative (Scaffaro et al. 2007) prepared in the frame of the studies reported in Pfaendner et al. (1998) as an alternative to classic peroxide compounds. The rebuilding effect is well evident even at the lowest additive concentrations. In Fig. 20.5 (Scaffaro et al. 2006), the viscosity curves are reported
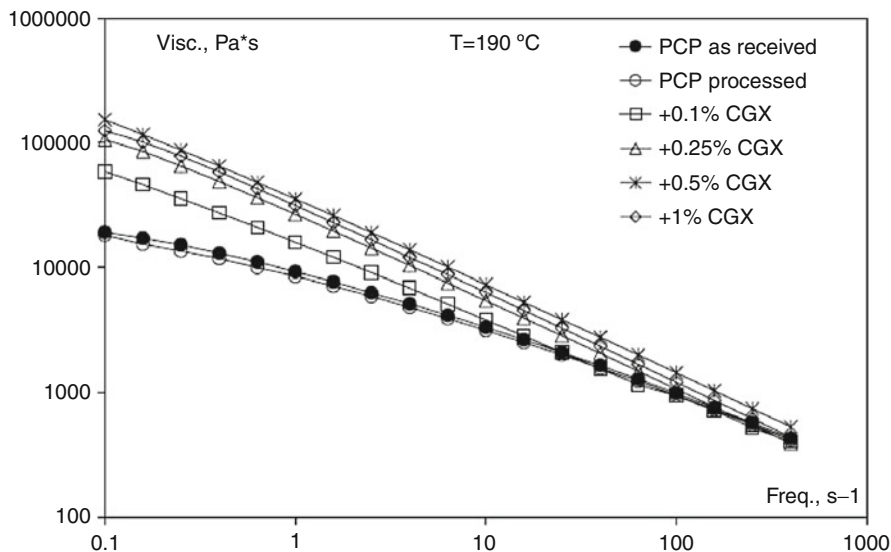
Fig. 20.5 Flow curves of as-received PCP and of PCP with and without CGX processed at 190 °C (Taken from R. Scaffaro, F.P. La Mantia, N. Dintcheva, Effect of the additive level and of the processing temperature on the re-building of post-consumer pipes from polyethylene blends, Europ. Polym. J. **43**, 2947 (2007); Fig. 2 with permission of Elsevier. Copyright © 2007 Elsevier)

as a function of frequency obtained at 190 °C in a parallel plate rheometer. PCP simply reprocessed with no additive shows a viscosity lower than that of as-received PCP due to some thermal degradation during processing. Adding 0.1 % of CGX causes a sharp increase of the melt viscosity, especially in the low-frequency region, and this phenomenon becomes more and more pronounced on increasing the CGX amount added to the blend. This rheological behavior can be explained considering the structural modification of the polyethylene phase in the presence of the nitroxyl compound. In brief, CGX forms nitroxyl radicals that induce the formation and subsequent recombination of free radicals to form branched and cross-linked structures. This structural change causes, of course, a change in the mechanical behavior. At lower additive concentration, the rebuilding causes an increase of the elastic modulus and of the ultimate properties. Above 0.2 % however, the increase of the cross-linked/branched fraction causes a progressive loss of deformability with worsening of the mechanical performance.

20.3.2 With the Formation of Composites

An interesting way to manage mixed plastic waste is to use it as matrix for composite materials. In this way it is possible to reinforce the otherwise poor secondary material with the potential side advantage of reducing the overall environmental impact by using natural fillers or fibers that can also be chemically

treated or added in the presence of a coupling agent to further improve the interaction with the polymeric matrix.

This method led to good results in the recycling of blends of LDPE/LLDPE coming from milk pouches (Choudory et al. 2007). In that case, coir fibers were added to the blend obtaining materials with properties only slightly inferior to those of the respective virgin materials. When pretreating the fibers with maleated styrene, the mechanical properties further improve together with the thermo-oxidative stability. On the other hand, the presence of natural fibers causes a dramatic increase of humidity sensitivity with obvious negative consequences on the mechanical performance.

Another study regarding composites based on natural filler and a mixed polymeric matrix focuses on the effect of reprocessing on the final properties (Lou et al. 2007). In particular, PET and PP have been blended, added with bamboo charcoal, and reprocessed up to three times to obtain extruded or injection molded materials. Injection molded samples showed the best mechanical properties, and the materials added with bamboo charcoal maintained almost the same mechanical properties even after three cycles of processing. For this system, however, the amount of PET plays a vital role in determining the behavior of the final composite as if it is above 20 %, the phase separation between the PP and the PET phase is predominant on the reinforcing action of the filler.

Other interesting results were found by adding cellulose compound to a commingled plastic stream containing HDPE, PP, PS, and PVC (Sik Ha et al. 1999); in this case a maleated rubber (SEBS-g-MA) was found to promote the compatibility between the phases and to enhance the mechanical performance, the thermal stability, and the aging properties. More in detail, adding 20 % of cellulose together with as low as 5 phr of SEBS-g-MA caused a doubling of the tensile strength that maintained approximately the same values even after 6 months aging at 100 °C.

One of the most appealing challenges in plastic recycling is managing complex systems such as Tetra Pak®. This material is a multicomponent layered composite made of paper, aluminum, and LDPE, with the latter two being kept together by a layer of an ethylene–methacrylic acid copolymer (EMAA). The paper part can be easily separated with water while the LDPE–EMAA–Al (PEAL) part must be processed together. Some authors (Lopes et al. 2004, 2006) studied the properties of directly reprocessed PEAL that is used as self-reinforced material as LDPE acts as a matrix, Al as the filler, and EMAA as coupling agent between the two. In another case (Lopes et al. 2006), PEAL was used in conjugation with another waste stream, i.e., PET coming from beverage bottles. The micromorphology of the composites put into evidence a good adhesion between the polymer and the aluminum, and the mechanical properties are consequently good. When PET is added to the system, impact strength and elongation at break decrease, while the elastic modulus is superior to the corresponding PET/LDPE blend from virgin polymers. In this case, the phase discontinuity of aluminum particles promotes crack propagation thus reducing the ultimate and impact

properties and suggesting, for these materials, use that can exalt the presence of the metallic phase such as in applications requiring thermal or electrical conductivity.

20.4   "In Blend" Recycling

20.4.1 With the Same Virgin Polymer (Homopolymer Blends)

The reuse of plastic scraps in the same processing line is a common industrial practice to reemploy materials with high purity otherwise destined for a landfill, with loss of money and negative environmental impact. It is well established, however, that recycled polymers have inferior properties compared with the virgin counterpart, with a magnitude depending on the chemical nature of the polymer, on the processing conditions, and on the number of reprocessing cycles. Of course, such blends must guarantee the same set of properties of the virgin material or, if they are lower, that the properties are still compatible with its final use.

Despite the chemical nature of the two components of the blend being theoretically similar, the processing may significantly change both the structure (e.g., from linear to branched polymer) and the composition (e.g., introduction of unsaturations or oxygenated moieties) that can prevent the formation of a homogeneous material. Moreover, on reprocessing, the recycled material is more sensitive to degradation and it is often necessary to use a stabilizing system that, of course, must be taken into account in the overall cost of the operation. In this direction, small amount of specific inorganic filler can be added to preserve both the material performance and the economic impact (1B, 94B). In some other cases, beyond the stabilizers, even a compatibilizing system must be added to overcome the incompatibility that arises between the virgin and the recycled polymer. When the use of recycled materials needs too expensive additives, the only way to reuse scraps is to decrease their amount in the blend. On the other hand, when the separation from other plastics is relatively easy, the recycling of post-consumer objects in homopolymer blends may have advantageous industrial applications. This is the case, for instance, of polyolefins (PE, PP) widely used for bottles, films, and packaging.

It was found (Sánchez-Soto et al. 2008) that the introduction of moderate (up to 20 wt%) amounts of HDPE from bottles or injection molded parts to virgin HDPE did not cause relevant changes in the mechanical behavior and better results were obtained adding small quantities of talc. In particular, the composites with r-HDPE showed higher deformation and energy absorption in impact tests especially when the provenance was post-consumer bottles. In any case, the results suggest that the conditions of r-HDPE and the reprocessing parameters generate a homogeneous material. Other authors (Ramırez-Vargas et al. 2006) found that homopolymer blends of r-HDPE/HDPE are substantially a single phase material even at high concentration of r-HDPE (70 wt%) even if a progressive drop of ductility is observed. This phenomenon in polyethylenes is common and due to structural changes that can go

from short-/long-chain branching to cross-linking. In this latter case, the recycled polymer tends to be brittle but adding EVA as modifier (3 %) can bring the mechanical properties back to those observed for virgin HDPE. In any case, the use of virgin polyethylene in blend with recycled polyethylene (also mixed) can guarantee mechanical properties comparable with that of the fresh material.

Recycled materials are often associated with scraps or mass consumer end-life appliances, but an important source of secondary materials comes from agricultural applications. Greenhouse covers are made of polyolefins that undergo a slight degradation during processing but a strong photodegradation during their use. It is well known that a photosensitive component in a polymer blend may sensitize the whole material (La Mantia 1986; La Mantia and Curto 1992; La Mantia 1992; Al-Malaika 2002), thus requesting a specific photostabilizing system for the corresponding monopolymer blends (La Mantia and Dintcheva 2004; Herbst et al. 1992; Pospisil et al. 1995; Pfaendner et al. 1995, 1996; Pospisil et al. 1997; Dintcheva et al. 1997; Pfaendner et al. 1998; Herbst et al. 1999; Kartalis et al. 2000a, b, 2001; Papaspyrides et al. 2001; Pfaender 2001). In this case, in fact, the recyclate behaves as a pro-degradant as the oxygenated groups generated by UV irradiation during the lifetime act as chromophore promoting further photodegradation processes. Commonly, a progressive embrittlement of the material and changes in the crystallinity are observed, especially if the new item is thin (below 1 mm) as the degradation rapidly advance from the skin to the core.

Blends of different r-HDPEs coming from post-consumer objects were prepared in order to obtain specific rheological properties and in particular to control the melt flow index (MFI) aiming at the control of the reprocessing operations (Brown et al. 2010). In another case (Miller et al. 2001), an attempt was made to correlate the relative shear viscosity and the relative stiffness of blends of r-PEs coming from different sources/applications. It was found that the difference of viscosity and stiffness are strictly related to factors such as branching content/length and nature of any side unit. With the same aim, morphological measurements with polarized optical microscopy and SEM were used to generate a model that was used to develop both processability windows and optimum blend conversion costs for a given balance of properties (Adewole et al. 1994).

Another plastic typically present in post-consumer waste streams is PET. This material can be advantageously recycled in homopolymer blends by extrusion, injection molding, spinning, or a combination of different processes. It was found (Pattabiraman et al. 2005) that adding r-PET causes a worsening of the mechanical properties, especially at high temperatures, but another study (Aldi 2010) reports that blends prepared by extrusion showed properties very similar to virgin PET after the addition of up to 50 wt% of r-PET. On the contrary, when injection molding is followed by injection molding, the differences are more relevant, likely due to the more intense degradation phenomena.

Beyond the composition of the homopolymer blends, also the processing conditions are essential for determining the behavior of the materials. In this view, it was reported (La Mantia and Scaffaro 1997) that the rheological and mechanical properties of blends of PET and r-PET remained very close to that of the virgin

material provided that a careful drying is carried out before any melt operation. However, even if the homopolymer blends generally showed properties between those of the two components, when the concentration of the two kinds of PET is almost the same, minima in the property–composition plot were observed. In this case, therefore, by a careful drying and the use of small amounts of r-PET, it is possible to obtain materials with properties substantially equal to those of virgin PET without the use of any other additive, with obvious positive impact from the industrial point of view.

Among the engineering plastics, ABS is widely used in electrical and electronic equipment, in the automotive industry, and in telecommunication instruments. Usually, the recycling of these materials causes only slight changes of the mechanical properties unless a high number of reprocessing cycles (more than 10) is applied (Scaffaro et al. 2012; Brennan et al. 2002; Kim and Kang 1995; Boldizar and Moller 2003; Bai et al. 2007; Karahaliou and Tarantili 2009; Arnold et al. 2009; Boronat et al. 2009; Pérez et al. 2010). However, adding r-ABS to virgin ABS causes different outcomes depending on the property, on the number of reprocessings, and on the amount of r-ABS of the blend. The rheological measurements showed that the viscosity of ABS blends was not substantially different by virgin ABS up to two reprocessing steps. Indeed, the third reprocessing cycle induced a slight decrease of the viscosity of all the blends. Up to two reprocessing steps and the presence of r-ABS did not influence significantly the HDT values of the materials. The tensile properties of ABS/r-ABS blends decreased during the first reprocessing, even by adding the smallest amount of r-ABS. Further increase of PC/ABS amount or further reprocessing did not cause significant changes. This was explained as a results of a balance between the opposite degradation effect of chain scission and cross-linking of the PB phase. On the contrary, the flexural properties were almost unaffected by the r-ABS amount and only slightly influenced by the number of recycling operations. The impact resistance significantly decreased both by adding r-ABS and by increasing the number of reprocessing steps. The worsening of this property was correlated with the photodegradation of the PB phase of r-ABS and further thermal degradation during the reprocessing.

Polyamide homopolymer blends were also studied (Scaffaro and La Mantia 2002) by changing humidity of the material and the presence or not of a stabilizer. Neither dry nor wet stabilized polyamide samples showed significant variations of the molecular weight even if the melt Newtonian viscosity is slightly different from that predicted with the rule of mixtures, despite the same chemical nature of the two components. This holds also even more for humid stabilized samples as its noticeably lower molecular weight implies values lower than those expected on a linearity basis. The situation is different for the mechanical properties. The morphology in the solid state determines a more rigid and brittle material, compared to the pure components, with relevant deviations from linearity for all the recycled samples used to prepare the blends. The blends containing dry and wet stabilized recycled PA6 showed almost the same behavior confirming the reduced degradation of these samples.

20.4.2 With Polymers Different from the Recycled One

As already said in the previous section, when the separation of plastics is simple, it could be extremely convenient to prepare homopolymer blends. When this is not possible or is economically disadvantageous, the polymers are recycled together or used as component in blends with virgin polymers different from the recycled one.

Polyolefins represent more than half of the whole polymer production and therefore their recycling attracts the interests of both industry and academia. The simple reprocessing of polyolefin waste leads to products with low mechanical properties because these polymers are frequently incompatible and contaminated by impurities (Mano et al. 1994). These features are evident even in blends between polyethylenes with different chemical structure (e.g., LDPE, LLDPE, HDPE) and can lead to extremely bad quality materials when processing different polyolefins like PE/PP. In this case, beyond the incompatibility of the couple, the strong thermal degradation sensitivity of PP and the higher density with respect to PE causes loss of the mechanical performance. The use of recycled HDPE in blend with PP was found to accelerate the degradation process at concentrations of r-HDPE higher than 20 % (Albano and Sanchez 1999; Albano et al. 1998), and the same threshold was found critical in terms of compatibility of the polymer couple. The incompatibility was demonstrated also by calorimetric tests (Madi 2013); blends of virgin PP and r-HDPE show two distinct peaks in differential scanning calorimetric tests, confirming the essentially biphasic nature of these blends. Moreover, the presence of PE disturbs the formation of PP crystallites thus causing lower crystallinity and worse crystal quality. Of course, the lack of compatibility has direct consequences on the morphology (gross, with evident separated domains of the two components) (Albano and Sanchez 1999) and on the mechanical properties that are far from the theoretical ones of the rule of mixtures (Madi 2013). The situation is better using EPDM, EPM, or PE-g-(2 methyl butadiene) copolymers as compatibilizing agents (Albano and Sanchez 1999; Albano et al. 1998; Bertin and Robin 2002). In this case the properties of the recycled blends are suitable to applications requiring good mechanical performances, but, of course, the costs of the operation are higher. Actually, an attempt was made (Bonelli et al. 2001) to compatibilize the blend with r-PP extracted by floatation. It was found that PP exposed to random/noncontrolled outdoor conditions provided spontaneous non-oxidative chemical modifications that brought a certain compatibilization action to the PE/PP blends.

Another system that attracts the interest of both industry and academia is PET with polyolefins. The two materials are completely different considering the synthesis method, the structure, the polarity, and the degradation behavior. This latter feature is maybe the most important aspect that must be controlled during reprocessing. PET generally undergoes hydrolytic degradation that results in poor mechanical properties, while polyolefins, especially PP, are extremely sensitive to high temperatures thus making complicated the contextual recycling as requested, for instance, for the heavy fraction of urban waste or in the recycling of caps and

bottles. On the other hand, the presence of polyolefins may have positive influence on processing and on the impact behavior of PET.

Some authors (Inoya et al. 2008; Inoya et al. 2012) studied the effect of the compatibilizer level (SEBS) on the mechanical properties of r-PET/PP blends. The addition of up to 15 phr of compatibilizer resulted in a size reduction of the dispersed phase, while a slight increase in density suggested an improvement on interfacial interactions. As expectable, adding the SEBS rubbery compatibilizer caused an increase of ductility and impact resistance. Since 15 phr of compatibilizer is a too high amount in terms of costs, another way is to change the PP molecular weight (Inoya et al. 2012). In this case, lower molecular weight PP helps with the diffusion of the compatibilizer inside the melt and the maximization of its concentration at the interface, allowing the reduction of the compatibilizer amount.

Blends based on r-HDPE and r-PET were prepared by reactive extrusion in the presence of PE-g-MA as compatibilizer, 4,4′-methylene(phenyl isocyanate) (MDI) as PET chain extender, and SEBS as toughening agent were prepared by high shear mixing (5,000 rpm). Only 2 % of PE-g-MA allowed improving the compatibility of the blends toughened with SEBS. In particular, when r-HDPE is the major phase (70 wt%), the maleated additive causes a significant reduction of the domain size (in the range of micron) with a consequent sharp increase of the impact strength. When r-PET is the major phase, the ultimate and the impact strength were improved by adding MDI through the extension of the PET molecular chains. r-HDPE and r-PET influence each other during crystallization and the presence of PE-g-MA or SEBS reduces the crystalline level of either r-PET or r-HDPE. Excess of MDI did not influence crystallization behavior of r-HDPE while reducing that of r-PET. MDI was also found to increase the thermal stability of the r-HDPE-based blend.

r-PET can be also used either with specific additives/modifiers or in conjugation with other engineering polymers (e.g., PA6, PC). r-PET from fabrics was melt blended with PA6 in the presence of LLDPE-g-MA as compatibilizing promoting agent (Jeziórska 2006). The interfacial adhesion was found improved as well as the static and impact mechanical properties: LLDPE-g-MA bridges the polyester and the polyamide forming in situ copolymers r-PET/LLDPE-g-MA/PA6 that locate at the interface acting as compatibilizers. The same modifier (LLDPE-g-MA) was used alone to improve the properties of r-PET also by adopting a low-temperature solid-state extrusion that consists in processing the r-PET above the cold crystallization temperature but slightly below the melting temperature (Zhang et al. 2008). The use of lower processing temperature allows reducing the hydrolytic degradation or r-PET, while the maleated polyethylene improves the ductility with a level-off above 10 wt%. FTIR demonstrated that r-PET and LLDPE-g-MA formed copolymers and SEM confirms that the adhesion between the two phases is excellent. PET/PC blends from post-consumer bottles show mechanical properties that are better than the respective pure component and similar to those of virgin PET (Fraısse et al. 2005). The presence of PC was found to improve the processability of the blend that needs to be extruded to achieve the desired properties. It cannot be excluded that the two recycled polymers react in the melt forming copolymers that are compatibilizers for the blend.

However, the use of maleated copolymers is common to improve the properties of r-PET/rPE blends. In a study, SEBS-g-MA was used to improve the thermal stability and the mechanical properties of r-PET/LLDPE blends (Zhang et al. 2009). In this case, therefore, instead of using distinct compounds – namely, the maleated one and the impact modifier – the functions of compatibilization and impact modification are committed to only one additive. The addition of maleated SEBS (10 wt%) led to the deformation of the dispersed phase from spherical to fibrous structures, with microfibrils formed at the interface between the two phases. The best compatibility was found when 20 wt% of maleated SEBS with positive effects on the elastic modulus and impact strength in agreement with the other studies (Zhang et al. 2008; Jeziórska 2006). SEBS-g-MA was also used as compatibilizer impact modifier for blends of r-PET with different polyethylenes (LLDPE, LDPE, m-PE) to evaluate the influence of the structural differences of the PE phase on the properties of the material (Zhang et al. 2011). In the work, moreover, the effect of the molecular weight of LLDPE was also evaluated. The authors found that the key factor to achieve a good set of properties was the miscibility/interactivity of SEBS-g-MA with the polyethylene phase. More in detail, when using LDPE, the coupling agent locates at the interface between the r-PET phase and the PE phase thus increasing the adhesion with consequent increase of the impact strength. On the contrary, when the miscibility of SEBS-g-MA is too high (m-PE, lower molecular weight LLDPE) or too low (LLDPE with higher molecular weight), the additive is segregated mainly in one phase and its compatibilizing effect is drastically reduced. The compatibilizer caused a reduction of PET crystallinity. Moreover, due to the massive penetration of the compatibilizer into the m-PE phase, its crystal structure is destroyed and no DSC peak is observed.

Similarly, r-PET from food packaging and bottles was melt blended with ethylene–propylene grafted with maleic anhydride (EP-g-MA) at various amounts ranging from 5 to 40 wt% (Alsewailem 2008). The results showed that EP-g-MA is a good impact modifier for r-PET, due to its rubbery status. In particular, adding 40 wt% of modifier allows producing a material tougher than neat virgin PET. Similarly, EGMA was added as reactive component to modify the morphology and the mechanical characteristics of r-PET. Up to 13.5 wt% EGMA content, the impact strength gradually increases while it drastically increases (to ten times of that measured for neat r-PET) for higher concentrations. SEM morphological analysis demonstrated that ductile deformation at the interface produced local fibrils with high energy absorption during the break. The density of the blends, as expected, progressively decreases with increasing the amount of EGMA.

r-PET was also used in combination with PCL (Malinconico et al. 1997; Qi and Nakayama 2000). In a case (Malinconico et al. 1997), the r-PET was first depolymerized and then copolymerized with PCL to form PET–PCL copolymers. Those copolymers were then used as compatibilizers for r-PET/PCL blends and a significant improvement of the morphology was observed. In another case (Qi and Nakayama 2000), r-PET and PCL was blended and hot drawn. Adding 5–10 wt% of PCL allowed achieving the hot drawing at temperature

10 °C lower than those necessary for preparing r-PET sheets. r-PET orientation increases on increasing the draw ratio, while no orientation was observed for PCL. As regards the thermal properties, PCL crystallization was found independent on the draw ratio, while r-PET crystallization was not affected by the presence of PCL.

PC was also used in blends with r-ABS to recover the mechanical performance of the latter up to that of the virgin polymer (Barthes et al. 2012). The authors found that at the highest concentrations of r-ABS, it is necessary to add up to 5 wt% of PP-g-MA as compatibilizer. However, if r-ABS is obtained from formulations containing flame retardants or if the residence time in the melt is too long (e.g., for multiple reprocessing steps), the efficiency of the compatibilizer is sensibly reduced. The use of maleated ABS had positive effects on the properties of r-PC (Elmaghor et al. 2004). In particular, the toughness of the waste was greatly improved, Fig. 20.6, due to the particular morphology developed in the presence of ABS-g-MA and consisting in domains connected together and forming a network that causes the increase of the energy absorbed during the impact.

The r-PC/r-ABS blends may also include PMMA as a third component (Laverty et al. 1996; Rybnicek et al. 2005). In this case, the chemical composition of the styrene–acrylonitrile matrix of ABS was found to have a dramatic effect on the morphology, while lubricant additives of ABS are adverse to the chemical stability. However, all the compositions rich in PMMA exhibited inferior mechanical performance (Laverty et al. 1996). A more detailed mechanical study (Rybnicek et al. 2005) demonstrated that the transition from ductile elastoplastic behavior to brittle linear elastic fracture behavior occurs when the PMMA is above 10 wt%.

Among the engineering plastics, it is worth mentioning the recycling of PPE (Nerkar et al. 2011). Two recyclates with different content of PPE were reprocessed with an injection molding machine. The molecular weight, the T_g, and the viscosity were found to be unaffected even after ten molding cycles and for both compositions of the blends investigated.

Several studies report on the use of styrenic polymers in blends with recycled polymers. PVC, for instance, may undergo severe degradation during reprocessing with rapid worsening of the mechanical performance (Scott 1993). The combination with other polymers may enhance the performance of the secondary materials and allow industrial applications (Robeson 1984; Maiti et al. 1992; Kulshreshtha 1993). SAN and ABS (virgin or recycled) were added to r-PVC exploring the whole composition range (Garcia et al. 2006). Despite the degradation level of r-PVC was not relevant, the incorporation of styrenic polymers causes, as expectable, an improvement of the impact resistance when using ABS, while it is worse if SAN is added; see Fig. 20.7.

Moreover, the virgin styrenic polymers offer a better performance than the recycled ones. The thermal analysis revealed a partial miscibility between r-PVC and the styrenic part. r-PVC was also used in blends with NBR together with glycidyl methacrylate (GMA) as coupling agent (Supri and Yusof 2005). The addition of GMA significantly improved the tensile stress while reducing the elongation at break. This toughening of the compatibilized blend was ascribed to

Fig. 20.6 TEM micrographs of PC and ABS-g-MA of different grafting degrees. Relative degree of grafting: (**a**) zero, (**b**) 1.75, (**c**) 2.75. PC/ABS-g-MA = 1/0.25 wt/wt (Taken from F. Elmaghor, L. Zhang, R. Fan, H.Li, Recycling of polycarbonate by blending with maleic anhydride grafted ABS, Polymer **45**, 6719 (2004); Fig. 2 with permission of Elsevier. Copyright © 2007 Elsevier)
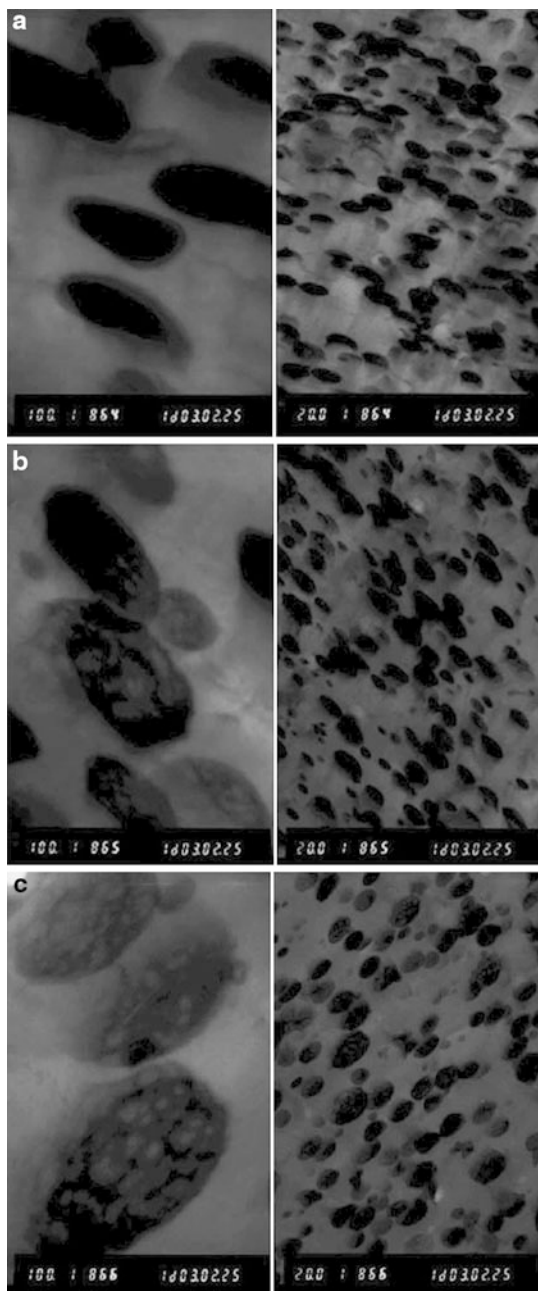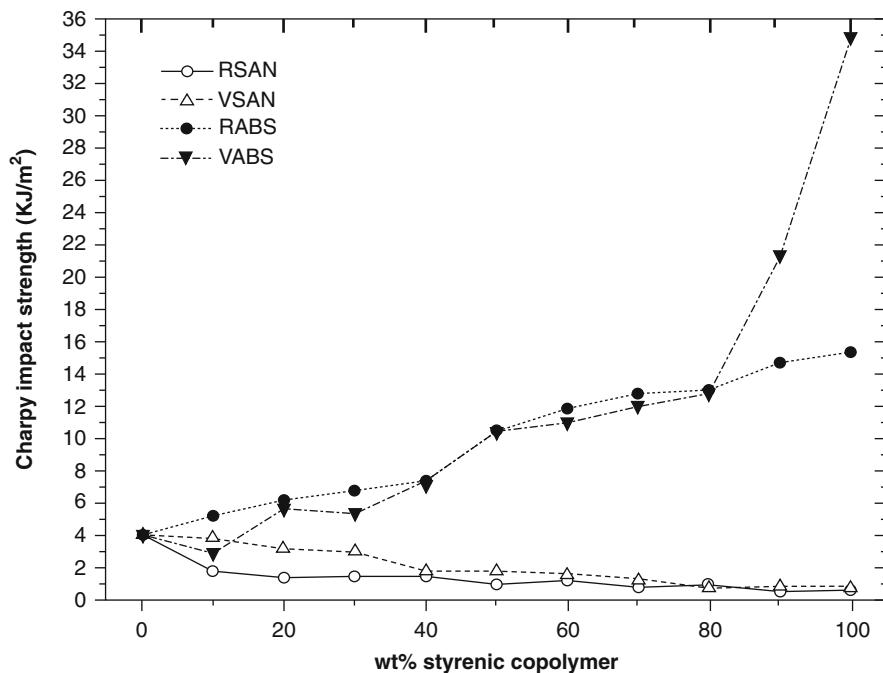
Fig. 20.7 Variation of Charpy impact strength versus styrenic polymers wt% incorporated to r-PVC (Taken from D. Garcia, R. Balart, J.E. Crespo, J. Juan Lopez, Mechanical properties of recycled PVC blends with styrenic polymers, J. Appl. Polym. Sci. **101**, 2464 (2006); Fig. 7. Copyright © 2000 John Wiley & Sons, Inc. Reproduced with permission)

the improved interfacial adhesion as confirmed by SEM analysis. However, GMA was found to decrease the overall thermal stability. Similar results were obtained for the same system using maleic acid to improve the compatibility between the phases (Ghani et al. 2005).

HIPS was added to r-LDPE aiming to the improvement of the mechanical performance. To achieve this goal, HIPS together with an impact modifier system composed by EPDM and styrene–1butadiene (SB) copolymer and with N,N' 1,4-phenylendiamine as stabilizer were added to LDPE coming from outdoor application (i.e., severely photodegraded) (Pospisil et al. 2005). The combination of the tough HIPS phase with the rubbery EPDM/SB phase and with the stabilizer improves the impact strength of the resulting blend.

PS/HDPE blends were prepared by melt processing using both virgin and recycled polymers (Joshi et al. 2006). The morphology of the blends was fine structured with co-continuity regions and average domain dimensions in the micron range. The blends show mechanical properties nearly obeying the rule of mixtures although the behaviors of virgin and recycled materials are quite different. Recycled blends show significant regions of incompatibility but a synergistic zone at around 40 wt% of PS corresponding with the co-continuity of the blends.

The crystallinity of HDPE is reduced in the recycled blend but not in the virgin ones, while the glass transition temperature of PS increases only in the virgin blends. Some modeling of the system was proposed but the full explanation of this behavior is still under study.

r-PS was also added with styrene–butadiene rubber (SBR) (up to 50 wt%) to modify the mechanical properties of the brittle styrenic phase (KGK-Kautschuk und Gummi Kunststoffe 2000). At 20 wt% of SBR, there is a significant increase of the elongation at break and of the impact strength. Conversely, the tensile stress, the hardness, and the T_g of r-PS decreased with increasing the SBR content. The blends showed a pronounced Newtonian behavior and decreased on increasing the SBR level.

Other challenging field in recycling polymer blends is the use of post-consumer ground tire rubber (GTR). Homogeneous dispersion of HDPE/GTR via solid-state mechanochemical milling (Zhang et al. 2012) showed excellent mechanical properties with an enhancement of the tensile strength of 60 % and an increase of the elongation at break of 14 times that of the conventional melt-mixing processed material. This behavior was correlated to the partial devulcanization of the blend as demonstrated by the decrease of the gel fraction.

In another study (Grigoryeva et al. 2008), the polyethylenic phase (either LDPE or HDPE) was pre-functionalized with maleic anhydride. The rubber component, as well, was functionalized with maleic anhydride or acrylamide using chemical methods or gamma-ray irradiation. Additional coupling agents such as p-phenylenediamine or polyamide fibers were used to produce thermoplastic elastomeric materials. As a result, the impact strength and the elongation at break of the resulting materials were drastically improved.

The effect of particles and matrix properties on the shear viscosity of LDPE/GTR blend was also studied by developing a theoretical model to predict the viscosity of the composites as a function of the rheological properties of the matrix, solid concentration, particle size distribution, particle shape, and deformability (Bhattacharya and Sbarski 1998). The real viscosity measurements were found in good agreement with the values predicted below the maximum packing fraction.

As a general conclusion, it is not possible to predict exactly the physical properties of a mixture containing recycled materials. Consequently, when degraded polymers are used, it is a good idea to add only limited amounts to the virgin material to maintain the mechanical properties of the virgin polymer.

20.5   Conclusions

Recycling aims to recover the added value of scraps or post-consumer materials, otherwise irremediably lost. Technically speaking, even the recycling of materials with an initial identical chemical structure should be considered as a blend recycling. Secondary materials can be obtained by blending with the same virgin polymer (homopolymer blends) or by blending with other polymers (virgin or present in the same post-consumer stream), in the presence, or less, of fillers.

Homopolymer blends represent a simple, effective, and cost-efficient way to reuse scraps. Using relatively low amounts (up to 20 wt% or even more for certain polymers) of scraps or post-consumer plastic with the same virgin polymer does not significantly alter the mechanical performance. If higher amount must be added, either a stabilizing system or the concurrent addition of a filler may grant a good set of final properties.

When the scraps or end-use materials are added to a virgin one, the main problems are as follows: the higher thermal sensitivity to reprocessing, the presence of humidity while reprocessing polycondensation polymers, and the incompatibility between the different phases. In this case a stabilizing and/or compatibilizing system is required to obtain materials with properties adequate for the use in new applications.

Of course, these troubles are exalted when recycling commingled plastics. In this case, beyond the problems highlighted above, there is generally no chance to choose the composition, and the presence of small quantities of contaminants can compromise the whole process. To avoid or at least to reduce these phenomena, stabilizers and compatibilizers are not optional.

20.6   Cross-References

▶ Applications of Polymer Blends
▶ Commercial Polymer Blends
▶ Compounding Polymer Blends
▶ Degradation, Stabilization, and Flammability of Polymer Blends
▶ Interphase and Compatibilization by Addition of a Compatibilizer
▶ Morphology of Polymer Blends
▶ Polyethylenes and their Blends
▶ Reactive Compatibilization
▶ Rheology of Polymer Alloys and Blends

Abbreviations

CPE Chlorinated polyethylene
EMAA Ethylene–metacrylic acid copolymer
EPR Ethylene–propylene rubber
GMA Glycidyl methacrylate
HDPE High-density polyethylene
LDPE Low-density polyethylene
LLDPE Linear low-density polyethylene
PA Generically for polyamides
PA6 Polyamide 6
PB Polybutadiene
PB-MA Maleated (liquid) polybutadiene

PC Polycarbonate
PE-g-MA Polyethylene grafted maleic anhydride
PE-g-MB Polyethylene grafted (2-methyl-1,3-butadiene)
PP-g-MA Polypropylene grafted maleic anhydride
PET Polyethyleneterephtalate
PP Polypropylene
PS Polystyrene
PU Polyurethane
PVC Polyvinylchloride
SBR Styrene–butadiene rubber
SEBS Styrene–ethylene–butadiene–styrene rubber
SEBS g-MA styrene–ethylene–butadiene–styrene grafted maleic anhydride rubber
SEP Styrene–ethylene–propylene copolymer

References

A. Adewole, K. Dackson, M. Wolkowicz, Adv. Polym. Techn. **13**, 219 (1994)

C. Albano, G. Sanchez, Polym. Eng. Sci. **39**, 1456 (1999)

C. Albano, G. Sanchez, A. Ismayel, J. Macromol. Sci. Pure Appl. Chem. **35**, 1349 (1998)

R. Aldi, *Society of Plastics Engineers – Global Plastics Environmental Conference*, 2010

S. Al-Malaika, S. Chohan, M. Coker, G. Scott, R. Arnaud, P. Dabin, A. Fauve, J. Lemaire, J. Pure Appl. Chem. **A32**, 709 (1995)

F.D. Alsewailem, Technical papers, regional technical conference. Soc. Plast. Eng. **2**, 659 (2008)

G.D. Andrews, P.M. Subramanian, Emerging technologies, in *Plastics Recycling*. ACS Symposium Series (Washington, DC, 1992)

J.C. Arnold, S. Alston, A. Holder, Polym. Degrad. Stab. **94**, 693 (2009)

V.M. Aslaniam, V.I. Vardanian, M.H. Avetisian, S.S. Felekian, S.R. Ayvasyan, Polymer **28**, 755 (1987)

X. Bai, D.H. Isaac, K. Smith, Polym. Eng. Sci. **47**, 120 (2007)

B. Ballauri, M. Trabuio, F.P. La Mantia, Compatibilization of recycled polyethyleneterephthalate/polypropylene blends using a functionalized rubber, in *Recycling of PVC and Mixed Plastics*, ed. by F.P. La Mantia (Chemtec Publishing, Toronto, 1993)

M.-L. Barthes, O. Mantaux, M. Pedros, E. Lacoste, M. Dumon, Adv. Polym. Technol. **31**, 343 (2012)

S. Bertin, J.J. Robin, Europ. Polym. J. **38**, 2255 (2002)

S.N. Bhattacharya, I. Sbarski, Plast. Rubber Compos. **27**, 317 (1998)

A. Boldizar, K. Moller, Polym. Degrad. Stab. **81**, 359 (2003)

C.M.C. Bonelli, A.F. Martins, E.B. Mano, C.L. Beatty, J. Appl. Polym. Sci. **80**, 1305 (2001)

T. Boronat, V.J. Segui, M.A. Peydro, M.J. Reig, J. Mater. Process. Technol. **209**, 2735 (2009)

J. Brandrup, M. Bittner, W. Michaeli, G. Menges, *Recycling and Recovery of Plastics* (Hanser, Munchen, 1995)

L.B. Brennan, D.H. Isaac, J.C. Arnold, J. Appl. Polym. Sci. **86**, 572 (2002)

G. Brown, G. Mcnally, J. Grabowska, P. Beaney, S. Cherry, ANTEC, Conf. Proc. **1**, 30 (2010)

B.I. Chaudhary, L. Chopin, J. Klier, Polym. Eng. Sci. **47**, 50 (2007)

R. Choudhury, S. Kumar, B. Adhikari, J. Appl. Polym. Sci. **106**, 775 (2007)

KGK-Kautschuk und Gummi Kunststoffe, **53**, 273 (2000)

I.H. Craig, J.R. White, J. Mater. Sci. **41**, 993 (2006)

S. Daren, Polimery **43**, 379 (1998)

N.T. Dintcheva, N. Jilov, F.P. La Mantia, Polym. Degrad. Stab. **57**, 191 (1997)

B. Dubrulle D'Orhcel, A new process for recycling of mixed plastics waste, in *Recycling of PVC and Mixed Plastics*, ed. by F.P. La Mantia (Chemtec Publishing, Toronto, 1993)

F. Elmaghor, L. Zhang, R. Fan, H. Li, Polymer **45**, 6719 (2004)

N. Equiza, W. Yave, R. Quijada, M. Yazdani-Pedram, Macromol. Mater. Eng. **292**, 1001 (2007)

I. Fortelny, Z. Krulis, D. Michalkova, Die Angew. Makromol. Chem. **238**, 97 (1996)

I. Fortelny, Z. Krulis, D. Michalkova, Polimery **47**, 534 (2002)

F. Fraısse, V. Verney, S. Commereuc, M. Obadal, Polym. Degrad. Stab. **90**, 250 (2005)

D. Garcia, R. Balart, J.E. Crespo, J. Lopez, J. Appl. Polym. Sci. **101**, 2464 (2006)

S.A. Ghani, H. Ismail, A.M.M. Yusof, Progr. Rubber Plast. Re. **21**, 85 (2005)

O. Grigoryeva, A. Fainleib, O. Starostenko, A. Tolstov, W. Brostow, Polym. Int. **53**, 1693 (2004)

O. Grigoryeva, A. Fainleib, L. Stepanenko, L. Sergeeva, P. Pissis, Polym. Eng. Sci. **45**, 801 (2005)

O. Grigoryeva, A. Fainleib, J.B. Grenet, J.M.B. Saiter, Rubber Chem. Technol. **81**, 737 (2008)

A. Gugliemotti, C. Lucignano, F. Quadrini, Plast. Rubber Compos. **41**, 40 (2012)

C.S. Sik Ha, H.D. Park, W.J. Cho, J. Appl. Polym. Sci. **74**, 1531 (1999)

C.-S. Ha, H.-D. Park, W.-J. Cho, Polym. Recycl. **5**, 1 (2000)

H. Herbst, R. Pfaendner, Polym. Recycl. **4**, 75 (1999)

H. Herbst, K. Hoffmann, R. Pfaendner, F. Sitek, Kunstst. Ger. Plast. **82**, 783 (1992)

P.S. Hope, J.G. Bonner, A.F. Miles, Plast. Rubber Compos. Proc. Appl. **22**, 147 (1994)

H. Inoya, W.B. Klinklai, Y.W.C. Leong, H.C. Hamada, Technical papers, regional technical conference. Soc. Plast. Eng. **3**, 1815 (2008)

H. Inoya, Y.W.C. Leong, W.B. Klinklai, S. Thumsorn, Y. Makata, H. Hamada, J. Appl. Polym. Sci. **124**, 3947 (2012)

R. Jeziórska, Pigm. Resin Technol. **35**, 3 (2006)

C. Jiang, G.J. Zhong, Z.M. Li, Macromol. Mater. Eng. **292**, 362 (2007)

Y. Joshi, R. Lehman, T. Nosker, J. Appl. Polym. Sci. **99**, 2044 (2006)

E.-K. Karahaliou, P.A. Tarantili, Polym. Eng. Sci. **49**, 2269 (2009)

J. Karger-Kocsis, L. Mészáros, T. Bárány, J. Mater. Sci. **48**, 1 (2013)

C.N. Kartalis, C.D. Papaspyrides, R. Pfaendner, Polym. Degrad. Stab. **70**, 189 (2000a)

C.N. Kartalis, C.D. Papaspyrides, R. Pfaendner, K. Hoffman, H. Herbst, J. Appl. Polym. Sci. **77**, 1118 (2000b)

C.N. Kartalis, C.D. Papaspyrides, R. Pfaendner, K. Hoffman, H. Herbst, Polym. Eng. Sci. **41**, 771 (2001)

K. Khait, J.M. Thorkelson, Polym. Plast. Technol. Eng. **38**, 445 (1999)

K. Khait, S.H. Carr, H. Martin, M.H. Mack, *Solid-State Shear Pulverization* (Technomic, Lancaster, 2001)

J.K. Kim, C.K. Kang, Polym. Plast. Technol. Eng. **34**, 875 (1995)

G.H. Kim, S.S. Hwang, B.G. Cho, S.M. Hong, Macromol. Symp. **249–250**, 485 (2007)

A.K. Kulshreshtha, Polym. Plast. Technol. Eng. **32**, 551 (1993)

F.P. La Mantia, Polym. Degrad. Stab. **14**, 241 (1986)

F.P. La Mantia, Degradation of polymer blends, in *Handbook of Polymer Degradation*, ed. by S. Halim Hamid, M.B. Amin, A.G. Maadhah (Marcel Dekker, New York, 1992a)

F.P. La Mantia, Polym. Degrad. Stab. **37**, 145 (1992b)

F.P. La Mantia, Polym. Degrad. Stab. **42**, 213 (1993a)

F.P. La Mantia, Basic concepts on the recycling of homogeneous and heterogeneous plastics, in *Recycling of PVC and Mixed Plastics* (Chemtec Publishing, Toronto, 1993b)

F.P. La Mantia (ed.), *Hanbook of Plstics Recycling* (RAPRA, Shrewbury, 2002)

F.P. La Mantia (ed.), *Recycling of Plastics Materials* (Chemtec Publishing, Toronto, 1995)

F.P. La Mantia, Polym. Recycl. **20**, 11 (2004)

F.P. La Mantia, Polym. Degrad. Stab. **95**, 285 (2010)

F.P. La Mantia, L. Capizzi, Polym. Degrad. Stab. **71**, 285 (2001)

F.P. La Mantia, D. Curto, Polym. Degrad. Stab. **36**, 131 (1992)

F.P. La Mantia, N.T. Dintcheva, J. Appl. Polym. Sci. **91**, 2244 (2004)

F.P. La Mantia, N.T. Dintcheva, Macromol. Rapid Commun. **26**, 361 (2005a)

F.P. La Mantia, N.T. Dintcheva, Macromol. Mat. Eng. **290**, 970 (2005b)

F.P. La Mantia, R. Scaffaro, Polym. Recycl. **3**, 209 (1997)

F.P. La Mantia, M. Marrone, B. Dubrulle D'Orhcel, Polym. Recycl. **2**, 3 (1996)

O. Laguna Castellanos, E.P. Collar, Resour. Conserv. Rec. **2**, 37 (1988)

O. Laguna, E.P. Collar, J. Taranco, J. Appl. Polym. Sci. **38**, 667 (1989)

J.J. Laverty, R.L. Bullach, T.S. Ellis, T.E. Mcminn, Polym. Recycl. **2**, 159 (1996)

Y.K. Lee, H.K. Lee, T.W. Yoo, H.G. Yoon, W.N. Kim, J. Appl. Polym. Sci. **127**, 1416 (2012)

X. Liu, H. Bertilsson, Polym. Recycl. **3**, 107 (1997)

X. Liu, H. Bertilsson, *Doktorsavhandlingar* (Chalmers Tekniska, Hogskola, 2000)

X. Liu, A. Boldizar, M. Rigdahl, H. Bertilsson, J. Appl. Polym. Sci. **86**, 2535 (2002)

C.M.A. Lopes, M.I. Felisberti, Polym. Test. **23**, 637 (2004)

C.M.A. Lopes, M.I. Felisberti, J. Appl. Polym. Sci. **101**, 3183 (2006)

C.M.A. Lopes, M.C. Goncalves, M.I. Felisberti, J. Appl. Polym. Sci. **106**, 2524 (2007)

C.-W. Lou, C.-W. Lin, C,-W, C.-H. Lei, K.-U. Su, K,-U, Suh, Z.-H. Liu, Z.-H. Lin, J. Mater. Process. Technol. **428**, 192–193 (2007)

N.K. Madi, Mater. Des. **46**, 435–441 (2013)

S.N. Maiti, U.K. Saroop, A. Misra, Polym. Eng. Sci. **32**, 27 (1992)

M. Malinconico, M.G. Volpe, F. Pota, Polym. Recycl. **3**, 281 (1997)

E.B. Mano, C.M.C. Bonelli, M.A. Guadagnini, S.J. Moyses-Luiz, Polim Ciéncia Tecnol **4,** 19 (1994)

J.C. Martinez, R. Benavides, C. Guerrero, J. Appl. Polym. Sci. **108**, 2597 (2008)

L. Mészáros, M. Fejos, T. Bárány, J. Appl. Polym. Sci. **125**, 512 (2012)

P. Miller, I. Sbarski, E. Kosior, S. Masood, P. Iovenitti, J. Appl. Polym. Sci. **82**, 3505 (2001)

V. Mital, Polym. Recycl. **2**, 173 (1996)

C.L Moad, D.J. Windzor, Prog. Polym. Sci. **23**, 759 (1998)

L.S. Montagna, R.M.C. Santana, Plast. Rubber Compos. **41**, 256 (2012)

T. Nedkov, F. Lednicky, M. Mihailova, J. Appl. Polym. Sci. **109**, 226 (2008)

M. Nerkar, S. Bandyopahyay, R. Kamalakaran, S. Gupta, H. Guo, J. Appl. Polym. Sci. **120**, 2921 (2011)

T.J. Nosker, R.W. Renfree, D.R. Morrow, Plast. Eng. **33**, 90 (1990)

C.D. Papaspyrides, C.N. Kartalis, R. Pfaendner, Polym. Recycl. **6**, 1 (2001)

H.D. Park, K.P. Park, W.J. Cho, C.S. Ha, S.K. Kwon, Polym. Recycl. **2**, 277 (1996a)

H.D. Park, K.P. Park, W.J. Cho, H. Chang-Sik, K. Soon-Ki, Polym. Recycl. **2**, 283 (1996b)

G.N. Patel, A. Keller, J. Polym. Sci. Phys. Ed. **13**, 303 (1975)

P. Pattabiraman, I. Sbarski, T. Spurling, E. Kosior, ANTEC, Conf. Proc. **8**, 301 (2005)

D.R. Paul, C.E. Vison, C.E. Locke, Polym. Eng. Sci. **12**, 157 (1972)

D.R. Paul, C.E. Locke, C.E. Vinson, Polym. Eng. Sci. **13**, 202 (1973a)

D.R. Paul, C.E. Vison, C.E. Locke, Polym. Eng. Sci. **13**, 308 (1973b)

A. Pawlak, J. Morawiec, F. Pazzagli, M. Pracella, A. Galeski, J. Appl. Polym. Sci. **86**, 1473 (2002a)

A. Pawlak, J. Morawiec, A. Galeski, Polimery **47**, 491 (2002b)

J.M. Pérez, J.L. Vilas, J.M. Laza, S. Arnáiz, F. Mijangos, E. Bilbao, M. Rodriguez, L.M. Leon, J. Polym. Environ. **18**, 71 (2010)

R. Pfaender, in *Plastics Additives Handbook*, ed. by H. Zweifel, 5th edn. (Hanser, Munich, 2001). Chap.19

R. Pfaendner, H. Herbst, K. Hoffmann, F. Sitek, Angew. Makromol. Chem. **232**, 193 (1995)

R. Pfaendner, H. Herbst, K. Hoffmann, Eng. Plast. **9**, 249 (1996)

R. Pfaendner, H. Herbst, K. Hoffmann, Macromol. Symp. **135**, 97 (1998)

M. Pluta, Z. Barczak, A. Pawlak, A. Galeski, M. Pracella, J. Appl. Polym. Sci. **82**, 1423 (2001)

J. Pospisil, F. Sitek, R. Pfaendner, Polym. Degrad. Stab. **48**, 351 (1995)

J. Pospisil, S. Nespurek, R. Pfaendner, H. Zweifel, Trends Polym. Sci. **5**, 294 (1997)

J. Pospisil, I. Fortelny, D. Michalkova, Z. Krulis, M. Slouf, Polym. Degrad. Stab. **90**, 244 (2005)

K. Qi, K. Nakayama, Polym. Polym. Compos. **8**, 187 (2000)

E. Ramırez-Vargas, Z. Sandoval-Arellano, J.S. Hernández-Valdez, J.G. Martınez-Colunga, S. Sánchez-Valdés, J. Appl. Polym. Sci. **100**, 3696 (2006)

M.J. Reig, V.J. Segui, S. Ferrandiz, J.D. Zamanillo, J. Polym. Eng. **27**, 29 (2007)

L.M. Robeson, Polym. Eng. Sci. **24**, 587 (1984)

J. Rybnicek, J. Steidl, Z. Krulis, R. Lach, W. Grellmann, *Global Plastics Environmental Conference 2005: GPEC 2005 – Creating Sustainability for the Environment*, 2005, p. 157

E.M.S. Sanchez, Polym. Test. **26**, 378 (2007)

M. Sánchez-Soto, A. Rossa, A.J. Sánchez, J. Gámez-Pérez, Waste Manag. **28**, 2565 (2008)

A.S.F. Santos, R.C. Santana, J.A.M. Agnelli, S. Manrich, Polym. Recycl. **6**, 57 (2001)

R. Scaffaro, L. Botta, G. Di Benedetto, Europ. Polym. J. **48**, 637 (2012)

R. Scaffaro, F.P. La Mantia, Polym. Eng. Sci. **42**, 2412 (2002)

R. Scaffaro, F.P. La Mantia, L. Botta, M. Morreale, N. Tz. Dintcheva, P. Mariani Polym. Eng. Sci **49**, 1316 (2009)

R. Scaffaro, N.T. Dintcheva, M.A. Nocilla, F.P. La Mantia, Polym. Degrad. Stab. **90**, 281 (2005)

R. Scaffaro, F.P. La Mantia, N.T. Dintcheva, Polym. Degrad. Stab. **91**, 3110 (2006)

R. Scaffaro, F.P. La Mantia, N.Tz. Dintcheva Eur. Polym. J. **43**, 2947 (2007)

J. Scheirs, *Polymer Recycling* (Wiley, New York, 1998)

G. Scott, Recycling of PVC: effect of the processing operations, in *Recycling of PVC and Mixed Plastics*, ed. by F.P. La Mantia (Chemtec Publishing, Toronto, 1993)

R. Sonnier, E. Leroy, L. Clerc, A. Bergeret, J.M. Lopez-Cuesta, Polym Testing, **26**, 274 (2007)

J.C.M. Suarez, E.B. Mano, Polym. Test. **19**, 607 (2000)

J.C.M. Suarez, E.B. Mano, Polym. Degrad. Stab. **72**, 217 (2001)

J.C.M. Suarez, E.B. Mano, C.M.C. Bonelli, Polym. Eng. Sci. **39**, 398 (1999)

J.C.M. Suarez, E.B. Mano, R.A. Pereira, Polym. Degrad. Stab. **69**, 217 (2000a)

J.C.M. Suarez, E.B. Mano, M.I.B. Tavares, J. Appl. Polym. Sci. **78**, 899 (2000b)

I.H. Supri, A.M.M. Yusof, Iran. Polym. J. Engl. Ed. **14**, 565 (2005)

Y. Wyser, Y. Leterrier, J.-A.E. Mânson, J. Appl. Polym. Sci. **78**, 910 (2000)

M. Xanthos, A. Patel, S. Dey, S.S. Dagli, C. Jacos, T.J. Nosker, R.W. Renfree, Adv. Polym. Technol. **13**, 231 (1994)

M. Xanthos, J. Grenci, S.H. Patel, A. Patel, C. Jacos, S. Dey, S.S. Dagli, Polym. Compos. **16**, 204 (1995)

L. Yam Kit, K.L. Nichols, S.E. Selke, Technical papers, regional technical conference – Soc. Plast. Eng. **77** (1998)

H. Zhang, Y. Zhang, W. Guo, D. Xu, C. Wu, J. Appl. Polym. Sci. **109**, 3546 (2008)

Y. Zhang, H. Zhang, Y. Yu, W. Guo, C. Wu, J. Appl. Polym. Sci. **114**, 1187 (2009)

H. Zhang, Y. Zhang, W. Guo, C. Wu, Polym. Adv. Technol. **22**, 1851 (2011)

X.A. Zhang, C.B. Chen, C.A. Lu, Progr. Rubber Plast. Restor. **28**, 81 (2012)

Miscible Polymer Blends

21

Suat Hong Goh

Contents

Abstract

Miscible polymer blends were once considered a rarity. However, extensive research has led to the discovery of a large number of miscible polymer blends. This Chapter is a compilation of miscible polymer blends reported in literature up to 2012.

21.1   Introductory Remarks

Miscible polymer blends were once considered a rarity. Flory (1953) wrote the following statement in his book *Principles of Polymer Chemistry*:

> It is permissible to state as a principle of broad generality that two high polymers are mutually compatible with one another only if their free energy of interaction is favorable, i.e., negative. Since the mixing of a pair of polymers, like the mixing of simple liquids, in the great majority of cases is endothermic, incompatibility of chemically dissimilar polymer is observed to be the rule and compatibility is the exception.

S.H. Goh
Department of Chemistry, National University of Singapore, Singapore, Singapore
e-mail: chmgohsh@nus.edu.sg

Indeed, in the early 1970s, only a dozen of miscible polymer blends were known to exist (Krause 1972). However, extensive research has led to the discovery of a large number of miscible polymer blends. By 1995, some 1,320 pairs of miscible polymer blends had been reported (Krause and Goh 2002).

What gives rise to miscibility between two chemically dissimilar polymers? Since the entropy gain upon mixing two polymers is negligibly small, a negative Gibbs energy of mixing requires a negative heat of mixing. Therefore, the formation of a miscible polymer blend requires attractive specific interactions (hydrogen bonding, dipole-dipole, ion-dipole, and charge transfer) between the two constituent polymers. Various spectroscopic techniques such as Fourier transform infrared spectroscopy (Coleman and Painter 1995; He et al. 2004a), nuclear magnetic resonance spectroscopy (Takegoshi 1995), and X-ray photo-electron spectroscopy (Chan and Weng 2000) have shown the existence of interpolymer interactions in miscible polymer blends. When polymer-polymer interaction is stronger than polymer-solvent interaction, the two polymers form interpolymer complexes (or simply complexes) by coprecipitating from their common solvent, in which both polymers are initially soluble. It has been commonly observed that through the introduction of increasing amounts of suitable functional groups to polymer chains, an immiscible polymer blend system can be transformed to a miscible polymer blend system and eventually leads to the formation of complexes (Jiang et al. 1999). For a blend containing one or more copolymers, intramolecular interactions between two different types of segments in a copolymer are also important in determining the miscibility (Kambour et al. 1983; Ten Brinke et al. 1983; Paul and Barlow 1984).

The miscibility of polymer blends is dependent on temperature. There are a large number of miscible polymer blends which undergo phase separation upon heating, showing lower critical solution temperature (LCST) behavior. On the other hand, some immiscible polymer blends at room temperature become miscible upon heating, showing upper critical solution temperature (UCST) behavior. There are also examples of polymer blends showing both LCST and UCST behaviors. While solution casting method is widely used to prepare polymer blends, it should be noted that the choice of solvent can affect the miscibility of the blends. A well-known example is the polystyrene/poly(vinyl methyl ether) system (Bank et al. 1971). Blends cast from toluene or benzene are miscible, but those cast from chloroform or trichloroethane are immiscible. Similarly, the formation of interpolymer complexes is also dependent on the choice of solvent. For example, poly(methacrylic acid) forms complexes with poly (4-vinylpyridine) in ethanol/water (1:1) solution but not in dimethylformamide (Yi and Goh 2001).

21.1.1 Determination of Miscibility

The miscibility of a polymer blend is usually ascertained by studying the optical, morphological, and glass transition behavior of the blend. When two amorphous polymers with different refractive indices mix intimately to form a miscible blend, the refractive index of the blend is uniform, and the blend appears transparent. On the other hand, when the two polymers do not mix intimately, the resulting blend is opaque. It must be cautioned that a two-phase immiscible blend may appear transparent if the refractive indices of the two polymers are closely matched or the domain size is smaller than the wavelength of the visible light. For a blend containing a crystallizable polymer, the blend may appear opaque even when the amorphous phases of the two polymers mix intimately.

The most commonly used method to determine miscibility is the measurements of glass transition temperatures (T_g's) by thermoanalytical techniques such as differential scanning calorimetry and dynamic mechanical thermal analysis. The existence of a single composition-dependent T_g indicates intimate mixing of the two polymers on a scale of about 10–30 nm. The appearance of two T_g's indicates a two-phase immiscible blend. For a blend of two polymers with sufficiently close T_g values (difference less than 10–15 °C), it is often difficult to ascertain whether the observed single glass transition is really one glass transition or two overlapping glass transitions. In this type of situation, examination of the enthalpy recovery behavior of the blend after annealing offers a way to determine miscibility (Ten Brinke et al. 1994). A more stringent criterion for miscibility is based on nuclear magnetic resonance spectroscopy (Takegoshi 1995). If two polymer chains in a blend mix intimately, spin diffusion occurs quickly among the chemically different components, and so single values of spin-lattice relaxation times in the laboratory frame, $T_1(H)$, and in the rotating frame, $T_{1\rho}(H)$, are obtained. A single $T_{1\rho}(H)$ value indicates mixing to a scale of about 1–3 nm, whereas a single $T_1(H)$ value mixing to a scale of about 20–30 nm.

For a blend containing a crystallizable polymer, the melting point depression of the crystalline polymer by the amorphous polymer can be used to evaluate polymer-polymer interaction parameter using the Nishi-Wang equation (Nishi and Wang 1975).

21.1.2 Arrangement of Tables

Lists of miscible polymer blends were previously prepared by Krause (1972, 1978, 1989) and Krause and Goh (1999, 2002). The list appeared in the first edition of this handbook covered literature up to 1995. The present compilation extends the coverage to 2012.

The eight tables in the present compilation adopt the same format as that in the first edition of the handbook. The column labeled Polymer I of is an alphabetical listing. The column labeled Polymer II of is an alphabetical listing of polymers miscible with the appropriate polymer from the first column. Because of space constraint, each table contains a particular polymer mixture only once. Readers are advised to look for the names of both polymers for a particular blend system.

The column labeled Methods briefly lists the method(s) used by the researchers in their works. The Comments column mainly lists the compositions of copolymers and other relevant information. For a polymer blend system reported by a number of research groups, comments on selected works are listed.

The eight tables are the following:

1. Chemically dissimilar polymer pairs miscible in the amorphous state at room temperature. Some of these polymers may be copolymers, but the polymer pairs may not have any monomer units in common. One or both of the polymers may be semicrystalline.
2. Polymer pairs containing one monomer in common (at least one of these must be a copolymer), miscible in the amorphous state at room temperature. One or both of the polymers may be semicrystalline.
3. Chemically dissimilar polymer triads and tetrads miscible in the amorphous state at room temperature.
4. Polymer pairs miscible in the amorphous state at room temperature. Molecular weight dependence investigated. These are usually polymer pairs that are miscible when the molecular weights are low and immiscible as when the molecular weights are increased.
5. Polymer pairs that appear to have high temperature miscibility although immiscible at or below room temperature (upper critical solution temperature [UCST] behavior).
6. Polymer pairs miscible at room temperature that appear to have a lower critical solution temperature (LCST) above room temperature. These polymer pairs are also listed in one of the earlier Tables, usually Table 21.1 or 21.2.
7. Polymer pairs that appear to have both lower and upper critical solution temperatures.
8. Polymer pairs that co-crystallize and form mixed crystals. These blends are generally composed of polymers with similar subunits that can substitute for each other in the same unit cells; this is generally called "isomorphous replacement." This table is probably incomplete even though co-crystallization is expected to be rare.

Table 21.1 Chemically dissimilar polymer pairs miscible in the amorphous state at room temperature

Polymer I of	Polymer II of	Method	Comments	Refs.
Acetoxystyrene	γ-Benzyl-L-glutamate	Single T_g; FTIR; NMR; WAXD	–	Kuo and Chen (2012)
	Novolac	Single T_g; FTIR; NMR	–	Kuo and Chang (2002b)
Acetoxystyrene-co-styrene	Novolac	Single T_g; FTIR	II had >45 mol% acetoxystyrene	Kuo and Chang (2001e)
2-Acrylamido-2-methylpropane sulfonic acid	Hexafluoropropylene-co-vinylidene fluoride	Single T_g; TEM	II had 10 wt% hexafluoropropylene	Gibon et al. (2008)
	Vinylpyridine	Single T_g	II was 2- or 4-vinylpyridine; formed complexes	Huglin and Rego (1990)
Acrylic acid	Acrylamide	FTIR; NMR	Formed complexes	Garces et al. (1994), Moharram et al. (1996)
	Acrylamide-co-N,N-dimethylacrylamide	Fluorescence study	Formed complexes; II had 6.0–55 mol% acrylamide	Wang and Morawetz (1989)
	Caprolactam	Single T_g; WAXD	Semicrystalline	Nishio et al. (1993)
	Dextran	Single T_g; transparency; SEM	–	Cascone et al. (1997)
	N,N-Dimethylacrylamide	Fluorescence study	Formed complexes; II had 6.0–55 mol% acrylamide	Wang and Morawetz (1989)
	Ethylene glycol	Single T_g; FTIR; clear films; NMR	Semicrystalline when >50 % II	Chu and Berner (1993), Jeon and Ree (1988), Lu and Weiss (1995), Maunu et al. (1993), Miyoshi et al. (1997), Smith et al. (1959)
	Hydroxypropylcellulose	Single T_g; SEM	Miscible when blends were prepared by coprecipitation	Khutoryansky et al. (2004)
	Vinyl alcohol	FTIR; T_m-depression; SEM	Semicrystalline	Diniluc et al. (1992), Herrera-Kao and Agular-Vega (1999), Nurkeeva et al. (2005), Vazquez-Torres et al. (1993)
	Vinylmethylether	Single T_g; FTIR; NMR	Formed 1:1 complexes	Cowie et al. (1989b)
	N-Vinyl pyrrolidone	Single T_g; FTIR; NMR	Formed complexes	Lau and Mi (2002), Maunu et al. (1993)
	Vinylpyridine	Single T_g; FTIR; XPS	II was 2- or 4-vinylpyridine; formed complexes	Zhou et al. (1998)

(continued)

Table 21.1 (continued)

Polymer I of	Polymer II of	Method	Comments	Refs.
Acrylic acid-butyl acrylate	Styrene-*co*-4-vinylpyridine	Single T_g	I was K-neutralized; II was quaternized with methyl iodide	Pen and Shen (1998)
Acrylic acid-*co*-ethylene	Caprolactam (PA-6)	Single T_g	I had 19 wt% acrylic acid	Matzner et al. (1979)
Acrylic acid-*co*-isobutyl methacrylate	*N,N*-Dimethylaminoethyl methacrylate-*co*-styrene	Single T_g; IGC	I had 10.5 or 22 mol% acrylic acid; II had 88 mol% styrene	Djadoun et al. (1996), Hadj-Hamou et al. (1997)
Acrylic acid-*co*-methyl methacrylate	*n*-Butyl methacrylate-*co*-4-vinylpyridine	Single T_g; FTIR	II had 26 mol% vinylpyridine	Iguerb et al. (1999)
	Vinyl chloride	Single T_g; FTIR	–	Iguerb et al. (1999)
Acrylic acid-*co*-styrene	Acrylonitrile-*co*-methyl methacrylate	Single T_g	–	Brannock et al. (1990)
	11-Aminoundecanoic acid (PA-11)	Single T_g	I had 20 % acrylic acid	Yu et al. (1991)
	Caprolactam (PA-6)	Single T_g	I had 20 % acrylic acid	Kuphal et al. (1991)
	Caprolactone	Single T_g	I had 11.4–20.8 wt% acrylic acid	Jo and Kim (1991)
	Dimethylacrylamide	Single T_g; FTIR	I had 22 mol% acrylic acid	Hadj-Hamou and Djadoun (2006)
	Ethyl methacrylate	Single T_g	I had 2.65–20 wt% acrylic acid	Brannock et al. (1990), Feraz et al. (1995)
	Ethyl methacrylate-*co*-4-vinylpyridine	Single T_g; IGC	I had 20 mol% acrylic acid; II had 8 mol% vinylpyridine	Feraz et al. (1995)
	Ethylene glycol	Single T_g	I had 21 wt% acrylic acid	Jo et al. (1991b)
	Isobutyl methacrylate-*co*-4-vinylpyridine	Single T_g; IGC; FTIR	I had 20 mol% acrylic acid; II had 32 mol% vinylpyridine	Feraz et al. (1995), Hadj-Hamou (2010)
	Methyl methacrylate	Single T_g	I had 8–20 wt% acrylic acid	Brannock et al. (1990), Jo et al. (1989a, b)
	Lauryllactam (PA-12)	Single T_g	I had 20 % acrylic acid	Yu et al. (1991)

	N-Methyldodecano-12-lactam	Single T_g; FTIR	I had 25.7 wt% acrylic acid	Kratochivil et al. (2005, 2007)
	n-Propyl methacrylate	Single T_g	I had 2.65–8.84 wt% acrylic acid	Bowner and Tondii (1986)
	Vinylmethylether	Single T_g	I had 8–20 wt% acrylic acid	Min and Paul (1988)
Acrylonitrile	Tertiary amide	Single T_g; FTIR	II was dimethylacrylamide, N-methyl-N-vinylacetamide or N-vinylpyrrolidone	Yeo et al. (1997)
	p-Vinylphenol	Single T_g; FTIR; XPS	–	Goh et al. (1999b)
Acrylonitrile-co-butadiene	Cellulose acetate butyrate	Some compositions appeared homogeneous	–	Asimova et al. (1962), Gesner (1969), Kosai and Higashino (1975), Peterson et al. (1969)
	Chloroprene	Single T_g when I had 18 % acrylonitrile; sorption of solvent vapors	Two phases in electron micrograph when I had 18 % acrylonitrile may indicate a crystalline phase; two torsional transitions when I had ≥28 % acrylonitrile	Casper and Morbitzer (1977), Tager et al. (1987)
	Epichlorohydrin	Single T_g	I had 26–54 wt% AN	Cowie and Harris (1994)
	Ethylene, chlorinated	Single T_g	I was hydrogenated and had 36.3 or 49.9 wt% AN; II had 42.1 wt% Cl (Severe and White (2000)); I had 34 wt% AN; and II had 35 wt% Cl (Zhang et al. (2002))	Severe and White (2000), Zhang et al. (2011)
	Nitrocellulose	Transparent films when I had 28.6–44.4 % acrylonitrile	Immiscible when I had 18.4 % acrylonitrile	Casper and Morbitzer (1977), Grose and Friese (1965), Kalinina et al. (1956a, b), Kosai and Higashino (1975)
	Vinyl acetate-co-vinyl chloride	Single loss peak when ≤40 % vinyl acetate in II; clear films for some mixtures of commercial polymers	Two loss peaks when ≥50 % vinyl acetate in II	Grose and Friese (1965), Kosai and Higashino (1975), Manabe et al. (1969), Peterson et al. (1969)

(continued)

Table 21.1 (continued)

Polymer I of	Polymer II of	Method	Comments	Refs.
	Vinyl chloride	Single T_g; IGC	I had 29–45 wt% acrylonitrile	Aivazov et al. (1970), Breuers et al. (1954), Buchdahl and Nielson (1955), Cowie and Harris (1992), Dimitrova et al. (1971), Kosai and Higashino (1975), Landi (1974), Livingston and Rongone (1967), Matsuo et al. (1969), Nielson (1955), Nielson and Chinai (1962), Oganesov et al. (1969), Reznikova et al. (1955), Shur and Ranby (1975b), Sen and Mukherjee (1993), Takayanagi et al. (1963), Wang and Chen (1981), Wolff (1957), Zahrzewski (1973)
	Vinyl chloride, head-to-head	Single T_g	I had 23.5–56.6 wt% acrylonitrile; II was made from chlorination of poly (1,4-butadiene)	Cowie et al. (1992d)
Acrylonitrile-*co*-butadiene, hydrogenated	Vinyl chloride	Single T_g; microscopy	I had 38 wt% AN	Sotiropoulou et al. (1993)
Acrylonitrile-*co*-butadiene-methyl acrylate	Ethylene-alt-maleic anhydride	Single T_g; microscopy	I was made from a copolymer of AN/MA (75/25) grafted onto BD/AN (70/30) copolymer	Percec and Melamud (1993)
Acrylonitrile-*co*-butadiene-*co*-styrene	Propylene-*co*-vinyl chloride	Single T_g	I was Blendex 701; II had 3.2 or 3.8 % propylene; electron micrographs may indicate two phases	Cheng and Mantell (1979)
Acrylonitrile-*co*-methyl methacrylate	N,N-Dimethylacrylamide	Single T_g; transparency	I had 70 wt% acrylonitrile (AN)	Percec and Melamud (1990)
	Maleic anhydride	Single T_g; transparency	I had 70 wt% AN	Percec and Melamud (1990)
	Vinyl chloride	Single T_g; transparency	II had 2–17 wt% AN	Lath et al. (1993)
	N-Vinylpyrrolidone	Single T_g; transparency	I had 70 wt% AN	Percec and Melamud (1990)

Acrylonitrile-*co*-methyl methacrylate-*co*-α-methylstyrene	Vinyl chloride	Single T_g	I had 8/58/34/acrylonitrile/methyl methacrylate/-methylstyrene	Casper and Morbitzer (1977)
Acrylonitrile-*co*-α-methylstyrene	Alkyl methacrylate	Single T_g; transparency	I had 30 wt% AN; II had an alkyl group of acetonyl, chloromethyl, 2-chloroethyl, 2-hydroxyethyl, 2-hydroxypropyl, methoxymethyl, methylthiomethyl, or tetrafurfuryl	Goh and Lee (1990d), Goh et al. (1991b, 1992b), Goh and Siow (1986a)
	n-Butyl methacrylate	Single T_g	I had 12 wt% AN	Cowie and Elexpuru (1992)
	n-Butyl methacrylate-*co*-methyl methacrylate	Single T_g; transparency	I had 30 wt% AN; II had 70 wt% methyl methacrylate	Goh et al. (1984)
	Carbonate of tetramethylbisphenol-A	Single T_g	I had 4–16.5 wt% AN	Gan et al. (1994a)
	Ethyl methacrylate	Single T_g	I had 10–28 wt% AN	Cowie and Elexpuru (1992), Goh et al. (1982b)
	Ethyl methacrylate-*co*-methyl methacrylate	Single T_g; transparency	I had 30 wt% AN; II had 30 or 60 wt% methyl methacrylate	Goh et al. (1985)
	Ethylene, chlorinated	Single T_g	Depended on AN and Cl contents	Cowie et al. (1991a)
	Methyl methacrylate	Single T_g; XPS; SALS	I had 10–37 wt% AN; I had 30 wt% AN; and II was atactic or isotactic (Goh et al. (1982b))	Bebin and Prud'homme (2004), Cowie and Elexpuru (1992), Goh et al. (1982b), Gan et al. (1994), Zuo et al. (2006)
	Methyl methacrylate-*co*-2,2,6,6-tetramethyl-piperidinyl methacrylate	Single T_g; transparency	I had 30 wt% AN; II had ≥76.2 wt% methyl methacrylate	Goh et al. (1986b, 1987)

(continued)

Table 21.1 (continued)

Polymer I of	Polymer II of	Method	Comments	Refs.
	n-Propyl methacrylate	Single T_g	I had 17–20 wt% AN	Cowie and Elexpuru (1992a)
	Vinyl chloride	Single T_g; FTIR	I had 30 wt% AN; miscible when melt blended or cast from methyl ethyl ketone; immiscible when cast from tetrahydrofuran	Gan et al. (1994a), Kim et al. (1989d, 1996), Moon et al. (2007), Rink et al. (1983)
Acrylonitrile-co-p-methylstyrene	Acetonyl methacrylate	Single T_g; transparency	I had 43–61 wt% AN	Chong and Goh (1992a)
	Alkyl methacrylate	Single T_g	II had an alkyl group of 1-chloroethyl and I had 10–40 wt% AN; II had an alkyl group of 2,2-dichloroethyl and I had 8–44 wt% AN; II had an alkyl group of 2,2,2-trichloroethyl and I had 78–88 wt% AN	Goh et al. (1996c)
	2-Bromoethyl methacrylate	Single T_g; transparency	I had 14–61 wt% AN	Neo and Goh (1991a)
	n-Butyl methacrylate	Single T_g; transparency	I had 13.6 wt% AN	Goh et al. (1991a)
	2-Chloroethyl methacrylate	Single T_g; transparency	I had 18.3–46 wt% AN	Neo et al. (1991a)
	Chloromethyl methacrylate	Single T_g; transparency	I had 13–42 wt% AN	Goh and Lee (1990a)
	Cyclohexyl methacrylate	Single T_g; transparency	I had ≤22 wt% AN	Chong and Goh (1992d)
	2,6-Dimethyl-1,4-phenylene ether	Single T_g; transparency	I had ≤5.0 wt% AN	Goh and Lim (1990)
	Ethyl methacrylate	Single T_g; transparency	I had 12–33 wt% AN	Goh et al. (1991a)
	Methyl methacrylate	Single T_g; transparency	I had 12–34 wt% AN	Goh et al. (1991a)
	Methylthiomethyl methacrylate	Single T_g; transparency	I had 19–34 wt% AN	Goh et al. (1992b)
	n-Propyl methacrylate	Single T_g; transparency	I had 6–28 wt% AN	Goh et al. (1991a)
	Tetrahydrofurfuryl methacrylate	Single T_g; transparency	I had 12–48 wt% AN	Goh et al. (1992a)
	Tetrahydropyranyl-2-methyl methacrylate	Single T_g; transparency	I had 5–29 wt% AN	Chong and Goh (1992b)
Acrylonitrile-co-α-methylstyrene-co-styrene	Vinyl chloride	Single T_g; SEM	I had 25 wt% AN	Zhang et al. (2008a, b)

Acrylonitrile-co-styrene				
Acetonyl methacrylate	Single T_g; transparency	I had 33–58 wt% AN	Chong and Goh (1992c)
Alkyl acrylate-co-methyl methacrylate	Single T_g	II had an alkyl group of ethyl or n-butyl; miscibility depended on compositions of I and II; miscibility increased and then decreased with increasing size of alkyl group of II (Zhao et al. (1991)3)	Chu and Paul (1999)
Alkyl methacrylate	Single T_g	II had an alkyl group of 1-chloroethyl and I had 9–30 wt% AN; II had an alkyl group of 2,2-dichloroethyl and I had 9–41 wt% AN; II had an alkyl group of 2,2,2-trichloroethyl and I had 64–93 wt% AN	Goh et al. (1996c)
Alkyl methacrylate-co-methyl methacrylate	Single T_g	II had an alkyl group of t-butyl, phenyl or cyclohexyl; miscibility depended on compositions of I and II	Chu and Paul (1999)
Arylate	Single T_g	Miscibility the greatest when AN = 25 %	Ahn and Jeong (1987)
Arylate of bisphenol-A-co-arylate of tetramethylbisphenol-A	Single T_g	I had 4.2–17.8 wt% AN	Ahn et al. (1997c)
Arylate of tetrabromobisphenol-A-co-arylate of tetramethylbisphenol-A	Single T_g	Miscibility depended on compositions of I and II	Jeong et al. (1994)
Benzyl methacrylate	Single T_g	I had 3.9–7.8 and 24.3–26.6 wt % AN	Sankarapandian and Kishore (1994), Woo et al. (2000b)
2-Bromoethyl methacrylate	Single T_g; transparency	I had 10–58 wt% AN	Neo and Goh (1991a)

(continued)

Table 21.1 (continued)

Polymer I of	Polymer II of	Method	Comments	Refs.
	Butylene adipate	Single T_g	I had 13–32.3 wt% AN	Fernandes et al. (1986a)
	Butylene sebacate	Single T_g	I had 13–20 wt% AN	Fernandes et al. (1986a)
	n-Butyl methacrylate-co-methyl methacrylate	Single T_g; transparency	I had 22 wt% AN; II had 70 wt% methyl methacrylate	Goh et al. (1984a), Kammer (1989)
	t-Butyl methacrylate-co-methyl methacrylate	Single T_g	Miscibility depended on compositions of I and II	Nishimoto et al. (1990)
	Caprolactone	Single T_g; light scattering; FTIR; OM; dielectric spectroscopy	I had 10–30 wt% AN; II was linear or 6-arm star polymer (Gorda and Peiffer 1993)	Fernandes et al. (1986a), Groeninckx et al. (1988), Gorda and Peiffer (1993), Janarthanan et al. (1993), Kressler and Kammer (1988), Keyzlarovi and Saha (1999), Li and Woo (2008c), McMaster (1973), Madbouly et al. (2006), Princi and Vicini (2010), Seefried and Koleske (1976), Schulze et al. (1993)
	Carbon monoxide-alt-propene	Single T_g; transparency	I had 25 wt% AN	De Vos et al. (1999)
	Carbonate of bisphenol-A-co-tetramethylbisphenol-A	Single T_g	I had ≤18 wt% acrylonitrile; II had ≤22 wt% bisphenol-A	Kim and Paul (1992e)
	Carbonate of dimethylbisphenol-A-co-carbonate of tetramethylbisphenol-A	Single T_g	I had 2–24 wt% AN; II had 41–83 wt% tetramethylbisphenol-A	Kim et al. (2003a), Yoo et al. (2003)
	2-Chloroethyl methacrylate	Single T_g; transparency	I had 12.5–43 wt% AN	Neo et al. (1991a)
	Chloromethyl methacrylate	Single T_g; transparency	I had 12–37 wt% AN	Goh and Lee (1990e)
	Cyclohexyl methacrylate	Single T_g; transparency	I had ≤20 wt% AN	Chong and Goh (1992b)
	Cyclohexyl methacrylate-co-methyl methacrylate	Single T_g	Miscibility depended on compositions of I and II	Nishimoto et al. (1990)
	2,6-Dimethyl-1,4-phenylene ether	Single T_g	I had ≤10.5 wt% AN	Gottschalk et al. (1994), Kressler and Kammer (1987)

2,6-Dimethyl-1,4-phenylene ether, benzoylated	Single T_g	I had 18 mol% AN; II had 35 or 86 % benzoylated units	Song et al. (1991)
Ethylene adipate	Single T_g	I had 25–28 wt% AN	Fernandes et al. (1986a)
Ethyl methacrylate	Single T_g; transparency; NMR	I had 5.5–28.0 wt% AN (Fowler et al. (1987)); I had 9–34 wt% AN (Chiou et al. (1982))	Chiou et al. (1982), Fowler et al. (1987), Feng et al. (1996b), Lath et al. (1992)
Ethyl methacrylate-co-methyl methacrylate	Single T_g; transparency	I had 22 wt% AN; II had 30 or 50 wt% methyl methacrylate	Goh et al. (1984b)
Ethyl methacrylate-co-2,2,6,6-tetramethyl-piperidinyl methacrylate	Single T_g; transparency	I had 30 wt% AN; II had $\leq$13.3 wt% 2,2,6,6-tetramethyl-piperidinyl methacrylate	Goh et al. (1987)
2-E thyl-2-oxazoline	Single T_g; transparency	I had 25–40 wt% AN; two T_g's when I had 8, 23.5, or 70 % AN	Keskkula and Paul (1986), Pfennig et al. (1986)
Hexamethylene sebacate	Single T_g	I had 16.2 wt% AN	Fernandes et al. (1986a)
2-Hydroxyethyl methacrylate	Transparency	I had 22 wt% AN	Goh et al. (1982b)
2-Hydroxyethyl methacrylate-co-methyl methacrylate	Single T_g	II had <8wt% hydroxyethyl methacrylate; miscibility depended on composition of I	Chu and Paul (2000)
2-Hydroxypropyl methacrylate	Single T_g; transparency	I had 22 wt% AN	Goh and Siow (1986a)
Isobutene-alt-N-methylmaleimide	Single T_g; transparency	I had 25 or 30 wt% AN	Doi et al. (1997)
4-Methacryloxyethyl trimellitic anhydride-co-methyl methacrylate	Single T_g	II had >97 wt% methyl methacrylate; miscibility depended on composition of I	Chu and Paul (2000)
Methoxymethyl methacrylate	Single T_g; transparency	I had 30 wt% AN	Goh et al. (1992b)

(continued)

Table 21.1 (continued)

Polymer I of	Polymer II of	Method	Comments	Refs.
	Methyl methacrylate	Transparency; NMR; AFM; XPS	I had 9.4–34.4 wt% AN (Suess et al. 1987); I had 9.5–28 wt% AN (Fowler et al. 1987); I had 9–39 wt% AN (Cowie et al. 1988); II was atactic or syndiotactic (Hsu 1999)	Bernstein et al. (1977), Cowie et al. (1988), Fowler et al. (1987), Feng et al. (1996b), Hsu (1999), Jung and Stein (1973), McMaster (1975), Naito et al. (1978), Peterson et al. (1969), Ramaswamy and Weber (1973), Robertson and Wilkes (2001a), Shaw (1974), Stein et al. (1974), Suess et al. (1987), Wen et al. (2003)
	Methyl methacrylate-co-itaconic anhydride	Single T_g	–	Bell et al. (1994)
	Methyl methacrylate-co-N-phenylitaconimide	Single T_g	Miscibility depended on compositions of I and II	Cowie et al. (1990b)
	Methyl methacrylate-co-phenyl methacrylate	Single T_g	Miscibility depended on compositions of I and II	Nishimoto et al. (1990)
	Methyl methacrylate-co-phenylmaleimide	Single T_g	Miscibility depended on compositions of I and II	Merfeld et al. (1999)
	Methyl methacrylate-co-tribromophenyl maleimide	Single T_g	Miscibility depended on compositions of I and II	Merfeld et al. (1999)
	Methyl methacrylate-co-2,2,6,6-tetramethyl-piperidinyl methacrylate	Single T_g; transparency	I had 22 or 30 wt% AN; II had ≤31.4 wt% 2,2,6,6-tetramethyl-piperidinyl methacrylate	Goh et al. (1986b), Goh et al. (1987)
	Methylthiomethyl methacrylate	Single T_g; transparency	I had 9–36 wt% AN	Goh et al. (1991c)
	Novolac	Single T_g	I had 25 wt% AN; II was formaldehyde + 13/17/70 mol% p-t-butylphenol/m-cresol/o-cresol	Fahrenhlotz and Kwei (1981)

	Oxy-1,4-phenylene-sulfonyl-1,4-phenylene oxy-2,6-diisopropyl-1,4-phenylene isopropylidene 3,5-diisopropyl-1,4-phenylene	Modulus-temperature	I had 13–16 % AN	R17
	Phenyl acrylate	Single T_g	I had 14.6–34.1 wt% AN; width of miscibility window dependent on choice of solvent (Rana et al. (1993))	Rana et al. (1993), Sankarapandian and Kishore (1991), Sankarapandian and Kishore (1994)
	n-Propyl methacrylate	Single T_g	I had 5.7–19.5 wt% AN	Fowler et al. (1987), Lath and Lathova (1994)
	Tertiary amide	Single T_g	II was N-methyl-N-vinylacetamide and I had 67–88 wt% AN; II was N,N'-dimethylacrylamide and I had 70–88 wt% AN; II was N-vinylpyrrolidone and I had 64–88 wt% AN	Yeo et al. (1996)
	Tetrahydrofurfuryl methacrylate	Single T_g; transparency	I had 9–48 wt% AN	Goh and Siow (1987), Goh et al. (1992a)
	Tetrahydropyranyl-2-methyl methacrylate	Single T_g; transparency	I had ≤31 wt% AN	Chong and Goh (1991a)
	Tetramethyl sulfone	Single T_g	I had 11.5–19.5 wt% AN	Ahn et al. (1994)
	Vinyl acetate-co-vinyl chloride	Single T_g	I had 22 wt% AN; miscibility depended on choice of solvent	Das and Banerjee (1996), Das et al. (1996)
	Vinyl chloride	Single T_g	I had 11.5–26 wt% AN	Kim et al. (1989)
Acrylonitrile-co-styrene-co-p-vinylphenol	Carbonate of bisphenol-A	Single T_g; FTIR	I had 25–80 mol% vinylphenol	Li et al. (2007)
Acrylonitrile-co-p-vinylphenol	Carbonate of bisphenol-A	Single T_g; FTIR	I had 12–50 mol% acrylonitrile	Li et al. (2007)

(continued)

Table 21.1 (continued)

Polymer I of	Polymer II of	Method	Comments	Refs.
Acrylonitrile-*co*-vinylidene chloride	Caprolactone	Single T_g	I was usually Saran F (80 % vinylidene chloride); semicrystalline when ≤70 wt% I	Aubin et al. (1983), Varnell et al. (1983), Zhang and Prud'homme (1987)
	Hexamethylene terephthalate	Single T_g	Probably semicrystalline; I was Saran F (80 % vinylidene chloride)	Aubin and Prud'homme (1984)
	Methyl methacrylate	Single T_g; FTIR; NMR	I had 20 wt% AN	Feng et al. (1996c)
N-Acryloyl-*N'*-methylpiperazine	Acid	FTIR; XPS	II was acrylic acid, methacrylic acid, styrenesulfonic acid, or vinylphosphonic acid; formed complexes	Liu et al. (2000)
	p-Vinylphenol	Single T_g; FTIR; XPS	–	Liu et al. (1999)
N-Acryloyl-*N'*-phenylpiperazine	Acid	FTIR; XPS	II was acrylic acid, styrenesulfonic acid, or vinylphosphonic acid; formed complexes	Goh et al. (1999d)
	p-Vinylphenol	Single T_g; FTIR; XPS	–	Goh et al. (1999d)
N-1-Alkylitaconamic acid	*p*-Vinylphenol	Single T_g; FTIR	I had an alkyl group of ethyl, propyl, butyl, hexyl, octyl, decyl, or dodecyl	Urzua et al. (2002)
	2-Vinylpyridine	Single T_g; FTIR	I had an alkyl group of ethyl, propyl, butyl, hexyl, octyl, decyl, or dodecyl	Urzua et al. (2002)

N-1-Alkylitaconamic acid-co-styrene	N-Vinylpyrrolidone	Single T_g; FTIR	I had an alkyl group of ethyl, propyl, butyl, hexyl, octyl, decyl, or dodecyl; I had 50 or 80 wt% styrene	Urzua et al. (2006)
	Vinylpyridine	Single T_g; FTIR	I had an alkyl group of ethyl, propyl, butyl, hexyl, octyl, decyl, or dodecyl; I had 50 or 80 wt% styrene; II was 2- or 4-vinylpyridine	Urzua et al. (2006)
Allyl alcohol-co-styrene	Alkyl methacrylate	Single T_g; FTIR; NMR	I had 5.7 wt% OH; II had an alkyl group of ethyl or methyl	Feng and Feng (1997)
	Ester	Single T_g	I had M_w = 1.4–2.1 kg/mol and had 1.3–7.7 wt% OH groups; II was butylene adipate, butylene sebacate, caprolactone, 1,4-cyclohexane dimethylene succinate, decamethylene sebacate, and 2,2-dimethyl-1,3-propylene adipate of hexamethylene sebacate; high OH content of I favored miscibility	Bamum et al. (1981), Woo et al. (1984a)
Amic acid	3,3-Diamino-4,4'-benzidine isophthalamide	Transparency; FTIR	I was LaRC-TPI	Kim et al. (1993b)
	Phenol-formaldehyde	Clear before and after curing	I was made from 4,4'-methylene-dianiline and pyromellitic dianhydride	Adduci et al. (1981)
	Imide	Single T_g	II was Polyimide Prashantha et al. (2008); miscible over certain composition range	Makhija et al. (1992)

(continued)

Table 21.1 (continued)

Polymer I of	Polymer II of	Method	Comments	Refs.
Amide	Ester	Single T_g	I was MXDS made from *m*-xylylenediamine and adipic acid; II was made from hexamethylene diamine and a mixture of iso- and terephthalic acid	Nagasawa et al. (2000)
Amide enaminonitrile	*N*-Vinylpyrrolidone	Single T_g; transparency	–	Moore and Kaur (1998)
	4-Vinylpyridine	Single T_g; transparency	–	Moore and Kaur (1998)
Amideimide	Benzimidazole	Single T_g; FTIR; SEM; POM	I was Torlon 4,000T	Wang et al. (2007)
	Novolac	Single T_g	I was made from rosin	Kundu et al. (1986a)
	Imide	Single T_g; FTIR; SEM; POM	I was Torlon 4,000T; II was Matrimid 5218	Wang et al. (2007)
	Resol	Single T_g	I was made from rosin maleic anhydride Diels–Alder adduct with 4,4′-diaminodiphenylmethane	Kundu et al. (1986b)
	Shellac	Single T_g	I was made from rosin-imidoamino acid with 4,4′-diaminodiphenylmethane	Kuo et al. (1990)
n-Amyl methacrylate	Vinyl chloride	Single T_g; transparency	–	Ha et al. (1990a), Perrin and Prud'homme (1991), Tremblay and Prud'homme (1984), Walsh and McKeown (1980)
	Vinyl chloride, chlorinated	Single T_g; transparency	II had 65 or 68 wt% Cl	Ha et al. (1990a), Trask and Roland (1988)
	Vinyl chloride-*co*-vinylidene chloride	Single T_g; transparency	II was Saran; ≥80 % vinylidene chloride	Kang and Cho (1989), Tremblay and Prud'homme (1984)

Aniline	2-Ethyl-2-oxazoline	Single T_g; XPS	I was doped with p-phenolsulfonic acid; blend had 5–60 wt% I	Ong et al. (1996b)
	Tertiary amide	Single T_g; FTIR	I was doped with p-phenolsulfonic acid or 5-sulfosalicylic acid; blend had $\leq$50 wt% I; II was N-vinylpyrrolidone, N-methyl-N-vinylacetamide, N,N-dimethylacrylamide, or 2-methyl-2-oxazoline	Goh et al. (1998a)
	Vinyl acetate	Single T_g; FTIR; XPS	I was doped with p-phenolsulfonic acid; blend had $\leq$50 wt% I	Goh et al. (1996a)
o-Anisidine	2-Alkyl-2-oxazoline	Single T_g; FTIR	Blend had $\leq$50 wt% I; II had an alkyl group of methyl or ethyl	Ong et al. (1996a)
Aramide	Amide	Single T_g; T_m-depression	I was Trogamid T; II was PA-6, PA-4,6, PA-6,6, PA-6,9, PA-6,10, or PA-11, PA-6,12	Ellis (1988, 1989), Garlund (1993), Myers et al. (1990)
	Butylene terephthalate	Single T_g	I was made from 2,2,4-trimethyl-1,6-hexanediamine and terephthalic acid (Trogamid T); semicrystalline	Nadkarni et al. (1988)
	Caprolactam-co-laurolactam	Single T_g	I was Trogamid T; II had 43.8–55.6 mol% caprolactam; semicrystalline	Ellis (1990a, b)
	Caprolactam-co-2-pyrrolidinone	Single T_g	I was Trogamid T; II had 93.5 mol% caprolactam; semicrystalline	Ellis (1990a, b)

Table 21.1 (continued)

Polymer I of	Polymer II of	Method	Comments	Refs.
	Ester	Single T_g	I was Trogamid T; II was made from 1,4-cyclohexanedimethanol/ethylene glycol/terephthalic acid (PETG 6763)	Nadkarni et al. (1988)
	Cycloaliphatic amide	Single T_g	I was Trogamid T; II was made from 1,4- and 1,3-benzenedicarboxylic acids and a mixture of 1,6-hexanediamine and bis (4-aminocyclohexyl)methane (Bexloy AP C-803)	Ellis (1989)
	Ethylene terephthalate	Single T_g	I was Trogamid T; semicrystalline	Nadkarni et al. (1988)
	Amide	Single T_g	II was PA-4,6, PA-6, PA-6,6, or PA-6,9; I was made from 1,6-hexanediamine and a mixture of isophthalic and terephthalic acids (Zytel 330); semicrystalline	Ellis (1989, 1990b)
	Cycloaliphatic amide	Single T_g	I was Zytel 330; II was Bexloy AP C-803	Ellis (1989)
	Vinyl chloride	Single T_g; FTIR; SEM	I was made from 4,4′-oxydianiline and isophthaloyl chloride	Shabbir et al. (2008)
Aryl ether ether ketone	Aryl ether ether ketone	Single T_g; POM; AFM	–	Chen and Yang (2005)
	Etherimide	Single T_g; microscopy	–	Tseng and Woo (1998)

Arylate				
	Aramide	Single T_g	I was made from bisphenol-A and a mixture of terephthalic acid/isophthalic acid/5-t-butyl-isophthalic acid = 44/44/12 (Polyarylate C); II was Trogamid T	Dean (1987b)
	Aramide-S	Single T_g	I was Polyarylate C; II was made from 5-t-butylisophthalic acid/isophthalic acid 90/10 and 1,12-diaminododecane (Aramide-S)	Dean and Harris (1992)
	Aramide-M	Single T_g	I was made from bisphenol-A and a mixture of terephthalic acid/isophthalic acid/5-t-butyl-isophthalic acid = 42.5/42.5/15 (Polyarylate D); II was made from adipic acid and m-xylene-diamine/hexamethylene diamine 80/20 (Aramide-M)	Dean and Harris (1992)
	Aramide	Single T_g	I was Polyarylate D; II was Trogamid T	Dean and Harris (1992)
	Aramide-S	Single T_g	I was Polyarylate D; II was Aramide-S	Dean and Harris (1992)
	Aramide-M	Single T_g	I was made from bisphenol-A and a mixture of terephthalic acid/isophthalic acid/5-t-butyl-isophthalic acid = 37.5/37.5/25 (Polyarylate E); II was Aramide-M	Dean and Harris (1992)
	Aramide	Single T_g	I was Polyarylate E; II was Trogamid T	Dean and Harris (1992)

(continued)

Table 21.1 (continued)

Polymer I of	Polymer II of	Method	Comments	Refs.
	Aramide-S	Single T_g	I was Polyarylate E; II was Aramide-S	Dean and Harris (1992)
	Aramide	Single T_g	I was made from bisphenol-A and a mixture of terephthalic acid/5-t-butylisophthalic acid 50/50 (Polyarylate F); II was Trogamid T	Dean and Harris (1992)
	Aramide	Single T_g	I was Polyarylate F; II was Aramide-S	Dean and Harris (1992)
	Carbonate of bisphenol-A	Single T_g	I was made from bisphenol-A and a mixture of terephthalic acid/isophthalic acid 50/50 (Ardel D-100); miscibility arose from transesterification	Robeson (1985)
	Ester	Single T_g	I was Ardel D-100; II was made from cyclohexane dimethanol and terephthalic acid/isophthalic acid (80–87 % tere) (Kodar A-150) and another copolymer with tere/iso ratio of 70/30	Robeson (1985)
	Ester	Single T_g; positron annihilation lifetime spectroscopy	I was Ardel D-100; II was made form cyclohexane dimethanol and 1,4-cyclohexane dicarboxylic acid	Zipper et al. (1995)
	Ester	Single T_g	I was Ardel D-100; II was made from cyclohexane dimethanol, ethylene glycol, and terephthalic acid (molar ratio 1:2:3, PETG-6763)	Golovoy and Cheung (1989), Robeson (1985)

		Methods	Comments	Reference
	1,4-Cyclohexamethylene terephthalate	Single T_g	II was arylate of bisphenol-A and iso/terephthalic acid	Hwang (2000)
	Ethylene terephthalate	Single T_g	I was Ardel D-100; miscibility arose from transesterification	Robeson (1985)
	Hydroxyether of bisphenol-A (Phenoxy)	Single T_g	I was Ardel D-100; miscibility arose from transesterification	Robeson (1985)
Arylate of tetramethylbisphenol-A	Butylene sebacate	Single T_g	Semicrystalline	Ahn et al. (1995)
	Ester	Single T_g; T_m-depression	II was caprolactone, butylene sebacate, hexamethylene sebacate, hexamethylene decamethylene decarboxylate, or decamethylene sebacate	Ahn et al. (1998)
	Hexamethylene sebacate	Single T_g	Semicrystalline	Ahn et al. (1993a)
Aryletherketone	Etherimide	Single T_g	I was made from 4,4′-difluoro-benzophenone and hydroquinone; II was Ultem 1000	Harris and Robeson (1988)
	Etherimide	Single T_g	I was made from p-phenoxybenzoyl chloride; II was Ultem 1000	Harris and Robeson (1988)
Arylsulfone	Imide	Single T_g	I was Radel A; II was XU-218	Jeremic et al. (1992)
	3-Bromo-2,6-dimethyl-1,4-phenylene ether p-bromostyrene	Single T_g; microscopy	–	Kambour et al. (1983)
	p-Bromostyrene-co-styrene	Single T_g; microscopy	II had ≤85 mol% styrene	Kambour et al. (1983)
γ-Benzyl glutamate		Dynamic mechanical methods; DSC	Miscible as random coil, but not as α-helics	Tsujita et al. (1985)
Benzimidazole	Phenylsulfone, sulfonated	Single T_g; FTIR; SEM	II was Na-neutralized	Sun et al. (2004)
	Sulfone, sulfonated	Single T_g; FTIR; SEM	II was Na-neutralized	Sun et al. (2004)
	Vinylidene fluoride	Single T_g; FTIR; T_m-depression	–	Dhamodaran et al. (2008)
Benzyl methacrylate	Phenyl methacrylate	Single T_g; FTIR; transparency; SEM	–	Lee and Woo (2000)

(continued)

Table 21.1 (continued)

Polymer I of	Polymer II of	Method	Comments	Refs.
Bismaleimide	Imide	Single T_g; transparency	I was based on bisphenol-A; II was alkyl terminated and hyperbranched	Qin et al. (2006)
Bis(methoxyethoxyethoxy) phosphazene	Acrylic acid-co-methyl methacrylate	Single T_g; transparency	II had 10, 20, or 30 mol% acrylic acid	Landry et al. (1993d)
	Methylic acid-co-methyl methacrylate	Single T_g; transparency	II had 20 mol% methacrylic acid	Landry et al. (1993d)
	Styrene-co-styrene-4-carboxylic acid	Single T_g; transparency	II had 75 mol% styrene	Landry et al. (1993d)
	Styrene-co-p-vinylphenol	Single T_g; transparency	II had 78 mol% styrene	Landry et al. (1993d)
	p-Vinylphenol	Single T_g; transparency	–	Landry et al. (1993d)
Bis(methoxyethox yethoxyethoxy)phosphazene	p-Vinylphenol	Single T_g; transparency	–	Landry et al. (1993d)
3-Bromo-2,6-dimethyl-1,4-phenylene oxide-co-2,6-dimethyl-1,4-phenylene ether	p-Bromostyrene	Single T_g; microscopy	I had $\leq$22 mol% 2,6-dimethyl-1,4-phenylene ether	Kambour et al. (1983)
	Styrene	Single T_g; microscopy	Miscible up to full bromination of I when I had $M_w \leq$40 kg/mol and II had $M_w \leq$30 kg/mol	Kambour et al. (1983), Maconnachie et al. (1984)
2-Bromoethyl methacrylate	Ester	Single T_g	II was ethylene adipate, caprolactone, butylene adipate, 2,2-dimethyl-1,3-propylene adipate, 2,2-dimethyl-1,3-propylene sebacate, or hexamethylene sebacate	Neo and Goh (1993)
	Tetrahydrofurfuryl methacrylate	Single T_g; transparency	–	Neo and Goh (1991c)

Bromohydroquinone-co-4,4'-(decamethylenedioxy) bibenzoic acid	(Decamethylenedioxy)-bibenzoic acid-co-4,4'-(ethylenedioxy) diphenol	Single T_g; microscopy	Transition temperature from a mesophase to an isotopic phase changed continuously and smoothly depending on the composition	Jin et al. (1986)
	p-Hydroxybenzoic acid-co-3-methyl-1,6-hexanediol-terephthalic acid	Single T_g; microscopy	Transition temperature from a mesophase to an isotopic phase changed continuously and smoothly depending on the composition	Jin et al. (1986)
p-Bromostyrene-co-styrene	2,6-Dimethyl-1,4-phenylene ether	Single T_g; microscopy	I had ≥ 53 mol% styrene	Kambour et al. (1983)
Butadiene	Butadiene	Single T_g	I was 1,4-polybutadiene; II had 63 % 1,2-	Roovers and Toporowski (1992)
	Diene-co-ethylene-co-propylene	Single T_g	Commercial samples; many mixtures had two T's	Caspary (1972), Kleintjens "unpublished results", Koningsveld et al. (1974)
	Isoprene	Single T_g; microscopy; light scattering; NMR	Depended on microstructure; immiscible when I and II were both highly cis; I was deuterated (Hasegawa et al. (1991))	Bartenev and Kongarov (1963), Briber and Khoury (1987), Corish (1967), Fujimoto and Yoshimiya (1968), Gesner (1969), Hasegawa et al. (1991), Heffner and Mirau (1994), Kawahara et al. (1994), Livingston and Rongone (1970) Marei and Sidorovich (1965), Marsh et al. (1967, 1968), Shutilin and Vysokomol (1991), Slonimskii (1958), Slonimskii and Komskaia (1956), Struminskii and Slonimskii (1956), Walters and Keyte (1965), Zlatkevich and Nikolskii (1973)

(*continued*)

Table 21.1 (continued)

Polymer I of	Polymer II of	Method	Comments	Refs.
Butadiene-*co*-styrene	t-Butylstyrene	Single dynamic mechanical loss peak	I had 25 % styrene; II had $M_w = 835$	Class and Chu (1985a)
	Glycerol ester of hydrogenated rosin	Single dynamic mechanical loss peak	I had 25 % styrene; II had $M_w = 500$	Class and Chu (1985c)
Butadiene-*co*-vinyl ethylene	Hydrogenated terpene resin	Light scattering; SEM	I had 47.4 or 60 wt% vinyl content	Kano et al. (1993)
1-Butene	1-Pentene	Single T_g	–	Decroix and Piloz (1977)
	Propylene	Single T_g; T_m-depression	Semicrystalline	Decroix and Piloz (1977), Lee and Marand (1991), Lee and Chen (1996), Piloz et al. (1976)
Butyl acrylate	Alkyl methacrylate	Single T_g	II had an alkyl group of 1-chloroethyl or dichloroethyl	Peng et al. (1996)
	Ethylene, chlorinated	Single T_g; transparency	II had 49.8 or 62.1 % Cl; immiscible when II had 48.0 % Cl	Chai and Walsh (1983)
	Hexafluoroacetone-*co*-vinylidene fluoride	Single T_g; XPS	II had 8 mol% hexafluoroacetone	Kano et al. (1997b)
	4-Hydroxystyrene-*co*-styrene	Single T_g	I was t-butyl; II had 28–66 mol% 4-hydroxystyrene	Zhu et al. (1990)
	Vinyl chloride	Single T_g; transparency	Some papers showed two T_g's (refs. Tremblay and Prud'homme (1984), Wolf (1963)) or phase separation in solution (Kern (1958))	Kern (1958), Piglowski and Kammer (1990), Tremblay and Prud'homme (1984), Walsh and Cheng (1982, 1984a), Walsh and McKeown (1980), Walsh and Sham (1989), Wolf (1963)
	Vinyl chloride-*co*-vinylidene chloride	Single T_g; transparency	II was Saran ($\geq$80 % vinylidene chloride)	Tremblay and Prud'homme (1984)

Butyl acrylate-*co*-methyl methacrylate	Ethylene, chlorinate	Single T_g; FTIR	I had 13–82 wt% butyl acrylate	Piglowski et al. (1996)
	Vinyl chloride	Single T_g; electron microscopy; FTIR	II was Degalan VanderHart (1994) (90 % methyl methacrylate) (Zelinger et al. (1976)); I had 75 % butyl acrylate (Piglowski (1990)); II was head-to-tail or head-to-head (Piglowski et al. (1996))	Piglowski (1990), Piglowski et al. (1996), Zelinger et al. (1976)
Butyl methacrylate	*p*-(2-Hydroxy-hexafluoroisopropyl) styrene-*co*-styrene	Single T_g; transparency	II had 83.3–98.25 mol% styrene; immiscible when II had 99.0 mol% styrene	Adduci et al. (1981), Chen and Morawetz (1989), Min et al. (1983), Pearce et al. (1984), Ting et al. (1980)
	p-(2-Hydroxy-hexafluoroiso-propyl)-α-methylstyrene-*co*-styrene	NMR	II had 1.5 mol% OH-containing monomer	Campbell et al. (1992)
	Vinyl chloride	Single T_g; transparency; miscible in solution	I was *n*-butyl, isobutyl, or sec-butyl	Ha et al. (1990a), Kern (1958), Perrin and Prud'homme (1991), Piglowski (1988), Walsh and Cheng (1984a), Walsh and McKeown (1980), Trask and Roland (1988)
	Vinyl chloride-*co*-vinylidene chloride	Single T_g; transparency	II was Saran, ≥80 % vinylidene; I was *n*-butyl, isobutyl, or sec-butyl	Kang et al. (1988), Tremblay and Prud'homme (1984)
Butyl methacrylate-*co*-vinylbenzyl thymine	Styrene-*co*-2-vinyl-4,6-diamino-1,3,5-triazine	Single T_g; FTIR	I had <93 mol% butyl methacrylate; II had <93 mol% styrene	Kuo and Hsu (2010)
N-Butyl-3-hydroxymethyl carbazoyl methacrylate	ω-Hydroxybutyl-3,5-dinitrobenzoyl methacrylate	Single T_g	–	Rodriguez-Parada and Percec (1986b)

(continued)

Table 21.1 (continued)

Polymer I of	Polymer II of	Method	Comments	Refs.
n-Butyl methacrylate-co-methacrylic acid	N,N-Dimethylacrylamide-co-styrene	Single T_g; FTIR	I had 18 mol% methacrylic acid and II had 17 mol% dimethylacrylamide; formed complexes when II had 32 mol% dimethylacrylamide	Siham and Said (2006)
	Styrene-co-4-vinylpyridine	Single T_g; FTIR	I had 8 or 18 mol% methacrylic acid; II had 15, 22, or 28 mol% 4-vinylpyridine	Djadoun et al. (1996)
n-Butyl methacrylate-co-4-vinylpyridine	Methacrylic acid-co-styrene	Single T_g; FTIR	I had 10.6, 18.9, or 26 mol% 4-vinylpyridine; II had 12, 24, or 29 mol% methacrylic acid (Djadoun et al. (1996)); I had 6.50 mol% 4-vinylpyridine; II had 10.50 mol% methacrylic acid (Djadoun (1983))	Djadoun (1983), Djadoun et al. (1996)
t-Butylstyrene	Cyclohexyl acrylate	Single T_g; transparency	–	Siol (1991)
	Cyclohexyl methacrylate	Single T_g; transparency	–	Siol (1991)
	Isoprene	Single dynamic mechanical loss peak	I had $M_w = 835$; II was natural rubber	Class and Chu (1985a)
	3,3,5-Trimethyl-cyclohexyl methacrylate	Single T_g; transparency	–	Siol (1991)
Butylene adipate	Arylate	WAXD; DMA	–	Huo et al. (1993)
	Epichlorohydrin	Single T_g	Semicrystalline	Fernandes et al. (1984)
	Hydroxyether of bisphenol-A (Phenoxy)	Single T_g; melt transparent; IGC	Semicrystalline when ≤60 wt% II	Harris et al. (1982), Uriate et al. (1995)
	Trifluoroethylene-co-vinylidene fluoride	Single T_g	–	Kim and Kyu (1999), Kim and Kyu (2003)
	Vinyl acetate-co-vinylidene chloride	Single T_g	II was Saran C (≥80 % vinylidene chloride); semicrystalline	Aubin et al. (1983)

	Vinyl bromide	Single T_g	–	Cousin and Prud'homme (1982)
	Vinyl chloride	Single T_g	Semicrystalline when ≤70 wt% II	Ziska et al. (1981)
Butylene dodeca methylene dicarboxylate	Vinylidene fluoride	Single T_g; FTIR	Exhibited double T_m	Penning and Manley (1996)
Butylene 2,6-naphthalate	Vinyl chloride	Single T_g	Semicrystalline	Woo et al. (1985b)
	Etherimide	Single T_g; T_m-depression	–	Huang (2004)
	Ethylene 2,6-naphthalate	Single T_g	Blend had ≥80 wt% I	Yoon et al. (1994)
	Ethylene 2,6-naphthalate, phosphorus containing	Single T_g	Blend had ≤40 wt% and ≥90 wt% II	
Butylene sebacate	Epichlorohydrin	Single T_g	Semicrystalline	Fernandes et al. (1984)
	Vinyl chloride	Single T_g	Semicrystalline	Woo et al. (1985b)
Butylene succinate	Vinylidene fluoride	T_m-Depression; OM	Semicrystalline	Lee et al. (1998c)
Butylene terephthalate	Arylate	Single T_g; FTIR	Semicrystalline	Jang and Won (1998), Lee et al. (2000)
	Arylate	Single T_g; T_m-depression	II was arylate of bisphenol-A and 3 different acids	Liau et al. (1999)
	Arylate	Single T_g; T_m-depression	II was arylate of bisphenol-A and a mixture of isophthalic and terephthalic acid	Liau et al. (2006)
	Arylate of bisphenol-A	Single T_g; T_m-depression	Semicrystalline	Liu et al. (1998)
	Butylene oxide-g-butylene terephthalate	Single T_g; dielectric loss measurements; microscopy	II had 84 wt% butylene terephthalate	Martynowicz-Hans and Runt (1986), Runt et al. (1989)
	Caprolactone	Single T_g; FTIR; OM	Miscible when II was oligomeric	Di Lorenzo et al. (2007), Righetti et al. (2007)
	Decamethylene-4,4'-terephthaloyl dioxydibenzoate	Single T_g; microscopy; T_m-depression	0–50 % II in blend	Pracella et al. (1986, 1987, 1989)
	Epoxy	Single T_g; T_m-depression	–	Zhang et al. (2006b)
	Ester	Single T_g	Semicrystalline when ≥25 wt% I; II was CP-350(bisphenol-A-neopentyl glycol terephthalate)	Slagowski et al. (1981)

(continued)

Table 21.1 (continued)

Polymer I of	Polymer II of	Method	Comments	Refs.
	Ester	Single T_g	Semicrystalline; II was made from bisphenol-A and 1/1 or 1/3 terephthaloyl chloride/isophthaloyl chloride	Kimura and Porter (1981), Kimura et al. (1983)
	Ester	Single T_g; SEM	II was made from ethylene glycol and cyclohexane-1,4-dimethanol terephthalate	Papadopoulou and Kalfoglou (1997a)
	Ester carbonate	Single T_g	II had 29.1 wt% carbonate unit	Lee et al. (2000)
	Ester carbonate	Single T_g	II had 42 or 70 mol% aromatic ester group	Rodriguez et al. (1996)
	Ester ether	Single crystallization peak	II was a segmental block copolymer	Gallagher et al. (1993)
	Ethylene naphthalene-2,6-dicarboxylate	Single T_g; T_m-depression; NMR	–	Guo and Zachmann (1997)
	Ethylene terephthalate	Single T_g	Semicrystalline	Avramova (1995), Escala et al. (1978), Escala et al. (1979)
	Hydroxyether of bisphenol-A (Phenoxy)	Single T_g; melt transparent	Semicrystalline	Robeson and Furtek (1977, 1979), Seymour and Zehner (1980)
	Vinyl acetate-co-vinylidene chloride	Single T_g	II had ≥80 % vinylidene chloride	Aubin and Prud'homme (1984)
	Vinyl butyral	Single T_g; FTIR; NMR	Miscible when blend was prepared by in situ polymerization of oligomer I in II	Tripathy et al. (2003)
	Vinyl chloride	Single T_g	Semicrystalline	Aubin and Prud'homme (1984), Robeson (1978)
	Vinyl chloride, chlorinated	Single T_g	Semicrystalline	Aubin and Prud'homme (1984)

Caprolactam (PA-6)	Acrylic acid	Single T_g	Semicrystalline	Jiang et al. (1986)
	Amide	Single T_g; OM	II was made from hexamethylene diamine with tere and isophthalic acid	Siciliano et al. (1996)
	Aramide	Single T_g	II was aramide from 5-(4-aminobenzoylamino) isophthalic acid	Monticelli et al. (2003)
	Aramide, hyperbranched	Single T_g; T_m-depression	–	Monticelli et al. (2005)
	Etheretherketone, sulfonated	Single T_g; FTIR	II had 19.2 mol% sulfonation	Lu and Weiss (1996a)
	Etheretherketone, sulfonated and metal-neutralized	Single T_g; FTIR	II had 19.2 mol% sulfonation and neutralized with Li or Zn	Lu and Weiss (1996a)
	Hexamethylene adipamide	Single T_g; enthalpy recovery kinetics	Semicrystalline	Ellis (1992), Tomova et al. (2000), Verma et al. (1986), Wei et al. (2004)
	Maleic anhydride-*co*-vinyl acetate	Single T_g; FTIR, transparency; WAXD	II was hydroxylated	Lee et al. (1996a)
	Methacrylic acid	SAXS	Semicrystalline	Janicke and Wlochowicz (1989)
	Novolac	Single T_g; SAXS	II was chlorinated	Huang et al. (2001)
	Styrene, sulfonated and Li-neutralized	Single T_g	II had 9,8 mol% sulfonated groups; semicrystalline	Molner and Eisenberg (1991), Molner and Eisenberg (1992)
	Styrene, sulfonated and Mn-neutralized	Single T_g; T_m-depression	II had 10.2 mol% sulfonated groups; semicrystalline	Lu and Weiss (1991)
	Styrene, sulfonated and Zn-neutralized	Single T_g; T_m-depression	II had 10.1 mol% sulfonated groups; semicrystalline	Lu and Weiss (1992)
	Vinyl alcohol	Single T_g; T_m-depression	Blend had ≤50 wt% II (Kang et al. (1989))	Cui et al. (2008), Koulouri and Kallitsis (1998)
	Vinyl butyral	Single T_g	Semicrystalline; II had 50–65 vol% residual vinyl alcohol unit	Jeong et al. (2000a)
	p-Vinylphenol	Single T_g; SAXS	Semicrystalline	Huang et al. (2001)
	m-Xylene adipamide	T_m-Depression	Semicrystalline	Shibayama et al. (1995)

(*continued*)

Table 21.1 (continued)

Polymer I of	Polymer II of	Method	Comments	Refs.
Caprolactone	Acrylonitrile-*co*-t-butylstyrene	Single T_g; SALS; microscopy	II had 19.8–39.6 wt% acrylonitrile	Hseih and Peiffer (1993)
	Benzoxazine	Single T_g; FTIR; NMR	–	Ishida and Lee (2001), Huang and Yang (2005)
	Benzyl methacrylate	OM	–	Woo et al. (2000d)
	3,3-Bis(chloromethyl)oxetane	Single T_g	Semicrystalline; II was Penton	Guo (1990c), Koleske (1978)
	Bisphenol-A	Single T_g; FTIR	Semicrystalline	He et al. (2001)
	t-Butylphenol	Single T_g; FTIR	Semicrystalline	He et al. (2001)
	Caprolactone-*co*-ethylene terephthalate	Single T_g	II had 13 or 28 wt% ethylene terephthalate	Ma et al. (1996)
	Cellulose alkyl ester	Single T_g; transparency	II was cellulose butyrate, cellulose propionate, or cellulose valerate	Kusumi et al. (2008)
	Chlorostyrene	Single T_g; FTIR; SEM; T_m-depression	II was *o*-chlorostyrene or mixed *o*- and *p*-isomers; semicrystalline when ≥21 % I	Allard (1982), Aubin et al. (1982), Aroguz et al. (2007)
	4,4′-Dihydroxydiphenyl ether	Single T_g; FTIR; T_m-depression	–	Li et al. (2006)
	Epichlorohydrin	Single T_g	Semicrystalline	Brode and Koleske (1972), Fernandes et al. (1984)
	Epoxy	Single T_g; FTIR; NMR	Miscible before and after curing with 2,2′-bis[4-(4-aminophenoxy)phenyl] propane (Zheng et al. (2003d))	Guo nad Groeninckx (2001), Ni and Zheng (2005), Zheng et al. (2003a, c, d)
	Ester	DSC; SALS; X-ray diffraction; microscopy	II was made from terephthaloyl chloride and 4,4′-bis (6-hydroxyhexyloxy)biphenyl	Van Ende et al. (1992)
	Ester, unsaturated	Single T_g; FTIR; T_m-depression	–	Salom et al. (2006)

Ethylene, chlorinated	Single T_g; WAXS; SAXS; TEM	Semicrystalline when ≤90 % II; II had ≥30 % Cl; two T_g's when II had 25 % Cl	Aubin et al. (1982), Belorgey and Prud'homme (1982), Defieuw et al. (1989c), Groeninckx et al. (1988), Plivelic et al. (2007)
Hydroxyether of bisphenol-A (Phenoxy)	Single T_g; melt transparent; IGC; FTIR	Semicrystalline when >50 wt% I	Brode and Koleske (1972), Defieuw et al. (1989b), De Juann et al. (1994), Harris et al. (1982), Kuo et al. (2001a)
Hydroxyether of bisphenol-A, partially acetylated	Single T_g; T_m-depression, FTIR	I had a degree of acetylation of 5–90 mol%	Ma et al. (1999), Zheng et al. (1997c)
Methoxystyrene-*co*-*p*-vinylphenol	Single T_g; T_m-depression, FTIR	I had 60 mol% methoxystyrene	Sanchis et al. (1998)
Nitrocellulose	Single T_g	≥50 % I; semicrystalline when ≥50 % I	Brode and Koleske (1972), Hubbell and Copper (1977, 1979)
Novolac	Single T_g; T_m-depression, FTIR	–	Kuo and Chang (2001a), Kuo et al. (2001a)
Phenol catechin	Single T_g; T_m-depression, FTIR	–	Zhu et al. (2003)
Phenyl methacrylate	Single T_g; FTIR; OM	–	Woo and Mandal (1999), Woo et al. (2000d)
Propylene, chlorinated	Single T_g	I had 66 wt% Cl; semicrystalline when ≥50 wt% I	Allard and Prud'homme (1982), Aubin et al. (1982)
Vinyl acetate-*co*-vinylidene chloride	Single T_g	II was Saran C (≥80 mol% vinylidene chloride); semicrystalline	Aubin et al. (1983), Chiu and Min (2000), Zhang and Prud'homme (1987)
Vinyl bromide	Single T_g	Semicrystalline when >30 % I	Coleman et al. (1991a), Vogl et al. (1997)

(continued)

Table 21.1 (continued)

Polymer I of	Polymer II of	Method	Comments	Refs.
	Vinyl chloride	Single T_g; NMR; FTIR; T_m-depression	Semicrystalline when ≥ 30 % I; II was head-to-head or head-to-tail (Vogl et al. (1997))	Brode and Koleske (1972), Chiu and Min (2000), Hubbell and Copper (1977, 1979), Koleske and Lundberg (1969), Kwak (1994), Ma et al. (1999), Nojima et al. (1986a), Ong and Price (1978), Vogl et al. (1997), Woo et al. (1985b), Ziska et al. (1981)
	Vinyl chloride, chlorinated	Single T_g	II had 67.2 wt% Cl; semicrystalline when ≥ 50 wt% I	Belorgey et al. (1982)
	Vinyl chloride-co-vinylidene chloride	Single T_g	Semicrystalline; II had 79 % or 88 % vinylidene chloride; some samples of II were Saran B	Aubin et al. (1983), Varnell et al. (1983), Woo et al. (1983, 1986), Zhang and Prud'homme (1987)
	Vinylidene fluoride	T_m-Depression	Semicrystalline	Jo et al. (1992b)
Caprolactone-co-ethylene terephthalate	Carbonate of bisphenol-A	Single T_g	I had <60 wt% ethylene terephthalate	Ma et al. (1995)
	Ethylene, chlorinated	Single T_g	I had 33–89 wt% ethylene terephthalate; II had 67.2 wt% Cl	Ma and Prud'homme (1990), Zhao et al. (1991)
	Hydroxyether of bisphenol-A	Single T_g; FTIR	I had 48, 58, 72, and 82 wt% ethylene terephthalate	Zhang et al. (1995b)
	Vinyl chloride	Single T_g	I had 33 or 44 wt% ethylene terephthalate	Ma and Prud'homme (1990)
	Vinyl chloride, chlorinated	Single T_g	I had 33 wt% ethylene terephthalate	Ma and Prud'homme (1990)

Carbon monoxide-*co*-ethyl acrylate-*co*-ethylene	Vinyl chloride	Single T_g	Semicrystalline when I had >60 % ethylene; I had 4.0–19.6 % carbon monoxide, 5.5–35.4 % ethyl acetate, and 34.2–79.6 % ethylene	Robeson and McGrath (1977)
Carbon monoxide-*co*-2-ethylhexyl acrylate-*co*-ethylene	Vinyl chloride	Single T_g	I had 17.8/34.2/47.9 or 18.6/ 39.6/41.8 = carbon monoxide/ 2-ethylhexyl acrylate/ethylene	Robeson and McGrath (1977)
Carbon monoxide-*co*-ethylene-*co*-vinyl acetate	Chlorostyrene	Single T_g	I was Elvaloy 741; II was a mixture of *o*- and *p*- isomers	Allard and Prud'homme (1982)
	Propylene, chlorinated	Single T_g	I was Elvaloy 741	Allard and Prud'homme (1982)
	Vinyl chloride	Single T_g	Semicrystalline when I had >60 % ethylene; I was Elvaloy 741 or 10.5/66.7/22.8 or 10.2/ 58.2/31.5 = carbon monoxide/ ethylene/vinyl acetate	Anderson et al. (1979), Bair et al. (1978), Robeson and McGrath (1977)
Carbon monoxide-alt-phenylacetylene	Caprolactone	Single T_g	Semicrystalline	Chen et al. (1996)
	Styrene	Single T_g	–	Chen et al. (1996)
Carbonate of bisphenol-A	Benzoyl paraphenylene	Single T_g; SEM	–	Ha et al. (2001)
	Biphenyl-4,4'ylene sebacate	Single T_g	Up to 40 wt% II in blend	Jo et al. (1992a)
	p-t-Butylphenol formaldehyde	Single T_g	–	Kalkar and Roy (1993)
	Butylene adipate	Single T_g; FTIR	Semicrystalline	Cruz et al. (1979b, c), Mishra and Venkidusamy (1995)
	Caprolactone	Single T_g; SAXS; SANS; NMR; T_m-depression	Semicrystalline, especially when ≥25 wt% II	Balsamo et al. (2001), Cruz et al. (1979b, c), Cheung and Stein (1994), Cheung et al. (1993, 1994), Chun et al. (2000), Herrera et al. (2005), Ma et al. (1999), Paul et al. (1977)
	Caprolactone-*co*-ethylene terephthalate	Single T_g	II had 48 or 58 wt% ethylene terephthalate	Zhang et al. (1995c)

(continued)

Table 21.1 (continued)

Polymer I of	Polymer II of	Method	Comments	Refs.
	Carbonate	Single T_g; transparency	II was carbonate of bisphenol-E, bisphenol-F, bisphenol-Z, bisphenol chloral, dimethylbisphenol-A, dimethylbisphenol-A, or tetramethylbisphenol-F	Kim and Paul (1992a)
	1,4-Cyclohexane-dimethylene succinate	Single T_g	Semicrystalline	Cruz et al. (1979c, 1980)
	1,4-Cyclohexane-dimethylene terephthalate	Single T_g; melt transparent	Semicrystalline	Cruz et al. (1979c), Landry and Hendrichs (1989), Mohn et al. (1979)
	Cyclohexyl methacrylate-co-methyl methacrylate	Single T_g; NMR	II had 6.1–43.8 wt% cyclohexyl methacrylate	Hung et al. (1994), Min et al. (1990), Nishimoto et al. (1991)
	Cyclohexyl methacrylate-co-methyl methacrylate-co-2,4,6-tribromophenyl methacrylate	Single T_g; light scattering	II had 70 mol%methyl methacrylate and 10 mol% cyclohexyl methacrylate	Ohnaga et al. (1997)
	Ester	Single T_g; melt transparent	Semicrystalline when cast form solvent up to 80 wt% II; II was prepared from bisphenol-A and 1/1 = terephthalic/isophthalic acid	Mondragon et al. (1983)
	Ester	Single T_g; FTIR	II was prepared from bisphenol-A and 1/1 = terephthalic/isophthalic acid	Sakar et al. (2010)

Ester	Single T_g	II was made from terephthalic acid and 1,4-cyclohexanedimethanol and up to 60 mol% ethylene glycol	A23
Ester	Single T_g; melt transparent	Semicrystalline; II was KODAR Alexandrovich et al. (1980)0, made from 1,4-cyclohexanedimethanol and 1/4 = isophthalic/terephthalic acid	Cruz et al. (1979c), Lee et al. (2006), Masi et al. (1980), Mohn et al. (1979), Zipper et al. (1995)
Ester	Single T_g	II was Hytrel 5556, a multiblock copolymer with poly(tetramethylene ether) glycol terephthalate soft segment and tetramethylene terephthalate hard segment	Gaztelumendi et al. (1988)
Ester	Single T_g; positron annihilation lifetime spectroscopy	II was made from 1,4-cyclohexanedimethanol and 1,4-cyclohexanedicarboxylic acid	Zipper et al. (1995)
Ester	Single T_g	4 different polyesters	Kollodge and Porter (1993)
Ester	Single T_g	I had 2–7 methylene segment per ester group	Ellis (1998)
Ester, liquid crystalline	Single T_g; positron annihilation lifetime spectroscopy; SEM	II was made from p-hydroxybenzoic acid and phenylene isophthalate	Hsieh et al. (1999)
Ethylene adipate	Single T_g	Semicrystalline	Cruz et al. (1979b, c)
Ethylene succinate	Single T_g	Semicrystalline	Cruz et al. (1979b, c)

(continued)

Table 21.1 (continued)

Polymer I of	Polymer II of	Method	Comments	Refs.
	Ethylene terephthalate	Single T_g	Semicrystalline; ≥50 or 75 % II; two T_g's when ≤60 % II	Hendrichs et al. (1988), Murff et al. (1984), Nassar et al. (1979), Pellow-Jarman et al. (1995)
	p-(2-Hydroxy-hexafluoroisopropyl) styrene-co-styrene	Single T_g; transparency	II had 29–78 mol% styrene; immiscible when II had 83 mol % styrene	Min and Pearce (1981), Pearce et al. (1984), Ting et al. (1980)
	Maleic anhydride-co-styrene	Light scattering	II had 8 % maleic anhydride	Saito and Inoue (1987)
	Methacrylic acid-co-styrene	Single T_g	II had 2–23 wt% methacrylic acid	Akiyama et al. (1987, 1991)
	Methyl methacrylate	Single T_g; WAXD; NMR	Blends prepared by precipitation of THF solutions in n-heptane or cast from hot THF solutions; phase behavior governed by kinetics of solvent evaporation rate (Woo and Su (1996b))	Asano et al. (1992), Chiow et al. (1987), Kyu and Saldanha (1988, 1989), Landry and Hendrichs (1989), Park and Hong (1998), Saldanha and Kyu (1987), Uyar et al. (2005), Woo and Su (1996a, b)
	Methyl methacrylate-co-p-methylstyrene	Single T_g	II had ≥70 wt% methyl methacrylate	Ikawa and Hosoda (1991)
	Methyl methacrylate-co-N-phenylmaleimide	Single T_g	II had ≥70 wt% methyl methacrylate	Ikawa and Hosoda (1991), Merfeld et al. (1999)
	Methyl methacrylate-co-phenyl methacrylate	Single T_g	II had 16–63 wt% phenyl methacrylate	Nishimoto et al. (1991), Ohnaga et al. (1997)
	Methyl methacrylate-co-styrene	Single T_g	II had ≤14 wt% styrene	Min and Paul (1989)
	Methyl methacrylate-co-2,4,6-tribromophenyl methacrylate	Single T_g; light scattering	II had 52.3–90 wt% methyl methacrylate	Ohnaga et al. (1997), Merfeld et al. (1999)

Novolac	Single T_g	II had $M_w = 1$ kg/mol and was made from formaldehyde and 13/17/70 mol% = p-t-butylphenyl/m-cresol/o-cresol	Fahrenhlotz and Kwei (1981)
Phenyl methacrylate	Single T_g	–	Kyu et al. (1992), Nishimoto et al. (1991)
Pyrrole	Single T_g	Blend had 7 % II	Wang et al. (1990)
Styrene, sulfonated and metal neutralized	Single T_g; FTIR	II had various degrees of sulfonation and neutralized by Na or Li	Lu and Weiss (1996b)
Urethane	Single T_g	II was based on 3,3'-diphenylmethane diisocyanate and aliphatic polycarbonate diols and/or polytetramethylene glycol	Fambri et al. (1997)
Vinyl acetate	Single T_g; WAXD; NMR	Formed by coalescence of gamma-cyclodextrin inclusion complex	Uyar et al. (2005)
Vinylidene chloride-co-vinyl chloride	Single T_g	II had 13.5 wt% vinyl chloride; semicrystalline when ≤25 wt% I	Woo et al. (1985a)
Carbonate of bisphenol-A, cyclic oligomer			
Acrylonitrile-co-styrene	Single T_g; transparency	II had 16–35 wt% acrylonitrile	Kambour et al. (1994)
Carbonate of bisphenol chloral	Single T_g; transparency	–	Kambour et al. (1994)
Carbonate of tetramethylbisphenol-A	Single T_g; transparency	–	Kambour et al. (1994)
Ethersulfone	Single T_g; transparency	–	Kambour et al. (1994)
Etherimide	Single T_g; transparency	–	Kambour et al. (1994)
Formal of bisphenol-A	Single T_g; transparency	–	Kambour et al. (1994)
Methyl methacrylate	Single T_g; transparency	–	Kambour et al. (1994)
Phenyl sulfone	Single T_g; transparency	–	Kambour et al. (1994)
Sulfone	Single T_g; transparency	–	Kambour et al. (1994)
Vinyl acetate	Single T_g; transparency	–	Kambour et al. (1994)
Xylylene ether	Single T_g; transparency	–	Kambour et al. (1994)

Table 21.1 (continued)

Polymer I of	Polymer II of	Method	Comments	Refs.
Carbonate of dimethylbisphenol-A	Styrene	Single T_g	–	Park et al. (2001b)
Carbonate of hexafluorobisphenol-A	Ethyl methacrylate	Single T_g; transparency	–	Fernandes et al. (1986d)
	Isopropyl methacrylate	Single T_g; transparency	$\leq$70 wt% I in blend	Kim and Paul (1992d)
	Methyl methacrylate	Single T_g; transparency	–	Kim and Paul (1992d)
	n-Propyl methacrylate	Single T_g; transparency	–	Kim and Paul (1992d)
Carbonate of 2,2-propane-bis(4-(2-methylphenyl))-co-carbonate of 2,2-propane-bis(4-(2,6-dimethylphenyl))	Methyl methacrylate-co-styrene	Single T_g	I had $\geq$60 wt% carbonate of 2,2-propane-bis(4-(2,6-dimethylphenyl)); II had $\leq$37 wt% methyl methacrylate	Yoo and Kim (2004a)
Carbonate of tetrachlorobisphenol-A	Vinyl chloride	Single T_g	–	Neill and Karasz (2000)
	Vinyl chloride, chlorinated	Single T_g	II had $\leq$70.2 wt% Cl	Neill and Karasz (2000)
Carbonate of tetramethylbisphenol-A	Acrylonitrile-co-styrene	Single T_g; FTIR	II had <13 % acrylonitrile	Ahn et al. (1991b), Fernandes et al. (1986d), Kim et al. (1993a)
	Alkyl methacrylate-co-styrene	Single T_g	II had an alkyl group of methyl, ethyl, n-propyl, n-butyl, cyclohexyl, or phenyl	Kim et al. (2002c), Moon et al. (2002)
	Allyl alcohol-co-styrene	Single T_g	II had <19.1 wt% allyl alcohol	Fernandes et al. (1986d)
	Butylene sebacate	Single T_g	Semicrystalline	Fernandes et al. (1986e)
	Caprolactone	Single T_g; dielectric spectroscopy	Semicrystalline	Fernandes et al. (1986e), Madbouly et al. (2006)
	Carbonate of bisphenol-A	Single T_g; transparency	–	Belaribi et al. (1986), Kim and Paul (1992a)

	Carbonate of bisphenol-AP	Single T_g; transparency; dielectric spectroscopy	–	Kim and Paul (1992a), Mansour and Madbouly (1995)
	Carbonate	Single T_g; transparency	II was carbonate of bisphenol-E, bisphenol-F, bisphenol-S, bisphenol-Z, bisphenol chloral, dimethylbisphenol-A, dimethylbisphenol-Z, norbornane, tetramethylbisphenol-F, or tetramethylbisphenol-P	Kim and Paul (1992a)
	Ester	Single T_g	II was decamethylene decamethylene dicarboxylate, decamethylene sebacate, ethylene adipate, hexamethylene decamethylene dicarboxylate, or hexamethylene sebacate	Fernandes et al. (1986e)
	Maleic anhydride-co-styrene	Single T_g	II had 8 % maleic anhydride	Fernandes et al. (1986d)
	Methyl methacrylate-co-styrene	Single T_g	II had <50 wt% methyl methacrylate	Min and Paul (1987), Yu et al. (1991)
	α-Methylstyrene	Single T_g	–	Fernandes et al. (1986e)
	p-Methylstyrene-co-tetrahydrofurfuryl methacrylate	Single T_g	II had ≤50 mol% tetrahydrofurfuryl methacrylate	Goh et al. (1992c)
	Styrene-co-tetrahydrofurfuryl methacrylate	Single T_g	II had ≤53 mol% tetrahydrofurfuryl methacrylate	Goh et al. (1992c)
3-Carboxypropylmethyl siloxane	Vinylpyridine	Single T_g, FTIR; XPS	II was 2- or 4-vinylpyridine	Li et al. (2001b)
3-Carboxypropylmethyl siloxane-co-dimethylsiloxane	Vinylpyridine	Single T_g, FTIR; XPS	II was 2- or 4-vinylpyridine; I had ≥23 mol% acid groups	Li et al. (2001b)

(continued)

Table 21.1 (continued)

Polymer I of	Polymer II of	Method	Comments	Refs.
Cellulose	Acrylonitrile	NMR; single T_g; microscopy; WAXD	–	Masson and Manley (1992), Nishio et al. (1987), VanderHart et al. (1994)
	Caprolactone	NMR	–	Masi et al. (1980)
	Ethylene glycol	Single T_g; FTIR; WAXD	–	Guo and Liang (1999), Kondo et al. (1994), Nishio et al. (1989a)
	Vinyl acetate	Single T_g	≥70 % I in blend	Nishio and Manley (1988)
	Vinyl alcohol	NMR; FTIR; T_m-depression	–	Kondo et al. (1994), Masson and Manley (1992), Nishio et al. (1989b), Radloff et al. (1996), Shibayama et al. (1991), Schartel et al. (1996)
	4-Vinylpyridine	Single T_g; NMR	–	Masson and Manley (1991), VanderHart et al. (1994)
Cellulose acetate	2,6-Dimethyl-1,4-phenylene ether, phosphonate derivative	Single T_g	II had 9.5 % P	Cabasso et al. (1977)
	2,6-Dimethyl-3-bromo-1,4-phenylene ether, phosphonate derivative	Single T_g	II had 10.5 % P	Cabasso et al. (1977)
	Ethylene succinate	Single T_g; NMR	Blend had ≥70 % I	Buchanan et al. (1997)
	Methyl methacrylate	Single T_g	I had a degree of substitution of 2.95	Ohno and Nishio (2007)
	Methyl methacrylate-co-N-vinylpyrrolidone	FTIR; NMR	Miscibility depended on degree of substitution of I and composition of II	Ohno and Nishio (2007)
	Styrene, phosphonate derivative	Single T_g	II had 8.0 % P	Cabasso et al. (1977)
	Styrene, phosphorylated	Single T_g	II had more than 1 phosphoryl group per 4 styrene units	Martuscelli et al. (1991)

	Styrenephosphonate ester	Single T_g	Blend initially prepared was heterogeneous and became miscible when annealed above T_g	Sun et al. (1989)
	Vinylidene chloride-co-styrene, phosphonylated, chloromethylated	Single T_g; electron microscopy	I was Eastman 394-45; II had 7 % P, 14.5 % Cl	Cabasso et al. (1974)
	Vinylidene chloride-co-styrene, phosphonylated	Single T_g	II had 8.6 % P	Cabasso et al. (1977)
	Vinyl acetate-co-N-vinylpyrrolidone	Single T_g; FTIR	II had >25 mol% vinylpyrrolidone	Miyashita et al. (2002), Ohno et al. (2005)
	N-Vinylpyrrolidone	Single T_g; FTIR	–	Miyashita et al. (2002), Ohno et al. (2005)
	4-Vinylpyridine	Single T_g; cast films transparent	Semicrystalline; I had 39.4 % acetyl content or had 10H/2 glucose	Aptel and Cabasso (1980), Cabasso (1981)
Cellulose acetate butyrate	Ethylene-co-vinyl acetate	Single T_g; transparent films	I had 18.5/45 = acetic acid/ butyric acid and II had 80 % vinyl acetate; two T_g's when II had 70 % vinyl acetate	Casper and Morbitzer (1977), Kosai and Higashino (1975)
	Ethylene glycol	Single T_g; OM; SAXS	–	Park and Kim (2002)
	Hydroxybutyrate-co-valerate	Single T_g; WAXD; NMR	II had 10 mol% valerate; miscible when blend had 20–50 % II, and partially miscible when blend had 60–80 % II	Buchannan et al. (1992)
	Vinyl acetate-co-N-vinylpyrrolidone	Single T_g; transparency	Miscibility depended on degree of substitution of I and composition of II	Ohno and Nishio (2006)
	p-Vinylphenol	Single T_g; FTIR	–	Gaibler et al. (2004)
Cellulose acetate hydrogen phthalate	Methyl methacrylate	Single T_g	–	Rao et al. (1999)
	N-Vinylpyrrolidone	Single T_g	–	Rao et al. (2000)

(continued)

Table 21.1 (continued)

Polymer I of	Polymer II of	Method	Comments	Refs.
Cellulose butyrate	Vinyl acetate-*co*-*N*-vinylpyrrolidone	Single T_g; transparency	II had >80 mol% vinylpyrrolidone	Ohno and Nishio (2006)
	N-Vinylpyrrolidone	Single T_g; transparency	I had a degree of substitution of 2.41; immiscible if degree of substitution >2.5	Ohno and Nishio (2006)
Cellulose acetate propionate	Alkylene glutarate	Single T_g; transparency	The alkylene group was ethylene, diethylene, hexamethylene, pentamethylene, tetramethylene, or trimethylene	Buchanan et al. (1993)
	Epichlorohydrin	Single T_g; transparency	–	Yamaguchi and Masuzawa (2008)
	p-Vinylphenol	Single T_g; FTIR	–	Gaibler et al. (2004)
Cellulose diacetate	*N*-Vinyl pyrrolidone	Single T_g	–	Yin et al. (1997)
Cellulose triacetate	Cyanoethyl cellulose	Single T_g; SEM; FTIR	–	Guo et al. (1993b)
Chitin	Glycidyl methacrylate	Single T_g	–	Miyashita et al. (1997)
	2-Hydroxyethyl methacrylate	Single T_g; FTIR	–	Castro et al. (2005)
	Tertiary amide	Single T_g; transparency	I was 47 % deacetylated; II was *N*-vinylpyrrolidone, *N*-vinylacetamide, or acrylamide	Nishio et al. (1999)
	Vinyl acetate	FTIR; transparency	–	Lee et al. (1996b)
	Vinyl alcohol	Single T_g; T_m-depression	I had a degree of deacetylation of 28 %	Castro et al. (2005), Cho et al. (2001)
	N-Vinylpyrrolidone	Single T_g; FTIR; transparency	–	Miyashita et al. (1995)
Chitin, acyl derivative	Caprolactone	Single T_g; FTIR	Miscibility depended on the nature of carbon atoms in acyl group	Sugimoto et al. (2010)
Chitin-g-2-methyl-2-oxazoline	Vinyl chloride	Single T_g; FTIR	Blend had ≤10 wt% I	Aoi et al. (1995a)

			Formed complexes	
Chitosan	2-Acryloylamino-2-methylpropane sulfonic acid	–		Stoilova et al. (1999)
	Caprolactone	Single T_g; T_m-depression	–	Sarasam and Madihally (2005)
	Ethylene glycol	T_m-Depression; FTIR; WAXD	–	Rakkapao et al. (2011), Zhao et al. (1995)
	Tertiary amide	Single T_g; FTIR	II was N-vinylpyrrolidone, N-methyl-N-vinylacetamide, 2-ethyl-2-oxazoline, or 2-methyl-2-oxazoline	Fang and Goh (2000)
	N-Vinylpyrrolidone	FTIR; transparency; WAXD	–	Cao et al. (1999), Demirci et al. (2009), Sakurai et al. (2000), Yilmaz et al. (2005)
Chitosan acetate	Ethylene glycol	FTIR; SEM	–	Wrzyszczynski et al. (1995)
p-Chloro-(3-ethenoxypropyl) cinnamate	p-Methoxy-(6-ethenoxyhexyl) cinnamate	Single T_g	–	Lin et al. (1989)
	p-Methoxy-(6-ethenoxypropyl) cinnamate	Single T_g	–	Lin et al. (1989)
	p-Methyl-(3-ethenoxypropyl) cinnamate	Single T_g	–	Lin et al. (1989)
1-Chloroethyl methacrylate	Alkyl methacrylate	Single T_g; transparency	II had an alkyl group of methyl, ethyl, n-propyl, isopropyl, n-butyl, or tetrahydrofurfuryl	Peng et al. (1993)
	Ester	Single T_g; transparent melt	II was butylene adipate, caprolactone, 2,2-dimethyl-1,3-propylene adipate, 2,2-dimethyl-1,3-propylene sebacate, ethylene adipate, or hexamethylene sebacate	Peng et al. (1993, 1994a)

Table 21.1 (continued)

Polymer I of	Polymer II of	Method	Comments	Refs.
2-Chloroethyl methacrylate	Alkyl methacrylate	Single T_g; transparent melt	II had an alkyl group of methyl, ethyl, or tetrahydrofurfuryl	Neo et al. (1991b)
	Ester	Single T_g; transparent melt	II was butylene adipate, caprolactone, 2,2-dimethyl-1,3-propylene adipate, 2,2-dimethyl-1,3-propylene sebacate, ethylene adipate, or hexamethylene sebacate	Neo and Goh (1991b, 1992b)
	N-Vinylpyrrolidone	Single T_g	–	Neo and Goh (1991d)
Chloromethyl methacrylate	Alkyl methacrylate	Single T_g	II had an alkyl group of methyl, ethyl, n-propyl, isopropyl, acetonyl, or tetrahydrofurfuryl	Chong et al. (1990b), Goh et al. (1990a)
	Carbonate of bisphenol-A	Single T_g	Miscibility depended on method of preparation	Goh et al. (1990b)
	Ester	Single T_g; transparent melt	II was butylene adipate, caprolactone, 2,2-dimethyl-1,3-propylene adipate, 2,2-dimethyl-1,3-propylene sebacate, 2,2-dimethyl-1,3-propylene succinate, ethylene succinate, ethylene adipate, ethylene succinate, or hexamethylene sebacate	Neo and Goh (1991b, 1992b)
	N-Vinylpyrrolidone	Single T_g	–	Neo and Goh (1991d)
Chloroprene	Ethylene-co-methyl acrylate	Single T_g; phase contrast microscopy; WAXD	Semicrystalline; II had 21 wt% methyl acrylate (Kundu et al. (1996c))	Kalfoglou and Margaritis (1984), Kundu et al. (1996a), Kundu et al. (1996c)
	Isoprene, epoxidized	Single T_g; FTIR	II had 50 mol% epoxidation (Kim et al. (1998))	Kim et al. (1998), Nagode and Roland (1991)

3-Chloropropyl methacrylate	Acrylonitrile-*co*-*p*-methylstyrene	Single T_g	II had 15–33 wt% AN	Low et al. (1993a)
	Acrylonitrile-*co*-styrene	Single T_g	II had 12–35 wt% AN	Low et al. (1993a)
	Ester	Single T_g	II was butylene adipate, caprolactone, 2,2-dimethyl-1,1,3-propylene adipate, or hexamethylene sebacate	Low et al. (1994c)
	Tetrahydrofurfuryl methacrylate	Single T_g	–	Low et al. (1993c)
o-Chlorostyrene	Styrene	Single T_g	–	Kalfoglou and Margaritis (1984)
o-Chlorostyrene-*co*-*p*-chlorostyrene	2,6-Dimethyl-1,4-phenylene ether	Single T_g; transparency	I had 23–64 % *p*-chlorostyrene	Alexandrovich et al. (1977)
	Styrene	Single T_g	After quenching from 145 °C; I had 71–92 mol% *o*-chlorostyrene; two T_g's when I had $\leq$62 mol% *o*-chlorostyrene	Cimmino et al. (1992), Ten Brinke et al. (1984)
o-Chlorostyrene-*co*-*o*-fluorostyrene	2,6-Dimethyl-1,4-phenylene ether	Single T_g; transparency; NMR	I had 14–40 mol% *o*-chlorostyrene; two T_g's when I had >36 mol% *o*-chlorostyrene	Andreis et al. (1992), Vukovic et al. (1982a), Vukovic et al. (1983c)
p-Chlorostyrene-*co*-*o*-fluorostyrene	2,6-Dimethyl-1,4-phenylene ether	Single T_g; transparency; NMR	I had 13–74 mol% *p*-chlorostyrene; two T_g's when I had >74 mol% *p*-chlorostyrene	Andreis et al. (1992), Vukovic et al. (1982a), Vukovic et al. (1983c)
p-Chlorostyrene-*co*-styrene	2,6-Dimethyl-1,4-phenylene ether	Single T_g	I had $\geq$34.7 mol% styrene; two T_g's when I had <34.7 mol% styrene	Fried et al. (1978), Karasz et al. (1974), Shultz and Beach (1974)

Table 21.1 (continued)

Polymer I of	Polymer II of	Method	Comments	Refs.
Cinnamic acid-*co*-styrene	2-Diaminomethylaminoethyl methacrylate	Single T_g; FTIR	I had 5, 8, or 23 mol% cinnamic acid	Boulash et al. (1999b)
	Ethyl methacrylate	Single T_g; IGC	I had 5, 8, or 23 mol% cinnamic acid	Boulash and Amrani (2001)
	Ethyl methacrylate-*co*-4-vinylpyridine	Single T_g	I had 5, 8, or 21 mol% cinnamic acid; II had 13 or 23 mol% vinylpyridine	Boulash et al. (1999a)
	Methyl methacrylate	Single T_g; FTIR	I had 23 mol% cinnamic acid	Boulash and Amrani (2007)
	Methyl methacrylate-*co*-vinylpyridine	Single T_g; FTIR	I had 23 mol% cinnamic acid; II was 2- or 4-vinylpyridine; II had 15 or 16 mol% vinylpyridine	Boulash and Amrani (2007)
	4-Vinylpyridine	Single T_g; FTIR	Formed complexes	Boulash et al. (2008)
Collagen hydrolysate	Ethyl acrylate	Single T_g	–	Mindru et al. (1983)
2-Cyanoethyl methacrylate	Alkyl methacrylate	Single T_g	II had an alkyl group of methyl, acetonyl, 2-hydroxyethyl, 2-hydroxypropyl, or tetrahydrofurfuryl	Yeo et al. (1994a, b, 1995a)
	2-Ethyl-2-oxazoline	Single T_g; FTIR	Blend had >80 wt% I	Yeo et al. (1995b)
	Tertiary amide	Single T_g; FTIR	II was *N*-vinylpyrrolidone, *N*, *N*-dimethylacrylamide, or *N*-methyl-*N*-vinylacetamide; formed complexes	Yeo et al. (1995b)
Cyanomethyl methacrylate	Alkyl methacrylate	Single T_g; FTIR	II had an alkyl group of acetonyl, 2-hydroxyethyl, or 2-hydroxypropyl	Yeo et al. (1995a)
	2-Ethyl-2-oxazoline	Single T_g	Blend had ≥60 wt% I	Yeo et al. (1995b)
	Tertiary amide	Single T_g	II was *N*-vinylpyrrolidone, *N*, *N*-dimethylacrylamide, or *N*-methyl-*N*-vinylacetamide; formed complexes	Yeo et al. (1995b)

Component 1	Component 2	Method	Comments	Reference
Cyclohexyl methacrylate-co-methyl methacrylate	Carbonate of bisphenol-A	Single T_g	I had 9.5–40.4 wt% CHMA	Park et al. (2001)
	Carbonate of dimethylbisphenol-A	Single T_g	I had 28.5–66.7 wt% CHMA	Park et al. (2001)
	Carbonate of tetramethylbisphenol-A	Single T_g	I had 0–36.7 wt% CHMA	Park et al. (2001)
1,4-Cyclohexane dimethylene succinate	Epichlorohydrin	Single T_g	Semicrystalline	Fernandes et al. (1984)
	Vinyl chloride-co-vinylidene chloride	Transparent melt; large T_m-depression	II was Saran (86.5 % vinylidene chloride)	Woo et al. (1983)
	Hydroxyether of bisphenol-A (Phenoxy)	Single T_g; transparent melt	Semicrystalline ≥50 wt% I	Harris et al. (1982)
	Vinyl chloride	Single T_g	Semicrystalline ≤30 wt% II	Zhuang et al. (1988)
Cyclohexyl methacrylate	Methyl methacrylate-co-styrene	Single T_g	–	Pomposo et al. (1998)
	Vinyl chloride	Single T_g; NMR	–	Parmer et al. (1988)
	Vinyl chloride-co-vinylidene chloride	Single T_g	Semicrystalline ≥75 % II; II had 86.5 wt% vinylidene chloride	Kang et al. (1988), Woo et al. (1984b)
	2-Vinylnaphthalene	Single T_g; excimer fluorescence	I had low M_w; II had M_w = 70 kg/mol	Frank and Zin (1987)
Decamethylene decamethylene dicarboxylate	Vinyl chloride	Single T_g	Semicrystalline	Woo et al. (1985b)
Decamethylene sebacate	Epichlorohydrin	Single T_g	Semicrystalline	Fernandes et al. (1984)
2,6-Dibromo-1,4-phenylene ether	Styrene, sulfonated and metal neutralized	Single T_g; SEM	II had 3.8 mol% sulfonation and Zn- or Mn-neutralized	Alkan and Aras (2001)
2,3-Dichloro-1-propyl acrylate	Ethyl acrylate-co-glycidyl methacrylate	Single T_g	II had 65 % ethyl acrylate	Davis et al. (1981)
2,2-Dichloroethyl methacrylate	Alkyl methacrylate	Single T_g; transparency	II had an alkyl group of methyl, ethyl, n-propyl, isopropyl, n-butyl, isoamyl, cyclohexyl, or tetrahydrofurfuryl	Low et al. (1994b)
2,6-Dichloro-1,4-phenylene ether	Styrene, sulfonated and metal-neutralized	Single T_g	II had 4.8 mol% sulfonation and Zn-neutralized	Mfih et al. (2003)

(continued)

Table 21.1 (continued)

Polymer 1 of	Polymer II of	Method	Comments	Refs.
2,6-Diethyl-1,4-phenylene ether	Styrene	Single T_g	–	Cizek (1968)
N,N-Dimethyl acrylamide	Alkyl methacrylate	Single T_g; FTIR	II had an alkyl group of chloromethyl, 2-chloroethyl, 3-chloropropyl, 2-bromoethyl, or 2-iodoethyl	Low et al. (1994d)
	Ethylene-co-vinyl alcohol	Single T_g; FTIR	II had 56, 68, or 78 mol% vinyl alcohol	Katime et al. (2000)
	Monoalkyl itaconate	Single T_g; FTIR	II had an alkyl group of methyl, ethyl, propyl, butyl, pentyl, hexyl, decyl, or dodecyl	Meaurio et al. (1997, 1998)
	Vinyl acetate-co-vinyl alcohol	Single T_g; FTIR	II had 15–84 mol% vinyl alcohol	Parada et al. (1998b)
	Vinyl alcohol	Single T_g; FTIR	–	Parada et al. (1998b)
	Vinylidene fluoride	Single T_g	Semicrystalline $\geq$60 wt% II	Galin (1984)
N,N-Dimethylacrylamide-co-ethylene	Vinyl chloride	Single T_g	I had 71.4 or 73.1 wt% ethylene; two T_g's when I had $\geq$75.1 wt% ethylene	Matzner et al. (1982)
2,6-Dimethyl-1,4-phenylene ether	Acrylic acid-co-t-butyl acrylate-co-potassium acrylate-co-styrene	Single T_g	II had 1.53 mol% butyl acrylate, 2.14 mol% acrylic acid, and 0.52 mol% potassium acrylate	Leung et al. (2001)
	Acrylic acid-co-styrene	Single T_g	II had 4.7–8.5 wt% acrylic acid	Benabdelghani et al. (1995), Gottschalk et al. (1994)
	p-Bromostyrene	Single T_g; transparency	Blend had $\leq$25 et% II	Aroguz and Baysal (2000)
	p-Bromostyrene-co-fluorostyrene	Single T_g; FTIR	II had 11–73 mol% p-bromostyrene	Mariam et al. (1986), Vukovic et al. (1988)
	t-Butyl acrylate-co-styrene	Single T_g	II had $\geq$76.6 mol% styrene	Leung et al. (2001)
	Cyclohexylmaleimide-co-styrene	Light scattering	I had 83 wt% styrene	Saito and Inoue (1987)

Dinitrostyrene-*co*-styrene	Single T_g	II had 3–14 mol% dinitrostyrene	Fernandez et al. (1997)
Ester	Single T_g; IGC	II was made from bisphenol-A and a mixture of isophthalic acid and terephthalic acid	Sakar et al. (2009)
o-Fluorostyrene-*co*-*p*-fluorostyrene	Single T_g; transparency	II had 10–38 % para isomer; two T_g's when II had 5 or ≥43 % para isomer	Karasz and MacKnight (1986), Vukovic et al. (1983b)
o-Fluorostyrene-*co*-styrene	Single T_g; transparency	II had ≥9 mol% styrene	Vukovic et al. (1981, 1982, 1983a)
p-Fluorostyrene-*co*-styrene	Single T_g; transparency	II had ≥44 mol% styrene	Maeda et al. (1986, 1989), Vukovic et al. (1981, 1982, 1983a)
p-(2-Hydroxy-hexafluoroisopropyl) styrene-*co*-styrene	Single T_g	II had 77.9–90.3 mol% styrene	Min and Pearce (1981), Min et al. (1983), Pearce et al. (1984), Ting et al. (1980)
Luloylmaleimide-*co*-styrene	Light scattering	II had 81 wt% styrene	Saito and Inoue (1987)
Maleic anhydride-*co*-styrene	Single T_g; transparency	II had 8 wt% maleic anhydride; two T_g's when II had 14 wt% maleic anhydride	Fried and Hanna (1982), Fried et al. (1982), Gottschalk et al. (1994), Witteler et al. (1993)
Methacrylic acid-*co*-styrene	DMA; FTIR: OM; IGC	II had 5.9 mol% methacrylic acid; immiscible when II had ≥7.2 mol% methacrylic acid	Akiba et al. (2000), Benabdelghani et al. (1995, 2006), Bazuin et al. (1993)
2-Methyl-6-benzyl-1,4-phenylene ether	Single T_g; transparency	–	Shultz and Gendron (1973)
Methyl methacrylate-*co*-styrene	Single T_g	II had ≤16.5 wt% methyl methacrylate	Goh and Lee (1988b), Gottschalk et al. (1994), Kressler et al. (1990b)
2-Methyl-6-phenyl-1,4-phenylene ether	Single T_g	–	Shultz and Gendron (1974a, b)

(*continued*)

Table 21.1 (continued)

Polymer I of	Polymer II of	Method	Comments	Refs.
	α-Methylstyrene	Single T_g	–	Cizek (1968), Kressler et al. (1990a), Robeson et al. (1974)
	α-Methylstyrene-co-styrene	Single T_g	All compositions of II	Kressler et al. (1990a), Shultz and Young (1983)
	o-Methylstyrene	NMR	NMR showed heterogeneity on a 3-nm scale	Dickinson et al. (1987)
	p-Methylstyrene	Single T_g	–	Dickinson et al. (1987), Fried et al. (1985), Su and Fried (1986)
	p-Nitrostyrene-co-styrene	Single T_g	II had <22 mol% nitrostyrene	Cowie et al. (1992a)
	Phenylmaleimide-co-styrene	Light scattering	II had 84 wt% styrene	Lokaj et al. (1995), Saito and Inoue (1987)
	Styrene	Single T_g; transparency; NMR; XPS	Older work showed some ambiguous results; II was syndiotactic (Duff et al. (2001))	Bair (1970), Balsamo et al. (2001), Drioli et al. (1978), Duff et al. (2001), Goh et al. (1999a), MacKnight et al. (1971), Mucha et al. (1981), Prest and Porter (1972), Shultz and Gendron (1972), Shultz and Gendron (1974a, b), Stoelting et al. (1970), VanderHart (1994), Wu and Woo (1999)
	Styrene, head-to-head	Single T_g	–	Kryszewski et al. (1982)
	Styrene, iodinated	Single T_g	II had ≤47 % iodination	Goh and Lee (1989b)
	Styrene, sulfonated and metal-neutralized	Single T_g	II had up to 7.8 mol% sulfonation (Register and Bell (1992)); metal was Zn, Mn, or Ni	Mih et al. (2003), Register and Bell (1992), Tomita and Register (1993)
	Styrene, syndiotactic	Single T_g	–	Cimmino et al. (1993)

	Styrene-b-isoprene-b-styrene	II had block M_w 15-51-17 and 78-52-80 kg/mol	Single T_g; with styrene blocks of II	Meyer and Tritscher (1978)
	2,2,6,6-Tetramethyl-piperidinyl methacrylate-co-styrene	II had ≤24 wt% 2,2,6,6-tetramethylpiperidinyl methacrylate	Single T_g	Goh and Lee (1987)
2,6-Dimethyl-1,4-phenylene ether, carboxylated	Urethane acrylate	I and II formed interpenetrating network	Single T_g; FTIR	Mengujoh and Frisch (1989)
	Styrene	11.8 mol% of repeat units in I carboxylated; two T_g's when 35.0 mol% repeat units in I carboxylated	Single T_g; FTIR	Liao et al. (1996), Xie et al. (1984)
	Styrene, sulfonated and metal-neutralized	II was neutralized with Li, Na, or Cs; miscible when I and II had similar amounts of functional groups	Single T_g	Pan et al. (1997)
2,6-Dimethyl-1,4-phenylene ether, brominated phosphonylated	Cellulose acetate	II was Eastman 394-45	Single T_g; electron microscopy	Cabasso et al. (1974)
2,6-Dimethyl-1,4-phenylene ether, modified	Epichlorohydrin, modified	Both I and II had at least 25 % carbazolyl or 3,5-dinitrobenzoyl groups	Single T_g	Pugh and Percec (1986)
2,6-Dimethyl-1,4-phenylene ether, modified with C_{60}	Acrylonitrile-co-styrene	I had 6.9 or 19.5 wt% C_{60}; II had ≤6.3 wt% AN	Single T_g	Goh et al. (2000a)
	p-Methylstyrene-co-styrene	I had 6.9 or 19.5 wt% C_{60}	Single T_g	Goh et al. (2000a)
	Styrenic monomer	I had 6.9 or 19.5 wt% C_{60}; II was styrene, α-methylstyrene, or p-methylstyrene	Single T_g	Goh et al. (2000a)
2,6-Dimethyl-1,4-phenylene ether, phenylsulfonated	o-Bromostyrene-co-styrene	I had 10.9–88 mol% o-bromostyrene	Single T_g	Vukovic et al. (1998)
	p-Bromostyrene-co-styrene	I had 10.6–90.4 mol% p-bromostyrene	Single T_g	Vukovic et al. (1998)
	p-Chlorostyrene-co-o-fluorostyrene	–	Single T_g	Vukovic et al. (1995)

Table 21.1 (continued)

Polymer I of	Polymer II of	Method	Comments	Refs.
	o-Chlorostyrene-*co*-*p*-fluorostyrene	Single T_g	–	Vukovic et al. (1995)
	o-Fluorostyrene-*co*-*p*-fluorostyrene	Single T_g	I had a degree of phenylsulfonation of 4–92 mol %; II had 14–93 mol% *o*-fluorostyrene	Vukovic et al. (1994a)
2,6-Dimethyl-1,4-phenylene ether, sulfonylated	Acrylonitrile-*co*-styrene	Single T_g	I had 20–26 wt% sulfonylation	Kang et al. (1987)
	p-Bromostyrene	Single T_g	I had >12 mol% sulfonylation	Vukovic et al. (1994c)
	o-Bromostyrene-*co*-*p*-bromostyrene	Single T_g	High *p*-bromostyrene content and high degree of sulfonylation favored miscibility	Vukovic et al. (1996b)
	o-Bromostyrene-*co*-*o*-fluorostyrene	Single T_g	Miscibility depended on compositions of I and II	Vukovic et al. (1996b)
	o-Bromostyrene-*co*-*p*-fluorostyrene	Single T_g	Miscibility depended on compositions of I and II	Vukovic et al. (1996b)
	p-Bromostyrene-*co*-*o*-fluorostyrene	Single T_g	Miscibility depended on compositions of I and II	Vukovic et al. (1996b)
	p-Bromostyrene-*co*-*p*-fluorostyrene	Single T_g	Miscibility depended on compositions of I and II	Vukovic et al. (1996b)
	o-Chlorostyrene-*co*-*p*-chlorostyrene	Single T_g	Miscibility not favored when I had high degree of sulfonylation and II had high *o*-chlorostyrene content	Vukovic et al. (1994b)
	o-Chlorostyrene-*co*-*p*-fluorostyrene	Single T_g	Miscibility depended on compositions of I and II	Vukovic et al. (1996a)
	p-Chlorostyrene	Single T_g	Degree of sulfonylation = 4–17 mol%	Vukovic et al. (1993, 1994b, 1996a)
	o-Fluorostyrene	Single T_g	Degree of sulfonylation = 4–17 mol%	Vukovic et al. (1993)

	Component	Method	Notes	References
	p-Fluorostyrene	Single T_g	Degree of sulfonylation = 4–17 mol%	Vukovic et al. (1993, 1996a)
	p-Fluorostyrene-co-styrene	Single T_g	I had 20–26 wt% sulfonylation	Kang et al. (1987)
	Phenylvinyl sec-butyl ether-alt-N-phenylmaleimide	Single T_g	I had 68–87 % sulfonylation	Vukovic et al. (1994d)
	Phenylvinyl ethyl ether-alt-N-phenylmaleimide	Single T_g	I had 61–91 % sulfonylation	Vukovic et al. (1994d)
	Styrene	Single T_g	I had <31 wt% sulfonylation	Kang et al. (1987)
	Styrene-co-4-vinylpyridine	Single T_g; FTIR; NMR	I had 3–12 mol% sulfonation; II had 3–10 mol% vinylpyridine; formed complexes when I had 12 mol% sulfonation and II had 10 mol% vinylpyridine (Pan et al. (2001))	Pan et al. (2001), Pan and Xue (2001)
α,α-Dimethyl-β-propiolactone (pivalolactone)	Vinyl chloride	T_m-Depression	Semicrystalline	Aubin et al. (1982), Aubin and Prud'homme (1980)
Dimethylsiloxane	Ethylene-co-methyl acrylate	Single T_g; FTIR	II had 21 wt% methyl acrylate; I had a small amount of vinyl groups	Santra et al. (1993a)
Dimethylsiloxane, modified	Butyl methacrylate	Single T_g; FTIR	One of the methyl groups in the repeating unit of I was changed to 4-hydroxy-4,4-bis (trifluoromethyl) butyl group	Chu et al. (1991)
	Ethylene glycol	Single T_g; FTIR	One of the methyl groups in the repeating unit of I was changed to 4-hydroxy-4,4-bis (trifluoromethyl) butyl group	Chu et al. (1991)
2,6-Dimethyl-4-vinylphenol	Alkyl methacrylate	Single T_g; FTIR	II had an alkyl group of ethyl, n-propyl, n-hexyl, or n-butyl	Coleman et al. (1996), Pehlert et al. (1996)
	Ethylene-co-vinyl acetate	Single T_g; FTIR	II had 45 or 70 wt% vinyl acetate	Coleman et al. (1996), Pehlert et al. (1996)
	Vinyl acetate	Single T_g; FTIR	–	Coleman et al. (1996), Pehlert et al. (1996)

(continued)

Table 21.1 (continued)

Polymer I of	Polymer II of	Method	Comments	Refs.
2,6-Diisopropyl-4-vinylphenol	Alkyl methacrylate	Single T_g; FTIR	II had an alkyl group of ethyl, *n*-butyl, *n*-hexyl, *n*-octyl, or *n*-decyl	Coleman et al. (1996), Pehlert et al. (1996)
	Ethylene-*co*-vinyl acetate	Single T_g; FTIR	II had 33, 45, or 70 wt% vinyl acetate	Coleman et al. (1996), Pehlert et al. (1996)
	Vinyl acetate	Single T_g; FTIR	–	Coleman et al. (1996), Pehlert et al. (1996)
2,6-Dipropyl-1,4-phenylene ether	Styrene	Single T_g	–	Cizek (1968)
Dodecamethylene adipamide, *N*, *N*-dimethyl substituted	*p*-(2-Hydroxy-hexafluoroisopropyl) styrene-*co*-styrene	Single T_g	Semicrystalline when ≤50 % substitution on I	Kotzev et al. (1984)
Dodecamethylene adipate	Epichlorohydrin	Single T_g	Semicrystalline	Fernandes et al. (1984)
	Vinyl chloride	Single T_g	Semicrystalline	Woo et al. (1985b)
Dodecamethylene decamethylene dicarboxylate	Vinyl chloride	Single T_g	Semicrystalline	Woo et al. (1985b)
Dodecamethylene dodecamethylene dicarboxylate	Vinyl chloride	Single T_g	Semicrystalline	Woo et al. (1985b)
Enaminonitrile	Ethylene glycol	Single T_g	–	Moore and Kim (1992)
	Tertiary amide	Single T_g	II was *N*, *N*-dimethylacrylamide, 2-ethyl-2-oxazoline, or *N*-vinylpyrrolidone	Moore and Kim (1992)
	4-Vinylpyridine	Single T_g	–	Moore and Kim (1992)
Epichlorohydrin	Acrylonitrile-*co*-styrene	Single T_g	II had 18 or 25 wt% acrylonitrile	Guo (1991)
	Alkyl acrylate	Single T_g	II had an alkyl group of ethyl or *n*-propyl	Fernandes et al. (1986b, c)
	Alkyl methacrylate	Single T_g	II had an alkyl group of ethyl, *n*-propyl, *n*-butyl, or cyclohexyl	Fernandes et al. (1986b)
	Butyl acrylate rubber	Single T_g	II was Hycar 4043	Fernandes et al. (1986c)

	Ester	Single T_g; T_m-depression	II was made from aliphatic glycols and aliphatic dicarboxylic acids	Fernandes et al. (1984), Kim et al. (1999b), Wetton and Williams (1988)
	Ethyl acrylate rubber	Single T_g	II was Hycar 4051EP	Fernandes et al. (1986c)
	Glycidyl methacrylate	Single T_g	–	Wetton and Williams (1988)
	Glycidyl methacrylate-co-methyl methacrylate	Single T_g	II had 76 % glycidyl methacrylate	Wetton and Williams (1988)
	Methacrylonitrile-co-methyl methacrylate	Single T_g	II had 30–40 mol% methacrylonitrile	Wetton and Williams (1988)
	Methyl methacrylate	Single T_g	Broad T_g might be due to separate phases with differing T_g's within the mixture	Akiyama et al. (1987), Clark et al. (1992), Fernandes et al. (1986b)
	Neopentyl glycol adipate	Single T_g; transparency	–	Fernandes et al. (1984), Goh et al. (1982a)
	Vinyl acetate	Single T_g; NMR; FTIR	–	Cheung et al. (2000), El Shafee (2002b), Guo (1990a)
Epichlorohydrin-co-ethylene glycol	Neopentyl glycol adipate	Transparency	I was Hydrin 200; refractive indices not equal in the temperature range investigated	Goh et al. (1984b)
Ester	Ester	Single T_g; microscopy	I and II were various linear aliphatic polyesters (13 miscible blend systems)	Braun et al. (1993)
	Ester	Melting behavior	Both polymers I and II were liquid crystalline; II had one more ethylene unit in the main chain	Darragas et al. (1994)
Ester, hyperbranched and 3,5-dihydroxyphenyl-terminated	Amide	Single T_g	II was PA-6	Massa et al. (1995)
	Aramide	Single T_g	II was Trogamid T or MXD-6	Massa et al. (1995)
	Butylene adipate	Single T_g	–	Massa et al. (1995)
Ester, hyperbranched and 3,5-diacetoxylphenyl-terminated	Butylene terephthalate	Single T_g	–	Massa et al. (1995)
	Ester	Single T_g	II was made from terephthalic acid and a mixture of ethylene glycol and 1,4-cyclohexane dimethanol	Massa et al. (1995)

(continued)

Table 21.1 (continued)

Polymer I of	Polymer II of	Method	Comments	Refs.
4-Ethenylpheno lmethylsiloxane	Acrylonitrile-*co*-styrene	Single T_g; AFM; transparency; XPS	II had 24–31 wt% acrylonitrile	Duan et al. (2001)
	N,N-Dimethylacrylamide	Single T_g; AFM; transparency; XPS	–	Duan et al. (2001)
	N-Vinylpyrrolidone	Single T_g; AFM; transparency; XPS	–	Duan et al. (2001)
	4-Vinylpyridine	Single T_g; AFM; transparency; XPS	–	Duan et al. (2001)
Etheretherketone	Aryl ether ketone	Single T_g; WAXD; FTRI; SEM	–	Woo and Tseng (1999)
	Arylketone	Single T_g	II had 25, 50, or 57 % ketone content	Harris and Robeson (1987)
	Etherdiphenyl ether ketone	Single T_g; WAXD	–	Jo et al. (1994c)
	Etherketone	Single T_g	I was poly(oxy-1,4-phenyleneoxy-1,4-phenylenecarbonyl-1,4-phenylene); II was poly (oxy-1,4-phenylenecarbonyl-1,4-phenylene); semicrystalline	Sham et al. (1988a)
	Etherimide	Single T_g	I was Victrex 450G; II was Ultem 1000; semicrystalline	Crevecoeur and Groeninckx (1991), Chen and Porter (1993), Chun et al. (1999), Goodwin and Simon (1996), Hsiao and Sauer (1993), Jenkins (2001), Lee and Kim (1997), Sauer and Hsiao (1993a)
	Ethersulfone	Single T_g	–	Yu et al. (1990)
	Ethylene terephthalate-*co*-*p*-hydroxybenzoic acid	Single T_g	–	Acierno and Naddo (1994)
	Imide	Single T_g	II was YS-30 (Kong et al. 1998)	Kong et al. (1998), Kong et al. (1996)

Etheretherketone, sulfamidated	Amideimide	Single T_g; FTIR	I had a degree of sulfamidation of 1.33; II was Torlon 4,000T	Karcha and Porter (1993)
Etheretherketone, sulfonated	Amideimide	Single T_g; FTIR	I had a degree of sulfonation of 0.42, 0.53, and 1.00; II was Torlon 4,000T	Karcha and Porter (1989), Karcha and Porter (1993)
	Etherimide	Single T_g	II was Ultem 1000	Karcha and Porter (1989), Karcha and Porter (1993)
Etherethersulfone	Epoxy	Single T_g; microscopy	Miscible when II was cured by amine; immiscible when cured by anhydride	Guo (1993)
Etherimide	Amideimide	Single T_g	I was Ultem 1000; II was Torlon; 4,203 L; miscible when blend had 15, 60, 70, 75, or 85 wt% I; immiscible when blend had 25, 30, or 50 wt% I	Palsule and Cowie (1994), Ryu et al. (2000)
	Arylate	Single T_g	I was Ultem 1000; blend had 10 or 20 wt% II	Bastida et al. (1996a, b)
	Benzimidazole	Single T_g; FTIR	II was nitro-substituted	Cho et al. (2001b)
	Butylene naphthalate	Single T_g; FTIR; SEM	–	Lin and Wang (2001)
	Butylene terephthalate	Single T_g; OM	–	Woo and Yau (1997)
	Ether diphenylether ketone	Single T_g; FTIR	–	Huang and Woo (2000)
	Etheretherketoneketone	Single T_g	Semicrystalline	Shibata et al. (2001)
	Etherimide	Single T_g	I was Ultem 1000; II was made from isophthaloyl chloride and bis-[(4-aminophenoxy)-4-phenyl]propane	Etxeberria et al. (1998)
	Ethylene-1,6-naphthalene dicarboxylate	Single T_g; OM	I was Ultem 1000	Chen et al. (1998c)
	Ethylene terephthalate	Single T_g; T_m-depression; OM; SAXS	I was Ultem 1000	Chen (1995), Chen and Hsiao (1998), Jo et al. (1994c), Martinez et al. (1993)

(continued)

Table 21.1 (continued)

Polymer I of	Polymer II of	Method	Comments	Refs.
	Imide	Single T_g	I was Ultem 1000; II was made from diphenylpyromellitic dianhydride (DPPMDA) and 4,4'-diaminodiphenylether	Fukai et al. (1992)
	Imide	Single T_g	I was Ultem 1000; II was made from DPPMDA and 6,6'-perfluoromethylbenzidine	Fukai et al. (1992)
	Imide	Single T_g	I was Ultem 1000; II was made from DPPMDA and 3,3'-dimethoxybenzidine	Fukai et al. (1992)
	Phenylsulfone	Single T_g; SEM	–	Ramiro et al. (2006)
	Trimethylene terephthalate	Single T_g; SEM	–	Huang and Chang (2002), Kuo et al. (2001b)
Etherimide ether	Thioetherimide ether	NMR	–	Feng et al. (1995a)
Etherketone	Terephthaloylimide	Single T_g; WAXS; SAXS	Semicrystalline	Cser and Goodwin (2001)
Etherketoneketone	Etherimide	Single T_g; WAXD; microscopy	II was Ultem 1000	Hsiao and Sauer (1993), Sauer and Hsiao (1993a)
	Imide	Single T_g	II was made from 3,4'-oxydianiline and oxydiphthalic dianhydride	Sauer and Hsiao (1993a)
	Imide	Single T_g	II was made from 4,4'-bis (3-aminophenoxy)biphenyl and pyromellitic anhydride	Sauer et al. (1996)
	Imide	Single T_g; WAXD; FTIR	–	Chun and Weiss (2004)
Ethersulfone	Aramide	Single T_g	II was made from isophthaloyl chloride and bis (4-aminophenyl) ether	Matsuura et al. (1992), Nakata et al. (1990)
	Epoxy	Single T_g; SEM; transparency	–	Francis et al. (2006)
	Etheretherketone	Single T_g; SEM	–	Nandan et al. (2002)

	Imide	Single T_g; NMR	II was Polyimide XUeda and Karasz (1985)18	Janusz et al. (1990)
	Imide	Single T_g; transparency	II was Matrimide	Cha et al. (1994)
	Imide	Single T_g	II was Matrimide 5218; miscibility was a metastable phenomenon achieved by rapid solvent removal	Liang et al. (1992)
	N,N'-(Oxydi-p-phenylene) isophthalamide	Single T_g; transparency	I was Victrex PES 300P	Hayashi et al. (1993)
	Phenylene ether ether ketone	Single T_g	–	Schneider et al. (1995)
	Phenylene ether sulfone ketone	Single T_g	–	Schneider et al. (1995)
	Phenylene sulfone ether sulfone ketone	Single T_g	–	Schneider et al. (1995)
	Phenylene thioether ether ketone	Single T_g	–	Schneider et al. (1995)
	Tertiary amide	Single T_g	II was N-methyl-N-vinylacetamide or N,N-dimethylacrylamide	Goh et al. (1997)
Ethersulfoneetherketone	Epoxy	Single T_g; SEM; transparency	–	Francis et al. (2006)
Ether urethane	Vinyl chloride	Single T_g	20 or 40 wt% II; I was Adiprene L-100 and 4,4'-methylene-bis-2-chloroaniline	Hourston and Hughes (1981)
3-Ethenoxypropyl cinnamate	p-Methyl-(3-ethenoxypropyl) cinnamate	Single T_g	–	Lin et al. (1989)

(continued)

Table 21.1 (continued)

Polymer I of	Polymer II of	Method	Comments	Refs.
Ethyl acrylate	Alkyl methacrylate	Single T_g	II had an alkyl group of chloromethyl, 1-chloroethyl, 2-chloroethyl, 2,2-dichloroethyl, 2,2,2-trichloroethyl, or 1,3-difluoroisopropyl	Peng et al. (1996)
	Novolac	Single T_g	II had M_w about 1 kg/mol; II was formaldehyde and 13/17/70 mol% = p-t-butylphenol/m-cresol/o-cresol or formaldehyde and 15/17/68 mol% = 2-t-butylphenol/m-cresol/o-cresol	Fahrenhlotz and Kwei (1981)
	Hexafluoroacetone-co-vinylidene fluoride	Single T_g; XPS	II had 8 mol% hexafluoroacetone	Kano and Akiyama (1992), Kano et al. (1997a)
	Styrene, sulfonated	Single T_g; FTIR	Degree of sulfonation of II = 7.2 %	Taylor-Smith and Register (1993)
	Styrene-co-p-vinylphenol	Single T_g; FTIR	II had >4.46 mol% vinylphenol	Taylor-Smith and Register (1993)
	Vinyl chloride	Single T_g	In situ polymerized II; other mixtures formed two phases (e.g., refs. Grose and Friese (1965), Keskkula and Paul (1986))	Grose and Friese (1965), Keskkula and Paul (1986), Walsh and Cheng (1984a)
	Vinyl chloride-co-vinylidene chloride	Single T_g; transparency	II was Saran ($\leq$80 % vinylidene chloride); I had $M_w = 50$ kg/mol; two T_g's when I had $M_w = 140$ kg/mol; and II was Saran (86.5 wt% vinylidene chloride)	Tremblay and Prud'homme (1984), Woo et al. (1984b)
	Vinylidene fluoride	Single T_g; transparency	Semicrystalline $\geq$25 wt% II	Bernstein et al. (1977), Briber and Khoury (1987), Wahrmund et al. (1978)

Ethyl acrylate, modified with C$_{60}$	Vinylidene fluoride	Single T_g; T_m-depression	I had 19.3 wt% C$_{60}$	Zheng et al. (2001)
Ethyl acrylate-co-methacrylonitrile-co-α-methylstyrene	Vinyl chloride	Single T_g; transparency	I had 2/40/58 = ethyl acrylate/methacrylonitrile/-methylstyrene or unknown composition	Kenney (1976, 1977)
Ethyl acrylate-co-methyl methacrylate	Vinyl chloride	Single T_g; electron microscopy	I was Polaroid Kammer (1989) 0N (95 % methyl methacrylate)	Zelinger et al. (1976)
Ethyl acrylate-co-4-vinylpyridine	Perfluorinated acid copolymer	FTIR	I had 5–21 mol% vinylpyridine; II was Nafion	Tannenbaum et al. (2003)
	Styrene-co-styrene sulfonic acid	Single T_g; transparency	I and II both ≥5 % of second monomer (data obtained ≤10 % substitution)	Eisenberg et al. (1982), Smith and Eisenberg (1983)
	Vinyl chloride	Single T_g	I had 2–14 mol% 4-vinylpyridine	Clas and Eisenberg (1984)
	Vinyl chloride, sulfonated	Single T_g	I had 6.2 mol% 4-vinylpyridine; II had 3.7 mol% sulfonic acid	Clas and Eisenberg (1984)
(N-Ethylcarbazole-3-yl)methyl acrylate	2-(3,5-Dinitrobenzoyl) oxyethyl methacrylate	Single T_g; NMR	–	Simmons and Natansohn (1992a)
(N-Ethylcarbazole-3-yl)methyl methacrylate	2-(3,5-Dinitrobenzoyl) oxyethyl methacrylate	Single T_g; NMR	–	Simmons and Natansohn (1992b)
Ethyl cellulose	Amide	Single T_g; FTIR	II was a copolyamide with PA-6, PA-6,6, and PA-10,10 units	Zhang et al. (2012b)
Ethyl methacrylate	Novolac	Single T_g; FTIR	II had M_w about 1 kg/mol and was formaldehyde and 13/17/70 mol% = p-t-butylphenol/m-cresol/o-cresol	Fahrenhlotz and Kwei (1981), Kim et al. (1991)
	Butyl acrylate-co-styrene	Single T_g	II had 23–63 wt% styrene	Rana et al. (2000)
	Ethyl acrylate	Single T_g	–	Cowie et al. (1992f)
	p-(2-Hydroxy-hexafluoroisopropyl) styrene-co-styrene	Single T_g; transparency	II had 90.3–98.9 mol% styrene	Chen and Morawetz (1989), Min and Pearce (1981), Pearce et al. (1984)

(continued)

Table 21.1 (continued)

Polymer I of	Polymer II of	Method	Comments	Refs.
	Vinyl acetate	Transparency	Transparent film when I <25 wt% or when content of I toward 100 wt%	Olayemi and Ibiyeye (1986)
	Vinyl chloride	Single T_g; transparency	–	Fried et al. (1978), Ha et al. (1990a), Perrin and Prud'homme (1991), Tremblay and Prud'homme (1984), Walsh and Cheng (1984a)
	Vinyl chloride-co-vinylidene chloride	Single T_g; transparency	II was Saran (≥80 % vinylidene chloride) or 86.5 wt% vinylidene chloride; semicrystalline ≤30 % I	Kang et al. (1988), Tremblay and Prud'homme (1984), Woo et al. (1984b)
	Vinylidene fluoride	Single T_g	Semicrystalline when ≥40 % II; two T_g's when >60 % II	Galin and Maslinko (1987), Imken et al. (1976), Kwei et al. (1976), Noland et al. (1971), Roerdink and Challa (1980)
Ethyl methacrylate, modified with C_{60}	Vinylidene fluoride	Single T_g; T_m-depression	I had 4.9–14.8 wt% C_{60}	Zheng et al. (2001)
Ethylene, chlorinated	Acrylonitrile-co-butadiene	Single T_g	Depended on Cl content and acrylonitrile content	Chai and Karasz (1992), Cowie and Harris (1992)
	Caprolactam-co-caprolactone	Single T_g	I had 35.2 wt% Cl; II had 17 mol% caprolactam	Van Ekenstein et al. (1997)
	Hexamethylene terephthalate	Single T_g	I had 48 % Cl; immiscible with I had 36 % Cl	Aubin and Prud'homme (1984)
	Methyl methacrylate	Single T_g; transparency; electron microscopy	I had ≥50 wt% Cl; two T_g's when I had 48 wt% Cl	Chai et al. (1983), Grose and Friese (1965), Tremblay and Prud'homme (1984), Walsh et al. (1982)

Polymer I	Polymer II	Method	Comment	Reference
	Neopentyl glycol adipate	Single T_g	I had 42 or 48 wt% Cl; immiscible when I had ≤36 wt% Cl	Goh et al. (1984b)
	Vinyl chloride, chlorinated	Single T_g	I and II with identical chlorine content were immiscible	Ueda and Karasz (1992)
Ethylene, chlorosulfonated	Vinyl chloride	Single T_g	I had 1 % S as SO_2Cl and 42 wt % Cl; stated immiscible when I had 30 wt% Cl in Grose and Friese (1965)	Doube and Walsh (1979)
Ethylene adipate	Hydroxyether of bisphenol-A (Phenoxy)	Single T_g; transparent melt	Semicrystalline when ≥50 wt% I	Harris et al. (1982)
Ethylene-co-methacrylic acid	Ethylene glycol	FTIR	I had 55 wt% methacrylic acid	Coleman et al. (1989b)
	Ethylene glycol-co-propylene glycol	Single T_g; FTIR	I had 18, 32, 44, or 55 wt% methacrylic acid; II had 70 wt% ethylene oxide	Lee et al. (1988c)
	Ethyloxazoline	FTIR	I had 44 wt% methacrylic acid	Lichkus et al. (1988)
	Styrene-co-2-vinylpyridine	FTIR	I had 32 wt% methacrylic acid; II had 70 wt% 2-vinylpyridine	Lee et al. (1988d)
	Tetramethylene glycol	FTIR	I had 55 wt% methacrylic acid	Lee et al. (1988c)
	Vinylethylether	FTIR	I had 55 wt% methacrylic acid	Lee et al. (1988c)
	Vinylmethylether	Single T_g; FTIR	I had 18, 32, 44, or 55 wt% methacrylic acid	Lee et al. (1988a)
	2-Vinylpyridine	FTIR	Miscible when I had 18 wt% methacrylic acid and formed complexes when I had 44 or 55 wt% methacrylic acid; formed complexes when I had 32 wt% methacrylic acid and was ≤35 % I in blend	Lee et al. (1988a)
Ethylene-co-methacrylic acid, zinc neutralized	Vinylmethylether	FTIR	I had 44 wt% methacrylic acid	Serman et al. (1988)
	4-Vinylpyridine	NMR	I had 15 wt% methacrylic acid and 60 % zinc-neutralized	Belfiore (1988)

(continued)

Table 21.1 (continued)

Polymer I of	Polymer II of	Method	Comments	Refs.
Ethylene-*co*-methyl acrylate-*co*-unspecified acid	Vinyl chloride	Single T_g	I was Vamac *N*-123	Kalfoglou (1983)
Ethylene-2,6-naphthalene dicarboxylate	Ester	Single T_g; T_m-depression	II was made from hydroxybenzoic acid and ethylene terephthalate	Park and Kim (2003)
	Oxybenzoate-*co*-ethylene terephthalate	Single T_g; T_m-depression	II had 40 mol% ethylene terephthalate	Ho et al. (2000)
Ethylene orthophthalate	Vinyl acetate	Single T_g	–	Vazquez-Torres and Cruz-Ramos (1986)
Ethylene glycol	Acetoxystyrene	Single T_g; T_m-depression; FTIR	–	Kuo et al. (2004b)
	Benzoxazine	Single T_g; T_m-depression	Miscible before curing; phase separation after curing	Lu and Zheng (2003)
	Benzyl methacrylate	Single T_g; FTIR; SEM; OM; NMR	Semicrystalline	Lin et al. (2001), Maekawa et al. (1999)
	Bisphenol-A-*co*-epichlorohydrin	Single T_g; T_m-depression; FTIR	–	Rocco et al. (2003b)
	n-Butyl methacrylate	Single T_g	–	El Shafee and Ueda (2002)
	Butylene adipate-*co*-butylene succinate	Single T_g; T_m-depression; OM	–	Ikehara et al. (2005)
	Butylene succinate	Single T_g; T_m-depression; WAXD, SAXS; NMR; AFM		He et al. (2004b), Hexig et al. (2005), Ikehara et al. (2009), Qiu et al. (2003b)
	Copolyester-polyurethane	Single T_g	–	Iriarte et al. (1991)
	Diethylene glycol-*co*-ethylene terephthalate	Single T_g	II had 37 mol% diethylene glycol	Barcellos et al. (1998)
	Epichlorohydrin	Single T_g; T_m-depression	–	Silva et al. (1988)
	Epoxy resin	Single T_g; FTIR	Miscible when II was uncured; immiscible when II was cured (Guo et al. (1991b)); miscible before and after curing (Luo et al. (1994))	Guo et al. (1991b, 2001), Chen et al. (2008), Hu et al. (2004), Luo et al. (1994, 1995a), Zheng et al. (2003c)

Ester	Single T_g; T_m-depression; POM	II was ethylene adipate, propylene adipate, butylene adipate, or ethylene azelate	Lin and Woo (2006)
Ethersulfone	Single T_g; light scattering; SAX; OM	–	Dreezen et al. (1999), Guo and Higgins (1991), Maejima et al. (1988), Shibanov and Radzhabov (1988)
Ethyl methacrylate	Single T_g	–	Chung et al. (1991)
Ethyl methacrylate-co-methyl methacrylate	Single T_g; NMR	Blend had ≤20 wt% I	Pomposo et al. (1996)
Ethylene-co-vinyl acetate	Single T_g	II had 87.1 wt% vinyl acetate (Cimmino et al. (1991)); II had 73.4 wt% vinyl acetate, miscible with I of $M_w = 20$ and 100 kg/mol (Han et al. (1992))	Cimmino et al. (1991), Han et al. (1992)
Ethylene succinate	Single T_g	–	Lu et al. (2008)
Hydroxyether of bisphenol-A (Phenoxy)	Single T_g; NMR	Semicrystalline when >40 % I	Iriarte et al. (1989, 1991), Robeson et al. (1981)
Hydroxyether terephthalate ester	Single T_g; T_m-depression; FTIR	–	Liu et al. (2005b)
p-(2-Hydroxy-hexafluoroiso-propyl)-α-methylstyrene-co-styrene	ESR	II had 4.88–27.28 mol% OH	Chen et al. (2004a)
p-(2-Hydroxy-hexafluoroisopropyl) styrene-co-styrene	Single T_g	II had 77.9 mol% styrene, and I/II was 1/8–1/2; semicrystalline and no amorphous phase	T80
Hydroxyether sulfone	Single T_g; OM; FTIR; NMR	–	H194
2-Hydroxyethyl methacrylate	Single T_g	–	Prashantha et al. (2008)
2-Hydroxyethyl methacrylate-co-p-vinylphenol	T_m-Depression; WAXD; SAXS	II had 55 mol% vinylphenol (Silva et al. (2009))	Pereira and Rocco (2005), Silva et al. (2009)
3-Hydroxypropionate	Single T_g; NMR	Semicrystalline	He et al. (2000)
Lactide	Single T_g; OM; T_m-depression	Blend had up to 50 wt% I	Lai et al. (2004), Nijenhuis et al. (1996), Yang et al. (1997)

(continued)

Table 21.1 (continued)

Polymer I of	Polymer II of	Method	Comments	Refs.
	Maleic acid-alt-methylvinylether	Single T_g; FTIR	Semicrystalline	Rocco et al. (2001)
	Maleic anhydride-co-styrene	Single T_g; T_m-depression	Semicrystalline	Al-Salah (2000), Al-Salah and Qudah (1997)
	Methacrylic acid	Single T_g; NMR	Formed complexes in water and dimethylsulfoxide	Jeon and Ree (1988), Maunu et al. (1993), Miyoshi et al. (1996)
	Methacrylic acid-co-styrene	FTIR	II had 5.6, 11.0, or 17.9 mol% acid and Na-neutralized	Lim et al. (1994)
	Methyl methacrylate	Single T_g; NMR; SAXS; dielectric spectroscopy	I was miscible with atactic or syndiotactic II and immiscible with isotactic II; semicrystalline when >20 wt% I	Baldrian et al. (1999), Chow (1990), John and Ree (1990), Jin et al. (2004b), Liberman et al. (1984), Martuscelli and Demma (1980), Martuscelli et al. (1986), Silvestre et al. (1987), Straka et al. (1995)
	Methyl methacrylate-co-p-vinylphenol	Single T_g; T_m-depression; FTIR; NMR	I had 51 mol% vinylphenol (Kuo and Chang (2001b)); I had 30–92 mol% vinylphenol (Lin et al. (2006b))	Kuo and Chang (2001b), Lin et al. (2006b)
	Phenyl methacrylate	Single T_g; FTIR; SEM	Semicrystalline	Woo et al. (2000c)
	Resorcinol	NMR	–	Belaribi et al. (1986)
	Styrene, sodium salt of sulfonated polystyrene	Single T_g	II had 2.9–8.8 mol% sulfonation; miscible when blend had low I content	Lee et al. (1991)
	Styrene-co-p-vinylphenol	Single T_g; ESR; dielectric spectroscopy	II had 13.1 mol% styrene, and I/II was 1/8-1/1; semicrystalline at higher I content and no amorphous phase miscibility; II had 2.1–48.4 mol% vinylphenol (Tan et al. 2004)	Jin et al. (2004a), Ting et al. (1981), Tan et al. (2004)

Styrene-*co*-vinylphenol trifluoromethyl carbinol	Single T_g	II had 84.4 mol% styrene and I/II had 54.5 mol% styrene and I/II was 1/8–1/4 or II had 1/8–1/2; semicrystalline at higher I content and no amorphous phase miscibility	Ting et al. (1981)
Sulfone	Transparency; light scattering	I had M_n = 3.5–4.0 kg/mol; immiscible when I had M_n = 200 kg/mol	Swinyard et al. (1987)
Vinyl acetate	Single T_g	Kalfoglou et al. (1988) stated miscible when ≥40 wt% II in blend; Guo et al. (1990b) stated completely miscible if I had M_w = 20 kg/mol, and miscible up to 50 wt% II if I had M_w = 100 kg/mol	Chen et al. (1999), Guo et al. (1990b), Kalfoglou et al. (1988), Martuscelli et al. (1985)
Vinyl alcohol	T_m-Depression; FTIR; WAXD; OM	II was hydroxypropylated	Sawatari and Kondo (1999)
Vinyl chloride	T_m-Depression; NMR; IGC	Semicrystalline	Castro et al. (2003), Etxeberria et al. (1993), Katsaros et al. (1986), Marco et al. (1993), Marentette and Brown (1998)
Vinylmethylether	Single T_g; FTIR	–	Pedrosa et al. (1994)
Vinylnaphthalene	Single T_g	Semicrystalline when >50 % I; two amorphous phases when 25–50 % I	Cuddkhy et al. (1965), Moacanin et al. (1965), Rembaum et al. (1963)
p-Vinylphenol	Single T_g; FTIR; NMR; WAXD; POM	–	Lin et al. (2006a), Pedrosa et al. (1995), Qin et al. (1990), Sotele et al. (1997), Tang and Liau (2000), Zhang and Hikichi (1992)
Vinylphosphonic acid	Single T_g; OM	–	Jiang et al. (2010)

(*continued*)

Table 21.1 (continued)

Polymer I of	Polymer II of	Method	Comments	Refs.
Ethylene glycol, modified with C_{60}	Acrylic acid	Single T_g; FTIR	I was linear or 4-arm and end-capped with C_{60}	Song et al. (2002)
	Lactide	Single T_g	I was capped with C_{60} at both ends	Kai et al. (2006)
	Methacrylic acid	Single T_g; FTIR	I was end-capped with C_{60}; formed complexes	Huang and Goh (2000)
	Vinyl chloride	Single T_g; T_m-depression; XPS	One or both ends of I were end-capped with C_{60}	Huang and Goh (2002)
	p-Vinylphenol	Single T_g; FTIR	I was end-capped with C_{60}	Huang et al. (2000)
Ethylene succinate	p-Dioxanone	Single T_g; T_m-depression; WAXD; POM	–	Zeng et al. (2010)
	Propylene succinate	Single T_g; T_m-depression; WAXD; POM	–	Papageorgious and Bikiaris (2006)
Ethylene-co-sulfur dioxide-co-vinyl acetate	Vinyl chloride	Single T_g; transparency	I had 72.7/8.8/18.5 = ethylene/sulfur dioxide/vinyl acetate; immiscible when I had 89.0/3.2/7.8 = ethylene/sulfur dioxide/vinyl acetate	Hickman and Ikeda (1973)
Ethylene terephthalate	Ester-carbonate	Single T_g	I was from 1/2 = terephthalate/bisphenol-A with ester and carbonate linkages	Aharoni (1983)
	Ethylene-co-cyclohexane 1,4-dimethanol terephthalate	Single T_g	–	Papadopoulou and Kalfoglou (1997b)
	Ethylene-2,6-naphthalene dicarboxylate	Single T_g; WAXD; NMR	Miscibility arose from transesterification	Andresen and Zechmann (1994), Ihn et al. (1996), Shi and Jabarin (2001)
	Hydroxyether of 4,4′-dihydroxy-α-methylstilbene	Single T_g	Blend had I:II = 1:1	Bruggeman and Tinnemans (1999)
	Hydroxyether of bisphenol-A (Phenoxy)	Single T_g	T_g's of I and II were close; semicrystalline	Robeson and Furtek (1979)

	Ester, liquid crystalline	Single T_g	II was made from ethylene terephthalate (40 %) and hydroxybenzoic acid (60 %) (Zhuang et al. (1988)) or segmental block copolyester (Lin et al. (1983))	Lin et al. (1993), Park and Kim (2003), Zhuang et al. (1988)
	Trimethylene terephthalate	Single T_g; T_m-depression; SEM	–	Liang et al. (2008)
	Vinylidene fluoride	Single T_g, T_m-depression	–	Rahman and Nandi (2002)
Ethylene-co-vinyl acetate	Acrylic acid-co-alkyl acrylate	Single T_g	II had an alkyl group of n-butyl, ethyl, ethylhexyl, or methyl; miscibility depended on compositions of I and II	Bott et al. (1995)
	Alkylthiophene	Microscopy	II had an alkyl group of 3-octyl or 3-dodecyl; I had 20 mol% vinyl acetate; miscible when blend had <30 wtt II	Ho et al. (1993)
	Aniline, N-octadeceylated	OM; T_m-depression	I had 20 wt% vinyl acetate; II had a degree of alkylation of 60.2 wt%	Zheng et al. (1995)
	Chloroprene	Single T_g; SEM; NMR; FTIR	I had 28 wt% vinyl acetate	Kundu et al. (1996b), Kundo et al. (1995)
	2,2-Dimethylbutadiene-co-p-vinylphenol	Single T_g; FTIR	–	Pehlert et al. (1997)
	Hexafluoroacetone-co-vinylidene fluoride	Single T_g	I had $\geq$70 % vinyl acetate; II had 8.9 mol% hexafluoroacetone	Hasegawa and Akiyama (1988)
	Lactide	Single T_g; T_m-depression	II had 85 wt% vinyl acetate	Yoon et al. (1999)
	Novolac	Single T_g; FTIR	I had 14–50 wt% vinyl acetate	Mekhilef and Hadjiandreou (1995)
	3-Octylthiophene	UV-vis spectroscopy; NMR; T_m-depression	I had 20 mol% vinyl acetate	Leung and Lo (1995), Monedero et al. (1999)

(continued)

Table 21.1 (continued)

Polymer I of	Polymer II of	Method	Comments	Refs.
	Propylene, chlorinated	Single T_g	I had 40, 44.3, or 45 wt% vinyl acetate; II had 40 or 50 wt% Cl	Lee et al. (1988a, 1989a)
	Vinyl chloride	Single T_g; T_m-depression; SEM	I had 65–75 wt% vinyl acetate; two T_g's when I had 40–45 wt% vinyl acetate; ambiguous when I had 45–65 wt% vinyl acetate	Corradini et al. (1997), Da Silva Neiro et al. (2000), Elmqvist and Svanson (1975), Feldman and Rusu (1974), Hammer (1971), Hardt (1969), Kosai and Higashino (1975), Marcincin et al. (1972), Ranby (1975), Shur and Ranby (1975a), Thaumaturgo and Monteiro (1997a, b)
	Vinyl chloride, chlorinated	Single T_g	Stated that there was a miscible region when I had 0.4–0.75 mol% ethylene and II had 0.4–0.8 mol% vinyl chloride	Shiomi et al. (1986b)
Ethylene-*co*-vinyl acetate-*co*-unnamed monomer	Vinyl chloride	Single T_g	Semicrystalline; I was du Pont de Nemours PBosma et al. (1988)41 (>60 % ethylene)	Bair et al. (1977)
Ethylene-*co*-vinyl alcohol	Alkyl methacrylate	Single T_g; FTIR	I had 21 mol% vinyl alcohol; II had an alkyl group of methyl, *n*-octyl, or *n*-decyl	Coleman et al. (1993b)
	Amide	Single T_g; FTIR; WAXD	II was PA-4,6, PA-6, PA-6,12, PA-12, or copolyamide of PA-6 and PA-12	Ahn and Jeong (1987), Akiba and Akiyama (1994), Ha et al. (1997), Yamaguchi et al. (1996)
	n-Butyl methacrylate	Single T_g; FTIR	I had 56 mol% vinyl alcohol	Keskin and Elliot (2003)
	N-Vinylpyrrolidone	Single T_g; FTIR	I had 45 or 57 mol% vinyl alcohol	Ahn and Jeong (1998)
	4-Vinylpyridine	Single T_g; FTIR	I had 68 mol% vinyl alcohol (Isasi et al. (1994)) or 56 mol% vinyl alcohol (Keskin and Elliot (2003))	Isasi et al. (1994) , Keskin and Elliot (2003)

Polymer I	Polymer II	Methods	Comments	Reference
2-Ethylhexyl methacrylate	Styrene-co-hexyl methacrylate	Single T_g	I had 3–5 % acrylic acid; II had 30 % styrene and 5–15 % 3-(dimethylamino)-2,2-dimethylpropyl methacrylate	Siol and Terbrack (1991)
N-Ethyl-3-hydroxymethylcarbazoyl methacrylate	o-Hydroxyalkyl-3,5-dinitrobenzoyl methacrylate	Single T_g	II had an alkyl group of butyl, hexyl, pentyl, or propyl	Rodriguez-Parada and Percec (1986a)
2-Ethyl-2-oxazoline	Acrylic acid	Single T_g	Formed complexes in water, methanol, or dioxane	Lin et al. (1988)
	Acrylic acid-co-ethylene	Single T_g	II had 20 wt% acrylic acid	Nuno-Donlucas et al. (2001b)
	Acrylic acid-co-styrene	Single T_g	II had 74 mol% acrylic acid	Lin et al. (1988)
	Alkyl methacrylate	Single T_g; FTIR	II had an alkyl group of 2-hydroxyethyl or 2-hydroxypropyl	Isasi et al. (1996)
	Allyl alcohol-co-styrene	Single T_g; FTIR	II had 4.5 or 6.5 wt% OH	Dai et al. (1994b)
	Aramide	Optical microscopy; light scattering	–	Maejima et al. (1989)
	Ethersulfone	Light scattering, transparency	–	Nakamura et al. (1990)
	Ethylene-co-vinyl alcohol	Single T_g; FTIR	II had 68 or 78 mol% vinyl alcohol	Parada et al. (1998a)
	Hydroxyether of bisphenol-A (Phenoxy)	Single T_g; transparency; FTIR; NMR	–	Keskkula and Paul (1986), Lau et al. (1998)
	Maleimide-co-styrene	Single T_g	II had 9.5–48.2 mol% maleimide	Dean (1987b)
	Monoalkyl itaconate	Single T_g; FTIR	II had an alkyl group of methyl, ethyl, propyl, butyl, pentyl, hexyl, decyl, or dodecyl	Meaurio et al. (1997, 1998)
	Novolac	Single T_g	Formed complexes in methanol or acetone	Lin et al. (1988)
	Styrenesulfonic acid, Zn-neutralized	Single T_g; FTIR; XPS	–	G144
	Sulfone, carboxylated	Single T_g	II had $\geq$0.93° of carboxylation	Goh et al. (1991e)

(continued)

Table 21.1 (continued)

Polymer I of	Polymer II of	Method	Comments	Refs.
	Vinyl acetate-*co-co*-vinyl alcohol	Single T_g; FTIR	II had 15.3–84.4 mol% vinyl alcohol	Parada et al. (1997)
	Vinyl alcohol	Single T_g; FTIR	–	Aoi et al. (1998)
	p-Vinylphenol	Single T_g; NMR	Formed complexes in dioxane	Lin et al. (1988), Wang et al. (1991, 2001b)
	Vinylidene fluoride	Single T_g	>50 wt% II	Galin (1987b)
2-Ethyl-6-propyl-1,4-phenylene ether	Styrene	Single T_g	–	Cizek (1968)
2-Fluoroethyl methacrylate	Alkyl methacrylate	Single T_g	II had an alkyl group of methyl or ethyl	Peng et al. (1993)
3-Fluoropropyl methacrylate	Alkyl methacrylate	Single T_g	II had an alkyl group of methyl or tetrahydrofurfuryl	Peng et al. (1995)
	Ester	Single T_g	II was butylene adipate, 2,2-dimethyl-1,3-propylene adipate	Peng et al. (1995)
Glutarimide	Maleic anhydride-*co-co*-styrene	Single T_g; SEM	II had 8 wt% maleic anhydride	Bikiaris et al. (2004)
Glycidyl methacrylate	Acrylonitrile-*co*-styrene	Single T_g	II had 32.3–58.8 wt% AN	Gan and Paul (1994b)
	Methyl methacrylate	Single T_g	II had $M_w \leq 4.25$ kg/mol	Gan and Paul (1994b)
	α-Methylstyrene	Single T_g	II had $M_w = 3.5$ kg/mol	Gan and Paul (1994b)
Glycidyl methacrylate-*co*-methyl methacrylate	Acrylonitrile-*co*-styrene	Single T_g	Miscibility depended on compositions of I and II	Gan and Paul (1994b)
	Vinylidene fluoride	Single T_g	Semicrystalline	Gan and Paul (1995)
Glycidyl methacrylate-*co*-styrene	Carbonate of tetramethylbisphenol-A	Single T_g	I had 1.6–37.1 wt% GMA	Gan and Paul (1994b)
	2,6-Dimethyl-1,4-phenylene ether	Single T_g	I had 1.6–18.6 wt% GMA	Gan and Paul (1994b)

Glycolide-co-lactide	(Ethyl glycinato)(p-methylphenoxy)phosphazene	Single T_g; SEM	II had 3 different ratios of ethyl glycinato to p-methylphenoxy	Ibim et al. (1997)
	(Ethyl alanato) (p-phenylp henoxy) phosphazene	Single T_g; SEM	I had 15 mol% glycolide; blend had 25 wt% I	Deng et al. (2008)
	Phosphazene	Single T_g	I had 15 or 50 mol% glycolide; II was choline-substituted	Weikel et al. (2010)
	Phosphazene	Single T_g; SEM	I had 15 or 50 mol% clycolide; II contained alanyl glycine ethyl ester group	Krogman et al. (2010)
Heptamethylene terephthalate	Hexamethylene terephthalate	Single T_g; POM	–	Yen et al. (2009)
	Pentamethylene terephthalate	POM; T_m-depression	–	Yen and Woo (2009)
Hexadecamethylene dodecamethylene dicarboxylate	Vinyl chloride	Single T_g	Semicrystalline	Woo et al. (1985b)
Hexafluoroisopropanol-modified vinyl ether-alt-tetrafluoroethylene	Alkyl methacrylate	Single T_g; FTIR	II had an alkyl group of methyl, ethyl, or n-butyl	Guigley et al. (2002)
	Ethylene-co-vinyl acetate	Single T_g; FTIR	II had 70 wt% vinyl acetate	Guigley et al. (2002)
Hexafluoroisopropyl methacrylate	Alkyl methacrylate	Single T_g	II had an alkyl group of methyl or ethyl	Peng et al. (1993)
Hexamethylene adipamide (PA-6,6)	Ethylene terephthalate	FTIR; NMR	Blends prepared by coprecipitation; blends prepared by melt blending showed no sign of hydrogen bonding	Pillon et al. (1987)
Hexamethylene isophthalamide	Amide	Single T_g	II was PA-6,5, PA-6,7, PA-6,8, or PA-6,9	Cote and Brisson (1994)
	Caprolactam-co-caprolactone	Single T_g	II had varying composition	Ellis (1997)
Hexamethylene sebacate	Vinyl acetate-co-vinylidene chloride	Single T_g	Semicrystalline; II was Saran C ($\geq$80 % vinylidene chloride)	Aubin et al. (1983)
	Vinyl bromide	Single T_g	–	Cousin and Prud'homme (1982)
	Vinyl chloride	Single T_g	Semicrystalline when $\geq$50 % I	Woo et al. (1985b), Ziska et al. (1981)

(continued)

Table 21.1 (continued)

Polymer I of	Polymer II of	Method	Comments	Refs.
Hexamethylene terephthalate	Hydroxyether of bisphenol-A (Phenoxy)	Single T_g	Semicrystalline when ≥75 % I	Seymour and Zehner (1980)
	Pentamethylene terephthalate	Single T_g; POM; WAXD; SAXS	–	Yan et al. (2007)
	Vinyl chloride	Single T_g	Semicrystalline; deposited from some solvents as two phases	Aubin and Prud'homme (1984)
Hexanoyl chitosan	Lactide	Single T_g; T_m-depression	Semicrystalline	Peesan et al. (2005)
1-Hexene	1-Pentene	Single T_g	–	Decroix and Piloz (1977), Peesan et al. (2007)
Hexyl methacrylate	Vinyl chloride	Single T_g; transparency	Especially when II was polymerized in situ (Walsh and Cheng (1984a)); stated as immiscible in Tremblay and Prud'homme (1984)	Walsh and Cheng (1984a), Walsh and McKeown (1980)
	Vinyl chloride-co-vinylidene chloride	Single T_g; transparency	II was Saran (≥80 % vinylidene chloride)	Kang et al. (1988), Tremblay and Prud'homme (1984)
3-Hydroxybutyrate	Acrylonitrile-co-vinylidene chloride	Single T_g; T_m-depression	II had 20 wt% (Lee et al. (1997)) or 32 mol% (Gonzalez et al. (2002)) acrylonitrile	Gonzalez et al. (2002), Lee et al. (1997)
	Caprolactone-co-lactide	Single T_g	II had 41 or 68 mol% lactide	Koyama and Doi (1996)
	Cellulose acetate butyrate	Single T_g; OM; SAXS; T_m-depression	Semicrystalline	Ceccorulli et al. (1993), El Shafee et al. (2001), Scandola et al. (1992), Scandola (1995)
	Cellulose acetate-proprionate	Single T_g; microscopy	Semicrystalline	Scandola et al. (1992), Scandola (1995)
	Cellulose proprionate	Single T_g; microscopy; T_m-depression	Semicrystalline	Maekawa et al. (1999)
	Cellulose tributyrate	Single T_g; microscopy	–	Scandola (1995)
	Chitosan	Single T_g; T_m-depression; NMR	–	Cheung et al. (2002)

Epichlorohydrin	Single T_g; microscopy; T_m-depression; dielectric spectroscopy	Semicrystalline	Dubini Paglia et al. (1993), El Shafee (2002a), Finelli et al. (1997), Scandola (1995), Tsukada et al. (1992)
Epichlorohydrin-*co*-ethylene glycol	Single T_g; T_m-depression	II had 30 wt% ethylene glycol (Gonzalez et al. (2003)); II had 48 mol% ethylene glycol (Zhang et al. (2000))	Gonzalez et al. (2003), Zhang et al. (2000)
Ethylene glycol	Single T_g; SAXS	Semicrystalline	Avella and Martuscelli (1988), Chiu and You (2003), He et al. (2000), Kumagai and Doi (1992a), Yoon et al. (1993), You et al. (2003)
Ethylene succinate	Single T_g; microscopy; T_m-depression	Semicrystalline	Al-Salah (1998b)
Ethylene-*co*-vinyl acetate	Single T_g; T_m-depression; POM	Semicrystalline; II had 9–91 mol% vinyl acetate	Ellis (1993), Yoon et al. (1998)
Ethyl cellulose	Single T_g; SEM	Semicrystalline	Zhang et al. (1997)
Hydroxyether of bisphenol-A	Single T_g; FTIR	Semicrystalline; blend had ≤20 wt% I	Yuan and Ruckenstein (1998)
2-Hydroxyethyl methacrylate-*co*-4-vinylphenol	Single T_g; FTIR; OM	II had 55 mol% vinylphenol	Rocco et al. (2003a)
Lactide	Single T_g; microscopy; WAXD	Miscible when II had M_n = 1,759 kg/mol, immiscible when II had M_n = 159.4 kg/mol (Blumm and Owen (1995)); I had M_w = 650 kg/mol, and II had M_w <18 kg/mol (Koyama and Doi (1997))	Blumm and Owen (1995), Focarete et al. (2002), Koyama and Doi (1995, 1997), Ohkoshi et al. (2000), Zhang et al. (2006b)
Methyl acrylate	Single T_g; T_m-depression	–	An et al. (2000)
Methyl methacrylate	Single T_g	Miscible when blend had <20 wt% I	Ceccorulli and Scandola (1999), Cimmino et al. (2000), Lotti et al. (1993)

(continued)

Table 21.1 (continued)

Polymer I of	Polymer II of	Method	Comments	Refs.
	Styrene-*co*-*p*-vinylphenol	Single T_g; T_m-depression; FTIR; NMR	II had 20–80 mol% vinylphenol	Gonzalez et al. (2004a, b), Kuo and Liu (2011)
	Vinyl acetate	Single T_g	Semicrystalline	Grece and Martuscelli (1989), Hay and Sharma (2000), Kumagai and Doi (1992b)
	Vinyl acetate-*co*-vinyl alcohol	Single T_g; OM; SASX; WAXD	II had 9, 15, or 22 mol% vinyl alcohol	Xing et al. (1998b)
	Vinyl alcohol	Single T_g; FTIR; NMR	II was 80 % hydrolyzed (Huang et al. (2005)); blend had large amount of II (Yoshie et al. (1995))	Huang et al. (2005), Yoshie et al. (1995)
	Vinylidene fluoride	Single T_g; T_m-depression; SAXS	Semicrystalline	Chiu et al. (2001), Kang and Cho (1989), Karcha and Porter (1989), Liu et al. (2005c)
	p-Vinylphenol	Single T_g; FTIR; WAXD; SAXS; T_m-depression	–	Ding et al. (2011), Guo et al. (2010, 2011), Iriondo et al. (1995, 1996), Xing et al. (1997), Zhang et al. (1999)
3-Hydroxybutyrate-*co*-3-hydroxyhexanoate	Butylene succinate	Single T_g; T_m-depression; FTIR	I had 4 mol% hydroxyhexanoate	Lim et al. (2008)
	Ethylene glycol	Single T_g; FTIR	I had 7.5, 12.3, or 31.2 mol% hydroxyhexanoate; miscible when blend had <17 wt% II	Yu et al. (2010)
3-Hydroxybutyrate-*co*-hydroxyvalerate	Acrylonitrile-*co*-butadiene-*co*-styrene	Single T_g	I had 16 % hydroxyvalerate	Dave et al. (1990)
	Caprolactone	Single T_g; T_m-depression; FTIR	I had 18 mol% hydroxyvalerate	Cho et al. (2001a)
	Chitosan	Single T_g; T_m-depression; NMR	I had 30 mol% hydroxyvalerate	Cheung et al. (2002)
	Epichlorohydrin-*co*-ethylene glycol	Single T_g; T_m-depression	I had 14 mol% hydroxyvalerate and II had 48 mol% ethylene glycol	Zhang et al. (2000)

Ethylene glycol	Single T_g; T_m-depression	II had 12 mol% hydroxyvalerate	Tan et al. (2006)
Methyl methacrylate	Single T_g; T_m-depression; OM; SAXS	I had 10 mol% hydroxyvalerate	Chiu (2004), Chiu and Shu (2005)
Novolac	Single T_g; T_m-depression; POM	I had 5 wt% hydroxyvalerate	Yang et al. (2012)
Vinyl acetate	Single T_g; T_m-depression; FTIR; POM; AFM	I had 9 or 10 mol% hydroxyvalerate	Chang et al. (2011), Chiu (2006), Kwang et al. (1998)
Vinyl chloride	Single T_g	I had 16 % hydroxyvalerate	Dave et al. (1990)
Vinylidene fluoride	OM	I had 14 mol% hydroxyvalerate	Qiu et al. (2004)
p-Vinylphenol	Single T_g; T_m-depression; FTIR; POM; NMR	I had 15 or 20 mol% hydroxyvalerate	Alata et al. (2007), Cai et al. (2012), Xing et al. (1998a)
Hydroxyether of bisphenol-A (Phenoxy) Aryleneetherphenyl phosphine oxide-co-sulfone	Single T_g; FTIR	II was based on bisphenol-A or hydroquinone	Wang et al. (1999b)
Biphenol poly(arylene ether phenyl phosphine oxide)	Single T_g; FTIR; NMR	–	Wang et al. (2001a)
n-Butyl methacrylate-co-methyl methacrylate	Single T_g	II had 18 wt% butyl methacrylate	Erro et al. (2000)
2,2-Dichloroethyl methacrylate	Single T_g; FTIR	–	Goh et al. (1994b)
2,2-Dichloroethyl methacrylate-co-methyl methacrylate	Single T_g; FTIR	II had ≤62 wt% methyl methacrylate	Goh et al. (1994b)
Ester	Single T_g	I was cyclohexylene dimethylene tere/isophthalate	Robeson and Furtek (1979)
Etherester	Single T_g	Interchange reaction took place	Gan and Paul (1995)
Etheretherketone-co-phenolphthalein etheretherketone	Single T_g; FTIR	II had 6.2 or 12.3 mol% etheretherketone	Guo et al. (1996c)
Ethylene oxide-co-propylene oxide	Single T_g	II had >22 mol% ethylene oxide	Guo et al. (1993a)
Ethersulfone	Light scattering	–	Saito et al. (1990)
Hexafluorobisphenol-A poly (arylene ether phenyl phosphine oxide)	Single T_g; FTIR; NMR	–	Wang et al. (2001a)

Table 21.1 (continued)

Polymer I of	Polymer II of	Method	Comments	Refs.
	1,1,1,3,3,3-Hexafluoroisopropyl methacrylate	Single T_g; FTIR; XPS; ToF-SIMS	–	Huang et al. (2004b)
	Imide	Single T_g; FTIR; NMR	II were two different imides	Wang et al. (2001a)
	Methyl acrylate-*co*-methyl methacrylate	Single T_g; FTIR	II had 72 or 91 mol% methyl methacrylate	Wu et al. (1998)
	Methyl methacrylate	Single T_g; NMR; FTIR; Raman spectroscopy	II was atactic, isotactic, or syndiotactic (Alberdi et al. (1994), Hsu and Yeh (2000b))	Alberdi et al. (1994), Chiou et al. (1982), Erro et al. (1992, 2000), Hsu and Yeh (2000b), Kim and Choi (1996), Soh (1992b), Ward and Mi (1999)
	Tertiary amide	Single T_g; FTIR	II was *N*-methyl-*N*-vinylacetamide, *N*, *N*-dimethylacrylamide, or 2-methyl-2-oxazoline; formed complexes	Dai et al. (1996)
	Thiodithiophenol poly(arylene ether phenyl phosphine oxide)	Single T_g; FTIR; NMR	–	Wang et al. (2001a)
	Vinylmethylether	Single T_g; IGC	–	Etxeberria et al. (1994, 1995), Robeson et al. (1981), Uriarte et al. (1987, 1989)
	Vinylpyridine	Single T_g; FTIR; NMR	II was 2- or 4-vinylpyridine	De Ilarduya et al. (1993), Zheng and Mi (2003)

Component 1	Component 2	Method	Comments	References
	N-Vinylpyrrolidone	Single T_g; transparency; FTIR; NMR	–	De Ilarduya et al. (1995), Eguiazabal et al. (1984), Zheng et al. (1999a)
	Urethane	Single T_g	II was made from 1/1/2 = polycaprolactone diol (M_n = 2.1 kg/mol)/1,4-butanediol/4,4′-diphenylmethane diisocyanate	Seefried et al. (1976)
Hydroxyether of bisphenol-A, benzoylated	N-Vinylpyrrolidone	Single T_g; FTIR	–	Fernandez-Berridi et al. (1993)
Hydroxyether of bisphenol-A, modified	2-Vinylpyridine	Single T_g; FTIR	OH groups in I were converted to benzoate, acetate, or methoxy	Eguiburu et al. (1994)
Hydroxyether of phenolphthalein	Butylene terephthalate	Single T_g	–	Guo et al. (1990d)
	Carbonate of bisphenol-A	Single T_g	–	Guo et al. (1990d)
	Ethersulfone	Single T_g; FTIR	–	Guo (1992b)
	Ethylene glycol	Single T_g	–	Guo et al. (1990c)
Hydroxyethyl cellulose	Maleic acid-alt-methylvinylether	Single T_g; FTIR	–	Khutoryanskaya et al. (2005)
β-Hydroxyethyl-3,5-dinitrobenzoyl methacrylate	N-Alkyl-3-hydroxymethylcarbazoyl methacrylate	Single T_g	II had an alkyl group of butyl, decyl, dodecyl, ethyl, hexadecyl, hexyl, methyl, octyl, or tetradecyl	Rodriguez-Parada and Percec (1986b)
	N-(2-Hydroxyethyl)carbazoyl methacrylate	Single T_g	–	Rodriguez-Parada and Percec (1986b)
2-Hydroxyethyl methacrylate	Acrylamide-co-styrene	Single T_g; NRET	II had 40, 47, 52, or 57 mol% acrylamide	Chu and Ji (1995), Zhu et al. (1995)
	Dialkyl itaconate-co-styrene	Single T_g	II had an alkyl group of methyl or ethyl; II had 18–80 wt% styrene	Opazo et al. (1996)
	Methacrylic acid	Single T_g; NMR	–	Asano et al. (1999), Eguchi et al. (1998)

(continued)

Table 21.1 (continued)

Polymer I of	Polymer II of	Method	Comments	Refs.
2-Hydroxyethyl methacrylate, modified	1-Vinylimidazole	Single T_g; FTIR	I had 0.6–2.6 wt% C_{60}	Goh et al. (2002a, b)
	4-Vinylpyridine	Single T_g; FTIR	I had 0.6–2.6 wt% C_{60}	Goh et al. (2002a, b)
p-(2-Hydroxy-hexafluoroisopropyl)-α-methylstyrene-co-styrene	Butyl acrylate	Single T_g	I had ≥1.2 mol% OH-containing monomer	Cao et al. (1989)
	Methyl methacrylate	Single T_g; NRET; NMR	I had ≥1.9 mol% OH-containing monomer; formed complexes when I had 24 mol% OH	Cao et al. (1989), Jiang et al. (1995c), Qiu and Jiang (1994)
	Methyl methacrylate-co-2-vinylpyridine	Single T_g	I had ≥6 mol% OH-containing monomer	Jiang et al. (1989)
	Propyl carbonate	ESR	I had 19.4 or 27.28 mol% OH	Chen et al. (2004c)
	4-Vinylpyridine	Single T_g; XPS; TOF-SIMS; AFM	Miscible when I had ≥5.1 mol % OH; formed complexes when I had ≥8.3 mol% OH	Liu et al. (2002), Liu et al. (2004a)
p-(2-Hydroxy-hexafluoroisopropyl) styrene	Ethylene-co-vinyl acetate	Single T_g; FTIR; dielectric spectroscopy	II had 45 or 70 mol% vinyl acetate	Masser et al. (2010)
	Vinyl acetate	Single T_g; FTIR; dielectric spectroscopy	–	Masser et al. (2010)
p-(2-Hydroxy-hexafluoroisopropyl) styrene-co-styrene	Aramide	Single T_g; transparency	I had 60 mol% styrene; two T_g's when I had 83 mol% styrene; II was poly(iminotrimethylhexa-methyleneiminoterephthaloyl)	Min and Pearce (1981), Pearce et al. (1984)
	n-Butyl methacrylate	Single T_g; NRET	Miscible with I had 1 mol% OH; formed complexes when I had 18 mol% OH	Qiu and Jiang (1995)

	Ester	Single T_g; transparency	II was KODAR PETG (made from terephthalic and isophthalic acid and ethylene glycol and 1,4-dihydroxymethyl cyclohexane); II had 60 mol% styrene; immiscible when II han >83 mol% styrene	Min and Pearce (1981), Pearce et al. (1984)
	Ester	Single T_g; transparency	I was VITEL PE-307; II had 83–90.3 mol% styrene	Pearce et al. (1984)
	Ester	Single T_g	I was VITEL VPE-5545; II had 83 mol% styrene; immiscible when II had 90.3 mol% styrene	Pearce et al. (1984)
	Hexanediamine-*co*-,-decanedicarboxylic acid	Single T_g	Semicrystalline	Kotzev et al. (1984)
	Hydroxypropyl L-glutamine	Single T_g; light scattering; microscopy	Blend had >50 vol% II	Dadmun and Han (1993)
	Methyl methacrylate	Single T_g; transparency; NMR; FTIR; WAXD; NRET	I had >8 mol% OH; formed complexes when I had 24 mol% OH; II was syndiotactic or isotactic (Luo et al. (1995))	Luo et al. (1993, 1995b), Min and Pearce (1981), Pearce et al. (1984),
	Vinyl acetate	Single T_g; transparency	I had 90.3 mol% styrene	Min and Pearce (1981), Pearce et al. (1984)
	Vinylmethylether	Single T_g; transparency	I had 83.3–99.9 mol% styrene	Min and Pearce (1981), Min et al. (1983), Pearce et al. (1984)
	Vinylmethylketone	Transparency	I had 90.3 mol% styrene	Mengujoh and Frisch (1989)
2-Hydroxypropyl methacrylate	Tertiary amide	Single T_g; FTIR	Formed complexes; II was dimethylacrylamide, *N*-methyl-*N*-vinylacetamide, or 2-ethyl-2-oxazoline	Dai et al. (1994a)
	N-Vinylpyrrolidone-*co*-4-vinylpyridine	Single T_g	–	Radic et al. (2001)
	N-Vinylpyrrolidone-*co*-vinyltrimethylsilane	Single T_g	II had <25 wt% VTMS	Radic et al. (2001)

(continued)

Table 21.1 (continued)

Polymer I of	Polymer II of	Method	Comments	Refs.
Hydroxypropyl methyl cellulose	Vinyl acetate-*co*-1-vinylpyrrolidone	Single T_g; FTIR	II had 43 mol% vinyl acetate	Zaccaron et al. (2005)
Imide	Amide	Single T_g; SEM	I was made from 1,6-hexamethylenediamine and a mixture of isophthalic acid and terephthalic acid; II was two different amides	Endo et al. (2006)
	Benzimidazole	Single T_g; FTIR	I was 8 different types of imides	Ahn et al. (1997b)
	Ether ketone	Single T_g	I was made from pyromellitic dianhydride and 4,4'-bis(3-aminophenoxy)biphenyl; II was Victrex 220P	Sauer and Hsiao (1993b)
	Ether ketone ketone	Single T_g	I was the same as the previous system	Sauer and Hsiao (1993b)
	Imide	X-ray diffraction	I was made from pyromellitic dianhydride (PMDA) and oxydianiline; II was made from PMDA and *p*-phenylenediamine; <90 % II in blend	Jou and Huang (1990)
	Imide	Single T_g	I was made from PMDA and 1,4-phenylenediamine; II was made from 6FDA and 2,2'-bis[4-(4-aminophenoxy)phenyl]propane	Tong et al. (2001)

Imide	Single T_g	I was made from 2,2′-bis(3,4′-dicarboxyphenyl)hexafluoro-propane dianhydride (6FDA) and 2,2′-bis(3-aminophenyl)hexafluoropropane (3,3′-6 F-diamine); II was made from 6FDA and 2,2′-bis(4-aminophenyl)hexafluoropropane (4,4′-6F-diamine)	Chung et al. (1991)
Imide	Single T_g	I was made from 4,4′-biphthalic anhydride (BPDA) and 3,3′-6F-diamine; II was made from BPDA and 4,4′-6F-diamine	Chung et al. (1991)
Imide	Single T_g	I was made from 3,3′4,4′-benzophenonetetra-carboxylic dianhydride (BTDA) and 3,3′-6F-diamine; II was made from BTDA and 4,4′-6F-diamine	Chung et al. (1991)
Imide	Single T_g	I was made from 3,3′4,4′-diphenylet hercarboxylic dianhydride (OPDA) and 3,3′-6F-diamine; II was made from OPDA and 4,4′-6F-diamine	Chung et al. (1991)
Imide	Single T_g	I was made from PMDA/BPDA/3,3′-6F-diamine = 25/25/50; II was made from PMDA/BPDA/4,4′-6F-diamine = 25/25/50	Chung et al. (1991)

(continued)

Table 21.1 (continued)

Polymer 1 of	Polymer II of	Method	Comments	Refs.
	Imide	Single T_g	I was made from PMDA/BTDA/3,3'-6F-diamine = 25/25/50; II was made from PMDA/BTDA/4,4'-6F-diamine = 25/25/50	Chung et al. (1991)
	Imide	Single T_g	I was made from PMDA/OPDA/3,3'-6F-diamine = 25/25/50; II was made from PMDA/BTDA/4,4'-6F-diamine = 25/25/50	Chung et al. (1991)
	Imide	Single T_g; WAXD, SAXS	I was made from 3,4:3'4'-biphenyltetra carboxylic dianhydride and 4,4'-oxydianiline; II was made from 4,4'-thiophthalic anhydride and 4,4'oxydianiline	Zhang et al. (1993)
	Imide	Single T_g	I and II were isomeric; 3 blend systems	Coleman et al. (1993a)
	Imide	Single T_g	I and II were different imides, but both had hexafluoroisopropylidene group	Chung and Kafchinski (1996)
	Imide	Single T_g	I and II were different imides	Tang et al. (1997)
	Imide	Single T_g	I was a liquid crystalline imide	Konda et al. (1998)
	Imide	Single T_g	Two pairs of different imides	Khalid et al. (2007)
2-Iodoethyl methacrylate	Acrylonitrile-co-p-methylstyrene	Single T_g	I had 21–42 wt% AN	Low et al. (1993b)
	Acrylonitrile-co-styrene	Single T_g	I had 13–51 wt% AN	Low et al. (1993b)
	Ester	Single T_g	II was butylene adipate, caprolactone, 2,2-dimethyl-1,3-propylene adipate, or hexamethylene sebacate	Low et al. (1994c)
	Tetrahydrofurfuryl methacrylate	Single T_g	–	Low et al. (1993d)

Isobutylene	Dimethylsilylenemethylene	Single T_g; OM	–	Maier et al. (1998)
	Propylene	NMR	II was head-to-head	Wachowicz and White (2007), Walak and White (2005)
Cis-isoprene	Butadiene-*co*-1,2-vinylbutadiene	Single T_g	II had $\geq$32.3 % vinylbutadiene	Kawahara et al. (1989)
	Cis-pentenamer	Single T_g	–	Braun and Rehage (1985)
	Vinylethylene	Single T_g; NMR	II had 86 % 1,2-butadiene	Miller et al. (1990), Roland (1987), Roland and Trask (1989), Trask and Roland (1988), Trask and Roland (1989)
Isoprene, chlorinated	Ethylene-*co*-vinyl acetate	Single T_g; transparency	Semicrystalline; commercial samples	Leffingwell et al. (1973), Purcell and Thies (1968)
Isoprene, modified by hexafluoroisopropanol group	Alkyl methacrylate	Single T_g; FTIR	II had an alkyl group of methyl or *n*-butyl	Coleman et al. (1994)
	Ethylene-*co*-methyl acrylate	Single T_g; FTIR	II had 40 or 75 wt% methyl acrylate	Coleman et al. (1994)
	Ethylene-*co*-methyl methacrylate	Single T_g; FTIR	II had 50 wt% methyl methacrylate	Coleman et al. (1994)
	Ethylene-*co*-vinyl acetate	Single T_g; FTIR	II had 35 or 70 wt% vinyl acetate	Coleman et al. (1994)
	Methyl acrylate	Single T_g; FTIR	–	Coleman et al. (1994)
	Methyl acrylate-*co*-styrene	Single T_g; FTIR	II had 28 wt% methyl acrylate	Coleman et al. (1994)
Isoprene-stat-*N*-(2-hydroxyethyl) carbazole methacrylate	*N*-Itaconimidyl-3,5-dinitrobenzoate-*co*-styrene	Single T_g	I and II had at least 20 mol% of electron donor or acceptor	Cowie and Demaude (1994)
Isoprene-*co*-b-methyl methacrylate	Acrylonitrile-*co*-styrene	Single T_g; TEM	II had 22 wt% AN	Jiang et al. (1995b)
	p-(2-Hydroxyhexafluoroiso-propyl)-α-methystyrene-*co*-styrene	TEM	II had >1.6 mol% OH	Jiang et al. (1995a)

Table 21.1 (continued)

Polymer I of	Polymer II of	Method	Comments	Refs.
N-Isopropylacrylamide	Acrylic acid	Single T_g; SEM; FTIR	Formed complexes	Garay et al. (1997, 2000), Mano et al. (2004b), Mayo-Pedrosa et al. (2004)
	Ethylene-co-vinyl alcohol	Single T_g; SEM; T_m-depression	II had 60 mol% vinyl alcohol	Mano et al. (2004a)
	2-Hydroxyethyl methacrylate	Single T_g	–	Garay et al. (2004)
	Methacrylic acid	Single T_g	Formed complexes	Garay et al. (1997, 2000)
	p-Vinylphenol	Single T_g	Formed complexes	Garay et al. (2004)
Isopropyl acrylate	Isopropyl methacrylate	Single T_g; transparency	–	Kosai et al. (1977)
Lactide	Butylene carbonate-co-butyl succinate	Single T_g; POM	–	Hirano et al. (2002)
	Butylene succinate	Single T_g; WAXD; SAXD	Semicrystalline	Park and Im (2002)
	Diethylene adipate	Single T_g; SEM	I had $\leq$20 wt% II	Okamoto et al. (2009)
	Ethylene adipate	Single T_g; SEM	I had $\leq$20 wt% II	Okamoto et al. (2009)
	Hydroxyesterether	Single T_g	Miscibility achieved after several heating-cooling cycles	Cao et al. (2003)
	Methyl acrylate	Single T_g	–	Eguiburu et al. (1998)
	Methyl methacrylate	Single T_g	–	Eguiburu et al. (1998), Shirahase et al. (2006)
	Sebacic anhydride	Single T_g; surface analysis	I had M_w less than 3 kg/mol	Davies et al. (1996)
	Vinyl acetate-co-vinyl alcohol	Single T_g; T_m-depression	II had 11.7–31.4 mol% vinyl alcohol	Park and Im (2003)
Maleic anhydride-alt-α-methylstyrene	2,6-Dimethyl-1,4-phenylene ether, sulfonylated	Single T_g	II had <55 mol% sulfonylation	Vukovic et al. (1992b)
Maleic anhydride-co-styrene	Caprolactone	Single T_g; T_m-depression; WAXD; TEM	I had 14 or 25 wt% maleic anhydride; semicrystalline	Balsamo et al. (2006), Defieuw et al. (1989a)
	Carbonate of bisphenol-A-co-carbonate of tetramethylbisphenol-A	Single T_g	I had 9, 10.7, or 12.2 wt% maleic anhydride	Merfeld and Paul (1998)

	Carbonate of tetramethylbisphenol-A	Single T_g	I had <12 mol% MA	Gan and Paul (1994a)
	2,6-Dimethyl-1,4-phenylene ether	Single T_g	I had <10 mol% MA	Gan and Paul (1994a)
	2,6-Dimethyl-1,4-phenylene ether, sulfonylated	Single T_g	I was alternating copolymer and had <55 mol% sulfonylation	Vukovic et al. (1992b)
	Ethyl methacrylate	Single T_g	I had 0–33 wt% maleic anhydride	Brannock et al. (1991)
	Glutarimide	Single T_g; FTIR; OM	I had 25, 33, or 50 mol% maleic anhydride	Prinos et al. (1999)
	N-Methyl-glutarimide	Single T_g; FTIR	I had 14 wt% maleic anhydride	Prinos et al. (1997)
	Methyl methacrylate	Single T_g; FTIR; NMR	I had 8–33 wt% maleic anhydride	Brannock et al. (1991), Fang et al. (2007), Feng et al. (1995b)
	n-Propyl methacrylate	Single T_g	I had 0–18.1 wt% maleic anhydride	Brannock et al. (1991)
	Methyl methacrylate-co-phenylmaleimide	Single T_g	Miscibility depended on compositions of I and II	Merfeld et al. (1999)
	Methyl methacrylate-co-tribromophenyl maleimide	Single T_g	Miscibility depended on compositions of I and II	Merfeld et al. (1999)
	Vinylmethylether	Single T_g	I had 4.7 wt% maleic anhydride	Wendland et al. (1989)
Maleimide-co-methyl methacrylate	7-(2-Methacryloyloxy)ethyl adenine	Single T_g	I and II had ≥15 mol% hydrogen bonding unit site	Cowie and Love (2001)
Maleimide-alt-α-methylstyrene	2,6-Dimethyl-1,4-phenylene ether, sulfonylated	Single T_g	Depended on degree of sulfonylation of II	Vukovic et al. (1992a)
Maleimide-co-methyl acrylate	Acrylonitrile-co-styrene-co-vinyl 2,4-diamino-1,3, 5-triazine	Single T_g	I had 9–14 mol% maleimide; II had ≥ triazine unit	Cowie and Cocton (1999)
Methacrylate, liquid crystalline	Methacrylate, liquid crystalline	Single T_g, microscopy	I had electron-donating group; II had electron accepting group	Kosaka and Uryu (1995)
Methacrylic acid	Ester of dehydrated castor oil	Single T_g; SEM	Blend had ≤40 wt% I	Ashraf et al. (2007)
	4-Vinylpyridine	NMR	–	Yi and Goh (2001b)
	Vinylpyridine	Single T_g; FTIR; XPS	II was 2- or 4-vinylpyrdine; formed complexes in ethanol/water (1:1)	Zhou et al. (1998)

Table 21.1 (continued)

Polymer I of	Polymer II of	Method	Comments	Refs.
Methacrylic acid-*co*-α-methylstyrene	Butyl methacrylate-*co*-4-vinylpyridine	Single T_g; FTIR	I had 50.6 mol% methacrylic acid (MA); II had 18 or 26 mol % vinylpyridine (VP)	Metref and Djadoun (1995)
	Ethyl methacrylate-*co*-4-vinylpyridine	Single T_g; FTIR	I had 50.6 mol% MA; II had 23 mol% VP	Metref and Djadoun (1995)
	Methyl methacrylate-*co*-4-vinylpyridine	Single T_g; FTIR	I had 50.6 mol% MA; II had 8 mol% VP	Metref and Djadoun (1995)
Methacrylic acid-*co*-styrene	Ethyl methacrylate	Single T_g	I had 22 mol% methacrylic acid	Abdellaoui and Djadoun (2005)
	Isobutyl methacrylate-*co*-2-(N,N'-dimethylamino)ethyl methacrylate	Single T_g; IGC	I had 12–45 mol% methacrylic acid; II had 12 or 20 mol% dimethylaminoethyl methacrylate	Habi and Djadoun (1999)
	Isobutyl methacrylate-*co*-4-vinylpyridine	Single T_g; IGC; FTIR	I had 12–45 mol% methacrylic acid; II had 10 mol% vinylpyridine	Habi and Djadoun (1999, 2008)
	Tetrahydrofuran	FTIR	I had 9 mol% methacrylic acid	Cleveland et al. (2000)
Methacrylonitrile-*co*-α-methylstyrene	Vinyl chloride	Single T_g	I was azeotropic; I had 31–43 wt% MAN (Kim et al. (1996))	Kenney (1974), Kim et al. (1996)
Methacrylonitrile-*co*-*p*-methylstyrene	*n*-Butyl methacrylate	Single T_g	I had 12–28 wt% MAN	Chen and Porter (1993)
	Ethyl methacrylate	Single T_g	I had 12–55 wt% MAN	Chen and Porter (1993)
	Methyl methacrylate	Single T_g	I had 19–70 wt% MAN	Chen and Porter (1993)
	Isopropyl methacrylate	Single T_g	I had 19–34 wt% MAN when II had $M_n = 161$ kg/mol; I had 16–34 wt% MAN when II had $M_n = 41.6$ kg/mol	Chen and Porter (1993)
	n-Propyl methacrylate	Single T_g	I had 12–43 wt% MAN	Chen and Porter (1993)
	Vinyl chloride	Single T_g	I had 20–43 wt% methacrylonitrile	Chen et al. (1998d)

Methacrylonitrile-co-styrene	t-Butyl methacrylate-co-methyl methacrylate	Single T_g	Miscibility depended on compositions of I and II	Nishimoto et al. (1995)
	Cyclohexyl methacrylate-co-methyl methacrylate	Single T_g	Miscibility depended on compositions of I and II	Nishimoto et al. (1995)
	Ethyl methacrylate	Single T_g	I had 4.5–44 wt% methacrylonitrile (MAN)	Chen et al. (1994)
	Methyl methacrylate	Single T_g; transparency; fluorescence spectroscopy	Miscibility range varied in various studies especially at low MAN end	Dong et al. (1994), Goh et al. (1993), Nishimoto et al. (1995)
	Isopropyl methacrylate	Single T_g	I had 12–38 wt% MAN when II had $M_n = 161$ kg/mol; I had 8–43 wt% MAN when II had $M_n = 41.6$ kg/mol	Chen et al. (1994)
	n-Propyl methacrylate	Single T_g	I had 2–32 wt% MAN	Chen et al. (1994)
4-[[6-(Methacryloyloxy)hexyl]oxy]-N-[9-methyl-2-carbazolyl]methylene]aniline	4-[[6-(Methacryloyloxy)hexyl]oxy-N-(4'-nitrobenzylidene)aniline	Single T_g	Both polymers I and II were liquid crystalline	Kosaka and Uryu (1994)
4-[[1-[(4-Methoxyphenyl)azo]phenyl-4]oxy-3-propyl]oxy]styrene	[4-[-[[(4-Cyanobiphenyl)-4']oxy]-3-propyl]oxy]styrene	Single T_g	Blends showed liquid crystallinity	Imrie and Paterson (1994)
p-Methoxystyrene-co-p-vinylphenol	Alkyl acrylate	Single T_g; FTIR	II had an alkyl group of methyl or ethyl	Sanchis et al. (1995)
	Vinyl acetate	Single T_g; FTIR	–	Sanchis et al. (1995)
Methyl acrylate	Alkyl methacrylate	Single T_g	II had an alkyl group from 2-chloroethyl, 2-fluoroethyl, 1,3-difluoroisopropyl	Peng et al. (1996)
	Epichlorohydrin	Single T_g; IGC	–	Etxeberria et al. (1995), Fernandes et al. (1986c)
	Epichlorohydrin-co-ethylene glycol	Single T_g	I had 50 mol% epichlorohydrin (Hydrin 200)	Fernandes et al. (1986c)
	Ethylene glycol	Single T_g	–	Fernandes et al. (1986c)
	Hexafluoroacetone-co-vinylidene fluoride	Single T_g; XPS	II had 8 mol% of hexafluoroacetone	Kano et al. (1997c)

(continued)

Table 21.1 (continued)

Polymer I of	Polymer II of	Method	Comments	Refs.
	p-Methoxystyrene-co-p-vinylphenol	Dielectric analysis	II had 67 mol% methoxystyrene	Prolongo et al. (1997)
	Nitrocellulose	Single T_g	–	Kargin (1963)
	Vinyl acetate	Single T_g; transparency; NMR	Probably formed two phases when deposited from some solvents (Refs. Nandi et al. (1985), Djadoun (1983))	Casarino et al. (1996), Nandi et al. (1985), Nielson and Chinai (1962), Kosai et al. (1977), Song et al. (1999), Takegoshi et al. (1995)
	Vinyl chloride-co-vinylidene chloride	Single T_g; transparency	II was Saran ($\geq$80 % vinylidene chloride); I had $M_w = 1.0$ kg/mol; two T_g's when I had $M_w = 576$ kg/mol in Woo et al. (1984b)	Tremblay and Prud'homme (1984)
	Vinylidene fluoride	Single T_g; transparent melt	Semicrystalline	Maiti and Nandi (1995), Wahrmund et al. (1978)
Methyl acrylate, modified with C_{60}	Vinylidene fluoride	Single T_g; T_m-depression	I had 10.1 or 19.8 wt% C_{60}	Zheng et al. (2001)
Methyl acrylate-co-vinylcarbazole	Methyl methacrylate-co-2(3,5-dinitrobenzoyl)oxyethyl methacrylate	Single T_g	Both I and II had >27 mol% monomer with interactive groups	Russell et al. (1991)
	Styrene-co-2(3,5-dinitrobenzoyl) oxyethyl methacrylate	Single T_g	Both I and II had >12 mol% monomer with interactive groups	Crone and Natansohn (1991)
Methyl 1-bicyclobutane-carboxylate	Acrylonitrile-co-styrene	Single T_g; transparency	II had 24–38 wt% acrylonitrile	Drujon et al. (1992)
	Ethylene glycol	Single T_g; transparency	$\leq$20 wt% II	Drujon et al. (1992)
2-Methyl-6-ethyl-1,4-phenylene ether	Styrene	Single T_g	–	Cizek (1968)
α-Methyl-α-ethyl-β- propiolactone	Vinyl chloride	Single T_g	Semicrystalline when 75 % I	Aubin and Prud'homme (1980)

Methyl methacrylate	Acrylonitrile-*co*-methyl methacrylate-*co*-styrene	Single T_g	II had 40/39.1/20.9 or 61.1/19.6/19.3 = styrene/methyl methacrylate/acrylonitrile	Nishimoto et al. (1989)
	4'-[[2-(Acryloyloxy)ethyl] ethylamino]-3-chloro-4-nitroazobenzene	Single T_g; NMR	–	Xie et al. (1994)
	4'-[[2-(Acryloyloxy)ethyl] ethylamino]-4-nitroazobenzene	Single T_g; NMR	–	Xie et al. (1994)
	p-t-Butylphenol formaldehyde	Single T_g; FTIR; WAXD	II had M_n = 1,500–1,600	Kalkar et al. (1995)
	Carbon monoxide-alt-propylene	Single T_g; FTIR; NMR	–	Xu and Chien (1994)
	Carbonate of bisphenol-A-*co*-hexafluorobisphenol-A	Single T_g; transparency	II had 4.5–14.0 wt% hexafluorobisphenol-A	Kim and Paul (1992d)
	Carbonate of bisphenol-F	Single T_g; transparency	–	Keskkula and Paul (1986)
	Carbonate of bisphenol-AF	Single T_g; transparency	–	Keskkula and Paul (1986)
	Carbonate of bisphenol chloral	Single T_g; NMR	–	Chiou and Paul (1987), De Los Santos Jones et al. (1984), Keskkula and Paul (1986), Raymond and Paul (1990)
	Epichlorohydrin-*co*-ethylene glycol	Single T_g	–	Fernandes et al. (1986b)
	Ethyl acrylate	Single T_g	–	Cowie et al. (1992f)
	Ethyl methacrylate	Single T_g	Made from slurries of poly (ethyl methacrylate) and methyl methacrylate; inherently unstable, phase separation upon heating	Singh et al. (1988)
	Ethylene, chlorinated	Single T_g	I was atactic, syndiotactic, or isotactic	Ueda and Karasz (1994)
	Formaldehyde-*co*-*p*-tert-butylphenol	Single T_g; FTIR	–	Pennacchia et al. (1986)
	Formaldehyde-*co*-*p*-chlorophenol	Single T_g; FTIR	–	Pennacchia et al. (1986)

(continued)

Table 21.1 (continued)

Polymer I of	Polymer II of	Method	Comments	Refs.
	Formaldehyde-*co*-*p*-nitrophenol	Single T_g; FTIR	–	Pennacchia et al. (1986)
	Formaldehyde-*co*-phenol	Single T_g; FTIR	–	Pennacchia et al. (1986)
	Hexafluoropropene-*co*-vinylidene fluoride	Single T_g	II had 10 or 20 mol% hexafluoropropene	Jauannet et al. (1997)
	N-Maleimide-*co*-styrene	Single T_g; FTIR	II had 45 wt% *N*-maleimide	Vermeesch and Groeninckz (1995)
	Methacrylic acid	Single T_g; FTIR; NMR	–	Huang and Chang (2003)
	Methoxymethyl methacrylate	Single T_g	–	Goh and Lee (1990c)
	Methyl acrylate	Single T_g	–	Cowie et al. (1992f)
	α-Methylstyrene	Single T_g	–	Cowie and Miachon (1992), Siol (1991)
	Nitrocellulose	No phase separation in solution or films	–	Dobry and Boyer-Kawenoki (1974), Grose and Friese (1965), Kosai and Higashino (1975), Peterson et al. (1969)
	Novolac	Single T_g; FTIR; NMR	II had M_w about 1.0 kg/mol and was formaldehyde and 13/17/70 mol% = *p*-t-butylphenol/ *m*-cresol/*o*-cresol or formaldehyde and 15/17/68 mol% = 2-t-butylphenol/ *m*-cresol/*o*-cresol; I was isotactic, atactic, or syndiotactic	Fahrenhlotz and Kwei (1981), Huang et al. (2004d), Kim et al. (1991), Kwei (1984)
	Propylene glycol	Single T_g; SAXS	I had M_w = 550 kg/mol; II had M_w = 1.0–3.9 kg/mol	Macchi et al. (1986)
	Silyl ether	Single T_g; NMR	–	Zheng et al. (2003e)
	Trifluoroethylene-*co*-vinylidene fluoride	Single T_g	II had 25 or 50 mol% trifluoroethylene	Jauannet et al. (1997)
	Trifluoroethylene-*co*-vinylidene fluoride	FTIR; T_m-depression	II had 25 mol% trifluoroethylene	Kim et al. (1993c)

Tetrafluoroethylene-*co*-vinylidene fluoride	Single T_g; T_m-depression	II had 80 mol% vinylidene fluoride	Cho (1991), Hamazaki et al. (1991)
Trifluoroethylene-*co*-vinylidene fluoride	Single T_g; T_m-depression; light scattering	II had 58 mol% vinylidene fluoride	Faria and Moreira (1999), Saito et al. (1988)
Vinyl acetate	Single T_g; FTIR; NMR	Miscible when cast from chloroform or cyclohexanone; immiscible when cast from tetrahydrofuran or melt blended	Crispim et al. (1999), Crispim et al. (2000), Guo (1990e), Lee and Ha (1994a), Nandi et al. (1986), Schnek et al. (1990), Song et al. (1990), Song and Long (1991), Uyar et al. (2005)
Vinyl acetate-*co*-vinyl chloride	Single T_g; transparency	II had 5.9–15.1 vol% vinyl acetate	Friese (1968), Grose and Friese (1965), Kosai and Higashino (1975), Lee et al. (1992), Peterson et al. (1969)
Vinyl alcohol	T_m-Depression	Blend had 60, 80, or 90 wt% II	Adoor et al. (2006)
Vinyl chloride	Single T_g; transparency; NMR	Especially when II was polymerized in situ (Walsh and Cheng 1984a); I of all tacticities miscible with II (Hendrioulle-Granville et al. 1990); increase in isotactic content and mol. wt. of I reduced miscibility with II (Zhao and Prud'homme 1990)	Bosma et al. (1988b), Hendrioulle-Granville et al. (1990), Jager et al. (1983), Kamira and Naima (2006), Karlou and Schneider (2000), Lau and Mi (2001), Parmer et al. (1986, 1988), Piglowski (1988), Tremblay and Prud'homme (1984), Walsh and Cheng (1984a), Walsh and McKeown (1980), Zhao et al. (1991), Zhao and Prud'homme (1990), Zheng and Kyu (1992)

(*continued*)

Table 21.1 (continued)

Polymer I of	Polymer II of	Method	Comments	Refs.
	Vinyl chloride, chlorinated	Single T_g; FTIR	II had 63–68 wt% Cl; I was atactic, isotactic, or syndiotactic (Ueda and Karasz (1994))	Lemieux et al. (1988), Ueda and Karasz (1994), Voremkamp and Challa (1988)
	Vinyl chloride-*co*-vinylidene chloride	Single T_g; transparency	II was Saran (>80 % vinylidene chloride) or 86.5 wt% vinylidene chloride; semicrystalline when ≥20 % II and I was isotactic and when ≥75 % II and I was atactic for the second II	Kang et al. (1988), Lemieux et al. (1988), Tremblay and Prud'homme (1984), Woo et al. (1984b)
	Vinyl chloroacetate	Single T_g	–	Das and Rodriguez (1987)
	Vinylidene fluoride	Single T_g; NMR; dielectric study; T_m-depression; Raman spectroscopy	Semicrystalline when >35–65 % II; I was isotactic, atactic, or syndiotactic; I was linear or 4-arm (Fan and Zheng (2007))	Aihara et al. (1998), Chow (1990), Fan and Zheng (2007), Grinsted and Koenig (1990), Hahn and Wendroff (1985), Hourston and Hughes (1977b), Imken et al. (1976), Mijovic et al. (1982), Nishi and Wang (1975), Noland et al. (1971), Patterson et al. (1976), Paul et al. (1975), Roerdink and Challa (1978), Walker et al. (2003), Zhou and Cakmak (2007)
	Vinylidene fluoride-*co*-hexafluoroacetone	Single T_g	–	Kobayashi et al. (1987)
Methyl methacrylate, imidized	Acrylonitrile-*co*-styrene	Single T_g	I had 53–91 wt% imidized units; II had 5.7–33 wt% acrylonitrile; miscibility depended on extent of imidization of I and acrylonitrile content of II	Fowler et al. (1989), Majumdar et al. (1994)
	Vinyl chloride	Single T_g	I had 53–85 wt% imidized units	Fowler et al. (1989)

Methyl methacrylate, modified with C_{60}	Vinylidene fluoride	Single T_g; T_m-depression	I had 2.6 or 7.4 wt% C_{60}	Zheng et al. (2000)
Methyl methacrylate-*co*-styrene	Carbonate of bisphenol-A-*co*-tetramethylbisphenol-A	Single T_g; transparency	I had ≤33 wt% methyl methacrylate; II had ≤15 wt% bisphenol-A	Kim and Paul (1992e)
	Carbonate of hexafluorobisphenol-A-*co*-tetramethylbisphenol-A	Single T_g	I had 9, 20, or 33 wt% methyl methacrylate; II had 20 wt% hexafluorobisphenol-A	Takakuwa et al. (1994)
Methyl methacrylate-*co*-2,4,5-tribromostyrene	Acrylonitrile-*co*-styrene	Single T_g	I had ≤51 wt% tribromostyrene; II had 10–30 wt% AN	Chu et al. (2000)
	Maleic anhydride-*co*-styrene	Single T_g	I had ≤51 wt% tribromostyrene; II had 10–33 wt% maleic anhydride	Chu et al. (2000)
Methyl methacrylate-*co*-trifluoroethyl methacrylate	Hexafluoropropene-*co*-vinylidene fluoride	Single T_g	I had 33 or 66 mol% trifluoroethyl methacrylate: II had 10 or 20 mol% hexafluoropropene	Jauannet et al. (1997)
	Vinylidene fluoride	Single T_g	I had 33 or 66 mol% trifluoroethyl methacrylate	Jauannet et al. (1997)
Methyl methacrylate-*co*-vinylpyridine	Acrylic acid-*co*-butyl acrylate	Single T_g; FTIR	I had 13–20 mol% vinylpyridine; II had 13–20 mol % acrylic acid	Jo et al. (1989b)
Methyl methacrylate-*co*-4-vinylpyridine	Triphenylene oxide	Single T_g; FTIR	I had 11 mol% vinylpyridine; II was sulfonated or phenylated	Rajagopalan et al. (2003)
2-Methyl-2-oxazoline	Allyl-*co*-styrene	Single T_g; FTIR	II had 6.5 wt% OH	Dai et al. (1995a)
	Hexamethylene sulfoxide	Single T_g	Blend had 20 wt% I	Oyama et al. (1998)
	Hydroxyether of bisphenol-A	Single T_g; FTIR	–	Dai et al. (1995a)
	2-Hydroxypropyl methacrylate	Single T_g; FTIR	–	Dai et al. (1995a)
	Vinyl alcohol	Single T_g; FTIR	–	Aoi et al. (1995b)
	Vinyl chloride	Single T_g	I <50 wt% in blend	Kobayashi et al. (1988)
	Vinyl fluoride	Single T_g	I <50 wt% in blend	Kobayashi et al. (1988)
	p-Vinylphenol	Single T_g; FTIR	–	Dai et al. (1995a)

Table 21.1 (continued)

Polymer I of	Polymer II of	Method	Comments	Refs.
2-Methyl-1-pentene sulfone	Novolac	Single T_g	II had $M_w = 1.0$ kg/mol and was formaldehyde and 13/17/ 70 mol% = p-t-butylphenol/ m-cresol/o-cresol or formaldehyde and 15/17/68 mol % = 2-t-butylphenol/m-cresol/ o-cresol	Fahrenhlotz and Kwei (1981)
N-Methyl-4-piperidinyl methacrylate	Acid	Single T_g, FTIR; XPS	II was acrylic acid, methacrylic acid, styrenesulfonic acid, or vinylphosphonic acid	Luo et al. (1998)
	p-Vinylphenol	Single T_g; FTIR; XPS	–	Goh et al. (2001)
2-Methyl-6-propyl-1,4-phenylene ether	Styrene	Single T_g		Cizek (1968)
α-Methyl-α-n-propyl-β-propiolactone	Vinyl chloride	Single T_g	Semicrystalline when >50 % I	Aubin et al. (1982), Aubin and Prud'homme (1980)
α-Methylstyrene	Cyclohexyl acrylate	Single T_g, transparency	–	Siol (1991)
	Cyclohexyl methacrylate	Single T_g, transparency	–	Chong and Goh (1991a), Chang and Woo (2001b), Siol (1991)
	Ethyl methacrylate	Single T_g, transparency	–	Siol (1991)
	n-Propyl methacrylate	Single T_g, transparency	–	Siol (1991)
p-Methylstyrene	Cyclohexyl acrylate	Single T_g, transparency	–	Siol (1991)
	Cyclohexyl methacrylate	Single T_g, transparency; OM	–	Chong and Goh (1991a), Siol (1991), Woo and Jang (1999)
	2,6-Dimethyl-1,4-phenylene ether, bromobenzylated	Single T_g, transparency	II had 9, 16, or 37 % bromination	Goh and Lee (1989b)
4-Methyl-5-vinylthiazole	Acrylic acid	Single T_g; FTIR; XPS	–	Luo et al. (2003)
	p-Vinylphenol	Single T_g; FTIR; XPS	–	Luo et al. (2003)
	Vinylphosphonic	Single T_g; FTIR; XPS	–	Luo et al. (2003)

N-1-Monoalkyl itaconamide	2-Hydroxypropyl methacrylate	Single T_g; FTIR	I had an alkyl group of butyl, hexyl, or octyl	Urzua et al. (2000)
	4-Vinylpyridine	Single T_g; FTIR	I had an alkyl group of butyl, hexyl, or octyl	Urzua et al. (2000)
Monomethyl itaconate	Thiocarbonate	Single T_g	II had methyl, ethyl, or propyl side groups	Radic and Gargallo (1991)
α-Methylstyrene-co-4-(2-hydroxyethyl)-α-methylstyrene	Alkyl acrylate	Single T_g	I had 6, 41, 72, or 89 mol% α-methylstyrene; II had alkyl group of methyl, ethyl, or t-butyl	Cowie and Reilly (1993a)
	Alkyl methacrylate	Single T_g	I had 6, 41, 72, or 89 mol% α-methylstyrene; II had alkyl group of methyl, ethyl, or t-butyl	Cowie and Reilly (1993a)
	Dialkyl itaconate	Single T_g	I had 6, 41, 72, or 89 mol% α-methylstyrene; II had dialkyl group of dimethyl, diethyl, or di-t-butyl or di-n-propyl	Cowie and Reilly (1993a)
	Vinyl acetate	Single T_g	I had 6, 41, 72, or 89 mol% α-methylstyrene	Cowie and Reilly (1993b)
	4-Vinylpyridine	Single T_g	I had 6, 41, 72, or 89 mol% α-methylstyrene	Cowie and Reilly (1993b)
	N-Vinyl pyrrolidone	Single T_g	I had 6, 41, 72, or 89 mol% α-methylstyrene	Cowie and Reilly (1993b)
α-Methylstyrene-co-4-(1,1,1-trifluoro-2-hydroxyethyl)-α-methylstyrene	Alkyl acrylate	Single T_g	I had 23, 47, 60, 84, or 93 mol% α-methylstyrene; II had an alkyl group of methyl, ethyl, or t-butyl	Cowie and Reilly (1993a)
	Alkyl methacrylate	Single T_g	I had 23, 47, 60, 84, or 93 mol% α-methylstyrene; II had an alkyl group of methyl, ethyl, or t-butyl	Cowie and Reilly (1993a)

(continued)

Table 21.1 (continued)

Polymer I of	Polymer II of	Method	Comments	Refs.
	Dialkyl itaconate	Single T_g	I had 23, 47, 60, 84, or 93 mol% α-methylstyrene; II had dialkyl group of dimethyl, diethyl, or di-t-butyl or di-n-propyl	Cowie and Reilly (1993a)
	Vinyl acetate	Single T_g	I had 23, 47, 60, 84, or 93 mol% α-methylstyrene	Cowie and Reilly (1993b)
	4-Vinylpyridine	Single T_g	I had 23, 47, 60, 84, or 93 mol% α-methylstyrene	Cowie and Reilly (1993b)
	N-Vinyl pyrrolidone	Single T_g	I had 23, 47, 60, 84, or 93 mol% α-methylstyrene	Cowie and Reilly (1993b)
Methylthiomethyl methacrylate	Vinyl alcohol	Single T_g; FTIR; XPS; NMR	–	Yi and Goh (2003)
N-Methyl-N-vinylacetamide	Allyl alcohol-co-styrene	Single T_g; FTIR	II had 4.5 or 6.5 wt% OH; formed complexes in butanone	Dai et al. (1994b)
Mono-n-alkyl itaconate	Vinylpyridine	Single T_g; FTIR	I had an alkyl group of methyl, ethyl, n-propyl, n-butyl, n-pentyl, or n-hexyl; II was 2- or 4-vinylpyridine	Velada et al. (1996a, b)
Monomethyl itaconate	Tertiary amide	Single T_g	II was N,N-dimethylacrylamide or 2-ethyl-2-oxazoline; formed complexes	Meaurio et al. (1996)
2,2'-(2,6-Naphthalene) bisbenzimidazole	Imide	Single T_g; FTIR	II was made from 1,4-phenylene and 3,3',4,4'-benzo-phenolic dianhydride	Kao and Chen (1997)
Natural rubber, epoxidized	Acrylic acid-co-ethylene	Single T_g	I had 50 mol% epoxidation; II had 6 wt% acrylic acid	Mohanty et al. (1995, 1996)
	Ethylene, chlorinated	Single T_g	I had 50 mol% epoxidation; II had 25 or 48 % Cl	Margaritis et al. (1987)
	Ethylene, chlorosulfonated	Single T_g	I had 25 mol% epoxidation; II was Hypalon 40	Mukhopadhyay and De (1990)
	Novolac	Single T_g	I had 50 mol% epoxidation	Kallistsis and Kalfoglou (1989)

Neopentyl glycol adipate (2,2-dimethyl-1,3-propylene adipate)	Propylene, chlorinated	Single T_g	I had 50 mol% epoxidation	Kallistsis and Kalfoglou (1987)
	Vinyl chloride	Single T_g	I had 50 mol% epoxidation	Leung et al. (1986), Varughese et al. (1986, 1989)
	Vinyl chloride, plasticized	Single T_g	I had 50 mol% epoxidation; II had 40 phr dioctyl phthalate	Varughese (1990)
	Vinylidene chloride-*co*-alkyl acrylate	Single T_g	I had 50 mol% epoxidation; II had 10 % alkyl acrylate	Kallistsis and Kalfoglou (1987)
	Hydroxyether of bisphenol-A (Phenoxy)	Single T_g; transparency	–	Harris et al. (1982)
	Vinyl acetate-*co*-vinyl chloride	Single T_g; transparency	II had 2 or 17 wt% vinyl acetate	Goh et al. (1984c)
	Vinyl chloride	Single T_g; transparency	–	Goh et al. (1982b)
	Vinyl chloride-*co*-vinylidene chloride	Single T_g	Semicrystalline; II was Saran (86.5 wt% vinylidene chloride)	Woo et al. (1983)
	Vinylidene fluoride	Clear melt although refractive indices very different; T_{m}-depression	Semicrystalline	Goh et al. (1985)
Neopentyl glycol succinate (2,2-dimethyl-1,3-propylene succinate)	Epichlorohydrin	Single T_g; transparency	–	Fernandes et al. (1984)
	Hydroxyether of bisphenol-A (Phenoxy)	Single T_g; transparency	Semicrystalline ≤20 wt% II	Harris et al. (1982)
	Vinyl chloride	Single T_g; transparency	–	Ziska et al. (1981)
	Vinyl chloride-*co*-vinylidene chloride	Single T_g	≤60 wt% I; possible second T_g when >60 wt% I; semicrystalline	Woo et al. (1983)
Nitrocellulose	Butylene adipate	Single T_g; FTIR	I had 12.62 or 13.42 % N	Jutier et al. (1988)
	Caprolactone	Single T_g; FTIR	I had 12.62 or 13.42 % N	Jutier et al. (1988)
	Ethylene adipate	Single T_g; FTIR	I had 12.62 or 13.42 % N	Jutier et al. (1988)
	Valerolactone	Single T_g; FTIR	I had 12.62 or 13.42 % N	Jutier et al. (1988)
	Vinyl acetate	Single T_g; clear films	–	Friese (1968), Kawai (1956), Kosai and Higashino (1975)

(*continued*)

Table 21.1 (continued)

Polymer I of	Polymer II of	Method	Comments	Refs.
Norbornene	Carbonate of bisphenol-A	Single T_g, FTIR	I was hydrogenated	Yang and Han (2008)
	Styrene-*co-p*-vinylphenol	Single T_g, FTIR	II had 5–28 mol% vinylphenol	Tanaka et al. (2009)
	2-Vinylpyridine	Single T_g, FTIR	I was hydrogenated	Yang and Han (2008)
Novolac	Amide	Single T_g, FTIR	II was PA-6 or PA-6,6	Wang et al. (1999a)
	n-Butyl methacrylate	Single T_g, FTIR	–	Kim et al. (1991)
	Butylene adipate	FTIR	–	Ma et al. (1997b)
	Dimethylsiloxane adipamide	Single T_g, FTIR	–	Hung et al. (2002)
	Ethylene adipate	FTIR	–	Ma et al. (1997b)
	Ethylene glycol	Single T_g, FTIR; T_m-depression	–	Ma and Wu (2001), Sotele et al. (1997), Zhong and Guo (1998)
	Vinyl acetate	Single T_g	I had M_w about 1.0 kg/mol and was formaldehyde and 15/17/68 mol% = 2-t-butylphenol/*m*-cresol/*o*-cresol	Fahrenhlotz and Kwei (1981)
	Vinylmethylether	Single T_g	I had M_w about 1.0 kg/mol and was formaldehyde and 13/17/70 mol% = *p*-t-butylphenol/*m*-cresol/*o*-cresol	Fahrenhlotz and Kwei (1981)
	Vinylpyridine	Single T_g, FTIR	II was 2- or 4-vinylpyridine	Kuo et al. (2002b)
(2-Oxo-1,3-dioxolan-4-yl)methyl methacrylate	Ethyl acrylate-*co*-methyl methacrylate	Single T_g, FTIR; transparency	II had 2 or 5 wt% ethyl acrylate	Park et al. (2001a)
(2-Oxo-1,3-dioxolan-4-yl)methyl methacrylate-*co*-acrylonitrile	Ethyl acrylate-*co*-methyl methacrylate	Single T_g, transparency	I had 24.5 wt% AN; II had 7 wt % ethyl acrylate	Park et al. (2002a)
(2-Oxo-1,3-dioxolan-4-yl)methyl methacrylate-*co*-ethyl acrylate	Methyl methacrylate	Single T_g, FTIR; transparency	I had 19.7 wt% ethyl acrylate	Park et al. (2001c)
(2-Oxo-1,3-dioxolan-4-yl)methyl methacrylate-*co*-ethyl acrylate	Vinyl chloride	Single T_g, FTIR; transparency	I had 19.7 wt% ethyl acrylate	Park et al. (2001c)
(2-Oxo-1,3-dioxolan-4-yl)methyl methacrylate-*co*-styrene	Vinyl chloride	Single T_g, FTIR; transparency	I had 19.5 wt% styrene	Park et al. (2002b)

(2-Oxo-1,3-dioxolan-4-yl)methyl vinyl ether-co-N-phenylmaleimide	Acrylonitrile-co-styrene	Single T_g; transparency	I had 67.7 wt% N-phenylmaleimide; II had 40 wt% acrylonitrile	Moon et al. (2000)
	Vinyl chloride	Single T_g; transparency	–	Moon et al. (2000)
Oxy-2,2-bis(butylsulfonylmethyl)-trimethylene	Oxy-(alkylsulfonylmethyl)ethylene-co-oxyethylene	Single T_g	II had an alkyl group of n-butyl or pentyl	Lee et al. (1998b)
	Oxy-(pentylsulfonylmethyl)ethylene	Single T_g	–	Lee et al. (1998b)
Oxy-2,2-bis(ethylsulfonylmethyl)-trimethylene	Oxy-(alkylsulfonylmethyl)ethylene	Single T_g	II had an alkyl group of ethyl, n-propyl, or isopropyl	Lee et al. (1998b)
	Oxy-(alkylsulfonylmethyl)ethylene-co-oxyethylene	Single T_g	II had an alkyl group of methyl, ethyl, n-propyl, or isopropyl	Lee et al. (1998b)
Oxy-2,2-bis(isopropylsulfonylmethyl)-trimethylene	Oxy-(2-alkylsulfonylmethyl)-ethylene-co-oxyethylene	Single T_g	II had an alkyl group of n-butyl, 2-butyl, or isopropyl	Lee et al. (1998b)
	Oxy-(2-butylsulfonylmethyl)ethylene	Single T_g	–	Lee et al. (1998b)
Oxy-2,2-bis(methylsulfonylmethyl)-trimethylene	Epichlorohydrin	Single T_g	–	Lee and Litt (2001)
	Epichlorohydrin-co-oxy(methylsulfonylmethyl)ethylene	Single T_g	II had 34, 18, or 0 mol% epichlorohydrin	Lee and Litt (2001)
	Oxy(methylsulfonylmethyl)ethylene-co-oxyethylene	Single T_g	–	Lee et al. (2001)
Oxy-2,2-bis(n-propylsulfonylmethyl)-trimethylene	Oxy-(alkylsulfonylmethyl)ethylene	Single T_g	II had an alkyl group of n-butyl or 2-butyl	Lee et al. (1998b)
	Oxy-(alkylsulfonylmethyl)ethylene-co-oxyethylene	Single T_g	II had an alkyl group of n-propyl, isopropyl, n-butyl, 2-butyl, or pentyl	Lee et al. (1998b)
Oxy(methylsulfonylmethyl)ethylene-co-oxyethylene	Epichlorohydrin-co-oxy(methylsulfonylmethyl)ethylene	Single T_g	II had 34 or 46 mol% epichlorohydrin	Lee and Litt (2001)
Pentabromobenzyl methacrylate-co-methyl methacrylate	Acrylonitrile-co-styrene	Single T_g	Miscibility depended on compositions of I and II	Merfeld et al. (2000)
	Maleic anhydride-co-co-styrene	Single T_g		Merfeld et al. (2000)

(continued)

Table 21.1 (continued)

Polymer I of	Polymer II of	Method	Comments	Refs.
Pentabromobenzyl methacrylate-co-styrene	Carbonate of tetramethylbisphenol-A	Single T_g; light scattering	II had ≤33.9 wt% pentabromobenzyl methacrylate	Merfeld et al. (2000)
	2,6-Dimethyl-1,6-phenylene ether	Single T_g; light scattering	I had ≤54 wt% pentabromobenzyl methacrylate	Merfeld et al. (2000)
	Methyl methacrylate	Single T_g; light scattering	Miscibility depended on M_w of II and blend composition	Merfeld et al. (2000)
	Styrene	Single T_g; light scattering	Miscibility depended on M_w of II and blend composition	Merfeld et al. (2000)
2,2,3,3,3-Pentafluoropropyl methacrylate-co-4-vinylpyridine	Methacrylic acid co-methyl methacrylate	Single T_g; FTIR; XPS; ToF-SIMS	I had 28–54 mol% vinypyridine	Huang et al. (2004a, c)
Phenolphthalein polyaryletherketone	Ethylene glycol	Single T_g	–	Zheng et al. (2004)
Phenolphthalein polyetheretherketone	Epoxy	Single T_g; FTIR; SEM	–	Guo et al. (1991a), Song et al. (2001), Zhong and Guo (1998)
	Hydroxyether of bisphenol-A (Phenoxy)	Single T_g	–	Guo et al. (1988, 1991a)
	Sulfone	Single T_g	–	Guo et al. (1988, 1990b)
	N-Vinylpyrrolidone	Single T_g	–	Guo (1992a)
Phenolphthalein polyetherethersulfone	Ethylene glycol	Single T_g		
	N-Vinylpyrrolidone	Single T_g	–	Guo (1992a)
Phenolphthalein polyetherketone	Imide	Single T_g	Blend had <90 wt% I	Tang et al. (1996)
Phenolphthalein polyethersulfone	Hydroxyether of bisphenol-A	Single T_g; FTIR; SEM	–	Zheng et al. (2003b)

Phenol-formaldehyde	N,N-Dimethylacrylamide	Single T_g	Formed complexes from acetone, dioxane, and ethyl acetate	Yang et al. (1989)
	Methyl methacrylate-co-styrene	Single T_g	II had >20 wt% methyl methacrylate	Kim et al. (1989a)
Phenyl acrylate	Vinyl benzoate	Single T_g; transparency	–	Maiti et al. (1988)
N-phenyl-2-hydroxytrimethylene amine	Caprolactone	Single T_g; FTIR	Semicrystalline	Guo et al. (1997)
	Ethylene glycol	Single T_g; FTIR	Semicrystalline	Guo et al. (1997)
	Vinylmethylether	Single T_g; FTIR	–	Guo et al. (1997)
Phenylene	Phenyl sulfone	Single T_g; AFM	I was made from phenylketone-substituted p-phenylene and m-phenylene	J76
Phenylene, sulfonated	Ethyl acrylate-co-4-vinylpyridine	Single T_g	–	Murali et al. (1986)
2,2-(m-Phenylene)-5,5'-bisbenzimidazole	Arylate	Single T_g	–	Christiansen et al. (1987)
	Carbonate of bisphenol-A	FTIR	–	Musto et al. (1991)
	Imide	Single T_g; FTIR	II was made from 3,3',4,4'-benzophenone-tetracarboxylic dianhydride (BDTA) and 3,3'-diaminobenzophenone (LARC TPI)	Guerra et al. (1988a)
	Imide	Single T_g; FTIR; transparency	II was made from BDTA and 2,4-toluenediamine or 4,4'-methylene dianiline	Ahn and Choe (1995)
	Imide	Single T_g; FTIR	II was poly[2,2'-bis(3,4-dicarboxyphenoxy) phenylpropane-2-phenylene bisimide] (Ultem 1000)	Leung et al. (1986), Liang et al. (1991), Shiomi et al. (1989), Vanderhart et al. (1992)

Table 21.1 (continued)

Polymer I of	Polymer II of	Method	Comments	Refs.
	Imide	Single T_g; FTIR	II was made from 3,3',4,4'-benzophenonetetra-carboxylic dianhydride and 5,6-amino-1-(4'-aminophenyl)-1,3,3'-trimethylindane (XU 218)	Choe et al. (1987), Leung et al. (1986), Shiomi et al. (1989)
	Imide	Single T_g; FTIR	II was made from benzophenone-tetracarboxylic dianhydride and 4/1 mixture of 2,4-toluenediisocyanate and 4,4'-diphenylmeth anediisocyanate (PI 2080)	Leung et al. (1986), Stankovic et al. (1988)
	Imide sulfone	Single T_g; FTIR	II was made from 3,3',4,4'-benzophenonetetra-carboxylic dianhydride and 3,3'-diaminodiphenyl sulfone	Chen et al. (1988b), Janarthanan et al. (1992), Lee and Quin (1989)
	Imide sulfone, fluorinated	Single T_g; FTIR	≥80 % I	Janarthanan et al. (1992)
	Siloxaneimide, segmental copolymer	Single loss tangent peak	II was 3,3',4,4'-benzophenonetetra-carboxylic dianhydride and 3,3'-diaminodiphenyl sulfone-based polyimide and dimethylsiloxane segmental copolymer	Chen et al. (1988a)
m-Phenylene-isophthalamide	Aramide	Single T_g	II was a copolyamide Ultramid T or Selar 3426	Ellis (1995)
	Ethersulfone	Single T_g; transparency	–	Hayashi et al. (1995)
	Hexamethylene isophthalamide	Single T_g	Semicrystalline	Brisson and Breault (1991), Ellis (1995)
	Heptamethylene isophthalamide	Single T_g	Semicrystalline	Brisson and Breault (1991)
	m-Xylene adipamide	Single T_g	Semicrystalline	Ellis (1995)

Phenylene sulfide	Phenylene sulfide ether	Single T_g	Semicrystalline	Brostow et al. (1995)
p-Phenylene terephthalamide	Caprolactam (nylon 6)	Single T_g; FTIR	Semicrystalline	Kyu et al. (1989b)
	Hexamethylene adipamide (nylon 6,6)	Single T_g; FTIR	Semicrystalline	Kyu et al. (1989b)
	p-Phenylene 1,3,4-oxadiazole	OM; FTIR	–	Kummerlowe et al. (1993)
	4-Vinylpyridine	Single T_g; TEM	N atom of I was modified to propanesulfonate or n-propyl group	Parker and Hara (1997)
o-Phenylphenol	Ethyl acrylate-co-methyl acrylate	Single T_g	II had 37 or 81 wt% ethyl acrylate	Kim et al. (1998)
Phosphazene	Glycolide-co-lactide	Single T_g; FTIR; SEM	II had 50 or 85 mol% lactide	Krogman et al. (2007)
n-Propyl acrylate	Alkyl methacrylate	Single T_g	II had an alkyl group of chloromethyl, 1-chloroethyl, 2-chloroethyl, dichloroethyl, or trichloroethyl	Peng et al. (1996)
	Vinyl chloride	Single T_g; transparency	–	Walsh and McKeown (1980)
n-Propyl methacrylate	Vinyl alcohol	Single T_g; FTIR; NMR	–	Yi and Goh (2005)
	Vinyl chloride	Single T_g; transparency	–	Ha et al. (1990a), Perrin and Prud'homme (1991), Tremblay and Prud'homme (1984), Walsh and McKeown (1980)
	Vinyl chloride-co-vinylidene chloride	Single T_g; transparency	Semicrystalline when $\geq$65 % II; II was Saran ($\geq$80 % vinylidene chloride) or 86.6 wt% vinylidene chloride	Kang et al. (1988), Tremblay and Prud'homme (1984), Woo et al. (1984b)
Propyloxazoline	Styrene	Single T_g	<25 wt% I in blend	Kobayashi et al. (1988)
Propylene	1-Butene-co-ethylene	NMR	I was atactic; II had 66 mol% butene	Wachowicz et al. (2008)
	Hydrogenated oligocyclopentadiene	Melting point depression; WAXS; SANS	–	Martuscelli et al. (1991)
Propylene, chlorinated	Neopentyl glycol adipate	Single T_g; transparency	I had 67 wt% Cl	Goh et al. (1985)
Rubber, chlorinated	Vinylmethylether	Phase diagram	–	Gevorkyan et al. (1978)

(continued)

Table 21.1 (continued)

Polymer I of	Polymer II of	Method	Comments	Refs.
Sebacic anhydride	2,2-Dimethyltrimethylene carbonate	T_m-Depression	Semicrystalline	Wang et al. (2002a)
	Tetramethylene carbonate	T_m-Depression	Semicrystalline	Wang et al. (2002a)
Styrene	5-Acetyl-2,6-dimethyl-1,4-phenylene ether	Single T_g; transparency; FTIR; light scattering	–	Liu et al. (2000)
	5-Benzoyl-2,6-dimethyl-1,4-phenylene ether	Single T_g; transparency; FTIR; light scattering	–	Liu et al. (2000)
	Carbonate of bisphenol-A	Single T_g; SEM	–	Jang and Lee (2003)
	Carbonate of tetramethylbisphenol-A	Single T_g; light scattering; FTIR	Semicrystalline after long annealing	Guo and Higgins (1990), Iler et al. (1984), Kim and Paul (1992b), Koh et al. (1998), Liu et al. (1995), Shaw (1974),Yang et al. (1993a, b)
	Carbonate of bisphenol-A-co-tetramethylbisphenol-A	Single T_g; transparency	II had ≥85 wt% tetramethylbisphenol-A	Kim and Paul (1992e)
	2-Chlorostyrene	Negative volume change of mixing	–	Tsujita et al. (1987)
	Cyclohexyl acrylate	Single T_g	–	Siol (1991)
	Cyclohexyl methacrylate	Single T_g; transparency; NMR	I was isotactic (Chang and Woo 2003b, Chang et al. 2004a)	Chong and Goh (1991a), Chang and Woo (2003b), Chang et al. (2004b), Friedrich et al. (1996), Nishimoto et al. (1990), Siol (1991), Wu et al. (2002)
	Cyclohexyl methacrylate-co-methyl methacrylate	Single T_g	II had ≥21.6 % cyclohexyl methacrylate	Nishimoto et al. (1990), Pomposo et al. (1998)
	2,6-Dimethyl-1,4-phenylene ether, bromobenzylated	Single T_g	II had ≤76 % bromination	Goh and Lee (1988a)
	2,6-Dimethyl-1,4-phenylene ether, sulfonated	Single T_g	II had <1.9 % sulfonation	Hsieh and Peiffer (1992)

2,6-Dimethyl-1,4-phenylene ether-co-2,3,6-trimethyl-1,4-phenylene oxide	Single T_g	I was atactic or isotactic; II had <20 mol% 2,3,6-trimethyl-1,4-phenylene oxide	Paduchewit et al. (1989)
Dimethylsilphenylene	Single T_g	–	Werlang et al. (1997)
Ethyl methacrylate	Single T_g	Miscible when melt blended	Brannock et al. (1990)
α-Methylstyrene	Single T_g	–	Saeki et al. (1983), Schneider and Dilger (1989), Van Tam Bui et al. (1988), Widmaier and Mignard (1987), Yang et al. (1991)
n-Propyl methacrylate	Single T_g	Miscible when melt blended	Brannock et al. (1990)
Sila-α-methylstyrene	Single T_g; OM	–	Maier et al. (1996)
Vinylmethylether	Single T_g; transparency; NMR; SANS	Two phases when deposited from some solvents	Asano et al. (1995), Bank et al. (1971, 1972), Bhowmick et al. (1986), Beaucage and Stein (1993), Chu et al. (1988), Cowie et al. (1993a), Hikichi et al. (1998), Kwei et al. (1974), McMaster (1973), Mandal and Woo (1999c), Nishi and Kwei (1975), Tezuka et al. (1995)
Styrene, modified with C$_{60}$			
2,6-Dimethyl-1,4-phenylene ether	Single T_g	I had 1.9–13.6 wt% C$_{60}$	Zheng et al. (1997a)
Vinylmethylether	Single T_g	I had 1.9 or 9.9 wt% C$_{60}$	Zheng et al. (1997a)
Styrene, sulfonated			
Amine-terminated polyalkylene glycol	FTIR	I had 4.5 mol% sulfonation; II had M_n = 900 (Jeffamine ED-900)	Gracia (1986)
Benzyl methacrylate-co-4-vinylpyridine	Single T_g; FTIR	I had 4–10.2 mol% sulfonation; II had 3.7–11.2 mol% 4-vinylpyridine	Sankarapandian and Kishore (1996a)
N,N-Dimethylacrylamide	Transparency	I had 12 mol% sulfonation	Landry and Teegarden (1991)

(continued)

Table 21.1 (continued)

Polymer I of	Polymer II of	Method	Comments	Refs.
	2,6-Dimethyl-1,4-phenylene ether	Single T_g	I had <2.6 % sulfonation	Hsieh and Peiffer (1992)
	Ethylene glycol	Single T_g	I had 1.35 or 4.51 mol% SOlayemi and Ibiyeye (1986)H; II end-capped with propylamine groups	Weiss et al. (1990)
	Methyl methacrylate	Single T_g; transparency	I had 12 mol% sulfonation	Landry and Teegarden (1991)
	Methyl methacrylate-*co*-4-vinylpyridine	FTIR; TEM; NMR	I had 6 mol% sulfonation and II had 6 mol% vinylpyridine (Chen et al. (2004b)); I had 9.9 % sulfonation; II had 11.1 % vinylpyridine (Natansohn and Eisenberg (1986))	Chen et al. (2004b), Natansohn and Eisenberg (1986)
	Phenylsilsesquioxane	Single T_g; SEM; WAXD	–	Li et al. (1996)
	Urethane	FTIR	I had 7.9 mol% sulfonation	Tannanbaum et al. (1986)
	Vinylpyridine	Single T_g; FTIR; XPS	II was 2- or 4-vinylpyridine	Zhou et al. (1997c)
Styrene, sulfonated and metal-neutralized	Amide	Single T_g; NMR; FTIR	I had 9.8 mol% sulfonation and Li-neutralized; II was PA-6,6 or PA-6,10 (Molnar and Eisenberg (1993)); II was PA-6 and I was Zn-neutralized or not neutralized (Kwei et al. (1993)); I had 5.4 or 9.8 mol% sulfonation and Li-neutralized, II was PA-6 (Rajagopalan et al. (1995))	Kwei et al. (1993), Molnar and Eisenberg (1993), Rajagopalan et al. (1995)
	Amide	Single T_g; WAXD	I had 9.7 mol% sulfonation and Li-neutralized; II was PA-4	Ng et al. (1994)
	Amide	Single T_g; FTIR; SAXS	I had 5.4 or 9.8 mol% sulfonation and Li-neutralized; II was PA-6	Weiss and Lu (1994)

	Amide	Single T_g; FTIR; NMR; SAXS	I had 6.5–9.0 mol% sulfonation and Zn-neutralized; II was PA-6	Weiss and Lu (1994)
	Amide	T_m–Depression	I had 20, 44, or 70 mol% sulfonation and Na-neutralized; II was PA-11	Deimede et al. (2000)
	N,N′-Dimethylene sebacamide	Single T_g; light scattering; NMR; SANS	I had 13.7 mol% sulfonation and neutralized by Zn, Cu, Mn, Cd, or Li	Feng et al. (1996a, e)
	N,N′-Dimethylethylene sebacamide	Single T_g	I had 7.4 mol% sulfonation and Li-neutralized	Feng et al. (1996d)
	Ester, liquid crystalline	Single T_g	I had 5 mol% sulfonation and Zn-neutralized	Dutta et al. (1996)
	Ester, liquid crystalline	Single T_g; FTIR; SEM	I had 6.9 mol% sulfonation and neutralized with Li, Na, Mn, or Zn; II was made from hydroxybenzoic acid and ethylene terephthalate (60:40)	He and Liu (1999)
	Ester, liquid crystalline	Single T_g; FTIR; SEM	I had 5.3 mol% sulfonation and Zn-neutralized; II was made from hydroxybenzoic acid and hydroxynaphthoic acid	Weiss et al. (2000)
	Ethyl acrylate-co-4-vinylpyridine	FTIR	I had 2.1–7.3 mol% sulfonation and Zn-neutralized; II had 2.4–10.6 mol% vinylpyridine	Sakurai et al. (1993)
	N-Methyl-4-piperidyl methacrylate	FTIR; XPS	I was neutralized with Zn; formed complexes	Goh et al. (2000b)
	4-Vinylpyridine	Single T_g; FTIR; XPS	I was Li- or Zn-neutralized; formed complexes	Goh et al. (1998b)
Styrene-co-o-acetyl-1,6-diisopropyl-4-vinylphenol	Ethylene glycol	Single T_g; FTIR	I had 7 mol% OH	Coleman et al. (1999)
	Vinylmethylether	Single T_g; FTIR;	I had 7 mol% OH	Coleman et al. (1999)
Styrene-co-p-(2-hydroxypropan-2-yl)styrene	n-Butyl methacrylate-co-4-vinylpyridine	Single T_g; light scattering	I had 8–58 mol% OH; II had 4.7–68 mol% vinylpyridine; formed complexes when OH and pyridine contents were high	Zhu et al. (1998a)

Table 21.1 (continued)

Polymer I of	Polymer II of	Method	Comments	Refs.
Styrene-*co*-maleic acid	Vinyl butyral	Transparency	I was Daidou Kogyo Styrite HS-2	Kosai and Higashino (1975)
Styrene-*co*-methacrylic acid	Ethyl methacrylate	Single T_g; fluorescence study	Miscible when cast from toluene or dioxane; immiscible when cast from chloroform; I had 93.4–96.7 mol% styrene	Chen and Morawetz (1989)
Styrene-*co*-methacryloyl glycine	Ethyl methacrylate	Fluorescence study	Miscible when cast from toluene; immiscible when cast from chloroform; I had 93.8–97.2 mol% styrene	Chen and Morawetz (1989)
Styrene-*co*-styrene-4-carboxylic acid	*N,N*-Dimethylacrylamide	Single T_g; transparency	I had 25 or 54 mol% acid groups	Landry and Teegarden (1991)
	Methyl methacrylate	Single T_g; transparency	I had 25 mol% acid units	Landry and Teegarden (1991)
Styrene-*co*-*p*-(2,2,2-trifluoro-1-hydroxy-1-trifluoromethyl) ethyl-α-methylstyrene	Caprolactone	Single T_g	I had $\geq$5 mol% OH	Zhou et al. (1997a)
	p-(Tert-butyl)phenylene fumarate	Single T_g	I had 3.9 or 8.0 mol% OH	Chen et al. (1998a)
Styrene-*co*-4-vinylbenzene phosphonic acid	Vinylmethylether	Single T_g; FTIR	I had 7.5 or 13.3 mol% VPBA;	Zhuang et al. (1995)
Styrene-*co*-4-vinylbenzoic acid	*n*-Butyl methacrylate-*co*-4-vinylpyridine	Single T_g	I had 1–20 mol% acid group; II had 4.7–68 mol% vinylpyridine; formed complexes when acid and pyridine contents were high	Zhu et al. (1998a)
	Ethyl methacrylate-*co*-4-vinylpyridine	Single T_g; FTIR	I had 7.4 mol% acid; II had 12.5 mol% vinylpyridine	Hammachin et al. (1999), Ourdani and Amrani (2000)
Styrene-*co*-4-vinylbenzoic acid, K-neutralized	5,7-Dodecadiyne-1,12-dicarboxylic acid, K-neutralized	Single T_g	I had 26 mol% acid group	Eisenbach et al. (1994a)
Styrene-*co*-4-vinylbenzoic acid, triethylammonium ionomer	5,7-Dodecadiyne-1,12-dicarboxylic acid, triethylammonium ionomer	Single T_g	I had 26 mol% acid group	Eisenbach et al. (1994a, b)

Styrene-*co*-*p*-vinylphenol	Acetoxystyrene	Single T_g; FTIR	I had 16–50 mol% vinylphenol	Kuo and Chang (2002a)
	Benzyl methacrylate	Single T_g; FTIR	II had 4.9, 9.2, or 23 mol% vinylphenol	Sankarapandian and Kishore (1996a)
	n-Butyl methacrylate	Transparency; FTIR; fluorescence study	I had 8, 25, 43, or 75 wt% vinylphenol	Chen and Morawetz (1989), Xu et al. (1991)
	N,N-Dimethylacrylamide	Transparency; FTIR; single T_g	I had 22, 42, or 82 mol% vinylphenol	Landry and Teegarden (1991)
	Caprolactone	Single T_g; FTIR	I had 10, 12.2, 15.4, or 20.4 wt% vinylphenol	Ahn et al. (1993b), Kuo and Chang (2001d), Vaidya et al. (1995)
	Carbonate of bisphenol-A	Single T_g; FTIR	I had 54 or 63 mol% vinylphenol	Li et al. (1999a)
	Carbonate of tetramethylbisphenol-A	Single T_g; FTIR	I had 20, 44, 55, or 100 mol% vinylphenol	Li et al. (1999a)
	Cyclohexyl methacrylate	Single T_g; FTIR; NMR	I had 16–50 mol% vinylphenol	Kuo and Chang (2002a), Mugica et al. (2005)
	Ethyl methacrylate	Transparency; fluorescence study; light scattering	I had >0.93 mol% vinylphenol; formed complexes when I had >9 mol% OH (Xiang et al. (1997b))	Chen and Morawetz (1989), Xiang et al. (1997b)
	n-Hexyl methacrylate	FTIR; light scattering	I had 8, 25, or 43 wt% vinylphenol	Bhagwagar et al. (1994), Xu et al. (1991)
	Lactide	Single T_g; FTIR; SEM	I had 16 or 33 mol% vinylphenol	Zuza et al. (2008)
	Methyl methacrylate	Single T_g; transparency; fluorescence study; FTIR	I had >0.93 mol% vinylphenol; II was syndiotactic (Jong et al. (1993)); I had 15 mol% vinylphenol, and II was atactic, isotactic, or syndiotactic (Hsu and Yeh (1999a))	Chen and Morawetz (1989), Hsu and Yeh (1999a), Jong et al. (1993), Landry and Teegarden (1991)
	Phenylimino-1,4-phenyleneoxyterephthaloyl	Single T_g; FTIR	I had 46 mol% vinylphenol	Cowie et al. (1996)

Table 21.1 (continued)

Polymer I of	Polymer II of	Method	Comments	Refs.
	Vinyl cinnamate	Single T_g	Miscible after I was thermally cross-linked	Hsu (2008)
	Vinylbutylether	FTIR	I had 48 wt% vinylphenol	Serman et al. (1991b)
	4-Vinylpyridine	Single T_g	I had 50 mol% vinylphenol	Vivas de Meftahi and Frechet (1988)
	N-Vinyl pyrrolidone	Single T_g; FTIR	II had >11 mol% OH; formed complexes in THF when I had >25 mol% vinylphenol (Prinos et al. (1998))	Prinos et al. (1998), Zhu et al. (1994)
Styrene-co-4-vinylphenyldimethylsilanol	n-Butyl methacrylate	Single T_g; FTIR	II had 9, 11, 18, or 34 mol% silanol group; formed complexes when II had 34, 60, 81, or 100 mol% VDPMS	Lu et al. (1994, 1995a, b)
Styrene-co-4-vinylphenylmethyl-phenylsilanol	n-Butyl methacrylate	Single T_g; FTIR	II had 9–56 mol% OH	Lu et al. (1996a)
	N-Vinylpyrrolidone	Single T_g; FTIR	Miscible when I had 9–18 mol% OH; formed complexes when I had 31–74 mol% OH	Lu et al. (1996b)
Styrene-co-2-vinylpyridine	n-Butyl methacrylate-co-p-vinylphenol	Single T_g; FTIR	I had 27 wt% vinylpyridine; II had 54 wt% vinylphenol	Coleman et al. (1998a)
	2,3-Dimethylbutadiene-co-p-vinylphenol	Single T_g; transparency	I had 17, 26, or 40 mol% 2-vinylpyridine; II had 38 mol% p-vinylphenol	Motzer et al. (2001a)
Styrene-co-4-vinylpyridine	2,6-Dimethyl-1,4-phenylene ether	Single T_g; SEM	I had 5 or 15 mol% 4-vinylpyridine	Benabdelghani et al. (2008)
	Isoprene, sulfonated	Single T_g; transparency	II had 5–10 % substituted and partly cyclized; immiscible when II had 2 % substituted	Eisenberg et al. (1982), Zhou and Eisenberg (1983)
	Methyl methacrylate-co-p-vinylphenol	Single T_g; FTIR; SEM	I had ≥30 mol% vinylpyridine; II had 50 mol% vinylphenol	Belabed et al. (2012)

N,N′-(Sulfo-p-phenylene terephthalamide)	Vinyl alcohol	Single T_g	–	Dai et al. (1994)
	Vinyl pyridine	Single T_g; NMR	II was 2- or 4-vinylpyridine	Dai et al. (1994)
Sulfone	Etheretherketone-co-phenolphthalein etheretherketone	Single T_g; FTIR	II had 6.2 mol% etheretherketone	Guo et al. (1996c)
	Styrene-co-1-vinylpyrrolidone	Single T_g; transparency	II had 12–32 wt% styrene	Kim et al. (2002b, 2003b)
1,2,2,2-Tetrachloroethyl methacrylate	Cyclohexyl methacrylate	Single T_g	–	Goh et al. (1997a)
	Ester	Single T_g	II was caprolactone or 2,2-dimethyl-1,3-propylene adipate	Goh et al. (1997a)
Tetrafluoroethylene, sulfonated	Ethyl acrylate-co-4-vinylpyridine	Single T_g	I had equivalent weight of 1155	Murali and Eisenberg (1988)
Tetrafluoroethylene-alt-vinyl alcohol	Alkyl methacrylate	Single T_g; FTIR	II had an alkyl group of methyl or ethyl	Coleman et al. (1993c)
	Methyl acrylate	Single T_g; FTIR	–	Coleman et al. (1993c)
	Vinyl acetate	Single T_g; FTIR	–	Coleman et al. (1993c)
Tetrahydrofurfuryl methacrylate	Allyl alcohol-co-styrene	Transparency	II had 5.4–6.0 % OH	Goh (1987)
	Epichlorohydrin	Single T_g; transparency	–	Chong and Goh (1991b)
	Hydroxyether of bisphenol-A (Phenoxy)	Single T_g; transparency	–	Goh (1987)
	Vinyl chloride	Single T_g; transparency	–	Goh and Siow (1987)
	Vinyl chloride-co-vinylidene chloride	Single T_g	II had 88 % vinylidene chloride	Chong and Goh (1991b)
Tetrahydropyranyl-2-methyl methacrylate	Allyl alcohol-co-styrene	Transparency	II had 5.4–6.0 wt% OH	Chong and Goh (1992a)
	Epichlorohydrin	Single T_g; transparency	–	Chong and Goh (1991b)
	Hydroxyether of bisphenol-A (Phenoxy)	Single T_g; transparency	–	Chong and Goh (1992a)
	Vinyl chloride	Single T_g; transparency	–	Chong and Goh (1991b)
	Vinyl chloride-co-vinylidene chloride	Single T_g	II had 88 % vinylidene chloride	Chong and Goh (1991b)
	p-Vinyl phenol	Single T_g; transparency	–	Chong and Goh (1992a)

(*continued*)

Table 21.1 (continued)

Polymer I of	Polymer II of	Method	Comments	Refs.
2,4,5-Tribromostyrene-*co*-styrene	Carbonate of tetramethylbisphenol-A	Single T_g	≤38.8 wt% tribromostyrene	Chu et al. (2000)
	2,6-Dimethyl-1,4-phenylene ether	Single T_g	I had ≤48.8 wt% tribromostyrene	Chu et al. (2000)
2,2,2-Trichloroethyl methacrylate	Alkyl methacrylate	Single T_g; transparency	II had an alkyl group of methyl, ethyl, *n*-propyl, isopropyl, cyclohexyl, or tetrahydrofurfuryl	Low et al. (1994b)
3,3,5-Trimethyl cyclohexyl methacrylate	3,3,5-Trimethyl-cyclohexyl acrylate	Single T_g; transparency	–	Siol (1991)
Trifluoroethylene	Vinylidene fluoride	Single T_g	Semicrystalline	Godovskii et al. (1981)
2,2,4-Trimethylhexamethylene terephthalamide	Caprolactam-*co*-caprolactone	Single T_g	II had varying composition	Ellis (1997)
Trimethylene adipate	Vinyl chloride	Single T_g; transparency	When ≥75 % II	Woo et al. (1985b)
Trimethylene terephthalate	Ester	Single T_g; microscopy; WAXD	II was ethylene terephthalate or butylene terephthalate	Chiu (2007), Kuo and Woo (2003), Supaphol et al. (2004)
	Ethylene naphthalate	Single T_g; T_m-depression	Semicrystalline	Krutphun and Supaphol (2005), Run et al. (2006)
	Carbonate of bisphenol-A	Single T_g; FTIR	Initially immiscible, became miscible after annealing	El Shafee et al. (2008), Lee and Woo (2004a)
4-Trimethylsilyl Styrene	Isoprene	Single T_g; SANS; OM	–	Harada et al. (2005a, b)
Urethane	Carbonate of bisphenol-A	Single T_g	Miscible when blend had 10–20 wt% I	Fambri et al. (1993)
	Ethylene-*co*-methacrylic acid-*co*-isobutyl acrylate	Single T_g; FTIR; OM	I was Desmopan 359; II had 78 mol% ethylene and 10 mol% methacrylic acid: II was 70 % neutralized with Zn	Papadopoulou and Kalfoglou (1998)
	Ethylene-*co*-methyl acrylate	Single T_g; FTIR	I was Estane 58311; II had 21 wt% methyl acrylate	Santra et al. (1993b)

Ethylene glycol	FTIR	I was made from a mixture of 2,4- and 2,6-tolyldiisocyanate and 1,4-butanediol	Coleman et al. (1988a), Hu et al. (1988)
Ethylene glycol-*co*-propylene glycol	Single T_g; FTIR	I was made from a mixture of 2,4- and 2,6-tolyldiisocyanate and 1,4-butanediol; II had 70 wt% ethylene glycol	Coleman et al. (1988b)
Methacrylic acid-*co*-styrene	Single T_g	I had polyether segment with M_w = 1.0 or 2.0 kg/mol; II had 10.5 % methacrylic acid, Li-neutralized	Rutkowska and Eisenberg (1984)
Styrene-*co*-p-vinylphenol	FTIR; SANS; FTIR	II had 5–50 mol% vinylphenol; I was liquid crystalline	Metha and Dadmun (2006), Viswanathan and Dadmun (2004)
Urethane	Single T_g	I and II were separate polymers; I was 4,4'-diisocyanate diphenyl methane (MDI)/dipropylene glycol = 9/10 mol ratio; II was poly Groeninckx et al. (1988)-56 polyoxyethylene-*co*-oxypropylene, 45 % ethylene oxide, M_w = 2000/MDI/1/1	Lockwood and Alberino (1981)
N-Vinylpyrrolidone	Single T_g; for II with hard segments of I; soft segment T_g's also observed; clear films	I was segmented, made from methylene bis(4-phenyl isocyanate) and poly(ethylene glycol) and *cis*-2-butene-1,4-diol and butane-1,4-diol	Egboh (1983)

(continued)

Table 21.1 (continued)

Polymer I of	Polymer II of	Method	Comments	Refs.
Urethane, functionalized	Styrene-*co*-2-methyl-5-vinylpyridine	Single T_g	I carried pendant carboxylated groups neutralized by ammonium ion	Rutkowska (1991)
	Styrene-*co*-acrylic acid	Single loss peak; microscopy	I had tertiary amine group; II had 15 or 30 mol% acrylic acid; linear blend of I and II or interpenetrating polymer network of I and II	Hsieh and Chou (1989)
Valerolactone	Vinyl acetate-*co*-vinylidene chloride	Single T_g	Semicrystalline; II was Saran C (≥80 % vinylidene chloride)	Aubin et al. (1983)
	Vinyl bromide	Single T_g	–	Cousin and Prud'homme (1982)
	Vinyl chloride	Single T_g	Semicrystalline when ≥50 % I	Aubin et al. (1982), Aubin and Prud'homme (1981a, b)
Vinyl acetate	Alkyl acrylate	Single T_g; FTIR	I had an alkyl group of methyl, ethyl, or butyl	Princi et al. (2009)
	2-Bromoethyl methacrylate	Single T_g; transparency	Miscible when cast from methyl ethyl ketone; immiscible when cast from tetrahydrofuran	Neo and Goh (1992a)
	2-Chloroethyl methacrylate	Single T_g; transparency	–	Neo and Goh (1992a)
	Chloromethyl methacrylate	Single T_g; transparency	–	Neo and Goh (1992a)
	Ester	Single T_g; SEM; OM	II was ethylene adipate, propylene adipate, or butylene adipate	Chang et al. (2006)
	Formaldehyde-melamine resin	Single T_g; FTIR; NMR	–	Kim and Kim (2007)
	Hexafluoroacetone-*co*-vinylidene fluoride	Single T_g	II had 8.9 mol% hexafluoroacetone	Shiomi et al. (1989)
	Lactide	Single T_g	–	Gajria et al. (1996)
	Methacrylic acid	NMR	–	Asano (2004), Asano et al. (2002)
	Novolac	Single T_g; FTIR; NMR	–	Huang et al. (2002b)

		Method	Comments	Reference
	Styrene-alt-maleic anhydride, hydrolyzed	Single T_g	1.8–43 % hydrolyzed	Bosma et al. (1988a)
	Trifluoroethylene-co-vinylidene fluoride	Single T_g; T_m-depression	II had 32 mol% trifluoroethylene	Tang and Scheinbeim (2003)
	Vinyl nitrate	Single T_g; phase contrast microscopy	–	Akiyama et al. (1969)
	Vinylidene fluoride	Single T_g	Semicrystalline	Belke and Cabasso (1988), Bernstein et al. (1978b)
Vinyl acetate-co-vinyl chloride	n-Butyl methacrylate-co-isobutyl methacrylate	Single T_g	Miscibility range depended on compositions of I and II; I had ≥81 wt% vinyl chloride	Shiomi et al. (1989)
	Hexyl acrylate-co-methyl acrylate	Single T_g	I had 5–23.7 vol% vinyl acetate; II had 15–88 vol% hexyl acrylate; miscibility depended on compositions of I and II	Jin et al. (1992)
	n-Butyl methacrylate	Single T_g	I had 5.9–15.1 wt% vinyl acetate	Lee et al. (1992)
Vinyl acetate-co-vinyl alcohol	4-Vinylpyridine	Single T_g; FTIR; OM	I had 35–70 mol% vinyl alcohol	Isasi et al. (1995), Lee et al. (1998a)
Vinyl acetate-co-N-vinylpyrrolidone	Methyl methacrylate-co-p-vinylphenol	Single T_g	Formed complexes	Akiba et al. (2002)
Vinyl alcohol	Acrylamide	Single T_g	–	El-Din et al. (2003)
	Ethylene imine	Single T_g; T_m-depression	Semicrystalline	Guo (1995)
	N-Methylglycine	Single T_g; FTIR; SEM; transparency	Blend had ≤40 wt% II	Aoi et al. (2000)
	Pyrrole	FTIR; SEM; X-ray	Blend lost crystallinity when less than 15–20 % II was present	Wang and Fernandez (1992)
	Sodium α,β-D,L-aspartate	FTIR; SEM; X-ray	–	Takasu et al. (1997)
	Sodium-4-styrenesulfonate	Single T_g; FTIR; SEM	–	Mbareck et al. (2009)
Vinyl alkanoate	Vinyl alkanoate	Single T_g; microscopy	The alkanoate was butyrate, caprate, caproate, caprylate, or laurate	Braun et al. (1993)

Table 21.1 (continued)

Polymer I of	Polymer II of	Method	Comments	Refs.
Vinyl butyral	N-Vinylpyrrolidone	Single T_g; transparency	≤50 % II	Eguiazabal et al. (1984)
	Urethane elastomer	Single T_g	II from methylene bisdiphenyl diurethane and polytetramethylene ether glycol; miscible with hard segment	Sincock and David (1992)
Vinyl chloride	Acetonyl methacrylate	Single T_g; transparency	–	Chong et al. (1990a, b)
	Acrylic acid-co-carbitylacrylate-co-methylstyrene-co-styrene	Single T_g	II was an oligomer with M_n = 1.07 and M_w = 3.32 kg/mol	Rim and Orler (1987)
	Acrylonitrile-co-n-butyl acrylate	Optical microscopy	II had 53, 67, or 84 mol% butyl acrylate	Piglowski and Kammer (1990)
	Acrylonitrile-co-methyl methacrylate-co-α-methylstyrene	Single T_g	II had 32.3 wt% AN and 8.1 wt% MMA	Kovacic et al. (1994)
	Arylate of tetramethylbisphenol-S	Single T_g; FTIR	–	Choi et al. (1998)
	Butadiene, epoxidized	Single T_g	II had 50 mol% epoxidation	Margaritis and kalfoglou (1988)
	Butadiene-co-styrene, epoxidized	Single T_g	II had 45 wt% styrene; epoxidation >40 mol%	Margaritis et al. (1989)
	Butyl acrylate-co-ethyl acrylate	Single T_g	II had 22.9, 43.5, or 52.8 % butyl acrylate	Walsh and Sham (1989)
	Butyl acrylate-co-hexyl acrylate	Single T_g	II had 47.8 % butyl acrylate	Walsh and Sham (1989)
	Butyl acrylate-co-methyl acrylate	Single T_g	II had 44.6 % butyl acrylate	Walsh and Sham (1989)
	Butyl methacrylate-co-methyl methacrylate	Single T_g	II had 30 or 70 % methyl methacrylate	Yang et al. (1986a)
	Butylene adipate	FTIR	II has linear of branched	Lindstrom and Hakkarainen (2007)
	Butylene adipate-co-terephthalate	Single T_g; FTIR	–	Ibrahim et al. (2011)

Caprolactam-*co*-caprolactone	Single T_g	II had 12.8 mol% caprolactam	Van Ekenstein et al. (1997)
Caprolactone-*co*-L-lactide	Single T_g	II had $\leq$40 wt% lactide	Vion et al. (1986)
Caprolactone-*co*-lignin	Single T_g; SEM; TEM	II was a 7-arm starlike polymer containing 20 wt% lignin derivative	De Oliveira and Glasser (1994)
Caprolactone-*co*-methylcaprolactone	Single T_g	Whatever composition of II	Vion et al. (1986)
Carbonate, liquid crystalline	Single T_g; SEM; FTIR	–	Sato and Ujiie (1996a)
Cyclohexyl methacrylate	Single T_g	–	Ha et al. (1990a)
2,2-Dimethyl-1,3-propylene sebacate	Single T_g; transparency	–	Neo and Goh (1992b)
Ester	Single T_g; FTIR	II was made from 1,4-butanediol and a mixture of isophthalic acid and adipic acid	Andrcic et al. (2006)
Ester	Single T_g	II was made from 1,4-butanediol and a mixture of terephthalic acid and adipic acid	Andrcic et al. (2008)
Ester	Single T_g; for I with soft segments of I	II was Hytrel, a multiblock copolymer with poly(tetramethylene ether) glycol terephthalate soft segments and tetramethylene terephthalate hard segments; hard segments crystalline; two T_g's after 130 °C annealing; Hourston and Hughes (1977a), Hourston and Hughes (1981) showed single T_g to 50 or 60 wt% I	Hourston and Hughes (1977a, 1981), Nishi et al. (1975a)

(*continued*)

Table 21.1 (continued)

Polymer I of	Polymer II of	Method	Comments	Refs.
	Ester	Single T_g	I was made from adipic acid, hexane-1,6-diol and neopentanediol and had M_n = 2 kg/mol	Hardt et al. (1982)
	Ester, liquid crystalline	Single T_g	II was made from p-hydroxybenzoic acid and ethylene terephthalate (60:40)	Meng and Tjong (1999)
	Ester carbonate	Single T_g	I was made from adipic acid and hexane-1,6-diol and neopentane-diol and diphenyl carbonate	Hardt et al. (1982)
	Ethyl acrylate-co-hexyl acrylate	Single T_g	II had 41.7 or 43.2 % ethyl acrylate	Walsh and Sham (1989)
	Ethyl acrylate-co-methyl methacrylate	Single T_g	II had 10 % ethyl acrylate	Xu et al. (1987)
	Ethylene-co-vinyl acetate	Permittivity measurements; single T_g and negative enthalpy of mixing (Righetti et al. (2002))	II had 70 % vinyl acetate; composition dependent; miscible when blend contained ≥25 % II	Rellick and Runt (1986), Righetti et al. (2002)
	Isopropyl methacrylate	Single T_g	–	Ha et al. (1990a)
	Methyl acrylate-co-hexyl acrylate	Single T_g	II had 9.7 % methyl acrylate	Walsh and Sham (1989)
	Methyl methacrylate-b-styrene	–	No gross phase separation when I had M_n = 43 kg/mol; PMMA and PS block had the same M_n = 40 kg/mol in II	Jerome et al. (1986)
	Methyl methacrylate-co-styrene	Single T_g, FTIR	II had 0–30 wt% styrene	Dompas et al. (1997)
	Methyl methacrylate-co-4-vinylpyridine	Single T_g, FTIR	II had 15 wt% vinylpyridine	Benmerad et al. (2011)
	Nitrile rubber, carboxylated	Single T_g	II was Krynac-221	Ramesh et al. (1993)
	Pentyl acrylate	Single T_g	–	Walsh and Sham (1989)

	Phenyl acrylate	Single T_g; NMR	—	Sankarapandian and Kishore (1996b)
	Propyl acrylate	Single T_g	—	Walsh and Sham (1989)
	Pentyl acrylate-*co*-propyl acrylate	Single T_g	II had 48.1 % propyl acrylate	Walsh and Sham (1989)
	Styrene	Single T_g; SEM	Blends were prepared by in situ polymerization of styrene in PVC with supercritical carbon dioxide as swelling agent	Dai et al. (2002)
	Urethane	Single T_g	II was a thermoplastic PU elastomer	Kim et al. (1994b)
	Vinyl acetate	Single T_g	Bhagwagar et al. (1989) stated miscible when cast from methyl ethyl ketone and immiscible when cast from tetrahydrofuran; De Jager and Ten Brinke (1991) stated blends cast from both THF and MEK were immiscible	De Jager and Ten Brinke (1991), Bhagwagar et al. (1989)
Vinyl chloride, chlorinated	Butadiene, epoxidized	Single T_g	II had 20 or 43 mol% epoxidation	Sotiropoulou et al. (1992)
	Butadiene-*co*-acrylonitrile	Single T_g	Depended on Cl-content and acrylonitrile content	Chai and Karasz (1992), Cowie and Elexpuru (1992), Huh and Karasz (1989, 1992)
	n-Butyl methacrylate	Single T_g; transparency	I had 65 or 68 wt% Cl	Ha et al. (1990a), Tremblay and Prud'homme (1984)
	Cyclohexyl methacrylate	Single T_g	I had 68 wt% Cl	Ha et al. (1990a)
	Ethyl methacrylate	Single T_g; transparency	I had 65 or 68 wt% Cl	Ha et al. (1990a), Tremblay and Prud'homme (1984)
	Ethylene terephthalate	Single T_g	Probably semicrystalline	Aubin and Prud'homme (1984)
	Hexamethylene sebacate	Single T_g	I had 67.2 wt% Cl; semicrystalline when ≥50 wt% II	Belorgey et al. (1982)
	Hexamethylene terephthalate	Single T_g	Semicrystalline	Aubin and Prud'homme (1984)

(*continued*)

Table 21.1 (continued)

Polymer I of	Polymer II of	Method	Comments	Refs.
	Isopropyl methacrylate	Single T_g	I had 68 wt% Cl	Ha et al. (1990a)
	n-Hexyl methacrylate	Single T_g	–	Ha et al. (1990a)
	Maleic anhydride-ran-styrene	Single T_g	I was Goodrich CPVC 3010; II had 86 % styrene	Bourland (1988), Bowland and Braunstein (1986)
	α-Methyl-α-n-propyl-β-propiolactone	Single T_g	I had 67.2 wt% Cl	Belorgey et al. (1982)
	n-Propyl methacrylate	Single T_g, transparency	I had 65 or 68 wt% Cl	Ha et al. (1990a), Tremblay and Prud'homme (1984)
	Urethane	Single T_g	I had 67 wt% Cl; II had a soft poly(tetramethylene adipate) segment capped with 2-hydroxyethyl acrylate	Gracia (1986), Wu et al. (1999)
	Valerolactone	Single T_g	I had 67.2 wt% Cl	Belorgey et al. (1982)
Vinyl chloride-co-vinylidene chloride	Ester	Single T_g	I had 13.5 wt% vinyl chloride; semicrystalline; II was butylene adipate, butylene sebacate, dodecamethylene adipate, dodecamethylene decamethylene dicarboxylate, dodecamethylene dodecamethylene dicarboxylate, hexadecamethylene dodecamethylene dicarboxylate, or hexamethylene sebacate	Woo et al. (1986)
	Phenyl methacrylate	Single T_g	I had 12 % vinyl chloride; semicrystalline	Kang et al. (1988)
	Isopropyl methacrylate	Single T_g	I had 12 % vinyl chloride; semicrystalline	Kang et al. (1988)
Vinyl cinnamate-co-ethylene	Dimethylbutadiene-co-p-vinylphenol	Single T_g, FTIR	I had 82 mol% ethylene; II had 18 mol% vinylphenol	Hu et al. (2002)

Polymer	Component	Method	Comment	Reference
Vinyl cinnamate-co-vinyl acetate	Dimethylbutadiene-co-p-vinylphenol	Single T_g; FTIR	I had 83, 90, or 96 mol% vinyl acetate; II had 33 mol% vinylphenol	Hu et al. (2002)
Vinyl fluoride	Vinylidene fluoride	Single T_g	Semicrystalline; later work found the blends immiscible (Guerra et al. (1986))	Godovskii et al. (1981), Guerra et al. (1986)
Vinyl p-methoxycinnamate	p-Chloro-(3-ethenoxypropyl) cinnamate	Single T_g	–	Lin et al. (1989)
	Vinyl p-chlorocinnamate	Single T_g	–	Lin et al. (1989)
	Vinyl cinnamate	Single T_g	–	Lin et al. (1989)
Vinyl p-methylcinnamate	Vinyl cinnamate	Single T_g	–	Lin et al. (1989)
	p-Chloro-(3-ethenoxypropyl) cinnamate	Single T_g	–	Lin et al. (1989)
	p-Cyano-(3-ethenoxypropyl) cinnamate	Single T_g	–	Lin et al. (1989)
	3-Ethyoxypropyl cinnamate	Single T_g	–	Lin et al. (1989)
	Vinyl p-chlorocinnamate	Single T_g	–	Lin et al. (1989)
N-Vinylimidazole	Acrylic acid	Single T_g, FTIR	Formed complexes	Luo et al. (1999)
	3-Carboxyprop ylmethylsiloxane-co-dimethylsiloxane	Single T_g, FTIR; XPS	II had 77 mol% dimethylsiloxane	Li et al. (2001a)
	2-Hydroxypropyl methacrylate	Single T_g; FTIR	Formed complexes	Luo et al. (1999b)
	Methacrylic acid	NMR	–	Ruhnau and Veeman (1996)
	Styrenesulfonic acid	FTIR; XPS	Formed complexes	Luo et al. (1999a)
	Styrenesulfonic acid, Zn-neutralized	FTIR; XPS	Formed complexes	Luo et al. (1999a)
	p-Vinylphenol	Single T_g; FTIR	Formed complexes	Luo et al. (1999b)
Vinylethylether	Butyl acrylate	Single T_g; FTIR; OM	–	Woo and Juang (2007)
Vinylmethylether	Alkyl acrylate	Single T_g	II had an alkyl of ethyl, n-propyl, or n-butyl	Chakraborty et al. (1993)
	Acrylonitrile-co-styrene	Single T_g	–	Lin et al. (1989)
	Benzyl methacrylate	Single T_g; FTIR; OM	–	Mandal and Woo (1999a)

(continued)

Table 21.1 (continued)

Polymer I of	Polymer II of	Method	Comments	Refs.
	Butadiene-*co*-styrene	Light scattering	II had 60 or 68 wt% styrene	Ahn et al. (1997d)
	Caprolactone	Single T_g; FTIR; OM	–	Bisso et al. (1998, 1999), Woo et al. (2010)
	2-Chlorostyrene	Single T_g; FTIR; light scattering; dielectric studies	–	Tran-Cong et al. (1994), Urakawa et al. (2001)
	Dinitrostyrene-*co*-styrene	Single T_g	II had 3–14 mol% dinitrostyrene	Fernandez et al. (1997)
	Epichlorohydrin	NMR; dielectric spectroscopy	–	Alegria et al. (1994, 1995) McGrath and Roland (1994)
	Ester	Single T_g; FTIR; OM	II was ethylene succinate, ethylene adipate, butylene adipate, trimethylene adipate, ethylene azelate, or hexamethylene sebacate	Chiang and Woo (2007)
	Ethyl methacrylate	Single T_g; transparency	–	Woo and Juang (2007)
	Hexamethylene adipate	Single T_g; OM; T_m-depression	–	Woo et al. (2010)
	Hydroxybutyrate	Single T_g; FTIR; OM	–	Chiang and Woo (2007)
	Hydroxyether of bisphenol-A	Single T_g	II was 11.7–42.3 mol% methylated or 7.5–30.1 mol% benzoylated	Etxeberria et al. (2001)
	Lactide	Single T_g; FTIR; OM	–	Chiang and Woo (2007)
	Maleic anhydride-*co*-styrene	Single T_g	II had <10–11 % acrylonitrile	Min and Paul (1988)
	Methyl methacrylate-*co*-styrene	Single T_g	II had 15 % maleic anhydride	Min and Paul (1988)
	α-Methylstyrene	Light scattering	II had <60 mol% methyl methacrylate	Halary et al. (1991), Chien et al. (1988)
	α-Methylstyrene-*co*-4-(2-hydroxyethyl)-α- methylstyrene	Single T_g	II had 6–89 mol% methylstyrene	Cowie and Reilly (1992), Ha et al. (1990b)
	α-Methylstyrene-*co*-4-(1,1,1-trifluoro-2-hydroxyethyl)-methylstyrene	Single T_g	II had 0–96 mol% methylstyrene	Cowie and Reilly (1992)

	α-Methylstyrene-co-styrene	Light scattering; FTIR;	II had 77.5 or 88 wt% styrene	Ha et al. (1990b, 1993)
	p-Methylstyrene-co-styrene	Light scattering; FTIR; single T_g	II had 78.5 or 87.3 wt% styrene; II had ≥61 mol% styrene (Goh et al. (1994))	Goh et al. (1994), Ha et al. (1990b, 1993)
	m-Methylstyrene-co-styrene	Light scattering; FTIR	II had 76.5 or 87.5 wt% styrene	Ha et al. (1993)
	Nitrostyrene-co-styrene	Single T_g	II had ≤25.6 mol% nitrostyrene	Cowie et al. (1990a), Defieuw et al. (1989a)
	Styrene-co-1-vinylnaphthalene	Light scattering	II had 17.4, 23, 50, or 80 wt% styrene; depended on composition of blend	Ha et al. (1990b), Kanakalatha et al. (1983)
	Styrene-co-2-vinylnaphthalene	Light scattering	II had 19.2, 51, or 84 wt% styrene	Ha et al. (1990b), Ryu et al. (2000)
	Vinyl alkanoate	Single T_g; IGC; transparency	II was vinyl propionate or vinyl butyrate	Dutta et al. (1993)
	1-Vinylnaphthalene	Single T_g; FTIR	II had M_n = 5.4 kg/mol; blend contained 65–85 wt% II	Kang and Cho (1989)
Vinylmethylketone	Epichlorohydrin	Single T_g; FTIR	–	Guo et al. (1996a)
	2-Hydroxyethyl methacrylate	Single T_g; FTIR	–	Guo et al. (1996a)
	Vinyl nitrate	Single T_g; FTIR	–	Kondo et al. (2002)
	Vinylidene fluoride	Single T_g; transparent melt	Semicrystalline	Bernstein et al. (1978a)
Vinylphenylketone, hydrogenated	2,6-Dimetyl-1,4-phenylene ether	Single T_g; FTIR	Blend had 10–40 wt% and 60–90 wt% II	Maldonado-Santoyo et al. (2004c)
	2-Ethyl-2-oxazoline	Single T_g; FTIR	–	Maldonado-Santoyo et al. (2004a)
	Styrene-co-4-vinylpyridine	Single T_g; FTIR	II had 50 wt% vinylpyridine	Maldonado-Santoyo et al. (2004b)
p-Vinylphenol	Acetonyl methacrylate	Single T_g; transparency	–	Chong and Goh (1992a)
	4-Acetoxystyrene	Single T_g; FTIR	–	Himuro et al. (1992)
	N-Acryloylmorphine	Single T_g; FTIR; XPS; NMR	–	Yi and Goh (2002)
	N-Acryloylthiomorphine	Single T_g; FTIR; XPS	–	Yi et al. (2001a)
	Amide	Single T_g	II PA-6, PA-6,6, or PA-11	Landry et al. (1993b)
	Butyl acrylate-co-t-butyl acrylate	Single T_g	II had 64 mol% butyl acrylate	Zhu et al. (1990)

(continued)

Table 21.1 (continued)

Polymer I of	Polymer II of	Method	Comments	Refs.
	Butylene adipate	Single T_g; NMR; WAXD	Semicrystalline	Belfiore et al. (1993), Landry et al. (1993b, c), Qin and Belfiore (1990), Sun et al. (2011)
	Butylene adipate-co-butylene succinate	Single T_g; T_m-depression; WAXD; SAXS	–	Yang et al. (2009)
	Butylene adipate-co-butylene terephthalate	Single T_g; FTIR	II had 44 mol% butylene terephthalate	Lee et al. (2010)
	Butylene 2,6-naphthalate	Single T_g; T_m-depression; FTIR	–	Lee and Han (2004), Lee and Yan (2002)
	Butylene succinate	Single T_g; T_m-depression	–	Qiu et al. (2003a)
	Butylene terephthalate	Single T_g; FTIR	Semicrystalline	Landry et al. (1993b)
	Caprolactone	Single T_g; FTIR; NMR; IGC	Semicrystalline	Belfiore et al. (1993), Coleman et al. (1989a), Kuo et al. (2001a), Lezcano et al. (1995, 1996), Qin and Belfiore (1990), Wang et al. (2002b)
	Cellulose tripropionate	Single T_g	–	Landry et al. (1993b)
	Copolyester	Single T_g; FTIR	Five different copolyesters	Landry et al. (1993c)
	Dialkyl itaconate	Single T_g; FTIR	II had a dialkyl group of methyl, ethyl, bis [2-[2-(2-methoxyethoxy) ethoxy]ethyl], or bis [2-(2-methoxyethoxy)ethyl]	Hong et al. (1995b), Landry et al. (1993a)
	N,N-Dimethylacrylamide	Single T_g	Formed complexes in dioxane or acetone	Landry and Teegarden (1991), Landry et al. (1993b), Suzuki et al. (1992), Wang et al. (1991)
	2-(Dimethylamino)ethyl methacrylate	Single T_g; FTIR; XPS	Formed complexes	Huang et al. (1999)
	2,2-Dimethylpropylene terephthalate	Single T_g; FTIR	–	Landry et al. (1993b, c)

Epoxy	Single T_g; FTIR; NMR	–	Huang and Woo et al. (2002)
Ester, liquid crystalline	Single T_g	II contained lateral pyridyl group	Sato et al. (1996b)
Ethoxyethyl methacrylate	Single T_g; FTIR; NMR	–	Hill et al. (1999)
Ethyl acrylate	FTIR	–	Coleman et al. (1989a), Parmer et al. (1988)
γ-Ethyl L-glutamate	FTIR; microscopy	–	Painter et al. (1991), Zucco and Painter (1988)
Ethyl methacrylate	Single T_g; FTIR	–	Coleman et al. (1991b), Goh and Siow (1988a), Pomposo et al. (1993b), Serman et al. (1991a)
Ethyl methacrylate-co-methyl methacrylate	Single T_g; FTIR	II had 30, 60, or 70 mol% MMA	Pomposo et al. (1993b, 1994a)
Ethylene adipate	Single T_g; NMR	Semicrystalline	Belfiore et al. (1993), Qin and Belfiore (1990)
Ethylene azelate	Single T_g; T_m-depression; FTIR	–	Woo and Chang (2004)
Ethylene imine	Single T_g; FTIR; OM	Formed complexes	Huang et al. (1997)
Ethylene sebacate	Single T_g; T_m-depression; FTIR	–	Papageorgiou et al. (2011)
Ethylene succinate	Single T_g; NMR	Semicrystalline	Belfiore et al. (1993)
Ethylene terephthalate	Single T_g; FTIR	–	Gestoso and Brisson (2003), Landry et al. (1993c)
Ethylene glycol-b-2-vinylpyridine	Single T_g; FTIR; NMR; TEM	–	Lee et al. (2006a)
Ethylene 2,6-naphthalenedicarboxylate	Single T_g; FTIR	–	Landry et al. (1993b, c)
Ethylene-co-vinyl acetate	Single T_g; FTIR	II had 70 % vinyl acetate	Coleman et al. (1989a), Coleman et al. (1987), Moskala et al. (1986)
Hexamethylene adipate	Single T_g	–	Chiang and Woo (2006)
Hexamethylene sebacate	Single T_g; T_m-depression; FTIR	Semicrystalline	Qin and Belfiore (1990), Woo and Chang (2004)

(continued)

Table 21.1 (continued)

Polymer I of	Polymer II of	Method	Comments	Refs.
	n-Hexyl methacrylate-co-methyl methacrylate	Single T_g; FTIR	II had 20, 38, or 48 wt% hexyl methacrylate	Coleman et al. (1993b)
	Hexylene-m-xylenedicarboxamide	Single T_g	–	Landry et al. (1993b)
	Hydroxyether of bisphenol-A	Single T_g; FTIR; NMR	–	Kuo et al. (2003)
	Isopropyl methacrylate	Single T_g	–	Goh and Siow (1986b)
	Lactide	Single T_g; T_m-depression; FTIR; SAXS; NMR	–	Chen et al. (2000), Meaurio et al. (2005a, b), Shirahase et al. (2007), Zhang et al. (1998), Zuza et al. (2006)
	γ-Methyl L-glutamate	FTIR; microscopy	–	Painter et al. (1991), Zucco and Painter (1988)
	Methyl acrylate	FTIR; NMR	–	Coleman et al. (1989a), Li and Brisson (1996), Parmer et al. (1988a), Prolongo et al. (1997), Takegoshi and Hikichi (1994), White and Mirau (1994), Zhang et al. (1991a), Zhao and Prud'homme (1991)
	Methyl methacrylate	Single T_g; FTIR	II was atactic, isotactic, or syndiotactic (Hsu et al. (1997, 2002a)	Coleman et al. (1991b), Goh and Siow (1988a), Hsu et al. (1997, 2002a), Landry and Teegarden (1991), Pomposo et al. (1993b), Serman et al. (1991a), White and Mirau (1994)
	Methyl methacrylate-b-N-vinylpyrrolidone	Single T_g; FTIR; NMR; TEM	Immiscible when blend had 2–60 wt% vinylphenol	Lee et al. (2006b)
	N-Methyl-4-piperidinyl methacrylate	Single T_g; FTIR; XPS	Formed complexes	Luo et al. (1997)
	Methylthiomethyl methacrylate	Single T_g; FTIR; XPS; NMR	–	Yi et al. (2001b)

n-Propyl acrylate	FTIR	–	Coleman et al. (1989a), Parmer et al. (1988)
2,2,3,3,3-Pentafluoropropyl methacrylate-co-4-vinylpyridine	Single T_g; FTIR; XPS	II had 28, 40, or 54 mol% vinylpyridine	Huang et al. (2002a)
Propylene carbonate	Single T_g; FTIR; XPS	–	Zhang et al. (2002)
n-Propyl methacrylate	Single T_g; FTIR	–	Coleman et al. (1991b), Goh and Siow (1988a), Serman et al. (1991a)
Styrene-co-4-vinylbenzenephosphonic acid diethyl ester	Single T_g; FTIR; NMR	II had >7.5 mol% phosphorus group	Zhuang et al. (1994)
Styrene-co-4-vinylpyridine	Single T_g	II had 50 mol% 4-vinylpyridine	Vivas de Meftahi and Frechet (1988)
Styrene-co-2-vinylpyridine	Single T_g; FTIR	II had 30 mol% styrene; formed complexes	Dai et al. (1994c)
Tetrahydrofuran	FTIR; transparency	–	Serman et al. (1991b)
Tetrahydrofurfuryl methacrylate	Single T_g	–	Goh and Siow (1988a)
2,2,5-Trimethylene terephthalamide	Single T_g	–	Landry et al. (1993b)
Trimethylene terephthalate	Single T_g; T_m-depression; FTIR	–	Lee and Woo (2004b)
Vinyl acetate	Single T_g; FTIR	–	Coleman et al. (1987, 1989a), Moskala et al. (1986)
Vinyl cinnamate	Single T_g; FTIR	–	Coleman et al. (1998b)
Vinylethylether	Single T_g; dielectric spectroscopy	–	Mpoukouvalas et al. (2005)
1-Vinylimidazole	Single T_g; FTIR	–	Goh et al. (1996)
Vinylmethylether	Single T_g; FTIR; IGC	–	Pedrosa et al. (1994), Lezcano et al. (1998)

(continued)

Table 21.1 (continued)

Polymer I of	Polymer II of	Method	Comments	Refs.
	Vinylphenylketone	Single T_g; FTIR	–	Rodriguez-Castro et al. (2006)
	Vinylpyridine	Single T_g; FTIR; NMR; XPS	Formed complexes; II was 2- or 4-pyridine	Dai et al. (1994c), Vivas de Meftahi and Frechet (1988), Wang et al. (2001c), Zhou et al. (1997b)
	N-Vinylpyrrolidone	Single T_g; FTIR; NMR	–	Akiba and Akiyama (2001), Kuo and Chang (2001c)
p-Vinylphenol, brominated	Caprolactone	Single T_g; T_m-depression	–	Prolongo et al. (2002)
	Vinylmethylether	Single T_g; T_m-depression	–	Prolongo et al. (2002)
Vinyl propionate	N-Vinylpyrrolidone	Single T_g	Formed complexes from methanol	Wang et al. (1991)
N-Vinylpyrrolidone	Acrylic acid-co-ethylene	FTIR; dielectric analysis	Blend had 12, 20, 30, 40, 50, or 90 wt% N-vinylpyrrolidone	Nuno-Donlucas et al. (2001a)
	Acrylonitrile	Single T_g	–	Guo et al. (1996b)
	N-1-Alkyl itaconic acid	Single T_g	II had an alkyl group of butyl, hexyl, or octyl	Urzua et al. (1998)
	Allyl alcohol-co-styrene	Single T_g; transparency	II had 5.4–6.0 or 7.3–8.0 wt% OH	Dai et al. (1995b), Goh and Siow (1990)
	Amide	Single T_g; FTIR; POM	–	Neelakandan and Kyu (2009)
	Amide	Single T_g	II had 1/1/1 = caprolactam/hexamethylene adipamide/hexamethylene sebacamide structural unit	Guo et al. (1992)
	Aramide	Single T_g; transparency	Five different aramides	Cherdron et al. (1994)
	Benzimidazole	Single T_g; transparency	–	Cherdron et al. (1994)
	n-Butyl methacrylate-co-2-hydroxyethyl methacrylate	Single T_g; transparency	II had ≥20.9 mol% 2-hydroxyethyl methacrylate	Lee et al. (1991c)
	Carbonate of bisphenol-A	NMR	–	Da Silva and Tavares (1998a)
	Chitosan acetate salt	FTIR; transparency	–	Cao et al. (1998)

2-Cyano-1,4-phenylene terephthalamide	FTIR; NMR	—	Oh et al. (2009)
Dialkyl itaconate	Single T_g	II had an alkyl group of methyl, 2-chloroethyl or 3-chloropropyl	Opazo et al. (1994)
Dialkyl itaconate-co-styrene	Single T_g	II had an alkyl group of methyl or ethyl	Opazo et al. (1996)
Epoxy resin	Single T_g; FTIR	—	Janarthanan and Thyagarajan (1992)
Ether amide	Single T_g; transparency	Studied up to 30 % II; I was made from isophthaloyl chloride and cis-4,4'-diamino-dibenzo-18-crown-6	Schchori and Jagur-Grodzinski (1976)
Ethersulfone	Single T_g	—	Guo (1992a)
Ethyl acrylate	Single T_g; transparency; IGC	—	Bhattacharyya et al. (1986, 1989)
Ethylene glycol	Single T_g; NMR	I had $M_w = 360$ kg/mol; II had $M_w = 0.3$ kg/mol	Da Silva and Tavares (1998b), Spindler and Shriver (1986)
Epichlorohydrin	Single T_g; NMR	—	C514, Guo (1990d)
Ethyl methacrylate-co-2-hydroxyethyl methacrylate	Single T_g; transparency	II had ≥ 7.5 mol% 2-hydroxyethyl methacrylate	Goh and Lee (1990b)
Haloalkyl methacrylate	Single T_g; FTIR	II had a haloalkyl group of chloromethyl, 2-chloroethyl, 3-chloropropyl, 2-bromoethyl, or 2-iodoethyl	Low et al. (1994a), Opazo et al. (1994)
Hydroxyether of bisphenol-A	Single T_g; FTIR	Formed complexes	Dai et al. (1995b)
Hydroxyether benzoate	Single T_g; FTIR	—	Wang et al. (2008)
Hydroxyether of phenolphthalein	Single T_g; FTIR	—	Guo et al. (1996b)
Hydroxyether terephthalate ester	Single T_g; FTIR	—	Wang et al. (2008)
2-Hydroxyethyl methacrylate	Single T_g; transparency	—	Goh and Siow (1990)
2-Hydroxyethyl methacrylate-co-methyl methacrylate	Single T_g; transparency	II had ≥ 1.9 mol% 2-hydroxyethyl methacrylate	Lee et al. (1991c)

(continued)

Table 21.1 (continued)

Polymer I of	Polymer II of	Method	Comments	Refs.
	2-Hydroxypropyl methacrylate	Single T_g; transparency	Formed complexes	Dai et al. (1995b), Goh and Siow (1990), Kuo et al. (2004a)
	Hydroxypropyl cellulose	T_m-Depression; SEM; FRIT; WAXD	–	Reddy et al. (2012)
	Hydroxypropylmethyl cellulose	Single T_g	–	Karavas et al. (2006)
	Isopropenyl methyl ketone	Single T_g; FTIR; NMR	–	Hong et al. (1995a)
	Methacrylic acid	NMR	Formed complexes	Maunu et al. (1993)
	Methyl methacrylate	Single T_g	II was atactic or syndiotactic	Hsu (2001)
	Monobenzyl itaconate	FTIR	Formed complexes	Cesteros et al. (1990)
	Monoethyl itaconate	FTIR	Formed complexes	Cesteros et al. (1994b)
	N-Phenyl-2-hydroxytrimethylene amine	Single T_g; NMR	–	Zhang and Mi (1999)
	Sulfone	Single T_g; transparency	–	Goh et al. (1991d)
	Sulfone, carboxylated	Single T_g; transparency	II had degree of carboxylation 0.43–1.93	Goh et al. (1991d)
	Vinyl alcohol	Single T_g; NMR; XPS; FTIR	–	Cassu and Felisberti (1997, 1999), Feng et al. (1993), Lewandowska (2005), Li et al. (1998b), Nishio et al. (1990), Ping et al. (1990), Thyagarajan and Janarthanan (1989), Wang et al. (1990)
	Vinyl alcohol, modified	Single T_g; FTIR	II was grafted with lactic acid, glycolic acid, or hydroxybutyric acid	Lejardi et al. (2011)
	Vinyl alcohol-co-vinyl acetate	Single T_g	II had ≥70 % vinyl alcohol	Eguiazabal et al. (1986a)
	Vinyl chloride	Single T_g; FTIR; NMR	–	Guo (1990d), Zheng et al. (1999b)
	Vinyl formal	Single T_g; FTIR	–	Huang and Guo (1990), Isasi et al. (1993)

Vinylidene fluoride	Acetonyl methacrylate	Single T_g	Semicrystalline	C37
	Acrylic acid-co-methyl methacrylate	Single T_g; T_m-depression	II had 5.7 mol% acrylic acid	Moussaif and Jerome (1999)
	Butylene succinate-co-butylene adipate	T_m-Depression; POM; WAXD	II had 20 mol% butylene adipate	Qiu et al. (2007a, b)
	N,N-Dimethylacrylamide	Single T_g	Semicrystalline	Galin (1987a)
	Ethyl 2-cyanoacrylate	T_m-Depression; SEM	–	Tiwari et al. (2009)
	Ethyl methacrylate-co-methyl methacrylate	T_m-Depression	II had 16–80 wt% methyl methacrylate	Goh and Siow (1988b)
	Methacrylic acid-co-methyl methacrylate	Single T_g; T_m-depression	II had 2.2–9.5 mol% methacrylic acid and K-neutralized	Leung and Lo (1995)
	Methyl methacrylate-co-styrene	Single T_g	II had <13 vol% styrene	Jo et al. (1991a)
	2-Methyl-2-oxazoline	Single T_g; T_m-depression	Miscible when II was a star polymer; immiscible when II was a linear polymer	Shen and Zheng (2006)
	N-Methyl-N-vinylacetamide	Single T_g	Semicrystalline	Galin (1987a)
	Methoxymethyl methacrylate	Single T_g	Semicrystalline	Goh et al. (1991c)
	Pivalolactone	T_m-Depression		Huang et al. (1994)
	Thiophene-g-methyl methacrylate	Single T_g; FTIR; WAXD; POM		Mandai and Nandi (2011)
	N-Vinylpyrrolidone	Single T_g	Semicrystalline	Alfonso et al. (1989), Ceccorulli et al. (1989), Galin (1984), Kang et al. (1989)
Vinylphosphonic acid	Vinylpyridine	Single T_g; FTIR; XPS	II was 2- or 4-vinylpyridine	Zhou et al. (1997d)
Vinylpyridine	Hydroxyalkyl methacrylate	Single T_g; FTIR	I was 2- or 4-vinylpyridine; II had an alkyl group of 2-hydroxyethyl or 3-hydropropyl	Cesteros et al. (1994a)
	Monoalkyl itaconate	T_g difficult to detect	I was 2- or 4- vinylpyridine; II had an alkyl group of methyl or ethyl	Gargallo et al. (1994)
	Monoethyl itaconate	FTIR	I was 2- or 4-vinylpyridine; formed complexes in ethanol	Cesteros et al. (1995), Velada et al. (1995)

(continued)

Table 21.1 (continued)

Polymer I of	Polymer II of	Method	Comments	Refs.
2-Vinylpyridine	Aramide	Single T_g; FTIR	II was made from hexamethylenediamine and a mixture of terephthaloyl and isophthaloyl dichlorides	Skrovanek and Coleman (1987)
4-Vinylpyridine	Benzimidazole	Single T_g; FTIR	–	Pu (2003)
	N-Cyclohexyl methacrylamide	Single T_g; FTIR; NMR	–	Lin et al. (2010)
	Ethylene-alt-maleic acid	FTIR	–	Villar et al. (2003)
	Hydroxyether ketone	Single T_g; T_m-depression; FTIR	–	Zhu et al. (2012)
	Hydroxyether terephthalate ester	Single T_g; FTIR	–	Liu et al. (2006b)
	Methylcellulose	Single T_g; NMR	–	Masson and Manley (1991)
	N-Phenyl methacrylamide	Single T_g; FTIR; NMR	–	Lin et al. (2010)
	p-Phenylene terephthalamide	Transparency; microscopy	–	Cowie et al. (1996), Hara and Parker (1992)
	Sulfone, carboxylated	Single T_g; transparency	II had degree of carboxylation 0.43–1.93	Goh et al. (1992d)
	Tyrosine	Single T_g; FTIR; WAXD; NMR	–	Lu et al. (2012)
	Vinyl acetate-*co*-vinyl alcohol	Single T_g; FTIR	II had 29–38 mol% vinyl alcohol	Cesteros et al. (1993, 1994c, d)
4-Vinylpyridinium chloride	Sodium (2-acrylamido-2-methyl propane sulfonate)	–	Formed complexes in dilute aqueous solutions; T_g difficult to detect	Huglin et al. (1996)
	Sodium phosphate	–	Formed complexes in aqueous solution	Acar and Tulun (1996)
2,3-Xylenyl methacrylate	2,6-Xylenyl methacrylate	Single T_g	–	Petrovic-Djakov et al. (1993)

Table 21.2 Polymer pairs containing one monomer in common, miscible in the amorphous state at room temperature

Polymer I of	Polymer II of	Method	Comments	Refs.
Acrylic acid-*co*-styrene	Dimethylacrylamide-*co*-styrene	Single T_g; FTIR	I had 27 mol% acrylic acid; II had 17 or 32 mol% dimethylacrylamide	El Miloudi et al. (2008, 2009) Hadj-Hamou and Djadoun (2006), Hadj-Hamou et al. (2009)
	Styrene-*co*-4-vinylpyridine	Single T_g	I had 14 mol% acrylic acid; II had 15 mol% vinylpyridine	El Miloudi et al. (2009)
Acrylonitrile-*co*-butadiene	Acrylonitrile-*co*-butadiene	Single T_g; clear films; electron microscopy	Difference in composition between I and II ≤22 % acrylonitrile	Ambler (1973), Bartenev and Kongarov (1963), Chandler and Collins (1969), Cheng and Kardos (1969), Corish (1967), Jorgenson et al. (1973), Kosai and Higashino (1975)
	Acrylonitrile-*co*-styrene	Single T_g	–	Cowie et al. (1992c)
	Acrylonitrile-*co*-vinylidene fluoride	Single T_g	I had 23.6–49.6 vol%AN; II had 19 wt% AN	Cowie and Harris (1994)
Acrylonitrile-*co*-maleic anhydride-*co*-styrene	Acrylonitrile-*co*-styrene	Single T_g	Miscibility dependent on compositions of I and II	Cowie et al. (1994b)
	Maleic anhydride-*co*-styrene	Single T_g	Miscibility dependent on compositions of I and II	Cowie et al. (1994b)
Acrylonitrile-*co*-methyl methacrylate	Acrylonitrile-*co*-N-phenylitaconimide	Single T_g	–	Cowie et al. (1990c)
	Methyl methacrylate-*co*-itaconic anhydride	Single T_g	Miscibility dependent on compositions of I and II	Bell et al. (1994)
	Methyl methacrylate-*co*-N-phenylitaconimide	Single T_g	–	Cowie et al. (1990c)
Acrylonitrile-*co*-methyl methacrylate-*co*-methylstyrene	Methyl methacrylate	Single T_g	I had 20/20/60 = acrylonitrile/methyl methacrylate/-methylstyrene	Olabisi and Farnham (1979)
Acrylonitrile-*co*-methyl methacrylate-*co*-styrene	Acrylonitrile-*co*-styrene	Light scattering	–	Ikawa and Hosoda (1990)
	Methyl methacrylate	Light scattering	–	Ikawa and Hosoda (1990)

(*continued*)

Table 21.2 (continued)

Polymer I of	Polymer II of	Method	Comments	Refs.
Acrylonitrile-co-α-methylstyrene	Acrylonitrile-co-methyl methacrylate	Single T_g	–	Cowie and Elexpuru (1992)
	Acrylonitrile-co-styrene	Single T_g; NMR	I had 32.3 wt% acrylonitrile; II had 27 wt% acrylonitrile	Aoki (2000), Cowie et al. (1992a), Ikawa et al. (1993), Lath et al. (2000), Rink et al. (1983)
Acrylonitrile-co-methylstyrene-co-styrene	Acrylonitrile-co-methylstyrene-co-styrene	Clear films	Difference in composition between I and II <12 % acrylonitrile	Slocombe (1957)
Acrylonitrile-co-styrene	Acrylic acid-co-styrene	Single T_g	–	Jin et al. (1986)
	Acrylonitrile-co-benzyl methacrylate	Single T_g	Miscibility dependent on compositions of I and II	Sankarapandian and Kishore (1994)
	Acrylonitrile-fumaronitrile-styrene	Single T_g	I had 32–40 wt% AN; II had 11–17 wt% fumaronitrile	Warakomski and Dion (1992)
	Acrylonitrile-co-methyl methacrylate	Single T_g	–	Cowie et al. (1988), Nishimoto et al. (1989)
	Acrylonitrile-co-(2-oxo-1,3-dioxolane-4-yl)methyl methacrylate	Single T_g	I had 25 wt% AN; II had 24.5 wt% AN	Park et al. (2002a)
	Acrylonitrile-co-N-phenylitaconimide	Single T_g	–	Cowie et al. (1990c)
	Acrylonitrile-co-styrene	Single T_g; no visible phase separation	Difference in composition between I and II <3.5 % acrylonitrile	Landi (1972), Molau (1965)
	Acrylonitrile-co-vinylidene chloride	Single T_g	I had 25 wt% AN; II had 20 wt% AN	Hsu (2004a)
	Benzyl methacrylate-co-styrene	Single T_g	Miscibility dependent on compositions of I and II	Sankarapandian and Kishore (1994)
	p-(2-Hydroxy-hexafluoro-isopropyl)styrene-co-styrene	Single T_g; clear film	I had 70 % styrene; II had 90.3 % styrene	Min and Pearce (1981), Pearce et al. (1984)

	Itaconic anhydride-stat-styrene	Single T_g	Miscibility dependent on compositions of I and II	Bell et al. (1994)
	Maleic anhydride-co-styrene	Single T_g	I had 44.4–94.6 wt% styrene; II had 50–91.5 wt% styrene	Aoki (1988), Heinen et al. (1998), Kressler et al. (1988), Martynowicz-Hans and Runt (1986), Shiomi et al. (1986a), Wastlund et al. (1998)
	Methyl methacrylate-co-styrene	Light scattering	–	Tang et al. (2002)
	N-Phenylitaconimide-co-styrene	Single T_g	–	Cowie et al. (1988)
	N-Phenylmaleimide-co-styrene	Single T_g	–	Aoki (1988, 1990)
	Styrene-co-p-vinylphenol	Single T_g; FTIR	I had 6–30 wt% acrylonitrile; II had 27–92 wt% vinylphenol; miscibility depended on compositions of I and II	Ahn et al. (1997a)
3-Bromo-2,6-dimethyl-1,4-phenylene ether	3-Bromo-2,6-dimethyl-1,4-phenylene ether-co-2,6-dimethyl-1,4-phenylene ether	Single T_g; microscopy	II had ≥48 mol% 3-bromo-2,6-dimethyl-1,4-phenylene oxide	Kambour et al. (1983)
3-Bromo-2,6-dimethyl-1,4-phenylene ether-co-2,6-dimethyl-1,4-phenylene ether	2,6-Dimethyl-1,4-phenylene ether	Single T_g; microscopy	I had ≥62 mol% 2,6-dimethyl-1,4-phenylene ether	Kambour et al. (1983)
p-Bromostyrene-co-styrene	Styrene	Single T_g	I had ≥90 mol% styrene	Kambour et al. (1983), Strobl et al. (1986)
Butadiene	Butadiene	Single T_g	Semicrystalline; I was SKD (87 % cis-1,4) and II was SKBM (Godovskii et al. (1979); I had 50 % vinyl-1,2, 35 % cis-1,4, and 15 % trans-1,4, and II had 98 % cis-1,4 (Shah et al. (1988)); I had 50 % vinyl-1,2, 35 % cis-1,4, and 15 % trans-1,4, and II had 55 % trans-1,4, 35 % cis-1,4, and 10 % vinyl-1,2 (Shah et al. (1988))	Godovskii et al. (1979), Shah et al. (1988)

(continued)

Table 21.2 (continued)

Polymer I of	Polymer II of	Method	Comments	Refs.
Butadiene-*co*-styrene	Butadiene-*co*-styrene	Single T_g	II had >70 % butadiene; immiscible when II had <60 % butadiene	Caspary (1972), Corish (1967), De Decker and Sabatine (1967), Fujimoto and Yoshimiya (1968a, b), Livingston and Rongone (1967), Marsh et al. (1967), Marsh et al. (1968), Shah et al. (1989), Slonimskii (1958), Slonimskii and Komskaia (1956), Struminskii and Slonimskii (1956), Yoshimura et al. (1968)
Butadiene-*co*-styrene	Butadiene-*co*-styrene	Single T_g; microscopy	Difference in composition between I and II <20 % styrene; two T_g's when composition difference >20 %	De Decker and Sabatine (1967), Livingston and Brown (1968, 1970), Livingston and Rongone (1967), Kraus and Rollman (1971), Shutilin and Vysokomol (1991), Slonimskii and Komskaia (1956)
	Styrene	Single dynamic mechanical loss peak	I had 25 % styrene; II had M_w ≤917; ≤50 % II; two loss peaks when 75 % II	Class and Chu (1985a, c)
Butene-*co*-ethylene	Ethylene-*co*-styrene	Phase contrast optical microscopy	I had 15 mol% butane; II had 1.0–3.9 mol% styrene	Hu et al. (2005)
Butyl acrylate-*co*-butyl methacrylate	Butyl acrylate-*co*-butyl methacrylate	Clear films	Difference in composition between I and II 25 % butyl acrylate; immiscible when composition difference 50 % butyl acrylate	Kosai et al. (1977)
Butyl acrylate-*co*-N-hydroxyethylcarbozolyl acrylate	Butyl acrylate-*co*-β-hydroxyethyl-3,5-dinitrobenzoyl acrylate	Single T_g	I had 6 or 48 mol% electron donating carbozoyl groups; II had 10 or 63 mol% electron withdrawing dinitrobenzoyl groups	Schneider et al. (1992)

Butyl acrylate-co-ethyl acrylate	Butyl acrylate-co-ethyl acrylate	Clear films	Difference in composition between I and II 25 % ethyl acrylate; immiscible when composition difference 50 % ethyl acrylate	Kosai et al. (1977)
	Ethyl acrylate	Clear films	I had 75 % ethyl acrylate; immiscible when I had ≤50 % ethyl acrylate	Kosai et al. (1977)
Butyl acrylate-co-methyl methacrylate	Butyl acrylate-co-methyl methacrylate	Single T_g; clear films	Difference in composition between I and II ≤10 % methyl methacrylate	Kollinsky and Markert (1969, 1971)
n-Butyl methacrylate	n-Butyl methacrylate-co-styrene	Single T_g; clear films	II had ≥90 wt% n-butyl methacrylate	Fujimoto and yoshimura (1968)
n-Butyl methacrylate-co-p-chlorostyrene	n-Butyl methacrylate-co-p-chlorostyrene	Single T_g; microscopy	–	Braun et al. (1992)
n-Butyl methacrylate-co-N-hydroxyethylcarbazoyl acrylate	n-Butyl methacrylate-co-hydroxyethyl-3,5-dinitrobenzoyl acrylate	Single T_g	I had 9 mol% carbazoyl groups; II had 9 mol% dinitrobenzoyl groups	Schneider et al. (1992)
Butyl methacrylate-co-methacrylic acid	Methacrylic acid-co-styrene	Single T_g	MAA contents of I and II were 20.2 and 13.7 mol%, respectively; MAA was Na-neutralized	Jiang et al. (1993)
Butyl methacrylate-co-methyl methacrylate	Butyl methacrylate-co-methyl methacrylate	Clear films	Difference in composition between I and II ≤20–30 % butyl methacrylate, depending on compositions of I and II	Braun et al. (1992), Kollinsky and Markert (1969)
n-Butyl methacrylate-co-styrene	n-Butyl methacrylate-co-styrene	Single T_g; microscopy	–	Braun et al. (1992)
	Styrene	Single T_g; microscopy	II had ≥90 wt% styrene	Fujioka et al. (1984)
Caprolactam-co-caprolactone-co-laurolactam	Caprolactam-co-laurolactam	Single T_g	I and II had varying compositions	Ellis (1993)
Caprolactone	Butylene terephthalate-co-caprolactone	Single T_g; microscopy	II had <60 mol%butylene terephthalate	Ma et al. (1997a)
Carbonate of bisphenol-A	Carbonate of bisphenol-A-co-1,1-bis(4-hydroxyphenyl)-3,3,5-trimethylcyclohexane	Single T_g; transparency	II had 36–89 wt% bisphenol-A	Haggard and Paul (2004)

(continued)

Table 21.2 (continued)

Polymer I of	Polymer II of	Method	Comments	Refs.
p-Chlorostyrene-co-hexyl methacrylate	p-Chlorostyrene-co-hexyl methacrylate	OM	Closely match compositions of I and II favored miscibility	Sato et al. (2004)
Cyclohexyl methacrylate-co-methyl methacrylate	Cyclohexyl methacrylate-co-methyl methacrylate	Single T_g	Miscibility depended on compositions of I and II	Pomposo et al. (1998)
Cinnamic acid-co-styrene	Styrene-co-4-vinylpyridine	Single T_g; FTIR	I had 15 mol% cinnamic acid; II had 16.6 mol% 4-vinylpyridine	Boulash et al. (2008)
	Methyl methacrylate-co-styrene	Single T_g		Pomposo et al. (1998)
1,8-Dibromooctane-co-bisphenol-A	1,8-Dibromooctane-co-4,4′-(hexafluoroisopropylidene) diphenol	Single T_g; AFM; XPS; TOF-SIMS	I:II = 80:20 in blend	Lei et al. (2003)
2,6-Dimethyl-1,4-phenylene ether, sulfonylated	2,6-Dimethyl-1,4-phenylene ether, sulfonylated	Single T_g	Difference in degree of sulfonylation between I and II in the range of 20–26 wt%	Kang et al. (1987)
2,3-Dimethylbutadiene-stat-p-vinylphenol	2,3-Dimethylbutadiene-stat-alkyl methacrylate	Single T_g; transparency	II had an alkyl group of methyl, ethyl, n-propyl, n-butyl, n-decyl, or n-hexadecyl	Pehlert et al. (1998)
Dimethylsiloxane, functionalized	Dimethylsiloxane, functionalized	Single T_g	I had 4–15 mol% electron-donating carbazoyl or N-methylaniline groups; II had 4–15 mol% electron-accepting dinitrobenzoyl groups; donor/acceptor = 1/1	Schneider et al. (1992)
Epichlorohydrin	Epichlorohydrin-co-ethylene glycol	Single T_g	I was Hydrin 100; II was Hydrin 200	Jaroszynska and Gaczynski (1976)
Etheretherketone	Etheretherketone	Single T_g	I was linear and II was hyperbranched	Li et al. (2011)
Ethyl acrylate-co-ethyl methacrylate	Ethyl acrylate-co-ethyl methacrylate	Clear films	I and II had 25, 50, or 75 % ethyl acrylate	Kosai et al. (1977)
	Ethyl methacrylate	Clear films	I had 75 wt% ethyl methacrylate; immiscible when I had ≤50 wt% ethyl methacrylate	Kosai et al. (1977)

Polymer I	Polymer II	Method	Comments	References
Ethyl acrylate-*co*-methyl methacrylate	Ethyl acrylate-*co*-methyl methacrylate	Clear films	Difference in composition between I and II <20–27 % ethyl acrylate depending on compositions of I and II	Kollinsky and Markert (1969)
Ethylene	Ethylene	Rheological studies; IGC	I and II were LDPE, HDPE, or LLDPE; miscibility depended on branch content and composition distribution	Hameed and Hussein (2004), Hussein (2003), Hussein et al. (2003), Hussein and William (2004a, b), Zhao and Choi (2004)
Ethylene-*co*-propylene	Ethylene-*co*-propylene	AFM	Difference in ethylene content in I and II was less than 18 mol%	Kamdar et al. (2006)
Ethylene, chlorinated	Ethylene, chlorinated	Single T_g; clear films	Difference in composition between I and II $\leq$1.2–13.3 wt% Cl depending on compositions of I and II	Chai and Sun (1983), Chai et al. (1992), Oswald and Kubu (1963), Ueda and Karasz (1990a)
	Ethylene-*co*-methyl acrylate	Single T_g; phase contrast microscopy	Semicrystalline when I had 25 wt% Cl; I had 25 or 48 wt% Cl	Kalfoglou and Margaritis (1984)
	Ethylene-*co*-vinyl acetate	Single T_g; microscopy	I had 35.4–52.6 wt% Cl; II had 50–60 wt% ethylene	Walsh et al. (1983)
	Ethylene-*co*-styrene	Single T_g	Miscible when the difference in styrene content was less than 10 wt%	Cheung and Guest (2000)
Ethylene-*co*-vinyl acetate	Ethylene, low density	Single T_g	I:II = 50:50	Ray et al. (1993)
	Ethylene acetate-*co*-vinyl acetate	Single T_g; microscopy	I and II had 7–100 wt% vinyl acetate	Braun et al. (1993)
	Ethylene-*co*-vinyl alcohol	Single T_g; FTIR	I and 21 mol% vinyl acetate; II had 21 mol% vinyl alcohol	Coleman et al. (1993b)
	Vinyl acetate-*co*-vinyl chloride	Single T_g	–	Shiomi et al. (1986, 1990)
Ethylene-*co*-vinyl alcohol	Ethylene-alt-maleic anhydride	Single T_g; T_m-depression	I had 38 mol% ethylene	Aouak et al. (2012)
Ethylene-*co*-vinyl chloride	Ethylene-*co*-vinyl chloride	Single T_g	Difference in vinyl chloride or ethylene content of I and II <15 mol%	Bowmer and Tondli (1986a, b)
Vinyl chloride	Vinyl chloride	Single T_g; T_m-depression	I had >80 mol% vinyl chloride	Bowmer and Tondli (1986a)
Ethylene glycol	Epichlorohydrin-*co*-ethylene glycol	Single T_g; T_m-depression	–	Silva et al. (1988)
Ethylene naphthalene-2,6-dicarboxylate	Ethylene naphthalene-2,6-dicarboxylate-*co*-4-hydroxybenzoate	NMR	II had 20 mol% 4-hydroxybenzoate	Guo and Zachmann (1993)
Ethyl methacrylate-*co*-methyl methacrylate	Ethyl methacrylate-*co*-methyl methacrylate	Single T_g	–	Chai et al. (1992)

(*continued*)

Table 21.2 (continued)

Polymer I of	Polymer II of	Method	Comments	Refs.
o-Fluorostyrene-co-p-styrene	o-Fluorostyrene-co-p-styrene	Single T_g	I and II had 10 and 23 mol% p-fluorostyrene, respectively	Oudhuis et al. (1993)
o-Fluorostyrene-co-styrene	o-Fluorostyrene-co-styrene	Single T_g	I had 18 or 49 % o-fluorostyrene; II had 40 or 77 % o-fluorostyrene	Oudhuis et al. (1993), Salomons et al. (1991)
	Styrene	Single T_g	I had 18, 40, or 49 % o-fluorostyrene and II had M_n = 15 kg/mol; I had 18 % o-fluorostyrene and II had M_n = 110 kg/mol	Oudhuis et al. (1993), Salomons et al. (1991)
p-Fluorostyrene-co-styrene	Styrene	Single T_g	I had 8 or 16 mol% p-fluorostyrene; II had M_n = 40 or 326 kg/mol	Oudhuis et al. (1993)
Hexyl methacrylate-co-methyl methacrylate	Hexyl methacrylate-co-methyl methacrylate	OM	Closely match compositions of I and II favored miscibility	Sato et al. (2004)
Hexyl methacrylate-co-styrene	Hexyl methacrylate-co-styrene	OM	Closely match compositions of I and II favored miscibility	Sato et al. (2004)
Hydrocarbon polymer, chlorinated	Hydrocarbon polymer, chlorinated	Clear films	One series derived from reduction of polyvinyl chloride and one series derived from chlorination of polyethylene	Braun et al. (1989)
p-Hydroxybenzoic acid-co-6-hydroxy-2-naphthoic acid-co-terephthalic acid-co-hydroquinone	p-Hydroxybenzoic acid-co-6-hydroxy-2-naphthoic acid	Single T_g; X-ray diffraction	X-ray diffraction showed no significant transesterification occurred in the mixture	DeMeuse and Jaffe (1989)
Hydroxybutyrate	Hydroxybutyrate	OM; SAXS	I was isotactic. II was atactic	Abe et al. (1994)
	3-Hydroxybutyrate-co-4-hydroxybutyrate	Single T_g; FTIR	I had 41 mol% 4-hydroxybutyrate; miscible when blend had 1- = 50 wt% II	Luo et al. (2007)
	Hydroxybutyrate-co-hydroxyhexanoate	Single T_g	II had 10 or 20 mol% hydroxyhexanoate	Feng et al. (2003)
	Hydroxybutyrate-co-hydroxyvalerate	Microscopy; melting behavior; WAXS	II had 3.8–22.3 mol% hydroxyvalerate	Organ (1994), Organ and Barham (1993), Scandola et al. (1997)

Hydroxybutyrate-co-hydroxyhexanoate	Hydroxybutyrate-co-hydroxyhexanoate	Single T_g	Hydroxyhexanoate contents of I and II were 10 and 20 mol%, respectively	Feng et al. (2003)
3-Hydroxybutyrate-co-hydroxypropionate	3-Hdroxybutyrate-co-hydroxypropionate	Single T_g	II had hydroxypropionate content less than 40 mol%	Na et al. (2001)
Imide	Imide	Single T_g; transparency	I and II had a common monomer but different flexibility	Cosutchi et al. (2012)
Isoprene	Isoprene-styrene block copolymer	Electron microscopy	I had M_n = 6.5–53.9 kg/mol; II was diblock, triblock, or four-arm star copolymer having total M_n = 26–622 kg/mol	Jiang et al. (1986)
Maleic anhydride-co-styrene	Acrylonitrile-co-styrene	Single T_g, transparency, microscopy	I had 15.3 wt% maleic anhydride; II had 15.0, 19.5, or 25.0 wt% acrylonitrile	Gan and Paul (1994a) Kim et al. (1989b), Maruta et al. (1988)
	Maleic anhydride-co-styrene	Single T_g	Miscible when the difference in MA content of I and II was less than 2.5 vol %	Pinoit and Prud'homme (2002)
	Methyl methacrylate-co-styrene	Single T_g	Miscibility dependent on compositions of I and II	Gan and Paul (1994a)
	Styrene-co-4-vinylpyridine	Single T_g; FTIR	I had 28 or 50 mol% maleic anhydride; II had 32 mol% vinylpyridine	Haddadine-Rahmoun et al. (2008)
N-Maleimide-co-methyl methacrylate	Methyl methacrylate-co-7-[2-methacryloyloxy]ethyladenine	Single T_g	I and II had ≥10 mol% hydrogen bonding unit site	Cowie and Love (2001)
N-Maleimide-co-styrene	Styrene-co-2-vinylpyridine	Single T_g; FTIR	II had 30 wt% styrene	Vermeesch et al. (1993)
Methacrylic acid-co-methyl methacrylate	Methyl methacrylate-co-4-vinylpyridine	Phase diagram	I had 91.48 or 77.7 mol% methyl methacrylate; II had 80.2 mol% methyl methacrylate	Djadoun (1983)

(continued)

Table 21.2 (continued)

Polymer I of	Polymer II of	Method	Comments	Refs.
Methacrylic acid-*co*-styrene	2-(*N*,*N*-Dimethylamino)ethyl methacrylate-*co*-styrene	Single T_g	Formed complexes when I had 22 mol% acid and II had 79 or 88 mol% styrene	Abdellaoui and Djadoun (2005)
	Styrene-*co*-4-vinylpyridine	Single T_g; phase diagram; FTIR	Formed complexes when I had 12 or 29 mol% acid and II had 6 or 15 mol% vinylpyridine (Bennour et al. (2005)); I had 89.5 mol% styrene; II had 83.9 mol% styrene (Djadoun (1983))	Benabdelghani et al. (2008), Benabdelghani and Etxeberria (2011), Bennour et al. (2005), Djadoun (1983)
	Styrene-*co*-2-vinylpyridine	Single T_g; FTIR	I had 9 mol% methacrylic acid; II had 17 mol% vinylpyridine	Motzer et al. (2001b)
	Styrene-*co*-N-vinylpyrrolidone	Single T_g; FTIR	I had 9 mol% methacrylic acid; II had 13 mol% N-vinylpyrrolidone	Motzer et al. (2001b)
[4-(Methacryloyloxy)-butyl] pentamethyldisiloxane	[4-(Methacryloyloxy)-butyl] pentamethyldisiloxane-*co*-methyl methacrylate	Single T_g; clear films	II had 67 % methyl methacrylate	Blahovici et al. (1982)
[4-(Methacryloyloxy)-butyl] pentamethyldisiloxane-*co*-methyl methacrylate	Methyl methacrylate	Single T_g; clear films	I had 67 or 75 % methyl methacrylate	Blahovici et al. (1982)
Methacrylonitrile-*co*-styrene	Methacrylonitrile-*co*-methyl methacrylate	Single T_g	Miscibility dependent on compositions of I and II	Cowie et al. (1993b)
	Methacrylonitrile-*co*-styrene	Single T_g	Miscibility dependent on compositions of I and II	Cowie et al. (1993b)
Methyl acrylate	Methyl acrylate-*co*-vinyl acetate	Clear films	II had 25–75 % methyl acrylate	Kosai et al. (1977)
Methyl acrylate-*co*-methyl methacrylate	Methyl acrylate-*co*-methyl methacrylate	Clear films	Difference in composition between I and II 28–48 % methyl acrylate when I and II had degree of polymerization = 400 and 20–35 % methyl acrylate when I and II had degree of polymerization = 3,000, depending on compositions of I and II	Kollinsky and Markert (1969)

Methyl acrylate-*co*-vinyl acetate	Vinyl acetate	Clear films	I had 25–75 % vinyl acetate	Kosai et al. (1977)
Methyl methacrylate	Ethyl methacrylate-*co*-methyl methacrylate	Single T_g	I was isotactic; II had ≤45 % ethyl methacrylate	Schroeder et al. (1985)
	Methyl methacrylate	Single T_g	I was isotactic; II was syndiotactic; I and II were atactic, isotactic, or syndiotactic (Chang and Woo (2010))	Chang and Woo (2010), Ragupathy et al. (2007), Schroeder et al. (1985)
	Methyl methacrylate-*co*-phenylmaleimide	Single T_g	Miscibility depended on M_w of I and composition of II	Merfeld et al. (1999)
	Methyl methacrylate-*co*-tribromophenyl maleimide	Single T_g	Miscibility depended on M_w of I and composition of II	Merfeld et al. (1999)
	Methyl methacrylate-*alt*-styrene	Single T_g; TEM	–	Galvin et al. (1994)
Methyl methacrylate-*co*-2-[(3,5-dinitrobenzoyl)oxy] ethyl methacrylate	Methyl methacrylate-*co*-(N-ethylcarbazole-3-yl)methyl methacrylate	Single T_g	I was mixed with II with similar acceptor or donor content and D:A = 1	Pionteck et al. (1995)
Methyl methacrylate-*co*-styrene	Acrylonitrile-*co*-styrene	Single T_g	–	Cowie and Lath (1988), Kammer et al. (1989)
	Maleic anhydride-*co*-styrene	Single T_g	–	Kammer et al. (1989)
	Methyl methacrylate-*co*-N-phenylitaconimide	Single T_g	–	Cowie et al. (1990c)
	Methyl methacrylate-*co*-styrene	Single T_g; microscopy	Miscibility depended on compositions of I and II	Braun et al. (1992), Kohl et al. (1990), Zhu and Paul (2003)
	Methyl methacrylate-*co*-2,4,5-tribromostyrene	Single T_g	I had ≤29.1 wt% styrene; II had ≤13.6 wt% tribromostyrene	Chu et al. (2000)
	N-Phenylitaconimide-*co*-styrene	Single T_g	–	Cowie et al. (1990c)
Methyl methacrylate-*co*-trifluoroethyl methacrylate	Trifluoroethyl methacrylate-*co*-vinylidene fluoride	Single T_g	I had 33 or 66 mol% trifluoroethyl methacrylate; II had 25 or 50 mol% trifluoroethyl methacrylate	Jauannet et al. (1997)
α-Methylstyrene	*p*-Methylstyrene	Single T_g; SEM	I had M_w = 70 kg/mol; miscible when II had M_w = 7.5 kg/mol, immiscible when II had M_w = 31.4 kg/mol	Chang and Woo (2000)
p-Nitrostyrene-*co*-styrene	*p*-Nitrostyrene-*co*-styrene	Single T_g	–	Cowie et al. (1992d)

Table 21.2 (continued)

Polymer I of	Polymer II of	Method	Comments	Refs.
Novolac resin	Novolac resin	Single T_g	I was formaldehyde and 13/17/70 mol% = p-t-butyl phenol/m-cresol/o-cresol; II was formaldehyde and 15/85 mol% = 2-t-butyl phenol/o-cresol; I and II had M_w 0.8–1.6 kg/mol	Fahrenhlotz and Kwei (1981)
2,2,3,3,3-Pentafluoropropyl methacrylate-co-4-vinylpyridine	2,2,2-Trifluoroethyl methacrylate-co-4-vinylpyridine	Single T_g; FTIR; XPS; ToF-SIMS	I had 28–54 mol% pyridine; II had 27 or 42 mol% vinylpyridine	Huang et al. (2004a)
N-Phenylmaleimide-co-styrene	4-Cyanostyrene-co-styrene	Single T_g	I had 39 wt% styrene; II had 58.5–83.1 mol% styrene	Dean (1987a)
	2-Cyanostyrene-co-4-cyanostyrene-co-styrene	Single T_g	II had 23.5 or 22.7 mol% styrene; ratios of 2-cyanostyrene/4-cyano-styrene were 25:75 or 78:22	Dean (1987a)
Propylene	Ethylene-co-propylene	Single T_g	Miscible when I and II had low M_w	Lohse et al. (1993)
	Propylene	T_m-Depression; OM	I and II had different tacticities	Woo et al. (2007)
Styrene	Alkyl methacrylate-co-styrene	Single T_g	II had an alkyl group of methyl or ethyl; II had 22 mol% styrene; blend had 5, 20, or 95 wt% II	De Andrade and Atvars (2004)
	α-Methylstyrene-co-styrene	Single T_g; T_m-depression	I was syndiotactic; II had 44 wt% styrene	Chiu and Li (2003)
	2-Oxo-1,3-dioxolane-4-yl)methyl methacrylate-co-styrene	Single T_g	II had 19.5 wt% styrene	Park et al. (2002b)
	Styrene	Single T_g	I had M_w = 0.8 kg/mol; II had M_w = 8420 kg/mol; I/II = 31.7/68.5	Chang (1988)
	Styrene	Single T_g	I was linear; II was multibranched	Tsukahara et al. (1994)
	Styrene	Single T_g; OM; T_m-depression	I and II had different tacticity	Ahn et al. (1997e), Bonnet et al. (1998), Hong et al. (1998), Li and Woo (2006), Wang et al. (2005), Woo et al. (2000a), Wu and Woo (1999)

Styrene-*co*-styrenesulfonic acid	Styrene, iodinated	Transparency	II had a degree of iodination of 6 or 15 %	Goh and Lee (1989b)
	Styrene-*co*-*p*-vinylphenol	FTIR; NMR	I had 86 mol% styrene; II had 22 mol% vinylphenol	Huang and Guo (1990), Kelts et al. (1993), Landry et al. (1993a)
	Styrene-*co*-4-vinylpyridine	FTIR; XPS	I had 1.8–9.9 mol% acid; II had 1.9–9.9 mol% pyridine (Smith and Eisenberg (1994); I had 17 or 27 mol % acid and II had 17 or 30 mol% vinylpyridine (Goh et al. (1996b))	Goh et al. (1996b), Smith and Eisenberg (1994)
Styrene-*co*-2,4,5-tribromostyrene	Acrylonitrile-*co*-styrene	Single T_g	I had $\leq$29 wt% tribromostyrene; II had $\leq$6.3 wt% acrylonitrile	Chu et al. (2000)
	Maleic anhydride-*co*-styrene	Single T_g	I had $\leq$29 wt% tribromostyrene; II had $\leq$8 wt% maleic anhydride	Chu et al. (2000)
Styrene-*co*-*p*-vinylphenol	Styrene-*co*-4-vinylpyridine	Light scattering; NRET; XPS; TOF-SIMA	I had 3–70 mol% vinylphenol; II had 14–75 mol% vinylpyridine; formed complexes	Li et al. (1998a), Liu et al. (2004b, 2005a), Xiang et al. (1997a)
Sulfone	Sulfone, carboxylated	Single T_g	Degree of carboxylation of II <1.3	Lau et al. (1993)
Vinyl acetate-*co*-vinyl chloride	Vinyl chloride	Single T_g; microscopy of fibers	I had 78 or 86 wt% vinyl chloride	Kolowski and Laskawski (1980)
	Vinyl chloride, chlorinated	Single T_g	–	Shiomi et al. (1986)
Vinyl acetate-*co*-vinyl stearate	Vinyl acetate-*co*-vinyl stearate	Single T_g; microscopy	I and II had 21–98 wt% vinyl acetate	Braun et al. (1993)
Vinyl chloride	Propylene-*co*-vinyl chloride	Single T_g; microscopy of fibers	II had 89 or 91 wt% vinyl chloride	Kolowski and Laskawski (1980)
Vinyl chloride, chlorinated	Vinyl chloride	Single T_g	Up to 61.3 or 65.2 % Cl in I with dependence on mol% CCl_2 groups	Carmoin et al. (1977), Lehr (1985, 1986)
	Vinyl chloride, chlorinated	Single T_g	Difference in composition between I and II $\leq$3–4 % Cl depending on composition of I and II with dependence on number of CCl2 groups	Chai et al. (1992), Lehr (1985)

Table 21.3 Chemically dissimilar polymer triads (and tetrads) miscible in the amorphous state at room temperature

Polymer I of	Polymer II of	Polymer III of and Polymer IV of	Method	Comments	Refs.
Acetoxystyrene	Ethylene glycol	p-Vinylphenol	Single T_g; FTIR	Existence of an immiscibility loop	Kuo et al. (2005b)
Acrylic acid-co-methyl methacrylate	n-Butyl methacrylate-co-4-vinylpyridine	Vinyl chloride	Single T_g	Miscible when blend had >50 wt% II	Iguerb et al. (1999)
Acrylic acid-co-styrene	N,N-Dimethylacrylamide-co-styrene	Styrene-co-4-vinylpyridine	Single T_g	I had 14 mol% acrylic acid; II had 25 mol% dimethylacrylamide; III had 15 mol% vinylpyridine	El Miloudi et al. (2009)
	Ethylene glycol	Methyl methacrylate	Single T_g	I had 12.2, 20.8, or 33.1 mol% acrylic acid	Jo et al. (1991b)
Acrylonitrile-co-butadiene	Vinyl chloride	Vinyl chloride-co-vinylidene chloride	Single T_g	Semicrystalline; I had 30 or 40 wt% acrylonitrile; III had 65 wt% vinylidene chloride	Wang and Chen (1981)
Acrylonitrile-co-butadiene-co-styrene	Carbonate of bisphenol-A	Propylene-co-vinyl chloride	Single T_g	I was Blendex 701; II was Merlon Matzner et al. (1982), M-60; III had 3.2 or 3.8 % propylene; I/II/III = 1/1/2; two T_g's when I/II/III = 3/7/10	Cheng and Mantell (1979)
Acrylonitrile-co-methyl acrylate	Ethylene glycol	2-Hydroxyethyl methacrylate-co-4-vinylphenol	Single T_g; T_m-depression; FTIR	III had 55 mol% vinylphenol	Silva et al. (2009)
Acrylonitrile-co-methyl methacrylate	Acrylonitrile-co-styrene	Maleic anhydride-co-styrene	Single T_g	I had 12 % acrylonitrile; II had 25 % acrylonitrile; III had 25 % maleic anhydride	Brannock and Paul (1990)
	Acrylonitrile-co-styrene	Methyl methacrylate-co-styrene	Single T_g	I had 2.7–7.4 vol% acrylonitrile; II had 14.5–49.5 vol% acrylonitrile; III had 11.2–16.0 vol% styrene	Cowie and Lath (1987), Cowie et al. (1992b)
	Acrylonitrile-co-styrene	Methyl methacrylate-co-N-phenylitaconimide	Single T_g	I had 68 or 95 vol% MMA; II had 63 or 70 vol% styrene; II had 12 or 45 vol% MMA	Cowie et al. (1994a)

Acrylonitrile-co-methylstyrene	Vinyl chloride	Single T_g	I had 32.3 wt% acrylonitrile; II had 27 wt% acrylonitrile; >25 % I	Rink et al. (1983)
	Ethyl methacrylate	Single T_g	I had 30 wt% acrylonitrile	Goh et al. (1986a)
Acrylonitrile-co-N-phenylitaconimide	Acrylonitrile-co-styrene	Single T_g	I had 6 or 9 vol% acrylonitrile; II had 22, 44, or 65 vol% acrylonitrile; III had 12 or 42 vol% styrene	Cowie et al. (1991b)
Acrylonitrile-co-styrene	Maleic anhydride-co-styrene	Single T_g	I and I had different compositions; III had 22–34 mol% maleic anhydride	Tacx et al. (2002)
	Butylene adipate	Single T_g	I had 12 or 25 % acrylonitrile	Shah et al. (1986)
	Caprolactone	Single T_g	–	Shah et al. (1986)
	Hydroxyether of bisphenol-A	Single T_g	I had 15 wt% AN	Jo et al. (1994a), Vanneste and Groeninckx (1994), Vanneste et al. (1997)
	Maleic anhydride-co-styrene	Single T_g; transparency	I had 15 wt% AN; II had 14 wt % MA	Vanneste and Groeninckx (1995)
	Caprolactone	Single T_g	Miscible when I/II/III = 68/16/16	Huang et al. (1988b)
	Cyclohexane dimethylene succinate	Single T_g	–	Shah et al. (1986)
	Carbonate of tetramethylbisphenol-A	Single T_g	All blends were miscible and exhibited LCST	Yoo and Kim (2004b), Yoo et al. (2003)
	Maleic anhydride-co-styrene	Single T_g	Miscible at all blend compositions	Reichelt et al. (1996a, b)
	Maleic anhydride-co-styrene	Single T_g	I had 25 % acrylonitrile; III had 14–25 % acrylonitrile	Brannock and Paul (1990)
	Methyl methacrylate	Single T_g	I had 30 wt% acrylonitrile; some blends showed LCST	Goh and Siow (1986b)
Ethylene-co-vinyl acetate	Vinyl chloride	Single T_g; SEM; PALS	I had 25 wt% AN; II had 45 wt % vinyl acetate	Meghala and Ranganathaiah (2012)
	Methyl methacrylate	Single T_g	II was atactic; III was isotactic	Hsu and Yeh (1999b)

(continued)

Table 21.3 (continued)

Polymer I of	Polymer II of	Polymer III of and Polymer IV of	Method	Comments	Refs.
	Methyl methacrylate	Vinyl chloride	Single T_g	I had 23 or 25 wt% acrylonitrile	Huang and Guo (1990), Meghala and Ranganathaiah (2012)
Acrylonitrile-*co*-vinylidene chloride	Methyl methacrylate	Methyl methacrylate	Single T_g	I had 20 wt% AN; I and II were atactic and isotactic, respectively	Hsu and Yeh (2000a)
	Methyl methacrylate	*p*-Vinylphenol	Single T_g	Miscible when blend had ≤20 wt% III	Hsu (2004a)
Acrylonitrile-*co*-vinylidene fluoride	Methyl methacrylate	Methyl methacrylate	Single T_g	II and II were atactic and sydiotactic, respectively; blend had >12.5 wt% II	Hsu (2000)
Amide	Methyl methacrylate	*p*-Vinylphenol	Single T_g; FTIR	I was amorphous; miscibility required a high content of III	Hosokawa and Akiyama (1999)
n-Amyl methacrylate	*n*-Butyl methacrylate	Vinyl chloride	Single T_g	Miscible when blend had >30 wt% III	Perrin and Prud'homme (1993)
n-Amyl methacrylate	*n*-Propyl methacrylate	Vinyl chloride	Single T_g	Miscible when blend had >70 wt% III	Perrin and Prud'homme (1993)
Arylate	Butylene terephthalate	Hydroxyether of bisphenol-A (Phenoxy)	Single T_g	I was Arilef U-100; III >30 wt%	Ahn et al. (1990), Eguiazabal et al. (1986b), Iruin et al. (1989)
Benzyl methacrylate	Caprolactone	Acrylonitrile-*co*-styrene	Single T_g; microscopy	III had 17 or 25 wt% AN; blend exhibited LCST	Su et al. (2003)
	Caprolactone	Phenyl methacrylate	Single T_g	Miscible at all compositions; all blends exhibited LCST	Lee and Woo (2002)
	Caprolactone	Vinylmethylether	Single T_g; microscopy	Blend exhibited LCST	Woo et al. (2003b)

3-Bromo-2,6-dimethyl-1,4-phenylene ether-co-2,6-dimethyl-1,4-phenylene ether	2,6-Dimethyl-1,4-phenylene ether	Single T_g; microscopy	≤37 mol% brominated monomer in I and II	Kambour et al. (1983)
	Styrene	Single T_g; microscopy	≤16 mol% brominated monomer in I and II	Kambour et al. (1983)
	Styrene	Single T_g; microscopy	≤45 mol% brominated monomer in I	Kambour et al. (1983)
	2,6-Dimethyl-1,4-phenylene ether	Single T_g; microscopy	≤26 mol% brominated monomer in I and in II	Kambour et al. (1983)
Bromostyrene	2,6-Dimethyl-1,4-phenylene ether (polymer IV of styrene)	Single T_g	Blend had ≥33 wt% II	Aroguz and Baysal (2000)
p-Bromostyrene-co-styrene	Styrene	Single T_g; microscopy	≤29 mol% p-bromostyrene in I	Kambour et al. (1983)
n-Butyl methacrylate	Propylene glycol	Transparency	–	Duffy et al. (2005)
Butylene adipate	p-Vinylphenol	Single T_g; OM: FTIR	Blend had ≥60 wt% III	Lee et al. (2010)
Butylene succinate	Ethylene succinate	Single T_g; OM	–	Ikehara et al. (2010)
	Hydroxybutyrate-co-hydroxyvalerate	Single T_g; SEM; TEM	–	Zhang et al. (2012a)
Butylene terephthalate	Carbonate of bisphenol-A (Phenoxy)	Single T_g	Blend had ≥33 wt% II	Remiro and Nazabal (1991a, b)
	Etherimide	Single T_g	–	Yau and Woo (1996)
	Etherimide	Single T_g	–	Woo and Lee (2003)
	Ethylene terephthalate (polymer IV of trimethylene adipate)	Single T_g	Completely miscible (Woo and Kuo (2003))	Run et al. (2007), Woo and Kuo (2003)
Ethylene terephthalate	Trimethylene terephthalate	Single T_g	Completely miscible	Lee et al. (2006)
Ethylene terephthalate	p-Vinylphenol	Single T_g; T_m-depression; FTIR	Completely miscible	Lee et al. (2006)
Trimethylene terephthalate	p-Vinylphenol	Single T_g; T_m-depression; FTIR		
Hydroxyether of bisphenol-A	Methyl methacrylate	Single T_g; SEM	Miscible when blend had >50 wt% III	Jo et al. (1994b)

(continued)

Table 21.3 (continued)

Polymer I of	Polymer II of	Polymer III of and Polymer IV of	Method	Comments	Refs.
Caprolactam	Vinyl alcohol	Vinyl butyral	Single T_g; SEM	Miscible when blend had 40–60 wt% II	Jeong et al. (2000b)
Caprolactone	Ethylene glycol	Hydroxybutyrate	Light scattering	–	Chee et al. (2004)
	Ethylene glycol	Lactide	Single T_g; OM	–	Buddhiranon et al. (2011)
	Ethylene glycol	Novolac	Single T_g; FTIR;	3 Miscible binary pairs; existence of an immiscibility loop	Kuo et al. (2002a)
	Hydroxyether of bisphenol-A (Phenoxy)	Novolac	Single T_g; FTIR;	Miscible at all compositions	Kuo et al. (2005a)
	Hydroxyether of bisphenol-A (Phenoxy)	Vinylmethylether	Single T_g	Miscible at all compositions; all blends showed LCST	Guo (1990a)
	Carbonate of bisphenol-A	Hydroxyether of bisphenol-A (Phenoxy)	Single T_g	Generally miscible when >60 wt% I in blend	Christiansen et al. (1987)
	Carbonate of bisphenol-A	Carbonate of tetramethylbisphenol-A	Single T_g	Miscible at all compositions	Kim and Paul (1994)
	Vinyl chloride	Vinyl chloride, chlorinated	Single T_g	II had 67.2 wt% Cl; generally miscible when I >40 % at high II/III ratio and miscible when I >26 % at low II/III ratio	Ameduri and Prud'homme (1988)
Carbonate of bisphenol-A	Carbonate of bisphenol chloral	Methyl methacrylate	Single T_g	–	Kim and Paul (1992a)
	Carbonate of tetramethylbisphenol-A	Acrylonitrile-co-styrene	Single T_g	III had 2.7–19.7 wt% AN	Kim et al. (1994a)
	Carbonate of tetramethylbisphenol-A	Methyl methacrylate-co-styrene	Single T_g	III had 4.5–58.5 wt% MMA	Kim et al. (1994a)
	Carbonate of tetramethylbisphenol-A	Styrene	Single T_g	–	Kim et al. (1994a), Landry et al. (1991)
	Methyl methacrylate	Vinyl acetate	Single T_g; NMR	I:II:III = 1:4.5:4.5	Rusa et al. (2004)

Carbonate of dimethylbisphenol-A	Styrene	Single T_g; OM	–	Kim et al. (2005)
Carbonate of tetramethylbisphenol-A	Methyl methacrylate-co-styrene	Single T_g; OM	III had 15 or 30 wt% methyl methacrylate	Kim et al. (2005)
Carbonate of tetramethylbisphenol-A	Methyl methacrylate-co-styrene	Single T_g	–	Yu et al. (1991)
2-Chlorostyrene	Styrene	Single T_g; light scattering	Three miscible binary blend systems; existence of an immiscibility loop in the ternary system	Rabeony et al. (1994)
o-Chlorostyrene-co-p-chlorostyrene	Styrene	Single T_g	I had 50 mol% p-chlorostyrene; miscible when blend had $\geq$10 wt% II	Aroguz and Karasz (2004)
Copolyester	Hydroxyether of bisphenol-A (Phenoxy)	Single T_g; microscopy	II/III = 1/1; I was made from 65/30/5 = terephthalate/isophthalate/sebacate and 70/20/10 = ethylene glycol/resorcinol di-(hydroxy ethyl) ether/poly(tetra-methylene ether)glycol; II was 4/1 by wt = Araldite 6099/Araldite 6010	Aharoni (1978)
Cyclohexyl methacrylate	p-Methylstyrene	Single T_g; OM; SEM	Immiscibility loop present at the center of the phase diagram; all blends exhibited LCST	Chang and Woo (2003c)
	Methyl methacrylate	SIMS	–	Harton et al. (2005)
	Styrene	Single T_g; POM	II was atactic; III was isotactic; miscible at all compositions; blends exhibited LCST	Chang et al. (2004a)

(continued)

Table 21.3 (continued)

Polymer I of	Polymer II of	Polymer III of and Polymer IV of	Method	Comments	Refs.
2,6-Dimethyl-1,4-phenylene ether	Methacrylic acid-co-styrene	Styrene-co-4-vinylpyridine	Single T_g; SEM	I:II:III = 25:25:50; II had 20 mol% methacrylic acid and III had 15 mol% vinylpyridine	Benabdelghani et al. (2008)
	Styrene	Styrene	Single T_g; POM	II was atactic; III was isotactic; miscible at all compositions	Chang et al. (2004a)
Epichlorohydrin	Ethylene glycol	3-Hydroxybutyrate	Single T_g	Miscible at all compositions	Goh and Ni (1999)
	Ethylene glycol	Methyl methacrylate	Single T_g	Miscible at all compositions	Min et al. (1987)
	Methyl methacrylate	Vinyl acetate	Single T_g	Miscible at all compositions; all blends showed LCST	Guo (1990b), Pinoit and Prud'homme (2002)
Etherimide	Amideimide	Etheretherketone, sulfonated	Single T_g	I was Ultem 1000; II was Torlon 4,000T; III had a degree of sulfonation of 0.53 or 1.00	Karcha and Porter (1992)
	Etheretherketone	Etherdiphenyletherketone	Single T_g; FTIR;	–	Woo and Tseng (2000)
	Etheretherketone	Liquid crystalline polymer	Single T_g	I was Ultem 1000; II was Victrex 450G; III was HXiang et al. (1997)000	Bretas and Baird (1992), Morales and Bretas (1996a, b)
	Ethylene naphthalate	Pentamethylene naphthalate	Single T_g; OM; WAXD	Miscible after annealing	Su and Shih (2006)
Ether urethane	Oxytetramethylene-co-oxyditetramethylene-co-terephthalic acid	Vinyl chloride	Single T_g	I was Adiprene L-100 and 4,4'-methylene-bis-2-chloroaniline; I/II/III = 1/1/2; two T_g's when I/II/III = 1/2/1 and 1/1/1	Hourston and Hughes (1981)
Ethyl methacrylate	Methyl methacrylate	Styrene-co-p-vinylphenol	Single T_g	III had 5 or 15 mol% vinylphenol	Hsu (2003)
	Methyl methacrylate	p-Vinylphenol	Single T_g; FTIR; microscopy	Blend had >60 wt% III	Pomposo et al. (1993a, 1994b)
	Vinyl acetate	p-Vinylphenol	Single T_g	–	Hsu (2006a)

Ethylene, chlorinated	Natural rubber, epoxidized	Vinyl chloride	Single T_g	II was 50 mol% epoxidized	Kaklas et al. (1991)
Ethylene, chlorosulfonated	Natural rubber, epoxidized	Nitrile rubber, carboxylated	Single T_g	I had 35 % Cl and 1 % S (Hypalon-40); II was 50 mol % epoxidized; III was Krynac-211	Roychoudhury et al. (1992)
Ethyl methacrylate	Methyl methacrylate	Vinylidene fluoride	Single T_g	>30 and <80 wt% III	Kwei et al. (1977)
Ethylene glycol	Ethyl acrylate-co-methacrylic acid	N-Vinylpyrrolidone	Single T_g; FTIR	–	Kireeva et al. (2007)
	Hydroxyether of bisphenol-A	Vinylethylether	Single T_g; FTIR	–	Rocco et al. (2010)
	Vinyl acetate	p-Vinyl phenol	Single T_g; FTIR	Existence of an immiscibility loop (Zhang et al. (1994))	Le Menestrel et al. (1992), Zhang et al. (1994)
	p-Vinylphenol	2-Vinylpyridine	Single T_g; SEM; NMR; FTIR	I:III = 22:77; blend had 20, 30, 50, or 80 wt% II	Lee et al. (2006a)
	Hydroxyether of bisphenol-A	Methyl methacrylate	Single T_g	Three miscible binary pairs; existence of an immiscibility loop	Hong et al. (1997)
Ethylene-2,6-naphthalene	Etheretherketone	Etherimide	Single T_g; SEM	–	Bicakci and Cakmak (1998)
Ethylene terephthalate	Trimethylene terephthalate	p-Vinylphenol	Single T_g; T_m-depression; FTIR	Completely miscible	Lee and Woo (2006)
Hexafluoroacetone-co-vinylidene fluoride	Methyl methacrylate	Vinyl acetate	Single T_g	I had 9 mol% hexafluoroacetone	Kobayashi et al. (1994)
Imide	Imide	Imide	Single T_g	I, II, and III were different	Chung et al. (1997)
Hydroxyether of bisphenol-A	Methyl methacrylate	p-Vinylphenol	Single T_g	II was atactic, isotactic, or syndiotactic	Hsu (2002b)
	Novolac	p-Vinylphenol	Single T_g; OM; FTIR	–	Kuo (2009)
Maleic acid-co-maleic anhydride-co-styrene	Urethane	Vinyl chloride	Single T_g	I had 6.25 wt% maleic acid and 25 wt% maleic anhydride	Al-Salah (1998a)
Methyl acrylate	Vinyl acetate	p-Vinyl phenol	Single T_g	Completely miscible at all compositions	Zhang et al. (1994)

(continued)

Table 21.3 (continued)

Polymer I of	Polymer II of	Polymer III of and Polymer IV of	Method	Comments	Refs.
Methyl acrylate-*co*-styrene	Vinyl acetate	*p*-Vinyl phenol	Single T_g	–	Zhang et al. (1994)
Methyl methacrylate	Methyl methacrylate-*co*-styrene	Styrene	Single T_g	–	Winey et al. (1966)
	Methyl methacrylate-alt-styrene	Styrene	Single T_g	–	Winey et al. (1966)
	Styrene-*co*-*p*-vinylphenol	N-Vinylpyrrolidone	Single T_g	II had 5 or 15 mol% vinylphenol	Hsu (2005)
	Vinyl acetate	Vinylidene fluoride	Single T_g	All ternary blends showed LCST (Guo (1996))	Classen et al. (1995), Guo (1996)
	Vinyl acetate	*p*-Vinylphenol	Single T_g; FTIR	I was isotactic or syndiotactic (Hsu (2006b))	Hsu (2004b, 2006b), Liu et al. (2006a)
	Vinyl cinnamate	*p*-Vinylphenol	Single T_g	Three miscible binary pairs; existence of an immiscibility loop	Hsu (2007)
	N-Vinylpyrrolidone	Vinylidene fluoride	Single T_g; FTIR; WAXD	–	Cheng et al. (2012)
α-Methylstyrene	*p*-Methylstyrene	Styrene	Single T_g; OM; NMR	Miscibility at high I (≥80 wt%) content	Chang et al. (2004c)
Natural rubber, epoxidized	Nitrile rubber, carboxylated	Chloroprene	Single T_g	I was 50 mol% epoxidized; II was Krynac-211; I/II/III =1/1/1	Alex et al. (1990)
Natural rubber, epoxidized	Nitrile rubber, carboxylated	Vinyl chloride	Single T_g	I was 50 mol% epoxidized; II was Krynac-211	Ramesh and De (1993)
Neopentyl glycol adipate	Vinyl chloride	Vinylidene fluoride	Single T_g	III <50 wt%	Lau et al. (1988)
Styrene-*co*-4-vinylpyridine	Vinyl acetate	*p*-Vinyl phenol	Single T_g	I had 70 wt% vinylpyridine	Zhang et al. (1994)

Table 21.4 Polymer pairs miscible in the amorphous state at room temperature. Molecular weight dependence investigated

Polymer I of	Polymer II of	Method	Comments	Refs.
Acrylonitrile-co-α-methylstyrene	Carbonate of bisphenol-A	Single T_g; transparency	I had 9–12 wt% AN; miscible when II had $M_w = 3.8$ kg/mol, immiscible when II had $M_w = 9.9$ kg/mol	Callaghan and Paul (1994a)
	Maleic anhydride-co-styrene	Single T_g	Region of miscibility was sensitive to M_w	Gan et al. (1994b)
Acrylonitrile-co-styrene	Carbonate of bisphenol-A	Single T_g; transparency	I had 24.6 wt% AN and II had $M_w = 3.8$ kg/mol; miscible when I had $M_w = 3.317$ kg/mol and immiscible when I had $M_w = 6.085$ kg/mol	Callaghan et al. (1993)
	Acrylonitrile-co-α-methylstyrene	Single T_g	Region of miscibility was sensitive to M_w	Gan et al. (1994b)
3-Bromo-2,6-dimethyl-1,4-phenylene ether	Styrene	Single T_g; transparency	I had $M_w \leq 40$ kg/mol; II had $M_w \leq 30$ kg/mol	Machado and French (1992b)
n-Butyl methacrylate	Styrene	Single T_g; transparency	I had $M_w = 320$ kg/mol; II had $M_w = 1.71$ kg/mol; two T_g's when II had $M_w = 1,100$ kg/mol	Defieuw et al. (1989b)
Carbonate of bisphenol-A	Ester	Single T_g	II was made from 4,4′ (2-norbornylidene)diphenol and terephthalic acid and azelaic acid; miscible when I had $M_w = 28.1$ kg.mol; immiscible when I had $M_w = 73.2$ kg/mol	Yang and Yetter (1994)
2,6-Dimethyl-1,4-phenylene ether	Alkylstyrene	Transparency	I had $M_w = 5$ to 500 kg/mol, and II was a ring-alkyl (with various carbon atoms) styrene. Raising M_w of II eventually produced a transition from clear to hazy or cloudy films in each system except that containing poly-α-methylstyrene. With this resin, clear single-T_g films were obtained even with M_w of I = 500 kg/mol and M_w of II = 800 kg/mol	Kambour et al. (1988)
	p-Bromostyrene	Transparency	II had $M_n = 29.1$ kg/mol and $M_w = 32$ kg/mol; M_w limit for miscibility in 50/50 blend of I with II was 6.2 ± 2.4 kg/mol. When II had $M_n = 6.4$ kg/mol and $M_w = 7.04$ kg/mol, M_w limit for miscibility of I was 14.0 ± 4.0 kg/mol	Kambour et al. (1988)

(continued)

Table 21.4 (continued)

Polymer I of	Polymer II of	Method	Comments	Refs.
	p-Tert-butylstyrene	Transparency	II had $M_n = 113$ kg/mol and $M_w = 289$ kg/mol; M_w limit for miscibility in 50/50 blend of I with II was 4.50 ± 0.7 kg/mol	Kambour et al. (1988)
	4-Ethylstyrene	Transparency	II had $M_n = 139$ kg/mol and $M_w = 158$ kg/mol; M_w limit for miscibility in 50/50 blend of I with II was 22.4 kg/mol	Kambour et al. (1988)
	4-Methoxystyrene	Transparency	II had $M_n = 282$ kg/mol and $M_w = 457$ kg/mol; M_w limit for miscibility in 50/50 blend of I with II was 3.6 kg/mol	Kambour et al. (1988)
	4-Methylstyrene	Transparency	II had $M_n = 118$ kg/mol and $M_w = 265$ kg/mol; M_w limit for miscibility in 50/50 blend of I with II was 35.5 kg/mol	Kambour et al. (1988)
	4-n-Propylstyrene	Transparency	II had M_n 128 kg/mol and $M_w = 267$ kg/mol; M_w limit for miscibility in 50/50 blend of I with II was 14.0 ± 4.0 kg/mol	Kambour et al. (1988)
	Vinylbenzylchloride	Transparency	II had $M_n = 16.8$ kg/mol and $M_w = 29.3$ kg/mol; M_w limit for miscibility in 50/50 blend of I with II was 14.0 ± 4.0 kg/mol	Kambour et al. (1988)
	4-Vinylbiphenyl	Transparency	II had $M_n = 79$ kg/mol and $M_w = 153$ kg/mol; M_w limit for miscibility in 50/50 blend of I with II was 7.0 ± 1.6 kg/mol	Kambour et al. (1988)
	Vinylnaphthalene	Transparency	II had $M_n = 13$ kg/mol and $M_w = 32.6$ kg/mol; M_w limit for miscibility in 50/50 blend of I with II was 10.2 kg/mol	Kambour et al. (1988)
	Vinyltoluene	Transparency	II had $M_n = 20.7$ and $M_w = 40.4$ kg/mol; M_w limit for miscibility in 50/50 blend of I with II was 69 ± 25 kg/mol	Kambour et al. (1988)
Ethylene	Dimethylsiloxane	Cloud point curve	I was oligomeric polyethylene with $M_w = 0.254$–2.234 kg/mol, and II was oligomeric polydimethylsiloxane with $M_w = 0.505$–4.5 kg/mol	Molner and Eisenberg (1992)

Table 21.4 (continued)

Polymer I of	Polymer II of	Method	Comments	Refs.
Ethylene glycol	Propylene glycol	Miscibility stated	I and II both had $M_w <1,000$	Booth and Pickles (1973)
	Vinyl acetate	Single T_g	I had $M_w = 20$ kg/mol miscible with II; I had $M_w = 100$ kg/mol miscible with II when blend had ≤ 50 % II	Han et al. (1992)
	Sulfone	Scattering turbidimetry	Blends with II >40 wt% were homogeneous when I had $M_w = 3.5–4.5$ kg/mol and II had $M_w = 35.6$ kg/mol. Blends were heterogeneous at all compositions when I had $M_w = 200$ kg/mol	Swinyard et al. (1987)
Hydroxybutyrate	Lactide	Microscopy	Miscible when II had $M_n = 1.759$ kg/mol; immiscible when II had $M_n = 159.4$ kg/mol	Blumm and Owen (1995)
Cis-isoprene	Styrene	Single dynamic mechanical loss peak	I was natural rubber; II had $M_w \leq 0.375$ kg/mol; two peaks when II had $M_w \geq 0.600$ kg/mol	Class and Chu (1985b)
	Vinyl cyclohexane	Single dynamic mechanical loss peak	I was natural rubber; II had $M_w \leq 0.375$ kg/mol; two peaks when II had $M_w \geq 0.65$ kg/mol	Class and Chu (1985b)
Methyl methacrylate	Carbonate of bisphenol-A	Single T_g; transparency	Miscible when M_w of I/II were 2.4/38, 10.55/38, 60/9.9, and 105/99 kg/mol; immiscible when M_w of I/II were 20.3/38, 33.5/25.9, 33.5/38, and 60/38 kg/mol	Callaghan and Paul (1994a)
	Carbonate of hexafluor obisphenol-A-co-carbonate of tetramethy lbisphenol-A	Single T_g; transparency	II had 60 wt% HFPC and $M_w = 33$ kg/mol, and miscible when I had $M_w = 4–99$ kg/mol; when II had $M_w = 103$ kg/mol, it was miscible with I having $M_w = 4$ and 11 kg/mol only	Takakuwa et al. (1994)
	Styrene	Transparency	I was "high" M_w; ≤ 15 or 20 wt% II when II had $M_n = 2.1$ kg/mol; ≤ 5 or 10 wt% II when II had $M_n = 3.1$ kg/mol	Parent and Thompson (1978), Thompson (1980)
Methyl methacrylate-co-styrene	Styrene	Single T_g; transparency	I had 26 % styrene and II had 0.6 kg/mol or I had 62.6 % styrene and II had $M_w \leq 2.1$ kg/mol or I had 80 % styrene and II had $M_w \leq 4.0$ kg/mol	Massa (1979), Thompson (1980)

(continued)

Table 21.4 (continued)

Polymer I of	Polymer II of	Method	Comments	Refs.
α-Methylstyrene	Styrene	Single T_g; transparency; neutron scattering	I had M_n = 4–80 kg/mol; II had M_n = 55–300 kg/mol	Baer (1964), Ballard et al. (1976), Black and Worsfold (1974), Cowie et al. (1992e), Dunn and Krause (1974), Robeson et al. (1974), Saeki et al. (1983), Schelten et al. (1976), Van Tam Bui et al. (1988), Widmaier and Mignard (1987)
	Styrene, deuterated	Single T_g	I had M_n = 25.8–78.3 kg/mol; II had M_n = 36.1–84.1 kg/mol	Rameau et al. (1989)
α-Methylstyrene-co-styrene	Styrene	Single T_g	I had M_n = 59–818 kg/mol; II had 3–79 mol% α-methylstyrene	Cowie et al. (1992e)
Styrene	Carbonate of bisphenol-A	Single T_g; transparency	I had M_w = 0.58, 0.68, 0.95, or 2.95 kg/mol; II had M_w = 3.8, 9, 25.9, or 38 kg/mol; miscibility depended on M_w and blend composition	Callaghan and Paul (1994a)
	Carbonate of tetramethylbisphenol-A	Single T_g; transparency	II had M_w = 30 kg/mol; miscible when I had M_w = 0.58, 0.68, or 9.5 kg/mol; immiscible when I had M_w = 2.95 kg/mol	Callaghan and Paul (1994a)
	Carbonate of tetramethylbisphenol-P	Single T_g; transparency	II had M_w = 31 kg/mol; miscible when I had M_w = 2.95 kg/mol; partially miscible when I had M_w = 9.2 or 17.5 kg/mol; immiscible when I had M_w = 341 kg/mol	Callaghan and Paul (1994a)
	o-Chlorostyrene-co-p-chlorostyrene	Single T_g	I had M_n = 2.2–93 kg/mol; II had 7–100 mol% o-chlorostyrene	Cimmino et al. (1992)
	Vinylmethylether	Single T_g	I had mol. wt. 0.8–233 kg/mol; II had MW 1.0–97.5 kg/mol	Yang et al. (1991), Schneider and Leikauf (1987)
	2-Vinyl naphthalene	Single T_g	I had M_w = 2.2 kg/mol; II had M_w ≤70 kg/mol	Semerek and Frank (1984)
p-Vinylphenol	Diethyl itaconate	Single T_g	II had M_w = 9.4 kg/mol and was miscible with I having M_w = 1.5–7, 9–11, 22, or 30 kg/mol; II had M_w = 61 kg/mol and was miscible with I having M_w = 1.5–7 and 9–11 kg/mol	Hong et al. (1995b)

Table 21.5 Polymer pairs that appear to have high temperature miscibility although immiscible at or below room temperature (UCST behavior)

Polymer I of	Polymer II of	Comments	Refs.
Acrylonitrile-co-styrene	N-Phenylmaleimide-co-styrene	I had 22–28 wt% AN and II had 56.2 wt% N-phenylmaleimide; I had 20–24 wt% AN and II had 49 wt% N-phenylmaleimide	Park et al. (2008)
	Styrene	I had 4–20 vol% acrylonitrile	Yang et al. (2004)
	Sulfone of tetramethylbisphenol-A	I had 9 wt% AN and II had M_w = 4.8 kg/mol; I had 11 wt% AN and II had M_w = 12.4 kg/mol	Callaghan and Paul (1994b), Pfefferkorn et al. (2012)
Aramide	Imide	I was Aramide 34I and II was polyimide UR	Nakata et al. (1993)
2-Bromoethyl methacrylate	2,2-Dimethyl-1,3-propylene sebacate	–	Neo and Goh (1993)
Butadiene	Butadiene	I had 98 % cis-1,4; II had 71 % vinyl-1,2 and 19 % trans-1,4	Shah et al. (1988)
	Butadiene, perdeuterated	Both I and II were cis-1,4	Bates et al. (1986)
	Butadiene-co-styrene	I was cis-1,4; II had 23–30 wt% styrene	Inoue et al. (1985), Maier et al. (1994), Pestov et al. (1978), Shah et al. (1989), Tager et al. (1987)
	Styrene	II was hydrogenated or partly deuterated; I and II had M_w = 2.0 kg/mol (Lin et al. 1985); I had M_w = 0.96 kg/mol and II had M_w = 9.0 kg/mol (Tomlins and Higgins 1989)	Lin et al. (1985), Lipson et al. (2003), Tomlins and Higgins (1989)
	Terpene, hydrogenated	I had 10–70.4 % 1,2-content	Kawahara and Akiyama (1993)
Butadiene-co-styrene	Styrene	II was hydrogenated or partly deuterated; II was 68.4 wt% styrene and had M_w of 10 kg/mol and II had M_w of 100 kg/mol	Lin et al. (1985)
n-Butyl methacrylate	n-Butyl methacrylate-co-methyl methacrylate	II had 29, 56, or 71 mol% methyl methacrylate	Sato et al. (1996a)
	Isobutyl methacrylate-co-methyl methacrylate	II had 23, 42, 58, or 75 mol% methyl methacrylate	Sato et al. (1996a)
Isobutyl methacrylate	n-Butyl methacrylate-co-methyl methacrylate	II had 29, 56, or 71 mol% methyl methacrylate	Sato et al. (1996a)
	Isobutyl methacrylate-co-methyl methacrylate	II had 23, 42, 58, or 75 mol% methyl methacrylate	Sato et al. (1996a)

Table 21.5 (continued)

Polymer I of	Polymer II of	Comments	Refs.
n-Butyl methacrylate-*co*-isobutyl methacrylate	Isobutyl methacrylate-*co*-methyl methacrylate	I had 13–87 mol% isobutyl methacrylate; II had 75 mol% methyl methacrylate	Sato et al. (1996b)
Caprolactone	Ester	II was made from adipoyl chloride and 4,4′-bis (6-hydrohexyloxy) biphenyl	Van Ende et al. (1992)
Carbonate of bisphenol-A	Biphenyl-4,4′ylene sebacate	II was liquid crystalline and blend had 50–80 wt % II	Jo et al. (1992a)
	1,4-Dimethylcyclohexane-*co*-ethylene terephthalate	II had 32–80 mol% dimethylcyclohexane	Kim et al. (2006)
	Etherester	II had a hard tetramethylene terephthalate segment and a soft polytetramethylene ether-glycol terephthalate segment	Gaztelumendi and Nazabal (1995)
	Methacrylic acid-*co*-styrene	II had 4–23 wt% methacrylic acid	Akiyama et al. (1991, 2001)
	Styrene	I had M_w = 6 kg/mol; II had M_w = 2.7 kg/mol; blend had 10–30 wt% I	Li et al. (1999b)
	Styrene, sulfonated	II had 6.5 mol% sulfonation and Li-neutralized	Lu and Weiss (1996b)
2-Chloroethyl methacrylate	2,2-Dimethyl-1,3-propylene sebacate	–	Neo and Goh (1992b)
3-Chloropropyl methacrylate	2,2-Dimetyl-1,3-propylene sebacate	–	Low et al. (1994c)
Chlorostyrene-*co*-styrene	2,6-Dimethyl-1,4-phenylene ether	I had 32.9 mol% styrene	Fried et al. (1978), Wetton et al. (1978)
Cyclohexyl methacrylate	Cyclohexyl acrylate	–	Siol (1991)
2,6-Dimethyl-1,4-phenylene ether	*p*-Methylstyrene	–	Woo et al. (2002)
	p-Methylstyrene + styrene	The ternary blend system exhibited UCST	Chou et al. (2002)
Dimethylsiloxane	Hexylmethylsiloxane	–	Stammer and Wolff (1998)
	Methylethylsiloxane	–	Horiuchi et al. (1991)
	Phenylmethylsiloxane	–	Kuo and Clarson (1990)
Epoxy	Acrylonitrile-*co*-butadiene, carboxyl terminated	I was Epon 828, M_n = 380; II had 17 wt% acrylonitrile, M_n = 3,500	Lee and Quin (1989)
	2,6-Dimethyl-1,4-phenylene ether	Optical and electron microscopy	Pearson and Yee (1993)

(*continued*)

Table 21.5 (continued)

Polymer I of	Polymer II of	Comments	Refs.
Etherethersulfone	Etheretherketone-*co*-etherethersulfone	II had 50 % etherethersulfone	Sham et al. (1988a)
Etherimide	Butylene terephthalate	–	Chen et al. (1997)
	Ethylene naphthalate-*co*-ethylene terephthalate	The higher the ethylene naphthalate content in II, the lower the UCST	Kinami et al. (1995)
Etherketone	Imide, thermoplastic	–	Sauer et al. (1996)
Ethyl methacrylate	*n*-Butyl acrylate-*co*-styrene	II had 63 wt% styrene	Rana et al. (2000)
	Ethyl acrylate	–	Siol and Terbrack (1991)
Ethylene	Butane-*co*-ethylene	I was LLDPE; II had 26 mol% butene	Li et al. (2004)
	Ethylene	I was HDPE; II was LLDPE containing 5.3 mol% octene	Stephens et al. (2003)
	Ethylene-*co*-propylene	II was alternate copolymer (Choi et al. (2006))	Choi et al. (2006), Lipson et al. (2003)
	Propylene	II was atactic; no UCST when II was isotactic; from high temperature phase diagrams (Kosai and Higashino (1975)); II was head-to-head (Lipson et al. (2003)); I was LLDPE (Lo et al. (2004))	Kosai and Higashino (1975), Lipson et al. (2003), Lo et al. (2004)
Ethylene, chlorinated	Ethylene, chlorinated	Cl contents = 40–50 wt%	Ueda and Karasz (1985)
Ethylene glycol	Caprolactone	–	Chuang et al. (2005)
	2-Ethylhexyl methacrylate-*co*-methyl methacrylate	II had 7.7–31.0 mol% 2-ethylhexyl methacrylate	Takeshita et al. (2005)
	n-Hexyl methacrylate-*co*-methyl methacrylate	II had 7.8–21.1 mol% *n*-hexyl methacrylate	Takeshita et al. (2005)
Hemicellulose	Lignin	Blend had 10, 80, or 90 vol% of II	Shiyematsu et al. (1994)
3-Hydroxybutyrate	Ethylene adipate	–	Hsieh and Woo (2011)
	Ethylene succinate	–	Hsieh and Woo (2011)
2-Iodoethyl methacrylate	2,2-Dimethyl-1,3-propylene sebacate	–	Low et al. (1994c)
Isophthalamide-6I (iminoisophthaloyl-iminohexamethylene)	Hexamethylene adipamide	Interchange reaction slow	Zimmerman et al. (1973)
Isoprene	Vinylethylene	II was syndiotactic and had 92 % vinyl-1,2-	Iriarte et al. (1991)
Lactide	Ethylene succinate	–	Hsieh et al. (2012)
	Trimethylene adipate	–	Hsieh et al. (2012)
Maleic anhydride-*co*-styrene	Sulfone of tetramethylbisphenol-A	I had 14 wt% maleic anhydride; II had $M_w = 4.8$ kg/mol	Callaghan and Paul (1994b)
	Alkyl methacrylate	I had an alkyl group of *n*-butyl or isobutyl	Sato et al. (1996a)

(*continued*)

Table 21.5 (continued)

Polymer I of	Polymer II of	Comments	Refs.
Methyl methacrylate	Carbonate of bisphenol-A	I had M_w = 1.21 or 2.4 kg/mol; II had M_w = 33 kg/mol	Callaghan and Paul (1994a)
	Carbonate of tetrachlorobisphenol-A	I had M_w = 1.21 kg/mol; II had M_w = 41 kg/mol	Callaghan and Paul (1994a)
	Carbonate of tetramethylbisphenol-P	I had M_w = 1.21 or 2.4 kg/mol; II had M_w = 31 kg/mol	Callaghan and Paul (1994a)
	Ester	II was ethylene adipate, 1,3-trimethylene adipate, 1,4-butylene adipate, ethylene azelate, caprolactone, or hexamethylene adipate	Li and Woo (2008a)
	Hydroxybutyrate	–	Siciliano et al. (1995)
	Lactide	I was atactic or syndiotactic	Li and Woo (2008c)
	Styrene	II had M_n = 600; M_w of I was 1,950, 2,950, or 9,200 and M_w of II was 2,030, 2,400, 4,250, 10,550, or 60,000 (Callaghan and Paul (1993))	Callaghan and Paul (1993), Ougizawa and Walsh (1993), Massa (1988)
	Sulfone of tetramethylbisphenol-A	I had M_w = 1.21 or 2.4 kg/mol; II had M_w = 4.8 or 12.4 kg/mol	Callaghan and Paul (1994b)
	Sulfone of tetramethylhexafluorobisphenol-A	I had M_w = 1.21 kg/mol; I had M_w = 40 kg/mol	Callaghan and Paul (1994b)
	Sulfone of tetramethylbisphenol-P	I had M_w = 1.21 kg/mol; II had M_w = 40 kg/mol	Callaghan and Paul (1994b)
	Vinyl butyral	–	Chen et al. (2001)
	Vinyl chloride	–	Razinskaya et al. (1985)
Methyl methacrylate-co-styrene	Ethylene glycol	–	Sato et al. (1998)
	Styrene	–	Sato et al. (1998)
1,3-Phenylene adipamide	Hexamethylene adipamide	I was made from m-phenylenediamine and adipic acid; interchange reaction slow	Zimmerman et al. (1973)
Propylene	Propylene	I and II had different tacticities	Woo et al. (2007)
Sebacic acid	1,6-Bis(p-carboxyphenoxy) hexane	–	Kipper et al. (2004)
Styrene	3-Alkylthiophene	II had an alkyl group of butyl, hexyl, octyl, or dodecyl	Lee et al. (2009)
	Caprolactone	I had M_n = 950	Nojima et al. (1986b)
	Carbonate of bisphenol-A	I was sulfonated and Zn-neutralized; I had 8.7–13.7 mol% sulfonation	Xie and Weiss (1998)

<div align="right">(continued)</div>

Table 21.5 (continued)

Polymer I of	Polymer II of	Comments	Refs.
	Carbonate of bisphenol chloral	I had M_w = 0.58 or 0.68 kg/mol; II had M_w = 30 kg/mol	Callaghan and Paul (1994a)
	Isoprene	I had low M.W.; UCST was depressed in the presence of supercritical carbon dioxide	Walker et al. (1999)
	α-Methylstyrene	UCST increased with molecular weight	Lim and Roe (1988)
	o-Methylstyrene	–	Antonietti et al. (1986)
	p-Methylstyrene	–	Antonietti et al. (1986), Chang and Woo (2001a, 2003a), Stroeks et al. (1991)
	m-Methylstyrene	–	Antonietti et al. (1986)
	Styrene, brominated	II had 27 or 29 mol% brominated units	Stoelting et al. (1970)
	Styrene, deuterated	–	Bates and Wignall (1968), Yang et al. (1986b)
	Styrene, sulfonated	II had 0.7 mol% sulfonated and neutralized with Na, Ba, or Zn	Zhou et al. (2007)
	Sulfone of tetramethylbisphenol-A	I had M_w = 1.21 or 2.4 kg/mol; II had M_w = 4.8 or 12.4 kg/mol	Callaghan and Paul (1994b)
	Sulfone of tetramethylbisphenol-P	I had M_w = 1.21 kg/mol; II had M_w = 40 kg/mol	Callaghan and Paul (1994b)
	Sulfone of tetramethylhexafluorobisphenol-A	I had M_w = 1.21 kg/mol; II had M_w = 40 kg/mol	Callaghan and Paul (1994b)
	Vinylmethylether	By SANS and by extrapolation of solution data	Cowie et al. (1990c), Kim et al. (2002b)
Urethane	Styrene-co-p-vinylphenol	I was liquid crystalline; II had 5–50 mol% vinylphenol	Viswanathan and Dadmun (2003)
Vinyl chloride	Acrylonitrile-co-methyl methacrylate-co-α-methylstyrene	II had 32.3 wt% AN, 8.1 wt% MMA; blend had 50–80 wt% II	Kovacic et al. (1994)
Vinylidene fluoride	Methyl methacrylate	–	Tomura et al. (1992)
Vinylidene fluoride-co-tetrafluoroethylene	Vinylidene fluoride-co-hexafluoroacetone	I had 80 mol% vinylidene fluoride; II had 92 mol% vinylidene fluoride	Cho et al. (1993)
Vinylmethylether	Alkyl methacrylate	II had an alkyl group of n-propyl or isopropyl	Woo and Juang (2007)

Table 21.6 Polymer pairs miscible at room temperature that appear to have a lower critical solution temperature (LCST) above room temperature

Polymer I of	Polymer II of	Comments	Refs.
Acrylic acid, Li-neutralized	Ethylene glycol	0.1–0.4 mol fraction of I was neutralized	Lu and Weiss (1995)
Acrylic acid-*co*-styrene	Ethyl methacrylate	I had 8.84 wt% acrylic acid	Brannock et al. (1990)
	Methyl methacrylate	I had 2.65–20.0 wt% acrylic acid	Wang et al. (1990), Jo et al. (1991b)
	n-Propyl methacrylate	I had 2.65–8.84 wt% acrylic acid	Wang et al. (1990)
Acrylonitrile-butadiene-methyl acrylate	Ethylene-alt-maleic anhydride	I was Barex 210	Percec and Melamud (1993)
Acrylonitrile-*co*-α-methylstyrene	Acetonyl methacrylate	I had 30 wt% acrylonitrile (AN)	Goh and Lee (1990d)
	Acrylonitrile-*co*-styrene	II had 28–40 wt% AN	Aoki (2000), Lath et al. (2000)
	n-Butyl methacrylate	I had 12 wt% AN	Cowie and Elexpuru (1992)
	n-Butyl methacrylate-*co*-methyl methacrylate	I had 30 wt% AN; II had 70 wt% methyl methacrylate	Goh et al. (1984a)
	Carbonate of tetramethylbisphenol-A	I had 4–16.5 wt% AN	Gan et al. (1994a)
	Ethyl methacrylate	I had 30 wt% AN (Goh et al. 1982b); II had 10–28 wt% AN (Cowie and Elexpuru (1992))	Cowie and Elexpuru (1992), Goh et al. (1982b)
	Ethyl methacrylate-*co*-methyl methacrylate	I had 30 wt% AN; II had 60 wt% methyl methacrylate	Goh et al. (1984a)
	Methoxymethyl methacrylate	I had 30 wt% AN	Goh and Lee (1990d)
	Methyl methacrylate	I had 30 wt% AN and II was atactic or isotactic (Goh et al. 1982b); I had 31.3, 33.1, 34.8, or 41.3 wt% AN (Suess et al. 1986); I had 10–37 wt% AN (Cowie et al. 1991a)	Cowie and Elexpuru (1992), Goh et al. (1982b), Gan et al. (1994a), Suess et al. (1986)
	Methyl methacrylate-*co*-2,2,6,6-tetramethylpiperidinyl methacrylate	I had 30 wt% AN; II had ≥76.2 wt% methyl methacrylate	Goh et al. (1986b, 1987)
	Methylthiomethyl methacrylate	I had 30 wt% AN	Goh et al. (1991b)
	n-Propyl methacrylate	I had 17–20 wt% AN	Cowie and Elexpuru (1992)
	Tetrahydrofurfuryl methacrylate	I had 30 wt% AN	Goh and Siow (1987)
	Vinyl chloride	I had 11.9–30 wt% AN	Gan et al. (1994a)

Acrylonitrile-*co*-*p*-methylstyrene	Acetonyl methacrylate	I had 43.0–61.0 wt% AN	Chong and Goh (1992c)
	Alkyl methacrylate	II had an alkyl group of 1-chloroethyl and I had 10–40 wt% AN; II had an alkyl group of 2,2-dichloroethyl and I had 8–44 wt% AN	Goh et al. (1996c)
	n-Butyl methacrylate	I had 13.6 wt% AN	Goh et al. (1991a)
	Cyclohexyl methacrylate	I had 15.8–21.3 wt% AN	Chong and Goh (1992d)
	Ethyl methacrylate	I had 26.5–32.3 wt% AN	Goh et al. (1991a)
	n-Propyl methacrylate	I had 21.3–26.5 wt% AN	Goh et al. (1991a)
	Tetrahydrofurfuryl methacrylate	I had 32.3–46.5 wt% AN	Goh et al. (1991a)
	Tetrahydropyranyl-2-methyl methacrylate	I had 23.8–26.5 wt% AN	Chong and Goh (1992b)
Acrylonitrile-*co*-styrene	Copolycarbonate of bisphenol-A and tetramethylbisphenol-A	Some blends showed LCST, depending on compositions of I and II	Kim and Paul (1992e)
	Acetonyl methacrylate	I had 33–58 wt% AN	Chong and Goh (1992c)
	Acrylonitrile-*co*-methyl methacrylate	Some blends showed LCST	Nishimoto et al. (1989)
	Alkyl methacrylate	II had an alkyl group of 1-chloroethyl and I had 9–30 wt% AN; II had an alkyl group of 2,2-dichloroethyl and I had 9–41 wt% AN	Goh et al. (1996c)
	Benzyl methacrylate	I had 3.5–24.4 wt% AN	Woo et al. (2000b)
	Butyl methacrylate-*co*-methyl methacrylate	Some blends showed LCST	Kammer and Piglowski (1989)
	Caprolactone	I had 28 % AN	McMaster (1973), Madbouly et al. (2006), Oudhuis et al. (1994)
	Carbonate of dimethylbisphenol-A-*co*-carbonate of tetramethylbisphenol-A	I had 2, 10, or 15 wt% AN; II had 60, 74, or 83 wt% tetramethylbisphenol-A	Kim et al. (2003a)
	Cyclohexyl methacrylate	I had 13.4–19.8 wt% AN	Chong and Goh (1992d)

(continued)

Table 21.6 (continued)

Polymer I of	Polymer II of	Comments	Refs.
	2,6-Dimethyl-1,4-phenylene ether, benzoylated	I and 18 mol% AN; II had 35 % benzoylated unit	Song et al. (1991)
	Ethyl methacrylate	I had 5.5–28 wt% AN	Fowler et al. (1987), Lath et al. (1992)
	2-Hydroxyethyl methacrylate	I had 28.4 or 30 wt% AN; II had 1.4 or 2 wt% hydroxyethyl methacrylate	Chu and Paul (2000)
	Maleic anhydride-*co*-styrene	Some blends showed LCST	Fang et al. (2007), Kim et al. (1989b), Kressler et al. (1988), Maruta et al. (1988)
	Methoxymethyl methacrylate	I had 30 wt% AN	Goh and Lee (1988b)
	Methyl methacrylate	I had 9.4, 9.8, 27.0, 28.2, 30.5, or 34.4 wt% AN (Lemieux et al. 1988); I had 29.4–39.3 wt% AN (Cowie et al. 1988)	Bernstein et al. (1977), Cowie et al. (1988), Kressler et al. (1986), Lemieux et al. (1988), McMaster (1975)
	Methyl methacrylate-*co*-2,2,6,6-tetramethylpiperidinyl methacrylate	I had 22 or 30 wt% AN; II had 69, 74, or 85.5 wt% methyl methacrylate	Goh et al. (1986b, 1987)
	Methyl methacrylate-*co*-N-phenylmaleimide	I had 24.6 wt% AN; II had 23.5 wt% N-phenylmaleimide	DeMeuse and Jaffe (1989)
	Methyl methacrylate-*co*-2,4,5-tribromostyrene	I had 33 wt% AN; II had 8 or 14 wt% tribromostyrene	Chu et al. (2000)
	Methylthiomethyl methacrylate	I had 34.5 wt% AN	Goh et al. (1992b)
	Phenyl acrylate	I had 14.6, 29.9, or 34.1 wt% AN	Sankarapandian and Kishore (1991), Rana et al. (1993)
	n-Propyl methacrylate	I had 5.7–19.5 wt% AN	Fowler et al. (1987), Lath and Lathova (1994)
	Tetrahydrofurfuryl methacrylate	I had 34.5–46.6 wt% AN	Goh et al. (1992a)
	Tetrahydropyranyl-2-methyl methacrylate	I had 2.2 or 22–30.5 wt% AN	Chong and Goh (1992b)
	Vinyl chloride	I had 11.5–26 wt% AN	Kim et al. (1989)

Aramide	Caprolactam-*co*-laurolactam	I was Trogamid T; II had 43.8 mol% caprolactam	Ellis (1990b)
Arylsulfone	Imide	I was Radel A; II was XU 218	Jeremic et al. (1992)
2-Bromoethyl methacrylate	Vinyl acetate	Blends cast from methyl ethyl ketone	Neo and Goh (1992a)
Butadiene	Butadiene	I had 50 % vinyl-1,2, 35 % *cis*-1,4, and 15 % *trans*-1,4; II had 55 % *cis*-1,4, 35 % *trans*-1,4, and 10 % vinyl-1,2	Shah et al. (1988)
	Isoprene	I had £ 59 % 1,4 content and II was *cis*-1,4 isomer (Trask and Roland 1988); I was deuterated and II was protonated (Hasegawa et al. 1991); I had 32.3 mol% 1,2 (Kawahara et al. 2002)	Hasegawa et al. (1991), Kawahara et al. (2002), Trask and Roland (1988)
Butyl acrylate	Alkyl methacrylate	II had an alkyl group of 1-chloroethyl or dichloroethyl	Peng et al. (1996)
	Ethylene, chlorinated	–	Chai and Walsh (1983)
	Hexafluoroacetone-*co*-vinylidene fluoride	–	Kano et al. (1997b)
	Vinyl chloride	–	Piglowski and Kammer (1990), Walsh and Cheng (1982), Walsh and McKeown (1980), Walsh and Sham (1989)
Butyl methacrylate	*p*-(2-Hydroxy hexafluoroisopropyl) styrene-*co*-styrene	II had 90.3–90.8 mol% styrene	Pearce et al. (1984)
N-Butyl-3-hydroxymethyl-carbazoyl methacrylate	o-Hydroxybutyl-3,5-dinitrobenzoyl methacrylate	–	Guerra et al. (1986)
Butylene adipate	Trifluoroethylene-*co*-vinylidene fluoride	–	Kim and Kyu (1999, 2003)
	Vinylidene fluoride	–	Penning and Manley (1996)
p-Tert-butylstyrene	1,2-Butadiene	–	Yurekli and Krishnamoorti (2004)
	Cyclohexyl acrylate	–	Siol (1991)
	Cyclohexyl methacrylate	–	Siol (1991)
	Isoprene	–	Yurekli and Krishnamoorti (2004)

(*continued*)

Table 21.6 (continued)

Polymer I of	Polymer II of	Comments	Refs.
Caprolactone	Benzyl methacrylate	–	Mandal and Woo (1998, 1999c)
	Ethylene, chlorinated	II had 30 or 42.1 wt% Cl	Belke and Cabasso (1988), Defieuw et al. (1989c)
	Lactide	–	Meredith and Amis (2000)
	Vinylidene fluoride	Blends rich in I showed LCST	Jo et al. (1992b)
Carbon monoxide-*co*-ethyl acrylate-*co*-ethylene	Vinyl chloride	I had 13.8/7.41/78.8 = carbon monoxide/ethyl acrylate/ethylene	Robeson and McGrath (1977)
Carbonate of bisphenol-A	Benzoyl methacrylate	–	Ha et al. (2001)
	Caprolactone	Thermal diffusivity measurements (Tsutsumi and Kano 1999)	Bernstein et al. (1977), Cruz et al. (1979a), Paul et al. (1977), Tsutsumi and Kano (1999)
	Cyclohexyl methacrylate-*co*-methyl methacrylate	II had £ 3.3 wt% cyclohexyl methacrylate (Min et al. 1990); II had 14.7–34.3 wt% cyclohexyl methacrylate (Brisson and Breault 1991)	Brisson and Breault (1991), Min et al. (1990)
	Cyclohexyl methacrylate-*co*-methyl methacrylate-*co*-2,4,6-tribromophenyl methacrylate	II had 70 wt% methyl methacrylate, and 10 wt% cyclohexyl methacrylate	Ohnaga et al. (1997)
	Methyl methacrylate	Blends prepared by precipitation of tetrahydrofuran solutions by *n*-heptane or by solution casting from tetrahydrofuran at high temperature	Chiow et al. (1987), Landry and Hendrichs (1989), Kyu and Saldanha (1988)
	Methyl methacrylate-*co*-*p*-methylstyrene	II had $\geq$70 wt% methyl methacrylate	Ikawa and Hosoda (1991)
	Methyl methacrylate-*co*-*N*-phenylmaleimide	II had $\geq$70 wt% methyl methacrylate	Ikawa and Hosoda (1991)
	Methyl methacrylate-*co*-phenyl methacrylate	II had 16–63 wt% phenyl methacrylate	Brisson and Breault (1991), Ohnaga et al. (1997)

	Methyl methacrylate-co-styrene	II had £ 14 wt% styrene	Min and Paul (1989)
	Methyl methacrylate-co-2,4,6-tribromophenyl methacrylate	II had 52.3–90 wt% methyl methacrylate	Ohnaga et al. (1997)
Carbonate of dimethylbisphenol-A	Styrene	Blend had <60 wt% I	Park et al. (2001b)
Carbonate of hexafluorobisphenol-A	Alkyl methacrylate	II had an alkyl group of ethyl, n-propyl, or isopropyl	Kim and Paul (1992a, d)
Carbonate of 2,2-propane-bis(4-(2-methylphenyl))-co-carbonate of 2,2-propane-bis(4-(2,6-dimethylphenyl))	Methyl methacrylate-co-styrene	I had $\geq$60 wt% carbonate of 2,2-propane-bis(4-(2,6-dimethylphenyl)); II had $\leq$37 wt% methyl methacrylate	Yoo and Kim (2004a)
Carbonate of tetramethylbisphenol-A	Acrylonitrile-co-styrene	II had 2 or 11.5 % acrylonitrile	Fernandes et al. (1986d)
	Methyl methacrylate-co-styrene	II had 4.5, 32.5, 33.5, or 35 wt% methyl methacrylate (Min and Paul 1987); II had 4.5–33.5 wt% methyl methacrylate (Kim and Paul 1992c)	Kim and Paul (1992c), Min and Paul (1987), Yu et al. (1991)
	Pentabromobenzyl acrylate-co-styrene methacrylate	II had 19.8 or 33.9 wt% pentabromobenzyl methacrylate	Merfeld and Paul (2000)
	Styrene	I had M_w = 341 kg/mol; II had M_w = 33 kg/mol (Callaghan and Paul 1994a)	Callaghan and Paul (1994a), Iller et al. (1984), Kim and Paul (1992b), Shaw (1974)
Carbonate of tetramethylbisphenol-P	Styrene	I had M_w = 9.2 kg/mol; II had M_w = 31 kg/mol	Callaghan and Paul (1994a)
Cellulose acetate	4-Vinyl pyridine	I was 10H/2 glucose	Cabasso (1981)
Cellulose acetate butyrate	Ethylene glycol	–	Park and Kim (2002)
1-Chloroethyl methacrylate	Alkyl methacrylate	The alkyl group of II was ethyl, n-propyl, isopropyl, or n-butyl	Peng et al. (1993)
2-Chloroethyl methacrylate	Ethyl methacrylate	–	Neo et al. (1991b)
Chloromethyl methacrylate	Alkyl methacrylate	II had an alkyl group of ethyl, n-propyl, or isopropyl	Goh et al. (1990a)
o-Chlorostyrene	Styrene	–	Alexandrovich et al. (1980)
o-Chlorostyrene-co-p-chlorostyrene	2,6-Dimethyl-1,4-phenylene ether	–	Alexandrovich et al. (1977)
	Styrene	I had 71–92 mol% ortho isomer	Ten Brinke et al. (1984)

(continued)

Table 21.6 (continued)

Polymer I of	Polymer II of	Comments	Refs.
o-Chlorostyrene-co-o-fluorostyrene	2,6-Dimethyl-1,4-phenylene ether	I had about 14–40 mol% ortho-chloro isomer	Vukovic et al. (1982a, 1985)
p-Chlorostyrene-co-o-fluorostyrene	2,6-Dimethyl-1,4-phenylene ether	I had 66–74 mol% para isomer	Vukovic et al. (1982a, 1985)
Cyclohexyl methacrylate-co-methyl methacrylate	Carbonate of bisphenol-A	I had 9.5–40.4 wt% CHMA	Park et al. (2001b)
	Carbonate of dimethylbisphenol-A	I had 28.5–66.7 wt% CHMA	Park et al. (2001b)
	Carbonate of tetramethylbisphenol-A	I had 0–36.7 wt% CHMA	Park et al. (2001b)
2,2-Dichloroethyl methacrylate	Alkyl methacrylate	II had an alkyl group of n-propyl, isopropyl, n-butyl, or isoamyl	Low et al. (1994b)
2,6-Dimethyl-1,4-phenylene ether	Acrylic acid-co-styrene	II had 6.3 or 8.5 wt% acrylic acid	Gottschalk et al. (1994)
	Acrylonitrile-co-styrene	II had 6.3 wt% acrylonitrile	Gottschalk et al. (1994)
	o-Fluorostyrene-co-p-fluorostyrene	II had 10–38 % para isomer	Vukovic et al. (1983b)
	o-Fluorostyrene-co-p-bromostyrene	II had 68 or 73 mol% bromostyrene	Vukovic et al. (1988)
	o-Fluorostyrene-co-styrene	II had 9–20 mol% styrene	Vukovic et al. (1981, 1982)
	p-Fluorostyrene-co-styrene	II had about 22–54 mol% styrene	Maeda et al. (1989), Vukovic et al. (1981, 1982)
	Maleic anhydride-co-styrene	II had 4.6, 8.0, or 9.9 wt% maleic anhydride (Witteler et al. (1993)); II had 7.3, 8.5, 10, or 12.5 wt% maleic anhydride (Gottschalk et al. (1994))	Gottschalk et al. (1994), Witteler et al. (1993)
	Methyl methacrylate-co-styrene	II had 12.5, 15, or 20 wt% methyl methacrylate	Gottschalk et al. (1994)
	α-Methylstyrene	–	Woo et al. (2003a)
2,6-Dimethyl-1,4-phenylene ether, sulfonylated	Phenylvinyl sec-butyl ether-alt-N-phenylmaleimide	I had 87 % sulfonylation	Vukovic et al. (1994d)
	Phenylvinyl ethyl ether-alt-N-phenylmaleimide	I had 87 or 91 % sulfonylation	Vukovic et al. (1994d)
Dodecamethylene decamethylene dicarboxylate	Vinyl chloride	–	Woo et al. (1985b)
Dodecamethylene dodecamethylene dicarboxylate	Vinyl chloride	–	Woo et al. (1985b)
	Vinyl chloride-co-vinylidene chloride	II had 13.5 wt% vinyl chloride	Woo et al. (1986)

Epichlorohydrin	Alkyl acrylate	II had an alkyl group of ethyl or n-propyl	Fernandes et al. (1986c)
	Alkyl methacrylate	II had an alkyl group of methyl, ethyl, n-propyl, n-butyl, or cyclohexyl	Fernandes et al. (1986b)
	Vinyl acetate	–	El Shafee (2002b), Guo (1991)
	N-Vinylpyrrolidone	–	Guo (1990d)
Etherimide	Amideimide	Examined by thermo-optical analysis	Ryu et al. (2000)
	Etheretherketone	–	Nandan et al. (2002)
	Ethylene glycol	Examined by thermo-optical analysis	Ryu et al. (2000)
	Styrene	Examined by thermo-optical analysis	Ryu et al. (2000)
Ethersulfone	N,N-Dimethylacrylamide	–	Goh et al. (1997)
	Imide	II was Matrimide 5218	Liang et al. (1992)
Ethyl acrylate	Alkyl methacrylate	II had an alkyl group of chloromethyl, 1-chloroethyl, 2-chloroethyl, 1,3-difluoroisopropyl	Peng et al. (1996)
	Vinylidene fluoride	–	Bernstein et al. (1977), Wahrmund et al. (1978)
	Hexafluoroacetone-co-vinylidene fluoride	II had 8 mol% hexafluoroacetone	Kano and Akiyama (1992), Kano et al. (1995), Kano et al. (1997a)
2-Ethylhexyl methacrylate	Hexyl methacrylate-co-styrene	I had 3–5 % acrylic acid; II had 30 % styrene and 5–15 % 3-(dimethylamino) 2,2-dimethylpropyl methacrylate	Siol and Terbrack (1991)
N-Ethyl-3-hydroxymethylcarbazoyl methacrylate	ω-Hydroxyalkyl-3,5-dinitrobenzoyl methacrylate	II had an alkyl group of butyl, hexyl, propyl of pentyl	Rodriguez-Parada and Percec (1986a)
Ethyl methacrylate	n-Butyl methacrylate-co-styrene	II had 23 or 34 wt% styrene	Rana et al. (2000)
	p-(2-Hydroxy hexafluoroisopropyl) styrene-co-styrene	II had 90.3–98.8 mol% styrene	Pearce et al. (1984)
	Vinyl chloride-co-vinylidene chloride	II had 86.5 wt% vinylidene fluoride	Woo et al. (1984b)
	Vinylidene fluoride	I was syndiotactic or atactic; LCST below T_m of II if I had high M_w isotactic	Bernstein et al. (1977), Roerdink and Challa

Table 21.6 (continued)

Polymer I of	Polymer II of	Comments	Refs.
			(1980), Ten Brinke et al. (1982)
2-Ethyl-2-oxazoline	Aramide	–	Maeda et al. (1986)
	Ethersulfone	–	Nakamura et al. (1990)
Ethylene, chlorinated	Ethylene-co-vinyl acetate	I had 35.4–52.6 wt% Cl; II had 40–45 wt% vinyl acetate	Walsh et al. (1983)
	Methyl methacrylate	I had 50–52 wt% Cl	Chai et al. (1983), Walsh et al. (1982)
Ethylene orthophthalate	Vinyl acetate	I had M_n = 9.5 kg/mol; no LCST when I had M_n = 5.1 kg/mol	Vazquez-Torres and Cruz-Ramos (1986)
Ethylene glycol	n-Butyl methacrylate	–	El Shafee and Ueda (2002)
	Enaminonitrile	–	Mondragon et al. (1983)
	Ethersulfone	–	Dreezen et al. (1991), Guo and Higgins (1991), Maejima et al. (1998), Shibanov and Radzhabov (1988), Walsh and Singh (1984)
	Ethylene-co-vinyl acetate	–	Chung and Chen (1990)
	Hydroxyether sulfone	–	H194
	Sulfone	M_n of I = 3,500–4,500; II was Udel Piglowski (1990)00	Swinyard et al. (1987)
	Vinyl acetate	LCST decreased with increasing M_w of II	Chen et al. (1999)
	Vinylphosphonic acid	Blend had ≤50 wt% I	Jiang et al. (2010)
Ethylene-co-vinyl acetate	Aniline, N-octadecylated	I had 20 wt% vinyl acetate; II had a degree of alkylation of 60.2 wt%	Zheng et al. (1995)
	Hexafluoroacetone-co-vinylidene fluoride	I had 70 % vinyl acetate; II had 8.9 mol% hexafluoroacetone	Hasegawa and Akiyama (1988)
	Vinyl chloride	I had 30 or 37 wt% ethylene	Nolley et al. (1979), Rellick and Runt (1986), Thaumaturgo and Monteiro (1997b)

Ethylene-*co*-vinyl alcohol	Amide	II was a copolyamide of PA-6 and PA-12	Akiba and Akiyama (1994)
2-Fluoroethyl methacrylate	Alkyl methacrylate	II had an alkyl group of methyl or ethyl	Peng et al. (1993)
3-Fluoropropyl methacrylate	Methyl methacrylate	–	Peng et al. (1995)
Hexadecamethylene dodecamethylene dicarboxylate	Vinyl chloride	–	Woo et al. (1985b)
Hydroxyether of bisphenol-A (Phenoxy)	Alkyl methacrylate	II had an alkyl group of methyl, tetrahydrofurfuryl or tetradropyranyl-2-methyl	Chiou and Paul (1991), Chong and Goh (1992a), Goh (1987)
	Ester	II was neopentyl glycol adipate or neopentyl glycol succinate	Harris et al. (1982)
	Ethersulfone	–	Saito et al. (1990), Singh and Walsh (1986)
	Ethylene oxide-*co*-propylene oxide	EO content of II = 22, 50, or 56 mol%	Guo et al. (1993a)
	Vinylmethylether	–	Ueda and Karasz (1992)
Hydroxyether of phenolphthalein	Butylene terephthalate	–	Guo et al. (1990d)
	Ethersulfone	–	Guo (1992b)
	Ethylene glycol	–	Guo et al. (1990c)
β-Hydroxyethyl-3,5-dinitrobenzoyl methacrylate	*N*-Alkyl-3-hydroxymethylcarbazoyl methacrylate	II had an alkyl group of butyl, decyl, dodecyl, ethyl, hexadecyl, hexyl, octyl, or tetradecyl	Rodriguez-Parada and Percec (1986b)
2-(Hydroxyl-hexafluoroisopropyl) styrene-*co*-styrene	Hydroxypropyl L-glutamine	I had 98.5 mol% styrene; blend had <50 vol% II	Dadmun and Han (1993)
	Methyl methacrylate	I had 90.3–96.1 mol% styrene	Pearce et al. (1984)
	Vinylmethylether	I had 90.3–99.9 mol% styrene	Pearce et al. (1984)
2-Iodoethyl methacrylate	Tetrahydrofurfuryl methacrylate	–	Low et al. (1993d)
Isoprene	*Cis*-butadiene-*co*-1,2-vinylbutadiene	II had £ 24.3 % vinylbutadiene	Kawahara et al. (1989)
Maleic anhydride-*co*-styrene	Ethyl methacrylate	I had 0–33 wt% maleic anhydride	Brannock et al. (1991)
	N-Methyl glutarimide	I had 14 wt% maleic anhydride	Prinos et al. (1997)
	Methyl methacrylate	I had 8, 10, 13, or 33 wt% maleic anhydride	Brannock et al. (1991)
	n-Propyl methacrylate	I had 0–18.1 wt% maleic anhydride	Brannock et al. (1991)

(continued)

Table 21.6 (continued)

Polymer I of	Polymer II of	Comments	Refs.
Methacrylonitrile-*co-p*-methylstyrene	*n*-Butyl methacrylate	I had 15, 17, 22, 23, or 25 wt% methacrylonitrile (MAN)	Chen and Porter (1993)
	Ethyl methacrylate	I had 40, 46, or 53 wt% MAN	Chen and Porter (1993)
	Isopropyl methacrylate	I had 22, 23, 25, or 31 wt% MAN when II had $M_n = 161$ kg/mol; I had 17, 22, 23, 25, or 31 wt% MAN when II had $M_n = 41.6$ kg/mol	Chen and Porter (1993)
	Methyl methacrylate	I had 34, 53, 56, or 68 wt% MAN	Chen and Porter (1993)
	n-Propyl methacrylate	I had 37 or 40 wt% MAN	Chen and Porter (1993)
Methacrylonitrile-*co*-styrene	Methyl methacrylate	I had 46.6–62.8 wt% MAN	Goh et al. (1993)
	n-Propyl methacrylate	I had 2–32 wt% methacrylonitrile	Chen et al. (1994)
Methyl acrylate	1,3-Difluoroisopropyl methacrylate	–	Peng et al. (1996)
	Hexafluoroacetone-*co*-vinylidene fluoride	II had 8 mol% hexafluoroacetone	Kano et al. (1997c)
	Vinylidene fluoride	–	Bernstein et al. (1977), Wahrmund et al. (1978)
Methyl methacrylate	Acrylonitrile-*co*-methyl methacrylate-*co*-styrene	II had 40.0/39.1/20.9 or 61.1/19.6/19.3 of S/MMA/AN	Nishimoto et al. (1989)
	Carbonate of bisphenol-A-*co*-hexafluorobisphenol-A	II had 5.3–14 wt% hexafluorobisphenol-A	Kim and Paul (1992d)
	Carbonate of bisphenol chloral	–	Chiou and Paul (1987), Callaghan and Paul (1994a)
	Epichlorohydrin-*co*-ethylene glycol	II had 50 mol% ethylene glycol	Fernandes et al. (1986b)
	Ethylene, chlorinated	I had 56–68 wt% Cl	Ueda and Karasz (1994)
	Ethylene glycol	–	Fernandes et al. (1986b)
	Hexafluoroacetone-*co*-vinylidene fluoride	–	Kobayashi et al. (1987)
	Maleic anhydride-*co*-styrene	–	Chopra et al. (1998)

	N-Maleimide-co-styrene	II had 45 wt% N-maleimide	Vermeesch and Groeninckx (1995)
	Tetrafluoroethylene-co-vinylidene fluoride	II had 80 mol% vinylidene fluoride	Hamazaki et al. (1991)
	Vinyl acetate	Blends cast from chloroform and cyclohexanone	Burdin and Tager (1993), Guo (1990e), Lee and Ha (1994a), Song et al. (1990), Song and Long (1991)
	Vinyl chloride	–	Jager et al. (1983), Lemieux et al. (1988), Piglowski (1988), Shen and Torkelson (1992)
	Vinyl chloride, chlorinated	II had 63, 65, or 68 wt% Cl	Lemieux et al. (1988), Ueda and Karasz (1994), Voremkamp and Challa (1988)
	Vinyl chloride-co-vinylidene chloride	I was atactic or isotactic; II had 86.5 wt% vinylidene chloride	Lemieux et al. (1988), Woo et al. (1983, 1984b)
	Vinylidene fluoride	LCST above decomposition temperature of I	Belorgey and Prud'homme (1982)
Methyl methacrylate, imidized	Acrylonitrile-co-styrene	I had 53–91 wt% imidized unit; II had 5.7–33 wt% acrylonitrile; some blends showed LCST	Fowler et al. (1989)
Methyl methacrylate-co-styrene	Vinylmethylether	–	Sato et al. (1998)
α-Methylstyrene	Carbonate of bisphenol-A	I had M_w = 3.5 or 6.7 kg/mol; II had M_w = 33 kg/mol	Callaghan and Paul (1994a)
	Carbonate of bisphenol-P	I had M_w = 3.5 or 6.7 kg/mol; II had M_w = 31 kg/mol	Callaghan and Paul (1994a)
	Cyclohexyl methacrylate	–	Chang and Woo (2001b)
	Ethyl methacrylate	–	Siol (1991)
	Methyl methacrylate	Effect of M_w on LCST was reported in Callaghan and Paul (1993)	Cowie and Miachon (1992), Callaghan and Paul (1993), Siol (1991)

(continued)

Table 21.6 (continued)

Polymer I of	Polymer II of	Comments	Refs.
	p-Methylstyrene	–	Chang and Woo (2000)
	n-Propyl methacrylate	–	Siol (1991)
	Styrene	–	Saeki et al. (1983), Schneider and Dilger (1989), Widmaier and Mignard (1987)
	Tetrahydropyranyl-2-methyl methacrylate	–	Chong and Goh (1991a)
p-Methylstyrene	Cyclohexyl methacrylate	–	Woo and Jang (1999)
α-Methylstyrene-co-4-(2-hydroxyethyl)-α-methylstyrene	Alkyl acrylate	I had an alkyl group of methyl, ethyl, or t-butyl	Cowie and Reilly (1993a)
	Alkyl methacrylate	I had an alkyl group of methyl, ethyl, or t-butyl	Cowie and Reilly (1993a)
	Dialkyl itaconate	I had an alkyl group of methyl, ethyl, n-propyl, n-butyl, or t-butyl	Cowie and Reilly (1993a)
	Vinyl acetate	–	Cowie and Reilly (1993b)
	4-Vinylpyridine	–	Cowie and Reilly (1993b)
	N-Vinyl pyrrolidone	–	Cowie and Reilly (1993b)
α-Methylstyrene-co-4-(1,1,1-trifluoro-2-hydroxyethyl)-α-methylstyrene	Alkyl acrylate	I had an alkyl group of methyl, ethyl, or t-butyl	Cowie and Reilly (1993a)
	Alkyl methacrylate	I had an alkyl group of methyl, ethyl, or t-butyl	Cowie and Reilly (1993a)
	Dialkyl itaconate	I had an alkyl group of methyl, ethyl, n-butyl, or t-butyl	Cowie and Reilly (1993a)
	Vinyl acetate	–	Cowie and Reilly (1993b)
	4-Vinylpyridine	–	Cowie and Reilly (1993b)
	N-Vinyl pyrrolidone	–	Cowie and Reilly (1993b)
Novolac	Ethylene-co-vinyl acetate	II had 50 wt% vinyl acetate; LCST decreased with increasing degree of cure	Chen et al. (1998b)
Oxymethylene	Novolac	–	Wang et al. (1991b)
Pentabromobenzyl methacrylate-co-methyl methacrylate	Carbonate of bisphenol-A	II had ≤23.7 wt% pentabromobenzyl methacrylate	Merfeld et al. (2000)

Pentabromobenzyl methacrylate-*co*-styrene	Carbonate of tetramethylbisphenol-A	I had ≤33.9 wt% pentabromobenzyl methacrylate	Merfeld et al. (2000)
	2,6-Dimethyl-1,4-phenylene ether	I had 54 or 44.9 wt% pentabromobenzyl methacrylate	Merfeld et al. (2000)
Phenol-formaldehyde	Methyl methacrylate-*co*-styrene	II had 30.4–83.5 % MMA	Kim et al. (1989a)
Phenolphthalein polyaryletherketone	Ethylene glycol	–	Zheng et al. (2004)
Phenolphthalein polyetherethersulfone	Ethylene glycol	–	Zheng et al. (1997a)
p-Phenylene benzobisoxazole	Amide	II was PA-6,6 (Kyu and Chen (1993)) or an amorphous polyamide Zytel 330 (Chen and Kyu (1993))	Chen and Kyu (1993), Kyu and Chen (1993)
2,2′-(*m*-Phenylene)- 5,5′-bisbenzimidazole	Imide	II was Ultem 1000	Choe et al. (1988)
	Imide	II was XU 218	Choe et al. (1988)
o-Phenylphenol	Ethyl acrylate-*co*-methyl methacrylate	II had 37 or 81 wt% ethyl acrylate	Kim et al. (1998)
n-Propyl acrylate	Alkyl methacrylate	II had an alkyl group of chloromethyl, 1-chloroethyl, 2-chloroethyl, dichloroethyl. or trichloethyl	Peng et al. (1996)
n-Propyl methacrylate	Vinyl chloride-*co*-vinylidene chloride	II had 86.5 wt% vinylidene chloride	Woo et al. (1984b)
Styrene	5-Acetyl-2,6-dimethyl-1,4-phenylene ether	–	Kim et al. (1993c)
	5-Benzoyl-2,6-dimethyl-1,4-phenylene ether	–	Kim et al. (1993c)
	Carbonate of bisphenol-A-*co*-tetramethylbisphenol-A	II had ≥85 wt% tetramethylbisphenol-A	Kim and Paul (1992e)
	Carbonate of dimethylbisphenol-A-*co*-carbonate of bisphenol-A	II had 60–90 wt% tetramethylbisphenol-A	Kim et al. (2003a)
	Cyclohexyl methacrylate	I was isotactic (Chang and Woo (2003b))	Chang and Woo (2003b), Friedrich et al. (1996)
	o-Fluorostyrene-*co*-*p*-fluorostyrene	II had 10 or 23 mol% *p*-fluorostyrene	Oudhuis et al. (1991, 1993)
	Vinylmethylether	–	Mandal and Woo (1999c)
Styrene, sulfonated	Caprolactam (PA-6)	I had 6.5, 8.1, or 9.0 mol% sulfonated unit and Zn-neutralized	Kwei et al. (1993)
Styrene, modified with C$_{60}$	Vinylmethylether	I had 1.9 or 9.9 wt% C$_{60}$	Zheng et al. (1997b)

(continued)

Table 21.6 (continued)

Polymer I of	Polymer II of	Comments	Refs.
Styrene, sulfonated and metal-neutralized	Caprolactam (PA-6)	I was neutralized by Li, Mg, or Zn	Weiss and Lu (1994)
	N,N′-Dimethylene sebacamide	I had 4.0, 5.2, or 9.5 mol% sulfonation and neutralized by Li	Feng et al. (1996a, e), Tucker et al. (2003)
	N,N′-Dimethylethylene sebacamide	I had 7.4 mol% sulfonation and Li neutralized	Feng et al. (1996d)
Styrene-*co*-*p*-(2,2,2-trifluoro-1-hydroxy-1-trifluoromethyl)ethyl-*α*-methylstyrene	*p*-(Tert-butyl)phenylene fumarate	I had 3.9 or 8.0 mol% OH	Chen et al. (1998a)
Styrene-*co*-vinylphenol	Caprolactone	I had 10 wt% vinylphenol	Ahn et al. (1993)
	n-Hexyl methacrylate	–	Bhagwagar et al. (1994)
	Methyl methacrylate	I had 5 mol% vinylphenol; II was syndiotactic	Jong et al. (1993)
Sulfone	Styrene-*co*-1-vinylpyrrolidone	II had 12–32 wt% styrene	Kim et al. (2003b)
1,2,2,2-Tetrachloroethyl methacrylate	Ester	II was caprolactone or 2,2-dimethyl-1,3-propylene adipate	Goh et al. (1997a)
4-Trimethylsilylstyrene	Isoprene	–	Harada et al. (2005a, b)
Vinyl acetate	Maleic anhydride-alt-styrene, hydrolyzed	II was 1.8–43 % hydrolyzed; LCST increased with increasing degree of hydrolysis	Bosma et al. (1988a)
Vinyl acetate-*co*-vinyl chloride	*n*-Butyl methacrylate	I had 5.9–15.1 vol% vinyl acetate	Lee et al. (1992)
	Hexyl acrylate-*co*-methyl acrylate	I had 5–23.7 vol% vinyl acetate; II had 15–88 vol% hexyl acrylate; some blends showed LCST	Jin et al. (1992)
	Methyl methacrylate	I had 5.9–15.1 vol% vinyl acetate	Lee et al. (1992)
	4-Vinylpyridine	I had 32–55 mol% vinyl alcohol	Isasi et al. (1995)
Vinyl alcohol	Amide	I composed of 1:1:1 (wt%) of PA-6, PA-6,6, and PA-6,10 units	Zheng et al. (1996)
Vinyl butyral	Vinylpyridine	II was 2- or 4-pyridine	Franzen et al. (1995)

Vinyl chloride	Acrylonitrile-*co*-*n*-butyl acrylate	II had 53, 67 or 84 mol% butyl acrylate	Piglowski and Kammer (1990)
	n-Amyl methacrylate	–	Perrin and Prud'homme (1991), Piglowski (1988)
	Butyl acrylate-*co*-ethyl acrylate	II had 22.9, 43.5, or 52.8 % butyl acrylate	Walsh and Sham (1989)
	Butyl acrylate-*co*-hexyl acrylate	II had 47.8 % butyl acrylate	Walsh and Sham (1989)
	Butyl acrylate-*co*-methyl acrylate	II had 44.6 % butyl acrylate	Walsh and Sham (1989)
	Butyl acrylate-*co*-methyl methacrylate	II had 75 % butyl acrylate	Piglowski (1990)
	n-Butyl methacrylate	–	Perrin and Prud'homme (1991), Piglowski (1988)
	Butyl methacrylate-*co*-methyl methacrylate	II had 30 or 70 % methyl methacrylate	Piglowski (1988)
	Ethyl acrylate-*co*-hexyl acrylate	II had 41.7 or 43.2 % ethyl acrylate	Walsh and Sham (1989)
	Methyl acrylate-*co*-hexyl acrylate	II had 9.7 % methyl acrylate	Walsh and Sham (1989)
	Methyl methacrylate-*co*-styrene	II had 30 wt% styrene	Dompas et al. (1997)
	Pentyl acrylate	–	Walsh and Sham (1989)
	Pentyl acrylate-*co*-propyl acrylate	II had 48.1 % propyl acrylate	Walsh and Sham (1989)
	Propyl acrylate	–	Walsh and Sham (1989)
Vinyl chloride-*co*-vinylidene chloride	Neopentyl glycol succinate	I was Saran with 86.5 wt% vinylidene chloride; LCST above T_m when blend had ≤50 wt% II	Cowie and Reilly (1993a)
Vinylmethylether	Acrylonitrile-*co*-styrene	II had £ 10–11 % acrylonitrile	Min and Paul (1987)

(continued)

Table 21.6 (continued)

Polymer I of	Polymer II of	Comments	Refs.
	Alkyl acrylate	II had an alkyl group of ethyl or *n*-propyl	Chakraborty et al. (1993)
	Benzyl methacrylate	–	Mandal and Woo (1999a)
	Butadiene-*co*-styrene	II had 60 or 68 wt% styrene	Ahn et al. (1997d)
	Caprolactone	–	Bisso et al. (1998), Bisso et al. (1999), Oudhuis et al. (1994)
	2-Chlorostyrene	–	Tran-Cong et al. (1994), Urakawa et al. (2001)
	Dinitrostyrene-*co*-styrene	II had 3–14 mol% dinitrostyrene	Fernandez et al. (1997)
	Hydrogenous-block-deuterated styrene	–	Gomez-Elvira et al. (1994)
	Maleic anhydride-*co*-styrene	II had <15 % maleic anhydride	Min and Paul (1987)
	Hydroxyether of bisphenol-A	II was 11.7–42.3 mol% methylated or 7.5–30.1 mol % benzoylated	Etxeberria et al. (2001)
	α-Methylstyrene	–	Ha et al. (1990b)
	α-Methylstyrene-*co*-4-(2-hydroxyethyl)–methylstyrene	II had 6–89 mol% methylstyrene	Cowie and Reilly (1992)
	α-Methylstyrene-*co*-4-(1,1,1-trifluoro-2-hydroxyethyl)-methylstyrene	II had 0–93 mol% methylstyrene	Cowie and Reilly (1992)
	α-Methylstyrene-*co*-styrene	II had 77.5 or 88 wt% styrene	Ha et al. (1990b, 1993)
	p-Methylstyrene-*co*-styrene	II had 78.5 or 87.3 wt% styrene; II had 61, 72, 80, 90, or 95 mol% styrene (Goh et al. (1994a))	Goh et al. (1994a), Ha et al. (1990b, 1993)
	m-Methylstyrene-*co*-styrene	II had 76.5 or 87.5 wt% styrene	Ha et al. (1993)
	o-Methylstyrene-*co*-styrene	II had 76.2 or 86.8 wt% styrene	Ha et al. (1993)
	Methyl methacrylate-*co*-styrene	II had <60 mol% methyl methacrylate	Chien et al. (1988)
	Nitrostyrene-*co*-styrene	II had £ 25.6 mol% nitrostyrene	Cowie et al. (1992b), Defieuw et al. (1989a)
	Styrene-*co*-1-vinyl naphthalene	II had 17.4 wt% styrene	Ha et al. (1990b)
	Styrene-*co*-2-vinyl naphthalene	II had 19.2 wt% styrene	Ha et al. (1990b)
	Trimethylene adipate	–	Chiang and Woo (2007)

Vinylmethylketone	Styrene-*co*-4-vinylstilbene	Cloud point was sensitive to the *cis*-fraction of 4-stilbenzyl groups	Irie and Iga (1986)
p-Vinylphenol	4-Acetoxystyrene	–	Himuro et al. (1992)
	Trimethylene terephthalate	–	Lee and Woo (2004b)
2-Vinylpyridine	Aramide	II made from hexamethylenediamine and a mixture of isomers of phthalic acid	Skrovanek and Coleman (1987)
	2-Hydroxyethyl methacrylate	–	Cesteros et al. (1994a)
Vinylidene fluoride	Butylene adipate	–	Lee et al. (2008)
	Methoxymethyl methacrylate	–	Goh et al. (1991c)
	Pentamethylene adipate	–	Li and Woo (2008b)
	Trimethylene adipate	–	Li and Woo (2008b)

Table 21.7 Polymer pairs appear to have both a lower critical solution temperature and an upper critical solution temperature

Polymer I of	Polymer II of	Comments	Refs.
Acrylonitrile-*co*-styrene	Acrylonitrile-*co*-butadiene	I had 25 wt% acrylonitrile; II had 40 wt% acrylonitrile	Oswald and Kubu (1963)
	Caprolactone	II had 12.4–26.4 wt% AN; blends showed an LCST-UCST loop	Svoboda et al. (1994)
	Carbonate of bisphenol-A	I had 25 wt% AN; II had $M_w = 6$ kg/mol; blend had 20–25 wt% II	Li et al. (1999b)
Butadiene	Butadiene-*co*-styrene	II had 45 wt% styrene	Tager et al. (1987)
4-t-Butoxystyrene-stat-4-t-butylstyrene	Isoprene	I had 30–66 mol% t-butylstyrene	Rahman et al. (2009)
Carbonate of bisphenol-A	Methyl methacrylate	Blends showed an LCST-UCST loop	Brannock et al. (1990), Kyu and Lim (1989), Kyu et al. (1993)
Dimethylsiloxane	Methylphenylsiloxane	–	kundu et al. (1986c)
Etherimide	Imide	II was made from 4,4′-bis(3,3′-aminophenoxy)biphenyl and pyromellitic anhydride	Ma and Takahashi (1996)
2-Hydroxyethyl acrylate-*co*-liquid crystalline acrylate	2-Hydroxyethyl acrylate-*co*-liquid crystalline acrylate	Both I and II had 6 % 2-hydroxyethyl acrylate; the liquid crystalline acrylate of I and II had different space groups	Guo and Mitchell (1994)
o-Methylated phenol formaldehyde	Methyl methacrylate	I had 20 or 50 % of OH group methylated	Kim et al. (1989b)
	Methyl methacrylate-*co*-styrene	I had 20 or 50 % of OH group methylated; II had 50 or 60 % methyl methacrylate	Kim et al. (1989b)
Styrene	2,6-dimethyl-1,4-phenylene ether, carboxylated	II had 8.0–10.3 mol% carboxyl group	Cong et al. (1986)
	n-Pentyl methacrylate	–	Kim et al. (2004)

Table 21.8 Polymer pairs that co-crystallize

Polymer I of	Polymer II of	Method	Comments	Refs.
Butylene terephthalate	Butylene glycol-b-butylene terephthalate	T_g and T_m by DSC, dielectric loss measurements	Two T_g's when I was Valox 310 (General Electric) having $M_n = 20$ kg/mol and II contained 44–67 wt% butylene terephthalate; single T_g and single T_m when II contained 85 wt% butylene terephthalate; single T_m indicated that only one type of crystal was present	Martynowicz-Hans and Runt (1986)
	Butylene glycol-b-butylene terephthalate	T_g and T_m by DSC, dielectric loss measurements, microscopy	Single T_g and single T_m when I was Valox 310 (General Electric) with $M_n = 33$ kg/mol, II contained 84 wt% butylene terephthalate and I/II = 1/3–3/1; thermal analysis and morphological evidence pointed to extensive co-crystallization in this mixture; two T_g's when II contained 50 wt% butylene terephthalate	Runt et al. (1989)
	Ester–ether segmented polymer	Dielectric loss peak and T_m by DSC	I was Valox 310 (General Electric) with $M_n = 20$ kg/mol; II was comprised of a poly(butylene oxide) soft segment and a hard segment 4GT-butylene terephthalate and had total $M_w = 25$–30 kg/mol; single beta dielectric loss peak and single T_m were found when II was 44 or 67 wt% 4GT; single T_m between the T_ms of the pure components indicated co-crystallization; two dielectric loss peaks and two T_m when II was 84 wt% 4GT	Runt et al. (1987)
Etheretherketone	Ether ether ether ketone	T_g and T_m by DSC	Single T_g and single T_m when I contained 33 % ketone linkages and had melt flow = 3.0 dg/min at 400° C and II had melt flow = 10 dg/min; I/II = 1/1	Harris and Robeson (1987)
	Etheretherketone ketone	T_g and T_m by DSC	Single T_g and single T_m when I contained 33 % ketone linkages and had melt flow = 3.0 dg/min at 400° C and II contained 50 % ketone linkages and had melt flow = 4.0 dg/min; I/II = 1/1	Harris and Robeson (1987)
	Ether ketone	T_g and T_m by DSC	Single T_g and single T_m when I contained 33 % ketone linkages and had melt flow = 3.0 dg/min and II contained 50 % ketone linkages and had melt flow = 1.5 dg/min; I/II = 1/1	Harris and Robeson (1987), Nandan et al. (2001)

(continued)

Table 21.8 (continued)

Polymer I of	Polymer II of	Method	Comments	Refs.
	Ether ketone	T_g and T_m by DSC; WAXD	Single composition-dependent melting endotherms obtained upon quenching when I had intrinsic viscosity = 1.124 dl/g in sulfuric acid at 30° C and II had intrinsic viscosity = 1.107 dl/g in sulfuric acid at 30° C, but it did not happen when other thermal histories were imposed	Sham et al. (1988b)
	Ether-*co*-ketone	T_g and T_m by DSC	Single T_g and single T_m when I contained 33 % ketone linkages and had melt flow = 3.0 dg/min and II contained 57 % ketone linkages and had melt flow = 1.5 dg/min; I/II = 1/1	Harris and Robeson (1987)
	Ether ketone (polymer II), etherimide (polymer III)	T_g and T_m by DSC	I had reduced viscosity = 1.05 dl/g in 1 wt% conc. sulfuric acid at 23° C; II had reduced viscosity = 1.9 dl/g in the same condition as for I; III was Ultem 1000 from GE with reduced viscosity = 0.5 dl/g in 0.2 wt% chloroform at 25° C; single T_g and single T_m for I/II/III = 25/25/50	Harris and Robeson (1988)
Ethylene	Butadiene, hydrogenated	DSC, SALS, and SEM	I was narrow M_w fraction with M_w = 113 kg/mol and M_n = 105 kg/mol; II contained 2.2–5.5 mol% ethyl branches and had M_w = 103–420 kg/mol and M_n = 83–156 kg/mol; stated that I and II co-crystallized upon rapid crystallization from the melt when II contained up to 2 mol% of ethyl branches	Alamo et al. (1988)
Ethylene	Ethylene	DSC and SALS	I was polyethylene and II was UHMWPE with M_w = 5,000 kg/mol; I was LLDPE (GRSN-7047 from Union Carbide with M_w = 134 kg/mol and M_w/M_n = 4), or I was HDPE (Chemplex 6186 with M_w = 134.8 kg/mol and M_w/M_n = 7.4); only a single composition-dependent T_m was observed; SALS showed the co-crystallization took place; but when I was LDPE (M_w = 114 kg/mol and M_w/M_n = 5.2), separate crystals were formed	Kyu and Vadhar (1986)

Ethylene	DSC, SAXS, and X-ray diffraction	I was linear LLDPE and II was HDPE; co-crystallization was evidenced by a single T_m by DSC; stated that X-ray diffraction peak width, SAXS and Raman spectra were all consistent with a single crystallizing species; but for HDPE/LDPE and LLDPE/LDPE, separate crystals were seen with two T_ms being found by DSC	Stein et al. (1989)
Ethylene	DSC, SAXS, and X-ray diffraction	I was HDPE with $M_w = 100$ kg/mol and $M_n = 11$ kg/mol and II was LLDPE with $M_w = 350$ kg/mol and $M_n = 16$ kg/mol; after the blend with I/II $= 25/75$ by weight was cross-linked either by irradiation or by peroxides in the liquid state above a critical degree of cross-linkage, the DSC curve of the blend showed only one single melting point on heating and only one single crystallization peak on cooling; references B8, Hahn and Wendroff (1985)1, Machado and French (1992b)5, Kallistis and Kalfoglou (1989)5, and R8 also discussed the miscibility of PE/PE blends	Illers and Koehnlein (1986)
Ethylene	DSC; SANS; SAXS	I was HDPE and II was LDPE; blends were homogeneous in the melt	Wignall et al. (1995)
Ethylene	SANS	I was LDPE and II was LLDPE	Shin et al. (2009)
Ethylene, deuterated	T_m by DSC	Single T_m varying smoothly with composition and no gross segregation occurred	English et al. (1985)
Ethylene-co-vinyl acetate	DSC, SALS, and SEM	I was narrow M_w fraction with $M_w = 113$ kg/mol and $M_n = 105$ kg/mol; II contained 1.12–6.6 mol% of acetate branches and had $M_w = 60.3$–105 kg/mol and $M_n = 23.5$–43.6 kg/mol; stated that I and II co-crystallized upon rapid crystallization from the melt contained up to 2 mol% of acetate branches	Alamo et al. (1988)
Ethylene-co-vinyl acetate	Ethylene-co-vinyl acetate	DSC, SALS, and SEM	I and II had $M_w = 60.3$–105 kg/mol, $M_n = 23.5$–43.6 kg/mol, and they were different in the content of acetate branches; stated that these copolymers containing about 1–2 mol% of acetate branches were found to co-crystallize with one another	Alamo et al. (1988)

Table 21.8 (continued)

Polymer I of	Polymer II of	Method	Comments	Refs.
Glutamate	Glutamate	Dynamic mechanical measurements, X-ray diffraction	I or II was poly(L-glutamate) or poly(D-glutamate) having m number of methylene group in the ester group of a general formula as -CH$_2$CH$_2$COO-(CH$_2$)$_m$-C$_6$H$_5$-, m might be 1, 2, or 3, so the component polymer would be represented as L_m or D_m; the M_w of both components were 135–380 kg/mol and M_w/M_n = 1.1–1.2; stated that binary blends of Landi (1972), Dave et al. (1990), Landry and Hendrichs (1989), and Davis et al. (1981) were miscible and formed isomorphous mixed crystals at all compositions, whereas other pairs, with the exception of Landi (1974)/Das and Rodriguez (1987), were immiscible	Sankarapandian and Kishore (1991)
Hexafluoroacetone-co-vinylidene fluoride	Tetrafluoroethylene-co-vinylidene fluoride	DSC	I had 92 mol% VDF and II had 80 mol% VDF; blends of difference compositions showed single melting peak	Cho et al. (1993)
Hexafluoropropylene-co-tetrafluoroethylene	Perfluoromethyl vinyl ether-co-tetrafluoroethylene	DSC	I had 1 mol% hexafluoropropylene; II had 2 mol% perfluoromethyl vinyl ether	Pucciariello and Angioletti (1999)
Isopropylvinylether, isotactic	Sec-butylvinylether, isotactic	Unit cell dimension from X-ray diffraction	Co-crystallization at all compositions	Natta et al. (1969)
Lactide	Lactide	DSC	I was linear and II was branched; I and II co-crystallized in one lamellae type	Zuideveld et al. (2006)
4-Methyl-1-hexene, isotactic	4-Methyl-1-pentene, isotactic	Unit cell dimensions from X-ray diffraction	Co-crystallization only below 25 wt% I and above 75 wt% I	Natta et al. (1969)
Propylene	Ethylene-co-propylene	–	I was isotactic	Kim et al. (1999a)
Tetrafluoroethylene	Tetrafluoroethylene-co-perfluoroalkyl vinyl ether	Dynamic mechanical studies	II had 98 or 99 mol% tetrafluoroethylene	Runt et al. (1995)
	Tetrafluoroethylene-co-perfluoropropyl vinyl ether	WAXD; SEM	II had 98 mol% tetrafluoroethylene	Endo et al. (2000)

Trifluoroethylene-co-vinylidene fluoride	Trifluoroethylene-co-vinylidene fluoride	DSC, X-ray, and phase-contrast microscopy	No phase separation by phase-contrast microscopy, a sharp single X-ray peak, intermediate in spacing between those of the individual copolymers, and clearly different from their superposition, and only one ferroelectric transition and only one melting point by DSC, indicated co-crystallization within the same lattice when I was 52/48 mol% vinylidene fluoride (VDF)/trifluoroethylene (TFE), II was 65/35 mol% VDF/TFE, or I was 65/35 mol% VDF/TFE, and II was 73/27 mol% VDF/TFE; but two X-ray peaks and two ferroelectric transitions and two melting points when I was 52/48 and II was 73/27 mol% VDF/TFE	Tanaka and Lovinger (1987)
Vinyl alcohol	Vinyl alcohol	DSC	I and II had a diad syndiotacticity of 54 and 58 mol%, respectively	Tanigami et al. (1994)
Vinylidene fluoride	Tetrafluoroethylene-co-vinylidene fluoride	DSC	II had 9.1, 14.3, or 17.6 mol% tetrafluoroethylene	Datta and nandi (1996)

Notations and Abbreviations

AFM Atomic force microscopy
DSC Differential scanning calorimetry
FTIR Fourier transform infrared spectroscopy
HDPE High-density polyethylene
IGC Inverse gas chromatography
LCST Lower critical solution temperature
LDPE Low-density polyethylene
LLDPE Linear low-density polyethylene
M_n Number-average molecular weight
M_w Weight-average molecular weight
NMR Nuclear magnetic resonance spectroscopy
NRET Non-radiative energy transfer
OM Optical microscopy
PA Polyamide
PALS Positron annihilation light spectroscopy
POM Polarized optical microscopy
SALS Small angle light scattering
SANS Small angle neutron scattering
SAXS Small angle X-ray scattering
SEM Scanning electron microscopy
T_g Glass transition temperature
T_m Melting temperature
TEM Transmission electron microscopy
ToF-SIMS Top of flight secondary ion mass spectrometry
UCST Upper critical solution temperature
UHMWPE Ultra high molecular weight polyethylene
WAXD Wide angle X-ray diffraction
XPS X-ray photoelectron spectroscopy

References

M. Abdellaoui, S. Djadoun, J. Appl. Polym. Sci. **98**, 658 (2005)
H. Abe, Y. Doi, M.M. Satowski, I. Noda, Macromolecules **27**, 50 (1994)
N. Acar, T. Tulun, J. Polym. Sci. A: Polym. Chem. **34**, 1251 (1996)
D. Acierno, C. Naddo, Polymer **35**, 1994 (1994)
J. Adduci, D.K. Dandge, J. Kops, Am. Chem. Soc., Polym. Prepr **22**(2), 109 (1981)
S.G. Adoor, L.S. Manjeshwar, K.S.V. Khrisna Rao, B.V.K. Naidol, T.M. Aminabhavi, J. Appl.
   Polym. Sci. **100**, 2415 (2006)
S.M. Aharoni, J. Macromol. Sci. Phys. **B22**, 813 (1983)
S.M. Aharoni, Macromolecules **11**, 277 (1978)
T.K. Ahn, S. Choe, Polymer (Korea) **19**, 633 (1995)
T.O. Ahn, H.M. Jeong, Pollimo **11**, 112 (1987)
S.B. Ahn, H.M. Jeong, Korean Polym. J. **6**, 389 (1998)
T.O. Ahn, S. Lee, H.M. Jeong, Eur. Polym. J. **25**, 95 (1989)

T.O. Ahn, Y.J. Lee, S.M. Lee, H.M. Jeong, J. Macromol. Sci., Phys **B29**, 91 (1990)

T.O. Ahn, S. Lee, H.M. Jeong, K. Cho, Angew. Makromol. Chem. **192**, 133 (1991a)

T.O. Ahn, B.V. Nam, S. Lee, H.M. Jeong, Polym. Commun. **32**, 415 (1991b)

T.O. Ahn, H.S. Eum, H.M. Jeong, J.Y. Park, Pollimo **17**, 242 (1993a)

T.O. Ahn, H.S. Eum, H.M. Jeong, J.Y. Park, Polym. Bull. **30**, 461 (1993b)

T.O. Ahn, C.Y. Ryu, J.H. Sunwoo, H.M. Jeong, Macromol. Rapid Commun. **15**, 265 (1994)

T.O. Ahn, M. Lee, H.M. Jeong, K. Cho, J. Polym. Sci. B: Polym. Phys. **33**, 327 (1995)

T.O. Ahn, K. Kim, H.M. Park, H.M. Jeong, Eur. Polym. J. **33**, 781 (1997a)

T.K. Ahn, M. Kim, S. Choe, Macromolecules **30**, 3369 (1997b)

T.O. Ahn, B.U. Nam, M. Lee, H.M. Jeong, Polymer **38**, 577 (1997c)

J.H. Ahn, C.K. Kang, W.C. Zin, Eur. Polym. J. **33**, 1113 (1997d)

S.B. Ahn, Y.C. Ha, S.W. Park, D.H. Lee, H.M. Jeong, Polymer (Korea) **21**, 871 (1997e)

T.O. Ahn, M. Lu, H.M. Jeong, K. Cho, J. Polym. Sci. B: Polym. Phys. **36**, 201 (1998)

T. Aihara, H. Saito, T. Inoue, H.P. Wolff, B. Stuhn, Polymer **39**, 129 (1998)

A.B. Aivazov, K.G. Mindiyarov, Y.V. Zelenev, Y.G. Oganesov, V.G. Raevskii, Vyosokomol. Soedin. Ser. B. **12**, 10 (1970)

I. Akiba, S. Akiyama, Polym. J. **26**, 873 (1994)

I. Akiba, S. Akiyama, J. Macromol. Sci.: Phys. **B40**, 157 (2001)

I. Akiba, Y. Ohba, Y. Kobori, S. Akiyama, Polym. J. **32**, 402 (2000)

I. Akiba, T. Seki, S. Akiyama, E-Polymers, Art. 008 (2002)

S. Akiyama, N. Inaba, R. Kaneko, Chem. High Polym. Jpn. **26**, 529 (1969)

S. Akiyama, W.J. MacKnight, F.E. Karasz, J. Nambu, Polym. Commun. **28**, 236 (1987)

S. Akiyama, K. Ishikawa, H. Fujiishi, Polymer **32**, 1673 (1991)

S. Akiyama, K. Ishikawa, S. Kawahara, I. Akiba, Polymer **42**, 6657 (2001)

R.G. Alamo, R.H. Glaser, L. Mendelkern, J. Polym. Sci., Polym. Phys. Ed **26**, 2169 (1988)

H. Alata, B. Zhu, Y. Inoue, J. Appl. Polym. Sci. **106**, 2025 (2007)

M. Alberdi, E. Espi, J.J. Fernandez-Berridi, Polym. J. **26**, 1037 (1994)

A. Alegria, I. Telleria, J. Celmenero, J. Non-Cryst. Solid **172**, 961 (1994)

A. Alegria, C. Elizetxea, I. Cendoya, J. Colmenro, Macromolecules **28**, 8819 (1995)

R. Alex, P.P. De, S.K. De, Polym. Commun. **31**, 366 (1990)

P.S. Alexandrovich, F.E. Karasz, W.J. MacKnight, Polymer **18**, 1022 (1977)

P.S. Alexandrovich, F.E. Karasz, W.J. MacKnight, J. Macromol. Sci., Phys **B17**, 501 (1980)

G.C. Alfonso, A. Turturro, M. Pizzoli, M. Scandola, G. Ceccorulli, J. Polym. Sci., Polym. Phys. Ed **27**, 1195 (1989)

C. Alkan, L. Aras, J. Appl. Polym. Sci. **82**, 3558 (2001)

D. Allard, R.E. Prud'homme, J. Appl. Polym. Sci. **27**, 559 (1982)

H.A. Al-Salah, Polym. Bull. **40**, 477 (1998a)

H.A. Al-Salah, Polym. Bull. **41**, 593 (1998b)

H.A. Al-Salah, J. Appl. Polym. Sci. **77**, 1 (2000)

H.A. Al-Salah, A.M.A. Qudah, Polym. Int. **42**, 429 (1997)

A.M. Ambler, J. Polym. Sci., Polym. Chem. Ed **11**, 1505 (1973)

B. Ameduri, R.E. Prud'homme, Polymer **29**, 1052 (1988)

Y. An, L. Dong, G. Li, Z. Mo, Z. Feng, J. Polym. Sci. B: Polym. Phys. **38**, 1860 (2000)

E.W. Anderson, H.E. Bair, G.E. Johnson, T.K. Kwei, F.J. Padden Jr., D. Williams, in *Multiphase Polymers*, ed. by S.L. Cooper, G.M. Estes. Advances in Chemistry Series, vol. 176 (American Chemical Society, Washington, DC, 1979)

B. Andrcic, T. Kovacic, I. Klaric, J. Appl. Polym. Sci. **100**, 2158 (2006)

B. Andrcic, T. Kovacic, S. Perinovic, I. Klaric, J. Appl. Polym. Sci. **109**, 1002 (2008)

M. Andreis, Z. Veksli, R. Vukovic, New Polym. Mater. **3**, 197 (1992)

E. Andresen, H.G. Zechmann, Colloid Polym. Sci. **272**, 1352 (1994)

Anonymous, Res. Discl. **229**, 182 (1983)

M. Antonietti, S. Lang, H. Sillescu, Makromol. Chem., Rapid Commun **7**, 415 (1986)

K. Aoi, A. Takasu, M. Okada, Macromol. Rapid Commun. **16**, 53 (1995a)

K. Aoi, A. Takasu, M. Okada, Macromol. Rapid Commun. **16**, 757 (1995b)

K. Aoi, A. Takasu, M. Tsuchiya, M. Okada, Macromol. Chem. Phys. **199**, 2805 (1998)

K. Aoi, R. Nakamura, M. Odaka, Macromol. Chem. Phys. **201**, 1059 (2000)

Y. Aoki, Macromolecules **21**, 1277 (1988)

Y. Aoki, Macromolecules **23**, 2309 (1990)

Y. Aoki, Macromolecules **33**, 6006 (2000)

T. Aouak, A.S. Al-Arifi, M. Ouladsmane, J. Appl. Polym. Sci. **125**, 2262 (2012)

P. Aptel, I. Cabasso, J. Appl. Polym. Sci. **25**, 1969 (1980)

C.A. Arnold, D.H. Chen, Y.P. Chen, R.A. Waldbauer, M.E. Rogers, J.E. McGrath, High Performance Polym. **2**, 83 (1990)

A.Z. Aroguz, B.M. Baysal, J. Appl. Polym. Sci. **75**, 225 (2000)

A.Z. Aroguz, F.E. Karasz, Polymer **45**, 2685 (2004)

A.Z. Aroguz, H.H. Engin, B.M. Baysal, Eur. Polym. J. **43**, 403 (2007)

A. Asano, Polym. J. **36**, 23 (2004)

A. Asano, K. Takegoshi, K. Hikichi, Polym. J. **24**, 555 (1992)

A. Asano, K. Takegoshi, K. Hikichi, Polymer **35**, 5630 (1995)

A. Asano, M. Eguchi, T. Kurotsu, J. Thermal. Anal. Calorim. **56**, 1059 (1999)

A. Asano, M. Eguchi, M. Shimizu, T. Kurotsu, Macromolecules **35**, 8819 (2002)

S.M. Ashraf, S. Ahmad, U. Riaz, M. Alam, H.O. Sharma, J. Appl. Polym. Sci. **103**, 1367 (2007)

R.M. Asimova, P.V. Kozlov, V.A. Kargin, S.M. Vtorygin, Vysokomol. Soedin. **4**, 544 (1962)

M. Aubin, R.E. Prud'homme, Macromolecules **13**, 365 (1980)

M. Aubin, R.E. Prud'homme, J. Polym. Sci., Polym. Phys. Ed **19**, 1245 (1981a)

M. Aubin, R.E. Prud'homme, Polymer **22**, 1223 (1981b)

M. Aubin, R.E. Prud'homme, Polym. Eng. Sci. **24**, 350 (1984)

M. Aubin, D. Bussieres, D. Duchesne, R.E. Prud'homme, in *Polymer Compatibility and Incompatibility. Principles and Practices*, ed. by K. Solc (MMI Press, Harwood, 1982)

M. Aubin, Y. Bedard, M.F. Morrissette, R.E. Prud'homme, J. Polym. Sci., Polym. Phys. Ed **21**, 233 (1983)

M. Avella, E. Martuscelli, Polymer **29**, 1731 (1988)

A. Avramova, Polymer **36**, 801 (1995)

M. Baer, J. Polym. Sci. A **2**, 417 (1964)

H.E. Bair, Polym. Eng. Sci. **10**, 247 (1970)

H.E. Bair, D. Williams, T.K. Kwei, F.J. Padden Jr., Org. Coat. Plast. Chem. Prepr. **37**, 240 (1977)

H.E. Bair, E.W. Anderson, G.E. Johnson, T.K. Kwei, Am. Chem. Soc. Polym. Prepr. **19**, 143 (1978)

J. Baldrian, M. Horky, A. Sikora, M. Steinhart, P. Vlcek, H. Amenitsch, S. Bernstorff, Polymer **40**, 439 (1999)

D.G.H. Ballard, M.G. Rayner, J. Schelten, Polymer **17**, 640 (1976)

V. Balsamo, N. Calzadilla, G. Mora, A.J. Muller, J. Polym. Sci. B: Polym. Phys. **39**, 771 (2001)

V. Balsamo, D. Newman, L. Gouveia, L. Herrera, M. Grimau, E. Laredo, Polymer **47**, 5810 (2006)

M. Bank, J. Leffingwell, C. Thies, Macromolecules **4**, 43 (1971)

M. Bank, J. Leffingwell, C. Thies, J. Polym. Sci. A **2**, 1097 (1972)

I.O. Barcellos, V. Soldi, A.T.N. Pires, Polymer **39**, 6073 (1998)

P.J. Barham, M.J. Hill, A. Keller, C.C.A. Rosney, J. Mater. Sci. Lett. **7**, 1271 (1988)

R.S. Barnum, S.H. Goh, D.R. Paul, J.W. Barlow, J. Appl. Polym. Sci. **26**, 3917 (1981)

G.M. Bartenev, G.S. Kongarov, Rubber Chem. Technol. **36**, 668 (1963)

S. Bastida, J.I. Equiazabal, J.N. Etxeberria, Eur. Polym. J. **32**, 1229 (1996a)

S. Bastida, J.I. Equiazabal, J.N. Etxeberria, Polymer **37**, 2317 (1996b)

F.S. Bates, G.D. Wignall, Macromolecules **19**, 269 (1968)

F.S. Bates, G.D. Wignall, S.B. Dierker, Macromolecules **19**, 1938 (1986)

C.G. Bazuin, L. Rancourt, S. Villeneuve, A. Soldera, J. Polym. Sci. B: Polym. Phys. **31**, 1431 (1993)

G. Beaucage, R.S. Stein, Macromolecules **26**, 1617 (1993)

G. Beaucage, R.S. Stein, T. Hashimoto, H. Hasegawa, Macromolecules **24**, 3443 (1991)

P. Bebin, R.E. Prud'homme, J. Polym. Sci. B: Polym. Phys. **42**, 1408 (2004)

C. Belabed, Z. Benabdelghani, A. Granado, A. Etxeberria, J. Appl. Polym. Sci. **125**, 3811 (2012)

C. Belaribi, G. Marin, P. Monge, Eur. Polym. J. **22**, 481 (1986)

L.A. Belfiore, Am. Chem. Soc., Polym. Prepr **29**(1), 17 (1988)

L.A. Belfiore, C. Qin, E. Ueda, A.T.N. Pires, J. Polym. Sci. B: Polym. Phys. **31**, 409 (1993)

R.E. Belke, I. Cabasso, Polymer **29**, 1831 (1988)

S.Y. Bell, J.M.G. Cowie, I.J. McEwen, Polymer **35**, 786 (1994)

G. Belorgey, R.E. Prud'homme, J. Polym. Sci., Polym. Phys. Ed **20**, 191 (1982)

G. Belorgey, M. Aubin, R.E. Prud'homme, Polymer **23**, 1051 (1982)

Z. Benabdelghani, A. Etxeberria, J. Appl. Polym. Sci. **121**, 462 (2011)

Z. Benabdelghani, R. Belkhiri, S. Djadoun, Polym. Bull. **35**, 329 (1995)

Z. Benabdelghani, A. Etxeberria, S. Djadoun, J.J. Iruin, C. Uriarte, J. Chromatogr. A **1127**, 237 (2006)

Z. Benabdelghani, S. Djadoun, A. Etxeberria, J. Iruin, C. Uriarte, J. Appl. Polym. Sci. **108**, 220 (2008)

M.F. Benmerad, S. Djadoun, Z.A. Alothman, J. Aouak, J. Appl. Polym. Sci. **119**, 173 (2011)

S. Bennour, F. Metref, S. Djadoun, J. Appl. Polym. Sci. **98**, 806 (2005)

R.E. Bernstein, C.A. Cruz, D.R. Paul, J.W. Barlow, Macromolecules **10**, 681 (1977)

R.E. Bernstein, D.C. Wahrmund, J.W. Barlow, D.R. Paul, Polym. Eng. Sci. **18**, 1220 (1978a)

R.E. Bernstein, D.R. Paul, J.W. Barlow, Polym. Eng. Sci. **18**, 683 (1978b)

D.E. Bhagwagar, C.J. Serman, P.C. Painter, M.M. Coleman, Macromolecules **22**, 4654 (1989)

D.E. Bhagwagar, P.C. Painter, M.M. Coleman, Macromolecules **27**, 7139 (1994)

C. Bhattacharyya, S.N. Bhattacharyya, B.M. Mendal, J. Indian Chem. Soc. **63**, 157 (1986)

C. Bhattacharyya, M. Maiti, B.M. Mandal, S.N. Bhattacharyya, Macromolecules **22**, 4062 (1989)

A.K. Bhowmick, C.C. Kuo, A. Manzur, A. MacArthur, D. McIntyre, J. Macromol. Sci., Phys **B25**, 283 (1986)

S. Bicakci, M. Cakmak, Polymer **39**, 4001 (1998)

D. Bikiaris, J. Prinos, M. Botev, C. Betchev, C. Panayiotou, J. Appl. Polym. Sci. **93**, 726 (2004)

G. Bisso, P. Casarino, E. Pedemonte, Thermochim. Acta **321**, 81 (1998)

G. Bisso, P. Casarino, E. Pedemonte, Macromol. Chem. Phys. **200**, 376 (1999)

P. Black, D.J. Worsfold, J. Appl. Polym. Sci. **18**, 2307 (1974)

T.F. Blahovici, G.R. Brown, L.E. St, Pierre. Polym. Eng. Sci. **22**, 1123 (1982)

E. Blumm, A.J. Owen, Polymer **36**, 4077 (1995)

M. Bonnet, M. Buhk, G. Trogner, K.D. Rogausch, J. Petermann, Acta Polym. **49**, 174 (1998)

C. Booth, C.J. Pickles, J. Polym. Sci., Polym. Phys. Ed **11**, 595 (1973)

M. Bosma, E.J. Voremkamp, G. Ten Brinke, G. Challa, Polymer **29**, 1694 (1988a)

M. Bosma, G. Ten Brinke, T.S. Ellis, Macromolecules **21**, 1465 (1988b)

R.H. Bott, J.A. Kuphal, L.M. Robeson, D. Sagl, J. Appl. Polym. Sci. **58**, 1593 (1995)

N. Boulash, F. Amrani, Polym. Int. **50**, 1384 (2001)

N. Boulash, F. Amrani, Expr. Polym. Lett. **1**, 44 (2007)

N. Boulash, N. Haddadine, D. Bendiabdallah, F. Amrani, Polym. Bull. **42**, 701 (1999a)

N. Boulash, R. Hammachin, F. Amrani, Macromol. Chem. Phys. **200**, 678 (1999b)

N. Boulash, N. Haddadine, F. Amrani, R. Hammachin, J. Appl. Polym. Sci. **108**, 3256 (2008)

L.G. Bourland, J. Vinyl Technol. **10**, 183 (1988)

L.G. Bowland, D.M. Braunstein, J. Appl. Polym. Sci. **32**, 6151 (1986)

T.N. Bowmer, A.E. Tonelli, J. Vinyl Technol. **8**, 98 (1986a)

T.N. Bowmer, A.E. Tonelli, Macromolecules **19**, 498 (1986b)

G.R. Brannock, D.R. Paul, Macromolecules **23**, 5240 (1990)

G.R. Brannock, J.W. Barlow, D.R. Paul, J. Polym. Sci., Polym. Phys. Ed **28**, 871 (1990)

G.R. Brannock, J.W. Barlow, D.R. Paul, J. Polym. Sci., Polym. Phys. Ed **29**, 413 (1991)

H.G. Braun, G. Rehage, Angew. Makromol. Chem. **131**, 107 (1985)

D. Braun, J. Herth, G.P. Hellmann, Angew. Makromol. Chem. **171**, 53 (1989)

D. Braun, D. Yu, P.R. Kohl, X. Gao, L.N. Andradi, E. Manager, G.P. Hellmann, J. Polym. Sci., Polym. Phys. Ed **30**, 577 (1992)

D. Braun, D. Leiss, M.J. Bergmann, G.P. Hellmann, Eur. Polym. J. **29**, 225 (1993)

R.E.S. Bretas, D.G. Baird, Polymer **33**, 5233 (1992)

W. Breuers, W. Hild, H. Wolff, W. Burmeister, H. Hoyer, Plast. Katusch. **1**, 170 (1954)

R.M. Briber, F. Khoury, Polymer **28**, 38 (1987)

J. Brisson, B. Breault, Macromolecules **24**, 495 (1991)

G.L. Brode, J.V. Koleske, J. Macromol. Sci., Chem **A6**, 109 (1972)

W. Brostow, K.H. Seo, J.B. Back, J.C. Lim, Polym. Eng. Sci. **35**, 1016 (1995)

A. Bruggeman, A.H.A. Tinnemans, J. Appl. Polym. Sci. **71**, 1125 (1999)

N.Y. Buben, V.J. Goldanskii, L.Y. Zlatkevich, V.G. Nikolskii, V.G. Raevskii, Polym. Sci. USSR **9**, 2575 (1967)

C.M. Buchannan, S.C. Gedon, A.W. White, M.D. Wood, Macromolecules **25**, 7373 (1992)

C.M. Buchanan, S.C. Gedon, B.G. Pearcy, A.W. White, M.D. Wood, Macromolecules **26**, 5704 (1993)

C.M. Buchanan, B.G. Pearcy, A.W. White, M.D. Wood, J. Environ. Polym. Degrad. **5**, 209 (1997)

R. Buchdahl, L.E. Nielson, J. Polym. Sci. **15**, 1 (1955)

S. Buddhiranon, N. Kim, T. Kyu, Macromol. Chem. Phys. **212**, 1379 (2011)

A.B. Burdin, A.A. Tager, Vysokomol. Soedin, Ser. A **35**, 1290 (1993)

I. Cabasso, Am. Chem. Soc., Org. Coatings Chem. Prepr **45**, 359 (1981)

I. Cabasso, J. Jagur-Gordinski, D. Vofsi, J. Appl. Polym. Sci. **18**, 1969 (1974)

I. Cabasso, J. Jagur-Gordinski, D. Vofsi, in *Polymer Alloys, Blends, Blocks, Grafts and IPN's*, ed. by D. Klempner, K.C. Frisch (Plenum Press, New York, 1977)

H.Y. Cai, J. Yu, Z.B. Qiu, Polym. Eng. Sci. **52**, 233 (2012)

T.A. Callaghan, D.R. Paul, J. Polym. Sci. B: Polym. Phys. **32**, 1813 (1994a)

T.A. Callaghan, D.R. Paul, J. Polym. Sci. B: Polym. Phys. **32**, 1847 (1994b)

T.A. Callaghan, D.R. Paul, Macromolecules **26**, 2439 (1993)

T.A. Callaghan, K. Takakuwa, D.R. Paul, A.R. Padwa, Polymer **34**, 3796 (1993)

G.C. Campbell, D.L. Vanderhart, Y. Feng, C.C. Han, Macromolecules **25**, 2107 (1992)

X. Cao, M. Jiang, T. Yu, Makromol. Chem. **190**, 117 (1989)

S.G. Cao, Y.Q. Shi, G.W. Chen, Polym. Bull. **41**, 553 (1998)

S. Cao, Y. Shi, G. Chen, J. Appl. Polym. Sci. **74**, 1452 (1999)

X. Cao, A. Mohamed, S.H. Gordon, J.L. Sessa, D.J. Willett, Thermochim. Acta **406**, 115 (2003)

B. Carmoin, G. Villoutreix, R. Berlot, J. Macromol. Sci., Phys **B14**, 307 (1977)

P. Casarino, A. Brunacci, E. Pedemonte, Macromol. Chem. Phys. **197**, 3773 (1996)

M.G. Cascone, G. Polacco, L. Lazzeri, N. Barbani, J. Appl. Polym. Sci. **66**, 2089 (1997)

R. Caspary, Kautschuk Gummi Kunst. **25**, 249 (1972)

R. Casper, L. Morbitzer, Angew. Makromol. Chem **58/59**, 1 (1977)

S.N. Cassu, M.I. Felisberti, Polymer **38**, 3907 (1997)

S.N. Cassu, M.I. Felisberti, Polymer **40**, 4845 (1999)

R.E.N. Castro, E.A. Toledo, A.F. Rubria, E.C. Muniz, J. Mater. Sci. **38**, 699 (2003)

C. Castro, L. Gargallo, A. Leiva, D. Radic, J. Appl. Polym. Sci. **97**, 1953 (2005)

G. Ceccorulli, M. Pizzoli, M. Scandola, G.C. Alfonso, A. Turturro, Polymer **30**, 1251 (1989)

G. Ceccorulli, M. Pizzoli, M. Scandola, Macromolecules **26**, 6722 (1993)

G. Ceccorulli, M. Scandola, J. Macromol. Sci.: Pure Appl. Chem. **A36**, 327 (1999)

L.C. Cesteros, J.M. Rego, J.J. Vazquez, I. Katime, Polym. Commun. **31**, 152 (1990)

I.C. Cesteros, I.R. Isasi, I. Katime, Macromolecules **26**, 7256 (1993)

I.C. Cesteros, E. Meaurio, I. Katime, Macromolecules **26**, 2323 (1994a)

I.C. Cesteros, E. Meaurio, I. Katime, Polym. Int. **34**, 97 (1994b)

I.C. Cesteros, I.R. Isasi, I. Katime, J. Polym. Sci. B: Polym. Phys. **32**, 223 (1994c)

I.C. Cesteros, I.R. Isasi, I. Katime, Macromolecules **27**, 7887 (1994d)

I.C. Cesteros, J.L. Velada, I. Katime, Polymer **36**, 3183 (1995)

Y.T. Cha, E.T. Kim, T.K. Ahn, S. Choe, Polym. J. **26**, 1227 (1994)

Z. Chai, F.E. Karasz, Macromolecules **25**, 4716 (1992)

Z. Chai, R. Sun, Polymer **24**, 1279 (1983)

Z. Chai, D.J. Walsh, Makromol. Chem. **184**, 1459 (1983)

Z. Chai, R. Sun, D.J. Walsh, J.S. Higgins, Polymer **24**, 263 (1983)

Z. Chai, R. Sun, F.E. Karasz, Macromolecules **25**, 6113 (1992)

S.S. Chakraborty, N. Maiti, B.M. Mandal, S.N. Bhattacharyya, Polymer **34**, 111 (1993)

C.M. Chan, L.T. Weng, Rev. Chem. Eng. **16**, 341 (2000)

L.A. Chandler, E.A. Collins, J. Appl. Polym. Sci. **13**, 1585 (1969)

S.S. Chang, Polym. Commun. **29**, 33 (1988)

L.L. Chang, E.M. Woo, Macromolecules **33**, 6892 (2000)

L.L. Chang, E.M. Woo, Macromol. Chem. Phys. **202**, 636 (2001a)

L.L. Chang, E.M. Woo, Polym. J. **33**, 13 (2001b)

L.L. Chang, E.M. Woo, Colloid Polym. Sci. **281**, 1149 (2003a)

L.L. Chang, E.M. Woo, J. Polym. Sci. B: Polym. Phys. **41**, 772 (2003b)

L.L. Chang, E.M. Woo, Polym. Int. **52**, 249 (2003c)

L. Chang, E.M. Woo, Polym. Chem. **1**, 198 (2010)

L.L. Chang, E.M. Liu, H.L. Woo, Polym. J. **36**, 909 (2004a)

L.L. Chang, E.M. Woo, C.P. Chiang, Macromol. Chem. Phys. **205**, 611 (2004b)

L.L. Chang, E.M. Woo, H.L. Liu, Polymer **45**, 6909 (2004c)

C.S. Chang, E.M. Woo, J.H. Lin, Macromol. Chem. Phys. **207**, 1404 (2006)

L. Chang, Y.H. Chou, E.M. Woo, Colloid Polym. Sci. **289**, 199 (2011)

M.J.K. Chee, C. Kummerlowe, M.D. Lechner, H.W. Kammer, Macromol. Chem. Phys. **205**, 1108 (2004)

H.L. Chen, Macromolecules **28**, 2845 (1995)

H.L. Chen, M.S. Hsiao, Macromolecules **31**, 6579 (1998)

S.S. Chen, T. Kyu, J. Macromol. Sci.: Phys. **B32**, 63 (1993)

H.L. Chen, R.S. Porter, J. Polym. Sci. B: Polym. Phys. **31**, 1845 (1993)

J. Chen, D.C. Yang, Macromolecules **38**, 3371 (2005)

Y.P. Chen, D.H. Chen, C.A. Arnole, D.A. Lewis, J.F. Pollard, J.S. Graubeal, T.C. Ward, J.E. McGrath, Am. Chem. Soc., Polym. Prepr **29**(2), 370 (1988a)

F.L. Chen, E.M. Pearce, T.K. Kwei, Polymer **29**, 2285 (1988b)

C.T. Chen, H. Morawetz, Macromolecules **22**, 159 (1989)

J. Chen, S.H. Goh, S.Y. Lee, K.S. Siow, Polymer **35**, 1477 (1994)

J. Chen, S.H. Goh, S.Y. Lee, K.S. Siow, J. Appl. Polym. Sci. **56**, 761 (1995)

H.L. Chen, D.J. Liaw, J.S. Tsai, J.S. Shyu, J.M. Yang, Polym. J. **28**, 976 (1996)

H.L. Chen, J.C. Hwang, C.C. Chen, R.C. Wang, D.M. Fang, M.J. Tsai, Polymer **38**, 2747 (1997)

W. Chen, J. Wu, M. Jiang, Macromol. Chem. Phys. **199**, 1683 (1998a)

W. Chen, J. Wu, M. Jiang, Polymer **39**, 2867 (1998b)

H.L. Chen, J.C. Hwang, R.C. Wang, Polymer **39**, 6067 (1998c)

J. Chen, S.H. Goh, S.Y. Lee, K.S. Siow, Malaysian J. Chem. **1**, 20 (1998d)

X. Chen, L. An, L. Li, J. Yin, Z. Sun, Macromolecules **32**, 5905 (1999)

H.L. Chen, H.H. Liu, J.S. Lin, Macromolecules **33**, 4856 (2000)

W. Chen, D.J. David, W.J. MacKinight, F.E. Karasz, Macromolecules **34**, 4277 (2001)

S.M. Chen, F.R. Qiu, L. Tan, J. Appl. Polym. Sci. **92**, 2312 (2004a)

W. Chen, J.A. Sauer, M. Hara, Polymer **45**, 7219 (2004b)

Q. Chen, J.F. Shen, Y.Z. Hu, W.S. Huang, M.X. Ye, Polym. Eng. Sci. **48**, 556 (2008)

S.M. Chen, L. Tan, F.R. Qiu, X.L. Jiang, M. Wang, H.D. Zhang, Polymer **45**, 3045 (2004c)

F.S. Cheng, J.L. Kardos, Am. Chem. Soc. Polym. Prepr. **10**, 615 (1969)

J.T. Cheng, G.J. Mantell, J. Appl. Polym. Sci. **23**, 1733 (1979)

J. Cheng, S.C. Wang, S.J. Chen, J. Zhang, X.L. Wang, Polym. Int. **61**, 477 (2012)

H. Cherdron, M. Haubs, F. Herold, A. Schneller, P. Hermann-Schonherr, R. Wagener, J. Appl. Polym. Sci. **53**, 507 (1994)

Y.W. Cheung, R.S. Stein, Macromolecules **27**, 2512 (1994)

Y.W. Cheung, R.S. Stein, J.S. Lin, G.D. Wignall, H.E. Yang, Macromolecules **26**, 5365 (1993)

Y.W. Cheung, R.S. Stein, J.S. Lin, G.D. Wignall, Macromolecules **27**, 2520 (1994)

M.K. Cheung, S. Zheng, Y. Mi, Q. Guo, Polymer **39**, 6289 (1998)

M.K. Cheung, J. Wang, S. Zheng, Y. Mi, Polymer **41**, 1469 (2000)

Y.W. Cheung, M.J. Guest, J. Polym. Sci. B: Polym. Phys. **38**, 2976 (2000)

M.K. Cheung, K.P.Y. Wan, P.H. Yu, J. Appl. Polym. Sci. **86**, 1253 (2002)

C.P. Chiang, E.M. Woo, Eur. Polym. J. **42**, 1875 (2006)

C.P. Chiang, E.M. Woo, J. Polym. Sci. B: Polym. Phys. **45**, 2899 (2007)

Y.Y. Chien, E.M. Pearce, T.K. Kwei, Macromolecules **21**, 1616 (1988)

J.S. Chiou, D.R. Paul, J. Appl. Polym. Sci. **33**, 2935 (1987)

J.S. Chiou, D.R. Paul, J. Appl. Polym. Sci. **42**, 279 (1991)

J.S. Chiou, D.R. Paul, J.W. Barlow, Polymer **23**, 1543 (1982)

J.S. Chiou, J.W. Barlow, D.R. Paul, J. Polym. Sci., Polym. Phys. Ed **25**, 1459 (1987)

H.J. Chiu, J. Appl. Polym. Sci. **91**, 3595 (2004)

H.J. Chiu, J. Appl. Polym. Sci. **100**, 980 (2006)

H.J. Chiu, Polym. Eng. Sci. **47**, 2005 (2007)

F.C. Chiu, M.T. Li, Polymer **44**, 8013 (2003)

F.C. Chiu, K. Min, Polym. Int. **49**, 223 (2000)

H.J. Chiu, W.J. Shu, J. Polym. Res. **12**, 149 (2005)

H.J. Chiu, J.W. You, J. Polym. Res. **10**, 79 (2003)

H.J. Chiu, H.L. Chen, J.S. Lin, Polymer **42**, 5749 (2001)

J.W. Cho, Polym. Int. **24**, 173 (1991)

J.W. Cho, J. Tasaka, S. Miyata, Polym. J. **25**, 1267 (1993)

Y.W. Cho, C.W. Nam, J. Jang, S.W. Ko, J. Macromol. Sci.: Phys. **B40**, 93 (2001a)

J. Cho, M.S. Park, J.H. Choi, B.C. Jim, S.S. Han, W.S. Lyoo, J. Polym. Sci. B: Polym. Phys. **39**, 1778 (2001b)

S. Choe, D.J. Williams, W.J. MacKnight, F.E. Karasz, Polym. Mater. Sci. Eng. **56**, 827 (1987)

S. Choe, W.J. MacKnight, F.E. Karasz, Am. Chem. Soc. Polym. Mater. Sci. Eng. **59**, 702 (1988)

S. Choe, Y.J. Cha, H.S. Lee, J.S. Yoon, H.J. Choi, Polymer **36**, 4977 (1995)

J.H. Choi, S.Y. Kwak, S.Y. Kim, J.S. Kim, J.J. Kim, J. Appl. Polym. Sci. **70**, 2173 (1998)

P. Choi, S.S. Rane, W.L. Mattice, Macromol. Theory Simul. **15**, 563 (2006)

Y.F. Chong, S.H. Goh, Eur. Polym. J. **27**, 501 (1991a)

Y.F. Chong, S.H. Goh, J. Appl. Polym. Sci. **43**, 437 (1991b)

Y.F. Chong, S.H. Goh, J. Appl. Polym. Sci. **44**, 633 (1992a)

Y.F. Chong, S.H. Goh, Polymer **33**, 127 (1992b)

Y.F. Chong, S.H. Goh, Polymer **33**, 1289 (1992c)

Y.F. Chong, S.H. Goh, Polymer **33**, 132 (1992d)

Y.F. Chong, S.Y. Lee, S.H. Goh, Eur. Polym. J. **26**, 1145 (1990a)

Y.F. Chong, S.Y. Lee, S.H. Goh, Eur. Polym. J. **26**, 1207 (1990b)

D. Chopra, D. Vlassopoulos, S.G. Hatzikiriakos, J. Rheol. **42**, 1227 (1998)

I.C. Chou, P.L. Wu, E.M. Woo, Colloid Polym. Sci. **280**, 410 (2002)

T.S. Chow, Macromolecules **23**, 333 (1990)

W.H. Christiansen, D.R. Paul, J.W. Barlow, J. Appl. Polym. Sci. **34**, 537 (1987)

C.H. Chu, B. Berner, J. Appl. Polym. Sci. **47**, 1083 (1993)

K.J. Chu, W. Ji, Makromol. Chem. Phys. **196**, 479 (1995)

J.H. Chu, D.R. Paul, Polymer **40**, 2687 (1999)

J.H. Chu, D.R. Paul, Polymer **41**, 7193 (2000)

E.Y. Chu, E.M. Pearce, T.K. Kwei, T.F. Yeh, Y. Okamoto, Makromol. Chem., Rapid Commun **12**, 1 (1991)

C.W. Chu, L.C. Dickinson, J.C.W. Chien, Polym. Bull. **19**, 265 (1988)

J.H. Chu, H.K. Tilakaratne, D.R. Paul, Polymer **41**, 5393 (2000)

H.H. Chuah, T. Kyu, T. Helminiak, Polym. Mater. Sci. Eng. **56**, 58 (1987)

W.T. Chuang, K.S. Shih, P.D. Hong, J. Polym. Res. **12**, 197 (2005)

Y.S. Chun, R.A. Weiss, J. Appl. Polym. Sci. **94**, 1227 (2004)

Y.S. Chun, H.S. Lee, H.C. Jung, W.N. Kim, J. Appl. Polym. Sci. **72**, 733 (1999)

Y.S. Chun, J. Park, J.B. Sun, W.N. Kim, J. Polym. Sci. B: Polym. Phys. **38**, 2072 (2000)

T.S. Chung, P.N. Chen Sr., J. Appl. Polym. Sci. **40**, 1209 (1990)

T.S. Chung, E.R. Kafchinski, Polymer **37**, 1635 (1996)

T.S. Chung, R.H. Vora, M. Jaffe, J. Polym. Sci., Polym. Chem. Ed **29**, 1207 (1991)

T.S. Chung, P. Foley, M. Jaffe, Polym. Adv. Technol. **8**, 537 (1997)

S. Cimmino, E. Martuscelli, C. Silvestre, M. Canetti, C. Dedalla, A. Seves, J. Polym. Sci., Polym. Phys. Ed **27**, 1781 (1989)

S. Cimmino, E. Martuscelli, M. Saviano, C. Silvestre, Polymer **32**, 1461 (1991)

S. Cimmino, F.E. Karasz, W.J. MacKnight, J. Polym. Sci., Polym. Phys. Ed **30**, 49 (1992)

S. Cimmino, E. Dipace, E. Martuscelli, C. Silvestre, Polymer **34**, 2799 (1993)

S. Cimmino, P. Iodice, C. Silvestre, F.E. Karasz, J. Appl. Polym. Sci. **75**, 746 (2000)

E.P. Cizek, U.S. Patent 3,383,435 to General Electric Co., 1968

M.B. Clark Jr., C.A. Burkhardt, J.A. Gardella Jr., Macromolecules **22**, 4495 (1989)

J.N. Clark, J.S. Higgins, C.K. Kim, D.R. Paul, Polymer **33**, 3137 (1992)

S.D. Clas, A. Eisenberg, J. Polym. Sci., Polym. Phys. Ed **22**, 1529 (1984)

J.B. Class, S.G. Chu, J. Appl. Polym. Sci. **30**, 805 (1985a)

J.B. Class, S.G. Chu, J. Appl. Polym. Sci. **30**, 815 (1985b)

J.B. Class, S.G. Chu, J. Appl. Polym. Sci. **30**, 825 (1985c)

S. Classen, M. Vogt, J.H. Wendorff, Polym. Adv. Technol. **6**, 616 (1995)

C.S. Cleveland, K.S. Guigley, P.C. Painter, M.M. Coleman, Macromolecules **33**, 4278 (2000)

M.M. Coleman, P.C. Painter, Prog. Polym. Sci. **20**, 1 (1995)

M.M. Coleman, C.J. Serman, P.C. Painter, Macromolecules **20**, 226 (1987)

M.M. Coleman, J. Hu, Y. Park, P.C. Painter, Macromolecules **29**, 1659 (1988a)

M.M. Coleman, P.J. Shrovanek, P.C. Painter, Macromolecules **21**, 59 (1988b)

M.M. Coleman, A.M. Lichkus, P.C. Painter, Macromolecules **22**, 586 (1989a)

M.M. Coleman, J.Y. Lee, C.J. Serman, Z. Wang, P.C. Painter, Polymer **30**, 1298 (1989b)

M.M. Coleman, H. Zhang, Y. Xu, P.C. Painter, Am. Chem. Soc., Polym. Prepr **32**(2), 44 (1991a)

M.M. Coleman, Y. Xu, P.C. Painter, Am. Chem. Soc. Polym. Mater. Sci. Eng. **64**, 28 (1991b)

M.R. Coleman, R. Kohn, W.J. Koros, J. Appl. Polym. Sci. **50**, 1059 (1993a)

M.M. Coleman, X. Yang, H. Zhang, P.C. Painter, J. Macromol. Sci.: Phys. **32**, 295 (1993b)

M.M. Coleman, X. Yang, H. Zhang, P.C. Painter, K.V. Scherer Jr., J. Polym. Sci. A: Polym. Chem. **31**, 2039 (1993c)

M.M. Coleman, Y. Xu, S.R. Macio, P.C. Painter, Macromolecules **26**, 3457 (1993d)

M.M. Coleman, X. Yang, P.C. Painter, Y.H. Kim, J. Polym, Sci. A: Polym. Chem. **32**, 1817 (1994)

M.M. Coleman, G.J. Pehlert, X. Yang, J.B. Stallman, P.C. Painter, Polymer **37**, 4753 (1996)

M.M. Coleman, L.A. Narvett, Y.H. Park, P.C. Painter, J. Macromol. Sci.: Phys. **B37**, 283 (1998a)

M.M. Coleman, Y. Hu, M. Sobkowiak, P.C. Painter, J. Polym. Sci. B: Polym. Phys. **36**, 1579 (1998b)

M.M. Coleman, M. Mock, P.C. Painter, J. Macromol. Sci.: Phys. **B38**, 403 (1999)

G. Cong, Y. Huang, W.J. MacKnight, F.E. Karasz, Macromolecules **19**, 2675 (1986)

P.J. Corish, Rubber Chem. Technol. **40**, 324 (1967)

E. Corradini, A.F. Rubira, E.C. Muniz, Eur. Polym. J. **33**, 1651 (1997)

A.I. Cosutchi, S.L. Nica, C. Hulubei, M. Homocianu, S. Ioan, Polym. Eng. Sci. **52**, 1429 (2012)

P. Cote, J. Brisson, Macromolecules **27**, 7329 (1994)

P. Cousin, R.E. Prud'homme, Eur. Polym. J. **18**, 957 (1982)

P. Cousin, R.E. Prud'homme, in *Multicomponent Polymer Materials*, ed. by D.R. Paul, L.H. Sperling. Advances in Chemistry Series, vol. 211 (American Chemical Society, Washington, DC, 1986)

J.M.G. Cowie, D. Cocton, Polymer **40**, 227 (1999)

J.M.G. Cowie, A. Demaude, Polym. Adv. Technol. **5**, 178 (1994)

J.M.G. Cowie, E.M. Elexpuru, Eur. Polym. J. **28**, 623 (1992)

J.M.G. Cowie, J.H. Harris, Polymer **33**, 4592 (1992)

J.M.G. Cowie, J.H. Harris, Eur. Polym. J. **30**, 707 (1994)

J.M.G. Cowie, D. Lath, Polym. Commun. **28**, 300 (1987)

J.M.G. Cowie, D. Lath, Makromol. Chem. Macromol. Symp. **16**, 103 (1988)

J.M.G. Cowie, C. Love, Polymer **42**, 4783 (2001)

J.M.G. Cowie, S. Miachon, Macromolecules **25**, 3295 (1992)

J.M.G. Cowie, A.A.N. Reilly, Polymer **33**, 4814 (1992)

J.M.G. Cowie, A.A.N. Reilly, Eur. Polym. J. **29**, 455 (1993a)

J.M.G. Cowie, A.A.N. Reilly, J. Appl. Polym. Sci. **47**, 1155 (1993b)

J.M.G. Cowie, S. Saeki, Polym. Bull. **6**, 75 (1981)

J.M.G. Cowie, E.M. Elexpuru, J.H. Harris, I.J. McEwen, Makromol. Chem., Rapid Commun **10**, 691 (1989a)

J.M.G. Cowie, M.T. Garay, D. Lath, I.J. McEwen, Brit. Polym. J. **21**, 81 (1989b)

J.M.G. Cowie, I.J. McEwen, L. Nadvornik, Macromolecules **23**, 5106 (1990a)

J.M.G. Cowie, V.M.C. Reid, I.J. McEwen, Polymer **31**, 486 (1990b)

J.M.G. Cowie, V.M.C. Reid, I.J. McEwen, Polymer **31**, 905 (1990c)

J.M.G. Cowie, E.M. Elexpuru, I.J. McEwen, J. Polym. Sci., Polym. Phys. Ed **29**, 407 (1991a)

J.M.G. Cowie, R. Ferguson, I.J. McEwen, Polym. Commun. **32**, 293 (1991b)

J.M.G. Cowie, E.M. Elexpuru, I.J. McEwen, Polymer **33**, 1993 (1992a)

J.M.G. Cowie, G. Li, R. Ferguson, I.J. McEwen, J. Polym. Sci., Polym. Phys. Ed **30**, 1351 (1992b)

J.M.G. Cowie, J.H. Harris, I.J. McEwen, Macromolecules **25**, 5287 (1992c)

J.M.G. Cowie, M.D. Fernandez, M.J. Fernandez, I.J. McEwen, Eur. Polym. J. **28**, 145 (1992d)

J.M.G. Cowie, M.D. Fernandez, M.J. Fernandez, I.J. McEwen, Polymer **33**, 2744 (1992e)

J.M.G. Cowie, R. Ferguson, M.D. Fernandez, M.J. Fernandez, I.J. McEwen, Macromolecules **25**, 3170 (1992f)

J.M.G. Cowie, B.G. Devlin, I.J. McEwen, Polymer **34**, 501 (1993a)

J.M.G. Cowie, L.M. Watson, I.J. McEwen, Polym. Bull. **32**, 729 (1993b)

J.M.G. Cowie, G. Li, I.J. McEwen, Polymer **35**, 5518 (1994a)

J.M.G. Cowie, R. Ferguson, I.J. McEwen, V.M.C. Reid, Polymer **35**, 1473 (1994b)

J.M.G. Cowie, S. Nakata, G.W. Adams, Macromol. Symp. **112**, 207 (1996)

G. Crevecoeur, G. Groeninckx, Macromolecules **24**, 1190 (1991)

E.G. Crispim, A.F. Rubira, E.C. Muniz, Polymer **40**, 5129 (1999)

E.G. Crispim, I.T.A. Schuquel, A.F. Rubira, E.C. Muniz, Polymer. **41**, 933 (2000)

G. Crone, A. Natansohn, Polym. Bull. **27**, 73 (1991)

C.A. Cruz, D.R. Paul, J.W. Barlow, J. Appl. Polym. Sci. **23**, 589 (1979a)

C.A. Cruz, D.R. Paul, J.W. Barlow, J. Appl. Polym. Sci. **24**, 2101 (1979b)

C.A. Cruz, J.W. Barlow, D.R. Paul, Macromolecules **12**, 726 (1979c)

C.A. Cruz, J.W. Barlow, D.R. Paul, J. Appl. Polym. Sci. **25**, 1549 (1980)

F. Cser, A. Goodwin, J. Therm. Anal. Calorim. **65**, 69 (2001)

E. Cuddkhy, J. Moacanin, A. Rembaum, J. Appl. Polym. Sci. **9**, 1385 (1965)

L. Cui, J.T. Yeh, K. Wang, Q. Fu, J. Polym. Sci. B: Polym. Phys. **46**, 1360 (2008)

E.P. Da Silva, M.I.B. Tavares, J. Appl. Polym. Sci. **67**, 449 (1998a)

E.P. Da Silva, M.I.B. Tavares, Polym. Testing **17**, 43 (1998b)

S.M. Da Silva Neiro, D.C. Dragunski, A.F. Rubira, E.C. Muniz, Eur. Polym. J. **36**, 583 (2000)

M.D. Dadmun, C.C. Han, Mater. Res. Soc. Symp. Proc. **305**, 171 (1993)

J. Dai, S.H. Goh, S.Y. Lee, K.S. Siow, Polymer **34**, 4314 (1993)

Y.K. Dai, E.Y. Chu, Z.S. Xu, E.M. Pearce, Y. Okamoto, T.K. Kwei, J. Polym. Sci. A: Polym. Chem. **32**, 397 (1994)

J. Dai, S.H. Goh, S.Y. Lee, K.S. Siow, J. Appl. Polym. Sci. **53**, 837 (1994a)

J. Dai, S.H. Goh, S.Y. Lee, K.S. Siow, Polymer **35**, 2174 (1994b)

J. Dai, S.H. Goh, S.Y. Lee, K.S. Siow, Polym. J. **26**, 905 (1994c)

J. Dai, S.H. Goh, S.Y. Lee, K.S. Siow, J. Polym. Res. **2**, 209 (1995a)

J. Dai, S.H. Goh, S.Y. Lee, K.S. Siow, Polym. J. **27**, 558 (1995b)

J. Dai, S.H. Goh, S.Y. Lee, K.S. Siow, Polymer **37**, 3259 (1996)

X.H. Dai, Z.M. Liu, B.Z. Han, G.Y. Yang, X.L. Zhang, J. He, J. Xu, M.L. Yao, Macromol. Rapid Commun. **23**, 626 (2002)

K. Darragas, G. Groeninckx, H. Reynaers, C. Samyn, Eur. Polym. J. **30**, 1165 (1994)

G. Das, A.N. Banerjee, B.C. Mitra, Eur. Polym. J. **32**, 179 (1996)

G. Das, A.N. Banerjee, New Polym. Mater. **5**, 61 (1996)

S. Das, F. Rodriguez, Am. Chem. Soc., Polym. Prepr. **28**(2), 140 (1987)

J. Datta, A.K. Nandi, Polymer **35**, 4804 (1994)

J. Datta, A.K. Nandi, Polymer **37**, 5179 (1996)

P.B. Dave, N.J. Ashar, R.A. Gross, S.P. McCarthy, Am. Chem. Soc., Polym. Prepr. **31**(1), 442 (1990)

M.C. Davies, K.M. Shakesheff, A.G. Shard, A. Domb, C.J. Roberts, S.J.B. Tendler, P.M. Williams, Macromolecules **29**, 2205 (1996)

D.D. Davis, G.H. Taylor, T.K. Kwei, J. Appl. Polym. Sci. **26**, 2001 (1981)

M.L. De Andrade, T.D.Z. Atvars, Macromolecules **37**, 9096 (2004)

H.K. De Decker, D.J. Sabatine, Rubber Age **99**(4), 73 (1967)

A.M. De Ilarduya, J.L. Eguiburu, E. Espi, J.J. Iruin, M.J. Fernandez-Berridi, Macromol. Chem. **194**, 501 (1993)

A.M. De Ilarduya, J.J. Iruni, Fernandez-Berridi. Macromolecules **28**, 3707 (1995)

H. De Jager, G. Ten Brinke, Macromolecules **24**, 3454 (1991)

R. De Juann, A. Etxeberria, M. Cortazar, J.J. Iruin, Macromolecules **27**, 1395 (1994)

H. De Los Santos, Jones, Y. Liu, P.T. Inglefield, A.A. Jones, C.K. Kim, D.R. Paul. Polymer **35**, 57 (1994)

W. De Oliveira, W.G. Glasser, J. Appl. Polym. Sci. **51**, 563 (1994)

S.C. De Vos, W. Huhn, B. Rieger, M. Moller, Polym. Bull. **42**, 611 (1999)

B.D. Dean, J. Appl. Polym. Sci. **30**, 4193 (1985)

B.D. Dean, J. Appl. Polym. Sci. **33**, 2259 (1987a)

B.D. Dean, J. Appl. Polym. Sci. **34**, 887 (1987b)

B.D. Dean, J.E. Harris, J. Appl. Polym. Sci. **46**, 745 (1992)

J.Y. Decroix, A. Piloz, Rev. Caoutsch. Plast. **54**, 91 (1977)

G. Defieuw, G. Groeninckx, H. Reynaers, Polymer **30**, 2158 (1989a)

G. Defieuw, G. Groeninckx, H. Reynaers, Polymer **30**, 2164 (1989b)

G. Defieuw, G. Groeninckx, H. Reynaers, Polymer **30**, 595 (1989c)

V.A. Deimede, K.V. Fragou, E.G. Koulouri, J.K. Kallitsis, G.A. Voyiatzis, Polymer **41**, 9095 (2000)

M.T. DeMeuse, E.C. Chenevey, Z.H. Ophir, J.J. Rafalko, M.I. Haider, Am. Chem. Soc. Polym. Mater. Sci. Eng. **59**, 1714 (1988)

M.T. DeMeuse, M. Jaffe, Am. Chem. Soc., Polym. Prepr. **30**(2), 540 (1989)

S. Demirci, A. Alaslan, T. Caykara, Appl. Surf. Sci. **255**, 5979 (2009)

M. Deng, L.S. Nair, S.P. Nukavarapu, S.G. Kumbar, T. Jiang, N.R. Krogman, A. Singh, H.R. Allcock, C.T. Laurencin, Biomaterials **29**, 337 (2008)

A. Dhamodaran, S. Arindam, J. Tushar, J. Phys. Chem. B **112**, 5305 (2008)

M.L. Di Lorenzo, P.L. Pietra, Errico, M.C. Righetti, M. Angiuli. Polym. Eng. Sci. **47**, 323 (2007)

L.C. Dickinson, H. Yang, C.W. Chu, R.S. Stein, J.C.W. Chien, Macromolecules **20**, 1757 (1987)

D. Dimitrova, A. Aivazov, Y. Zelenev, God. Vissh. Khim. Tekhnol. Inst., Burgas. Bulg. **8**, 57 (1971) [Chem. Abstr., **79**, 127188d (1973)]

G.Z. Ding, K. Cui, J.P. Liu, J. Appl. Polym. Sci. **122**, 617 (2011)

L. Diniliuc, C. DeKesel, C. David, Eur. Polym. J. **28**, 1365 (1992)

G. DiPaola-Baranyi, P. Degre, Macromolecules **14**, 1456 (1981)

S. Djadoun, Polym. Bull. **9**, 313 (1983)

S. Djadoun, F.E. Karasz, F. Metref, Macromol. Symp. **78**, 155 (1994)

S. Djadoun, F.E. Karasz, A.S.H. Hamou, Thermochim. Acta **282/283**, 399 (1996)

A. Dobry, F. Boyer-Kawenoki, J. Polym. Sci. **2**, 90 (1974)

T. Doi, S. Yukioka, H. Inoue, A. Akimoto, J. Appl. Polym. Sci. **63**, 925 (1997)

D. Dompas, G. Groeninckx, M. Isogawa, T. Hasegawa, M. Kadokura, Polymer **38**, 421 (1997)

L. Dong, D.J.T. Hill, A.K. Whittaker, K.P. Ghiggino, Macromolecules **27**, 5912 (1994)

C.P. Doube, D.J. Walsh, Polymer **20**, 1115 (1979)

G. Dreezen, Z. Fang, G. Groeninckx, Polymer **40**, 5907 (1999)

E. Drioli, A. Apicella, H.B. Hopfenberg, E. Martuscelli, L. Nicolais, Chim. Ind. (Milan) **60**, 975 (1978)

X. Drujon, G. Reiss, H.K. Hall Jr., New Polym. Mater. **3**, 283 (1992)

Y. Duan, E.M. Pearce, T.K. Kwei, X. Hu, M. Rafailovich, J. Sokolov, K. Zhou, S. Schwarz, Macromolecules **34**, 6761 (2001)

E. Dubini Paglia, P.L. Beltrame, M. Canetti, A. Seves, B. Marcandalli, E. Martuscelli, Polymer **34**, 996 (1993)

S. Duff, S. Tsuyama, T. Iwamoto, F. Fujibayashi, C. Birkinshaw, Polymer **42**, 991 (2001)

D.J. Duffy, A.M. Heintz, H.D. Stidham, S.L. Hsu, W. Suen, C.W. Paul, Int. J. Adhesion Adhesives **25**, 39 (2005)

D.J. Dunn, S. Krause, J. Polym. Sci., Polym. Lett. Ed. **12**, 591 (1974)

S. Dutta, S.S. Chakraborty, B.M. Mandal, S.N. Bhattacharyya, Polymer **34**, 3499 (1993)

D. Dutta, R.A. Weiss, J.S. He, Polymer **37**, 429 (1996)

M. Ebert, R.W. Garbella, J.H. Wendroff, Makromol. Chem., Rapid Commun. **7**, 65 (1986)

S.L. Edie, H. Marand, Am. Chem. Soc., Polym. Prepr. **32**(3), 329 (1991)

S.H. Egboh, Am. Chem. Soc. Polym. Mater. Sci. Eng. **49**, 45 (1983)

M. Eguchi, A. Asano, T. Kurotu, Kobushi Ronbunshu **55**, 284 (1998)

J.I. Eguiazabal, J.J. Iruin, M. Cortazar, G.M. Guzman, Makromol. Chem. **185**, 1761 (1984)

J.I. Eguiazabal, E. Calahorra, M. Cortazar, G.M. Guzman, Makromol. Chem. **187**, 2439 (1986a)

J.I. Eguiazabal, J.J. Iruin, M. Cortazar, J. Appl. Polym. Sci. **32**, 5945 (1986b)

J.L. Eguiburu, A.M. de Ilarguya, J.J. Iruin, M.J. Fernandez-Berridi, Polym. Int. **33**, 393 (1994)

J.L. Eguiburu, J.J. Iruin, M.J. Fernandez-Berridi, J. San Roman, Polymer **39**, 6891 (1998)

A. Eisenberg, P. Smith, Z.L. Zhou, Polym. Eng. Sci. **22**, 1117 (1982)

C.D. Eisenbach, J. Hofmann, K. Fischer, Macromol. Rapid Commun. **15**, 117 (1994a)

C.D. Eisenbach, J. Hofmann, W.J. MacKnight, Macromolecules **27**, 3162 (1994b)

K. El Miloudi, A.S. Hadj Hamou, S. Djadoun, Polym. Eng. Sci. **48**, 458 (2008)

K. El Miloudi, S. Djaroun, N. Sbirrazzuoli, S. Geribaldi, Thermochim. Acta **483**, 49 (2009)

E. El Shafee, Eur. Polym. J. **38**, 413 (2002a)

E. El Shafee, Polymer **43**, 921 (2002b)

E. El Shafee, W. Ueda, Eur. Polym. J. **38**, 1327 (2002)

E. El Shafee, G.R. Saad, S.M. Fahmy, Eur. Polym. J. **37**, 2091 (2001)

E. El Shafee, G.R. Saad, M. Zaki, J. Polym. Res. **15**, 47 (2008)

H.M.N. El-Din, A.W.M. El-Naggar, F.I. Ali, Polym. Int. **52**, 225 (2003)

T.S. Ellis, Polymer **29**, 2015 (1988)

T.S. Ellis, Macromolecules **22**, 742 (1989)

T.S. Ellis, Polym. Eng. Sci. **30**, 998 (1990a)

T.S. Ellis, Polymer **31**, 1058 (1990b)

T.S. Ellis, Polymer **33**, 1469 (1992)

T.S. Ellis, J. Polym. Sci. B: Polym. Phys. **31**, 1109 (1993)

T.S. Ellis, Polymer **36**, 3919 (1995)

T.S. Ellis, Polymer **38**, 3837 (1997)

T.S. Ellis, Polymer **39**, 4741 (1998)

C. Elmqvist, S.E. Svanson, Eur. Polym. J. **11**, 789 (1975)

S.H. El-Taweei, B. Stroll, C. Schick, E-Polymers, Art. No. 018 (2011)

M. Endo, K. Yamada, K. Tadano, Y. Yishino, S. Yano, Macromol. Rapid Commun. **21**, 396 (2000)

M. Endo, Y. Morishima, S. Yano, K. Tadano, Y. Murata, K. Tsunashima, J. Appl. Polym. Sci. **101**, 3971 (2006)

A.D. English, P. Smith, D.E. Avelson, Polymer **26**, 1523 (1985)

R. Erro, M. Gaztelumendi, J. Nazabal, New Polym. Mater. **3**, 87 (1992)

R. Erro, M. Gaztelumendi, J. Nazabal, J. Appl. Polym. Sci. **77**, 2978 (2000)

A. Escala, R.S. Stein, in *Multiphase Polymers*, ed. by S.L. Cooper, G.M. Estes. American Chemical Society, Advances in Chemistry Series, vol. 176 (Washington, DC, 1979)

A. Escala, E. Balitzer, R.S. Stein, Am. Chem. Soc., Polym. Prepr. **19**(1), 152 (1978)

A. Etxeberria, J.M. Elorza, J.J. Iruin, C. Macro, M.A. Gomez, J.G. Faton, Eur. Polym. J. **29**, 1483 (1993)

A. Etxeberria, C. Uriarte, M.J. Fernandez-Berridi, J.J. Iruin, Polymer **35**, 2128 (1994)

A. Etxeberria, M. Iriarte, C. Uriarte, J.J. Iruin, Macromolecules **28**, 7188 (1995)

A. Etxeberria, S. Guezala, J.J. Iruin, J.G. de la Campa, J. de Abajo, J. Appl. Polym. Sci. **68**, 2141 (1998)

A. Etxeberria, J.J. Iruin, A. Unanue, P.J. Iriondo, M.J. Fernandez-Berridi, A.M. de Ilarduya, Eur. Polym. J. **37**, 1943 (2001)

S.R. Fahrenhlotz, T.K. Kwei, Macromolecules **14**, 1076 (1981)

L. Fambri, A. Penati, J. Kolarik, Angew, Makromol. Chem. **209**, 119 (1993)

L. Fambri, A. Penati, J. Kolarik, Polymer **38**, 835 (1997)

W.C. Fan, S.X. Zheng, J. Polym. Sci. B: Polym. Phys. **45**, 2580 (2007)

L. Fang, S.H. Goh, J. Appl. Polym. Sci. **76**, 1785 (2000)

H.X. Fang, F. Mighri, A. Ajji, J. Appl. Polym. Sci. **105**, 2955 (2007)

L.O. Faria, R.L. Moreira, Polymer **40**, 4465 (1999)

D. Feldman, M. Rusu, Eur. Polym. J. **10**, 41 (1974)

H. Feng, Z. Feng, L. Shen, Polymer **34**, 2516 (1993)

H. Feng, C. Ye, P. Zhang, Z. Sun, Z. Feng, Macromol. Chem. Phys. **196**, 2587 (1995a)

H.Q. Feng, L.F. Shen, Z.L. Feng, Eur. Polym. J. **31**, 243 (1995b)

Y. Feng, A. Schmidt, R.A. Weiss, Macromolecules **29**, 3909 (1996a)

H. Feng, C. Ye, Z. Feng, Polym. J. **28**, 661 (1996b)

H. Feng, C. Ye, Z. Feng, Polym. J. **28**, 678 (1996c)

Y. Feng, R.A. Weiss, A. Karim, C.C. Han, J.F. Ankner, H. Kaiser, D.G. Peiffer, Macromolecules **29**, 3918 (1996d)

Y. Feng, R.A. Weiss, C.C. Han, Macromolecules **29**, 3925 (1996e)

H. Feng, C. Ye, Z. Feng, Eur. Polym. J. **33**, 743 (1997)

L. Feng, T. Watanabe, Y. He, Y. Wang, T. Kichise, T. Fukuchi, G.Q. Chen, Y. Doi, Y. Inoue, Macromol. Biosci. **3**, 310 (2003)

F. Feraz, A.S.H. Hamou, S. Djadoun, Eur. Polym. J. **31**, 665 (1995)

A.C. Fernandes, J.W. Barlow, D.R. Paul, J. Appl. Polym. Sci. **29**, 1971 (1984)

A.C. Fernandes, J.W. Barlow, D.R. Paul, J. Appl. Polym. Sci. **32**, 5357 (1986a)

A.C. Fernandes, J.W. Barlow, D.R. Paul, J. Appl. Polym. Sci. **32**, 5481 (1986b)

A.C. Fernandes, J.W. Barlow, D.R. Paul, J. Appl. Polym. Sci. **32**, 6073 (1986c)

A.C. Fernandes, J.W. Barlow, D.R. Paul, Polymer **27**, 1788 (1986d)

A.C. Fernandes, J.W. Barlow, D.R. Paul, Polymer **27**, 1799 (1986e)

M.D. Fernandez, M.J. Fernandez, McEwen. Polymer **38**, 2767 (1997)

M.J. Fernandez-Berridi, M. Valero, A.M. de Ilarduya, E. Espi, J.J. Iruin, Polymer **34**, 38 (1993)

L. Finelli, B. Sarti, M. Scandola, J. Macromol. Sci. Pure Appl. Chem. **A33**, 13 (1997)

P.J. Flory, *Principles of Polymer Chemistry* (Cornell University Press, Ithaca, 1953), p. 555

M.L. Focarete, M. Scandola, P. Dobrzynski, M. Kowalczuk, Macromolecules **35**, 8472 (2002)

M.E. Fowler, J.W. Barlow, D.R. Paul, Polymer **28**, 1177 (1987)

M.E. Fowler, D.R. Paul, L.A. Cohen, W.T. Freed, J. Appl. Polym. Sci. **37**, 513 (1989)

B. Francis, S. Thomas, S.P. Thomas, R. Ramaswamy, V.L. Rao, Colloid Polym. Sci. **285**, 83 (2006)

C.W. Frank, W. Zin, in *Photophysics of Polymers*, ed. by C.E. Hoyle, J.M. Torkelson. American Chemical Society, Symposium Series, vol. 358 (Washington, DC, 1987)

M.L. Franzen, J.R. Elliott Jr., T. Kyu, Macromolecules **28**, 5147 (1995)

J.R. Fried, G.A. Hanna, Polym. Eng. Sci. **22**, 705 (1982)

J.R. Fried, F.E. Karasz, W.J. MacKnight, Macromolecules **11**, 150 (1978)

J.R. Fried, G.A. Hanna, H. Kalkanoglu, in *Polymer Compatibility and Incompatibility. Principles and Practices*, ed. by K. Solc (MMI Press, Harwood, 1982)

J.R. Fried, T. Lorenz, A. Ramdas, Polym. Eng. Sci. **25**, 1048 (1985)

C. Friedrich, C. Schwarzwaelder, R.E. Riemann, Polymer **37**, 2499 (1996)

F. Friese, Plaste Kautsch. **15**, 646 (1968)

K. Fujimoto, N. Yoshimiya, Nippon Gomu Kyokaishi **38**, 284 (1965); Rubber Chem. Technol. **41**, 669 (1968)

K. Fujimoto, N. Yoshimura, Nippon Gomu Kyokaishi **39**, 919 (1966); Rubber Chem. Technol. **41**, 1109 (1968)

K. Fujioka, N. Noethiger, C.L. Beatty, Y. Baba, A. Kagemoto, in *Polymer Blends and Composites in Multiphase Systems*, ed. by C.D. Han. American Chemical Society, Advances in Chemistry Series, vol. 206 (Washington, DC, 1984)

T. Fukai, J.C. Yang, T. Kyu, S.Z.D. Cheng, S.K. Lee, S.L.C. Hsu, F.W. Harris, Polymer **33**, 3621 (1992)

D.W. Gaibler, W.E. Rochefort, J.B. Wilson, S.S. Kelley, Cellulose **11**, 225 (2004)

A.M. Gajria, V. Dave, R.A. Gross, S.P. McCarthy, Polymer **37**, 437 (1996)

M. Galin, Makromol. Chem. Rapid. Commun. **5**, 119 (1984)

M. Galin, Makromol. Chem. **188**, 1391 (1987a)

M. Galin, Makromol. Chem. Rapid. Commun. **8**, 411 (1987b)

M. Galin, L. Maslinko, Eur. Polym. J **23**, 923 (1987)

K.P. Gallagher, X. Zhang, J.P. Runt, G. Huynh-ba, J.S. Lin, Macromolecules **26**, 588 (1993)

M.E. Galvin, Macromolecules **24**, 6354 (1991)

M.E. Galvin, S. Heffner, K.I. Winey, Macromolecules **27**, 3520 (1994)

P.P. Gan, D.R. Paul, A.R. Padwa, Polymer **35**, 1487 (1994a)

P.P. Gan, D.R. Paul, A.R. Padwa, Polymer **35**, 3351 (1994b)

P.P. Gan, D.R. Paul, J. Appl. Polym. Sci. **54**, 317 (1994a)

P.P. Gan, D.R. Paul, Polymer **35**, 3513 (1994b)

P.P. Gan, D.R. Paul, J. Polym. Sci. B: Polym. Phys. **33**, 1693 (1995)

M.T. Garay, M.C. Llamas, E. Iglesins, Polymer **38**, 5091 (1997)

M.T. Garay, C. Alava, M. Rodriguez, Polymer **41**, 5799 (2000)

M.T. Garay, M. Rodriguez, J.L. Vilas, L.M. Leon, J. Macromol. Sci. B **B43**, 437 (2004)

F.O. Garces, K. Sivadasan, P. Somasundaran, N.J. Turro, Macromolecules **27**, 272 (1994)

Z.G. Gardlund, Polymer **34**, 1850 (1993)

L. Gargallo, N. Gatica, D. Radic, Int. J. Polym. Mater. **27**, 107 (1994)

A. Garton, S. Wang, R.A. Weiss, J. Polym. Sci. Polym. Phys. Ed. **26**, 1545 (1988)

M. Gaztelumendi, J. Nazabal, J. Appl. Polym. Sci. **70**, 185 (1998)

M. Gaztelumendi, I. Mondragon, J. Nazabal, Makromol. Chem. Macromol. Symp. **20/21**, 269 (1988)

M. Gaztelumendi, J. Nazabal, J. Polym. Sci. B: Polym. Phys. **33**, 603 (1995)

B.D. Gesner, in *Encyclopedia of Polymer Science and Technology*, ed. by N.M. Bikales, vol. 10 (Wiley-Interscience, New York, 1969), p. 694

P. Gestoso, J. Brisson, Polymer **44**, 7765 (2003)

A.V. Gevorkyan, M.E. Ovsepyan, A.S. Safarov, Arm. Khim. Zh. **31**, 107 (1978)

C.M. Gibon, S. Norvez, S. Tence-Girault, J.T. Goldbach, Macromolecules **41**, 5744 (2008)

Y.K. Godovskii, N.P. Bessonova, Vysokomol. Soedin. Ser. A **21**, 2293 (1979); Polym. Sci. USSR **21**, 2531 (1979)

Y.K. Godovskii, Z.F. Zharikova, Y.M. Malinskii, Vysokomol. Soedin. Ser. A **23**, 133 (1981); Polym. Sci. USSR **23**, 149 (1981)

S.H. Goh, Polym. Bull. **17**, 221 (1987)

S.H. Goh, S.Y. Lee, Eur. Polym. J **23**, 315 (1987)

S.H. Goh, S.Y. Lee, Eur. Polym. J. **24**, 923 (1988a)

S.H. Goh, S.Y. Lee, Thermochim. Acta **123**, 3 (1988b)

S.H. Goh, S.Y. Lee, Eur. Polym. J. **25**, 571 (1989a)
S.H. Goh, S.Y. Lee, Eur. Polym. J. **25**, 997 (1989b)
S.H. Goh, S.Y. Lee, Eur. Polym. J. **26**, 715 (1990a)
S.H. Goh, S.Y. Lee, Makromol. Chem. **191**, 3081 (1990b)
S.H. Goh, S.Y. Lee, Polym. Bull. **23**, 643 (1990c)
S.H. Goh, S.Y. Lee, Polym. Commun. **31**, 463 (1990d)
S.H. Goh, S.Y. Lee, J. Appl. Polym. Sci. **41**, 1391 (1990e)
S.H. Goh, L.S. Lim, Eur. Polym. J. **26**, 711 (1990)
S.H. Goh, X.P. Ni, Polymer **40**, 5733 (1999)
S.H. Goh, K.S. Siow, J. Appl. Polym. Sci. **32**, 3407 (1986a)
S.H. Goh, K.S. Siow, Thermochim. Acta **105**, 191 (1986b)
S.H. Goh, K.S. Siow, J. Appl. Polym. Sci. **33**, 1849 (1987)
S.H. Goh, K.S. Siow, Polym. Bull. **17**, 453 (1988a)
S.H. Goh, K.S. Siow, Polym. Bull. **20**, 393 (1988b)
S.H. Goh, K.S. Siow, Polym. Bull. **23**, 205 (1990)
S.H. Goh, D.R. Paul, J.W. Barlow, J. Appl. Polym. Sci. **27**, 1091 (1982a)
S.H. Goh, D.R. Paul, J.W. Barlow, Polym. Eng. Sci. **22**, 34 (1982b)
S.H. Goh, K.S. Siow, K.S. Yap, J. Appl. Polym. Sci. **29**, 99 (1984a)
S.H. Goh, K.S. Siow, T.T. Nguyen, A. Nam, Eur. Polym. J. **20**, 65 (1984b)
S.H. Goh, T.T. Nguyen, K.S. Siow, J. Appl. Polym. Sci. **29**, 1463 (1984c)
S.H. Goh, K.S. Siow, Y.H. Leong, Eur. Polym. J. **21**, 915 (1985)
S.H. Goh, K.S. Siow, K.S. Yap, Thermochim. Acta **102**, 281 (1986a)
S.H. Goh, S.Y. Lee, K.S. Siow, J. Appl. Polym. Sci. **31**, 2055 (1986b)
S.H. Goh, S.Y. Lee, K.S. Siow, C.L. Pua, J. Appl. Polym. Sci. **33**, 353 (1987)
S.H. Goh, S.Y. Lee, K.S. Siow, M.K. Neo, Polymer **31**, 1065 (1990a)
S.H. Goh, S.Y. Lee, M.K. Neo, J. Appl. Polym. Sci. **40**, 2243 (1990b)
S.H. Goh, K.S. Siow, S.Y. Lee, Eur. Polym. J. **27**, 921 (1991a)
S.H. Goh, S.Y. Lee, Y.F. Chong, M.K. Neo, C.L. Leong, Macromolecules **24**, 806 (1991b)
S.H. Goh, S.Y. Lee, Y.F. Chong, Polym. Bull. **25**, 257 (1991c)
S.H. Goh, W.W.Y. Lau, C.S. Lee, Polym. Bull. **26**, 319 (1991d)
S.H. Goh, W.W.Y. Lau, C.S. Lee, Polym. Commun. **32**, 202 (1991e)
S.H. Goh, K.S. Siow, S.Y. Lee, Eur. Polym. J. **28**, 657 (1992a)
S.H. Goh, S.Y. Lee, C.L. Leong, J. Appl. Polym. Sci. **44**, 199 (1992b)
S.H. Goh, S.Y. Lee, S.M. Low, Eur. Polym. J. **28**, 661 (1992c)
S.H. Goh, W.W.Y. Lau, C.S. Lee, Polym. Bull. **29**, 524 (1992d)
S.H. Goh, S.Y. Lee, K.S. Siow, J. Chen, Polymer **34**, 2898 (1993)
S.H. Goh, S.Y. Lee, A.S.H. Ho, Bull. Singapore Natl. Inst. Chem. **22**, 47 (1994a)
S.H. Goh, S.Y. Lee, S.M. Low, Macromolecules **27**, 6736 (1994b)
S.H. Goh, H.S.O. Chan, C.H. Ong, Polymer **37**, 2675 (1996a)
S.H. Goh, S.Y. Lee, J. Dai, K.L. Tan, Polymer **37**, 5305 (1996b)
S.H. Goh, S.Y. Lee, L.I.K Tan. Polym. Bull. **37**, 253 (1996)
S.H. Goh, S.Y. Lee, S.M. Low, J. Peng, X.P. Ni, Polym. Polym. Compos. **4**, 541 (1996c)
S H. Goh, S.Y. Lee, H.W. Goh, X.P. Ni, Polym. Bull. **38**, 197 (1997)
S.H. Goh, S.Y. Lee, S.M. Low, Polym. Networks Blends **7**, 19 (1997a)
S.H. Goh, H.S.O. Chan, C.H. Ong, J. Appl. Polym. Sci. **68**, 1839 (1998a)
S.H. Goh, S.Y. Lee, X. Zhou, K.L. Tan, Macromolecules **31**, 4260 (1998b)
S.H. Goh, S.Y. Lee, X. Zhou, K.L. Tan, Macromolecules **32**, 942 (1999a)
S.H. Goh, S.Y. Lee, Y.T. Yeo, X. Zhou, K.L. Tan, Macromol. Rapid Commun. **20**, 148 (1999b)
S.H. Goh, S.Y. Lee, X. Zhou, K.L. Tan, Polymer **40**, 2667 (1999c)
S.H. Goh, Y. Liu, S.Y. Lee, C.H.A. Huan, Macromolecules **32**, 8595 (1999d)
S.H. Goh, J.W. Zheng, S.Y. Lee, Polymer **41**, 8721 (2000a)
S.H. Goh, S.Y. Lee, X.F. Luo, C.H.A. Huan, Polymer **41**, 211 (2000b)
S.H. Goh, S.Y. Lee, X.F. Luo, M.W. Wong, K.L. Tan, Macromol. Chem. Phys. **202**, 31 (2001)

H.W. Goh, S.H. Goh, G.Q. Xu, J. Polym. Sci. A: Polym. Chem. **40**, 1157 (2002a)

H.W. Goh, S.H. Goh, G.Q. Xu, J. Polym. Sci. A: Polym. Chem. **40**, 4316 (2002b)

A. Golovoy, M.F. Cheung, Polym. Eng. Sci. **29**, 85 (1989)

J.M. Gomez-Elvira, J.L. Halary, L. Monnerie, L.J. Fetters, Macromolecules **27**, 3370 (1994)

A. Gonzalez, L. Irusta, M.J. Fernandez-Berridi, M. Iriarte, J.J. Iruin, Polymer **45**, 1477 (2004a)

A. Gonzalez, M. Iriarte, P.J. Iriondo, J.J. Iruin, Polymer **43**, 6205 (2002)

A. Gonzalez, M. Iriarte, P.J. Iriondo, J.J. Iruin, Polymer **44**, 7701 (2003)

A. Gonzalez, M. Iriarte, P.J. Iriondo, J.J. Iruin, Polymer **45**, 4139 (2004b)

A.A. Goodwin, G.P. Simon, Polymer **37**, 991 (1996)

K.R. Gorda, D.J. Peiffer, J. Appl. Polym. Sci. **50**, 1977 (1993)

A. Gottschalk, K. Muhlbach, F. Seitz, R. Stadler, C. Auschra, Macromol. Symp. **83**, 127 (1994)

D. Gracia, J. Polym. Sci. Polym. Phys. Ed. **24**, 1577 (1986)

P. Grece, E. Martuscelli, Polymer **30**, 1475 (1989)

R.A. Grinsted, J.L. Koenig, J. Polym. Sci. Polym. Phys. Ed. **28**, 177 (1990)

J. Grobelny, D.M. Rice, F.E. Karasz, W.J. MacKnight, Macromolecules **23**, 2139 (1990)

G. Groeninckx, M. Vandermaliene, G. Defieuw, H. Reynaers, Am. Chem. Soc. Polym. Prepr. **29** (1), 438 (1988)

G. Grose, K. Friese, quoted in K. Friese, Plaste. Kaut. **12**, 90 (1965)

G. Guerra, D.J. Williams, F.E. Karasz, W.J. MacKnight, J. Polym. Sci. Polym. Phys. Ed. **26**, 301 (1988a)

G. Guerra, F.E. Karasz, W.J. MacKnight, Macromolecules **19**, 1935 (1986)

G. Guerra, S. Choe, D.J. Williams, F.E. Karasz, W.J. MacKnight, Macromolecules **21**, 231 (1988b)

K.S. Guigley, A.E. Feiring, P.C. Painter, M.M. Coleman, J. Macromol. Sci.: Phys. **41**, 207 (2002)

Q. Guo, Eur. Polym. J. **26**, 1329 (1990a)

Q. Guo, Eur. Polym. J. **26**, 1333 (1990b)

Q. Guo, Makromol. Chem. **191**, 2639 (1990c)

Q. Guo, Makromol. Chem. Rapid Commun. **11**, 279 (1990d)

Q. Guo, Polym. Commun. **31**, 217 (1990e)

Q. Guo, Polym. Commun. **32**, 62 (1991)

Q. Guo, Eur. Polym. J. **28**, 1049 (1992a)

Q. Guo, Eur. Polym. J. **28**, 1395 (1992b)

Q. Guo, Polymer **34**, 70 (1993)

Q. Guo, Macromol. Rapid Commun. **16**, 785 (1995)

Q. Guo, Eur. Polym. J. **32**, 1409 (1996)

Q. Guo, G. Groeninckx, Polymer **42**, 8647 (2001)

W. Guo, J.S. Higgins, Polymer **31**, 699 (1990)

W. Guo, J.S. Higgins, Polymer **32**, 2115 (1991)

Y.Q. Guo, X.H. Liang, J. Macromol. Sci.: Phys. **B38**, 439 (1999)

W. Guo, G.R. Mitchell, Polymer **35**, 3706 (1994)

M. Guo, H.G. Zachmann, Polymer **34**, 2503 (1993)

M. Guo, H.G. Zachmann, Macromolecules **30**, 2746 (1997)

Q. Guo, J. Huang, T. Chen, Polym. Bull. **20**, 517 (1988)

Q. Guo, H. Xu, D. Ma, S. Wang, Eur. Polym. J. **26**, 67 (1990a)

Q. Guo, J. Huang, T. Chen, H. Zhang, Y. Yang, C. Hou, Z. Feng, Polym. Eng. Sci. **30**, 44 (1990b)

Q. Guo, J. Huang, T. Chen, Polym. Commun. **31**, 115 (1990c)

Q. Guo, J. Huang, T. Chen, Z. Feng, Polym. Commun. **31**, 240 (1990d)

Q. Guo, J. Huang, B. Li, T. Chen, H. Zhang, Z. Feng, Polymer **32**, 58 (1991a)

Q. Guo, X. Peng, Z. Wang, Polymer **32**, 53 (1991b)

Q. Guo, M. Yu, Z. Feng, Polymer **33**, 893 (1992)

Q. Guo, K. Sun, T. Fang, Y. Qi, Z. Feng, J. Appl. Polym. Sci. **48**, 547 (1993a)

Q.H. Guo, X.J. Yuan, L.K. Chen, N. Sun, Cellul. Chem. Technol. **27**, 369 (1993b)

Q. Guo, J. Huang, X. Li, Eur. Polym. J. **32**, 321 (1996a)

Q. Guo, J. Huang, X. Li, Eur. Polym. J. **32**, 423 (1996b)

Q. Guo, J.Y. Huang, T.L. Chu, J. Appl. Polym. Sci. **60**, 807 (1996c)

Q. Guo, S. Zheng, J. Li, Y. Mi, J. Polym. Sci. A: Polym. Chem **35**, 211 (1997)

Q. Guo, C. Harrats, G. Groeninckx, Polymer **42**, 4127 (2001)

L.H. Guo, H. Sato, T. Hashimoto, Y. Ozaki, Macromolecules **43**, 3897 (2010)

L.H. Guo, H. Sato, T. Hashimoto, Y. Ozaki, Macromolecules **44**, 2229 (2011)

C.S. Ha, R.E. Prud'homme, W.J. Cho, Pollimo **14**, 506 (1990a)

C.S. Ha, W.J. Cho, R.J. Roe, Pollimo **14**, 322 (1990b)

C.S. Ha, W.J. Cho, J.H. Ryou, R.J. Roe, Polymer **34**, 505 (1993)

C.S. Ha, M.G. Ko, W.J. Cho, Polymer **38**, 1243 (1997)

Y.H. Ha, C.E. Scott, E.L. Thomas, Polymer **42**, 6463 (2001)

A. Habi, S. Djadoun, Eur. Polym. J. **35**, 483 (1999)

A. Habi, S. Djadoun, Thermochim. Acta. **469**, 1 (2008)

N. Haddadine-Rahmoun, F. Amrani, V. Arrighi, J.M.G. Cowie, Eur. Polym. Sci. **44**, 821 (2008)

A.S. Hadj-Hamou, S. Djadoun, J. Appl. Polym. Sci. **103**, 1011 (2006)

A.S. Hadj-Hamou, A. Habi, S. Djadoun, Eur. Polym. J. **33**, 1105 (1997)

A.S. Hadj-Hamou, A. Habi, S. Djadoun, Thermochim. Acta. **497**, 117 (2010)

A.S. Hadj-Hamou, K. El Miloudi, S. Djadoun, J. Polym. Sci. B: Polym. Phys. **47**, 2074 (2009)

H.W. Haggard, D.R. Paul, Polymer **45**, 2313 (2004)

B.R. Hahn, J.H. Wendroff, Polymer **26**, 1619 (1985)

J.L. Halary, J.M. Ubrich, J.M. Nunzi, L. Monnerie, R.S. Stein, Polymer **25**, 956 (1984)

J.L. Halary, J.M. Ubrich, L. Monnerie, H. Yang, R.S. Stein, Polym. Commun. **26**, 73 (1985)

J.L. Halary, M.H. Leviet, T.K. Kwei, E.M. Pearce, Macromolecules **24**, 5939 (1991)

N. Hamazaki, J.W. Cho, S. Miyata, Polym. J. **23**, 333 (1991)

T. Hameed, I.A. Hussein, Macromol. Mater. Eng. **289**, 198 (2004)

R. Hammachin, F. Amrani, R.E. Prud'homme, D. Pinoit, Polym. Bull. **42**, 595 (1999)

C.F. Hammer, Macromolecules **4**, 69 (1971)

C.C. Han, H.H. Yang, J. Appl. Polym. Sci. **33**, 1199 (1987)

C.D. Han, H.S. Chung, J.K. Kim, Polymer **33**, 546 (1992)

C.C. Han, M. Okada, Y. Muroga, B.J. Bauer, Q. Tran-Cong, Polym. Eng. Sci. **26**, 1208 (1986)

J.T. Haponiuk, A. Balas, J. Therm. Anal. **43**, 215 (1995)

M. Hara, G.J. Parker, Polymer **33**, 4650 (1992)

M. Harada, T. Suzuki, M. Ohya, D. Kawaguchi, A. Takano, Y. Matsushita, Macromolecules **38**, 1868 (2005a)

M. Harada, T. Suzuki, M. Ohya, D. Kawaguchi, A. Takano, Y. Matsushita, N. Torikai, J. Polym. Sci. B: Polym. Phys. **43**, 1486 (2005b)

D. Hardt, Brit. Polym. J. **1**, 225 (1969)

D. Hardt, C. Sueling, C. Linder, L. Morbitzer, Angew. Chem. Int. Ed. **21**, 174 (1982)

J.E. Harris, L.M. Robeson, J. Polym. Sci. Polym. Phys. Ed. **25**, 311 (1987)

J.E. Harris, L.M. Robeson, J. Appl. Polym. Sci. **35**, 1877 (1988)

J.E. Harris, S.H. Goh, D.R. Paul, J.W. Barlow, J. Appl. Polym. Sci. **27**, 839 (1982)

S.E. Harton, T. Koga, F.A. Stevie, J. Araki, H. Ade, Macromolecules **38**, 10511 (2005)

M. Hasegawa, S. Akiyama, Polymer J. **20**, 471 (1988)

M. Hasegawa, S. Sakurai, M. Takenaka, T. Hashimoto, C.C. Han, Macromolecules **24**, 1813 (1991)

J.N. Hay, L. Sharma, Polymer **41**, 5749 (2000)

H. Hayashi, S. Nakata, M. Kakimoto, Y. Imai, J. Appl. Polym. Sci. **49**, 1241 (1993)

H. Hayashi, M. Kakimoto, Y. Imai, Polymer **36**, 2797 (1995)

J. He, J. Liu, Polymer **40**, 959 (1999)

Y. He, N. Asakawa, Y. Inoue, Polym. Int. **49**, 609 (2000)

Y. He, J. Li, H. Uyama, S. Kobayashi, Y. Inoue, J. Polym. Sci. B: Polym. Phys. **39**, 2898 (2001)

Y. He, B. Zhou, Y. Inoue, Prog. Polym. Sci. **29**, 1021 (2004a)

Y. He, B. Zhu, W.H. Kai, Y. Inoue, Macromolecules **37**, 3337 (2004b)

S.A. Heffner, P.A. Mirau, Macromolecules **27**, 7283 (1994)

W. Heinen, C.B. Wenzel, C.H. Rosenmoller, F.M. Mulder, G.J. Boender, J. Lugtenburg, H.J.M. de Groot, M. van Duin, B. Klemperman, Macromolecules **31**, 7404 (1998)

P.M. Hendrichs, J. Tribone, D.J. Massa, J.M. Hewitts, Macromolecules **21**, 1282 (1988)

M. Hendrioulle-Granville, K. Kyuda, R. Jerome, P. Teyssie, F.C. De Schryver, Macromolecules **23**, 1202 (1990)

W. Herrera-Kao, M. Agular-Vega, Polym. Bull. **42**, 449 (1999)

D. Herrera, J.C. Zamora, A. Bello, M. Grimau, F. Laredo, A.J. Muller, T.P. Lodge, Macromolecules **38**, 5109 (2005)

H. Hexig, H. Alata, N. Asakawa, Y. Inoue, J. Polym. Sci. B: Polym. Phys. **43**, 368 (2005)

J.J. Hickman, R.M. Ikeda, J. Polym. Sci. Polym. Phys. Ed. **11**, 1713 (1973)

K. Hikichi, A. Tezuka, K. Takegoshi, Polym. J. **30**, 356 (1998)

D.J.T. Hill, A.K. Whittaker, K.W. Wong, Macromolecules **32**, 5285 (1999)

S. Himuro, N. Sakamoto, S. Arichi, Polym. J. **24**, 1371 (1992)

S. Hirano, Y. Nishikawa, Y. Terada, T. Ikehara, T. Nishi, Polym. J. **34**, 85 (2002)

K.S. Ho, K. Levon, J. Mao, W.Y. Zheng, J. Laakso, Synth. Met. **57**, 3591 (1993)

J.C. Ho, T.C. Lin, K.H. Wei, Polymer **41**, 9299 (2000)

J. Hong, S.H. Goh, S.Y. Lee, K.S. Siow, Polym. Networks Blends **5**, 101 (1995a)

J. Hong, S.H. Goh, S.Y. Lee, K.S. Siow, Polymer **36**, 143 (1995b)

B.K. Hong, J.Y. Kim, W.H. Jo, S.C. Lee, Polymer **38**, 4373 (1997)

B.K. Hong, W.H. Jo, J. Kim, Polymer **39**, 3753 (1998)

H. Horiuchi, S. Irie, T. Nose, Polymer **32**, 1970 (1991)

M. Hosokawa, S. Akiyama, Polym. J. **31**, 13 (1999)

D.J. Hourston, I.D. Hughes, J. Appl. Polym. Sci. **21**, 3099 (1977a)

D.J. Hourston, I.D. Hughes, Polymer **18**, 1175 (1977b)

D.J. Hourston, I.D. Hughes, J. Appl. Polym. Sci. **26**, 3467 (1981)

D.T. Hseih, D.G. Peiffer, J. Appl. Polym. Sci. **47**, 1469 (1993)

B.S. Hsiao, B.B. Sauer, J. Polym. Sci. B: Polym. Phys. **31**, 901 (1993)

K.H. Hsieh, L.M. Chou, J. Appl. Polym. Sci. **38**, 645 (1989)

D.T. Hsieh, D.G. Peiffer, Polymer **33**, 1210 (1992)

T.T. Hsieh, C. Tiu, K.H. Hsieh, G.P. Simon, J. Polym. Res. **6**, 211 (1999)

Y.T. Hsieh, E.M. Woo, Expr. Polym. Lett. **5**, 570 (2011)

Y.T. Hsieh, N.T. Kuo, E.M. Woo, J. Therm. Anal. Calorim. **107**, 745 (2012)

W.P. Hsu, C.F. Yeh, J. Appl. Polym. Sci. **73**, 431 (1999a)

W.P. Hsu, C.F. Yeh, Polym. J. **31**, 574 (1999b)

W.P. Hsu, C.F. Yeh, J. Appl. Polym. Sci. **75**, 1313 (2000a)

W.P. Hsu, C.F. Yeh, Polym. J. **32**, 127 (2000b)

W.P. Hsu, J. Appl. Polym. Sci. **66**, 1773 (1997)

W.P. Hsu, J. Appl. Polym. Sci. **74**, 2894 (1999)

W.P. Hsu, Polym. J. **32**, 849 (2000)

W.P. Hsu, J. Appl. Polym. Sci. **81**, 3190 (2001)

W.P. Hsu, J. Appl. Polym. Sci. **83**, 1425 (2002a)

W.P. Hsu, J. Appl. Polym. Sci. **86**, 2720 (2002b)

W.P. Hsu, J. Appl. Polym. Sci. **89**, 2088 (2003)

W.P. Hsu, J. Appl. Polym. Sci. **91**, 3068 (2004a)

W.P. Hsu, J. Appl. Polym. Sci. **92**, 2797 (2004b)

W.P. Hsu, J. Appl. Polym. Sci. **96**, 2064 (2005)

W.P. Hsu, J. Appl. Polym. Sci. **101**, 643 (2006a)

W.P. Hsu, Thermochim. Acta **441**, 137 (2006b)

W.P. Hsu, Thermochim. Acta **454**, 50 (2007)

W.P. Hsu, J. Appl. Polym. Sci. **108**, 900 (2008)

S.R. Hu, T. Kyu, R.S. Stein, J. Polym. Sci. Polym. Phys. Ed. **25**, 71 (1987)

J. Hu, Y. Park, P.C. Painter, M.M. Coleman, Am. Chem. Soc. Polym. Prepr. **29**(1), 321 (1988)

Y. Hu, V. Gamble, P.C. Painter, M.M. Coleman, Macromolecules **35**, 1289 (2002)

L.D. Hu, H. Lu, S.X. Zheng, J. Polym. Sci. B: Polym. Phys. **42**, 2567 (2004)

H.Q. Hu, C.B. Chong, A.H. He, C.G. Zhang, G.Q. Fan, J.Y. Dong, C.C. Han, Macromol. Rapid Commun. **26**, 973 (2005)

J.M. Huang, J. Polym. Sci. B: Polym. Phys. **42**, 1694 (2004)

J.M. Huang, F.C. Chang, J. Appl. Polym. Sci. **84**, 850 (2002)

C.F. Huang, F.C. Chang, Polymer **44**, 2965 (2003)

X.D. Huang, S.H. Goh, Macromolecules **33**, 8894 (2000)

X.D. Huang, S.H. Goh, Polymer **43**, 1417 (2002)

J. Huang, Q. Guo, Makromol. Chem. Rapid Commun. **11**, 613 (1990)

B.S. Huang, E.M. Woo, Colloid. Polym. Sci. **278**, 392 (2000)

Y.P. Huang, E.M. Woo, Polymer **43**, 6795 (2002)

H.M. Huang, S.J. Yang, Polymer **46**, 8068 (2005)

J. Huang, A. Prasad, H. Marand, Polymer **35**, 1896 (1994)

W. Huang, Y. Li, J. Xu, M. Ding, Polymer **38**, 4261 (1997)

X.D. Huang, S.H. Goh, S.Y. Lee, Z.D. Zhao, M.W. Wong, C.H.A. Huan, Macromolecules **32**, 4327 (1999)

X.D. Huang, S.H. Goh, S.Y. Lee, Macromol. Chem. Phys. **201**, 281 (2000)

P.T. Huang, T.K. Kwei, E.M. Pearce, S.V. Levchik, J. Polym. Sci. A: Polym. Chem. **39**, 841 (2001)

H.L. Huang, S.H. Goh, A.T.S. Wee, Polymer **43**, 2861 (2002a)

M.W. Huang, S.W. Kuo, H.D. Wu, F.C. Chang, S.Y. Fang, Polymer **43**, 2479 (2002b)

H.L. Huang, S.H. Goh, D.M.Y. Lai, A.T.S. Wee, C.H.A. Huan, J. Polym. Sci. B: Polym. Phys. **42**, 1145 (2004a)

H.L. Huang, S.H. Goh, D.M.Y. Lai, C.H.A. Huan, A.T.S. Wee, J. Appl. Polym. Sci. **91**, 1798 (2004b)

H.L. Huang, S.H. Goh, D.M.Y. Lai, C.H.A. Huan, Appl. Surf. Sci. **227**, 373 (2004c)

C.F. Huang, S.W. Kuo, H.C. Lin, J.K. Chen, Y.K. Chen, H.Y. Xu, F.C. Chang, Polymer **45**, 5913 (2004d)

H. Huang, Y. Hu, J.M. Zhang, H. Sato, H.T. Zhang, I. Noda, Y. Ozaki, J. Phys. Chem. B. **109**, 19175 (2005)

J.C. Huarng, K. Min, J.L. White, Polym. Eng. Sci. **28**, 1085 (1988a)

J.C. Huarng, K. Min, J.L. White, Polym. Eng. Sci. **28**, 1590 (1988b)

D.S. Hubbell, S.L. Copper, J. Appl. Polym. Sci. **21**, 303 (1977)

D.S. Hubbell, S.L. Copper, in *Multiphase Polymers*, ed. by S.L. Cooper, G.M. Estes. American Chemical Society, Advances in Chemistry Series, vol. 176 (Washington, DC, 1979)

M.B. Huglin, J.M. Rego, Polymer **31**, 1269 (1990)

M.B. Huglin, L. Webster, I.D. Robb, Polymer **37**, 1211 (1996)

W. Huh, F.E. Karasz, Polym. Mater. Sci. Eng. **60**, 792 (1989)

W. Huh, F.E. Karasz, Macromolecules **25**, 1057 (1992)

C.C. Hung, W.G. Carson, S.P. Bohan, J. Polym. Sci. B: Polym. Phys. **32**, 141 (1994)

A.Y.C. Hung, F.Y. Wang, C.C.M. Ma, Y.M. Sun, J. Appl. Polym. Sci. **86**, 984 (2002)

P.P. Huo, P. Cebe, M. Capel, Macromolecules **26**, 4275 (1993)

I.A. Hussein, Macromolecules **36**, 2024 (2003)

I.A. Hussein, M.C. William, Polym. Eng. Sci. **44**, 660 (2004a)

I.A. Hussein, M.C. William, Rheol. Acta. **43**, 602 (2004b)

I.A. Hussein, T. Hameed, B.F. Abu Sharkh, K. Mezgali, Polymer **44**, 4665 (2003)

S.H. Hwang, J. Appl. Polym. Sci. **76**, 1947 (2000)

S.E.M. Ibim, A.M.A. Ambrosio, M.S. Kwon, S.F. El-Amin, H.R Allock, C.T. Laurecia. Biomaterials **18**, 1565 (1997)

N.A. Ibrahim, N.M. Rahim, W.Z.W. Yunus, J. Sharif, J. Polym. Res. **18**, 891 (2011)

O. Iguerb, R. Bouyahia, F. Bouzouia, S. Djadoun, R. Legras, Eur. Polym. J. **35**, 1345 (1999)

D.W. Ihn, S.Y. Park, C.G. Chang, Y.S. Kim, H.K. Lee, J. Polym. Sci. A: Polym. Chem. **34**, 2841 (1996)

K. Ikawa, S. Hosoda, Polym. J. **22**, 643 (1990)

K. Ikawa, S. Hosoda, Polym. Networks Blends **1**, 103 (1991)

K. Ikawa, S. Tanaka, K. Ueno, Polym. Networks Blends **3**, 31 (1993)

T. Ikehara, H. Kimura, T. Kataoka, J. Polym. Sci. B: Polym. Phys. **48**, 706 (2010)

T. Ikehara, H. Kimura, Z.B. Qiu, Macromolecules **38**, 5104 (2005)

T. Ikehara, H. Kurihara, T. Kataoka, J. Polym. Sci. B: Polym. Phys. **47**, 539 (2009)

K.H. Iller, W. Heckmann, J. Hambrecht, Colloid Polym. Sci. **262**, 557 (1984)

K.H. Illers, E. Koehnlein, Makromol. Chem. **187**, 2725 (1986)

R.L. Imken, D.R. Paul, J.W. Barlow, Polym. Eng. Sci. **16**, 593 (1976)

C.T. Imrie, B.J.A. Paterson, Macromolecules **27**, 6673 (1994)

T. Inoue, F. Shomura, T. Ougizawa, K. Miyasaka, Rubber Chem. Technol. **58**, 873 (1985)

M. Iriarte, E. Espi, A. Etxeberria, M. Valero, M.J. Fernandez-Berridi, Macromolecules **24**, 5546 (1991)

M. Iriarte, J.I. Iribarreu, A. Etxeberria, J.J. Iruin, Polymer **30**, 1160 (1989)

M. Irie, R. Iga, Makromol. Chem. Rapid Commun. **7**, 751 (1986)

P. Iriondo, J.J. Iruin, M.J. Fernandez-Berridi, Polymer **36**, 3235 (1995)

P. Iriondo, J.J. Iruin, M.J. Fernandez-Berridi, Macromolecules **29**, 5605 (1996)

J.J. Iruin, J.I. Eguiazabal, G.M. Guzman, Eur. Polym. J. **25**, 1169 (1989)

J.R. Isasi, E. Meaurio, L.C. Cesteros, I. Katime, Macromol. Chem. Phys. **197**, 641 (1996)

I.R. Isasi, L.C. Cesteros, I. Katime, Polymer **34**, 2374 (1993)

I.R. Isasi, L.C. Cesteros, I. Katime, Polymer **36**, 1235 (1995)

H. Ishida, Y.H. Lee, J. Polym. Sci. B: Polym. Phys. **39**, 736 (2001)

K. Ishikawa, S. Kawahara, S. Akiyama, Polym. Networks Blends **1**, 1 (1991)

H. Jager, E.J. Vorenkamp, G. Challa, Polym. Commun. **24**, 290 (1983)

V. Janarthanan, G. Thyagarajan, Polymer **33**, 3593 (1992)

V. Janarthanan, F.E. Karasz, W.J. MacKnight, Polymer **33**, 3388 (1992)

V. Janarthanan, J. Kressler, F.E. Karasz, W.J. MacKnight, J. Polym. Sci. B: Polym. Phys. **31**, 1013 (1993)

L.W. Jang, D.C. Lee, J. Appl. Polym. Sci. **87**, 1610 (2003)

J. Jang, J. Won, Polymer **39**, 4335 (1998)

J. Janicke, A. Wlochowicz, Angew. Makromol. Chem. **168**, 9 (1989)

G. Janusz, D.M. Rice, F.E. Karasz, W.J. MacKnight, Polym. Commun. **31**, 86 (1990)

D. Jaroszynska, R. Gaczynski, Plaste Kautsch. **23**, 581 (1976)

D. Jauannet, T.N. Pham, S. Pimbert, G. Levesque, Polymer **38**, 5137 (1997)

M.J. Jenkins, Polymer.**42**, 1981 (2001)

S.H. Jeon, T. Ree, J. Polym. Sci. Polym. Chem. Ed. **26**, 1419 (1988)

S.C. Jeong, H.M. Jeong, M.H. Oh, B.K. Kim, Polym. Bull. **33**, 237 (1994)

H.K. Jeong, M. Rooney, D.J. David, W.J. MacKnight, F.E. Karasz, T. Kajiyama, Polymer **41**, 6003 (2000a)

H.K. Jeong, M. Rooney, D.J. David, W.J. MacKnight, F.E. Karasz, T. Kajiyama, Polymer **41**, 6671 (2000b)

K. Jeremic, F.E. Karasz, W.J. MacKnight, New Polym. Mater. **3**, 163 (1992)

R.J. Jerome, B. Albert, Teyssie, Ph. Am. Chem. Soc. Polym. Prepr. **27**(1), 72 (1986)

X.L. Ji, W.J. Zhang, Z.W. Wu, Polymer **37**, 4205 (1996)

M. Jiang, X. Cao, T. Yu, Polymer **27**, 1923 (1986)

M. Jiang, X. Cao, W. Chen, T. Yu, Polym. Bull. **21**, 599 (1989)

M. Jiang, C. Zhou, Z. Zhang, Polym. Bull. **30**, 449 (1993)

M. Jiang, T. Huang, J. Xie, Macromol. Chem. Phys. **196**, 787 (1995a)

M. Jiang, T. Huang, J. Xie, Macromol. Chem. Phys. **196**, 803 (1995b)

M. Jiang, X. Qiu, W. Qin, L. Fei, Macromolecules **28**, 730 (1995c)

M. Jiang, M. Li, M. Xiang, H. Zhou, Adv. Polym. Sci. **146**, 121 (1999)

F.J. Jiang, H.J. Zhu, R. Graf, W.H. Meyer, H.W. Spiess, G. Wegner, Macromolecules **43**, 3876 (2010)

J.I. Jin, E.J. Choi, K.Y. Lee, Polym. J. **18**, 99 (1986)

Y. Jin, R.Y.M. Huang, J. Appl. Polym. Sci. **36**, 1799 (1988)

B.S. Jin, S.C. Kim, D.S. Lee, Polym. J. **24**, 1189 (1992)

X. Jin, S.H. Zhang, J. Runt, Macromolecules **37**, 4808 (2004a)

X. Jin, S.H. Zhang, J. Runt, Macromolecules **37**, 8110 (2004b)

W.H. Jo, C.A. Cruz, D.R. Paul, J. Polym. Sci. Polym. Phys. Ed. **27**, 1057 (1989a)

W.H. Jo, S.C. Lee, M.S. Lee, Polym. Bull. **21**, 183 (1989b)

W.H. Jo, H.G. Kim, J. Polym. Sci. Polym. Phys. Ed. **29**, 1579 (1991)

W.H. Jo, J.T. Yoon, S.C. Lee, Polym. J. **23**, 1243 (1991a)

W.H. Jo, Y.K. Kwon, I.H. Kwon, Macromolecules **24**, 4708 (1991b)

W.H. Jo, H. Yim, I.H. Kwon, T.W. Son, Polym. J. **24**, 519 (1992a)

W.H. Jo, S.J. Park, I.H. Kwon, Polym. Int. **29**, 173 (1992b)

W.H. Jo, J.Y. Kim, M.S. Lee, J. Polym. Sci. B: Polym. Phys. **32**, 1321 (1994a)

W.H. Jo, J.Y. Kim, M.S. Lee, Polym. J. **26**, 465 (1994b)

W.H. Jo, M.R. Lee, B.G. Min, M.S. Lee, Polym. Bull. **33**, 113 (1994c)

E. John, T. Ree, J. Polym. Sci. Polym. Chem. Ed. **28**, 385 (1990)

P.J. Jones, L.C. Paslay, S.E. Morgan, Polymer **51**, 738 (2010)

L. Jong, E.M. Pearce, T.K. Kwei, Polymer **34**, 48 (1993)

A.H. Jorgenson, L.A. Chandler, E.A. Collins, Rubber Chem. Technol. **46**, 1087 (1973)

J.H. Jou, P.T. Huang, Polym. J. **22**, 909 (1990)

R.H. Jung, D.J. Stein, Prepr. IUPAC Symp. Aberdeen. **411** (1973)

J.J. Jutier, E. Lemieaux, R.E. Prud'homme, J. Polym. Sci. Polym. Phys. Ed. **26**, 1313 (1988)

C.K. Kim, J.J. Lim, D.R. Paul, Polym. Eng. Sci. **34**, 1788 (1994a)

W.H. Kai, L. Zhao, B. Zhu, Y. Inoue, Macromol. Chem. Phys. **207**, 746 (2006)

S.N. Kaklas, D.D. Sotiropoulou, J.K. Kallitsis, N.K. Kalfoglou, Polymer **32**, 66 (1991)

N.K. Kalfoglou, Angew. Makromol. Chem. **118**, 19 (1983)

N.K. Kalfoglou, A.G. Margaritis, Angew. Makromol. Chem. **125**, 135 (1984)

N.K. Kalfoglou, D.D. Sotiropoulu, A.G Margartis. Eur. Polym. J. **24**, 389 (1988)

L.E. Kalinina, V.I. Alekseenko, S.S. Voyutskii, Z. Kolloid, **18**, 691 (1956); Colloid J. USSR **18**
    (689) (1956a)

L.E. Kalinina, V.I. Alekseenko, S.S. Voyutskii, Z. Kolloid, **18**, 180 (1956); Colloid J. USSR **18**
    (171) (1956b)

A.K. Kalkar, N.K. Roy, Eur. Polym. J. **29**, 1391 (1993)

A.K. Kalkar, P.S. Parkhi, J. Appl. Polym. Sci. **57**, 233 (1995)

J.K. Kallistsis, N.K. Kalfoglou, Angew. Makromol. Chem. **148**, 103 (1987)

J.K. Kallistsis, N.K. Kalfoglou, J. Appl. Polym. Sci. **37**, 453 (1989)

R.P. Kambour, J.T. Bendler, R.C. Bopp, Macromolecules **16**, 753 (1983)

R.P. Kambour, P.E. Gundlach, I.C.W. Wang, D.M. White, G.W. Yeager, Polym. Commun. **29**,
    170 (1988)

R.P. Kambour, W.L. Nachlis, J.D. Carbeck, Polymer **35**, 209 (1994)

A.R. Kamdar, Y.S. Hu, P. Ansems, S.P. Chun, A. Hiltner, E. Baer, Macromolecules **39**, 1496
    (2006)

A. Kamira, B.B. Naima, Polym. Testing **25**, 1101 (2006)

H.W. Kammer, J. Piglowski, Acta Polym. **40**, 363 (1989)

H.W. Kammer, J. Kressler, B. Kressler, D. Scheller, H. Kroschwitz, G. Schmidt-Naake, Acta
    Polym. **40**, 75 (1989)

P. Kanakalatha, K. Vijayan, M.K. Sridhar, A.K. Singh, Polymer **24**, 621 (1983)

D.P. Kang, W.J. Cho, Pollimo **13**, 638 (1989)

H.S. Kang, W.J. MacKnight, F.E. Karasz, Am. Chem. Soc., Polym. Prepr. **28**(2), 134 (1987)

D.P. Kang, C.S. Ha, R.E. Prud'homme, W.J. Cho, Pollimo **12**, 634 (1988)

D.P. Kang, C.S. Ha, W.J. Cho, J. Polym. Sci., Polym. Chem. Ed. **27**, 1401 (1989)

Y. Kano, S. Akiyama, Polym. Bull. **29**, 97 (1992)

Y. Kano, S. Kawahara, S. Akiyama, J. Adhes. **41**, 25 (1993)

Y. Kano, S. Akiyama, T. Kasemura, Int. J. Adhesion and Adhesives **15**, 219 (1995)

Y. Kano, S. Akiyama, T. Kasemura, Int. J. Adhesion and Adhesives **17**, 207 (1997a)

Y. Kano, S. Akiyama, T. Kasemura, J. Adhes. Sci. Technol. **11**, 407 (1997b)

Y. Kano, S. Akiyama, T. Kasemura, Polym. Networks Blends **7**, 97 (1997c)

Y.H. Kao, L.W. Chen, Mater. Chem. Phys. **47**, 51 (1997)

F.E. Karasz, W.J. MacKnight, J. Appl. Polym. Sci. **32**, 4423 (1986)

F.E. Karasz, W.J. MacKnight, J.J. Tkacik, Am. Chem. Soc. Polym. Prepr. **15**, 415 (1974)

E. Karavas, E. Georgarakis, D. Bikiaris, Eur. J. Pharmaceu. Biopharm. **64**, 115 (2006)

R.J. Karcha, R.S. Porter, Polymer **33**, 4866 (1992)

R.J. Karcha, R.S. Porter, J. Polym. Sci., Polym. Phys. Ed. **27**, 2153 (1989)

R.J. Karcha, R.S. Porter, J. Polym. Sci. B: Polym. Phys. **31**, 821 (1993)

V.A. Kargin, J. Polym. Sci. C **4**, 1601 (1963)

K. Karlou, H.A. Schneider, J. Therm. Anal. Calorim. **59**, 59 (2000)

I.A. Katime, M.S. Anasagasti, M.C. Peleteiro, R. Valenciano, Eur. Polym. J. **23**, 907 (1987)

I. Katime, L.G. Parada, E. Meaurio, L.C. Cesteros, Polymer **41**, 1369 (2000)

J.D. Katsaros, M.F. Malone, H.H. Winter, Polym. Bull. **16**, 83 (1986)

S. Kawahara, S. Akiyama, Polym. J. **22**, 361 (1990)

S. Kawahara, S. Akiyama, Macromolecules **26**, 2428 (1993)

S. Kawahara, S. Akiyama, K. Ueda, Polym. J. **21**, 221 (1989)

S. Kawahara, K. Sato, A. Akiyama, J. Polym. Sci. B: Polym. Phys. **32**, 15 (1994)

S. Kawahara, Y. Asada, Y. Isono, K. Muraoka, Y. Minagawa, Polym. J. **34**, 1 (2002)

T. Kawai, Kogyo Kagaka Zasshi **59**, 779 (1956)

L.W. Kelts, C.J.T. Landry, D.M. Teegarden, Macromolecules **29**, 2941 (1993)

J.F. Kenney, in *Recent Advances in Polymer Blends, Grafts, and Blocks*, L.H. Sperling, (ed.),
    (Plenum Press, New York, 117 1974)

J.F. Kenney, J. Polym. Sci., Chem. Ed. **14**, 123 (1976)

J.F. Kenny, Am. Chem. Soc., Org. Coatings Plastics Chem. Prepr. **37**, 615 (1977)

R.J. Kern, J. Polym. Sci. **33**, 524 (1958)

S. Keskin, J.R. Elliot, Ind. Eng. Chem. Res. **42**, 6331 (2003)

H. Keskkula, D.R. Paul, J. Appl. Polym. Sci. **31**, 1189 (1986)

L. Keyzlarova, P. Saha, Int. Polym. Process **14**, 228 (1999)

M. Khalid, S. Saeed, Z. Zhmad, J. Macromol. Sci. A: Pure Appl. Chem. **44**, 55 (2007)

O.V. Khutoryanskaya, V.V. Khutoryanskiy, R.A. Pethrick, Macromol. Chem. Phys. **206**, 1497 (2005)

D.V. Khutoryansky, M.G. Cascone, L. Lazzen, N. Barbani, Z.S. Nurkeeva, G.A. Mun, A.V.
    Dubolazov, Polym. Int. **53**, 307 (2004)

B.K. Kim, C.H. Choi, Polymer **37**, 807 (1996)

B.K. Kim, I.H. Kim, Polym. Plast. Technol. Eng. **32**, 167 (1993)

S. Kim, H.J. Kim, Macromol. Mater. Eng. **292**, 339 (2007)

J.K. Kim, T. Kyu, Polymer **40**, 6125 (1999)

J.K. Kim, T. Kyu, Fiber Polym. **4**, 188 (2003)

C.K. Kim, D.R. Paul, Macromolecules **25**, 3097 (1992a)

C.K. Kim, D.R. Paul, Polym. Eng. Sci. **34**, 24 (1994)

C.K. Kim, D.R. Paul, Polymer **33**, 1630 (1992b)

C.K. Kim, D.R. Paul, Polymer **33**, 2089 (1992c)

C.K. Kim, D.R. Paul, Polymer **33**, 4929 (1992d)

C.K. Kim, D.R. Paul, Polymer **33**, 4941 (1992e)

H.I. Kim, E.M. Pearce, T.K. Kwei, Macromolecules **22**, 3374 (1989a)

H.I. Kim, E.M. Pearce, T.K. Kwei, Macromolecules **22**, 3498 (1989b)

J.H. Kim, J.W. Barlow, D.R. Paul, J. Polym. Sci., Polym. Phys. Ed. **27**, 2211 (1989)

J.H. Kim, J.W. Barlow, D.R. Paul, J. Polym. Sci., Polym. Phys. Ed. **27**, 223 (1989)

J.H. Kim, J.W. Barlow, D.R. Paul, Polym. Eng. Sci. **29**, 581 (1989d)

H.I. Kim, J.R. Pennachia, T.K. Kwei, E.M. Pearce, Am. Chem. Soc., Polym. Prepr. **32**(3), 343
    (1991)

J.H. Kim, C.J. Lim, K.E. Min, Pollimo **17**, 654 (1993a)

S.H. Kim, E.M. Pearce, T.K. Kwei, J. Polym. Sci. A: Polym. Chem. **31**, 3167 (1993b)

K.J. Kim, G.B. Kim, S.H. Han, J. Appl. Polym. Sci. **49**, 7 (1993c)

S.J. Kim, B.K. Kim, H.M. Jeong, J. Appl. Polym. Sci. **51**, 2187 (1994b)

C.H. Kim, J.K. Park, T.S. Hwang, Polym. Eng. Sci. **36**, 535 (1996)

B.S. Kim, G. Nakamura, T. Inoue, J. Appl. Polym. Sci. **68**, 1829 (1998)

M.H. Kim, R.G. Alamo, J.S. Lin, Polym. Eng. Sci. **39**, 2117 (1999a)

J. Kim, T.K. Shin, H.J. Choi, M.S. Jhon, Polymer **40**, 6873 (1999b)

G.H. Kim, H.G. Shin, W.J. Cho, C.S. Ha, J. Appl. Polym. Sci. **86**, 1071 (2002a)

J.H. Kim, J.E. Yoo, C.K. Kim, Macromol. Res. **10**, 209 (2002b)

M.J. Kim, J.E. Yoo, H.K. Choi, C.K. Kim, Macromol. Res. **10**, 91 (2002c)

Y. Kim, J.E. Yoo, C.K. Kim, Polymer **44**, 5439 (2003a)

J.H. Kim, Y. Kim, C.K. Kim, J.W. Lee, S.B. Seo, J. Polym. Sci. B: Polym. Phys. **41**, 1401 (2003b)

J.K. Kim, J. Jang, D.H. Lee, D.Y. Ryu, Macromolecules **37**, 8599 (2004)

J.W. Kim, J.E. Yoo, C.K. Kim, Polym. Int. **54**, 130 (2005)

L.U. Kim, m.Y. Jeon, C.K. Kim, C.G. Kum. Ind. Eng. Chem. **45**, 8921 (2006)

M. Kimura, R.S. Porter, Am. Chem. Soc., Org. Coatings Plastics Chem. Prepr. **45**, 84 (1981)

M. Kimura, R.S. Porter, G. Salee, J. Polym. Sci., Polym. Phys. Ed. **21**, 367 (1983)

N. Kinami, T. Okuyama, M. Okamoto, T. Inoue, Polymer **36**, 4449 (1995)

M.J. Kipper, S. Seifert, P. Thiyagarajan, B. Narasimhan, Polymer **45**, 3329 (2004)

P.E. Kireeva, G.A. Shandryuk, J.V. Kostina, G.N. Bondarendo, P. Singh, G.W. Cleary, M.M. Feldstein, J. Appl. Polym. Sci. **105**, 3017 (2007)

L.A. Kleintjens, unpublished results, quoted in Koningsveld et al. (1947)

S. Klotz, R.H. Schuster, H.J. Cantow, Makromol. Chem. **187**, 1491 (1986)

S. Kobayashi, S. Tasaka, S. Miyata, Kobunshi Ronbunshu **44**, 695 (1987)

S. Kobayashi, M. Kaku, T. Saegusa, Macromolecules **21**, 334 (1988)

S. Kobayashi, J.W. Cho, S. Miyata, Polym. J. **26**, 235 (1994)

K.A. Koh, J.H. Kim, D.O. Lee, M. Lee, H.M. Jeong, Eur. Polym. J. **34**, 1229 (1998)

P.R. Kohl, A.M. Seifert, G.P. Hellmann, J. Polym. Sci., Polym. Phys. Ed. **28**, 1309 (1990)

S. Koizumi, Soft Matter **7**, 3984 (2011)

J.V. Koleske, in *Polymer Blends*, ed. by D.R. Paul, S. Newman, vol. 2, Chap. 22 (Academic, New York, 1978)

J.V. Koleske, R.D. Lundberg, J. Polym. Sci. A-2 **7**, 795 (1969)

F. Kollinsky, G. Markert, in *Multicomponent Polymer Systems*, ed. by N.A.J. Platzer. American Chemical Society, Advances in Chemistry Series, vol. 99 (Washington, DC, 1971)

F. Kollinsky, G. Markert, Makromol. Chem. **121**, 117 (1969)

J.S. Kollodge, R.S. Porter, Polymer **34**, 4990 (1993)

M. Kolowski, W. Laskawski, Angew. Makromol. Chem. **91**, 29 (1980)

M. Konda, M. Tanaka, M. Miyamoto, Y. Kimura, A. Yamaguchi, High Perform. Polym. **10**, 93 (1998)

T. Kondo, C. Sawatari, R.St. Manley, D.G. Gray, Macromolecules **27**, 210 (1994)

M. Kondo, I. Akiba, S. Akiyama, E-Polymers Art. 050 (2002)

X. Kong, F. Teng, H. Tang, L. Dong, Z. Feng, Polymer **37**, 1751 (1996)

X. Kong, H. Tang, L. Dong, F. Teng, Z. Feng, J. Polym. Sci. B: Polym. Phys. **36**, 2267 (1998)

R. Koningsveld, H.A.G. Chermin, M. Gordon, Proc. R. Soc., A **319**, 331 (1970)

R. Koningsveld, L.A. Kleintjens, H.M. Schoffeleers, Pure Appl. Chem. **39**, 1 (1974)

K. Kosai, T. Higashino, Nippon Setchaku Kyokai Shi **11**, 2 (1975)

K. Kosai, T. Higashino, N. Nishioka, Shikizai Kyokaishi **50**, 76 (1977)

Y. Kosaka, T. Uryu, Macromolecules **27**, 6286 (1994)

Y. Kosaka, T. Uryu, J. Polym. Sci. A: Polym. Chem. **33**, 2221 (1995)

D.L. Kotzev, E.M. Pearce, T.K. Kwei, J. Appl. Polym. Sci. **29**, 4443 (1984)

E.G. Koulouri, J.K. Kallitsis, Polymer **39**, 2373 (1998)

T. Kovacic, B. Baric, I. Klaric, Thermochim. Acta **231**, 215 (1994)

N. Koyama, Y. Doi, Can. J. Microbiol. **41**, 316 (1995)

N. Koyama, Y. Doi, Macromolecules **29**, 5843 (1996)

N. Koyama, Y. Doi, Polymer **38**, 1589 (1997)

J. Kratochivil, A. Sikora, Eur. Polym. J. **43**, 2155 (2007)

J. Kratochivil, A. Sikora, Labsky, R. Puffr. Eur. Polym. J. **46**, 1681 (2005)

S. Krause, in *Polymer Blends*, ed. by D.R. Paul, S. Newman (Academic, New York, 1978)

S. Krause, in *Polymer Handbook*, ed. by J. Braudrup, E.H. Immergut, 3rd edn. (Wiley Interscience, New York, 1989)

S. Krause, J. Macromol. Sci.: Rev. Macromol. Chem. **C7**, 251 (1972)

G. Kraus, K.W. Rollman, in *Multicomponent Polymer Systems*, ed. by N.A.J. Platzer. American Chemical Society, Advances in Chemistry Series, vol. 99 (Washington, DC, 1971)

S. Krause, N. Roman, J. Polym. Sci. A **3**, 1631 (1965)

S. Krause, S.H. Goh, in *Polymer Blends Handbook*, ed. by L.A. Utracki, vol. 2 (Kluwer Academic Publishers, Dordrecht, 2002)

S. Krause, S.H. Goh, in *Polymer Handbook*, ed. by J. Braudrup, E.H. Immergut, E.A. Grulke, 4th edn. (Wiley Interscience, New York, 1999)

J. Kressler, H.W. Kammer, Acta Polym. **38**, 600 (1987)

J. Kressler, H.W. Kammer, Polym. Bull. **19**, 283 (1988)

J. Kressler, H.W. Kammer, K. Klostermann, Polym. Bull. **15**, 113 (1986)

J. Kressler, H.W. Kammer, G. Schmidt-Naake, K. Herzog, Polymer **29**, 686 (1988)

J. Kressler, H.W. Kammer, K. Herzog, H. Heyde, Acta Polym **41**, 1 (1990a)

J. Kressler, H.W. Kammer, U. Morgenstern, B. Litauszki, W. Berger, Makromol. Chem. **191**, 243 (1990b)

N.R. Krogman, A. Singh, L.S. Nair, C.T. Laurencin, H.R. Allcock, Biomacromolecules **8**, 1036 (2007)

N.R. Krogman, A.L. Weikei, N.Q. Nguyen, K.A. Kristhart, S.P. Nukavarapu, L.S. Nair, C.T. Laurencin, H.R. Allcock, J. Appl. Polym. Sci. **115**, 431 (2010)

P. Krutphun, P. Supaphol, Eur. Polym. J. **41**, 1561 (2005)

M. Kryszewski, J. Jachowciz, M. Malanga, O. Vogl, Polymer **23**, 271 (1982)

Y. Kumagai, Y. Doi Polym, Deg. Stab. **35**, 87 (1992)

Y. Kumagai, Y. Doi, Polym. Deg. Stab. **36**, 241 (1992)

C. Kummerlowe, H.W. Kammer, M. Malinconico, E. Martuscelli, Polymer **34**, 1677 (1993)

P.P. Kundo, D.K. Tripathy, B.K. Samanthroy, Polym. Networks Blends **5**, 11 (1995)

P. Kundu, D.K. Tripathy, S. Banerjee, Polymer **37**, 2423 (1996a)

P.P. Kundu, S. Banerjee, D.K. Tripathy, Int. J. Polym. Mater. **32**, 125 (1996b)

P.P. Kundu, S. Banerjee, D.K. Tripathy, Polymer **37**, 2423 (1996c)

A.K. Kundu, S.S. Ray, B. Adhikari, S. Maiti, Eur. Polym. J. **22**, 369 (1986a)

A.K. Kundu, S.S. Ray, R.N. Mukherjea, S. Maiti, Angew. Makromol. Chem. **143**, 197 (1986b)

A.K. Kundu, S.S. Ray, S. Maiti, Eur. Polym. J. **22**, 821 (1986c)

S.W. Kuo, J. Appl. Polym. Sci. **114**, 116 (2009)

S.W. Kuo, F.C. Chang, Macromol. Chem. Phys. **202**, 3112 (2001a)

S.W. Kuo, F.C. Chang, Macromolecules **34**, 4089 (2001b)

S.W. Kuo, F.C. Chang, Macromolecules **34**, 5224 (2001c)

S.W. Kuo, F.C. Chang, Macromolecules **34**, 7737 (2001d)

S.W. Kuo, F.C. Chang, Polymer **42**, 9843 (2001e)

S.W. Kuo, F.C. Chang, J. Polym. Sci. B: Polym. Phys. **40**, 1661 (2002a)

S.W. Kuo, F.C. Chang, Macromol. Chem. Phys. **203**, 868 (2002b)

S.W. Kuo, C.J. Chen, Macromolecules **45**, 2442 (2012)

C.M. Kuo, S.J. Clarson, Am. Chem. Soc. Polym. Prepr. **31**, 550 (1990)

C.M. Kuo, S.J. Clarson, Macromolecules **25**, 2192 (1992)

S.W. Kuo, C.H. Hsu, Polym. Int. **59**, 998 (2010)

S.W. Kuo, W.C. Liu, J. Appl. Polym. Sci. **119**, 300 (2011)

Y.H. Kuo, E.M. Woo, Polym. J. **35**, 236 (2003)

S.W. Kuo, C.F. Huang, F.C. Chang, J. Polym. Sci. B: Polym. Phys. **39**, 1348 (2001a)

Y.H. Kuo, E.M. Woo, T.Y. Kuo, Polym. J. **33**, 920 (2001b)

S.W. Kuo, C.L. Lin, F.C. Chang, Macromolecules **35**, 278 (2002a)

S.W. Kuo, C.L. Lin, F.C. Chang, Polymer **43**, 3943 (2002b)

S.W. Kuo, C.L. Lin, H.D. Wu, F.C. Chang, J. Polym. Res. **10**, 87 (2003)

S.W. Kuo, C.C. Shih, J.S. Shieh, F.C. Chang, Polym. Int. **53**, 218 (2004a)

S.W. Kuo, W.J. Huang, C.F. Huang, S.C. Chan, F.C. Chang, Macromolecules **37**, 4164 (2004b)

S.W. Kuo, S.C. Chan, H.D. Wu, F.C. Chang, Macromolecules **38**, 4729 (2005a)

S.W. Kuo, W.P. Liu, F.C. Chang, Macromol. Chem. Phys. **206**, 2307 (2005b)

J.A. Kuphal, L.H. Sperling, L.M. Robeson, J. Appl. Polym. Sci. **42**, 1525 (1991)

R. Kusumi, Y. Inoue, M. Shirakawa, Y. Miyashita, Y. Nishio, Cellulose **15**, 1 (2008)

N. Kuwahara, M. Ishizawa, S. Saeki, M. Kaneko, Rept. Prog. Polym. Phys. Jpn. **19**, 9 (1976)

S.Y. Kwak, J. Appl. Polym. Sci. **53**, 1823 (1994)

S.H. Kwang, J.C. Jung, S.W. Lee, Eur. Polym. J. **34**, 949 (1998)

T.K. Kwei, T. Nishi, R.F. Roberts, Macromolecules **7**, 667 (1974)

T.K. Kwei, G.D. Patterson, T.T. Wang, Macromolecules **9**. 780 (1976)

T.K. Kwei, H.L. Frisch, W. Radigan, S. Vogel, Macromolecules **10**, 157 (1977)

T.K. Kwei, J. Polym. Sci., Polym. Lett. Ed. **22**, 307 (1984)

T.K. Kwei, Y.K. Dai, X. Lu, R.A. Weiss, Macromolecules **26**, 6583 (1993)

T. Kyu, S.S. Chen, J. Macromol. Sci.: Phys. **B32**, 55 (1993)

T. Kyu, D.S. Lim, J. Polym. Sci., Polym. Lett. Ed. **27**, 421 (1989)

T. Kyu, J.M. Saldanha, J. Polym. Sci., Polym. Lett. Ed. **26**, 33 (1988)

T. Kyu, J.M. Saldanha, J. Polym. Sci., Polym. Phys. Ed. **28**, 97 (1990)

T. Kyu, P. Vadhar, J. Appl. Polym. Sci. **32**, 5575 (1986)

T. Kyu, S.R. Hu, R.S. Stein, J. Polym. Sci., Polym. Phys. Ed, **25**, 89 (1987)

T. Kyu, T.J. Chen, H.S. Park, J.L. White, J. Appl. Polym. Sci. **37**, 201 (1989b)

T. Kyu, D. Park, W. Cho, J. Appl. Polym. Sci. **44**, 2233 (1992)

T. Kyu, C.C. Ko, D.S. Lim, S.D. Smith, I. Noda, J. Polym. Sci. B: Polym. Phys. **31**, 1641 (1993)

W.C. Lai, W.B. Liau, T.S. Lin, Polymer **45**, 3073 (2004)

V. Landi, Rubber Chem. Technol. **45**, 222 (1972)

V. Landi, Appl. Polym. Symp. **25**, 223 (1974)

C.J.T. Landry, P.M. Hendrichs, Macromolecules **22**, 2157 (1989)

C.J.T. Landry, D.M. Teegarden, Macromolecules **24**, 4310 (1991)

C.J.T. Landry, B.K. Coltrain, D.M. Teegarden, W.T. Ferrar, Macromolecules **26**, 5543 (1993a)

M.R. Landry, D.J. Massa, C.J.T. Landry, D.M. Teegarden, R.H. Colby, T.E. Long, P.M. Henrichs,
    J. Appl. Polym. Sci. **54**, 991 (1993b)

C.J.T. Landry, D.J. Massa, D.M. Teegarden, M.R. Landry, P.M. Henrichs, R.H. Colby, T.E. Long,
    Macromoleules **26**, 6299 (1993c)

C.J.T. Landry, H. Yang, J.S. Machell, Polymer **32**, 44 (1991)

C.J.T. Landry, W.T. Ferrar, D.M. Teegarden, B.K. Coltrain, Macromolecules **26**, 35 (1993d)

D. Lath, E. Lathova, Chem. Papers **48**, 226 (1994)

D. Lath, J.M.G. Cowie, E. Lathova, Polym. Bull. **28**, 361 (1992)

D. Lath, E. Lathova, J.M.G. Cowie, Makromol. Chem. **194**, 3087 (1993)

D. Lath, E. Lathova, J.M.G. Cowie, Polymer **41**, 3871 (2000)

C. Lau, Y. Mi, J. Polym. Sci. B: Polym. Phys. **39**, 2390 (2001)

C. Lau, Y. Mi, Polymer **43**, 823 (2002)

C. Lau, S. Zheng, Z. Zhong, Y. Mi, Macromolecules **31**, 7291 (1998)

W.W.Y. Lau, S.H. Teoh, S.H. Goh, Brit. Polym. J. **20**, 323 (1988)

W.W.Y. Lau, Y.Q. Jiang, P.P.K. Tan, Polym. Int. **31**, 163 (1993)

C. Le Menestrel, D.E. Bhagwagar, P.C. Painter, M.M. Coleman, J.F. Graf, Macromolecules **25**,
    7107 (1992)

M.S. Lee, S.A. Chen, J. Polym. Res. **3**, 235 (1996)

W.K. Lee, C.S. Ha, Pollimo **18**, 935 (1994a)

W.K. Lee, C.S. Ha, Polymer (Korea) **18**, 935 (1994b)

J.Y. Lee, J.Y. Han, Macromol. Res. **12**, 94 (2004)

H.S. Lee, W.N. Kim, Polymer **38**, 2657 (1997)

J.C. Lee, M.H. Litt, Eur. Polym. J. **37**, 603 (2001)

T.H. Lee, H. Marand, Am. Chem. Soc., Polym. Prepr. **32**(3), 316 (1991)

D.S. Lee, G. Quin, Polym. J. **21**, 751 (1989)

S.C. Lee, E.M. Woo, Macromol. Rapid Commun. **21**, 1196 (2000)

S.C. Lee, E.M. Woo, J. Polym. Sci. B: Polym. Phys. **40**, 747 (2002)

L.T. Lee, E.M. Woo, Colloid Polym. Sci. **282**, 1308 (2004a)

L.T. Lee, E.M. Woo, Polym. Int. **53**, 1813 (2004b)

J.Y. Lee, J.Y. Yan, Polymer (Korea) **26**, 737 (2002)

S.S. Lee, K.H. Chung, K.S. Kim, J.C. Jung, Angew. Makromol. Chem. **164**, 171 (1988a)

J.Y. Lee, P.C. Painter, M.M. Coleman, Am. Chem. Soc., Polym. Prepr. **29**(1), 313 (1988)

J.Y. Lee, P.C. Painter, M.M. Coleman, Macromolecules **21**, 346 (1988c)

J.Y. Lee, P.C. Painter, M.M. Coleman, Macromolecules **21**, 954 (1988d)

S.S. Lee, K.H. Chung, K.S. Kim, J.C. Jung, Angew. Makromol. Chem. **165**, 89 (1989a)

S.C. Lee, M.S. Lee, W.H. Jo, J. Polym. Sci., Polym. Phys. Ed. **29**, 759 (1991)

S.Y. Lee, M.Y. Low, S.H. Goh, Eur. Polym. J. **27**, 1379 (1991c)

J.S. Lee, H.J. Kim, D.S. Lee, Polym. Bull. **30**, 229 (1993)

H.S. Lee, T. Kyu, Am. Chem. Soc., Polym. Prepr., **30**(1), 308 (1989)

M.S. Lee, S.C. Lee, S.H. Chae, W.H. Jo, Macromolecules **25**, 4339 (1992)

S.W. Lee, C.S. Ha, W.J. Cho, Polymer **37**, 3347 (1996a)

Y.M. Lee, S.H. Kim, S.J. Kim, Polymer **37**, 5897 (1996b)

J.C. Lee, K. Nakajima, T. Ikehara, T. Nishi, J. Polym. Sci. B: Polym. Phys. **35**, 2645 (1997)

J.Y. Lee, H. Lee, D.H. Choi, Polymer (Korea) **22**, 501 (1998a)

J.C. Lee, M.H. Litt, C.E. Rogers, Macromolecules **31**, 4232 (1998b)

J.C. Lee, H. Tazawa, T. Ikehara, T. Nishi, Polym. J. **30**, 327 (1998c)

L.T. Lee, E.M. Woo, J. Polym. Sci. B: Polym. Phys. **44**, 1339 (2006)

L.T. Lee, E.M. Woo, S.S. Hou, S. Forster, Polymer **47**, 8350 (2006a)

H.F. Lee, S.W. Kuo, C.F. Hunag, J.S. Lu, S.C. Chan, C.F. Wang, F.C. Chang, Macromolecules **39**, 5458 (2006b)

S.S. Lee, H.M. Jeong, J.Y. Jho, T.O. Ahn, J. Polym. Sci. B: Polym. Phys. **38**, 803 (2000)

J.S. Lee, A.A. Prabu, K.J. Kim, C. Park, Macromolecules **41**, 3598 (2008)

Y. Lee, J.K. Kim, C.H. Chiu, Y.K. Lau, C.I. Huang, Polymer **50**, 4944 (2009)

L.T. Lee, E.M. Woo, W.T. Chen, L. Chang, K.C. Yen, Colloid Polym. Sci. **288**, 439 (2010)

J. Leffingwell, C. Thies, H. Gertzman, Am. Chem. Soc. Polym. Prepr. **14**, 596 (1973)

M.H. Lehr, Polym. Eng. Sci. **25**, 1056 (1985)

M.H. Lehr, Polym. Eng. Sci. **26**, 947 (1986)

Y.G. Lei, Z.L. Cheung, K.M. Ng, L. Li, L.T. Weng, C.M. Chan, Polymer **44**, 3883 (2003)

A. Lejardi, E. Meaurio, J. Fernandez, J.R. Sarasua, Macromolecules **44**, 7351 (2011)

E. Lemieux, R.E. Prud'homme, R. Forte, R. Jerome, P. Teyssie, Macromolecules **21**, 2148 (1988)

L.M. Leung, K.K.C. Lo, Polym. Int. **36**, 339 (1995)

L. Leung, D.J. Williams, F.E. Karasz, W.J. MacKnight, Polym. Bull. **16**, 457 (1986)

L.M. Leung, C.T. Lau, L. Chang, Y. Huang, B. Liao, M.C. Chen, G. Cong, Polymer **42**, 539 (2001)

K. Levon, E. Chu, K.S. Ho, T.K. Kwei, J. Mao, W.Y. Zheng, J. Laakso, J. Polym. Sci. B: Polym. Phys. **33**, 537 (1995)

K. Lewandowska, Eur. Polym. J. **41**, 55 (2005)

E.G. Lezcano, M.G. Prolongo, C.S. Coll, Polymer **36**, 595 (1995)

E.G. Lezcano, C. Salom Coll, M.G. Prolongo, Polymer **37**, 3603 (1996)

E.G. Lezcano, D.R. de Arellano, M.G. Prolongo, C.S. Coll, Polymer **39**, 1583 (1998)

D. Li, J. Brisson, Macromolecules **29**, 868 (1996)

W. Li, R.E. Prud'homme, J. Polym. Sci. B: Polym. Phys. **31**, 719 (1993)

S.H. Li, E.M. Woo, Macromol. Mater. Eng. **291**, 1397 (2006)

S.H. Li, E.M. Woo, Colloid Polym. Sci. **286**, 253 (2008a)

S.H. Li, E.M. Woo, J. Appl. Polym. Sci. **107**, 766 (2008b)

S.H. Li, E.M. Woo, J. Polym. Sci. B: Polym. Phys. **46**, 2355 (2008c)

W. Li, L. Shi, D. Shen, Y. Wu, J. Zheng, Polymer **30**, 604 (1989)

G. Li, Y. Jin, L. Shi, M. Ye, F. Bai, J. Polym. Sci. B: Polym. Phys. **34**, 1079 (1996)

L. Li, C.M. Chan, L.T. Weng, M.L. Xiang, M. Jiang, Macromolecules **31**, 7248 (1998a)

L. Li, C.M. Chan, L.T. Weng, Polymer **39**, 2355 (1998b)

G. Li, J.M.G. Cowie, V. Arrighi, J. Appl. Polym. Sci. **74**, 639 (1999a)

H. Li, Y. Yang, R. Fujitsuka, T. Ougizawa, T. Inoue, Polymer **40**, 927 (1999b)

X. Li, S.H. Goh, Y.H. Lai, A.T.S. Wee, Polymer **42**, 5463 (2001a)

X. Li, S.H. Goh, Y.H. Lai, A.T.S. Wee, Polymer **42**, 6563 (2001b)

C.X. Li, J. Zhao, D.L. Zhao, Q.R. Fan, J. Polym. Res. **11**, 323 (2004)

J.C. Li, T. Fukuoka, Y. He, H. Urama, S. Kobayashi, Y. Inoue, J. Appl. Polym. Sci. **101**, 149 (2006)

G.X. Li, S.Y. Mong, S.J. Jiang, L. Ragupathy, J.M.G. Cowie, R. Ferguson, V. Arrighi, J. Appl. Polym. Sci. **106**, 944 (2007)

X.J. Li, S.L. Zhang, H. Wang, C.F. Zhang, J.H. Pang, J.X. Mu, G. Ma, G.B. Wang, Z.H. Jiang, Polym. Int. **60**, 607 (2011)

K. Liang, G. Banhegyi, F.E. Karasz, W.J. MacKnight, J. Polym. Sci., Polym. Phys. Ed. **29**, 649 (1991)

K. Liang, J. Grebowicz, F.E. Karasz, W.J. MacKnight, J. Polym. Sci., Polym. Phys. Ed. **30**, 465 (1992)

H. Liang, F. Xie, B. Chen, F.Q. Guo, Z. Jin, F.S. Luo, J. Appl. Polym. Sci. **107**, 431 (2008)

B. Liao, Y.H. Huang, M.C. Cheng, G.M. Cong, Polym. Bull. **36**, 79 (1996)

W.B. Liau, A.S. Liu, W.Y. Chiu, J. Polym. Res. **6**, 27 (1999)

W.B. Liau, S.H. Tung, W.C. Lai, L.Y. Yang, Polymer **47**, 8360 (2006)

S.A. Liberman, A de S. Gomes, E.M. Macchi, J. Polym. Sci., Polym. Chem. Ed. **22**, 2809 (1984)

A.M. Lichkus, P.C. Painter, M.M. Coleman, Macromolecules **21**, 2636 (1988)

D.S. Lim, T. Kyu, J. Chem. Phys. **92**, 3944 (1990)

J.L. Lim, R.J. Roe, Polymer **29**, 1227 (1988)

J.C. Lim, J.K. Park, H.Y. Song, J. Polym. Sci. B: Polym. Phys. **32**, 29 (1994)

J.S. Lim, I. Noda, S.S. Im, Eur. Polym. J. **44**, 1428 (2008)

C.H. Lin, C.S. Wang, Polym. Bull. **46**, 191 (2001)

J.H. Lin, E.M. Woo, Polymer **47**, 6826 (2006)

J.L. Lin, D. Rigby, R.J. Roe, Macromolecules **18**, 1609 (1985)

P. Lin, C. Clash, E.M. Pearce, T.K. Kwei, M.A. Aponte, Solid-state phase behavior and molecular-level mixing phenomena in a strongly interacting polymer blend. J. Polym. Sci., Polym. Phys **26**, 603 (1988)

A.A. Lin, T.K. Kwei, A. Reiser, Macromolecules **22**, 4112 (1989)

Y.G. Lin, H.W. Lee, H.H. Winter, S. Dashevsky, K.S. Kim, Polymer. **34**, 4703 (1993)

R.H. Lin, E.M. Woo, J.C. Chiang, Polymer **42**, 4289 (2001)

J.H. Lin, E.M. Woo, Y.P. Huang, J. Polym. Sci. B: Polym. Phys. **44**, 3357 (2006a)

C.L. Lin, W.C. Chen, S.W. Kuo, F.C. Chang, Polymer **47**, 3436 (2006b)

C.T. Lin, S.W. Kuo, J.C. Lo, F.C. Chang, J. Phys. Chem. B. **114**, 1603 (2010)

A. Lindstrom, M. Hakkarainen, J. Polym. Sci. B: Polym. Phys. **45**, 1552 (2007)

J.E.G. Lipson, M. Tambasco, K.A. Willets, J.S. Higgins, Macromolecules **36**, 2977 (2003)

B. Litauszki, G. Schmidt-Naake, J. Kressler, H.W. Kammer, Polym. Commun. **30**, 359 (1989)

J. Liu, Y.C. Jean, H. Yang, Macromolecules **28**, 5774 (1995)

A.S. Liu, W.B. Liau, W.Y. Chiu, Macromolecules **31**, 6593 (1998)

Y. Liu, S.H. Goh, S.Y. Lee, C.H.A. Huan, Macromolecules **32**, 1967 (1999)

Y. Liu, S.H. Goh, S.Y. Lee, C.H.A. Huan, J. Polym. Sci. B: Polym. Phys. **38**, 501 (2000)

S. Liu, C.M. Chan, L.T. Weng, L. Li, M. Jiang, Macromolecules **35**, 5623 (2002)

S.Y. Liu, C.M. Chan, L.T. Weng, M. Jiang, Anal. Chem. **76**, 5165 (2004a)

S.Y. Liu, C.M. Chan, L.T. Weng, M. Jiang, Polymer **45**, 4945 (2004b)

S.Y. Liu, C.M. Chan, L.T. Weng, M. Jiang, J. Polym. Sci. B: Polym. Phys. **43**, 1924 (2005a)

B.Q. Liu, W. Zhang, S.X. Zheng, Polymer. **46**, 10574 (2005b)

J.P. Liu, Z.B. Qiu, B.J. Jungnickel, J. Polym. Sci. B: Polym. Phys. **43**, 287 (2005c)

H.L. Liu, S.H. Li, E.M. Woo, J. Polym. Sci. B: Polym. Phys. **44**, 1147 (2006a)

B.Q. Liu, W.A. Zhang, S.X. Zheng, Q.P. Guo, J. Polym. Sci. B: Polym. Phys. **44**, 1618 (2006b)

D.I. Livingston, J.E. Brown Jr., Proc. Int. Congr. Rheol. **4**, 25 (1968, 1970)

D.I. Livingston, R.L. Rongone, Proc. 5th Int. Rubber Technol. Conf. Brighton, 337 (1967); Chem. Abstr., **72**, 67965y (1970)

C.T. Lo, S. Seifert, P. Thiyagarajan, B. Narasimhan, Polymer **45**, 3671 (2004)

R.J. Lockwood, L.M. Alberino, in *Urethane Chemistry and Applications*, ed. by K.N. Edwards, W. F. Gum. American Chemical Society, Symposium Series, vol. 172 (Washington, DC, 1981)

D.J. Lohse, Polym. Eng. Sci. **26**, 1500 (1986)

D.J. Lohse, L.J. Fetters, M.J. Doyle, H.C. Wang, C. Kow, Macromolecules **26**, 3444 (1993)

J. Lokaj, A. Sikora, Z. Pientka, M. Bleha, J. Appl. Polym. Sci. **58**, 1485 (1995)

N. Lotti, M. Pizzoli, G. Ceccorulli, M. Scandola, Polymer **34**, 4935 (1993)

S.M. Low, S.Y. Lee, S.H. Goh, Eur. Polym. J. **29**, 1075 (1993a)

S.M. Low, S.Y. Lee, S.H. Goh, Eur. Polym. J. **29**, 1543 (1993b)

S.M. Low, S.Y. Lee, S.H. Goh, Eur. Polym. J. **29**, 909 (1993c)

S.M. Low, S.Y. Lee, S.H. Goh, Macromolecules **26**, 2631 (1993d)

S.M. Low, S.H. Goh, S.Y. Lee, M.K. Neo, Polym. Bull. **32**, 187 (1994a)

S.M. Low, S.H. Goh, S.Y. Lee, Macromolecules **27**, 3764 (1994b)

S.M. Low, S.H. Goh, S.Y. Lee, Polymer **35**, 3290 (1994c)

S.M. Low, S.Y. Lee, S.H. Goh, Eur. Polym. J. **30**, 139 (1994d)

X. Lu, R.A. Weiss, Macromolecules **24**, 4381 (1991)

X. Lu, R.A. Weiss, Macromolecules **25**, 6185 (1992)

X. Lu, R.A. Weiss, Macromolecules **28**, 3022 (1995)

X. Lu, R.A. Weiss, J. Polym. Sci. B: Polym. Phys. **34**, 1795 (1996a)

X. Lu, R.A. Weiss, Macromolecules **29**, 1216 (1996b)

H. Lu, S.X. Zheng, Polymer **44**, 4689 (2003)

S. Lu, E.M. Pearce, T.K. Kwei, J. Polym. Sci. A: Polym. Chem. **32**, 2607 (1994)

S. Lu, E.M. Pearce, T.K. Kwei, Polym. Eng. Sci. **35**, 1113 (1995a)

S. Lu, E.M. Pearce, T.K. Kwei, Polymer **26**, 2435 (1995b)

S. Lu, E.M. Pearce, T.K. Kwei, E. Chu, J. Polym. Sci. B: Polym. Phys. **34**, 3163 (1996a)

S. Lu, E.M. Pearce, T.K. Kwei, Polym. Adv. Technol. **7**, 553 (1996b)

H. Lu, S.X. Zheng, G.H. Tian, Polymer **45**, 2897 (2004)

J.M. Lu, Z.B. Qiu, W.T. Yang, Macromolecules **41**, 141 (2008)

Y.S. Lu, Y.C. Lin, S.W. Kuo, Macromolecules **45**, 6547 (2012)

D. Luo, E.M. Pearce, T.K. Kwei, Macromolecules **26**, 6220 (1993)

X. Luo, S. Zheng, N. Zhang, D. Ma, Polymer **35**, 2619 (1994)

X. Luo, S. Zheng, D. Ma, K. Hu, Chinese J. Polym. Sci. **13**, 144 (1995a)

D. Luo, T.K. Kwei, E.M. Pearce, Macromol. Symp. **98**, 769 (1995b)

X.F. Luo, S.H. Goh, S.Y. Lee, Macromolecules **30**, 4934 (1997)

X.F. Luo, S.H. Goh, S.Y. Lee, K.L. Tan, Macromolecules **31**, 3251 (1998)

X.F. Luo, S.H. Goh, S.Y. Lee, C.H.A. Huan, Macromol. Chem. Phys. **200**, 874 (1999a)

X.F. Luo, S.H. Goh, S.Y. Lee, Macromol. Chem. Phys. **200**, 399 (1999b)

X.F. Luo, X. Hu, X.Y. Zhao, S.H. Goh, X.D. Li, Polymer **44**, 5285 (2003)

R.C. Luo, K.T. Xu, G.Q. Chen, J. Appl. Polym. Sci. **105**, 3402 (2007)

D. Ma, R.E. Prud'homme, Polymer **31**, 917 (1990)

S.P. Ma, T. Takahashi, Polymer **37**, 5589 (1996)

C.C.M. Ma, W.J. Wu, J. Mater. Sci. **36**, 943 (2001)

D. Ma, R. Zhang, X. Luo, Polymer **36**, 3963 (1995)

D. Ma, X. Luo, R. Zhang, T. Nishi, Polymer **37**, 1575 (1996)

D. Ma, X. Xiang, X. Luo, T. Nishi, Polymer **38**, 1131 (1997a)

C.C.M. Ma, H.D. Wu, P.P. Chu, H.T. Tseng, Macromolecules **30**, 5443 (1997b)

D. Ma, H. Cai, J. Zhang, X. Luo, Macromol. Chem. Phys. **200**, 2040 (1999)

E.M. Macchi, S.A. Liberman, A.S. Gomes, Makromol. Chem. **187**, 573 (1986)

J.M. Machado, R.N. French, Polymer **33**, 439 (1992)

J.M. Machodo, R.N. French, Polymer **33**, 760 (1992)

W.J. MacKnight, J. Stoelting, F.E. Karasz, in *Multicomponent Polymer Systems*, ed. by N.A.J. Platzer. American Chemical Society, Advances in Chemistry Series, vol. 99 (Washington, DC, 1971)

A. Maconnachie, R.P. Kambour, R.C. Bopp, Polymer **25**, 357 (1984)

S.A. Madbouly, N.Y. Abdou, A.A. Mansour, Macromol. Chem. Phys. **207**, 978 (2006)

Y. Maeda, F.E. Karasz, W.J. MacKnight, R.J. Vukovic, Polym. Sci. Polym. Phys. Ed. **24**, 2345 (1986)

Y. Maeda, F.E. Karasz, W.J. MacKnight, Netsu Sokutei **16**, 65 (1989)

M. Maejima, Y. Takeda, T. Inoue, T. Sakai, Sen'i Gakkaishu **44**, 444 (1988)

M. Maejima, H. Nakamura, T. Inoue, T. Sakai, Sen'i Gakkaishu **45**, 516 (1989)

M. Maekawa, R. Pearce, R.H. Marchessault, R.S.J. Manley, Polymer **40**, 1501 (1999)

T.R. Maier, A.M. Jamieson, R. Simha, J. Appl. Polym. Sci. **51**, 1053 (1994)

R.D. Maier, J. Kressler, B. Rudolf, P. Reichert, F. Koopman, H. Frey, R. Mulhaupt, Macromolecules **29**, 1490 (1996)

R.D. Maier, M. Kopf, D. Maeder, F. Koopman, H. Frey, J. Kressler, Acta Polym. **49**, 356 (1998)

P. Maiti, A.K. Nandi, Macromolecules **28**, 8511 (1995)

N. Maiti, S. Dutta, S.N. Bhattacharyya, B.M. Mandel, Polym. Commun. **29**, 363 (1988)

B. Majumdar, H. Keskkula, D.R. Paul, N.G. Harvey, Polymer **35**, 4263 (1994)

S. Makhija, E.M. Pearce, T.K. Kwei, F. Liu, Polym. Eng. Sci. **30**, 798 (1990a)

S. Makhija, E.M. Pearce, T.K. Kwei, Polym. Mater. Sci. Eng. **63**, 498 (1990b)

S. Makhija, E.M. Pearce, T.K. Kwei, J. Appl. Polym. Sci. **44**, 917 (1992)

M. Maldonado-Santoyo, C. Ortiz-Estrada, G. Luna-Barcenas, I.C. Sanchez, L.C. Cesteros, I. Katime, S.M. Nuno-Donlucas, J. Polym. Sci. B: Polym. Phys. **42**, 636 (2004a)

M. Maldonado-Santoyo, L.C. Cesteros, I. Katime, S.M. Nuno-Donlucas, Polymer **45**, 5591 (2004b)

M. Maldonado-Santoyo, S.M. Nuno-Donlucas, L.C. Cesteros, I. Katime, J. Appl. Polym. Sci. **91**, 1887 (2004c)

S. Manabe, P. Murakami, M. Takayanagi, Mem. Faculty Eng. Kyushu Univ. **28**, 295 (1969)

A. Mandai, A.K. Nandi, Macromol. Chem. Phys. **212**, 1636 (2011)

T.K. Mandal, E.M. Woo, J. Polym. Res. **5**, 205 (1998)

T.K. Mandal, E.M. Woo, Macromol. Chem. Phys. **200**, 1143 (1999a)

T.K. Mandal, E.M. Woo, Polym. J. **31**, 226 (1999b)

T.K. Mandal, E.M. Woo, Polymer **40**, 2813 (1999c)

T.K. Mandal, J.F. Kuo, E.M. Woo, J. Polym. Sci. B: Polym. Phys. **38**, 562 (2000)

V. Mano, M.E.S.R.E. Silva, N. Barbani, P. Giusti, J. Appl. Polym. Sci. **91**, 501 (2004a)

V. Mano, M.E.S.R.E. Silva, N. Barbani, P. Giusti, J. Appl. Polym. Sci. **92**, 743 (2004b)

A.A. Mansour, S.A. Madbouly, Polym. Int. **36**, 269 (1995)

H. Marand, M. Collins, Am. Chem. Soc. Polym. Prepr. **31**(1), 552 (1990)

K. Marcincin, A. Ramonov, V. Pollak, J. Appl. Polym. Sci. **16**, 2239 (1972)

C. Marco, M.A. Gomez, J.G. Fatou, A. Etxeberria, M.M. Elorza, J.J. Iruin, Eur. Polym. J. **29**, 1477 (1993)

A.I. Marei, E.A. Sidorovich, Polym. Mechanics **1**(5), 55 (1965)

J.M. Marentette, G.R. Brown, Polymer **39**, 1415 (1998)

A.G. Margaritis, N.K. Kalfoglou, Polymer **28**, 497 (1987)

A.G. Margaritis, N.K. Kalfoglou, Eur. Polym. J. **29**, 1043 (1988)

A.G. Margaritis, J.K. Kallitisis, N.K. Kalfoglou, Polymer **28**, 2122 (1987)

A.G. Margaritis, J.K. Kallitisis, N.K. Kalfoglou, Polymer **30**, 2253 (1989)

Y.H. Mariam, K.P.W. Pemawansa, K.B. Bota, Am. Chem. Soc. Polym. Prepr. **27**(1), 271 (1986)

P.A. Marsh, A. Voet, L.D. Price, Rubber Chem. Technol. **40**, 359 (1967)

P.A. Marsh, A. Voet, L.D. Price, T.J. Mullens, Rubber Chem. Technol. **41**, 344 (1968)

J.M. Martinez, J.I. Eguiazabal, J. Nazabal, J. Appl. Polym. Sci. **48**, 935 (1993)

E. Martuscelli, G.B. Demma, in *Polymer Blends: Processing, Morphology and Properties*, ed. by E. Martuscelli, R. Palumbo, M. Kryszewski (Plenum, New York, 1980), p. 101

E. Martuscelli, C. Silvestre, C. Gismondi, Makromol. Chem. **186**, 2161 (1985)

E. Martuscelli, C. Silvestre, M.L. Addonizio, L. Amelino, Makromol. Chem. **187**, 1557 (1986)

E. Martuscelli, M. Canetti, A.M. Bonfatti, A. Seves, Polymer **32**, 641 (1991)

L.M. Martynowicz-Hans, J. Runt, Am. Chem. Soc. Polym. Prepr. **27**(1), 269 (1986)

J. Maruta, T. Ougizawa, T. Inoue, Polymer **29**, 2056 (1988)

P. Masi, D.R. Paul, J.W. Barlow, Rheol. Proc. **3**, 315 (1980)

D.J. Massa, in *Multiphase Polymers*, ed. by S.L. Cooper, G.M. Estes. American Chemical Society, Advances in Chemistry Series, vol. 176 (Washington, DC, 1979), p. 433

D.J. Massa, Am. Chem. Soc. Polym. Prepr. **29**(1), 434 (1988)

D.J. Massa, K.A. Shriner, S.R. Turner, B.I. Voit, Macromolecules **28**, 3214 (1995)

K.A. Masser, H.Q. Zhao, P.C. Painter, J. Runt, Macromolecules **43**, 9004 (2010)

J.F. Masson, R.S.J. Manley, Macromolecules **24**, 5914 (1991)

J.F. Masson, R.S.J. Manley, Macromolecules **25**, 589 (1992)

M. Matsuo, C. Nozaki, Y. Jyo, Polym. Eng. Sci. **9**, 197 (1969)

M. Matsuura, H. Saito, S. Nakata, Y. Imai, T. Inoue, Polymer **33**, 3210 (1992)

M. Matzner, D.L. Schoher, R.N. Johnson, L.M. Robeson, J.E. McGrath, in *Permeability of Plastic Films and Coatings to Gases, Vapors, and Liquids*, ed. by H.B. Hopfenberg (Plenum, New York, 1979), p. 125

M. Matzner, L.M. Robeson, E.W. Wise, J.E. McGrath, Makromol. Chem. **183**, 2871 (1982)

S.L. Maunu, J. Kinnunen, K. Soljamo, F. Sundholm, Polymer **34**, 1141 (1993)

M. Mayo-Pedrosa, C. Alvarez-Lorenzo, A. Concheiro, J. Therm. Anal. Calorim. **77**, 681 (2004)

C. Mbareck, T.Q. Nguyen, J.M. Saiter, J. Appl. Polym. Sci. **114**, 2261 (2009)

K.G. McGrath, C.M. Roland, Rubber Chem. Technol. **67**, 629 (1994)

L.P. McMaster, Macromolecules **6**, 760 (1973)

L.P. McMaster, in *Copolymers, Polyblends and Composites*, ed. by N.A.J. Platzer. American Chemical Society, Advances in Chemistry Series, vol. 142 (Washington, DC, 1975), p. 43

E. Meaurio, J.L. Velada, L.C. Cesteros, I. Katime, Macromolecules **29**, 4598 (1996)

E. Meaurio, L.C. Cesteros, I. Katime, Macromolecules **30**, 4567 (1997)

E. Meaurio, L.C. Cesteros, I. Katime, Polymer **39**, 379 (1998)

E. Meaurio, E. Zuza, J.R. Sarsua, Macromolecules **38**, 1027 (2005a)

E. Meaurio, E. Zuza, J.R. Sarsua, Macromolecules **38**, 9221 (2005b)

D. Meghala, C. Ranganathaiah, Polymer **53**, 842 (2012)

N. Mekhilef, P. Hadjiandreou, Polymer **36**, 2165 (1995)

Y.Z. Meng, S.C. Tjong, Polymer **40**, 2711 (1999)

P.C. Mengujoh, H.L. Frisch, J. Polym. Sci. Polym. Chem. Ed. **27**, 3363 (1989)

J.C. Meredith, E.J. Amis, Macromol. Chem. Phys. **201**, 733 (2000)

G.D. Merfeld, D.R. Paul, Polymer **39**, 1999 (1998)

G.D. Merfeld, D.R. Paul, Polymer **41**, 649 (2000)

G.D. Merfeld, K. Chan, D.R. Paul, Macromolecules **32**, 429 (1999)

G.D. Merfeld, T.T. Maa, K. Chan, D.R. Paul, Polymer **41**, 663 (2000)

R. Metha, M.D. Dadmun, Macromolecules **39**, 8799 (2006)

F. Metref, S. Djadoun, Polym. Bull. **34**, 485 (1995)

G.C. Meyer, G.E. Tritscher, J. Appl. Polym. Sci. **22**, 719 (1978)

M. Mih, L. Aras, C. Alkan, Polym. Bull. **50**, 191 (2003)

J. Mijovic, H.L. Luo, C.D. Han, Polym. Eng. Sci. **22**, 234 (1982)

J.B. Miller, K.J. McGrath, C.M. Roland, C.A. Trask, Macromolecules **23**, 4543 (1990)

B.Y. Min, E.M. Pearce, Am. Chem. Soc. Org. Coatings Plastics Chem. Prepr **45**, 58 (1981)

K.E. Min, D.R. Paul, Macromolecules **20**, 2828 (1987)

K.E. Min, D.R. Paul, J. Polym. Sci. Polym. Phys. Ed. **26**, 2257 (1988)

K.E. Min, D.R. Paul, J. Appl. Polym. Sci. **37**, 1153 (1989)

B.Y. Min, E.M. Pearce, T.K. Kwei, Am. Chem. Soc. Polym. Prepr. **24**(2), 441 (1983)

K.E. Min, J.S. Chiou, J.W. Barlow, D.R. Paul, Polymer **28**, 1721 (1987)

K.E. Min, D.H. Lee, H.M. Jung, Polym. Bull. **24**, 221 (1990)

I. Mindru, M. Olteanu, L. Dehe, V. Trandafir, Rev. Roum. Chim. **28**, 683 (1983)

L. Minkova, M. Mikhailov, Colloid Polym. Sci. **265**, 1 (1987)

S.P. Mishra, P. Venkidusamy, J. Appl. Polym. Sci. **58**, 2229 (1995)

Y. Miyashita, Y. Yamada, N. Kimura, Y. Nishio, H. Suzuki, Seni Gakkaishi **51**, 396 (1995)

Y. Miyashita, Y. Yamada, N. Kimura, H. Suzuki, Polymer **38**, 6181 (1997)

Y. Miyashita, T. Suzuki, Y. Nishio, Cellulose **9**, 215 (2002)

T. Miyoshi, K. Takegoshi, K. Hikichi, Polymer **37**, 11 (1996)

T. Miyoshi, K. Takegoshi, K. Hikichi, Polymer **38**, 2315 (1997)

J. Moacanin, E. Cuddihy, A. Rembaum, in *Plasticization and Plasticizer Processes*, ed. by N.A.J. Platzer. American Chemical Society, Advances in Chemistry Series, vol. 48 (Washington, DC, 1965), p. 159

S. Mohanty, S. Roy, R.N. Santra, G.B. Nando, J. Appl. Polym. Sci. **58**, 1947 (1995)

S. Mohanty, G.B. Nando, K. Vijayan, N.R. Neelakanthan, Polymer **37**, 5387 (1996)

M.A. Moharram, L.S. Balloomal, H.M. El-Gendy, J. Appl. Polym. Sci. **59**, 987 (1996)

R.N. Mohn, D.R. Paul, J.W. Barlow, C.A. Cruz, J. Appl. Polym. Sci. **23**, 575 (1979)

G.E. Molau, J. Polym. Sci. B **3**, 1007 (1965)

A. Molnar, A. Eisenberg, Polym. Commun. **32**, 370 (1991)

A. Molnar, A. Eisenberg, Macromolecules **25**, 5774 (1992)

A. Molnar, A. Eisenberg, Polymer **34**, 1918 (1993)

I. Mondragon, M. Cortazar, G.M. Guzman, Makromol. Chem. **184**, 1741 (1983)

I. Mondragon, M. Gaztelumendi, J. Nazabal, Polym. Eng. Sci. **28**, 1126 (1988)

M.A. Monedero, G.S. Luengo, S. Moreno, F. Ortega, R.G. Rubio, M.G. Prolongo, R.M. Masegosa, Polymer **40**, 5833 (1999)

O. Monticelli, D. Oliva, S. Russo, C. Clausnitzer, P. Potschke, B. Boit, Macromol. Mater. Eng. **288**, 318 (2003)

O. Monticelli, S. Russo, R. Campagna, B. Voit, Polymer **46**, 3597 (2005)

J.Y. Moon, H.J. Jang, K.H. Kim, D.W. Park, C.S. Ha, J.K. Lee, J. Appl. Polym. Sci. **77**, 1809 (2000)

E.J. Moon, M.J. Kim, H.K. Choi, C.K. Kim, J. Polym. Sci. B: Polym. Phys. **40**, 1288 (2002)

H.S. Moon, W.M. Choi, M.H. Kim, O.O. Park, J. Appl. Polym. Sci. **104**, 95 (2007)

J.A. Moore, J.H. Kim, Macromolecules **25**, 1427 (1992)

J.A. Moore, S. Kaur, Macromolecules **31**, 328 (1998)

A.R. Morales, R.E.S. Bretas, Eur. Polym. J. **32**, 349 (1996a)

A.R. Morales, R.E.S. Bretas, Eur. Polym. J. **32**, 365 (1996b)

E.J. Moskala, J.P. Runt, M.M. Coleman, in *Multicomponent Polymer Materials*, ed. by D.R. Paul, L.H. Sperling. American Chemical Society, Advances in Chemistry Series, vol. 211 (Washington, DC, 1986), p. 77

H.R. Motzer, P.C. Painter, M.M. Coleman, Macromolecules **34**, 8388 (2001a)

H.R. Motzer, P.C. Painter, M.M. Coleman, Macromolecules **34**, 8390 (2001b)

N. Moussaif, R. Jerome, Polymer **40**, 6831 (1999)

K. Mpoukouvalas, G. Floudas, S.H. Zhang, J. Runt, Macromolecules **38**, 552 (2005)

M. Mucha, J. Jachowicz, M. Kryszewski, Acta Polym. **32**, 156 (1981)

A. Mugica, M.E. Calahorra, M. Cortazar, Macromol. Chem. Phys. **203**, 1088 (2002)

A. Mugica, J.A. Pomposo, E. Calahorra, M. Cortazar, Polymer **46**, 10741 (2005)

S. Mukhopadhyay, S.K. De, J. Mater. Sci. **25**, 4027 (1990)

R. Murali, A. Eisenberg, J. Polym. Sci. Polym. Phys. Ed. **26**, 1385 (1988)

R. Murali, A. Eisenberg, R.K. Gupta, F.W. Harris, Am. Chem. Soc. Polym. Prepr. **27**(1), 343 (1986)

S.R. Murff, J.W. Barlow, D.R. Paul, J. Appl. Polym. Sci. **29**, 3231 (1984)

P. Musto, L. Wu, F.E. Karasz, W.J. MacKnight, Polymer **32**, 3 (1991)

M.E. Myers, A.M. Wims, T.S. Ellis, J. Barnes, Macromolecules **23**, 2807 (1990)

Y.H. Na, Y. Arai, N. Asakawa, N. Yoshie, Y. Inoue, Macromolecules **34**, 4834 (2001)

V.M. Nadkarni, V.L. Shingankuli, J.P. Jog, Polym. Eng. Sci. **28**, 1326 (1988)

T. Nagasawa, Y. Murata, K. Tsunashima, Y. Morishima, S. Yano, N. Koizumi, Macromolecules **33**, 2302 (2000)

J.B. Nagode, C.M. Roland, Polymer **32**, 505 (1991)

K. Naito, G.E. Johnson, D.L. Allara, T.K. Kwei, Macromolecules **11**, 1260 (1978)

H. Nakamura, J. Maruta, T. Ohnaga, T. Inoue, Polymer **31**, 303 (1990)

S. Nakata, M. Kakimoto, Y. Imai, T. Inoue, Polym. J. **22**, 80 (1990)

S. Nakata, M. Kakimoto, Y. Imai, Polym. J. **25**, 569 (1993)

B. Nandan, B. Lal, K.N. Pandey, S. Alam, L.D. Kandpal, G.N. Mathur, Eur. Polym. J. **37**, 2147 (2001)

B. Nandan, L.D. Kandpal, G.N. Mathur, J. Polym. Sci. B: Polym. Phys. **40**, 1407 (2002)

A.K. Nandi, B.M. Mandal, S.N. Bhattacharyya, Macromolecules **18**, 1454 (1985)

A.K. Nandi, B.M. Mandal, S.N. Bhattacharyya, S.K. Roy, Polym. Commun. **27**, 151 (1986)

T.R. Nassar, D.R. Paul, J.W. Barlow, J. Appl. Polym. Sci. **23**, 85 (1979)

A. Natansohn, A. Eisenberg, Am. Chem. Soc. Polym. Prepr. **27**(1), 349 (1986)

G. Natta, G. Allegra, I.W. Bassi, C. Carlini, E. Chiellini, Montagnoli, Macromolecules **2**, 311 (1969)

C. Neelakandan, T. Kyu, Polymer **50**, 2885 (2009)

J.T. Neill, F.E. Karasz, J. Therm. Anal. Calorim. **59**, 33 (2000)

M.K. Neo, S.H. Goh, Eur. Polym. J. **27**, 915 (1991a)

M.K. Neo, S.H. Goh, Eur. Polym. J. **27**, 927 (1991b)

M.K. Neo, S.H. Goh, Macromolecules **24**, 2564 (1991c)

M.K. Neo, S.H. Goh, Polym. Commun. **32**, 200 (1991d)

M.K. Neo, S.H. Goh, Polymer **33**, 2012 (1992a)

M.K. Neo, S.H. Goh, Polymer **33**, 3203 (1992b)

M.K. Neo, S.H. Goh, Polym. Networks Blends **3**, 131 (1993)

M.K. Neo, S.Y. Lee, S.H. Goh, Eur. Polym. J. **27**, 831 (1991a)

M.K. Neo, S.Y. Lee, S.H. Goh, J. Appl. Polym. Sci. **43**, 1301 (1991b)

C.W.A. Ng, M.A. Bellinger, W.J. MacKnight, Macromolecules **27**, 6942 (1994)

Y. Ni, S.X. Zheng, Polymer **46**, 5828 (2005)

L.E. Nielson, J. Am. Chem. Soc. **75**, 1435 (1955)

L.E. Nielson, S.N. Chinai, *unpublished work, quoted in Mechanical Properties of Polymers, ed. by L.E. Nielson* (Reinhold, New York, 1962), p. 173

A.J. Nijenhuis, E. Colstee, D.W. Grijpma, A. Pennings, J. Polymer **37**, 5849 (1996)

T. Nishi, T.K. Kwei, Polymer **16**, 285 (1975)

T. Nishi, T.T. Wang, Macromolecules **8**, 909 (1975)

T. Nishi, T.K. Kwei, T.T. Wang, J. Appl. Phys. **46**, 4157 (1975a)

T. Nishi, T.T. Wang, T.K. Kwei, Macromolecules **8**, 227 (1975b)

M. Nishimoto, H. Keskkula, D.R. Paul, Polymer **30**, 1279 (1989)

M. Nishimoto, H. Keskkula, D.R. Paul, Macromolecules **23**, 3633 (1990)

M. Nishimoto, H. Keskkula, D.R. Paul, Polymer **32**, 1274 (1991)

M. Nishimoto, Y. Takami, A. Tohara, H. Kasahara, Polymer **36**, 1441 (1995)

Y. Nishio, Macromolecules **21**, 1270 (1988)

Y. Nishio, S.K. Roy, R.S.J. Manley, Polymer **28**, 1385 (1987)

Y. Nishio, N. Hirose, T. Takahashi, Polym. J. **21**, 347 (1989a)

Y. Nishio, T. Haratani, T. Takahashi, R.S.J. Manley, Macromolecules **22**, 2547 (1989b)

Y. Nishio, T. Haratari, T. Takahashi, J. Polym. Sci. Polym. Phys. Ed. **28**, 355 (1990)

Y. Nishio, H. Suzuki, K. Morisaki, Polym. Int. **31**, 15 (1993)

Y. Nishio, T. Koide, Y. Miyashita, N. Kimura, J. Polym. Sci. B: Polym. Phys. **37**, 1533 (1999)

S. Nojima, H. Tsutsui, M. Urushihara, W. Kosaka, N. Kato, T. Ashida, Polym. J. **18**, 451 (1986a)

S. Nojima, Y. Terashima, T. Ashida, Polymer **27**, 1007 (1986b)

J.S. Noland, N.N. Hsu, R. Saxon, J.M. Schmitt, in *Multicomponent Polymer Systems*, ed. by N.A.J. Platzer. American Chemical Society, Advances in Chemistry Series, vol. 99 (Washington, DC, 1971), p. 15

E. Nolley, D.R. Paul, J.W. Barlow, J. Appl. Polym. Sci. **23**, 623 (1979)

S. Nuno-Donlucas, J. Puig, I. Katime, Macromol. Chem. Phys. **202**, 3106 (2001a)

S. Nuno-Donlucas, L.C. Cesteros, J.E. Puig, I. Katime, Macromol. Chem. Phys. **202**, 663 (2001b)

Z.S. Nurkeeva, G.A. Mun, A. Dubolazov, V.A. Khutoryanskiy, Macromol. Biosci. **5**, 424 (2005)

Y.G. Oganesov, V.S. Osipchuk, K.G. Mindiyarov, V.G. Rayevskii, S.S. Voyutskii, A. Vysokomol. Soedin. Ser. **11**, 896 (1969); Polym. Sci. USSR. **11**, 1012 (1969)

T.J. Oh, J.H. Nam, Y.M. Jung, Vibr. Spectrosc. **51**, 15 (2009)

I. Ohkoshi, H. Abe, Y. Doi, Polymer **41**, 5985 (2000)

T. Ohnaga, T. Sato, S. Nagata, Polymer **38**, 1073 (1997)

T. Ohno, Y. Nishio, Cellulose **13**, 245 (2006)

T. Ohno, Y. Nishio, Macromol. Chem. Phys. **208**, 622 (2007)

T. Ohno, S. Yoshizawa, Y. Miyashita, Y. Nishio, Cellulose **12**, 281 (2005)

K. Okamoto, T. Ichikawa, T. Yokohara, M. Yamaguchi, Eur. Polym. J. **45**, 2304 (2009)

O. Olabisi, A.G. Farnham, in *Multiphase Polymers*, ed. by S.L. Copper, G.M. Estes. American Chemical Society, Advances in Chemistry Series, vol. 176 (Washington, DC, 1979), p. 559

J.Y. Olayemi, M.K. Ibiyeye, J. Appl. Polym. Sci. **31**, 237 (1986)

C.J. Ong, F.P. Price, J. Polym. Sci. Symp. **63**, 45 (1978)

C.H. Ong, S.H. Goh, H.S.O. Chan, J. Appl. Polym. Sci. **65**, 391 (1996a)

C.H. Ong, S.H. Goh, H.S.O. Chan, Polymer **38**, 1065 (1996b)

A. Opazo, L. Gargallo, D. Radic, Int. J. Polym. Mater. **27**, 117 (1994)

A. Opazo, L. Gargallo, D. Radic, Polym. Bull. **36**, 511 (1996)

S.J. Organ, Polymer **35**, 86 (1994)

S.J. Organ, P.J. Barham, Polymer **34**, 459 (1993)

H.J. Oswald, E.T. Kubu, SPE Trans. **3**, 168 (1963)

A.A.C.M. Oudhuis, G. ten Brinke, F.E. Karasz, *Polymer 34 (1991*, 1993

A.A.C.M. Oudhuis, H.J. Thiewes, P.F. van Hutten, G. ten Brinke, Polymer **35**, 3936 (1994)

T. Ougizawa, T. Inoue, J. Polym **18**, 521 (1986)

T. Ougizawa, D.J. Walsh, Polym. J. **25**, 1315 (1993)

S. Ourdani, F. Amrani, Macromol,Chem. Phys. **201**, 2458 (2000)

T. Oyama, J. Ozaki, Y. Chujo, Polym. Bull. **40**, 503 (1998)

P. Padunchewit, D.R. Paul, J.W. Barlow, in Multiphase Polymers: Blends and Ionomers, ed. by L. A. Utracki, R.A. Weiss. American Chemical Society, Symposium Series, vol. 395 (Washington, DC, 1989), p. 84

P.C. Painter, W.L. Tang, J.F. Graf, B. Thomson, M.M. Coleman, Macromolecules **24**, 3929 (1991)

S. Palsule, J.M.G. Cowie, Polym. Bull. **33**, 241 (1994)

Y. Pan, F. Xue, Eur. Polym. J. **37**, 247 (2001)

Y. Pan, Y. Huang, B. Liao, M. Chen, G. Cong, L.M. Leung, J. Appl. Polym. Sci. **65**, 341 (1997)

Y. Pan, W. Fu, F. Xue, Y. Luo, J.J. Gu, Appl. Polym. Sci. **81**, 2843 (2001)

C.P. Papadopoulou, N.K. Kalfoglou, Eur. Polym. J. **33**, 191 (1997a)

C.P. Papadopoulou, N.K. Kalfoglou, Polymer **38**, 631 (1997b)

C.P. Papadopoulou, N.K. Kalfoglou, Polymer **39**, 7015 (1998)

G.A. Papageorgious, D.N.J. Bikiaris, Polym. Sci. B: Polym. Phys. **44**, 584 (2006)

G.Z. Papageorgiou, D.N. Bikiaris, C.G. Panayiotou, Polymer **52**, 4553 (2011)

L.G. Parada, L.C. Cesteros, E. Meaurio, I. Katime, Macromol. Chem. Phys. **198**, 2505 (1997)

L.G. Parada, E. Meaurio, L.C. Cesteros, I. Katime, Macromol. Chem. Phys. **199**, 1597 (1998a)

L.G. Parada, L.C. Cesteros, E. Meaurio, I. Katime, Polymer **39**, 1019 (1998b)

R.R. Parent, E.V.J. Thompson, Configurational statistics of polymer chains accounting for all rotational states. General extension to finite chains and copolymers. Polym. Sci., Polym. Phys **16**, 1829 (1829)

D. Park, J.W. Hong, Polym. J. **29**, 970 (1998)

J.W. Park, S.S. Im, J. Appl. Polym. Sci. **86**, 647 (2002)

J.W. Park, S.S. Im, Polymer **44**, 4341 (2003)

M.S. Park, J.K.J. Kim, Polym. Sci. B: Polym. Phys. **40**, 1673 (2002)

D.S. Park, S.H.J. Kim, Appl. Polym. Sci. **87**, 1842 (2003)

S.Y. Park, H.S. Lee, C.S. Ha, D.W. Park, J. Appl. Polym. Sci. **81**, 2161 (2001a)

D.S. Park, J.H. Kim, M.J. Kim, C.K. Kim, J.W. Lee, J. Polym. Sci. B: Polym. Phys. **39**, 1948 (2001b)

S.Y. Park, H.Y. Park, H.S. Lee, S.W. Park, C.S. Ha, D.W. Park, J. Polym. Sci. A: Polym. Chem. **39**, 1472 (2001c)

S.Y. Park, H.Y. Park, D.W. Park, C.S.J. Ha, Macromol. Sci. Pure Appl. Chem. **A39**, 573 (2002a)

S.Y. Park, H.Y. Park, H.S. Woo, C.S. Ha, D.W. Park, Polym. Adv. Technol. **13**, 513 (2002b)

I.K. Park, Y.S. Chung, C.K.J. Kim, Polym. Sci. B: Polym. Phys. **46**, 1131 (2008)

G.J. Parker, M. Hara, Polymer **38**, 2773 (1997)

J.F. Parmer, L.C. Dickinson, R.S. Porter, Am. Chem. Soc. Polym. Prepr. **27**(1), 295 (1986)

J.F. Parmer, L.C. Dickinson, J.C.W. Chien, R.S. Porter, Am. Chem. Soc., Polym Prepr. **29**(1)), 476 (1988)

G.D. Patterson, T. Nishi, T.T. Wang, Macromolecules **9**, 603 (1976)

D.R. Paul, J.O. Altamirano, in *Copolymers, Polyblends and Composites*, ed. by N.A.J. Platzer. American Chemical Society, Advances in Chemistry Series, vol. 142 (Washington, DC, 1975), p. 371

D.R. Paul, J.W. Barlow, Polymer **25**, 487 (1984)

D.R. Paul, J.W. Barlow, C.A. Cruz, R.N. Mohn, T.R. Nassar, D.C. Wahrmund, Am. Chem. Soc., Org. Coatings. Plastics Chem. Prepr. **37**(1)), 130 (1977))

E.M. Pearce, T.K. Kwei, B.Y.J. Min, Macromol. Sci., Chem **A21**, 1181 (1984)

R.A. Pearson, A.F. Yee, J. Appl. Polym. Sci. **48**, 1051 (1993)

P. Pedrosa, J.A. Pomposo, E. Calahorra, M. Cortazar, Macromolecules **27**, 102 (1994)

P. Pedrosa, J.A. Pomposo, E. Calahorra, M. Cortazar, Polymer **36**, 3889 (1995)

M. Peesan, P. Supaphol, R. Rujiravanit, Carbohyd. Polym. **60**, 343 (2005)

M. Peesan, P. Supaphol, R.J., Rujirava, Appl. Polym. Sci **105**, 1844 (2007)

G.J. Pehlert, X. Yang, P.C. Painter, M.M. Coleman, Polymer **37**, 4763 (1996)

G.J. Pehlert, P.C. Painter, B. Veytsman, M.M. Coleman, Macromolecules **30**, 3671 (1997)

G.J. Pehlert, P.C. Painter, M.M. Coleman, Macromolecules **31**, 8423 (1998)

M.V. Pellow-Jarman, P.J. Hendra, M.J.J. Hetem, Spectrochim. Acta A. **51A**, 2107 (1995)

X. Pen, J. Shen, Polym. Int. **46**, 106 (1998)

J. Peng, S.H. Goh, S.Y. Lee, K.S. Siow, Polymer **34**, 4930 (1993)

J. Peng, S.H. Goh, S.Y. Lee, K.S. Siow, Polym. Netw. Blends **4**, 139 (1994a)

J. Peng, S.H. Goh, S.Y. Lee, K.S. Siow, Polymer **35**, 1482 (1994b)

J. Peng, S.H. Goh, S.Y. Lee, K.S. Siow, Polym. Netw. Blends **5**, 19 (1995)

J. Peng, S.H. Goh, S.Y. Lee, S.M. Low, Polym. Adv. Technol. **8**, 234 (1996)

J.R. Pennacchia, E.M. Pearce, T.K. Kwei, B.J. Bulkin, J.P. Chen, Macromolecules **19**, 973 (1986)

J.P. Penning, R.S.J. Manley, Macromolecules **29**, 77 (1996)

S. Percec, L.J. Melamud, Appl. Polym. Sci. **41**, 1853 (1990)

S. Percec, L. Melamud, J. Appl. Polym. Sci. **47**, 723 (1993)

R.P. Pereira, A.M. Rocco, Polymer **46**, 12493 (2005)

P. Perrin, R.E. Prud'homme, Polymer **32**, 1468 (1991)

S. Perrin, R.E. Prud'homme, Acta Polym. **44**, 307 (1993)

S.S. Pestov, V.N. Kuleznev, V.A. Shershnew, Zh. Kolloid. **40**, 705 (1978); Colloid J. USSR, **40**, 581 (1978)

R.J. Peterson, R.D. Corneliussen, L.T. Rozelle, Polym. Prepr. **10**, 385 (1969)

D.M. Petrovic-Djakov, J.M. Filipovic, L.P. Vrhovac, J.S.J. Velickovic, Thermal Anal. **40**, 741 (1993)

D. Pfefferkorn, D. Browazik, H. Steininger, M. Weber, C. Gibbon, H.W. Kammer, J. Kressler, Eur. Polym. J. **48**, 200 (2012)

J.L.G. Pfennig, H. Keskkula, D.R.J. Paul, Appl. Polym. Sci. **32**, 3657 (1986)

J. Piglowski, Eur. Polym. J. **24**, 905 (1988)

J. Piglowski, Acta Polym. **41**, 518 (1990)

J. Piglowski, K.H. Kammer, Acta Polym. **41**, 431 (1990)

J. Piglowski, P. Drozdzewski, M. Trelinska-Wlazlak, Polym. Netw. Blends **6**, 161 (1996)

L.Z. Pillon, L.A. Utracki, D.W. Pillon, Polym. Eng. Sci. **27**, 562 (1987)

A. Piloz, J.Y. Decroix, J.F. May, Angew. Makromol. Chem. **54**, 77 (1976)

Z.H. Ping, Q.T. Nguyen, J. Neel, Makromol. Chem. **190**, 437 (1989)

Z.H. Ping, Q.T. Nguyen, J. Neel, Makromol. Chem. **191**, 185 (1990)

D. Pinoit, R.E. Prud'homme, Polymer **43**, 2321 (2002)

J. Pionteck, V. Reid, W.J. MacKnight, Acta Polym. **46**, 156 (1995)

M.C. Piton, A. Natasohn, Macromolecules **28**, 1197 (1995)

T. Plivelic, S.N. Cassu, M. do Carmo Goncalves, I.L. Torriani, Macromolecules **40**, 253 (2007)

J.A. Pomposo, E. Calahorra, I. Eguiazabal, M. Cortazar, Macromolecules **26**, 2104 (1993a)

J.A. Pomposo, I. Equiazabal, E. Calahorra, M. Cortazar, Polymer **34**, 95 (1993b)

J.A. Pomposo, M. Cortazar, E. Calahorra, Macromolecules **27**, 245 (1994a)

J.A. Pomposo, M. Cortazar, E. Calahorra, Macromolecules **27**, 252 (1994b)

J.A. Pomposo, R. de Juana, A. Mugica, M. Cortazar, M.A. Gomez, Macromolecules **29**, 7038 (1996)

J.A. Pomposo, A. Mugica, J. Areizaga, M. Cortazar, Acta Polym. **49**, 301 (1998)

M. Pracella, D. Dainelli, G. Gralli, E. Chielline, Makromol. Chem. **187**, 2387 (1986)

M. Pracella, E. Chiellini, G. Gralli, D. Dainelli, Mol. Cryst. Liq. Cryst. **153(A)**, 525 (1987)

M. Pracella, E. Chielline, D. Dainelli, Makromol. Chem. **190**, 175 (1989)

K. Prashantha, K.V.K. Pai, B.S.J. Sherignava, Macromol. Sci. A: Pure Appl. Chem. **45**, 238 (2008)

W.M. Prest, R.S.J. Porter, Polym. Sci **A-2**(10), 1639 (1972)

E. Princi, S.J. Vicini, Polym. Sci. B: Polym. Phys. **48**, 2129 (2010)

E. Princi, S. Vicini, E. Pedemote, Polym. Int. **58**, 656 (2009)

J. Prinos, C. Tselios, D. Bikiaris, C. Panayiotou, Polymer **38**, 5921 (1997)

J. Prinos, A. Dompros, C. Panayiotou, Polymer **39**, 3011 (1998)

J. Prinos, D. Bikiaris, C. Panayiotou, Polymer **40**, 4741 (1999)

M.G. Prolongo, C. Salom, R.M. Masegosa, S. Moreno, R.G. Rubio, Polymer **38**, 5097 (1997)

M.G. Prolongo, C. Salom, R.M. Masegosa, Polymer **43**, 93 (2002)

H.T. Pu, Polym. Int. **52**, 1540 (2003)

R. Pucciariello, C.J. Angioletti, Polym. Sci. B: Polym. Phys. **37**, 679 (1999)

C. Pugh, V. Percec, Macromolecules **19**, 65 (1986)

A. Purcell, C. Thies, Am. Chem. Soc.,Polym. Prepr. **9**, 115 (1968)

R. Qian, X. Gu, Angew. Makromol. Chem. **141**, 1 (1986)

C. Qin, L.A. Belfiore, Am. Chem. Soc., Polym. Prepr. **31**((1), 263 (1990)

C. Qin, A.T.N. Pires, L.A. Belfiore, Polym. Commun. **31**, 177 (1990)

H.H. Qin, P.T. Mather, J.B. Baek, L.S. Tan, Polymer **47**, 2813 (2006)

X. Qiu, M. Jiang, Polymer **35**, 5084 (1994)

X. Qiu, M. Jiang, Polymer **36**, 3601 (1995)

Z.B. Qiu, M. Komura, T. Ikehara, T. Nishi, Polymer **44**, 8111 (2003a)

Z.B. Qiu, T. Ikehara, T. Nishi, Polymer **44**, 2799 (2003b)

Z.B. Qiu, S. Fujinami, M. Komura, K. Nakajima, T. Ikehara, T. Nishi, Polymer **45**, 4355 (2004)

Z.B. Qiu, C.Z. Yan, J.M. Lu, W.T. Yang, Macromolecules **40**, 5047 (2007a)

Z.B. Qiu, C.Z. Yan, J.M. Lu, W.T. Yang, T. Ikehara, T.J. Nishi, Phys. Chem. B. **111**, 2783 (2007b)

M. Rabeony, D.B. Siano, D.H. Peiffer, E. Siakali-Koulafa, N. Hadjichristidis, Polymer **35**, 1033 (1994)

D. Radic, L. Gargallo, Thermochim. Acta **180**, 241 (1991)

D. Radic, N. Gastica, L. Gargallo, Polimery **46**, 823 (2001)

D. Radloff, C. Boeffel, H.W. Spiess, Macromolecules **29**, 1528 (1996)

L. Ragupathy, V. Arrighi, J.M.G. Cowie, R. Ferguson, I.J. McEwen, S.L. Shenoy, Macromolecules **40**, 1667 (2007)

M.H. Rahman, A.K. Nandi, Macromol. Chem. Phys. **203**, 653 (2002)

S.S.A. Rahman, D. Kawaguchi, D. Ito, A. Takano, Y. Matsushita, J. Polym. Sci. B: Polym. Phys. **47**, 2272 (2009)

P. Rajagopalan, J.S. Kim, H.P. Brack, X. Lu, A. Eisenberg, R.A. Weiss, W.M. Risen Jr., J. Polym. Sci. B: Polym. Phys. **33**, 495 (1995)

M. Rajagopalan, A. Natansohn, A. Eisenberg, R. Tannenbaum, J. Appl. Polym. Sci. **89**, 728 (2003)

N. Rakkapao, V. Vao-Soongnern, Y. Masubuchi, H. Watanabe, Polymer **52**, 2618 (2011)

V. Ramaswamy, H.P. Weber, Appl. Optics **12**, 1581 (1973)

A. Rameau, Y. Gallot, P. Marie, B. Farnoux, Polymer **30**, 386 (1989)

P. Ramesh, S.K. De, J. Appl. Polym. Sci. **50**, 1369 (1993)

P. Ramesh, D. Khastgir, S.K. De, Plast. Rubber Compos. Process Appl. **20**, 35 (1993)

J. Ramiro, J.I. Eguiazabal, J. Nazabal, Macromol. Mater. Eng. **291**, 707 (2006)

D. Rana, B.M. Mandal, S.N. Bhattacharyya, Polymer **34**, 1454 (1993)

D. Rana, K. Bag, S.N. Bhattacharyya, B.M. Mandal, J. Polym. Sci. B: Polym. Phys. **38**, 369 (2000)

B.G. Ranby, J. Polym. Sci., Polym. Symp **51**, 89 (1975)

V. Rao, P.V. Ashokan, M.H. Shridhar, Polymer **40**, 7167 (1999)

V. Rao, P.V. Ashokan, M.H. Shridhar, J. Appl. Polym. Sci. **76**, 859 (2000)

L. Ray, S. Roy, D. Khastgir, Polym. Bull. **30**, 685 (1993)

P.C. Raymond, D.R. Paul, J. Polym. Sci., Polym. Phys **28** (1990)

I.N. Razinskaya, L.I. Vidyakina, T.I. Radbil', B.P. Shtarkman, Vysokomol. Soedin. Ser A **14**, 968 (1974); Polym. Sci. USSR **14**, 1079 (1972)

I.N. Razinskaya, B.P. Shtarkman, A.E. Chalykh, I.N. Sapozhnikova, Vysokomol. Soedin, Ser **B** **27**, 871 (1985)

K.S. Reddy, M.N. Prabhakar, V.N. Reddy, G. Sathyamaiah, Y. Maruthi, M.C.S. Subha, K.C. Rao, J. Appl. Polym. Sci. **125**, 2289 (2012)

M. Ree, T. Kyu, R.S. Stein, J. Polym. Sci., Polym. Phys. Ed **25**, 105 (1987)

R.A. Register, T.R. Bell, J. Polym. Sci., Polym. Phys. Ed **30**, 569 (1992)

K. Reichelt, C. Kummerlowe, H.W. Kammer, Polym. Networks Blends **6**, 117 (1996a)

K. Reichelt, C. Kummerlowe, H.W. Kammer, Polym. Networks Blends **6**, 21 (1996b)

G.S. Rellick, J.P. Runt, J. Polym. Sci., Polym. Phys. Ed **24**, 1986 (279)

A. Rembaum, J. Mocanin, E. Cuddihy, J. Polym. Sci. C **4**, 529 (1963)

P.M. Remiro, J. Nazabal, J. Appl. Polym. Sci. **42**, 1639 (1991a)

P.M. Remiro, J. Nazabal, J. Appl. Polym. Sci. **42**, 1475 (1991b)

R.A. Reznikova, A.D. Zaionchkovskii, S.S. Voyutskii, Zh.Tekh.Fiz. **25**, 1045 (1955)

M.C. Righetti, C. Cardelli, M. Scalari, E. Tombari, G. Conti, Polymer **43**, 5035 (2002)

M.R. Righetti, M.L. Di Lorenzo, M. Angiuli, E. Tomban, Eur. Polym. J. **43**, 4726 (2007)

P.B. Rim, E.B. Orler, Macromolecules **20**, 433 (1987)

M. Rink, L. Monfrini, P. Gasparini, A. Pavan, Rubber Process. Appl. **3**, 145 (1983)

C.G. Robertson, G.L. Wilkes, Polymer **42**, 1581 (2001a)

C.G. Robertson, G.L. Wilkes, J. Polym. Sci. B: Polym. Phys. **39**, 2118 (2001b)

L.M. Robeson, quoted in reference Shaw (1974)

L.M. Robeson, J. Polym. Sci., Polym. Lett. Ed. **16**, 261 (1978)

L.M. Robeson, J. Appl. Polym. Sci. **30**, 4081 (1985)

L.M. Robeson, A.B. Furtek, Am. Chem. Soc., Org. Coat. Plast. Chem. Prepr **37**, 136 (1977)

L.M. Robeson, A.B. Furtek, J. Appl. Polym. Sci. **23**, 645 (1979)

L.M. Robeson, J.E. McGrath, Polym. Eng. Sci. **17**, 300 (1977)

L.M. Robeson, M. Matzner, L.J. Fetters, J.E. McGrath, in *Recent Advances in Blends, Grafts and Blocks*, ed. by L.H. Sperling (Plenum, New York, 1974), p. 281

L.M. Robeson, W.F. Hale, C.N. Merriman, Macromolecules **14**, 1644 (1981)

A.M. Rocco, R.P. Pereira, M.I. Felisberti, Polymer **42**, 5199 (2001)

A.M. Rocco, C.E. Bielschowsky, R.P. Pereira, Polymer **44**, 361 (2003a)

A.M. Rocco, D.P. Moreira, R.P. Pereira, Eur. Polym. J. **39**, 1925 (2003b)

A.M. Rocco, A. de Assis Carias, R.P. Pereira, Polymer **51**, 5151 (2010)

J.L. Rodriguez, J.I. Eguiazabal, J. Nazabal, Polym. J. **28**, 501 (1996)

M. Rodriguez-Castro, L.C. Cesteros, I. Katime, S.M. Nuno-Donlucas, J. Polym. Sci. B: Polym. Phys. **44**, 2404 (2006)

J. Rodriguez-Parada, V. Percec, J. Polym. Sci., Polym. Chem. Ed **24** (1986a)

J. Rodriguez-Parada, V. Percec, Macromolecules **19**, 55 (1986b)

E. Roerdink, G. Challa, Polymer **19**, 173 (1978)

E. Roerdink, G. Challa, Polymer **21**, 1161 (1980)

C.M. Roland, Macromolecules **20**, 2557 (1987)

C.M. Roland, J. Polym. Sci., Polym. Phys. Ed **26**, 839 (1988a)

C.M. Roland, Rubber Chem. Technol. **61**, 866 (1988b)

C.M. Roland, C.A. Trask, Rubber Chem. Technol. **62**, 896 (1989)

J. Roovers, P.M. Toporowski, Macromolecules **25**, 1096 (1992)

A. Roychoudhury, P.P. De, A.K. Bhowmick, S.K. De, Polymer **33**, 4737 (1992)

F.C. Ruhnau, W.S. Veeman, Macromolecules **29**, 2916 (1996)

M.T. Run, Y.J. Wang, C.G. Yao, J.G. Gao, Thermochim. Acta **447**, 13 (2006)

M.T. Run, A.J. Song, Y.J. Wang, C.G. Yao, J. Appl. Polym. Sci. **104**, 3459 (2007)

J. Runt, L.M. Martynowicz-Hans, L. Du, M. Mayo, Am. Chem. Soc., Polym. Prepr. **28**((2), 153 (1987)

J. Runt, L. Du, L.M. Martynowicz, D.M. Brezny, M. Mayo, Macromolecules **22**, 3908 (1989)

J. Runt, L. Jin, S. Talibuddin, C.R. Davis, Macromolecules **28**, 2781 (1995)

C.C. Rusa, T. Uyar, M. Rusa, M.A. Hunt, X.W. Wang, A.E. Toneli, J. Polym. Sci. B: Polym. Phys. **42**, 4182 (2004)

E. Russell, G. Crone, A. Natansohn, Polym. Bull. **27**, 67 (1991)

M. Rutkowska, J. Appl. Polym. Sci. **42**, 1695 (1991)

M. Rutkowska, A. Eisenberg, Macromolecules **17**, 821 (1984)

M. Rutkowska, A. Eisenberg, J. Appl. Polym. Sci. **33**, 2833 (1987)

J.H. Ryou, H.D. Kim, D.S. Lim, C.S. Ha, W.J. Cho, Pollimo **16**, 225 (1992)

J.H. Ryou, C.S. Ha, W.J. Cho, J. Polym. Sci. A: Polym. Chem. **31**, 325 (1993)

C.H. Ryu, Y.H. Kim, C.Y. Bae, Eur. Polym. J. **36**, 495 (2000)

S. Saeki, J.M.G. Cowie, I.J. McEwen, Polymer **24**, 60 (1983)

H. Saito, T. Inoue, J. Polym. Sci., Polym. Phys. Ed **25**, 1629 (1987)

H. Saito, Y. Fujita, T. Inoue, Polym. J. **19**, 405 (1987)

M. Saito, T. Takahashi, J. Inoue, Polym. Sci., Polym. Phys. Ed **26**, 1761 (1988)

H. Saito, D. Tsutsumi, T. Inoue, Polym. J. **22**, 128 (1990)

D. Sakar, O. Cankurtaran, F. Karaman, Polym. Adv. Technol **20**, 291 (2009)

D. Sakar, F. Cakar, O. Cankurtaran, F. Karaman, J. Appl. Polym. Sci. **117**, 309 (2010)

K. Sakurai, E. Douglas, W.J. MacKnight, Macromolecules **26**, 208 (1993)

K. Sakurai, T. Maegawa, T. Takahashi, Polymer **41**, 7051 (2000)

J.M. Saldanha, T. Kyu, Macromolecules **20**, 2840 (1987)

C. Salom, D. Nava, M.G. Prolongo, R.M. Masegosa, Eur. Polym. J. **42**, 1798 (2006)

W. Salomons, G. Ten Brinke, F.E. Karasz, Polym. Commun. **32**, 185 (1991)

A. Sanchis, M.G. Prolongo, R.G. Rubio, R.M. Masegosa, Polym. J. **27**, 10 (1995)

A. Sanchis, M.G. Prolongo, R.M. Masegesa, Salom, J. Polym. Sci. B: Polym. Phys **36**, 95 (1998)

M. Sankarapandian, K. Kishore, Macromolecules **24**, 3090 (1991)

M. Sankarapandian, K. Kishore, Macromolecules **27**, 7278 (1994)

M. Sankarapandian, K. Kishore, J. Appl. Polym. Sci. **61**, 507 (1996a)

M. Sankarapandian, K. Kishore, Polymer **37**, 2957 (1996b)

R.N. Santra, S. Roy, A.K. Bhowmick, G.B. Nando, Polym. Eng. Sci. **33**, 1352 (1993a)

R.N. Santra, T.K. Chaki, S. Roy, G.B. Nando, Angew. Makromol. Chem. **213**, 7 (1993b)

A. Sarasam, S.V. Madihally, Biomaterials **26**, 5500 (2005)

S. Sasaki, M. Nagao, M. Gotoh, J. Polym. Sci., Polym. Phys. Ed **26**, 637 (1988)

I.R. Sasi, L.C. Cesteros, I. Katime, Macromol. Rapid Commun. **15**, 903 (1994)

M. Sato, S. Ujiie, Macromol. Rapid Commun. **17**, 439 (1996)

T. Sato, M. Endo, T. Shiomi, K. Imai, Polymer **37**, 2131 (1996a)

A. Sato, T. Kato, T. Uryu, J. Polym. Sci. A: Polym. Chem. **34**, 503 (1996b)

T. Sato, K. Katayama, T. Suzuki, T. Shiomi, Polymer **39**, 773 (1998)

T. Sato, M. Ikeda, A. Sugawara, Polym. Int. **53**, 951 (2004)

B.B. Sauer, B.S. Hsiao, J. Polym. Sci. B: Polym. Phys. **31**, 917 (1993a)

B.B. Sauer, B.S. Hsiao, Polymer **34**, 3315 (1993b)

B.B. Sauer, B.S. Hsiao, K.L. Faron, Polymer **37**, 445 (1996)

C. Sawatari, I. Kondo, Macromolecules **32**, 1949 (1999)

M. Scandola, Can. J. Microbiol. **41**(Suppl. 1), 310 (1995)

M. Scandola, G. Ceccorulli, M. Pizzoli, Macromolecules **25**, 6441 (1992)

M. Scandola, M.L. Focarete, G. Adamus, W. Sikorska, I. Baranowska, S. Swierczek, M. Gnatowski, M. Kowalczuk, Z. Jedlinski, Macromolecules **30**, 2568 (1997)

B. Schartel, J. Wendling, J.H. Wendorff, Macromolecules **29**, 1521 (1996)

E. Schchori, J. Jagur-Grodzinski, J. Appl. Polym. Sci. **20**, 1665 (1976)

J. Schelten, W. Schamtz, D.G.H. Ballard, G.W. Longman, M.G. Rayner, G.D. Wignall, Prepr. Int. Microsymp. Crystal. Fusion Polym., Louvain-la-Neuve **1** (1976)

I.A. Schneider, E.M. Calugaru, Eur. Polym. J. **11**, 861 (1975)

H.A. Schneider, P. Dilger, Polym. Bull. **21**, 265 (1989)

H.A. Schneider, B. Leikauf, Thermochim. Acta **114**, 165 (1987)

H.A. Schneider, U. Epple, B. Leikauf, H.N. Neto, New Polym. Mater. **3**, 115 (1992)

H.A. Schneider, F. Glatz, R. Mulhaupt, New Polym. Mater. **4**, 289 (1995)

W. Schnek, D. Reichert, H. Schneider, Polymer **31**, 329 (1990)

J.A. Schroeder, F.E. Karasz, W.J. MacKnight, Polymer **26**, 1795 (1985)

K. Schulze, J. Kressler, H.W. Kammer, Polymer **34**, 3704 (1993)

J.W. Schurer, A. DeBoer, G. Challa, Polymer **16**, 201 (1975)

C.G. Seefried Jr., J.V. Koleske, J. Testing Eval. **4**, 220 (1976)

C.G. Seefried Jr., J.V. Koleske, F.E. Critchfield, Polym. Eng. Sci. **16**, 771 (1976)

S.N. Semerek, C.W. Frank, in *Polymer Blends and Composites in Multiphase Systems*, ed. by C.D. Han. American Chemical Society, Advances in Chemistry Series, vol. 206 (Washington, DC, 1984), p. 77

A.K. Sen, G.S. Mukherjee, Polymer **34**, 2386 (1993)

C.J. Serman, P.C. Painter, M.M. Coleman, Am. Chem. Soc., Polym. Prepr **29**(1), 315 (1988)

C.J. Serman, P.C. Painter, M.M. Coleman, Polymer **32**, 1049 (1991a)

C.J. Serman, Y. Xu, P.C. Painter, M.M. Coleman, Polymer **32**, 516 (1991b)

G. Severe, J.L. White, J. Appl. Polym. Sci. **78**, 1521 (2000)

R.W. Seymour, B.E. Zehner, J. Polym. Sci., Polym. Phys. Ed. **18**, 2299 (1980)

S. Shabbir, S. Zulfiqar, M. Ishaq, M.I. Sarwar, Colloid Polym. Sci. **286**, 673 (2008)

V.S. Shah, J.D. Keitz, D.R. Paul, J.W. Barlow, J. Appl. Polym. Sci. **32**, 3863 (1986)

K. Shah, K. Min, J.L. White, Polym. Eng. Sci. **28**, 1277 (1988)

K. Shah, J.L. White, K. Min, Polym. Eng. Sci. **29**, 586 (1989)

C.K. Sham, C.H. Lau, D.J. Williams, F.E. Karasz, W.J. MacKnight, Brit. Polym. J. **20**, 149 (1988a)

C.K. Sham, G. Guerra, F.E. Karasz, W.J. MacKnight, Polymer **29**, 1016 (1988b)

M.T. Shaw, J. Appl. Polym. Sci. **18**, 449 (1974)

S. Shen, J.M. Torkelson, Macromolecules **25**, 721 (1992)

J. Shen, S.X. Zheng, J. Polym. Sci. B: Polym. Phys. **44**, 942 (2006)

Y. Shi, S.A. Jabarin, J. Appl. Polym. Sci. **81**, 11 (2001)

D. Shibanov, T.M. Radzhabov, Vysokomol. Soedin., Ser. **B 30**, 281 (1988)

M. Shibata, Z. Fang, R. Yosomiya, J. Appl. Polym. Sci. **80**, 769 (2001)

M. Shibayama, T. Yamamoto, C.F. Xiao, S. Sakurai, A. Hayami, S. Nomura, Polymer **32**, 1010 (1991)

M. Shibayama, K. Uenoyama, J. Okura, S. Nomura, T. Iwamoto, Polymer **36**, 4811 (1995)

T.J. Shin, B. Lee, J. Lee, S. Jin, B.S. Sung, Y.S. Han, C.H. Lee, R.S. Stein, M. Ree, J. Appl. Crystollgraphy **42**, 161 (2009)

T. Shiomi, F.E. Karasz, W.J. MacKnight, Macromolecules **19**, 2274 (1986a)

T. Shiomi, F.E. Karasz, W.J. MacKnight, Macromolecules **19**, 2644 (1986b)

T. Shiomi, M. Suzuki, M. Tohyama, K. Imai, Macromolecules **22**, 3578 (1989)

T. Shiomi, T. Eguchi, I. Ishimatsu, K. Imai, Macromolecules **23**, 4978 (1990)

T. Shirahase, Y. Komatsu, Y. Tominaga, S. Asai, M. Sumita, Polymer **47**, 4839 (2006)

T. Shirahase, Y. Komatsu, H. Marubayashi, Y. Tominaga, S. Asai, M. Sumita, Polym. Degrad. Stab. **92**, 1626 (2007)

M. Shiyematsu, M. Morita, I. Sakata, Macromol. Chem. Phys. **195**, 2827 (1994)

A.R. Shultz, B.M. Beach, Macromolecules **7**, 902 (1974)

A.R. Shultz, B.M. Gendron, J. Appl. Polym. Sci. **16**, 461 (1972)

A.R. Shultz, B.M. Gendron, J. Polym. Sci., Symp. Ed. **43**, 89 (1973)

A.R. Shultz, B.M. Gendron, in *Polymer Characterization by Thermal Methods of Analysis*, ed. by J. Chiu (Dekker, New York, 1974a), p. 175

A.R. Shultz, B.M. Gendron, J. Macromol. Sci., Chem. **A8**, 175 (1974b)

A.R. Shultz, A.L. Young, J. Appl. Polym. Sci. **28**, 1677 (1983)

Y.J. Shur, B. Ranby, J. Appl. Polym. Sci. **19**, 1337 (1975a)

Y.J. Shur, B. Ranby, J. Appl. Polym. Sci. **19**, 2143 (1975b)

Y.F. Shutilin, Vysokomol. Soedin., Ser. **B 23**, 708 (1991)

A. Siciliano, A. Seves, T. de Marco, S. Cimmino, E. Martuscelli, C. Silvestre, Macromolecules **28**, 8065 (1995)

A. Siciliano, D. Severgnini, A. Seves, T. Pedrelli, L. Vicini, J. Appl. Polym. Sci. **60**, 1757 (1996)

A. Siegmann, G. Cohen, Z. Baraam, J. Appl. Polym. Sci. **37**, 1481 (1989)

H.H.A. Siham, D. Said, J. Appl. Polym. Sci. **102**, 2717 (2006)

M.A. Silva, M.A. de Paoli, M.I. Felisberti, Polymer **39**, 2551 (1998)

E.S. Silva, R.P. Pereira, A.M. Rocco, Eur. Polym. J. **45**, 3127 (2009)

C. Silvestre, S. Cimmino, E. Martuscelli, F.E. Karasz, W.J. MacKnight, Polymer **28**, 1190 (1987)

A. Simmons, A. Natansohn, Macromolecules **25**, 3881 (1992a)

A. Simmons, A. Natansohn, Macromolecules **25**, 1272 (1992b)

T.F. Sincock, D.J. David, Polymer **33**, 4515 (1992)

V.B. Singh, D.J. Walsh, J. Macromol. Sci., Phys **B25**, 65 (1986)

D.P. Singh, S. Kalachandra, D.T. Turner, J. Polym. Sci., Polym. Phys. Ed. **26**, 1795 (1988)

W. Siol, Makromol. Chem.,Macromol. Symp. **44**, 47 (1991)

W. Siol, U. Terbrack, Angew. Makromol. Chem **185/186**, 259 (1991)

D.J. Skrovanek, M.M. Coleman, Polym. Eng. Sci. **27**, 857 (1987)

E.L. Slagowski, E.P. Chang, J.J. Tkacik, Polym. Eng. Sci. **21**, 513 (1981)

R.J. Slocombe, J. Polym. Sci. **26**, 9 (1957)

G.L. Slonimskii, J. Polym. Sci. **30**, 625 (1958)

G.L. Slonimskii, N.K. Komskaia, Zhur. Fiz. Khim. **30**, 1746 (1956)

P. Smith, A. Eisenberg, J. Polym. Sci., Polym. Lett. Ed. **21**, 223 (1983)

P. Smith, A. Eisenberg, Macromolecules **27**, 545 (1994)

K.L. Smith, A.E. Winslow, D.E. Peterson, Ind. Eng. Chem. **51**, 1361 (1959)

S.Y. Soh, J. Appl. Polym. Sci. **44**, 371 (1992a)

S.Y. Soh, J. Appl. Polym. Sci. **45**, 1831 (1992b)

M. Song, F. Long, Eur. Polym. J. **27**, 983 (1991)

M. Song, H. Liang, B. Jiang, Polym. Bull. **23**, 615 (1990)

M. Song, Y. Huang, G. Cong, Polym. Commun. **32**, 155 (1991)

M. Song, D.J. Hourston, H.M. Pollock, A. Hammiche, Polymer **40**, 4763 (1999)

X. Song, S. Zheng, J. Huang, P. Zhu, Q. Guo, J. Appl. Polym. Sci. **79**, 598 (2001)

T. Song, S.H. Goh, S.Y. Lee, Macromolecules **35**, 4133 (2002)

J.J. Sotele, V. Soldi, A.T.N. Pires, Polymer **38**, 1179 (1997)

D.D. Sotiropoulou, K.G. Gravalos, N.K. Kalfoglou, J. Appl. Polym. Sci. **45**, 273 (1992)

D.D. Sotiropoulou, O.E. Avramidou, N.K. Kalfoglou, Polymer **34**, 2297 (1993)

R. Spindler, D.F. Shriver, Macromolecules **19**, 347 (1986)

A. Stammer, B.A. Wolff, Polymer **39**, 2065 (1998)

S. Stankovic, G. Guerra, D.J. Williams, F.E. Karasz, W.J. MacKnight, Polym. Commun. **29**, 14 (1988)

D.J. Stein, R.H. Jung, K.H. Iller, H. Hendus, Angew. Makromol. Chem. **36**, 89 (1974)

R.S. Stein, S. McGuire, M. Satkowski, D. Esnault, Am. Chem. Soc., Polym. Prepr. **30**(2), 270 (1989)

C.H. Stephens, A. Hiltner, E. Baer, Macromolecules **36**, 2733 (2003)

J. Stoelting, F.E. Karasz, W.J. MacKnight, Polym. Eng. Sci. **10**, 133 (1970)

O. Stoilova, N. Koseva, N. Manolova, I. Rashkov, Polym. Bull. **43**, 67 (1999)

J. Straka, P. Schmidt, J. Dybal, B. Schneider, J. Speracek, Polymer **36**, 1147 (1995)

G.R. Strobl, J.T. Bendler, R.P. Kambour, A.R. Shultz, Macromolecules **19**, 2683 (1986)

A. Stroeks, R. Paquail, E. Nies, Polymer **32**, 2653 (1991)

G.V. Struminskii, G.L. Slonimskii, Zhur. Fiz. Khim. **30**, 1941 (1956)

A.C. Su, J.R. Fried, in *Multicomponent Polymer Materials*, ed. by D.R. Paul, L.H. Sperling. American Chemical Society, Advances in Chemistry Series, vol. 211 (DC, Washington, 1986), p. 59

C.C. Su, C.K. Shih, J. Appl. Polym. Sci. **100**, 3840 (2006)

C.C. Su, J.H. Lin, E.M. Woo, Polym. Int. **52**, 1209 (2003)

M. Suess, J. Kressler, H.W. Kammer, K. Heinemann, Polym. Bull. **16**, 371 (1986)

M. Suess, J. Kressler, H.W. Kammer, Polymer **28**, 957 (1987)

M. Sugimoto, M. Kawahara, Y. Teramoto, Y. Nishio, Carbohyd. Polym. **79**, 948 (2010)

J. Sun, I. Cabasso, Macromolecules **24**, 3603 (1991)

J. Sun, H.L. Frisch, I. Cabasso, J. Polym. Sci., Polym. Phys. Ed. **27**, 2657 (1989)

Z. Sun, H. Li, Y. Zhuang, M. Ding, Z. Feng, Polym. Bull. **26**, 557 (1991)

H. Sun, N. Venkatasubramanian, M.D. Houtz, J.E. Mark, S.C. Tan, F.E. Arnold, C.Y.C. Lee, Colloid Polym. Sci. **282**, 502 (2004)

X.L. Sun, F.W. Pi, J.M. Zhang, I. Takahashi, F. Wang, S.K. Yau, Y. Ozaki, J. Phys. Chem. B **115**, 1950 (2011)

P. Supaphol, N. Dangseeyun, P. Thanomkiat, M. Nithitanakul, J. Polym. Sci. B: Polym. Phys. **42**, 676 (2004)

L. Suspene, T.M. Lam, J.P. Pascault, J. Appl. Polym. Sci. **39**, 1347 (1990)

T. Suzuki, E.M. Pearce, T.K. Kwei, Polymer **33**, 198 (1992)

P. Svoboda, J. Kressler, T. Chiba, T. Inoue, H.W. Kammer, Macromolecules **27**, 1154 (1994)

B.T. Swinyard, J.A. Barrie, D.J. Walsh, Polym. Commun. **28**, 331 (1987)

J.C.J.F. Tacx, H. Roolant, R.T.G. Francken, V.M.C. Reid, Polymer **43**, 737 (2002)

A.A. Tager, L.V. Adamova, V.S. Blinov, N.Ye. Klimova, Ye.N. Racheiskova, T.Ye. Chudinovskikh, T.V. Litvinova, L.A. Mazyrina, Vysokomol. Soedin., Ser. A **29**, 2327 (1987); Polym. Sci. USSR **29**, 2557 (1987)

Y. Takagi, T. Ougizawa, T. Inoue, Polymer **28**, 103 (1987)

K. Takakuwa, S. Gupta, D.R. Paul, J. Polym. Sci. B: Polym. Phys. **32**, 1719 (1994)

A. Takasu, K. Aoi, M. Okada, Macromol. Rapid Commun. **18**, 497 (1997)

M. Takayanagi, H. Harima, Y. Iwata, Mem. Faculty Eng. Kyushu Univ. **23**, 1 (1963)

K. Takegoshi, Annu. Rep. NMR Spectrosc. **30**, 97 (1995)

K. Takegoshi, K. Hikichi, Polym. J. **26**, 1377 (1994)

K. Takegoshi, K. Tsuchiya, K. Hikichi, Polym. J. **27**, 284 (1995)

T. Takeshita, T. Shiomi, T. Suzuki, T. Sato, M. Miya, K. Takenaka, S. Wacharawichanant, S. Damrongsakkul, S. Rimdusit, S. Thongyai, V. Taepaisitphongse, Polymer **46**, 11463 (2005)

L. Tan, S.M. Chen, Z.H. Ping, Y.M. Shen, Polym. Int. **53**, 204 (2004)

S.M. Tan, J. Ismail, C. Kummerlowe, H.W. Kammer, J. Appl. Polym. Sci. **101**, 2776 (2006)

H. Tanaka, A.J. Lovinger, Macromolecules **20**, 2638 (1987)

S. Tanaka, H. Nishida, T. Endo, Macromol. Chem. Phys. **210**, 1235 (2009)

M. Tang, W.R. Liau, Eur. Polym. J. **36**, 2597 (2000)

Y. Tang, J. Scheinbeim, J. Polym. Sci. B: Polym. Phys. **41**, 927 (2003)

H. Tang, L. Dong, J. Zhang, M. Ding, Z. Feng, J. Appl. Polym. Sci. **60**, 725 (1996)

H. Tang, H. Feng, L. Dong, Z. Feng, Eur. Polym. J. **33**, 183 (1997)

P. Tang, G.X. Li, J.S. Higgins, A. Arrighi, J.T. Cabral, Polymer **43**, 6661 (2002)

T. Tanigami, Y. Shirai, K. Yamaura, S. Matsuzawa, Polymer. **35**, (1970 (1994)

R. Tannanbaum, M. Rutkowska, A. Eisenberg, Am. Chem. Soc., Polym. Prepr **27**(1), 345 (1986)

R. Tannenbaum, M. Rajagopalan, A. Eisenberg, J. Polym. Sci. B: Polym. Phys. **41**, 4814 (2003)

R.E. Taylor-Smith, R.A. Register, Macromolecules **26**, 2802 (1993)

G. Ten Brinke, E. Roerdink, G. Challa, in *Polymer Compatibility and Incompatibility: Principles and Practices*, ed. by K. Solc (MMI Press, Harwood, 1982), p. 77

G. Ten Brinke, F.E. Karasz, W.J. MacKnight, Macromolecules **16**, 1827 (1983)

G. Ten Brinke, E. Rubinstein, F.E. Karasz, W.J. MacKnight, R. Vukovic, J. Appl. Phys. **56**, 2440 (1984)

G. Ten Brinke, L. Oudhuis, T.S. Ellis, Thermochim. Acta **238**, 75 (1994)

A. Tezuka, K. Takegoshi, K. Hikichi, J. Mol. Struct. **355**, 9 (1995)

C. Thaumaturgo, E.C. Monteiro, J. Thermal. Anal. **49**, 235 (1997a)

C. Thaumaturgo, E.C. Monteiro, Polym. Bull. **39**, 495 (1997b)

E.V. Thompson, in *Polymer Alloys II: Blends, Blcoks, Grafts and IPN's*, ed. by D. Klempner, K.C. Frisch (Plenum, New York, 1980)), p. 1

E.V. Thompson, in Polymer Alloys II: Blends, Blcoks, Grafts and IPN's, ed. by D. Klempner, K.C. (Frisch, Plenum, New York, 1980), p. 1

G. Thyagarajan, V. Janarthanan, Polymer **30**, 1797 (1989)

S.P. Ting, E.M. Pearce, T.K. Kwei, J. Polym. Sci., Polym. Lett. Ed. **18**, 201 (1980)

S.P. Ting, B.J. Bulkin, E.M. Pearce, T.K. Kwei, J. Polym. Sci.,Polym. Chem. **19**, 1451 (1981)

M.K. Tiwari, I.S. Bayer, G.M. Jursich, T.M. Schutzius, C.M. Megaridis, Macromol. Mater. Eng. **294**, 775 (2009)

H. Tomita, R.A. Register, Macromolecules **26**, 2796 (1993)

P.E. Tomlins, J.S. Higgins, J. Chem. Phys. **90**, 6691 (1989)

D. Tomova, J. Kressler, H.J. Raduseh, Polymer **41**, 7773 (2000)

H. Tomura, H. Saito, T. Inoue, Macromolecules **25**, 1161 (1992)

Y.J. Tong, X.D. Huang, T.S. Chung, Macromolecules **34**, 5748 (2001)

Q. Tran-Cong, H. Nakano, J. Okinaka, R. Kawakubo, Polymer **35**, 1242 (1994)

C.A. Trask, C.M. Roland, Polym. Commun. **29**, 332 (1988)

C.A. Trask, C.M. Roland, Macromolecules **22**, 256 (1989)

C. Tremblay, R.E. Prud'homme, J. Polym. Sci., Polym. Phys. Ed **22**, 1857 (1984)

A.R. Tripathy, W.J. Chen, S.N. Kukureka, W.J. MacKnight, Polymer **44**, 1835 (2003)

Y.C. Tseng, E.M. Woo, Macromol. Rapid Commun. **19**, 215 (1998)

Y. Tsujita, T. Higaki, A. Takizawa, T. Kiroshita, J. Polym. Sci., Polym. Chem. Ed. **23**, 1255 (1985)

Y. Tsujita, K. Iwakiri, T. Kiroshita, A. Takizawa, W.J. MacKnight, J. Polym. Sci., Polym. Phys. Ed. **25**, 415 (1987)

M. Tsukada, M. Romano, A. Seves, Acta Polym. **43**, 327 (1992)

Y. Tsukahara, J. Inoue, Y. Ohta, S. Kohjiya, Polymer **35**, 5785 (1994)

N. Tsutsumi, K. Kano, J. Polym. Sci. B: Polym. Phys. **37**, 745 (1999)

R.T. Tucker, C.C. Han, A.V. Dobrynin, R.A. Weiss, Macromolecules **36**, 4404 (2003)

J.M. Ubrich, F.B.C. Larbi, J.L. Halary, L. Monnerie, B. Bauer, C.C. Han, Macromolecules **19**, 810 (1986)

H. Ueda, F.E. Karasz, Macromolecules **18**, 2719 (1985)

H. Ueda, F.E. Karasz, J. Macromol. Sci., Chem. **A27**, 1693 (1990a)

H. Ueda, F.E. Karasz, J. Macromol. Sci., Chem **A27**, 1693 (1990b)

H. Ueda, F.E. Karasz, Polym. J. **24**, 1363 (1992)

H. Ueda, F.E. Karasz, Polym. J. **26**, 771 (1994)

O. Urakawa, Y. Fuse, H. Hori, Q. Tran-Cong, O. Yano, Polymer **42**, 765 (2001)

C. Uriarte, I.J. Eguiazabal, M. Llanos, J.I. Iribarren, J.J. Iruin, Macromolecules **20**, 3038 (1987)

C. Uriarte, J.J. Iruin, M.J. Fernandez-Berridi, J.M. Elorza, Polymer **30**, 1155 (1989)

C. Uriate, J. Alfageme, A. Etxeberria, J.J. Iruin, Eur. Polym. J. **31**, 609 (1995)

M. Urzua, A. Opazo, L. Gargallo, D. Radic, Polym. Bull. **40**, 63 (1998)

M. Urzua, L. Gargallo, D. Radic, J. Macromol. Sci.: Phys. **B39**, 143 (2000)

M. Urzua, L. Gargallo, D. Radic, J. Appl. Polym. Sci. **84**, 1245 (2002)

M. Urzua, C. Sandoval, F. Gonzalez-Nilo, A. Leiva, L. Gargallo, D. Radic, J. Appl. Polym. Sci. **102**, 2512 (2006)

T. Uyar, C.C. Rusa, X.W. Wang, M. Rusa, J. Hacaloglu, A.E. Tonelli, J. Polym. Sci. B: Polym. Phys. **43**, 2578 (2005)

M.M. Vaidya, K. Levon, E.M. Pearce, J. Polym. Sci. B: Polym. Phys. **33**, 2093 (1995)

G. Van Ekenstein, H. Deuring, G. ten Brinke, T.S. Ellis, Polymer **38**, 3025 (1997)

P. Van Ende, G. Groeninckx, H. Reynaers, C. Samyn, Polymer **33**, 3598 (1992)

D.L. VanderHart, Macromolecules **27**, 2837 (1994)

D.L. Vanderhart, G.C. Campbell, R.M. Briber, Macromolecules **25**, 4734 (1992)

D.L. VanderHart, St. R.J. Manley, J.D. Barnes, Macromolecules **27**, 2826 (1994)

J. Vanderschueren, A. Janssens, M. Ladang, J. Niezette, Polymer **23**, 395 (1982)

M. Vanneste, G. Groeninckx, Polymer **35**, 1051 (1994)

M. Vanneste, G. Groeninckx, Polymer **36**, 4253 (1995)

M. Vanneste, G. Groeninckx, H. Reynaers, Polymer **38**, 4407 (1997)

D.F. Varnell, J.P. Runt, M.M. Coleman, Polymer **24**, 37 (1983)

K.T. Varughese, J. Appl. Polym. Sci. **39**, 205 (1990)

K.T. Varughese, G.B. Nando, P.P. De, S.K. De, J. Mater. Sci. **23**, 3894 (1986)

K.T. Varughese, P.P. De, S.K. Sanyal, S.K. De, J. Appl. Polym. Sci. **37**, 2537 (1989)

H. Vazquez-Torres, C.A. Cruz-Ramos, J. Appl. Polym. Sci. **32**, 6095 (1986)

H. Vazquez-Torres, J.V. Canich-Rodriguez, C.A. Cruz-Ramos, J. Appl. Polym. Sci. **50**, 777 (1993)

J.L. Velada, L.C. Cesteros, E. Meaurio, I. Katime, Polymer **36**, 2765 (1995)

J.L. Velada, L.C. Cesteros, I. Katime, Appl. Spectrosc. **50**, 893 (1996a)

J.L. Velada, L.C. Cesteros, I. Katime, Macromol. Chem. Phys. **197**, 2247 (1996b)

A. Verma, B.L. Deopura, A.K. Sengupta, J. Appl. Polym. Sci. **31**, 747 (1986)

J.M. Vermeesch, G. Groeninckz, Polymer **36**, 1039 (1995)

J.M. Vermeesch, G. Groeninckz, M.M. Coleman, Macromolecules **26**, 6643 (1993)

V. Villar, L. Irusta, M.J. Fernandez-Berridi, M. Iriarte, L. Gargallo, D. Radic, Thermochim. Acta **402**, 209 (2003)

J.M. Vion, R. Jerome, P. Teyssie, M. Aubin, R.E. Prud'homme, Macromolecules **19**, 1828 (1986)

S. Viswanathan, M.D. Dadmun, Macromolecules **36**, 3196 (2003)

S. Viswanathan, M.D. Dadmun, J. Polym. Sci. B: Polym. Phys. **42**, 1010 (2004)

M. Vivas de Meftahi, J.M.J. Frechet, Polymer **29**, 477 (1988)

O. Vogl, T.K. Kwei, M. Qin, J. Macromol. Sci.: Pure Appl. Chem. **A34**, 1747 (1997)

E.J. Voremkamp, G. Challa, Polymer **29**, 86 (1988)

R. Vukovic, V. Kuresevic, F.E. Karasz, W.J. MacKnight, Proc. 2nd Eur. Symp. Thermal Analysis **243** (1981) [Chem. Abstr., **96**, 36064v (1982)]

R. Vukovic, V. Kuresevic, F.E. Karasz, W.J. MacKnight, Thermochim. Acta. **54**, 349 (1982)

R. Vukovic, V. Kuresevic, F.E. Karasz, W.J. MacKnight, Proc. 7th Int. Conf. Therm. Anal. **2**, 1078 (1982a) [Chem. Abstr., 99, 176649b (1983)]

R. Vukovic, F.E. Karasz, W.J. MacKnight, J. Appl. Polym. Sci. **28**, 219 (1983a)

R. Vukovic, F.E. Karasz, W.J. MacKnight, Polymer **24**, 529 (1983b)

R. Vukovic, V. Kuresevic, N. Segudovic, F.E. Karasz, W.J. MacKnight, J. Appl. Polym. Sci. **28**, 1379 (1983c)

R. Vukovic, V. Kuresevic, F.E. Karasz, W.J. MacKnight, J. Appl. Polym. Sci. **30**, 317 (1985)

R. Vukovic, G. Bogdanic, V. Kuresevic, F.E. Karasz, W.J. MacKnight, Eur. Polym. J. **24**, 123 (1988)

R. Vukovic, V. Kuresevic, G. Bogdanic, D. Fles, Thermochim. Acta. **195**, 351 (1992a)

R. Vukovic, V. Kuresevic, G. Bogdanic, N. Segudovic, Polym. Bull. **28**, 473 (1992b)

R. Vukovic, M. Zuanic, G. Bogdanic, F.E. Karasz, W.J. MacKnight, Polymer **34**, 1449 (1993)

R. Vukovic, G. Bogdanic, V. Kuresevic, N. Segudovic, F.E. Karasz, W.J. MacKnight, Polymer **35**, 3055 (1994a)

R. Vukovic, G. Bogdanic, V. Kuresevic, N. Segudovic, M. Thomaskovic, F.E. Karasz, W.J. MacKnight, J. Polym. Sci. B: Polym. Phys. **32**, 1079 (1994b)

R. Vukovic, G. Bogdanic, V. Kuresevic, N. Segudovic, V. Srica, F.E. Karasz, W.J. MacKnight, J. Appl. Polym. Sci. **52**, 1499 (1994c)

R. Vukovic, V. Kuresevic, G. Bogdanic, D. Fles, Thermochim. Acta **233**, 75 (1994d)

R. Vukovic, G. Bogdanic, V. Kuresevic, N. Segudovic, D. Fles, F.E. Karasz, W.J. MacKnight, Thermochim. Acta **264**, 125 (1995)

R. Vukovic, G. Bogdanic, A. Erceg, D. Fles, F.E. Karasz, W.J. MacKnight, Thermochim. Acta **275**, 259 (1996a)

R. Vukovic, G. Bogdanic, A. Erceg, D. Fles, F.E. Karasz, W.J. MacKnight, Thermochim. Acta **285**, 141 (1996b)

R. Vukovic, G. Bogdanic, A. Erceg, D. Fles, F.E. Karasz, W.J. MacKnight, Polymer **39**, 2847 (1998)

M. Wachowicz, J.L. White, Macromolecules **40**, 5433 (2007)

M. Wachowicz, L. Gill, J. Wolak, J.L. White, Macromolecules **41**, 2832 (2008)

D.C. Wahrmund, R.E. Bernstein, J.W. Barlow, D.R. Paul, Polym. Eng. Sci. **18**, 677 (1978)

J.E. Walak, J.L. White, Macromolecules **28**, 10466 (2005)

T.A. Walker, S.R. Raghavan, J.R. Royer, S.D. Smith, G.D. Wignall, Y. Melnichenko, S.A. Khan, R.J. Spontak, J. Phys. Chem. B. **103**, 5472 (1999)

T.A. Walker, Y.B. Melnichenko, G.D. Wignall, J.S. Lin, R.J. Spontak, Macromol. Chem. Phys. **204**, 2064 (2003)

D.J. Walsh, G.L. Cheng, Polymer **23**, 1965 (1982)

D.J. Walsh, G.L. Cheng, Polymer **25**, 495 (1984)

D.J. Walsh, J.G. McKeown, Polymer **21**, 1330 (1980)

D.J. Walsh, C.K. Sham, Macromolecules **22**, 3799 (1989)

D.J. Walsh, V.B. Singh, Makromol. Chem. **185**, 1979 (1984)

D.J. Walsh, L. Shi, Z. Chai, Polymer **22**, 1005 (1981)

D.J. Walsh, J.S. Higgins, Z. Chai, Polymer **23**, 336 (1982)

D.J. Walsh, J.S. Higgins, S. Rostami, Macromolecules **16**, 388 (1983)

D.J. Walsh, G.T. Dee, J.T. Halary, Macromolecules **22**, 3385 (1989)

M.H. Walters, D.N. Keyte, Rubber Chem. Technol. **38**, 62 (1965)

Y.Y. Wang, S.A. Chen, Polym. Eng. Sci. **21**, 47 (1981)

C.B. Wang, S.L. Cooper, J. Polym. Sci. Polym. Phys. Ed. **21**, 11 (1983)

H.L. Wang, J.E. Fernandez, Macromolecules **26**, 3336 (1993)

C.S. Wang, C.H. Lin, Polymer **41**, 4029 (2000)

Y. Wang, H. Morawetz, Macromolecules **22**, 164 (1989)

H.L. Wang, L. Toppare, J.E. Fernandez, Macromolecules **23**, 1053 (1990)

L.F. Wang, E.M. Pearce, T.K. Kwei, J. Polym. Sci. Polym. Phys. Ed. **29**, 619 (1991a)

X. Wang, H. Saito, T. Inoue, Kobunshi Ronbushu. **48**, 443 (1991b)

F.Y. Wang, C.C.M. Ma, H.D. Wu, J. Appl. Polym. Sci. **74**, 2283 (1999a)

S. Wang, Q. Ji, C.N. Tchatchoua, A.R. Schultz, J.E. McGrath, J. Polym. Sci. B: Polym. Phys. **37**, 1849 (1999b)

S. Wang, H. Zhuang, H.K. Shobha, T.E. Glass, M. Sankarapandian, Q. Ji, A.R. Schultz, J.E. McGrath, Macromolecules **34**, 8051 (2001a)

J. Wang, M.K. Cheung, Y. Mi, Polymer **42**, 2077 (2001b)

J. Wang, M.K. Cheung, Y. Mi, Polymer **42**, 3087 (2001c)

L.Q. Wang, J. Jing, C. Xiao, K.J. Zhu, J. Mater. Sci. Lett. **21**, 45 (2002a)

J. Wang, M.K. Cheung, Y. Mi, Polymer **43**, 1357 (2002b)

C. Wang, M.L. Wang, Y.D. Fan, Macromol. Chem. Phys. **206**, 1791 (2005)

Y. Wang, S.H. Goh, T.S. Chung, Polymer **48**, 2901 (2007)

P.Y. Wang, B.Q. Liu, L. Li, S.X. Zheng, J. Macromol. Sci. B: Phys. **47**, 800 (2008)

J.M. Warakomski, R.P. Dion, J. Appl. Polym. Sci. **46**, 1057 (1992)

Y. Ward, Y. Mi, Polymer **40**, 2465 (1999)

C. Wastlund, H. Berndtsson, F.H.J. Maurer, Macromolecules **31**, 3322 (1998)

M. Wei, I.D. Shin, B. Urban, A.E. Tonelli, J. Polym. Sci. B: Polym. Phys. **42**, 1369 (2004)

A.L. Weikel, S.G. Owens, N.L. Morozowich, M. Deng, L.S. Nair, C.T. Laurencin, H.R. Allcock, Biomaterials **31**, 8507 (2010)

R.A. Weiss, X. Lu, Polymer **35**, 1963 (1994)

R.A. Weiss, C. Beretta, S. Sasongko, A. Garton, J. Appl. Polym. Sci. **41**, 91 (1990)

R.A. Weiss, Y. Ghebremeski, L. Charbonneau, Polymer **41**, 3471 (2000)

G. Wen, X. Li, Y. Liao, L. An, Polymer **44**, 4035 (2003)

C. Wendland, S. Klotz, V. Krieger, H.J. Cantow, Am. Chem. Soc. Polym. Prepr. **30**(2), 109 (1989)

M.M. Werlang, M.A. de Aranjo, S.P. Nunes, I.V.P. Yoshida, J. Polym. Sci. B: Polym. Phys. **35**, 2609 (1997)

R.E. Wetton, P. Williams, J. Polym. Mater. Sci. Eng. **59**, 846 (1988)

R.E. Wetton, W.J. MacKnight, J.R. Fried, F.E. Karasz, Macromolecules **11**, 158 (1978)

J.L. White, P.A. Mirau, Macromolecules **27**, 1648 (1994)

J.M. Widmaier, G. Mignard, Eur. Polym. J. **23**, 989 (1987)

G.D. Wignall, J.D. Londono, J.S. Lin, G. Alamo, M.J. Galante, L. Mandelkern, Macromolecules **28**, 3156 (1995)

K.L. Winey, M.L. Berba, M.E. Galvin, Macromolecules **29**, 2868 (1996)

H. Witteler, G. Lieser, M. Droscher, Makro. Chem. Rapid Commun. **14**, 401 (1993)

K.A. Wolf, J. Polym. Sci. C **4**, 1626 (1963)

H. Wolff, Plast. Kautsch. **4**, 244 (1957)

E.M. Woo, C.P. Chang, Polymer **45**, 8415 (2004)

E.M. Woo, F.H. Jang, Polymer **40**, 3803 (1999)

E.M. Woo, Y.T. Juang, J. Polym. Sci. B: Polym. Phys. **45**, 1521 (2007)

E.M. Woo, Y.H. Kuo, J. Polym. Sci. B: Polym. Phys. **41**, 2394 (2003)

E.M. Woo, L.T. Lee, Polym. Bull. **50**, 33 (2003)

E.M. Woo, T.K. Mandal, Macromol. Rapid Commun. **20**, 46 (1999)

E.M. Woo, C.C. Su, Polymer **37**, 4111 (1996a)

E.M. Woo, C.C. Su, Polymer **37**, 5189 (1996b)

E.M. Woo, Y.C. Tseng, J. Polym. Sci. B: Polym. Phys. **37**, 1455 (1999)

E.M. Woo, Y.C. Tseng, Macromol. Chem. Phys. **201**, 1877 (2000)

E.M. Woo, S.N. Yau, Macromolecules **30**, 3626 (1997)

E.M. Woo, J.W. Barlow, D.R. Paul, J. Appl. Polym. Sci. **28**, 1347 (1983)

E.M. Woo, J.W. Barlow, D.R. Paul, J. Appl. Polym. Sci. **29**, 3837 (1984a)

E.M. Woo, J.W. Barlow, D.R. Paul, J. Polym. Sci. Polym. Symp. **71**, 137 (1984b)

E.M. Woo, J.W. Barlow, D.R. Paul, J. Appl. Polym. Sci. **30**, 4243 (1985a)

E.M. Woo, J.W. Barlow, D.R. Paul, Polymer **26**, 763 (1985b)

E.M. Woo, J.W. Barlow, D.R. Paul, J. Appl. Polym. Sci. **32**, 3889 (1986)

E.M. Woo, M.L. Lee, Y.S. Sun, Polymer **41**, 883 (2000a)

E.M. Woo, T.K. Mandal, L.L. Chang, Macromolecules **33**, 4186 (2000b)

E.M. Woo, T.K. Mandal, L.L. Chang, S.C. Lee, Polymer **41**, 6663 (2000c)

E.M. Woo, T.K. Mandal, S.C. Lee, Colloid Polym. Sci. **278**, 1032 (2000d)

E.M. Woo, I.C. Cho, L.T. Lee, Polymer **43**, 4225 (2002)

E.M. Woo, I.C. Chou, L.L. Chang, H.M. Kao, Polym. J. **35**, 372 (2003a)

E.M. Woo, Y.J. Mao, P.L. Wu, C.C. Su, Polym. Eng. Sci. **43**, 543 (2003b)

E.M. Woo, K.Y. Cheng, Y.F. Chen, C.C. Su, Polymer **48**, 5753 (2007)

E.M. Woo, Y.H. Chou, W.J. Chiang, I.T. Chen, I.H. Huang, N.T. Kuo, Polym. J. **42**, 396 (2010)

A. Wrzyszczynski, X. Qu, L. Szosland, E. Adamczak, L.A. Linden, J.F. Rabek, Polym. Bull. **34**, 493 (1995)

F.S. Wu, E.M. Woo, Polym. Eng. Sci. **39**, 825 (1999)

C. Wu, Y. Wu, R. Zhang, Eur. Polym. J. **34**, 1261 (1998)

W. Wu, X.L. Luo, D.Z. Ma, Eur. Polym. J. **35**, 985 (1999)

R.R. Wu, H.M. Kao, J.C. Chiang, E.M. Woo, Polymer **43**, 171 (2002)

M. Xiang, M. Jiang, Y.B. Zhang, C. Wu, L. Feng, Macromolecules **30**, 2313 (1997a)

M. Xiang, M. Jiang, Y.B. Zhang, C. Wu, Macromolecules **30**, 5339 (1997b)

R. Xie, R.A. Weiss, Polymer **39**, 2851 (1998)

S. Xie, W.J. MacKnight, F. Karasz, J. Appl. Polym. Sci. **29**, 2679 (1984)

S. Xie, A. Natasohn, P. Rochon, Macromolecules **27**, 1489 (1994)

P. Xing, L. Dong, Y. An, Z. Feng, M. Avella, E. Martuscelli, Macromolecules **30**(2726) (1997)

P. Xing, L. Dong, Z. Feng, H. Feng, Eur. Polym. J. **34**, 1207 (1998a)

P. Xing, X. Ai, L. Dong, Z. Feng, Macromolecules **31**, 6898 (1998b)

F.Y. Xu, J.C.W. Chien, Macromolecules **27**, 6589 (1994)

X. Xu, L. Zhang, H. Li, Polym. Eng. Sci. **27**, 398 (1987)

Y. Xu, J.F. Graf, P.C. Painter, M.M. Coleman, Polymer **31**, 3103 (1991)

M. Yamaguchi, K. Masuzawa, Cellulose. **15**, 17 (2008)

N. Yamaguchi, S. Akiyama, M. Tokoh, Kobunshi Ronbunshu. **53**, 842 (1996)

A. Yamanaka, A. Kaji, M. Murano, Polym. J. **30**, 210 (1998)

K.C. Yan, E.M. Woo, Y.F. Chen, Polym. J. **39**, 935 (2007)

Z.Y. Yang, C.D. Han, Polymer **23**, 5128 (2008)

H. Yang, W. Yetter, Polymer **35**, 2417 (1994)

H. Yang, G. Hadziioannou, R.S. Stein, J. Polym. Sci. Polym. Phys **21**, 159 (1983)

H. Yang, M. Shibayama, R.S. Stein, N. Shimizu, T. Hashimoto, Macromolecules **19**, 1667 (1986a)

H. Yang, S. Richard, C.C. Han, B.J. Bauer, E. Kramer, J. Polym. Commun. **27**, 132 (1986b)

T.P. Yang, E.M. Pearce, T.K. Kwei, N.L. Yang, Macromolecules **22**, 1813 (1989)

H. Yang, S. Ricci, M. Collins, Macromolecules **24**, 5218 (1991)

H. Yang, E.Y. Ni, W. McKenna, Compos. Interf. **1**, 439 (1993a)

H. Yang, T.K. Kwei, Y. Dai, Macromolecules **26**, 842 (1993b)

J.M. Yang, H.L. Chen, J.W. You, J.C. Hwang, Polym. J. **29**, 657 (1997)

Q. Yang, Y.M. Mao, G.X. Li, Y.J. Huang, P. Tang, C.H. Lei, Mater. Lett. **58**, 3999 (2004)

F. Yang, Z.B. Qiu, W.T. Yang, Polymer **50**, 2328 (2009)

F. Yang, Z.S. Li, Z.B. Qiu, J. Appl. Polym. Sci. **123**, 2781 (2012)

S.N. Yau, E.M. Woo, Macromol. Rapid Commun. **17**, 615 (1996)

K.C. Yen, E.M. Woo, Polym. Int. **58**, 1380 (2009)

K.C. Yen, E.M. Woo, K. Tashiro, Polymer **50**, 6312 (2009)

Y.T. Yeo, S.H. Goh, S.Y. Lee, Eur. Polym. J. **30**, 1117 (1994a)

Y.T. Yeo, S.H. Goh, S.Y. Lee, Eur. Polym. J. **30**, 495 (1994b)

Y.T. Yeo, S.H. Goh, S.Y. Lee, Eur. Polym. J. **31**, 39 (1995a)

Y.T. Yeo, S.H. Goh, S.Y. Lee, J. Appl. Polym. Sci. **55**, 1651 (1995b)

Y.T. Yeo, S.H. Goh, S.Y. Lee, Polym. Polym. Compos. **4**, 235 (1996)

Y.T. Yeo, S.H. Goh, S.Y. Lee, J. Macromol. Sci.: Pure Appl. Chem. **34**, 597 (1997)

J.Z. Yi, S.H. Goh, Polymer **42**, 9313 (2001a)

J.Z. Yi, S.H. Goh, Polymer **42**, 9319 (2001b)

J.Z. Yi, S.H. Goh, Polymer **43**, 4515 (2002)

J.Z. Yi, S.H. Goh, Polymer **44**, 1973 (2003)

J.Z. Yi, S.H. Goh, Polymer **46**, 9170 (2005)

J.Z. Yi, S.H. Goh, A.T.S. Wee, Macromolecules **34**, 4662 (2001a)

J.Z. Yi, S.H. Goh, A.T.S. Wee, Macromolecules **34**, 7411 (2001b)

E. Yilmaz, D. Ozalp, O. Yilmaz, Int. J. Polym. Anal. Charac. **10**, 329 (2005)

J. Yin, C. Xue, G.C. Alfonso, A. Turturro, E. Pedemonte, Polymer **38**, 2127 (1997)

J.E. Yoo, C.K. Kim, Polym. Int. **53**, 1950 (2004a)

J.E. Yoo, C.K. Kim, Polymer **45**, 287 (2004b)

J.E. Yoo, Y. Kim, C.K. Kim, Macromol. Res. **11**, 303 (2003)

J.S. Yoon, C.S. Choi, S.J. Maing, H.J. Choi, H.S. Lee, S.J. Choi, Eur. Polym. J. **29**, 1359 (1993)

K.H. Yoon, C.S. Lee, O.O. Park, Polym. J. **26**, 816 (1994)

J.S. Yoon, S.H. Oh, M.N. Kim, Polymer **39**, 2479 (1998)

J.S. Yoon, S.H. Oh, M.N. Kim, I.J. Chiu, Y.H. Kim, Polymer **40**, 2303 (1999)

N. Yoshie, Y. Azuma, M. Sakurai, T. Inoue, J. Appl. Polym. Sci. **56**, 17 (1995)

N. Yoshimura, K. Fujimoto, Nippon Gomu Kyokaishi, **41**, 161 (1968); Rubber Chem. Technol. **42** 1009 (1968)

J.W. You, H.J. Chiu, T.M. Don, Polymer **44**, 4355 (2003)

D. Yu, Y. Zheng, Z. Wu, X. Tang, B. Jiang, J. Appl. Polym. Sci. **41**, 2649 (1990)

D. Yu, E.H. Hellmann, G.P. Hellmann, Makromol. Chem. **192**, 2749 (1991)

F. Yu, Nakamura, Y. Inoue, Polymer **51**(5556) (2010)

Y. Yuan, E. Ruckenstein, Polymer **39**, 1893 (1998)

K. Yurekli, R. Krishnamoorti, J. Polym. Sci. B: Polym. Phys. **42**, 3204 (2004)

C.M. Zaccaron, R.V.B. Oliveira, M. Guiotoku, A.T.N. Pires, V. Soldi, Polym. Degrad. Stab. **90**, 21 (2005)

G.A. Zakrzewski, Polymer **14**, 347 (1973)

J. Zelinger, E. Volfova, H. Zahraknikova, Z. Pelzbauer, Int. J. Polym. Mater. **5**, 99 (1976)

J.B. Zeng, Q.Y. Zhu, Y.D. Li, Z.C. Qiu, Y.Z. Wang, J. Phys. Chem. B **114**, 14827 (2010)

X. Zhang, K. Hikichi, Macromolecules **25**, 2336 (1992)

Z. Zhang, Y. Mi, J. Polym. Sci. B: Polym. Phys. **37**, 237 (1999)

H. Zhang, R.E. Prud'homme, J. Polym. Sci. Polym. Phys. Ed. **25**, 723 (1987)

X. Zhang, K. Takegoshi, K. Hikichi, Macromolecules **24**, 5756 (1991a)

X. Zhang, K. Takegoshi, K. Hikichi, Polym. J. **23**, 79 (1991b)

X. Zhang, K. Takegoshi, K. Hikichi, Polym. J. **23**, 87 (1991c)

X. Zhang, K. Takegoshi, K. Hikichi, Polymer **33**, 712 (1992a)

X. Zhang, K. Takegoshi, K. Hikichi, Polymer **33**, 718 (1992b)

X. Zhang, K. Takegoshi, K. Kikichi, Polym. J. **24**, 1403 (1992c)

P. Zhang, Z. Sun, G. Li, Y. Zhuang, M. Ding, Z. Feng, Makromol. Chem. **194**, 1871 (1993)

H. Zhang, D.E. Bhagwagar, J.F. Graf, P.C. Painter, M.M. Coleman, Polymer **35**, 5379 (1994)

L. Zhang, C. Xiong, X. Deng, J. Appl. Polym. Sci. **56**, 105 (1995a)

R. Zhang, X. Luo, D. Ma, Eur. Polym. J. **31**, 1011 (1995b)

R. Zhang, X. Luo, D. Ma, J. Appl. Polym. Sci. **55**, 455 (1995c)

L.L. Zhang, Z.M. Deng, Z.T. Huang, Polymer **38**, 5379 (1997)

L.L. Zhang, S.H. Goh, S.Y. Lee, Polymer **39**, 4841 (1998)

L.L. Zhang, S.H. Goh, S.Y. Lee, J. Appl. Polym. Sci. **74**, 383 (1999)

L.L. Zhang, S.H. Goh, S.Y. Lee, G.R. Hee, Polymer **41**, 1429 (2000)

Z. Zhang, Z. Mo, H. Zhang, Y. Zhang, T. Na, Y. An, X. Wang, X. Zhao, J. Polym. Sci. B: Polym. Phys. **40**, 1957 (2002)

J.M. Zhang, H. Sato, T. Furukawa, H. Tsuji, I. Noda, Y. Ozaki, J. Phys. Chem. B **110**, 24463 (2006a)

H.L. Zhang, M.Q. Ren, Q.Y. Chen, S.L. Sun, X.H. Sun, H.X. Zhang, Z.S. Mo, J. Polym. Sci. B: Polym. Phys. **44**, 1320 (2006b)

L.X. Zhang, S.L. Sun, L. Ren, F.F. Zhang, M.Y. Zhang, H.X. Zhang, J. Appl. Polym. Sci. **108**, 3016 (2008a)

L.X. Zhang, S.L. Sun, X.W. Li, M.Y. Zhang, H.X. Zhang, Polym. Bull. **61**, 99 (2008b)

Z.X. Zhang, C.H. Chen, X.W. Gao, J.K. Kim, Z.X. Xin, J. Appl. Polym. Sci. **120**, 1180 (2011)

K.Y. Zhang, A.K. Mohanty, M. Misra, ACS Appl. Mater. Interf. **4**, 3091 (2012a)

X.Z. Zhang, Y.H. Shen, A.J. Xie, S.L. Gao, Polym. Testing **31**, 171 (2012b)

L.Y. Zhao, P. Choi, J. Appl. Polym. Sci. **91**, 1827 (2004)

Y. Zhao, R.E. Prud'homme, Macromolecules **23**, 713 (1990)

Y. Zhao, R.E. Prud'homme, Polym. Bull. **26**, 101 (1991)

Y. Zhao, D. Ma, R.E. Prud'homme, Polymer **32**, 791 (1991)

W. Zhao, L. Yu, X. Zhong, Y. Zhang, J. Sun, J. Macromol. Sci.: Phys. **B34**, 231 (1995)

J.Q. Zheng, T. Kyu, Polym. Eng. Sci. **32**, 1004 (1992)

S.X. Zheng, Y.L. Mi, Polymer **44**, 1067 (2003)

W. Zheng, K. Levon, T. Taka, J. Lankso, J.E. Osterholm, J. Polym. Sci. B: Polym. Phys. **33**, 1289 (1995)

S. Zheng, J. Huang, W. Liu, X. Yang, Q. Guo, Eur. Polym. J. **32**, 757 (1996)

S. Zheng, J. Huang, Y. Li, Q. Guo, J. Polym. Sci. B: Polym. Phys. **35**, 1383 (1997a)

J.W. Zheng, S.H. Goh, S.Y. Lee, Macromolecules **30**, 8069 (1997b)

S. Zheng, W. Zhang, D. Ma, Eur. Polym. J. **33**, 937 (1997c)

S. Zheng, Q. Guo, Y. Mi, J. Polym. Sci. B: Polym. Phys. **36**, 2291 (1999a)

S. Zheng, Q. Guo, Y. Mi, J. Polym. Sci. B: Polym. Phys. **37**, 2412 (1999b)

J.W. Zheng, S.H. Goh, S.Y. Lee, J. Appl. Polym. Sci. **75**, 1393 (2000)

J.W. Zheng, S.H. Goh, S.Y. Lee, Fullerene Sci. Technol. **9**, 487 (2001)

S.X. Zheng, G.Q. Guo, C.M. Chan, J. Polym. Sci. B: Polym. Phys. **41**, 1099 (2003a)

S.X. Zheng, G.Q. Guo, Y.L. Mi, Polymer **44**, 867 (2003b)

S. Zheng, H. Lu, C. Chen, K. Nie, Q. Guo, Colloid Polym. Sci. **281**, 1015 (2003c)

S.X. Zheng, H.F. Zheng, G.P. Guo, J. Polym. Sci. B: Polym. Phys. **41**, 1085 (2003d)

S.X. Zheng, J.H. Li, R. Gao, G.P. Guo, J. Macromol. Sci. B Phys. **B42**, 351 (2003e)

S.X. Zheng, K.M. Nie, G.P. Guo, Thermochim. Acta **419**, 267 (2004)

Z. Zhong, Q. Guo, J. Polym. Sci. A: Polym. Chem. **36**, 401 (1998)

Z. Zhong, S. Zheng, J. Huang, X. Cheng, Q. Guo, J. Wei, Polymer **39**, 1075 (1998)

X.X. Zhou, M. Cakmak, J. Macromol. Sci. B: Phys. **46**, 667 (2007)

Z.L. Zhou, A. Eisenberg, J. Polym. Sci. Polym. Phys. Ed. **21**, 595 (1983)

H. Zhou, M. Xiang, W. Chen, M. Jiang, Macromol. Chem. Phys. **198**, 809 (1997a)

X. Zhou, S.H. Goh, S.Y. Lee, K.L. Tan, Appl. Surf. Sci. **119**, 60 (1997b)

X. Zhou, S.H. Goh, S.Y. Lee, K.L. Tan, Appl. Surf. Sci. **126**, 141 (1997c)

X. Zhou, S.H. Goh, S.Y. Lee, K.L. Tan, Polymer **38**, 5333 (1997d)

X. Zhou, S.H. Goh, S.Y. Lee, K.L. Tan, Polymer **39**, 3631 (1998)

N.C. Zhou, W.R. Burghardt, K.I. Winey, Macromolecules **40**, 6401 (2007)

S. Zhu, D.R. Paul, Polymer **44**, 3009 (2003)

K.J. Zhu, S.F. Chen, T. Ho, E.M. Pearce, T.K. Kwei, Macromolecules **23**, 150 (1990)

K.J. Zhu, L. Wang, J. Wang, S. Yang, Macromol. Chem. Phys. **195**, 1965 (1994)

K.J. Zhu, L. Wang, S. Yang, Polym. Int. **36**, 293 (1995)

L. Zhu, M. Jiang, L. Liu, H. Zhou, L. Fan, Y. Zhang, J. Macromol. Sci.: Phys. **B37**, 805 (1998a)

L. Zhu, M. Jiang, L. Liu, H. Zhou, L. Fan, Y. Zhang, J. Macromol. Sci.: Phys. **B37**, 827 (1998b)

B. Zhu, J. Li, Y. He, N. Yoshie, Y. Inoue, Macromol. Biosci. **3**, 684 (2003)

L.L. Zhu, L. Li, X.T. Yang, R.T. Yu, S.X. Zheng, J. Macromol. Sci. B: Polym. Phys. **51**, 368 (2012)

P. Zhuang, T. Kyu, J.L. White, Polym. Eng. Sci. **28**, 1095 (1988)

H. Zhuang, E.M. Pearce, T.K. Kwei, Macromolecules **27**, 6398 (1994)

H. Zhuang, E.M. Pearce, T.K. Kwei, Polymer **36**, 2237 (1995)

J. Zimmerman, E.M. Pearce, I.K. Miller, J.A. Muzzio, I.E. Epstein, E.A.J. Hosegood, Appl. Polym. Sci. **17**, 849 (1973)

M.D. Zipper, G.P. Simon, M.R. Tant, J.D. Small, G.M. Stack, A.J. Hill, Polym. Int. **36**, 127 (1995)

J.J. Ziska, J.W. Barlow, D.R. Paul, Polymer **22**, 918 (1981)

L.Y. Zlatkevich, V.G. Nikolskii, Rubber Chem. Technol. **46**, 1210 (1973)

P. Zucco, P.C. Painter, Am. Chem. Soc. Polym. Prepr. **29**(1), 341 (1988)

M. Zuideveld, C. Gottschalk, H. Kropfinger, R. Thomann, M. Rusu, H. Frey, Polymer **47**, 3740 (2006)

M. Zuo, M. Peng, Q. Zheng, J. Polym. Sci. B: Polym. Phys. **44**, 1547 (2006)

E. Zuza, E. Meaurio, A. Etxeberria, J.R. Sarasua, Macromol. Rapid Commun. **27**, 2026 (2006)

E. Zuza, A. Lejardi, J.M. Ugartemedia, N. Monasterio, E. Meaurio, J.R. Sarasua, Macromol. Chem. Phys. **209**, 2423 (2008)

Appendices

Appendix I: International Abbreviations for Polymers and Polymer Processing

AA	Acrylic acid (monomer)
AAS, ASA	Copolymer of acrylonitrile, acrylate (ester), and styrene
ABA	Acrylonitrile-butadiene-acrylate copolymer
ABM	Copolymer of acrylonitrile-butadiene-methyl acrylate
ABMA	Copolymer of acrylonitrile-butadiene-methacrylic acid
ABR	Elastomeric copolymer from an acrylate (ester) and butadiene, a rubber
ABS	Thermoplastic terpolymer, an acrylonitrile-butadiene-styrene copolymer
ABSM	Graft copolymer of acrylonitrile-butadiene-styrene-methyl methacrylate
ABSMA	Graft copolymer of acrylonitrile-butadiene-styrene-maleic anhydride
ABS-MA	Maleated acrylonitrile-butadiene-styrene copolymer
ABVC	Thermoplastic terpolymer, an acrylonitrile-butadiene-vinyl chloride copolymer
ACM	Acrylate rubber, based on ethyl acrylate with other acrylics
ACM	Acrylic elastomer, e.g., alkyl acrylate-2-chloroethyl vinyl ether copolymer
ACPES	Acrylonitrile-chlorinated polyethylene-styrene copolymer
ACRYL	Poly- or copoly-methyl methacrylate (acrylic)
ACS	Thermoplastic blend of acrylonitrile-styrene-chlorinated PE terpolymer
ACS, ACPES	Acrylonitrile-chlorinated polyethylene-styrene copolymer
AEM	Elastomeric ethyl (or other) acrylate-ethylene copolymer
AES	Terpolymer from acrylonitrile, ethylene-propylene elastomer, and styrene
AF	Aniline-formaldehyde molding resins

AFMU	Terpolymer of tetrafluoroethylene, trifluoro-nitrosomethane, and nitrosoperfluorobutyric acid
AK	Alkyd resin
AMAB	Copolymer from acrylonitrile, methyl acrylate, and butadiene rubber
AMC	Alkyd molding compound
AMMA	Thermoplastic copolymer from acrylonitrile and methyl methacrylate
AMS	α-Methyl styrene
AN	Acrylonitrile
ANM	Acrylate rubber, based on ethyl acrylate with acrylonitrile
AP, APR	Elastomeric ethylene-propylene-diene copolymer, now EPDM
APET	Amorphous polyethyleneterephthalate
aPP	Amorphous polypropylene
aPP	Atactic PP
AR	Elastomeric copolymer from acrylates and olefins
ARP	Polyarylterephthalate liquid crystal copolymers, also PAT
AS	Acrylonitrile-styrene copolymer (see also SAN)
ASA, AAS	Thermoplastic copolymer from acrylonitrile, styrene, and acrylates
ASR	Alkylene sulfide rubber
AU	Elastomeric polyester or polyurethane with polyester segments
BA, PBA	Polybutylacrylate (incorrectly used for acrylic elastomer, ACM)
BAAN	Butyl acrylate-acrylonitrile copolymer
BAMM	Butyl acrylate-methyl methacrylate copolymer
BFE	Bromotrifluoroethylene polymers
BIIR	Brominated elastomer from isobutene and isoprene, bromobutyl rubber
BMC	Bulk molding compound (UP resins)
BMI	Bismaleimide
BMMM	Butyl methacrylate-methyl methacrylate copolymer
BOPP	Biaxially oriented polypropylene film
BP, BR	Polybutadiene or an isobutene-isoprene copolymer, butyl or butadiene rubber
BPA	Bisphenol-A
bPC	Branched polycarbonate of bisphenol-A
BR	Butadiene rubber
Bu-ABS	Graft copolymer of butylacrylate and triallyl isocyanurate on polybutadiene, in turn emulsion grafted with styrene and acrylonitrile

CA	Cellulose acetate
CAB	Cellulose acetate-butyrate
CAN	Cellulose acetate-nitrate
CAP	Cellulose acetate-propionate
CB	Cellulose butyrate (also carbon black reinforcing pigment)
CBR	Chlorinated butadiene rubber
CDB	Conjugated diene butyl elastomer
CE	Cellulose plastics in general
CEM	Polychlorotrifluoroethylene (also CFM, CTFEP, PCTFE)
CF	Cresol-formaldehyde resins (also reinforcing carbon fiber)
CFM	Polychlorotrifluoroethylene (also CEM, CTFEP, PCTFE)
CHR	Elastomeric copolymer from epichlorohydrin and ethylene oxide
CIIR	Post chlorinated elastomeric copolymer from isobutene and isoprene
CM	Chloro-polyethylene (also compression molding)
CMC	Carboxymethyl cellulose (or critical micelle concentration)
CMHEC	Carboxymethyl hydroxyethyl cellulose
CMPS	Poly(chloromethyl styrene)
CN	Cellulose nitrate (celluloid)
CNR	Elastomeric terpolymer from tetrafluoroethylene, trifluoronitrosomethane, and a small amount of an unsaturated monomer, e.g., nitrosoperfluorobutyric acid and nitroso or carboxy nitroso rubber
CO	Polychloromethyl oxirane elastomer, epichlorohydrin rubber
COP	Cycloolefin polymers or copolymers
CO-PAI	Copolyamideimide
COPE	Copolyester elastomer
CO-PI	Copolyimide
COPO	Poly(carbon monoxide-co- polyolefin), a linear, alternating terpolymer: ethylene-co- propylene-co-carbon monoxide
COX	Carboxylic rubber
CP	Cellulose propionate, or chlorinated polyethylene, also CPE
CP2	Alternating copolymer from vinyl ether and maleic acid
CP4	Copolymer from acrylic acid and maleic acid
CPE	Chlorinated polyethylene
CPET	Crystallizable (or chlorinated) polyethyleneterephthalate
CPI	*cis*-Polyisoprene, also IR
CPVC	Chlorinated polyvinyl chloride
CR	Chloroprene, or neoprene, rubber
CRM	Chlorosulfonated polyethylene
CRP	Carbon fiber reinforced plastics
CS	Casein

CSM, CSPE	Chlorosulfonated polyethylene, also CSPE or CSR
CSR	Chlorosulfonated polyethylene (also CSPE or CSM)
CT, CTA	Cellulose triacetate
CTBN	Carboxy-terminated nitrile rubber
CTFE	Polychlorotrifluoroethylene
CTFEP	Polychlorotrifluoroethylene (also CFM, CEM, PCTFE)
CUT	Continuous use temperature
CV	Viscose, also VI
DAC	Diallylchlorendate
DAF	Diallylfumarate
DAIP	Diallylisophthalate
DAP	Diallylphthalate
DCA	Dichloroacetic acid
DMA	Dynamic mechanical analysis
DMC	Dough molding compound
DMF	*N*,*N*-dimethylformamide (solvent, also DMT)
DMSO	Dimethyl sulfoxide (solvent)
DSC	Differential scanning calorimetry
E/B	Copolymers of ethylene and 1-butene
E/P	Ethylene-propylene copolymer EA
EAA	Ethylene acrylic acid copolymer
EAM	Elastomeric copolymer of ethylene and vinyl acetate
EBA	Ethylene-butyl acrylate copolymer
EBA-AA	Ethylene-butyl acrylate-acrylic acid copolymer
EBA-GMA	Ethylene-butyl acrylate-glycidyl methacrylate copolymer
EBA-MA	Ethylene (50–90 parts)-co-butyl acrylate (5 to 49 parts)-co-maleic anhydride (0.5 to 10 parts) copolymer
EBM	Extrusion blow molding
EC	Ethyl cellulose
ECA	Ethylene-carbonate copolymer
ECB	Blends from ethylene copolymers with bitumen
ECO, CO	Elastomeric copolymer from ethylene oxide and epichlorohydrin (also EO-ECH)
ECPE	Extended chain polyethylene
ECTF, ECTFE	Poly(ethylene-co-chlorotrifluoroethylene)
EEA	Elastomeric copolymer from ethylene and ethyl acrylate
EEAAA	Polyethylene grafted with ethyl acrylate and acrylic acid
EEA-GMA	Ethylene-ethyl acrylate-glycidyl methacrylate copolymer
EGMA	Ethylene-glycidyl methacrylate copolymer
EHEC	Hydroxyethyl cellulose
ELAST	Elastomer
EMA	Copolymer from ethylene and maleic anhydride or ethylene-methyl acrylate
EMAc	Copolymer from ethylene and methacrylic acid

EMAC	Ethylene methacrylate copolymer
EMI	Electromagnetic interference
EMM	Copolymer from ethylene and methyl methacrylate
EMP	Ethylene-propylene copolymers (ethylene-modified polypropylene)
ENR	Epoxidized natural rubber
EO-ECH	Copolymer of ethylene oxide and epichlorohydrin (also ECO, CO)
EP	Epoxy resins
EPD	Ethylene-propylene-diene copolymer
EPD, EPDM	Elastomeric terpolymer from ethylene, propylene, and a non-conjugated diene
EPDM-MA	Maleic anhydride-modified ethylene-propylene-diene terpolymer
EPE	Ester of an epoxy resin
EP-G-G	Prepreg from epoxy resin and glass fabric (German literature)
EP-K-L	Prepreg from epoxy resin and carbon fiber fabric (German literature)
EPR, EPM	Elastomeric copolymer of ethylene and propylene
EPR-MA	Maleated ethylene-propylene rubber, EPR
EPS	Polystyrene foam, expanded PS
EPT, EPTR	Ethylene, propylene, and a non-conjugated diene terpolymer, also EPDM
E-PVC	Emulsion polyvinyl chloride, PVC polymerized in emulsion
ES	Ethylene-styrene block copolymer
E-SBR	Polymerized in emulsion styrene/butadiene copolymer
ESCR	Environmental stress crack resistance
ESD	Electrostatic dissipation
ETE	Engineering thermoplastic elastomer
ETFE	Copolymer from ethylene and tetrafluoroethylene
EtOH	Ethanol
EU	Polyether urethane
EVA	Ethylene-vinyl acetal copolymer
EVAc	Copolymer from ethylene and vinyl acetate
EVAc-AA	Ethylene-vinyl acetate-acrylic acid graft copolymer
EVAc-CO	Ethylene-vinyl acetate-carbon monoxide copolymer
EVAc-MA	Copolymer from ethylene, vinyl acetate, and methacrylic acid
EVA-GMA	Ethylene-vinyl acetate-glycidyl methacrylate copolymer
EVAl, EVAL	Copolymer of ethylene and vinyl alcohol
EVAVC	Ethylene-vinyl acetate-vinyl chloride copolymer
EVC	Copolymer from ethylene and vinylene carbonate
EVE	Ethylene-vinyl ether copolymer
EVM	Ethylene-vinyl acetate copolymer, a thermoplastic elastomer
EVOH	Ethylene-vinyl alcohol copolymer (also EVAl, EVAL)

EVP	Ethylene-vinyl pyrrolidinone copolymer
FA	Formic acid
FE	Fluorine-containing elastomer
FEP	Fluorinated EPR, tetrafluoroethylene/hexa-fluoro propylene rubber
FF	Resin from furan and formaldehyde
FFKM	Perfluoro rubbers of the polymethylene type, having all substituent fluoro, perfluoroalkyl, or perfluoroalkoxy groups on the polymer chain
FK, FRP, GRP	Fiber reinforced plastic
FKM	Hexa-fluoro propylene- vinylidene fluoride copolymer
FMQ	Methyl fluoro silicone rubber
FP	Fluoroplastic
FPM	Vinylidene fluoride/hexa-fluoro propylene elastomer, rubbers with fluoro and fluoroalkyl or fluoroalkoxy groups
FPVC	Flexible PVC film
FQ	Elastomeric silicone with fluorine-containing substituents
FRE	Fiber reinforced epoxy
FRP, GRP, FK	Glass fiber reinforced polyester
FTIR	Fourier transform infrared spectroscopy
FVMQ	Silicone rubber with fluorine, vinyl, and methyl substituents
GC	Gas chromatograph
GECO	Epichlorohydrin-ethylene glycol- glycidyl ether elastomeric copolymer
GEP	Glass fiber reinforced epoxy resin
GF	Glass fiber, or glass fiber reinforced plastic
GF-PF	Glass fiber reinforced phenolic resin
GF-UP	Glass fiber reinforced unsaturated polyester resin
GMA	Glycidyl methacrylate (monomer)
GMT	Glass mat reinforced plastics
GP	Gutta-percha
GPC	Gel permeation chromatograph (now: size exclusion chromatography, SEC)
GPO	Elastomeric copolymer from propylene oxide and allyl glycidyl ether
GPPS	General-purpose polystyrene (also PS)
GPSMA	General-purpose styrene-maleic anhydride copolymer (also SMA)
GR	Government rubber from state-owned factories in the USA during the Second World War
GR-1	Butyl rubber
GR-N	Nitrile rubber, now NBR
GR-S	Styrene-butadiene rubber

GRP	Glass reinforced polyester (thermoset)
GUR	Ultrahigh molecular weight polyethylene (UHMWPE)
HALS	Hindered amines (antioxidants)
HAO	Higher alpha-olefins
HBV	Poly(3-hydroxy butyrate- co-valerate)
HDPE	High-density polyethylene (ca. 960 kg/m^3)
HDT	Heat deflection temperature
HEC	Hydroxyethyl cellulose
HIPS	High-impact polystyrene
HISMA	High-impact styrene-maleic anhydride copolymer
HM	Hot melt adhesive
HMC	Sheet molding compound with high glass fiber content
HMW	High molecular weight
HMW-PE	Polyethylene with high molecular weight
H-NBR, HNBR	Hydrogenated acrylonitrile- butadiene elastomer
HPC	Hydroxy propyl cellulose
HPMC	Hydroxy propyl-methyl cellulose
HR	High resiliency foams
HTE	Hydroxyl-terminated polyether
ICP	Intrinsically conductive (or connecting) polymer
IEN	Interpenetrating elastomeric network
IGC	Inverse gas chromatograph
IHPN	Interpenetrating homopolymer network
IIR	Isobutene-isoprene rubber (butyl rubber)
IM	Polyisobutene, also PIB
IO	Ionomer
IPN	Interpenetrating polymer network
IPS	Impact resistant polystyrene
IR	Synthetic *cis*-1,4-polyisoprene, synthetic isoprene rubber
IR, FTIR	Infrared spectroscopy (or Fourier transform infrared spectroscopy)
LCP	Liquid crystal polymer
LDPE	Low-density polyethylene (ca. 918 kg/m^3)
LIM	Liquid impingement molding (now reactive injection molding, RIM)
LIPN	Latex interpenetrating polymer network
LLDPE	Linear low-density polyethylene
LMDPE	Linear medium-density polyethylene
LPE	Linear polyethylene
LRM	Liquid reaction molding (now reactive injection molding, RIM)
LRMR	Reinforced liquid reaction molding (now reinforced reactive injection molding, RRIM)
L-SBR	Solution-polymerized SBR

LSR	Liquid silicone rubber
LTG	Low-temperature zinc phosphate glasses
MA or MAH	Maleic anhydride (monomer)
MABS	Copolymer from methyl methacrylate, acrylonitrile, butadiene, and styrene
MAN	Copolymer from methyl methacrylate and acrylonitrile
MAS	Copolymer from methyl methacrylate, acrylonitrile, and styrene
MBA	Copolymer from methyl methacrylate, butadiene, and acrylonitrile
MBS	Copolymer from methyl methacrylate, butadiene, and styrene
MC	Methyl cellulose
MC	Methylene chloride (solvent)
MDI	Methyl di-isocyanate
MDPE	Medium-density polyethylene (ca. 930 to 940 kg/m^3)
MEK	Methyl ethyl ketone (solvent)
MeSAN	Copolymer from α-methyl styrene and acrylonitrile
MF	Melamine-formaldehyde resins
MFI	Melt flow index
MFK	Metal fiber reinforced plastic
MFQ	Silicone rubbers with methyl and fluorine substituent groups, also FMQ
MFR	Melt flow rate
MI	Melt index
MIPS	Medium-impact-strength polystyrene
MMA	Methyl methacrylate (monomer)
MMA-MAc-EA	Copolymer of methyl methacrylate, methacrylic acid, and ethyl acrylate
MMBA	Copolymer from methyl methacrylate and butyl acrylate
MMBA-TPT	Copolymer from methyl methacrylate, butyl acrylate, diallyl maleate, and trimethylol propane triacrylate
MMEA	Methyl methacrylate-ethyl acrylate copolymer
MMMA	Methyl methacrylate-methyl acrylate copolymer
MMPMI	Methyl methacrylate-co-*N*-phenylmaleimide copolymer
MMS	Copolymer from methyl methacrylate and α-methyl styrene
MMVAc	Methyl methacrylate-vinyl acetate copolymer
MMVAc-AA	Copolymer of methyl methacrylate, vinyl acetate, and acrylic acid
MMW	Medium molecular weight
MPC	Tetramethyl polycarbonate (also TMPC, TMBPA-PC)
MPF	Melamine-phenol-formaldehyde resin
MPQ	Silicone rubbers having both methyl and phenyl substituent groups, also PMQ
MPR	Melt-processable rubber poly(α-methyl styrene)

M-PVC	Polymerized in bulk polyvinyl chloride
MPVQ	Silicone rubbers with methyl, phenyl, and vinyl groups, also PVMQ
MQ	Elastomeric silicones with methyl substituents
MSABS	Methylstyrene-styrene-acrylonitrile-grafted polybutadiene
MSAN	Thermoplastic copolymer from α-methyl styrene and acrylonitrile
MSMA	Copolymer of methyl methacrylate, *p*-methyl-styrene, and maleic anhydride
MVQ	Silicone rubbers having both methyl and vinyl substituent groups, also VMQ
MWR	Molding with rotation
n-C$_6$	n-Hexane
n-C$_7$	n-Heptane
n-C$_{10}$	n-Decane
NBR	Elastomeric copolymer from butadiene and acrylonitrile, nitrile rubber
NC	Cellulose nitrate, also CN
NCR	Elastomeric copolymer from acrylonitrile and chloroprene
NDPE	Low-density polyethylene (see also LDPE)
NIR	Elastomeric copolymer from acrylonitrile and isoprene
NK	Natural rubber, also NR
NP	Network polymer
NR	Natural rubber, also NK
OEP	Oil-extended polymer
OPET	Oriented polyethyleneterephthalate
OPP	Oriented polypropylene, film, or bottles, also PP
OPR	Elastomeric polymer from propylene oxide
OPS	Oriented polystyrene films
OPVC	Oriented polyvinyl chloride
OSA	Olefin-modified styrene-acrylonitrile copolymer
P3FE	Poly(trifluoroethylene)
PA	Polyamide; the abbreviation PA is normally followed by a number, a combination of numbers, a letter, or a combination of letters and numbers. A single number refers to the polyamide from an α,ω-amino acid or its lactam. A combination of two numbers is often separated by a comma. The first number following the symbol PA indicates the number of methylene groups of aliphatic diamines and the second number the number of carbon atoms of aliphatic dicarboxylic acids. An I stands for isophthalic acid and a T for terephthalic acid. For example, co-polyamide from caprolactam, hexamethylenediamine condensed with isophthalic and terephthalic acids

	is abbreviated as PA-6IT6, or that from caprolactam, m-xylylenediamine, and adipic acid as PA-mXD6, etc.
PA-6	Poly-ε-caprolactam
PA-46	Poly(tetramethylene adipamide), also PTA
PA-66	Poly(hexamethylenediamine-adipic acid), polyhexa-methylene adipamide
PA-6IT6	Poly(caprolactam-co-hexamethylenediamine-isophthalic and terephthalic acids)
PAA	Polyacrylic acid
PAAE	Polyarylamide-polyether
PAAM	Polyacrylamide
PABM	Polyaminobismaleimide
PAC	Polyacrylonitrile fiber (also PAN), polyacrylate
PACE	Polyacetylene
PADC	Poly(allyl diglycol carbonate)
PAE	Polyarylether
PAEB	Poly(*p*-aminoethyl benzoate)
PAEI	Polyacrylic ester imide
PAEK	Polyaryletherketone
PAES	Polyarylethersulfone
PAI	Polyamide-imide
PAK	Polyester alkyd
PALL	Polyallomer – a block copolymer of propylene, ethylene (1.5 to 3%), butene (8%), and hexene (5%)
PAMS	Poly-α-methyl styrene
PA-mXD	Poly(*m*-xylylene adipamide)
PA-mXD6	Poly(*m*-xylylenediamine and adipic acid-co-caprolactam)
PAN	Polyacrylonitrile
PANI	Polyaniline
PAPA	Polyazelaic polyanhydride
PAPI	Polymethylenepolyphenylene isocyanate, also PMPPI
PAr, PAR	Polyarylate $[-\varphi\text{-}C(CH_3)_2\text{-}\varphi\text{-}CO_2-\varphi\text{-}CO_2\text{-}]_n$, amorphous polyester of bisphenol-A with isophthalic and terephthalic acids
PARA	Polyaryl amide (aromatic, usually amorphous polyamide)
PARS	Polyaryloxysiloxane
PArSi	Poly(aryloxysiloxane), e.g., poly(dimethylsiloxane biphenylene-oxide)
PAS	Polyarylsulfide copolymers (esp. in German and Japanese literature)
PAS, PASU	Polyarylsulfone $[-\varphi\text{-}SO_2\text{-}\ \varphi\text{-}O-]_{0.875}\ [-\varphi\text{-}O-]_{0.125}$
PAT	Polyaminotriazole, also polyarylterephthalate, aromatic LCP polyester
PAUR	Polyester urethane
PB	Poly-1-butene, polybutylene, elastic polydiene fiber

PBA	Polybutylacrylate, also poly(1,4- benzamide)
PBAN	Poly(butadiene-co-acrylonitrile)
PBCD	Poly(butylene cyclohexane dicarboxylate)
PBD	Polybutadiene
PBE	Poly(1-butene-co-ethylene)
PBG	Polybutylene glycol, also known as polytetrahydrofuran, PTHF
PBI	Polybenzimidazoles
PBMA	Poly-*n*-butyl methacrylate
PBMI	Polybismaleimide
PBN	Poly(butylene-2,6-naphthalene dicarboxylate)
PBNDC	Poly(butylene-2,5-naphthalene dicarboxylate)
PBO	Polybutylene oxide
PBR	Copolymer from butadiene and vinyl pyridine
PBS	Copolymer from butadiene and styrene (see also GR-S, SBR)
PB-SMA	Styrene-maleic anhydride-grafted polybutadiene
PBT, PBTP	Polybutyleneterephthalate
PBT-PBG	Copolymer of 1,4-butanediol- polybutylene glycol-terephthalic acid
PBZ	Polybenzobisoxazole
PBzMA	Poly(benzyl methacrylate)
PBZT	Poly(p-phenylenebenzobisthiazole)
PC	Polycarbonate of bisphenol-A
PCA	Polycarbonate-acrylic
PCD	Polycarbodiimide
PCDP	Polydicyclopentadiene
PCDT	Poly(1,4-cyclohexylene dimethylene terephthalate)
PCE	Polycycloenes
PCF	Polychlorotrifluoroethylene fiber
PCHMA	Polycyclohexyl methacrylate
PCI	Poly(1,4-cyclohexylenedimethylene isophthalate)
PCME	Poly(2,2-dichloro- methyltrimethylene ether)
PCN	Poly(2-cyano-5-norbornene)
PCO	Polycycloolefin
PC-Ph	Co-polycarbonate from phosgene with bisphenol-A and phenolphthalein
PCT, PCTG	Poly(cyclohexane terephthalate- glycol), copolymer of cyclohexanedimethanol (66 mol%), ethylene glycol, (34 mol%), and terephthalic acid
PCTFE	Polychlorotrifluoroethylene (also CEM, CFM, CTFE)
PCU	Polyvinyl chloride (old German literature)
PDAP	Polydiallylphthalate (also DAP, FDAP)
PDCP	Polydicyclopentadiene
PDMDPhS	Poly(dimethyl-diphenylsiloxane)

PDMS	Polydimethylsiloxane
PDPS	Polydiphenylsiloxane
PE	Polyethylene
PEA	Polyetheramide
PEAc	Polyethylacrylate
PEB	Polyethylene-*p*-oxybenzoate
PEBA	Thermoplastic elastomer, polyether block amide
PEC	Polyestercarbonate or chlorinated polyethylene, usually CPE
PeCe	Chlorinated PVC (also CPVC, PC, PVCC)
PECO	Polyethylene carbonate
PEE	Polyester ether fibers (containing diol and *p*-hydroxy benzoate units, e.g., polyethylene-*p*-oxybenzoate
PEEI	Polyesteretherimide
PEEK	Polyetheretherketone
PEG	Polyethyleneglycol
PEH	High-density polyethylene, also HDPE
PEI	Polyetherimide
PEIE	Polyetherimide ester copolymer
PEIm	Polyetherimine
PEK	Polyetherketone
PEKEKK	Poly(ether-ketone-ether-ketone-ketone)
PEL	Low-density polyethylene, also LDPE
PEM	Medium-density polyethylene, also MDPE
PENDC, PEN	Poly(ethylene 2,6-naphthalene dicarboxylate) or polyethylenenaphthalate
PENi	Polyethernitrile
PEO	Polyethylene glycol, usually PEG
PEOX	Poly(2-ethyl-2-oxazoline)
PEP	Thermoplastic copolymer from ethylene and propylene
PEPA	Polyether-polyamide copolymer
PES	Polyethersulfone $[-\varphi\text{-}SO_2\text{-}\varphi\text{-}O\text{--}]_n$
PEsA	Polyesteramide
PESK	Polyarylenethioetherketone
PEST	Thermoplastic polyesters, e.g., PBT, PET, also TPES
PET, PETP	Polyethyleneterephthalate
PETG	Polyethyleneterephthalate glycol, copolymer with 66 mol% ethylene glycol and 34 mol% cyclohexylene dimethanol
PEtI	Polyethyleneimine
PEUR	Polyether urethane
PF	Phenol-formaldehyde resin
PFA	Polyfluoroalcoxyalkane, copolymer of tetrafluoroethylene and perfluorinated
PFEP	Copolymer from tetrafluoroethylene and hexa-fluoro propylene, also FEP

PFF	Phenol-furfural resin
PG	Poly-α-hydroxy acrylic acid
PGI	Polyglutarimide
PH	Phenolics
PHB, POB	Poly(p-hydroxybenzoic acid)
PHBA	Poly(β-hydroxybutyric acid)
PHEMA	Poly-2-hydroxyethyl methacrylate
PHIT	Poly(hexylene-isophthalate-terephthalate)
PHMT, PHT	Polyhexamethylene terephthalate PHP Physiological hydrophilic polymers PhPS Poly(p-phenyl styrene)
PHP	Physiological hydrophilic polymers
PhPS	Poly(p-phenyl styrene)
PHT, PHMT	Polyhexamethylene terephthalate
PHZ	Polyphosphazene
PI	Polyimide but also *trans*-1,4- polyisoprene, gutta-percha (UK)
PIAN	Isoprene – acrylonitrile oil-resistant elastomer
PIB	Polyisobutene
PIBI	Copolymer from isobutene and isoprene, butyl rubber (also butyl, GR-I, IIR)
PIBO	Polyisobuteneoxide
PIP	Synthetic *cis*-1,4-polyisoprene (also CPI, IR)
PIPO	Polyimidazipyrolone
PIR	Polyisocyanurate (foam) PIS Polyisobutylene
PISU	Polyimidesulfone
PL	Polyethylene (EWG), also PE
PLA	Polylactic acid
PMA	Polymethyl acrylate
PMAC	Polymethoxy acetal
PMAN	Polymethyl acrylonitrile
PMB	Poly-methylenebenzoate
PMCA	Polymethyl-α-chloro acrylate
PMI	Polymethacrylimide
PMMA- GMA	Poly(methyl methacrylate-co-glycidyl methacrylate)
PMMA	Polymethyl methacrylate
PMMA-MA	Poly(methyl methacrylate-co-acrylic acid)
PMMI	Polypyromellitimide
PMP	Poly-4-methyl-1-pentene (see also TPX)
PMPhS	Polymethylphenylsiloxane
PMPPI	Polymethylenepolyphenylene isocyanate, also PAPI
PMQ	Silicone rubbers with methyl and phenyl substituents
PMS	Poly-α-methyl styrene
PNA	Polynuclear aromatics
PNF	Polyfluoroalcoxyphosphazene
PNR	Polynorbornene rubber

PO	Polyolefin but also elastomeric polypropylene oxide and phenoxy resin
POB, PHB	Poly-*p*-hydroxy benzoate
POBA	Polyoxybenzoyl acid, rigid-rod polymer
POBI	Polyoxadiazobenzimidazole
POCA	Poly(oxy(cyanoarylene)) or polyoxycyanoarylene
POD	Polyoctadecene
PODZ	Poly(*p*-phenylene 1,3,4-oxadiaxole)
POM	Polyoxymethylene, polyformaldehyde, polyacetal, or "acetal resin"
POMA	Poly(oxetane methacrylate)
POP	Polyoxypropylene, usually PPG
POR	Elastomeric copolymer from propylene oxide and allyl glycidyl ether
POT	Polyoctyl thiophene
PP	Polypropylene or oriented polypropylene (see also OPP)
PPA	Polyphthalamide, also polypropyleneadipate
PPAc	Polypropyl acrylate
PPBA	Polyparabanic acid
PPC	Chlorinated polypropylene
PPC	Polyphthalate-carbonate, High heat PC with HDT $= 160°C$
PPCA	Poly(polycyclic (meth)acrylate)
PPD-T, PPTA	Poly(*p*-phenylene terephthalamide) Kevlar™
PPE	Poly(2,6-dimethyl 1,4-phenylene ether) (see also PPO)
PPeA	Poly(*n*-pentyl acrylate)
PPE-MA	Maleic anhydride-modified poly(2,6-dimethyl 1,4-phenylene ether)
PPG	Polypropylene glycol
PPhA	Polyphthalamide
PPI	Polymeric polyisocyanate
PP-MA	Maleic anhydride-modified polypropylene
PPMA	Poly(phenyl methacrylate)
PPMS, PpMS	Poly(*para*-methyl styrene)
PPO	GE Co., Polymer Products Operation, trade name for poly (2,6-dimethyl 1,4-phenylene ether) (see PPE)
PPOEA	Poly(phenoxyethoxyethyl acrylate)
PPOX, PPO	Polypropylene glycol, usually PPG
PPP	Poly-*p*-phenylene
PPR	Polypyrrole
PPrA	Poly(*n*-propyl acrylate)
PPS	Polyphenylsulfide
PPSK, PKS	Polyketonesulfide $[-φ-S-φ-CO-]_n$
PPSS	Polyphenylenesulfidesulfone
PPS-S	polythioethersulfone

PPSU, PSF, PSO	Polyphenylene sulfone, polysulfone
PPT, PPTP	Polypropyleneterephthalate; (see also PTT)
PPTA, PPD-T	Poly(1,4-phenylene terephthalamide)
PPX	Poly(*p*-xylylene)
PPy	Polypyrrole
PPZ	Polyorganophosphazene
PQ	Elastomeric silicone with phenyl substituents
PS	Polystyrene
P-S, PSA	Pressure-sensitive adhesive
PSAB	Copolymer from styrene and butadiene (also SB, S/B)
PSAN	Thermoplastic copolymer from styrene and acrylonitrile, also SAN
PSB	Styrene-butadiene rubber, also GS-R, SBR
PSBR	Elastomeric terpolymer from vinyl pyridine, styrene, and butadiene
PSF	Polysulfone, also PSUL, PSU, PSO
PS-GMA	Styrene-glycidyl methacrylate copolymer
PSI	Polymethylphenylsiloxane
PSL	Polyspirodilactone
PS-MA	Styrene-maleic anhydrite copolymer
PSO	Polysulfone, also PSUL, PSU, PSF
PSOX	Styrene polymer having reactive (2-oxazoline) groups
PST	Polystyrene fiber with at least 85% styrene units
PS-TSG	Polystyrene foam, processed by injection (German literature)
PSU	Polysulfone $[-\varphi\text{-}SO_2\text{-}\varphi\text{-}O\text{--}\varphi\text{-}C(CH_3)_2\text{-}\varphi\text{-}O\text{--}]_n$
PSUL	Polysulfone, also PSF, PSU, PSO
PS-VPh	Poly(styrene-b-vinyl phenol) block copolymer
PTA	Polytetramethylene adipamide
PTF	Polytetrafluoroethylene fiber
PTFE	Polytetrafluoroethylene (also TFE)
PTHF	Polytetrahydrofuran [also known as polybutylene glycol, PBG]
PTMA	Polytetramethyleneadipate
PTMC	Poly(trimethylene carbonate)
PTMEG	Poly(tetramethylene ether glycol)
PTMG	Polytetramethylene glycol
PTMT	Poly(tetramethylene terephthalate) or polybutyleneterephthalate, PBT
PTO	Polytransoctanylene
PTR	Polysulfide rubber
PTT	Poly(trimethylene terephthalate), also PPT
PU, PUR	Polyurethane elastomer
PVA	Polyvinyl acetal
PVAc, PVAC	Polyvinyl acetate

PVAl, PVAL	Polyvinyl alcohol
PVBO	Polyvinyl butyral
PVBu	Polyvinyl butyrate
PVC	Polyvinyl chloride
PVCA, PVCAc	Copolymer from vinyl chloride and vinyl acetate
PVCC	Chlorinated PVC, also CPVC, PeCe
PVC-DC	Poly(vinyl chloride-co-vinylidene chloride)
PVD	Polyvinylidene chloride fiber with 50 wt% vinylidene chloride
PVDC	Polyvinylidene chloride, also PVC_2
PVDF	Polyvinylidene fluoride, also PVF_2
PVE	Polyvinylethylene
PVF	Polyvinyl fluoride
PVFM, PVFO	Polyvinyl formal
PVI	Poly(vinyl isobutyl ether)
PVID	Polyvinylidenecyanide
PVIE	Polyvinyl isobutyl ether
PVK	Poly-*N*-vinylcarbazole
PVM	Copolymer from vinyl chloride and vinyl methyl ether
PVME	Polyvinyl methyl ether
PVMQ	Silicone rubber with methyl, phenyl, and vinyl substituents
PVOH	Polyvinyl alcohol (also PVAL, PVAl)
PVP	Poly-*N*-vinylpyrrolidone
PVPh	Poly(4-vinylphenol), poly(*p*-hydroxy styrene)
PVSI	Polydimethylsiloxane with phenyl and vinyl substituents
PY	Unsaturated polyester resins, also UP
Q	Silicone elastomer
QA	Quality assurance
QC	Quality control
QDS	Quality data statistics
QMC	Quick molding change
RAM	Restricted area molding
RCF	Refractory ceramic fiber
REX	Reactive extrusion
RF	Resorcinol-formaldehyde resin
RH	Relative humidity (in %)
RHB	Reheat blow molding
RIM	Reaction injection molding
RLM	Reactive liquid polymer
RMPS	Rubber-modified polystyrene
RP, RTP	Reinforced plastics, reinforced thermoplastic, also RP/C
RPBT	Reinforced polybutyleneterephthalate
RPET	Reinforced polyethyleneterephthalate
RPVC	Rigid PVC film

RRIM	Reinforced reaction injection molding
RTD	Residence time distribution
RTM	Resin transfer molding
RTP	Reinforced thermoplastic
RTPO	Reactor-blended thermoplastic olefinic elastomer
RTS	Reinforced thermoset
RTV	Room temperature vulcanization (of silicone rubber)
RUC	Chlorinated rubber
SAA	Styrene-acrylic acid copolymer
SAMA	Styrene-acrylonitrile-methacrylic acid copolymer
SAN	Styrene-acrylonitrile
SAN	Thermoplastic copolymer from styrene and acrylonitrile, also AS, PSAN
SANGMA	Styrene-acrylonitrile-glycidyl methacrylate copolymer
SANMA	Styrene-acrylonitrile-maleic anhydride copolymer
SAXS	Small-angle X-ray scattering
SB, SBR	Thermoplastic copolymer from styrene and butadiene, also PASB, S/B
SB/BA	Styrene-butadiene-butyl acrylate copolymer
SBCL	Styrene-butadiene-caprolactone copolymer
SBMA	Styrene-butadiene-maleic anhydride copolymer
SBMI	Styrene-butadiene-maleimide
SBP	Styrene-butadiene polymer
SBR	Styrene-butadiene elastomer
SBS	Styrene-butadiene-styrene
SBS	Styrene-butadiene-styrene triblock polymer
SCR	Elastomeric copolymer from styrene and chloroprene
SEBS	Styrene-ethylene/butylene-styrene triblock polymer
SEM	Scanning electron microscopy
SEP	Styrene-ethylene-propylene block copolymer
S-EPDM	Sulfonated ethylene- propylene-diene terpolymer
SF, SFM	Structural foam, structural foam molding
SFK	Synthetic fiber reinforced plastic (German literature)
SFP	Scrapless forming process
SHIPS	Super-high-impact polystyrene
SI	Thermoplastic silicone
SIN	Simultaneous interpenetrating network or semi-interpenetrating network
SIPN	Sequential interpenetrating polymer network
SIR	Elastomeric copolymer from styrene and isoprene
SIS	Styrene-isoprene-styrene triblock polymer
SMA	Copolymer from styrene and maleic anhydride
SMAA	Copolymer from styrene and methacrylic acid
SMA-AA	Styrene-maleic anhydride-acrylic acid copolymer

SMC	Sheet molding compound
SMI	Copolymer from styrene and maleimide
SMMA, SMM	Styrene-methyl methacrylate copolymer
SMM-GM	Styrene-methyl methacrylate- glycidyl methacrylate copolymer
SMM-MA	Styrene-methyl methacrylate-maleic anhydride copolymer
SMS	Copolymer from styrene and α-methyl styrene
SP	Saturated polyester plastics
SPC	Statistical process control
sPP	Syndiotactic polypropylene
SPPF	Solid-phase pressure forming
SPSF	Solid-phase stretch forming
S-PVC	Suspension PVC
SR	Synthetic rubber, polysulfide rubber
SRIM	Structural reactive injection molding
SRP	Styrene-rubber plastics
SSE	Single-screw extruder
SVA	Styrene-vinyl-acrylonitrile copolymer
SVPh	Styrene-*p*-vinyl phenol copolymer
SWP	Solvent-welded plastics pipe
TA	Cellulose triacetate, also CT, CTA
TC	Technically classified natural rubber
TCE	Tetrachloroethane
TDI	Toluene di-isocyanate
TE	Thermoplastic elastomer of any type
TEEE	Thermoplastic elastomer, ether-ester
TEO	Thermoplastic elastomer, olefinic
TES	Thermoplastic elastomer, styrenic
TFE	Polytetrafluoroethylene (also PTFE)
TGA	Thermogravimetric analysis
TGIC	Triglycidyl isocyanurate
THF	Tetrahydrofuran (solvent)
TM	Thioplasts, transfer molding
TMA	Thermomechanical analyzer
TMBA-PC	Tetramethyl bisphenol-A polycarbonate (or MPC, TMPC)
TMC	Thick molding compound
TMPC	Tetramethyl bisphenol-A polycarbonate (TMBPA-PC)
TOR	*Trans*-polyoctenamer rubber TP Thermoplastic
TPA, TPR	1,5-*trans*-polypentenamer
TPE, TPEL	Thermoplastic elastomer
TPE-A	Thermoplastic elastomer-amide
TPE-E	Thermoplastic elastomer-ester
TPE-S	Thermoplastic elastomer-polystyrene
TPES	Thermoplastic polyesters, e.g., PBT, PET (see also PEST)

TPI	Thermoplastic polyimide
TPO	Thermoplastic olefinic elastomer
TPS	Toughened PS (in the UK for HIPS)
TPU, TPUR	Thermoplastic urethanes
TPV	Thermoplastic vulcanizate
TPX	Poly(4-methyl-1-pentene) (see also PMP)
TR	Thermoplastic elastomer or thio rubber (UK)
TREF	Temperature-rising elution fractionation
TS	Thermoset
TSE	Thermoset elastomer
TSI	Thermoset polyimide
TSUR	Thermoset polyurethane
UE	Polyurethane elastomer
UF	Urea-formaldehyde resin
UFS	Urea-formaldehyde foam
UHMW-PE	Ultrahigh molecular weight polyethylene (over 3 Mg/mol)
ULDPE	Ultralow-density polyethylene (ca. 900–915 kg/m^3)
UP	Unsaturated polyester
UP-G-G	Prepreg from unsaturated polyesters and textile glass fibers
UP-G-M	Prepreg from unsaturated polyesters and textile glass mats
UP-G-R	Prepreg from unsaturated polyesters and textile glass rovings
UPVC	Unplasticized PVC
UR	Polyurethane elastomers, also UP
VAc	Vinyl acetate
VAc-AN	Copolymer from vinyl acetate and acrylonitrile
VAcE	Vinyl acetate-ethylene copolymer
VC/E, VCE	Vinyl chloride-ethylene copolymer
VCE	Copolymer from ethylene and vinyl chloride
VCEMA	Copolymer from vinyl chloride, ethylene, and methyl acrylate (or maleic anhydride)
VCEV	Copolymer from vinyl chloride, ethylene, and vinyl acetate
VCM	Vinyl chloride (monomer), also VC
VCMA	Copolymer from vinyl chloride and methyl acrylate
VCMMA	Copolymer from vinyl chloride and methyl methacrylate
VCOA	Copolymer from vinyl chloride and octyl acrylate
VCVAc	Copolymer from vinyl chloride and vinyl acetate
VCVDC	Copolymer from vinyl chloride and vinylidene chloride
VDC	Vinylidene chloride
VDC/AN	Copolymer from vinylidene chloride and acrylonitrile
VF/HFP	Copolymer from vinylidene fluoride and hexa-fluoro propylene
VLDPE	Very low-density polyethylene (ca. 885 kg/m^3)
VMQ	Silicone rubber with methyl and vinyl substituents
VOC	Volatile organic compound

VPE	Vulcanized (cross-linked) polyethylene, also XLPE
VQ	Elastomeric silicone with vinyl substituents
VSI	Polydimethylsiloxane with vinyl groups
WAXS	Wide-angle X-ray scattering
WR	Woven rovings
XABS	Acrylonitrile-butadiene-styrene/acidic monomer, an elastomeric copolymer
XLPE	Cross-linked polyethylene
XMC	Extra-strength molding compound
XNBR	Acrylonitrile-butadiene/acidic monomer, an elastomeric copolymer
XPS	Expandable or expanded PS
XSBR	Butadiene-styrene/acidic monomer, an elastomeric copolymer
YBPO	Elastomeric polyetherester: $[((CH_2)_4\text{-}O)_n\text{-}CO\text{-}\phi\ CO\text{-}O\text{-}]_m$
YSBR	Thermoplastic, elastomeric block copolymer from styrene and butadiene
YXSBR	Block copolymer from styrene and butadiene containing carboxylic groups

Note: This list is based on the nomenclature proposed by diverse standardizing organizations, as well as on the acronyms used in technical literature, viz., American Society for Testing Materials, Standard Terminology for Abbreviated Terms Relating to Plastics, ASTM D1418-01a, ASTM D1600-99, and their referenced standards; British Standards, schedule of common names, and abbreviations for plastics and rubbers, BS 3502–1978; Deutsches Institut für Normung, plastics, symbols and codes for polymers and their special characteristics, DIN 7728 Teil 1 01.88; symbols for reinforced plastics, DIN 7728 Teil 2 03.80; plastics molding materials DIN 7742 Teil 1 01.88; molding techniques for molding materials, definitions, DIN 16700 09.67; Association Française de Normalisation, plastics, vocabulary, T 50–100 08.90; plastics, symbols, T 50-050-1, T 50-050-2, T 50-050-3 06.89; International Organization for Standardization, plastics, symbols, ISO 1043–1; 1987, ISO 1043–2; 1988, ISO 1043–3; International Union for Pure and Applied Chemistry, Pure Appl. Chem. **18**, 583 (1969); Pure Appl. Chem. **40**, 473 (1974).

Appendix II: Examples of Commercial Polymer Blends

	Polymer				
No.	A	B	Name	Supplier	Comments
1.	PS	PB(BR) or PE	Hostyren	Hoechst	The blends are formulated for extrusion, injection and blow molding
			Limera R	Dainippon Ink and Chemicals	They show excellent processability, low moisture absorption and shrinkage, improved impact strength. Composition-dependent modulus, toughness, ductility, transparency, and gloss
			Polysar	Bayer Miles	
			Polystyrol	BASF AG	
			Styroblend	BASF AG	
			Styroplus	BASF AG	
2.	ABS or ASA	Elastomer or SMA*	Cadon*	Monsanto Chem.	Blends of ABS or ASA with either acrylic rubber (800) or PB (900 series) were formulated for extrusion, thermoforming, injection, and blow molding. They show excellent processability, weatherability, impact strength, HDT, scratch resistance, paintability, and plateability
			Centrex	Monsanto Chem.	
			Luran S	BASF AG	
			Magnum	Dow Chem. Co.	
			Rovel	Uniroyal	
			Starflam ABS	Ferro Plastics	
			Terluran	BASF AG	

No.	Polymer A	B	Name	Supplier	Comments
3.	TPU	ABS	Prevail	Dow Chem. Co.	The blends can be injection molded, extruded, blow molded, or thermoformed. Transfer or compression molding, calendering, and solid state may also be used. They show hardness between that of TPU and ABS, superb toughness, chemical resistance, appearance
			Techniace TU	Sumitomo Dow	
4.	LDPE	PIB	Lupolen O 250	BASF AG	The 1:1 blends are flexible and resistant to cracking under stress and show good water-vapor properties. The blends are formulated for extrusion, injection, and blow molding. The weld-line strength, resistance to warpage, and shrinkage depend on processing conditions
			Pax-Plus	Paxon Polymer Co.	
5.	NBR	EPDM or CPE or PVC	Geolast JSR NE *	Monsanto JSR	The blends are formulated for extrusion, calendering, injection, and blow molding. They have either co-continuous or (less frequently) dispersed morphology. They show good processability; ozone, oil, and heat resistance; low compression set; low-temperature flexibility; nearly total elastic recovery; and excellent weather resistance. Principal use includes automotive weather stripping, interior moldings, tubings, hoses, seals, gaskets, expansion joints, cable sheathings, conveying belts, roofing, pond liners, geomembranes, floorings, etc.
			Chemigum TPE[#]	Goodyear Tire & Rubber Co.	
			Krynac NV	Polysar, Inc.	
			[#]Nipol	Nippon Zeon	
			[#]Paracril OZO	Uniroyal Chemical	

	Polymer				
No.	A	B	Name	Supplier	Comments
6.	PP	TPO or EPR or EPDM	BK 891	Mitsui Chemical	The blends are formulated mainly for injection molding, but they can also be extruded, thermo- or vacuum-formed (e.g., Optum), compression or transfer molded, calendered, and blow molded. Several have dynamic properties, viz., hardness and heat resistance. Some blends are vulcanized, showing toughness, and are composition dependent (30 wt%) (e.g., Kelburon) and reactor made. Reinforced and filled grades (containing glass fiber, talc, $CaCO_3$, or mineral filler) are available. These blends show good processability, low-temperature modulus and impact strength, dimensional stability, low shrinkage, good mechanical properties at temperatures from −40 to 150 °C, ozone resistance, dynamic fatigue and abrasion resistance, as well as high good weather ability (especially carbon-black filled grades) tear strength and paintability. Over 200 applications have been found for these materials, e.g., they are used in appliances, hardware and plumbing, automotive industry (arm rests, pillar trim, door panels, radiator grilles, dashboards, children seats, side protectors, bumpers, spoilers), etc.
			Deflex	A. Schulman	
			Dynaflex	JSR	
			Ferrolene	Ferro Plastics	
			Ferro Flex	Ferro Plastics	
			HiFax	Himont Adv. Mat.	
			Hostalen PP	Hoechst	
			IPCL JSA1986	IPCL	
			Kelburon, Keltan TP	DSM Polymer International	
			Milastomer	Mitsui Petrochem.	
			Modylen	Tiszagi Vergi Kom.	
			Moplen SP	Himont	
			Oleflex	Showa Denko Co.	
			Optum	Ferro Plastics	
			Polytrope	A. Schulman, Inc.	
			Propathene	ICI	
			PU-21713	Ferro Plastics	
			RPI 507 EP	Research Polym.	
			RxLOY	Ferro Plastics	
			Santoprene	Monsanto	
			Sarlink	Novacor	
			Sumitomo TPE	Sumitomo Chem.	
			Thermolan 2000	Mitsubishi Petrochemicals	
			TPO 900	Reichhold Chem.	
			Vestolen EM	Hüls A.-G.	

	Polymer				
No.	A	B	Name	Supplier	Comments
7.	PVC	Acrylics	Acrylivin	General Tire & Rubber	Suspension PVC modified by 5–15 wt% acrylic elastomer. The blends are are formulated for extrusion, injection, and blow molding, vacuum- or thermoforming, and calendering. They show high impact strength, rigidity, resilience, dimensional stability, flame retardancy, excellent outdoor performance, and good flame, abrasion, electrical, chemical, and solvent resistance. These blends are used in industrial, commercial, consumer (e.g., as wall coverings, corner guards, column covers, shelving, counter laminates, ceiling tiles), medical, food or beverage equipment, aircraft or mass transit interior components, and applications requiring good resistance to weathering
			Cladux	R. Daleman	
			Decoloy	GE Plastics	
			Fiberloc HTX	The Geon Company	
			Haibulen	Nippon Zeon	
			Kane-ace	Kanegafuchi Chem.	
			Kydex	Rohm and Haas	
			Metabulen	Mitsubishi Rayon	
			Polycast	Royalite	
			Sunloid KD	Tsutsunaka	
			Vinidur	BASF AG	
8.	PVC	NBR	Carloy	Cary Chem. Inc.	These blends (containing 30–60 wt% PVC) are formulated mainly for extrusion and calendering, but injection, blow, compression, and transfer molding can also be used. They show good processability, fast calendering and extrusion, impact and tear strength, and oil, fuel, improved chemical, abrasion, weathering, ozone, antistatic, flame, and moisture resistance. Their applications include cables and hoses, printing plates and rollers, shoe soles, bottles for cosmetics and edible oils, profiles, etc.
			Geon/Hycar	B. F. Goodrich	
			Denka LCS	Showa Denko Co.	
			JSR NV	Jap. Synth. Rub.	
			Krynac NV	Miles-Polysar	
			Nipol	Nippon Zeon	
			Oxyblend	OxyChem	
			Paracril OZO	Uniroyal Chem.	
			Vynite	Alpha Chem. Plast.	

No.	Polymer A	B	Name	Supplier	Comments
9.	PVC	ABS or ASA*	Abson 042	Abtec Chem. Co.	These blends are formulated for injection molding, extrusion, and thermo-or vacuum forming, but calendering can also be used. The blends show superior processability to component polymers, impact strength, flame retardance, and cost-to-performance ratio. The blends with ASA show superior weatherability, while those containing SMA high HDT. The main use is for business machines, electrical and electronic equipment housings, automotive applications, swimming pool fittings, irrigation, etc.
			Cycovin K-29	The Geon Co.	
			Denka Taimel.	Denki Kagaku	
			*Geloy XP2003	GE Plastics	
			Kaneka Enplex	Kanegafuchi Corp.	
			Kralastic	Uniroyal/Sumitomo	
			Lustran ABS 860	Monsanto Chem.	
			Nipeon AL	Zeon Kasei Co.	
			Polyman 500	A. Schulman, Inc. DSM	
			Ronfaloy V	DSM	
			Tufrex VB	Mittsubishi	
			Triax CBE (discontinued)	Monsanto Chem.	
10.	PA-6		Grilon BT	EMS-Chemie	Miscible blends show improved processability, solvent resistance, elongation, low-temperature impact and tensile strength
		PA	Wellamid MR	Wellman, Inc.	
			Zytel 3100	E. I. du Pont	
11.	PA	PA	Akuloy RM	DSM Eng. Plast.	The blends are formulated mainly for injection molding and extrusion. Polyamides PA-6, PA-66, PA-mXD6, and PARA. In most blends PA is the matrix phase, but those with PP as a matrix are also available (e.g., from Solvay). The blends show good processability; reduced water absorption; dimensional stability; low density (i.e., low cost per volume); low liquid and vapor permeability; moderate impact strength; good resistance to alcohols, glycols, and gasohol; improved heat aging; primer-less paintability; and resistance to cracking when exposed to metal halides (e.g., CaCl$_2$). Some grades are reinforced. Principal blend uses include appliances, automotive, tools, building, furniture, and industrial
			Dexpro, Dexlon	Dexter Corp.	
			Eref	Solvay	
			Flexloy	Sumitomo Chem.	
			Gapex	Ferro Plastics	
			LAX 23	Ube, Inc.	
			MCX-Q	Mitsui Petrochem.	
			NB	Toyobo	
			Novamid AC	Mitsubishi Chem.	
			Orgalloy R-6	Atochem	
			Poliblend NH	Poliresins SA	
			Snialoy	Nylon Corp. Amer.	
			Systemer S	Showa Denko Co.	
			Thermocomp	LNP	
			Ube Alloy CA	Ube Inc.	
			Ultramid KR	BASF AG	
			UTX	Unitika	

No.	Polymer A	B	Name	Supplier	Comments
12.	PA-6, P PA-66, PARA, or PA-666	E, EPR, acrylic elastomers, or ionomers	Albis	Albis Plastics	The blends are formulated for extrusion, co-extrusion, injection, compression, transfer, and blow molding. They can also be thermoformed. Grades containing up to 40 wt% mineral or glass fibers are available. Some may contain PTFE. The blends have good processability, low-temperature impact strength, rigidity, stiffness, high heat resistance, lower service temperature. The molded articles can suppress vibration, even when dry and at sub-zero temperatures. The blends find use in a broad range of applications, viz., automotive (stone and splash guards, under-the-hood moldings, seals, hoses, tubes, clips, fasteners, fuel doors, gears), appliances, sport (e.g., ski bindings, roller skates), business equipment, consumer products (office chair seats, housings, casters, wheels, rollers, pulleys, gears), etc.
			Bexloy C	E. I. du Pont	
			Brilion BT-40	Emser Ind.	
			Capron	AlliedSignal	
			Durethan	Bayer A.-G	
			Dynyl	Rhône Poulenc	
			Fiberfil TN	DSM Eng. Plast.	
			Grilon A	EMS-Chem. A.-G.	
			Maranyl	ICI	
			Minlon	E. I. du Pont	
			Nybex	Ferro Plastics	
			Nycoa	Nylon Corp. Amer.	
			Nydur	Bayer A.-G	
			Nylafil	Wilson-Fiberfil Int.	
			Nylon	Celanese Eng. Res.	
			Star X	Ferro Plastics	
			Technyl A and B	Rhône Poulenc	
			Ultramid A, B, C, and T	BASF AG	
			Vydyne	Monsanto Chem.	
			Wellamid 22 L	Wellman Inc.	
			Zytel ST	E. I. du Pont	
			Zytel 300, 400	E. I. du Pont	
13.	PA-66, or PA-6	Brominated PS	Akulon K228	DSM	These fire-resistant, unreinforced blends designed for injection molding or extrusion are used in automotive and electrical applications. They show good flame retardance, mechanical properties, and dimensional stability
			Latamid 66	Lati	
			Starflam PA6	Ferro Plastics	
			Ultramid A3X	BASF AG	
			Zytel FR	E. I. du Pont	

No.	Polymer A	Polymer B	Name	Supplier	Comments
14.	PA-6 or PA-66	ABS	Alphaloy MPA	Kanegafuchi Chem.	The compatibilized blends (with either PA as matrix or co-continuity of both phases) are formulated for injection molding, extrusion, and thermoforming, but blow and compression molding also can be used. The blends show good processability and flow; high heat and chemical resistance; high resistance to oil, wear, and abrasion; dimensional stability; low-temperature impact strength; reduced moisture sensitivity; and economy. Main application is in automotive, chemical, electrical, customer, and sport industries. Some grades are glass fiber reinforced. The material has been also used in anti-vibration damping structures
			Elemid	GE Plastics	
			Diaaloy N	Mitsubishi Rayon	
			Kane ace MUH	Kanegafuchi Chem.	
			Malecca S	Denki Kagaku K.	
			Maxloy A	JSR	
			Monkalloy N	Monsanto Kasei	
			N5	Thermofil Inc.	
			Novaloy-A	Daicel Chem. Ind.	
			Stapron N	DSM Polymer Int.	
			SX	Toray Ind., Inc.	
			Techniace TA	Sumitomo Dow	
			Toyolac alloy	Toray Ind., Inc.	
			Triax 1000	Monsanto	
			Ultramid	BASF AG	
15.	PA	Cyclic - PO	Elmit ZF	Mitsui Petrochemicals	Processability, impact strength, moisture insensitivity
16.	PA	PC	Dexcarb	D & S Int.	Processability, HDT > 200 °C, impact strength, low mold shrinkage, solvent, and moisture sensitivity
			Iupilon	Mitsubishi Gas	
			SC 720	Idemitsu	
			Petrochemicals		
17.	PC	TPU	Texin 3000	Bayer/Miles	PC blends with polyester urethane were designed for extrusion or molding articles used in automotive and consumer goods' industries
			Texin 4000		
18.	PC	Elastomer	Idemitsu SC-150	Idemitsu Petrochemicals	The blends for extrusion or injection molding contain < 6 wt% elastomer (e.g., butyl acrylate-co-methacrylate) and thus are opaque. They show low temperature toughness, high impact strength, good weld-line strength, and HDT
			Makrolon T-78	Bayer/Miles	
			Novarex AM	Mitsubishi Chem.	

No.	Polymer A	B	Name	Supplier	Comments
19.	PC	ABS (and SAN in some blends)	Alphaloy	Kanegafuchi Chem.	The blends are formulated for injection molding, extrusion, and thermo-or vacuum forming, but they can also be compression or transfer molded. They show good processability, excellent plating, HDT and impact strength, high stiffness and strength, dimensional stability, toughness, delamination resistance, low-temperature impact strength, good weld-line strength, and solvent and chemical resistance. These are three-phase blends, with 30–65 wt% PC usually being the matrix. Grades with glass fiber reinforcement are available. The blends are used for housings of computers, business machines and electrical appliances, electrical and electronic parts, connectors, carriages, switches, fans, power and agricul-tural, garden and lawn tools, cameras, optical instruments, exterior automotive components, electronic or telecommunication parts, sporting goods, etc.
			Bayblend T	Bayer/Miles	
			Cycoloy	GE Plastics	
			Denka HS	Denki Kagaku	
			Dialoy C	Mitsubishi Rayon	
			Exceloy	JSR	
			Iupilon MB	Mitsubishi Gas	
			Lynex B	Asahi Chem.	
			Malecca P	Denka	
			Multilon PX	Teijin Chem. Ltd.	
			Novaloy-S	Daicel Chem. Ind.	
			Proloy/Lexan	GE Plastics	
			Pulse	Dow Chem. Co.	
			Ronfalin	DSM	
			Royalite R11	Uniroyal	
			Ryulex	Dainippon	
			SC 250	Idemitsu Petrochem.	
			Techniace TC	Sumitomo Dow	
			Toplex	Multibase, Inc.	
			Terblend B	BASF AG	
			Triax 2000	Monsanto Chem.	
			ABS/PC 7901	Diamond Polymers	
20.	PC	ASA, or AAS*	Baitaloy*	Hitachi Chem. high-	High impact strength, thermal stability, improved resistance to temperature aging and UV degradation, excellent weatherability, rigidity, and dimensional stability. The blends are formulated mainly for extrusion, injection molding, and thermoforming
			Dialoy A	Mitsubishi Rayon	
			Geloy XP4001	GE Plastics	
			Terblend S	BASF AG	
21.	PC	PS	Novadol	Mitsubishi Chem.	Impact strength, thermal stability, and weatherability
			SC 200	Idemitsu Petrochemicals	

No.	Polymer A	B	Name	Supplier	Comments
22.	PC	SMA	Arloy 1000	ARCO Chem. Co.	The blends are designed for extrusion, thermoforming, or injection molding. They show excellent processability, toughness, and heat resistance
			Ektar MB	Eastman Kodak	
			R4 9900	Thermofil Inc.	
23.	PC	PBT or PET or PCTG (and 10–20 wt% impact modifier)	Azloy	Azdel, Inc.	The blends are formulated for injection molding, extrusion, and blow molding, but they can be transfer or compression molded, formed in solid state, or thermoformed. In most blends PC is the matrix phase. The impact modifier can be PE, ABS, or acrylic copolymer, e.g., MBS. The blends show good processability; heat resistance; ductility; HDT; high modulus, impact, tensile, and flexural strength over a wide temperature range; good adhesion; solvent, chemical, and UV resistance. They can be painted, hot stamped, metallized, and plated. Some blends (containing polybutadiene as impact modifier) may have poor weather-ability. The blends are mainly used in automotive industry
			BCT 4201	Toray	
			Defsan	Russia	
			Dialoy P	Mitsubishi Rayon	
			Ektar MB,	Eastman Chemical Company	
			Eastalloy DA (PCTG)	Eastman Chemical Company	
			Idemitsu SC 600	Idemitsu Petrochem.	
			Makroblend	Bayer A.-G.	
			MB4300	Mitsubishi Gas	
			Novadol	Mitsubishi Chem.	
			Pocan	Bayer	
			R2-9000	Thermofil Inc.	
			Sabre	Dow	
			Stapron E	DSM Polymer Int.	
			Ultrablend KR	BASF	
			Valox	GE Plastics	
			Xenoy 1000	GE Plastics	

No.	Polymer A	Polymer B	Name	Supplier	Comments
24.	PET	Elastomer or SMA*	Arloy 2000*	ARCO Chem. Co.	The blends are formulated for extrusion, injection, compression, blow, and transfer molding. The blends contain up to 35 wt% glass fiber. They show good processability, rigidity, impact and tensile strength, as well as excellent weatherability
			Celanex	Celanese Eng. Res.	
			Rynite	E. I. du Pont	
			SC-150	Idemitsu Petrochemicals	
25.	PET or PCTG*	PC (and 15–20 wt% impact modifier)	*Ektar MB	Eastman	These blends can be injection molded or extruded. They are partially miscible, with co-continuous morphology showing improved processability, solvent resistance, elongation, low-temperature impact and tensile strength (possible reduction of crystallinity upon blending) Ektar resins are based on poly(cyclohexane-terephthalate-glycol) mixed with PC and/or with SMA. They are primarily used in business machines, appliances, consumer goods, garden tools, lightning, automotive, sports equipment, fluid handling, etc.
			Hyperlite	Kanegafuchi Chem.	
			Impact	AlliedSignal	
			Makroblend UT	Mobay	
			MB 3500	Mitsubishi Gas	
			Petsar	Polysar	
			Sabre 1600	Dow	
			SC	Idemitsu Petrochemicals	
			Xenoy 2000	GE Plastics	
26.	PBT	PET	C, CN	Teijin	Good surface properties, HDT, impact strength, dimensional stability, and economy
			Celanex	Hoechst Celanese	
			EMC	Toyobo	
			Valox	GE Plastics	
27.	PBT	Acrylic rubber	BU	Dai Nippon Ink	Improved processability and impact resistance
			BX	Toray	
			Novadol	Mitsubishi Chem.	
			Vandar	Hoechst	
28.	PBT	Elastomer	Bexloy J	E. I. du Pont	These impact-modified PBT blends are formulated for injection molding, but they can also be extruded and thermoformed. They show good processability, electrical properties, high stiffness and strength, HDT, dimensional stability, impact strength, and solvent and chemical resistance
			Celanex	Hoechst Celanese	
			Gafite	GAF	
			Macroblend	Bayer Miles	
			Pibiter HI	Montedipe	
			Starflam PBT	Ferro Plastics	
			Techster T	Rhône Poulenc	
			Ultradur KR	BASF AG	

(continued)

	Polymer				
No.	A	B	Name	Supplier	Comments
29.	PBT	ABS or AAS*	A, AN	Teijin	The blends contain 0–30 wt% glass fiber or mineral fillers. They are formulated for injection molding but can be extruded, thermoformed, or solid state formed. They show excellent processability, high gloss, stiffness at high temperature, good electrical properties, thermal stability, mechanical strength, HDT, low shrinkage, good dimensional stability, impact strength, as well as solvent (e.g., to gasoline and motor oils) and chemical resistance. The main consumption includes electronics, automotive and electrical industry, as well as office, sports, and household equipment
			Alphaloy MPB	Kanegafuchi Chem.	
			BA	Dai Nippon Ink	
			Baitaloy VL*	Hitachi Chem.	
			Cycolin	GE Plastics	
			Diaaloy B	Mitsubishi Rayon	
			Lumax	Lucky Co., Ltd.	
			Malecca B	Denka Kagaku K.	
			Maxloy B	JSR	
			Novaloy-B	Daicel Chem. Ind.	
			Techniace TB	Sumitomo Dow	
			Triax 4000	Monsanto	
			Ultrablend S	BASF AG	
			VX	Toray	
30.	PAr	PET or PC	Ardel D-240	Amoco Corp.	Processability, high HDT, tough, high impact strength
			U-8000	Unitika	
31.	POM	PBT	Duraloy	Celanese	HDT, toughness, softness, high impact strength
			Lynex T	Asahi Chem.	
32.	POM	TPU	Celcon	Celanese Eng. Res.	The blends are formulated for extrusion, injection, compression, blow, and transfer molding. They show excellent processability; rigidity; high impact strength; high fatigue, flexural, and tensile strength; high toughness; low water absorbency; gloss; and resistance to chemicals. In most blends POM is impact-modified with 10–30 wt% TPU. Some grades contain PTFE. Co-continuous morphology gives especially good performance. These blends find use in sports equipment, plumbing, electronic/mechanical parts, automotive, appliances, hinges, etc.
			Delrin	E. I. du Pont	
			Duraloy	H.-Celanese	
			Formaldafil	Wilson-Fiberfil	
			Fulton KL	LNP Corp.	
			Hostaform S	Hoechst A.-G.	
			RTP 800	RTP Corp.	
			TC	Polyplastics	
			Thermocomp	LNP	
			Ultraform	BASF AG	

(continued)

No.	Polymer A	B	Name	Supplier	Comments
33.	PPE	PS (HIPS, SBS, SEBS, ABS, SB,. . .)	Gepax	GE Plastics	These blends, with 25–60 wt% PPE, were designed for injection or blow molding, calendering, thermoforming, and extrusion. Some grades are rein-forced with < 30 wt% glass fibers. They show good processability, heat resistance, HDT = 90–150 °C, toughness, good dimensional stability, resistance to hot water, flame retardance, low density, cost/performance ratio, and low moisture absorption
			Luranyl	BASF AG	
			Noryl	GE Plastics	
			Prevex	GE Plastics	
			Verton	Hüls	
			Vestoran 1900 and 2000	Hüls-Nuodex	
			Xyron 200	Asahi Chem. Ind.	
34.	PPE	PA	Artley	Sumitomo Chem.	The blends are designed for extrusion, thermoforming, or injection molding. They are compatibilized, with 40–60 wt% PA, showing moderate processability and impact strength; good tensile and flexural strength; high-temperature creep, solvent, and chemical resistance; and low moisture absorption. They are dimensionally stable, paintable, and palatable
			Dimension	AlliedSignal	
			Lynex A	Asahi Chem. Ind.	
			Noryl GTX	GE Plastics	
			Remaloy	Mitsubishi Petrochemicals	
			Ultranyl	BASF AG	
			Vestoblend	Hüls A.-G.	
			Xyron A and G	Asahi Chem. Ind.	
35.	PPE	PBT (+ PC + impact modifier)	Dialoy X	Mitsubishi Rayon	Excellent processability, high solvent and temperature resistance, and dimensional stability
			BE	Dai Nippon Ink	
			Gemax	GE Plastics	
			Iupiace	Mitsubishi Gas	
36.	PPE	PPS	DIC PPS	Dainippon Ink & Chemicals	The blends are designed for injection molding, but extrusion, compression molding, or thermoforming can also be used. The blends have to be compatibilized and contain up to 40 wt% glass fibers. They show good compatibilized and contain up to 40 wt% glass fibers. They show good processability, reduced flash, toughness, and high heat resistance
			Iupiace	Mitsubishi Gas	
			Noryl APS	GE Plastics	

(continued)

	Polymer				
No.	A	B	Name	Supplier	Comments
37.	PVDF	PMMA	Polycast	Royalite	Used for electrets or as outdoor films with good clarity and chemical and UV stability
38.	PSF	ABS	Arylon	Uniroyal	The blends can be either extruded or injection molded. They show good processability, toughness, dimensional stability, high HDT, hot water resistance, plateability, and paintability. The applications include plumbing, food service, and fiber optics controlled system
			Mindel A	Amoco Corp.	
39.	PSF	PET	Mindel B	Amoco Corp.	The blends can be either extruded or injection molded. They show improved processability and impact strength, low shrinkage and warpage, high HDT, good stress crack chemical and solvent resistance, and good economy. The blends find applications as molded electrical parts, viz., connectors, relays, switches, motor starters, control housings, etc.
40.	PSF	PA	Reo-alloy	Riken Vinyl	Processability, low viscosity, and low water absorption
41.	SMI	SAN	Malecca A	Denka	High heat and impact resistanc
42.	SMI	ABS	Malecca K	Denka	High heat and impact resistance
43.	SMI	PA	Malecca N	Denka	High heat, solvent, and impact resistance
44.	PEEK	PES	Sumiploy SK	Sumitomo Chem.	The blends are designed for injection molding, but extrusion, compression molding, or thermoforming can also be used. SK 1660 grade contains glass fibers. The materials show good processability, excellent high temperature, and chemical and hot water resistance

No.	Polymer		Name	Supplier	Comments
	A	B			
45.	PEEK	LCP	Sumiploy EK	Sumitomo Chem.	The blends are designed for injection molding, but extrusion, compression molding, or thermoforming can also be used. They show good process- ability, high strength, modulus, and HDT
46.	PEI	PC	Ultem LTX	GE Plastics	Designed for injection molding and extrusion. Processability; HDT; flexural, tensile, and impact strength; flame retardancy; long-term hydrolytic stability; stain and chemical resistance; and lower cost than PEI
47.	PI	LCP	Aurum	Mitsui Toatsu	Good processability, low viscosity, HDT, and low water absorption
48.	HIPS	Hydrophilic polymer		Toray	Permanent antistatic properties

Appendix III: Dictionary of Terms Used in Polymer Science and Technology

A-, B-, and C-stages	Expressions used by Baekeland to differentiate polymerization steps of phenolic resins. A-stage, initial; resins are still fusible and soluble. B-stage, advanced degree of condensation; resins are still capable of swelling but no longer soluble. C-stage; complete cross-linking and insolubility.
AB, AABB polymerization	Step-growth polymerization, in which the two types of functional group (A and B) are attached to the same or two different monomers, viz., hydroxy acid (AB) and diol-diacid (AABB).
Ablation	Decomposition of a material caused by heat friction.
Abrasion	The wearing away of some surface area by its contact with another material.
Abrasion resistance	Ability of material to withstand mechanical action such as rubbing, scraping, or erosion that tends to progressively remove material from its surface; to resist surface wear.
ABS	A thermoplastic classified as an elastomer-modified styrene-acrylonitrile copolymer.
Accelerated aging	Aging by artificial means to obtain an indication on how a material will behave under normal conditions over long period. Also tests in which conditions are intensified to reduce the time required to obtain deteriorating effects, similar to these resulting from normal service conditions.
Accelerated weathering	Duplicating or reproducing weather conditions by machine-made means. Test in which the normal weathering conditions are accelerated by means of a device.

Accumulator	A device for conserving energy in hydraulic systems of molding equipment, or an auxiliary ram extruder used to provide fast material delivery in a molding machine.
Acetal resins	Polyoxymethylene – a crystalline thermoplastic material made from formaldehyde, viz., Delrin™ or Celcon™.
Acrylic elastomer	An elastomer based on polyethylacrylate and/or poly-n-butylacrylate with thermal stability up to T = 200 °C, usually cross-linked by heating with peroxides or with alkali. To improve the solvent resistance, 20–50 wt% of ethoxy or methoxyethyl-acrylate may be added.
Acrylics	Name given to plastics produced by the polymerization of acrylic acid derivatives, usually including methyl methacrylate. An amorphous thermoplastic material. In technological jargon polymethylmethacrylate (PMMA) or polyacrylonitrile fiber with at least 85 wt% of PAN.
Adapter	A mechanical reducing mechanism between the barrel and either a nozzle or a die.
Additive	A material added to a polymer during the final synthesis stages or in subsequent processing to improve or alter some characteristics of the polymer. Additives, as a class of materials, are not intended to increase strength properties. Examples of additive include pigments, lubricants, antistatic agents, flame retardants, and plasticizers.
Adhesion	The state in which two surfaces are held together at an interface by mechanical or chemical forces, by interlocking action, etc.
Adhesive	A substrate capable of holding two materials together by surface attachment. Adhesive can be in film, liquid, or paste form.
Advanced composites	Composite materials that are reinforced with continuous fibers having a modulus higher than that of glass fibers. The term includes polymeric matrix, metal matrix, and ceramic matrix composites, as well as carbon-carbon composites.
Aging	The change of a material over time under defined natural or synthetic environmental conditions, leading to improvement or deterioration of properties. Also, changes caused by exposure to physical and chemical factors (viz., light, temperature, chemicals, weather), leading to irreversible deterioration. A process of exposing plastics to natural or artificial environmental

	conditions for a prolonged time. See also "Accelerated aging," "Artificial aging," "Chemical aging," and "Physical aging."
Alkyd resins	Name given to synthetic, thermosetting resins processed from polyhydric alcohols and polybasic acid or anhydrides. These unsaturated polyesters are prepared by esterification of a polyfunctional alcohol (e.g., glycerin) with phthalic anhydride in combination with fatty acids or rosin acids (molecular weight about 2,000 to 5,000). These resins are frequently modified by incorporation of, e.g., nitrocellulose, NC, or phenolics. Alkyds are used mainly as lacquers.
Alloy	A material made by blending polymers or copolymers with other polymers or elastomers under selected conditions, e.g., styrene-acrylonitrile copolymer (SAN) blended with butadiene-acrylonitrile elastomer (NBR). A mixture of two chemically different polymers to form a material having properties different from but often comprising those of the original resins. Also see "Polymer alloy."
Allyl resin	Low-molecular-weight polymerization product of allyl monomer, $CH_2 = CHCH_2X$, where, for example, $X = -OH, -OOCCH_3$.
Ambient temperature	Temperature of the medium surrounding an object. Used to denote prevailing room temperature (RT).
Amino resin	Collective term for resins that are capable of being cross-linked. Terms, aminoplast and amino plastic, are also used. The materials are based on compounds containing NH_2 group and formaldehyde. The representatives are urea-, melamine-, and dicyanodiamide-based resins used for laminating and molding.
Amorphous polymer	A noncrystalline polymeric material that has no definite order or crystallinity. A polymer in which the macromolecular chain has a random conformation in solid (glassy or rubbery) state. On the one hand, an amorphous polymer may show a short range order, while on the other, a crystalline polymer may be quenched to the amorphous state (viz., polyethylene terephthalate (PET)).
Amplitude	The maximum value of a periodically varying function, e.g., used to describe the energy transmitted from the ultrasonic welding horn to the weld joint.
Analysis of variance	A statistical technique where the total variation of the investigated response is being analyzed or divided into meaningful components, such as a portion due to regression and a portion due to error.

Anionic polymerization	Chain polymerization in which the active center is an anion, usually carbanion. The method is mostly used to polymerize vinyl monomers carrying electron-withdrawing substituents (e.g., $-CN$, $-COOR$, $-COR$, $-aryl$). The polymerization is frequently initiated by n-butyllithium.
Anisometry	The difference in the magnitude of the dimensions of a particle that depend on the direction. Thus, sphere is isometric – it has a minimum of anisometry. It is customary to define anisometry in terms of the aspect ratio, p. For platelets, p is defined as the thickness divided by the longest orthogonal dimension; thus, for platelets, $p \leq 1$. By contrast, for fiber-like particles, p is the length-to-diameter ratio, i.e., $p \geq 1$. Macromolecules show high anisometry with a typical value $p = 1,000$.
Anisotropy	The material properties being dependent on the direction. Most multiphase polymeric systems show some degree of anisometry. The mechanical performance in the machine direction can be as much as a hundred times higher than those in the transverse direction. In homopolymers, the anisotropy is a reflection of the molecular orientation in either a glassy or a semicrystalline state (see "Birefringence").
Annealing	To heat a molded plastic article to a predetermined temperature and slowly cool it to relieve stresses. Annealing of molded or machined parts may be done dry, as in an oven, or wet, as in a heated tank of mineral oil. To relieve the stresses without introducing major change of the molecular structure in the formed article, the annealing is frequently carried out at a temperature being few degrees *below* the glass transition temperature, T_g. The treatment is also used to increase polymer crystallinity. The process requires keeping the polymer at a temperature $T < T_d$ (where T_d is the thermal degradation temperature). The best results are usually obtained when $(T_g + T_m)/2 \leq T < T_m$, where T_m is the melting temperature.
Antioxidant	A substance that, when added in small quantities to the resin during mixing, prevents its oxidative degradation and contributes to the maintenance of its properties.
Antiplasticization	An increase of stiffness, tensile strength, and/or the glass transition temperature and a decrease of the elongation at break caused by addition of small amount of a plasticizer. For example, maximum hardness of

	polyvinylchloride was observed at 5–10 phr of diethylhexyl phthalate, PVC/DOP, and minimum impact strength at 12 phr. Antiplasticization occurs in many polymers, viz., PVC, polymethylmethacrylate (PMMA), polystyrene (PS), polycarbonate (PC), polyamides (PA), and silk (by water).
Antistatic agents (antistats)	Substances that, when added to the molding material or applied on the surface of the molded part, make it less able to store static electrical charge.
Apparent or bulk density	Weight of unit volume of material including voids (air) inherent in the material.
Arc resistance	The time required for a given electrical current to render the plastic surface of a material conductive because of carbonization by the arc flame. Also ability to resist the action of a high voltage electrical arc, usually in terms of time required to render the material electrically conductive. The total time (in sec) that intermittent arc may play across the plastic surface with rendering the surface conductive.
Aromatic	Description used for chemicals that have at least one ring structure derived from benzene in their chemical structure. Benzene rings are made by six carbon atoms forming a hexagonal structure with alternating single and double bonds. The description is general and covers a wide range of chemicals. The word "aromatic" is used because of the strong smell of benzene. Many of the chemicals classified as aromatics have a very different smell or no smell at all. A benzene ring structure with one bonding site is a "phenyl" ring or group. See also "Benzene."
Aromatic polymer	A polymer containing aromatic ring structures, viz., polyamides, polyesters, polyethers, polysulfides, polysulfones, polysiloxanes.
Artificial aging	The exposure of a plastic to conditions that accelerate the effects of time, such as heating, exposure to cold, flexing, application of electrical field, immersion in water, exposure to chemicals and solvents, ultraviolet, light stability, and resistance to fatigue. The accelerated testing of plastic specimens to determine their changes in properties carried out over a short time. The tests indicate what may be expected of a material under service conditions over extended periods. Typical investigations include those for dimensional stability, mechanical fatigue, chemical resistance, stress cracking resistance, dielectric strength, and so forth, under the

	conditions that reflect the conditions under which the article will be used. Usually, the time the article is exposed to these test conditions is relatively short. See also "Aging."
Ashing	The reduction of a polymer by high heat to yield any inorganic material, e.g., fillers or reinforcements, used to verify the percentage of nonorganic content in the resin.
Aspect ratio	The relative comparison of one dimension of an object to another. For fibers, the aspect ratio is the length divided by the diameter. For mica, it is the shorter of the length and width of a platelet to its thickness. For complex objects like a particle of clay, it is a relative number approximating the ratio of the longer of two dimensions to the shorter. This ratio is key in how effective a reinforcement is within a matrix of polymer molecules. Given uniform composition and coupling agents, higher aspect ratio reinforcement results in a higher increase in strength. The aspect ratio determines how much stress can be transferred to the fibers or platelets before being transferred back into polymer matrix.
ASTM	Abbreviation for American Society for Testing and Materials.
Atactic polymer	A polymer in which at least one chain atom in a mer can exhibit stereoisomerism (e.g., $-CH_2C*HX-$), but has no preference for one particular configuration, e.g., atactic vinyl polymers (PVC or PS), atactic polypropylene, and PP.
Atom	The most basic compositional unit of the elements composed of protons, electrons, and neutrons. Elements are any substance composed solely of chemically identical atoms, viz., carbon, hydrogen, oxygen, sulfur, nitrogen, iron, and aluminum.
Attenuation	The diminution of vibrations or energy over time or distance. The term is also used to describe a process of making thin and slender articles, e.g., the formation of fiber from molten glass.
Autoclave	A closed vessel for conducting either a chemical reaction or other operation (e.g., cooling) under pressure and heat. Autoclaves are widely used for bonding and curing reinforced plastic laminates.
Autoclave molding	A process in which after lay-up, winding, or warping, an entire assembly is placed in a heated autoclave, usually at 340–1,380 kPa (50–200 psi). The pressure results in higher density and improved removal of volatiles.

	The lay-ups are usually vacuum bagged with a bleeder and release cloth.
Automatic mold	A mold or die in injection or compression molding that repeatedly goes through the entire cycle without human assistance.
Auxiliary equipment	Refers to equipment, other than the principal processing unit (e.g., an extruder or an injection molding machine), required to ensure that the manufactured part would be made correctly. The auxiliary equipment comprises dryers, chillers, material and part conveyors, robots, process monitoring and controlling units, etc.
Average molecular weight	Summation over the distribution of molecular weights of a polymeric substance, e.g., with respect to the number, M_n, weight, M_w, or higher moments. Depending on the method of determination, M_n, M_w, or higher average molecular weight is obtained.
Back pressure	A pressure against the free flow of material during extrusion that causes the material to have a high mixing action. Also resistance of a material caused by its viscosity to flow when mold is closing.
Back taper or draft	Reverse draft used in mold to prevent molded articles from drawing freely.
Backing plate	In mold construction, a plate used as a support for the cavity blocks, guide pins, bushings, etc.
Ball valve	A screw melt seal or valve, similar to a check ring valve, but designed differently. Uses a roundball to seal off the melt so it does not flow back over the screw flights during the injection cycle.
Banbury	An internal mixer for compounding, composed of a pair of counterrotating rotors that masticate the materials.
Barrel	In extrusion, injection molding, or blow molding machine a hollow tube in which the plastic material is gradually heated and melted and from which it is extruded.
Batch	A quantity of materials formed during the same process or in one continuous process and having identical characteristics throughout.
Benzene	A chemical structure composed of six carbon atoms arranged in a stable cyclic structure. Each carbon atom is single bonded to the next carbon atom on one side and double bonded to the carbon atom on the other side. Each also has a hydrogen atom bonded to it. Phenyl groups are benzene rings where one of the carbon atoms is bonded to another molecule, making the entire cyclic structure a substituent or side group of that molecule.

Bezel	A grooved rim or flange.
Binder	The resin or a cementing constituent that holds the other components together. The agent applied to mats or preforms to bond the fibers before molding.
Binomial distribution	A discrete probability distribution based on two possible outcomes, which may be labeled success (with probability p) or failure (with probability q = 1 − p); the probability function expresses the number of X successes in n independent trials.
Bimodal distribution	A probability distribution in which the differential distribution function has two maxima.
Biopolymer	Polymer produced by biosynthesis in nature, viz., polysaccharides, nucleic acids, proteins, cellulose, lignin, and natural rubber.
Binodal	The line on the temperature vs. composition phase diagram for a mixture of two components, which separates the metastable region from the single-phase regions. Hence, it represents the limits of stability in a two-phase system, viz., a polymer solution or polymer blend.
Birefringence (double refraction)	The difference between index of refraction in two directions, measured with polarized light. The birefringence originates in the molecular orientation in either a glassy or crystalline phase. Positive birefringence occurs when the principal optic axis lies along the chain and negative when it is perpendicular. See also "Dichroism."
Bleed	To give up color when in contact with water or a solvent. Also a "migration," undesired movement of additives in a plastic (e.g., plasticizers in PVC) to the surface of the finished article or into an adjacent material. The term is also used to describe a passage at the parting line of a mold (such as a vent, but deeper) that makes it possible for the material to escape or bleed.
Bleeding	Diffusion of an additive in or out of a plastic part. See "Bleed."
Blending	Preparation of polymer blends or alloys, usually involving mixing of two polymeric liquids.
Blends	see "Polymer blends."
Blister	A raised area on the surface of a molded part caused by the pressure of gases inside it.
Blister packaging	Packaging method based on sealing articles inside thermoformed, transparent cases.
Block copolymers	Copolymer synthesized from two or more monomers in such a way that monomers of the same kind are arranged in homopolymeric blocks.

Block polymerization	An older expression for bulk or mass polymerization.
Blocking	The adhesion between layers of plastic that may develop under pressure during storage or use.
Bloom	A visible exudation or efflorescence on the surface of a plastic – it may be caused by lubricant, plasticizer, etc.
Blow film extrusion	Techniques for making film by extruding the plastic through a circular die, followed by expansion (by the pressure of internal air admitted though the center of the mandrel), cooling, and collapsing the bubble.
Blow molding	A molding process used to produce hollow objects in which a hollow tube (parison) is forced into a shape of the mold cavity using internal air pressure. The two primary types are injection blow molding and extrusion blow molding. Blow molding is a method of fabrication in which a warm plastic parison is placed between the two halves of a mold and forced to assume the shape of that mold cavity by use of air pressure introduced through the inside of the parison that forces the melt against the surface of the mold.
Blow pin	A hollow pin inserted or made to contact the blowing mold so that the blowing media can be introduced into the parison or hollow form and expanded to conform to the mold cavity.
Blowing agent	Additive capable of producing a cellular structure in a plastic or rubber mass.
Blueing off	Checking the accuracy of mold cutoff surfaces by putting a thin coating of Prussian blue on one-half and checking the blue transfer to the other half.
Blush	The tendency of a plastic to turn white or chalky in areas that are highly stressed (viz., gate blush).
Bonds	Forces between atoms that hold them in relative proximity to each other resulting in larger structures called molecules. Primary bonds result from the sharing of two electrons of two atoms of the same molecule and are strongest. Secondary bonds are between atoms of different molecules or remote sections of the same molecule. They are the result of attractions due to polarity, induced polarity due to displaced electrons, and temporary polarity due to vibration and spinning. These bond forces are weak in comparison to primary bonds.
Boss	A projection on a plastic part designed to add strength, facilitate alignment during assembly, and provide for fastening.
Bottom plate	Part of the mold containing the heel radius and push-up.

Branched chains	Side chains attached to the main, original chain.
Branched polymer	A nonlinear polymer in which the molecules consist of linear main chain to which there are randomly attached secondary chain branches, viz., low density polyethylene. A fraction of repeat units in a polymer that statistically contain one branch is defined as the branching density: $\lambda = \alpha b/n$, where α is the branching coefficient (dependent on functionality of the branch point), b is the number of branch points, and n is the number of repeat units.
Breaker plate	A perforated plate located at the end of an extruder or at the nozzle end of an injection cylinder. It often supports the screens that prevent foreign particles from entering the die.
Breathing or degassing	The opening and closing of a mold to allow gases to escape early in the molding cycle. When referring to plastic film, "breathing" indicates permeability.
Brittle failure	Failure resulting from inability of material to absorb energy, resulting in instant fracture upon mechanical loading.
Brittle or brittleness temperature	Temperature at which plastics and elastomers exhibit brittle failure under impact conditions – the lowest temperature at which the material withstands given condition without failure.
Brittle point	The highest temperature at which a material fractures in a prescribed impact test procedure.
Buckling	Crimping of the fibers in a composite material, often occurring in glass-reinforced thermosets due to resin shrinkage during cure.
Bulk or apparent density	Average density of material in a loose or powdered form of plastic (granular, nodular, etc.) expressed as a ratio of weight to volume.
Bulk factor	Ratio of volume of any given quantity of the loose plastic material to the volume of the same quantity of the material after molding or forming. It is a measure of volume change that may be expected in fabrication.
Bulk polymerization	Polymerization where only the monomer and initiator (or catalyst) are involved. Owing to heat of polymerization and difficulty of safe dissipation of generated heat, the conversion rarely exceeds 50 %. Older terms: block or mass polymerization.
Burning	Overheating the resin in the barrel causing discoloration and, if long enough, charring the material. Burning can be caused by trapped gases in poor or nonvented area of the mold. The gases may ignite, due to pressure and

temperature (as in a diesel engine) and discolor or char the part.

Burst strength	The internal pressure required to break a pressure vessel such as a pipe or fitting. The pressure (and therefore the burst strength) varies with the rate of pressure buildup and the time during which the pressure is held.
Butadiene	A common name of a synthetic elastomer, polybutadiene – BR, e.g., used in butadiene-styrene, butadiene-acrylonitrile, and acrylonitrile-butadiene-styrene copolymers.
Butt fusion	A method of joining similar forms of thermoplastic materials using heat.
Buttress thread	A type of thread used for transmitting power in only one direction. It has the efficiency of the square thread and the strength of the V-thread.
Calendering	The passing of sheet materials between sets of pressure rollers to produce a smooth finish sheet of desired thickness.
Calorimeter	An instrument capable of making absolute measurements of energy absorbed in a material by measuring changes of temperature.
Capillary rheometer	Instrument for measuring the flow properties (viscosity) of polymer melts. Composed of a capillary tube of specified diameter and length, means for applying a pressure to force molten polymer through the capillary, means for maintaining the desired temperature of the apparatus, and means for measuring differential pressures and flow rates.
Carbon black	A black pigment or filler produced by the incomplete burning of natural gas or oil. It is widely used in the rubber industry and for wire/cable applications. Since it possesses ultraviolet protective properties, it is also used in formulations intended for outside weathering applications.
Carbon fiber	Fibers produced by the pyrolysis of organic precursor fibers, such as rayon, polyacrylonitrile (PAN), and pitch, in an inert environment. The term is often used interchangeably with the term graphite; however, carbon fibers and graphite fibers differ. The differences lie in the temperature at which the fibers are made and heat-treated, as well as in the amount of elemental carbon produced. Carbon fibers typically are carbonized at around 1,315 °C and contain 94 $\pm$ 1 % carbon, while graphite fibers are graphitized at 1,900–2,480 °C and contain 99 % carbon.

Carborane polymer | A polymer containing carborane structures, viz., $-C(B_{10}H_{10})C-$, known for their high decomposition temperature $T_d \S 500\ °C$. Owing to the hydrogen presence, the oxidative stability is limited to about 300 °C.

Carreau-Yasuda equation | Relation between viscosity, η, and the deformation rate, y, was originally derived for monodisperse polymers:

$$\eta = \eta_0 \left[1 + (\tau y)^2 \right]^{-(1-n)/2}$$

where η_o is the zero-shear viscosity, τ is the principal relaxation time, and n is the power-law exponent. For polydispersed systems, the above equation was later modified by other authors to read:

$$\eta = \eta_0 \left[1 + (\tau y)^{m_1} \right]^{-m_2}$$

where m_1 and m_2 are polydispersity parameters:

$$n = 1 - m_1 \cdot m_2$$

Cartridge heaters | Electrical heaters enclosed in a jacket that can be selectively located to heat the surrounding metal.

Catalyst | A substrate that changes the rate of a chemical reaction without itself undergoing permanent change in composition or becoming a part of the molecular structure of the product. By contrast, either curing agents or hardeners may not only catalyze the reaction but also participate in it. Also accelerator, curing agent, hardener, inhibitor, and promoter.

Cationic polymerization | Chain polymerization in which the active center is a cation, usually carbonium ion, $-C^+$. Generally, the method is used to polymerize vinyl monomers carrying electron-releasing substituents (e.g., alkyl or alkoxy groups). The polymerization is initiated by an initiator and co-initiator, viz., $BH_3 + H_2O$.

Cavity | A depression in the mold that usually forms the outer surface of the part. Depending on the number of such depressions, molds are designated as a single cavity, a multicavity, or a family cavity mold.

Cavity number | A sequential number engraved in a mold cavity and reproduced on the molded part for later reference in case a problem ever occurs with the part.

Cavity retainer plates | Plates in a mold that hold the cavities and usually contain the guide pins and bushings.

Ceiling temperature	Temperature at which the free polymerization energy is zero. Thus, above this temperature, no further polymerization takes place.
Cellular plastic	A plastic with greatly decreased density because of the presence of numerous cells or bubbles dispersed throughout its mass. Also foamed plastics and synthetic cellular plastics.
Cellulose acetate	An acetic acid ester of cellulose, obtained by the action of acetic acid or acetic anhydride on purified cellulose (e.g., from cotton linters). All three hydroxyl groups of each glucose unit can be acetylated. For plastics' applications, it is usual to acetylate fully and then lower the acetyl value to 54 ± 2 % by partial hydrolysis.
Cellulosic plastics	Plastics based on cellulose derivatives, such as esters (cellulose acetate) or ethers (ethyl cellulose).
Cementing	A process of joining two similar plastic materials to themselves or to dissimilar materials by means of solvents.
Center-gated mold	An injection or transfer mold in which the cavity is filled with molding material through a sprue or gate directly into the center of the part.
Chain member number	Number of atoms involved in building a macromolecule.
Chain polymerization	An addition polymerization in which a monomer is converted to polymer in a chain reaction. Here initiator activates the monomer to which other monomers are added:

$$I^* + M \rightarrow IM^*$$
$$IM^* + M \rightarrow IMM^*$$
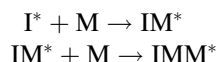
	preserving the active status of the terminal mer. The active center may be a free radical, an anion or a cation.
Chalking	A dry, whitish, powdery chalk-like appearance or deposit on the surface of a plastic caused by material degradation (usually from weather). See also "Haze" and "Bloom."
Change request	A request to modify or alter the dimensions, material, tolerances, or manufacture of a part now in or soon to be in production. Used to ensure all interested and involved department personnel are informed and can comment and approve or disapprove of the pending change.
Charpy	A common name of a type of pendulum tests for toughness.
Charpy impact test	A test for shock loading in which a centrally notched sample bar is held at both ends and broken by striking

	the back face in the same plane as the notch. A destructive test measuring impact resistance, consisting of placing the specimen in a horizontal position between two supports, then striking the specimen with a pendulum striker swung from a fixed height. The magnitude of the blow is increased until specimen breaks.
Check ring	A material shutoff ring mounted on the front of the screw, behind the screw tip, that allows melt to flow past it when the screw is retracting so that a supply of melt builds up in front of the screw. When the screw moves forward to inject melt into the mold, the check ring moves rearward and seals off the screw flights so that the melt is pushed into the mold.
Chemical aging	The long-term deleterious effects on a material under defined natural or artificial environmental conditions (viz., light, temperature, humidity), leading to irreversible deterioration of properties. A process of exposing plastics to natural or artificial factors for prolonged time. See also "Aging," "Accelerated aging," "Artificial aging," and "Physical aging."
Chemical resistance	Ability of a material to retain utility and appearance following contact with chemical agents.
Chi-square (χ^2) test	Test of normality of distribution or a goodness of fit.
Chromatography	The separation, especially of closely related compounds, caused by allowing a solution or mixture to seep through an absorbent, such that each compound becomes adsorbed in a separate layer.
Chromium plating	An electrolytic process that deposits a hard film of chromium metal onto working surfaces of other metals. Used when resistance to corrosion, abrasion, and/or erosion is needed.
Clamping area	The largest rate molding area an injection or transfer press can hold closed under full molding pressure.
Clamping force or pressure	In injection molding, the pressure applied to the mold to keep it closed despite the fluid pressure of the compressed molding material within the cavity and runner system.
Clamping plate	A plate used to fasten the mold to a molding machine.
Clarity or transparency	Frequently considered as evidence of blends miscibility or at least that of fine domains. This, however, is misleading when the refractive indices of the two polymers approach each other. Also material clearness or lack of haze.
Closed loop	A feedback system used with microprocessor for control of a processing unit operation.

Coefficient of expansion or thermal expansion	The fractional change in a specified dimension or volume of a material for a unit change in temperature. Values for plastics range from 10 to 200 ppm per 1 °C (ASTM D696).
Coefficient of friction	A measure of the resistance to sliding of one surface in contact with another. The value calculated under a known set of conditions, such as pressure, surface, speed, temperature, and material, to develop a number, either static or dynamic, of the resistance of the material to slide – the lower the value, the higher the material's lubricity.
Coefficient of linear expansion	A measure of the change in dimension of an object caused by a change in temperature; specifically measured by the increase in length of an object per one degree.
Coefficient of regression, or coefficient of correlation, R	Measure of the degree of relationship between a model obtained by regression (curve fitting) and the independent variables; if reported as $100R^2$ (%), it can be interpreted as the percentage variation explained by the postulated model.
Coefficient of thermal expansion	The change in volume per unit volume produced by a one degree rise in temperature.
Coining	The peening over or compressing of a material to change its original shape or form.
Cold flow	A plastic exhibits cold flow when it does not return to its original dimensions after being subjected to stress. See also "Creep."
Cold shot	Incomplete parts formed while cycling a molding machine during heating.
Cold slug	The first material to enter an injection mold so called because in passing through sprue orifice, it is cooled below the effective molding temperature.
Cold slug well	Space provided directly opposite the sprue opening in an injection mold to trap the cold slug.
Colloid	A system in which at least one component exists in state of fine dispersion with particle diameter d = 1 to 1,000 nm. Three types, colloidal dispersions, lyophilic colloids, and colloidal associations, are distinguished.
Colloidal molecules	A discrete macromolecule is the colloidal particle.
Color concentrate	A mixture of a measured amount of dye or pigment and a specific plastic material base. A more precise color can be obtained using concentrates than using neat colors. Note: Care should be taken to verify that the color concentrate base is miscible with the plastic it is to color. Color concentrate may contain up to 60 wt% of

	pigment and it is normally used at 1–4 % of the plastic material to be colored.
Color standard	The exact color a plastic resin or part must match to be acceptable. Resin suppliers often submit color chip samples of the matched resin color to be compared to the molded part. The color chip, or standard, is usually 51 × 76 mm with one polished surface and various textured surfaces on the opposite side. Suppliers use similar standards to verify the color of each lot of resin shipped to their customer.
Colorfast	The ability to resist change in color.
Colorimeter	Instrument for matching colors with results approximately the same as those of visual inspection but more consistently.
Commodity resin	The term associated with the high-volume low-price resins having low-to-medium physical properties, used for less critical applications. The principal five resin types are polyethylenes (PE), polypropylenes (PP), styrenics (PS, HIPS, ABS, MBS, etc.), acrylics, and vinyls (PVC, EVAc, etc.).
Compatibility	Ill-defined term pertaining to ability of one material to coexist with another without undesirable effects – to be avoided.
Compatibilization	A process of modification of interfacial properties of an immiscible polymer blend, leading to creation of a polymer alloy.
Compatible polymer blend	Ill-defined, utilitarian term indicating a commercially attractive polymer mixture, normally homogenous to the eye, frequently with enhanced physical properties over the constituent polymers – to be avoided.
Complex modulus	The ratio of stress to strain in which each is a vector that may be represented by a complex number. It may be measured in tension or flexure, E*; compression, K*; or shear, G*.
Compliance	Tensile compliance is the reciprocal of Young's modulus. Shear compliance is the reciprocal of shear modulus. The term is also used in the evaluation of stiffness and deflection.
Composites	Any solid material that consists of a combination of two or more types retaining their separate identity. In polymer technology, the term is reserved for these polymeric systems in which additions of solid particles result in reinforcing effect. The composites are divided into reinforced filled systems (with a particle size:

	d = 50 nm), short fiber composites, long fiber composites, and continuous fiber composites.
Compound	A mixture of polymer(s) with all materials necessary for the finished product. In reinforced plastics and composites, the intimate admixture of a polymer with other ingredients, such as fillers, softeners, plasticizers, reinforcements, catalysts, pigments, dyes, etc.
Compounding	Preparation of a compound.
Compression molding	A molding technique in which the preheated compound is placed in the heated open mold cavity, the mold is closed, pressurized (what causes the material to flow and fill the cavity), and then pressure is held until the material has cured.
Compression ratio	In an extruder is a ratio of volume available in the first flight (at the feed) to the last flight at the end of the screw (near the die).
Compressive strength	The ability of a material to resist a compressive force. It is expressed as maximum load sustained by a test specimen in a compressive test divided by original cross-sectional area of the specimen or, in other words, a crushing load at the failure divided by the original sectional area of the specimen (ASTM D695).
Concentricity	The relationship of all circular surfaces with the same center. Deviation from concentricity is often referred to as a runout.
Condensation polymer	A polymer obtained in step-growth polymerization, often accompanied by elimination of small molecules (e.g., water). Polyesters, polyamides, phenol-, melamine-, and urea-formaldehyde resins are typical condensation polymers.
Conditioning	The subjection of a material to standard environmental and/or stress history before testing, so that it will respond in a uniform way to subsequent testing or processing. The term is frequently used to refer to the treatment given before testing. ASTM standard conditions for a plastic testing laboratory are 23 ± 2 °C and 50 + 5 % relative humidity.
Conditioning chamber	An enclosure used to prepare parts for their next step in the assembly or decorating process. Parts can be stress relieved, humidity or moisture conditioned, or impregnated with another element.
Configuration	Spatial arrangement of atoms in a molecule. The chemical constitution of a polymer chain, which can be changed only by breaking the chemical bonds.

Conformation	Arrangements of the chain elements in space, which may be changed by rotation about bonds. The conformation depends on the internal and external forces, e.g., interactions, pressure, temperature, and stresses. For polymers with the carbon-carbon main chain, two conformations are important: trans or t and gauche or g:

gauche   trans
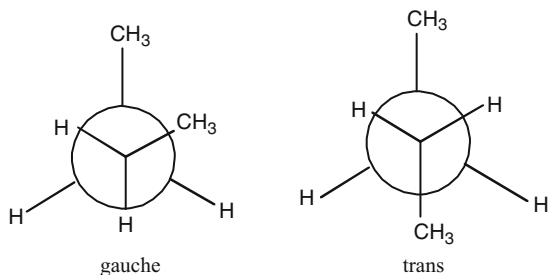
	The helical conformations are defined by the long sequences of these two, viz., tgtgtgtgtgt and tggtggtggtggt.
Conjugated polymer	A polymer with sequence of conjugated double bonds, such as polyacetylene, polyphenylene, and dehydrogenated polyvinyl chloride.
Continuous use temperature (CUT)	Maximum temperature at which material may be subjected to continuous use without fear of premature thermal degradation.
Cooling channels	Passageways within the body of a mold through which a cooling or heating medium (e.g., chilled water, steam, hot oil, or other fluids) can be circulated to control temperature on the mold surface.
Cooling or shrink fixture	A block of steel, wood, or composite material that is similar to the shape of the molded piece. The hot molded part is taken from the mold, placed on it, and allowed to cool, without distorting.
Cooling time	The time required after the gate freezes for the part to cool and becomes rigid enough for ejection from the mold cavity.
Copolycondensation	Polycondensation of different monomers having either a different constitution or different functional groups following different reaction mechanisms.
Copolymer	A polymer obtained from polymerization of two or more monomers, where the repeating structural units of both are present within each molecule, thus comprising more than one chemical species. In most cases, the term refers

	to a polymer containing two monomer types, e.g., styrene and butadiene (SBR). When a copolymer contains three or four different mer species terms, terpolymer, tetrapolymer, or multipolymer may be used. Seven types of copolymers are recognized: statistical, random, alternating, periodic, graft, block, and core-shell. The copolymers may be prepared in reactive blending, with properties intermittent between those of polymers of the two composing monomers.
Copolymerization parameter	Ratio of the velocity constants during copolymerization.
Copolymerization	Polymerization with more than one species of monomer, which can react with one another, forming a copolymer.
Core	Either a male element in die that produces a hole or recess in a part, a part of a complex mold that molds undercut parts (cores are usually withdrawn to one side before the main sections of the mold open), a channel in a mold for circulation of a heat-transfer medium or the central part of a laminate.
Coring	Removal of excess material from the cross section of a molded part to attain a more uniform wall thickness.
Corona treatment	Exposing a plastic part to a corona discharge increases receptivity to inks, lacquers, paints, and adhesives. See also "Surface treatment."
Corrosion	Material that is eaten away by chemical reactions at the surface.
Corrosion resistance	The ability of a material to withstand contact with ambient natural factors or those of a particular artificially created atmosphere.
Coupling agent	A material used to improve the interfacial properties between two phases. The term most frequently refers to the material used to improve an adhesion between polymer matrix and filler or reinforcing particles.
Covalent bond	A bond where electrons are equally shared between two atoms producing a stable electron configuration and a very stable molecule. Covalent bonds are the strongest of the molecular bonds.
Crack	A fracture, a separation of material, visible on opposite surfaces of the part, and extending through the thickness.
Crazing	A series of or the forming of very fine cracks in the surface of a material, usually a polymeric substance. The cracks may extend in a network on or under the surface or through a layer of plastic material. These are

	undesirable defects, characterized by distinct cracks or minute, frost-like internal cracks, resulting from stresses within the article. These stresses result from molding shrinkage, machining, flexing, impact shocks, temperature changes, or action of solvents. Crazing is generally caused by chemical attack or other degrading agents such as ultraviolet radiation.
Creep	The change in dimension of a plastic under load over a period of time (excluding the initial instantaneous elastic deformation). Owing to viscoelastic nature, a plastic subjected to a load for a period of time tends to deform more than it would from the same load released immediately after application. The degree of this deformation depends on the load duration. Creep is the permanent deformation resulting from prolonged application of stress below the elastic limit. Data obtained in creep test are presented as creep vs. time, with stress and temperature constant. Slope of the curve is the creep rate, and the end point of the curve is the time for rupture. Creep at room temperature is called cold flow (ASTM D674).
Creep modulus (apparent modulus)	Ratio of initial applied stress to creep strain.
Creep rupture strength	Stress required to cause fracture in a creep test.
Creep strength	Maximum stress required to cause specific creep in specific time.
Cross-links	Covalent bonds, or a short sequence of chemical bonds, joining two macromolecules to form a cross-linked or network polymer.
Cross-linking	The chemical reaction between polymeric molecules to form covalently bonded three-dimensional macromolecules. The reaction progresses from a linear chain to branched elastomeric macromolecules, than to hard and brittle resin. When extensive, as in most thermosetting resins, cross-linking engenders a single, infusible supermolecule of all the chains. Cross-linking can be achieved by irradiation with high energy electron beams or by chemical means.
Cross-linked polymer	A polymer in which initially linear macromolecules are joined by a covalent bond or a short sequence of chemical bonds either during the polymerization [e.g., poly(styrene-co-divinylbenzene)] or in a post-polymerization cross-linking reaction (cross-linking, curing, or vulcanization). The cross-linked materials are insoluble and they do not flow when heated.

Crystalline polymer	A material having an internal structure in which the atoms are arranged in an orderly three-dimensional configuration. More accurately a semicrystalline polymer, since only a portion of the macromolecules is in crystalline form.
Crystallinity	A state of molecular structure attributed to existence of solid crystals with a definite geometric form. Such structures are characterized by uniformity and compactness. A regular arrangement of the atoms of a solid in space.
	In most polymers, including cellulose, this state is imperfect. The crystalline regions are submicroscopic volumes in which there is a degree of regularity sufficient to obtain X-ray diffraction patterns. High crystallinity causes a polymer to be less transparent or opaque.
Cup flow test	Test for measuring the flow properties of thermosetting materials. A standard mold is charged with preweighed material, and the mold is closed using sufficient pressure to form a required cup. Minimum pressures required to mold a standard cup and the time required to close the mold fully are determined.
Cup viscosity test	Test for making flow comparison under strictly comparable conditions. The cup viscosity test employs a cup-shaped gravity device that permits the timed flow of a known volume of liquid passing through an orifice located at the bottom of the cup.
Cure	That portion of the molding cycle during which the plastic material in the mold becomes sufficiently rigid to permit ejection.
Curing	Cross-linking or vulcanizing a polymer to improve such properties as modulus, strength, thermal stability, etc.
Cushion	The 5–10 mm of resin in front of the screw tip that remains at the end of the injection cycle. It is used to maintain packing pressure on the melt until the cavity gate freezes.
Curing time	The time between the end of injection pressure and the opening of the mold.
Cycle	Complete, repetitive sequence of operations in a process or part of a process. In molding, the cycle time is the period, between a certain point in one cycle and the same point in the next.
Cyclopolymerization	Polymerization leading to ring structures, with usually low molecular weight and low viscosity. These prepolymers or cyclomers can be used at a higher temperature in the subsequent catalyzed reaction to generate a high molecular weight, linear polymers, viz.,

	polycarbonates and polyesters. The cyclomer technology facilitates preparation of polymer alloys, composites, or nanocomposites.
Damping	The loss in energy, as dissipated heat, that results when a material system is subjected to an oscillatory load or displacement.
Daylight opening	Clearance between two platens of a press in the open position. Mold daylight describes the opening distance of mold halves for part removal.
Deboss(ed)	Indent or cut in design, or lettering of a surface.
Decompression	The removal of the melt pressure by an increase in screw flight depth and a positive vent opening in the barrel of a vented barrel extruder or injection molding machine.
Deflashing	The term is used for a variety of finishing methods used to remove the flash (excess, unwanted material), viz., filing, sanding, milling, tumbling, and vibrating.
Deflection temperature under load (DTUL)	The temperature at which a simple beam has deflected a given amount under load (formerly called heat distortion temperature (HDT)).
Deformation	Any change of form or shape in a body, in particular a linear change of dimension of a body in a given direction produced by the action of external forces.
Degating	The removal of the part from the runner system.
Degradation	A deleterious change in the chemical structure, physical properties, and/or appearance of a plastic, usually caused by exposure to heat. Also any undesirable change of polymer chemical structure leading to deleterious change of properties, viz., thermal, hydrolytic, oxidative, photo, bio, and radiation.
Degree of polymerization	The number of mers in a macromolecule, i.e., the number of repeat units in the chain of a molecule, DP. In a condensation polymer, a repeating unit is composed of a monomer group from each reactive species.
Delaminate	To split or separate a laminated plastic material along the plane of its layers.
Density	The weight per unit volume of a substance, expressed in kilograms per cubic meter.
Depropagation or unzipping	A degradation reaction in which the consecutive mers are gradually removed from one macromolecular chain end to another. Few polymers undergo this reverse kinetics process, viz., PMMA, POM, and PTFE.
Desiccant	A substance that can be used for drying purposes because of its affinity to water.
Design of experiments (DOE)	Process of planning the experiment so that sufficient data will be collected for the statistical analysis, to

provide valid and objective conclusions. It includes the choice of the factors, levels, and treatments, as well as the use of certain tools called randomization and replication. The term is frequently used to indicate a problem-solving technique developed by Taguchi, i.e., by using a testing process with an orthogonal array to analyze data and determine the main contributing factors in the solution to the problem.

Degree of freedom	The number of degree of freedom in statistical analysis is the number of independent elements used in the computation of that statistic.
Design stress	The long-term stress, including creep factors and safety factors, that is used in designing structural fabrication.
Destaticization	Treating plastic materials to minimize their accumulation of static electricity.
Destructive test	Any test performed on a part in an attempt to destroy it; often performed to see how much abuse the part can tolerate without failing.
Deterioration	Permanent change in the physical properties of a plastic evidenced by impairment of these properties.
Devolatilization	The removal of volatile components during processing.
Diaphragm gate	The gate used in molding annular or tubular articles that forms a solid web across the opening of the part.
Diblock copolymer	A block copolymer made of two blocks, one having a chain of AAAAA mers and the other of BBBBB to form AAAAAA BBBBBBB polymer. The two block copolymers are used as compatibilizers in the poly-A + poly-B mixtures.
Dichroism	The dependence of absorbency of polarized radiation on the direction of polarization. For polymers the magnitude of dichroism, expressed as dichroic ratio, depends on the orientation of the radiation absorbing groups, thus the macromolecules. In consequence, the infrared dichroism is a powerful method to measure the molecular orientation.
Dichroic ratio	The ratio of absorbencies of polarized radiation, usually the infrared region. The dichroic ratio is used as a measure of molecular orientation in oriented polymers. The dichroic ratio may provide information on the orientation in the glassy and at the same time in the crystalline phase.
Die	A metal form in making or punching plastic products.
Die adapter	The part of an extrusion die that holds the die block.
Die drips	Carbonized resin drool formed on the face of an extrusion die face during the resin production cycle. If the die

	face is not kept clean, it can solidify, break off, and contaminate the product.
Dielectric constant or permittivity	Normally the relative dielectric constant, in practice, a ratio of the capacitance of a given configuration of electrodes with a material as dielectric to the capacitance of the same electrodes' configuration with a vacuum or air as dielectric. A relative measure of nonconductance. Capacitance is the ability of a material to store electrical charge when exposed to electrical current. A low dielectric constant is desired for plastic components used to insulate and isolate electrical components from each other. High dielectric constant materials are desirable for use as the insulator portion of capacitors, so that the electrical energy can be stored in as small a volume of material as possible.
Dielectric heating (also electronic, or R.F. heating)	The plastic to be heated forms the dielectric of a condenser to which a high frequency (20–80 MHz) voltage is applied. Dielectric loss in the material is the basis of the process (e.g., used for sealing vinyl films).
Dielectric strength	The maximum electrical voltage a material can sustain before it is broken down, or "arced through." Also an electrical voltage gradient at which an insulating material is broken down or "arced through."
Dielectrometry	An electrical technique to measure changes in loss factor and capacitance during cure of the resin. Also called dielectric spectroscopy.
Differential scanning calorimetry (DSC)	Thermal analysis technique that measures the quantity of energy absorbed or evolved (given off by a specimen as its temperature is changed). Also measurements of the energy absorbed (endotherm) or produced (exotherm) while undergoing glass transition, melting, crystallizing, curing, evaporating of solvents, and other processes involving energy change.
Differential shrinkage	Nonuniform material shrinkage in part caused by nonuniform distribution of stresses, thus orientation.
Differential thermal analysis (DTA)	An analytical method in which a specimen and a control are simultaneously heated and the difference in their temperatures is monitored. The difference provides information on the relative heat capacities, presence of solvents, changes in structure, and chemical reactions. See also DSC.
Diffusion	The movement of a material, such as a gas or liquid, in the body of a polymer. If the gas or liquid is adsorbed on one side of a test piece and given off on the other, the phenomenon is related to permeability. Diffusion and

	permeability are controlled by the chemical not physical mechanisms.
Digital device	Numerical output device that must index from the initial to the final output reading. More accurate than a similar analog device, but slower.
Dimensional stability	Ability to retain the precise shape to which it was molded, cast, or otherwise fabricated.
Discoloration	Either a change from an initial color possessed by a plastic or lack of uniformity in color over the whole area of an object caused either by overheating, light exposure, irradiation, or chemical attack.
Dished	Showing a symmetrical distortion of a flat or curved section of a plastic object, so that as normally viewed, it appears concave or more concave than intended. See "Warpage."
Dispersion	Finely divided particles of one material suspended in another.
Dispersive mixing	A mixing process in which agglomerates are reduced in size by fracture due to stresses generated during mixing and/or drops of the dispersed phase are deformed and broken.
Dissipation factor	Ratio of the conductance of a capacitor in which the material is dielectric to its substance, or the ratio of its parallel reactivity to its parallel resistance. Most plastics have a low dissipation factor, a desirable property because it minimizes the waste of electrical energy as heat.
Distribution	A method of describing the variation of a stable system, in which individual values are not predictable but in which the outcome as a group forms a pattern that can be described in terms of its location, spread, and shape.
Distribution function	A differential or integral description of population. For the polymer molecular weight a mathematical description of the polydispersity.
Distributive mixing	A mixing process in which the dispersed phase domains are uniformly distributed – a reduction of nonuniformity.
Domain	A morphological term used in noncrystalline systems, such as block copolymers, in which the chemically different sections of the chain separate, generating amorphous phases.
Domed	Showing a symmetrical distortion of a flat or curved section of a plastic object, so that as normally viewed, it appears convex or more convex than intended. See "Warpage."

Double strand polymer	Rigid rod "ladder polymer," consisting of two parallel chains of polymer regularly joined by covalent bonding, viz., pyrrones, polyquinoxalines, and polyphenylsilsesquioxane.
Double-shot molding	A method of producing two-color pieces in thermoplastic materials by successive injection molding operations.
Draft	A taper or slope in a mold that facilitates removal of the molded piece. The opposite of this is called back draft, q.v.
Drool	Melt oozing from a nozzle that is not correctly temperature controlled, or presence of drip on the face of extruder die.
Drop impact test	Impact resistance test in which a predetermined weight is allowed to fall freely onto the specimen from varying heights.
Dry as molded (DAM)	Term used to describe a part immediately after it is removed from a mold and allowed cooling down. All physical, chemical, and electrical property tests are performed on nonconditioned test bars and the results recorded on the data sheets. Parts and test bars in this DAM state are felt to be their weakest in some properties as they have not had time to condition or relieve the molded-in stresses.
Dry blend	Molding compound containing all necessary ingredients mixed in a way that produces a dry, free flowing, particulate material (commonly used for PVC formulations).
Dry coloring	A method commonly used to color plastic by tumble blending uncolored particles of the plastic material with selected dyes and pigments.
Dryers	Auxiliary equipment used to dry resins before processing to ensure that surface properties are within manufacturer specifications. There are several styles of dryers, including ovens, microwave, hot-air desiccant bed, and refrigeration types.
Ductility	The amount of plastic strain that a material can withstand without fracturing, the extent to which a solid material can be drawn into a thinner cross section without breaking. Also, the ability of material to deform plastically before fracturing.
Duromer	Old German name for thermosets, i.e., strongly cross-linked, insoluble polymer.
Durometer hardness	Measure of the indentation hardness of plastics, usually understood as hardness measured by the Shore

	Durometer as an extent to which a spring-loaded steel indenter protrudes into the material.
Dwell	A pause in the application of pressure to a mold, just before the mold is completely closed, to allow the escape of gas from the thermoset molding material. Also the time between when the injection ram is fully forward holding pressure on the material within the mold and the time the ram retracts.
Dyes	Intensely colored synthetics or natural chemicals that are soluble in most common solvents and can be dissolved in a resin to impart color. Dyes are characterized by good transparency, high tinctorial strength, and low specific gravity.
Dynamic mechanical measurement	A technique in which either the modulus or damping of a substance under oscillatory load or displacement is measured as a function of temperature, frequency, time, or their combination.
Ebonite	A material consisting of rubber cured with large quantity with sulfur (one sulfur atom per 4–8 main chain carbons).
Ejection	The removal by mechanical means of the finished part from the mold cavity.
Ejection time	Time in the cycle when the mold opens, the part is ejected, the mold closes, and clamping pressure is applied.
Ejector pin (ejector sleeve)	A rod, pin, or sleeve that pushes a molding off a core or out of a cavity. It is attached to an ejector bar or plate that can be activated by the ejector rod(s) or the press or by auxiliary hydraulic or air cylinders.
Ejector pin retainer Plate	A retainer plate onto which ejector pins are assembled.
Ejector return pins	Projections that push the ejector assembly back as the mold closes. Also called safety pins or position push backs.
Ejector rod or bar	A bar that activates the ejector assembly when the mold is open.
Elastic deformation	A deformation in which a substance returns to its original dimensions on release of the deforming stress – any portion of the total deformation of a body that occurs immediately when load is applied and disappears immediately and completely when the load is removed.
Elastic limit	The greatest stress a material is capable of sustaining without permanent strain remaining after the complete release of the stress. A material is said to have passed its

	elastic limit when the load is sufficient to initiate plastic, or non-recoverable, deformation.
Elastic recovery	The fraction of a given deformation that behaves elastically. A perfectly elastic material has an elastic recovery of one, while a perfectly plastic material has an elastic recovery of zero.
Elasticity	That property of plastic materials because of which they tend to recover their original size and shape after removal of a force causing deformation. If the strain is proportional to the applied stress, the material is said to exhibit Hookean or ideal elasticity.
Elastomers	A customary name for substances showing the plastic–elastic behavior, characteristic for vulcanized rubberlike synthetic or natural polymers, viz., rubbers and weakly cross-linked polyether and polyester urethanes.
Elastomeric	The property of a material that at room temperature can be stretched under low stress to at least twice its original length and, upon immediate release of the stress, will return with force to its approximate original length.
Electric discharge machining (EDM)	A metal-working process applicable to mold construction in which controlled sparking is used to erode the workpiece.
Electrical strength [dielectric strength]	That property of an insulating material that enables it to withstand electrical stress. The electrical strength is defined as the highest electrical stress that an insulating material can withstand for a specified time without the occurrence of electrical breakdown.
Electroformed molds	A mold made by electroplating metal on the reverse pattern of the cavity. Molten steel may be then sprayed on the back of the mold to increase its strength.
Electronic data interchange (EDI)	Exchange of data by customer and supplier computers, usually through a third neutral company that safeguards the host computers from unwanted entry. Used for order placement, shipment, receiving, billing, and payment.
Electroplating	A deposition of metals on certain plastics and mold for finish.
Elongation at break	Elongation recorded at the moment of rupture of a specimen, often expressed as a fraction or percentage of the original length.
Elongation	Deformation caused by stretching, or fractional increase in length of a material in tension, expressed as a percentage difference between the original length and the length at the moment of the break – higher elongation indicates higher ductility.

Embossing	Techniques used to create depressions of a specific pattern in plastics' films or sheeting. Also development of surface patterns on the molded part by photoengraving or a similar process.
Embrittlement	Reduction in ductility due to physical or chemical changes.
Emulsion	A stable dispersion of one liquid in another created in the presence of an emulsifying agent (that has affinity with both phases). The emulsifying agent, discontinuous phase, and continuous phase produce the third phase, the interphase, which serves as an enveloping protective layer around each dispersed drop.
Emulsion polymerization	Free radical polymerization of an emulsion, consisting of aqueous phase containing an initiator and emulsified oil phase containing the monomer.
Endothermic	An action or reaction that absorbs heat.
Endurance or fatigue lifetime	Maximum fluctuating stress a material can endure for infinite number of cycles – determined from the S-N diagram.
End use	Function the part or assembly was originally designed and manufactured to perform.
Engineering polymer alloy	A processable engineering material containing two or more compatibilized polymers, capable of being formed to precise and stable dimensions, exhibiting high performance at the continuous use temperature above 100 °C, and having tensile strength exceeding 40 MPa.
Engineering polymer	A processable polymeric material capable of being formed to precise and stable dimensions, exhibiting high performance at high temperature and high tensile strength. Usually to qualify for the term, the material must have the continuous use temperature above 100 °C and the strength exceeding 40 MPa. Five types of polymers are customarily qualified as engineering resins: polyamide (PA), polycarbonates (PC), thermoplastic polyesters (EST), polyoxymethylene (POM), and modified polyphenylene ethers (PPE).
Engineering polymer blend	A polymer blend either containing engineering polymer(s) or having properties of an engineering polymer.
Engineering resin	Term associated with plastics having medium to high physical properties used for structural and demanding applications. Five types of resins belong to this group: PA, PEST (viz., PBT, PET, PAr), PC, PPE, and POM.
Environmental stress cracking (ESC)	The susceptibility of a thermoplastic resin to crack or craze when in the presence of surface-active agents or other environments, e.g., under the influence of certain chemicals or aging, weather, and stress.

Epoxide	A compound containing 1,2-epoxide, $CH_2(O)CH–R$, or its derivative.
Epoxy plastics	A thermoset polymer containing one or more epoxide groups and curable by reaction with amines, alcohols, phenols, carboxylic acids, acid anhydrides, and mercaptans. It has been primarily used as a matrix resin in composites and adhesives.
Epoxy resin	An oligomer containing two or more epoxide groups per molecule cross-linked with a hardener, usually diglycidyl ether of bisphenol A or pentaerythritol:

$$RH + CH(O)CH- \rightarrow -C(R)H - C(OH)H-$$
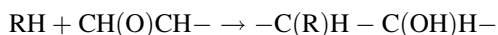
	The OH group may further react with the hardener, which leads to highly cross-linked thermoset polymer.
Etch	To treat with an acid, leaving parts of the surface in relief to form the desired design.
Ethylene plastics	Plastics based on polymers of ethylene or copolymers of ethylene with other monomer, the ethylene being in greatest amount by mass.
Ethylene-propylene rubber (EPR)	An elastomeric copolymer based on ethylene and propylene prepared in Ziegler-Natta polymerization. When small amount of a diene monomer is added, the resulting polymer becomes ethylene-propylene terpolymer, EPDM.
Ethylene-vinyl acetate (EVAc)	A thermoplastic copolymer made from ethylene and vinyl acetate. This copolymer is similar to polyethylene but has considerably increased flexibility.
Exfoliated clay	Individual clay platelets dispersed in a matrix polymer with the interlayer distance $d_{001} > 8.8$ nm. The platelets can be randomly dispersed individually or as short stacks or tactoids.
Exfoliation	Chemical and/or mechanical means of dispersing clay platelets in a polymer matrix. The process usually starts with intercalated clay (q.v.).
Exothermic	Pertaining to an action or reaction that gives off heat.
Extensibility (or extendibility)	The ability of a material to extend or elongate upon application of sufficient force, expressed as a percentage of the original length.
Extensometer	Instrument for measuring changes in linear dimensions (also called strain gauge).
Extrudate swell (sometimes improperly called die swell)	The ratio of the outer parison diameter to the inner diameter of the die. The swell is influenced by polymer nature, die construction, land length, extrusion speed, additives (viz., external lubricants), and temperature.

Extruder	A machine that accepts solid (pellets or powder) or liquid feed, conveys it through a surrounding barrel by means of a rotating screw(s), and pumps it, under pressure, through an orifice called "die."
Extrusion blow molding	Most often the process, in which a parison is extruded from a polymeric melt and is then entrapped between the halves of a mold. The parison is expanded by compressed air against the mold cavity, and then it is cooled, removed, and trimmed.
Extrusion	Compacting a plastic material (powders or granules) into a uniform melt and forcing it through an orifice in a continuous fashion to yield a desired shape. While held in the desired shape, the melt must be cooled to solidify. The term also describes plasticization of a resin in an extruder (barrel-and-screw or plunger assembly) and forcing of the molten material or extrudate through a die or into a mold. Extrusion is the initial part of the molding process.
Extrusion plastometer or melt indexer	A primitive viscometer used for determining the melt flow index, MFI. It is composed of a vertical cylinder with two longitudinal bored holes (one for measuring temperature and one for containing the specimen, the latter having an orifice of stipulated diameter at the bottom and a plunger from the top). The cylinder is heated by external bands, and weight is placed on the plunger to force the polymer specimen through the orifice. The result is reported in g/10 min. See also "Melt index."
Exudation	Formation of liquid plasticizer on the surface of a plasticized (usually PVC) resin.
Fabricate	To work a material into a finished form by machining, forming, or other operation. In the broadest sense, it means to manufacture.
Fading	Any lightning of an initial color possessed by a plastic.
Fadometer	Apparatus for determining the resistance of materials to fading by exposing them to ultraviolet rays of approximately the same wavelength as those found in sunlight.
Family mold	A multicavity mold in which each cavity forms a part that often has a direct relationship in usage to the other parts in the mold. Family molds can have more than one cavity making the same part, but they will still always have the same direct relationship to usage. The term is often applied to molds in which parts for different customers are grouped for economy of production. Sometimes called a combination mold.

Fan gate	A shallow gate somewhat wider than the runner from which it originates.
Fatigue	Permanent structural changes that occur in a material subjected to fluctuating stress and strain, which cause decay of mechanical properties. See "S-N diagram."
Fatigue ductility	The ability of a material to plastically deform before fracturing in constant strain amplitude and low-cycle fatigue tests. See "S-N diagram."
Fatigue failure	The failure or rupture of a plastic under repeated cyclic stress, at a point below the normal static breaking strength. See "S-N diagram."
Fatigue limit	The stress below which a material can be stressed cyclically for an infinite number of times without failure. See "S-N diagram."
Fatigue strength	Magnitude of fluctuating stress required to cause failure in a fatigue test specimen after specified number of cyclic loading – determined from the S-N diagram. Also the maximum cyclic stress a material can withstand for a given number of cycles before failure. The residual strength after being subjected to fatigue. See "S-N diagram."
Feathered thread	A thread that is thin at one end and does not end abruptly. Usually found in screw machine parts.
Feed throat	The section of the hopper mounted on the extruder to feed resin into the feed section of the barrel and screw.
Feedback	Information returned to a system or process to maintain the output within specified limits. See also "Closed loop."
Fiber	Often the term is used synonymously with filament having a finite length, $L = 100d$, where the diameter is typically $d = 100–130$ μm. In most cases, it is prepared by drawing from a molten bath, spinning, or depositing on a substrate. Fibers can be continuous, long (10–50 mm) or short (about 3 mm). In the plastics industry almost synonymous with thin strands of glass used to reinforce both thermoplastic and thermosetting materials.
Fiber-reinforced plastic (FRP)	A general term for a plastic that is reinforced with cloth, mats, strands, or any other fiber form.
Fiberglass	Filaments made by drawing molten glass. Continuous filaments have indefinite length. Staple fiber mat is made of glass fibers of the length generally 430 mm, the length depending on the forming or spinning process used.
Fiberglass reinforcement	Major material used to reinforce plastic, available as mat, roving, fabric, and so forth. It is incorporated into both thermosets and thermoplastics.

Filament	The smallest unit of a fibrous material. The basic units formed during drawing and spinning, which are gathered into strands of fiber for use as reinforcements. Filaments usually are of great length and small diameter, $d < 25$ μm.
Filler	A relatively inert substance added to plastics to improve their physical, mechanical, thermal, electrical, or other properties or to lower cost or density. A compound or substance added to a polymer during the initial synthesis process or in subsequent processing to decrease the volume of resin needed to produce a given product. Fillers are generally much lower in cost than the resins they are used in, thus reducing resin cost per part. Fillers or extenders are generally not used with engineering resins.
Fillet	A rounded inside corner of a plastic piece. The rounded outside corner is called a bevel.
Fines	Small particles mixed in with larger particles.
Finish	The secondary work on a part so that it is ready for use: filing, deflashing, buffing, drilling, tapping, and degating are commonly called finishing operations.
Finite element analysis	A stress analysis technique of a part using a computer-generated model that can take finite sections of the part for analysis of the forces and loads the part will experience in service. It generates a part-section analysis that shows the force concentrations in the section and determines if the material selected will be suitable for the part.
First surface	The front surface of a plastic part, nearest the eye.
Fisheye	A small, globular mass that has not completely blended into the surrounding polymeric material. This condition is particularly evident in a transparent or translucent film, fiber, or sheet.
Fishbone diagram	A problem analysis technique used to list all the variables and steps in the solution to a problem. All contributing elements are associated with each factor and taken back to their starting point to ensure that all variable elements are considered.
Fissure	A narrow opening crack in a material.
Fixture	Means of holding a part during a machine or other operation.
Flakes	A term used to describe resin residue formed on the inside of pipes during material transfer, created by the friction of the pellets against the surface of the transfer piping. With time, they build up, flake off, and can cause feed problems at the throat of the extruder.

Flame resistance	Ability of a material to extinguish flame once the source of heat is removed.
Flame retardants	Chemicals used to reduce the tendency of a polymer to burn.
Flame retarded	A resin modified by flame-inhibiting additives so that exposure to a flame will not burn or will self-extinguish. Some resins will not burn and others can be modified to meet flame burning specifications, while others may not be able to be modified.
Flame treatment	A type of surface treatment that oxidizes a plastic surface for better reception of paint, inks, and adhesives. See also "Surface treatment."
Flammability	Measure of the extent to which a material will support combustion.
Flash	Extra plastic attached to a molding along the parting line. Under most conditions, it is objectionable and must be removed before parts are judged acceptable.
Flash gate	Usually a long gate extending from a runner parallel to an edge of a molded part along the flash or parting line of the mold.
Flash line	A raised line appearing on the surface of a mold and formed at the junction of mold faces. "See Parting line."
Flash mold	A mold in which the faces are perpendicular to the clamping action of the press. The higher the clamping force, the tighter the mold seam.
Flash trap	A molded-in lip or blind recess on a part that is used for trapping excess molten material during an assembly operation. It negates flash trimming secondary operations.
Flex life	The time of heat aging that an insulating material can withstand before failure when bent around a specific radius (used to evaluate thermal endurance).
Flexural modulus	The ratio within the elastic limit of the applied stress to specimen's strain during flexural deformation mode testing – a measure of relative stiffness.
Flexural strength	Ability of a material to flex without permanent distortion or breaking. The resistance of a material to being broken by bending stresses.
Flock	Short fibers of cotton, wood, glass, etc., used as inexpensive filler.
Flocking	A decorating and/or sound-deadening technique where fibers of different materials are attached to the surface of a plastic part. Fibers can be oriented in specific directions and patterns determined by the techniques used, and adhesive patterns lay down on the surface of the part.

Flow	A qualitative description of the fluidity of a plastic material during processing. A quantitative value of fluidity may be expressed by the flow curve, melt index (MI), or melt flow index (MFI).
Flow chart	A line chart that traces the whole process.
Flow curve	A log-log plot of the isothermal viscosity as a function of the deformation rate.
Flow length	The actual distance a material will flow under a set of molding machine conditions. Influenced by the processing and mold design variables, the composition of the polymer, and any additives in the polymer.
Flow line	A mark on a molded piece made by the meeting of two flow fronts during molding. Also called weld line or weld mark.
Flow marks	Wavy surface appearance of an object molded from thermoplastic resins, caused by improper flow of the resin into the mold. Also see "Splay marks."
Flow coating	A painting process in which the article to be painted is drenched under a curtain of lacquer. The part is withdrawn and rotated until the coating dries.
Fluidized bed coating	Process in which small particles of a thermoplastic resin are suspended in a gas stream (generally air) and behave like a liquid. A heated article is immersed in this fluidized bed of powder. The particles melt and fuse to the heated surface, forming a smooth coating.
Fluoropolymer	A polymer whose mers contain fluorine, F.
Fluoropolymers	The family of fluorinated polymers that include polytetrafluoroethylene, (PTFE), polychlorotrifluoroethylene (PCTFE), polyvinylidenefluoride (PVDF), and fluorinated ethylene-propylene. These resins are characterized by good thermal and chemical resistance, nonadhesiveness, low dissipation factor, and low dielectric constant. They are available in a variety of forms, such as moldings, extrudates, dispersions, films, or tapes.
Foamed plastics or cellular plastics	Plastics with numerous cells disposed throughout its mass. Cells are formed by a blowing agent or by the reaction of the constituents. Resins in sponge form may be flexible or rigid; the cells may be open or closed.
Foil decorating	Molding paper, textile, or plastic foils printed with compatible inks directly onto a plastic part so that the foil is visible below the surface of the part as an integral decoration.
Force	That which changes the state of rest or motion in matter, measured by the rate of change of momentum.

Forming	The term usually applied to a process in which the shape of plastic pieces such as sheets, rods, or tubes is changed to a desired form. Usually the term does not include extrusion, molding, or casting, in which forms are made from molten polymers or solutions.
Fourier transform	An analytical method used in advanced forms of spectroscopic analysis such as infrared and nuclear magnetic resonance spectroscopy.
Fractionation	Experimental methods for separating and isolating fractions, each with the more uniform molecular weight, and thus of low polydispersity. The process also serves for ascertaining the distribution function.
Fracture strength	The normal stress at the beginning of fracture. Calculated from the load at the beginning of fracture during a tension test, and the original cross-sectional area of the specimen.
Fracture	The separation of a body, defined both as rupture of the surface without complete separation of the laminate and as complete separation of a body because of external or internal forces.
Free radical polymerization	Polymerization in which the active centers of reaction are radicals. The polymerization can be initiated by thermally activated or redox initiator, by irradiation, or through thermal activation of monomer.
Freeze drying	A method of removing volatiles from solidified material at low temperatures.
Freeze-off	Refers to the gate area when polymer solidifies, as well as any area in the flow system when the melt becomes too cool to flow and solidifies.
Frequency	The number of times a specified phenomenon occurs within a specified interval, e.g., number of completed energy transmissions imparted to the welding horn in a vibratory motion.
Friction welding	A means of assembling thermoplastic parts by melting them along their line of contact through friction. See also "Spin welding."
Full IPN	Any material containing two or more polymers in an intimate network form without induced cross-links between the individual polymers.
Fusion bond	The joining of two melt fronts that meet and solidify in a mold cavity. A bond formed during the assembly operation where the joint line is melted before assembly. See "Hot-plate welding," "Induction welding," and "Ultrasonic sealing."

Fusion	Heating of a vinyl dispersion to produce a homogeneous material.
Galling	A surface area that is worn away by another by rubbing against it.
Gas-assisted injection molding (GAM)	An injection molding process that introduces a gas (usually nitrogen) into the plasticized material, to form voids in strategic locations.
Gaseous blowing agent	A compressed gas, such as compressed air or nitrogen, used to create a cellular structure or controlled voids in a rubber or plastic's mass.
Gate	In injection and transfer molding, the orifice through which the melt enters the cavity.
Gauges	Measuring devices used to determine if the part meets customer specifications, including micrometers and vernier calipers.
Gaussian (or normal) distribution	A symmetrical, bell-shaped distribution function: $$y = \left[1/\sigma(2\pi)^{1/2}\right]\exp\left\{-[(x-\bar{x})/\sigma]^2/2\right\}$$ where x is a variable and σ is the standard deviation.
Gaylord	A term used to identify a box of resin vs. a bag or drum. Box size and weight of resin can vary depending on the density of the resin and the supplier's box size. Box size usually conforms to the size of a standard pallet on which it is shipped.
Gel or Trommsdorff effect	Auto-acceleration at the end of chain growth polymerization. With increasing size of the macroradicals, their mobility decreases and terminations are less frequent. However, the diffusion of the monomer remains unhindered and the polymerization proceeds exothermally, resulting in auto-acceleration.
Gel permeation chromatography (GPC, more recently size exclusion chromatography, SEC)	A form of liquid chromatography in which the polymers are separated by their ability or inability to penetrate the material in the separation columns. Column chromatography technique employing a series of columns containing closely packed rigid gel particles. The polymer to be analyzed is introduced at the top of the column and then is eluted with a solvent. The polymer molecules diffuse through the gel at rates depending on their molecular size. As they emerge from the columns, they are detected by differential refractometer, viscometer, FTIR device, etc. From the output of these detectors, a molecular weight distribution curve can be obtained.

Gel point	The stage at which a liquid begins to exhibit pseudo-elastic properties. Also known as "gel time."
Gel solutions	Concentrated solutions; intermediate state between gel and sol.
Gel	That cross-linked part of polymer in liquid state, which having its network character may swell but not dissolve.
Generic	Descriptive of an entire type or class of plastic resins. The base resin is one of a family of polymers, but there may be hundreds of product combinations.
Glass	A material that solidifies from the molten state without crystallization, a supercooled liquid whose shear viscosity is $\eta \geq 10^{12.5}$ Pas, a liquid whose rigidity is great enough to be put to use, or a glassy state of matter. A typical glassy material is hard and brittle (tensile modulus E § 70 GPa, tensile strength σ § 0.5 GPa). Typical polymeric glasses are atactic polystyrene, atactic polymethylmethacrylate, polycarbonate, etc.
Glass-mat thermoplastics, (GMT)	A mat consisting of long glass fibers that are impregnated with a thermoplastic resin to produce a flat, homogeneous, semifinished composite blank.
Glass transition temperature, or glass transition point, T_g	The center of the temperature range in which a noncrystalline solid changes from being glass brittle to being viscous or rubbery. The temperature, or a range of temperatures, separating the rigid (glassy) from elastic (rubbery or liquid) state of a polymer. For the transition to occur, 20 to 50 main chain atoms must be able to move in a cooperative manner. For the organic polymers -160 "T_g" 400 °C depending on the intrinsic flexibility of the polymeric chain and its molecular weight. Since the transition is kinetic in nature, it depends on the rate or frequency. The measured T_g value depends considerably on the test rate, frequency, or mechanical deformation.
Gloss	Brightness or luster of a plastic resulting from a smooth surface. The shine or luster of the surface of a material (ASTM D 673). See "Specular gloss" and "Surface finish."
Grades	Polymers that belong to the same chemical family and are produced by the same manufacturer. They may vary in processing or performance due to differences in molecular weight, additives, or other structural features. For example, a supplier of PC may have flame-resistant grades, glass fiber-reinforced grades, a conductive grade, and easy flowing grades.

Graft copolymers	A copolymer whose macromolecules consist of two or more macromolecular parts of different composition, covalently joined in such a way that one of the parts forms the main chain (polymer A) and the other(s) the side chains (polymer B). In a sense the block copolymers are graft copolymers in which the graft block B is attached to the end of main chain A. Graft copolymers are frequently used as compatibilizers.
Graining	The term refers to wood graining on plastics. This can be done by hand, roller coating, hot stamping, or printing.
Graphite	A crystalline allotropic form of carbon.
Graphite fiber	A fiber from either pitch or polyacrylonitrile (PAN) precursor by an oxidation, carbonization, and graphitization processes. See also "Carbon fiber."
Grinder or granulator	A machine (in many sizes, styles, and capacities) with a series of knife blades and a sizing screen to chop up plastic materials for reuse.
Grit blasted	A surface treatment of a mold in which grit or sand materials are blown onto the walls of the cavity to produce a roughened surface. Air escape from mold is improved and special appearance of the molded article is often obtained by this method.
Guide or leader pins	Devices that maintain proper alignment of parts.
Guideway	Usually a T-shaped slot in a mold.
Gusset	An angular piece of material used to support or strengthen two adjoining walls.
Hand molds	Molds that are removed from the press by the operator, who opens the mold and extracts the part by hand.
Hardenable substance	Thermoset resin that, under the influence of temperature and/or reactive agent, undergoes cross-linking that irreversibly changes the chemical constitution and thereby physical properties.
Hardeners	Polyfunctional substances that are able to cause cross-linking in thermosets.
Hardening, curing	A chemical cross-linking of material, initially soft or that can be made so by warming, into a more viscous form or hard solid.
Hardness	The resistance to compression and surface indentation, usually measured by the depth of penetration of a blunt point under a given load using a particular instrument according to a prescribed procedure. Among the most important methods of testing are Barcol hardness, Brinell hardness, Knoop hardness, Mohs hardness, Rockwell hardness, and Shore hardness.

Haze	The degree of cloudiness in a plastic material. The cloudy or turbid aspect of appearance of an otherwise transparent specimen caused by light scattered from within the specimen or from its surface.
Head	The end section of the molding machine that consists of the core, die, mandrel, mold, and other parts necessary to form the plastic.
Head-to-head structure	A structure of the type $-CH_2CHX-CHXCH_2-$ in polymers where the monomer placement in the growing chain has two isomeric possibilities: head-to-head (as shown) or head-to-tail, viz., $-CH_2CHX-CH_2CHX-$. The latter structure predominates.
Heading	The mechanical, thermal, or ultrasonic deformation of a pin to form a locking attachment.
Heat resistance	The property or ability of plastics and elastomers to resist the deteriorating effects of elevated temperatures.
Heat sealing	A process of joining two or more thermoplastic films or sheets by heat.
Heat stability	The resistance of a plastic material to chemical deterioration caused by exposure to heat during processing.
Heat stabilizer	An ingredient added to a polymer to improve its processing or end-use resistance to elevated temperatures. The term is used in different contexts depending on the benefit to be derived from the additive. For processing, it retards changes of color. For end use, it protects the surface of the part exposed to elevated temperatures. It does not imply that a resin can be used beyond its recommended end-use temperature rating if it is heat stabilized.
Heat distortion temperature (HDT)	The temperature at which a standard test bar deflects by an arbitrary value under a stated load. In ASTM D648, it is defined as a total deflection of 250 μm in a rectangular bar supported at both ends under a load of 0.5 or 1.8 MPa. The temperature is increased at a rate 2 °C/min.
Heated manifold mold	A hot-runner mold that is both heated and insulated; an insulated mold is a hot-runner mold that does not contain heaters.
Heater bands	The heat source for the barrel and nozzle. The temperature control is usually divided into rear, middle, front, and nozzle sections. The bands are accurate resistance heaters with high heat output.
Heating chamber	In injection molding that part of the machine in which the cold feed is reduced to a hot melt. Also called heating cylinder.

Helix	A helical conformation of polymeric chain in which all main chain atoms can be placed on a cylindrical surface in such a way that all elements on that surface are cut at constant angle or, in other words, that the conformation is exactly repeated at constant intervals. For example, 31 helix in polypropylene has three repeating units per one helix turn.
Hermetic	As in seal, to form a bond that is pressure tight, so that air or gases cannot enter or escape.
Heterogeneous	Materials consisting of identifiable dissimilar constituents separated by internal boundaries. It is noteworthy that not all nonhomogeneous materials are necessarily heterogeneous.
Hiding power	The opacity that can be effected with a coating.
High-density polyethylene (HDPE)	Linear polyethylene copolymers with low branching, having density $\rho = 940$–960 kg/m^3. The regular structure engenders material with greater strength, rigidity, chemical resistance, and higher softening temperature than the branched one.
High-impact polystyrene (HIPS)	A thermoplastic resin from a styrene and elastomer. It has good dimensional stability and low-temperature impact strength, high rigidity, and ease of processing.
Histogram	A bar chart with the height of each bar indicating how many data points were collected within certain interval. The width of the bar provides a measure of the interval.
Hob	A master model in hardened steel used to sink the shape of a mold cavity into a soft steel block.
Hobbing	Forming multiple mold cavities by forcing a hob into soft steel cavity blanks. Also called sinking.
Holding pressure	The pressure maintained on the melt after the cavity is filled until the gate is filled and freezes.
Homologous polymer blend	A mixture of two or more homologous polymers, usually narrow molecular weight distribution fractions of the same polymer.
Homologous polymers	Polymers identical in structure and composition and differing only in molecular weight. A polydispersed polymer is a miscible blend of homologous polymers.
Homopolymer	The product of the polymerization of a single monomer, i.e., a polymer containing one type of repeating units, viz.

$$-[\mathrm{CH_2CHX - CH_2CHX}]_n^-.$$
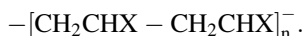
Hone, honing, honed	To impart a precise accuracy to the surface finish by using a fine-grained whetstone.

Hooke's solid	An ideal elastic material where stress is directly proportional to strain.
Hoop stress	The circumferential stress in a material of cylindrical form subjected to internal or external pressure.
Hopper	A conical reservoir from which the molding powders or pellets are fed into the extruder.
Hopper feeder	Usually part of the resin drying system that also can be an independent unit, to convey material to the machine's feed hopper using vacuum or pressure.
Hot stamping or branding	Engraving operation in which roll leaf is stamped with heated metal dies onto the face of the plastics.
Hot tip	The precise controller and gating mechanism of a hot-runner mold.
Hot-plate welding	The use of a heated tool to cause surface melting of a part at the joint area. It is then removed before the joint surfaces being pressed together to form a fusion bond.
Hot-runner mold	A thermoplastic injection mold in which the runners are insulated from the chilled cavities and remain hot so that the center of the runner never cools in normal cycle operation. Runners are not usually ejected with the molded pieces.
Hot/heated manifold mold	A thermoplastic injection mold in which the mold that contains the runner system has its own heating elements to keep the molding material in a plastic state ready for injection into the cavities, from which the manifold is insulated.
Hydrolysis	Chemical decomposition of a substance involving the addition of water.
Hydrophilic	Capable of absorbing water.
Hydrophobic	Capable of repelling water.
Hygroscopic	Material capable of absorbing and retaining atmospheric moisture from air. Plastics such as PA, PEST, or ABS are hygroscopic and must be dried before molding.
Hysteresis	The failure of a property that has been changed to return to its original value when the cause of the change was removed. The cyclic noncoincidence of the elastic loading and the unloading curves under cyclic stressing. The area of the resulting elliptical hysteresis loop is equal to the heat generated in the system.
Immiscible polymer blend	Any polymer blend whose free energy of mixing is positive: $\Delta G_m > 0$.
Impact strength	The ability of a material to withstand shock loading, expressed as an amount of energy required to fracture a specimen subjected to impact. The work done in fracturing, under shock loading, using a specified test

	specimen and a specified procedure. Also, the relative susceptibility of plastic articles to fracture under stress applied at high speeds.
Impact test	Often associated with the Gardner (ball or falling dart) test, with a known weight falling at a known distance and hitting a part, thereby subjecting it to an instantaneous high load. ASTM impact tests for material properties are the Izod, Charpy, and tensile impact tests. The test can also be a pendulum type.
Induction welding	The use of radio, magnetic, or electrical energy to form a melt through the application of a foreign medium at the joint line to form a fusion bond.
Inert pigment	A pigment that does not react with any component of paint.
Infrared (IR or FTIR)	Pertaining to that part of the electromagnetic spectrum between the visible light range and the radar range. Radiant heat is in this range, and infrared heaters are frequently used in the thermoforming and curing of plastics and composites. Infrared analysis is used for identification of polymer constituents. The powerful Fourier transform infrared spectroscopy, FTIR, uses a method of splitting a beam into two waves, and the spectral information is obtained from the phase difference between the two waves, recombining them in the Michelson interferometer. The interferogram is obtained by digitizing the detector signal and transforming it from the time domain by means of the Fourier transform operation into a conventional IR spectrum. See "Infrared spectroscopy."
Infrared spectroscopy or spectrometry	A technique used to observe the wavelengths in the electromagnetic spectrum lying beyond the red, from about 750 nm to a few mm.
Inhibitor	A substance that reacts with the active polymerization site either to form a totally nonreactive product or to reduce the system reactivity. In radical polymerization, the radical scavengers, viz., diphenylpicrylhydrazyl and quinones, are used as inhibitors.
Initiator	Either an additive mixed in a material to cause a chemical or physical reaction in the melt or a substance able to engender reaction of a monomer, radical or ionic.
Injection blow molding	Blow molding in which the parison is directly formed by injection molding.
Injection molding	A method of forming a plastic to the desired shape by forcing the softened plastic into a relative cool cavity

	using a screw or ram – used with thermoplastics or thermosets. See "Thermoplastic injection molding" and "Thermoset injection molding."
Injection pressure	The pressure in the mold during the injection of plasticized material into the mold cavity.
Injection ram	See "Ram."
Injection time	The time it takes for the screw's forward motion to fill the mold cavity with melt.
Inorganic	A mineral compound not composed of carbon atoms.
Inorganic pigments	Natural or synthetic metallic oxides, sulfides, and other salts that impart color, as well as heat and light stability, and weathering resistance.
Inorganic polymer	A polymer with high proportions of non-carbon atoms. In principle, most inorganic materials can be considered inorganic polymers, viz., silicates. In polymer science, the inorganic materials containing organic groups are considered inorganic polymers, e.g., polysiloxanes (silicones), phosphonitrilic elastomers, polycarboranes, organometallic polymers, polymetaphosphates, polyphosphazenes, and sulfurnitride polymers. See also "Organic polymers."
Insert	An integral part of plastics molding. It consists of metal or other material that may be molded into position or may be pressed into the molding after the molding is completed. Also a removable or interchangeable component of the mold.
Intercalated clay	Clay having organic or inorganic molecules inserted between its platelets, thus increasing the interlayer spacing between them to at least 1.5 nm.
Intercalation	Process of inserting organic or inorganic molecules between platelets of a layered material, thus increasing the interlayer spacing.
Interface	The boundary or surface between two different, physically distinguishable media. With fibers, the contact area between the fibers and sizing or finish. In laminates, the contact area between the reinforcements and the laminating resin.
Interpenetrating polymer network, (IPN)	Historically, any material containing two or more polymers, each in network form, without induced cross-links between the individual polymers, usually produced by polymerizing and/or cross-linking at least one component in the immediate presence of the other, thus thermoset in character. Currently, the term IPN encompasses the thermoplastic co-continuous polymer blends, as well as ionomers and block and graft

	copolymers. The later materials are known as thermoplastic IPN.
Interphase	The boundary region between two phases in polymer blends, the matrix polymer and the dispersed phase, or (in case of phase co-continuity) between two polymeric phases. In compatibilized blends, the interphase contains the compatibilizer as well as low-molecular-weight additives and fractions.
Intrinsic viscosity	The limiting value (at infinite dilution) of the ratio of specific viscosity of the polymer solution to concentration.
Ion exchange resins	Cross-linked polymers that form salts with ions from aqueous solutions.
Ionic polymers or ionomers	Polymers of linear or network structure with ionic groups which by addition of the appropriate counterions can be ionically cross-linked. A copolymer of ethylene and acrylic acid is used as a compatibilizer in polyamide blends. Converted to ethylene-zinc acrylate copolymer, Surlyn™ is used as packaging film. Other ionic polymers are applied as polyelectrolytes, ion exchange resin, etc.
Ionomer	Polyethylene that contains both covalent and ionic bonds. The polymer exhibits strong interchain ionic forces. The anions hang from the hydrocarbon chain, and the cations are metallic, e.g., Na, K, Li, Zn, and Mg. The resins have similar properties as polyethylenes, with high transparency, tenacity, resilience, and increased resistance to oils, greases, and solvents.
Ishakawa	See Fishbone diagram.
Isomeric polymers	Polymers that are basically homogeneous but in which, by secondary alterations or by a small number of different kinds of linking of the primary molecules (e.g., branching), variations are introduced.
Isotactic polymer	A polymer in which the constitutional repeating units have the same stereochemical configuration, for example, isotactic polypropylene.
Izod impact test	A type of pendulum impact test in which a notched sample bar is held at one end and broken by a blow. This is a test for shock loading.
Izod impact strength	Determination of the resistance of a plastic material to a shock loading, in which a notched specimen bar is held at one end and broken by striking, and the energy absorbed is measured.
Jetting	Turbulent flow of plastic from an undersized gate or thin section into a thicker mold section, as opposed to

	laminar flow of material progressing radially from a gate to the extremities of the cavity. May also result from shooting material into a mold cavity where there is no core or immediate cavity wall to break up the flow of the material coming through the gate.
Just-in-time (JIT)	A practice developed to minimize customer inventory. The supplier provides the product, at predetermined intervals, so that it can proceed directly to the customer's assembly line. This practice demands excellent quality control and production schedules. Customers who use JIT must demand the same care and treatment from their own suppliers. Suppliers and customers are usually located within a few hours shipping time of each other.
Kirksite	An alloy of aluminum and zinc used for the construction of prototype molds. It imparts a high degree of heat conductivity to the mold
Kneading elements, kneading blocks	Three types of elements are used to assemble screws in a twin-screw extruder: kneading, mixing, and transporting. The kneading elements are mostly two- or three-lobe self-wiping that mainly provide for the dispersive mixing by pressing, stretching, and folding actions. An assembly of kneading elements is known as a kneading block, characterized by the individual disk length, number of disks, and stagger angle between the disks in the kneading block. See also "Mixing elements."
Knit line	A line on a part where opposing melt fronts meet. Created by material flow around obstructions or multiple gating. See "Weld line."
Knockout or ejector pin	A pin that pushes a cured molded article out of a mold.
Kurtosis	The state or quality of peakedness or flatness of the graphic representation of a statistical distribution expressed as $\alpha_4 = m_4/m_2^2$, where m_4 and m_2 are the fourth and second moment of the distribution function. The excess of kurtosis is given as $\alpha_4 - 3$. The kurtosis is large when on a distribution function there is a relatively high concentration in the middle and out on the tails, with a relatively steep drop in between.
Lack of fill-out	An area occurring usually at the edge of a laminated plastic, where the reinforcement has not been wetted with resin.
Ladder polymer	A rigid rod polymer, consisting of two parallel macromolecular chains regularly joined by covalent bonding, forming a sequence of interconnecting rings, e.g.,

	pyrrone, polyquinoxalines, polyphenylsilsesquioxane, and poly(bisbenzimid-azobenzo-phenanthroline).
Lamella	The basic morphological unit of a crystalline polymer, usually ribbonlike or platelike in shape. Generally (if ribbonlike), about 10–50 nm thick, 100 nm wide, and 1,000 nm long.
Lamellar thickness	A characteristic morphological parameter, usually estimated from X-ray studies or electron microscopy, usually 10–50 nm.
Laminar flow	Flow of thermoplastic resins accompanied by solidification of the layer in contact with the mold surface that acts as an insulating tube through which material flows to fill the remainder of the cavity. This type of flow is essential to duplication of the mold surface.
Land	Either a horizontal bearing surface of a semipositive or flash mold by which excess material escapes, a bearing surface along the top of the flights of a screw in an extruder, or the surface of an extrusion die parallel to the direction of the melt flow. In injection molding, the gate, when entering a part, has always the length of the gate itself that is called the land.
Latex, lattices	Aqueous dispersion of polymeric particles, a polymer emulsion, a product of emulsion polymerization used in paints, adhesives, coatings, etc.
LCST (lower critical solution temperature)	The lowest temperature of immiscibility, where binodal and spinodal curves meet. This type of phase separation predominates in polymer blends.
Let-down ratio	The quantity of one ingredient to be mixed with a base material to obtain the desired results.
Level of significance, "a"	The probability of committing the error of rejecting a given hypothesis when it is true; "a" is usually set to 0.05 for most of the statistical tests.
Light resistance	The ability of a plastic material to resist fading after exposure to sunlight or ultraviolet light (ASTM D1501). Light stability is the measure of this resistance.
Limit switch	An electromechanical switch positioned to stop or start an action. It is operated by mechanical action on a movable control arm.
Liquid crystal polymer (LCP)	A thermoplastic polymer (polyamide or polyester) that contains primarily benzene rings in its backbone, is melt processable, and can be highly oriented during processing. Available with or without fiber reinforcement.
Living polymer	An ionic polymer in which, in the absence of a monomer, the active centers of polymerization are

	preserved. Formation of living polymers in anionic or Ziegler-Natta polymerizations makes it possible to produce block copolymers.
Loading or charging tray	A device used to load the charge of material or metal inserts simultaneously into each cavity of a multicavity mold by the withdrawal of a sliding bottom from the tray.
London dispersion forces	Weak intermolecular forces based on dipole-dipole interactions.
Long chain branching	Branches of comparable length as the main polymer chain as in low-density polyethylene, polyvinylchloride, etc.
Loss modulus	A quantitative measure of energy dissipation, defined as the ratio of stress $90°$ out of phase with oscillating strain to the magnitude of strain. The loss modulus may be measured in tension of flexure, E", compression, K", or shear, G" (see also "Complex modulus").
Lubricants	Processing aids to assist material flow during extrusion or injection molding. The internal and external lubricants are recognized. Internally lubricated resins use oils, Teflon™, MoS_2, or other materials to give the molded part a lower coefficient of friction. The external lubricant can be a solid, such as sodium or zinc stearate, a fluoropolymer, or silicone resin or liquid.
Macbeth	A lighting system used for checking color.
Macromer	An oligomeric or telomeric chain capable of entering into a polymerization reaction.
Macromolecule	A large molecule in which neither the end groups nor the substitution of a group has any significant influence on the material properties.
Manifold	A pipe channel, or mold, with several inlets or outlets.
Mass spectrometer	An instrument capable of separating ionized molecules of different mass/charge ratios and measuring the respective ion currents.
Master curve	The acceptable or required curve that all subsequent test curves must match.
Matched metal, or die, molding	A method of molding reinforced plastics between two close-fitting metal molds mounted in a press.
Matrix	Either the base resin used for a molded part or the main phase in polymer blends.
Matte finish	A type of dull, nonreflective finish. See "Surface finish."
Mean or average	The sum of values divided by their number.
Mechanical properties	The properties related to the relationships between stress and strain, such as compressive and tensile strengths and moduli, associated with elastic and inelastic reaction to the applied force.

Median	The middle value when all values are arrayed in order of magnitude.
Melt fracture	An elastic strain set up in a molten polymer as the polymer flows through the die. It may show up as irregularities on the surface of the plastic. Several stages (and different mechanisms responsible for these) are recognized, viz., shark skin, pressure oscillation (or spurt), and gross distortions.
Melt front	The exposed surface of molten resin as it flows into a mold. The melt front advances as the molten resin is continuously pushed through its center section.
Melt index (MI), melt flow index (MFI), or melt flow rate (MFR)	The amount in grams of a thermoplastic resin forced through a 2.10 mm (0.0825 in. orifice when subjected to the prescribed force, e.g., 2.16 kg force during 10 min at the prescribed temperature ($^{\circ}$C) using an extrusion plastometer (ASTM D1238). It is customary to refer to the flow rate of polyethylene as "melt index." However, for all other materials, the term "melt flow rate" should be used.
Melt strength	The strength of a plastic while in the molten state.
Melt temperature	The temperature at which a resin melts or softens and begins to flow. The temperature of resin melt taken with a pyrometer melt probe.
Melting point	The temperature at which a resin changes from a solid to a liquid.
Metal plating	The process of plating a plastic part by chemically etching the surface to accept a base metal on which the subsequent layers of metal are deposited. Usually a multistep process. Not all plastics can be metallized.
Metallizing	A general term used to cover all processes by which plastics are coated with metal.
Metallocenes	Metallo-organic sandwich compounds in which two cyclopentadienlidene, Cp, rings form a sandwich around a metallic ion of, e.g., Fe, Co, Ni, Cr, Ti, V, and Zr. They have been used to catalyze the coordination polymerization of olefinic or vinylic monomers into highly regular macromolecules, viz., with narrow molecular weight, high regularity of comonomer placement, and/or high tactic purity. For example, ethylene was catalyzed with $R'_s(Cp)_2MeQ$ [Me is metal from group 4b, 5b, or 6b (preferably Zr); R' is a C_1–C_4 alkylene radical, a dialkyl germanium, or silicone; Q is an alkylidene radical having from 1 to about 20 carbon atoms, s = 0–1, p = 0–2, m = 4–5], in combination with alumoxanes.

Meter	SI length unit equal to 100 cm molecular dimension, or 39.37 in.
Metering equipment	A machine or system to accurately meter additives to the machine's hopper or feed throat. Comes in many sizes and types to suit each particular application, including augers, shuttle plates, photoelectric eyes, and positive or negative weight loss belt feeders.
Metering screw	An extrusion or injection molding screw that has constant shallow depth and pitch section, usually over the last three to four flights.
Micelle colloids	Low-molecular-weight, mainly homogeneous molecules, held together by secondary forces to form a colloidal particle.
Microcracking	Cracks formed when local stresses exceed the strength of the matrix. In composites, because microcracks do not penetrate the reinforcing fibers, in cross-ply or cloth prepreg tape laminates, they are usually limited to the thickness of a single ply.
Micro-morphology	Structural constitution on a submicron scale as related to crystallinity, viz., crystalline unit cells, lamellae shape and size, and stress-induced shish kebab crystals.
Microprocessor	Computer system that stores, analyzes, and adjusts the controls of a machine based on the parameters established during the operation of the machine it is controlling. It continuously analyzes output data to adjust and maintain the machine's cycle within programmed limits. Can also store data and output it as directed by programming.
Microstructure	The molecular structural features of a single polymer chain: tacticity, isomerism, chain branching, structural irregularities, etc.
Migration of plasticizer	Loss of plasticizer from a polymeric compound, with subsequent absorption by an adjacent medium that lowers its concentration and induces brittleness.
Migration	The transfer of a material from a plastic to other contacting solids.
Mil	English unit of length equal to 0.001 in. or 25.4 μm.
Miscible polymer blend	A polymer blend, homogenous down to the molecular level, in which the domain size is comparable to macromolecular dimension, associated with the negative value of the free energy and heat of mixing, ΔG_m and $\Delta H_m < 0$, and $\partial^2 \Delta G_m / \partial \varphi^2 > 0$. Operationally, it is a blend whose domain size is comparable to the dimension of the macromolecular statistical segment.

Mixing	General term associated with the physical act of homogenization (e.g., mixing of fractions). Mixing of liquids is usually called blending (e.g., preparation of polymer blends or alloys), while incorporation of solids into molten polymer is usually called compounding (e.g., preparation of a compound).
Mixing elements	Three types of elements are used to assemble screws in a twin-screw extruder: kneading, mixing, and transporting. The mixing elements of different types are provided by the equipment manufacturers, viz., turbine, gear, notched disk, and blister rings. Depending on the type, these elements are responsible for either or for both the distributive and dispersive actions. Several authors consider kneading and mixing elements as belonging to the same class, alternatively labeled as kneading or as mixing blocks. See also "Kneading elements."
Modified natural products	Plastics or fibers that are prepared by chemical transformation of natural substances, e.g., cellulose nitrate or acetate and casein or gelatin hardened by formaldehyde.
Modifiers	Any additive that improves the processing or end-use properties of the polymer, e.g., PVC plasticizers added to make it soft and pliable and improve its impact strength. Almost all plastic resins use different modifiers to meet desired product requirements.
Modulus of elasticity	The ratio of the stress to the strain produced in a material that is elastically deformed (ASTM D790). If a tensile stress of 20 MPa results in an elongation of 1 %, the modulus of elasticity is 2 GPa.
Modulus of resilience	The energy that can be absorbed per unit volume without creating a permanent distortion. Calculated by integrating the stress–strain curve from zero to the elastic limit and dividing by the original volume of the specimen.
Moisture absorption	The pickup of water vapor from the atmosphere by bulk of a material. It relates only to vapor withdrawn from the air by a material and must be distinguished from water absorption, which is the gain in weight due to the take-up of water by immersion.
Moisture adsorption	Surface retention of moisture from the atmosphere.
Moisture vapor transmission rate (MVTR)	The rate at which water vapor permeates through a plastic film or wall at a specified temperature and relative humidity (ASTM E96).

Mold deposits	Material build up on a cavity's surface due to plate out of resin, usually in a gaseous state. Can be attributed to additives in a resin adhering to the mold's surface.
Mold release agent	A lubricant, liquid, or powder (often silicon oils and waxes) used to coat a mold cavity to prevent the molded piece from sticking to it, thereby facilitating its removal from the mold. Additives put into a material to serve as a mold release.
Mold shrinkage	Shrinking a molded part while it is removed from a mold and cooled to room temperature. The difference in dimensions between a piece and the mold cavity. The incremental difference between the dimensions of the molding and the mold from which it was made, expressed as percentage of the mold dimensions.
Molding	A group of plastics processes used to form polymers or composites into solids with shape and size defined by the mold cavity, by the application of pressure and heat for a given time.
Molding cycle	The time required to complete a cycle and produce a part.
Molding compound powder or material	Plastic material, often comprising resin, filler, pigments, plasticizers, and other ingredients, ready for molding operation.
Molding pressure	The pressure applied directly or indirectly on the compound to allow the complete transformation to a solid dense part. The pressure developed by a ram or screw to push molten plastic into a mold cavity. See "Injection pressure."
Molding shrinkage	See "Mold shrinkage."
Molecular weight, or an average molecular weight (MW)	The sum of the atomic masses of the elements forming the molecule expressed in units of 1/12 the mass of ^{12}C atom, or a mass of one mole of the substance (kg/mol), indicating the relative size typical chain length of the polymer molecule. Owing to polydispersity the molecular weight of a polymer is expressed as an average:

$$M_k = \frac{\sum_i N_i M_i^{k+1}}{\sum_i N_i M_i^k}$$

For $k = 1$, the number average; for $k = 2$, the weight average; for $k = 3$, the z-average; for $k = 4$ ($z + 1$), average molecular weight is generated; etc. (viz., M_n, M_w, M_z, $M_z + 1$, respectively).

Molecularly homogeneous	A polymer in which all the molecules possess the same chemical structure.
Molecular weight distribution (MWD)	A statistical description of the sizes and frequency of occurrence of different molecular chain lengths within a given sample or lot of polymers, i.e., the distribution of molecular sizes in a polydispersed polymer. Several analytical functions f(M) have been proposed. Some of them are general statistical expressions (e.g., log-normal distribution, q.v.) and the others are based on assumed kinetics of polymerization (e.g., Schultz-Flory distribution). MWD is normally determined using a size exclusion chromatography, SEC (an old GPC). Wide and skewed distributions result in significant variation of properties. Narrow distributions are more consistent.
Molecule	A group of atoms bonded together which forms the fundamental structural unit of most organic substances. The number of atoms can range from two to millions. A molecule is the smallest unit of a substance that still retains the properties of that substance.
Monomer (monomer = single unit)'	A small molecule of an organic substance capable of entering into a polymerization reaction with itself or with other similar molecules or compounds, viz., vinyl monomers, dienes, α,ω-lactams, and diamines. A low-molecular-weight-reactive chemical that polymerizes to form a polymer. Monomers are generally gases or liquids. When bonded together in long chains, they form solid materials or polymers.
Morphology	The study of the physical form and structure of a material. The overall physical form of the physical structure of a material on a submicron and micron scale. Common units are dispersed phase domains, lamellae, spherulites, etc. The term comprises notion of the global structure (e.g., stress-induced skin core), as well as shape, size, orientation, and distribution of the dispersed phase (solid, liquid, or gaseous).
Mottle	The desired or accidental mixture of colors or shades of a color giving approximately distinct or complicated patterns or specks, spots, or streaks of color.
Movable platen	The moving platen of an injection or compression molding machine to which half of the mold is secured during operation. The platen is moved either by a hydraulic ram or a toggle mechanism.
Multiblock copolymer	A block copolymer with more than three blocks, e.g., $-[AB]_n-$.

Multicavity mold	A mold having more than one cavity or impression for forming finished items during one machine cycle.
Multichain polymer	A polymer with more than two chains extending from a center, e.g., comb or star polymer.
Multiple-screw extruder	An extruder machine that has two or more screws, as contrasted with conventional single-screw extruders.
Nanocomposite (NC)	A matrix material (metallic, ceramic, or polymeric in nature) having dispersed particles, with at least one dimension that does not exceed 10 nm. Polymeric nanocomposites (PNC) of commercial interest comprise 2–5 wt% of exfoliated clay.
Necking	Localized reduction in cross section that may occur in a material under tensile loading during a tensile test. Necking is disregarded in calculation of the engineering stress, but is taken into account in determining the true stress.
Network polymer	A cross-linked polymer forming infinite network, obtained in a step-growth polymerization with multifunctional monomers.
Newtonian fluid	An ideal fluid characterized by a constant ration of the shear stress to the rate of shearing in a simple shear deformation and with zero normal stress difference (nonelastic).
Nondestructive evaluation (NDE) or nondestructive inspection (NDI)	An analysis to determine whether the material is acceptable for its function.
Nondestructive inspection (NDI)	A process or procedure, such as ultrasonic or radiographic inspection, for determining the quality or characteristics of a material, part, or assembly, without permanently altering the subject or its properties. Used to find internal anomalies in a structure without degrading its properties.
Nonpolar	Incapable of having a significant dielectric loss. Polystyrene and polyethylene are nonpolar.
Nonreturn valve	See "Ball or checking valve."
Nonrigid plastic	A plastic that has a modulus of elasticity (either in flexure or in tension) of not over 69 MPa (10,000 psi) at 25 °C and 50 % relative humidity (ASTM D747).
Normal distribution	See "Gaussian distribution."
Notch sensitive	A plastic material is said to be notch sensitive if it will break when it has been scratched, notched, or cracked. Glass is considered to be highly notch sensitive.
Notch sensitivity	A measure of reduction in load-carrying ability caused by stress concentration in a specimen. Brittle plastics are more notch sensitive than ductile.

Nozzle	A hollow metal nose screwed into the extrusion end of either the heating cylinder of an injection machine or a transfer chamber (where this is a separate structure).
Nuclear magnetic resonance (NMR)	Relates to the radio frequency-induced transitions between magnetic energy levels of atomic nuclei. NMR instrument consists essentially of a magnet, radio frequency accelerator, sample holder, and detector, capable of producing an oscilloscope image or line recording of NMR spectrum. See also "Nuclear magnetic resonance spectroscopy."
Nuclear magnetic resonance (NMR) spectroscopy	When an organic molecule containing certain atoms (e.g., ^{13}C, H, D, F) is placed in a strong magnetic field and irradiated with radio frequency, transition between different nuclear spin orientational states takes place, and energy is absorbed at specific frequencies. Several different types of NMR measurements have been developed for characterization of polymer molecules, viz., high-resolution NMR of polymer solutions, wide-line solid-state NMR, magic-angle spinning NMR, and pulse-induced NMR.
Nucleating agent	A foreign substance, often crystalline, usually added to a crystallizable polymer to increase its rate of solidification and reduce size of spherulites.
Nucleation	Any additive that assists or acts as a starting site for crystallization of a polymer. These initiators can reduce cycle time by speeding up the crystalline formations, thereby causing the part to solidify faster so its ejection from the mold can occur sooner.
Nylon™	A generic term for polyamides (a trademark of E. I. du Pont de Nemours, adduct of New York and London). To be avoided – use polyamide, PA, instead.
Olefins	Plastics produced from olefins, viz., polyethylene or polypropylene.
Oligomer	Low-molecular-weight polymeric material with the degree of polymerization, $10 < DP < 50$; from Greek oligos = few, little.
Opalescence	Limited clarity of vision through a sheet of transparent plastic at any angle, caused by light scattering within or on the surface of the plastic.
Opaque	A material that will not transmit light and is not transparent.
Open-hole insert	An insert having a hole drilled completely through it.
Optical comparator	An inspection machine using optics to compare the outline of a part to its required dimensions on a graphic screen.

Optical distortion	Any apparent alteration of the geometric pattern of an object when observed through a plastic or as reflection from a plastic surface.
Orange peel	An unintentional rugged surface that gives an appearance resembling the skin of an orange.
Ordered polymer	A polymer with monomers arranged in regular sequence, viz., alternating or block copolymers.
Organic	The term refers to a general class of substances whose composition is based on the element carbon. Organic infers some relationship to materials, which at some point in time were alive.
Organosol	Fine PVC suspension in a volatile, organic liquid. At room temperature, the resin is swollen, but not appreciably dissolved. At elevated temperatures, the liquid evaporates, and the residue upon cooling forms homogenous plastics. Plasticizers may be dissolved in the volatile liquid. See also "Plastisols."
Orientation	The alignment of the molecular structure in polymeric materials to produce anisometric material properties. It can be accomplished by drawing or stretching during fabrication, especially at low temperatures.
Orifice	An opening in a die or other metal piece used to meter the flow of fluid material.
Out-of-round	Nonuniform radius or diameter.
Overflow Tab	A small, localized extension of a part at a weld-line junction to allow a longer material flow path for the purpose of obtaining a better fusion bond of the meeting melt fronts.
Overlay sheet	See "Foil decorating."
Oxidation	Any chemical reaction in which electrons are transferred. The chemical reaction involving oxygen to form an oxide; the deterioration of an adhesive film due to atmospheric exposure; the breakdown of a hot melt adhesive due to prolonged heating and oxide formation. Degradation of a material through contact with air. A chemical reaction involving a combination with oxygen to form new compounds.
Oxygen index	The minimum concentration oxygen expressed as a volume percentage in a mixture of oxygen and nitrogen that will just support flaming combustion of a material initially at room temperature under the specified conditions. An indication of flammability.
Pack time	The amount of time that packing pressure is kept on the screw until the gate freezes. It takes time immediately after the injection stroke ends.

Packing pressure	The pressure applied just before the part cavity fills, which is about 50 % of the injection pressure required to continue filling the mold without flashing it. Packing pressure is maintained until the gate freezes.
Pad	See "Cushion."
Paint line	The point where two colors meet.
Paint step	Break in a smooth surface that allows a mask to rest.
Parallel to the draw	The axis of the cored position or insert parallel to the up-and-down movement of the mold as it opens and closes.
Parallels (risers or support fillers)	The support spacers between the mold and press platen or clamping plate.
Pareto analysis	An analytical and statistical technique used to determine part defect type and quantity. Ranks each type of defect as a percentage of the total number of defects found, based on the quantity of each type of defect.
Parison	Hollow plastic tube from which a part is blow molded.
Part separator	A machine or system used to automatically separate parts from the runner system after molding. Separated parts go to their next station and the runner moves to a granulator for reuse if permitted. The system may use blades, rigid pins, or a degating station with parts placed by a robot for separation.
Parting agent	See "Mold release."
Parting line	The point in the mold where two or more metal surfaces meet creating a shutoff. Mark on a molding or casting where halves of a mold met in closing.
Partitioned mold cooling	See "Bubbler."
Pastel	A tint, a tone to which white has been added.
Paucimolecular	Polymers that consist of only a few different molecular weight components. Also called the paucidisperse polymers.
Peak exothermic temperature	The maximum temperature reached by reacting thermosetting plastic composition is called peak exothermic temperature.
Permeability	The passage or diffusion of a gas, vapor, liquid, or solid through a barrier without affecting it. The rate of the passage.
pH	Negative logarithm of concentration of hydrogen ions, $-\log [H^+]$, a measure of the acidity or alkalinity of a substance. Acid solutions have $pH < 7$, at neutrality $pH = 7$, and in alkaline solutions $pH > 7$.
Phase	A separate, but not necessarily separable, portion of a system.

Phenolic resins	Cross-linked resins based on phenol and formaldehyde of a complex, not fully known, structure.
Photodegradation	Degradation caused by long wavelength ultraviolet radiation that is the main cause of outdoor weathering.
Photoelasticity	Experimental technique for the measurement of stresses and strains in material objects by means of the mechanical birefringence.
Physical aging	The relaxation process that takes place in plastics after fabrication. Upon cooling a melt, the molecular mobility decreases, and when the relaxation time exceeds the experimental time scale, the melt becomes a glass in nonequilibrium thermodynamic state (density, enthalpy, etc.). Thus, the value of the thermodynamic parameters continues to change toward an equilibrium state. The process may lead to development of cracks and crazes that initiate critical failure. See also "Aging," "Accelerated aging," "Artificial aging," and "Chemical aging."
Physical cross-link	A physical bond that joins two or more chains together. They may arise from crystalline portions of a semicrystalline polymer, the glassy or crystalline portion of a block copolymer, or the ionic portion of an ionomer. The physical cross-link forces are affected by the temperature.
Physical cross-linking	An existence of restraining force between polymer chains other than covalent bonding; viz., entanglements, presence of microcrystallinity, and glassy blocks in block copolymer.
Piece part price	Calculated finished part cost based on material, processing, assembly, decorating, and packaging, including productivity and overhead costs.
Pigment	Imparts color to plastic while remaining a dispersion of undissolved particles.
Pigmented	A plastic resin comprising pigments to produce a desired color after molding. The pigments can be either organic or inorganic based.
Pinpoint or restricted gate	A restricted orifice through which molten plastic flows into a mold cavity.
Pit	Small regular or irregular crater in the surface of a plastic, usually with width approximately of the same order of magnitude as its depth.
Pitch	With respect to extruder or injection molding, the distance from any point on the flight of a screw line to the corresponding point on an adjacent flight, measured parallel to the axis of the screw line or threading.

Plastic	A synthetic or natural organic substance (exclusive of adhesives and rubbers) formable or pliable at some stage during its formation or subsequent manufacturing process, thus a polymeric material that is capable of being shaped through plastic flow under influence of deforming forces, a thermoplastic or thermoset material. It either melts and flows with heat and pressure, as with a thermoplastic, or it chemically "sets," as with a thermoset material. Many materials, such as glass, become plastic under the right conditions.
Plastic deformation	Any portion of the total deformation of a body that occurs immediately when load is applied but that remains permanently when the load is removed. The deformation of a material under load that is not recoverable after the load is removed. Opposite of elastic deformation.
Plastic memory	A phenomenon of a plastic to return, in some degree, to its original form upon heating.
Plasticate	To soften by heating and/or kneading.
Plasticating extruder	An extruder fed with solid polymer that melts and plasticates it while conveying toward the die.
Plasticity	A property of plastics that upon the application of a force allows the material to be deformed continuously and permanently without rupture (the opposite of "elasticity").
Plasticization	Softening, enhancement of flexibility engendered by incorporation of low-molecular-weight liquid, a plasticizer, such as 2-ethylhexylphthalate (DOP).
Plasticize	To make a material soft and moldable with the addition of heat, pressure, or a plasticizer.
Plasticizer	A material incorporated in a thermoplastic to reduce its glass transition temperature, thus to increase its flexibility.
Plastisols	Mixtures of PVC and plasticizers that can be molded, cast, or converted to continuous films by the application of heat. The mixtures that contain volatile thinners are known as organosols, q.v.
Plate dispersion plug	See "Breaker plate."
Platens	The mounting plates of a press to which the entire mold assembly is bolted.
Plunger	The part of a transfer or injection press that applies pressure to the unmelted plastic material to push it into the chamber. This, in turn, forces the melt out through the nozzle.
Poisson distribution	Discrete probability function, derived by Simeon Poisson in 1837, for the situation when the probability

	of a single event is very small, but the number of events approaches infinity.
Poisson's ratio, r	The ratio of lateral strain to the corresponding axial strain in axially loaded specimens, below the proportional limit. It is a material constant that relates the modulus of rigidity, G, to Young's modulus, E, in the relation: $E = 2G(r + 1)$, viz., ASTM E1321.
Polarized light	Polarized electromagnetic radiation whose frequency is in the optical region.
Polarizer	A medium or a device used to polarize the incoherent light.
Polyacrylonitrile (PAN)	Product of free radical polymerization in solution or suspension. Used primarily for production of fibers (it may contain up to 10 % comonomer to improve dyeability). Homopolymer of PAN is a base material in the manufacture of carbon fibers.
Polyaddition	A step-growth polymerization from two types of bi- or polyfunctional primary molecules, e.g., polyurethane formation. This irreversible, rapid process is caused, usually through heteroatoms, by bond displacement without the splitting off any component.
Polyallomers	Crystalline thermoplastic polymers made from two or more different monomers, usually ethylene and propylene.
Polyamide-imide (PAI)	A family of polymers based on the combination of trimellitic anhydride with aromatic diamines. In the uncured form (ortho-amic acid), the polymers are soluble in polar organic solvents. The imide linkage is formed by heating, producing an infusible resin with thermal stability up to 290 °C. These resins are used for laminates, prepregs, and electrical components.
Polyamides (PA)	A group of semicrystalline thermoplastics containing the amide group (−NHCO−) in the main chain, resulting from polycondensation of either α,ω-lactam or a diacid with a diamine. Natural polyamides, polypeptides, and synthetic polyamides belong to this family.
Polyarylates (PAr)	Wholly aromatic polyesters from dihydric phenols and dicarboxylic acid chlorides. They are characterized by high melting point (up to 500 °C), good thermal stability, and solubility in chlorinated solvents. Commercial polymers are produced by polycondensation of iso- and terephthalic acids with bisphenol A, having glass transition temperatures near 170 °C and the continuous use temperature of 140–150 °C.
Polyarylsulfone (PAS)	Alternative name for aromatic polyethersulfone. See "Polyethersulfone."

Polybenzimidazole (PBI)	The polycondensation product of tetraaminobiphenyl with terephthalic acid has the highest thermal stability of all commercial organic polymers. Its continuous use temperature is 400 °C, and it has good chemical stability.
Polybutylene terephthalate (PBT)	Polycondensation product of dimethylterephthalate and 1,4 butanediol, with melting temperature T_m § 224 °C. PBT can be easily blended with number of other thermoplastics. Major uses include automotive parts (interior, under-the-hood, and exterior), electrical connectors, small appliances, and pump housings.
Polybutylenes, BR	A group of polymers consisting of isotactic, stereoregular, highly crystalline polymers based on butene-1. Their properties are similar to those of polypropylene and linear polyethylene, with superior toughness, creep resistance, and flexibility.
Polycarbonate (PC)	An amorphous thermoplastic derived from the direct reaction between aromatic and aliphatic dihydroxy compounds with phosgene or by the ester exchange reaction with appropriate phosgene-derived precursors. Highest impact resistance of any transparent plastic. It is transparent and can be injection molded, extruded, thermoformed, or blow molded (esp. branched PC).
Polycondensation	A polymer synthesis from bi- or multifunctional monomers with liberation of a low-molecular, volatile by-product.
Polyesters	Polymers containing the ester group (−COO−) in the main chain, products of polycondensation of α,ω-lactones or diacid with diols. Both unsaturated (alkyd) polyesters and thermoplastic polyesters (including PC, PET, PBT, and PNT) enjoy wide commercial use.
Polyether-imide (PEI)	An aromatic polymer containing both ether and imide groups in the polymeric chain. It has a heat distortion temperature of 200 °C, continuous use temperature of 170 °C, and low flammability. It can be blended with several engineering thermoplastics for a wide range of properties and applications (mainly in automotive and electronic/electrical industries).
Polyethersulfone (PES)	An aromatic polymer containing benzene rings linked by both ether and sulfone groups in the polymeric chain. Several commercial products of this type have been developed. Their glass transition temperature varies from 190 to 285 °C. The materials have high rigidity, low creep, high electrical resistance, transparent, self-extinguishing, and low flammability. They can be

	blended with several engineering thermoplastics. The applications include printed circuit boards, TV components, and diverse electronic/electrical parts.
Polyethylenes (PE)	Thermoplastic materials composed of ethylene units. They are normally translucent, tough, waxy solids that are unaffected by water and by a large range of chemicals. These plastics have >85 % ethylene and >95 % of total olefins.
Polyethylene terephthalate (PET)	Polycondensation product of dimethylterephthalate and ethylene glycol, with $T_m = 260$–270 °C. Oriented PET has outstanding tensile strength. Its principal use includes bottles, X-ray films, electrical insulation, and food packaging.
Polyimide (PI)	Polymer produced by reacting an aromatic dianhydride with an aromatic diamine. It is highly heat-resistant (at $T = 315$ °C) resin, similar to a polyamide, differing only in the number of hydrogen atoms per mer. The polymer is suitable for the use a binder or adhesive and may be either a thermoplastic or a thermoset. Initially, it could not be processed by conventional molding methods. The polymer has rings of four carbon atoms tightly bound together. It has excellent resistance to heat.
Poly-liner	A perforated, longitudinally ribbed sleeve that fits inside the cylinder of an injection molding machine. Used as a replacement for conventional injection cylinder torpedoes/older machines. Also a plastic bag placed inside a carbon or box to prevent material contamination during shipment.
Polymer	Material composed of many (Greek poly) units (Greek meros). A high molecular weight organic compound – natural or synthetic, formed by a chemical reaction in which two or more small organic units join to form large units composed of repeating small units. Its structure can be represented by repeated small units, the mers. Synthetic polymers are formed by addition or condensation polymerization of monomers. Some polymers are elastomeric, and others thermoplastic or thermoset. The term was coined by Berzelius in 1832 to describe hydrocarbons of a general formula $(CH_2)_n$ with $n = 1$ to 4 (sic!). Today a substance may be called polymer if it shows high degree of polymerization, DP >50.
Polymer alloy	An immiscible polymer blend having a modified interface and/or morphology.

Polymer blend	A mixture of at least two macromolecular materials: two or more polymers, polymer with copolymers, two or more copolymers, etc. Polymer blends are either miscible or immiscible. See "Miscible polymer blend" and "Immiscible polymer blend."
Polymer conversion	Preparation of polymer derivatives during which the number of macromolecules or the degree of polymerization is preserved.
Polymerization	The process or chemical reaction in which the molecules of a monomer are linked together to form macromolecules whose molecular weight is a multiple of that of the original substance $nM \rightarrow [M]_n$, where n is a degree of polymerization, DP. It is said that the polymerization leads to oligomer if $10 < DP < 50$ and to polymer if $DP > 50$. When two or more monomers are involved, the process is called copolymerization. Most polymerization processes are classified as condensation (step) reactions or addition (chain) reactions.
Polymethylme-thacrylate (PMMA)	Crystal-clear radical polymerization product of methyl methacrylate. PMMA has the glass transition temperature of 105 °C, excellent weatherability, and scratch resistance, as well as useful combination of stiffness, density, and toughness. It can be easily modified by co-reacting or blending.
Polymolecularity	Practically all polymers are mixtures of impossible to separate homologues or fractions. Mathematically the polymolecularity is expressed by a molecular weight distribution, MWD, q.v.
Polyphenylene ether (PPE)	An amorphous thermoplastic with useful temperature range that depending on composition varies from 135°C to 190 °C.
Polypropylenes (PP)	A crystalline thermoplastic made by polymerizing propylene gas. It has the lowest density of all plastics, except methylpentene. Tough, lightweight thermoplastics made by the polymerization of propylene in the presence of an organometallic catalyst at relatively low pressures and temperatures.
Polystyrenes (PS)	An amorphous thermoplastic made by polymerizing styrene. Thermoplastics produced by the polymerization of styrene, having outstanding electrical properties and good thermal and dimensional stability. Because it is somewhat brittle, it is often copolymerized or blended with other materials to obtain desired properties (see HIPS).

Polysulfones (PSF or PSU)	A family of engineering thermoplastics with excellent high-temperature properties, high strength, high service temperature, low creep, and self-extinguishing properties, produced either by a Friedel-Crafts reaction of sulfonyl chloride groups with aromatic nuclei or by reacting dichlorosulfone with diphenyls. The continuous use temperature is about 160 °C. They can be formed by extrusion and molding method, directly competing with metals and more expensive materials for electronic circuitry.
Polytetrafluoroethylenes (PTFE)	A linear polymer obtained by radical polymerization of tetrafluoroethylene. PTFE has a melting point of 327 °C and outstanding resistance to chemical attacks or dissolution. Its uses include liners for chemical processing equipment, high-temperature cable insulation, bushings, seals, and nonstick surfaces.
Polyurethanes (PU)	Polymers containing urethane groups ($-$NHCOO$-$) in the main chain. Thermoplastic or thermoset materials made from isocyanates and polyols. The linear polyurethanes (thermoplastic polyurethanes, TPU) are formulated with rigid and soft segments, thus (as block copolymers) showing interesting elastomeric character. However, most polyurethanes are produced as cured rubbers (polyurethane rubber, PUR) by means of combining isocyanate having functionality about 2.7 with diols. The principal use of PUR is in manufacture of rigid and flexible foams.
Polyvinyl chloride (PVC)	A thermoplastic material composed of polymers of vinyl chloride. It is a colorless solid with outstanding resistance to water, alcohols, and concentrated acids and alkalis. It is obtainable as granules, solutions, lattices, and pastes. Compounded with plasticizers, it yields a flexible material superior to rubber in aging properties. It is widely used for cable and wire coverings, in chemical plants, and in the manufacture of protective garments. The pure polymer is brittle and difficult to process. It yields a flexible material when compounded with plasticizers.
Polyvinylidene chloride (PVDC)	A thermoplastic material composed of polymers of vinylidene chloride. Its principal uses are in flexible films and coatings.
Porosity	A condition of trapped pockets of air, gas, or vacuum within a solid material, expressed as percentage of the total nonsolid volume to the total volume.

Post annealing	Stress relieving of molded parts by external means, hot air or oil, humidity chambers, or submersion in a fluid.
Post mold shrinkage	The shrinkage occurring after a part has been removed from the mold is influenced by the material properties of the resin and its molding conditions.
Post-forming	A process used to impart a shape to a previously molded article.
Pot life	The time span during which a cross-linking resin-hardener system can still be processed.
Potentiometer	An electrical control device that senses changes in voltage or a potential difference by comparison to a standard voltage and can transmit a signal to a control switch.
Preplastication	Technique of premelting injection molding powders in a separate chamber and then transferring the melt to the injection cylinder. The device used for preplastication is known as a preplasticizer.
Prepolymer	A chemical intermediate with a molecular weight between that of the monomer or monomers and the final polymer.
Press fit	An interference assembly between two mating parts, with friction holding the parts together under considerable stress.
Pressure drop	The decrease in pressure of a fluid related to the number of turns it has to make and the distance it must flow to fill a cavity.
Pressure gradient lines	A hypothetical set of pressure lines in a part created by the material's pressure drop as the part is filled. The further the material flows from the gate, the lower the packing pressure.
Pressure pads	Reinforcements distributed around the dead areas in the faces of a mold to help the land absorb the final pressure of closing.
Primary molecule, monomer	The smallest molecular unit from which the macromolecule is built.
Printing on plastics	The decoration of plastics by means of various printing processes, e.g., offset, silk screen, letterpress, electrostatic, or photographic methods.
Process control procedures	A separate document, often included as an attachment to the quality control manual that provides detailed description of the methods to be followed in the manufacture of a product. A copy may be attached to the work order for reference and revision as required should changes in the product occur.
Processing aid	An additive that improves processing characteristics.

Product certification	The certificate or letter stating that the material or product meets or exceeds customer requirements. Values are often listed for the tested or measured results. To be signed by a key representative of the company to verify accuracy.
Projected surface area	The exposed resin area of a mold on the parting line that transmits the injection pressure on the closed mold halves. It includes part, runner, and sprue surfaces.
Propagation	A series of reaction steps in a chain polymerization in which the monomers are being added to the active polymerization center.
Proportional limit	The greatest stress that a material is capable of sustaining without deviation from proportionality of stress and strain (Hooke's law).
Prototype mold	A simplified mold construction often made from a light metal casting alloy or from an epoxy resin to obtain information for the final mold and/or part design.
Pseudo-IPN	Simultaneous IPN in which one polymer is in network form and the other linear.
Pultrusion	A continuous process for manufacturing composites that have a constant cross-sectional shape. The process consists of pulling a fiber-reinforcing material through a resin impregnation bath and then through a shaping die, where the resin is subsequently cured.
Purging	Cleaning one color or type of material from the processing machine by forcing it out with the new color or material to be used in subsequent production. Special purging materials are also available.
Pyrometer	An electrical thermometer for measuring high temperatures. The units come with two probes to measure melt and surface temperatures.
Quality assurance	A separate department established to direct the quality function of the business areas. Major efforts are directed to assisting and auditing the activities of the quality control department in their efforts to ensure that quality products are manufactured.
Quality circles	A quality analysis group consisting of employees with specific departmental knowledge used to provide suggestions and ways to solve a procedural or manufacturing quality problem. If found acceptable, the group's findings and solutions are then passed on to upper management for implementation.
Quality control (QC)	A department set up to be technically involved in the control of product quality. Involved in the principal

	inspection and testing of a product, with limited systems responsibility.
Quality control manual	A document that states the company's quality objectives, and how they will be implemented, documented, and followed in the manufacture of products.
Quality rated	See "Approved supplier."
Quenching	A method of rapidly cooling thermoplastic parts when they are removed from the mold, usually by submerging the parts in water.
Radical polymerization	Polymerization in which the active centers of reaction are radicals. The polymerization can be initiated by thermally activated or redox initiator, irradiation, or through thermal activation of monomer (also known as free radical polymerization).
Radio frequency, RF, preheating	A method of preheating used to mold materials to facilitate the molding operation and/or reduce the molding cycle. The frequencies commonly used are between 10 and 100 MHz/s.
Ram	The press member that enters the cavity block and exerts pressure on the molding compound designated as the "top force" or "bottom force" by position in the assembly. See "Plunger."
Ram travel	Distance ram moves during a complete molding cycle.
Random copolymer	A copolymer in which the different monomers are randomly placed in the main chain. A perfectly random copolymer is produced by polymerization of different mers having identical reactivity ratios, $r_A = r_B = r_C$.
Randomness	A condition in which individual values are not predictable, although they may come from a definable distribution.
Reactive extrusion	Execution of chemical reactions during extrusion of polymers and/or polymerizable monomers. The reactants must be in a physical form suitable for extrusion processing. Reactions have been performed on molten polymers, on liquefied or dispersed monomers, or on polymers dissolved or suspended in or plasticized by a solvent (also reactive compounding or reactive processing).
Reactive injection molding (RIM)	A semicontinuous manufacturing process in which two liquid components are metered in the calculated ratio by high pressure piston pumps, mixed by impingement mixing and injected into a mold cavity or cavities, where the reactants are polymerized or cured. The process has been used to polymerize polyamides, elastomeric polyurethanes, and polyurethane foams.

Reactivity ratio	A ratio of two kinetic constants $r = k_{AA}/k_{AB}$ where k_{AA} represents the self-propagation and k_{AB} the transfer from A* active center to B* active center caused by addition of monomer-B to a growing copolymer chain.
Real time	The present time or as an activity is occurring.
Reciprocating screw	A combination injection and plasticizing unit in which an extrusion device with a reciprocating screw is used to plasticize the material. Injection of material into a mold can take place by direct extrusion into the mold, by reciprocating the screw as an injection plunger, or by a combination of the two. When the screw serves as an injection plunger, this unit acts as a holding, measuring, and injection chamber.
Recycled plastics	A plastic material prepared from previously used or processed plastic materials that have been cleaned and reground.
Redox initiator	An initiator capable of generating free radicals at low temperature by oxidation-reduction reaction between two components, viz., $H_2O_2 + FeSO_4$.
Regrind	Waste material from industrial operations that has been reclaimed by shredding or granulating. Regrind is usually incorporated, at a predetermined percentage, with virgin material.
Reinforced molding compound	A material reinforced with special fillers to meet specific requirements, such as rag or glass.
Reinforced polypropylene	Polypropylene that is reinforced with mineral fillers, such as talc, mica, and calcium carbonate, as well as with glass and carbon fibers. The maximum concentration is about 5 wt%, although concentrates with higher levels of filler or reinforcement are available.
Reinforcement	A substance or material added to a polymer during the final synthesis stages or in subsequent processing to improve the strength properties of the polymer. Usually, a high strength material bonded into a matrix to improve its mechanical properties. Reinforcements are usually long fibers (glass, carbon or aramid), chopped fibers, whiskers, particulates (glass beads, mica, clay, and organic fibers), and so forth. The term is *not* synonymous with filler.
Relative viscosity	Ratio of the kinematic viscosity of a polymer solution to the kinematic viscosity of the pure solvent.
Relaxation time	The time required for a stress under a sustained constant strain to diminish by a stated fraction of its initial value.
Release agent	See "Mold release."

Release or parting agent	A material that is applied in a thin film to the surface of a mold to keep the resin from bonding (also mold release agent).
Relief angle	The angle of the cutaway portion of the pinch-off blade from a line parallel to the pinch-off land. In a mold, the angle between the pitch-off land and the cutaway portion adjacent to the pinch-off land.
Repeatability	The variation obtained when one person measures the same quantity several times using the same instrument.
Reprocessed plastic	A thermoplastic material, prepared from melt-processed scrap or reject parts, or from nonstandard or nonuniform virgin material. The term scrap does not necessarily connote feedstock that is less desirable or usable than the virgin material from which it may have been generated. Reprocessed plastic may or may not be reformulated by the addition of fillers, plasticizers, stabilizers, or pigments.
Reproducibility	The variation in measured averages obtained when several persons measure the quantity using the same instrument or when one person measures the quantity using different instruments.
Residence time	Time a resin spends in a given processing machine (an extruder, injection molding unit, etc.) and is subjected to heat and stress.
Residence time distribution	The distribution of residence time provides information how long different parts of the resin reside in the processing equipment. The spread of the residence times reflects, on the one hand, the uniformity of flow inside the processing unit and, on the other, the quality of the product, the degree of mixing, or the extent of a chemical reaction.
Residual stress	The stresses remaining in a plastic part as a result of thermal or mechanical treatment.
Resin	An organic material, usually of high molecular weight, that tends to flow when subjected to stress. Any of a large class of synthetic substances that have some of the properties of natural resin (or rosin) but differ chemically. "Resin" is often used as a general term for polymers or plastics and denotes a class of material. It usually has a softening or melting range and fractures conchoidally. Most resins are polymers. Also any of a class of solid or semisolid organic products of natural or synthetic origin, generally of high molecular weight with no definite melting point (also see "Polymer").

	In reinforced plastics, the material used to bind together the reinforcement material; the matrix.
Resin pocket	An apparent accumulation of excess resin in a small localized section that is visible on cut edges of molded surfaces. Also called resin segregation.
Resin transfer molding (RTM)	A fabrication process that involves the transfer of catalyzed resin into an enclosed mold cavity containing a previously positioned reinforcement preform. The process has been used for manufacturing from components consisting of glass fiber mats and polyester resins.
Restricted gate	Sometimes referred to as pinpoint gate. A small opening between the runner and cavity in an injection or transfer mold.
Retainer plate	The plate, usually drilled for steam or water, on which demontable pieces, such as mold cavities, ejector pins, guide pins, and bushings, are mounted.
Retaining pin	A pin on which an insert is placed and located before molding.
Rheology	The study of the deformation and flow of materials of the interrelations between the force and its effects. The science considers deformation of all materials from the elastic deformation of Hookean solids to the flow of Newtonian liquids.
Rib	An object designed into a plastic part to provide lateral, longitudinal, or horizontal support.
Rigid plastics	A plastic that has a modulus of elasticity either in flexure or in tension greater than 690 MPa at 23 °C and 50 % relative humidity, RH.
Ring gate	A gate or annular opening that circles around a core pin or molded part.
Rockwell hardness	A common method of testing materials for resistance to indentation in which a diamond or steel ball, under pressure, is used to pierce the test specimen.
Rubbers	Cross-linked polymers having glass transition temperatures below the room temperature that exhibit highly elastic deformation and have high elongation.
Runner	In an injection or transfer mold, the channel that connects the sprue with the gate to the cavity.
Runner system	The sprues, runners, and gates that lead the material from the nozzle of an injection machine to the mold cavity.
Rupture	A cleavage or break resulting from physical stress. Work of rupture is the integral under the stress–strain curve between the origin and the point of rupture.

Salt and pepper blends	Resin blends of different concentrate additives, in pellet form, mixed with virgin resin to make a different product. Usually associated with color concentrate blends, that, when melted and mixed by the injection molding machine's screw, yield a uniform colored melt for a part.
SAN	An abbreviation for styrene-acrylonitrile copolymers.
Scanning electron microscopy (SEM)	Electron microscopy that uses the secondary emission of electrons from a surface when bombarded with an electron beam. The main advantage is the depth of field. Technique in which the surface of a specimen is scanned, point by point, with a finely focused electron beam. Image formation is made by detecting the secondary electrons emitted by the specimen's surface. Even though resolution in modern SEM can be as high as 4 nm, the main advantage of SEM over the other microscopy techniques is its very large depth of field.
Scanning probe microscopy (SPM)	a microscopy technique in which the surface of a specimen is scanned, point by point, using a very sharp probe (d = 10 nm). Accurate piezoelectric devices are utilized to maintain the separation distance between the lowest atom on the probe tip and the highest atom on the specimen constant and in the range of 1–100 nm. In this range of tip-to-sample spacing, phenomena like tunneling current (scanning tunneling microscopy (STM)) or interatomic repulsion/attraction (atomic force microscopy (AFM)) can be used for determining specimen topography with resolution ranging from a few microns, down to atomic level.
Scanning transmission electron microscopy (STEM)	a microscopy technique in which an ultrathin specimen is scanned, point by point, with a finely focused electron beam. Image formation is made by detecting the electrons transmitted through the specimen.
Scrap	A product or material that is out of specification to the point of being unusable.
Screw plasticating injection molding	See "Injection molding."
Screw	The main component of the "reciprocating screw" injection molding machine. It may have various sizes, lengths, and compression ratios. It is used to feed, compress, melt, and meter the resin for injecting into the mold cavity. Basically divided into 3 major sections: feed section, deep screw depths to convey the resin into the next screw's section; transition section, gradually decreasing screw depths when resin is compressed, forced against the barrel's surface, and melts; and

	metering section, the molten melt that is further compressed in a shallow, uniform screw depth conveying forward as the screw turns.
Scuff mark	An imperfection on a part's show surface caused by dragging the part against the mold's surface during ejection from the mold cavity.
Sealant	A material applied to a joint in paste or liquid form that hardens or cures in place, forming a seal.
Sealing diameter	That portion of a metal insert that is free of knurl and is allowed to enter the mold to prevent the flow of plastic material.
Secant modulus	The ratio of total stress to corresponding strain at any specific point on the stress–strain curve.
Second-surface decorating	A method of decorating a transparent plastic part from the back or reverse side. The decoration is visible through the part, but is not exposed.
Semiautomatic molding machine	A molding machine in which only part of the operation is controlled by direct human action. The automatic part of the operation is controlled by the machine according to a predetermined program.
Semi-I IPN	An intimate combination of two polymers in network form. Sequential IPN in which polymer-1 is cross-linked and polymer-2 linear.
Semi-II IPN	An intimate combination of two polymers in network form. Sequential IPN in which polymer-1 is linear and polymer-2 cross-linked.
Semicrystalline	Polymers that exhibit localized, partial crystallinity (see "Crystalline plastic").
Sequential polymerization	Formation of an alternating or block copolymer through careful control of addition of different monomers at specific stages of the reaction.
Sequential IPN (SIPN)	An intimate combination of two polymers in network form. During preparation of SIPN, the first polymer-A is swollen in a mixture of monomer-B, cross-linking agent, and initiator and then polymerizing in situ.
Servomotor	An electrical motor or hydraulic piston that supplies power to a feedback system that consists of a sensing element and an amplifier used in the automatic control of a mechanical device.
Shear heat	The rise in temperature created by the compression and longitudinal pressure on the resin in the barrel by the screw's pumping action.
Shear joint	An ultrasonic welding joint design where the welding action is parallel to each part surface.

Shear rate	The overall velocity over the cross section of a channel with which molten polymer layers is gliding along each other or along the wall in laminar flow. A change of shear strain within one second.
Shear strain	Deformation relative to the reference configuration of length, area, or volume. Tangent of the angular change, caused by a force between two lines originally perpendicular to each other through a point in a body is called angular strain.
Shear strength	The maximum shear stress that a material is capable of sustaining. The maximum load required to shear a specimen in such a volume manner that the resulting pieces are completely clear of each other. Shear strength (engineering) is calculated from the maximum load during a shear or torsion test and is based on the original cross-sectional area of the specimen.
Shear stress	Stress developed because of the action of the layers in the material attempting to glide against or separate in a parallel direction. In other words, the stress developed in a polymer melt when the layers in a cross section are gliding along each other or along the wall of the channel (in laminar flow).
Shearing	Breaking caused by the action of equal and opposed forces, located in the same plane.
Shelf-life	The time a material, such as a molding compound, can be stored without loss of its original physical or functional properties.
Shore hardness	A method of determining the hardness of a plastic material using a scleroscope or sclerometer. The device consists of a small conical hammer fitted with a diamond point and acting in a glass tube. The hammer is made to strike the material under test and the degree of rebound is noted on a graduated scale. Generally, the harder the material, the greater the rebound (ASTM D2240).
Short or short shot	A molded part produced when the mold has not been filled completely.
Shot capacity	The maximum volume of material that a machine can produce from one forward motion of the plunger or screw.
Shot peening	Impacting the surface of the material with hard, small, round beads of materials to disrupt the surface flatness. Used to stress relieve welds and to improve the release of plastic resins on smooth core surfaces.
Shot	The yield from one complete molding cycle, including cull, runner, and flash.

Shrink fixture	See "Cooling fixture."
Shrinkage allowance	The additional dimensions that must be added to a mold to compensate for shrinkage of a plastic material on cooling.
Shrinkage	In a plastic, the reduction in dimensions after cooling. The relative change in dimension from the length measured on the mold when it is cold to the length of the molded object 24 h after it has taken out of the mold.
SI units	International System of Units.
Side actions (side coring or side draw pins)	An action built into a mold that operates at an angle to the normal open-and-close action and facilitates the removal of parts that would not clear a cavity or core on the normal press action. Projections used to core a hole in a direction other than the line of closing of a mold and which must be withdrawn before the part is ejected.
Sigma (σ)	The Greek letter used to indicate the standard deviation of a population, defined as the square root of the variance, e.g., for the normal (Gaussian) distribution:

$$y = \left[1/\sigma(2\pi)^{1/2}\right]\exp\left\{-[(x - \bar{x})/\sigma]^2/2\right\}$$
$$\text{Variance} \equiv \sigma^2 = \Sigma(x - \bar{x})/(N - 1)$$

Silicones	Chemicals derived from silica used in molding as a release agent and general lubricant. A silicon-based thermoset plastic material. Polyorganosiloxanes of different composition (e.g., polydimethylsiloxane, silicone rubber), structures (linear or network), and molecular weight, used as "high-temperature oil," resin, or elastomer.
Silk screen printing	In its basic form, it involves laying a pattern of an insoluble material, in outline, on a finely woven fabric. When ink is drawn across the material, it passes through the screen only in the designed areas. Also called screen process decorating.
Simultaneous IPN (SIN)	IPN is prepared by mixing together the two monomers, their respective cross-linking agents, and initiators and then polymerizing simultaneously by way of noninterfering modes.
Sink mark	A depression or dimple on the surface of an injection molded part formed as a result of collapsing of the surface following local internal shrinkage after the gate seals. May also be an incipient short shot.

Size exclusion chromatography, SEC	Recent name for what has been known as gel permeation chromatography, GPC, q.v.
Skewness	The degree to which a distribution is asymmetrical; negative or positive skewness is observed when the distribution peak is shifted to the upper or lower side.
Skins	See "Flakes."
Slides	Sections of a mold cavity that form complex three-dimensional parts that must move before the molding can be ejected. Used to form openings and sections of parts 90° to the part's release from the mold cavity.
S-N diagram	Plot of stress, S, vs. number of cycles, N, required to cause failure of similar specimens in fatigue test. Data for each curve on the S-N diagram are obtained by determining fatigue life of a number of specimens subjected to various amounts of fluctuating stress. The stress axis may represent stress amplitude, maximum stress, or minimum stress. A log scale is usually used, especially for the N-axis.
Snap fit	An assembly of two mating parts, with one or both parts deflecting under stress, mating the parts together.
Softening temperature	Temperature at which amorphous polymer (or the amorphous part of crystalline polymer) passes from the hard glass to the soft elastic or liquid state.
Sol solutions	Solutions of macromolecules so diluted that they do not hinder each other free rotation. The limiting concentration depends on the hydrodynamic volume of the macromolecule, usually expressed by the intrinsic viscosity, $[\eta]$.
Solid-state polymerization	Polymerization of crystalline monomer, usually vinyl, using high energy radiation. Topochemical, topotactic, and canal polymers belong to this group.
Solvent	Any substance, but usually a liquid, that dissolves other substance.
Solvent welding, cementing, or bonding	A method of bonding thermoplastic articles of like materials to each other by using a solvent capable of softening the surfaces to be bonded. Thermoplastic materials that can be bonded by this method are ABS, PA, PC, PS, acrylics, cellulosics, and vinyls.
Solvent casting	A process that consists of mixing and dissolving the ingredients in a suitable carrier that conveys the solution of "dope" through a drier where the solvent is subsequently evaporated; the resulting film is removed from the substrate surfaces and wound into rolls.
Specific gravity	The ratio of the mass of a given volume of a substance to the mass of an equal volume of a reference substance,

	usually water, at a specified temperature (ASTM D792). Also, dimensionless ratio of a substance density to that of a reference material.
Specific heat	The quantity of heat required to raise the temperature of a unit mass of a substance by one degree (1 °C) at constant pressure or volume.
Specific volume	Reciprocal of density.
Specification	A written statement that dictates the material, dimensions, and workmanship of a manufactured product.
Spectrometry	A method based on designation of the wavelengths within a particular portion of a range of radiation or absorption, for example, ultraviolet (UV), emission, and absorption spectrometry.
Spectrophotometer	An instrument that measures transmission of apparent reflectance of visible light as a function of wavelength, permitting accurate analysis of color or accurate comparison of luminous intensities of two sources of specific wavelengths.
Spectroscopy	The study of spectra using an instrument for dispersing radiation for visual observation of emission or absorption. See also "Infrared," "Nuclear magnetic resonance," "NMR," and "Spectroscopy."
Specular gloss	The relative luminous reflectance factor of a specimen at the specular direction.
Spherocolloids	The colloidal particle has a spherical shape, formed either by single macro-molecule or an association of low-molecular weight species.
Spider gate	Multi-gating of a part through a system of radial runners from the sprue.
Spin welding	The process of fusing two objects by forcing them together while one of the pair is spinning, until frictional heat melts the interface. Spinning is then stopped and pressure held until they are frozen together.
Spinodal	The line on the temperature vs. composition phase diagram for a mixture of two components, which separates the region from the two-phase regions. Hence, with binodal, it represents the limits of metastability of a two-phase system, viz., in polymer solutions or polymer blends. See also "Binodal."
Spinodal decomposition	The phase separation that occurs when the single-phase system is abruptly brought into the spinodal region of phase diagram, by either a rapid change of temperature, pressure, or flash evaporation of a solvent, viz., in polymer blends. Owing to spontaneous phase separation in

the system (no nucleation!), the morphology generated is co-continuous.

Spiral flow test
A method for determining the flow properties of a plastic material based on the distance it will flow under controlled conditions, pressure, and temperature along the path of a spiral cavity using a controlled charge. The length of the material that flows into the cavity and its weight gives a relative indication of the flow properties of the resin.

Splay marks or splay
Marks or lines found on the surface of the part after molding that may be caused by overheating the material, moisture in the material, or flow paths in the part. Usually white, silver, or gold in color. Also called silver streaking.

Split cavity
A cavity of a mold that has been made in sections.

Split-ring mold
A mold in which a split cavity block is assembled in a chase to permit the forming of undercuts in a molded piece. These parts are ejected from the mold and then separated from the molded piece.

Spot welding
The localized fusion bonding of two adjacent plastic parts that does not require a molded protrusion or hole in the parts. To be effective, use where two parallel and flat surfaces meet.

Spray drying
The transformation of feed from a fluid state into a dried particulate form by spraying the feed into a hot drying medium. It is used for the continuous production of dry solids in powder, granulate, or agglomerate form from liquid feedstocks as solutions, emulsions, pastes, and pumpable suspensions, viz., PVC lattices.

Spreader/torpedo
A streamlined metal block placed in the path of flow of the plastics material in the heating cylinder of extruders and injection molding machines to spread it into intimate contact with the heating areas.

Sprue bushing
A hardened steel insert in an injection mold that contains the tapered sprue hole and has a suitable seat for the nozzle of the injection cylinder. Sometimes called an adapter.

Sprue
Feed opening provided in the injection or transfer mold. Also, a slug formed at this hole.

Sprue gate
A passageway through which molten plastic flows from the nozzle to the mold cavity.

Sprue lock or puller
In injection molding, a portion of the plastic composition held in the cold slug well by an undercut, used to pull the sprue out of the bushing as the mold is opened.

	The sprue lock itself is pushed out of the mold by an ejector pin.
Stabilizer	An ingredient used in the formulation of some plastics to assist in maintaining the physical and chemical properties of the compounded materials at their initial values throughout the processing and service life of the material.
Staking	A term used in fastening – forming of a head on a protruding stud to hold component parts together. Staking may be done by cold staking, hot staking, or ultrasonic heating.
Standard deviation, or sigma (σ)	The standard deviation of a population, labeled as the Greek letter sigma, is defined as the square root of the variance:

$$\sigma \equiv (\text{Variance})^{1/2} = \sqrt{\Sigma(x - \bar{x})/(N-1)}$$

Starve feeding	A method of feeding an extruder where the polymer is metered in a rate below the full capability of the machine. Thus, the output is determined by the feeder not the extruder or process variables. The controlled metering of resin into the machine's feed section to fill the screw flights is not necessarily from the hopper, but from auger, feed belt, or by hand.
Stationary platen	The plate of an injection or compression molding machine to which the front plate of the mold is secured during operation. This platen does not move during the normal operation.
Statistical chain (Kuhn)	Hypothetical free rotating polymer chain units with length ls, defined to reproduce the chain length; viz., the square end-to-end distance can be expressed as:

$$< r^2 > = N_s l_s^2$$

Statistical process control (SPC)	The use of statistical methods to monitor and control a process.
Stereolithography	A three-dimensional printing process that produces copies of solid or surface models in plastic. This process uses a moving laser beam, directed by computer, to print or draw across sections of the model onto the surface of photo-curable liquid plastic.
Stereoregular polymers	Tactic polymers exhibiting tacticity, i.e., regularity in the stereochemical configuration of its constitutional repeating units: isotactic, syndiotactic, erythro, and threo.

Storage life	See "Shelf-life."
Storage modulus	A quantitative measure of elastic properties, defined as the ratio of the stress inphase with strain, to the magnitude of the strain. The storage modulus may be measured in tension or flexure, E', compression, K', or shear, G'.
Strain	The charge in length per unit of original length, expressed as a fraction of the original length, $\lambda = (L - L_o)/L_o$, in percent, $\Delta l = 100\lambda$, or in extensional flow as $\varepsilon = (L - L_o)/L$. The dimensionless numbers that characterize the change of dimensions of a specimen during controlled deformation. In tensile testing, the elongation divided by the original gage length of the test specimen.
Strength of material	Refers to the structural engineering analysis of a part to determine its strength properties.
Stress concentration	Magnification of the level of applied stress in the region of a notch, crack, void, inclusion, or other stress raisers. Sections or areas in a part where the molded-in or physical forces are high or magnified – all sharp corners have high stresses.
Stress concentration factor (SCF)	Ratio of the maximum stress in the region of a notch, or another stress raiser, to the nominal corresponding stress. SCF is a theoretical indication of the effect of stress concentration on mechanical behavior. Since it does not take into account the stress relief due to plastic deformation, its value is usually larger than the empirical fatigue notch factor or strength reducing ratio.
Stress crack	External or internal cracks in a plastic caused by imposed stresses.
Stress cracking	A process of cracking under induced mechanical stress. Stress cracking generally starts with microscopic surface cracks, caused by chemical attack or other degrading influence such as ultraviolet radiation. Under mechanical stress, the microcracks propagate eventually producing a localized failure.
Stress optical sensitivity	The ability of materials to exhibit double refraction of light when placed under stress.
Stress relaxation	The gradual decrease in stress with time under a constant deformation (strain) and temperature. Stress relaxation is determined in creep test. Data is often presented as stress vs. time plot. The stress relaxation rate is given by the slope of the curve at any point.
Stress	The force applied to produce a deformation in the material. The ratio of applied load to the original

	cross-sectional area of a test specimen, or force per unit area that resists a change in size or shape of a body.
Stress-induced crystallization	The production of crystals in a polymer by the action of stress, usually in the form of an elongation. It occurs in fiber spinning, or during rubber elongation, and is responsible for enhanced mechanical properties.
Stress–strain curve	Simultaneous readings of load and deformation, converted to stress and strain, plotted as ordinates and abscissas, respectively, to obtain a stress–strain diagram.
Stress–strain diagram	Graph of stress as a function of strain constructed from data obtained in any mechanical test in which a load is applied to a material and continuous measurements of stress and strain are made simultaneously. It is constructed for tensile, creep, or torsional loadings.
Striation	A separation of colors resulting in a linear effect or color variation. In blow molding, the rippling of thick parisons. Also a longitudinal line in a plastic created by a disturbance in the melt path.
Stripper-Plate	A plate that strips a molded piece from core pins or cores.
Structural reaction injection molding (SRIM)	A molding process that is similar in practice to resin transfer molding, RTM. SRIM derives its name from the RIM process from which the resin chemistry and injection techniques have added to indicate the reinforced nature of the composite components manufactured by this process.
Styrene-acrylonitrile copolymers (SAN)	A thermoplastic copolymer of styrene and acrylonitrile. If it comprises either SAN-grafted butadiene or is blended with nitrile rubber, NBR, a terpolymer is known as ABS.
Styrenics	A group of plastic materials that are either whole or partially polymerized from styrene monomer.
Submarine gate	A type of edge gate where the opening from the runner into the mold is located below the parting line or mold surface, as opposed to conventional edge gating where the opening is machined into the surface of the mold. With submarine gates, the item is broken from the runner system on opening of the mold or ejection from the mold.
Substituted macromolecules	Linear macromolecules with the side chains consisting of definite and usually homogeneous substituents. (In branched macromolecules, the side chains consist of the same primary molecules as in the main chain and are of varied length and irregularly arranged.)

Substrate	A material upon the surface of which an adhesive-containing substance is spread for any purpose, such as bonding or coating.
Suck-back	A slight retracting of the screw, usually no more than 5–7 mm as the mold opens to suck-back any resin that might have drooled out of the nozzle after the sprue was pulled. Correct nozzle type and temperature control can eliminate a need for this step, even when using very fluid resins.
Surface finish	Finish of a molded product. Refer to the SPI-SPE Mold Finishes Comparison Kit.
Surface treatments	Any method of treating a material so as to alter the surface and render it receptive to inks, paints, lacquers, and adhesives such as chemical, flame, and electronic treatments.
Surfactant	A compound that affects (usually reduces) interfacial tension between two liquids.
Surging	Unstable pressure buildup in an extruder leading to variable throughput.
Suspension polymerization	Chain polymerization of vinyl monomer dispersed in form of large drops in aqueous medium. The polymerization is initiated by monomer-soluble initiator; thus, each drop can be treated as individual bulk polymerizing volume.
Swaging	An assembly technique, similar to heading, where the plastic material is deformed to a specific shape to assemble one or more parts.
Sweating	Exudation of drops of liquid, usually a plasticizer, on the surface of a plastic part.
Swell	A dimensional increase caused by exposure to liquids and/or vapors.
Swelling	Swelling is the ability of a body to take up liquids. It depends on the size and shape of the macromolecule. Linear or lightly branched polymers immersed in a good solvent first swell without limit and then dissolve. The cross-linked polymers show limited swelling capability.
Syndiotactic polymer	A stereoregular polymer in which at least one monomeric carbon atom exhibits stereochemical configurational isomerism and in which the configurations alternate between the neighboring units, viz., syndiotactic PVC and isotactic or syndiotactic PP.
Tab gated	A small removable tab of approximately the same thickness as the mold item, usually located perpendicular to the item. The tab is used as a site for edge gate location, usually on items with large flat areas.

Tacticity	A regularity of configurational isomeric unit placement in the polymeric chain. See "Isotactic, stereoregular, and syndiotactic polymer."
Taguchi method	Problem-solving technique developed by Taguchi, which employs a testing process with an orthogonal array to analyze data and determine the main contributing factors in the solution of the problem.
Tapered block copolymer	Gradient block copolymer in which there is a gradual change of composition at the junction between the two blocks from pure AAAAAAAA type to pure BBBBBBBB type. The tapered block copolymers are reported to be more efficient than pure AB block copolymers as compatibilizers of polymer blends. Tapping cutting threads in the walls of a circular hole.
Tear resistance	The force required to tear completely across a notched specimen tested according to prescribed procedures, expressed in pounds per inch of specimen thickness.
Telechelic polymer	A polymer with purposely introduced chain end groups of a specific type, e.g., ionic, hydroxyl, acidic, etc.
Telomer	Low-molecular-weight radical polymerization product obtained in a reaction in which extensive chain transfer to a solvent (or specifically introduced chain transfer agent) has occurred, so that the telomer contains fragments of these reactants as end groups.
Telomerization	Primarily, a radical solution polymerization with high transfer constant, leading to products of relatively low molecular weight (telomers, with MW § 10,000) containing built-in fragments of the solvent.
Temperature gradient	The slope of a temperature curve. An increasing or decreasing temperature profile on the barrel of the molding machine is an example.
Tensile impact energy	The energy required to break a plastic specimen in tension by a single swing of a calibrated pendulum.
Tensile impact test	A test whereby the sample is clamped in a fixture attached to a swinging pendulum. The swinging pendulum strikes a stationary anvil causing the test sample to rupture. This is similar to the Izod test.
Tensile strength	The pulling stress at any given point on the stress vs. strain curve, usually just before the material tears or breaks. Area used in computing the engineering strength is the original, rather than the necked-down area.
Tensile strength or stress	The maximum tensile load per unit area of original cross section, within the gage boundaries, sustained by the

	specimen during a tension test. Ultimate strength of a material subjected to tensile loading.
Terpolymers	A copolymer composed of three different repeat units or monomers, where the repeating structural units of all three are present within each molecule. The influence of all three types of monomer is evident in the property profile of the polymer. Common terpolymers include ABS and ASA.
Tetrapolymers	Copolymers that contain four different monomers.
Texturizing	The etching or cutting of a pattern on a mold surface to be reproduced on the molded part.
Thermal conductivity	Ability of a material to conduct heat. The coefficient of thermal conductivity is expressed as the quantity of heat that passes through a unit cube of the substance in a given unit of time when the difference in temperature of the two faces is 1 °C.
Thermal degradation	Degradation caused by exposure to an elevated temperature. In the absence of oxygen, the term pyrolysis, while in its presence, the term thermo-oxidative are frequently used.
Thermal expansion	The linear rate at which a material expands or contracts due to a rise or fall in temperature. Each material is unique and has its own rate of expansion and contraction.
Thermal polymerization	Free radical polymerization initiated either by thermal homolysis of an initiator (e.g., azo compound) or caused by action of heat on the monomer itself.
Thermal stress cracking (TSC)	Crazing and cracking of some thermoplastic resins that results from overexposure to elevated temperatures.
Thermocouple	A thermoelectric heat-sensing element mounted in or on machinery and the mold to transmit accurate temperature signals to a control and readout unit.
Thermoelasticity	Rubberlike elasticity exhibited by a rigid plastic and resulting from an increase of temperature.
Thermoforming	The process of forming a thermoplastic sheet into a three-dimensional shape after heating it to the point at which it is soft and flowable and then applying differential pressure to make the sheet conform to the shape of a mold or die positioned below the frame. Thermoforming variations include vacuum forming, air-assist vacuum forming, plug-assist forming, drape forming, plug-and-ring forming, ridge forming, slip forming, bubble forming, matched-mold forming, and scrapless thermoforming.

Thermogravimetric analysis (TGA)	The study of the change in mass of a material, either in oxygen, air, or an inert atmosphere. The test can be conducted under various conditions of time, temperature, and pressure. A testing procedure in which changes in the weight of a specimen are recorded as the specimen is progressively heated.
Thermomechanical analysis (TMA)	An analytical technique consisting of measuring physical dimensions of a material or changes in its moduli as a function of temperature and/or frequency.
Thermoplastics (TP)	A class of plastic materials that is capable of being repeatedly softened by heating and hardened by cooling, viz., ABS, PVC, PS, and PE. Generally, a polymer that, upon heating softens, changing from a solid into elastic or liquid moldable state without having undergone chemical changes. The process is reversible and can be repeated many times.
Thermoplastic elastomer (TPR)	An elastomer which upon heating turns into regularly behaving linear polymer. Polystyrene-polybutadiene block copolymers, polypropylene blends with ethylene-propylene-diene terpolymer provide examples.
Thermoplastic injection molding	A process in which melted plastic is injected into a mold cavity, where it cools and takes the shape of the cavity. Bosses, screw threads, ribs, and other details can be integrated, which allows the molding operation to be accomplished in one step. The finished part usually does not require additional work before assembling.
Thermoplastic (IPN)	Any IPN in which the individual polymers are thermoplastic. The polymers may contain physical cross-links as in ionomers where ionic clusters join two or more chains together. Nowadays, phase-separated polymeric systems, e.g., block and graft copolymers or thermoplastic polyurethanes, are frequently considered thermoplastic IPNs.
Thermoplasticity	The ability of material to be deformed without breaking with a relatively fast flow, when (at a suitable temperature) this material is properly stressed.
Thermosets (TS)	Materials that undergo a chemical reaction by the action of heat and pressure, catalysts, ultraviolet light, etc., leading to a relatively infusible state. Typical of the plastics in the thermosetting family are the amines (melamine and urea), unsaturated polyesters, alkyds, epoxies, and phenolics. A common thermoset goes through three stages.
	A-stage An early stage when the material is soluble in certain liquids and fusible and will flow.

| | B-stage | An intermediate stage at which the material softens when heated and swells in contact with certain liquids, but does not dissolve or fuse. Molding compound resins are in this stage. |
| | C-stage | The final stage is the TS reaction when the material is insoluble, infusible, and cured. |

Thermoset injection molding
A process in which thermoset material that has been heated to a liquid state is caused to flow into a cavity or several cavities and held at an elevated temperature for a specific time. After cross-linking is complete, the hardened part is removed from the open mold.

Thermosetting plastics
See "Thermosets."

Thinner
A liquid that can extend a solution, but not reduce the power of the solvent.

Thixotropy
A decrease of apparent viscosity under shear stress, followed by a gradual recovery when the stress is removed. The effect is time dependent. Its antonym is rheopexy.

Thread plug, ring, or core
A part of the mold that shapes a thread.

Tie bars
Bars that provide structural rigidity to the clamping mechanism of an injection molding press and usually guide platen movement.

Toggle or toggle action
A mechanism that exerts pressure developed by the application of force on a knee joint. It is used as a method of closing presses and serves to apply pressure at the same time.

Tolerance
A specified allowance for deviation in weighing and measuring or for deviations from the standard dimensions of weight.

Topochemical polymerization
Solid-state polymerization of crystalline monomer without any intermediate loss of order. The topotactic oligomers have been produced, but the order is lost as the polymerization progresses beyond a low degree of polymerization.

Torsion pendulum
Test equipment used for determining the dynamic mechanical properties of plastics.

Torsion
Stress caused by twisting a material.

Torsional
The twisting or turning motion of a part. Torsional stress is created when one end of a part is twisted in one direction while the other is held rigid or twisted in the other direction.

Toughness
The extent to which a material absorbs energy without fracture. A measure of the ability of a material to absorb energy. The actual work per unit volume or unit mass of

	material that is required to rupture it. Toughness is proportional to the area under the load-elongation curve from the origin to the breaking point.
Transesterification	An ester interchange reaction occurring when ester is heated in the presence of hydroxy compound (alcoholysis) or acid compound (acidolysis). Since esterification is reversible, the transesterification occurs between mixed esters in the presence of (thermally activated) low concentration of volatile reaction by-products. Ester-amide exchange can also be accomplished by similar (catalyzed) process.
Transfer molding	A method of molding thermosetting materials in which the plastic is first softened by heat and pressure in a transfer chamber and then forced by high pressure through suitable spruces, runners, and gates into a closed mold for final shaping and curing.
Translucent	The quality of transmitting light without being transparent.
Transmission electron microscopy (TEM)	a microscopy technique in which an ultrathin specimen is illuminated by an electron beam. Image formation is made by detecting the electrons transmitted through the specimen. The short wavelength of electrons allows a much higher resolution in TEM (0.2 nm) than in its visible light analogous: the optical microscopy
Transparent	A material with a high degree of light transmission that can be easily seen through.
Triblock polymer	A block copolymer consisting of three $A_nB_mA_n$ blocks.
Tristimulus colorimeter	The instrument for color measurement based on spectral tristimulus values. The color is expressed in terms of three primary colors: red, green, and blue.
Tumbling	Finishing operation for small plastic article by which gates, flash, and fins are removed and/or surfaces are polished by rotating them in a barrel together with wooden pegs, sawdust, and polishing compounds. Adding color to a material through tumble blending.
Tunneling	Release of longitudinal portions of the substrate in incompletely bonded laminates and deformation of these portions to form tunnellike structures.
UCST (upper critical solution temperature)	The highest temperature of immiscibility, where binodal and spinodal curves meet. This type of phase separation predominates in solutions.
Ultimate strength	Strength at the break point in tensile test.
Ultimate tensile strength	The highest stress sustained by a specimen in a tension test. Rupture and ultimate stress may *not* be the same.

Ultrasonic insertion	The inserting of metal into a thermoplastic part by the application of vibratory mechanical pressure at ultrasonic frequencies.
Ultrasonic sealing, bonding, or welding	A method in which sealing is accomplished through the application of vibratory mechanical pressure at ultrasonic frequencies (16–4,000 kHz). Electrical energy is converted to ultrasonic vibrations through the use of a piezoelectric transducer. The vibratory pressures at the interface in the sealing area develop localized heat losses that melt the plastic surfaces effecting the seal.
Ultrasonic testing	Measurement of ultrasonic velocity and absorption (dissipation of sonic energy as a result of conversion to heat) to determine such structure-related factors as glass transition temperature, cross-link density, branching, morphology, composition, etc. Also a nondestructive test applied to materials to locate internal flaws or structural discontinuities by high-frequency reflection or attenuation ultrasonic beam.
Ultrasonics	Branch of acoustics dealing with periodic waves with frequencies above the audible range, i.e., greater than 16 kHz.
Ultraviolet, UV	The region of the electromagnetic spectrum between the violet end of visible light and the X-ray region, including wavelengths from 10 to 390 nm. Because UV wavelengths are shorter than visible wavelengths, their photons have more energy, which initiates some chemical reactions and degrades most plastics, particularly aramids and polypropylenes.
Unbalanced mold	A nonuniform layout of mold cavities and runner system, fill rate, packing pressure, and part quality will vary from cavity to cavity. Used only for noncritical, stand-alone parts.
Undercut	Having a protuberance or indentation that impedes withdrawal from a mold in its normal open/closed movement. Flexible materials can be ejected intact even with slight undercuts.
Unimodal distribution	Distribution with a single peak.
Unit mold	Mold designed for quick-changing interchangeable cavity parts. A mold that comprises only a single cavity, frequently a pilot for the production set of molds.
Universal testing machine	A machine used to determine tensile, flexural, or compressive properties.
Unsaturated polyester	A low-molecular-weight polyester with unsaturated, double bonds able to enter into cross-linking reaction

	with added unsaturated monomer by the radical mechanism. The latter reaction is usually initiated by solution of methyl ethyl ketone peroxide. Also a family of polyesters characterized by vinyl unsaturation in the polyester backbone, which enables subsequent hardening or curing by copolymerization with a reactive monomer in which the polyester constituent has been dissolved.
Unzipping	Depropagation – a degradation reaction in which the consecutive mers are gradually removed from one macromolecular chain end to another. Few polymers undergo such a reverse propagation reaction, viz., PMMA, POM, and PTFE.
UV stabilizer	Any chemical compound that, when added to thermoplastic material, selectively absorbs ultraviolet rays.
Vacuum metallizing	Process in which surfaces are thinly coated with metal by exposing them to the vapor of metal that has been evaporated under vacuum (one millionth of normal atmospheric pressure).
Variance	See "Standard deviation."
Vent	In a mold, a shallow channel or minute hole cut in the cavity to allow air to escape as the melt enters.
Vertical flash ring	The clearance between the force plug and the vertical wall of the cavity in a positive or semipositive mold. Also the ring of excess material that escapes from the cavity into this clearance space.
Vicat softening point	The temperature at which a flat-ended needle of 1 mm, circular or square cross section, will penetrate a thermoplastic specimen to a depth of 1 mm under a specified load using a uniform rate of temperature rise. The temperature at which a plastic is penetrated to 1 mm depth by a flat-ended circular metal pin, while in a controlled temperature silicone fluid bath.
Vinyl	Usually polyvinyl chloride, PVC, but may be used to identify other polyvinyl plastics.
Vinyl chloride plastics	Plastics based on polyvinyl chloride, PVC, or copolymers of vinyl chloride with other monomers, the vinyl chloride being the major component.
Virgin plastics or virgin material	A material not previously used or processed and meeting manufacturer's specifications.
Viscoelasticity	A property involving a combination of elastic and viscous behavior. A material having this property is considered to combine the features of an elastic solid and Newtonian liquid.

Viscosity	The property of resistance to flow exhibited within the body of a material, expressed in terms of relationship between applied shearing stress and resulting rate of strain in shear. A measurement of resistance of flow due to internal friction when one layer of fluid is caused to move in relationship to another layer. Viscosity is quantitatively defined as a ratio of shear stress to shear rate.
Viscometer	An instrument used for measuring the viscosity and flow properties of fluids.
Viscous deformation	Any portion of the total deformation of a body that remains permanently when the load is removed, also referred to as nonelastic deformation.
Void	A void or bubble occurring in the center of a heavy thermoplastic part, usually caused by excessive shrinkage.
Volume resistivity	The electrical resistance between opposite faces of a 1 cm cube of insulating material. It is measured under prescribed conditions using a direct current potential after a specified time of electrification. Also called specific insulation resistance (ASTM D257).
Vulcanization	Process of converting of raw rubber compounds into lightly cross-linked network elastomer. Vulcanization of diene rubbers involves compounding it with sulfur or sulfur compounds and then heating at about 140 °C for sometimes several hours. The process can be sped up by addition of catalyst, viz., ZnO.
Warpage	Dimensional distortion in a plastic object after molding.
Water absorption	The amount of water absorbed by a polymer when immersed in water for stipulated periods of time.
Weathering	A term encompassing exposure of polymers to solar or ultraviolet light, temperature, oxygen, humidity, snow, wind, pollutants (e.g., ozone, NO_2, CO_2), cyclical changes of temperature and moisture, etc. Outdoor degradation of material, exposed to adverse weather factors.
Weatherometer	An instrument used for studying the accelerated effects of weather on plastics, using artificial light sources and simulated weather conditions.
Weibull distribution function:	$$y = (\beta/\alpha)(x - y)^{b-1} \exp\left\{ -(x - \gamma)^{\beta/\alpha} \right\}$$ $$\text{for} : x \geq \gamma; y = 0$$ $$\text{for} : x \leq \gamma$$ where x is a variable and α, β, and γ are the distribution parameters.

Welding	Joining thermoplastic pieces by one of several heat-softening processes. Butt fusion, spin welding, ultrasonic, and hot gas are examples of such methods.
Welding horn	The sonic-energy transmission and pressure-transmitting tool used for ultrasonic welding. Each welding horn is tuned to specific amplitudes to efficiently perform the welding operation.
Wetting agent	An ingredient or solution used to lower the surface tension between two materials, so that good coverage and bonding occur.
Wheel abrading	Deflashing molded parts by abrasion with small particles at high velocity.
Witness lines	Lines left on a molded part by poor mating and fit of side action cores.
WLF equation	Williams-Landel-Ferry equation that relates the value of the shift factor, a_T (associated with time-temperature superposition of viscoelastic data), required to bring log-modulus (or log-compliance) vs. time or frequency curves measured at different temperatures onto a master curve at a particular reference temperature, T_0, usually taken at 50 °C above the glass transition temperature ($T_0 = T_g + 50$ °C): $$a_T = \frac{C_1(T - T_0)}{[C_2 + (T - T_0)]}$$ where the constants, C_1 and C_2, are approximately identical for all polymers: -8.86 and 101.6 K, respectively. Later, the WLF equation has been interpreted in terms of the Doolittle's free volume theory.
Yellowness index	Measure of the tendency of plastics to turn yellow upon long-term exposure to light.
Yield point elongation	In materials that exhibit a yield point, the difference between the elongation at the completion and the start of discontinuous yielding.
Yield point	The point at which permanent deformation of a stressed specimen begins to take place. Stress at which strain increases without accompanying increase in stress. Only materials that exhibit yielding have a yield point.
Yield strength	The stress at the yield point – stress at which a material exhibits a specified limiting deviation from the proportionality of stress to strain or the lowest stress at which a material undergoes plastic deformation. When the material is elastic at lower stresses and viscoelastic at higher, unless otherwise specified, the stress at the

	border of this change is the yield stress. Yield stress is often defined as the stress needed to produce a specified amount of plastic deformation, usually a 0.2 % change in length. In tensile testing, the yield stress is taken as that at which there is no increase in stress with a corresponding increase in strain – usually the first peak on the curve. It may also be defined as a specific limiting deviation from the proportional stress–strain curve.
Young's modulus	The ratio of normal stress to corresponding strain under tensile or compressive loading at stresses below the linearity limit of the material (also modulus of elasticity).
Zero defects	A quality control method where anyone in the production cycle who discovers a quality problem can stop the assembly line or manufacturing process until it is corrected. The problem associated with this method is that upper management is often never made aware that a problem occurred. This lack of knowledge may prevent a complete repair from being initiated and the problem continues to occur.
Ziegler-Natta polymerization	Chain polymerization on a Ziegler-Natta catalyst, Z-N. The Z-N catalysts are based either on $TiCl_4$, VCl_5, or $CoCl_3$ mixed with either $Al(C_2H_5)_3$ or $Al(C_2H_5)_2Cl$, e.g., reacting AlR_3 (R is an alkyl group) with crystalline $TICl_3$ in an inert solvent. For example, three catalytic systems led to polymerization of high-density polyethylene, HDPE, (1) molybdena-alumina, (2) hexavalent CrO_3 on silica, and (3) aluminum trialkyl (e.g., $AlEt_3$) with $TiCl_4$. The polymerization occurs at relatively mild conditions. Z-N polymerization is frequently used to obtain stereoregular polymers, viz., either to an isotactic or a syndiotactic polypropylene.

References

M.S.M. Alger, *Polymer Science Dictionary* (Elsevier Applied Science, London, 1989)

H. Batzer, F. Lohse, *Einführung in die makromoleculare* (Chemie Hütingt & Wepf Verlag, Basel, 1976)

J. Brandrup, E.H. Immergut, *Polymer Handbook* (Intersc Pub, New York, 1966)

P.J. Flory, *Statistical Mechanics of Chain Molecules* (Intersc Pub, New York, 1969)

J. Frado (ed.), *Plastics Engineering Handbook*, 4th edn. (Reinhold Pub Corp, New York, 1976)

C.A. Harper (ed.), *Handbook of Plastics and Elastomers* (McGraw-Hill, New York, 1975)

H.E. Pebly, Glossary of terms in composites, in *Engineering Materials Handbook*, vol. 1 (ASM International, Ohio, 1987)

T.A. Richardson, *Industrial Plastics: Theory and Application* (Cincinnati, South-Western, 1983)

Standard Abbreviation of Terms Relating to Plastics, D1600, Annual Book of ASTM Standards, American Society for Testing and Materials

Standard Definitions and Descriptions of Terms Relating to Conditioning, E41, Annual book of ASTM Standards, American Society for Testing and Materials

Standard Definitions and Descriptions of Terms Relating to Dynamic Mechanical Measurements on plastics, D4092, Annual book of ASTM Standards, American Society for Testing and Materials

Standard Definitions and Descriptions of Terms Relating to Methods of Mechanical Testing, E6, Annual book of ASTM Standards, American Society for Testing and Materials

Standard Definitions and Descriptions of Terms Relating to Plastics, D883, Annual book of ASTM Standards, American Society for Testing and Materials

Standard Definitions and Descriptions of Terms Relating to Reinforced Plastic Pultruded Products, D3918, Annual book of ASTM Standards, American Society for Testing and Materials

Standard Definitions and Descriptions of Terms Relating to Resinography, E375-75 (reproved in 1986), Annual book of ASTM Standards, American Society for Testing and Materials

Standard Guide for Identification of Plastic Materials, D4000, Annual book of ASTM Standards, American Society for Testing and Materials

Standard Terminology Relating to Radiation Measurements and Dosimetry, E170, Annual book of ASTM Standards, American Society for Testing and Materials

J. Thewlis, R.C. Glass, A.R. Meetham (eds.), *Encyclopaedic Dictionary of Physics* (Pergamon Press, Oxford, 1967)

L.A. Utracki, *Commercial Polymer Blends* (Chapman & Hall, London, 1998)

L.A. Utracki, *Encyclopaedic Dictionary of Commercial Polymer Blends* (ChemTec Pub, Toronto, 1994)

L.A. Utracki, *Polymer Alloys and Blends – Thermodynamics and Rheology* (Hanser Pub, Munich, 1989)

Van Nostrand's Scientific Encyclopaedia. (D. Van Nostrand Co. Inc., Princeton, 1958)

L.R. Whittington, *Whittington's Dictionary of Plastics*, 2nd edn. (Technomic, Lancaster, 1978)

Appendix IV: Trade Names of Polymers and Their Blends

A		
A-C	Low molecular weight polyethylene, PE	Allied-Signal Inc.
A-FAX	Amorphous polypropylene, PP	Himont
A-fax	Polypropylene, PP	Himont
A-Tell	Polyethylene-*p*-oxybenzoate for fibers	ICI
Abbey #100	Poly(vinyl chloride) compound, PVC	Abbey Plastic Corp.
Abbey #400	Polypropylene, PP	Abbey Plastic Corp.
Absafil	Acrylonitrile-butadiene-styrene terpolymer, ABS	Fiberfil/Akzo/DSM
Abson	ABS/PVC blends	Abtec/BF Goodrich
Abstrene	Acrylonitrile-butadiene-styrene terpolymer, ABS	Distillers
Accpro	Polypropylene blends	Amoco Chemical
Acctuf	High-impact ethylene-propylene copolymers	Amoco Chemical
Acculloy	Polymer alloys	Aclo Compounders
Accutech	Reinforced resins	Aclo Compounders
Acetabel	Cellulose acetate, CA	Ponceblanc
Acetron GP Acetal	POM reinforced or not (rods or sheets)	Polymer Corp.
Acetron NS Acetal	POM. lubricated (rods or sheets)	Polymer Corp.
Achieve	Metallocene-grade isotactic polypropylene, PP	Exxon
Acihr	Fluoropolymer film	Allied-Signal Inc.
Aclar, Aclon	Fluorocarbon PCTFE film	Allied-Signal Inc.
Aclyn	Low molecular weight EVAc ionomers	Allied-Signal Inc.
Acme	Epoxy resins and molding compounds	Allied Products Corp.
Acpol	Acrylic or thermoset polyesters; acrylic/urethane/styrene IPN	Freeman Chem Co.
Acraldon	Ethylene-vinyl acetate copolymer, EVAc	Bayer AG

(*continued*)

Acralen	Elastomers	Bayer AG
Acrifix	PMMA, poly(methyl methacrylate)	Röhm AG
Acrilan	Polyacrylonitrile, PAN	Chemstrand Corp.
Acronal	Acrylic esters; homo- and copolymers	BASF Plastics
Acrylafil	Glass fiber-reinforced SAN	Akzo/DSM
Acrylan	Acrylic fiber	Monsanto
Acrylan-Rubber	Butyl acrylate-acrylonitrile copolymer	Monomer Corp.
Acrylite	Acrylic (PMMA)	Cyro Industries
Acrylite FF	Poly(methyl methacrylate) powder, sheets, PMMA	Cyro Industries
Acrylite GP	Cast acrylic sheet, PMMA	Chemacryl Plastics, Ltd.
Acrylite SDP	Double-skinned acrylic sheet, PMMA	Chemacryl Plastics, Ltd.
Acrylivin	Poly(vinyl chloride)/Acrylic alloy	Gen. Tire & Rubber
Acryloid	Poly(methyl methacrylate)-butadiene-styrene	Rohm and Haas
Acrylyn	Melt-processable rubber	E. I. du Pont de Nemours
Acrypanel	PMMA, poly(methyl methacrylate)	Mitsubishi Rayon Co.
Acrypoly	Acrylic extruded sheet, PMMA	Chi Mei Ind. Co. Ltd.
Acryrex	Acrylic resin, PMMA	Chi Mei Ind. Co. Ltd.
ACS	Chlorinated polyolefins, e.g., PE, cross-linked or not	Showa Denko K. K.
ACS Resin NS	Styrene-acrylonitrile copolymer, SAN	Biddle Sawyer Corp.
Acsium	Alkylated chlorosulfonated polyethylene, CSR	DuPont/Safic-Alcan
ACter	Low molecular weight terpolymers	Allied-Signal Inc.
ACumist	Micronized polyolefins, PO	Allied-Signal Inc.
ACX	Polyoxymethylene, POM	United Composites
Addylene	Polypropylene, PP	Addiplast
Addylon	Polyamides, PA	Addiplast
Adell A, B	Polyamide-6 or polyamide-66; reinforced or not, PA-6	Adell Plastics, Inc.
Adell F	Polypropylene; reinforced or not, PP	Adell Plastics, Inc.
Adell H	Poly(butylene terephthalate); reinforced or not, PBT	Adell Plastics, Inc.
Adell K	Polyethylene; reinforced or not, PE	Adell Plastics, Inc.
Adflex	Reactor PP alloy; soft PP/EP copolymer	Himont Inc.
Adion A	ABS/hydrophilic-PA; antistatic, for medical uses	Asahi Chemical Ind.
Adion H	HIPS/hydrophilic-PA; antistatic, for cassettes	Asahi Chemical Ind.
Adiprene	Diisocyanates, polyurethanes, PU	E. I. du Pont de Nemours
Admer	Polyolefins, PO	Mitsui Petrochem.
Adpro AP	Reactor olefinic thermoplastic elastomers, RTPO	Genesis Polymers
Adpro	Polypropylene, PP	Novacor/Genesis Polymers
Adstif	Rigid polypropylene made in *Catalloy* process	Himont Inc.
Aerolam, Aerolite	Epoxy resin and molding compounds	Ciba-Geigy Ltd.
Aeroweb, Aracast	Honeycomb materials	
Afcolène	Styrene-acrylonitrile copolymer, SAN	Rhône Poulenc

Afcoryl	Acrylonitrile-butadiene-styrene terpolymer, ABS	Pechiney-Saint-Gobain
Affinity	Polyolefin plastomer, containing 0–20 wt% comonomer based on Insite™ metallocene technology, with long chain branching	Dow Chem. Co.
Aflas FA	Fluoropolymers	3M Ind. Chem.
Aflas	PTFE + PP + cure site monomer terpolymer	Asahi Glass
Aflon	Poly(tetrafluoroethylene-co-ethylene)	Asahi Glass
Ahane	Ultra low-density polyethylene, ULDPE	Dow Chem. Co.
Aim	–	Dow Plastics
Airflex	Ethylene-vinyl acetate copolymer, EVAc	AP&C
Akulon	PA-6, PA-66, blends with PO, reinforced or not	Akzo/DSM Plastics
Akuloy J	Polyamide-66 with PP and 30 % glass fiber	DSM Plastics Int.
Akuloy RM	Polyamide-6 or polyamide-66 blend with functionalized-PP; glass fiber or mineral filled or not	DSM Plastics Int.
Akuloy XT	Polyamide-6/thermoset elastomer alloy	DSM Plastics Int.
Alathon	Polyethylene resins, PE	Occidental
Alathon	Polyethylenes, PE	Cain Chem. Inc.
Albertol	Phenol-formaldehyde resins, PF	Chem. Werke Albert
Albidur	Thermosetting resins; PU, epoxides, polyesters	OFACI
Albis	Polyamide-6/Polyolefin (10 %) blend	Albis Plastics
Alcotex	Poly(vinyl alcohol), PVAl	Revertex
Alcryn	Chlorinated olefin/EVAl/acrylate ester blends; PVC/ethylene-carbon monoxide-vinyl chloride copolymer; TP elastomers	E. I. du Pont de Nemours
Alcudia	Polyethylene, PE	Repsol Quimica SA
Alcupol	Polyols, polyurethanes, PU	Repsol Quimica SA
Alfon Cop.	Modified ethylenetetrafluoroethylene copolymer	Asahi Glass
Alftalat	Alkyd resins	Chem. Werke Albert
Algoflon	Fluorinated resins	Enimont
Algoflon	Polytetrafluoroethylene, PTFE	Montecatini/Ausimont
Alkapols	Polyfunctional PPO polyols	Rhône-Poulenc
Alkathene	High-density polyethylene, HDPE	ICI Adv. Mater.
Alkox	Polyethylene oxide	Meisei Chemical Works
Alkydal	Alkyd, polyester resins, UP	Bayer AG/Miles
Alkyde	Polyester polyurethanes, TPU	Synres-Almoco
Alkynol	Polyester resins for paints and varnishes, UP	Bayer
Allied CM-X	Polytetrafluoroethylene, PTFE	Allied-Signal Corp.
Allobec	Polyesterimide, PEI	Dr. Beck & Co.
Alloprene	Chlorinated rubber	ICI Adv. Mater.
Alpha-PVC	Flexible PVC – CPD	Alpha Chem. & Plastics
Alphaseal	TPO elastomer for packaging	Alpha Chem. & Plastics

(*continued*)

Alphatec	TPE for medical products	Alpha Chem. & Plastics
Alphon	Fluoroelastomer, PTFE/elastomer blends	Custom M.P.
Alton	Poly(phenylene sulfide)/polytetrafluoroethylene	Intl. Polym. Corp.
Altuchoc	Polycarbonate, PC	Societe Altulor SA
Altuglas	Acrylic, poly(methyl methacrylate), PMMA; sheets	Societe Altulor SA/ Elf Atochem
Altuglas	PUR/PMMA interpenetrating polymer networks	Elf Atochem
Altulite	Poly(methyl methacrylate); powder, PMMA	Societe Altulor SA
Alulon	Polyamide-66, PA-66	Akzo/DSM
Amberlite	Synthetic ion exchanger	Rohm and Haas
Ameripol CB	Polybutadiene, PB	BF Goodrich
Ameripol	Polyisoprene, CPI	Firestone
Ameripol	Polyisoprene, CPI	Firestone
Ameripol SM	cis-1,4-Polyisoprene, CPI	Firestone
Amidel	Polyamide, amorphous, transparent	Union Carbide
Amidel	Polyamide-6, PA-6	Toray Industries
Amilan	Glass fiber- or mineral-reinforced polyamide-6	Toray Industries
Amilon	Polyamide-6 or polyamide-66, PA-6 or PA-66	Toray Industries
Amoco 10	Polypropylenes, PP	Amoco Chem. Corp.
Amoco 20	Polyethylenes, PE	Amoco Chem. Corp.
Amoco A-I	Polyimide; insulative and conductive coatings	Amoco Chem. Corp.
Amoco G	Polystyrene, PS	Amoco Chem. Corp.
Amodel A-	Polyphthalamide, reinforced	Amoco Performance Products
Amodel AD-	Polyphthalamide, PPA, semicrystalline-PA	Amoco Performance Products
Amodel ET-	Polyphthalamide, impact modified	Amoco Performance Products
Amoron	Polythioethersulfone, block copolymer with 53 % PPS and poly(phenylene sulfide)sulfone, PPSS, filled with 0, 30, and 40 wt% glass and PTFE	Dainippon Ink & Chem.
Ampal	Polyester, unsaturated, UP	Ciba-Geigy Ltd.
Ampec	Ethyl cellulose, EC	American Polymers
Ampol	Cellulose propionate, CP, or cellulose acetate-butyrate, CAB	American Polymers
Antron	Polyamide fiber	E. I. du Pont de Nemours
Apec	Aromatic, "high heat," polyester carbonate, PEC	Bayer AG/Miles
Apex	Poly(vinyl chloride) compounds; PVC	Teknor Apex
Apiax	Polyether compound	Polymix
Apiflex	Poly(vinyl chloride), semirigid, plastified; PVC	Polymix
Apilon	Polyurethanes, PU, or poly(vinyl chloride), PVC	Polymix
Aplical	Polyimide film, PI	Allied Signal Inc.
APP	Polypropylenes, PP	Reichhold Chem., Inc.
Applied Comp 8000	Thermoset polyester-based composites, UP	Applied Composites

(*continued*)

Appryl	Polypropylene, PP	Elf Atochem
Apscom	Speciality thermoplastics (ABS, Acrylics, SAN, Akzo/DSM POM, PC, PEI, PP, PPE, PPS, etc.)	
Aqua Keep	Superabsorbent polymers	Elf Atochem
Aqualoy 100	Polypropylenes, PP	CoAlloy Intl. Corp.
Aqualoy 600	Polyamide-66	CoAlloy Intl. Corp.
Aquathene	Polyethylene	Quantum
Arakote	Thermoset polyesters, UP	Ciba-Geigy Corp.
Araldite	Epoxy resins, EP	Ciba-Geigy Ltd.
Arcel	Polyethylene copolymers	ARCO Chemical
Arcol	Polyols	ARCO Chemical
Ardel D-100	Polyarylate, bisphenol-A iso-/terephthalate	Amoco Chem. Co.
Ardel	PAr/PET blends	Amoco Chem. Co.
Areca	Reinforced polypropylene, PP	SPCI
Ariloks	Poly(phenylene ether)/HIPS; PPE/HIPS blends	USSR
Arimax	Polyurethanes, PU	Ashland Chem. Co
Aristech	Polypropylene, PP	Aristech Chem Corp.
Arlon	Polyetheretherketone; reinforced or not, PEEK	Du Pont/Green, Tweed
Arloy 1000	Polycarbonate, PC/SMA blend	Arco Chem. Co.
Arloy 2000	Styrene maleic anhydride, SMA/PET alloys	Arco Chem. Co.
Arloy	PC/SMA/HIPS blends	Amoco
Arnel	Cellulose triacetate	Celanese
Arnite PBTP	Poly(butylene terephthalate), reinforced or not	Akzo/DSM
Arnite	Poly(ethylene terephthalate), reinforced or not	Akzo/DSM
Arnitel	Thermoplastic ether-ester elastomer, TPE	Akzo/DSM
Aropol	Unsaturated polyesters, UP	Ashland Chem.
Aroset	Acrylic copolymers (P-sensitive adhesives)	Ashland Chem.
Arpak/Arpro	Polyethylene-expanded beads	ARCO Chemical/JSP
Arpro/Arpak	Polypropylene-expanded beads	ARCO Chemical/JSP
Arradur	Acrylonitrile-butadiene-styrene terpolymer, ABS	Elf Atochem
Arum	Polyimide for injection molding	Mitsui Toatsu Chem., Inc.
Arylef	Polyarylate	Solvay
Arylon	Polyarylate, PAr, PET blends	E. I. du Pont de Nemours
Asahi PPS RE	Poly(phenylene sulfide), PPS alloy	Asahi Glass
Ashlene	Polyamide-6, polyamide-612, or polyamide-66; reinforced or not	Ashley Polymers Inc
Aspect	Thermoplastic polyester; PET-based blends	Phillips 66 Co.
Asplit	Phenol-formaldehyde resins, PF	Hoechst
Aspun	Fiber-grade polyethylene resins, PE	Dow Chem. Co.
Asterite	Acrylic dispersion	ICI Chem. Polym. Ltd.
Astrel	Polyarylethersulfone, PAES, $[-\phi-O-\phi-SO_2-\phi-\phi-SO_2-]$	Carborundum
Astryn	Filled polypropylene, PP	Himont

(*continued*)

Astyr	Butadiene rubber, BR	Montecatini
Atlac	Unsaturated polyester resin, UP	DSM/Koppers Co., Inc.
Atlantic Polybead	Expanded polystyrene, PS	Atlantic Gypsum
Atlas	Acrylate and methacrylate resins	Degussa
Attane	Ultra low-density linear polyethylene copolymers	Dow Chem. Co.
Aurum	Polyimide; for injection molding, recyclable	Mitsui Toatsu
Avimid	Thermoplastic polyimide	E.I. du Pont de Nemours
AVP	Engineering thermoplastic resins and blends	Polymerland, Inc.
AVP Resin	Recycled thermoplastic resins	Polymerland, Inc.
Avron	Acrylic dispersion	ICI Chem. Polym. Ltd.
Avtel	Advanced composites	Phillips 66 Co.
AX-500	Amorphous polyarylate/PA-6 alloy + 40 % glass	Unitika
Azdel	Continuous glass fiber-filled PP	Azdel Inc.
Azloy	Continuous glass fiber-reinforced PC/PBT blends	Azdel Inc.
Azmet	Crystalline polyester-based composite	Azdel Inc.
B		
Bakelite DFD	Polyethylenes, PE	Bakelite/Union Carbide
Bakelite DHDA	Ethylene-vinyl acetate copolymers, EVAc	Bakelite/Union Carbide
Bakelite DPD	Acrylic resins	Bakelite/Union Carbide
Bakelite DQDA	Ethylene-vinyl acetate copolymers, EVAc	Bakelite/Union Carbide
Bakelite ERL, ERR	Epoxy resins, EP	Bakelite/Union Carbide
Bakelite HFD	Polyethylenes, PE	Bakelite/Union Carbide
Bapolan 1000	Polyethylenes; reinforced or not, PE	Bamberg Polymers
Bapolan 4000, 5000	Polypropylenes, PP	Bamberg Polymers
Bapolan 6000	Polystyrenes, PS	Bamberg Polymers
Bapolan 7000	Styrene-acrylonitrile copolymer, SAN	Bamberg Polymers
Bapolan 8445	Acrylonitrile-butadiene-styrene terpolymer, ABS	Bamberg Polymers
Bapolene	Polyethylene	Bamberger
Barex	Polyacrylonitrile and acrylonitrile copolymers transparent for bottles, films, etc.	BP Chemicals, Intl.
Basopor	Urea-formaldehyde resin, UF	BASF Plastics
Basotect	Elastic melamine foam, MPF	BASF Plastics
Bayblend DP2	PC/ABS alloy; molding, structural foam, etc.	Bayer AG/Miles
Bayblend	PC/ABS alloys, reinforced, flame retard or not	Bayer AG/Miles
Baycoll/Baymer	Polyurethanes, PU	Bayer AG/Miles
Baycomp	Fiber-reinforced plastic	Bay Mills
Baydur	Polyurethanes, PU	Bayer AG/Miles
Bayer LCP	Liquid crystal polymers, LCP	Bayer AG/Miles

Bayer Silicone	Silicones	Bayer AG/Miles
Bayfill/Bayfit	Polyurethanes, PU	Bayer AG/Miles
Bayflex	Polyurea for reactive injection molding, RIM	Bayer AG/Miles
Bayfol CR	PC/PBT blends	Bayer AG/Miles
Bayfol	Films made of PC blends	Bayer AG/Miles
Baygal/Baymidur	Polyurethane casting resins, PU	Bayer AG/Miles
Baylon	Ethylene-vinyl acetate copolymer, EVAc	Bayer AG/Miles
Baylon	Polycarbonate PC	Bayer AG/Miles
Baylon	Polyamide-66	Bay Resins
Baymer/Baysport	Polyurethanes, PU	Bayer AG/Miles
Baymoflex	Acrylonitrile-styrene-acrylic rubber blend	Bayer AG/Miles
Baynat/Baytec	Polyurethane, PU	Bayer AG/Miles
Baypren	Chloroprene rubber, CR; for molding	Polysar/Bayer AG
Baypren Latex	Anionic lattices of chloroprene rubber, CR	Polysar/Bayer AG
Baypren/Bystal	Polychloroprene elastomers	Bayer AG/Miles
Baysilone	Silicones	Bayer AG/Miles
Baytac	Laminating adhesives (hot melt)	IGI Baychem, Inc.
Baytec 800	Polyurethanes, PU	Bayer AG/Miles
Beckacite	Phenol-formaldehyde resins, PF	Reichhold Ltd.
Beckopox	Epoxy resins, EP	Reichhold Ltd.
Beetle	α-cellulose-reinforced urea-formaldehyde, UF	BIP Chemicals Ltd.
Beetle	PBT, PET compounds	BIP Chemicals Ltd.
Beetle	Polyamide-6, polyamide-66 compounds, PA-6	BIP Chemicals Ltd.
Beetle	Polycarbonate compounds, PC	BIP Chemicals Ltd.
Beetle	Polyester compounds (PMC)	BIP Chemicals Ltd.
Beetle	Polyoxymethylene, POM	BIP Chemicals Ltd.
Beetle	Unsaturated polyester resins, UP	BIP Chemicals Ltd.
Beetle	Urea-formaldehyde molding powders UF	BIP Chemicals Ltd.
Benvic	PVC blends with ABS, NBR, MBS, CPE, etc. with glass fiber or not	Solvay & Cie SA
Bergacell	Cellulose acetates, CA	Th. Bergmann
Bergadur	Thermoplastic polyesters	Th. Bergmann
Bergamid	Polyamides reinforced or not, PA	Th. Bergmann
Bergaprop	Reinforced polypropylene, PP	Th. Bergmann
Beta	–	Beta Polymers
Bexel	SAN/acrylic alloys	Bakelite Xylonite
Bexloy	Automotive engineering resins (an ionomer)	E. I. du Pont de Nemours
Bexloy C	Amorphous polyamide blend, PA	E. I. du Pont de Nemours
Bexloy J	Poly(butylenes terephthalate), PBT, blend	E. I. du Pont de Nemours
Bexloy K	Reinforced PET blend	E. I. du Pont de Nemours
Bexloy M	Aromatic polyester blend	E. I. du Pont de Nemours

(*continued*)

Bexloy	Polyarylate, PAr, PET blends	E. I. du Pont de Nemours
Bexloy V	Thermoplastic copolyester elastomer blend	E. I. du Pont de Nemours
Bexloy W	Ionomer engineering blend	E. I. du Pont de Nemours
Bexoid	Cellulose acetate, CA	British Xylonite
Bexone F	Poly(vinyl formal), PVFM	British Xylonite
Bextrene	Polystyrene, PS	British Xylonite
Bioform	Acrylic-based IPN for artificial teeth	Dentsply International
Biopol	Poly(β-hydroxybutyric acid), PHBA	
Biresin	Thermoset resins, UP	SPCI
Blane	Poly(vinyl chloride), PVC; with clay or not	BP Performance
Blendex	ABS modifier/processing aid for rigid PVC	GE Speciality Chemicals
Blendur	PU-based thermoset blend	Bayer AG/Miles
Blendur-E	Epoxides, EP	Bayer AG/Miles
Blueboard	Plastic foam insulation	Dow Chem. Co.
BMC	Unsaturated polyester; reinforced or not, UP	BMC Inc.
Boltaron	Poly(vinyl chloride)/acrylic alloy sheets	GenCorp Polymer Prod.
Bond 811B	Epoxy resins, EP	Furane Products
Bonoplex	Poly(methyl methacrylate), PMMA	AB Bofors, Sweden
Bonvic	Rigid PVC formulation based on emulsion resin	Solvay & Cie SA
Bovidur/Bovil	Poly(vinyl chloride) compounds, PVC	Maprac
BP D, H	Polyethylenes, PE	BP Chemicals Ltd.
BP Polystyrene	Polystyrene, PS	BP Chemicals Ltd.
BR	Poly(phenylene sulfide), PPS/PTFE blend	Phillips 66 Co.
Brilion BT 40	Polyamide alloys, PA	EMS
Bristrend	Poly(vinyl chloride)/Poly(vinyl acetate)	Polymers Inc.
Bromo XP-50	Brominated poly(isobutylene-*co*-*p*-methylstyrene)	Exxon Chem.
Bromobutyl	Elastomers	Exxon Chem.
BT resin	Thermosetting polyimide	Mitsubishi Gas Chem.
Budd Cast	Polyamide-6, PA-6	Budd Co.
Budene	*cis*-1,4-Polybutadiene, PB	Goodyear, USA
Buna AP	Thermoplastic elastomers: EPR or EPDM	Bunawerke Hüls
Buna BL	Styrene-butadiene block copolymer, for impact modification of PS, leading to HIPS	Polysar/Bayer AG
Buna CB	Butadiene rubber, BR; polymerized with Ti-, Nd-, or Li-based catalyst	Polysar/Bayer AG
Buna EM	Expandable SBR, E-SBR	Bunawerke Hüls
Buna Hüls butacryl	Butadiene-acrylonitrile copolymer, MBR	Plastugil, France
Buna N	Poly(butadiene-*co*-acrylonitrile), MBR	Chem. Werke Hüls
Buna	Polybutadiene, PB	Buna AG
Buna S	Butadiene-styrene copolymer, SB	Chem. Werke Hüls

Bur-A-Loy	PVC/nitrile rubber blends	Mach-1 Compounding
Butacite	Poly(vinyl butyral) sheeting; safety glass sheeting E. I. du Pont de Nemours	
Butaclor	Polychloroprene, CR	Distugil
Butacon	Butadiene copolymers	ICI
Butaprene	Styrene-butadiene copolymers	Firestone
Buton	Cross-linked butadiene-styrene copolymer	Exxon, GB
Butvar	Poly(vinyl butyral)	Shawinigan Chemicals
Butylkautschuk	Polyisobutylene with 5 % isoprene, PIB	Bayer AG/Miles
BVC	Poly(vinyl chloride), PVC	Bayshore Vinyl
BXL	Polysulfone, PSU	Union Carbide Co., Inc.
Bynel (CXA)	Coextrudable adhesive resins	E. I. du Pont de Nemours
C		
C-020	Polypropylene, PP	Aristech Chem.
C-Flex	Thermoplastic elastomers; SEBS/PDMS blends	Concept Polymer
Cadon	SMA and SMA/ABS elastomeric blends with glass fibers or not	Monsanto Chem. Co.
Calatrava	High-density polyethylene, HDPE	Repsol Quimica
Caleprene	Elastomers	Repsol Quimica
Calibre	Polycarbonate, PC, and its blends	Dow Chem. Co.
Calibre CR	PC blended with PBT and PET	Sumitomo Dow Ltd.
Calibre IM	PC blended with an elastomer	Sumitomo Dow Ltd.
Calprene	Synthetic rubber	Repsol Quimica SA
Capran	Polyamide-6; resins, films, fibers, laminates, PA	Allied-Signal Inc.
Caprolan	Thermoplastic elastomers	Elastogran
Capron	Polyamide-6 and blends; reinforced or not, PA	Allied-Signal Inc.
Capron	Polyamide/PO or elastomer blend	Allied-Signal Inc.
Capron AB	Polyamide-6/elastomer; food grade barrier resin	Allied-Signal Inc.
Caradate	Polyurethanes, isocyanates, PU	Shell Chem. Co.
Caradol	Polyols for PU	Shell Chem. Co.
Carapor	Additive for polyurethane	Shell Chem. Co.
Carbopol	Acrylic acid polymers, PAA	BF Goodrich
Carboset	Acrylic polymers	BF Goodrich
Carbowax	Poly(ethylene glycol), PEO	Union Carbide Co., Inc.
Carbres	Reinforced polypropylene, PP	SIC Plastic
Cardura	Chemical intermediates	Shell Chem. Co.
Cariflex I	*cis*-1,4-Polyisoprene	Shell Chem. Co.
Cariflex	Styrene-butadiene block copolymer, SB	Shell Chem. Co.
Caril	Poly(phenylene ether), PPE blend	Shell Chem. Co.
Carilon	Linear, alternating olefin/CO copolymer, COPO, engineering resin with good barrier properties [based on Pd catalyst; introduced in 1995]	Shell Chem. Co.

(continued)

Carina	Poly(vinyl chloride), PVC	Shell Chem. Co.
Carinex	Polystyrene, PS	Shell Chem. Co.
Caristar	Plastic packaging material	Shell Chem. Co.
Carloy	Poly(vinyl chloride), PVC/elastomer blend	Cary Chem. Inc.
Cast Nylon	Polyamide, PA	Commercial Plastic
Castethane	Elastomer systems	Dow Chem. Co.
Catalloy	Polypropylene copolymer alloy	Himont
Cefor	Polypropylene	Shell Chem. Co.
Celanese Nylon 6	Polyamide-6, PA-6 impact modified	Hoechst Celanese Corp.
Celanese Nylon 6/6	Polyamide-66 and polyamide-66/TPU alloys glass fiber reinforced or not	Hoechst Celanese Corp.
Celanese	Polyamide-6, polyamide-66, PA-6 or PA-66	Hoechst Celanese Corp.
Celanex	PBT/elastomer; blends reinforced or not	Hoechst Celanese Corp.
Celanex	PBT/PET/elastomer; blends reinforced or not	Hoechst Celanese Corp.
Celazole	Thermoplastic polyimides, reinforced or not	Hoechst Celanese Corp.
Celcon	Copolyoxymethylene, POM, glass-reinforced, impact-modified elastomer blends	Hoechst Celanese Corp.
Celion	Carbon fibers	BASF Plastics
Cellasto	Cellular PUR elastomers	BASF Plastics
Cellatherm	Polyesterimide, PEI	Reichhold Chemie
Cellidor B	Cellulose acetate-butyrate, CAB	Bayer AG/Miles
Cellidor CP	Cellulose propionate, CP	Bayer AG/Miles
Cellit	Cellulose acetate or cellulose propionate	Bayer AG/Miles
Cellon	Cellulose acetate, CA	Dynamit Nobel
Cellophan	Cellulose hydrate from pulp	Kalle
Cellosize	Hydroxyethyl cellulose	Union Carbide
Celltrek 3000	Polyol for PU foam without CFC	Dow Europe
Celluloid	Cellulose nitrate plasticized with camphor, CN	Hoechst Celanese
Celstran	Long glass fiber-reinforced thermoplastics, viz., POM, PBT, PET, PA, etc.	Hoechst Celanese Corp.
Centrex 800	ASA-based, weatherable polymers	Monsanto Chem. Co.
Centrex	Acrylonitrile-styrene-acrylate copolymers, ASA/AES rubber modified blends	Monsanto Chem. Co.
Cevian	ABS	Hoechst Celanese Co.
Chem-AD	Epoxy and polyurethane industrial adhesive	Chemque
Chem-POT	Encapsulating resins of epoxy and polyurethane	Chemque
Chemfluor	Polytetrafluoroethylene compounds, PTFE	Norton Performance
Chemigum	Nitrile rubber, NBR; TP elastomers	Goodyear Chem.
Chemigum TPE	NBR blend with PVC, CPE, TPU, and/or PA	Goodyear Chem.
Chemorset	Epoxy adhesives, EP	Chemor Inc
Chemplex 1000, 3000	Polyethylenes, PE	Norchem, Inc.

Chemplex 5000, 6000	Polyethylenes, PE	Norchem, Inc.
Chemplex EVA	EVAc for extrusion coating, laminating	Norchem, Inc.
Chemplex PE	EVAc for tough film applications	Norchem, Inc.
Chen-Lon	Polyimide, PI, adhesive	Chemtronics
Chevron	Polypropylene, PP	Chevron
Chlorkautschuk	Chlorinated natural rubber	Bayer AG/Miles
Chlorobutyl	Elastomers	Exxon Chem.
Cibamin	UF, MF-lacquer resins	Ciba-Geigy Ltd.
Cibanoid	Urea-formaldehyde, UF, molding material	Ciba-Geigy Ltd.
CIL 100	Low-density polyethylenes and copolymers	CIL Inc.
CIL 1000	Ethylene-vinyl acetate copolymers, EVAc	CIL Inc.
Cis-4	*cis*-1,4-Polyisoprene	Phillips
Cladlux	Acrylic/PVC alloy	Richard Daleman
Claradex	ABS	Shin-A
Clarene	Poly(ethylene-*co*-vinyl alcohol); EVAl or EVOH	Solvay & Cie SA
Clariflex TR	Styrene-butadiene-styrene copolymer, SBS	Shell Chem. Co.
Clear 01	PVC alloy with glutarimide acrylic copolymer for hot-fill bottles	Georgia Gulf
Cleartuf 7000	Poly(ethylene terephthalate), PET	Goodyear
Clysar	PO shrink films	E. I. du Pont de Nemours
Cobex	Poly(vinyl chloride)	Bakelite Xylonite
Codabs	ABS reinforced or not	Codiplast
Codica	Reinforced polypropylene, PP	Codiplast
Codimel	Reinforced poly(vinyl chloride), PVC	Codiplast
Codix	Polypropylene, PP	Codiplast
Comalloy 110	Polypropylenes; reinforced or not, PP	Comalloy Intl. Corp.
Comalloy 210	Polystyrenes; reinforced or not, PS	Comalloy Intl. Corp.
Comalloy 220	ABS; reinforced	Comalloy Intl. Corp.
Comalloy 240	SAN; glass fiber reinforced	Comalloy Intl. Corp.
Comalloy 260	Polystyrene; glass fiber reinforced, PS	Comalloy Intl. Corp.
Comalloy 310	Poly(vinyl chloride); glass fiber reinforced, PVC	Comalloy Intl. Corp.
Comalloy 410	Poly(butylene terephthalate); glass fiber reinforced	Comalloy Intl. Corp.
Comalloy 510	Polycarbonate; mineral/glass fiber reinforced	Comalloy Intl. Corp.
Comalloy 610	Polyamide-6; glass fiber reinforced, PA-6	Comalloy Intl. Corp.
Comalloy 620	Polyamide-66; glass fiber reinforced, PA-66	Comalloy Intl. Corp.
Comalloy 640	Polyamide-612; glass fiber reinforced, PA-612	Comalloy Intl. Corp.
Comalloy 710	Poly(phenylene sulfide); mineral/GF reinforced	Comalloy Intl. Corp.
Comalloy 740	Polysulfone; glass fiber reinforced, PSU	Comalloy Intl. Corp.
Comalloy 832	ABS/PVC alloy	Comalloy Intl. Corp.
Comalloy 862	Polyamide-66; glass fiber reinforced, PA-66	Comalloy Intl. Corp.
Comalloy 940	Polypropylene; 50 % copper filled, PP	Comalloy Intl. Corp.
Comalloy	Polycarbonates, PC	Comalloy Intl. Corp.
Comco Nylon 6	Polyamide-6, PA-6	Commercial Plastic
Comco Nylon 6	Polyamide-6, PA-6	Commercial Plastic

(*continued*)

Comco Nylon 6/6	Polyamide-66, PA-66	Commercial Plastic
Comco PVC	Poly(vinyl chloride), PVC	Commercial Plastic
Comco UHMW-PE	Ultrahigh molecular weight PE, UHMWPE	Commercial Plastic
Comp Armor	Unsaturated polyester, UP	Haysite Reinforced Plastics
Compodic	Polyamides, PA	DIC Trading
Compound No. 1000	Unsaturated polyester, UP	Resinoid Engr. Corp.
Comshield	Filled polypropylene, PP	Comalloy Intl. Corp.
Comtuf 100	Reinforced polypropylene, PP	Comalloy Intl. Corp.
Comtuf 400	Reinforced polyesters, PBT, PET	Comalloy Intl. Corp.
Comtuf 600	Reinforced polyamides-6, PA-612, or PA-66	Comalloy Intl. Corp.
Conap CE-1132	Unsaturated polyesters, UP	Conap, Inc.
Conap CE-1170	Acrylic resins	Conap, Inc.
Conap UC-21	Polyurethanes, PU	Conap, Inc.
Conapoxy	Epoxy resins, reinforced or not, EP	Conap, Inc.
Conathane	Polyurethanes (TS)	Conap, Inc.
Condux 8000A	Poly(vinyl chloride)/ABS alloy, PVC/ABS	Advanced Dynamics
Conex	Aramid	Teijin/Hoechst
Conoptic	Polyurethanes (TS)	Conap, Inc.
Contrex	Acrylonitrile-styrene-acrylate terpolymer, ASA	Monsanto Europe SA
Coral rubber	*cis*-1,4-Polyisoprene	BF Goodrich
Cordura	Polyamide fiber	DuPont de Nemours
Corezyn	Unsaturated vinyl esters or polyesters, UP	Interplastic Corp.
Corovin	Polypropylene, PP	J. H. Benecke
Corton	Mineral-filled resins	PolyPacific
Corvic	Poly(vinyl chloride) polymers, PVC	European Vinyls Corp.
Cosmic DAP	Diallyl phthalate (TS), DAP	Cosmic Plastics
Courlene	Polyethylene, PE fiber	Courtaulds Fibers Ltd.
Courlene PY	Polypropylene, PP-fiber	Courtaulds Fibers Ltd.
Courtelle	Polyacrylonitrile, PAN	Courtaulds Fibers Ltd.
CP 41	Acrylates	Continental Poly.
CP D33	Diallyl phthalate (TS); reinforced or not, DAP	Cosmic Plastics
CP	PMMA/elastomer blend	Continental
CPP30GF	Mineral-reinforced polypropylene, PP	Ferro Corp.
Crastin	Poly(butylene terephthalate), PBT	Ciba-Geigy Ltd.
Crastin	Poly(ethylene terephthalate), PET	Ciba-Geigy Ltd.
Crastin XMB	Poly(butylene terephthalate)/ABS blends	DuPont
Crastone	Poly(ethylene sulfide), PES	Ciba-Geigy/Phillips
Crealan	Thermoset resins	Bayer
Creslan	Acrylic fiber	Cyanamid
CRI	Polyamide-6, PA-6	Custom Resins
Crystalor PMP	Poly(4-methylpentene-1), PMP	Phillips 66 Co.
Crystic	Unsaturated polyesters, UP	Ashland Chem
CTE	Acrylics	Richardson Polymer
CTI AN	Glass fiber-reinforced polyamide, PA	CTI

CTI AS	Glass fiber-reinforced ABS	CTI
CTI AT	Glass fiber-reinforced polyoxymethylene, POM	CTI
CTI ES	Glass fiber-reinforced polyethersulfone, PES	CTI
CTI NH	Glass fiber-reinforced polyamide-11, PA-11	CTI
CTI NI	Glass fiber-reinforced polyamide-610, PA-610	CTI
CTI NJ	Glass fiber-reinforced polyamide-12, PA-12	CTI
CTI NL	Glass fiber-reinforced polyamide-612, PA-612	CTI
CTI NN	Glass fiber-reinforced polyamide-66, PA-66	CTI
CTI NY	Glass fiber-reinforced polyamide-6, PA-6	CTI
CTI PC	Fiber-reinforced polycarbonate, PC	CTI
CTI PF	Fiber-reinforced polysulfone, PSU	CTI
CTI PI	Fiber-reinforced polyetherimide, PEI	CTI
CTI PK	Fiber-reinforced polyetheretherketone, PEEK	CTI
CTI PS	Glass fiber-reinforced poly(butylenes terephthalate)	CTI
CTI SF	Glass fiber-reinforced poly(phenylene sulfide), PPS	CTI
CTI SN	Glass fiber-reinforced SAN	CTI
Cyanacryl	Alkyl-*co*-alkoxyalkyl acrylates, elastomers	Akzo/DSM
Cyanaprene	Castable urethane, PU	Cyanamid Co.
Cycogel	ABS	Nova Polymers
Cycolac	Acrylonitrile-butadiene-styrene terpolymers, ABS	GE Plastics
Cycolac EHA	ABS/PC alloys	GE Plastics
Cycolac G	ABS/PBT	GE Plastics
Cycolac GCT/M	ABS/PBT automotive blends	GE Plastics
Cycolac SDB	ABS/engineering polymer blends	GE Plastics
Cycolac SDM	ABS/electrostatic dissipation polymer blends	GE Plastics
Cycolin	ABS/PBT alloy	GE Plastics
Cycoloy	ABS/PC; ABS/PVC; or ABS/TPU blends	GE Plastics
Cycoloy EHA	PC/ABS alloys with varying PC content	GE Plastics
Cycoloy LG9000	PC/ABS low-gloss alloy	GE Plastics
Cycopac	Acrylonitrile-butadiene-styrene terpolymers, ABS	GE Plastics
Cycovin	Acrylonitrile-butadiene-styrene terpolymer, ABS	BF Goodrich
Cycovin K25	Poly(vinyl chloride)/ABS high impact alloy	BF Goodrich
Cycovin KAB	ABS/PVC alloys	BF Goodrich
Cyglas	Unsaturated polyesters; reinforced or not	American Cyanamid
Cymel	Alpha cellulose-reinforced melamine-formaldehyde	American Cyanamid
Cyrex 200	PMMA/PC opaque, high-impact-strength alloys	Cyro Industries
Cyrex	SAN/PC opaque blends	Cyro Industries
Cyrolite	Acrylic-based, impact-modified highly transparent multipolymer	Cyro Industries
D		
D-007	Polypropylene, PP	Aristech Chem.
D-10FG	Glass fiber-reinforced ABS	Thermofil, Inc.
D.E.R.	Epoxy resins, EP	Dow Chem. Co.
D7	Acrylonitrile-butadiene-styrene terpolymer, ABS	Thermofil, Inc.

(*continued*)

D8	Styrene-acrylonitrile copolymer, SAN	Thermofil, Inc.
Dacron	Poly(ethylene terephthalate), PET fibers	E. I. du Pont de Nemours
Dai El	PTFE/PHFP/PVDF or PVDF/PHFP elastomers	Daikin/Chevassus
Daki Polistyren	Styrene-butadiene copolymer, SBR	INA
Dalpen	Polyolefins: PE or PP	Kingsley & Keith/PCD
Daltoflex I	Polyurethane rubber	ICI
Dalvor	Fluorinated EPR rubber, FEP	Dow Chem. Co.
Dapex RX	Diallyl phthalate, DAP	Rogers Corp.
Daplen	LDPE, HDPE, PP, GMT, PCD	Polymere Gesellschaft
Dapon	Diallyl phthalate resin	FMC Corp.
Daramelt	Hot melt adhesives/sealants	W R Grace
Dararay	Microwave fluxed plastisols	W R Grace
Daraseal	Poly(vinyl chloride) plastisols, PVC	W R Grace
Darawave	Microwave curable plastisols, PVC	W R Grace
Daron 40	Unsaturated polyester/polyurethane thermosetting blends for fiber-filled systems	DSM
Daron	Hybrid polyester resin; HT resistance	DSM
Dart PS-100	Polystyrene, PS	Dart Polymers, Inc.
Darvic	Poly(vinyl chloride)	ICI
Decaplast	Polyamide-6, -10, PA-610	Montefibre
Decargias	Extruded polycarbonate sheet, PC	Degussa AG
Decoloy	Acrylic/PVC alloy	Borg-Warner/Ube
Deerlon	Polyamides	Deer Polymer
Defsan	Polycarbonate, PC/PET alloy	USSR
Degalan	Acrylates and methacrylates, PMMA powder	Degussa AG
Deglas	Extruded acrylic sheet, PMMA	Degussa AG
Delrin	Polyoxymethylene (*acetal*) resins, POM, some grades contain PTFE	E. I. du Pont de Nemours
Delrin T, ST	POM toughened by addition of TPU elastomer	E. I. du Pont de Nemours
Demospan	Polyurethanes	Bayer
DEN	Epoxy resins, EP	Dow Chem.
Denka HS	Acrylonitrile-butadiene-styrene terpolymer/PC	Denki Kagaku
Denka LCS	Poly(vinyl chloride)/NBR blends	Denki Kagaku/Chevassus
Denka Taimelan	Acrylonitrile-butadiene-styrene terpolymer/PVC	Denki Kagaku
DER	Epoxy resins, EP	Dow Chem. Co.
Derakane	Thermoset vinyl ester epoxy resins	Dow Chem. Co.
Desmodur	Polyurethanes, isocyanates	Bayer AG/Miles
Desmopan	Polycarbonate, PC, with TPU blends	Bayer AG/Miles
Desmopan	Thermoplastic polyurethanes, TPU, isocyanates	Bayer AG/Miles
Desmophen A	TPU ether or ester elastomers	Bayer AG/Miles
Dexcarb	Polycarbonate/polyamide, PC/PA alloys	Dexter Corp.
Dexter RPI	Polycarbonate/ABS alloys	Dexter Corp.

(*continued*)

Dexel	Cellulose acetate	Courtaulds Fibers Ltd.
Dexflex	PO alloys	Dexter Corp.
Dexlon	Polyamide/polypropylene, PA/PP alloy	Dexter Corp.
Dexloy	Customized alloys	Dexter Corp.
Dexpro	Polypropylene/polyamide, PP/PA alloy	Dexter Corp.
Dexter RPI 101EP	Polypropylene/polyolefins, PP/PO alloy	Dexter Corp.
Dexter RPI 101EP	Polypropylene/polyolefins; reinforced or not	Dexter Corp.
Dexter RPI 201EP	Acrylonitrile-butadiene-styrene terpolymer, ABS	Dexter Corp.
Dexter RPI 207EP	ABS/polycarbonate alloys	Dexter Corp.
Dexter RPI 310	Poly(butylene terephthalate); reinforced or not, PBT	Dexter Corp.
Dexter RPI 424, 600	Glass fiber-reinforced polyamide-6 or polyamide-66, PA	Dexter Corp.
Dexter RPI 500EP	Polycarbonates; reinforced or not, PC	Dexter Corp.
Dexter RPI BEE-15	Polyesters	Dexter Corp.
Dexter RPI BEE-18	Polyamides, PA	Dexter Corp.
Dexter RPI BEE-23	Polyesters	Dexter Corp.
Dia Alloy	ABS/PC alloys	Mitsubishi Rayon
Diacon	PMMA, acrylic/elastomer blends (powder)	ICI Adv. Mater.
Diamond	–	Diamond Polymers
Diarex	Styrene-butadiene copolymer, SBR	Mitsubishi Monsanto
Diathon	Acrylic coatings	ICI Polyurethanes
DIC-PPS SE-730	Poly(phenylene sulfide), PPS, alloys with PPE for high HDT and low flash	Dainippon Ink &Chem.
Dielectrite	Unsaturated polyesters, UP	Industrial Dielect.
Diene	Polybutadiene	Firestone
Difan	Poly(vinylidene chloride), PVDC	BASF A.-G.
Dimension	PA-6 blends with PPE; reinforced or not with up to 30 wt% GF	AlliedSignal
Diolen	Poly(ethylene terephthalate), PET	ENKA-Glanzstoff
Dion	Unsaturated vinyl esters, UP	Koppers Co., Inc.
Dispercoll	Polyurethanes, water dispersions	Bayer
Distifoam/Distitron	Polyester resins, UP	Maprac
Distugil	Polyurethane elastomers, PUR	Arnaud Promecome
DK	Epoxy resins, EP	Dexter Corp.
DKE 450	Poly(methyl methacrylate)/PVC alloy	E. I. du Pont de Nemours
Dolan	Polyacrylonitrile, PAN	Südd. Zellwolle
Dorlastan	Spandex fiber	Bayer
Dow ABS	Acrylonitrile-butadiene-styrene terpolymer, ABS	Dow Chem. Co.
Dow CG	Polyethylenes, PE	Dow Chem. Co.
Dow Corning 1	Silicones	Dow Corning
Dow D.E.H./D.E.R.	Epoxy resins, EP	Dow Chem. Co.
Dow HDPE	High-density polyethylene, HDPE	Dow Chem. Co.
Dow LDPE	Low-density polyethylene, LDPE	Dow Chem. Co.
Dow SAN	Styrene-acrylonitrile copolymer, SAN	Dow Chem. Co.

(*continued*)

Dow Tyrin	Chlorinated polyethylene, CPE	Dow Chem. Co.
Dowex	Ion-exchange resin	Dow Chem. Co.
Dowlex IP-2580	Linear low-density polyethylene, LLDPE	Dow Chem. Co.
Dowlex IP-90	High-density polyethylene, HDPE	Dow Chem. Co.
Dowlex	Linear low-density polyethylene, LLDPE	Dow Chem. Co.
Dowlex NG	Poly(ethylene-*co*-octene) LLDPEs	Dow Chem. Co.
Dralon	Polyacrylonitrile, PAN, fiber	Bayer AG/Miles
Drexflex	TP elastomer	D&S Plastics
Driscopipe pipe	Polyethylene pipe, PE	Phillips 66 Co.
DS6CO1K	Polypropylene, PP	Shell Chem. Co.
Dualite	Poly(vinylidene chloride), PVDC, microspheres	Pierce & Stevens
Duct 2.5	Epoxy resins, EP	Furane Products
Duethan BC	Elastomer modified PA-6 blends	Bayer AG/Miles
Duocel	Epoxy coating, EP	Duochem Inc.
Duoclad	Epoxy flooring systems, EP	Duochem Inc.
Duodeck	Polyurethane membrane, PU	Duochem Inc.
Duolite	Ion-exchange resin	Chemical Processing Co.
DuPont LCP	Liquid crystal polymers, LCP	E. I. du Pont de Nemours
Duracon	Polyoxymethylene, POM	Daicel-Polyplastics
Duracryn	TPE: ethylene interpolymers/PP or PE	E. I. du Pont de Nemours
Duraflex	Polyisobutylene, PIB	Shell Chem.
Duraflex 8000	Polyethylenes, PE	Shell Chem.
Dural	Reinforced rigid poly(vinyl chloride), CPD	Dexter Corp./Alpha Chemical
Dural 776/X6	Poly(vinyl chloride)/ABS high impact alloy	Alpha Chem. & Plastics
Duralex	Poly(vinyl chloride)/PU/NBR alloy	Alpha Chem. & Plastics
Duralon	Polyamide-11, PA-11	Thermoclad Co.
Duraloy 1000	Polyoxymethylene, POM, with elastomer	Hoechst Celanese Corp.
Duraloy 2000	Poly(butylene terephthalate), PBT, with elastomer	Hoechst Celanese Corp.
Duraloy	PBT blended with elastomers or POM	Hoechst Celanese Corp.
Duraloy/Vandar	POM/TPU or PBT/elastomer blends	Hoechst Celanese Corp.
Durastrength	Acrylic impact modifier for outdoor PVC siding and window profiles	Elf Atochem
Duratop	Industrial coatings	Thermoclad Co.
Duravin	Poly(vinyl chloride), PVC	Thermoclad Co.
Durel	Polyarylate, PAr, and PAr/PBT blends, glass fiber reinforced or not	Hoechst Celanese Corp.

Durethan	PA-6, PA-66, blended with PO or elastomer, modified and/or reinforced	Bayer AG/Miles Inc.
Durethan BC	PA-6 blended with ethylene-butyl acrylate-acrylic acid	Bayer AG/Miles Inc.
Durethan RM	PA-6 blended with methacrylate-butyl acrylate-bisphenol-A copolymer, with glass fiber or not	Bayer AG/Miles Inc.
Durethan U	Polyurethane, thermoplastic, TPU	Bayer AG/Miles Inc.
Durez 111	Thermoset phenolic compounds; filled or not	Cain Chem. Inc.
Durez SI-75	Thermoset diallyl phthalate compounds, DAP	Cain Chem. Inc.
Durodet	GRP application and SMC	Mitras Kunstoffe
Durolito	GRP syntactical foam	Mitras Kunstoffe
Durolon	Polycarbonate, PC	Polymix
Dutral	EPR copolymers	Himont/Enimont
Dutralene	Thermoplastic elastomer, TPO	Himont/Montedison
Duval	Polypropylene, PP, graft for high-temperature steel pipes	E. I. du Pont de Nemours
Dycryl	Photopolymer system	DuPont de Nemours
Dyflor 2000	Poly(vinylidene fluoride), PVDF	Dynamit Nobel
DYGL	Styrene maleic anhydride copolymer, SMA	Polymer Composites
Dylark	SMA and its blends (with, e.g., PBT, HIPS)	Arco Chem. Co.
Dylene	Polystyrene, PS; styrene-butadiene rubber, SBR	Arco Chem. Co.
Dylite	Polystyrene – expandable, EPS	Arco Chem. Co.
Dylite EPS	Polystyrene – expandable, EPS (25 % recycles)	Arco Chem. Co.
Dym	Polyester elastomer	E. I. du Pont de Nemours
Dymetrol	Elastomeric type	E. I. du Pont de Nemours
Dynacoll	Polyesters	Hüls AG
Dynaflex	PP/EPDM/NBR blends	
Dynalit	Poly(butylene terephthalate), PBT	Dynamit Nobel
Dynamar	Fluoroelastomer processing aid for LLDPE film	3M Canada Inc
Dynapol	Polyester resins	Hüls AG
Dynapor	Phenolic resin foams, PF	Dynamit Nobel
Dynaset	Phenolic compounds, PF	Reichhold Ltd.
Dyneema	UHMWPE gel-spun fibers	DSM
Dynel	Vinyl chloride-acrylonitrile copolymer	Union Carbide Co., Inc.
Dynyl	Polyblockamides: PA-66-*mb*-PA-636	Rhône Poulenc
Dyphene	Phenolic resins, PF	PMC Specialties Group
Dytherm	Expandable copolymer for rigid foam	Arco Chem. Co.
Dytherm	Expandable copolymers	Arco Chem. Co.
Dytron XL	Polyolefins/elastomer blends	Monsanto Chem. Co.
E		
E-08, 9900	Reinforced poly(butylene terephthalate), PBT	Thermofil, Inc.
E-260H, 2748	Epoxy; reinforced or not, EP	ICI/Fiberite
E1-	Glass fiber-filled PET/PBT polyesters	Thermofil, Inc.

<div align="right">(continued)</div>

E484	Glass-filled epoxy, EP	Cosmic Plastics
EA 3000	Polystyrene, PS	Chevron Chem.
Eagle Picher EP	Unsaturated polyesters with glass fibers, UP	Eagle Picher Plas.
EB 6000	Polystyrene, PS	Chevron Chem.
Eastalloy DA003	Transparent copolyester/PC alloy	Eastman
Ebaco	Ethylene-vinyl acetate copolymers, EVAc	Neste Chim.
Ebecryl	Acrylates and methacrylates	UCB Soc.
EC 6000	Polystyrene, PS	Chevron Chem.
Ecavyl	Poly(vinyl chloride), PVC	Kuhlmann/Fr.
Eccogel	Epoxy resins, EP	Emerson & Cuming
Eccoseal	Epoxy resins, EP	Emerson & Cuming
Eccothane	Polyurethane, PU	Emerson & Cuming
Econit SHF-MR	Polypropylene/nitrile rubber	Resine Sintet. Adamoli
Econol	Poly(p-hydroxybenzoic acid ester)	Sumitomo Chem.
Ecothene	HDPE containing 28 % postconsumer resin	Quantum Chem. Corp.
Edistir	High-impact polystyrene, HIPS, PS	ECP Enimont Polymeri
Editer	Glass fiber-reinforced ABS	ECP Enimont Polymeri
EE4000	Mineral-filled epoxy, EP	Dexter Corp.
EFK	Aromatic polyester	Sumitomo Chemical
Ekkcel	Aromatic polyester	Carborundum
Ekonol	Poly(p-hydroxybenzoic acid), $T_m = 550\ °C$	Carborundum
Ektar	Thermoplastic polyesters and copolyesters: PET, PBT, PCT, PCTG polyesters	Eastman Chem. Prod.
Ektar DN	Thermoplastic polyesters	Eastman Chem. Prod.
Ektar FB	TP elastomers	Eastman Chem. Prod.
Ektar FB CG	Glass fiber-filled polyarylate	Eastman Chem. Prod.
Ektar FB DG	Glass fiber-filled poly(ethylene terephthalate), PET	Eastman Chem. Prod.
Ektar FB PG	Glass fiber-filled polypropylene, PP	Eastman Chem. Prod.
Ektar MB DA003	PCTG/PC or SMA transparent alloys	Eastman Chem. Prod
Elastalloy	TP elastomers	GLS Corporation
Elastocell	Polyurethane foam compounds, PU	BASF Plastics
Elastocoat	Polyurethane casting systems, PU	BASF Plastics
Elastoflex	Soft PUR foam system	BASF Plastics
Elastofoam	Soft integral-skin PUR foam	BASF Plastics
Elastogran	Family of polyurethanes, PU	BASF Plastics
Elastolan	Thermoplastic polyurethane, TPE	BASF Plastics
Elastolit	Hard integral-skin PUR foam	BASF Plastics
Elastopal	Polyurethane elastomers, PUR	BASF Plastics
Elastopor	Hard PUR foam systems	BASF Plastics
Elastopreg	Semifinished product glass-mat	BASF Plastics
Elastorob	Polyurethane elastomers, PUR	Robbe

(*continued*)

Elastosil	Silicone rubbers	Wacker Chemie
Elastotec	Polyester thermoplastic elastomers	BASF Plastics
Elastron	PU vapor barriers	ICI Polyurethanes
Elastuff	Urethane coatings, PU	ICI Polyurethanes
Electrafil 55-EC	Carbon black-filled EVAc	Akzo/DSM
Electrafil ABS	ABS, aluminum filled	Akzo/DSM
Electrafil CF	Polyamide-66, carbon fiber filled; PA-66	Akzo/DSM
Electrafil	Electrically conductive plastics	Wilson-Fiberfil Inc./ DSM
Electrafil G-1100	Polyethersulfone, stainless steel filled, PES	Akzo/DSM
Electrafil G-50	Polycarbonate, carbon fiber filled, PC	Akzo/DSM
Electrafil J-1	Polyamide-66, carbon fiber filled, PA-66	Akzo/DSM
Electrafil J-1105	Polyetheretherketone, carbon fiber filled, PEEK	Akzo/DSM
Electrafil J-1106	Polyetherimide, carbon fiber filled, PEI	Akzo/DSM
Electrafil J-1200	ABS, carbon fiber filled	Akzo/DSM
Electrafil J-1300	Poly(phenylene sulfide), carbon fiber filled, PPS	Akzo/DSM
Electrafil J-1400	FTFE, carbon fiber filled	Akzo/DSM
Electrafil J-1500	Polysulfone, carbon fiber filled, PSU	Akzo/DSM
Electrafil J-3	Polyamide-6, carbon fiber filled, PA-6	Akzo/DSM
Electrafil J-30	Polystyrene, carbon fiber filled, PS	Akzo/DSM
Electrafil J-50	Polycarbonate, carbon fiber filled, PC	Akzo/DSM
Electrafil J-60	Polypropylene, carbon fiber filled, PP	Akzo/DSM
Electrafil SMA	SMA plastics, aluminum filled	Akzo/DSM
Elemid	ABS/polyamide alloys; PA/ABS	GE Plastics
Elexar	Triblock SEBS or SBS thermoplastic elastomers	Shell Chem.
Elix	Polymer modifiers: elastomer with either PB, SAN, SMA, ASA, or MSAN	Monsanto Chem. Co.
Eltex P	Polypropylenes, PP; also highly isotactic PP	Solvay & Cie SA
Eltex	Polyethylenes, PE	Solvay & Cie SA
Elvacet	Poly(vinyl acetate), PVAc	E. I. du Pont de Nemours
Elvacite	Acrylic resins	E. I. du Pont de Nemours
Elvamide	Polyamide resins, PA	E. I. du Pont de Nemours
Elvanol	PVAl, ethylene-vinyl alcohol copolymers, EVAl	E. I. du Pont de Nemours
Elvax	Ethylene-vinyl acetate copolymers, EVAc	Du Pont/Safic-Alcan
Elvic	Poly(vinyl chloride), PVC	Solvay & Cie SA
EM-7302	Epoxy resins, EP	Industrial Dielect.
Emac	EMA copolymer	Chevron
EMI-X	PA-6 or PA-66 with Al flakes for EMI control	LNP Eng. Plastics
Emiclear	–	Toshiba
EMPEE PE	Polyethylenes, PE	Monmouth Plastics
EMPEE PP	Glass fiber-reinforced polypropylene, PP	Monmouth Plastics
EMPEE PP	Polypropylenes, PP	Monmouth Plastics

(*continued*)

EMPEE PS	Polystyrenes, PS	Monmouth Plastics
Empee	Polyethylene, polypropylene	Monmouth
Enathene	Ethylene butyl acrylate	Quantum
Encron	Polyester fiber	Akzo/DSM
Enduran	High-density PBT resin	GE Plastics
Engage	Poly(ethylene-*co*-octene) a polyolefin elastomer, POE, based on Insite™ metallocene technology	Dow Chem. Co.
Enjay Butyl	Isobutylene-isoprene copolymer, IIR	Enjay
Envex	PI, PI lubricated by PTFE, MoS_2, or graphite	Rogers Corp.
EP Total	EPDM, thermoplastic polyolefins	Total Elastomers
EP Total SL 180	Silicones	Total Elastomers
EP	Unsaturated polyesters, UP	Eagle Picher Plas.
Epalex	–	PolyPacific
EPDM XG 006	Ethylene-propylene oil extended rubber	Polysar-Miles
Epi-Rez	Epoxy resins, EP	Celanese
Epi-Rez	Ethylene-propylene elastomer, EPR	Devoe-Raynolds
Epiall	Epoxy resins, EP	Rogers Corp
Epic	Epoxy/unsaturated polyesters, UP	Epic Resins
Epikote	Epoxy resins, EP	Shell Chem.
Epilox	Ethylene-propylene elastomer, EPR	Soprochim
EPM XF 004	Ethylene-propylene impact modifier for TPO	Polysar-Miles
Epo-Tek	Epoxy resins, EP	Epoxy Technology
Epocast	Ethylene-propylene elastomer, EPR	Elastomer Chem./USA
Epodite	Epoxy resin	Showa Highpolymer
Epolan	Acrylonitrile-butadiene-styrene terpolymer, ABS	Industrial Resistol
Epolene	Oxidized polyolefin, PO	Van Waters & Rogers Ltd.
Epolite	Epoxy; filled or not, EP	Hexcel Corp.
Epon	Epoxy resins, EP	Shell Chem. Co.
Eponite	Epoxy resin-based materials, EP	Shell Chem. Co.
Eposir	Epoxy resins, EP	Kingsley & Keith/SIR
Epoxilrub	Epoxy resins, EP	Furane Products
Epoxylite	Epoxy resins, EP	Epoxylite Corp.
Eraclear	LLDPE and VLLDPE	ECP EniChem Polymeri
Eraclene	High-density polyethylene, HDPE	ECP EniChem Polymeri
Eref LS	PP modified, with 40 % or 50 % glass fiber	Solvay SA
Eref	PA-66 or PA-mXD6 blends with 40–60 % PP; ≤50 % glass fiber	Solvay SA
Ertacetal	Polyoxymethylene (acetal), POM	Polymer Corp.
Ertalon	PA-6, internally lubricated, cast in rods and plates	Polymer Corp.
Ertalyte PET-P	PET rods or plates	Polymer Corp.
ES0002	Epoxy resins, EP	Dexter Corp.
Esall	Polypropylene, PP	Sumitomo Chem. Co.

<div align="right">(continued)</div>

Esbrid	Polyamide-6 with 50 % ceramic and glass reinforced	Thermofil, Inc.
Esbrite	Polystyrene, PS	Sumitomo Chem. Co.
Escalloy	Polypropylene, PP	Comalloy Intl. Corp.
Escor	Ethylene-acrylic acid, EAA, copolymers	Exxon Chem
Escorene Micro	Ethylene-vinyl acetate copolymers, EVAc	Exxon Chem/Esso Chem
Escorene	Polyolefins (PO): LDPE, LLDPE, MDPE, PP	Exxon Chem/Esso Chem.
Escorene Ultra	Ethylene-vinyl acetate copolymers, EVAc	Exxon Chem/Esso Chem
Esso-PVC	Poly(vinyl chloride), PVC	Esso Chemical
Estalloy DA	Polyester/polycarbonate blends	Eastman Kodak
Estane	Thermoplastic polyurethanes, TPU, and TPU/SAN or TPU/ABS blends	BF Goodrich/ Polyplastic
Estar	Polyester film	Eastman Kodak
Esthane	Polyurethane TPE	BF Goodrich
ET-Polymer	Butyl-grafted polyethylene, PE	ABB Polymer Comp.
ET-Semicon	Conductive butyl-grafted PE	ABB Polymer Comp.
ETA-Polymer	PP/EPDM, TPO alloys, thermoplastic elastomers	Republic Plastics
Ethavin	Olefinic/poly(vinyl chloride) alloy	Vi-Chem Corp.
Ethocel	Cellulose ethers: ethyl and methyl	Dow Chem. Co.
Ethofil	Polyethylenes; glass fiber filled, PE	Akzo/DSM
Ethron	Polyethylenes, PE	Dow Chem. Co.
ETP	Polyamide/acrylic thermoplastic elastomer blend	E. I. du Pont de Nemours
Euredur/Eurelon	Polyamide resins, PA	Schering AG
Euremelt	Polyamide and polyester resins	Schering AG
Eurepox	Epoxy resins, EP	Schering AG
Europrene SOL T	Triblock SBS or SIS thermoplastic elastomers	EniChem
Evaclene	Ethylene-vinyl acetate copolymer, EVAc	Anic
Evaco	Ethylene-vinyl acetate copolymers, EVAc	Neste Chim.
Evaflex	Ethylene-vinyl acetate copolymer, EVAc	Mitsui
EVAL	Ethylene-vinyl alcohol copolymers, EVAc	EVAL Co. of America
Evalca	EVA copolymer	EVAL Co. of America
Evatane	Ethylene-vinyl acetate copolymers, EVAc	ICI
Evatate	Ethylene-vinyl alcohol copolymers, EVAl	Sumitomo Chem. Co.
Evathane	Ethylene-vinyl acetate copolymers, EVAc	Elf Atochem
Ever-Flex	Thermoplastic elastomers, TPO formulations	Quality Service Technology
Evoprene	Thermoplastic elastomers, TPE	Evode Plastics Ltd.
Exac CTFE	CTFE fluorocarbon	Norton Performance
Exac ECTFE	ECTFE fluorocarbon	Norton Performance
Exac ETFE	ETFE fluorocarbon	Norton Performance
Exac FEP	FEP fluorocarbon	Norton Performance
Exac PFA	PFA fluorocarbon	Norton Performance
Exac PTFE	PTFE fluorocarbon	Norton Performance

Exac PVDF	PVDF fluorocarbon	Norton Performance
Exact PE	Polyethylene (medical grade) prepared using the metallocene catalyst, Exxpol	Exxon Chem. Co.
Exprima	Rigid poly(vinyl chloride) compounds, PVC	European Vinyls Corp.
Extir	Expandable polystyrene, EPS	ECP Enimont Polymeri
Extron	Glass-filled resins	PolyPacific
Exxelor	Polymeric modifiers	Exxon Chem.
Exxon Butyl 077	IIR, also chlorobutyl and bromobutyl rubbers	Exxon Chem.
Exxtral	Reactor olefinic thermoplastic elastomers, RTPO	Exxon Chem.
F		
F-007	Polypropylene; glass filled or not, PP	Aristech Chem.
F-40MF	Polyethylene; glass filled or not, PE	Aristech Chem.
F-9900	Polyethylenes, PE	Thermofil, Inc.
F6	Glass fiber-filled polyethylenes, PE	Thermofil, Inc.
Fascat	Alkydes, polyesters, silicones	Ceca
Faskene	Poly(vinyl chloride) compounds, PVC	Technicompound
Fastool	Filled epoxy resins, EP	REN Plastics
Fenilin	Poly(*m*-phenyleneisophthalamide), PPA	USSR
Fenochem	Phenol-formaldehyde resins, PF	C.P.R.I.
Ferrene	Filled polyolefins, PO	Ferro Corp.
Ferrex	Mineral-filled polypropylenes, PP	Ferro Corp.
Ferro Flex	Polypropylene, PP, PP/EPDM or EPM blends	Ferro Corp.
Ferrocon	Polypropylenes, PP	Ferro Corp.
Ferroflo	Polyolefins, PO, polystyrene, PS	Ferro Corp.
Ferrolene	PP, rubber modified, containing 20 % mineral	Ferro-Eurostar
Ferrolene TPE	IPN-type PP/EPDM blends	Ferro Corp.
Ferropak	PP/PE alloy	Ferro Corp.
Fertene	Low-density polyethylene, LDPE	Montecatini
FF-020	Polypropylene, PP	Aristech Chem.
Fibercore	Glass-filled unsaturated polyesters, UP	American Cyanamid
Fiberfil	Fiber-reinforced material	DSM
Fiberfil G-1	Polyamide-66 with glass fiber, PA-66	Akzo/DSM
Fiberfil G-1500	Fiber-filled polysulfone, PSU	Akzo/DSM
Fiberfil G-40	Fiber-filled SAN	Akzo/DSM
Fiberfil G-50	Fiber-filled polycarbonate, PC	Akzo/DSM
Fiberfil G-60	Fiber-filled polypropylene, PP	Akzo/DSM
Fiberfil J-1106	Glass fiber-filled polyetherimide, PEI	Akzo/DSM
Fiberfil J-1300	Glass fiber-filled poly(phenylene sulfide), PPS	Akzo/DSM
Fiberfil J-1850	Glass fiber-filled poly(butylene terephthalate), PBT	Akzo/DSM
Fiberfil J-7	Fiber-filled polyamide, PA	Akzo/DSM
Fiberfil NY-12	Glass fiber-filled polyamide-612, PA-6,12	Akzo/DSM
Fiberfil NY-7	Glass fiber-filled polyamide, PA	Akzo/DSM

Fiberfil TN	Polyamide-6, 12 impact modified blends containing PO; GF reinforced or not	Akzo/DSM
Fiberfil VO	Flame-retarded plastics	Wilson-Fiberfil Intl.
Fiberite FM	Phenolic compounds, PF	Fiberite/ICI
Fiberite PI	Graphite-filled polyimide, PI	Fiberite/ICI
Fiberite SI	Filled thermoset silica compounds	Fiberite/ICI
Fiberloc	Poly(vinyl chloride) rigid formulation, PVC fiber reinforced	BF Goodrich/Geon
Fiberstran	Long glass-reinforced thermoplastics	Akzo/DSM
Fiberstran	Long fiber-reinforced material	DSM
Fibredux	Epoxy prepregs, EP	Ciba-Geigy Ltd.
Fibrela	Honeycomb sandwich panels	Ciba-Geigy Ltd.
Filabond	Unsaturated polyester, UP	Reichhold Ltd.
Filmex	Cast film extrusion	Windmoeller/ Hoelscher
Filmon	Cast polyamide, PA, films	SNIA Tecnopolimeri SpA
Fina	Polystyrenes, PS	Fina Oil & Chem.
Finaclear	SBS, linear Poly(styrene-b-butadiene-b-styrene) with 75 wt% styrene (lamellar structure)	Fina Oil & Chem.
Finaprene	Elastomers, TPE	Fina Chem.
Finaprop	Polypropylene, PP	Fina Chem.
Finathene	Polyethylenes: LDPE, MDPE, HDPE	Fina Chem.
Firestone	Polyamide-6, PA-6	Firestone Canada Inc.
Flemion	Carboxylated fluoropolymer	Asahi Glass
Flex-Line	Polyamide monofilaments, PA	Elf Atochem Deutschland
Flexel	Thermoplastic elastomers, TPE	BF Goodrich
Flexomer	Ultra low-density linear polyethylene ULDPE	Union Carbide Co., Inc.
Flexomer DFDA	ULDPE high flow processing aid for injection	Union Carbide Co., Inc.
Flexorob/Flexothane	Polyurethane, PU	Robbe
Flexthane	Urethane-acrylate water-based coatings	Air Products & Chem.
Flo-Well	PP/PVC copolymer blends	Air Products & Chem.
Flovic	Poly(vinyl acetate), PVAc	ICI Adv. Mater.
Fluon	Polytetrafluoroethylene, PTFE	ICI Adv. Mater.
Fluorel	Thermoset fluoropolymers; PVDF/PHFP blend	3M Ind. Chem.
Fluorocomp	60 % bronze-filled PTFE	LNP Engineering
Fluorofil	Carbon/glass-filled PVDF	Akzo/DSM
Fluorogold	Polytetrafluoroethylene filled or not, PTFE	Fluorocarbon
Fluoromelt	Fluoropolymers, melt processable	ICI Adv. Mater.
Fluoromelt FP-CC	ECTFE, glass or carbon fiber filled	LNP Engineering
Fluoromelt FP-EC	FTFE, glass or carbon fiber filled	LNP Engineering
Fluoromelt FP-FC	FEP, glass or carbon fiber filled	LNP Engineering
Fluoromelt FP-PC	PFA, glass or carbon fiber filled	LNP Engineering
Fluoromelt FP-VC	PVDF, glass or carbon fiber filled	LNP Engineering
Fluorosint PTFE	PTFE + mica composites (rods or plates)	Polymer Corp.

<div align="right">(continued)</div>

Fluorotemp 103	Polyetheretherketone, PEEK, filled	Fluorocarbon
Fluorothene	Polychlorotrifluoroethylene, PCTFE	DuPont de Nemours
Fomrez/Formrez	Polyurethane, PU	Witco
Foraflon 51	Fluorocarbon PTFE	Elf Atochem
Foraflon 1000	Fluorocarbon PVDF	Elf Atochem
Foraflon	Poly(vinylidene fluoride), PVDF	Elf Atochem
Formacast	Epoxy/polyurethane casting blends	Formulated Resins
Formaldafil	Polyoxymethylene; filled or not, POM	Akzo/DSM
Formaldafil	Polyoxymethylene, POM/PTFE blend	Fiberfil
Formica	Melamine-formaldehyde resin	Cyanamid
Formion	Ionomer	A. Schulman, Inc.
Formion	Ionomer compounds; PO/ionomer blends	A. Schulman, Inc.
Forprene	Olefinic thermoplastic elastomers, TPO	Ferro Corp.
Forticel	Propyl cellulose, CP	Hoechst Celanese Corp.
Fortiflex	Polyethylenes, PE	Soltex Polymer Co.
Fortiflex	Polyethylenes, PE	Solvay & Cie SA
Fortilene	Polypropylene, PP	Soltex Polymer Co.
Fortilene	Polypropylene, PP	Solvay & Cie SA
Fortron	Poly(phenylene sulfide), linear PPS, glass and mineral reinforced or not	Kureha Chem./ Hoechst Celanese
Fosta Tuf-Flex	Styrene-butadiene copolymer, SBR	Hoechst AG
FP-200	Polypropylene, PP	Aristech Chem.
FPC 18MI	Styrene-acrylonitrile copolymer, SAN	Federal Plastics
FPC 30	Polypropylene, PP	Federal Plastics
FPC 40	Polyethylene, PE	Federal Plastics
FPC 75	Acrylonitrile-butadiene-styrene terpolymer, ABS	Federal Plastics
FPC 500, 600	Polyethylenes, PE	Federal Plastics
FPC	Polystyrene, PS	Federal Plastics
Freshtuff	Ionomer/polyamide alloys	American Can Co.
FT-015	Polypropylene, PP	Aristech Chem.
Fulton 404	POM lubricated with PTFE	LNP Eng. Plastics
FurCarb	Furan-based TS resins; reinforced or not	QC Chem., Inc.
FyRid	Flame-retardant polystyrene, PS	GE Plastics
G		
G-2-	Polyoxymethylene, filled: glass bead, graphite, etc.	Thermofil, Inc.
G-Resin	Polyethylenes, PE	Union Carbide Co., Inc.
G1	Glass fiber-filled polyoxymethylene, POM	Thermofil, Inc.
Gabrite	Phenol-formaldehyde, PF, molding material	Montecatini
Gafite	PBT/elastomer alloys, reinforced or not	GAF Corp.
Gaflex	TPU, ester/ether thermoplastic elastomer	GAF Corp.
Gaflon	Polytetrafluoroethylene, PTFE	Gachot, France
Gaftuf	High-impact PBT/elastomer alloys	GAF Corp.
Galalith	Plastics from milk protein, CS	Int. Galalith-Ges.

Gantrez	Poly(methyl vinyl ether-*co*-maleic anhydride)	GAF Corp
Gapex	PP/PA-6 or PA-66 compatibilized alloy, reinforced or not	Ferro-Eurostar
Garamed	Poly(vinyl chloride), PVC	Ferro Corp.
Garaprene E	Thermoplastic elastomers	Ferro Corp.
Garaprene O	TPO for wire and cable applications	Ferro Corp.
Garaprene	Thermoplastic alloy compounds	Evode Plastics Ltd.
Garaprene	Thermoplastic elastomer	Ferro Corp.
Gary PVC	PVC compounds for cables	Evode Plastics Ltd.
GC 480	Polyurethanes, PU	Gallagher Corp.
GECET	PPE/PS foams	GE Plastics
Gedamine	Unsaturated polyester, UP	Norsolor, France
Gedelite	Phenol-formaldehyde resins, PF	Norsolor, France
Gedex	Polystyrene, PS	Elf Atochem
Gedexcel	Expanded polystyrene, PS	Elf Atochem
Gel 151	Epoxy resins, EP	Furane Products
Gelon	Amorphous polyamide, PA	GE Plastics
Geloy GY1020	Acrylic acid-styrene-acrylonitrile terpolymer, ASA	GE Plastics
Geloy GY1220	ASA/PVC alloys in pellet form	GE Plastics
Geloy SCC 1320	ASA/Poly(methyl methacrylate), PMMA blends	GE Plastics
Geloy XP 2003	ASA/Poly(vinyl chloride), PVC alloy	GE Plastics
Geloy XP 4001	ASA/polycarbonate, PC blends for automobile	GE Plastics
Geloy XP 4025	ASA/PC blends	GE Plastics
Gelvatol	Poly(vinyl alcohol)	Shawinigan Chemicals
Gemax	Poly(phenylene ether)/PBT, PPE/PBT blends	GE Plastics
Gemon	Maleimide	GE Plastics
Geolast	Thermoplastic elastomer blends; NBR/EPDM or PP/NBR blends	Advanced Elastom. Syst.
Geon	Poly(vinyl chloride) and blends, viz., PVC/NBR	BF Goodrich/Geon
Geon HTX	Poly(vinyl chloride)-based high performance alloy	BF Goodrich/Geon
Georgia-Gulf	Poly(vinyl chloride) resins and alloys, PVC	Georgia-Gulf
Gepax	PPE/crystalline PS alloys	GE Plastics
Getem	Amorphous cyclomer-type polymers	GE Plastics
Glaskyd	Thermoset alkyd resins; filled or not, UP	American Cyanamid
Glastic	Unsaturated polyesters; filled or not, UP	Glastic Co.
Glendion/Tercarol	Polyether and polyester polyols	ECP EniChem Polymeri
Glyptal	Alkyd resin, UP	GE Plastics
Goodrite Latex	SB and vinyl pyridine	BF Goodrich
Goodrite	Polyacrylic acid, PAA	BF Goodrich
GPC DELTA	Styrene-acrylonitrile copolymer, SAN	Grand Pacific
GR7	Glass-reinforced Zytel polyamides, PA	Du Pont Canada
Grafoil	Foils of pure graphite	Union Carbide Co., Inc.
Granular Compound	Urea-formaldehyde resin; cellulose filled, UF	Plastics Mfg. Co.

(*continued*)

Granular	Liquid crystal polyester, LCP	Granmont Inc./ Montedison
Granulation Comp.	Filled melamine-formaldehyde resin, MF	Plastics Mfg. Co.
Grilamid	Polyamide-12, reinforced or not, PA-12; also blends with aromatic-aliphatic polyamides	EMS-American Grilon
Grilamid ELY-60	Polyetheramide, PEA	EMS-American Grilon
Grilamid TR	Polyamide, transparent, amorphous	EMS-American Grilon
Grilesta	Powder coating resins	EMS-American Grilon
Grilet	PBT-extrusion and PET-molding resins	EMS-American Grilon
Grilon	PA-6 or PA-612 blended with PB or EPR	EMS-American Grilon
Grilon A	Polyamide-6, PA-6, with PB or EPR; filled or not	Emser Ind.
Grilon BT	PA-6/aromatic-aliphatic polyamide, PA alloys	EMS-American Grilon
Grilon T	Polyamide-66, PA-66	EMS-Chemie AG
Grilon XE	Polyamide-66/610 copolymer	EMS-Chemie AG
Grilon XE3404	Polyamide-polyethylene blend	EMS-Chemie AG
Grilonit	Ethylene-propylene copolymers, EPR	Emser-Werke
Grilpet	PET, PBT; reinforced or not	EMS-Chemie AG
Griltex	Copolyamides, copolyesters	EMS-Chemie AG
Grivory	Amorphous engineering resin, reinforced or not	EMS-American Grilon
Grivory G	Amorphous polyamide, PA	EMS-Chemie AG
Grilamid TR	Amorphous polyamide, PA	EMS-Chemie AG
Grilesta	Copolyester resin for powder coating	EMS-Chemie AG
Gumiplast	Poly(vinyl chloride) compounds, PVC	Saplast
GX-200	ASA/polycarbonate, PC, alloys	GE Plastics
H		
H-Film	PI (pyromellitic anhydride/ diaminodiphenylether)	E. I. du Pont de Nemours
Halar	ECTFE fluoropolymers	Ausimont Inc.
Halon	Fluoropolymer	Ausimont Inc.
Halon 1000R	Polytetrafluoroethylene, ETFE; glass fiber filled	Ausimont Inc.
Halon 2000R	Polytetrafluoroethylene, ETFE; graphite filled	Ausimont Inc.
Halon 3000R	Polytetrafluoroethylene, ETFE; bronze filled	Ausimont Inc.
Halon 4000R	Polytetrafluoroethylene, ETFE; graphite filled	Ausimont Inc.
Halon ET	Filled ETFE fluorocarbon	Ausimont Inc.
Hanalac	ABS	Miwon
Hannam ABS	Acrylonitrile-butadiene-styrene terpolymer, ABS	Hannam
Haysite BMC	Unsaturated polyesters, glass filled, UP	Haysite Reinforced Plastics
HC-3	Polyethylene; filled, PE	CCA Compounding
HCPP	High crystallinity polypropylene with isotacticity ≤99 %, broad MWD	Chiso Corp.
HDPEX	Auto cross-linkable PE	ABB Polymer Comp.
Heatlok	Polyurethane elastomer, PUR resins	ICI Polyurethanes
Herclor	Elastomers	Hercules
Hercocel	Cellulose acetate, CA	Hercules

(*continued*)

Hercules K-type	Ethyl cellulose, EC	Hercules
Herculoid	Cellulose nitrate, CN	Hercules
Hercuprene	Thermoplastic rubber, TPE	J-Von
Hetron	Unsaturated polyester, UP	Ashland Chem. Co.
Hevea-Plus	NR/PMMA interpenetrating polymer networks	Malaysia
HF-2230	Poly(vinyl chloride), PVC/ABS blends	Georgia Gulf
HHW, HHP	Poly(vinyl chloride) rigid formulations, PVC	Georgia Gulf
Hi-D	Polyethylenes, PE	Chevron Chem.
Hi-Fax	High-density polyethylene, HDPE	Hercules
Hi-Zex	Polyethylenes, PE	Mitsui Petrochem.
Hicond-2000	HDPE/PP electrically conductive alloy	United Composites
Hicond-X	Polyethylene, PE	United Composites
HiFax	Reactor olefinic thermoplastic elastomers, RTPO	Himont Adv. Materials
HiGlass	Glass-filled polypropylene Himont	
Hiloy 100	Glass fiber filled polypropylene, PP	Comalloy Intl. Corp.
Hiloy 400	Glass fiber filled poly(butylene terephthalate), PBT	Comalloy Intl. Corp.
Hiloy 440	Glass fiber filled poly(ethylene terephthalate), PET	Comalloy Intl. Corp.
Hiloy 600	Glass fiber-filled polyamide-6, polyamide-612 or polyamide-66, PA	Comalloy Intl. Corp.
Himod PU GL	Thermoplastic polyurethane, TPU, alloys	Polymer Compos.
Histat-X	Electrically conductive polyethylenes, PE	United Composites
Hitalex	Polyethylene	Hitachi
Hitanol	Phenol-formaldehyde resin	Hitachi
HiVal	Polyethylenes, HDPE	General Polymers
HMS 1000	Conductive styrenic alloy	HMS Compounds, Inc.
Hoslapren	Chlorinated polyethylene, CPE	Hoechst Celanese Corp.
Hostacom	Filled or reinforced polypropylene, PP	Hoechst Celanese Corp.
Hostadur	Poly(ethylene terephthalate), PET	Hoechst Celanese Corp.
Hostadur X	PBT/PET alloy	Hoechst Celanese Corp.
Hostaflon	Fluoropolymers (PTFE, PFA, ETFE)	Hoechst Celanese Corp.
Hostaflon C2	Polychlorotrifluoroethylene	Hoechst Celanese Corp.
Hostaflon ET	Ethylene-*co*-tetrafluoroethylene, ETFE	Hoechst Celanese Corp.
Hostaflon FEP	Tetrafluoroethylene-*co*-hexafluoropropylene	Hoechst Celanese Corp.
Hostaflon TF	Polytetrafluoroethylene, PTFE	Hoechst Celanese Corp.
Hostaflon TFM	Modified suspension PTFE	Hoechst Celanese Corp.

(*continued*)

Hostaform C	POM/TPU alloys	Hoechst Celanese Corp.
Hostaform	POM copolymer, impact modified, reinforced, etc.	Hoechst Celanese Corp.
Hostalen GUR	Ultrahigh molecular weight PE, UHMWPE	Hoechst Celanese Corp.
Hostalen	UHMWPE, HDPE, PP/EPDM, resins and prod.	Hoechst Celanese Corp.
Hostalen PP	Polypropylene, PP	Hoechst Celanese Corp.
Hostalit	Poly(vinyl chloride), PVC	Hoechst Celanese Corp.
Hostalit Z	High-impact PVC/CPE blends	Hoechst Celanese Corp.
Hostalloy 731	Polyolefin alloy, with high abrasion resistance	Hoechst Celanese Corp.
Hostamid	Polyamide, transparent, amorphous	Hoechst Celanese Corp.
Hostaphan	Poly(ethylene terephthalate), PET	Kalle, Germany
Hostapren	Chlorinated polyethylene, CPE	Hoechst Celanese Corp.
Hostatec	Polyetheretherketoneketone, PEK	Hoechst Celanese Corp.
Hostyren	Polystyrene, PS; PS/elastomer blends	Hoechst Celanese Corp.
HPP30GR	Mineral/glass fiber-filled polypropylene, PP	Ferro Corp.
HTX	Polyetherketone	ICI
Hycar PA	Modified acrylic elastomers	BF Goodrich
Hycar	PVC/nitrile rubber	BF Goodrich
Hydrin	Polyepichlorohydrin elastomer, can be blended with any elastomer, sulfur or peroxide curable	Zeon Chemicals, Inc.
Hylar 5000	Poly(vinylidene fluoride), PVDF	Ausimont
Hylar	Poly(ethylene terephthalate), PET	E. I. du Pont de Nemours
Hypalon	Chlorosulfonated PE (CSM) synthetic rubber	E. I. du Pont de Nemours
HyTemp	Polyacrylate elastomer, curable or not	Nippon Zeon Co., Ltd.
Hytrel	Thermoplastic polyether-ester block copolymer elastomers, 1,4-butanediol-polybutylene glycol-terephthalic acid copolymer, TPE	E. I. du Pont de Nemours
Hytrel HA	Copolyester/polyacrylate/PET	E. I. du Pont de Nemours
I		
Icdal Ti40	Polyesterimide	Dynamit Nobel
Idemitsu LCP	Liquid crystal polyester, LCP	Idemitsu Petro Chem
Idemitsu Polycarb.	Polycarbonates, PC	Idemitsu Petro Chem
Idemitsu SC	PC/ABS, PES blends	Idemitsu Petro Chem
Igelit	Poly(vinyl chloride), PVC	Bitterfeld, Germany

(*continued*)

Illen	Poly(butylene terephthalate), PBT/elastomer blend	Dr. Illing GmbH
Imidex	Polyesterimide, PEI	General Electric Co.
Impet	Poly(ethylene terephthalate), PET, glass reinforced	Hoechst Celanese Corp.
Implex	High-impact acrylic blends	Rohm and Haas
Imprez	Resins	ICI Polymers
Indopol	Polybutenes, PB	Amoco Chem. Co.
Innovex	Linear low-density polyethylene, LLDPE	BP Chem. Ltd.
Inprima	Rigid poly(vinyl chloride), PVC	European Vinyls Corp.
Insite	Ethylene/octene copolymers prepared using the *constrained-geometry* metallocene catalyst	Dow Plastics
Instant-Set Polym.	Thermosetting polyurethane, PU	Dow Chem. Co.
Insultruc P-	Unsaturated polyesters with glass fiber, UP	Industrial Dielect.
Intene/Intex	Elastomers	Enimont
Intol/Intolene	Elastomers	Enimont
Ionac	Ion-exchange resin	Ionac
Iotek	Ionomers	Exxon Chem.
IPC	Glass fiber-filled poly(phenylene sulfide), PPS	IPC
IPN-Compound	Interpenetrating polymer	ABB Polymer Comp.
Iporka	Urea-formaldehyde, UF, plastic foam	BASF Plastics
Iropol	Polyester resin	Armkem Iroquois Chem.
Irostic	Polyurethane, TPU-adhesive resins	Monon International Inc
IRPS	Polystyrene, PS	Huntsman Chem.
Irrathene	Polyethylenes cross-linked by radiation, XLPE	GE Plastics
Isobam	Copolymer of isobutylene and maleic anhydride water soluble (protective colloids)	Kuraray Co., Ltd.
Isolic	Acrylic resins	Great Eastern
Isomid	Polyesterimide, PEI	Schenectady Chem.
Isoplast	Polyurethanes	Dow Plastics
Isorob/Isothanne	Polyurethanes, PU	Robbe
Isplen	Polypropylene, PP	Repsol Quimica
Isplen	Polypropylene, PP	Repsol Quimica SA
ITP	PU/polyester/polystyrene IPN	ICI
Iupiace	PPE alloys	Mitsubishi
Iupilon	Polycarbonate, PC	Mitsubishi Gas
Iupilon Polym. All.	Polycarbonate/ABS alloys	Mitsubishi Gas
Iupirex	Polyimide	Ube Industries
Iupital F40-03	Polyoxymethylene, POM	Mitsubishi Gas Chem.
Iupital-FL	Polyoxymethylene, POM, fluoropolymer blends	Mitsubishi Gas Chem./Franklin
Iupital-FU	Polyoxymethylene, POM, elastomer blends	Mitsubishi Gas Chem./Franklin
Ixan	Poly(vinylidene chloride) copolymers, PVDC	Solvay & Cie SA

(*continued*)

Ixef	Semi-aromatic polyamide, PA, polyarylamides, with GF or mineral	Solvay & Cie SA
Ixol	Polyetherpolyol halogened (for PU)	Solvay & Cie SA
Iztavil	Poly(vinyl chloride), PVC	Polimeros de Mexico
J		
J-Plast.	Thermoplastic elastomer, TPE	J-Von
Jet-Flex	Acrylonitrile-ethylene/propylene-styrene copolymer	Multibase, Inc.
Jonylon	Polyamide-6, polyamide-66, PA	BIP Chem. Ltd./ Polymix
JSR Excelloy CB	ABS/polycarbonate, alloys	Japan Synth. Rubber
JSR Excelloy GE	Polycarbonate/AES, alloys	Japan Synth. Rubber
JSR NE	NBR/EPDM blends	Japan Synth. Rubber
JSR NV	NBR/poly(vinyl chloride), alloys	Japan Synth. Rubber
Jupilon	Polycarbonate, PC MBS (now *Paraloid*™)	Mitsubishi Chem.
K		
K-15NF	Graphite fiber-filled polyethersulfone, PES	Thermofil, Inc.
K-20NF	Glass fiber-filled polyethersulfone, PES	Thermofil, Inc.
K-Resin	Butadiene-styrene copolymer, SBR	Phillips Chemicals
K-Resin SB Plastic	Styrene-butadiene copolymer, SB	Phillips 66 Co.
K-Resin	Styrene-butadiene copolymer, SB	Phillips Petrol. Chem.
K-Resin	Styrene/butadiene bl. copolymer Phillips	
K2-30FG	Glass-reinforced polyetheretherketone, PEEK	Thermofil, Inc.
K2-30NF	Graphite fiber-reinforced polyetheretherketone	Thermofil, Inc.
K2-50FG	Graphite fiber-reinforced polyetheretherketone	Thermofil, Inc.
Kadel	Polyetherketone, aromatic, PEAK	Amoco Performance Products
Kadon	ABS/SMA blends	Monsanto Chem. Co.
Kaladex	Poly(ethylene 2,6-naphthalene dicarboxylate)	ICI Films
Kalrez	Perfluoro elastomer parts, TFE/PVME blend	E. I. du Pont de Nemours
Kamax	Polyacrylates, polymethacrylates, and imidized poly(methyl methacrylate)s	Rohm and Haas/Ato Haas
Kane Ace B	Methacrylate-butadiene-styrene, MBS, modifiers for clear PVC (impact strength improvers)	Kanegafuchi Chemicals
Kane Ace	MBS acrylics	Kanegafuchi Chemicals
Kane Ace PA	Acrylic processing aids	Kanegafuchi Chemicals
Kane Ace	Polyamide chlorinated	Kanegafuchi Chemicals
Kane Ace XEL	Poly(vinyl chloride) cross-linked, XLPVC	Kanegafuchi Chemicals
Kane Ace-FM	Acrylic low gloss impact modifiers for PVC	Kanegafuchi Chemicals
Kaneka CPVC	Poly(vinyl chloride) chlorinated resins, XLPVC	Kanegafuchi Chemicals

Kaneka Enplex	ABS/PVC alloys compatibilized with α-methyl styrene-methyl methacrylate copolymer	Kanegafuchi Chemicals
Kaneka	Poly(vinyl chloride) chlorinated resins, XLPVC	Kanegafuchi Chemicals
Kaneka	Teralloy, PVC HDT modifiers	Kanegafuchi Chemicals
Kapton 300H	Polyimide, PI, electrical and thermal insul. film	E. I. du Pont de Nemours
Kapton H	PI, (pyromellitic anhydride/diaminodiphenylether)	E. I. du Pont de Nemours
Kasobond	Polyurethane elastomers for adhesives, PUR	Lu-Kas Polym. Chemie
Kasothan	Polyurethane thermoplastic, TPU	Lu-Kas Polym. Chemie
Kaurit-Leim	Urea-formaldehyde glue, UF	BASF Plastics
Kayocel	Cellulose compounds	Henley-McKenzie Feimann
KC 1257	PVC alloy with glutarimide acrylic copolymer for hot-fill bottles	Keysor-Century
KC1000	Poly(vinyl chloride), PVC, rigid, high impact	Keysor-Century
Kel-F Elastomer	Poly(vinylidene fluoride/chlorotrifluoroethylene)	Kellogg, USA
Kel-F	PCTFE fluoroelastomer	3M Ind. Chem.
Kel-F	Polychlorotrifluoroethylene, PCTFE	3M
Kel-F	PVDF/PCTFE blend	3M
Kelanex	Glass-filled poly(butylene terephthalate), PBT	Hoechst Celanese Corp.
Kelburon	Reactor-blended PP/EPDM; RTPO for self-supporting car bumpers	DSM Polymers Int.
Keldax	Filled polyethylenes, PE	E. I. du Pont de Nemours
Kelon	Mineral-reinforced polyamides, PA	Lati Eng. Thermoplast.
Kelprox	Thermoplastic olefinic elastomers, TPO	DSM Polymers Int.
Kelrinal	Chlorinated, rubber (CM)	DSM Polymers Int.
Keltan	Thermoplastic elastomers, EPDM, PP/EPDM	DSM Polymers Int.
Keltan TP	PP/EPDM blends with fillers	DSM Polymers Int.
Kematal	Polyoxymethylene (acetal), POM	Hoechst Celanese Corp.
Kenflex	Hydrocarbon resins	Kenrich
Kerimide	Polyimide, PI, for laminating and molding (TS)	Nippon Polyimide
Keripol	Polyester resins	Vynckier
Kermel	Poly(m-phenyleneisophthalamide), PPA	Rhône Poulenc
Kermel	Polyamide-imide; fibers, PAI	Rhône Poulenc
Kevlar	Poly(p-phenylene terephthalamide); fibers, resins	E. I. du Pont de Nemours
Keysor	Poly(vinyl chloride), PVC	Keysor-Century
KF Polymer	Poly(vinylidene fluoride), PVDF	Kureha
Kibisan PN	Acrylonitrile-styrene-acrylate copolymer, ASA	Chi Mei Ind. Co. Ltd.

(continued)

Kibisan	Styrene-acrylonitrile copolymer, SAN	Chi Mei Ind. Co. Ltd.
Kinel	Filled *bis*-maleimide-based molding polyimides	Rhône-Poulenc
KN-220	Polyethylenes, PE	Chevron Chem.
Koblend	Polycarbonate/AES and PC/ABS alloys	ECP Enimont Polym./ EniChem
Koblend PCA	Polycarbonate/ABS blends	Montedipe Milano
Kodapak PET	Poly(ethylene terephthalate), PET	Eastman Chem. Prod.
Kodapak	Poly(butylene terephthalate), PBT	Eastman Chem. Prod.
Kodar PETG	PETG, a thermoplastic copolyester of 1,4 cyclohexylene glycol and mixture of iso- and terephthalic acids	Eastman Chem.
Kodar	Thermoplastic polyesters	Eastman Chem.
Kodel	Polyester fiber	Eastman Chem.
Kodel-10	Poly(ethylene terephthalate), PET	Eastman Chem.
Kodel-2	Polybishydroxymethylcyclohexaneterephthalate	Eastman Chem.
Kollidon	Polyvinylpyrrolidone, PVP	BASF Plastics
Koppers	Unsaturated polyesters, UP	Koppers Co., Inc.
Koroseal	Poly(vinyl chloride)/PVF blends	BF Goodrich
Korton	Thermoplastic fluoropolymer alloy	Norton Performance Plast.
Kostil BV	Styrene-acrylonitrile copolymer, SAN, reinforced	Montepôlimeri
Kostil	Styrene-acrylonitrile copolymer, SAN	Montepôlimeri
Kralastic	Acrylonitrile-butadiene-styrene terpolymers, ABS	Uniroyal
Kralastic FVM	ABS/Poly(vinyl chloride) alloys	Uniroyal/Sumitomo
Kraton	Thermoplastic elastomers, TPE	Shell Chem. Co.
Kraton D1101	SBS three block thermoplastic elastomer	Shell Chem. Co.
Kraton D1107	SIS three block thermoplastic elastomer	Shell Chem. Co.
Kraton D1116	$(SB)_n$ multi block thermoplastic elastomer	Shell Chem. Co.
Kraton D1320X	$(SI)_n$ multi block thermoplastic elastomer	Shell Chem. Co.
Kraton D2103	SBS/HIPS alloys	Shell Chem. Co.
Kraton FG	SEBS functionalized with maleic or succinic anhydride (a PA impact modifier)	Shell Chem. Co.
Kraton G	SEBS blends	Shell Chem. Co.
Kraton G1650	SEBS three block thermoplastic elastomer	Shell Chem. Co.
Kraton G1701	SEP three block thermoplastic elastomer	Shell Chem. Co.
K-Resin	Styrene/butadiene block copolymer	Phillips Petrol.
Krystaltite	Poly(vinyl chloride) film, PVC	Allied Signal Inc
Krynac	Nitrile rubber, NBR; AN = 19–50 %	Polysar/Bayer AG
Krynac NV	NBR/Poly(vinyl chloride) alloys (34 % AN)	Polysar/Bayer AG
Krynac Xi	Carboxylated NBR with i = 1–9 % carboxylic	Polysar/Bayer AG
Krynac XN	NBR lightly cross-linked with AN = 29–35 %	Polysar/Bayer AG
KUI	Liquid crystal polyester, LCP	Bayer
Kureha KF	PVDF fluorocarbon, poly(vinylidene fluoride)	Kureha Corp.
Kydene/Kydex	Poly(vinyl chloride)/Poly(methyl methacrylate) alloys	Rohm and Haas

(continued)

Kydex lOO	Poly(vinyl chloride)/acrylic alloy sheets	Kleerdex Co.
Kynar	Poly(vinylidene fluoride), PVDF	Elf Atochem
L		
L-030 Z	Polypropylene, PP	Aristech Chem.
L-20 FG	Poly(phenylene ether), PPE, glass fiber filled	Thermofil, Inc.
L-20 NF	Poly(phenylene ether), PPE, graphite filled	Thermofil, Inc.
L-30 FG	Poly(phenylene ether), PPE, glass fiber filled	Thermofil, Inc.
L-30 NF	Poly(phenylene ether), PPE, graphite filled	Thermofil, Inc.
L-40 AF	Poly(phenylene ether), PPE, aluminum filled	Thermofil, Inc.
L-9900	Poly(phenylene ether), PPE, filled	Thermofil, Inc.
L.C.P.	Liquid crystal polymers, LCP	E. I. du Pont de Nemours
L1, L2. L3	Poly(phenylene ether), PPE, glass fiber filled	Thermofil, Inc.
Lacovyl	Poly(vinyl chloride), PVC, bulk polymerized	Elf Atochem
Lacovyl	Poly(vinyl chloride), PVC, emulsion polymerized	Elf Atochem
Lacovyl	Poly(vinyl chloride), PVC, suspension polymerized	Elf Atochem
Lacovyl	Vinyl chlorine-*co*-vinyl acetate, VC/VAc	Elf Atochem
Lacqrene	Crystal, high-impact polystyrene, HIPS	Elf Atochem
Lacqrene	Polystyrene, PS	Elf Atochem
Lacqrene	Styrene-acrylonitrile copolymer, SAN	Elf Atochem
Lacqsan	Styrene-acrylonitrile copolymer, SAN	Aquitaine, France
Lacqtene HD	High-density polyethylene, HDPE	Elf Atochem
Lacqtene	Low-density polyethylene, LDPE	Elf Atochem
Lacqtene LX	Linear low-density polyethylene, LLDPE	Elf Atochem
Lacqvyl	Polyvinylchloride, PVC	Elf Atochem
Ladene	LLDPE, MDPE, PS resins (all grades)	SABIC Marketing Ltd.
Laminac	Polyester resin	Cyanamid
Lanital	Fiber from milk protein, CS	SNIA Viscosa, Italy
LARC-TPI	Polyimides, PI	NASA/Mitsui Toatsu Chem.
LARC-13	Polyimides, PI, for structural adhesives to metal	NASA Langley RC
Laril	Modified poly(phenylene ether), *m*-PPE, alloys	Lati Eng. Thermoplast.
Larodur	Acrylic resins	BASF Plastics
Larton	Reinforced poly(phenylene sulfide), PPS	Lati Eng. Thermoplast.
Lastane	Polyurethane elastomers, PUR	Lati Eng. Thermoplast.
Lastiflex	Poly(vinyl chloride)/terpolymer alloy	Lati Eng. Thermoplast.
Lastil	SAN; reinforced or not	Lati Eng. Thermoplast.
Lastilac 09-11	ABS/polycarbonate alloy	Lati Eng. Thermoplast.
Lastilac	ABS; reinforced or not	Lati Eng. Thermoplast.
Lastirol	Polystyrene, HIPS	Lati Eng. Thermoplast.
Lasulf	Polysulfone, PSU	Lati Eng. Thermoplast.
Latamid 6	Polyamide-6; reinforced or not, PA-6	Lati Eng. Thermoplast.
Latamid 12	Polyamide-12; reinforced or not, PA-12	Lati Eng. Thermoplast.
Latamid 66	Polyamide-66; reinforced or not, PA-66	Lati Eng. Thermoplast.
Latamid 68	Polyamide-68; reinforced or not, PA-68	Lati Eng. Thermoplast.

Latan	Polyoxymethylene; reinforced or not, POM	Lati Eng. Thermoplast.
Latene EP	Impact modified polypropylene, PP	Lati Eng. Thermoplast.
Latene HD	High-density polyethylene, HDPE	Lati Eng. Thermoplast.
Latene	Polypropylene; reinforced or not, PP	Lati Eng. Thermoplast.
Later	Reinforced polyester resins	Lati Eng. Thermoplast.
Latilon	Polycarbonate; reinforced or not, PC	Lati Eng. Thermoplast.
Lavasint	Ethylene-vinyl alcohol copolymer, EVAl	Bayer AG
LCP	Liquid crystal polymers, LCP	RTP Co.
LDPE	Low-density polyethylene, LDPE	Dow Chem. Co.
Le Vinychlore	Poly(vinyl chloride) compounds, PVC	Saplast
Leacril	Polyacrylonitrile, PAN	ACSA, Italy
Leguval	Unsaturated polyester, UP, for SMC or BMC	Bayer AG/Miles
Leguval	Unsaturated polyester resin, UP	DSM
Leguval	Unsaturated polyester, UP	Bayer AG/Miles
Lekutherm	Epoxy resins, EP	Bayer AG/Miles
Leona HR100	Polyamide-6,6, foam grade + 30 % glass fiber	Asahi Chemical
Levaflex	Thermoplastic elastomers, TPE	Bayer AG/Miles
Levapren	Ethylene-vinyl acetate copolymer, EVAc	Polysar/Bayer AG
Lewatit	Ion-exchange resins	Bayer AG/Miles
Lexan	Polycarbonate resins or blends, toughened by PO or elastomers; reinforced or not	GE Plastics
Lexan PPC	Polyphthalate-carbonate resins or blends, PPC	GE Plastics
Lexan WR	Fluorocarbon polytetrafluoroethylene, PTFE	GE Plastics
Lexan XT	Poly(carbonate-*co*-silicone) copolymer	GE Plastics
LF-1	Thermoplastic polyesters	GE Plastics
Limera	Styrenic blends with a variety of polymers: PS, PVC, PMMA, ABS, PPE; reinforced or not	Dainippon Ink & Chem.
LISA	Polycarbonate-based light conducting polymers	Bayer AG/Miles
Litrex	Low-density polyethylene, LDPE	PCD France
LLD	Linear low-density polyethylene, LLDPE	Dow Chem. Co.
Lomod	Copolyetherimide esters elastomer blends, PBT/SBS, TPE	GE Plastics
Lonox	Polyethylene, PE	Union Carbide Co., Inc.
Lotader AX	EEVA-glycidylmethacrylate, E-EA-GMA GMA content ca. 8 wt%	Norsolor/Elf Atochem
Lotader	Ethylene-ethylacrylate-vinyl acetate, EEVA	Norsolor/Elf Atochem
Lotrene	Low-density polyethylene, LDPE	S.F.PE
Lotrex	LLDPE and VLLDPE	S.F.PE
Lotryl	EBA and EDA copolymers	Elf Atochem
LP	Polyethylenes, PE	Aristech Chem.
LPP	Calcium carbonate-filled polypropylene, PP	Ferro Corp.
LR 3320	Thermoplastic elastomer, TPE	GE Plastics
Lubricom	–	Comalloy
Lubricomp	Lubricated, wear-resistant engineering polymers, filled or not, viz., PAs	ICI/LNP Eng. Plastics

(continued)

Lubricomp A	ABS/PTFE or PDMS with 0–30 % glass fiber	ICI/LNP Eng. Plastics
Lubricomp Fulton/K	POM + 0–25 PTFE, 0–2 % PDMS, filler	ICI/LNP Eng. Plastics
Lubriloy	Internally lubricated resins	ICI/LNP Eng. Plastics
Lucalen	Ethylene/acrylic acid/acrylate copolymers, EAA	BASF Plastics
Lucalor	Chlorinated poly(vinyl chloride), CPVC	Elf Atochem
Lucel	Polyoxymethylene (acetal), POM	S.P.C.I.
Lucite	Poly(methyl methacrylate) and copolymers, PMMA	E. I. du Pont de Nemours
Lucky ABS	Acrylonitrile-butadiene-styrene terpolymer, ABS	Standard Polymers
Lucobit	Ethylene copolymer/bitumen blend	BASF Plastics
Lucoflex	Poly(vinyl chloride), PVC	Péchiney, France
Lucolene/Lucorex	Poly(vinyl chloride) compounds, PVC	Elf Atochem
Lucovyl	Poly(vinyl chloride) resin, PVC	Elf Atochem Canada
Lucryl	Poly(methyl methacrylate), PMMA	BASF Plastics
Luparen	Polypropylene, PP	BASF Plastics
Luphen	Phenol-formaldehyde resins, PF	BASF Plastics
Lupolen	Ethylene-vinyl acetate copolymer, EVAc	BASF A.-G.
Lupolen O 250H	LDPE blends with polyisobutylene	BASF Plastics
Lupolen	Polyethylenes: LDPE, LLDPE, MDPE, HDPE	BASF Plastics
Lupox	Thermoplastic polyesters; reinforced or not	S.P.C.I.
Lupoy	ABS alloys	S.P.C.I.
Lupragen/Lupranat	Polyurethanes, PU	Elastogran France
Lupranol/Lupraphen	Polyurethanes, PU	Elastogran France
Luprenal	Acrylic resin	BASF Plastics
Luran	Styrene-acrylonitrile copolymers and blends, SAN, ASA	BASF Plastics
Luran S	SAN blended with grafted acrylic ester elastomer, ASA, and its blends	BASF Plastics
Luranyl	PPE/styrene-butadiene copolymer blend, reinforced with up to 30 wt% glass fiber or not	BASF Plastics
Lustran	ABS, SAN, alloys with PVC, etc.	Monsanto Chem. Co.
Lustran ABS	Acrylonitrile-butadiene-styrene terpolymer, ABS, high gloss, general purpose	Monsanto Chem. Co.
Lustran Elite	ABS, low gloss, high flow grades	Monsanto Chem. Co.
Lustran FRABS	ABS, flame-retardant grades	Monsanto Chem. Co.
Lustran SAN	Styrene-acrylonitrile copolymer	Monsanto Chem. Co.
Lustran Ultra	ABS, for injection molding	Monsanto Chem. Co.
Lustrex	Polystyrene, PS	Monsanto Chem. Co.
Lustropak	Acrylonitrile-butadiene-styrene terpolymers, ABS	Monsanto Chem. Co.
Lutonal	Polyvinyl ethers	BASF Plastics
Luvican	Polyvinylcarbazole, PVK	BASF Plastics
Luvitherm	Poly(vinyl chloride) foil, PVC	BASF Plastics
Luxis	Polyamides, PA-66	Westover Color Chem.
Lycra	Diisocyanates/polyether elastomeric fibers	E. I. du Pont de Nemours
Lynex	PPE/polyamide blends	Asahi Chemical

(continued)

M

M-2014	Thermoset melamine, MF	ICI/Fiberite
M-511, M-521	MBS modifiers for PC, PEST, PVC	Kaneka
MA 5000	Polystyrene, PS	Chevron Chem.
Mablex	ABS/polycarbonate alloys	Mazzucchelli Cell.
MABS	Glass fiber-reinforced ABS	Modified Plastics
MAC	Glass fiber-reinforced polyoxymethylene, POM	Modified Plastics
Macepreg	Preimpregnated polyesters	Mecelec Holding
Maflex	Butadiene-styrene copolymer, SB	Sic Plastics France
Magnacomp	Polyamide-6 filled with barium ferrite	LNP Engineering
Magnum	Acrylonitrile-butadiene-styrene terpolymer, ABS	Dow Chem. Co.
Makroblend DP	Polycarbonate/PET/HDPE alloys; general purpose	Bayer AG/Miles, Inc.
Makroblend EC 900	PVC/elastomer, high-impact blends	Bayer AG/Miles, Inc.
Makroblend	PBT/elastomer	Bayer AG/Miles, Inc.
Makroblend PR	Polycarbonate/PBT or PET alloys	Bayer AG/Miles, Inc.
Makroblend UT	Polycarbonate/PET/ABS alloys, filled or not	Bayer AG/Miles, Inc.
Makrofol	Polycarbonate films, PC or PC/PVF	Bayer AG/Miles, Inc.
Makrolon	Polycarbonate, PC, and impact-modified PC, containing <6 % butyl acrylate-methacrylate elastomer; blends reinforced or not	Bayer AG/Miles, Inc.
Malecca	SMI blends with ABS or PBT	Denki Kagaku
Malon	Thermoplastic polyesters	MA Industries
Maragla	Epoxy resins, EP	Acme Div. of Allied
Maranyl	Impact modified, PA-66 or PA-6/elastomer blends, mineral filled	ICI Adv. Mater.
Marlex	Polyethylenes, PE	Phillips 66 Co.
Marlex BMN	Polyethylene, PE	Phillips 66 Co.
Marlex CL	Polyethylene, PE	Phillips 66 Co.
Marlex CP	Polypropylene, PP	Phillips 66 Co.
Marlex EHM	Polyethylene, PE	Phillips 66 Co.
Marlex ER	Mineral-filled polyethylene, PE	Phillips 66 Co.
Marlex GP	Polypropylene, PP	Phillips 66 Co.
Marlex HGL	Polypropylene, PP	Phillips 66 Co.
Marlex PE	Polyethylene, PE	Phillips 66 Co.
Marnyte	Poly(ethylene terephthalate); glass filled or not, PET	Bamberger Polymers
Marvalloy	Acrylic-modified polystyrene	Marval Industries
Marvylan	Poly(vinyl chloride) compounds, PVC	L.V.M. France
Marvyloy	ABS/poly(vinyl chloride) alloys	DSM
MAT-20FG	Glass fiber-filled polyoxymethylene, POM	Modified Plastics
Mater-Bi	Starch-based biodegradable thermoplastics	Novamont
MB 1000	Unsaturated polyesters, UP	Mar Bal Inc.
MC 2100	Polystyrene, PS	Chevron Chem.
MDI	Polyurethane, PU	Dow
Megarad	Polycarbonate, PC	Dow Chem. Co.
Megol	Elastomeric compounds	Polymix

Melacoll	Melamine-formaldehyde resins, MF	Piesteritz
Melan	Melamine-formaldehyde, urea-formaldehyde	Henke
Meldin 2001	Polyimide, PI; for high-temperature electrical parts	Furon Dixon
Meldin 2021	PI + 15 % graphite; high-temperature applications	Furon Dixon
Meldin 2030	PI + 30 % PTFE; high-temperature bearings	Furon Dixon
Melinar PET	Poly(ethylene terephthalate), PET	ICI Adv. Mater.
Melinex	Poly(ethylene terephthalate) films, PET	ICI Films
Melinite	Poly(ethylene terephthalate), PET	ICI Adv. Mater.
Melmex	Melamine-formaldehyde molding powders, MF	BIP Chemicals Ltd.
Melochem	Melamine-formaldehyde, MF	C.P.R.I.
Melolam	Melamine-formaldehyde laminating resins, MF	Ciba-Geigy Ltd.
Melopas	Melamine molding compound, MF	Ciba-Geigy Ltd.
Meraklon	Polypropylene, PP	Montecatini
Merlon	Polycarbonate, PC; PC/PO blends	Bayer AG/Miles
Mertex	TPU blends	Bayer AG/Miles
Metablen P-522	Acrylic processing aid for PVC blow molding	Mitsubishi Rayon Co., Metco
Metablen P-570	Acrylic processing aid for PVC siding	Mitsubishi Rayon Co., Metco
Metamarble	Polycarbonate/PMMA alloy	Teijin Chem. Ltd.
Methafil	Mica- or glass fiber-filled polymethylpentene	Akzo/DSM
Methocel	Ethyl and methyl cellulose	Dow
Methylon	Phenolic resin, PF	Cain Chem. Inc.
MG-6	Silica-filled epoxy resins, EP	Dexter Corp.
Mikrothene FE, MU	Ethylene-vinyl acetate copolymer, EVAc	Quantum Chem.
Mikrothene FN	Polyolefins, PO	Quantum Chem.
Mikrothene HD, MD	Polyethylenes, PE	Quantum Chem.
Milastomer	TP elastomer	Mitsui
Milkon	PPS/PTFE blend	Tribol. Ind. Inc.
Millathane	Thermoplastic polyurethane elastomer, TPE	TSE Industries, Inc.
Mindel	Polysulfone, PSF or PSO, blends; filled or not	Amoco Performance Product
Mindel A	Polysulfone/ABS blends; filled or not	Amoco Chem. Co.
Mindel B	Polysulfone/PET blends; filled or not	Amoco Chem. Co.
Minlon	PA-66 or PA-66/ionomer alloy + mineral/glass	E. I. du Pont de Nemours
Mipolam	Poly(vinyl chloride), PVC	Dynamit Nobel
Miramid	Polyamides, PA	Soprochim
Miraspin	Polyethylenes, PE	Mitsui Petrochem.
Mirathen	Low-density polyethylene, LDPE	Soprochim
Mirlon	Polyamide, PA	Viscose Suisse
MN-6	Glass fiber-filled polyamide-6, PA-6	Modified Plastics
MN-6/6	Glass fiber-filled polyamide-66, PA-66	Modified Plastics
Moatek	Ethylene-butene-1, or octene-1, copolymer	Idemitsu Petrochem.

(*continued*)

Mobil MX	Polystyrenes, PS	Mobil Chem. Co.
Mobil	Polyethylenes, PE	Mobil Chem. Co.
Mobil PS	Polystyrenes, PS	Mobil Chem. Co.
Modar	Urethane-modified acrylic resin	ICI Chem. Polym.
Modylen	PP copolymer/EPDM blends	Tiszai Vegyi Komb.
Moldex A	ABS/polycarbonate alloy	Anic
Moltopren	Foam material based on polyurethane, PU	Bayer AG/Miles
Monkalloy P	PC/ABS alloys with glass fiber	Monsanto-Kasei Co.
Monocast	PA directly polymerized into shapes	Polymer Corp.
Moplen	PP homopolymers and copolymers with ethylene	Himont/Montedison
Mor-Thane	Thermoplastic polyurethanes, TPU	Morton Thiokol
Morthane	Thermoplastic polyurethane, TPU	Morton International, Inc
Morvanflex	Thermoplastic elastomers, TPE	S.P.2.I
Mowicoll	Poly(vinyl acetate) dispersions, PVAc	Hoechst Celanese Corp.
Mowilith	Poly(vinyl acetate), PVAc	Hoechst Celanese Corp.
Mowiol	Poly(vinyl alcohol), PVAl	Hoechst Celanese Corp.
Mowital	Poly(vinyl butyral), PVB	Hoechst Celanese Corp.
MPBT-FG	Glass fiber-filled polybutylene terephthalate, PBT	Modified Plastics
MPC	Phenolic resin, PF	Rogers Corp
MPC-FG	Glass fiber filled polycarbonate, PC	Modified Plastics
MPP-FG	Glass fiber filled polypropylene, PC	Modified Plastics
MPPE	PA/PPE alloys	Asahi Chem. Ind.
MPPO-FG	Glass fiber-filled poly(phenylene ether), PPE	Modified Plastics
MPSL-FG	Glass fiber-filled polysulfone, PSU	Modified Plastics
Multi-Flam	Polypropylene	Multibase, Inc.
Multi-Flex	SEBS (Kraton G)-based TPEs	Multibase, Inc.
Multi-Hips	Polystyrene, PS, HIPS	Multibase, Inc.
Multi-Pro	Polypropylene	Multibase, Inc.
Multi-San	SAN copolymer	Multibase, Inc.
Multibase ABS	Acrylonitrile-butadiene-styrene copolymer	Multibase, Inc.
Multibase	ABS	Multibase, Inc.
Multibase	Reinforced polypropylene, PP	Multibase, Inc.
MultiChem	Vinyl compounds	Colorite Plastics
Multilon	Polycarbonates and PC/ABS alloys	Teijin Chem. Ltd.
Multipet	Polyethylene-polyester multilayer film	Wihuri Oy Wipak
MX-5350	Polystyrene/elastomer blends	Mobil
Mylar	Poly(ethylene terephthalate) film, PET	E. I. du Pont de Nemours

N

N05FG	Polyamide-6 with 5 % glass fiber, PA-6	Thermofil, Inc.
N15-40NF	Polyamide-610 with 40 % graphite fiber, PA-610	Thermofil, Inc.
N3-20FG	Polyamide-66 with 20 % glass fiber, PA-66	Thermofil, Inc.
N40fm	Polyamide-6 with 40 % glass fiber and mineral	Thermofil, Inc.
N40MF	Polyamide-6 with 40 % mineral, PA-6	Thermofil, Inc.
N5	PA/ABS alloys containing up to 30 wt% GF	Thermofil, Inc.
N6-30MF	Polyamide-612 with 30 % mineral, PA-612	Thermofil, Inc.
N66G-30	Polyamide-66 with 30 % glass fiber, PA-66	Polymer Composites
N8-30FG	Polyamide-11 with 30 % glass fiber, PA-11	Thermofil, Inc.
N9-30FG	Polyamide-12 with 30 % glass fiber, PA-12	Thermofil, Inc.
Nafion	Perfluorinated membranes	E. I. du Pont de Nemours
Nalcite	Ion-exchange resin	National Aluminate
NAP	Polyarylate, amorphous; 3,3′, 5,5′-tetramethyl-dihydroxydiphenylmethane copolymer	Kanegafuchi Chem.
Napryl	Polypropylene, PP	Péchiney, France
NAS 30	Poly(styrene-*co*-methyl methacrylate), transparent	Novacor Chemicals
NAS 50	Poly(methyl methacrylate-*co*-styrene), transparent	Novacor Chemicals
Natene	Polyethylenes, PE	Péchiney, France
Natsyn	Polyisoprene	Goodyear
Naxell	Polycarbonate (recycled)	MRC Polymers
Naxols/Naxoreses	Polyester resins for paints and varnishes	Convert
NCH	"Nylon-Clay Hybrid"; polyamide-6 with montmorillonite particles 0.1–0.2 nm diameter; *nanometer composite* developed by Toyota Research Corp.	Ube Industries, Ltd.
Neo Cis	Elastomers	Enimont/Safic-Alcan
Neo-zex	Polyethylenes, PE	Mitsui Petrochem.
Neoflon FEP	Fluorinated ethylene-propylene, FEP	Daikin
Neoflon PCTFE	Polychlorotrifluoroethylene, PCTFE	Daikin
Neoflon PFE	Perfluoroalkoxyether, PFE	Daikin
Neoflon PVDF	Poly(vinylidene fluoride), PVDF	Daikin
Neopolen	PE/polypropylene foam	BASF Plastics
Neopolen	Polystyrene/polyethylene, PS/PE, blend	BASF Plastics
Neoprene	Polychloroprene, CR	E. I. du Pont de Nemours
Neoprene	Synthetic polychloroprene rubber	E. I. du Pont de Nemours
Neosepta F	Ionic fluoropolymer membrane	Tokoyama Soda
Neoxil	Unsaturated polyester resin, UP	DSM
Neste Oxo	Plastisols, PVC	Neste Chim.
Neste Polystyrene	Polystyrene, PS	Neste Chim.
Neste PP	Polypropylene, PP	Neste Chim.

Newcon	Reactor made TPO/PP alloys for car bumpers	Chiso Corp.
New TPI	Polyimides; reinforced or not, PI	S.P.C.I.
Niax	Polyether from glycerin or hexane-1,2,6-triol	Union Carbide Co.
Nike	Cellulose nitrate, CN	Punda Inc.
Nipoflex	Ethylene-vinyl acetate copolymer	Toyo Soda
Niopolon	Polyethylene	Toyo Soda
Nipeon AL	ABS/poly(vinyl chloride) (50 %) alloy	Zeon Kasei Co.
Nipol AR	Polyacrylate elastomers	Nippon Zeon Co., Ltd.
Nipol Carboxylated	Nitrile rubbers lightly carboxylated, NBR	Nippon Zeon Co., Ltd.
Nipol DP 5120P	NBR modifiers for clear PVC	Nippon Zeon Co., Ltd.
Nipol	Nitrile elastomers, NBR, AN = 21–51 % also liquids, powders, or crumbs	Nippon Zeon Co., Ltd.
Nipol Polyblends	NBR/PVC (30–50 %) elastomeric alloys plasticized or not	Nippon Zeon Co., Ltd.
Nipol Terpolymer	Acrylonitrile-butadiene-isoprene elastomers; grade DN-224 contains 50 % DOP	Nippon Zeon Co., Ltd.
Nissan 1000–3000	Polyethylenes, PE	Nissan Chem. Ind.
Nitriflex	Acrylonitrile-butadiene-styrene copolymer, ABS	A. Schulman, Inc.
Nitrilene	Poly(vinyl chloride)/BR/ABS alloys	Rhein Chemie
Nitron	Cellulose nitrate, CN	Monsanto Chem. Co.
Nitrovin	Nitrile or polyurethane rubber/PVC, alloys	Vi-Chem Corp.
Nivionplast	Polyamides, PA-6, PA-66	ECP Enimont Polymeri
Nivionplast	Polyamide-6, PA-6	EniChem
Noblen	Polypropylene, PP	Mitsubishi Petrochem.
Noblen	Polypropylene; filled or not, PP	Sumitomo Chem. Co.
Nolimid 32	Polyimides; for junction coatings, PI	Rhône-Poulenc
Nomex	Poly(*m*-phenyleneisophthalamide) fibers, PPA	E. I. du Pont de Nemours
Norasol	Polycarboxylate, water soluble	Elf Atochem
Norchem	Polyethylenes, PE	Quantum Chem.
Norchem	Polyethylenes, reinforced or not, PE	Norchem, Inc.
Norchem	Polyolefins: LDPE, HDPE, LLDPE, PP	Enron Chem. Co.
Nordbak 7451	Epoxy or polyurethane	Rexnord Chem.
Nordel	EPDM, hydrocarbon rubbers	E. I. du Pont de Nemours
Norsodyne	Polyester resins	Norsolor/Please
Norsoflex	Polyethylenes: LLDPE and VLLDPE	S.F.PE
Norsolene	C-9 hydrocarbon resins, PE	Elf Atochem
Norsomix	Polyester resin compounds	Norsolor
Norsophen	Phenol-formaldehyde resins, PF	Norsolor
Norsorex	Polynorbornene elastomers	Cyanamid/Atochem/ Nippon Zeon Co.
Nortuff	Polypropylene, PP	Quantum Chem. Co.
Norvinyl	Poly(vinyl chloride), PVC	Norsk Hydro/Hydro PLast

(*continued*)

Noryl	PPE thermoplastic blends, reinforced or not	GE Plastics
Noryl BN	PPE/HIPS alloys; reinforced or not	GE Plastics
Noryl FN	Foamable PPE/HIPS alloys	GE Plastics
Noryl GFN	Glass fiber-filled PPE/HIPS alloys	GE Plastics
Noryl GTX	PA/PPE(30 %) blend, reinforced or not	GE Plastics
Noryl Plus	PPE/HIPS/PA alloys	GE Plastics
Nova PC	Polycarbonate, PC; with flame retardant or not	Nova Polymers, Inc.
Novablend	Poly(vinyl chloride), PVC; rigid	Novcor
Novablend 4510	PVC alloy with glutarimide acrylic copolymer for hot-fill bottles	Novatech Plastics & Chem.
Novacor	–	Novacor
Novaccurate	Liquid crystal polyester with glass fiber or not	Mitsubishi Chem.
Novadur	Poly(butylene terephthalate), PBT	Mitsubishi Chem.
Novadur ST520	Poly(butylene terephthalate) with 20 % acrylic rubber	Mitsubishi Chem.
Novalar	Elastomeric grafting copolymer to be used in ABS, PVC, PC, PBT, TPU, EP, acrylics, etc., for improvement of impact strength and ductility	Nova Polymers, Inc.
Novalast	Thermoplastic olefins, TPE	Nova Polymers, Inc.
Novalene	TPO compound from recycled PE or PP; 50–90 Shore A durometer	Nova Polymers, Inc.
Novalene RF	TPO/TPE impact modifier for PE or PP	Nova Polymers, Inc.
Novalloy 9000	Poly(vinyl chloride)/ABS alloy, PVC/ABS	Novatech Plastics & Chem.
Novalloy-A	PA-6 or PA-66 blends with ABS	Daicel Chem. Ind., Ltd.
Novalloy-B	PBT blends with ABS, reinforced or not	Daicel Chem. Ind., Ltd.
Novalloy-S	ABS/polycarbonate blends, reinforced or not	Daicel Chem. Ind., Ltd.
Novamate A	AAS/polycarbonate blends	Mitsubishi Chem.
Novamate B	ABS/polycarbonate blends	Mitsubishi Chem.
Novamid	Polyamides	Mitsubishi Chem.
Novamid ST220	Polyamide/elastomer blends	Mitsubishi Chem.
Novamid X21	Semi-aromatic amorphous polyamide	Mitsubishi Chem.
Novapet	Poly(ethylene terephthalate) with glass fiber or not	Mitsubishi Chem.
Novapol	Polyethylenes	Novacor
Novapol LD	Low-density polyethylene, LDPE	Novacor
Novapol LL	Linear low-density polyethylene, LLDPE	Novacor
Novapol, HD	High-density polyethylene, HDPE	Novacor
Novapps	Poly(phenylene sulfide) blends	Mitsubishi Chem.
Novarex AM	PC/elastomer with glass fiber or not	Mitsubishi Chem.
Novarex	Polycarbonates, PC	Mitsubishi Chem.
Novatec P	Polypropylenes, PP	Mitsubishi Chem.
Novatec	Polyethylenes, PE	Mitsubishi Chem.
Novex	Low-density polyethylene, LDPE	BP Chemicals Limited
Novimide	Epoxy resins, EP	Furane Products
Novodur	Acrylonitrile-butadiene-styrene terpolymer, ABS	Bayer AG/Miles
Novolac	Phenol-formaldehyde resins, PF	Perstorp Bakelite S.A.

Novolen KR	Polypropylene/EPR blend	BASF Plastics
Novolen	Polypropylene, PP, also filled and reinforced	BASF Plastics
Novolen	Rubber modified PP/PE blend	BASF Plastics
Novon	Based on starch, biodegradable polymers for extrusion, injection molding, or thermoforming	Warner-Lambert/ Novon Co.
Nucrel	Ethylene-methacrylic acid copolymer, EMAA	E. I. du Pont de Nemours
Nupol	Thermoset acrylics	Freeman Chem. Corp.
NX-7000	PPE/PA-6 alloys for automobile applications	Mitsubishi Gas Chem.
NX-9000	PPE/polyamide-66 alloys	Mitsubishi Gas Chem.
Ny-Kon	PA-6 or PA-66 internally lubricated with MoS_2	LNP Eng. Plastics
Nybex	Polyamides, PA-6,PA-66, impact modified	Ferro Corp.
Nycoa 1485	Polyamide-6 with PE toughened blends	Nylon Corp. of America
Nycoa 2084	Polyamide-6 with EEA toughened blends	Nylon Corp. of America
Nycoa 7551	Polyamide-6 with EPR toughened blends	Nylon Corp. of America
Nydur	Polyamide, PA/PO blends, fiber reinforced or not	Bayer AG/Miles
Nylafil G	Polyamide-6/elastomer; glass or carbon fibers	Akzo/DSM/Wilson-Fiberfil
Nylafil J-1	Polyamide-66/elastomer; glass or carbon fibers	Akzo/DSM/Wilson-Fiberfil
Nylafil J-2	Polyamide-610/elastomer blend; glass fibers	Akzo/DSM/Wilson-Fiberfil
Nylamid	Polyamide-6 or polyamide-66; reinforced or not, PA	Polymer Service
Nylatron GS Nylon	Polyamides; glass, mineral, or MoS_2, in shapes	Polymer Corp.
Nylon 6T	Poly(hexamethylenediamine-terephthalic acid)	Hoechst Celanese Corp.
Nylon 7000	Polyamide/elastomer blend	Hoechst Celanese Corp.
Nylon Celanese	Polyamides; reinforced or not, PA	Hoechst Celanese Corp.
Nylon	Generic name for polyamides, PA	E. I. du Pont de Nemours
Nylon MXD	Polyamides, PA	Mitsubishi Gas
Nyltex	Polyamides, PA	Vecoplas
Nypel	Polyamide-6; reinforced or not, PA-6	Allied Signal Inc
Nyref	Semicrystalline polyamides N-MXD6, PA-N	Solvay & Cie SA
Nyrim	PA-block copolymers	DSM
O		
Oldodur	Integral-skin-rigid foams	Buesting & Fasch Co.
Oldofill	Packing foams	Buesting & Fasch Co.
Oldoflex	Integral skin, flexible foams	Buesting & Fasch Co.
Oldotherm	Rigid foams	Buesting & Fasch Co.

Oleflex	TPO blend of PE, PP, and α-olefin random copolymer.	Showa Denko K. K.
Olehard	Filled polypropylene	Chiso America
Ontex ABX, APE	PP/EPDM – elastomer/binder blends	Dexter Corporation.
Oppanol B	Polyisobutylene, PIB	BASF Plastics.
Oppanol C	Polyvinylisobutyl ether, PVI	BASF Plastics.
Oppanol O	Isobutylene-styrene copolymer (9:1)	BASF Plastics
Oppanol	Polyisobutylene, PIB	BASF Plastics
Optema	Ethylene-maleic anhydride, EMA copolymers	Exxon Chem.
Optix	Acrylic resins	Plaskolite
Opto 90	Epoxy resins, EP	ICI/Fiberite
Optum	Polypropylene/TPO alloys, reinforced	Ferro Corp.
Orevac	Ethylene-vinyl acetate copolymers, EVAc	Elf Atochem
Orgablend	Polyamide/polypropylene recycled alloys, PA/PP	Elf Atochem
Orgaflex	Polyphosphazene	Elf Atochem
Orgalan	Polycarbonate, PC	Elf Atochem
Orgalloy R 60ES	Polypropylene/polyamide-6, CO_2, H_2O barrier	Elf Atochem
Orgalloy R 6000	Polypropylene/polyamide-6 alloys, PP/PA-6 with up to 30 wt% GF	Elf Atochem
Orgalloy R 6600	Polypropylene/polyamide-66 alloys, PP/PA-66	Elf Atochem
Orgamide	Polyamide-6, PA-6	Elf Atochem
Orgasol	Ultrafine powder polyamides, PA	Elf Atochem
Orgater	PBT, PBT/EVA/PEBA alloys	Elf Atochem
Orlon	Polyacrylonitrile, PAN	E. I. du Pont de Nemours
Oroglas	Polyacrylates and polymethacrylates	Rohm and Haas
OS0100	Epoxy resins, EP	Dexter Corp.
OS2000	Epoxy resins, EP	Dexter Corp.
Owens-Corning E-	Unsaturated polyesters, UP	Owens/Corning
Oxy 3700	Poly(vinyl chloride), PVC	Occidental Chem. Corp.
Oxyblend	Poly(vinyl chloride), PVC, elastomer blends	Occidental Chem. Corp.
Oxyclear	Poly(vinyl chloride) rigid formulation, PVC	Occidental Chem. Corp.
Oxyclear 4190	PVC alloy with glutarimide acrylic copolymer for hot-fill bottles	Occidental Chem. Corp.
Oxyester	Polyurethanes, PU	Hüls AG
Oxytuf	Poly(vinyl chloride), PVC/EPDM blends	Occidental Chem. Corp.
P		
P-2000	Unsaturated polyesters, UP	Industrial Dielect.
P-9900-	Polypropylene; filled or not, PP	Thermofil, Inc.
P-xyBG	Polypropylene with xy wt% glass beads, PP	Thermofil, Inc.
P-xyCC	Polypropylene with xy wt% $CaCO_3$, PP	Thermofil, Inc.
P-xyFG	Polypropylene with xy wt% glass fibers, PP	Thermofil, Inc.

P-xyMF	Polypropylene with xy wt% mineral, PP	Thermofil, Inc.
P-xyMI	Polypropylene with xy wt% mica, PP	Thermofil, Inc.
P-xyTC	Polypropylene with xy wt% talc, PP	Thermofil, Inc.
P.M.C.	Gel coats	Synres-Almoco
P1-xyFG	Polypropylene with xy wt% of glass fiber, PP	Thermofil, Inc.
P1120	Polypropylene filled with mineral and glass, PP	MA Industries
PA66-110	Polyamide-66; filled or not, PA-66	MRC Polymers Inc.
PAF-200 to 600	Polyoxymethylene with 10–30 wt% glass, POM	Polyfil, Inc.
Palapreg	SMC/BMC resins, resin system	BASF Plastics
Palatal	Unsaturated polyester resins, UP	BASF Plastics
Palesit	Silicones	S.P.C.I.
Panapol	Polybutylene, PB	Exxon Chem.
Panlite	Polycarbonates; filled or not, PC	Teijin Chem. Ltd.
Pantalast	Poly(vinyl chloride), PVC/EVAc alloys	Pantasote Inc.
Paracril AZO	Nitrile rubber/Poly(vinyl chloride), NBR/PVC alloy	Uniroyal Chemical
Parad	Photopolymer, resistant and dielectric	E. I. du Pont de Nemours
Paraglas	Cast acrylic sheet, PMMA	Degussa AG
Paralac	Polyester resin, UP	ICI Adv. Mater.
Paraloid EXL-3361	Acrylic impact modifier for PC and its blends	Rohm and Haas
Paraloid EXL-3657	MBS impact modifier for PC and its blends	Rohm and Haas
Paraloid EXL-4151	Polyglutarimide for alloying PC with polyamide	Rohm and Haas
Paraloid HT-510	Polyacrylic-imide modifier for PVC bottles	Rohm and Haas
Paraloid	Poly(methyl methacrylate-butadiene-styrene) MBS (old *Acryloid*™)	Rohm and Haas
Paraplast 8000	Epoxy resins, EP	Hexcel Corp.
Paraplex	Polyester resin	Rohm and Haas
Parastyren	Styrene-butadiene copolymer, SBR	Paraisten Kalkki Oy
Parel	Polypropylene oxide elastomers	Nippon Zeon Co., Ltd.
Parlon	Chlorinated rubber, RUC	Hercules
Parylene C	Poly(monochloro-*p*-xylene)	Union Carbide Co., Inc.
Parylene D	Poly(dichloro-*p*-xylene)	Union Carbide Co., Inc.
Parylene N	Polyparaxylene	Union Carbide Co., Inc.
PAS-2	Polyphenylsulfide-sulfone	Phillips
Pax-Plus	HDPE/polyisobutylene blends	Allied-Signal Corp.
Paxon	Polyethylene/polyisobutylene, PE/PIB, blends	Allied-Signal Corp./ Paxon
Paxon Pax-Plus	PE/elastomer blends	Allied-Signal Corp./ Paxon
PBF-300	Poly(butylene terephthalate), glass filled, PBT	Polyfil, Inc.
PBT-5008	Poly(butylene terephthalate); filled or not, PBT	Mitsubishi Chem.
PBTGL-30	Poly(butylene terephthalate), 30 % glass filled, PBT	Polymer Compos.
PC-00B	Polycarbonate; filled or not, PC	Plastic Materials
PC-100	Polycarbonate; filled or not, PC	MRC Polymers, Inc.
PC-12	Epoxy resins, EP	Dexter Corp.

<div align="right">(continued)</div>

PC-18	Polyurethane (TS)	Dexter Corp.
PCC-800	Polycarbonate; carbon fiber filled, PC	Polyfil, Inc.
PCCE-5154	Thermoplastic polyester	Eastman Chem. Prod.
PCF-800	Polycarbonate; glass fiber filled, PC	Polyfil, Inc.
PCGL-30	Polycarbonate, 30 % glass filled, PC	Polymer Compos.
PDC-400	Poly(phenylene sulfide) with carbon fibers, PPS	Polyfil, Inc.
PDF-400	Poly(phenylene sulfide) with glass fibers, PPS	Polyfil, Inc.
PE-1007 to 5976	Polyethylenes, PE	Chevron Chem.
PE-2FR	Polyethylenes; filled or not, PE	Reichhold Chem., Inc.
Pebar	Blends of polyolefins (HDPE, PP) with high nitrile resin, _Barex_™	BP Chemicals
Pebax	TPE polyether block amide; GF filled or not	Elf Atochem
Pedigree 433	Unsaturated polyester, UP	P. D. George Co.
PEF-400	Polyethylene with glass fibers, PE	Polyfil, Inc.
Pekema	Poly(vinyl chloride), PVC	Punda Inc.
Pelaspan	Polystyrene, expandable	Dow Chem. Co.
Pellethane	Polyurethane TPU, ABS/TPU, TPE	Upjohn/Dow Chem.
Pellethane 2102	Polyester-polycaprolactone	Dow Chem. Co.
Pellethane 2103	Polyether TPU	Dow Chem. Co.
Pellethane 2352	Thermoplastic elastomer, TPU	Dow Chem. Co.
Pellethane 2355	Polyester TPU	Dow Chem. Co.
Pellethane 2363	Thermoplastic polyurethane, TPU	Dow Chem. Co.
Pellets	Polyurethane, TPU	Fimor
Pelprene	Aliphatic-b-aromatic polyester copolymer	Toyobo Corp.
Pensrene EN	IPN of poly(phenylene sulfide) and TS resin	Dainippon Ink & Chem.
Penton	Poly(2,2-dichloromethyltrimethylene ether)	Hercules
PEO	Polyethylene oxide	Seitetsu Kagaku
Perbunan C	Polychloroprene elastomer, CR	Bayer AG/Miles
Perbunan N Latex	Anionic latices of nitrile rubber, NBR; 45–50 % solids; AN = 18–48 %	Polysar/Bayer AG
Perbunan N	Nitrile rubber, NBR; AN = 18–48 %	Polysar/Bayer AG
Pergut	Diverse resins	Bayer AG
Periston	Polyvinylpyrrolidone	Bayer AG/Miles
Perlenka	Polyamide-6, PA-6	AKU, Netherlands
Perlon	Generic name for polyamide-6, PA-6	Bayer AG/Miles
Perlon U	Polyurethane, PU	Bayer AG/Miles
PermaStat 100	Polypropylene, with 0 % and 10 % glass fiber	RTP Co.
PermaStat 2500	Polycarbonate/ABS alloys	RTP Co.
PermaStat 2700	Styrenic elastomer resins	RTP Co.
PermaStat 4000	Polyphthalamide with 0 % and 30 % glass fiber	RTP Co.
Permutit	Ion-exchange resin	Permutit Co.
Perspex	Cast, extruded PMMA sheet	ICI Chem. Polym. Ltd.
Perstorp Grade 151	Urea-formaldehyde, UF	Perstorp, Inc.
Perstorp Grade 751	Melamine-formaldehyde, MF	Perstorp, Inc.

PET Azdel	Polypropylene with 35 % glass fiber, PP	Azdel Inc.
Pet	Thermoplastic polyesters	ICI
PETGL-30	Poly(ethylene terephthalate), 30 % glass filled, PET	Polymer Compos.
Petlon	Poly(ethylene terephthalate) glass/mineral filled	Bayer AG/Miles
Petra	Poly(ethylene terephthalate), PET	Allied Signal Inc
Petra 130	Poly(ethylene terephthalate), glass filled, PET	Allied Signal Inc
Petra 230	Poly(ethylene terephthalate), glass/mineral filled	Allied-Signal Inc.
Petrarch PTFP	Polytetrafluoroethylene, PTFE	Petrarch Systems
Petron	Poly(ethylene terephthalate)	Mobay
Petrothene	LDPE, LLDPE, HDPE, PP, EVAc; filled or not	Quantum Chem. Co.
Petsar	PET/PC/acrylic blends with 30 % glass fiber	Novacor Chemicals Inc.
Pevalon	Poly(vinyl alcohol)	May & Baker
Pevikon	Poly(vinyl chloride) resins, PVC	Norsk Hydro/Hydro PLast
PGF-400	Glass-filled poly(phenylene ether), PPE	Polyfil, Inc.
PHC-600	Carbon fiber-filled polysulfone, PSU	Polyfil, Inc.
Phenoxy	Bisphenol-A/epichlorohydrin copolymer	Amoco Performance
PHF-400	Glass-filled polysulfone, PSU	Polyfil, Inc.
Philprene	Styrene-butadiene thermoplastic copolymer, SBR	Phillips 66 Co.
PI-730	Polyimide; glass or carbon fiber filled, PI	ICI/Fiberite
Pibiflex	Poly(butylene terephthalate), PBT copolymers	Enimont
Pibiter	PBT homopolymers or blends; filled or not	Montepolimeri/ EniChem
Pioloform	Polyvinyl acetal, butyral, and formal	Wacker-Chemie
PIQ	Polyimide, electronic coatings, PI	Hitachi
PKF-400	Glass-filled ABS	Polyfil, Inc.
PL-25	Acrylics	Plaskolite, Inc.
Plaper	Styrene-butadiene copolymer, SBR	Mitsubishi Monsanto
Plaskon	Thermoset resins: alkyd, DAP, epoxy, phenolic	Plaskon Electronic
Plaslube	Lubricated resins	Akzo/DSM
Plaslube AC	Polyoxymethylene with 15 % fluorocarbon, POM	Akzo/DSM
Plaslube J	PC, PA-66, PSU; lubricated materials with GF	Akzo/DSM
Plaslube NY	Polyamide-66 with 5 % MoS_2, PA-66	Akzo/DSM
Plastadur	Phenol-formaldehyde, PF	Soprochim
Plastalloy	Polysulfone alloys with short glass fiber, PSU	Akzo/DSM
Plastylene	Polyethylene, PE	Pichney-Saint-Gobain
Platabond	Copolyamides, hot melts	Elf Atochem
Platamid	Copolyamides, hot melts	Elf Atochem
Plathen	Polyethylene hot melt, PE	Elf Atochem Deutschland
Platherm	Copolyamides, hot melts	Elf Atochem
Platilon	TPU and nylon films	Elf Atochem Deutschland
Platon	PET, polyamide-6 monofilaments	Elf Atochem Deutschland

(*continued*)

Plenco	Diallyl phthalate, phenolics, polyesters	Plastics Engineering Co.
Plexalloy	PMMA/ABS alloys	Rohm and Haas
Plexar	PO-based adhesives	DSM
Plexidur	Poly(acrylonitrile-*co*-methyl methacrylate)	Rohm and Haas
Plexiglas	Acrylic, methacrylic resins and blends	Roehm GmbH/ AtoHaas
Plexiglas G, V, MC	Acrylic, methacrylic resins and copolymers	Rohm and Haas
Plexigum	Acrylate and methacrylate resins	Rohm and Haas
Pliocord VP Latex	Vinylpyridine copolymer	Goodyear Chemicals
Pliofilm	Hydrochloride rubber	Goodyear Chemicals
Pliogrip	Polyurethane adhesives, PU	Ashland Chemicals
Pliolite	Styrene-butadiene copolymers	Goodyear Chemicals
Pluracol	Polyether polyols	BASF Plastics
Pluronics	Ethylene oxide-propylene oxide copolymers, EPO	Wyandotte Chem.
Plyophen	Phenolic resin,	Cain Chem. Inc.
PMF-400	Glass-filled polyamide-66, PA-66	Polyfil, Inc.
PNC-400	Carbon fiber-filled polyamide-66, PA-66	Polyfil, Inc.
PO	Polypropylene, PP	MA Industries
Pocan 7913	PBT/PC/elastomer alloys	Bayer AG/Miles
Pocan	Poly(butylene terephthalate), PBT, PBT/ABS	Bayer AG/Miles/Albis
Pocan-S	PBT/elastomer blends	Bayer AG/Miles
POF-400	Glass-filled polyamide-6, PA-6	Polyfil, Inc.
Polane T, HST	Urethane coatings	Sherwin-Williams Co
Poliblend NH	Polypropylene/polyamide blend; reinforced or not	Poliresins SpA
Polidux	ABS, SAN, polystyrenes	Aiscondel
Polifil	Polypropylene + mineral, talc, calcium carbonate	Polifil, Inc.
Pollopas	Urea-formaldehyde resins, UF	Dynamit Nobel
Polloplas	Urea-based cellulose-containing compound	Dynamit Nobel
Poly BD	Polybutene, hydroxyl terminated	Elf Atochem
Poly G	Specialty polyols	Olin Chemicals
Poly-Dap	Diallyl phthalate; glass or mineral filled	Industrial Dielect.
Poly-Eth	Polyethylene, PE	Gulf Oil
Polyac	Acrylonitrile-butadiene-styrene terpolymer, ABS	Primex
Polybatch	PE, PP, PVC, PA, ABS color concentrates	A. Schulman, Inc.
Polyblak	Carbon black concentrates	A. Schulman, Inc.
Polybond	Chemically modified POs	PB Performance Polymers
Polycarbafil G	Polycarbonate; filled with glass, metal, carbon	Akzo/DSM
Polycast	Poly(vinylidene fluoride)/poly(methyl methacrylate) blends for electrets	Royalite
Polychem 100	Phenolic resins filled with glass, wood, etc.	Budd Co.
Polyclear	Polyethylene terephthalate, PET	Hoechst Celanese Corp.
Polycol	Poly(vinyl chloride) compound, PVC	Elf Atochem

<div align="right">(continued)</div>

Polycomp	PPS or PET/PTFE blends	LNP Corp.
Polycomp	PTFE filled with PPS or PAr blends	LNP Corp.
Polydene	Poly(methyl methacrylate)/PVC alloy	A. Schulman, Inc.
Polydet	GRP plates (polyester)	Mitras Kunstoffe GmbH
Polydur	Thermoplastic polyurethane, TPU	Dynamit Nobel/A. Schulman
Polyfil	–	Polyfil
Polyfine	–	Tokuyama Soda
Polyflam X	Flame-retarded resins; X = ABS, PS, PE, PP, etc.	A. Schulman, Inc.
Polyflon	Polytetrafluoroethylene, PTFE	Daikin
Polyfort	Polypropylene; filled with mineral, glass, PP	A Schulman Inc.
Polyimide	Polyimide, PI	Upjohn Co.
Polylac	Acrylonitrile-butadiene-styrene terpolymer, ABS	Chi Mei Industrial Co.
Polylite	Unsaturated polyester resin, UP	Reichhold Ltd.
Polyloy	Polyamide-6 or polyamide-6,6/PO or TPO blends	Dr. Illing GmbH
Polyman	ABS or SAN/PVC compounds	A. Schulman, Inc.
Polyman *506, 509*, etc.	Poly(vinyl chloride)/ABS high-temperature alloys	A. Schulman, Inc.
Polyman *551*	Polyolefin, PO	A. Schulman, Inc.
Polyman *552*	SAN/PO blends	A. Schulman, Inc.
Polymer XE *3055*	Polyamide blends, PA	EMS-Chemie AG
Polymin	Polyethyleneimine	BASF Plastics
Polyox	Polyethylene oxide	Union Carbide
Polypenco Acrylic	Cast acrylic rods	Polymer Corp.
Polypenco Nylon 101	PA-66 reinforced or not (rods or sheets)	Polymer Corp.
Polypenco Q200.5	Cross-linked PS (rods or sheets)	Polymer Corp.
Polypenco Torlon	Polyamide-imide in rods or plates	Polymer Corp.
Polypro J	Polypropylene; filled or not, PP	Mitsui Petrochem.
Polypro KS	Polypropylene; filled or not, PP	Tokuyama Soda Co.
Polypur APU	Long fiber-reinforced TPU alloys	A. Schulman, Inc.
Polyrex P	Polystyrene, PS	Chi Mei Industrial
Polyrite PP	Unsaturated polyester with glass fiber, UP	Polyply, Inc.
Polysar Bromobutyl	Bromobutyl rubber, BIIR	Polysar/Bayer AG
Polysar Butyl	Butyl rubber, BR	Polysar/Bayer AG
Polysar Chlorobutyl	Chlorobutyl rubber, CIIR	Polysar/Bayer AG
Polysar EPDM	EPDM rubbers with ethylene/propylene ratio = 58/42 to 75/25	Polysar/Bayer AG
Polysar	Polystyrene, PS	Novacor
Polysar	PS with 4–8 % polybutadiene blend	Novacor
Polysar S	Emulsion SBR with 23.5 % bound styrene	Polysar/Bayer AG
Polysar SS	Emulsion SBR with 64 % bound styrene	Polysar/Bayer AG
Polysizer	Poly(vinyl alcohol), PVAl	Showa Highpolymer
Polystyrol	Polystyrene/polybutadiene alloys, HIPS, styrene-butadiene copolymer, SBR, etc.	BASF Plastics
Polysulfon	Poly(bisphenol-A/dichlorodiphenylsulfone)	Shell Chem. Co.

<div align="right">(continued)</div>

Polythene	Polyethylenes, PE (high pressure)	E. I. du Pont de Nemours
Polytron	Electroconductive Poly(vinyl chloride) alloys	BF Goodrich
Polytrope TPP	TPO alloys, PP/EPDM	A. Schulman, Inc.
Polyval	Poly(vinyl alcohol), PVAl	Unitika Kasei
Polyvest	Polybutadiene, PB	Hüls AG
Polyvin	Poly(vinyl chloride) compounds, PVC	A. Schulman, Inc.
Polyviol	Poly(vinyl alcohol), PVAl	Wacker-Chemie
Poticon	PA-66, POM, PBT, PA-6 with potassium titanate	Biddle Sawyer Corp.
PP-C1CC	Polypropylene with calcium carbonate, PP	Reichhold Chem., Inc.
PP-C2TF	Polypropylene with talc, PP	Reichhold Chem., Inc.
PP-G2MF	Polypropylene with mica, PP	Reichhold Chem., Inc.
PP-HFG	Polypropylene with glass fiber, PP	Reichhold Chem., Inc.
PPO	Poly(2,6-dimethyl-phenyl ether), PPE	GE Plastics
Prester	Polyester polyurethanes, TPU	SPRA Neste Polyesters
Prevail	TPU/ABS alloys	Dow Plastics
Prevex	PPE alloys	GE Plastics
Prevex P2A, V3A	PA/PPE-copolymer blends with glass fiber	GE Plastics
Prevex PMA, PQA	PPE-copolymer-based blends with HIPS	GE Plastics
Prevex *S33*	Polyamide/PPE-copolymer alloys	GE Plastics
Primacor	EAA copolymer, EEA-type adhesives	Dow Chem. Co.
Primef	Poly(phenylene sulfide), PPS, with GF, CF, or mineral fillers	Solvay & Cie SA
Primex	Poly(vinyl chloride), PVC	Primex
PRL-ABS	ABS; glass filled or not	Polymer Resources
PRL-Acetal	Acetal; glass filled or not, POM	Polymer Resources
PRL-Nylon	Polyamide-6 or polyamide-66; glass filled or not, PA	Polymer Resources
PRL-PC	Polycarbonate; glass filled or not, PC	Polymer Resources
PRM	Polymer reflective material; PC/acrylic multilayer metallic-like sheets	Dow Plastics
Pro-Fax	PP homopolymers, copolymers with ethylene and PP/EPR blends	Himont Canada
Pro-Seal	Epoxy resins, EP	Prod. Res.& Chem.
Procom	Polypropylene, PP, PP/PA semi-IPNs	ICI Materials – Plast.
Procond-H	Polypropylene, PP	United Composites
Profil	Polypropylene + $CaCO_3$, talc, mica, carbon, etc.	Wilson-Fiberfil
Profil	Polypropylene with glass or carbon fiber, PP	Akzo/DSM
Proloy	ABS/polycarbonate alloys	GE Plastics
Propafilm	Oriented PP film, OPP	ICI Films
Propak	Polypropylene	PolyPacific
Propathene	Polypropylene, PP, toughened PP/EPR blends	ICI Materials – Plast.
Propathene PP	Polypropylene, PP	ICI Materials – Plast.
Propiofan	Polyvinylpropionate	BASF Plastics
PS 50	Polystyrene, PS	Huntsman Chem.

(*continued*)

PSF	Styrene-acrylonitrile copolymer with glass, SAN	Polyfil, Inc.
PU-21713	Polypropylene, PP, rubber modified alloy	Ferro-Eurostar
PUGL	Polyurethane with glass fiber, TPU	Polymer Composites
Pulse	Polycarbonate/ABS, PC/ABS (30 %) alloy	Sumitomo Dow Ltd.
PVC-Semicon	Conductive PVC	ABB Polymer Comp.
PVC360	Poly(vinyl chloride), PVC	Exxon Chem.
PXM	Polyetherketone	Amoco
Pyralin	Polyimide; laminates and electronics coating, PI	E. I. du Pont de Nemours
Pyratex	Elastomers	Bayer
Pyre-ML	Polyimide, PI; wire enamel	E. I. du Pont de Nemours
Pyrotex	Phenolic resins with asbestos	Raymark Indust. Div.
Q		
Q 2	PA from 1,4-bis-aminomethylcyclohexane and suberic acid	Eastman/USA
Q-TEL	Encapsulating EP or PU resins	Chemque
QuaCorr Resin	Thermoset furan resins with glass fiber	QC Chem., Inc
Quatrex	Electronic grade epoxy resins, EP	Dow Chem. Co.
Quiana	Polyamide fiber from trans, trans diamino-dicyclohexylmethane and dodecanedioic acid	E. I. du Pont de Nemours
Quimcel	Cellulose nitrate, CN	Punda Inc.
Quirvil	Poly(vinyl chloride), PVC	Rumianca SpA
R		
R-570	Acrylic resins	Richardson Polymer
R-9900	Polycarbonate, PC	Thermofil, Inc.
R-xyAF	Polycarbonate with xy wt% aluminum, PC	Thermofil, Inc.
R-xyFG	Polycarbonate with xy wt% glass fiber, PC	Thermofil, Inc.
R-xyMF	Polycarbonate with xy wt% mineral, PC	Thermofil, Inc.
R-xyNF	Polycarbonate with xy wt% graphite fiber, PC	Thermofil, Inc.
R2-9900	Polycarbonate, PC/PBT alloy	Thermofil, Inc.
R2-xyFG	Polycarbonate with xy wt% glass fiber, PC	Thermofil, Inc.
R2-xyNF	Polycarbonate with xy wt% graphite fiber, PC	Thermofil, Inc.
R4-9900	Polycarbonate, PC/SMA alloy	Thermofil, Inc.
R9-2039	Epoxy resins, EP	Dexter Corp.
RA-059	Polyolefin, PO	Himont, Inc.
Radel A	Polyarylethersulfone, PAES, $[-\phi-O-\phi-SO_2-\phi-\phi-SO_2-]$	Amoco Performance Products
Radel AG	Polyarylsulfone; filled, PAS	Amoco Performance Products
Radel R	Polyphenylsulfone, PSU	Amoco Performance Products
Radlite	Glass fiber-reinforced PC/PBT blends	Azdel Inc.
Raplan	Elastomers	Polymix
Ravemul	Poly(vinyl acetate), PVAc	Enimont
Ravikral	Acrylonitrile-butadiene-styrene terpolymer, ABS	EniChem

Ravinil	Poly(vinyl chloride), PVC, suspension polymers	European Vinyls Corp.
RBC 2000	Epoxy resins, EP; filled or not	RBC Ind.
RDZ	Acrylics/PC opaque blends	Cyro Industries
RE2038/9	Epoxy resins, EP	Dexter Corp.
Reapox	Epoxy resins, EP	Rea Industrie
Regulus	Thermoplastic polyimides; thermoformable film	Mitsui Toatsu Chem., Inc.
Reichhold TPR	Thermoplastic elastomers: PO/EPDM blend	Reichhold Chem., Inc.
Ren RP-1774	Epoxy resins, EP; filled or not	Dexter Corp.
Ren-Flex	Thermoplastic elastomers, TPO, PP/EPDM	Dexter Corp.
Ren-Flex-726	Polyolefins, PO	Dexter Corp.
Renalal	Acetal copolymer, POM	Hoechst Celanese Corp.
Reny	Polyamides, PA-66	Mitsubishi
Replay	Polystyrene	Huntsman
Repolem, Ecocryl	Acrylic and vinylic emulsions	Elf Atochem
Reprean	Ethylene copolymers	Discas
Resarit	Poly(methyl methacrylate), PMMA powder	Resart-IHM AG
Resartglas	Poly(methyl methacrylate), PMMA sheets	Resart-IHM AG
Resiglas	Unsaturated polyester with glass fiber, UP	Kristal Kraft, Inc.
Resin 18	Poly-alpha-methylstyrene	Amoco Chem. Co.
Resin PVC	Poly(vinyl chloride), PVC	Georgia Gulf
Resin S, trans, etc.	Epoxy resins, EP; filled or not	Furane Products
Resinmec	Polyamides, polypropylene	Amoco Chem. Co.
Resinol Type A, F, etc.	Polyethylenes, PE	Allied Resinous
Resolite	Urea-formaldehyde, UF	Ciba-Geigy, GB
Restirolo	Polystyrene, PS	Societa Italiana Resine
Retain	Polyethylene/polystyrene-based recycled blends	Dow Plastics
Revinex	Carboxylated rubber	Doverstrand
Rex Flex-D	Thermoplastic elastomers; filled or not, TPO	Dexter Corp.
Rexene PE	Polyethylenes, PE	Rexene/El Paso Prod.
Rexene PP	Polypropylenes, PP	Rexene/El Paso Prod.
Rexflex	Polypropylene	Rexene
Rhodester	Cellulose acetate, CA	Rhône-Poulenc
Rhodia	Cellulose-2.5 acetate, CA	Soc. Rhodiaceta, France
Rhodiaceta-nylon	Polyamide-6,6, PA-66	Soc. Rhodiaceta, France
Rhodopas	Styrene-butadiene copolymer, SBR	Rhône-Poulenc
Rhodorsil	Silicones	Rhône-Poulenc
Rhodoviol	Poly(vinyl alcohol), PVAl	Rhône-Poulenc
Rhovyl	Poly(vinyl chloride), PVC	Soc. Rhodiaceta, France

(*continued*)

Riblene	Ethylene-vinyl acetate copolymers, EVA	ECP EniChem Polymeri
Riblene	Polyethylenes: LDPE, LLDPE, and VLLDPE	ECP EniChem Polymeri
Rigidex	High-density polyethylene, HDPE	BP Chemicals Limited
Rigidite	Carbon, aramid, glass fiber filled	BASF PLASTICS
Rigipore	Expandable polystyrene, PS	BP Chemicals Limited
Rigolac	Polyester resins	Showa Highpolymer
Rilsan A	Polyamide-12, PA-12, or blends with PEBA	Elf Atochem
Rilsan AVR	Polyamide-11 with $T_m = 175\ °C$ (rotomolding)	Elf Atochem
Rilsan B	Polyamide-11, PA-11	Elf Atochem
Rilsan ESY	Polyamide-11 for electrostatic spraying	Elf Atochem
Rilsan	Polyamide-11, polyamide-12, PA-6.6/PEBA	Elf Atochem
Rimplast	PA-6,6 or PA-12/silicone, reinforced or not	LNP Corp./Petrarch Sys.
Rimplast	Polyurethane/silicone IPN, reinforced or not	LNP Corp./Petrarch Sys.
Rimplast PTUE	Silicone-modified TPU, aromatic ether	Hüls AG
Risilan AZM	Polyamide-12 with glass/graphite fibers, PA-12	Elf Atochem
Risilan BZM	Polyamide-11 with glass/graphite fibers, PA-11	Elf Atochem
Riston	Photopolymer film resistant	E. I. du Pont de Nemours
Riteflex	Thermoplastic elastomer and blends	Hoechst Celanese Corp.
Riteflex BP	Poly(butylene terephthalate), PBT, alloys with a thermoplastic elastomer	Hoechst Celanese Corp.
RNYxy	Polyamide-6 with xy wt% glass fiber, PA-6	Ferro Corp.
Robetanche	Polyurethanes, PU	Robbe
Robfill/Robflex	Polyurethanes, PU	Robbe
Robinsectisol	Polyurethanes, PU	Robbe
Rocalene	Reinforced polypropylene, PP	R.M.P.
Rodran	Liquid crystal polyester, LCP	Unitika
Rogers HT	Phenolics with glass fiber	Rogers Corp.
Rogers RX 1	Diallyl phthalate with filler, DAP	Rogers Corp.
Rogers RX 300	Phenolics; filled with glass, wood, mineral, etc.	Rogers Corp.
Ronfalin	Acrylonitrile-butadiene-styrene copolymer, ABS	DSM
Ronfalin	Acrylonitrile-butadiene-styrene/polycarbonate	DSM
Ronfaloy E	Acrylonitrile-butadiene-styrene/EPDM alloy	DSM
Ronfaloy P	Acrylonitrile-butadiene-styrene/PET alloy	DSM
Ronfaloy V	Acrylonitrile-butadiene-styrene/Poly(vinyl chloride)	DSM
Ropet	Poly(ethylene terephthalate), PET/PMMA alloys	Rohm and Haas
Rosite 3250 BMC	Unsaturated polyester with glass fiber, UP	Rostone Corp.
Roskydal	UP lacquer resins	Bayer AG/Miles
Roto Flame	Polyethylene, PE	Rototron Corp.
Rotothene R-	Polyethylenes; filled or not, PE	Rototron Corp.

Rotothon XP-I	Polypropylene, PP for rotational molding	Rototron Corp
Rovel 747	Polycarbonate, PC/AES blends	Dow Chem. Co.
Rovel	Styrene-acrylonitrile copolymer, SAN, blended with saturated olefinic elastomer, EPR	Dow Chem. Co.
Royalcast	Elastomers	Safic-Alcan
Royalcast	Polyurethanes, thermoset (TS)	Uniroyal Chemical
Royalene	EPDM for modification of HDPE	Uniroyal Chemical
Royalene	Polyethylene, PE, or polypropylene, PP	US-Rubber, USA
Royalite	Acrylonitrile-butadiene-styrene terpolymers, ABS	Uniroyal Chemical
Royalite	Poly(vinyl chloride)/PMMA alloys	Uniroyal Chemical
Royalite R 11	Polycarbonate/ABS alloys	Uniroyal Chemical
Royaltherm	EPDM modified with silicone	Uniroyal Chemical
Royaltuf 372	EPDM grafted with SAN	Uniroyal Chemical
Royaltuf 465	EPDM functionalized with maleic anhydride	Uniroyal Chemical
Royaltuf	Modified EPDM	Uniroyal Chemical
Royaltuf XN6G	EPDM grafted with polyamide-6	Uniroyal Chemical
Roylar A-863	Polyether-polyurethenes, PU	Uniroyal Chemical
RPC-440	Acrylic, PMMA	Richardson Polymer
RPI 504 EP	Polycarbonate-based alloys	Research Polymers Intl.
RPI 507 EP	Polypropylene/EPDM-type TPO blends	Dexter Corp.
RPI 602 EP	Polyamide-66-based alloys	Research Polymers Intl.
RPI	Polyolefin, PO/EPDM blends	Dexter Corp.
RPPxy	Polypropylene with xy wt% glass fiber, PP	Ferro Corp.
RPS	Polystyrene, PS-reactive	Dow Chem. Co.
RT 700	Cellulose (Viscose)	Glanzstoff, Germany
RT/duroid	Polytetrafluoroethylene with glass fiber, PTFE	Rogers Corp.
RTA-Polymer	Rigid TP alloys	Republic Plast. Co.
RTD	Impact-modified acrylics	Cyro Industries
RTP 200 TFE	Polyamide-66/PTFE/PDMS; filled or not	RTP Co.
RTP 200C	Polyamide-11/PTFE (20 %); filled or not	RTP Co.
RTP 200D	Polyamide-612/PTFE ($\leq$ 20 %); filled or not	RTP Co.
RTP 200H	Polyamide/PTFE ($\leq$ 20 %); filled or not	RTP Co.
RTP 300 TFE	Polycarbonate/PTFE/PDMS; filled or not	RTP Co.
RTP 600	ABS/PTFE or PDMS; filled or not	RTP Co.
RTP 800	POM/PTFE or PDMS; filled or not	RTP Co.
RTP 900	PSF/PTFE (15 %); filled or not	RTP Co.
RTP 1000	PBT/PTFE(15 %); filled or not	RTP Co.
RTP 1300	PPS/PTFE ($\leq$ 20 %); filled or not	RTP Co.
RTP ESD	Polyarylsulfone with glass fiber	RTP Co.
RTP PWB	Polyarylsulfone with glass fiber	RTP Co.
Rucon	Poly(vinyl chloride), PVC	Hooker
Rucothane	TPU, polyurethane thermoplastic elastomers	Hooker Chem. Corp.

Rulan	Polyethylene with filler, PE	E. I. du Pont de Nemours
Rumiten	Polyethylenes, PE	Rumianca SpA
Runite SST	Poly(ethylene terephthalate) + 35 wt% glass, PET	E. I. du Pont de Nemours
Rütaform	Aminoplasts: MF, MPF, melamine-polyester, etc.	Hoechst Celanese Corp.
Rutapal	Polyester resins, UP	Bakelite GmbH
Rutaphen	Phenol-formaldehyde, resorcinol-formaldehyde	Bakelite GmbH
Rutapox	Epoxy resins, EP	Bakelite GmbH
Rutapur	Polyurethane resins, PU	Bakelite GmbH
RX	Acrylonitrile-butadiene-styrene copolymer, ABS	Resin Exchange
RX ENG. TS	Phenolic and diallyl phthalate molding materials	Rogers Corp
RX	Poly(phenylene sulfide), PPS/PTFE blend	Intl. Polym. Corp.
RxLoy	Polyolefin alloys for medical applications	Ferro Corp.
Rylon	Polyphenylene sulfide, PPS	Phillips Petrol. Co.
Rylon PPS	Polyphenylene sulfide, PPS	Phillips Petrol. Co.
Rynite PBT	Poly(butylene terephthalate)/elastomer alloys with up to 30 wt% glass fibers	E. I. du Pont de Nemours
Rynite	PBT or PET/elastomer with up to 35 wt% mica and glass fibers	E. I. du Pont de Nemours
Rynite SST	Poly(ethylene terephthalate)/elastomer alloys	E. I. du Pont de Nemours
Ryton	Poly(*p*-phenylene sulfide); filled or not, PPS	Phillips Petrol. Co.
Ryulex C	Polycarbonate/acrylonitrile-butadiene-styrene	Dainippon Ink & Chem.
S		
S-660	Unsaturated polyester with glass fiber, UP	ICI/Fiberite
S-xyFG	Polysulfone with xy wt% glass fiber, PSU	Thermofil, Inc.
S-xyMF	Polysulfone with xy wt% mineral, PSU	Thermofil, Inc.
S-xyNF	Polysulfone with xy wt% graphite fiber, PSU	Thermofil, Inc.
Sabre	Polycarbonate, PC, alloys with PET or PBT	Dow Chem. Co.
Sadisol	Polyurethanes, polyols, isocyanates	Robbe
Saflex	Polyvinylacetal, PVAc	Monsanto, USA
Sanrex	Styrene-acrylonitrile copolymer, SAN	Mitsubishi Monsanto
Santoprene	Polypropylene/EPDM or EPM, dynamically vulcanized thermoplastic elastomers, TPO	Monsanto Chem. Co.
Sapedur	Poly(vinyl chloride) compounds, PVC	Saplast
Saran	PVDC with at least 80 % vinylidene chloride	(generic name)
Saran	PVDC with at least 80 % vinylidene chloride	Dow Chem. Co.
Saranex	Poly(vinylidene chloride), PVDC, and PVDC/PO	Dow Chem. Co.
Sarlink 1000	TPE; oil-resistant PP/PB blends	DSM; Novacor
Sarlink 2000	TPE; low permeability PP/BR blends	DSM; Novacor
Sarlink 3000	TPE; multipurpose PP/EPDM	DSM; Novacor
Sarlink TPE	Thermoplastic elastomers, TPE	DSM; Novacor
Sarnylene	Poly(vinyl chloride) compounds, PVC	Plastic Auvergne

Sarnymousse	Poly(vinyl chloride) compounds, PVC	Plastic Auvergne
Satellite	HDPE blown film system	Filmaster Inc.
Satinflex	Poly(vinyl chloride) super elastomers, PVC	Alpha Chem. & Plastics
Scarab	Urea-formaldehyde, UF, molding powders	BIP Chemicals Ltd.
Schulamid GB	Polyamide-6 with glass beads, PA-6	A. Schulman, Inc.
Schulamid GF	Polyamide-6 or polyamide-66 with glass fibers, PA-6 or PA-66	A. Schulman, Inc.
Schulamid MF	Polyamide-66 with mineral, PA-66	A. Schulman, Inc.
Schulamid MWG	Polyamide-6 with glass fiber/mineral, PA-6	A. Schulman, Inc.
Schulman 9HD	Polyethylene resins, PE	A. Schulman, Inc.
Schulman 9PE	Polyethylene resins, PE	A. Schulman, Inc.
Schulman ABS	Acrylonitrile-butadiene-styrene copolymer, ABS	A. Schulman, Inc.
Schulman CP	Polyethylene resins, PE	A. Schulman, Inc.
Sclair	Polyethylene resins, PE	Du Pont Canada
Sclar	Polyamide/polyolefin, PA/PO, blends	Du Pont Canada
Scolefin	High-density polyethylene, HDPE	Buna AG
Sconapor	Polystyrene foam, EPS	Buna AG
Sconatex	Acrylonitrile-butadiene-styrene copolymer, ABS	Buna AG
Scopyrol	Polystyrene, PS	Buna AG
Scotch-Grip	Adhesives	3M Canada Inc
Scotchcast	Epoxy resins, EP	3M, USA
Scotchcote	Epoxy resin, EP	3M Canada Inc
Scotchpak	Polyester film	3M Canada Inc
Scovinat	Poly(vinyl acetate), PVAc	Buna AG
Scovinyl	Poly(vinyl chloride), PVC	Buna AG
Scuranate	Polyurethanes, isocyanates	Rhône-Poulenc
SEBS-Compound	Thermoplastic elastomer, TPE	ABB Polymer Comp.
SEBS-Semicon	Conductive TPE	ABB Polymer Comp.
Selar Barrier Resin	Polyamide blend	E. I. du Pont de Nemours
Selar OH	EVAl resins for oxygen barrier film (blend)	E. I. du Pont de Nemours
Selar PA	Amorphous PA for oxygen barrier film (blend)	E. I. du Pont de Nemours
Selar PT	Polyester resins for barrier films (blend)	E. I. du Pont de Nemours
Selar PT	Polyethylene terephthalate blend, PET, (blend)	E. I. du Pont de Nemours
Selar RB	PA/HDPE concentrates for O_2 barrier PO films	E. I. du Pont de Nemours
SFP	Polystyrene, PS	Huntsman Chem.
Shell DP	Polyisobutylene resins, PIB	Shell Chim.
Shell	PP, PS, PVC resins	Shell Chim.
Shinko-Lac G	Poly(butylene terephthalate); filled or not, PBT	Mitsubishi Rayon Co.
Shinko-Lac GH	Acrylonitrile-butadiene-styrene copolymer, ABS	Mitsubishi Rayon Co.

(*continued*)

Shinkolite A	Acrylic sheets, PMMA	Mitsubishi Rayon Co.
Sholex	Polyethylene	Showa Denko K. K.
Shore	Polyester elastomers, TPE	E. I. du Pont de Nemours
Shuman 500	Polypropylene, PP	Philip Shuman & Sons
Shuman 700	Acrylonitrile-butadiene-styrene copolymers, ABS	Philip Shuman & Sons
Shuman 780	Poly(vinyl chloride)/ABS alloy, PVC/ABS	Philip Shuman & Sons
Shuman 800	Polystyrene, PS	Philip Shuman & Sons
Shuman 900	Polycarbonate, PC	Philip Shuman & Sons
Shuman 6000	Polyethylene, PE	Philip Shuman & Sons
Shuman SP	Poly(phenylene ether), PPE alloy	Philip Shuman & Sons
Shutane	Poly(vinyl chloride)/TPU alloy	Reichhold Chem., Inc.
Shuvinite	Poly(vinyl chloride)/ABS alloy	Reichhold Chem., Inc.
Sicalit	Cellulose acetate, CA	Sic Plastics
Sicoflex	Acrylonitrile-butadiene-styrene copolymers, ABS	Sic Plastics
Sicol	Plastisols, PVC	Enimont
Sicostrol	Polystyrene; reinforced or not, PS	Sic Plastics
Sicron	Poly(vinyl chloride) compositions, PVC	European Vinyls/ Montedison
Silastic	Silicones	Dow Chem. Co.
Silastomer	Silicones	Dow Chem. Co.
Silflex	Silicone, TS	Furane Products
Silixol	Silicones, MQ	Convert
Silmar	Unsaturated polyesters, UP	Silmar
Silopren	Silicone rubber, MQ	Bayer AG/Miles
Siltem	Siloxane-etherimide copolymers and blends	GE Plastics
Sinkral	Acrylonitrile-butadiene-styrene copolymers, ABS	ECP Enimont Polym./ EniChem
Sinvet	Polycarbonate, PC	Anic; ECP EniChem Polymeri
Sirester	Polyester resins	SIR France
Sirester	Polyester resins	SIR France
Sirfen	Phenol-formaldehyde resins, PF	SIR France
Sirit	Urea-formaldehyde resins, UF	SIR France
Siritle	Urea-formaldehyde resins, UF	SIR France
Sirotherm	Ampholytic polyelectrolyte	ICI
Sirtene	Polyethylene, PE	Societa Italiana Resine
SKS	Copolymers from butadiene	USSR
Skybond 700	Polyimides; laminating varnish, PI	Monsanto
Skygreen	Biodegradable polyethylene succinate/adipate for injection or extrusion	Sukyong Industries
Skyprene	CR elastomers	Tosoh, Harcros Chemicals
SMA	Styrene maleic anhydride, SMA	Elf Atochem
Snevyl	Poly(vinyl chloride) compositions, PVC	Sebuca

Snialene	Polypropylene, PP	SNIA Tecnopolimeri SpA
Snialoy AP06	Polyamide-66 with PP toughened blends	Nylon Corp. of America
Snialoy BP06	Polyamide-6 with PP toughened blends	Nylon Corp. of America
Sniamid	Polyamide-6, polyamide-66, PA-6, PA-66	SNIA Tecnopolimeri SpA
Sniater	Poly(butylene terephthalate), PBT	SNIA Tecnopolimeri SpA
Snissan	Acrylonitrile-butadiene-styrene copolymer, ABS	SNIA Tecnopolimeri SpA
Snlatal	Polyoxymethylene (acetal), POM	SNIA Tecnopolimeri SpA
Soablen/Soarlex	Ethylene-vinyl acetate copolymer, EVAc	Nippon Synthetic
Soarnol	EVA copolymer	Nichimen
Soarnol EVOH SF	Ethylene-vinyl alcohol, EVAl	Elf Atochem
Soetene	Low-density polyethylene, LDPE	Sogo
Sokalan CP2	Polyelectrolyte	BASF
Sol T	SBS and SIS block copolymers	Enarco Elastomers Co.
Solef 1000	Poly(vinylidene fluoride), PVDF	Solvay & Cie SA
Solef 8800	Poly(vinylidene fluoride), PVDF, with filler	Soltex/Solvay & Cie SA
Solimide	Polyimide foam, PI	Ethyl Corp
Solprene	Branched $(SB)_n$ or $(SI)_n$ block copolymers	Phillips Petrol.
Solucryl	Acrylates and methacrylates	UCB Soc.
Solvic	Poly(vinyl chloride), PVC	Solvay & Cie SA
Somel	TPO thermoplastic elastomer, PP/EPDM	Colonial
Soreflon	Polytetrafluoroethylene, PTFE	Rhône-Poulenc
Sowpren	Polychloroprene, CR	USSR
Spandex	Elastic PU fibers	(generic name)
Spanzelle	Spandex fiber	Courtaulds
Specflex	PU elastomer	Dow Chem. Co.
Spectra	UHMWPE gel-spun fibers	AlliedSignal Inc.
Spectrim HF	Thermoplastic polyurea	Dow Chem. Co.
Spectrim HF-80	Thermoplastic polyurethane, TPU	Dow Chem. Co.
Spectrim HT	Thermoplastic polyurea	Dow Chem. Co.
Spectrim RD	Polyurethane; filled or not, TPU	Dow Chem. Co.
SPX	PP/EPR elastomer	Mitsubishi
SRIM	Polyurethane, PU	Mobay Corp.
ST-801	Polyamide elastomer blends	DuPont
ST-Nylon	Polyamide/ionomer(?) blends	Toray
Stabar	PES and PEEK films	ICI Films
Stadlite	Phenol-formaldehyde resin, PF	Hitachi
Staloy N	Acrylonitrile-butadiene-styrene/PA alloys	DSM Polymer Int.
Stamylan HD or LD	High or low-density polyethylene, PE	DSM Polymer Int.

(*continued*)

Stamylan LD	Low-density polyethylene, LDPE	DSM Polymer Int.
Stamylan P	Polypropylene, PP	DSM Polymer Int.
Stamylex	Linear low-density polyethylene, LLDPE	DSM Polymer Int.
Stamyroid	Modified amorphous polypropylene, PP	DSM Polymer Int.
Stanuloy ST	Poly(ethylene terephthalate), PET, modified or blended with polycarbonate	MRC Polymers, Inc.
Stanyl	Polyamide-4,6 and its blends, PA-46	DSM Polymer Int.
Stapron	Rubber-modified SMA polymers	DSM Polymer Int.
Stapron C	Polycarbonate/acrylonitrile-butadiene-styrene	DSM Polymer Int.
Stapron E	Polycarbonate/PET or PBT with PB as impact-modifier; for interior automobile door panels	DSM Polymer Int.
Stapron N	Polyamide-6, PA-6, alloys with ABS with impact-modified PA-phase	DSM Polymer Int.
Stapron S	Rubber modified amorphous SMA with glass fiber reinforcements or not	DSM Polymer Int.
Star	Reinforced thermoplastic resins, e.g., ABS, SAN	Ferro-Eurostar
Star X	PA-6,PA-46, or PA-66 with an impact modifier, glass fiber reinforced or not	Ferro-Eurostar
Staramide-Glass	Glass fiber-filled polyamide-6, PA-6	Ferro Corp.
Staramide-Mineral	Mineral-filled polyamide-6, PA-6	Ferro Corp.
Starcoat	Gel-coat	Chanet Paints
Starflam ABS	ABS blend, flame retarded, glass reinforced or not	Ferro-Eurostar
Starflam PA6; PA66	PA-6 or PA-66/brominated polystyrene, impact modified, glass or mineral reinforced or not	Ferro-Eurostar
Starflam PBT	PBT blend, flame retarded, glass reinforced	Ferro-Eurostar
Starglas ABS	Acrylonitrile-butadiene-styrene with glass fiber	Ferro Corp.
Starglas PBT	Glass fiber filled poly(butylene terephthalate), PBT	Ferro Corp.
Starglas PC	Glass fiber filled polycarbonate, PC	Ferro Corp.
Starglas PE	Glass fiber filled HDPE	Ferro Corp.
Starglas POM	Reinforced polyoxymethylene, POM	Ferro Corp.
Starglas PSU	Glass fiber-filled polysulfone, PSU	Ferro Corp.
Starglas SAN	Reinforced SAN	Ferro Corp.
Starpylen	Glass fiber-filled thermoplastic resins	Ferro-Eurostar
Stat-Kon M	PP with electrostatic discharge	LNP Eng. Plastics
Statcon	Electrostatic dissipative materials	LNP
Stereon	Triblock SBS thermoplastic elastomer	Firestone Co.
Stilon	Acrylonitrile-butadiene-styrene/polycarbonate	USSR
Strathox	Epoxy resins, EP	Technibat
Stratyl	Unsaturated polyester, UP	Péchiney, France
Stycast	Epoxy; filled or not, EP	Emerson & Cuming
Stycone	Polystyrene, PS alloys	United Compos.
Sterpon	Polyester resins, UP	Convert
Stypol	Unsaturated polyesters; filled or not, UP	Freeman Chem. Corp.
Styrafil	Polystyrene with fillers, PS	Akzo/DSM
Styroblend	Polystyrene, PS, blends with PE or PB	BASF Plastics
Styrocell	Expandable polystyrene, EPS	Shell Chem.

Styrodur	Extruded rigid polystyrene, PS	BASF Plastics
Styroflex	PS fiber	Ndd. Seekabelwerke
Styrofoam	Polystyrene, PS plastic foam	Dow Chem. Co.
Styrol	Polystyrene, PS	Idemitsu
Styrolux	Styrene-butadiene copolymer, SBR	BASF Plastics
Styron	Polystyrene, PS, and impact-modified PS, HIPS	Dow Chem. Co.
Styroplus	Polystyrene, PS, blends with polybutadiene, PB	BASF Plastics
Styropol	Styrene-butadiene copolymer, SBR	Carl Gordon Ind.
Styropor	Expandable polystyrene, EPS	BASF Plastics
Styruvex	Styrene-acrylonitrile copolymer, SAN	Coplex
Sulfil G	Polysulfone with long glass fibers, PSU	Akzo/DSM
Sulfil J-1100	Polyethersulfone with glass fibers, PES	Akzo/DSM
Sulfil J-1300	Poly(phenylene sulfide) with fillers, PPS	Akzo/DSM
Sulfil J-1800	PET or PBT with glass fibers	Akzo/DSM
Sumigraft	Poly(vinyl chloride), PVC	Sumitomo Chem. Co.
Sumikathene	Polyethylenes, PE	Sumitomo Chem. Co.
Sumikon	Epoxy resins	Sumitomo Bakelite
Sumilit SX	Poly(vinyl chloride), PVC	Sumitomo Chem. Co.
Sumipex	Acrylic resins, PMMA	Sumitomo Chem. Co.
Sumiploy	PES, PES/PEEK-modified blends	Sumitomo Chem. Co.
Sunloid	Acrylonitrile-butadiene-styrene terpolymers, ABS	Tsutsunaka Plastics
Sunloid KD	Poly(vinyl chloride)/PMMA alloy	Tsutsunaka Plastics
Sunloid New Ace	Poly(vinyl chloride) sheets, PVC	Tsutsunaka Plastics
Sunloid PC	Polycarbonate, PC sheet, films	Tsutsunaka Plastics
Sunprene	Poly(vinyl chloride)-based elastomers, PVC/elastomer	Mitsubishi Kasei/A. Schulman
Suntec	Polyethylene	Asahi Chemical Co.
Suntra	Poly(phenylene sulfide), PPS resin	Sunk Yong
Supec	Poly(phenylene sulfide) and blends with PEI, PPE	GE Plastics/Toso Susteel
Supec CTX530	Poly(phenylene sulfide)/PEI blends with 30 % GF	GE Plastics
Supec CTX540	Poly(phenylene sulfide)/PEI blends with 40 % GF	GE Plastics
Superec P	Acrylonitrile-butadiene-styrene/polycarbonate	Mitsubishi-Monsanto
Supec W331	Poly(phenylene sulfide)/PTFE blends with 30 % GF	GE Plastics
Superohm	Ethylene-propylene copolymer, EPR	A. Schulman, Inc.
Supralen	Polyethylenes, PE (pipes)	Mannesmann, Germany
Supraplast	Thermoset resins: resorcinol-formaldehyde, etc.	O.F.A.C.I.
Suprel	Styrene-acrylonitrile grafted on PVC, SAN or ABS/PVC alloys	Vista Chemical Co.
Suprel SVA	Poly(vinyl chloride)/α-methyl styrene-ABS	Vista Chemical Co.
Surlyn	Ionomer resins	E. I. du Pont de Nemours
Surlyn 7930	Lithium grade ionomer resin	E. I. du Pont de Nemours

(*continued*)

Surlyn 8020	Sodium grade ionomer resin	E. I. du Pont de Nemours
Surlyn 9020	Zink grade ionomer resin	E. I. du Pont de Nemours
Surlyn A	Ionomer, ethylene-acrylic acid copolymer	E. I. du Pont de Nemours
Susteel	Poly(phenylene sulfide), PPS	Toso Susteel
SVM	Aromatic polyamides	USSR
Sylon FX	Fluoropolymer, thermoset (TS)	3M Ind. Chem.
Syn-Flex	Polyolefin compounds, PO	Synergistics Ind
Synergy	Polyamide-6/PPE blends	Allied-Signal Inc.
Synolite	Unsaturated polyester resin, UP	DSM Plastics
Synprene	Thermoplastic rubber compounds, TPE	Synergistics Ind
Synres	Specialty olefins, PO	Quality Service Technology
Syntewax	Acrylonitrile-butadiene-styrene terpolymer, ABS	Comiel SpA
Synthetic ABS	Polypropylene with calcium carbonate, PP	Reichhold Chem., Inc.
Syspur/Systanat	Polyurethane, PU	Soprochim
Systemer S	Polypropylene/polyamides, reinforced or not	Showa Denko K. K.
Systol	Polyurethane, PU	Soprochim
T		
T-xyCF	Polyphenylene sulfide, PPS + xy% graphite fiber	Thermofil, Inc.
T-xyCG	Polyphenylene sulfide with xy% carbon/glass	Thermofil, Inc.
T-xyFG	Polyphenylene sulfide with xy wt% glass fiber	Thermofil, Inc.
T-xyNF	Polyphenylene sulfide with xy wt% graphite fiber	Thermofil, Inc.
T-xyNG	Polyphenylene sulfide with xy% glass/graphite	Thermofil, Inc.
Tactix	High performance EP elastomeric resins	Dow Chem. Co.
Taffen	Thermoplastic composites	Exxon Chem.
Taflite	Polystyrene, PS-g-EPDM blends	Mitsui Toatsu
Tafmer	Metallocene-made linear low-density polyolefin with strictly controlled comonomer placement	Mitsui Petrochemicals
Tafmer A	Metallocene-made linear low-density polyolefin with 1 % acidic groups, used for compatibilization	Mitsui Petrochemicals
Taitalac	Acrylonitrile-butadiene-styrene terpolymer, ABS	Taita Chem. Co.
Taktene	Butadiene rubber, BR; based on co-catalyst	Polysar/Bayer AG
Tallerand	Poly(vinyl chloride), PVC	Tallerand Chem.
Tamcin PP	Polypropylene, PP	Reichhold Chem., Inc.
TAP-MR	Polyisocyanate thermoplastics	Urylon Development
Tarpee	Polyethylene laminated sheet, PE	Hagihara Industries Inc.
TDI	Polyurethane, PU	Dow
TE-1004	Epoxy with metallic fillers, EP	Dexter Corp.
Techniace TA	Polyamide/ABS alloys	Sumitomo Dow, Ltd.
Techniace TB	Poly(butylene terephthalate)/ABS alloys	Sumitomo Dow, Ltd.

Techniace TC	ABS/polycarbonate alloys, T-series = heat and impact resistant, H-series = high heat and impact resistant, W-series = weather and impact resistant, F-series = flame and impact resistant	Sumitomo Dow, Ltd.
Techniace TU	Thermoplastic polyurethane/ABS alloys	Sumitomo Dow, Ltd.
Technora	Poly(p-phenylene diphenylether terephthalamide)	Teijin Ltd.
Technyl A	Polyamide-66/elastomer, with filler or not, PA-66	Rhône Poulenc
Technyl B	Polyamide-66, 6/elastomer, with filler or not	Rhône Poulenc
Technyl C	Polyamide-6/elastomer, with filler or not	Rhône Poulenc
Technyl D	Polyamide-610/elastomer, with filler or not	Rhône Poulenc
Technyl	Polyamide-6, polyamide-66, polyamide-610 impact modified, glass fiber or mineral reinforced or not	Rhône Poulenc
Techster	Polyesters: PBT, PET, and blends	Rhône Poulenc
Techster T	Poly(butylene terephthalate), PBT/elastomer blends	Rhône Poulenc
Techtron PPS	Polyphenylene sulfide, PPS rods or plates	Polymer Corp.
Tecnoflon	Fluoroelastomers; PVDF/PHFP blends	Enimont
Tecnoprene	Glass fiber-reinforced polypropylene	Enimont
Tecoflex	Polyurethane, PU	Thermedics, Inc.
Tecolite KM	Phenolic-filled thermosets, PF	Toshiba Chem. Prod.
Tediflex/Tedilast	Polyurethane, PU, formulated systems	ECP Enimont Polymeri
Tedipur	Polyurethane, PU, formulated systems	ECP Enimont Polymeri
Teditherm/Tedirim	Polyurethane, PU, formulated systems	ECP Enimont Polymeri
Tedlar	Polyvinyl fluoride, PVF, film	E. I. du Pont de Nemours
Tedur	Polyphenylene sulfide, PPS, with glass/mineral	Bayer AG/Miles
Tefabloc/Tefaprene	Elastomers	Thermoplastiques C. T.
Tefanyl	Poly(vinyl chloride) compounds, PVC	Thermoplastiques C. T.
Teflon	Fluoropolymers; PTFE, PFA, FEP	E. I. du Pont de Nemours
Teflon FEP	Tetrafluoroethylene-co-hexafluoropropylene, FEP	E. I. du Pont de Nemours
Teflon PFA	Fluorocarbon, perfluoroalkoxy resin, PFA	E. I. du Pont de Nemours
Teflon TFE	Polytetrafluoroethylene, PTFE	E. I. du Pont de Nemours
Tefzel	Modified ethylenetetrafluoroethylene copolymer	E. I. du Pont de Nemours
Teijinconex	Poly(m-phenyleneisophthalamide), PPA	Teijin, Ltd.
Teknor Apex	Poly(vinyl chloride), PVC	Teknor Apex
Telcar	PP/EPDM, TPO elastomeric blends	Teknor Apex
Tempalloy	Polypropylene with fillers, PP	Comalloy Intl. Corp.
Temprene	Poly(vinyl chloride)/nitrile rubber (15–40 phr)	Piltec Group
TempRite	Chlorinated PVC, CPVC	BF Goodrich

(*continued*)

Temprite LC	Poly(vinyl chloride) compounds, PVC	Polyplastic
Tenac	Polyoxymethylene, POM	Asahi Chemical Ind.
Tenite	Polyolefins, cellulosics, CAB	Eastman Chem. Prod.
Tenite 000	Cellulose acetate, CA	Eastman Chem. Prod.
Tenite 200	Cellulose butyrate, CB	Eastman Chem. Prod.
Tenite 300	Cellulose propionate, CP	Eastman Chem. Prod.
Tenite 5000	Polyallomer	Eastman Chem. Prod.
Tenite Acetate	Cellulose acetate, CA	Eastman Chem. Prod.
Tenite Butyrate	Cellulose acetate-butyrate, CAB	Eastman Chem. Prod.
Tenite P7673	Polyallomer	Eastman Chem. Prod.
Tenite Pet	Thermoplastic polyesters, PET	Eastman Chem. Prod.
Tenite Polypropion	Cellulose acetate-propionate, CAP	Eastman Chem. Prod.
Tenite Propionate	Cellulose propionate, CP	Eastman Chem. Prod.
Tenite PTMT	Polytetramethylene terephthalate, PTMT	Eastman Chem. Prod.
Tenite	PVAc, PVB, PVPr	Eastman Chem. Prod.
Tenneco 2710	Polyallomer	Tenneco Polymers
Tenneco	Poly(vinyl chloride)/EVA blends	Tenneco Polymers
Teracol	Polyoxytetramethylene glycol	E. I. du Pont de Nemours
Terathane	Polyether glycol, PEO	E. I. du Pont de Nemours
Terblend B	ABS/polycarbonate, PC, blend	BASF Plastics
Terblend S	ASA/polycarbonate, PC, blend	BASF Plastics
Terblend	Styrene copolymer blends	BASF Plastics
Terital	Poly(ethylene terephthalate), PET	Montefibre, Italy
Teritherm	Polyesterimide, PEI	P. D. GeorgeÉ. Co.
Terlenka	Poly(ethylene terephthalate), PET	AKU, Netherlands
Terluran	ABS blends with acrylic rubber	BASF Plastics
Terluran	Acrylonitrile-butadiene-styrene terpolymers, ABS	BASF Plastics
Terlux	Clear methyl methacrylate-acrylonitrile-butadiene-styrene, MABS	BASF Plastics
Terphane	Polyester film	Rhône Poulenc
Terylene	Poly(ethylene terephthalate), PET	ICI Adv. Mater.
Tetra-Temp PEEK	Polyetheretherketone, PEEK	Tetrafluor, Inc.
Tetrafil J-1800	Poly(ethylene terephthalate) filled, PET	Akzo/DSM
Tetrafluor	Polytetrafluoroethylene, PTFE	Tetrafluor, Inc.
Tetralene UHMW	Polyethylene, PE	Tetrafluor, Inc.
Texalon/Texapol	Polyamide-6; PA-66, with filler or not, PA-6; PA-66	Texapol Corp.
Texicote	Poly(vinyl acetate)	Scott Bader
Texigels	Acrylic polyelectrolyte	Scott Bader
Texin	Polyurethanes	Bayer AG/Miles, Inc.
Texin 3000	Polycarbonate/polyester-PU, PC/TPU alloys	Bayer AG/Miles, Inc.
Texin 4000	Polyester-PU alloys with PC	Bayer AG/Miles, Inc.
Therban/Tornac	Fully or partially hydrogenated nitrile rubber, NR, with AN = 33–43 %	Polysar/Bayer A

<div align="right">(continued)</div>

Therban	Elastomers	Bayer
Thermaflo	Poly(vinyl chloride) footwear compounds, PVC	Evode Plastics Ltd.
Thermaflo	Thiorubber, TR, compound	Evode Plastics Ltd.
Thermalloy	Acrylonitrile-butadiene-styrene, ABS blends	CdF Chimie
Thermid IP-600	Polyimide, PI, structural adhesive	Nat. Starch @ Chem.
Thermocomp	Reinforced engineering polymer compounds with either glass or carbon fibers	LNP Engineering
Thermocomp AF	Acrylonitrile-butadiene-styrene, ABS, with fillers	LNP Corp.
Thermocomp BF	Styrene-acrylonitrile cop., ABS, with fillers	LNP Corp.
Thermocomp DL	Polycarbonate, PC/PTFE 13 %/silicone 2 %	LNP Corp.
Thermocomp PDX	PEEK/PTFE (20 %) alloys	LNP Corp.
Thermocomp RFL	Polyamide-66/silicone 5 % blends	LNP Corp.
Thermocomp RL	Polyamide-66/PTFE 13 %/Rimplast	LNP Corp.
Thermolan 2000	Polypropylene/EPDM blends	Mitsubishi Petrochem.
Thermolan 3000	EPDM/polypropylene blends	Mitsubishi Petrochem.
Thermomanto	Extruded EPS insulation boards	Dow Europe
Thermoset	Epoxy resins with fillers, EP	Thermoset Plastics
Thiokol	Poly(ethylene chloride-*co*-sodium sulfide)	E. I. du Pont de Nemours
Thornel	Graphite yarn	Union Carbide Co.
THV-Fluoroplastic	Terpolymer of tetrafluoroethylene, hexafluoropropylene and vinylidene fluoride (processing at 130 °C)	3M
TI-4000	Polypropylene, PP	Aristech Chem.
Tinolex	Poly(vinyl chloride); rigid, calendered, PVC	Tins Ind. Co. Ltd.
Tivar (Series)	Ultrahigh molecular weight PE, UHMWPE	Menasha Corporation
Tivar-Thane	Polyurethane sheet, PU	Menasha Corporation
Tonen Polyeth	Polyethylenes, filled or not, PE	Tonen Petrochem./ TCA Plastics
Tool WDC	Epoxy resin with aluminum, EP	Furane Products
Topalloy	–	TCA Plastics
Topas	Cyclic, amorphous *co*-polyolefin, COC, optical grade for compact disks (metallocene based)	Hoechst/Mitsui Petrochemicals
Toplex	Polycarbonate/ABS alloy	Multibase, Inc.
Toprene	Poly(phenylene sulfide), PPS	Tonen Petrochem.
Toray PBT	Poly(butylene terephthalate), with glass or not, PBT	Toray Industries
Torelina	Poly(phenylene sulfide), PPS	Toray Industries
Torlon	Polyamide-imide, PAI; modified PAI with PTFE, for electrical connectors, valves, bushings, parts, etc.	Amoco Chem. Co.
Torlon 4000	Polyamide-imide + PTFE + graphite	Amoco Chem. Co.
Torlon 7000	Polyamide-imide + PTFE + glass/graphite fiber	Amoco Chem. Co.
Torolithes	Thermoset polyester resins, UP	Routhan Soc. Nouv.
Toso LCP	Liquid crystal polyester, LCP	Toso

(continued)

Total Butyl	Elastomers	Total Chim.
Total Plast	Thermoplastic elastomers; EPDM/PO blends, etc.	Total Chim.
Toyarac	Acrylonitrile-butadiene-styrene, ABS	Toyo, Japan
Toyoflon	Polytetrafluoroethylene, PTFE	Toyo, Japan
Toyolac	Acrylonitrile-butadiene-styrene, ABS also polycarbonate/ABS	Toray Industries
Toyolac ASG20	Styrene-acrylonitrile, SAN with glass fiber	Toray Industries
TPO 900	Polypropylene/EPDM blends	Reichhold Chem., Inc.
TPP 10GB	Polypropylene alloy with talc, paintable	Ferro Corp.
TPR	Thermoplastic cross-linked rubber for PP	Uniroyal Chemical
TPX	Polymethylpentene, PMP	Mitsui Petrochem.
Trans-4	*trans*-1,4-Polybutadiene	Phillips
Traytuf	Poly(ethylene terephthalate) with TiO_2, PET	Goodyear
Trefsin	Thermoplastic elastomers, TPR, PP/BR	Advanced Elastomer Systems
Trespaphane	Biaxially oriented polypropylene film, BOPP	Hoechst Celanese Corp.
Trevira	Poly(ethylene terephthalate) fiber, PET	Hoechst
Triax 1000	Polyamide-6 or polyamide-66, PA-6 or PA-66 blends with acrylonitrile-butadiene-styrene, ABS	Monsanto Chem. Co.
Triax 1120	Polyamide-6/ABS blends	Monsanto Chem. Co.
Triax 1125	Polyamide-66/ABS = 1:1 blends	Monsanto Chem. Co.
Triax 1180	Polyamide-6,66/acrylonitrile-butadiene-styrene	Monsanto Chem. Co.
Triax 2000	PC/acrylonitrile-butadiene-styrene, ABS	Monsanto Chem. Co.
Triax CBE	Poly(vinyl chloride)/α-methyl styrene-ABS (available as Suprel SVA from Vista Chemical Co.)	Monsanto Chem. Co.
Tribolon	Polyimide/polytetrafluoroethylene, PI/PTFE	Tribol. Ind. Inc.
Tribolon XT	Poly(phenylene sulfide)/polytetrafluoroethylene	Tribol. Ind. Inc.
Tricel	Cellulose acetate, CA	Bayer AG/Miles
Triplus TPR 178	Silicone-based paints and coatings	GE Plastics
Typlax	–	Typlax
Trivin	Poly(vinyl chloride) alloys, PVC	Vi-Chem
Trogamid	Polyamide resins, PA	Kingsley & Keith
Trogamid	Polyamide-63-T, PA-63-T	Hüls AG
Trogamid T	Poly(trimethylhexamethylene terephthalamide)	Dynamit Nobel
Trolen	Polyethylene, PE	Dynamit Nobel
Trolit AE	Cellulose ether	Dynamit Nobel
Trolit F	Cellulose nitrate, CN	Dynamit Nobel
Trolitan	Phenol-formaldehyde resins, PF	Dynamit Nobel
Trolitul	Polystyrene, PS	Dynamit Nobel
Trolon	Phenolic resins	Hüls AG
Trolon	Phenolic-based binder	Dynamit Nobel
Trosiplast	Poly(vinyl chloride), rigid or plasticized, PVC	Dynamit Nobel
Trovicel	Poly(vinyl chloride), foamed, PVC	Hüls AG
Trovidur	Poly(vinyl chloride), PVC	Dynamit Nobel

(*continued*)

Trovitherm	Poly(vinyl chloride) sheets, PVC	Dynamit Nobel
Trubyte	Acrylic-based IPN for artificial teeth	Dentsply International
Tuffak	Polycarbonate sheet, PC	Rohm and Haas
Tuffax	Polycarbonate, PC	Rohm and Haas
Tuflin	Second-generation Unipol-type LLDPE	Union Carbide
Tufpet	Poly(ethylene terephthalate)	Toyobo Corp.
Tufprene	Triblock SBS thermoplastic elastomer	Asahi
Tufrex VB	ABS/Poly(vinyl chloride), PVC alloys	Mitsubishi-Monsanto
Twaron	Poly(p-phenyleneisophthalamide), PPA	Akzo NV
Tybrene	Acrylonitrile-butadiene-styrene terpolymer	Dow Chem. Co.
Tylac	Poly(vinyl chloride), PVC/BR blends	Standard Brands Chemicals
Tylose	Cellulose ether	Kalle, Germany
Tynex	Polyamide-6,6, PA-66	E. I. du Pont de Nemours
Typlax	Thermoplastic Elastomers	Typlax Products
Tyril	Styrene-acrylonitrile copolymer, SAN	Dow Chem. Co.
Tyrin	Chlorinated PE elastomers and resins, CPE	Dow Chem. Co.
Tyvek	Spunbonded olefin fiber, PO	E. I. du Pont de Nemours
U		
U-Polymer	Polyarylate, amorphous	Unitika
U-polymer	Polyarylate	Unitika
U-xyFG	Polyurethane with xy wt% glass fiber, PU	Thermofil, Inc.
Ube	–	Ube Industries Inc.
Ube 3000	Polyamide-12, modified, PA-12	Ube Industries Inc.
Ube Alloy CA700	Polypropylene/polyamide, PP/PA blend	Ube Industries Inc.
Ube Nylon	Polyamide-6 or polyamide-66, modified, PA-6, PA-66	Ube Industries Inc.
Ube Polypro	Polypropylene, PP	Ube Industries Inc.
Ube, Ubec	Polyethylenes, PE	Ube Industries Inc.
Ucardel P4174	Polysulfone/SAN blend	Amoco Performance
Ucecoat	Polyurethane, PU	UCB Soc. Com.
Ucecryl	Acrylates and methacrylates	UCB Soc. Com.
Ucefix	Polyurethane, PU	UCB Soc. Com.
Uceflex	Polyurethane, PU	UCB Soc. Com.
Udel	Bisphenol-A polysulfone, PSF (or PSO)	Amoco Chem. Co.
Udel GF	Polysulfone with glass fiber, PSF	Amoco Chem. Co.
Udel P	Bisphenol-A polysulfone, PSF	Amoco Chem. Co.
Udel P-1700	PSF + 10 % anhydride-terminated PSF + 50 % PA-6 (or PA-66), with PA being the matrix	Amoco Chem. Co.
Udel-X	PSU/PA-6 or PA-66 experimental alloys, with 10 wt% anhydride-terminated PSU	Amoco Chem. Co.
Ugikral	Acrylonitrile-butadiene-styrene copolymer, ABS	GE Plastics
UHMWPE 900	Ultrahigh molecular weight PE, UHMWPE	Himont

Ultem	Polyetherimide, PEI, and its blends, e.g., with PC, TP	GE Plastics
Ultem 2000	Polyetherimide with glass fiber, PEI	GE Plastics
Ultem 5000	Polyetherimide copolymer, PEI	GE Plastics
Ultem 6000	Polyetherimide copolymer, PEI	GE Plastics
Ultem 8000	Polyetherimide/polycarbonate alloy, PEI/PC	GE Plastics
Ultem LTX	PEI/PC blends (unreinforced)	GE Plastics
Ultem ATX	PEI/PC blends (unreinforced)	GE Plastics
Ultem HTX	PEI/PPC blends (unreinforced)	GE Plastics
Ultem PEI/PPO	PEI blends with polyphenylene ether	GE Plastics
Ultra-Wear	Polyethylene, PE	Polymer Corp.
Ultrablend	ASA/PBT blend	BASF Plastics
Ultrablend KR	PET or PBT/PC/elastomer blends	BASF Plastics
Ultrablend S	PBT/SAN, ABS, or ASA blends, with up to 30 wt% glass fiber	BASF Plastics
Ultradur B	Poly(butylene terephthalate), PBT, and impact-modified PBT	BASF Plastics
Ultraform	Polyoxymethylene, POM, acetal	BASF
Ultraform	Polyoxymethylene/thermoplastic polyurethane, POM/TPU, alloys, with 10–30 wt% TPU	BASF Plastics
Ultralastic	Polyurethane sheet, PU	Menasha Corporation
Ultramid A	Polyamide-66, PA-66/elastomer, with glass fiber, mineral filler or not	BASF Plastics
Ultramid B	Polyamide-6, PA-6/elastomer; with glass fiber, mineral filler or not	BASF Plastics
Ultramid C	Copolyamide-6/66, PA-6,66/elastomer; 15 or 30 wt% mineral filled	BASF Plastics
Ultramid Lurans	Polyamide, PA-66/ASA alloys	BASF Plastics
Ultramid	PA-6, PA-66, PA-610; blends, reinforced	BASF Plastics
Ultramid S	Polyamide-610; with glass fiber or not	BASF Plastics
Ultramid T	Semi-aromatic polyamide-6/66, PA-66 T, or PARA with elastomer; 30 wt% glass fiber or mineral filled	BASF Plastics
Ultramid Terluran	Polyamide, PA-66/ABS alloys	BASF Plastics
Ultranyl	PA-66/PPE alloys, reinforced or not	BASF Plastics
Ultrapas	Melamine-based molding compound	Dynamit Nobel
Ultrapek	Polyaryletherketone, PAEK (PEKEKK, PEK)	BASF Plastics
Ultrason E	Polyether sulfone, PES	BASF
Ultrason S	Polysulfone, PSF (or PSO)	BASF
Ultrason E	Polyethersulfone, ≤30 wt% glass fiber, PES	BASF Plastics
Ultrason	Polyethersulfone, PES, alloys	BASF Plastics
Ultrason S	Polysulfone, ≤30 wt% glass fiber, PSU	BASF Plastics
Ultrastyr OSA	SAN-EPDM/ABS or PC alloys	ECP Enimont Polymeri
Ultrastyr	Special styrene copolymers	ECP Enimont Polymeri

Ultrathene	Ethylene-vinyl acetate, reinforced or not, EVAc	USI Chemicals Co./ Quantum
Ultrax	Liquid crystal polymers, LCP	BASF Plastics
Ultryl	Poly(vinyl chloride)	Phillips
Ultzex	Ethylene-4-methylpentene-1 copolymer	Mitsui Petrochem
Unichem	Poly(vinyl chloride); with glass fiber or not, PVC	Colorite Plastics
Unidene	Elastomers	Enimont
Union Carbide	Polyethylenes; with carbon fibers or not	Union Carbide Co., Inc. Corp.
Unipol PP	Polypropylene, PP	Shell Chem. Co.
Unirez	Polyacrylic resin emulsions	Unocal
Unitika	Polyamide-6, filled or not, PA-6	Unitika Co.
Unival DMDA	Polyethylene; PE	Union Carbide Co., Inc. Corp.
UP	Polyarylate/Poly(ethylene terephthalate) blend	Unitika
Upilex	Polyimide films; PI	ICI Films
Uradil	Polyester resins for paints (aqu. dispersions), UP	DSM
Urafil J	Polyurethane; glass or carbon fiber filled, PU	Akzo/DSM
Uraflex	Polyester resins for paints, UP	DSM
Uralac	Polyester resins for paints, UP	DSM
Uralite	Polyurethane prepolymer resin, PU	Kingsley & Keith
Uramex	Polyester resins for paints, UP	DSM
Uramul	Poly(vinyl acetate) latices for paints, PVAc	DSM
Uravin	TPU/PVC alloy	Vi-Chem
Urecoll	Urea-formaldehyde, UF	BASF Plastics
Ureol	Polyurethane resins, PU	Ciba-Geigy Ltd.
Urepan	Polyurethane, PU	Bayer
Urochem	Urea-formaldehyde resins, UF	C.P.R.I.
Urtal	Acrylonitrile-butadiene-styrene copolymer, ABS	Montepolimeri
Urylon	Polyisocyanate thermoplastic, PPI	Urylon Development
US0028	Polyurethane; filled or not, PU	Dexter Corp.
Uvecryl	Acrylic and methacrylic resins	UCB Soc. Com.
V		
V440	Poly(vinyl chloride) compounds, PVC	Vi-Chem Corp.
Vacrel	Photopolymer film soldermask	E. I. du Pont de Nemours
Valox	PBT or PET or PCT, resins or blends	GE Plastics
Valox 200	Poly(butylene terephthalate); unreinforced, PBT	GE Plastics
Valox 300	Poly(butylene terephthalate); unreinforced, PBT	GE Plastics
Valox 400	Poly(butylene terephthalate); glass reinforced, PBT	GE Plastics
Valox 500	PBT/PET alloy; glass reinforced	GE Plastics
Valox 700	Poly(butylene terephthalate); glass/mineral filled	GE Plastics
Valox 800	Poly(butylene terephthalate) alloy; glass reinforced	GE Plastics
Valox 815	PBT/PET alloy; with glass fiber or not	GE Plastics
Valox 9000	Poly(ethylene terephthalate); glass reinforced, PBT	GE Plastics

Valox 9700	Polycyclohexyleneterephthalate; glass reinforced	GE Plastics
Valox HV7000	Poly(butylene terephthalate) alloy; mineral filled	GE Plastics
Valox VCT	PBT or PET toughened with elastomer	GE Plastics
Valtel, Valtec	Polypropylene, PP	Himont
Valtra	Polystyrene, PS, and blends	Chevron Chemicals
Valtra 7023	Rubber-modified styrenic blends	Chevron Chemicals
Valtra HG-200	Styrenic copolymer for injection molding	Chevron Chemicals
Vamac	Ethylene-acrylic elastomer, curable with diamines	E. I. du Pont de Nemours & Co.
Vandar	PBT/acrylic alloys, reinforced or not	Hoechst Celanese Corp.
VB-510	Polypropylene with talc, PP	Reichhold Chem., Inc.
VC	Poly(vinyl chloride), PVC	Borden Chem.
VE	Unsaturated vinyl ester, with glass or carbon fiber	ICI/Fiberite
Vector 6000	SB, SBS, SI, and SIS block copolymers	Dexco Polymers
Vectra A	Liquid crystal polymer, LCP; reinforced or not a copolyester from hydroxy benzoic acid with hydroxynaphthoic acid	Hoechst Celanese Corp.
Vectra B950	LCP copolymer comprising 20 mol% of terephthalic acid, 20 mol% 4-aminophenol, and 60 mol% of 2-hydroxy-6-naphthoic acid	Hoechst Celanese Corp.
Vectra V140	LCP/PPS blends for electrical/electronic parts	Hoechst Celanese Corp.
Vedril	Poly(methyl methacrylate)s powder, sheets, PMMA	Montedison SpA
Vekton 6	Polyamide-6; filled or not, PA-6	Norton Performance
Vekton 11	Polyamide-11, PA-11	Norton Performance
Vekton 66	Polyamide-66; filled or not, PA-66	Norton Performance
Velponyl/Velporex	Printing resins	DSM
Venyl	Polyamides; reinforced or not, PA	Vecoplas
Versamid	Polyamide; vegetable oils condensed with amines	General Mills
Versamid	Polyamides, PA	Henkel Corp
Versicol	Acrylic polyelectrolyte	Allied Colloids
Verton	Long fiber reinforced resins	ICI Materials – Plast./ LNP
Verton DF	Long fiber reinforced polyamide-66	ICI Materials – Plast./ LNP
Verton KA	Long fiber reinforced polyoxymethylene, POM	ICI Materials – Plast./ LNP
Verton NF	Long fiber reinforced SMA	ICI Materials – Plast./ LNP
Verton OF	Long fiber reinforced poly(phenylene sulfide), PPS	ICI Materials – Plast./ LNP
Verton PF	Long fiber reinforced polyamide-66, PA-66	ICI Materials – Plast./ LNP
Verton QA	Long fiber reinforced polyamide-610	ICI Materials – Plast./ LNP

Verton RF	Long fiber reinforced polyamide-66	ICI Materials – Plast./LNP
Verton TF	Long fiber reinforced polyurethane, PU	ICI Materials – Plast./LNP
Verton WF	Long fiber reinforced poly(butylene terephthalate)	ICI Materials – Plast./LNP
Verton YA	Long fiber reinforced polycarbonate, PC	ICI Materials – Plast./LNP
Verton YF	Long fiber reinforced polyester	ICI Materials – Plast./LNP
Vespel ST	Super-tough polyimide with high-impact strength	E. I. du Pont de Nemours
Vespel-SP	Polyimide (polypyromellitimide); electrical parts	E. I. du Pont de Nemours
Vestamelt	Copolyesters	Hüls AG
Vestamid	Polyamide-12, polyamide-6,12, PA-12 elastomer	Hüls AG
Vestamid D; X	Polyamide-612; filled or not, PA-612	Hüls AG
Vestamid L	Polyamide-12; filled or not	Hüls AG
Vestenamer	*Trans*-polyoctenamer, thermoplastic elastomer	Hüls AG
Vestoblend	Polyamide/PPE alloys, reinforced or not	Hüls/Nuodex Inc.
Vestodur	Poly(butylene terephthalate), PBT; reinforced or not	Hüls AG
Vestolen A	High-density polyethylene, HDPE	Hüls AG
Vestolen BT	Polybutene, PB	Hüls AG
Vestolen EM	EPR- or EPDM-modified polypropylene, PP, containing talc, $CaCO_3$, glass fibers, mineral, or not	Hüls AG
Vestolen P	Polypropylene, PP	Hüls AG
Vestolit	Poly(vinyl chloride), PVC, rigid and flexible	Hüls AG
Vestopal	Unsaturated polyester resins, UP	Hüls AG
Vestoplast	Amorphous olefin copolymers, TPO	Hüls AG
Vestopren	Polyolefin impact modifier, PO	Hüls AG
Vestoran	PPE blends with HIPS and elastomer	Hüls AG
Vestosint	Polyamides, PA	Hüls AG
Vestypor	Expandable polystyrene, EPS	Hüls AG
Vestyron	GP-PS, HIPS	Hüls AG
VFR-10248	Poly(ethylene terephthalate) with TiO_2, PET	Goodyear
Vibraspray	Elastomers	Safic-Alcan
Vibrathane	Urethane prepolymers, TS	Uniroyal Chemical Ltd.
Vibrin	Polyester resins, UP	Fiberglas Canada
Viclan	Vinylidene chloride copolymers, PVDC	ICI
Vicotex 260	Phenolic prepreg resins	Ciba-Geigy
Vicotex	Epoxy preimpregnates, EP	Brochier
Victrex D	Polyetheretherketone, with glass or carbon fiber	ICI Materials – Plastics/Victrex
Victrex J	Polyethersulfone, PES; filled	ICI/LNP Eng. Plastics
Victrex PEEK	Polyetheretherketone, PEEK; reinforced or not	ICI/LNP Eng. Plastics

Victrex PES	Polyethersulfone, PES; filled, lubricated	ICI/LNP Eng. Plastics
Victrex SRP	Liquid crystal polyester, LCP	ICI Materials – Plast.
Victrex VKT	Polyetheretherketone, PEEK/PTFE blend	ICI Materials – Plast.
Victrex VST	Polyethersulfone, PES/PTFE blends	ICI Materials – Plast.
Vidar	Poly(vinylidene fluoride), PVDF coating powders	Solvay & Cie SA
Vifnen VN	AAS/Poly(vinyl chloride), PVC alloys	Hitachi Chem.
Vilit	Poly(vinylidene chloride) copolymers, PVDC	Hüls A.-G
Vinapas	Poly(vinyl acetate), PVAc	Wacker Chemie
Vinavil	Poly(vinyl acetate), PVAc	Montecatini
Vinavol	Poly(vinyl alcohol), PVAl	Hoechst AG
Vinex	Poly(vinyl alcohol), PVAl	Air Products & Chem.
Vinidur	Poly(vinyl chloride), PVC, and impact-modified PVC with 5–15 wt% acrylate-graft copolymer	BASF Plastics
Vinika	Poly(vinyl chloride)-based elastomers, PVC	A. Schulman, Inc.
Viniproz	Poly(vinyl chloride)/PMMA alloys	USSR
Vinnapas	Poly(vinyl acetate), PVAc	Wacker-Chemie
Vinnol	Poly(vinyl chloride), *homo*, *g* and *r* copolymer., PVC	Wacker-Chemie
Vinoflex	Poly(vinyl chloride), suspension grade, PVC	BASF Plastics
Vinoflex	Vinyl chloride-vinyl ether copolymer, PVCAc	BASF Plastics
Vinuran	MBS modifier for poly(vinyl chloride)	BASF Plastics
Vipla	Poly(vinyl chloride) paste polymers, PVC	European Vinyls Corp.
Viplast	Poly(vinyl chloride) compositions, PVC	European Vinyls Corp.
Viscose	Fibers from cellulose	(generic name)
Vista	Poly(vinyl chloride); filled or not, PVC	Vista Chem. Co.
Vistaflex	Thermoplastic elastomers, TPO, PP/EPDM	Advanced Elastomer System
Vistalon 404	Ethylene-propylene copolymer, EPM	Exxon Chem.
Vistalon 2504	EPDM terpolymer	Exxon Chem.
Vistanex	Polyisobutene, PIB	Exxon Chem.
Vistel	Rigid PVC blends for injection molding	Vista Chemical Co.
Vithane	Polyurethanes, PU	Goodyear
Viton A	Vinylidene fluoride/fluoridehexafluoropropylene	E. I. du Pont de Nemours
Viton B	PTFE/PHFP/PVDF	E. I. du Pont de Nemours
Viton	Fluoroelastomers	E. I. du Pont de Nemours
Vitrofi	Vetrotex trademark for tissue	Vetrotex International
Vituf	Poly(ethylene terephthalate), PET; with TiO_2	Goodyear
Vivypak/Lighter	Poly(ethylene terephthalate), PET bottle grades	ECP EniChem Polymeri
Vixrex PES	Polyethersulfone, PES; glass/mineral filled	LNP Engineering
Vodcum	Phenolic resin, PF	Cain Chem. Inc.
Volara	EVA/PP or PE blends	Seiksui/Voltek
Volex 410	Poly(butylene terephthalate), PBT; glass/mineral	Comalloy Intl. Corp.

(*continued*)

Volex 440	Poly(ethylene terephthalate), PET; glass/mineral	Comalloy Intl. Corp.
Volex 600	Polyamides-6, polyamide-66, polyamide-612, PA; with glass/mineral	Comalloy Intl. Corp.
Voloy 100	Polypropylene; with glass/mineral, PP	Comalloy Intl. Corp.
Voloy 680	Polyamide-6,6; with glass/mineral, PA-66	Comalloy Intl. Corp.
Voltalef 300	Polychlorotrifluoroethylene, PCTFE	Elf Atochem
Voralast	Tailored PU elastomers	Dow Chem. Co.
Voranol	Polyether PU elastomers	Dow Chem. Co.
Vulcaprene	Polyurethanes, PU	ICI
Vulkollan	Polyurethanes, PU	Bayer AG/Miles
Vulta Foam	Rigid urethane foam, EPU	General Latex
Vultex	Latex and compounds	General Latex
Vybak	Poly(vinyl chloride), PVC	Bakelite Xylonite
Vydyne	Polyamide-66 or polyamide-69	Monsanto Chem. Co.
Vydyne M	Polyamide-66, PA-66	Monsanto Chem. Co.
Vydyne R	Polyamide-66 with glass or mineral, PA-66	Monsanto Chem. Co.
Vygen	Poly(vinyl chloride), PVC	Vygen Corp.
Vynathene	Ethylene-vinyl acetate copolymer, EVAc	Quantum Chem.
Vyncolite	Phenol-formaldehyde resins, PF	Vynckier
Vynite	Poly(vinyl chloride)/nitrile rubber alloy	Dexter Corp.
Vyram	PP/diene – TPE elastomeric blends	Advanced Elastomers
Vythene	Poly(vinyl chloride), PVC/PU alloy	Dexter Corp.
W		
W-xyFG	Polyetherimide with xy wt% glass fiber, PEI	Thermofil, Inc.
W-xyNF	Polyetherimide with xy wt% graphite fiber, PEI	Thermofil, Inc.
Wacke VAE	Ethylene-vinyl acetate copolymer, EVAc	Wacker Chimie A.-G.
Wacker PU	Polyurethane or silicone elastomers, PU	Arnaud Promecome
Wellamid	Polyamide-6, polyamide-66, PA-66	Wellman Inc.
Wellamid 22 LHI	Polyamide-66/elastomer, PA-66 blend	Wellman Inc.
Wellamid FR	Polyamide-66 with glass spheres, PA-66	Wellman Inc.
Wellamid GF	Polyamide-6 or polyamide-66 with glass fiber, PA-6, PA-66	Wellman Inc.
Wellamid MR	Polyamide-6 or polyamide-66 with glass or mineral, PA-66	Wellman Inc.
Wellamid MR	Polyamide-66/polyamide-6, PA-6 alloys	Wellman Inc.
Wellite	Poly(butylene terephthalate), PBT; with glass	Wellman Inc.
Wellpet GF	Poly(butylene terephthalate), PBT; with glass	Wellman Inc.
Welvic	Poly(vinyl chloride) compositions, PVC	European Vinyls Corp.
Wingtack	Synthetic polyterpene	Goodyear Chem. Eur.
Witcast	Polyurethane elastomers, PUR	Witco
Witcothane	Polyurethane elastomers, PUR	Witco
Wofatit	Ion-exchange resin	VEB Farbenfabrik
WRM	Elastomers	Safic-Alcan
WRS	Polypropylene, PP	Shell Chem. Co.
Wydyne	Polyamides; reinforced or not, PA	Monsanto

X

X-28057	Epoxy resins with mineral, EP	ICI/Fiberite
Xantar	Polycarbonate, PC	DSM
XB-4000	Polyamide-6 with or without glass, PA-6	Allied Signal Corp.
Xenoy	PC/PBT/MBA alloys, reinforced or not	GE Plastics
Xenoy 1000, 5000	Polycarbonate, PC:PBT = 1:1 alloys	GE Plastics
Xenoy 2000	Polycarbonate, PC/PET/MBA alloys	GE Plastics
Xenoy 3000	Polycarbonate, PC/TPE alloy	GE Plastics
Xenoy 6125	PET/PC, impact mod.; 0–30 wt% glass fiber	GE Plastics
Xenoy DX6302	Polycarbonate/polyester alloy with carbon fiber	GE Plastics
XL-030	Polypropylene, PP	Aristech Chem.
XP-50	Poly(*p*-methylstyrene-*co*-isobutylene)-based compatibilizing system	Exxon Chem. Co.
XT	Acrylic-based multipolymer blends	Cyro Industries
XT 3055	Polyamide alloys, PA	EMS-American Grilon
XT Polymer	Acrylic-based transparent, high-impact blend	Cyro Industries
Xtcon	Polyester/polyurethane hybrid resin	Amoco Chem. Co.
XTPE	Cross-linkable elastomers and olefins	Quality Service Technology
XTPL NFR-6000	Thermoplastic elastomer, TPE	E. I. du Pont de Nemours
XU	TPU/acrylonitrile-butadiene-styrene, ABS alloys	Dow Chem. Co.
XU61513	Polyethylene, PE	Dow Chem. Co.
Xycon	TPEs/TPU alloys	Amoco Chem. Co.
Xydar	Liquid crystal polymer, LCP	Amoco Performance Products
Xydar FC	Liquid crystal polymer, LCP; glass/mineral	Amoco Chem. Co.
Xydar FSR-315	Liquid crystal polymer, LCP; 50 % talc	Amoco Chem. Co.
Xydar RC	Liquid crystal polymer, LCP; glass/mineral	Amoco Chem. Co.
Xylok	Aralkyl thermoset resins	O.F.A.C.I.
Xylon	Polyamide-66 with a filler, PA-66	Akzo/DSM
Xyron 200	Poly(phenylene ether) PPE/HIPS alloys	Asahi Chem. Ind.
Xyron A	Polyamide/PPE/alloys, reinforced or not	Asahi Chem. Ind.
Xyron G	Polyamide/poly(phenylene ether) PPE alloys	Asahi Chem. Ind.

Y

Y-xyFG	Polystyrene with xy wt% glass fiber, PS	Thermofil, Inc.
Y1-xyFG	Polystyrene with xy wt% glass fiber, PS	Thermofil, Inc.
Yukalon	Polyethylenes, PE	Mitsubishi Petrochem.

Z

Zemid	–	E. I. du Pont de Nemours
Zenite	Polyamide-66, with glass fiber, PA-66	E. I. du Pont de Nemours
Zenite	Wholly aromatic polyester, LCP, HDT = 295 °C	E. I. du Pont de Nemours

(*continued*)

Zeo-karb	Ion-exchange resin	Permutit Co.
Zeonex	Polymethylpentene, PMP	Nippon Zeon
Zeonex	Polyolefin, amorphous, transparent for optical applications: disks, lenses, prism, LCD films, etc.	Nippon Zeon Co., Ltd.
Zeospan	Polyether elastomer	Nippon Zeon Co., Ltd.
Zerlon	Polystyrene, PS/PMMA alloys	Dow Chem. Co.
Zetabond	Plastic clad metal for fiber optic cables	Dow Europe
Zetafin	Ethylene-vinyl acetate copolymer, EVAc	Dow Chem. Co.
Zetpol	Hydrogenated, nitrile elastomer (HNBR), highly saturated for fuel and solvent resistance	Nippon Zeon Co., Ltd.
Zetpol PBZ	HNBR/PVC blends	Nippon Zeon Co., Ltd.
Zitex G	PTFE porous films	Norton Performance Plast.
Zylar	High transparency acrylic terpolymers	Novacor Chemicals Inc.
Zylar ST	SAN/polybutadiene high transparency alloy	Novacor Chemicals Inc.
Zytel	Polyamide-6,10, PA-610	E. I. du Pont de Nemours
Zytel 71G	Polyamide-66/ionomer, PA-66 alloys	E. I. du Pont de Nemours
Zytel 77G	Polyamide-6,12/ionomer, PA-612 alloys	E. I. du Pont de Nemours
Zytel 101	Polyamide-66, PA-66	E. I. du Pont de Nemours
Zytel 105	Polyamide-66, with carbon black, PA-66	E. I. du Pont de Nemours
Zytel 150	Polyamide-6,12, PA-612	E. I. du Pont de Nemours
Zytel 300, 400	Polyamide-6,6/ionomer, PA-66 alloys	E. I. du Pont de Nemours
Zytel 3100	Polyamide-6/polyamide-66 alloys	E. I. du Pont de Nemours
Zytel FN	Flexible polyamide alloys	E. I. du Pont de Nemours
Zytel GRZ	Glass fiber-reinforced PA-66 or PA-612	E. I. du Pont de Nemours
Zytel ST	Impact-modified PA-6 or PA-66	E. I. du Pont de Nemours
Zytel ST-350	Polyamide-612/elastomer, PA-612 alloys	E. I. du Pont de Nemours

Appendix V: Commercialization Dates of Selected Polymers

Year	Code	Polymer	Producer
1868	NC	Cellulose nitrate; *Nixon*	Hyatt Bros.
1900	CS	Casein; *Galalith*	Kritische (France)
1909	PF	Phenol-formaldehyde; *Bakelit*	Bakelit Gesellschaft
1915	PS	Polystyrene; *Trolitul*	I. G. Farbenindustrie
1926	AK	Alkyd resins; *Glyptal*	General Electric Company
1927	CA	Cellulose acetate fibers; *Lumarith*	Canadian Celanese/Eastman
1927	PMA	Poly(methyl acrylate)	O. Röhm
1928	PVAc	Poly(vinyl acetate); *Elvacet*	Shawinigan Chemical Ltd.
1928	PVC/Ac	Poly(vinyl chloride-co-vinyl acetate)	I. G. Farbenindustrie
1928	PMMA	Poly(methyl methacrylate), *Plexiglas*	Röhm and Haas
1929	GRS/SBR	Styrene-butadiene rubber; *Styrolux*	I. G. Farbenindustrie
1929	UF	Urea/formaldehyde resins; *Pollopas*	Stein Hall Mfg. Company
1930	PAN	Polyacrylonitrile	I. G. Farbenindustrie
1930	CR	Chloroprene rubber; *Neoprene*	E. I. du Pont de Nemours & Co.
1930	TR	Polysulfide rubbers; *Thiokol*	Thiokol Chemical Corporation
1931	PVC	Poly(vinyl chloride); *Trovidur, Vestolit*	I. G. Farbenindustrie
1931	PEG	Poly(ethylene glycol)	I. G. Farbenindustrie
1931	PVAl	Poly(vinyl alcohol)/formaldehyde fibers	I. G. Farbenindustrie
1932	Buna-S	Styrene-butadiene rubber	I. G. Farbenindustrie
1932	Buna-N	Acrylonitrile-butadiene rubber	I. G. Farbenindustrie

(continued)

Year	Code	Polymer	Producer
1932	UM	Urea/melamine	American Cyanamid Company
1933	PEMA	Poly(ethyl methacrylate)	Röhm and Haas
1933	EC	Ethyl cellulose; *Methocel*	ICI
1933	AF	Aniline/formaldehyde resins; *Cibanite*	Ciba
1934	PCTFE	Polychlorotrifluoroethylene; *Hostaflon*	I. G. Hoechst
1934	PVFO	Poly(vinyl formal)	Shawinigan Chemical Ltd.
1935	PVBO	Poly(vinyl butyral)	Shawinigan Chemical Ltd.
1936	ABS-A	Acrylonitrile-butadiene-styrene; *Royalite*	Naugatuck Chemical Company
1936	MF	Melamine/formaldehyde resins	Ciba
1937	PA-66	Polyamide-66; *Nylon*	E. I. du Pont de Nemours & Co.
1937	SAN	Styrene-acrylonitrile copolymer; *Luran*	I. G. Farbenindustrie
1937	TPU	Thermoplastic polyurethane elastomers	O. Bayer
1937	TS	Thermoset polyesters	Marco Chemical Company
1937	PVK	Poly-N-vinylcarbazole; *Luvican*	I. G. Farbenindustrie (BASF)
1938	MF	Melamine-formaldehyde resin; *Resart*	Henkel AG
1938	CAB	Cellulose acetate butyrate; *Tenite*	Eastman Kodak Company
1938	PA-6	Poly-ε-caprolactam; *Perlon*	I. G. Farbenindustrie
1938	PA-66	Polyhexamethyleneadipamide; *Nylon*	E. I. du Pont de Nemours & Co.
1939	LDPE	Low-density polyethylene; *Alketh*	ICI Ltd.
1939	PVDC	Poly(vinylidene chloride); *Saran*	Dow Chemical Company
1939	PVP	Poly-N-vinylpyrrolidone	Farbenindustrie
1939	PU	Polyurethane fibers, *Perlon U*	I. G. Farbenindustrie, Wolfen
1940	DAC	Diallyl glycol carbonate; *CR-38*	PPG Company
1942	UP	Unsaturated polyester; *Vestopal*	United States Rubber Company
1942	PTFE	Polytetrafluoroethylene; *Teflon TFE*	E. I. du Pont de Nemours & Co.
1943	EP	Epoxy; *Araldite*	Ciba-Geigy
1943	BR	Butyl rubber	St. Claire Processing Corporation
1943	HDPE	High-density polyethylene; *Vestolen*	BASF A.-G.
1943	PDMS	Polydimethylsiloxane; *Dow Corning*	Dow Corning Corporation
1943	PVAl	Poly(vinyl alcohol); *Vinaviol*	Shawinigan Chemical Ltd.

Year	Code	Polymer	Producer
1943	PVCAc	Vinyl copolymers; *Vinidur*	Shawinigan Chemical Ltd.
1945	CP	Cellulose propionate; *Forticel*	Celanese
1947	PU	Polyurethanes; *Perlon U*	Bayer A.-G.
1948	ABS-G	Acrylonitrile-butadiene-styrene latex	Röhm & Haas
1948	ACM	Acrylic elastomer; *Hycar PA*	B. F. Goodrich Chemical Co.
1950	EVA	Ethylene-vinyl acetate copolymer	ICI
1950	CSR	Chlorosulfonated PE; *Hypalon*	E. I. du Pont de Nemours & Co.
1950	PCTFE	Polychlorotrifluoroethylene	Hoechst A.-G.
1952	OPET	Oriented polyethyleneterephthalate film	E. I. du Pont de Nemours & Co.
1953	PET	Poly(ethylene terephthalate); *Melinite*	ICI
1954	PVAc/Ph	Poly(vinyl acetate)/phthalate	C. E. Frosst & Company
1955	PA-11	Polyamide-11; *Risilan*	Thann & Mulhouse
1956	PC	Bisphenol-A polycarbonate; *Macrolon*	Bayer A.-G.; General Electric Co.
1956	PCME	Polydichloromethyltrimethylene ether; *Penton*	Hercules
1957	PEG	Poly(ethylene glycol); *Carbowax*	Union Carbide Canada Ltd.
1957	PP	Isotactic Polypropylene; *Pro-Fax*	Hoechst/Montecatini/Hercules
1958	DAP/DAIP	Allyl unsaturated polyester; *Dapon*	FMC Corporation
1958	SMM	Poly(styrene-co-methylmethacrylate); *Kamax*	Röhm & Haas A.-G.
1958	UHMWPE	Ultrahigh molecular weight polyethylene; *Hostalen GUR*	Hoechst A.-G./Himont
1959	CPE	Chlorinated polyethylene; *Hostapren*	Hoechst A.-G.
1959	POM	Polyoxymethylene (Acetal); *Delrin*	E. I. du Pont de Nemours & Co.
1959	POM	Poly(oxymethylene/ethylene); *Celcon*	Celanese
1959	TPU	Thermoplastic polyurethane; *Estane*	B. F. Goodrich
1960	EVAc	Ethylene-vinyl acetate; *Elvacet*	E. I. du Pont de Nemours & Co.
1960	CAP	Cellulose acetate propionate; *Tenite*	Eastman Kodak
1960	CBR	Chlorobutyl rubber; *Exxon Butyl*	Exxon
1960	EPR	Ethylene-propylene elastomer; *Vistalon*	Exxon
1960	LLDPE	Linear low-density polyethylene; *Sclair*	DuPont-Canada
1960	–	Chlorinated polyether; *Penton*	Hercules Inc.
1961	–	Polyamide-epichlorohydrin; *Hydrin*	Hercules Powder Company
1961	Aramid	Poly(m-phenyleneisophthalamide); *Nomex*	E. I. du Pont de Nemours & Co.

<div align="right">(continued)</div>

Year	Code	Polymer	Producer
1961	FEP	Fluorinated-ethylene propylene; *Teflon FEP*	E. I. du Pont de Nemours & Co.
1961	PVDF	Poly(vinylidene fluoride); *Kynar*	Pennwalt Chemical Company
1962	SB	Styrene-butadiene block copolymer	Phillips
1962	ACM	Acrylate rubber	Polymer Corp. Ltd. (Polysar)
1962	Phenoxy	Polyhydroxyether of bisphenol-A; *Phenoxy*	Union Carbide
1962	PI	Polyimides; *Kapton*	E. I. du Pont de Nemours & Co.
1963	EPDM	Ethylene-propylene-diene; *Nordel*	E. I. du Pont de Nemours & Co.
1963	SMA	Styrene-maleic anhydride; *Dylark*	Sinclair Petrochemicals Company
1963	IO	Ethylene copolymer ionomers; *Surlyn*	E. I. du Pont de Nemours & Co.
1964	EVAc	Ethylene-vinyl acetate copolymer; *Elvax*	E. I. du Pont de Nemours & Co.
1964	EVAc	Ethylene-vinyl acetate cop.; *Ultrathene*	U. S. Industrial Chemicals
1964	PIAN	Isoprene/acrylonitrile rubber	Polymer Corp. Ltd. (Polysar)
1964	PPE	Poly(phenylene ether); *PPE*	General Electric Company
1964	PB	Polybutylene, *Vestolen BT*	Hüls A.-G.
1965	PAI	Polyamide-imide; *Torlon*	Amoco Chemical Corporation
1965	PBIA	Polybenzimidazole	Naramco, Materials Div.
1965	PSF	Polysulfone of bisphenol-A; *Udel*	Union Carbide Corp./ Amoco
1965	SBS	Poly(styrene-b-butadiene); *Kraton D*	Shell Chemical Company
1965	EP	Poly(ethylene-b-propylene); *Polyallomer*	Eastman Chemical Products
1965	(blend)	PU/polyester; *Corfam*	E. I. du Pont de Nemours & Co.
1965	PPX	Polyparaxylene; *Parylene*	Union Carbide Company, Inc.
1965	PMP	Poly-4-methyl pentene-1; *TPX*	ICI/Mitsui Petrochemical Ind.
1966	PPE blend	Poly(phenylene ether); *Noryl*	General Electric Company
1966	PA-12	Polyamide-12; *Vestamid*	Hüls A.-G./Emser Werke
1969	–	Amorphous, aromatic PARA; *Trogamid*	Dynamit Nobel
1969	PB	Polybutene-1; *Duraflex*	Hüls A.-G.

Year	Code	Polymer	Producer
1969	PBT	Poly(butylene terephthalate); *Celanex*	Celanese
1969	PBT	Poly(butylene terephthalate); *Hostadur*	Hoechst A.-G.
1970	PO	*Unipol process*	Union Carbide Company, Inc.
1970	LCP	Poly(p-oxybenzoyl); *Ekonol*	Carborundum
1970	BIIR	Bromobutyl rubber	Polysar
1970	PA-612	Polyamide-6,12; *Zytel 150*	E. I. du Pont de Nemours & Co.
1970	Aramid	Poly(p-phenyleneisophthalamide); *Kevlar*	E. I. du Pont de Nemours & Co.
1971	PASU	Polyarylsulfone; *Astrel*	3M Company
1971	PPS	Poly(phenylene sulfide); *Rayton R*	Phillips Petroleum Company
1971	PAE	Polyarylether; *Arylon T*	Uniroyal
1972	EVAl	Ethylene-vinyl alcohol; *Elvanol*	Kuraray Company Ltd.
1972	LCP	Liquid crystal polymers; *Ekkcel I-2000*	Carborundum
1972	PES	Polyethersulfone; *Victrex*	ICI Ltd.
1972	PFA	Perfluoro alkoxy polymer; *Teflon PFA*	E. I. du Pont de Nemours & Co.
1972	ETFE	Poly(ethylene-co-tetrafluoroethylene); *Tefzel*	E. I. du Pont de Nemours & Co.
1972	SB	Styrene-butadiene blocks; *K-resin*	Phillips Petroleum Company
1972	SEBS	Poly(styrene-b-ethylene butylene); *Kraton G*	Shell Chemical Company
1973	PVDF	Poly(vinylidene fluoride); *Dyflon*	Dynamit Nobel
1973	PAr	Polyarylate (mixture of *i*- and *t*-phthalic acid with bisphenol-A); *U-polymer*	Unitika
1976	PPSU	Polyphenylsulfone; *BXL, Radel R*	Union Carbide/Amoco
1978	PEEK	Polyetheretherketone; *Victrex*	ICI Ltd.
1980	APEC	Aromatic polyestercarbonate; *Apec*	Chemical Werke Albert; Bayer
1981	PEBA	Polyether-block-amide; *Pebax*	Atochem
1981	TPO	Dynamically vulcanized PO blend; *Santoprene*	Monsanto Company
1982	PEI	Polyetherimide; *Ultem*	General Electric Company
1983	PAS	Polyarylsulfone; *Radel*	Amoco
1983	PBI	Polybenzimidazole; *PBI*	Celanese Corporation
1985	PAE	Polyarylether; *Parylen*	Union Carbide
1985	MPR	Melt-processable rubber; *Acrylyn*	E. I. du Pont de Nemours & Co.
1986	PISO	Polyimidesulfone	Celanese
1987	PTES	Polythioethersulfone; *Amoroon*	Dainippon Ink & Chemicals
1987	PA-46	Polyamide-4,6; *Stanyl*	DSM
1987	PPMB	Poly-*p*-methylenebenzoate	Amoco

Year	Code	Polymer	Producer
1989	sPS	Syndiotactic polystyrene	Idemitsu/Dow
1991	PPA	Polyphthalamide; *Amodel*	Amoco
1992	sPP	Syndiotactic polypropylene	Sumitomo Chemical
1994	PENi	Polyethernitrile	Idemitsu Materials Company
1995	COPO	Ethylene-carbon monoxide copolymer	Shell Chemicals

Appendix VI: Notation and Symbols

The following list of commonly used notation and symbols is used in the *Encyclopedia*. They are based on those listed in *American National Standard Abbreviations for Use on Drawings and in Text (ANSI Yl.l)*, *American National Standard Letter Symbols for Units in Science and Technology (ANSI Y10)*, and *The Society of Rheology [J. Rheol., 28, 181 (1984)]*.

Abbreviations

A	Amorphous polymer
a-c	Alternating current
abs	Absolute
aq	Aqueous
av	Average
BC	Block copolymer
bcc	Body-centered cubic
bct	Body-centered tetragonal
bp	Boiling point
C	Crystalline polymer
ca	Circa (about as much)
cgs	Old units: centimeter-gram-second
CH	Centrifugal homogenizer
CMC	Critical micelle concentration
conc	Concentration
cp	Chemically pure
CPC	Cloud point curve
cryst	Crystalline
CST	Critical solution temperature
CTM	Cavity transfer mixer

d-c	Direct current, adj.
dB	Decibel
dec	Decompose
detd	Determined
detn	Determination
dia	Diameter
dil	Diluted
dl -; DL-	Racemic
DMA	Dimethylacetamide
DMF	Dimethylformamide
DMG	Dimethylglyoxime
DMSO	Dimethyl sulfoxide
DP	Degree of polymerization
dp	Dew point
DPH	Diamond pyramid hardness
DR	Draw ratio
DS	Degree of substitution
dsc	Differential scanning calorimetry
dta	Differential thermal analysis
ECU	Electrochemical unit
ED	Effective dose
ed.	Edited, edition, editor
em	Electron microscopy
emf	Electromotive force
emu	Electron magnetic unit
EP	Engineering polymer
EPB	Engineering polymer blends
epr	Electron paramagnetic resonance
Eq	Equation
esca	Electron-spectroscopy for chemical analysis
esp	Especially
esr	Electron-spin resonance
est(d)	Estimate(d)
estn	Estimation
esu	Electrostatic unit
exp	Experiment, experimental
ext(d)	Extract(ed)
fcc	Face-centered cubic
fp	Freezing point
frz	Freezing
FTIR	Fourier transform IR
g-mol	Gram-molecular weight
gc	Gas chromatography
glc	Gas–liquid chromatography

gpc	In old terminology, gel-permeation chromatography; modern term, size exclusion chromatography, sec, should be used instead
grd	Ground
hcp	Hexagonal close-packed
hex	Hexagonal
HPB	Homologous polymer blend
hplc	High-pressure liquid chromatography
HRC	Rockwell hardness (C scale)
HV	Vickers hardness number
hyg	Hygroscopic
ICT	International Critical Table
ID	Inside diameter
Im	Imaginary part of a complex function
im	Immiscible
intl.	International
ir	Infrared
IU	International Unit
IUPAC	International Union of Pure and Applied Chemistry
l.c.	Lower case (in printing)
LALLS	Low-angle laser light scattering
LCB	Long-chain branching
LCD	Liquid crystal display
LCST	Lower critical solution temperature
LED	Light-emitting diode
liq	Liquid
ln	Logarithm (natural)
log	Logarithm (common)
m	Miscible
max	Maximum
MEK	Methyl ethyl ketone
meq	Milliequivalent
mfd	Manufactured
mfg	Manufacturing
mfr	Manufacturer
MIBC	Methyl isobutyl carbinol
MIBK	Methyl isobutyl ketone
min	Minute; minimum
mol	Mole
mol wt	Molecular weight
mp	Melting point (also T_m)
MPB	Miscible polymer blend
ms	Mass spectrum
MTT	Melt titration technique
MW	Molecular weight

MWD	Distribution of MW
mxt	Mixture
na	Not available
nat	Natural
NDB	Negatively deviating blends
neg	Negative
NG	Nucleation-and-growth
NI	Notched Izod impact strength
NIRT	Notched Izod impact strength at room temperature
nmr	Nuclear magnetic resonance
no.	Number
NRET	Non-radiative energy transfer
NTP	Normal temperature and pressure (25 °C and 101.3 kPa or 1 atm)
o-	Ortho
OD	Outside diameter
OM	Optical microscopy
p-	Para
p-i-n	Positive-intrinsic-negative
p., pp.	Page, pages
PAB	Polymer alloys and blends
PDB	Positively deviating blends
Pe	Peclet number
pH	Negative logarithm of the effective hydrogen ion concentration
phr	Concentration in parts per hundred of resin
PICS	Pulse-induced critical scattering
pm	Partially miscible
pmr	Proton magnetic resonance
PNDB	Positively and negatively deviating blends (sigmoidal)
pos	Positive
ppb	Parts per billion (10^9)
pph	Parts per hundred
ppm	Parts per million (10^6)
ppmv	Parts per million by volume
ppmwt	Parts per million by weight
PRC	Particular rheological composition
pt	Point; part
pwd	Powder
qv	Quod vide (which see)
r-f, rf	Radio frequency; adj. and n., respectively
rad	Radian
rds	Rate-determining step
Re	Real part of complex function
Ref.	Reference
rh	Relative humidity

rms	Root-mean square
rpm	Rotations per minute
rps	Revolutions per second
RT	Room temperature
SANS	Small-angle neutron scattering
satn	Saturation
SAXS	Small-angle X-ray scattering
SCB	Short-chain branching
SCF	Self-consistent field
SD	Spinodal decomposition
SEC	Size-exclusion chromatography
SEM	Scanning electron microscope
SH	Strain hardening
SI	Le Système International d'Unités (International System of Units)
SIS	Solvent-induced shift
sol	Soluble
soln	Solution
soly	Solubility
sp	Specific
sp gr	Specific gravity
sr	Steradian
std	Standard
TEM	Transmission electron microscopy
tex	Tex, linear density
THF	Tetrahydrofuran
tlc	Thin-layer chromatography
trans	Isomer in which substituents are on opposite sides of double $C = C$ bond
TREF	Temperature rising elution fractionation
TW	Glass temperature width (°C)
UCST	Upper critical solution temperature
uv	Ultraviolet
v sol	Very soluble
var	Variable
vol	Volume
vs.	Versus, against
WAXS	Wide-angle X-ray scattering
yr	Year

Notation: Roman Letters

A	Chemical affinity
a	Drop curvature

A_2	Second virial coefficient
a_c, a_T	Concentration and temperature shift factors
A_j, a_j	Equation constants
a_s	Distance from spinodal condition; $a_s = 2[(\chi N)_s - (\chi N)]$
B	Thermodynamic interaction parameter; $B = \chi_{12} RT/V_{1u}$
B	Mobility
B, B_o	Extrudate swell and its value for Newtonian liquid
$C = \omega/\dot{\gamma}$	Sprigg's constant
c_i^o	Universal constants in WLF equation
c_2, C	Concentration (g/dl)
C_p	Heat capacity at constant pressure
C_v	Heat capacity at constant volume
$c \times 3$, $(3c)$	Number of external degrees of freedom per macromolecular segment
D^c	Cahn-Hilliard diffusion constant
D	Droplet deformability; $D = (l-b)/(l+b)$
D	Diffusion coefficient
D	Tensile compliance
$D(t, \sigma_E)$	Tensile creep compliance
d, d_i	Diameter, diameter of ith generation of particles in polydisperse suspensions
D_c, D_e	Capillary and extrudate diameter, respectively
D_E	Droplet deformability in extensional flow
D_r	Rotational Brownian diffusion coefficient
$D_s(\sigma_E)$	Steady-state tensile compliance
$d_{v/s}$	Volume-to-surface average particle diameter
E	Elasticity of the interphase
E_i	Interaction energy
E	Tensile, or Young's, modulus
e	Electron
$E(t)$	Tensile relaxation modulus
$E(t, \varepsilon)$	Tensile stress relaxation modulus
E^+	Threshold energy of coagulation
E_j	Activation energy
E_{ij}	Exchange energy of i-j contact
F	Helmholtz free energy (F = E—TS)
f	Free volume fraction
$f(x)$	Function of a parameter x
f_O	Onsager coefficient
G	Gibb's free energy (G = E — TS + pV = H — TS)
G	Shear modulus (modulus of rigidity)
G	Gravitational constant, G = 6.67 3 1011 N m^2/kg^2
Gy	Gray
g	Acceleration due to gravity; g = 9.80621 m/s^2 (see level, lat. 45°)
g^*	Concentration gradient at the interface

$G'(\omega)$	Shear storage modulus
G'_y, G''_y	Yield values for G' and G''
$G(t)$	Shear relaxation modulus
$G(t, \gamma)$	Shear stress relaxation modulus
$G''(\omega)$	Shear loss modulus
$G^*(\omega)$	Complex shear modulus
H	Enthalpy
H	Henry
h	Hydrodynamic shielding parameter
$H(t)$	Relaxation spectrum
h_c	Critical separation distance for drop coalescence
$\tilde{H}_G$	Reduced Gross relaxation spectrum
h_g	Partial (or specific) molar enthalpy of component g
$H_G(s)$	Gross frequency relaxation spectrum
h_T	Vertical time-temperature shift factor
Hz	Hertz
I	Scattering intensity ratio
I_D, I_M	Intensity of emission of the excimer and monomer
J	Hear compliance
J	Joule
$J'(\omega)$	Shear storage compliance
$J(t)$	Shear creep compliance
$J(t, \sigma)$	Shear creep compliance
$J''(\omega)$	Shear loss compliance
$J^*(\omega)$	Complex shear compliance
J, J_o, J_c°	Creep compliance, its value at t = 0 and at steady state
J_e	Equilibrium shear compliance
J_s	Steady-state shear compliance
$J_s(\sigma)$	Steady-state compliance
K	Bulk modulus
K	Kelvin
k_B	Boltzmann s universal constant
k	Rate constants
k_H, k_M	Huggins, Martin constants of solution viscosity
L	Length of a dispersed particle
$L(t)$	Retardation spectrum
L, L*	Lamellar thickness
l, b	Prolate drop half length and half width
M	Mobility constant
m	Strain ratio in asymmetric extension
M, M_w, M_n	Molecular weight and its weight and number averages
M_e	Entanglement molecular weight
M_n	Number-average molecular weight
M_v	Viscosity-average molecular weight

$\mathbf{M_w}$	Weight-average molecular weight
$\mathbf{N_e}$	Number of polymer segments between entanglements
$\mathbf{N}$	Newton (force)
n_i^D	Index of refraction (for 20 °C and sodium light)
$\mathbf{n}$	"Power law" exponent between melt viscosity and the deformation rate
N_1, N_2	First and second normal stress difference, respectively
$N_1^+(t, \dot{\gamma})$	First normal stress growth function
$N_1^-(t, \dot{\gamma})$	First normal stress decay function
$N_1(t, \dot{\gamma})$	First normal stress relaxation function
$N_2(t, \dot{\gamma})$	Second normal stress relaxation function
$N_2^+(t, \dot{\gamma})$	Second normal stress growth function
$N_2^-(t, \dot{\gamma})$	Second normal stress decay function
$\mathbf{P}$	Pressure
P	Probability
$\mathbf{P(q)}$	One-particle scatter function
$\mathbf{p, p^*}$	Anisometric particle aspect ratio and its generalized value
$\mathbf{Pa}$	Pascal (pressure)
P_e	Entrance-exit pressure drop in capillary flow
$\mathbf{Q}$	Heat received by the system
$\mathbf{q}$	Wavevector
R, r	Radius, position variable radius
$\mathbf{R}$	Universal gas constant; 8.31432 J/mol deg
$\mathbf{r^2}$	Correlation coefficient squared, precision of data
$\mathbf{kr^2l}$	Mean square end-to-end distance
$R(t, \sigma)$	Ecoil function, $R(t, \sigma) = \gamma_r/\sigma$
$\mathbf{r, r_c}$	Radial position of a particle and its critical value
$\mathbf{R_c}$	Particle diameter-to-capillary diameter ratio
$\mathbf{Re}$	Reynolds number
$\mathbf{R_R}$	Rao constant
R_T	Trouton ratio; ratio of the extensional to shear viscosity
$\mathbf{R_g}$	Radius of gyration
$R_\infty(\sigma)$	Ultimate recoil function
$\mathbf{S}$	Entropy
$\mathbf{S}$	Siemens
$\mathbf{s}$	Number of statistical segments per macromolecule
$\mathbf{s}$	Second
$S(t, \sigma_E)$	Tensile recoil coefficient; $S(t, \sigma_E) = \varepsilon_r/\sigma_E$
$\mathbf{s_g}$	Specific molar entropy of g
S_i	Initial slope of the stress growth function in uniaxial extension
$\mathbf{s_i}$	Specific surface area of ith particle
$\mathbf{S_v}$	Entropy per unit volume
T	Temperature
t	Time

T_g	Glass transition temperature
T_m, T_g	Melting point; glass transition temperature
t_p	Period of rotation for anisometric particles
U	Total energy of the system
V	Volume
v	Specific volume
v_g	Partial molar (or specific) volume of g
v_i	Velocity in direction i
V_L, V_S	Ultrasonic velocity; transverse and shear
W	Heat flow (components W_i, i = x, y, z)
w	Weight fraction
w_i	Weight fraction of specimen i
x	Variable
x_1 or x	Direction of flow
x_2 or y	Direction of velocity gradient
x_3 or z	Neutral direction
x_i	Mole fraction
z	Coordination number

Greek Alphabet (Lower Case, Capital Letter)

α, ς	alpha	ν, N	nu
β, B	beta	ξ, Ξ	xi
γ, Γ	gamma	π, Π	pi
δ, Δ	delta	ρ, P	rho
ε, E	epsilon	σ, Σ	sigma
ζ, Z	zeta	τ, T	tau
η, H	eta	φ, (ω), Φ	phi
θ, (ϑ), Θ	theta	χ, X	chi
κ, K	kappa	ψ, Ψ	psi
λ, Λ	lambda	ω, Ω	omega
μ, M	mu		

Notation: Greek Letters

α_i	Thermal expansion coefficient
2α	Convergence angle
β_{12}	Slip factor in Lin's equation
Γ_{ij}	Nonrandomness parameter for ij segment placement
Γ_o	Critical parameter for droplet breakup

$\boldsymbol{\gamma}$	Shear strain
$\dot{\boldsymbol{\gamma}}_c, \dot{\boldsymbol{\gamma}}_y$	Critical value of $\dot{\gamma}$ for onset of dilatancy or yield
$\boldsymbol{\gamma}_R$	Recoverable shear strain
$\dot{\boldsymbol{\gamma}}$	Shear rate
$\boldsymbol{\gamma}_r(t, \boldsymbol{\sigma})$	Recoil strain
$\boldsymbol{\gamma}_\infty(\boldsymbol{\sigma})$	Ultimate recoil
$\boldsymbol{\Delta}$	Increment
$\boldsymbol{\Delta E_\eta}$	Activation energy of flow
$\boldsymbol{\Delta G_m}, \boldsymbol{\Delta G_{el}}$	Gibbs free energy of mixing and an elastic contribution
$\boldsymbol{\Delta H_m}$	Heat of mixing
$\boldsymbol{\Delta l}$	Thickness of the interphase
$\boldsymbol{\delta}$	Solubility parameter
$\boldsymbol{\varepsilon}$	Dielectric parameter
$\boldsymbol{\varepsilon}$	Tensile Hencky strain
$\dot{\boldsymbol{\varepsilon}}$	Strain rate (≥ 0)
$\boldsymbol{\varepsilon}_b$	Maximum Hencky strain at break
$\boldsymbol{\varepsilon}_{\max}$	Maximum filament shrinkage
$\boldsymbol{\varepsilon}_r(t, \dot{\boldsymbol{\varepsilon}})$	Tensile recoil function
$\boldsymbol{\varepsilon}_\infty(\boldsymbol{\sigma}_E)$	Ultimate tensile recoil
$\boldsymbol{\varepsilon}_B/\dot{\boldsymbol{\varepsilon}}_B$	Biaxial strain/strain rate (≥ 0)
$\boldsymbol{\zeta}$	Correlation length; domain size
$\boldsymbol{\eta}$	Viscosity
$\boldsymbol{\eta}_o$	Limiting viscosity at zero shear rate, i.e., at the upper Newtonian plateau
$\boldsymbol{\eta}_\infty$	Limiting viscosity at infinite shear rate, i.e., at the lower Newtonian plateau
$\boldsymbol{\eta}_s$	Viscosity of solvent or of continuous medium
$\boldsymbol{\eta}_r$	Relative viscosity (η/η_s)
$\boldsymbol{\eta}_{sp}$	Specific viscosity ($\eta_r - 1$)
$[\boldsymbol{\eta}]$	Intrinsic viscosity
$[\boldsymbol{\eta}]_E, [\boldsymbol{\eta}]_{E,d}$	Emulsion and deformable droplet emulsion intrinsic viscosity, respectively
$\boldsymbol{\eta}_d, \boldsymbol{\eta}_m$	Viscosity of dispersed and matrix liquid; also η_1, η_2, respectively
$\boldsymbol{\eta}_i, \boldsymbol{\eta}_{si}, \boldsymbol{\eta}_{ei}$	Interface viscosity and its shear and extensional components
$\boldsymbol{\eta}_{app}$	Apparent viscosity
$\boldsymbol{\eta}_{o,M}$	Maxwellian viscosity
$\boldsymbol{\eta}^*(\boldsymbol{\omega})$	Complex viscosity
$\boldsymbol{\eta}'(\boldsymbol{\omega})$	Dynamic viscosity
$\boldsymbol{\eta}''(\boldsymbol{\omega})$	Out-of-phase component of complex viscosity
$\boldsymbol{\eta}^+(t, \dot{\boldsymbol{\gamma}})$	Shear stress growth coefficient
$\boldsymbol{\eta}^-(t, \dot{\boldsymbol{\gamma}})$	Shear stress decay coefficient
$\boldsymbol{\eta}_E^+(t, \dot{\boldsymbol{\varepsilon}})$	Tensile stress growth coefficient
$\boldsymbol{\eta}_E^-(t, \dot{\boldsymbol{\varepsilon}})$	Tensile stress decay coefficient

$\boldsymbol{\eta_E}$	Elongational or tensile viscosity
$\boldsymbol{\eta_B}$	Biaxial extensional viscosity
$\boldsymbol{\eta_B^+(t, \dot{\varepsilon}_B)}$	Biaxial stress growth coefficient
$\boldsymbol{\eta_B^-(t, \dot{\varepsilon}_B)}$	Biaxial stress decay coefficient
$\boldsymbol{\Theta}$	Scattering angle
$\boldsymbol{\vartheta}$	Distortion wavelength in capillary instability
$\boldsymbol{\kappa}$	Ratio of rheological to interface forces; capillarity factor $\kappa = \sigma d / v$
$\boldsymbol{\Lambda}$	Wavelength
$\boldsymbol{\lambda}$	Thermal conductivity
$\boldsymbol{\lambda = \eta_d / \eta_m}$	Viscosity ratio of the dispersed to the matrix phase liquids in polymer blend flow
$\boldsymbol{\mu}$	Chemical potential
$\boldsymbol{\mu_i}$	Chemical potential of i
$\boldsymbol{\mu}$	Poisson ratio
$\boldsymbol{\nu}$	Interfacial tension coefficient
$\boldsymbol{\nu, \nu_o}$	Dynamic interfacial tension coefficient and its equilibrium value
$\boldsymbol{\nu_s, \nu_e}$	Side and interfacial energies of a polymeric crystal
$\boldsymbol{\sigma}$	Shear stress
$\boldsymbol{\sigma_{ij}}$ ij	component of the stress tensor
$\boldsymbol{\sigma_y, \sigma_{yc}, \sigma_{yE}}$	Yield shear stress, its value in compression and extension
$\boldsymbol{\sigma_c}$	Critical shear stress for droplet break-up
$\boldsymbol{\sigma_m}$	Critical shear stress for melt fracture
$\boldsymbol{\sigma^+(t, \dot{\gamma})}$	Shear stress growth function
$\boldsymbol{\sigma^-(t, \dot{\gamma})}$	Shear stress decay function
$\boldsymbol{\sigma(t, \gamma)}$	Shear stress relaxation function
$\boldsymbol{\sigma_E}$	Net tensile stress
$\boldsymbol{\sigma_B^+(t, \dot{\varepsilon})}$	Tensile stress growth function
$\boldsymbol{\sigma_B^-(t, \dot{\varepsilon})}$	Tensile stress decay function
$\boldsymbol{\sigma_E^-}$	Tensile stress decay coefficient
$\boldsymbol{\sigma_B}$	Net stretching stress
$\boldsymbol{\rho}$	Density
$\boldsymbol{\tau}$	Relaxation time
$\boldsymbol{\tau_y}$	Characteristic time of the yield cluster
$\boldsymbol{\tau_\zeta}$	Lifetime of the density fluctuation
$\boldsymbol{\Phi_\iota}$	Farris volume fraction of component i in the mixture
$\boldsymbol{\phi, \phi_m}$	Volume fraction; maximum packing volume fraction
$\boldsymbol{\phi_{mo}, \phi_{m\infty}}$	Maximum packing volume fraction at shear stress $\sigma \to 0$ and $\sigma \to \infty$
$\boldsymbol{\chi_{ij}}$	Thermodynamic interaction coefficient between species i and j
$\boldsymbol{\Psi(t)}$	Retardation function
$\boldsymbol{\Psi_1}$	First normal stress coefficient
$\boldsymbol{\Psi_2}$	Second normal stress coefficient
$\boldsymbol{\psi_1^+(t, \dot{\gamma})}$	First normal stress growth coefficient
$\boldsymbol{\psi_2^+(t, \dot{\gamma})}$	Second normal stress growth coefficient

$\psi_1^-(t, \dot{\gamma})$	First normal stress decay coefficient
$\psi_2^-(t, \dot{\gamma})$	Second normal stress decay coefficient
Ω	Distortion wavelength
Ω	Vorticity
ω	Frequency (rad/s)

Subscripts

app, a	Apparent
B	Binodal
E	Uniaxial extension
g	Glass
i	Counting subscript, inversion or dispersed phase
L	Linear viscoelastic function
m	Mixing, melt, matrix
R	Reference variable
S	Strain hardening
S	Spinodal
s	Suspension
y	Yield

Superscripts

E	Excess value
L	Lattice gas model
+	Stress growth function
−	Decay function
∼ (tilde)	Reduced variable
*	Complex or reducing variable

Mathematical Symbols

<>	Average
Π	Multiplication
π	3.1415926536
Σ	Summation

Index